

A total of 484 articles published in *World Journal of Gastroenterology* are cited by 361 ISI-SCI covered journals distributed in 38 countries during 1998-2003

Lian-Sheng Ma, Bo-Rong Pan

Lian-Sheng Ma, Bo-Rong Pan, The WJG Press, PO Box 2345, Beijing 100023, China

Supported by the National Natural Science Foundation of China, No.30224801

Correspondence to: Lian-Sheng Ma, M.D., The WJG Press, PO Box 2345, Beijing 100023, China. wjg@wjgnet.com

Telephone: +86-10-85381901 **Fax:** +86-10-85381893

Received: 2004-03-20 **Accepted:** 2004-04-11

Abstract

Articles published in the *World Journal of Gastroenterology* (WJG) have been cited by 361 SCI covered journals, 44.59% of which are journals in the USA and 3.60% in China. Authors from 484 institutions have cited WJG, in which 22.58% of them are in the USA and 18.84% in China. The highest impact factor of SCI journals that have cited WJG is 28.740 (*Nature Medicine*), with 52.95% ($n=170$) of journals with an impact factor over 2.0. The total citation times of articles published in WJG during 1998-2003 were 484. The total citation times in 2003 were 2736 with 73.24% (2004) self-citation, 1486 in 2002 with 94.27% (1401) self-citation, 537 in 2001 with 92.92% (499) self-citation, 238 in 2000 with 92.43% (220) self-citation and 24 in 1999 with 33.33% (8) self-citation. Articles published in WJG in 2002 were cited 85 times by other SCI covered journals, and 82 articles were cited. The number was increased to 372 and 332 for articles published in 2003, respectively, with increase rates of 337.64% and 304.87%, respectively. Authors who have cited WJG are from 37 countries, and the journals that have cited WJG are from 21 countries. A total of 1 020 (57.46%) articles published in WJG were supported by international or national grants. Authors of WJG articles are from 40 countries. Articles published in issues 5-12 in 2003 have been downloaded 53 476 times online. In 2002, WJG was awarded a special grant from National Natural Science Foundation of China. Generally, the percentage of the self-citation times of articles published in WJG declined from 94.27% in 2002 to 73.24% in 2003. Meanwhile, article numbers and times cited by other SCI covered journals rose to 304.87% and 337.64% respectively. The above data suggested that the WJG underwent rapid development in 2003 with a significant increase in both numbers of cited articles and times of citation.

Ma LS, Pan BR. A total of 484 articles published in *World Journal of Gastroenterology* are cited by 361 ISI-SCI covered journals distributed in 38 countries during 1998-2003. *World J Gastroenterol* 2004; 10(9): 1233-1237

<http://www.wjgnet.com/1007-9327/10/1233.asp>

INTRODUCTION

World Journal of Gastroenterology (WJG ISSN-1007-9327) is an international academic journal in digestology published in China. The WJG was established in 1995 under the name

of China National Journal of New Gastroenterology, and adapted its present title in 1998^[1]. The WJG, now published semimonthly by the WJG Press, is a 210×297 mm-sized journal with 160 pages in each issue. The Journal is distributed by the Beijing Newspaper and Periodical Subscription and Distribution Bureau (Postal Issuance Code 82-261). In response to continuing growth in both basic and clinical studies on digestive diseases and the increasing demands for the international exchange in science and technology, the WJG will be published weekly from January 2005, with 160 pages in each issue. The publication dates are on the 7th, 14th, 21th and 28th of each month. Center for Information Analysis, Institute of Scientific and Technical Information of China conducted a general assessment on the SCI citation, source of manuscripts, and grant support of the articles published in the WJG during 1998-2004(issues 1-6), based on the information from ISI SCI, ISI JCR and Citation Report of Chinese Journals of Science and Technology. The assessment report is as follows.

CITATIONS OF ARTICLES PUBLISHED IN WJG BY SCI COVERED JOURNALS

Articles published in WJG have been cited 5 021 times, of which the total citation times in 2003 were 2 736 with 73.24% (2004) self-citation, 1 486 in 2002 with 94.27% (1 401) self-citation, 537 in 2001 with 92.92% (499) self-citation, 238 in 2000 with 92.43% (220) self-citation and 24 in 1999 with 33.33% (8) self-citation. Citations have been consistently increasing. However, the increase in self-citations is significantly lower than the increase in total citations (Figure 1).

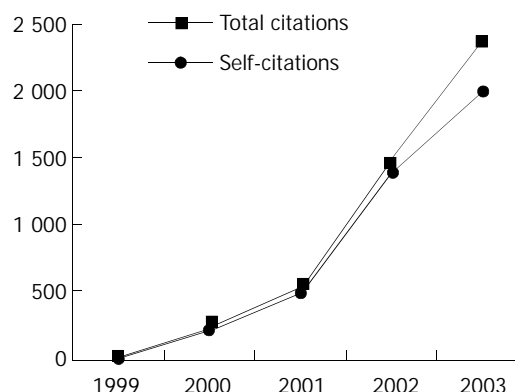


Figure 1 Increase in self-citations is significantly lower than the increase in total citations.

CHANGING TREND IN OVERALL TIMES AND NUMBERS OF ARTICLES PUBLISHED IN WJG CITED BY SCI COVERED JOURNALS

Articles published in WJG in 2002 were cited by other SCI covered journals 85 times, and 82 articles were cited. The numbers were increased to 372 and 332 for articles published in 2003, respectively, with an increase rate of 338% and 305%, respectively (Figure 2, Table 1).

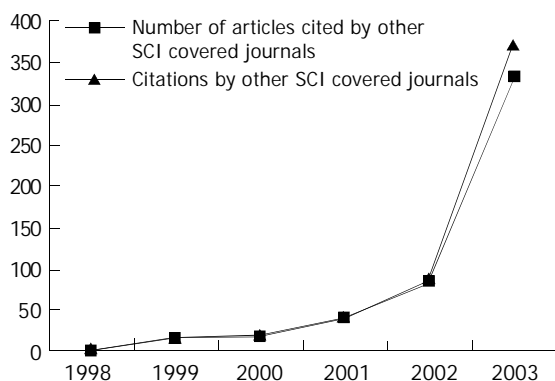


Figure 2 Changing trend in overall times and numbers of articles published in WJG between 1998 and 2003 cited by other SCI covered journals.

Table 1 Overall times and numbers of articles cited by other SCI covered journals

Year	2003	2002	2001	2000	1999	1998
Number of cited articles	332	82	38	17	16	0
Number of citations	372	85	38	18	16	0

GEOGRAPHIC DISTRIBUTION AND NUMBERS OF SCI COVERED JOURNALS THAT HAVE CITED ARTICLES PUBLISHED IN WJG

Overall, 361 SCI covered journals in 21 countries including 161 (44.59%) journals in the USA have cited articles published in WJG (Table 2).

Table 2 Geographic distribution and numbers of SCI covered journals that have cited articles published in WJG between 1998 and February 2004

List	Country	Number of journals
1	USA	161
2	UK	78
3	Netherlands	24
4	Germany	15
5	China	13
6	Switzerland	8
7	Denmark	7
8	France	7
9	Greece	6
10	Australia	5
11	Japan	5
12	Ireland	4
13	Poland	3
14	Italy	3
15	Spain	3
16	Norway	2
17	Brazil	2
18	South Korea	2
19	Singapore	1
20	India	1
21	Austria	1

Of the 361 journals, 10 journals' publishing countries are unknown.

IMPACT FACTORS OF SCI COVERED JOURNALS THAT HAVE CITED ARTICLES PUBLISHED IN WJG

Overall, 361 SCI covered journals have cited articles published in WJG between 1998 and February 2004 (Table 3). Of these journals 321 (88.92%) with an impact factor ranged from 0.160 (*Progress in Biochemistry and Biophysics*) to 28.740

(*Nutare Medicine*). The impact factor was not available for other 40 journals. The impact factors of the 321 journals are shown in Figure 3.

Table 3 Impact factors of SCI covered journals that have cited articles published in WJG

Impact factor	Number of journals (%)
20.699-28.740	4 (1.24)
10.321-18.772	12 (3.73)
6.073-9.825	20 (6.23)
5.095-5.991	14 (6.30)
4.039-4.974	19 (7.88)
3.008-3.991	46 (14.33)
2.013-2.980	55 (17.13)
1.000-1.990	78 (24.29)
0.160-0.996	73 (22.74)

GEOGRAPHIC DISTRIBUTION OF AUTHORS AND ARTICLES IN OTHER SCI COVERED JOURNALS THAT HAVE CITED ARTICLES PUBLISHED IN WJG

Overall, 484 articles by authors of SCI covered journals from 37 countries have cited articles published in WJG, of which 133 (22.58%) were from the USA and 111 (18.84%) from China (Figure 3 and Table 4).

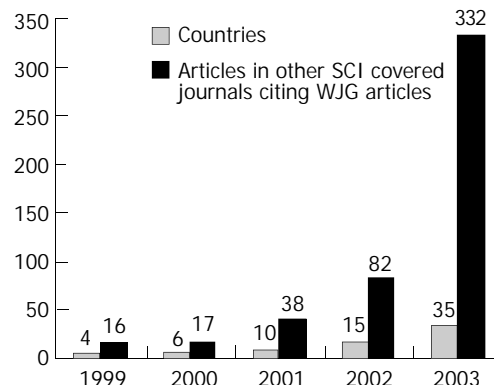


Figure 3 Geographic distribution of authors and articles in other SCI covered journals that have cited articles published in WJG.

Table 4 Geographic distribution of authors and articles in other SCI covered journals that have cited articles published in WJG

List	Country of authors	Number of articles
1	USA	133
2	China	111
3	Japan	38
4	Germany	35
5	UK	35
6	Italy	17
7	France	15
8	Australia	11
9	Spain	10
10	Sweden	8
11	Poland	7
12	South Korea	7
13	Netherlands	7
14	Canada	7
15	Belgium	5
16	Singapore	4
17	Austria	3

18	Greece	3
19	Hungary	3
20	Ireland	2
21	Brazil	2
22	Finland	2
23	Norway	2
24	Switzerland	2
25	Turkey	2
26	India	2
27	Czech Republic	1
28	Croatia	1
29	Slovakia	1
30	Argentina	1
31	Pakistan	1
32	Denmark	1
33	Cuba	1
34	Malaysia	1
35	South Africa	1
36	Thailand	1
37	New Zealand	1

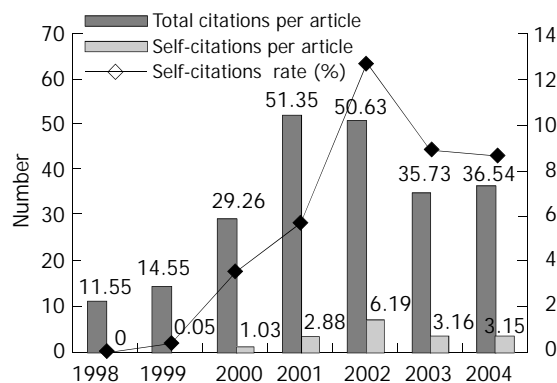


Figure 4 Citing status of articles published in WJG.

GEOGRAPHIC DISTRIBUTION AND GRANT INFORMATION OF MANUSCRIPTS ACCEPTED FOR PUBLICATION IN WJG

Of the 1775 articles published from 1998 to issue 6, 2004, 1020 (57.46%) were supported by various international and national research grants (Figures 5-7).

DISTRIBUTION OF INSTITUTIONS OF AUTHORS WHO HAVE CITED ARTICLES PUBLISHED IN WJG

The authors who have cited articles published in WJG between 1998 and 2003 are from 484 institutions, including the world famous universities and institutes such as Washington University, Yale University, Cornell University, University of Minnesota, Stanford University, University of California, National Institute of Health and University of London (Table 5).

CITING STATUS OF ARTICLES PUBLISHED IN WJG

Self-citations have been decreased from 6.19 per article published in WJG in 2002 to 3.16 in 2003 and 3.15 in February 2004. The rate decreased from 12.68% in 2001 to 8.84% and 8.61%, respectively, in 2003 and 2004 (Figure 4 and Table 6).

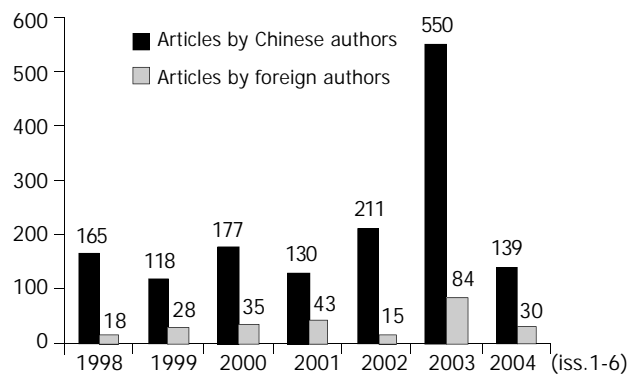


Figure 5 Geographic distribution of authors of manuscripts accepted for publication in WJG.

Table 5 Distribution of institutions of authors who have cited articles published in WJG

List	Country	Higher educational institutions	Research institutions	Medical institutions	Companies	Number of articles
1	USA	91	13	18	11	133
2	China	89	13	6	3	111
3	Japan	30	4	2	2	38
4	Germany	27	4	3	1	35
5	UK	24	2	3	4	33
6	Italy	13	3	0	1	17
7	France	5	5	5	0	15
8	Australia	7	1	3	0	11
9	Spain	7	1	2	0	10
10	Canada	2	2	1	2	7

Table 6 Citing status of articles published in WJG

Year	Volume	Issue	Articles	Total citations	Average citations per article	Self citations	Average self citation per article	Self citation rate (%)
1998	4	1-6	183	2 115	11.55	0	0	0
1999	5	1-6	146	2 125	14.55	8	0.05	0.37
2000	6	1-6	212	6 205	29.26	220	1.03	3.54
2001	7	1-6	173	8 884	51.35	499	2.88	5.61
2002	8	1-6	226	11 444	50.63	1 401	6.19	12.68
2003	9	1-12	634	22 657	35.73	2 004	3.16	8.84
2004	10	1-6	201	7 309	36.54	630	3.15	8.61

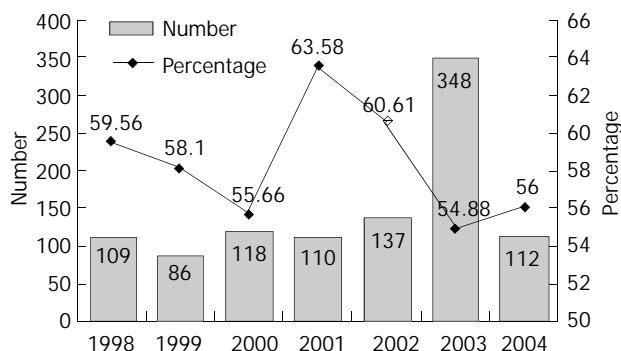


Figure 6 Numbers and percentage of articles with research grants published in WJG.

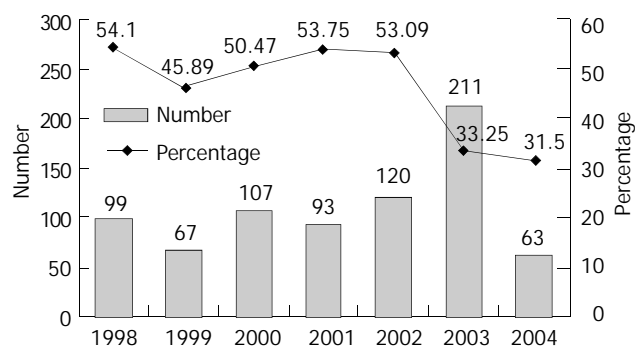


Figure 7 Number and percentage of the National Natural Science Foundation of China articles supported by published in WJG.

Table 7 Online visiting and downloading of articles published in WJG

Total articles	Articles visited	Articles downloaded	Total visits	Total downloads	Average visits per article	Average downloads per article
603	582	582	127 760	64 145	219.51	110.21

Table 8 Geographic distribution and numbers of authors of articles published in WJG

List	Country	Number
1	China	8 232
2	Japan	198
3	USA	190
4	Germany	125
5	Turkey	116
6	Italy	106
7	UK	69
8	Singapore	50
9	South Korea	39
10	Hungary	35
11	Australia	32
12	Poland	29
13	Belgium	23
14	India	21
15	South africa	20
16	Netherlands	17
17	Brazil	16
18	Greece	16
19	Sweden	15
20	Finland	14
21	Thailand	14
22	Canada	13
23	Iran	13
24	Pakistan	11
25	Yugoslavia	11
26	Spain	11
27	Israel	11
28	Argentina	9
29	Russia	9
30	Croatia	8
31	Ireland	6
32	Saudi Arabia	5
33	France	4
34	Norway	4
35	Switzerland	3
36	New Zealand	2
37	Egypt	1
38	Estonia	1
39	Denmark	1
40	Dominica	1

ONLINE VISITING AND DOWNLOADING OF ARTICLES PUBLISHED IN WJG

A total of 436 articles published in issues 5-12, 2003 have been downloaded online with a total downloading number of 53 476 times. One article has been downloaded 2 255 times^[2] (Table 7).

GEOGRAPHIC DISTRIBUTION OF AUTHORS OF ARTICLES PUBLISHED IN WJG

Authors of WJG are from 40 countries (Table 8).

HONORS AWARDED TO WJG

The WJG is nationally recognized as a core journal in national natural science and an outstanding journal in science and technology, with an honor of the 2nd National Journal Award, and was listed as one of the 100 most important journals in China. In 2001, it was selected into the China Journal Square consisting of "200" journals. It was awarded a specific project grant as one of the key academic journals by the National Natural Science Foundation of China in 2002 (Project Grant No. 30224801).

OVERALL ASSESSMENT COMMENTS

- Total citation times of articles published in WJG in January and February 2004 by SCI covered journals were 560, in which self-citation rate was 77.67% (435). The total citation times in 2003 were 2736 with 73.24% (2004) self-citation, 1486 in 2002 with 94.27% (1401) self-citation, 537 in 2001 with 92.92% (499) self-citation, 238 in 2000 with 92.43% (220) self-citation and 42 in 1999 with 33.33% (8) self-citation. No data were available in 1998.
- Article number and times cited by other SCI covered journals were 82 and 85 in 2002, 332 and 372 in 2003, and 104 and 125 in January and February 2004, respectively.
- Overall, 361 SCI covered journals in 21 countries including 161 (44.59%) journals in the USA have cited articles published in WJG.
- Journals that have cited WJG include 11 SCI covered journals with a high impact factor; i.e. *Nature Medicine* (IF 28.740), *Cell* (IF 27.254), *Nature Reviews Neuroscience* (IF 24.047), *Nature Cell Biology* (IF 20.699), *Gene and Development* (IF 18.772), *Lancet* (IF 15.397), *Nature Neuroscience* (IF 14.857), *Neuron* (IF 13.846), *Nature Reviews*

Cancer (IF 13.625), *Gastroenterology* (IF 13.440) and *Hepatology* (IF 9.825). The impact factors of the journals that have cited WJG are as follows: 20.699-28.740 (4, 1.24%), 10.321-18.772 (12, 3.73%), 6.073-9.825 (20, 6.23%), 5.095-5.991 (14, 6.30%), 4.039-4.974 (19, 7.88%), 3.008-3.991 (46, 14.33%), 2.013-2.980 (55, 17.13%), 1.000-1.990 (78, 24.29%) and 0.160-0.996 (73, 22.74%).

- Overall, 484 articles by authors of SCI covered journals from 37 countries have cited articles published in WJG; 133 (22.58%) from the USA and 111 (18.84%) from China.
- The authors who have cited WJG are from 484 research institutions, including the world famous universities and institutes, such as Washington University School of Medicine, Yale University, Cornell University, University of Minnesota, Stanford University Center of Medicine, University of California at San Francisco, National Institute of Health and Imperial College, University of London.
- Self-citations have decreased from 6.19 per article published in WJG in 2002 to 3.16 in 2003 and 3.15 in February 2004.
- Of the 1 775 articles published from 1998 to issue 6, 2004, 1 020 (57.46%) were supported by various international

and national research grants.

- Authors of WJG are from 40 countries.
- A total of 436 articles published in issues 5-12, 2003 have been downloaded online with a total downloading number of 53 476 times. One article has been downloaded 2 255 times^[2].
- In 2002, WJG was awarded a special grant (No. 30224801) from National Natural Science Foundation of China.

In conclusion, WJG has been established its position as a regional and international English journal in gastroenterology, with increasing international influence. Despite high self citations over the past years, it appears that both self citations and self citation rate are rapidly decreasing.

REFERENCES

- 1 **Ma LS**, Pan BR, Ma JY, Xu JY, Wu XN, Wang XL, Lu HM, Xia HHX, Liu HX, Zhang JZ, Su Q, Ren SY, Zhu L, Zhu LH, Lu YY. Towards a higher international standard - *World Journal of Gastroenterology* will be published semimonthly in 2004. *World J Gastroenterol* 2004; **10**: 1-4
- 2 **Wang QC**, Nie QH, Feng ZH. RNA interference: Antiviral weapon and beyond. *World J Gastroenterol* 2003; **9**: 1657-1661

Edited by Xia HHX, Wang XL and Zhang JZ **Proofread by** Xu FM

Wireless capsule video endoscopy: Three years of experience

Rami Eliakim

Rami Eliakim, Department of Gastroenterology, Rambam Medical Center, Technion School of Medicine, Haifa, Israel

Correspondence to: Rami Eliakim, M.D., Department of Gastroenterology, Rambam Medical Center, Bat Galim, Haifa, PO Box 9602, Israel 31096. r_eliakim@rambam.health.gov.il

Telephone: +972-4-8542504 **Fax:** +972-4-8543058

Received: 2004-03-06 **Accepted:** 2004-04-01

Abstract

AIM: To review and summarize the current literature regarding M2A wireless capsule endoscopy.

METHODS: Peer reviewed publications regarding the use of capsule endoscopy as well as our personal experience were reviewed.

RESULTS: Review of the literature clearly showed that capsule endoscopy was superior to enteroscopy, small bowel follow through and computerized tomography in patients with obscure gastrointestinal bleeding, iron deficiency anemia, or suspected Crohn's disease. It was very sensitive for the diagnosis of small bowel tumors and for surveillance of small bowel pathology in patients with Gardner syndrome or familial adenomatous polyposis syndrome. Its role in celiac disease and in patients with known Crohn's disease was currently being investigated.

CONCLUSION: Capsule video endoscopy is a superior and more sensitive diagnostic tool than barium follow through, enteroscopy and entero-CT in establishing the diagnosis of many small bowel pathologies.

Eliakim R. Wireless capsule video endoscopy: Three years of experience. *World J Gastroenterol* 2004; 10(9): 1238-1239
<http://www.wjgnet.com/1007-9327/10/1238.asp>

INTRODUCTION

The M2A video capsule endoscope (CE) (Given Imaging LTD; Yokneam, Israel) is a wireless capsule (11 mm×27 mm) comprised of a light source, lens, CMOS imager, battery and a wireless transmitter. The slippery outside coating of the capsule allows easy ingestion and prevents adhesion of intestinal contents, while the capsule moves via peristalsis from mouth to anus. The battery provides 7-8 h of work in which the capsule photographs 2 images per second (between 50 000-60 000 images all together), which are transmitted to a recorder which is worn on the belt. The recorder is downloaded into a computer and seen as a continuous video film. Since its development additional support systems have been added- a localization system, a blood detector and a double picture viewer. All meant to assist the interpreter of the film and to shorten the reviewing period.

INDICATIONS

The full range of indications for CE became apparent with time. The initial device was invented to address a need for a better diagnostic tool for small bowel pathologies.

Obscure gastrointestinal bleeding

The most obvious and the first indication to be tested was obscure gastrointestinal bleeding (OGIB), which occurred in 5-10% of patients with any type of gastrointestinal (GI) bleeding. Several peer reviewed articles and many abstracts have compared the diagnostic yield of CE to push enteroscopy and other modalities in patients with OGIB^[1-4]. The added diagnostic yield of enteroscopy was in the range of 25-30%, while that of CE was significantly better (50-67%). This led Cave to propose an algorithm in which the first method to evaluate the small bowel in a patient with gastrointestinal bleeding with negative gastroscopy and colonoscopy would be CE, and then according to its results, the evaluation was continued with either push enteroscopy, angiography or intra-operative enteroscopy^[5]. Cave suggested that the closer the study was performed to the time of actual bleeding, the greater the diagnostic yield of CE.

Crohn's disease

The 2nd obvious indication was in patients with suspected Crohn's disease. Three peer reviewed studies published in journal and some more in abstract form demonstrated the superiority of CE compared to small bowel follow through and entero CT in these patients^[6-8]. The diagnostic yield of CE in these patients ranged between 43-71%, significantly better than small bowel follow through or entero CT (<30%). Moreover CE diagnosed Crohn's disease in 6-9% of patients that had OGIB^[9]. In patients with undetermined colitis the use of CE changed the diagnosis into Crohn's disease in 50% of patients (5/10)^[9].

Costamagna *et al.* compared CE and small bowel radiographs in patients with any suspected small bowel disease, another indication for CE^[10]. CE was diagnostic in 45% patients, and suspicious in another 40% patients, while X-ray was diagnostic in only 20% patients.

Other indications for CE

Diagnosis of celiac disease, extent of Crohn's disease, GI tumors, NSAID induced small bowel damage and surveillance of polyposis syndromes were currently investigated.

We have recently looked at CE in real life. We looked at the charts of the first 160 patients referred for CE by various doctors to 4 centers in Israel. We found that CE was of value in patients with OGIB (65%), Crohn's disease (55%) and chronic diarrhea (100%), but not in patients with chronic abdominal pain.

Future probable indications

These indications may include monitoring of small bowel damage due to drugs and chemicals (NSAID, *etc.*), monitoring of mucosal healing after various treatments (Crohn's for example), assessing the extent of diseases (Crohn's, celiac) and monitoring/surveillance of upper or lower GI damage (esophagitis, Barrett's, polyps).

CONTRAINDICATIONS

The only definite contraindication for CE was a patient with a history of intestinal obstruction or known stricture, or a patient who was a non surgical candidate.

Severe motility problems, or swallowing abnormalities could also preclude the use of CE. Initially patients with pacemakers were excluded from CE trials, but recent data mostly in abstract form, revealed that CE could be safely performed in patients with pacemakers.

COMPLICATIONS

The major complication with CE was capsule retention or non natural excretion (NNE) which was usually proximal to a stricture. This happened many times despite normal small bowel X-rays. History of NSAID usage, ischemic bowel event or known Crohn's disease, carried higher risk for NNE. NNE that necessitated surgery occurred in less than 1% of all patients and in 1.25% of patients with Crohn's disease^[9]. Usually, there were no clinical signs or symptoms and NNE was found when doing a plain abdominal film. Retrieval of the capsule and resection of narrowed segment via surgery, usually resolved the medical problem which was detected by the retained capsule.

CONCLUSIONS

M2A CE is a safe, valuable, non-invasive, innovative tool for the diagnosis and management of small bowel lesions like OGIB, Crohn's disease, chronic diarrhea and probably other small bowel diseases.

Newer versions of CE software allow us to get better localization and blood detection. Advanced versions will allow us to get therapeutic modalities and a shorter reading time.

REFERENCES

- 1 **Lewis BS**, Swain P. Capsule endoscopy in the evaluation of patients with suspected small intestinal bleeding: Results of a pilot study. *Gastrointest Endosc* 2002; **56**: 349-354
- 2 **Scapa E**, Jacob HJ, Lewkowicz S, Migdal M, Gat D, Glukhovskiy A, Guttman N, Fireman Z. Initial experience of wireless capsule endoscopy for evaluating occult gastrointestinal bleeding and suspected small bowel pathology. *Amer J Gastroenterol* 2002; **97**:2776-2779
- 3 **Eli C**, Remke S, May A, Helou L, Henrich R, Mayer G. The first prospective controlled trial comparing wireless capsule endoscopy with push enteroscopy in chronic gastrointestinal bleeding. *Endoscopy* 2002; **34**: 685-689
- 4 **Saurin JC**, Delvaux M, Gaudin JL, Fassler I, Villarejo J, Vahedi K, Bitoun A, Canard JM, Souquet JC, Ponchon T, Florent C, Gay G. Diagnostic value of endoscopic capsule in patients with obscure digestive bleeding: Blinded comparison with video push-enteroscopy. *Endoscopy* 2003; **35**: 576-584
- 5 **Cave DR**. Wireless video capsule endoscopy. *Clin Perspectives Gastroenterol* 2002; **5**: 203-207
- 6 **Eliakim R**, Fischer D, Suijsa A, Yassin K, Katz D, Migdal M, Guttman N. Wireless capsule video endoscopy is a superior diagnostic tool compared to barium follow through and CT in patients with suspected Crohn's disease. *Europ J Gastroenterol Hepatol* 2003; **15**: 363-367
- 7 **Fireman Z**, Mahajna E, Broude E, Shapiro M, Fich L, Sternberg A, Kopelman Y, Scapa E. Diagnosing small bowel Crohn's disease with wireless capsule endoscopy. *Gut* 2003; **52**: 390-392
- 8 **Herrerias JM**, Caunedo A, Rodriguez-Tellez M, Pellicer F, Herrerias JM Jr. Capsule endoscopy in patients with suspected Crohn's disease in negative endoscopy. *Endoscopy* 2003; **35**: 1-5
- 9 **Eliakim R**, Adler SN. Capsule endoscopy in Crohn's disease – the European experience. *Gastrointest Endoscopy Clin N Amer* 2004; **14**: 129-137
- 10 **Costamagna G**, Shah SK, Riccioni ME, Foschia F, Mutignani M, Perri V. A prospective trial comparing small bowel radiographs and video capsule endoscopy for suspected small bowel disease. *Gastroenterology* 2002; **123**: 999-1005

Edited by Xu XQ and Wang XL **Proofread by** Xu FM

GSTT1, *GSTM1* and *CYP2E1* genetic polymorphisms in gastric cancer and chronic gastritis in a Brazilian population

Jucimara Colombo, Andréa Regina Baptista Rossit, Alaor Caetano, Aldenis Albanese Borim, Durval Wornrath, Ana Elizabete Silva

Jucimara Colombo, Ana Elizabete Silva, Departamento de Biologia, UNESP-Campus de São José do Rio Preto-SP, Brazil

Andréa Regina Baptista Rossit, Departamento de Doenças Dermatológicas, Infeciosas e Parasitárias, Faculdade de Medicina, FAMERP, São José do Rio Preto, SP, Brazil

Alaor Caetano, Aldenis Albanese Borim, Hospital de Base, Faculdade de Medicina, FAMERP, São José do Rio Preto, SP, Brazil
Durval Wornrath, Fundação Pio XII, Barretos, Brazil

Supported by the Brazilian Agency CAPES

Correspondence to: Ana Elizabete Silva, Departamento de Biologia, UNESP - Campus de São José do Rio Preto, Rua Cristovão Colombo, 2265, 15054-000 - São José do Rio Preto, SP-Brazil. anabete@bio.ibilce.unesp.br

Telephone: +55-17-2212384 **Fax:** +55-17-2212390

Received: 2003-09-23 **Accepted:** 2003-12-30

Abstract

AIM: To test the hypothesis that, in the Southeastern Brazilian population, the *GSTT1*, *GSTM1* and *CYP2E1* polymorphisms and putative risk factors are associated with an increased risk for gastric cancer.

METHODS: We conducted a study on 100 cases of gastric cancer (GC), 100 cases of chronic gastritis (CG), and 150 controls (C). Deletion of the *GSTT1* and *GSTM1* genes was assessed by multiplex PCR. *CYP2E1/PstI* genotyping was performed using a PCR-RFLP assay.

RESULTS: No relationship between *GSTT1/GSTM1* deletion and the *c1/c2* genotype of *CYP2E1* was observed among the three groups. However, a significant difference between CG and C was observed, due to a greater number of *GSTT1/GSTM1* positive genotypes in the CG group. The *GSTT1* null genotype occurred more frequently in Negroid subjects, and the *GSTM1* null genotype in Caucasians, while the *GSTM1* positive genotype was observed mainly in individuals with chronic gastritis infected with *H pylori*.

CONCLUSION: Our findings indicate that there is no obvious relationship between the *GSTT1*, *GSTM1* and *CYP2E1* polymorphisms and gastric cancer.

Colombo J, Rossit ARB, Caetano A, Borim AA, Wornrath D, Silva AE. *GSTT1*, *GSTM1* and *CYP2E1* genetic polymorphisms in gastric cancer and chronic gastritis in a Brazilian population. *World J Gastroenterol* 2004; 10(9): 1240-1245

<http://www.wjgnet.com/1007-9327/10/1240.asp>

INTRODUCTION

In Brazil, gastric cancer occupies the fifth position, with an estimates of 20 640 new cases and 11 145 deaths in 2003, as a consequence of late diagnosis, and also of its high recurrence rate^[1]. Gastric carcinogenesis is a multi-step process, involving both genetic and environmental factors^[2]. Among the latter,

the most outstanding are dietary factors^[3], smoking^[4], drinking^[5], *Helicobacter pylori* infection^[6], and the occurrence of previous gastric injuries^[7]. Correa^[8] and Stemmermann^[9] suggested, in separate studies, a general hypothesis of pre-cancerous sequences for gastric carcinogenesis, especially for the intestinal types, namely superficial gastritis, chronic atrophic gastritis, intestinal metaplasia, dysplasia, and cancer.

Over the last decades, several studies have revealed the participation of polymorphisms in metabolic and DNA repair enzymes, that might confer different degrees of susceptibility to cancer. Among these metabolic enzyme polymorphisms, the most outstanding are those of cytochrome P-450 (CYPs), glutathione-S-transferases (GSTs), and N-acetyltransferases (NATs)^[10-12].

Concerning the superfamily of metabolic enzymes, both *CYP2E1* gene, a member of the cytochrome P-450 superfamily, and the *GSTT1* and *GSTM1* genes, that catalyze the conjugation reaction of glutathione with electrophilic compounds, exhibit polymorphisms which have been considered as potentially important modifiers of the individual risk for environmentally induced cancers, including cancer of stomach^[13-17]. Subjects with null *GSTT1* and *GSTM1* have a decreased capability of detoxifying some carcinogens, among wich N-nitrous compounds are involved in stomach carcinogenesis^[14].

Previous studies have shown inconclusive or controversial findings on associations between polymorphism of these genes and cancer susceptibility, due to the different types of cancer investigated and the diverse ethnic origin of the populations studied. Increased risk for oral^[18], nasopharyngeal^[19], and pulmonary^[20] cancer was observed in carriers of the rare allele *CYP2E1*, while an increased risk for esophageal cancer was observed in carriers of the common allele^[21]. On the other hand, *GSTT1* and *GSTM1* null genotypes have been linked to an increased risk for cancer of the lung, bladder and colon, and other specific sites^[11,17].

The relationship between *GSTT1*, *GSTM1* and *CYP2E1* gene polymorphisms and the risk for gastric cancer is not obvious. Many investigations were conducted on Asian populations^[22-36]. The Brazilian population is characterized by heterogeneous ethnic groups, emphasizing the need to investigate the frequency of these metabolizing genes and their association with gastric cancer.

We performed a case-control study to evaluate the association between the *GSTT1*, *GSTM1* and *CYP2E1* polymorphisms in patients from the Brazilian Southeast with gastric cancer or chronic gastritis, a lesion that increases the risk for gastric cancer by 10%^[37]. We also explored the potential interactions between the *GSTT1*, *GSTM1* and *CYP2E1* polymorphisms and demographic risk factors.

MATERIALS AND METHODS

Subjects

We conducted a simultaneous case-control study for gastric cancer and chronic gastritis. The case groups comprised 100 patients with histopathologically confirmed diagnosis of gastric

adenocarcinoma (73 men and 27 women) with a mean age of 60 years (ranging from 28 to 93 years), and 100 patients with histopathologically confirmed diagnosis of chronic gastritis (54 men and 46 women) with a mean age of 53 years (ranging from 19 to 86 years), respectively. These subjects were recruited from the "Hospital de Base", São José do Rio Preto, SP, and from the Pio XII Foundation, Barretos, SP, Brazil. The pathological diagnoses of gastric cancer and chronic gastritis were made according to criteria proposed by Lauren^[38] and the Sidney classification^[39], respectively. *H. pylori* infection was histologically established by Giemsa staining. The control group consisted of 150 healthy volunteers (90 men and 60 women), with a mean age of 54 years (ranging from 20 to 93 years), with no previous history of gastric disease, matched to the patients with respect to age, gender and ethnicity. Most controls were blood donors. Epidemiological data on the study population were collected through a standard interviewer-administered questionnaire, which included questions about current and past occupation, ethnicity, life-long smoking habits and alcohol consumption, and family history of cancer.

The human subject protocol was approved by the Research Ethics Committee of the IBILCE-UNESP, and written informed consent was obtained from all subjects.

Blood sampling and DNA extraction

Whole blood was collected and put into EDTA-coated tubes. Lymphocytes were isolated, transferred to tubes, and assigned a unique identifier code. DNA was then extracted using a non-organic extraction procedure, and stored at -20 °C until use for genotyping^[40].

Genotype analysis

The *GSTT1* and *GSTM1* genes were determined simultaneously in a single assay, using a PCR multiplex protocol, where part of exon 7 of the constitutional gene *CYP1A1* was co-amplified as an internal control.

PCR was performed in 25 µL reaction buffer containing 0.5 mmol/L of dNTPs, 2.0 mmol/L of MgCl₂, 12.5 pmol of each primer, about 150 ng DNA, and 1.25 U of thermostable Taq DNA polymerase, using a programmable thermocycler. The primers used for *GSTM1* were 5'- GAACTCCCTGAAAAGCTA AGC and 5'- GTTGGGGCTCAAATATACGGTGG. The primers used for *GSTT1* were 5'-TTCCTTACTGGTCCCTCACATCTC and 5' TCACCGGATCAGGCCAGCA. The primers used for *CYP1A1* were 5' GAACTGCCACTTCAGCTGTCT and 5' CAGCTGCATT TGGAAAGTGCTC.

PCR conditions were 94 °C for 5 min, followed by 40 denaturation cycles of 2 min at 94 °C, 1 min annealing at 59 °C, and 1 min extension at 72 °C. The PCR products were then analyzed by electrophoresis on ethidium bromide-stained 20 g/L agarose gel.

The presence or absence of *GSTT1* and *GSTM1* genes was detected by the presence or absence of a band at 480 bp and at 215 bp, respectively. A band at 312 bp (*CYP1A1*) was documented successful amplification^[41].

This technique could not distinguish between heterozygote and homozygote positive genotypes, but it could conclusively identify the null genotypes.

PCR-RFLP was performed to investigate the *CYP2E1**c2 allele. PCR was used to amplify the transcription regulation region of *CYP2E1* that includes the *PstI* enzyme recognition site. PCR was performed in 25 µL reaction buffer containing 0.28 mmol/L of dNTPs, 1.5 mmol/L of MgCl₂, 10 pmol of each primer, about 200 ng DNA, and 1.5 units of thermostable Taq DNA polymerase, using a programmable thermocycler. The *CYP2E1* primers were 5' CCAGTCGACTCTACATTGTCA and 5' TTCATTCTGTCTTCTAACTGG. After 5 min of pretreatment

at 94 °C, 35 denaturation cycles of 1 min at 94 °C, 30 s annealing at 60 °C, and 1 min extension at 72 °C were performed. After amplification, the PCR products were subjected to restriction digestion by enzyme *PstI* for 16 h at 37 °C. The PCR-RFLP fragments were then analyzed by electrophoresis on ethidium bromide-stained 20 g/L agarose gel^[42].

All the experiments included positive and negative controls for each studied polymorphism.

Statistical analysis

Statistical analyses were performed using Statdisk, Statistica, Minitab Release 10.1 computer software programs. The probability level (*P*) of 0.05 was used as significance criterion. Student's *t*-test and ANOVA *F*-test tests were used to compare continuous variables between the groups. Chi-square test or Fisher's exact test was utilized as appropriate to compare the groups with regard to genotype frequencies and putative risk factors such as gender, ethnicity, smoking, drinking, *H. pylori* infection, occupational pesticide exposure, and histological type of adenocarcinoma. In order to investigate gene-environment interactions, we also calculated the odds ratios (OR) and their 95% confidence intervals (95% CI), according to combinations of the *GSTT1*, *GSTM1* and *CYP2E1* polymorphisms with putative risk factors.

RESULTS

Figure 1 (PCR) and Figure 2 (PCR-PFLP) show the genotype analysis results. Table 1 shows the frequency distributions of the *GSTT1* and *GSTM1* genotypes among the groups. With respect to the genotype frequencies, considering the combinations between the *GSTT1/GSTM1* genes, no statistically significant differences were observed between the gastric cancer and chronic gastritis patients (*P*=0.189), nor between gastric cancer patients and controls (*P*=0.448). However, a significant difference (*P*=0.048) was observed between chronic gastritis patients and controls, due to a higher frequency of combination *GSTT1/GSTM1* positive genotypes in the chronic gastritis patients.

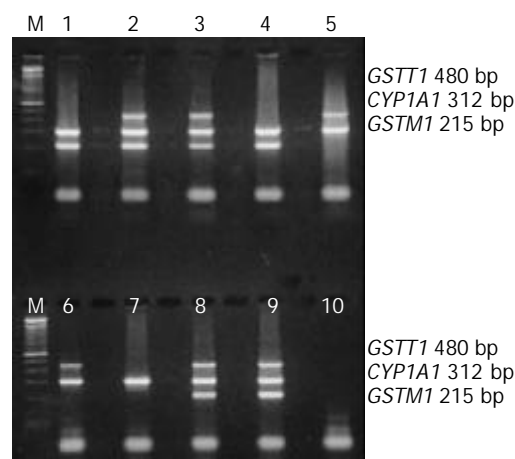


Figure 1 Polymerase chain reaction of the *GSTT1* and *GSTM1* genes. Lanes M: molecular weight maker; Lanes 1 and 4: patients homozygously null for *GSTT1*; Lanes 2, 3, 8 and 9: patients with positive *GSTT1* and *GSTM1* genotypes; Lanes 5 and 6: patients homozygously null for *GSTM1*; Lane 7: patient homozygously null for *GSTT1* and *GSTM1*; Lane 10 negative control.

The associations of the different genotypes with demographic risk factors (gender, ethnicity, smoking, drinking, pesticide-exposure, *H. pylori* infection and histological type of gastric cancer) in each group evidenced that the *GSTT1* null genotype occurred more frequently in Negroid controls (*P*=0.003), and

Table 1 *GSTT1* and *GSTM1* genotype frequencies among gastric cancer (GC) and chronic gastritis (CG) patients and controls (C)

Groups	n	<i>GSTT1</i> Null (%)	<i>GSTM1</i> Null (%)	<i>GSTT1/GSTM1</i>			
				+/+ (%)	+ / 0 (%)	0 / + (%)	0 / 0 (%)
GC	100	17 (17.0)	47 (47.0)	43 (43.0)	40 (40.0)	10 (10.0)	7 (7.0)
CG	100	12 (12.0)	38 (38.0)	57 (57.0)	31 (31.0)	5 (5.0)	7 (7.0)
C	150	28 (18.6)	62 (41.3)	64 (42.7)	58 (38.7)	24 (16.0)	4 (2.6)

+ / +=presence of *GSTT1* and *GSTM1*, + / 0=presence of *GSTT1* and absence of *GSTM1*, 0 / +=absence of *GSTT1* and presence of *GSTM1*, 0 / 0=absence of *GSTT1* and *GSTM1*.

Table 2 Associations of *GSTT1* and *GSTM1* genotypes with demographic risk factors in gastric cancer (GC) and chronic gastritis (CG) cases and controls (C)

Groups	Categories	Genotype			
		<i>GSTM1</i> positive (%)	<i>GSTM1</i> null (%)	<i>GSTT1</i> positive (%)	<i>GSTT1</i> null (%)
C	Ethnicity				
	Caucasian	75 (55.6)	60 (44.4)	114 (84.4)	21 (15.6)
	Negroid	13 (86.7)	2 (13.3)	8 (53.3)	7 (46.7)
		<i>P</i> =0.020		<i>P</i> =0.003	
GC	Ethnicity				
	Caucasian	42 (46.3)	45 (51.7)	73 (83.9)	14 (16.1)
	Negroid	11 (84.6)	2 (15.4)	10 (76.9)	3 (23.1)
		<i>P</i> =0.017		<i>P</i> =0.690	
CG	<i>H. pylori</i> Infection				
	No	43 (71.7%)	17 (28.3%)	54 (90.0%)	6 (10.0%)
	Yes	19 (48.7%)	20 (51.3%)	34 (87.2%)	5 (12.8%)
		<i>P</i> =0.032		<i>P</i> =0.748	

the *GSTM1* null genotype in Caucasian controls (*P*=0.020) and gastric cancer patients (*P*=0.017). The *GSTM1* positive genotype was observed mainly in chronic gastritis cases with *H. pylori* infection (*P*=0.032) (Table 2).

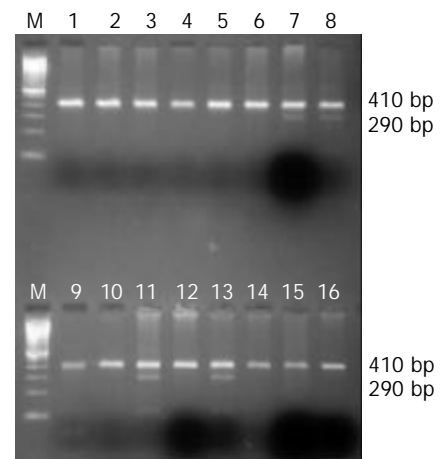
The frequencies of the *GSTT1* and *GSTM1* polymorphisms were compared among the groups by χ^2 tests and estimated OR (data not shown), according to the pattern of the gastric cancer risk factors represented by gender, ethnicity, smoking, drinking, pesticide-exposure, and *H. pylori* infection. Thus, comparing the GC and CG groups, multivariate analysis revealed that smoking was not associated with increased OR's for stomach cancer in the *GSTM1* positive subjects (1.54, 95% CI=0.71-3.33), whereas it was associated with elevated OR's in the *GSTM1* null subjects (2.7, 95% CI=1.04-7.14).

Table 3 shows the frequency distributions of *CYP2E1* genotypes among the groups. The frequencies of *CYP2E1* (*c1/c2*) variant genotypes in the gastric cancer, chronic gastritis and control groups were 11.0%, 9.0% and 10.7%, respectively. The rare homozygous genotype (*c2/c2*) was not found. The results showed no statistical difference (*P*=0.878) between the groups, nor was there any relationship with the investigated etiological factors, according to the χ^2 test and estimated OR's (data not shown).

Table 3 *CYP2E1* genotype frequencies among gastric cancer (GC) and chronic gastritis (CG) patients and controls (C)

Groups	Genotype	
	<i>c1/c1</i> (%)	<i>c1/c2</i> (%)
GC	89 (89.0)	11 (11.0)
CG	91 (91.0)	9 (9.0)
C	134 (89.3)	16 (10.7)

c1/c1=homozygote for the common allele, *c1/c2*=heterozygote.

**Figure 2** PCR-RFLP of *CYP2E1*/PstI. Lanes M: molecular weight maker; Lanes 1, 2, 3, 4, 5, 6, 10, 12, 14, 15 and 16 patients homozygote for the common allele of *CYP2E1*/PstI; Lanes 7, 8, 9, 11 and 13 heterozygote for the rare allele of *CYP2E1*/PstI.

DISCUSSION

Interindividual differences in the cellular mechanisms of activation and detoxification of carcinogenic chemicals could confer different degrees of susceptibility to cancer^[43]. However, the results have not always been consistent, due to a number of possible reasons for anomalous findings, such as interaction between environmental and genetic factors, which is a complicating factor that needs to be taken into account^[32].

GSTT1, *GSTM1* and *CYP2E1* genetic polymorphisms have shown pronounced interethnic variations^[10]. Brazil is a large country with a very heterogeneous population, resulting from the cross-mating of the native population with immigrants from

Europe, Africa and Asia. Therefore, descriptive studies of the frequencies of genetic polymorphisms in the Brazilian population could be useful in verifying genetic variability in relation to xenobiotic metabolism, since this variability may influence cancer susceptibility. This is the first study that simultaneously evaluated the *GSTT1*, *GSTM1* and *CYP2E1* polymorphisms in Brazilian patients with gastric cancer and chronic gastritis.

The *GSTM1* genotype was absent in 35-65% of individuals^[44], while *GSTT1* was deleted in 10-65% of the human population^[17]. The prevalence of the *CYP2E1* *c2* allele was shown to be 2-8% in both Caucasians and African Americans^[13], but higher in Asian populations, ranging from 17 to 26%^[45].

The frequencies of *GSTT1* (18.6%) and *GSTM1* (41.3%) null genotypes and the *CYP2E1/PstI* (10.7%) polymorphism observed in the control group were not different from other studies in Brazilian populations^[46-49]. We showed that the frequency of the *GSTT1* null genotype was higher in Negroid subjects, and that the *GSTM1* null genotype was higher in Caucasians. Other studies described similar results in Brazilian^[46,50] and also in American populations^[51].

Although studies of the *GSTT1* and *GSTM1* polymorphisms were performed previously, their association with gastric cancer susceptibility has not been established. Most of them showed no association between the *GSTT1* null genotype and risk for gastric cancer^[25,32,36,52,53]. However, two others suggested that the *GSTT1* null genotype might confer an increased risk for gastric cancer^[39,54].

The correlation between the *GSTM1* null genotype and gastric cancer appeared to be more consistent^[22,25,27,28,30,55]. On the other hand, other authors failed to demonstrate any statistically significant difference in the *GSTM1* polymorphism distribution of gastric cancer patients and controls^[24,26,32,36,52,55,56].

Several case-control studies also failed to find a significant association between the *CYP2E1/PstI* polymorphism and gastric cancer^[23,24,26,34]. However, while Nishimoto *et al.*^[51] observed that the rare variant *c2/c2* was associated with a reduced risk for gastric cancer in non-Japanese Brazilians, Wu *et al.*^[35] observed that the distribution of the *c2/c2* genotype, detected by *PstI* or *RsaI* digestion, differed significantly between gastric cancer cases and controls. These authors suggested that the *CYP2E1* genotype could be a determinant of gastric cancer. The reason for these inconsistent results is not clear, but one problem is the lack of sufficient investigation of the gene-environment interactions. Thus, Cai *et al.*^[31] and Gao *et al.*^[33] suggested that gene-environment interactions between the *CYP2E1* polymorphism and smoking might have the potential to alter the susceptibility for cancer development in the stomach.

Our current data corroborate the hypothesis of there being no association between *GSTT1* and *GSTM1* deletions and *CYP2E1/PstI* polymorphism with gastric cancer and chronic gastritis. However, smoking raised the OR's for stomach cancer in *GSTM1* null subjects. Our findings suggest that *GSTM1* null carriers may be more susceptible to the action of tobacco with regard to stomach cancer. Polycyclic aromatic hydrocarbons and N-nitrosamines found in cigarette smoke are potential human carcinogens. Thus, a deficiency of the detoxifying enzymes may affect the metabolic fates of these chemicals and raise cancer risk in subjects with a *GSTM1* null genotype. Cai *et al.*^[30] reported an increased frequency of the *GSTM1* null genotype in smokers with gastric cancer, that may modulate tobacco-related gastric carcinogenesis.

We also observed that a *GSTM1* positive genotype was more prevalent in chronic gastritis patients with *H pylori* infection. In the multi-step carcinogenesis of the stomach, chronic gastritis preceded the formation of gastric cancer, and a great proportion of the clinical tumors occurred in connection

with advanced forms of this pathology^[57]. *H pylori* has been reported to be a Class I human carcinogen^[58], and chronic *H pylori* infection was shown to increase the risk for gastric carcinoma from 2.8 to 9 fold^[59-64]. Ng *et al.*^[27] observed that the absence of the *GSTM1* enzyme might increase the risk of developing gastric cancer in patients with *H pylori* infection. Thus, chronic gastritis patients with *H pylori* infection, but with a *GSTM1* positive genotype, might benefit from a protective effect and exhibit a smaller predisposition to developing gastric cancer.

In this study, no association between the *CYP2E1/PstI* polymorphism and overall risk for gastric cancer was observed. Different from the study of Nishimoto *et al.*^[51] in a Brazilian population, the rare variant *c2/c2* was not observed. Moreover, the risk for gastric cancer as related to demographic risk factors was also not affected by the *CYP2E1/PstI* polymorphisms.

In conclusion, the present work does not show any obvious relationship between *GSTT1*, *GSTM1* and *CYP2E1* polymorphisms and the development of gastric cancer in a Brazilian population. However, smoking and the *GSTM1* null genotype may be associated with an increased OR for stomach cancer. We emphasize that studies with negative findings also need to be reported, so as to avoid a publication bias leading to an overestimate of positive findings. We also suggest that the investigation of a greater number of biometabolism genes associated with DNA repair genes might bring a broader view of the process.

ACKNOWLEDGEMENTS

We wish to thank Dr. Adriana Barbosa Santos and Dr. Antônio José Manzato for their help in the statistical analysis.

REFERENCES

- 1 **INCA** - Instituto Nacional do Câncer, Ministério da Saúde. Estimativa da incidência e mortalidade por câncer no Brasil, Rio de Janeiro, 2003. Disponível em <http://www.inca.org.br>.
- 2 **Stadländer CT**, Waterbor JW. Molecular epidemiology, pathogenesis and prevention of gastric cancer. *Carcinogenesis* 1999; **20**: 2195-2208
- 3 **Galanis DJ**, Kolonel LN, Lee J, Nomura A. Intakes of selected foods and beverages and the incidence of gastric cancer among the Japanese residents of Hawaii: a prospective study. *Int J Epidemiol* 1998; **27**: 173-180
- 4 **Brenner H**, Arndt V, Bode G, Stegmaier C, Ziegler H, Stümer T. Risk of gastric cancer among smokers infected with *Helicobacter pylori*. *Int J Cancer* 2002; **98**: 446-449
- 5 **Zaridze D**, Borisova E, Maximovitch D, Chkhikvadze V. Alcohol consumption, smoking and risk of gastric cancer: case-control study from Moscow, Russia. *Cancer Causes Control* 2000; **11**: 363-371
- 6 **Pakodi F**, Abdel-Salam OM, Debreceni A, Mózsik G. *Helicobacter pylori*. One bacterium and a broad spectrum of human disease! An overview. *J Physiol Paris* 2000; **94**: 139-158
- 7 **Sipponen P**, Hyvärinen H, Seppälä K, Blaser MJ. Review article: pathogenesis of transformation from gastritis to malignancy. *Aliment Pharmacol Ther* 1998; **12**: 61-71
- 8 **Correa P**. A human model of gastric carcinogenesis. *Cancer Res* 1988; **48**: 3554-3560
- 9 **Stermmermann GN**. Intestinal metaplasia of the stomach. A status report. *Cancer* 1994; **74**: 556-564
- 10 **Wormhoudt LW**, Commandeur JN, Vermeulen NP. Genetic polymorphisms of human N-acetyltransferase, cytochrome P450, glutathione S-transferase, and epoxide hydrolase enzymes: relevance to xenobiotic metabolism and toxicity. *Crit Rev Toxicol* 1999; **29**: 59-124
- 11 **Autrup H**. Genetic polymorphisms in human xenobiotic metabolizing enzymes as susceptibility factors in toxic response. *Mutat Res* 2000; **464**: 65-76
- 12 **Rothman N**, Wacholder S, Caporaso NE, Garcia-Closas M,

- Buetow K, Fraumeni JF. The use of common genetic polymorphisms to enhance the epidemiologic study of environmental carcinogens. *Biochim Biophys Acta* 2001; **1471**: 1-10
- 13 **Liu S**, Park JY, Schantz SP, Stern JC, Lazarus P. Elucidation of *CYP2E1* 5' regulatory *RsaI/PstI* allelic variants and their role in risk for oral cancer. *Oral Oncol* 2001; **37**: 437-445
 - 14 **Pavanello S**, Clonfero E. Biological indicators of genotoxic risk and metabolic polymorphisms. *Mutat Res* 2000; **63**: 285-308
 - 15 **AICR** - American Institute for Cancer Research. World Cancer Research Fund. Food, Nutrition and the Prevention of Cancer: a Global Perspective. Washington: *Banta Book Group* 1997: 670p
 - 16 **Sheweita SA**, Tilmisany AK. Cancer and phase II drug-metabolizing enzymes. *Curr Drug Metab* 2003; **4**: 45-58
 - 17 **Landi S**. Mammalian class theta GST and differential susceptibility to carcinogens: a review. *Mutat Res* 2000; **463**: 247-283
 - 18 **Hung HC**, Chuang J, Chien YC, Chern HD, Chiang CP, Kuo YS, Hi Desheim A, Chen CJ. Genetic polymorphisms of *CYP2E1*, *GSTM1* and *GSTY1*: environmental factors and risk of oral cancer. *Cancer Epidemiol Biomarkers Prev* 1997; **6**: 901-905
 - 19 **Hildesheim A**, Chen CJ, Caporaso NE, Cheng YJ, Hoover RN, Hsu MM, Levine PH, Chen IH, Chen JY, Yang CS, Daly AK, Idle JR. Cytochrome P450IIE1 genetic polymorphisms and risk of nasopharyngeal carcinoma. Results from a case-control study conducted in Taiwan. *Cancer Epidemiol Biomarkers Prev* 1995; **4**: 607-610
 - 20 **Le Marchand LL**, Sivaraman L, Pierce L, Seifried A, Lum A, Wilkens LR, Lau AF. Association of *CYP1A1*, *GSTM1* and *CYP2E1* polymorphisms with lung cancer suggest cell type specificities to tobacco carcinogens. *Cancer Res* 1998; **58**: 4858-4863
 - 21 **Lin DX**, Tang YM, Peng Q, Lu SX, Ambrosone CB, Kadlubar FF. Susceptibility to esophageal cancer and genetic polymorphisms in Glutathione S-Transferases T1, P1 and M1 and Cytochrome P4502E1. *Cancer Epidemiol Biomarkers Prev* 1998; **7**: 1013-1018
 - 22 **Harada S**, Misawa S, Nakamura T, Tanaka N, Ueno E, Nozoe M. Detection of *GST1* gene deletion by the polymerase chain reaction and its possible correlation with stomach cancer in Japanese. *Hum Genet* 1992; **90**: 62-64
 - 23 **Kato S**, Onda M, Matsukura N, Tokunaga A, Tajiri T, Kim DY, Tsuruta H, Matsuda N, Yamashita K, Shields PG. Cytochrome P4502E1 (*CYP2E1*) genetic polymorphism in a case-control study of gastric cancer and liver disease. *Pharmacogenetics* 1995; **5**: 141-144
 - 24 **Kato S**, Onda M, Matsukura N, Tokunaga A, Matsuda N, Yamashita K, Shields PG. Genetic polymorphisms of the cancer related gene and *Helicobacter pylori* infection in Japanese gastric cancer patients: An age and gender matched case-control study. *Cancer* 1996; **77**(8 Suppl): 1654-1661
 - 25 **Katoh T**, Nagata N, Kuroda Y, Itoh H, Kawahara A, Kuroki N, Ookuma R, A'bell D. Glutathione S-transferase M1 (*GSTM1*) and T1 (*GSTT1*) genetic polymorphism and susceptibility to gastric and colorectal adenocarcinoma. *Carcinogenesis* 1996; **17**: 1855-1859
 - 26 **Kato S**, Onda M, Matsukura N, Tokunaga A, Matsuda N, Yamashita K, Shields GP. *Helicobacter pylori* infection and genetic polymorphisms to cancer related genes in gastric carcinogenesis. *Biomed Pharmacother* 1997; **51**: 145-149
 - 27 **Ng EK**, Sung JJ, Ling TK, Ip SM, Lau JY, Chan AC, Liew CT, Chung SC. *Helicobacter pylori* and the null genotype of glutathione-S-transferase-m in patients with gastric adenocarcinoma. *Cancer* 1998; **82**: 268-273
 - 28 **Oda Y**, Kobayashi M, Ooi A, Muroishi Y, Nakanishi I. Genotypes of glutathione S-transferase M1 and N-acetyltransferase 2 in Japanese patients with gastric cancer. *Gastric Cancer* 1999; **2**: 158-164
 - 29 **Setiawan VW**, Zhang ZF, Yu GP, Li ML, Tsai CJ, Cordova D, Wang MR, Guo CR, Yu SZ, Kurtz RC. *GSTT1* and *GSTM1* null genotypes and the risk of gastric cancer: a case-control study in a chinese population. *Cancer Epidemiol Biomarkers Prev* 2000; **9**: 73-80
 - 30 **Cai L**, Yu SZ, Zhang ZF. Glutathione S-transferase M1, T1 genotypes and the risk of gastric cancer: A case-control study. *World J Gastroenterol* 2001; **7**: 506-509
 - 31 **Cai L**, Yu SZ, Zhang ZF. Cytochrome P450 2E1 genetic polymorphism and gastric cancer in Changle, Fujian Province. *World J Gastroenterol* 2001; **7**: 792-795
 - 32 **Gao CM**, Takezaki T, Wu JZ, Li ZF, Liu YT, Li SP, Ding JH, Su P, Hu X, Xu TL, Sugimura H, Tajima K. Glutathione-S-transferases M1 (*GSTM1*) and *GSTT1* genotype, smoking, consumption of alcohol and tea and risk of esophageal and stomach cancers: a case-control study of a high-incidence area in Jiangsu Province, China. *Cancer Lett* 2002; **188**: 95-102
 - 33 **Gao CM**, Takezaki T, Wu JZ, Li ZY, Wang J, Ding J, Liu YT, Hu X, Tajima K, Sugimura H. Interaction between Cytochrome P-450 2E1 polymorphisms and environmental factors with risk of esophageal and stomach cancers in chinese. *Cancer Epidemiol Biomarkers Prev* 2002; **11**: 29-34
 - 34 **Tsukino H**, Kuroda Y, Qiu D, Nakao H, Imai H, Katoh T. Effects of cytochrome P450 (*CYP*) 2A6 gene deletion and *CYP2E1* genotypes on gastric adenocarcinoma. *Int J Cancer* 2002; **100**: 425-428
 - 35 **Wu MS**, Chen CJ, Lin MT, Wang HP, Shun CT, Shen JC, Liu JT. Genetic polymorphisms of cytochrome p450 2E1, glutathione S-transferase M1 and T1, and susceptibility to gastric carcinoma in Taiwan. *Int J Colorectal Dis* 2002; **17**: 338-343
 - 36 **Choi SC**, Yun KJ, Kim TH, Kim HJ, Park SG, Oh GT, Chae SC, Oh GJ, Nah YH, Kim JJ, Chung HT. Prognostic potential of glutathione S-transferase M1 and T1 null genotypes for gastric cancer progression. *Cancer Lett* 2003; **195**: 169-175
 - 37 **Genta RM**. Gastric atrophy and atrophic gastritis - nebulous concepts in search of a definition. *Aliment Pharmacol Ther* 1998; **12**: 17-23
 - 38 **Lauren J**. The two histological main types of gastric carcinoma: diffuse and so-called intestinal type carcinoma: na attempt at a histo clinical classification. *Acta Pathol Microbiol Scand* 1965; **64**: 31-49
 - 39 **Price AB**. The Sydney system: histological division. *J Gastroenterol Hepatol* 1991; **6**: 209-222
 - 40 **Abdel-Rahman SZ**, Nouraldean AM, Ahmed AE. Molecular interaction of [2,3-14C] acrylonitrile with DNA in gastric tissue of rat. *J Biochem Toxicol* 1994; **9**: 191-198
 - 41 **Abdel-Rahaman SZ**, El-Zein RA, Anwar WA, Au WW. A multiplex PCR procedure for genetic polymorphism of the *GSTM1* and *GSTT1* genes in human. *Cancer Lett* 1996; **107**: 229-233
 - 42 **Kato S**, Shields PG, Caporaso NE, Hoover RN, Trump BF, Sugimura H, Weston A, Harris CC. Cytochrome P450IIE1 genetic polymorphisms, racial variation, and lung cancer risk. *Cancer Res* 1992; **52**: 6712-6715
 - 43 **van Iersel ML**, Verhagen H, van Bladeren PJ. The role of biotransformation in dietary (anti) carcinogenesis. *Mutat Res* 1999; **443**: 259-270
 - 44 **Mizoue T**, Tokui N, Nishisaka K, Nishisaka S, Ogimoto I, Ikeda M, Yoshimura T. Prospective study on the relation of cigarette smoking with cancer of the liver and stomach in an endemic region. *Int J Epidemiol* 2000; **29**: 232-237
 - 45 **De Stefani E**, Boffetta P, Carzoglio J, Mendilaharsu S, Deneo-Pellegrini H. Tobacco smoking and alcohol drinking as risk factors for stomach cancer: a case-control study in Uruguay. *Cancer Causes Control* 1998; **9**: 321-329
 - 46 **Ekström AM**, Eriksson M, Hansson LE, Lindgren A, Signorello LB, Nyrén O, Hardell L. Occupational exposures and risk of gastric cancer in a population-base case-control study. *Cancer Res* 1999; **59**: 5932-5937
 - 47 **Mikelsaar AV**, Tasa G, Parlist P, Uuskula M. Human glutathione S-transferase *GSTM1* genetic polymorphism in Estonia. *Hum Hered* 1994; **44**: 248-251
 - 48 **Persson I**, Johansson I, Lou YC, Yue QY, Duan LS, Bertilsson L, Ingelman-Sundberg M. Genetic polymorphism of xenobiotic metabolizing enzymes among Chinese lung cancer patients. *Int J Cancer* 1999; **81**: 325-329
 - 49 **Gattas GJ**, Soares-Vieira JA. Cytochrome P450-2E1 and glutathione S-transferase mu polymorphisms among caucasians and mulattoes from Brazil. *Occup Med* 2000; **50**: 508-511
 - 50 **Hatagima A**, Klautau-Guimarães MN, Silva FP. Glutathione S-transferase M1 (*GSTM1*) polymorphism in two Brazilian populations. *Genet Mol Biol* 2000; **23**: 709-713
 - 51 **Nishimoto IN**, Hanaoka T, Sugimura H, Nagura K, Ihara M, Li XJ, Arai T, Hamada GS, Kowalski LP, Tsugane S. Cyto-

- chrome P450 2E1 polymorphism in gastric cancer in Brazil: case-control studies of Japanese Brazilians and non-Japanese Brazilians. *Cancer Epidemiol Biomarker Prev* 2000; **9**: 675-580
- 52 **Losi-Guembarovski R**, D'Arce LPG, Cólus IMS. Glutathione S-transferase Mu (GSTM1) null genotype in relation to gender, age and smoking status in a healthy Brazilian population. *Genet Mol Biol* 2002; **25**: 357-360
- 53 **Arruda VR**, Grignolli CE, Gonçalves MS, Soares MC, Menezes R, Saad ST, Costa FF. Prevalence of homozygosity for the deleted alleles of glutathione S-transferase um (GSTM1) and theta (GSTT1) among distinct ethnic groups from Brazil: relevance to environmental carcinogenesis? *Clini Genet* 1998; **54**: 210-214
- 54 **Chen CL**, Liu Q, Relling WV. Simultaneous characterization of glutathione S-transferase M1 and T1 polymorphisms by polymerase chain reaction in American whites and blacks. *Pharmacogenetics* 1996; **6**: 187-191
- 55 **Deakin M**, Elder J, Hendrickse C, Peckham D, Baldwin D, Pantin C, Wild N, Leopard P, Bell DA, Jones P, Duncan H, Brannigan K, Aldersea J, Fryer A, Strange ARC. Glutathione S-transferase GSTT1 genotypes and susceptibility to cancer: studies of interactions with GSTM1 in lung, oral, gastric and colorectal cancers. *Carcinogenesis* 1996; **17**: 881-884
- 56 **Saadat I**, Saadat M. Glutathione S-transferase M1 and T1 null genotypes and the risk of gastric and colorectal cancers. *Cancer Lett* 2001; **169**: 21-26
- 57 **Lan Q**, Chow WH, Lissowska J, Hein DW, Buetow K, Engel LS, Ji B, Zatonski W, Rothman N. Glutathione S-transferase genotypes and stomach cancer in a population-based case-control study in Warsaw, Poland. *Pharmacogenetics* 2001; **11**: 655-661
- 58 **Martins G**, Alves M, Dias J, Santos R, Costa-Neves J, Mafra M, Marins AP, Ramos S, Ramos M, Mexia J, Quina M, Rueff J, Montero C. Glutathione S-transferase mu polymorphism and gastric cancer in the portuguese population. *Biomarkers* 1998; **3**: 441-447
- 59 **Conde AR**, Martins G, Saraiva C, Rueff J, Monteiro C. Association of p53 genomic instability with the glutathione S-transferase null genotype in gastric cancer in the portuguese population. *Mol Pathol* 1999; **52**: 131-134
- 60 **Sipponen P**, Hyvärinen H, Seppälä K, Blaser MJ. Review article: pathogenesis of transformation from gastritis to malignancy. *Aliment Pharmacol Ther* 1998; **12**: 61-71
- 61 International Agency for Research on Cancer. World Health Organization. The evaluation of carcinogenic risks to humans, Monograph N° 61. Lyon, France, 1994
- 62 **Kuipers EJ**. Exploring the link between *Helicobacter pylori* and gastric cancer. *Aliment Pharmacol Ther* 1999; **13**: 3-11
- 63 **El-Omar EM**, Oien K, Murray LS, El-Nujumi A, Wirz A, Gillen D, Williams G, Fullarton G, Mccoll KEL. Increased prevalence of precancerous changes in relatives of gastric cancer patients: critical role of *H pylori*. *Gastroenterology* 2000; **118**: 22-30
- 64 **Uemura N**, Okamoto S, Yamamoto S, Matsumura N, Yamaguchi S, Yamakido M, Taniyama K, Sasaki N, Schlemper RJ. *Helicobacter pylori* infection and the development of gastric cancer. *N Engl J Med* 2001; **345**: 784-789

Edited by Wang X L Proofread by Xu FM

Role of nucleostemin in growth regulation of gastric cancer, liver cancer and other malignancies

Si-Jin Liu, Zi-Wei Cai, Ya-Jun Liu, Mei-Yu Dong, Li-Qiu Sun, Guo-Fa Hu, Ying-Yun Wei, Wei-De Lao

Si-Jin Liu, Guo-Fa Hu, Ying-Yun Wei, Wei-De Lao, Institute of Genetics and Developmental Biology, Chinese Academy of Sciences, Beijing 100080, China

Zi-Wei Cai, Li-Qiu Sun, Institute of Biology of Self-protection, Mudanjiang Medical College, Mudanjiang 157011, Heilongjiang Province, China

Ya-Jun Liu, Department of Spine, Beijing Jishuitan Hospital, Peking University, Beijing 100035, China

Mei-Yu Dong, Tianjin Institute of Urologic Surgery, Tianjin Medical University, Tianjin 300211, China

Correspondence to: Professor Wei-De Lao, No. 3 Zhongguancun Road, Haidian District, Beijing 100080, China. wdlao@genetics.ac.cn

Telephone: +86-10-62552956 **Fax:** +86-10-62551951

Received: 2003-12-23 **Accepted:** 2004-01-15

Abstract

AIM: To examine the role of nucleostemin in the growth regulation of gastric cancer, liver cancer and other cancers.

METHODS: RT-PCR was used to clone the fragment of nucleostemin cDNA from HEK 293 cells. Eighteen kinds of malignant tumor tissues including gastric adenocarcinoma and liver cancer tissues, 3 kinds of benign tumor tissues, 3 kinds of benign hyperplastic tissues and normal tissues were employed to examine nucleostemin gene expression by RT-PCR, Slot blot, Northern blot and *in situ* hybridization.

RESULTS: We successfully cloned a 570 bp fragment of nucleostemin-cDNA from HEK-293 cells. All detected malignant tumor tissues, benign tumor tissues, and benign hyperplastic tissues had high levels of nucleostemin expression. Nucleostemin was also expressed in human placenta tissue at a high level. In terminally differentiated normal human adult kidney and mammary gland tissues, no nucleostemin expression could be detected.

CONCLUSION: Nucleostemin can help regulate the proliferation of both cancer cells and stem cells. It might play an important role in the growth regulation of gastric cancer, liver cancer and other cancers.

Liu SJ, Cai ZW, Liu YJ, Dong MY, Sun LQ, Hu GF, Wei YY, Lao WD. Role of nucleostemin in growth regulation of gastric cancer, liver cancer and other malignancies. *World J Gastroenterol* 2004; 10(9): 1246-1249

<http://www.wjgnet.com/1007-9327/10/1246.asp>

INTRODUCTION

Perhaps the most important and useful property of stem cells is self-renewal. Through this property, striking parallels can be found between stem cells and cancer cells: tumor may originate from the transformation of normal stem cells. Similar signaling pathways may regulate self-renewal in stem cells, and cancer cells^[1]. McKay and Tsai found a novel gene nucleostemin (NS) in rat embryo stem cells, the rat central nervous system (CNS)

stem cells and rat primitive bone marrow cells. NS gene was apparently involved in regulating the proliferation of both stem cells and at least some types of cancer cells^[2]. The protein encoded by NS was abundantly expressed while the cells were proliferating in an early multipotential state, but it abruptly and almost entirely disappeared at the start of differentiation. The fact that NS expressed in stem cells and several cancer cell lines, but not in the differentiated cells of adult tissues, suggested its role in maintaining self-renewal of stem cells and cancer cells. Our recent data also showed that NS expressed in human gastric cancer (SGC-7901) cells, human hepatocarcinoma (HepG2) cells, human cervical cancer (Hela) cells, human osteosarcoma (OS-732) cells, human mammary (MMK-7) cells and human embryo kidney (HEK-293) cells^[3]. Coordinated control of self-renewal and commitment to differentiation is key to maintaining the homeostasis of the stem cell compartment^[4,5], when deregulated it may contribute to cancer pathogenesis^[6,7]. The identification of stem-cell-specific proteins and the elucidation of novel regulatory pathways that ensure the integration of these processes, are therefore of fundamental importance^[8,9]. It seems that NS is involved in the regulatory pathways, but the fundamentals about NS are still unknown. For example, why does NS express in stem cells and cancer cells but not in differentiated cells? What are the tumor types that misexpress NS and the underlying mechanism? And what is the timing of NS reactivation in cancer cells.

Gastric cancer is common in China, and its early diagnosis and treatment are difficult^[10,11]. To investigate the mechanism of carcinogenesis of gastric cancer would facilitate its diagnosis and treatment. Therefore, NS may take part in the growth regulation of tumor tissues and hyperplastic tissues. So we employed a number of malignant tumor tissues, benign tumor tissues, benign hyperplastic tissues and normal tissues to examine the expression of NS gene by RT-PCR, Slot blot, Northern blot and *in situ* hybridization, which would help illuminate the mechanism of self-renewal of cancer cells.

MATERIALS AND METHODS

Materials

We collected tens of tumor tissue samples including gastric adenocarcinoma, liver cancer, bladder carcinoma, pancreatic cancer and esophagus squamous carcinoma samples. We also collected several kinds of normal tissue samples such as normal kidney tissues and muscle tissues. Human embryo kidney (HEK-293) cells were cultured in DMEM containing 100 mL/L FCS at 37 °C in 50 mL/L CO₂^[12,13]. The cells were kept in logarithmic growth phase by trypsin digestion and reinoculation every 2-4 d^[14,15]. DMEM cell culture medium was purchased from Gibco Corporation; fetal calf serum (FCS) and trypsin from Hyclone Corporation; restriction enzymes and T4 DNA ligase from Promega Corporation. PCR primers were synthesized by Shanghai Shenyou Company and DNA sequencing was also performed by this company.

Cloning of NS cDNA fragment

Total RNA in HEK 293 cells was isolated using total RNA

isolation kit (Promega Corporation). A 2 µg total RNA was used in reverse transcription (RT) reaction. Up-stream primer, 5' -ggatccatgaaaaggcctaagttaaagaaagc (*Bam*HI site underlined); Down-stream primer, 5' -aagcttgctctccaaattctcttggta (*Hind*III site underlined). PCR protocol (94 °C 30 s → 50 °C 30 s → 72 °C 30 s) was run for 30 cycles and PCR product was about 570 bp. PCR product was separated by agarose gel electrophoresis, recovered with gel extraction kit (Omega Corporation), and ligated with pGEM-T vector. The ligate was transformed into competent *E.coli* JM 109 cells. The correct transformant was identified by restriction enzyme analysis and DNA sequencing.

Isolation of total RNA in tissue samples and RT-PCR

About 100 mg tissues of each sample was used to isolate total RNA using total RNA isolation kit (Promega Corporation). RT protocol and PCR protocol including PCR primers are the same as the above. GAPDH was used as a loading control, its up-stream primer, 5' -ggtggacctgacctgccgtctaga, and its down-stream primer, 5' -ttactcctggaggccatgtggg. PCR protocol (94 °C 30 s → 55 °C 30 s → 72 °C 20 s) was run for 25 cycles.

Analysis of slot blot

Twenty µg total RNA of each sample was added into slots, and transferred onto nylon membrane. Slot blot analysis was carried out using ³²P-labeled NS fragments and human 18S RNA as probes in the hybridization.

Analysis of Northern blot

Equal volume of total RNA of each sample was used in denaturing agarose gel electrophoresis, and after that RNA was transferred onto nylon membrane. Northern blot analysis was made using ³²P labeled NS fragments and human 18S RNA as probes in the hybridization.

Preparation of cRNA probes

Nucleostemin cDNA fragment was inserted into pGEM-T vector, and large quantities of plasmid was harvested with Plasmid Extraction Kit (Promega Corporation). After linearization by *Nco*I restriction enzyme, SP6 promoter was used to drive the transcription of NS-cRNA probes *in vitro* and in this system Biotin labeled rUTPs was introduced into NS-cRNA probes. In the same way, after linearization by *Not* I restriction enzyme, T7 promoter was used to drive the transcription of sense NS-cRNA probes *in vitro*, which acted as the negative control.

Detection of *in situ* hybridization histochemistry

The expression of NS mRNA was detected *in situ* by Biotin SP-HRP method^[16,17]. Pretreatment of paraffin-embedded specimens referred to the previously used methods^[13]. In brief, before *in situ* hybridization, sections were deparaffinized in xylene (7.5 min, twice) and rehydrated in graded ethanol. Sections were then rinsed in 2 changes of diethylpyrocarbonate-treated distilled water and rinsed in 10 mmol/L citrate buffer, pH 6.0. Sections were placed in glass racks (20 slides/rack) and submerged in approximately 250 mL citrate buffer in covered glass tubes. Sections were then microwaved in a 900-watt microwave (Panasonic Matsushita Electric, Danville, MA) 3 times for 5 min each time at full power, topped up with additional citrate buffer to compensate for evaporation. Slides were allowed to cool slightly, then were rinsed in 2 changes of diethylpyrocarbonate-treated distilled water, dehydrated in graded ethanol, and dried. Hybridization of the labeled probes to the tissue sections was carried out using a previously described method^[18]. Sense NS-cRNA probes and SP-HRP solution were used as negative controls. And the tissue sections were counterstained by hematoxylin.

RESULTS

Gain of NS-cDNA fragment

We successfully cloned a 570 nt fragment by RT-PCR in HEK-293 cells. Then the fragment was ligated with pGEM-T vector and the recombinant vector was named pGEM-T-NS. pGEM-T-NS was digested by *Bam*HI and *Hind*III enzymes, yielding a 3.0 kb fragment of vector and a 570 bp fragment of NS cDNA (Figure 1). The result of sequencing indicated our sequence of NS cDNA was completely identical to the sequence in Genebank. Sequencing revealed that no base mutation occurred in the sequence of our cloned NS-cDNA fragment.

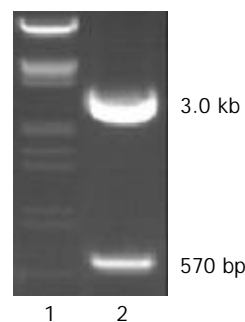


Figure 1 Molecular cloning of nucleostemin cDNA fragment. 1. DNA marker: λ DNA, *Eco*RI+ *Hind* III. 2. pGEM-T-NS, *Bam*HI+*Hind* III.

NS expression detected by RT-PCR

According to the results of RT-PCR, all above malignant tumor tissues, benign tumor tissues, and benign hyperplastic tissues had high levels of NS expression, so did the normal human placenta tissues. And a lower level of NS expression in normal human adult muscle tissues could also be detected. However, no NS expression could be detected in normal human adult kidney tissues and mammary gland tissues. Partial results of RT-PCR are shown in Figure 2.

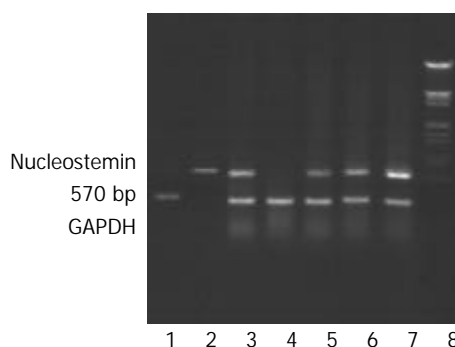


Figure 2 Detection of NS expression in various tumor tissues and normal human adult kidney tissues using RT-PCR. 1. GAPDH cDNA-fragment sample. 2. NS-cDNA fragment sample. 3. Renal carcinoma tissue. 4. Normal human adult kidney tissue. 5. Bladder carcinoma tissue. 6. Liver cancer tissue. 7. Gastric adenocarcinoma tissue. 8. DNA marker: λ DNA, *Eco*RI+*Hind* III.

NS expression by slot blot

Slot blot analysis indicated that NS expressed in all above malignant tumor tissues, benign tumor tissues, and benign hyperplastic tissues, which was in agreement with the results of RT-PCR. However, no NS expression could be detected in normal human adult kidney tissues, mammary gland tissues and muscle tissues. Partial results of Slot blot analysis are shown in Figure 3.

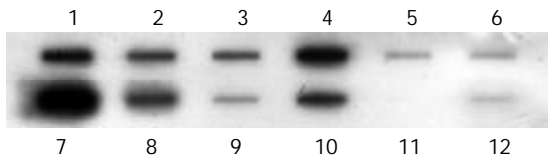


Figure 3 Detection of NS expression in various tumor tissues and normal human adult kidney tissues by Slot blot. 1. Liver cancer tissue. 2. Bladder carcinoma tissue. 3. Pancreatic cancer tissue. 4. Cardia adenocarcinoma tissue. 5. Gastric adenocarcinoma tissue. 6. Esophagus squamous carcinoma tissue. 7. Denatured NS-cDNA sample. 8. Ovary serous cystadenocarcinoma. 9. Ampulle carcinoma tissue. 10. Renal carcinoma tissue. 11. Normal human adult kidney tissue. 12. Benign hyperplasia tissue of prostate.

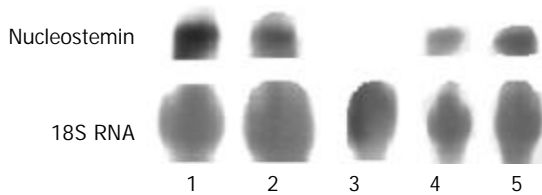


Figure 4 Detection of NS expression in various tumor tissues and normal human adult kidney tissues by Northern blot. 1. Gastric adenocarcinoma tissue. 2. Renal carcinoma tissue. 3. Normal human adult kidney tissue. 4. Liver cancer tissue. 5. Bladder carcinoma tissue.

Detection of NS expression by Northern blot

The results of Slot blot were further confirmed by Northern blot analysis. NS misexpressed in all these malignant tumor tissues, benign tumor tissues, and benign hyperplastic tissues. But the results of Northern blot analysis showed NS did not express in normal human adult kidney tissues, mammary gland tissues and muscle tissues. Partial results of Northern blot analysis are shown in Figure 4.

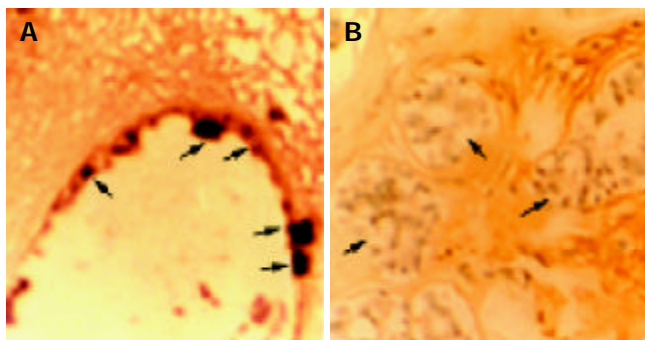


Figure 5 *In situ* hybridization detection of nucleostemin mRNA in invasive ductal breast carcinoma and normal mammary gland tissue by SP-HRP method. Counterstained with hematoxylin. A: Ductal carcinoma cells showed strong staining *in situ* (arrows). B: Normal mammary glandular epithelial cells showed no positive staining, only with azury nuclear counterstaining (arrows).

NS expression in tumor tissues confirmed by *in situ* hybridization

The Biotin SP-HRP (streptavidin-biotin-peroxidase-DAB) system reacted with 0.05% DAB (3-3', 4-4' -diaminobenzidine tetrahydrochloride) containing 0.1 mL/L H₂O₂, producing brown positive staining. And counterstain was performed by hematoxylin, producing azury nuclear staining. The results of *in situ* hybridization conformed to those of Slot blot analysis and Northern blot analysis. Positive staining was located in cytoplasm of cancer cells, but no positive staining was in cytoplasm of normal adult tissue cells such as normal kidney cells and mammary gland cells. The results of *in situ* hybridization

detection of nucleostemin mRNA in invasive ductal breast carcinoma and normal mammary gland tissue are indicated in Figure 5. Ductal carcinoma cells showed strong staining in cytoplasm (Figure 5A), while normal mammary glandular epithelial cells showed no positive staining, only with azury nuclear counterstaining (Figure 5B).

DISCUSSION

Nucleostemin (NS) is a newly found p53-binding protein, which exists mainly in the nucleoli of stem cells and some various cancer cells, but does not express in committed and terminally differentiated cells^[2]. The expression level of NS declined obviously during embryo and adult development due to the differentiation of stem cells. For example, it was expressed preferentially in neuroepithelial precursors during embryogenesis and diminished during the central nervous system (CNS) differentiation. The expression of NS was also found in adult bone marrow hematopoietic stem cells, however could not be found in committed B-lymphocytes and granulocytes. *In vivo* experiments displayed that the NS expression could not even be detected after CNS stem cells were induced to differentiate. Recently, it was confirmed that NS expression also existed in ES cells and mesenchymal stem cells of mice^[19]. *In vivo*, NS expression disappeared before the changes of cell cycle markers during the development of CNS, which indicated the disappearance of NS expression induced the cell cycle arrest, but not the reverse. Moreover, non-cycling cells increased by silencing NS expression with small interfering RNA (siRNA) in CNS stem cells and U2OS cancer cells^[2].

We successfully cloned a 570 bp fragment of NS-cDNA from HEK-293 cells. The full length of NS-cDNA was 1 650 bp and the cloned fragment was located in the 5' -terminal of the full length. The fragment had high specificity and non-homology with other genes by BLAST analysis, so it was equal to probes in the screening of gene expression. From the results of RT-PCR, Northern blot and Slot blot analysis, we found that all these malignant tumor tissues, benign tumor tissues, and benign hyperplastic tissues had high levels of NS expression, which indicated that NS played an important role in the self-renewal of these cancer cells and hyperplastic cells. At the same time, NS expressed in human placental tissues also at a high level, possibly due to the existence of a mass of placental stem cells^[20-23]. A small quantity of NS expression could be found in normal human muscle tissues by RT-PCR, however no expression could be detected by Slot blot and Northern blot analysis. The reason might be that a few of myoblasts with the characteristic of stem cells existed in muscle tissues^[24,25], so only by the sensitive RT-PCR technique could a very small volume of NS expression be detected (figures not provided). In terminally differentiated normal human adult kidney tissues and mammary gland tissues, no NS expression could be detected as no cells possess the characteristics of stem cells or cancer cells in these tissues. The analysis of *in situ* hybridization indicated that NS gene expressed in cancer cells, but not in normal adult tissue cells, such as normal kidney cells and mammary gland cells. These results were in agreement with McKay's^[2].

All these results displayed that NS might play an important role in the proliferation regulation of cancer cells and stem cells. A working hypothesis of NS deduced from all information involved displayed that NS accumulated predominantly in the nucleolus and NS localized into nucleoplasm after binding with GTP^[26]. In the nucleoplasm, NS and p53 existed in a protein complex, and subsequently the growth-suppressive function of p53 was inhibited. During cell differentiation, when NS expression was downregulated, p53 was released from the protein complex, which allowed the stabilization or activation of p53 and induction of target genes critical for cell cycle exit

and differentiation, such as p21^{CIP}. Members of the E2F family of transcription factors play a crucial role in cell proliferation control by regulating the expression of genes important for DNA synthesis and cell cycle progression^[27]. A functional E2F factor is composed of a heterodimer between an E2F polypeptide (E2F1- E2F6) and a DP polypeptide (DP1 and DP2). The transcriptional activities of E2F factors are regulated through association with the Rb (retinoblastoma) tumor suppressor protein and the other pocket proteins, p107 and p130. Binding of a pocket protein inhibits the transcriptional activation capacity of E2F factors and, in at least some cases, can convert E2F to repressors of transcription. The activity of Rb is regulated during the cell cycle by cdks (cyclic dependent kinase), primarily by cdk4 and cdk6, in association with D-type cyclin and cyclin E in association with cdk2. Phosphorylation of Rb by these cdks results in the dissociation of Rb from E2F and the depression/activation of E2F-regulated genes. The E2F-DP transcription complex determined the start of S phase and induced the expression of some genes which were necessary for the progress of S phase, such as Cyclin E, Cyclin A, proliferating cell nuclear antigen (PCNA) and dihydrofolate reductase (DHFR). The product of Cip1, p21^{CIP1}, blocked the process of phosphorylation of Rb by cdks and Cyclin complex, so E2F-DP in non-phosphorylation state still bound with RB and could not be freed. Only freed E2F-DP could gain its activity to promote the expression of these genes, and as a result, DNA synthesis was carried out and cells would pass through S phase.

Our results were in agreement with the working hypothesis mentioned above. There were high levels of NS expression in cancer cells, hyperplastic tissue cells and stem cells, so NS inhibited the p53-induced cell differentiation or apoptosis and these cells could easily pass through cell cycles. NS helped regulate the proliferation of both cancer cells and stem cells, although the precise mechanism was not yet clear. The focus on NS has potential therapeutic implications. For example, the growth of gastric cancer may be suppressed by silencing the NS expression with some molecular techniques, which would greatly improve the validity of its treatment.

ACKNOWLEDGEMENT

We want to thank Dr. Hong Gao and Dr. Siguo Liu in our group for their helpful discussions and research suggestions. We also thank Ms. Lin Hou from pathological center of Peking University for her help with *in situ* hybridization experiments and Professor. Hongwei Zhang and her colleagues from Beijing Haidian Hospital for their help with the pathological analysis.

REFERENCES

- 1 **Reya T**, Morrison SJ, Clarke MF, Weissman IL. Stem cells, cancer, and cancer stem cells. *Nature* 2001; **414**: 105-111
- 2 **Tsai RY**, McKay RD. A nucleolar mechanism controlling cell proliferation in stem cells and cancer cells. *Genes Dev* 2002; **16**: 2991-3003
- 3 **Liu SJ**, Cai ZW, Liu YJ, Dong MY, Zhang HW, Hu GF, Liu SG, Gao H, Zhang ZH, Liu XL, Wei YY, Xue Y, Lao WD. The effect of Knocking-down Nucleostemin Gene Expression on the *in vitro* Proliferation and *in vivo* tumorigenesis of HeLa cells. *J Exp Clin Canc Res* 2004; in press
- 4 **Sparger JM**, Chen X, Draper JS, Antosiewicz JE, Chon CH, Jones SB, Brooks JD, Andrews PW, Brown PO, Thomson JA. Gene expression patterns in human embryonic stem cells and human pluripotent germ cell tumors. *Proc Natl Acad Sci U S A* 2003; **100**: 13350-13355
- 5 **Goldschmidt-Clermont PJ**. Loss of bone marrow-derived vascular progenitor cells leads to inflammation and atherosclerosis. *Am Heart J* 2003; **146**: S5-12
- 6 **Hori Y**, Rulifson IC, Tsai BC, Heit JJ, Cahoy JD, Kim SK.

- Growth inhibitors promote differentiation of insulin-producing tissue from embryonic stem cells. *Proc Natl Acad Sci U S A* 2002; **99**: 16105-16110
- 7 **Wang N**, Liu ZH, Ding F, Wang XQ, Zhou CN, Wu M. Down-regulation of gut-enriched Kruppel-like factor expression in esophageal cancer. *World J Gastroenterol* 2002; **8**: 966-970
- 8 **Fiorini M**, Ballaro C, Sala G, Falcone G, Alema S, Segatto O. Expression of RALT, a feedback inhibitor of ErbB receptors, is subjected to an integrated transcriptional and post-translational control. *Oncogene* 2002; **21**: 6530-6539
- 9 **Zhou J**, Gurates B, Yang S, Sebastian S, Bulun SE. Malignant breast epithelial cells stimulate aromatase expression via promoter II in human adipose fibroblasts: an epithelial-stromal interaction in breast tumors mediated by CCAAT/enhancer binding protein beta. *Cancer Res* 2001; **61**: 2328-2334
- 10 **Lu JB**, Sun XB, Dai DX, Zhu SK, Chang QL, Liu SZ, Duan WJ. Epidemiology of gastroenterologic cancer in Henan Province, China. *World J Gastroenterol* 2003; **9**: 2400-2403
- 11 **Zhang C**, Liu ZK. Gene therapy for gastric cancer: A review. *World J Gastroenterol* 2003; **9**: 2390-2394
- 12 **Nadeau I**, Sabatie J, Koehl M, Perrier M, Kamen A. Human 293 cell metabolism in low glutamine-supplied culture: interpretation of metabolic changes through metabolic flux analysis. *Metab Eng* 2000; **2**: 277-292
- 13 **Liu SJ**, Hu GF, Liu YJ, Liu SG, Gao H, Zhang CS, Wei YY, Xue Y, Lao WD. The effect of human osteopontin on the proliferation, transmigration and expression of matrix metalloproteinase-2 and 9 of osteosarcoma cells *in vitro*. *Chin Med J* 2004; **117**: 235-240
- 14 **Christoffers AB**, Kreisler M, Willershausen B. Effects of estradiol and progesterone on the proliferation of human gingival fibroblasts. *Eur J Med Res* 2003; **8**: 535-542
- 15 **Song J**, Rolfe BE, Hayward IP, Campbell GR, Campbell JH. Effects of collagen gel configuration on behavior of vascular smooth muscle cells *in vitro*: association with vascular morphogenesis. *In Vitro Cell Dev Biol Anim* 2000; **36**: 600-610
- 16 **Palumbo A**, Napolitano A, Carraturo A, Russo GL, d'Ischia M. Oxidative conversion of 6-nitrocatecholamines to nitrosating products: a possible contributory factor in nitric oxide and catecholamine neurotoxicity associated with oxidative stress and acidosis. *Chem Res Toxicol* 2001; **14**: 1296-1305
- 17 **Duran N**, Bromberg N, Kunz A. Kinetic studies on veratryl alcohol transformation by horseradish peroxidase. *J Inorg Biochem* 2001; **84**: 279-286
- 18 **Busuttil BE**, Frauman AG. Extrathyroidal manifestations of Graves disease: the thyrotropin receptor is expressed in extraocular, but not cardiac, muscle tissues. *J Clin Endocrinol Metab* 2001; **86**: 2315-2319
- 19 **Baddoo M**, Hill K, Wilkinson R, Gaupp D, Hughes C, Kopen GC, Phinney DG. Characterization of mesenchymal stem cells isolated from murine bone marrow by negative selection. *J Cell Biochem* 2003; **89**: 1235-1249
- 20 **Chambers I**, Colby D, Robertson M, Nichols J, Lee S, Tweedie S, Smith A. Functional expression cloning of Nanog, a pluripotency sustaining factor in embryonic stem cells. *Cell* 2003; **113**: 643-655
- 21 **Bernatchez R**, Belkacemi L, Rassart E, Daoud G, Simoneau L, Lafond J. Differential expression of membrane and soluble adenylyl cyclase isoforms in cytotrophoblast cells and syncytiotrophoblasts of human placenta. *Placenta* 2003; **24**: 648-657
- 22 **Dhot PS**, Nair V, Swarup D, Sirohi D, Ganguli P. Cord blood stem cell banking and transplantation. *Indian J Pediatr* 2003; **70**: 989-992
- 23 **Alvarez-Silva M**, Belo-Diabangouaya P, Salaun J, Dieterlen-Lievre F. Mouse placenta is a major hematopoietic organ. *Development* 2003; **130**: 5437-5444
- 24 **Berendse M**, Grounds MD, Lloyd CM. Myoblast structure affects subsequent skeletal myotube morphology and sarcomere assembly. *Exp Cell Res* 2003; **291**: 435-450
- 25 **Chen JC**, Goldhamer DJ. Skeletal muscle stem cells. *Reprod Biol Endocrinol* 2003; **1**: 101-107
- 26 **Bernardi R**, Pandolfi PP. The nucleolus: at the stem of immortality. *Nat Med* 2003; **9**: 24-25
- 27 **Nevins JR**. Toward an understanding of the functional complexity of the E2F and retinoblastoma families. *Cell Growth Differ* 1998; **9**: 585-593

Significance of vascular endothelial growth factor expression and its correlation with inducible nitric oxide synthase in gastric cancer

Zhen-Ya Song, Shu-Qun Wen, Jia-Ping Peng, Xuan Huang, Ke-Da Qian

Zhen-Ya Song, Xuan Huang, Ke-Da Qian, Department of Digestive Medicine, Second Affiliated Hospital of Medical College of Zhejiang University, Hangzhou 310009, Zhejiang Province, China

Shu-Qun Wen, Department of Neurology, Second Affiliated Hospital of Medical College of Zhejiang University, Hangzhou 310009, Zhejiang Province, China

Jia-Ping Peng, Cancer Institute, Zhejiang University, Hangzhou 310009, Zhejiang Province, China

Supported by Science and Technology Fund of Medicine and Health of Zhejiang Province, No.2000A116

Correspondence to: Dr. Zhen-Ya Song, Department of Digestive Medicine, Second Affiliated Hospital of Medical College of Zhejiang University, Hangzhou 310009, Zhejiang Province, China. sz2700@hzcmc.com

Telephone: +86-571-87783715

Received: 2003-10-15 **Accepted:** 2003-12-06

analysis showed the immunoreactive grades of VEGF were not associated with that of iNOS.

CONCLUSIONS: The expression of VEGF₁₆₅mRNA is well related with lymph node metastasis and TNM stages of UICC in gastric cancer, and is concerned with the invasiveness and metastasis of gastric cancer. The relationship can be observed between the expression of VEGF and iNOS in gastric cancer.

Song ZY, Wen SQ, Peng JP, Huang X, Qian KD. Significance of vascular endothelial growth factor expression and its correlation with inducible nitric oxide synthase in gastric cancer. *World J Gastroenterol* 2004; 10(9): 1250-1255

<http://www.wjgnet.com/1007-9327/10/1250.asp>

Abstract

AIM: To investigate the clinical significance of the expression of VEGF₁₆₅mRNA and the correlation with vascular endothelial growth factor (VEGF) protein and inducible nitric oxide synthase (iNO) in human gastric cancer.

METHODS: We tested VEGF₁₆₅mRNA expression in 31 cases of resected gastric cancer specimens and normal paired gastric mucosae by RT-PCR. Total RNA was extracted with TRIzol reagents, transcribed into cDNA with oligo (dT)₁₅ priming, inner controlled with β -actin expression and agarose gel isolated after PCR. VEGF expression was quantitated with IS1000 imaging system. Meanwhile we also examined expression levels of VEGF protein and iNOS in 85 cases of gastric cancer. All paraffin-embedded samples were immunohistochemically stained by streptavidin-peroxidase method (SP).

RESULTS: The mean expression of VEGF₁₆₅mRNA in gastric cancer was 1.125 ± 0.356 , significantly higher than that of normal paired mucosae, which was 0.760 ± 0.278 . The data indicated that the expression level of VEGF₁₆₅mRNA was well related to lymph node metastasis and TNM stages of UICC. The expression levels in patients with lymph node metastasis and without lymph node metastasis were 1.219 ± 0.377 and 0.927 ± 0.205 respectively ($P < 0.05$). The expression in stages I, II, III, IV was 0.934 ± 0.194 , 1.262 ± 0.386 respectively ($P < 0.01$). Further analysis showed the lymph node metastasis rate in the group with over-expression of VEGF was higher than that in the group with low expression of VEGF (83.3% vs 46.2%), and the ratio of stage III+IV in the group with over-expression of VEGF was also higher than that in the group with low expression with VEGF (77.8% vs 33.8%) ($P < 0.05$). The positive rates of expression of VEGF protein and iNOS in 85 cases of gastric cancer were 75.4% and 58.8% respectively, and 50.1% of the patients showed positive staining both for iNOS and VEGF, the correlation with the two factors was significant ($P = 0.018$). But more intensive

INTRODUCTION

Many observations have shown that angiogenesis plays an important role in the growth, progression and metastasis of solid tumors. Several potential angiogenic factors have been identified, vascular endothelial growth factor (VEGF) is known as one of the most powerful and specific molecules in vascularization. VEGF₁₆₅ is the major isoform among the five different VEGF species^[1,2]. Studies have demonstrated that tumor cells could produce and secrete VEGF periodically by themselves, which binding with the VEGF receptor in the vascular endothelial cells and then promote the angiogenesis in tumors^[3]. Inducible nitric oxide synthase (iNOS) is one of the isoforms of nitric oxide synthase that catalyzes the formation of nitric oxide, a regulator of vascular permeability. Expression of VEGF protein and iNO has been shown by immunohistochemistry in gastric cancer^[4-8]. However, the relationship has not been well evaluated between the VEGF₁₆₅mRNA and the clinical pathological features, and between VEGF and iNO, the two angiogenic regulators in gastric cancer.

The present study detected the expression of VEGF₁₆₅mRNA by RT-PCR and the expression of VEGF protein and iNO by immunohistochemistry in surgically resected human gastric cancer specimens, and characterized the correlation that mentioned above.

MATERIALS AND METHODS

Materials

Specimens of cancer tissue from 85 cases of gastric cancer were confirmed pathologically and at the second Affiliated Hospital of Medical College of Zhejiang University from August 1998 to January 2002. Of these, 54 patients were male, and 23 female, with a median age of 54 (31-77) years. All the cases were classified by WHO criteria histologically and TNM staging of UICC. Fresh cancerous and normal paired gastric mucosae obtained from 31 cases of them were frozen quickly by liquid nitrogen and stored at -80 °C until used for RT-PCR. All the specimens from 85 cases were fixed in 40 g/L buffered formaldehyde and embedded in paraffin for immunohistochemistry.

RT-PCR

Total RNA was extracted from 100 mg each frozen tissue using TRIzol reagents according to the manufacturer's instructions (GIBCO BRL) and the purity and quality were identified by an ultraviolet spectrometer and denatural gel electrophoresis.

First-strand cDNA was synthesized from 2 µg of total RNA in a 40 µL reaction volume by reverse transcription (RT) using 50 pmol oligo (dT)₁₅ 2 µL, RNasin 40 U, 10 mmol/L dNTP 2 µL, M-MLV reverse transcriptase 10 U (PROMEGA). The RNA template and oligo (dT)₁₅ were incubated at 65 °C for 10 min first, and were then added to the total reaction system at 37 °C for 1 h, stored at -20 °C for PCR. cDNA of 5 µL was amplified by PCR in a 25 µL reaction volume, containing 10 mmol/L dNTP 0.5 µL, Taq 1.5 U, per primer 10 pmol, and was inner controlled with β-actin. VEGF primers according to Tishcer's design^[9] were the upper primer: 5' -CAAGGATCCATGAAC TTTCTGCTGTCTT-3', the lower primer: 5' -CTTAAGCTTGC TCCTTCC TCCTGCCCGGC-3'. The upper primer of β-actin: 5' -TCGACAACGGCTCCGGCA-3', the lower primer of β-actin: 5' -CGTACATGGCTGGGGTGT-3'. The recombinant plasmid pGEM- T-VEGF₁₆₅ was used as positive control (provide by the Surgery Laboratory in our hospital). PCR condition of VEGF₁₆₅: pre-denaturation 94 °C for 5 min, then 30 cycles of amplification at 94 °C for 45 s, at 60 °C for 45 s, and at 72 °C for 45 s, extension at 72 °C for 10 min.

Aliquots of the PCR products (10 µL) were separated and visualized with ethidium bromide staining after electrophoresis in a 15 g/L agarose gel in Tris acetate ethylenediaminetetraacetic acid buffer at 100 V for 20 min, and quantitated with IS 1000 imaging system (Alpha Inotech). The expression of VEGF₁₆₅mRNA was expressed as follow: numeral value of VEGF₁₆₅=scanning data of VEGF₁₆₅ band/ scanning data of β-actin band. The value greater than 1 was regarded as higher expression of VEGF₁₆₅mRNA, and the value less than 1 was regarded as lower expression of VEGF₁₆₅mRNA. Statistical analysis was performed by means of SPSS10.0.

Immunohistochemical analysis

Paraffin-embedded samples were serially sectioned at 4 µm, and mounted onto the histosticked-coated slides. Sections were dewaxed in xylene, and dehydrated in ethanol, and then heated at 98 °C in EDTA retrieved solution for the antigens. Endogenous peroxidase was blocked by incubation of samples in hydrogen peroxide blocking reagent (Maixin Bio, Fuzhou). After washed with phosphate-buffered saline solution, the samples were incubated for 60 min with the primary antibodies. The anti-VEGF antibody is a polyclonal mouse anti-serum against VEGF of human origin and recognizes an amino-terminal epitope found in VEGF_{121,165,189}, and the anti-iNOS antibody is a monoclonal mouse anti-serum against the C-terminal domain of iNOS of human origin (The two antibodies were from Santa Cruz Biotechnology, Inc., CA). Location of the primary antibodies was achieved by subsequent application of a biotinylated anti-primary antibody, an avidin-biotin complex conjugated to horseradish peroxidase. The reaction products were visualized with diaminobenzidine. The slides were counter-stained by hematoxylin. Negative controls were established by replacing the primary antibody with PBS and normal rabbit serum. Known immunostaining-positive slides were used as positive controls. Immunoreactivity was diagnosed depending on the shade of cells staining assigned to 0-3 scores (0: negative reaction, 1: weak brown-color staining, 2: moderate brown-color staining, 3: strong brown-color staining), and the percent of positive staining cells, the average percentage of positive cells was determined in at least 5 areas

at ×400 and assigned to 0-3 scores (0: negative or equivocal staining, 1: weakly positive expression, cells were staining in 1-25%, 2: moderately positive expression, cells were staining in 25-50%, 3: strongly positive expression, the cells were stained over 50%). The diagnosed grades accorded to the sum of two scores, -: 0-1, +: 2, ++: 3-4, +++: >5. Statistical analysis was performed by means of SPSS10.0.

RESULTS

Expression of VEGF₁₆₅mRNA in gastric cancer

As shown by RT-PCR, the amplification products of VEGF and β-actin were 655 bp and 370 bp, respectively. Over-expression of VEGF₁₆₅ was detected in gastric cancer mucosae, and the over-expression rate was 58%, whereas 16% in normal paired mucosae. The mean value of the VEGF₁₆₅mRNA expression in gastric cancer tissues was significantly higher than that in normal paired tissues, which was 1.125±0.356 and 0.760±0.278 respectively (Figure 1 and Table 1).

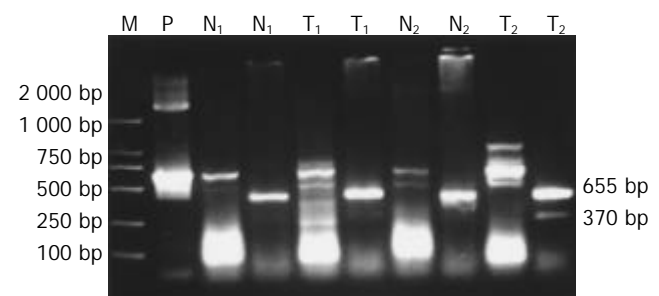


Figure 1 RT-PCR products of VEGF₁₆₅mRNA by 20 g/L agarose gel electrophoresis. M, marker; P, recombinant plasmid of VEGF₁₆₅; T, gastric cancer mucosae; N, non-gastric cancer mucosae; β-actin. The product of VEGF₁₆₅ mRNA was 655 bp, and the product of β-actin was 370 bp.

Relationship between expression of VEGF₁₆₅mRNA and clinical pathological features of gastric cancer

As shown in Table 2, the expression level of VEGF₁₆₅mRNA in the group of positive lymph node metastasis was higher than that in the group of negative lymph node metastasis ($P<0.05$), and the expression level in stages III and IV was also higher than that in stages I and II ($P<0.05$). The expression levels had no correlation with age, sizes of tumors and degree of histological differentiation.

Another observation shown in Table 3 and Table 4 was that the rate of lymph node metastasis and the ratio of stages III and IV in the group with over-expression of VEGF₁₆₅ mRNA were also higher than those in the group with low-expression of VEGF₁₆₅mRNA (83.3% vs 46.2%, 77.8% vs 30.8% respectively, $P<0.05$).

Correlation between VEGF and iNOS in gastric cancer

Positive immunostaining for iNOS and VEGF was observed in cancer cells, and weakly positive or negative staining was observed in the normal gastric epithelial tissues. VEGF and iNOS immunoreactivity was located mainly in the cytoplasm and cell membrane (Figure 2). The positive expression rate of iNOS was 58.8% (50/85), and that of VEGF was 75.4% (64/85). There were 50.1% (43/85) patients showing positive staining both for iNOS and VEGF, 16.5% (14/85) showing negative staining both for iNOS and VEGF. Correlation with the two factors was significant ($P<0.05$). But more intensive analysis by Kendall test showed that the immunoreactive grades of VEGF had no association with that of iNOS ($P>0.05$, see Table 5).

Table 1 Expression of VEGF₁₆₅mRNA in gastric cancer and non-cancerous mucosa by RT-PCR

No.	Sex	Age (yr)	Histological type	Depth of invasion	Lympho node metastasis	Stage of TNM	VEGFmRNA	
							T	N
1	M	67	PD	musclaris	-	I	1.286	0.782
2	M	67	WD	extraserosa	+	III	1.568	1.086
3	F	41	PD	serosa	+	III	1.624	0.925
4	M	54	PD	extraserosa	+	IV	0.815	0.729
5	M	35	PD	extraserosa	+	III	1.204	0.627
6	M	50	MD	extraserosa	+	III	1.111	0.335
7	F	34	WD	extraserosa	+	III	1.347	0.845
8	M	46	MD	serosa	+	III	0.785	0.701
9	M	60	WD	submucosae	-	I	0.833	0.807
10	F	70	WD	serosa	-	I	0.627	0.525
11	M	62	WD	serosa	+	IV	0.850	0.646
12	F	31	WD	mucosae	-	I	0.815	1.136
13	M	55	MD	extraserosa	+	IV	1.545	0.872
14	M	70	WD	serosa	+	II	0.765	0.577
15	M	64	MD	serosa	-	III	1.082	0.842
16	M	66	MD	serosa	+	III	1.069	0.422
17	M	77	PD	serosa	+	IV	1.383	10.28
18	M	40	PD	serosa	+	II	1.156	1.381
19	F	50	PD	serosa	+	II	0.989	0.874
20	M	52	PD	serosa	+	III	1.895	0.356
21	F	38	PD	extraserosa	+	III	1.667	0.759
22	F	68	WD	mucosae	-	I	0.884	0.682
23	F	53	WD	extraserosa	+	III	1.456	0.682
24	M	61	MD	extraserosa	+	III	1.574	0.098
25	M	43	PD	serosa	-	I	1.198	0.429
26	M	43	PD	serosa	+	III	0.368	0.994
27	M	57	PD	serosa	+	II	1.052	0.661
28	F	44	PD	mucosae	-	I	0.952	0.793
29	M	71	WD	extraserosa	-	II	0.750	0.728
30	M	77	PD	extraserosa	+	IV	1.375	10.105
31	F	50	PD	mucosae	-	I	0.842	0.794
Mean value							1.125	0.760

Table 2 Relationship between expression of VEGF₁₆₅mRNA and clinical pathological features in gastric cancer tissue

Variable	No	Expression of VEGF (mean±SD)	
Age (yr)			
<55	16	1.139±0.393	P>0.05
>55	15	1.139±0.393	
Sizes of tumor			
≤2 cm	2	0.993±0.271	P>0.05
2-3 cm	6		
>3 cm	23	1.171±0.375	
Histological type			
Well differentiated	10	0.979±0.339	P>0.05
Moderate or poorly differentiated	21	1.1937±0.350	
Lymph node metastasis			
Positive	21	1.219±0.377	P=0.03
Negative	10	0.927±0.205	
Stage of UICC			
I	8	0.934±0.194	P=0.009
II	5		
III	13	1.262±0.386	
IV	5		

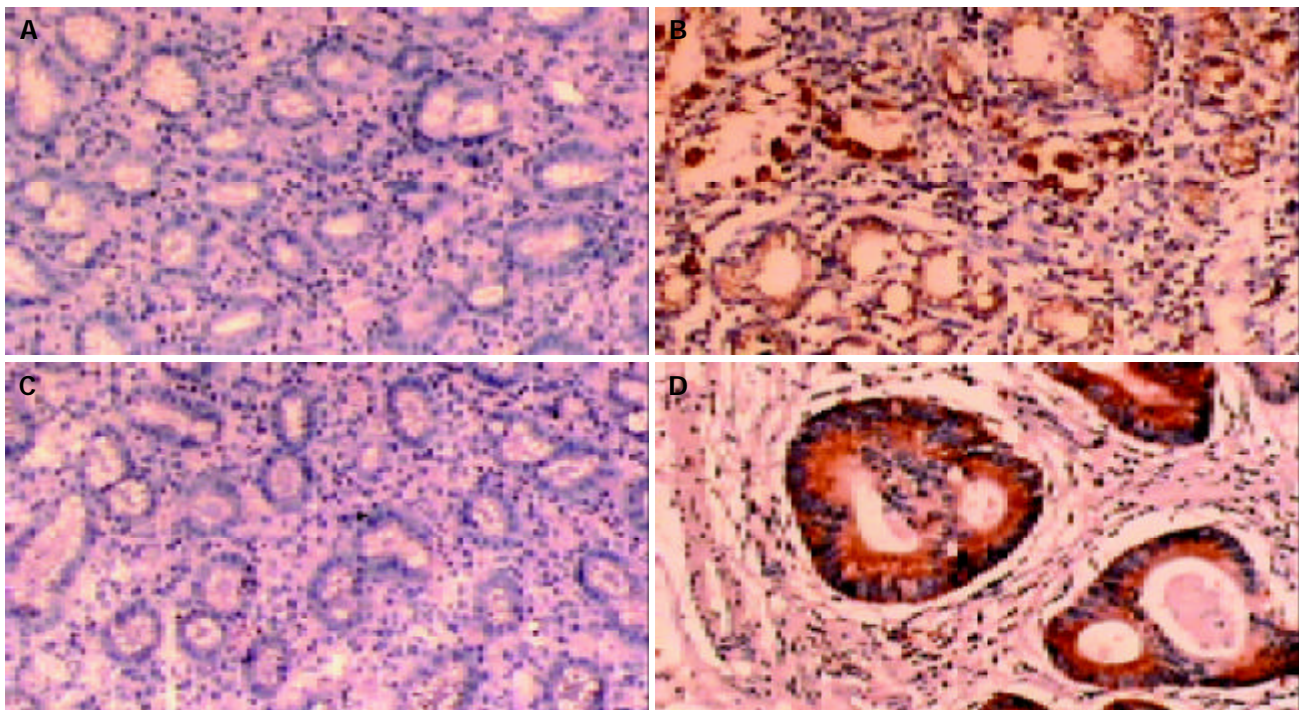


Figure 2 Immunostaining of VEGF and iNOS in gastric cancer and normal paired tissues. A: Negative staining of VEGF in normal paired gastric mucosae (×100), B: Positive staining of VEGF in gastric cancer (×100), C: Negative staining of iNOS in normal paired gastric mucosae (×100), D: Positive staining of iNOS in gastric cancer (×100).

Table 3 Relationship between level of VEGF₁₆₅mRNA expression and lymph node metastasis

Variable	Lymph node metastasis			Metastasis
	Positive cases	Negative cases	Total rate	
Over-expression	15	3	18	83.3%
Low-expression	6	7	13	46.2%
Total	19	10	31	

$\chi^2=4.775, P=0.02.$

Table 4 Relationship between level of VEGF₁₆₅mRNA expression and stages of UICC

Variable	Stages of UICC		Total	Ratio of III+IV
	I+II	III+IV		
Over-expression	4	14	18	77.8%
Low-expression	9	4	13	30.8%
Total	13	18	31	

$\chi^2=6.85, P=0.009.$

Table 5 Association with immunoreactive grades of VEGF protein and iNOS in gastric cancer

iNOS (N)	VEGF (N)				Total
	-	+	++	+++	
-	14	12	6	3	35
+	5	9	8	2	24
++	2	5	11	1	19
+++	0	2	3	2	7
Total	21	28	28	8	85

$\chi^2=5.615, P=0.132.$

DISCUSSION

VEGF is well characterized by its potent, specific angiogenesis-promoting effect. Native VEGF is a basic, heparin-binding, homodimeric glycoprotein of M_r 43 000-46 000. Five human VEGF mRNA species encoding VEGF isoforms of 121, 145, 165, 189, and 206 amino acids have been identified by alternative splicing of VEGFmRNA. An important biological property that distinguishes the different VEGF isoforms is their heparin and heparin-sulfate binding ability. VEGF₁₆₅ is the predominant form. VEGF has been found to be a highly specific mitogen for endothelial cells, and a prime regulator of angiogenesis and vasculogenesis, and could also contribute to the development of tumors because of its ability to induce permeabilization of blood vessels^[1,2,10,11]. Numerous studies have demonstrated that the high expression level of VEGF in many kinds of tumor cells^[12-14]. The same observations have also been seen in gastric cancer cells by *in vitro* and *in vivo*^[3-6,15,16]. We tested VEGF₁₆₅mRNA expression in 31 cases of resected gastric cancer specimens and normal paired gastric mucosae by RT-PCR, the results showing that the mean expression of VEGF₁₆₅mRNA in gastric cancer was significantly higher than that of normal paired mucosae. VEGF in high expression could combine with its receptors Flt-1 or KDR to exert its powerful function of promoting angiogenesis^[1,2,10]. Furthermore, some studies showed the high expression of Flt-1 and KDR in gastric tumor specimens by RT-PCR and immunohistochemistry, and exogenous VEGF₁₆₅ stimulated the growth of KDR positive carcinoma cells^[17,18]. These findings indicate there is a possible autocrine pathway for VEGF in gastric cancer, which is very important in the development of gastric cancer.

VEGF induces the formation of fenestrations in blood vessels and vesiculo-vacuolar organelles that form channels through which blood-borne proteins can extravasate. This could lead to the formation of an extravascular fibrin gel, which provides a matrix that supports the growth of endothelial cells and tumor cells and allows invasion of stromal cells into the development of tumors^[2]. A substantial number of studies have demonstrated a strong association between elevated tumor

expression of VEGF and advanced disease or poor prognosis in various cancers^[1,2]. In our study, the expression of VEGF₁₆₅mRNA was well related with lymph node metastasis and TNM stage, VEGF₁₆₅mRNA elevated in lymph node positive or stages III and IV patients, and was consistent with many immunohistochemical results. Kakeji *et al.*^[4] also revealed VEGF to be an independent prognostic factor and independent risk factor for liver metastasis. Karayiannakis *et al.*^[19] showed there was a significant association between serum VEGF levels and disease stage, as well as invasion depth of the tumor and the presence of distant metastasis. It was concerned with the invasiveness and metastasis of gastric cancer, and might be predictive of tumor status and prognosis in advanced gastric cancer patients, and could provide new prognostic information not afforded by conventional clinicopathologic prognostic indicators^[20-24].

Early gastric cancer patients have high survival rates, but there is lymph node metastasis in early gastric cancer, especially in submucosa, the rate of lymph node metastasis was about 20%, resulting in the decrease of 5-year survival of early gastric cancers. In our study, the expression of VEGF₁₆₅mRNA in the 5 cases of early gastric cancer had no difference with the normal paired mucosae, which the mucosae or submucosae were invaded, and lymph node metastasis was negative in the 5 cases. Recently Amioka *et al.* demonstrated VEGF was associated with lymphatic invasion and lymph node metastasis in early gastric cancer^[25-27]. The clinical significance of VEGF expression in early gastric cancer should be intensively studied.

VEGF production has been found to be regulated by growth factors, cytokines, oncogenes, anti-oncogenes and other extra cellular molecules, such as hypoxia, p53 gene, TGF- α ^[28-32]. But few investigations have been concerned with relationship between VEGF and iNOS. Nitric oxide produced through iNOS induction could enhance vasodilation, increase vascular permeability and accelerate nutrient supply of tumor tissues and promote neovascularization, thereby facilitating tumor growth^[7,8]. It has been shown that the expression of iNOS in most tumor tissues was higher than that in normal tissues. There were many reports concerning the high expression of iNOS in gastric cancer, which increased with the stage of the cancer and lymph node metastasis^[7,8,33]. We found the expression rate of iNOS in gastric cancer was 58.8%, and iNOS and VEGF had co-expressions in 50.1% of the patients, there was a correlation between the two factors. According to some reports^[34], VEGF could induce the release of NO from endothelial cells, on the other hand, endogenous NO enhanced VEGF synthesis in rat vascular smooth muscle cells; Host expression of NOS could contribute to induction of NOS in tumor and melanoma growth in mice, possibly by regulating the amount and availability of VEGF. The positive interaction between endogenous NO and VEGF might have implications for endothelial regeneration^[35]. Kisley *et al.*^[36] examined the effect of iNOS deficiency on VEGF protein concentration in mouse lung tumors, and showed VEGF concentration was lower than 54% in lung tumors isolated from iNOS(-/-)mice versus controls(wild-type +/+). NO enhanced the transcription of VEGF gene by inducing HIF-1 (hypoxia -inducible factor-1) binding activity in glioblastoma A-172 cells and hepatoma Hep3B cells. HIF was the best-characterized regulator of VEGF gene transcription^[37]. The high coincidental expression of iNOS and VEGF protein accumulation may be important events to enhance gastric carcinogenesis and poor clinical features. But in our present work, more intensive analysis showed that the immunoreactive grades of VEGF were no association with that of iNOS, indicating that many other factors may induce the production and angiogenesis of VEGF besides iNOS in gastric cancer.

REFERENCES

- Ferrara N.** Role of Vascular Endothelial Growth Factor in the Regulation of Angiogenesis. *Kidney International* 1999; **56**: 794-814
- Neufeld G,** Cohen T, Gaengrinovitch S, Poltorak AZ. Vascular endothelial growth factor (VEGF) and its receptors. *The FASEB Journal* 1999; **13**: 9-22
- Tian X,** Song S, Wu J, Meng L, Dong Z, Shou C. Vascular endothelial growth factor: acting as an autocrine growth factor for human gastric adenocarcinoma cell MGC803. *Biochem Biophys Res Commun* 2001; **286**: 505-512
- Kakeji Y,** Koga T, Sumiyoshi Y, Shibahara K, Oda S, Maehara Y, Sugimachi K. Clinical significance of vascular endothelial growth factor expression in gastric cancer. *J Exp Clin Cancer Res* 2002; **21**: 125-129
- Liu DH,** Zhang XY, Fan DM, Huang YX, Zhang JS, Huang WQ, Zhang YQ, Huang QS, Ma WY, Chai YB, Jin M. Expression of vascular endothelial growth factor and its role in oncogenesis of human gastric carcinoma. *World J Gastroenterol* 2001; **7**: 500-505
- Ichikura T,** Tomimatsu S, Ohkura E, Mochizuki H. Prognostic significance of the expression of vascular endothelial growth factor (VEGF) and VEGF-C in gastric cancer. *J Surg Oncol* 2001; **78**: 132-137
- Rajnakova A,** Mochhala S, Goh PM, Ngoi S. Expression of nitric oxide synthase, cyclooxygenase, and p53 in different stages of human gastric cancer. *Cancer Lett* 2001; **172**: 177-185
- Feng CW,** Wang LD, Jiao LH, Liu B, Zheng S, Xie XJ. Expression of p53, inducible nitric oxide synthase and vascular endothelial growth factor in gastric precancerous lesion: correlation with clinical features. *BMC Cancer* 2002; **2**: 8-15
- Tisher E,** Mitchell R, Hartman T, Silva M, Gospodarowicz D, Fiddes JC, Abraham JA. The human gene for vascular endothelial growth factor. Multiple protein forms are encoded through alternative exon splicing. *J Biol Chem* 1991; **266**: 11947-11954
- Ferrara N,** Gerber H, LeCouter J. The biology of VEGF and its receptors. *Nat Med* 2003; **9**: 669-676
- Bates DO,** Harper SJ. Regulation of vascular permeability by vascular endothelial growth factors. *Vascul Pharmacol* 2002; **39**: 225-237
- Whang YE,** Godley PA. Renal cell carcinoma. *Curr Opin Oncol* 2003; **15**: 213-216
- Shinkaruk S,** Bayle M, Lain G, Deleris G. Vascular endothelial growth factor (VEGF), an emerging target for cancer chemotherapy. *Curr Med Chem Anti Canc Agents* 2003; **3**: 95-117
- Mesters RM.** Angiogenesis in hematologic malignancies. *Ann Hematol* 2002; **81**: S72-74
- Song ZY,** Pang JP, Zhu YL, Qian KD, Zheng S. O-chloroacetylcarbonyl fumagillol combined with 5-fluorouracil in suppression of the growth of gastric cancer. *Chin J Pharmacol Toxicol* 2003; **17**: 24-28
- Du JR,** Jiang Y, Zhang YM, Fu H. Vascular endothelial growth factor and microvascular density in esophageal and gastric carcinomas. *World J Gastroenterol* 2003; **9**: 1604-1606
- Ren J,** Dong L, Xu CB, Pan BR. The role of KDR in the interactions between human gastric carcinoma cell and vascular endothelial cell. *World J Gastroenterol* 2002; **8**: 596-601
- Zhang H,** Wu J, Meng L, Shou CC. Expression of vascular endothelial growth factor and its receptors KDR and Flt-1 in gastric cancer cells. *World J Gastroenterol* 2002; **8**: 994-998
- Karayannakis AJ,** Syrigos KN, Polychronidis A, Zbar A, Kouraklis G, Simopoulos C, Karatzas G. Circulating VEGF levels in the serum of gastric cancer patients: correlation with pathological variables, patient survival, and tumor surgery. *Ann Surg* 2002; **236**: 37-42
- Kimura H,** Konishi K, Nukui T, Kaji M, Maeda K, Yabushita K, Tauji M, Miwa A. Prognostic significance of expression of thymidine phosphorylase and vascular endothelial growth factor in human gastric carcinoma. *J Surg Oncol* 2001; **76**: 31-36
- Maehara Y,** Kabashima A, Koga T, Tokunaga E, Takeuchi H, Kakeji Y, Sugimachi K. Vascular invasion and potential for tumor angiogenesis and metastasis in gastric carcinoma. *Surgery* 2000; **128**: 408-416

- 22 **Saito H**, Tsujitani S, Kondo A, Ikeguchi M, Maeta M, Kaibara N. Expression of vascular endothelial growth factor correlated with hematogenous recurrence in gastric carcinoma. *Surgery* 1999; **125**: 195-201
- 23 **Ohta M**, Konno H, Tanaka T, Baba M, Kamiya K, Syouji T, Kondoh K, Watanabe M, Terada M, Nakamura S. The significance of circulating vascular endothelial growth factor (VEGF) protein in gastric cancer. *Cancer Lett* 2003; **192**: 215-225
- 24 **Poon RT**, Fan ST, Wong J. Clinical significance of angiogenesis in gastrointestinal cancers: a target for novel prognostic and therapeutic approaches. *Ann Surg* 2003; **238**: 9-28
- 25 **Amioka T**, Kitadai Y, Tanaka S, Haruma K, Yoshihara M, Yasui W, Chayama K. Vascular endothelial growth factor-C expression predicts lymph node metastasis of human gastric carcinomas invading the submucosa. *Eur J Cancer* 2002; **38**: 1413-1419
- 26 **Maeda K**, Kang SM, Onoda N, Ogawa M, Kato Y, Sawada T, Chung KH. Vascular endothelial growth factor expression in preoperative biopsy specimens correlates with disease recurrence in patients with early gastric carcinoma. *Cancer* 1999; **86**: 566-571
- 27 **Konno H**, Baba M, Tanaka T, Kamiya K, Ota M, Oba K, Shoji A, Kaneko T, Nakamura S. Overexpression of vascular endothelial growth factor is responsible for the hematogenous recurrence of early-stage gastric carcinoma. *Eur Surg Res* 2000; **32**: 177-181
- 28 **Kim YB**, Han JY, Kim TS, Kim PS, Chu YC. Overexpression of c-H-ras p21 is correlated with vascular endothelial growth factor expression and neovascularization in advanced gastric carcinoma. *J Gastroenterol Hepatol* 2000; **15**: 1393-1399
- 29 **Saito H**, Tujitani S, Ikeguchi M, Ikeguchi M, Maeta M, Kaibara N. Neoagogenesis and relationship to nuclear p53 accumulation and vascular endothelial growth factor expression in advanced gastric carcinoma. *Oncology* 1999; **57**: 164-172
- 30 **Yamakawa M**, Liu LX, Date T, Belanger AJ, Vincent KA, Akita GY, Kuriyama T, Cheng SH, Gregory RJ, Jiang C. Hypoxia-inducible factor-1 mediates activation of cultured vascular endothelial cells by inducing multiple angiogenic factors. *Circ Res* 2003; **93**: 664-673
- 31 **Joo TE**, Sohn YH, Joo SY, Lee WS, Min SW, Park CH, Rew JS, Choi SK, Park CS, Kim YJ, Kim SJ. The role of vascular endothelial growth factor (VEGF) and p53 status for angiogenesis in gastric cancer. *Korean J Intern Med* 2002; **17**: 211-219
- 32 **Joo YE**, Rew JS, Seo YH, Choi SK, Kim YJ, Park CS, Kim SJ. Cyclooxygenase-2 overexpression correlates with vascular endothelial growth factor expression and tumor angiogenesis in gastric cancer. *J Chin Gastroenterol* 2003; **37**: 28-33
- 33 **Song ZJ**, Gong P, Wu YE. Relationship between the expression of iNOS, VEGF, tumor angiogenesis and gastric cancer. *World J Gastroenterol* 2002; **8**: 591-595
- 34 **DulaK J**, Jozkowicz A, Dembinska KA, Guevara I, Zdzienicka A, Zmudzinska GD, Florek I, Wojtowicz A, Szuba A, Cooke JP. Nitric oxide induces the synthesis of vascular endothelial growth factor by rat vascular smooth muscle cells. *Arterioscler Thromb Vasc Biol* 2000; **20**: 659-666
- 35 **Konopka TE**, Barker JE, Bamford TL, Guida E, Anderson RL, Stewart AG. Nitric oxide synthase II gene disruption—Implications for tumor growth and vascular endothelial growth factor production. *Cancer Res* 2001; **61**: 3182-3187
- 36 **Kisley LR**, Barrett BS, Bauer AK, Dwyer Nield LD, Barthel B, Meyer AM, Thompson DC, Malkinson AM. Genetic ablation of inducible nitric oxide synthase decreases mouse lung tumorigenesis. *Cancer Res* 2002; **62**: 6850-6856
- 37 **Kimura H**, Weisz A, Kurashima Y, Hashimoto K, Ogura T, D'Acquisto F, Addeo R, Makuuchi M, Esumi H. Hypoxia response element of the human vascular endothelial growth factor gene mediates transcriptional regulation by nitric oxide: control of hypoxia-inducible factor-1 activity by nitric oxide. *Blood* 2000; **95**: 189-197

Edited by Zhao M and Wang XL Proofread by Xu FM

Association of tumor necrosis factor genetic polymorphism with chronic atrophic gastritis and gastric adenocarcinoma in Chinese Han population

Bao-Ying Fei, Bing Xia, Chang-Sheng Deng, Xiao-Qing Xia, Min Xie, J Bart A Crusius, A Salvador Pena

Bao-Ying Fei, Department of Gastroenterology, Zhejiang Provincial People's Hospital, Hangzhou 310014, Zhejiang Province, China

Bing Xia, Chang-Sheng Deng, Department of Gastroenterology, Wuhan University Zhongnan Hospital, Wuhan 430071, Hubei Province, China

Xiao-Qing Xia, Min Xie, Department of Tumor Surgery, Hubei Provincial Tumor Hospital, Wuhan 430071, Hubei Province, China

J Bart A Crusius, A Salvador Pena, Laboratory of GI immunogenetics Vrije Universiteit Medical Center, Amsterdam, The Netherlands

Supported by a grant from provincial public health bureau, Hubei Province, No. 97420

Correspondence to: Dr Bao-Ying Fei, Department of Gastroenterology, Zhejiang Provincial People's Hospital, Hanzhou 310014, Zhejiang Province, China. feibaoying6924@tom.com

Telephone: +86-571-85239988 **Fax:** +86-571-85131448

Received: 2003-11-18 **Accepted:** 2003-12-16

Abstract

AIM: To investigate the association of TNF polymorphisms with chronic atrophic gastritis (CAG) and gastric adenocarcinoma in Chinese Han patients.

METHODS: The TNF- α 5 microsatellites and 3 RFLP sites were typed using PCR technique, followed by high-voltage denaturing PAGE with silver staining and restriction enzyme digestion respectively in specimens from 53 patients with CAG and 56 patients with gastric adenocarcinoma and 164 healthy controls. The PCR products were cloned and sequenced.

RESULTS: The frequency of TNF- β NcoI*1/2 genotype was higher in patients with chronic atrophic gastritis than in healthy controls, but no significant difference was observed (60.38% vs 46.34%, $P=0.076$). The frequency of TNa10 allele was significantly higher in patients with chronic atrophic gastritis than in healthy controls (19.81% vs 11.89%, $P=0.04$). However, it did not relate to age, gender, atrophic degree or intestinal metaplasia in patients with chronic atrophic gastritis. The frequency of TNF- β NcoI*1/2 and d2/d6 genotypes were significantly higher in patients with gastric adenocarcinoma than in healthy individuals ($P>0.05$). However, TNF- β NcoI*1/2 and d2/d6 genotypes did not relate to age, gender, grade of differentiation and clinicopathologic stage in patients with gastric adenocarcinoma. The frequency of TNFa6b5c1 haplotype homozygote was significantly lower in patients with gastric adenocarcinoma than in healthy controls (1.79% vs 15.85%, $P=0.006$).

CONCLUSION: TNFa10 allele may be a risk factor for chronic atrophic gastritis. TNF- β NcoI*1/2 and d2/d6 genotypes are associated with the susceptibility to gastric adenocarcinoma, whereas TNFa6b5c1 haplotype homozygote may contribute to the resistance against gastric adenocarcinoma.

Fei BY, Xia B, Deng CS, Xia XQ, Xie M, Crusius JBA, Pena AS.

Association of tumor necrosis factor genetic polymorphism with chronic atrophic gastritis and gastric adenocarcinoma in Chinese Han population. *World J Gastroenterol* 2004; 10(9): 1256-1261

<http://www.wjgnet.com/1007-9327/10/1256.asp>

INTRODUCTION

Gastric adenocarcinoma is one of the most frequent malignant diseases in the world, but the causes of gastric cancer remains unclear. The crude mortality rate of stomach cancer in China was 25.2 per 10⁵ (32.8 per 10⁵ for males and 17.0 per 10⁵ for females), which comprised 23.2% of the total death of cancer from 1990 to 1992, making stomach cancer the leading cause of the death among cancers^[1].

Tumor necrosis factor (TNF) is a multifunctional cytokine and its anti-tumor effect has attracted particular attention. TNF was found at a higher concentration in patients with malignant tumor. Forones *et al.*^[2] reported increased TNF- α expression in the sera of patients with advanced gastric cancer. TNF- α mRNA was markedly increased in gastric carcinoma tissue^[3]. Recombinant TNF has been demonstrated to have considerable treatment effect on gastric cancer *in vitro*^[4,5].

The gene for TNF- α and lymphotoxin- α (TNF- β), referred to as the TNF locus, are tandemly arranged within a 7-kilobase region in the HLA on the short arm of chromosome 6. HLA has recently been found to contribute to cancer development^[6-9]. Several RFLP sites and 5 microsatellites within the TNF gene have been identified. Some studies have shown that TNF individual alleles were correlated to secretion from activated monocytes^[10-13]. Furthermore, some experiments found that TNF secretion was also associated with TNF haplotypes, not only individual alleles^[14]. These findings suggest that TNF polymorphisms may play a role in the pathogenesis of several autoimmune, infectious and neoplastic diseases.

Chronic atrophic gastritis (CAG) is believed to be the precancerous lesion of gastric adenocarcinoma. In the present study, we examined whether TNF genetic polymorphisms were associated with CAG and gastric adenocarcinoma in Chinese Han population. Additionally, we determined whether the associations between TNF genetic polymorphisms and CAG and gastric adenocarcinoma varied with clinicopathologic features of the 2 diseases.

MATERIALS AND METHODS

Patients and genomic DNA extraction

The subjects of this study included 56 patients with gastric adenocarcinoma (43 males, 13 females; mean age 55.6 \pm 12.2 years), 53 patients with CAG (32 males, 21 females; mean age 53.5 \pm 11.4 years), and 164 unrelated healthy individuals (113 males, 51 females; mean age 52.5 \pm 11.3 years) from Chinese Han population in Hubei province of China. The diagnoses of gastric adenocarcinoma and CAG were confirmed by histopathology examinations. Genomic DNA was extracted

from venous blood by a salting out procedure with minor modifications.

TNF polymorphism typing

Five microsatellites were amplified using a single step PCR reaction with primers described by Pociot *et al.*^[15]. TNF microsatellite alleles were typed by a 60 g/L polyacrylamide, 0.4-mm sequencing gel, followed by silver nitrate staining. Fragments were sized using DNA markers and simultaneously typed with known alleles derived from the cloned PGEM-T vector.

The sites in the first intron of TNF-β marked by AspH1 and Nco1 were analyzed using PCR and endonuclease digestion. BSIHKA1, an isoschizomer of AspH1 (New England Biolabs, Beverley, MA) was used instead of AspH1. The digested products were electrophoresed in 1 g/L ethidium bromide-stained 15 g/L agarose gels. Similarly, the TNF-308 polymorphism was examined by PCR amplification and Nco1 digestion. The digested products were separated on a 100 g/L non-denaturing polyacrylamide gel. Alleles were visualized as described for TNF microsatellite typing.

Cloning and sequencing

The PCR products of 5 microsatellites were purified and ligated with PGEM-T vector. High efficiency JM 109 competent cells were used in the process of transformation. Needed transformants were obtained by blue/white color screening and standard ampicillin selection. Recombinant plasmid DNA were isolated and identified. Sequencing was done on ABI 377 DNA sequencer.

Statistical analysis

Allele frequencies in patients and control groups were calculated by direct counting. The Chi-square test and Fisher’s exact test were used for statistical analysis. Hardy-Weiberg equilibrium was tested in a 2×n analysis using Chi-Square.

RESULTS

The frequencies of the various alleles at 8 TNF polymorphic sites in 3 groups are shown in Table 1. The frequency of TNFa10 allele was significantly higher in patients with CAG than in healthy controls (19.81% vs 11.89%, *P*=0.04, OR=1.83, 95%CI

Table 1 Distribution frequency of TNF alleles at 8 polymorphic loci in CAG, gastric adenocarcinoma and healthy controls

TNF locus	Allele	Size (bp)	Controls (n=164)	CAG (n=53)	Gastric adenocarcinoma (n=56)	<i>P</i>
TNFa	a1	97	0.0183	0.0094	0.0089	0.040
	a2	99	0.1583	0.1698	0.2054	
	a3	101	0.0000	0.0094	0.0268	
	a4	103	0.0061	0.0094	0.0178	
	a5	105	0.0396	0.0378	0.0089	
	a6	107	0.3811	0.3585	0.3928	
	a7	109	0.0793	0.0378	0.0536	
	a8	111	0.0061	0.0094	0.0000	
	a9	113	0.0335	0.0566	0.0152	
	a10	115	0.1189	0.1981*	0.1161	
	a11	117	0.0945	0.0660	0.0803	
	a12	119	0.0091	0.0000	0.0000	
	a13	121	0.0549	0.0378	0.0152	
TNFb	b1	125	0.1006	0.0755	0.1339	
	b2	126	0.0000	0.0000	0.0000	
	b3	127	0.1128	0.0943	0.0536	
	b4	128	0.3293	0.3585	0.3482	
	b5	129	0.4512	0.4717	0.4643	
	b6	130	0.0000	0.0000	0.0000	
	b7	131	0.0061	0.0000	0.0000	
TNFc	c1	159	0.2104	0.7264	0.7679	
	c2	161	0.7896	0.2736	0.2321	
TNFd	d1	124	0.0061	0.0094	0.0000	
	d2	126	0.0548	0.0755	0.0536	
	d3	128	0.0457	0.0566	0.0446	
	d4	130	0.3537	0.3774	0.3393	
	d5	132	0.1341	0.1226	0.1786	
	d6	134	0.3018	0.2925	0.2857	
	d7	136	0.0000	0.0000	0.0000	
	d8	138	0.1037	0.0660	0.0982	
TNFe	e1	99	0.0640	0.0755	0.0000	
	e3	103	0.8110	0.8302	0.7768	
	e4	105	0.1159	0.0660	0.1250	
TNF-α 308	1		0.9329	0.9434	0.9732	
	2		0.0671	0.0566	0.0268	
TNF-β Nco1	1		0.4817	0.4528	0.4464	
	2		0.5183	0.5472	0.5536	
TNF-β AspH1	1		0.3079	0.3302	0.3571	
	2		0.6921	0.6698	0.6429	

1.02-3.27). However, it was not related to age, gender, atrophic degree and intestinal metaplasia in patients with CAG (Table 2). The frequency of TNF- β NcoI*1/2 genotype was higher in patients with chronic atrophic gastritis than in healthy controls (Table 3). However no significant difference was observed (60.38% vs 46.34%, $P=0.076$).

The frequency of TNF- β NcoI*1/2 genotype was significantly higher in patients with gastric adenocarcinoma than in healthy controls (64.29% vs 46.34%, $P=0.020$, OR=2.08, 95%CI 1.12-3.86). The frequency of d2/d6 genotype was also significantly higher in patients with gastric adenocarcinoma than in healthy individuals (10.71% vs 2.44%, $P=0.028$, OR=4.8, 95%CI 1.18-19.47). However, TNF- β NcoI*1/2 and d2/d6 genotypes were not related to age, gender, grade of differentiation and clinicopathologic stage in patients with gastric adenocarcinoma (Table 4).

Based on maximum likelihood estimate, 4 most frequent 3-locus haplotypes have been described in 4 European

populations: TNFa11b4c1, TNFa2b1c2, TNFa6b5c1, TNFa10b4c1. These haplotypes have also been observed in our study. By analysis of 2 locus association, we established 5 extended haplotypes which integrated alleles across the TNF locus in our population: TNFa6b5c1d8e4TNF308-1TNF β Nco1-1TNFAspH1-2, TNFa2b1c2d5e1TNF308-1TNF β Nco1-2TNFAspH1-2, TNFa11b4c1d4e3TNF308-1TNF β Nco1-2TNFAspH1-1, TNFa10b4c1d4e3TNF308-1TNF β Nco1-2TNFAspH1-1, TNFa2b3c1d2e3TNF308-2TNFAspH1-2. There were no significant differences in haplotype frequencies between CAG, gastric adenocarcinoma, and control groups for these haplotypes. However the frequency of TNFa6b5c1 haplotype homozygote was significantly lower in patients with gastric adenocarcinoma than in healthy individuals (1.79% vs 15.85%, $P=0.006$). It was not related to age, gender, grade of differentiation and clinicopathologic stage in patients with gastric adenocarcinoma.

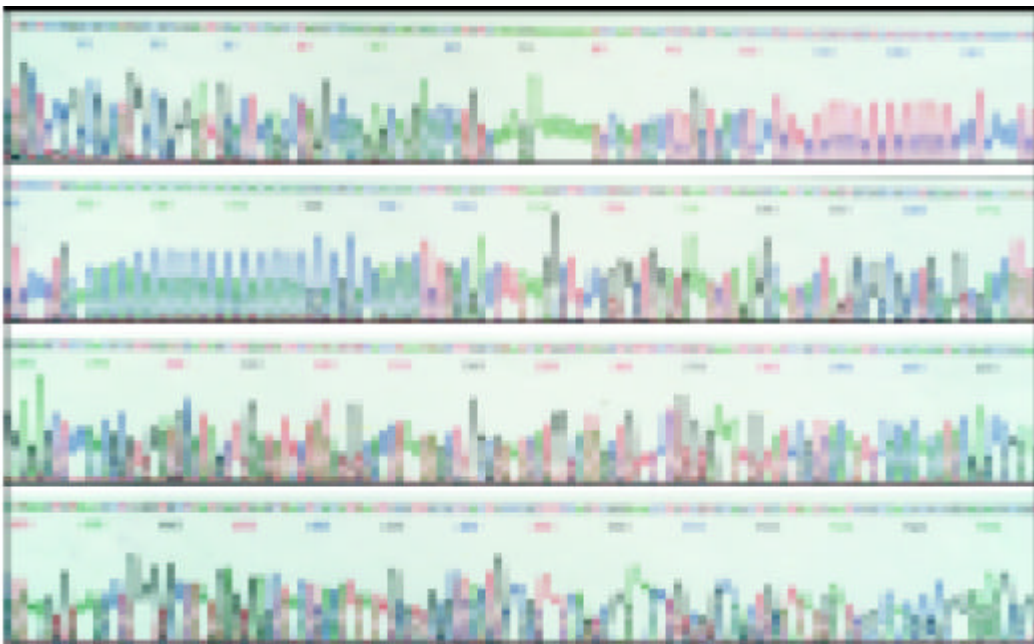


Figure 1 Nucleotide sequence of the cloned PGEM-T vector comprising TNFa6 allele (135→241) and TNFb5 allele (29→157), 150→179 fragment is 15 (AC/GT) repeats, 107→127 fragment is 10.5 (TC/GA) repeats.

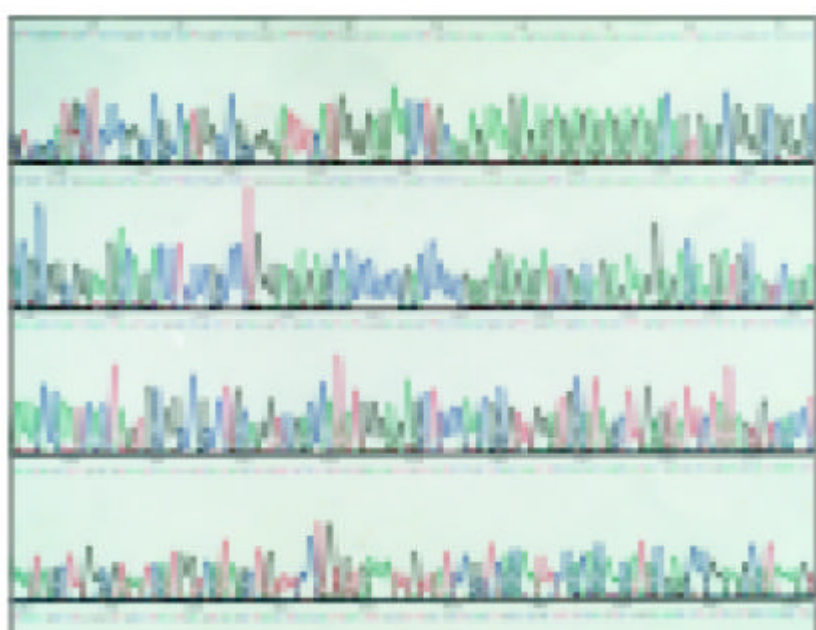


Figure 2 Nucleotide sequence of the cloned PGEM-T vector comprising TNFc1 allele (35→193), 59→76 fragment is 9 (TC/GA) repeats.

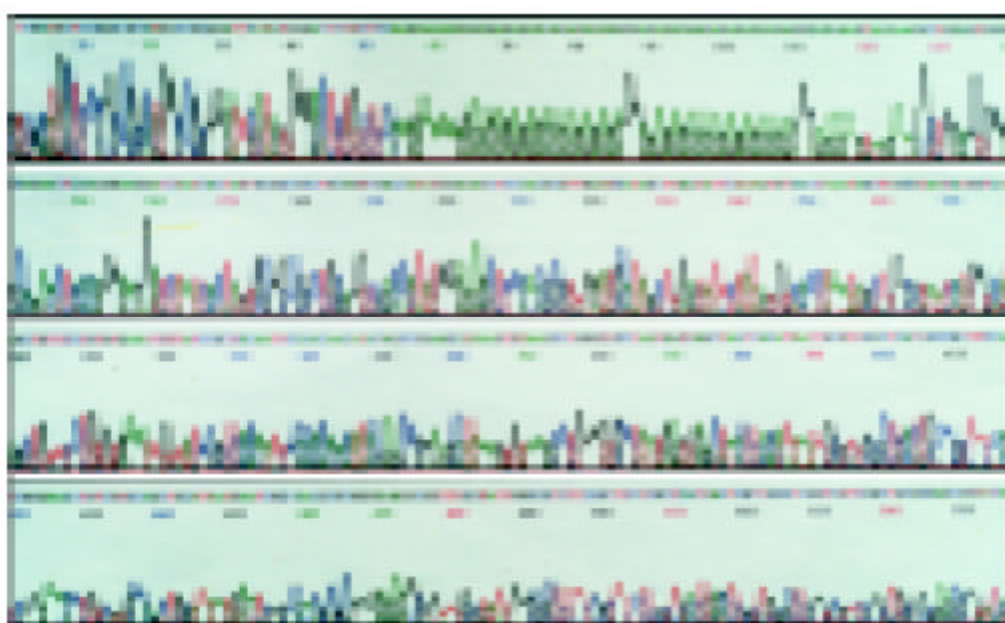


Figure 3 Nucleotide sequence of the cloned PGEM-T vector comprising TNFd4 allele (34→163), 64→85 fragment is 11 (TC/GA) repeats.

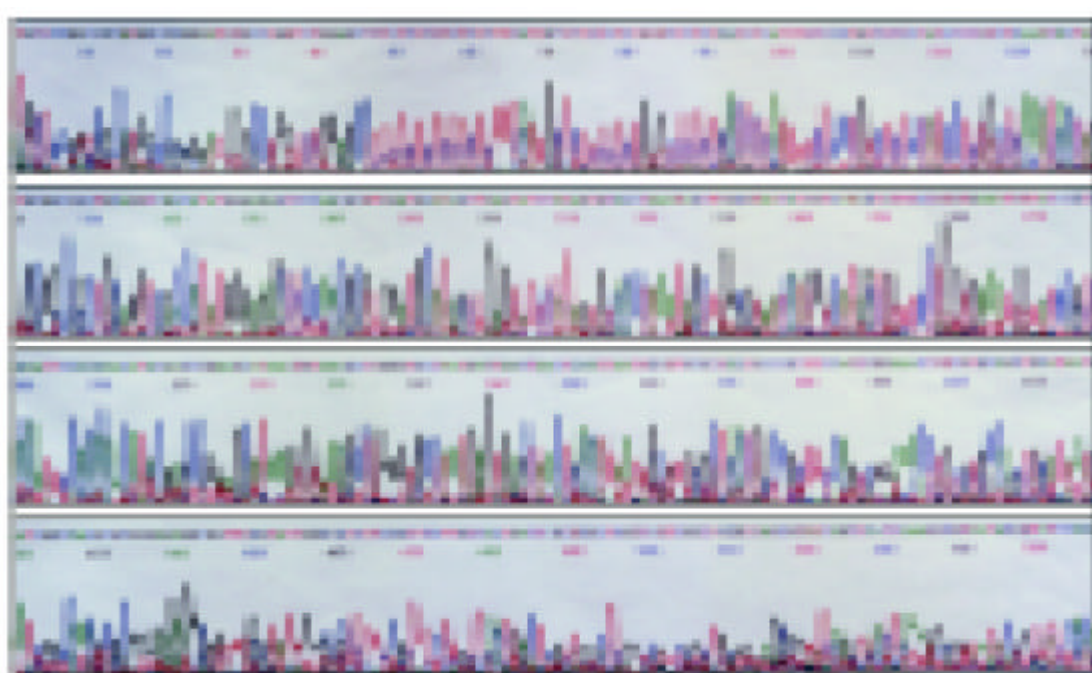


Figure 4 Nucleotide sequence of the cloned PGEM-T vector comprising TNFe3 allele (29→131), 47→62 fragment is 8 (TC/GA) repeats.

Table 2 Association between TNFa10 allele and clinical features of CAG

Groups	Age (yr)	Gender		Atrophic degree			Intestinal metaplasia	
		M	F	Mild	Moderate	Severe	Positive	Negative
TNFa10+	53.9±9.6	13	8	3	12	6	14	7
TNFa10-	53.2±12.5	19	13	6	18	8	22	10

Table 3 Distribution frequency of TNF TNF-β Ncol*1/2 and TNFd2/d6 genotypes in CAG, gastric adenocarcinoma and healthy controls

Group	TNF-β Ncol*1/2		TNFd2/d6	
	+	-	+	-
Controls	76	88	4	160
CAG	32	21	2	51
Gastric adenocarcinoma	36 ^a	20	6 ^c	50

^aP<0.05 vs compared with control group of TNF-β Ncol*1/2, ^cP<0.05 vs compared with control group of TNFd2/d6.

Table 4 Association between d2/d6 and TNF- β Ncol*1/2 genotypes and clinical features of gastric adenocarcinoma

Group	Age (yr)	Gender		Grade of differentiation		Clinicopathologic stage	
		M	F	High and moderate	Low	I-II	III-IV
d2/d6+	59.7±9.5	5	1	0	6	4	2
d2/d6-	55.1±12.5	38	12	13	37	21	29
1/2+	56.7±12.2	26	10	9	27	15	21
1/2-	53.6±11.5	17	3	4	16	10	10

The sequences of five TNF microsatellites (Figures 1-4) were consistent with that from a GeneBank database. However, several base exchanges were noted as following: TNFa at position 218 T→G, TNFc at 129 G→C, 170 A→G, TNFd at 87 G→A, 91 A→G, and TNFe at 81 C→T.

DISCUSSION

Genetic predisposition appears to be important in the pathogenesis of gastric adenocarcinoma. Genetic factors determining cancer risk have been postulated for the last decades and seem to be more apparent for gastric adenocarcinoma^[16-21]. The relevant genes mediating the risk of gastric adenocarcinoma have not been identified until now. Progress of CAG towards gastric adenocarcinoma seems to be influenced by genetic factors^[22,23].

A diallelic TNF- β polymorphism detected using the enzyme Ncol influences the TNF- α and/or - β secretion of peripheral blood mononuclear cells^[24]. Park *et al.*^[25] found that TNF- β Ncol*1/1 genotypes showed an increased risk for colorectal cancer, and that TNF- β *1 allele played some role in the initial step of tumorigenesis or activation of dormant tumor cells, whereas TNF- β *2 allele mediated some functions associated with cytotoxicity of tumor cells. Our result showed that the frequency of TNF- β Ncol*1/2 genotype was significantly higher in patients with gastric adenocarcinoma than in healthy individuals. It suggested that TNF- β Ncol*1/2 genotype was related to the pathogenesis of gastric cancer. At the same time we found the frequency of TNF- β Ncol*1/2 genotype was also high in patients with CAG. However, the association between TNF- β Ncol*1/2 genotype and CAG did not show a significant difference. Further studies are necessary to elucidate if TNF- β Ncol*1/2 genotype is a risk factor for CAG. The frequency of d2/d6 genotype was also significantly higher in patients with gastric adenocarcinoma than in healthy individuals. It indicated that d2/d6 genotype might have some effect on pathogenesis of gastric adenocarcinoma.

Azuma *et al.*^[23] reported that the DQA1*0102 might contribute to resistance against *H pylori* associated gastric atrophy and immunogenetic factors were important in the etiology of *H pylori* associated gastric atrophy. Proinflammatory IL-1beta polymorphisms are associated with hypochlorhydria and atrophic gastritis in Japan^[24]. The presence of the IL-1*C allele may also indicate a risk of mucosal atrophy of the stomach in the Japanese population^[26]. Our study has shown an association between TNFa10 allele and CAG, but not between TNFa10 allele and gastric adenocarcinoma. It suggested that TNFa10 allele might be a host risk factor for CAG. However, it was not related to age, gender, atrophic degree and intestinal metaplasia in patients with CAG.

A significant reduction in high expressing haplotypes was found in patients with follicular lymphoma^[27]. Hajeer *et al.*^[28] reported the TNF a2-b4-d5 haplotype was significantly associated with the number of basal cell carcinoma (BCC) lesions. It provides the evidence that TNF microsatellite haplotype may influence the pathogenesis of multiple BCC. We found negative association between TNFa6b5c1 haplotype homozygote and gastric adenocarcinoma. The frequency of

TNFa6b5c1 haplotype homozygote was lower in patients with gastric adenocarcinoma. It suggested that TNFa6b5c1 haplotype homozygote might contribute to the resistance against gastric adenocarcinoma. The absence of TNFa6b5c1 haplotype homozygote might increase the risk of gastric adenocarcinoma.

The TNF- α 308A allele has been associated with enhanced TNF- α expression^[10]. Machado *et al.* proposed that individuals carrying TNF- α 308A allele had an increased risk for gastric cancer with an OR of 1.9^[29]. However our results showed that there was no association between TNF- α 308 allele and gastric adenocarcinoma. Similarly, Wu *et al.* reported no association was noted between gastric cancer and controls in the distribution of TNF- α genotypes in Taiwanese Chinese population^[30]. The discrepancy may be attributable to ethnic difference.

Onishi *et al.*^[31] demonstrated a significantly favorable prognosis in the renal carcinoma patients with TNF- β 1/1 homozygote compared with other zygotes of TNF-beta polymorphism. The patients with TNF- β 1/1 homozygote showed much lower stage and/or grade than those of other zygotes. TNF polymorphisms TNF+488A and TNF-859T were associated with grade of tumour in patients with bladder cancer^[32]. However, in our study TNF- β Ncol*1/2 and d2/d6 genotypes and TNFa6b5c1 haplotype were not related to age, gender, grade of differentiation and clinicopathologic stage in patients with gastric adenocarcinoma. Patients with d2/d6 genotype were present with a lowly differentiated tumor, however the difference did not reach statistical significance. Larger sample studies are needed.

The association between TNF genetic polymorphisms and CAG and gastric adenocarcinoma is not clear. However, 2 distinct potential mechanisms can be proposed. First, TNF alleles may be involved in genetically controlled variations in TNF production as previously described. Another possible explanation is that these genes are not responsible for the pathophysiological mechanisms but are linked closely to other responsible genes. TNF has been reported to be in linkage disequilibrium with HLA genes^[33-35]. The negative association of TNFa3-e1 with rheumatoid arthritis may be secondary to the negative linkage disequilibrium between TNFa3-e1 and HLA-DR4^[36]. Additional studies will be necessary to investigate whether TNF genes are independent of other linked genes to play a role.

With regard to several base exchanges in our sequencing result, more studies should be done to verify whether they are caused by ethnic difference or other factors.

REFERENCES

- 1 Sun X, Mu R, Zhou Y, Dai X, Qiao Y, Zhang S, Huangfu X, Sun J, Li L, Lu F. 1990-1992 mortality of stomach cancer in China. *Zhonghua Zhongliu Zazhi* 2002; **24**: 4-8
- 2 Forones NM, Mandowsky SV, Lourenco LG. Serum levels of interleukin-2 and tumor necrosis factor-alpha correlate to tumor progression in gastric cancer. *Hepatogastroenterology* 2001; **48**: 1199-1201
- 3 Izutani R, Katoh M, Asano S, Ohyanagi H, Hirose K. Enhanced expression of manganese superoxide dismutase mRNA and increased TNF alpha mRNA expression by gastric mucosa

- in gastric cancer. *World J Surg* 1996; **20**: 228-233
- 4 **Wei XC**, Wang XJ, Chen K, Zhang L, Liang Y, Lin XL. Killing effect of TNF-related apoptosis inducing ligand regulated by tetracycline on gastric cancer cell line NCI-N87. *World J Gastroenterol* 2001; **7**: 559-562
 - 5 **Buell JF**, Reed E, Lee KB, Parker RJ, Venzon DJ, Amikura K, Arnold S, Fraker DL, Alexander HR. Synergistic effect and possible mechanisms of tumor necrosis factor and cisplatin cytotoxicity under moderate hyperthermia against gastric cancer cells. *Ann Surg Oncol* 1997; **4**: 141-148
 - 6 **Ghaderi M**, Nikitina Zake L, Wallin K, Wiklund F, Hallmans G, Lenner P, Dillner J, Sanjeevi CB. Tumor necrosis factor A and MHC class I chain related gene A (MIC-A) polymorphisms in Swedish patients with cervical cancer. *Hum Immunol* 2001; **62**: 1153-1158
 - 7 **Juszczynski P**, Kalinka E, Bienvenu J, Woszczek G, Borowiec M, Robak T, Kowalski M, Lech-Maranda E, Baseggio L, Coiffier B, Salles G, Warzocha K. Human leukocyte antigens class II and tumor necrosis factor genetic polymorphisms are independent predictors of non-Hodgkin lymphoma outcome. *Blood* 2002; **100**: 3037-3040
 - 8 **Gelder CM**, Williams OM, Hart KW, Wall S, Williams G, Ingrams D, Bull P, Bunce M, Welsh K, Marshall SE, Borysiewicz L. HLA class II polymorphisms and susceptibility to recurrent respiratory papillomatosis. *J Virol* 2003; **77**: 1927-1939
 - 9 **Matsumoto K**, Yasugi T, Nakagawa S, Okubo M, Hirata R, Maeda H, Yoshikawa H, Taketani Y. Human papillomavirus type 16 E6 variants and HLA class II alleles among Japanese women with cervical cancer. *Int J Cancer* 2003; **106**: 919-922
 - 10 **Wilson AG**, Symons JA, McDowell TL, McDevitt HO, Duff GW. Effects of a polymorphism in the human tumor necrosis factor α promoter on transcriptional activity. *Proc Natl Acad Sci U S A* 1997; **94**: 3195-3199
 - 11 **Kaluza W**, Reuss E, Grossmann S, Hug R, Schopf RE, Galle PR, Maerker-Hermann E, Hoehler T. Different transcriptional production in psoriasis patients carrying the TNF- α 238A promoter polymorphism. *J Invest Dermatol* 2000; **114**: 1180-1183
 - 12 **Fargion S**, Valenti L, Dongiovanni P, Scaccabarozzi A, Fracanzani AL, Taioli E, Mattioli M, Sampietro M, Fiorelli G. Tumor necrosis factor alpha promoter polymorphisms influence the phenotypic expression of hereditary hemochromatosis. *Blood* 2001; **97**: 3707-3712
 - 13 **Baseggio L**, Bienvenu J, Charlot C, Picollet J, Felman P, Coiffier B, Salles G. Higher LPS-stimulated TNF-alpha mRNA levels in peripheral blood mononuclear cells from non-Hodgkin's lymphoma patients. *Exp Hematol* 2001; **29**: 330-338
 - 14 **Bouma G**, Crusius JB, Oudkerk Pool M, Kolkman JJ, von Blomberg BM, Kostense PJ, Giphart MJ, Schreuder GM, Meuwissen SG, Pena AS. Secretion of tumor necrosis factor alpha and lymphotoxin alpha in relation to polymorphisms in the TNF genes and HLA-DR alleles. Relevance for inflammatory bowel disease. *Scand J Immunol* 1996; **43**: 456-463
 - 15 **Pociot F**, Briant L, Jongeneel CV, Molvig J, Worsaae H, Abbal M, Thomsen M, Nerup J, Cambon-Thomsen A. Association of tumor necrosis factor (TNF) and class II major histocompatibility complex alleles with the secretion of TNF- α and TNF- β by human mononuclear cells: a possible link to insulin-dependent diabetes mellitus. *Eur J Immunol* 1993; **23**: 224-231
 - 16 **Artunedo Pe P**, Moreno Azcoita M, Alonso A, Fernandez-Peralta A, Gonzalez-Aguilera JJ. Prognostic significance of high microsatellite instability in a Spanish series of gastric adenocarcinomas. *Anticancer Res* 2000; **20**: 4009-4014
 - 17 **Cai L**, Yu SZ, Zhang ZF. Glutathione S-transferases M1, T1 genotypes and the risk of gastric cancer: A case-control study. *World J Gastroenterol* 2001; **7**: 506-509
 - 18 **El-Omar EM**, Carrington M, Chow WH, McColl KE, Bream JH, Young HA, Herrera J, Lissowska J, Yuan CC, Rothman N, Lanyon G, Martin M, Fraumeni JF Jr, Rabkin CS. Interleukin-1 polymorphisms associated with increased risk of gastric cancer. *Nature* 2000; **404**: 398-402
 - 19 **Machado JC**, Pharoah P, Sousa S, Carvalho R, Oliveira C, Figueiredo C, Amorim A, Seruca R, Caldas C, Carneiro F, Sobrinho-Simoes M. Interleukin 1B and interleukin 1RN polymorphisms are associated with increased risk of gastric carcinoma. *Gastroenterology* 2001; **21**: 823-829
 - 20 **Oue N**, Matsumura S, Nakayama H, Kitadai Y, Taniyama K, Matsusaki K, Yasui W. Reduced expression of the TSP1 gene and its association with promoter hypermethylation in gastric carcinoma. *Oncology* 2003; **64**: 423-429
 - 21 **El-Omar EM**, Rabkin CS, Gammon MD, Vaughan TL, Risch HA, Schoenberg JB, Stanford JL, Mayne ST, Goedert J, Blot WJ, Fraumeni JF Jr, Chow WH. Increased risk of noncardia gastric cancer associated with proinflammatory cytokine gene polymorphisms. *Gastroenterology* 2003; **124**: 1193-1201
 - 22 **Furuta T**, El-Omar EM, Xiao F, Shirai N, Takashima M, Sugimura H, Sugimura H. Interleukin 1beta polymorphisms increase risk of hypochlorhydria and atrophic gastritis and reduce risk of duodenal ulcer recurrence in Japan. *Gastroenterology* 2002; **123**: 92-105
 - 23 **Azuma T**, Ito S, Sato F, Yamazaki Y, Miyaji H, Ito Y, Suto H, Kuriyama M, Kato T, Kohli Y. The role of the HLA-DQA1 gene in resistance to atrophic gastritis and gastric adenocarcinoma induced by Helicobacter pylori infection. *Cancer* 1998; **82**: 1013-1018
 - 24 **Whichelow CE**, Hitman GA, Raafat I, Bottazzo GF, Sachs JA. The effect of TNF* β gene polymorphism on TNF-alpha and -beta secretion levels in patients with insulin-dependent diabetes mellitus and healthy controls. *Eur J Immunogenet* 1996; **23**: 425-435
 - 25 **Park KS**, Mok JW, Rho SA, Kim JC. Analysis of TNFB and TNFA NcoI RFLP in colorectal cancer. *Mol Cells* 1998; **8**: 246-249
 - 26 **Kato S**, Onda M, Yamada S, Matsuda N, Tokunaga A, Matsukura N. Association of the interleukin-1 beta genetic polymorphism and gastric cancer risk in Japanese. *J Gastroenterol* 2001; **36**: 696-699
 - 27 **Fitzgibbon J**, Grenzelias D, Matthews J, Lister TA, Gupta RK. Tumour necrosis factor polymorphisms and susceptibility to follicular lymphoma. *Br J Haematol* 1999; **107**: 388-391
 - 28 **Hajeer AH**, Lear JT, Ollier WE, Naves M, Worthington J, Bell DA, Smith AG, Bowers WP, Jones PW, Strange RC, Fryer AA. Preliminary evidence of an association of tumour necrosis factor microsatellites with increased risk of multiple basal cell carcinomas. *Br J Dermatol* 2000; **142**: 441-445
 - 29 **Machado JC**, Figueiredo C, Canedo P, Pharoah P, Carvalho R, Nabais S, Castro Alves C, Campos ML, Van Doorn LJ, Caldas C, Seruca R, Carneiro F, Sobrinho-Simoes M. A proinflammatory genetic profile increases the risk for chronic atrophic gastritis and gastric carcinoma. *Gastroenterology* 2003; **125**: 364-371
 - 30 **Wu MS**, Wu CY, Chen CJ, Lin MT, Shun CT, Lin JT. Interleukin-10 genotypes associate with the risk of gastric carcinoma in Taiwanese Chinese. *Int J Cancer* 2003; **104**: 617-623
 - 31 **Onishi T**, Ohishi Y, Goto H, Asano K, Makino H, Hatano T, Tomita M, Abe K, Imagawa K, Kinoshita M, Fukui T. Study on the relationship between tumour necrosis factor gene polymorphism and prognosis in the patients with renal cell carcinoma. *Nippon Hinyokika Gakkai Zasshi* 1998; **89**: 413-420
 - 32 **Marsh HP**, Haldar NA, Bunce M, Marshall SE, le Monier K, Winsey SL, Christodoulos K, Cranston D, Welsh KI, Harris AL. Polymorphisms in tumour necrosis factor (TNF) are associated with risk of bladder cancer and grade of tumour at presentation. *Br J Cancer* 2003; **89**: 1096-1101
 - 33 **Oturai A**, Larsen F, Ryder LP, Madsen HO, Hillert J, Fredrikson S, Sandberg-Wollheim M, Laaksonen M, Koch-Henriksen N, Sawcer S, Fugger L, Sorensen PS, Svejgaard A. Linkage and association analysis of susceptibility regions on chromosomes 5 and 6 in 106 Scandinavian sibling pair families with multiple sclerosis. *Ann Neurol* 1999; **46**: 612-616
 - 34 **Louka AS**, Lie BA, Talseth B, Ascher H, Ek J, Gudjonsdottir AH, Sollid LM. Coeliac disease patients carry conserved HLA-DR3-DQ2 haplotypes revealed by association of TNF alleles. *Immunogenetics* 2003; **55**: 339-343
 - 35 **Di Somma C**, Charron D, Deichmann K, Buono C, Ruffilli A. Atopic asthma and TNF-308 alleles: linkage disequilibrium and association analyses. *Hum Immunol* 2003; **64**: 359-365
 - 36 **Yen JH**, Chen CJ, Tsai WC, Lin CH, Ou TT, Lin SC, Dai ZK, Liu HW. Tumor necrosis factor microsatellite alleles in patients with rheumatoid arthritis in Taiwan. *Immunol Lett* 2002; **81**: 177-182

Significance of effector protease receptor-1 expression and its relationship with proliferation and apoptotic index in patients with primary advanced gastric adenocarcinoma

Xue-Quan Yao, Fu-Kun Liu, Jie-Shou Li, Xiao-Ping Qi, Bo Wu, Hong-Lin Yin, Heng-Hui Ma, Qun-Li Shi, Xiao-Jun Zhou

Xue-Quan Yao, Fu-Kun Liu, Jie-Shou Li, Xiao-Ping Qi, Bo Wu, Hong-Lin Yin, Heng-Hui Ma, Qun-Li Shi, Xiao-Jun Zhou, School of Medicine, Nanjing University. Department of General Surgery, Jinling Hospital, 305 Zhongshangdong Road, Nanjing, 210002, Jingsu Province, China

Correspondence to: Xue-Quan Yao, Department of General Surgery, Jinling Hospital, 305 Zhongshangdong Road, Nanjing, 210002, Jingsu Province, China. yaoxuequan@yahoo.com

Telephone: +86-25-84826808-860005

Received: 2003-04-02 **Accepted:** 2003-06-07

Abstract

AIM: To investigate the expression of effector protease receptor-1 (EPR-1), proliferative index ki-67 and apoptosis index in patients with primary advanced gastric adenocarcinoma and to clarify the significance of EPR-1 expression and its correlation with the proliferation and apoptosis indexes.

METHODS: Using immunohistochemical staining and terminal deoxynucleotidyl transferase mediated nick end labelling (TUNEL) technique, we determined the expression of EPR-1, proliferative index (Ki-67) and apoptotic index (AI) in 120 paraffin-embedded specimens of primary advanced gastric adenocarcinoma as well as lymph node metastasis and adjacent normal tissues.

RESULTS: EPR-1 expression was distributed in the cytoplasm of normal gastric mucosa, carcinoma cells and smooth muscle cells. The positive rate of EPR-1 expression in the primary gastric adenocarcinomas, invasion tumor node and lymph node metastasis was 65.83%, 55.29% and 68%, respectively. While the positive rate in normal gastric mucosa and smooth muscle cells was 46.7% and 53.3%, respectively. The average positive rate of ki-67 in EPR-1-positive tumors was 7.00% which was significantly lower than that of 8.53% in EPR-1-negative tumors, but the average AI in EPR-1-positive tumors was 1.25%, which was significantly higher than that of 1.00% observed in EPR-1-negative tumors. On the other hand, the average positive labeling index for Ki-67 (ki-67) in EPR-1-positive lymph node metastasis was 7.65%, which was significantly lower than that of 9.44% observed in EPR-1-negative lymph node metastasis. However, the average AI in EPR-1-positive lymph node metastasis tumors was 0.99%, which was significantly higher than that of 0.67% observed in EPR-1-negative lymph node metastasis.

CONCLUSION: The frequency of EPR-1 expression was significantly higher in primary gastric adenocarcinoma and in its lymph node metastasis than that in normal gastric mucosa. Expression of EPR-1 was significantly correlated with tumor histological subtypes and tumor differentiation. Weighted EPR-1 Score is positively correlated with apoptosis

index, but is negatively related with proliferative index. Thus, Weighted EPR-1 Score and EPR-1 expression in gastric adenocarcinoma cells maybe a potential marker in clinical setting.

Yao XQ, Liu FK, Li JS, Qi XP, Wu B, Yin HL, Ma HH, Shi QL, Zhou XJ. Significance of effector protease receptor-1 expression and its relationship with proliferation and apoptotic index in patients with primary advanced gastric adenocarcinoma. *World J Gastroenterol* 2004; 10(9): 1262-1267

<http://www.wjgnet.com/1007-9327/10/1262.asp>

INTRODUCTION

Gastric cancer is the second most common malignancy worldwide. Approximately 95% of all malignant gastric neoplasms are adenocarcinoma. This study aimed to investigate the relationship among expression of EPR-1, proliferative index (PI, also referred to as ki-67) and apoptosis index (AI) in patients with primary advanced gastric adenocarcinoma and to clarify the significance of EPR-1 expression in human primary gastric adenocarcinoma, its lymph node metastasis and adjacent non-tumor tissues.

MATERIALS AND METHODS

Patients and tissue samples

Primary gastric adenocarcinoma specimens from 120 patients who had undergone gastrectomy in the period of January 1991 and December 1995 were selected from the files of the Pathology Department, Nanjing Jinling Hospital. None of the patients had received chemotherapy or radiotherapy before surgery. There were 72 males and 48 females, with a median age of 64.8 years (range, 45-78 years). Samples were taken from the representative cancerous lesions as well as lymph node metastasis and adjacent non-cancerous mucosa.

Specimens of the adenocarcinoma were classified into papillary adenocarcinoma, tubular adenocarcinoma, mucinous adenocarcinoma and signet-ring cell carcinoma. Each subclass had 30 cases.

For formalin-fixed and paraffin-embedded tissue specimens, consecutive 4- μ m thick sections were cut and representative sections were used for immunohistochemistry (IHC) and haematoxylin-eosin (H&E) staining as well as the terminal deoxynucleotidyl transferase (TdT)-mediated dUTP-biotin nick end-labeling (TUNEL) for apoptotic index. Using the H&E-stained sections, the tumor histology according to Lauren's grade of tumor differentiation and criteria of the World Health Organization were reassessed. Tumors were staged according to TNM classification.

Immunohistochemistry

The deparaffinized and rehydrated slides were boiled in a 10 mmol/L EDTA buffer (pH 8.0) for 5 min in an autoclave at 121 °C. The sections were immunohistochemically stained by

the labeled streptavidin-biotin peroxidase method (LSAB2 Kit; Dako Japan Inc., Kyoto, Japan) with the following primary antibodies: monoclonal antibodies EPR-1 (ADI, Alpha Diagnostic International, dilution 1:100), and Ki-67 (Maxim, China, dilution 1:50). The slides were immersed for 10 min in 3 mL/L hydrogen peroxide/methanol to deplete endogenous peroxidase. Then, nonspecific binding sites were blocked with 3 mL/L normal goat serum for 10 min. The primary antibody was then applied, and the sections were incubated overnight at 4 °C. After washed with PBS (0.01 mol/L pH7.4), biotinylated goat antimouse IgG was applied onto the tissue sections and incubated at room temperature for 10 min. After washed with PBS, a streptavidin peroxidase reagent was applied and incubated at room temperature for 10 min. Finally, the reaction product was visualized using developing color by incubating the slides in a solution of 3 mL/L hydrogen peroxide and AEC chromogen. The sections were counterstained slightly with hematoxylin. Negative controls included parallel sections treated without the primary antibody, in addition to negat an adjacent section of the same block in which the primary antibody was replaced by phosphate-buffered saline (PBS).

TUNEL staining

For detection of apoptotic cells, apoptotic index was examined by the terminal deoxynucleotidyl transferase-mediated deoxyuridine triphosphate fluorescence nick end labeling (TUNEL) method. TUNEL: *In situ* cell death detection kit POD (ISCCD, Boehringer Mannheim, Germany) was used to detect the apoptotic cell. The procedures was according to the protocol of the kit and other references. Briefly, the sections were deparaffinized, rehydrated, and washed in distilled water (DW). The tissues were digested with 20 g/mL proteinase K (Boehringer Mannheim, Mannheim, Germany) at room temperature for 15 min. Endogenous peroxidase activity was blocked by incubating it in 3 mL/L hydrogen peroxide/methanol in PBS at 37 °C for 30 min. The sections then were incubated with terminal deoxynucleotidyl transferase at 37 °C for 60 min, and dioxigenin-conjugatd dUTP was added to the 3' -OH ends of fragmented DNA. Anti-dioxigenin antibody peroxidase was applied to the sections to detect the labeled nucleotides. The sections were stained with DAB and counterstained slightly with hematoxylin. The positive cells were identified, counted and analyzed under the light microscope.

Evaluation of EPR-1 expression

Two experienced pathologists in a blinded fashion (without knowledge of the clinico-pathological features of the tumors) examined the expression of EPR-1 and Ki-67 independently in terms of intensity and positive rate of the immunostaining in each specimen tissue section. The positive staining for EPR-1 protein was expressed as red brown granules, which were mainly located in cell cytoplasm at microscopy. At least 5 high-power ($\times 400$ field) fields were chosen randomly and 1 000 cells were counted. The ratio of EPR-1-positive cells was calculated by dividing the number of positive cells over the total number of cells, and was expressed as percentage.

For quantitation of the EPR-1 expression in various samples examined, a semi-quantitative scoring system was used as previously described^[1]. An average percentage of positive tumor cells was determined in at least five areas at $\times 400$ magnification and assigned to one of the five categories: (a) $0 \leq 5\%$, (b) $1 = 5-25\%$, (c) $2 = 25-50\%$, (d) $3 = 50-75\%$, and (e) $4 \geq 75\%$. The intensity of EPR-1 immunostaining was scored on a scale of 1-3 as following: (a) weak, 1+; (b) moderate, 2+; and (c) intense, 3+. The percentage of positive tumor cells and the staining intensity were multiplied to produce a weighted score for each case. The case with the weighted score less than 1 was defined as negative, otherwise as positive.

Ki-67-positive cells showed a distinct brown staining of the nuclei with strong intratumoral heterogeneity (Figure 1). The percentages of Ki-67-positive tumor cells were evaluated with a light microscope holding a $\times 100$ oil immersion objective by scoring a minimum of 1 000 tumor cells in randomly selected fields.

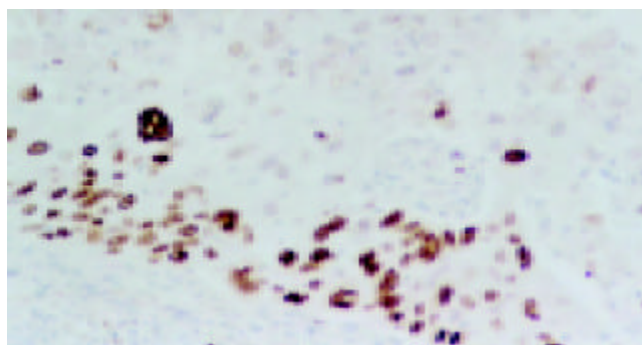


Figure 1 Immunohistochemical staining patterns of Ki-67 in gastric adenocarcinomas. Positive nuclear staining in LSAB, $\times 200$. Poorly-differentiated adenocarcinoma, demonstrated cell proliferative activity.

The percentage of apoptotic cells was calculated as the number of TUNEL-positive cancer cells per 1 000 cancer cells in the most frequently identified areas, and determined as the apoptotic index (AI). Under microscopy, morphological evidences of cell shrinkage, nuclear chromatin condensation, formation of cytoplasmic blebs and apoptotic bodies were frequently observed as the characteristic changes of apoptosis cells (Figure 2).

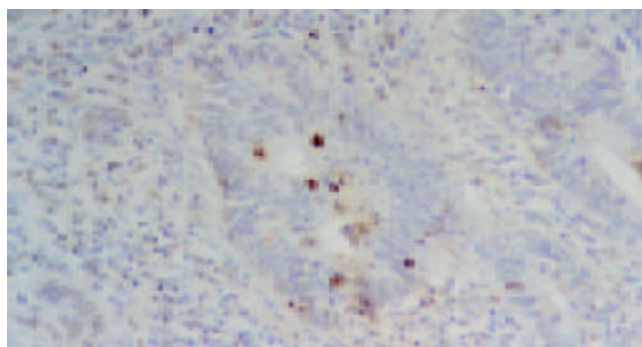


Figure 2 Apoptotic cancer cells in well-differentiated adenocarcinoma detected by TUNEL method. LSAB, $\times 200$.

Statistical analysis

Data were expressed as mean \pm SD. The two-tailed χ^2 test was used to examine the correlation between various clinical or pathologic parameters and the expression of EPR-1. Statistical significance between different groups was determined by independent Student's *t*-test (two-tailed). The Pearson test was used to examine linear correlation between Weighted EPR-1 Score and proliferative or apoptotic indexes. A *P* value less than 0.05 was considered statistically significant. All the calculations were performed by SPSS 10.0 for windows.

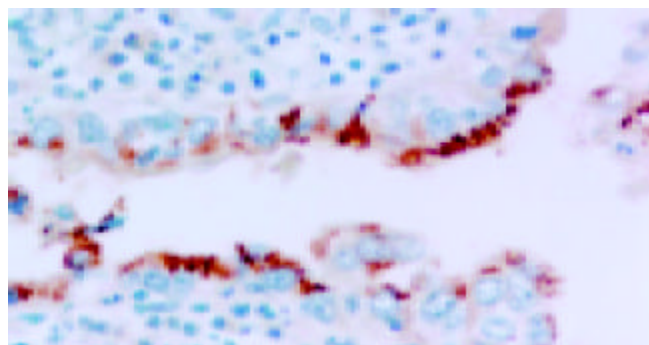
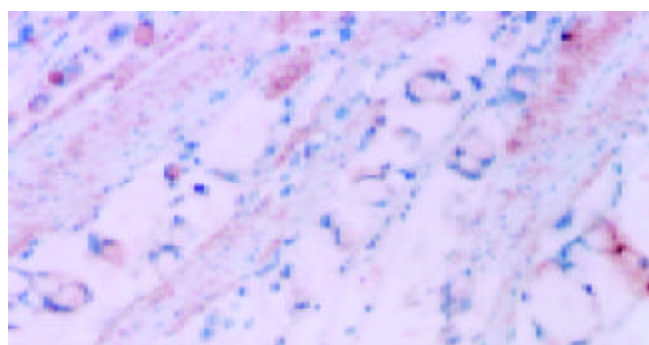
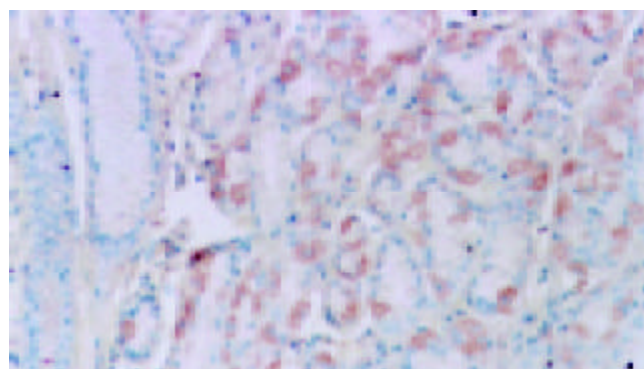
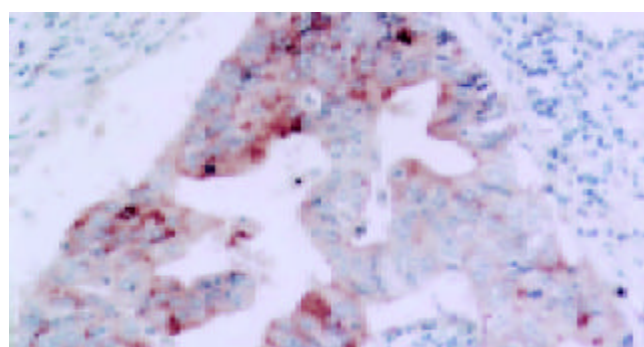
RESULTS

Correlation between EPR-1 protein expression and clinicopathological parameters

No significant relation was found between the expression of EPR-1 and patient age, sex, tumor location, lymph node metastasis or depth of invasion (Table 1, *P* > 0.05).

Table 1 No Correlation between EPR-1 protein expression and clinicopathological parameters

Clinico-pathological parameters	Cases	EPR-1 positive cases (%)	P value
Age (yr)			
<60	37	21 (56.8)	0.258
≥60	83	56 (67.5)	
Sex			
Male	72	43 (59.7)	0.214
Female	48	34 (70.8)	
Tumor location			
Upper 1/3	39	22 (56.4)	0.199
Middle 1/3	32	20 (62.5)	
Lower 1/3	19	11 (57.9)	
More than 2 locaitons	30	24 (80.0)	
Differentiation			
Well	60	46 (76.7)	0.004
Poorly	60	31 (51.7)	
Subtypes			
Papillary	30	24 (80.0)	0.017
Tubular	30	22 (73.3)	
Mucinous	30	13 (43.3)	
Signet-ring cell	30	18 (60.0)	
Invasion mucosa			
No	66	40 (60.6)	0.369
Yes	54	37 (68.5)	
Lymph node metastasis			
No	70	43 (61.4)	0.459
Yes	50	34 (68.0)	

**Figure 3** Strong Positive cytoplasmic staining of EPR-1 in gastric adenocarcinomas (LSAB×400).**Figure 4** Positive staining of EPR-1 in signet-ring cell carcinoma invasion in smooth muscle and smooth muscle cells (LSAB×200).**Figure 5** Moderate positive nuclear staining in benign gastric adenocytes (LSAB×200).**Figure 6** Positive cytoplasmic staining in well-differentiated lymph node metastasis (LSAB×200).

Expression of EPR-1 between histological subtypes

There were a variety of positive rates of EPR-1 protein in different histological subtypes (Figures 3, 4, 5, 6 and Table 2). The positive rate of EPR-1 expression nodes was significantly different in the invasive tumor ($P=0.007$), while it was differently expressed among the 4 subtypes and adjacent non-tumor tissues in the primary carcinoma and its lymph node metastasis ($P<0.05$). But there was no difference of EPR-1 expression in the adjacent normal gastric mucosa cells and smooth muscle cells among the 4 histological subtypes ($P=0.849$ and 0.720).

Expression of EPR-1 in the highly-differentiated adenocarcinomas

The positive rate of EPR-1 expression in the primary gastric adenocarcinoma was significantly higher than that in normal gastric mucosa (Table 3, $P=0.006$), while no significant difference was found in the invasion tumor nodes, lymph node metastasis and smooth muscle ($P=0.20, 0.632, 0.088$), respectively. However, in the primary highly-differentiated gastric adenocarcinomas, the positive expression rate of EPR-1 was significantly different from that of normal gastric mucosa, invasive tumor node, lymph node metastasis and smooth muscle while no significant difference was found in the poorly-differentiated adenocarcinomas.

Relation of EPR-1 expression with AI and PI in primary adenocarcinoma

The apoptotic index for EPR-1 positive in primary adenocarcinoma group was 1.25% and was 1.00% for EPR-1 negative group, while the proliferative index for the two groups was 7.00% and 8.53%, respectively. The difference of the two indexes between the EPR-1 positive and negative groups was statistically significant (Table 4, $P<0.05$). The relation of EPR-1 score with AI and PI is shown in Figure 7.

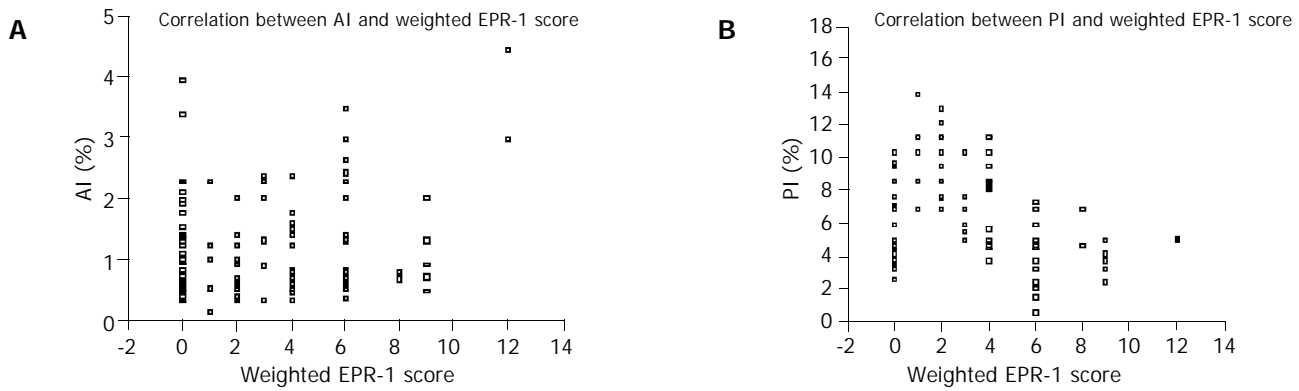


Figure 7 Significant difference of AI and PI with EPR-1 score in primary adenocarcinoma. A: The results of Pearson correlation coefficient, $r=-0.296$, $P=0.001<0.05$; B: The results of Pearson correlation coefficient, $r=-0.204$, $P=0.025<0.05$. Weighted EPR-1 Score was positively correlated with apoptotic index, but negatively related with proliferative index in primary adenocarcinoma.

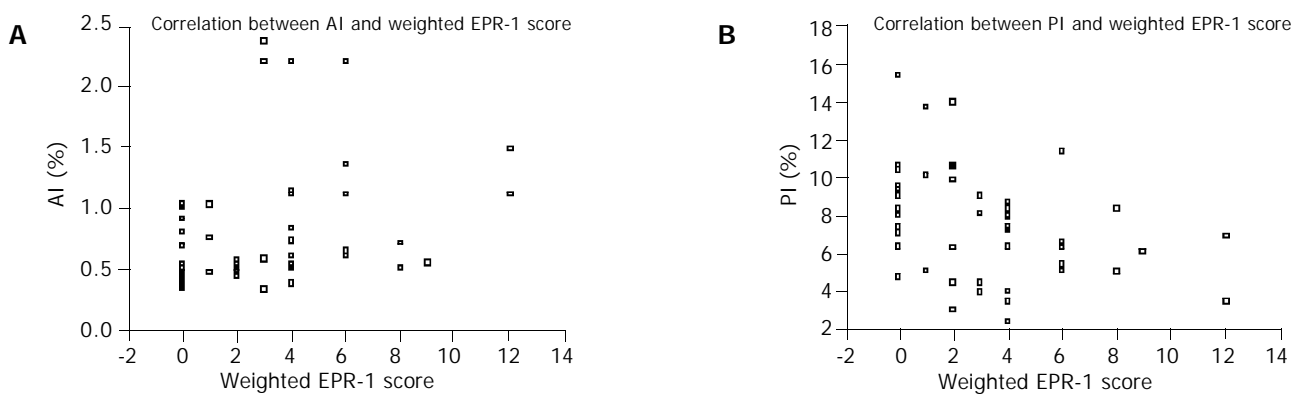


Figure 8 Significant difference of AI and PI with EPR-1 score in lymph node metastasis. A: The results of Pearson correlation coefficient, $r=0.332$, $P=0.019<0.05$. B: The results of Pearson correlation coefficient, $r=-0.336$, $P=0.017<0.05$. Weighted EPR-1 score is positively correlated with apoptosis index, but negatively related with proliferative index in lymph node metastasis.

Table 2 Different expression of EPR-1 between histological subtypes

Subtypes	Primary carcinoma	P value	Normal gastric mucosa	P value	Invasion node	P value	Lymph node metastasis	P value	Smooth muscle cell	P value
Papillary	24/30 (80.0)		14/30 (46.7)		14/17 (82.4)		11/13 (84.6)		17/30 (56.7)	
Tubular	22/30 (73.3)		15/30 (50.0)		12/16 (75.0)		11/15 (73.3)		15/30 (50.0)	
Mucinous	13/30 (43.3)		12/30 (40.0)		10/24 (41.7)		3/10 (30.0)		14/30 (46.7)	
Signet-ring cell	18/30 (60.0)	0.017	15/30 (50.0)	0.849	11/28 (39.3)	0.007	9/12 (75.0)	0.033	18/30 (60.0)	0.720

Table 3 Different expression of EPR-1 in the highly-differentiated adenocarcinomas

Differentiation	Primary gastric adenocarcinoma	Normal gastric mucosa cells	Invasion node adenocarcinoma	Lymph node metastasis	Smooth muscle cell	P value
Well	46/60 (76.7)	29/60 (48.3)	26/33 (78.8)	22/28 (78.6)	32/60 (53.3)	0.002
Poorly	31/60 (51.7)	27/60 (45.0)	21/52 (40.4)	12/22 (54.5)	32/60 (53.3)	0.594

Table 4 Significant expression difference of the AI and PI between EPR-1 positive and negative groups in primary adenocarcinomas

	n	AI (%)	P value	PI (%)	P value
EPR-1		mean±SD		mean±SD	
+	77	1.25±0.86		7.00±3.28	
-	43	1.00±0.80	0.024	8.53±2.70	0.010

Relation of EPR-1 expression with AI or PI in cancer with lymph node metastasis

The apoptotic index for EPR-1 positive lymph node metastasis group was 0.99% and was 0.67% for EPR-1 negative lymph node metastasis group, while the proliferative index for the two

groups was 7.65% and 9.44%, respectively. The difference of the two indexes between the EPR-1 positive and negative groups was statistically significant ($P<0.05$). The EPR-1 score was showed with the AI and PI in (Table 5, Figure 8).

Table 5 Significant expression difference of the AI and PI between EPR-1 positive and negative groups in lymph node metastasis

	n	AI (%)	P	PI (%)	P
EPR-1					
+	34	0.99±0.58		7.65±2.60	
-	16	0.67±0.24	0.010	9.44±3.05	0.037

DISCUSSION

Effector cell Protease Receptor-1 (EPR-1) has been recognized as a receptor of the transmembrane glycoprotein coagulation factor Xa and its transcripts are present in terminally differentiated adult tissues^[2-9]. Survivin gene was identified by Ambrosini *et al.* during hybridization screening of a human EPR-1 genomic library with the cDNA of EPR-1^[10,11]. The gene spanned nearly 15 kb and was co-located at 17q25 with EPR-1^[12]. Survivin has been found to be a new member of the inhibitors of apoptosis proteins (IAP) family^[13-16], and is selectively overexpressed in common human cancers but not in normal adult tissues.

Transfecting with EPR-1 mRNA into cells could inhibit endogenous expression of survivin gene and induce apoptosis as well as inhibit cell proliferation^[17]. Shinozawa *et al.*^[18] used RT-PCR method to detect the expression of Survivin and EPR-1 in leukemia and lymphoma, and found that the abnormality of the expression ratio of EPR-1 and Survivin might exert anti-colon tumor proliferation functions. Yamamoto *et al.*^[19] reported that EPR-1 in a human colon cancer cell line downregulated survivin expression, with a similar decrease in cell proliferation and an increase in apoptosis. This antitumor efficacy was further enhanced in combination with anticancer agents 5-Fu and CDDP. These findings suggest that regulation of survivin by induction of EPR-1 may have a significant potential as a therapy for human cancer. But to our knowledge, EPR-1 expression in gastric adenocarcinoma has not been reported.

In order to gain insight into the role of EPR-1 in gastric adenocarcinoma, we investigated the expression of EPR-1 in a group of gastric adenocarcinomas, and examined the relationship of its expression with cell proliferation and apoptosis index. By immunohistochemical analysis performed in 120 cases, our study shows that positive staining for EPR-1 protein was expressed as red brown granules, which were mainly located in cell cytoplasm. There was no significant relationship between the expression of EPR-1 and patient age, sex, tumor location, lymph node metastasis or depth of invasion. However, a significantly difference in expressions of EPR-1 was found between histological subtypes.

Our study also explored the potential relationship between the Weighted EPR-1 expression score and apoptotic, proliferative indexes. Ki-67 has been regarded as a parameter of tumor proliferation^[20-29] and the TUNEL method has become a popular way to detect apoptotic cells^[30-32]. Using these two reliable methods, we found that the positive rate of EPR-1 expression in the primary gastric adenocarcinoma was significantly higher than that in normal gastric mucosa and in terms with degree of differentiation, the positive expression rate of EPR-1 was significantly different among the primary gastric adenocarcinoma, normal gastric mucosa, tumor invasive node, lymph node metastasis and smooth muscle in the highly-differentiated adenocarcinomas while no significant difference was found in the poorly-differentiated adenocarcinomas.

In conclusion, EPR-1 can influence the biological behaviors of tumor cells not only by inducing their apoptosis, but by inhibiting their proliferation. Whether EPR-1 can be used as a new anti-cancer therapeutics strategy is still waiting for more evidence.

REFERENCES

- 1 **Lu CD**, Altieri DC, Tanigawa N. Expression of a novel antiapoptosis gene, survivin, correlated with tumor cell apoptosis and p53 accumulation in gastric carcinomas. *Cancer Res* 1998; **58**: 1808-1812
- 2 **Altieri DC**. Molecular cloning of effector cell protease receptor-1, a novel cell surface receptor for the protease factor Xa. *J Biol Chem* 1994; **269**: 3139-3142
- 3 **Bouchard BA**, Silveira JR, Tracy PB. On the role of EPR-1 or an EPR-1-like molecule in regulating factor Xa incorporation into platelet prothrombinase. *Thromb Haemost* 2001; **86**: 1133-1135
- 4 **McLean K**, Schirm S, Johns A, Morser J, Light DR. FXa-induced responses in vascular wall cells are PAR-mediated and inhibited by ZK-807834. *Thromb Res* 2001; **103**: 281-297
- 5 **Blanc-Brude OP**, Chambers RC, Leoni P, Dik WA, Laurent GJ. Factor Xa is a fibroblast mitogen via binding to effector-cell protease receptor-1 and autocrine release of PDGF. *Am J Physiol Cell Physiol* 2001; **281**: C681-689
- 6 **Cirera S**, Fredholm M. Isolation and mapping the pig homologs survivin (BIRC5) and effector cell protease receptor 1 (EPR1) genes. *Cytogenet Cell Genet* 2001; **92**: 351-352
- 7 **Kawabata A**, Kuroda R, Nakaya Y, Kawai K, Nishikawa H, Kawao N. Factor Xa-evoked relaxation in rat aorta: involvement of PAR-2. *Biochem Biophys Res Commun* 2001; **282**: 432-435
- 8 **Monno R**, Grandaliano G, Faccio R, Ranieri E, Martino C, Gesualdo L, Schena FP. Activated coagulation factor X: a novel mitogenic stimulus for human mesangial cells. *J Am Soc Nephrol* 2001; **12**: 891-899
- 9 **Shinozawa I**, Inokuchi K, Wakabayashi I, Dan K. Disturbed expression of the anti-apoptosis gene, survivin, and EPR-1 in hematological malignancies. *Leuk Res* 2000; **24**: 965-970
- 10 **Altieri DC**. Splicing of effector cell protease receptor-1 mRNA is modulated by an unusual retained intron. *Biochemistry* 1994; **33**: 13848-13855
- 11 **Altieri DC**. Molecular cloning of effector cell protease receptor-1, a novel cell surface receptor for the protease factor Xa. *J Biol Chem* 1994; **269**: 3139-3142
- 12 **Ambrosini G**, Adida C, Sirugo G, Altieri DC. Induction of apoptosis and inhibition of cell proliferation by survivin gene targeting. *J Biol Chem* 1998; **273**: 11177-11182
- 13 **Zaffaroni N**, Daidone MG. Survivin expression and resistance to anticancer treatments: perspectives for new therapeutic interventions. *Drug Resist Updat* 2002; **5**: 65-72
- 14 **Takai N**, Miyazaki T, Nishida M, Nasu K, Miyakawa I. Survivin expression correlates with clinical stage, histological grade, invasive behavior and survival rate in endometrial carcinoma. *Cancer Lett* 2002; **184**: 105-116
- 15 **Fortugno P**, Wall NR, Giodini A, O'Connor DS, Plescia J, Padgett KM, Tognin S, Marchisio PC, Altieri DC. Survivin exists in immunochemically distinct subcellular pools and is involved in spindle microtubule function. *J Cell Sci* 2002; **115** (Pt 3): 575-585
- 16 **Kanwar JR**, Shen WP, Kanwar RK, Berg RW, Krissansen GW. Effects of survivin antagonists on growth of established tumors and B7-1 immunogene therapy. *J Natl Cancer Inst* 2001; **93**: 1541-1552
- 17 **Adida C**, Crotty PL, McGrath J, Berrebi D, Diebold J, Altieri DC. Developmentally regulated expression of the novel cancer anti-apoptosis gene survivin in human and mouse differentiation. *Am J Pathol* 1998; **152**: 43-49
- 18 **Shinozawa I**, Inokuchi K, Wakabayashi I, Dan K. Disturbed expression of the anti-apoptosis gene, survivin, and EPR-1 in hematological malignancies. *Leuk Res* 2000; **24**: 965-970
- 19 **Yamamoto T**, Manome Y, Nakamura M, Tanigawa N. Downregulation of survivin expression by induction of the effector cell protease receptor-1 reduces tumor growth potential and results in an increased sensitivity to anticancer agents in human colon cancer. *Eur J Cancer* 2002; **38**: 2316-2324
- 20 **Scholzen T**, Gerdes J. The Ki-67 protein: from the known and the unknown. *J Cell Physiol* 2000; **182**: 311-322
- 21 **Aoki T**, Inoue S, Imamura H, Fukushima J, Takahashi S, Urano T, Hasegawa K, Ogushi T, Ouchi Y, Makuuchi M. EBAG9/RCAS1 expression in hepatocellular carcinoma: correlation with tumour dedifferentiation and proliferation. *Eur J Cancer* 2003; **39**: 1552-1561
- 22 **Nieto A**, Perez-Alenza MD, Del Castillo N, Tabanera E, Castano M, Pena L. BRCA1 expression in canine mammary dysplasias and tumours: relationship with prognostic variables. *J Comp Pathol* 2003; **128**: 260-268
- 23 **Friedrich RE**, Hagel C, Brehme Z, Kluwe L, Mautner VF. Ki-67 proliferation-index (MIB-1) of neurofibromas in neurofibro-

- matosis type 1 patients. *Anticancer Res* 2003; **23**: 953-955
- 24 **Sredni ST**, Alves VA, Latorre Mdo R, Zerbini MC. Adrenocortical tumours in children and adults: a study of pathological and proliferation features. *Pathology* 2003; **35**: 130-135
- 25 **Grabsch H**, Takeno S, Parsons WJ, Pomjanski N, Boecking A, Gabbert HE, Mueller W. Overexpression of the mitotic checkpoint genes BUB1, BUBR1, and BUB3 in gastric cancer—association with tumour cell proliferation. *J Pathol* 2003; **200**: 16-22
- 26 **Furuya Y**, Kawauchi Y, Fuse H. Cell proliferation, apoptosis and prognosis in patients with metastatic prostate cancer. *Anticancer Res* 2003; **23**: 577-581
- 27 **Watanabe J**, Sato H, Kanai T, Kamata Y, Jobo T, Hata H, Fujisawa T, Ohno E, Kameya T, Kuramoto H. Paradoxical expression of cell cycle inhibitor p27 in endometrioid adenocarcinoma of the uterine corpus - correlation with proliferation and clinicopathological parameters. *Br J Cancer* 2002; **87**: 81-85
- 28 **Rudolph P**, Bonichon F, Gloeckner K, Collin F, Chassevent A, Schmidt D, Coindre JM, Parwaresch R, Kloppel G. Comparative analysis of prognostic indicators for sarcomas of the soft parts and the viscerae. *Verh Dtsch Ges Pathol* 1998; **82**: 246-252
- 29 **Janicke F**. Value of tumor biological prognostic factors in adjuvant therapy of node-negative breast cancer. *Zentralbl Gynakol* 1994; **116**: 449-455
- 30 **Kase S**, Osaki M, Honjo S, Adachi H, Ito H. Tubular adenoma and intramucosal intestinal-type adenocarcinoma of the stomach: what are the pathobiological differences? *Gastric Cancer* 2003; **6**: 71-79
- 31 **Uysal H**, Cevik IU, Soylemezoglu F, Elibol B, Ozdemir YG, Evrenkaya T, Saygi S, Dalkara T. Is the cell death in mesial temporal sclerosis apoptotic? *Epilepsia* 2003; **44**: 778-784
- 32 **Bendardaf R**, Ristamaki R, Kujari H, Laine J, Lamlum H, Collan Y, Pyrhonen S. Apoptotic index and bcl-2 expression as prognostic factors in colorectal carcinoma. *Oncology* 2003; **64**: 435-442

Edited by Zhang JZ and Wang XL **Proofread by** Xu FM

1 α , 25-dihydroxyvitamin D₃ prevents DNA damage and restores antioxidant enzymes in rat hepatocarcinogenesis induced by diethylnitrosamine and promoted by phenobarbital

Mahendrakumar Chandrasekharappa Banakar, Suresh Kanna Paramasivan, Mitali Basu Chattopadhyay, Subrata Datta, Prabir Chakraborty, Malay Chatterjee, Kalaiselvi Kannan, Elayaraja Thygarajan

Mahendrakumar Chandrasekharappa Banakar, Suresh Kanna Paramasivan, Mitali Basu Chattopadhyay, Subrata Datta, Prabir Chakraborty, Malay Chatterjee, Division of Biochemistry, Department of Pharmaceutical Technology, Jadavpur University, Kolkata 700032, India

Kalaiselvi Kannan, Elayaraja Thygarajan, Department of Environmental Science, PSG College of Arts and Science, Coimbatore 641014, Tamilnadu, India

Supported by: All India Council for Technical Education (AICTE), Govt of India and Veerasaiva Vidya Vardhaka Sangha (VVS), Bellary Karnataka, India

Correspondence to: Malay Chatterjee, PO 17028, Division of Biochemistry, Department of Pharmaceutical Technology, Jadavpur University, Kolkata-700032, India. mcbiochem@yahoo.com

Telephone: +91-33-24146393 **Fax:** +91-33-24146393

Received: 2003-10-31 **Accepted:** 2003-12-30

Abstract

AIM: To investigate the chemopreventive effects of 1 α , 25-dihydroxyvitamin D₃ in diethylnitrosamine induced, phenobarbital promoted rat hepatocarcinogenesis.

METHODS: The rats were randomly divided into 6 different groups (A-F). Groups A, C and E rats received a single intraperitoneal (i.p) injection of diethylnitrosamine (DEN) at a dose of 200 mg/kg body mass in 9 g/L NaCl solution at 4 wk of age, while group B served as normal vehicle control received normal saline once. After a brief recovery of 2 wk, all the DEN treated rats were given phenobarbital (PB) at 0.5 g/L daily in the basal diet till wk 20. Group A was DEN control. Treatment of 1 α , 25-(OH)₂D₃ in group C was started 4 wk prior to DEN injection and continued thereafter till wk 20 at a dose of 0.3 μ g/100 μ L propylene glycol per one single dose (os) twice a week. Group E received the treatment of 1 α , 25-(OH)₂D₃ at the same dose mentioned as above for 15 wk. The rats in group D and F received 1 α , 25-(OH)₂D₃ alone as in group C without DEN injection.

RESULTS: The comet assay showed statistically higher mean values for length to width ratios (L: W) of DNA mass and tailed cells ($P < 0.01$; $P < 0.01$ respectively) in DEN treated rats as compared to their normal controls. Continuous supplementation of 1 α , 25-dihydroxyvitaminD₃ showed a significant ($P < 0.01$) decrease in L:W ratio of DNA mass tailed cells. Furthermore, 1 α , 25-(OH)₂D₃ supplementations elevated the super oxide dismutase (SOD) activity, hepatic malondialdehyde (MDA) level, reduced glutathione (GSH) and glutathione S-transferase (GST) activity ($P < 0.01$, $P < 0.05$, $P < 0.05$ and $P < 0.05$ respectively). As an endpoint marker histological changes were observed to establish the chemopreventive effects of 1 α , 25-dihydroxyvitaminD₃.

CONCLUSION: Supplementations of 1 α , 25-(OH)₂D₃ has

a marked protection against hepatic nodulogenesis, antioxidant enzymes and DNA damages in DEN induced rat hepatocarcinogenesis promoted by phenobarbital.

Banakar MC, Paramasivan SK, Chattopadhyay MB, Datta S, Chakraborty P, Chatterjee M, Kannan K, Thygarajan E. 1 α , 25-dihydroxyvitamin D₃ prevents DNA damage and restores antioxidant enzymes in rat hepatocarcinogenesis induced by diethylnitrosamine and promoted by phenobarbital. *World J Gastroenterol* 2004; 10(9): 1268-1275

<http://www.wjgnet.com/1007-9327/10/1268.asp>

INTRODUCTION

1 α , 25dihydroxyvitaminD₃ plays an important role in reducing the incidence of carcinomas of breast, prostate and colon in human as well as in experimental animals^[1,2]. 1 α , 25(OH)₂D₃ has been shown to promote the differentiation of cancer cells and cell lines *in vitro*^[3,4]. Little information is available for the antioxidant property of 1 α , 25(OH)₂D₃ in the inhibition of chemical rat hepatocarcinogenesis^[5]. A number of micronutrients, macronutrients and non-nutrients have been reported as the chemopreventive agents in the carcinogenesis^[6]. Vitamin D₃ treatment of mice with GM-CSF-secreting tumors can interrupt the myelopoiesis-associated immunosuppressor cascade and reduce tumor metastasis^[7]. Various new vitamin D analogues are developed with increased growth inhibitory and reduced calcemic activity, but significant antiproliferative and differentiation-inducing agents have now been synthesized and may be used as anticancer drugs^[8,9]. Polychlorinated biphenyls, phenobarbital and many other compounds that induce hepatic biotransformation enzymes promote experimental hepatocarcinogenesis in rodents previously exposed to initiating carcinogens^[10]. Several mechanisms for liver tumor promotion by PB and other inducing xenobiotics have been documented^[11].

Number of methods are available for detecting DNA damage, as opposed to the biological effects of DNA damaging agents (*e.g.*, micronuclei, mutations, structural chromosomal aberrations) have been used to identify substances with genotoxic activity. The alkaline elution assay ignores the critical importance of intercellular differences in DNA damage and requires relatively large numbers of cells. The full approach for assessing DNA damage is the single-cell gel electrophoresis (SCG) or comet assay^[12]. Identification of different cell populations can be made by a modified alkaline comet assay^[13,14]. Comet assay can be used to identify possible human mutagens and carcinogens^[15] and DNA damage of human hepatoma cells irradiated by heavy ions^[16]. The alkaline comet assay has been very popular for the analysis of DNA damage caused by various chemical and physical agents^[17-20]. The genetic damages in leprosy patients undergoing multidrug treatment are also measured by comet assay^[21].

Free radical species are involved in carcinogenesis, superoxide dismutases catalyze the dismutation of super-oxide

radical to hydrogen peroxide and oxygen^[22]. Chemical induction of liver carcinoma is associated with changes in the oxygen radical metabolism in liver. The changes in hepatic oxygen radical metabolism were demonstrated by measurement of the antioxidant enzymes SOD. Tumour cells have abnormal activities of antioxidant enzymes, and decreased activities of SOD in tumour cells^[23,24]. The influence of oxygen-derived free radicals on survival in advanced colonic cancer was assessed in a prospective randomized controlled double-blind trial using the radical scavengers^[25]. Compounds that can scavenge excessive free radicals in the body are suggested to hinder the process of carcinogenesis.

The present study was undertaken to investigate the effectiveness of $1\alpha, 25(\text{OH})_2\text{D}_3$ on the development of hepatic nodules, the cytogenetic effects of DEN induced rat hepatocarcinogenesis determined by comet assay and the antioxidant enzymes in diethylnitrosamine induced rat hepatocarcinogenesis promoted by phenobarbital.

MATERIALS AND METHODS

Chemicals

All the reagents and biochemicals, unless otherwise mentioned, were obtained from Sigma Chemical Co. (St. Louis, MO, USA).

Animals

Male Sprague-Dawley rats (80-100 g) were purchased from the Indian Institute of Chemical Biology (CSIR), Kolkata, India. They were given the standard laboratory diet purchased from Lipton, India. The animals were housed in an air-conditioned room (22±1 °C, relative humidity 50±10%) with a 12-h light/dark cycle in Tarson cages (4 rats per cage) and were acclimatized for 1 wk before the start of the experiment. Guidelines for the care and use of the laboratory animals (National Institute of Health, USA) were followed during the experiment and approved by the Institutional Animal Ethics Committee (IAEC), Jadavpur University, Kolkata.

Experimental regime

The rats were randomly divided into 6 different groups with 10 rats in each as illustrated in Figure 1. Groups A, C and E rats received a single intraperitoneal (i.p) injection of DEN (Sigma) at a dose of 200 mg/kg body mass in 9 g/L NaCl solution at 4 wk of age while group B served as normal vehicle control (received normal saline once). After a brief recovery of 2 wk, all the DEN treated rats were given PB at 0.05% daily in the basal diet till wk 20. Group A was DEN control. Treatment of $1\alpha, 25(\text{OH})_2\text{D}_3$ in group C was started 4 wk prior to DEN injection and continued thereafter till wk 20 at a dose of 0.3 µg/100 µL propylene glycol *per os (opus sit)* twice a week. In group E $1\alpha, 25(\text{OH})_2\text{D}_3$ treatment at the same dose mentioned as above was started 1 wk after DEN injection and continued thereafter till the completion of the experiment. The animals of groups D and F served as $1\alpha, 25(\text{OH})_2\text{D}_3$ controls for groups C and E that received $1\alpha, 25(\text{OH})_2\text{D}_3$ (Sigma, MO, USA) at a dose of 0.3 µg/100 µL propylene glycol *per os* twice weekly for 20 wk. All the treatments were withdrawn at wk 20 and the rats were sacrificed at wk 21 under proper ether anaesthesia.

Comet assay

Comet assay was performed on liver tissue under alkaline conditions following the procedure of Ward *et al.*^[26], with minor modifications. All the steps of comet assay were conducted under yellow light to prevent the occurrence of additional DNA damage. After sacrifice, liver of either lobe was excised, minced and homogenized in 50 µL of phosphate-buffered saline (PBS; pH 7.5). Briefly, 4 µL of homogenized tissue samples was diluted

with 50 µL of PBS and mixed with 150 µL of 10 g/L low melting point agarose (37 °C) prepared in PBS and pipetted onto a 10 g/L normal melting agarose precoated slide, which had been dried overnight, and covered with a coverslip. After the slide was kept on a chilled plate for 10 min, the coverslip was removed and the slide was lowered into freshly made ice-cold lysis solution (2.5 mol/L NaCl, 100 mmol/L EDTA, 10 mmol/L Tris, 100 g/L DMSO, 10 g/L Triton X-100, pH 10) and kept at 4 °C in the dark for 60 min. After draining the lysis solution, the slide was rinsed with distilled water for 15 min. After washed twice in the prepared distilled water, the slide was placed in a horizontal electrophoresis tank containing freshly made buffer (300 mmol/L NaOH and 1 mmol/L EDTA, pH>13) for 30 min. Electrophoresis was performed in the same buffer for 20 min by applying an electric field of 25 V (0.8 V/cm) and adjusting the current to 300 mA by slowly changing the buffer level in the tray. After electrophoresis the slide was rinsed gently with 0.4 mol/L Tris-Hcl buffer (pH 7.5) for 5 min, this step was again repeated. Then the slide was dried at room temperature and kept in a refrigerator in a sealed container until analysis. Duplicate slides were prepared for all the samples.

The slides were immersed in distilled water for 30 min, then stained with 100 µL of ethidium bromide (5 µg/mL) and read at 250× using a Zeiss fluorescence microscope equipped with a green excitation filter and a 590 nm barrier filter. All slides were coded and examined blindly. Routinely 100 cells (50 cells/slide) were screened per sample. In selecting cells for measurements, straight line scanning of a slide was begun at an arbitrary point and cells were measured as they came into the field, provided there was no overlap with patterns from other cells. The length and width of the DNA mass were measured using an ocular micrometer disk. Under these conditions a DNA pattern with a ratio of one had a DNA length of -25 µm and a ratio of four had a DNA length of -100 µm. The length: width ratios of the DNA mass and the frequency of tailed (damaged) cells were used in all comparisons.

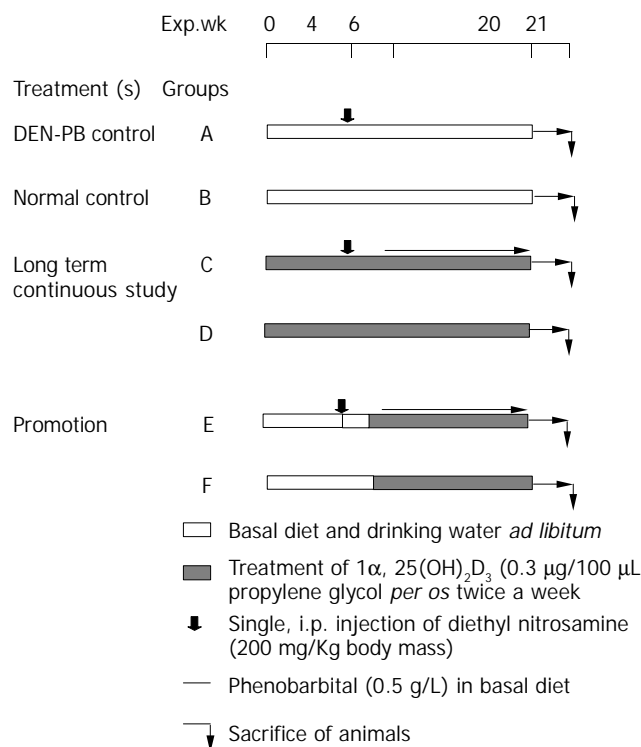


Figure 1 Basic experimental protocol.

Morphology and morphometry of liver tissue

After the rats were sacrificed, their livers were excised from all

treated and control rats, weighed and examined on the surface for subcapsular macroscopic lesions (hyperplastic nodules; HNs). The nodules with approximate spheres were measured in 2 perpendicular directions to the nearest millimeter into three categories namely ≥ 3 , $< 3 - > 1$ and ≤ 1 mm^[27].

Histopathological examination

For histopathological examination and morphometric analysis, tissues were fixed in 40 g/L buffered formaldehyde and the fixed paraffin embedded sections were stained with hematoxylin and eosin (H&E).

Histochemical detection of γ -glutamyl transpeptidase-positive foci

After sacrifice of the rats, each liver was examined of the right, left and caudate lobes. They were fixed in an ice-cold mixture of dehydrated ethanol and glacial acetic acid (19:1) for 4 h followed by an overnight incubation in 995 mL/L ethanol at 4 °C and then embedded in soft paraffin (melting point 47 °C). Two contiguous paraffin sections were made from each liver section for γ -glutamyl transpeptidase (GGT) histochemistry according to the method of Rutenberg^[28]. Quantitative evaluation of GGT-positive foci (lesions smaller than a liver lobule mainly visible microscopically) was performed according to the method of Campbell^[29].

Biochemical assays

The animals were sacrificed with proper anaesthesia. Liver of either lobes was minced and homogenized with 0.25 mol/L sucrose and the homogenate was centrifuged at 9 000 g (33 000 r/min) for 15 min in refrigerated centrifuge (Megafuge 1.0R). The pellet was discarded and an aliquot of supernatant was kept for the assay of cytosolic enzyme activities. The left portion was recentrifuge at 105 000 g for 90 min in refrigerated centrifuge (Megafuge 1.0R). The microsomal fraction was prepared separately from hyperplastic nodule (HNs) and non-nodular surrounding parenchyma (NNSP) liver area and untreated normal control liver. All the operations were done at 0-4 °C.

The activity of superoxide dismutase (SOD) was measured by following the method of Beyer and Fridovich^[30]. Hepatic cytosolic enzymatic lipid peroxidation was estimated according to the method of Okhaw *et al.*,^[31] based on the formation of malondialdehyde (MDA). The reduced glutathione (GSH) level was quantified by the method of Ellman^[32]. Hepatic cytosolic glutathione S-transferase (GST) activity was determined with 1-chloro 2,4-dinitrobenzene as the substrate according to the method of Habig *et al.*^[33].

Statistical analysis

Data were analyzed statistically for differences between the means using Dunnett's *t*-test when more than one group was compared against a control group. *P*-value <0.05 was considered statistically significant.

RESULTS

Dietary intake

Daily food and water intake of all the groups of rats was same. Daily intake of water was measured with a measuring cylinder and it was found that each rat took on an average of 8-10 mL water per day.

Body and liver mass

The effect of 1 α , 25(OH)₂D₃ on body and liver mass of different group of rats sacrificed after 20 wk is shown in Table 1. Body mass of DEN control group rats (group A) were slightly lower (*P*<0.05) than that of the normal control rats (group B). Treatment with 1 α , 25(OH)₂D₃ increased the final body mass of

the animals in groups C, D, E and F which received 1 α , 25(OH)₂D₃ as compared with group A carcinogen control. This suggested that treatment with 1 α , 25(OH)₂D₃ had no adverse effect on the growth response of rats. Liver masses of rats in various groups showed no significant differences. The relative liver mass of DEN control group rats (group A) was found to be significantly increased (*P*<0.01) than that of normal control rats (group B). Treatment with 1 α , 25(OH)₂D₃ significantly (*P*<0.05) reduced the relative liver masses of rats in groups C, D, E and F compared with group A. 1 α , 25(OH)₂D₃ supplied rats showed a better resistance against hepatocarcinogenesis.

Table 1 Body and liver masses in each group of rats at end of the study (after 20 wk) (mean \pm SE)

Group	No of rats	Body mass (g)	Liver mass (g)	Relative liver mass (g) (Liver/100 g body mass)
A	6	282.5 \pm 15.8 ^a	14.6 \pm 2.6	5.16 \pm 0.47 ^b
B	10	338.0 \pm 18.3	10.8 \pm 1.9	3.19 \pm 0.21
C	8	334.3 \pm 13.8 ^c	12.3 \pm 1.8	3.67 \pm 0.36 ^e
D	10	348.9 \pm 21.6	11.9 \pm 1.5	3.41 \pm 0.29
E	8	308.1 \pm 19.1	13.1 \pm 2.2	4.25 \pm 0.45
F	10	336.6 \pm 22.2	12.1 \pm 1.8	3.59 \pm 0.42

Statistical level of significance by using Dunnett's *t*-test. ^a*P*<0.05, ^b*P*<0.01, significantly different from normal control (group B), ^c*P*<0.05, ^d*P*<0.05, significantly different from DEN control (group A).

Effect of 1 α , 25(OH)₂D₃ on induction of GGT-positive foci

Table 2 shows that GGT-positive foci developed in all the DEN treated groups (Groups A, C and E), while the livers of rats in normal as well as 1 α , 25(OH)₂D₃ control groups (groups B, D and F respectively) were found to be normal in terms of histochemical observations of GGT-positive foci. In group E supplementation of 1 α , 25(OH)₂D₃ inhibited the appearance of GGT-positive foci (45.25%). But 1 α , 25(OH)₂D₃ treatment which was started 4 wk before DEN administration and continued till the end of the experiment minimized the appearance of GGT-positive foci most significantly in group C (68.80%) than in DEN treatment. Thus 1 α , 25(OH)₂D₃ decreased significantly (*P*<0.01) GGT-positive foci in group C compared to the DEN control (group A).

Table 2 Effect of 1 α , 25(OH)₂D₃ on inhibition of GGT-positive foci in DEN induced rat hepatocarcinogenesis promoted by phenobarbital (mean \pm SE)

Group	No. of rats	No. of GGT-positive foci/cm ²	Decrease (%)
A	06	26.16 \pm 2.16	
C	08	8.16 \pm 0.59 ^b	68.80
E	08	14.32 \pm 1.23 ^d	45.25

Statistical level of significance by using Dunnett's *t*-test, ^b*P*<0.01, ^d*P*<0.01 compared with group A.

Effect of 1 α , 25(OH)₂D₃ on hepatic histopathology

Histopathological examination of liver sections from normal untreated group B (Figure 5) revealed normal liver parenchymal cells with granulated cytoplasm and small uniform nuclei radially arranged around the altered cell foci with granulated cytoplasm and small uniform nuclei radially arranged around the central vein. In the DEN treated groups A, C and E, phenotypically altered hepatocytes in altered liver cell foci and nodules at varying extent were noticeable throughout the hepatic parenchyma. The hepatocellular architecture of DEN control (group A) was found to be grossly altered and the hepatocytes became oval

in shape. The altered liver cells in foci and nodules were considerably enlarged, vesiculated and binucleated (Figure 4). A substantial irregularity (enlargement) in the shape of nucleus and chromatin pattern (chromatin condensation) were also observed. The nucleo-cytoplasmic ratio was increased in sinuses and greatly dilated with hyperplastic Kupffer cells. The cytoplasm was extensively vacuolated, continued masses of acidophilic material were observed. Supplementation of 1 α , 25(OH)₂D₃ for the entire period study (group C) elicited a maximum protection against DEN induced hepatocarcinogenesis, which was reflected in almost normal hepatocellular architecture. In group C liver cells were found to contain compact cytoplasmic material with only clear cell foci (Figure 6). The nucleocytoplasmic ratio was decreased considerably as compared to group A. The configuration of sinuses appeared normal with normal Kupffer cells. The size of nuclei resembled that of normal cells and binucleated cells were extremely less. A moderate improvement of hepatic histological picture was observed in 1 α , 25(OH)₂D₃ supplemented group C in comparison to group E. A considerable vacuolation was still observed in the cytoplasm and the compactness of hepatocytes was somewhat disturbed in group C. The liver sections from these groups presented a predominance of clear cell foci rather than eosinophilic or basophilic foci. There was a slight decrement in nucleocytoplasmic ratio in the cells with respect to group A with slightly dilated sinuses. The number of binucleated cells was less as compared to group A with normal size nuclei.

Effect of 1 α , 25(OH)₂D₃ on incidence, number and size of hepatocellular lesions

The carcinogen treated rats showed 100% nodule incidence in group A as compared to the normal control rats (group B). The incidence of HNs was lower in the rats that received 1 α , 25(OH)₂D₃ and DEN in groups C and E (Table 3). The average number of nodules/nodule-bearing livers (nodule multiplicity) was also found to be less in 1 α , 25(OH)₂D₃ supplemented group C (60%) as compared to group A. The result was statically significant ($P<0.01$) in group C compared with group A. The total number of nodule 22 and the average nodule bearing livers (3.66 \pm 0.68) in group C were compared with the DEN control (group A). Group C rats showed the lowest value in each range compared with the other groups (groups A and E). In the present study the relative size distribution of nodules revealed that supplementation of 1 α , 25(OH)₂D₃ characteristically reduced the appearance of HNs more than 3 mm in size in group C compared to group A.

Effect of 1 α , 25(OH)₂D₃ on comet Assay

The results of comet assay based on mean tailed cells (TC) (%) and mean length: width ratios (L: W) in hepatic cells of rats treated with DEN are shown in Table 4. The mean length to width ratio of the DNA mass observed in DEN control rats (group A) was significantly greater ($P<0.01$) compared with the normal control group B. Similarly, the mean frequency of tailed cells was (84 \pm 0.020) in DEN control rats and significantly different ($P<0.01$) from the normal control (29 \pm 0.008). Figures 2 and 3 illustrate the distribution of L: W and TC in DEN control

(group A), normal (group B), long term study (group C), and promotion study (group E). For length: width ratio and tailed cells, the median values were higher in DEN control (group A) compared with the normal control (group B). The distribution of damage cells was also wider and the lengths of the boxes were greater in DEN control rats, indicating larger interquartile ranges than that of the normal controls rats. The median line in normal control rats (group B) were tailing towards smaller values. In group C and group E the median lines were in the middle of the boxes, the distribution of TC was more or less symmetrical. In group C 1 α , 25(OH)₂D₃ offered more than 54.09% in the length and width ratio and 53.37% of tailed cells compared to group A.

Table 4 Effect of 1 α , 25dihydroxyvitamin D₃ on DNA damage [based on mean tailed cells (%) and mean length: width ratios \pm SEM of DNA pattern] in hepatic cells of rats during DEN induced rat hepatocarcinogenesis promoted by phenobarbital (mean \pm SE, n=100)

Groups	Length and width ratio of DNA mass	Decrease (%)	Tailed cells (%)	Decrease (%)
A	2.44 \pm 0.0681		84 \pm 0.020	
B	1.029 \pm 0.005		29 \pm 0.008	
C	1.12 \pm 0.025 ^b	54.09	39 \pm 0.014 ^d	53.57
D	1.02 \pm 0.0005		29 \pm 0.008	
E	1.63 \pm 0.026 ^e	33.19	62 \pm 0.026 ^f	26.19
F	1.02 \pm 0.005		29 \pm 0.008	

Group A: DEN control; Group B: Normal control; Group C: Long term study; Groups D, F 1 α , 25(OH)₂D₃ control; Group E: promotion. Statistical level of significance by using Dunnett's *t*-test, ^b $P<0.01$, ^c $P<0.01$, ^d $P<0.01$ and ^e $P<0.01$ compared to group A.

Effect of 1 α , 25(OH)₂D₃ on hepatic super oxide dismutase activity

Table 5 depicts the SOD activity. A significant decrease ($P<0.01$) was found in SOD activity in HNs and NNSP tissues in DEN control (group A) compared with the normal control (group B). A significant increase ($P<0.05$) in SOD level was observed in both HNs and NNSP tissues in group C rats, where 1 α , 25(OH)₂D₃ treatment started 4 wk before DEN administration and continued till the end of the experiment. In group E 1 α , 25(OH)₂D₃ was supplemented only for 15 wk, starting the treatment 1 wk after DEN administration showed no statistical significance in SOD activity.

Table 5 Changes in activities of superoxide dismutase (units/mg protein) in different groups of rats treated with 1 α , 25(OH)₂D₃ during DEN induced rat hepatocarcinogenesis promoted by phenobarbital (mean \pm SE, n=5)

Groups	Nodules	Surrounding	Control
A	4.38 \pm 0.56 ^b	5.28 \pm 0.57 ^a	8.64 \pm 0.87
C	6.84 \pm 0.81 ^c	7.60 \pm 0.73	8.84 \pm 0.80
E	4.88 \pm 0.66	5.64 \pm 0.53	8.52 \pm 0.77

Statistical level of significance by using Dunnett's *t*-test. ^b $P<0.01$, ^a $P<0.05$, compared with control. ^c $P<0.05$ compared with group A.

Table 3 Effect of 1 α , 25(OH)₂D₃ on incidence, number and size of hepatocellular lesions during DEN induced rat hepatocarcinogenesis promoted by phenobarbital (mean \pm SE)

Group	No. of rats with nodules	Nodule incidence (%)	Total No. of nodule	Average No. of nodules per nodule bearing liver	Relative size		
					<1mm	>1mm<3mm	>3mm
A	10/10	100	168	16.80 \pm 1.33	94 (55.95)	48 (28.57)	26 (15.47)
C	6/10	60 ^b	22	3.66 \pm 0.88	11 (50.0)	6 (27.27)	05 (22.72)
E	8/10	80 ^d	72	8.00 \pm 1.05	28 (38.88)	24 (33.33)	20 (27.77)

Statistical level of significance by using Dunnett's *t*-test, ^b $P<0.01$, ^d $P<0.01$ compared with group A.

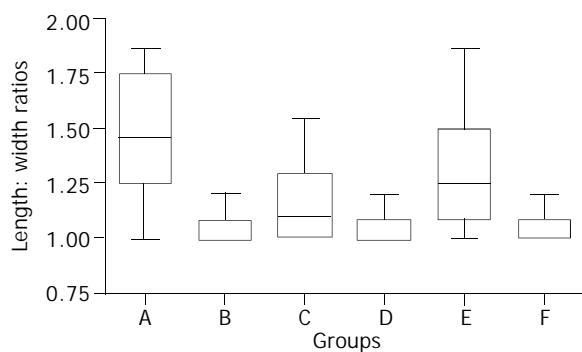


Figure 2 Box-and-whisker plot of the distribution of DNA damage treated with $1\alpha, 25(\text{OH})_2\text{D}_3$ in DEN induced rat hepatocarcinogenesis promoted by phenobarbital.

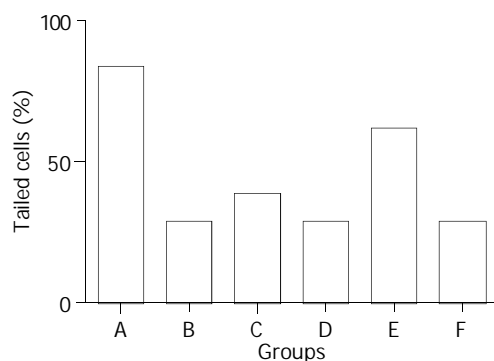


Figure 3 Tailed cells (%) in hepatic cells of rats treated with $1\alpha, 25(\text{OH})_2\text{D}_3$ in DEN induced rat hepatocarcinogenesis promoted by phenobarbital.

Effect of $1\alpha, 25(\text{OH})_2\text{D}_3$ on hepatic cytosolic lipid peroxidation

$1\alpha, 25(\text{OH})_2\text{D}_3$ had effect on hepatic cytosolic lipid peroxidation (Table 6) in different groups of rats treated with DEN, which was promoted by phenobarbital. A significant increase in the total content of MDA ($P<0.01$) was observed in DEN control rats (group A), both HNs and NNSP liver area in group A were compared with normal control. A significant decrease ($P<0.05$) in elevated hepatic MDA level was found in group C when compared with DEN control. Supplementation of $1\alpha, 25(\text{OH})_2\text{D}_3$ led to a significant reduction in total MDA production in DEN treated rats. The maximum effect was observed in group C rats whose $1\alpha, 25(\text{OH})_2\text{D}_3$ treatment was started 4 wk before DEN administration and continued till 20 wk, which offered a better protection in group E, in which $1\alpha, 25(\text{OH})_2\text{D}_3$ was supplemented for only 15 wk, starting 1 wk after DEN administration.

Table 6 Changes in total hepatic lipid peroxidation (nmol MDA/100 mg protein) level in different groups of rats treated with $1\alpha, 25(\text{OH})_2\text{D}_3$ during DEN induced rat hepatocarcinogenesis promoted by phenobarbital (mean \pm SE, $n=5$)

Groups	Nodules	Surrounding	Control
A	18.72 \pm 1.59 ^b	17.4 \pm 1.34 ^d	2.44 \pm 0.84
C	8.80 \pm 1.02 ^a	7.6 \pm 0.88	3.16 \pm 0.94
E	13.16 \pm 1.23	12.32 \pm 1.03	2.8 \pm 0.79

Statistical level of significance by using Dunnett's *t*-test. ^b $P<0.01$, ^d $P<0.01$ compared with control; ^a $P<0.05$ compared with group A.

Effect of $1\alpha, 25(\text{OH})_2\text{D}_3$ on hepatic cytosolic glutathione (GSH)

Table 7 shows the GSH content in different experimental groups. GSH content was found to be increased both in HNs and NNSP liver areas ($P<0.01$) in DEN control rats (group A) compared with normal control (group B). GSH content was decreased

significantly ($P<0.05$) in group C. GSH levels were marginally increased in groups D and F when compared with the normal control.

Table 7 Changes in total hepatic reduced glutathione (GSH) (mg/100 g tissue) level in different groups of rats treated with $1\alpha, 25(\text{OH})_2\text{D}_3$ during DEN induced rat hepatocarcinogenesis promoted by phenobarbital (mean \pm SE, $n=5$)

Groups	Nodules	Surrounding	Control
A	367.6 \pm 25.5 ^b	310.0 \pm 24.9 ^c	226.0 \pm 22.5
C	268.0 \pm 21.5 ^a	254.0 \pm 20.1	248.0 \pm 21.7
E	303.2 \pm 22.5	284.0 \pm 21.6	256.0 \pm 22.5

Statistical level of significance by using Dunnett's *t*-test. ^b $P<0.01$, ^c $P<0.05$ compared with control. ^a $P<0.05$ compared with group A.

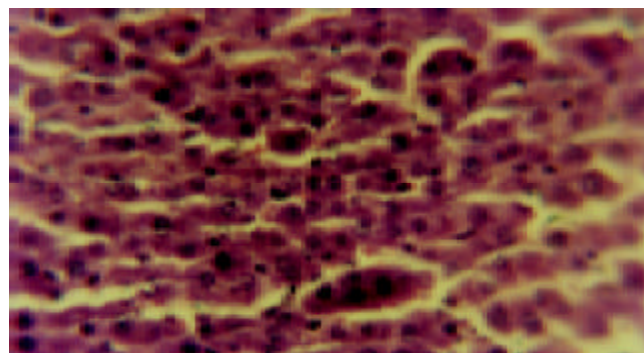


Figure 4 Shows the section of the rat liver (group A) showing abnormal hepatic architecture after a single i.p. Injection of DEN (200 mg/kg b.m.) (HE \times 325).

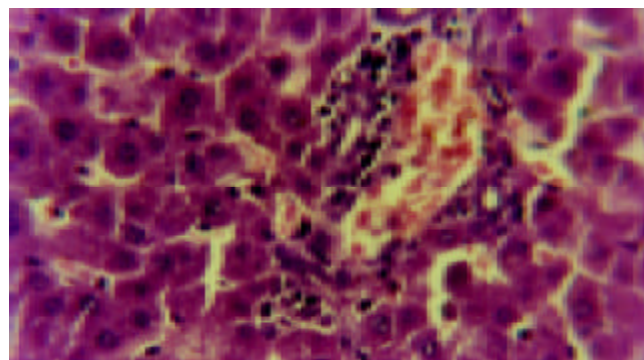


Figure 5 Shows the thin section of normal rat liver untreated (group B) showing hepatocellular architecture (HE \times 325).

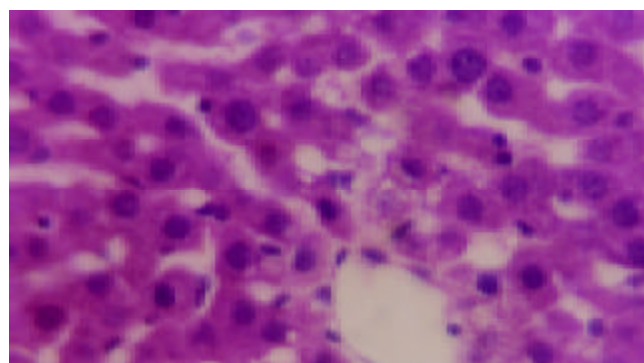


Figure 6 Shows section of rat liver (group C) initiated with DEN and supplemented with $1\alpha, 25(\text{OH})_2\text{D}_3$ [0.3 $\mu\text{g}/100 \mu\text{L}$ propylene glycol per os twice a week for 20 wk] showing almost normal hepatic architecture (HE \times 325).

Effect of 1 α , 25(OH)₂D₃ on 1-chloro-2, 4-dinitro benzene (CDNB) conjugated hepatic cytosolic glutathione S-transferase (GST) activity in different groups

Table 8 depicts the GST activity with CDNB in different experimental groups. DEN control rats showed (group A) a significantly increase ($P < 0.01$) more than 2-fold in NNSP compared with the normal control, but HNs showed a significantly decrease in value. Altered activity of 1 α , 25(OH)₂D₃ was found in group B. Groups C and E also showed higher altered activity of 1 α , 25(OH)₂D₃ than the normal control rats. 1 α , 25(OH)₂D₃ was found to be more effective in the inhibition of rat liver carcinogenesis ($P < 0.05$) in abating the GST activity. 1 α , 25(OH)₂D₃ control groups (groups D and F) had no statistical significance in the GST activity when compared with normal control.

Table 8 Changes in activity of 1-chloro-2, 4-dinitro benzene (CDNB) conjugated ($\mu\text{mol CDNB conjugated/mg protein/mL}$) hepatic cytosolic glutathione S-transferase (GST) in different groups of rats treated with 1 α , 25(OH)₂D₃ during DEN induced rat hepatocarcinogenesis promoted by phenobarbital (mean \pm SE, $n=5$)

Groups	Nodules	Surrounding	Control
A	2.52 \pm 0.23 ^b	1.54 \pm 0.23 ^c	0.9 \pm 0.10
C	1.45 \pm 0.27 ^a	1.24 \pm 0.11	1.12 \pm 0.13
E	1.76 \pm 0.29	1.48 \pm 0.19	1.10 \pm 0.11

Statistical level of significance by using Dunnett's *t*-test. ^b $P < 0.01$, ^c $P < 0.05$ compared with control. ^a $P < 0.05$ compared with group A.

DISCUSSION

The results of our present investigation clearly demonstrated that long term supplementation of 1 α , 25(OH)₂D₃ (at a dose of 0.3 $\mu\text{g}/100 \mu\text{L}$ propylene glycol twice a week) greatly reduced the incidence of hepatic nodulogenesis, antioxidant enzymes and genetic damage in DEN induced rat hepatocarcinogenesis promoted by phenobarbital. Previous studies in our laboratory have shown that long term supplementation of 1 α , 25(OH)₂D₃ in combination with vanadium could effectively inhibit DEN-induced rat liver carcinogenesis^[34-36].

DEN is a well-known hepatocarcinogen in rats, forming DNA-carcinogen adducts in the liver and inducing hepatocellular carcinomas without cirrhosis through the development of putative preneoplastic enzyme-altered hepatocellular focal lesions^[37]. After limited treatment with DEN, the rats ended up with a large benign hepatomas^[35,38], which were equivalent to neoplastic nodules and highly differentiated hepatocarcinomas. The preneoplastic lesions were thought to be the possible precursors of hepatic cancer in experimental animals and humans^[39]. Treatment with hepatocarcinogen could result in the proliferation of oval cells. These cells have been shown to have the ability to differentiate into hepatocytes^[40]. The results of our present investigation clearly indicated that long term supplementation of 1 α , 25(OH)₂D₃ could reduce the incidence, multiplicity and size of visible HNs more than 3 mm in size. Preneoplasia (γ -glutamyl transpeptidase -positive and glucose 6-phosphate negative) appeared in 1 α , 25(OH)₂D₃ treated animals 1 wk after carcinogen withdrawal, but livers from 1 α , 25(OH)₂D₃ depleted rats exhibited an increase in the number of GGT-positive foci. There was no change in the body masses among the groups under study. This is particularly important because nutritional deprivation causing body mass loss might result in a decrease in tumor volume^[41]. Thus 1 α , 25(OH)₂D₃ had the maximum effect in reducing the number and nodule growth, which were not mediated through the impairment of nutritional status in the experimental animals. 1 α , 25(OH)₂D₃ effect

observed in this study might be important for cancer prevention.

Comet assay is sensitive, a small number of cells and substances are required. It is inexpensive, and easy to apply to any tissues. The tissue selection in our study was based on a recent data analysis of the mice and rats^[42]. Comet assay can be applied to any tissues *in vivo*. In comet assay DNA is organized as loops, retaining the super coils and circular structure that are contained in the nucleosome. Epidemiological studies showed that comet tail was made up of relaxed loops and that the number of loops in the tail could indicate the number of DNA damages and tailed cells consisting of fragments of DNA^[43]. This study indicated a significantly higher incidence of DNA damage in the DEN-PB control compared with the normal control. In the present investigation, 1 α , 25(OH)₂D₃ protected against the DNA damage in DEN induced rat hepatocarcinogenesis.

SOD is the first line of defense of the cellular antioxidant system against the oxidative damage mediated by superoxide radicals. Life is continuously exposed to oxidative stress, cells are equipped with gene regulatory mechanism that can sense a high oxidative stress potential and consequently induce higher levels of several enzymes capable of reducing reactive oxygen species and repairing oxidative damage. The antioxidant enzymes are thus a major cell defense against acute oxygen toxicity. Their function is to protect membrane and cytosolic components against damage caused by free radicals. SOD, catalase and glutathione peroxidase (GPx) exemplify some of the most important ones. SOD, catalase could convert oxygen into hydrogen peroxides and water, SOD could diminish the damage caused by superoxide-producing agents as long as the generated hydrogen peroxide was removed by glutathione peroxidase and catalase does not become rate limiting^[44,45]. The enzyme GPx and glutathione reductase were then destroyed either by catalase or by enzyme system, these 2 systems could convert hydrogen peroxide into water at the expense of NADPH, using reduced GSH as an electron donor^[46]. Differences were found between normal and cancer cell superoxide dismutase activity in the treatment of cancer^[47]. The SOD ratio was lower in liver cells, and this might provide an explanation for the higher susceptibility of tumor cells to treatments likely to involve oxygen radicals^[48,49]. Our present results showed that 1 α , 25(OH)₂D₃ supplementation in group C inclined towards normal and in group E no change was found. Decreased antioxidant activity could cause the accumulation of free radicals. However, there was no change in SOD activities in group E rats, which might be due to the inactivated gene not reactivated by 1 α , 25(OH)₂D₃ supplementation, the physiological characterization and the genetic mapping of the mutant should identify the gene.

Lipid peroxidation plays an important role in carcinogenesis, treatment with inhibitors of lipid peroxidation, such as vitamins D, E, C, as well as selenium and vanadium and beta-carotene are protective agents^[36,50-52]. Stimulation of NADPH-dependent microsomal lipid peroxidation was proposed to be mediated by ADP/Fe²⁺, NADPH-cytochrome P-450 reductase and cytochrome P-450^[53]. Therefore, the increase of one of these modulators in the liver could explain the reduced lipid peroxidation. Previous studies in our laboratory showed that a significant increase in the total content of MDA was observed in DEN control compared to normal control^[50,54]. In our present study a significant increase in lipid peroxidation was observed in DEN PB-treated rats (group A) when compared with normal control rats (group B). But it was found in group C most significant ($P < 0.05$) compared to DEN-PB control. Treatment with 1 α , 25(OH)₂D₃ abated the production of MDA in different DEN-PB treated rats (groups C and E). The ability of 1 α , 25(OH)₂D₃ to inhibit iron dependent lipid peroxidation in liposomes might be important in protecting the membranes of normal cells against free radical induced oxidative damage^[55]. Thus, the oxygen

radical formation and detoxification, which result in lipid peroxidation and tissue damage, may be prevented.

GSH occurred primarily in the soluble phase, part of it conjugated with foreign compounds or their metabolites for detoxification and transport from body in the precancerous stage, GSH concentration in rat liver increased^[56-58]. From our study increased level of GSH in DEN control rats (group A), might be that GGT catalysed the degradation of extracellular GSH that can be used in the intracellular GSH synthesis^[59]. $1\alpha, 25(\text{OH})_2\text{D}_3$ supplemented groups C and F rats showed decrease in GSH levels. The significantly decreased GSH level in group C reflected the chemopreventive mechanism, by promoting the formation of additional pyridine nucleotides to provide hepatocytes with reduced properties and to inhibit the growth and spread of neoplastic nodules.

GST catalyzes the reaction of compounds with -SH group and thus neutralizes their electrophilic sites and produces more water soluble products. The evolution of thiol dependent detoxification pathways was initially the result of the availability of molecular oxygen^[60]. The cellular defence against oxygen free radicals and peroxides is of considerable importance to cell survival. Since the initial report of elevated expression of GST activity in nitrogen mustard resistant cell line^[61], a number of different tumors have been found to overexpress GST isoenzymes. In MCF-7 human breast cancer cell line, there appeared to have a coordinately increased expression of both GST- π and other enzymes including selenium dependent glutathione peroxidase and SOD^[62]. An increased GST activity was observed in metabolic inactivation and resistance to several anticancer drugs^[63]. In the present study, an increased activity of GST was observed in DEN control rats (group A). Decreased activity of GST was observed in groups C and F. But the significant decrease ($P < 0.05$) in GST activity was found in group C supplemented with $1\alpha, 25(\text{OH})_2\text{D}_3$. The increased anti-cancer drug resistance of one or more of the GST isoenzymes in resistant cells was compared with normal cells^[64].

$1\alpha, 25(\text{OH})_2\text{D}_3$ is very much effective in preventing DEN-PB induced changes in hepatocytes possibly through the inhibition of nodular growth, GGT-positive foci development, normalization of DEN induced changes in enzyme activities and prevention DNA damages in DEN-induced rat hepatocarcinogenesis. The results of our present study strongly suggest that $1\alpha, 25(\text{OH})_2\text{D}_3$ may be important for cancer prevention.

ACKNOWLEDGEMENTS

Mr. Mahendrakumar C.B is highly indebted to All India Council for Technical Education (AICTE), Government of India, and New Delhi for financial assistance to carry out this work and Veerasaiva Vidhya Vardhaka Sangha's T V M College of Pharmacy (VVS) Bellary, Karnataka, India. Mr. P Suresh Kanna is highly indebted to Department of Science & Technology, Government of India.

REFERENCES

- 1 **Blutt SE**, Allegretto EA, Pike JW, Weigel NL. $1,25$ -dihydroxyvitamin D_3 and 9-cis-retinoic acid act synergistically to inhibit the growth of LNCaP prostate cells and cause accumulation of cells in G1. *Endocrinology* 1997; **138**: 1491-1497
- 2 **Beatty MM**, Lee EY, Glauert HP. Influence of dietary calcium and vitamin D on colon epithelial cell proliferation and 1,2-dimethylhydrazine-induced colon carcinogenesis in rats fed high fat diets. *J Nutr* 1993; **123**: 144-152
- 3 **Welsh J**. Induction of apoptosis in breast cancer cells in response to vitamin D and antiestrogens. *Biochem Cell Biol* 1994; **72**: 537-545
- 4 **Chouvet C**, Vicard E, Devonec M, Saez S. $1,25$ -Dihydroxyvitamin D_3 inhibitory effect on the growth of two human breast cancer cell lines (MCF-7, BT-20). *J Steroid Biochem* 1986; **24**: 373-376
- 5 **Sardar S**, Chakraborty A, Chatterjee M. Comparative effectiveness of vitamin D_3 and dietary vitamin E on peroxidation of lipids and enzymes of the hepatic antioxidant system in Sprague-Dawley rats. *Int J Vitam Nutr* 1996; **66**: 39-45
- 6 **Wattenberg LW**. Inhibition of carcinogenesis by minor dietary constituents. *Cancer Res* 1992; **52**(7 Suppl): 2085s-2091s
- 7 **Young MR**, Ihm J, Lozano Y, Wright MA, Prechel MM. Treating tumor-bearing mice with vitamin D_3 diminishes tumor-induced myelopoiesis and associated immunosuppression, and reduces tumor metastasis and recurrence. *Cancer Immunol Immunother* 1995; **41**: 37-45
- 8 **Vink-Van Wijngaarden T**, Pols HA, Buurman CJ, van den Bemd GJ, Dorssers LC, Birkenhager JC, van Leeuwen JP. Inhibition of breast cancer cell growth by combined treatment with vitamin D_3 analogues and tamoxifen. *Cancer Res* 1994; **54**: 5711-5717
- 9 **James SY**, Mackay AG, Binderup L, Colston KW. Effects of a new synthetic vitamin D analogue, EB1089, on the oestrogen-responsive growth of human breast cancer cells. *J Endocrinol* 1994; **141**: 555-563
- 10 **Goldsworthy TL**, Pitot HC. The quantitative analysis and stability of histochemical markers of altered hepatic foci in rat liver following initiation by diethylnitrosamine administration and promotion with Phenobarbital. *Carcinogenesis* 1985; **6**: 1261-1269
- 11 **Kolaja KL**, Stevenson DE, Walborg EF Jr, Klaunig JE. Dose dependence of phenobarbital promotion of preneoplastic hepatic lesions in F344 rats and B6C3F1 mice: effects on DNA synthesis and apoptosis. *Carcinogenesis* 1996; **17**: 947-954
- 12 **Ostling O**, Johanson KJ. Microelectrophoretic study of radiation-induced DNA damages in individual mammalian cells. *Biochem Biophys Res Commun* 1984; **123**: 291-298
- 13 **Godard T**, Gauduchon P, Debout CA. First step in visual identification of different cell populations by a modified alkaline comet assay. *Mutation Res* 2002; **520**: 207-211
- 14 **McNamee JP**, McLean JR, Ferrarotto CL, Bellier PV. Comet assay: rapid processing of multiple samples. *Mutat Res* 2000; **466**: 63-69
- 15 **Anderson D**, Yu TW, McGregor DB. Comet assay responses as indicators of carcinogen exposure. *Mutagenesis* 1998; **13**: 539-555
- 16 **Qiu LM**, Li WJ, Pang XY, Gao QX, Feng Y, Zhou LB, Zhang GH. Observation of DNA damage of human hepatoma cells irradiated by heavy ions using comet assay. *World J Gastroenterol* 2003; **9**: 1450-1454
- 17 **Li WJ**, Gao QX, Zhou GM, Wei ZQ. Micronuclei and cell survival in human liver cancer cells irradiated by 25MeV/u (40Ar^{14+}). *World J Gastroenterol* 1999; **5**: 365-368
- 18 **Mohankumar MN**, Paul SF, Venkatachalam P, Jeevanram RK. Influence of in vitro low-level gamma-radiation on the UV-induced DNA repair capacity of human lymphocytes—analysed by unscheduled DNA synthesis (UDS) and comet assay. *Radiat Environ Biophys* 1998; **37**: 267-275
- 19 **Koppen G**, Angelis KJ. Repair of X-ray induced DNA damage measured by the comet assay in roots of *Vicia faba*. *Environ Mol Mutagen* 1998; **32**: 281-285
- 20 **Mayer C**, Popanda O, Zelezny O, von Brevern MC, Bach A, Bartsch H, Schmezer P. DNA repair capacity after gamma-irradiation and expression profiles of DNA repair genes in resting and proliferating human peripheral blood lymphocytes. *DNA Repair* 2002; **1**: 237-250
- 21 **Kalaiselvi K**, Rajaguru P, Palanivel M, Usharani MV, Ramu G. Re: Chromosomal aberration, micronucleus and Comet assays on peripheral blood lymphocytes of leprosy patients undergoing multidrug treatment. *Mutagenesis* 2003; **18**: 309-312
- 22 **McCord JM**, Fridovich I. The utility of superoxide dismutase in studying free radical reactions. I. Radicals generated by the interaction of sulfite, dimethyl sulfoxide, and oxygen. *J Biol Chem* 1969; **244**: 6056-6063
- 23 **Halliwell B**, Gutteridge JMC. Free Radicals in Biology and medicine (2nd edn). Clarendon Press: Oxford, UK, 1989: 543
- 24 **Oberley LW**, Oberley TD. Free radicals, cancer and aging. In free radicals, aging and degenerative Diseases Johnson Jr JE, Walford R, Harman D, Miquies J (eds). *Alan R Liss, Inc: New*

- York 1986; 325-371
- 25 **Salim AS.** Scavengers of oxygen-derived free radicals prolong survival in advanced colonic cancer. A new approach. *Tumour Biol* 1993; **14**: 9-17
- 26 **Ward TH,** Butler J, Shahbakhti H, Richards JT. Comet assay studies on the activation of two diaziridinylbenzoquinones in K562 cells. *Biochem Pharmacol* 1997; **53**: 1115-1121
- 27 **Moreno FS,** Rizzi MB, Dagli ML, Penteado MV. Inhibitory effects of beta-carotene on preneoplastic lesions induced in Wistar rats by the resistant hepatocyte model. *Carcinogenesis* 1991; **12**: 1817-1822
- 28 **Rutenburg AM,** Kim H, Fischbein JW, Hanker JS, Wasserkrug HL, Seligman AM. Histochemical and ultrastructural demonstration of gamma-glutamyl transpeptidase activity. *J Histochem Cytochem* 1969; **17**: 517-526
- 29 **Campbell HA,** Pitot HC, Potter VR, Laishes BA. Application of quantitative stereology to the evaluation of enzyme-altered foci in rat liver. *Cancer Res* 1982; **42**: 465-472
- 30 **Beyer WF Jr,** Fridovich I. Assaying for superoxide dismutase activity: some large consequence of minor changes in conditions. *Anal Biochem* 1987; **161**: 559-566
- 31 **Okhawa H,** Ohishi N, Yagi K. Assay for lipid peroxides in animal tissues by thiobarbituric acid reaction. *Anal Biochem* 1979; **95**: 351-358
- 32 **Ellman GL.** Tissue sulfhydryl groups. *Arch Biochem Biophys* 1959; **82**: 70-77
- 33 **Habig WH,** Pabst MJ, Jakoby WB. Glutathione S-transferase: the first enzymatic step in mercapturic acid formation. *J Biol Chem* 1974; **249**: 7130-7139
- 34 **Bishayee A,** Chatterjee M. Inhibitory effect of vanadium on rat liver carcinogenesis initiated with diethylnitrosamine and promoted by Phenobarbital. *Br J Cancer* 1995; **71**: 1214-1220
- 35 **Bishayee A,** Chatterjee M. Inhibition of altered liver cell foci and persistent nodule growth by vanadium during diethylnitrosamine induced hepatocarcinogenesis in rats. *Anticancer Res* 1995; **15**: 455-462
- 36 **Basak R,** Basu M, Chatterjee M. Combined supplementation of vanadium and 1 α , 25(OH)₂D₃ inhibit diethylnitrosamine-induced rat liver carcinogenesis. *Chem Biol Interact* 2000; **128**: 1-18
- 37 **Singer B,** Crundrger D. Molecular Biology and Mutagens and Carcinogens, Plenum Press, New York, 1984
- 38 **Scherer P,** Van Dijk WF, Emmelot P. Effect of antilymphocytic and normal serum on growth of precancerous foci and development of tumors induced by diethyl nitrosamine. *Eur J Cancer* 1976; **12**: 25-31
- 39 **Farber E.** Clonal adaptation during carcinogenesis. *Biochem Pharmacol* 1990; **39**: 1837-1846
- 40 **Sell S.** Is there a liver stem cell? *Cancer Res* 1990; **50**: 3811-3815
- 41 **Waltzberg DL,** Goncalves EL, Faintuch J, Bevilacqua LR, Rocha CL, Cologni AM. Effect of diets with different protein levels on the growth of Walker 256 carcinosarcoma in rats. *Braz J Med Biol Res* 1989; **22**: 447-455
- 42 **Sasaki YF,** Sekihashi K, Izumiyama F, Nishidate E, Saga A, Ishida K, Tsuda S. The comet assay with multiple mouse organs: comparison of comet assay results and carcinogenicity with 208 chemicals selected from the IARC monographs and U.S. NTP Carcinogenicity Database. *Crit Rev Toxicol* 2000; **30**: 629-799
- 43 **Collins AR,** Dobson VL, Dusinska M, Kennedy G, Stetina R. The comet assay: what can it really tell us? *Mutation Res* 1997; **375**: 183-193
- 44 **Fridovich I.** Superoxide radical: an endogenous toxicant. *Annu Rev Pharmacol Toxicol* 1983; **23**: 239-257
- 45 **Fridovich I.** Superoxide dismutases. *Adv Enzymol Relat Areas Mol Biol* 1986; **58**: 61-97
- 46 **Gaetani GF,** Galiano S, Canepa L, Ferraris AM, Kirkman HN. Catalase and glutathione peroxidase are equally active in detoxification of hydrogen peroxide in human erythrocytes. *Blood* 1989; **73**: 334-339
- 47 **Oberley LW,** Buettner GR. Role of superoxide dismutase in cancer. *Cancer Res* 1979; **39**: 1141-1149
- 48 **Bozzi A,** Mavelli I, Finazzi A, Strom R, Wolf AM, Mondovi B, Rotilio G. Enzyme defense against reactive oxygen derivatives. II. Erythrocytes and tumor cells. *Mol Cell Biochem* 1976; **10**: 11-16
- 49 **Thirunavukkarasu C,** Sakthisekaran D. Effect of selenium on N-nitrosodiethylamine-induced multistage hepatocarcinogenesis with reference to lipid peroxidation and enzymic antioxidants. *Cell Biochem Funct* 2001; **19**: 27-35
- 50 **Sarkar A,** Bishayee A, Chatterjee M. Beta-carotene prevents lipid peroxidation and red blood cell membrane protein damage in experimental hepatocarcinogenesis. *Cancer Biochem Biophys* 1995; **15**: 111-125
- 51 **Appel MJ,** Roverts G, Woutersen RA. Inhibitory effects of micronutrients on pancreatic carcinogenesis in azaserine treated rats. *Carcinogenesis* 1991; **2**: 2157-2161
- 52 **Eskelson CD,** Odeleye OE, Watson RR, Earnest DL, Mufti SI. Modulation of cancer growth by vitamin E and alcohol. *Alcohol Alcohol* 1993; **28**: 117-125
- 53 **Cajelli E,** Ferraris A, Brambilla G. Mutagenicity of 4-hydroxynonenal in V79 Chinese hamster cells. *Mutat Res* 1987; **190**: 169-171
- 54 **Basak R,** Bhattacharya R, Chatterjee M. 1 α , 25-Dihydroxyvitamin D(3) inhibits rat liver ultrastructural changes in diethylnitrosamine-initiated and phenobarbital promoted rat hepatocarcinogenesis. *J Cell Biochem* 2001; **8**: 357-367
- 55 **Wiseman H.** Vitamin D is a membrane antioxidant. Ability to inhibit iron-dependent lipid peroxidation in liposomes compared to cholesterol, ergosterol and tamoxifen and relevance to anticancer action. *FEBS Lett* 1993; **326**: 285-288
- 56 **Fiala S.** Intracellular changes in levels of polarographically active sulphhydryl groups in rat liver during carcinogenesis. *Nature* 1958; **182**: 257-258
- 57 **Neish WJ,** Rylett A. effect of alpha-tocopheryl acetate on liver glutathione of male rats injected with 3'-methyl-4-dimethylaminoazobenzene. *Biochem Pharmacol* 1963; **12**: 1147-1150
- 58 **Dijkstra J.** The contents of trichloroacetic acid-soluble sulphhydryl compounds and ascorbic acid in the liver of rats fed aminoazo dyes: the effect of a single large dose of dye. *Br J Cancer* 1964; **13**: 608-617
- 59 **Reiners JJ Jr,** Kodari E, Cappel RE, Gilbert HF. Assessment of the antioxidant/prooxidant status of murine skin following topical treatment with 12-O-tetradecanoylphorbol-13-acetate and throughout the ontogeny of skin cancer. Part II: Quantitation of glutathione and glutathione disulfide. *Carcinogenesis* 1991; **12**: 2345-2352
- 60 **Boylard E,** Chasseaud LF. The role of glutathione and glutathione S-transferases in mercapturic acid biosynthesis. *Adv Enzymol Relat Areas Mol Biol* 1969; **32**: 173-219
- 61 **Wang AL,** Tew KD. Increased glutathione-S-transferase activity in a cell line with acquired resistance to nitrogen mustards. *Cancer Treat Rep* 1985; **69**: 677-682
- 62 **Mimnaugh EG,** Dusre L, Atwell J, Myers CE. Differential oxygen radical susceptibility of adriamycin-sensitive and -resistant MCF-7 human breast tumor cells. *Cancer Res* 1989; **49**: 8-15
- 63 **Kulkarni AA,** Kulkarni AP. Retinoids inhibit mammalian glutathione transferases. *Cancer Lett* 1995; **91**: 185-189
- 64 **Fahey RC.** Biologically important thiol-disulfide reactions and the role of cyst(e)ine in proteins: an evolutionary perspective. *Adv Exp Med Biol* 1977; **86**: 1-30

Association of low p16INK4a and p15INK4b mRNAs expression with their CpG islands methylation with human hepatocellular carcinogenesis

Yang Qin, Jian-Yu Liu, Bo Li, Zhi-Lin Sun, Ze-Fang Sun

Yang Qin, Jian-Yu Liu, Zhi-Lin Sun, Ze-Fang Sun, Department of Biochemistry and Molecular Biology, School of Preclinical and Forensic Medicine, West China Medical Center, Sichuan University, Chengdu, 610041, Sichuan Province, China

Bo Li, Department of General Surgery, West China Hospital, Sichuan University, Chengdu, 610041, Sichuan Province, China

Supported by the National Natural Science Foundation of China. No. 39670702

Correspondence to: Yang Qin, Department of Biochemistry and Molecular Biology, School of Preclinical and Forensic Medicine, West China Medical Center, Sichuan University, Chengdu, 610041, Sichuan Province, China. qin_1@sina.com

Telephone: +86-28-85501265 **Fax:** +86-28-85501257

Received: 2003-11-27 **Accepted:** 2003-12-22

Abstract

AIM: To study the significance of p16 and p15 transcription suppression with hypermethylation of their genes' 5' CpG islands during human hepatocellular carcinogenesis.

METHODS: The mRNA expression levels of p16 and p15 genes were evaluated in cancerous, para-cancerous and non-cancerous tissues of 20 HCC, 3 normal liver tissues from 3 accidentally died healthy adults using semi-quantitatively Northern blot. The methylation status was also assessed with methylation specific PCR.

RESULTS: p16 mRNA expression level was decreased in the cancerous tissues in 60% (12/20) of HCC patients, of which 2 cases had no p16 mRNA detected, 5 cases (25%) displayed variation in the order of cancerous<para-cancerous<non-cancerous liver tissues. p15 mRNA expression level was decreased in the cancerous tissues in 50% (10/20) HCC patients, of which one case had no p15 mRNA detected, 4 cases (20%) displayed variation in the order of cancerous <para-cancerous<non-cancerous liver tissues. In cancerous, para-cancerous and non-cancerous tissues, p16 promoter CpG islands hypermethylation occurred 65%, 60% and 35%, while p15 promoter CpG islands hypermethylation occurred 50%, 40% and 25%. Of 12 HCCs with lower p16 mRNA expression level, 11 cases showed p16 promoter CpG islands methylation (91.6%). Hundred percent (10/10) HCCs with lower p15 mRNA expression level showed p15 promoter CpG islands methylation. Significant correlation between 5' CpG islands methylation and p16/p15 mRNA expression suppression was found. The decreased expression of p16/p15 mRNA or methylation of p16/p15 promoters 5' CpG island was significantly correlate with poor differentiation of HCC ($P=0.0083, 0.0102, 0.00271, 0.0218$, respectively, $P<0.05$).

CONCLUSION: p16 and p15 genes transcriptional inactivation might play an important role in hepatocarcinogenesis. 5' CpG islands methylation might be the major mechanism of p16 and p15 genes inactivation in primary HCC in the studied

population. 5' CpG islands methylation of p16 and p15 genes might be an early event in hepatocarcinogenesis.

Qin Y, Liu JY, Li B, Sun ZL, Sun ZF. Association of low p16INK4a and p15INK4b mRNAs expression with their CpG islands methylation with human hepatocellular carcinogenesis. *World J Gastroenterol* 2004; 10(9): 1276-1280

<http://www.wjgnet.com/1007-9327/10/1276.asp>

INTRODUCTION

Hepatocellular carcinoma (HCC) is one of the most common causes of death from cancer in China. The mechanisms of hepatocellular carcinogenesis are not yet expounded although alterations of some cell cycle tumor suppressor genes have been revealed to be involved in hepatocellular carcinogenesis. p16INK4a and p15INK4b are homologous cell cycle tumor suppressors, which are within 30 kb of one another on chromosome 9p21 region and in the same transcription orientation. p16INK4a has 3 exons whereas p15INK4b is encoded by 2 exons. They act as competitive inhibitors by binding directly to CDK4 and CDK6 and prevent their association with a cyclin, which in turn arrest the cells in late G1 phase of the cycle with pRB in a hypophosphorylated state^[1-4].

Although the high frequency of P16 protein expression deficiency or low expression in HCC was reported, the rate of p16 gene homozygous deletion and mutation is much lower than P16 protein expression deficiency. This suggested that there might be another mechanism inactivating p16 and p15 genes in human primary hepatocarcinoma^[5-9].

It has been demonstrated that aberrant methylation of CpG islands, which are CpG dinucleotide rich region located mainly in the promoter regions of many gene, serves as an alternative mechanism for inactivation of the tumor suppressor gene in cancers^[10]. Recently, aberrant methylation of the p16 and p15 promoters has been reported^[11-16]. The discordant events in which low P16 protein expression was not accompanied with deletion or mutation could be resulted from the low mRNA expression level of p16 gene due to hypermethylation of its CpG islands. To further study the association of hypermethylation of CpG islands in p16 and p15 genes with disrupted transcription of the corresponding genes in hepatocarcinogenesis, and to address the question whether the expression of p16 and p15 genes, as well as CpG island methylation of p16 and p15 genes is related to the differentiation degrees of HCC, the mRNA expression of p16 and p15 genes, as well as their CpG island methylation status in 20 HCCs was studied.

MATERIALS AND METHODS

Samples and extraction of total RNA and DNA

With informed consent of patients and ethics committee approval, surgically resected tumor, adjacent cancerous as well as non-cancerous tissue samples from 20 HCC patients, and

normal liver tissues from 3 accidentally died healthy adults were collected in West China Hospital of Sichuan University. The diagnosis of HCC was confirmed histologically in all cases.

Total RNA was extracted from 100 mg frozen tissue specimen with one-step guanidine thiocyanate-phenol method and dissolved in 5 g/L SDS solution. Genomic DNA was isolated from 100 mg frozen tissue specimen by digestion with proteinase K, followed by standard phenol-chloroform extraction and ethanol precipitation. The concentration of RNA and DNA was calculated according to their A_{260} values.

The genomic DNA of human plasmacytoma cell line HS-Sultan, which had p16 and p15 CpG islands methylation, was kindly gifted by Dr. Lo YM in Chinese University of Hong Kong. It was used as a methylation control for methylation specific PCR.

Northern blot hybridization

The plasmid that contained complete sequences of p16 cDNA or p15 cDNA was kindly gifted by Dr. D Beach in Cold Spring Harbor Laboratory. The 0.8 kb cDNA fragment of p16 and 2 kb cDNA fragment of p15 were nick translated with non-radiated digoxin using Boehringer Mannheim random primer DNA labeling kit. A 0.9 kb cDNA fragment of γ -actin was used as control probe. The total RNA (20–30 μ g) was fractionated on 1% agarose-formaldehyde gel and blotted onto nylon membrane (Bio-Rad) by capillary transfer. The hybridization was carried out in a solution containing 70 g/L SDS, 500 g/L formamide, 20 mL/L blocking reagent, 50 mmol/L sodium phosphate, pH7.0, 1 g/L sarcosyl, 5 \times SSC, 80 ng/mL probe. The hybridization and the subject signal chemiluminescent imaging were performed according to the manufacturer's manual. Every membrane was sequentially hybridized with p16, p15 and γ -actin cDNA probe after the bound probe was washed with 5 g/L SDS.

The intensity of the hybridization signal was scanned with UVP GDS8000 and quantited with Gelworks of UVP. To calculate the relative expression level of p16 or p15 gene, the hybridization signal intensity of γ -actin was employed as internal control to correct the unidentical amount of RNA loaded in electrophoresis, because γ -actin gene has a stable expression in various tissues.

Bisulfite conversion of DNA

Bisulfite modification and methylation specific PCR were conducted based on the principle that bisulfite treatment of DNA would convert unmethylated cytosine residues into uracil, whereas methylated cytosine residues would remain unmodified. Thus, the sequence-specific primers would distinguish the bisulfite converted unmethylation sequences and the unmodified methylation sequences by U and C.

The chemical modification was performed essentially as described previously with minor modification^[17]. DNA (1–2 μ g) in a volume of 50 μ L was denatured by NaOH (final concentration, 0.2 mol/L) for 10 min at 37 °C. Totally 520 μ L of 3 mol/L sodium bisulfite at pH5.0 and 30 μ L of 10 mmol/L hydroquinone, both freshly prepared, were added. After being mixed, the samples were incubated under the cover of mineral oil at 56 °C for 16 h. The modified DNA was desalted with the Wizard DNA purification resin and eluted in 50 μ L of water. For alkali desulphonation, an equal volume of 0.6 mol/L NaOH was added to an eluted DNA and incubated for 5 min at room temperature, modified DNA was precipitated with sodium acetate and ethanol and resuspended in 30 μ L of water. The DNA was stored at -70 °C.

Methylation specific PCR

The primers were designed for the CpG islands in promoter

and the first exon region of both p16 and p15 genes. All bisulfite-converted DNA samples were amplified with primers specific for methylated p16 or p15 sequence, and also amplified with primers specific for unmethylated p16 or p15 sequence. The sense and antisense primers for methylated p16 sequence were 5' TTATTAGAGGGGTGGGGCGGATCGC3' and 5' GACCCCGAACCGCGACCGTAA3'. The sense and antisense primers for unmethylated p16 sequence were 5' TTATTAGAGGGTGGGGTGGATTGT3' and 5' CAACCCCAAACCACAACCATAA3'. The sense and antisense primers for methylated p15 sequence were 5' GCGTTCGTATTTTGCGGTT3' and 5' CGTACAATAACCGAACGACCGA3'. The sense and antisense primers for the unmethylated p15 sequence were 5' TGTGATGTGTTTGTATTTTGTGGTT3' and 5' CCATACAATAACCAAACAACCAA3'. The 25 μ L of PCR mixture contained 50 ng of modified DNA, 200 μ mol/L each dATP, dGTP, dCTP and dTTP, 1 μ mol/L each primer, 50 g/L DMSO, 2.5 mmol/L MgCl₂, 1 \times reaction buffer and 1.5 U Taq polymerase. The PCR conditions were as follows: one cycle of at 95 °C for 5 min, 35 cycles of at 95 °C for 30 s, at 65 °C for 30 s (p16 methylation primers) or at 60 °C for 30 s (p16 unmethylation primers, p15 methylation and unmethylation primers), at 72 °C for 45 s, and 1 cycle of at 72 °C for 7 min. A 10 μ L of PCR products was then electrophoresed on a 25 g/L agarose gel, stained with ethidium bromide, and visualized under UV illumination in UVP GDS8000 gel imaging system^[17].

Statistical analysis

The difference in the p16 and p15 mRNA expression between cancer and noncancer tissue was analyzed using *t* test. The correlation of p16 or p15 gene mRNA expression level with its corresponding methylation of CpG islands was analyzed using Fisher's exact test. The correlation of between mRNA expression, and methylation of p16 and p15 genes with pathologic characteristics was also analyzed with Fisher's exact test. A *P* value <0.05 was considered statistically significant.

RESULTS

p16 and p15 mRNA expression in human hepatocarcinoma

After Northern blot hybridization, the 1.3 kb transcript of p16 mRNA, 3.8 kb transcript of p15 mRNA, 2.1 kb transcript of γ -actin mRNA were detected.

As shown in Figure 1, there was a decrease in p16 mRNA expression level in the cancerous tissues in 60% (12/20) of HCC compared with their corresponding para-cancerous and non-cancerous liver tissues, and p16 mRNA signal was not detected in 2 cases (10%). Five cases (25%) displayed variation in the order of cancerous <para-cancerous <non-cancerous tissues. The mRNA expression level of p16 gene in cancerous tissues was significantly lower than that of non-cancerous liver tissues (*P*<0.05).

p15 mRNA expression level was decreased within the cancerous tissues in 50% (10/20) of HCC, and p15 mRNA was not detected in 1 case. Four cases displayed variation in the order of cancerous <para-cancerous <non-cancerous tissue. The mRNA expression level of p15 gene in cancerous tissues was significantly lower than that of non-cancerous liver tissues (*P*<0.05).

Methylation status of the 5'CpG islands of p16 and p15 genes

Hypermethylation of p16 promoter CpG islands occurred in cancerous tissues (65%, 13/20), and also in para-cancerous tissues (60%, 11/20,) and non-cancerous tissues (35%, 7/20). Four cancerous tissues exhibited only the methylation band,

while the others showed methylation and unmethylation bands, suggesting partial methylation (Figure 2)^[11,13,18].

Aberrant promoter methylation of p15 gene was detected in 50%(10/20) of patients with HCC. Among them, the methylation was found only in cancerous tissues in 2 cases, in both cancerous and para-cancerous tissues in 3 cases, in all of cancerous, para-cancerous and non-cancerous tissues in 5 cases. The partial methylation occurred in all of the non-cancerous tissues. None of the 3 healthy subjects displayed p16 or p15 methylation, whereas they displayed unmethylated p16 and p15 alleles (Figure 3).

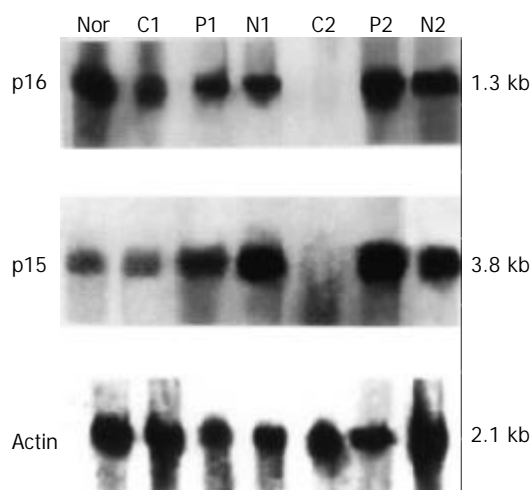


Figure 1 Northern blot analysis of the p16 and p15 genes in human primary hepatocarcinoma. Total RNA from tissues of human primary hepatocarcinoma was hybridized with cDNA fragment probes of p16, p15 and γ -actin labeled with non-radiated digoxinin. N: Normal liver tissue control; C, P, N represent RNA from cancerous, para-cancerous, non-cancerous liver tissues respectively; 1, 2 represent the No. of HCC patient.

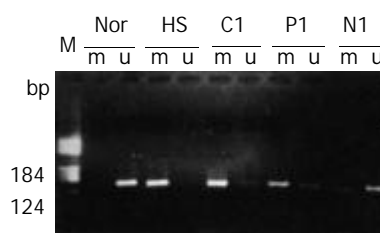


Figure 2 Methylation analysis of p16 gene in human primary hepatocarcinoma. MSP product of p16 gene from HCC tissues was electrophoresed on a 25 g/L agarose gel. M: pBR322/HeaIII DNA molecular marker; N: Normal liver tissue DNA; HS: HS-Sultan DNA (positive control); C, P, N represent RNA from cancerous, para-cancerous, non-cancerous liver tissue respectively; 1, 2 mark the HCC patient number; m: PCR products from methylation specific primers, u: PCR products from unmethylation specific primers.

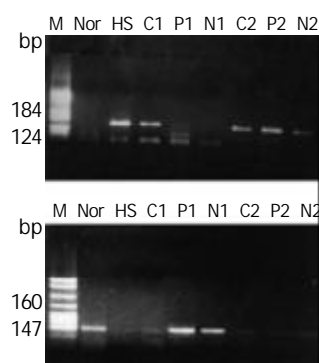


Figure 3 Methylation analysis of p15 gene in human primary hepatocarcinoma. MSP product of p15 gene from HCC tissues was electrophoresed on a 2.5% agarose gel. M: pBR322/HeaIII DNA molecular marker (in graph m) or PBR322/Msp I DNA marker (in graph u); N: Normal liver tissue DNA; HS: HS-Sul-

Table 1 CpG island methylation status and expression of p16 and p15 genes and clinical information of 20 HCC patients

Cases	p16 methylation ¹	p16 expression	p15 methylation ¹	p15 expression	HBsAg ⁴	Cirrhosis ⁵	Differentiation ⁶
1	±	D	+	D	+	Y	L
2	+	D	+	D	+	Y	L
3	±	D	+	D	+	N	M
4	±	N	±	D	+	Y	M
5	±	D	+	D	+	N	L
6	+	D	-	N	+	N	L
7	-	N	-	N	-	N	H
8	±	N	±	D	-	N	M
9	±	D	±	D	+	Y	M
10	-	N	-	N	-	N	H
11	+	D	N ²	N	+	Y	L
12	±	D	-	I	+	Y	M
13	-	D	±	D	+	Y	M
14	-	N	-	I	-	N	M
15	+	D	-	N	+	N	L
16	±	N	±	D	-	Y	L
17	-	D	-	N	-	N	H
18	-	I	-	I	+	N	H
19	±	D	±	D	-	Y	L
20	-	N	-	N	+	N	H

¹+Positively amplified with methylation primers only; - positively amplified with unmethylation primers only; ± positively amplified with methylation and unmethylation primers; ²N: Negatively amplified with methylation or unmethylation primers, ³D: Decreased; I: Increased; N: No significant difference; compared with non-cancer tissue, ⁴+: Positive; -: Negative; ⁵Y: Cirrhosis; N: No cirrhosis, ⁶H: High differentiation; M: moderate differentiation; L: Low differentiation.

tan DNA(positive control); C, P, N represent RNA from cancerous, para-cancerous, non-cancerous liver tissue respectively; 1, 2 mark the HCC patient number; m: PCR products from methylation specific primers, u: PCR products from unmethylation specific primers.

Reciprocal relationship between mRNA expression of p16/p15 and their promoter methylation status

Significant correlation between 5' CpG island methylation and low mRNA expression of p16/p15 was found in the 20 HCCs ($P<0.05$). Among 12 HCCs, which displayed lower p16 mRNA expression level in cancerous tissue, 11 cases showed p16 promoter 5' CpG island methylation (91.6%). Similar event took place in p15 gene. All of 10 HCCs with decreased p15 mRNA expression in cancerous tissue had 5' CpG island hypermethylation (100%), while unmethylation occurred in non-cancerous liver tissue. Interestingly, 1 case displayed no detectable transcript p15 gene in cancerous tissue with hypermethylation (Table 1).

The relationship between mRNA expression, or methylation and pathologic characteristics

Significant correlation either between decreased p16/p15 mRNA expression and poor cellular differentiation of HCC, or between p16/p15 promoters 5' CpG islands methylation and poor differentiation of HCC was found ($P=0.0083$, 0.0102 , 0.00271 , 0.0218 , respectively, $P<0.05$). However, there was no significant correlation between p16/p15 mRNA expression and HBV infection or cirrhosis, or between their promoter methylation and HBV infection or cirrhosis (Table 1).

DISCUSSION

Our study showed that a decreased p16 mRNA expression level was detected within cancerous tissues in 60% of HCCs compared with their corresponding non-cancerous tissues, 5 of which displayed in turn variation in cancerous tissue less than in para-cancerous tissue, then in non-cancerous liver tissues. It was interesting that among the 12 cases with lower p16 mRNA expression, 9 cases were accompanied with p16 gene promoter partial methylation in cancerous tissues, while 2 cases were accompanied with complete methylation. In contrast, methylation was not detected in normal liver tissues from 3 accidentally died subject. The partial methylation of p16 gene promoter may explain why the p16 mRNA expression just decreased but not loss in majority of HCCs. It has been reported that partial loss of expression of p16 was associated with low level of methylation rather than complete loss^[11,19,20]. The relationship between p16 mRNA expression and its promoter CpG island methylation has been demonstrated in other studies. Kaneto *et al.*, using methylation specific PCR and immunohistochemistry, had detected methylation of p16 promoter in HCC (72.6%, 16/22) and loss of expression in all methylation positive HCC^[13]. Roncalli *et al.* reported that methylation of p16 promoter with complete loss of immunoreactivity occurred in 27 of 33 HCC (82%)^[15]. Thus, our result, which was consistent with other reports, suggested that association of p16 gene 5' CpG island methylation with transcription inactivation might play an important role in hepatocarcinogenesis, and 5' CpG island methylation was the major mechanism of p16 gene inactivation.

Like the alteration of p16 gene, a decreased p15 mRNA expression level was found within cancerous tissue in 50% of HCC compared with their corresponding non-cancerous liver tissues. All cases that had a lower transcription level of p15 were in conjunction with the hypermethylation of p15 promoter CpG island. Roncalli *et al.* detected methylation of p15 islands in 42% of HCC (14/33), and methylation positive HCC had a

complete loss of immunocytochemical expression of p15. Wong *et al.* reported a high frequency of p15 methylation (64%, 15/25) in HCC. Yang *et al.* showed methylation of p15 in 49% of HCC^[14-16]. Based on Northern blot analysis, our study found that a complete loss of p15 mRNA expression accounted for a small portion of the p15 methylation positive cases, while the majority had decreased transcription level. This discrepancy of our result with other studies might be due to the high sensitivity of Northern blot analysis. Nevertheless, our result provided further evidence from different aspect for the contribution of the epigenetic alteration to inactivation of p15 gene in hepatocarcinogenesis.

In our present study, partial methylation of p16 and/or p15 promoter was detected in 50% of non-cancerous liver tissues (10/20). However, the p16/p15 positive liver tissue still expressed mRNA of p16/p15 genes. It was very interesting to note that a complete methylation of p16 promoter CpG island was present in cancerous tissue while partial methylation in non-cancerous tissues. A similar phenomenon of p15 gene alteration occurred in 2 cases. This supported the hypothesis that methylation of cell cycle inhibitor gradually accumulate in the transition from cirrhosis or chronic hepatitis to HCC^[13,15]. Yu *et al.* detected that hypermethylation of the p16 promoter CpG islands occurred overwhelmingly in HCC samples (56.6%, 17/29) and less frequently in adjacent non-cancerous tissues (21.9%, 6/29) after analyzing the methylation profiling of 20 promoter-CpG islands of genes in human primary hepatocellular carcinoma. Therefore, they thought that hypermethylation of p16 promoter CpG islands may occur at very late stage of the hepatocarcinogenesis^[21]. Edamoto *et al.* showed that higher rate of promoter methylation of p16 in HCCs (59%) than in cirrhotic liver (21%) or chronic hepatitis lesions (0/10)^[22].

Our study also showed that in the non-cancerous liver tissues, the frequency of p15 partial methylation was higher in cirrhosis (44%, 4/9) than non-cirrhosis (9%, 1/11). Also the rate of p16 partial methylation was higher in cirrhosis (44%, 4/9) than non-cirrhosis 27%, 3/11), although these results had no statistical significance probably due to the few studied cases (Data not shown). The percentage of p16 methylation in cirrhosis was reported 29.4% by Kaneto *et al.*, and 39% by Roncalli *et al.*^[13,15]. The frequency of p15 methylation reported by Roncalli *et al.* was 33%^[15]. Roncalli *et al.* noted that p15 was responsible for the early methylation pattern in cirrhosis but not in HCC. They proposed that p15 but not p16 was necessary for the inactivation of other genes in the transition from cirrhosis to HCC^[15]. Nevertheless, the methylation of p16 and p15 might be the major mechanism to inactive cell-cycle inhibitor in preneoplastic stage.

The correlation between either decreased p16/p15 mRNA expression or p16/p15 promoter CpG island methylation and poor differentiation of HCC was determined in our present study. Interestingly, the correlation of loss of p16 protein expression with the cellular differentiation of HCC and gastric cancer has been reported^[23,24]. Park *et al.* also noted that inactivation of p16 exon 1 by DNA hypermethylation occurred during the progression of tumor cells to poorly differentiated HCC, which was induced by diethylnitrosamine plus thioacetamide in Fischer 344 rats^[25]. These studies suggested that the aberrant alteration of mRNA expression and methylation of p16 and p15 genes might be not only involved HCC carcinogenesis but also associated with its progress.

Although the mechanism of methylation in cancers remains to be explained clearly, it has been generally recognized that two methyltransferases, Dnmt1 and Dnmt3b cooperatively maintain DNA methylation and gene silencing in human cancer cells^[26-28]. It has been reported that higher expression of methyltransferases was associated with methylation of p16

and p15 genes in HCC^[29]. It has been noted that either the inhibitors of methyltransferase, such as 5-aza-2'-deoxycytidine and tea-polyphenol (-)-epigallocatechin-3-gallate or antisense inhibitors of DNA methyltransferases, reactivated silenced tumor suppressor genes and inhibited the growth of cancer cells^[30-33].

Thus, methylation of 5' CpG islands of p16 and p15 genes might be an early event in hepatocarcinogenesis. The methylation of p16 and p15 genes could be a biomarker for monitoring HCC and other tumors, which was demonstrated by recent studies^[14,34,35,36]. It also provides an insight into therapy of the high risky patients and prevention of HCC.

REFERENCES

- 1 **Ortega S**, Malumbres M, Barbacid M. Cyclin D-dependent kinase, INK4 inhibitors and cancer. *Biochim Biophys Acta* 2002; **1602**: 73-87
- 2 **Serrano M**, Hannon GJ, Beach D. A new regulatory motif in cell-cycle control causing specific inhibition of cyclin D/CDK4. *Nature* 1993; **366**: 704-707
- 3 **Hannon GJ**, Beach D. p15INK4B is a potential effector of TGF-beta-induced cell cycle arrest. *Nature* 1994; **371**: 257-261
- 4 **Weinberg RA**. The retinoblastoma protein and cell cycle control. *Cell* 1995; **81**: 323-330
- 5 **Hui AM**, Sakamoto M, Kanai Y, Ino Y, Gotoh M, Yokota J, Hirohashi S. Inactivation of p16INK4 in hepatocellular carcinoma. *Hepatology* 1996; **24**: 575-579
- 6 **Kita R**, Nishida N, Fukuda Y, Azechi H, Matsuoka Y, Komeda T, Sando T, Nakao K, Ishizaki K. Infrequent alterations of the p16INK4A gene in liver cancer. *Int J Cancer* 1996; **67**: 176-180
- 7 **Bonilla F**, Orlow I, Cordon-Cardo C. Mutational study of p16CDKN2/MTS1/INK4A and p57KIP2 genes in hepatocellular carcinoma. *Int J Oncol* 1998; **12**: 583-588
- 8 **Qin Y**, Li B, Tan YS, Sun ZL, Zho FQ, Sun ZF. Polymorphism of p16INK4a gene and rare mutation of p15INK4b gene exon2 in primary hepatocarcinoma. *World J Gastroenterol* 2000; **6**: 411-414
- 9 **Huang J**, Shen W, Li B, Luo Y, Liao S, Zhang W, Cheng N. A study on the inactivation of p16 and the expression of P16 protein in primary hepatocellular carcinomas. *Huaxi Yike Daxue Xuebao* 2000; **31**: 306-309
- 10 **Baylin SB**, Herman JG. DNA hypermethylation in tumorigenesis: epigenetics joins genetics. *Trends Genet* 2000; **16**: 168-174
- 11 **Matsuda Y**, Ichida T, Matsuzawa J, Sugimura K, Asakura H. p16 (INK4) is inactivated by extensive CpG methylation in human hepatocellular carcinoma. *Gastroenterology* 1999; **116**: 394-400
- 12 **Liew CT**, Li HM, Lo KW, Leow CK, Chan JY, Hin LY, Lau WY, Lai PB, Lim BK, Huang J, Leung WT, Wu S, Lee JC. High frequency of p16INK4A gene alterations in hepatocellular carcinoma. *Oncogene* 1999; **18**: 789-795
- 13 **Kaneto H**, Sasaki S, Yamamoto H, Itoh F, Toyota M, Suzuki H, Ozeki I, Iwata N, Ohmura T, Satoh T, Karino Y, Toyota M, Satoh M, Endo T, Omata M, Imai K. Detection of hypermethylation of the p16(INK4A) gene promoter in chronic hepatitis and cirrhosis associated with hepatitis B or C virus. *Gut* 2001; **48**: 372-377
- 14 **Wong IH**, Lo YM, Yeo W, Lau WY, Johnson PJ. Frequent p15 promoter methylation in tumor and peripheral blood from hepatocellular carcinoma patients. *Clin Cancer Res* 2000; **6**: 3516-3521
- 15 **Roncalli M**, Bianchi P, Bruni B, Laghi L, Destro A, Gioia SD, Gennari L, Tommasini M, Malesci A, Coggi G. Methylation framework of cell cycle gene inhibitors in cirrhosis and associated hepatocellular carcinoma. *Hepatology* 2002; **36**: 427-432
- 16 **Yang B**, Guo M, Herman JG, Clark DP. Aberrant promoter methylation profiles of tumor suppressor genes in hepatocellular carcinoma. *Am J Pathol* 2003; **163**: 1101-1107
- 17 **Herman JG**, Graff JR, Myohanen S, Nelkin BD, Baylin SB. Methylation-specific PCR: a novel PCR assay for methylation status of CpG islands. *Proc Natl Acad Sci U S A* 1996; **93**: 9821-9826
- 18 **Baek MJ**, Piao Z, Kim NG, Park C, Shin EC, Park JH, Jung HJ, Kim CG, Kim H. p16 is a major inactivation target in hepatocellular carcinoma. *Cancer* 2000; **89**: 60-68
- 19 **Gonzalzo ML**, Hayashida T, Bender CM, Pao MM, Tsai YC, Gonzales FA, Nguyen HD, Nguyen TT, Jones PA. The role of DNA methylation in expression of the p19/p16 locus in human bladder cancer cell lines. *Cancer Res* 1998; **58**: 1245-1252
- 20 **Herman JG**. p16(INK4): involvement early and often in gastrointestinal malignancies. *Gastroenterology* 1999; **116**: 483-485
- 21 **Yu J**, Ni M, Xu J, Zhang H, Gao B, Gu J, Chen J, Zhang L, Wu M, Zhen S, Zhu J. Methylation profiling of twenty promoter-CpG islands of genes which may contribute to hepatocellular carcinogenesis. *BMC Cancer* 2000; **2**: 29
- 22 **Edamoto Y**, Hara A, Biernat W, Terracciano L, Cathomas G, Riehle HM, Matsuda M, Fujii H, Scoazec JY, Ohgaki H. Alterations of RB1, p53 and Wnt pathways in hepatocellular carcinomas associated with hepatitis C, hepatitis B and alcoholic liver cirrhosis. *Int J Cancer* 2003; **106**: 334-341
- 23 **Wang ZW**, Peng ZH, Li K, Qiu GQ, Zhang Y, Gu W. Effect of p16 gene on carcinogenesis of hepatitis B virus related hepatocellular carcinoma. *Zhonghua Zhongliu Zazhi* 2003; **25**: 356-358
- 24 **Rocco A**, Schandl L, Nardone G, Tulassay Z, Staibano S, Malfertheiner P, Ebert MP. Loss of expression of tumor suppressor p16(INK4) protein in human primary gastric cancer is related to the grade of differentiation. *Dig Dis* 2002; **20**: 102-105
- 25 **Park TJ**, Kim HS, Byun KH, Jang JJ, Lee YS, Lim IK. Sequential changes in hepatocarcinogenesis induced by diethylnitrosamine plus thioacetamide in Fischer 344 rats: induction of gankyrin expression in liver fibrosis, pRB degradation in cirrhosis, and methylation of p16(INK4A) exon 1 in hepatocellular carcinoma. *Mol Carcinog* 2001; **30**: 138-150
- 26 **Rhee I**, Bachman KE, Park BH, Jair KW, Yen RW, Schuebel KE, Cui H, Feinberg AP, Lengauer C, Kinzler KW, Baylin SB, Vogelstein B. DNMT1 and DNMT3b cooperate to silence genes in human cancer cells. *Nature* 2002; **416**: 552-556
- 27 **Kim GD**, Ni J, Kelesoglu N, Roberts RJ, Pradhan S. Co-operation and communication between the human maintenance and de novo DNA (cytosine-5) methyltransferases. *EMBO J* 2002; **21**: 4183-4195
- 28 **Robert MF**, Morin S, Beaulieu N, Gauthier F, Chute IC, Barsalou A, MacLeod AR. DNMT1 is required to maintain CpG methylation and aberrant gene silencing in human cancer cells. *Nat Genet* 2003; **33**: 61-65
- 29 **Saito Y**, Kanai Y, Sakamoto M, Saito H, Ishii H, Hirohashi S. Expression of mRNA for DNA methyltransferases and methyl-CpG-binding proteins and DNA methylation status on CpG islands and pericentromeric satellite regions during human hepatocarcinogenesis. *Hepatology* 2001; **33**: 561-568
- 30 **Fang MZ**, Wang Y, Ai N, Hou Z, Sun Y, Lu H, Welsh W, Yang CS. Tea polyphenol (-)-epigallocatechin-3-gallate inhibits DNA methyltransferase and reactivates methylation-silenced genes in cancer cell lines. *Cancer Res* 2003; **63**: 7563-7570
- 31 **Liu LH**, Xiao WH, Liu WW. Effect of 5-Aza-2'-deoxycytidine on the P16 tumor suppressor gene in hepatocellular carcinoma cell line HepG2. *World J Gastroenterol* 2001; **7**: 131-135
- 32 **Stewart DJ**, Donehower RC, Eisenhauer EA, Wainman N, Shah AK, Bonfils C, MacLeod AR, Besterman JM, Reid GK. A phase I pharmacokinetic and pharmacodynamic study of the DNA methyltransferase 1 inhibitor MG98 administered twice weekly. *Ann Oncol* 2003; **14**: 766-774
- 33 **Zhang H**, Xiao W, Liang H, Fang D, Yang S, Luo Y. Demethylation in the promoter area by the antisense of human DNA MTase gene. *Zhonghua Zhongliu Zazhi* 2002; **24**: 444-447
- 34 **Wong IH**, Zhang J, Lai PB, Lau WY, Lo YM. Quantitative analysis of tumor-derived methylated p16INK4a sequences in plasma, serum, and blood cells of hepatocellular carcinoma patients. *Clin Cancer Res* 2003; **9**: 1047-1052
- 35 **Deligezer U**, Yaman F, Erten N, Dalay N. Frequent copresence of methylated DNA and fragmented nucleosomal DNA in plasma of lymphoma patients. *Clin Chim Acta* 2003; **335**: 89-94
- 36 **Siu LL**, Chan JK, Wong KF, Choy C, Kwong YL. Aberrant promoter CpG methylation as a molecular marker for disease monitoring in natural killer cell lymphomas. *Br J Haematol* 2003; **122**: 70-77

Correlation of expression of multidrug resistance protein and messenger RNA with ^{99m}Tc-methoxyisobutyl isonitrile (MIBI) imaging in patients with hepatocellular carcinoma

Hai Wang, Xiao-Ping Chen, Fa-Zu Qiu

Hai Wang, Xiao-Ping Chen, Fa-Zu Qiu, Hepatic Center of Tongji Hospital, Tongji Medical College, Huazhong University of Science and Technology, Wuhan 430030, HuBei Province, China

Supported by the Clinical Focal Point Subject Foundation of Ministry of Public Health, No.3212001

Correspondence to: Dr. Xiao-Ping Chen, Hepatic Surgery Center of Tongji Hospital, Tongji Medical College, Huazhong University of Science and Technology, Wuhan 430030, Hubei Province, China. chenxp53@sina.com

Telephone: +86-27-83662599 **Fax:** +86-27-83662851

Received: 2003-03-12 **Accepted:** 2003-08-16

Abstract

AIM: To explore whether P-glycoprotein (Pgp) and other pumps, multidrug resistance-associated protein (MRP) and lung resistance protein (LRP), could affect tumor accumulation and efflux of ^{99m}Tc-MIBI in liver cancer.

METHODS: Surgically treated 78 liver cancer patients were included in this study. Before surgery, ^{99m}Tc-MIBI SPECT was performed 15 min and 120 min after injection of 20 mCi ^{99m}Tc-MIBI, respectively. Early uptake, delayed uptake (L/Nd), and washout rate (L/Nwr) of ^{99m}Tc-MIBI were obtained. Expressions of Pgp, MRP and LRP were investigated with Western blotting and immunohistochemistry. Messenger RNA (mRNA) level of Pgp, MRP and LRP was determined by RT-PCR.

RESULTS: No ^{99m}Tc-MIBI uptakes in tumor lesions of 68 of 78 (87.2%) patients with hepatocellular carcinoma were found on ^{99m}Tc-MIBI SPECT. P-gp expression was observed in tumor tissues of the patients with no uptake of ^{99m}Tc-MIBI ($P < 0.017$). No appreciable correlation was found between liver cancer ^{99m}Tc-MIBI images and expression of MRP or LRP on the level of protein or mRNA.

CONCLUSION: ^{99m}Tc-MIBI SPECT is noninvasive, and useful in predicting the presence of MDR1 gene-encoded Pgp in patients with hepatocellular carcinoma.

Wang H, Chen XP, Qiu FZ. Correlation of expression of multidrug resistance protein and messenger RNA with ^{99m}Tc-methoxyisobutyl isonitrile (MIBI) imaging in patients with hepatocellular carcinoma. *World J Gastroenterol* 2004; 10 (9): 1281-1285

<http://www.wjgnet.com/1007-9327/10/1281.asp>

INTRODUCTION

Multidrug resistance (MDR) is the main barrier to efficient chemotherapy of human malignancies. MDR has been closely associated with overexpression of multidrug resistance genes (MDR1)^[1] and has been observed in hepatocellular carcinomas (HCC)^[2]. The MDR phenotype has been defined on the basis

of cellular drug targets involved Pgp, MRP, LRP and atypical MDR (mediated through altered expression of topoisomerase type II)^[3-6]. Pgp, encoded by MDR1 gene, is a 170-ku transmembrane glycoprotein and acts as an adenosine triphosphate (ATP)-driven drug efflux pump to reduce drug accumulation^[7]. MRP is a 190-ku membrane-bound glycoprotein and can act as a glutathione S-conjugate efflux pump by transporting drugs that are conjugated or cotransported with glutathione^[8,9]. Both Pgp and MRP are integral membrane proteins belonging to the ATP-binding cassette (ABC) superfamily of transporter proteins, which appear to confer resistance by decreasing intracellular drug accumulation^[10]. In contrast, LRP is not an ABC transporter protein. LRP has recently been identified as a vault protein, which is a typical multisubunit structure involved in nucleocytoplasmic transporter^[11]. Determination of these MDR proteins at the time of diagnosis is imperative to the development of rational therapeutic strategies for preventing drug resistance.

^{99m}Tc-MIBI is a cationic lipophilic agent, widely used for myocardial perfusion imaging to detect various tumors^[12-18]. Recent evidence has shown that ^{99m}Tc-MIBI is a suitable transport substrate for Pgp and may provide additional information about the Pgp status of tumor cells^[19,20]. It has been reported that MIBI is accumulated within mitochondria and cytoplasm of cells based on transmembrane electrical potentials. Malignant tumors show increased transmembrane potential as a result of increased metabolic requirements that induce increased accumulation of MIBI in tumors^[21]. The potential advantage of ^{99m}Tc-MIBI imaging lies in its superiority in detecting the presence of Pgp overexpression *in vivo* noninvasively^[22,23]. Recently, ^{99m}Tc-MIBI efflux has been shown to be a substrate for MRP *in vivo*^[24].

^{99m}Tc-MIBI imaging or SPECT was performed in various cancers^[25,26], but no clinical studies in HCC have been found. The aim of this study was to determine whether Pgp and other pumps, MRP and LRP, could affect tumor accumulation and efflux of ^{99m}Tc-MIBI in hepatocellular carcinoma.

MATERIALS AND METHODS

Patients

Seventy-eight patients (30 women, 48 men, aged 24-71 years, mean 54±11.6 years) with HCC were enrolled in the study, 70 of 78 (89.7%) patients were hepatitis B surface antigen positive, 2 (2.6%) were anti-hepatitis C virus positive, and the remaining had no known cause of HCC. No patients previously received chemotherapy. All patients underwent ^{99m}Tc-MIBI SPECT prior to surgery. All tumor samples were analyzed with RT-PCR, Western blotting and immunohistochemistry.

^{99m}Tc-MIBI SPECT

Liver imaging was performed with a double-head gamma camera equipped with a high-resolution parallel-hole collimator (PRISM 2000; Marconi Medical Systems, Cleveland, OH). Images were obtained 15 and 120 min after injection of 20 mCi ^{99m}Tc-MIBI, respectively. Early and delayed SPECT of the liver was performed

on all patients. For SPECT of the liver, 72 projections were obtained using 64×64 matrix at 45 s per view. Image reconstruction was performed using filtered back projection with Butter-worth and ramp filters. Transverse, coronal, and sagittal sections were reconstructed. Attenuation correction was not applied.

SPECT images were compared with liver CT images, and accumulation in liver tumors was interpreted by nuclear medicine physicians. The findings on ^{99m}Tc-MIBI livers were measured semiquantitatively. Regions of interest (ROIs) were manually defined on the transaxial tomograms showing the lesion's highest uptake in center of the tumor. ROIs placed on the lesions (L) encompassed all pixels that had uptake values of >90% of the maximum uptake in that slice, and the average rate in each ROI was calculated. Another ROI of the same size was then drawn over the normal lung (N) on the same transverse section. The early uptake (L/Ne) and the delayed uptake (L/Nd) were obtained. The washout rate (L/Nwr) was calculated using the following formula: $L/Nwr = (L/Ne - L/Nd) \times 100 / (L/Ne)$.

Immunohistochemical study

After resection of HCC, immunohistochemical study of the biopsy or resected tumor tissues and surrounding nontumorous liver parenchyma was performed. Four-micrometer-thick, formalin-fixed, paraffin-embedded tissue sections were cut from the specimens and mounted on poly-L-lysine-coated glass slides (Sigma Chemical Co., St. Louis, MO). The standard avidin-biotin-peroxidase complex (ABC) technique was used for immunostaining using a LSAB kit (Dako Co., Carpinteria, CA).

After deparaffinization and rehydration, the sections were treated with 1 mL/L methanol hydrogen peroxide for 20 min to block endogenous peroxidase activity, incubated with normal horse serum for 30 min at 37 °C, and with primary antibody, JSB-1 (1:20), MRP1 (1:10), LRP-56 (1:10) overnight in a moist chamber at 4 °C. The tissue sections were incubated with avidin-biotin-peroxidase complex. The final reaction product was

revealed by exposure to 0.3 g/L diaminobenzidine, and the nuclei were counterstained with Mayer's hematoxylin.

A negative control was obtained by staining the sample with secondary antibody and a positive control by inclusive of a normal liver. The results of immunostaining were interpreted independently by two pathologists who were unaware of the imaging studies. Expressions of Pgp, MRP and LRP were scored as follows: -, negative; +, ≤10% positive tumor cells; ++, ≤30% positive tumor cells; +++, >30% positive tumor cells.

Quantitative RT-PCR

RT was performed with random primers with a complementary DNA (cDNA) synthesis kit (Promega, Madison, WI). RT-reaction reagents were added as follows: 2 μL of MgCl₂ (50 mmol/L), 2 μL of reverse transcription buffer (Tris-HCL [PH8.3], 100 mmol/L, KCL 500 mmol/L and Triton X-100 10 g/L), 2 μL of deoxynucleotide mixture (10 mmol/L), 0.5 μL of RNase inhibitor (20U), 2 (15U) of avian myeloblastoma virus reverse transcriptase, 1 μL of random primers (500 μg/mL) and 5 μg substrate RNA. The final volume of the reaction (20 μL) was completed with RNase free water. First strand cDNA synthesis was carried out at 42 °C for 30 min in the DNA thermal cycler (PTC-100, MJ Reserch Inc., Watertown, MA). Afterwards, the tubes were incubated at 99 °C for 5 min to stop the reaction. Then each tube was kept at 4 °C until PCR was performed. Expression of the target genes (MDR1, MRP and LRP) and endogenous reference β-actin was quantified using the primers and standards. The primers were designed using the software Primer Express (Applied Biosystems) (Table 1).

RT-PCR

Expressions of the target genes (MDR1, MRP and LRP) and GAPDH gene were quantified using the primers and standards. The primers were designed using the software Primer Express (Applied Biosystems) (Table 2).

RT-PCR was performed according to the TaqMan 2-step

Table 1 MDR1, MRP, LRP primers for RT-PCR amplifications

Gene	Quantification method	Sequence	cDNA
MDR1	Forward primer	5- CATTGGTGTGGTGAGTCAGG-3	1523-1542
	Reverse primer	5- CTCTCTCTCCAACCAGGGTG-3	1679-1698
MRP	Forward primer	5- CTACCGAGAGGACCTGGACT-3	4099-4118
	Reverse primer	5- GTCTAGCTTGTACGGAAGGG-3	4437-4456
LRP	Forward primer	5- TAAGGGCTTCCAGCACCAAC-3	148-167
	Reverse primer	5- GGAGTTCTCGCTTCTCGTCC-3	520-539
β-actin	Forward primer	5- GTGTTGGCCGAGTCCTACC-3	
	Reverse primer	5- CTCCTGCAAGGAAAAGCTCTG-3	

Table 2 Oligonucleotides used for PCR amplifications

Gene	Quantification method	Sequence	cDNA
MDR1	Forward primer	5' - CCCAGGAGCCCATCCTGT-3'	3774-3791
	Reverse primer	5' - CCCGGCTGTTGTCTCCATA-3'	3838-3821
	Probe	5' -(FAM)TGACTGCAGCATTGCTGAGAACATTGC(TAMRA)-3'	3793-3819
MRP	Forward primer	5' - AAGCGCTCGAGTCGGT-3'	3617-3633
	Reverse primer	5' - TCGAATGACGCTGACCCC-3'	3694-3677
	Probe	5' -(FAM)AGCCGCTCCCCGGTCTATTCCC-(TAMRA)-3'	3635-3656
LRP	Forward primer	5' - TTTCGATGACTTCCATAAGAACTCA-3'	1881-1905
	Reverse primer	5' - TTCCGAGGTCTCAAAGCCAA-3'	1950-1931
	Probe	5' (FAM)-CCCGCATCATTGCACTGCTGT- (TAMRA)3'	1907-1928
GAPDH	Forward primer	5' - GAAGGTGAAGGTCGGAGTCA-3'	
	Reverse primer	5' - GAAGATGGTGATGGGA-3'	
	Probe	5' -(JOE)CAAGCTTCCCGTCTCAGCC(TAMRA)-3'	

method using the ABI PRISM 7 700 sequence detection system (Applied Biosystems). The nontemplate controls, standard dilutions, and samples were assayed. A 25- μ l volume of PCR reaction mixture was used, containing 200 ng of the sample cDNA, TaqMan buffer, 200 μ mol/L deoxy-ATP, deoxycytidine triphosphate, and deoxy-guanosine triphosphate, 400 μ mol/L deoxyuridine triphosphate, 5.5 mmol/L magnesium chloride, 0.025 U/mL AmpliTaq Gold DNA polymerase (Applied Biosystems), 0.01 U/mL AmpErase uracil N-glycosylase (Applied Biosystems), 200 nmol/L forward and reverse primers, and 100 nmol/L probe. PCR cycling conditions included an initial phase at 50 °C for 2 min, followed by at 95 °C for 10 min for AmpErase, 40 cycles at 95 °C for 15 s, and at 60 °C for 1 min. Quantification of the PCR products was based on the TaqMan 5' nuclease assay using the ABI PRISM 7 700 sequence detection system. The starting quantity of a specific mRNA in an unknown sample was determined by preparing a standard cDNA. The standard curve was generated on the basis of the linear relationship between CT value (corresponding to the cycle number at which a significant increase in fluorescence signal was first detected) and logarithm of the starting quantity. The unknown samples were quantified by the software of the ABI PRISM 7 700 sequence detector system, which calculated the CT value for each sample and then determined the initial quantity of the target using the standard curve. The amount of expressed target gene was normalized to that of GAPDH.

Western blotting

Liver cancer samples were analyzed for the presence of Pgp, MRP and LRP protein. Samples were washed in PBS and homogenized in a lysis buffer^[27]. Protein supernatants were quantitated using the Lowry assay, and equal amounts of protein from each sample were separated by SDS-PAGE and electroblotted onto nitrocellulose membranes. Membranes were probed with mAb recognizing Pgp, MRP and LRP (Sigma, Co), respectively. Enhanced chemiluminescence was used for protein detection.

Statistical analysis

The results of L/Ne, L/Nd, and L/Nwr were expressed as mean \pm SD. The differences in L/Ne, L/Nd, and L/Nwr between patients with (-), (+), and (++) Pgp, MRP, and LRP expressions were determined using Student *t* test. The differences in L/Ne, L/Nd, and L/Nwr between patients with high and low Pgp mRNA, MRP mRNA, and LRP mRNA expressions were determined using Student *t* test. If *P* was <0.05, the difference was considered statistically significant.

RESULTS

All the 78 surgically obtained tissue samples were assessed to estimate the levels of Pgp, MRP, and LRP expression on protein and mRNA. Table 3 summarizes the immunohistochemical results and RT-PCR data.

Correlation of ^{99m}Tc-MIBI results with immunohistochemical results

Significant MIBI uptake on ^{99m}Tc-MIBI SPECT was noted in tumor lesions of 10 (12.8%) patients with HCC, but not in tumor lesions of 68 (87.2%) patients with HCC. In patients with MIBI uptake, immunohistochemical analysis of tumor tissues showed no detectable P-glycoprotein-positive cells. But immunohistochemical analysis of tumor lesions in patients without MIBI uptake revealed uniformly distributed P-gp-positive cells. We noted a significant correlation between ^{99m}Tc-MIBI SPECT findings and P-gp expression in tumors of patients with HCC.

MRP and LRP protein expression was found in tumor lesions of 7 and 4 patients, respectively, and no correlation was found with ^{99m}Tc-MIBI.

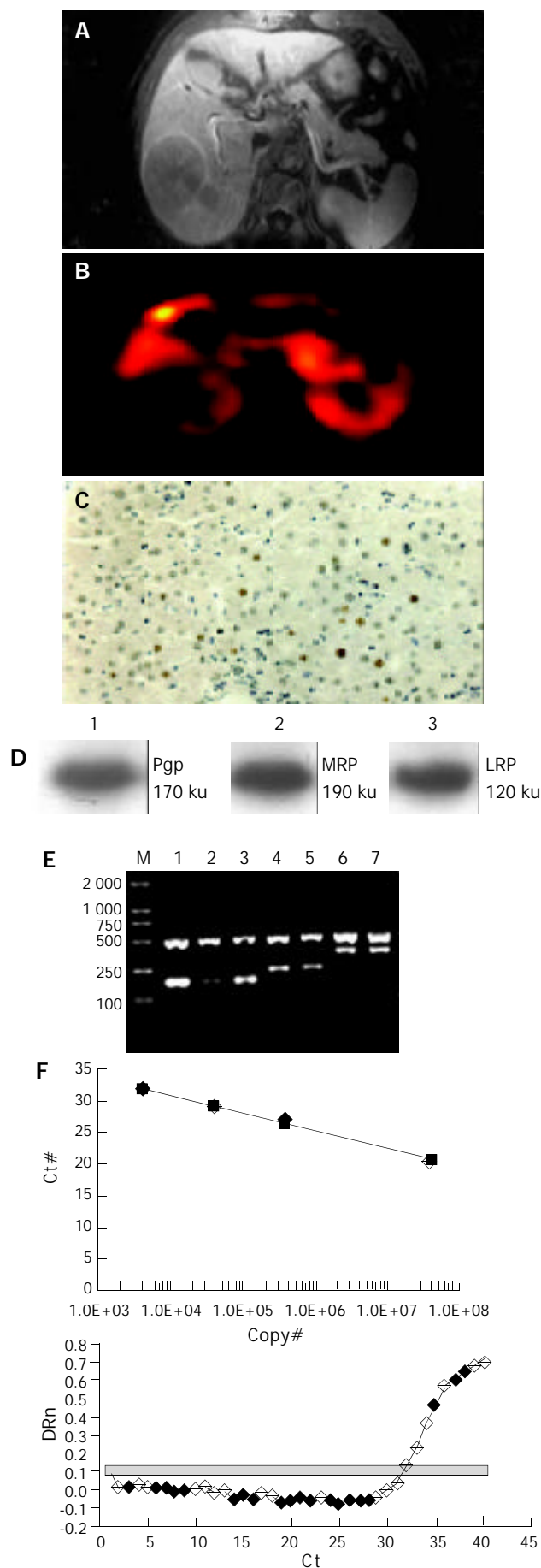


Figure 1 A: CT image of one patient with liver carcinoma. B: ^{99m}Tc-MIBI SPECT Liver image of the patient. C: Immunohistochemical expression of Pgp. D: Western blotting images of Pgp, MRP and LRP. E: MDR1 176 bp, MRP 358 bp, LRP 492 bp shown by RT-PCR image. F: Real time RT-PCR image of Pgp.

Table 3 Patient characteristics and radionuclide imaging

Group	Cases	Tumor size (cm)	^{99m} Tc-MIBI SPECT			Immunohistochemistry			RT-PCR		
			L/Ne	L/Nd	L/Nwr(%)	Pgp	MRP	LRP	mdr1	MRP	LRP
I	68	2.5-15	2.09±0.67	1.25±0.42	54.94±10.23	68 (+)	4 (+)	3 (+)	0.38±0.16	0.04±0.02	0.02±0.01
II	10	1.5-7	1.98±0.56	2.78±0.53	3.07±0.57	10 (-)	3 (+)	1 (+)	0	0.06±0.03	0.03

Correlation of ^{99m}Tc-MIBI with RT-PCR results

No correlation was found between L/Ne and the level of Pgp mRNA, MRP mRNA, and LRP mRNA. The mean L/Nd (2.78±0.64) of the Pgp mRNA low expression group was significantly higher than that (1.25±0.43) of the Pgp high-expression group ($P=0.0115$, Figure 1). L/Nd was not related to the level of MRP mRNA or LRP mRNA. Statistical support was found toward a significant difference in L/Nwr between the Pgp mRNA high-expression group and the Pgp mRNA low-expression group. L/Nwr was not related to the level of MRP mRNA or LRP mRNA.

The grouping was according to the positive immunohistochemistry of Pgp, there were 4 cases positive of MRP and 3 cases positive of LRP in group I, there were 3 cases positive of MRP and 1 case positive of LRP in group II.

DISCUSSION

The resistance of tumors to multiple drugs is a major problem in cancer chemotherapy. Pgp, a transmembrane ATP-dependent efflux pump encoded by MDR1 gene, has a central role in multidrug resistance. Increased amounts of Pgp may confer multidrug resistance to cells by preventing intracellular accumulation of a variety of cytotoxic drugs. A unique feature of multidrug resistance is the apparent capacity of Pgp for recognizing and transporting a large group of cytotoxic compounds sharing little structural or functional similarity other than being relatively small hydrophobic and cationic agents, including anthracyclines, Vinca alkaloids, and actinomycin D. Evidence has shown that Pgp as a drug efflux pump extrudes ^{99m}Tc-MIBI and other drugs from cells and that Pgp expression and enhanced efflux of ^{99m}Tc-MIBI from these cells are closely connected^[28,29]. In animal models, faster clearance of ^{99m}Tc-MIBI was observed in tumors with or without Pgp expression^[30,31]. Our study revealed that the mean L/Nd in Pgp (-) patients was significantly higher than that in Pgp (++) patients ($P=0.035$). Pgp (++) patients had a higher L/Nwr than Pgp (-) patients ($P=0.027$). No correlation was found between L/Ne and Pgp expression. The same results were obtained from mRNA level. Moreover, no correlation was found between MRP and ^{99m}Tc-MIBI SPECT. The same result was obtained from LRP protein and mRNA level. ^{99m}Tc-MIBI uptake by tumor is associated with many factors, including direct mechanisms such as negative transmembrane potential and drug efflux pump and indirect mechanisms such as blood flow and capillary permeability. We considered L/Ne to be more affected by blood flow. In contrast, L/Nd and L/Nwr clearly reflected Pgp expression of intrinsic properties of the tumor.

Until now, there have been some reports about the expression of Pgp in tumor tissues of patients with HCC^[32,33]. Resistance to cancer chemotherapy in HCC resulted from Pgp expression. The specific localization of Pgp and the incidence of Pgp expression in each histological type of HCC were observed. The analysis indicated that the incidence was the lowest in the compact type of HCC, and it was significantly lower than that in the pseudo glandular and trabecular types^[34]. But in our study, mRNA and protein level of Pgp revealed no significant difference in the incidence of Pgp expression in each histological type.

It has been established that MRP belongs to the superfamily of ABC transmembrane transporter proteins and can act as a glutathione S-conjugate efflux pump^[35]. ^{99m}Tc-MIBI was shown

to be a substrate for MRP *in vitro*^[36]. The abilities of Pgp and MRP transporters to wash out ^{99m}Tc-MIBI have been reported to be similar in cell lines, in spite of different possible mechanisms of transport^[37]. However, cardiac muscle showed a low L/Nwr of ^{99m}Tc-MIBI and a low level of Pgp expression but a high level of MRP expression^[38]. In our study, we did not observe any correlation between tumor accumulation or efflux of ^{99m}Tc-MIBI and expression of MRP on protein level or mRNA level in liver cancer. The mechanisms are also unclear.

LRP has been identified as the vault protein involved in nucleocytoplasmic transport. Recently, subcellular accumulation of drugs was found to be localized in cytoplasm and minimally in nuclei in LRP overexpression cells^[39]. As increased cytoplasm concentration of the drug could intensify its contact with the membrane, we proposed that efflux of the drug might be enhanced in LRP overexpression cells. However, we did not find a correlation between tumor accumulation or efflux of ^{99m}Tc-MIBI and expression of LRP. Subcellular accumulation of ^{99m}Tc-MIBI within mitochondria and cytoplasm of cells has been reported to be based on transmembrane electric potentials^[40]. Therefore, efflux of ^{99m}Tc-MIBI was rarely affected by expression of LRP.

Until now, there have been few clinical studies on the relation between Pgp expression and ^{99m}Tc-MIBI uptake in HCC. As ^{99m}Tc-MIBI is cleared through the liver, and it is not easy to detect liver tumors. To the best of our knowledge, our study was the first to show an inverse correlation in MDR1/Pgp expression and ^{99m}Tc-MIBI uptake in HCC. But ^{99m}Tc-MIBI SPECT has some limitations, because it depends on the optimal perfusion of tumor tissues. Poor MIBI penetration could be attributable to poor tumor perfusion in tumors larger than 2.5 cm, where tumor necrosis would be expected. Therefore, perfusion studies such as a Tl-201 scan could be used to eliminate the possibility of poor penetration.

In conclusion, our results suggest that L/Nd and L/Nwr of ^{99m}Tc-MIBI are noninvasive and useful in detecting the expression of Pgp in patients with HCC

REFERENCES

- 1 **McGrath MS**, Rosenblum MG, Philips MR, Scheinberg DA. Immunotoxin resistance in multidrug resistant cells. *Cancer Res* 2003; **63**: 72-79
- 2 **Huesker M**, Folmer Y, Schneider M, Fulda C, Blum HE, Hafkemeyer P, Huesker M, Folmer Y, Schneider M, Fulda C, Blum HE, Hafkemeyer P. Reversal of drug resistance of hepatocellular carcinoma cells by adenoviral delivery of anti-MDR1 ribozymes. *Hepatology* 2002; **36**(4Pt 1): 874-884
- 3 **Ogiso Y**, Tomida A, Tsuruo T. Nuclear localization of proteasomes participates in stress-inducible resistance of solid tumor cells to topoisomerase II-directed drugs. *Cancer Res* 2002; **62**: 5008-5012
- 4 **Masanek U**, Stammer G, Volm M. Modulation of multidrug resistance in human ovarian cancer cell lines by inhibition of P-glycoprotein 170 and PKC isoenzymes with antisense oligonucleotides. *J Exp Ther Oncol* 2002; **2**: 37-41
- 5 **Volm M**. Multidrug resistance and its reversal. *Anticancer Res* 1998; **18**: 2905-2918
- 6 **Scaglioui GV**, Novello S, Selvaggi G. Multidrug resistance in non-small-cell lung cancer. *Ann Oncol* 1999; **10**(Suppl 5): 583-586
- 7 **Molinari A**, Calcabrini A, Meschini S, Stringaro A, Crateri P, Tocciaeli L, Marra M, Colone M, Cianfriglia M, Arancia G. Subcellular detection and localization of the drug transporter.

- Curr Protein Pept Sci* 2002; **3**: 653-670
- 8 **Sharma KG**, Mason DL, Liu G, Rea PA, Bachhawat AK, Michaelis S. Localization, regulation, and substrate transport properties of Bpt1p, a *Saccharomyces cerevisiae* MRP-type ABC transporter. *Eukaryot Cell* 2002; **1**: 391-400
 - 9 **Jin J**, Huang M, Wei HL, Liu GT. Mechanism of 5-fluorouracil required resistance in human hepatocellular carcinoma cell line Bel(7402). *World J Gastroenterol* 2002; **8**: 1029-1034
 - 10 **Hsia TC**, Lin CC, Wang JJ, Ho ST, Kao A. Relationship between chemotherapy response of small cell lung cancer and P-glycoprotein or multidrug resistance-related protein expression. *Lung* 2002; **180**: 173-179
 - 11 **Damiani D**, Michelutti A, Michieli M, Masolini P, Stocchi R, Geromin A, Ermacora A, Russo D, Fanin R, Baccarani M. P-glycoprotein, lung resistance-related protein and multidrug resistance-associated protein in de novo adult acute lymphoblastic leukaemia. *Br J Haematol* 2002; **116**: 519-527
 - 12 **Vergote J**, Moretti JL, Kouyoumdjian JC, Garnier-Suillerot A. MRP1 modulation by PAK-104P: detection with technetium-99m-MIBI in cultured lung tumor cells. *Anticancer Res* 2002; **22** (1A): 251-256
 - 13 **Zhou J**, Higashi K, Ueda Y, Kodama Y, Guo D, Jisaki F, Sakurai A, Takegami T, Katsuda S, Yamamoto I. Expression of multidrug resistance protein and messenger RNA correlate with ^{99m}Tc-MIBI imaging in patients with lung cancer. *J Nucl Med* 2001; **42**: 1476-1483
 - 14 **Kim YS**, Cho SW, Lee KJ, Hahm KB, Wang HJ, Yim H, Jin YM, Park CH. ^{99m}Tc-MIBI SPECT is useful for noninvasively predicting the presence of MDR1 gene-encoded P-glycoprotein in patients with hepatocellular carcinoma. *Clin Nucl Med* 1999; **24**: 874-879
 - 15 **Andrews DW**, Das R, Kim S, Zhang J, Curtis M. Technetium-MIBI as a glioma imaging agent for the assessment of multidrug resistance. *Neurosurgery* 1997; **40**: 1323-1332
 - 16 **Fukumoto M**, Yoshida D, Hayase N, Kurohara A, Akagi N, Yoshida S. Scintigraphic prediction of resistance to radiation and chemotherapy in patients with lung carcinoma: technetium 99m-tetrofosmin and thallium-201 dual single photon emission computed tomography study. *Cancer* 1999; **86**: 1470-1479
 - 17 **Bom HS**, Kim YC, Song HC, Min JJ, Kim JY, Park KO. Technetium-99m-MIBI uptake in small cell lung cancer. *J Nucl Med* 1998; **39**: 91-94
 - 18 **Cayre A**, Cachin F, Maublant J, Mestas D, Feillel V, Ferriere JP, Kwiaktowski F, Chevillard S, Finat-Duclos F, Verrelle P, Penault-Llorca F. Single static view 99mTc-sestamibi scintimammography predicts response to neoadjuvant chemotherapy and is related to MDR expression. *Int J Oncol* 2002; **20**: 1049-1055
 - 19 **Ramachandran C**, Khatib Z, Escalon E, Fonseca HB, Jhabvala P, Medina LS, D' Souza B, Ragheb J, Morrison G, Melnick SJ. Molecular studies in pediatric medulloblastomas. *Brain Tumor Pathol* 2002; **19**: 15-22
 - 20 **Capella LS**, Gefe MR, Silva EF, Affonso-Mitidieri O, Lopes AG, Rumjanek VM, Capella MA. Mechanisms of vanadate-induced cellular toxicity: role of cellular glutathione and NADPH. *Arch Biochem Biophys* 2002; **406**: 65-72
 - 21 **Vergote J**, Moretti JL, de Vries EG, Garnier-Suillerot A. Comparison of the kinetics of active efflux of ^{99m}Tc-MIBI in cells with P-glycoprotein-mediated and multidrug-resistance phenotypes. *Eur J Biochem* 1998; **252**: 140-146
 - 22 **Heiba SI**, Santiago J, Mirzaitehrane M, Jana S, Dede F, Abdel-Dayem HM. Transient postischemic stunning evaluation by stress gated Tl-201 SPECT myocardial imaging: Effect on systolic left ventricular function. *J Nucl Cardiol* 2002; **9**: 482-490
 - 23 **Yuksel M**, Cermik F, Doganay L, Karlikaya C, Cakir E, Salan A, Berkarda S. 99mTc-MIBI SPET in non-small cell lung cancer in relationship with Pgp and prognosis. *Eur J Nucl Med Mol Imaging* 2002; **29**: 876-881
 - 24 **Kao A**, Shiun SC, Hsu NY, Sun SS, Lee CC, Lin CC. Technetium-99m methoxyisobutylisonitrile chest imaging for small-cell lung cancer. Relationship to chemotherapy response (six courses of combination of cisplatin and etoposide) and p-glycoprotein or multidrug resistance related protein expression. *Ann Oncol* 2001; **12**: 1561-1566
 - 25 **Blocklet D**, Schoutens A, Kentos A, Feremans W. Bone marrow uptake of 99mTc-MIBI in patients with multiple myeloma. *Eur J Nucl Med* 2001; **28**: 1430-1432
 - 26 **Ceriani L**, Giovannella L, Bandera M, Beghe B, Ortelli M, Roncari G. Semi-quantitative assessment of ^{99m}Tc-sestamibi uptake in lung cancer: relationship with clinical response to chemotherapy. *Nucl Med Commun* 1997; **18**: 1087-1097
 - 27 **Wiest R**, Shah V, Sessa WC, Groszmann RJ. Nitric oxide overproduction by eNOS precedes hyperdynamic splanchnic circulation in portal hypertensive rats. *Am J Physiol* 1999; **276**: G1043-G1051
 - 28 **Kostakoglu L**, Elahi N, Kiratli P. Clinical validation of the influence of P-glycoprotein on technetium-99m-sestamibi uptake in malignant tumors. *J Nucl Med* 1997; **38**: 1003-1008
 - 29 **Kostakoglu L**, Kiratli P, Ruacan S. Association of tumor wash-out rates and accumulation of ^{99m}Tc-MIBI with the expression of P-glycoprotein in lung cancer. *J Nucl Med* 1998; **39**: 228-234
 - 30 **Vecchio SD**, Ciarmiello A, Potena MI, Carriero MV, Mainolfi C, Botti G, Thomas R, Cerra M, D' Aiuto G, Tsuruo T, Salvatore M. *In vivo* detection of multidrug resistant (MDR1) phenotype by technetium-99m-sestamibi scan in untreated breast cancer patients. *Eur J Nucl Med* 1997; **24**: 150-159
 - 31 **Hendrikse NH**, Franssen EJ, van der Graaf WT, Meijer C, Piers DA, Vaalburg W, de Vries EG. ^{99m}Tc-sastamibi is a substrate for P-glycoprotein and the multidrug resistance associated protein. *Br J Cancer* 1998; **77**: 353-358
 - 32 **Nagasue N**, Dhar DK, Makino Y, Yoshimura H, Nakamura T. Overexpression of P-glycoprotein in adenomaous hyperplasia of human liver with cirrhosis. *J Hepatol* 1995; **22**: 197-201
 - 33 **Soini Y**, Virkajarvi N, Raunio H, Paakko P. Expression of P-glycoprotein in hepatocellular carcinoma: a potential marker of prognosis. *J Clin Pathol* 1996; **49**: 470-473
 - 34 **Itsubo M**, Ishikawa T, Toda G, Tanaka M. Immunohistochemical study of expression and cellular localization the multidrug resistance gene product P-glycoprotein in primary liver carcinoma. *Cancer* 1994; **73**: 298-303
 - 35 **Versantvoort CH**, Broxterman HJ, Bagrij T, Schepere RJ, Twentyman PR. Regulation by glutathione of drug transport in multidrug-resistant human lung cell lines overexpressing multidrug resistant-associated protein. *Br J Cancer* 1995; **72**: 82-89
 - 36 **Hendrikse NH**, Franssen EJ, van der Graaf WT, Meijer C, Piers DA, Vaalburg W, de Vries EG. ^{99m}Tc-sestamibi is a substrate for P-glycoprotein and the multidrug resistance associated protein. *Br J Cancer* 1998; **77**: 353-358
 - 37 **Vergote J**, Morreti JL, de Vries EG, Garnier-Suillcrot A. Comparison of the kinetics of active efflux of ^{99m}Tc-MIBI in cells with P-glycoprotein-mediated and multidrug-resistance protein-associated phenotypes. *Eur J Biochem* 1998; **252**: 140-146
 - 38 **Flens MJ**, Zaman GJ, van der Valk P, Izquierdo MA, Schroeijers AB, Scheffer GL, van der Groep P, de Haas M, Meijer CJ, Schepere RJ. Tissue distribution of the multidrug resistance protein. *Am J Pathol* 1996; **148**: 1237-1247
 - 39 **Cheng SH**, Lam W, Lee ASK, Fung KP, Wu RS, Fong WF. Low-level doxorubicin resistance in benzo[α] pyrene-treated κ B-3-1 cells is associated with increased LRP expression and altered subcellular drug distribution. *Toxicol Appl Pharmacol* 2000; **164**: 134-142
 - 40 **Piwnica-Worms D**, Kronauges JF, Chiu ML. Uptake and retention of hexakis (2-methoxyisobutyl isonitrile) technetium (1) in cultured chick myocardial cells: mitochondrial and plasma membrane potential dependence. *Circulation* 1990; **82**: 1826-1838

Differential gene expression in human hepatocellular carcinoma Hep3B cells induced by apoptosis-related gene *BNIP-2*

Li Xie, Wen-Xin Qin, Xiang-Huo He, Hui-Qun Shu, Gen-Fu Yao, Da-Fang Wan, Jian-Ren Gu

Li Xie, Wen-Xin Qin, Xiang-Huo He, Hui-Qun Shu, Gen-Fu Yao, Da-Fang Wan, Jian-Ren Gu, National Laboratory for Oncogenes and Related Genes, Shanghai Cancer Institute, Shanghai 200032, China

Wen-Xin Qin, Da-Fang Wan, Jian-Ren Gu, Cancer Institute, Shanghai Jiaotong University, Shanghai 200032, China

Supported by a grant from the National Key Basic Research Program (973) of China, No. 2002CB513100 and grants from the National 863 High Technology Research and Development Program of China, No. 2001AA221141, 2002BA711A02, and 2001AA227121

Co-correspondents: Da-Fang Wan

Correspondence to: Dr. Wen-Xin Qin, National Laboratory for Oncogenes and Related Genes, Shanghai Cancer Institute, Shanghai Jiaotong University, Shanghai 200032, China. nlog@public.sta.net.cn

Telephone: +86-21-64177401 **Fax:** +86-21-64177401

Received: 2003-09-06 **Accepted:** 2003-10-27

Abstract

AIM: Bcl-2/adenovirus E1B 19 ku interacting protein 2-like (BNIP-2) is a novel protein recently identified in our laboratory. BNIP-2 is homologous to human BNIP-2, a potentially proapoptotic protein, and can interact with Bcl-2 and Cdc42GAP and promote apoptosis in BEL-7402 cells. Here we report the gene-expression profile regulated by BNIP-2 in human hepatocarcinoma Hep3B cells and the analysis of its potential roles in cell apoptosis.

METHODS: BNIP-2 was overexpressed in Hep3B cells using tetracycline inducible or Tet-on system. Screened by Western blot, the cells with low background and high induction fold of BNIP-2 were obtained. We performed Atlas human cDNA expression array hybridization on these cells and analyzed the data with Quantarray® software to identify *BNIP-2*-regulated genes and their expression profile. RT-PCR was used to confirm the altered expression level of part of genes identified by the Atlas array hybridization.

RESULTS: Fifteen of 588 genes spotted on the Atlas membrane showed altered expression levels in BNIP-2-transfected Hep3B-Tet-on cells, in which 8 genes involved in cell apoptosis or growth inhibition were up-regulated and 7 genes involved in cellular proliferation were down-regulated following overexpression of BNIP-2.

CONCLUSION: cDNA array is a powerful tool to explore gene expression profiles under inducible conditions. The data obtained using the cDNA expression microarray technology indicates that BNIP-2 may play its roles in apoptosis through regulating the expression of genes associated with cell apoptosis, growth inhibition and cell proliferation.

Xie L, Qin WX, He XH, Shu HQ, Yao GF, Wan DF, Gu JR. Differential gene expression in human hepatocellular carcinoma Hep3B cells induced by apoptosis-related gene *BNIP-2*. *World J Gastroenterol* 2004; 10(9): 1286-1291
<http://www.wjgnet.com/1007-9327/10/1286.asp>

INTRODUCTION

Bcl-2/adenovirus E1B 19 ku interacting protein 2-like (BNIP-2) is recently identified and characterized as an apoptosis-associated protein^[1-3]. BNIP-2 shares 72% homology (46% identity) with BNIP-2^[4] and has 2 variants BNIP-1 and BNIP-2. Full-length amino acid sequence of BNIP-1 is shorter by 82 amino acids at N-terminus than that of BNIP-2. Our previous experiment showed that BNIP-1 could inhibit MIF-mediated proliferation of BEL-7402 cells and BNIP-2 could inhibit cell growth and promote apoptosis in BEL-7402 cells. However, the molecular mechanisms by which BNIP-1 suppresses the cell growth and BNIP-2 commits the cell to die are not known^[1,2].

In 1992, Gossen and Bugard developed the tetracycline (or doxycycline)-induced gene expression (Tet-on) system, which is useful for controlling the expression of targeted genes in a quantitative manner and for determining the roles of gene products in cellular functions^[5,6]. In the present study, Hep3B-Tet-on cells were transfected with *BNIP-2* using lipofectamine transfection reagent. In order to obtain cells with low background and high induction fold of *BNIP-2*, transfected cells were screened by Western blot. Using this system, we established Hep3B cell line with doxycycline-regulated BNIP-2 expression.

The microarray technique was first reported in 1995 by Schena *et al.*^[7] and allows simultaneous parallel expression analysis of thousands of genes. Information provided by cDNA microarray analysis might be useful for tumor classification, elucidation of key factor in tumors, and identification of genes which might be applied to diagnostic purposes or as therapeutic targets^[8,9]. The Atlas human cDNA expression system provides a convenient and quick method for profiling the expression of 588 genes at the same time. In this study, we used cDNA expression microarray technology to analyze the differentially expressed genes regulated by cell apoptosis-related gene *BNIP-2*.

MATERIALS AND METHODS

Materials

cDNA microarray Atlas human cDNA expression array membranes (#7740-1) were purchased from Clontech Laboratories Inc (Palo Alto, California, USA). The membrane contained 10 ng of each gene-specific cDNA from 588 known genes and 9 housekeeping genes. Several plasmid and bacteriophage DNAs and blank spots were also included as negative and blank controls to confirm hybridization specificity. The 588 known genes spotted on the Atlas membrane consist of cDNAs for cell-cycle control proteins, stress response proteins, apoptosis-associated proteins, DNA transcription factors, cell receptors, extracellular cell signaling and communication proteins, *etc.* A complete list of the genes with the array positions and GeneBank accession numbers spotted on the array is available at Clontech's web site (<http://www.clontech.com>).

Enzyme and other reagents

Restriction endonucleases *Bam*HI and *Cla*I were purchased from New England Biolabs Inc (Beverly, Maryland, USA).

Lambda DNA/*Hind*III Markers were from Sino-American Biotechnology Company (Shanghai, China). Tet system approved fetal bovine serum, doxycycline, hygromycin, pTRE2hyg, and Atlas human cDNA expression array trial kit were from BD Biosciences Clontech (Palo Alto, California, USA). Lipofectamine and SuperScript™ first strand synthesis system for RT-PCR were from Invitrogen™ Life Technologies (Carlsbad, California, USA). High glucose Dulbecco's modified Eagle's medium (DMEM) was from Gibco/BRL (Carlsbad, California, USA). Monoclonal antibody actin pan Ab-5, horseradish peroxidase-coupled second antibodies anti-rabbit IgG, and anti-mouse IgG were from Santa Cruz Biotechnology (Santa Cruz, California, USA). SuperSignal west femto maximum sensitivity substrate and T-PER™ tissue protein extraction reagent was from Pierce Chemical Company (Rockford, Illinois, USA). PROTRAN nitrocellulose transfer membrane was from Schleicher & Schuell (Keene, New Hampshire, USA). Hep3B-Tet-on cell line was constructed by Wang *et al.*^[10].

Methods

Plasmid construction For construction of plasmid pTRE2hyg-BNIP1-2, human *BNIP1-2* DNA fragment encoding the full-length protein was amplified by PCR using the primers containing *Bam*HI and *Cla*I restriction sites and HA-tag sequence (Table 1). The PCR product was subcloned into the Tet-on expression vector pTRE2hyg which contains hygromycin-resistance gene. The recombinant plasmid construct, pTRE2hyg-BNIP1-2, was confirmed by *Bam*HI/*Cla*I digestion and DNA sequencing.

Cell culture and transfection

Hep3B-Tet-on cells were cultured in DMEM containing 150 mL/L tetracycline-free fetal bovine serum at 37 °C in a 50 mL/L CO₂ incubator. They were grown in 6-well plates to 70% confluence and transfected with pTRE2hyg-BNIP1-2 plasmid DNA using lipofectamine reagents under conditions recommended by the manufacturer. After 48 h, the medium was replaced with fresh DMEM containing 100 mg/L hygromycin to select the stable cell lines. Two weeks later, hygromycin-resistant clones were obtained. Thirty-seven clones were selected and cultured continuously. After further selection in the medium containing 25 mg/L hygromycin for more than 3 wk, they were analyzed by Western blot using anti-BNIP1-2 polyclonal antibody (the rabbit anti-BNIP1-2 polyclonal antibody was prepared by National Laboratory for Oncogenes and Related Genes, Shanghai Cancer Institute, Shanghai, China). BNIP1-2 expression in the cell line was induced by incubating cells with doxycycline (Dox), which is a tetracycline analogue.

Western blot

Cells were washed twice with ice-cold PBS and lysed with T-PER™ tissue protein extraction reagent. Equal amounts of protein (10 µg) were electrophoresed on 100 g/L SDS-PAGE and blotted to PROTRAN nitrocellulose transfer membrane by a semi-dry transfer unit (Amersham Pharmacia Biotech AB, Piscataway, New Jersey, USA). The transferred membranes were blocked with 50 g/L non-fat milk in PBST buffer (20 mmol/L Tris-HCl, pH 7.6; 130 mmol/L NaCl, 1 g/L Tween 20) for 1 h at room temperature and subsequently incubated with the primary antibody anti-BNIP1-2 at 1:500 dilutions in PBST containing 40 g/L non-fat milk for 2 h. After several washes with PBST, the membranes were incubated with the corresponding horseradish peroxidase-coupled secondary antibody anti-rabbit IgG in the same buffer. The immunocomplexes were visualized using SuperSignal west femto maximum sensitivity substrate. For standardization and quantification, β-actin was used as an internal control.

cDNA synthesis, labeling and purification

Hep3B-Tet-on-BNIP1-2/13 cells were cultured in DMEM containing 150 mL/L tetracycline-free fetal bovine serum at 37 °C in a 50 mL/L CO₂ incubator. They were grown in 4 10-cm dishes to 80% confluence and 2 dishes were treated with Dox (2 mg/mL) for 24 h. Then total RNA samples were extracted from 1×10⁷ cells using TRIzol reagent. They were reverse-transcribed into cDNA and labeled with [α-³²P] dATP. Before labeling, total RNA of each sample was treated with DNase I (TaKaRa, Dalian, Shenyang, China) at 37 °C for 30 min to remove contaminated DNA. For each labeling, the treated 5 µg of total RNA was dissolved in 2 µL of diethyl pyrocarbonate (DEPC)-treated H₂O, incubated with 1 µL CDS Primer Mix at 70 °C for 2 min, and continued to incubate at 50 °C for 2 min. Then, 2 µL 5×reaction buffer, 0.5 µL 0.1 mol/L DTT, 1 µL dNTP mixture (containing dCTP, dGTP, and dTTP), 3.5 µL [α-³²P] dATP (10 µCi/µL), and 1 µL MMLV reverse transcriptase were added to each sample and incubated at 50 °C for 25 min. The reaction was stopped by adding 1 µL of 10× Termination Mix. The labeled first strand cDNA probes were purified by NucleoSpin extraction spin column to remove the unincorporated nucleotides. After purification, labeled cDNAs were denatured before use.

Membrane hybridization and exposure

Five milliliters ExpressHyb hybridization solution and 0.5 mg heat-denatured sheared salmon testes DNA were added to the tube containing Atlas human cDNA expression array membrane, which was pre-hybridized at 68 °C for 3 h. The different probes were then added to different tubes and hybridization was performed at 68 °C for 18 h in a rolling bottle. The membrane was washed twice at 68 °C in 2×SSC, 10 g/L SDS for 20 min, once at 68 °C in 0.1×SSC, 5 g/L SDS for 20 min, and once at room temperature in 2×SSC for 5 min, followed by exposure to x-ray films at -70 °C for 2-5 d.

Image analysis

The images were scanned with Cyclone™ storage phosphor system (Packard Bioscience Company, Meriden, Connecticut, USA) and saved as TIFF format files. The TIFF images were imported into the Quantarray® image system (Packard Bioscience Company) and analyzed. Housekeeping genes *ubiquitin* and *b-actin* were selected for normalization. The normalized intensity of each spot representing a unique gene expression level was acquired. Genes were considered to be up-regulated when the intensity ratio was >2 and down-regulated when the intensity ratio was <0.5.

Semi-quantitative RT-PCR

To confirm the cDNA array results, semi-quantitative RT-PCR was performed for 4 genes (*Rad*, *CLK-1*, *p38 MAP Kinase* and *p21*) that displayed expression alterations. Five micrograms of total RNA was reverse-transcribed into 20 µL of the first strand cDNA with SuperScript™ first strand synthesis system, then 2 µL of the product was used as the template to amplify each specific gene fragment in a 25 µL reaction mixture with corresponding primers (Table 1) under the following conditions: denaturation at 94 °C (3 min); 26 cycles at 94 °C (30 s), at 60 °C (30 s), and at 72 °C (30 s); then extension at 72 °C (3 min). In each PCR reaction, primers for the human *b-actin* gene were used as an internal control. PCR primer pairs were designed using Primer3 Internet software program. Their specificity was confirmed by a BLAST Internet software assisted search for a nonredundant nucleotide sequence database (National Library of Medicine, Bethesda, Maryland, USA). Ten microliters PCR reaction product was analyzed by electrophoresis on a 20 g/L agarose gel and visualized by ethidium bromide staining.

Table 1 Gene specific primers for PCR

Gene	GenBank accession number	Orientation	Sequence
BNIPL-2	AY033000	Forward	5' <u>CGGGATCC</u> <u>ACCATGT</u> <u>ACCCATACGATGTTCCAGATT</u> <u>ACGCTCTTGGAACTATAACAAGAG</u> 3'
		Reverse	5' CCATCGATCTATGTCCCTCCTGAGCCATGGAGATCCCGTCCAGCTGTCTGACAGC 3'
β -actin	NM_001101	Forward	5' AAGTACTCCGTGTGGATCGG 3'
		Reverse	5' TCAAGTTGGGGGACAAAAAG 3'
Rad	L24564	Forward	5' GCTGCCCTGCGAAGTGGCTC 3'
		Reverse	5' TCCCTCCAGGGCAGGCACAC 3'
CLK-1	L29222	Forward	5' GGGTGGTCCCAACCATGTGA 3'
		Reverse	5' CCGGCAGAAGTGTTCATCCCA 3'
p38 MAP kinase	L35253	Forward	5' GTTGAACCCAGGGGCTG 3'
		Reverse	5' GGCATGTGCAAGGGCTGGG 3'
p21	U09579	Forward	5' CTGTGGGGGTGAGGGTCCCA 3'
		Reverse	5' TGGGGAGGGATGGGGTGGAT 3'

Underlined sequences are restriction endonuclease recognition sites (single line) and HA-tag (double lines).

Table 2 Up-regulated genes in BNIPL-2-transfected Hep3B-Tet-on cells

Location	Gene description	Induction-fold
C5n	Rad (Ras associated with diabetes)	5.886
F3e	Insulin-like growth factor binding protein 1 (IGFBP-1)	2.594
D6f	p21; Cdk-interacting proteins (Cip1); mda-6/WAF1/SD11	2.574
E2m	Interleukin-2 receptor	2.5
D3n	Transcription factor (E2A)	2.115
F7m	Estrogen sulfotransferase (EST)	2.112
F1e	Transforming growth factor-beta (TGF-beta)	2.018
E7k	Ifa-1 alpha subunit	2.012

RESULTS

Construction and identification of pTRE2hyg-BNIPL-2 plasmid

Tet-on expression plasmid pTRE2hyg-BNIPL-2 was successfully constructed. Restriction endonucleases *Bam*HI and *Cla*I digestion showed that *BNIPL-2* gene was correctly inserted into the multicloning site. The *BNIPL-2* fragment and pTRE2hyg vector were about 1.1 kb and 5.3 kb, respectively (Figure 1).

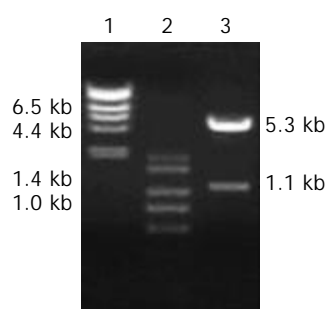


Figure 1 Agarose gel (10 g/L) electrophoresis analysis of recombinant pTRE2hyg-BNIPL-2 digested with *Bam*HI and *Cla*I. Lane 1: Lambda DNA/*Hind* III markers, Lane 2: SD 006 markers, Lane 3: pTRE2hyg-BNIPL-2 digested with *Bam*HI and *Cla*I.

Screening of stable Hep3B-Tet-on-BNIPL-2 cell line

After screening in the medium containing hygromycin for more than 8 wk, a total of 37 independent Hyg-resistant cell lines were obtained from the Hep3B-Tet-on cells, transfected with pTRE2hyg-BNIPL-2. Of the 37 clones, clone Hep3B-Tet-on-BNIPL-2/13 showed a low background and high induction fold expression of BNIPL-2 by Dox and was selected as the cell line for further investigations. The amount of BNIPL-2 induced in the Hep3B-Tet-on-BNIPL-2/13 cells treated with Dox (2 000 μ g/L) was 12-fold higher than that in the cells without Dox treatment (Figure 2A).

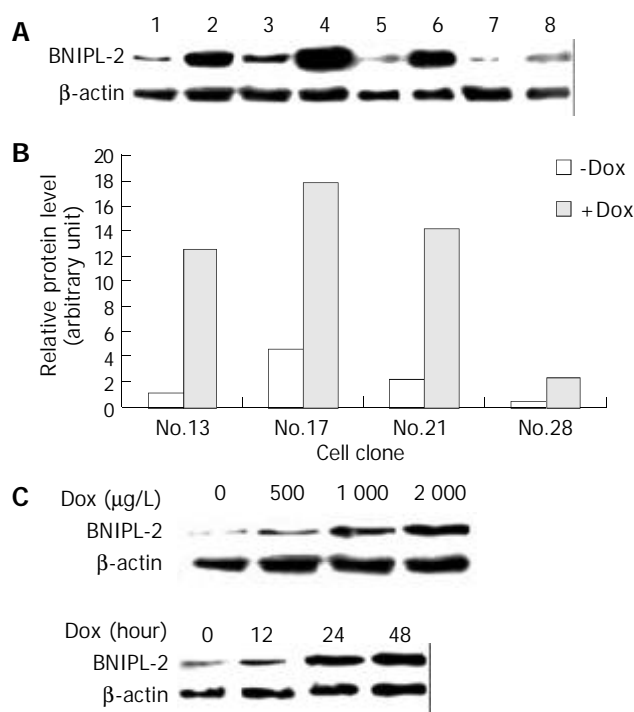


Figure 2 Western blot analysis of BNIPL-2 expression after Dox induction. A: Different cell protein was gotten from 37 clones after hygromycin selection. The clone Tet-on-BNIPL-2/13 showed a low background and high induction fold of BNIPL-2 regulated by Dox. The intensity of each band was quantified by densitometry. Lane 1: lysate of Tet-on-BNIPL-2/13, Lane 2: lysate of Tet-on-BNIPL-2/13+Dox, Lane 3: lysate of Tet-on-BNIPL-2/17, Lane 4: lysate of Tet-on-BNIPL-2/17+Dox, Lane 5: lysate of Tet-on-BNIPL-2/21, Lane 6: lysate of Tet-on-BNIPL-2/21+Dox, Lane 7: lysate of Tet-on-BNIPL-2/28, Lane

8: lysate of Tet-on-*BNIP1-2*/28+Dox. B: Hep3B-Tet-on-*BNIP1-2*/13 cells were treated with Dox at different concentrations (0, 500, 1 000, 2 000 $\mu\text{g/L}$) for 24 h. C: Hep3B-Tet-on-*BNIP1-2*/13 cells were treated with Dox (2 000 $\mu\text{g/L}$) for different time as indicated (0, 12, 24, 48 h). Equal amount of total cell protein was analyzed using *BNIP1-2* antibody. β -actin was used as an internal control.

Hep3B-Tet-on-*BNIP1-2*/13 cells were amplified and passaged (1.0×10^5 cells) into 35-mm dishes, and treated with varying amounts of Dox for different times. Equal amounts of total cell protein were detected by Western blot with *BNIP1-2* antibody. The level of *BNIP1-2* expression increased significantly after exposing the cells to Dox for 24 h over a range of Dox concentrations from 500 $\mu\text{g/L}$ to 2 000 $\mu\text{g/L}$ (Figure 2B). However, the level of *BNIP1-2* expression did not increase when Dox concentration was over 2 000 $\mu\text{g/L}$ (data not shown). On the other hand, after the cells were treated with Dox (2 000 $\mu\text{g/L}$) for 0, 12, 24, or 48 h, the level of the induction

increased with the treatment time and apparent increased induction was seen at 24 h (Figure 2C). Therefore, there was a direct correlation between the concentrations of Dox added to the cells or the time of treatment with Dox and the level of *BNIP1-2* induction. The above results obtained by Western blot screening with anti-*BNIP1-2* polyclonal antibody were confirmed by anti-HA McAb (data not shown).

Microarray analysis

Using a cDNA expression microarray technique we established the expression profile of 588 genes regulated by *BNIP1-2* (Figure 3) in Hep3B-Tet-on-*BNIP1-2*/13 cells. No signals were visible in the blank spots and negative control spots, indicating that Atlas human cDNA array hybridization was highly specific. The density of housekeeping genes was very similar between samples, indicating that the results were reliable. We used the housekeeping genes *Ubiquitin* and *b-actin* to normalize the intensities. The comparison results analyzed by Quantarray®

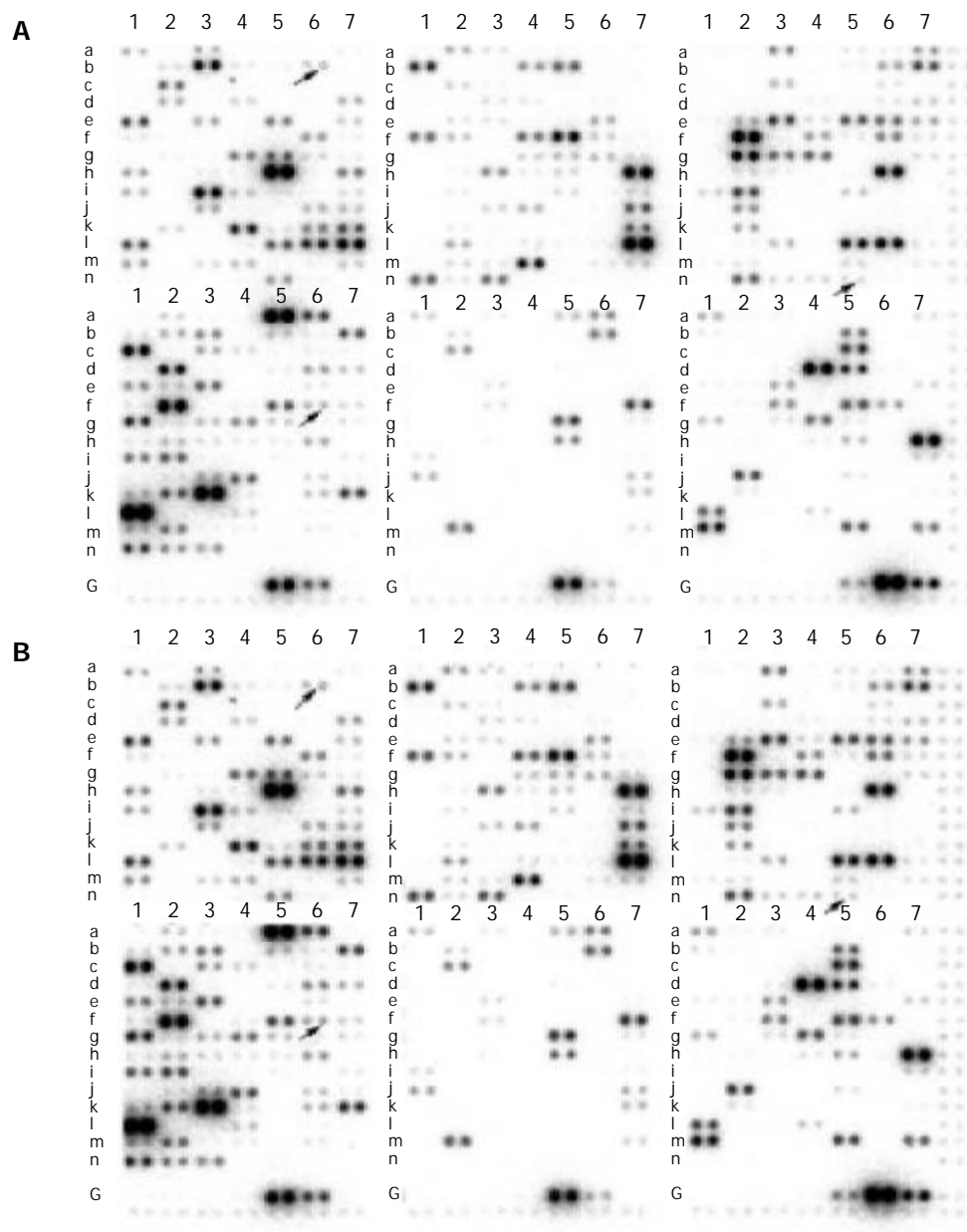


Figure 3 Parallel analysis of gene expression profiles in Hep3B-Tet-on-*BNIP1-2*/13 cells before or after *BNIP1-2* overexpression. Total RNA samples were purified from 1×10^7 cells using TRIzol reagent before (A) or after (B) *BNIP1-2* overexpression. They were reverse-transcribed into cDNA, labeled with $[\alpha\text{-}^{32}\text{P}]$ dATP, and hybridized to Atlas human cDNA expression array (#7740-1) according to the manufacturer's protocol. Notes: The genes in the row G are housekeeping genes. Arrows indicate the three examples of differentially expressed genes (*A6b*, *p120 antigen*; *C5n*, *Rad*; *D6f*, *p21*).

image system showed that there were 15 genes altered in terms of their expression levels, of which 8 were up-regulated (Table 2) and 7 were down-regulated (Table 3) following overexpression of BNIPL-2 in Hep3B cells.

Table 3 Down-regulated genes in BNIPL-2-transfected Hep3B-Tet-on cells

Location	Gene description	Induction-fold
B4f	Transducin beta-1 subunit 3' end	0.429
B1b	MAL protein	0.431
B5f	p38 MAP kinases/CSBP/Mxi2	0.442
A7e	Tob	0.447
A7h	CLK-1	0.457
B4b	GTP binding protein (RAB5)	0.48
A6b	p120 antigen	0.496

Semi-quantitative RT-PCR

Four genes were measured for their transcript levels by RT-PCR to verify the accuracy and universality of the hybridization data. The RT-PCR results were consistent with hybridization data in each of the genes measured (Figure 4), *i.e.* *Rad* and *p21* were up-regulated, *p38 MAPK* and *CLK-1* were down-regulated in BNIPL-2 overexpressed cells.

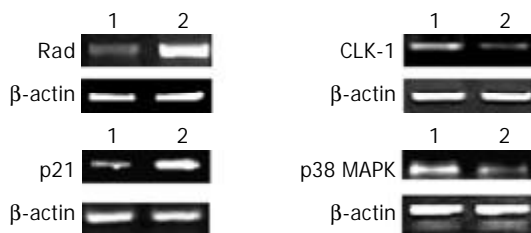


Figure 4 Semi-quantitative RT-PCR assays of *Rad*, *CLK-1*, *p21*, and *p38 MAPK* before or after BNIPL-2 overexpression, β -actin was also amplified as an internal control. The figure was consistent with the hybridization results. Lane 1: Before BNIPL-2 inducible expression, Lane 2: After BNIPL-2 inducible expression.

DISCUSSION

The Tet-on system, which utilizes an *E. coli* gene regulatory system^[11], has been found to have several advantages^[12-14]. Namely gene expression is easily regulated by administration of Dox, Dox is minimally toxic, and Dox acts specifically on the target gene, and does not activate other cellular genes. In the present study, we established a cell line Hep3B-Tet-on-BNIPL-2/13 in which *BNIPL-2* gene could be expressed conditionally by Dox treatment. Dox activated the Tet-response element and significantly enhanced the expression of *BNIPL-2* gene in Hep3B cells in a dose-dependent manner. The strategy used here, by which a stable cell line with a low background and high fold Dox-induced expression of BNIPL-2 was generated, seemed to be more efficient and rapid for regulating *BNIPL-2* gene expression.

The cDNA array technology was used to examine simultaneously the expression of specific genes on a single hybridization. Although expression analysis techniques such as differential display polymerase chain reaction (DD-PCR), Northern blot, serial analysis of gene expression (SAGE), and RT-PCR have been widely used, these studies are time-consuming and can only be used to deal with a limited number of genes. Thus a systematic approach to the examination of a large number of genes simultaneously is required. We therefore explored the gene expression profiles in human hepatocarcinoma

cell line Hep3B regulated by BNIPL-2 overexpression using Atlas human cDNA array.

Following overexpression of BNIPL-2 in Hep3B cells, the expression level of 15 genes was altered, of which 8 were up-regulated and 7 were down-regulated. Genes involved in growth inhibition (*IGFBP-1*, *TGF- β*) or cell apoptosis (*p21*, *E2A*) were up-regulated. IGFBP-1 is thought to be the major short-term modulator of IGF bioavailability. In most clinical studies, circulating IGFBP-1 has been associated with growth inhibition^[15]. Insulin-like growth factor I promotes muscle cell survival as an early event in differentiation through a pathway that involves Akt-dependent induction of p21^[16]. Transforming growth factor- β (TGF- β) is a potent growth inhibitor for a wide variety of cells, controlling growth, differentiation and apoptosis of cells, and having important functions during embryonic development^[17]. It has been found that Cdk inhibitor p21 is often responsible for stress-induced p53-dependent and p53-independent cell cycle arrest, and p21 plays an essential role in growth arrest after DNA damage and its overexpression leads to G1 and G2 or S-phase arrest. In addition, p21 is a negative regulator of p53-dependent apoptosis^[18]. Human gastric cells were initially arrested in G1 by TGF- β and then driven to apoptosis after caspase-3-induced cleavage of p21^[19]. Overexpression of E2A protein activity has been shown to induce either growth arrest or apoptosis, indicating that these proteins may regulate cell proliferation and survival^[20,21]. Genes involved in cellular proliferation (*p38 MAPK*, *Tob*, *CLK-1*) were down-regulated in Hep3B cells when BNIPL-2 was overexpressed. P38 MAPK participates in not only inflammatory responses but also stress-induced signaling, cell proliferation and apoptosis. The p38 MAPK pathway participates in p21 induction, which consequently leads to decrease of cyclin D1/cdk4 and cyclinE/cdk2 complexes^[22]. Tob is a member of the Tob and BTG anti-proliferative protein family. Recently, one report indicated that Tob functioned as a molecular switch that regulates cell cycle progression through early G1^[23]. In *CLK-1* mutants, the affected features included cell cycle, embryonic and post-embryonic development, rhythmic behaviors, reproduction, and life span, all of which were lengthened or slowed down on average^[24,25].

In conclusion, cDNA array is a powerful tool to explore gene expression profiles and the present results provide the basis for elucidating previous findings that BNIPL-2 might inhibit cell growth and promote apoptosis in BEL-7402 cells^[2]. Although the mechanism of this interaction between BNIPL-2 and other proteins is not clear, we suggest that BNIPL-2 maybe inhibited growth by inducing cell cycle arrest at the G1 phase by TGF- β and p21 and affecting G2/M checkpoint through the p38 MAP kinase pathway.

REFERENCES

- 1 **Shen L**, Hu J, Lu H, Wu M, Qin W, Wan D, Li YY, Gu J. The apoptosis-associated protein BNIPL interacts with two cell proliferation-related proteins, MIF and GFER. *FEBS Lett* 2003; **540**: 86-90
- 2 **Qin W**, Hu J, Guo M, Xu J, Li J, Yao G, Zhou X, Jiang H, Zhang P, Shen L, Wan D, Gu J. BNIPL-2, a novel homologue of BNIPL-2, interacts with Bcl-2 and Cdc42GAP in apoptosis. *Biochem Biophys Res Commun* 2003; **308**: 379-385
- 3 **Zhou YT**, Soh UJ, Shang X, Guy GR, Low BC. The BNIPL-2 and Cdc42GAP homology/Sec14p-like domain of BNIPL-2 is a novel apoptosis-inducing sequence. *J Biol Chem* 2002; **277**: 7483-7492
- 4 **Boyd JM**, Malstrom S, Subramanian T, Venkatesh LK, Schaeper U, Elangovan B, D' Sa-Eipper C, Chinnadurai G. Adenovirus E1B 19 kDa and Bcl-2 proteins interact with a common set of cellular proteins. *Cell* 1994; **79**: 341-351
- 5 **Lottmann H**, Vanselow J, Hessabi B, Walther R. The Tet-On

- system in transgenic mice: inhibition of the mouse *pdx-1* gene activity by antisense RNA expression in pancreatic beta-cells. *J Mol Med* 2001; **79**: 321-328
- 6 **Milo-Landesman D**, Surana M, Berkovich I, Compagni A, Christofori G, Fleischer N, Efrat S. Correction of hyperglycemia in diabetic mice transplanted with reversibly immortalized pancreatic beta-cells controlled by the tet-on regulatory system. *Cell Transplant* 2001; **10**: 645-650
- 7 **Schena M**, Shalon D, Davis RW, Brown PO. Quantitative monitoring of gene expression patterns with a complementary DNA microarray. *Science* 1995; **270**: 467-470
- 8 **Selaru FM**, Zou T, Xu Y, Shustova V, Yin J, Mori Y, Sato F, Wang S, Oлару A, Shibata D, Greenwald BD, Krasna MJ, Abraham JM, Meltzer SJ. Global gene expression profiling in Barrett's esophagus and esophageal cancer: a comparative analysis using cDNA microarrays. *Oncogene* 2002; **21**: 475-478
- 9 **Rew DA**. DNA microarray technology in cancer research. *Eur J Surg Oncol* 2001; **27**: 504-508
- 10 **Wang JR**, Qin WX, Shu HQ, Pan Y, Zhang YY, Wan DF. Establishment of Hep3B cell line controlled by the Tet-On regulatory system. *Tumor* 2002; **22**: 191-193
- 11 **Sonntag KC**, Haller GW, Giauffret D, Germana S, Reeves SA, Levy J, Sachs D, LeGuern C. Regulated expression of an MHC class II gene from a promoter-inducible retrovirus. *Hum Gene Ther* 2000; **11**: 1961-1969
- 12 **Kashima Y**, Miki T, Minami K, Seino S. Establishment of a tet-on gene expression system in glucose-responsive and -unresponsive MIN6 cells. *Diabetes* 2001; **50**(Suppl): S133
- 13 **Wang D**, Grammer JR, Cobbs CS, Stewart JE Jr, Liu Z, Rhoden R, Hecker TP, Ding Q, Gladson CL. P125 focal adhesion kinase promotes malignant astrocytoma cell proliferation *in vivo*. *J Cell Sci* 2000; **113**(Pt 23): 4221-4230
- 14 **Kobayashi T**, Sawa H, Morikawa J, Zhang W, Shiku H. Bax induction activates apoptotic cascade via mitochondrial cytochrome c release and Bax overexpression enhances apoptosis induced by chemotherapeutic agents in DLD-1 colon cancer cells. *Jpn J Cancer Res* 2000; **91**: 1264-1268
- 15 **Kajantie E**, Hytinantti T, Koistinen R, Risteli J, Rutanen EM, Seppala M, Andersson S. Markers of type I and type III collagen turnover, insulin-like growth factors, and their binding proteins in cord plasma of small premature infants: relationships with fetal growth, gestational age, preeclampsia, and antenatal glucocorticoid treatment. *Pediatr Res* 2001; **49**: 481-489
- 16 **Lawlor MA**, Rotwein P. Insulin-like growth factor-mediated muscle cell survival: central roles for Akt and cyclin-dependent kinase inhibitor p21. *Mol Cell Biol* 2000; **20**: 8983-8995
- 17 **Derynck R**, Akhurst RJ, Balmain A. TGF- β signaling in tumor suppression and cancer progression. *Nat Genet* 2001; **29**: 117-129
- 18 **Zhang Y**, Fujita N, Tsuruo T. Caspase-mediated cleavage of p21Waf1/Cip1 converts cancer cells from growth arrest to undergoing apoptosis. *Oncogene* 1999; **18**: 1131-1138
- 19 **Kim DK**, Cho ES, Lee SJ, Um HD. Constitutive hyperexpression of p21(WAF1) in human U266 myeloma cells blocks the lethal signaling induced by oxidative stress but not by Fas. *Biochem Biophys Res Commun* 2001; **289**: 34-38
- 20 **Park ST**, Nolan GP, Sun XH. Growth inhibition and apoptosis due to restoration of E2A activity in T cell acute lymphoblastic leukemia cells. *J Exp Med* 1999; **189**: 501-508
- 21 **Engel I**, Murre C. Ectopic expression of E47 or E12 promotes the death of E2A-deficient lymphomas. *Proc Natl Acad Sci U S A* 1999; **96**: 996-1001
- 22 **Moon SK**, Jung SY, Choi YH, Lee YC, Patterson C, Kim CH. PDTC, metal chelating compound, induces G1 phase cell cycle arrest in vascular smooth muscle cells through inducing p21Cip1 expression: involvement of p38 mitogen activated protein kinase. *J Cell Physiol* 2004; **198**: 310-323
- 23 **Suzuki T**, K-Tsuzuku J, Ajima R, Nakamura T, Yoshida Y, Yamamoto T. Phosphorylation of three regulatory serines of Tob by Erk1 and Erk2 is required for Ras-mediated cell proliferation and transformation. *Genes Dev* 2002; **16**: 1356-1370
- 24 **Gems D**. Nematode ageing: Putting metabolic theories to the test. *Curr Biol* 1999; **9**: R614-616
- 25 **Levavasseur F**, Miyadera H, Sirois J, Tremblay ML, Kita K, Shoubridge E, Hekimi S. Ubiquinone is necessary for mouse embryonic development but is not essential for mitochondrial respiration. *J Biol Chem* 2001; **276**: 46160-46164

Edited by Liu HX and Wang XL Proofread by Xu FM

Effects of recombinant human growth hormone on remnant liver after hepatectomy in hepatocellular carcinoma with cirrhosis

Shi-Min Luo, Li-Jian Liang, Jia-Ming Lai

Shi-Min Luo, Li-Jian Liang, Jia-Ming Lai, Department of Hepatobiliary Surgery, The First Affiliated Hospital of Sun Yat-Sen University, Guangzhou 510080, Guangdong Province, China

Correspondence to: Dr. Li-Jian Liang, Department of Hepatobiliary Surgery, The First Affiliated Hospital of Sun Yat-Sen University, 56 Zhongshan Er Lu, Guangzhou 510080, Guangdong Province, China. liangpw@gzsums.edu.cn

Telephone: +86-20-87755766 Ext 8096

Fax: +86-20-87755766 Ext 8663

Received: 2003-11-17 **Accepted:** 2003-12-16

Abstract

AIM: To explore the effects of recombinant human growth hormone (rhGH) on the remnant liver after hepatectomy in hepatocellular carcinoma with liver cirrhosis.

METHODS: Twenty-four patients with hepatocellular carcinoma who underwent hepatectomy were randomly divided into 2 groups: parenteral nutrition (PN) group ($n=12$) and rhGH+PN group ($n=12$). Liver function, blood glucose, AFP, serum prealbumin and transferrin were detected before operation, at post-operative d 1 and d 6. Albumin (ALB) mRNA in liver biopsy specimens was detected by RT-PCR at post-operative d 6. Liver Ki67 immunohistochemical staining was studied.

RESULTS: On post-operative d 6, compared with PN group, the levels of blood glucose, serum prealbumin, transferrin, the expression of hepatic ALB mRNA and liver Ki67 labeling index were higher in rhGH+PN group.

CONCLUSION: rhGH can improve protein synthesis and liver regeneration after hepatectomy in hepatocellular carcinoma with liver cirrhosis.

Luo SM, Liang LJ, Lai JM. Effects of recombinant human growth hormone on remnant liver after hepatectomy in hepatocellular carcinoma with cirrhosis. *World J Gastroenterol* 2004; 10(9): 1292-1296

<http://www.wjgnet.com/1007-9327/10/1292.asp>

INTRODUCTION

Hepatocellular carcinoma (HCC) is one of the most common malignant tumors of mankind. Since 1990s HCC has become the second killer among various cancers in China^[1]. Surgical resection of the tumor is considered the only potentially curative therapy, and is regarded as the first choice of treatment of HCC. However, 80% of HCC are complicated with liver cirrhosis in China. After partial hepatectomy, the risk of hemorrhage, infection, and liver failure is very high, as the liver function is usually impaired before surgery in patients with cirrhosis. For safer hepatic resection in patients with cirrhosis, the reserve of hepatic function and rapid regeneration of the remnant liver are crucial. Because liver function is usually impaired in patients with cirrhosis, and because cirrhotic livers are less able to regenerate, it is important to

stimulate both the regeneration and function of the remnant cirrhotic liver after hepatectomy.

The prognosis of severe liver failure depends on the ability of the remaining hepatocytes to regenerate. Improvement of hepatic tissue repair can increase the survival rate of patients suffering from acute hepatic failure and reduce the recovery period after massive liver resection. Nutritional support is undoubtedly the most physiologic manner of treatment and it is clear that adequate nutrition should significantly speed up liver regeneration and patient recovery. The composition of parenteral nutrition (PN) for the postoperative nutritional management of patients with liver cirrhosis might be extremely important because of their metabolic disorders and hemodynamic disturbance following surgical intervention.

Considering that the provision of branched-chain amino acids (BCAA) may improve nutritional status and liver regeneration and ameliorate hepatic encephalopathy, increased provision of BCAA in patients with liver disease seems to be a reasonable approach to various forms of liver injury^[2-4]. While a decline in liver protein synthesis was induced by the surgical procedure^[5]. In patients given short-term PN, plasma insulin concentrations were increased 5-fold compared with control, but no effect on liver protein synthesis rates was observed^[6]. Growth hormone (GH) has important direct and indirect effects on protein, carbohydrate and lipid metabolism. Potential areas of further research may include the combination of BCAA supplements with other anabolic factors (*e.g.* GH) in managing patients with catabolic disease states^[7]. The aim of this study was to investigate the effects of treatment with amino acids enriched BCAA and recombinant human GH (rhGH) for 5 d on the remnant liver after hepatectomy in HCC with liver cirrhosis.

MATERIALS AND METHODS

Patients

All the patients were from our department who underwent curative resection for HCC with liver cirrhosis between September 2002 and June 2003. Curative resection was defined as complete resection of all macroscopically detectable tumors with histological tumor clearance (the entire tumor mass was included in the surgical specimen without exposure of tumor cells on the cut edge). At the time of entry, the inclusion criteria were no evidence of endocrine disease. The study protocol conformed to the ethical guidelines and the patients were enrolled after informed consent was obtained. Twenty-four patients were recruited and were randomly using sealed envelopes divided into 2 groups: PN group ($n=12$) and rhGH+PN group ($n=12$) using sealed envelopes. Between the 2 groups, there were no differences in age, sex, body mass, operative methods, operation time, intraoperative blood loss and intraoperative blood transfusion (Table 1). At the same time, 12 patients with cholelithiasis or hemangioma who underwent operation served as normal controls. None had liver cirrhosis or endocrine disease.

Nutritional support and rhGH administration

Nutritional support and rhGH administration were started on the first day after surgery and continued until d 5. PN was

initiated through a percutaneously placed subclavian vein catheter threaded into the superior vena cava. The formula provided non-protein calorie 25 kcal/kg·d. Each patient was provided 250 mL 200 mL/L MCT/LCT lipid emulsion (Guangzhou Qiaoguang Pharmaceutical Co. Ltd) and 750 mL 100 g/L aminoplasmal Hepa (Braun Co. Ltd) containing 20 kinds of amino acids, 330 g/L branched-chain amino acids and 15.3 g/L nitrogen. Nonprotein calories were provided 310 mL/L as lipid emulsion. The formula provided nitrogen 0.19 g/kg·d. The ratio of nonprotein calories to nitrogen was 132:1. The ratio of glucose (g) to insulin (IU) was 6:1. Vitamins, trace minerals, and electrolytes were supplied according to the daily requirement. This parenteral nutrition was tolerated by all patients without complications, and no patient showed symptoms of sepsis during the treatment period.

Patients in the rhGH+PN group received 10 U rhGH (Saizen, Serono Biotech&Beyond) additionally per day subcutaneously.

Table 1 Patient characteristics

	PN group (n=12)	rhGH+PN group (n=12)
General conditions		
Age (years)	46.1±13.6	50.3±10.6
Sex (M/F)	11/1	10/2
Body weight (kg)	59.7±9.3	64.3±7.7
Operative methods		
Hepatic left lateral lobectomy	0	1
Left hemihepatectomy	2	2
Right hemihepatectomy	1	1
Tumor or segmentectomy	9	8
Intraoperative information		
Operation time (min)	250.8±126.4	203.3±73.2
Intraoperative blood loss (mL)	1 331.7±1 704.8	966.7±1031.4
Intraoperative blood transfusion (mL)	1 100.0±1 334.2	408.3±609.7

Collection of samples

Blood samples were collected from antecubital veins in the morning after an overnight fast prior to operation in the normal, PN and rhGH+PN groups, on postoperative day (POD) 1 and 6 in the PN and rhGH+PN groups. Aliquots were transferred into different tubes placed for the determination of liver function, blood glucose, prealbumin, transferrin and α -fetoprotein (AFP). Blood samples were centrifuged at 4 °C and then frozen at -70 °C until assay.

Liver specimens from PN and rhGH+PN group, including hepatocellular carcinomas and adjacent non-tumor tissues were excised at the operation and percutaneous liver biopsies were taken on d 6 after operation in the PN group and rhGH+PN group, immediately frozen with liquid nitrogen, and stored at -70 °C for analysis of ALB mRNA. Liver biopsy specimens were obtained with Tru-Cut biopsy needles. The needle-biopsy specimens ranged in length from 15 to 20 mm. For histological examination, some liver specimens were fixed in 40 g/L neutrally-buffered formaldehyde and embedded in paraffin.

Biochemical examinations

Liver function, including serum aspartate aminotransferase (AST), alanine aminotransferase (ALT), alkaline phosphatase (ALP), total bilirubin (TBIL), albumin (ALB) and blood glucose were analyzed by an autoanalyzer. Serum prealbumin and transferrin were detected quantitatively by immunoturbidity assay. Serum AFP was detected quantitatively by microparticle enzyme immunoassay. The normal values were <20 μ g/L.

Measurement of ALB mRNA in liver tissue

RT-PCR was performed to measure the expression levels of

ALB mRNA in liver tissue. The primers used were deduced from the cDNA sequence. The sequences of the primers for ALB sense and antisense were as 5' -CCCAAGTGTC AACTCCA ACT-3' (sense) and 5' - GCAGGTCTCCTTATCGTCAG-3' (antisense), a 456-bp long fragment was amplified. The sequences of the primers for β -actin sense and antisense were as 5' -ACTCTTCCAGCCTTCCTTCCT-3' (sense) and 5' -TCACCTTACCGTTCCAGTTT-3' (antisense), a 513-bp long fragment was amplified.

Total RNA was extracted from frozen liver specimens by the guanidinium isothiocyanate method. The RNA was quantified and checked for purity by spectrophotometry at 260 and 280 nm. Aliquots of total RNA were reversely transcribed using SpermSriptII Reverse Transcriptase (Invitrogen Corp) and subsequently amplified by PCR using the Taq DNA polymerase (Promega).

The PCR was carried out in 25 mL of reaction mixture containing 0.5 μ L cDNA template, 2.5 μ L 10 \times PCR-Buffer, 1.5 μ L 25 mmol/L MgCl₂, 0.5 μ L 10 mmol/L dNTPs, 0.5 μ L 10 μ mol/L ALB, 0.15 μ L 10 μ mol/L β -actin primers, 0.5 μ L 5 U/ μ L Taq DNA polymerase. The mixture was heated for 5 min. at 94 °C for initial DNA denaturation, followed by 30 cycles of denaturation at 94 °C for 45 s, annealing at 50 °C for 45 s, polymerization at 72 °C for 1 min. and then a final extension of 10 min at 7 °C. PCR reactions were stored frozen until analysis by agarose gel electrophoresis.

PCR reactions were electrophoresed on 15 g/L agarose gel, stained with ethidium bromide and quantitated using the interactive build analysis system (IBAS). The band intensity of the ALB was compared with the band intensity of the β -actin, and the amount of ALB mRNA was estimated.

Immunohistochemical staining of Ki67 in liver tissue

Two-step immunohistochemical staining technique was used. Main reagents included rabbit polyclonal antibody Ki67 Ab-4 (Neomarkers) and PV-6000 PicTure™ kits. Briefly, sections were deparaffinized, rehydrated, and then immersed in 0.1 mol/L citric acid buffer (pH 6.0) and boiled for 5-10 min in a microwave oven. The slides were then rinsed gently with phosphate buffered saline (PBS) at pH 7.2-7.4, and treated with 3 mL/L hydrogen peroxide in absolute methanol for 1 h at room temperature (RT) to remove endogenous peroxidase. The sections were then incubated with the primary antibody Ki67 Ab-4 (1:200 dilution) for 30 min at 37 °C. After rinsed with PBS for 3 times, each for 2 min, the sections were incubated with PV-6000 for 30 min at 37 °C. They were then rinsed 3 times with PBS for 2 min each and visualized with DAB. Finally, the sections were counterstained with hematoxylin.

On each slide, Ki67-positive nuclei were estimated by means of light microscopy at 400 magnifications. At least 1 000 cells were evaluated in 5 different fields each containing a minimum of 200 cells. The Ki67 labeling index (Ki67 LI) is the percentage (%) of positive cells.

Recording doses of albumin infusions within 5 d after operation

Plasma contained 4.5 g/L albumin. Doses of plasma infusion were converted into doses of albumin.

Statistical analysis

Data were expressed as mean \pm SD. The statistical software SPSS 10.0 was used. Statistical significance was set at $P<0.05$.

RESULTS

Surgery outcome and albumin doses within 5 d after operation

There was no surgical mortality in this series. The postoperative

hospital stay showed no difference between the PN group and rhGH+PN group (14.7±6.2 d vs 13.5±4.5 d, $P>0.05$). In the PN group, 2 patients had right pleural effusion. In the rhGH+PN group, 1 patient had right pleural effusion, another patient had subcutaneous fat liquefaction. The postoperative complication related morbidity was not different between the 2 groups ($P>0.05$). Albumin doses within 5 d after operation were not different between the PN and rhGH+PN group (57.0±48.8 g vs 52.4±24.4 g, $P>0.05$).

The decreased percentage of serum AFP within 5 d after operation

The decreased percentage of serum AFP within 5 d after operation were calculated by (POD 1 serum AFP- POD 6 serum AFP)/POD 1 serum AFP. In the PN group, 6 patients had preoperative serum AFP<20 µg/L. In the rhGH+PN group, 3 patients had preoperative serum AFP<20 µg/L and at POD 6, 3 patients whose preoperative serum AFP were <50 µg/L had their serum AFP<20 µg/L. Those patients were excluded from the statistics. For the other 6 patients in the 2 groups, the decrease percentage of serum AFP within 5 d after operation was not different between the PN group and rhGH+PN group (0.536±0.182 vs 0.579±0.193, $P>0.05$).

The changes of liver function and blood glucose

Compared with normal control group, serum AST, ALT of HCC patients with cirrhosis were significantly increased, while serum ALP, TBIL, ALB, blood glucose were not different. Serum AST, ALT, ALP, TBIL, ALB, blood glucose on preoperative day and POD 1 were not different between the PN group and rhGH+PN group. Compared with PN group, serum AST, ALT, ALP, TBIL, ALB on POD 6 in the rhGH+PN group were not different, but blood glucose was significantly increased (Table 2).

The changes of serum prealbumin and transferrin

In HCC patients with cirrhosis, serum prealbumin and

transferrin were lower than the normal control group. Serum prealbumin and transferrin on preoperative day and POD 1 were not different between PN group and rhGH+PN group, but serum prealbumin and transferrin on POD 6 in the rhGH+PN group were significantly increased compared with the PN group (Table 2).

The changes of hepatic ALB mRNA and liver Ki67 labeling index

In HCC patients with cirrhosis, hepatic ALB mRNA of tumor tissues was lower than in adjacent non-tumor tissues, while in adjacent non-tumor tissues it was lower than the normal liver tissues. Compared with the PN group, hepatic ALB mRNA on POD 6 was significantly increased in the rhGH+PN group. Liver Ki67 labeling index in tumor tissues was higher than adjacent non-tumor tissues. Liver Ki67 labeling index on POD 6 in the rhGH+PN group was higher than the PN group (Table 3).

DISCUSSION

The prevalence of malnutrition in patients with liver cirrhosis is high^[8]. Nutritional status affects prognosis, and cirrhotic patients with malnutrition are prone to develop major complications and infections. A poor nutritional status negatively influences survival, while appropriate nutritional intervention has been found to improve liver function and survival. Because the liver is the metabolic workhouse of the body, alteration in liver function clearly affects the whole body metabolism. In addition, the goals of nutritional support should include maintenance of adequate nutrition and prevention and/or amelioration of liver damage. Major resection of portions of the liver for primary hepatic or metastatic malignancy and the repair of hepatic injury associated loss of liver tissue are performed with such a frequency as to require careful consideration of the consequences of the postoperative nutritional care of the patients. Often, the recovery from such surgery involves a prolonged period of delayed oral intake.

Table 2 Comparison of liver function, blood glucose, serum prealbumin and transferrin

	Normal control group (n=12)	PN group (n=12)			rhGH+PN group (n=12)		
		Preoperative	POD 1	POD 6	Preoperative	POD 1	POD 6
AST (IU/L)	26.0±5	56.0±27 ^a	761.0±578	62.0±32	55.0±25 ^a	578.0±206	56.0±25
ALT (IU/L)	27.0±17	60.0±36 ^a	749.0±571	153.0±95	42.0±17 ^a	590.0±273	154.0±71
ALP (IU/L)	94.0±55	151.0±87	145.0±80	148.0±65	105.0±27	100.0±33	113.0±46
TBIL (µmol/L)	17.4±6.4	22.6±9.0	52.5±48.1	43.1±37.4	20.5±9.3	42.1±41.6	30.2±21.0
ALB (g/L)	42.8±4.0	39.8±4.7	31.5±3.3	34.0±3.4	40.7±3.5	32.4±3.6	37.1±5.0
Blood glucose (mmol/L)	4.6±0.6	4.8±0.9	7.3±3.5	5.3±1.5	4.5±0.6	7.0±3.2	8.8±5.2 ^c
Serum prealbumin (mg/L)	279.8±43.0	202.4±32.3 ^a	158.3±25.4	127.2±13.4	204.5±31.9 ^a	157.2±23.0	156.4±20.0 ^c
Serum transferrin (g/L)	3.5±0.5	2.5±0.2 ^a	2.1±0.3	1.8±0.2	2.5±0.2 ^a	2.2±0.3	2.2±0.3 ^c

^a $P<0.05$, preoperative vs normal control group; ^c $P<0.05$, between rhGH+PN group and PN group.

Table 3 Comparison of hepatic ALB mRNA and liver Ki67 labeling index

	Normal control group (n=12)	PN group (n=12)			rhGH+PN group (n=12)		
		Tumor tissues	Adjacent non-tumor tissues	Liver biopsy specimens POD 6	Tumor tissue	Adjacent non-tumor tissues	Liver biopsy specimens POD 6
ALB mRNA	0.69±0.05	0.38±0.01 ^a	0.50±0.06 ^{a,c}	0.63±0.05	0.38±0.01 ^a	0.50±0.06 ^{a,c}	0.71±0.06 ^c
Liver Ki67 LI(%)	0	17.4±6.1 ^a	0.20±0.1 ^{a,c}	4.60±0.5	17.2±5.9 ^a	0.20±0.1 ^{a,c}	5.50±0.5 ^c

^a $P<0.05$, tumor tissues or adjacent non-tumor tissues vs normal control group; ^c $P<0.05$, adjacent non-tumor tissues vs tumor tissues in the same group, ^b $P<0.05$, of the same tissues comparison between the PN group and rhGH+PN group.

Although the liver normally has considerable reserve function and regeneration potential, an acute reduction in hepatic mass can significantly affect liver function, its metabolic activity, and substrate metabolism. The trauma caused by moderate or large operation may result in disturbance of glucose, lipid and protein metabolism including hypermetabolism and increased catabolism, which may lead to acute protein malnutrition, decline of immunological function and dysfunction of multiple organs^[9-11]. Postoperative maintenance of protein synthesis is one measure to preserve a satisfactory quality of life after hepatectomy^[12].

The amino acids that comprise the various parenteral feeding formulations are the important components of these regimens, because they provide the precursors for the synthesis of numerous structural and functional body proteins. BCAA appears to act favorably in albumin metabolism. Early oral supplementation of BCAA for HCV-related cirrhosis with serum albumin level between 3.5 and 3.9 g/dL and branched-chain tyrosine ratio (BTR) less than 4.0, improves serum albumin levels and thus might improve prognosis^[13].

Liver protein synthesis is usually estimated in humans by measuring the synthesis rates of major exported liver proteins. Albumin is a ubiquitous protein synthesized only by hepatocytes. Albumin is a polypeptide chain of 580 amino acids that is produced by hepatocytes^[14]. The expression of ALB gene is reduced in various liver diseases and the degree of reduction in the hepatic ALB mRNA level is generally correlated with the severity of the disease^[15]. This study showed that hepatic ALB mRNA in tumor tissues was lower than in adjacent non-tumor tissues, and it was lower in adjacent non-tumor tissues than normal liver tissues. Serum ALB whose long half-life of approximately 20 d makes it a late index of nutritional status, and its exclusive use may delay implementation of appropriate nutritional interventions. Serum prealbumin and transferrin have been proposed as earlier nutritional markers. Clinically significant changes in albumin can be reliably predicted by earlier changes in serum transferrin and prealbumin^[16]. In this study, serum AST, ALT, ALP, TBIL, ALB on POD 6 were not different between the PN group and rhGH+PN group, but blood glucose, serum prealbumin, transferrin, hepatic ALB mRNA, and liver Ki67 labeling index were significantly increased in the rhGH+PN group. Thus, rhGH can promote liver protein synthesis and liver regeneration. Moreover, liver function recovered faster in the rhGH+PN group. It has been demonstrated that PN is not able to support protein synthesis sufficiently in patients with or without malnutrition^[17]. Long-term conventional PN is unable to increase or even maintain body protein; the anabolic response to PN is often suboptimal because of the concomitant presence of catabolism and/or alterations in the hormonal regulation of metabolism^[18,19]. GH is anabolic in protein metabolism. Gu and Wu also demonstrated that the administration of rhGH could result in significant anabolic effects on body growth and improve the efficiency of PN^[20].

An important but unresolved question is intrahepatic recurrence after resection of HCC^[21-26]. Metastasis and recurrence of HCC after surgical removal is still high. The frequency of 5-year recurrence after radical resection was 61.5% overall^[27]. The recurrence, especially at an early period after hepatectomy, is the major cause of poor prognosis in patients with HCC^[28]. This is of relevance in determining preventive and therapeutic strategies for recurrence. Although all patients in this study underwent curative tumor resection, the potential tumor-promoting effect of GH must be addressed. This study showed that the decreased percentage of serum AFP within 5 d after operation was not different between the PN group and rhGH+PN group. Furthermore, liver function recovered faster in the rhGH+PN group. However, hepatic

functional damage immediately after hepatectomy is a significant risk factor for early intrahepatic recurrence in cirrhotic HCC. Careful perioperative management of hepatic function may therefore be important in preventing early recurrence and prolonging survival^[29]. Tacke *et al* demonstrated no evidence for an increased risk of tumor recurrence after rhGH treatment for a short period of time after removal of a gastrointestinal adenocarcinoma^[30]. Moreover, rhGH attenuated the depression in cellular immunity following surgical stress^[31]. Therefore, short-term use of rhGH in HCC patients with cirrhosis after operation may be safe.

In conclusion, rhGH+PN can promote liver recovery, liver protein synthesis and liver regeneration after hepatectomy in HCC with liver cirrhosis. It may not promote HCC recurrence, but may increase blood glucose.

REFERENCES

- 1 **Tang ZY.** Hepatocellular carcinoma-cause, treatment and metastasis. *World J Gastroenterol* 2001; **7**: 445-454
- 2 **Holecck M.** Nutritional modulation of liver regeneration by carbohydrates, lipids, and amino acids: a review. *Nutrition* 1999; **15**: 784-788
- 3 **Freund HR, Hanani M.** The metabolic role of branched-chain amino acids. *Nutrition* 2002; **18**: 287-288
- 4 **James JH.** Branched chain amino acids in hepatic encephalopathy. *Am J Surg* 2002; **183**: 424-429
- 5 **Barle H, Essen P, Nyberg B, Olivecrona H, Tally M, McNurlan MA, Wernerman J, Garlick PJ.** Depression of liver protein synthesis during surgery is prevented by growth hormone. *Am J Physiol* 1999; **276**(4 Pt 1): E620-627
- 6 **Barle H, Nyberg B, Andersson K, Essen P, McNurlan MA, Wernerman J, Garlick PJ.** The effects of short-term parenteral nutrition on human liver protein and amino acid metabolism during laparoscopic surgery. *J Parenter Enteral Nutr* 1997; **21**: 330-335
- 7 **Platell C, Kong SE, McCauley R, Hall JC.** Branched-chain amino acids. *J Gastroenterol Hepatol* 2000; **15**: 706-717
- 8 **Donaghy A.** Issues of malnutrition and bone disease in patients with cirrhosis. *J Gastroenterol Hepatol* 2002; **17**: 462-466
- 9 **Antonio J, Sanders MS, Ehler LA, Uelmen J, Raether JB, Stout JR.** Effects of exercise training and amino-acid supplementation on body composition and physical performance in untrained women. *Nutrition* 2000; **16**: 1043-1046
- 10 **Wang SJ, Wen DG, Zhang J, Man X, Liu H.** Intensify standardized therapy for esophageal and stomach cancer in tumor hospitals. *World J Gastroenterol* 2001; **7**: 80-82
- 11 **Dionigi P, Alessiani M, Ferrazi A.** Irreversible intestinal failure, nutrition support, and small bowel transplantation. *Nutrition* 2001; **17**: 747-750
- 12 **Ueno S, Tanabe G, Nuruki K, Yoshidome S, Kubo F, Kihara K, Aoki D, Aikou T.** Quality of life after hepatectomy in patients with hepatocellular carcinoma: implication of change in hepatic protein synthesis. *Hepatogastroenterology* 2002; **49**: 492-496
- 13 **Habu D, Nishiguchi S, Nakatani S, Kawamura E, Lee C, Enomoto M, Tamori A, Takeda T, Tanaka T, Shiomi S.** Effect of oral supplementation with branched-chain amino acid granules on serum albumin level in the early stage of cirrhosis: a randomized pilot trial. *Hepatol Res* 2003; **25**: 312-318
- 14 **Yamaguchi K, Nalesnik MA, Carr BI.** *In situ* hybridization of albumin mRNA in normal liver and liver tumors: identification of hepatocellular origin. *Virchows Arch B Cell Pathol Incl Mol Pathol* 1993; **64**: 361-365
- 15 **Ozaki I, Motomura M, Setoguchi Y, Fujio N, Yamamoto K, Kariya T, Sakai T.** Albumin mRNA expression in human liver diseases and its correlation to serum albumin concentration. *Gastroenterol Jpn* 1991; **26**: 472-476
- 16 **Neyra NR, Hakim RM, Shyr Y, Ikizler TA.** Serum transferrin and serum prealbumin are early predictors of serum albumin in chronic hemodialysis patients. *J Ren Nutr* 2000; **10**: 184-190
- 17 **Warnold I, Eden E, Lundholm K.** The inefficiency of total parenteral nutrition to stimulate protein synthesis in moderately malnourished patients. *Ann Surg* 1988; **208**: 143-149

- 18 **Ziegler TR**, Rombeau JL, Young LS, Fong Y, Marano M, Lowry SF, Wilmore DW. Recombinant human growth hormone enhances the metabolic efficacy of parenteral nutrition: a double blind, randomized controlled study. *J Clin Endocrinol Metab* 1992; **74**: 865-873
- 19 **Wilmore DW**. Growth factors and nutrients in the short bowel syndrome. *J Parenter Enteral Nutr* 1999; **23**(5 Suppl): S117-120
- 20 **Gu Y**, Wu ZH. The anabolic effects of recombinant human growth hormone and glutamine on parenterally fed, short bowel rats. *World J Gastroenterol* 2002; **8**: 752-757
- 21 **Qin LX**, Tang ZY. The prognostic significance of clinical and pathological features in hepatocellular carcinoma. *World J Gastroenterol* 2002; **8**: 193-199
- 22 **Ezaki T**, Yamamoto K, Yamaguchi H, Sasaki Y, Ishida T, Mori M, Aimitsu S. Hepatic resection for hepatocellular carcinoma existing with liver cirrhosis. *Hepatogastroenterology* 2002; **49**: 1363-1368
- 23 **Sun HC**, Tang ZY. Preventive treatments for recurrence after curative resection of hepatocellular carcinoma-a literature review of randomized control trials. *World J Gastroenterol* 2003; **9**: 635-640
- 24 **Takada Y**, Otsuka M, Todoroki T, Fukao K. Accompanying liver cirrhosis as a risk factor for recurrence after resection of solitary hepatocellular carcinoma. *Hepatogastroenterology* 2003; **50**: 1991-1995
- 25 **Grazi GL**, Cescon M, Ravaioli M, Ercolani G, Gardini A, Del Gaudio M, Vetrone G, Cavallari A. Liver resection for hepatocellular carcinoma in cirrhotics and noncirrhotics. Evaluation of clinicopathologic features and comparison of risk factors for long-term survival and tumour recurrence in a single centre. *Aliment Pharmacol Ther* 2003; **17**(Suppl): 119-129
- 26 **Imamura H**, Matsuyama Y, Tanaka E, Ohkubo T, Hasegawa K, Miyagawa S, Sugawara Y, Minagawa M, Takayama T, Kawasaki S, Makuuchi M. Risk factors contributing to early and late phase intrahepatic recurrence of hepatocellular carcinoma after hepatectomy. *J Hepatol* 2003; **38**: 200-207
- 27 **Niu Q**, Tang ZY, Ma ZC, Qin LX, Zhang LH. Serum vascular endothelial growth factor is a potential biomarker of metastatic recurrence after curative resection of hepatocellular carcinoma. *World J Gastroenterol* 2000; **6**: 565-568
- 28 **Shimada M**, Takenaka K, Gion T, Fujiwara Y, Kajiyama K, Maeda T, Shirabe K, Nishizaki T, Yanaga K, Sugimachi K. Prognosis of recurrent hepatocellular carcinoma: a 10-year surgical experience in Japan. *Gastroenterology* 1996; **111**: 720-726
- 29 **Hanazaki K**, Wakabayashi M, Sodeyama H, Kajikawa S, Amano J. Hepatic function immediately after hepatectomy as a significant risk factor for early recurrence in hepatocellular carcinoma. *Hepatogastroenterology* 1999; **46**: 3201-3207
- 30 **Tacke J**, Bolder U, Herrmann A, Berger G, Jauch KW. Long-term risk of gastrointestinal tumor recurrence after postoperative treatment with recombinant human growth hormone. *J Parenter Enteral Nutr* 2000; **24**: 140-144
- 31 **Liu W**, Jiang Z, Wang X, Shu H, Cui W, Wilmore DW. Impact of perioperative treatment of recombinant human growth hormone on cell immune function and intestinal barrier function: randomized, double-blind, controlled trial. *World J Surg* 2003; **27**: 412-415

Edited by Zhu LH and Xu FM

Amino acid uptake in arterio-venous serum of normal and cancerous colon tissues

Lin-Bo Wang, Jian-Guo Shen, Su-Zhan Zhang, Ke-Feng Ding, Shu Zheng

Lin-Bo Wang, Jian-Guo Shen, Department of Surgical Oncology, Sir Run Run Shaw Hospital, Zhejiang University Medical College, Hangzhou 310016, Zhejiang Province, China

Su-Zhan Zhang, Ke-Feng Ding, Shu Zheng, Department of Surgical Oncology, the Second Hospital, Zhejiang University Medical College, Hangzhou 310016, Zhejiang Province, China

Supported by Oncology Research Institute, Medical College, Zhejiang University

Correspondence to: Dr. Lin-Bo Wang, Department of Surgical Oncology, Sir Run Run Shaw Hospital, Zhejiang University Medical College, Hangzhou 310016, Zhejiang Province, China. wanglinbo@medmail.com.cn

Telephone: +86-571-86090073 **Fax:** +86-571-86044817

Received: 2003-08-02 **Accepted:** 2003-10-12

Abstract

AIM: To investigate the difference of amino acid uptake between normal and cancerous colon tissues.

METHODS: Sixteen patients with colon cancer were enrolled in our study. Blood samples were taken during operations, serum amino acid concentrations of blood from cancerous or normal colon were analyzed. Amino acid uptake rate was calculated by the A-V difference and evaluated statistically.

RESULTS: Except for methionine, the uptake rate of amino acids in cancer was higher than that in normal colon (25.01% vs -2.29%, $P < 0.01$). The amino acid uptake rate did not correlate to the size of tumor mass ($P > 0.05$). There was no statistical significance in the amino acid uptake rate according to the Dukes stage, though it was higher in patients with Dukes stage C or D than that with Dukes stage B ($P > 0.05$).

CONCLUSION: Abnormal synthetic metabolism of colon cancer may contribute to its higher amino acid uptake rate than that of normal colon.

Wang LB, Shen JG, Zhang SZ, Ding KF, Zheng S. Amino acid uptake in arterio-venous serum of normal and cancerous colon tissues. *World J Gastroenterol* 2004; 10(9): 1297-1300
<http://www.wjgnet.com/1007-9327/10/1297.asp>

INTRODUCTION

Studies note the significance of amino acid metabolism in neoplasms, though there are lots of questions that remain to be answered^[1-5]. It is helpful to improve the life quality if we take patients' nutrition into account according to their characteristic amino acid metabolism before we treat cancer patients. Studies^[6,7,8,9] demonstrated that the amino acid concentrations in serum, especially essential amino acids (EAAs) but not leucine, were decreased in colon cancer patients with weight loss, but not in patients without weight changes, of which the non-essential amino acids (NEAAs), like asparagic

acid, glutamine, glycine, alanine, taurine and ornithine, were slightly elevated in serum. Zheng^[10] studied the changes of free amino acids in colon cancer tissue and revealed that the serum concentration of most EAAs (leucine, isoleucine, phenylalanine, threonine, lysine) and some NEAAs (tyrosine, proline, glutamine) in cancer tissue were obviously higher than those in normal tissue ($P < 0.01$), while the serum concentration of most NEAAs and some EAAs (methionine, valine, histamine) was slightly elevated. There was no statistical significance. The ammonia serum concentration in cancer tissue decreased significantly ($P < 0.05$). To make further investigations of the amino acid metabolism in colon cancer, we analyzed the arterial and venous (A-V) serum free amino acid uptake rates in tumor region, and tried to find the difference of amino acid metabolism between normal and cancerous colon tissue.

MATERIALS AND METHODS

Clinical materials

Sixteen patients were enrolled in this study from Department of Surgical Oncology, Sir Run Run Shaw Hospital, Zhejiang University Medical College. Patients with a median age of 57 years (range from 37 to 77) were diagnosed having colon cancer pathologically. Nine (66.7%) patients were males and in 9 patients, the mass was larger than 5 cm in size. According to Dukes stage, 10 patients were in stage B, 5 in stage C, and 1 in stage D. Before operation, hormone, blood, albumin and amino acid intake were prohibited. Five-day doses of sulfaguanidine and metronidazol were given for bowel preparations.

Sample collection and processing

A 3 mL arterial blood as sample A was collected before making division of the mesentery vessels during laparotomy, and 3 mL reflux venous blood from the tumor region was collected as sample C, another 3 mL mesentery venous blood in normal colon tissue, which was about 7 cm from the tumor margin, was collected as sample E. After incubation at 37 °C for an hour, the serum was collected by centrifugation, and 1 mL serum mixed with 50 mg sulfosalicylic acid was placed for an hour at 4 °C, then centrifuged at 16 000 g for 6 min. The supernatant was diluted with 0.02 mol/L hydrochloric acid before analysis. Each sample was analyzed twice with automatic amino-acid analyzer (Japan 835-50) 18 standard amino acids including ammonia were placed as control.

Statistical analysis

The A-V amino acid uptake rate in colon cancer (R1) was calculated by the following formula ($R1 = (A-C)/A \times 100\%$) and that in normal tissue (R2) was calculated as the following: $R2 = (A-E)/A \times 100\%$ [A, C and E refer to the amino acid concentrations of samples A, C and E]. The rate was compared by means of *t* test, statistical significance was defined as $P < 0.05$.

RESULTS

We measured 16 patients with 48 samples. The uptake rates of amino acids in normal and cancerous colon tissue were calculated. As is shown in Table 1, except for methionine, the uptake rates of all amino acids in cancer were higher than those

in normal colon (25.01% vs -2.29%, $P < 0.01$). The EAAs uptake rates in cancer tissue were between 25.44% and 39.75% with a mean of 31.7% and between -8.01% and 13.5% in normal colon tissue ($P < 0.01$). Methionine was 11.55% in cancer tissue but -0.13% in normal tissue. The ketogenic or ketogenic and glucogenic amino acid uptake rates had a mean of 30.86%, which was higher than that of glucogenic acids (18.7%). Sulfur-bearing amino acid uptake rates in colon cancer tissue, which were comparatively lower than the other amino acids, were higher than those in normal tissue, though there was no statistical significance. The uptake rates of some amino acids (lysine, arginine, proline, glutamine, glycine, alanine, cystine, methionine and ammonia) were negative in normal tissue, and the serum concentration of asparagic acid could not be detected in more than 10 patients.

Table 1 A-V amino acid uptake rates in normal and cancerous colon tissue

Amino acid	Sample number	R2 (%)	R1 (%)	P value
Threonine ^{1,3}	16	13.50±3.76	39.25±7.59	<0.01
Phenylalanine ^{1,3}	16	6.37±1.77	26.26±4.31	<0.01
Leucine ^{1,4}	16	8.21±2.13	36.55±6.11	<0.01
Isoleucine ^{1,3}	15	11.39±3.55	30.63±5.50	<0.01
Methionine ¹	16	-0.13±1.20	11.55±5.22	>0.05
Valine ¹	16	7.67±2.42	33.46±5.56	<0.01
Lysine ^{1,4}	16	-8.01±1.85	25.44±4.41	<0.01
Histidine ¹	16	1.06±0.94	29.83±6.37	<0.01
Proline ²	11	-26.86±8.36	6.49±1.69	<0.02
Glutamine ²	16	-12.42±3.12	18.70±5.23	<0.01
Ammonia ²	16	-23.61±4.58	4.70±1.97	<0.05
Alanine ²	16	-9.65±2.47	18.16±2.29	<0.01
Glycine ²	16	-1.50±0.98	29.18±4.41	<0.01
Cystine ²	13	-10.01±3.37	8.89±1.58	<0.01
Arginine ²	16	-1.74±0.88	29.02±4.93	<0.01
Serine ²	16	2.39±1.02	37.26±5.67	<0.01
Tyrosine ^{2,3}	16	6.57±1.45	26.33±3.39	<0.01

¹Refers to essential amino acids, ²refers to non-essential amino acids, ³refers to ketogenic and glucogenic amino acids, ⁴refers to ketogenic amino acids.

Table 2 Relationship between A-V amino acid uptake rates and tumor size in colon cancer

Amino acid	Tumor size<5.0 cm		Tumor size>5.0 cm		P value
	Sample number	R1 (%)	Sample number	R1 (%)	
Threonine	7	35.25±10.13	9	42.37±7.81	0.580
Phenylalanine	7	25.44±10.63	9	26.89±3.81	0.889
Leucine	7	33.02±12.85	9	39.30±6.53	0.648
Isoleucine	6	30.09±16.48	9	30.99±4.34	0.950
Methionine	7	13.53±7.47	9	9.99±8.79	0.772
Valine	7	27.63±8.37	9	37.99±8.50	0.408
Lysine	7	21.17±14.07	9	28.76±7.36	0.618
Histidine	7	25.41±10.03	9	33.26±7.26	0.528
Proline	4	10.05±9.81	7	4.45±7.19	0.653
Glutamine	7	25.45±8.69	9	13.44±11.93	0.455
Ammonia	7	13.92±9.08	9	2.47±7.08	0.179
Alanine	7	14.97±1.56	9	20.64±7.72	0.679
Glycine	7	30.04±1.14	9	28.52±11.24	0.926
Cystine	7	20.82±0.69	8	7.23±10.54	0.329
Arginine	7	21.68±7.09	9	34.73±9.06	0.485
Serine	7	25.40±3.22	9	38.71±9.36	0.836
Tyrosine	7	24.90±0.66	9	27.44±4.56	0.815

Table 3 Relationship between A-V amino acid uptake rates and Dukes stage in colon cancer

Amino acid	Dukes stage B		Dukes stage C or D		P value
	Sample number	R1 (%)	Sample number	R1 (%)	
Threonine	10	35.75±8.85	6	45.10±7.10	0.476
Phenylalanine	10	24.26±7.02	6	29.60±6.47	0.616
Leucine	10	29.73±9.68	6	47.93±4.07	0.184
Isoleucine	9	22.74±10.23	6	42.47±4.41	0.158
Methionine	10	2.44±6.39	6	26.72±8.30	0.036
Valine	10	34.85±9.53	6	31.15±3.37	0.776
Lysine	10	20.10±11.03	6	34.34±4.90	0.356
Histidine	10	25.32±8.83	6	37.35±5.08	0.341
Proline	6	-2.70±6.43	5	17.50±7.25	0.066
Glutamine	10	26.30±9.92	6	6.02±10.95	0.209
Ammonia	10	5.44±7.74	6	3.47±10.07	0.879
Alanine	10	21.57±9.65	6	12.50±6.66	0.516
Glycine	10	29.37±8.65	6	28.87±15.91	0.976
Cystine	9	11.46±10.67	6	16.73±6.03	0.715
Arginine	10	23.12±13.84	6	38.85±4.80	0.409
Serine	10	34.32±9.75	6	42.16±12.82	0.632
Tyrosine	10	23.08±7.78	6	31.74±4.30	0.432

Relationships between the uptake rates of amino acids and the size of tumor mass or the Dukes stage are shown in Table 2 and Table 3.

DISCUSSION

Studies have noted the amino acid uptake changes in blood and tumor tissue, but the results were controversial^[8,11-13]. More factors, such as ages, food intake, consumption and digestion, liver and kidney functions, could influence the amino acid concentrations in serum, and different sample treatment was also confirmed as an important factor^[14-17]. In our study, we compared the amino acid concentrations in cancer tissue with those in normal colon as self-control to eliminate the factors that influenced the results.

Tumor cells needed more glucose and amino acids than normal body cells^[1]. Limited data were found in *in vivo* studies. We analyzed the amino acid uptake rates in cancer tissue and revealed that the uptake rates of amino acids, especially EAAs, ketogenic, ketogenic and glucogenic amino acids, but not methionine, were significantly higher than those in normal tissue, suggesting that colon cancer might need more of these amino acids.

Protein synthesis was more active in tumor tissue^[18-21], and enzymes such as protein kinase were more active in hepatic cancer cells than those in normal cells. Michael *et al.* demonstrated that the protein concentration in cancer tissue (hepatic cancer, digestive cancer and breast cancer) was elevated continuously with tumor progression. Hagmuller *et al.*^[22] revealed that, not only the protein synthesis, but the uptake of EAAs and branched-chain amino acids (BAAs) in cancer tissue were more significant than those in arm tissue, as in our study. Khirallah *et al.* suggested that the sources of amino acids in cell protein synthesis came from the plasma and cell protein degradation, though it was not clear which would be the major source. According to our study, amino acids, especially EAAs, might come from the plasma because colon cancer cells were inadequate to synthesize EAAs.

Asparagic acid, glycine, glutamine, folic acid and ammonia were the basic substrates in pyrimidine and purine nucleosides

synthesis^[23]. Our data showed that asparagic acid was too low to be detected in most patients, which might be due to its total utilization in nucleosides synthesis, as was reported by Norton^[6]. Methionine is one of the important amino acids in cancer metabolism, and total parenteral nutrition (TPN) with cystine and methionine deficiency has been shown to decrease the tumor growth by inhibiting DNA and RNA synthesis in cancer cells^[24,25]. Our data showed that the cystine and methionine uptake rates in cancer tissue were not higher than those in normal tissue, it might be resulted from its repetitive utilization in methylation by s-adenomethionine circulation. On the other hand, lower methylation in nucleosides metabolism might also decrease the cystine/methionine requirement in tumor.

Tumor growth consumes a large amount of energy. Glycolysis was ascertained as the major source of energy especially in archaeocytes and poorly differentiated cells because the enzymes in glycolysis in tumor tissue were elevated, which increased the lactic acid concentration and reduced the pH value. Because a little adenosine triphosphate (ATP) could be released by glycolysis, a lot of glucose should be consumed to get adequate energy. Most studies showed that alanine, glycine and glutamine might be involved in glyconeogenesis for their concentrations in blood were higher than the other amino acids. On the other hand, liver glyconeogenesis increased in tumor tissue, and the enzymes involved in glyconeogenesis were more activated, though they were lower in liver cancer than in normal tissue in some studies^[1,26]. The glucogenic amino acid concentrations were not obviously changed in tumor tissue in our study, though the uptake rates were higher than those in normal tissue, suggesting these amino acids were utilized during glyconeogenesis.

Aerobic metabolism was present in tumor tissue. Whether any enzyme deficiency occurs in tumor aerobic metabolism is still controversial. Kern *et al.*^[27] reported that the fat, but not the liver starch, was the primary substrate in energy metabolism when fasting. Compared with anaerobic metabolism, it could produce eighteen to nineteen times of ATP. The amino acid concentrations in colon cancer tissue (threonine, isoleucine, leucine, phenylalanine, proline, tyrosine and lysine) were higher than those in normal tissue in our study, suggesting that tumor colon tissue utilized these amino acids as a fuel to get more energy in Krebs cycle. There might be a more active and flawless aerobic metabolism in colon cancer tissue, and further studies should be conducted.

It seems that the poorer the cell differentiation, the more elevated ability the more amino acid uptake in tumor. The samples we selected in our study were moderately differentiated globular adenocarcinomas. It was difficult to reveal the differences according to their differentiation, and more samples are needed in further study. Several studies^[28-32] demonstrated that there was a correlation between the amino acid concentrations and the tumor volume. On the contrary, in our study, there was no obvious correlation between the size of tumor and the uptake rates of amino acids in tumor tissue, which might probably due to tumor necrosis or lower metabolism. The amino acid uptake rates of patients in Dukes stage C or D were higher than those in Dukes stage B, but only methionine had statistical significance.

The uptake rates of EAAs (methionine and lysine) and NEAAs (glutamine, glycine, alanine, cystine, arginine, proline and ammonia) were negative in normal colon tissue, suggesting that normal colon tissue has the ability to synthesize these amino acids or produce them by tissue protein degradation. Studies^[26,33] demonstrated that malignant neoplasms had the ability to enhance the degradation of proteins in surrounding normal tissue or muscles and absorb some part of amino acids to glyconeogenesis, though its function was ignored in general

conditions. Whether it is significant in short gut patients needs further studies.

REFERENCES

- 1 **Shrivastava GC**, Quastel JH. Malignancy and tissue metabolism. *Nature* 1962; **196**: 876-880
- 2 **Christensen HN**. Interorgan amino acid nutrition. *Physiol Rev* 1982; **62**(4 Pt 1): 1193-1233
- 3 **Heys SD**, Park KG, McNurlan MA, Keenan RA, Miller JD, Eremin O, Garlick PJ. Protein synthesis rates in colon and liver: stimulation by gastrointestinal pathologies. *Gut* 1992; **33**: 976-981
- 4 **Smith TK**, Gibson CL, Howlin BJ, Pratt JM. Active transport of amino acids by gamma-glutamyl transpeptidase through Caco-2 cell monolayers. *Biochem Biophys Res Commun* 1991; **178**: 1028-1035
- 5 **Johnstone RM**, Scholefield PG. Amino acid transport in tumor cells. *Adv Cancer Res* 1965; **9**: 143-226
- 6 **Norton JA**, Gorschboth CM, Wesley RA, Burt ME, Brennan MF. Fasting plasma amino acid levels in cancer patients. *Cancer* 1985; **56**: 1181-1186
- 7 **Liu HL**, Wang YB, Nie L. The amino acids difference between cancer and normal gastric tissue: a 22 cases study. *Acad J PLA Postgrad Med Sch* 2001; **22**: 105-108
- 8 **Zhang PC**, Pang CP. Plasma amino acid patterns in cancer. *Clin Chem* 1992; **38**: 1198-1199
- 9 **Tamemasa O**, Goto R, Takeda A, Maruo K. High uptake of 14C-labeled D-amino acids by various tumors. *Gann* 1982; **73**: 147-152
- 10 **Wang LB**, Zhang SZ, Ding KF, Zheng S. A study of the free amino acids uptake in colon cancer. *Zhejiang Yixue* 1997; **19**: 208-209
- 11 **Becker W**, Konstantinides F, Eyer S, Ward H, Fath J, Cerra F. Plasma amino acid clearance as an indicator of hepatic function and high-energy phosphate in hepatic ischemia. *Surgery* 1987; **102**: 777-783
- 12 **Sahai S**, Uhlhaas S. Stability of amino acids in human plasma. *Clin Chim Acta* 1985; **148**: 255-259
- 13 **Watanabe A**, Higashi T, Sakata T, Nagashima H. Serum amino acid levels in patients with hepatocellular carcinoma. *Cancer* 1984; **54**: 1875-1882
- 14 **Yang H**, Jiang J, Hu P. Metabolism of protein and amino acids during chronic renal failure. *Zhongguo Linchuang Yingyang Zazhi* 2001; **9**: 175-177
- 15 **Garibotto G**, Deferrari G, Robaudo C, Saffiotti S, Salvidio G, Paoletti E, Tizianello A. Effect of amino acid ingestion on blood amino acid profile in patients with chronic renal failure. *Am J Clin Nutr* 1987; **46**: 949-954
- 16 **Upton JD**, Hindmarsh P. More pitfalls in human plasma amino acid analysis. *Clin Chem* 1990; **36**: 157-158
- 17 **Rattenbury JM**, Townsend JC. Establishment of an external quality-assessment scheme for amino acid analyses: results from assays of samples distributed during two years. *Clin Chem* 1990; **36**: 217-224
- 18 **Smith SR**, Pozefsky T, Chhetri MK. Nitrogen and amino acid metabolism in adults with protein-calorie malnutrition. *Metabolism* 1974; **23**: 603-618
- 19 **Steiger E**, Oram-Smith J, Miller E, Kuo L, Vars HM. Effects of nutrition on tumor growth and tolerance to chemotherapy. *J Surg Res* 1975; **18**: 455-466
- 20 **Torosian MH**, Mullen JL, Stein TP, Miller EE, Zinsser KR, Buzby GP. Enhanced tumor response to cycle-specific chemotherapy by pulse total parenteral nutrition. *J Surg Res* 1985; **39**: 103-113
- 21 **Heys SD**, Park KG, McNurlan MA, Calder AG, Buchan V, Blessing K, Eremin O, Garlick PJ. Measurement of tumour protein synthesis *in vivo* in human colorectal and breast cancer and its variability in separate biopsies from the same tumour. *Clin Sci* 1991; **80**: 587-593
- 22 **Hagmuller E**, Kollmar HB, Gunther HJ, Holm E, Trede M. Protein metabolism in human colon carcinomas: *in vivo* investigations using a modified tracer technique with L-[1-13C] leucine. *Cancer Res* 1995; **55**: 1160-1167

- 23 **Cascino A**, Muscaritoli M, Cangiano C, Conversano L, Laviano A, Ariemma S, Meguid MM, Rossi Fanelli F. Plasma amino acid imbalance in patients with lung and breast cancer. *Anti-cancer Res* 1995; **15**: 507-510
- 24 **He YC**, Wang YH, Cao J, Chen JW, Pan DY, Zhou YK. Effect of complex amino acid imbalance on growth of tumor in tumor-bearing rats. *World J Gastroenterol* 2003; **9**: 2772-2775
- 25 **He YC**, Cao J, Chen JW, Pan DY, Zhou YK. Influence of methionine/valine-depleted enteral nutrition on nucleic acid and protein metabolism in tumor-bearing rats. *World J Gastroenterol* 2003; **9**: 771-774
- 26 **Waterhouse C**, Jeanpretre N, Keilson J. Gluconeogenesis from alanine in patients with progressive malignant disease. *Cancer Res* 1979; **39**(6 Pt 1): 1968-1972
- 27 **Kern KA**, Norton JA. Cancer cachexia. *J Parenter Enteral Nutr* 1988; **12**: 286-298
- 28 **Wang L**, Tong XQ, Li QR. The study on interrelation between colonic carcinoma tissue free amino acid and tumor volume. *Parenteral Enteral Nutrition* 2001; **8**: 221-223
- 29 **Wang L**, Li BY, Li QR. The study on interrelation between gastric cancer tissue free amino acid and tumor volume. *Parenteral Enteral Nutrition* 2000; **7**: 41-44
- 30 **Yamanaka H**, Kanemaki T, Tsuji M, Kise Y, Hatano T, Hioki K, Yamamoto M. Branched-chain amino acid-supplemented nutritional support after gastrectomy for gastric cancer with special reference to plasma amino acid profiles. *Nutrition* 1990; **6**: 241-245
- 31 **Nishizaki T**, Matsumata T, Taketomi A, Yamamoto K, Sugimachi K. Levels of amino acids in human hepatocellular carcinoma and adjacent liver tissue. *Nutr Cancer* 1995; **23**: 85-90
- 32 **Ye SL**, Tang ZY, Liu H, Zhao QC. The changes of amino acids concentration in hepatocellular carcinoma. *Zhonghua Yixue Zazhi* 1989; **69**: 319-320
- 33 **Goodlad GA**, Clark CM. Leucine metabolism in skeletal muscle of the tumour-bearing rat. *Eur J Cancer* 1980; **16**: 1153-1162

Edited by Wang XL and Zhang JZ **Proofread by** Xu FM

Construction of a metastasis-associated gene subtracted cDNA library of human colorectal carcinoma by suppression subtraction hybridization

Li Liang, Yan-Qing Ding, Xin Li, Guang-Zhi Yang, Jun Xiao, Li-Chun Lu, Jin-Hua Zhang

Li Liang, Yan-Qing Ding, Xin Li, Guang-Zhi Yang, Li-Chun Lu, Jin-Hua Zhang, Department of Pathology, the First Military Medical University, Guangzhou 510515, Guangdong Province, China
Jun Xiao, Department of Tropic Medicine, the First Military Medical University, Guangzhou 510515, Guangdong Province, China
Supported by the Military Medical Foundation of China, No. 01MA128

Correspondence to: Professor Yan-Qing Ding, Department of Pathology, the First Military Medical University, Guangzhou 510515, Guangdong Province, China. wjgd@public.bta.net.cn
Telephone: +86-20-61642148 **Fax:** +86-20-61642148
Received: 2002-08-26 **Accepted:** 2003-04-11

Abstract

AIM: To construct a differentially-expressed gene subtracted cDNA library from two colorectal carcinoma (CRC) cell lines with different metastatic phenotypes by suppression subtractive hybridization.

METHODS: Two cell lines of human CRC from the same patient were used. SW620 cell line showing highly metastatic potential was regarded as tester in the forward subtractive hybridization, while SW480 cell line with lowly metastatic potential was treated as tester in the reverse hybridization. Suppression subtractive hybridization (SSH) was employed to obtain cDNA fragments of differentially expressed genes for the metastasis of CRC. These fragments were ligated with T vectors, screened through the blue-white screening system to establish cDNA library.

RESULTS: After the blue-white screening, 235 white clones were picked out from the positive-going hybridization and 232 from the reverse. PCR results showed that 200-700 bp inserts were seen in 98% and 91% clones from the forward and reverse hybridizations, respectively.

CONCLUSIONS: A subtractive cDNA library of differentially expressed genes specific for metastasis of CRC can be constructed with SSH and T/A cloning techniques.

Liang L, Ding YQ, Li X, Yang GZ, Xiao J, Lu LC, Zhang JH. Construction of a metastasis-associated gene subtracted cDNA library of human colorectal carcinoma by suppression subtraction hybridization. *World J Gastroenterol* 2004; 10 (9): 1301-1305

<http://www.wjgnet.com/1007-9327/10/1301.asp>

INTRODUCTION

CRC is one of the most common malignant tumors in the world and its metastasis is the major cause of mortality in patients with colorectal carcinoma. More than hundreds of genes have been reported to be involved in the regulations of metastasis in colorectal carcinoma. However, they are still not sufficient for

fully explaining the complexity and diversity of metastasis. Besides, current investigations of these genes that mostly focused on the expression analysis of one or several genes make it difficult to understand the genes' interactions and find the new genes. Cloning and identification of metastasis-associated genes have been hypothesized to be beneficial to the elucidation of the molecular mechanisms underlying the metastasis and finding gene targets for metastatic forecast, therapy and prognosis of CRC patients. In our study, SSH and bacterial culture PCR screening were used to construct a differentially-expressed gene subtracted cDNA library specific for metastasis of human CRC with the hope to screen new metastasis associated genes.

MATERIALS AND METHODS

Cell lines

Highly metastatic cell line SW620 and lowly metastatic cell line SW480 from human colorectal carcinoma were purchased from ATCC with the number of CCL-227 and CCL-228 respectively. Both of the paired cell lines were from one colonic adenocarcinoma patient and had the same genetic backgrounds. Cell lines were routinely cultured with DMEM supplemented with 10% bovine serum under the atmosphere containing 50 mL/L CO₂ at 37 °C.

PCR primers and adaptors

cDNA synthesis primer (5' -TTTTGTACAAGCTT₃₀N₁N-3') was used for the first-strand cDNA synthesis. Adaptor1 (5' -CTAATACGACTCACTATAGGGCTCGAGCGGCCGCCGGG CAGGTACCTGCCCGG-3') and adaptor2R (5' -CTAATACGAC TCACTATAGGGCAGCGTGGTTCGCGGCCGAGGTACCTCGGC CG-3') have the same sequence of the 5' region and the different palindromic structures in the 3' end. Only the differentially expressed fragments digested by RsaI restriction enzyme could be ligated with two adaptors. Primary PCR was performed to amplify these fragments with primer1 (5' -CTAATACGACTCAC TATAGGGC-3') that corresponds to the outer common sequence of the adaptors. After that, nested primer1 (5' -TCGAGCGGCC GCCCGGCCAGGT-3') and nested primer2R (5' -AGCGTGG TCGCGGCCGAGGT-3') designed from the inner sequences of the adaptors respectively were used for the further enrichment of these fragments in secondary PCR. The underlines in the sequences indicated the sites of RsaI restriction enzyme. The above primers and adaptors were provided by PCR-Select™ cDNA Subtraction Kit (Clontech Laboratories Inc, USA).

mRNA isolation

Total mRNA was isolated from the two cell lines respectively using QuickPrep micro mRNA purification kit (Pharmacia, USA) following the recommendations of the manufacturer.

Suppression subtractive hybridization

SSH was performed by using PCR-Select™ cDNA subtraction kit (Clontech Laboratories Inc, USA) according to the

recommendations of the manufacturer. The highly metastatic cell line SW620 was used as the tester while the lowly metastatic cell line SW480 was used as the driver in the forward hybridization, and vice versa in the reverse hybridization.

Double strand cDNA synthesis

A total of 2 μg (4 μL) mRNA with 1 μL oligo (dT₃₀) primer was heated to 70 °C for 2 min and rapidly cooled on ice. The reaction mixture was made up to 10 μL by adding 1 μL cDNA synthesis primer (10 $\mu\text{mol/L}$), 2 μL 5 \times the first strand reaction buffer, 1 μL dNTP mix (10 mmol/L each) and 1 μL sterile H₂O. Reverse transcription was started by adding 1 μL AMV reverse transcriptase (20 U/ μL). The reaction mixture was incubated at 42 °C for 1.5 h to synthesize the first strand cDNA. The second strand cDNA synthesis was performed by immediately adding 48.4 μL sterile H₂O, 16 μL 5 \times the second strand buffer, 1.6 μL dNTP mix, 4 μL 20 \times the second strand enzyme cocktail. The reaction mixture was incubated at 16 °C for 2 h. Double strand cDNA was blunted by adding of 2 μL T4 DNA polymerase and incubated at 16 °C for 20 min. The reaction was stopped by adding 20 \times EDTA/glycogen mix into the reactive mixture. cDNAs were then extracted, precipitated, and resuspended in 50 μL of deionized water.

Ligation of cDNA fragments

For the ligation of cDNA fragments, 43.5 μL of ds cDNA from the tester and driver was digested respectively with 1.5 μL of RsaI (10 U/ μL) at 37 °C for 1.5 h. The reaction was terminated by adding 20 \times EDTA/glycogen mix. The resulting fragments of cDNAs were extracted, precipitated and finally resuspended in 5.5 μL of deionized water. Adaptor 1 and adaptor 2R were ligated separately to 2 μL of RsaI digested tester cDNA with 1:6 dilution in the presence of T4 DNA ligase at 16 °C overnight followed by heating at 70 °C for 5 min to inactivate the ligase. In order to determine whether the ligation efficiency was high or not, 1 μL of adaptor 1-ligated and adaptor 2R-ligated cDNAs of the tester was diluted into 200 μL H₂O respectively and amplified in two separate 50 μL reactions. One reaction used G3PDH3' , 5' primer, while the other used G3PDH3' primer and PCR primer 1. PCR parameters were as follows: 30 cycles at 94 °C for 30 s, at 65 °C for 30 s and at 68 °C for 2.5 min. The products were examined by electrophoresis on a 20 g/L agarose/EB gel.

Two subtractive hybridizations

In the first hybridization, 1.5 μL of RsaI digested driver cDNA was mixed with 1.5 μL of diluted adaptor 1- or adaptor 2R-ligated tester cDNA. The samples were denatured at 98 °C for 1.5 min and immediately incubated in a thermal cycler at 68 °C for 8 h. In the second hybridization, two kinds of sample resulting from the first hybridization were mixed in the presence of a freshly denatured driver cDNA. The samples were incubated at 68 °C for 18 h. After 200 μL of dilution buffer was added, the samples were incubated for an additional 7 min. Analysis of the subtraction efficiency was carried out using PCR amplification of G3PDH in diluted subtracted cDNA versus unsubtracted cDNA. PCR was performed for 33 cycles at 94 °C for 30 s, at 60 °C for 30 s and at 68 °C for 2 min. The products were monitored on a 20 g/L agarose/EB gel for an aliquot which was removed from each reaction after 18, 23, 28, 33 cycles.

Two suppression PCRs (nested PCR)

A 1 μL of diluted subtraction mixture was amplified with PCR primer 1 in the primary PCR. The reaction mixture was incubated at 75 °C for 5 min to extend the adaptors and followed in turn at 94 °C for 25 s, 30 cycles at 94 °C for 10 s, at 64 °C for 30 s and at 71 °C for 1.5 min. The primary PCR mixture was diluted 10-fold and 1 μL from that was used in secondary PCR with nested

PCR primer 1 and primer 2R. The conditions of the reaction were 15 cycles at 94 °C for 10 s, at 68 °C for 30 s and at 72 °C for 1.5 min. Eight μL products from each PCR reaction of the secondary PCR was analyzed on a 20 g/L agarose/EB gel.

Screening for subtraction library

The second PCR products were purified and their concentrations were measured by a spectrophotometer. The T/A cloning method was performed by using pGEM-T vector system I (Promega, USA) according to the recommendations of the manufacturer. The PCR product was cloned into the vector with a molar ratio of 6:1 (insert: vector). A 2 μL purified PCR products (25 ng/ μL) was used in a 10 μL -ligation-reaction system including 5 μL 2 \times Rapid ligation buffer, 1 μL pGEM-T Easy Vector (50 ng/ μL), 1 μL T4 DNA ligase (3 Weiss units/ μL) and 1 μL deionized water. The mixture was incubated at 4 °C overnight. The positive control was made by using the control insert DNA from the kit instead of the PCR products. The background control was made without inserting any fragments. The recombinant plasmids were transformed respectively into the competent JM109 E-coli cell with the CaCl₂ method. A 100 μL of transformants was grown on 8 cm \times 8 cm agar plates containing 100 $\mu\text{g/mL}$ ampicillin, 100 $\mu\text{mol/L}$ IPTG and 100 $\mu\text{g/mL}$ X-gal at 37 °C for 20 h when the blue/white staining could be clearly distinguished. White clones were counted, inoculated into 3 mL of LB liquid medium containing ampicillin and shaken overnight at 37 °C. The resulting bacterial culture was directly used as PCR templates to amplify the inserts in 50 μL reaction mixture containing 10 \times PCR buffer 5.0 μL , Mg²⁺ (25 mmol/L) 3 μL , nested primer 1 (20 $\mu\text{mol/L}$) 1 μL , nested primer 2R (20 $\mu\text{mol/L}$) 1 μL , dNTP mix (10 mmol/L) 1 μL , Taq enzyme mix (5 U/ μL) 0.5 μL and bacterial culture 0.5 μL . PCR consisted of an initial denaturation step at 94 °C for 5 min, followed by 25 cycles at 94 °C for 30 s, at 68 °C for 30 s and at 72 °C for 2 min each. The PCR products were analyzed on an 10 g/L agarose/EB gel.

RESULTS

Quality identification of extracted mRNA

The extracted mRNA that was electrophoresed on 10 g/L agarose gel exhibited as a clear smear with over 0.5 kb length (Figure 1). Their absorbances ($A_{260}/A_{280} > 1.8$) in spectrophotometry suggested that extracted mRNAs were in a highly purified quality.



Figure 1 Quality identification of mRNA extracted from two cell lines, Lane 1: SW480 cell line, Lane 2: SW620 cell line.

RsaI digestion analysis of synthesized cDNA

The results of 10 g/L agarose electrophoresis showed that cDNA before digested with RsaI, displayed a zonal smear with a length from 0.5 kb to 10 kb. After the digestion, the cDNA length became shorter with fragments from 0.1 kb to 2 kb, suggesting that cDNAs were completely digested (Figure 2).

Analysis of ligation efficiency

The high ligation efficiency was the most important factor for

success of SSH. Figure 3 shows that the intensity of band 2/ band1, band4/ band3 was over 80%, indicating that subtracted cDNA library had the high ligation efficiency, 80% of the tester' ds cDNA fragments were ligated with adaptors1 or 2R.

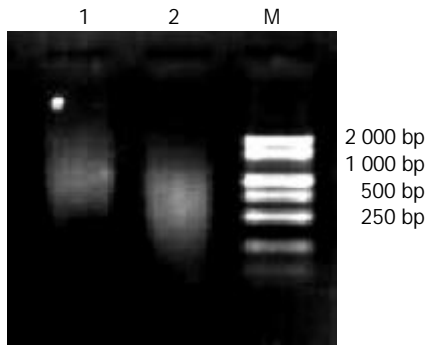


Figure 2 RsaI digestion analysis of synthesized cDNA, Lane 1: Synthesized cDNA digested with RsaI, Lane 2: Synthesized cDNA, Lane M: Marker DGL2000.

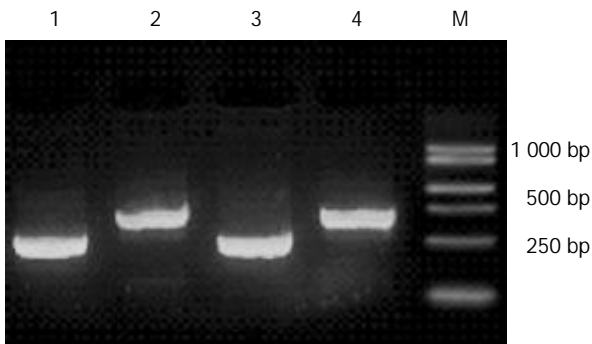


Figure 3 Ligation efficiency analysis of ds cDNA, Lane 1: PCR products using tester1-1 (adaptor1-ligated-cDNA fragment) as the template and the G3PDH3', 5' primer; Lane 2: PCR products using tester1-1 as the template and the G3PDH3' primer, PCR primer1; Lane 3: PCR products using tester1-2 (adaptor2R-ligated-cDNA fragments) as the template and the G3PDH3', 5' primer; Lane 4: PCR products using tester1-2 as the template and the G3PDH3' primer, PCR primer1; Lane M: Marker DGL2000.

Analysis of secondary PCR products

Nested primers from the inner sequences of adaptors were used to amplify the primary PCR products, and the smear was increased obviously after 15 cycles, in which some obscure bands with the lengths between 0.2 and 1.5 kb were observed (Figure 4).

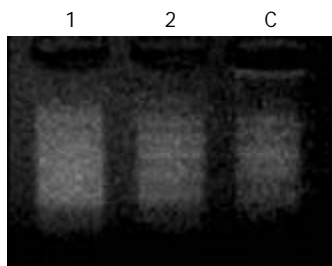


Figure 4 Electrophoresis of secondary PCR products, Lane C: Positive control cDNA supplied with the kit, Lane 1: Unsubtracted cDNA, Lane 2: Subtracted cDNA.

Subtractive efficiency

Figure 5 shows that obvious bands were seen after 23 cycles in

unsubtracted cDNA and after 33 cycles in diluted subtracted cDNA. The amount of G3PDH was significantly decreased after subtraction, indicating that the subtracted cDNA library had the high subtraction efficiency.

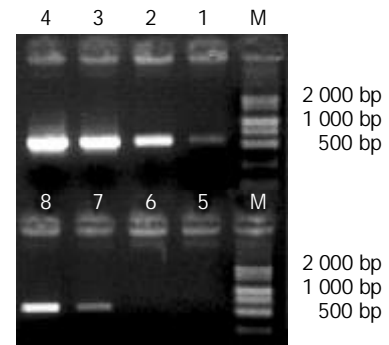


Figure 5 Reduction of G3PDH by PCR subtraction, Lanes 1-4: Unsubtracted secondary PCR products, Lanes 5-8: Subtracted secondary PCR products, Lanes 1, 5: 18 cycles Lane 2, 6: 23 cycles, Lanes 3, 7: 28 cycles, Lane 4, 8: 33 cycles, Lane M: Marker DGL2000.

Screening for subtraction cDNA library

On the agar plates with 100 μ L of transformants, 235 white clones were obtained in the forward hybridization (group A) while 232 white clones were obtained in the reverse hybridization (group R) (Figure 6). White clones accounted for more than 80% of the total clones. Ninety-eight percent and 91% of the white clones were demonstrated by PCR having the inserts with a length of 200-700 bp in groups A and R, respectively (Figure 7), indicating that a subtracted cDNA library specific for metastasis in CRC was successfully constructed.

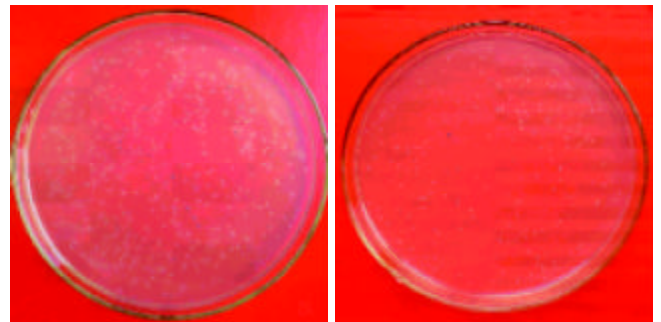


Figure 6 Blue/white screening for target clones, Two hundred and thirty-five white clones (86%) and 37 blue clones were seen on the agar plates in group A, and 232 white clones (91%) and 21 blue clones were seen in group R.

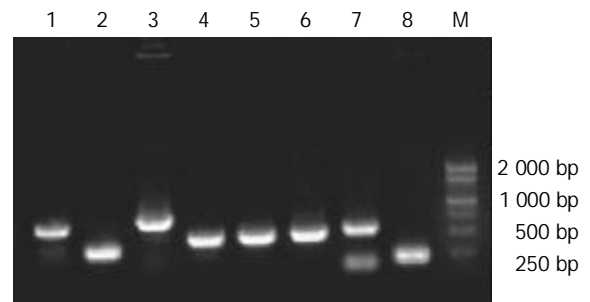


Figure 7 Different lengths of cDNA fragments from white clones amplified by PCR, Lanes 1-8: Randomly-selected white clones, Lane M: Marker DGL2000.

DISCUSSION

Metastasis is the major cause of mortality in CRC patients. The molecular basis for metastasis has not been fully elucidated yet. Available studies have shown that many specific genes are involved in the process of metastasis, which may accelerate or suppress metastasis by a mechanism of cooperative or inhibitive interactions between genes^[1]. Till now hundreds of genes have been reported to be involved in the regulation of metastasis in colorectal carcinoma. However, the existent methods for investigating the molecular mechanism of metastasis are mostly limited to the analysis of expressions of only one or several genes, which makes it difficult to understand the genes' interactions and their relations to the metastasis.

One of the most important ways to understand the carcinogenesis and development of tumors is to clone and identify the differentially expressed genes. In recent years several cloning techniques for the differentially expressed genes have been established, including differential display PCR (DD-PCR), representational difference analysis (RDA), SSH and cDNA microarray. Until now, these techniques have been widely applied in the study of pathology^[2], immune^[3], embryo development^[4], as well as the specific expression of tissue protein^[5]. Although it is rapid, easy to perform and sensitive, DD-PCR has also some limitations, such as the higher false positive rate and the truncated length of obtained specific cDNA that is usually located in non-translated regions of 3' poly(A). Likewise, RDA needs less amount of mRNAs samples and has lower false positive rate. But it is troublesome to perform more complicated steps of hybridization or PCR. Microarray-based methods have the potentials to revolutionize the study of differential gene expression under parallel conditions with higher automation. While a number of drawbacks of this approach have been found such as the higher expense and less sensitive than that of PCR-based techniques.

SSH was first put forward by Diatchenko *et al.* in 1996. The basic principle was that common cDNAs in the paired materials were subtracted by subtractive hybridization and then suppressive PCR was carried out to amplify cDNA fragments specially expressed in tester. The advantage of SSH was the design of two different adaptors and the introduction of suppression PCR with the result that the differentially expressed cDNA fragments were amplified. It allows two subtractive hybridizations in the forward or reverse direction. Some mRNA expressed with low abundance could be detected, which provided clues for the further gene sequencing and identification^[6-9]. With the development and improvement of SSH technique, it has become one of the most effective techniques for cloning differentially expressed genes. Since it was established, more than two hundred papers have been published concerning about carcinogenesis^[10], tumor metastasis^[11], signal transduction^[12], apoptosis^[13] and tumor therapy^[14]. Combined with other molecular biological techniques such as DNA chip, it could clone tumor associated genes^[15] and metastasis-associated genes in lung carcinoma, breast carcinoma and other malignancies^[16-20]. Zhang *et al.*^[21] carried out SSH in human NCI-H69 cell line and its variant, a more aggressive NCI-N417 SCLC cell line, to characterize the variable expression of genes between the two cell lines, in which 42 genes were screened by the forward and reverse hybridizations. Wang *et al.*^[22] have identified five cDNA fragments with SSH that were expressed at much higher levels in the poorly metastatic cancer cell clone than in the highly metastatic variety. Until now studies on separating metastasis-associated genes in human CRC have not been reported.

In our study, SSH and bacterial culture PCR were performed to construct a subtracted cDNA library specific for the metastasis-related genes of human CRC, in which a pair of

human colorectal carcinoma cell lines SW620 and SW480 was used. The SW480 cell line was derived from a Dukes' stage B colon carcinoma that arose in a 50-year-old male patient with liver and mesenteric lymph node metastases. The SW620 cell line was derived from one of the lymph node metastases. The monoclonal origin of the two cell lines that was confirmed by the presence of shared marker chromosomes on cytogenetic analysis makes it suitable to study the genetic basis of their phenotypic differences. Hewitt *et al.*^[23] have also found that the phenotypic differences of both SW620 and SW480 cell lines were retained, despite long-term culture *in vitro*.

Both the forward and reverse hybridizations were performed in this study. In the forward hybridization (group A), the highly metastatic cell line SW620 was treated as the tester, while the lowly metastatic cell line SW480 was treated as the driver in the reverse hybridization (group R). As a result, the total cDNAs in the tester and driver were subtracted efficiently. cDNA fragments appearing only in SW620 cells were amplified specially in group A and those only in SW480 cells were amplified in group R. After that, the second PCR products were inserted into T vectors and then screened by the blue/white screening system. Two hundred and thirty-five or 232 white clones were obtained in group A or group R respectively. The resultant subtractive cDNA library that was rich in metastasis-associated gene fragments of CRC was superior to that obtained by other methods for 4 reasons: (1) High specificity. Two subtractive hybridizations and two suppressive PCR were carried out to amplify the differentially expressed cDNA fragments, and suppress the amplification of unspecific cDNA fragments. Thus, the specificity of the subtractive library was greatly increased. (2) High sensitivity. The normalization of tester ss cDNA by SSH could make the differentially expressed genes with high or low abundance separated efficiently. (3) High efficiency. One SSH reaction could separate hundreds and thousands differentially expressed genes simultaneously. (4) More information. The differentially expressed fragments in the forward hybridization might have a role in accelerating metastasis, and those in the reverse hybridization might be metastasis suppressor genes. The forward and reverse hybridizations could provide more information of the screening results.

However, the subtracted cDNA library constructed by SSH had some limitations. One of them was the requirement of large quantities of mRNA samples. The other was that differentially expressed cDNAs obtained from SSH were cDNA fragments digested by restrictive enzyme and needed to be amplified to get the full length. These drawbacks could be overcome by other methods such as the multi-cycle linear amplification based on cDNA synthesis and template-guided *in vitro* transcription, in which enough mRNA for the continual research could be amplified with less than 1-50 ng RNA samples^[24]. Thus, it is especially suitable for tissues that are hard to get or too little to provide enough RNAs. In addition, the full length of differential fragments could be obtained by the rapid amplification of cDNA ends (RACE)^[25].

After the blue/white screening, bacterial culture PCR was used in the present study to screen the positive recombinants. Compared with the routine methods, bacterial culture PCR was not only simple but also helpful for the further identifications. Our results showed that there were 98% clones with 200-700 bp inserts in group A and 91% positive clones of recombinants in group R, suggesting that these clones may contain metastasis-related cDNA fragments. The construction of this library is therefore of significance in screening and identifying the genes associated with metastasis of CRC, which would be beneficial to the elucidation of the molecular mechanism of metastasis and provide new gene targets for metastasis forecast, gene therapy and prognosis estimation in clinical practice.

REFERENCES

- 1 **Welch DR**, Rinker-Schaeffer CW. What defines a useful marker of metastasis in human cancer? *J Natl Cancer Inst* 1999; **91**: 1351-1353
- 2 **Sharma R**, Samantaray S, Shukla NK, Ralhan R. Transcriptional gene expression profile of human esophageal squamous cell carcinoma. *Genomics* 2003; **81**: 481-488
- 3 **Dunphy JL**, Balic A, Barcham GJ, Horvath AJ, Nash AD, Meeusen EN. Isolation and characterization of a novel inducible mammalian galectin. *J Biol Chem* 2000; **275**: 32106-32113
- 4 **Li P**, Li JL, Hou R, Han QD, Zhang YY. Changes in the gene expression profile of the left heart ventricle during growth in the rat. *Shengli Xuebao* 2003; **55**: 191-196
- 5 **Ito H**, Akiyama H, Iguchi H, Iyama K, Miyamoto M, Ohsawa K, Nakamura T. Molecular cloning and biological activity of a novel lysyl oxidase-related gene expressed in cartilage. *J Biol Chem* 2001; **276**: 24023-24029
- 6 **Sandhu H**, Dehnen W, Roller M, Abel J, Unfried K. mRNA expression patterns in different stages of asbestos-induced carcinogenesis in rats. *Carcinogenesis* 2000; **21**: 1023-1029
- 7 **Zhu NX**, Zheng S, Xu RZ, Gao RL, Shen JP, Yu RX. Identification of multidrug resistance related genes in leukemia by suppression subtractive hybridization. *Zhonghua Yexue Zazhi* 2003; **24**: 14-17
- 8 **Ai JK**, Huang X, Wang YJ, Bai Y, Lu YQ, Ye XJ, Xin DQ, Na YQ, Zhang ZW, Guo YL. Screening of novel genes differentially expressed in human renal cell carcinoma by suppression subtractive hybridization. *Aizheng* 2002; **21**: 1065-1069
- 9 **Shen C**, Hui-Zhao, Wang D, Jiang G, Wang J, Zhang G. Molecular cloning, identification and analysis of lung squamous cell carcinoma-related genes. *Lung Cancer* 2002; **38**: 235-241
- 10 **Hufton SE**, Moerkerk PT, Brandwijk R, de Bruine AP, Arends JW, Hoogenboom HR. A profile of differentially expressed genes in primary colorectal cancer using suppression subtractive hybridization. *FEBS Lett* 1999; **463**: 77-82
- 11 **Asai T**, Tomita Y, Nakatsuka S, Hoshida Y, Myoui A, Yoshikawa H, Aozasa K. VCP (p97) regulates NFkappaB signaling pathway, which is important for metastasis of osteosarcoma cell line. *Jpn J Cancer Res* 2002; **93**: 296-304
- 12 **Kostic C**, Shaw PH. Isolation and characterization of sixteen novel p53 response genes. *Oncogene* 2000; **19**: 3978-3987
- 13 **Sakamoto H**, Mashima T, Kizaki A, Dan S, Hashimoto Y, Naito M, Tsuruo T. Glyoxalase I is involved in resistance of human leukemia cells to antitumor agent-induced apoptosis. *Blood* 2000; **95**: 3214-3218
- 14 **Zhang Z**, DuBois RN. Detection of differentially expressed genes in human colon carcinoma cells treated with a selective COX-2 inhibitor. *Oncogene* 2001; **20**: 4450-4456
- 15 **Schlingemann J**, Hess J, Wrobel G, Breitenbach U, Gebhardt C, Steinlein P, Kramer H, Furstenberger G, Hahn M, Angel P, Lichter P. Profile of gene expression induced by the tumour promoter TPA in murine epithelial cells. *Int J Cancer* 2003; **104**: 699-708
- 16 **Yin J**, Fan Q, Hao X, Fan D. Identification of genes associated with human osteosarcoma metastasis suppression using suppression subtractive hybridization. *Zhonghua Yixue Yichuanxue Zazhi* 2002; **19**: 213-217
- 17 **Yin JN**, Fan QY, Hao XB, Yang N. Apoptosis antagonizing transcription factor is a gene highly expressed in highly metastatic human osteosarcoma cell lines. *Aizheng* 2002; **21**: 127-131
- 18 **Koo TH**, Lee JJ, Kim EM, Kim KW, Kim HD, Lee JH. Syntenin is overexpressed and promotes cell migration in metastatic human breast and gastric cancer cell lines. *Oncogene* 2002; **21**: 4080-4088
- 19 **Goldberg SF**, Miele ME, Hatta N, Takata M, Paquette-Straub C, Freedman LP, Welch DR. Melanoma metastasis suppression by chromosome 6: evidence for a pathway regulated by CRSP3 and TXNIP. *Cancer Res* 2003; **63**: 432-440
- 20 **Devoogdt N**, Hassanzadeh Ghassabeh G, Zhang J, Brys L, De Baetselier P, Revets H. Secretory leukocyte protease inhibitor promotes the tumorigenic and metastatic potential of cancer cells. *Proc Natl Acad Sci U S A* 2003; **100**: 5778-5782
- 21 **Zhang L**, Cilley RE, Chinoy MR. Suppression subtractive hybridization to identify gene expressions in variant and classic small cell lung cancer cell lines. *J Surg Res* 2000; **93**: 108-119
- 22 **Wang T**, Lu Y, Liu S. Suppression subtractive hybridization in the cloning of gene fragments in relation to lung cancer metastasis. *Zhonghua Zhongliu Zazhi* 2001; **23**: 296-300
- 23 **Hewitt RE**, McMarlin A, Kleiner D, Wersto R, Martin P, Tsokos M, Stamp GW, Stetler-Stevenson WG, Tsoskas M. Validation of a model of colon cancer progression. *J Pathol* 2000; **192**: 446-454
- 24 **Wang E**, Miller LD, Ohnmacht GA, Liu ET, Marincola FM. High-fidelity mRNA amplification for gene profiling. *Nat Biotechnol* 2000; **18**: 457-459
- 25 **Xu CS**, Li YC, Lin JT, Zhang HY, Zhang YH. Cloning and analyzing the up-regulated expression of transthyretin-related gene (LR1) in rat liver regeneration following short interval successive partial hepatectomy. *World J Gastroenterol* 2003; **9**: 148-151

Edited by Wang XL and Zhu L Proofread by Xu FM

Helicobacter pylori L-form and patients with chronic gastritis

Ke-Xia Wang, Lin Chen

Ke-Xia Wang, Lin Chen, School of Medicine, Anhui University of Science & Technology Huainan 232001, Anhui Province, China
Supported by The Education Department of Anhui Province, China No.2003kj111

Correspondence to: Dr. Ke-Xia Wang, School of Medicine, Anhui University of Science & Technology, Huainan, 232001, Anhui Province, China. kexiawang2003@yahoo.com.cn

Telephone: +86-554-6658770 **Fax:** +86-554-6662469

Received: 2003-10-20 **Accepted:** 2003-12-08

Abstract

AIM: To study the relationship between infection with *Helicobacter pylori* L-forms and chronic gastritis and its association with possible changes of cellular immune function.

METHODS: Gastric mucosal biopsies were taken from 428 patients with chronic gastritis to detect *H pylori* L-form by Gram staining and immunohistochemistry staining. Peripheral venous blood samples of patients were taken to detect the percentage of CD3+, CD4+ and CD8+ by the biotin-streptavidin (BSA) assay and the levels of IL-2, IL-6 and IL-8 by ELISA.

RESULTS: The rate of infection with *H pylori* L-forms was 48.83% (209/428). The rate was 50.47% (216/428) and 52.80% (226/428), respectively, as detected by immunohistochemistry staining and Gram staining ($P>0.05$). The rate of *H pylori* L-forms in males and females was 57.8% (136/235) and 37.28% (73/193), respectively, ($\chi^2=17.05$, $P<0.01$). Furthermore, the rate increased with age, with the rate being significantly greater in patients ≥ 40 years old than in those <40 years old ($P<0.01$). The percentage of CD3+, CD4+, CD8+, the ratio of CD4+ / CD8+, and the levels of IL-2, IL-6, IL-8 in *H pylori*-positive patients were 47.58 \pm 4.44%, 25.51 \pm 4.74%, 22.77 \pm 7.46%, 1.44 \pm 0.51%, 1.56 \pm 0.47 mg/L, 103.62 \pm 5.85 ng/L, and 109.79 \pm 7.18 ng/L, respectively. Compared with *H pylori*-negative patients, the percentage of CD3+, CD4+ and the ratio of CD4+ / CD8+ and the IL-2 level decreased, but the levels of IL-6, IL-8 increased ($P<0.001$ - $P<0.01$). Moreover, the percentage of CD3+, CD4+, CD8+, the ratio of CD4+ / CD8+, and the levels of IL-2, IL-6 and IL-8 in patients infected with both *H pylori* L-forms and vegetative forms were 46.67 \pm 5.21%, 30.75 \pm 4.89%, 22.15 \pm 6.45%, 1.32 \pm 0.47%, 1.16 \pm 0.38 mg/L, 116.45 \pm 5.44 ng/L, and 118.64 \pm 6.24 ng/L, respectively. Compared with patients infected with only vegetative forms, the percentage of CD4+, the ratio of CD4+ / CD8+ and IL-2 level decreased, but the levels of IL-6 and IL-8 increased ($P<0.001$ or $P<0.01$).

CONCLUSION: L-form variation often occurs in patients with chronic gastritis and is commonly found in male patients and associates with ages. The L-form variation may be an important factor causing disorder of cellular immune function in the patients with *H pylori*-induced chronic gastritis.

Wang KX, Chen L. *Helicobacter pylori* L-form and patients

with chronic gastritis. *World J Gastroenterol* 2004; 10(9): 1306-1309

<http://www.wjgnet.com/1007-9327/10/1306.asp>

INTRODUCTION

Helicobacter pylori infection of the gastric mucosa can be found in approximately 50% of the world's population, and is associated with a range of pathologies, including chronic gastritis, peptic ulcer, atrophic gastritis, and gastric cancer^[1-6]. Infection of *H pylori* is life-long that elicits a marked host inflammatory response^[7-9]. However, natural infection fails to yield protective immunity^[10,11]. *H pylori* is a gram-negative, spiral and microaerophilic bacterium that colonizes the gastric epithelium of humans^[12-15]. Under some hostile conditions, *H pylori* changes from vegetative forms into L-forms by which *H pylori* can escape the body's immune response and live in the body for a long time. Once conditions return to normal *H pylori* reverts into vegetative forms, which further deteriorates the pathological changes. Therefore, *H pylori* L-forms appear to be more pathogenic and virulent than vegetative forms^[16-18]. Animal experiments and clinical studies have demonstrated that damages induced by *H pylori* are associated with Th1 cell-mediated immune response^[19-23]. The aim of this study was to confirm the occurrence of L-forms variation of *H pylori* vegetative forms, and to determine the relationship between *H pylori* L-form infection and chronic gastritis, and its association with possible changes of cellular immune function in the patients. In the study, gastric mucosal biopsies were taken from 428 patients with chronic gastritis to detect *H pylori* L-form by Gram staining and immunohistochemistry staining, and T lymphocyte subsets and serum levels of IL-2, IL-6 and IL-8 of patients were also detected.

MATERIALS AND METHODS

Patients

A total of 428 patients (aged from 14 to 67 years, 235 males and 193 females) with chronic gastritis diagnosed in our affiliated hospital from September 2000 to December 2002 were included in this study. Patients with other diseases were excluded.

Reagents

Gram staining and immunohistochemistry staining were used in this study. The biotin-streptavidin (BSA) reagents for T lymphocyte subset classification were provided by Jin' an Medical Laboratory Institute in Shanghai. Separating medium for lymphocyte was supplied by The Second Biochemical Reagent Factory in Shanghai (batch No.011215), and the test kits for IL-2 (batch No.1002-21), IL-6 (batch No.1006-32) and IL-8 (batch No.1008-25), were offered by Besancon Company (France).

Detection of *H pylori* L-forms

Biopsies of gastric antrum and gastric corpus were taken from 428 patients during upper endoscopy, fixed in 40 g/L formaldehyde, then embedded in paraffin and cut into section in 4 μ m thickness. The sections were used for Gram staining and immunohistochemistry staining separately. Gram stained slide was observed under oil lens (10 \times 100), and a total of 10-15

fields were randomly counted for *H pylori* L-forms. We regarded it as positive only when the average number was greater than 20. The antigen and antibody used in immunohistochemistry staining for *H pylori* L-forms were made in our laboratory, and the concentration of first antibody is 1:80. Other steps were performed according to the instruction of manufacturer (Dako company), using the known positive slide as a positive control and using PBS instead of first antibody as a negative control. A specimen was defined to be infected with *H pylori* L-forms when both staining methods produced a positive result.

Detection of cellular immune function

To investigate the possible changes of cellular immune function in *H pylori*-infected individuals, including the patients infected by *H pylori* L-forms and vegetative forms, the percentage of CD3+, CD4+, CD8+, ratio of CD4+/CD8+, and the levels of IL-2, IL-6, IL-8 in peripheral blood of *H pylori*-positive individuals were tested with the biotin-streptavidin (BSA) method. The peripheral venous blood of the subjects was taken, anticoagulated with heparin, and diluted with a solution free of Ca²⁺, Mg²⁺. Then, peripheral blood mononuclear cells were separated with lymphocytes separating medium and cleaned, and the number of cells was adjusted to (1-3)×10⁹/L of which 10 μL was taken and smeared in an acidproof varnish circle on the surface of a slide. When it dried naturally, McAb of anti-CD3+, anti-CD4+ and anti-CD8+, and sheep anti-guinea pig IgG, and SA-HRP. Cells were regarded as positive when the membrane was stained in brown color. A total of 200 cells were counted, and the positive percentages of cells were calculated. In addition, the serum levels of IL-2, IL-6 and IL-8 were detected by ELISA following the procedures detailed in the product instructions.

Statistical analysis

Data were expressed as mean±SD. Multiple comparison tests were performed with the χ^2 test and *t*-test.

RESULTS

Examination of *H pylori* L-forms with gram staining

Of the 428 patients studied, 226 (52.80%) were positive for both *H pylori* vegetative forms and L-forms, and other 17 (3.97%) were positive for vegetative forms only by Gram staining. The morphology of *H pylori* L-forms was highly variable, such as spheroid, coccoid form, big body, elementary body, long filament body, as seen on the smears under microscope.

Comparison between gram staining and immunohistochemistry staining

H pylori L-forms was detected in 216 (50.47%) patients by immunohistochemistry staining, of whom 209 (48.83%) were also detected *H pylori* L-forms by Gram staining. There was no significant difference in detection rate of *H pylori* L-forms between the 2 methods ($P>0.05$) (Table 1).

Relationship between infection of *H pylori* L-forms and gender as well as age of patients with chronic gastritis

H pylori L-forms were present in 57.87% (136/235) of males and 37.82% (73/193) of females ($\chi^2=17.05, P<0.01$). Furthermore, the rate of *H pylori* L-forms was significant difference between patients <40 years old and those ≥ 40 years old ($P<0.01$) (Table 2).

Detection of cellular immune function

The percentages of CD3+, CD4+ and the ratio of CD4+/CD8+ and IL-2 decreased, but the levels of IL-6 and IL-8 increased in *H pylori*-positive patients, compared with *H pylori*-negative patients, (Tables 3 and 4). In addition, the percentage of CD4+, the ratio of CD4+/CD8+ and the levels of IL-2 decreased, but

the levels of IL-6 and IL-8 increased in the patients infected by both L-forms and vegetative forms of *H pylori*, compared with those only infected by vegetative forms (Tables 3, 4).

Table 1 Comparison of Gram staining and immunohistochemistry staining in detection of *H pylori* L-forms

Gram staining (n)	Immunohistochemistry staining (n)		Total (n)
	Positive	Negative	
Positive	209	17	226
Negative	7	195	202
Total	216	212	428

$\chi^2=0.46779, P>0.05$ between the 2 methods.

Table 2 Relationship of infection of *H pylori* L-forms with gender and age of patients with chronic gastritis

Age(yr)	n	Male		Female		Total	
		n	Detection rate (%)	n	Detection rate (%)	n	Detection rate (%)
14-	62	31 (50.00)		75	17 (22.67)	137	48 (35.04) ^b
30-	37	14 (37.84)		48	18 (37.50)	85	32 (37.65) ^b
40-	55	35 (63.64)		23	12 (52.17)	78	47 (60.26) ^b
50-	81	56 (69.14)		47	26 (55.32)	128	82 (64.06) ^b
Total	235	136 (57.87) ^d		193	73 (37.82) ^d	428	209 (48.83)

^d $\chi^2=17.05, P<0.01$; ^b $\chi^2=33.74, P<0.01$.

Table 3 Detection of T lymphocyte subsets in patients with chronic gastritis in relation to infection with *H pylori* (Hp) and its L-forms

Group	n	CD3+ (%)	CD4+ (%)	CD8+ (%)	CD4+/CD8+
Hp (-)	202	60.72±8.38 ^b	36.33±3.68 ^d	25.83±6.93	1.55±0.34 ^j
Hp (+)	226	47.58±4.44 ^b	25.51±4.74 ^d	22.77±7.46	1.44±0.51 ^j
Hp-L (-)	17	50.81±6.20	33.74±5.34 ^f	25.04±10.48	1.68±0.58 ^h
Hp-L (+)	209	46.67±5.21	30.75±4.89 ^f	22.15±6.45	1.32±0.47 ^h
Total	428	52.20±6.21	34.31±4.18	23.49±6.86	1.16±0.466

^b $P<0.001, t=20.61$; ^d $P<0.001, t=26.21$; ^j $P<0.001, t=4.36$; ^f $P<0.001, t=7.78$; ^h $P<0.01, t=2.99$.

Table 4 Detection of serum IL-2, IL-6 and IL-8 in patients with chronic gastritis in relation to infection with *H pylori* (Hp) and its L-forms

Group	n	IL-2 (mg/L)	IL-6 (ng/L)	IL-8 (ng/L)
Hp (-)	202	6.14±0.65 ^b	36.82±3.15 ^d	48.35±3.63 ^f
Hp (+)	226	1.56±0.47 ^b	103.62±5.85 ^d	109.79±7.18 ^f
Hp-L (-)	17	3.39±0.57 ^h	63.35±6.51 ^j	82.33±8.45 ^j
Hp-L (+)	209	1.16±0.38 ^h	116.45±5.44 ^j	118.64±6.24 ^j
Total	428	3.27±0.52	81.83±4.73	87.53±5.68

^b $P<0.001, t=83.06$; ^d $P<0.001, t=145.3$; ^f $P<0.001, t=110.3$; ^h $P<0.001, t=21.08$; ^j $P<0.001, t=38.45$; ⁱ $P<0.001, t=22.61$.

DISCUSSION

Helicobacter pylori was first isolated by Warren and Marshall in 1983 from gastric mucosa of patients with gastritis. It is now accepted to be an etiological agent of chronic gastritis, peptic ulcer and gastric cancer. It is a Gram-negative, spiral-shaped, microaerophilic bacterium that colonizes human gastric epithelium, with a curved, S or arc-like appearance in the stomach. When exposed to factors such as gastric juice, bile,

antibiotics and other hostile conditions, some bacterial cells turn into pleomorphic variations^[24-26] of which L-forms (spheroid) is the most common one^[27-30]. In this study, gastric mucosal biopsy specimens from 428 patients with chronic gastritis were taken for the detection of *H pylori* L-forms. Gram staining showed that 226 patients were infected with both *H pylori* L-forms and vegetative forms, and 17 patients were infected with *H pylori* vegetative forms only. This indicates that L-forms variation of *H pylori* is common in patients with chronic gastritis. Due to the loss of cell walls, or certain components and antigens of cell walls, *H pylori* L-forms differ from the vegetative forms in antigenicity, which may affect the result of serology diagnoses and, more importantly, enables the bacteria to live in the stomach for a long time by escaping the body's immunity. Moreover, when conditions improve, L-form can revert to typical vegetative forms, which may be an important factor leading to deterioration and relapse of infection. Therefore, *H pylori* L-forms are more adhesive, invasive and pathogenic, and the variation of *H pylori* results in the deferment and recurrence of chronic gastritis^[9,31].

In this study, the detection rate of *H pylori* L-forms was significantly greater in males than in female (57.87% vs 37.82%). This may be related to some male habits, such as smoking, drinking, irregular diets that might damage gastric mucosa and change the gastric internal environment^[9,30-35]. In addition, the presence of *H pylori* L-forms seems to be related to patients' ages, as the detection rate of *H pylori* L-forms increases with age.

Cellular immune function of patients with *H pylori* has been described in recent years. The chronic inflammatory responses associated with natural infection do not provide protection, but contribute to tissue damages and pathogenesis of gastroduodenal diseases, including atrophic gastritis, peptic ulcer, and gastric cancer. These immune responses are likely to attribute to a subject of T helper lymphocytes, so-called Th1 cells, which enhance cell-mediated immunity and induce damage to the gastric epithelium. To investigate the mechanisms for Th1 immune response caused by *H pylori* based on the variation of L forms, T lymphocyte subsets and the levels of IL-2, IL-6, and IL-8 in peripheral blood of the patients were detected. The results showed that in *H pylori*-positive patients, CD3+, CD4+, CD4+/CD8 and IL-2 decreased, but IL-6 and IL-8 increased, compared with those in *H pylori*-negative, indicating that *H pylori* infection may weaken the immune function of the host and cause a predominant Th1 cellular response. Moreover, the percentage of CD4+, the ratio of CD4+/CD8 and the level of IL-2 were lower but the levels of IL-6 and IL-8 were higher in the patients infected with both L-forms and vegetative forms, compared with those infected with vegetative forms only. Thus, *H pylori* L-forms infection may be closely related to disorder of the immune function, and may be one of the crucial factors causing Th1 immune response. We postulate that *H pylori* L-forms may invade into the host cells where they may serve as a pronounced inducer for Th1-type CD4 (+) T cell response, leading to the decrease in the percentage of CD4+ and the ratio of CD4+/CD8. Active CD4+-T cell may also inhibit the activation of Th1 cells cytokines, and the outcome of IL-2 is a risk factor of cellular immune response.

In addition, in this study, the levels of IL-6 and IL-8 in peripheral blood of the patients increased significantly, which is likely to be associated with ulceration inflammation, blood macrophage stimulation and active secretion by the neutrophils and vascular endothelial cells. Once attached to the gastric epithelial cells, *H pylori* incites an immune response characterized by the increased pro-inflammatory cytokine of IL-8, IL-12 and TNF-alpha. Activated inflammatory and immunologically competent cells such as neutrophils, lymphocytes and monocytes release cytokines such as IL-6, IL-8 and IFN-gamma. As a result, the serum levels of IL-6 and IL-8 increase^[18].

In conclusion, Co-infection with both *H pylori* vegetative forms and L-forms is common in patients with chronic gastritis. The rate of infection with *H pylori* L-forms in males is higher than in females, and the rate increases with age. Once *H pylori* L-forms occurs, the morphology and microstructure of the organisms change, *i.e.*, the cell walls of the L-forms are partly or completely lost, the charge of the bacterial surface increases, and the adherence and invasiveness of the bacteria become more powerful. All of these changes may play an important role in the deferment and relapse of chronic gastritis and in the disordered cellular immune function in patients with *H pylori* infection.

REFERENCES

- 1 **Pineros DM**, Riveros SC, Marin JD, Ricardo O, Diaz OO. *Helicobacter pylori* in gastric cancer and peptic ulcer disease in a Colombian population. Strain heterogeneity and antibody profiles. *Helicobacter* 2001; **6**: 199-206
- 2 **Takeuchi K**, Ohno Y, Tsuzuki Y, Ando T, Sekihara M, Hara T, Kuwano H. *Helicobacter pylori* infection and early gastric cancer. *J Clin Gastroenterol* 2003; **36**: 321-324
- 3 **So JB**, Yeoh KG, Moochala S, Moolchani N, Ho J, Wong WK, Mack P, Goh PM. Serum pepsinogen levels in gastric cancer patients and their relationship with *Helicobacter pylori* infection: a prospective study. *Gastric Cancer* 2003; **5**: 228-232
- 4 **Vandenplas Y**. *Helicobacter pylori* infection. *World J Gastroenterol* 2000; **6**: 20-31
- 5 **Miehlke S**, Yu J, Schuppler M, Frings C. *Helicobacter pylori vacA, iceA, and cagA* status and pattern of gastritis in patients with malignant and benign gastroduodenal disease. *Am J Gastroenterol* 2001; **96**: 1008-1013
- 6 **Ayhan S**, Demir MA, Kandiloglu AR, Saruc M, Kucuketin N. Features of chronic inflammation at the gastric cardia and the relationship with *Helicobacter pylori* infection and oesophagitis. *Acta Gastroenterol Belg* 2003; **66**: 144-149
- 7 **Atisook K**, Kachinthorn U, Luengrojankul P, Yanwandee T, Pakdirat P, Pupairoj A. Histology of gastritis and *Helicobacter pylori* infection in Thailand: a nationwide study of 3776 cases. *Helicobacter* 2003; **8**: 132-141
- 8 **Nguyen TN**, Barkun AN, Fallone CA. Host determinants of *Helicobacter pylori* infection and its clinical outcome. *Helicobacter* 1999; **4**: 185-197
- 9 **Hahn KB**, Kim DH, Lee KM, Lee JS, Surh YJ, Kim YB, Kim JH, Joo HJ, Cho YK, Nam KT, Cho SW. Effect of long-term administration of rebamipide on *Helicobacter pylori* infection in mice. *Aliment Pharmacol Ther* 2003; **18**(Suppl): 24-38
- 10 **Kotloff KL**, Sztein MB, Wasserman SS, Losonsky GA, DiLorenzo SC, Walker RI. Safety and immunogenicity of oral inactivated whole-cell *Helicobacter pylori* vaccine with adjuvant among volunteers with or without subclinical infection. *Infect Immun* 2001; **69**: 3581-3590
- 11 **Hwang IR**, Hsu PI, Peterson LE, Gutierrez O, Kim JG, Grahsam DY, Yamaoka Y. Interleukin-6 genetic polymorphisms are not related to *Helicobacter pylori*-associated gastroduodenal diseases. *Helicobacter* 2003; **8**: 142-148
- 12 **Chatzaki E**, Charalampopoulos I, Leontidis C, Mouzas IA, Tzardi M, Tastsanis C, Margioris AN, Gravanis A. Urocortin in human gastric mucosa: relationship to inflammatory activity. *J Clin Endocrinol Metab* 2003; **88**: 478-483
- 13 **Holck S**, Norgaard A, Bennedsen M, Permin H, Norn S, Andersen LP. Gastric mucosal cytokine responses in *Helicobacter pylori*-infected patients with gastritis and peptic ulcers. Association with inflammatory parameters and bacteria load. *FEMS Immunol Med Microbiol* 2003; **36**: 175-180
- 14 **Megraud F**. *Helicobacter pylori*, gastric inflammation and its consequences. *Ann Pharm Fr* 2003; **61**: 282-287
- 15 **Touati E**, Michel V, Thiberge JM, Wuscher N, Huerre M, Labigne A. Chronic *Helicobacter pylori* infections induce gastric mutations in mice. *Gastroenterology* 2003; **124**: 1408-1419
- 16 **Schmidtke LM**, Carson J. Induction, characterization and pathogenicity in rainbow trout *Oncorhynchus mykiss* (Walbaum) of *Lactococcus garvieae* L-forms. *Vet Microbiol* 1999; **69**: 287-300

- 17 **Dominis M**, Dzebro S, Gasparov S. Morphology of gastritis and *Helicobacter pylori* infection. *Lijec Vjesn* 2002; **124**(Suppl 1): 36-42
- 18 **Londono-Arcila P**, Freeman D, Kleanthous H, O' Dowd AM, Lewis S, Turner AK, Rees EL, Tibbitts TJ, Greenwood J, Monath TP, Darsley MJ. Attenuated *Salmonella enterica* serovar Typhi expressing urease effectively immunizes mice against *Helicobacter pylori* challenge as part of a heterologous mucosal priming-parenteral boosting vaccination regimen. *Infect Immun* 2002; **70**: 5096-5106
- 19 **Scheiman JM**, Greenson JK, Lee J, Cryer B. Effect of cyclooxygenase-2 inhibition on human *Helicobacter pylori* gastritis: mechanisms underlying gastrointestinal safety and implications for cancer chemoprevention. *Aliment Pharmacol Ther* 2003; **17**: 1535-1543
- 20 **Smith MF Jr**, Mitchell A, Li G, Ding S, Fitzmaurice AM, Ryan K, Crowe S, Goldberg JB. Toll-like receptor (TLR) 2 and TLR5, but not TLR4, are required for *Helicobacter pylori*-induced NF-kappa B activation and chemokine expression by epithelial cells. *J Biol Chem* 2003; **278**: 32552-32560
- 21 **Stromberg E**, Lundgren A, Edebo A, Lundin S, Svennerholm AM, Lindholm C. Increased frequency of activated T-cells in the *Helicobacter pylori*-infected antrum and duodenum. *FEMS Immunol Med Microbiol* 2003; **36**: 159-168
- 22 **Su B**, Ceponis PJ, Lebel S, Huynh H, Sherman PM. *Helicobacter pylori* activates Toll-like receptor 4 expression in gastrointestinal epithelial cells. *Infect Immun* 2003; **71**: 3496-3502
- 23 **Ernst PB**, Pappo J. T-cell-mediated mucosal immunity in the absence of antibody: lessons from *Helicobacter pylori* infection. *Acta Odontol Scand* 2001; **59**: 216-221
- 24 **Kusters JG**. Recent developments in *Helicobacter pylori* vaccination. *Gastroenterol* 2001; **234**(Suppl): 15-21
- 25 **Nilsson I**, Utt M, Nilsson HO, Ljungh A, Wadstrom T. Two-dimensional electrophoretic and immunoblot analysis of cell surface proteins of spiral-shaped and coccoid forms of *Helicobacter pylori*. *Electrophoresis* 2000; **21**: 2670-2677
- 26 **Wen M**, Zhang Y, Yamada N, Matsuhisa T, Matsukura N, Sugisaki Y. An evaluative system for the response of antibacterial therapy: based on the morphological change of *Helicobacter pylori* and mucosal inflammation. *Pathol Int* 1999; **49**: 332-337
- 27 **Khin MM**, Ringner M, Aleljung P, Wadstrom T, Ho B. Binding of human plasminogen and lactoferrin by *Helicobacter pylori* coccoid forms. *J Med Microbiol* 1996; **45**: 433-439
- 28 **She FF**, Su DH, Lin JY, Zhou LY. Virulence and potential pathogenicity of coccoid *Helicobacter pylori* induced by antibiotics. *World J Gastroenterol* 2001; **7**: 254-258
- 29 **Brenner H**, Bode G, Adler G, Hoffmeister A, Koenig W, Rothenbacher D. Alcohol as a gastric disinfectant? The complex relationship between alcohol consumption and current *Helicobacter pylori* infection. *Epidemiology* 2001; **12**: 209-214
- 30 **Guarner J**, Mohar A, Parsonnet J, Halperin D. The association between *Helicobacter pylori* and gastric neoplasia. Epidemiologic evidence. *Rev Gastroenterol Mex* 2000; **65**: 20-24
- 31 **Bergin IL**, Sheppard BJ, Fox JG. *Helicobacter pylori* infection and high dietary salt independently induce atrophic gastritis and intestinal metaplasia in commercially available outbred Mongolian gerbils. *Dig Dis Sci* 2003; **48**: 475-485
- 32 **Touati E**, Michel V, Thiberge JM, Wuscher N, Huerre M, Labigne A. Chronic *Helicobacter pylori* infections induce gastric mutations in mice. *Gastroenterology* 2003; **124**: 1408-1419
- 33 **Genta RM**, Rindi G, Fiocca R, Magner DJ, D'Amico D, Levine DS. Effects of 6-12 months of esomeprazole treatment on the gastric mucosa. *Am J Gastroenterol* 2003; **98**: 1257-1265
- 34 **Kaise M**, Miwa J, Iihara K, Suzuki N, Oda Y, Ohta Y. *Helicobacter pylori* stimulates inducible nitric oxide synthase in diverse topographical patterns in various gastroduodenal disorders. *Dig Dis Sci* 2003; **48**: 636-643
- 35 **Jang J**, Lee S, Jung Y, Song K, Fukumoto M, Gould VE, Lee I. Malgun (clear) cell change in *Helicobacter pylori* gastritis reflects epithelial genomic damage and repair. *Am J Pathol* 2003; **162**: 1203-1211

Edited by Xia HHX and Xu FM

C-kit gene mutation in human gastrointestinal stromal tumors

Ying-Yong Hou, Yun-Shan Tan, Meng-Hong Sun, Yong-Kun Wei, Jian-Fang Xu, Shao-Hua Lu, Su-Jie A-Ke-Su, Yan-Nan Zhou, Feng Gao, Ai-Hua Zheng, Tai-Ming Zhang, Wen-Zhong Hou, Jian Wang, Xiang Du, Xiong-Zeng Zhu

Ying-Yong Hou, Yun-Shan Tan, Jian-Fang Xu, Shao-Hua Lu, Su-Jie A-Ke-Su, Yan-Nan Zhou, Feng Gao, Department of Pathology, Zhongshan Hospital, Fudan University, Shanghai 200032, China
Meng-Hong Sun, Yong-Kun Wei, Ai-Hua Zheng, Tai-Ming Zhang, Wen-Zhong Hou, Jian Wang, Xiang Du, Xiong-Zeng Zhu, Department of Pathology, Cancer Hospital, Fudan University, Shanghai 200032, China

Supported by the National Natural Science Foundation of China, No. 30300152

Correspondence to: Dr. Xiong-Zeng Zhu, Department of Pathology, Cancer Hospital, Fudan University, Shanghai 200032, China

Telephone: 86-21-64175590-3204

Received: 2003-09-09 **Accepted:** 2003-10-22

Abstract

AIM: To investigate the significance of c-kit gene mutation in gastrointestinal stromal tumors (GIST).

METHODS: Fifty two cases of GIST and 28 cases of other tumors were examined. DNA samples were extracted from paraffin sections and fresh blocks. Exons 11, 9 and 13 of the c-kit gene were amplified by PCR and sequenced.

RESULTS: Mutations of exon 11 were found in 14 of 25 malignant GISTs (56%), mutations of exon 11 of the c-kit gene were revealed in 2 of 19 borderline GISTs (10.5%), and no mutation was found in benign tumors. The mutation rate showed significant difference ($\chi^2=14.39$, $P<0.01$) between malignant and benign GISTs. Most of mutations consisted of the in-frame deletion or replication from 3 to 48 bp in heterozygous and homozygous fashions, None of the mutations disrupted the downstream reading frame of the gene. Point mutations and frame deletions were most frequently observed at codons 550-560, but duplications were most concentrated at codons 570-585. No mutations of exons 9 and 13 were revealed in GISTs, Neither c-kit gene expression nor gene mutations were found in 3 leiomyomas, 8 leiomyosarcomas, 2 schwannomas, 2 malignant peripheral nerve sheath tumors, 2 intra-abdominal fibromatoses, 2 malignant fibrous histiocytomas and 9 adenocarcinomas.

CONCLUSION: C-kit gene mutations occur preferentially in malignant GISTs and might be a clinically useful adjunct marker in the evaluation of GISTs and can help to differentiate GISTs from other mesenchymal tumors of gastrointestinal tract, such as smooth muscle tumors, schwannomas, etc.

Hou YY, Tan YS, Sun MH, Wei YK, Xu JF, Lu SH, A-Ke-Su SJ, Zhou YN, Gao F, Zheng AH, Zhang TM, Hou WZ, Wang J, Du X, Zhu XZ. C-kit gene mutation in human gastrointestinal stromal tumors. *World J Gastroenterol* 2004; 10(9): 1310-1314
<http://www.wjgnet.com/1007-9327/10/1310.asp>

INTRODUCTION

GISTs are the most common mesenchymal tumors of the human

gastrointestinal tract, previously uniformly classified as smooth muscle tumors. Recently, GISTs have been defined as cellular spindle cell, epithelioid, or occasionally pleomorphic mesenchymal tumors of the gastrointestinal tract (GI) that express the c-kit protein (CD117), as detected using immunohistochemistry. GISTs are strongly and nearly uniformly CD117 positive^[1-4].

Recently, the c-kit mutations in GISTs have been shown to lead to ligand-independent activation of the tyrosine kinase of c-kit^[5]. So several questions were suggested: what are the possible relationship of c-kit expression and mutations, the relationship of mutations and malignancy, and the possible specificity of the mutations for GISTs?

A study of larger series of GISTs, revealed that these tumors had a spectrum of clinical behaviors at all sites of their occurrence^[6]. Some GISTs are typical benign tumors, and most of them are found incidentally in other conditions, for example, during gall bladder or gynecologic surgery. In contrast, other GISTs metastasize to the liver and disseminate in the peritoneal cavity. Large tumor size, presence of intratumoral necrosis, infiltrative growth pattern in muscularis propria, invasion of mucosa, and high mitotic figures are considered as malignant. However, there is a definite percentage of mitotically inactive tumors that subsequently metastasize, emphasizing the fact that low mitotic count does not rule out a malignant behavior. Therefore, the designation "uncertain malignant potential" applies to a significant number of GISTs.

In this study, we further explored whether the c-kit gene mutations were valuable as an adjunct malignant marker in GISTs and could help to differentiate GISTs from other tumors.

MATERIALS AND METHODS

Cases

Archival paraffin-embedded and frozen tissue samples of 52 GISTs were immunohistochemically analysed for CD117 and CD34. They were mainly obtained from the Department of Pathology, Zhongshan Hospital, Fudan University, and from other pathology departments in Cancer Hospital, Huadong Hospital, and Chongming Center Hospital, etc. Additionally, 28 other tumors were investigated, including 8 leiomyosarcomas of retroperitoneum, 3 leiomyomas of esophagus, 2 schwannomas of stomach, 2 malignant peripheral nerve sheath tumors of intra-abdomen, 2 intra-abdominal fibromatoses of intestine, 2 malignant fibrous histiocytomas of intra-abdomen, and 9 adenocarcinomas of GI (of which, 4 were accompanied by GISTs).

Histologic evaluation

One to 14 hematoxylin and eosin-stained slides (median, 4 slides) were reviewed for each case. The following features were recorded in all cases: type of the majority cells (spindle vs epithelioid), skeinoid fibers (extracellular collagen globules), mucosal ulceration. Additionally, other important features included mitoses counted from 50 consecutive high-power fields (HPFs), coagulation necrosis, infiltrative growth pattern, and lymph node involvement. According to the histologic observation, GISTs were divided into 3 groups: small incidental tumors with less 5 cm in diameter or fewer mitoses per 50 HPF

were designated as benign, mitotically inactive tumors larger than 5 cm or cellular tumors which had no necrosis and infiltration were designated as uncertain malignant potential, and tumors with active mitotic counts over five per 50HPF or with necrosis, infiltrative growth pattern were designated as malignant.

Immunohistochemistry

Antibodies to the following antigens were used. CD117 (c-kit protooncogene product, polyclonal, 1:70) was purchased from Santa Cruz Biotechnology, Santa Cruz, CA, USA, CD34 (QBEND-10, monoclonal, 1:150, DAKO), α -SMA (1A4 monoclonal, 1:200), MSA (HHF35 monoclonal, 1:200), desmin (D33, monoclonal, 1:150), S-100 protein (polyclonal, 1:300), and protein gene product 9.5 (PGP9.5, polyclonal, 1:300) were purchased from Dako Corp. Epitope retrieval was used for antibodies. The slides were immersed in 10 mmol/L citrate buffer, pH 6.0 and heated in a microwave oven at a high setting for 5 min. The EnVision staining technique was used followed by incubation with 3,3'-diaminobenzidine tetrahydrochloride and counterstained with hematoxylin.

DNA extraction

Ten micrometers of tissue sections were cut from freshly frozen tumors or paraffin embedded, and then incubated in extraction buffer (50 mmol/L KCl, 10 mmol/L Tris[pH8.3], 2.5 mmol/L MgCl₂) containing 60 μ g/mL proteinase K overnight at 55 °C. The proteinase K was inactivated by a 10-min incubation at 95 °C. The resulting lysate was spun in a microcentrifuge for 5 min to pellet debris, and then stored at -20 °C.

PCR amplification of exons 11, 9, and 13 of c-kit gene

PCR assays were developed to amplify exons 11, 9, and 13. The 3 primer pairs were designed based on the human c-kit gene. Exons 9, 11 and 13 of the c-kit gene were amplified by PCR using the following oligonucleotide primer pairs: for exon 9, 5' - TCCTAGAGTAAGCCAGGGCTT-3' /5' -TGGTAGACAGAGCCTAAACATCC-3'; for exon 11, 5' -CCAGAGTGCTCTAATGACTG-3' /5' -TGACATGGAAAGCCCCTGTT-3'; and for exon 13, 5' -GCTTGACATCAGTTTGCCAG-3' /5' -AAAGGCAGCTTGGACACGGCTTTA-3'. The lengths of PCR products were

261 bp, 225 bp, and 193 bp, respectively. The PCR reaction conditions were the standard ones recommended by Perkin Elmer. The annealing temperature was 55 °C. The PCR products were size fractionated on 50 g/L polyacrylamide gels and stained with ethidium bromide.

DNA sequencing

Direct sequencing was performed on the ABI Prism 310 DNA sequencer, using the same primers as were used for amplification. Sequencing reactions were conducted with the big dye terminator sequencing ready reaction kit (Perkin-Elmer) according to the manufacturer's instructions.

Statistical analysis

χ^2 test was used.

RESULTS

Clinicopathological features of GISTs

There were 27 gastric, 7 small intestine, 6 rectal, 5 extra-GI, 2 abdominal disseminated primary tumors, with 5 intraabdominal recurrences. Of these tumors, 8 were classified as histologically benign, 19 as histologically uncertain malignant potential of borderline tumor, and 25 as malignant based on high mitotic activity, coagulative necrosis, infiltrative growth pattern. These tumors displayed a wide variety of cell types and histologic patterns, of which, 34 tumors had a predominant spindle cell pattern, 8 were epithelioid, and 10 were spindle/epithelioid mixed. The spindle cells were most often arranged in interlacing fascicles, The epithelioid cells were characterized by sheets. However, they often showed focally a storiform pattern, mimicked large rosettes, or palisaded the nuclei.

Immunohistochemical findings

CD117 positivity was detected in 50 of 52 cases (96.2%), typically in most of tumor cells in a strong membrane of apparently diffuse cytoplasm. CD34 positivity was seen in 38 of 52 cases (73%), including focal reactive cases. Two CD117-negative cases were CD34 positive. A small number were focal positive for α -SMA (10 of 52), MSA (9 of 52), desmin (2 of 52). Additionally, 6 and 3 cases were reactive for S-100 and PGP9.5.

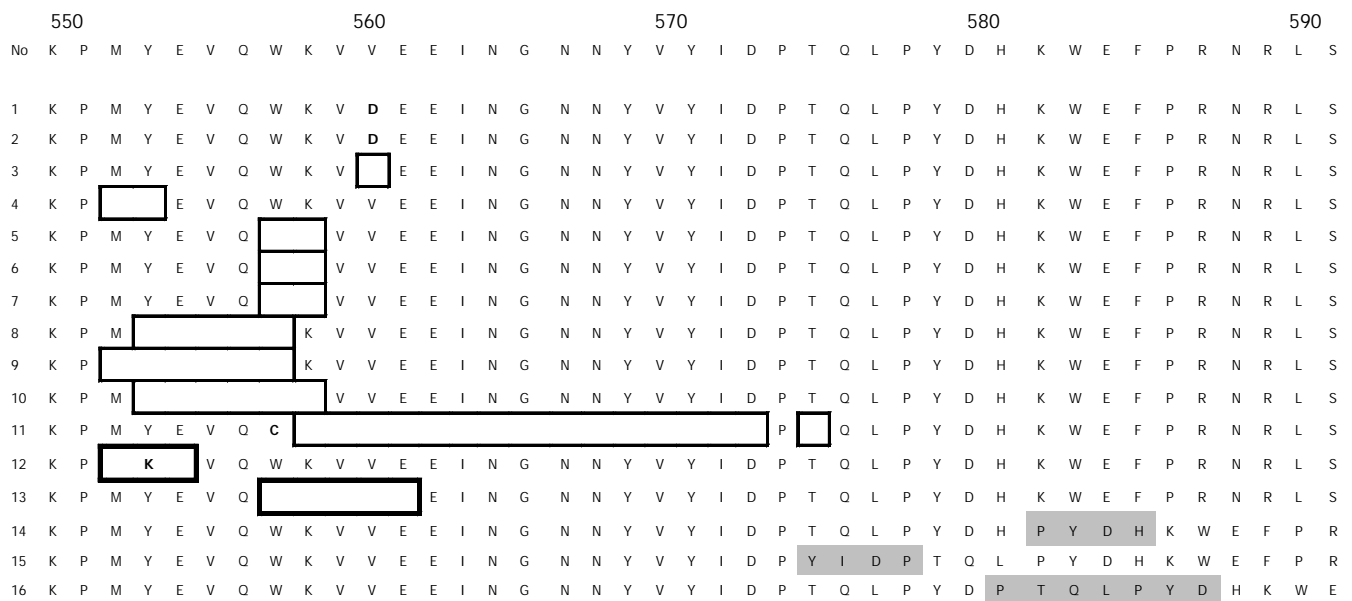


Figure 1 Exon 11 of c-kit mutations in 16 GIST samples. The wild-type sequence of amino acids encoded by exon 11 is shown at the top. The sequence starting at codon 550 and ending at 590. The wild-type sequence is shown above, the numbers are shown at the left. Point mutation is shown in black type, deletion is shown in the thin line indicates heterozygote mutation and thick line indicates homozygote ones. the shaded areas correspond to insertion or duplication mutations.

Evaluation of mutations in exons 11, 9, and 13 of c-kit gene

PCR amplification and DNA sequencing revealed exon 11 mutation in 14 malignant GISTs, in 2 borderline GISTs, and in no benign GISTs. Sequence analysis showed in-frame deletions of 3 to 48 bp, point mutations, and duplications. Point mutations and deletions were most frequently observed at codons 550-560, but duplications were most concentrated at codon 570-585. Of the 16 mutated GISTs, 2 had a homozygous mutation and 14 heterozygous mutation, which did not result in any amino acid change. The sequence corresponding to these mutations are shown in Figure 1. Figure 2 shows a case of duplication by DNA direct sequencing.

Five non-tumor tissue samples from the stomach or intestine adjacent to mutation-bearing GISTs demonstrated neither deletions nor point mutations.

The conservation of c-kit mutation pattern was observed in a relapse lesion from the same patients (Figure 3).

No exon 9 and exon 13 mutation were detected.

χ^2 test showed that the c-kit mutation of GISTs demonstrated a statistical ($\chi^2=14.39$, $P<0.01$) significance between the malignant group and the borderline and benign groups.

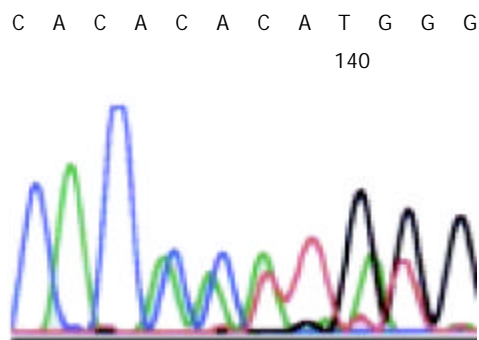


Figure 2 Duplication of codons from 581 to 584 (PYDHH) in one case of GIST by direct sequencing of c-kit exon 11.

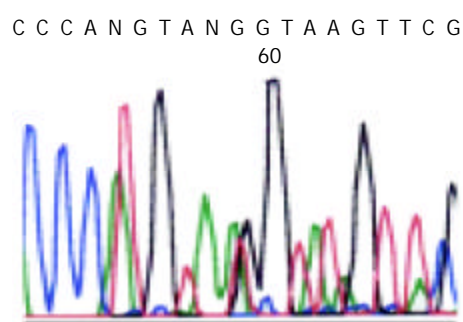


Figure 3 Deletion of codon from 553 to 557 (YEVQW) by direct sequencing of c-kit exon 11.

Other tumors

The three esophageal leiomyomas were histologically paucicellular spindle cell neoplasms with distinctly eosinophilic cytoplasm, and lack of mitotic activity. All cases were positive for α -SMA, MSA and desmin, and negative for CD117 and CD34, and only mast cells in the stroma showed positive CD117.

The 8 retroperitoneal leiomyosarcomas were spindle cell tumors that resembled smooth muscle tumor with oval to mildly elongated nuclei and variably eosinophilic cytoplasm. Four tumors showed focal pleomorphism and high mitotic activity ($>50/50$ HPF). Coagulation necrosis was present in 4 tumors. All cases were positive for α -SMA, MSA, and 7 cases positive for desmin. All cases were negative for CD34 but 1 case was focal weak positive for CD117.

The 2 cases of schwannomas showed slender spindle cells

and a characteristic lymphoid cuff. Two cases were diffusely and strongly positive for S-100 and 1 case was positive for PGP9.5. Both of them were negative for CD117 and CD34. The 2 cases malignant peripheral nerve sheath tumor showed spindle cells and active mitosis. Two cases were positive for S-100 and weak positive for PGP9.5 and negative for CD117 and CD34.

The 2 cases of intro-abdominal fibromatosis of intestine and 2 cases of malignant fibrous histiocytoma were negative for all antigens but 1 case of intro-abdominal fibromatosis was focal positive for α -SMA.

There were no mutations of the c-kit gene in the above 28 control tumors and one case of adenocarcinoma accompanied by mutation-bearing GIST also had wild-type c-kit gene.

DISCUSSION

Most of the GISTs examined expressed both CD117 and CD34, which was consistent with the literature reports^[7-12]. The rates of CD117 and CD34 expression had no difference between benign, borderline, and malignant GISTs, so the expressions were not useful markers for evaluating malignancy.

In this study, we examined the sequence and expression of c-kit gene in the spectrum of GISTs, including benign, borderline, and malignant variants from different sites. The sequences of c-kit gene were also evaluated in typical smooth muscle tumors, schwannomas and other tumors, especially in 4 adenocarcinomas accompanied by GISTs.

Our series of 52 benign, borderline, and malignant GISTs showed that 96.2% of the GISTs expressed CD117 and only some of the GISTs had mutations. The results indicated a considerable proportion of GISTs expressed CD117 with no mutation. In other words, most of c-kit mutations did not affect the proportion of GISTs with CD117 expression. Mutations in exon 11 of the c-kit gene were observed in 56% of malignant cases. In contrast, only 2 borderline GISTs (10.5%) showed mutations, and no benign GISTs showed mutations, suggesting that the mutations of exon 11 of the c-kit gene may represent a genotypic marker with a correlation to malignancy.

Lasota and colleagues^[13] reported the mutation of exons 9 and 13, but the mutation rate seemed to be very low, and they only detected the small portion (8%) of mutations of GISTs in exons 9 and 13, which did not have mutations in exon 11 of the c-kit gene. In our series, no mutations were detected. The result also indicated the rates of mutations in other regions of the c-kit gene were very low.

Our present results were in accordance with those previously reported^[14-16]. In hot spot region of exon 11 involving codons 550-560, point mutation and frame deletion were mainly detected at these codons, and 2 cases showed homozygous deletions.

In addition to the change at codons of 550-560, however, the duplication mutation fashion was found in 3 cases to cluster at codons 570 to 585, which was rarely detected in the previously reports.

Analysis of c-kit mutation pattern in relapse lesions showed the persistence of the mutation that remained identical in the primary lesion. Therefore, the c-kit mutation pattern could be tumor-specific.

C-kit mutations were never observed in smooth muscle tumors or nerve sheath tumors or other soft tissue tumors. Furthermore, one adenocarcinoma accompanied by mutation-positive GIST was the wild-type c-kit gene. Therefore, c-kit mutations may also represent a genotypic lineage marker for GISTs.

Previous and present molecular studies have revealed the gain-of-function mutations of the c-kit gene could be observed in mast cell neoplasms^[17,18], human germ cell tumors^[19] and GISTs, but the location of c-kit mutations differs in them. The particular aspartic acid in the tyrosine kinase domain would

changes into valine in mast cell neoplasms, The aspartic acid at amino acid position 816 would change into histidine, whereas deletion, point mutation, or both in the juxtamembrane domain were observed in GISTs mutations. Specially, the mutations were located within codons 550 to 560 in exon 11, and rare mutations are detectable in other domains of the c-kit gene, such as exons 9, 13. Clustering of c-kit mutations in the same region of GISTs and in different region with mast cell neoplasm supported their specific biological significance.

The occurrence of activating mutations involving exon 11 of the c-kit gene in sporadic GIST and the association of exon 11 germline mutations in familial GISTs indicated they were important in GIST's tumorigenesis^[20]. Especially, c-kit mutations could be detected only in some of GISTs^[21,22], so the value of the c-kit gene mutation in GISTs inspired the researchers, but there are no concordant conclusions, reports regarding the frequency of mutations in exon 11 varied widely, and prognostic significance of c-kit mutations with respect to the association between exon 11 mutations and malignant histology and/or aggressive malignant behavior were conflicting, and the reported frequency of these mutations varied over a wide range^[23-29]. Taniguchi and colleagues^[23] found that c-kit mutation-positive GIST were worse than c-kit mutation-negative GISTs. But other studies showed that c-kit exon 11 mutation analysis did not correlate well with histological assessment of malignant potential, and could not be regarded as a reliable objective marker for poor prognosis in GISTs.

Some malignant GISTs lack of exon 11 mutation suggested that mutations in exon 11 of c-kit gene were not the only mechanisms related to malignancy and there must exist other molecular mechanisms^[30-33], which may include mutations in other regions of the c-kit gene. But previous report and our study indicated other region mutation of the c-kit gene was few. Recently, Heihrich and colleagues^[34] have made an important finding in GISTs, they reported that 35% (14/40) of GISTs lacking c-kit mutations had intragenic activation mutations in tyrosine kinase, platelet-derived growth factor (PDGFRA). C-kit gene and PDGFRA mutations appeared to be alternative and mutually exclusive in GISTs, further study is needed to understand the role of PDGFRA in GISTs.

In summary, the results showed a consistent c-kit expression in GISTs with or without detectable mutations. The mutations occurred more preferentially in malignant GISTs than versus in benign GISTs, but not in smooth muscle tumor and other tumors. These observations suggest that mutations in exon 11 of the c-kit gene might represent useful molecular genetic markers for malignant GISTs and help to differentiate GIST from other tumors. Whether the c-kit gene mutation can indicate bad prognosis of malignant GISTs needs to be further studied.

ACKNOWLEDGMENTS

We thank Dr. Lu X,Y. and Dr. Yu M. for kindly providing the cases.

REFERENCES

- 1 **Chan JKC.** Mesenchymal tumors of the gastrointestinal tract: a paradise for acronyms (STUMP, GIST, GANT, and now GIPACT) implication of *c-kit* in genesis, and yet another of the many emerging roles of the interstitial cell of Cajal in the pathogenesis of gastrointestinal disease? *Advances Anatomic Pathol* 1999; **6**: 19-40
- 2 **Tworek JA,** Goldblum JR, Weiss SW, Greenson JK, Appelman HD. Stromal tumors of the abdominal colon. A clinicopathologic study of 20 cases. *Am J Surg Pathol* 1999; **23**: 937-945
- 3 **Sircar K,** Hewlett BR, Huizinga JD, Chorneyko K, Berezin I, Riddell RH. Interstitial cells of Cajal as precursors of gastrointestinal stromal tumors. *Am J Surg Pathol* 1999; **23**: 377-389
- 4 **Miettinen M,** Lasota J. Gastrointestinal stromal tumors- definition, clinical, histological, immunohistochemical, and molecular genetic features and differential diagnosis. *Virchows Arch* 2001; **438**: 1-12
- 5 **Moskaluk CA,** Tian Q, Marshall CR, Rumpel CA, Franquemont DW, Frierson HF. Mutations of *c-kit* JM domain are found in a minority of human gastrointestinal stromal tumors. *Oncogene* 1999; **18**: 1897-1902
- 6 **Miettinen M,** Sarlomo-Rikala M, Lasota J. Gastrointestinal stromal tumors: recent advances in understanding of their biology. *Human Pathol* 1999; **30**: 1213-1220
- 7 **Seidal T,** Edvardsson H. Expression of c-kit (CD117) and *ki67* provides information about the possible cell of origin and clinical course of gastrointestinal stromal tumours. *Histopathology* 1999; **34**: 416-424
- 8 **Robinson TL,** Sircar K, Hewlett BR, Chorneyko K, Riddell RH, Huizinga JD. Gastrointestinal stromal tumors may originate from a subset of CD34-positive interstitial cells of Cajal. *Am J Pathol* 2000; **156**: 1157-1163
- 9 **Miettinen M,** Sobin LH, Sarlomo-Rikala M. Immunohistochemical spectrum of GISTs at different sites and their differential diagnosis with a reference to CD117(KIT). *Mod Pathol* 2000; **13**: 1134-1142
- 10 **Miettinen M,** Furlong M, Sarlomo-Rikala M, Burke A, Sobin LH, Lasota J. Gastrointestinal stromal tumors, Intramural leiomyomas, and leiomyosarcomas in the rectum and anus. A clinicopathologic, immunohistochemical, and molecular genetic study of 144 cases. *Am J Surg Pathol* 2001; **25**: 1121-1133
- 11 **Smitley BE,** Pappo AS, Hill DA. C-kit expression in pediatric solid tumors. *Am J Surg Pathol* 2002; **26**: 486-492
- 12 **Hornick JL,** Fletcher CDM. Immunohistochemical staining for KIT (CD117) in soft tissues sarcomas is very limited in distribution. *Am J Clin Pathol* 2002; **117**: 188-193
- 13 **Lasota J,** Wozniak A, Sarlomo-Rikala M, Rys J, Kordek R, Nassar A, Sobin LH, Miettinen M. Mutations in exons 9 and 13 of KIT gene are rare events in gastrointestinal stromal tumors A study of 200 cases. *Am J Pathol* 2000; **157**: 1091-1095
- 14 **Allander SV,** Nupponen NN, Ringnér M, Hostetter G, Maher GW, Goldberger N, Chen Y, Carpten J, Elkahloun AG, Meltzer PS. Gastrointestinal stromal tumors with kit mutations exhibit a remarkably homogeneous gene expression profile. *Cancer Res* 2001; **61**: 8624-8628
- 15 **Miettinen M,** Sarlomo-Rikala M, Sobin LH, Lasota J. Esophageal stromal tumors: a clinicopathologic, immunohistochemical, and molecular genetic study of 17 cases and comparison with esophageal leiomyomas and leiomyosarcomas. *Am J Surg Pathol* 2000; **24**: 211-222
- 16 **Wardelmann E,** Neidt I, Bierhoff E, Speidel N, Manegold C, Fischer HP, Pferfer U, Pietsch T. c-kit mutations in gastrointestinal stromal tumors occur preferentially in the spindle rather than in the epithelioid cell variant. *Mod Pathol* 2002; **15**: 125-136
- 17 **Jordan JH,** Fritsche-Polanz R, Sperr WR, Mitterbauer G, Födinger M, Scherthaner GH, Bankl HC, Gebhart W, Chott A, Lechner K, Valent P. A case of 'smouldering' mastocytosis with high mast cell burden, monoclonal myeloid cells, and C-KIT mutation Asp-816-Val. *Leuk Res* 2001; **25**: 627-634
- 18 **Sotlar K,** Escribano L, Landt O, Möhrle S, Herrero S, Torrelo A, Lass U, Horny HP, Bültmann B. One-step detection of c-kit point mutations using peptide nucleic acid-mediated polymerase chain reaction clamping and hybridization probes. *Am J Pathol* 2003; **162**: 737-746
- 19 **Tian Q,** Frierson HF Jr, Krystal GW, Moskaluk CA. Activating c-kit gene mutations in human germ cell tumors. *Am J Pathol* 1999; **154**: 1643-1647
- 20 **Maeyama H,** Hidaka E, Ota H, Minami S, Kajiyama M, Kuraishi A, Mori H, Matsuda Y, Wada S, Sodeyama H, Nakata S, Kawamura N, Hata S, Watanabe M, Lijima Y, Katsuyama T. Familial gastrointestinal stromal tumor with hyperpigmentation: association with a germline mutation of the c-kit gene. *Gastroenterology* 2001; **120**: 210-215
- 21 **Lasota J,** Jasinski M, Sarlomo-Rikala M, Miettinen M. Mutations in exon 11 of c-kit occur preferentially in malignant vs benign gastrointestinal stromal tumors and do not occur in leiomyomas or leiomyosarcomas. *Am J Pathol* 1999; **154**: 53-60

- 22 **Miettinen M**, Sarlomo-Rikala M, Sobin LH, Lasota J. Gastrointestinal stromal tumors and leiomyosarcomas in the colon. *Am J Surg Pathol* 2000; **24**: 1339-1352
- 23 **Taniguchi M**, Nishida T, Hirota S, Isozaki L, Ito T, Nomura T, Matuda H, Kitamura Y. Effect of *c-kit* mutation on prognosis of gastrointestinal stromal tumors. *Cancer Res* 1999; **59**: 4297-4300
- 24 **Rubin BP**, Singer S, Tsao C, Duensing A, Lux ML, Ruiz R, Hibbard MK, Chen CJ, Xiao S, Tuveson DA, Demetri GD, Fletcher CDM, Fletcher JA. KIT activation is ubiquitous feature of gastrointestinal stromal tumors. *Cancer Res* 2001; **61**: 8118-8121
- 25 **Corless CL**, McGreevey L, Haley A, Town A, Heinrich MC. KIT mutation are common in incidental gastrointestinal stromal tumors one centimeter or less in size. *Am J Pathol* 2002; **160**: 1567-1572
- 26 **Miettinen M**, El-Rifai W, Sobin LH, Lasota J. Evaluation of malignancy and prognosis of gastrointestinal stromal tumors: A review. *Hum Pathol* 2002; **33**: 478-483
- 27 **Andersson J**, Sjögren H, Meis-Kidblom JM, Stenman G, Aman P, Kindblom LG. The complexity of KIT gene mutations and chromosome rearrangements and their clinical correlation in gastrointestinal stromal (pacemaker cell) tumors. *Am J Pathol* 2002; **160**: 15-22
- 28 **Miettinen M**, Kopczynski J, Makhoul H, Sarlomo-Rikala M, Gyorffy H, Burke A, Sobin LH, Lasota J. Gastrointestinal stromal tumors, intramural leiomyomas, and leiomyosarcomas in the duodenum. A clinicopathologic, immunohistochemical, and molecular genetic study of 167 cases. *Am J Surg Pathol* 2003; **27**: 625-641
- 29 **O'Leary T**, Ernst S, Przygodzki R, Emory T, Sobin L. Loss of heterozygosity at 1p36 predicts poor prognosis in gastrointestinal stromal/smooth muscle tumors. *Lab Invest* 1999; **79**: 1461-1467
- 30 **O'Leary T**, Berman JJ. Gastrointestinal stromal tumors: answers and questions. *Hum Pathol* 2002; **33**: 456-458
- 31 **El-Rifai W**, Sarlomo-Rikala M, Andersson LC, Knuutila S, Miettinen M. DNA sequence copy number changes in gastrointestinal stromal tumors: tumor progression and prognostic significance. *Cancer Res* 2000; **60**: 3899-3903
- 32 **Heinrich M**, Rubin BP, Longley BJ, Fletcher JA. Biology and genetic aspects of gastrointestinal stromal tumors: KIT activation and cytogenetic alterations. *Hum Pathol* 2002; **33**: 484-495
- 33 **Kim NG**, Kim JJ, Ahn JY, Seong CM, Noh SH, Kim CB, Min JS, Kim H. Putative chromosomal deletions on 9P, 9Q and 22Q occur preferentially in malignant gastrointestinal stromal tumors. *Int J Cancer* 2000; **85**: 633-638
- 34 **Heinrich MC**, Corless CL, Duensing A, McGreevey L, Chen CJ, Joseph N, Singer S, Griffith DJ, Haley A, Town A, Demetri GD, Fletcher CDM, Fletcher JA. PDGFRA activating mutations in gastrointestinal stromal tumors. *Science* 2003; **299**: 708-710

Edited by Wang XL and Xu FM

Suppressive effects of 17 β -estradiol on hepatic fibrosis in CCl₄-induced rat model

Qing-Hua Liu, Ding-Guo Li, Xin Huang, Chun-Hua Zong, Qin-Fang Xu, Han-Ming Lu

Qing-Hua Liu, Ding-Guo Li, Xin Huang, Chun-Hua Zong, Qin-Fang Xu, Han-Ming Lu, Department of Gastroenterology, Xinhua Hospital of Shanghai Secondary Medical University, Shanghai 200092, China

Supported by the National Natural Science Foundation of China, No. 30170411

Correspondence to: Dr. Ding-Guo Li, Department of Gastroenterology, Xinhua Hospital of Shanghai Secondary Medical University, Shanghai 200092, China. dingguo_li@yahoo.com.cn

Telephone: +86-21-65790000-5316 **Fax:** +86-21-55055127

Received: 2003-08-11 **Accepted:** 2003-10-12

Abstract

AIM: To investigate the pathway via which 17 β -estradiol (β -Est) exerts suppressive effects on rat hepatic fibrosis.

METHODS: *In vivo* study was done in CCl₄-induced female hepatofibrotic rats. Fibrosis-suppressive effect of β -Est (20 μ g/kg·d) was evaluated in intact and ovariectomized rat models. Six weeks after the treatment, all the rats were sacrificed and specimens of serum or liver tissue were collected for the studies. Serum liver enzymes, fibrosis markers and estradiol levels were determined by standard enzymatic methods, ELISA and RIA, respectively. Degrees of fibrosis and areas of hepatic stellate cells (HSCs) positive for alpha-smooth muscle actin (α -SMA) in the liver were determined by van Gieson (VG) stain and immunohistochemistry. *In vitro* studies, HSCs were isolated by a combination of pronase-collagenase perfusion and density gradient centrifugation. First-passage HSCs were randomly divided into 10 groups, and different concentrations of β -Est, 2-hydroxyestradiol (2OHE) or 2-methoxyestradiol (2MeOE) were separately added to the cell groups. After incubation for 72 h, the degree of cell proliferation, collagen production, α -SMA or estrogen receptor (ER) expression was determined by MTT assay, ELISA and immunohistochemistry, respectively.

RESULTS: β -Est treatment reduced aspartate aminotransferase (AST), alanine aminotransferase (ALT), hyaluronic acid (HA) and type IV collagen (C IV) in sera, suppressed hepatic collagen content, decreased the areas of HSCs positive for α -SMA significantly in both intact and ovariectomized female hepatofibrotic rats. There was a negative correlation between the percentage of fibrotic area of liver tissue and the serum estradiol level; the calculated correlation coefficient was -0.57 ($P < 0.01$). β -Est and its metabolites concentration-dependently (10^{-9} mol/L- 10^{-7} mol/L) inhibited HSC proliferation and collagen synthesis. At the concentration of 10^{-7} mol/L, they could inhibit α -SMA expression. The order of potency was 2MeOE > 2OHE > β -Est.

CONCLUSION: β -Est may suppress hepatic fibrosis probably via its biologically active metabolites.

Liu QH, Li DG, Huang X, Zong CH, Xu QF, Lu HM. Suppressive

effects of 17 β -estradiol on hepatic fibrosis in CCl₄-induced rat model. *World J Gastroenterol* 2004; 10(9): 1315-1320
<http://www.wjgnet.com/1007-9327/10/1315.asp>

INTRODUCTION

Several epidemiological studies demonstrated a lower incidence of hepatic cirrhosis and its complications in women than in men^[1-3]. But as menopause comes, the morbidity of the disease increases gradually. So, endogenous estrogen may take part in the protective effects on hepatic fibrosis. *In vivo*, 17 β -estradiol (β -Est) is the most active estrogen and can be converted to several metabolites, some of which are known to possess biological activities. Of the various metabolites, 2-hydroxyestradiol (2OHE) and 2-methoxyestradiol (2MeOE) are the biologically active substances, which have been investigated in depth^[4,5]. 2OHE is one of the hydroxylated metabolites of β -Est converted by cytochrome P-450 enzymes (CYP450) and can be rapidly catalyzed by enzyme catechol-O-methyl-transferase (COMT) to 2MeOE^[6-8]. Recent studies have shown that 2OHE and 2MeOE could inhibit DNA synthesis, cell proliferation, collagen synthesis and mitogen activated protein kinase activity in vascular smooth muscle cells (VSMCs), cardiac fibroblasts (CFs) and glomerular mesangial cells (GMCs) with the potency stronger than β -Est^[9-13]. Hence, the fibrosis-suppressive effects of β -Est not only reflect the biological effects of β -Est per se but also those of its biologically active metabolites.

Hepatic stellate cells (HSC), the key cells responsible for hepatic fibrogenesis, are VSMC, CF or GMC analogs and belong to the pericytes generically^[14]. So, they may have many properties in common, including a prominent role in fibrosing injury and the same reaction to metabolites of β -Est.

The present study was initiated to investigate the role of β -Est in the female rat model of carbon tetrachloride (CCl₄)-induced hepatic fibrosis. Moreover, the effects of β -Est, 2OHE and 2MeOE on the first-passage rat HSCs were assessed.

MATERIALS AND METHODS

In vivo study

Fifty female Sprague-Dawley rats aged 10 wk (Laboratory Animal Center affiliated to Chinese Academy of Sciences, Shanghai, China) were divided into 5 groups ($n=10$). All the rats were initiated with either a bilateral ovariectomy (Ovx) or a sham operation 3 wk before the studies. Control group received subcutaneous injection of olive oil (3 mL/kg every 3 d and first dosage doubled), CCl₄ group was given the same dose of 400 g/L CCl₄, Ovx+CCl₄ group was treated with the same dose of 400 g/L CCl₄ after ovariectomy, β -Est+CCl₄ group along with CCl₄ injection described above was treated with 0.002% β -Est (1 mL/kg·d, Sigma-Aldrich Corporation, St Louis, Missouri, USA), Ovx+ β -Est+CCl₄ group was treated the same as β -Est+CCl₄ group with the addition of ovariectomy.

At the end of 6 wk, the number of alive rats in the groups was 10, 7, 8, 10, 9 respectively. Several rats died of infection at the site of injection or hepatic crack by unsuitable handling.

After an overnight fast, all the rats were sacrificed. Serum samples obtained were treated with proteinase inhibitor and stored at -20°C . Liver tissue specimens were rinsed with normal saline containing 0.1 g/L DEPC, some were stored at -80°C , and the others were fixed in neutral formalin and embedded in paraffin.

Serum activities of aspartate aminotransferase (AST) and alanine aminotransferase (ALT) were assayed by standard enzymatic methods, hyaluronic acid (HA) and type IV collagen (C IV) concentrations were measured by enzyme-linked immunosorbent assay (ELISA) using a commercial kit (Navy Medical Institute, Shanghai, China).

The embedded liver specimens were sliced 5 μm in thickness, mounted on slides, deparaffinised in xylene, and dehydrated in alcohol. For histopathological studies, the liver sections were stained with van Gieson (VG). For alpha-smooth muscle actin (α -SMA) immunohistochemistry, the sections were incubated with 3% (v/v) hydrogen peroxide in methanol for 15 min to block endogenous peroxidase, and then with 1 g/L Triton-X plus 1 g/L BSA in phosphate-buffered saline (PBS) to block non-specific antigens. After absorption of surplus liquid, the samples were incubated with a 1:100 dilution of a polyclonal antibody against α -SMA (Boster Biological Technology Corporation, Wuhan, China) at 37°C for 2 h. Then the samples were rinsed and incubated with a 1:100 dilution of biotin-conjugated goat anti-rabbit IgG (Boster Biological Technology Corporation, Wuhan, China) at 37°C for 30 min. Finally, the antigen-antibody complexes were visualized with 3,3'-diaminobenzidine (DAB).

For morphometric analysis, the mean value of collagen content or α -SMA positive cells in six ocular fields per specimen was used as the percentage area at 100x magnification using Zeiss KS400 image analysis system (Kontron Electronics, Eching, Germany).

Serum estradiol concentrations were measured with radioimmunoassay (RIA) using a commercial kit (Diagnostic Products Corporation, Tianjin, China).

In vitro study

HSCs were isolated and purified from the livers of normal female rats weighing about 400 g to 450 g by a combination of pronase-collagenase perfusion and density gradient centrifugation^[15-19]. Briefly, the liver was perfused *in situ* through the portal vein, first with $\text{Ca}^{2+}/\text{Mg}^{2+}$ -free Krebs-Ringer (KR) solution at a flow rate of 20 mL/min, followed by pronase and then with collagenase (Sigma-Aldrich Corporation, St Louis, Missouri, USA) in KR solution. The digested liver was excised, minced with scissors, and incubated in KR solution containing pronase and DNase (Sigma-Aldrich Corporation, St Louis, Missouri, USA) for 30 min. The resulting suspension was filtered through nylon mesh (200 μm in diameter) and then washed 3 times by centrifugation in D-Hanks solution at 1 700 r/min for 7 min. An HSC-enriched fraction was obtained by centrifugation of the filtrate in an 180 g/L nycodenz (Sigma-Aldrich Corporation, St Louis, Missouri, USA) solution with the volume ratio of 1:2 at 3 200 r/min for 17 min. The cells in the upper layer were washed by centrifugation at 1 700 r/min for 7 min and suspended in Dulbecco's modified Eagle medium (DMEM, GIBCO BRL Life Technologies Corporation, USA) supplemented with 200 mL/L fetal bovine serum (FBS, GIBCO BRL Life Technologies Corporation, USA). Both cell viability and purity were over 90%, examined by trypan blue (Sigma-Aldrich Corporation, St Louis, Missouri, USA) exclusion and autofluorescence respectively.

Cells were plated at a density of 1×10^6 cells in 1 mL culture medium on uncoated plastic culture dishes. The culture medium was changed after 24 h and then every 3 d. After cultured for 14 d, the cells were passaged.

The first-passage HSCs were plated at a density of 2×10^5

cells in 1 mL DMEM supplemented with 100 g/L FBS on an uncoated plastic culture dish. Subconfluent HSCs were divided into 10 groups, and different concentrations of β -Est, 2OHE, 2MeOE (Sigma-Aldrich Corporation, St Louis, Missouri, USA) or vehicle were added to the cells. After incubated for 24 h, experiments were done to assess the functional state of HSCs.

HSC proliferation was measured by MTT assay. The cells were continually cultivated with 3-(4,5-dimethylthiazol-2yl)-2,5-diphenyl tetrazolium bromide (MTT, Sigma-Aldrich Corporation, St Louis, Missouri, USA) in a 96-well plate for 4 h. After the supernatant in each well was aspirated and discarded, the cells were agitated with dimethylsulfoxide (DMSO, Sigma-Aldrich Corporation, St Louis, Missouri, USA) 150 μL for 10 min. Finally, the optical density of each well was read in an auto reader using a 492 nm filter with a reference at 630 nm.

The levels of HA and C IV in the supernatants of cell were measured as afore-mentioned.

For immunohistochemical examination of α -SMA, estrogen receptor (ER) α and ER β , the cells were mounted on slides and fixed with 40 g/L paraformaldehyde for 5 min at 4°C . Following incubation with 30 mL/L H_2O_2 for 15 min, the cells were blocked by 1 g/L Triton-X plus 1 g/L BSA in PBS for 15 min at room temperature. They were incubated for 2 h at 37°C with a 1:100 dilution of polyclonal antibody against α -SMA, ER α or ER β (Santa Cruz Biotechnology Incorporation, California, USA) in a humid chamber. After the samples were rinsed, they were incubated with a 1:200 dilution of biotin-conjugated goat anti-rabbit IgG, and then visualized with DAB. Integral light density (ILD) analysis was performed on 20 cells in up, down, left, right quadrant of each section, data were calculated from average of 4 ILDs.

Statistical analysis

Data are presented as mean \pm SE unless otherwise indicated. Parametric data were compared using one-way analysis of variance, followed by multiple pair-wise comparisons according to the least-significant difference *t*-test. Pearson's analysis was performed to compare the correlation between serum estradiol and fibrotic area percentage. A *P* value less than 0.05 was accepted as statistically significant.

RESULTS

In vivo effect of β -Est on hepatic fibrosis

Table 1 shows the liver enzymes and fibrosis markers in CCl_4 -treated female rats. Treatment with CCl_4 caused a significant increase in the activities of serum ALT and AST compared with the control animals. The enzyme levels in ovariectomized model rats were higher than those in CCl_4 model group, whereas CCl_4 plus β -Est group showed a significant decrease in enzyme levels compared with CCl_4 group. There was no significant difference between CCl_4 group and Ovx+ β -Est+ CCl_4 group.

The changes of fibrosis markers, HA and C IV, were in parallel with those of the enzyme levels in all groups.

The control livers showed a distinct lobular architecture with collagens only surrounding the central and portal veins (Figure 1A). Administration of CCl_4 induced inflammation, necrosis and collagen deposition in the livers. Ovariectomy significantly increased hepatic fibrosis induced by CCl_4 (Figure 1B), whereas β -Est had the opposite effect. The fibrotic area percentage of Ovx+ CCl_4 + β -Est group was similar to that of CCl_4 group (Figure 1C).

Immunohistochemistry of α -SMA, an activation marker of rat HSC^[20-22], showed strong staining around vascular wall, but not the sinusoids in control female rat livers (Figure 2A). After administration of CCl_4 , fibrotic change was evident with significant increases of α -SMA positive cells in centrilobular

and periportal fibrotic bands. Ovariectomy significantly increased the percentage area of staining (Figure 2B), whereas β -Est had the opposite effect. There was no significant difference in the fibrotic area percentage of staining between CCl₄ and OvX+CCl₄+ β -Est groups (Figure 2C).

Figure 3 summarizes the histopathological and immunohistochemical changes in CCl₄-treated female rats.

Figure 4 shows the serum estradiol levels in the rats. The levels did not change in animals treated with CCl₄ alone. Ovariectomy produced significantly lower serum estradiol levels. In rats model treated with exogenous β -Est, the levels increased significantly as compared with those of control or CCl₄ model groups. Twenty μ g/kg·d β -Est could rectify the low serum estradiol levels in ovariectomized rats.

Table 1 Change of liver enzymes and serum fibrosis indicators

	ALT (nkat/L)	AST (nkat/L)	HA (μ g/L)	C IV (μ g/L)
Control	275.50 \pm 32.05	84.80 \pm 11.83	155.50 \pm 10.41	17.10 \pm 1.77
CCl ₄	1 070.71 \pm 82.95 ^b	806.00 \pm 82.43 ^b	481.43 \pm 24.68 ^b	49.57 \pm 2.47 ^b
Ovx+CCl ₄	1 403.88 \pm 120.30 ^{ab}	1 102.88 \pm 84.91 ^{bd}	583.75 \pm 37.50 ^{ab}	61.00 \pm 3.30 ^{ab}
CCl ₄ + β -Est	789.40 \pm 58.61 ^{ab}	606.70 \pm 45.68 ^{ab}	389.30 \pm 29.77 ^{ab}	38.80 \pm 2.59 ^{ab}
Ovx+CCl ₄ + β -Est	1 008.44 \pm 93.07 ^b	794.89 \pm 70.93 ^b	474.56 \pm 32.57 ^b	46.22 \pm 3.06 ^b

^a*P*<0.05 vs CCl₄, ^b*P*<0.01 vs Control, ^d*P*<0.01 vs CCl₄

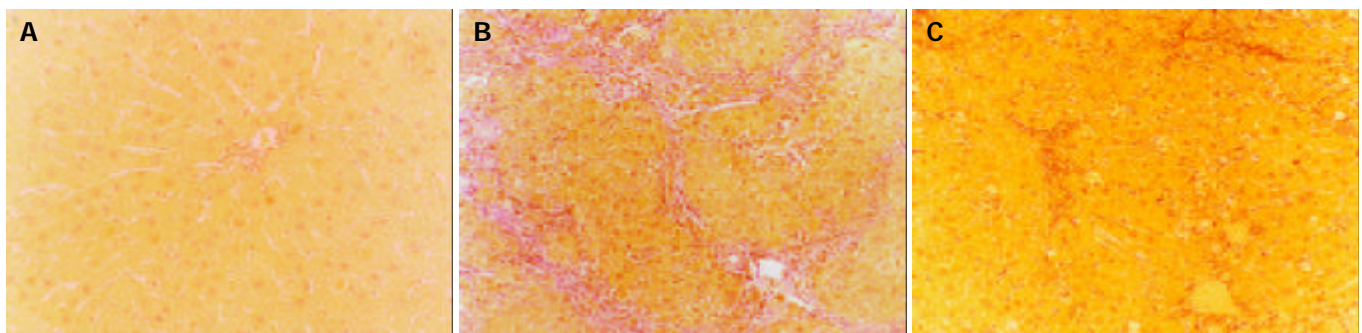


Figure 1 Histopathological findings of representative liver sections from female rats treated with CCl₄, VG staining, original magnification \times 100, A: Control group; B: OvX+CCl₄ group; C: OvX+CCl₄+ β -Est group.

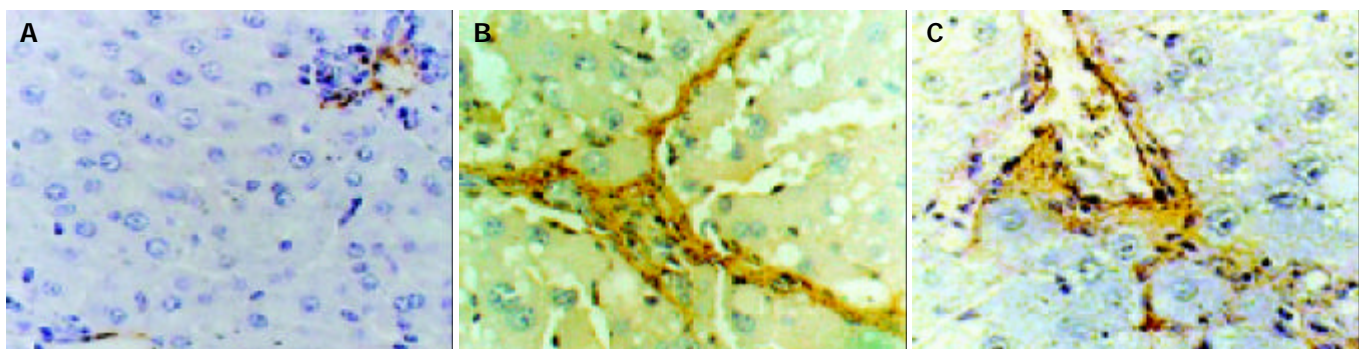


Figure 2 Immunohistochemistry of α -SMA in representative liver sections from female rats treated with CCl₄, DAB staining, A: control group, original magnification \times 200; B: OvX+CCl₄ group, original magnification \times 400; C: OvX+CCl₄+ β -Est group, original magnification \times 400.

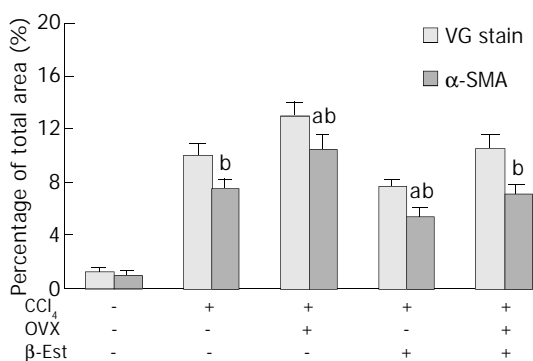


Figure 3 Histopathological and immunohistochemical changes in CCl₄-treated female rats (fibrotic area percentage of total field), ^a*P*<0.05 vs CCl₄; ^b*P*<0.01 vs control.

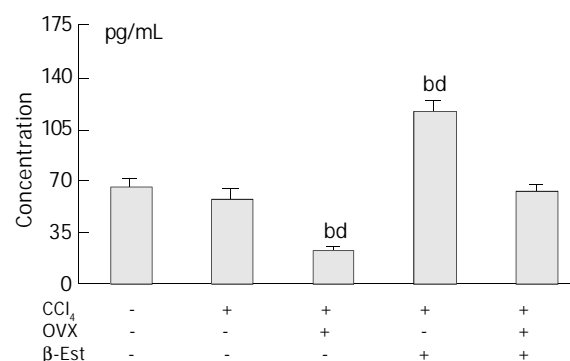


Figure 4 Serum estradiol levels in CCl₄-treated female rats, ^b*P*<0.01 vs control, ^d*P*<0.01 vs CCl₄.

In 34 CCl₄-treated rats, there was a negative correlation between the fibrotic area percentage and serum estradiol level, the calculated correlation coefficient was -0.57 ($P < 0.01$, Figure 5).

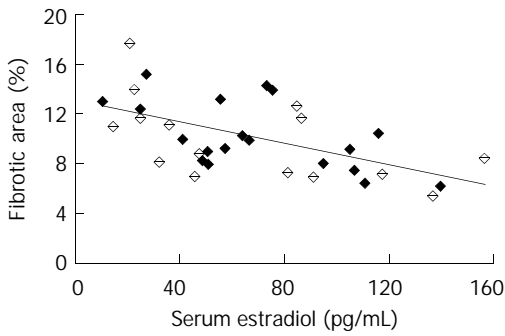


Figure 5 Negative correlation between fibrotic area percentage and serum estradiol level ($r = -0.57$, $P < 0.01$).

In vitro effect of β -Est and its metabolites on activation of rat HSCs
 β -Est, 2OHE and 2MeOE (10^{-9} - 10^{-7} mol/L) inhibited HSC proliferation (Figure 6A) and ECM secretion (Figures 6B and

6C) in a dose-dependent manner. Only the high concentration ($\geq 10^{-7}$ mol/L) of β -Est exerted inhibitory effects, while a concentration of 2MeOE as low as 10^{-9} mol/L had a similar effect. The order of potency was 2MeOE > 2OHE > β -Est. At a concentration of 10^{-7} mol/L, β -Est, 2OHE and 2MeOE all could inhibit HSCs in expressing α -SMA, and the potency of 2MeOE was significantly stronger than that of β -Est (Figure 6D)

A representative immunohistochemistry showed the expression of ER- β (Figure 7B) but not ER- α (Figure 7A) on rat HSCs.

DISCUSSION

Hepatic fibrosis, which is often associated with hepatocellular necrosis and inflammation, occurs as a repair process in many chronic liver diseases and is considered to be a forerunner of cirrhosis. HSCs are regarded as the primary target cells for inflammatory stimuli in the injured liver. Once activated, HSCs would be transformed into α -SMA positive myofibroblast-like cells, which are responsible for much of the collagen hypersecretion during hepatic fibrogenesis^[23-28].

In vivo study showed that β -Est at physiological doses could suppress the development of hepatic fibrosis in CCl₄-

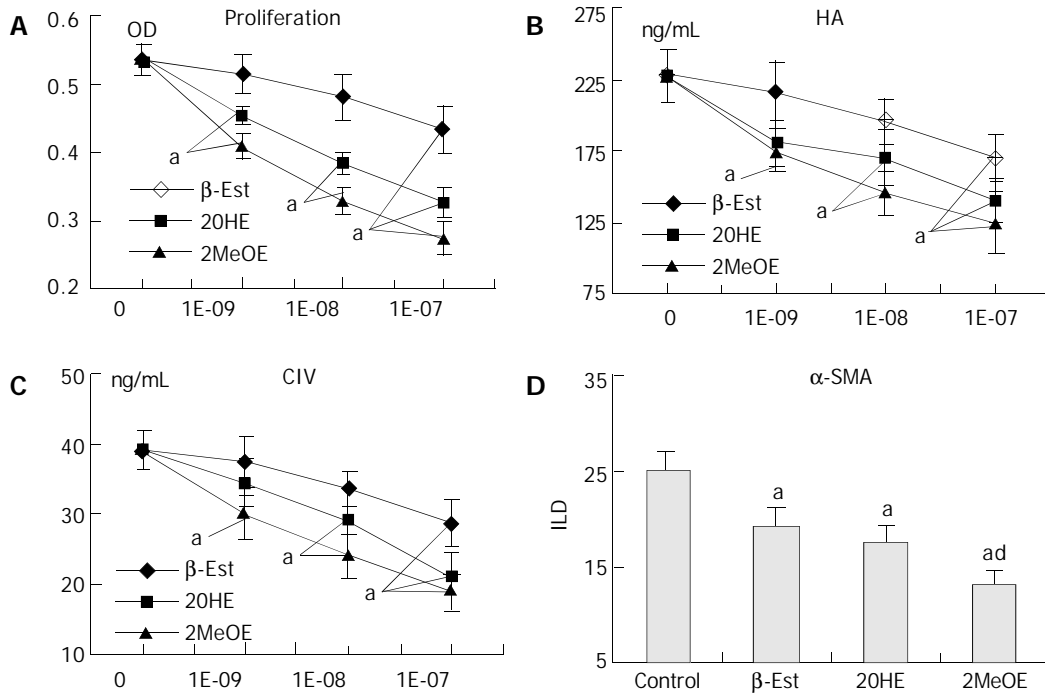


Figure 6 Effects of estradiol metabolites on function of HSCs proliferation (A), HA (B) and C IV (C) secretion in HSCs, effects of 10^{-7} mol/L estradiol metabolites on α -SMA expression (D) of HSCs, Values for each point represent mean \pm SD from 5 separate experiments, ^a $P < 0.05$ vs control, ^d $P < 0.05$ vs 10^{-7} mol/L β -Est.

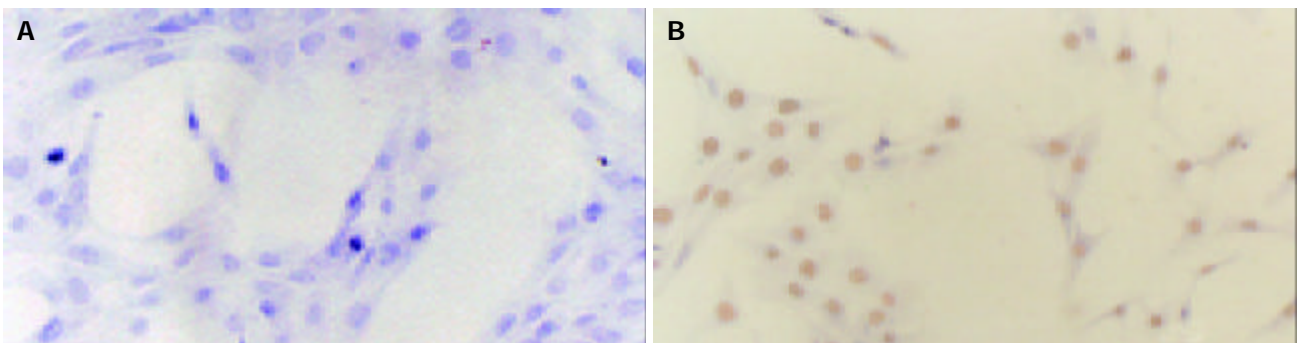


Figure 7 Representative immunohistochemistry showing expression of ER on HSCs used for studies, original magnification $\times 200$, No expression of ER- α (A) but ER- β (B) was observed.

induced hepatofibrotic rat models along with decreased serum liver enzymes, reduced collagen content and smaller areas of fibrosis in the liver. There was a negative correlation between the percentage of fibrotic area and the serum estradiol level with a calculated correlation coefficient of -0.57. Additionally, in cultured rat HSCs, β -Est inhibited cell proliferation, ECM secretion and α -SMA expression in a dose-dependent manner. These findings support β -Est as a potent inhibitor of HSCs transformation, thus, playing an antifibrogenic role in the progression from hepatic fibrosis to cirrhosis.

The pathway by which β -Est inhibits HSC activation is not clear. As HSCs contain ERs, it is presumed that ERs mediate the fibrosuppressive effects of β -Est. However, several lines of evidence do not support the hypothesis. In this regard, high levels of ER β but low or no levels of ER α expression were observed in normal and fibrotic livers and also in quiescent and activated HSCs from both male and female rats^[29], but β -Est in physiological doses was unable to suppress hepatic fibrosis in male rats following dimethylnitrosamine or pig serum administration^[30-32]. Our preliminary studies also suggested a sexually dimorphic response pattern of the injured liver to β -Est. Besides, the male patients expressed high serum levels of estradiol parallel to the stage of liver cirrhosis.

HSCs are VSMC, CF or GMC analogs that belong to the pericytes generically, so they may have many properties in common including a prominent role in repairing fibrosis against injury and similar reactions to β -Est. Recent studies by Iafrati *et al.*^[33] and Karas *et al.*^[34,35] showed that β -Est inhibited injury-induced VSMC proliferation in arteries of mice that lacked either ER α or ER β as well as in double knockout mice that lacked both ER α and ER β , suggesting that the effects might be mediated via an ER-independent pathway. Furthermore, 2OHE and 2MeOE, the biologically active metabolites of β -Est, could inhibit DNA synthesis, cell proliferation, collagen synthesis and mitogen activated protein kinase activity in VSMCs, CFs or GMCs with a potency stronger than β -Est^[9-13,36,37]. Liver is the main locus where β -Est metabolizes, so it is possible that the antifibrogenic actions of β -Est are mediated in part by local conversion of β -Est to biologically active metabolites.

In the present study, we attempted to testify this hypothesis by comparing the inhibitory effects of β -Est and its metabolites on the activation of rat HSCs *in vitro*. We found that treatment of HSCs with β -Est or its metabolites differentially inhibited FCS-induced cell proliferation, ECM secretion and α -SMA expression in the following order of potency: 2MeOE>2OHE> β -Est. Only the pharmacological concentration (>10⁻⁷ mol/L) of β -Est could significantly inhibit HSC proliferation and collagen synthesis, while the concentration of 2MeOE or 2OHE as low as 10⁻⁹ mol/L gave similar effects. β -Est, 2OHE and 2MeOE at a concentration of 10⁻⁷ mol/L each inhibited α -SMA expression by 24%, 30% and 47%, respectively.

The findings of this study provided evidence in rat HSC experiments that the metabolites of β -Est with little or no affinity for ERs could mediate the fibrosuppressive effects of β -Est via an ER-independent pathway. The results suggest that β -Est metabolism in the liver may be an important determinant of fibrosuppressive effects of circulating estradiol and that sexual differences in the liver metabolism of β -Est could determine a sexually dimorphic response pattern of liver cirrhosis. Moreover, genetic or acquired differences in β -Est metabolism may determine the fibrosuppressive benefits a patient receives from β -Est replacement therapy. Finally, the results also imply that nonfeminizing β -Est metabolites may afford antifibrogenic protection regardless of gender.

REFERENCES

- 1 **Poynard T**, Bedossa P, Opolon P. Natural history of liver fibrosis progression in patients with chronic hepatitis C. The OBSVIRC, METAVIR, CLINIVIR, and DOSVIRC groups. *Lancet* 1997; **349**: 825-832
- 2 **Poynard T**, Ratziu V, Charlotte F, Goodman Z, McHutchison J, Albrecht J. Rates and risk factors of liver fibrosis progression in patients with chronic hepatitis C. *J Hepatol* 2001; **34**: 730-739
- 3 **el-Serag HB**. Epidemiology of hepatocellular carcinoma. *Clin Liver Dis* 2001; **5**: 87-107
- 4 **Zhu BT**, Conney AH. Functional role of estrogen metabolism in target cells: review and perspectives. *Carcinogenesis* 1998; **19**: 1-27
- 5 **Zhu BT**, Conney AH. Is 2-methoxyestradiol an endogenous estrogen metabolite that inhibits mammary carcinogenesis? *Cancer Res* 1998; **58**: 2269-2277
- 6 **Cheng ZN**, Shu Y, Liu ZQ, Wang LS, Ou-Yang DS, Zhou HH. Role of cytochrome P450 in estradiol metabolism *in vitro*. *Acta Pharmacol Sin* 2001; **22**: 148-154
- 7 **Lee AJ**, Cai MX, Thomas PE, Conney AH, Zhu BT. Characterization of the oxidative metabolites of 17 β -estradiol and estrone formed by 15 selectively expressed human cytochrome p450 isoforms. *Endocrinology* 2003; **144**: 3382-3398
- 8 **Goodman JE**, Jensen LT, He P, Yager JD. Characterization of human soluble high and low activity catechol-O-methyltransferase catalyzed catechol estrogen methylation. *Pharmacogenetics* 2002; **12**: 517-528
- 9 **Dubey RK**, Gillespie DG, Zacharia LC, Barchiesi F, Imthurn B, Jackson EK. CYP450- and COMT-derived estradiol metabolites inhibit activity of human coronary artery SMCs. *Hypertension* 2003; **41**(3 Pt 2): 807-813
- 10 **Barchiesi F**, Jackson EK, Gillespie DG, Zacharia LC, Fingerle J, Dubey RK. Methoxyestradiols mediate estradiol-induced antimitogenesis in human aortic SMCs. *Hypertension* 2002; **39**: 874-879
- 11 **Dubey RK**, Gillespie DG, Keller PJ, Imthurn B, Zacharia LC, Jackson EK. Role of methoxyestradiols in the growth inhibitory effects of estradiol on human glomerular mesangial cells. *Hypertension* 2002; **39**(2 Pt 2): 418-424
- 12 **Dubey RK**, Gillespie DG, Zacharia LC, Rosselli M, Imthurn B, Jackson EK. Methoxyestradiols mediate the antimitogenic effects of locally applied estradiol on cardiac fibroblast growth. *Hypertension* 2002; **39**(2 Pt 2): 412-417
- 13 **Dubey RK**, Gillespie DG, Zacharia LC, Rosselli M, Korzekwa KR, Fingerle J, Jackson EK. Methoxyestradiols mediate the antimitogenic effects of estradiol on vascular smooth muscle cells via estrogen receptor-independent mechanisms. *Biochem Biophys Res Commun* 2000; **278**: 27-33
- 14 **Bissell DM**. Sex and hepatic fibrosis. *Hepatology* 1999; **29**: 988-989
- 15 **Friedman SL**, Rockey DC, McGuire RF, Maher JJ, Boyles JK, Yamasaki G. Isolated hepatic lipocytes and Kupffer cells from normal human liver: morphological and functional characteristics in primary culture. *Hepatology* 1992; **15**: 234-243
- 16 **Riccaltan-Banks L**, Bhandari R, Fry J, Shakesheff KM. A simple method for the simultaneous isolation of stellate cells and hepatocytes from rat liver tissue. *Mol Cell Biochem* 2003; **248**: 97-102
- 17 **Ratziu V**, Lalazar A, Wong L, Dang Q, Collins C, Shaulian E, Jensen S, Friedman SL. Zf9, a Kruppel-like transcription factor up-regulated *in vivo* during early hepatic fibrosis. *Proc Natl Acad Sci U S A* 1998; **95**: 9500-9505
- 18 **Reynaert H**, Vaeyens F, Qin H, Hellemans K, Chatterjee N, Winand D, Quartier E, Schuit F, Urbain D, Kumar U, Patel YC, Geerts A. Somatostatin suppresses endothelin-1-induced rat hepatic stellate cell contraction via somatostatin receptor subtype 1. *Gastroenterology* 2001; **121**: 915-930
- 19 **Williams EJ**, Benyon RC, Trim N, Hadwin R, Grove BH, Arthur MJ, Unemori EN, Iredale JP. Relaxin inhibits effective collagen deposition by cultured hepatic stellate cells and decreases rat liver fibrosis *in vivo*. *Gut* 2001; **49**: 577-583
- 20 **Ikeda K**, Wakahara T, Wang YQ, Kadoya H, Kawada N, Kaneda K. *In vitro* migratory potential of rat quiescent hepatic stellate cells and its augmentation by cell activation. *Hepatology* 1999; **29**: 1760-1767
- 21 **Kim KY**, Choi I, Kim SS. Progression of hepatic stellate cell

- activation is associated with the level of oxidative stress rather than cytokines during CCl₄-induced fibrogenesis. *Mol Cells* 2000; **10**: 289-300
- 22 **Sato M**, Suzuki S, Senoo H. Hepatic stellate cells: unique characteristics in cell biology and phenotype. *Cell Struct Funct* 2003; **28**: 105-112
- 23 **Friedman SL**. Molecular regulation of hepatic fibrosis, an integrated cellular response to tissue injury. *J Biol Chem* 2000; **275**: 2247-2250
- 24 **Gabele E**, Brenner DA, Rippe RA. Liver fibrosis: signals leading to the amplification of the fibrogenic hepatic stellate cell. *Front Biosci* 2003; **8**: D69-D77
- 25 **Mann DA**, Smart DE. Transcriptional regulation of hepatic stellate cell activation. *Gut* 2002; **50**: 891-896
- 26 **McCrudden R**, Iredale JP. Liver fibrosis, the hepatic stellate cell and tissue inhibitors of metalloproteinases. *Histol Histopathol* 2000; **15**: 1159-1168
- 27 **Dooley S**, Delvoux B, Lahme B, Mangasser-Stephan K, Gressner AM. Modulation of transforming growth factor beta response and signaling during transdifferentiation of rat hepatic stellate cells to myofibroblasts. *Hepatology* 2000; **31**: 1094-1106
- 28 **Brenner DA**, Waterboer T, Choi SK, Lindquist JN, Stefanovic B, Burchardt E, Yamauchi M, Gillan A, Rippe RA. New aspects of hepatic fibrosis. *J Hepatol* 2000; **32**(1 Suppl): 32-38
- 29 **Zhou Y**, Shimizu I, Lu G, Itonaga M, Okamura Y, Shono M, Honda H, Inoue S, Muramatsu M, Ito S. Hepatic stellate cells contain the functional estrogen receptor beta but not the estrogen receptor alpha in male and female rats. *Biochem Biophys Res Commun* 2001; **286**: 1059-1065
- 30 **Yasuda M**, Shimizu I, Shiba M, Ito S. Suppressive effects of estradiol on dimethylnitrosamine-induced fibrosis of the liver in rats. *Hepatology* 1999; **29**: 719-727
- 31 **Shimizu I**, Mizobuchi Y, Yasuda M, Shiba M, Ma YR, Horie T, Liu F, Ito S. Inhibitory effect of oestradiol on activation of rat hepatic stellate cells *in vivo* and *in vitro*. *Gut* 1999; **44**: 127-136
- 32 **Xu JW**, Gong J, Chang XM, Luo JY, Dong L, Hao ZM, Jia A, Xu GP. Estrogen reduces CCL₄- induced liver fibrosis in rats. *World J Gastroenterol* 2002; **8**: 883-887
- 33 **Iafrati MD**, Karas RH, Aronovitz M, Kim S, Sullivan TR Jr, Lubahn DB, O' Donnell TF Jr, Korach KS, Mendelsohn ME. Estrogen inhibits the vascular injury response in estrogen receptor alpha deficient mice. *Nat Med* 1997; **3**: 545-548
- 34 **Karas RH**, Hodgin JB, Kwoun M, Kregel JH, Aronovitz M, Mackey W, Gustafsson JA, Korach KS, Smithies O, Mendelsohn ME. Estrogen inhibits the vascular injury response in estrogen receptor beta-deficient female mice. *Proc Natl Acad Sci U S A* 1999; **96**: 15133-15136
- 35 **Karas RH**, Schulten H, Pare G, Aronovitz MJ, Ohlsson C, Gustafsson JA, Mendelsohn ME. Effects of estrogen on the vascular injury response in estrogen receptor alpha, beta (double) knockout mice. *Circ Res* 2001; **89**: 534-539
- 36 **Dubey RK**, Jackson EK. Cardiovascular protective effects of 17beta-estradiol metabolites. *J Appl Physiol* 2001; **91**: 1863-1883
- 37 **Dubey RK**, Jackson EK. Estrogen-induced cardiorenal protection: potential cellular, biochemical, and molecular mechanisms. *Am J Physiol Renal Physiol* 2001; **280**: F365-F388

Edited by Kumar M and Wang XL Proofread by Xu FM

Hyperammonemia, brain edema and blood-brain barrier alterations in prehepatic portal hypertensive rats and paracetamol intoxication

Camila Scorticati, Juan P. Prestifilippo, Francisco X. Eizayaga, José L. Castro, Salvador Romay, María A. Fernández, Abraham Lemberg, Juan C. Perazzo

Camila Scorticati, Juan P. Prestifilippo, Francisco X. Eizayaga, Salvador Romay, María A Fernández, Abraham Lemberg, Juan C. Perazzo, Cátedra de Fisiopatología, Facultad de Farmacia y Bioquímica, Universidad de Buenos Aires, Buenos Aires, Argentina
José L. Castro, Cátedra de Farmacología, Facultad de Farmacia y Bioquímica, Universidad de Buenos Aires, Buenos Aires, Argentina
Supported by Grant # TB 56 from the University of Buenos Aires, Argentina

Correspondence to: Professor. Dr. J. C. Perazzo, Cátedra de Fisiopatología, Junín 956, 5° Piso, (1113), Ciudad Autónoma de Buenos Aires, Argentina. jperazzo@ffyb.uba.ar

Fax: +54-11-4964 8268

Received: 2003-09-23 **Accepted:** 2003-12-24

Abstract

AIM: To study the blood-brain barrier integrity, brain edema, animal behavior and ammonia plasma levels in prehepatic portal hypertensive rats with and without acute liver intoxication.

METHODS: Adults male Wistar rats were divided into four groups. Group I: sham operation; II: Prehepatic portal hypertension, produced by partial portal vein ligation; III: Acetaminophen intoxication and IV: Prehepatic portal hypertension plus acetaminophen. Acetaminophen was administered to produce acute hepatic injury. Portal pressure, liver serum enzymes and ammonia plasma levels were determined. Brain cortex water content was registered and trypan blue was utilized to study blood brain barrier integrity. Reflexes and behavioral tests were recorded.

RESULTS: Portal hypertension was significantly elevated in groups II and IV. Liver enzymes and ammonia plasma levels were increased in groups II, III and IV. Prehepatic portal hypertension (group II), acetaminophen intoxication (group III) and both (group IV) had changes in the blood brain-barrier integrity (trypan blue) and hyperammonemia. Cortical edema was present in rats with acute hepatic injury in groups III and IV. Behavioral test (rota rod) was altered in group IV.

CONCLUSION: These results suggest the possibility of another pathway for cortical edema production because blood brain barrier was altered (vasogenic) and hyperammonemia was registered (cytotoxic). Group IV, with behavioral altered test, can be considered as a model for study at an early stage of portal-systemic encephalopathy.

Scorticati C, Prestifilippo JP, Eizayaga FX, Castro JL, Romay S, Fernández MA, Lemberg A, Perazzo JC. Hyperammonemia, brain edema and blood-brain barrier alterations in prehepatic portal hypertensive rats and paracetamol intoxication. *World J Gastroenterol* 2004; 10(9): 1321-1324

<http://www.wjgnet.com/1007-9327/10/1321.asp>

INTRODUCTION

Portal hypertension (PH) is a major syndrome that frequently accompanies chronic liver diseases such as cirrhosis. Prehepatic

PH creates a splanchnic hyperdynamic circulation and hyperemia with increased splanchnic resistance and production of collateral vessels that drive splanchnic blood flow to systemic circulation^[1].

Portal-systemic encephalopathy (PSE), the most commonly encountered form of hepatic encephalopathy (HE), describes a wide spectrum of reversible and irreversible neuropsychiatric abnormalities that appear as a complication in patients with acute or chronic liver disease. HE is usually found as an overt form or in a mild form with lesser neuropsychiatric symptoms, which can be misdiagnosed^[2].

Acetaminophen (APAP) is a non-steroid anti-inflammatory drug (NSAID), frequently used in adults and children. At high concentration of APAP, the glutathione-dependent conjugation system generates a toxic metabolite that binds covalently to cellular proteins and macromolecules followed by cell destruction^[3,4].

Finally, ammonia originated from the gut protein metabolism has been implicated as an important factor in the production of HE. In chronic liver disease, ammonia evades liver catabolism to urea through portal systemic shunts and collaterals, and reaches the brain in high blood concentration^[5].

In previous experiments we documented different aspects of the relationship between prehepatic PH in rats and central nervous system: alterations in uptake and release of norepinephrine and modification and tyrosine hydroxylase activity in discrete regional mesencephalic nucleus^[6,7]. Furthermore, we considered that PH rats underwent a subclinical HE^[8].

The aim of this experiment was to study the blood-brain barrier (BBB) integrity, brain cortical edema, ammonia plasma levels and behavior in rats with different liver injuries.

MATERIALS AND METHODS

Animals and surgical procedures

Male Wistar rats (240-260 g of body mass, 12 h of light cycle: 8 a.m.-8 p.m.) were used and animal welfare was in accordance with guidelines of the Faculty of Pharmacy and Biochemistry of Buenos Aires and approved by ethical committee according to Helsinki's Declaration. Animals were placed in individual cages and allowed to recover from surgery. Rats were fed standard laboratory chow and water *ad libitum*.

Group II (chronic PH): Portal hypertensive (PH) animals were obtained by calibrated stenosis of the portal vein according to Chojkier *et al.*^[1]. Rats were lightly anesthetized with ether and then midline abdominal incision was made. The portal vein was located and isolated from surrounding tissues. A ligature of 3.0 silk suture was placed around the vein, and snugly tied to a 20-gauge blunt-end needle placed along the side of the portal vein. The needle was subsequently removed to yield a calibrated stenosis of portal vein, after which the abdomen was sutured. Operations were performed at 2 p.m. to obey circadian rhythm and fourteen days later the animals developed PH.

Group III (acute intoxication): Acetaminophen was injected i.p. at a dose of 750 mg/kg.d per rat on the 13th and 14th day, considering as the start day or day zero, the day of the surgical procedure of group II.

Group IV (chronic PH plus acute intoxication): Rats underwent partial portal vein ligation as in group II and then

received acetaminophen the same dose as in group III.

Group I: Shamly operated rats underwent the same experimental procedure like group II, except that portal vein was isolated but not stenosed.

All groups received a subcutaneous injection (25 mL/Kg of body mass) of a 50 g/L dextrose, 4.5 g/L saline solution, containing 20 mEq/L of potassium chloride, every 12 h after the first injection of APAP, as a supportive therapy to prevent hypoglycemia and renal failure^[9]. Rats were sacrificed on d 14, 6 to 8 h after the last acetaminophen injection.

Experimental procedures

Following experiment were performed in four groups of animals (I: SHAM, II: HP, III: APAP and IV: HP+APAP, $n=6/8$ per group).

Portal pressure measurement

Rats were anesthetized with sodium pentobarbital (40 mg/kg, ip). The spleen was cannulated with a polyethylene cannula (PE 50) filled with heparinized saline solution (25 U/mL) to measure portal pressure by Statham Gould P23ID pressure transducer (Statham, Hato Rey, Puerto Rico) coupled to a Grass 79 D polygraph (Grass Instruments, Quincy, MA).

Biochemical determination

Blood samples were obtained by abdominal aortic artery puncture for the determination of biochemical parameters. Plasma aminotransferase activity was determined using standardized and optimized commercial Boehringer-Mannheim kits (Germany). Ammoniac Enzymatique UV kits (Biomerieux-France) were used to determine plasma ammonia concentration. Plasma levels of urea, glucose and creatinine were measured by current biochemical colorimetric UV methods (Wiener, Argentine).

Microscopy

High resolution optical microscopy (HROM): sections of liver were fixed in buffered formalin and embedded in paraplast. Routine stains were used: hematoxylin-eosin, PAS and Masson's trichrome for light microscopy and toluidine blue stain for HROM.

Brain water content

Rats were sacrificed by exsanguination under complete ether anesthesia, their brains cortex water content was measured to quantify possible brain edema according to Marmorou^[10].

One cerebral hemisphere was quickly removed after rats were sacrificed and stored at 4 °C to be processed within 30 min. The hemisphere was cut into coronal slices and eight samples taken from the cerebral cortex, approximately 10 mg in weight, was placed in a bromobenzene-kerosene density gradient column to measure brain water^[10]. The column was previously calibrated with varying concentrations of potassium sulfate to ensure a linear relation (>0.997) between the K₂SO₄ and readings in the density gradient. The equilibration point of the samples was read at 2 min and averaged, conversion from specific gravity to brain water was done as previously reported^[10].

Trypan blue transcardial perfusion

Rats were perfused with trypan blue (TB) solution and then fixed in paraformaldehyde. TB solution (5 g/L) was made by dissolving 1 g of TB in 200 mL of PBS with gentle heat. The solution was allowed to cool room temperature and then added to the filtrate, then the solution was placed on ice and used immediately. The temperature of TB solution was 10-12 °C at the time of perfusion. Rats were anesthetized with ethyl urethane (1 mg/kg) and perfused transcardially with 200 mL of TB solution, followed by 300 mL of ice-cold paraformaldehyde (20 g/L in PBS), the low rate of perfusate was maintained at 25 mL/min. Brains were dissected and post-fixed overnight in

0.3 Kg/L sucrose for 2 d. Subsequently, brains were frozen in powdered dry ice and stored at -80 °C until processed for microscopic studies. Slices of brain hippocampus were obtained with cryostat in sections of 300 microns according to Watson and Paxinos (Hippocampus fig 24, bregma 4.8, interneuron 4.2). Hippocampal slices were evaluated under light microscopy and the results were expressed as positive (+) or negative (-) for TB staining. Medial eminence and choroids plexus staining were used as control of TB appropriated perfusion^[11].

Pharmacological and behavioral test

Corneal, pain-response and right reflexes were performed. Automated open field (Animex) and rota-rod tests (to study motor coordination) were realized. Rota-rod speed was fixed at 25 turns/min. Rats were trained 48 h before the experiment until they fell down less than 3 times in 5 min. The number of falls during the experiment and time elapsed to the first fall were recorded^[12,13].

Statistical methods

Results were expressed as mean±SE. Statistical analysis was performed by means of repeated measurement analysis of variance (ANOVA) followed by Newman-Keuls' s test. Dunn' s test was used for non-parametric data, *P* values less than 0.05 were considered statistically significant.

RESULTS

Portal pressure (PP) was significant higher in groups II and IV ($^aP<0.01$) when compared to control group. There was no significant difference when compared PP of group I (Sham) with group III (APAP) (Table 1).

Table 1 Portal pressure (PP) and plasma aminotranferase levels

	Sham (I)	PH (II)	APAP (III)	PH+APAP (IV)
PP (mmHg)	8.5±0.5	12.1±1 ^a	8.1±0.2	11.9±0.9 ^a
AST (UI/L)	155±25	316±23 ^b	426±36 ^b	380±34 ^b
ALT (UI/L)	39±4	63±9	134±20 ^a	308±27 ^b

PP was significantly increased in groups II and IV ($^aP<0.05$ vs control and APAP group). AST plasma levels were significantly increased in groups II, III and IV ($^bP<0.001$ vs sham group). ALT was significantly increased in groups III and IV ($^aP<0.05$ and $^bP<0.001$ vs sham group, respectively).

AST plasma levels were significant increased in groups II, III and IV when compared with group I ($^bP<0.001$). ALT plasma levels were significant increased in groups III and IV when compared with control group (Table 1).

Plasma levels of urea, glucose and creatinine were normal in all groups of rats (data not shown).

Ammonia blood concentrations (μmol/L) showed significant increase in PH rats, APAP group and PH plus APAP ($P<0.05$ and $P<0.001$ respectively) (Figure 1).

Light microscopy and HROM showed normal histology in liver parenchyma in group I, minimal focal necrosis in group II; diffuse hemorrhagic necrosis in group III and focal hemorrhage and confluent necrosis in group IV. (Figure 2 A-D).

Brain cortical water content (H₂O/ g brain weight %) showed significant increase in rats injected with APAP ($P<0.001$) and in those with PH+APAP ($P<0.01$) (Figure 3).

In Groups II, III and IV trypan blue was positive in the perivascular space in the hippocampus area (Figure 4).

All reflexes studied including the Animex were normal for all groups except for rota-rod test that showed in group IV a significant difference at the time elapsed to the first fall (not in number of falls), when compared to shamly operated animals (Table 2).

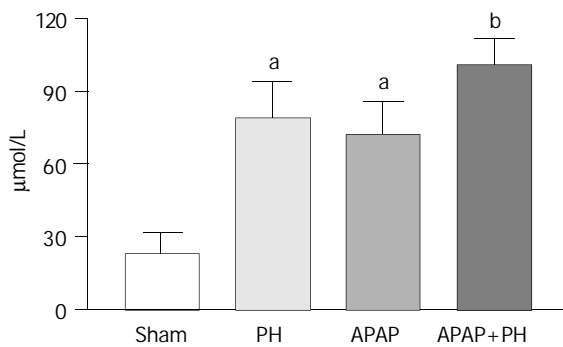


Figure 1 Significantly increased ammonia plasma levels in all groups of rats ^a $P < 0.05$ and ^b $P < 0.01$ when compared with sham group.

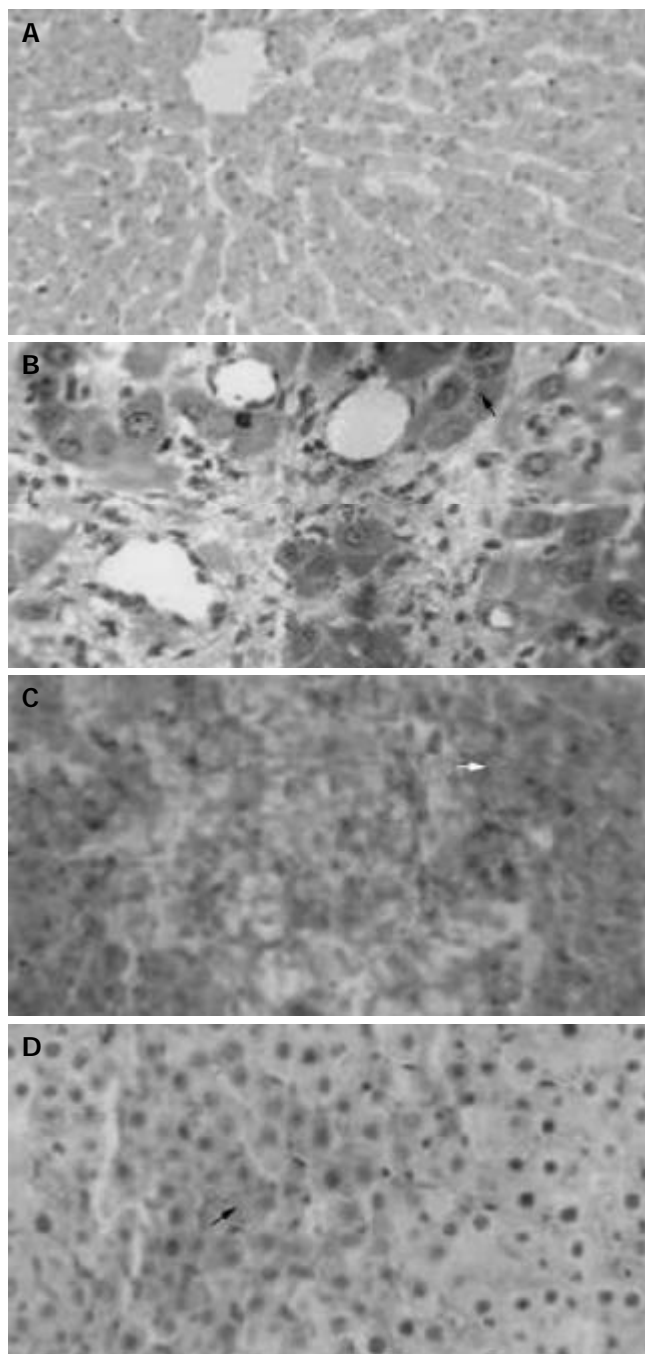


Figure 2 Liver Microscopy. A: Shows a normal liver histology corresponding to a rat in sham group (HE, 100×), B: Minimal focal necrosis in group II (HE, asterisk, 500×), C: Diffuse hemorrhagic necrosis in group III (HE, arrows, 400×), D: Focal hemorrhagic confluent necrosis in group IV (HE, asterisk, 400×).

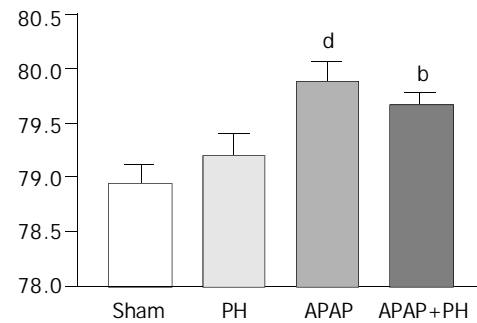


Figure 3 Significantly increased brain water content in groups III and IV ^d $P < 0.01$, ^b $P < 0.001$ when compared with sham group.

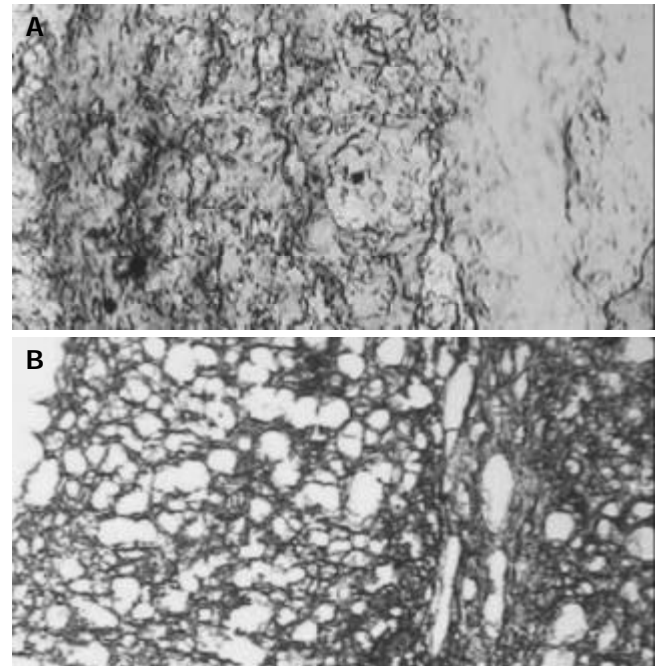


Figure 4 Trypan blue and BBB. A: Trypan blue dye in hippocampus of a sham rat. No breakdown of BBB was observed. Trypan blue was only positive in vascular space (100×), B: Trypan blue dye diffusion due to the breakdown of BBB as an example of what was observed in hippocampus in groups II, III and IV (100×).

Table 2 Rota rod test: First fall time

	Sham (I)	PH (II)	APAP (III)	PH+APAP (IV)
Median	300 ^a	300 ¹	205 ¹	45 ¹
Confidence interval (Lower 95%-Upper 95%)	(172-356)	(63-316)	(45-318)	(-13.9-108) ^a

¹: expressed in seconds. Rota rod test was significantly different in group IV compared with all the others groups (^a $P < 0.05$ Dunnett's test).

DISCUSSION

Experimental prehepatic portal hypertension produces a hyperdynamic redistribution of splanchnic circulation and minimal liver damage. It could be considered that prehepatic PH is a subclinical PSE stage^[8]. In this study APAP was used to produce liver injury because of its aggressive effect on liver parenchyma^[3,4]. It was administered to two groups that reflected different situations, namely an acute form of liver injury (group III) and a chronic liver PH group plus an acute liver intoxication.

Portal pressure (PP) was significantly increased in group II, as it was described elsewhere^[8] and in group IV. PP in group III (APAP) had normal values. This agreed with acute intoxications

and specifically with acute APAP intoxication^[14]. Group IV and group II had similar PP values, and it might be due to a chronic PH induced shunt (groups II and IV).

Liver enzymes reflected hepatocyte damage. When liver parenchyma was injured, the enzymes increased as it could be seen in early stages of PSE. Plasma enzyme levels were higher in group III than those in APAP induced acute liver damage. In addition, liver histopathology was concordant with these data as a diffuse hemorrhagic necrosis was observed in group III^[14].

Ammonia plasma level data showed normal values in group I and significantly increased values in groups II, III and IV. The values registered were remarkably lower than those observed in different models of acute liver failure (ALF). It is important to point out that in group II hyperammonemia was produced by opened shunts due to the splanchnic blood flow redistribution^[15]. It is also interesting that in this experimental model the hepatic blood flow was reduced, but not completely shunted as in other models (e.g. porto-caval shunts, PCS). Ammonia was markedly increased as the major responsible molecule related to HE^[16] had several pathways, lately the cGMP-NO-glutamate that leads to cytotoxic brain edema characterized by swelling of astrocytes and their processes, raised intracranial pressure and as a consequence, to brain herniation^[5]. This was the main cause of mortality in ALF and it could be predicted by increased arterial ammonia plasma levels^[17]. Besides this, PSE could lead to increased nNOS activity^[18], associated with L-arginine uptake in a PCS model^[19].

In this model of PH, brain edema was not correlated with ammonia increase. Furthermore brain edema was documented in group III and ammonia level was lower than that in group II and no cerebral edema was observed. Besides this, brain edema was lower in group IV than in group III and the highest recorded ammonia was recorded. What is the major mechanism involved in the development of brain edema in this experiment? One of the pathways of brain edema is the vasogenic and if that mechanism was involved in groups III and IV, why in group II BBB integrity was broken-down and ammonia plasma levels were increased, and no cortical brain edema was documented? Although a mixed mechanism (vasogenic and cytotoxic) was proposed for brain edema in ALF^[20], in this experiment no brain edema was present in the chronic group without acute hepatocyte injury. In the chronic group plus acute liver injury brain edema was registered and the cytotoxic mechanism could be mostly responsible. Under these experimental conditions another mechanism of brain edema might involve aquaporins. The aquaporin-type water channels are integral membrane proteins that have been found to function as conduits for osmotically driven transport of water across cell plasma membranes^[21]. In this experiment BBB integrity was altered and thus endothelial cells were involved. AQP4 presented in both, endothelia and astrocytes might play an active role in regulation of astrocyte swelling and the presence of brain edema^[22].

TB demonstrated altered integrity of the BBB at the hippocampus areas involved in learning and memory consolidation in groups II, III and IV. Furthermore, the only group with an altered behavioral test, at first fall in rota rod test, was group IV. These might be related with the observation in the only group with PH, elevated enzymes, hepatocyte injury, hyperammonemia, brain edema, positive TB and altered rota rod test. Dixit^[23] demonstrated that in rats with galactosamine-induced ALF BBB breakdown evidenced by TB dye infusion studies began in grade III coma. Despite this, under the present experimental conditions no clinical evidence of coma could be registered in any group. Therefore, group IV can be considered as an experimental model of subclinic PSE.

REFERENCES

1 **Chojkier M**, Groszmann RJ. Measurement of portal-systemic

- shunting in the rat by using gamma-label microspheres. *Am J Physiol* 1981; **240**: G371-375
- 2 **Watanabe A**. Cerebral changes in hepatic encephalopathy. *J Gastroenterol Hepatol* 1998; **13**: 752-760
- 3 **Kelly JH**, Koussayes T, Da-hertte HE, Chong MG, Shang TA, Wissenbrot HH, Sussman NC. An improved model of acetaminophen-induced fulminant hepatic failure in dogs. *Hepatol* 1992; **15**: 329-335
- 4 **Francavilla A**, Makowka L, Polimeno L, Barone M, Demetris J, Prelich J, Van Thiel DH, Starzl TE. A dog model for acetaminophen-induced fulminant hepatic failure. *Gastroenterology* 1989; **96**(2 Pt 1): 470-478
- 5 **Felipo V**, Butterworth RF. Neurobiology of ammonia. *Prog Neurobiol* 2002; **67**: 259-279
- 6 **Lemberg A**, Eizayaga F, Vatta M, Dominguez A, Romay S, Bianciotti L, Sanso G, Fernandez B. Prehepatic portal hypertension in rats modifies norepinephrine metabolism in hypothalamus, medulla oblongata and portal vein. *Dig Dis Sci* 1993; **38**: 1259-1262
- 7 **Lemberg A**, Rubio M, Bengochea L, Romay S, Eizayaga F, Diez A, Perazzo JC. Tyrosine hydroxylase activity in discrete brain regions from prehepatic portal hypertensive rats. *Hepatogastroenterology* 1998; **45**: 547-550
- 8 **Scorticati C**, Prestifilippo P, Murer G, Lemberg A, Perazzo JC. Functional alterations in central nervous system of prehepatic portal hypertensive rats. *Medicina* 2001; **61**: 673-675
- 9 **Gammal SH**, Basile AS, Heller D, Skolnick P, Jones LA. Reversal of the behavioral and electrophysiological abnormalities of an animal model of hepatic encephalopathy by benzodiazepines receptor ligands. *Hepatology* 1990; **11**: 371-378
- 10 **Marmarou A**, Poll W, Shulman K, Banagavem H. A simple gravimetric technique for measurement of cerebral edema. *J Neurosurg* 1978; **49**: 530-537
- 11 **Reynolds DS**, Morton AJ. Changes in Blood Brain Barrier permeability following neurotic lesions of rat brain can be visualized with Trypan Blue. *J Neurosci Methods* 1998; **79**: 115-121
- 12 **Dunham NW**, Miya TS. A note on a simple apparatus for detection neurological deficit in rats and mice. *J Am Pharm Assoc* 1957; **46**: 208-209
- 13 **Maynert EW**. A test group for central depressants. RA Turner (Ed) screening methods in pharmacology. New York: Academic Press 1965: 80-86
- 14 **Bengochea L**, Ghanem C, Perazzo JC, Ghisolfi C, Marabotto L, Acevedo C, Mino J, Lemberg A, Rubio M. Drug glucuronidation and hepatic lipid microsomal membrane profile in cholestatic rats followed paracetamol intoxication. *Pharmacol Res* 1999; **40**: 369-376
- 15 **MacMathuna P**, Vlavianos P, Westaby D, Williams R. Pathophysiology of Portal Hypertension. *Dig Dis* 1992; **10**(Suppl 1): 3-15
- 16 **Kramer E**, Tribl B, Gendo A, Zauner C, Schneider B, Ferenci P, Madl C. Partial pressure of ammonia versus ammonia in hepatic encephalopathy. *Hepatology* 2000; **31**: 30-34
- 17 **Clemmensen JO**, Larsen FS, Kondrup J, Hansen BA, Ott P. Cerebral herniation in patients with acute liver is correlated with arterial ammonia concentration. *Hepatol* 1999; **29**: 648-653
- 18 **Rao VL**, Audet RM, Butterworth RF. Increased nitric oxide synthase activities and l- [3 H] arginine uptake in brain following portacaval anastomosis. *J Neurochem* 1995; **65**: 677-678
- 19 **Rao VL**, Audet RM, Butterworth RF. Portacaval shunting and hyperammonemia stimulate the uptake of l- [3 H] arginine but not of l- [3 H] nitroarginine into rat brain synaptosomes. *J Neurochem* 1997; **68**: 337-343
- 20 **Swain M**, Butterworth RF, Blei AT. Ammonia and related amino acids in the pathogenesis of brain edema in acute ischemic liver failure in rats. *Hepatol* 1992; **15**: 449-453
- 21 **Verkman AS**. Role of aquaporin water channels in eye function. *Exp Eye Res* 2003; **76**: 137-143
- 22 **Papadopoulos MC**, Krishna S, Verkman AS. Aquaporin water channels and brain edema. *Mt Sinai J Med* 2002; **69**: 242-248
- 23 **Dixit V**, Chang TM. Brain edema and blood brain barrier in galactosamine-induced fulminant hepatic failure rats. An animal model for evaluation of liver support systems. *ASAIO Trans* 1990; **36**: 21-27

Modulation of Kupffer cells on hepatic drug metabolism

Hong Ding, Jing Tong, Shi-Cheng Wu, Deng-Ke Yin, Xian-Fen Yuan, Jian-Yuan Wu, Jun Chen, Gang-Gang Shi

Hong Ding, Gang-Gang Shi, Medical College, Shantou University, Shantou 515031, Guangdong Province, China

Jing Tong, Shi-Cheng Wu, Deng-Ke Yin, Xian-Fen Yuan, Jian-Yuan Wu, Jun Chen, Department of Pharmacology, College of Pharmacy, Wuhan University, Wuhan 430072, Hubei Province, China
Supported by the Postdoctor Science Foundation of China, No. 2002032238 the Major State Basic Research Development Program of China, No. 2002ccc00300

Correspondence to: Jing Tong, College of Pharmacy, Wuhan University, Wuhan 430072, Hubei Province, China. tongjing2002@etang.com

Telephone: +86-27-87682339 **Fax:** +86-27-87682339

Received: 2003-08-26 **Accepted:** 2003-10-07

Abstract

AIM: To observe the effects of Kupffer cells on hepatic drug metabolic enzymes.

METHODS: Kunming mice were ip injected with $GdCl_3$ 10, 20, 40 mg/kg to decrease the number and block the function of kupffer cells selectively. The contents of drug metabolic enzymes, cytochrome P450, NADPH-cytochrome C reductase (NADPH-C), aniline hydroxylase (ANH), aminopyrine N-demethylase (AMD), erythromycin N-demethylase (EMD), and glutathione s-transferase (mGST) in hepatic microsome and S9-GSTpi, S9-GST in supernatant of 9 000 g were accessed 1 d after the injection. The time course of alteration of drug metabolic enzymes was observed on d 1, 3, and 6 treated with a single dose $GdCl_3$. Mice were treated with *Angelica sinensis* polysaccharides (ASP) of 30, 60, 120 mg/kg, ig, qd \times 6 d, respectively and the same assays were performed.

RESULTS: P450 content and NADPH-C, ANH, AMD, and EMD activities were obviously reduced 1 d after Kupffer cell blockade. However, mGST and S9-GST activities were significantly increased. But no relationship was observed between $GdCl_3$ dosage and enzyme activities. With single dose $GdCl_3$ treatment, P450 content, NADPH-C, and ANH activities were further decreased following Kupffer cell blockade lasted for 6 d, by 35.7%, 50.3%, 36.5% after 3 d, and 57.9%, 57.9%, 63.2% after 6 d, respectively. On the contrary, AMD, EMD, mGST, and S9-GST activities were raised by 36.5%, 71.9%, 23.1%, 35.7% after 3 d, and 155%, 182%, 21.5%, 33.7% after 6 d, respectively. Furthermore, the activities of drug metabolic enzymes were markedly increased after 30 mg/kg ASP treatment, and decreased significantly after 120 mg/kg ASP treatment. No change in activity of S9-GSTpi was observed in the present study.

CONCLUSION: Kupffer cells play an important role in the modulation of drug metabolic enzymes. The changes of drug metabolic enzyme activities depend on the time of kupffer cell blockade and on the degree of Kupffer cells activated. A low concentration of ASP increases the activities of drug metabolic enzymes, but a high concentration of ASP decreases the activities of drug metabolic enzymes.

Ding H, Tong J, Wu SC, Yin DK, Yuan XF, Wu JY, Chen J, Shi

GG. Modulation of Kupffer cells on hepatic drug metabolism. *World J Gastroenterol* 2004; 10(9): 1325-1328
<http://www.wjgnet.com/1007-9327/10/1325.asp>

INTRODUCTION

Drug metabolic enzymes can detoxify endogenous and exogenous compounds and also generate potentially carcinogenic or toxic compounds in the process of catalyzing the metabolism of xenobiotics, and inhibition and induction of their activities are also the key mechanisms in drug-drug interactions^[1,2]. The induction or inhibition of metabolizing enzyme activities by a great deal of substances (including drugs, foods, inflammatory factors, etc.) influences their toxicological or pharmacological outcomes as well as those of other xenobiotics or drugs^[3-5].

The role of sinusoidal cells in hepatic metabolism has been greatly underestimated until now. However, Kupffer cells, despite their size represents 80% to 90% of all fixed macrophages in the body and approximately 14% of the hepatic cellular mass, the function in hepatic metabolism of Kupffer cells is unknown. Some reports suggested that Kupffer cells might play an important role in xenobiotic-induced hepatotoxicity, which is often dependent on their metabolism. Although hepatocytes are the major site of xenobiotic metabolism, several enzymatic activities such as glutathione s-transferase, UDP-glucuronosyltransferase and cytochrome P450-dependent oxidase have been found in nonparenchymal cells (mainly Kupffer cells) and may play an important role in the metabolism and cellular effects of paracetamol^[6,7]. Only a small number of reports demonstrated the relationship between drug metabolic enzymes and activities of Kupffer cells. The aim of this work was to investigate the effects of kupffer cell mediated metabolism as demonstrated by hepatic drug metabolic enzymes.

MATERIALS AND METHODS

Reagents

Gadolinium chloride ($GdCl_3$), glutathione (GSH), erythromycin, aniline, NADPH, aminophenazone, isocitric acid, isocitric acid dehydrogenase, 1-chloro-2,4-dinitrobenzene (CDNB), ethacrynic acid (EA) were purchased from Sigma, USA. All other reagents used in this study were of AR grade.

Animals and treatment

Kunming strain male mice (aged 4-6 wk) weighing 18-24 g were obtained from the Experimental Animal Center, Wuhan University School of Medicine. The animals were fed with a standard diet in pellets, and allowed free access to water. The mice were randomly divided into 9 groups, 10 per group: control group; $GdCl_3$ 10-1d group; $GdCl_3$ 20-1d group; $GdCl_3$ 40-1d group: mice received ip injection of $GdCl_3$ 10, 20, 40 mg/kg, respectively, and killed after 1 d; $GdCl_3$ 20-3 d group; $GdCl_3$ 20-6 d group: mice were treated with $GdCl_3$ at a single dose of 20 mg/kg, and killed after 3 d, and 6 d, respectively; ASP1 group; ASP2 group; ASP3 group: mice were given ASP 30, 60, and 120 mg/kg, respectively, i.g, qd \times 7 d, and were then killed on the 7th d. The livers were collected for the assay of drug metabolic enzyme activities.

Preparation of liver sample S9 and microsomal fractions

Microsomal fractions were prepared as previously described^[8]. Total protein concentration in mice liver microsomes was determined by the method of Lowry *et al.*^[9] (1951) using BSA as the standard. All operations were performed at 4 °C.

Assays for metabolic enzyme activities

Total cytochrome P450 (P450) content was based on the use of the extinction coefficient of 105 mmol/L·cm for reduced cytochrome P450 minus oxidized P450 with a UV-1601 spectrophotometer^[10].

NADPH-cytochrome C reductase (NADPH-C) activity was determined with a spectrophotometer at 550 nm by monitoring the reduction of cytochrome C (0.5 mg/mL) at 37 °C in an incubation mixture containing potassium phosphate (300 mmol/L, pH7.7) EDTA (0.1 mmol/L), liver microsomes (20 µg/mL) and NADPH (2 mg/L)^[11].

Aminopyrine N-demethylase (AMD) and erythromycin N-demethylase (EMD) were detected by measuring the production of formaldehyde. Its reaction system contained Tris-HCl 50 mmol/L, MgCl₂ 10 mmol/L, KCl 50 mmol/L and an NADPH-generating system (including NADP⁺ 0.4 mmol/L, isocitric acid 10 mmol/L, and isocitric acid dehydrogenase 0.6 units). Erythromycin 0.4 mmol/L or aminopyrine 8 mmol/L was added, the reaction was initiated by the NADPH-generating system, the supernatant was incubated with the Nash reagent at 60 °C for 20 min and the color absorbance was measured at 415 nm with a UV-1601 spectrophotometer^[12].

Aniline hydroxylase (ANH) was assessed with aniline as substrate as previously described^[13].

Microsome glutathione s-transferase (mGST) and S9 glutathione s-transferase (S9-GST) activities were measured with CDNB as substrate ($\epsilon=9.6$ mmol/L·cm)^[14]. The assay mixture contained 850 µL of 0.1 mol/L sodium phosphate-1 mmol/L EDTA (pH6.5), 50 µL of 20 mmol/L GSH, 50 µL of 50 mmol/L CDNB, and 50 µL of sample. The absorbance at 340 nm was continuously recorded for 1 min^[15]. S9-GSTpi was determined

with EA and GSH as substrates ($\epsilon=5.0$ mmol/L·cm)^[14]. The assay mixture contained 850 µL of 0.1 mol/L sodium phosphate, 1 mmol/L EDTA (pH6.8), 50 µL of 50 mmol/L GSH, 50 µL of 50 mmol/L EA, and 50 µL of sample. The absorbance at 340 nm was continuously recorded for 1 minute.

Statistical analysis

The data were presented as mean±SD. Comparisons were performed using one-way analysis of variance (ANOVA) followed by the *posteriori* Student-Newman-Keuls' *t*-test. *P*<0.05 was considered statistically significant.

RESULTS

Influence of different dose of GdCl₃ on P450 content and P450 isoform activities

The content of P450 and the activities of NADPH-C, ANH, AMD, and EMD were obviously reduced after 1 d after GdCl₃ treatment, and no relationship was found between the enzyme activities and the dose of GdCl₃ (Table 1).

Time course of alterations of P450 content, activities of P450 isoforms, S9-GSTpi, S9-GST and mGST by Kupffer cell blockade

The content of P450 and activities of NADPH-C and ANH were reduced by 35.7%, 50.3%, 36.8% after Kupffer cell blockade for 3 d, and 57.9%, 57.9%, 63.2% for 6 d, respectively. However, the activities of AMD, EMD were raised by 36.5%, 71.9% after 3 d, and 155%, 181% after 6 d, respectively. S9-GST, mGST were markedly increased by Kupffer cell blockade. However, the changes were not related with the time of Kupffer cell blockade. No changes in S9-GST were observed (Table 2).

Influence of ASP on P450, activities of P450 isoforms, S9-GSTpi, S9-GST and mGST

The content of P450 and the activities of NADPH-C, ANH,

Table 1 Influence of different dose of GdCl₃ on P450 content and P450 isoform activities

Group	P-450 (nmol/mg·pro)	NADPH-C (nmol/min·mg·pro)	ANH (nmol/min·mg·pro)	AMD (nmol/min·mg·pro)	EMD (nmol/min·mg·pro)
Control	1.4±0.4	14.5±2.8	0.038±0.009	0.96±0.07	0.89±0.06
GdCl ₃ 10-1 d	1.13±0.25	10.9±1.0 ^b	0.032±0.016	0.76±0.07 ^b	0.78±0.12
GdCl ₃ 20-1 d	0.87±0.28 ^b	10.5±1.8 ^b	0.033±0.006	0.82±0.03 ^a	0.74±0.13 ^a
GdCl ₃ 40-1 d	1.01±0.29 ^a	6.0±1.0 ^b	0.036±0.010	0.77±0.17 ^a	0.74±0.18 ^a

GdCl₃10-1 d, GdCl₃20-1 d, GdCl₃40-1 d: Mice were intraperitoneally injected with GdCl₃ 10, 20, 40 mg/kg respectively, and sacrificed after 1 d. The hepatic microsome was prepared to assess the content of P450 and the activities of P450 isoforms. P450: cytochrome P450; NADPH-C: NADPH-cytochrome c reductase; ANH: aniline hydroxylase; AMD: aminopyrine N-demethylase; EMD: erythromycin N-demethylase (*n*=8, mean±SD, ^a*P*<0.05, ^b*P*<0.01 compared with control group).

Table 2 Time course of alterations of P450 content, activities of P450 isoforms, S9-GSTpi, S9-GST and mGST by Kupffer cell blockade

Group	Control	GdCl ₃ 20-1 d	GdCl ₃ 20-3 d	GdCl ₃ 20-6 d
P-450 (nmol/mg·pro)	1.4±0.4	0.87±0.28 ^b	0.90±0.21 ^b	0.59±0.24 ^b
NADPH-C (nmol/min·mg·pro)	14.5±2.8	10.5±1.8 ^b	7.2±1.0 ^b	6.1±0.8 ^b
ANH (nmol/min·mg·pro)	0.038±0.009	0.033±0.006	0.024±0.006 ^b	0.024±0.006 ^b
AMD (nmol/min·mg·pro)	0.96±0.07	0.82±0.03 ^a	1.31±0.24 ^b	1.31±0.24 ^b
EMD (nmol/min·mg·pro)	0.89±0.06	0.74±0.13 ^a	1.53±0.26 ^b	2.5±0.3 ^b
S9-GSTpi (nmol/min·mg·pro)	1.07±0.28	0.93±0.17	1.1±0.4	0.98±0.23
S9-GST (nmol/min·mg·pro)	8.3±0.91	0.2±1.5 ^a	11.4±0.9 ^b	11.1±1.3 ^b
mGST (nmol/min·mg·pro)	0.25±0.03	0.28±0.06	0.31±0.04 ^b	0.305±0.015 ^b

GdCl₃20-1 d, GdCl₃20-3 d, GdCl₃20-6 d: Mice were intraperitoneally injected with a signal dose of 20 mg/kg of GdCl₃, and sacrificed after 1 d, 3 d, and 6 d of GdCl₃ treatment. The hepatic microsome was prepared to assay the P450 content, and activities of P450 isoforms, S9-GSTpi, S9-GST and mGST. (*n*=8, mean±SD, ^a*P*<0.05, ^b*P*<0.01 compared with control group).

Table 3 Influence of ASP on P450 content, P450 isoform activities and activities of S9-GSTpi, S9-GST and mGST

Group	Control	ASP1	ASP2	ASP3
P-450 (nmol/mg·pro)	1.4±0.4	2.1±0.4 ^b	1.2±0.4	0.60±0.13 ^b
NADPH-C (nmol/min·mg·pro)	14.5±2.8	19.7±2.2 ^b	19.1±4.3 ^a	7.6±1.1 ^b
ANH (nmol/min·mg·pro)	0.038±0.009	0.045±0.009 ^b	0.018±0.006 ^b	0.010±0.003 ^b
AMD (nmol/min·mg·pro)	0.96±0.07	1.29±0.11 ^b	1.11±0.19	0.61±0.16 ^b
EMD (nmol/min·mg·pro)	0.89±0.06	1.30±0.21	1.14±0.33	0.41±0.09 ^b
S9-GSTpi (nmol/min·mg·pro)	1.07±0.28	1.2±0.3	1.15±0.26	0.78±0.19 ^a
S9-GST (nmol/min·mg·pro)	8.3±0.9	0.5±1.9 ^a	11.8±1.5 ^a	7.9±0.7 ^a
mGST (nmol/min·mg·pro)	0.25±0.03	0.29±0.03 ^a	0.35±0.08 ^b	0.155±0.016 ^b

ASP1, ASP2, ASP3: Mice were given 30, 60, and 120 mg/kg ASP, ig, qd×7 d, respectively and sacrificed on day 7. The hepatic microsome was prepared to assay the content of P450, and activities of P450 isoforms, S9-GSTpi, S9-GST and mGST. ($n=8$, mean±SD, ^a $P<0.05$, ^b $P<0.01$ compared with control group).

AMD, EMD were obviously increased by 50.0%, 35.9%, 18.4%, 34.4%, and 46.1% after 30 mg/kg ASP treatment, and obviously decreased by 57.1%, 47.6%, 73.7%, 36.5%, and 53.9% after 120 mg/kg ASP treatment, respectively. Thirty and 60 mg/kg of ASP could increase the activity of S9-GST by 26.5%, 42.3%, respectively. The alterations of mGST activity were similar to those of S9-GST. The activities of S9-GST and mGST were reduced by 4.8%, 38.0% after administration of 120 mg/kg ASP, respectively. No changes in S9-GSTpi were observed (Table 3).

Influence of different dose of GdCl₃ on activities of S9-GSTpi, S9-GST and mGST

S9-GST activity was increased by 18.1%, 22.9% after 10 mg and 20 mg/kg of GdCl₃ treatment, respectively, and the alterations in mGST activity were similar to those of S9-GST. No changes in S9-GSTpi were observed (Table 4).

Table 4 Influence of different dose of GdCl₃ on activities of S9-GSTpi, S9-GST and mGST

Group	S9-GSTpi	S9-GST	mGST
	(nmol/min·mg·pro)		
Control	1.07±0.28	8.3±0.9	0.25±0.03
GdCl ₃ 10-1d	1.16±0.019	9.8±1.5 ^a	0.289±0.026 ^a
GdCl ₃ 20-1d	0.93±0.17	10.2±1.5 ^a	0.28±0.06
GdCl ₃ 40-1d	0.91±0.12	7.9±0.8	0.264±0.012

The administration of GdCl₃ and the treatment of animals were the same as described in Table 1. S9-GST: glutathione s-transferase in S9; S9-GSTpi: glutathione s-transferase pi in S9; mGST: glutathione s-transferase in microsome. ($n=8$, mean±SD, ^a $P<0.05$ compared with control group).

DISCUSSION

Neyrinck *et al.*^[16,17] reported that Kupffer cells might play a role of xenobiotic metabolism in hepatocytes *in vitro*, and treatment of GdCl₃ could decrease the total hepatic content of cytochrome P450. Kupffer cells were involved in some liver diseases in which the activities of drug metabolic enzymes changed^[18,19]. Few studies until now have reported an effect of GdCl₃ injection on the activities of specific CYP isoforms and GST, and on the time course of developmental changes of their activities after Kupffer cells blocked by GdCl₃ *in vivo*. The present study showed that Kupffer cell blockade indicated a tendency to decrease cytochrome P450 content and its isoform activities, and to increase GST (including S9-GST, and mGST) activities. However, CYP isoforms and GST activities showed different changes following different time of Kupffer cell blockade. The total cytochrome P450 content, NADPH-C and ANH (as marker of CYP2E1) activities had a sustained decrease following

prolonged Kupffer cell blockade, but AMD, EMD (as marker of CYP3A) activities obviously raised 3 d after Kupffer cell blockade, and GST activities kept a high level 6d after Kupffer cell blockade. Some authors have already reported that the treatment of GdCl₃ causing inactivation of Kupffer cells could protect liver against damage induced by some toxic chemicals (such as ethanol, CCl₄, *etc.*) through inhibiting CYP2E1^[20,21]. The present study offered further support for a relevant role of Kupffer cells through the control of hepatocyte metabolism mediated liver injury. CYP3A contributed significantly to the biotransformation of xenobiotic chemicals such as drugs, and toxic chemicals^[22]. GSTs constitute a multigene family of phase II conjugating enzymes broadly distributed phylogenetically. Detoxification of electrophilic compounds by GSTs may occur via catalytic conjugation of electrophilic intermediates with GSH, via GSH-dependent reduction of organic peroxides, or via direct binding to lipophilic compounds. GST might have an important cytoprotective function^[23]. The current study showed CYP3A and GST activities were rapidly recovered, which might be a self-regulated and self-protected mechanism of the body.

The changes in CYP and GST activities were related with the state of Kupffer cells activated by *Angelica sinensis* polysaccharides (ASP). Now, some new functions of ASP have been reported. ASP could promote ulcer healing, protect hepatic injury and might have antitumor effects^[24-26]. Immunoactivity is the most important function of ASP. It could enhance the proliferative response of lymphocytes *in vitro* and differential expression of genes in the liver of immunological injury mice^[27,28]. In the present study, 30 mg/kg ASP could increase cytochrome P450 content, P450 isoform activities and GST activities. However, 120 mg/kg ASP could obviously decrease the activities of these enzymes. This phenomenon might be concerned with the immunoactivity of ASP. Its mechanism remains to be further studied.

GSTpi, a glutathione s-transferase of placenta type, often presented high expression in tumor tissues related with drug resistance^[29]. The present study indicated that GSTpi activity was not influenced by Kupffer cell blockade or activated, suggesting that GSTpi activity is not easily induced in normal tissues.

In conclusion, Kupffer cells and their adjacent hepatocytes capable of regulating interactions could be demonstrated^[30], suggesting that Kupffer cells may mediate hepatic functions including drug metabolism.

REFERENCES

- Jarin C, Ute MK, Rachel MM, Lawrence MS, Paul FH. Mechanism-based inactivation of cytochromes P450 2B1 and P450 2B6 by 2-phenyl-2 (1-piperidinyl) propane. *Drug Metab Dispos* 2000; **8**: 905-911
- Li AP, Maurel P, Gomez-lechon MJ, Cheng LC, Jurima-Romet

- M. Preclinical evaluation of drug-drug interaction potential: present status of the application of primary human hepatocytes in the evaluation of cytochrome P450 induction. *Chem Biol Interact* 1997; **2**: 5-16
- 3 **Harris R**, Jang G, Tsunoda S. Dietary effects on drug metabolism and transport. *Clin Pharmacokinet* 2003; **13**: 1071-1088
- 4 **Paolini M**, Biagi GL, Cantelli-Forti G. The many consequences of chemical- and genetic-based modulation of drug metabolizing enzyme activities. *Life Sci* 1999; **8**: 75-79
- 5 **Nicholson TE**, Renton KW. Modulation of cytochrome P450 by inflammation in astrocytes. *Brain Res* 1999; **8**: 12-18
- 6 **Bennis RK**, Bethany K, Yuji I, Ronald GT. Gadolinium chloride blocks alcohol-dependent liver toxicity in rats treated chronically with inytagastric alcohol despite the induction of CYP2E1. *Mol Pharma* 1997; **2**: 944-950
- 7 **Kim SG**, Choi SH. Gadolinium chloride inhibition of rat hepatic microsomal epoxide hydrolase and glutathione S-transferase gene expression. *Drug Metab Dispos* 1997; **12**: 1416-1423
- 8 **Lake BG**. Preparation and characterisation of microsomal fractions for studies of xenobiotic metabolism. *Biochemical Toxicology: A Practical Approach*. IRL Press, Oxford 1987; 189-215
- 9 **Lowry OH**, Rosebrough NJ, Farr AL, Randall RJ. Protein measurement with the Folin phenol reagent. *J Biol Chem* 1951; **193**: 265-275
- 10 **Badger DA**, Sauer JM, Hoglen NC, Jolley CS, Sipes IG. The role of inflammatory cells and cytochrome P450 in the potentiation of CCl4-induced liver injury by a single dose of retinol. *Toxicol Appl Pharmacol* 1996; **2**: 507-519
- 11 **Williams CH Jr**, Kamin H. Microsomal triphosphopyridine nucleotide-cytochrome c reductase of liver. *J Biol Chem* 1962; **237**: 587-595
- 12 **Wang H**, Peng RX, Zhang YH, Chen JH, Li QX, Kong R, Ding H, Yu JP. Demethylation capacity of human fetal adrenal mitochondrial cytochrome P-450 *in vitro*. *Acta Pharmacol Sin* 1999; **4**: 358-367
- 13 **Badger DA**, Kuester RK, Sauer JM, Sipes IG. Gadolinium chloride reduces cytochrome P450: relevance to chemical-induced hepatotoxicity. *Toxicology* 1997; **2**: 143-153
- 14 **Kim SG**, Chung HC, Cho JY. Molecular mechanism for alkyl sulfide-modulated carbon tetrachloride-induced hepatotoxicity: the role of cytochrome P450 2E1, P450 02B and glutathione S-transferase expression. *J Pharmacol Exp Ther* 1996; **2**: 1058-1066
- 15 **Sundberg K**, Jernstrom B, Swedmark S. Studies on the differential inhibition of glutathione conjugate formation of (+)-anti-benzo(a) pyren 7,8-dihydrodiol 9,10-epoxide and 1-chloro-2,4-dinitrobenzene in V79 Chinese hamster cells. *Biochem J* 2000; **349**: 693-696
- 16 **Neyrinck A**, Eeckhoudt SL, Meunier CJ, Pampfer S, Taper HS, Verbeeck R. Modulation of paracetamol metabolism by Kupffer cells: a study on rat liver slices. *Lif Sci* 1999; **26**: 2851-2859
- 17 **Milosevic N**, Schawalder H, Maier P. Kupffer cell-mediated differential down-regulation of cytochrome P450 metabolism in rat hepatocytes. *Eur J Pharmacol* 1999; **1**: 75-87
- 18 **Lee WY**, Lee SM. The roles of Kupffer cells in hepatocellular dysfunction after femur fracture trauma in rats. *Arch Pharm Res* 2003; **1**: 47-52
- 19 **Niemela O**, Parkkila S, Bradford B, Iimuro Y, Pasanen M, Thurman RG. Effect of Kupffer cell inactivation on ethanol-induced protein adducts in the liver. *Free Radic Biol Med* 2002; **3**: 350-355
- 20 **Gouillon ZQ**, Miyamoto K, Sonohue TM, Wan YJ, French BA, Nagao Y, Fu P, Reitz RC, hagbjork A, Yap C, Yuan QX, Ingelman-Sundberg M, French SW. Role of CYP2E1 in the pathogenesis of alcoholic liver disease: modifications by cAMP and ubiquitin-proteasome pathway. *Front Biosci* 1999; **4**: A16-25
- 21 **Badger DA**, Sauer JM, Hoglen NC, Jooney CS, Sipes IG. The role of inflammatory cells and cytochrome P450 in the potentiation of CCl4-induced liver injury by a single dose of retinol. *Toxicol Appl Pharmacol* 1996; **2**: 507-519
- 22 **Zhang W**, Parentau II, Greenly RL, Metz CA, Affarwal S, Wainer IW, Tracy TS. Effect of protein-calorie malnutrition on cytochromes P450 and glutathione S-transferase. *Eur J Drug Metab Pharmacokinet* 1999; **2**: 141-147
- 23 **Choi SH**, Kim SG. Lipopolysaccharide inhibition of rat hepatic microsomal epoxide hydrolase and glutathione S-transferase gene expression irrespective of nuclear factor-kappaB activation. *Biochem Pharmacol* 1998; **11**: 1427-1436
- 24 **Ye YN**, So HL, Liu ES, Shin VY, Cho CH. Effect of polysaccharides from *Angelica sinensis* on gastric ulcer healing. *Life Sci* 2003; **8**: 925-932
- 25 **Ye YN**, Liu ES, Li Y, So HL, Cho CC, Sheng HP, Lee SS, Cho CH. Protective effect of polysaccharides-enriched fraction from *Angelica sinensis* on hepatic injury. *Life Sci* 2001; **6**: 637-646
- 26 **Shang P**, Qian AR, Yang TH, Jia M, Mei QB, Cho CH, Zhao WM, Chen ZN. Experimental study of anti-tumor effects of polysaccharides from *Angelica sinensis*. *World J Gastroenterol* 2003; **9**: 1963-1967
- 27 **Shan JJ**, Wang Y, Wang SC, Liu D, Hu ZB. Effect of *Angelica sinensis* polysaccharides on lymphocyte proliferation and induction of IFN-gamma. *Yaoxue Xuebao* 2002; **7**: 497-500
- 28 **Ding H**, Shi GG, Yu X, Yu JP, Huang JA. Modulation of GdCl3 and *Angelica sinensis* polysaccharides on differentially expressed genes in liver of hepatic immunological injury mice by cDNA microarray. *World J Gastroenterol* 2003; **5**: 1072-1076
- 29 **Mayr D**, Pannekamp U, Baretton GB, Gropp M, Meier W, Flens MJ, Scheper R, Biebold J. Immunohistochemical analysis of drug resistance-associated proteins in ovarian carcinomas. *Pathol Res Pract* 2000; **7**: 469-475
- 30 **Milosevic N**, Schawalder H, Maier P. Kupffer cell-mediated differential down-regulation of cytochrome P450 metabolism in rat hepatocytes. *Eur J Pharmacol* 1999; **8**: 75-87

Edited by Zhang JZ and Wang XL Proofread by Xu FM

Peroxisome proliferator activated receptor- γ in pathogenesis of experimental fatty liver disease

Cai-Yan Zhao, Ling-Ling Jiang, Li Li, Zhuo-Jun Deng, Bao-Li Liang, Jian-Mei Li

Cai-Yan Zhao, Ling-Ling Jiang, Department of Biochemistry, Hebei Medical University, Shijiazhuang 050017, Hebei Province, China
Li Li, Zhuo-Jun Deng, Bao-Li Liang, Jian-Mei Li, Department of Liver Disease, Third Affiliated Hospital of Hebei Medical University, Shijiazhuang 050051, Hebei Province, China

Correspondence to: Ling-Ling Jiang, Department of Biochemistry, Hebei Medical University, Shijiazhuang 050017, Hebei Province, China. zhaoyy63811@sohu.com

Telephone: +86-13313012898

Received: 2003-10-29 **Accepted:** 2004-01-08

Abstract

AIM: To study the expression of peroxisome proliferator activated receptor- γ (PPAR γ) in the liver of rats with fatty liver disease (FLD) and to explore the role of PPAR γ in the pathogenesis of FLD to provide the basis for using PPAR γ ligand to treat patients with FLD.

METHODS: Forty Wistar rats were divided into 4 groups of ten rats each randomly: normal group (group A), alcohol group (group B), fat-rich diet group (group C), alcohol and fat-rich diet group (group D). The rats were sacrificed at the end of the 16th week from the feeding day. Alanine aminotransferase (ALT), tumor necrosis factor- α (TNF α) in serum and malondialdehyde (MDA) in liver homogenate were determined; livers were collected for observing pathologic changes by HE, Sudan IV, Masson stain under microscope. The morphologic results were analyzed by picture quantitative analysis technique. The changes of ultrastructure were also examined under electron microscope. The expression of PPAR γ in liver was detected by immunohistochemistry and RT-PCR. The correlations between the expression of PPAR γ and biochemical indexes, and liver histology were analyzed.

RESULTS: The steatosis, inflammation, necrosis and fibrosis were present in livers of different experimental groups, especially in livers of alcohol and fat-rich diet group. The content of immunodetectable PPAR γ was decreased remarkably in the livers of model rats (group B-D); the level in alcohol and fat-rich diet group (3.43 ± 1.48) was significantly lower than that in normal group (18.34 ± 3.73), alcohol group (8.82 ± 2.52) and fat-rich diet group (11.73 ± 2.51) (all $P < 0.01$). The level of PPAR γ mRNA was also lower in the livers of model rats (group B-D) than in livers of controls. The expression of PPAR γ in rat liver correlated negatively with the degree of its inflammation, necrosis and fibrosis, as well as the level of serum TNF α and the content of MDA in liver homogenates, but not with steatosis or serum ALT.

CONCLUSION: Decreased expression of PPAR γ may play an important role in the development of hepatocellular inflammation, necrosis and fibrosis of rats with FLD. Thus, activating PPAR γ by its ligand can be anticipated to provide a therapy target for FLD.

Zhao CY, Jiang LL, Li L, Deng ZJ, Liang BL, Li JM. Peroxisome

proliferator activated receptor- γ in pathogenesis of experimental fatty liver disease. *World J Gastroenterol* 2004; 10(9): 1329-1332
<http://www.wjgnet.com/1007-9327/10/1329.asp>

INTRODUCTION

Fatty liver disease (FLD) includes alcoholic liver disease (ALD) caused by alcohol and non-alcoholic fatty liver disease (NAFLD) due to obesity, hypertriglyceridemia and other factors. The pathogenesis is not clear now. Some scholars put forward the tale of two or multiple "hits"^[1]. The first hit is steatosis by ethanol or insulin resistance which offers substrates for lipid peroxidation. The second hit is alcoholic hepatitis or nonalcoholic steatohepatitis (NASH) caused by oxidative stress and lipid superoxidation. The release of the inflammation mediator, inflammation and necrosis can be found in hepatocytes^[2-6]. Liver fibrosis or cirrhosis is the third hit because the synthesis of extracellular matrix exceeds the decomposition of it or inflammation is continuous. Why excess hepatocellular fat can induce inflammation or even fibrosis in the liver? The pathogenesis is not clarified up now. Peroxisome proliferator-activated receptor-gamma (PPAR γ), is one member of the nuclear hormone receptor superfamily that can be activated by various ligands. Recent studies showed that this transcription factor associated not only with adipocyte differentiation, insulin resistance, sugar and lipid metabolism^[7-10], but also with the regulation of inflammation, hepatocyte proliferation and the apoptosis in human liver cancer cells^[11-17]. The role of PPAR γ in FLD has not been well addressed and some studies even showed contrary results. The present study was designed to characterize PPAR γ activity in liver of rats with FLD so to explore whether PPAR γ ligand could be used as a potential therapeutic agent for FLD.

MATERIALS AND METHODS

Rat model of fatty liver disease

Forty female Wistar rats (from the Animal Center of Hebei Medical University) were divided into 4 groups of ten rats each randomly. Rats in normal group (group A) received standard diet and intragastric saline (1.5 mL/100 g body mass) twice daily. Rats in alcohol group (group B) were intragastrically fed twice a day initially with 400 mL/L ethanol (1.5 mL/100 g body weight) for 4 wk, with 500 mL/L ethanol for 4 wk and then with 60% ethanol for 8 wk on the basis of standard diet. Rats in fat-rich diet group (group C) were fed with high fat diet (standard diet with 10% lard and 2% cholesterol) and given intragastrically with saline twice a day. Rats in alcohol and fat-rich diet group (group D) had the same high fat diet as rats in group C and took the same ethanol as rats in group B.

Preparation of samples

Serum from rats fasted for 12 h was isolated and stored at -70 °C for alanine aminotransferase (ALT) and tumor necrosis factor α (TNF α) determination. Liver was homogenized in 10 volumes of 0.01 mol/L sucrose containing 10 mmol/L Tris-Cl, pH 7.4, and 0.1 mmol/L ethylenediaminetetraacetic acid and

centrifuged at 3 000 r/min for 10 min at 4 °C and the supernatant was stored at -70 °C for MDA assay. A small sample of liver was stored in liquid nitrogen for isolation of total RNA. The others were fixed in 40 g/L formaldehyde for light microscopy or in 40 g/L paraformaldehyde for immunohistochemistry and in 40 g/L glutaraldehyde for electron microscopy.

Biochemical indexes

Serum ALT, TNF α were measured using an auto-biochemical analyzer (Olympus AU 2700) and radio-immuno- assay (Beijing Furu) respectively. MDA in liver homogenates was detected using TBA kit (Nanjing Jiancheng).

Liver histology

Livers were fixed in 40 g/L buffered formaldehyde, embedded in paraffin, sectioned, and stained with hematoxylin-eosin for routine examination and with Sudan IV for steatosis or with Masson for fibrosis. The steatosis and collagen were quantified as the percentage of positive area by multifunctional pathological image analyzer (Beijing Aerospace University). The activity of necro- inflammation was scored between 1 to 4 blindly by an independent pathologist. The ultrastructure of the livers was observed by HITACHI H7500 transmission electron microscope (TEM) after the samples underwent 40 g/L glutaraldehyde-osmic acid fixation, epoxy resin embedding and ultrathin section.

Immunohistochemistry

In brief, paraffin-embedded tissue specimens and controls were sectioned at a thickness of 4 μ m, deparaffinized, and rehydrated. The slides were incubated with 30 mL/L hydrogen peroxide in methanol for 10 min to block endogenous peroxidase activity and then washed twice in phosphate -buffered saline (PBS) for 5 min. Antigen in sections was retrieved by microwave. Sections were then blocked with 10% goat serum and incubated (12 h at 4 °C) with the primary antibody (mouse anti-rat monoclonal antibody of PPAR γ , E-8, 1:100, Santa Cruz). After being washed twice for 15 min in PBS, sections were incubated (30 min at 37 °C) with the secondary antibody (goat anti -mouse IgG marked by biotin), with streptavidin marked by horseradish peroxidase, and then with DAB (Beijing Zhongshan). Then, 0.01 mol/L PBS was substituted for primary antibody as the negative control. The positive cells presented brownish yellow. Quantitative analysis was done by a multifunctional pathological image analyzer. Ten high power fields were examined randomly per sample.

Reverse transcriptase-polymerase chain reaction

Total RNA was isolated from liver using a modification of the single -step guanidinium-phenol-chloroform method. cDNA was obtained by reverse transcription (Promega kit) and then subjected to PCR amplification with GAPDH as standard reference (452 bp). A 403 bp PPAR γ gene fragment was amplified with the following primers: up 5' -TATCATAAATAAGCTT CAATCGGATG GTTC -3' and down 5' -ACCACAGTCCATG CCATCAC -3'. The primers were designed according to the published sequences^[18] and synthesized by Shanghai Biology Engineering Corporation. Thirty-two cycles of amplification were performed at 94 °C for 5 min, then at 94 °C for 30 s, at 57 °C for 45 s, and at 72 °C for 1 min, with a final extension at 72 °C for 5 min. The PCR reaction mixture was electrophoresed in 5% SDS-polyacrylamide gel, and observed by EB staining under UV light. The optical density of EB-stained DNA bands was analyzed by BIO-PROFIL picture analysis system and the ratio of PPAR γ to GAPDH was calculated.

Statistical analysis

SAS8.0 package was used to process all data. Results were

expressed as mean \pm SD. Student's *t*-test was used for the comparison between two groups. Group means were compared by ANOVA followed by the Student-Newman-Keuls test if the former was significant. Differences were considered significant when $P < 0.05$. Linear regression analysis was used for relativity analysis.

RESULTS

Biochemistry

The biochemical features are outlined in Table 1. Serum ALT, TNF α and MDA in liver homogenates were elevated significantly, particularly in group D.

Table 1 Biochemical features of rats with fatty liver disease

Group	n ¹	ALT (U/L)	TNF α (μ g/L)	MDA (μ mol/g)
A	10	34 \pm 9.02	1.36 \pm 0.35	5.71 \pm 0.25
B	9	119 \pm 17.15 ^a	3.39 \pm 0.42 ^a	7.26 \pm 0.32 ^a
C	10	103 \pm 17.24 ^a	3.02 \pm 0.37 ^a	6.72 \pm 0.31 ^a
D	9	125 \pm 16.51 ^a	5.01 \pm 0.52 ^{a,b,d}	9.12 \pm 0.42 ^{a,b,d}

^a $P < 0.05$ vs the normal control; ^b $P < 0.01$ vs the alcohol group; ^c $P < 0.01$ vs the fat-rich diet group, ¹ One rat died in groups B, D respectively in the process of experiment.

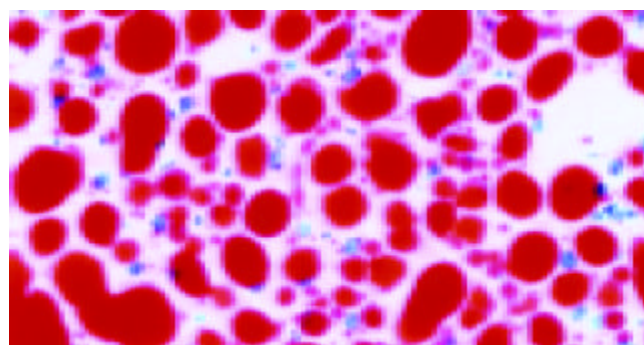


Figure 1 Swelling, diffusible steatosis of hepatocytes (SudanIV 40 \times).

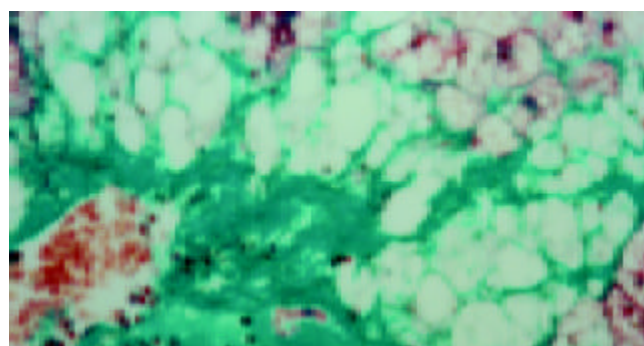


Figure 2 Central vein fibrosis (Masson 40 \times).

Liver histology

The quantitative evaluation of the liver histology of rats in each group is shown in Table 2. The livers of model rats (group B-D) were engorged with microvesicular and macrovesicular fat, particularly in alcohol and high-fat group (group D) (Figure 1). The hepatocytes of rats in alcohol group presented inflammation, and centrilobular (zone 3) cloudy swelling, ballooning degeneration, spotty necrosis with either pericellular fibrosis or Mallory body. The hepatic sinusoids became narrowed significantly. The infiltration of inflammatory cells, especially

neutrophilic granulocytes could be seen in the portal areas, and there was fibrosis around the hepatic sinusoids. Focal necrosis or piecemeal necrosis (PN) even bridge necrosis (BN) in alcohol and fat-rich diet group could be found. Around these areas there were a large number of inflammatory cells. Perisinusoid fibrosis and central vein fibrosis could be seen (Figure 2) and the vein wall became thick even occluded. The portal area was enlarged, the fibrous tissue proliferated and extended to interlobular area. Under TEM, the nuclear membrane was tortuous, the nuclear chromatin agglutinated into blocks in hepatocytes of the model rats (groups B-D). The cytoplasm was loose and had more or less fat. The mitochondria swelled and proliferated and sometimes huge mitochondria could be seen. Some of the sinusoids were capillarized. Activated stellate cells and perisinusoid fibrosis could be observed distinctly (Figure 3).

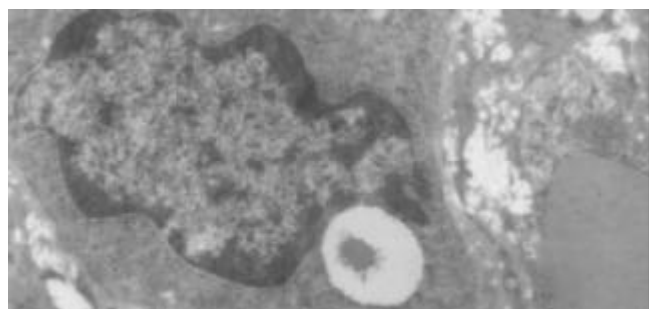


Figure 3 Activated stellate cells and perisinusoid fibrosis (TEM $\times 8\ 000$).

Table 2 Quantitative evaluation of liver histology of rats (%)

Groups	n	Steatosis	Inflammation and necrosis	Collagen
A	10	1.34 \pm 0.33	0.67 \pm 0.66	2.03 \pm 0.87
B	9	12.79 \pm 2.73 ^a	4.35 \pm 0.56 ^a	11.85 \pm 3.89 ^a
C	10	35.82 \pm 8.52 ^{a,b}	3.05 \pm 0.72 ^a	7.90 \pm 2.79 ^{a,b}
D	9	37.97 \pm 11.48 ^{a,b}	5.71 \pm 1.03 ^{a,c}	19.02 \pm 4.01 ^{a,b,c}

^a $P < 0.01$ vs the normal control; ^b $P < 0.05$ vs the alcohol group; ^c $P < 0.05$ vs the fat-rich diet group.

Expression of PPAR γ

The level of PPAR γ protein and mRNA in rat livers detected by immunohistochemistry and RT-PCR respectively is shown in Table 3. The levels of PPAR γ expression were decreased significantly in model groups (groups B-D), especially in group D (Figure 4).

Table 3 Level of PPAR γ protein and mRNA in rat livers (%)

Group	n	PPAR γ protein	PPAR γ mRNA
A	10	18.34 \pm 3.73	0.8097 \pm 0.098
B	9	8.82 \pm 2.52 ^a	0.2530 \pm 0.072 ^a
C	10	11.73 \pm 2.51 ^a	0.3647 \pm 0.084 ^a
D	9	3.43 \pm 1.48 ^{a,b,d}	0.1226 \pm 0.054 ^{a,b,d}

^a $P < 0.05$ vs the normal control; ^b $P < 0.01$ vs the alcohol group; ^d $P < 0.01$ vs the fat-rich diet group.

Relationship between levels of PPAR γ protein and biochemical and histological parameters

The correlation analysis showed that the expression of PPAR γ protein in the liver of model rats (group B-D) was associated negatively with the level of serum TNF α , the content of MDA in the liver, the degree of liver inflammation, necrosis, and

fibrosis, but not associated with the degree of liver steatosis and the level of serum ALT (Table 4).

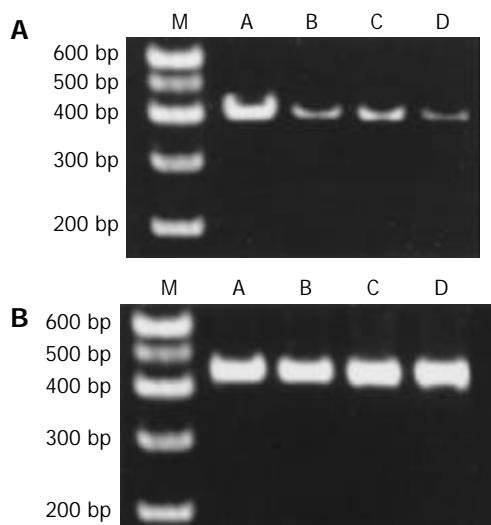


Figure 4 Expression of PPAR γ mRNA and GAPDH mRNA in the liver of rats with FLD (Note: from left to right M: PCR marker; lane A: normal control; lane B: alcohol group; lane C: fat-rich diet group. Lane D: alcohol and fat-rich diet group). A: Expression of PPAR γ mRNA in the liver of rats with FLD, B: Expression of GAPDH mRNA in the liver of rats with FLD.

Table 4 Correlation between levels of PPAR γ protein and biochemical, histological parameters in model rats (*r* value)

Groups	ALT	TNF α	MDA	Steatosis	Inflammation	Fibrosis
B	-0.263	-0.745 ^b	-0.560 ^a	-0.437	-0.568 ^b	-0.728 ^a
C	-0.493	-0.662 ^a	-0.772 ^b	-0.323	-0.671 ^a	-0.812 ^b
D	-0.352	-0.624 ^b	-0.781 ^b	-0.329	-0.891 ^b	-0.679 ^b

^a $P < 0.05$ vs the normal control the alcohol group ^b $P < 0.01$.

DISCUSSION

It is well known that PPAR γ is one of the nuclear transcription factors activated by ligands and belongs to type II nuclear receptor superfamily. It includes 3 subtypes as PPAR α , PPAR δ and PPAR γ . PPAR α is expressed abundantly in liver associated with lipid deposition and certain amount of PPAR γ could be found in liver possibly related to the inflammation^[19-30]. The experiment *in vitro* proved that the activation of PPAR γ could inhibit the secretion of cytokines and chemokines. For example, the activation of PPAR γ could inhibit the secretion of IL-6, IL-1 and TNF α induced by lipopolysaccharide (LPS)^[31]. Kon proved that pioglitazone (1 mg/kg body weight), the ligand of PPAR γ could prevent liver from inflammation, necrosis and increase of serum TNF α caused by carbon tetrachloride. At the same time pioglitazone could inhibit the expression of α -SMA and type I precollagenin of primary cultured hepatic stellate cells (HSCs)^[11,32]. The activation of HSC was the basis of liver fibrosis. Everett's research also proved that activation of PPAR γ could inhibit the activation of cultured HSC *in vitro*^[19]. We speculated that decreased expression and dysfunction of PPAR γ might correlate with the release of inflammatory mediator and fibrosis during the process of liver injury due to alcohol and high fat diet.

Our data showed that there were steatosis, inflammation and centrolobular ballooning degeneration, necrosis with fibrosis in the livers of rats fed with either alcohol or high fat diet, especially in the rats fed with both alcohol and high fat. The expression of PPAR γ in the liver of rats with FLD (groups

B, C, D) decreased significantly particularly in group D compared to the normal control ($P < 0.05$). The correlation analysis indicated that except for steatosis, the expression of PPAR γ correlated negatively with the levels of liver MDA, serum TNF α and the degree of inflammation and fibrosis in livers of rats with FLD. These suggested that the weaker the PPAR γ expressed, the more severe the liver would be damaged. High-fat diet could deteriorate liver damage and promote liver fibrosis by increasing the lipid deposition, lipid peroxidation and inhibiting PPAR γ expression in the liver. It proved that PPAR γ played a very important role in the cascade reaction of lipid peroxidation - release of inflammation cytokines - damage of liver - liver fibrosis of rats with FLD. It might be one of the initiation factors. Therefore, the ligand of PPAR γ might block the development of inflammation, necrosis and fibrosis of FLD and be potentially used for FLD treatment.

REFERENCES

- 1 **Day CP**, James OF. Steatohepatitis: a tale of two "hits". *Gastroenterology* 1998; **114**: 842-845
- 2 **Chitturi S**, George J. Interaction of iron, insulin resistance, and nonalcoholic steatohepatitis. *Curr Gastroenterol Rep* 2003; **5**: 18-25
- 3 **Gao ZQ**, Lu FE. Free fatty acid, insulin resistance and nonalcoholic steatohepatitis. *Shijie Huaren Xiaohua Zazhi* 2003; **11**: 1043-1045
- 4 **Fan JG**. Steat ohepatitis studies. *Shijie Huaren Xiaohua Zazhi* 2001; **9**: 6-10
- 5 **Chitturi S**, Abeygunasekera S, Farrell GC, Holmes-Walker J, Hui JM, Fung C, Karim R, Lin R, Samarasinghe D, Liddle C, Woltman M, George J. NASH and insulin resistance: Insulin hypersecretion and specific association with the insulin resistance syndrome. *Hepatology* 2002; **35**: 373-379
- 6 **Wu Q**, Cheng J, Li L. Study on alcoholic fatty liver disease. *Shijie Huaren Xiaohua Zazhi* 2002; **10**: 1037-1038
- 7 **Bedoucha M**, Atzpodien E, Boelsterli UA. Diabetic KKAY mice exhibit increased hepatic PPAR gamma 1 gene expression and develop hepatic steatosis upon chronic treatment with antidiabetic thiazolidinediones. *J Hepatol* 2001; **35**: 17-23
- 8 **Kersten S**. Peroxisome proliferator activated receptors and obesity. *Eur J Pharmacol* 2002; **440**: 223-234
- 9 **Clarke SD**, Thuillier P, Baillie RA, Sha X. Peroxisome proliferator-activated receptors: a family of lipid-activated transcription factors. *Am J Clin Nutr* 1999; **70**: 566-571
- 10 **Kersten S**, Mandard S, Escher P, Gonzalez FJ, Tafuri S, Desvergne B, Wahli W. The peroxisome proliferator-activated receptor alpha regulates amino acid metabolism. *FASEB J* 2001; **15**: 1971-1978
- 11 **Kon K**, Ikejima K, Hirose M, Yoshikawa M, Enomoto N, Kitamura T, Takei K, Sato N. Pioglitazone prevents early-phase hepatic fibrogenesis caused by carbon tetrachloride. *Biochem Biophys Res Commun* 2002; **291**: 55-61
- 12 **Marra F**, Efsen E, Romanelli RG, Caligiuri A, Pastacaldi S, Batignani G, Bonacchi A, Caporale R, Laffi G, Pinzani M, Gentilini P. Ligands of peroxisome proliferator-activated receptor gamma modulate profibrogenic and proinflammatory actions in hepatic stellate cells. *Gastroenterology* 2000; **119**: 466-478
- 13 **Li MY**, Deng H, Zhao JM, Dai D, Tan XY. Peroxisome proliferator-activated receptor gamma ligands inhibit cell growth and induce apoptosis in human liver cancer BEL-7402 cells. *World J Gastroenterol* 2003; **9**: 1683-1688
- 14 **Li MY**, Deng H, Zhao JM, Dai D, Tan XY. PPARgamma pathway activation results in apoptosis and COX-2 inhibition in HepG2 cells. *World J Gastroenterol* 2003; **9**: 1220-1226
- 15 **Kersten S**, Desvergne B, Wahli W. Roles of PPARs in health and disease. *Nature* 2000; **405**: 421-424
- 16 **Rao MS**, Peters JM, Gonzalez FJ, Reddy JK. Hepatic regeneration in peroxisome proliferator-activated receptor alpha-null mice after partial hepatectomy. *Hepatol Res* 2002; **22**: 52-57
- 17 **Yu S**, Rao S, Reddy JK. Peroxisome proliferator-activated receptors, fatty acid oxidation, steatohepatitis and hepatocarcinogenesis. *Curr Mol Med* 2003; **3**: 561-572
- 18 **Braissant O**, Foufelle F, Scotto C, Dauca M, Wahli W. Differential expression of peroxisome proliferator-activated receptors (PPARs): tissue distribution of PPAR- α , - β , and - γ in the adult rat. *Endocrinology* 1996; **137**: 354-366
- 19 **Everett L**, Galli A, Grabb D. The role of hepatic peroxisome proliferator-activated receptors (PPARs) in health and disease. *Liver* 2000; **20**: 191-199
- 20 **Reddy JK**, Hashimoto T. Peroxisomal beta-oxidation and peroxisome proliferator-activated receptor alpha: an adaptive metabolic system. *Annu Rev Nutr* 2001; **21**: 193-230
- 21 **Qi C**, Zhu Y, Reddy JK. Peroxisome proliferator-activated receptors, coactivators, and downstream targets. *Cell Biochem Biophys* 2000; **32**: 187-204
- 22 **Qi C**, Zhu Y, Pan J, Usuda N, Maeda N, Yeldandi AV, Rao MS, Hashimoto T, Reddy JK. Absence of spontaneous peroxisome proliferation in enoyl-CoA Hydratase/L-3-hydroxyacyl-CoA dehydrogenase-deficient mouse liver. Further support for the role of fatty acyl CoA oxidase in PPARalpha ligand metabolism. *J Biol Chem* 1999; **274**: 15775-15780
- 23 **Yu S**, Matsusue K, Kashireddy P, Cao WQ, Yeldandi V, Yeldandi AV, Rao MS, Gonzalez FJ, Reddy JK. Adipocyte-specific gene expression and adipogenic steatosis in the mouse liver due to peroxisome proliferator-activated receptor gamma1 (PPARgamma1) overexpression. *J Biol Chem* 2003; **278**: 498-505
- 24 **Hashimoto T**, Cook WS, Qi C, Yeldandi AV, Reddy JK, Rao MS. Defect in peroxisome proliferator-activated receptor alpha-inducible fatty acid oxidation determines the severity of hepatic steatosis in response to fasting. *J Biol Chem* 2000; **275**: 28918-28928
- 25 **Kersten S**, Seydoux J, Peters JM, Gonzalez FJ, Desvergne B, Wahli W. Peroxisome proliferator-activated receptor alpha mediates the adaptive response to fasting. *J Clin Invest* 1999; **103**: 1489-1498
- 26 **Reddy JK**. Nonalcoholic steatosis and steatohepatitis. III. Peroxisomal beta-oxidation, PPAR alpha, and steatohepatitis. *Am J Physiol Gastrointest Liver Physiol* 2001; **281**: G1333-1339
- 27 **Rao MS**, Reddy JK. Peroxisomal beta-oxidation and steatohepatitis. *Semin Liver Dis* 2001; **21**: 43-55
- 28 **Fan CY**, Pan J, Usuda N, Yeldandi AV, Rao MS, Reddy JK. Steatohepatitis, spontaneous peroxisome proliferation and liver tumors in mice lacking peroxisomal fatty acyl-CoA oxidase. Implications for peroxisome proliferator-activated receptor alpha natural ligand metabolism. *J Biol Chem* 1998; **273**: 15639-15645
- 29 **Clarke SD**. Nonalcoholic steatosis and steatohepatitis. I. Molecular mechanism for polyunsaturated fatty acid regulation of gene transcription. *Am J Physiol Gastrointest Liver Physiol* 2001; **281**: G865-869
- 30 **Chitturi S**, Farrell GC. Etiopathogenesis of nonalcoholic steatohepatitis. *Semin Liver Dis* 2001; **21**: 27-41
- 31 **Reginato MJ**, Krakow SL, Bailey ST, Lazar MA. Prostaglandins promote and block adipogenesis through opposing effects on peroxisome proliferator-activated receptor gamma. *J Biol Chem* 1998; **273**: 1855-1858
- 32 **Miyahara T**, Schrum L, Rippe R, Xiong S, Yee HF Jr, Motonura K, Anania FA, Willson TM, Tsukamoto H. Peroxisome proliferator-activated receptors and hepatic stellate cell activation. *J Biol Chem* 2000; **275**: 35715-35722

Dexamethasone and dextran 40 treatment of 32 patients with severe acute pancreatitis

Zi-Fa Wang, Chang Liu, Yi Lu, Rui Dong, Jun Xu, Liang Yu, Ying-Min Yao, Qing-Guang Liu, Cheng-En Pan

Zi-Fa Wang, Chang Liu, Yi Lu, Rui Dong, Jun Xu, Liang Yu, Ying-Min Yao, Qing-Guang Liu, Cheng-En Pan, Department of Surgery, First Hospital, Xi'an Jiaotong University, Xi'an 710061, Shaanxi Province, China

Zi-Fa Wang, Now is in the Department of Surgery, University of Pittsburgh School of Medicine, Pittsburgh, PA 15213, USA

Correspondence to: Dr. Zi-Fa Wang, Department of Surgery, University of Pittsburgh, NW607, Montefiore University Hospital, 3459 Fifth Avenue, Pittsburgh, PA 15213, United States. ziw3@pitt.edu

Telephone: +1-412-343-9407 **Fax:** +1-412-647-5959

Received: 2003-05-10 **Accepted:** 2004-01-29

Abstract

AIM: Based on the pathogenesis of severe acute pancreatitis and our experimental studies, to investigate the effect of dexamethasone and dextran in treatment of patients with severe acute pancreatitis.

METHODS: Thirty-two patients with severe acute pancreatitis were treated with 0.5-1 mg/kg per day dexamethasone for 3-5 d, and 500-1 000 mL/d of dextran 40 for 7 d, besides the routine therapy.

RESULTS: After 4-8 h of treatment, abdominal pain began to be relieved; range of tenderness began to be localized in 27 patients. They were cured with nonsurgical treatment. Five of them were deteriorated, and treated with surgery. Four patients in this group died.

CONCLUSION: Dexamethasone and dextran 40 block the pathologic process of severe acute pancreatitis through inhibition of inflammatory mediators and improvement of microcirculation disorders respectively.

Wang ZF, Liu C, Lu Y, Dong R, Xu J, Yu L, Yao YM, Liu QG, Pan CE. Dexamethasone and dextran 40 treatment of 32 patients with severe acute pancreatitis. *World J Gastroenterol* 2004; 10 (9): 1333-1336

<http://www.wjgnet.com/1007-9327/10/1333.asp>

INTRODUCTION

Acute pancreatitis (AP) is usually mild and self-limiting. However, 15-20% of cases deteriorate and develop organ failure or local complications (including necrosis, pseudocyst and abscess)^[1]. Many patients with severe AP develop organ failure during the first few days of illness, and this accounts for the majority of early deaths^[2]. The rate of severe AP approaches 40 per cent^[3]. Although a number of treatments are currently available to treat AP, they have failed to have a significant impact on the overall disease progression^[1,4-6]. It is known that the activation of trypsin is the trigger of AP. The key to understand the pathophysiology of AP lies in discovering why a proportion of patients progress from a limited local inflammation to a potentially dangerous systemic inflammatory response. Recent studies^[6-21] showed that inflammatory

mediators and microcirculation disorders (MCD) play very important roles in the pathogenesis of severe acute pancreatitis. It has been proposed that the systemic sequelae of AP arise from excessive leukocyte activation with the release of secondary inflammatory mediators, such as interleukin (IL)-1 α , IL-6, IL-8, IL-10; tumor necrosis factor- α (TNF- α); platelet-activating factor (PAF); nitric oxide (NO); and phospholipase A₂^[6-14]. Excessive production of these mediators contributes to the induction of the systemic inflammatory response syndrome, acute phase response, and multiple organ failure^[7,14]. On the other hand, the pancreatic microcirculation is impaired in acute pancreatitis^[15]. Local release of acinar enzyme, vasoactive mediators, vasoconstriction, increase in vascular permeability, ischaemia, intravascular coagulation, and capillary stasis result in pancreatic edema and hemoconcentration, and impaired capillary and venous drainage consequently lead to hemorrhagic pancreatic necrosis^[16-21]. Furthermore, MCD in severe AP are not confined to the pancreas but can also be found in the colon, liver, and lungs; they extend beyond the early stage of AP and persist for 48 h or longer. They not only affect capillary blood flow but also involve prolonged changes of capillary permeability and leukocyte endothelial interaction^[22]. There is no strict correlation between necrosis and organ failure in AP. Patients with pancreatic necrosis are not necessarily at risk of having initial organ failure or later organ failure during the total hospital stay and *vice versa*^[23].

Therefore, the therapeutic strategy for severe AP should focus on inhibiting inflammatory mediators and improving systemic MCD. Based on our previous experimental studies^[24,25], 32 patients with severe AP were treated with the new therapeutic approach.

MATERIALS AND METHODS

General data of patients

According to the definition of the International Symposium on Acute Pancreatitis held in 1992 in Atlanta^[26], 32 patients with severe AP were treated in our hospital. Eighteen of them were males and fourteen females. The mean age was 42.8 (range 26-63) years. The treatment began from 8 h to 4 d after the symptoms onset.

Diagnosis

The patients had an epigastric pain of visceral nature that radiated to the back. The pain was constant and at times could be poorly localized. Other clinical findings included fever, nausea, vomiting, ileus, and abdominal distention, hyperamylasemia, and hypotension. Ultrasonography demonstrated edema of the pancreas, retroperitoneal edema, and pancreatic ascites. Sixteen patients represented biliary systemic problems (cholecystitis, cholelithiasis or biliary ductal dilatation). Findings on CT (or contrast-enhanced dynamic CT) included edema of the pancreas, peripancreatic fluid collections, and edema of the surrounding viscera and pancreatic necrosis. Twelve patients had abnormal findings on chest radiographs at the time of diagnosis, including segmental atelectasis, an elevated hemidiaphragm, pleural effusions, or the presence of

early pulmonary parenchyma infiltrates.

Treatment

After severe AP was diagnosed, the patients were treated with following routine methods: (1) Nasogastric tube decompression; (2) Supplemental oxygen, mechanical ventilation instituted in the event of respiratory insufficiency, (3) Aggressive fluid and electrolyte resuscitation to prevent hypovolemia and prerenal azotemia; and (4) Prophylactic antibiotics (Imipenem).

Besides above routine therapy, 0.5-1.0 mg/kg of dexamethasone was administered daily for 3-5 d, and 500-1 000 mL of dextran 40 was daily administered for 7 d.

RESULTS

After for 4-8 h of treatment, the abdominal pain began to be relieved, and the range of tenderness began to be localized in 27 patients. They were cured with nonsurgical treatment. Five patients were deteriorated, and 4 patients were treated with surgery (necrosectomy). The necrotic peripancreatic and pancreatic tissues were removed, and the lesser sac was drained with multiple drains (closed drainage), or lavaged with a large volume of dialysate (closed lavage). Cholecystectomy was performed in 21 patients with biliary pancreatitis, after pancreatitis was completely relieved. Operative cholangiography was performed in 18 patients. Gallstone was found in 5 cases of them, and their common bile ducts were explored. Four cases died, and 2 of them died from acute respiratory distress syndrome, 1 died from postoperative intraabdominal hemorrhage and sepsis and, 1 died from severe intraabdominal infection and organ failure.

DISCUSSION

It is now becoming much better understood that inflammatory mediators and MCD play a dominant role in the pathogenesis of systemic inflammatory response syndrome and organ dysfunction of AP. In addition, there is little doubt that inhibition or blockage of the inflammatory mediators or improvement of MCD can dramatically alter the expected course of experimental AP^[30-33]. In our observation, the patients were treated with dexamethasone and dextran 40 for 4-8 h, then, their symptoms and signs began to be improved. Twenty-seven out of 32 patients were cured with this non-surgical approach. The mortality rate was lower (12.5%) compared with literature (40%)^[3].

It has been shown in recent studies that inflammatory mediators, including IL-1, IL-6, PAF, and arachidonic acid metabolites were excessively produced during AP. These mediators play an active role in initiating or amplifying the cytokines cascade^[9,10], and a central role in the progression of AP from a local to a systemic disease^[11,27-29]. It is the cumulative effect of each of these mediators that eventually leads to vascular leakage, hypovolemia, systemic inflammatory response syndrome, shock, and organ failure^[27,28]. Therefore, recent advances in understanding of the pathophysiology of the early systemic illness have led to the development of a new therapeutic approach in AP. Many specific inhibitors of these mediators have beneficial effects in experimental AP^[33-40]. However, few specific inhibitors can be used in clinic. A recent randomized, controlled study showed that antagonist of PAF activity is not sufficient to ameliorate systemic inflammatory response syndrome in severe AP^[41]. One of main reasons is that many inflammatory mediators may be involved in the pathophysiology of AP, and any one specific antagonist can not successfully down-regulate this inflammatory response, systemic effects, and organ failure. Dexamethasone is a non-specific anti-inflammatory agent, can inhibit or block several

inflammatory mediators' production, including inhibition of synthesis of TNF- α , IL-1 α , IL-6, IL-8, and prostaglandins^[42-44]. In our previous study, we found that dexamethasone attenuated the inflammatory mediators, 6-keto-PGI $_2$, TXB $_2$, and cytokine IL-6, and then improved the survival rate of experimental AP^[24]. The mechanism by which dexamethasone inhibits arachidonic acid and its metabolites is that dexamethasone can induce phospholipase A $_2$ inhibitor lipocortin. Other studies also indicated that exogenous glucocorticoids have beneficial effects in experimental AP^[42-47]. Now it is also clear that, the earlier glucocorticoids used, the better the results obtained. However, the optimal dose of glucocorticoids is not known. We used a high dose of dexamethasone short time interval, and found significant results. Although glucocorticoids have a positive impact on AP, Gomez *et al*^[48] found that survival rate decreased and pancreatic necrosis increased in mice after 7 d of pretreatment with hydrocortisone. Therefore, in our clinic, dexamethasone was used for 3-5 d to prevent its potential side reactions.

MCD is another important factor in the pathogenesis of multiple organ dysfunction syndromes in AP^[49,50]. MCD involve a series of changes including vasoconstriction, ischaemia, increased vascular permeability, impairment of nutritive tissue perfusion, ischaemia/reperfusion, leukocyte adherence, hemorrhheological changes and impaired lymphatic drainage. In addition, MCD in AP is not confined to the pancreas but appear to be a systemic disorder. Increased capillary permeability results in ascites and/or pleural effusion. Above mentioned ultrasonography demonstrated ascites in all patients with severe AP. In our previous experimental study, we found that blood viscosity, plasma viscosity, hematocrit, erythrocyte osmotic fragility elevated, while erythrocyte sedimentation rate and fibrinogen decreased significantly in AP^[25]. MCD affect organs other than the pancreas and persist after pancreatic necrosis is manifested and enzyme levels have returned to normal values^[22]. Therefore, MCD are not only an initiating or aggravating factor to pancreatic injury, but considered as a systemic reaction that contributes to pancreatitis-associated multiple organ dysfunction syndrome. Dextran 40 has numerous pharmacologic effects when infused intravenously: anti-platelet activity, anti-fibrin activity, and plasma volume expansion in hypovolemia, improvement of microcirculation by decreasing blood viscosity and impeding erythrocyte aggregation. The principal effect of dextran 40 is plasma volume expansion, resulting from the drug's colloidal osmotic effect in the drawing fluid from the interstitial to the intravascular spaces. Plasma volume expansion is accompanied by an increase in central venous pressure, cardiac output, stroke volume, blood pressure, urinary output, capillary perfusion, and pulse pressure, and by a decrease in heart rate, peripheral resistance, blood viscosity, and mean transit time. Dextran 40 also enhances blood flow through correction of hypovolemia and improved microcirculation. Dextran 40 may coat erythrocytes, thus reducing bonding forces and maintaining the erythrocytes in a state of electronegativity, and mutual repellancy; dextran 40 may also coat other formed elements. In addition, the drug may decrease erythrocyte rigidity, thereby facilitating passage of erythrocytes through small blood vessels^[51]. In experimental studies, it has been shown that dextran not only limited the progression of pancreatic necrosis by improving pancreatic microcirculation, reduced trypsinogen activation, prevented acinar necrosis, and improved survival in necrotizing rodent pancreatitis^[52-56], but also reduced blood viscosity, hematocrit and erythrocyte osmotic fragility, and elevated fibrinogen significantly^[25]. The colon, liver, and lungs affected by the AP associated systemic inflammatory response may still benefit from improved microcirculation at a time when pancreatic necrosis can no longer be reversed^[22].

In conclusion, treatment of severe AP with dexamethasone and dextran is an effective and practical approach. Dexamethasone can inhibit multiple inflammatory mediators and dextran can improve MCD. We emphasize that high dose of dexamethasone should be used in a short time interval to ensure the pharmacological effect and avoid its potential side reactions. Of course, when patients represent acute respiratory distress syndrome or severe intraabdominal infection, other therapeutic approaches, such as, mechanical ventilation, surgery should be considered.

REFERENCES

- Beger HG**, Rau B, Isenmann R. Prevention of severe change in acute pancreatitis: prediction and prevention. *J Hepatobiliary Pancreat Surg* 2001; **8**: 140-147
- Mutinga M**, Rosenbluth A, Tenner SM, Odze RR, Sica GT, Banks PA. Does mortality occur early or late in acute pancreatitis? *Int J Pancreatol* 2000; **28**: 91-95
- Yousaf M**, McCallion K, Diamond T. Management of severe acute pancreatitis. *Br J Surg* 2003; **90**: 407-420
- Slavin J**, Ghaneh P, Sutton R, Hartley M, Rowlands P, Garvey C, Hughes M, Neoptolemos J. Management of necrotizing pancreatitis. *World J Gastroenterol* 2001; **7**: 476-481
- Ulrich CD 2nd**. Medical management of acute pancreatitis: strategies, reality, and potential. *Curr Gastroenterol Rep* 2000; **2**: 115-119
- Norton ID**, Clain JE. Optimising outcomes in acute pancreatitis. *Drugs* 2001; **61**: 1581-1591
- Wang ZF**, Pan CE, Liu SG. Role of inflammatory mediators in acute pancreatitis. *Huaren Xiaohua Zazhi* 1998; **7**: 170-171
- Kingsnorth A**. Role of cytokines and their inhibitors in acute pancreatitis. *Gut* 1997; **40**: 1-4
- Makhija R**, Kingsnorth AN. Cytokine storm in acute pancreatitis. *J Hepatobiliary Pancreat Surg* 2002; **9**: 401-410
- McKay CJ**, Gallagher G, Brooks B, Imrie CW, Baxter JN. Increased monocyte cytokine production in association with systemic complication in acute pancreatitis. *Br J Surg* 1996; **83**: 919-923
- Uhl W**, Schrag HJ, Schmitter N, Aufenanger J, Nevalainen TJ, Buchler MM. Experimental study of a novel phospholipase A₂ inhibitor in acute pancreatitis. *Br J Surg* 1998; **85**: 618-623
- Uhl W**, Schrag HJ, Schmitter N, Wheatley AM, Büchler MW, Nevalainen TJ, Aufenanger J. Pathophysiological role of secretory type I and II phospholipase A₂ in acute pancreatitis: an experimental study in rats. *Gut* 1997; **40**: 386-392
- Abe T**, Shimsegawa T, Satoh A, Abe R, Kikuchi Y, Koizumi M, Toyota T. Nitric oxide modulate pancreatic edema formation in rat caerulein-induced pancreatitis. *J Gastroenterol* 1995; **30**: 636-642
- de Beaux AC**, Goldie AS, Ross JA, Carter DC, Fearon KC. Serum concentrations of inflammatory mediators related to organ failure in patients with acute pancreatitis. *Br J Surg* 1996; **83**: 349-353
- Zhou ZG**, Chen YD. Influencing factors of pancreatic microcirculatory impairment in acute pancreatitis. *World J Gastroenterol* 2002; **8**: 406-412
- Chen HM**, Hwang TL, Chen MF. The effect of gabexate mesilate on pancreatic and hepatic microcirculation in acute experimental pancreatitis in rats. *J Surg Res* 1996; **66**: 147-153
- Yuan YZ**, Lou KX, Gong ZH, Tu SP, Zhai ZK, Xu JY. Effects and mechanisms of emodin on pancreatic tissue EGF expression in acute pancreatitis in rats. *Shijie Huaren Xiaohua Zazhi* 2001; **9**: 127-130
- Sunamura M**, Yamauchi J, Shibuya K, Chen HM, Ding L, Takeda K, Kobari M, Matsuno S. Pancreatic microcirculation in acute pancreatitis. *J Hepatobiliary Pancreat Surg* 1998; **5**: 62-68
- Zhou ZG**, Chen YD, Sun W, Chen Z. Pancreatic microcirculatory impairment in experimental acute pancreatitis in rats. *World J Gastroenterol* 2002; **8**: 933-936
- Schmidt J**, Ebeling D, Ryschich E, Werner J, Gebhard MM, Klar E. Pancreatic capillary blood flow in an improved model of necrotizing pancreatitis in the rat. *J Surg Res* 2002; **106**: 335-341
- Bong JJ**, Ammori BJ, McMahon MJ, Kumar A, Turney JH, Norfolk DR. Thrombotic microangiopathy in acute pancreatitis. *Pancreas* 2002; **25**: 107-109
- Foitzik T**, Eibl G, Hotz B, Hotz H, Kahrau S, Kasten C, Schneider P, Buhr HJ. Persistent multiple organ microcirculatory disorders in severe acute pancreatitis: experimental findings and clinical implications. *Dig Dis Sci* 2002; **47**: 130-138
- Lankisch PG**, Pflüchthofer D, Lehnick D. No strict correlation between necrosis and organ failure in acute pancreatitis. *Pancreas* 2002; **20**: 319-322
- Wang ZF**, Xu J, Pan CE, Liu SG, Dong R. Dexamethasone inhibits inflammatory mediators and improves the prognosis of severe acute pancreatitis. *Shijie Huaren Xiaohua Zazhi* 2000; **8**: 239
- Wang ZF**, Pan CE, Liu SG. Treatment for acute necrotizing pancreatitis with correcting abnormal hemorheology. *Zhonghua Gandan Waiké Zazhi* 2000; **6**: 89
- Bradley EL 3rd**. A clinically based classification system for acute pancreatitis. Summary of the International symposium on Acute Pancreatitis, Atlanta, Ga, September 11 through 13, 1992. *Arch Surg* 1993; **128**: 586-590
- Norman J**. The Role of cytokines in the pathogenesis of acute pancreatitis. *Am J Surg* 1998; **175**: 76-83
- Sandoval D**, Gukovskaya A, Reavey P, Gukovsky S, Sisk A, Braquet P, Pandol SJ, Poucell-Hatton S. The role of neutrophils and platelet-activating factor in mediating experimental pancreatitis. *Gastroenterology* 1996; **111**: 1081-1091
- Norman JG**, Fink GW, Denham W, Yang J, Carter G, Sexton C, Falkner J, Gower WR, Franz MG. Tissue-Specific cytokine production during experimental acute pancreatitis (a probable mechanism for distant organ dysfunction). *Dig Dis Sci* 1997; **42**: 1783-1788
- Hughes CB**, Gaber LW, Mohey el-Din AB, Grewal HP, Kotb M, Mann L, Gaber AO. Inhibition of TNF alpha improves survival in an experimental model of acute pancreatitis. *Am Surg* 1996; **62**: 8-13
- Windsor AC**, Mullen PG, Walsh CJ, Fisher BJ, Blocher CR, Jesmok G, Fowler AA 3rd, Sugerman HJ. Delayed tumor necrosis factor a blockade attenuates pulmonary dysfunction and metabolic acidosis associated with experimental gram-negative sepsis. *Arch Surg* 1994; **129**: 80-89
- Norman J**, Franz M, Messina J, Riker A, Fabri PJ, Rosemurgy AS, Gower WR Jr. Interleukin-1 receptor antagonist decreases severity of experimental acute pancreatitis. *Surgery* 1995; **117**: 648-655
- Guice K**, Oldham KT, Remick DG, Kunkel SL, Ward PA. Anti-tumor necrosis factor antibody augments edema formation in caerulein-induced acute pancreatitis. *J Surg Res* 1991; **51**: 495-499
- Osman MO**, Kristensen JU, Jacobsen NO, Lausten SB, Deleuran B, Deleuran M, Gesser B, Matsushima K, Larsen CG, Jensen SL. A monoclonal anti-interleukin 8 antibody (WS-4) inhibits cytokine response and acute lung injury in experimental severe acute necrotizing pancreatitis in rabbits. *Gut* 1998; **43**: 232-239
- McKay CJ**, Curran F, Sharples C, Baxter JN, Imrie CW. Prospective placebo-controlled randomized trial of lexipafant in predicted severe acute pancreatitis. *Br J Surg* 1997; **84**: 1239-1243
- Kusske AM**, Rongione AJ, Ashley SW, McFadden DW, Reber HA. Interleukin-10 prevents death in lethal necrotizing pancreatitis in mice. *Surgery* 1996; **120**: 284-288
- Norman J**, Franz M, Fink GS, Messina J, Fabri PJ, Gower WR, Carey LC. Decreased mortality of severe acute pancreatitis following proximal cytokines blockade. *Ann Surg* 1995; **221**: 625-631
- Hughes CB**, Grewal HP, Gaber LW, Kotb M, El-din AB, Mann L, Gaber AO. Anti-TNF- α therapy improves survival and ameliorates the pathophysiology sequelae in acute pancreatitis in the rat. *Am J Surg* 1996; **171**: 274-280
- Kingsnorth AN**, Galloway SW, Formela PJ. Randomized double blind phase trial of lexipafant, a platelet-activating factor antagonist, in human acute pancreatitis. *Br J Surg* 1995; **82**: 1414-1420
- Grewal HP**, Mohey el Din A, Gaber L, Kotb M, Gaber AO. Amelioration of the physiologic and biochemical changes of acute pancreatitis using an anti-TNF-alpha polyclonal antibody. *Am J Surg* 1994; **167**: 214-218
- Johnson CD**, Kingsnorth AN, Imrie CW, McMahon MJ, Neoptolemos JP, McKay C, Toh SK, Skaife P, Leeder PC, Wilson P, Larvin M, Curtis LD. Double blind, randomized, placebo controlled study of a platelet activating factor antagonist, lexipafant, in the treatment and prevention of organ failure in predicted severe acute pancreatitis. *Gut* 2001; **48**: 62-69

- 42 **Yao XL**, Cowan MJ, Gladwin MT, Lawrence MM, Angus CW, Shelhamer JH. Dexamethasone alters arachidonate release from human epithelial cells by induction of p11 protein synthesis and inhibition of phospholipase A₂ activity. *J Biol Chem* 1999; **274**: 17202-17208
- 43 **Wang ZF**, Pan CE, Lu Y, Liu SG, Zhang GJ, Zhang XB. The role of inflammatory mediators in severe acute pancreatitis and regulation of glucocorticoids. *Hepatobil Pancreas Dis Int* 2003; **2**: 458-462
- 44 **Takaoka K**, Kataoka K, Sakagami J. The effect of steroid pulse therapy on the development of acute pancreatitis induced by closed duodenal loop in rats. *J Gastroenterol* 2002; **37**: 537-542
- 45 **Rakoczay Z**, Duda E, Kaszaki J, Ivanyi B, Boros I, Lonovics J, Takacs T. The anti-inflammatory effect of methylprednisolone occurs down-stream of nuclear factor-kappaB DNA binding in acute pancreatitis. *Eur J Pharmacol* 2003; **464**: 217-227
- 46 **Osman MO**, Jacobsen NO, Kristensen JU, Larsen CG, Jensen SL. Beneficial effects of hydrocortisone in a model of experimental acute pancreatitis. *Dig Surg* 1999; **16**: 214-221
- 47 **Gloor B**, Uhl W, Tcholakov O, Roggo A, Muller CA, Worni M, Buchler MW. Hydrocortisone treatment of early SIRS in acute experimental pancreatitis. *Dig Dis Sci* 2001; **46**: 2154-2161
- 48 **Gomez G**, Townsend CMJ, Green D, Rajaraman S, Uchida T, Thompson JC. Involvement of cholecystokinin receptors in the adverse effect of glucocorticoids on diet-induced necrotizing pancreatitis. *Surgery* 1989; **106**: 230-236
- 49 **Gullo A**, Beriot G. Ingredients of organ dysfunction or failure. *World J Surg* 1996; **20**: 430-436
- 50 **Eibl G**, Buhr HJ, Foitzik T. Therapy of microcirculatory disorders in severe acute pancreatitis: what mediators should we block? *Intens Care Med* 2002; **28**: 139-146
- 51 **McEvoy GK**. AHFS Drug Information. 45th ed. Bethesda: American Society of Health-System Pharmacists, Inc 2003: 2487-2489
- 52 **Schmidt J**, Huch K, Mithofer K, Hotz HG, Sinn HP, Buhr HJ, Warshaw AL, Herfarth C, Klar E. Benefits of various dextrans after delayed therapy in necrotizing pancreatitis of the rat. *Intens Care Med* 1996; **22**: 1207-1213
- 53 **Klar E**, Foitzik T, Buhr H, Messmer K, Herfarth C. Isovolemic hemodilution with dextran 60 as treatment of pancreatic ischemia in acute pancreatitis. Clinical practicability of an experimental concept. *Ann Surg* 1993; **217**: 369-374
- 54 **Schmidt J**, Fernandez-del Castillo C, Rattner DW, Lewandrowski KB, Messmer K, Warshaw AL. Hyperoncotic ultrahigh molecular weight dextran solutions reduce trypsinogen activation, prevent acinar necrosis, and lower mortality in rodent pancreatitis. *Am J Surg* 1993; **165**: 40-44
- 55 **Kusterer K**, Enghofer M, Poschmann T, Usadel KH. The effect of somatostatin, gabexate mesilate and dextran 40 on the microcirculation in sodium taurocholate-induced pancreatitis. *Acta Physiol Hung* 1992; **80**: 407-415
- 56 **Klar E**, Herfarth C, Messmer K. Therapeutic effect of isovolemic hemodilution with dextran 60 on the impairment of pancreatic microcirculation in acute biliary pancreatitis. *Ann Surg* 1990; **211**: 346-353

Edited by Xu CT and Pan BR Proofread by Xu FM

Detection of K-ras point mutation and telomerase activity during endoscopic retrograde cholangiopancreatography in diagnosis of pancreatic cancer

Guo-Xiong Zhou, Jie-Fei Huang, Zhao-Shen Li, Guo-Ming Xu, Feng Liu, Hong Zhang

Guo-Xiong Zhou, Jie-Fei Huang, Hong Zhang, Department of Gastroenterology, Affiliated Hospital of Nantong Medical College, Nantong 226001, Jiangsu Province, China

Zhao-Shen Li, Guo-Ming Xu, Feng Liu, Changhai Hospital, Second Military Medical University, Shanghai 200433, China

Correspondence to: Dr. Guo-Xiong Zhou, Department of Gastroenterology, Affiliated Hospital of Nantong Medical College, Nantong 226001, Jiangsu Province, China. zhouguoxiong@pub.nt.jsinfo.net

Telephone: +86-513-5052079

Received: 2003-06-05 **Accepted:** 2003-08-16

Abstract

AIM: To study the value of monitoring K-ras point mutation at codon 12 and telomerase activity in exfoliated cells obtained from pancreatic duct brushings during endoscopic retrograde cholangiopancreatography (ERCP) in the diagnosis of pancreatic cancer.

METHODS: Exfoliated cells obtained from pancreatic duct brushings during ERCP were examined in 27 patients: 23 with pancreatic cancers, 4 with chronic pancreatitis. K-ras point mutation was detected with the polymerase chain reaction and restriction fragment-length polymorphism (PCR-RFLP). Telomerase activity was detected by PCR and telomeric repeat amplification protocol assay (PCR-TRAP-ELISA).

RESULTS: The telomerase activities in 27 patients were measured in 21 exfoliated cell samples obtained from pancreatic duct brushings. D_{450} value of telomerase activities in pancreatic cancer and chronic pancreatitis were 0.446 ± 0.27 and 0.041 ± 0.0111 , respectively. Seventy-seven point eight percent (14/18) of patients with pancreatic cancer and none of the patients with chronic pancreatitis showed telomerase activity in cells collected from pancreatic duct brushings when cutoff value of telomerase activity was set at 2.0. The K-ras gene mutation rate (72.2%) in pancreatic cancer was higher than that in chronic pancreatitis (33.3%) ($P < 0.05$). In considering of both telomerase activities and K-ras point mutation, the total positive rate was 83.3% (15/18), and the specificity was 100%.

CONCLUSION: Changes of telomerase activities and K-ras point mutation at codon 12 may be an early event of malignant progression in pancreatic cancer. Detection of telomerase activity and K-ras point mutation at codon 12 may be complementary to each other, and is useful in diagnosis of pancreatic cancer.

Zhou GX, Huang JF, Li ZS, Xu GM, Liu F, Zhang H. Detection of K-ras point mutation and telomerase activity during endoscopic retrograde cholangiopancreatography in diagnosis of pancreatic cancer. *World J Gastroenterol* 2004; 10(9): 1337-1340

<http://www.wjgnet.com/1007-9327/10/1337.asp>

INTRODUCTION

Pancreatic cancer has a poor prognosis, its early diagnosis remains unsatisfactory. Even serum tumor markers, such as CA19-9, are associated with pancreatic cancer, but lack sensitivity and tumor specificity. Recent studies have shown that K-ras oncogene is often activated by specific point mutations restricted to codon 12 in human pancreatic ductal adenocarcinoma. In pancreatic adenocarcinoma, K-ras mutations were found in 75% to 100% of the cases^[1-8]. We and others previously showed that k-ras analysis from specimens obtained during ERCP was a sensitive (around 80% to 85%) and specific (close to 100%) method in differentiating benign from malignant pancreatic diseases. Therefore, k-ras mutation identification has been claimed as an useful and early marker in diagnosis of pancreatic cancer^[9-12]. Telomerase is a key enzyme with regard to immortalization of cancer cells and increased activity has been demonstrated in various human malignant neoplasms^[13-16]. We previously detected telomerase activity in 87% of surgically resected human pancreatic cancers. While in adjacent tissues, the positive rate of telomerase activity was only 10%. Detection of telomerase activity was useful in diagnosis of pancreatic cancer^[17].

In the present study, we evaluated the diagnostic role of K-ras mutation and telomerase activity in exfoliated cells obtained from pancreatic duct brushings alone and in combination, in differentiating chronic pancreatitis from pancreatic cancer.

MATERIALS AND METHODS

Patients

From April 1999 to December 2000, 27 patients undergoing ERCP were prospectively investigated at Changhai Hospital, 23 of them were patients with pancreatic cancer, 4 were patients with chronic pancreatitis. There were 17 men, 10 women with a mean age of 58.5 years (range: 22 to 75). The diagnosis of pancreatic cancer was confirmed histologically. The locations of the cancer were pancreatic head ($n=13$), body ($n=5$) and tail ($n=1$), and diffusion over the pancreas ($n=4$). Chronic pancreatitis was diagnosed by clinical history, ERCP and CT findings. All patients with chronic pancreatitis were followed up clinically and radiologically for at least six months.

Sampling technique

ERCP was performed using Olympus JF-240, 230 and TJF200 duodenoscope (Olympus, Japan). Lesions were identified after injection of iodinated contrast agent, a wire (0.035 inch in length) was introduced carefully into the main pancreatic duct and advanced to the suspected abnormal areas under guidance of fluoroscopic monitoring. Then a pancreatic duct brush (BC-24Q, Olympus) was introduced through the guide wire to the suspicious lesion, and the guide wire was withdrawn. The brush was moved rigorously back and forth across the suspicious lesion, brushes were retracted into the guiding catheter tip and removed together with the catheter to avoid losing a portion of the specimen inside the catheter. Specimens were immediately

collected in 5 mL of sterile saline solution at 4 °C for analysis of telomerase activity and DNA or smeared on glass slides, fixed in 95% alcohol and stained by HE for cytological examination, the order of brushing samples studied was always kept consistent.

Detection of K-ras point mutations at codon 12

Samples were centrifuged at 2000 r/min for 15 min and the pellet was collected. Genomic DNA was isolated using DNA lysis buffer and proteinase K digestion, followed by extraction with phenol and chloroform. K-ras point mutations were detected using PCR and restriction fragment-length polymorphism (PCR-RFLP). Primers were synthesized and supplied by Shanghai Bio-Engineering Research Center. The sequences of primers were: P1=5' -CTTGTGGTAGTTGGACCT-3' containing a mismatched base indicated by the underline, P2=5' -GTCAGAGAAACCTTTATCTG-3' , P3=5' -TGCACAGTAATATG-CATAT-3' . The reaction volume was 50 µL containing 5 µL of 10×Ex Taq buffer, 4 µL of dNTP mixture, 0.5 µL of each primer, 0.25 µL (5 U/µL) of Taq DNA polymerase. The primers for the first PCR were P1 (sense) and P2 (antisense) that flanked codon 12 of the K-ras gene. The first PCR amplification was performed for 30 cycles using a DNA thermal cycler, and each cycle consisted of denaturation at 94 °C for 30 s, annealing at 52 °C for 30 s, and extension at 72 °C for 45 s. A 5 µL sample of the first PCR product was digested with 1 µL (10 U/µL) of Mva I at 37 °C for 1 h under the conditions recommended by the supplier of mismatched sense primer described above. Subsequently, 5 µL of the reaction mixture was subjected to a second round of PCR and amplified for 30 cycles under the same conditions using the following primers: sense: P1; antisense: P3. The second PCR products were also digested with 1 µL (10 U/µL) of Mva I for 1 h. Mutations were confirmed by electrophoresis of 10 µL of the second digested sample on a 20 g/L agarose gel.

Detection of telomerase activity

Telomerase activity was detected with telomerase PCR-ELISA (Boehringer Mannheim, Germany). Exfoliated cells obtained from pancreatic duct brushings were collected and washed with PBS, and centrifuged at 10 000 g for 10 min. Then the cells in PBS containing 200 µL Lysis reagent were incubated on ice for 30 min, and centrifuged at 16 000 g for 20 min at 4 °C. Next, the supernatants (175 µL) were transferred to a Eppendorf tube, and tested for telomerase activity assay. Protein concentration was determined by Coomassie protein assay. Each of TRAP reactions contained 2 µL of cell extract (5-6 µg total protein) and sterile water with a final volume of 50 µL. The reaction mixture was incubated at 25 °C for 30 min, heated at 94 °C for 5 min. Then PCR amplification was performed for 33 cycles using a DNA thermal cycler, and each cycle consisted of denaturation at 94 °C for 30 s, annealing at 50 °C for 30 s, and extension at 72 °C for 90 s followed by 72 °C for 10 min. After PCR, 5 µL of the PCR products was dispensed into a reaction tube and incubated with 20 µL of denaturation reagent at room temperature for 10 min, and then mixed thoroughly by overtaking briefly with 225 µL hybridization buffer per tube. By transferring 100 µL of the mixture per well of percolated MTP modules, MTP modules were incubated at 37 °C on a shaker (300 r/min) for 2 h and washed 3 times with PBS, and enzyme reactions were incubated at room temperature on a shaker (300 r/min) for 30 min by addition of 100 µL anti-Dig-POD per well. After washed 5 times with PBS, 100 µL TMB substrate solution was added to each well and incubated for color development at room temperature for 20 min while shaking at 300 r/min. Using a ELISA reader, the absorbance value of samples was measured at 450 nm within 30 min after termination of reaction.

Statistical analysis

Statistical analysis was performed using the unpaired *t* test and χ^2 test or Fisher's exact test. $P < 0.05$ was considered statistically significant. Data were expressed as mean±SD.

RESULTS

Detection of K-ras point mutations at codon 12

K-ras point mutations at codon 12 were detected in 21 exfoliated cell samples obtained from pancreatic duct brushings by PCR-RFLP. Normal DNA had a 114 base pair (bp) band and k-ras DNA mutation remained as a 131 bp band since it was not digested by MvaI (Figures 1,2). K-ras gene mutation rate in pancreatic cancer was 72.2%, which was higher than that of chronic pancreatitis (33.3%, $P < 0.05$).

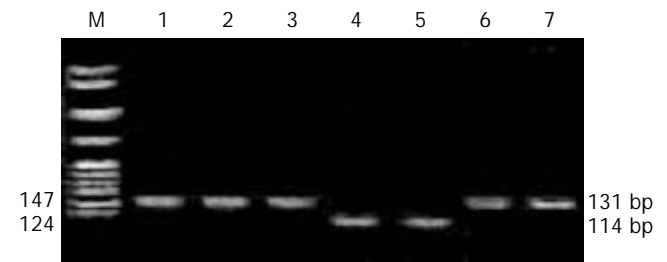


Figure 1 PCR products after restriction enzyme digestion, M: Marker; 1: Positive control; 2-7: Pancreatic cancer.

Detection of telomerase activity

Telomerase activities in 27 patients were measured in 21 exfoliated cell samples obtained from pancreatic duct brushings. D450 values of telomerase activity in carcinoma and chronic pancreatitis were 0.446 ± 0.27 and 0.041 ± 0.0111 , respectively. Seventy-seven point eight percent (14/18) of the patients with pancreatic cancer and none of patients with chronic pancreatitis showed telomerase activity in cells from pancreatic duct brushings when cutoff value of telomerase activity was set at 2.0. Both telomerase activity and cytological examination were detected in 66.7% (12/18) of patients.

Table 1 Location of pancreatic cancer and K-ras mutation or telomerase activity

Location	n	K-ras mutation		Telomerase activity	
		(+)	%	(+)	%
Head	11	8	72.7	9	81.8
Body	3	2	66.7	2	66.7
Tail	1	1	100	1	100
Diffuse	3	2	66.7	2	66.7
Total	18	13	72.2	14	77.8

Table 2 Comparison of K-ras point mutations and telomerase activity

	K-ras mutation	Telomerase	Both
Pancreatic cancer (n=18)	13	14	12
Chronic pancreatitis (n=3)	1	0	0
Sensitivity (%)	72.2	77.8	66.7
Specificity (%)	66.7	100	100

Relationship between K-ras gene or telomerase activity and location of tumors

No significant correlation of positivity of K-ras gene or telomerase activity with tumor location was observed (Table 1).

Comparison of K-ras point mutations with telomerase activity

The total rate of positive telomerase activity and K-ras mutation was 83.3% (15/18). The sensitivity and specificity of K-ras mutation and telomerase in differential diagnosis of pancreatic cancer and chronic pancreatitis was compared (Table 2).



Figure 2 Agarose gel of PCR products, P1, P2, P3 : after restriction enzyme digestion; P1a, P2a, P3a: before restriction enzyme digestion, P1 and P1a, P2 and P2a, P3 and P3a represent same samples, respectively.

DISCUSSION

Recent application of molecular biologic techniques, such as detection of K-ras mutation, has been proposed for the diagnosis of pancreatic cancer^[18-22]. K-ras gene mutation was found in greater than 90% of pancreatic cancers, and detection of K-ras gene mutation-positive cells in pure pancreatic juice or duodenal juice were reported to be useful in the diagnosis of pancreatic cancer^[23-26]. K-ras mutation was detected in ERCP brush samples. We used the sensitive RFLP method and found 72.2% of patients with pancreatic cancer had K-ras mutation, which was relatively higher than that in other reports. K-ras mutation was also detected in 1 patient with chronic pancreatitis. Although K-ras mutation has been detected mainly in malignancy, it could be detected in nonmalignant pancreatic lesions^[27-29]. However, a recent long-term follow-up report suggested that K-ras mutation in chronic pancreatitis might represent false-positive results^[30]. Studies including ours showed that this mutation could also occur in benign condition. Queneau *et al.*^[31] found 27.8% (10/36) chronic pancreatitis patients had k-ras mutations. Recently, several investigators failed to detect K-ras mutations in chronic pancreatitis even though they used highly sensitive methods^[32,33] and suggested that K-ras mutation was an extremely specific event in pancreatic cancer. Unfortunately, the reason for this discrepancy is not clear.

Telomerase is an enzyme that was found containing an RNA template complementary to the short DNA sequence repeats at chromosomal ends^[34]. Telomerase activity has been found in the majority of malignant tissues, such as pancreatic cancers, but not in somatic tissues except for reproductive and hematopoietic cells. Moreover, telomerase activity was detected in an extremely early stage of pancreatic cancer when the tumor could not be detected by other diagnostic methods^[35]. Hiyama *et al.*^[36] reported that 95% of pancreatic carcinomas but none of 11 benign pancreatic tumors showed telomerase activity. Suehara *et al.*^[37] reported that 100% of pancreatic carcinomas had high levels of telomerase activity. None of pancreatitis or normal pancreas extracts had detectable telomerase activity. However, some pancreatic adenomas demonstrated weak telomerase activity. Telomerase activity in pancreatic juice reflected the activity of the enzyme in tissue specimens^[38,39]. The telomerase activity in pancreatic juice from patients with pancreatic ductal carcinomas was lower than that in resected tissues. It is possible that various digestive enzymes in pancreatic juice might disturb telomerase assay by inhibiting Taq polymerase^[40]. Myung *et al.*^[41] and Uehara *et al.*^[42]. Have reported their study results in the diagnosis of pancreatic cancer by detecting K-ras mutations and telomerase activity alone

and in combination in pancreatic juice. We compared these two methods and evaluated their usefulness alone and in combination for the differentiation of pancreatic cancer from chronic pancreatitis. Using PCR-TRAP-ELISA method, we could give a more accurate diagnosis of pancreatic cancer by evaluating both K-ras mutations and telomerase activity in cells obtained from pancreatic duct brushings, and found that K-ras mutations in cells obtained from pancreatic duct brushings were useful for detecting neoplastic lesions and that telomerase activity was useful for differentiating malignancy from benign lesions of the pancreas, when telomerase activity cutoff was set at 2.0. The sensitivity and specificity of K-ras mutations for the diagnosis of pancreatic cancer were 72.2% and 66.7%, respectively, whereas those of telomerase activity were 77.8% and 100%, respectively. By combining these two methods, the sensitivity was 66.7% and the specificity was 100%.

In conclusion, detection of K-ras mutation and telomerase activity in cells obtained from pancreatic duct brushings may be complementary to each other, and may prove to be a potent tool for the diagnosis of pancreatic cancer.

REFERENCES

- Inoue S**, Tezel E, Nakao A. Molecular diagnosis of pancreatic cancer. *Hepatogastroenterology* 2001; **48**: 933-938
- Yoshizawa K**, Nagai H, Sakurai S, Hironaka M, Morinaga S, Saitoh K, Fukayama M. Clonality and K-ras mutation analyses of epithelia in intraductal papillary mucinous tumor and mucinous cystic tumor of the pancreas. *Virchows Arch* 2002; **441**: 437-443
- Raimondo M**, Tachibana I, Urrutia R, Burgart LJ, DiMagno EP. Invasive cancer and survival of intraductal papillary mucinous tumors of the pancreas. *Am J Gastroenterol* 2002; **97**: 2553-2558
- Nakata B**, Yashiro M, Nishioka N, Aya M, Yamada S, Takenaka C, Ohira M, Ishikawa T, Nishino H, Wakasa K, Hirakawa K. Genetic alterations in adenoma-carcinoma sequencing of intraductal papillary-mucinous neoplasm of the pancreas. *Int J Oncol* 2002; **21**: 1067-1072
- Mizumoto K**, Tanaka M. Genetic diagnosis of pancreatic cancer. *J Hepatobiliary Pancreat Surg* 2002; **9**: 39-44
- Tada M**, Komatsu Y, Kawabe T, Sasahira N, Isayama H, Toda N, Shiratori Y, Omata M. Quantitative analysis of K-ras gene mutation in pancreatic tissue obtained by endoscopic ultrasonography-guided fine needle aspiration: clinical utility for diagnosis of pancreatic tumor. *Am J Gastroenterol* 2002; **97**: 2263-2270
- Pabst B**, Arps S, Binmoeller K, Thul R, Walsemann G, Fenner C, Klapdor R. Analysis of K-ras mutations in pancreatic tissue after fine needle aspirates. *Anticancer Res* 1999; **19**: 2481-2483
- Luttges J**, Schlehe B, Menke MA, Vogel I, Henne-Bruns D, Kloppel G. The K-ras mutation pattern in pancreatic ductal adenocarcinoma usually is identical to that in associated normal, hyperplastic, and metaplastic ductal epithelium. *Cancer* 1999; **85**: 1703-1710
- Futakawa N**, Kimura W, Yamagata S, Zhao B, Ilsoo H, Inoue T, Sata N, Kawaguchi Y, Kubota Y, Muto T. Significance of K-ras mutation and CEA level in pancreatic juice in the diagnosis of pancreatic cancer. *J Hepatobiliary Pancreat Surg* 2000; **7**: 63-71
- Tateishi K**, Tada M, Yamagata M, Isayama H, Komatsu Y, Kawabe T, Shiratori Y, Omata M. High proportion of mutant K-ras gene in pancreatic juice of patients with pancreatic cystic lesions. *Gut* 1999; **45**: 737-740
- Watanabe H**, Yamaguchi Y, Ha A, Hu YX, Motoo Y, Okai T, Yoshimura T, Sawabu N. Quantitative determination of K-ras mutations in pancreatic juice for diagnosis of pancreatic cancer using hybridization protection assay. *Pancreas* 1998; **17**: 341-347
- Watanabe H**, Sawabu N, Songur Y, Yamaguchi Y, Yamakawa O, Satomura Y, Ohta H, Motoo Y, Okai T, Wakabayashi T. Detection of K-ras point mutations at codon 12 in pure pancreatic juice for the diagnosis of pancreatic cancer by PCR-RFLP analysis. *Pancreas* 1996; **12**: 18-24

- 13 **Pearson AS**, Chiao P, Zhang L, Zhang W, Larry L, Katz RL, Evans DB, Abbruzzese JL. The detection of telomerase activity in patients with adenocarcinoma of the pancreas by fine needle aspiration. *Int J Oncol* 2000; **17**: 381-385
- 14 **Yeh TS**, Cheng AJ, Chen TC, Jan YY, Hwang TL, Jeng LB, Chen MF, Wang TC. Telomerase activity is a useful marker to distinguish malignant pancreatic cystic tumors from benign neoplasms and pseudocysts. *J Surg Res* 1999; **87**: 171-177
- 15 **Tsutsumi M**, Tsujuchi T, Ishikawa O, Majima T, Yoshimoto M, Sasaki Y, Fukuda T, Oohigashi H, Konishi Y. Increased telomerase activities in human pancreatic duct adenocarcinomas. *Jpn J Cancer Res* 1997; **88**: 971-976
- 16 **Mizumoto K**, Suehara N, Muta T, Kitajima S, Hamasaki N, Tominaga Y, Shimura H, Tanaka M. Semi-quantitative analysis of telomerase in pancreatic ductal adenocarcinoma. *J Gastroenterol* 1996; **31**: 894-897
- 17 **Zhou GX**, Li ZS, Xu GM, Huang JF. Telomerase activity and Telomerase gene expression in pancreatic cancer. *Shiyong Aizheng Zazhi* 2003; **18**: 32-34
- 18 **Mulcahy H**, Farthing MJ. Diagnosis of pancreatico-biliary malignancy: detection of gene mutations in plasma and stool. *Ann Oncol* 1999; **10**(Suppl 4): 114-117
- 19 **Wenger FA**, Zieren J, Peter FJ, Jacobi CA, Muller JM. K-ras mutations in tissue and stool samples from patients with pancreatic cancer and chronic pancreatitis. *Langenbecks Arch Surg* 1999; **384**: 181-186
- 20 **Castells A**, Puig P, Mora J, Boadas J, Boix L, Urgell E, Sole M, Capella G, Lluís F, Fernandez-Cruz L, Navarro S, Farre A. K-ras mutations in DNA extracted from the plasma of patients with pancreatic carcinoma: diagnostic utility and prognostic significance. *J Clin Oncol* 1999; **17**: 578-584
- 21 **Mulcahy HE**, Lyautey J, Lederrey C, Qi Chen X, Anker P, Alstead EM, Ballinger A, Farthing MJ, Stroun M. A prospective study of K-ras mutations in the plasma of pancreatic cancer patients. *Clin Cancer Res* 1998; **4**: 271-275
- 22 **Lu X**, Xu T, Qian J, Wen X, Wu D. Detecting K-ras and p53 gene mutation from stool and pancreatic juice for diagnosis of early pancreatic cancer. *Chin Med J* 2002; **115**: 1632-1636
- 23 **Kimura W**, Zhao B, Futakawa N, Muto T, Makuuchi M. Significance of K-ras codon 12 point mutation in pancreatic juice in the diagnosis of carcinoma of the pancreas. *Hepatogastroenterology* 1999; **46**: 532-539
- 24 **Nakamura Y**, Onda M, Uchida E. Analysis of K-ras codon 12 point mutations using duodenal lavage fluid for diagnosis of pancreatic carcinoma. *Pancreas* 1999; **18**: 133-140
- 25 **Ha A**, Watanabe H, Yamaguchi Y, Ohtsubo K, Wang Y, Motoo Y, Okai T, Wakabayashi T, Sawabu N. Usefulness of supernatant of pancreatic juice for genetic analysis of K-ras in diagnosis of pancreatic carcinoma. *Pancreas* 2001; **23**: 356-363
- 26 **Wilentz RE**, Chung CH, Sturm PD, Musler A, Sohn TA, Offerhaus GJ, Yeo CJ, Hruban RH, Slebos RJ. K-ras mutations in the duodenal fluid of patients with pancreatic carcinoma. *Cancer* 1998; **82**: 96-103
- 27 **Tada M**, Ohashi M, Shiratori Y, Okudaira T, Komatsu Y, Kawabe T, Yoshida H, Machinami R, Kishi K, Omata M. Analysis of K-ras gene mutation in hyperplastic duct cells of the pancreas without pancreatic disease. *Gastroenterology* 1996; **110**: 227-231
- 28 **Rivera JA**, Rall CJ, Graeme-Cook F, Fernandez-del Castillo C, Shu P, Lakey N, Tepper R, Rattner DW, Warshaw AL, Rustgi AK. Analysis of K-ras oncogene mutations in chronic pancreatitis with ductal hyperplasia. *Surgery* 1997; **121**: 42-49
- 29 **Berndt C**, Haubold K, Wenger F, Brux B, Muller J, Bendzko P, Hillebrand T, Kottgen E, Zanol J. K-ras mutations in stools and tissue samples from patients with malignant and nonmalignant pancreatic diseases. *Clin Chem* 1998; **44**: 2103-2107
- 30 **Furuya N**, Kawa S, Akamatsu T, Furihata K. Long-term follow-up of patients with chronic pancreatitis and K-ras gene mutation detected in pancreatic juice. *Gastroenterology* 1997; **113**: 593-598
- 31 **Queneau PE**, Adessi GL, Thibault P, Cleau D, Heyd B, Mantion G, Carayon P. Early detection of pancreatic cancer in patients with chronic pancreatitis: diagnostic utility of a K-ras point mutation in the pancreatic juice. *Am J Gastroenterol* 2001; **96**: 700-704
- 32 **Hsiang D**, Friess H, Buchler MW, Ebert M, Butler J, Korc M. Absence of K-ras mutations in the pancreatic parenchyma of patients with chronic pancreatitis. *Am J Surg* 1997; **174**: 242-246
- 33 **Orth M**, Gansauge F, Gansauge S, Beger HG, Adler G, Schmid RM. K-ras mutations at codon 12 are rare events in chronic pancreatitis. *Digestion* 1998; **59**: 120-124
- 34 **Greider CW**, Blackburn EH. Identification of a specific telomere terminal transferase activity in Tetrahymena extracts. *Cell* 1985; **43**: 405-413
- 35 **Suehara N**, Mizumoto K, Kusumoto M, Niiyama H, Ogawa T, Yamaguchi K, Yokohata K, Tanaka M. Telomerase activity detected in pancreatic juice 19 months before a tumor is detected in a patient with pancreatic cancer. *Am J Gastroenterol* 1998; **93**: 1967-1971
- 36 **Hiyama E**, Kodama T, Shinbara K, Iwao T, Itoh M, Hiyama K. Telomerase activity is detected in pancreatic cancer but not in benign tumors. *Cancer Res* 1997; **57**: 326-331
- 37 **Suehara N**, Mizumoto K, Muta T, Tominaga Y, Shimura H, Kitajima S, Hamasaki N, Tsuneyoshi M, Tanaka M. Telomerase elevation in pancreatic ductal carcinoma compared to nonmalignant pathological states. *Clin Cancer Res* 1997; **3**: 993-998
- 38 **Suehara N**, Mizumoto K, Tanaka M, Niiyama H, Yokohata K, Tominaga Y, Shimura H, Muta T, Hamasaki N. Telomerase activity in pancreatic juice differentiates ductal carcinoma from adenoma and pancreatitis. *Clin Cancer Res* 1997; **3**: 2479-2483
- 39 **Iwao T**, Tsuchida A, Hiyama E, Kajiyama G. Telomerase activity in pancreatic juice for the preoperative diagnosis of pancreatic cancer. *Nippon Rinsho* 1998; **56**: 1229-1233
- 40 **Piatyszek MA**, Kim NW, Wwinrich SL, Hiyama K, Hiyama E, Wright WE, Shay JW. Detection telomerase activity in human cells and tumors by a telomeric repeat amplification protocol (TRAP). *Methods Cell Sci* 1995; **17**: 1-15
- 41 **Myung SJ**, Kim MH, Kim YS, Kim HJ, Park ET, Yoo KS, Lim BC, Wan Seo D, Lee SK, Min YI, Kim JY. Telomerase activity in pure pancreatic juice for the diagnosis of pancreatic cancer may be complementary to K-ras mutation. *Gastrointest Endosc* 2000; **51**: 708-713
- 42 **Uehara H**, Nakaizumi A, Tatsuta M, Baba M, Takenaka A, Uedo N, Sakai N, Yano H, Iishi H, Ohigashi H, Ishikawa O, Okada S, Kakizoe T. Diagnosis of pancreatic cancer by detecting telomerase activity in pancreatic juice: comparison with K-ras mutations. *Am J Gastroenterol* 1999; **94**: 2513-2518

Edited by Ren SY and Wang XL Proofread by Xu FM

Epidemiology and outcome of Crohn's disease in a teaching hospital in Riyadh

Abdullah S. Al-Ghamdi, Ibrahim A. Al-Mofleh, Rashed S. Al-Rashed, Saleh M. Al-Amri, Abdulrahman M. Aljebreen, Arthur C. Isnani, Reda El-Badawi

Abdullah S. Al-Ghamdi, Ibrahim A. Al-Mofleh, Rashed S. Al-Rashed, Saleh M. Al-Amri, Abdulrahman M. Aljebreen, Reda El-Badawi, Gastroenterology Division, Department of Medicine (38), King Khalid University Hospital, Riyadh, Kingdom of Saudi Arabia
Arthur C. Isnani, King Khalid University Hospital, College of Medicine and Research Center (74), PO Box 2925, Riyadh, Kingdom of Saudi Arabia

Correspondence to: Professor Ibrahim A. Al-Mofleh, Gastroenterology Division, Department of Medicine (38), King Khalid University Hospital, PO Box 2925 Riyadh 11461, Kingdom of Saudi Arabia
Telephone: +966-1-4671215 **Fax:** +966-1-4672558
Received: 2003-10-15 **Accepted:** 2004-01-09

Abstract

AIM: To know the epidemiology and outcome of Crohn's disease at King Khalid University Hospital, Riyadh, Saudi Arabia and to compare the results from other world institutions.

METHODS: A retrospective analysis of patients seen for 20 years (between 1983 and 2002). Individual case records were reviewed with regard to history, clinical, findings from colonoscopy, biopsies, small bowel enema, computerized tomography scan, treatment and outcome.

RESULTS: Seventy-seven patients with Crohn's disease were revisited, 13% presented the disease in the first 10 years and 87% over the last 10 years. Thirty-three patients (42.9%) were males and 44 (57.1%) were females. Age ranged from 11–70 years (mean of 25.3 ± 11.3 years). Ninety-two (92%) were Saudi. The mean duration of symptoms was 26 ± 34.7 mo. The mean annual incidence of the disease over the first 10 years was 0.32:100 000 and 1.66:100 000 over the last 10 years with a total mean annual incidence of 0.94:100 000 over the last 20 years. The chief clinical features included abdominal pain, diarrhea, weight loss, anorexia, rectal bleeding and palpable mass. Colonoscopic findings were abnormal in 58 patients (76%) showing mostly ulcerations and inflammation of the colon. Eighty nine percent of patients showed nonspecific inflammation with chronic inflammatory cells and half of these patients revealed the presence of granulomas and granulations on bowel biopsies. Similarly, 69 (89%) of small bowel enema results revealed ulcerations (49%), narrowing of the bowel lumen (42%), mucosal thickening (35%) and cobblestone appearance (35%). CT scan showed abnormality in 68 (88%) of patients with features of thickened loops (66%) and lymphadenopathy (37%). Seventy-eight percent of patients had small and large bowel disease, 16% had small bowel involvement and only 6% had colitis alone. Of the total 55 (71%) patients treated with steroids at some point in their disease history, a satisfactory response to therapy was seen in 28 patients (51%) while 27 (49%) showed recurrences of the condition with mild to moderate symptoms of abdominal pain and diarrhea most of which were due to poor compliance to medication. Seven patients (33%) remained with active Crohn's disease. Nine (12%)

patients underwent surgery with resections of some parts of bowel, 2 (2.5%) had steroid side effects, 6 (8%) with perianal Crohn's disease and five (6.5%) with fistulae.

CONCLUSION: The epidemiological characteristics of Crohn's disease among Saudi patients are comparable to those reported from other parts of the world. However the incidence of Crohn's disease in our hospital increased over the last 10 years. The anatomic distribution of the disease is different from other world institutions with less isolated colonic affection.

Al-Ghamdi AS, Al-Mofleh IA, Al-Rashed RS, Al-Amri SM, Aljebreen AM, Isnani AC, El-Badawi R. Epidemiology and outcome of Crohn's disease in a teaching hospital in Riyadh. *World J Gastroenterol* 2004; 10(9): 1341-1344
<http://www.wjgnet.com/1007-9327/10/1341.asp>

INTRODUCTION

Crohn's disease is a chronic recurrent inflammatory disorder of the bowel of unknown cause that can affect any gastrointestinal site from mouth to the anal canal. It results in long-term morbidity and the need for medical treatment and surgical interventions with resection of bowels. Slight increase in mortality plays significant demands upon healthcare resources^[1,2]. Epidemiological studies have shown that Crohn's disease tends to increase^[3-5]. These may be due to improvement of diagnostic procedures and practices and increasing awareness of the disease. Crohn's disease varies with geographical location^[6-15]. Diet and genetic predisposition triggered by environmental factors may play a significant role^[16].

The aim of this study was to know the epidemiology and outcome of Crohn's disease at our institution and to compare the results with reports from other world institutions.

MATERIALS AND METHODS

All patients attending the Gastroenterology Unit of King Khalid University Hospital, Riyadh, Saudi Arabia with a diagnosis of Crohn's disease between 1983 and 2002 were enrolled into the study. Seventy-seven patients with Crohn's disease were qualified (based on completeness of the data). The files of these patients were thoroughly reviewed from the time when the diagnosis of Crohn's disease was made based on history, colonoscopic findings, colonic biopsies, small bowel enema and CT scan of abdomen up to the date of each patient's last follow-up. Significant data collected included epidemiological points of Crohn's disease patients, age and gender at presentation, smoking history, the common clinical features of the disease, diagnostic modalities used for confirmation of the disease and their corresponding results, laboratory tests at initial and last visits, current status of the patient, treatment protocols used, their responses to treatment and outcome of management.

Data were entered systematically into computer with Microsoft Excel. Statistical analyses and correlations were done

using Stat Pac Gold analysis software. *P* values less than 0.05 were considered statistically significant.

RESULTS

A total of 77 patients with Crohn's disease over the last 20 years were reviewed. Ten (13%) patients presented the disease in the first 10 years and 67 (87%) patients over the last 10 years (Figure 1). Thirty-three (42.9%) patients were males and 44 (57.1%) were females. Age ranged from 11 to 70 years with a mean age of 25.3 ± 11.3 years. Seventy-one (92%) were Saudi nationals (Figure 2). The mean duration of symptoms was 26 ± 34.7 mo (range 1-180 mo). Table 1 shows the demographic characteristics of all patients with Crohn's disease.

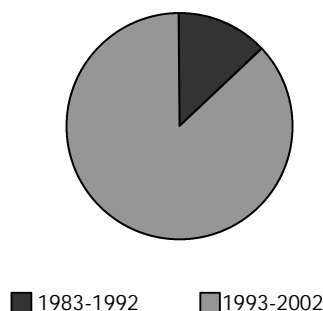


Figure 1 Number of patients with Crohn's disease over the last 20 years.

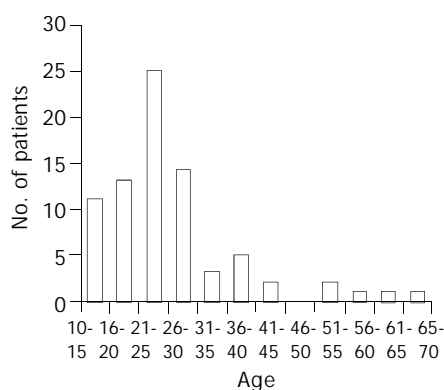


Figure 2 Age of patients at presentation.

Table 1 Demographic characteristics of patients with Crohn's disease in KKHU, Riyadh, Saudi Arabia (*n*=77)

	All patients	Active	On remission
Number	77	34 (44%)	43 (56%)
Total males	33 (42.9%)	15 (44%)	18 (42%)
Total females	44 (57.1%)	19 (56%)	25 (58%)
Age (range)	11-70 years	11-55 years	11-70 years
Mean age	25.3 ± 11.3 years	22.9 ± 8.3 years	27.3 ± 13.2 years
Nationality	71/6	32/2	39/4
(Saudi/non-Saudi)			

The mean annual incidence of the disease in the first 10 years was 0.32:100 000 and 1.66:100 000 in the last 10 years with total a mean annual incidence of 0.94:100 000 in the last 20 years.

Table 2 illustrates the chief clinical features of patients with Crohn's disease, showing abdominal pain in 67 patients (87%), diarrhea in 60 (78%), weight loss in 41 (53%), anorexia in 22 (29%) and rectal bleeding in 19 patients (25%). Fifty eight percent of patients had abdominal tenderness and 10% had palpable mass while 42% had negative physical examination findings.

Table 2 Clinical features of Crohn's disease in KKHU

	All patients <i>n</i> =77 (%)	Active Crohn's <i>n</i> =34 (%)	Remission <i>n</i> =43 (%)
Abdominal pain	67 (87)	29 (85)	38 (88)
Diarrhea	60 (78)	27 (79)	33 (77)
Weight loss	41 (53)	23 (68)	18 (42)
Anorexia	22 (29)	10 (29)	12 (28)
Fever	20 (26)	8 (24)	12 (28)
Rectal bleeding	19 (25)	5 (15)	14 (32)
Normal physical examination	32 (42)	10 (29)	22 (51)
Abdominal tenderness	45 (58)	24 (71)	21 (49)
Palpable mass	8 (10)	3 (9)	5 (12)

Table 3 shows the colonoscopic, biopsy results, enteroclysis findings and CT scan results. Colonoscopy was abnormal in 58 patients (76%) showing features of ulcerations in 40 patients (52%), inflammation in 25 (33%), thickened mucosa in 18 (24%), pseudopolyps in 13 (17%) and nodularity in 8 (11%). Biopsy showed abnormal results in all patients with chronic inflammatory cell infiltration in 69 patients (90%), ulceration and granuloma in 31 patients (40%), crypt abscess in 19 (25%), edema in 15 (19.5%), granulations in 11 (14%) and goblet cell depletion in 10 (13%). Small bowel enema showed abnormal findings in 69 patients (89%) with ulceration in 34 (49%), narrowed lumen in 29 (42%), mucosal thickening in 24 (35%), nodularity in 18 (23%), loop separation in 15 (19%) and filling defect in 6 (8%). CT scan results showed abnormal findings in 68 patients (88%) with thickened loops in 45 patients (66%), small mesenteric nonspecific lymphadenopathy in 25 (37%), hypervascularity in 18 (23%) and presence of mass in 15 (19%).

Table 3 Colonoscopic, biopsy, small bowel enema findings and CT scan results of Crohn's disease in KKHU

	All patients <i>n</i> =77	Active Crohn's <i>n</i> =34	Remission <i>n</i> =43
Colonoscopy	<i>n</i> =76	<i>n</i> =33	<i>n</i> =43
Normal	18 (24%)	8 (24%)	10 (23%)
Abnormal	58 (76%)	25 (76%)	33 (77%)
Biopsy	<i>n</i> =77	<i>n</i> =34	<i>n</i> =43
Normal	0	0	0
Abnormal	77 (100%)	34 (100%)	43 (100%)
Enteroclysis	<i>n</i> =77	<i>n</i> =34	<i>n</i> =43
Normal	8 (11%)	5 (15%)	3 (7%)
Abnormal	69 (89%)	29 (85%)	40 (93%)
CT scan	<i>n</i> =77	<i>n</i> =34	<i>n</i> =43
Normal	9 (12%)	9 (26%)	0
Abnormal	68 (88%)	25 (74%)	43 (100%)

The anatomic distribution of Crohn's disease in our patients was as follows, namely 16% had small bowel disease without colonic involvement, 78% had both small and large bowel disease and 6% had colitis alone.

Of the 77 patients, 55 were treated with steroids. A satisfactory response was seen in 28 patients (51%) while 27 (49%) showed recurrences of the condition, most of which were due to poor compliance to medication. Twenty-one (27%) patients however, did not receive steroids, of them seven (33%) remained with active Crohn's disease.

Nine (12%) patients underwent surgery with resections of parts of their bowel, two (2.5%) with steroid side effects, 6 (8%) with perianal disease (*e.g.* fissure, sinuses or fistulae), and 3 (4%) with fistulae between the bowel and 2 (2.5%) with perianal fistulae.

Table 4 Initial laboratory results of Crohn's disease patients at KKUH (all patients vs active vs on remission)

	All patients	Active Crohn's	Remission
WBC count	9.06±3.95	8.57±4.43	9.42±3.58
Hemoglobin	10.8±1.89	10.97±1.61	10.72±2.12
Platelets	429.9±161	422.5±145.2	435.4±176.1
ESR	42.8±27.8	34.4±22.9	49.5±26.6
Albumin	30.7±8.9	30.4±9.9	30.97±8.21

Table 5-A Comparison of initial and last follow-up laboratory results of Crohn's disease patients who went into remission

	Initial visit	Last follow-up	P value
WBC count	9.42±3.58	8.36±3.4	0.1629
Hemoglobin	10.72±2.12	12.4±1.78	0.0001
Platelets	435.4±176.1	396.4±132.02	0.2485
ESR	49.5±26.6	29.9±26.01	0.0009
Albumin	30.97±8.21	33.5±7.97	0.1508

Table 5-B Comparison of initial and last follow-up laboratory results of Crohn's disease patients who remained active

	Initial visit	Last follow-up	P value
WBC count	8.57±4.43	8.35±3.04	0.8120
Hemoglobin	10.97±1.61	11.2±2.3	0.6344
Platelets	422.5±145.2	388.5±122.5	0.3005
ESR	34.4±22.9	33.05±24.4	0.8148
Albumin	30.4±9.9	30.55±7.67	0.9445

Table 4 illustrates the comparison of the initial laboratory results in all patients with active Crohn's disease and those with remission. Of these initial laboratory results, the hemoglobin level in patients with remission was statistically significantly higher than those patients with active Crohn's disease (P value =0.0118). Table 5-A shows the comparison of initial and last follow-up laboratory results of 43 patients with remission. In patients with remission, the hemoglobin level was significantly increased from an initial level of 10.72±2.12 g/L to 12.4±1.78 g/L at the last follow-up (P value=0.0001). Furthermore, erythrocyte sedimentation rate (ESR) of 49.5±26.6 on the initial visit was significantly dropped to 29.9±26.01 at the last follow-up (P value 0.0009). Whereas, in patients with active Crohn's, there was no significant change in their laboratory results from initial to last follow-up (Table 5-B).

DISCUSSION

Before 1982, Kirsner and shorter observed that inflammatory bowel disease was rare or non existent in Saudi Arabia and Morocco^[16]. In 1982 Mokhtar and his group from King Abdul-Aziz University in Jeddah reported the first two cases of Crohn's disease in Saudi's^[6]. In 1984 Al-Nakib *et al* in Kuwait reported 14 patients with Crohn's disease and suggested that inflammatory bowel disease was uncommon in our population was wrong^[17]. El Sheik *et al* from Riyadh Armed Force Hospital reported three cases of Crohn's disease between 1979 and 1985^[18]. In 1990 Hossain and his group from King Khalid University Hospital in Riyadh reported seven cases of Crohn's disease, three patients were Saudis and the remaining were of different Arab nationalities and concluded that Crohn's disease did exist among Arabs^[7]. Hubler and Isbister from King Faisal Specialist and Research Hospital in Riyadh reported 28 patients with Crohn's disease between 1976 and 1994^[19]. From the previous reports we noticed that Crohn's disease was present among Saudi nationals in the 1980s but in a few numbers.

The present study was a retrospective study done in a referral, teaching hospital where we noticed an increase in the number of patients with Crohn's disease over the last a few years (Figure 1).

The total number of patients with Crohn's disease in KKUH from 1983 till 2002 was seventy-seven. Some of them were diagnosed after admission to the hospital for investigation and management of acute problems and the remaining as outpatients for investigations of chronic problems, *e.g.* diarrhea, abdominal pain and loss of weight.

There was an increase in the number and incidence of patients with Crohn's disease over the last 10 years in comparison to the first 10 years of the study. This is not definitely related to the accuracy of diagnostic tools because the same investigations were applied to all patients, *e.g.* colonoscopy and radiological investigations from the start of the study. These may reflect an actual increase in the number of patients since 1993.

The mean annual incidence of the disease over the last 20 years was 0.94:100 000 and this is more than that in Japan and some other Far East countries, less than that of Western countries and similar to that in the Province of Granada in Spain^[8-13,20].

It appeared that there was a slight female preponderance to the disease and the female to male ratio was 1.33. This is similar to that of North American population and some European countries, while in some studies from various areas of Asia and Europe suggested that there was a marked male preponderance, *e.g.* 1.6:1-2.2:1 in Japan and Korea respectively and 1.3:1 in Italy^[1,8-14].

In many European studies, the age distribution showed a bimodal pattern, with peaks at the ages of 20-29 and 60-69 years^[12]. Many other studies, however, have demonstrated a unimodal distribution and some a trimodal distribution^[15]. The peak age at diagnosis in our study was between 20 and 30 years and this is similar to the results of other institutions (Figure 3).

The clinical manifestations of Crohn's disease are variable depending on the involved part of the bowel and the extent of disease. In our center more than two thirds of our patients presented had abdominal pain and diarrhea, half of all our patients had weight loss and tenderness, less than one third had fever and rectal bleeding and a few percent had a palpable mass. These presentations were investigated and the diagnosis of Crohn's disease was confirmed by endoscopies, biopsies and radiological investigations. The above presentations are the usual manifestations of Crohn's disease in most of the communities.

The worldwide anatomic distribution of Crohn's disease ranged from 30-40% in those with small bowel disease, 40-55% in those with both small and large intestine involvement and 15-25% in those with colitis alone^[20,21]. In our study the distribution of the disease was different, most of the patients had small and large intestinal involvement and less than a quarter of patients had small bowel disease, while colonic disease alone represented only 6%.

It is difficult to predict which patients with Crohn's disease will go into remission. Localization of the disease, age, sex or even clinical symptoms did not significantly correlated with outcome of the treatment. Prolonged steroid response could occur in nearly half of patients receiving steroid^[22]. In this review, 55 patients (71%) received steroids and 28 of them (51%) went into remission with good response to therapy while the remaining did not, mainly due to poor compliance to treatment. During the long-term follow-up of this study, 42 patients (54.5%) were in remission at any time.

It was estimated that 75% of patients with Crohn's disease require surgery within the first 20 years after onset or appearance of symptoms. The most common operation performed is a resection of a diseased segment of small intestine and colon^[23,24]. Only 12% of our patients had surgeries with resections of parts

of their colon and small bowel.

In general, perianal Crohn's disease is present in as many as 25% of patients and develops in 31% to 94% of patients over the course of their illness. Manifestations of perianal disease include skin involvement (maceration, erosions, skin tags, ulceration, and abscesses), lesions of the anal canal (fissures, ulcers, and stenosis), and fistulae. Approximately two thirds of patients with Crohn's colitis have perianal fissures.

Unlike ordinary anal fissure, typical fissures associated with Crohn's disease are multiple, painless, and non-midline in location. Fistulae have been found to develop in 20% to 40% of patients with Crohn's disease and were difficult to be managed medically^[25-27]. More than half of patients with colonic involvement will have anal complications, whereas in less than 20% of patients with small-bowel disease, anal symptoms were likely to develop^[28,29]. Only 6% of our patients had perianal disease with fissures, sinuses and fistulae, all of them had involvement solely of the colon.

Patients with Crohn's disease who went into remission showed significant improvement in their hemoglobin and erythrocyte sedimentation rate (ESR) while other laboratory results remained statistically insignificant as that before remission.

Those who remained active showed no changes in all laboratory results.

The epidemiological characteristics of Crohn's disease among Saudi patients are comparable to those reported from other parts of the world. There is an increase in the incidence of Crohn's disease in our hospital over the last 10 years. However, the anatomic distribution of the disease is entirely different from other world institutions, with less isolated colonic disease and, all patients with perianal disease have colonic inflammation.

REFERENCES

- 1 **Loftus EV**, Schoenfeld P, Sandborn WJ. The epidemiology and natural history of Crohn's disease in population-based patient cohorts from North America: a systematic review. *Aliment Pharmacol Ther* 2002; **16**: 51-60
- 2 **Rubin GP**, Hungin AP, Kelly PJ, Ling J. Inflammatory bowel disease: epidemiology and management in an English general practice population. *Aliment Pharmacol Ther* 2000; **14**: 1553-1559
- 3 **Loftus EV**, Sandborn WJ. Epidemiology of inflammatory bowel disease. *Gastroenterol Clin North Am* 2002; **31**: 1-20
- 4 **Loftus EV**. A matter of life or death: mortality in Crohn's disease. *Inflamm Bowel Dis* 2002; **8**: 428-429
- 5 **Card T**, Hubbard R, Logan RF. Mortality in inflammatory bowel disease: a population-based cohort study. *Gastroenterology* 2003; **125**: 1583-1590
- 6 **Mokhtar A**, Khan MA. Crohn's disease in Saudi Arabia. *Saudi Med J* 1982; **3**: 207-208
- 7 **Hossain J**, Al-Mofleh IA, Laajam MA, Al-Rashed RS, Al-Faleh FZ. Crohn's disease in Arab. *Ann Saudi Med* 1991; **11**: 40-46
- 8 **Yang SK**, Loftus EV Jr., Sandborn WJ. Epidemiology of inflammatory bowel disease in Asia. *Inflammatory bowel disease* 2001; **7**: 260-270
- 9 **Probert CS**, Jayanthi V, Mayberry JF. Inflammatory bowel disease in Indian migrants in Fiji. *Digestion* 1991; **50**: 82-84
- 10 **Munkholm P**, Langholz E, Nielsen OH, Kreiner S, Binder V. Incidence and prevalence of Crohn's disease in the country of Copenhagen, 1962-87: a sixfold increase in incidence. *Scand J Gastroenterol* 1992; **27**: 609-614
- 11 **Loffler A**, Glados M. Data on the Epidemiology of Crohn's disease in the city of Cologne. *Med Klin* 1993; **88**: 516-519
- 12 **Martinez-Salmeron JF**, Rodrigo M, de Teresa J, Noguera F, Garcia-Montero M, de Sola C, Salmeron J, Caballero M. Epidemiology of inflammatory bowel disease in the Province of Granada, Spain: a retrospective study from 1979 to 1988. *Gut* 1993; **34**: 1207-1209
- 13 **Cottone M**, Cipolla C, Orlando A, Oliva L, Salerno G, Pagliaro L. Hospital incidence of Crohn's disease in the province of Palermo. A preliminary report. *Scand J Gastroenterol* 1989; **170**: 27-28
- 14 **Cottone M**, Cipolla C, Orlando A, Oliva L, Aiala R, Puleo A. Epidemiology of Crohn's disease in Sicily: a hospital incidence study from 1987 to 1989. "The Sicilian Study Group of Inflammatory Bowel Disease." *Eur J Epidemiol* 1991; **7**: 636-640
- 15 **Kaerle L**, Teglbjaerg PS, Sabroe S, Kolstad HA, Ahreas W, Eriksson M, Guenel P, Hardell L, Launoy G, Merler E, Merletti F, Stang A. Medical risk factors for small bowel adenocarcinoma with focus on Crohn's disease: a European population-based case-control study. *Scand J Gastroenterol* 2001; **36**: 641-646
- 16 **Kirsner JB**, Shorter RG. Recent developments in non-specific inflammatory bowel disease. *N Engl J Med* 1982; **306**: 837-848
- 17 **Al-Nakib B**, Radhakrishnan S, Jacob GS, Al-Liddawi H, Al-Ruwaih A. Inflammatory bowel disease in Kuwait. *Am J Gastroenterol* 1984; **79**: 191-194
- 18 **El Sheikh MAR**, Dip Ven Al Karawi MA, Hamid MA, Yasawy I. Lower gastrointestinal endoscopy. *Ann Saudi Med* 1987; **7**: 306-311
- 19 **Hubler M**, Isbister W. Inflammatory bowel disease in Saudi Arabia presentation and initial. *J Gastroenterol Hepatol* 1998; **13**: 1119-1124
- 20 **Moum B**, Ekblom A. Epidemiology of inflammatory bowel disease-methodological considerations. *Dig Liver Dis* 2002; **34**: 364-369
- 21 **Nakahara T**, Yao T, Sakurai T, Okada M, Iida M, Fuchigami T, Tanaka K, Okada Y, Sakamoto K, Sata M. Long-term prognosis of Crohn's disease. *Nippon Shokakibyo Gakkai Zasshi* 1991; **88**: 1305-1312
- 22 **Munkholm P**, Langholz E, Davidsen M, Binder V. Frequency of glucocorticoid resistance and dependency in Crohn's disease. *Gut* 1994; **35**: 360-362
- 23 **Becker JM**. Surgical therapy for ulcerative colitis and Crohn's disease. *Gastroenterol Clin North Am* 1999; **28**: 371-390
- 24 **Iida M**, Yao T, Okada M. Long-term follow-up study of Crohn's disease in Japan. The research committee of Inflammatory Bowel Disease in Japan. *J Gastroenterol* 1995; **30**(Suppl 8): 17-19
- 25 **Brown MO**. Inflammatory bowel disease. *Prim Care* 1999; **26**: 141-170
- 26 **Rubesin SE**, Scotinotis I, Birnbaum BA, Ginsberg GC. Radiologic and endoscopic diagnosis of Crohn's disease. *Surg Clin North Am* 2001; **81**: 39-70
- 27 **Thuraisingam A**, Leiper K. Medical management of Crohn's disease. *Hosp Med* 2003; **64**: 713-718
- 28 **McClane SJ**, Rombeau JL. Anorectal Crohn's disease. *Surg Clin North Am* 2001; **81**: 169-183
- 29 **Tersigni R**, Alessandrini L, Kohn A, Speziale G. Treatment of perianal Crohn's disease (Abstract). *Chir Ital* 2000; **52**: 155-164

Edited by Wang XL Proofread by Xu FM

Catheter-related infection in gastrointestinal fistula patients

Ge-Fei Wang, Jian-An Ren, Jun Jiang, Cao-Gan Fan, Xin-Bo Wang, Jie-Shou Li

Ge-Fei Wang, School of Medicine, Nanjing University, Nanjing, 210093, Jiangsu Province, China

Jian-An Ren, Jun Jiang, Cao-Gan Fan, Xin-Bo Wang, Jie-Shou Li, Department of General Surgery, Jinling Hospital, Clinical School of Nanjing University, Nanjing 210002, Jiangsu Province, China

Correspondence to: Dr. Ge-Fei Wang, School of Medicine, Nanjing University, 27 Hankou Road, Nanjing, 210093, Jiangsu Province, China. wang_gefei@hohmail.com

Telephone: +86-25-4825110 **Fax:** +86-25-4803956

Received: 2003-08-06 **Accepted:** 2003-10-07

Abstract

AIM: To study the incidence, bacterial spectrum and drug sensitivity of catheter-related infection (CRI) in gastrointestinal fistula patients.

METHODS: A total of 216 patients with gastrointestinal fistulae during January 1998 to April 2001 were studied retrospectively. Two hundred and sixteen catheters of the 358 central venous catheters used in 216 gastrointestinal fistula patients were sent for microbiology analysis.

RESULTS: Ninety-five bacteria were cultivated in 88 catheters (24.6%). There were 54 Gram-negative bacteria (56.8%), 35 Gram-positive bacteria (36.8%), and 6 fungi (6.4%). During the treatment of CRI, 20 patients changed to use antibiotics or antifungal, and all patients were cured. The mean time of catheters used was 16.9±13.0 d.

CONCLUSION: CRI is still the common complication during total parenteral nutrition (TPN) treatment in patients with gastrointestinal fistulae, and Gram-negative bacteria are the main pathogens, and bacterial translocation is considered the common reason for CRI.

Wang GF, Ren JA, Jiang J, Fan CG, Wang XB, Li JS. Catheter-related infection in gastrointestinal fistula patients. *World J Gastroenterol* 2004; 10(9): 1345-1348

<http://www.wjgnet.com/1007-9327/10/1345.asp>

INTRODUCTION

Total parenteral nutrition (TPN) support is one of the main treatments for gastrointestinal fistula patients, and central venous catheters (CVC) are widely used as the major route. Catheter-related infection (CRI) is a serious complication during TPN. This paper retrospectively reviewed patients with gastrointestinal fistulae complicated by CRI during TPN during January 1998 to April 2001, and studied the incidence, bacterial spectrum and drug sensitivity of CRI. There were special characteristics of CRI in gastrointestinal fistula patients.

MATERIALS AND METHODS

Patient data

Patient data were obtained from a retrospective review of 216 CVC of 358 CVC from 216 patients with gastrointestinal fistulae

in the surgical unit of Nanjing Jinling Hospital during January 1998 to April 2001.

Intervention

The catheters were removed and sent for microbiological culture and analysis, when the patients were clinically considered as CRI because of infection signs (e.g. tremble and fever) during TPN.

Diagnosis of CRI

Patients who had signs of infection and positive culture of CVC were diagnosed as CRI.

Statistical analysis

Patient data, culture of central venous catheters and drug sensitivity were collected and analyzed by the softwares of WHONET 5.0 and SPSS 10.0

RESULTS

Clinical data

In this study, 358 catheters were inserted in 216 gastrointestinal fistula patients. The number of male patients was 129, mean age was 42.5±16.6 years, and that of female was 87, mean age was 43.9±16.5 years. Two hundred and sixteen catheters were removed, and then the catheter tips and concurrent peripheral venous blood were sent for microbiological analysis when the patients had such infection signs as phricasmus, chill and fever. Of the catheters sent for microbiological analysis, 88 (24.6%) were confirmed to have infection by positive culture. Ninety-five bacteria were cultivated, and 8% were polymicrobes. Of the concurrent peripheral venous blood culture, 50 (14.0%) were confirmed to be positive. Fifty-two bacteria were cultivated, and 4% were polymicrobes. Twenty-four bacteria were cultivated from catheters and concurrent peripheral venous blood. The mean time of catheters used was 16.9±13.0 d.

Treatment and outcome

All the 88 patients who were confirmed having CRI were cured. Five patients were self-cured without treatment of any antibiotics after CVC was removed. Among the other 83 patients who were treated by antibiotics, 63 were cured by antibiotics in 1-3 d, 16 changed to use antibiotics, and 4 were treated by antifungal drugs according to the drug sensitivity because of persistent infection.

Microbiological analysis

Ninety five bacteria were cultivated from 88 catheters. The bacterial spectrum is shown in Table 1. There were 54 Gram-negative bacteria (56.8%), 35 Gram-positive bacteria (36.8%), and 6 fungi (6.4%). Drug sensitivity test was performed in 77 of 95 bacteria. Drug sensitivity of 48 Gram-negative bacteria and 29 Gram-positive bacteria is shown in Table 2 and Table 3, respectively. The result of drug sensitivity test indicated severe drug resistance. The preferably sensitive antibiotics for Gram-negative bacteria were imipenem, amikacin, ciprofloxacin, ceftazidime and cefoperazone/sulbactam in turn, and those for Gram-positive bacteria were vancomycin, norfloxacin and ciprofloxacin.

Table 1 Organisms present in 88 catheters

Species of bacteria	No of bacteria	Percent (%)
Gram-negative bacteria		56.8
Enterobacteriaceae		
Enterobacter cloacae	6	6.3
Escherichia coli	5	5.3
Non- identified Gram-negative bacteria	4	4.2
Klebsiella pneumoniae	1	1.1
Non-ferment gram negative rods		
Pseudomonas	20	21.1
Acinetobacter baumannii	7	7.3
Bacterium aeruginosa	5	5.3
Corynebacterium diphtheriae	4	4.2
Acinetobacter lwoffii	2	2.1
Gram-positive bacteria		36.8
Staphylococcus epidermidis	9	9.4
Staphylococcus haemolyticus	7	7.3
Tetrads	4	4.2
Staphylococcus aureus	4	4.2
Enterococcus sp.	4	4.2
Streptococcus viridans	2	2.1
Staphylococcus hominis	2	2.1
Staphylococcus warneri	2	2.1
Staphylococcus simulans	1	1.1
Fungus		6.4
Candida	5	5.3
Saccharomyces	1	1.1
Total	95	100.0

DISCUSSION

Characteristics of CRI in gastrointestinal fistula patients

As the serious complication during TPN support, the incidence of CRI was as high as 23% in simple malnutrition patients in the early years of TPN^[1]. Due to the development in nurse technology and catheter materials, the incidence of CRI has gradually decreased to 2-6%^[2-4]. However, the CRI incidence in surgical critical patients was still as high as 21.1-34%, and its mortality was increased^[5,6]. Based on this report, the CRI incidence in gastrointestinal fistula patients was similar to that in critical patients, and higher than that in simple malnutrition patients. The mean time of catheters used was 16.9±13.0 d, and it was 17 d in other reports^[2,5,6]. So it is important to supervise the symptoms of gastrointestinal fistula patients during TPN, especially 17 d after catheters were inserted.

In most literature reports, Gram-positive bacteria like *S. epidermidis* and *S. aureus* were most frequently cultivated from catheters^[5-8]. Bacterial skin colonization at the catheter-skin interface at the time of insertion or afterward distal spread of the bacteria along the external catheter surface is the basic pathogenesis. However, Gram-negative bacteria are the most common organisms causing CRI of gastrointestinal fistula patients, and the orderly are Gram-positive bacteria and Fungi. Three reasons were considered for this phenomenon. First, the importance of catheter nursing has been cognized and the means for decreasing bacterial skin colonization, such as disinfection and dressing replacement were performed 3 times per week. Second, gastrointestinal fistula patients always were complicated with inflammation of abdomen, microorganisms especial Gram-negative bacteria could broadcast from abdominal abscess to blood and adhere to catheter-hub and colonize. Third, patient were commonly fasting once gastrointestinal fistula occurred. If long-term lack of food stimulation and direct lumen nutrition, mucous atrophy, height of villus decrease and

Table 2 Drug sensitivity test of 48 Gram-negative bacteria (%S)

Species of bacteria	n	AMK	AMP	CFP	CSL	PIP	CAZ	CRO	CXA	CIP	IPM
Pseudomonas	20	75	12.5	0	25	25	70	45	0	70.5	75
Acinetobacter baumannii	7	100	16.7	0	100	0	60	60	0	85.7	100
Enterobacter cloacae	6	75	0	100	75	50	75	80	33.3	50	100
Escherichia coli	5	0	0	0	100	0	0	0	0	0	100
Bacterium aeruginosa	5	40	0	20	80	20	60	20	0	60	80
Corynebacterium diphtheriae	4	75	0	50	100	0	75	50	25	75	100
Klebsiella pneumoniae	1	0	0	0	0	100	0	0	100	100	100
Summary	48	80	7.5	30	69.2	21.1	70.3	55.6	8.9	75.6	90

%S indicates drug sensitivity. AMK: Amikacin, AMP: Ampicillin, CFP: Cefoperazone, CSL: Cefoperazone/Sulbactam, PIP: Piperacillin, CAZ: Ceftazidime, CRO: Ceftriaxone, CXA: Cefuroxime axetil, CIP: Ciprofloxacin, IPM: Imipenem.

Table 3 Drug sensitivity test of 29 Gram-positive bacteria (%S)

Species of bacteria	n	AMK	AMP	SAM	CEP	CIP	ERY	NOR	PEN	PIP	VAN
Staphylococcus epidermidis	9	0	0	0	0	66.7	0	66.7	0	0	100
S. haemolyticus	7	50	0	20	25	50	16.7	60	0	0	100
S. aureus	4	100	0	0	0	25	33.3	75	0	0	100
Enterococcus sp.	4	0	0	0	0	100	0	0	0	0	100
S. hominis	2	0	0	0	0	50	0	0	0	60	100
S. warneri	2	0	0	100	0	100	100	0	0	100	100
S. simulans	1	0	0	100	100	0	0	0	0	0	100
Summary	29	50	0	18.2	16.7	56.2	21.4	66.7	11.8	10.2	100

%S indicates drug sensitivity. AMK: Amikacin, AMP: Ampicillin, SAM: Ampicillin/Sulbactam, CEP: cephalothin, CIP: Ciprofloxacin, ERY: Erythromycin, NOR: Norfloxacin, PEN: Penicillin, PIP: Piperacillin, VAN: Vancomycin.

barrier damage would arise, followed by bacterial translocation from gastrointestinal tract to the mesenteric lymph nodes even blood^[9-11]. Gram-negative bacterial translocation was considered to be the most common reason for the high incidence of CRI in gastrointestinal fistula patients. Several researches indicated that gut bacterial translocation might be the pathogenesis of catheter-related infection during TPN. Pierro *et al* found that in neonates and infants who were receiving long-term parenteral nutrition, enteric microorganisms including *Escherichia coli*, *Klebsiella*, *Candida species* and *enterococci* were the main microorganisms cultured from blood sample, and they figured out that CRI might be a gut-related phenomenon^[12]. Pappo *et al.* speculated that Candida sepsis during TPN might be the result of Candida translocation from the gut due to the combination of high-density Candida colonization and favorable local conditions in the gut induced by TPN and bowel rest^[13]. Another research indicated that patients with an extremely short remaining small bowel (shorter than 50 cm) receiving home TPN had a higher frequency of catheter-related sepsis, particularly by enteric microorganisms^[14]. Based on our research, Gram-negative bacterial translocation was considered to be the pathogenesis of CRI in gastrointestinal fistula patients. Absence of gastrointestinal integrality and extravasations of intestinal succus would induce abdominal or systemic infection once fistula occurs, and the best treatment to deal with fistulae and infection is more effective drainage. Without effective drainage, it is very difficult to control infection, even with antibiotics from low to high grade or narrow to broad spectrum. Abuse of antibiotic would result in arouse increase of drug resistance. Our study demonstrated that drug resistance of gastrointestinal fistula patients was high, and the preferably sensitive antibiotics for Gram-negative bacteria were imipenem, ceftazidime and cefoperazone/sulbactam, and those for Gram-positive bacteria were vancomycin, norfloxacin and ciprofloxacin.

Prevention and treatment of CRI

The methods for prevention of CRI included skin cleanout and antisepsis before catheter inserted, strictly disinfection system and operation during inserting, catheter nursing and dressing replacement after insertion, decreasing manipulation of catheter, and avoiding unnecessary device^[15-22]. Catheters must be removed once CRI occurred or clinically suspected to be, subsequently therapies of experiential antibiotics were supposed to utilize, though part of patients could self-cure without treatment of any antibiotics^[23-29]. Imipenem, ceftazidime and cefoperazone/sulbactam are the perfect choice for therapy of experiential antibiotics based on the result of drug sensitivity. If the infective symptom persisted after catheters were removed and antibiotics were utilized, drug resistance or Candida infection should be considered, and effective antibiotics or antifungal drugs should apply according to drug sensitivity. Intravenous glutamine or short-chain fatty acids could reduce central venous catheter related infection by reducing bacterial translocation from gut lumen^[30,31]. According to the advancement of gastrointestinal physiology, enteral nutrition has been confirmed to improve gut mucosa barrier and liver function and nutrition, reduce bacterial translocation and avoid infection complication of TPN^[32-34]. For avoiding CRI, enteral nutrition (EN) should be utilized, and the time of TPN should be reduced in gastrointestinal fistula patients. CRI is a severe complication in gastrointestinal fistula patients, and attention should be paid to its high incidence based on this retrospective study. Gram-negative bacteria with high drug resistance are the most common organisms causing CRI. Catheters must be removed and sent for microbiological analysis once CRI occurs, sensitive antibiotics for Gram-negative bacteria should be utilized. If the infective symptom persists, drug resistance or Candida infection should be considered, and effective antibiotics or antifungal

drugs should be applied according to drug sensitivity.

REFERENCES

- 1 **Adal KA**, Farr BM. Central venous catheter-related infections: a review. *Nutrition* 1996; **12**: 208-213
- 2 **Peterson KK**. Central line sepsis. *Clin J Oncol Nurs* 2003; **7**: 218-221
- 3 **Safdar N**, Kluger DM, Maki DG. A review of risk factors for catheter-related bloodstream infection caused by percutaneously inserted, noncuffed central venous catheters: implications for preventive strategies. *Medicine* 2002; **81**: 466-479
- 4 **Memish ZA**, Arabi Y, Cunningham G, Kritchevsky S, Braun B, Richards C, Weber S, Pereira CR. Comparison of US and non-US central venous catheter infection rates: evaluation of processes and indicators in infection control study. *Am J Infect Control* 2003; **31**: 237-242
- 5 **Charalambous C**, Swoboda SM, Dick J, Perl T, Lipsett PA. Risk factors and clinical impact of central line infections in the surgical intensive care unit. *Arch Surg* 1998; **133**: 1241-1246
- 6 **Clarke DE**, Raffin TA. Infectious complication of indwelling long-term central venous catheters. *Chest* 1990; **97**: 966-972
- 7 **Page S**, Abel G, Stringer MD, Puntis JW. Management of septicemic infants during long-term parenteral nutrition. *Int J Clin Pract* 2000; **54**: 147-150
- 8 **Reimund JM**, Arondel Y, Finck G, Zimmermann F, Duclos B, Baumann R. Catheter-related infection in patients on home parenteral nutrition: results of a prospective survey. *Clin Nutr* 2002; **21**: 33-38
- 9 **Alverdy JC**, Aoye E, Moss GS. Total parenteral nutrition promotes bacterial translocation from the gut. *Surgery* 1988; **104**: 185-190
- 10 **Odetola FO**, Moler FW, Dechert RE, Van Der Elzen K, Chenoweth C. Nosocomial catheter-related bloodstream infections in a pediatric intensive care unit: Risk and rates associated with various intravascular technologies. *Pediatr Crit Care Med* 2003; **4**: 432-436
- 11 **Eizaguirre I**, Aldamiz L, Aldazabal P, Garcia Urkia N, Asensio AB, Bachiller P, Garcia Arenzana JM, Ruiz JL, Sanjurjo P, Perez Nanclares G. Tissue antioxidant capacity and bacterial translocation under total parenteral nutrition. *Pediatr Surg Int* 2001; **17**: 280-283
- 12 **Pierro A**, van Saene HK, Donnell SC, Hughes J, Ewan C, Nunn AJ, Lloyd DA. Microbial translocation in neonates and infants receiving long-term parenteral nutrition. *Arch Surg* 1996; **131**: 176-179
- 13 **Pappo I**, Polacheck I, Zmora O, Feigin E, Freund HR. Altered gut barrier function to Candida during parenteral nutrition. *Nutrition* 1994; **10**: 151-154
- 14 **Terra RM**, Plopper C, Waitzberg DL, Cukier C, Santoro S, Martins JR, Song RJ, Gama-Rodrigues J. Remaining small bowel length: association with catheter sepsis in patients receiving home total parenteral nutrition: evidence of bacterial translocation. *World J Surg* 2000; **24**: 1537-1541
- 15 **Wang FD**, Cheng YY, Kung SP, Tsai YM, Liu CY. Risk factors of catheter-related infections in total parenteral nutrition catheterization. *Zhonghua Yixue Zazhi* 2001; **64**: 223-230
- 16 **Rijnders BJ**, Vandecasteele SJ, Van Wijngaerden E, De Munter P, Peetermans WE. Use of semiautomatic treatment advice to improve compliance with Infectious Diseases Society of America guidelines for treatment of intravascular catheter-related infection: a before-after study. *Clin Infect Dis* 2003; **37**: 980-983
- 17 **Bong JJ**, Kite P, Ammori BJ, Wilcox MH, McMahon MJ. The use of a rapid *in situ* test in the detection of central venous catheter-related bloodstream infection: a prospective study. *J Parenter Enteral Nutr* 2003; **27**: 146-150
- 18 **Kamala F**, Boo NY, Cheah FC, Birinder K. Randomized controlled trial of heparin for prevention of blockage of peripherally inserted central catheters in neonates. *Acta Paediatr* 2002; **91**: 1350-1356
- 19 **Chang L**, Tsai JS, Huang SJ, Shih CC. Evaluation of infectious complications of the implantable venous access system in a general oncologic population. *Am J Infect Control* 2003; **31**: 34-39
- 20 **Shin JH**, Kee SJ, Shin MG, Kim SH, Shin DH, Lee SK, Suh SP,

- Ryang DW. Biofilm production by isolates of *Candida* species recovered from nonneutropenic patients: comparison of bloodstream isolates with isolates from other sources. *J Clin Microbiol* 2002; **40**: 1244-1248
- 21 **Buchman AL**. Complications of long-term home total parenteral nutrition: their identification, prevention and treatment. *Dig Dis Sci* 2001; **46**: 1-18
- 22 **Widmer AF**. Management of catheter-related bacteremia and fungemia in patients on total parenteral nutrition. *Nutrition* 1997; **13**(4 Suppl): 18S-25S
- 23 **Dinc L**, Erdil F. The effectiveness of an educational intervention in changing nursing practice and preventing catheter-related infection for patients receiving total parenteral nutrition. *Int J Nurs Stud* 2000; **37**: 371-379
- 24 **McConnell SA**, Gubbins PO, Anaissie EJ. Do antimicrobial-impregnated central venous catheters prevent catheter-related bloodstream infection? *Clin Infect Dis* 2003; **37**: 65-72
- 25 **Shorr AF**, Humphreys CW, Helman DL. New choices for central venous catheters: potential financial implications. *Chest* 2003; **124**: 275-284
- 26 **Kaplan SL**, Deville JG, Yogev R, Morfin MR, Wu E, Adler S, Edge-Padbury B, Naberhuis-Stehouwer S, Bruss JB. Linezolid versus vancomycin for treatment of resistant Gram-positive infections in children. *Pediatr Infect Dis J* 2003; **22**: 677-686
- 27 **Harbarth S**, Sax H, Gastmeier P. The preventable proportion of nosocomial infections: an overview of published reports. *J Hosp Infect* 2003; **54**: 258-266
- 28 **Beathard GA**. Catheter management protocol for catheter-related bacteremia prophylaxis. *Semin Dial* 2003; **16**: 403-405
- 29 **Hanna HA**, Raad II, Hackett B, Wallace SK, Price KJ, Coyle DE, Parmley CL. Antibiotic-impregnated catheters associated with significant decrease in nosocomial and multidrug-resistant bacteremias in critically ill patients. *Chest* 2003; **124**: 1030-1038
- 30 **Ding LA**, Li JS. Effects of glutamine on intestinal permeability and bacterial translocation in TPN-rats with endotoxemia. *World J Gastroenterol* 2003; **9**: 1327-1332
- 31 **McAndrew HF**, Lloyd DA, Rintala R, van Saene HK. Intravenous glutamine or short-chain fatty acids reduce central venous catheter infection in a model of total parenteral nutrition. *J Pediatr Surg* 1999; **34**: 281-285
- 32 **Fatkenheuer G**, Buchheidt D, Cornely OA, Fuhr HG, Karthaus M, Kisro J, Leithauser M, Salwender H, Sudhoff T, Szelenyi H, Weissinger F. Central venous catheter (CVC)-related infections in neutropenic patients. Guidelines of the Infectious Diseases Working Party (AGIHO) of the German Society of Hematology and Oncology (DGHO). *Ann Hematol* 2003; **82**(Suppl 2): S149-157
- 33 **Alpers DH**. Enteral feeding and gut atrophy. *Curr Opin Clin Nutr Metab Care* 2002; **5**: 679-683
- 34 **Wang XB**, Ren JA, Li JS. Sequential changes of body composition in patients with enterocutaneous fistula during the 10 days after admission. *World J Gastroenterol* 2002; **8**: 1149-1152

Edited by Wang XL and Kumar M Proofread by Xu FM

Capsule endoscopy in diagnosis of small bowel Crohn's disease

Zhi-Zheng Ge, Yun-Biao Hu, Shu-Dong Xiao

Zhi-Zheng Ge, Yun-Biao Hu, Shu-Dong Xiao, Department of Gastroenterology, Renji Hospital, Shanghai Institute of Digestive Disease, Shanghai Second Medical University, Shanghai 200001, China
Correspondence to: Dr. Zhi-Zheng Ge, Department of Gastroenterology, Renji Hospital, Shanghai Institute of Digestive Disease, Shanghai Second Medical University, 145 Shandong Zhong Road, Shanghai 200001, China. gezheng@public8.sta.net.cn
Telephone: +86-21-63260930 **Fax:** +86-21-63200879
Received: 2003-06-05 **Accepted:** 2003-08-16

Abstract

AIM: To evaluate the effectiveness of wireless capsule endoscopy in patients with suspected Crohn's disease (CD) of the small bowel undetected by conventional modalities, and to determine the diagnostic yield of M2A Given Capsule.

METHODS: From May 2002 to April 2003, we prospectively examined 20 patients with suspected CD by capsule endoscopy. The patients had the following features: abdominal pain, weight loss, positive fecal occult blood test, iron deficiency anaemia, diarrhoea and fever. All the patients had normal results in small bowel series (SBS) and in upper and lower gastrointestinal endoscopy before they were examined. Mean duration of symptoms before diagnosis was 6.5 years.

RESULTS: Of the 20 patients, 13 (65%) were diagnosed as CD of the small bowel according to the findings of M2A Given Capsule. The findings detected by the capsule were mucosal erosions (2 patients), aphthas (5 patients), nodularity (1 patient), large ulcers (2 patients), and ulcerated stenosis (3 patients). The distribution of the lesions was mainly in the distal part of the small bowel, and the mild degree of lesions was 54%.

CONCLUSION: Wireless capsule endoscopy is effective in diagnosing patients with suspected CD undetected by conventional diagnostic methods. It can be used to detect early lesions in the small bowel of patients with CD.

Ge ZZ, Hu YB, Xiao SD. Capsule endoscopy in diagnosis of small bowel Crohn's disease. *World J Gastroenterol* 2004; 10 (9): 1349-1352
<http://www.wjgnet.com/1007-9327/10/1349.asp>

INTRODUCTION

Crohn's disease (CD) is a systemic granulomatous disease that may involve any part of the alimentary tract. The small bowel is the affected site in 30-40% of cases^[1]. Recent studies have reported a worldwide rise in the incidence of CD. The "gold standard" for the diagnosis of CD includes the presence of following features: abdominal pain, weight loss, positive fecal occult blood test, iron deficiency anaemia, diarrhoea, fever, and typical evidence of pathological processes on conventional imaging techniques, such as, small bowel X ray, computerized tomography (CT) of the abdomen, enteroscopy, colonoscopy and ileoscopy. The small bowel is the most difficult part to be

examined by endoscopy because of its distance from the mouth and anus. Small bowel series (SBS) therefore remains the first line approach in the diagnosis of small bowel Crohn's disease. When the disease is mild, with inflammatory changes confined to the mucosa, CD lesions can be missed by SBS.

Wireless capsule endoscopy (CE)^[2-7] has now made painless imaging of the entire small bowel possible. In some trials, CE proved to have a higher diagnostic yield in patients with suspected small bowel diseases^[8-19]. It can be used to detect early lesions in the small bowel of patients with CD. The current study represented our initial experience with the M2A Capsule in diagnosing CD in patients undergone conventional investigations in which no characteristic abnormalities were detected.

MATERIALS AND METHODS

Patients

From May 2002 to April 2003, we prospectively examined 20 patients with suspected CD by capsule endoscopy. They were 5 women and 15 men, aged 16-78 years (mean 45.2). They had the following manifestations such as abdominal pain, weight loss, positive fecal occult blood test, iron deficiency anaemia, diarrhoea and fever. All patients had normal results in SBS and in upper and lower gastrointestinal endoscopy within 6 mo before they were examined. Exclusion criteria included a history of bowel obstruction, X ray evidence of small bowel stricture, evidence of any pathological abnormalities of the small bowel, any use of non-steroidal anti-inflammatory drugs during the past year.

The pertinent characteristics of the study population are shown in Table 1. The symptoms of the 20 patients enrolled in the study were consistent with suspected CD. Fourteen had abdominal pain, 13 had positive fecal occult blood test, 10 had iron deficiency anaemia (mean 81 g/L haemoglobin), 4 had diarrhoea, 3 had weight loss, and 2 had fever, some had more than one symptoms. Mean duration of the symptoms before diagnosis was 6.5 years (SD6.5).

Table 1 Clinical data of patients with suspected Crohn's disease

	Total patients	CD	Patients based on CE
Patients (n)	20		13
Age (yr)	45.2 (16-78)		44.2 (16-78)
(mean (range))			
Sex(%):	75 / 25		85 / 15
male / female			
Positive fecal	13 / 20 (65)		11 / 13 (85)
occult blood test ¹			
Anaemia ¹ (%)	10 / 20 (55)		9 / 13 (77)
Haemoglobin (g%)	8.1 (2.0)		7.8 (1.9)
(mean (SD))			
Abdominal pain ¹ (%)	14 / 20 (70)		7 / 13 (54)
Diarrhoea ¹ (%)	4 / 20 (20)		2 / 13 (15)
Weight loss ¹ (%)	3 / 20 (15)		3 / 13 (23)
Fever ¹ (%)	2 / 20 (10)		2 / 13 (15)
Duration of disease (y)	6.5 (6.5)		7.0 (7.8)
(mean±SD)			

¹Some of the patients had more than one symptoms.

Instrument^[2-7]

Wireless capsule endoscope (CE) (Given M2A, Given Imaging Ltd, Yoqneam, Israel) measures 11 mm×26 mm, has a battery life of approximately 6-8 h, and is propelled by peristalsis, not requiring air insufflation. CE is used in conjunction with an imaging system which includes a data recorder and interpretive workstation. CE is disposable and contains a complementary metal-oxide semiconductor (CMOS) chip camera, a transmitter, a light-emitting diode (LED) to provide illumination, and silver oxide batteries. Continuous video images were transmitted from the capsule to an antenna worn over the patient abdomen at a rate of two frames per second during passage of the CE through the gastrointestinal tract. The hemispheric lens yielded a 140-degree field of view. During the procedure, approximately 50 000 images were recorded by a solid-state recorder that was worn as a belt by the patient. The recorder was later connected to a computer workstation, in which the images were processed and then viewed on a monitor using a specifically designed reporting and processing of images and data (RAPID) software package.

Procedures

After an overnight fast for 8-12 h, the patients ingested CE with a small amount of water. They were then free to remain active as outpatients. After the study interval, the patients returned to the clinic and the recorded digital information was then downloaded into a computer. Images from the stomach and the length of small bowel were analyzed using the proprietary RAPID software. The images transmitted by the capsule were interpreted by two independent gastroenterologists. All patients were interviewed after completing the study to evaluate the tolerance or complications.

RESULTS

All the 20 patients described that the capsule was easy to swallow, painless, and preferable to conventional endoscopy. No complications were observed. The images displayed were considered to be good (Figure 1). Retention of the capsule was observed in three patients with small bowel stenosis caused by Crohn's disease (5, 7 and 22 d after capsule ingestion, respectively). One of them had a transient abdominal pain on the third and fourth day after capsule ingestion. None of the three patients with retention of the capsule showed any symptoms of acute or subacute obstruction during the follow-up. The capsule failed to reach the colon in 2 patients during the 8-h acquisition time.

Based on the results of the Given M2A Capsule, we diagnosed CD of the small bowel in 13/20 patients (65%) and normal small bowel mucosa in the remaining 6 of 7 (30%), a jejunal carcinoid confirmed by surgery in the other one. The findings detected by the capsule were mucosal erosions (2 patients), aphthas (5 patients), nodularity (1 patient), large ulcers (2 patients), and ulcerated stenosis (3 patients) (Figure 1). The distribution of the lesions was mainly in the distal part of small bowel (9 in ileum and 2 in the distal part of jejunum) which could not be reached with push endoscopy. The mild lesions or early stages of the disease accounted for 54% (2 mucosal erosions and 5 aphthas). Most of the patients underwent total colonoscopy (16/20), ileoscopy (the ileoscopy succeeded in only five patients) and gastroscopy (20/20). Fourteen out of 20 patients had abdominal CT and all had small bowel X ray series. Some of the patients underwent the procedures more than once. The mean number of procedures undergone previously was 5.4 (SD2.3).

Of the 13 patients who received medications, 11 showed a good clinical improvement after 5-ASA (mean 4 g/d) and a short term steroid treatment while the other two showed some

improvement in their clinical symptoms with the same treatment. Follow up ranged from one to eleven months (mean 4 mo).

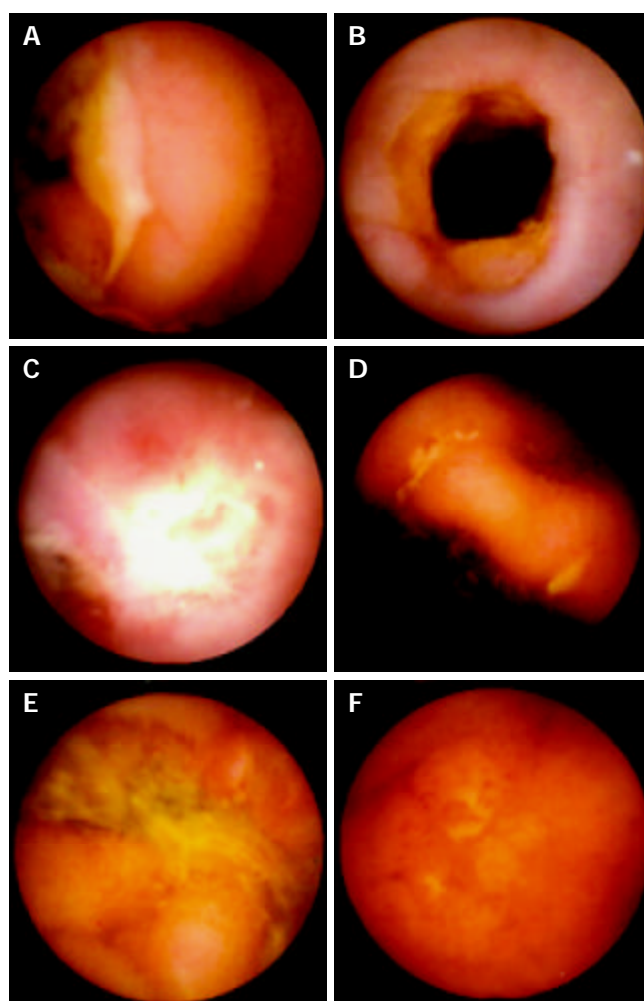


Figure 1 Capsule endoscopic findings of Crohn's disease in small bowel. A: A large ulcer in the distal part of jejunum, B: Ulcerations in a narrow ring caused by Crohn's disease in jejunum, C: A large ulcer in ileum, D: Ileal ulcers, E: Aphthas in the distal part of ileum, F: Ileal mucosal erosions.

DISCUSSION

It is generally accepted that the current visualization and imaging methods available to gastroenterologists in identifying small bowel pathology, particularly inflammatory diseases, were unsatisfactory^[19,20].

The reliability of radiological studies is highly influenced by the skill and experience of the operator and how fine is the detail of the mucosa on the film. Neither enteroclysis nor small bowel follow-through (SBFT) X-ray series were able to detect flat mucosal lesions^[14,21-23]. CT of the abdomen could not detect mucosal inflammation, it could show transmural thickening and extramural complications but is incapable of discerning CD in early stages of the disease.

Push enteroscopy requires an experienced and skillful endoscopist, the procedure requires between 15 and 45 min and is often uncomfortable for patients. In addition, the instrument could only examine between 80 cm and 120 cm beyond the ligament of Treitz, and occasional complications might occur^[24-27].

Sonde endoscopy in theory, has the potential to examine the entire small bowel. The procedure time is often 8 h or longer and can be associated with significant patient discomforts. Among patients referred for Sonde examination, 10% had

complications, and up to 75% of the distal ileum was not reached. For these reasons, Sonde- enteroscopy was seldom performed and available in only a few diagnostic centers worldwide^[25-28].

Another approach to small bowel imaging is examination of the entire small bowel by intraoperative endoscopy. The limitations of this option were the drawbacks associated with exploratory laparotomy and general anaesthesia^[29].

The alternative solution should be relatively comfortable for patients, easy to use by gastroenterologists, and one that could provide a reasonable level of visual imaging for the detection of small bowel abnormalities. The Given diagnostic imaging system (M2A Capsule)^[2-7] is a new modality designed to accommodate these requirements.

Capsule endoscopy has now made imaging of the entire small bowel possible. Its indications^[30] are obscure gastrointestinal bleeding, abnormal imaging of small intestine, chronic abdominal pain with reasonable suspicion of organic cause in small intestine, chronic diarrhea, evaluation of extent of Crohn's disease and celiac disease and visualization of surgical anastomoses, surveillance of polyposis syndromes of small intestine.

The cost of the technology per test is about ¥8 500. In order to answer what is the cost of capsule endoscopy in comparison with the cost of traditional examinations, one must consider the diagnostic yield and *cost-effectiveness* of capsule endoscopy compared with traditional diagnostic tools. The diagnostic rate of wireless capsule endoscopy in patients with suspected small bowel diseases was about 70% in our experience^[8,9]. It was similar to some other reports and significantly superior to the traditional diagnostic tools^[10,19]. The potential for cost savings includes (1) improved diagnostic rate and reduction in recurrence, conclusive testing associated not only with the clarity of the images obtained by the Capsule, but also with the Capsule's ability to traverse the entire small bowel (whereas endoscopic examinations leave part of the small bowel unexamined); (2) improved diagnostic precision able to confirm the source of bleeding, and/or rule-out certain etiologies; (3) earlier diagnosis of potentially adverse conditions such as malignancies of the small bowel; (4) reduced complications associated with the diagnostic procedure such as intestinal tears resulting from placement of the enteroscope and/or infection; (5) reduced loss in productivity associated with undergoing testing and repetitive examinations, and reduced loss in quality of life associated with both testing and worry; (6) reduced pain and discomfort associated with the diagnostic procedures.

A significant advantage of wireless capsule endoscopy is its ability to detect small bowel abnormalities, including those areas not reached by traditional endoscopy. The current battery life of 8 h could allow a reliable examination of the upper GI tract and small bowel in most patients. This was our experience as well because the complete small bowel could be studied in 18 of the 20 (90%) patients (except for the three patients with small bowel stenosis caused by Crohn's disease). The lesions in the distal jejunum and ileum were identified in 11 of 13 patients (85%) with abnormal capsule endoscopy beyond the reach of push enteroscope.

The only definite contraindication to the procedure is a patient who is a nonsurgical candidate or who refuses to entertain the idea of surgery. A retained capsule then would present the problem of retrieval with laparotomy. Severe motility disorders, including untreated achalasia and gastroparesis, should preclude CE, unless the capsule could be delivered endoscopically to the duodenum^[30].

In our study, retention of the capsule occurred in three patients with small bowel stenosis caused by Crohn's disease and delayed passage of the capsule was observed in two CD patients, possibly because of slow transit time due to the inflamed small bowel mucosa. Although the capsule failed to

reach the caecum, we could still identify typical lesions of CD from the recordings that emerged before the battery ran out. The information gained was helpful in further treatment planning for all these patients.

Possible complications existed with any procedure, CE was no exception. The major issue was capsule retention proximal to a stricture. The narrowed area might be anticipated or completely unexpected. Even enteroclysis could not preclude the possibility of a stricture. Our initial experience suggests the capsule does not itself cause intestinal obstruction, but proximal to a stricture it would tumble around and either eventually passes or rarely needs surgical retrieval. A retained capsule usually is asymptomatic and can be detected on the video when reviewed. Plain abdominal films could be obtained after several days to see whether the capsule passed spontaneously. The transient abdominal pain usually signals the passage of the capsule. Barkin *et al.*^[31] reported that surgical intervention to remove a non-passed capsule was only 0.75% (7/937). Therefore, capsule endoscopy should not be used in patients with a history of small bowel obstruction or evidence of significant bowel stenosis.

Our study demonstrated a high diagnostic rate in patients with clinical symptoms indicative of CD who had previously undergone several diagnostic procedures that showed normal results. The patients had long intervals from the onset of disease to diagnosis. The wireless capsule might have been able to provide a correct diagnosis during early stages of the disease as well as in cases of less severe forms. We propose the wireless capsule as an effective modality for diagnosing patients with suspected CD.

In conclusion, wireless capsule endoscopy is a valuable diagnostic tool in the evaluation of obscure GI bleeding and a variety of other small bowel disorders. It illustrates the power of innovative technology to advance our diagnostic capabilities that can be applied safely to patients in the outpatient setting. In our opinion, CE should become the initial diagnostic choice in patients with suspected small bowel diseases and negative upper and lower gastrointestinal endoscopic studies.

REFERENCES

- 1 **Delaney CP**, Fazio VW. Crohn's disease of the small bowel. *Surg Clin North Am* 2001; **81**: 137-158
- 2 **Iddan G**, Meron G, Glukhovsky A, Swain P. Wireless capsule endoscopy. *Nature* 2000; **405**: 417
- 3 **Gong F**, Swain P, Mills T. Wireless endoscopy. *Gastrointest Endosc* 2000; **51**: 725-729
- 4 **Swain P**. Wireless capsule endoscopy. *Gut* 2003; **52**: 48-50
- 5 **Fritscher-Ravens A**, Swain CP. The wireless capsule: new light in the darkness. *Dig Dis* 2002; **20**: 127-133
- 6 **Bar-Meir S**, Bardan E. Wireless capsule endoscopy—pros and cons. *Isr Med Assoc J* 2002; **4**: 726
- 7 **Fireman Z**, Glukhovsky A, Jacob H, Lavy A, Lewkowicz S, Scapa E. Wireless capsule endoscopy. *Isr Med Assoc J* 2002; **4**: 717-719
- 8 **Ge ZZ**, Hu YB, Gao YJ, Xiao SD. Clinical application of wireless capsule endoscopy. *Zhonghua Xiaohua Zazhi* 2003; **23**: 7-10
- 9 **Ge ZZ**, Hu YB, Xiao SD. An evaluation of capsule endoscopy and push enteroscopy in the diagnosis of obscure gastrointestinal bleeding. *Zhonghua Xiaohua Neijing Zazhi* 2003; **20**: 223-226
- 10 **Ang TL**, Fock KM, Ng TM, Teo EK, Tan YL. Clinical utility, safety and tolerability of capsule endoscopy in urban South-east Asian population. *World J Gastroenterol* 2003; **9**: 2313-2316
- 11 **Appleyard M**, Fireman Z, Glukhovsky A, Jacob H, Shreiver R, Kadirkamanathan S, Lavy A, Lewkowicz S, Scapa E, Shofti R, Swain P, Zaretsky A. A randomized trial comparing wireless capsule endoscopy with push enteroscopy for the detection of small-bowel lesions. *Gastroenterology* 2000; **119**: 1431-1438

- 12 **Appleyard M**, Glukhovskiy A, Swain P. Wireless-capsule diagnostic endoscopy for recurrent small-bowel bleeding (letter). *N Engl J Med* 2001; **344**: 232-233
- 13 **Lewis BS**, Swain P. Capsule endoscopy in the evaluation of patients with suspected small intestinal bleeding: Results of a pilot study. *Gastrointest Endosc* 2002; **56**: 349-353
- 14 **Costamagna G**, Shah SK, Riccioni ME, Foschia F, Mutignani M, Perri V, Vecchioli A, Brizi MG, Picciocchi A, Marano P. A prospective trial comparing small bowel radiographs and video capsule endoscopy for suspected small bowel disease. *Gastroenterology* 2002; **123**: 999-1005
- 15 **Ell C**, Remke S, May A, Helou L, Henrich R, Mayer G. The first prospective controlled trial comparing wireless capsule endoscopy with push enteroscopy in chronic gastrointestinal bleeding. *Endoscopy* 2002; **34**: 685-689
- 16 **Van Gossum A**, Francois E, Hittelet A, Schmit A, Deviere J. A prospective, comparative study between push enteroscopy and wireless video capsule in patients with obscure digestive bleeding. *Gastroenterology* 2003; **125**: 276
- 17 **Scapa E**, Jacob H, Lewkowicz S, Migdal M, Gat D, Gluckhovskiy A, Gutmann N, Fireman Z. Initial experience of wireless-capsule endoscopy for evaluating occult gastrointestinal bleeding and suspected small bowel pathology. *Am J Gastroenterol* 2002; **97**: 2776-2779
- 18 **Bardan E**, Nadler M, Chowers Y, Fidler H, Bar-Meir S. Capsule endoscopy for the evaluation of patients with chronic abdominal pain. *Endoscopy* 2003; **35**: 688-689
- 19 **Schreyer AG**, Golder S, Seitz J, Herfarth H. New diagnostic avenues in inflammatory bowel diseases. Capsule endoscopy, magnetic resonance imaging and virtual enteroscopy. *Dig Dis* 2003; **21**: 129-137
- 20 **Tibble JA**, Bjarnason I. Non-invasive investigation of inflammatory bowel disease. *World J Gastroenterol* 2001; **7**: 460-465
- 21 **Lewis B**. Radiology versus endoscopy of the small bowel. *Gastrointest Clin North Am* 1999; **9**: 13-27
- 22 **Chong AK**. Comments regarding article comparing small bowel radiographs and video capsule endoscopy. *Gastroenterology* 2003; **125**: 276
- 23 **Liangpunsakul S**, Chadalawada V, Rex DK, Maglinte D, Lappas J. Wireless capsule endoscopy detects small bowel ulcers in patients with normal results from state of the art enteroclysis. *Am J Gastroenterol* 2003; **98**: 1295-1298
- 24 **MacKenzie J**. Push enteroscopy. *Gastrointest Endosc Clin North Am* 1999; **1**: 29-36
- 25 **Swain CP**. The role of enteroscopy in clinical practice. *Gastrointest Endosc Clin N Am* 1999; **9**: 135-144
- 26 **Lewis BS**. The history of enteroscopy. *Gastrointest Endosc Clin N Am* 1999; **9**: 1-11
- 27 **Gay GJ**, Delmotte JS. Enteroscopy in small intestinal inflammatory diseases. *Gastrointest Endosc Clin N Am* 1999; **9**: 115-123
- 28 **Seensalu R**. The sonde exam. *Gastrointest Endosc Clin N Am* 1999; **9**: 37-59
- 29 **Delmotte JS**, Gay GJ, Houcke PH, Mesnard Y. Intraoperative endoscopy. *Gastrointest Endosc Clin North Am* 1999; **1**: 61-69
- 30 **Ge ZZ**, Xiao SD. Prospects for wireless capsule endoscopy. *Wei Chang Bing Xue* 2002; **7**: 326-330
- 31 **Barkin J**, Friedman S. Wireless capsule endoscopy (WCE) requiring surgical intervention: The world's experience [abstract]. *2nd conference on capsule endoscopy, Berlin* 2003: 171

Edited by Zhang JZ and Wang XL Proofread by Xu FM

Plasma erythropoietin levels in anaemic and non-anaemic patients with chronic liver diseases

Cosimo Marcello Bruno, Sergio Neri, Claudio Sciacca, Gaetano Bertino, Pietro Di Prima, Danila Cilio, Rinaldo Pellicano, Luciano Caruso, Raffaello Cristaldi

Cosimo Marcello Bruno, Sergio Neri, Claudio Sciacca, Gaetano Bertino, Pietro Di Prima, Danila Cilio, Luciano Caruso, Raffaello Cristaldi, Department of Internal Medicine and Systemic Diseases, University of Catania, Italy

Rinaldo Pellicano, Department of Gastro-Hepatology, Molinette Hospital, Torino, Italy

Correspondence to: Professor C.M. Bruno, Dip. Medicina Interna e Patologie Sistemiche, Osp. S. Marta, via G. Clementi 36, 95124 Catania, Italy. cmbruno@unict.it

Telephone: +39-95-7435706 **Fax:** +39-95-7435706

Received: 2003-10-08 **Accepted:** 2003-12-24

Abstract

AIM: To investigate the serum erythropoietin (Epo) levels in patients with chronic liver diseases and to compare to subjects with iron-deficiency anaemia and healthy controls.

METHODS: We examined 31 anaemic (ALC) and 22 non-anaemic (NALC) cirrhotic patients, 21 non-anaemic subjects with chronic active hepatitis (CAH), 24 patients with iron-deficiency anaemia (ID) and 15 healthy controls. Circulating Epo levels (ELISA; R&D Systems, Europe Ltd, Abingdon, UK) and haemoglobin (Hb) concentration were determined in all subjects.

RESULTS: Mean±SD of Epo values was 26.9±10.8 mU/mL in ALC patients, 12.5±8.0 mU/mL in NALC subjects, 11.6±6.3 mU/mL in CAH patients, 56.4±12.7 mU/mL in the cases of ID and 9.3±2.6 mU/mL in controls. No significant difference ($P>0.05$) was found in Epo levels between controls, CAH and NALC patients. ALC individuals had higher Epo levels ($P<0.01$) than these groups whereas ID subjects had even higher levels ($P<0.001$) than patients suffering from ALC.

CONCLUSION: Increased Epo values in cirrhotics, are only detectable when haemoglobin was lesser than 12 g/dL. Nevertheless, this rise in value is lower than that observed in anaemic patients with iron-deficiency and appears blunted and inadequate in comparison to the degree of anaemia.

Bruno CM, Neri S, Sciacca C, Bertino G, Di Prima P, Cilio D, Pellicano R, Caruso L, Cristaldi R. Plasma erythropoietin levels in anaemic and non-anaemic patients with chronic liver diseases. *World J Gastroenterol* 2004; 10(9): 1353-1356

<http://www.wjgnet.com/1007-9327/10/1353.asp>

INTRODUCTION

Chronic anaemia is often observed in patients with liver disease, especially in advanced stages, and an inverse relation has been reported between haemoglobin (Hb) concentration or hematocrit value and survivorship^[1]. Inapparent gastrointestinal bleeding, folate and vitamin B₁₂ deficiency, autoimmune haemolysis, altered oxide-reductive balance and hypersplenism are

underlying mechanisms responsible for the anaemic state^[2-4].

Moreover, a reduced proliferation of erythroid precursor cells has been described in the bone marrow of these patients^[4,5].

Erythropoietin (Epo) is an endogenous glycoprotein stimulating erythrocytosis which interacts with erythroid progenitor cells to promote their proliferation and maintain their viability as they differentiate^[6,7]. The regulation of erythropoiesis is a biological feedback loop whereby the degree of tissue oxygenation sets the amount of Epo production, the concentration of erythropoietin in turn drives the bone marrow to produce a level of red cells at which oxygen delivery is sufficient to lower Epo production^[8]. The gene codifying for this growth factor has been isolated and a regulatory region involved with oxygen sensing has been defined. Expression in response to hypoxia is mediated via a DNA-binding complex^[8].

Since literature data^[9,10] suggest an emerging role of this hormone in causing haematological changes in chronic diseases, suboptimal production of, or response to, Epo might contribute to the pathogenesis of chronic anaemia in cirrhotics. Some studies regarding the association between Epo levels and cirrhosis have appeared in literature^[11-16] but reported data are controversial.

The aim of this study was to investigate the circulating Epo levels in patients suffering from chronic liver disease of various degrees, with and without concomitant anaemia, compared to subjects with iron-deficiency uncomplicated anaemia as well as to healthy controls, in order to assess the relationship between serum Epo and Hb concentration.

MATERIALS AND METHODS

We examined 74 patients suffering from chronic liver diseases (21 chronic active hepatitis [CAH] and 53 cirrhosis), 24 patients with iron-deficiency (ID) uncomplicated anaemia and 15 healthy control subjects, comparable to sex and age. Haematology, albumin concentration, aspartate aminotransferase (AST) and alanine aminotransferase (ALT) levels, serum bilirubin and prothrombin time (as percentage of prothrombin activity), were measured in all patients and controls.

Diagnosis of patients with liver disease, was based on clinical (medical history, physical examination), instrumental (ultrasonography, endoscopy) and laboratory (liver function tests) data. In 47 out of these cases, hepatic damage was confirmed by liver biopsy (in the remaining subjects the procedure was not necessary, as diagnosis was clinically evident).

In 6 out of 21 CAH patients, the etiological agent was hepatitis B virus (HBV) while in the remaining 15, hepatitis C virus (HCV). Of the 53 cirrhotic subjects, 19 were infected with HBV, 31 with HCV while 3 had a history of alcohol abuse.

According to accepted criteria^[8], thirty-one cirrhotic patients had normocromic normocytic anaemia (ALC group, mean±SD Hb 10.2±0.9 gr/dL) and twenty-two were non anaemic (NALC group, mean±SD Hb 13.6±0.7 gr/dL).

None of anaemic cirrhotics had signs of iron-deficiency (serum iron ≥ 70 µg/dL, serum ferritin ≥ 50 ng/mL and transferrin saturation $\geq 30\%$).

Table 1 Main characteristics of investigated subjects

	Controls n=15	CAH patients n=21	NALC patients n=22	ALC patients n=31	ID patients n=24
Age (yr, mean \pm SD)	52 \pm 6	54 \pm 8	59 \pm 3	60 \pm 5	54 \pm 5
Males	8	10	9	12	10
Females	7	11	13	19	14
Albumin (g/dL)	3.6 \pm 0.2	3.3 \pm 0.3	3.0 \pm 0.3	2.9 \pm 0.2	3.5 \pm 0.3
AST (U/L)	14.2 \pm 1.5	73.7 \pm 19.2	41.9 \pm 12.6	40.6 \pm 16.4	16.1 \pm 3.5
ALT (U/L)	15.6 \pm 2.7	69.7 \pm 8.4	39.8 \pm 10.1	37.9 \pm 12.5	14.2 \pm 3.1
Bilirubin (mg/dL)	0.6 \pm 0.1	0.8 \pm 0.1	1.1 \pm 0.2	1.3 \pm 0.2	0.7 \pm 0.1
Prothrombin time (%)	98.2 \pm 5.0	81.1 \pm 6.2	72.4 \pm 8.9	70.3 \pm 10.2	95.1 \pm 3.1

In agreement with Child-Pugh's classification^[17], 12 of NALC patients were in class B and 10 belonged to class C. In the ALC group, 13 patients were in class B whereas 18 in class C.

Cirrhotic subjects affected by gastrointestinal bleeding in the previous 3 mo (as confirmed by endoscopy and fecal occult blood testing) and those with suspected hepatocellular carcinoma (on the basis of ultrasonography, alpha-foetoprotein and carcinoembryonic antigen levels performed during the screening) were excluded from the study.

Diagnosis in patients with iron-deficiency anaemia, was based on clinical (medical history, physical examination), and laboratory (Hb concentration <12 g/dL, serum ferritin <40 ng/dL and transferrin saturation <16%) data. None of them had clinical or laboratory (C-reactive protein) evidence of inflammatory condition.

All subjects had normal renal function (serum creatinine <1.2 mg/dL, creatinine clearance \geq 70 mL/min). The main characteristics of our study groups are summarised in Table 1.

The study was conformed to Helsinki Declaration and informed consent was obtained from the whole study series.

A blood sample was obtained from all subjects and ethylenediaminetetraacetic acid (EDTA) was added. Samples were centrifuged and plasma was stored at -25 °C. Erythropoietin was determined by a commercial ELISA kit (R&D Systems Europe Ltd, Abingdon, UK). The sensitivity of assay was less than 0.6 mU/mL. Non specific binding was <1%. Intra and inter-assay variability averaged 3.1% and 3.5%, respectively. Epo concentrations were expressed as mU/mL.

Analysis of variance and Kruskal-Wallis test were used to compare mean \pm SD between various groups. Relationship between continuous variables was investigated by correlation test or multiple regression test when they were more than two. Covariance analysis was performed to assess the difference in Epo values for adjusted Hb, between ALC and ID patients. The regression lines between Hb concentration and Epo values in these two groups were compared by *t*-test, according to current statistical procedures^[18].

RESULTS

No significant difference ($P>0.05$) in Hb concentration was observed between controls (13.9 \pm 0.3 gr/dL), CAH (13.7 \pm 0.5 gr/dL) and NALC (13.6 \pm 0.7 gr/dL) patients. Subjects suffering from ALC (10.2 \pm 0.9 gr/dL) and ID (10.1 \pm 0.8 gr/dL) had values significantly lower than others ($P<0.05$), but Hb concentration was similar in these two groups ($P>0.05$). Among cirrhotic subjects, Hb concentration was similar ($P>0.05$) in Child-Pugh class B and class C patients both in ALC (10.4 \pm 0.7 gr/dL *versus* 10.1 \pm 0.9 gr/dL, respectively) and in NALC (13.8 \pm 0.4 gr/dL *versus* 13.5 \pm 0.9 gr/dL, respectively) groups.

Mean \pm SD of plasma Epo was 9.3 \pm 2.6 mU/mL in controls, 11.6 \pm 6.3 mU/mL in CAH patients, 12.5 \pm 8.0 mU/mL in NALC

subjects, 26.9 \pm 10.8 mU/mL in ALC patients and 56.4 \pm 12.7 mU/mL in ID individuals.

Regarding Child-Pugh related allocation, mean \pm SD of plasma Epo was 24.18 \pm 9.56 mU/mL for patients in class B *versus* 30.71 \pm 10.82 mU/mL for those in class C of the ALC group, 12.3 \pm 7.8 mU/mL in class B *versus* 12.9 \pm 8.1 mU/mL in class C patients of the NALC group, respectively.

Statistical analysis did not show any significant difference between controls, CAH patients and NALC patients ($P>0.05$). ALC subjects had significantly higher Epo levels than these three groups ($P<0.01$) and patients suffering from ID had significantly higher Epo levels than ALC patients ($P<0.001$). In both NALC and ALC groups, no significant difference ($P>0.05$) was observed between class B and class C patients.

Epo levels were not related ($P>0.05$) to albumin concentration, AST and ALT values, serum bilirubin and prothrombin time in any group of patients with liver disease.

An inverse significant relationship between Epo and Hb was found in ID patients ($r=-0.61$, $P=0.001$) but not in ALC patients ($r=-0.22$, $P>0.05$). Covariance analysis revealed a significant difference ($P<0.001$) in Epo values for adjusted Hb concentration between ALC and ID patients.

Finally, the regression lines between Epo and Hb in ALC and ID patients, were compared and a significant difference was found (ALC patients: slope -2.47, ES 2.02, y-intercept 52.39; ID patients: slope -9.79, ES 2.7, y-intercept 155.48; $t=2.23$, $fd=53$, $P=0.03$).

DISCUSSION

Anaemia is a multifactorial complication of liver cirrhosis^[2-5]. Papers regarding abnormalities of circulating Epo in patients with liver diseases were few and results were contradictory^[11-18]. Some authors have reported higher Epo levels in cirrhotic patients when compared to healthy controls. An inverse relation between Epo values and the haematological indices has been described by some groups.

We assessed plasma Epo levels in anaemic and non-anaemic patients with chronic liver disease compared to healthy controls and iron-deficiency anaemic subjects.

Our results showed that non-anaemic patients with liver disease and controls had similar Epo values, in cirrhotic patients, circulating Epo was not related to Child-Pugh score. Moreover, multiple regression test documented that Epo levels were not related to concentration of albumin, bilirubin, ALT or AST values and prothrombin time in any of these three groups of patients with liver disease.

This was in part conflicting with the findings of other authors^[12,13,15] and suggested that liver damage itself, independent of the degree of dysfunction, was not able to alter circulating Epo levels.

On the other hand, we detected a significant increase in levels of this hormone both in ALC patients and in ID patients.

However, a significant inverse correlation between Epo and Hb was found in ID group ($r=-0.61$, $P<0.05$) but not in ALC group ($r=-0.22$, $P>0.05$).

Nevertheless, increased Epo level in anaemic patients *versus* healthy controls was not enough to assess Epo production.

In fact, the definition of defective Epo production has relied on a low Epo value in comparison to reference patients with similar Hb^[19]. Consequently, circulating Epo cannot be simply compared with normal values and levels found must be evaluated in relation to the degree of anaemia.

As it has been widely accepted that adequate Epo production occur in patients with iron-deficiency anaemia^[19], we chosen ID patients as reference group.

Mean±SD of Hb values was similar in the two groups of anaemic patients, but mean±SD of Epo concentrations in ALC group was much lower than that in ID patients.

Analysis of covariance showed a significant difference in Epo values between the two groups ($P<0.001$). Moreover, we also compared the regression lines between Epo and Hb in ALC and ID patients. The slope and y-intercept of two regression lines (Figure 1) were significantly different ($P<0.05$).

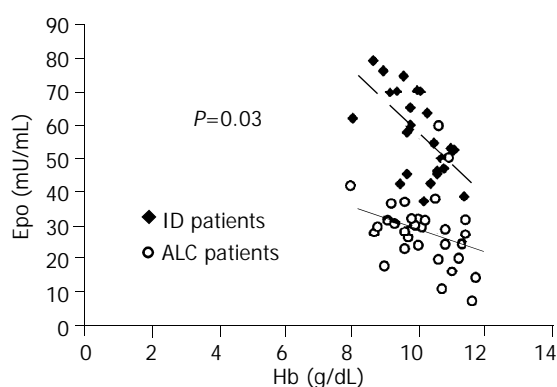


Figure 1 Comparison between regression lines of Epo and Hb in ALC and ID patients.

Therefore, although circulating Epo levels in ALC patients, were higher than that in non anaemic individuals with liver disease, they were significantly lower in healthy subjects, than in ID patients. The reason of this finding is unclear. It seems that an altered Epo clearance did not result in the difference because normal metabolism of this hormone was maintained in cirrhotics^[20].

Cazzola *et al.*^[21] described an inverse relationship between red blood precursor mass and serum Epo. As in cirrhosis, a reduction of erythroid cells has been reported^[4,5], the finding of lower Epo values in our ALC patients than in ID patients was not due to an increased utilization by precursor cells.

Therefore, lower Epo values in ALC subjects, are likely provoked by an impaired synthesis rather than by an increased metabolism.

Consequently, we think that Epo production occurred in different quantitative patterns in these two groups, and other factors besides Hb concentration, could affect its output in cirrhotic patients.

This can explain why no relationship was found between Hb and Epo in our ALC patients.

In adults, Epo has been found to be synthesised by the kidney and to a lesser extent by the liver^[22]. Thus, liver failure could endanger the hepatic residual share of Epo synthesis, even though in this study, the absence of relation between Epo values and investigated indices of liver dysfunction did not support this hypothesis. Alternatively, a reduced sensitivity of renal cells to hypoxic stimuli could be hypothesized. Furthermore, the inhibitory action of reactive oxygen species

and nitric oxide as well as malnutrition of cirrhotic patients might contribute to reduction in Epo synthesis^[23-26].

Finally, inflammatory cytokines, namely interleukin-1, tumor necrosis factor and transforming growth factor, are enhanced in liver diseases and have been found to inhibit hypoxia-induced erythropoietin production *in vitro* and *in vivo*^[27-29].

Whatever the cause of blunted and unsuitable rise in circulating Epo is the levels of this hormone in anaemic cirrhotics, appear defective and inadequate with regard to the degree of anaemia.

Even though Epo deficiency is not only the cause of anaemia in cirrhotics, its insufficient concentration could play a role in the persistence of anaemic status, worsening the outcome of cirrhotic patients.

In conclusion, non-anaemic patients with chronic liver disease have normal Epo levels. During cirrhosis, elevated Epo values are detectable in patients with Hb concentration lesser than 12 g/dL and are not related to the degree of both Hb concentration and severity of liver dysfunction. In addition, such an increase is lower than that observed in patients with iron-deficiency anaemia and appears blunted and inadequate in comparison to the degree of anaemia.

REFERENCES

- 1 **Pignon JP**, Poynard T, Naveau S, Marteau P, Zourabichvili O, Chaput JC. Multidimensional analysis by Cox's model of the survival of patients with alcoholic cirrhosis. *Gastroenterol Clin Biol* 1986; **10**: 461-467
- 2 **Tymofieiev VV**, Kolomoiets' MIW. The pathogenetic characteristics of the anemic syndrome in liver cirrhosis. *Lik Sprava* 1997; **5**: 66-71
- 3 **Mehta AB**, McIntyre N. Hematological disorders in liver disease. *Forum* 1998; **8**: 8-25
- 4 **Sherlok S**, Dooley J. "The haematology of liver disease" in *Diseases of the Liver and Biliary System*, 11th edition. UK 2002: 47, Oxford: Blackwell Publishing
- 5 **Korolko IUR**, Sarycheva TG, Kotelnikov VM, Kozinets GI, Zherebtsov LA. Anemic syndrome in chronic hepatitis and liver cirrhosis. *Klin Med* 1993; **71**: 45-48
- 6 **Spivak JL**, Pham T, Isaacs M, Hankins WD. Erythropoietin is both a mitogen and survival factor. *Blood* 1991; **77**: 1228-1233
- 7 **Koury MJ**, Bondurant MD. Erythropoietin retards DNA breakdown and prevents programmed death in erythroid progenitor cells. *Science* 1990; **248**: 378-381
- 8 **Weatherall DJ**, Provan AB. Red cells I: inherited anaemias. *Lancet* 2000; **355**: 1169-1175
- 9 **Scudla V**, Adam Z, Scudlova M. Diagnosis and therapy of anemia in chronic diseases. *Vnitř Lek* 2001; **47**: 400-406
- 10 **Spivak JL**. The blood in systemic disorders. *Lancet* 2000; **355**: 1707-1712
- 11 **Siciliano M**, Tomasello D, Milani A, Ricerca BM, Storti S, Rossi L. Reduced serum levels of immunoreactive erythropoietin in patients with cirrhosis and chronic anemia. *Hepatology* 1995; **22**: 1132-1135
- 12 **Pirisi M**, Fabris C, Falletti E, Soardo G, Toniutto P, Gonano F, Bartoli E. Evidence for a multifactorial control of serum erythropoietin concentration in liver disease. *Clin Chim Acta* 1993; **219**: 47-55
- 13 **Mady E**, Wissa G, Khalifa A, el-Sabbagh M. Assessment of erythropoietin levels and some iron indices in chronic renal failure and liver cirrhosis patients. *Dis Markers* 1999; **15**: 229-236
- 14 **Vasilopoulos S**, Hally R, Caro J, Martin P, Westerberg S, Moritz M, Jarrel B, Munoz S. Erythropoietin response to post-liver transplantation. *Liver Transpl* 2000; **6**: 349-355
- 15 **Tacke F**, Schoffski P, Gausser A, Manus MP. Erythropoietin plasma levels are elevated in chronic liver disease and correlate with anemia, liver dysfunction, bleeding episodes and interleukin-6 (Abstract). *J Hepatol* 2002; **36**: 65
- 16 **Obczko-Grzesik B**, Weicek A, Kokot F. Influence of IFN-alpha on plasma erythropoietin levels in patients with hepatitis B virus-

- associated chronic active hepatitis. *J Interferon Cytokine Res* 2001; **21**: 669-676
- 17 **Pugh RNH**, Murray-Lyon IM, Dawson JL, Pietrosi MC, Williams R. "Transection of the esophagus for bleeding esophageal varices". *Br J Surg* 1973; **60**: 646
- 18 **Colton T**. Statistics in Medicine. *Boston: Little, Brown and Company*, 1973: 201
- 19 **Cazzola M**, Mercuriali F, Brugnara C. Use of recombinant human erythropoietin outside the setting of uremia. *Blood* 1997; **89**: 4248-4267
- 20 **Jensen JD**, Jensen LW, Madsen JK, Poulsen L. The metabolism of erythropoietin in liver cirrhosis patients compared with healthy volunteers. *Eur J Haematol* 1995; **54**: 111-116
- 21 **Cazzola M**, Guarnone R, Cerani P, Centenara E, Rovati A, Beguin Y. Red blood cell precursor mass as an independent determinant of serum erythropoietin level. *Blood* 1998; **91**: 2139-2145
- 22 **Krantz SB**. Erythropoietin. *Blood* 1991; **77**: 419-434
- 23 **Canbolat O**, Fandrey J, Jelkmann W. Effects of modulators of the production and degradation of hydrogen peroxide on erythropoietin synthesis. *Respir Physiol* 1998; **114**: 175-183
- 24 **Fandrey J**, Frede S, Jelkmann W. Role of hydrogen peroxide in hypoxia-induced erythropoietin production. *Biochem J* 1994; **303**: 507-510
- 25 **Schobersberger W**, Hoffmann G, Fandrey J. Nitric oxide donors suppress erythropoietin production *in vitro*. *Pflugers Arch* 1996; **432**: 980-985
- 26 **Genius J**, Fandrey J. Nitric oxide affects the production of reactive oxygen species in hepatoma cells: implications for the process of oxygen sensing. *Free Radic Biol Med* 2000; **29**: 515-521
- 27 **Faquin WC**, Schneider TJ, Goldberg MA. Effect of inflammatory cytokines on hypoxia-induced erythropoietin production. *Blood* 1992; **79**: 1987-1994
- 28 **Jelkmann WE**, Fandrey J, Frede S, Pagel H. Inhibition of erythropoietin production by cytokines. Implications for the anemia involved in inflammatory states. *Ann N Y Acad Sci* 1994; **718**: 300-309
- 29 **Poveda Gomez F**, Camacho Siles J, Quevedo Morales E, Fernandez Zamorano A, Codoceo Alquinta R, Arnalich Fernandez F, Sempere Alcocer M. Pattern of blood levels of erythropoietin and proinflammatory cytokines in patients with anemia of chronic disorders secondary to infection. *An Med Interna* 2001; **18**: 298-304

Edited by Wang XL and Xu FM

Effect of cyclin G2 on proliferative ability of SGC-7901 cell

Jie Liu, Ze-Shi Cui, Yang Luo, Li Jiang, Xiao-Hui Man, Xue Zhang

Jie Liu, Ze-Shi Cui, Experimental Technology Center, China Medical University, Shenyang 110001, Liaoning Province, China

Yang Luo, Li Jiang, Xiao-Hui Man, Xue Zhang, Medical Gene Group of Cell Biology Laboratory, Key Laboratory of the Ministry of Health, China Medical University, Shenyang 110001, Liaoning Province, China

Supported by a grant for Distinguished Young Teachers of Higher Education of the Ministry of Education of the Teaching and Research Encouragement Plan

Correspondence to: Dr. Xue Zhang, Medical Gene Group of Cell Biology Laboratory, Key Laboratory of the Ministry of Health, China Medical University, Shenyang 110001, Liaoning Province, China. zhangxuenew@yahoo.com

Telephone: +86-24-23256666-5532 **Fax:** +86-24-23265492

Received: 2003-10-10 **Accepted:** 2003-12-16

Abstract

AIM: To study the effect of cyclin G2 on proliferation of gastric adenocarcinoma cell line-SGC-7901 cell *in vitro*.

METHODS: By use of cation lipofectamine transfection reagent, the pIRES-G2 and pIRESneo plasmids were transferred into SGC-7901 cell line. Anticlonal cells were selected by G418. Positive clones were observed and counted using Giemsa staining. Cell proliferative ability was assayed by MTT.

RESULTS: (1) The clone number of pIRES-G2 group decreased, clone volume reduced. The number of cell clones in pIRESneo group was 87 ± 3 , that of pIRES-G2 group was 53 ± 4 , occupying 60.1% of pIRESneo group, there was significant difference obviously ($P < 0.01$, $t = 15.45$). (2) The average absorbance of clone cell obtained by stable transfection of pIRES-G2 at 570 nm was 1.6966 ± 0.2125 , the average absorbance of clone cell obtained by stable transfection of pIRESneo at 570 nm was 2.1182 ± 0.3675 , there was significant difference between them ($P < 0.01$, $t = 3.412$).

CONCLUSION: Cyclin G2 can inhibit SGC-7901 cell proliferative ability obviously, it may be a negative regulator in cell cycle regulation.

Liu J, Cui ZS, Luo Y, Jiang L, Man XH, Zhang X. Effect of cyclin G2 on proliferative ability of SGC-7901 cell. *World J Gastroenterol* 2004; 10(9): 1357-1360

<http://www.wjgnet.com/1007-9327/10/1357.asp>

INTRODUCTION

Cell cycle regulation is the core part in cell proliferation, which has a close relationship with cell carcinogenesis. In recent years, the study of cell cycle regulation is the forefront and hotspot field in cell biology and genetics. At present, research on the formation, activation, inactivation of cyclin-CDK (cyclin-dependent kinase) holo-enzyme complex is the main molecular basis of cell cycle regulation^[1,2]. All the 12 type different cyclins found in mammalian cells contain a 100 amino-acid homologous region named cyclin box, which is the molecular structure marker of cyclins^[3]. Cyclin G is a new member of cyclin family, which

includes cyclin G1 and cyclin G2. Although the identity of amino acid sequence and nucleotide sequence of cDNA of cyclin G1 and cyclin G2 was 53% and 60% respectively, their biological function and distribution in tissue and organ differ greatly^[4,5]. Research shows that cyclin G1 is located mainly in nucleus, whose expression is induced by the damage of DNA and depends on the expression level of p53^[6,7]. Cyclin G2 is located mainly in cytoplasm, whose expression can be induced by the VHL protein and to some degree is independent of p53^[8]. We have known that cyclin G1 is a positive regulator in cell cycle regulation. But we still do not know if cyclin G2 is connected with CDKs and with which kind of CDKs. The expression of cyclin G2 induced by cancer-suppressing gene hints that it may act as a negative regulator in cell proliferation^[9]. Moreover, we purified oral squamous carcinoma cell by laser capture micro-dissection, and found that 4 cases showed low expression of cyclin G2 in 5 cases in the gene expression pedigree research with gene chip analysis^[10]. Thus, it is much more likely for cyclin G2 to have the negative regulating effect on the cell proliferation.

In this article, we transfected pIRES-G2 into SGC-7901 cell and studied the effect of cyclin G2 expression on the cell proliferation *in vitro*.

MATERIALS AND METHODS

Materials

The eukaryotic plasmid expression vector contains the whole length of cyclin G2 and selective marker gene, neo was constructed by the Medical Gene Group of China Medical University^[11]. pIRESneo vector was purchased from Clontech. *E. Coli* JM109 competent cell was the product of TaKaRa, plasmid extraction and purification kits were from Qiagen. Lipofectamine PlusTM and G418 were the products of Invitrogen. MTT was from Huamei. SABC kit and DAB kit were from Boster.

The human gastric adenocarcinoma cell line SGC-7901 (Cell Biology Laboratory of China Medical University) was grown in DMEM (Gibco) supplemented with 100 mL/L heat-inactivated fetal calf serum (Hyclone), 100 U/mL of penicillin sodium and 100 µg/mL streptomycin sulfate, cultured at 37 °C, with 50 mL/L CO₂.

Methods

Plasmid amplification reaction and evaluation *E. Coli* JM109 competent cells were transformed by pIRES-G2 plasmid, cultured in LB medium supplemented with Amp⁺ (100 µg/mL). The positive clones were selected and cultured. Abundant plasmids were produced and purified by alkaline lysis method, identified by 10 g/L agarose gel electrophoresis after restriction endogenous enzyme digestion. The concentration and purity were determined by ultraviolet scanning spectrophotometer.

Gene transfection Exponentially growing SGC-7901 cells were seeded using 2 mL non-antibiotics culture medium into 6-well plates. After 24 h when cells grew to 60-80% confluence transfection began. Cells were transiently transfected according to the protocol of Lipofectamine PlusTM. Briefly, the plasmid DNA was premixed with the Plus reagent by diluting 1 µg DNA into 100 µL transfection DMEM (serum-free, non-antibiotics) and adding 6 µL Plus reagents in polystyrene tubes. Solutions

were combined, gently mixed, and incubated for 15 min at room temperature to allow formation of DNA/Plus complexes. Meanwhile, 4 μ L Lipofectamine reagents were diluted in 100 μ L transfection DMEM. The DNA/Plus reagent was mixed with the diluted Lipofectamine reagent and incubated for 15 min again at room temperature. The growth medium was removed from the cells and replaced with 800 μ L transfection DMEM. The complexes were added to the cells and incubated for 3 h at 37 $^{\circ}$ C, with 50 mL/L CO₂. Then 1 mL of non-antibiotics DMEM containing 200 mL/L FCS was added to it. Transfection of the pIRESneo vector into SGC-7901 cell was the same.

Cell clone At 24 h after gene transfection, cells were trypsin digested and transferred into 100 mm culture dish, and cultured for another 2 wk in G418 (400 μ g/mL) selective culture medium. The clone formation and cell morphology were observed under an inverted microscope (Olympus IX70). Images were acquired using a cool charge-coupled device (Spot) and transferred into computer. Cells were fixed in methanol/ice acetic acid (3:1) and stained in 50-100 g/L Giemsa. Cell clones were observed and counted.

Immunocytochemistry staining for exogenous cyclin G2 expression Cell transfection and G418 selection were done as above. After fourteen days, cell clones could be seen in pIRES-G2 and pIRESneo group. After PBS washing, the cell clones were circled, separated with sterile tip and cultured in G418 (250 μ g/mL) selective culture medium for another 2 wk. The stably transfected cell lines were obtained after passage by 2-3 generations. Cells were seeded into 6-well culture plates containing coverslips allowed to grow until they were 60-80% confluence and coverslips were picked up, washed with PBS, then fixed in ice cold acetone for 30 min at room temperature, washed 3 times (5 min each) in PBS. Cytochemistry staining was performed by the avidin-biotin peroxidase complex method using the SABC kit as follows: cells were treated to remove endogenous peroxidase activity, blocked with rabbit serum for 30 min at room temperature, and then incubated in primary goat anti-cyclin G2 polyclonal antibody (American Santa Cruz Company) for 1 h at 37 $^{\circ}$ C or overnight at 4 $^{\circ}$ C, washed 3 times with PBS, then incubated with a rabbit-anti-goat secondary antibody conjugated to horseradish peroxidase for 1 h. Following PBS washing, the coverslips were incubated with SABC elite reagent for 30 min at room temperature and washed 3 times in PBS. The bound horseradish peroxidase complexes were developed using DAB kit. The coverslips were counterstained with hematoxylin, for colored by 10 mL/L hydrochloric acid ethanol, dehydrated by graded ethanol, and enveloped by neutral resin, negative contrast was made by using PBS instead of primary antibody.

MTT assay The stably transfected cells were seeded into 24-well culture plates and cultured for 24 h at 37 $^{\circ}$ C, with 50 mL/L CO₂. Cells were seeded into 96-well culture plates at 4 000-6 000 cells/well. After 48 h culture, the culture solution was poured out and washed twice with PBS. 150 μ L (0.5 mg/mL) MTT was added at 37 $^{\circ}$ C for 4 h, the culture medium solution was poured out and 150 μ L/ each well DMSO was added again, shaken for 10 min in horizontal shaker. The absorbance at 570 nm was read by enzyme-labelling analysis equipment. The average absorbance reflected the cell proliferative ability. Data showed in mean \pm SD format and statistic significance was analyzed by *t* test.

RESULTS

Plasmid appraisal

The cyclin G2 fragment was inserted between the *Bam*HI and *Bst*XI restriction sites, the restriction enzyme digestion and gel electrophoresis results were the same as predicted.

Selection of the stable transfection cell line and exogenous cyclin G2 gene expression

After 14 d of selection by G418 in transfected cells, several cell clones could be seen in pIRES-G2 and pIRESneo group. After PBS washing, the cell clones were circled, and the larger single cell clones were separated with sterile tip, cultured in G418 (250 μ g/mL) selective culture medium for another 2 wk, the stable transfection cell lines were obtained after passage by 2-3 generations.

Immunocytochemistry staining result showed that a large number of gray positive granules appeared in SGC-7901 cell cytoplasm after pIRES-G2 transfection, while pIRESneo cell cytoplasm only appeared blue and no positive granule was seen in negative contrast cell.

The effect of cyclin G2 overexpression on the colony-formation of SGC-7901 cell

Observing the stably transfected SGC-7901 cell obtained by G418 selection under microscope, the clone number of pIRES-G2 group decreased, clone volume reduced and the cells in clone changed irregularly, many granules and bubbles appeared in cytoplasm. The 5 repeated experimental results were the same. The number of pIRESneo group was 87 \pm 3, that of pIRES-G2 group was 53 \pm 4, occupying 60.1% of pIRESneo group, there was significant difference obviously ($P < 0.01$, $t = 15.45$) (Figures 1, 2).

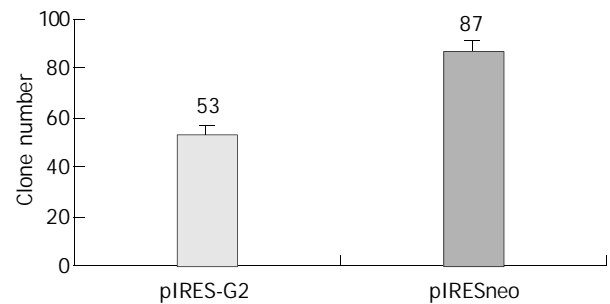


Figure 1 The positive clone number obtained with pIRES-G2 and pIRESneo plasmids after stable transfection in SGC-7901 cell line.

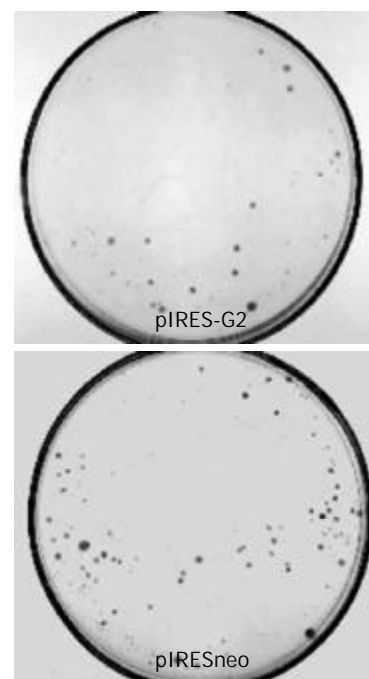


Figure 2 Effect of cyclin G2 overexpression on the colony-formation ability of SGC-7901.

Effects of cyclin G2 overexpression on SGC-7901 proliferative ability

By MTT assay analysis the proliferative ability change of stably transfected SGC-7901 cell obtained by G418 selection was as following: the average absorbance of clone cell obtained by stably transfected pIRES-G2 at 570 nm was 1.6966 ± 0.2125 , the average absorbance of clone cell obtained by stably transfected pIRESneo at 570 nm was 2.1182 ± 0.3675 , there was statistical difference between them ($P < 0.01$, $t = 3.412$) (Table 1).

Table 1 The proliferative ability compared between 2 clone-cell

Group	Well number	Average absorbance
pIRESneo	96	2.1182 ± 0.3675^b
pIRES-G2	96	1.6966 ± 0.2125

^b $P < 0.01$, $t = 3.412$ vs pIRES-G2.

DISCUSSION

There are many kind of cyclins and CDKs in mammalian cells, which combine with each other forming active cyclin-CDK complex as a triggering factor in the regulation of cell cycle. The expression level of cyclins shows phase specificity, which is obviously regulated by transcription and the rate of protein hydrolysis. Cyclin G, a recent addition to the cyclin family, has homology to fission yeast Cig1, B-type cyclins, and human cyclin A and I. The molecular structure of cyclin G differs from other cyclins. NH₂ terminus lacks a "destruction box" sequence controlling the ubiquitin-dependent degradation mitotic cyclins, while contains an epidermal growth factor receptor (EGF-R/ ErbB) like autophosphorylation motif in its carboxyl terminus^[12]. The structure suggested that a role for cyclin G in signal transduction. Cyclin G has not yet been matched with a CDK binding partner, and its biologic function is still elusive. Cyclin G is the only known cyclin that is transcriptionally activated by the p53 tumor suppressor gene. Cyclins G1 and G2 share the highest sequence identity and similarity to the fission yeast B-type cyclins Cig1 and Cig2 respectively, while cyclin G2 exhibits high sequence identity to the S-phase cyclin Clb-5 of budding yeast. Cloning and sequencing a partial cDNA sequence revealed the cyclin G1 transcript does not encode motifs which resemble known degradation signals. In contrast, the cyclin G2 protein contains a prototypic protein destabilizing (PEST) rich sequences which may be responsible for its potential regulated degradation in cell cycle. The cyclin G1 mRNA expression does not fluctuate with cell cycle phase, whereas the expression of cyclin G2 mRNA oscillated with cell cycle and reached peak in the mid-late S phase. In contrast to cyclin G1, cyclin G2 mRNA weakly expressed in skeletal muscles and heart. It showed high expression in cerebrum, thymus, spleen, prostate gland and kidney^[13]. Notably cyclin G2 transcripts are abundant in tissue rich in either terminally differentiated cells or cells reacting to growth inhibitory signals and apoptosis^[5]. Cyclin G1 is a positive regulator and prompts cell proliferation, so far, neither the physiological role nor the biochemical function of cyclin G2 has been defined. The mRNA expression of cyclin G1 and cyclin G2 can be induced by DNA-damage drug actinomycin-D, which has the p53 dependency for cyclin G1 but the p53 independency for cyclin G2^[14]. Cyclin G2 can be induced by negative growth regulators such as TGF- β 1 and dexamethasone. In the growth inhibition state of B cell, the transcription level of cyclin G2 is up-regulated. Re-conducting the VHL cancer-suppressing gene into renal cancer cells with VHL gene defect can induce cyclin G2 expression. The newest research also showed that lack of cyclin G2 plays an important role in the malignant transformation of papillary carcinoma of the thyroid. It may play an adjuvant role in the transformation of follicular

adenoma to carcinoma^[15]. So cyclin G2 most likely appears to be a negative regulator of the cell cycle.

The result showed that compared with the control group, the clones formed by transfected pIRES-G2 group were smaller and fewer, cells became wrinkled and irregular, which proved that the high expression of cyclin G2 inhibited the cell proliferation. In this research we had the gene transfection experiment through cloning cyclin G2 cDNA into bicistronic eukaryotic expression vector pIRESneo, the 2 open reading frame (ORF) of inserted gene cyclin G2 and selective label gene neo were separated by the inserted brain cardiomyoditis virus IRES^[16,17]. So the recombinant plasmid pIRES-G2 in host cells only produced a single transcriptional template, which made the 2 proteins to be translated simultaneously to ensure all positive cells after G418 selection express target genes, overcame the shortcoming that these 2 genes could not be transcribed and translated at the same time when using other eukaryotic expression vectors^[18,19]. The positive clones formed by G418 selection in the experimental group of pIRES-G2 should have the expression of cyclin G2. Thus, the difference of clones between the experimental and control groups was only caused by the high expression of cyclin G2. The MTT assay also testified that the average absorbance of pIRES-G2 group cell was lower than that of pIRESneo group, it showed that the proliferative ability decreased after pIRES-G2 transfection. Because by MTT assay, the cell numbers in pIRES-G2 group and pIRESneo group were the same and they also grew at the exponentially growing state, thus the average absorbance difference between them was merely caused by the difference of transfected genes. From this we could draw the conclusion that cyclin G2 overexpression makes the proliferative ability decrease.

Our experiment indicates that cyclin G2 could inhibit the SGC-7901 cell proliferation. Unlike other cyclins, it may be a negative regulating factor of cell cycle.

REFERENCES

- 1 **Hunter T**, Pines J. Cyclins and cancer. *Cell* 1991; **66**: 1071-1074
- 2 **Pines J**, Hunter T. Cyclin-dependent kinases : a new cell cycle motif ? *Trends Cell Biol* 1991; **1**: 117-121
- 3 **Pines J**. Cyclins and cyclin-dependent kinases: theme and variations. *Adv Cancer Res* 1995; **66**: 181-212
- 4 **Draetta GF**. Mammalian G1 cyclins. *Curr Opin Cell Biol* 1994; **6**: 842-846
- 5 **Horne MC**, Goolsby GL, Donaldson KL, Tran D, Neubauer M, Wahl AF. Cyclin G1 and cyclin G2 comprise a new family of cyclins with contrasting tissue-specific and cell cycle-regulated expression. *J Biol Chem* 1996; **271**: 6050-6061
- 6 **Zauberman A**, Lupo A, Oren M. Identification of p53 target genes through immune selection of genomic DNA: the cyclin G gene contains two distinct p53 binding sites. *Oncogene* 1995; **10**: 2361-2366
- 7 **Kimura SH**, Ikawa M, Ito A, Okabe M, Nojima H. Cyclin G1 is involved in G2/M arrest in response to DNA damage and in growth control after damage recovery. *Oncogene* 2001; **20**: 3290-3300
- 8 **Wykoff CC**, Pugh CW, Maxwell PH, Harris AL, Ratcliffe PJ. Identification of novel hypoxia dependent and independent target genes of the von Hippel-Lindau(VHL) tumor suppressor by mRNA differential expression profiling. *Oncogene* 2000; **19**: 6297-6305
- 9 **Horne MC**, Donaldson KL, Goolsby GL, Tran D, Mulheisen M, Hell JW, Wahl AF. Cyclin G2 is up-regulated during growth inhibition and B cell antigen receptor-mediated cell cycle arrest. *J Biol Chem* 1997; **272**: 12650-12661
- 10 **Alevizos I**, Mahadevappa M, Zhang X, Ohshima H, Kohno Y, Posner M, Gallagher GT, Varvares M, Cohen D, Kim D, Kent R, Donnoff RB, Todd R, Yung CM, Warrington JA, Wang DT. Oral cancer *in vivo* gene expression profiling assisted by laser capture microdissection and microarray analysis. *Oncogene* 2001;

- 20:** 6196-6204
- 11 **Tian YL**, Liu FR, Liu J, Jiang L, Luo Y, Zhang X. Ectopic expression of cyclin G2 inhibits cell proliferation in HeLa cancer cell line. *Aizheng* 2002; **21**: 577-581
 - 12 **Tamura K**, Kanaoka Y, Jinno S, Nagata A, Ogiso Y, Shimizu K, Hayakawa T, Nojima H, Okayama H. Cyclin G: a new mammalian cyclin with homology to fission yeast Cig1. *Oncogene* 1993; **8**: 2113-2118
 - 13 **Jensen MR**, Audolfsson T, Keck CL, Zimonjic DB, Thorgeirsson SS. Gene structure and chromosomal localization of mouse cyclin G2 (Ccng2). *Gene* 1999; **230**: 171-180
 - 14 **Bates S**, Rowan S, Vousden KH. Characterisation of human cyclin G1 and G2: DNA damage inducible genes. *Oncogene* 1996; **13**: 1103-1109
 - 15 **Ito Y**, Yoshida H, Uruno T, Nakano K, Takamura Y, Miya A, Kobayashi K, Yokozawa T, Matsuzuka F, Kuma K, Miyauchi A. Decreased expression of cyclin G2 is significantly linked to the malignant transformation of papillary carcinoma of the thyroid. *Anticancer Res* 2003; **23**: 2335-2338
 - 16 **Rees S**, Coote J, Stables J, Goodson S, Harris S, Lee MG. Bicistronic vector for the creation of stable mammalian cell lines that predisposes all antibiotic-resistant cells to express recombinant protein. *Biotechniques* 1996; **20**: 102-110
 - 17 **Gaines P**, Wojchowski DM. PIRES-CD4t, a dicistronic expression vector for MACS- or FACS- based selection of transfected cells. *Biotechniques* 1999; **26**: 683-688
 - 18 **Felgner PL**. Improvements in cationic liposomes for *in vivo* gene transfer. *Hum Gene Ther* 1996; **7**: 1791-1793
 - 19 **Bennett CF**, Chiang MY, Chan H, Shoemaker JE, Mirabelli CK. Cationic lipids enhance cellular uptake and activity of phosphorothioate antisense oligonucleotides. *Mol Pharmacol* 1992; **41**: 1023-1033

Edited by Zhu LH and Xu FM

Expression of tumor related gene NAG6 in gastric cancer and restriction fragment length polymorphism analysis

Xiao-Mei Zhang, Shou-Rong Sheng, Xiao-Yan Wang, Liang-Hua Bin, Jie-Ru Wang, Gui-Yuan Li

Xiao-Mei Zhang, Department of Digestive Medicine, Xiangya Hospital, Central South University, Changsha 410008, Hunan Province, China

Shou-Rong Sheng, Xiao-Yan Wang, Department of Digestive Medicine, the Third Xiangya Hospital, Central South University, Changsha 410013, Hunan Province, China

Liang-Hua Bin, Jie-Ru Wang, Gui-Yuan Li, Cancer Research Institute, Xiangya Medical College, Central South University, Changsha 410078, Hunan Province, China

Supported by the Natural Science Foundation of Hunan Province, No.02JJY2049 and the National "863" Program of China, No.102-10-01-05

Correspondence to: Dr. Shou-Rong Sheng, Department of Digestive Medicine, the Third Xiangya Hospital, Central South University, Changsha 410013, Hunan Province, China. tangyy@public.cs.hn.cn
Telephone: +86-731-4316667

Received: 2003-04-12 **Accepted:** 2003-09-18

Abstract

AIM: NAG6 gene is a novel tumor related gene identified recently. This study was designed to examine the expression of this gene in gastric cancer and corresponding normal tissues, and to investigate its role in the occurrence and development of gastric cancer, also to study if the genetic structure of NAG6 was altered in gastric cancer.

METHODS: Reverse transcription-polymerase chain reaction (RT-PCR), Northern blot analysis and dot hybridization were used to compare the expression level of NAG6 gene in 42 cases of gastric cancer tissues with their corresponding normal tissues of the same patients respectively. In addition, restriction fragment length polymorphism (RFLP) analysis was adopted to study if the genetic structure of NAG6 was altered in gastric carcinomas.

RESULTS: The expression of NAG6 in 57.1% gastric cancer tissues (25/42) was absent by RT-PCR analysis. The down-regulation rate of NAG6 in gastric cancer tissues was significantly higher than that in corresponding normal tissues ($P < 0.01$). However no correlation between the down-regulation of NAG6 and lymph-node and/or distance metastasis was found in this study ($P > 0.05$). Dot hybridization confirmed the results of RT-PCR. Furthermore, the results of *EcoRI* RFLP analysis of NAG6 gene demonstrated that 3 of 7 cases of gastric cancer showed loss of 5 kb fragment in comparison with their corresponding normal tissues.

CONCLUSION: NAG6 gene is significantly down regulated in gastric cancer. The loss of genetic materials may be the cause of down-regulation of NAG6 expression. This seems to suggest that NAG6 may represent a candidate of putative tumor suppressor gene at 7q31-32 loci associated with gastric carcinoma. The down-regulation of this gene may play a role in occurrence and development of this disease, however it may not be associated with lymph node and/or distance metastasis.

Zhang XM, Sheng SR, Wang XY, Bin LH, Wang JR, Li GY. Expression of tumor related gene NAG6 in gastric cancer and restriction fragment length polymorphism analysis. *World J Gastroenterol* 2004; 10(9): 1361-1364

<http://www.wjgnet.com/1007-9327/10/1361.asp>

INTRODUCTION

Gastric cancer (GC) is one of the leading causes of cancer death in the world, although its incidence has gradually declined in recent years^[1,2]. However, in the Far East, including China and Japan, gastric cancer remains a prevalent cancer with a high mortality^[3,4]. It is well known that carcinogenesis and progression of human gastric cancer are related to multiple genetic aberrations including activation of oncogenes and inactivation of tumor suppressor genes. The latter involves the loss of heterozygosities (LOH) of several chromosomal loci and mutations in tumor suppressor genes, such as *p53* and *DCC* genes. However, the mechanism of the process of multistage carcinogenesis is still not well understood^[5-12]. Recently, a number of cytogenetic and molecular genetic studies have revealed that LOH on the long arm of chromosome 7 occurs frequently in many types of primary cancers including nasopharyngeal, gastric, breast, ovarian, and oral carcinomas, and investigators have identified the most common site of LOH as 7q31-32, implying the existence of at least one multi-tissue tumor suppressor gene (TSG) at this locus^[13-22]. Based on these findings, in our previous studies, we have cloned a novel tumor related gene from this common deletion region in 7q31-32 by positional candidate cloning strategy, we named it NAG6, and its GenBank accession number was AF156971. It was found to be a potential tumor suppressor gene associated with NPC^[23-26]. To investigate whether the expression of NAG6 was also altered in GC and whether NAG6 gene also played a role in the pathogenesis of gastric carcinoma, we analyzed the expression level of NAG6 in 42 cases of human gastric carcinoma and their matched normal tissues by RT-PCR, Northern blot analysis and dot hybridization. Furthermore, to study if the genetic structure alteration of NAG6 was the reason of its abnormal expression in GC, RFLP analysis was adopted. These studies can lead to a better understanding of the molecular mechanism of gastric cancer.

MATERIALS AND METHODS

Tumor specimens

Fresh surgical specimens of forty-two gastric carcinoma (GC) and corresponding normal tissues were obtained from the Affiliated Xiangya Hospital of Central South University from January 2000 to July 2000. All tumor specimens were confirmed by pathological diagnosis. Each freshly resected specimen was frozen immediately and stored in liquid nitrogen until analyzed. Histologically, in the 42 cases of gastric carcinoma, 4 were well-differentiated adenocarcinomas, 30 poorly-differentiated adenocarcinomas, 6 signet ring cell carcinomas and 2 mucoid carcinomas. There were 22 males and 20 females, their age ranged from 30 to 68 years (mean

age, 51.7 years). Six cases had lymph node or distance metastases. No patient had received chemotherapy or radiation therapy before surgery.

RT-PCR

Total RNA was isolated using Trizol reagent (Gibco-BRL, Gaithersburg, MD, USA) according to the protocol provided by the manufacturer. After treated with DNase-I (Promega), 1-2 µg of total RNA was reversely transcribed into complementary DNA (cDNA) with oligo(dT) using cDNA synthesis kit (Promega). Then 1 µL product was used as the template to amplify specific fragments in a 25 µL reaction mixture. The subsequent PCR was performed using Taq polymerase and the buffer (Promega) supplied with 0.2 mmol/L dNTPs and 0.2 µmol/L primers. Primers corresponding to NAG6 sequences were designed with WWW Primer Picking (Primer 3) and synthesized by TaKaRa. Gene-specific forward and reverse primers for NAG6 were designed to produce a PCR product of 680 bp. RT-PCR reaction was carried out with an initial denaturation at 95 °C for 5 min, followed by 35 cycles at 94 °C for 50 s, annealing at 56 °C for 50 s, at 72 °C for 60 s, and a final extension at 72 °C for 10 min. At the same time, a housekeeping gene, GAPDH was amplified as internal control to normalize the relative levels of cDNA, which generated a PCR product of 475 bp. An aliquot (10 µL) of each reaction product was analyzed by 10 g/L agarose gel electrophoresis.

The sequences of primers were as follows: NAG6F1, 5'-GGCACTGGAGTACAAAGACA-3'; NAG6R1, 5'-TTACTTTTCCCATTGCTCA-3'; GAPDHF1, 5'-GTCATCCATGACAACCTTTGGTATC-3'; GAPDHR1, 5'-CTGTAGCCAAATTCGTTGTCATAC-3'.

Northern blot analysis

Total RNA was isolated from human gastric carcinoma and corresponding normal tissues by Trizol reagent (Gibco-BRL), and hybridization was performed as described. A 30 µg RNA was separated by electrophoresis by denaturing agarose gels and blotted onto nylon membrane (Clontech). RNA was permanently attached to the membrane by UV illumination for 150 s (GS Gene Linker, Bio-Rad, USA), and the membrane was dried in a vacuum at 80 °C for 2 h and sealed in a plastic bag for use. The hybridization probes were obtained by RT-PCR amplification. NAG6 cDNA probe was random-prime labeled with [α -³²P]dCTP using primer-a-gene random labeling kit (Promega, USA) and following the protocol. Hybridization with the RNA blots was carried out at 68 °C overnight in Express Hyb™ hybridization solution (Clontech) in a rolling bottle. The membranes were washed twice at room temperature in 2×saline sodium citrate (SSC), 0.5 g/LSDS for 10 min, once at 42 °C in 1×SSC, 1 g/L SDS for 15 min and once at 50 °C in 0.1×SSC, 1 g/L SDS for 30 min. Then, they were exposed to film (Eastman Kodak, Rochester, NY, USA) for 4 d at -70 °C. After exposure, the blot was again hybridized with a GAPDH probe.

Dot blot analysis

GAPDH and NAG6 cDNA fragments containing open reading frames from cDNA of gastric carcinoma samples were obtained by RT-PCR. These cDNAs were reclaimed and purified by using a kit according to the instructions of its manufacturer (Shanghai Huashun Co.). After alkali dissolution, GAPDH and NAG6 cDNA were blotted onto nylon membranes. cDNA was permanently attached to the membrane by UV illumination for 150 s, and the membranes were dried in a vacuum at 80 °C for 2 h to fix the cDNA. Ten µg total RNA was isolated from 10 cases of human gastric carcinomas and 10 cases of each corresponding normal tissues, and reversely-transcribed into

cDNA probe with oligo (dT) and [α -³²P] dCTP using cDNA synthesis kit after treated with DNase I and RNasin at 37 °C for 1 h to remove contaminated DNA (1 µg total RNA of each case was used). Then the two cDNA probes were hybridized with GAPDH and NAG6 cDNA blots respectively as Northern hybridization described above.

Southern-based RFLP analysis

Genomic DNA was extracted from gastric cancer and corresponding normal tissues by using sodium dodecyl sulphate (SDS), EDTA, proteinase K, dispelled protein and phenol-chloroform methods, removing RNA with RNA enzyme, precipitating DNA with alcohol of two times in volume, mixed in proper TE buffer solution, and kept for use at 4 °C. Genomic DNA was digested with the stated restriction endonuclease *EcoRI* and electrophoresed on 7 g/L agarose (TAE) gel. After electrophoresis, DNAs were denatured, neutralized and transferred to nylon membranes. Then DNAs were permanently attached to the membrane by UV illumination and the membrane was dried in a vacuum at 80 °C for 2 h. The nylon membrane was hybridized with the radiolabelled NAG6 cDNA probe according to the method of Southern blot. After washed and autoradiographed at -70 °C for 3 to 5 d, hybridizing was carried out.

Statistical analysis

Chi-square test was used. A *P* value less than 0.05 was considered statistically significant.

RESULTS

Expression of NAG6 in gastric cancer and corresponding normal tissues

In 42 pairs of GC and corresponding normal tissues, NAG6 expression was undetectable in 24 tumors (57.1%), while it was detectable in all corresponding normal tissues. The expression of NAG6 in gastric carcinomas was significantly down-regulated than that in normal tissues ($\chi^2=33.6, P<0.005$). Representative cases of NAG6 expression detected by RT-PCR are shown in Figure 1. The down-regulation rate of NAG6 in patients with lymph node and/or distance metastases and those without lymph-node and/or distance metastases was 66.7%(4/6) and 47.2%(17/36) respectively. There was no apparent relevance between NAG6 down-expression and lymph node and/or distance metastasis of gastric carcinomas ($P>0.05$).

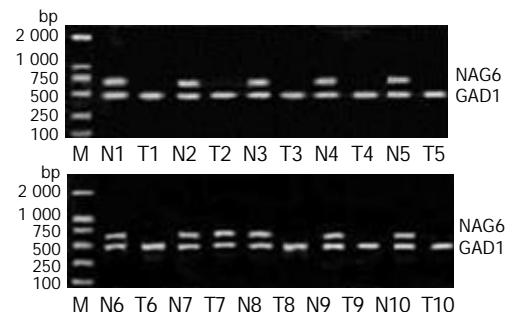


Figure 1 Expression of NAG6 in gastric carcinoma and corresponding normal tissues examined by RT-PCR. The RT products were examined by PCR with NAG6 primers, producing a 680 bp fragment and with GAPDH primers, producing a 466 bp fragment. Lane M: 2 000 bp marker, Lane N: normal epithelium tissues, Lane T: gastric carcinoma tissues.

In order to verify the results of RT-PCR, Northern hybridization was performed. Northern blot analysis did not detect NAG6 expression in both gastric carcinoma and

corresponding normal tissues, whereas GAPDH was strongly expressed in both of them. We speculated that the expression abundance of NAG6 gene in gastric cancer and corresponding normal tissues might be too low to be detected by Northern blot analysis. So, we used dot hybridization analysis to verify the reliability of RT-PCR on the other hand. The results of dot hybridization confirmed the results of RT-PCR that the expression of NAG6 was significantly down-regulated in gastric carcinoma tissues (Figure 2).

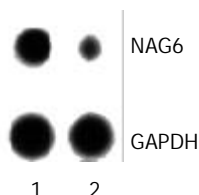


Figure 2 Dot hybridization analysis of NAG6 gene expression profiles in human gastric carcinoma and corresponding normal tissues. NAG6 cDNA obtained by RT-PCR was blotted onto nylon membranes. The membranes were hybridized with ^{32}P -labeled cDNA probes obtained from total RNA of human gastric carcinoma (1) and corresponding normal gastric epithelial (2) tissues. After stringent washes, membranes were exposed to X-ray film for 4 d at -70°C . NAG6 was down-regulated in gastric carcinoma tissues.

RFLP analysis

*Eco*RI RFLP analysis of NAG6 gene was performed in 7 cases of gastric cancer and corresponding normal tissues. The results showed that there were two kinds of common allelic fragments (11.5 Kb, 5.0 Kb) in all corresponding normal tissues and 4 cases of gastric cancer, but 3 cases of gastric cancer tissues showed loss of 5 Kb fragment in comparison with their matched normal tissues.

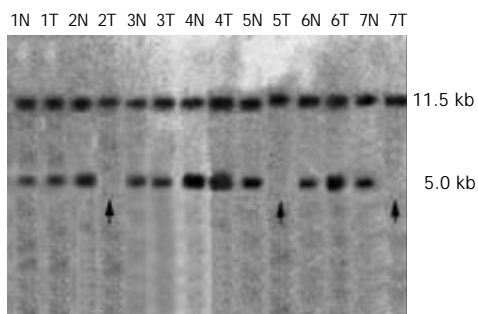


Figure 3 RFLP analysis using Southern hybridization. Gastric cancer and normal epithelium genome DNAs were digested with *Eco*RI and hybridized with NAG6 cDNA probe. Three cases of gastric cancer tissues showed loss of 5Kb fragment (N: normal epithelium tissues, Lane T: gastric carcinoma tissues).

DISCUSSION

NAG6 gene has been recently identified and cloned by our group at chromosome 7q31-32, the common deletion site in various human malignancies. Comparison with GenBank and EMBO database using the BLAST program the cDNA sequence of NAG6 gene was a unique gene with no homology to any previously reported human genes, and its GenBank accession number is AF156971. The predicted NAG6 protein contained four protein kinase C (PKC) phosphorylation sites, suggesting that the activity of NAG6 protein can be regulated by phosphorylation. Its mRNA expression level in NPC biopsies was significantly lower than that in normal nasopharyngeal epithelium, and the down-regulation of NAG6

in NPC was attributable to several factors including loss of genetic materials and hypermethylation. All these findings supported NAG6 as a candidate tumor suppressor gene at 7q31-32. The down-regulation of this gene might play a role in occurrence and development of NPC^[23-26].

Cytogenetic and molecular analyses demonstrated that frequent LOH on the long arm of chromosome 7 could also be observed in a high proportion of gastric cancer cases^[13-16]. Nishizuka *et al* reported LOH at any locus on 7q occurred in 34% (18 out of 53) of primary gastric carcinomas^[14]. Kuniyasu *et al* examined LOH on the long arm of chromosome 7 using 5 polymorphic marker probes in 98 gastric carcinomas^[15]. The results showed twenty-six of 82(32%) informative cases showed LOH on 7q at least one locus of 5 loci. Xia *et al* studied a total of 28 primary gastric cancer specimens, and they found that deletion of 7q (21/26) was one of the characteristic structural changes of primary gastric cancer^[16]. Furthermore, investigators have identified the most common site of LOH as 7q32-qter, and concluded that in the 7q32-qter segments, at least one tumor suppressor gene probably existed and it might have a close relation to the development and progression of gastric cancer^[13-16]. NAG6 gene located at 7q31-32 locus. We were interested in whether expression of NAG6 was altered in GC and whether NAG6 was also a possible tumor suppressor in human gastric carcinoma. In this study, RT-PCR, Northern blot and dot hybridization were used to detect the expression abundance of the gene in gastric carcinoma and corresponding normal tissues. The results of RT-PCR showed that the down-regulation rate of NAG6 in gastric carcinoma tissues was significantly higher than that in corresponding normal tissues ($P<0.005$). Dot hybridization confirmed the results of RT-PCR. However the expression of NAG6 was not relevant to lymph node and/or distance metastasis of gastric carcinomas. This seems to suggest that down-regulation of NAG6 might play a role in the occurrence and progression of GC.

In order to study the possible cause of down-regulation of NAG6 in gastric cancers, we studied on the restriction fragment length polymorphisms (RFLPs) of NAG6 gene in gastric cancer and corresponding normal tissues to detect if the genetic structure of NAG6 was changed in GC. We used restriction enzymes to cut DNA at specific recognition sites, fragments of restricted DNA separated by gel electrophoresis and detected by subsequent Southern blot hybridization to a radiolabeled DNA probe. In recent twenty years, the application value of restriction fragment length polymorphism (RFLP) analysis in the detection of genetic structure change and genetic polymorphisms of candidate gene has called attention of the scholars at home and abroad^[27-29]. Polymorphic sequences that result in RFLPs are used as markers on both physical maps and genetic linkage maps. In this study, *Eco*RI RFLP analysis of NAG6 gene was performed in 7 cases of gastric cancer and corresponding normal tissues. The results demonstrated that 3 of 7 cases of gastric cancer showed loss of 5 kb fragment in comparison with their corresponding normal tissues. In the previous study, RFLP analysis also found that 6 of 14 NPC cases lost the fragment of 3 kb in comparison with their matched peripheral blood lymphocytes. These results demonstrated that the genetic structure of NAG6 was changed in both NPC and GC. A preliminary conclusion was drawn that loss of genetic materials might be the cause of down-regulation of NAG6 expression.

To summarize, our data showed that NAG6 was down-regulated in gastric cancer, and loss of genetic materials of NAG6 was also found in GC. It is reasonable to predict that NAG6 may represent a candidate of putative tumor suppressor gene at 7q31-32 locus associated with GC and NPC, and this gene may play an important role in suppressing GC tumorigenesis, losses of its function may contribute to the occurrence and

development of GC. The mechanism of this gene is still unclear. Further studies on a large patient population are needed to verify these initial observations and to characterize the mechanism of down-regulation of NAG6 in tumors. It is important to examine the possible relationship between loss or preservation of NAG6 expression and clinical outcome in patients with tumor.

REFERENCES

- Stadlander CT**, Waterbor JW. Molecular epidemiology, pathogenesis and prevention of gastric cancer. *Carcinogenesis* 1999; **20**: 2195-2208
- Palli D**. Epidemiology of gastric cancer: an evaluation of available evidence. *J Gastroenterol* 2000; **35**(Suppl): 84-89
- Maehara Y**, Kakeji Y, Oda S, Takahashi I, Akazawa K, Sugimachi K. Time trends of surgical treatment and the prognosis for Japanese patients with gastric cancer. *Br J Cancer* 2000; **83**: 986-991
- Deng DJ**. Progress of gastric cancer etiology: Nnitrosamides in the 1990s. *World J Gastroenterol* 2000; **6**: 613-618
- Becker KF**, Keller G, Hoefler H. The use of molecular biology in diagnosis and prognosis of gastric cancer. *Surg Oncol* 2000; **9**: 5-11
- Boussioutas A**, Taupin D. Towards a molecular approach to gastric cancer management. *Intern Med J* 2001; **31**: 296-303
- Yasui W**, Oue N, Kuniyasu H, Ito R, Tahara E, Yokozaki H. Molecular diagnosis of gastric cancer: present and future. *Gastric Cancer* 2001; **4**: 113-121
- Maltoni M**, Volpi A, Nanni O, Bajorko P, Belletti E, Vecchi AM, Liverani M, Danesi S, Calistri D, Ricotti L, Amadori D. Gastric cancer: epidemiologic and biological aspects. *Forum* 1998; **8**: 199-207
- Xu AG**, Li SG, Liu JH, Gan AH. Function of apoptosis and expression of the proteins *Bcl-2*, *p53* and *C-myc* in the development of gastric cancer. *World J Gastroenterol* 2001; **7**: 403-406
- Liu LX**, Liu ZH, Jiang HC, Qu X, Zhang WH, Wu LF, Zhu AL, Wang XQ, Wu M. Profiling of differentially expressed genes in human gastric carcinoma by cDNA expression array. *World J Gastroenterol* 2002; **8**: 580-585
- Meltzer SJ**. Tumor genomics vs tumor genetics: a paradigm shift? *Gastroenterology* 2001; **121**: 726-729
- Nishizuka S**, Tamura G, Terashima M, Satodate R. Loss of heterozygosity during the development and progression of differentiated adenocarcinoma of the stomach. *J Pathol* 1998; **185**: 38-43
- Zenklusen JC**, Conti CJ. Cytogenetic, molecular and functional evidence for novel tumor suppressor genes on the long arm of human chromosome 7. *Mol Carcinog* 1996; **15**: 167-175
- Nishizuka S**, Tamura G, Terashima M, Satodate R. Commonly deleted region on the long arm of chromosome 7 in differentiated adenocarcinoma of the stomach. *Br J Cancer* 1997; **76**: 1567-1571
- Kuniyasu H**, Yasui W, Yokozaki H, Akagi M, Akama Y, Kitahara K, Fujii K, Tahara E. Frequent loss of heterozygosity of the long arm of chromosome 7 is closely associated with progression of human gastric carcinomas. *Int J Cancer* 1994; **59**: 597-600
- Xia J**, Xiao S, Zhang J. Direct chromosome analysis and FISH study of primary gastric cancer. *Zhonghua Zhongliu Zazhi* 1999; **21**: 345-349
- Tan G**, Xiao J, Tian Y, Dong L, Jiang N, Zhan F, Li G. Microsatellite analyses of loci at 7q31.3-q36 reveal a minimum of two common regions of deletion in nasopharyngeal carcinoma. *Otolaryngol Head Neck Surg* 2002; **126**: 296-300
- Zenklusen JC**, Weintraub LA, Green ED. Construction of a high-resolution physical map of the approximate 1-Mb region of human chromosome 7q31.1-q31.2 harboring a putative tumor suppressor gene. *Neoplasia* 1999; **1**: 16-22
- Liu JC**, Scherer SW, Tougas L, Traverso G, Tsui LC, Andrulis IL, Jothy S, Park M. Detailed deletion mapping with a refined physical map of 7q31 localizes a putative tumor suppressor gene for breast cancer in the region of MET. *Oncogene* 1996; **13**: 2001-2008
- Koike M**, Takeuchi S, Yokota J, Park S, Hatta Y, Miller CW, Tsuruoka N, Koeffler HP. Frequent loss of heterozygosity in the region of the D7S523 locus in advanced ovarian cancer. *Genes Chromosomes Cancer* 1997; **19**: 1-5
- Koike M**, Tasaka T, Spira S, Tsuruoka N, Koeffler HP. Allelotyping of acute myelogenous leukemia: loss of heterozygosity at 7q31.1 (D7S486) and q33-34 (D7S498, D7S505). *Leuk Res* 1999; **23**: 307-310
- Wang XL**, Uzawa K, Miyakawa A, Shiiba M, Watanabe T, Sato T, Miya T, Yokoe H, Tanzawa H. Localization of a tumour-suppressor gene associated with human oral cancer on 7q31.1. *Int J Cancer* 1998; **75**: 671-674
- Jiang N**, Zhan F, Tan G, Deng L, Zhou M, Cao L, Qiu Y, Xie Y, Li G. A cDNA located on chromosome 7q32 shows loss of expression in epithelial cell line of nasopharyngeal carcinoma. *Chin Med J* 2000; **113**: 650-653
- Jiang N**, Zhan F, Xie Y, Zeng Z, Zhou M, Deng L, Li G. Establishment of partial gene expression map of 7q32 in nasopharyngeal carcinoma and primary culture normal nasopharyngeal epithelial cells. *Zhonghua Yixue Yichuanxue Zazhi* 1998; **15**: 267-270
- Jiang N**, Deng LW, Tan GL, Zhan FH, Zhou M, Cao L, Qiu YZ, Xie Y, Li GY. A nasopharyngeal carcinoma negatively related EST on 7q32. *Yichuan Xuebao* 1999; **26**: 301-308
- Zhang XM**, Sheng SR, Wang XY, Xiang Q, Li J, Tan C. Expression of tumor related gene NAG6, NAG-7, BRD7 in gastric cancer. *Zhonghua Xiaohua Zazhi* 2002; **22**: 733-736
- Yuan Y**, Dong M, Lu P, Wang XJ, Jin CL, He AG. Restriction fragment length polymorphism of pepsinogen C gene in patients with stomach carcinoma and in its high risk population. *China Natl J New Gastroenterol* 1996; **2**: 223-225
- Byrne M**, Parish TL, Moran GF. Nuclear RFLP diversity in *Eucalyptus nitens*. *Heredity* 1998; **81**: 225-233
- Butcher PA**, Moran GF, Perkins HD. RFLP diversity in the nuclear genome of *Acacia mangium*. *Heredity* 1998; **81**: 205-213

Edited by Zhang JZ and Wang XL Proofread by Xu FM

Establishment of a P-glycoprotein substrate screening model and its preliminary application

Yi Wang, Jiang Cao, Su Zeng

Yi Wang, Su Zeng, College of Pharmaceutical Sciences, Zhejiang University, Hangzhou 310031, Zhejiang Province, China

Jiang Cao, Cancer Institute, Zhejiang University, Hangzhou 310009, Zhejiang Province, China

Supported by the National Natural Science Foundation of China, No. 30225047

Correspondence to: Dr. Su Zeng, College of Pharmaceutical Sciences, Zhejiang University, Hangzhou 310031, Zhejiang Province, China. zengsu@cps.zju.edu.cn

Telephone: +86-571-87217060

Received: 2003-08-11 **Accepted:** 2003-10-12

Abstract

AIM: To establish a high P-glycoprotein (P-gp) expressing cell line as a model for studying drug absorption and distribution, and to explore the preliminary application of this screening model.

METHODS: A full-length MDR1 cDNA fragment in plasmid pMDRA1 was first subcloned into plasmid pET28a(+), then MDR1 cDNA was cut from the recombinant plasmid with double-digestion and ligated into the mammalian expression vector pcDNA3.1(+). The recombinant plasmid pcDNA3.1(+)/MDR1 was transfected into breast cancer cell line Bcap37 using the Superfect transfection reagent. Several stably transfected clones were obtained after selection with G418. Real-time fluorescent quantitative RT-PCR and Western blot methods were used to detect the expression of P-gp, and the cellular location of the expressed protein was determined by immunohistochemical staining. Drug sensitivity assay was used to evaluate the biological function of expressed P-gp. Concentration of quercetin in cells was determined by high-performance liquid chromatography (HPLC).

RESULTS: The recombinant plasmid was confirmed to be inserted in the correct orientation by restrictive enzyme digestion and DNA sequencing. Real-time fluorescent quantitative RT-PCR showed a higher level of P-gp mRNA in transfected cells compared to that in the control cells, and the Western blot result also indicated that P-gp expression in transfected cells was higher than that in control cells. The immunohistochemical staining showed that the expressed P-gp was localized on cell membranes. Drug sensitivity assay showed that the IC₅₀ for adriamycin and colchicine of the transfected cells was higher than that of the control cells. The concentration of quercetin in model cells was lower than that in control cells by HPLC. After P-gp inhibitor verapamil was administered, the concentration of quercetin in model cells was increased.

CONCLUSION: A high P-gp expressing cell line can be established, which could provide a suitable *in vitro* model system for studying drug intestinal absorption mechanism, predicting the drug permeability characteristics and screening new multi-drug resistance reversing agents. With this model, quercetin can be found to be transported by P-gp, and it is a P-gp substrate.

Wang Y, Cao J, Zeng S. Establishment of a P-glycoprotein substrate screening model and its preliminary application. *World J Gastroenterol* 2004; 10(9): 1365-1368

<http://www.wjgnet.com/1007-9327/10/1365.asp>

INTRODUCTION

P-glycoprotein (P-gp), a product of the multidrug resistance (MDR) gene, is widely distributed in normal tissues of the body, including intestinal mucosa, proximal tubule of the kidneys, placenta, testes, and blood-brain barrier^[1]. It is an ATP-dependent efflux transporter that affects the absorption, distribution, and excretion of a number of clinically important drugs^[2]. For example, in intestinal mucosa, P-gp serves as a biochemical barrier to drug delivery. Drugs or drug candidates are bound to P-gp and transported back to the apical surface of the tissue, thereby restricting the overall permeability of drugs and drug candidates.

Due to *in vivo* disposition and pharmacokinetics of drug efflux transporters, identification of compounds as P-gp substrates can aid the optimization and screening of new drug candidates. A variety of *in vitro* assays have been used to classify compounds as P-gp substrates^[3]. These assays can be classified into three groups. One is transport across polarized cell monolayers expressing P-gp on the apical membrane, the other is drug uptake into cells over-expressing P-gp, the third is direct binding to P-gp using inside-outside membrane vesicles or reconstituted P-gp.

Quercetin, a flavonoid and phytoestrogen, is present in a wide variety of fruits and vegetables^[4]. Quercetin is also a potent antioxidant *in vivo* and *in vitro*, and thus quercetin and other flavonoids have been considered as therapeutic agents for a wide range of diseases, including cancer, viral infection, inflammation/allergy, hypertension and atherosclerosis^[5-7].

In this study we constructed a P-gp expressing plasmid, established a P-gp high-expression cell model, and identified quercetin as a P-gp substrate with this cell model.

MATERIALS AND METHODS

Cell lines and cell culture

Breast cancer cell line Bcap37 (maintained by the Cancer Institute of Zhejiang University) was cultured in RPMI 1640 medium (Hyclone, USA) containing 100 ml/L heat-inactivated newborn calf serum (GIBCO), 100 U/mL penicillin and 100 µg/mL streptomycin. The cells were incubated at 37 °C in a humidified atmosphere with 50 mL/L CO₂ in air.

Construction of expression vector

Plasmid pMDRA1 containing a full-length MDR1 cDNA was kindly provided by Professor Kazumitsu Ueda^[8]. The plasmid was digested with *SacI* and *XhoI*, and the MDR1 cDNA fragment was ligated into pET28a(+) which was pre-cut with *SacI* and *XhoI*. The recombinant plasmid was digested with *BamHI* and *XhoI*, and the insert was purified by 0.8% agarose gel electrophoresis and ligated into the mammalian expression vector pcDNA3.1(+) pre-cut with *BamHI* and *XhoI*. The resulting pcDNA3.1(+)/MDR1 was digested with *EcoRI* to

check the orientation of the insert and DNA sequencing was used to verify the inserted sequence.

Transfection of Bcap37 cells

Bcap37 cells were transfected with the recombinant expression vector pcDNA3.1(+)/MDR1 using Superfect transfection reagent according to the manufacturer's instructions (QIAGEN). After 48 h of transfection, stable transfectants were isolated by selection with 800 µg/mL G418 for 10 d. G418-resistant stable clones were picked for further characterization. The transfectants were maintained in RPMI 1640 containing 100 mL/L newborn calf serum and 400 µg/mL G418. Bcap37 cells were also transfected with pcDNA3.1(+) vector as the control.

Real-time fluorescent quantitative RT-PCR

Total RNAs in Bcap37/MDR1 cells and control cells were extracted using TRIzol™ reagent (GIBCOBRL, Life Technologies) according to the user's guide. Real-time fluorescent quantitative RT-PCR was done with the MDR1 mRNA quantification kit (designed by the Cancer Institute of Zhejiang University and manufactured by Shanghai Jiusheng Medical Instrument Company) according to the manufacturer's instructions^[9].

Western blot

Total proteins in Bcap37/MDR1 and control cells were extracted with 1 g/L Triton X-100 and protein concentration was determined with a Bio-Rad protein assay kit and standardized with bovine serum albumin. The samples were electrophoresed (SDS-PAGE, 80 g/L) and electroblotted onto PVDF membrane (BioRad). The membrane was blocked in buffer with 50 mL/L fat free dry milk, detected with anti P-gp antibody (monoclonal F4, Sigma).

Immunohistochemical staining

Bcap37/MDR1 cells and control cells were harvested by centrifugation at 2 000 r/min for 5 min, washed twice with PBS, and mounted onto the slides. Immunohistochemical staining was done with the UltraSensitive™S-P mouse kit (Fuzhou Maxim Biotech, Inc). The protocol was accorded to the user guide. Primary antibody was monoclonal anti-human P-glycoprotein antibody purchased from Fuzhou Maxim Biotech (monoclonal number C494).

Drug sensitivity assay

Sensitivity of cells to anticancer drugs was examined by a colorimetric assay using MTT method. Cells (6×10^3 cells/well) were seeded on 96-well plates, and cultured in a humidified atmosphere with 50 mL/L CO₂ at 37 °C. Twenty-four hours later, drugs were added at various concentrations. Control wells were included for each drug that consisted of the respective solvents. Forty-eight hours later, 50 µL of 1 mg/mL MTT (in PBS) [3-[4,5-dimethylthiazol-2-yl]-2,5-diphenyltetrazolium bromide] was added to each well and incubated in a humidified atmosphere with for 4 h at 37 °C 50 mL/L CO₂. The supernatants were aspirated, and 200 µL /well of dimethyl sulfoxide was added to dissolve formazan crystals. Color intensity was measured at 570 nm using an ELISA reader. The 50% inhibitory concentration for a particular agent was defined as the drug concentration which resulted in a 50% reduction in cell number at 48 h relative to the control. Each experiment was performed in triplicate.

Accumulation of quercetin

Bcap37 and Bcap37/MDR1 cells were seeded at the density of 7.5×10^5 to a 35 mm i.d. tissue culture well. After twenty-four

hours, the culture medium was aspirated, and replaced by the medium containing 25 µmol/L quercetin. After 10 and 20 min, the medium was aspirated and the cells were washed 3 times with ice-cold PBS (pH7.4) to stop further uptake. A 1 mL of 1 g/L Triton X-100 was added to each well to lyse the cells. Drug concentration in lysis solution was determined by reverse-phase HPLC, and normalized with cellular protein content^[10].

Bcap37/MDR1 and control cells were seeded at the density of 7.5×10^5 to a 35 mm i.d. tissue culture well. After twenty-four hours, the culture medium was aspirated, and replaced by the medium containing 25 µmol/L quercetin with/without 6.6 µmol/L verapamil. After 30 min, the media were aspirated and the cells were washed 3 times with ice-cold PBS (pH7.4) to stop further uptake. A 1 mL of 1 g/L Triton X-100 was added to each well to lyse the cells. Drug concentration in lysis solution was determined by reverse-phase HPLC, and normalized with cellular protein content.

The HPLC system used was Agilent 1100 system (Agilent Technologies). Separation was done on a conLichrospher ODS-C18 (4.6 mm i.d. × 250 mm) column. The mobile phase consisted of pH2.0 phosphate buffer-tetrahydrofuran-methanol-isopropanol (65:15:10:20, v:v:v:v) at a flow rate of 0.5 mL/min, and the wavelength of UV detector was 380 nm. Morin was used as internal standard. Cell protein was quantitated by Bio-Rad DC protein assay kit.

RESULTS

Analysis of plasmid expression

After digestion with *EcoRI*, the recombinant plasmid pcDNA3.1(+)/MDR1 showed three DNA fragments about 1.2 kb, 3.4 kb and 5.4 kb as expected (Figure 1). DNA sequencing result further confirmed the correct construction of this P-gp expression vector.



Figure 1 Analysis of pcDNA3.1(+)/MDR1 digested by *EcoRI*. M: DNA ladder; A: pcDNA3.1(+)/MDR1 digested by *EcoRI*.

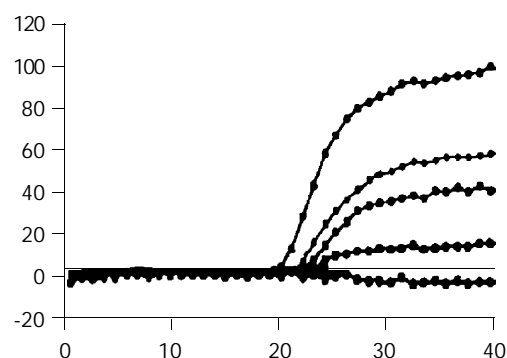


Figure 2 Map of real-time fluorescent quantitative RT-PCR. Blue curve: Bcap37; Other color curves: Bcap37 cell clones transfected with pcDNA3.1(+)/MDR1; Red curve stands for the clone expressing higher P-gp level than others.

Real-time fluorescent quantitative RT-PCR

The C_T of Bcap37/MDR1 and control cells was 19 and 40 cycles (Figure 2). It showed a significant increase of MDR1 mRNA levels in Bcap37/MDR1 than in control cells.

Western blot

The Bcap37/MDR1 cells showed significantly higher level of P-gp at 170 ku compared with control cells (Figure 3).



Figure 3 Western blot analysis of P-gp expression in Bcap37 and Bcap37/MDR1 cells. A: Bcap37; B, C, D, E: Bcap37 cell clones transfected with pcDNA3.1(+)/MDR1.

Immunohistochemical staining

The nuclei and plasma of control cells were stained blue (Figure 4A), demonstrating that the cells did not express P-gp. The Bcap37/MDR1 cells showed brown staining on cell membrane (Figure 4B). This indicated that P-gp was expressed on the transfected cell membrane.

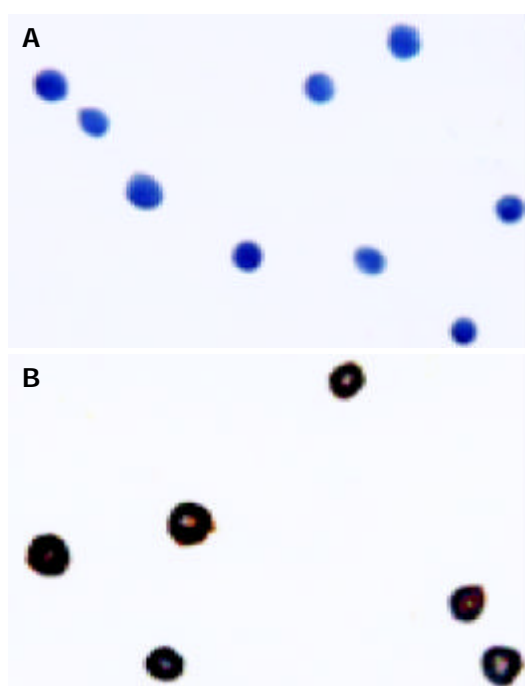


Figure 4 P-gp immunohistochemical staining in Bcap37 (A) and Bcap37/MDR1 (B) cells.

The cells were stained using a human anti-Pgp primary antibody, biotinylated anti-rabbit IgG secondary antibody, followed by the avidin and horseradish containing Vector ABCD reagent. The sections were then stained with 3,3'-diaminobenzidine (DAB) and counterstained with hematoxylin. The brown color represented Pgp expression and the blue color was the non-specific counterstaining.

Drug sensitivity assay

Resistance to anticancer drugs was determined using MTT assay. Bcap/MDR1 exhibited multidrug resistant phenotypes characterized by cross-resistance to two unrelated antitumor agents (Table 1) including adriamycin and colchicine. The results confirmed the expressed Pgp in transfected cells played a role as an efflux pump.

Table 1 Relative resistance of multidrug resistant Bcap37 transfected cells

Cell line	IC ₅₀ (μg/mL)	
	Adriamycin	Colchicine
Bcap37	0.047	0.028
Bcap37/MDR1	2.203	0.391

Logarithmically growing cells were incubated for 48 h in the presence of the drug. IC₅₀ referred to the drug concentration that resulted in a 50% reduction in cell number.

Quercetin accumulation in cells

Quercetin was incubated with Bcap37/MDR1 and Bcap37 for 10 min and 20 min, and the drug accumulation in cells is listed in Table 2. After P-gp inhibitor verapamil was administered the concentration of quercetin in model cells was increased (Figure 5). All values were normalized with protein content. The results demonstrated that quercetin was accumulated in Bcap37 much more than in Bcap37/MDR1 ($P < 0.05$).

Table 2 Quercetin accumulation over different periods ($n=3$)

Cell line	10 min	20 min
Bcap37(μmol/L.mg)	2.44	3.33
Bcap37/MDR1(μmol/mg)	1.47 ^a	1.82 ^a

^a $P < 0.05$ vs Bcap37 cells.

The amount of quercetin accumulation in cells was determined by reverse phase HPLC through a standard curve, and the values were normalized with cellular protein content. There was a significantly higher concentration of quercetin accumulated in MDR1 transgenic cells ($P < 0.05$).

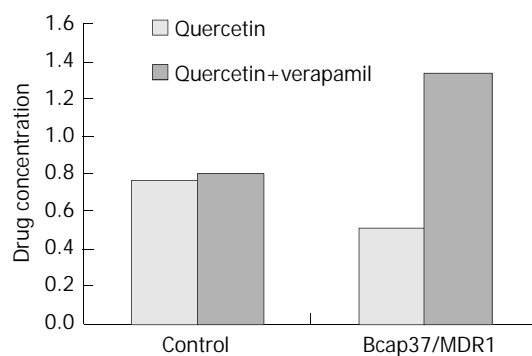


Figure 5 Amount of quercetin accumulation in cells with/without verapamil.

DISCUSSION

In recent years, it has become apparent that transport proteins play a major role in controlling the distribution, elimination and potentially the metabolism of some drugs, including organic cation transporters, organic anion transporters, MRP related transporters, and P-glycoprotein. P-gp has received considerable attention in recent years both as a barrier to drug absorption and distribution, and as a potential source for variability in drug pharmacokinetics and pharmacodynamics. In the intestine, P-gp could actively transport drugs counter-current to the absorptive transport of drugs, thus posing a barrier to absorption of exogenous compounds^[11]. This activity has been proposed to act in concert with intestinal cytochrome P-450 3A4 to increase pre-systemic metabolism of drugs, further minimizing systemic exposure to other drugs and xenobiotics^[12,13]. For

example, Pgp limited intestinal absorption of digoxin, talinolol, and cyclosporine after oral dosing, limited the central nervous system penetration of human immunodeficiency virus protease inhibitors, and helped excrete paclitaxel into intestine^[14-18].

A P-gp over-expressing cell line was established and characterized by Western blot, drug sensitivity assay and flow cytometry (data not shown). The results showed that the P-gp over-expressing cell line had biological functions.

In cellular drug accumulation assays, drug accumulation in P-gp expressing cells was compared with accumulation in cells from the parental cell line. Since the accumulation of P-gp substrates in P-gp over-expressing cells was restricted by P-gp mediated efflux of the compound back into the extracellular fluid, P-gp substrates showed less accumulation in P-gp expressing cells than in P-gp deficient cells. Similarly, drug accumulation was increased under conditions when P-gp was inhibited. In our experiment, quercetin showed less accumulation in Bcap37/MDR1 than in Bcap37. After P-gp inhibitor verapamil was administered, the concentration of this flavonoid in model cells increased. This implied the compound was a P-gp substrate. The result was similar to that of Walgren *et al*^[19].

A high P-gp expressing cell line can be established which provides a suitable *in vitro* model system for studying drug intestinal absorption mechanism, predicting the drug permeability characteristics and screening new multi-drug resistant reversing agents.

REFERENCES

- 1 **Hugger ED**, Novak BL, Burton PS, Audus KL, Borchardt RT. A comparison of commonly used polyethoxylated pharmaceutical excipients on their ability to inhibit P-glycoprotein activity *in vitro*. *J Pharm Sci* 2002; **9**: 1991-2002
- 2 **Schinkel AH**. P-glycoprotein, a gatekeeper in the blood-brain barrier. *Adv Drug Deliv Rev* 1999; **36**: 179-194
- 3 **Hochman JH**, Yamazaki M, Ohe T, Lin JH. Evaluation of drug interactions with P-glycoprotein in drug discovery: *in vitro* assessment of the potential for drug-drug interactions with p-glycoprotein. *Curr Drug Metab* 2002; **3**: 257-273
- 4 **Jovanovic SV**, Simic MG. Antioxidants in nutrition. *Ann N Y Acad Sci* 2000; **899**: 326-334
- 5 **Wiseman H**. The bioavailability of non-nutrient plant factors: dietary flavonoids and phyto-oestrogens. *Proc Nutr Soc* 1999; **58**: 139-146
- 6 **Graefe EU**, Derendorf H, Veit M. Pharmacokinetics and bioavailability of the flavonol quercetin in humans. *Int J Clin Pharmacol Ther* 1999; **37**: 219-233
- 7 **Lamson DW**, Brignall MS. Antioxidants and cancer 3: quercetin. *Altern Med Rev* 2000; **5**: 196-208
- 8 **Kioka N**, Tsubota J, Kakehi Y, Komano T, Gottesman MM, Pastan I, Ueda K. P-glycoprotein gene (MDR1) cDNA from human adrenal: normal P-glycoprotein carrier Gly¹⁸⁵ with an altered pattern of multidrug resistance. *Biochem Biophys Res Commun* 1989; **162**: 224-231
- 9 **Becker K**, Pan D, Whitley CB. Real-time quantitative polymerase chain reaction to assess gene transfer. *Hum Gene Ther* 1999; **10**: 2559-2566
- 10 **Takara K**, Tanigawara Y, Komada F, Nishiguchi K, Sakaeda T, Okumura K. Cellular pharmacokinetic aspects of reversal effect of itraconazole on P-glycoprotein-mediated resistance of anticancer drugs. *Biol Pharm Bull* 1999; **22**: 1355-1359
- 11 **Lown KS**, Mayo RR, Leichtman AB, Hsiao HL, Turgeon DK, Schmiedlin-Ren P, Brown MB, Guo W, Rossi SJ, Benet LZ, Watkins PB. Role of intestinal P-glycoprotein (mdr1) in interpatient variation in the oral bioavailability of cyclosporine. *Clin Pharmacol Ther* 1997; **62**: 248-260
- 12 **Shapiro AB**, Ling V. Stoichiometry of coupling of rhodamine 123 transport to ATP hydrolysis by P-glycoprotein. *Eur J Biochem* 1998; **254**: 189-193
- 13 **Ambudkar SV**, Dey S, Hrycyna CA, Ramachandra M, Pastan I, Gottesman MM. Biochemical, cellular, and pharmacological aspects of the multidrug transporter. *Annu Rev Pharmacol Toxicol* 1999; **39**: 361-398
- 14 **Sparreboom A**, van Asperen J, Mayer U, Schinkel AH, Smit JW, Meijer DK, Borst P, Nooijen WJ, Beijnen JH, van Tellingen O. Limited oral bioavailability and active epithelial excretion of paclitaxel (Taxol) caused by P-glycoprotein in the intestine. *Proc Natl Acad Sci U S A* 1997; **94**: 2031-2035
- 15 **Kim RB**, Fromn MF, Wandel C, Leake B, Wood AJ, Roden DM, Wilkinson GR. The drug transporter P-glycoprotein limits oral absorption and brain entry of HIV-1 protease inhibitors. *J Clin Invest* 1998; **101**: 289-294
- 16 **Polli JW**, Jarrett JL, Studenberg SD, Humphreys JE, Dennis SW, Brouwer KR, Woolley JL. Role of P-glycoprotein on the CNS disposition of amprenavir (141W94), an HIV protease inhibitor. *Pharm Res* 1999; **16**: 1206-1212
- 17 **Verschraagen M**, Koks CH, Schellens JH, Beijnen JH. P-glycoprotein system as a determinant of drug interactions: the case of digoxin-verapamil. *Pharmacol Res* 1999; **40**: 301-306
- 18 **Schwarz UI**, Gramatte T, Krappweis J, Oertel R, Kirch W. P-glycoprotein inhibitor erythromycin increases oral bioavailability of talinolol in humans. *Int J Clin Pharmacol Ther* 2000; **38**: 161-167
- 19 **Walgren RA**, Walle UK, Walle T. Transport of quercetin and its glucosides across human intestinal epithelial Caco-2 cells. *Biochem Pharmacol* 1998; **55**: 1721-1727

Edited by Zhu LH and Wang XL Proofread by Xu FM

Diagnosis of intestinal acariasis with avidin-biotin system enzyme-linked immunosorbent assay

Rong-Bo Zhang, Yong Huang, Chao-Pin Li, Yu-Bao Cui

Rong-Bo Zhang, Chao-Pin Li, Yu-Bao Cui, Department of Etiology and Immunology, School of Medicine, Anhui University of Science and Technology, Huainan 232001, Anhui Province, China
Yong Huang, Shandong Institute of Parasitic Diseases, Jining 272033, Shandong Province, China

Correspondence to: Dr. Chao-Pin Li, Department of Etiology and Immunology, School of Medicine, Anhui University of Science and Technology, Huainan 232001, Anhui Province, China. cpli@aust.edu.cn

Telephone: +86-554-6658770 **Fax:** +86-554-6662469

Received: 2003-08-02 **Accepted:** 2003-09-18

Abstract

AIM: To explore the value of avidin-biotin system enzyme-linked immunosorbent assay (ABC-ELISA) in diagnosis of intestinal acariasis.

METHODS: Mite-specific IgG levels in serum of 48 patients with intestinal acariasis were measured with ABC-ELISA. The sensitivity of this method was compared with that of staphylococcal protein A enzyme-linked immunosorbent assay (SPA-ELISA).

RESULTS: The positive rate of mite-specific IgG detected with ABC-ELISA and SPA-ELISA was 89.58% (43/48) and 56.25% (27/48), respectively. The positive rate with ABC-ELISA was statistically higher than that with SPA-ELISA ($\chi^2=13.50$, $P<0.01$).

CONCLUSION: ABC-ELISA is an effective method for the diagnosis of intestinal acariasis.

Zhang RB, Huang Y, Li CP, Cui YB. Diagnosis of intestinal acariasis with avidin-biotin system enzyme-linked immunosorbent assay. *World J Gastroenterol* 2004; 10(9): 1369-1371
<http://www.wjgnet.com/1007-9327/10/1369.asp>

INTRODUCTION

Mites could live in intestinal tract and cause intestinal acariasis with most frequent symptoms of abdominal pain, diarrhea and pyohemofecia^[1-3]. Intestinal acariasis is traditionally diagnosed by identification of adult or larval mites, eggs or hypopus in either single or multiple fecal specimens under microscopy. The detection of the parasites is increased on examination of multiple fecal samples obtained on three different days. However, it is not easy to detect mites technically. Thus, the present study intended to develop and evaluate an enzyme-linked immunosorbent assay for mite-specific antibody detection in serum samples using *Dermatophagoides farinae* extract.

MATERIALS AND METHODS

Serum

A total of 78 serum specimens were collected from 48 patients with intestinal acariasis and 30 health blood donors. All of the

subjects investigated were asked to provide stools for detection of mites by saturated saline floatation method. The 48 patients with mites in stools were grouped as experimental group, while the health blood donors without mites as control group.

Reagents

Reagents for ABC-ELISA and SPA-ELISA were provided by Shanghai Institute of Biological Products (Batch No. 990004 and 990012). *Dermatophagoides farinae* extract was made according to NIBSC82/518 approved by World Health Organization (WHO) in 1984. The mites were cultured in the initial medium for several months. A 48-h maceration in a borate buffer (pH 8.5) was centrifuged. The supernatant was neutralized and precipitated with a series of acetone. The precipitated fraction at 800 mL/L acetone was isolated, washed and dried. This purified extract was lyophilized or stored as a solution in the presence of 500 mL/L glycerol and 50 mL/L phenol^[4-7].

Methods

ABC-ELISA procedure Initially 0.1 mL *Dermatophagoides farinae* extract with protein concentrations of 62.5 µg/mL was added in each well on a 40-well plate coated with enzyme, and the plate was placed at 4 °C overnight. Then the plate was washed with PBS (pH=7.4), sera of the patients with intestinal acariasis were diluted at 1:40 and added in duplicated wells, and incubated in water bath at 37 °C for 60 min. Following washing of the plate, bio-SAH IgG at the concentration of 1:40 was added and incubated at 37 °C for 60 min, avidin-HRP at the concentration of 1:20 was added for reaction at 37 °C for 30 min, and the substrate OPD-H₂O₂ was added and incubated at 37 °C for 30 min. Lastly, 2 mol/L H₂SO₄ was added to terminate the reaction. Sera of the control group were detected with the same procedure^[8,9].

SPA-ELISA procedure Concentrations of antigen and sera dilution in SPA-ELISA method were similar to those in ABC-ELISA. SPA-ELISA was performed as routine. Values of optic densities (OD) in each well were determined, the value of 2.1 times or more of the negative control was considered as positive.

RESULTS

General data

A total of 48 patients (male 32 and female 16) with intestinal acariasis were selected as mites were found in their stools. The 48 patients consisted of 13 workers in traditional Chinese medical storehouses, 22 workers in rice storehouse or mill, 8 miners, 2 workers in machine factory and 3 with other occupations. The mites in stool samples included *Acarus siro*, *Tyrophagus putrescentiae*, *Dermatophagoides farinae*, *D. pteronyssinus*, *Glycyphagus domesticus*, *G. ornatus*, *Carpoglyphus lactis* and *Tarsonemus granaries*.

ABC-ELISA data

In ABC-ELISA, the mean OD value of mite-specific IgG in sera of the 48 patients was 0.358±0.124 (0.176-0.615), while that in 30 controls was 0.112±0.065 (0.085-0.253). The Absorbent values in 43 of 48 patients were at least 2.1 times of 0.112, the positive

rate of the patients detected by ABC-ELISA was 89.58%. Interestingly, the A value of one case in normal control group was 0.253, and the false positive rate was 3.33%.

SPA-ELISA data

In SPA-ELISA, the mean OD value of mite-specific IgG in sera of the 48 patients was 0.225 ± 0.147 (0.133-0.574) and that in the control group was 0.078 ± 0.047 (0.043-0.172). The A values in 37 patients were at least 2.1 times of 0.078, the positive rate of the patients detected by SPA-ELISA was 56.25%. However, the A values of 2 cases in control group were 0.168 and 0.172, respectively, which were higher than 0.1638. The false positive rate in SPA-ELISA was 6.67%.

Comparison between ABC-ELISA data and SPA-ELISA data

The positive rate of the patients detected by ABC-ELISA and SPA-ELISA was 89.58% (43/48) and 56.25% (27/48) with a significant difference ($\chi^2=13.50, P<0.01$). Although only 25 cases were positive in both ABC-ELISA and SPA-ELISA, the positive number of patients was 45 (93.75%) by ABC-ELISA or SPA-ELISA (Table 1).

Table 1 Intestinal acariasis detected with ABC-ELISA and SPA-ELISA

Methods	ABC-ELISA method (+)	ABC-ELISA method (-)	Total
SPA-ELISA method (+)	25	2	27 ^b
SPA-ELISA method (-)	18	3	21
Total	43 ^b	5	48

^b: $\chi^2=13.50, P<0.01$.

DISCUSSION

ABC-ELISA and SPA-ELISA were used to detect mite-specific antibody IgG in serum samples from 48 patients with intestinal acariasis, and the positive rate in ABC-ELISA and SPA-ELISA was 89.58% and 56.25%, respectively. ABC-ELISA had high specificity in diagnosis of intestinal acariasis. Moreover, ABC-ELISA in detection of mite-specific antibody was easy to perform, inexpensive, and numerous samples could be performed simultaneously. The test could be carried out quickly for the diagnosis, particularly for individuals who suffered from recurrent diarrhea, chronic abdominal pain, malabsorption and stunting due to infection.

The occurrence of false positive in two methods in diagnosis of intestinal acariasis might be associated with mites' invasive locus, stool examination techniques and dilution of sera. In addition to gastrointestinal tract, acaroid mites could infest other organs of the human body such as respiratory tract and urinary tract, no matter where they were parasitized, mite-specific antibody would occur in peripheral blood^[10-18]. Although saturated saline floatation method is useful in examination of feces, some large and heavy mites may be missed because of difficult drift. Sera dilution at 1:40 in the present study was lower than that in routine ELISA with dilution at 1:100 to 1:200. It was suggested that much more times repeating stool examination should be carried out in the normal control group to avoid false positive detection^[19-24].

Our study showed 8 species of mites in human stools. We used *Dermatophagoides farinae* extract as coating antigen only, which might decrease the detectable rates of mite-specific antibody, because common antigen might exist in *Dermatophagoides farinae* and other seven species of mites^[25-28]. In addition, the number of mites in intestinal tract might affect the levels of mite-specific antibodies and detectable rates. In

conclusion, ABC-ELISA method is effective in diagnosis of intestinal acariasis.

REFERENCES

- 1 **Li CP**, Wang J. Intestinal acariasis in Anhui Province. *World J Gastroenterol* 2000; **6**: 597-600
- 2 **Li CP**, Cui YB, Wang J, Yang QG, Tian Y. Acaroid mite, intestinal and urinary acariasis. *World J Gastroenterol* 2003; **9**: 874-877
- 3 **Li CP**, Wang KX. A study on treatment of intestinal acariasis. *Shijie Huaren Xiaohua Zazhi* 2000; **8**: 919-920
- 4 **Nuttall TJ**, Lamb JR, Hill PB. Characterization of major and minor *Dermatophagoides* allergens in canine atopic dermatitis. *Res Vet Sci* 2001; **71**: 51-57
- 5 **Basomba A**, Tabar AI, de Rojas DH, Garcia BE, Alamar R, Olaguibel JM, del Prado JM, Martin S, Rico P. Allergen vaccination with a liposome-encapsulated extract of *Dermatophagoides pteronyssinus*: a randomized, double-blind, placebo-controlled trial in asthmatic patients. *J Allergy Clin Immunol* 2002; **109**: 943-948
- 6 **Akcakaya N**, Hassanzadeh A, Camcioglu Y, Cokugras H. Local and systemic reactions during immunotherapy with adsorbed extracts of house dust mite in children. *Ann Allergy Asthma Immunol* 2000; **85**: 317-321
- 7 **Hillier A**, Kwochka KW, Pinchbeck LR. Reactivity to intradermal injection of extracts of *Dermatophagoides farinae*, *Dermatophagoides pteronyssinus*, house dust mite mix, and house dust in dogs suspected to have atopic dermatitis: 115 cases (1996-1998). *J Am Vet Med Assoc* 2000; **217**: 536-540
- 8 **Guo H**, Zhao ZF, Shi DZ. A study on the culture medium antigens of *Cystercercus cellulosa* for detecting antibodies of cysticercosis by means of ABC-ELISA. *Southeast Asian J Trop Med Public Health* 1997; **28**(Suppl 1): 125-127
- 9 **Koldas M**, Uras F. Avidin-biotin ELISA for measurement of prothrombin in human plasma. *Thromb Res* 2001; **102**: 221-227
- 10 **Beco L**, Petite A, Olivry T. Comparison of subcutaneous ivermectin and oral moxidectin for the treatment of notoedric acariasis in hamsters. *Vet Rec* 2001; **149**: 324-327
- 11 **Hiraoka E**, Sato T, Shirai W, Kimura J, Nogami S, Itou M, Shimizu K. A case of pulmonary acariasis in lung of Japanese macaque. *J Vet Med Sci* 2001; **63**: 87-89
- 12 **van der Geest LP**, Elliot SL, Breeuwer JA, Beerling EA. Diseases of mites. *Exp Appl Acarol* 2000; **24**: 497-560
- 13 **Hammerberg B**, Bevier D, DeBoer DJ, Olivry T, Orton SM, Gebhard D, Vaden SL. Auto IgG anti-IgE and IgG x IgE immune complex presence and effects on ELISA-based quantitation of IgE in canine atopic dermatitis, demodectic acariasis and helminthiasis. *Vet Immunol Immunopathol* 1997; **60**: 33-46
- 14 **Morris DO**, Dunstan RW. A histomorphological study of sarcoptic acariasis in the dog: 19 cases. *J Am Anim Hosp Assoc* 1996; **32**: 119-124
- 15 **Jungmann P**, Guenet JL, Cazenave PA, Coutinho A, Huerre M. Murine acariasis: I. Pathological and clinical evidence suggesting cutaneous allergy and wasting syndrome in BALB/c mouse. *Res Immunol* 1996; **147**: 27-38
- 16 **Jungmann P**, Freitas A, Bandeira A, Nobrega A, Coutinho A, Marcos MA, Minoprio P. Murine acariasis. II. Immunological dysfunction and evidence for chronic activation of Th-2 lymphocytes. *Scand J Immunol* 1996; **43**: 604-612
- 17 **Ponsonby AL**, Kemp A, Dwyer T, Carmichael A, Couper D, Cochrane J. Feather bedding and house dust mite sensitization and airway disease in childhood. *J Clin Epidemiol* 2002; **55**: 556-562
- 18 **Paufler P**, Gebel T, Dunkelberg H. Quantification of house dust mite allergens in ambient air. *Rev Environ Health* 2001; **16**: 65-80
- 19 **Gonin P**, Trudel L. Detection and differentiation of *Entamoeba histolytica* and *Entamoeba dispar* isolates in clinical samples by PCR and enzyme-linked immunosorbent assay. *J Clin Microbiol* 2003; **41**: 237-241
- 20 **Molinari JL**, Garcia-Mendoza E, de la Garza Y, Ramirez JA, Sotelo J, Tato P. Discrimination between active and inactive

- neurocysticercosis by metacestode excretory/secretory antigens of *Taenia solium* in an enzyme-linked immunosorbent assay. *Am J Trop Med Hyg* 2002; **66**: 777-781
- 21 **Levett PN**, Branch SL. Evaluation of two enzyme-linked immunosorbent assay methods for detection of immunoglobulin M antibodies in acute leptospirosis. *Am J Trop Med Hyg* 2002; **66**: 745-748
- 22 **Van Gool T**, Vetter H, Vervoort T, Doenhoff MJ, Wetsteyn J, Overbosch D. Serodiagnosis of imported schistosomiasis by a combination of a commercial indirect hemagglutination test with *Schistosoma mansoni* adult worm antigens and an enzyme-linked immunosorbent assay with *S. mansoni* egg antigens. *J Clin Microbiol* 2002; **40**: 3432-3437
- 23 **Odashima NS**, Takayanagui OM, Figueiredo JF. Enzyme linked immunosorbent assay (ELISA) for the detection of IgG, IgM, IgE and IgA against *Cysticercus cellulosae* in cerebrospinal fluid of patients with neurocysticercosis. *Arq Neuropsiquiatr* 2002; **60**: 400-405
- 24 **Starke-Buzetti WA**, Machado RZ, Zocoller-Seno MC. An enzyme-linked immunosorbent assay (ELISA) for detection of antibodies against *Toxocara vitulorum* in water buffaloes. *Vet Parasitol* 2001; **97**: 55-64
- 25 **Varela J**, Ventas P, Carreira J, Barbas JA, Gimenez-Gallego G, Polo F. Primary structure of Lep d I, the main *Lepidoglyphus destructor* allergen. *Eur J Biochem* 1994; **225**: 93-98
- 26 **Kemp SF**, Lockey RF, Fernandez-Caldas E, Arlian LG. Skin test and crossreactivity studies with *Euroglyphus maynei* and *Dermatophagoides pteronyssinus*. *Clin Exp Allergy* 1997; **27**: 893-897
- 27 **Garcia-Robaina JC**, Eraso E, De la Torre F, Guisantes J, Martinez A, Palacios R, Martinez J. Extracts from various mite species contain cross-reactive and noncross-reactive IgE epitopes. A RAST inhibition study. *J Investig Allergol Clin Immunol* 1998; **8**: 285-289
- 28 **Smith W**, Mills K, Hazell L, Hart B, Thomas W. Molecular analysis of the group 1 and 2 allergens from the house dust mite, *Euroglyphus maynei*. *Int Arch Allergy Immunol* 1999; **118**: 15-22

Edited by Ren SY and Wang XL **Proofread by** Xu FM

Catheterization-associated complications of intraperitoneal chemotherapy in advanced gastric cancer

Meng Ye, Hong-Ming Pan, Hai-Yun Wang, Fang Lou, Wei Jin, Yu Zheng, Jin-Ming Wu

Meng Ye, Hong-Ming Pan, Hai-Yun Wang, Fang Lou, Wei Jin, Yu Zheng, Jin-Ming Wu, Center for Oncology, Sir Run Run Shaw Hospital, Zhejiang University, Hangzhou 310016, Zhejiang Province, China

Correspondence to: Professor Hong-Ming Pan, Center for Oncology, Sir Run Run Shaw Hospital, Zhejiang University, Hangzhou 310016, Zhejiang Province, China. panhongming@163.net

Telephone: +86-571-86090073-3121 **Fax:** +86-571-86044817

Received: 2003-06-30 **Accepted:** 2003-07-30

Abstract

AIM: To assess the catheterization-associated complications during intraperitoneal chemotherapy (IPCT) for advanced gastric cancer.

METHODS: From 1998 to 2002, 80 patients with advanced gastric cancer received a total of 320 courses of IPCT using a large bore central venous catheter and associated complications were analyzed.

RESULTS: Catheterization-associated complications occurred in 11 of the 80 patients (13.8%), including abdominal pain caused by catheter in 2 cases (0.63%), insertion failure in 2 cases (0.63%), bowel perforation in 1 case (0.31%) and abdominal pain during chemotherapy in 6 cases (1.88%). No serious complications required surgical intervention.

CONCLUSION: IPCT using central venous catheters can be performed safely and simply without severe associated complications.

Ye M, Pan HM, Wang HY, Lou F, Jin W, Zheng Y, Wu JM. Catheterization-associated complications of intraperitoneal chemotherapy in advanced gastric cancer. *World J Gastroenterol* 2004; 10(9): 1372-1374

<http://www.wjgnet.com/1007-9327/10/1372.asp>

INTRODUCTION

Gastrointestinal tumor is quite common. In China, the morbidity of gastric cancer is the leading cause of malignant tumors. For non-advanced gastric cancer, surgical removal is the first choice, but for advanced gastric cancer, the outcome of surgical resection remains unsatisfactory. Fifty percent of gastric cancer patients have local recurrence or long distance metastasis after radical surgery within 5 years. The common sites of gastric cancer recurrence or metastasis are the resection site, liver and peritoneal surfaces^[1-4]. It was reported that intraperitoneal chemotherapy could result in markedly increased local drug concentration, and had favorable clinical results in preventing recurrence and metastasis of gastric cancer after surgical treatment, but some complications were reported by using Tenckhoff catheter in IPCT^[5-7]. From March 1998 to June 2002, 80 patients with advanced gastric cancer were treated by central venous catheterization during intraperitoneal chemotherapy (IPCT) after radical gastrectomy in SRRSH Cancer Center. The

main purpose of this study was to analyze the complications of central venous catheterization during IPCT.

MATERIALS AND METHODS

Patients

Between March 1998 and June 2002, 80 patients with advanced gastric cancer were treated in SRRSH Cancer Center. Forty-eight cases were males and 31 females aged 29 to 71 years (median 43.5 years). Patients in stage III_A were 18 cases, stage III_B 29 cases, stage IV 33 cases. The patients were treated with a total of 320 courses of IPCT. Each patient received at least 3 courses of IPCT (mean 4 courses for each patient).

Peritoneal catheters and methods

Single cavity central venous catheters were produced by Arrow Raulerson Syring Ltd, USA. Transparent protecting patches and heparin caps were produced by 3 mol/L Health Care Ltd, USA. As there are no large vessels in this site, puncture site is usually chosen at the cross-point of left midclavicular line and navel line, which is located at outer edge of rectus abdominis muscle. Two percent lidocaine was used for local anesthesia, then a conducting needle was put into the peritoneal cavity, after a steel string was put into peritoneal cavity though the conducting needle. The needle was taken out and the central venous catheter was put into the peritoneal cavity following the steel string after the abdominal wall was dilated. Then 100 mL normal saline was administrated though the catheter, if nothing abnormal was observed, and a heparin cap was put on the top of the catheter and the catheter was fixed to the abdominal wall.

The regimen of intraperitoneal chemotherapy was HCPT+5-FU+CF+VP-16, the dose of chemotherapeutic agents was 8 mg/m² for HCPT, 375 mg/m² for 5-FU, 100 mg for leucovorin (CF), 80 mg/m² for etoposide (VP-16) for three days. HCPT was administrated though peritoneal cavity, other agents were administrated though peripheral vein. Before chemotherapy started, 1 000 mL warm (42 °C) normal saline was administrated into the peritoneal cavity together with 10 mg DXM and 20 mL 20 g/L lidocaine. HCPT was dissolved in 500 mL of normal saline and instilled in the peritoneal cavity though the implanted catheter. Then 42 °C normal saline was instilled to the peritoneal cavity again, until the total volume reached 1 500 mL/m². Patients were asked to change their position every 15 min for 2 h after drug administration. Chemotherapy was given 2 wk after surgery, and repeated every 3 wk with the same regimen. The central venous catheter was taken out after each cycle of chemotherapy, a new catheter was put into peritoneal cavity just before the next cycle of IPCT started.

RESULTS

The complications associated with catheterization during IPCT in this series were common and mild. Moderate to severe pain induced by catheterization occurred in 2 cases (0.63%). Failure in catheterization because of intraabdominal adhesion occurred in 2 cases (0.63%), but the catheter was successfully put into peritoneal cavity through the other side of abdominal wall. Bowel perforation occurred in one case (0.31%) possibly due

to severe intraabdominal adhesion after surgery, and the catheter was put into bowel cavity. This patient received systemic chemotherapy instead of IPCT afterwards, and antibiotics were given to him. He had no signs of peritonitis during the procedure. Moderate pain during chemotherapy occurred in 6 cases (1.88%). There was no incidence of severe complications such as intestinal obstruction, peritonitis, intestinal hemorrhage, leakage of peritoneal fluid and anastomotic stoma fistula (Table 1).

Table 1 Catheterization-associated complications

Complications	Cases (n=320, %)
Pain by catheterization	2 (0.63)
Insertion failure	2 (0.63)
Bowel perforation	1 (0.31)
Pain during chemotherapy	6 (1.88)

DISCUSSION

Postoperative IPCT should be started early^[8-11]. Because surgery for gastrointestinal cancer is associated with an extremely high rate of dissemination within the peritoneal cavity and seeding on peritoneum, the resection site and abraded peritoneal surfaces are common sites of tumor cell seeding, early postoperative IPCT lets all intraabdominal surfaces expose to intraperitoneal chemotherapy agents. Because all adhesions are lysed at this time, the response rate of minor metastatic lesions on peritoneal surface to the chemotherapy agents can be 100%. Besides, tumor burden is light at this time according to tumor cell proliferative kinetics, chemotherapy agents can not only kill dissociative tumor cells in peritoneal cavity, but also kill inflammatory cells in peritoneal cavity, thus decreasing the releasing of cellular factors and preventing their effect on tumor cell proliferation. Regional chemotherapy could result in markedly increased local responses without compromising systemic effects^[12-14]. Studies of pharmacokinetics of IPCT also showed advantages. Sugarbaker^[15] summarized the pharmacokinetics of 4 kinds of chemotherapy agents often used in IPCT, the area under the curve (AUC) within peritoneal fluid compared with plasma of these agents was as follows, 5-FU 150/1, MMC 72/1, ADM 205/1, and DDP 20/1. There was an obvious difference between AUC within peritoneal fluid and AUC within plasma.

Several methods could be used in IPCT^[7,16]. The catheters commonly used are Tenckhoff catheter and single peritoneal cavity catheter. Tenckhoff catheter is popular in Western countries. After completing the surgical procedure and prior to closing the abdominal wall, Tenckhoff catheter is placed through the abdominal wall and then a Dacron cuff is fixed subcutaneously. A needle is inserted into the Dacron cuff during chemotherapy. The disadvantage of this method is that the catheter is left in the peritoneal cavity for a long period, and there are some complications. Esquivel *et al.*^[17] reported that in 44 patients who received IPCT during the first day to fifth day after surgery, 13% of the patients had pneumonia, 9% bleeding after surgery, 9% intestinal fistula, 7% a prolonged duration of intubation, 2% biliary fistula, 2% anastomotic stoma fistula, and 2% pancreatitis. The total complication morbidity was 37%, 17% of the complications were related to bowel function. Topuz *et al.*^[18] also reported that there were 39 patients in 205 cycles of intraperitoneal chemotherapy, severe abdominal pain was in 4 patients (10.3%), peritonitis and coloperitoneal fistula each in 1 patient (2.6%), catheter obstruction in 3 patients (7.7%) and colon puncture in 4 patients (10.3%). Sakuragi *et al.*^[19] did IPCT in 78 patients using Tenckhoff catheter, the total cycles were 365. Among them, 27 (34.6%) experienced IPCT related complications, 17 (21.8%) had extensive intraabdominal

adhesion, 13 (16.7%) had local infection around the reservoir, 3 (3.8%) had an abscess at the site of the implanted port of the catheter, 3 (3.8%) had catheter obstruction, one (1.3%) had ileus, one (1.3%) had perforation of small intestine, one (1.3%) underwent opening of the wound at the site of catheter implantation due to bleeding.

We used central venous catheter in IPCT, the procedure of catheterization was easy to master. Meanwhile it was not necessary to leave the catheter for a long time, the catheter could be taken out 2-3 d after chemotherapy, which could improve the life quality of patients. Moreover, central venous catheter was used only one time with few complications. In fact, our patients had no severe complications such as intestinal perforation, intestinal bleeding, peritonitis, anastomotic stoma fistula and implantation site infection. The morbidity of complications in our group was 13.75%, much lower than reported in other documents. Pain after catheterization was due to the length of catheter into the peritoneal cavity, and the pain could be relieved after pulling out the catheter. The pain during chemotherapy could be relieved by administrating lidocaine and DXM into peritoneal cavity.

The reasons why our group has a low morbidity of complications are as follows. Chemotherapy was started two weeks after surgery instead of 5 d after surgery. Since surgical incision was healed 2 wk after surgery, many complications of IPCT were avoided by starting chemotherapy 2 wk after surgery. Besides, statistical analysis showed that there was no difference in response rate (data not shown). Tenckhoff catheter used by Sakuragi *et al.*^[19] had to put in the peritoneal cavity for a long period and there also must be a drainage system or an outflow tube. But we used central venous catheter only one time and did not need an outflow tube and the chemotherapy agents of IPCT were spontaneously absorbed by peritoneum. Clinical observation revealed that intraperitoneal fluid could be absorbed spontaneously 2 or 3 d after chemotherapy. Radical gastrectomy has a great surgical scope and can cause severe intraabdominal adhesion which can limit intraperitoneal fluid to flow freely. Sugarbaker *et al.*^[15] thought this would affect the distribution of chemotherapy agents in peritoneal cavity, and would affect chemotherapy agents to contact with peritoneum. If there was not enough fluid in the peritoneal cavity, the fluid could not flow freely in peritoneal cavity because of resistance. Though patients changed their position frequently, chemotherapy agents could not distribute to the whole peritoneal cavity, thus decreasing the response rate. Only a large volume of fluid causing abdominal distension could make chemotherapy agents distribute evenly in peritoneal cavity^[20]. Therefore, 1 500-2 000 mL fluid should be given to patients every time during chemotherapy, and the patients should change their position frequently in order to achieve chemotherapeutic effect. Besides, a large volume of fluid can decrease the incidence of complications such as abdominal pain, intestinal perforation, intestinal bleeding, ileus, peritonitis and anastomotic stoma fistula.

In conclusion, it is safe and convenient to use central venous catheters in intraperitoneal chemotherapy and it also has less side effects and fewer complications.

REFERENCES

- 1 Earle CC, Maroun J, Zuraw L. Neoadjuvant or adjuvant therapy for resectable gastric cancer? A practice guideline. *Can J Surg* 2002; **45**: 438-446
- 2 Hu JK, Chen ZX, Zhou ZG, Zhang B, Tian J, Chen JP, Wang L, Wang CH, Chen HY, Li YP. Intravenous chemotherapy for resected gastric cancer: meta-analysis of randomized controlled trials. *World J Gastroenterol* 2002; **8**: 1023-1028
- 3 Jeung HC, Rha SY, Jang WI, Noh SH, Chung HC. Treatment of advanced gastric cancer by palliative gastrectomy,

- cytoreductive therapy and postoperative intraperitoneal chemotherapy. *Br J Surg* 2002; **89**: 460-466
- 4 **Yagi Y**, Seshimo A, Kameoka S. Prognostic factors in stage IV gastric cancer: univariate and multivariate analyses. *Gastric Cancer* 2000; **3**: 71-80
- 5 **Fu QG**, Meng FD, Shen XD, Guo RX. Efficacy of intraperitoneal thermochemotherapy and immunotherapy in intraperitoneal recurrence after gastrointestinal cancer resection. *World J Gastroenterol* 2002; **8**: 1019-1022
- 6 **Witkamp AJ**, de Bree E, Van Goethem R, Zoetmulder FA. Rationale and techniques of intra-operative hyperthermic intraperitoneal chemotherapy. *Cancer Treat Rev* 2001; **27**: 365-374
- 7 **Averbach AM**, Jacquet P. Strategies to decrease the incidence of intra-abdominal recurrence in resectable gastric cancer. *Br J Surg* 1996; **83**: 726-733
- 8 **Noh SH**, Yoo CH, Chung HC, Roh JK, Shin DW, Min JS. Early postoperative intraperitoneal chemotherapy with mitomycin C, 5-fluorouracil and cisplatin for advanced gastric cancer. *Oncology* 2001; **60**: 24-30
- 9 **Jeung HC**, Rha SY, Jang WI, Noh SH, Chung HC. Treatment of advanced gastric cancer by palliative gastrectomy, cytoreductive therapy and postoperative intraperitoneal chemotherapy. *Br J Surg* 2002; **89**: 460-466
- 10 **Maehara Y**, Baba H, Sugimachi K. Adjuvant chemotherapy for gastric cancer: a comprehensive review. *Gastric Cancer* 2001; **4**: 175-184
- 11 **Tsujitani S**, Fukuda K, Saito H, Kondo A, Ikeguchi M, Maeta M, Kaibara N. The administration of hypotonic intraperitoneal cisplatin during operation as a treatment for the peritoneal dissemination of gastric cancer. *Surgery* 2002; **131**(1Suppl): S98-104
- 12 **Yu W**, Whang I, Chung HY, Averbach A, Sugarbaker PH. Indications for early postoperative intraperitoneal chemotherapy of advanced gastric cancer: results of a prospective randomized trial. *World J Surg* 2001; **25**: 985-990
- 13 **Ceelen WP**, Hesse U, de Hemptinne B, Pattyn P. Hyperthermic intraperitoneal chemoperfusion in the treatment of locally advanced intra-abdominal cancer. *Br J Surg* 2000; **87**: 1006-1015
- 14 **Fujimoto S**, Takahashi M, Mutou T, Kobayashi K, Toyosawa T. Successful intraperitoneal hyperthermic chemoperfusion for the prevention of postoperative peritoneal recurrence in patients with advanced gastric carcinoma. *Cancer* 1999; **85**: 529-534
- 15 **Sugarbaker PH**. Peritoneal carcinomatosis: natural history and rational therapeutic interventions using intraperitoneal chemotherapy. *Cancer Treat Res* 1996; **81**: 149-168
- 16 **Yu W**, Whang I, Averbach A, Chang D, Sugarbaker PH. Morbidity and mortality of early postoperative intraperitoneal chemotherapy as adjuvant therapy for gastric cancer. *Am Surg* 1998; **64**: 1104-1108
- 17 **Esquivel J**, Vidal-Jove J, Steves MA, Sugarbaker PH. Morbidity and mortality of cytoreductive surgery and intraperitoneal chemotherapy. *Surgery* 1993; **113**: 631-636
- 18 **Topuz E**, Basaran M, Saip P, Aydinler A, Argon A, Sakar B, Tas F, Uygun K, Bugra D, Aykan NF. Adjuvant intraperitoneal chemotherapy with cisplatin, mitoxantrone, 5-fluorouracil, and calcium folinate in patients with gastric cancer: a phase II study. *Am J Clin Oncol* 2002; **25**: 619-624
- 19 **Sakuragi N**, Nakajima A, Nomura E, Noro N, Yamada H, Yamamoto R, Fujimoto S. Complications relating to intraperitoneal administration of cisplatin or carboplatin for ovarian carcinoma. *Gynecol Oncol* 2000; **79**: 420-423
- 20 **Sugarbaker PH**. Intraperitoneal chemotherapy and cytoreductive surgery for the prevention and treatment of peritoneal carcinomatosis and sarcomatosis. *Semin Surg Oncol* 1998; **14**: 254-261

Edited by Wang XL Proofread by Xu FM

Protective effect of doxorubicin induced heat shock protein 72 on cold preservation injury of rat livers

Hao Chen, Ying-Yan Yu, Ming-Jun Zhang, Xia-Xing Deng, Wei-Ping Yang, Jun Ji, Cheng-Hong Peng, Hong-Wei Li

Hao Chen, Xia-Xing Deng, Wei-Ping Yang, Cheng-Hong Peng, Hong-Wei Li, Department of Surgery and Center of Organ Transplantation, Ruijin Hospital, Shanghai Second Medical University, Shanghai 200025, China

Ying-Yan Yu, Jun Ji, Center of Organ Transplantation, Ruijin Hospital, Shanghai Second Medical University, Shanghai 200025, China

Ming-Jun Zhang, Animal Laboratory, Ruijin Hospital, Shanghai Second Medical University, Shanghai 200025, China

Correspondence to: Hao Chen, Department of Surgery and Center of Organ Transplantation, Ruijin Hospital, Shanghai Second Medical University, Shanghai 200025, China. chenhaodr@sohu.com

Telephone: +86-21-64370045 **Fax:** +86-21-64333548

Received: 2003-08-26 **Accepted:** 2003-10-22

Abstract

AIM: To observe the protective effect of heat shock protein 72 (HSP 72) induced by pretreatment of doxorubicin (DXR) on long-term cold preservation injury of rat livers.

METHODS: Sprague-Dawley rats were administered intravenously DXR at a dose of 1 mg/kg body mass in DXR group and saline in control group. After 48 h, the rat liver was perfused with cold Linger's and University of Wisconsin (UW) solutions and then was preserved in UW solution at 4 °C for 24, 36 and 48 h. AST, ALT, LDH and hyaluronic acid in preservative solution were determined. Routine HE, immunohistochemical staining for HSP 72 and electron microscopic examination of hepatic tissues were performed.

RESULTS: After 24, 36 and 48 h, the levels of AST, ALT and hyaluronic acid in preservative solution were significantly higher in control group than in DXR group ($P < 0.05$), while LDH level was not significantly different between the 2 groups ($P > 0.05$). Hepatic tissues in DXR group were morphologically normal and significantly injured in control group. HSP 72 was expressed in hepatocytes and sinusoidal endothelial cells in DXR group but not in control group.

CONCLUSION: Pretreatment of DXR may extend the time of rat liver cold preservation and keep liver alive. The expression of HSP 72 in liver can prevent hepatocytes and sinusoidal endothelial cells from long-term cold preservation injury.

Chen H, Yu YY, Zhang MJ, Deng XX, Yang WP, Ji J, Peng CH, Li HW. Protective effect of doxorubicin induced heat shock protein 72 on cold preservation injury of rat livers. *World J Gastroenterol* 2004; 10(9): 1375-1378

<http://www.wjgnet.com/1007-9327/10/1375.asp>

INTRODUCTION

The term of organ preservation has been extended enormously since Belzer invented University of Wisconsin (UW) solution in 1988^[1]. In liver transplantation, the use of UW solution doubles the time of liver cold preservation compared with the

use of Euro-Collins solution. But hepatic cold preservation reperfusion injury remains the important reason for the failure of liver transplantation^[2-5]. It was reported that cold preservation reperfusion injury in liver, kidney and lung could be prevented by the expression of heat shock protein, which was induced by heat shock reaction (HSR)^[6-8]. Kume *et al*^[9] reported that doxorubicin (DXR) could induce HSR, which attenuated hepatic warm ischemia reperfusion injury. DXR is a kind of cytotoxic agent and may induce HSR^[10]. Being administered intravenously, DXR was accumulated and metabolized in liver. As a result, semiquinone free radicals were produced, which could induce stress oxidative reaction and expression of HSP 72^[11]. Hela cells and cardiac cells could express HSP 72 by pretreatment of DXR *in vitro* in experiments^[12,13]. The aim of this study was to observe the protective effect of HSR induced by DXR on long-term hepatic cold preservation injury.

MATERIALS AND METHODS

Reagents

Doxorubicin was purchased from Shenzhen Main Luck Pharmaceuticals. Inc., China-Merian Corp., Japan. University of Wisconsin solution was purchased from Dupan Co., USA. HA RIA kit was purchased from Shanghai Ocean Research Biomedical Technology Center, China. Monoclonal antibody of HSP 72 was purchased from Oncogene Co. DAKO Envision™ kit was from Dako Co.

Animals

Male Sprague-Dawley rats weighing 200-300 g were purchased from Sino-British Sippr/BK Lab Animal Ltd. All rats were kept in animal quarters with controlled temperature (18-25 °C) and light (light on from 7 a.m. to 7 p.m.) and were fed with a standard laboratory chow and water in accordance with institutional animal care policies. Prior to the experimental procedure, the rats were fasted for 12 hours but allowed free access to water.

Experimental design

Thirty-six rats were randomly assigned into DXR group and control group. The rats in DXR group were injected intravenously DXR at a dose of 1 mg/kg body mass 48 h before the operation^[9], while those in control group were treated with 1 mL normal saline (NS). After being cold perfused orthotopically, the livers were preserved in UW solution for 24, 36 and 48 h.

Liver procurement and cold storage

Rat orthotopic liver cold perfusion was used according to the method described by Kamada and Calne^[14]. Under ether anesthesia, 2 mL of heparinized saline solution (250 units/mL) was injected intravenously. Laparotomy was performed via a midline incision. After the abdominal aorta was cannulated with a 14-gauge angiocatheter, the liver was flushed with 10 mL of Linger's solution at 4 °C. Simultaneously, the supra and infrahepatic vena cava were cut to enhance flushing of the liver. Then, 5 mL of Linger's solution, followed by 10 mL of

UW solution at 4 °C was progressively injected into portal vein. Finally the liver was excised and preserved in 40 mL of UW solution at 4 °C.

Hepatic enzyme assays of preservative solution

Alanine aminotransferase (ALT), aspartate aminotransferase (AST) and lactic dehydrogenase level (LDH) in the preservative solutions, collected at 24, 36 and 48 h after cold preservation, were determined by a standard biochemistry autoanalyzer (Backman DU 640).

Assessment of hyaluronic acid (HA) of preservative solution

HA in the preservative solutions collected at 24, 36 and 48 h after cold preservation was determined using a HA RIA kit according to the manufacturer's protocols.

Histology and immunohistochemical analysis for HSP 72

The liver specimens collected at 24, 36 and 48 h after cold preservation were fixed in buffered 10% formalin and embedded in paraffin. Tissue sections (4-µm thick) were stained with hematoxylin-eosin.

Immunohistochemical analysis was performed by using a mouse anti-HSP 72 monoclonal antibody at a dilution of 1:100, and rabbit anti-mouse IgG as a secondary antibody. Then the specimens were incubated with horseradish peroxidase-conjugated streptavidin complex. Diaminobenzidine was used as the substrate. The specimens were counterstained with hematoxylin. All specimens were examined under an optical microscope (Olympus BX51).

Transmission electron microscopical analysis

Liver fragments of approximately 1 mm×1 mm×2 mm were fixed in 20 g/L glutaraldehyde at 4 °C. After washed in phosphate buffer solution, fragments were postfixed with 10 g/L osmium tetroxide, dehydrated in graded alcohols, replaced in epoxy ethane and stained with uranyl acetate. All specimens were examined under an electron microscope (Hitachi 500).

Statistical analysis

Values are expressed as mean±SE. Intragroup analysis was performed by paired Student's *t* test. *P* value less than 0.05 was considered statistically significant.

RESULTS

ALT, AST and LDH level

ALT and AST levels were significantly higher in control group after preservation for 24, 36 and 48 h than in DXR group (*P*<0.05), but LDH level was not different between the 2 groups (*P*>0.05) (Table 1).

Table 1 Comparison of ALT, AST and LDH levels between two groups

Group	<i>n</i>	Term of storage	ALT (IU/L)	AST (IU/L)	LDH (IU/L)
Control	6	24 h	337.3±163.4 ^b	417.2±247.5 ^a	3 369.1±851.9 ^c
	6	36 h	589.8±237.3 ^a	744.5±317.6 ^a	3 623.2±907.1 ^c
	6	48 h	713.3±191.8 ^a	1 160.2±321.3 ^a	3 771.7±733.5 ^c
DXR	6	24 h	140.5±58.5	148.8±110.6	3 162.5±1442
	6	36 h	347.3±89	340.5±139.4	3 468.7±815.7
	6	48 h	406.0±79	733.3±394.4	3 549.8±894.1

^a*P*<0.05, ^b*P*<0.01, ^c*P*>0.05 vs DXR.

HA level

HA level was significantly higher in control group after

preservation for 24, 36 and 48 h than in DXR group (*P*<0.05) (Table 2).

Table 2 Comparison of HA levels between two groups

Group	<i>n</i>	Term of storage	HA (ng/mL)
Control	6	24 h	43.1±17.0 ^a
	6	36 h	91.2±19.8 ^b
	6	48 h	143.7±23.2 ^a
DXR	6	24 h	26.2±6.0
	6	36 h	44.2±7.8
	6	48 h	90.2±13.5

^a*P*<0.05, ^b*P*<0.01 vs DXR.

Histology and immunohistochemistry for HSP 72

After cold storage for 24 to 48 h, hepatocytes in control group were swelling, ballooning, vacuolizing and partly autolyzing while the majority of sinusoidal endothelial cells (SECs) also became swollen, rounded and detached from basement membrane and hepatic sinusoids were narrowed. In DXR group, hepatocytes remained normal and few SECs appeared swollen, rounded or detached.

After cold storage for 24 to 48 h, some hepatocytes and SECs expressed HSP 72 in DXR group but not in control group.

Transmission electron microscopical analysis

After cold storage for 24 to 48 h, hepatocytes in control group showed swollen mitochondria, fatty dots, and while cellular swelling, rounding, detachment from the matrix and nuclear condensation were seen in part of SECs. In DXR group, hepatocytes remained normal and few SECs appeared swollen, rounded or detached.

DISCUSSION

The use of University of Wisconsin solution extended the time of organ cold preservation to 24 h in theory^[15]. UW solution was designed to attenuate cell swelling, inhibit reactive oxygen intermediates (ROIs), offer substrates for synthesizing adenosine triphosphates (ATP) and prevent cells from absorbing ions of sodium and calcium^[16,17]. But in the course of cold storage, cells remained to be injured in different degrees with the extension of preservation time. In the period of liver cold storage, hepatocytes and SECs were all injured, especially the latter^[18,19].

During warm ischemia hepatocytes were the most vulnerable cells whereas SECs were less sensitive^[20]. But hepatocytes were less damaged during cold preservation^[21]. However, along with the extension of the time of cold storage, hepatocytes were also injured in different degrees. The mechanisms underlying hepatocyte injury during hypothermia storage were intracellular acidosis due to anaerobic glycolysis and lactate accumulation, drawback of protein synthesis and exhaustion of heparin and ATP which lessen the ability to resist rewarm ischemia and reperfusion damage^[21]. In morphology, changes of hepatocytes included swelling, ballooning and vacuolization. Although little loss of cell viability occurred after 24 h of storage in UW solution, the cellular functions were already injured^[22]. In this study, histological results showed that hepatocytes were apparently damaged in control group after cold storage for 36 to 48 h. In contrast, the shapes of hepatocytes were normal in DXR group. In preservation solution, ALT and AST levels in DXR group were significantly lower than in control group (*P*<0.05). These data indicated that pretreatment with DXR could evidently protect hepatocytes.

During hepatic cold ischemia, SECs were most susceptible

to hypothermia injury. Injuries of SECs were due to angiogenic factors and proteases, resulting in digestion of fibronectin, a key molecule linking collagen to the sinusoidal lining cell membrane integrin^[23]. In morphology, SECs became rounded, detached, and sloughed into the sinusoidal lumen^[24-26]. These changes were more distinct along with the prolongation of cold storage^[27]. But little loss of viability of SECs occurred after 24 h of storage in UW solution^[28]. This study indicated that SECs in both groups were injured after 24 to 48 h of cold storage in UW solution, but the degree of injury was significantly attenuated in DXR group than in control group. The shape of SECs was normal after 24 h and a small quantity of SECs became rounded, and detached after 36 to 48 h in DXR group. But in control group, SECs were obviously rounded and detached after 24 h, and the morphological changes became more significant after 36 to 48 h. On the other hand, hyaluronic acid level was significantly higher in control group than in DXR group ($P < 0.05$). Hyaluronic acid is a high-molecular-weight polysaccharide that could be rapidly and specifically degraded by SEC^[29]. Hyaluronic acid level was a sensitive index of SECs' injury^[30]. These results showed that pretreatment with DXR could protect SECs.

Cold storage of livers for more than 12 to 18 h carried the risk for graft failure^[31-34] and post-transplantation infection^[35]. In recent years, preconditioning has been used to prolong hepatic cold ischemia^[6,36-38]. The liver graft was subjected to an acute sublethal stress and this preconditioning could offer resistance to subsequent lethal injury by inducing the expression of heat shock proteins (HSPs). One of the important functions of HSPs was to protect cells and organs from a wide variety of damages such as hypothermia, ischemia, and ROIs^[39-41]. Cheng^[42] reported that pretreated by Zinc and heat shock, the expression of HSP 72 was markedly elevated after rat livers were stored in UW solution for 24 h. It was also reported that rat kidneys were preserved well successively for 45 h in cold UW solution^[43]. In our study, the protective effect of pretreatment of DXR on hepatic long-term cold storage injury might be attributed to induction of HSR and expression of HSP 72 in rat livers. HSR induced by DXR extended the time of hepatic cold storage to 48 h while morphological shape and functions of both hepatocytes and SECs remained commendable. The expressions of HSP 72 in hepatocytes and SECs were confirmed by immunohistochemical staining. It was clear that induction of HSP 72 in advance could make rat livers enter into stress state ahead of schedule and endure long-term cold ischemia injury afterwards.

In conclusion, these results demonstrate that pretreatment with doxorubicin could induce the expression of HSP 72 in rat livers. Thus pharmacological induction of HSR may be a successful method to prevent liver from long-term hypothermia preservation injury.

REFERENCES

- 1 **Belzer FO**, Kalayoglu M, D' Alessandro AM, Pirsch JD, Sollinger HW, Hoffmann R, Boudjema K, Southard JH. Organ preservation: experience with University of Wisconsin solution and plans for the future. *Clin Transplant* 1990; **4**: 73-77
- 2 **Bilzer M**, Gerbes AL. Preservation injury of the liver: mechanisms and novel therapeutic strategies. *J Hepatol* 2000; **32**: 508-515
- 3 **Jaeschke H**. Molecular mechanisms of hepatic ischemia-reperfusion injury and preconditioning. *Am J Physiol Gastrointest Liver Physiol* 2003; **284**: G15-26
- 4 **Serracino-Ingloff F**, Habib NA, Mathie RT. Hepatic ischemia-reperfusion injury. *Am J Surg* 2001; **181**: 160-166
- 5 **Kang KJ**. Mechanism of hepatic ischemia/reperfusion injury and protection against reperfusion injury. *Transplant Proc* 2002; **34**: 2659-2661
- 6 **Redaelli CA**, Tian YH, Schaffner T, Ledermann M, Baer HU, Dufour JF. Extended preservation of rat liver graft by induction of heme oxygenase-1. *Hepatology* 2002; **35**: 1082-1092
- 7 **Wagner M**, Cadetg P, Ruf R, Mazzucchelli L, Ferrari P, Redaelli CA. Heme oxygenase-1 attenuates ischemia/reperfusion induced apoptosis and improves survival in rat renal allografts. *Kidney Int* 2003; **63**: 1564-1573
- 8 **Hiratsuka M**, Yano M, Mora BN, Nagahiro I, Cooper JD, Patterson GA. Heat shock pretreatment protects pulmonary isografts from subsequent ischemia-reperfusion injury. *J Heart Lung Transplant* 1998; **17**: 1238-1246
- 9 **Kume M**, Yamamoto Y, Yamagami K, Ishikawa Y, Uchinami H, Yamaoka Y. Pharmacological hepatic preconditioning: involvement of 70-kDa heat shock proteins (HSP72 and HSP73) in ischaemic tolerance after intravenous administration of doxorubicin. *Br J Surg* 2000; **87**: 1168-1175
- 10 **Yee SB**, Pritsos CA. Comparison of oxygen radical generation from the reductive activation of doxorubicin, streptonigrin, and menadione by xanthine oxidase and xanthine dehydrogenase. *Arch Biochem Biophys* 1997; **347**: 235-241
- 11 **Trost LC**, Wallace KB. Stimulation of myoglobin-dependent lipid peroxidation by adriamycin. *Biochem Biophys Res Commun* 1994; **204**: 23-29
- 12 **Lee EK**, Regenold WT, Shapiro P. Inhibition of aldose reductase enhances HeLa cell sensitivity to chemotherapeutic drugs and involves activation of extracellular signal-regulated kinases. *Anticancer Drugs* 2002; **13**: 859-868
- 13 **Huber SA**. Heat-shock protein induction in adriamycin and picornavirus-infected cardiocytes. *Lab Invest* 1992; **67**: 218-224
- 14 **Kamada N**, Calne RY, Wight DG, Lines JG. Orthotopic rat liver transplantation after long-term preservation by continuous perfusion with fluorocarbon emulsion. *Transplantation* 1980; **30**: 43-48
- 15 **Belzer FO**, Southard JH. Principles of solid-organ preservation by cold storage. *Transplantation* 1988; **45**: 673-676
- 16 **Lemasters JJ**, Thurman RG. Reperfusion injury after liver preservation for transplantation. *Annu Rev Pharmacol Toxicol* 1997; **37**: 327-338
- 17 **Southard JH**, van Gulik TM, Ametani MS, Vreugdenhil PK, Lindell SL, Pienaar BL, Belzer FO. Important components of the UW solution. *Transplantation* 1990; **49**: 251-257
- 18 **Urata K**, Nguyen B, Brault A, Lavoie J, Rocheleau B, Huet PM. Decreased survival in rat liver transplantation with extended cold preservation: role of portal vein clamping time. *Hepatology* 1998; **28**: 366-373
- 19 **Otto G**, Wolff H, David H. Preservation damage in liver transplantation: electron-microscopic findings. *Transplant Proc* 1984; **16**: 1247-1248
- 20 **Noack K**, Bronk SF, Kato A, Gores GJ. The greater vulnerability of bile duct cells to reoxygenation injury than anoxia. Implications for the pathogenesis of biliary strictures after liver transplantation. *Transplantation* 1993; **56**: 495-500
- 21 **Clavien PA**, Harvey PR, Strasberg SM. Preservation and reperfusion injuries in liver allografts. An overview and synthesis of current studies. *Transplantation* 1992; **53**: 957-978
- 22 **Lichtman SN**, Lemasters JJ. Role of cytokines and cytokine-producing cells in reperfusion injury to the liver. *Semin Liver Dis* 1999; **19**: 171-187
- 23 **Upadhyia AG**, Harvey RP, Howard TK, Lowell JA, Shenoy S, Strasberg SM. Evidence of a role for matrix metalloproteinases in cold preservation injury of the liver in humans and in the rat. *Hepatology* 1997; **26**: 922-928
- 24 **McKeown CM**, Edwards V, Phillips MJ, Harvey PR, Petrunka CN, Strasberg SM. Sinusoidal lining cell damage: the critical injury in cold preservation of liver allografts in the rat. *Transplantation* 1988; **46**: 178-191
- 25 **Hansen TN**, Dawson PE, Brockbank KG. Effects of hypothermia upon endothelial cells: mechanisms and clinical importance. *Cryobiology* 1994; **31**: 101-106
- 26 **Marsh DC**, Lindell SL, Fox LE, Belzer FO, Southard JH. Hypothermic preservation of hepatocytes. Role of cell swelling. *Cryobiology* 1989; **26**: 524-534
- 27 **Fratte S**, Gendraut JL, Steffan AM, Kirn A. Comparative ultrastructural study of rat livers preserved in Euro-Collins or Uni-

- versity of Wisconsin solution. *Hepatology* 1991; **13**: 1173-1180
- 28 **Clavien PA**. Sinusoidal endothelial cell injury during hepatic preservation and reperfusion. *Hepatology* 1998; **28**: 281-285
- 29 **Laurent TC**, Fraser JR, Pertoft H, Smedsrod B. Binding of hyaluronate and chondroitin sulphate to liver endothelial cells. *Biochem J* 1986; **234**: 653-658
- 30 **Reinders ME**, van Wagenveld BA, van Gulik TM, Frederiks WM, Chamuleau RA, Endert E, Klopper PJ. Hyaluronic acid uptake in the assessment of sinusoidal endothelial cell damage after cold storage and normothermic reperfusion of rat livers. *Transpl Int* 1996; **9**: 446-453
- 31 **Figueras J**, Busquets J, Grande L, Jaurieta E, Perez-Ferreiro J, Mir J, Margarit C, Lopez P, Vazquez J, Casanova D, Bernardos A, De-Vicente E, Parrilla P, Ramon JM, Bou R. The deleterious effect of donor high plasma sodium and extended preservation in liver transplantation. A multivariate analysis. *Transplantation* 1996; **61**: 410-413
- 32 **Ploeg RJ**, D' Alessandro AM, Knechtle SJ, Stegall MD, Pirsch JD, Hoffmann RM, Sasaki T, Sollinger HW, Belzer FO, Kalayoglu M. Risk factors for primary dysfunction after liver transplantation-a multivariate analysis. *Transplantation* 1993; **55**: 807-813
- 33 **Furukawa H**, Todo S, Imventarza O, Casavilla A, Wu YM, Scotti-Foglieni C, Broznick B, Bryant J, Day R, Starzl TE. Effect of cold ischemia time on the early outcome of human hepatic allografts preserved with UW solution. *Transplantation* 1991; **51**: 1000-1004
- 34 **Adam R**, Bismuth H, Diamond T, Ducot B, Morino M, Astarcioglu I, Johann M, Azoulay D, Chiche L, Bao YM. Effect of extended cold ischaemia with UW solution on graft function after liver transplantation. *Lancet* 1992; **340**: 1373-1376
- 35 **Nuno J**, Cuervas-Mons V, Vicente E, Turrion V, Pereira F, Mora NP, Barrios C, Millan I, Ardaiz J. Prolonged graft cold ischemia: a risk factor for early bacterial and fungal infection in liver transplant recipients. *Transplant Proc* 1995; **27**: 2323-2325
- 36 **Takahashi Y**, Tamaki T, Tanaka M, Konoeda Y, Kawamura A, Katori M, Kakita A. Efficacy of heat-shock proteins induced by severe fasting to protect rat livers preserved for 72 hours from cold ischemia/reperfusion injury. *Transplant Proc* 1998; **30**: 3700-3702
- 37 **Kiemer AK**, Gerbes AL, Bilzer M, Vollmar AM. The atrial natriuretic peptide and cGMP: novel activators of the heat shock response in rat livers. *Hepatology* 2002; **35**: 88-94
- 38 **Kiemer AK**, Kulhanek-Heinze S, Gerwig T, Gerbes Vollmar AM. Stimulation of p38 MAPK by hormonal preconditioning with atrial natriuretic peptide. *World J Gastroenterol* 2002; **8**: 707-711
- 39 **Leppa S**, Sistonen L. Heat shock response-pathophysiological implications. *Ann Med* 1997; **29**: 73-78
- 40 **Morimoto RI**, Santoro MG. Stress-inducible responses and heat shock proteins: new pharmacologic targets for cytoprotection. *Nat Biotechnol* 1998; **16**: 833-838
- 41 **Santoro MG**. Heat shock factors and the control of the stress response. *Biochem Pharmacol* 2000; **59**: 55-63
- 42 **Cheng Y**, Liu Y, Liang J. Zinc is a potent heat shock protein inducer during liver cold preservation in rats. *Chin Med J* 2002; **115**: 1777-1779
- 43 **Redaelli CA**, Tien YH, Kubulus D, Mazzucchelli L, Schilling MK, Wagner AC. Hyperthermia preconditioning induces renal heat shock protein expression, improves cold ischemia tolerance, kidney graft function and survival in rats. *Nephron* 2002; **90**: 489-497

Edited by Zhu LH and Wang XL Proofread by Xu FM

Evaluation of effect of hybrid bioartificial liver using end-stage liver disease model

Qing Liu, Zhong-Ping Duan, Chun Huang, Chun-Hui Zhao

Qing Liu, Zhong-Ping Duan, Chun Huang, Chun-Hui Zhao, Artificial Liver Treatment and Training Center, Beijing Youan Hospital, Beijing 100054, China

Correspondence to: Qing Liu, Artificial Liver Treatment and Training Center, Beijing Youan Hospital, Beijing 100054, China. lqlq8@yahoo.com

Telephone: +86-10-63292211-2517

Received: 2002-08-06 **Accepted:** 2002-11-04

Abstract

AIM: To study the role of hybrid bioartificial liver (HBL) in clearing proinflammatory cytokines and endotoxin in patients with acute and sub-acute liver failure and the effects of HBL on systemic inflammatory syndrome (SIRS) and multiple organ dysfunction syndrome (MODS).

METHODS: Five cases with severe liver failure (3 acute and 2 subacute) were treated with HBL. The clinical signs and symptoms, total bilirubin (TBIL), serum ammonia, endotoxin TNF- α , IL-6 and prothrombin activity (PTA), cholinesterase (CHE) were recorded before, during and after treatment. The end-stage liver disease (MELD) was used for the study.

RESULTS: Two patients were bridged for spontaneous recovery and 1 patient was bridged for OLT successfully. Another 2 patients died on d 8 and d 21. The spontaneous recovery rate was 30.0%. PTA and CHE in all patients were significantly increased ($P < 0.01$), while the serum TBIL, endotoxin, TNF- α , IL-6 were decreased. MELD score (mean 43.6) predicted 100% deaths within 3 mo before treatment with HBL. After treatment with HBL, four out of 5 patients had decreased MELD scores (mean 36.6). The MELD score predicted 66% mortalities.

CONCLUSION: The proinflammatory cytokines (TNF α , IL-6 and endotoxin) can be significantly removed by hybrid bioartificial liver and HBL appears to be effective in blocking SIRS and MODS in patients with acute and sub-acute liver failure. MELD is a reliable measure for predicting short-term mortality risk in patients with end-stage liver disease. The prognostic result also corresponds to clinical outcome.

Liu Q, Duan ZP, Huang C, Zhao CH. Evaluation of effect of hybrid bioartificial liver using end-stage liver disease model. *World J Gastroenterol* 2004; 10(9): 1379-1381
<http://www.wjgnet.com/1007-9327/10/1379.asp>

INTRODUCTION

About 80% ICU deaths may be attributable to progressive multiple organ dysfunction (MODS). MODS is also a major cause of death in patients suffering from severe hepatitis. The sequela of systemic inflammatory syndrome (SIRS) is MODS. Hybrid bioartificial liver (HBL) is a well-known liver support system that is close to native liver in function. In the present

study our primary goals were to investigate the role of HBL in removing serum proinflammatory cytokines such as TNF α , IL-6, endotoxin and in blocking SIRS to MODS.

In this report, we used the validity of end-stage liver disease model as a disease severity index for patients with end-stage liver disease treated with bioartificial liver support system. The model was considered to be able to provide a reliable estimate of short-term survival over a wide range of liver diseases.

MATERIALS AND METHODS

Subjects

The Beijing Youan Hospital Ethics Committee approved the study and informed consent was obtained from all patients or their relatives. Five patients with severe hepatitis treated with HBL in our center from March, 2000 to June 2001 were involved in the study. Three of 5 patients were acute severe hepatitis and 2 of them were sub-acute hepatitis. All the 5 patients suffered from SIRS, 4 of them were complicated with 2-organ failure and only one patient were with 3-organ failure (Table 1). The criteria for severe hepatitis, SIRS and MODS were based on the recommendations of references 1-3^[1-3].

HBL

HBL system consists of a bioreactor (MicrognInc, Laguna Hills, CA with a pore size 0.2 μ m, total fiber internal surface area 6 000 cm², external surface area 7 000 cm², volume 200 mL loaded with fresh isolated hepatocytes ($2-4 \times 10^{10}$), a single-use plasma circuit, and a machine to control the fluid flow through these components. At first, plasma exchange was achieved by a membrane separation method (PLASAUTO-IQ, Asahi, Tokyo). The amount of plasma removal was set at 3 000 mL. In the following HBL treatment (SYBIOL, U.S.A), patients' plasma was separated using a plasma separation system (COBE-Spectra, Lakewood, CO) and was then perfused through an HBL system. The plasma was separated at a rate of 70-100 mL/min and perfused through the bioreactor at a rate of 28-30 mL/min; flow rate of porcine cell suspension was 60 mL/min. After exchange of patients' plasma with porcine cells across the hollow-fiber membranes, patients' blood was returned to the superficial femoral vein. Evaluation of the viability of hepatocytes in circuit of porcine liver cells was done by cell membrane exclusion of trypan blue dye.

Clinical assessments

All patients were managed in a specialized intensive care unit and received standard supportive care. The following parameters were monitored before, during and after treatment: vital signs (blood pressure, heart rate, breath rate and SaO₂), hemodynamics (mean artery pressure, central venous pressure) and urinary output. Liver biochemistry (bilirubin, transaminases, Creatinine, BUN, serum ammonia, prothrombin activity (PTA)), cytokines TNF α , IL-6 (ELISA, Bangding Co) and endotoxin were analysed. The mental state of hepatic encephalopathy was graded into five stages. When the patients regained consciousness or hepatic encephalopathy decreased by I stage, the treatments was considered as effective.

MELD score assessment system

According to Kamath *et al.*, the score was multiplied by 10 and then rounded to the nearest integer. The formula for the MELD scores $3.8 \cdot \log_e(\text{bilirubin}[\text{mg/dL}]) + 11.2 \cdot \log_e(\text{INR}) + 9.6 \cdot \log_e(\text{creatinine}[\text{mg/dL}])$. We used on-line available worksheet to compute MELD scores (www.mayo.edu/int-med/gi/model/mayomodl.htm).

Statistical analysis

Statistical comparisons were carried out using chi-square and Student *t*-tests. A *P* value <0.05 was considered statistically significant.

RESULTS

Patients' response to treatment

All treatments were completed as scheduled. Each treatment lasted for 8-10 h and all were well tolerated. All patients remained hemodynamically stable throughout the treatment period. No gastrointestinal coagulopathy, fever, allergy and other severe adverse reactions were observed.

HBL treatment outcome

Gastrointestinal symptoms such as anorexia, nausea and fatigue were significantly improved in 4 out of 5 patients. Three patients who suffered from hepatic encephalopathy (HE) experienced remarkable neurological improvement with reversal of the decerebrate state after HBL treatment. Two of

3 HE at grades III and II became respectively grades II and I, another one at grade IV regained consciousness. Four patients who were complicated with 2-organ failure recovered spontaneously, one died 8 and 21 d after HBL treatment. The patient who was complicated with 3-organ failure (liver, cardiovascular, and gastrointestinal coagulopathy) was successfully bridged until an organ became available for orthotopic liver transplantation 1 wk after HBL treatment. The spontaneous recovery rate was 40.0%.

The treatment with the PE lowered TBIL in all patients (from 23.08 ± 12.50 mg/dL to 12.34 ± 4.39 mg/dL). At the end of treatment TBIL was reduced about 50%. Post evaluation showed that TBIL had a significant difference before and after HBL treatment at 0, 24 and 72 h (*P*<0.05). No statistically significant improvement in albumin and blood ammonia levels noted (*P*<0.05). CHE and PTA were significantly increased in all patients at 0, 24, 72 h and at the end of HBL treatment (*P*<0.05-0.01). The serum chemistry changes are shown in Table 2.

A significant decrease in serum endotoxin levels was observed by the end of PE (*P*<0.05) and it was declined during the period of HBL treatment. By the end of HBL, endotoxin level was the lowest (*P*<0.001). TNF- α and IL-6 were reduced rapidly, the clearance rate of TNF- α was approximately 45% and IL-6 was 55% (*P*<0.001) (Figure 1).

Evaluation of effect of HBL with MELD

MELD was used for predicting the outcome of HBL before and after treatment (Table 3).

Table 1 General data of patients

No	Sex	Age(yr)	Diagnosis	Multi-organs failure	Outcome
1	Female	43	ALF, HBV	Liver, brain	Spontaneous recovery
2	Male	31	SALF, HBV	Liver, brain	Recovery spontaneous
3	Male	33	SALF, HBV and alcoholic liver disease	Liver, coagulopathy, cardiovascular	Orthotopic liver transplantation
4	Female	27	ALF, drug induced liver injury	Liver, brain	Death
5	Male	31	ALF, HBV	Liver, kidney	Death

ALF: acute liver failure, SALF: sub-acute liver failure, HBV: hepatitis B virus.

Table 2 Changes of partial biochemical indices pre- and post-treatment of HBL(mean \pm SD)

Item	TBIL (mg/dL)	NH ₃ (μ g/dL)	ALB (g/L)	CHE (U/L)	PTA%
Pre-treatment	23.08 \pm 12.50	116.6 \pm 23.1	29.79 \pm 4.35	3 801.5 \pm 1710.6	17.25 \pm 10.11
Post-treatment at 0 h	12.34 \pm 4.39 ^b	98.3 \pm 19.5	32.57 \pm 4.76	5 560.9 \pm 1067.6 ^a	38.60 \pm 10.25 ^b
Post-treatment at 24 h	14.10 \pm 6.08 ^b	103.2 \pm 23.5	33.13 \pm 4.34	5 438.5 \pm 1024.3 ^a	34.31 \pm 11.75 ^a
Post-treatment at 72 h	17.24 \pm 8.34 ^a	110.8 \pm 30.6	31.42 \pm 4.07	5 676.2 \pm 957.9 ^a	35.20 \pm 9.78 ^b

^a*P*<0.05, ^b*P*<0.01, vs pre-treatment, TBIL: total bilirubin, NH₃: serum ammonia, ALB: albumin, CHE: cholinesterase, PTA: prothrombin activity.

Table 3 Changes of MELD score before and after treatment of HBL

Patients	Before-treatment						After-treatment					
	1	2	3	4	5	(mean \pm SD)	1	2	3	4	5	(mean \pm SD)
PTA%	22.4	21	18	11	14.37	17.35 \pm 4.7	40.2	43	45	30.1	18.2	35.3 \pm 20.87
INR	2.42	2.51	2.61	4.14	3.74	3.08 \pm 1.27	1.58	1.55	1.50	2.08	2.71	1.8 \pm 1.02
Creatinine (mg/dL)	13	16.9	7.9	16.6	42.4	19.36 \pm 15.3	5.9	5.0	4.3	8.9	35.2	11.8 \pm 13.1
Bilirubin (mg/dL)	20.4	17	15.1	22.2	40.46	23.03 \pm 10.1	20.4	17	15.1	22.2	40.46	17.4 \pm 12.66
MELD	41	41	41	47	48	43.6	34	33	32	39	45	33.6

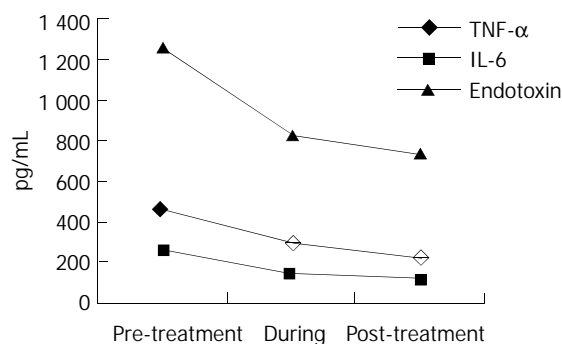


Figure 1 Change of cytokines and LPS in different points.

DISCUSSION

In the present study we demonstrated that the patients with severe hepatitis and hepatic failure might benefit from HBL for temporary liver support. HBL could maintain patients with hepatic failure alive, neurologically intact and metabolic state improved until a donor organ was available^[4]. It could also allow the native liver to regenerate, thus avoiding liver transplantation. The study showed that TNF- α and IL-6 were reduced rapidly about 45% and 55% ($P < 0.001$) after HBL treatment. The alteration of serum endotoxin levels was similar to TNF α and IL-6. Four of 5 patients responded to HBL treatment and 3 of them survived. Since the case number was limited, there were not enough data in our study to show that HBL could improve the survival rate of patients with multiple organ dysfunction. However the beneficial effect of HBL on the systemic concentration of cytokines was definite and the efficacy was not reached by drug treatment in such a short period. Just as Stephen described^[5,6], a success liver support device was likely to depend on their ability to modify factors influencing liver cell death and regeneration and on the extent to which multi-organ failure could be prevented or reversed. Hybrid liver support devices replace the lost liver function through a combination of mechanical and biologic effects. Mechanical parts use activated charcoal or plasma exchange before the hepatocyte bioreactor, which may not only provide a "protective" effect on the porcine hepatocytes from possible toxic effect of hepatic failure plasma, but also strengthen the effect of plasma detoxification. HBL treatment could remarkably improve SIRS signs and symptoms. Also it slowed down the progression from SIRS to MODS and protected MODS from further deterioration.

The mechanism of HBL to block the progression from SIRS to MDOS was to support failed liver. In our study, It was observed that CHE and PTA were significantly increased in all patients at 0, 24 and 72 h after HBL treatment ($P < 0.05-0.01$). Plasma cholinesterase, an enzyme with a short half-life, is not usually changed by the substitution of clotting factors or by freshly frozen plasma and therefore is a good parameter of synthesis. Increased cholinesterase level in plasma may reflect improvement of liver synthesis function. The metabolic ability of liver for various nervous toxicity implicates liver detoxification function. Similar to the previous report, 3 patients with hepatic encephalopathy were improved by HBL treatment in our study, but it was different from previous report, in that the blood ammonia

levels were not changed after HBL treatment. Impairment of central nervous system in hepatic encephalopathy is probably multifactorial in origin. Except ammonia, other neuroexcitatory factors like amino acid imbalance, mercaptans, phenols, fatty acids, GABA, and benzodiazepine, also play a role in hepatic encephalopathy. Therefore consciousness improvement may cause removal of other neuroexcitatory factors. There are two mechanisms blocking the progression from SIRS to MODS related to liver function improvement. First, liver is an amplifier of the systemic acute-phase reaction, proinflammatory cytokines enter the liver through the portal vein, eventually passing the smallest functional unit of the liver, the acinus. The special architecture of sinusoids ensures that cytokines in the liver primarily reach the nonparenchymal liver cells such as endothelial cells and kupffer cells. Because these cells express not only receptors of IL-1 β , TNF- α and IL6, but also modulators of cytokines^[7]. Also the most active cells have the potential for the systemic response to the intrahepatic release of inflammatory cytokines. They might function as intrahepatic amplifiers of the systemic acute-phase reaction by liberating a second wave of proinflammatory cytokines which could enhance the effect of injuring agents and accelerate or maintain development of liver fibrosis^[8]. Second, it has been found that LBP/CD14 is an endotoxin strengthening system. LBP is produced in liver. When under stress the production of LBP from liver would increase many times. Trace endotoxin binding to LBP and interacting with target cells would increase the sensitivity of target cells to endotoxin up to 10 000 times and stimulate the synthesis and secretion of a large number of proinflammatory cytokines, mainly IL1B and TNF α ^[8]. Therefore the improvement in liver function is the basis for decreasing proinflammatory cytokine levels.

MELD is a reliable measure and predictive of short-term mortality risk in patients with end-stage liver disease^[9].

REFERENCES

- 1 Fifth conference of national contagious disease and parasitic disease Guideline: prevention and treatment of virus hepatitis (draft). *Zhonghua Neike Zazhi* 1995; **34**: 788-791
- 2 Qiu HB, Zhou SX, Yang Y. Multiple organ dysfunction syndrome predictors of mortality and clinical therapeutic strategies. *Linchuang Jijiyu Yixue* 2001; **10**: 13-16
- 3 Fry DE, Pearlstein L, Fulton RL. Multiple system organ failure: the role of uncontrolled infection. *Arch Surg* 1980; **115**: 136-139
- 4 Xue YL, Zhao SF, Zhang ZY. Effects of bioartificial liver support system on acetaminophen-induced acute liver failure canines. *World J Gastroenterol* 1999; **5**: 308-311
- 5 Zimminerman JE, Knauus WA, Sun X, Wagner DP. Severity stratification and outcome prediction for multisystem organ failure and dysfunction. *World J Surg* 1996; **20**: 401-409
- 6 Riordan SM, Williams R. Acute liver failure: targeted artificial and hepatocyte-based support of liver regeneration and reversal of multiorgan failure. *J Hepatol* 2000; **32**(Suppl 1): 63-67
- 7 Ramadori G, Christ B. Cytokines and the hepatic acute-phase response. *Seminars In Liver Disease* 1999; **19**: 141-156
- 8 Stange J, Mitzner SR, Risler T. Molecular adsorbent recycling system: Clinical results of a new membrane-based blood purification system for bioartificial liver support. *Artificial Organs* 1999; **23**: 319-330
- 9 Kamath PS, Wiesner RH, Malinchoc M. A Model to predict survival in patients with end-stage Liver disease. *Hepatology* 2001; **33**: 467-470

Expression and significance of angiopoietin-2 in gastric cancer

Xiao-Dong Sun, Xing-E Liu, Jin-Min Wu, Xiu-Jun Cai, Yi-Ping Mou, Jun-Da Li

Xiao-Dong Sun, Xiu-Jun Cai, Yi-Ping Mou, Jun-Da Li, Department of General Surgery, the Affiliated Sir Run Run Shaw Hospital, Medical College, Zhejiang University, Hangzhou 310016, Zhejiang Province, China

Xing-E Liu, Jin-Min Wu, Center of Oncology, the Affiliated Sir Run Run Shaw Hospital, Medical College, Zhejiang University, Hangzhou 310016, Zhejiang Province, China

Correspondence to: Dr. Xiao-Dong Sun, Department of General Surgery, the Affiliated Sir Run Run Shaw Hospital, Medical College, Zhejiang University, Hangzhou 310016, Zhejiang Province, China. s.xiaodong@sohu.com

Telephone: +86-571-86090073 **Fax:** +86-571-86044817

Received: 2003-09-18 **Accepted:** 2003-10-12

Abstract

AIM: To investigate the expression and pathological factors of Angiopoietin-2 (Ang-2) in primary gastric cancers and adjacent normal tissues.

METHODS: The expression of Angiopoietin-2 and VEGF were studied in 72 primary gastric cancers and adjacent normal tissues from the same patients by semi-quantitative reverse transcriptase-polymerase chain reaction (RT-PCR) and immunohistochemistry.

RESULTS: Ang-2 was mainly expression in tumor cells. There were significantly difference between expression of Ang-2 in primary gastric cancer and in adjacent normal tissue samples ($P=0.003$). It was statistically correlation between Ang-2 and VEGF expression in tumors ($P=0.0055$). With regard to Ang-2 expression in tumors, there were significant difference between early stage and advanced stage ($P=0.017$), and significant difference between positive vascular involvement and negative vascular involvement ($P=0.032$). However, there was no significant difference between moderate-poor differential type and high differential type ($P=0.908$), between positive lymph node metastasis and negative lymph node metastasis ($P=0.752$), between positive serosal invasion and negative serosal invasion ($P=0.764$). The cases with expression of Ang-2 were increasing with advanced stage and vascular involvement.

CONCLUSION: The results manifested that Angiopoietin-2, coordinated with VEGF, play role in regulating tumor angiogenesis of gastric cancer.

Sun XD, Liu XE, Wu JM, Cai XJ, Mou YP, Li JD. Expression and significance of angiopoietin-2 in gastric cancer. *World J Gastroenterol* 2004; 10(9): 1382-1385

<http://www.wjgnet.com/1007-9327/10/1382.asp>

INTRODUCTION

Angiogenesis is required for the growth and metastasis of malignant tumor, and is defined as the sprouting of blood vessels from pre-existing vessels that migrate into the tumor and form a new vascular network. Many factors attend the process of angiogenesis. Recently, several studies have shown

that, the expression of angiopoietin-2 (Ang-2) probably correlates to tumor angiogenesis^[1,2]. However, the role and mechanism of Ang-2 in tumor angiogenesis still remain to be determined. Here, we investigate the expression and significance of angiopoietin-2 in gastric cancer.

MATERIALS AND METHODS

Materials

Reagents Trizol liquid, AMV reverse transcriptase, Oligd(T)₁₄, RNAsin, dNTP, Taq DNA polymerase were purchased from shanghai sangon biological engineering technology and service co.Ltd, PCR primers were synthesized by shanghai sangon biological engineering technology and service co.Ltd. N-18 and P-20, the monoclonal antibodies of Ang-2 and VEGF respectively, were purchased from santa cruz company.

Clinical data Total of 72 patients with respectable primary gastric cancer were analysed. There were 46 males and 26 females with primary gastric cancer. Age varied from 38 to 72 years, with a mean age of 53.5 years. Routine pathological diagnosis showed that 53 cases were adenocarcinoma, 19 cases were signet carcinoma. Of these 72 patients, 48 individuals had lymph nodes metastasis, and 26 others had no lymph node metastasis.

Methods

Detection of expression of Ang-2 AND VEGF Expressions of Ang-2 and VEGF were assessed in every gastric cancer sample and its adjacent normal tissue by semi-quantitative RT-PCR.

RNA extraction Total RNA was extracted by Trizol one step procedure, and suspended in DEPC-treated reverse osmosis-H₂O, and conserved at -70 °C for reverse transcription. RNA yield and purity were determined by standard UV spectrophotometric assay. The ratio of A₂₆₀/A₂₈₀ is 1.80.

First strand cDNA synthesis A 5 µg of the total RNA was dissolved in 20 µL of a mixture containing 2 µL of 10× first-strand buffer, 20 µL of AMV reverse transcriptase, 2 µL of dNTP, 20 µL of RNAsin, 500 ng of Oligd(T)₁₄, and DEPC-treated reverse osmosis-H₂O. The reaction conditions were as following: at 42 °C for 60 min, at 95 °C for 5 min. The first strand cDNA was stored at -20 °C until use.

PCR amplification Primers of Ang-2, VEGF and β-actin were synthesized according to primer design principles, all primer sets used span an intron to control amplification of genomic DNA sequences. A 3 µL of the first strand cDNA were amplified in 20 µL volume. The primers of Ang-2 were yielded 921-bp product and as following: 5' -end primer: 5' -GGGGGAGGACTG GTGACAGCCACGG-3', 3' -end primer: 5' -GAAATCTGCTGGC CGGATCATCAT-3'. Following an initial denaturation at 94 °C for 5 min, the samples were amplified by 30 cycles of denaturation at 94 °C for 30 s, annealing at 58 °C for 30 s, extension at 72 °C for 30 s, and ended by extension at 72 °C for 10 min. The primers of VEGF were yielded 356-bp product and as following: 5' -end primer: 5' -ACCATGAACTTTCTGCTCTCTTGG-3', 3' -end primer: 5' -CCGCCTTGGCTTGTCACATCTGCA-3'. Following an initial denaturation at 94 °C for 5 min, the samples were amplified by 28 cycles of denaturation at 94 °C for 30 s, annealing at 58 °C for 1 min, extension at 72 °C for 1 min, and ended by extension at 72 °C for 10 min. The primers of β-actin, which was

amplified with Ang-2 and VEGF as internal control, were yielded 644 bp product and as following: 5' -end primer: 5' -ACGTTATG GATGATGATATCGC-3' , 3' -end primer: 5' -CTTAATGTCACG CACGATTTCC-3' . PCR products were separated on 1.7% agarose gel , stained with ethidium bromide, and analysed with Quantity one 4.1.0 software. The ratios of Ang-2/ β -actin, AEGF/ β -actin were used to semiquantify the levels of Ang-2 and VEGF.

Immunohistochemical staining The immunohistochemical study of expression of Ang-2 and VEGF in gastric cancer and adjacent normal tissue was performed by the avidin-biotin-peroxidase technique using monoclonal antibody N-18 and P-20, as previously described^[3,4]. Briefly, after formaldehyde-fixed paraffin-embedded tissue sections were deparaffinized in xylene and rehydrated in alcohol, they were incubated in 3 mL/L H₂O₂ to block endogenous peroxidase activity. Each slide was incubated with normal horse serum for 20 min at room temperature, and then monoclonal antibody N-18 or P-20, the working dilution were 1:100 and 1:200 respectively, was incubated on the tissue section overnight at 4 °C. After incubated in biotinylated mouse anti-goat IgG (the working dilution were 1:200) for 30 min at room temperature, each slide was rinsed in phosphate-buffered saline and was incubated in the avidin-biotin peroxidase complex for 40 min at 37 °C. The peroxidase was visualized with 3-3' -diamino-benzidine-tetrahydrochloride solution and then counterstained with methyl green.

Expressions of Ang-2 and VEGF in primary gastric cancers and adjacent normal tissues were detected under microscopy. **Statistical analysis** Results are calculated as mean \pm SD for each group. *t* test groups or *chisq* test was used to analyze the variables. Statistical analyses were performed with SPSS software, version 10.0.

RESULTS

Results of RT-PCR

Seventy-two primary gastric cancers and adjacent normal tissues from the same patients were examined for the expression of Ang-2 and VEGF by RT-PCR. In 72 cases of primary tumors, Ang-2 and VEGF were expressed in 46 (63.9%) and 48 cases (66.7%) respectively. However, in 72 adjacent normal samples, Ang-2 and VEGF were expressed in 10 (13.9%) and 16 (22.2%) respectively. The expression of Ang-2 in primary gastric cancer has significant differences from that in adjacent normal tissues ($P=0.003$), (Figure 1, Table 1).

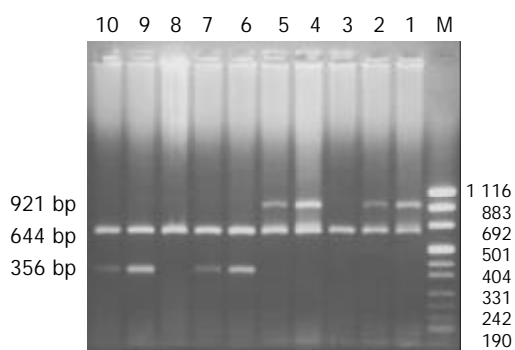


Figure 1 Semi-quantitative RT-PCR amplified products of Ang-2 and VEGF in primary gastric cancer and adjacent normal tissue 644 bp: internal standards, 921 bp: Ang-2 expression, 365 bp: VEGF expression, Lane-M: puc mix marker (1116, 883, 692, 501, 404, 331, 242, 190, 147, 110, 67, 34, 26, 19) bp, Lanes 1-5: Ang-2 expression, Lanes 6-10: VEGF expression.

Meanwhile, in 46 cases of gastric cancers with Ang-2

positive expression, VEGF was coexpressed in 36 cases (78.26%), but 26 cases of gastric cancers with Ang-2 negative expression showed VEGF expression in 12 cases (46.15%). The expressions of Ang-2 and VEGF in the primary tumors were significantly correlated ($P=0.0055$), (Table 2).

Table 1 Expression of Ang-2 in primary gastric cancers and adjacent normal tissues detected by semi-quantitative RT-PCR

	Cases	Ang-2 (mean \pm SD)
Primary gastric cancers	72	0.497 \pm 0.393 ^a
Adjacent normal tissues	72	0.088 \pm 0.224

a: $P=0.003$ vs adjacent normal tissues.

Table 2 Correlation between expression of Ang-2 and VEGF in 72 primary gastric cancer detected by semi-quantitative RT-PCR

Ang-2 expression (Cases)	VEGF expression (Cases)		<i>P</i>
	Positive	Negative	
Positive	36	10	0.0055
Negative	12	14	

Result of immunohistochemistry

Positive control included human placenta. Positive expression of Ang-2 and VEGF show brown staining in the cytoplasm of tumor or normal cells, Ang-2 was mainly expression in tumor cells (Figures 2,3).

Pathologic factors affecting expression of VEGF-C

Several pathological factors, including tumor stage, histological type, lymph node metastasis, serosal invasion and vascular involvement, were investigated to predicting expression of Ang-2 in gastric cancer. The results show that, in expression of Ang-2, there were significant difference between early stage and advanced stage ($P=0.017$), and significant difference between positive vascular involvement and negative vascular involvement ($P=0.032$). However, there was no significant difference between moderate-poor differential type and high differential type ($P=0.908$), no significant difference between positive lymph node metastasis and negative lymph node metastasis ($P=0.752$), and no significant difference between positive serosal invasion and negative serosal invasion ($P=0.764$), (Table 3).

Table 3 Correlation between pathological factors and Ang-2 expression in 72 primary gastric cancer

Pathological factors	No. of cases	Ang-2 mRNA (mean \pm SD)	<i>P</i> value
Tumor stage			
Early stage	26	0.222 \pm 0.310	0.017
Advanced stage	46	0.593 \pm 0.318	
Histological type			
Moderate-Poor differential type	45	0.425 \pm 0.350	0.908
High differential type	27	0.203 \pm 0.290	
Lymph node metastasis			
Positive	48	0.413 \pm 0.346	0.752
Negative	24	0.490 \pm 0.450	
Serosal invasion			
Positive	43	0.404 \pm 0.327	0.764
Negative	29	0.334 \pm 0.459	
Vascular involvement			
Positive	46	0.640 \pm 0.335	0.032
Negative	26	0.272 \pm 0.298	

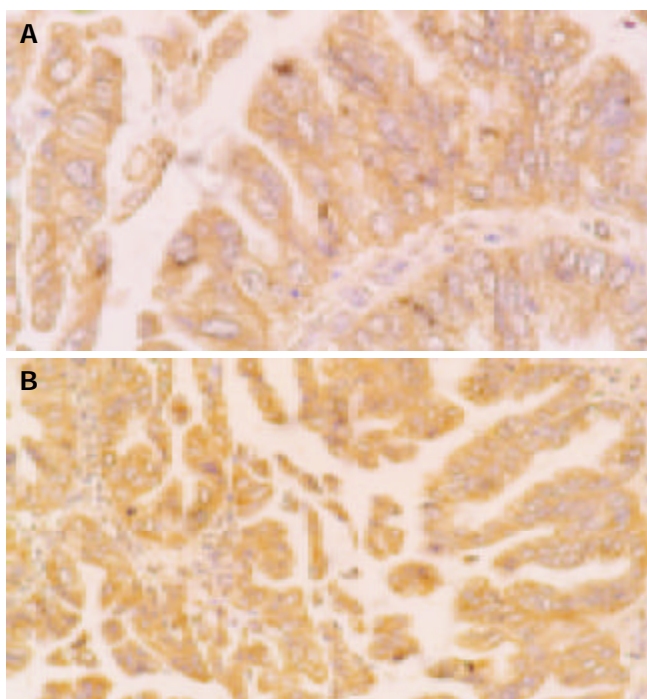


Figure 2 Expression of Ang-2 and VEGF in gastric cancer, A: Ang-2 positive expression in gastric cancer ($\times 400$), B: VEGF positive expression in gastric cancer ($\times 400$).

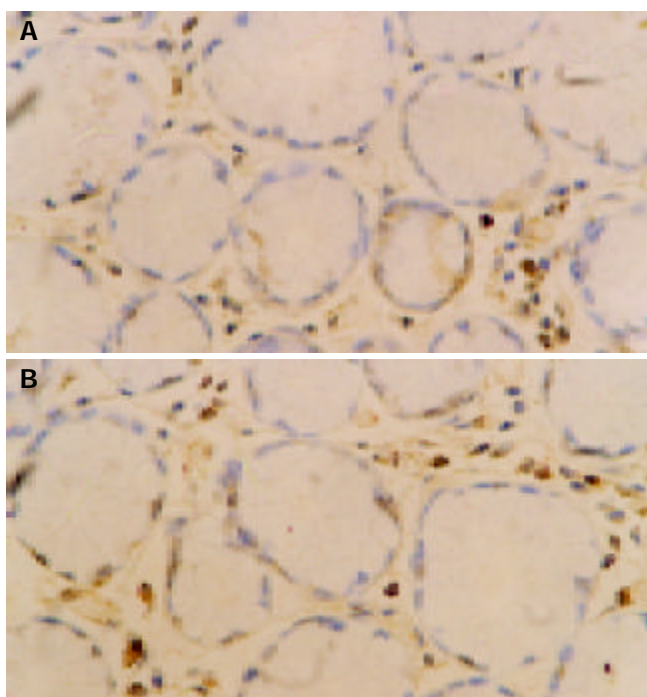


Figure 3 Expression of Ang-2 and VEGF in adjacent normal tissue, A: Ang-2 negative expression in adjacent normal tissue ($\times 400$), B: VEGF negative expression in adjacent normal tissue ($\times 400$).

DISCUSSION

Solid tumors could recruit blood vessels from the neighboring tissue by angiogenesis, and adequate blood supply could promote solid tumor growth to a clinically relevant size^[5]. The ability of a tumor to induce angiogenesis could determine its rate of growth and its likelihood of metastasis^[6-8]. It has been found angiogenesis is dependent on a tightly regulated balance between angiogenic promoters and inhibitors^[9]. Numerous factors have been implicated in regulate angiogenesis, including

growth factors and their receptors, a variety of proteases, adhesion receptors and ECM component^[10,11].

Angiopoietins, novel endothelial factors, were found to be ligands for the endothelium-specific tyrosin kinase receptor Tie-2^[12]. Angiopoietins (Ang) included Ang-1, Ang-2, Ang-3 and Ang-4, the best characterized were Ang-1 and Ang-2. Ang-1 and Ang-2 were soluble 70-ku factors, which consist of an amino-terminal coiled-coil domain and a carboxy-terminal fibrinogen-like domain^[13,14].

Both of Ang-1 and Ang-2 could bind to the Tie-2 receptors. Ang-1 could bind to the Tie-2 receptor and activate it by inducing phosphorylation, and help to maintain and stabilize mature vessels by promoting interactions between endothelial cells and supporting cells^[15-17]. Ang-2 could also bind to the Tie-2, but not activate phosphorylation. Ang-2 could block the action of Ang-1^[18]. That is to say, Ang-2 was an antagonist of Ang-1 and induces the loosening of the interactions between endothelial and perivascular support cells and ECM, reducing vascular integrity and facilitating access to angiogenic inducers^[19,20]. Recent studies have shown that the expression pattern of Ang-2 is strongly associated with that of VEGF in the process of tumor angiogenesis, VEGF and Ang-2 seemed to play complementary and coordinated roles in the development of new blood vessels^[21,22]. Angiopoietins were mainly produced by endothelial cells and pericytes, and their receptor Tie-2 was also expressed in endothelial cells and partly in hematopoietic cells^[23]. Ang-2 was selectively expressed in endothelial cells of tumors, ovaries, uterus and placenta, which are known to have extensive vascularization patterns^[24-26].

The role and mechanism of Ang-2 in tumor angiogenesis have not been clarified. Some studies suggested that the production of VEGF and Ang-2 must be coordinated in development of tumor angiogenesis^[27,28]. Ang-2 could produce destabilization and induce angiogenic response in the presence of VEGF, but lead to vessel regression in the absence of VEGF^[13,29]. While other studies manifested that VEGF upregulates expression of Ang-1, but not Ang-2^[30]. The expression of Ang-2 correlated with tumor size, but had no correlation with expression of VEGF^[31]. Kuroda's results showed that upregulation of Ang-1, Ang-2 and Tie-2 is closely associated with the development of microvascular proliferation in psoriasis, and the angiopoietin-Tie-2 system might act coordinately with VEGF to promote angiogenesis^[32]. Hatanaka's results suggested that tumor-produced IL-10 promotes stromal vascularization through expression of Ang-1, Ang-2 and Tie-2^[33]. Angiopoietin-Tie-2 system, particularly Ang-2, played critical role in the vascularization of prostate carcinoma, breast cancer, colon cancer, astrocytoma, gastric carcinoma, etc^[23,34-37]. Ang-2 expression was highest during the early stages of angiogenesis, perhaps reducing Tie-2 activity to allow the established vasculature to respond to angiogenic stimuli, consequently, Ang-2 expression was decreased and superseded by Ang-1 expression, perhaps activating Tie-2 and resulting in the stabilization and maturation of neovessel^[13].

We studied the expression of Ang-2 in 72 primary gastric cancer and adjacent normal tissues by semi-quantitative reverse transcriptase-polymerase chain reaction (RT-PCR) and immunohisto-chemistry. The results showed that Ang-2 was mainly expression in tumor cells, and there were significantly difference in Ang-2 expression between primary tumor and adjacent normal tissue samples. The present study also clearly manifested that it was statistically correlated between Ang-2 and VEGF expression in tumors. The expression of Ang-2 was related with tumor stage and vascular involvement. Ang-2 overexpression by newly formed tumor blood vessels may lead to vessel destabilization and relative hypoxia, which could drive the release of VEGF, leading to robust angiogenesis^[37].

REFERENCES

- 1 **Tanaka S**, Mori M, Sakamoto Y, Makuuchi M, Sugimachi K, Wands JR. Biologic significance of angiopoietin-2 expression in human hepatocellular carcinoma. *J Clin Invest* 1999; **103**: 341-345
- 2 **Yu Q**, Stamenkovic I. Angiopoietin-2 is implicated in the regulation of tumor angiogenesis. *Am J Pathol* 2001; **158**: 563-570
- 3 **Flens MJ**, Zaman GJ, van der Valk P, Izquierdo MA, Schroeijers AB, Scheffer GL, van der Groep P, de Haas M, Meijer CJ, Scheper RJ. Tissue distribution of the multidrug resistance protein. *Am J Pathol* 1996; **148**: 1237-1247
- 4 **Itsubo M**, Ishikawa T, Toda G, Tanaka M. Immunohistochemical study of expression and cellular localization of the multidrug resistance gene product P-glycoprotein in primary liver carcinoma. *Cancer* 1994; **73**: 298-303
- 5 **Folkman J**. Tumor angiogenesis. *Adv Cancer Res* 1985; **43**: 175-203
- 6 **Weidner N**, Semple JP, Welch WR, Folkman J. Tumor angiogenesis and metastasis—correlation in invasive breast carcinoma. *N Engl J Med* 1991; **324**: 1-8
- 7 **Weidner N**, Carroll PR, Flax J, Blumenfeld W, Folkman J. Tumor angiogenesis correlates with metastasis in invasive prostate carcinoma. *Am J Pathol* 1993; **143**: 401-409
- 8 **Macchiarini P**, Fontanini G, Hardin MJ, Squartini F, Angeletti CA. Relation of neovascularisation to metastasis of non-small-cell lung cancer. *Lancet* 1992; **340**: 145-146
- 9 **Mustonen T**, Alitalo K. Endothelial receptor tyrosine kinases involved in angiogenesis. *J Cell Biol* 1995; **129**: 895-898
- 10 **Hanahan D**, Folkman J. Patterns and emerging mechanisms of the angiogenic switch during tumorigenesis. *Cell* 1996; **86**: 353-364
- 11 **Risau W**. Mechanisms of angiogenesis. *Nature* 1997; **386**: 671-674
- 12 **Peters KG**. Vascular endothelial growth factor and the angiopoietins: working together to build a better blood vessel. *Circ Res* 1998; **83**: 342-343
- 13 **Maisonpierre PC**, Suri C, Jones PF, Bartunkova S, Wiegand SJ, Radziejewski C, Compton D, McClain J, Aldrich TH, Papadopoulos N, Daly TJ, Davis S, Sato TN, Yancopoulos GD. Angiopoietin-2, a natural antagonist for Tie2 that disrupts *in vivo* angiogenesis. *Science* 1997; **277**: 55-60
- 14 **Davis S**, Aldrich TH, Jones PF, Acheson A, Compton DL, Jain V, Ryan TE, Bruno J, Radziejewski C, Maisonpierre PC, Yancopoulos GD. Isolation of angiopoietin-1, a ligand for the TIE2 receptor, by secretion-trap expression cloning. *Cell* 1996; **87**: 1161-1169
- 15 **Papapetropoulos A**, Garcia-Cardena G, Dengler TJ, Maisonpierre PC, Yancopoulos GD, Sessa WC. Direct actions of angiopoietin-1 on human endothelium: evidence for network stabilization, cell survival, and interaction with other angiogenic growth factors. *Lab Invest* 1999; **79**: 213-223
- 16 **Witzenbichler B**, Maisonpierre PC, Jones P, Yancopoulos GD, Isner JM. Chemotactic properties of angiopoietin-1 and -2, ligands for the endothelial-specific receptor tyrosine kinase Tie2. *J Biol Chem* 1998; **273**: 18514-18521
- 17 **Suri C**, Jones PF, Patan S, Bartunkova S, Maisonpierre PC, Davis S, Sato TN, Yancopoulos GD. Requisite role of angiopoietin-1, a ligand for the TIE2 receptor, during embryonic angiogenesis. *Cell* 1996; **87**: 1171-1180
- 18 **Kampfer H**, Pfeilschifter J, Frank S. Expressional regulation of angiopoietin-1 and -2 and the tie-1 and -2 receptor tyrosine kinases during cutaneous wound healing: a comparative study of normal and impaired repair. *Lab Invest* 2001; **81**: 361-373
- 19 **Lauren J**, Gunji Y, Alitalo K. Is angiopoietin-2 necessary for the initiation of tumor angiogenesis? *Am J Pathol* 1998; **153**: 1333-1339
- 20 **Beck H**, Acker T, Wiessner C, Allegrini PR, Plate KH. Expression of angiopoietin-1, angiopoietin-2, and tie receptors after middle cerebral artery occlusion in the rat. *Am J Pathol* 2000; **157**: 1473-1483
- 21 **Stratmann A**, Risau W, Plate KH. Cell type-specific expression of angiopoietin-1 and angiopoietin-2 suggests a role in glioblastoma angiogenesis. *Am J Pathol* 1998; **153**: 1459-1466
- 22 **Holash J**, Wiegand SJ, Yancopoulos GD. New model of tumor angiogenesis: dynamic balance between vessel regression and growth mediated by angiopoietins and VEGF. *Oncogene* 1999; **18**: 5356-5362
- 23 **Etoh T**, Inoue H, Tanaka S, Barnard GF, Kitano S, Mori M. Angiopoietin-2 is related to tumor angiogenesis in gastric carcinoma: possible *in vivo* regulation via induction of proteases. *Cancer Res* 2001; **61**: 2145-2153
- 24 **Zagzag D**, Hooper A, Friedlander DR, Chan W, Holash J, Wiegand SJ, Yancopoulos GD, Grumet M. *In situ* expression of angiopoietins in astrocytomas identifies angiopoietin-2 as an early marker of tumor angiogenesis. *Exp Neurol* 1999; **159**: 391-400
- 25 **Wulff C**, Wilson H, Rudge JS, Wiegand SJ, Lunn SF, Fraser HM. Luteal angiogenesis: prevention and intervention by treatment with vascular endothelial growth factor trap(A40). *J Clin Endocrinol Metab* 2001; **86**: 3377-3386
- 26 **Otani A**, Takagi H, Oh H, Koyama S, Honda Y. Angiotensin II induces expression of the Tie2 receptor ligand, angiopoietin-2, in bovine retinal endothelial cells. *Diabetes* 2001; **50**: 867-875
- 27 **Takahashi Y**, Kitadai Y, Bucana CD, Cleary KR, Ellis LM. Expression of vascular endothelial growth factor and its receptor, KDR, correlates with vascularity, metastasis, and proliferation of human colon cancer. *Cancer Res* 1995; **55**: 3964-3968
- 28 **Woolf AS**, Yuan HT. Angiopoietin growth factors and Tie receptor tyrosine kinases in renal vascular development. *Pediatr Nephrol* 2001; **16**: 177-184
- 29 **Sato TN**, Tozawa Y, Deutsch U, Wolburg-Buchholz K, Fujiwara Y, Gendron-Maguire M, Gridley T, Wolburg H, Risau W, Qin Y. Distinct roles of the receptor tyrosine kinases Tie-1 and Tie-2 in blood vessel formation. *Nature* 1995; **376**: 70-74
- 30 **Hangai M**, Murata T, Miyawaki N, Spee C, Lim JJ, He S, Hinton DR, Ryan SJ. Angiopoietin-1 upregulation by vascular endothelial growth factor in human retinal pigment epithelial cells. *Invest Ophthalmol Vis Sci* 2001; **42**: 1617-1625
- 31 **Holash J**, Maisonpierre PC, Compton D, Boland P, Alexander CR, Zagzag D, Yancopoulos GD, Wiegand SJ. Vessel cooption, regression, and growth in tumors mediated by angiopoietins and VEGF. *Science* 1999; **284**: 1994-1998
- 32 **Kuroda K**, Sapidin A, Shoji T, Fleischmajer R, Lebwohl M. Altered expression of angiopoietins and Tie2 endothelium receptor in psoriasis. *J Invest Dermatol* 2001; **116**: 713-720
- 33 **Hatanaka H**, Abe Y, Naruke M, Tokunaga T, Oshika Y, Kawakami T, Osada H, Nagata J, Kamochi J, Tsuchida T, Kijima H, Yamazaki H, Inoue H, Ueyama Y, Nakamura M. Significant correlation between interleukin 10 expression and vascularization through angiopoietin/TIE2 networks in non-small cell lung cancer. *Clin Cancer Res* 2001; **7**: 1287-1292
- 34 **Wurmbach JH**, Hammerer P, Sevinc S, Huland H, Ergun S. The expression of angiopoietins and their receptor Tie-2 in human prostate carcinoma. *Anticancer Res* 2000; **20**: 5217-5220
- 35 **Currie MJ**, Gunningham SP, Han C, Scott PA, Robinson BA, Harris AL, Fox SB. Angiopoietin-1 is inversely related to thymidine phosphorylase expression in human breast cancer, indicating a role in vascular remodeling. *Clin Cancer Res* 2001; **7**: 918-927
- 36 **Ding H**, Roncari L, Wu X, Lau N, Shannon P, Nagy A, Guha A. Expression and hypoxic regulation of angiopoietins in human astrocytomas. *Neuro Oncol* 2001; **3**: 1-10
- 37 **Ahmad SA**, Liu W, Jung YD, Fan F, Wilson M, Reinmuth N, Shaheen RM, Bucana CD, Ellis LM. The effects of angiopoietin-1 and -2 on tumor growth and angiogenesis in human colon cancer. *Cancer Res* 2001; **61**: 1255-1259

Alterations in expression, proteolysis and intracellular localizations of clusterin in esophageal squamous cell carcinoma

Hong-Zhi He, Zhen-Mei Song, Kun Wang, Liang-Hong Teng, Fang Liu, You-Sheng Mao, Ning Lu, Shang-Zhong Zhang, Min Wu, Xiao-Hang Zhao

Hong-Zhi He, Liang-Hong Teng, Fang Liu, You-Sheng Mao, Ning Lu, Min Wu, Xiao-Hang Zhao, National Laboratory of Molecular Oncology, Department of Thoracic Surgery and Department of Pathology, Cancer Institute and Hospital, Chinese Academy of Medical Sciences and Peking Union Medical College, Beijing 100021, China

Zhen-Mei Song, Shang-Zhong Zhang, Qilu Hospital, School of Medicine, Shandong University, Qindao 250012, Shandong Province, China

Kun Wang, Xiao-Hang Zhao, Beijing Yanjing Hospital, Beijing 100037, China

Supported by National Natural Science Foundation, No.30225045, No.39990570, No.30171049 and No.30370713, and National High Tech and Major State Basic R & D Program of China, No.G1998051205 and No.2001AA227091

Co-first-authors: Hong-Zhi He and Zhen-Mei Song

Correspondence to: Xiao-Hang Zhao, M.D., Ph.D. National Laboratory of Molecular Oncology, Cancer Institute and Hospital, Chinese Academy of Medical Sciences and Peking Union Medical College, Beijing 100021, China. zhaoxh@pubem.cicams.ac.cn

Telephone: +86-10-67709015 **Fax:** +86-10-67709015

Received: 2004-01-09 **Accepted:** 2004-02-24

Abstract

AIM: To investigate biogenesis and intracellular localizations of clusterin to elucidate the potential molecular mechanisms implicated in tumorigenesis of esophageal mucosa.

METHODS: Semi-quantitative RT-PCR for multi-region alteration analysis, Western blot for different transcriptional forms and immunohistochemical staining for intracellular localizations of clusterin were carried out in both tissues and cell lines of ESCC.

RESULTS: The N-terminal deletions of the clusterin gene and the appearance of a 50-53 ku nuclear clusterin, an uncleaved, nonglycosylated, and disulfide-linked isoform, were the major alterations in cancer cells of esophagus. Naturally the 40 ku clusterin was located in the connective tissue of the lamina *propria* of epithelial mucosa and right under the basal membrane of epithelia, but it was disappeared in stromal mucosa of esophagus and the pre-matured clusterin was found positive in cancerous epithelia.

CONCLUSION: The N-terminal deletion of clusterin may be essential for its alterations of biogenesis in ESCC.

He HZ, Song ZM, Wang K, Teng LH, Liu F, Mao YS, Lu N, Zhang SZ, Wu M, Zhao XH. Alterations in expression, proteolysis and intracellular localizations of clusterin in esophageal squamous cell carcinoma. *World J Gastroenterol* 2004; 10(10): 1387-1391
<http://www.wjgnet.com/1007-9327/10/1387.asp>

INTRODUCTION

Clusterin, a 70-80 ku heterodimeric, disulfide-linked glycoprotein is expressed in a wide variety of tissues and secreted in all

human fluids^[1-3]. Human clusterin is encoded by a single copy gene located on chromosome 8p12 and 8p21 with nine exons and eight introns, spanning approximately 17 kb^[4,5]. Clusterin gene has a single functional promoter and a single transcript mRNA, 1.6 kb in length, containing an N-terminal hydrophobic leader sequence. There are two forms of clusterin: one set of proteins is directly for secreted into humour, and the other forms are expressed in the cytoplasm and nucleus. The secretory form of the clusterin protein is produced by translation on membrane-bound ribosomes from the first AUG codon of the full-length clusterin mRNA and is targeted to the endoplasmic reticulum (ER) by an initial leader peptide. Subsequently, this -60 ku pre-clusterin protein containing 427 amino acids has to be further glycosylated in the ER and proteolytically cleaved between R205 and S206 into a mature protein discrete α - and β -chains, held together by disulfide bonds in Golgi^[1,6]. External secretory clusterin is a 70-80 ku heterodimeric glycoprotein that appears as a -40 ku α - and β -subunits smear by sodium dodecyl sulfate-polyacrylamide gel (SDS-PAGE) electrophoresis under reducing conditions^[7-9]. Recent data suggest that secretory clusterin acts as a molecular chaperone to scavenge denatured proteins and cellular debris outside cells following specific stress-induced injury such as heat shock^[10-14].

Clusterin has been found highly conserved and implicated in a variety of biological processes including lipid transport, epithelial cell differentiation, transformation, and regulation of apoptosis in numerous models of epithelial cells during hormone ablation^[15-20]. It is induced during regression of most hormone-dependent secretory epithelial cells as one of the most potent proteins of the rat ventral prostate or mammary gland^[9,20-23]. Overexpression of secretory clusterin in human cancer cells caused drug resistance and protection against certain cytotoxic agents that induce apoptosis^[24-26]. In human prostate cancer cells, overexpression of clusterin provides protection against TNF α -induced cell death and oligonucleotide directed antisense inhibition enhances spontaneous cell death in untreated cultures^[24]. Clusterin may have a cytoprotective role in epithelial cell death. There are significant alterations in the biogenesis of clusterin during apoptosis, which lead to the appearance of a 50-53 ku uncleaved, nonglycosylated, disulfide-linked isoform that accumulates in the nucleus of MCF-7 cells^[20]. Nuclear clusterin synthesis is a product of alternative splicing, in which the exon II, containing the first AUG and encoding the ER-targeting peptide, was omitted. This "death" form of the clusterin protein was proposed to be synthesized from a second in-frame AUG codon in exon III as translation start site. The short mRNA produces the 49 ku precursor nuclear clusterin which overexpression acts as a pro-death signal, inhibiting cell growth and survival^[27-29].

Clusterin mRNA and protein was recently shown to be down-regulated in esophageal squamous cell carcinoma (ESCC), the major malignant tumor occurred in epithelium of esophagus^[7]. Thus, to the author's knowledge, it is unclear whether alternative splicing clusterin is also involved and the possible roles of clusterin in process of the ESCC. We additionally studied, by multi-regional RT-PCR, Western blot

and immunohistochemical staining, the levels of expression and cellular distribution of clusterin in both tissues and cell lines of human ESCC.

MATERIALS AND METHODS

Tissue sample

The esophageal specimens were obtained from patients diagnosed with ESCC by the pathologists that assisted in our previous work in Cancer Hospital of Chinese Academy of Medical Sciences and Beijing Yanjing Hospital^[7]. The study was approved by the Institutional Review Board. Briefly, immediately the specimens were dissected manually into several aliquots (about 0.3 cm³ in size), quickly frozen in the liquid nitrogen and, then stored at -80 °C until analysis. Carcinoma tissues were obtained from poorly, moderate, and well differentiated ESCC. The corresponding normal tissues were obtained from the distant edge of dissected esophagus. For immunohistochemical (IHC) staining, tissues were fixed in 700 mL/L ethanol or 40 mg/L neutral formalin and embedded in paraffin.

Cell lines

Human ESCC cell lines, EC0156 and EC0132, were generated in our laboratory from ESCC tissues.

RNA isolation and semi-quantitative RT-PCR

Total RNAs were isolated from ESCC specimens and cell lines with RNeasy MinElute cleanup kit (QIAGEN, Valencia, CA) according to the manufacture's instruction. RNA quality was assessed on agarose gel electrophoresis and spectrophotometric analysis. Reverse transcription reactions were performed on 5 µg of total RNAs using SuperScript™ First-Strand synthesis for RT-PCR II kit (Invitrogen, Carlsbad, CA) at 42 °C for 80 min, and 0.5-1 µg aliquots of the cDNA were then subjected to RT-PCR. Based on probable splice sites, the following primers were used to investigate different regions whether alternative splice forms or deleted fragments of clusterin could be found (Table 1).

The PCR step was performed using Taq DNA polymerase (Invitrogen, Carlsbad, CA). As an internal control, *GAPDH* was amplified to ensure cDNA quality and quantity for each RT-PCR reactions. The amplified multiproducts were analyzed on 12-20 g/L agarose gels. Each PCR reaction was down triplicate.

Protein extraction and western blot

The tumor tissues and cell lines were lysed in the lysis buffer (50mmol/L Tris-HCl, pH7.4, 150mmol/L NaCl, 10 g/L TritonX-100, 1 g/L SDS, 1 mmol/L AEBSF, 20 µg/mL Aprotinin and 20 µg/mL Leupeptin) for soluble protein extraction or in the extraction/labeling buffer (BD Biosciences, San Jose, CA) for whole

proteins extraction, and then placed on ice for 20 min. Then they were sonicated and centrifuged at 12 000 g at 4 °C for 30 min. The supernatants were transferred and the protein concentration was measured by Bradford method^[30].

Equal amount of proteins were separated on 100 g/L of SDS-PAGE gels and transferred to polyvinylidene difluoride (PVDF) membranes. After being blocked with 10 g/L non-fat milk, the membranes were incubated with anti-clusterin monoclonal antibody B-5 (sc-5289, Santa Cruz Biotechnology, Santa Cruz, CA) (1:1 000 dilution) at 4 °C overnight. After washing for 3 times, the membranes were incubated with rabbit anti-mouse IgG at room temperature for 1 h. The signals were developed with the ECL kit (Amersham Pharmacia Biotechnology, Piscataway, NJ) and using anti- α -tubulin antibody (Santa Cruz Biotechnology, Santa Cruz, CA) as an internal loading control.

Rabbit anti-human clusterin polyclonal H-330 antibody (sc-8354, Santa Cruz Biotechnology, Santa Cruz, CA) was used to detect the truncated forms of clusterin in whole extracts from EC0156 and EC0132 cells and tissues. A 1:500 dilution of primary H-330 antibody was used, followed by a 1:3 000 dilution of horseradish peroxidase-conjugated anti-rabbit secondary antibody (Santa Cruz Biotechnology, Santa Cruz, CA).

Immunohistochemical analysis

The streptavidin-peroxidase method was used for the immunohistochemical staining of clusterin. Briefly, after deparaffinization in xylene and rehydration in grade ethanol, endogenous peroxidase activity was blocked by incubation with 30 mL/L hydrogen peroxide for 10 min. Tissue sections were then heated at 100 °C in citrate buffer (10 mmol/L, pH 6.0) to retrieve antigens for 10 min. After being incubated with anti-human clusterin monoclonal/polyclonal antibodies, clusterin was visualized by adding biotinylated secondary antibody and streptavidin-horseradish peroxidase (Zymed Laboratories, South San Francisco, CA). Counterstaining was performed with hematoxylin and 3,3'-diaminobenzidine used as a chromogen. Negative controls, made by PBS excluding mono- or polyclonal anti-human clusterin antibodies from the reaction, showed no specific staining and. Experiments performed using polyclonal and monoclonal anti-human clusterin antibodies from the same commercial source gave the same pattern of specific distributions. Cover slips were mounted with Eukitt (O. Kindler GmbH & Co., Freiburg, Germany).

RESULTS

N-terminal deletions of the clusterin transcription in ESCC

To detect the alterations of clusterin expression, a multi-region cDNA fragments of ESCC were analyzed by semi-quantitative

Table 1 Primers and PCR reactions for multi-region amplifications of clusterin

Amplified fragments (bp)	Sense primers	Antisense primers	PCR conditions
1-1 350	5'-CCGGATCCTTATGATGA AGACTCTGCTGCTG-3'	5'-GCCTCGAGTCACTCC CGCTGCTTTTTG-3'	95 °C for 40 s, 62 °C for 40 s, and 72 °C for 90 s
1-1 056	5'-CCGGATCCTTATGATG AAGACTCTGCTGCTG-3'	5'-GTGTTGAGCATCTTCC ACTG-3'	95 °C for 30 s, 60 °C for 40 s, and 72 °C for 60 s
1-321	5'-CCGGATCCTTATGATGA AGACTCTGCTGCTG-3'	5'-CATCATGGTCTCATT GCACAC-3'	95 °C for 30 s, 56 °C for 30 s, and 72 °C for 30 s
437-1 056	5'-GAGCTCGCCCTTCTACTTCT-3'	5'-GTGTTGAGCATCTTCCACTG-3'	95 °C for 30 s, 56 °C for 30 s, and 72 °C for 30 s
437-1 350	5'-GAGCTCGCCCTTCTACTTCT-3'	5'-GCCTCGAGTCACTC CCGCTGCTTTTTG-3'	95 °C for 40 s, 60 °C for 40 s, and 72 °C for 60 s
1 120-1 350	5'-ACCTCACGCAAGGC GAAGACC-3'	5'-TCTCACTCCTCCGGTGCTT-3'	95 °C for 30 s, 56 °C for 25 s, and 72 °C for 25 s
GAPDH	5'-ACCACAGTCCATGCCATCAC-3'	5'-TCCACCACCTGTTGCTGTA-3'	

RT-PCR (Figure 1). The clusterin cDNA derived from the total RNA of both ESCC tissues and their matched dissected normal esophageal mucosa. The results of various fragments are shown in Figure 2. Comparing with the tumor matched normal epithelia of esophagus, the expressions of full-length and N-terminal fragment (1-320 bp) of clusterin were deleted obviously, however, there were no differences between the middle (437-1 056 bp) and C-terminal fragments (1 120-1 350 bp). By this approach, additionally using the primer containing the start codon of clusterin and the -3' end of the middle fragment obtained the same result with the one from full-length (1-1 056 bp), and also found the same expression level between the cancer tissue and normal epithelia from 437 to the end of clusterin (437-1 350 bp). The exceptional transcription area of clusterin was narrowed in the region of 1-437 bp, which contained the abnormal translation start site of the "death" form clusterin (nuclear clusterin) and omitted the region encoding the endoplasmic reticulum (ER)-targeting peptide of clusterin protein. These results indicated that clusterin was truncated at 5' end of gene.

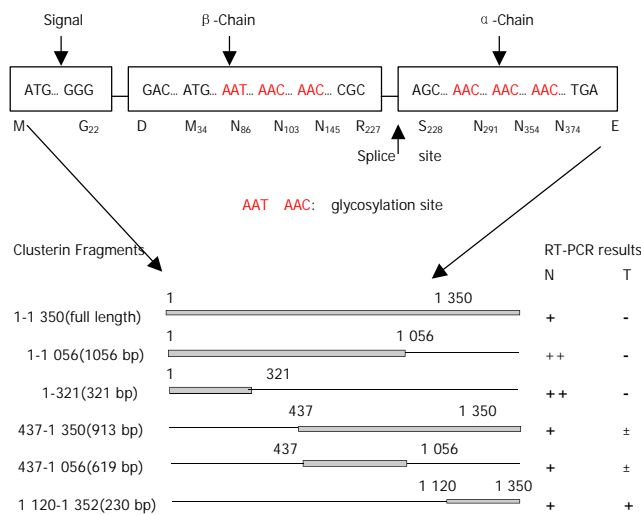


Figure 1 Schematic diagram of analyzed fragments of clusterin. A: structural map of the human clusterin protein. Letters and boxes signify the following: ER-targeting signal, endoplasmic reticulum-targeting hydrophobic leader peptide; splice site, α/β -cleavage site (amino acid 205 and 206) of cytoplasmic -60 ku pre-secreted clusterin which was glycosylated and cleaved into α and β chains to form an 80 ku matured secretory clusterin protein; rectangles, hydrophobic leader peptide (N-terminal 66 bp encode aa M1 to G22, 22 aa), β -chain (5' end) and α -chain (3' end); Red letters, the glycosylation sites. B: Schematic diagram of analyzed fragments of clusterin and their RT-PCR results.

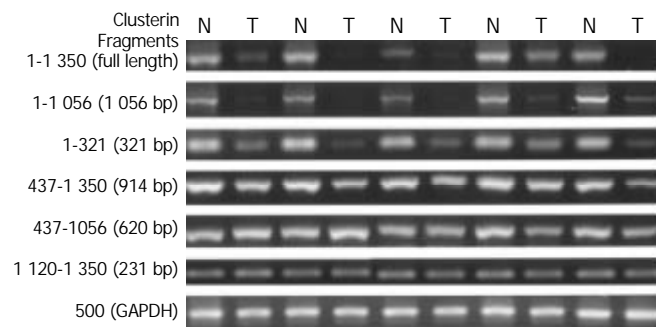


Figure 2 N-terminal truncated clusterin was analyzed by RT-PCR. GAPDH was used as internal control. N: tumor matched far edge normal esophageal mucosa. T: ESCC specimens. The expression of full-length and different of clusterin fragments

were analyzed comparing with the tumor matched normal esophageal mucosa. The truncated region was narrowed down at the 5' end of clusterin (1-437 bp).

Down-regulation of nuclear clusterin and secreted clusterin in ESCC

According to the results of RT-PCR, anti-clusterin antibodies were used to detect the expression of clusterin protein both in the tissues and cell lines of ESCC (Figure 3). The predominant form of clusterin in tumor tissues was the secreted heterodimeric glycoprotein with MW of 75-80 ku (37-40 ku smear in reducing SDS-PAGE), which was down-regulated in ESCC tissues compared with the normal epithelia of esophagus (100%, 21/21), but was absent in the ESCC cell lines (EC0516 and EC0132). The results confirmed our previous data that the clusterin gene is generally down-regulated in esophageal cancer^[7]. Meanwhile, an about 50 ku nuclear clusterin was appeared in both the ESCC tissues (100%, 21/21) and cell lines (100%, 2/2), and sometimes in normal epithelia. It was highly expressed in the tumor tissues and cells. Additionally, an about 35 ku band was detected by anti-clusterin antibody H-330 in the EC0132 cell line. Under these experimental conditions, it must be noticed that, as shown in Figure 3, the monoclonal antibody used (Clusterin- β , B-5 from Santa Cruz Biotechnology, Santa Cruz, CA) might react with the carboxy terminus of clusterin β chain of human origin and not react with uncleaved nuclear clusterin. However, the polyclonal antibody used (Clusterin- α/β , H-330 from Santa Cruz Biotechnology Inc., Santa Cruz, CA) recognized the major part of clusterin from 120 to 449 amino acids at the carboxy terminus of clusterin- α/β chains, including the 60 ku precursor (cytoplasmic clusterin), from which all clusterin isoforms are supposed to be derived, uncleaved nuclear clusterin (-50 ku) and the matured secreted clusterin (-37-40 ku, cleaved in - α and - β chains).

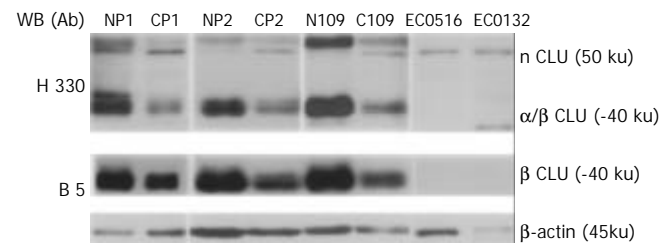


Figure 3 Western blot analysis of expression of multiple forms of clusterin in ESCC. nCLU: the nonglycosylated uncleaved nuclear clusterin; α/β CLU: cleaved and glycosylated secreted clusterin protein; β CLU: cleaved and glycosylated clusterin β chain; B-5: monoclonal antibody (Santa Cruz Biotechnology, Santa Cruz, CA) reacted with the C-terminus of clusterin- β of human origin and did not react with the nuclear clusterin; H-330: polyclonal antibody (Santa Cruz Biotechnology, Santa Cruz, CA) recognized the major part of clusterin from 120 to 449 aa at the C-terminus of clusterin- α/β chains including uncleaned nuclear clusterin (-50 ku and the matured secreted clusterin (-37-40 ku); Np: pooled normal esophageal mucosa from 10 cases; Cp: pooled ESCC tumor tissues from 10 cases; N109: normal esophageal mucosa from a single individual; C109: ESCC tumor tissue from a single individual. β -actin was used as loading control.

Intracellular localizations of clusterin in ESCC

Immunohistochemistry analysis was performed in the tissue sections of ESCC specimen and matched normal counterparts using the same antibody (B 5, Santa Cruz Biotechnology, Santa Cruz, CA) as previously used for Western blot analysis (Figure 4). In normal esophageal mucosa, clusterin protein localized prevalently to the stroma of esophageal mucosa, while the squamous epithelial cells and basal lamina were negative. Very

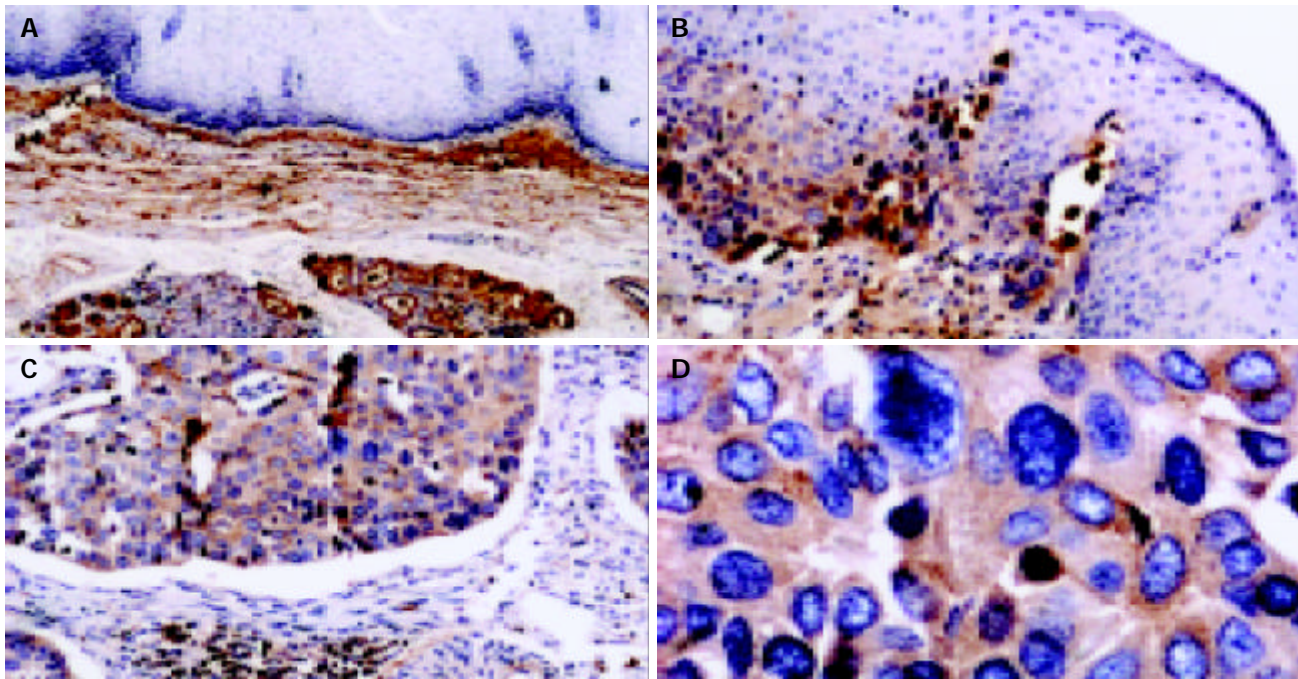


Figure 4 Detection of clusterin protein in tissue sections of human ESCC by immunohistochemistry. In normal esophageal mucosa, the expression of clusterin in squamous epithelial cells and basal lamina was negative, while clusterin immunostaining was visualized obviously in the stroma of epithelial mucosa (A, 100 \times); clusterin was positive in middle dysplasia, while the vast majority of stromal cells were negative in normal squamous epithelia of esophagus (B, 100 \times); clusterin was strong positive in the remnants of stromal extracellular matrix invaded by tumor cells in well-differentiated ESCC (C, 100 \times). D show that stromal and basal membrane are almost completely disrupted and invaded by tumor cells. (D, same section, different field of that of C, 400 \times). Counterstaining was performed with hematoxylin.

high levels of clusterin expression were found in the connective tissue of the lamina *propria* of epithelial mucosa, in which clusterin was confined to what appeared to be the remnants of the extra cellular matrix right under the basal membrane of epithelia, the cytoplasm of esophageal glandular cells, plasma membrane and cytoplasm of duct glandular epithelia, and plasma membrane and cytoplasm of lymphocytes in lymphatic follicle were detected positive by IHC (Figure 4A). During tumorigenesis the intracellular localizations of clusterin was translocated from stroma to the squamous epithelial cells at very early states. It was even found positive in middle dysplasia, a kind of very early lesion of esophagus versus negative in normal squamous epithelia (Figure 4B). However, clusterin and its pre-matured form were distributed in cancerous epithelia of ESCC (the antibody B 5 is able to detect the 60-ku secretory clusterin precursor by Western blot analysis, data not show here) and then, disappeared in stromal mucosa of esophagus (Figure 4C and D).

DISCUSSION

Based on our previous data, clusterin is markedly down-regulated in both serum and tissues of ESCC^[7]. To further clarify the mechanisms of clusterin alterations during tumorigenesis, we first analyzed the gene transcription using semi-quantitative RT-PCR by amplifying different regions from 5' end to 3' end of the gene. We found the same expression results from 437 to 1 350 bp of clusterin between cancer and their matched normal. However, comparing with the cDNA reverse-transcribed from the total mRNA of normal epithelial mucosa, using the cDNA of tumor tissues, no fragment was amplified completely by the N-terminus of 5' -primer which contains the start codon located in the first exon (see underline sequences of the primer 5' - CCGGATCCTTATGATGAAGACTCTGCTGCTG-3'). Those suggested that there was an N-terminal deletion or miss splicing located on 1-437 bp that induced a wrong transcription

forms of the clusterin in ESCC. A miss splicing site repeated in breast cancer cell line MCF 7 was right in this area^[29]. At protein expression level, this region is naturally corresponding to the β chain of clusterin protein. According this rationale, an N-terminal truncated form of clusterin protein would be also detectable. The different protein forms of clusterin in ESCC also describe the biogenesis of multi-transcription forms of clusterin.

The significance of alterations of clusterin gene expression during tumorigenesis remains a mystery. Our data indicated that human esophageal epithelial cells synthesized at least two forms of clusterin, secretory and nuclear clusterins, and their expression levels were changed during tumorigenesis. The secretory clusterin was down-regulated both in serum and tissues of ESCC; while, nuclear clusterin was induced in tumor cells. We also found a 60 ku secretory clusterin precursor protein in ESCC and normal epithelial cells (data not shown). Previous data indicated the existence of a mature about 55 ku nuclear clusterin protein, as a cell death protein and lack ER-signaling peptides, which did not appear to be either glycosylated or cleaved at its α/β site, a site cleaved during maturation of the 60 ku secretory clusterin precursor protein^[12,28,29]. Yang *et al*^[27], described nuclear clusterin was induced by relatively high levels of cytotoxic stress in direct proportion to lethality after growth stimulation of ionizing radiation (IR). Utilization of an in-framed secondary downstream AUG as a translation start site was proposed to result in the synthesis of an about 50 ku precursor nuclear clusterin protein that resided in cytoplasm of undamaged cells by confocal microscopy. Overexpression of this nuclear clusterin, even without IR treatment, caused cell death^[12]. In our immunoblotting results, an about 50 ku nuclear clusterin was detected in both ESCC tissues and cell lines, and occasionally in normal esophageal epithelia using H-330 anti-clusterin antibody. This form of nuclear clusterin could not be detected with B-5 anti-clusterin antibody. As Leskov *et al*^[29] used, H-330 anti-clusterin antibody recognizes the major part of clusterin from 120 to 449 amino acid at the

carboxy terminus of clusterin α/β chains, including the 60 ku precursor and a -49 ku nuclear clusterin precursor (pnCLU). These results were consistent with our findings by RT-PCR that deletion at 5' end or appearance of a splicing at different sites of clusterin gene resulted in N-terminal truncated forms of clusterin transcription. These abnormal forms of clusterin undergo alien post-translational modification compared to secretory clusterin.

Nuclear clusterin is associated with Ku70^[8], a DNA double-strand break repair protein. Its Ku70 binding activity was localized to the C-terminal coiled-coil domain of nuclear clusterin^[30]. The C-terminal coiled-coil domain of nuclear clusterin was the minimal region required for Ku binding and apoptosis. We also found that Ku70 altered in ESCC (data not shown). Although we do not yet know whether nuclear clusterin binding to Ku70 is essential for lethality, we could speculate that enhanced clusterin binding to Ku70 may hinder the formation of Ku70/Ku80 heterodimer, consequently interfere with non-homologous DNA repair, resulting in genomic instability or cell death.

Our studies suggested, on the other hand, the alterations of the localizations and intracellular localizations of clusterin. It was translocated from stroma to the epithelial cells by disrupting the basal membrane of epithelial mucosa during carcinogenesis.

In general, our results demonstrated that the alterations in the expression, proteolysis and intracellular localizations of clusterin and an N-terminus truncated form of clusterin were found in ESCC. Its possible roles in cell survival, cell death and neoplastic transformation remain an additional debate.

ACKNOWLEDGEMENTS

Professor Xin-Yu Zhang and Dr. Li-Yong Zhang are thanked for their help with clusterin primers design.

REFERENCES

- Trougakos IP**, Gonos ES. Clusterin/apolipoprotein J in human aging and cancer. *Int J Biochem Cell Biol* 2002; **34**: 1430-1448
- Polihronis M**, Paizis K, Carter G, Sedal L, Murphy B. Elevation of human cerebrospinal fluid clusterin concentration is associated with acute neuropathology. *J Neurol Sci* 1993; **115**: 230-233
- Law GL**, Griswold MD. Activity and form of sulfated glycoprotein 2 (clusterin) from cultured Sertoli cells, testis, and epididymis of the rat. *Biol Reprod* 1994; **50**: 669-679
- Purrello M**, Bettuzzi S, Di Pietro C, Mirabile E, Di Blasi M, Rimini R, Grzeschik KH, Ingletti C, Corti A, Sichel G. The gene for SP-40, 40, human homolog of rat sulfated glycoprotein 2, rat clusterin, and rat testosterone-repressed prostate message 2, maps to chromosome 8. *Genomics* 1991; **10**: 151-156
- Wong P**, Taillefer D, Lakins J, Pineault J, Chader G, Tenniswood M. Molecular characterization of human TRPM-2/clusterin, a gene associated with sperm maturation, apoptosis and neurodegeneration. *Eur J Biochem* 1994; **221**: 917-925
- Kapron JT**, Hilliard GM, Lakins JN, Tenniswood MP, West KA, Carr SA, Crabb JW. Identification and characterization of glycosylation sites in human serum clusterin. *Protein Sci* 1997; **6**: 2120-2133
- Zhang LY**, Ying WT, Mao YS, He HZ, Liu Y, Wang HX, Liu F, Wang K, Zhang DC, Wang Y, Wu M, Qian XH, Zhao XH. Loss of clusterin both in serum and tissue correlates with the tumorigenesis of esophageal squamous cell carcinoma via proteomics approaches. *World J Gastroenterol* 2003; **9**: 650-654
- Yang CR**, Yeh S, Leskov K, Odegaard E, Hsu HL, Chang C, Kinsella TJ, Chen DJ, Boothman DA. Isolation of Ku70-binding proteins (KUBs). *Nucleic Acids Res* 1999; **27**: 2165-2174
- Wong P**, Pineault J, Lakins J, Taillefer D, Leger J, Wang C, Tenniswood M. Genomic organization and expression of the rat TRPM-2 (clusterin) gene, a gene implicated in apoptosis. *J Biol Chem* 1993; **268**: 5021-5031
- Humphreys DT**, Carver JA, Easterbrook-Smith SB, Wilson MR. Clusterin has chaperone-like activity similar to that of small heat shock proteins. *J Biol Chem* 1999; **274**: 6875-6881
- Clark AM**, Griswold MD. Expression of clusterin/sulfated glycoprotein-2 under conditions of heat stress in rat Sertoli cells and a mouse Sertoli cell line. *J Androl* 1997; **18**: 257-263
- Kimura K**, Asami K, Yamamoto M. Effect of heat shock treatment on the production of variant testosterone-repressed prostate message-2 (TRPM-2) mRNA in culture cells. *Cell Biochem Funct* 1997; **15**: 251-257
- Michel D**, Chatelain G, North S, Brun G. Stress-induced transcription of the clusterin/apoJ gene. *Biochem J* 1997; **328**(Pt 1): 45-50
- Viard I**, Wehrli P, Jornot L, Bullani R, Vechietti JL, Schifferli JA, Tschopp J, French LE. Clusterin gene expression mediates resistance to apoptotic cell death induced by heat shock and oxidative stress. *J Invest Dermatol* 1999; **12**: 290-296
- Witte DP**, Aronow BJ, Dry JK, Harmony JA. Temporally and spatially restricted expression of apolipoprotein J in the developing heart defines discrete stages of valve morphogenesis. *Dev Dyn* 1994; **201**: 290-296
- Wunsche W**, Tenniswood MP, Schneider MR, Vollmer G. Estrogenic regulation of clusterin mRNA in normal and malignant endometrial tissue. *Int J Cancer* 1998; **76**: 684-688
- Correa-Rotter R**, Ibarra-Rubio ME, Schwochau G, Cruz C, Silksen JR, Pedraza-Chaverri J, Chmielewski D, Rosenberg ME. Induction of clusterin in tubules of nephrotic rats. *J Am Soc Nephrol* 1998; **9**: 33-37
- Calvo EL**, Mallo GV, Fiedler F, Malka D, Vaccaro MI, Keim V, Morisset J, Dagorn JC, Iovanna JL. Clusterin overexpression in rat pancreas during the acute phase of pancreatitis and pancreatic development. *Eur J Biochem* 1998; **254**: 282-289
- May PC**. Sulfated glycoprotein-2: an emerging molecular marker for neurodegeneration. *Ann N Y Acad Sci* 1993; **679**: 235-244
- O'Sullivan J**, Whyte L, Drake J, Tenniswood M. Alterations in the post-translational modification and intracellular trafficking of clusterin in MCF-7 cells during apoptosis. *Cell Death Differ* 2003; **10**: 914-927
- Guenette RS**, Corbeil HB, Leger J, Wong K, Mezl V, Mooibroek M, Tenniswood M. Induction of gene expression during involution of the lactating mammary gland of the rat. *J Mol Endocrinol* 1994; **12**: 47-60
- Bettuzzi S**, Hiipakka RA, Gilna P, Liao ST. Identification of an androgen-repressed mRNA in rat ventral prostate as coding for sulphated glycoprotein 2 by cDNA cloning and sequence analysis. *Biochem J* 1989; **257**: 293-296
- Strange R**, Li F, Saurer S, Burkhardt A, Friis RR. Apoptotic cell death and tissue remodelling during mouse mammary gland involution. *Development* 1992; **115**: 49-58
- Sensibar JA**, Sutkowski DM, Raffo A, Buttyan R, Griswold MD, Sylvester SR, Kozlowski JM, Lee C. Prevention of cell death induced by tumor necrosis factor alpha in LNCaP cells by overexpression of sulfated glycoprotein-2 (clusterin). *Cancer Res* 1995; **55**: 2431-2437
- Steinberg J**, Oyasu R, Lang S, Sintich S, Rademaker A, Lee C, Kozlowski JM, Sensibar JA. Intracellular levels of SGP-2 (Clusterin) correlate with tumor grade in prostate cancer. *Clin Cancer Res* 1997; **3**: 1707-1711
- Miyake H**, Nelson C, Rennie PS, Gleave ME. Acquisition of chemoresistant phenotype by overexpression of the antiapoptotic gene testosterone-repressed prostate message-2 in prostate cancer xenograft models. *Cancer Res* 2000; **60**: 2547-2554
- Yang CR**, Leskov K, Hosley-Eberlein K, Criswell T, Pink JJ, Kinsella TJ, Boothman DA. Nuclear clusterin/XIP8, an x-ray-induced Ku70-binding protein that signals cell death. *Proc Natl Acad Sci U S A* 2000; **97**: 5907-5912
- Reddy KB**, Jin G, Karode MC, Harmony JA, Howe PH. Transforming growth factor beta (TGF beta)-induced nuclear localization of apolipoprotein J/clusterin in epithelial cells. *Biochemistry* 1996; **35**: 6157-6163
- Leskov KS**, Klokov DY, Li J, Kinsella TJ, Boothman DA. Synthesis and functional analyses of nuclear clusterin, a cell death protein. *J Biol Chem* 2003; **278**: 11590-11600
- Bradford MM**. A rapid and sensitive method for the quantitation of microgram quantities of protein utilizing the principle of protein-dye binding. *Anal Biochem* 1976; **72**: 248-254

Effects of *c9,t11*-conjugated linoleic acid on adhesion of human gastric carcinoma cell line SGC-7901

Bing-Qing Chen, Yan-Mei Yang, Qi Wang, Yan-Hui Gao, Jia-Ren Liu, Jing-Shu Zhang, Xuan-Lin Wang, Rui-Hai Liu

Bing-Qing Chen, Qi Wang, Jia-Ren Liu, Jing-Shu Zhang, Xuan-Lin Wang, Department of Nutrition and Food Hygiene, Public Health College, Harbin Medical University, Harbin 150001, Heilongjiang Province, China

Yan-Mei Yang, Medical College of Shantou University, Shantou 515031, Guangdong Province, China

Yan-Hui Gao, Chinese Center for Disease Control and Prevention, the Center for Endemic Disease Control, Beijing, China

Rui-Hai Liu, Food Science and Toxicology, Department of Food Science, 108 Stocking Hall, Cornell University, Ithaca, NY 14853-7201, USA

Supported by the National Natural Science Foundation of China, No. 30070658

Correspondence to: Professor Bing-Qing Chen, Department of Nutrition and Food Hygiene, Public Health College, Harbin Medical University, Harbin 150001, Heilongjiang Province, China. bingqingchen@sina.com

Telephone: +86-451-3608014 **Fax:** +86-451-3648617

Received: 2003-10-08 **Accepted:** 2003-12-08

Abstract

AIM: To investigate the effect of *c9,t11*-conjugated linoleic acid (*c9,t11*-CLA) on the adhesion of human gastric carcinoma cell line (SGC-7901).

METHODS: SGC-7901 cells were at first treated with different concentrations (25, 50, 100, 200 $\mu\text{mol/L}$) of *c9,t11*-CLA and 1 mL/L ethanol (as a negative control) for 24 h. Using adhesion assay and Western blot, we investigated the ability of SGC-7901 cells to adhere to intracellular matrix and examined the expression of E-cadherin (ECD), α -catenin, intercellular adhesion molecule 1 (ICAM-1) and vascular cell adhesion molecule 1 (VCAM-1) in these cells.

RESULTS: The attachment rate to laminin of SGC-7901 cells treated with different concentrations of *c9,t11*-CLA (0, 25, 50, 100, and 200 $\mu\text{mol/L}$) was 100.0 ± 3.3 , 95.7 ± 4.0 , 89.2 ± 4.6 , 87.9 ± 6.1 , and 65.9 ± 5.8 , respectively. The attachment rate to fibronectin was 100.0 ± 4.7 , 96.8 ± 3.8 , 94.5 ± 4.1 , 76.5 ± 4.3 , and 61.8 ± 4.8 , respectively. The attachment rate to Matrigel was 99.9 ± 6.6 , 91.4 ± 6.8 , 85.5 ± 7.4 , 79.3 ± 5.6 , and 69.6 ± 5.1 , respectively. Besides, *c9,t11*-CLA could increase the level of ECD and α -catenin, and decrease the level of ICAM-1 and VCAM-1 in SGC-7901 cells.

CONCLUSION: *c9,t11*-CLA can reduce the adhesion of human gastric carcinoma cells to laminin, fibronectin and Matrigel. *c9,t11*-CLA can increase the level of ECD and α -catenin, and decrease the level of ICAM-1 and VCAM-1 in human gastric carcinoma cells.

Chen BQ, Yang YM, Wang Q, Gao YH, Liu JR, Zhang JS, Wang XL, Liu RH. Effects of *c9,t11*-conjugated linoleic acid on adhesion of human gastric carcinoma cell line SGC-7901. *World J Gastroenterol* 2004; 10(10): 1392-1396
<http://www.wjgnet.com/1007-9327/10/1392.asp>

INTRODUCTION

Although the incidence of gastric cancer is decreasing worldwide, it remains one of the most common tumors in China^[1-4] and is a major cause of cancer deaths in some countries^[5,6]. Most of gastric cancer patients die from metastasis. Although the mechanism of gastric cancer metastasis is not fully elucidated, the abnormal adhesion ability of cells has been reported to play a pivotal role. Cell-cell and cell-matrix adhesions are essential for establishing and maintaining normal cell morphology and function. Disturbance of cell adhesion may result in the malignant transformation of cells. Furthermore, cell adhesion molecules are important ingredients in maintaining cell-cell adhesion and cell-matrix interactions. The abnormality of cell adhesion molecules closely correlates with neoplastic transformation and metastasis^[7,8]. Cell adhesion molecules mediate tumor cell-cell, tumor cell-endothelial cell and tumor cell-matrix interactions. In tumor metastasis, cell-cell and cell-matrix interactions are determined by functional status of cell adhesion molecules. Glycoproteins are the cell adhesion molecules and can be classified into several classes according to their structure: cadherins, selectins, CD44, immunoglobulin family, and integrin family.

Conjugated linoleic acid (CLA) is a class of positional and stereoisomers of octadecadienoate (18:2) with conjugated double bonds. The predominant isomer in foods is the *c9,t11*-CLA isomer^[9-16]. In 1979, Pariza *et al.*^[17] detected mutagenic inhibitory activity in both cooked and uncooked ground beef. Then in 1985, they observed that the crude extracts could protect rats against tumors^[18]. In 1987, Ha *et al.*^[19] identified four isomers of CLA from cooked beef. In several animal models of chemical carcinogenesis, it has been reported that CLA was a potent cancer preventive agent. For example, CLA could inhibit skin papillomas^[18,20], forestomach neoplasia^[21-23], mammary tumors^[24-30], and colon aberrant crypt foci^[31]. Moreover, CLA was also effective in reducing the size and metastasis of transplanted human breast cancer cells and prostate cancer cells in SCID mice^[32,33]. Several studies^[34-43] suggested that CLA was cytostatic and cytotoxic to a variety of human cancer cells *in vitro*, including hepatoma, malignant melanoma, colorectal cancer, breast carcinoma, and gastric cancer.

One of our previous studies showed that *c9,t11*-CLA could inhibit the invasion of mouse melanoma cells (B16-MB) through reducing their adhesion ability to extracellular matrix^[44]. Two other studies of ours showed that *c9,t11*-CLA could decrease the invasive ability of human gastric carcinoma cells (SGC-7901)^[45,46]. However, it is unclear whether CLA influences the adhesive ability of SGC-7901 cells and the expression of their adhesion molecules. Therefore, in this study, we investigated the effect of *c9,t11*-CLA on the adhesive ability of SGC-7901 cells and detected the expression of E-cadherin (ECD), α -catenin, intercellular adhesion molecule 1 (ICAM-1) and vascular cell adhesion molecule 1 (VCAM-1) in SGC-7901 cells using adhesion and Western blot assays.

MATERIALS AND METHODS

Materials

c9,t11-CLA with 98% purity, was provided by Dr. Rui-Hai

Liu at Food Science and Toxicology, Department of Food Science, Cornell University, Ithaca, NY, USA. The *c9,t11*-CLA was dissolved in ethanol, then diluted to the following concentrations: 25, 50, 100, and 200 $\mu\text{mol/L}$.

To examine the expression of ECD, α -catenin, ICAM-1, and VCAM-1, we used four primary antibodies: rabbit polyclonal antibody for ECD, mouse monoclonal antibody for α -catenin, and goat polyclonal antibodies for ICAM-1 and VCAM-1, respectively. These antibodies were purchased from Zhongshan Co., China.

Methods

Cell culture Human gastric adenocarcinoma cells (SGC-7901), purchased from Cancer Research Institute of Beijing (China), were cultured in RPMI 1640 (Gibco) medium, supplemented with 100 mL/L fetal calf serum (FCS), 100×10^3 U/L penicillin, 100 mg/L streptomycin and 2 mmol/L L-glutamine under 50 mL/L CO_2 in a humidified incubator. The pH was maintained at 7.2-7.4 and the temperature at 37 °C. After sub-cultured with EDTA, the SGC-7901 cells were incubated with different concentrations (25, 50, 100, and 200 $\mu\text{mol/L}$) of *c9,t11*-CLA and 1ml/L ethanol (as a negative control) for 24 h.

Cell adhesion assay A total of 96-well plates (Nunc. Co.) were incubated at 37 °C with laminin, fibronectin or Matrigel for 1 h and then blocked with phosphate-buffered saline (PBS) containing 100 g/L BSA at the same temperature for another 1 h. After exposed to different concentrations (25, 50, 100, and 200 $\mu\text{mol/L}$) of *c9,t11*-CLA for 24 h, the SGC-7901 cells were suspended in serum-free medium at a density of 8×10^5 cells/ml. Then, 0.1 mL of SGC-7901 cells suspension was added to each well and incubated at 37 °C for 1 h. The plates were washed three times with PBS to remove unattached cells. The remaining SGC-7901 cells in 96-well plates were reacted with MTT for 4 h at 37 °C, then solved with DMSO. The absorbance of each well was measured at 570 nm with an ELX800 microplate reader (Bio-TEK Co.). Results were expressed as the percentage of total cells assuming that the adhesion of cells in control was 100%.

Protein extract and western blot The SGC-7901 cells treated with different concentrations of *c9,t11*-CLA were harvested, washed twice times with PBS and lysed at 4 °C in lysis buffer containing 150 mmol/L NaCl, 1 mL/L NP-40, 5 mg/L sodium deoxycholate, 100 g/L SDS, 50 mmol Tris (pH 7.4), 1 mmol/L DTT, 0.5mmol/L Na_3VO_4 , 10 mmol/L phenylmethylsulfonyl fluoride (PMSF), 10 mg/L aprotinin, and 5 mg/L leupeptin. Following the centrifugation of 10 000 *g* for 30 min at 4 °C, the amount of protein in the supernatant was determined using DUR 640 nucleic acid and protein analyzer. Equal amount of protein was separated on SDS-polyacrylamide gel electrophoresis and transferred to nitrocellulose membrane (Gibco BRL, USA) overnight. Blocked with 50 g/L defatted milk, the membrane was hybridized with rabbit anti-E-cadherin, mouse anti- α -catenin, goat anti-ICAM-1 and goat anti-VCAM-1 antibody, then incubated with horseradish peroxidase- conjugated IgG. Finally, the immunoreactive bands were detected using diaminobenzidine tetrahydrochloride (DAB) substrate and analyzed with a ChemiImager™ 4000 low light imaging system (Alpha Innotech Corporation). At the same time GAPDH was used as house-keeping protein.

RESULTS

Effect of *c9,t11*-CLA on adhesion of SGC-7901 cells

As shown in Table 1, *c9,t11*-CLA could reduce the cell attachment to FN, LN or Matrigel in a dose dependent manner after SGC-7901 cells were pre-incubated for 24 h with different concentrations of *c9,t11*-CLA.

Table 1 Effects of *c9,t11*-CLA on adhesion of SGC-7901 cells (*n*=3)

Doses ($\mu\text{mol/L}$)	Attachment rate to LN (%)	Attachment rate to FN (%)	Attachment rate to matrigel (%)
200	100.0 \pm 3.3	100.0 \pm 4.7	99.9 \pm 6.6
100	95.7 \pm 4.0	96.8 \pm 3.8	91.4 \pm 6.8
50	89.2 \pm 4.6 ^b	94.5 \pm 4.1	85.5 \pm 7.4 ^a
25	87.9 \pm 6.1 ^b	76.5 \pm 4.3 ^b	79.3 \pm 5.6 ^b
Negative control group	65.9 \pm 5.8 ^b	61.8 \pm 4.8 ^b	69.6 \pm 5.1 ^b

^a*P*<0.05 vs negative control, ^b*P*<0.01 vs negative control.

Effect of *c9,t11*-CLA on ECD and α -catenin in SGC-7901 cells

As shown in Figure 1, the level of ECD and α -catenin protein in SGC-7901 cells treated with different concentrations of *c9,t11*-CLA was increased in comparison with that in the negative control group. The level of ECD and α -catenin protein in SGC-7901 cells treated with 200 $\mu\text{mol/L}$ *c9,t11*-CLA increased 65.9% and 80.5% respectively, compared with those in the negative control group.

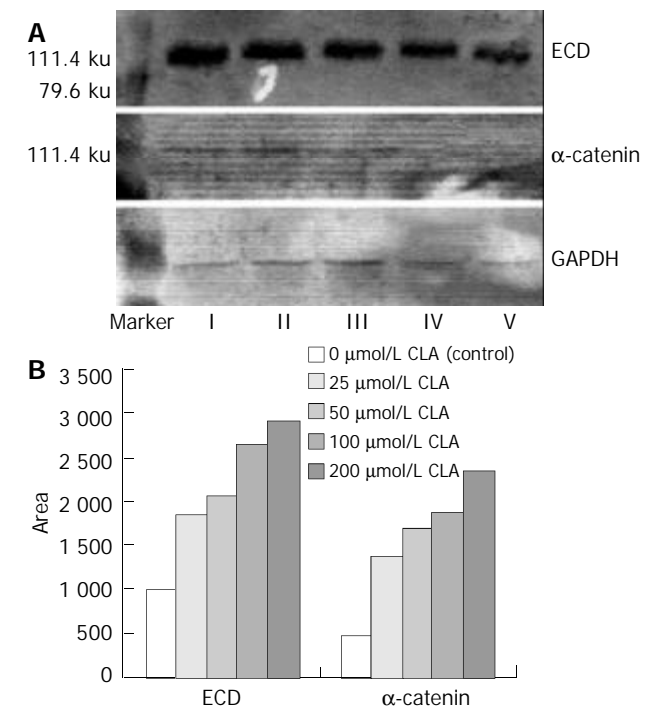


Figure 1 Effect of *c9,t11*-CLA on ECD and α -catenin in SGC-7901 cells detected by Western blot. A: Top: The expression of ECD in SGC-7901 cells treated with different concentrations of *c9,t11*-CLA. Middle: The expression of α -catenin protein in SGC-7901 cells treated with different concentrations of *c9,t11*-CLA. I - IV are 200, 100, 50, 25 $\mu\text{mol/L}$ *c9,t11*-CLA; V is the control group. B: the result of quantitation of ECD and α -catenin levels in SGC-7901 cells by ChemiImager™ 4000 digital system.

Effect of *c9,t11*-CLA on ICAM-1 and VCAM-1 in SGC-7901 cells

As shown in Figure 2, the expression of ICAM-1 and VCAM-1 protein in SGC-7901 cells treated with different concentrations of *c9,t11*-CLA was decreased in comparison with that in the negative control group. Analyzed by ChemiImager 4000 digital system, the level of ICAM-1 and VCAM-1 protein in SGC-7901 cells treated with 200 $\mu\text{mol/L}$ *c9,t11*-CLA increased 70.2% and 65.4% respectively, compared with that in the negative control group.

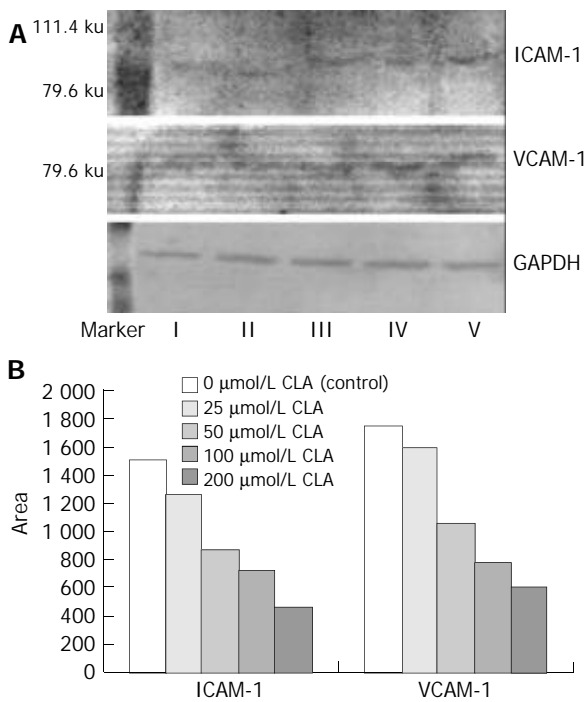


Figure 2 Effect of *c9,t11*-CLA on ICAM-1 and VCAM-1 in SGC-7901 cells detected by Western blot. A: Top: The expression of ICAM-1 in SGC-7901 cells treated with different concentrations of *c9,t11*-CLA. Middle: The expression of VCAM-1 in SGC-7901 cells treated with different concentrations of *c9,t11*-CLA. I-IV are 200, 100, 50, 25 $\mu\text{mol/L}$ *c9,t11*-CLA, respectively; V is the control group. B: the result of quantitation of ICAM-1 and VCAM-1 levels in SGC-7901 cells by ChemiImagerTM 4000 digital system.

DISCUSSION

Many researches have indicated the importance of cancer cell-extracellular matrix (ECM) interaction in tumor metastasis. Cell and matrix interactions could promote cell migration, proliferation, and ECM degradation^[47-51]. It also has been shown that prevention of tumor cell adhesion and migration is related to inhibition of tumor cell invasion into the basement membrane. Laminin (LN), fibronectin (FN) and type IV collagen are the principal components of ECM. The *in vitro* assays of FN, LN, or Matrigel that mainly contain FN, LN and type IV collagen can better simulate the *in vivo* adhesive process. It was shown that agents that inhibited cell attachment *in vitro* decreased the invasion and metastatic potential of tumor cells *in vivo*. Therefore, cell adhesion assay not only is employed in determining the adhesive interaction between tumor cells and matrix components, but also is suitable in screening agents that can inhibit adhesion and metastasis of tumor cell. We demonstrated in our current study that after incubation with 200, 100, and 50 $\mu\text{mol/L}$ of *c9,t11*-CLA for 1 h, the attachment to extracellular matrix components of SGC-7901 cells was significantly reduced. The result was consistent with the findings in our previous study^[44]. Therefore, we could conclude that *c9,t11*-CLA could inhibit the attachment to extracellular matrix components of tumor cells and this process might be a mechanism for the inhibition of tumor invasion.

Before they can invade or metastasize, tumor cells have to dissociate from primary neoplasms. A loss of cell-cell adhesive interaction is required for the detachment. Thus, adhesion molecules play an important role in metastatic process. Cadherins have been found to be a class of calcium dependent cell adhesion molecules involved in homotypic cell-cell adhesion^[7,8]. E-cadherin is a member of the cadherin family that is expressed in all epithelial cells and is essential to the

maintenance of cell morphology, cell movement and cell adhesive function. Because E-cadherin can maintain cell adhesion, its abnormalities may be associated with tumorigenesis. It was proved that abnormalities of E-cadherin mRNA and E-cadherin protein expression existed in various human primary cancers, such as gastric, colon, pancreas, esophagus, liver, prostate, bladder, breast, and head and neck tumors^[52]. Recent studies showed that gene mutations or loss of heterozygous E-cadherin occurred in gastric carcinomas, ovary cancer, and cervix cancer. It was found that E-cadherin had strong expression in well-differentiated noninvasive cancers with tight cell-cell adhesion, and had markedly reduced, heterogeneous, or even no expression in undifferentiated invasive cancers with lack of cell-cell adhesion. Several studies have offered the evidence that reduction or structural alternation of E-cadherin expression plays a causal role in metastasis of gastric and colon cancers. The role of E-cadherin in metastasis and invasion was further demonstrated by the fact that the invasion of epithelial tumor cell lines was inhibited *in vitro* by transfection and expression of E-cadherin cDNA, and induced again by exposure to anti-E-cadherin monoclonal antibodies^[53]. Through its cytoplasmic sequence, E-cadherin was associated with a group of proteins called catenins, which are necessary for E-cadherin function^[54]. Dysfunction of catenin can cause instability of homotypic cell-cell adhesion mediated by E-cadherin. Therefore, in tumors with normal E-cadherin expression, alteration of cell adhesion may result from abnormal expression of catenins. Catenins have been classified into α -catenin, β -catenin, and γ -catenin. α -catenin links E-cadherin with cytoskeleton. Expression of α -catenin is essential to the function of E-cadherin in normal cells. Thus, in cancers with normal E-cadherin expression, decreased expression of α -catenin leads to impaired cell adhesion. Downregulation of α -catenin and E-cadherin expression in several cancer tissues has been found to be associated with differentiation degree, invasion and metastasis of cancer cells^[55-57]. Our current study demonstrated that after incubation with different concentrations of *c9,t11*-CLA for 24 h, expression of E-cadherin and catenin in SGC-7901 cells increased. Through upregulation of expression of E-cadherin and catenin, *c9,t11*-CLA also increased homotypic adhesion of cancer cells.

ICAM-1 is a 70-110 ku glycoprotein belonging to the immunoglobulin superfamily and is also a ligand for leukocyte-function associated antigen-1 (LFA-1). It has been reported that ICAM-1 could express on the surface of tumor cells, endothelial cells, keratinocytes, and mediate heterotypic cell-cell interaction^[58]. Several studies indicated that high expression of ICAM-1 in melanoma cells was associated with tumor metastasis, and expression on the surface of metastasizing cancer cells in lymph node increased significantly^[59]. It is suggested that high expression of ICAM-1 on the surface of metastasizing cancer cells in lymph node plays a role in evading immune destruction, thus helping these cancer cells retain in lymphatic sinus to form metastasis. VCAM-1 is a 90 ku cell surface glycoprotein belonging to the immunoglobulin superfamily. Studies also showed that VCAM-1 in renal cell carcinoma, melanoma, and malignant sarcoma linked tumor cells to endothelial cells via binding to integrin $\alpha_4\beta_1$, and contributed to penetration into blood vessels^[60]. We demonstrated here that different concentrations of *c9,t11*-CLA could decrease expression of ICAM-1 and VCAM-1 in SGC-7901 cells after incubation for 24 h and also decrease heterotypic adhesion of cancer cells via downregulation of expression of ICAM-1 and VCAM-1.

In conclusion, *c9,t11*-CLA can inhibit cell-matrix component interactions, increase expression of E-cadherin and catenin and reduce expression of ICAM-1 and VCAM-1 in

SGC-7901 cells. Through these effects, *c9,t11*-CLA may inhibit the invasion of SGC-7901 cells.

REFERENCES

- Liu LX, Liu ZH, Jiang HC, Qu X, Zhang WH, Wu LF, Zhu AL, Wang XQ, Wu M. Profiling of differentially expressed genes in human Gastric carcinoma by cDNA expression array. *World J Gastroenterol* 2002; **8**: 580-585
- Song ZJ, Gong P, Wu YE. Relationship between the expression of iNOS, VEGF, tumor angiogenesis and gastric cancer. *World J Gastroenterol* 2002; **8**: 591-595
- Shi XY, Zhao FZ, Dai X, Ma LS, Dong XY, Fang J. Effect of jianpiyiwei capsule on gastric precancerous lesions in rats. *World J Gastroenterol* 2002; **8**: 608-612
- Zhao AG, Zhao HL, Jin XJ, Yang JK, Tang LD. Effects of Chinese Jianpi herbs on cell apoptosis and related gene expression in human gastric cancer grafted onto nude mice. *World J Gastroenterol* 2002; **8**: 792-796
- Fuchs CS, Mayer RJ. Gastric carcinoma. *N Engl J Med* 1995; **333**: 32-41
- Hansson LE, Sparen P, Nyren O. Survival in stomach cancer is improving: results of a nationwide population-based Swedish study. *Ann Surg* 1999; **230**: 162-169
- Takeichi M. Cadherin cell adhesion receptors as a morphogenetic regulator. *Science* 1991; **251**: 1451-1455
- Hirohashi S. Inactivation of the E-cadherin-mediated cell adhesion system in human cancers. *Am J Pathol* 1998; **153**: 333-339
- Sebedio JL, Gnaedig S, Chardigny JM. Recent advances in conjugated linoleic acid research. *Curr Opin Clin Nutr Metab Care* 1999; **2**: 499-506
- Pariza MW, Park Y, Cook ME. Mechanisms of action of conjugated linoleic acid: evidence and speculation. *Proc Soc Exp Biol Med* 2000; **223**: 8-13
- Pariza MW, Park Y, Cook ME. Conjugated linoleic acid and the control of cancer and obesity. *Toxicol Sci* 1999; **52**(2 Suppl): 107-110
- Whigham LD, Cook ME, Atkinson RL. Conjugated linoleic acid: implications for human health. *Pharmacol Res* 2000; **42**: 503-510
- MacDonald HB. Conjugated linoleic acid and disease prevention: a review of current knowledge. *J Am Coll Nutr* 2000; **19**(2 Suppl): 111S-118S
- Banni S. Conjugated linoleic acid metabolism. *Curr Opin Lipidol* 2002; **13**: 261-266
- Belury MA. Dietary conjugated linoleic acid in health: physiological effects and mechanisms of action. *Annu Rev Nutr* 2002; **22**: 505-531
- Belury MA. Inhibition of carcinogenesis by conjugated linoleic acid: potential mechanisms of action. *J Nutr* 2002; **132**: 2995-2998
- Pariza MW, Ashoor SH, Chu FS, Lund DB. Effects of temperature and time on mutagen formation in pan-fried hamburger. *Cancer Lett* 1979; **7**: 63-69
- Pariza MW, Hargraves WA. A beef-derived mutagenesis modulator inhibits initiation of mouse epidermal tumors by 7,12-dimethylbenz[a]anthracene. *Carcinogenesis* 1985; **6**: 591-593
- Ha YL, Grimm NK, Pariza MW. Anticarcinogens from fried ground beef: heat-altered derivatives of linoleic acid. *Carcinogenesis* 1987; **8**: 1881-1887
- Belury MA, Nickel KP, Bird CE, Wu Y. Dietary conjugated linoleic acid modulation of phorbol ester skin tumor promotion. *Nutr Cancer* 1996; **26**: 149-157
- Ha YL, Storkson J, Pariza MW. Inhibition of benzo(a)pyrene-induced mouse forestomach neoplasia by conjugated dienoic derivatives of linoleic acid. *Cancer Res* 1990; **50**: 1097-1101
- Zhu Y, Qiou J, Chen B. The inhibitory effect of CLA on mice forestomach neoplasia induced by B(a). *Zhonghua Yufang Yixue Zazhi* 2001; **35**: 19-22
- Chen BQ, Xue YB, Liu JR, Yang YM, Zheng YM, Wang XL, Liu RH. Inhibition of conjugated linoleic acid on mouse forestomach neoplasia induced by benzo(a)pyrene and chemopreventive mechanisms. *World J Gastroenterol* 2003; **9**: 44-49
- Ip C, Jiang C, Thompson HJ, Scimeca JA. Retention of conjugated linoleic acid in the mammary gland is associated with tumor inhibition during the post-initiation phase of carcinogenesis. *Carcinogenesis* 1997; **18**: 755-759
- Ip C, Singh M, Thompson HJ, Scimeca JA. Conjugated linoleic acid suppresses mammary carcinogenesis and proliferative activity of the mammary gland in the rat. *Cancer Res* 1994; **54**: 1212-1215
- Ip C, Banni S, Angioni E, Carta G, McGinley J, Thompson HJ, Barbano D, Bauman D. Conjugated linoleic acid-enriched butter fat alters mammary gland morphogenesis and reduces cancer risk in rats. *J Nutr* 1999; **129**: 2135-2142
- Thompson H, Zhu Z, Banni S, Darcy K, Loftus T, Ip C. Morphological and biochemical status of the mammary gland as influenced by conjugated linoleic acid: implication for a reduction in mammary cancer risk. *Cancer Res* 1997; **57**: 5067-5072
- Banni S, Angioni E, Casu V, Melis MP, Carta G, Corongiu FP, Thompson H, Ip C. Decrease in linoleic acid metabolites as a potential mechanism in cancer risk reduction by conjugated linoleic acid. *Carcinogenesis* 1999; **20**: 1019-1024
- Kimoto N, Hirose M, Futakuchi M, Iwata T, Kasai M, Shirai T. Site-dependent modulating effects of conjugated fatty acids from safflower oil in a rat two-stage carcinogenesis model in female Sprague-Dawley rats. *Cancer Lett* 2001; **168**: 15-21
- Ip C, Ip MM, Loftus T, Shoemaker S, Shea-Eaton W. Induction of apoptosis by conjugated linoleic acid in cultured mammary tumor cells and premalignant lesions of the rat mammary gland. *Cancer Epidemiol Biomarkers Prev* 2000; **9**: 689-696
- Liew C, Schut HA, Chin SF, Pariza MW, Dashwood RH. Protection of conjugated linoleic acids against 2-amino-3-methylimidazo[4,5-f]quinoline-induced colon carcinogenesis in the F344 rat: a study of inhibitory mechanisms. *Carcinogenesis* 1995; **16**: 3037-3043
- Visonneau S, Cesano A, Tepper SA, Scimeca JA, Santoli D, Kritchevsky D. Conjugated linoleic acid suppresses the growth of human breast adenocarcinoma cells in SCID mice. *Anticancer Res* 1997; **17**: 969-973
- Cesano A, Visonneau S, Scimeca JA, Kritchevsky D, Santoli D. Opposite effects of linoleic acid and conjugated linoleic acid on human prostatic cancer in SCID mice. *Anticancer Res* 1998; **18**: 1429-1434
- Shultz TD, Chew BP, Seaman WR, Luedecke LO. Inhibitory effect of conjugated dienoic derivatives of linoleic acid and beta-carotene on the *in vitro* growth of human cancer cells. *Cancer Lett* 1992; **63**: 125-133
- Igarashi M, Miyazawa T. Newly recognized cytotoxic effect of conjugated trienoic fatty acids on cultured human tumor cells. *Cancer Lett* 2000; **148**: 173-179
- Igarashi M, Miyazawa T. The growth inhibitory effect of conjugated linoleic acid on a human hepatoma cell line, HepG2, is induced by a change in fatty acid metabolism, but not the facilitation of lipid peroxidation in the cells. *Biochim Biophys Acta* 2001; **1530**: 162-171
- Park Y, Allen KG, Shultz TD. Modulation of MCF-7 breast cancer cell signal transduction by linoleic acid and conjugated linoleic acid in culture. *Anticancer Res* 2000; **20**: 669-676
- O'Shea M, Devery R, Lawless F, Murphy J, Stanton C. Milk fat conjugated linoleic acid (CLA) inhibits growth of human mammary MCF-7 cancer cells. *Anticancer Res* 2000; **20**: 3591-3601
- O'Shea M, Stanton C, Devery R. Antioxidant enzyme defence responses of human MCF-7 and SW480 cancer cells to conjugated linoleic acid. *Anticancer Res* 1999; **19**: 1953-1959
- Cunningham DC, Harrison LY, Shultz TD. Proliferative responses of normal human mammary and MCF-7 breast cancer cells to linoleic acid, conjugated linoleic acid and eicosanoid synthesis inhibitors in culture. *Anticancer Res* 1997; **17**: 197-203
- Schonberg S, Krokan HE. The inhibitory effect of conjugated dienoic derivatives (CLA) of linoleic acid on the growth of human tumor cell lines is in part due to increased lipid peroxidation. *Anticancer Res* 1995; **15**: 1241-1246
- Liu J, Chen B, Liu R, Lu G. Inhibitory effect of conjugated linoleic acid on human gastric carcinoma cell line. *Weisheng Yanjiu* 1999; **28**: 353-355
- Liu JR, Li BX, Chen BQ, Han XH, Xue YB, Yang YM, Zheng YM, Liu RH. Effect of *cis*-9, *trans*-11-conjugated linoleic acid on cell cycle of gastric adenocarcinoma cell line (SGC-7901). *World J Gastroenterol* 2002; **8**: 224-229
- Xue Y, Chen B, Zheng Y, Yuan L. Effects of conjugated linoleic

- acid on the metastasis of mouse melanoma B16-MB. *Weisheng Yanjiu* 2001; **30**: 37-39
- 45 **Yang Y**, Chen B, Xue Y, Zheng Y. Effects of c9, t11-conjugated linoleic acid on the metastasis of human gastric carcinoma cell line. *Weisheng Yanjiu* 2003; **32**: 117-119
- 46 **Yang YM**, Chen BQ, Zheng YM, Wang XL, Liu JR, Xue YB, Liu RH. The effects of conjugated linoleic acid on the expression of invasiveness and metastasis-associated gene of human gastric carcinoma cell line. *Zhonghua Yufang Yixue Zazhi* 2003; **37**: 26-28
- 47 **Yoon SO**, Kim MM, Chung AS. Inhibitory effect of selenite on invasion of HT1080 tumor cells. *J Biol Chem* 2001; **276**: 20085-20092
- 48 **Ara T**, Deyama Y, Yoshimura Y, Higashino F, Shindoh M, Matsumoto A, Fukuda H. Membrane type 1-matrix metalloproteinase expression is regulated by E-cadherin through the suppression of mitogen-activated protein kinase cascade. *Cancer Lett* 2000; **157**: 115-121
- 49 **Seftor RE**, Seftor EA, Gehlsen KR, Stetler-Stevenson WG, Brown PD, Ruoslahti E, Hendrix MJ. Role of the alpha v beta 3 integrin in human melanoma cell invasion. *Proc Natl Acad Sci U S A* 1992; **89**: 1557-1561
- 50 **Nakahara H**, Nomizu M, Akiyama SK, Yamada Y, Yeh Y, Chen WT. A mechanism for regulation of melanoma invasion. Ligation of alpha6beta1 integrin by laminin G peptides. *J Biol Chem* 1996; **271**: 27221-27224
- 51 **Giancotti FG**, Ruoslahti E. Integrin signaling. *Science* 1999; **285**: 1028-1032
- 52 **Dogan A**, Wang ZD, Spencer J. E-cadherin expression in intestinal epithelium. *J Clin Pathol* 1995; **48**: 143-146
- 53 **Chan AO**, Lam SK, Chu KM, Lam CM, Kwok E, Leung SY, Yuen ST, Law SY, Hui WM, Lai KC, Wong CY, Hu HC, Lai CL, Wong J. Soluble E-cadherin is a valid prognostic marker in gastric carcinoma. *Gut* 2001; **48**: 808-811
- 54 **Jawhari A**, Farthing M, Pignatelli M. The importance of the E-cadherin-catenin complex in the maintenance of intestinal epithelial homeostasis: more than intercellular glue? *Gut* 1997; **41**: 581-584
- 55 **Jiang WG**. E-cadherin and its associated protein catenins, cancer invasion and metastasis. *Br J Surg* 1996; **83**: 437-446
- 56 **Yu J**, Ebert MP, Miehlke S, Rost H, Lendeckel U, Leodolter A, Stolte M, Bayerdorffer E, Malfertheiner P. Alpha-catenin expression is decreased in human gastric cancers and in the gastric mucosa of first degree relatives. *Gut* 2000; **46**: 639-644
- 57 **Shiozaki H**, Iihara K, Oka H, Kadowaki T, Matsui S, Gofuku J, Inoue M, Nagafuchi A, Tsukita S, Mori T. Immunohistochemical detection of alpha-catenin expression in human cancers. *Am J Pathol* 1994; **144**: 667-674
- 58 **Schwaeble W**, Kerlin M, Meyer zum Buschenfelde KH, Dippold W. De novo expression of intercellular adhesion molecule 1 (ICAM-1, CD54) in pancreas cancer. *Int J Cancer* 1993; **53**: 328-333
- 59 **Natali P**, Nicotra MR, Cavaliere R, Bigotti A, Romano G, Temponi M, Ferrone S. Differential expression of intercellular adhesion molecule 1 in primary and metastatic melanoma lesions. *Cancer Res* 1990; **50**: 1271-1278
- 60 **Tomita Y**, Saito T, Saito K, Oite T, Shimizu F, Sato S. Possible significance of VLA-4 (alpha4beta1) for hematogenous metastasis of renal-cell cancer. *Int J Cancer* 1995; **60**: 753-758

Edited by Chou LF and Wang XL Proofread by Xu FM

Diagnosis and surgical treatments of hepatocellular carcinoma with tumor thrombosis in bile duct: Experience of 34 patients

Lun-Xiu Qin, Zeng-Chen Ma, Zhi-Quan Wu, Jia Fan, Xin-Da Zhou, Hui-Chuan Sun, Qing-Hai Ye, Lu Wang, Zhao-You Tang

Lun-Xiu Qin, Zeng-Chen Ma, Zhi-Quan Wu, Jia Fan, Xin-Da Zhou, Hui-Chuan Sun, Qing-Hai Ye, Lu Wang, Zhao-You Tang, Liver Cancer Institute and Zhongshan Hospital, Fudan University former Shanghai Medical University, Shanghai 200032, China

Correspondence to: Zhao-You Tang, M.D., Professor and Chairman, Liver Cancer Institute, Fudan University, 136 Yi Xue Yuan Road, Shanghai 200032, China. zytang@srcap.stc.sh.cn

Telephone: +86-21-64037181 **Fax:** +86-21-64037181

Received: 2003-10-15 **Accepted:** 2003-12-16

Abstract

AIM: Hepatocellular carcinoma (HCC) with bile duct tumor thrombosis (BDT) is a rare event. The prognosis of this type of patients is very dismal. The aim of this study was to share the experience in the diagnosis and treatment of HCC with BDT, to further improve the prognosis of these patients.

METHODS: Thirty-four patients of HCC with BDT received surgical treatment in authors' institute from July 1987 to January 2003 were reviewed retrospectively. The experience in the diagnosis and treatment, and the outcome of this type of HCC patients were summarized.

RESULTS: Thirty of the 34 patients (88.2%) were positive for alpha-fetoprotein (AFP) ($>20 \mu\text{g/L}$), and 12 patients (35.3%) were found having obstructive jaundice before operation, 18 cases were suspected of "obstruction of bile duct" preoperatively. The primary tumors were frequently located at the left medial (13 cases) or right anterior lobe (14 cases). Thirty-one patients received liver resections and removal of BDT, while the other 3 patients received removal of BDT combined with hepatic artery ligation and cannulation (HAL+HAI), or only removal of BDT because their liver function reservation and general condition could not tolerate the primary tumor resection. The 1-year survival rate was 71.4%(20/28). The longest disease-free survival was over 15 years. The intrahepatic tumor recurrence within 1 year after operation was found in 14 patients (14/28, 50.0%).

CONCLUSION: Surgical removal of primary tumors and BDT is safe and beneficial to the HCC patients with BDT. Early detection, diagnosis, and surgical treatment are the key points to prolong the survival time of patients.

Qin LX, Ma ZC, Wu ZQ, Fan J, Zhou XD, Sun HC, Ye QH, Wang L, Tang ZY. Diagnosis and surgical treatments of hepatocellular carcinoma with tumor thrombosis in bile duct: Experience of 34 patients. *World J Gastroenterol* 2004; 10(10): 1397-1401 <http://www.wjgnet.com/1007-9327/10/1397.asp>

INTRODUCTION

Obstructive jaundice as the main presenting clinical feature is uncommon in patients with hepatocellular carcinoma (HCC). Only 1-12% of patients with HCC manifest obstructive jaundice as the initial complaint^[1-3]. Mallory *et al.* described

the first such case in 1947, in which HCC invaded the cystic duct and gave rise to obstructive jaundice caused by the tumor thrombosis^[4]. These kinds of patients were clinically classified as "icteric-type hepatoma"^[5] or "cholestatic type of HCC"^[6].

Tumor thrombus in bile duct (BDT) is one of the main reasons for obstructive jaundice. The incidence was 1.2-9% in previous reports^[2,3,5-8]. However, Huang *et al.* found the incidence was only 0.53%^[9]. It is usually difficult to make diagnosis before operation, because of the low incidence rate, ignorance of this disease, and the difficulty for the imaging diagnosis to find the BDT preoperatively. The prognosis of this type of HCC patients is very dismal, but is better than those with jaundice caused by hepatic insufficiency. Identification of this group of patients is clinically important, because surgical treatment may be beneficial. In this study, we summarized our experience in the diagnosis and treatment of 34 cases of this type of HCC during the past 15 years.

MATERIALS AND METHODS

Patients' information

From July 1987 to January 2003, totally 4 324 patients suffering from HCC received surgical treatment in Liver Cancer Institute and Zhongshan Hospital, Fudan University (former Shanghai Medical University), and 34 cases (0.79%) were found having tumor thrombosis in bile duct. Among of them, 28 cases were male, and 6 cases were female. The mean age of patients was 48.5 years (32- 76 years). The history of hepatitis B virus (HBV) infection or HBsAg positive was found in all of the patients, and liver cirrhosis in 94.1%(32/34) of patients. Thirty of them (30/34, 88.2%) were positive for alpha-fetoprotein (AFP) ($>20 \mu\text{g/L}$), and the highest was over 2 000 $\mu\text{g/L}$. Preoperative obstructive jaundice was found in 12 patients (12/34, 35.3%), and 2 of them had the history of "transient cholangitis" with the manifestation of transient jaundice. The history of "hemorrhage of upper digestive system" was found in 2 patients. Four patients had the history of preoperative transcatheter arterial chemoembolization (TACE) (Table 1).

Imaging diagnostic features

Ultrasonography (US) and CT scan were performed in all of the patients. Magnetic resonance cholangiography (MRCP) was also done in 12 patients in recent 3 years. (Figures 1, 2) Eighteen cases were suspected of "obstruction of bile duct" because of the occurrence of preoperative jaundice (12 cases), and/or dilation of intrahepatic bile duct shown in imaging diagnosis (in 6 cases without obstructive jaundice). Only 9 cases of them were obviously shown tumor thrombosis in the bile duct by US, CT scan or MRI preoperatively. One case with neoplasm in the bile duct, while no obvious intrahepatic lesion, was misdiagnosed as cholangiocarcinoma, in spite of the positive AFP.

Characteristics of the primary tumors and BDT

The size of primary tumors was 6.4 ± 2.5 cm in diameter (2-15 cm). All of the primary tumors had no capsule, with unclear tumor margin, and invasive pattern of growth. The primary tumors

were located at the segment IV in 13 cases, right anterior section (segments V and VIII) in 14 cases, segment I (caudate lobe) in 1 case, segment II-III in 4 cases, and segment VI in 2 cases. The tumor thrombus located at left hepatic duct (LHD) in 5 cases, LHD to common hepatic duct (CHD)/common bile duct (CBD) in 9 cases, right hepatic bile duct (RHD) in 5 cases, RHD to CHD/CBD in 8 cases, and CBD in 7 cases. According to Ueda classification^[10], 2 cases belonged to type I, 8 cases type II, 16 cases type IIIa, 1 case type IIIb, and 7 cases type IV. In 2 cases, the BDT was as long as 6 cm, and 9 cm, respectively (Table 1, Figure 1).

Treatment strategies

All of the patients received surgical treatment. Thirty-one patients received liver resection and removal of the tumor thrombosis (or thrombectomy). Among them, 12 patients received left hemihepatectomy, 2 cases received left lateral sectionectomy, 11 cases received limited partial resection of the liver, 5 cases received right hemihepatectomy, and 1 case received resection of the left lobe and caudate lobe of liver, and CHD, and RHD-jejunum anastomosis. Two patients received removal of CBD thrombosis combined with hepatic artery ligation and cannulation (HAL+HAI), and 1 patient

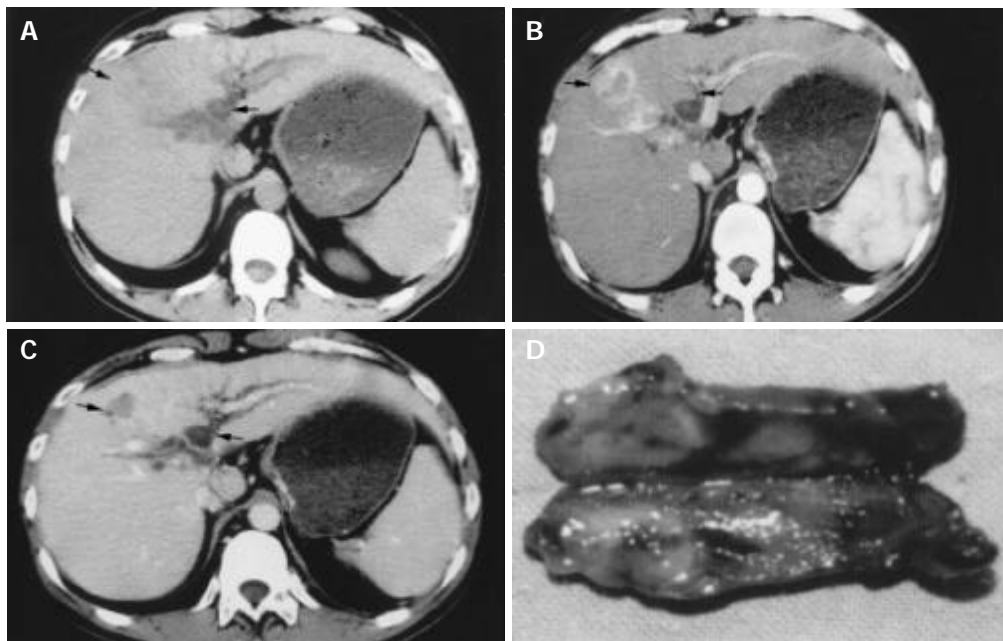


Figure 1 The hepatocellular carcinoma (HCC) with tumor thrombosis in common bile duct. A-C: The three phases of CT scan. One small HCC with rich arterial blood flow is shown in the left medial lobe of liver (arrow), with the intrahepatic bile duct of both sides and common hepatic duct dilated obviously (arrow). D: The tumor thrombosis removed from the common bile duct of this HCC patient.

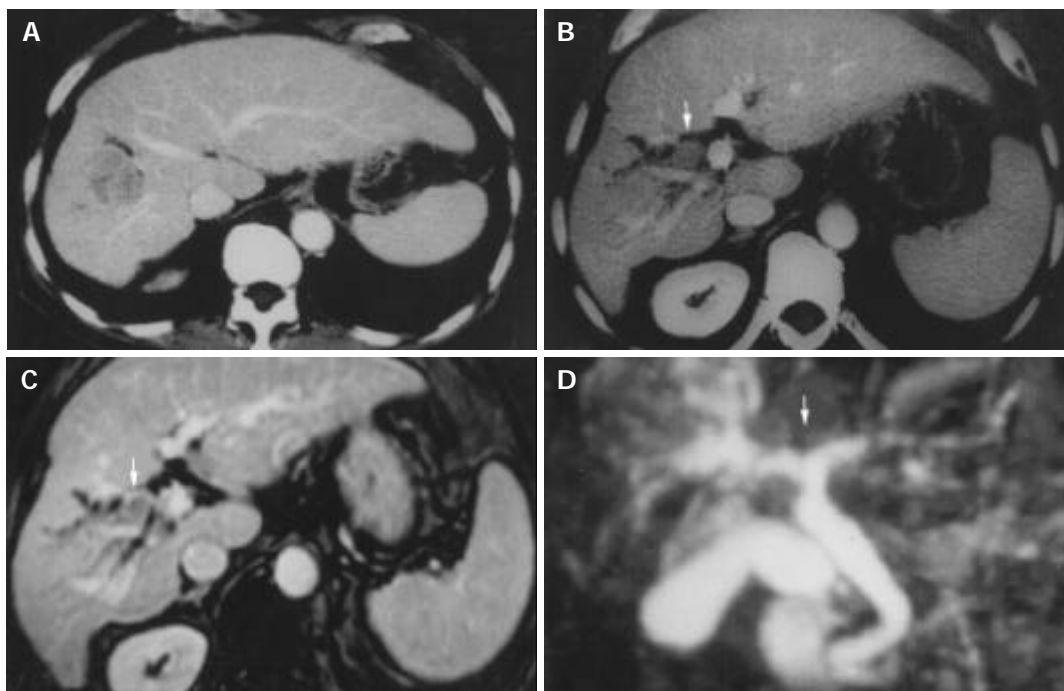


Figure 2 The imaging diagnosis of hepatocellular carcinoma with thrombosis in bile duct. A and B are pictures of CT scan, C and D are pictures of magnetic resonance cholangiography (MRCP). These pictures show the primary tumor in right anterior lobe of the liver, with tumor thrombosis in common hepatic duct (arrow).

received removal of BDT only because their liver function reservation and general condition could not tolerate the primary tumor resection.

The tumor thrombi were removed by the exploration of CBD in 14 cases, from the cut end of the bile duct after liver resection in 15 cases, and *en bloc* removal with the primary tumor in 5 patients. Intraoperative active bleeding from the CHD after removal of the thrombosis happened in 1 patient, and hemostasis was achieved finally by infusing noradrenalin in normal saline into the bile duct and oppressing locally.

The operations were well tolerated. After operation, the obstructive jaundice due to BDT was successfully relieved in all but 2 patients. One patient with severe liver cirrhosis and preoperative obstructive jaundice (the total serum bilirubin was 182 $\mu\text{mol/L}$) received partial resection of the right liver lobe, and died of liver failure at the 35th d after the operation. Another patient with severe preoperative obstructive jaundice (total serum bilirubin was 320 $\mu\text{mol/L}$, and the direct bilirubin was 210 $\mu\text{mol/L}$) received right hemihepatectomy and removal of thrombosis in CBD, the total serum bilirubin did not decrease although the general condition of the patient was good, the patient himself chose to give up the treatment and left the hospital at the 40th d after the operation. A third patient with obstructive jaundice (preoperative total serum bilirubin was 156 $\mu\text{mol/L}$) due to BDT in the CBD received left hemihepatectomy and removal of BDT. His total serum bilirubin rose to over 700 $\mu\text{mol/L}$ in 2 wk after operation, and finally returned to normal in 3 mo. By now, this patient has survived for 11 mo.

Table 1 The clinical information of the 34 HCC patients with tumor thrombosis in bile duct

Items	Cases (%)
Sex	
Male	28 (82.4%)
Female	6
HBV infection	
HBsAg+	34 (100%)
Liver cirrhosis	32 (94.1%)
AFP	
>20 $\mu\text{g/L}$	30 (88.2%)
$\leq 20 \mu\text{g/L}$	4
Obstructive jaundice	
+	12 (12, 35.3%)
-	
Ueda classification	
Type I	2
Type II	8
Type IIIa	16
Type IIIb	1
Type IV	7
Treatment	
Surgical resection	31 (91.2%)
Removal of BDT +HAL+HAI	2
Only removal of BDT	1
Survival	
>1 yr	20 (20/28, 71.4%)
>3 yr	3
>15 yr	1
HCC recurrence	
Within 1 yr	14 (14/28, 50.0%)
Within 3 mo	9 (9/31, 29.0%)

Survivals

The follow-up was up to February of 2003. Twenty-eight patients

were followed-up over 1 year. Twenty patients survived over 1 year. One-year survival rate was 71.4%(20/28). The longest disease-free survival time was over 15 years. It occurred in one female patient who received left hemihepatectomy and removal of the tumor thrombosis in CBD (Ueda type IV) in July of 1987. She was still alive without recurrence of cancer up to the last follow-up. Another female patient who received partial resection of right lobe and removal of BDT from the RHD (Ueda type II) in August of 1993 had survived over 9 years without recurrence. The third female patient received right hemihepatectomy and removal of CHD thrombosis (Ueda type IIIa) in May of 1995, and received the second operation due to HCC recurrence 3.5 years later. One male patient who received right hemihepatectomy in September of 1999 (Type II) had also survived over 2 years without recurrence. Fourteen patients (14/28, 50.0%) were found intrahepatic HCC recurrence within 1 year after operation. Nine of them (9/31, 29.0%) were found intrahepatic recurrence within 3 mo after operations. The survival times of the 3 patients received biliary decompression were only 2, 3, and 3.5 mo, respectively (Table 1).

DISCUSSION

Obstructive jaundice caused by BDT, especially as the initial presentation of HCC, is a rare event. And little is known about this type of HCC. However, there are more and more reports about this type of disease, and the incidence is increasing in patients with HCC^[11]. In this study, only 34 out of the 4 324 HCC patients who received surgical treatment in authors' institute were found BDT. The incidence was only 0.79%. And more, most of them (26/34, 76.5%) were treated in recent 5 years. This might be due to the increased understanding of this type of HCC, further improvement of diagnosis (particularly the imaging diagnosis), and more positive attitude towards the treatment to this kind of patients.

HCC invades into bile duct through the following different mechanisms: a distal tumor may grow continuously until it fills the entire extrahepatic biliary system; a fragment of necrotic tumor may separate from the proximal intraductal growth, migrate to the distal common bile duct and cause an obstruction; hemorrhage from the tumor may partially or completely fill the biliary tract with tumor-containing blood clots^[2,3,7-9,12,13]. These produce different types of BDT which will also affect the patients' prognosis^[10]. In this series, 4 patients without any obvious evidence of BDT at initial diagnosis were found BDT after TACE treatment, which suggested that TACE might increase the possibility of BDT^[11]. The exact mechanism is not clear yet.

Just as other types of HCC, no specific symptoms could be found in the early stage. Only when intraductal tumor growth occurs in the CHD and/or CBD does obstructive jaundice become a clinical concern. The common clinical features include high level of serum AFP, the history of cholangitis with dilation of intrahepatic bile duct, aggravating jaundice and rapidly developing into liver dysfunction. Unexplained hemobilia could be the initial complaint without any manifestation of primary tumor. And "hemorrhage of upper digestive system", which might be due to the hemorrhage of bile duct (hemobilia), could also be the first manifestation. The most important point is that we should think about the possibility of BDT when these manifestations are found in HCC patients.

There are still difficult and challenging problems in differential diagnosis of this type of HCC before operation. Despite remarkable recent improvements in the imaging techniques for diagnosis of HCC, such cases were still incorrectly diagnosed as cholangiocarcinoma or choledocholithiasis^[2,7-14]. In this series, only 9 out of the 18 cases suspected of "obstruction

of bile duct” were obviously shown BDT with US or CT scan preoperatively. The others were misdiagnosed as “bile duct stone” or cholangiocarcinoma, even though “neoplasm in CBD” was found. All of these suggest that deeper understanding of this type of disease is the key to further improving the diagnosis preoperatively. Further advanced imaging examination should be performed if the intrahepatic bile duct of one lobe or around the tumor is found dilated. The existence of tumor thrombosis in bile duct should be considered when an occupying lesion is found within bile duct. Fortunately, in recent years, more correct preoperative diagnosis could be made in this type of patients.

MR cholangiography (MRCP) is an absolutely noninvasive imaging modality, which has been shown to be superior to ERCP in detecting the presence of biliary obstruction. Both primary liver tumors and dilatation of biliary system could be demonstrated in MRCP^[15]. Presence of intraluminal soft tissue at the bile duct, and enhancement of the intraluminal soft tissue in the arterial phase are 2 typical features of HCC with BDT (Figure 2). However, these characteristic cholangiographic features should be differentially diagnosed with papillary type cholangiocarcinoma, intraductal polyps or mucin-hypersecreting intrahepatic biliary neoplasm, or intrahepatic cholangiocarcinoma with invasion of extrahepatic bile duct, and even the bile duct stones^[16]. It still relies on other information, such as the presence of liver cirrhosis, hepatitis markers, tumor markers (AFP, CEA), the fluctuation of jaundice, and hemobilia.

The prognosis of this type of HCC is generally dismal, particularly for those with obstructive jaundice^[2,3]. However, the prognosis of these patients is better than those HCC patients who have jaundice caused by hepatic insufficiency, which is closely related to the stage of disease, the location and extent of BDT. Different therapies also influence the prognosis of this type of patients. Surgical resection is the only way that possibly cures the patients. Jaundice is not necessarily a harbinger of advanced disease and a contraindication for surgery. The goals of operative intervention are biliary decompression with removal of tumor debris or tumor-containing blood clots, and, if possible, curative resection of the hepatic tumor. The usually used operative methods are lobectomy (including the primary tumor and the tumor thrombosis in bile duct), hepatectomy combined with thrombectomy, biliary decompression and drainage (choledochotomy with T-tube drainage alone, internal biliary stenting, or biliary diversion). The ideal treatment is hepatic resections^[17-19]. Patients who received curative liver resection had a much better survival rate than those without resection^[20-24]. In our series, the postoperative 1-year survival rate of patients was 71.4%, 1-year disease-free survival rate was 21.4%, and one patient has survived over 15 years. These are better than that of previous reports. It might be attributed to active attitude of the doctors and appropriate procedures of treatment taken. All of the 4 long-term survivors received major liver resection (hemihepatectomy) and removal of BDT, while the 3 patients who received biliary decompression only survived 2, 3, and 3.5 mo, respectively. So, to improve survival, if the patient's liver function and general condition could tolerate, it is suggested to perform major liver resection with removal of BDT. However, it should be very careful to perform major liver resection for those patients with both severe liver cirrhosis and severe obstructive jaundice, because their liver function reservation is very poor. In this series, one patient died of liver failure postoperatively even though his liver function test was good (except for obstructive jaundice). If hepatic resection cannot be accomplished with bile duct resection due to limited liver function, non-surgical modalities should be considered instead of surgery.

Surgical intervention is very effective to relieve the

obstruction of bile duct in this type of patients. It could take a long time (such as 3 mo in one case of this study) for the serum bilirubin of patients with obstructive jaundice to return to normal, or even transiently increase in short time after operation though the obstruction in bile duct has been dispelled completely. The altering pattern and the duration for the serum bilirubin to return to normal after operation, especially for those with severe preoperative obstructive jaundice, still need further studying.

The ideal way to remove BDT is *en bloc* resection with the primary tumor. It is also relatively easy to remove BDT either with the exploration of CBD or from the cut-end of bile duct after hepatectomy. However, active hemorrhage occurred during operation in some cases, possibly because of the continuity of the intraductal tumor debris with the main intrahepatic tumor. In this study, we met one patient with active bleeding during the operation after removing the thrombosis from the common hepatic duct. The hemostasis was achieved finally by infusing noradrenalin in normal saline into the bile duct and oppressing locally. Suturing, electrocauterization, compression, Pringle's maneuver, or hepatic arterial ligation are some alternative ways to achieve hemostasis.

BDT often grows faster than the primary cancer. We found in 2 cases, the BDT was as long as 6 cm, and 9 cm, respectively, while their primary HCC less than 6 cm. The primary tumor often has no capsule, with unclear tumor margin, and invasive growth. The infiltrative nature of this particular type of HCC may in part explain their invasion of the biliary tree early in their growth without regard to tumor size or type^[25,26], which might also be one of the reasons that the prognosis of this type of patients was very poor. In this series, the 1-year recurrence rate was 50.0%, and as high as 29.0% of the patients were found having tumor recurrence within 3 mo after operation. This might also indicate the poor malignant phenotype of this type of HCC. Combined chemotherapy or chemoembolization might be helpful to control the postoperative recurrence^[27].

In summary, HCC with tumor thrombosis in bile duct, particularly with obstructive jaundice as the main presenting clinical feature, is uncommon. The prognosis of this type of HCC is generally dismal, but is better than those HCC patients who have jaundice caused by hepatic insufficiency. Jaundice is not necessarily a harbinger of advanced disease and a contraindication for surgery. If appropriate procedures are selected and carried out safely, it can result in long-term relief of symptoms and occasional long-term survival. Deeper understanding, and active attitude to treatment of this type of disease are the keys to further improving survival of these patients.

REFERENCES

- 1 **Kew MC**, Paterson AC. Unusual presentations of hepatocellular carcinoma. *Trop Gastroenterol* 1985; **6**: 10-22
- 2 **Kojiro M**, Kawabata K, Kawano Y, Shirai F, Takemoto N, Nakashima T. Hepatocellular carcinoma presenting as intrabiliary duct tumor growth. A clinicopathological study of 24 cases. *Cancer* 1982; **49**: 2144-2147
- 3 **Qin LX**, Tang ZY. Hepatocellular carcinoma with obstructive jaundice: diagnosis, treatment and prognosis. *World J Gastroenterol* 2003; **9**: 385-391
- 4 **Mallory TB**, Castleman B, Parris EE. Case records of the Massachusetts General Hospital. *N Eng J Med* 1947; **237**: 673-676
- 5 **Lin TY**, Chen KM, Chen YR, Lin WS, Wang TH, Sung JL. Icteric type hepatoma. *Med Chi Dig* 1975; **4**: 267-270
- 6 **Okuda K**. Clinical aspects of hepatocellular carcinoma: analysis of 134 cases. In: Okuda K, Peters RL, eds. *Hepatocellular carcinoma*. New York: John Wiley 1976: 387-436
- 7 **Jan YY**, Chen MF. Obstructive jaundice secondary to hepatocellular carcinoma rupture into the common bile duct: choledochoscopic findings. *Hepatogastroenterology* 1999; **46**: 157-161
- 8 **Lau WY**, Leung JW, Li AK. Management of hepatocellular carcinoma

- noma presenting as obstructive jaundice. *Am J Surg* 1990; **160**: 280-282
- 9 **Huang JF**, Wang LY, Lin ZY, Chen SC, Hsieh MY, Chuang WL. Incidence and clinical outcome of icteric type hepatocellular carcinoma. *J Gastroenterol Hepatol* 2002; **17**: 190-195
- 10 **Ueda M**, Takeuchi T, Takayasu T, Takahashi K, Okamoto S, Tanaka A. Classification and surgical treatment of hepatocellular carcinoma (HCC) with bile duct thrombi. *Hepatogastroenterology* 1994; **41**: 349-354
- 11 **Spahr L**, Frossard JL, Felley C, Brundler MA, Majno PE, Hadengue A. Biliary migration of hepatocellular carcinoma fragment after transcatheter arterial chemoembolization therapy. *Eur J Gastroenterol Hepatol* 2000; **12**: 243-244
- 12 **Afroudakis A**, Bhuta SM, Ranganath KA, Kaplowitz N. Obstructive jaundice caused by hepatocellular carcinoma. *Dig Dis* 1978; **23**: 609-617
- 13 **Buckmaster MJ**, Schwartz RW, Carnahan GE, Strodel WE. Hepatocellular carcinoma embolus to the common hepatic duct with no detectable primary hepatic tumor. *Am Surg* 1994; **60**: 699-702
- 14 **Wang JH**, Chen TM, Tung HD, Lee CM, Changchien CS, Lu SN. Color Doppler sonography of bile duct tumor thrombi in hepatocellular carcinoma. *J Ultrasound Med* 2002; **21**: 767-772
- 15 **Fulcher AS**, Turner MA, Capps GW, Zfass AM, Baker KM. Half-Fourier RARE MR cholangiopancreatography: experience in 300 subjects. *Radiology* 1998; **207**: 21-32
- 16 **Yeh TS**, Jan YY, Tseng JH, Chiu CT, Chen TC, Hwang TL, Chen MF. Malignant perihilar biliary obstruction: magnetic resonance cholangiopancreatographic findings. *Am J Gastroenterol* 2000; **95**: 432-440
- 17 **Chen MF**, Jan YY, Jeng LB, Hwang TL, Wang CS, Chen SC. Obstructive jaundice secondary to ruptured hepatocellular carcinoma into the common bile duct. *Cancer* 1994; **73**: 1336-1340
- 18 **Jan YY**, Chen MF, Chen TJ. Long term survival after obstruction of the common bile duct by ductal hepatocellular carcinoma. *Eur J Surg* 1995; **161**: 771-774
- 19 **Tantawi B**, Cherqui D, Tran van Nhieu J, Kracht M, Fagniez PL. Surgery for biliary obstruction by tumour thrombus in primary liver cancer. *Br J Surg* 1996; **83**: 1522-1525
- 20 **Lau WY**, Leung KL, Leung TW, Liew CT, Chan MS, Yu SC, Li AK. A logical approach to hepatocellular carcinoma presenting with jaundice. *Ann Surg* 1997; **225**: 281-285
- 21 **Wang HJ**, Kim JH, Kim WH, Kim MW. Hepatocellular carcinoma with tumor thrombi in the bile duct. *Hepatogastroenterology* 1999; **46**: 2495-2499
- 22 **Hu J**, Pi Z, Yu MY, Li Y, Xiong S. Obstructive jaundice caused by tumor emboli from hepatocellular carcinoma. *Am Surg* 1999; **65**: 406-410
- 23 **Lau WY**, Leung KL, Leung TW, Ho S, Chan M, Liew CK. Obstructive jaundice secondary to hepatocellular carcinoma. *Surg Oncol* 1995; **4**: 303-308
- 24 **Nishio H**, Miyata K, Hanai M, Kato M, Yoneyama F, Kobayashi Y. Resection of an icteric type hepatoma with tumor thrombi filling the right posterior bile duct. *Hepatogastroenterology* 2002; **49**: 1682-1685
- 25 **Huang GT**, Sheu JC, Lee HS, Lai MY, Wang TH, Chen DS. Icteric type hepatocellular carcinoma: revisited 20 years later. *J Gastroenterol* 1998; **33**: 53-56
- 26 **Tseng JH**, Hung CF, Ng KK, Wan YL, Yeh TS, Chiu CT. Icteric-type hepatoma: magnetic resonance imaging and magnetic resonance cholangiographic features. *Abdom Imaging* 2001; **26**: 171-177
- 27 **Fukuda S**, Okuda K, Imamura M, Imamura I, Eriguchi N, Aoyagi S. Surgical resection combined with chemotherapy for advanced hepatocellular carcinoma with tumor thrombus: report of 19 cases. *Surgery* 2002; **131**: 300-310

Edited by Zhu LH Proofread by Xu FM

Construction of human liver cancer vascular endothelium cDNA expression library and screening of the endothelium-associated antigen genes

Xing Zhong, Yu-Liang Ran, Jin-Ning Lou, Dong Hu, Long Yu, Yu-Shan Zhang, Zhuan Zhou, Zhi-Hua Yang

Xing Zhong, Yu-Liang Ran, Dong Hu, Long Yu, Yu-Shan Zhang, Zhuan Zhou, Zhi-Hua Yang, Department of Cell and Molecular Biology, Cancer Institute (Hospital), Chinese Academy of Medical Sciences and Peking Union Medical College, Beijing, 100021, China
Jin-Ning Lou, Institute of Clinical Medical Sciences, China-Japan Friendship Hospital, Beijing 100029, China

Supported by the National 863 Program, No.2001AA221251 and the National Natural Science Foundation of China, No.30230150

Correspondence to: Professor Zhi-Hua Yang, Department of Cell and Molecular Laboratory, Cancer Institute (Hospital), Chinese Academy of Medical Sciences and Peking Union Medical College, Panjiayuan, Chaoyang Qu PO Box, Beijing, 100021, China. zhyang@public.bta.net.cn

Telephone: +86-10-87771740 **Fax:** +86-10-67713359

Received: 2003-10-15 **Accepted:** 2003-12-02

the functional genes associated with tumor endothelium or angiogenesis were identified. The modified SEREX, xenogeneic functional serum screening, was demonstrated to be effective for isolation and identification of antigen genes of tumor endothelium, and also for other tumor cell antigen genes. These antigen genes obtained in this study could be a valuable resource for basic and clinical studies of tumor angiogenesis, thus facilitating the development of anti-angiogenesis targeting therapy of tumors.

Zhong X, Ran YL, Lou JN, Hu D, Yu L, Zhang YS, Zhou Z, Yang ZH. Construction of human liver cancer vascular endothelium cDNA expression library and screening of the endothelium-associated antigen genes. *World J Gastroenterol* 2004; 10(10): 1402-1408

<http://www.wjgnet.com/1007-9327/10/1402.asp>

Abstract

AIM: To gain tumor endothelium associated antigen genes from human liver cancer vascular endothelial cells (HLCVECs) cDNA expression library, so as to find some new possible targets for the diagnosis and therapy of liver tumor.

METHODS: HLCVECs were isolated and purified from a fresh hepatocellular carcinoma tissue sample, and were cultured and proliferated *in vitro*. A cDNA expression library was constructed with the mRNA extracted from HLCVECs. Anti-sera were prepared from immunized BALB/c mice through subcutaneous injection with high dose of fixed HLCVECs, and were then tested for their specificity against HLCVECs and angiogenic effects *in vitro*, such as inhibiting proliferation and inducing apoptosis of tumor endothelial cells, using immunocytochemistry, immunofluorescence, cell cycle analysis and MTT assays, etc. The identified xenogeneic sera from immunized mice were employed to screen the library of HLCVECs by modified serological analyses of recombinant cDNA expression libraries (SEREX). The positive clones were sequenced and analyzed by bioinformatics.

RESULTS: The primary cDNA library consisted of 2×10^6 recombinants. Thirty-six positive clones were obtained from 6×10^5 independent clones by immunoscreening. Bio-informatics analysis of cDNA sequences indicated that 36 positive clones represented 18 different genes. Among them, 3 were new genes previously unreported, 2 of which were hypothetical genes. The other 15 were already known ones. Series analysis of gene expression (SAGE) database showed that *ERP70*, *GRP58*, *GAPDH*, *SSB*, *S100A6*, *BMP-6*, *DVS27*, *HSP70* and *NAC alpha* in these genes were associated with endothelium and angiogenesis, but their effects on HLCVECs were still unclear. *GAPDH*, *S100A6*, *BMP-6* and *hsp70* were identified by SEREX in other tumor cDNA expression libraries.

CONCLUSION: By screening of HLCVECs cDNA expression library using sera from immunized mice with HLCVECs,

INTRODUCTION

Angiogenesis is a critical event in solid tumor growth, invasion, and metastasis. Recently, more attractive targets are thought to be vasculature of tumor compared with tumor cells themselves in the therapy of solid tumor^[1]. Tumor endothelium is a key mediator during the complex process of tumor angiogenesis. There will not form new blood vessels in tumor if tumor vascular endothelia are lacking of the functions of proliferation, activation, adhering, migration and vessel formation. To date, the morphology, phenotype, functional aspects and gene expression observed in tumor-derived endothelial cells (TEC) were proven to be different from normal-derived endothelial cells (NEC)^[2,3]. Virtually, the therapeutic strategy of solid tumors targeting for tumor vasculature makes use of these differences. Various methods have been developed to identify the differences between TEC and NEC, such as serial analysis of gene expression (SAGE)^[4], suppression subtractive hybridization (SSH)^[5], antibody target^[6], immunohistochemical analysis of known endothelial adhesion molecules^[7] phage display peptide library^[8], and cDNA microarray^[9], etc. Due to the difficulty of isolating highly purified TEC, most studies now selected activated endothelial cells as a substitute, however, the activated endothelial cells cannot completely represent TEC.

SEREX has recently emerged as a powerful method for serological identification of tumor associated antigens (TAAs) and/or tumor rejection antigens (TRAs). Up to date, more than 1 000 candidate tumor antigens in various cancers have been identified^[10,11]. Tumor antigens identified by SEREX could provide valuable targets for cancer diagnosis, therapy and the study of cancer vaccines. Similarly, the proliferation-associated antigens on tumor endothelial cells may be more useful candidates for antiangiogenic therapy/vascular targeting therapy of tumor. However, up to the present, no data are available that associated antigen genes have been isolated from TEC.

The goal of this study was to define tumor endothelium associated antigen genes by the method of modified SEREX.

Therefore, we constructed and screened the HLCVECs cDNA expression library with murine immunosera of anti-HLCVECs, and identified 18 HLCVECs associated antigen genes. These genes may not only provide a valuable tool for study on the roles of endothelial cells in tumor angiogenesis, but also some potent candidate targets for antiangiogenic therapy of cancer. Our results in this report also indicated that the approach of screening cDNA expression library with functional xenogeneic sera, a modified SEREX, could be an effective strategy for isolation and identification of tumor endothelium associated antigen genes.

MATERIALS AND METHODS

Tumor tissue samples and cells

Human tumor tissue was obtained from therapeutic surgical resection of one patient with hepatocellular carcinoma (HCC) at the Cancer Hospital of Peking Union Medical College. After surgical removal, the tissue sample was immediately transferred to the laboratory in cold culture medium (DMEM, GIBCO) with penicillin (400 U/mL) and EDTA (1 g/L) and was isolated for 2 h. Human umbilical vein endothelial cells (HUVECs) were isolated as described^[12]. HUVECs were stimulated to generate activated HUVECs with endothelium growth medium (Clontech) containing EC growth factors and tumor tissues homogenate prepared in our laboratory.

Isolation, purification and culturing of HLCVECs

Isolation, purification and culturing of HLCVECs were performed by previously described method^[13,14] with some modifications. Briefly, the liver cancer tissue from patient with HCC was finely minced with curved scissors into approximately 2 mm × 2 mm × 2 mm pieces, then was re-suspended in 20 mL of 1 g/L trypsin (type II, Sigma) in DMEM containing 1 g/L EDTA and incubated for 10 min at 37 °C. After digestion, the whole suspension was filtered through a 200 μm melt mesh sieve and the filtrate was washed twice in DMEM by centrifugation at 450 r/min for 5 min at room temperature. The pellet was re-suspended in 5 mL of DMEM + 100 g/L FCS (Hyclon) added to 25 mL of 200 g/L percoll (Pharmacia Biotech) in DMEM and centrifuged at 1500 g for 15 min at 4 °C. Again, the cell pellet was washed twice. The isolated cells were resuspended in complete culture medium (DMEM containing 200 mL/L FCS, 2 mmol/L L-glutamin (GIBCO), 100 μg/mL antibiotic (penicillin/streptomycin), 100 μg/mL endothelial cell growth supplement and 40 U/mL heparin). The cells were seeded into a 20 g/L gelatin-coated 6-well plate (FALCON), and cultured at 37 °C in 50 mL/L CO₂ incubator and the medium was changed every 3 d, the purification could be carried out by the way of sub-cell colonies after 1 wk. The cells were cultured and proliferated in gelatin-coated T75 plastic tissue culture flasks (Falcon), and passaged by 1 g/L trypsin (1 g/L EDTA). The purified endothelial cells were identified by immunocytochemistry for von Willebrand factor (vWF), CD31 and uptake of Ac-LDL. Fenestration was demonstrated by transmission electron microscopy.

Preparation of the anti-HLCVECs immunosera

Female BALB/c mice (6-8 wk) were purchased from Experimental Animal Center of Peking Union Medical College. Six mice were immunized with HLCVECs (immunized), and 4 mice were treated with PBS alone (non-immunized). All studies on mice were approved by the institute's Animal Care and Use Committee.

Sera were obtained as described^[15]. For the generation of immunosera, mice were immunized subcutaneously with 1-6 × 10⁶ HLCVECs fixed with 30 g/L paraformaldehyde in PBS or PBS alone once weekly for 8 continuous weeks. Serum was obtained from each mouse of immunized and non-immunized on d 21, 28, 35, 42, 49 and 56 after the first immunization. Serum from each

mouse of immunized and non-immunized groups was serially diluted, and the reactivity against HLCVECs was examined by immunocytochemistry.

Immunofluorescence

To determine the reactivity of sera from immunized and non-immunized mice reacting to different endothelium, HLCVECs, HUVECs and activated HUVECs were seeded onto glass coverslips in 6-cm plates, then fixed in cold acetone and incubated with serially diluted sera isolated from immunized or non-immunized mice at 37 °C for 1 h, fluorescein-conjugated goat-anti-mouse IgG (H+L) (Sigma) was subsequently applied to them and incubated for another 1h, then to be restained by 0.1 g/L Evens Blue and washed 3 times by PBS. The results were observed under fluorescence microscope (Nicon)^[16].

MTT assay

Approximately 8 × 10³ cells in 200 μL DMEM were seeded in triplicate into each well of the 96-well tissue culture plates, and immunized or non-immunized sera diluted at 1:30, 1:90, 1:270, 1:810, 1:2430, 1:7290 and 1:21870 were added to corresponding wells. After 72 h of incubation, 10 μL MTT (100 mg/mL) reagent was added to each well (5 g/L), and incubated for 4 h at 37 °C, 50 mL/L CO₂. Subsequently, 180 μL medium was pipetted out from each well and 50 μL DMSO was added to it. The absorbency A₅₇₀, which correlates to the number of cells, was measured with micro-plate reader (Model 450, Bio-Rad)^[17].

Cell cycle analysis by flow cytometry

HLCVECs were serum starved for 24 h and then treated with immunized and non-immunized sera diluted at 1:100 for 6 h. Cells were trypsinized, washed twice in PBS. Totally 1 × 10⁶ cells were resuspended in 500 μL PBS and stained with 500 μL propidium iodide (10 μg/mL, Sigma) for 30 min. Flow Cytometry (Becton) was performed to determine DNA content and apoptosis^[18].

Construction of cDNA expression library

The mRNA was directly extracted from HLCVECs with mRNA extraction kit (mRNA Poly(A) Tract System 1 000, Promega, Madison, WI), Oligo (dT)-primed double-stranded cDNA was synthesized from 6 μg purified mRNA and ligated into the ZAP phage expression vector DNA according to the user's manual (including THERMO Script™ RT-PCR System Kit, ZAP-cDNA synthesis kit, ZAP-cDNA Gigapack III Gold Mrna Cloning kit, Stratagene).

Screening the HLCVECs cDNA expression library with immunosera

Immunoscreening of the HLCVECs cDNA expression library was performed as described previously^[19] with the following modifications. Sera from immunized mice were diluted 1:10 and preabsorbed with lysate from *Escherichia coli* (*E.coli*) strain XL-1 coupled to Sepharose 4B to remove antibodies reacting with *E.coli* components. XL-1 infected with recombinant phage vectors containing HLCVECs cDNA were plated onto NZY-tetracycline-agar plates. After induction of protein synthesis in *E.coli*, we transferred the expressed polypeptides onto nitrocellulose membranes (Gelman) and incubated them with 1:500 diluted pre-absorbed sera overnight at 4 °C in the first screening. After being washed, the filters were incubated with a 1:10 000 dilution of alkaline phosphatase-conjugated goat-anti-mouse IgG (H+L) (Secondary Ab, Sigma) for 1-2 h at room temperature. Reactive clones were visualized with 5-bromo-4-chloro-3-indolyl-phosphate/nitro blue tetrazolium tablets (BCIP/NBT, Sigma). Only clones that appeared blue were considered serum positive. The positive clones were picked out and plated on NZY-tetracycline agar plates for secondary screening with

1:5 000 diluted pre-absorbed immunosera. Subsequently, positive clones were subcloned 2 times to obtain monoclonality.

Sequence analyses of the reactive clones

Identified and subcloned positive clones were converted to pBluescript phagemid forms by *in vitro* excision, plasmid was purified and subjected to *EcoR* I and *Xho* I restriction enzyme digestion. Clones representing different cDNA inserts were sequenced with T3 primers by the dideoxy chain termination method using the Big Dye Terminator Cycle Sequencing Kit (PE Applied Biosystems, Foster city, CA) and an ABI PRISM automated DNA sequencer (Perkin-Elmer, Norwalk, CT). DNA and predicted amino acid sequences were compared with sequences in the GenBank and other public databases by using the BLAST program.

RESULTS

Identification of HLCVECs

The heterogeneity of human TEC is detectable at different levels and differentiates the behavior between different tumor tissues. HLCVECs here belong to micro-vascular ECs, and they grow in a monolayer and exhibit contact inhibition properties. Using electron microscopy, surface fenestrations and Weibel-Palade (W-P) bodies were observed in HLCVECs. Immunofluorescence staining showed that these cells expressed vWF, CD31 and took up large amounts of Ac-LDL (Figure 1). These results demonstrated that isolated and purified HLCVECs expressing specific markers of endothelial cells, especially fenestration, a tumor endothelium-specific structure, were also found in HLCVECs.

Detection of antibodies against endothelial cells in immunosera

The antibody titer in sera from immunized mice with HLCVECs are shown in Table 1. Titer of antibody reached 1:1 000 at 21 d after the first immunization, 1:9 000 at 42 d and 1:27 000 at 49 d as well as at 56 d. In contrast, the sera from non-immunized

mice were negative for anti-HLCVECs response. A similar antibody response, with a minimal variation in titer, was seen in all six immunized mice.

To determine whether differences existed in reactivity of sera from mice immunized with HLCVECs with human TEC versus NEC, immunofluorescence was applied to detect the reaction of anti-HLCVECs sera with HLCVECs, HUVECs and activated HUVECs. The results indicated that 1:500 dilution of the immunized serum showed the same degree fluorescence staining in HLCVECs and activated HUVECs, but the staining in HUVECs was distinctly weaker than that of the other 2 kinds of cells. The 1:5 000 dilutions of immunosera showed markedly stronger staining with HLCVECs than with activated HUVECs (Figures 2A and 2B), whereas the staining of HUVECs was completely negative in this dilution (Figure 2C). By comparison, the staining of all the 3 kinds of cells was negative when reacting with sera from non-immunized mice. Simultaneously, the fluorescence staining was observed in the membrane of positive endothelial cells. These data indicated that the murine anti-HLCVECs sera contained the specific antibodies with a high titer against TECs.

Table 1 Titer of anti-HLCVECs antibody in immunized animals

	D21	D28	D35	D42	D49	D56
HLCVEC	1:1 000	1:3 000	1:9 000-	1:9 000	1:27 000	1:27 000+

1:9 000- indicates that the titer is lower than 1:9 000, 1:27 000+ indicates that the titer is 1:27 000 or higher.

Identification of the effect of immunosera on ECs growth

To investigate whether the immunosera have any effects on the proliferation of HLCVECs, HLCVECs were treated with variously diluted sera isolated from mice immunized or non-immunized with HLCVECs. MTT assay demonstrated that the growth and proliferation of HLCVECs were apparently inhibited by the sera from immunized mice with HLCVECs, and there was

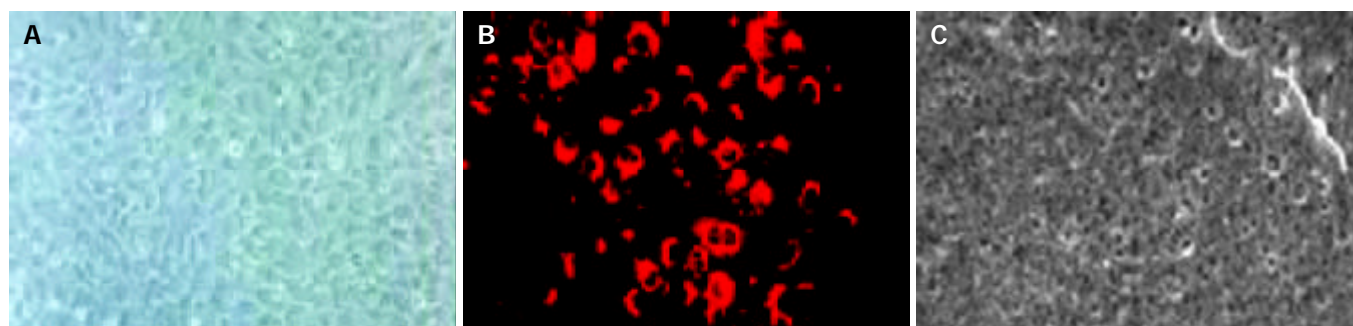


Figure 1 Cultured human liver cancer vascular endothelial cells. A: Morphology of cultured human liver cancer vascular endothelial cells; B: Uptake of Ac-LDL; C: Electron microscope for fenestration.

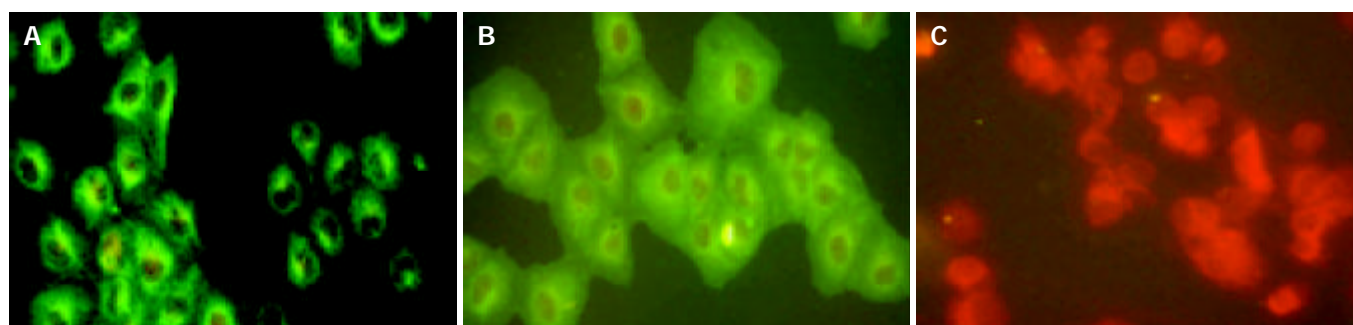


Figure 2 Immunofluorescence analysis of endothelial cells stained with the sera diluted 1:5 000 isolated from the mice immunized with HLCVECs. A: HLCVECs; B: Activated HUVECs; C: HUVECs.

Table 2 Construction of HLCVECs libraries in λ -ZAP expression vector and the number of SEREX-identified antigens

Patient	Age (years)	Primary size	Screening serum	Clones screened	Positive clones	cDNA fragment	Known genes	Unknown gene
HCC	56	2×10^6	immunized	6×10^5	36	18	15	3

Table 3 Results of immunoscreening of HLCVECs cDNA expression library by immunized BALB/C sera screening

Clone	Size (bp)	Gene	Localization	Identity	Accession number
EC19	2 100	HS.Protein disulfide isomerase related protein	7q35	99%	NM 004911.2
EC24	700	HS.Glucose regulated protein	15q15	98%	NM 005313.3
EC26	1 000	HS.Chemokine ligand 1	4q12-q13	99%	BC 011976
EC29	1 600	HS.Inner membrane protein	2p11.2	99%	NM 006839.1
EC30	1 800	HS.Hypothetical protein Loc283241	11q12.3	99%	XM 208579.1
EC31	1 700	HS.genomic DNA, clone	11q	98%	AP 002340.3
EC35	700	HS.BMP-6	15q13-q15	98%	NM 013372.1
EC36	2 200	HS.Glycerol dehyde-3-phosphate dehydrogenase	12p13.31	98%	BC 004109
EC38	1 900	HS.Replication factor C5	12q24.2	99%	NM 007370.2
EC39	2 100	HS.BAC, CloneRP11-1591120		99%	AC 010974.9
EC40	800	HS.Sjogren syndrome antigen B	2q31.1	98%	BC 020818
EC42	2 400	HS.X-ray repair complementing defective repair in Chinese	12q23	99%	AY 034001.1
EC51	400	HS.S100 calcium-binding protein A6	1q21	100%	BC 009017
EC52	1 500	HS.Protein kinase C	19p1.1	98%	NM 002743.1
EC53	1 700	HS.Heat shock 70 ku protein4	5q31.3	99%	XM 114482.2
EC59	1 900	HS.DVS27 related protein	9p24.1	99%	BC 04785.1
EC62	1 500	HS.NAC alpha mRNA	12q2	99%	AY 034001.1
EC63	1 500	HS.Hypothetical protein DJ1042k10.2	2 213.1	100%	HS1042k10

a dose dependent response from 1:30 to 1:2 430 dilution of the murine immunosera, while no inhibitory effects were observed in sera from non-immunized mice. Figure 3 shows the results of serum from one of six immunized mice and one of 4 non-immunized mice.

Using MTT assay, we observed that human TEC growth was inhibited when they were incubated with the immunosera, however, the underlying mechanism was unknown. We therefore studied further the effects of the sera on cell cycle of human TEC with Flow Cytometry. The results showed that the amount of apoptotic cells were increased in the group of immunosera compared with the group of non-immunosera at 6 h after treatment (Figure 4). Approximately 20.1% apoptotic cells were seen in the group of immunized serum and only 4.9% apoptotic cells were observed in the group of non-immunized serum. The results further indicated that, in terms of specificity and the effects on human TEC, the immunized sera were suitable to screen the HLCVECs cDNA expression library to obtain endothelium associated antigen genes.

Isolation of HLCVECs associated antigens genes by modified SEREX

HLCVEC cDNA expression library with 2×10^6 primary clones was established (Table 2). The 6×10^5 clones were immunoscreened with pooled sera from six immunized BALB/c mice collected on d 56 after inoculation of HLCVECs. Primary screening with 1:500 diluted pooled immunosera yielded 153 positive clones (named EC1 to EC153). After secondary screening with 1:5 000 immunosera and subcloning, a total of 36 positive clones were obtained (Figure 5). These 36 clones were then excised, to phagemide forms and purified *in vitro*. The size of inserts of these positive clones were determined by restriction enzyme digestion with *Eco*R I and *Xho*I, which yielded inserts sized from 900 bp to 3 600 bp, with an average of about 1 500 bp (Figure 6).

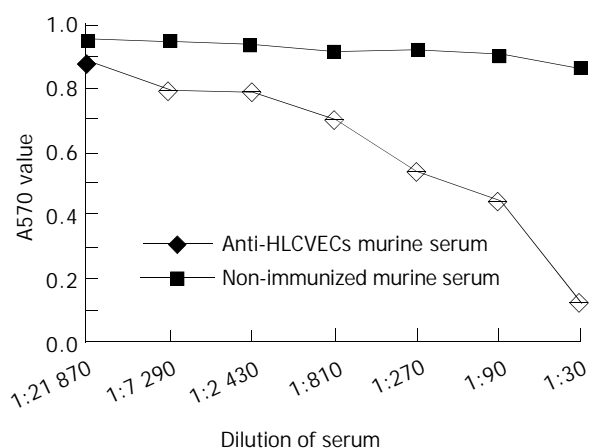


Figure 3 Inhibition of the HLCVECs proliferation by HLCVECs immunized murine serum from 1 of 6 immunized mice and 1 of 4 non-immunized mice. Points are the average of three wells.

Sequence analysis of the positive clones

Nucleotide sequences of cDNA inserts of 36 positive clones were sequenced. Sequence alignments were analyzed with DNASIS and BLAST software on EMBL and GeneBank. These 36 positive clones represented 18 different antigen genes (Table 3). EC36 was represented by 11 overlapping clones, EC42 by 6 overlapping clones, EC 62 by 4 overlapping clones and the others by a single clone. Of these 18 clones, 3 clones were new unknown genes, 2 of which may be functional genes encoding hypothetical proteins. The other 15 genes were known. However, all of them were first isolated and reported in the endothelial cells of human HCC here. By SAGE database analysis, the 15 genes can be grouped into different classes: (1) 9 of these genes are associated with endothelium and angiogenesis, such

as EC26, EC52, EC59, *etc.* (2) 4 of these genes have been reported previously as tumor antigen genes, such as NAPDH, S100A6, BMP-6 and hsp70, (3) The other genes are involved in genes transcription, protein translation and cell mitosis, such as inner membrane protein gene (IMMT).

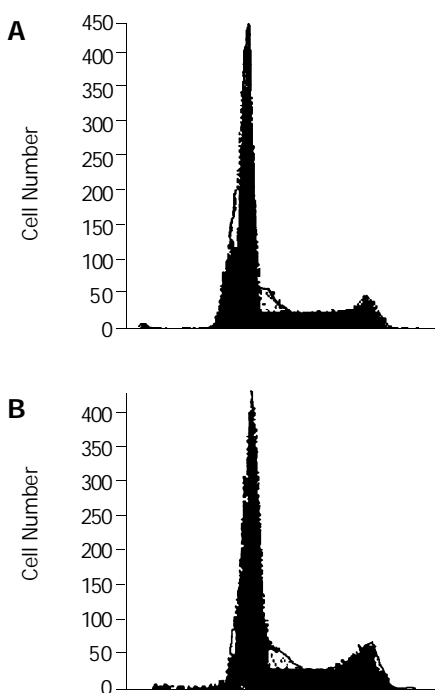


Figure 4 Cell cycle analysis of HLCVECs after treatment with immune sera or non-immune sera. A: HLCVECs treated with immune sera for 6 h; B: HLCVECs treated with non-immune sera for 6 h.

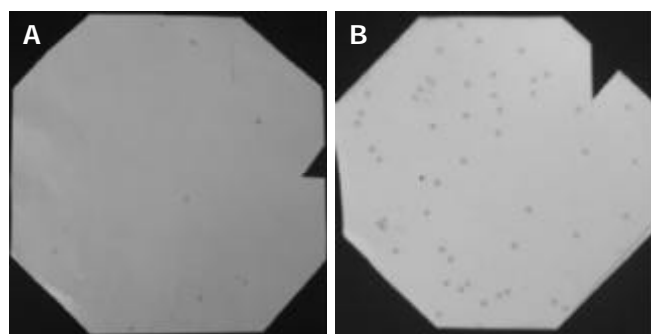


Figure 5 Positive dots of phage clone of screening by immune sera. A: The first cycle of screening by immune sera; B: The second cycle of screening by immune sera.

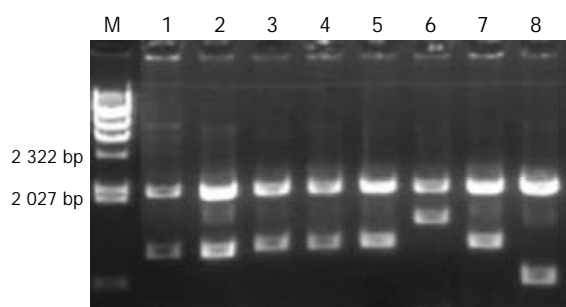


Figure 6 Electrophoresis analysis of enzymatic digestion of SEREX positive clones. M, λ Hind III marker, from above to below: 20 130, 9 416, 6 557, 4 316, 2 322, 2 027, 564 bp; Lanes 1-8, positive clones digested with *EcoR* I and *Xho* I.

DISCUSSION

Tumor angiogenesis is dependent on biochemical processes mediating the formation and development of the blood capillary network that supplies the tumor. In recent years, increasing evidence has indicated that targeting tumor vasculature is a very promising strategy for the therapy of solid tumor. Identifying molecular markers, target genes and antigen on endothelial cells of tumor vessels, in turn, is critical for the antiangiogenic therapeutic strategy of tumor. A number of researchers have gained some endothelia associated genes from activated HUVECs with cell growth factors and supernatant of cultured tumor cells. But it is difficult to determine tumor specific endothelial genes by these ways, because activated endothelium cannot completely represent tumor endothelium. In 2000, Croix^[4] first reported in *Science* that they successful isolated tumor endothelium from human colorectal cancer and gained tumor endothelium associated genes by the method of SAGE. In the present study, to obtain specific endothelium genes of human liver cancer vascular endothelial cells, we isolated and purified endothelial cells from liver tumor tissue of the patients with HCC. These endothelial cells were confirmed to have characteristics of endothelial cells with expressing vWF, CD31, W-P bodies and taking up high level of Ac-LDL, *etc.*, and also have the structure of fenestrations found only in tumor endothelial cells. From cDNA expression library constructed with above purified HLCVECs, we isolated 18 endothelia associated genes. Some of them were related to human TEC. Up to date, there have been no reports about the successful isolation of human liver cancer vascular endothelial cells and their specific genes.

Over the past years, efforts have been made to isolate and identify the proliferating TEC genes, including the methods of phage display peptide libraries, SSH and SAGE analysis, *etc.* However, the genes identified using these methods, in terms of their specificity and functions were rarely known. Therefore, in this study, to isolate and identify functional TEC associated antigen genes, we modified traditional SEREX and used it to screen cDNA expression library of HLCVECs. SEREX has recently emerged as a powerful method for identification of human tumor-associated antigen. The identification of tumor antigens with SEREX was based on the existence of autoantibodies in sera of patients^[10]. It is not unexpected that the method is applicable to only a limited number of patients because autoantibodies against most antigens can only be detected in 10-30% patients who bear tumors expressing the corresponding antigens. Therefore, a number of modifications have been made since the introduction of SEREX methodology to expand the range of antigens identified. These modifications include using established cell lines instead of tumor specimen to construct the cDNA library, and using allogeneic sera or xenogeneic sera instead of autologous sera as the antibody source. Hideho *et al.*, introduced the "cytokine-assisted SEREX (CAS)", which resulted in an enhanced capacity to identify glioma tumor associated antigens (TAAs) with characteristics similar to TAAs identified by traditional SEREX^[19-21]. Despite extensive screening of various tumor cDNA libraries with sera from tumor patients, however, identification of human tumor endothelium associated antigens by SEREX have not been reported up to date. To develop a method to screen the endothelium associated functional genes, we first immunized BALB/c mice by injection subcutaneously with high dose purified HLCVECs. Sera from the immunized mice were identified with several fixed methods for their specificity against HLCVECs and the effects on endothelial cells. For example, detection by immunocytochemistry and immunofluorescence showed that the ability of immunosera to bind HLCVECs were higher compared with activated HUVECs when sera were diluted at 1:5 000, whereas the staining of unactivated HUVECs were completely negative. These data

indicated that the immunosera still contained specific antibodies directed against HLCVECs in this dilution. By MTT assay and cell cycles analysis, we have also demonstrated that the growth and proliferation of HLCVECs were significantly inhibited when treated with anti-HLCVECs immunosera in range of 1:30-1:2430 dilution, while this inhibitory effect of sera from non-immunized (only injected by PBS) mice was not observed. To identify the possible mechanism about anti-HLCVECs proliferation activity of immunosera, we employed Flow Cytometry to analyse cell cycle of HLCVECs treated with the immunosera. The results showed that there was a 4-fold increase in the amount of apoptotic cells compared with the group of non-immunosera. These findings suggested that the anti-sera obtained from mice immunized with high dose of fixed HLCVECs presented some functional immunoglobulin with potent antiangiogenic activity. Similar results were also observed by Scappaticci *et al.*^[18], who recently demonstrated that vaccination of rabbits with murine endothelial cells yielded immunized sera with antiangiogenic effects *in vitro* and that the mechanism of antiangiogenic effect was proven to be through induction of apoptosis of ECs by polyclonal immunoglobulin in this serum. Furthermore, Wei *et al.*^[15] reported also that vaccination of mice with human ECs could induce a specific antiangiogenic immune response with broad anti-tumor activity. In our study, using xenogeneic functional anti-sera from mice immunized with HLCVECs to screen cDNA expression library of HLCVECs, a modified xenogeneic SEREX, we first isolated endothelium associated antigen genes from human liver cancer vascular endothelium.

To isolate TEC associated functional antigens genes, we immunoscreened HLCVECs cDNA expression library by a modified xenogeneic SEREX. Thirty-six positive clones were identified after screening of 6×10^5 clones. Sequencing analysis for homology with the GeneBank and other public databases indicated that these clones represented 18 different genes which were first isolated and identified to be the endothelial genes from human HCC tissues. Three of them were previously not reported new genes, 2 of which may be functional gene encoding hypothetical proteins. There other 15 genes were known. SAGE analysis revealed that 9 of the 15 genes, have been reported as endothelium associated genes and some of them were involved in the proliferation, migration of endothelia cells and the process of angiogenesis. For example, EC26 has 99% homology with chemokine ligand 1(CXCL1), which was implicated having effects on endothelial cells in angiogenesis^[22]. EC35 has 99% homology with bone morphogenetic protein-6 (BMP-6), which stimulates angiogenesis and induces migration^[23,24]. EC52 may be one of the factors that up-regulate VEGF gene expression during hypoxia^[25-27]. The expression of EC59 gene was mostly highly up-regulated in cerebral arteries^[28]. Camby *et al.* found that the level of EC51 expression differed markedly in the blood vascular walls according to whether these vessels originated from low- or high-grade astrocyte tumors^[29,30]. EC53 had 99% homology with heat shock 70 ku protein (HSP70) and is expressed in human microvascular endothelial cells. The expression of HSP70 is known to increase endothelial cells survival and growth^[31-33]. These data indicated that the genes identified in this study using specific and functional antiserum from mice immunized with human TEC, may be functional genes for human endothelial cells and angiogenesis. Furthermore, this approach through screening cDNA expression library with xenogeneic serum containing specific antibodies may serve as an effective strategy for isolation and identification of human TEC genes, which will provide useful marker and targets for tumor anti-angiogenesis therapy.

In summary, the screening of HLCVECs cDNA expression library by using murine immunosera of anti-tumor endothelium yielded 18 functional antigen genes associated with tumor endothelium. These antigen genes may be related to the

proliferation, migration and vessel formation of tumor vascular endothelium. Further exploration of these genes and their relationship with tumor angiogenesis would provide a valuable resource for basic and clinical studies of anti-angiogenesis targeting therapy of tumor.

REFERENCES

- 1 **Folkman J.** Angiogenesis inhibitors generated by tumors. *Mol Med* 1995; **1**: 120-122
- 2 **Hashizume H,** Baluk P, Morikawa S, Mclean JW, Thurston G, Roberge S, Jain RK, McDonald DM. Openings between defective endothelial cells explain tumor vessel leakiness. *Am J Pathol* 2000; **156**: 1363-1380
- 3 **Alessandri G,** Chirivi RG, Fiorentini S, Dossi R, Bonardelli S, Giulini SM, Zanetta G, Landoni F, Graziotti PP, Turano A, Caruso A, Zardi L, Giavazzi R, Bani MR. Phenotypic and functional characteristics of tumour-derived microvascular endothelial cells. *Clin Exp Metastasis* 1999; **17**: 655-662
- 4 **St Croix B,** Rago C, Velculescu V, Traverso G, Romans KE, Montgomery E, Lal A, Riggins GJ, Lengauer C, Vogelstein B, Kinzler KW. Genes expressed in human tumor endothelium. *Science* 2000; **289**: 1197-1203
- 5 **Liu C,** Zhang L, Shao ZM, Beatty P, Sartippour M, Lane TF, Barsky SH, Livingston E, Nguyen M. Identification of a novel endothelial-derived gene EG-1. *Biochem Biophys Res Commun* 2002; **290**: 602-612
- 6 **Huang X,** Molema G, King S, Wakins L, Edgington TS, Thorpe PE. Tumor infarction in mice by antibody-directed targeting of tissue factor to tumor vasculature. *Science* 1997; **275**: 547-550
- 7 **Nguyen M,** Corless CL, Kraling BM, Tran C, Atha T, Bischoff J, Barsky SH. Vascular expression of E-selectin is increased in estrogen-receptor-negative breast cancer: a role for tumor-cell-secreted interleukin-1 alpha. *Am J Pathol* 1997; **150**: 1307-1310
- 8 **Koivunen E,** Arap W, Valtanen H, Rainisalo A, Medina OP, Heikkila P, Kantor C, Gahmberg CG, Salo T, Kontinen YT, Sorsa T, Ruoslahti E, Pasqualini R. Tumor targeting with a selective gelatinase inhibitor. *Nat Biotechnol* 1999; **17**: 768-774
- 9 **Lee MJ,** Van Brocklyn JR, Thangada S, Liu CH, Hand AR, Menzeleev R, Spiegel S, Hla T. Sphingosine-1-phosphate as a ligand for the G protein-coupled receptor EDG-1. *Science* 1998; **279**: 1552-1555
- 10 **Chen YT.** Cancer vaccine: identification of human tumor antigens by SEREX. *Cancer J* 2000; **6**(Suppl 3): S208-S217
- 11 **Wang Y,** Han KJ, Pang XW, Vaughan HA, Qu W, Dong XY, Peng JR, Zhao HT, Rui JA, Leng XS, Cebon J, Burgess AW, Chen WF. Large scale identification of human hepatocellular carcinoma-associated antigens by autoantibodies. *J Immunol* 2002; **169**: 1102-1109
- 12 **Martinez J,** Rich E, Barsigian C. Transglutaminase-mediated cross-linking of fibrinogen by human umbilical vein endothelial cells. *J Biol Chem* 1989; **264**: 20502-20508
- 13 **Rupnick MA,** Carey A, Williams SK. Phenotypic diversity in cultured cerebral microvascular endothelial cells. *In Vitro Cell Dev Biol* 1988; **24**: 435-444
- 14 **Lou J,** Buhler L, Deng S, Mentha G, Montesano R, Grau GE, Morel P. Inhibition of leukocyte adherence and transendothelial migration in cultured human liver vascular endothelial cells by prostaglandin E1. *Hepatology* 1998; **27**: 823-828
- 15 **Wei YQ,** Wang QR, Zhao X, Yang L, Tian L, Lu Y, Kang B, Lu CJ, Huang MJ, Lou YY, Xiao F, He QM, Shu JM, Xie XJ, Mao YQ, Lei S, Luo F, Zhou LQ, Liu CE, Zhou H, Jiang Y, Peng F, Yuan LP, Li Q, Wu Y, Liu JY. Immunotherapy of tumors with xenogeneic endothelial cells as a vaccine. *Nat Med* 2000; **6**: 1160-1166
- 16 **Lou JN,** Mili N, Decrind C, Donati Y, Kossodo S, Spiliopoulos A, Ricou B, Suter PM, Morel DR, Morel P, Grau GE. An improved method for isolation of microvascular endothelial cells from normal and inflamed human lung. *In Vitro Cell Dev Biol Anim* 1998; **34**: 529-536
- 17 **Xin L,** Xu R, Zhang Q, Li TP, Gan RB. Kringle 1 of human hepatocyte growth factor inhibits bovine aortic endothelial cell proliferation stimulated by basic fibroblast growth factor and causes cell apoptosis. *Biochem Biophys Res Commun* 2000; **277**:

- 186-190
- 18 **Scappaticci FA**, Contreras A, Boswell CA, Lewis JS, Nolan G. Polyclonal antibodies to xenogeneic endothelial cells induce apoptosis and block support of tumor growth in mice. *Vaccine* 2003; **21**: 2667-2677
- 19 **Okada H**, Attanucci J, Giezeman-Smits KM, Brissette-Storkus C, Fellows WK, Gambotto A, Pollack LF, Pogue-Geile K, Lotze MT, Bozik ME, Chambers WH. Immunization with an antigen identified by cytokine tumor vaccine-assisted SEREX (CAS) suppressed growth of the rat 9L glioma *in vivo*. *Cancer Res* 2001; **61**: 2625-2631
- 20 **Chen YT**, Gure AO, Tsang S, Stockert E, Jager E, Knuth A, Old LJ. Identification of multiple cancer/testis antigens by allogeneic antibody screening of a melanoma cell line library. *Proc Natl Acad Sci U S A* 1998; **95**: 6919-6923
- 21 **Ono T**, Sato S, Kimura N, Tanaka M, Shibuya A, Old LJ, Nakayama E. Serological analysis of BALB/C methylcholanthrene sarcoma Meth A by SEREX: identification of a cancer/testis antigen. *Int J Cancer* 2000; **88**: 845-851
- 22 **Dhawan P**, Richmond A. Role of CXCL1 in tumorigenesis of melanoma. *Leukoc Biol* 2002; **72**: 9-18
- 23 **Valdimarsdottir G**, Goumans MJ, Rosendahl A, Brugman M, Itoh S, Lebrin F, Sideras P, ten Dijke P. Stimulation of Id1 expression by bone morphogenetic protein is sufficient and necessary for bone morphogenetic protein-induced activation of endothelial cells. *Circulation* 2002; **106**: 2263-2270
- 24 **Deckers MM**, van Bezooijen RL, van der Horst G, Hoogendam J, van Der Bent C, Papapoulos SE, Lowik CW. Bone morphogenetic proteins stimulate angiogenesis through osteoblast-derived vascular endothelial growth factor A. *Endocrinology* 2002; **143**: 1545-1553
- 25 **Zhou Z**, Yang XM, Xie YZ, Yin ZY. Vascular endothelial growth factor gene expression regulated by protein kinase C pathway in endothelial cells during hypoxia. *Space Med Med Eng* 2002; **15**: 322-326
- 26 **Siflinger-Birnboim A**, Johnson A. Protein kinase C modulates pulmonary endothelial permeability: a paradigm for acute lung injury. *Am J Physiol Lung Cell Mol Physiol* 2003; **284**: L435-451
- 27 **Feener EP**, King GL. Endothelial dysfunction in diabetes mellitus: role in cardiovascular disease. *Heart Fail Monit* 2001; **1**: 74-82
- 28 **Onda H**, Kasuya H, Takakura K, Hori T, Imaizumi T, Takeuchi T, Inoue I, Takeda J. Identification of genes differentially expressed in canine vasospastic cerebral arteries after subarachnoid hemorrhage. *J Cereb Blood Flow Metab* 1999; **19**: 1279-1288
- 29 **Ilg EC**, Schafer BW, Heizmann CW. Expression pattern of S100 calcium-binding proteins in human tumors. *Int J Cancer* 1996; **68**: 325-332
- 30 **Camby I**, Lefranc F, Titeca G, Neuci S, Fastrez M, Dedecken L, Schafer BW, Brotchi J, Heizmann CW, Pochet R, Salmon I, Kiss R, Decaestecker C. Differential expression of S100 calcium-binding proteins characterizes distinct clinical entities in both WHO grade II and III astrocytic tumours. *Neuropathol Appl Neurobiol* 2000; **26**: 76-90
- 31 **Oehler R**, Schmierer B, Zellner M, Prohaska R, Roth E. Endothelial cells downregulate expression of the 70 kDa heat shock protein during hypoxia. *Biochem Biophys Res Commun* 2000; **274**: 542-547
- 32 **Piura B**, Rabinovich A, Yavelsky V, Wolfson M. Heat shock proteins and malignancies of the female genital tract. *Harefuah* 2002; **141**: 969-972
- 33 **Gain P**, Thuret G, Chiquet C, Dumollard JM, Mosnier JF, Campos L. *In situ* immunohistochemical study of Bcl-2 and heat shock proteins in human corneal endothelial cells during corneal storage. *Br J Ophthalmol* 2001; **85**: 996-1000

Edited by Zhu LH and Xu FM

Effects of endostatin-vascular endothelial growth inhibitor chimeric recombinant adenoviruses on antiangiogenesis

Xin Pan, Yong Wang, Min Zhang, Wei Pan, Zhong-Tian Qi, Guang-Wen Cao

Xin Pan, Min Zhang, Wei Pan, Zhong-Tian Qi, Department of Microbiology, Second Military Medical University, Shanghai 200433, China

Yong Wang, Department of Ophthalmology of Changhai Hospital, Second Military Medical University, Shanghai 200433, China

Guang-Wen Cao, Department of Epidemiology, Second Military Medical University, Shanghai 200433, China

Supported by The National Natural Science Foundation of China, No. 30170891 and No.39970819

Correspondence to: Xin Pan, Department of Microbiology, Second Military Medical University, Shanghai 200433, China. panxinx@yahoo.com

Telephone: +86-21-25070314 **Fax:** +86-21-25070312

Received: 2003-10-08 **Accepted:** 2003-12-06

Abstract

AIM: To investigate the inhibitory effects of endostatin-vascular endothelial growth inhibitor (VEGI₁₅₁) recombinant adenoviruses on neovascularization.

METHODS: We used recombinant adenoviruses to treat human vascular endothelial cell line ECV304, human hepatocellular carcinoma cell line HepG2, and murine fibroblast cell line L929, in order to study the chimeric gene expression in these cell lines. Chick chorioallantoic membrane (CAM) model, rabbit inflammatory corneal neovascularization (CNV) model, and liver cancer-bearing nude mice model were employed to investigate the negative biological effect of fusion molecules on neovascularization *in vivo*.

RESULTS: Western blot showed that the molecular weight of fusion protein was about 41kD after infection of ECV304, HepG2 and L929 cells with supernatant of AdhENDO-VEGI₁₅₁. The fusion protein showed a specific inhibitory effect on the proliferation of ECV304 cells, but no inhibitory effect on the growth of HepG2 and L929 cells ($F=13112.13$, $P=0.0001$). In the chick chorioallantoic membrane (CAM) assay, the expressed fusion protein significantly inhibited neovascularization. Rabbit inflammatory corneal neovascularization (CNV) induced by intrastromal sutures resulted in a uniform neovascular response. In this model, direct subconjunctival injection of AdhENDO-VEGI₁₅₁ expressed the fusion protein *in vivo* and suppressed the development of CNV. Topical application of AdhENDO-VEGI₁₅₁ led to a significant suppression of CNV ($F=1413.11$, $P=0.0001$), as compared with the control group of AdLacZ. Immunohistochemical staining showed the fusion protein dominantly expressed in corneal epithelium. Compared with the control group of AdLacZ ($4075.9 \pm 1849.9 \text{ mm}^3$), the average tumor size of group AdhENDO-VEGI₁₅₁ reduced in size ($487.7 \pm 241.2 \text{ mm}^3$) ($F=14.80$, $P=0.0085$), with an inhibition rate of 88.03%. Immunohistochemical staining showed the adenoviruses carried the fusion gene expressed on liver cancer cell membrane. MVD decreased more significantly in treated mice ($30.75 \pm 3.31\%$) than in AdLacZ control ($50.25 \pm 8.65\%$) ($F=17.72$, $P=0.0056$) with an inhibition rate of 39%.

CONCLUSION: Fusion protein expressed by recombinant adenoviruses has a significant inhibitory effect on neovascularization.

Pan X, Wang Y, Zhang M, Pan W, Qi ZT, Cao GW. Effects of endostatin-vascular endothelial growth inhibitor chimeric recombinant adenoviruses on antiangiogenesis. *World J Gastroenterol* 2004; 10(10): 1409-1414

<http://www.wjgnet.com/1007-9327/10/1409.asp>

INTRODUCTION

Neovascularization plays a critical role in solid tumor growth and corneal opacification. Researches indicated that angiogenesis inhibitors were highly potent in suppressing angiogenesis which could enable the tumor mass to remain in a dormant state^[1-4] and inhibit the development of corneal neovascularization^[5-7]. Endostatin could cause G(1) cell cycle arrest in endothelial cells, inhibit endothelial cell proliferation and migration, and promote apoptosis^[8]. Vascular endothelial cell growth inhibitor (VEGI) belongs to the tumor necrosis factor superfamily. VEGI is another endothelial cell-specific gene and a potent inhibitor of endothelial cell proliferation, angiogenesis^[9]. VEGI could mediate early G(1) arrest in G(0)/G(1) endothelial cells responding to growth stimuli, and programmed death in proliferating endothelial cells^[10]. In our laboratory two recombinant proteins have been used to treat tumor-bearing nude mice, but the inhibitory effect was not satisfactory. A few groups have demonstrated that antiangiogenic gene therapy with viral vectors is a potentially useful approach for inhibiting tumor growth in mouse models^[11-15]. In the current study, we acquired recombinant adenoviruses carrying endostatin-vascular endothelial growth inhibitor fusion gene to investigate its inhibitory effect *in vitro* on endothelial cells and antiangiogenic activity *in vivo* on chicken chorioallantoic membrane, inflammatory corneal neovascularization (CNV) in rabbit and liver cancer in nude mice.

MATERIALS AND METHODS

Materials

AdhENDO-VEGI₁₅₁ and AdLacZ were prepared in our laboratory. Endostatin polyclonal antibody was a gift from Dr. Stanker (Hanover, Germany). VEGI polyclonal antibody was prepared in our laboratory. Ad5-transformed human embryo renal cell line 293, human vascular endothelial cell line ECV304, human hepatocellular carcinoma cell line HepG2, and murine fibroblast cell line L929 were purchased from the Institute of Cell Biology, Chinese Academy of Sciences. Cell culture media were obtained from GIBCO. Nine-day-old fertilized white Leghorn eggs, New Zealand white rabbits, liver cancer-bearing nude mice SMMC-LTNM, and BALB/c nude mice were purchased from the Center of Experiment Animals, Second Military Medical University (Shanghai, China). All cell lines and animals were maintained under standard conditions.

Methods

Recombinant adenovirus infectivity examination AdhENDO-

VEGI₁₅₁ and AdLacZ were acquired as described previously^[16,17]. In a 24-well plate, 6×10^5 293 cells were infected with 50 μ L of identified recombinant adenoviruses AdhENDO-VEGI₁₅₁ or AdLacZ in 150 μ L of Dulbecco's modified Eagle's medium (DMEM) containing 100 mL/L fetal bovine serum (200 μ L in total) for 72 h. The cells showed evidence of cytopathic effect (CPE) and its supernatant was harvested. After three freeze/thaw cycles, the mixtures were passed through a 0.45 μ m millipore filter. The filtrate was frozen at -70°C and stored. TCID₅₀ was used to determine the titer of recombinant adenoviruses^[18]. Ten thousand ECV304 cells were incubated in a 96-well plate for 5 h. Cells were infected with AdLacZ, covering a proper multiplicity of infection (MOI) range (0.1, 5, 10, 20, 50 and 100 MOI), and incubated for 48 h. X-gal staining was performed and blue stained cells were counted under a microscope.

Western blotting analysis Ad5-transformed human embryonic renal cell line 293, human vascular endothelial cell line ECV304, human hepatocellular carcinoma cell line HepG2, and murine fibroblast cell line L929 were used in this assay. In a 6-well plate, 1×10^6 cells were infected with recombinant adenoviruses at an MOI of 20 for 4 h, then the medium containing recombinant adenoviruses was replaced with 1 mL of normal medium and cells were incubated for 24 h. Cell extracts were separated by 100 g/L sodium dodecyl sulfate-polyacrylamide gel electrophoresis under reducing conditions and electroblotted onto nitrocellulose membrane followed by treatment with blocking buffer containing 50 g/L nonfat dry milk in TBST (20 mmol/L Tris [pH8.0], 150 mmol/L NaCl, 1 g/L Tween-20) for 1 h. The electroblotted membranes were incubated with rabbit polyclonal antibodies against VEGI proteins, then subsequently incubated with peroxidase horseradish-conjugated anti-rabbit immunoglobulin for 1 h at 37°C . The immune complexes were visualized with diaminobenzidine (DAB) staining.

In vitro bioactivity of fusion gene products 1×10^3 cells were incubated in the 96-well plates, cells were infected with recombinant adenoviruses at an MOI of 20 for 4 h. The cell lines were ECV304, HepG2, and L929, respectively. The recombinant adenoviruses were AdhENDO-VEGI₁₅₁ and AdLacZ, respectively. The medium containing recombinant adenoviruses was replaced with 100 μ L of normal medium and cells were incubated at 37°C for an appropriate period of time. The medium containing recombinant adenoviruses was removed, murine fibroblast cell line L929 was incubated with a normal medium containing 0.5 μ g/mL actinomycin D. Cell viability was determined by crystal violet vital staining^[19]. Cell viability (%) = (AdhENDO-VEGI₁₅₁ infected group $A_{570/630}$ / AdLacZ control group $A_{570/630}$) $\times 100$.

Inhibition of chick embryonic chorioallantoic membrane angiogenesis by recombinant adenoviruses A 1 cm \times 1 cm window in the shell was drilled over the air sac at the end of 9-day-old eggs. Chick embryonic chorioallantoic membrane was exposed by tearing up the egg membrane with a tip. A disk of methylcellulose was put on CAM, and 10 μ L recombinant adenoviruses was added at a titer of 1×10^{12} TCID₅₀/L. The windows were sealed with aseptic tapes and the eggs were incubated for 3 d. The membrane was cut around the air sac, which was turned upside down and observed by a stereomicroscope.

Suppression of rabbit inflammatory corneal neovascularization In this study, 4 female New Zealand white rabbits, weighing 4-5 kg, were used. Inflammatory CNV in rabbits induced by placement of intrastromal sutures resulted in a uniform neovascular response as described^[20]. On the first day after suturation, four rabbits were divided into AdlacZ control group and AdhENDO-VEGI₁₅₁ group. One hundred microliters of each recombinant adenovirus at a titer of 1×10^{12} TCID₅₀/L was injected into subconjunctiva. Then, gentamicin ointment was applied to the eyes once per day. Eyes were examined daily by

a slit-lamp biomicroscope and a surgical microscope was used to monitor angiogenic responses to recombinant adenoviruses. The area of corneal neovascularization was determined by measuring the vessel length (L) from the limbus and the number of clock hours (C) of limbus involved^[21-24]. Only the uniform contiguous band of neovascularization adjacent to the suture was measured. A formula was used to determine the area^[25]: $C/12 \times 3.1416 \times [r^2 - (r-L)^2]$, where $r=6$ mm (the measured radius of rabbit cornea). Rabbits were sacrificed on d 21. Rabbits' eyes were enucleated and inflammatory cornea was fixed in 40 g/L paraformaldehyde for 24 h.

Immunohistochemical staining of fusion protein in inflammatory cornea of rabbits Buffered formaldehyde fixed tissues were embedded in paraffin, 4- μ m thick sections were treated with 3 mL/L H₂O₂ in methanol for 20 min, and blocked with normal rabbit serum (1:20 dilution) for 20 min at room temperature. Then, the sections were incubated with rabbit polyclonal anti-endostatin (1:50 dilution) for 1 h at room temperature, followed by incubation with biotinylated goat anti-rabbit antibody IgG for 30 min and horseradish peroxidase-conjugated streptavidin at room temperature for 30 min. After completion of conjugation reaction, the slides were stained using 3,3'-diaminobenzidine (DAB)-H₂O₂. The sections were counterstained with hematoxylin, and viewed using a light microscope.

Treatment of liver cancer-bearing nude mice with recombinant adenoviruses Three SMMC-LTNM nude mice with liver cancer were sacrificed, and skin overlying the tumor was cleaned with ethanol. The tumors were resected under aseptic conditions. A suspension of tumor cells in Hank's was made by passage of viable tumor tissues small hypodermic needles. The final concentration was adjusted to 2×10^7 cells/mL. Female Balb/c nude mice, 3 wk of age, received injections sc into the dorsal midline in a 200 μ L volume. Tumors appeared approximately 10 d after implantation. The animals were randomized into 2 groups, and each group had four mice with comparable tumor size within and among the groups. Five hundred microliters of recombinant adenoviruses AdhENDO-VEGI₁₅₁ or AdLacZ at a titer of 1×10^{12} TCID₅₀/L was administered 10 times by sc every other day. The mice were sacrificed 24 h after the last injection, tumors from each mouse were removed and fixed in 40 g/L neutral buffered formaldehyde. Tumor size in all groups was measured, tumor volume was determined using the formula $\pi \times \text{width}^2 \times \text{length} / 6$. Tumor weight, inhibition rate and expression of target gene were evaluated, respectively.

Immunohistochemical staining of fusion protein in liver cancer of nude mice Tissues from liver cancer of nude mice were fixed in 40 g/L neutral buffered formaldehyde, embedded in paraffin, and sectioned into 4 μ m. The sections were treated with PBS, blocked with normal rabbit serum, incubated with rabbit polyclonal anti-endostatin (1:100 dilution) overnight at 4°C , washed with PBS, incubated with HRP-conjugated goat anti-rabbit antibody (1:500 dilution) for 1 h at 37°C , and stained using 3,3'-diaminobenzidine (DAB)-H₂O₂, counterstained with hematoxylin, and examined by a light microscope.

Determination of intratumor microvessel density Determination of microvessel density was carried out as described^[26-28]. Briefly, intratumor microvessels were immunostained with rat anti-human CD34 monoclonal antibody, and visualized with a biotinylated anti-rat IgG antibody by the Strept Avidin-Biotin Complex method. The sections were examined under low power to identify most vascular areas of the tumor. Within these areas, a maximum of 3 fields at $\times 200$ magnification was examined, and the mean values were calculated.

Statistical analysis Data were expressed as mean \pm SD. An analysis of variance was performed with Statview 4.0 statistical analysis software, and $P < 0.05$ was considered statistically significant.

RESULTS

Recombinant adenovirus infectivity

The titer of amplification of these two kinds of recombinant adenoviruses was 1×10^{12} TCID₅₀/L. When ECV304 cells were infected with AdLacZ at an MOI of 0.1, 20% cells showed LacZ-positive staining. If MOI was 20, 100% cells were stained blue (Figure 1). This result suggested recombinant adenoviruses had the highly efficient gene delivery.

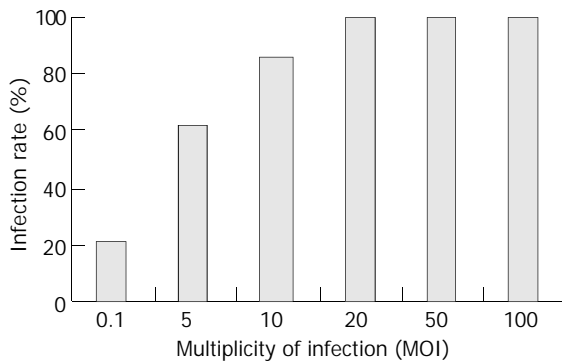


Figure 1 Infection efficiency of AdLacZ with different MOI.

Fusion protein expression of AdhENDO-VEGI₁₅₁ *in vitro*

Four kinds of cell lines infected with AdhENDO-VEGI₁₅₁ were immunoblotting stained with polyclonal antibodies against VEGI and visualized with DAB system. The results demonstrated that the fusion gene carried by AdhENDO-VEGI₁₅₁ could be *in vitro* expressed in all the cell lines, and the specific bands were located at about 41 ku, which was the expected size of ENDO-VEGI₁₅₁ fusion protein (Figure 2).

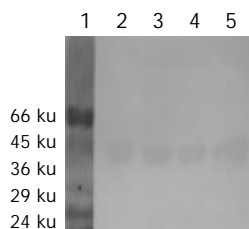


Figure 2 Western blot analysis of expressed fusion protein by AdhENDO-VEGI₁₅₁ with polyclonal antibody against VEGI₁₅₁. Lane 1: protein marker; lane 2: 293 cell; lane 3: ECV304 cell; lane 4: HepG2 cell; lane 5: L929 cell.

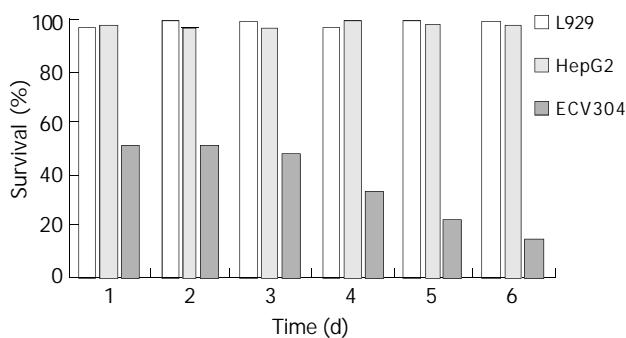


Figure 3 Viability of cells infected with AdhENDO-VEGI₁₅₁.

In vitro bioactivity of fusion gene on different cell lines

Human vascular endothelial cells ECV304 were sensitive to AdhENDO-VEGI₁₅₁, and cell proliferation was significantly inhibited. In contrast, no inhibitory activities on HepG2 and L929 *in vitro* growth were observed following AdhENDO-

VEGI₁₅₁ infection (Figure 3). Further analysis of variance showed there was a significant difference in viability between ECV304 cells and non-endothelial cells (HepG2 cells and L929 cells) ($F=13112.13$, $P=0.0001$). At different time points, there was a significant difference between the two groups ($F=72.75$, $P=0.0001$). There was no significant difference in viability between HepG2 cells and L929 cells neither for the hypothesis of no time effect ($F=7.17$, $P=0.0554$) nor at different time point ($F=1.74$, $P=0.2424$).

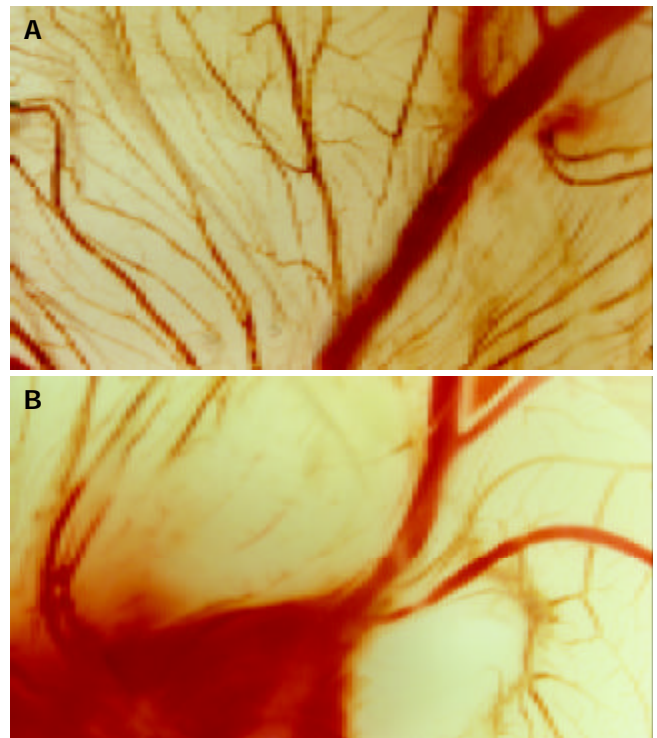


Figure 4 Inhibition of chick embryonic chorioallantoic membrane angiogenesis ($\times 7$). A: AdLacZ control; B: AdhENDO-VEGI₁₅₁.

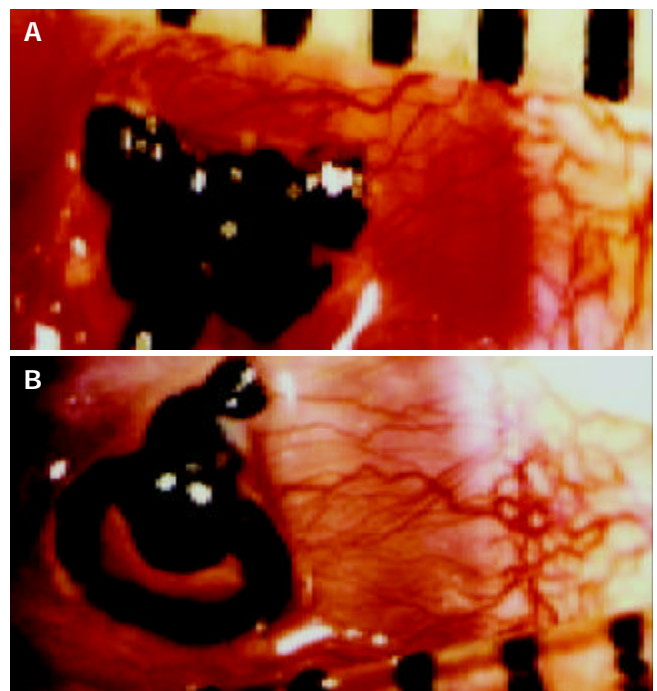


Figure 5 Suppression of rabbit corneal neovascularization ($\times 7$), CNV was examined on day 21. A: AdLacZ control; B: AdhENDO-VEGI₁₅₁.

Angiogenesis inhibition by AdhENDO-VEGI₁₅₁ in CAM

Nine-day old chick embryos were incubated with filter disks infected with AdhENDO-VEGI₁₅₁, or AdLacZ. The effect of AdhENDO-VEGI₁₅₁ on CAM angiogenesis was analyzed 3 d after incubation, by excising the membrane around the air sac and microscopy (Figure 4). At doses of 10-20 $\mu\text{L}/\text{disc}$ at a titer of 1×10^{12} TCID₅₀/L, there was a potent inhibition of angiogenesis of AdhENDO-VEGI₁₅₁ on the tested CAMs ($n=4/\text{group}$). In contrast, AdLacZ failed to suppress angiogenesis in CAM. There was no evidence of toxicity in any chick embryos tested.

Vessel inhibition in inflammatory cornea of rabbits

After direct subconjunctival injection of recombinant adenoviruses, rabbit eyes were examined by a surgical microscope daily. A few small capillary buds that arose from engorged limbal arcades were observed. CNV increased gradually, peaked on d 12-14, and degenerated on day 15 after suture induction. So we chose d 7, 10, 13, or 16 as time points to determine the number and length of vessels, and the area of neovascularization. Analysis of the CNV area found that local application of AdhENDO-VEGI₁₅₁ resulted in a significant suppression of CNV (Figure 5, Figure 6). Repeated measurement of two factors and multilevel analysis of variance showed there were significant differences between AdhENDO-VEGI₁₅₁ group and AdlacZ group ($F=1413.11$, $P=0.0001$) for the hypothesis of no time effect. At different time points, there was a significant difference between the two groups ($F=15517.87$, $P=0.0001$).

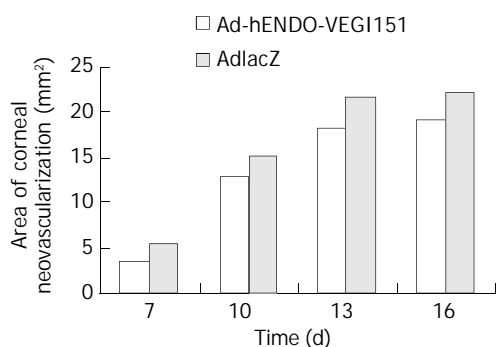


Figure 6 Comparison of corneal neovascularization in 2 groups.

AdhENDO-VEGI₁₅₁ expression in inflammatory cornea of rabbits

The fusion gene expression in inflammatory cornea of rabbits was detected by immunohistochemistry. Corneal endothelium was stained brown in AdLacZ group, others were stained negative. Corneal endothelium and epithelium were stained brown in AdhENDO-VEGI₁₅₁ group (Figure 7), and lasted for 21 d.

AdhENDO-VEGI₁₅₁ inhibited growth of liver cancer

Twenty-one days after therapy, the mice were sacrificed. Compared with AdLacZ control group ($4\,075.9 \pm 1\,849.9$ mm³), the average tumor size of AdhENDO-VEGI₁₅₁ group had confirmed regression (487.7 ± 241.2 mm³) ($F=14.80$, $P=0.0085$) with an inhibition rate of 88.03%.

Immunohistochemical features in liver cancer of nude mice

When we examined the sections stained by rabbit polyclonal anti-endostatin by a light microscope, strongly positive staining of fusion molecules presented in all cases of animals treated with AdhENDO-VEGI₁₅₁. The recombinant adenoviruses carrying chimeric gene could be expressed in liver cancer. Brown staining was mainly located on the membrane of liver cancer cells (Figure 8). There was no positive staining in tumor tissues of the control animals.

Determination of intratumor microvessel density

The antiangiogenesis effect of fusion protein producing adenoviruses was evaluated in tumor model. Tumor microvessel density (MVD) was reduced by the production of hENDO-VEGI₁₅₁ fusion gene. The MVD was decreased ($30.75 \pm 3.31\%$) more significantly in treated mice than in control ($50.25 \pm 8.65\%$) ($F=17.72$, $P=0.0056$).

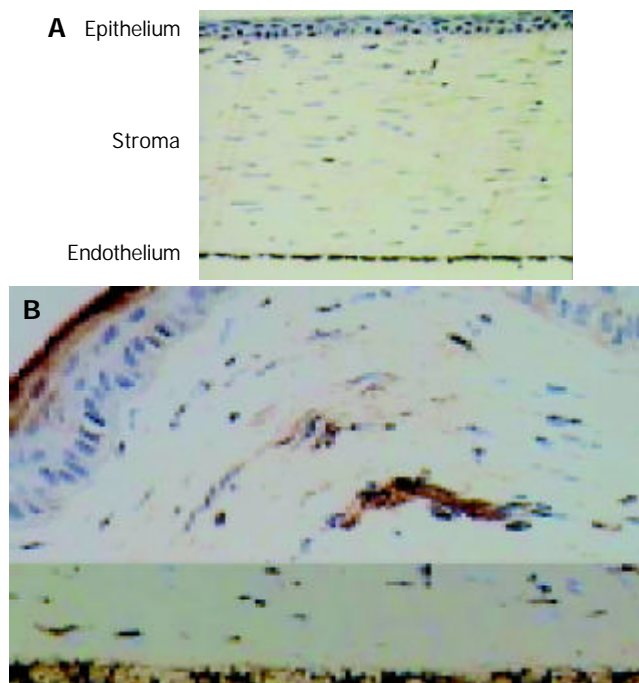


Figure 7 Immunohistochemical staining of rabbit cornea with polyclonal antibody against endostatin ($\times 200$). A: AdLacZ control; B: AdhENDO-VEGI₁₅₁.

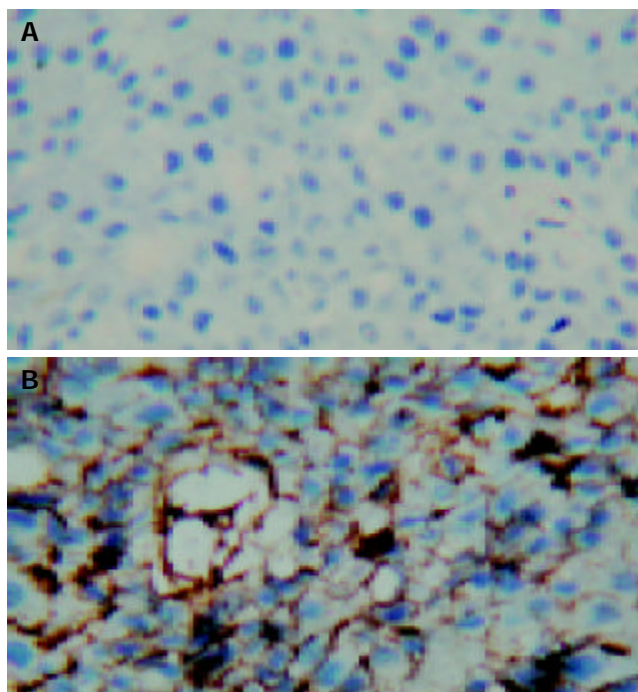


Figure 8 Immunohistochemical staining of nude mice liver cancer with polyclonal antibody against endostatin ($\times 200$). A: AdLacZ control; B: AdhENDO-VEGI₁₅₁.

DISCUSSION

Endostatin and vascular endothelial growth inhibitor are

endogenous angiostatic molecules. Both of them are angiogenesis inhibitors that could suppress the growth of endothelial cells^[29,30]. To achieve effectiveness, antiangiogenic therapy with endostatin or VEGI in tumor-bearing mice required prolonged administration and high doses of recombinant proteins^[31,32]. Production of functional polypeptides has proven difficult, perhaps because of its physical properties or variations in the purification procedures in different laboratories^[33,34]. In our laboratory (Department of Microbiology, Second Military Medical University, Shanghai, China) these two recombinant proteins were used respectively to treat tumor-bearing nude mice, but their bioactivities were not satisfactory. So we performed antiangiogenic gene therapy with adenoviral vectors. The results suggested recombinant adenoviruses AdhENDO-VEGI₁₅₁ could express fusion protein about 41 ku in ECV304, HepG2, L929 and 293 cells, and showed a specific inhibition on the proliferation of ECV304 cells, the inhibition rate reached 49% in 24 h and 86% in 144 h, respectively. But the AdhENDO-VEGI₁₅₁ showed no suppression on growth of HepG2 cells. VEGI belongs to the tumor necrosis factor (TNF) superfamily^[35] and was constitutively expressed in endothelial cells. Since murine fibroblast cell line L929 was used to determine the bioactivity of TNF, we also used this cell line to test the bioactivity of AdhENDO-VEGI₁₅₁. The results showed it had no suppression on growth of L929 cells, suggesting that fusion protein expressed by AdhENDO-VEGI₁₅₁ infection had no cytotoxicity to non-endothelial cells. Chick choriocallant membrane assay showed that fusion protein expressed by AdhENDO-VEGI₁₅₁ infection could significantly inhibit angiogenesis, and form no vessel regions. Because CAM was formed during embryogenic period, it was difficult to distinguish new vessels from previously established vascular networks. On the other hand, inflammatory CNV assay could avoid any confusion between new vessels and previously existed vessels, and any vessels penetrating into the corneal stroma could be identified as newly formed, as the cornea was avascular. For CNV was the main reason for corneal opacification, and also the main risk factor of immunologic rejection in allogeneous corneal transplantation, we tried to use AdhENDO-VEGI₁₅₁ as a safe and effective agent to inhibit CNV. We used intrastromal sutures to induce inflammatory CNV in rabbits. Neovascularization began sprouting into the corneal stroma from the limbus to the site of sutures within a few days after direct subconjunctival injection. Since small capillary vessels subsided gradually 16 d after suture induction, we selected d 7, 10, 13, or 16 as time points to measure vessel length and clock hours of circumferential neovascularization. Analysis of CNV area found there were significant differences between AdhENDO-VEGI₁₅₁ group and AdLacZ group. Local application of AdhENDO-VEGI₁₅₁ led to significant suppression of CNV, the inhibition rate was 36%, 16%, 17%, or 13% in turn. Our results suggested that in order to sustain the angiogenesis inhibition, AdhENDO-VEGI₁₅₁ should be administered every 7 d. Immunohistochemical staining showed that the positive reaction was predominant in corneal epithelium of AdhENDO-VEGI₁₅₁ group. These results suggested that the expression of recombinant adenoviruses was related with the site of injection. Positive staining in corneal endothelium was observed in two groups. This phenomenon might be caused by the endogenous endostatin expression of corneal endothelial cells. Compared with AdLacZ control group, the average tumor size of AdhENDO-VEGI₁₅₁ group was reduced with an inhibition rate of 88.03%. The gene of interest in adenoviruses could express in liver cancer. Since the fusion gene included IL-3 signal peptide coding sequence, the fusion protein might secrete out of the membrane of liver cancer cells. MVD was decreased more significantly in treated mice than that in control, the inhibition rate was 39%. These findings in combination with

the results of cell assay suggested that the antitumor activity of AdhENDO-VEGI₁₅₁ was not due to a direct effect on tumor cells, interference with the development of tumor microvessel density was responsible for tumor regression. However, up to now, we do not know whether the combination is more potent or not. Comparison of the effectiveness of fusion molecules with individual molecules has been under investigation.

REFERENCES

- 1 **Kleinman HK**, Liao G. Gene therapy for antiangiogenesis. *J Natl Cancer Inst* 2001; **93**: 965-967
- 2 **Tomanek RJ**, Schattman GC. Angiogenesis: new insights and therapeutic potential. *Anat Rec* 2000; **261**: 126-135
- 3 **Kim CW**, Lee HM, Lee TH, Kang C, Kleinman HK, Gho YS. Extracellular membrane vesicles from tumor cells promote angiogenesis via sphingomyelin. *Cancer Res* 2002; **62**: 6312-6317
- 4 **Oehler MK**, Bicknell R. The promise of anti-angiogenic cancer therapy. *Br J Cancer* 2000; **82**: 749-752
- 5 **Lai CM**, Brankov M, Zaknich T, Lai YK, Shen WY, Constable IJ, Kovacs I, Rakoczy PE. Inhibition of angiogenesis by adenovirus-mediated sFlt-1 expression in a rat model of corneal neovascularization. *Hum Gene Ther* 2001; **12**: 1299-1310
- 6 **Lai CM**, Spilsbury K, Brankov M, Zaknich T, Rakoczy PE. Inhibition of corneal neovascularization by recombinant adenovirus mediated antisense VEGF RNA. *Exp Eye Res* 2002; **75**: 625-634
- 7 **Ambati BK**, Jousen AM, Ambati J, Moromizato Y, Guha C, Javaherian K, Gillies S, O'Reilly MS, Adamis AP. Angiostatin inhibits and regresses corneal neovascularization. *Arch Ophthalmol* 2002; **120**: 1063-1068
- 8 **Hanai J**, Dhanabal M, Karumanchi SA, Albanese C, Waterman M, Chan B, Ramchandran R, Pestell R, Sukhatme VP. Endostatin causes G1 arrest of endothelial cells through inhibition of cyclin D1. *J Biol Chem* 2002; **277**: 16464-16469
- 9 **Zhang M**, Wang L, Wang HW, Pan X, Pan W, Qi ZT. Effect of N-terminal deletion on biological activity of vascular endothelial cell growth inhibitor. *Shengwu Huaxue Yu Shengwu Wuli Xuebao* 2003; **35**: 133-137
- 10 **Yu J**, Tian S, Metheny-Barlow L, Chew LJ, Hayes AJ, Pan H, Yu GL, Li LY. Modulation of endothelial cell growth arrest and apoptosis by vascular endothelial growth inhibitor. *Circ Res* 2001; **89**: 1161-1167
- 11 **Tanaka T**, Cao Y, Folkman J, Fine HA. Viral vector-targeted antiangiogenic gene therapy utilizing an angiostatin complementary DNA. *Cancer Res* 1998; **58**: 3362-3369
- 12 **Hampel M**, Tanaka T, Albert PS, Lee J, Ferrari N, Fine HA. Therapeutic effects of viral vector-mediated antiangiogenic gene transfer in malignant ascites. *Hum Gene Ther* 2001; **12**: 1713-1729
- 13 **Nguyen JT**. Adeno-associated virus and other potential vectors for angiostatin and endostatin gene therapy. *Adv Exp Med Biol* 2000; **465**: 457-466
- 14 **Nguyen JT**, Wu P, Clouse ME, Hlatky L, Terwilliger EF. Adeno-associated virus-mediated delivery of antiangiogenic factors as an antitumor strategy. *Cancer Res* 1998; **58**: 5673-5677
- 15 **Cao GW**, Qi ZT, Pan X, Zhang XQ, Miao XH, Feng Y, Lu XH, Kuriyama S, Du P. Gene therapy for human colorectal carcinoma using human CEA promoter controlled bacterial ADP-ribosylating toxin genes human CEA: PEA & DTA gene transfer. *World J Gastroenterol* 1998; **4**: 388-391
- 16 **Li Z**, Pan X, Pan W, Cao GS, Wen ZZ, Fang GE, Qi ZT, Bi JW, Hua JD. Packaging and identification of recombinant adenovirus carrying endostatin-soluble vascular endothelial growth inhibitor gene. *Shijie Huaren Xiaohua Zazhi* 2003; **11**: 741-744
- 17 **Pan X**, Li Z, Zhang M, Wang Y, Pan W, Qi ZT. Therapeutic effect of endostatin-vascular endothelial growth inhibitor recombinant adenoviruses on gastric carcinoma in nude mice. *Shijie Huaren Xiaohua Zazhi* 2003; **11**: 1282-1285
- 18 **Nyberg-Hoffman C**, Shabram P, Li W, Giroux D, Aguilar-Cordova E. Sensitivity and reproducibility in adenoviral infectious titer determination. *Nat Med* 1997; **3**: 808-811
- 19 **Michie J**, Akudugu J, Binder A, Van Rensburg CE, Bohm L.

- Flow cytometric evaluation of apoptosis and cell viability as a criterion of anti-tumour drug toxicity. *Anticancer Res* 2003; **23**: 2675-2679
- 20 **Zhao CS**, Zhang L, Shen YP. A preventive and therapeutic study of experimental corneal neovascularization. *Tongji Yike Daxue Xuebao* 1996; **25**: 399-401
- 21 **Cao Y**, Linden P, Farnebo J, Cao R, Eriksson A, Kumar V, Qi JH, Claesson Welsh L, Alitalo K. Vascular endothelial growth factor C induces angiogenesis *in vivo*. *Proc Natl Acad Sci U S A* 1998; **95**: 14389-14394
- 22 **Saita N**, Fujiwara N, Yano I, Soejima K, Kobayashi K. Trehalose 6,6'-dimycolate (cord factor) of *Mycobacterium tuberculosis* induces corneal angiogenesis in rats. *Infect Immun* 2000; **68**: 5991-5997
- 23 **Volpert OV**, Fong T, Koch AE, Peterson JD, Waltenbaugh C, Tepper RI, Bouck NP. Inhibition of angiogenesis by interleukin 4. *J Exp Med* 1998; **188**: 1039-1046
- 24 **Amin MA**, Volpert OV, Woods JM, Kumar P, Harlow LA, Koch AE. Migration inhibitory factor mediates angiogenesis via mitogen-activated protein kinase and phosphatidylinositol kinase. *Circ Res* 2003; **93**: 321-329
- 25 **Seo K**, Choi J, Park M, Rhee C. Angiogenesis effects of nerve growth factor (NGF) on rat corneas. *J Vet Sci* 2001; **2**: 125-130
- 26 **Chew LJ**, Pan H, Yu J, Tian S, Huang WQ, Zhang JY, Pang S, Li LY. A novel secreted splice variant of vascular endothelial cell growth inhibitor. *FASEB J* 2002; **16**: 742-744
- 27 **Nor JE**, Christensen J, Liu J, Peters M, Mooney DJ, Strieter RM, Polverini PJ. Up-Regulation of Bcl-2 in microvascular endothelial cells enhances intratumoral angiogenesis and accelerates tumor growth. *Cancer Res* 2001; **61**: 2183-2188
- 28 **Olewniczak S**, Chosia M, Kwas A, Kram A, Domagala W. Angiogenesis and some prognostic parameters of invasive ductal breast carcinoma in women. *Pol J Pathol* 2002; **53**: 183-188
- 29 **Wang L**, Pan W, Zhu FL, Jiao BH, Lou YH, Xiao Y, Qi ZT. Cloning, expression and biological activity of VEGI(151), a novel vascular endothelial cell growth inhibitor. *Shengwu Hua xue Yu Shengwu Wuli Xuebao* 2000; **32**: 485-489
- 30 **Cao MM**, Pan W, Chen QL, Ma ZC, Ni ZJ, Wu XL, Wu WB, Pan X, Cao GW, Qi ZT. Construction of the eukaryotic expression vector expressing the fusion protein of human endostatin protein and IL₃ signal peptide. *Shijie Huaren Xiaohua Zazhi* 2001; **9**: 43-46
- 31 **O'Reilly MS**, Boehm T, Shing Y, Fukai N, Vasios G, Lane WS, Flynn E, Birkhead JR, Olsen BR, Folkman J. Endostatin: an endogenous inhibitor of angiogenesis and tumor growth. *Cell* 1997; **88**: 277-285
- 32 **Zhai Y**, Yu J, Iruela-Arispe L, Huang WQ, Wang Z, Hayes AJ, Lu J, Jiang G, Rojas L, Lippman ME, Ni J, Yu GL, Li LY. Inhibition of angiogenesis and breast cancer xenograft tumor growth by VEGI, a novel cytokine of the TNF superfamily. *Int J Cancer* 1999; **82**: 131-136
- 33 **Dhanabal M**, Volk R, Ramchandran R, Simons M, Sukhatme VP. Cloning, expression, and *in vitro* activity of human endostatin. *Biochem Biophys Res Commun* 1999; **258**: 345-352
- 34 **Ding I**, Sun JZ, Fenton B, Liu WM, Kimsely P, Okunieff P, Min W. Intratumoral administration of endostatin plasmid inhibits vascular growth and perfusion in MCa-4 murine mammary carcinomas. *Cancer Res* 2001; **61**: 526-531
- 35 **Zhai Y**, Ni J, Jiang GW, Lu J, Xing L, Lincoln C, Carter KC, Janat F, Kozak D, Xu S, Rojas L, Aggarwal BB, Ruben S, Li LY, Gentz R, Yu GL. VEGI, a novel cytokine of the tumor necrosis factor family, is an angiogenesis inhibitor that suppresses the growth of colon carcinomas *in vivo*. *FASEB J* 1999; **13**: 181-189

Edited by Wang XL and Xu FM

Changes of tumor microcirculation after transcatheter arterial chemoembolization: First pass perfusion MR imaging and Chinese ink casting in a rabbit model

Jun-Gong Zhao, Gan-Sheng Feng, Xiang-Quan Kong, Xin Li, Ming-Hua Li, Ying-Sheng Cheng

Jun-Gong Zhao, Ming-Hua Li, Ying-Sheng Cheng, Department of Radiology, Sixth Affiliated Hospital of Shanghai Jiaotong University, Shanghai 200233, China

Gan-Sheng Feng, Xiang-Quan Kong, Xin Li, Department of Radiology, Union Hospital, Tongji Medical College, Huazhong University of Science and Technology, Wuhan 430022, Hubei Province, China

Correspondence to: Dr. Jun-Gong Zhao, Department of Radiology, Sixth Affiliated Hospital of Shanghai Jiaotong University, Shanghai 200233, China. zhaojun_gong@sohu.com

Telephone: +86-21-64369181 Ext 8882

Received: 2003-09-09 **Accepted:** 2003-10-22

Abstract

AIM: To observe the change of tumor microcirculation after transcatheter arterial chemoembolization (TACE) with *bletilla* microspheres by using first pass perfusion MR imaging (FP) and Chinese ink casting.

METHODS: VX2 carcinoma cells were surgically implanted into the left and right lobes of liver of 30 New Zealand white rabbits, which were divided into 3 groups at random. Emulsion of lipiodol mixed with mitomycin C, and 5-FU *bletilla* microspheres were injected into the hepatic artery respectively, and saline was used as control agent. MR imaging was performed with turbo-flash sequence 14 d after tumor implantation and 7 d after interventional therapy. The steepest slopes (SS) of the signal intensity versus time curves were created for quantitative analysis, 7.5% Chinese ink gelatin solution was injected through ascending artery (17 cases) or portal vein (2 cases) for lesion microvessel area (MVA) measurement after the last MRI examination. The correlation between perfusion imaging and MVA was studied blindly.

RESULTS: The SS values at the rim of tumor in lipiodol group (mean, 49% per second) and *bletilla* group (mean, 35% per second) were significantly decreased ($P < 0.05$) as compared with control group (mean, 124% per second), no difference was found between lipiodol and *bletilla* groups ($P > 0.05$). In lipiodol group, the MVAs ($24\ 974 \pm 11\ 836\ \mu\text{m}^2$) in the center of the tumor were significantly smaller than those of the control group ($35\ 510 \pm 15\ 675\ \mu\text{m}^2$) ($P < 0.05$), while the MVAs ($80\ 031 \pm 22\ 745\ \mu\text{m}^2$) around the tumor were significantly increased because small and dense plexuses appeared around the tumor which correlated to intense reaction of granulation tissue. None of the vessels was seen in the tumor in *bletilla* group, the peripheral MVAs of the tumor were significantly smaller than those of the control group ($P < 0.05$) and lipiodol group ($P < 0.05$). There was a good correlation between SS and MVAs in control group ($r_s, 0.985, P < 0.0001$) and *bletilla* group ($r_s, 0.743, P < 0.05$), the correlation was not significant in lipiodol group ($r_s, 0.527, P > 0.05$).

CONCLUSION: TACE with *bletilla* microspheres may

enhance its anti-tumor effect by inhibiting the angiogenesis, and FP-MRI provides useful information to assess the TACE effect by depicting tumor vascularization and perfusion.

Zhao JG, Feng GS, Kong XQ, Li X, Li MH, Cheng YS. Changes of tumor microcirculation after transcatheter arterial chemoembolization: First pass perfusion MR imaging and Chinese ink casting in a rabbit model. *World J Gastroenterol* 2004; 10(10): 1415-1420

<http://www.wjgnet.com/1007-9327/10/1415.asp>

INTRODUCTION

Transcatheter arterial chemoembolization (TACE) has been widely used and is considered to be an effective conservative treatment for hepatocellular carcinoma^[1,2]. Rapid development of small vessels after TACE resulting in incomplete necrosis, however, reduces therapeutic effectiveness^[1-9]. Therefore, inhibition of the development of arterial collaterals may be important in enhancing the therapeutic efficacy of this treatment. Recently, TACE with microspheres, microcapsules, cyanoacrylate and *bletilla* has been shown to improve the therapeutic results^[1,3,10-12]. *Bletilla* microspheres have also been shown to improve the therapeutic results because of its embolization of the hepatic artery and portal vein as well as controlled release systems, although changes at the level of hepatic microcirculation are not completely elucidated.

The purpose of this study was to observe the change of tumor microcirculation after TACE with *bletilla* microspheres by using first pass perfusion MR imaging (FP) and Chinese ink casting.

MATERIALS AND METHODS

Animals and tumor models

The VX2 tumor model used in this study was initially a virus-induced papilloma first seen in domestic rabbit in 1937. With sequential transplantations, the tumor line became increasingly anaplastic^[13]. VX2 carcinoma (Department of Radiology, Union Hospital, Tongji Medical College, Huazhong University of Science and Technology, Wuhan, China) was retained for approximately 4 years by repeated passage of tumor every 14-21 d by way of intramuscular or subcutaneous implantation into the thighs of male New Zealand white rabbits.

Twenty-five male and five female New Zealand white rabbits (Laboratory Center, Tongji Medical College) weighing 1-1.5 kg were used. Prior to all procedures, including tumor implantation and imaging, rabbits received an intramuscular injection of 1.0 mL/kg of body weight of ketamine hydrochloride injection (Shanghai Sino-west Pharmaceutical Company), intravenous access was then acquired via a marginal ear vein. Anesthesia was maintained by using the same dose of intravenously administered ketamine hydrochloride.

The technique for tumor implantation was basically similar to that described by Li *et al*^[14]. Briefly, the liver was exposed

by performing midline laparotomy, VX2 tumor fragments of approximately 1 mm³ were injected intraparenchymally into the right and left lobes of the rabbit liver. Thirty New Zealand white rabbits with tumors were divided into three groups at random. They were group A (control group, 8 rabbits), group B (lipiodol group, 12 rabbits) and group C (*bletilla* group, 10 rabbits). All three groups received their interventional therapy 14-21 d after tumor inoculation when MRI confirmed the successful implantation.

Interventional therapy

A polyethylene catheter (inner diameter 0.3 mm, outer diameter 0.5 mm) was retrogradely inserted into the gastroduodenal artery, the following agents were manually injected into the gastroduodenal artery, namely, saline only into group A, 0.4-0.6 mL lipiodol (Aulnay Sous-Bios, France) emulsion (lipiodol mixed with MMC) into group B, 0.3 mL ultravist mixed with 10 mg *bletilla* microspheres (Department of Radiology, Union Hospital, Wuhan, China, 40-200 μm in diameter, combined with 5-FU) into group C.

MR imaging and data analysis

Fourteen days after tumor implantation and 7 d after interventional therapy, MR imaging was undertaken by using a 1.5 T system (Magnetom Vision, Siemens Medical Systems) with a head coil. Transverse spin-echo T1-weighted images (repetition time was 525 ms, the echo time was 14 ms) and HASTE T2-weighted images (repetition time was 4.4 ms, the echo time was 90 ms) were obtained by using a 3 mm thick section, 0.5 mm intersection space, and four signals were acquired.

For the FP, a strongly T1-weighted, turbo-FLASH sequence was used with a high temporal resolution of 1.196 s per section, a single image was acquired sequentially with 65 repetitions, which resulted in an acquisition time of 2 min. The repetition time was 3.3 ms, the echo time was 1.4 ms, and time interval was 300 ms. At the end of the fourth acquisition, a dose of 0.1 mmol/kg body weight of gadopentetate dimeglumine (Bellona, Beijing, China) was administered via a marginal ear vein.

To quantitatively analyze FP, four circular ROIs were hand drawn, covering the center and rim of the lesion, signal intensity time curve was obtained over ROIs, and the steepest slope of the curve (SS) was calculated according to the previously described method^[15].

Evaluation of anti-tumor effect

Tumor size was measured with calipers. The size of each tumor on the liver surface was measured immediately before treatment and seven days after treatment on MR imaging. We evaluated the anti-tumor effect based on the tumor volume, which was calculated as follows: tumor volume (mm³)=0.5×a×b², where *a* is the length of major axis and *b* is the length of minor axis measured with calipers.

Chinese ink casting and histological evaluation

The tumor microvessels were demonstrated by perfusion of 75 g/L Chinese ink (Beijing Chinese Ink Company) gelatin solution into the ascending artery (17 cases) or portal vein (2 cases) after the last MR imaging examination. Before perfused with 75 g/L Chinese ink gelatin solution, 500 units of heparin was administered intravenously. After the rabbits were killed, the livers were removed and stored at -20 °C for 24 h. The specimens were immersed in 250-995 mL/L ethyl alcohol at increasing concentrations, and finally in a solution of methyl salicylate. When the oil penetrated the tissue, the specimens became transparent. The sections (50 μm) were observed first under a low power microscope (×40), then the sections with most dense area of microvessels were selected and observed under a high

power (×200). Micro-vessels filled with Chinese ink gelatin were evaluated under a microscope, micro-vessel areas (MVAs) in the center and rim of the lesion were calculated by an imaging analysis system (Beijing Aeronautic University). A 5 μm sections of the same specimens were stained with hematoxylin and eosin for light microscopy.

Statistical analysis

All data were expressed as mean±SD, the statistical differences between different groups were analyzed by ANOVA, and the correlation between SS and MVA was assessed by Spearman correlation analysis. Significance was accepted when *P*<0.05.

RESULTS

MR imaging

MR imaging depicted all tumors on pretreatment images. All untreated tumors had a low signal intensity on T1-weighted images and an intermediate signal intensity on T2-weighted images. Central areas of high signal intensity on T2-weighted images and low signal intensity on T1-weighted images were compatible with the central necrosis when tumors were larger than 1 cm. T1-weighted images after injection of gadolinium showed a slight enhancement in the center of lesion and a rim enhancement around the center of lesion in all tumors (Figure 1). No significant difference in tumor volume was observed among the three groups before therapy.

Tumor volumes in the lipiodol group and *bletilla* group after TACE were significantly decreased compared with the control group on d 7 after treatment, no significant difference in tumor volumes was observed between lipiodol group and *bletilla* group (Figure 2, Table 1). The central slight enhancement area was larger, and the peripheral arterial phase rim enhancement in the two groups was thinner. The SS values at the rim of tumor in lipiodol group (mean, 49% per second) and *bletilla* group (mean, 35% per second) were significantly decreased (*P*<0.05), as compared with the control group (mean, 124% per second), no difference was found between lipiodol group and *bletilla* one (*P*>0.05) (Table 2).

Table 1 Tumor volumes pre- and post-treatment (cm³)

Group	Pre-treatment	Post treatment
Control	0.430±0.067	1.620±0.327
Lipiodol	0.465±0.120	0.971±0.285 ^a
Bletilla	0.402±0.171	0.736±0.145 ^a

^a*P*<0.05 vs control.

Table 2 SS values at the rim of tumor in different groups

Group	SS (%·s ⁻¹)	<i>F</i>	<i>P</i>
Control	124±62		
Lipiodol	49±15	11.08	0.004 ^a
<i>Bletilla</i>	35±9	6.88	0.019 ^a

^a*P*<0.05 vs control.

Table 3 Correlation between SS values and MVA in different groups

Group	SS (%·s ⁻¹)	MVA (μm ²)	<i>r</i> _s	<i>P</i>
Control	124±62	35 510±15 675	0.985	<0.05
Lipiodol	49±15	80 031±22 745	0.527	>0.05
<i>Bletilla</i>	35±9	15 530±7 973	0.743	<0.05

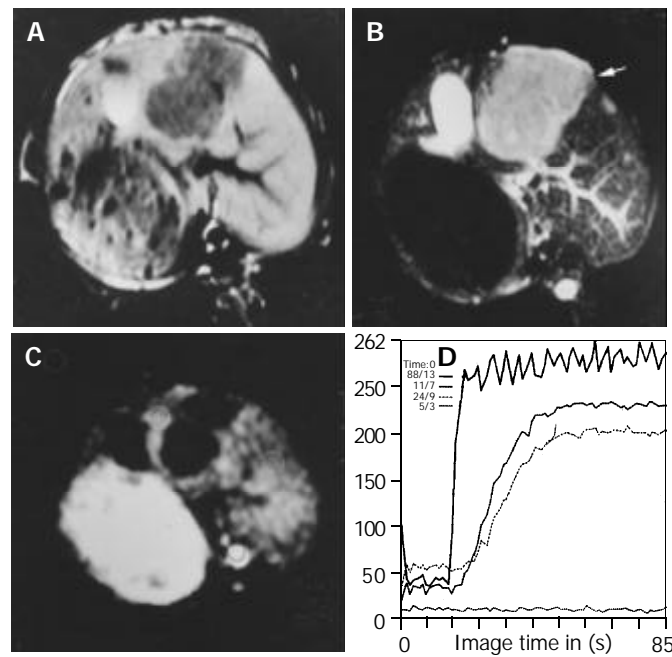


Figure 1 Images obtained before treatment in control group. A: T1WI shows hypointense lesions in left lobe of the liver. B: T2WI shows homogeneous hyperintense lesions in left lobe of the liver. C: FP T1-weighted image with gadolinium shows rim enhancement and no enhancement in the center of lesion. D: Signal intensity time curve derived from FP, SS of the curve in the border of the lesion is steeper than that of the normal liver.

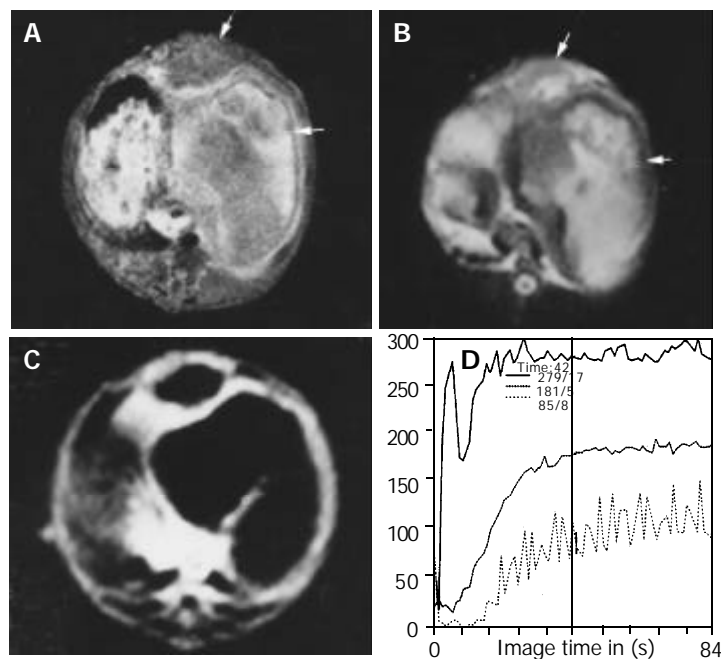


Figure 2 Images obtained after treatment in lipiodol group. Inhomogeneous hyperintense lesions with intermediate intense rim (arrow head) can be seen on T1WI (A) and T2WI (B), indicating the necrosis of the lesion and intratumor retention of lipiodol. (C) FP T1-weighted image with gadolinium shows thinner rim enhancement and no enhancement in the center of the lesion compared with control group although the lesion volume is increased. (D) SS of the curve in center of the lesion is decreased compared with those of the border.

Chinese ink casting

Investigation under microscope ($\times 40$) of the livers filled with Chinese ink in control group revealed networks of vessels or plexuses of dilated and tortuous course around and within the tumor originated from the arterioles, some sinusoid vessels were observed in the tumors, all these vessels were clearly distinct from the lobular architecture. In lipiodol group after TACE, the MVAs within the tumor ($24\,974 \pm 11\,836 \mu\text{m}^2$) were significantly smaller than those of the control group ($35\,510 \pm 15\,675 \mu\text{m}^2$) ($P < 0.05$), while the MVAs around the tumor ($80\,031 \pm 22\,745 \mu\text{m}^2$) were significantly increased, as

compared with the control group ($35\,510 \pm 15\,675 \mu\text{m}^2$) ($P < 0.05$). Small and dense plexuses appeared around the tumor, with unknown origin. None of the vessels was seen in the tumor in *bletilla* group after TACE (Figure 3). The peripheral MVAs of the tumor ($15\,530 \pm 7\,973 \mu\text{m}^2$) in *bletilla* group were significantly smaller than those of the control group ($35\,510 \pm 15\,675 \mu\text{m}^2$) ($P < 0.05$) and lipiodol group ($80\,031 \pm 22\,745 \mu\text{m}^2$) ($P < 0.05$). There was a good correlation between SS and MVA at the rim of tumor in control group ($r_s, 0.985, P < 0.0001$) and *bletilla* group ($r_s, 0.743, P < 0.05$), the correlation was not significant in lipiodol group ($r_s, 0.527, P > 0.05$) (Table 3).

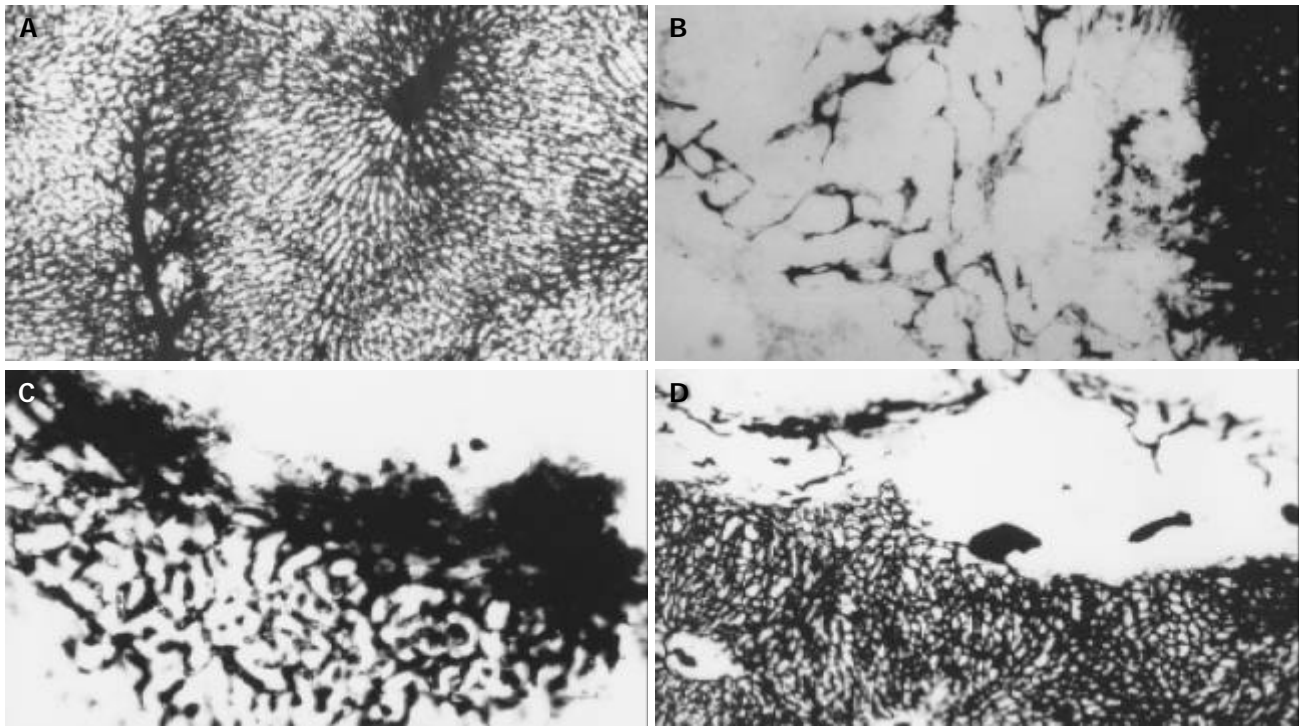


Figure 3 Micro-vessel casting with Chinese ink through ascending artery. A: The specimens show a lobular architecture of normal liver, magnification $\times 100$. B: In control group, hepatic artery perfusion shows networks of micro-vessels or plexuses of dilated and tortuous course around and within the tumor originated from the arterioles, some sinusoid vessels can be observed in this tumor, magnification $\times 100$. C: The original micro-vessels of the tumor are remarkably diminished, small and dense new plexuses appear around the tumor in lipiodol group, which are correlated to intense reaction of granulation tissue, magnification $\times 100$. D: micro-vessels are decreased in *betilla* group, no new micro-vessels can be seen at all, magnification $\times 100$.

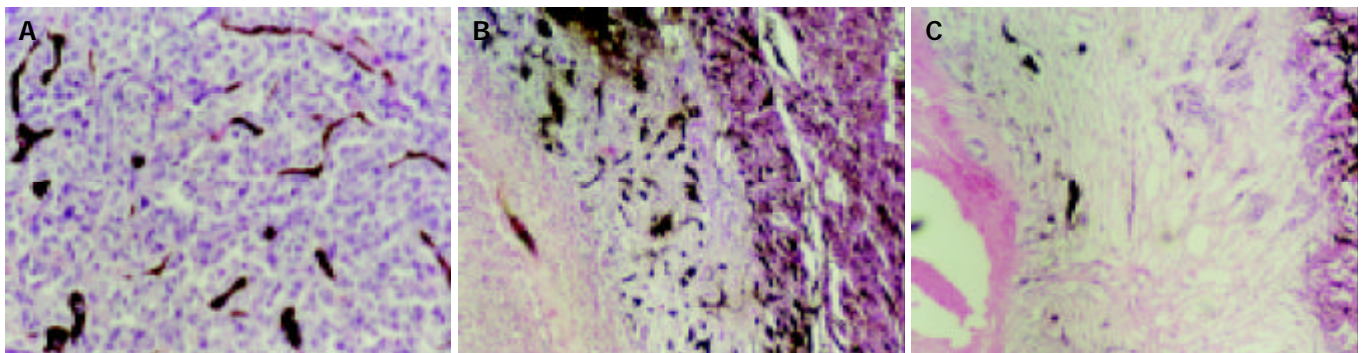


Figure 4 Histological examinations of hepatic lesion before and after treatment. A: HE stain shows nidus arrangement of VX2 cells as well as micro-vessels filled with Chinese ink before treatment, magnification $\times 200$. B: In lipiodol group, histological examination shows coagulation necrosis at the center of lesion, very few micro-vessels can be seen within this zone, residual tumor cells are seen at the periphery of lesions, moreover, an intense reaction of granulation tissue is seen within this area, small dense vessels are scattered at border of the lesion, and congested sinusoids are seen in the periphery of the tumor, magnification $\times 200$. C: Coagulation necrosis as well as large infarcts involving multiple adjacent lobules is seen in *betilla* group, few vessels are seen at the border of the lesion, magnification $\times 200$.

Pathologic correlation

The specimens did not show necrosis or infarct when the lesion was less than 1 cm in control group. In lipiodol group none lesions underwent complete necrosis, coagulation necrosis was demonstrated at the center of all lesions. Viable or residual cancerous tissues as well as an intense reaction of granulation tissue were seen at the periphery of all lesions in lipiodol groups after TACE, small and dense vessels were scattered at the border of the lesions, correlating with the irregular thick rim enhancement on MR image. In *betilla* group after TACE, all lesions demonstrated complete coagulation necrosis, large infarcts involving multiple adjacent lobules were seen as well, few vessels were seen at the border of the lesion, no granulation tissue was seen (Figure 4).

DISCUSSION

Bletilla inhibition of tumor micro-vessels

A previous study reported an intense reaction of granulation tissue at the periphery of all lesions in lipiodol group^[16], the dense angiogenic plexus in the granulation tissue is, to our knowledge, a new finding. Granulation tissue which resulted in capillary proliferation and permeability increase was correlated to arterial phase rim enhancement on MR image. Angiogenesis was central to tumor stroma formation and offered nutrition to the remaining viable tumor cells, which limited lipiodol embolization and anti-tumor effect. As a result, local tumor recurrence would occur sooner or later^[7-9,16].

TNP-470, cyanoacrylate and Pleg-mitomycin-microsphere have been used to inhibit capillary networks or to prolong

first-pass effect and to enhance the anti-tumor effect of TACE^[1,17-20]. Our experimental study indicated that *bletilla* could enhance the anti-tumor effect of TACE as well. *Bletilla*, as an anti-tumor and anti-inflammation agent, is a Chinese medicine^[10,12]. Its microspheres (mixed with 5-FU, 40-200 μm in diameter) can result in dual embolization (embolization of hepatic arterial and portal venous blood supply) and inhibit the microvessels around and in the tumor completely. The reason why no microvessels developed after TACE was partly due to its anti-tumor and anti-inflammation effect, partly through inhibition of the binding of vascular endothelial growth factor to its receptor^[10]. As a result, treatment with *bletilla* could necrose the tumor thoroughly. This was why *bletilla* could enhance the anti-tumor effect of TACE even the lesion was very large^[12].

VX2 microcirculation morphology

Many materials, including Chinese ink and microfil, have been used to demonstrate the vascular morphology of tumors^[17,21]. Among them, microfil is commonly used because of its different colors, which could identify the origin of vessels. But microfil was too viscous to get into the sinusoid, no vessel was visible inside the tumors less than 0.25 mm in diameter^[17]. So we selected less viscous materials to reveal microvessel morphology of VX2. Three percent of Chinese ink gelatin solution was used to explore the vascular architecture of cheek pouch carcinoma^[21]. To avoid overfilling the microvessels, we added gelatin to increase the viscosity of the solution to obtain 7.5% solution. As a result, all the microvessels of normal liver including arterioles and sinusoid were filled with black Chinese ink, so did those of tumor. Moreover, the pathologic change of the other part of the same specimens stained with HE could be observed. So microvessel casting correlating with pathologic change could assess the changes of tumor microcirculation at the same time. We believe that Chinese ink gelatin solution casting may be used as the golden standard to evaluate the microvessels in perfusion study with CT and MR imaging.

Value of FP-MRI

Although power Doppler US has been used to assess vascularity of tumors^[23-25], before contrast enhanced harmonic power Doppler US has widely been used, the major problems in the use of power Doppler are as follows. The detected velocities were too slow in the tumor, there were too many blooming artifacts associated with micro-bubble injection, the duration of enhancement was short and there were artifacts resulted from respiration^[23]. So the vascularity of tumors could not be evaluated in detail by power Doppler US. FP-MRI, with a high time resolution, can monitor the contrast agent first passing the target tissue by using signal intensity time curve, the steepest slope of which (SS, i.e. the maximum upward slope of the curve) correlates linearly with flow velocity and angiogenesis, and has been successfully used to quantify the myocardial perfusion reserve and to depict the tumor vascularization^[15,22], but no study has assessed the tumor microcirculation after TACE by FP^[26,27]. Our experimental result revealed that areas with the fastest contrast medium uptake (SS) colocalized significantly with focal hot spots of MVA in control group and *bletilla* group, but no significant correlation was observed between SS and MVA in lipiodol group, suggesting that factors beyond the MVA are involved in the gadopentetate dimeglumine-related signals enhanced in microvessels. We believed that the discrepancy could reflect the difference between small dense vessels newly developed at the border of the lesion after lipiodol treatment and tumor microvessels before treatment. The new vessels were hyperpermeable^[28], part of the small molecular contrast media (gadopentetate dimeglumine) might leak out of microvessels even at first pass

course. On the other hand, the new vessels might be too small to have the same flow velocity like those before treatment. So we believed that when the same categoric vessels were assessed by FP, the flow velocity might be constant, the SS was correlated linearly with MVA. When different categoric vessels were evaluated by FP, the flow velocity and permeability were different, and not dependent only on MVA.

In this study, *bletilla* microspheres were administered for 7 d only, and further studies of extended duration are needed. We conclude that tumor microvessels can be markedly inhibited by using *bletilla* microspheres in combination with 5-FU, which can explain and confirm its effectiveness in clinic. The SS derived from FP has a good correlation with MVA and may be used as a noninvasive method to quantitatively evaluate tumor angiogenesis after TACE.

REFERENCES

- 1 **Loewe C**, Cejna M, Schoder M, Thurnher MM, Lammer J, Thurnher SA. Arterial embolization of unresectable hepatocellular carcinoma with use of cyanoacrylate and lipiodol. *J Vasc Interv Radiol* 2002; **13**: 61-69
- 2 **Pacella CM**, Bizzarri G, Cecconi P, Caspani B, Magnolfi F, Bianchini A, Anelli V, Pacella S, Rossi Z. Hepatocellular carcinoma: long-term results of combined treatment with laser thermal ablation and transcatheter arterial chemoembolization. *Radiology* 2001; **219**: 669-678
- 3 **Tancredi T**, McCusky PA, Kan Z, Wallace S. Changes in rat liver microcirculation after experimental hepatic arterial embolization: comparison of different embolic agents. *Radiology* 1999; **211**: 177-181
- 4 **Park SI**, Lee do Y, Won JY, Lee JT. Extrahepatic collateral supply of hepatocellular carcinoma by the intercostal arteries. *J Vasc Interv Radiol* 2003; **14**: 461-468
- 5 **Tan LL**, Li YB, Chen DJ, Li SX, Jiang JD, Li ZM. Helical dual-phase CT scan in evaluating blood supply of primary hepatocellular carcinoma after transcatheter hepatic artery chemoembolization with lipiodol. *Zhonghua Zhongliu Zazhi* 2003; **25**: 82-84
- 6 **Won JY**, Lee do Y, Lee JT, Park SI, Kim MJ, Yoo HS, Suh SH, Park SJ. Supplemental transcatheter arterial chemoembolization through a collateral omental artery: treatment for hepatocellular carcinoma. *Cardiovasc Intervent Radiol* 2003; **26**: 136-140
- 7 **Yi J**, Liao X, Yang Z, Li X. Study on the changes in microvessel density in hepatocellular carcinoma following transcatheter arterial chemoembolization. *J Tongji Med Univ* 2001; **21**: 321-322
- 8 **Shao G**, Wang J, Zhou K, Yan Z. Intratumoral microvessel density and expression of vascular endothelial growth factor in hepatocellular carcinoma after chemoembolization. *Zhonghua Ganzangbing Zazhi* 2002; **10**: 170-173
- 9 **Huang J**, He X, Lin X, Zhang C, Li J. Effect of preoperative transcatheter arterial chemoembolization on tumor cell activity in hepatocellular carcinoma. *Chin Med J* 2000; **113**: 446-448
- 10 **Feng GS**, Li X, Zheng CS, Zhou CK, Liu X, Wu HP. Mechanism of inhibition of tumor angiogenesis by Bletilla colloid: an experimental study. *Zhonghua Yixue Zazhi* 2003; **83**: 412-416
- 11 **Furuse J**, Ishii H, Satake M, Onaya H, Nose H, Mikami S, Sakai H, Mera K, Maru Y, Yoshino M. Pilot study of transcatheter arterial chemoembolization with degradable starch microspheres in patients with hepatocellular carcinoma. *Am J Clin Oncol* 2003; **26**: 159-164
- 12 **Feng GS**, Zheng CS, Zhou RM, Liang B, Zhang YF. Arterial embolization of hepatocellular carcinoma with use of bletilla and gelatin powder. *Zhonghua Fangshexue Zazhi* 1996; **30**: 135-137
- 13 **Kuszyk BS**, Boitnott JK, Choti MA, Bluemke DA, Sheth S, Magee CA, Horton KM, Eng J, Fishman EK. Local tumor recurrence following hepatic cryoablation: radiologic-histopathologic correlation in a rabbit model. *Radiology* 2000; **217**: 477-486
- 14 **Li X**, Zheng CS, Feng GS, Zhuo CK, Zhao JG, Liu X. An implantable rat tumor model for experimental chemoembolization therapy and its imaging features. *World J Gastroenterol* 2002; **8**: 1035-1039
- 15 **Verstraete KL**, De Deene Y, Roels H, Dierick A, Uyttendaele D, Kunnen M. Benign and malignant musculoskeletal lesions: dy-

- namic contrast-enhanced MR imaging-parametric "first-pass" images depict tissue vascularization and perfusion. *Radiology* 1994; **192**: 835-843
- 16 **Han GH**, Guo QL, Huang GS, Guo YL. Distribution of lipiodol in hepatocellular carcinoma after hepatic arterial injection and its significance. *Zhonghua Fangshexue Zazhi* 1993; **27**: 828-831
- 17 **Mugitani T**, Taniguchi H, Takada A, Yamaguchi A, Masuyama M, Hoshima M, Takahashi T. TNP-470 inhibits collateralization to complement the anti-tumor effect of hepatic artery ligation. *Br J Cancer* 1998; **77**: 638-642
- 18 **Tanaka H**, Taniguchi H, Mugitani T, Koishi Y, Masuyama M, Higashida T, Koyama H, Suganuma Y, Miyata K, Takeuchi K, Takahashi T. Intra-arterial administration of the angiogenesis inhibitor TNP-470 blocks liver metastasis in a rabbit model. *Br J Cancer* 1995; **72**: 650-653
- 19 **Lund EL**, Bastholm L, Kristjansen PE. Therapeutic synergy of TNP-470 and ionizing radiation: effect on tumor growth, vessel morphology, and angiogenesis in human glioblastoma multiforme xenografts. *Clin Cancer Res* 2000; **6**: 971-978
- 20 **Qian J**, Truebenbach J, Graepler F, Pereira P, Huppert P, Eul T, Wiemann G, Claussen C. Application of poly-lactide-co-glycolide-microspheres in the transarterial chemoembolization in an animal model of hepatocellular carcinoma. *World J Gastroenterol* 2003; **9**: 94-98
- 21 **Zhou ZT**, Jin ZG, Zhang SL, Wang Z, Li WG. A morphic study on erigeron breviscapus (vant) hand-mazz affecting angiogenesis of golden hamster cheek pouch. *Linchuang Kouqiang Yixue Zazhi* 2000; **16**: 166-169
- 22 **Wilke N**, Jerosch-Herold M, Wang Y, Huang Y, Christensen BV, Stillman AE, Ugurbil K, McDonald K, Wilson RF. Myocardial perfusion reserve: assessment with multisection, quantitative, first-pass MR imaging. *Radiology* 1997; **204**: 373-384
- 23 **Du WH**, Yan WX, Wang X, Xiong XQ, Zhou Y, Li T. Vascularity of hepatic VX2 tumors of rabbits: assessment with conventional power Doppler US and contrast enhanced harmonic power Doppler US. *World J Gastroenterol* 2003; **9**: 258-261
- 24 **Kubota K**, Hisa N, Nishikawa T, Fujiwara Y, Murata Y, Itoh S, Yoshida D, Yoshida S. Evaluation of hepatocellular carcinoma after treatment with transcatheter arterial chemoembolization: comparison of Lipiodol-CT, power Doppler sonography, and dynamic MRI. *Abdom Imaging* 2001; **26**: 184-190
- 25 **Hosoki T**, Yosioka Y, Matsubara T, Minamitani K, Higashi M, Ohtani M, Choi S, Mitomo M, Tono T. Power Doppler sonography of hepatocellular carcinoma treated by transcatheter arterial chemoembolization. Assessment of the therapeutic effect. *Acta Radiol* 1999; **40**: 639-643
- 26 **Tsui EY**, Chan JH, Cheung YK, Cheung CC, Tsui WC, Szeto ML, Lau KW, Yuen MK, Luk SH. Evaluation of therapeutic effectiveness of transarterial chemoembolization for hepatocellular carcinoma: correlation of dynamic susceptibility contrast-enhanced echoplanar imaging and hepatic angiography. *Clin Imaging* 2000; **24**: 210-216
- 27 **Chan JH**, Tsui EY, Luk SH, Yuen MK, Cheung YK, Wong KP. Detection of hepatic tumor perfusion following transcatheter arterial chemoembolization with dynamic susceptibility contrast-enhanced echoplanar imaging. *Clin Imaging* 1999; **23**: 190-194
- 28 **Du JR**, Jiang Y, Zhang YM, Fu H. Vascular endothelial growth factor and microvascular density in esophageal and gastric carcinoma. *World J Gastroenterol* 2003; **9**: 1604-1606

Edited by Wang XL and Zhu LH Proofread by Xu FM

Expression of angiostatin cDNA in human hepatocellular carcinoma cell line SMMC-7721 and its effect on implanted carcinoma in nude mice

Kai-Shan Tao, Ke-Feng Dou, Xing-An Wu

Kai-Shan Tao, Ke-Feng Dou, Department of Hepatobiliary Surgery, Xijing Hospital, Fourth Military Medical University, Xi'an 710032, Shaanxi Province, China

Xing-An Wu, Department of Microbiology, Faculty of Basic Medicine, Fourth Military Medical University, Xi'an 710032, Shaanxi Province, China

Correspondence to: Kai-Shan Tao, Department of Hepatobiliary Surgery, Xijing Hospital, Fourth Military Medical University, Xi'an 710032, Shaanxi Province, China. tkaishan@fmmu.edu.cn

Telephone: +86-29-83375259 **Fax:** +86-29-83375255

Received: 2004-02-11 **Accepted:** 2004-02-21

Abstract

AIM: To transfect murine angiostatin cDNA into human hepatocellular carcinoma cell line SMMC-7721 and to investigate its effects on implanted carcinoma in nude mice.

METHODS: A eukaryotic expression vector of pcDNA3.1-mAST containing murine angiostatin was constructed. Then pcDNA3.1-mAST plasmid was transfected into cell line SMMC-7721 by Lipofectamine. The resistant clone was screened by G418 filtration and identified by RT-PCR and Western blotting. Nude mice were divided into three groups of 10 each. Mice in blank control group were only injected with SMMC-7721 cells. Mice in vector control group were injected with SMMC-7721 cells transfected with pcDNA3.1 (+) vector, whereas mice in angiostatin group were injected with SMMC-7721 cells transfected with pcDNA3.1-mAST plasmid. Volume, mass and microvessel density (MVD) of the tumors in different groups were measured and compared.

RESULTS: Murine angiostatin cDNA was successfully cloned into the eukaryotic expression vector pcDNA3.1 (+). pcDNA3.1-mAST was successfully transfected into SMMC-7721 cell line and showed stable expression in this cell line. No significant difference was observed in the growth speed of SMMC-7721 cells between groups transfected with and without angiostatin cDNA. Tumor volume, mass and MVD in the angiostatin group were significantly lower than those in the blank control group and vector control group ($P < 0.01$). The inhibitory rate of tumor reached 78.6%. Mass and MVD of the tumors only accounted for 34.6% and 48.9% respectively of those in the blank control group.

CONCLUSION: Angiostatin cDNA could be stably expressed in human hepatocellular carcinoma cell line SMMC-7721 without obvious inhibitory effects on the growth of SMMC-7721 cells. When implanted into nude mice, SMMC-7721 cells transfected with angiostatin cDNA show a decreased tumorigenic capability. It suggests that angiostatin can inhibit tumor growth through its inhibition on angiogenesis in tumors.

Tao KS, Dou KF, Wu XA. Expression of angiostatin cDNA in human hepatocellular carcinoma cell line SMMC-7721 and its effect on

implanted carcinoma in nude mice. *World J Gastroenterol* 2004; 10(10): 1421-1424

<http://www.wjgnet.com/1007-9327/10/1421.asp>

INTRODUCTION

The growth and metastasis of a tumor depend on the growth of blood vessels^[1-5], so anti-angiogenesis becoming a new way in treatment of tumors^[6-9]. Recently, angiostatin has been found to be one of the most effective inhibitory genes of angiogenesis. It can inhibit specifically the proliferation and migration of endothelial cells of blood vessels, and has been regarded as a very useful target gene in anti-angiogenesis-based cancer treatment^[10]. Liver cancer is one kind of cancers rich in blood vessels, so therapeutic angiogenesis represents a potential option in the therapy of primary liver cancer. We investigated the construction of an expression vector containing angiostatin cDNA and evaluated its effect on implanted tumor in nude mice.

MATERIALS AND METHODS

Transfection of pcDNA3.1-mAST into SMMC-7721

Eukaryotic expression vector of pcDNA3.1 (+) (Invitrogen, USA) and plasmid pRC-mAST containing full-length of angiostatin gene (a gift from Dr. Zhang DX in Folkman Laboratory, Yale University, USA) were digested by restriction enzymes *Xba* I and *Hind* III. The digested vector and angiostatin cDNA fragment were ligated. Recombinant clones were identified by *Xba* I and *Hind* III double digestion. Positive clones named pcDNA3.1-mAST were further confirmed by sequencing.

Cultured SMMC-7721 cells were divided into three groups: transfected with recombinant pcDNA3.1-mAST (group A), transfected with pcDNA3.1 (+) vector (group B), not transfected with pcDNA3.1 (+) vector (group C). Transfection was performed according to the instructions of Lipofectamine TM2000 reagent kit (Gibco). Cells were cultured in RPMI 1640 medium containing 200 mL/L fetal calf serum and 350 mg/L G418. Resistant clones could be detected two weeks later. Cell growth curve was also made.

RT-PCR and Western blotting

Total RNA was extracted following reversal transcriptase PCR. Primers used in PCR were designed according to the reported angiostatin cDNA sequence^[7]. The primer sequences were as follows: 5' end: 5' -ATGGACCATAAGGAAGTAA-3' ; 3' end 5' -GGTGGGCAATTCCACAA ACA-3' . The products of PCR were identified on 10 g/L agarose gel electrophoresis.

Cultured cells in the three groups were treated by adding 500 L solution containing 500 g/L lysine-Sepharose and 50 mmol/L Tris-HCl (pH 8.0) into the culture medium. Western blotting was then performed according to the reported methods^[11]. The primary antibody was anti-rabbit HA-tagged antibody (a gift from Dr. Zhang DX in Yale University).

Animal experiment

Thirty Balb/c nu/nu male mice aged 4-6 wk (body mass 18-20 g) were bred under SPF conditions. They were randomly divided into three groups of 10 each. The mice in blank control group were injected only with SMMC-7721 cells, the mice in vector-treated control group were injected with SMMC-7721 cells transfected with pcDNA3.1 (+) vector, the mice in angiostatin group received an injection of SMMC-7721 cells transfected with recombinant pcDNA3.1-mAST. After cancer cells were cultured into the stage of logarithmic growth phase, they were digested with trypsin to make cancer cell suspension of $5 \times 10^{10}/L$. Then, 0.2 mL of each suspension was subcutaneously injected into the right back of nude mice.

Tumor volume measurement

The survival of nude mice was observed every day. Tumor volume and inhibitory rate were measured on days 7, 14, 21, 28 and 35 after injection.

$$\text{Tumor volume} = \pi/6 \times (\text{long radius} \times \text{short radius}^2)^{12}$$

Inhibition rate = (tumor volume of blank control group - tumor volume of angiostatin group) / tumor volume of blank control group $\times 100\%$.

Microvessel density counting

Thirty-five days after cancer cell injection, the nude mice were killed and their tumors were removed. The surrounding fatty tissues were dissected and the tumors were weighed. CD34 immunohistochemical staining was carried out according to the previously reported methods^[11] to label endothelial cells of blood vessels. Five areas with the highest microvessel density (MVD) in each section were selected under $40 \times$ subjective lens. The number of blood vessels in each area was counted under a magnification of 200 fields ($0.708 \text{ mm}^2/\text{field}$). The data from 5 areas were averaged and the value was regarded as the tumor MVD of each nude mouse. The average MVD from 10 mice in each group was regarded as the MVD of implanted tumor of that group^[13].

Statistical analysis

All data were expressed as mean \pm SD and analyzed by Student's *t* test. A *P* value less than 0.05 was considered statistically significant.

RESULTS

Identification of recombinant plasmid pcDNA3.1-mAST

After digestion by *Xba* I and *Hind* III, bands at 1.4 kb could be detected for positive clones (Figure 1), which suggested that mAST fragment was inserted into the pcDNA3.1 (+) vector, named recombinant plasmid pcDNA3.1-mAST.

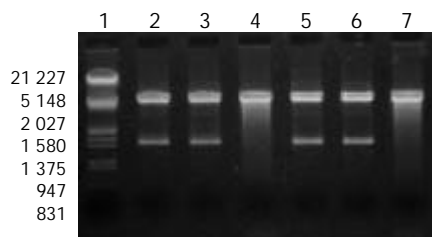


Figure 1 Restriction enzyme digestion of recombinant plasmid pcDNA3.1-mAST by *Xba* I and *Hind* III. Lane 1: DNA/*Eco*R I + *Hind* III Marker; Lanes 2, 3, 5, 6: positive clones; Lanes 4, 7: negative clones.

pcDNA3.1-mAST plasmid DNA was prepared and performed for sequencing. The sequence obtained was the same as the reported sequence of angiostatin cDNA, indicating that

the murine angiostatin gene was successfully cloned into the eukaryotic expression vector pcDNA3.1 (+).

Screening of angiostatin gene-transfected cells

No significant differences between the morphological characteristics of transfected cells and normal SMCC-7721 cells (Figure 2) were observed. No differences were detected in their growth rates (Figure 3).

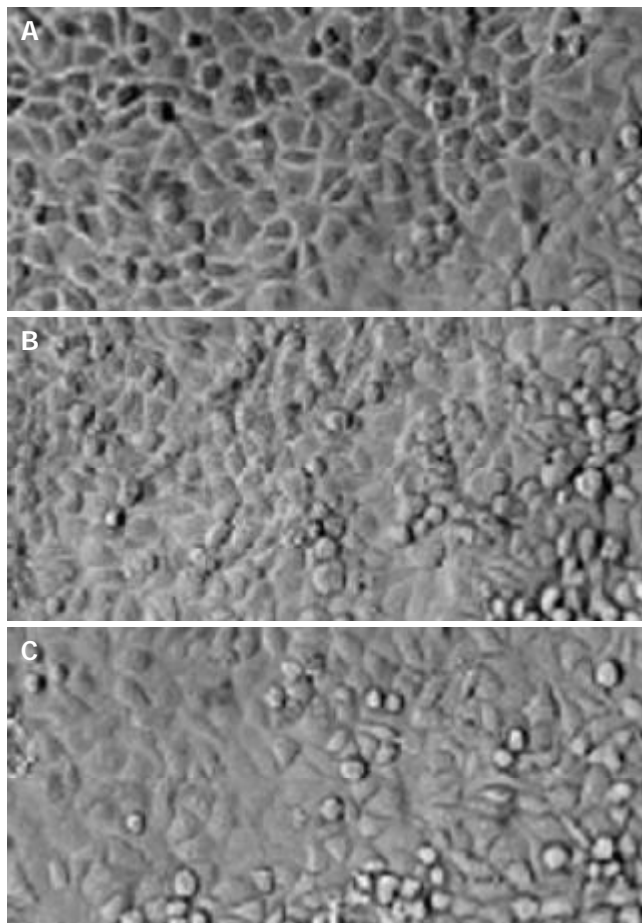


Figure 2 Morphology of HCC cells. A: SMMC-7721 cells; B: SMCC-7721 cells transfected with pcDNA3.1(+); C: SMCC-7721 cells transfected with pcDNA3.1-mAST.

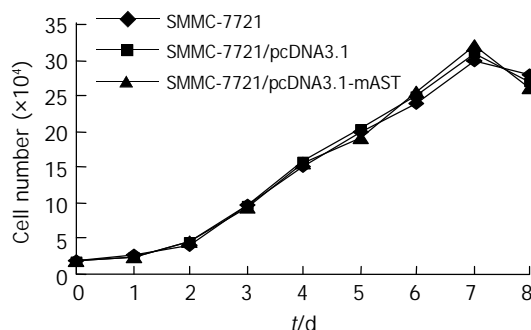


Figure 3 Growth curve of SMCC-7721 cells.

RT-PCR and Western blotting of angiostatin expression in transfected cells

SMMC-7721 cells transfected with pcDNA3.1-mAST were prepared and used as the template. By using angiostatin primers, a band was detected at 1.4 kb with PCR, indicating the presence of angiostatin cDNA in SMMC-7721 liver cancer cells (Figure 4).

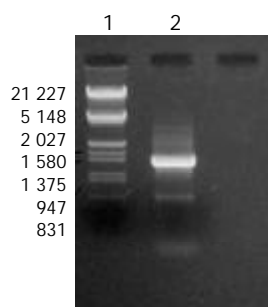


Figure 4 RT-PCR of transfected cells. Lane 1: DNA/*EcoR* I + *Hind* III Markers; Lane 2: positive clones.

Supernatants of cultured cells in three groups were collected and analyzed by Western blotting. A band in a molecular mass of 58 000 was detected with rabbit anti-HA-tagged antibody from the cells transfected with pcDNA3.1-mAST, but no bands were detected from blank control group or vector control group (Figure 5).

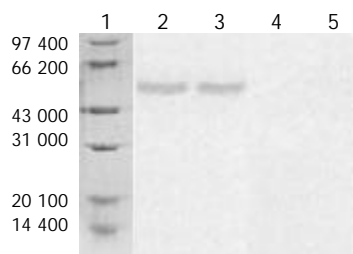


Figure 5 Western blotting of angiostatin expression. Lane 1: Marker protein; Lanes 2, 3: SMMC-7721/pcDNA3.1-mAST; Lane 4: SMMC-7721/pcDNA3.1 (+); Lane 5: SMMC-7721.

Tumor growth in nude mice

Tumors were observed in the nude mice just 5 d after they were implanted with cells in blank control group or vector control group. There was no significant difference in tumor volume between blank control group and vector control group ($t=1.53$, $P>0.05$). Mice had a visible tumor 10 d after cell injection in pcDNA3.1-mAST transfection group, and the tumor grew slowly. Tumor volumes among three groups were quite different, and a significant difference was observed when compared angiostatin group with blank control group or vector control group ($t=13.07$ and $t=12.91$, respectively, $P<0.01$, Table 1).

Table 1 Volume of implanted tumors in nude mice of three groups (mm^3)

Group	Time after implantation (d)				
	7	14	21	28	35
Blank control	20±5	91±25	624±139	1 631±363	3 538±643
Vector control	19±6	85±24	653±149	1 542±358	3 128±547
Angiostatin	0	23±6	112±20	237±46	755±198 ^b

^b $P<0.01$ vs blank control and vector control group.

On the 35th day, the tumor growth inhibition rate in angiostatin group reached 78.6% vs the control group. In addition, the speed of tumor growth in angiostatin group was significantly slower than that in blank control or vector control group (Figure 6).

On the other hand, the tumor mass in three groups was measured on day 35. It was found that the tumor mass in angiostatin group (2.1 ± 0.5 g) was significantly smaller than

that in blank control (6.0 ± 0.7 g) or vector control (5.9 ± 0.5 g) group ($t=14.98$ and 16.14 , respectively, $P<0.01$), whereas there was no significant difference in tumor mass between the blank control and vector control groups ($t=0.59$, $P>0.05$).

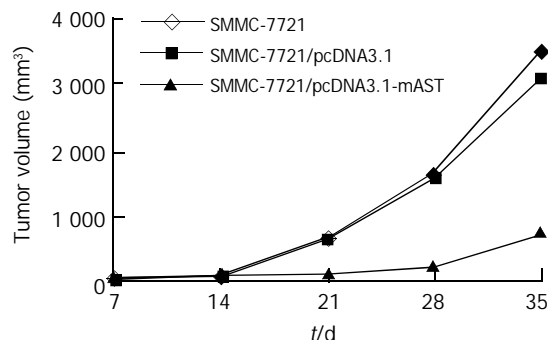


Figure 6 Growth curve of tumors.

MVD

Blood vessels were visualized by CD34 immunohistochemistry and endothelial cells were stained in brown color (Figure 7). There were no significant differences of MVD between the vector control group (49 ± 7 , mm^2) and the blank control group (52 ± 6 , mm^2) ($t=0.92$, $P>0.05$). But the tumor MVD in the angiostatin group (26 ± 4 , mm^2) was significantly lower than that in other two control groups ($t=9.33$, 10.94 , respectively, $P<0.01$), and was about 48.9% of that in the blank control group.

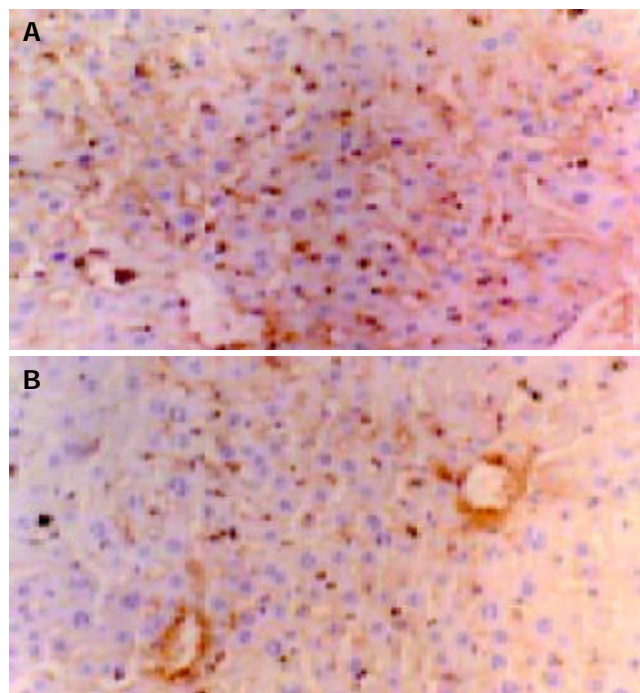


Figure 7 Immunohistochemical analysis of MVD in tumor tissue ($\times 200$). A: blank control group; B: angiostatin group

DISCUSSION

The growth and metastasis of a tumor depend upon the growth of blood vessels. Therefore, inhibition of blood vessel growth is a potential therapy for primary tumors, and it has become an important way to treat tumors by increasing the expression of inhibitory factors of angiogenesis in the tumor area. Angiostatin is one of the endogenous angiogenesis inhibitory factors^[10] and has been proved *in vitro* to inhibit the proliferation of endothelial cells. *In vivo* studies also confirmed

that angiostatin could inhibit the angiogenesis in solid tumors that could result in the inhibition of tumor growth^[14-20].

In the present study, we constructed a target fragment that contained a sequence encoding a secretory signal (SS) and a preactivation peptide (PA), the N-terminal kringle1-4 sequence of plasminogen and 11 amino acids in the C-terminal HA-tagged gene. The target gene fragment of 1.4 kb in length was cloned into *Xba* I and *Hind* III restriction sites of eukaryotic expression vector pcDNA3.1(+). Restriction digestion and sequencing analysis for positive clones indicated that a recombinant eukaryotic expression vector containing the angiostatin gene was successfully constructed. This recombinant vector was then transfected into human liver cancer cell line SMMC-7721 and screened by G418. The result of RT-PCR showed that the recombinant plasmid was stably integrated into the cells. By Western blotting, a protein ($M_r=38\ 000$) was detected, indicating that angiostatin protein was expressed in transfected SMMC-7721 cells. Furthermore, the growth curve showed that there was no significant difference in growth rate between transfected and non-transfected SMMC-7721 cells. This indicated that angiostatin had no inhibitory effect on the growth of SMMC-7721 cells.

CD34 is specifically located in endothelial cells. It was reported that CD34 could be regarded as a good marker of endothelial cells in liver cancer because of its high sensibility and specificity. Therefore, the expression of CD34 can reflect the angiogenesis of primary liver cancer and implanted liver tumors. So in this experiment we used CD34 antibody to label endothelial cells.

In this experiment, SMMC-7721 cells that stably expressed angiostatin cDNA (angiostatin group), SMMC-7721 cells alone (blank control group) and SMMC-7721 cells transfected with pcDNA3.1 (+) vector (vector control group) were subcutaneously implanted into nude mice respectively. We found that the implanted tumors appeared later in the angiostatin group, and the mass and volume of the tumor were significantly lower and smaller than those of the other two groups. The inhibitory rate reached 78.6%, and the mass was only 34.6% of that of the blank control group. These results suggested that angiostatin could significantly inhibit the growth of primary tumors. The MVD of the tumor in the angiostatin group was much less than that in the other two groups ($P<0.01$). These data indicated that angiostatin could upregulate the expression of angiogenic inhibitory factors and/or downregulate the expression of angiogenic stimulus factors after its cDNA was transfected into SMMC-7721 cells. This would change the balance between angiogenesis stimulus factors and angiogenic inhibitory factors, thus inhibiting of the angiogenesis and growth of tumors.

Gene therapy, concerning the special angiogenic inhibitory factor of endothelial cells of tumor tissue, is a new way of cancer treatment. We believe that this treatment in combination with chemotherapy and radiotherapy would definitely improve the effect of cancer treatment. Because liver cancer is more prevalent in the world^[21-23], especially in China^[24], our results have the significance in further research.

REFERENCES

- 1 **Compagni A**, Christofori G. Recent advances in research on multistage tumorigenesis. *Br J Cancer* 2000; **83**: 1-5
- 2 **Detmar M**. Tumor angiogenesis. *J Invest Dermatol Symp Proc* 2000; **5**: 20-23
- 3 **Maehara Y**, Kabashima A, Koga T, Tokunaga E, Takeuchi H, Kakeji Y, Sugimachi K. Vascular invasion and potential for tumor angiogenesis and metastasis in gastric carcinoma. *Surgery* 2000; **128**: 408-416
- 4 **Gervaz P**, Scholl B, Mainguene C, Poitry S, Gillet M, Wexner S. Angiogenesis of liver metastases: role of sinusoidal endothelial cells. *Dis Colon Rectum* 2000; **43**: 980-986
- 5 **Sabo E**, Boltenko A, Sova Y, Stein A, Kleinhaus S, Resnick MB. Microscopic analysis and significance of vascular architectural complexity in renal cell carcinoma. *Clin Cancer Res* 2001; **7**: 533-537
- 6 **Carmeliet P**, Jain RK. Angiogenesis in cancer and other diseases. *Nature* 2000; **407**: 249-257
- 7 **Cao Y**, O' Reilly MS, Marshall B, Flynn E, Ji RW, Folkman J. Expression of angiostatin cDNA in a murine fibrosarcoma suppresses primary tumor growth and produces long-term dormancy of metastases. *J Clin Invest* 1998; **101**: 1055-1063
- 8 **Luo YQ**, Wu MC, Cong WM. Gene expression of hepatocyte growth factor and its receptor in HCC and nontumorous liver tissues. *World J Gastroenterol* 1999; **5**: 119-121
- 9 **Barinaga M**. Designing therapies that target tumor blood vessels. *Science* 1997; **275**: 482-484
- 10 **O' Reilly MS**, Holmgren L, Shing Y, Chen C, Rosenthal RA, Moses M, Lane WS, Cao Y, Sage EH, Folkman J. Angiostatin: a novel angiogenesis inhibitor that mediates the suppression of metastases by a Lewis lung carcinoma. *Cell* 1994; **79**: 315-328
- 11 **Towbin H**, Staehelin T, Gordon T. Electrophoretic transfer of proteins from polyacrylamide gels to nitrocellulose sheets: procedure and some applications. *Proc Natl Acad Sci U S A* 1979; **76**: 4350-4354
- 12 **Hanahan D**, Folkman J. Patterns and emerging mechanisms of the angiogenic switch during tumorigenesis. *Cell* 1996; **86**: 353-364
- 13 **Araya M**, Terashima M, Takagane A, Abe K, Nishizuka S, Yonezawa H, Irinoda T, Nakaya T, Saito K. Microvessel count predicts metastasis and prognosis in patients with gastric cancer. *J Surg Oncol* 1997; **65**: 232-236
- 14 **O' Reilly MS**, Holmgren L, Shing Y, Chen C, Rosenthal RA, Cao Y, Moses M, Lane WS, Sage EH, Folkman J. Angiostatin: a circulating endothelial cell inhibitor that suppresses angiogenesis and tumor growth. *Cold Spring Harb Symp Quant Biol* 1994; **59**: 471-482
- 15 **Stack MS**, Gately S, Bafetti LM, Enghild JJ, Soff GA. Angiostatin inhibits endothelial and melanoma cellular invasion by blocking matrix-enhanced plasminogen activation. *Biochem J* 1999; **340** (Pt 1): 77-84
- 16 **Hari D**, Beckett MA, Sukhatme VP, Dhanabal M, Nodzenski E, Lu H, Mauceri HJ, Kufe DW, Weichselbaum RR. Angiostatin induces mitotic cell death of proliferating endothelial cell. *Mol Cell Biol Res Commun* 2000; **3**: 277-282
- 17 **Ijland SA**, Jager MJ, Heijdra BM, Westphal JR, Peek R. Expression of angiogenic and immunosuppressive factors by uveal melanoma cell lines. *Melanoma Res* 1999; **9**: 445-450
- 18 **Matsuda KM**, Madoiwa S, Hasumi Y, Saga Y, Kume A, Mano H, Ozana K, Matsuda M. A novel strategy for the tumor angiogenesis-targeted gene therapy: generation of angiostatin from endogenous plasminogen by protease gene transfer. *Cancer Gene Ther* 2000; **7**: 589-596
- 19 **Volm M**, Mattern J, Koomagi R. Angiostatin expression in non-small cell lung cancer. *Clin Cancer Res* 2000; **6**: 3236-3240
- 20 **Wu J**, Shi YQ, Wu KC, Zhang DX, Yang JH, Fan DM. Angiostatin up-regulation in gastric cancer cell SGC7901 inhibits tumorigenesis in nude mice. *World J Gastroenterol* 2003; **9**: 59-64
- 21 **El-Serag HB**, Davila JA, Petersen NJ, McGlynn KA. The continuing increase in the incidence of hepatocellular carcinoma in the United States: an update. *Ann Intern Med* 2003; **139**: 817-823
- 22 **Regimbeau JM**, Abdalla EK, Vauthey JN, Lauwers GY, Durand F, Nagorney DM, Ikai I, Yamaoka Y, Belghiti J. Risk factors for early death due to recurrence after liver resection for hepatocellular carcinoma: results of a multicenter study. *J Surg Oncol* 2004; **85**: 36-41
- 23 **Ku Y**, Iwasaki T, Tominaga M, Fukumoto T, Takahashi T, Kido M, Ogata S, Takahashi M, Kuroda Y, Matsumoto S, Obara H. Reductive surgery plus percutaneous isolated hepatic perfusion for multiple advanced hepatocellular carcinoma. *Ann Surg* 2004; **239**: 53-60
- 24 **Lin GY**, Chen ZL, Lu CM, Li Y, Ping XJ, Huang R. Immunohistochemical study on p53, H-rasp21, c-erbB-2 protein and PCNA expression in HCC tissues of Han and minority ethnic patients. *World J Gastroenterol* 2000; **6**: 234-238

Expression and altered subcellular localization of the cyclin-dependent kinase inhibitor p27^{Kip1} in hepatocellular carcinoma

Ke-Jun Nan, Zhao Jing, Ling Gong

Ke-Jun Nan, Zhao Jing, Department of Medical Oncology, First Hospital of Xi'an Jiaotong University, Xi'an 710061, Shaanxi Province, China

Ling Gong, Department of Infectious Diseases, First Hospital of Xi'an Jiaotong University, Xi'an 710061, Shaanxi Province, China

Correspondence to: Ke-Jun Nan, Department of Medical Oncology, First Hospital of Xi'an Jiaotong University, 1 Jiankang Xilu, Xi'an 710061, Shaanxi Province, China. jz96329@163.com

Telephone: +86-29-5324086 **Fax:** +86-29-5324086

Received: 2003-09-18 **Accepted:** 2003-12-08

Abstract

AIM: To investigate p27 expression in hepatocellular carcinoma (HCC), adjacent nontumoral and normal liver tissues, and to verify whether the subcellular localization of p27 was altered in HCC.

METHODS: The level of p27 in tumoral, nontumoral, and normal liver tissues were assessed by immunohistochemical (IHC) analysis. Parallel immunostaining was done for proliferating cell nuclear antigen (PCNA) to evaluate cell proliferation.

RESULTS: The labeling index (LI) of p27 in tumoral lesions was significantly lower than that in adjacent nontumoral lesions ($t=2.444$, $P=0.017$) and normal controls ($t=2.268$, $P=0.029$). The LI of p27 significantly decreased in patients with massive type ($t=2.227$, $P=0.037$) and infiltration ($t=2.197$, $P=0.036$). The prognosis of patients with higher p27 LI was longer than that of patients with lower p27 LI ($P=0.0247$, log-rank test). The LI of PCNA was significantly higher in HCC than that in adjacent nontumoral lesions ($t=2.092$, $P=0.041$) and normal controls ($t=3.533$, $P=0.002$). There was no significant correlation between p27 expression and cell proliferation in tumor samples. The level of p27 in the cytoplasmic fraction was higher in tumoral and nontumoral liver tissues, and was associated with clinical stage ($t=2.520$, $P=0.029$) and the degree of invasion ($t=2.640$, $P=0.019$). Survival analysis showed that p27 was an independent prognosis marker for HCC patients.

CONCLUSION: These results suggest that p27 underexpressing in patients with HCC is closely associated with infiltration, metastasis, and prognosis. Alterations in the subcellular localization of p27 protein may occur early during hepatocarcinogenesis.

Nan KJ, Jing Z, Gong L. Expression and altered subcellular localization of the cyclin-dependent kinase inhibitor p27^{Kip1} in hepatocellular carcinoma. *World J Gastroenterol* 2004; 10 (10): 1425-1430

<http://www.wjgnet.com/1007-9327/10/1425.asp>

INTRODUCTION

Abnormalities in various regulators of cell cycle frequently

occur in human cancers^[1-4]. Cell cycle is tightly controlled by the regulators, including cyclins, cyclin-dependent kinases (CDKs), and their inhibitors. Cyclin-dependent kinase inhibitors (CKIs) are potent negative regulators of cell cycle, and have two families on the basis of sequence homology. The inhibitors of CDK4 (INK4) family, including p16^{Ink4a}, p15^{Ink4b}, p18^{Ink4c}, and p19^{Ink4}, specifically binds to CDK4 and CDK6, and inhibits cyclin D binding. The Cip/Kip family, including p21^{Cip1}, p27^{Kip1}, and p57^{Kip2}, binds to and inhibits cyclin-bound CDKs^[5]. Among CKIs, p27 is thought to have crucial^[6] and important roles in a variety of fundamental cellular processes^[7-10]. The underexpression of p27 assessed by IHC analysis has been associated with more severe tumor grade and a negative prognostic marker in different carcinomas^[11-16].

Furthermore, studies showed that reduced p27 expression was correlated with advanced tumor stages and poorer disease-free survival in patients with HCC at a variety of evolutionary stages^[17-20]. However, most precious investigations are based on immunostaining of tumoral liver samples without comparing with surrounding nontumoral liver, which should be the best control tissue to be used for comparison.

In addition, p27 functions at the nuclear level by binding to and inhibiting cyclin/CDK complexes. It was recently reported that cytoplasmic displacement was an alternative way to inhibit p27 activity and might also play a role in tumor development^[21]. Indeed, positive immunostaining of cytoplasmic p27 has been previously reported in various human cancers^[22-25]. To address this hypothesis, the expression of p27 in tumoral, adjacent nontumoral, and normal liver tissues was evaluated by IHC analysis in patients with HCC, and the subcellular distribution of p27 was also investigated in this study.

MATERIALS AND METHODS

Patients and tumor samples

From January 2000 to December 2001, 32 liver samples were collected from patients who had HCC and underwent surgery in our institution. All liver tumors were histologically diagnosed. Tumor gross type and stage were diagnosed using Eggle's classification and Union International Contre Cancer (UICC) criteria. Tumor cellular differentiation was identified by Edmondson's classification. No patient received pre-operative chemotherapy or chemoembolization. The clinicopathologic characteristics of 32 patients with HCC are listed in Table 1. Normal livers were prepared from 10 patients who were died from the accident as the controls.

After curative surgery, all patients were followed up every 3 mo till death. They were followed from 2 to 32 mo (mean 15.2 mo). Actuarial survival was measured from the day of surgical operation to that of death or last follow-up.

Immunohistochemical study

Liver samples were routinely fixed in 40 g/L formaldehyde solution and embedded in paraffin. After slicing into 4 μ m-thick sections, IHC analysis was performed using Dako ElivisionTM plus two-step System. In brief, the sections were dewaxed in xylene, and rinsed in alcohol and graded alcohol/water mixtures. Then, 30 mL/L hydrogen peroxide was applied to block

endogenous peroxidase activity. The sections were subsequently treated in a microwave oven twice for 5 min in citrate buffer (pH 6.0) at high power. After blocking with goat serum, the mouse monoclonal antibodies against p27 (ZM-0340) and PCNA (ZM-0213) (Zymed Biotechnology, Zymed, CA) were applied on the slides at the dilution of 1:120 and 1:50, respectively. After rinsing, staining was performed by the Elivision™ plus two-step System (kit-9902, Dako, Carpinteria, CA). The color was developed by reacting with 3,3-diaminobenzidine. Slides were then counterstained with hematoxylin, dehydrated, cleared, and mounted. Negative controls were performed by replacing the primary antibody with nonimmune mouse serum or PBS (Figure 1). A human breast cancer specimen and the reactive tonsil were used as positive controls for p27 (Figure 2) and PCNA, respectively.

Table 1 Clinicopathologic characteristics of 32 Patients

Clinicopathologic parameters	Number	%
Age		
≤45 years	14	43.8
>45 years	18	56.2
Gender		
Male	26	81.2
Female	6	18.8
Gross type		
Massive	15	46.9
Nodular	17	53.1
Tumor size		
≤5 cm	5	15.6
>5 cm	27	84.4
Cellular differentiation		
I	4	12.5
II	17	53.1
III	5	15.6
IV	6	18.8
Degree of invasion		
T ₁ +T ₂	12	37.5
T ₃ +T ₄	20	62.5
Stage		
I+II	10	31.2
III+IV	22	68.8
Lymph node metastasis		
Present	4	87.5
Absent	28	12.5
Portal invasion		
With	3	9.4
Without	29	90.6
Infiltration		
Present	12	37.5
Absent	20	62.5

Immunostaining evaluation

Slides were mounted independently by 2 investigators without notifying any clinical or pathological information. The positive cells for p27 and PCNA were measured by counting at least 1 000 HCC cells from at least 5 randomly selected fields under the microscope. Then, LI was calculated as a percentage for each protein.

Statistical analysis

Values were expressed as mean±SD, The Student's *t* test was performed to analyze the relationship between the expression of the proteins and various clinicopathologic parameters. The

cumulative survival rate was computed and actuarial survival curves were constructed by the Kaplan-Meier method. The cumulative survival rate was compared between groups using the log-rank test. Relevant prognostic factors were identified by univariate and multivariate Cox proportional hazard regression analyses. Tests were considered significant when the *P* values were <0.05.

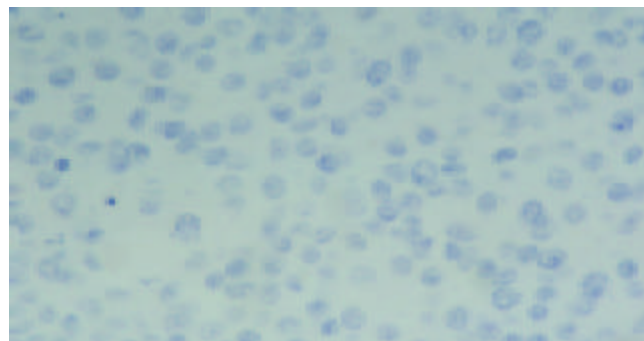


Figure 1 Negative control of p27 (×400).

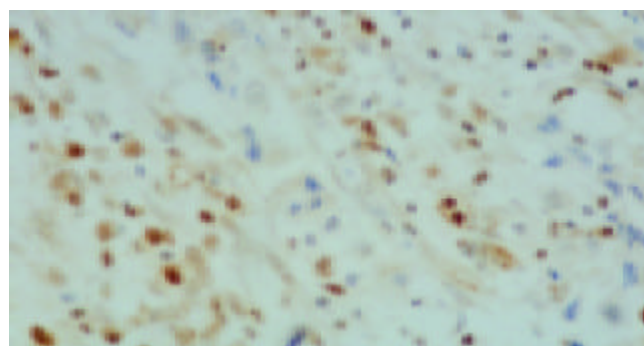


Figure 2 Positive control of p27 (×400).

RESULTS

Reduced expression of p27 in HCC

The mean LI of p27 in HCC was 27.7±19.9%, which was lower than that in adjacent nontumoral lesions (42.3±21.4%, *t*=2.444, *P*=0.017) and that in normal controls (39.1±17.5%, *t*=2.268, *P*=0.029). Furthermore, the LI of p27 in adjacent nontumoral lesions was not significantly different from that in normal controls (Figure 3). Table 2 shows the relationship between p27 expression and clinicopathologic characteristics. The LI of p27 significantly decreased in patients with massive type (*t*=2.227, *P*=0.037) and infiltration (*t*=2.197, *P*=0.036).

Proliferating activity in HCC

The mean LI of PCNA was 49.5±14.2% in HCC, which was higher than that in adjacent nontumoral lesions (42.8±11.2%, *t*=2.092, *P*=0.041) and normal controls (36.2±8.9%, *t*=3.533, *P*=0.002). The LI of PCNA in adjacent nontumoral lesions was not significantly different from that in normal controls (Figure 4). The LI of PCNA significantly increased in cases with poor differentiation (*t*=2.259, *P*=0.031, Table 2). The patients were divided into low p27 and high p27 groups with the cut-off value of the median LI. The LI of PCNA was 51.2±15.6% and 48.1±13.0% in low p27 and high p27 groups, respectively. There was no significant difference between these two groups (*t*=0.578, *P*=0.568).

Altered subcellular localization of p27 in HCC

The cytoplasmic expression of p27 was found in the HCC,

adjacent nontumoral, and normal liver tissues. Therefore, the cytoplasmic displacement of p27 might not be a specific phenomenon of tumor cells. However, the cytoplasmic sequestration of p27 was more frequent in HCC and adjacent nontumoral lesions (Figure 3).

The mean LI of cytoplasmic p27 was $31.0 \pm 12.6\%$ in adjacent nontumoral lesions, which was higher than that in HCC ($21.6 \pm 18.2\%$, $t=2.378$, $P=0.021$) and normal controls ($13.9 \pm 5.6\%$, $t=5.994$, $P<0.001$). The LI of cytoplasmic p27 in HCC was higher than that in normal controls ($t=2.106$, $P=0.042$).

Whereas, the nuclear LI in normal controls ($31.3 \pm 12.6\%$) was higher than that in HCC ($12.5 \pm 9.7\%$, $t=4.968$, $P<0.001$) and nontumoral lesions ($16.5 \pm 10.4\%$, $t=3.731$, $P=0.001$). Altered subcellular localization of p27 was correlated with clinical stage ($t=2.520$, $P=0.029$) and the degree of invasion ($t=2.640$, $P=0.019$) (Table 2).

Expression of p27 and PCNA and survival

The survival rate of 6, 12, and 24 mo was 71.9%, 47.8%, and 25.1%, respectively. The patients were divided into 2 groups according

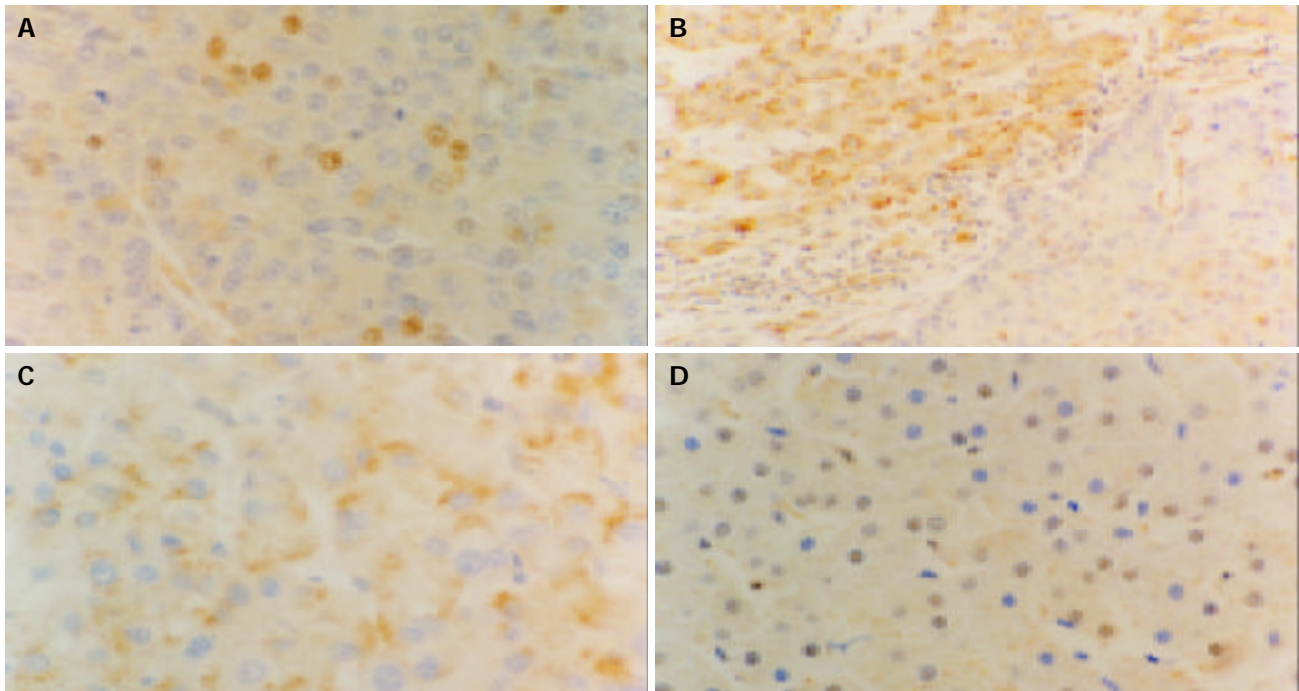


Figure 3 Immunohistochemical staining of p27 in different liver tissues(Elivision), A: p27 expression is decreased in HCC $\times 400$, B: Decreased p27 expression in HCC (right), the p27 expression is mostly located in the cytoplasm in nontumoral liver tissues (left) $\times 200$, C: Some tumor cells show cytoplasmic staining of p27 $\times 400$, D: p27 staining in normal controls is mostly located in nuclear $\times 400$.

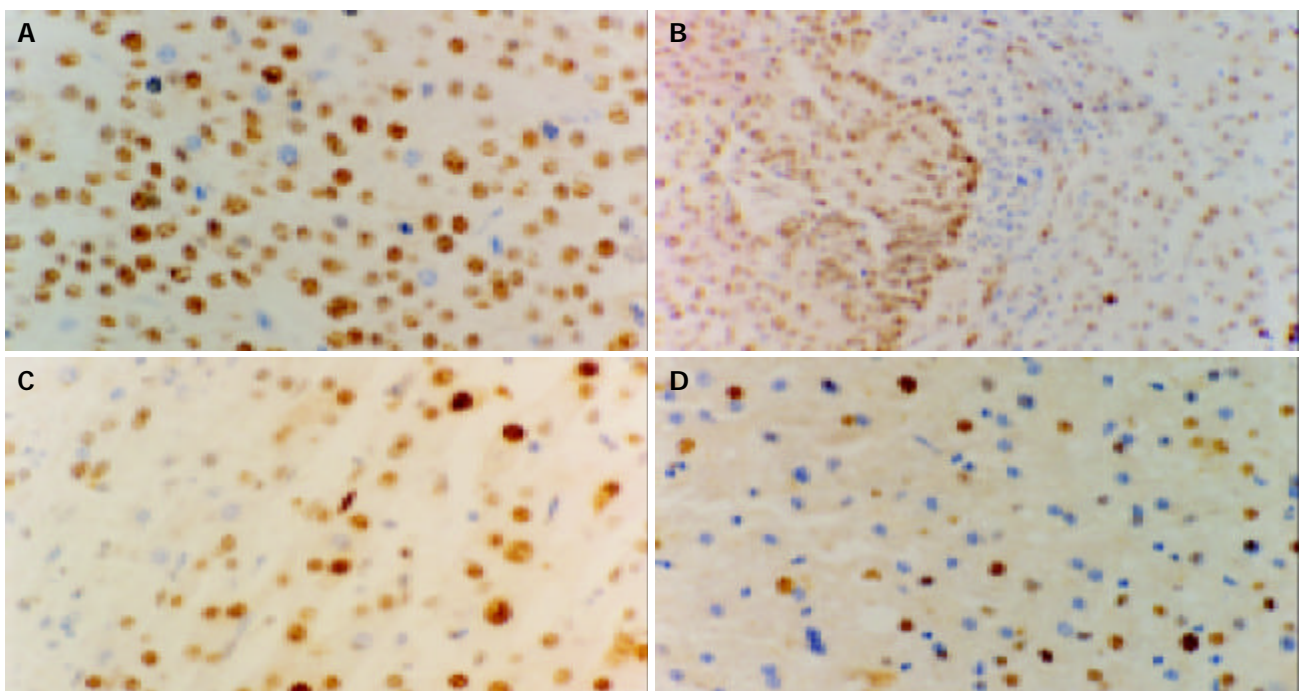
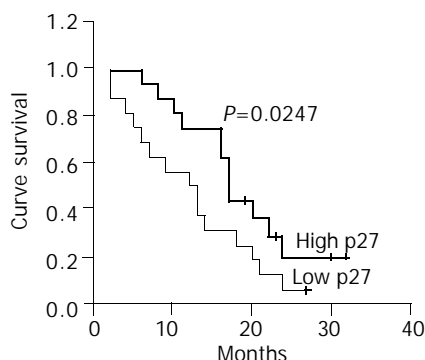


Figure 4 Expression of PCNA in different liver tissues(Elivision), A: Expression of PCNA in HCC $\times 400$, B: Expression of PCNA in HCC(left) and in nontumoral liver tissues(right) $\times 200$, C: Expression of PCNA in nontumoral liver tissues $\times 400$, D: in normal controls $\times 400$.

Table 2 Relationship among p27, PCNA, and cytoplasmic p27staining with clinicopathologic features

Parameters	p27 LI (%)	P	PCNA LI (%)	P	Cytoplasmic p27 LI (%)	P
Gross type						
Massive	20.5±13.1	0.037	46.4±13.4	0.249	25.9±18.9	0.221
Nodular	35.7±23.4		52.3±14.7		17.9±17.3	
Tumor size						
≤5 cm	23.8±14.4	0.645	38.1±10.7	0.047	27.0±24.1	0.481
>5 cm	28.4±20.9		51.7±13.9		20.6±17.4	
Cellular differentiation						
Well or moderate	29.7±21.4	0.438	45.7±13.8	0.031	23.2±18.0	0.498
Poor	23.8±17.1		56.9±12.6		18.6±19.1	
Degree of invasion						
T ₁ +T ₂	32.6±23.3	0.285	51.1±14.7	0.64	33.0±22.3	0.019
T ₃ +T ₄	24.7±17.5		48.6±14.4		14.8±11.1	
Stage						
I+II	33.6±25.6	0.261	48.0±12.9	0.688	35.3±23.9	0.029
III+IV	24.9±16.7		50.2±15.0		15.4±10.7	
Infiltration						
Present	18.3±18.8	0.036	44.4±12.3	0.117	19.0±18.3	0.536
Absent	33.3±18.7		52.6±14.7		23.2±18.5	
Lymphocyte metastasis						
With	25.5±2.6	0.565	56.0±14.9	0.339	16.0±10.6	0.518
Without	27.9±21.3		48.6±14.2		22.4±19.1	
Portal invasion						
Present	14.3±12.7	0.229	58.3±12.0	0.267	13.0±11.8	0.398
Absent	29.1±20.1		48.6±14.3		22.5±18.7	

to the median LI of p27, cytoplasmic p27, and PCNA. The survival analysis was performed on 32 patients and took into account for the following variables: age, gender, gross type, tumor size, UICC tumor stage, Edmondson's grade, portal invasion, lymph node metastasis, depth of invasion, infiltration, p27 LI, cytoplasmic p27 LI, and PCNA LI. In univariate analysis, a significant correlation with short survival was found only for present portal invasion ($P=0.021$) and low p27 expression ($P=0.033$). The prognosis of patients with higher p27 LI was longer than that of patients with lower p27 LI ($P=0.0247$, log-rank test, Figure 5). Multivariate analysis was performed by Cox proportional hazard regression model, age ≥ 45 years ($P=0.016$) and low p27 expression ($P=0.009$) were significantly associated with shorter survival. In addition, there was a trend of present lymphocyte metastasis ($P=0.05$) and advanced stage ($P=0.08$) correlated with poor prognosis (Table 3). For gross type, tumor size, Edmondson grade, depth of invasion, infiltration, cytoplasmic p27 LI, and PCNA LI, no significant correlations with overall survival were found.

**Figure 5** Kaplan-Meier curve for actuarial survival of patients in low p27 and high p27 groups.**Table 3** Univariate and multivariate analyses of individual parameters

Variables	P Values	
	Univariate	Multivariate
Age	0.150	0.016
Tumor size	0.513	0.678
Carcinoma differentiation	0.415	0.628
Stage	0.200	0.080
Lymphocyte metastasis	0.821	0.050
Infiltration	0.317	0.849
Portal invasion	0.021	0.619
p27	0.033	0.009
Cytoplasmic p27	0.114	0.624
PCNA	0.915	0.282

DISCUSSION

Hepatocellular carcinoma is one of the most common malignant tumors in China, and the incidence of HCC has increased in recent years^[26]. Cell proliferating activity is one of the prominent parameters for evaluating the biological aggressiveness of tumors. The study in cell proliferating status of HCC is very important for evaluating the biological aggressiveness^[27,28], because distant and lymph node metastasis are not very common.

The protein p27 is an important member of CKI family. It regulates G1 progression by binding to and inhibiting cyclin/CDKs^[29,30]. Loss or reduced expression of p27 has been found in a variety of human cancers and associated with more aggressive tumor behavior. The present study showed that p27 expression significantly decreased in HCC. The finding of p27 underexpression in HCC was similar to the previous reports^[31]. This study showed that the expression of p27 in

HCC was associated with gross type and direct liver invasion. Univariate analysis showed that portal invasion and p27 LI were related to survival in this study. In multivariate analysis, p27 expression was the strongest predictor of survival for HCC patients, which was independent of the other variables. Similar findings have also been observed in other cancers^[32-34]. It is therefore suggested that p27 should work as a negative regulator during hepatocarcinogenesis and may exert a useful prognostic marker. Interestingly, as reported by Milde-Langosch^[35], there was no correlation between p27 expression and proliferating level, indicating that reduced expression of p27 did not merely reflect high proliferating activity during tumor progression.

To our knowledge, this was the first study to report the altered subcellular localization of p27 in HCC. The protein p27 can bind to and inhibit the active cyclin/CDK complexes in the nucleus, so the cytoplasmic displacement may play an important role in inactivating this protein in tumor cells and in contributing to tumor development. Indeed, cytoplasmic localization of p27 immunostaining has been reported in various types of human cancers. In our study, we found that the cytoplasmic localization of p27 was more frequent in HCC and surrounding nontumoral livers. Furthermore, the cytoplasmic staining for p27 was more frequently accompanied with nuclear staining in normal controls. However, the increase in the cytoplasmic staining for p27 was often observed in the absence of a concomitant increase in the nuclear staining and was sometimes associated with a decrease in the nuclear staining. Some tumors expressed an increased level of p27 mainly because of an increase in the cytoplasmic level of this protein. The increase in the amount of cytoplasmic p27 was more frequent in early stage (I and II) tumors. Altered subcellular localization of p27 was also reported in Barrett's associated adenocarcinoma and colon cancer^[22,23]. In agreement with our results, cytoplasmic localization of p27 was an early event during carcinogenesis.

Although the mechanism responsible for the abnormal subcellular localization was not known, it may be due to loss of the tuberous sclerosis complex gene-2 (TSC2), the HER/Grb2/MAPK pathway which leads to nuclear export of p27^[36], overexpression of cyclin D3 which contributes to retaining p27 in the cytoplasm^[37], or PKB/Akt which phosphorylates p27 to impair its nuclear import^[38-40].

In conclusion, our results suggest that underexpression of p27 can contribute to the development of HCC. Cytoplasmic displacement is an alternative mechanism of inactivating p27 that acts early during hepatocarcinogenesis. Furthermore, studies on a large number of cases will reveal the significance of p27 subcellular localization in hepatocarcinogenesis and its relationship with clinicopathologic and prognostic parameters.

REFERENCES

- Ho A**, Dowdy SF. Regulation of G(1) cell-cycle progression by oncogenes and tumor suppressor genes. *Curr Opin Genet Dev* 2002; **12**: 47-52
- Sanchez-Beato M**, Sanchez-Aguilera A, Piris MA. Cell cycle deregulation in B-cell lymphomas. *Blood* 2003; **101**: 1220-1235
- Todd R**, Hinds PW, Munger K, Rustgi AK, Opitz OG, Suliman Y, Wong DT. Cell cycle dysregulation in oral cancer. *Crit Rev Oral Biol Med* 2002; **13**: 51-61
- Fiano V**, Ghimenti C, Schiffer D. Expression of cyclins, cyclin-dependent kinases and cyclin-dependent kinase inhibitors in oligodendrogliomas in humans. *Neurosci Lett* 2003; **347**: 111-115
- Polak J**, Pekova S, Schwarz J, Kozak T, Haskovec C. Expression of cyclin-dependent kinase inhibitors in leukemia. *Cas Lek Cesk* 2003; **142**: 25-28
- Slingerland J**, Pagano M. Regulation of the cdk inhibitor p27 and its deregulation in cancer. *J Cell Physiol* 2000; **183**: 10-17
- Philipp-Staheli J**, Payne SR, Kemp CJ. p27(Kip1): regulation and function of a haploinsufficient tumor suppressor and its misregulation in cancer. *Exp Cell Res* 2001; **264**: 148-168
- Tsukiyama T**, Ishida N, Shirane M, Minamishima YA, Hatakeyama S, Kitagawa M, Nakayama K, Nakayama K. Down-regulation of p27Kip1 expression is required for development and function of T cells. *J Immunol* 2001; **166**: 304-312
- Muraoka RS**, Lenferink AE, Simpson J, Brantley DM, Roebuck LR, Yakes FM, Arteaga CL. Cyclin-dependent kinase inhibitor p27(Kip1) is required for mouse mammary gland morphogenesis and function. *J Cell Biol* 2001; **153**: 917-932
- Alexander K**, Hinds PW. Requirement for p27(KIP1) in retinoblastoma protein-mediated senescence. *Mol Cell Biol* 2001; **21**: 3616-3631
- Nitti D**, Belluco C, Mammano E, Marchet A, Ambrosi A, Mencarelli R, Segato P, Lise M. Low level of p27(Kip1) protein expression in gastric adenocarcinoma is associated with disease progression and poor outcome. *J Surg Oncol* 2002; **81**: 167-175
- Hu YX**, Watanabe H, Li P, Wang Y, Ohtsubo K, Yamaguchi Y, Sawabu N. An immunohistochemical analysis of p27 expression in human pancreatic carcinomas. *Pancreas* 2000; **21**: 226-230
- Filipits M**, Puhalla H, Wrba F. Low p27Kip1 expression is an independent prognostic factor in gallbladder carcinoma. *Anticancer Res* 2003; **23**: 675-679
- Anastasiadis AG**, Calvo-Sanchez D, Franke KH, Ebert T, Heydthausen M, Schulz WA, Burchardt M, Gerharz CD. p27KIP1-expression in human renal cell cancers: implications for clinical outcome. *Anticancer Res* 2003; **23**: 217-221
- Tannapfel A**, Grund D, Katalinic A, Uhlmann D, Kockerling F, Haugwitz U, Wasner M, Hauss J, Engeland K, Wittekind C. Decreased expression of p27 protein is associated with advanced tumor stage in hepatocellular carcinoma. *Int J Cancer* 2000; **89**: 350-355
- Yue H**, Song FL, Zhang N, Feng XL, An TY, Yu JP. Expression of p27(kip1), Rb protein and proliferating cell nuclear antigen and its relationship with clinicopathology in human pancreatic cancer. *Hepatobiliary Pancreat Dis Int* 2003; **2**: 142-146
- Fiorentino M**, Altamari A, D'Errico A, Cukor B, Barozzi C, Loda M, Grigioni WF. Acquired expression of p27 is a favorable prognostic indicator in patients with hepatocellular carcinoma. *Clin Cancer Res* 2000; **6**: 3966-3972
- Zhou Q**, He Q, Liang LJ. Expression of p27, cyclin E and cyclin A in hepatocellular carcinoma and its clinical significance. *World J Gastroenterol* 2003; **9**: 2450-2454
- Qin LF**, Ng IO. Expression of p27(KIP1) and p21(WAF1/CIP1) in primary hepatocellular carcinoma: clinicopathologic correlation and survival analysis. *Hum Pathol* 2001; **32**: 778-784
- Ito Y**, Matsuura N, Sakon M, Miyoshi E, Noda K, Takeda T, Umeshita K, Nagano H, Nakamori S, Dono K, Tsujimoto M, Nakahara M, Nakao K, Taniguchi N, Monden M. Expression and prognostic roles of the G1-S modulators in hepatocellular carcinoma: p27 independently predicts the recurrence. *Hepatology* 1999; **30**: 90-99
- Blagosklonny MV**. Are p27 and p21 cytoplasmic oncoproteins? *Cell Cycle* 2002; **1**: 391-393
- Sgambato A**, Ratto C, Faraglia B, Merico M, Ardito R, Schinzari G, Romano G, Cittadini AR. Reduced expression and altered subcellular localization of the cyclin-dependent kinase inhibitor p27(Kip1) in human colon cancer. *Mol Carcinog* 1999; **26**: 172-179
- Singh SP**, Lipman J, Goldman H, Ellis FH Jr, Aizenman L, Cangi MG, Signoretti S, Chiaur DS, Pagano M, Loda M. Loss or altered subcellular localization of p27 in Barrett's associated adenocarcinoma. *Cancer Res* 1998; **58**: 1730-1735
- Masciullo V**, Sgambato A, Pacilio C, Pucci B, Ferrandina G, Palazzo J, Carbone A, Cittadini A, Mancuso S, Scambia G, Giordano A. Frequent loss of expression of the cyclin-dependent kinase inhibitor p27 in epithelial ovarian cancer. *Cancer Res* 1999; **59**: 3790-3794
- Masciullo V**, Susini T, Zamparelli A, Bovicelli A, Minimo C, Massi D, Taddei G, Maggiano N, De Iaco P, Ceccaroni M, Bovicelli L, Amunni G, Mancuso S, Scambia G, Giordano A. Frequent loss of expression of the cyclin-dependent kinase inhibitor p27(Kip1) in estrogen-related endometrial adenocarcinomas. *Clin Cancer Res* 2003; **9**: 5332-5338

- 26 **Tang ZY**. Hepatocellular carcinoma-cause, treatment and metastasis. *World J Gastroenterol* 2001; **7**: 445-454
- 27 **Qin LX**, Tang ZY. The prognostic significance of clinical and pathological features in hepatocellular carcinoma. *World J Gastroenterol* 2002; **8**: 193-199
- 28 **Zeng WJ**, Liu GY, Xu J, Zhou XD, Zhang YE, Zhang N. Pathological characteristics, PCNA labeling index and DNA index in prognostic evaluation of patients with moderately differentiated hepatocellular carcinoma. *World J Gastroenterol* 2002; **8**: 1040-1044
- 29 **Lloyd RV**, Erickson LA, Jin L, Kulig E, Qian X, Cheville JC, Scheithauer BW. p27kip1: a multifunctional cyclin-dependent kinase inhibitor with prognostic significance in human cancers. *Am J Pathol* 1999; **154**: 313-323
- 30 **McIntyre M**, Desdouets C, Senamaud-Beaufort C, Laurent-Winter C, Lamas E, Brechot C. Differential expression of the cyclin-dependent kinase inhibitor P27 in primary hepatocytes in early-mid G1 and G1/S transitions. *Oncogene* 1999; **18**: 4577-4585
- 31 **Armengol C**, Boix L, Bachs O, Sole M, Fuster J, Sala M, Llovet JM, Rodes J, Bruix J. p27(Kip1) is an independent predictor of recurrence after surgical resection in patients with small hepatocellular carcinoma. *J Hepatol* 2003; **38**: 591-597
- 32 **Zhang H**, Sun XF. Loss of p27 expression predicts poor prognosis in patients with Dukes' B stage or proximal colorectal cancer. *Int J Oncol* 2001; **19**: 49-52
- 33 **Hayashi H**, Ogawa N, Ishiwa N, Yazawa T, Inayama Y, Ito T, Kitamura H. High cyclin E and low p27/Kip1 expressions are potentially poor prognostic factors in lung adenocarcinoma patients. *Lung Cancer* 2001; **34**: 59-65
- 34 **Haitel A**, Wiener HG, Neudert B, Marberger M, Susani M. Expression of the cell cycle proteins p21, p27, and pRb in clear cell renal cell carcinoma and their prognostic significance. *Urology* 2001; **58**: 477-481
- 35 **Milde-Langosch K**, Hagen M, Bamberger AM, Loning T. Expression and prognostic value of the cell-cycle regulatory proteins, Rb, p16MTS1, p21WAF1, p27KIP1, cyclin E, and cyclin D2, in ovarian Cancer. *Int J Gynecol Pathol* 2003; **22**: 168-174
- 36 **Yang HY**, Zhou BP, Hung MC, Lee MH. Oncogenic signals of HER-2/neu in regulating the stability of the cyclin-dependent kinase inhibitor p27. *J Biol Chem* 2000; **275**: 24735-24739
- 37 **Baldassarre G**, Belletti B, Bruni P, Boccia A, Trapasso F, Pentimalli F, Barone MV, Chiappetta G, Vento MT, Spiezia S, Fusco A, Viglietto G. Overexpressed cyclin D3 contributes to retaining the growth inhibitor p27 in the cytoplasm of thyroid tumor cells. *J Clin Invest* 1999; **104**: 865-874
- 38 **Liang J**, Zubovitz J, Petrocelli T, Kotchetkov R, Connor MK, Han K, Lee JH, Ciarallo S, Catzavelos C, Beniston R, Franssen E, Slingerland JM. PKB/Akt phosphorylates p27, impairs nuclear import of p27 and opposes p27-mediated G1 arrest. *Nat Med* 2002; **8**: 1153-1160
- 39 **Shin I**, Yakes FM, Rojo F, Shin NY, Bakin AV, Baselga J, Arteaga CL. PKB/Akt mediates cell-cycle progression by phosphorylation of p27(Kip1) at threonine 157 and modulation of its cellular localization. *Nat Med* 2002; **8**: 1145-1152
- 40 **Viglietto G**, Motti ML, Bruni P, Melillo RM, D' Alessio A, Califano D, Vinci F, Chiappetta G, Tschlis P, Bellacosa A, Fusco A, Santoro M. Cytoplasmic relocation and inhibition of the cyclin-dependent kinase inhibitor p27(Kip1) by PKB/Akt-mediated phosphorylation in breast cancer. *Nat Med* 2002; **8**: 1136-1144

Edited by Chao JCJ Proofread by Xu FM

Loss of heterozygosity on chromosome 1 in sporadic colorectal carcinoma

Chong-Zhi Zhou, Guo-Qiang Qiu, Fang Zhang, Lin He, Zhi-Hai Peng

Chong-Zhi Zhou, Guo-Qiang Qiu, Fang Zhang, Zhi-Hai Peng,
Department of General Surgery, Shanghai Jiaotong University, First
People's Hospital, Shanghai 200080, China

Lin He, Shanghai Institute for Biological Science, Chinese Academy
of Sciences, Shanghai 200031, China

Supported by the National Natural Science Foundation of China,
No. 30080016

Correspondence to: Dr. Zhi-Hai Peng, Department of General
Surgery, Shanghai Jiaotong University, First People's Hospital, 85
Wujin Road, Shanghai 200080, China. pengpzhb@online.sh.cn

Telephone: +86-21-63240090 Ext 3102

Received: 2003-06-10 **Accepted:** 2003-08-16

Abstract

AIM: Loss of heterozygosity (LOH) on tumor suppressor genes is believed to play a key role in carcinogenesis of colorectal cancer. When it occurs at a tumor suppressor gene locus with abnormal allele, neoplastic transformation happens. In this study, we analyzed the LOH at 21 loci on chromosome 1 in sporadic colorectal cancer to identify additional loci involved in colorectal tumorigenesis.

METHODS: Twenty-one polymorphic micro-satellite DNA markers were analyzed with PCR both in 83 cases of colorectal cancer and in normal tissues. PCR products were electrophoresed on an ABI 377 DNA sequencer. Genescan 3.1 and Genotype 2.1 software were used for LOH scanning and analysis. χ^2 test was used to compare LOH frequency with clinicopathological data. $P < 0.05$ was considered as statistically significant.

RESULTS: The average LOH frequency of chromosome 1, short arm and long arm was 19.83%, 18.00% and 21.66%, respectively. The 2 highest LOH loci with a frequency of 36.54% and 32.50% were identified on D1S468 (1p36.33-p36.31) and D1S413 (1q31.3), respectively. On D1S2726 locus, LOH frequency of rectal cancer was 28.57% (6/21), which was higher than that of colon cancer (0.00%, 0/33) ($P = 0.002$), suggesting that the mechanism of carcinogenesis was different in both groups.

CONCLUSION: Putative tumor suppressor genes on chromosome 1 may relate to sporadic colorectal carcinomas. Tumor-suppressor-genes might locate on 1p36.33-36.31 and/or 1q31.3.

Zhou CZ, Qiu GQ, Zhang F, He L, Peng ZH. Loss of heterozygosity on chromosome 1 in sporadic colorectal carcinoma. *World J Gastroenterol* 2004; 10(10): 1431-1435

<http://www.wjgnet.com/1007-9327/10/1431.asp>

INTRODUCTION

Colorectal cancer is one of the three leading causes of cancer mortality worldwide. The progression of the cancer is due to an accumulation of genetic alteration in controlling growth

and proliferation at numerous loci. As a model for both multistep and multipathway carcinogenesis, colorectal neoplastic progression provides paradigms of both oncogenes and tumor suppressor genes^[1,2]. The loss of heterozygosity (LOH) on tumor suppressor genes is believed as one of the key steps to carcinogenesis of colorectal cancer^[3]. The loss of one allele at a specific locus is caused by a deletion mutation or loss of a chromosome from a chromosome pair^[4]. When this occurs at a tumor suppressor gene with an abnormal allele, neoplastic transformation occurs. In colorectal cancers, frequent allelic loss has been identified in chromosome 5q (30%), 8p (40%), 17p (75-80%), 18q (80%), and 22q (20-30%)^[5,6]. Tumor suppressor genes APC, p53, and DCC were found to be located on chromosome 5q, 17p, and 18q, respectively. LOH analysis became an effective way to find informative loci candidate tumor suppressor genes afterwards^[7,8]. In this study we analyzed the LOH at 21 loci on chromosome 1 in sporadic colorectal cancers to identify additional loci involved in colorectal tumorigenesis.

MATERIALS AND METHODS

Materials

From 1998 to 1999, 83 consecutively collected tumors were treated surgically at Surgical Department of First People's Hospital in Shanghai Jiaotong University. There were 40 males and 43 females with a median age of 66 years (range 31-84). The diagnosis was verified pathologically. The number of Dukes stages A, B, C, D was 8, 21, 40 and 14, respectively. The number of proximal colon cancer, distal colon cancer, and rectal cancer was 33, 21 and 29, respectively. Well-differentiated adenocarcinomas, moderately differentiated adenocarcinomas and poorly differentiated adenocarcinomas were 23, 39 and 6, respectively, and mucinous adenocarcinomas were 15. HNPCC patients were ruled out by Amsterdam criteria^[9,10]. Informed consent to use surgical specimens in this study was obtained from patients.

Methods

DNA extraction Thirty min after surgery, fresh cancerous and adjacent normal tissues were cut into approximately 2 mm³ and immediately frozen in liquid nitrogen. DNA was extracted using standard method with proteinase K digestion and phenol/chloroform purification.

Microsatellite markers and PCR Twenty-one fluorescence-labeled primers for polymorphic microsatellite markers (Perkin-Elmer, USA), at a density of approximately one marker every 10 cm (Figure 1), were used to amplify DNAs from normal and tumor tissues for LOH analysis. PCR for DNAs from normal and tumor tissue was done to analyze the polymorphic microsatellite markers. PCR conditions were as follows: 5 μ L total volume with approximately 1.4 ng of DNA as a template with 10 \times standard buffer, 0.3 μ L Mg²⁺, 0.8 μ L deoxynucleotide triphosphates, 0.3 unit of Hot-start taq polymerase and 0.06 μ L of each oligonucleotide primer, with the forward primer fluorescence labeled with HEX, FAM or NED. Cycling conditions consisted of 3 stages: an initial

denaturation at 96 °C for 12 min in stage I; 14 cycles each at 94 °C for 20 s, at 63-56 °C for 1 min (0.5 °C decreased per cycle), at 72 °C for 1 min in stage II; 35 cycles each at 94 °C for 20 s, at 56 °C for 1 min, at 72 °C for 1 min in stage III^[11-13].

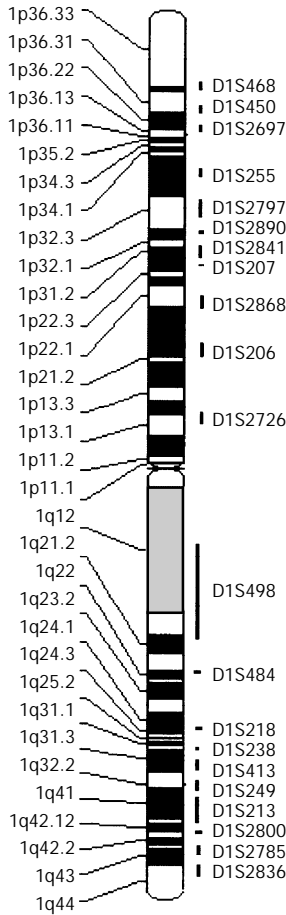


Figure 1 Twenty-one microsatellite markers on chromosome 1.

LOH analysis PCR product (0.5 μL) was mixed with 0.1 μL of Genescan 500 size standard (PE Applied Biosystems, USA) and 0.9 μL of formamide loading buffer. After denaturation

at 96 °C for 5 min, products were electrophoresed on 50 g/L polyacrylamide gels on an ABI 377 DNA sequencer (PE Applied Biosystems, USA) for 3 h. Genotype 2.1 software displayed individual gel lanes as electropherograms with a given size, height, and area for each detected fluorescent peak. Stringent criteria were used to score the samples. Alleles were defined as the two highest peaks within the expected size range. A ratio of T1:T2/N1:N2 less than 0.67 or greater than 1.50 was scored as a loss of heterozygosity (Figure 2). Most amplifications of normal DNA producing two PCR products indicated preserve of heterozygosity. A single fragment amplified from normal DNA (homozygote) and fragments not clearly amplified from PCR reactions were scored as not informative. The LOH frequency of a locus was equal to the ratio of the number between allelic loss and informative cases. The average LOH frequency of chromosome 1 was the mean of the LOH frequency in all loci^[14-17].

Statistics χ^2 test was used to compare LOH with clinicopathological data. $P < 0.05$ was considered statistically significant.

RESULTS

LOH of 21 microsatellite markers on chromosome 1

The average LOH frequency at chromosome 1, short arm and long arm was 19.83%, 18.00% and 21.66%, respectively. The two highest LOH loci with a frequency of 36.54% and 32.50% were identified on D1S468 (1p36.33-36.31) and D1S413 (1q31.3). Other loci also exhibited higher LOH frequencies, including D1S255 (1p34.1-32.3), D1S2868(1p22.1), D1S218 (1q24.1-24.3), D1S249 (1q32.2), D1S2800 (1q42.12-42.2) and D1S2836 (1q43-44) (Table 1).

Relationship of clinicopathological features and LOH on chromosome 1

On D1S2726 locus, LOH frequency of rectal cancer was 28.57% (6/21), which was higher than that of colon cancer (0%, 0/33) ($P=0.002$). No association between LOH of each marker on chromosome 1 and other clinicopathological data (patient sex, age, tumor size, growth pattern or Dukes stage) was observed. It indicated that LOH on chromosome 1 was a common phenomenon in all kinds of sporadic colorectal cancers (Tables 2A, 2B).

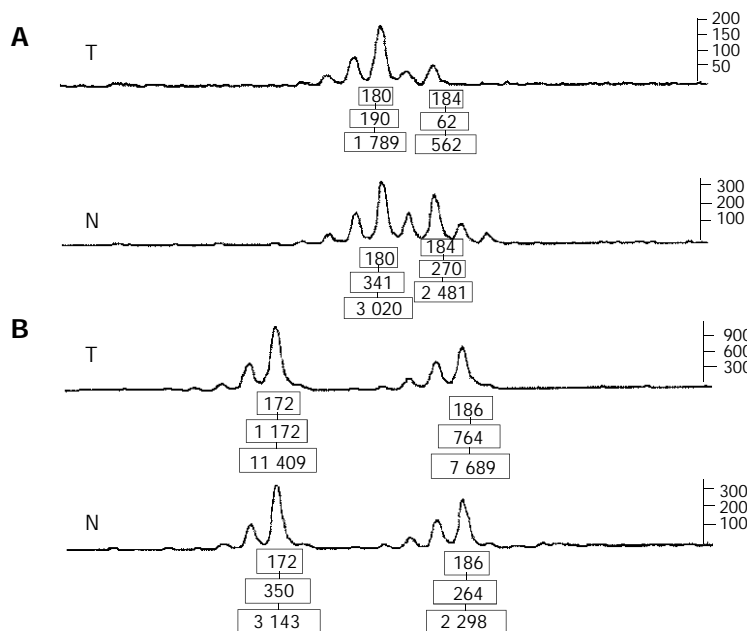


Figure 2 Typical peak and normal peak of LOH3. A: Typical peak of LOH: Allele ratio=(T1/T2)/(N1/N2)=(190/62)/(341/270)=2.43>1.5, B: The normal peak (no LOH): Allele ratio=(T1/T2)/(N1/N2)=(1172/764)/(350/264)=1.15, T: Tumor, N: Normal.

Table 1 LOH frequency of 21 microsatellite markers on chromosome 1

Locus	Location	LOH case	Normal case	LOH rate (%)	Informative rate (%)
D1S468	1p36.33-36.31	19	33	36.54	62.65
D1S450	1p36.31	7	41	14.58	57.83
D1S2697	1p36.22-36.13	5	25	16.67	36.14
D1S255	1p34.1-32.3	11	43	20.37	65.06
D1S2797	1p32.3	8	46	14.81	65.06
D1S2890	1p32.3-32.1	6	48	11.11	65.06
D1S2841	1p31.2	11	46	19.30	68.67
D1S207	1p31.2-22.3	5	63	7.35	81.93
D1S2868	1p22.1	10	39	20.41	59.04
D1S206	1p22.1-21.2	7	33	17.50	48.19
D1S2726	1p13.3-13.1	6	48	11.11	65.06
D1S498	1q12-21.2	11	48	18.64	71.08
D1S484	1q22	10	55	15.38	78.31
D1S218	1q24.1-24.3	16	42	27.59	69.88
D1S238	1q31.1	3	38	7.32	49.40
D1S413	1q31.3	13	27	32.50	48.19
D1S249	1q32.2	10	36	21.74	55.42
D1S213	1q41-42.12	8	41	16.33	59.04
D1S2800	1q42.12-42.2	12	45	21.05	68.67
D1S2785	1q43	10	48	17.24	69.88
D1S2836	1q43-44	12	36	25.00	57.83

Table 2a Relationship between clinicopathological features and LOH of 11 loci on short arm of chromosome 1

		D1S468		D1S450		D1S2697		D1S255		D1S2797		D1S2890		D1S2841		D1S207		D1S2868		D1S206		D1S2726	
		N	L	N	L	N	L	N	L	N	L	N	L	N	L	N	L	N	L	N	L	N	L
Gender	Male	18	8	20	4	13	2	19	7	20	5	21	4	20	6	31	2	15	3	17	3	19	5
	Female	15	11	21	3	12	3	24	4	26	3	27	2	26	5	32	3	24	7	16	4	29	1
Age (yr)	>60	26	13	30	7	19	4	32	8	36	7	37	6	34	11	46	5	32	7	27	5	33	6
	≤60	7	6	11	0	6	1	11	3	10	1	11	0	12	0	17	0	7	3	6	2	15	0
Location	Proximal colon	12	9	12	2	13	2	14	5	19	2	22	3	21	4	24	2	13	6	11	1	20	0
	Distal Colon	7	5	10	1	4	2	12	2	8	3	11	1	9	4	17	1	13	2	8	4	13	0
	Rectum	14	5	19	4	8	1	17	4	19	3	15	2	16	3	22	2	13	2	14	2	15	6 ¹
Gross pattern	Massive	15	9	16	2	10	1	15	7	21	3	17	5	20	4	23	2	17	3	17	1	19	2
	Ulcerative	13	5	16	3	9	3	22	4	19	3	20	1	18	4	27	3	15	3	10	3	20	3
	Encroaching	5	5	9	2	6	1	6	0	6	2	11	0	8	3	13	0	7	4	6	3	9	1
Size	≥5 (cm)	18	8	21	5	13	1	19	8	24	4	27	2	23	4	31	1	19	5	13	5	24	3
	<5 (cm)	15	11	20	2	12	4	24	3	22	4	21	4	23	7	32	4	20	5	20	2	24	3
LN metastasis	LN (+)	24	10	26	5	17	4	29	4	28	6	31	5	26	9	38	5	22	8	20	5	28	4
	LN (-)	9	9	15	2	8	1	14	7	18	2	17	1	20	2	25	0	17	2	13	2	20	2
Differentiation	Well	8	7	14	1	5	1	10	3	20	1	15	0	12	4	16	2	13	2	14	3	18	0
	Moderately	16	10	19	5	12	4	21	5	14	7	19	5	22	5	31	3	16	5	13	2	18	6
	Poorly	3	0	4	1	2	0	5	0	4	0	5	0	2	0	6	0	3	1	0	2	5	0
	Mucinous	6	2	4	0	6	0	7	3	8	0	9	1	10	2	10	0	7	2	6	0	7	0
Dukes stage	A	3	3	4	0	1	0	4	1	3	2	4	0	7	0	7	0	5	0	2	1	5	0
	B	6	6	11	2	7	1	10	6	15	0	13	1	13	2	18	0	12	2	11	1	15	2
	C	17	8	20	3	11	2	21	3	20	5	23	5	18	7	26	5	16	7	18	3	20	4
	D	7	2	6	2	6	2	8	1	8	1	8	0	8	2	12	0	6	1	2	2	8	0

¹P=0.002, LOH frequency of rectal cancer vs colon cancer.

Table 2b Relationship between clinicopathological features and LOH of 10 loci on long arm of chromosome 1

		D1S498		D1S484		D1S218		D1S238		D1S413		D1S249		D1S213		D1S2800		D1S2785		D1S2836	
		N	L	N	L	N	L	N	L	N	L	N	L	N	L	N	L	N	L	N	L
Gender	Male	25	6	25	7	22	6	20	1	14	7	16	6	17	3	19	9	25	3	19	5
	Female	23	5	30	3	20	10	18	2	13	6	20	4	24	5	26	3	23	7	17	7
Age (yr)	>60	37	10	43	6	30	14	28	3	18	10	28	7	33	6	33	10	39	10	26	9
	≤60	11	1	12	4	12	2	10	0	9	3	8	3	8	2	12	2	9	0	10	3
Location	Proximal colon	14	6	20	4	16	5	15	1	10	6	17	3	15	2	15	6	18	6	16	5
	Distal colon	14	3	14	4	14	4	10	1	7	3	4	2	12	3	14	1	14	2	6	5
	Rectum	20	2	21	2	12	7	13	1	10	4	15	5	14	3	16	5	16	2	14	2
Gross pattern	Massive	22	4	23	3	18	11	12	2	14	5	13	4	17	4	17	3	20	6	16	5
	Ulcerative	17	5	24	3	15	4	19	1	9	5	13	5	19	4	18	6	20	3	12	5
	Encroaching	9	2	8	4	9	1	7	0	4	3	10	1	5	0	10	3	8	1	8	2
Size	≥5 (cm)	21	7	27	7	22	6	18	3	11	6	16	5	21	4	21	8	23	7	17	8
	<5 (cm)	27	4	28	3	20	10	20	0	16	7	20	5	20	4	24	4	25	3	19	4
LN Metastasis	LN(+)	31	6	36	4	26	11	23	2	16	6	22	6	28	5	30	7	31	7	25	5
	LN(-)	17	5	19	6	16	5	15	1	11	7	14	4	13	3	15	5	17	3	11	7
Differentiation	Well	12	4	15	3	11	3	8	1	7	3	10	2	13	2	13	5	16	2	10	5
	Moderately	26	4	27	4	22	7	19	0	12	6	17	4	18	5	21	5	18	7	18	6
	Poorly	2	0	6	0	3	2	3	0	2	1	2	3	4	0	4	1	4	0	2	1
	Mucinous	8	3	7	3	6	4	8	2	6	3	7	1	6	1	7	1	10	1	6	0
Dukes stage	A	4	0	5	2	3	2	5	1	3	2	2	1	3	1	4	0	4	1	2	3
	B	13	5	14	4	13	3	10	0	8	5	12	3	10	2	11	5	13	2	9	4
	C	22	5	26	4	18	9	18	1	12	4	15	5	21	5	21	6	23	6	17	2
	D	9	1	10	0	8	2	5	1	4	2	7	1	7	0	9	1	8	1	8	3

DISCUSSION

During tumorigenesis, loss of wild-type alleles (inherited from the non-mutation-carrying parents) is frequently observed. Loss of heterozygosity (LOH) on tumor suppressor genes played a key role in colorectal cancer transformation, and LOH analysis of sporadic colorectal cancers could help discover unknown tumor suppressor genes^[7,8]. In this study, LOH scanning was analyzed by Genotyper software in 83 sporadic colorectal cancer samples with 21 highly polymorphic markers, the ratio of the fluorescence intensity of alleles was studied to identify additional loci involved in colorectal tumorigenesis.

In this study, the average LOH frequency at chromosome 1 (19.83%), short arm (18.00%) and long arm (21.66%) was consistent with the previous study^[5]. The two highest LOH loci with a frequency of 36.54% and 32.50% was identified on D1S468 (1p36.33-36.31) and D1S413 (1q31.3). There were few reports about the relationship between the long arm of chromosome 1 and colorectal cancer. But some previous studies showed that the 1q31-32 region frequently presented allelic loss in breast cancers and medulloblastomas. Pietsch *et al.*^[18] found that 36% of medulloblastomas showed loss of heterozygosity (LOH) on chromosome 1q. The study of Benitez J showed more than 60% of breast tumors exhibited allelic loss in the 1q31-32 region^[19]. These results suggested that putative tumor suppressor genes might locate on the 1q31-32 region. Our study also found that D1S413(1q31.3) exhibited a higher LOH frequency and that the LOH frequency of long arm of chromosome 1 was higher than that of short arm^[5]. If D1S413 could be excluded, the LOH frequency of long arm was nearly equal to that of short arm. Thus, we hypothesized that the higher LOH frequency of D1S413 might be the reason why the LOH frequency of long arm of chromosome 1 was higher than that of short arm, suggesting the presence of a tumor suppressor gene in this region. This gene might be involved in the neoplastic process of colorectal cancer, breast cancer and medulloblastoma.

Previous studies showed that the 1p36 region frequently presented allelic loss in various cancers, such as colon cancer^[20], neuroblastoma^[21], hepatocellular carcinomas^[22], lung cancer^[23], and breast cancer^[24]. But only NB gene was confirmed to be the tumor suppressor gene of neuroblastomas. In 1993, Tanaka *et al.* believed that a normal chromosome 1p36 might contain a tumor suppressor gene of colon carcinogenesis^[25]. By database referring, we found TP73 gene (1p36) might be the known candidate tumor-suppressor genes related to colon cancer in this region. TP73, a novel family member of p53, was predicted to encode a protein with significant amino acid sequence similarity to p53^[29]. TP73 could inhibit cell growth in a p53-like manner by inducing apoptosis^[27]. Kaghad *et al.*^[26] regarded TP73 as a tumor suppressor gene. But Sunahara found that allelic loss of p73 occurred only in 17% of colorectal carcinomas, and suggested that p73 might not play a role as a tumor suppressor in colorectal carcinoma at least not in a classic Knudson manner^[28]. In our study, the highest LOH frequency was exhibited in 1p36.33-36.31, and colorectal cancer related tumor suppressor gene (s) might locate in the region. TP73 gene is a member of p53 family, its effect on colorectal carcinogenesis is not certain and requires further study. Due to many genes located in the region of 1p36.33-36.31, further LOH scanning with high-density microsatellite markers in the region is necessary in order to find new candidate genes.

No association between LOH markers on chromosome 1 and the clinicopathological data was found, indicating that LOH was a common phenomenon in all sporadic colorectal cancers. However, we found that on D1S2726 locus, LOH frequency of rectal cancer was high, no LOH was found in colon cancer. In 2001, Kapiteijn *et al.*^[29] proposed that rectal cancer had more significant expression of p53 and more nuclear beta-catenin than colon cancer, and considered that the mechanism of carcinogenesis in distal colon was different from that in proximal colon. Our results could show that the mechanism of carcinogenesis in distal colon and rectum was not completely the same as in proximal colon.

In conclusion, colorectal cancer associated candidate genes are likely to locate on D1S468 and D1S413. Further LOH scanning with high-density microsatellite markers in the region may provide much more genetic information and discover novel tumor suppressor genes.

REFERENCES

- 1 **Fearon ER**, Vogelstein B. A genetic model for colorectal tumorigenesis. *Cell* 1990; **61**: 759-767
- 2 **Hardy RG**, Meltzer SJ, Jankowski JA. ABC of colorectal cancer: Molecular basis for risk factors. *BMJ* 2000; **321**: 886-889
- 3 **Kataoka M**, Okabayashi T, Johira H, Nakatani S, Nakashima A, Takeda A, Nishizaki M, Orita K, Tanaka N. Aberration of p53 and DCC in gastric and colorectal cancer. *Oncol Rep* 2000; **7**: 99-103
- 4 **Lengauer C**, Kinzler KW, Vogelstein B. Genetic instabilities in human cancers. *Nature* 1998; **396**: 643-649
- 5 **Vogelstein B**, Fearon ER, Kern SE, Hamilton SR, Preisinger AC, Nakamura Y, White R. Allelotype of colorectal carcinomas. *Science* 1989; **244**: 207-211
- 6 **Weber TK**, Conroy J, Keitz B, Rodriguez-Bigas M, Petrelli NJ, Stoler DL, Anderson GR, Shows TB, Nowak NJ. Genome-wide allelotyping indicates increased loss of heterozygosity on 9p and 14q in early age of onset colorectal cancer. *Cytogenet Cell Genet* 1999; **86**: 142-147
- 7 **Baker SJ**, Fearon ER, Nigro JM, Hamilton SR, Preisinger AC, Jessup JM, vanTuinen P, Ledbetter DH, Barker DF, Nakamura Y. Chromosome 17 deletions and p53 gene mutations in colorectal carcinomas. *Science* 1989; **244**: 217-221
- 8 **Kinzler KW**, Nilbert MC, Vogelstein B, Bryan TM, Levy DB, Smith KJ, Preisinger AC, Hamilton SR, Hedge P, Markham A. Identification of a gene located at chromosome 5q21 that is mutated in colorectal cancers. *Science* 1991; **251**: 1366-1370
- 9 **Vasen HF**, Mecklin JP, Khan PM, Lynch HT. The International Collaborative Group on Hereditary Non-Polyposis Colorectal Cancer (ICG-HNPCC). *Dis Colon Rectum* 1991; **34**: 424-425
- 10 **Vasen HF**, Watson P, Mecklin JP, Lynch HT. New clinical criteria for hereditary nonpolyposis colorectal cancer (HNPCC, Lynch syndrome) proposed by the International Collaborative group on HNPCC. *Gastroenterology* 1999; **116**: 1453-1456
- 11 **Zhou CZ**, Peng ZH, Zhang F, Qiu GQ, He L. Loss of heterozygosity on long arm of chromosome 22 in sporadic colorectal carcinoma. *World J Gastroenterol* 2002; **8**: 668-673
- 12 **Peng Z**, Zhou C, Zhang F, Ling Y, Tang H, Bai S, Liu W, Qiu G, He L. Loss of heterozygosity of chromosome 20 in sporadic colorectal cancer. *Chin Med J* 2002; **115**: 1529-1532
- 13 **Zhang F**, Zhou C, Ling Y, Qiu G, Bai S, Liu W, He L, Peng Z. Allelic analysis on chromosome 5 in sporadic colorectal cancer patients. *Zhonghua Zhongliu Zazhi* 2002; **24**: 458-460
- 14 **Xu SF**, Peng ZH, Li DP, Qiu GQ, Zhang F. Refinement of heterozygosity loss on chromosome 5p15 in sporadic colorectal cancer. *World J Gastroenterol* 2003; **9**: 1713-1718
- 15 **Peng Z**, Zhang F, Zhou C, Qiu G, Bai S, Liu W, He L. Loss of heterozygosity analysis to define putative region involved in tumor differentiation and metastases in sporadic colorectal cancer patients. *Zhonghua Waiké Zazhi* 2002; **40**: 776-779
- 16 **Peng Z**, Ling Y, Bai S. Loss of heterozygosity on chromosome 3 in sporadic colorectal carcinoma. *Zhonghua Yixue Zazhi* 2001; **81**: 336-339
- 17 **Zhang F**, Zhou C, Ling Y, Bai S, Liu W, Qiu G, He L, Peng Z. High frequency of LOH on chromosome 18 in Chinese sporadic colorectal cancer patients. *Zhonghua Shiyán Waiké Zazhi* 2002; **19**: 320-321
- 18 **Pietsch T**, Koch A, Wiestler OD. Molecular genetic studies in medulloblastomas: evidence for tumor suppressor genes at the chromosomal regions 1q31-32 and 17p13. *Klin Padiatr* 1997; **209**: 150-155
- 19 **Benitez J**, Osorio A, Barroso A, Arranz E, Diaz-Guillen MA, Robledo M, Rodriguez de Cordoba S, Heine-Suner D. A region of allelic imbalance in 1q31-32 in primary breast cancer coincides with a recombination hot spot. *Cancer Res* 1997; **57**: 4217-4220
- 20 **Praml C**, Finke LH, Herfarth C, Schlag P, Schwab M, Amler L. Deletion mapping defines different regions in 1p34.2-pter that may harbor genetic information related to human colorectal cancer. *Oncogene* 1995; **11**: 1357-1362
- 21 **White PS**, Maris JM, Beltinger C, Sulman E, Marshall HN, Fujimori M, Kaufman BA, Biegel JA, Allen C, Hilliard C. A region of consistent deletion in neuroblastoma maps within human chromosome 1p36.2-36.3. *Proc Natl Acad Sci USA* 1995; **92**: 5520-5524
- 22 **Yeh SH**, Chen PJ, Chen HL, Lai MY, Wang CC, Chen DS. Frequent genetic alterations at the distal region of chromosome 1p in human hepatocellular carcinomas. *Cancer Res* 1994; **54**: 4188-4192
- 23 **Nomoto S**, Haruki N, Tatematsu Y, Konishi H, Mitsudomi T, Takahashi T, Takahashi T. Frequent allelic imbalance suggests involvement of a tumor suppressor gene at 1p36 in the pathogenesis of human lung cancers. *Genes Chromosomes Cancer* 2000; **28**: 342-346
- 24 **Bieche I**, Khodja A, Lidereau R. Deletion mapping of chromosomal region 1p32-pter in primary breast cancer. *Genes Chromosomes Cancer* 1999; **24**: 255-263
- 25 **Tanaka K**, Yanoshita R, Konishi M, Oshimura M, Maeda Y, Mori T, Miyaki M. Suppression of tumorigenicity in human colon carcinoma cells by introduction of normal chromosome 1p36 region. *Oncogene* 1993; **8**: 2253-2258
- 26 **Kaghad M**, Bonnet H, Yang A, Creancier L, Biscan JC, Valent A, Minty A, Chalon P, Lelias JM, Dumont X, Ferrara P, McKeon F, Caput D. Monoallelically expressed gene related to p53 at 1p36, a region frequently deleted in neuroblastoma and other human cancers. *Cell* 1997; **90**: 809-819
- 27 **Jost CA**, Marin MC, Kaelin WG Jr. p73 is a human p53-related protein that can induce apoptosis. *Nature* 1997; **389**: 191-194
- 28 **Sunahara M**, Ichimiya S, Nimura Y, Takada N, Sakiyama S, Sato Y, Todo S, Adachi W, Amano J, Nakagawara A. Mutational analysis of the p73 gene localized at chromosome 1p36.3 in colorectal carcinomas. *Int J Oncol* 1998; **13**: 319-323
- 29 **Kapiteijn E**, Liefers GJ, Los LC, Kranenburg EK, Hermans J, Tollenaar RA, Moriya Y, van de Velde CJ, van Krieken JH. Mechanisms of oncogenesis in colon versus rectal cancer. *J Pathol* 2001; **195**: 171-178

Edited by Ren SY and Wang XL Proofread by Xu FM

Effect of Hejie decoction on T cell immune state of chronic hepatitis B patients

Shi-Jun Zhang, Ze-Xiong Chen, Shao-Xian Lao, Bi-Jun Huang

Shi-Jun Zhang, Ze-Xiong Chen, Department of Traditional Chinese Medicine, First Affiliated Hospital, Sun Yat-Sen University, Guangzhou 510080, Guangdong Province, China

Shao-Xian Lao, Institute of Digestive Diseases, Traditional Chinese Medicine University of Guangzhou, Guangzhou 510405, Guangdong Province, China

Bi-Jun Huang, Institute of Cancer, Sun Yat-Sen University, Guangzhou 510080, Guangdong Province, China

Supported by Guangdong Administrative Bureau of TCM and Chinese Drugs, No.98374 and No.100108

Correspondence to: Shi-Jun Zhang, Department of Traditional Chinese Medicine, First Affiliated Hospital, Sun Yat-Sen University, Guangzhou 510080, Guangdong Province, China. zhsjun1967@hotmail.com

Telephone: +86-20-87334505 **Fax:** +86-20-87334505

Received: 2003-08-06 **Accepted:** 2003-09-01

Abstract

AIM: To explore the effect of Hejie decoction (HJD) (mediation decoction) on T cellular immune state of chronic hepatitis B patients.

METHODS: Sixty-five patients with chronic hepatitis B were randomly divided into 2 groups. Forty patients in the treatment group were treated by HJD, and 25 patients in the control group were treated by routine Western medicine. The TCRV β_7 gene expression, T lymphocyte subsets (CD $_3^+$, CD $_4^+$, CD $_8^+$, CD $_4^+$ /CD $_8^+$) levels were observed before and after treatment.

RESULTS: The level of CD $_4^+$ cells was lower whereas the level of CD $_8^+$ cells was higher in patients than in the normal group. There was no significant difference between the levels of CD $_3^+$ cells in patients and normal persons. After 6 months of treatment, ALT, AST, TB levels of the 2 groups were obviously decreased, and the level of CD $_4^+$ cells was increased whereas the level of CD $_8^+$ cells was decreased in the treatment group. However, the level of CD $_4^+$ cells and CD $_8^+$ cells had no significant difference in the control group. TCRV β_7 expressions were detected in 6 patients of the treatment group, whose HBV-DNA and HBeAg turned negative and ALT became normal. HBeAg in another 3 patients turned negative while HBV-DNA did not, and TCRV β_7 expressions were not detectable. TCRV β_7 expression could not be detected in the control group, HBV-DNA of the control group did not turn negative. HBeAg in 1 patient turned negative while HBV-DNA did not, and TCRV β_7 expressions were not detectable. The total effective rate was not significantly different between the 2 groups and the markedly effective rate was significantly different ($P < 0.01$).

CONCLUSION: HJD is effective for treating chronic hepatitis B, and its effect seems to relate with the improvement of the TCRV β_7 expression of chronic hepatitis B patients, thus activating T cells and eliminating HBV. T cellular immune function plays an important role in HBV infection and virus elimination.

Zhang SJ, Chen ZX, Lao SX, Huang BJ. Effect of Hejie decoction on T cell immune state of chronic hepatitis B patients. *World J Gastroenterol* 2004; 10(10): 1436-1439
<http://www.wjgnet.com/1007-9327/10/1436.asp>

INTRODUCTION

T cells take charge of recognizing the cells infected with bacilli and virus, as well as cancer cells^[1]. Recent studies have demonstrated that the stimulating signal would be transferred to the inside of cells by CD $_3$ molecules when antigens are recognized by T cell receptor (TCR), sequentially activating T lymphocyte cells. TCR plays a crucial role in exerting T cellular immune function. Therefore it is very important to investigate the relation of T cellular function and clinical effect by studying the function of T cell receptor^[2-4]. We treated chronic hepatitis B patients with HJD from June 1999 to March 2003, and observed the relation between clinical effects and T lymphocyte subsets, TCRV β_7 gene expression. The results are reported as follows.

MATERIALS AND METHODS

Materials

All the 65 patients with chronic hepatitis B enrolled were outpatients from the special clinics of liver diseases, and were divided into 2 groups according to random number table. The 40 patients in the treatment group were 22 males and 18 females, aged 18-60 years, averaged 38.6 \pm 9.8 years, with an average course of illness of 0.8-12.5, 3.5 \pm 1.2 years. The 25 patients in the control group were 14 males and 11 females, aged 18-60 years, averaged 39.0 \pm 8.9 years, with an average course of illness of 0.6-11.1, 3.2 \pm 1.1 years. The difference of clinical data between the 2 groups was insignificant, so the 2 groups were comparable. Ten age-matched healthy donors from the Blood Center of our hospital were assigned as normal group.

Diagnostic criteria

The patient had a history of hepatitis B or HBsAg carrier for at least 6 mo and still had the symptoms and signs of hepatitis and abnormal liver function at the time when they were included in the trial. Their HBsAg, HBeAg and HBVDNA were positive.

Criteria of enrollment

The patients were aged 18-60 years, their serum levels of alanine aminotransferase (ALT) were between 80 U/L and 240 U/L, their serum HBeAg and HBV-DNA (quantitative PCR) were positive. The diagnostic criteria of hepatitis B were in accordance with the standards for chronic viral hepatitis issued in the Fifth National Conference on Infectious Diseases and Parasitosis in China (Beijing, China, 1995)^[5].

Criteria of exclusion

The patients who were over 60, or less than 18 years old, and those who were pregnant or in breast-feeding period, those who were complicated with hepatitis C or other hepatic viral infection, suspicious of autoimmune hepatitis, and drug hepatitis or alcoholic hepatitis, as well as those who had severe

complications of cardiovascular, renal or hematopoietic systems and mental diseases were excluded from the trial.

Methods

The treatment group was treated with Hejie decoction, consisting of Radix Bupleuri 10 g, Radix Scutellariae 12 g, Rhizoma Pinelliae 9 g, Radix Codonopsis Pilosulae 30 g, Radix Glycyrrhizae Praeparata 6 g, Fructus Ziziphi Jujubae 9 g, Rhizoma Polygoni Cuspidati 30 g, Radix Morindae Officinalis 8 g, Herba Hedyotis Diffusae 30 g. One dose was taken per day for 6 mo. The control group was treated with compound vitamin B₂, 2 tablets, vitamin C 100 mg, vitamin E 50 mg, Wuzhi capsules, 2 tablets, 3 times a day for 6 mo. Patients who had normal serum ALT, HBeAg and HBV DNA (quantitative PCR) after treatment were defined as responders, while those with negative results were taken as non-responders.

Patients' symptoms and signs were recorded in detail using "Clinical Observation Table" once a month before and during the treatment. HBV-M and anti-HAV, anti-HCV, anti-HDV and anti-EBV marks: Enzyme linked immunosorbent assay (ELISA) kit was obtained from Shanghai Kehua Corporation. HBV-DNA: Quantitative polymerized chain reaction (PCR) kit was from Diagnostic Center of Sun Yat-Sen University.

The patients had liver function examination (American Experiment Instrument Corporation) every month during the treatment, including contents of serum proteins, total bilirubin (TB), and activities of ALT and AST (aspartate aminotransferase). The kit was a product of American Experiment Instrument Corporation.

T-lymphocyte subsets were detected using single clone antibody APAAP method, the kits were purchased from Wuhan Boster Biological Technology Co. Ltd.

Peripheral blood mononuclear cells (PBMC) were prepared from 8 mL of freshly, heparinized blood by centrifugation at 400 r/min through a Ficoll-hypaque density gradient, washed 3 times with 10 g/L BSA in PBS and resuspended in 5 g/L BSA in PBS, stored on ice or at -70 °C for extraction of RNA.

Total cellular RNA was extracted from fresh PBMC with acid guanidinium thiocyanate-phenol-chloroform extraction according to the manufacturer's instructions, RNAs were purchased from Promega Corporation.

The primers were synthesized on an applied biosystems DNA synthesizer (Shanghai Shengong Company, China), and these sequences^[6] were (5' -3'): CCTGAATGCCCAACAGCTCTC,

expanding length: 235. β -actin was prepared as an internal standard to quantify the products. Three micrograms of total RNA was used to synthesize first-strand cDNA. RT-PCR was carried out according to the manufacturer's instructions (Promega, USA). The amplified products were then electrophoresed on 20 g/L agarose gel. The electrophoresis images were scanned by Fluor-S MultiImager (Bio-Rad, USA) and analyzed according to the $V\beta/\beta$ -actin ratios by computing densitometer and Image Quant software.

Statistical analysis

All statistics were performed by using statistical procedure of social science (SPSS), including chi-square test and Wilcoxon rank sum test. The probability values less than 0.05 were considered significant.

RESULTS

Standard for efficacy evaluation

The clinical efficacy of treatment was evaluated according to the following standards formulated by authors: (1) Markedly effective: Chief symptoms including right upper abdomen pain, poor appetite and abdominal distention disappeared, HBeAg and HBV-DNA turned negative, serum levels of ALT, AST, TBIL restored to normal. (2) Effective: Chief symptoms were alleviated or improved, the level of HBV-DNA decreased, HBeAg did not turn negative, serum levels of ALT, AST, TBIL decreased by >1/2 of the original levels. (3) Ineffective: Neither the chief symptoms nor the serum levels of ALT, AST and TBIL or HBeAg, HBV-DNA showed any improvement.

Clinical efficacy of treatment

In the treated group, the treatment was markedly effective in 6 cases, effective in 33 and ineffective in 1, the total effective rate was 97.5%. In the control group, the treatment was markedly effective in 0 cases, effective in 22 and ineffective in 3, the total effective rate was 88.0%. The difference of total effective rate was insignificant between the 2 groups ($P>0.05$) and that of markedly effective rate was significant ($P<0.01$).

ALT, AST, TB and HBVDNA levels before and after treatment, as well as TCRV β gene expression

After 6 mo of treatment, the ALT, AST, TB levels of the 2 groups

Table 1 ALT, AST, TB and HBVDNA levels before and after treatment (mean \pm SD)

	<i>n</i>	ALT (U/L)	AST (U/L)	TB (μ mol/L)	HBVDNA (copy/mL)
Normal	10	27.80 \pm 8.65	19.07 \pm 8.50	12.55 \pm 5.52	0
Treatment					
Pre-T	40	213.66 \pm 10.30	134.66 \pm 9.82	41.03 \pm 4.36	(1.52 \pm 0.72) \times 10 ^{8.25}
Post-T	40	37.01 \pm 9.75 ^b	29.07 \pm 8.97 ^b	20.55 \pm 5.52 ^b	(4.25 \pm 1.90) \times 10 ^{6.02 a}
Control					
Pre-T	25	195.70 \pm 11.11	125.12 \pm 9.21	40.87 \pm 6.78	(1.32 \pm 0.89) \times 10 ^{8.12}
Post-T	25	36.01 \pm 9.75 ^b	69.88 \pm 8.97 ^b	30.55 \pm 5.52 ^b	(6.95 \pm 2.39) \times 10 ^{7.82}

n: number; normal: normal group; treatment: treatment group; control: control group; Pre-T: before treatment; Post-T: after treatment; ^a $P<0.05$, vs before treatment in the same group, ^b $P<0.01$, vs before treatment in the same group.

Table 2 T lymphocyte subsets before and after treatment (mean \pm SD)

	<i>n</i>	CD ₃ (%)	CD ₄ (%)	CD ₈ (%)	CD ₄ /CD ₈
Normal	10	67.80 \pm 8.65	39.07 \pm 8.50	30.55 \pm 5.52	1.62 \pm 0.46
Treatment					
Pre-T	40	65.97 \pm 8.45	34.76 \pm 4.82 ^b	34.08 \pm 4.36 ^b	1.04 \pm 0.32
Post-T	40	67.01 \pm 9.75	37.39 \pm 8.97 ^a	32.35 \pm 5.52 ^a	1.20 \pm 0.30 ^a
Control					
Pre-T	25	65.70 \pm 9.11	35.02 \pm 5.21 ^b	34.87 \pm 6.78 ^b	1.02 \pm 0.29
Post-T	25	66.01 \pm 9.75	35.88 \pm 8.97	34.15 \pm 5.52	1.09 \pm 0.39

n: number; normal: normal group; treatment: treatment group; control: control group; Pre-T: before treatment; Post-T: after treatment; ^a $P<0.05$, vs before treatment in the same group, ^b $P<0.01$, vs control.

were obviously decreased ($P < 0.01$), HBVDNA levels of the treatment group were obviously decreased ($P < 0.05$, Table 1). TCRV β_7 expressions were detected in 6 patients of the treated group, and their HBV-DNA and HBeAg turned negative, and HBeAg in another 3 patients turned negative, but HBV-DNA did not turn negative, and TCRV β_7 expressions were not detectable. The TCRV β_7 expression could not be detected in the control group, HBV-DNA of the control group did not turn negative. HBeAg in 1 patient turned negative in the control group, but HBV-DNA did not turn negative, and TCRV β_7 expressions were not detectable. In patients without HBeAg negative conversion, or patients with HBeAg negative conversion and positive HBV-DNA and normal liver function, TCRV β_7 expression could not be detected.

T lymphocyte subsets before and after treatment

The level of CD $_4^+$ cells was lower whereas the level of CD $_8^+$ cells was higher in the patients than in the normal group ($P < 0.01$), there was no significant difference between the levels of CD $_3^+$ cells of the patients and normal persons. After 6 mo of treatment, the level of CD $_4^+$ cells increased whereas the level of CD $_8^+$ cells decreased ($P < 0.05$) in the treated group. However, the level of CD $_4^+$ cells and CD $_8^+$ cells had no significant difference in the control group ($P > 0.05$, Table 2).

Table 3 T lymphocyte subsets of responders and non-responders in treatment group before and after treatment (mean \pm SD)

		<i>n</i>	CD $_3$ (%)	CD $_4$ (%)	CD $_8$ (%)
Responders	Pre-T	6	66.62 \pm 8.86	35.10 \pm 4.76 ^b	34.02 \pm 4.86 ^b
	Post-T	6	66.80 \pm 9.11	38.85 \pm 8.85 ^a	30.15 \pm 5.82 ^a
Non-responders	Pre-T	34	65.86 \pm 9.08	34.62 \pm 6.30 ^b	34.17 \pm 6.56 ^b
	Post-T	34	66.09 \pm 9.35	35.72 \pm 8.70	33.85 \pm 5.52
Normal		10	67.80 \pm 8.65	39.07 \pm 8.50	30.55 \pm 5.52

n: number; responders: patients who had normal ALT and HBeAg and HBV DNA after treatment; non-responders: patients who had abnormal ALT, HBeAg and HBV DNA after treatment; normal: normal group; Pre-T: before treatment; Post-T: after treatment; ^a $P < 0.05$, vs before treatment in the same group, ^b $P < 0.01$, vs normal group.

T lymphocyte subsets of responders and non-responders in treatment group before and after treatment

The level of CD $_3^+$, CD $_4^+$, CD $_8^+$ cells in the 2 groups had no significant difference before treatment ($P > 0.05$). The level of CD $_4^+$ cells increased whereas the level of CD $_8^+$ cells decreased in the responders' group ($P < 0.01$). The level of CD $_4^+$ and CD $_8^+$ cells in the non-responders' group had no significant difference after treatment ($P > 0.05$, Table 3).

DISCUSSION

Although the pathogenesis of chronic hepatitis B has not been fully studied, the importance of cellular immune in the occurrence of chronic HBV infection and elimination of HBV has received more and more attention^[7]. CD $_3^+$, CD $_4^+$ and CD $_8^+$ are the major function subsets of T cells, many studies have discovered that CD $_3^+$, CD $_4^+$ of chronic hepatitis B with serum HBV positive are lower than those of chronic hepatitis B with serum HBV negative, and the higher the quantity of HBVDNA is, the lower the T cellular immune function is. Antiviral cellular immune response of CD $_4^+$ and CD $_8^+$ is the important mechanism of hepatocyte injury induced by HBV, the specific response of CD $_4^+$ and CD $_8^+$ to the virus antigen is closely related with the elimination of the virus. It is suggested that T cells could play a critical role in response to HBV infection, and their level and mutual relationship could be used to identify the cellular immune

level and could serve as one of the valuable immunologic targets to forecast the change of patients' condition^[8-12]. Some studies on chronic hepatitis B showed that T cell receptor function was the important cause of the obstacle to T cells, sequentially bringing about HBV escaping immune response, and finally resulting in standing HBV infection^[2,3,13-16]. Therefore, it is very important to study the antiviral effect of T cells starting with immune identification.

TCR has been found to be the receptor of T lymphocyte surface recognising extra antigen and the major histocompatibility complex I (MHC I), as well as the specific sign of T cells^[17-19]. The genes of the α and β chains which promote TCR α β reset formation of large amount of specific TCR to recognise the extra antigen when they meet antigen. TCR and CD $_3$ would inosculate on the surface cells and form TCRCD3 compounds, the stimulating signals would be transferred to the inside of cells by CD3 molecules when antigens were recognised by TCR, activating T lymphocyte cells^[20-26]. Some studies have indicated that the priority expression and employment of TCRV β_7 were related with the specific immune reaction of chronic hepatitis B^[27-29]. Therefore, it is a meaningful pathway to eliminate HBV and decrease the occurrence of liver cancer by screening experimental recipes to activate T cells by improving T cell recognising function under the present circumstances of low cure ratio and high recurrence. We discovered that in the outbreak period of chronic hepatitis B, TCRV β_7 gene expression was low. The level of CD $_4^+$ cells was lower whereas the level of CD $_8^+$ cells was higher in patients than in the normal group ($P < 0.01$). The serum TCRV β_7 gene expressions of non-responders were low, the level of CD $_4^+$ cells of non-responders was lower in patients than in normal persons whereas the level of CD $_8^+$ cells of non-responders was higher in patients than in the normal persons. After treatment, the TCRV β_7 gene expression was high in patients with the conversion of HBV-DNA and HBeAg, and the liver function, the level of CD $_4^+$ and CD $_8^+$ cells resumed to normal. The levels of CD $_4^+$ and CD $_8^+$ cells in the treatment group were significantly different from those before treatment ($P < 0.01$). The results showed that TCRV β_7 participated in the elimination of HBV and cytotoxic function, and the occurrence of chronic hepatitis B was related to the low expression of TCRV β_7 . The CTL could not be effectively activated to kill or injure HBV due to the obstacle of T cell receptor function, sequentially bringing about stable reproduction of HBV and resulting in chronic inflammation of hepatocytes. At the same time, we also discovered that TCRV β_7 expression of some patients in the palliating period was still low, indicating that recurrence might increase.

When HBeAg in chronic hepatitis B patients transforms to Anti-HBe, hepatocyte injury aggravates, which is considered to be mediated by CTL antiviral cellular immune response. The dynamic observation of 6 cases whose TCRV β_7 gene expressions were positive showed that the TCRV β_7 gene expression related with the HBeAg serum conversion, the decreased quantity of HBVDNA, and ALT levels experienced a period of acute exacerbation in the course of descending, suggesting that TCRV β_7 participated in the elimination of HBV and cytotoxic function. ALT fluctuation in patients with TCRV β_7 negative was small, and there was no obvious decrease in HBVDNA, or obvious HBeAg serum conversion, suggesting the cellular immune response of the patients was feeble. Thus TCRV β_7 might be an index to evaluate the cellular immune state of hepatitis B patients.

HBeAg is a good index that reflects the HBV replication. When HBeAg transforms to Anti-HBe, the reproduction of HBV will obviously weaken or cease, along with the relief of the state of illness. Among the 10 patients with HBeAg serum conversion, the quantity of HBVDNA in some patients did not alleviate or vanish after HBeAg serum conversion, and the

state of illness fluctuated, which should be treated continually. HJD is a proved recipe for treating hepatitis, in which cold and warm drugs are used to eliminate evils and restore healthy energy. Previous researches indicated that HJD had the effect to protect the liver, as well as the function of antiviral and immune regulation^[30-33]. We discovered that HJD could meliorate liver function, regulate TCRV β_7 gene expression, improve T cellular immune function of chronic hepatitis B in this study. The results suggest that the clinical effects of HJD on chronic hepatitis B, especially on the elimination of HBV, might relate with the improvement of TCR identifying function, and effectively activate CTL. However, HJD could not interrupt immune endurance of some patients, resulting in the failure of treatment, which needs further study to explore the cause and resolving methods.

REFERENCES

- 1 **Wang YX**, Ruan CP, Li L, Shi JH, Kong XT. Clinical significance of changes of perioperative T cell and expression of its activated antigen in colorectal cancer patients. *World J Gastroenterol* 1999; **5**: 181-182
- 2 **Guo Y**, Wu H, Li SY, Yan H. T cell receptor gene rearrangement of peripheral blood mononuclear cells from patients with chronic hepatitis B. *Zhonghua Chuanranbing Zazhi* 2000; **18**: 88-90
- 3 **Sugyo S**, Yuh K, Nakamura K, Emi K, Shijo H, Iida T, Kimura N, Tamura K. An analysis of T cell antigen receptor variable beta genes during the clinical course of patients with chronic hepatitis B. *J Gastroenterol Hepatol* 1999; **14**: 333-338
- 4 **Pardigon N**, Cambouris C, Bercovici N, Lemaitre F, Liblau R, Kourilsky P. Delayed and separate costimulation *in vitro* supports the evidence of a transient "excited" state of CD $_8^+$ T cells during activation. *J Immunol* 2000; **164**: 4493-4499
- 5 The infectious and parasitic disease institute of Chinese medical association. Diagnostic criteria of virus hepatitis. *Zhonghua Chuanranbing Zazhi* 1995; **13**: 242-247
- 6 **Yang LJ**, Li YQ, Chen SH, Han SF, Chen ST, Zhang XL, Zhang T. Comparison of the clonal expansion of TCR v β T cells in patients with acute promyelocytic leukemia *in vivo* and *in vitro*. *Zhongguo Shiyang Xueyexue Zazhi* 2003; **11**: 499-502
- 7 **Li L**, Gu CH, Li X. The significance of activation-induced cell death (AICD) in pathogenesis of hepatitis B. *Zhonghua Yixue Zazhi* 2003; **83**: 1146-1149
- 8 **Wang KX**, Peng JL, Wang XF, Tian Y, Wang J, Li CP. Detection of T lymphocyte subsets and mIL-2R on surface of PBMC in patients with hepatitis B. *World J Gastroenterol* 2003; **9**: 2017-2020
- 9 **Wang JP**, Li XH, Zhu Y, Wang AL, Lian JQ, Jia ZS, Xie YM. Detection of serum sIL-2R, IL-6, IL-8, TNF- α and lymphocytes subsets, mIL-2R in patients with chronic hepatitis B. *Shijie Huaren Xiaohua Zazhi* 2000; **8**: 763-766
- 10 **Crispe IN**. Hepatic T cells and liver tolerance. *Nat Rev Immunol* 2003; **3**: 51-62
- 11 **Sing GK**, Li D, Chen X, Macnaughton T, Lichanska AM, Butterworth L, Ladhams A, Cooksley G. A molecular comparison of T lymphocyte populations infiltrating the liver and circulating in the blood of patients with chronic hepatitis B: evidence for antigen-driven selection of a public complementarity-determining region 3 (CDR3) motif. *Hepatology* 2001; **33**: 1288-1298
- 12 **Zhang MX**, Zhang XY, Jin SG, Dong HF, Chen JJ, Wang LT. The changes of peripheral blood CD $_28^+$ T from patients with liver diseases. *Shijie Huaren Xiaohua Zazhi* 2000; **8**: 1432-1433
- 13 **Maru Y**, Yokosuka O, Imazeki F, Saisho H, Omata M. Analysis of T cell receptor variable regions and complementarity determining region 3 of infiltrating T lymphocytes in the liver of patients with chronic type B hepatitis. *Intervirology* 2003; **46**: 277-288
- 14 **Huang S**, Cao M, Luo L. Hepatitis B virus antigen-induced specific TCR V beta gene subfamily amplifications and their diversity. *Zhonghua Shiyang He Linchuang Bingdixue Zazhi* 1998; **12**: 318-321
- 15 **Soroosh P**, Shokri F, Azizi M, Jeddi-Tehrani M. Analysis of T-cell receptor beta chain variable gene segment usage in healthy adult responders and nonresponders to recombinant hepatitis B vaccine. *Scand J Immunol* 2003; **57**: 423-431
- 16 **Suzuki T**, Yamauchi K, Kuwata T, Hayashi N. Characterization of hepatitis B virus surface antigen-specific CD $_4^+$ T cells in hepatitis B vaccine non-responders. *J Gastroenterol Hepatol* 2001; **16**: 898-903
- 17 **Hodges E**, Krishna MT, Pickard C, Smith JL. Diagnostic role of tests for T cell receptor (TCR) genes. *J Clin Pathol* 2003; **56**: 1-11
- 18 **Hughes MM**, Yassai M, Sedy JR, Wehrly TD, Huang CY, Kanagawa O, Gorski J, Sleckman BP. T cell receptor CDR3 loop length repertoire is determined primarily by features of the V(D)J recombination reaction. *Eur J Immunol* 2003; **33**: 1568-1575
- 19 **Rezvany MR**, Jeddi-Tehrani M, Wigzell H, Osterborg A, Mellstedt H. Leukemia-associated monoclonal and oligoclonal TCR-BV use in patients with B-cell chronic lymphocytic leukemia. *Blood* 2003; **101**: 1063-1070
- 20 **Jiang H**, Curran S, Ruiz-Vazquez E, Liang B, Winchester R, Chess L. Regulatory CD $_8^+$ T cells fine-tune the myelin basic protein-reactive T cell receptor V beta repertoire during experimental autoimmune encephalomyelitis. *Proc Natl Acad Sci U S A* 2003; **100**: 8378-8383
- 21 **Hohn H**, Neukirch C, Freitag K, Necker A, Hitzler W, Seliger B, Maeurer MJ. Longitudinal analysis of the T-cell receptor (TCR)-VA and -VB repertoire in CD $_8^+$ T cells from individuals immunized with recombinant hepatitis B surface antigen. *Clin Exp Immunol* 2002; **129**: 309-317
- 22 **Vigan I**, Jouvin-Marche E, Leroy V, Pernollet M, Tongiani-Dashan S, Borel E, Delachanal E, Colomb M, Zarski JP, Marche PN. T lymphocytes infiltrating the liver during chronic hepatitis C infection express a broad range of T-cell receptor beta chain diversity. *J Hepatol* 2003; **38**: 651-659
- 23 **Turner SJ**, Diaz G, Cross R, Doherty PC. Analysis of clonotype distribution and persistence for an influenza virus-specific CD $_8^+$ T cell response. *Immunity* 2003; **18**: 549-559
- 24 **Raaphorst FM**, Schelonka RL, Rusnak J, Infante AJ, Teale JM. TCRBV CDR3 diversity of CD $_4^+$ and CD $_8^+$ T-lymphocytes in HIV-infected individuals. *Hum Immunol* 2002; **63**: 51-60
- 25 **Mitarnun W**, Saechan V, Pradutkanchana J, Suwiwat S, Takao S, Ishida T. Epstein-Barr virus-associated peripheral T-cell lymphoma with gastrointestinal tract involvement. *J Med Assoc Thai* 2003; **86**: 816-828
- 26 **Konig R**, Zhou W. Signal transduction in T helper cells: CD4 coreceptors exert complex regulatory effects on T cell activation and function. *Curr Issues Mol Biol* 2004; **6**: 1-15
- 27 **Abbott WG**, Geursen A, Fraser JD, Marbrook J, Skinner MA, Tan PL. The influence of a maternal chronic hepatitis B virus infection on the repertoire of transcribed T-cell receptor beta chain variable region genes in human cord blood. *Hepatology* 1995; **22**: 1034-1039
- 28 **Chen XH**, Cooksley G, Sing G. Distinct patterns of T cell receptor distribution of peripheral blood CD $_8^+$ cells during different stages of chronic infection with hepatitis B virus. *Human Immunol* 1998; **59**: 199-211
- 29 **Dou HY**, Wu JC, Peng WL, Chang C, Chi WK, Chu YD, Hu CP. Analysis of T cell receptor Vbeta gene usage during the course of disease in patients with chronic hepatitis B. *J Biomed Sci* 1998; **5**: 428-434
- 30 **Zhang SJ**, Chen ZX, Huang BJ. Effect of hejie decoction on T-cell receptor V beta 7 gene expression in patients of chronic hepatitis B. *Zhongguo Zhongxiyi Jiehe Zazhi* 2002; **22**: 499-500
- 31 **Zhang SJ**, Chen ZX, Huang JB, Li JB. Clinical study on the He Jie Decoction in keeping HBeAg negative conversion states of chronic hepatitis B patients after HBeAg negative conversion. *Zhongguo Zhongxiyi Jiehe Xiaohua Zazhi* 2001; **9**: 92-93
- 32 **Zhang SJ**, Chen ZX. Clinical study of He Jie Decoction on 37 chronic hepatitis B patients with HBeAg positive. *Shiyong Zhongyi Zazhi* 1999; **15**: 16-17
- 33 **Zhang SJ**, Chen ZX, Huang JB, Li JB, Qin J, Huang BJ, Huang DX, Liu XQ. Clinical study of He Jie Decoction on IL-8, sIL-2R of chronic hepatitis B patients. *Zhonghua Shiyong Zhongxiyi Zazhi* 2001; **14**: 725-726

Differential expression of cholangiocyte and ileal bile acid transporters following bile acid supplementation and depletion

N. Sertac Kip, Konstantinos N. Lazaridis, Anatoliy I. Masyuk, Patrick L. Splinter, Robert C. Huebert, Nicholas F. LaRusso

N. Sertac Kip, Konstantinos N. Lazaridis, Anatoliy I. Masyuk, Patrick L. Splinter, Robert C. Huebert, Nicholas F. LaRusso, Center for Basic Research in Digestive Diseases, Division of Gastroenterology and Hepatology, Department of Internal Medicine, Mayo Medical School, Clinic and Foundation, Rochester, MN 55905, USA
Nicholas F. LaRusso, Department of Biochemistry and Molecular Biology, Mayo Medical School, Clinic and Foundation, Rochester, MN, 55905, USA

Correspondence to: Nicholas F. LaRusso M.D., Center for Basic Research in Digestive Diseases, Mayo Clinic, 200 First Street, SW Rochester, MN 55905, USA. larusso.nicholas@mayo.edu

Telephone: +1-507 284-1006 **Fax:** +1-507 284-0762

Received: 2004-03-23 **Accepted:** 2004-04-09

ASBT and t-ASBT in cholangiocytes is regulated by a negative feedback loop while the expression of these transporters in terminal ileum is modified via positive feedback. Thus, while transcriptional regulatory mechanisms in response to alterations in bile acid pool size are operative in both cholangiocytes and ileocytes, each cell type responds differently to bile acid supplementation and depletion.

Kip NS, Lazaridis KN, Masyuk AI, Splinter PL, Huebert RC, LaRusso NF. Differential expression of cholangiocyte and ileal bile acid transporters following bile acid supplementation and depletion. *World J Gastroenterol* 2004; 10(10): 1440-1446 <http://www.wjgnet.com/1007-9327/10/1440.asp>

Abstract

AIM: We have previously demonstrated that cholangiocytes, the epithelial cells lining intrahepatic bile ducts, encode two functional bile acid transporters via alternative splicing of a single gene to facilitate bile acid vectorial transport. Cholangiocytes possess ASBT, an apical sodium-dependent bile acid transporter to take up bile acids, and t-ASBT, a basolateral alternatively spliced and truncated form of ASBT to efflux bile acids. Though hepatocyte and ileal bile acid transporters are in part regulated by the flux of bile acids, the effect of alterations in bile acid flux on the expression of t-ASBT in terminal ileocytes remains unclear. Thus, we tested the hypothesis that expression of ASBT and t-ASBT in cholangiocytes and ileocytes was regulated by bile acid flux.

METHODS: Expression of ASBT and t-ASBT message and protein in cholangiocytes and ileocytes isolated from paired rats given control (C) and 1% taurocholate (TCA) or 5% cholestyramine (CY) enriched diets, were assessed by both quantitative RNase protection assays and quantitative immunoblotting. The data obtained from each of the control groups were pooled to reflect the changes observed following TCA and CY treatments with respect to the control diets. Cholangiocyte taurocholate uptake was determined using a novel microperfusion technique on intrahepatic bile duct units (IBDUs) derived from C, TCA and CY fed rats.

RESULTS: In cholangiocytes, both ASBT and t-ASBT message RNA and protein were significantly decreased in response to TCA feeding compared to C diet. In contrast, message and protein of both bile acid transporters significantly increased following CY feeding compared to C diet. In the ileum, TCA feeding significantly up-regulated both ASBT and t-ASBT message and protein compared to C diet, while CY feeding significantly down-regulated message and protein of both bile acid transporters compared to C diet. As anticipated from alterations in cholangiocyte ASBT expression, the uptake of taurocholate in microperfused IBDUs derived from rats on TCA diet decreased 2.7-fold, whereas it increased 1.7-fold in those on CY diet compared to C diet fed groups.

CONCLUSION: These data demonstrate that expression of

INTRODUCTION

Bile acids are synthesized in hepatocytes from cholesterol, conjugated to either taurine or glycine, secreted into bile and reach the small intestine via the bile ducts to facilitate lipid absorption^[1]. Subsequently, bile acids are reclaimed at the terminal ileum, returned to the liver via the portal circulation, and resecreted into bile accomplishing their enterohepatic circulation^[1]. At the cellular level, this recycling of bile acids, important for conservation of the bile acid pool, is achieved by the coordinated activities of a series of apical and basolateral membrane bile acid transporters expressed on the epithelial cells of the terminal ileum and liver^[2].

The active recovery of conjugated bile acids in the terminal ileum is mediated by a Na⁺ driven bile acid transporter, ASBT, located at the luminal domain of the ileocyte^[2]. Following uptake into the ileocytes, bile acids bind to the intestinal bile acid binding protein (I-BABP) in the cytoplasm to be directed across the cell to the basolateral membrane where they enter into the portal venous circulation by a Na⁺-independent mechanism^[2]. Subsequently, the majority of conjugated bile acids are efficiently reabsorbed from portal vein blood into hepatocytes, mainly via the Na⁺-taurocholate cotransporter (ntcp)^[3] and then are secreted into the biliary system primarily via ATP-dependent export pumps located on the apical (*i.e.*, canalicular) domain of hepatocytes^[3].

As bile percolates through the intrahepatic bile ducts, it undergoes numerous modifications due to both secretory and absorptive activities of cholangiocytes. We and others, have previously shown that biliary epithelia can take up conjugated bile acids via ASBT^[4,5] expressed on the cholangiocyte apical membrane, a protein identical to that cloned from rat ileum and kidney^[6,7]. We have also recently identified an alternatively spliced and truncated transcript of ASBT, designated t-ASBT that allows cholangiocytes and possibly other bile-acid transporting epithelia (*i.e.*, ileum and kidney) to extrude bile acids at the basolateral domain^[8].

Despite these advances in our understanding of the physiology of bile acid transport, little is known about the regulation of ASBT and t-ASBT in bile acid transporting epithelia, especially in cholangiocytes. While recent studies have assessed the effects of ursodeoxycholic acid supplementation^[9], bile acid depletion and repletion in bile duct ligated rats^[10,11]

and bile acid feeding on different physiologic responses by cholangiocytes, including in some instances ASBT expression^[12]. No studies have addressed the regulation of t- ASBT or systematically compared the responses of the liver and ileum to bile acid expansion or depletion. We, therefore, designed the present study to further investigate the role of bile acids in the regulation of ASBT and t- ASBT in both the biliary tree and terminal ileum. For this purpose, we performed studies in non-surgically manipulated rats to determine the message and protein levels of ASBT and t- ASBT in both cholangiocytes and ileocytes following well-accepted experimental perturbations to either expand (*i.e.*, taurocholate feeding) or deplete (*i.e.*, cholestyramine feeding) the bile acid pool. To ensure that our molecular observations were physiologically relevant, we also employed functional studies using microperfusion of rat intrahepatic bile duct units (IBDUs), a technique recently developed in our laboratory.

MATERIALS AND METHODS

Materials

[α -³²P] UTP (specific activity 800 Ci/mmol) of >95% purity was purchased from Amersham (Arlington Heights, IL), taurocholate (TCA) of 98% purity was obtained from Calbiochem-Novabiochem Corp (La Jolla, CA). MAXIScript SP6/T7 high specific activity transcription kit and RPA III kit were purchased from Ambion Inc (Austin, TX). All sodium dodecyl sulfate-polyacrylamide gel reagents were purchased from Biorad (Hercules, CA). The ASBT antibody used in immunoblotting was a generous gift of Paul Dawson^[12]. The t-ASBT antibody was produced as described previously^[8]. The secondary antibody (goat anti-rabbit), a horseradish peroxidase (HRP) conjugate, was obtained from Biosource International. Enhanced chemiluminescence (ECL) Western blotting detection reagents were bought from Amersham (Arlington Heights, IL). X-ray films were purchased from Eastman Kodak Co (Rochester, NY). For measurement of biliary phospholipids and cholesterol, commercial kits were purchased from Wako Chemicals (Richmond, VA) and Boehringer Mannheim (Indianapolis, IN). All other commercially available reagents, including cholestyramine, were obtained from Sigma Chemical Co (St. Louis, MO).

Animals

All procedures involving rats were in compliance with guidelines of the Mayo Foundation Animal Care Committee, which approved the experimental protocols. Male Fischer 344 rats (225-275 g) purchased from Harlan Sprague Dawley Inc (Indianapolis, IN) were maintained in a temperature-controlled environment (22 °C) with alternating 12-h light-dark cycles. Rats had free access to water but were pair-fed for 10 d, either control diet (C), or diets enriched with 1% taurocholate (TCA) (wt/wt) or 5% cholestyramine (CY) (wt/wt) prepared by Dyets Inc (Bethlehem, PA). The feeding studies were conducted in two paired groups (*i.e.*, control and test) and four sets of rats (TCA vs C and CY vs C). However for data analysis, results from each of the control groups with respect to the message and protein data were pooled. To ensure equal chow consumption between the pair-fed groups, each rat was kept in an individual cage and its food intake and weight were monitored daily. According to the pair-feeding protocol, the amount of chow consumed by each one of the TCA or CY designated rats one day was provided the following day to the corresponding pair-fed C animal as control chow. At the end of each feeding study, rats were anesthetized with sodium pentobarbital (50 mg/kg) intraperitoneally, the common bile duct was cannulated and bile was collected continuously in timed aliquots to determine bile flow rate. Bile samples were extracted with 4 volumes of isopropanol and immediately frozen in liquid nitrogen for later

measurements of biliary bile acids, phospholipids and cholesterol. Subsequently, rats were euthanized consistently between 8 and 9 am to control possible circadian variation in ASBT and t- ASBT expression.

Isolation of cholangiocytes

Freshly isolated, highly purified cholangiocytes (>95%) were prepared from the livers of C, TCA, and CY fed rats using collagenase perfusion, enzymatic digestion, mechanical disruption and immunopurification as described^[13]. Cholangiocytes derived from animals of the same feeding group were pooled and kept at -70 °C until used for mRNA or protein extraction.

Isolation of ileocytes

The small intestine was prepped and 15 cm of terminal ileum was excised, flushed with cold 9 g/L NaCl solution and the luminal surface was scraped to harvest the epithelial cells. Ileocytes collected from animals of the same feeding group were pooled, centrifuged at 2 000 rpm for 5 min, and the pellet was kept at -70 °C until used for mRNA isolation and protein extraction.

Quantitative ribonuclease protection assay (Q-RPA)

Following extraction of total cellular RNA from freshly isolated cholangiocytes and ileocytes^[14], ASBT and t- ASBT mRNA were determined by Q-RPA using the RPA III kit, as previously described^[8]. Yeast and kidney RNA were used as a negative and positive control, respectively. Following RPA, the ASBT or t- ASBT mRNA content of the samples was measured both by scanning the X-ray film of the protected bands corresponding to either ASBT or t- ASBT and by comparing their arbitrary densitometric units to those obtained from their respective standard curves as described^[8]. The comparability of the total RNA used in this assay was determined both spectrophotometrically and by ultraviolet detection of the intensity of 28S and 14S ribosomal bands on ethidium bromide stained gels.

Quantitative immunoblotting (Q-IB)

Following cholangiocyte immunoisolation, the cells were sonicated twice for 7 s, using a Sonifier cell disrupter (Heat Systems-Ultrasonic, Inc. Plainview, NY) in a buffer containing 50 mmol/L Tris-HCl (pH 7.4), 50 mmol/L EDTA, 100 μ mol/L leupeptin, 1 μ mol/L pepstatin and 0.2 mmol/L PMSF. Cell fragments attached to immunomagnetic beads were removed by applying the samples to a magnet. The remaining cell lysate was centrifuged at 4 °C for 10 min at 2 500 rpm. Subsequently, the cholangiocyte post nuclear supernatant (PNS) was collected, protein concentration was determined and stored at -70 °C until used. To obtain PNS from ileocytes of the terminal ileum, the scraped ileocytes were sonicated in the same buffer and centrifuged as indicated above. In the PNS fraction of ileocytes, protein concentration was calculated and then it was stored at -70 °C until used.

Cholangiocyte and ileal PNS were run on a 120 g/L SDS-polyacrylamide gel. Electrophoresis was done at 100 volts (V) in the presence of a prestained low molecular range protein as a size marker (Biorad) and 40 μ g of kidney PNS as a positive control. Proteins were transferred overnight at 4 °C at 25 V onto nitrocellulose membranes (Micron Separations Inc., Westboro, MA) as described^[4]. Immunoblotting of ASBT and t- ASBT was performed using the well-characterized, specific, rabbit anti rat, polyclonal anti- ASBT^[6] and anti-t- ASBT^[8] antibodies. In brief, membranes were blocked in 50 mL/L milk and incubated at room temperature for 2 h with ASBT antibody (1:4 000) or t- ASBT antibody (1:1 000). Subsequently, membranes were washed 3 times and exposed to horseradish peroxidase conjugated secondary (goat anti-rabbit) antibody (1:7 000) for

1 h at room temperature. Following three additional washings of the membrane, the immunoreactive ASBT (48 kDa) and t-ASBT (19 kDa) bands were detected by enhanced chemiluminescence detection system (ECL).

Immunoblotting for β -actin (41 kDa), a housekeeping protein, was employed to demonstrate equal protein loading. Quantitative comparisons among experimental groups were made by determining the immunoreactive areas by densitometry using an imaging densitometer (Model GS-700) and the Molecular Analyst software program (Bio-Rad Laboratories, Hercules, CA) to calculate the ratios of ASBT or t-ASBT to that of β -actin. The immunoblotting data were also evaluated using another technique to exclude possible risk of β -actin being altered by any of the experimental perturbations. For this purpose, arbitrary densitometric units of each immunoreactive band were divided by the μ g of protein loaded and this value was further divided by the exposure time of the autoradiograph. The specificity of ASBT and t-ASBT antibodies and the bands observed in the immunoblots were evaluated by stripping the membranes and reprobing them with ASBT and t-ASBT antibodies (3 mg/mL) previously blocked with their respective peptides (2 mg/mL) for 1 h at 37°C^[4,8].

Isolation and microperfusion of rat intrahepatic bile duct units (IBDUs)

Isolation and microperfusion of IBDUs were performed, as previously described^[15]. Microperfusion of an IBDU was carried out using Ringer-HCO₃ (KRB solution) containing 40 mmol/L taurocholate at a perfusion rate of 436 nl/min and bile acid (*i.e.*, taurocholate) uptake by individual microperfused IBDU was calculated as published previously^[15].

Protein concentration

Concentrations of proteins were measured by the fluorescamine method using bovine serum albumin (BSA) as standard^[16]. Data were confirmed using the colorimetric Bradford method where vendor's (Sigma) instructions were applied. No differences were observed in protein recovery in TCA or CY groups when compared to controls for a specific cell type.

Measurements of biological samples

Biliary phospholipids and cholesterol were analyzed spectrophotometrically using commercial kits from Wako Chemicals and Boehringer Mannheim, respectively. Biliary bile acid concentration was determined spectrophotometrically according to the vendor's instructions (Sigma). Bile acid concentration of samples was derived from a calibration curve prepared using bile acid of known concentrations: 5, 10, 50, 100 and 200 μ mol/L.

Statistical analysis

All data were expressed as mean \pm SE. Statistical differences were analyzed by Student's *t*-test, and results were considered to be statistically different at $P < 0.05$.

RESULTS

Effect of TCA and CY feeding on body mass, bile flow, and biliary bile acids, phospholipids and cholesterol

The effects of TCA and CY feeding on rat body mass, bile flow and biliary lipid composition compared to C diet are provided in Table 1. Though an approximate 6% weight loss was observed following TCA and CY feedings, the differences in total body masses in experimental groups vs C diet were not significant. Bile flow was significantly higher (2.2-fold) in the TCA group, but similar in the CY group compared to the C group. As expected, the biliary bile acids in the TCA fed rats

were 3.2-fold higher, but 2-fold lower in the CY fed rats compared to the C fed rats. Biliary phospholipids of the TCA fed rats were significantly greater. In the CY group, biliary phospholipids were significantly lower than in the C group. Finally, biliary cholesterol levels of both the TCA and CY groups were similar compared to the C rats. These data indicated that the diets employed significantly altered bile flow and the biliary lipid parameters as anticipated.

Table 1 Alterations of weight and biliary constituents after TCA and CY feeding

	Control	TCA	CY
Body mass (g)	261(\pm 7)	247(\pm 3)	246(\pm 9)
Bile flow (μ L/min)	9.2(\pm 0.4)	19.8(\pm 0.3) ^a	9.7(\pm 0.8)
Biliary bile acids (mmol/L)	20(\pm 2)	65(\pm 3) ^a	10(\pm 1) ^a
Biliary phospholipids (mg/dL)	248(\pm 60)	470(\pm 87) ^a	127(\pm 76) ^a
Biliary cholesterol (g/L)	0.16(\pm 0.03)	0.16(\pm 0.01)	0.15(\pm 0.03)

^a $P < 0.05$.

Effect of TCA and CY feeding on ASBT and t-ASBT messages in cholangiocytes

Using Q-RPA, ASBT mRNA levels were significantly lower (2.3-fold) in cholangiocytes of the TCA fed rats than in cholangiocytes of the C fed rats (0.0035 \pm 0.002 ng mRNA/ μ g total RNA and 0.0081 \pm 0.002 ng mRNA/ μ g total RNA, respectively, $P = 0.009$) (Figure 1). Parallel to the down-regulation of ASBT in the TCA fed rats, t-ASBT mRNA of the same group was also 4.3-fold lower compared to the C fed rats (0.003 \pm 0.001 ng mRNA/ μ g total RNA and 0.013 \pm 0.003 ng mRNA/ μ g total RNA, respectively, $P = 0.01$) (Figure 1). ASBT mRNA levels were 1.5-fold higher in cholangiocytes of the CY fed rats than in those of the C fed rats (0.012 \pm 0.002 ng mRNA/ μ g total RNA and 0.0081 \pm 0.002 ng mRNA/ μ g total RNA, respectively, $P = 0.04$) (Figure 1). Corresponding to the upregulation of ASBT in the CY fed rats, t-ASBT mRNA of the same group was also 1.3-fold greater compared to the C fed rats. However, this was not statistically significant (0.015 \pm 0.004 ng mRNA/ μ g total RNA and 0.013 \pm 0.003 ng mRNA/ μ g total RNA, respectively, $P = 0.4$) (Figure 1). The insignificant increase in the t-ASBT message and the significant increase in the protein levels of t-ASBT (Figure 2) following CY treatment might indicate post-transcriptional modifications.

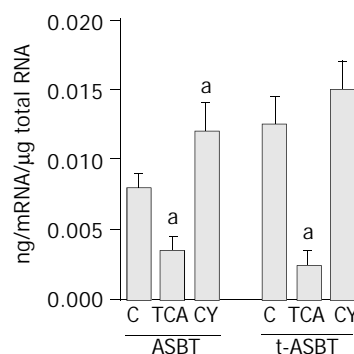


Figure 1 Q-RPA data demonstrating down-regulation of ASBT and t-ASBT message following TCA feeding and up-regulation of their expression following CY feeding in cholangiocytes. Bar graphs demonstrating ASBT and t-ASBT mRNA expression, in which 40 μ g total cellular RNA isolated from cholangiocytes obtained from rats fed regular chow (C), 1% TCA or 5% CY incorporated diets were used. Densitometric values shown here are expressed as mean \pm SE and represent 3 feeding studies in which 30 rats in total were analyzed per group (^a $P < 0.05$).

Effect of TCA and CY feeding on ASBT and t-ASBT proteins in cholangiocytes

ASBT protein in the TCA group decreased 2.2-fold compared to the C fed rats and that was statistically significant ($P=0.006$) (Figure 2). Protein levels of t-ASBT were also repressed 2.4-fold following TCA feeding compared to C fed rats that was also statistically significant ($P=0.004$) (Figure 2). The protein quantitative data were also analyzed using an additional approach to verify the above findings. In this case, to exclude the possibility of β -actin being affected by the bile acid feeding, quantitative analysis was made by determining the arbitrary densitometric units of each immunoreactive band and further dividing it by the amount of protein loaded and exposure time of the autoradiograph. Using this alternative approach, cholangiocyte ASBT protein from the TCA group was shown to be downregulated 2.2-fold compared to C fed rats. This finding reassured us about the accuracy of the data we obtained by the first quantitative method and provided evidence that actin was not affected by TCA feeding. In addition, following CY feeding, the ASBT protein was 2.3-fold higher and statistically significant compared to C fed rats ($P=0.003$) (Figure 2). Moreover, after CY feeding, the t-ASBT protein was also increased 2.4-fold compared to C fed rats ($P=0.04$) (Figure 2).

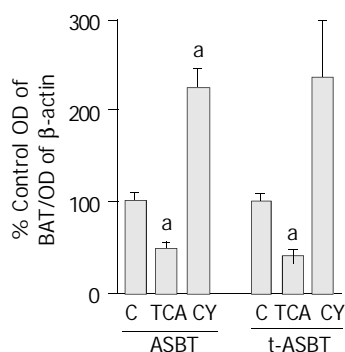


Figure 2 Effect of TCA and CY feeding on the expression of ASBT and t-ASBT protein in cholangiocytes. Bar graphs showing densitometric ratios of ASBT and t-ASBT standardized to β -actin in PNS fractions of freshly isolated cholangiocytes from rats fed control (C), 1% TCA or 5% CY incorporated diet. A 80 μ g for ASBT and 120 μ g for t-ASBT PNS protein were subjected to SDS-PAGE, immunoblotted for ASBT (48 kDa), t-ASBT (19 kDa) and β -Actin (41 kDa) and the bands were then visualized using enhanced chemiluminescence techniques. Densitometric values shown here are expressed as mean \pm SE ($^*P < 0.05$) and represent 3 feeding studies for ASBT protein analyses of the TCA and CY groups. Similarly, 3 feeding studies were performed to reflect the data obtained on t-ASBT protein following CY feeding, but only 2 feeding studies were done for t-ASBT protein analysis of the TCA group. Ten rats per group were analyzed in each of these feeding studies, thus a total of 30 rats per feeding study were used in all of the above groups, whereas 20 rats were incorporated into the analysis of t-ASBT in the TCA group.

Effect of TCA and CY feeding on ASBT and t-ASBT messages in ileum

Using Q-RPA, ASBT mRNA levels in ileum of the TCA fed rats were 2.1-fold higher than those in ileum of the C fed rats (0.073 ± 0.01 ng mRNA/ μ g total RNA and 0.036 ± 0.01 ng mRNA/ μ g total RNA, respectively, $P=0.01$) (Figure 3). Parallel to upregulation of ASBT message, t-ASBT mRNA of the TCA group was also 1.9 fold higher compared to the C fed rats (0.076 ± 0.015 ng mRNA/ μ g total RNA and 0.040 ± 0.004 ng mRNA/ μ g total RNA, respectively, $P=0.01$) (Figure 3). In addition, the ileal ASBT mRNA levels of the CY fed rats were 1.4-fold less and statistically

significant than those of the C fed rats (0.026 ± 0.003 ng mRNA/ μ g total RNA and 0.036 ± 0.007 ng mRNA/ μ g total RNA, respectively, $P=0.07$) (Figure 3). Corresponding to these findings, t-ASBT mRNA levels of the CY fed rats were 1.3-fold lower and statistically significant compared to the C fed rats (0.031 ± 0.002 ng mRNA/ μ g total RNA and 0.040 ± 0.004 ng mRNA/ μ g total RNA, $P=0.01$) (Figure 3).

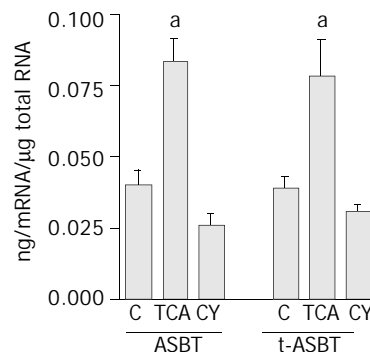


Figure 3 Q-RPA data demonstrating upregulation of ASBT and t-ASBT message following TCA feeding and downregulation of their message following CY feeding in ileum. Bar graphs demonstrating ASBT and t-ASBT mRNAs, in which 40 μ g total cellular RNA isolated from cholangiocytes obtained from rats fed regular chow (C), 1% TCA or 5% CY incorporated diets were used. Densitometric values demonstrated here are expressed as mean \pm SE and represent $n=3$ feeding studies in which 30 rats in total were analyzed for each group ($^*P < 0.05$).

Effect of TCA and CY feeding on ASBT and t-ASBT proteins in ileum

Parallel to increased ASBT transcript observed following bile acid feeding, ASBT protein expression was also 2.3-fold higher and statistically significant in the TCA fed rats compared to the C fed rats ($P=0.001$) (Figure 4). Moreover, the t-ASBT protein expression was also supportive of the mRNA data, t-ASBT protein was 2.7-fold higher and statistically significant in the TCA fed rats compared to the C fed rats ($P=0.02$) (Figure 4). Furthermore, following CY feeding, and parallel to decreased ASBT transcript, ileal ASBT protein was also 2.1-fold significantly down-regulated ($P=0.008$) compared to the C fed rats (Figure 4). Finally, the ileal t-ASBT protein was also in support of the message results for this transporter. Indeed, t-ASBT protein was 2.3-fold significantly decreased in the CY fed rats compared to the C fed rats ($P=0.01$) (Figure 4).

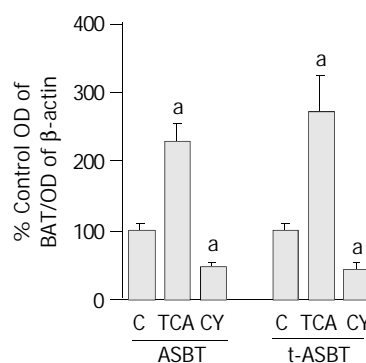


Figure 4 Effect of TCA and CY feeding on the amount of ASBT and t-ASBT protein in ileum. Bar graphs showing ratios of ASBT/ β -actin and t-ASBT/ β -Actin in PNS of ileal scrapings obtained from rats fed C, TCA and CY diets. Forty and 80 μ g of protein were subjected to SDS-PAGE and immunoblotted to visualize ASBT and t-ASBT, respectively. Data shown here are representative of $n=3$ feeding studies were analyzed per group

and expressed as mean \pm SE ($^*P<0.05$). For the analysis of ASBT and t-ASBT in the TCA treated groups, 7 and 3 rats in total were used, respectively. Whereas, the number of animals analyzed in the CY groups totaled 10 and 3 for ASBT and t-ASBT, respectively. Hence, the number of control rats was 17 for ASBT and 6 for t-ASBT in total.

Effect of TCA and CY feeding on bile acid uptake by IBDUs

To further verify and extend our observations at the functional level, taurocholate uptake was measured in IBDUs isolated from rats fed either TCA or CY diets and compared to those obtained from C fed animals using a novel microperfusion technique. Specifically, taurocholate uptake by IBDUs derived from the C diet group was 1.1 ± 0.2 nmol/min/mm². Taurocholate uptake was significantly lower in the TCA group (0.4 ± 0.1 nmol/min/mm², $P=0.002$, $n=4$ IBDU, 2 feeding studies) and significantly higher in CY group (1.95 ± 0.3 nmol/min/mm², $P=0.007$) (Figure 5).

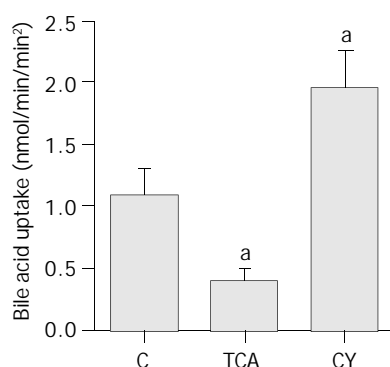


Figure 5 Effect of TCA and CY feeding on taurocholate uptake by ASBT in rat IBDUs. Bar graphs showing 2.7-fold decrease and 1.7-fold increase in taurocholate uptake in TCA and CY fed rats, respectively, compared to controls. Data shown here, and expressed as mean \pm SE, were obtained from $n=3$ feeding studies in which 11 control, 4 TCA and 5 CY IBDUs were analyzed ($^*P<0.05$).

DISCUSSION

The major findings described here are TCA feeding downregulates but CY feeding upregulates both ASBT and t-ASBT in cholangiocytes and TCA feeding upregulates whereas CY feeding downregulates both ASBT and t-ASBT in terminal ileum. Our findings suggested that both ASBT and t-ASBT in a specific cell type underwent parallel modes of regulation. On the other hand, reciprocal changes were observed between cholangiocytes and ileocytes in terms of ASBT and t-ASBT expression, suggesting organ-specific differences in regulation of these bile acid transporters.

Regulation of transporter expression to accommodate altered substrate loads is a well-recognized physiologic phenomenon. For example, adaptive up- or down-regulation of hepatic and ileal bile acid transporters occurred in response to changes in bile acid pool size^[3]. Moreover, a limited number of very recent studies addressed the problem of whether the same adaptive events could operate in cholangiocytes with respect to ASBT^[9-12]. However, no data exist regarding the regulation of t-ASBT in the liver or terminal ileum after bile acid supplementation or depletion. Regarding ASBT expression in terminal ileum, prior investigations have shown evidence of transcriptional regulation by bile acids^[17-19]. Nevertheless, results of these studies appeared to be species-specific given reported differences in ASBT regulation. For example, Lillienau *et al.* reported a negative feedback regulation of the ileal bile acid transporter in the guinea pig based on whole organ, ileal perfusion studies^[17]. Following cloning of ASBT in rats, Stravitz *et al.* described a positive

feedback regulatory mechanism of the ileal ASBT. These authors demonstrated induction of both mRNA and protein levels of ASBT after cholic acid feeding including supportive functional studies using ileal brush border membrane vesicles^[18]. More recently, Arrese *et al.* reported no change in ASBT expression and function following bile duct ligation and intestinal sequestration of bile acids^[19].

In the present study, we demonstrated that in cholangiocytes compared to C fed rats, TCA feeding downregulated both ASBT transcript and protein abundance as well as t-ASBT transcript and protein expression. On the other hand, CY feeding upregulated both ASBT transcript and protein abundance as well as t-ASBT transcript and protein expression compared to C fed rats. To support these molecular findings, microperfusion studies in rat IBDUs compared to C fed animals revealed 2.7-fold decrease and 1.7-fold increase in taurocholate uptake by IBDUs derived from TCA or CY fed rats, respectively. In terminal ileum, TCA feeding upregulated both ASBT transcript and protein abundance as well as t-ASBT transcript and protein expression. In contrast, CY feeding downregulated both ileal ASBT transcript and protein abundance as well as t-ASBT transcript and protein expression compared to C fed rats.

The pathophysiological significance of ASBT and t-ASBT adaptive changes in biliary epithelia and terminal ileum in response to bile acid pool perturbations described in this paper are intriguing. It appears that bile acid transporting epithelia of different organs (*i.e.*, bile ducts and ileum) respond differently to bile acid supplementation or depletion. ASBT and t-ASBT transcriptional down-regulation in cholangiocytes upon TCA feeding could diminish the cholehepatic shunt of conjugated bile acids. This pathway is believed to play a role in reclamation of bile acids from bile back to liver. Thus, during bile acid feeding, decreased expression of bile acid transporters in cholangiocytes and the ensuing reduction of bile acid shunting may provide protection to cholangiocytes and subsequently hepatocytes from the deleterious effects of excessive intracellular accumulation of bile acids. In fact, this protective mechanism became even more relevant given the fact that bile acid feeding increased the expression of bile acid transporters in terminal ileum as shown in the present and other studies^[18] and thus enhancing the uptake capacity of ileum for bile acids for delivery to the liver, perhaps to compensate the decreased cholehepatic shunt, and thus keeping the bile acid synthesis at a balance.

We have also observed that in CY fed rats, cholangiocyte ASBT and t-ASBT were up-regulated. These data should be reviewed in parallel with the reciprocal findings in the terminal ileum where CY feeding caused upregulation of both ASBT and t-ASBT. The potential pathophysiologic relevance of ASBT and t-ASBT induction in cholangiocytes after CY feeding may relate to increasing the biliary bile acid return to the liver via an enhanced cholehepatic shunt. This condition would potentially assist maintaining cholesterol homeostasis, given the concurrent observation of diminished expression of bile acid transporters in distal intestine and thus reducing absorption of bile acids from the terminal ileum. The experimental effect of CY on the expression of cholangiocyte bile acid transporters is analogous to the bile duct ligated (BDL) model, in which the enterohepatic circulation of bile acids is interrupted due to mechanical obstruction of the common bile duct. To this end, our observations in cholangiocytes were comparable to those reported by Lee *et al.*^[11]. These authors reported adaptive up-regulation and down-regulation of ASBT in biliary epithelia and kidney, respectively, in BDL rats, postulating that these changes might accommodate alternative pathways for secretion of excessive bile acids in cholestasis^[11]. However, others have shown in both BDL^[9,10] and bile acid fed rats^[12] that bile acid depletion and repletion could decrease and increase the expression of ASBT, respectively, in cholangiocytes. Differences

in results may very well reflect differences in study design (*e.g.*, feeding rats in a paired *vs* non-paired manner, feeding them until the surgical procedure *vs* fasting them overnight, feeding for 10 d *vs* 7 d, the age of the animals 225-275 g *vs* 125-150 g starting masses).

In our ileal studies, a significant increase in ASBT and t-ASBT occurred after TCA feeding, whereas a decrease in message and protein levels of both transporters was seen in bile acid depleted rats. These data suggest that changes in bile acid pool size could result in marked alterations in these bile acid carrier molecules. Our data agree with the work of Stravitz *et al.*^[18] who also reported a positive feedback mechanism on the regulation of ASBT in ileum. Arrese *et al.* reported that neither the pharmacological sequestration of bile acids nor common bile duct ligation affected the expression and function of ileal ASBT^[19]. Whether the different pharmacological agents used for bile acid depletion by Arrese (*i.e.*, the novel sequestrant GT31-104)^[19], and in our work, the well-established cholestyramine, accounted for these differences is unclear^[18].

Recently, the promoter region of the ASBT gene has been extensively analyzed^[20]. It appears that two AP-1 consensus sites have been identified in the proximal promoter of ASBT. At least four nuclear binding proteins, designated ABP 1-4, interacting with AP-1 sites, have been described. Of interest, formation of the ABP2 nuclear binding protein complex appeared to be correlated with regional and developmental stage-specific expression of ASBT in the rat intestine^[20]. In a study clarifying the transcriptional mechanisms involved in cytokine-mediated repression of rat ASBT, the authors observed reductions in ileal ASBT message and protein following proinflammatory cytokine and IL-1 beta treatment of IEC-6 and Caco-2 cells, along with significant increases in *c-fos* expression^[22]. The proinflammatory cytokines and interleukin-1 beta have thus been shown to repress the activity of the ASBT promoter via serine phosphorylation, and nuclear translocation of *c-fos*. Inflammation, associated with up-regulation, phosphorylation, and nuclear translocation of *c-fos*, which then represses ASBT promoter activity via binding to the 3' AP-1 element by a *c-fos/c-jun* heterodimer, may be operative following bile acid treatment, a stimulus known to increase inflammation in cholangiocytes. The inflammatory influence of bile acids might occur following directly activating eosinophils and inducing their effector functions^[23], or triggering interferon-gamma and tumor necrosis factor alpha production, which might in turn stimulate superoxide and interleukin release that resulted in disruption of the tight junctions in cholangiocytes^[24]. Bile acids, with the potential of altering the profile of cytokines, chemokines, and proinflammatory stimuli, which in turn were likely to activate fibrogenesis, stimulate apoptotic and proliferative responses, seemed to be important players in the pathophysiology of chronic cholestatic disorders^[25]. It is therefore imperative to begin to investigate the role of AP-1, ABP 1-4 and *c-fos* expression in bile acid transporting epithelia hoping to shed light on the adaptive and reciprocal expression of ASBT and t-ASBT. In a recent study, decreased expression of ileal ASBT protein and mRNA in mice following bile acid treatment was related to the presence of a potential liver receptor homologue-1 (LRH-1) cis acting element in the bile acid responsive region of the mouse but not the rat promoter. The mouse but not the rat promoter was activated by LRH-1 and this correlated with nuclear protein binding to the mouse but not rat LRH-1 element. Thus, species-specific negative feedback regulation of ASBT by bile acids was mediated by FXR via SHP-dependent repression of LRH-1 activation of the ASBT promoter^[21]. It is possible, therefore that, the reciprocal regulation pattern we have observed between cholangiocytes and ileocytes may reflect the role of FXR and LRH-1 in cholangiocytes.

In conclusion, we present data demonstrate that a bile acid enriched diet can down-regulate ASBT and t-ASBT in cholangiocytes but upregulate both transporters in terminal ileum. Conversely, bile acid depletion by sequestration can upregulate ASBT and t-ASBT in cholangiocytes, but down-regulate both transporters in terminal ileum. To have a better understanding of the mechanism (s) affecting the expression of bile acid transporters in relevant epithelia, a systematic comparative evaluation of their regulatory elements in different tissues known to be involved in bile acid homeostasis is required. Unraveling the presumed cell-specific regulatory mechanisms that affect bile acid transporter expression and function will help to develop novel rational options to treat cholestasis and chronic cholestatic liver diseases.

REFERENCES

- 1 **Hofmann AF**. Intestinal absorption of bile acids and biliary constituents: the intestinal component of the enterohepatic circulation and the integrated system. In: Physiology of the gastrointestinal tract, edited by LR Johnson. New York: Raven 1994; 1845-1865
- 2 **Dawson PA**, Oelkers P. Bile Acid transporters. *Curr Opin Lipidol* 1995; **6**: 109-114
- 3 **St-Pierre MV**, Kullak-Ublick GA, Hagenbuch B, Meier PJ. Transport of bile acids in hepatic and non-hepatic tissues. *J Exp Biol* 2001; **204**: 1673-1686
- 4 **Lazaridis KN**, Pham T, Tietz P, Marinelli RA, deGroen PC, Levine S, Dawson PA, LaRusso NF. Rat cholangiocytes absorb bile acids at their apical domain via the ileal sodium dependent bile acid transporter. *J Clin Invest* 1997; **100**: 2714-2721
- 5 **Alpini G**, Glaser SS, Rodgers R, Phinizy JL, Robertson WE, Lasater J, Caligiuri A, Tretjak Z, Lesage GD. Functional expression of the apical Na⁺-dependent bile acid transporter in large but not small rat cholangiocytes. *Gastroenterology* 1997; **113**: 1734-1740
- 6 **Shneider BL**, Dawson PA, Christie DM, Hardikar W, Wong MH, Suchy FJ. Cloning and molecular characterization of the ontogeny of a rat ileal sodium-dependent bile acid transporter. *J Clin Invest* 1995; **95**: 745-754
- 7 **Christie DM**, Dawson PA, Thevananther S, Shneider BL. Comparative analysis of the ontogeny of a sodium-dependent bile acid transporter in rat kidney and ileum. *Am J Physiol* 1996; **271**: G377-G385
- 8 **Lazaridis KN**, Tietz P, Wu T, Kip S, Dawson PA, LaRusso NF. Alternative splicing of the rat sodium/bile acid transporter changes its cellular localization and transport properties. *Proc Natl Acad Sci U S A* 2000; **97**: 11092-11097
- 9 **Alpini G**, Baiocchi L, Glaser S, Ueno Y, Marzioni M, Francis H, Phinizy JL, Angelico M, Lesage G. Ursodeoxycholate and tauroursodeoxycholate inhibit cholangiocyte growth and secretion of BDL rats through activation of PKC alpha. *Hepatology* 2002; **35**: 1041-1052
- 10 **Alpini G**, Glaser S, Alvaro D, Ueno Y, Marzioni M, Francis H, Phinizy JL, Angelico M, Lesage G. Bile acid depletion and repletion regulate cholangiocyte growth and secretion by a phosphatidylinositol 3-kinase-dependent pathway in rats. *Gastroenterology* 2002; **123**: 1226-1237
- 11 **Lee J**, Azzaroli F, Wang L, Soroka CJ, Gigliozzi A, Setchell KD, Kramer W, Boyer JL. Adaptive regulation of bile salt transporters in kidney and liver obstructive cholestasis in the rat. *Gastroenterology* 2001; **121**: 1473-1484
- 12 **Alpini G**, Ueno Y, Glaser SS, Marzioni M, Phinizy, Francis JL, LeSage G. Bile acid feeding increased proliferative activity and apical bile acid transporter expression in both small and large rat cholangiocytes. *Hepatology* 2001; **34**: 868-876
- 13 **Alpini G**, Philips JO, Vroman B, LaRusso NF. Recent advances in the isolation of liver cells. *Hepatology* 1994; **20**: 494-514
- 14 **Chomczynski P**, Sacchi N. The single-step method of RNA isolation by acid guanidium thiocyanate phenol-chloroform extraction. *Anal Biochem* 1987; **162**: 156-159

- 15 **Masyuk AI**, Gong AY, Kip S, Burke MJ, LaRusso NF. Perfused rat intrahepatic bile ducts secrete and absorb water, solute, and ions. *Gastroenterology* 2000; **119**: 1672-1680
- 16 **Udenfriend S**, Stein S, Bohlen P, Dairman W, Leimgruber W, Weigle M. Fluorescamine: a reagent for assay of amino acids, peptides, proteins and primary amines in the picomole range. *Science* 1972; **178**: 871-872
- 17 **Lillienau J**, Crombie DL, Munoz J, Longmire-Cook SJ, Hagey LR, Hofmann AF. Negative feedback regulation of the ileal bile acid transport system in rodents. *Gastroenterology* 1993; **104**: 38-46
- 18 **Stravitz RT**, Sanyal AJ, Pandak WM, Vlahcevic ZR, Beets JW, Dawson PA. Induction of sodium dependent bile acid transporter messenger RNA, protein, and activity in rat ileum by cholic acid. *Gastroenterology* 1997; **113**: 1599-1608
- 19 **Arrese M**, Trauner M, Sacchiero RJ, Crossman MW, Shneider BL. Neither intestinal sequestration of bile acids nor common bile duct ligation modulate the expression and function of the rat ileal bile acid transporter. *Hepatology* 1998; **28**: 1081-1087
- 20 **Chen F**, Ma L, Al-Ansari N, Shneider BL. The role of AP-1 in the transcriptional regulation of the rat apical sodium-dependent bile acid transporter. *J Biol Chem* 2001; **276**: 38703-38714
- 21 **Chen F**, Ma L, Dawson PA, Sinal CJ, Sehayek E, Gonzalez FJ, Breslow J, Ananthanarayanan M, Shneider BL. Liver-receptor homologue-1 mediates species and cell-line specific bile acid dependent negative feedback regulation of the apical sodium dependent bile acid transporter. *J Biol Chem* 2003; **22**: 19909-19916
- 22 **Chen F**, Ma L, Sartor RB, Li F, Xiong H, Sun AQ, Shneider B. Inflammatory-mediated repression of the rat ileal sodium-dependent bile acid transporter by c-fos nuclear translocation. *Gastroenterology* 2002; **123**: 2005-2016
- 23 **Yamazaki K**, Gleich GJ, Kita H. Bile acids induce eosinophil degranulation by two different mechanisms. *Hepatology* 2001; **33**: 582-590
- 24 **Hanada S**, Harada M, Koga H, Kawaguchi T, Taniguchi E, Kumashiro R, Ueno T, Ueno Y, Ishii M, Sakisaka S, Sata M. Tumor necrosis factor-alpha and interferon-gamma directly impair epithelial barrier function in cultured mouse cholangiocytes. *Liver Int* 2003; **23**: 3-11
- 24 **Strazzabosco M**. Transport systems in cholangiocytes: their role in bile formation and cholestasis. *Yale J Biol Med* 1997; **70**: 427-434

Edited by Wang XL Proofread by Xu FM

Transcriptional regulation of human $\alpha 1(I)$ procollagen gene in dermal fibroblasts

Chun-Fang Gao, Hao Wang, Ai-Hua Wang, Wei-Dong Wan, Yan-Aan Wu, Xian-Tao Kong

Chun-Fang Gao, Hao Wang, Ai-Hua Wang, Wei-Dong Wan, Yan-Aan Wu, Xian-Tao Kong, Department of Laboratory Medicine, Changzheng Hospital, Second Military Medical University, Shanghai 200003, China

Supported by the Natural Science Foundation of China, No. 39870301, No.30270605 and Project "208" of Shanghai Changzheng Hospital

Correspondence to: Dr. Chun-Fang Gao, Department of Laboratory Medicine, Changzheng Hospital, 415 Fengyang Road, Shanghai 200003, China. wanggaob@online.sh.cn

Telephone: +86-21-63610109-73641 **Fax:** +86-21-63520020

Received: 2003-12-10 **Accepted:** 2004-01-12

Abstract

AIM: To clarify the fractional activity of promoters from human $\alpha 1(I)$ procollagen gene, the interaction between cis-elements and consensus DNA-binding proteins responsible for high promoter activity, and the potential application of promoter competitors as well as cytokines for antifibrogenesis.

METHODS: Sequence between 2 483 bp upstream of the start of transcription and 42 bp downstream of this site was investigated with serial 5' -deletion. The 5' -deleted promoters recombined with chloramphenicol acetyltransferase (CAT) as reporter gene were transiently transfected to human dermal fibroblasts. Electrophoretic mobility shift assay was performed to show the DNA-protein binding capacity of the promoter sequence. Cytokines including tumor necrosis factor α (TNF α) and interferons (IFNs) were added to the culture medium of transiently transfected fibroblasts. Competitor DNA for the binding sites of Sp-1, Ap-1 and NF-1 was individually cotransfected transiently in order to block the promoter-driven CAT expression.

RESULTS: Sequences of -2 483 to +42 bp and -268 to +42 bp of human $\alpha 1(I)$ procollagen gene had high activity as promoters. Binding sites for Ap-1 and Sp-1 were among the cis-regulatory elements recognizing consensus transcription factors responsible for basal promoter activity of sequence -268 to +42 bp. TNF α , IFN α , IFN β showed inhibitory effects on sequence -2 483 to +42 bp as promoter with activities 43%, 62% and 60% of control respectively. Transfection of the promoter competitors could reverse the promoter activity of -268 to +42 bp 40-60%.

CONCLUSION: Sequences of -2 483 to +42 bp recombined with reporter gene provide an ideal construction for transcriptional study of $\alpha 1(I)$ procollagen gene. The anti-collagen capacity of TNF α and IFNs is associated with their transcriptional regulation. Ap-1 and Sp-1 mediate the basal transcriptional activation of human $\alpha 1(I)$ procollagen gene in dermal fibroblasts. Competitors for highly active promoters might be a novel potential candidate in fibrotic blockade.

Gao CF, Wang H, Wang AH, Wan WD, Wu YA, Kong XT. Transcriptional regulation of human $\alpha 1(I)$ procollagen gene in dermal fibroblasts. *World J Gastroenterol* 2004; 10(10): 1447-1451
<http://www.wjgnet.com/1007-9327/10/1447.asp>

INTRODUCTION

Excessive accumulation of extracellular matrix (ECM) following chronic impairment of tissue gives rise to the development of fibrosis which might occur in skin and other organs, such as liver, kidney and lung^[1]. Scarring or cirrhosis with the progression of fibrosis can cause functional failure of the organ due to the distortion of the structure. Type I collagen, composed of two chains of $\alpha 1(I)$ and one chain of $\alpha 2(I)$, is the most abundant component of ECM in most fibrotic tissues^[1]. The expression of genes coding for the $\alpha 1(I)$ and $\alpha 2(I)$ chains of type I collagen is regulated coordinatively^[2]. Researches on the expression of type I collagen in the past decades have been ascribed to fluctuations under various pathophysiological conditions at transcriptional and translational levels^[3]. Most of the recent available evidence suggest that the principal mechanisms operate at the level of transcription, although control and changes in mRNA processing and stability may also play a role^[4-7]. The mechanisms of transcriptional activation of collagen genes are poorly understood till now. Several putative regulatory elements that may determine the transcriptional efficiency of type I collagen gene have been identified in their corresponding promoters^[8-11]. Fine mapping of the cis-acting elements as well as the identification of their consensus DNA-binding proteins involved in the modulation of collagen gene expression is crucial for understanding the pathological regulation of collagen accumulation. In our previous work, we analyzed the promoter activity from mouse $\alpha 2(I)$ procollagen gene as well as its modulation by cytokines^[12,13]. In this study, we investigated the fractional activity of promoter from human $\alpha 1(I)$ procollagen gene and the interaction between cis-elements and consensus DNA-binding proteins responsible for high promoter activity. Sequence between 2 500 bp upstream of the start of transcription and 42 bp downstream of this site was studied with serial 5' -deletion. We report that regions from -2 483 to +42 bp, -268 to +42 bp of human $\alpha 1(I)$ procollagen gene have higher promoter activities. Binding sites for Ap-1, Sp-1 may be among the cis-regulatory elements recognizing consensus transcription factors responsible for basal promoter activity of sequence -268 to +42 bp. The anti-fibrotic capacities of TNF α and IFNs are associated with their transcriptional regulation of type I collagen. Transfection of the promoter competitors can partially reverse the promoter activity, suggesting that promoter competitors for highly active promoters may be a novel antifibrotic tool.

MATERIALS AND METHODS

Cell culture

Human dermal fibroblast culture was established by explanting tissue specimens obtained from the abdominal skin of a 3-year old male patient because of burn of his left arm and requiring skin transplantation. The cells were maintained under standard conditions in Dulbecco's modified Eagle's medium (DMEM, Gibco, USA) supplemented with 100 mL/L fetal calf serum (FCS, Gibco, USA). The cells in passages 3-8 were used for study.

Construction of plasmids

Plasmid pCAT3-enhancer (Promega, USA), a promoterless vector which contains SV40 enhancer and chloramphenicol

acetyltransferase (CAT) as reporter gene, was used as the recombinant plasmid backbone. The putative promoters in 6 constructions named pCOLH_{0.1}, pCOLH_{0.27}, COLH_{0.5}, pCOLH_{0.9}, pCOLH_{1.5} and pCOLH_{2.5} corresponded to sequences -105 to +42 bp, -268 to +42 bp, -496 to +42 bp, -829 to +42 bp, -1 448 to +42 bp, -2 483 to +42 bp, respectively in human $\alpha 1(I)$ procollagen gene with the same 3' ends. They were obtained by PCR with p5.3K $\alpha 1$ containing 5' flanking region -5 300 to +42 bp of human $\alpha 1(I)$ procollagen gene (gift from Dr. Sergio A. Jimenez) as template^[14]. Sense primers for PCR were as follows: pCOLH_{0.1}: 5' -ATGTCTACGCGTCTGATTGGCTGGGGCACGG-3', pCOLH_{0.27}: 5' -ATGTCTACGCGTCTGAGGACCCAGCTGCAC-3', pCOLH_{0.5}: 5' -ATGTCTACGCGTGGAGAGGTCCTCAGC ATGC-3', pCOLH_{0.9}: 5' -ATGTCTACGCGTGGCTGCTCCATCACCCAAC-3', pCOLH_{1.5}: 5' -ATGTCTACGCGTCTCAGGACGAGGTA GATTG-3', pCOLH_{2.5}: 5' -ATGTCTACGCGTACATCTT CAGCCTGGGCAC-3'. Antisense primers for the 6 putative promoters were the same: 5' -ATAGTACTCGAGCGTGCCTCCTGCTCCGAC-3'. The sense and antisense primers contained *Mlu*I and *Xho*I adaptors (underlined part) which were 6 bases away from the 5' end of the primers. PCR was performed as routine with high-fidelity PCR kit (Roche) and PE-9600 PCR amplifier. The PCR products were digested with *Mlu*I and *Xho*I and then ligated to *Mlu*I-*Xho*I linearized pCAT3 vector with T4 DNA ligase (Promega). The ligation mixtures were transformed to competent *E. coli* (JM109), and the ampicillin resistant positive clones were further identified by small-scale restriction enzyme digestion and DNA sequencing (ABI 377). The correct clones were amplified and recombinant plasmids were extracted and purified with plasmid isolation kit (Qiagen). The purity and yield rate were determined in UV spectrophotometer (Du 600, Beckman).

Synthesis of oligonucleotide for binding sites of Ap-1, Sp-1 and NF-1

Consensus binding sites for Ap-1, Sp-1, and NF-1 were first synthesized as single stranded DNA (Sangon, Shanghai) and sequences were: Ap-1, 5' CGCTTGATGACTCAGCCGGAA 3'; Sp-1, 5' ATCGATCGGGGCGGGGCGCGC3'; NF-1, 5' TTTTGGATTGAAGCCA ATATGATA3'. The synthesized sense and antisense single stranded DNAs were matched and mixed at a molar ratio of 1:1. After incubation of the mixtures at 95 °C for 10 min and then cooling slowly down to room temperature, the double stranded DNAs were stored at -20 °C.

DNA transfection

DNA transfection was performed with Dospere liposomal transfecting reagent (Roche, Germany) according to manufacturer's instruction. Briefly, the day before transfection, dermal fibroblasts were seeded at 5×10^5 /well in a 6-well plate (Nunc, USA) in 2 mL DMEM. The cells were incubated until 60-80% confluence. Then the medium was replaced with fresh culture medium without FCS shortly before adding transfection reagent. Two micrograms of construct plasmid together with 1 μ g of pSV β -gal (Promega, USA) as internal standard were cotransfected. CAT expression plasmid pCAT6.2 (Invitrogen, USA) was also transfected as CAT expression positive control. One milliliter medium containing 20 mL/L FCS was added to each well 6 h later. The medium was then replaced with fresh normal culture medium 24 h later. Two days after transfection, the cells were ready for reporter gene (CAT) expression measurement. For the cells transfected with pCOLH_{0.27}, 10 μ g of DNA for binding sites of Ap-1, Sp-1 or NF-1 was transfected to the cells 24 h after pCOLH_{0.27} transfection. Mock DNA transfection was included. The transfection was terminated 24 h later and ready for reporter gene detection.

To study the regulatory effect of cytokines, cells were starved for 4 h after being transfected with pCOLH_{2.5} for 24 h, then culture medium was replaced by fresh medium containing TNF α 10 μ g/L (R&D, USA), IFN α 1×10^5 U/L (PBL, England), IFN γ 1×10^5 U/L (Roche, USA) respectively. Another 24 h later, the transfection was terminated and ready for reporter gene detection.

Determination of CAT and β -galactosidase

Forty-eight hours after initial transfection, cells were washed with precooled phosphate buffered solution (PBS, 0.1 mol/L, pH7.4) and lysed with lysis buffer (Roche, USA). Aliquots of cell extracts were made for protein determination as described previously^[15]. CAT was measured by ELISA (Roche, USA) and β -galactosidase with enzyme activity analysis method (Promega, USA).

Electrophoretic mobility shift assay (EMSA)

EMSA was performed as described previously^[16]. Briefly, a fragment spanning -268 to +42 bp of the human $\alpha 1(I)$ procollagen gene was obtained by PCR with p5.3K $\alpha 1$ as template. The fragment obtained from PCR was purified, digested with *Eco*RII and 3' end-labeled with digoxigenin (Roche). Crude nuclear extracts from early passage confluent human fibroblasts were prepared according to the method described by Erdos *et al*^[17]. The protein concentration in nuclear extract was determined by Bradford method^[15]. DNA-protein binding reactions (20 μ L) were performed in a buffer containing 1 μ g of poly[d(A-T)], 1 μ g of poly L-lysine, 15 μ g of crude nuclear extract, 50 fmol of dig-labeled probes. Unlabeled probes and synthetic binding sites of Ap-1, Sp-1 and NF-1 were applied with 100-fold molar excess for competition tests. Following 20-min incubation at room temperature, DNA-protein complexes were resolved from free DNA probes by electrophoresis on 60 g/L non-denatured polyacrylamide gels. Transfer of DNA was finished by electroblotting. Signals were captured by chemiluminescent detection with alkaline phosphatase labeled anti-dig antibody and CSPD (Roche) as substrate.

RESULTS

Construction and transfection of 5'-deleted recombinant plasmids

Constructions of the 6 recombinant plasmids were verified by small-scale restriction enzyme digestion and DNA sequencing. Figure 1 shows the correct digestion of the constructs. The putative promoters in the constructions were 0.1 kb, 0.27 kb, 0.5 kb, 0.9 kb, 1.5 kb, and 2.5 kb, corresponding to -105 to +42 bp, -268 to +42 bp, -496 to +42 bp, -829 to +42 bp, -1 448 to +42 bp, -2 483 to +42 bp of human $\alpha 1(I)$ procollagen gene. DNA sequencing indicated that the inserted sequences of the putative promoters were the same as that published in GeneBank (accession No X98705). The 6 constructs containing serial 5'-deleted promoters were transiently transfected to early passage confluent human fibroblasts. Forty-eight hours after transfection, the expression of reporter gene CAT was determined by ELISA with the detection of β -galactosidase activity and protein for normalization. The expression of normalized CAT in the cells transfected with pCOLH_{2.5} was set as 1, the relative expression level of normalized CAT in cells transfected with other constructs is shown in Table 1 (mean \pm SD of three independent experiments), indicating that the highest CAT expressions were driven by -2 483 to +42 bp and -268 to +42 bp as promoters while the lowest by -105 to +42 bp.

Transfection of promoter competitors

For the cells transfected with pCOLH_{0.27}, 10 μ g of consensus recognition DNA for Ap-1, Sp-1 or NF-1 was transfected to

cells 24 h after pCOLH₁0.27 transfection. Reporter gene (CAT) was determined another 24 h later. Relative CAT expression values in different transfection groups were calculated relative to that of mock DNA transfection. The result shown in Figure 2 indicated that transfection of Ap-1 or Sp-1 DNA inhibited CAT expression approximately by 25% and 20% respectively compared to mock DNA transfection ($P < 0.05$). Transfection of NF-1 DNA did not show definite effect on reporter gene expression.

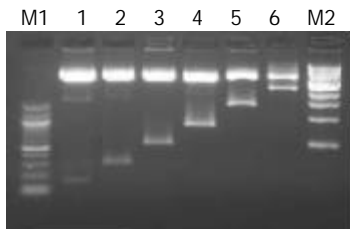


Figure 1 Electrophoresis of six constructs digested with *MluI* and *XhoI*. M1: 100 bp DNA ladder marker, M2: 1 kb DNA ladder marker, Lane1: pCOLH₁0.1, lane2: pCOLH₁0.27, lane3: pCOLH₁0.5, Lane4: pCOLH₁0.9, Lane5: pCOLH₁1.5, Lane6: pCOLH₁2.5. Six recombinant plasmids containing serial 5' -deleted flanking sequences of human $\alpha 1(I)$ procollagen gene as putative promoter were digested with *MluI* and *XhoI* at 37 °C for 1 h. The digested DNAs were fractionated on 15 g/L agarose gel showing vector DNA (4.3 kb) and insertion promoters with different sizes.

Table 1 Summary of CAT expression driven by various lengths of the 5' flanking sequence from human $\alpha 1(I)$ procollagen gene

Name of transfected constructions	Putative promoters' length (bp)	Relative activities of reporter gene (CAT, mean \pm SD) ¹
pCOLH ₁ 0.1	-105 to 42	0.10 \pm 0.02
pCOLH ₁ 0.27	-268 to 42	0.97 \pm 0.04
pCOLH ₁ 0.5	-496 to 42	0.20 \pm 0.05
pCOLH ₁ 0.9	-829 to 42	0.36 \pm 0.09
pCOLH ₁ 1.5	-1 448 to 42	0.73 \pm 0.11
pCOLH ₁ 2.5	-2 483 to 42	1.0

¹The expression of normalized CAT in the cells transfected with pCOLH₁2.5 was set as 1, the relative expression level of normalized CAT in the cells transfected with other constructs is shown in Table 1 (mean \pm SD of three independent experiments).

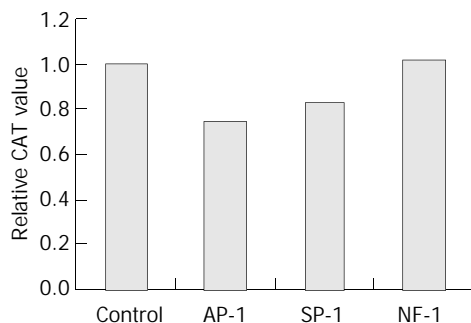


Figure 2 Effects of consensus DNA on CAT expression in pCOLH₁0.27 transfected cells. Control: mock DNA transfection, Ap-1: transfection of Ap-1 consensus DNA (10 μ g), Sp-1: transfection of Sp-1 consensus DNA (10 μ g), NF-1: transfection of NF-1 consensus DNA (10 μ g). For the cells transfected with pCOLH₁0.27, transfection of consensus recognition DNA for Ap-1, Sp-1 or NF-1 was performed 24 h after initial transfection. Reporter gene CAT was determined with ELISA after another 24 h. Relative CAT values in different transfection groups were calculated relative to that in mock DNA transfection. The

result represented three independent experiments. * $P < 0.05$ compared to control.

EMSA

The fragment spanning -268 to +42 bp in human $\alpha 1(I)$ procollagen gene was digested into three smaller ones (42 bp, 113 bp, 155 bp) with *EcoRII* (Figure 3). EMSA with these three labeled oligonucleotides mixture as probes showed that DNA-protein complexes were generated and detected in form of retardation bands. Competition with molar excesses of the same unlabeled probe prevented the formation of DNA-protein complexes, suggesting the specificity of the binding between DNA and protein. Excess consensus DNA for Sp-1, Ap-1 or NF-1 partially inhibited the occurrence of retardation differently, indicating the potential binding sites for Sp-1, Ap-1 and NF-1 in -268 to +42 bp of human $\alpha 1(I)$ procollagen gene (Figure 4).

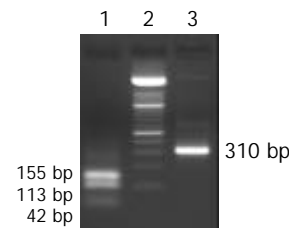


Figure 3 Electrophoresis (20 g/L agarose gel) of the fragment -268 to +42 bp digested with *EcoRII*. Lane1: *EcoRII*-digested fragment, Lane2: 100 bp DNA ladder, Lane3: 310 bp length of fragment spanning from -268 to +42bp. The 310 bp fragment spanning -268 to +42 bp of the human $\alpha 1(I)$ procollagen gene was obtained by PCR with p5.3K $\alpha 1$ as template. The fragment was digested with *EcoRII*. Electrophoresis (20 g/L agarose gel) of the digested mixture showed 3 bands with different sizes (42 bp, 113 bp, 155 bp) which were labeled and used as probes in EMSA.

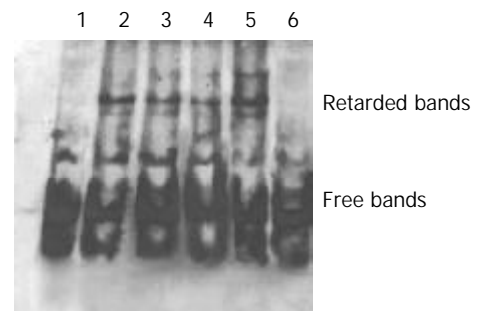


Figure 4 Result of EMSA with *EcoRII*-digested -268 to +42 bp as probe. Lane1: Labeled DNA, Lane2: Labeled DNA+ nuclear protein +NF-1 consensus DNA, Lane3: Labeled DNA + nuclear protein + Sp-1 consensus DNA, Lane4: Labeled DNA + nuclear protein + Ap-1 consensus DNA, Lane 5: Labeled DNA + nuclear protein, Lane 6: Labeled DNA + excess unlabeled DNA + nuclear protein. The existence of several retarded bands in EMSA indicated that there were several nuclear protein binding sites in sequence -268 to +42 bp (lane 5). No retardation occurred when excess unlabeled DNA probe was added to the DNA-protein reaction, confirming the specificity of the retardation (lane 6). Consensus DNAs for Sp1, Ap-1 and NF-1 were among the possible regulatory elements since the molar excess of the consensus unlabeled probe (Sp1, Ap-1, NF-1) inhibited partially the formation of retardation bands differently (lanes 2,3 and 4).

Effect of cytokines on reporter gene activity

TNF α , IFN α and IFN γ inhibited the reporter gene activity by 40-60% in the cells transfected with pCOLH₁2.5 ($P < 0.05$) compared to the control. The strongest inhibitory effect appeared in TNF α group (Table 2).

Table 2 Effect of cytokines on reporter gene activity in cells transfected with pCOLH₁2.5

Cytokines	Relative value of reporter gene activity ¹	P Value (compared to control)
Control	1.00±0.15	
TNFα 10 μg/L	0.43±0.17	<0.05
IFNα 1×10 ⁵ U/L	0.62±0.15	<0.05
IFNγ 1×10 ⁵ U/L	0.60±0.16	<0.05

¹The reporter gene activity of the cells transfected with pCOLH₁2.5 was set as 1, the relative expression level of normalized CAT in transfected cells treated with cytokines was expressed as mean±SD of three independent experiments.

DISCUSSION

The mechanisms involved in the regulation of collagen production under fibrotic conditions are not yet completely understood. The synthesis of collagen might be modulated transcriptionally and post-transcriptionally, similar to the regulation of most of the other proteins in eukaryotic cells. Evidence suggests that the stability of newly synthesized mRNA as well as some enzymes devoted to collagen synthesis and degradation may play important roles in excessive accumulation of collagen in tissues^[18]. Recently, studies focused on transcriptional regulation revealed that there existed several important cis-acting elements in the upstream region of human or rodent type I procollagen genes^[8-11,19]. Activation of type I collagen gene was regarded to be related to the MAP kinase cascade pathway^[6,20]. Newly identified tissue specific transcription factors for transcription of collagen genes have been increasing^[21-26]. Some responsive elements of cytokines, including TGFβ₁, TNFα and IFNγ have been reported to be located in procollagen genes^[7,27-29]. In previous work, we analyzed the promoter activity from mouse α2(I) procollagen gene as well as its modulation by cytokines and retinoic acid^[12,13,30]. Sequence spanning from -348 bp to +54 bp in mouse α2(I) procollagen was found to be of the highest promoter activity and partial cell specificity. The activity was influenced by TGFβ, TNFα and IFNs. In order to elucidate the transcriptional regulation of type I collagen in humans, especially the cis-acting elements and consensus transcription factors involved, six recombinant plasmids containing serial 5' -deleted flanking sequences of α1(I) procollagen gene as putative promoter were constructed here. Transient transfection of these constructions into human dermal fibroblasts showed that the sequences spanning from -2 483 bp to +42 bp and from -268 to +42 bp could drive the reporter gene with higher activity, while -105 to +42 bp had lower activity, indicating that there might be some positive and negative elements in the 2.5 kb flanking region. Our result was in agreement partially with that of Jimenez *et al.* though the fine mapping was different because of different constructs and host cells used^[14]. Further deduction from the ranked driving activity of the putative promoter suggests that positive elements may be localized at -2 483 to 1 448 bp, -1 448 to 829 bp, -829 to -498 bp, -268 to -105 bp and negative ones at -498 to 268 bp, -105 to +42 bp. Computer- based prediction (DNAssist 1.0) of this 2.5 kb flanking sequence revealed that there might be 5 binding sites for *Sp-1* (-123 bp, -1 615 bp, -1 628 bp, -2 170 bp, -2 176 bp), 1 for *NFκB* (-1 571 bp), 2 for *c-myc* (-1 118 bp, -2 406 bp), 2 for *Ap-1* (-103 bp, -1 985 bp), 1 for *NF-1* (-101 bp). Obviously, one site for *NF-1* (-101 bp), *Ap-1* (-103 bp) and *Sp-1* (-123 bp) might be located in -268+42 bp.

To further characterize the existence of Ap-1, Sp-1, and NF-1 as potential transcription factors transactivating α1(I) procollagen gene, we studied the DNA-binding capacity of sequence -268+42 bp, which showed a higher promoter activity

in transfection experiment with modified EMSA. Restriction enzyme *EcoR* II cut the target sequence into 3 smaller fragments with different sizes, *i.e.* -268 to -227 bp (42 bp), -226 to 114 bp (113 bp), and -113 to +42 bp (155 bp). The digested fragments were end-labeled with digoxigenin and used as probes in DNA-protein binding reaction (see details in MATERIALS AND METHODS). DNA-protein complexes were shown in form of DNA bands with low mobility. The existence of several retarded bands in EMSA indicates there are several nuclear protein binding sites in sequence -268 to +42 bp. No retardation could be found if excess unlabeled DNA probe was added to the DNA-protein reaction, confirming the specificity of the retardation. Consensus DNAs for Sp1, Ap-1 and NF-1 were among the possible regulatory elements since the molar excess of the consensus unlabeled probe (*Sp1*, *Ap-1*, *NF-1*) partially inhibited the formation of retardation bands differently (Figure 4).

In order to confirm the potential binding sites and their transcriptional regulatory effects on -268 to +42 bp flanking sequence, a set of competitors in forms of double stranded DNA consensus to Ap-1, Sp-1 and NF-1 were transfected to cells 24 h after pCOLH₁0.27 transfection. The competitive inhibitory effects were found in *Ap-1* (25%) and *Sp-1* (20%), indicating the positive effects of the sequences on *Ap-1* and *Sp-1* in -268 to +42 bp. The transfected sequence for *Ap-1* or *Sp-1* thus decreased -268 to +42 bp activity as promoter due to competition for binding of nuclear protein. The results were similar to those reported by Sugiura and Inagaki *et al.* who showed that some cytokines or calcium channel blockers could modulate the expression of collagen via Ap-1 and Sp-1^[9,31]. The anticipated inhibitory effect of *NF-1* competitor has not been found due to unknown reasons. No effect of *NF-1* on basal transcription or the weak effect of *NF-1* beyond detection limit might be the explanation.

The Sp1 is a ubiquitously expressed zinc-finger transcription factor recognizing GC rich sequence that is widely distributed in the promoters of various genes and is thought to be a target of intracellular signaling^[32]. It is regarded that Sp1 plays an important role in both basal and inducible regulation of type I collagen expression, and may be implicated in the increased production of collagen during the development of pathological fibrosis^[9]. Ap-1 consists of either Jun homodimers or Fos/Jun heterodimeric complexes which bind the palindromic TRE sequence TGA(C/G)TGA. Ap-1 is subjected to regulation by both phosphorylation and chemical oxidation of specific cysteine residues mapping within the DNA binding domains^[33]. In this study transfection of Ap-1 and Sp-1 oligonucleotides to pCOLH₁0.27 transfected cells inhibited the promoter activity of -268 to +42 bp, suggesting that Ap-1 and Sp-1 sites are important for the basal promoter activity of the α1(I) procollagen gene besides mediating the response of cytokines and chemicals^[31-34]. Increased promoter activity of procollagen α2(I) induced by TGFβ₁ or acetaldehyde is mediated through NF-1. The existence of NF-1 in -268 to +42 bp of human α1(I) gene has been shown by our competitive EMSA. Transfection of consensus DNA for NF-1 failed to inhibit the promoter activity of -268 bp to +42 bp in our experiment. The possible reason might be due to no or weak effect of NF-1 and thus its weak competition for the basal promoter activity.

The antifibrotic capacity of TNFα and IFNs has been reconfirmed in our study and their transcriptional regulation on collagen promoter definitely play a role in their anti-collagen production effect.

In conclusion, we find that sequences spanning from -2 483 bp to +42 bp and -268 to +42 bp in 5' -flanking region from α1(I) procollagen gene are highly active as promoters. The inhibitory cytokines including TNFα and IFNs downregulate collagen production via at least partially transcriptional regulation. The promoter activity of -268 bp to +42 bp shows

that binding sites for Sp-1, Ap-1 and NF-1 are existing candidate cis-element for transcriptional regulation in sequence -268 to +42 bp. Binding sites for Sp-1, Ap-1 are positive for basal transcription since transfections of their competitor oligo DNAs decrease the promoter activity of sequence -268 to +42 bp. Thus, transfection of competitor DNAs is applied for the first time to confirm that the sites for Sp-1 and Ap-1 are important for basal highly promoter activity. Competitors for the high active binding sites for transcription factors may be novel and promising tools for fibrotic blockade.

ACKNOWLEDGMENTS

We are especially grateful for the critical reading of the manuscript by Professor A.M. Gressner and Dr. Weiskirchen. We thank Dr. Sergio A. Jimenez for generously providing plasmid p5.3K $\alpha 1$.

REFERENCES

- Friedman SL.** Seminars in medicine of the Beth Israel Hospital, Boston. The cellular basis of hepatic fibrosis. Mechanisms and treatment strategies. *N Engl J Med* 1993; **328**: 1828-1835
- Slack JL, Liska DJ, Bornstein P.** Regulation of expression of the type I collagen genes. *Am J Med Genet* 1993; **45**: 140-151
- Rockey DC, Chung JJ.** Interferon gamma inhibits lipocyte activation and extracellular matrix mRNA expression during experimental liver injury: implications for treatment of hepatic fibrosis. *J Investig Med* 1994; **42**: 660-670
- Inagaki Y, Nemoto T, Kushida M, Sheng Y, Higashi K, Ikeda K, Kawada N, Shirasaki F, Takehara K, Sugiyama K, Fujii M, Yamauchi H, Nakao A, de Crombrughe B, Watanabe T, Okazaki I.** Interferon alfa down-regulates collagen gene transcription and suppresses experimental hepatic fibrosis in mice. *Hepatology* 2003; **38**: 890-899
- Buttner C, Skupin A, Rieber EP.** Transcriptional activation of the type I collagen genes COL1A1 and COL1A2 in fibroblasts by interleukin-4: analysis of the functional collagen promoter sequences. *J Cell Physiol* 2004; **198**: 248-258
- Papakrivopoulou J, Lindahl GE, Bishop JE, Laurent GJ.** Differential roles of extracellular signal-regulated kinase 1/2 and p38 (MAPK) in mechanical load-induced procollagen alpha(1)(I) gene expression in cardiac fibroblasts. *Cardiovasc Res* 2004; **61**: 736-744
- Kubota K, Okazaki J, Louie O, Kent KC, Liu B.** TGF-beta stimulates collagen (I) in vascular smooth muscle cells via a short element in the proximal collagen promoter. *J Surg Res* 2003; **109**: 43-50
- Ratziu V, Lalazar A, Wong L, Dang Q, Collins C, Shaulian E, Jensen S, Friedman SL.** Zf9, a Kruppel-like transcription factor up-regulated *in vivo* during early hepatic fibrosis. *Proc Natl Acad Sci U S A* 1998; **95**: 9500-9505
- Chen SJ, Artlett CM, Jimenez SA, Varga J.** Modulation of human alpha1(I) procollagen gene activity by interaction with Sp1 and Sp3 transcription factors *in vitro*. *Gene* 1998; **215**: 101-110
- Rippe RA, Schrum LW, Stefanovic B, Solis-Herruzo JA, Brenner DA.** NF-kappaB inhibits expression of the alpha1(I) collagen gene. *DNA Cell Biol* 1999; **18**: 751-761
- Bergeron C, Page N, Joubert P, Barbeau B, Hamid Q, Chakir J.** Regulation of procollagen I (alpha1) by interleukin-4 in human bronchial fibroblasts: a possible role in airway remodelling in asthma. *Clin Exp Allergy* 2003; **33**: 1389-1397
- Gao CF, Wang H, Huang C, Kong XT.** Study of activity of promoter from mouse $\alpha 2(I)$ procollagen gene. *Chin Med J* 1999; **112**: 316-320
- Gao CF, Wang H, Wu YA, Kong XT.** The effect of cytokines on promoter activity in mouse $\alpha 2(I)$ procollagen gene. *J Med Coll PLA* 1999; **14**: 12-16
- Jimenez SA, Varga J, Olsen A, Li L, Diaz A, Herhal J, Koch J.** Functional analysis of human alpha 1(I) procollagen gene promoter. Differential activity in collagen-producing and -nonproducing cells and response to transforming growth factor beta 1. *J Biol Chem* 1994; **269**: 12684-12691
- Bradford MM.** A rapid and sensitive method for the quantitation of microgram quantities of protein utilizing the principle of protein-dye binding. *Anal Biochem* 1976; **72**: 248-254
- Gao CF, Wang H, Gao GH, Mi QM, Kong XT.** Nonisotopic analysis of sequence specific DNA-binding proteins. *Shijie Huaren Xiaohua Zazhi* 2001; **9**: 499-503
- Erdos G, Lee YJ, Cho JM, Corry PM.** Heat-induced bFGF gene expression in the absence of heat shock element correlates with enhanced AP-1 binding activity. *J Cell Physiol* 1995; **164**: 404-413
- Yata Y, Takahara T, Furui K, Zhang LP, Jin B, Watanabe A.** Spatial distribution of tissue inhibitor of metalloproteinase-1 mRNA in chronic liver disease. *J Hepatol* 1999; **30**: 425-432
- Lindahl GE, Chambers RC, Papakrivopoulou J, Dawson SJ, Jacobsen MC, Bishop JE, Laurent GJ.** Activation of fibroblast procollagen alpha 1(I) transcription by mechanical strain is transforming growth factor-beta-dependent and involves increased binding of CCAAT-binding factor (CBF/NF-Y) at the proximal promoter. *J Biol Chem* 2002; **277**: 6153-6161
- Tharaux PL, Chatziantoniou C, Fakhouri F, Dussaulte JC.** Angiotensin II activates collagen I gene through a mechanism involving the MAP/ER kinase pathway. *Hypertension* 2000; **36**: 330-336
- Tanaka K, Matsumoto Y, Nakatani F, Iwamoto Y, Yamada Y.** A zinc finger transcription factor, alphaA-crystallin binding protein 1, is a negative regulator of the chondrocyte-specific enhancer of the alpha1(II) collagen gene. *Mol Cell Biol* 2000; **20**: 4428-4435
- Hasegawa T, Takeuchi A, Miyaishi O, Xiao H, Mao J, Isobe K.** PTRF (polymerase I and transcript-release factor) is tissue-specific and interacts with the BFCOL1 (binding factor of a type-I collagen promoter) zinc-finger transcription factor which binds to the two mouse type-I collagen gene promoters. *Biochem J* 2000; **347**(Pt 1): 55-59
- Zhao MK, Pretorius PJ, de Vries WN.** Characterization of a novel transcription factor binding to the regulatory regions of the human pro-alpha1(I) collagen gene. *Arch Biochem Biophys* 2000; **376**: 281-287
- Kanamaru Y, Nakao A, Tanaka Y, Inagaki Y, Ushio H, Shirato I, Horikoshi S, Okumura K, Ogawa H, Tomino Y.** Involvement of p300 in TGF-beta/Smad-pathway-mediated alpha2(I) collagen expression in mouse mesangial cells. *Nephron Exp Nephrol* 2003; **95**: e36-42
- Chen A, Davis BH.** The DNA binding protein BTEB mediates acetaldehyde-induced, jun N-terminal kinase-dependent alpha1(I) collagen gene expression in rat hepatic stellate cells. *Mol Cell Biol* 2000; **20**: 2818-2826
- Drissi MH, Li X, Sheu TJ, Zuscik MJ, Schwarz EM, Puzas JE, Rosier RN, O'Keefe RJ.** Runx2/Cbfa1 stimulation by retinoic acid is potentiated by BMP2 signaling through interaction with Smad1 on the collagen X promoter in chondrocytes. *J Cell Biochem* 2003; **90**: 1287-1298
- Falanga V, Zhou L, Yufit T.** Low oxygen tension stimulates collagen synthesis and COL1A1 transcription through the action of TGF-beta1. *J Cell Physiol* 2002; **191**: 42-50
- Kinbara T, Shirasaki F, Kawara S, Inagaki Y, de Crombrughe B, Takehara K.** Transforming growth factor-beta isoforms differently stimulate proalpha2(I) collagen gene expression during wound healing process in transgenic mice. *J Cell Physiol* 2002; **190**: 375-381
- Inagaki Y, Truter S, Tanaka S, Di Liberto M, Ramirez F.** Overlapping pathways mediate the opposing actions of tumor necrosis factor-alpha and transforming growth factor-beta on alpha 2(I) collagen gene transcription. *J Biol Chem* 1995; **270**: 3353-3358
- Gao CF, Wang H, Kong XT.** IFN effect on promoter activity in mouse $\alpha 2(I)$ procollagen gene. *Shijie Huaren Xiaohua Zazhi* 1998; **6**: 201-203
- Sugiura T, Imai E, Moriyama T, Horio M, Hori M.** Calcium channel blockers inhibit proliferation and matrix production in rat mesangial cells: possible mechanism of suppression of AP-1 and CREB activities. *Nephron* 2000; **85**: 71-80
- Ghayer C, Chadjichristos C, Herrouin JF, Ala-Kokko L, Suske G, Pujol JP, Galera P.** Sp3 represses the Sp1-mediated transactivation of the human COL2A1 gene in primary and de-differentiated chondrocytes. *J Biol Chem* 2001; **276**: 36881-36895
- Chung KY, Agarwal A, Uitto J, Mauviel A.** An AP-1 binding sequence is essential for regulation of the human alpha2(II) collagen (COL1A2) promoter activity by transforming growth factor-beta. *J Biol Chem* 1996; **271**: 3272-3278
- Greenwel P, Inagaki Y, Hu W, Walsh M, Ramirez F.** Sp1 is required for the early response of alpha2(II) collagen to transforming growth factor-beta1. *J Biol Chem* 1997; **272**: 19738-19745

In vitro cultivation of human fetal pancreatic ductal stem cells and their differentiation into insulin-producing cells

Zhong-Xiang Yao, Mao-Lin Qin, Jian-Jun Liu, Xing-Shu Chen, De-Shan Zhou

Zhong-Xiang Yao, Mao-Lin Qin, Jian-Jun Liu, Xing-Shu Chen, De-Shan Zhou, Department of Histology and Embryology, The Third Military Medical University, Chongqing 400038, China

Supported by the National Natural Science Foundation of China, No. 30370164 and Tenth-five-year Foundation of PLA, No.01J013

Correspondence to: Dr. De-Shan Zhou and Dr. Zhong-Xiang Yao, Department of Histology and Embryology, The Third Military Medical University, Chongqing 400038, China. yaozx@mail.tmmu.com.cn
Telephone: +86-23-68752231

Received: 2003-12-23 **Accepted:** 2004-01-08

Abstract

AIM: To isolate, culture and identify the human fetal pancreatic ductal stem cells *in vitro*, and to observe the potency of these multipotential cells differentiation into insulin-producing cells.

METHODS: The human fetal pancreas was digested by 1 g/L collagenase type IV and then 2.5 g/L trypsin was used to isolate the pancreatic ductal stem cells, followed by culture in serum-free, glucose-free DMEM media with some additional chemical substrates *in vitro* (according to the different stage). The cells were induced by glucose-free (control), 5 mmol/L, 17.8 mmol/L and 25 mmol/L glucose, respectively. The cell types of differentiated cells were identified using immunocytochemical staining.

RESULTS: The shape of human fetal pancreatic ductal stem cells cultured *in vitro* was firstly fusiform in the first 2 wk, and became monolayer and cobblestone pattern after another 3 to 4 wk. After induced and differentiated by the glucose of different concentrations for another 1 to 2 wk, the cells formed the pancreatic islet-like structures. The identification and potency of these cells were then identified by using the pancreatic ductal stem cell marker, cytokeratin-19 (CK-19), pancreatic β cell marker, insulin and pancreatic α cell marker, glucagons with immunocytochemical staining. At the end of the second week, 95.2% of the cells were positive for CK-19 immunoreactivity. Up to 22.7% of the cells induced by glucose were positive for insulin immunoreactivity, and less than 3.8% of the cells were positive for glucagon immunoreactivity in pancreatic islet-like structures. The positive ratio of immunoreactive staining was dependent on the concentration of glucose, and it was observed that the 17.8 mmol/L glucose stimulated effectively to produce insulin- and glucagons-producing cells.

CONCLUSION: The human fetal pancreatic ductal stem cells are capable of proliferation *in vitro*. These cells have multidifferentiation potential and can be induced by glucose and differentiated into insulin-producing cells *in vitro*.

Yao ZX, Qin ML, Liu JJ, Chen XS, Zhou DS. *In vitro* cultivation of human fetal pancreatic ductal stem cells and their differentiation into insulin-producing cells. *World J Gastroenterol* 2004; 10(10): 1452-1456

<http://www.wjgnet.com/1007-9327/10/1452.asp>

INTRODUCTION

Even 20 years ago, the accepted concept was that one was born with all the pancreatic β cells one ever had^[1]. However, now the concept that the pancreatic ductal stem cells exist and can differentiate into pancreatic endocrine cells are generally accepted^[2-7]. When the inability of the β cells to match the increased demand for insulin can be seen, diabetes occurs. One of the main obstacles to successful islet transplantation for diabetes is the limitation of available insulin-producing tissue^[8]. The lack of pancreatic insulin-producing tissue has given a high priority to efforts to stimulate the growth of pancreatic insulin-producing cells^[9-10].

It has been reported that the embryonic stem (ES) cells induce to generate cells expressing insulin and other pancreatic endocrine hormones^[11-15]. The cells self-assembled to form three-dimensional clusters similar in topology to normal pancreatic islets where pancreatic cell types were in close association with neurons. Glucose triggered insulin release from these cell clusters by mechanisms similar to those employed *in vivo*. When injected into diabetic mice, the insulin-producing cells underwent rapid vascularization and maintained a clustered, islet-like organization. Their use might lead to many clinical benefits but it was difficult that the differentiated cells derived from the ES cells were used to assemble functional organs^[10,16-21]. It was also shown that the duct tissue from adult human pancreas could be expanded in culture and then was directed to differentiate into glucose responsive islet-like tissue *in vitro*, but the quantities were limited, the amount would be expected to have little clinical impact^[22].

Herein we show it is easier to cultivate human fetal pancreatic ductal stem cells than adult human pancreatic ductal stem cells *in vitro* and the ductal stem cells can be induced by glucose and differentiate to insulin-producing cells.

MATERIALS AND METHODS

Specimens

The specimens ($n=5$) were collected from the Southwest Hospital of the Third Military Medical University. The samples were taken from the spontaneous abortion fetus of the embryonic age 8 stage (about 16-20 wk) of fetus according to the methods of Jirasek^[23].

Cell culture

Human fetal pancreas were digested in 1 g/L type IV collagenase for 40 min at 37 °C, naturally deposited for 10 min, the supernatant was removed. The cells were then digested in 2.5 g/L trypsin for 30 min at 37 °C, followed by centrifugation for 10 min at 1 000 r/min. The deposited cells were put into glucose-free DMEM culture medium containing 2 \times non-essential amino acid (NEAA), 1 \times B27, 100 U/mL penicillin, and 100 μ g/mL streptomycin. The cell suspensions were put into non-treated T-75 flasks having non-sticky glass coverslips inside and incubated at 37 °C in a humidified atmosphere containing 50 mL/L CO₂ in air. After 24 h the nonadherent tissue (both viable and dead) was removed, followed by the media change with additional keratinocyte growth factor (KGF, 10 ng/mL, F. Hoffmann-La

Roche Ltd, Basel, Switzerland), insulin-transferrin-selenium (ITS, 1 g/L, Sigma-Aldrich China Inc. Shanghai, China), and 2 g/mL BSA, 10 mmol/L nicotinamide (F. Hoffmann-La Roche Ltd, Basel, Switzerland). The adherent or residual cells were continuously cultured and expanded for 5-7 wk by changing the medium every 3 d. The cells were used for identification by immunostaining and further differentiation.

Cell induction and differentiation

For inducing the cells differentiation, the media with or without glucose were subdivided into 4 groups: glucose-free (control), 5 mmol/L, 17.8 mmol/L and 25 mmol/L glucose. Other elements of the media were the same as mentioned above.

Tissue fixation and immunocytochemical staining

Monolayer cells were fixed for 30 min in 40 g/L polyformaldehyde (PFA, in 0.1 mol/L phosphate buffer, pH 7.2), and then rinsed in 0.01 mol/L phosphate buffer saline (PBS, pH 7.2). The specimens were incubated with 30 mL/L H₂O₂ in pure methanol for 30 min at room temperature, followed by retrieval 3 times (1 min each time) on a microwave (750 W) in 0.1 mol/L pH 6.0 citrate buffer, and incubation with 10 g/L BSA plus 4 g/L Triton X-100 at 37 °C for 30 min. Then immunocytochemical staining was carried out by using primary antibodies of different species: monoclonal mouse anti-human cytokeratin 19 IgG1 antibody (1:100, Santa Cruz Biotechnology, Inc. California, United States of American), polyclonal rabbit anti-human insulin antibody (H-86, 1:200, Santa Cruz Biotechnology, Inc. California, United States of American), polyclonal goat anti-human glucagons IgG antibody (C-18, 1:100, Santa Cruz Biotechnology, Inc. California, United States of American). Horseradish peroxidase-labeled secondary antibody (Sigma-Aldrich China Inc. Shanghai, China) was detected by reaction with 30 mL/L H₂O₂ and 1 g/L 3, 3'-diaminobenzidine (DAB, Sigma) in solution at room temperature for 5 min, then the specimens were washed and dehydrated in a graded series by ethanol. Finally, the coverslips were mounted cell-side down on glass slides with a drop of DPX and then examined using an Olympus light microscope. Photographs were taken on Lekai-135 film. Positive cells were randomly counted on the montage of photographs generated.

RESULTS

Isolation, cultures and identification of human fetus pancreatic ductal stem cells

To promote the attachment of duct cells rather than islet cells, nonsticky culture flasks were used; these flasks had been used to maintain islets in suspension. The clumps of nonislet tissue could adhere to this nonsticky surface starting about 24 h after culture (Figure 1). Although there was considerable loss of floating tissue of pancreatic acinar tissue in culture, the quantity of cell clumps adhered increased with time. The nonadherent clumps were removed by changing the culture media. In the beginning, the adherent cells were seldom and fusiform. After the nonadherent clumps were removed, the media was changed by serum-free media with additional keratinocyte growth factor to stimulate the growth of only pancreatic ductal stem cells but not the growth of fibroblasts. The cells grew very slowly in the first 2 wk (Figure 2) and 95.2% (975/1024) of the cells were positive for CK-19 immunoreactivity (Figure 3). With additional time of 3 to 4 wk, the cells grew from the adherent clumps and formed monolayer with clear epithelial morphology. The cells were large, cobblestone patterns (Figures 4 and 5). There was a significant increase of the cultured tissue during the 5-6 wk of culture.

Differentiation of pancreatic ductal stem cells into insulin-producing cells

Once the clumps were attached and formed monolayers, the

media were changed by adding glucose in different concentration of 0, 5, 17.8 and 25 mmol/L, respectively. Over next 1-2 wk the plaques of epithelial cells became crowded, and formed a few pancreatic islet-like structures (Figure 6). Some of the cells in pancreatic islet-like structures were positive for insulin immunoreactivity (Figure 7), and a few cells were positive for glucagon immunoreactivity (Figure 8).

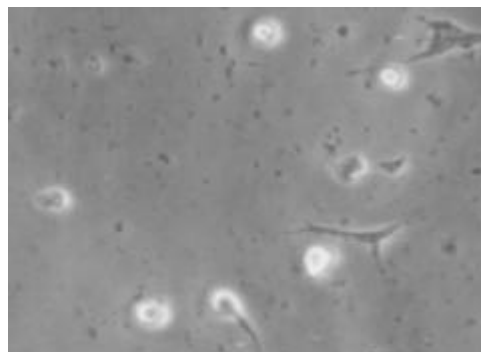


Figure 1 After being cultured for 24 h, a few cells were adhered on the bottom of non-sticky flasks, some of the cells processed protrusions ($\times 100$).



Figure 2 After being cultured for 2 wk in the media added the keratinocyte growth factor, the number of cells increased, the cells became fusiform with a few processes ($\times 100$).



Figure 3 Most cells of culture were positive for CK-19 immunoreactivity after being cultured for 2 wk ($\times 100$).

The stainings in immunopositive cells were located in the cytoplasm, but the immunonegative cells also revealed light stainings in the perinuclear region similar to those in control group. The intensity of the immunostaining varied from one cell to another. The shape of the positive cells also varied; most of the cells were polygonal in shape, but spherical or fusiform cells were also observed. The nucleus was unstained, and some cells seemed to have 2 nuclei. Analysis of the cells from randomly generated micrographs of 25 cultured coverslips revealed different percentages of the cells immunoreactivity

for CK-19, insulin and glucagons after the cells were induced by different concentration of glucose for 1-2 wk.

After induction for 2 wk with different concentrations of glucose, the numbers of positive cells for insulin and glucagon were different. The cells were CK-19 immunonegative, while the insulin immunopositive cells were obviously increased. When the concentration of glucose was 17.8 mmol/L, the ratio of insulin positive cells reached a very high level. In the media without glucose, 108 cells of total counting 1 325 (8.2%) were positive for insulin immunostaining, and 15 cells of total counting 1 187 (1.3%) were positive for glucagons immunostaining. When the concentration of glucose reached 5 mmol/L, the number of insulin-positive cells was 153 of total counting 1 142 (13.4%), while the number of glucagons-positive cells was 19 of total counting 1 092 (1.7%). In the medium containing 17.8 mmol/L glucose, 230 insulin-positive cells of total counting 1 079 (21.3%) and 40 glucagon-positive cells of total counting 1 046 (3.8%) were observed. When the concentration of glucose was 25 mmol/L, the insulin-positive cells were 255 of total counting 1 125 (22.7%) and the glucagons-positive cells were 39 of total counting 1 127 (3.5%) (Figure 9).

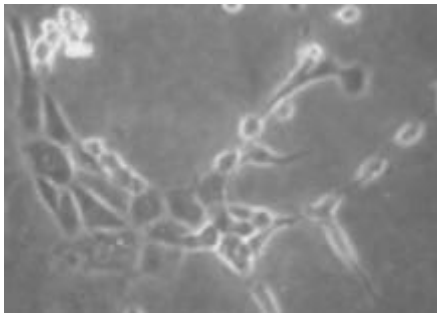


Figure 4 The cells were cobblestone pattern after being cultured for 4 wk ($\times 150$).

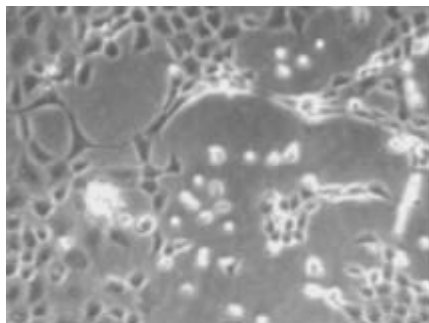


Figure 5 The cells were cobblestone pattern and formed monolayer after being cultured for 6 wk ($\times 100$).

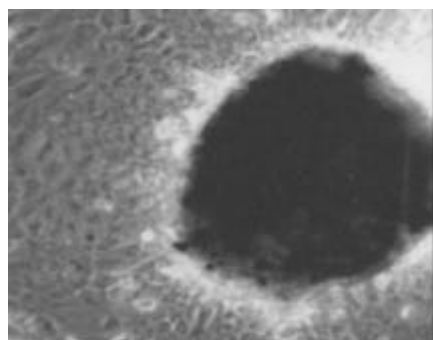


Figure 6 The cells were induced to form pancreatic islet-like structures after being cultured in the media containing 17.8 mmol/L glucose for 1 wk ($\times 100$).

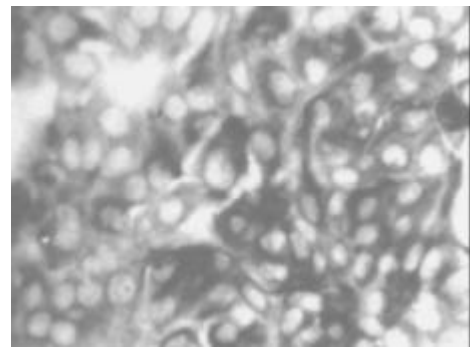


Figure 7 After being cultured in the medium containing 17.8 mmol/L glucose for 1 wk, many cells in islet-like structures were positive for insulin immunoreactivity ($\times 150$).

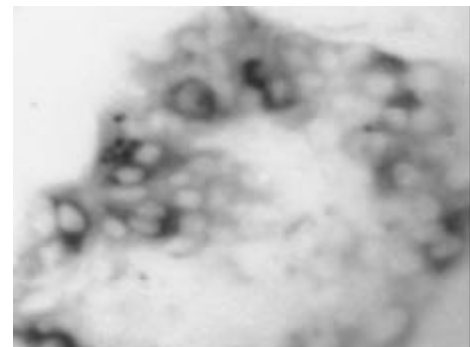


Figure 8 After being cultured in the medium containing 17 mmol/L glucose for 1 wk, a few cells in islet-like structures were positive for glucagon immunoreactivity ($\times 150$).

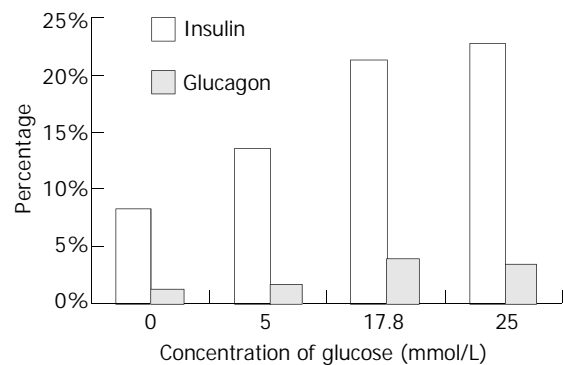


Figure 9 Percentage of immunopositive cells induced by glucose.

DISCUSSION

In pancreas, insulin is produced and secreted by specialized structures, islets of Langerhans. Diabetes, which affects thousands of million people in the world, results from abnormal function of pancreatic islets. The main obstacle to successful islet transplantation for diabetes is the limitation of available insulin-producing tissue^[24]. Herein, we introduced to generate cells expressing insulin from human fetal pancreas duct tissue. This approach may provide a potential new source of pancreatic islet cells for transplantation.

Most studies have shown there is limited *in vitro* growth of adult islet cells of any species^[25]. From the studies on rat pancreatic regeneration, it inferred that the capacity of adult pancreatic duct cells were strongly to both expand and differentiate^[26]. Bonner-Weir *et al.* showed the expansion of adult human pancreatic ductal tissue *in vitro* and its subsequent differentiation to islet cells after being overlaid with Matrigel, and over 3-4 wk culture there was a significant increase in

insulin as well as formation of islet-like structures called cultivated human islet buds^[27]. These data further provided proofs for the hypothesis that pancreatic ductal cells have the potential to lose their specific ductal epithelial cell phenotype with rapid proliferation *in vitro*, reverting to multipotent stem cells that then can differentiate into islet cells with the appropriate external stimuli^[28]. But the report showed the amount limitation and associated with loss of insulin production^[27]. In order to avoid these problems, we made use of human fetal pancreas from the spontaneous abortion human fetus, combined 2-enzyme digestion with mechanical dissection of the pancreas. The duct tissue could be dissected effectively and the single cells were rich in stem cells. The cell proliferation could be extended for at least 6 wk. The glucose can stimulate the pancreatic ductal stem cells to differentiate into insulin-producing cells.

Now, human islet isolations can yield maximum 400 000-600 000 islets per donor, which means that more than one donor may be requested for a successful transplant. In our study reported here that the pancreatic ductal stem cells, after *in vitro* expansion and glucose-induced differentiation, became organized into islet-like structures consisting of insulin- and glucagons-producing cells. Their use may lead to many clinical benefits. Because the pancreatic islets rarely adhered directly to the nonsticky flasks, and the culture medium was changed at time, the culture conditions did not favor the islets inclusion. These data provide evidence of the potential to expand and differentiate human pancreatic ductal stem cells to islet cells *in vitro*, but further optimization of conditions is needed to generate yields of islet tissue that will make an impact on islet transplantation. We have been able to expand human pancreatic ductal stem cells and then to direct its differentiation into insulin- and glucagons-producing cells, respectively. The ability to cultivate human islets from digested pancreatic ductal stem cells opens a new approach for β cell replacement therapy.

The culture condition's optimization could include further expansion of the ductal tissue or higher efficiency in differentiating cells. Of the cells adhered in the beginning, the most cells were ductal stem cells, some were fibroblasts. But the culture medium without serum and with keratinocyte growth factor favored the growth of ductal stem cells. The data from rodents suggested that *in vitro* culture of exocrine tissue (the ducts and acini) would result in ductal epithelial cells. Moreover, mouse pancreatic exocrine (acinar and ductular) tissue gave rise to epithelial cultures that were indistinguishable from cultures of isolated duct, raising the possibility that acinar cells could dedifferentiate to form duct cells^[29,30]. It is entirely possible that the cells from the smaller ducts/acini have a little capacity to differentiate into endocrine cells^[27]. Other studies suggested that between 50-95% of the rodent exocrine cells died in the initial culture condition with mainly the ductal stem cells left to replenish the cultures^[31].

In our study, the adherent cells during the early culture period seemed to be pancreatic ductal stem cells. The culture conditions were serum-free, glucose-free but including keratinocyte growth factor, and these media stimulated the proliferation of ductal stem cells but not fibroblasts. The CK-19 positive cells that formed in fusiform and cobblestone pattern were characteristic of pancreatic ductal stem cells. In contrast, the insulin-producing cells were CK-19 immunonegative and insulin immunopositive. The glucose could induce the ductal stem cells differentiation into insulin-producing cells, and the ratio of positive cells is dependent on the concentration of glucose.

Our study differs from previous work in several ways. In most other study, the human islets were isolated and expanded on an extracellular matrix substrate, in which islets were easily mixed with the ductal stem cells^[27,32,33]. With expansion as monolayers and culture in three-dimensional collagen gels,

human islets gradually lost endocrine phenotype^[27]. In the study of Bonner-Weir, mainly ductal tissue remaining after islet isolation was expanded and then coated with extracellular matrix to induce differentiation into islet cells^[27]. The potential of extracellular matrix to induce differentiation has been shown for other epithelial cell types. In the present study, we selected different concentration of glucose as the inducing element, which effectively induced the fetal ductal stem cells differentiation.

The expansion of duct tissue is effective and extensive, probably because of the removal of normal intercellular restraints found. Because the default pathway of differentiation of embryonic pancreas is thought to be that of islet formation, such restraint might be protective and necessary to prevent excessive islet formation that could produce too much insulin and even hypoglycemia^[29,30]. In the present experiment, we are able to generate new islet cells from duct stem cells, but the quantities are limited. Despite the limitations at this early stage, these findings raise the tantalizing possibility that this approach, once optimized, may generate meaningful amounts of new human insulin-producing cells from duct stem cells. This possibility has important implications for making β cell replacement therapy available to a larger number of patients with type 1 and 2 diabetes mellitus.

REFERENCES

- 1 **Bonner-Weir S.** Perspective: Postnatal pancreatic beta cell growth. *Endocrinology* 2000; **141**: 1926-1929
- 2 **Bonner-Weir S, Sharma A.** Pancreatic stem cells. *J Pathol* 2002; **197**: 519-526
- 3 **Lechner A, Habener JF.** Stem/progenitor cells derived from adult tissues: potential for the treatment of diabetes mellitus. *Am J Physiol Endocrinol Metab* 2003; **284**: E259-266
- 4 **Peshavaria M, Pang K.** Manipulation of pancreatic stem cells for cell replacement therapy. *Diabetes Technol Ther* 2000; **2**: 453-460
- 5 **Ramiya VK, Maraist M, Arfors KE, Schatz DA, Peck AB, Cornelius JG.** Reversal of insulin-dependent diabetes using islets generated *in vitro* from pancreatic stem cells. *Nat Med* 2000; **6**: 278-282
- 6 **Berna G, Leon-Quinto T, Ensenat-Waser R, Montanya E, Martin F, Soria B.** Stem cells and diabetes. *Biomed Pharmacother* 2001; **55**: 206-212
- 7 **Pattou F, Kerr-Conte J, Gmyr V, Vandewalle B, Vantuyghem MC, Lecomte-Houcke M, Proye C, Lefebvre J.** Human pancreatic stem cell and diabetes cell therapy. *Bull Acad Natl Med* 2000; **184**: 1887-1899
- 8 **Miyamoto M.** Current progress and perspectives in cell therapy for diabetes mellitus. *Hum Cell* 2001; **14**: 293-300
- 9 **Halvorsen T, Levine F.** Diabetes mellitus-cell transplantation and gene therapy approaches. *Curr Mol Med* 2001; **1**: 273-286
- 10 **Lumelsky N, Blondel O, Laeng P, Velasco I, Ravin R, McKay R.** Differentiation of embryonic stem cells to insulin-secreting structures similar to pancreatic islets. *Science* 2001; **292**: 1389-1394
- 11 **Kania G, Blyszczuk P, Czyz J, Navarrete-Santos A, Wobus AM.** Differentiation of mouse embryonic stem cells into pancreatic and hepatic cells. *Methods Enzymol* 2003; **365**: 287-303
- 12 **Kim D, Gu Y, Ishii M, Fujimiya M, Qi M, Nakamura N, Yoshikawa T, Sumi S, Inoue K.** *In vivo* functioning and transplantable mature pancreatic islet-like cell clusters differentiated from embryonic stem cell. *Pancreas* 2003; **27**: E34-41
- 13 **Kahan BW, Jacobson LM, Hullett DA, Ochoada JM, Oberley TD, Lang KM, Odorico JS.** Pancreatic precursors and differentiated islet cell types from murine embryonic stem cells: an *in vitro* model to study islet differentiation. *Diabetes* 2003; **52**: 2016-2024
- 14 **Blyszczuk P, Czyz J, Kania G, Wagner M, Roll U, St-Onge L, Wobus AM.** Expression of Pax4 in embryonic stem cells promotes differentiation of nestin-positive progenitor and insulin-producing cells. *Proc Natl Acad Sci U S A* 2003; **100**: 998-1003

- 15 **Shiroi A**, Yoshikawa M, Yokota H, Fukui H, Ishizaka S, Tatsumi K, Takahashi Y. Identification of insulin-producing cells derived from embryonic stem cells by zinc-chelating dithizone. *Stem Cells* 2002; **20**: 284-292
- 16 **Docherty K**. Growth and development of the islets of Langerhans: implications for the treatment of diabetes mellitus. *Curr Opin Pharmacol* 2001; **1**: 641-650
- 17 **Peck AB**, Cornelius JG, Chaudhari M, Shatz D, Ramiya VK. Use of *in vitro*-generated, stem cell-derived islets to cure type 1 diabetes: how close are we? *Ann N Y Acad Sci* 2002; **958**: 59-68
- 18 **Kaczorowski DJ**, Patterson ES, Jastromb WE, Shablott MJ. Glucose-responsive insulin-producing cells from stem cells. *Diabetes Metab Res Rev* 2002; **18**: 442-450
- 19 **Soria B**. *In-vitro* differentiation of pancreatic beta-cells. *Differentiation* 2001; **68**: 205-219
- 20 **Assady S**, Maor G, Amit M, Itskovitz-Eldor J, Skorecki KL, Tzukerman M. Insulin production by human embryonic stem cells. *Diabetes* 2001; **50**: 1691-1697
- 21 **Soria B**, Skoudy A, Martin F. From stem cells to beta cells: new strategies in cell therapy of diabetes mellitus. *Diabetologia* 2001; **44**: 407-415
- 22 **Peck AB**, Chaudhari M, Cornelius JG, Ramiya VK. Pancreatic stem cells: building blocks for a better surrogate islet to treat type 1 diabetes. *Ann Med* 2001; **33**: 186-192
- 23 **Jirasek JE**. Developmental stages of human embryos. *Czech Med* 1978; **1**: 156-161
- 24 **Path G**, Seufert J. Current status and perspectives of stem cell therapy for the treatment of diabetes mellitus. *Med Klin* 2003; **98**: 277-282
- 25 **Hayek A**, Beattie GM. Alternatives to unmodified human islets for transplantation. *Curr Diab Rep* 2002; **2**: 371-376
- 26 **Yamaoka T**. Regeneration therapy of pancreatic beta cells: towards a cure for diabetes? *Biochem Biophys Res Commun* 2002; **296**: 1039-1043
- 27 **Bonner-Weir S**, Taneja M, Weir GC, Tatarkiewicz K, Song KH, Sharma A, O'Neil JJ. *In vitro* cultivation of human islets from expanded ductal tissue. *Proc Natl Acad Sci U S A* 2000; **97**: 7999-8004
- 28 **Bonner-Weir S**. Stem cells in diabetes: what has been achieved. *Horm Res* 2003; **60**(Suppl 3): 10-12
- 29 **Means AL**, Leach SD. Lineage commitment and cellular differentiation in exocrine pancreas. *Pancreatology* 2001; **1**: 587-596
- 30 **Humphrey RK**, Smith MS, Kwok J, Si Z, Tuch BE, Simpson AM. *In vitro* dedifferentiation of fetal porcine pancreatic tissue prior to transplantation as islet-like cell clusters. *Cells Tissues Organs* 2001; **168**: 158-169
- 31 **Logsdon CD**, Williams JA. Pancreatic acinar cells in monolayer culture: direct trophic effects of caerulein *in vitro*. *Am J Physiol* 1986; **250**(4 Pt 1): G440-447
- 32 **Beattie GM**, Itkin-Ansari P, Cirulli V, Leibowitz G, Lopez AD, Bossie S, Mally MI, Levine F, Hayek A. Sustained proliferation of PDX-1⁺ cells derived from human islets. *Diabetes* 1999; **48**: 1013-1019
- 33 **Yuan S**, Rosenberg L, Paraskevas S, Agapitos D, Duguid WP. Transdifferentiation of human islets to pancreatic ductal cells in collagen matrix culture. *Differentiation* 1996; **61**: 67-75

Edited by Kumar M and Xu FM

Immune tolerance in pancreatic islet xenotransplantation

Tian-Hua Tang, Chun-Lin Li, Xin Li, Feng-Qin Jiang, Yu-Kun Zhang, Hai-Quan Ren, Shan-Shan Su, Guo-Sheng Jiang

Tian-Hua Tang, Feng-Qin Jiang, Yu-Kun Zhang, Hai-Quan Ren, Guo-Sheng Jiang, Department of Hemato-oncology, Institute of Basic Medicine, Shandong Academy of Medical Sciences, Jinan 250062, Shandong Province, China

Chun-Lin Li, Xin Li, Shan-Shan Su, Shandong Chinese Traditional Medical University, Jinan 250014, Shandong Province, China

Supported by Natural Science Foundation of Shandong Province, No. Y99C07

Correspondence to: Dr. Guo-Sheng Jiang, Department of Hemato-oncology, Institute of Basic Medicine, Shandong Academy of Medical Sciences, Jingshi Road 89, Jinan 250062, Shandong Province, China. jianggsh@hotmail.com

Telephone: +86-531-2919505 **Fax:** +86-531-2919978

Received: 2003-06-04 **Accepted:** 2003-09-18

Abstract

AIM: To observe the effect of tail vein injection with donor hepatocytes and/or splenocytes on the islet xenotransplantation rejection.

METHODS: New-born male pigs and BALB/C mice were selected as donors and recipients respectively. Islet xenotransplantation was performed in recipients just after the third time of tail vein injection with donor hepatocytes and/or splenocytes. Macrophage phagocytosis, NK(natural killing cell) killing activity, T lymphocyte transforming function of spleen cells, antibody forming function of B lymphocytes, and T lymphocyte subsets were taken to monitor transplantation rejection. The effects of this kind of transplantation were indicated as variation of blood glucose and survival days of recipients.

RESULTS: The results showed that streptozotocin (STZ) could induce diabetes mellitus models of mice. The pre-injection of donor hepatocytes, splenocytes or their mixture by tail vein injection was effective in preventing donor islet transplantation from rejection, which was demonstrated by the above-mentioned immunological marks. Each group of transplantation could decrease blood glucose in recipients and increase survival days. Pre-injection of mixture of donor hepatocytes and splenocytes was more effective in preventing rejection as compared with that of donor hepatocyte or splenocyte pre-injection respectively.

CONCLUSION: Pre-injection of donor hepatocytes, splenocytes or their mixture before donor islet transplantation is a good way in preventing rejection.

Tang TH, Li CL, Li X, Jiang FQ, Zhang YK, Ren HQ, Su SS, Jiang GS. Immune tolerance in pancreatic islet xenotransplantation. *World J Gastroenterol* 2004; 10(10): 1457-1461
<http://www.wjgnet.com/1007-9327/10/1457.asp>

INTRODUCTION

Insulin dependent diabetes mellitus (IDDM) so far is treated with a constant low dose insulin injection and immunosuppressive agents. But a large quantity of clinical data indicated that long-term insulin injection could induce insulin resistance and was

not favorable to prevent some serious complications^[1]. Long-term application of immunosuppressive drugs, for example, high-dose cyclosporine and tacrolimus, could bring about toxic effects on islets and normal liver and kidney^[2,3]. So in some cases, it is limited to use immunosuppressive drugs for a long period at high dose. However, islet transplantation has the potential to cure diabetes mellitus^[4], especially insulin-dependent diabetes mellitus^[5]. Islet transplantation could make insulin maintain normal level of blood glucose and prevent serious complications. In general, islet allotransplantation is safe and efficient to reduce hyperglycemia, and leads to insulin independence in patients with insulin dependent diabetes^[6,7]. But this kind of islets source is limited, which becomes the chief obstacle for treating patients. So it is necessary to find alternative islet sources, such as xenotransplantation of islets of new-born pigs. However, the rejection for xenotransplantation should be monitored efficiently. Usually, the way of preventing rejection lies in using high dose of immunosuppressive drugs, which gives rise to serious side effects. On the other hand, pre-injection of a suitable number of the same donor lymphocytes or blood cells could induce immune tolerance in different kinds of organ transplantations^[8-14]. Some other laboratories also reported that immunologic isolation, or transplantation of microencapsulated islets, could reduce rejection of islet xenotransplantation^[15,16]. In the present study, pig islet xenotransplantation in mice was performed after injection of donor hepatocytes, splenocytes or their mixture.

MATERIALS AND METHODS

Animals and induction of diabetes mellitus model

Eighty-four BALB/C female mice (22-24 g) and 6 new born male pigs were used as recipients and donors respectively. Each BALB/C mouse was injected 0.18-0.2 mL streptozotocin (STZ) (220 mg/kg) via tail vein. When blood glucose was increased to 11.1 mmol/L, the diabetes mellitus model of mice was used in the present experiments.

Isolation of islets, hepatocytes and splenocytes

Under sterile condition, Pig pancreases were washed three times with Hanks' solution. Trypsin digestion method was used to isolate single β cells or islets, referring to the method reported by Heiser^[17]. Activity of β cells was evaluated by dithiozon (DTZ) staining and the activity should be equal or over 90%. Under bacteria-free condition, pig livers or spleens were washed three times with serum-free RPMI1640, then ground on a 200 μ stainless steel net to make single cell suspension, washing two times (2 000 rpm/min, 5 min) with normal saline (N.S). The number of cells was adjusted to 2×10^7 /mL. The cell viability was detected by Hoechst/propidium iodine (Ho/PI), both hepatocytes and splenocytes were used as donor cells with viability of more than 95%.

Islet transplantation

For hepatocyte injection group, 0.2 mL liver single cell suspension was injected into diabetic mice via tail vein every 24 h for 3 times. After the last injection of donor hepatocytes, 0.5 mL pig islets (the number of islets was 980) was transplanted into peritoneal of mouse recipient.

For splenocyte injection group, 0.2 mL spleen single cell suspension was injected into diabetes mellitus mice via tail vein every 24 h for 3 times. After the last time of injection, 0.5 mL pig islets (the number of islets was 980) was transplanted into peritoneal mouse recipient.

For mixture injection group, 0.1 mL single hepatocyte cell suspension and 0.1 mL splenocyte single cell suspension were injected into model mice via tail vein every 24 h for 3 times. After the last time of injection, 0.5 mL pig islets (the number of islets was 980) was transplanted into their peritoneal.

For islets group, 0.2 mL serum-free RPMI1640 was injected into model mice via tail vein every 24 h for 3 times. After the last time of injection, 0.5 mL pig islets (the number of islets was 980) was transplanted into recipient peritoneal. Three mice in parallel were measured for each mark and the result was indicated as an average. Twelve mice in each group were observed in terms of their living days and survival rate.

Blood glucose measurement

The level of blood glucose in mice was measured every three days by a Glucose monitoring system before and after islet transplantation. The level of blood glucose in model mice before transplantation should be over 11.1 mmol/L. The survival of transplanted-islets was indicated as at least decreasing 2-fold as compared with that before transplantation, which was indicated as functional surviving. Rejection was monitored by the level of blood glucose in mice after islet transplantation with more than 16.5 mmol/L for a continuation of 2 times.

Macrophage phagocytosis assay

Candida albicans were used as targets, constant method in our laboratory was taken to detect phagocytosis of macrophages in abdominal cavity of mice.

Phagocytosis percent=(phagocytosis of macrophages/total macrophages)×100%,

Phagocytosis index=(number of phagocytotic *Candida albicans* in 100 macrophages /total macrophages)×100%.

Lymphocyte transformation assay

Pig spleens were washed three times with serum-free RPMI1640. The spleens were ground on a 200[#] stainless steel net. The number of cells was adjusted to 1×10⁶/mL with RPMI1640. Each well of the culture plate was added 100 μL cell suspension, 6 wells in parallel, 3 wells were added conA solution 50 μL, the other 3 wells were added RPMI 640 50 μL as control. The cells were incubated in 50 mL/L CO₂, at 37 °C for 56 h, then ³H-TdR 1 μCi/well was added and cultured cells for 72 h. Cpm value was detected with a β-liquid scintillation counter. Transformation function was evaluated as average Cpm value.

Assay of NK killing activity

For effector cells, mice spleens were made into single cell suspension as the same as above-mentioned method, and the cell density was adjusted to 1×10⁷/mL in 100 mL/L fetal calf serum(FCS) RPMI 640 medium. For target cells, exponentially growing YAC-1 cells were adjusted to 2×10⁵/mL cell suspension with 100 mL/L FCS RPMI1640. A 100 μL effector cell suspension and 100 μL target cell suspension were added into each well respectively in a 40-well plate as experimental group, 3 wells in parallel. On the other hand, 100 μL/well effector cells and 100 μL/well RPMI1640 were used as effector group, 100 μL 100 mL/L FCS RPMI1640 and 100 uL target cells as target group. They were cultured them in 50 mL/L CO₂, at 37 °C for 24 h. Then 3-(4,5-dimethylthiazol-2-yl)-2,5-diphenyl tetrazolium bromide(MTT) 20 μL/well, continually cultured

for another 4 h, centrifuged at 2 000 rpm/min 10 min, the supernatant was discarded, add 1 000 g/L dimethyl sulfoxide (MDS) 100 μL was added into each well, cells were lysed with vibration. After 10 min, A value was measured at 570 nm with an ELISA reader. NK killing activity=[1-(Experimental A-Effector A)/Target A]×100%.

T lymphocytes and subpopulations

The total number of lymphocytes was calculated directly under microscopy. T lymphocytes and its subpopulations were measured by constant strept avidin-biotin complex (SABC) staining. SABC kit was supplied by Wuhan Boshide Company.

Antibody-forming assay in vitro

Quantitative hemolytic spectrometry (QHS) was used to run antibody-forming assay. Mice spleens were washed three times with normal saline. A 200[#] stainless steel net was used to grind spleen tissues into single cell suspension. The cells were re-suspended and adjusted to a final concentration of 2×10⁷/mL Hanks buffer (pH 7.2). A 1 mL cell suspension and 1 mL 2 mL/L sheep red blood cell (SRBC) (1.5×10⁸/mL cells), then 1:10 complement 1 mL was added at 37 °C for 1 h, centrifuged at 3 000 rpm/min for 5 min, the A value of supernatant at 413 nm detected by 721 spectrophotometer. A value was indicated as the ability of antibody formation of B lymphocytes *in vitro*.

Pathological examination

Pathologic changes including inflammatory infiltration of local site of islet transplantation in different experimental groups were examined.

Statistical analysis

The experiments were repeated 3 times and the data were expressed as mean±SE, and significant difference was assessed by Student's *t* test.

RESULTS

The Variations of blood glucose level after islet transplantation is shown in Figure 1.

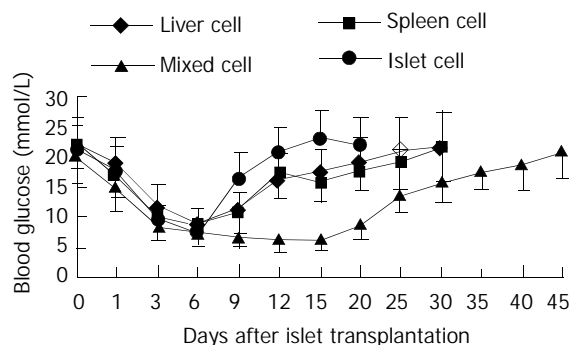


Figure 1 Variations of blood glucose after islet transplantation.

The survival time of hepatocyte injection group, splenocyte injection group, mixture group and islet group was 26.42±5.87 d, 29.56±4.52 d, 43.00±4.55 d and 16.92±2.47 d respectively (survival time of diabetic model mice was 3.86±0.85 d). The survival time of islet transplantation group was shorter than any other experimental group (*P*<0.05). So pre-injection of hepatocytes, splenocytes or their mixture from the same donor was effective in preventing rejection and delaying the time of death.

Macrophage phagocytosis in diabetic mice after pig islet xenotransplantation

Phagocytosis of macrophages in diabetic mice after pig islet xenotransplantation is summarized in Table 1.

Table 1 shows that phagocytosis percentage of islet group was increased, and the phagocytosis index of islet or hepatocyte group was obviously increased ($P<0.05$). There was no significant variation of phagocytosis percentage or index in other transplantation groups that received pre-injection of hepatocytes or mixture of hepatocytes and splenocytes 7 d after islet transplantation ($P<0.05$). After 14 d, phagocytosis percentage in hepatocyte, splenocyte and islet groups was significantly increased ($P<0.05$), phagocytosis index of islet or hepatocyte group was significantly increased ($P<0.05$).

Effect of pig islet xenotransplantation on splenic lymphocyte transforming function in mice

Seven days after transplantation, the cpm value of spleen lymphocytes in recipients of hepatocyte group, splenocyte group, mixture group or islet group was higher after pig islet

xenotransplantation than before transplantation ($P<0.05$). After 14 d, the value of hepatocyte group or islet group was still higher than that before transplantation ($P<0.05$). But there was no significant difference between splenocyte group and mixture group ($P>0.05$) (Table 2).

Effect of pig islet transplantation on NK activity of diabetic mice

NK activity of each experimental group, as compared with that before transplantation, was increased 7 d after islet transplantation ($P<0.05$), and their NK activity was continually higher than that before transplantation even 14 d after transplantation ($P<0.05$). As to the mixture group, there was no significant increase of NK activity 7 or 14 d after islet transplantation as compared with that before islet transplantation ($P>0.05$) (Table 3).

Variations of T lymphocytes in diabetic mice after pig islet xenotransplantation (Table 4)

CD₃ and CD₄ counts in hepatocyte, splenocyte or islet group

Table 1 Macrophage phagocytosis in diabetic mice after pig islet xenotransplantation

Group	Pre-treatment		7 d post-treatment		14 d post-treatment	
	Percent (%)	Index	Percent (%)	Index	Percent (%)	Index
Hepatocytes group	59.3±4.5	1.05±0.04	62.8±4.37	1.28±0.13	70.6±3.82	1.25±0.07
Splenocytes group	62.5±3.0	1.04±0.07	63.1±6.45	1.18±0.14	69.5±3.62	1.21±0.09
Mixture group	63.1±3.8	1.07±0.06	61.6±3.54	1.12±0.09	62.8±4.70	1.09±0.08
Islet group	62.0±3.3	1.06±0.08	73.5±5.51	1.41±0.18	72.7±5.71	1.47±0.10

Table 2 Effect of transplantation with pig islets on splenic lymphocyte transforming function in mice

Group	Pre-transplantation (cpm)	7 d post-transplantation (cpm)	14 d post-transplantation (cpm)
Hepatocytes group	11 437.56±1 137.55	23 453.74±4 157.28	20 178.56±4 159.74
Splenocytes group	11 437.56±1 137.55	25 834.66±3 763.37	15 336.25±3 782.38
Mixture group	11 437.56±1 137.55	21 920.05±600.08	14 345.53±2 653.28
Islets group	11 437.56±1 137.55	32 339.13±5 071.67	22 182.16±750.28

Table 3 Effect of pig islet xenotransplantation on NK activity (%) in diabetic mice

Group	Pre-treatment	7 d post-treatment	14 d post-treatment
Hepatocytes group	31.56±4.23	63.17±3.47	60.26±7.65
Splenocytes group	31.76±3.48	62.50±4.86	56.19±8.13
Mixture group	31.37±8.09	48.00±12.0	34.33±14.57
Islet group	35.67±3.51	76.23±12.50	71.00±3.0

Table 4 Variations of T lymphocytes in diabetic mice after pig islet xenotransplantation

Group	Pretreatment (%)			7 d post-treatment (%)			14 d post-treatment (%)		
	CD3	CD4	CD8	CD3	CD4	CD8	CD3	CD4	CD8
Hepatocyte group	61.6±4.5	42.0±4.6	24.3±1.5	72.7±5.5	51.6±4.5	28.0±3.6	70.0±2.0	52.7±4.9	26.7±4.2
Splenocyte group	66.0±3.6	46.3±4.0	24.6±2.5	73.0±4.4	53.3±4.5	31.3±4.1	68.7±5.7	45.3±4.1	33.0±3.6
Mixture group	64.7±2.5	44.3±6.7	25.3±4.9	65.0±5.3	47.6±3.8	28.3±2.5	61.6±3.5	47.0±4.4	27.7±2.1
Islet group	65.0±7.0	43.3±3.0	24.3±3.2	80.0±2.0	60.6±3.2	32.3±3.1	72.3±6.7	58.7±9.1	32.0±4.0

Table 5 B lymphocyte antibody-forming function (A value) in mice after transplantation (A)

Group	Pretransplantation	7 d post-transplantation	14 d post-transplantation
Hepatocyte group	0.34±0.06	0.44±0.02	0.63±0.07
Splenocyte group	0.34±0.06	0.55±0.02	0.63±0.08
Mixture group	0.34±0.06	0.55±0.01	0.50±0.06
Islet group	0.34±0.06	0.74±0.11	0.81±0.13

were up-regulated 7 days after islet transplantation. CD₈ counts in splenocyte or islet group was higher than that before islet transplantation ($P < 0.05$). Fourteen days after transplantation, CD₃ and CD₄ in hepatocyte and islet groups increased ($P < 0.05$), and CD₈ in splenocyte and islet groups became higher than that before transplantation ($P < 0.05$).

Antibody forming assay of B lymphocytes in mice after transplantation (Table 5)

Table 5 shows that antibody forming function of all four kinds of islet transplantation group was significantly increased as compared with that before islets transplantation 7 or 14 d after transplantation ($P < 0.05$).

Pathological examination

In islet transplantation group, there were a lot of lymphocyte infiltration, disruption of islets structure, or denaturation and necrosis of islet cells. Hepatocyte group with moderate lymphocyte infiltration. The mixture group had light lymphocytes infiltration.

DISCUSSION

Insulin dependent diabetes mellitus was considered as an autoimmune disease against beta cells^[18], which is usually treated with a low dose insulin injection and immunosuppressive agents. But a large quantity of clinical data indicated that long-term insulin injection could induce insulin resistance and could not prevent some serious complications^[11]. Recent studies focused on islet transplantation as a primary therapy for insulin dependent mellitus diabetes, accompanied by induction of immune tolerance to immunosuppressive agents^[19,20]. Islet allotransplantation could correct glucose imbalance and related complications, because successful islet transplantation could not only supplies the natural insulins but also other necessary biological factors. But most patients with insulin dependent diabetes mellitus could not be treated by this kind of islet transplantation because the source of allo-islets was limited. However, xenotransplantation, for example pig islet, could resolve the above-mentioned problems. Although xenotransplantation could renew the balance of glucose, rejection usually occurs, thus reducing the effect of transplantation. Islet transplantation combined with other organs or cells from the same donor could reduce rejection. Some laboratories have tried pancreas allotransplantation in combination with the same donor spleen transplantation. The results showed that the survival time of pancreas was significantly prolonged, which was attributed to the induced immunotolerance. It has been reported that bone marrow transplantation could induce the formation of hematopoiesis chimera, which could prevent acute or chronic rejection^[13-15,21,22]. So it is possible to use hematopoiesis chimera to treat insulin dependent diabetes mellitus.

T lymphocyte vaccine (TCV) could induce immunotolerance for transplantation^[23]. For example, TCV with recipient spleen cells pre-sensitized by donor antigen was used in rat heart transplantation, to observe the survival time of rat heart graft. The results showed that TCV could prolong the survival time of rat heart graft^[24]. As to the immune response, T lymphocyte proliferation reaction increased, B lymphocyte proliferation reaction was not affected, but mixed lymphocyte reaction (MLR) declined. The analysis of phenotype showed that CD₈ subpopulation increased, however there was no obvious change of antibody-dependent cell-mediated cytotoxicity (ADCC) reaction. Many other studies demonstrated that liver cells (or hepatocytes) and/or spleen cells (or splenocytes) could induce specific immune tolerance in different organ transplantations, such as kidney, marrow, heart, skin^[25-28]. In the aspect of islet transplantation, some scholars administrated pre-injection of

donor hepatocytes and/or splenocytes to induce the immune tolerance and got the positive result^[29-31].

In the present study, islet xenotransplantation was performed after pre-injection of donor hepatocytes, splenocytes, or their mixture. The results showed that the survival time of hepatocyte group, splenocyte group, mixture group was longer than islet group ($P < 0.05$). Pre-injection of hepatocytes, splenocytes or their mixture from the same donor was effective in preventing rejection and prolonging survival time. In the aspect of macrophage function, macrophage phagocytosis percent in islet transplantation group was increased, and the phagocytosis index in islet or hepatocyte group was increased ($P < 0.05$). There was no significant variation of phagocytosis percent or index in other transplantation groups 7 d after transplantation. After 14 d, phagocytosis in hepatocyte, splenocyte and islet group was significantly increased, phagocytosis index in islet or hepatocyte group was increased. The antibody-forming function of spleen B lymphocytes of recipients in hepatocyte group, splenocyte group, mixture group or islet group was increased 7 d after pig islet xenotransplantation. After 14 d, the B lymphocyte function in hepatocyte group or islet group was still higher than that before transplantation ($P < 0.05$). As to NK cells, NK killing activity of each experimental group, as compared with before transplantation, was increased 7 d after islet transplantation, and their NK activity maintained higher than that before transplantation 14 d after transplantation. As to the mixture group, there was no significant increase in NK activity 7 or 14 d after islet transplantation as compared with that before islet transplantation ($P > 0.05$). T lymphocyte subpopulation was also analyzed, the results showed that CD₃ and CD₄ percent of hepatocyte, splenocyte or islet group increased 7 d after islet transplantation. CD₈ percent of splenocyte or islet group was higher than that before islet transplantation. Fourteen days after transplantation, CD₃ and CD₄ percent of hepatocyte and islet group was still higher, and CD₈ percent of splenocyte and islet groups was higher than that before transplantation. To further examine immune tolerance in different experimental groups, pathological examination was performed. In islet transplantation group, lymphocyte infiltration was extensive, disruption of islet structure and necrosis of islet cells were also obvious. Hepatocyte group had moderate lymphocyte infiltration. The mixture group has slight lymphocyte infiltration. The results indicate that pre-injection of hepatocytes, splenocytes or mixture of them could reduce rejection by inducing immunotolerance. Although the concrete mechanism is not completely clear, pre-injection of hepatocytes and splenocytes from the same donor could induce immunotolerance of islet xenotransplantation, and prolong the survival time of islets.

REFERENCES

- 1 **Oluwole OO**, Depaz HA, Gopinathan R, Ali A, Garrovillo M, Jin MX, Hardy MA, Oluwole SF. Indirect allorecognition in acquired thymic tolerance: induction of donor-specific permanent acceptance of rat islets by adoptive transfer of allopeptide-pulsed host myeloid and thymic dendritic cells. *Diabetes* 2001; **50**: 1546-1552
- 2 **Contreras JL**, Eckhoff DE, Cartner S, Bilbao G, Ricordi C, Neville DM Jr, Thomas FT, Thomas JM. Long-term functional islet mass and metabolic function after xenotransplantation in primates. *Transplantation* 2000; **69**: 195-201
- 3 **Montori VM**, Basu A, Erwin PJ, Velosa JA, Gabriel SE, Kudva YC. Posttransplantation diabetes: a systematic review of the literature. *Diabetes Care* 2002; **25**: 583-592
- 4 **White SA**, James RF, Swift SM, Kimber RM, Nicholson ML. Human islet cell transplantation—future prospects. *Diabet Med* 2001; **18**: 78-103
- 5 **Pileggi A**, Ricordi C, Alessiani M, Inverardi L. Factors influenc-

- ing Islet of Langerhans graft function and monitoring. *Clin Chim Acta* 2001; **310**: 3-16
- 6 **Horton PJ**, Hawthorne WJ, Walters SN, Patel AT, O'Connell PJ, Chapman JR, Allen RD. Induction of allogeneic islet tolerance in a large-animal model. *Cell Transplant* 2000; **9**: 877-887
 - 7 **Kahl A**, Bechstein WO, Frei U. Trends and perspectives in pancreas and simultaneous pancreas and kidney transplantation. *Curr Opin Urol* 2001; **11**: 165-174
 - 8 **Deng YM**, Tuch BE, Rawlinson WD. Transmission of porcine endogenous retroviruses in severe combined immunodeficient mice xenotransplanted with fetal porcine pancreatic cells. *Transplantation* 2000; **70**: 1010-1016
 - 9 **Wennberg L**, Song Z, Bennet W, Zhang J, Nava S, Sundberg B, Bari S, Groth CG, Korsgren O. Diabetic rats transplanted with adult porcine islets and immunosuppressed with cyclosporine A, mycophenolate mofetil, and leflunomide remain normoglycemic for up to 100 days. *Transplantation* 2001; **71**: 1024-1033
 - 10 **Li H**, Ricordi C, Inverardi L. Effects of graft-versus-host reaction on intrahepatic islet transplants. *Diabetes* 1999; **48**: 2292-2299
 - 11 **Ikebukuro K**, Adachi Y, Yamada Y, Fujimoto S, Seino Y, Oyaizu H, Hioki K, Ikehara S. Treatment of streptozotocin-induced diabetes mellitus by transplantation of islet cells plus bone marrow cells via portal vein in rats. *Transplantation* 2002; **73**: 512-518
 - 12 **Kawai T**, Sogawa H, Koulmanda M, Smith RN, O'Neil JJ, Wee SL, Boskovic S, Sykes M, Colvin RB, Sachs DH, Auchincloss H Jr, Cosimi AB, C-Ko DS. Long-term islet allograft function in the absence of chronic immunosuppression: a case report of a non-human primate previously made tolerant to a renal allograft from the same donor. *Transplantation* 2001; **72**: 351-354
 - 13 **Wu T**, Levay YB, Heuss N, Sozen H, Kirchhof N, Sutherland DER, Hering B, Guo Z. Inducing tolerance to MHC-matched allogeneic islet grafts in diabetic NOD mice by simultaneous islet and bone marrow transplantation under nonirradiative and nonmyeloablative conditioning therapy. *Transplantation* 2002; **74**: 22-27
 - 14 **Girman P**, Kriz J, Dovolilova E, Cihalova E, Saudek F. The effect of bone marrow transplantation on survival of allogeneic pancreatic islets with short-term tacrolimus conditioning in rats. *Ann Transplant* 2001; **6**: 43-45
 - 15 **Maria-Engler SS**, Mares-Guia M, Correa ML, Oliveira EM, Aita CA, Krogh K, Genzini T, Miranda MP, Ribeiro M, Vilela L, Noronha IL, Eliaschewitz FG, Sogayar MC. Microencapsulation and tissue engineering as an alternative treatment of diabetes. *Braz J Med Biol Res* 2001; **34**: 691-697
 - 16 **Gamian E**, Kochman A, Rabczynski J, Burczak K. Biocompatibility testing and function of a pancreatic prosthesis consisting of viable pancreatic islets encapsulated in PVA macrocapsules. *Polim Med* 1999; **29**: 3-20
 - 17 **Heiser A**, Ulrichs K, Muller-Ruchholtz W. Isolation of porcine pancreatic islets: low trypsin activity during the isolation procedure guarantees reproducible high islet yields. *J Clin Lab Anal* 1994; **8**: 407-411
 - 18 **Petruzzo P**, Andreelli F, McGregor B, Lefrancois N, Dawahra M, Feitosa LC, Dubernard JM, Thivolet C, Martin X. Evidence of recurrent type I diabetes following HLA-mismatched pancreas transplantation. *Diabetes Metab* 2000; **26**: 215-218
 - 19 **Thomas JM**, Contreras JL, Smyth CA, Lobashevsky A, Jenkins S, Hubbard WJ, Eckhoff DE, Stavrou S, Neville DM Jr, Thomas FT. Successful reversal of streptozotocin-induced diabetes with stable allogeneic islet function in a preclinical model of type 1 diabetes. *Diabetes* 2001; **50**: 1227-1236
 - 20 **Sutherland DE**, Gruessner RW, Dunn DL, Matas AJ, Humar A, Kandaswamy R, Mauer SM, Kennedy WR, Goetz FC, Robertson RP, Gruessner AC, Najarian JS. Lessons learned from more than 1,000 pancreas transplants at a single institution. *Ann Surg* 2001; **233**: 463-501
 - 21 **Good RA**, Verjee T. Historical and current perspectives on bone marrow transplantation for prevention and treatment of immunodeficiencies and autoimmunities. *Biol Blood Marrow Transplant* 2001; **7**: 123-135
 - 22 **Ciancio G**, Miller J, Garcia-Morales RO, Carreno M, Burke GW, Roth D, Kupin W, Tzakis AG, Ricordi C, Rosen A, Fuller L, Esquenazi V. Six-year clinical effect of donor bone marrow infusions in renal transplant patients. *Transplantation* 2001; **71**: 827-835
 - 23 **Lakey JR**, Singh B, Wamock GL, Elliott JF, Rajotte RV. Long-term survival of syngeneic islet grafts in BCG-treated diabetic NOD mice can be reversed by cyclophosphamide. *Transplantation* 1995; **59**: 1751-1753
 - 24 **Shanqi Y**, Suisheng X. Study on the mechanisms of T cell vaccination-induced survival prolongation of cardiac allograft in rats. *Zhonghua Qiguan Yizhi Zazhi* 2000; **21**: 303-305
 - 25 **Motoyama K**, Arima T, Yu S, Lehmann M, Flye MW. The kinetics of tolerance induction by nondepleting anti-CD4 monoclonal antibody (RIB 5/2) plus intravenous donor alloantigen administration. *Transplantation* 2000; **69**: 285-293
 - 26 **Smyk-Pearson SK**, Bakke AC, Held PK, Wildin RS. Rescue of the autoimmune scurfy mouse by partial bone marrow transplantation or by injection with T-enriched splenocytes. *Clin Exp Immunol* 2003; **133**: 193-199
 - 27 **Nakafusa Y**, Goss JA, Mohanakumar T, Flye MW. Induction of donor-specific tolerance to cardiac but not skin or renal allografts by intrathymic injection of splenocyte alloantigen. *Transplantation* 1993; **55**: 877-882
 - 28 **Dono K**, Maki T, Wood ML, Monaco AP. Induction of tolerance to skin allografts by intrathymic injection of donor splenocytes. Effect of donor-recipient strain combination and supplemental rapamycin. *Transplantation* 1995; **60**: 1268-1273
 - 29 **Sun J**, Wang X, Wang C, Sheil AG. Sequential transplantation induces islet allograft tolerance. *Microsurgery* 2001; **21**: 148-152
 - 30 **Sutherland DE**, Gruessner RW, Gruessner AC. Pancreas transplantation for treatment of diabetes mellitus. *World J Surg* 2001; **25**: 487-496
 - 31 **Sakuma Y**, Uchida H, Nagai H, Kobayashi E. High-dose tacrolimus and lengthy survival of the combined rat pancreas/spleen graft in a high-responder combination. *Transpl Immunol* 2001; **9**: 37-42

Establishment and characterization of human hepatocellular carcinoma cell line FHCC-98

Chao-Yang Lou, Ying-Ming Feng, Ai-Rong Qian, Yu Li, Hao Tang, Peng Shang, Zhi-Nan Chen

Chao-Yang Lou, Ying-Ming Feng, Department of Oncology, Tangdu Hospital, Fourth Military Medical University, Xi'an 710038, Shaanxi Province, China

Peng Shang, Ai-Rong Qian, Yu Li, Hao Tang, Zhi-Nan Chen, Department of Cell Biology, Fourth Military Medical University, Xi'an 710032, Shaanxi Province, China

Supported by the National High-Tech Research and Development Program of China, NO. 2001AA215061

Co-correspondents: Zhi-Nan Chen

Correspondence to: Dr. Peng Shang, Department of Cell Biology, Fourth Military Medical University, Xi'an 710032, Shaanxi Province, China. chcerc7@fmmu.edu.cn

Telephone: +86-29-83374547

Received: 2004-03-15 **Accepted:** 2004-04-10

Abstract

AIM: To establish a novel human hepatocellular carcinoma (HCC) cell line FHCC-98 from HCC tissue and to provide a suitable model for studying HCC occurrence, progress and metastasis.

METHODS: Serially passaged cells were cultured and their morphologies were observed under light and electron microscope. Cytogenetic study was conducted by using flow cytometry and chromosome analysis. Expressions of tumor markers such as α -fetoprotein (AFP), cytokeratin (CK) and hepatoma metastasis-associated factor HAb18G/CD147 on the FHCC-98 cells were detected by immunocytochemistry or Western blotting. Lactic dehydrogenase (LDH) isoenzymes were detected by polyacrylamide gel electrophoresis (PAGE). Xenograft was performed by inoculating FHCC-98 cells into the flanks of nude mice.

RESULTS: Morphology of FHCC-98 cells was the same as that of other malignant cells. The expressions of the cells were positive for HAb18G/CD147 and CK, and negative for AFP. Its population doubling time was 21.4 h. The cell DNA was tetraploid and the major chromosomes were triploid by cytogenetics analysis. The tumorigenicity in nude mice was 100%. PAGE showed four bands representing LDH₂, LDH₃, LDH₄ and LDH₅.

CONCLUSION: FHCC-98 is a novel HCC cell line and an ideal cell model for further exploring the mechanism of hepatocellular carcinoma invasion and metastasis.

Lou CY, Feng YM, Qian AR, Li Y, Tang H, Shang P, Chen ZN. Establishment and characterization of human hepatocellular carcinoma cell line FHCC-98. *World J Gastroenterol* 2004; 10 (10): 1462-1465

<http://www.wjgnet.com/1007-9327/10/1462.asp>

INTRODUCTION

Hepatocellular carcinoma (HCC) is one of the most common malignant tumors. It ranks fifth in frequency worldwide among

all malignancies and causes 1 million deaths annually^[1], yet its incidence is increasing steadily in various countries^[2-4]. Epidemiology studies showed that primary liver cancer is the second mortality in China^[5] and it accounts for 53% of all liver cancer death worldwide^[6]. Though with great development in diagnosis and therapy, the prognosis of patients with HCC remains dismal for its high rate of metastasis and recurrence. For patients in advanced stages, the median survival is less than 6 mo, no matter what kinds of therapy were managed^[7-11]. So it is urgent to further explore the mechanism of HCC occurrence, progress and metastasis. HCC cell lines are powerful tools. Until now, ten of human HCC cell lines^[12-27] have been established, and every cell line has its own characteristics and offers convenience for various experiments. Stability, homogeneity and easy to culture are important parameters for good cell lines. Here we report a new HCC cell line, which has been maintained for five years through 500 passages.

MATERIALS AND METHODS

Patient

Tumor tissue obtained from a 39-year-old male HCC patient who lived in northwest China was used to establish a cell line. His family history of oncology was unknown, but there was no history of hepatitis or blood transfusions. There was no operation history. Investigations showed AST of 86 U/L, α -fetoprotein 8 ng/mL, carcinoembryonic antigen (CEA) 2.8 ng/mL and HBsAg(-). In 1998, the patient complained of upper right abdominal tender pain. A computerized-tomography demonstrated a 10 cm×11 cm space-occupying lesion in the right lobe of liver. A partial liver resection was performed. Pathologic diagnosis confirmed HCC with middle differentiation. The patient died of lung metastasis after 3 mo.

Primary culture

A slice portion of sample was obtained under sterile conditions and washed by RPMI 1640 (Life Technology) 3 times and minced with surgical blades into pieces smaller than 1 mm³, then these pieces were put into tissue-culture flasks and incubated at 37 °C and 50 mL/L CO₂ (Heraeus, Germany) with RPMI 1640 medium supplemented with 100 U/mL penicillin, 100 μ g/mL streptomycin and 200 mL/L FBS. One week later, cells migration was observed and some colonies were formed. Those colonies were detached with 2.5 g/L trypsin and pulled into 25 cm² flasks in RPMI 1640 medium with 200 mL/L FBS. The medium was renewed two or three times a week. After stable growth, the same medium with 100 mL/L FBS was used as maintenance medium. When cells were confluent, they were detached with 2.5 g/L trypsin and passaged at the ratio of 1:2 or 1:3. At the 80th passage (about 30 mo after the sample was got), a stable cell line was considered to be established.

Morphological observations

Cells were observed daily under an invert microscope (Olympus). Cells coated on tissue-culture slides were washed with PBS (pH 7.4) 3 times, then fixed with cool pure acetone for 10 min and stained with hematoxylin and eosin (HE

staining). For electron microscope observation, 4×10^6 cells were centrifuged at 1 000 r/min for 10 min, then fixed in 30 g/L glutaraldehyde for 30 min and embedded in paraffin and ultra-thin sectioned. The section was observed with a JEM 2000 transmission electron microscope (JEOL)^[22].

Growth properties

Growth curve was analyzed by modified MTT assay^[24]. Cells in exponential growth phase at 16th passage were collected. Single-cell suspension (5×10^4 /mL) was added to (200 μ L/well) a 24-well plate, incubated at 37 °C with 50 mL/L CO₂, then MTT (5 mg/mL) was added to the wells (20 μ L/well) every 24 h for 7 consecutive days. The plate was incubated in cell incubator for 4 h, and then the supernatants were removed and 150 μ L DMSO was added into each well. After incubation for 30 min, the dye-stained liquid was removed to a 96-well plate. Absorbency at 490 nm ($A_{490\text{nm}}$) was determined by M450 (Bio-Rad) enzyme-linked reader. The growth curve was plotted by half-height method.

FHCC-98 cells were incubated in another 24-well plate (1.2×10^4 /mL). Attachment efficiency was measured by counting the cell number every 2 h.

Attachment efficiency=(number of cells/120 000) \times 100%.

To determine the cloning rate, 1.5×10^2 cells in suspension in a culture medium containing 8 g/L agar were applied to a base layer of a culture medium containing 1.7% agar. The Petri dish was incubated for 12 d at 37 °C in a humidified atmosphere containing 50 mL/L CO₂, and colonies containing more than 5 cells were counted.

$$\text{Cloningrate} = \frac{\text{Number of clones}}{150} \times 100\%$$

Flow cytometry

Single-cell suspensions containing 2×10^6 cells were treated following the standardized protocol and cell cycle analysis were performed by flow-cytometry (ELITE ESP Coulter)^[22].

Chromosome analysis

Cells were cultured for 2 h in the culture medium containing 0.05 μ g/mL of colcemid and trypsinized, swollen with 0.075 mol/L KCl solution for 15 min and fixed with methanol: acetic acid (3:1) 3 times. Following air-drying, metaphase smears were stained with Giemsa. Samples were observed with oil immersion objective and photographed^[18].

Immunocytochemistry

Cells cultured on slides for 24 h were washed 3 times with PBS and then fixed in acetone for 10 min at room temperature. AFP and cytokeratin were detected by immunocytochemistry using SP method. The slides were viewed under light microscope and the degree of staining was assessed.

Western blotting

Tumor metastasis-associated factor HAb18G/CD147^[28,29] was detected by western blotting. Single-cell suspension (1.0×10^5 /mL) was collected, and centrifuged at 800 r/min. The cell pellets were collected and resuspended in lysis buffer of 50 mmol/L Tris-HCl (pH 8.0), 150 mmol/L NaCl, 0.2 g/L azido sodium, 1 g/L SDS, 100 μ g/mL PMSF, 10 g/L Triton X-100, 5 g/L deoxycholic acid and protease inhibitor for 10 min on the ice. The lysis solution was centrifuged at 16 000 g for 10 min at 4 °C and the supernatants were collected, and the protein concentration was detected with Lowery's method. SDS-PAGE was carried out. Western blotting was performed with secondary antibodies coupled to horseradish peroxidases and detected using ECL reagents (Amersham, Freiburg, German).

ConA coagulation test

Single-cell suspension (5.0×10^5 /mL) was mixed with the same volume of ConA and the mixture were diluted and incubated at 37 °C in 50 mL/L CO₂ for 20 min. Human embryonic lung cell was used as contrast. Assembling reaction was observed.

Isoenzyme analysis

LDH isoenzymes were detected by PAGE. FHCC-98 cells were trypsinized and 8.0×10^6 cells were re-suspended in sterile saline. The cell suspension was centrifuged at 1 000 r/min for 10 min twice and then re-suspended in 0.5 mL Tris-HCl (150 mmol/L, pH 7.6). The sample was repeatedly frozen and thawed at -40 °C and 37 °C for 6 times, then centrifuged at 3 000 r/min 4 °C for 20 min. The supernatant was stored under -20 °C for using. The SDS-PAGE sample buffer was 100 mmol/L Tris-HCl (pH 6.8) supplemented with 200 mL/L glycerite and 2 g/L bromphenol blue. The sample was mixed with an equal volume of buffer and used for PAGE. The stacking gel was 50 g/L while separation gel 60 g/L. The staining solution was composed of oxidized NAD⁺ (5 mg/mL), NBT (2 mg/mL), PMS (1 mg/mL) and sodium lactate (60 g/L). The minigels were run at a constant voltage (100 V) for 2 h and then stained for 1 h. The gel was fixed in 70 mL/L acetic acid over 16 h and photographed.

Xenograft

Ten 4-6-week-old nude mice (supplied by the animal center of Fourth Military Medical University) of both sexes bred under specific pathogen-free (SPF) conditions were used in the heterotransplantation experiments. Cells (2.0×10^6) suspended in medium (0.2 mL) were injected subcutaneously into flanks of each mouse.

Mycoplasma detection

Mycoplasma was detected by transmission electron microscopy.

RESULTS

Morphology

Polygonal epithelial-like cells in culture were identified to have large nuclei and the ratio of nuclear/cytoplasmic increased. Cells grew well at a high density ($>1 \times 10^6$ /mL). Electron microscopy revealed that abundant microvilli distributed on the cell surface (Figure 1). Desmosomes and gap junction could be seen between cells (Figure 2). Glycogen granules were rich in cytoplasm and mitochondria were in a round shape. Ribosome and rough endoplasmic reticulum were moderate. Atypical nuclei were conspicuous and euchromatin was rich. Karyokinesis and pathologic mitosis were frequently uncoupled.

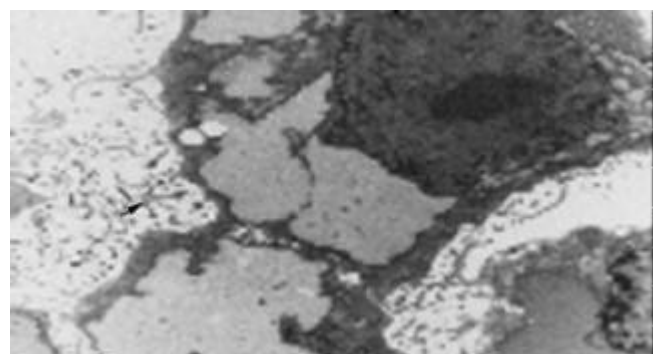


Figure 1 Ultrastructure of FHCC-98 illustrating the clear and abundant microvilli (Original magnification: $\times 4\ 000$).

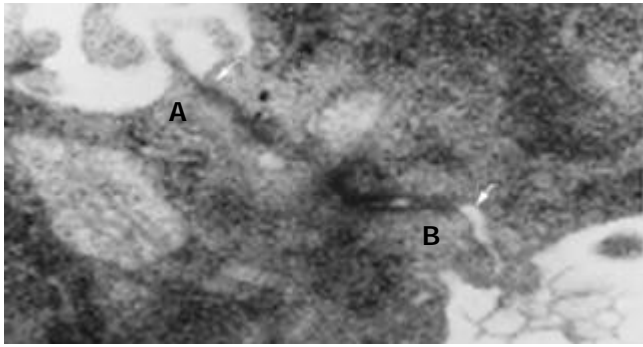


Figure 2 Desmosomes (A) and gap junction (B) between cells (Original magnification: $\times 30\ 000$).

Growth kinetics

The growth curve at the sixteenth passage (Figure 3) showed a stationary-phase at the beginning and at the end of the experiment, the exponential growth lasted about 3 d. The population doubling time of FHCC-98 was 21.4 h. At the time points of 2, 4, 6 and 8 h, the attachment efficiencies were 54.2%, 83.3%, 89.2% and 93.7%, respectively. The percentage of colony-forming cells in soft agar was an average of 32.6%.

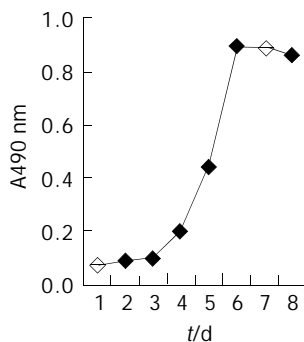


Figure 3 Growth curve of FHCC-98 cells in RPMI 1640+100 mL/LFBS at the 16th passage.

Cytogenetics studies

Chromosome analysis revealed the number of chromosomes per cell varied from 58 to 80 with a number in the triploid of 91%. FHCC-98 cell DNA became tetraploid. 75.0% cells were in G₁ phase, while 7.0% cells were in G₂ phase and 18.0% in S phase. The DNA index was 1.857.

Immunological characteristics

The FHCC-98 cell line was positive for CK and negative for AFP.

Western blotting

Western blotting showed that FHCC-98 was positive for HAB18G/CD147 and the band showed a single one with M_r 61 000 (Figure 4).

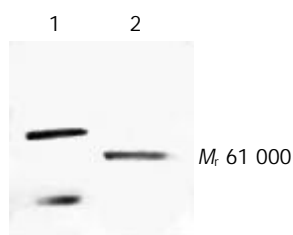


Figure 4 Western blotting of HAB18G/CD147 on FHCC-98 cell line. Lane 1: HAb18 mAb; Lane 2: HAb18G.

ConA test

The FHCC-98 cells were coagulated in 3.91 $\mu\text{g/mL}$ of ConA while human embryonic lung cells had no response to 250 $\mu\text{g/mL}$ of ConA.

Isoenzyme analysis

PAGE analysis revealed that FHCC-98 had tumor typical isoenzymes of LDH without LDH₁ (Figure 5). LDH₂, LDH₃, LDH₄ and LDH₅ isoenzymes were separated to relative activities (percentage of total LDH) of 3%, 19%, 49% and 29%, respectively.

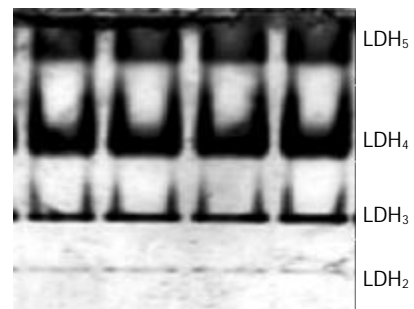


Figure 5 LDH isoenzyme analysis of FHCC-98.

Xenograft

Ten days after heterotransplantation of FHCC-98 cells into nude mice, subcutaneous tumors appeared at the sites of inoculation and grew rapidly in size during the next 20 d. Average tumor volumes on d 10, 14 and 30 were 42.4 ± 17.8 , 76.6 ± 43.4 , and 471.4 ± 187.5 mm³, respectively.

Mycoplasma detection

No mycoplasma contamination was detected in FHCC-98 cells from passages 16 and 28.

DISCUSSION

It is well known that heterogeneous tumors have diverse biologic behaviors, outcomes, and responses to therapy whether *in vivo* or *in vitro*. Malignant tumors show their genetic heterogeneities, differentiation and metastasis, which have been demonstrated in various kinds of tumors^[30-34], and even in permanent cell lines with different biological characteristics^[22,23,34]. Since the establishment of the first human HCC cell line in 1963 (Chen *et al.* *Chin Med J*, 1963; 82: 228), more than ten human HCC cell lines have been established, most of which are positive for either HBV, HCV or AFP, yet they differed in biological properties. HBV is the main viral cause of HCC in China. Unfortunately, there are about 30% HCC patients are AFP or HBV negative, partially due to the extensive necrosis of tumor mass. As a tumor marker, AFP's sensitivity and specificity for HCC detection depend on the diagnostic level and the cutoff level^[35]. Different detection approaches may have different results. In this study, immunocytochemical method was applied to detect AFP and the result was consistent with that by RIA. Up to now, human HCC cell lines with both AFP negative and HBV negative have been rarely reported. Fortunately, we established a HCC cell line, which was negative for both AFP and HBV.

FHCC-98 demonstrated the same epithelial-type morphology as other HCC cell lines. FHCC-98 showed no contact inhibition when the cell density was high. As important metabolic parameters of HCC, LDH₄ and LDH₅ had high activities, and LDH₁ had no, suggesting the existence of anaerobic respiration in HCC. Hypoxia and overgrowth of

cancerous tissue specifically repressed the activity of AFP, and the target was c-Myc, suggesting that c-Myc regulated AFP gene expression^[36]. Such changes in LDH₅ might be a factor hindering the synthesis of AFP and resulting in AFP-negative patients. FHCC-98 may be used as a model for anti-oxidant therapy of tumors. FHCC-98 has its own characteristics. The first prominent characteristic of the cell line is its biological properties of high concordance and little variation among different passages including its morphology, growth kinetics, chromosome, AFP and LDH isoenzyme; The second one is that its population doubling time was relatively shorter and it grew more rapidly compared with other human HCC cell lines^[12,14,18,20,23,25]. High coagulation of the cells showed that it could proliferate rapidly without contact inhibition. The third one is its high tumorigenicity in nude mice. And the last one of the cell line is that it can grow in various medium cultures, such as RPMI 1640 and DMEM with different concentrations of FBS.

In conclusion, we believe that FHCC-98 is a novel HCC cell line and a valuable cell model for studying HCC *in vitro* and *in vivo*, especially for AFP- and HBV-negative HCC.

REFERENCES

- 1 **Yu AS**, Keeffe EB. Management of hepatocellular carcinoma. *Rev Gastroenterol Disord* 2003; **3**: 8-24
- 2 **El Serag HB**, Mason AC. Rising incidence of hepatocellular carcinoma in the United States. *N Engl J Med* 1999; **340**: 745-750
- 3 **Kiyosawa K**, Tanaka E. Characteristics of hepatocellular carcinoma in Japan. *Oncology* 2002; **62**(Suppl 1): 5-7
- 4 **Tang ZY**. Hepatocellular carcinoma-cause, treatment and metastasis. *World J Gastroenterol* 2001; **7**: 445-454
- 5 **Zhang S**, Li L, Lu F. Mortality of primary liver cancer in China from 1990 through 1992. *Zhonghua Zhongliu Zazhi* 1999; **21**: 245-249
- 6 **Pisani P**, Parkin DM, Bray F, Ferlay J. Estimates of the worldwide mortality from 25 cancers in 1990. *Int J Cancer* 1999; **83**: 18-29
- 7 **Johnson PJ**. Hepatocellular carcinoma: is current therapy really altering outcome? *Gut* 2002; **51**: 459-462
- 8 **Watanabe T**, Omori M, Fukuda H, Takada H, Miyao M, Mizuno Y, Ohsawa I, Sato Y, Hasegawa T. Analysis of sex, age and disease factors contributing to prolonged life expectancy at birth, in cases of malignant neoplasms in Japan. *J Epidemiol* 2003; **13**: 169-175
- 9 **Ziparo V**, Balducci G, Lucandri G, Mercantini P, Di Giacomo G, Fernandes E. Indications and results of resection for hepatocellular carcinoma. *Eur J Surg Oncol* 2002; **28**: 723-728
- 10 **Kanematsu T**, Furui J, Yanaga K, Okudaira S, Shimada M, Shirabe K. A 16-year experience in performing hepatic resection in 303 patients with hepatocellular carcinoma: 1985-2000. *Surgery* 2002; **131**(1 Suppl): S153-158
- 11 **Aguayo A**, Patt YZ. Liver cancer. *Clin Liver Dis* 2001; **5**: 479-507
- 12 **Yano H**, Maruiwa M, Murakami T, Fukuda K, Ito Y, Sugihara S, Kojiro M. A new human pleomorphic hepatocellular carcinoma cell line, KYN-2. *Acta Pathol Jpn* 1988; **38**: 953-966
- 13 **Dor I**, Namba M, Sato J. Establishment and some biological characteristics of human hepatoma cell lines. *Gann* 1975; **66**: 385-392
- 14 **Alexander JJ**, Bey EM, Geddes EW, Lecatsas G. Establishment of a continuously growing cell line from primary carcinoma of the liver. *S Afr Med J* 1976; **50**: 2124-2128
- 15 **Tang ZY**, Sun FX, Tian J, Ye SL, Liu YK, Liu KD, Xue Q, Chen J, Xia JL, Qin LX, Sun HC, Wang L, Zhou J, Li Y, Ma ZC, Zhou XD, Wu ZQ, Lin ZY, Yang BH. Metastatic human hepatocellular carcinoma models in nude mice and cell line with metastatic potential. *World J Gastroenterol* 2001; **7**: 597-601
- 16 **Murakami T**, Yano H, Maruiwa M, Sugihara S, Kojiro M. Establishment and characterization of a human combined hepatocarcinoma cell line and its heterologous transplantation in nude mice. *Hepatology* 1987; **7**: 551-556
- 17 **Saito H**, Morizane T, Watanabe T, Kagawa T, Iwabuchi MN, Kumagai N, Inagaki Y, Tsuchimoto K, Tsuchiya M. Establishment of a human cell line (HCC-T) from a patient with hepatoma bearing no evidence of hepatitis B or A virus infection. *Cancer* 1989; **64**: 1054-1060
- 18 **Sing GK**, Pace R, Prior S, Scott JS, Shield P, Martin N, Searle J, Battersby C, Powell LW, Cooksley WG. Establishment of a cell line from a hepatocellular carcinoma from a patient with hemochromatosis. *Hepatology* 1994; **20**(1 Pt 1): 74-81
- 19 **Le Jossic C**, Glaise D, Corcos L, Diot C, Dezier JF, Fautrel A, Guguen-Guillouzo C. Trans-Acting factors, detoxication enzymes and hepatitis B virus replication in a novel set of human hepatoma cell lines. *Eur J Biochem* 1996; **238**: 400-409
- 20 **Lee JH**, Ku JL, Park YJ, Lee KU, Kim WH, Park JG. Establishment and characterization of four human hepatocellular carcinoma cell lines containing hepatitis B virus DNA. *World J Gastroenterol* 1999; **5**: 289-295
- 21 **Seki S**, Kitada T, Kawada N, Sakaguchi H, Kadoya H, Nakatani K, Satake K, Kuroki T. Establishment and characteristics of human hepatocellular carcinoma cells with metastasis to lymph nodes. *Hepatogastroenterology* 1999; **46**: 2812-2817
- 22 **Tian J**, Tang ZY, Ye SL, Liu YK, Lin ZY, Chen J, Xue Q. New human hepatocellular carcinoma (HCC) cell line with highly metastatic potential (MHCC97) and its expressions of the factors associated with metastasis. *Br J Cancer* 1999; **81**: 814-821
- 23 **Li Y**, Tang ZY, Ye SL, Liu YK, Chen J, Xue Q, Chen J, Gao DM, Bao WH. Establishment of cell clones with different metastatic potential from the metastatic hepatocellular carcinoma cell line MHCC97. *World J Gastroenterol* 2001; **7**: 630-636
- 24 **Yang JX**, Tang WX. Establishment of a cisplatin-induced human hepatocellular carcinoma drug-resistant cell line and its biological characteristics. *Aizheng* 2002; **21**: 872-876
- 25 **Wu X**, Wang Z, Liu B, Liu J, Gao Y, Li Z, Liu C. Establishment and characterization of human extrahepatic growing hepatocellular carcinoma cell line EGHC-9901. *Zhonghua Waike Zazhi* 2002; **40**: 616-617
- 26 **Li Y**, Tang Z, Ye S, Liu Y, Chen J, Xue Q, Huang X, Chen J, Bao W, Yang J, Gao D. Establishment of human hepatocellular carcinoma cell line with spontaneous pulmonary metastasis through *in vivo* selection. *Zhonghua Yixue Zazhi* 2002; **82**: 601-605
- 27 **Wen JM**, Huang JF, Hu L, Wang WS, Zhang M, Sham JS, Xu JM, Zeng WF, Xie D, Liang LJ, Guan XY. Establishment and characterization of human metastatic hepatocellular carcinoma cell line. *Cancer Genet Cytogenet* 2002; **135**: 91-95
- 28 **Jiang JL**, Zhou Q, Yu MK, Ho LS, Chen ZN, Chan HC. The involvement of HAB18G/CD147 in regulation of store-operated calcium entry and metastasis of human hepatoma cells. *J Biol Chem* 2001; **276**: 46870-46877
- 29 **Li Y**, Shang P, Qian AR, Wang L, Yang Y, Chen ZN. Inhibitory effects of antisense RNA of HAB18G/CD147 on invasion of hepatocellular carcinoma cells *in vitro*. *World J Gastroenterol* 2003; **9**: 2174-2177
- 30 **Kim GJ**, Cho SJ, Won NH, Sung JM, Kim H, Chun YH, Park SH. Genomic imbalances in Korean hepatocellular carcinoma. *Cancer Genet Cytogenet* 2003; **142**: 129-133
- 31 **Shindo-Okada N**, Takeuchi K, Nagamachi Y. Establishment of cell lines with high- and low-metastatic potential from PC-14 human lung adenocarcinoma. *Jpn J Cancer Res* 2001; **92**: 174-183
- 32 **Tammen H**, Kreipe H, Hess R, Kellmann M, Lehmann U, Pich A, Lamping N, Schulz-Knappe P, Zucht HD, Lilischkis R. Expression profiling of breast cancer cells by differential peptide display. *Breast Cancer Res Treat* 2003; **79**: 83-93
- 33 **Nelson SJ**, Cha S. Imaging glioblastoma multiforme. *Cancer J* 2003; **9**: 134-145
- 34 **Yang J**, Qin LX, Ye SL, Liu YK, Li Y, Gao DM, Chen J, Tang ZY. The abnormalities of chromosome 8 in two hepatocellular carcinoma cell clones with the same genetic background and different metastatic potential. *J Cancer Res Clin Oncol* 2003; **129**: 303-308
- 35 **Mazure NM**, Chauvet C, Bois-Joyeux B, Bernard MA, Nacer-Cherif H, Danan JL. Repression of alpha-fetoprotein gene expression under hypoxic conditions in human hepatoma cells: characterization of a negative hypoxia response element that mediates opposite effects of hypoxia inducible factor-1 and c-Myc. *Cancer Res* 2002; **62**: 1158-1165
- 36 **Taketa K**, Okada S, Win N, Hlaing NK, Wind KM. Evaluation of tumor markers for the detection of hepatocellular carcinoma in Yangon General Hospital, Myanmar. *Acta Med Okayama* 2002; **56**: 317-330

Overexpression of annexin 1 in pancreatic cancer and its clinical significance

Xiao-Feng Bai, Xiao-Guang Ni, Ping Zhao, Shang-Mei Liu, Hui-Xin Wang, Bing Guo, Lan-Ping Zhou, Fang Liu, Jin-Sheng Zhang, Kun Wang, Yong-Qiang Xie, Yong-Fu Shao, Xiao-Hang Zhao

Xiao-Feng Bai, Xiao-Guang Ni, Ping Zhao, Shang-Mei Liu, Hui-Xin Wang, Lan-Ping Zhou, Fang Liu, Jin-Sheng Zhang, Yong-Qiang Xie, Yong-Fu Shao, Xiao-Hang Zhao, National Laboratory of Molecular Oncology, Department of Abdominal Surgery, Department of Pathology, Cancer Institute and Hospital, Chinese Academy of Medical Sciences and Peking Union Medical College, Beijing 100021, China

Kun Wang, Xiao-Hang Zhao, Beijing Yanjing Hospital, Beijing 100037, China

Bing Guo, Department of Head, Neck and Breast, Mudanjiang Tumor Hospital, Mudanjiang 157009, Heilongjiang Province, China

Supported by National Natural Science Foundation of China NO. 30240050, 30225045, 39990570, 30171049, and 30370713 and National High Tech R & D Program of China, 2001AA227091

Co-first-authors: Xiao-Guang Ni

Correspondence to: Xiao-Hang Zhao, M.D., Ph.D. National Laboratory of Molecular Oncology, Cancer Institute and Hospital, Chinese Academy of Medical Sciences and Peking Union Medical College, Beijing 100021, China. zhaoxh@pubem.cicams.ac.cn

Telephone: +86-10-67709015 **Fax:** +86-10-67709015

Received: 2004-01-15 **Accepted:** 2004-02-24

Abstract

AIM: To investigate the expression of annexin I in pancreatic cancer and its relationship with the clinicopathologic factors, and to evaluate its potential clinical significance.

METHODS: Annexin I expression was analyzed by Western blot and immunohistochemical staining in pancreatic adenocarcinoma and multi-tissue microarrays (MTAs).

RESULTS: Western blot analysis showed that annexin I was overexpressed in 84.6% (11/13) pancreatic ductal adenocarcinomas. Immunohistochemistry analysis of pancreatic cancer in MTAs showed that annexin I protein was 71.4%(30/42) positive which was markedly increased compared with that in the tumor matched normal pancreas tissues 18.4%(7/38) ($P < 0.01$). In the meantime, the high expression of annexin 1 was correlated with the poor differentiation of pancreatic adenocarcinoma.

CONCLUSION: Annexin 1 overexpression is a frequent biological marker and correlates with the differentiation of pancreatic cancer during tumorigenesis.

Bai XF, Ni XG, Zhao P, Liu SM, Wang HX, Guo B, Zhou LP, Liu F, Zhang JS, Wang K, Xie YQ, Shao YF, Zhao XH. Overexpression of annexin 1 in pancreatic cancer and its clinical significance. *World J Gastroenterol* 2004; 10(10): 1466-1470
<http://www.wjgnet.com/1007-9327/10/1466.asp>

INTRODUCTION

Pancreatic cancer is one of the most lethal malignancies with less than 3-5% of the overall five-year survival rate, and the patients normally die within six months after diagnosis^[1]. There

are some indications that the incidence of pancreatic cancer following an upward increase, in recent years it has reached a plateau and in some countries there is even a slight decrease. But in China the incidence and mortality rates of this disease have taken an upward trend countrywide. Based on the data of demography and death collected through Chinese Disease Surveillance Point System (DSPS) over the period of 1991-2000, the age-standardized mortality rate due to pancreatic cancer increased from 2.18 in 1991 to 3.26 in 2000 per 1000 000 populations and the peak mortality of pancreatic cancer might arrive in China in the next few decades^[2]. In the United States, more than >30 000 people were diagnosed and died of pancreatic cancer in 2003, representing the fourth leading cause of cancer death^[1]. The significant factor for the poor prognosis of pancreatic cancer may be attributed to its biological aggressiveness, the difficulty of early diagnosis, and poor response to conventional therapeutics, those reflect a fact that pancreatic cancer is a poorly understood disease and the etiologic factors and the molecular basis for these characteristics are unknown. Comparisons of global gene and protein expression profiles between pancreatic cancer and normal pancreas using high-throughput methods could provide important information about the molecular characteristics and reveal some new specific or associated biomarkers of pancreatic cancer with promise for development into novel diagnostic or therapeutic targets^[3-7].

Annexin 1, a member of annexin family, was found with expression alterations in different kinds of malignant tumors. The molecular mechanisms and the clinical significance of annexin I altered expression still remain a debate. In this study, we investigated annexin I expression and distributions in a large number of pancreatic cancer specimens via Western blot and immunohistochemistry analysis based on multi-tissue microarrays (MTAs).

MATERIALS AND METHODS

Patients and specimens

Fresh tissue samples of 13 pancreatic cancers and their corresponding normal counterparts were obtained at the time of resection with informed consent from Cancer Institute and Hospital (CIH), Chinese Academy of Medical Sciences (CAMS) and Peking Union Medical College (PUMC) during November 2001 and November 2003. The samples were cut into two parts, one was snap-frozen in liquid nitrogen before storage at -80 °C, and the other was fixed with 10% formalin for histopathological diagnosis. Histological diagnosis of these samples was all pancreatic ductal adenocarcinomas. This group consisted of 8 males and 5 females with a median age of 64 years (range, 39-75 years). None of them received preoperative radiotherapy or chemotherapy.

Formalin-fixed paraffin-embedded tissue blocks of pancreatic cancer and normal pancreatic tissue were collected from the archives of the Department of Surgery at CIH, CAMS and Mudanjiang Tumor Hospital between January 1991 and August 2002 and subjected to tissue microarray construction. There were 32 pancreatic ductal adenocarcinomas, 6 mucinous

adenocarcinomas, 4 acinar cell carcinomas, 7 islet cell carcinomas, 8 ampulla of Vater carcinomas. The median age of these patients (37 males and 20 females) at the diagnosis was 60 years (range, 19-71 years).

Human pancreatic cancer cell lines BxPC-3 and PANC-1 were purchased from American Type Culture Collection (Manassas, VA). BxPC-3 and PANC-1 cells were cultured in RPMI 1640 and Dulbecco's modified Eagle's medium, respectively, and supplemented with 100 g/L heat-inactivated fetal bovine serum, 100 U/mL penicillin, and 100 µg/mL streptomycin.

Western blot analysis

Total tissue and cell lysate were prepared in extraction buffer containing 50 mmol/L Tris-HCl (pH 7.4), 150 mmol/L NaCl, 10 g/L Triton-100, 1 g/L SDS, 1 mmol/L EDTA, 1 mmol/L AEBSF, 20 µg/mL aprotinin, and 20 µg/mL leupeptin. After centrifugation at 12 000 g for 15 min at 4 °C, the supernatant was collected, and protein concentration was determined by Bradford method^[8]. Equal amounts of total protein (10 µg) from each sample were loaded and separated by 120 g/L SDS-polyacrylamide gel electrophoresis, and then transferred to Hybond-P polyvinylidene difluoride (PVDF) membrane (Amersham Pharmacia Biotech, Piscataway, NJ). After blocked with 50 g/L nonfat dry milk in PBS (pH 7.4) with 1 g/L Tween-20, membranes were probed with a mouse anti-annexin I monoclonal antibody (1:1 000 dilution, BD Biosciences Pharmingen, Chicago, IL), followed by subsequent incubation with horseradish peroxidase-conjugated goat anti-mouse secondary antibody (1:3 000 dilution, Santa Cruz Biotechnology, Santa Cruz, CA). Visualization of the protein bands was performed by the enhanced chemiluminescence kit (Santa Cruz Biotechnology). Parallel Western blot was probed with an anti- α -tubulin monoclonal antibody (Santa Cruz Biotechnology) as a loading control.

MTAs construction and immunohistochemistry analysis

Formalin-fixed paraffin-embedded tissue blocks containing pancreatic adenocarcinoma and normal pancreatic tissues were identified on the hematoxylin and eosin stained slide and marked. The marked areas in the corresponding paraffin block (donor block) were used for tissue microarray construction. From these defined areas of each specimen, triplicate tissue cores with a diameter of 0.6 mm were taken from donor block and arrayed into a recipient paraffin block using a tissue puncher/arrayer (Beecher Instruments, Silver Spring, MD) as previously described^[9]. Five micrometer sections of the tissue array block were cut and placed on Fisherbrand Colorfrost/Plus microscope slides (Fisher scientific, Pittsburgh, PA) for immunohistochemical staining.

The streptavidin-peroxidase method was used for the immunostaining of annexin I. Briefly, after deparaffinization in xylene and rehydration in grade ethanol, endogenous peroxidase activity was blocked by incubation with 3% hydrogen peroxide for 10 min. Tissue sections were then heated at 100 °C in 10 mmol/L citrate buffer (pH 6.0) for 10 min to retrieve antigens and pre-incubated with normal horse serum for 20 min at room temperature. Mouse anti-annexin I monoclonal antibody (BD Biosciences Pharmingen) diluted 1:100 was used as the primary antibody, and the specimens were incubated with it overnight at 4 °C, followed by addition of biotinylated anti-mouse secondary antibody and streptavidin-horseradish peroxidase (Zymed Laboratories, South San Francisco, CA). 3,3'-diaminobenzidine was used as a chromogen, and hematoxylin was used for counterstaining. For negative control purposes, the same procedure was followed except that the primary antibody was replaced by PBS. Known immunostaining-positive slides were used as positive controls.

The level of annexin I expression was calculated by combining an estimate of the percentage of immunoreactive cells (quantity score) with an estimate of the staining intensity (staining intensity score) as follows. No staining was scored as 0, 1-10% of cells with positive staining were scored as 1, 10-50% as 2, 50-70% as 3, and 70-100% as 4. Staining intensity was rated on a scale of 0 to 3 as follows: 0=negative (no color); 1=weak (weak yellow), 2=moderate (yellow), and 3=strong (brown). The raw data were converted to the immunohistochemical score (IHS) by multiplying the quantity and staining intensity scores. Therefore, the score could range from 0 to 12. The IHS score >3 was considered as positive expression^[10].

Statistical analysis

Statistical analysis was performed using the SPSS 10.0 software package (SPSS, Chicago, IL). The annexin I expression in different groups was analyzed using Mann-Whitney *U* test. The correlation between annexin I and each clinicopathologic factor was assessed with the Spearman rank correlation test. *P* value of less than 0.05 was considered statistically significant.

RESULTS

Western blot analysis of annexin I expression

Ten micrograms of protein extracts of pancreatic ductal adenocarcinoma tissues and their corresponding normal pancreas tissues from 13 different patients was prepared for Western blot analysis using monoclonal anti-annexin I antibody. This antibody could detect specific bands migrating at 37 ku (Figure 1). Western blot revealed that the expression of annexin I was low or undetectable in normal pancreas tissues. The level of annexin I expression was markedly increased in pancreatic ductal adenocarcinoma. Annexin I overexpression was found in 84.6% (11/13) pancreatic ductal adenocarcinoma tissues. There was also a strong expression of annexin I in pancreatic cancer cell lines.

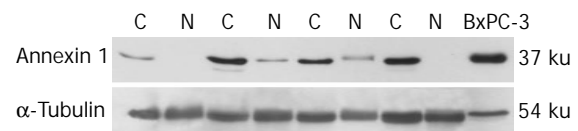


Figure 1 Western blot analysis of annexin I in pancreatic ductal adenocarcinoma. Ten micrograms of total protein extracts from pancreatic tissues and cell lines were run on 120 g/L SDS-PAGE, and annexin I protein expression was probed with mouse anti-annexin I monoclonal antibody and visualized by chemiluminescence (*top panel*). C: pancreatic ductal adenocarcinoma tissues; N: normal pancreas tissues; BxPC-3: human pancreatic adenocarcinoma cell line. α -Tubulin was used as an internal control (*bottom panel*).

Immunohistochemistry analysis of annexin I using pancreatic cancer MTAs

We carried out immunohistochemical studies for annexin I on the paraffin-embedded pancreatic cancer tissue microarray (Figure 2. A, B). This tissue microarray contained a total of 256 tissue spots consisting of 32 pancreatic ductal adenocarcinomas, 6 mucinous adenocarcinomas, 4 acinar cell carcinomas, 7 islet cell carcinomas, 8 ampulla of Vater carcinomas, and 38 normal pancreas tissues. In the normal pancreas, the positive rate of annexin I expression was 18.4% (7/38). It was found that most of normal pancreatic acinar and ductal cells did not express annexin I. There were only a small number of acinar cells that were observed. Annexin I cytoplasmic positive and the scattered positive cells were mainly located on the outside of acinar lumen (Figure 2. C, D). In contrast, positive expression of annexin I in

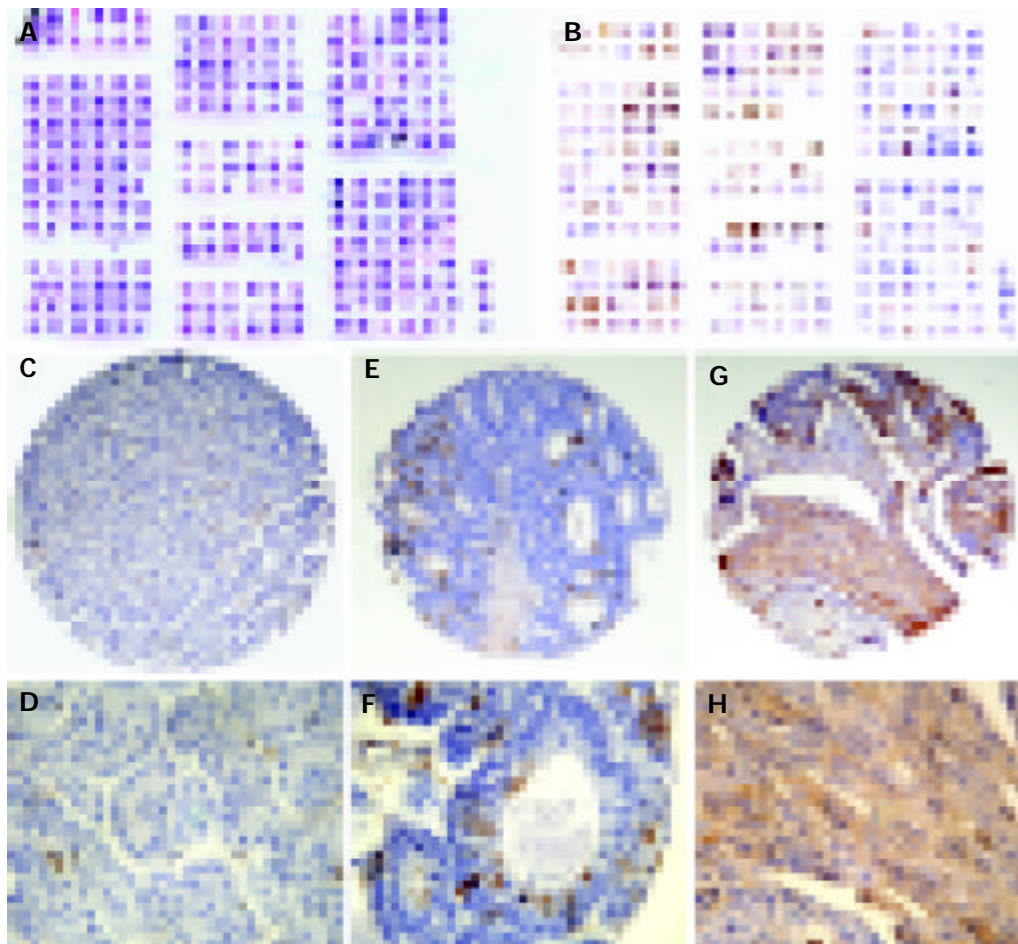


Figure 2 Immunohistochemical analysis of annexin I expression on pancreatic cancer MTAs. A and B: Overview of the H & E staining and immunohistochemical staining of annexin I on pancreatic cancer MTAs; C ($\times 200$) and D ($\times 400$): normal pancreas; E ($\times 200$) and F ($\times 400$): well differentiated ductal adenocarcinoma; G ($\times 200$) and H ($\times 400$): poorly differentiated ductal adenocarcinoma.

pancreatic cancer (71.4%, 30/42) was up-regulated significantly ($P < 0.01$). The different subtypes of the tumor were observed partially positive (Table 1). The possible relationships between annexin I expression with some clinicopathologic factors were additionally analyzed. It was found that the positive expression rate of annexin I in poorly differentiated pancreatic ductal adenocarcinomas (81.8%, 9/11) increased markedly compared with the well and moderately differentiated types (71.4%, 15/21) ($P < 0.05$). According to the progress of tumorigenesis, the distributions of annexin I were found altered from the outside of normal acinar lumen to the inside cancerous acinar lumen in the well differentiated ductal adenocarcinomas, and then to the most of poorly differentiated ductal adenocarcinomas separately (Figure 2. C, D, E, F, G, H). There were no statistically significant correlations between annexin I expression and lymph node metastasis and TNM stages (Table 2).

Table 1 Annexin I expression in normal pancreas and cancer tissues

Group	n	Positive rate of annexin I expression (%)	P value
Normal pancreas	38	18.4(7/38)	<0.0001
Pancreatic cancer	42	71.4(30/42)	
Ductal adenocarcinoma	32	75(24/32)	
Mucinous adenocarcinoma	6	83.3(5/6)	
Acinar cell carcinoma	4	25(1/4)	
Islet cell carcinoma	7	57.1(4/7)	
Ampulla of Vater carcinoma	7	57.1(4/7)	

Table 2 Correlation of annexin I expression with clinicopathologic factors of pancreatic adenocarcinoma on tissue microarray

Clinicopathologic factors	n	Positive expression rate of annexin I (%)	P value
Histological differentiation			0.012
High and moderate	21	71.4(15/21)	
Poor	11	81.8(9/11)	
Lymph node metastasis			0.810
Yes	8	75(6/8)	
No	34	73.5(25/3)	
TNM stage			0.551
I	15	66.7(10/15)	
II	21	81(17/21)	
III	5	60(3/5)	

DISCUSSION

Annexin I belongs to the family of the calcium and phospholipid-binding proteins, called annexins. Annexins are cytosolic or associated with the membrane or the cytoskeleton in a calcium-dependent manner. Annexin I is one of the more extensively studied annexins, which was initially cloned as phospholipase A2 (PLA2) inhibitor^[11]. Annexin I is a steroid-regulated protein and thus implicated in some actions of glucocorticoids, including inhibition of cell proliferation, anti-inflammatory effects, the regulation of cell migration, differentiation, death and the hypothalamic-pituitary axis^[12-16]. To date, there are some contradictory descriptions on annexin I expression in human

cancers. It has been reported that annexin I is up-regulated in human breast cancer^[17], hepatocellular carcinoma^[18], and pituitary adenoma^[19] and down-regulated in human esophageal squamous cell carcinoma^[20], prostate cancer^[21], and endometrial carcinoma^[22]. In this study, we found that annexin I was significantly overexpressed in pancreatic cancer by Western blot and immunohistochemistry, which was consistent with the results of gene expression profile analysis.

Annexin I is expressed in a tissue-specific manner in rodents. The highest annexin I expression level was found in lung and placenta; moderate in spleen, thymus, prostate, and submaxillary gland; and low (or absent) in muscle, brain, and liver^[23]. However, it was found that annexin I expression and phosphorylation were not only up-regulated during liver regeneration and transformation in antithrombin III SV40 T large antigen transgenic mice, but also overexpressed at both the transcriptional and translational levels in tumorous and nontumorous regions of hepatocellular carcinoma (HCC)^[18,24]. Annexin I up-regulation has been found to be correlated with increased synthesis of epidermal growth factor (EGF) and consequently with increased phosphorylation of EGF receptor (EGFR). Annexin I is a substrate for tyrosine kinases such as EGFR^[23,25] and for serine/threonine kinases such as protein kinase C^[26]. Annexin I can specifically modulate the extracellular signal-regulated kinase (ERK) signal cascade at an upstream site probably by associating with key signal components including the adaptor protein Grb2. Increased expression of annexin I could lead to constitutive activation of ERK1/2 kinase in macrophages^[27]. These findings implicated that annexin I might involve in mitogenic signal transduction and regulate cell growth. It was found that the level of annexin I expression increased three to four fold when quiescent human diploid foreskin fibroblasts (HFF) cells were stimulated to proliferate^[28]. This observation suggested that annexin I might be directly or indirectly involved in cellular proliferation. Pancreatic cancer demonstrated abnormally high expression of a number of important tyrosine kinase growth factors and receptors, particularly of the EGF family, which may contribute to the neoplasm's growth by autocrine and paracrine effects^[29]. Because annexin I is a substrate protein of EGFR, we can postulate that activated EGFR pathway promotes the annexin I up-regulation and then might associate with pancreas malignant transformation. We evaluated the relationship between annexin I and the clinicopathological factors of pancreatic cancer, and found that higher annexin I expression was correlated with the poorly differentiated type of pancreatic cancer, which was similar to the finding in HCC^[18]. These results suggest that annexin I is also involved in histological differentiation. It is interesting that the location of annexin I expression in different histologically differentiated types was changed, the reason for this change is not clear, which might be due to the role of annexin I in different places^[30].

On the other hand, enhanced expression of annexin I could reduce *in vitro* peripheral blood lymphocyte response to mitogens and might involve in the immunosuppressive mechanism of tumor-bearing hosts^[31]. Annexin I-derived peptides could inhibit antigen-driven human T cell proliferation and cytokine production^[32]. High constitutive levels of annexin I in leukaemic cells might protect them against immune-mediated killing^[33]. These evidences suggested that elevated annexin I might influence the immune defence system of body and might serve as a poor prognostic marker.

In conclusion, the present results show that overexpression of annexin I is a frequent event in pancreatic cancer, which may be one of the factors that link with the malignant transformation, lower differentiation and poor prognosis of pancreatic cancer. Detection of annexin I expression may be assistant to clinical diagnosis and can assess the prognosis of

pancreatic cancer. However, more efforts need to address the molecular mechanisms.

ACKNOWLEDGMENTS

We thank professor You-Yong Lu, Ms. Min Zhao and Dr. Zhuo-Bin Tang, Beijing Laboratory of Molecular Oncology, Beijing Institute for Cancer Research of Peking University for their help with tissue microarray construction.

REFERENCES

- 1 **Jemal A**, Murray T, Samuels A, Ghafoor A, Ward E, Thun MJ. Cancer statistics, 2003. *CA Cancer J Clin* 2003; **53**: 5-26
- 2 **Wang L**, Yang GH, Lu XH, Huang ZJ, Li H. Pancreatic cancer mortality in China (1991-2000). *World J Gastroenterol* 2003; **9**: 1819-1823
- 3 **Tan ZJ**, Hu XG, Cao GS, Tang Y. Analysis of gene expression profile of pancreatic carcinoma using cDNA microarray. *World J Gastroenterol* 2003; **9**: 818-823
- 4 **Rosty C**, Christa L, Kuzdzal S, Baldwin WM, Zahurak ML, Carnot F, Chan DW, Canto M, Lillemoe KD, Cameron JL, Yeo CJ, Hruban RH, Goggins M. Identification of hepatocarcinoma-intestine-pancreas/pancreatitis-associated protein I as a biomarker for pancreatic ductal adenocarcinoma by protein biochip technology. *Cancer Res* 2002; **62**: 1868-1875
- 5 **Iacobuzio-Donahue CA**, Maitra A, Shen-Ong GL, van Heek T, Ashfaq R, Meyer R, Walter K, Berg K, Hollingsworth MA, Cameron JL, Yeo CJ, Kern SE, Goggins M, Hruban RH. Discovery of novel tumor markers of pancreatic cancer using global gene expression technology. *Am J Pathol* 2002; **160**: 1239-1249
- 6 **Han H**, Bearss DJ, Browne LW, Calaluce R, Nagle RB, Von Hoff DD. Identification of differentially expressed genes in pancreatic cancer cells using cDNA microarray. *Cancer Res* 2002; **62**: 2890-2896
- 7 **Iacobuzio-Donahue CA**, Maitra A, Olsen M, Lowe AW, van Heek NT, Rosty C, Walter K, Sato N, Parker A, Ashfaq R, Jaffee E, Ryu B, Jones J, Eshleman JR, Yeo CJ, Cameron JL, Kern SE, Hruban RH, Brown PO, Goggins M. Exploration of global gene expression patterns in pancreatic adenocarcinoma using cDNA microarrays. *Am J Pathol* 2003; **162**: 1151-1162
- 8 **Bradford MM**. A rapid and sensitive method for the quantitation of microgram quantities of protein utilizing the principle of protein-dye binding. *Anal Biochem* 1976; **72**: 248-254
- 9 **Kononen J**, Bubendorf L, Kallioniemi A, Barlund M, Schraml P, Leighton S, Torhorst J, Mihatsch MJ, Sauter G, Kallioniemi OP. Tissue microarrays for high-throughput molecular profiling of tumor specimens. *Nat Med* 1998; **4**: 844-847
- 10 **Friedrichs K**, Gluba S, Eidtmann H, Jonat W. Overexpression of p53 and prognosis in breast cancer. *Cancer* 1993; **72**: 3641-3647
- 11 **Wallner BP**, Mattaliano RJ, Hession C, Cate RL, Tizard R, Sinclair LK, Foeller C, Chow EP, Browning JL, Ramachandran KL, Pepinsky RB. Cloning and expression of human lipocortin, a phospholipase A2 inhibitor with potential anti-inflammatory activity. *Nature* 1986; **320**: 77-81
- 12 **Flower RJ**, Rothwell NJ. Lipocortin-1: cellular mechanisms and clinical relevance. *Trends Pharmacol Sci* 1994; **15**: 71-76
- 13 **Parente L**, Solito E. Annexin I: more than an anti-phospholipase protein. *Inflamm Res* 2004; **53**: 125-132
- 14 **Perretti M**, Gavins FN. Annexin 1: an endogenous anti-inflammatory protein. *News Physiol Sci* 2003; **18**: 60-64
- 15 **de Coupade C**, Solito E, Levine JD. Dexamethasone enhances interaction of endogenous Annexin 1 with L-selectin and triggers shedding of L-selectin in the monocytic cell line U-937. *Br J Pharmacol* 2003; **140**: 133-145
- 16 **Buckingham JC**, Flower RJ. Lipocortin 1: a second messenger of glucocorticoid action in the hypothalamo-pituitary-adrenocortical axis. *Mol Med Today* 1997; **3**: 296-302
- 17 **Ahn SH**, Sawada H, Ro JY, Nicolson GL. Differential expression of annexin I in human mammary ductal epithelial cells in normal and benign and malignant breast tissues. *Clin Exp Metastasis* 1997; **15**: 151-156
- 18 **Masaki T**, Tokuda M, Ohnishi M, Watanabe S, Fujimura T, Miyamoto K, Itano T, Matsui H, Arima K, Shirai M, Maeba T,

- Sogawa K, Konishi R, Taniguchi K, Hatanaka Y, Hatase O, Nishioka M. Enhanced expression of the protein kinase substrate annexin in human hepatocellular carcinoma. *Hepatology* 1996; **24**: 72-81
- 19 **Mulla A**, Christian HC, Solito E, Mendoza N, Morris JF, Buckingham JC. Expression, subcellular localization and phosphorylation status of annexins 1 and 5 in human pituitary adenomas and a growth hormone-secreting carcinoma. *Clin Endocrinol* 2004; **60**: 107-119
- 20 **Paweletz CP**, Ornstein DK, Roth MJ, Bichsel VE, Gillespie JW, Calvert VS, Vocke CD, Hewitt SM, Duray PH, Herring J, Wang QH, Hu N, Linehan WM, Taylor PR, Liotta LA, Emmert-Buck MR, Petricoin EF 3rd. Loss of annexin I correlates with early onset of tumorigenesis in esophageal and prostate carcinoma. *Cancer Res* 2000; **60**: 6293-6297
- 21 **Xin W**, Rhodes DR, Ingold C, Chinnaiyan AM, Rubin MA. Dysregulation of the annexin family protein family is associated with prostate cancer progression. *Am J Pathol* 2003; **162**: 255-261
- 22 **Da J**, Meng X, Wang P, Yang Z, Zhu Y. Significance on expressions of Annexin-I and its correlative gene proteins in endometrial hyperplasia, atypical hyperplasia and endometrial carcinoma. *Zhonghua Binglixue Zazhi* 2001; **30**: 256-259
- 23 **De BK**, Misono KS, Lukas TJ, Mroczkowski B, Cohen S. A calcium-dependent 35-kilodalton substrate for epidermal growth factor receptor/kinase isolated from normal tissue. *J Biol Chem* 1986; **261**: 13784-13792
- 24 **de Coupade C**, Gillet R, Bennoun M, Briand P, Russo-Marie F, Solito E. Annexin I expression and phosphorylation are upregulated during liver regeneration and transformation in antithrombin III SV40 T large antigen transgenic mice. *Hepatology* 2000; **31**: 371-380
- 25 **Fava RA**, Cohen S. Isolation of a calcium-dependent 35-kilodalton substrate for the epidermal growth factor receptor/kinase from A-431 cells. *J Biol Chem* 1984; **259**: 2636-2645
- 26 **Khanna NC**, Tokuda M, Chong SM, Waisman DM. Phosphorylation of p36 *in vitro* by protein kinase C. *Biochem Biophys Res Commun* 1986; **137**: 397-403
- 27 **Allidridge LC**, Harris HJ, Plevin R, Hannon R, Bryant CE. The annexin protein lipocortin 1 regulates the MAPK/ERK pathway. *J Biol Chem* 1999; **274**: 37620-37628
- 28 **Schlaepfer DD**, Haigler HT. Expression of annexins as a function of cellular growth state. *J Cell Biol* 1990; **111**: 229-238
- 29 **Coppola D**. Molecular prognostic markers in pancreatic cancer. *Cancer Control* 2000; **7**: 421-427
- 30 **Liu Y**, Wang HX, Lu N, Mao YS, Liu F, Wang Y, Zhang HR, Wang K, Wu M, Zhao XH. Translocation of annexin I from cellular membrane to the nuclear membrane in human esophageal squamous cell carcinoma. *World J Gastroenterol* 2003; **9**: 645-649
- 31 **Koseki H**, Shiiba K, Suzuki Y, Asanuma T, Matsuno S. Enhanced expression of lipocortin-1 as a new immunosuppressive protein in cancer patients and its influence on reduced *in vitro* peripheral blood lymphocyte response to mitogens. *Surg Today* 1997; **27**: 30-39
- 32 **Kamal AM**, Smith SF, De Silva Wijayasinghe M, Solito E, Corrigan CJ. An annexin I (ANXA1)-derived peptide inhibits prototype antigen-driven human T cell Th1 and Th2 responses *in vitro*. *Clin Exp Allergy* 2001; **31**: 1116-1125
- 33 **Wu YL**, Jiang XR, Lillington DM, Newland AC, Kelsey SM. Upregulation of lipocortin 1 inhibits tumour necrosis factor-induced apoptosis in human leukaemic cells: a possible mechanism of resistance to immune surveillance. *Br J Haematol* 2000; **111**: 807-816

Edited by Kumar M and Wang XL Proofread by Xu FM

Mesenteric artery remodeling and effects of imidapril and irbesartan on it in spontaneously hypertensive rats

Zhong-Sheng Zhu, Jin-Ming Wang, Shao-Liang Chen

Zhong-Sheng Zhu, Jin-Ming Wang, Department of Cardiovascular Medicine, People's Hospital of Wuhan University, Wuhan 430060, Hubei Province, China

Shao-Liang Chen, Department of Cardiovascular Medicine, Third Affiliated Hospital of Nanjing Medical University, Nanjing 210006, Jiangsu Province, China

Supported by the Natural Science Foundation of Education Office of Hubei Province, No. 2000B03023/3011400802

Correspondence to: Dr. Zhong-Sheng Zhu, Department of Cardiovascular Medicine, Third Affiliated Hospital of Nanjing Medical University, Nanjing 210006, Jiangsu Province, China. zhuzhongsheng6966@hotmail.com

Telephone: +86-13016973706

Received: 2003-10-24 **Accepted:** 2003-12-08

Abstract

AIM: To investigate the remodeling of mesenteric artery and the expression of TGF- β_1 , c-Jun in mesenteric artery and effects of imidapril and irbesartan on the remodeling in spontaneously hypertensive rats (SHR).

METHODS: Thirty SHR (male/female, 21/9), aged 13 wk, were randomly divided into 3 groups (7 male rats and 3 female rats each group): SHR group, imidapril group (imidapril 3 mg/kg·d was given in drinking water for 14 wk), and irbesartan group (irbesartan 50 mg/kg·d was given in drinking water for 14 wk). Ten homogenous Wistar Kyoto rats, 5 males and 5 females, weighing 206±49 g, were selected as normal control group (WKY group). Systolic pressure was measured on d 1, 2, 4, 6, 8, 10, 12 and 14 during the experiment and the rats were killed at the end of the experiment. Angiotensin II (Ang II) level in plasma and mesenteric arteries was measured by radioimmunoassay. The morphology of the secondary branches of mesenteric artery were examined by light microscopy and electron microscopy. Reverse transcription polymerase chain reaction (RT-PCR) was used to detect the expression of transforming growth factor TGF- β_1 and c-Jun mRNA.

RESULTS: Compared with imidapril group and irbesartan group, the blood pressure was remarkably increased in SHR group. Ang II level in plasma and mesenteric arteries in SHR group was the same or lower than that in WKY group, and was higher in irbesartan group and lower in imidapril group. The remodeling of mesenteric arteries in SHR group was mostly obvious among the 4 groups. The ratio of TGF- β_1 absorbed light value to GAPDH absorbed light value in the SHR group was 0.887±0.019, which was significantly higher than that in WKY group, imidapril group, and irbesartan group with the ratios of 0.780±0.018, 0.803±0.005, and 0.847±0.017, respectively ($P<0.01$). Ang II level in plasma and mesenteric arteries in imidapril group was significantly lower than that in irbesartan group ($P<0.05$). The c-Jun absorbed light value/GAPDH absorbed light value of mesenteric arteries in the SHR group was 0.850±0.015, which was significantly higher than that in the WKY, imidapril, and irbesartan groups (0.582±0.013,

0.743±0.012, and 0.789±0.013, respectively, $P<0.01$), and was significantly lower in imidapril group than in irbesartan group ($P<0.05$).

CONCLUSION: Imidapril and irbesartan can not only control blood pressure but also inhibit mesenteric arteries remodeling and mRNA expression of TGF- β_1 , c-Jun in SHR. Imidapril is more effective than irbesartan.

Zhu ZS, Wang JM, Chen SL. Mesenteric artery remodeling and effects of imidapril and irbesartan on it in spontaneously hypertensive rats. *World J Gastroenterol* 2004; 10(10): 1471-1475

<http://www.wjgnet.com/1007-9327/10/1471.asp>

INTRODUCTION

It has been reported^[1-3] that angiotensin-converting enzyme inhibitor (ACEI) and angiotensin II type 1 (AT1) receptor antagonist can inhibit resistance blood vessel remodeling, but their action mechanism is still unknown. We selected irbesartan and imidapril to interfere mesenteric artery remodeling in spontaneously hypertensive rats (SHR) to investigate the expression of c-Jun and TGF- β_1 mRNA in resistance blood vessel of each group rats with reverse transcription polymerase chain reaction (RT-PCR) and to illustrate the mechanism of resistance blood vessel remodeling in hypertension and possible mechanism of these two drugs inhibiting mesenteric artery remodeling and possible effect on the inhibition of mesenteric artery remodeling.

MATERIALS AND METHODS

Materials

Thirty 13-wk old SHR (male/female, 21/9, provided by Fuwai Hospital in Beijing) with an average body mass of 228±39 g were randomly divided into 3 groups: SHR positive control group, imidapril treatment group (3 mg/kg·d), irbesartan treatment group (50 mg/kg·d). Ten homogenous Wistar-Kyoto rats [provided by Fuwai Hospital in Beijing, in which female rats were 5, male rats were 5, their average body mass was 206±49 g.] were selected as normal control group. During the 14-wk trial, all rats were in the breeding conditions: temperature 18-25 °C, humidity 40-60%, protein feed concentration 22-25%.

Methods

Irbesartan (presented by Hengrui Pharmacy Factory of Jiangsu Province) 50 mg/kg·d^[4] and imidapril (presented by Tianbian Pharmacy Factory of Tianjin) 3 mg/kg·d^[5] were dissolved in drinking water for 14 successive wk, respectively. Index observed included tail artery systolic blood pressure, angiotensin II (Ang II), histology of mesenteric artery. Fourteen weeks after irbesartan and imidapril interfering, all rats were killed and the second grade embranchment of mesenteric artery (about 2 mm) was taken and put into 25/L of glutaral for fixing, then transmission electron microscope (H-600, Hitachi in Japan) was used. About 1 mm of the artery was put into 100 g/L of neutral

formaldehyde and stained with HE, then observed by light microscope. Morphology of mesenteric artery was by a computer-assisted image analysis system. RT-PCR analysis was performed for TGF- β_1 ^[6] and c-Jun^[7] mRNA level in mesenteric artery.

SPSS 10.0 statistically analyzed the data and results were expressed as mean \pm SD.

RESULTS

Blood pressure from 4 groups was recorded in Table 1

Concentration of Ang II in plasma is shown in Table 2

Morphology of mesenteric artery (Figure 1)

Intima, vessel media, vessel wall were not increased in WKY group. Vessel lumen was relatively wider (A). Intima, vessel media and vessel wall were increased. Vessel lumen was relatively narrow in SHR (B), imidapril (C) and irbesartan (D) groups. The ratios of intima-media thickness / lumen radius, media / lumen area, lumen / vessel radius in 4 groups are shown in Table 3.

Microstructure of mesenteric arteries (transmission electron microscope, Figure 2)

As shown in A for WKY group, endothelial cells of intima were

abundant and normal, media had more smooth muscle cells. As shown in B for SHR group, endothelial cells of intima had vacuoles and fibrous tissues with adventitial hyperplasia, the thickness of adventitia was increased, media was severely fibrous and the fibrous tissue extended to smooth muscle layer and invaded internal elastic lamina, internal elastic lamina was tortuous and atrophic, some of smooth muscle cells were replaced by fibrous tissue. As shown in C for irbesartan group, endothelial cells of intima had vacuoles and marrow type corpses, internal elastic lamina was tortuous and atrophic and infiltrated by collagen fibers, but fibrosis in whole blood vessel wall relieved as compared with SHR group. The number of smooth muscle cells in media was slightly more than that in SHR group. As shown in D for imidapril group, endothelial cells of intima had marrow type corpses but no vacuole, the number of smooth muscle cells in media was more than that in irbesartan group, internal elastic lamina had a close-to-normal distribution, local internal elastic lamina was narrowed, fibrosis did not occur on blood vessel walls.

RT-PCR analysis of TGF- β_1 and c-Jun mRNA level in mesenteric artery (Figure 3)

mRNA expression levels of TGF- β_1 and c-Jun were analyzed by RT-PCR. Agarose gel electrophoresis of the PCR products was carried out to measure the relative intensity of the expression (A and B, Table 4).

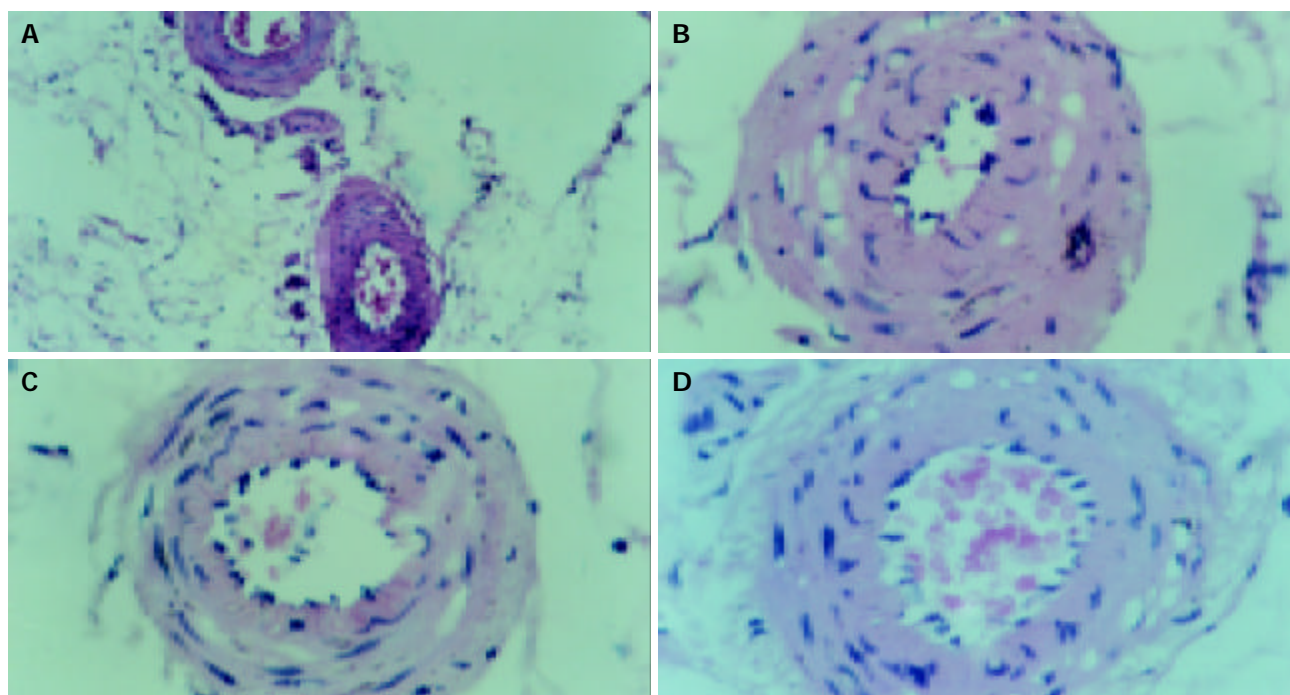


Figure 1 Morphology of mesenteric artery, A: Intima, media of vessel wall are not increased in WKY group and vessel lumen is relatively wider (HE, $\times 100$). B: Intima, media of vessel wall are increased in SHR group and vessel lumen is relatively narrow (HE, $\times 400$). C: Intima, media of vessel wall are increased in imidapril group and lumen of vessel is relatively narrow (HE, $\times 400$). D: Intima, media of vessel wall are increased in irbesartan group and lumen of vessel is relatively narrow (HE, $\times 400$).

Table 1 Blood pressure measured in WKY, SHR, imidapril and irbesartan groups (mean \pm SD, $n=10$)

Group	Blood pressure (mmHg)							
	13-wk-old	14-wk-old	15-wk-old	17-wk-old	19-wk-old	21-wk-old	24-wk-old	26-wk-old
WKY	105.90 \pm 16.10 ^d	115.70 \pm 9.19	112.00 \pm 7.53	90.00 \pm 9.13	125.50 \pm 7.62	116.00 \pm 6.99	116.00 \pm 11.25	121.50 \pm 4.74
SHR	134.40 \pm 7.72	140.00 \pm 17.48	151.00 \pm 24.59 ^b	160.00 \pm 14.90 ^f	177.00 \pm 16.19 ^f	177.50 \pm 14.39 ^f	190.00 \pm 19.00 ^f	198.10 \pm 14.04 ^f
Imidapril	131.50 \pm 6.68	124.30 \pm 7.02	127.50 \pm 8.58	125.00 \pm 7.45	130.80 \pm 15.16	138.00 \pm 12.52	127.00 \pm 11.10	142.00 \pm 6.32
Irbesartan	140.10 \pm 5.90	132.50 \pm 15.14	124.00 \pm 18.83	122.50 \pm 20.17	128.00 \pm 12.06	138.00 \pm 6.32	126.00 \pm 6.15	141.00 \pm 14.87

^b $P<0.01$ vs WKY, imidapril, irbesartan groups; ^d $P<0.01$ vs SHR, imidapril, irbesartan groups; ^f $P<0.01$ vs WKY, imidapril, irbesartan groups.

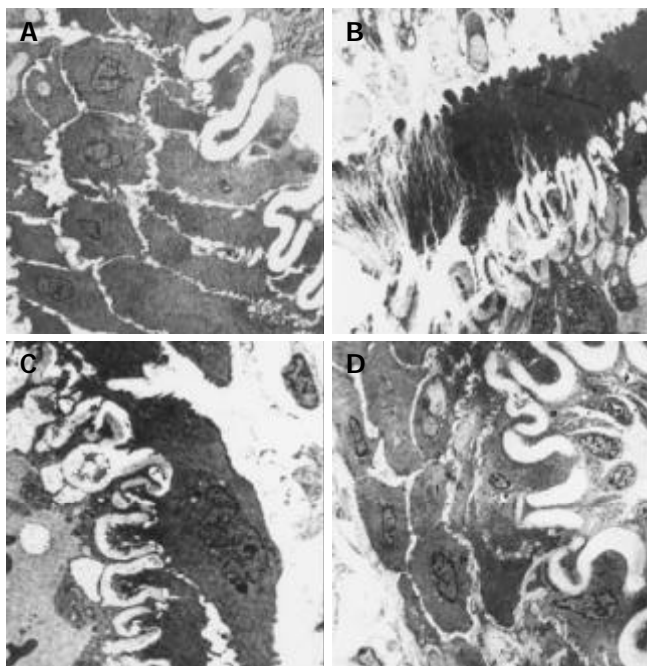


Figure 2 Microstructure of mesenteric arteries (transmission electron microscope), A: WKY group, endothelial cells of intima were abundant and normal, Media has more smooth muscle cells, internal elastic lamina is normal ($\times 2\ 000$). B: SHR group, endothelial cells of intima had vacuole and fibrous tissue with adventitial hyperplasia; thickness of the adventitia was increased; media was severely fibrous and the fibrous tissue extended to smooth muscle layer and invaded internal elastic lamina; internal elastic lamina was tortuous and atrophic; some of smooth muscle cells were replaced by fibrous tissue ($\times 2\ 500$). C: Irbesartan group, endothelial cells of intima have vacuole and marrow type corpses, internal elastic lamina was tortuous and atrophic and infiltrated by collagen fibers ($\times 2\ 500$). D: Imidapril group, endothelial cells of intima have marrow type corpses but no vacuole, numbers of smooth muscle cells in media were more than those in irbesartan group; internal elastic lamina got a close-to-normal distribution; local internal elastic lamina got narrow, fibrosis did not occur on blood vessel wall ($\times 2\ 000$).

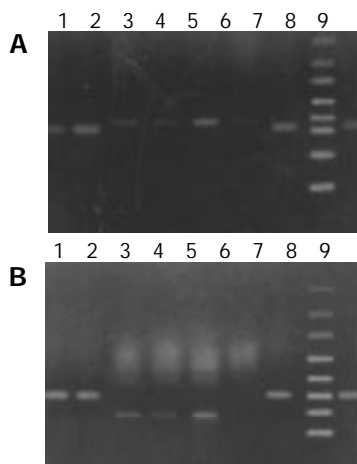


Figure 3 Agarose gel electrophoresis of TGF- β_1 and c-Jun mRNA RT-PCR product of mesenteric arteries. A: Agarose gel (2%) electrophoresis of TGF- β_1 mRNA RT-PCR product of mesenteric arteries of 4 groups. 1: WKY group GAPDH, 2: SHR group GAPDH, 3: irbesartan group, 4: imidapril group, 5: SHR group, 6: WKY group, 7: irbesartan group GAPDH, 8: pGEM-7Zf(+)/Hae III markers (from top to bottom: 102, 142, 174, 267, 289, 328, 434, 657 bp), 9: imidapril group GAPDH. B: Agarose gel (2%) electrophoresis of c-Jun mRNA RT-PCR product of

mesenteric arteries of 4 groups. 1: SHR group GAPDH, 2: WKY group GAPDH, 3: irbesartan group, 4: imidapril group, 5: SHR group, 6: WKY group, 7: irbesartan group GAPDH, 8: pGEM-3Zf(+)/Hae III markers (from top to bottom: 18, 80, 102, 174, 267, 314, 434, 587 bp), 9: imidapril group GAPDH.

Table 2 Concentration of Ang II in plasma (mean \pm SD, $n=7$)

Group	Plasma (pg/mL)	Mesenteric artery (pg/100 mg)
WKY	303.15 \pm 16.99	2 218.63 \pm 242.37
SHR	318.77 \pm 16.83	2 138.48 \pm 110.56 ^a
Imidapril	307.43 \pm 25.20	1 888.92 \pm 147.46 ^{ce}
Irbesartan	571.38 \pm 57.89 ^b	3 509.18 \pm 168.44 ^{bf}

^a $P<0.05$ vs WKY, ^b $P<0.01$ vs WKY, SHR, imidapril group, ^c $P<0.05$ vs WKY; ^e $P<0.05$ vs SHR; ^f $P<0.01$ vs SHR; ^b $P<0.01$ vs WKY; ^g $P<0.05$ vs imidapril.

Table 3 Comparisons of ratios of intima-media thickness / lumen radius, media / lumen area, lumen / vessel radius in four groups (mean \pm SD, $n=7$)

Group	Media thickness (mm)/lumen radius (mm)	Media area (mm ²)/lumen area (mm ²)	Lumen radius (mm)/vessel radius (mm)
WKY	0.75 \pm 0.09	0.35 \pm 0.04	0.65 \pm 0.01
SHR	2.67 \pm 0.20 ^a	1.21 \pm 0.14 ^a	0.46 \pm 0.01 ^a
Imidapril	1.67 \pm 0.13 ^{ec}	0.71 \pm 0.05 ^{ec}	0.51 \pm 0.01 ^{ec}
Irbesartan	1.47 \pm 0.27 ^{se}	0.65 \pm 0.14 ^{se}	0.53 \pm 0.01 ^{se}

^a $P<0.05$ vs WKY; ^c $P<0.05$ vs SHR; ^e $P<0.05$ vs WKY; ^e $P<0.05$ vs SHR; ^g $P<0.05$ vs WKY.

Table 4 Absorbance of c-Jun/absorbance of GAPDH, absorbance of TGF- β_1 /absorbance of GAPDH (mean \pm SD, $n=5$)

Group	Absorbance of c-Jun /absorbance of GAPDH	Absorbance of TGF- β_1 /absorbance of GAPDH
WKY group	0.582 \pm 0.013	0.780 \pm 0.018
SHR group	0.850 \pm 0.015 ^b	0.887 \pm 0.019 ^d
Imidapril group	0.743 \pm 0.012 ^a	0.803 \pm 0.005 ^c
Irbesartan group	0.789 \pm 0.013	0.847 \pm 0.017

$F=1\ 340$ in the ratio of absorbance of c-Jun/absorbance of GAPDH. ^a $P<0.05$ vs irbesartan group, ^b $P<0.01$ vs WKY, imidapril, irbesartan group. $F=198$ in the ratio of Absorbance of TGF- β_1 /absorbance of GAPDH. ^c $P<0.05$ vs irbesartan group, ^d $P<0.01$ vs WKY, imidapril, irbesartan group.

DISCUSSION

It is known that elevated blood pressure in essential hypertension patients and spontaneously hypertensive rats (SHR) related to the renin-angiotensin system (RAS)^[8-10]. The main effector peptide of RAS was Ang II^[11], which played an essential role in the pathogenesis of hypertension through the regulation of cell growth, inflammation, and fibrosis^[12]. The main biological effects of Ang II has been found to be the enhancement of smooth muscle contraction, aldosterone release^[13], arginine vasopressin release, cell proliferation, adjustment of body fluid balance. It had a close relation to blood vessel remodeling^[14]. There were 2 main angiotensin II receptors, AT1 and AT2^[15,16]. The AT1 receptor was responsible for most of the pathophysiologic actions of angiotensin II^[17], including cell proliferation, production of growth factors and cytokines, and fibrosis. AT2 could cause antiproliferation and counteract the cell growth induced by AT1 activation^[18]. In addition, pressure-lowering agent also had actions on blood vessel remodeling^[19]. Both

ACEI and AT1 receptor antagonists have been shown to act selectively on different cycles and they not only had satisfactory decompression effect, but also might inhibit blood vessel remodeling^[20,21].

These results suggest that imidapril and irbesartan have ideal decompression effects and inhibiting action upon angiotensin-converting enzymes and AT1 receptors. Blood pressure gradually rose and arrived to 200 mmHg in 26 wk-old SHR, but blood pressure in imidapril and irbesartan groups fluctuated within normal ranges and no obvious difference was observed between the 2 groups. Ang II level in plasma gradually increased in SHR group and slowly decreased in imidapril group compared with that in WKY group performed with radioimmunoassay, but there was no statistical significance between them. Ang II level in plasma increased in irbesartan group and it had a significant difference when compared with that in WKY group. Ang II level decreased in mesenteric artery in SHR group and it was obvious in imidapril group. Ang II level increased in mesenteric artery in irbesartan group and it had a significant difference. Campbell *et al.*^[22] made clear with experiment that Ang II levels in SHR plasma, lung, kidney, heart, adrenal, aorta, brown adipose tissue were lower than the levels in Donryu rats. In this experiment, Ang II levels in plasma of SHR group and WKY group and mesenteric artery were consistent with Duncan's experiment. Moreover, imidapril decreased Ang II levels and irbesartan increased Ang II levels^[23] in SHR plasma and mesenteric artery in this experiment.

Light microscopy and electron microscopy displayed that imidapril and irbesartan might inhibit structure alterations especially interstitial fibrosis. Furthermore, the effect of imidapril was better than that of irbesartan. It should be pointed out that electron microscopy of mesenteric artery displayed that the pathology of mesenteric artery remodeling in SHR possibly involved in fibrous tissue hyperplasia in adventitia, fibrosis in media, structure and function damage in endothelial cells. Castro *et al.*^[24] believed that extracellular matrix (ECM) accumulation in blood vessel walls could be attributable to constriction of artery lumen in hypertension. The pathological changes of resistance vessels could relate to the synthesis and excretion reduction of proteoglycan in blood vessel smooth muscle cells.

Several experiments have shown that Ang II could induce vascular smooth muscle cell proliferation *in vivo*. Griffin suggested that Ang II infusion in rats increased mesenteric vascular media width, media cross-sectional area and media/lumen ratio, and these changes were not inhibited by hydralazine despite normalization of blood pressure. Kim *et al.*^[25] also revealed that aortic ERK and JNK activities were significantly increased with the development of hypertension, and in particular, these activities were gradually and chronically enhanced in the development of hypertension and associated with an increase in aortic weight. *In vitro* experiments have also shown that Ang II stimulated protein synthesis and induced cellular hypertrophy in cultured vascular smooth muscle cells via AT1 receptors. More and more evidences have shown that AT1 receptors couple to a heterotrimeric G protein Gq. The activation of AT1 receptors could not only lead to the activation of PLC- β and increases of diacylglycerol and Ca²⁺ in cells but also activate intracellular signal transduction in cultured vascular smooth muscle cells. Schmitz *et al.*^[26] reported that Ang II could also activate JNK of vascular smooth muscle cells. JNK is well known to increase c-Jun transactivation by phosphorylating c-Jun on 2 critical N-terminal serine residues and inducing *c-fos* gene expression. Therefore, it has been well known that JNK is involved in the activation of transcription factor, AP-1^[27]. AP-1 is bound to TPA response component (TRE) of nucleus DNA to accelerate transcription and to increase proliferation and protein synthesis of vascular smooth

muscle cells. In vascular smooth muscle cells, activation of ERK and AP-1 could increase expression of TGF- β_1 mRNA^[28]. Both vascular endothelial cells and vascular smooth muscle cells could synthesis TGF- β_1 ^[29]. TGF- β_1 has been found to be one kind of multi-function proteins^[30] and to adjust hypertrophy and polyploidy of many kinds of cells and to stimulate and inhibit hyperplasia. In a word, it relates to vessel remodeling. TGF- β_1 is bound to specific receptors in cell surface to initiate the intracellular p53-dependent signaling cascade, resulting in down regulation or inhibition of cyclin-dependent kinases 2 and 4, and inducing cell cycle arrest in G₁. Ang II can mediate intracellular signal transduction of vascular smooth muscle cells. Remodeling of mesenteric artery in SHR would be inhibited if the expression of c-Jun and/or TGF- β_1 could be inhibited. Therefore, this experiment used AT1 receptor antagonist irbesartan and ACE inhibitor imidapril to interfere mesenteric artery remodeling in SHR in order to investigate the expression difference of c-Jun and TGF- β_1 mRNA in mesenteric artery with RT-PCR and to illustrate the intervention action and effect difference of these two kinds of drugs on inhibiting mesenteric artery remodeling.

Compared with WKY group, the mRNA level of TGF- β_1 and c-Jun in mesenteric arteries of SHR group was obviously increased. Imidapril and irbesartan might inhibit the expression of c-Jun and TGF- β_1 mRNA in mesenteric artery of SHR. Imidapril was better than irbesartan in preventing mesenteric arteries from structure modulation especially fibrosis and expression of TGF- β_1 , -Jun mRNA. Ohta *et al* proved that aortic TGF- β_1 , fibronectin, and collagen type IV WmRNA levels were higher in SHR than in WKY, and all of these elevated mRNAs in the aorta of SHR were significantly reduced by an ACE inhibitor, alacepril (50 mg/kg·d), or an AT1 receptor antagonist, SC-52458 (50 mg/kg·d). Kim *et al.*^[31] also showed that treatment with AT1 receptor antagonist (E4177, 20 mg/kg·d) significantly inhibited the activation of JNK and ERK in injured arteries. These experiments illuminate that the results in our investigation are acceptable. Further study should be done for the combined action of imidapril and irbesartan.

REFERENCES

- 1 **Kawano H**, Cody RJ, Graf K, Goetze S, Kawano Y, Schnee J, Law RE, Hsueh WA. Angiotensin II enhances integrin and alpha-actinin expression in adult rat cardiac fibroblasts. *Hypertension* 2000; **35**(1 Pt 2): 273-279
- 2 **Touyz RM**, He G, El Mabrouk M, Diep Q, Mardigyan V, Schiffrin EL. Differential activation of extracellular signal-regulated protein kinase 1/2 and p38 mitogen activated-protein kinase by AT1 receptors in vascular smooth muscle cells from Wistar-Kyoto rats and spontaneously hypertensive rats. *J Hypertens* 2001; **19**(3 Pt 2): 553-559
- 3 **Ledingham JM**, Phelan EL, Cross MA, Laverty R. Prevention of increases in blood pressure and left ventricular mass and remodeling of resistance arteries in young New Zealand genetically hypertensive rats: the effects of chronic treatment with valsartan, enalapril and felodipine. *J Vasc Res* 2000; **37**: 134-145
- 4 **Intengan HD**, Thibault G, Li JS, Schiffrin EL. Resistance artery mechanics, structure, and extracellular components in spontaneously hypertensive rats: effects of angiotensin receptor antagonism and converting enzyme inhibition. *Circulation* 1999; **100**: 2267-2275
- 5 **Yokota S**, Naito Y, Yoshida H, Ohara N, Adachi T, Narita H. Cardioprotective effects of an angiotensin-converting-enzyme inhibitor, imidapril, and Ca²⁺ channel antagonist, amlodipine, in spontaneously hypertensive rats at established stage of hypertension. *Jpn J Pharmacol* 1998; **77**: 79-87
- 6 **Ando T**, Okuda S, Tamaki K, Yoshitomi K, Fujishima M. Localization of transforming growth factor-beta and latent transforming growth factor-beta binding protein in rat kidney. *Kidney Int* 1995; **47**: 733-739

- 7 **Kreisberg JI**, Radnik RA, Ayo SH, Garoni J, Saikumar P. High glucose elevates c-fos and c-jun transcripts and proteins in mesangial cell cultures. *Kidney Inte* 1994; **46**: 105-112
- 8 **Umemura S**. Genetic aspect of essential hypertension. Article in Japanese. *Rinsho Byori* 2003; **51**: 813-817
- 9 **Petrovic D**, Bidovec M, Peterlin B. Gene polymorphisms of the renin-angiotensin-aldosterone system and essential arterial hypertension in childhood. *Folia Biol* 2002; **50**: 53-56
- 10 **Lijnen PJ**, Petrov VV. Role of intracardiac renin-angiotensin-aldosterone system in extracellular matrix remodeling. *Methods Find Exp Clin Pharmacol* 2003; **25**: 541-564
- 11 **Unger T**. Blood pressure lowering and renin-angiotensin system blockade. *J Hypertens Suppl* 2003; **21**(Suppl 6): S3-7
- 12 **Ruiz-Ortega M**, Ruperez M, Esteban V, Egido J. Molecular mechanisms of angiotensin II-induced vascular injury. *Curr Hypertens Rep* 2003; **5**: 73-79
- 13 **Fritsch Neves M**, Schiffrin EL. Aldosterone: a risk factor for vascular disease. *Curr Hypertens Rep* 2003; **5**: 59-65
- 14 **Williams B**. Angiotensin II and the pathophysiology of cardiovascular remodeling. *Am J Cardiol* 2001; **87**(8A): 10C-17C
- 15 **Rizkalla B**, Forbes JM, Cooper ME, Cao Z. Increased renal vascular endothelial growth factor and angiotensin II infusion is mediated by both AT1 and AT2 receptors. *J Am Soc Nephrol* 2003; **14**: 3061-3071
- 16 **Zhou Y**, Dirksen WP, Babu GJ, Periasamy M. Differential vasoconstrictions induced by angiotensin II: role of AT1 and AT2 receptors in isolated C57BL/6J mouse blood vessels. *Am J Physiol Heart Circ Physiol* 2003; **285**: H2797-2803
- 17 **Touyz RM**, Tabet F, Schiffrin EL. Redox-dependent signalling by angiotensin II and vascular remodeling in hypertension. *Clin Exp Pharmacol Physiol* 2003; **30**: 860-866
- 18 **Hannan RE**, Davis EA, Widdop RE. Functional role of angiotensin II AT2 receptor in modulation of AT1 receptor-mediated contraction in rat uterine artery: involvement of bradykinin and nitric oxide. *Br J Pharmacol* 2003; **140**: 987-995
- 19 **Iizuka K**, Murakami T, Kawaguchi H. Pure atmospheric pressure promotes an expression of osteopontin in human aortic smooth muscle cells. *Biochem Biophys Res Commun* 2001; **283**: 493-498
- 20 **Contreras F**, de la Parte MA, Cabrera J, Ospino N, Israili ZH, Velasco M. Role of angiotensin II AT1 receptor blockers in the treatment of arterial hypertension. *Am J Ther* 2003; **10**: 401-408
- 21 **Yavuz D**, Koc M, Toprak A, Akpınar I, Velioglu A, Deyneli O, Haklar G, Akalin S. Effects of ACE inhibition and AT1-receptor antagonism on endothelial function and insulin sensitivity in essential hypertensive patients. *J Renin Angiotensin Aldosterone Syst* 2003; **4**: 197-203
- 22 **Campbell DJ**, Duncan AM, Kladis A, Harrap SB. Angiotensin Peptides in spontaneously Hypertensive and Normotensive Donryu rats. *Hypertension* 1995; **25**: 928-934
- 23 **Duke LM**, Paull JR, Widdop RE. Cardiovascular status following combined angiotensin-converting enzyme and AT1 receptor inhibition in conscious spontaneously hypertensive rats. *Clin Exp Pharmacol Physiol* 2003; **30**: 317-323
- 24 **Castro CM**, Cruzado MC, Miatello RM, Risler NR. Proteoglycan production by vascular smooth muscle cells from resistance arteries of hypertensive rats. *Hypertension* 1999; **34**(4 Pt 2): 893-896
- 25 **Kim S**, Murakami T, Izumi Y, Yano M, Miura K, Yamanaka S, Iowa H. Extracellular signal-regulated kinase and c-Jun NH2-terminal kinase activities are continuously and differentially increased in aorta of hypertensive rats. *Biochem Biophys Res Commun* 1997; **236**: 199-204
- 26 **Schmitz U**, Ishida T, Ishida M, Surapishchat J, Hasham MI, Pelech S, Berk BC. Angiotensin II stimulates p21-activated kinase in vascular smooth muscle cells: role in activation of JNK. *Circ Res* 1998; **82**: 1272-1278
- 27 **Yano M**, Kim S, Izumi Y, Yamanaka S, Iwao H. Differential activation of cardiac c-jun amino-terminal kinase and extracellular signal-regulated kinase in angiotensin II-mediated hypertension. *Circ Res* 1998; **83**: 752-760
- 28 **Hamaguchi A**, Kim S, Izumi Y, Zhan Y, Yamanaka S, Iwao H. Contribution of extracellular signal-regulated kinase to angiotensin II-induced transforming growth factor- β_1 expression in vascular smooth muscle cells. *Hypertension* 1999; **34**: 126-131
- 29 **Ebisui O**, Dilley RJ, Li H, Funder JW, Liu JP. Growth factors and extracellular signal-regulated kinase in vascular smooth muscle cells of normotensive and spontaneously hypertensive rats. *J Hypertens* 1999; **17**: 1535-1541
- 30 **Gekle M**, Knaus P, Nielsen R, Mildenerger S, Freudinger R, Wohlfarth V, Sauvant C, Christensen EL. Transforming growth factor-beta1 reduces megalin-and cubilin-mediated endocytosis of albumin in proximal-tubule-derived opossum kidney-cells. *J Physiol* 2003; **552**(Pt 2): 471-481
- 31 **Kim S**, Izumi Y, Yano M, Hamaguchi A, Miura K, Yamanaka S, Miyazaki H, Iwao H. Angiotensin blockade inhibits activation of mitogen-activated protein kinases in rat balloon-injured artery. *Circulation* 1998; **97**: 1731-1737

Edited by Wang XL and Xu FM

Signal pathways involved in emodin-induced contraction of smooth muscle cells from rat colon

Tao Ma, Qing-Hui Qi, Jian Xu, Zuo-Liang Dong, Wen-Xiu Yang

Tao Ma, Qing-Hui Qi, Jian Xu, Zuo-Liang Dong, Department of Surgery, General Hospital of Tianjin Medical University, 300052, Tianjin, China

Wen-Xiu Yang, Division of Biophysics, Department of Physics, Nankai University, Tianjin 300071, China

Supported by the National Natural Science Foundation of China, No.30171198

Correspondence to: Dr. Qing-Hui Qi, Department of Surgery, General Hospital of Tianjin Medical University, Tianjin 300052, China. mataoemail@yahoo.com.cn

Telephone: +86-22-84283767

Received: 2003-06-04 **Accepted:** 2003-11-19

Abstract

AIM: To investigate the effects induced by emodin on single smooth muscle cells from rat colon *in vitro*, and to determine the signal pathways involved.

METHODS: Cells were isolated from the muscle layers of Wistar rat colon by enzymatic digestion. Cell length was measured by computerized image micrometry. Intracellular Ca^{2+} ($[Ca^{2+}]_i$) signals were studied using the fluorescent Ca^{2+} indicator fluo-3 and confocal microscopy. PKC α distribution at rest state or after stimulation was measured with immunofluorescence confocal microscopy.

RESULTS: (1) Emodin dose-dependently caused colonic smooth muscle cells contraction; (2) emodin induced an increase in intracellular Ca^{2+} concentration; (3) the contractile responses induced by emodin were respectively inhibited by preincubation of the cells with ML-7 (an inhibitor of MLCK) and calphostin C (an inhibitor of PKC); (4) Incubation of cells with emodin caused translocation of PKC α from cytosolic area to the membrane.

CONCLUSION: Emodin has a direct contractile effect on colonic smooth muscle cell. This signal cascade induced by emodin is initiated by increased $[Ca^{2+}]_i$ and PKC α translocation, which in turn lead to the activation of MLCK and the suppression of MLCP. Both of them contribute to the emodin-induced contraction.

Ma T, Qi QH, Xu J, Dong ZL, Yang WX. Signal pathways involved in emodin-induced contraction of smooth muscle cells from rat colon. *World J Gastroenterol* 2004; 10(10): 1476-1479
<http://www.wjgnet.com/1007-9327/10/1476.asp>

INTRODUCTION

Gastrointestinal dysmotility underlies frequent clinical entities such as diabetes mellitus, chronic constipation, irritable bowel syndrome, postoperative ileus *etc.* Currently few drugs have been proven to be efficient at improving motility. Emodin is a naturally occurring anthraquinone present in the roots and bark of numerous plants of the genus *Rhamnus*^[1]. Extracts from the roots, bark, and/or dried leaves of buckthorn, senna, cascara,

aloe, frangula, and rhubarb have been used as laxatives since ancient times and currently are widely used in the preparation of herbal laxative preparations in China^[2-5]. Anthraquinone glycosides are poorly absorbed from the gastrointestinal tract but are cleaved by gut bacteria to produce aglycones, including emodin which are more readily absorbed and thought to be responsible for the purgative properties of these preparations^[1]. The reported biological effects of emodin include antitumor, antibacterial and anti-inflammatory actions^[6-9]. Emodin also possesses prokinetic effect on gastrointestinal tract. Stimulatory actions of emodin on gastrointestinal smooth muscle have been described in several studies^[10-12]. However, its mechanism in accelerating gastrointestinal motion is not yet clarified.

It is now understood that the contraction of smooth muscle cells involves two processes^[13-16]: (a) The concentration of intracellular Ca^{2+} increases; this Ca^{2+} increase results in phosphorylation of myosin and consequently an increased contractility. (b) The sensitivity of the myofilaments to Ca^{2+} increases. Pharmacological agents can stimulate smooth muscle cell contractions by mobilizing intracellular Ca^{2+} and/or enhancing Ca^{2+} sensitivity.

Because of the potential therapeutic implications of emodin in gastrointestinal hypomotility disorders, this study was then designed to further characterize the effects of emodin on smooth muscle cells from rat colon *in vitro* and to investigate the signal transduction cascade leading to cell contraction induced by emodin.

MATERIALS AND METHODS

Materials

Fluo-3 AM and Pluronic F-127 were from Molecular Probes (USA). Rabbit anti-PKC α IgG and goat anti-rabbit IgG FITC were from Santa Cruz Biotechnology (USA). Collagenase type II, emodin, trypsin inhibitor and HEPES were all purchased from Sigma Co (USA). DMEM was purchased from GIBCO Co., USA. FBS was from Hyclone (USA). All other reagents were from LianXing Co., Ltd (China). Emodin was dissolved in dimethyl sulfoxide and ethanol mixture (2:8) to make stock solution and the final concentration of the vehicle in the solution did not exceed 0.1%.

Methods

Isolation of smooth muscle cells Smooth muscle cells from rat distal colon were isolated as described previously^[13]. Briefly, a segment of 5-cm long distal colon was dissected and digested to yield isolated smooth muscle cells. The tissue was incubated for 2 successive 30-min periods at 31 °C in 10 mL of HEPES (pH7.4) containing 1 g/L collagenase type II and 0.1 g/L soybean trypsin inhibitor. After the second enzymatic incubation, the medium was filtered through 500 μ m Nitex mesh. The partially digested tissue left on the filter was washed with collagenase-free buffer solution, and muscle cells were allowed to disperse spontaneously for 30 min. The cells were harvested by centrifugation at 350 r/min for 10 min. After a hemocytometric cell count, the harvested cells were resuspended in collagenase-free buffer solution and diluted as needed.

Measurement of smooth muscle cell contraction Individual cell length was measured by scanning micrometry as described previously^[13]. Aliquots consisting of 1×10^4 cells in 0.25 mL of medium were added to 50 μ L of a solution containing emodin with or without prior incubation with ML-7 (10^{-5} mol/L) or Calphostin C (10^{-6} mol/L). The reaction was allowed to proceed for 1 min and terminated by the addition of acrolein at a final concentration of 10 mL/L. The lengths of 30 consecutive intact healthy cells were measured through a phase-contrast microscope fitted with a video camera and connected to a Legend computer. The CIMAS program was used to measure the length. The contractile response was defined as the decrease in the average length of the 30 cells and was expressed as the percent change relative to control length.

Single cell intracellular Ca^{2+} measurements Changes in $[Ca^{2+}]_i$ were estimated as described elsewhere by using laser scanning confocal microscopy (Radiance 2000; Bio-rad, Hertfordshire, UK)^[17] linked to an inverted epifluorescence microscope (Olympus, Japan). The scanning box was set at a resolution of 256×256 . Only one fixed combination of laser intensity (20% maximum) and photomultiplier gain (1 800 of a maximum of 4 096) was used during scanning.

To load the cells with fluorescent Ca^{2+} indicator fluo-3, smooth muscle cells on the coverslips were incubated with 5 μ mol/L of the membrane permeant acetoxymethyl ester of the dye (fluo-3 AM; Molecular Probes, USA) and Pluronic F-127 (0.4 g/L; Molecular Probes, USA) dissolved in HEPES-ringer buffer [containing (mmol/L): NaCl 135, KCl 5.9, $CaCl_2$ 1.5, $MgCl_2$ 1.2, HEPES 11.6 and glucose 11.5, at pH 7.3] for 30 min at 37 °C. Cells were subsequently washed twice with HEPES-ringer buffer and further incubated for 20 min to allow de-esterification of the dye.

Coverglass chambers were then mounted on the microscope stage and continuously superfused with HEPES-ringer buffer. The cells loaded with fluo-3 were illuminated at 488 nm, and fluorescent emissions of 525/30 nm were recorded at an intensity of fluo-3. Digital Ca^{2+} images were collected at 10 s intervals. Because fluo-3 is a single wavelength indicator, it is not possible to apply the ratiometric method to quantitative determination of $[Ca^{2+}]_i$. Therefore, the intensity of fluo-3 fluorescence was normalized in the temporal analysis. The relative values of fluorescence intensity of the dye (Ft) were used to represent the $[Ca^{2+}]_i$.

Cell culture and confocal imaging of PKC α cell culture After enzymatic incubation, the dispersed cells were collected in DMEM with 100 mL/L FBS-medium, then transferred to coverslips coated with poly-L-lysine, and allowed to settle overnight in a humidified 50 mL/L CO_2 environment.

Cell fixation and permeabilization Cells were either untreated or treated with emodin (50 μ mol/L), and the reaction was stopped by removing the medium and adding 40 g/L formaldehyde to PBS. Cells were fixed in PBS for 10 min. Then the fixative was removed, and the cells were washed with PBS. Thereafter the cells were permeabilized by adding the permeabilization solution [(0.1 mL TritonX-100, 90 mL distilled water, and 10 mL PBS (10 \times)] for 10 min. After permeabilization, the cells were rinsed 3 times with PBS.

Labeling with PKC α antibody and confocal microscopy Cells were incubated for 1 h with normal goat serum, followed by 3 washes in PBS with gentle agitation. Subsequently, the cells were incubated for 1 h with the primary antibody, a rabbit anti-PKC α IgG followed by 3 washes with PBS with gentle agitation. This step was followed by incubation of the cells for 1 h with secondary antibody (goat anti-rabbit IgG FITC). Then the cells were washed 3 times with PBS with gentle agitation. Finally, the cells on the coverslip were mounted onto a slide. Control slides were made by incubating cells with the secondary antibody only. The excitation parameter for fluorescent probes

was as follows: FITC excitation at 488 nm and emission at 520 nm. Immunostained cells were visualized with an Olympus $\times 40$ objective by confocal laser scanning microscopy (Bio-Rad radiance 2000). Image restoration and analysis were performed in Lasersharp2000 and Laserpix.

Statistical analysis

The data are presented as mean \pm SD, and n represents the number of experiments. Statistical analysis was made by Student's unpaired *t* test when applicable. *P* values less than 0.05 were considered to be significant.

RESULTS

Effect of emodin on colonic smooth muscle cell length

Freshly isolated colonic smooth muscle cells appeared in spindle shape with diverse length (range from 44–121 μ m). Some of them were relaxed while others were at different phases of contraction (Figure 1). In resting state, the average cell length was 84.26 μ m. The application of emodin to freshly isolated smooth muscle cells induced a reduction in cell length. This reduction in cell length reflected contraction of the smooth muscle cells. Emodin at concentrations of 5 to 100 μ mol/L induced a concentration-dependent contraction (Figure 2). Maximal contraction of $19.17 \pm 2.59\%$ was observed with 50 μ mol/L of emodin.



Figure 1 Freshly isolated colonic smooth muscle cells appeared in spindle shape with diverse length. Some of them were relaxed while others were at different phases of contraction.

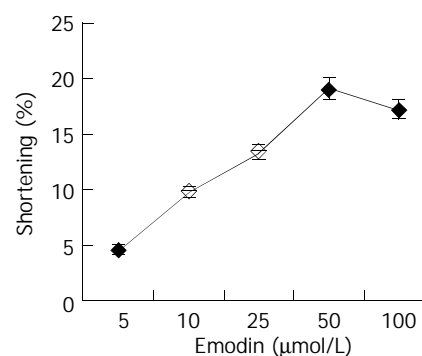


Figure 2 Dose-response curve representing the effects of emodin on the length of isolated colonic smooth muscle cell. Values are mean \pm SD of 3 experiments.

Effect of emodin on $[Ca^{2+}]_i$

Basal $[Ca^{2+}]_i$ levels were not significantly different between cells and the relative fluorescence intensity ranged from 38.46 to 52.59 (46.56 ± 3.79). At each concentration of emodin, the $[Ca^{2+}]_i$ response of 20 cells was determined. The application of emodin at concentrations from 5 to 100 μ mol/L could trigger

an increase in $[Ca^{2+}]_i$. The $[Ca^{2+}]_i$ responses to varying emodin concentrations are shown in Figure 3.

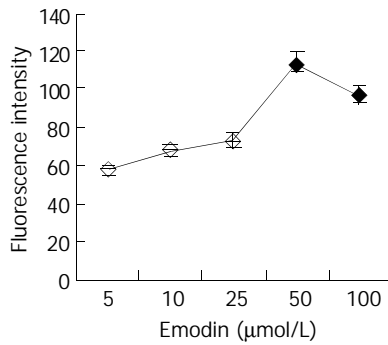


Figure 3 $[Ca^{2+}]_i$ response of colonic smooth muscle cells to emodin.

Effect of ML-7 and Calphostin C on emodin-induced contraction of colonic smooth muscle cells

Freshly isolated smooth muscle cells were treated with emodin (50 μmol/L) for 1 min with or without prior incubation with ML-7 (an inhibitor of MLCK, 10⁻⁵ mol/L) or Calphostin C (an inhibitor of PKC, 10⁻⁶ mol/L). The application of 50 μmol/L emodin to freshly isolated colonic smooth muscle cells induced a reduction in cell length (19.17±2.59%). And 42.93±6.16% of the contractile response induced by emodin was inhibited by preincubation of the cells with ML-7 ($P<0.05$). Similarly, 51.12±3.87% of the contractile response induced by emodin was inhibited by Calphostin C ($P<0.05$). (Figure 4).

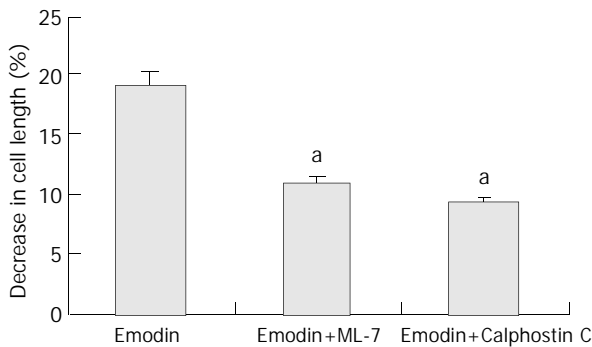


Figure 4 Effect of ML-7 and calphostin C on emodin-induced contraction of colonic smooth muscle cells. Emodin-induced cell shortening was 19.17±2.59%. Preincubation of the cells with ML-7 and calphostin C resulted in a decrease in cell contraction. ^a $P<0.05$ vs Emodin group.

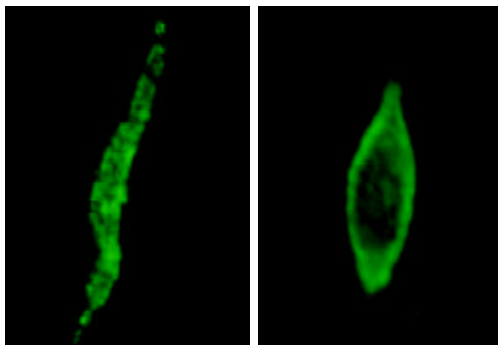


Figure 5 Membrane translocation of PKC α in response to emodin stimulation in smooth muscle cells of rat colon. Confocal microscopy showed PKC α distributed throughout the cell at rest state (left). When cells were stimulated with emodin (50 μmol/L), PKC α translocated to the membrane (right).

Emodin-induced translocation of PKC α in colonic smooth muscle cell

PKC α is thought to be inactive in the cytoplasm and therefore must translocate to the plasma membrane to be activated. Recent studies have demonstrated that PKC α can translocate from the cytoplasm to membrane on stimulation by contractile agonists during smooth muscle cell contraction^[18-21]. To determine whether activation of PKC α is involved in contraction of smooth muscle cells induced by emodin, we performed immunofluorescent labeling of PKC α in isolated smooth muscle cells, followed by confocal microscopy. Our data indicate that, at resting state, PKC α is mainly distributed throughout the cytoplasm. This is in contrast to the distribution of PKC α following emodin stimulation, as shown in Figure 5, PKC α translocated from the cytosolic part and aligned itself along the membranes of contracted cells.

DISCUSSION

Previous studies have indicated that emodin possesses prokinetic effect on gastrointestinal tract^[10-12]. Using confocal microscopy and cell isolation technique, the present study focused on emodin's cellular effect on smooth muscle cells from rat colon *in vitro* and investigated the signal mechanisms underlying its effect.

Our study showed that some of the action of emodin on gastrointestinal tract is exerted on the smooth muscle cells, as application of emodin to colonic smooth muscle cells resulted in a decrease in cell length. To our knowledge, this is the first study to show a direct contractile effect of emodin on gastrointestinal smooth muscle cells.

It is well established that Ca²⁺/calmodulin-mediated phosphorylation of the light chain of smooth muscle myosin is a major regulatory mechanism for smooth muscle contraction^[22-26]. Stimulation of smooth muscle cells by specific agonists induces Ca²⁺ mobilization and activation of myosin light chain (MLC) kinase, which subsequently phosphorylates MLC and activates the myosin ATPase. The cascade of events described above leads to contraction of smooth muscle. Yang *et al.* have demonstrated that emodin could evoke increases in $[Ca^{2+}]_i$ in guinea-pigs taenia coli cells^[12]. In the present study, we observed the changes in $[Ca^{2+}]_i$ induced by emodin in single smooth muscle cell by using confocal microscopy and fluo-3 loading technique. Our data showed that, when applied to isolated smooth muscle cells, emodin induced a significant increase in $[Ca^{2+}]_i$. The effect of emodin on $[Ca^{2+}]_i$ indicated that emodin-mediated contractions were Ca²⁺-dependent and MLCK pathways might be involved in emodin-induced contractions. We then carried out contraction studies in which we tested the effect of ML-7, a MLCK inhibitor, on emodin-induced contraction. As shown in Figure 4, the emodin-mediated contraction was significantly attenuated by ML-7. Taken together, these observations suggested that incubation of smooth muscle cells with emodin seemed to trigger a cascade of events including increase in $[Ca^{2+}]_i$, activation of MLCK and then cell contraction.

However, only (42.93±6.16)% of the contractile effect elicited by emodin was inhibited by ML-7. Therefore, it is possible that the rest of the emodin-induced contraction is mediated through an alternative pathway different from myosin light chain phosphorylation. Indeed, the rising of $[Ca^{2+}]_i$ has been found to be insufficient to explain excitation-contraction of smooth muscle cell, because the cytosolic concentration of Ca²⁺ is not always proportional to the extent of MLC phosphorylation and the force of contraction in smooth muscle cells. Other regulatory mechanisms have been proposed^[22,2-30]. Evidence accumulated that PKC α activation may contribute to the contraction of smooth muscle cells through a kinase cascade involving suppressing the activity of myosin light

chain phosphatase (MLCP) and increasing the sensitivity of contractile apparatus to Ca^{2+} . Therefore, we attempted to study the role of PKC α in emodin-induced contraction. The results of our contractile experiments showed that calphostin C, a PKC inhibitor, significantly suppressed the contraction induced by emodin, which suggested that PKC α might play a role in emodin-induced cell contraction. Lee has demonstrated that PKC α plays a critical role in emodin-induced apoptosis in CH27 and H460 cells^[7]. In order to verify the role of PKC α in emodin-induced contraction, we next examined the effect of emodin on the activity of PKC α . Previous studies have demonstrated that PKC α is activated by agonist and translocated from the cytoplasm to the plasma membrane through a complex mechanism during smooth muscle cell contraction. Although the exact nature of the translocation is still unclear, it has been suggested that the recruitment of cytosolic PKC α to the membrane is a pivotal component of signal mechanism which mediates the contraction of smooth muscle cell^[31-33]. In our study, it was shown that PKC α distribution at rest appeared homogeneous throughout the cell, which is in agreement with previous studies. After stimulation of colonic smooth muscle cells with emodin, PKC α underwent a distinct translocation to the membrane. These data above strongly suggest that emodin may exert its contractile effects on smooth muscle cells via PKC α activation.

On the basis of our findings, we propose the existence of an intracellular signaling cascade leading to cell contraction in colonic smooth muscle induced by emodin. This cascade is initiated by increased $[Ca^{2+}]_i$ and PKC α translocation, which in turn lead to the activation of MLCK and the suppression of MLCP, both of which contribute to the emodin-induced contraction. And these results provide evidence for an excitatory role of emodin in colonic smooth muscle cells contraction and indicate that emodin may be a promising prokinetic agent in ameliorating colonic hypomotility.

REFERENCES

- Liang JW, Hsiu SL, Wu PP, Chao PD. Emodin pharmacokinetics in rabbits. *Planta Med* 1995; **61**: 406-408
- Xie WL, Lin XZ, Ma DL, Li H. Effect of DACHENGQITANG* on phosphodiesterase in enteral smooth muscle cell in rats. *Chin Traditional Herbal Drug* 2001; **4**: 339-341
- Chen H, Wu X, Guan F. Protective effects of tongli gongxia herbs on gut barrier in rat with multiple organ dysfunction syndrome. *Chin J Int Traditional Western Med* 2000; **2**: 120-122
- You SY, Wu XZ, Liu ML. Effects of dachengqi decoction on gut hormones and intestinal movement after cholecystectomy. *Chin J Int Traditional Western Med* 1994; **9**: 522-524
- Xia Q, Jiang JM, Gong X, Chen GY, Li L, Huang ZW. Experimental study of Tong Xia purgative method in ameliorating lung injury in acute necrotizing pancreatitis. *World J Gastroenterol* 2000; **6**: 115-118
- Lee HZ. Effects and mechanisms of emodin on cell death in human lung squamous cell carcinoma. *Br J Pharmacol* 2001; **1**: 11-20
- Lee HZ. Protein kinase C involvement in aloe-emodin- and emodin-induced apoptosis in lung carcinoma cell. *Br J Pharmacol* 2001; **5**: 1093-1103
- Srinivas G, Anto RJ, Srinivas P, Vidhyalakshmi S, Senan VP, Karunakaran D. Emodin induces apoptosis of human cervical cancer cells through poly(ADP-ribose) polymerase cleavage and activation of caspase-9. *Eur J Pharmacol* 2003; **473**: 117-125
- Kuo YC, Meng HC, Tsai WJ. Regulation of cell proliferation, inflammatory cytokine production and calcium mobilization in primary human T lymphocytes by emodin from Polygonum hypoleucum Ohwi. *Inflamm Res* 2001; **2**: 73-82
- Jin ZH, Ma DL, Lin XZ. Study on effect of emodin on the isolated intestinal smooth muscle of guinea-pigs. *Zhongguo Chin J Int Traditional Western Med* 1994; **14**: 429-431
- Li J, Yang W, Hu W, Wang J, Jin Z, Wang X, Xu W. Effects of emodin on the activity of K channel in guinea pig taenia coli smooth muscle cells. *Acta Pharmaceutica Sinica* 1998; **5**: 321-325
- Yang WX, Wang J, Li JY. Characteristics of emodin evoked $[Ca^{2+}]_i$ and inhibition of GDP in guinea pig taenia coli cells. *Acta Biophysica Sinica* 2001; **1**: 165-169
- Wang P, Bitar KN. RhoA regulates sustained smooth muscle contraction through cytoskeletal reorganization of HSP27. *Am J Physiol* 1998; **274**(6 Pt 1): G1454-1462
- Fan J, Byron KL. Ca^{2+} signalling in rat vascular smooth muscle cells: a role for protein kinase C at physiological vasoconstrictor concentrations of vasopressin. *J Physiol* 2000; **524**(Pt 3): 821-831
- Taggart MJ, Lee YH, Morgan KG. Cellular redistribution of PKC α , rhoA and ROK α following smooth muscle agonist stimulation. *Exp Cell Res* 1999; **251**: 92-101
- Ibitayo AI, Sladick J, Tuteja S, Louis-Jacques O, Yamada H, Groblewski G, Welsh M, Bitar KN. HSP27 in signal transduction and association with contractile proteins in smooth muscle cells. *Am J Physiol* 1999; **277**(2 Pt 1): G445-454
- Claing A, Shbaklo H, Plante M, Bkaily G, D'Orleans-Juste P. Comparison of the contractile and calcium-increasing properties of platelet-activating factor and endothelin-1 in the rat mesenteric artery and vein. *Br J Pharmacol* 2002; **135**: 433-443
- Li L, Eto M, Lee MR, Morita F, Yazawa W, Kitazawa T. Possible involvement of the novel CPI-17 protein in protein kinase C signal transduction of rabbit arterial smooth muscle. *J Physiol* 1998; **508**(Pt 3): 871-881
- Sanders KM. Invited review: Mechanisms of calcium handling in smooth muscles. *J Appl Physiol* 2001; **3**: 1438-1449
- Cao W, Sohn UD, Bitar KN, Behar J, Biancani P, Harnett KM. MAPK mediates PKC-dependent contraction of cat esophageal and lower esophageal sphincter circular smooth muscle. *Am J Physiol Gastrointest Liver Physiol* 2003; **285**: G86-95
- Ratz PH, Meehl JT, Eddinger TJ. RhoA kinase and protein kinase C participate in regulation of rabbit stomach fundus smooth muscle contraction. *Br J Pharmacol* 2002; **137**: 983-992
- Somlyo AP, Somlyo AV. Signal transduction and regulation in smooth muscle. *Nature* 1994; **372**: 231-236
- Vorotnikov AV, Krymsky MA, Shirinsky VP. Signal transduction and protein phosphorylation in smooth muscle contraction. *Biochemistry* 2002; **67**: 1309-1328
- Makhlof GM, Murthy KS. Signal transduction in gastrointestinal smooth muscle. *Cell Signal* 1997; **9**: 269-276
- Bolton TB, Prestwich SA, Zholos AV, Gordienko DV. Excitation-contraction coupling in gastrointestinal and other smooth muscles. *Annu Rev Physiol* 1999; **61**: 85-115
- Harnett KM, Biancani P. Calcium-dependent and calcium-independent contractions in smooth muscles. *Am J Med* 2003; **115** (Suppl): 24S-30S
- Kitazawa T, Eto M, Woodsome TP, Brautigan DL. Agonists trigger G protein-mediated activation of the CPI-17 inhibitor phosphoprotein of myosin light chain phosphatase to enhance vascular smooth muscle contractility. *J Biol Chem* 2000; **7**: 9897-9900
- Sato A, Hattori Y, Sasaki M, Tomita F, Kohya T, Kitabatake A, Kanno M. Agonist-dependent difference in the mechanisms involved in Ca^{2+} sensitization of smooth muscle of porcine coronary artery. *J Cardiovasc Pharmacol* 2000; **5**: 814-821
- Yamada A, Ohya S, Hirano M, Watanabe M, Walsh MP, Imaizumi Y. Ca^{2+} sensitization of smooth muscle contractility induced by ruthenium red. *Am J Physiol* 1999; **276**(3 Pt 1): C566-575
- Gokina NI, Osol G. Temperature and protein kinase C modulate myofilament Ca^{2+} sensitivity in pressurized rat cerebral arteries. *Am J Physiol* 1998; **274**(6 Pt 2): H1920-1927
- Bitar KN. HSP27 phosphorylation and interaction with actin-myosin in smooth muscle contraction. *Am J Physiol Gastrointest Liver Physiol* 2002; **282**: G894-903
- Li C, Fultz ME, Wright GL. PKC-alpha shows variable patterns of translocation in response to different stimulatory agents. *Acta Physiol Scand* 2002; **174**: 237-246
- Taggart MJ, Leavis P, Feron O, Morgan KG. Inhibition of PKC α and rhoA translocation in differentiated smooth muscle by a caveolin scaffolding domain peptide. *Exp Cell Res* 2000; **258**: 72-81

Characterization and enrichment of hepatic progenitor cells in adult rat liver

Ai-Lan Qin, Xia-Qiu Zhou, Wei Zhang, Hong Yu, Qin Xie

Ai-Lan Qin, Xia-Qiu Zhou, Wei Zhang, Hong Yu, Qin Xie,
Department of Infectious Diseases, Ruijin Hospital, Shanghai Second
Medical University, Shanghai 200025, China

Supported by Shanghai Science Development Foundation, No.
004119044

Correspondence to: Dr. Ai-Lan Qin, Department of Infectious Diseases,
Ruijin Hospital, Shanghai 200025, China. ellen2111@sina.com.cn

Telephone: +86-21-64311242

Received: 2003-08-26 **Accepted:** 2003-10-27

Abstract

AIM: To detect the markers of oval cells in adult rat liver and to enrich them for further analysis of characterization *in vitro*.

METHODS: Rat model for hepatic oval cell proliferation was established with 2-acetylaminofluorene and two third partial hepatectomy (2-AAF/PH). Paraffin embedded rat liver sections from model (11 d after hepatectomy) and control groups were stained with HE and OV6, cytokeratin19 (CK19), albumin, alpha fetoprotein (AFP), connexin43, and c-kit antibodies by immunohistochemistry. Oval cell proliferation was measured with BrdU incorporation test. C-kit positive oval cells were enriched by using magnetic activated cell sorting (MACS). The sorted oval cells were cultured in a low density to observe colony formation and to examine their characterization *in vitro* by immunocytochemistry and RT-PCR.

RESULTS: A 2-AAF/PH model was successfully established to activate the oval cell compartment in rat liver. BrdU incorporation test of oval cell was positive. The hepatic oval cells coexpressed oval cell specific marker OV6, hepatocyte-marker albumin and cholangiocyte-marker CK19. They also expressed AFP and connexin 43. C-kit, one hematopoietic stem cell receptor, was expressed in hepatic oval cells at high levels. By using c-kit antibody in conjunction with MACS, we developed a rapid oval cell isolation protocol. The sorted cells formed colony when cultured *in vitro*. Cells in the colony expressed albumin or CK19 or coexpressed both and BrdU incorporation test was positive. RT-PCR on colony showed expression of albumin and CK19 gene.

CONCLUSION: Hepatic oval cells in the 2-AAF/PH model had the properties of hepatic stem/progenitor cells. Using MACS, we established a method to isolate oval cells. The sorted hepatic oval cells can form colony *in vitro* which expresses different combinations of phenotypic markers and genes from both hepatocytes and cholangiocyte lineage.

Qin AL, Zhou XQ, Zhang W, Yu H, Xie Q. Characterization and enrichment of hepatic progenitor cells in adult rat liver. *World J Gastroenterol* 2004; 10(10): 1480-1486

<http://www.wjgnet.com/1007-9327/10/1480.asp>

INTRODUCTION

It has ever been disputed whether there are stem/progenitor

cells in liver, because the liver is a quiescent organ and the adult liver can regenerate by hepatocytes reentering into cell cycle after surgical resection or injury^[1-3]. But it is now generally accepted that the liver contains hepatic stem cells/progenitor cells. When the ability of hepatocytes to divide and replace damaged tissues is compromised under the condition of severe and chronic liver injury caused by drugs, viruses and toxins, a subpopulation of liver cells termed oval cells, is induced to proliferate. Extensive studies in rodent models of hepatocarcinogenesis and other non-carcinogenic injury models suggest that oval cells may represent a facultative hepatic progenitor/stem cell compartment. These cells not only can be activated to proliferate but also differentiate both into mature hepatocytes and biliary epithelial cells under certain conditions^[4-7]. So these hepatic stem/progenitor cells (HSCs/HPCs) are ideal sources for cell therapy such as cell transplantation or tissue engineered bioartificial organs and identification of HSCs/HPCs has become increasingly important.

Hematopoiesis and hepatic development share common stages. During fetal development, hematopoietic stem cells move out of the yolk sac and into the developing liver. Simultaneous with the appearance of hematopoiesis, hematopoietic stem cells can be detected in the fetal liver (data not shown). It is increasingly apparent that HSCs/HPCs share common characteristics with stem cells of the hematopoietic system^[8,9]. C-kit is a hematopoietic stem cell receptor, and it is also expressed in hepatic oval cells^[10,11]. 2-Acetylaminofluorene and partial hepatectomy (2-AAF/PH) are a traditional model to activate oval cells in rat liver^[12]. We were also successful in establishment of an oval cell proliferation model treated with 2-AAF/PH. The current studies were performed to detect the markers expressed in rat oval cells and used c-kit antibody as well as magnetic activated cell sorting (MACS) to highly enrich the population of hepatic oval cells for further analysis of colony formation and characterization *in vitro*.

MATERIALS AND METHODS

Oval cell compartment proliferation/activation

Male SD rats (about 150 g) were supplied by Laboratory Animal Center of Chinese Academy of Sciences. They were fed 5, 10, 15 and 20 mg/kg body mass 2-AAF (dissolved in polyethylene glycol, Sigma) daily by oral gavage for 6 d and up to 7 d after operation and the control rats were fed saline. On the 7th d, rats were partially hepatectomized under general ether anesthesia and were not fed 2-AAF on the same day. The time points of this study were counted when partial hepatectomy was performed. One hour before the animals were killed, they received an intraperitoneal injection of BrdU (100 mg/kg body weight) (Sigma) to detect proliferation of oval cells (BrdU incorporation test). Liver tissue obtained was processed in the same manner described in immunohistochemistry methods.

Immunohistochemistry

Liver tissue was divided and fixed in 40 g/L buffered formaldehyde. All staining procedures for light microscopy

Table 1 First and second antibodies for immunohistochemistry

First antibody	Dilution	Second antibody	Dilution	Chromogen
OV6 (mouse IgG) ¹	1:100	Goat anti-mouse IgG (HRP or FITC)	1:150 1:200	DAB(brown) green fluorescence
CK19(mouse IgG) ²	1:150	Goat anti-mouse IgG (HRP)	1:150	DAB (brown)
Albumin (rabbit IgG)	1:400	Goat anti-rabbit IgG (AP)	1:50	Fuch sine (red) or NBT/BCIP(blue)
AFP (mouse IgG)	1:400	Goat anti-mouse IgG (HRP)	1:200	DAB(brown)
Connexin 43(mouse IgM) ²	1:400	Goat anti-mouse IgM (HRP)	1:200	DAB (brown)
C-kit (rabbit IgG) ³	1:50	Goat anti-rabbit IgG (AP)	1:50	Fuch sine(red) or NBT/BCIP(blue)
BrdU (mouse IgG)	1:50	Goat anti-mouse IgG (HRP)	1:150	DAB(brown)

Note:1=a gift from professor Sell S, 2=from Sigma, 3=from Santa Cruz, others were from DAKO Company.

were performed on paraffin-embedded 4 μ m sections. The sections were deparaffinized in xylene and rehydrated through graded alcohol. Routine histological examinations were made for liver sections stained with hematoxylin-eosin. Antigen retrieval was made by microwave - citrate buffer method, and then they were digested with trypsin (1 g/L trypsin, 1 g/L calcium chloride) at 37 °C for 30 min. For BrdU staining, the sections were immersed in 4N HCl for 15 min for DNA degeneration and neutralized with TBS. Single cells from suspensions were collected on glass slides by cytocentrifugation and air dried. All cells were fixed in methanol at 4 °C for 20 min. Endogenous peroxidase was inactivated by DAKO peroxidase blocking reagent for 10 min. The sections were incubated with 100 mL/L normal goat serum in TBS at room temperature for 20 min to block non-specific binding. For immunostaining, the primary antibody and second antibody are shown in Table 1. Double immunostaining for studies of antigen colocalization was performed with selected antibodies (OV6 *vs* albumin, CK19 *vs* albumin) using different chromogens (DAB and Fuch sine or NTB/BCIP). All antibodies were diluted with DAKO antibody diluent. Specimens were incubated with first antibody at 4 °C overnight, and then incubated with second antibody at room temperature for 1 h. For each antibody negative controls were performed by either blocking with appropriate nonimmune serum or by omitting the primary antibody from the protocol.

Cell sorting and culture

Rat liver cells were isolated by a two-step collagenase IV digestion method according to the protocol established by Seglen^[13]. The nonparenchymal cell fraction was determined to contain the hepatic oval cell population as described by Yaswen *et al*^[14]. Hepatocytes were separated from the nonarenchymal cell portion by low-speed centrifugation (50 r/min \times 1 min). About one third of the total liver cells were nonparenchymal cells.

Immunohistochemistry was performed on the parenchymal and nonparenchymal fractions to ensure that the cells of interest were in the nonparenchymal cell fraction. The portion of nonparenchymal cells was further purified using magnetic activated cell sorting (MACS). Cells were incubated with CD45 antibody (1:50) and rat erythroid cell antibody (1:200) (BD Pharmingen) at 4 °C for 10 min and incubated with magnetic goat anti-mouse IgG (1:5) at 4 °C for 15 min. MACS was performed according to the manufacturer's recommendations (Miltenyi Biotec). The depleted fraction was incubated with c-kit antibody (1:50) and then incubated with magnetic goat anti-rabbit IgG (1:50). The c-kit+ fraction was collected for immunohistochemistry and culture *in vitro*.

The sorted c-kit+ cells were resuspended in DMEM/F-12

medium supplemented with 100 g/L fetal bovine serum, insulin-transferrin-sodium selenite, dexamethasone (1×10^{-7} mol/L), nicotinamide (10 mmol/L), L-glutamine (2 mmol/L), β -mercaptoethanol (0.1 mmol/L), HEPES (10 mmol/L) and penicillin/streptomycin. They were placed in 96-well plates, the same volume of supernatant from cultured ED13 fetal liver cells was added and incubated at 37 °C with 50 mL/L CO₂. Human recombinant hepatocyte growth factor (HGF, 50 ng/mL), epidermal growth factor (EGF, 20 ng/mL) and α -transforming growth factor (TGF- α , 20 ng/mL) were added 24-48 h after initiation of culture.

Phenotypic characterization of cultured cells

After 7 days, BrdU with a final concentration of 10 μ M/L was added to the medium and incubated for 3 h. The cells were fixed with methanol at 4 °C for 20 min, and washed with PBS containing 0.5 g/L polyoxyethylene sorbitan monolaurate (Tween 20). Cytochemical staining was performed with BrdU, c-kit, albumin, and CK19 antibodies. The staining method was the same as immunohistochemistry.

Reverse-transcription polymerase chain reaction analysis

Characteristics of cultured cells were evaluated by reverse-transcription polymerase chain reaction (RT-PCR). mRNA was extracted from the cell colonies using a QuickPrep micro mRNA purification kit (Qiagen) according to the supplier's recommended protocol. cDNA was synthesized using oligo-d (T)15 and Omniscript RT kit. A 20 μ L of reaction mixture containing 1 \times Buffer RT, 0.5 mmol/L dNTP, 10 unit RNazin, 4 unit Omniscript reverse transcriptase and 1-2 μ g RNA template was incubated at 37 °C for 1 h. PCR was done using HotStarTaq DNA polymerase in 25 μ L of the reaction mixture (1 \times PCR buffer, 0.5 unit HotStar Taq DNA polymerase, 200 μ mol/L dNTP) with hepatocyte-specific primers for albumin (5' -GAG AAG TGC TGT GCT GAA GG-3' and 5' -TCA GAG TGG AAG GTG AAG GT-3'), α -fetoprotein (5' -AAC ACA TCC AGG AGA GCC AG-3' and 5' -TTC TCC AAG AGG CCA GAG AA-3'), cholangiocyte-specific primers for CK19 (5' -CTG TCT TGG TCC GGT CAC TG-3' and 5' -GGC ATC TTG GTC TGT GTC AT-3'). PCR cycles were as follows: initial denaturation at 95 °C for 15 min, followed by 35 cycles at 94 °C for 45 s, at 55 °C for 1 min, at 72 °C for 45 s, and final extension at 72 °C for 10 min. PCR products were separated in 20 g/L agarose gel.

RESULTS

Activation of oval cell proliferation

Oval cells could be seen in 2-AAF treated rat liver at the dosage from 10 mg/kg to 20 mg/kg weight mass 7 to 13 d after partial

hepatectomy. The peak of oval cell proliferation occurred 11 d after hepatectomy. The histologic changes in liver sections from rats exposed to 2-AAF at the dosage of 10 mg/kg body mass for 6 d, followed by partial hepatectomy and sacrifice 11 d posthepatic injury are shown in Figure 1. The proliferated oval cells were small in size (approximately 10 μm) with a large nuclei to cytoplasm ratio, radiating from the periportal region forming primitive ductular structures with poorly defined lumen. The control rat liver showed complete lobular structure without oval cell proliferation (Figures 1C and D). DNA synthesis in the oval cells was examined by BrdU incorporation test, and many of the oval cells were in S-phase with their nuclei stained positive by nuclear immunohistochemical staining for BrdU. DNA synthesis in epithelial cells of the portal bile ductules was also examined by BrdU incorporation (Figure 2).

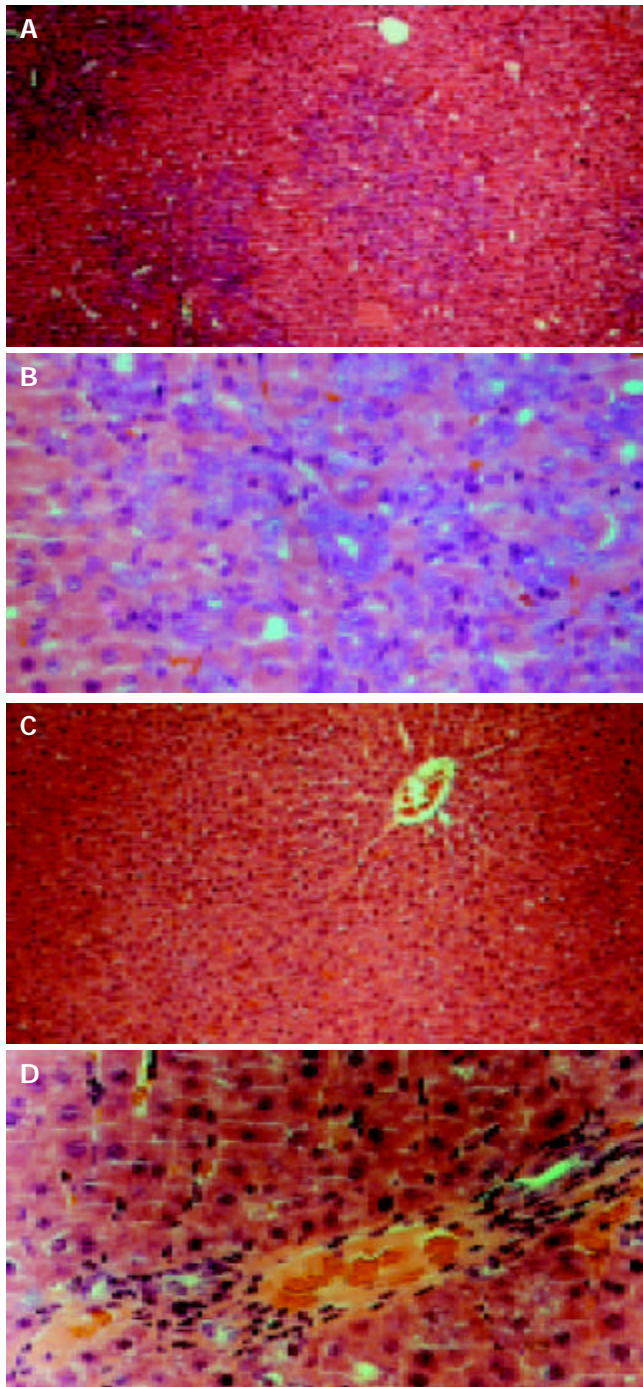


Figure 1 Rat liver sections obtained from 2-AAF/PH (11 d after operation) and control. Sections were stained with hematoxylin-eosin. (A and B) show liver sections obtained from

2-AAF/PH-treated rats at low ($\times 100$) and high ($\times 400$) magnification. Small oval cells (arrows) can be seen close proximity to proliferating bile ducts and in areas of ductular proliferation or in acinar arrangements around hepatocytes. The oval cells radiate from the periportal region, forming primitive ductular structures with poorly defined lumen. (C and D) show liver tissue from control rats at low and high magnification. Hepatocyte proliferation can be seen in the typical liver architecture. Central vein (CV) and portal triad region can be seen.

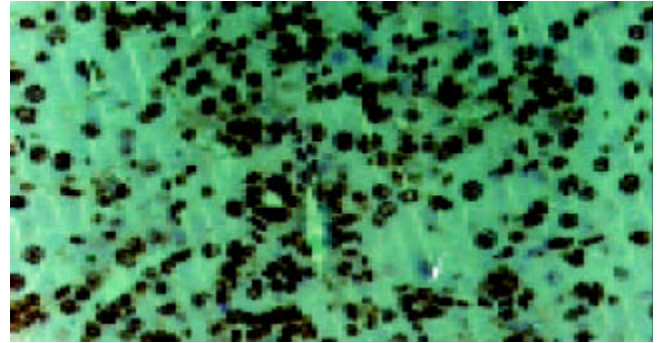
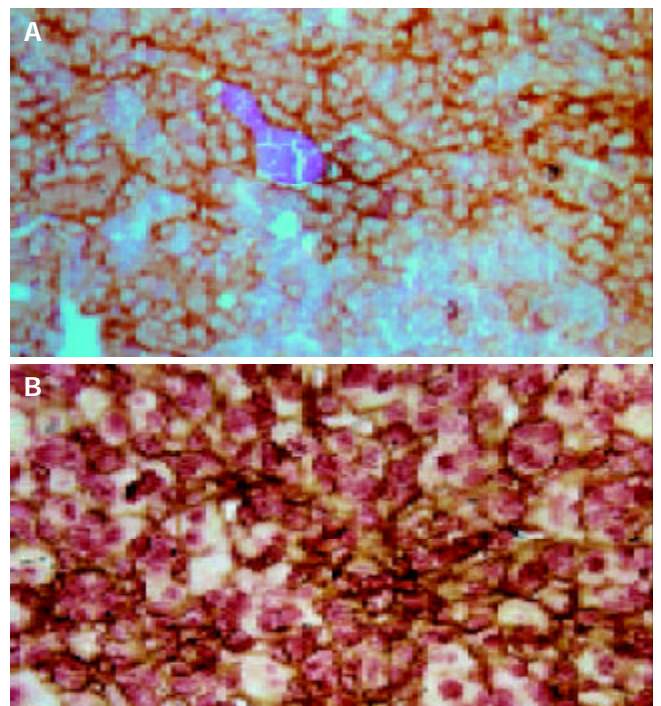


Figure 2 Immunohistochemistry of liver sections obtained from 11 2-AAF/PH rats. BrdU staining of oval cells in proliferative state. Arrows indicate oval cells.

Immunohistochemistry for marker on activated hepatic oval cells

The sections were stained with antibodies for oval specific marker, biliary lineage marker and hepatocyte lineage markers (OV6, CK19, albumin and AFP). The oval cells generated from 2-AAF/PH treated rat liver were positive for OV6 (Figure 3A), CK19 (Figure 3C), albumin (Figures 3B and D) and AFP (Figure 3E). Double immunohistochemistry showed that oval cells coexpressed OV6 and albumin or CK19 and albumin (Figures 3B and D). The oval cells were stained positive for connexin 43, but the sections from control rats were negative for connexin 43 (Figure 3F). In Figure 3G, oval cells expressed c-kit antigen, the ductular cells appeared to be positive with little to no staining for c-kit. No liver sections from control rat were stained positive for c-kit (Figure 3H).



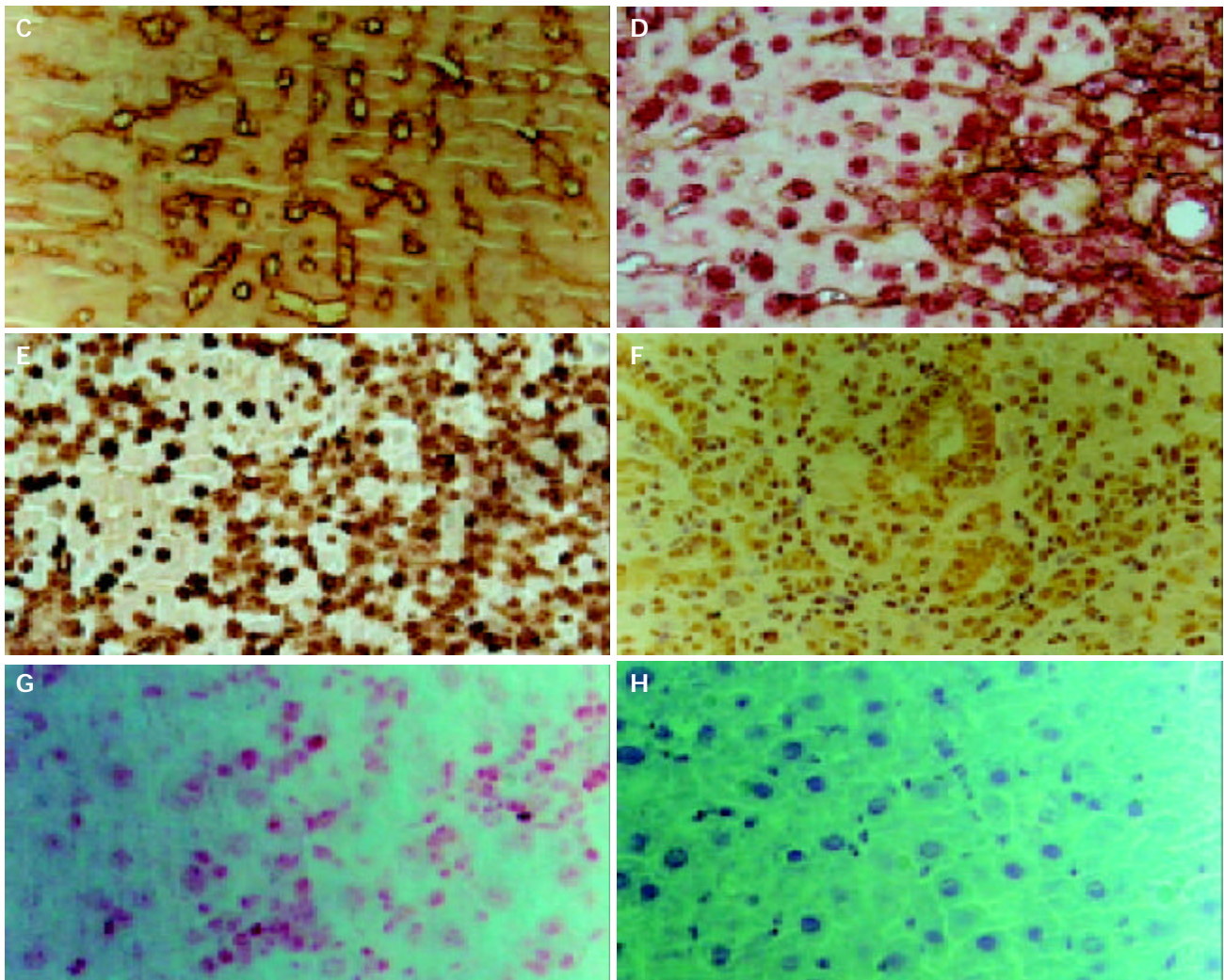


Figure 3 Immunohistochemical staining of liver sections from rat liver exposed to 2-AAF/PH (d 11) at high magnification. A: Staining for OV6, Arrows point to OV6-positive oval cells. B: Double immunohistochemical staining for OV6 (brown) and albumin (red). C: Staining for cytokeratin19(CK19). Ductular lumen face and oval cells were positive. Arrows point of CK19-positive cells. D: Double immunohistochemical staining for CK19 (brown) and albumin (red). Arrows point to oval cells with tow markers. E: Staining for AFP. F: Staining for connexin43, Arrows point to connexin43 positive oval cells. G: Staining for C-kit, Oval cells were stained with red. H: Negative control.

Purification and proliferation of *c-kit*⁺ oval cells

In order to define the phenotype, growth, and differentiation potential of individual *c-kit*⁺ cells, we used an immunoselection and cell culture strategy. After parenchymal cells were separated from nonparenchymal cells, antibody against *c-kit* was used to purify *c-kit*⁺ cells from nonparenchymal fraction by MACS. Immunohistochemical staining for OV6 showed that more than 90% sorted cells were positive (Figure 4).

After incubated for 24 h, most sorted *c-kit*⁺ cells adhered to collagen IV coated plate. By day 3 single cells proliferated to form colonies which expanded up to several hundred cells at 2 wk (Figures 5A, B). Figure 6 shows BrdU incorporation of a cultured *c-kit*⁺ oval cell colony, most cells were positive with their nuclei stained brown.

Characterization of *c-kit*⁺ oval cells

To determine the characterization of the colonies, we studied constituent cells by immunohistochemistry using albumin and CK19 as lineage markers as well as *c-kit*. After 1 wk, some progeny of *c-kit*⁺ oval cells in the colony lost the *c-kit* marker of parental generation (Figure 6). Most colonies at 2 wk contained 3 types of cells, namely albumin positive cells, CK19 positive cells, both albumin and CK19 positive cells (Figure 7). RT-PCR was performed to identify the expression

of genes encoding markers in both hepatocyte and cholangiocyte lineages (hepatocytes: albumin, α -fetoprotein; cholangiocytes: CK19). Almost all colonies contained mRNA of both hepatocyte-specific and cholangiocyte-specific genes at 2 wk (Figure 8). These results of RT-PCR and immunocytochemistry showed the bipotent differentiation ability of the sorted *c-kit*⁺ oval cells.

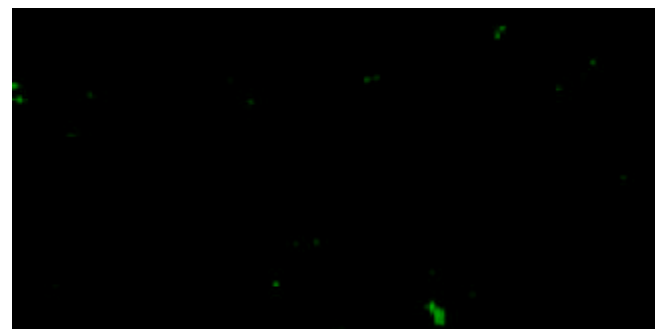


Figure 4 Immunocytochemistry for OV6 on cytocentrifuged preparations of *C-kit*⁺ MACS sorted cells from 2-AAF/PH treated rats. The sorted *C-kit*⁺ cells were stained with oval cell-specific antibody OV6 (green).

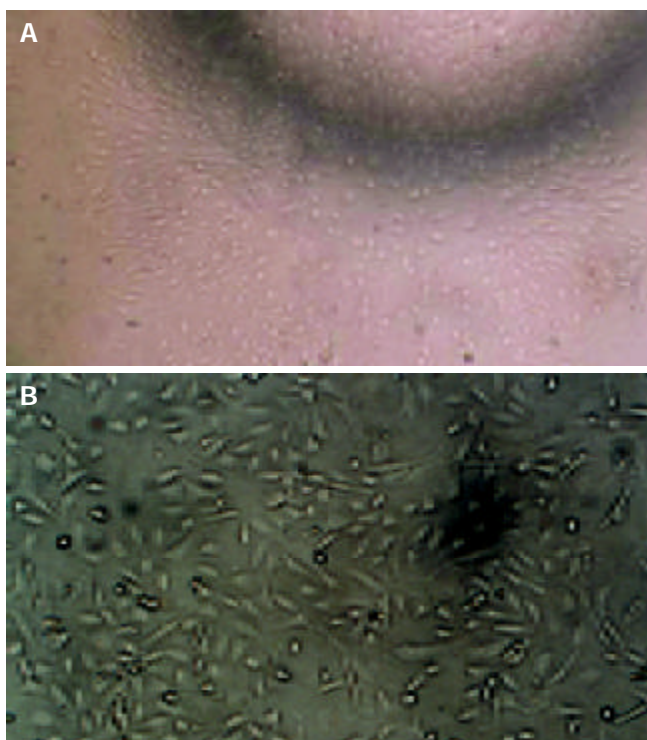


Figure 5 Phase contrast photomicrographs showing formation of a colony by a sorted C-kit⁺ oval cell after cultured *in vitro* for 2 wk. (A: $\times 100$; B: $\times 200$).

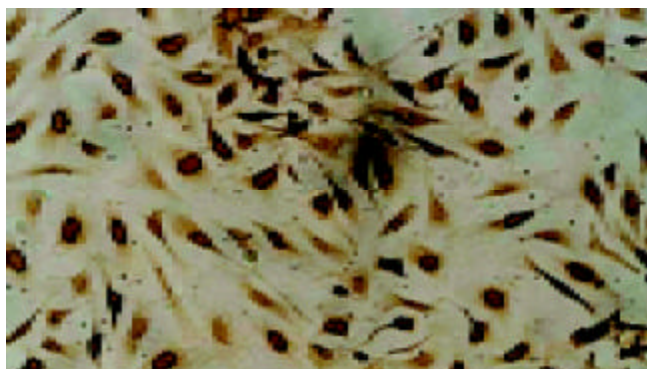


Figure 6 Double immunocytochemistry for BrdU incorporation and C-kit staining on sorted c-kit⁺ oval cell colony on d 7. Most cells had their nuclei stained with BrdU (arrow). Though they came from one precursor, many cells lost c-kit marker, just some of them were still c-kit positive stained blue. (arrowheads). ($\times 400$).

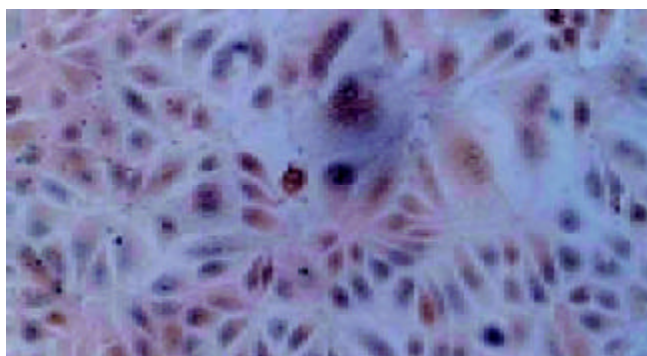


Figure 7 Dual staining of cultured sorted oval cell colony with albumin (dark blue) and CK19 (brown). Some cells were stained with both markers (Arrows) and the others were stained only one marker. ($\times 400$).

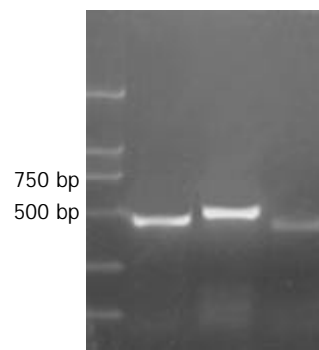


Figure 8 RT-PCR analysis of gene expression. RNA was isolated from sorted cell colony.

DISCUSSION

Since liver transplantation is the only available current therapy for end-stage liver failure and there is an ever-increasing shortage of donor livers, cell therapy from alternative cell source might offer a new therapeutic approach against liver disease^[15]. In recent years, such studies have been conducted successfully using primary hepatocytes in rodent models, and current research is being conducted to isolate progenitor or stem cells that should have the highest potential for effective liver repopulation. Therefore, identification of hepatic/progenitor cells has become increasingly important. Stem cells are defined as the cells with the self-renewing activity and capability of generating multiple types of lineage committed cells. As for the hepatocytic lineage, stem cells had to possess the ability to generate both parenchymal hepatocytes and bile duct epithelial cells^[16]. After debated for many years, it has been generally accepted that the liver contains cells with stem-like properties and that these cells can be activated to proliferate and differentiate into mature hepatocytes and cholangiocytes under certain pathophysiologic circumstances^[17,18]. These cells might be related to the so-called “oval cells”, originally identified by Farber as immature epithelial cells with oval shaped nuclei and scant cytoplasm^[19].

Activation of the oval cell proliferation could be induced by many rodent models^[20-22], we chose modified Solt-Farber model to activate oval cells^[12]. The model could be successfully established by 2-AAF at the dosage from 10 mg to 20 mg and the peak of oval cell proliferation was on d11 after partial hepatectomy. Immunohistochemical staining showed that the oval cells expressed oval cell-specific marker OV6, cholangiocyte lineage marker CK19 and hepatocyte lineage marker albumin and AFP. OV6 and albumin or CK19. Albumin was coexpressed in the same oval cells by double immunohistochemistry. These data suggest that the oval cells may represent a facultative hepatic progenitor/stem cell compartment. The oval cells also expressed connexin 43, but the liver cells in the control rat liver expressed connexin 32 instead of connexin 43 (data not shown). Gap junctional intercellular communication (GJIC) was considered to play a key role in the maintenance of tissue independence and homeostasis in multicellular organisms by controlling the growth of GJIC-connected cells. Gap junction channels are composed of connexin molecules, connexin 43 is expressed on immature liver cells or cholangiocytes, connexin 26 and connexin 32 are expressed on hepatocytes. As hepatocytes differentiate, the proportions of connexin 43 then 26 mRNAs decrease while that of connexin 32 mRNA increases. Connexin 43 was also expressed in fetal liver cells and the expression of connexin 43 declined after birth^[23]. Neveu reported that proliferating oval cells expressed diffuse connexin 43 immunoreactivity. Differentiation of oval cells into basophilic hepatocytes resulted in their alterations in Cx32 and

Cx26 expression^[24]. Since the oval cells were generated by the proliferation of terminal bile ducts, they formed structures representing an extension of the canals of Hering^[25], and there are many common features between immature embryonic hepatic cells and oval cells such as expression of AFP and connexin 43. It is reasonable to assume that oval cells may be a direct progeny of resident undifferentiated liver stem cells. Suzuki *et al.* have identified a population of hepatic stem cells that exist in developing mouse liver, and these cells may represent the resident hepatic stem cells which possess multilineage differentiation potential and self-renewing capability^[26,27]. Chen also^[28] reported that transfused oval cells through caudal vein can migrate into the parenchyma of the liver and are settled there.

Hepatic progenitor cells share common characteristics with stem cells of the hematopoietic system. Classical hematopoietic markers, including Thy-1, CD34, c-kit were expressed on the surface of oval cells^[8-11]. After bone marrow transplantation, a proportion of the regenerated hepatic cells was shown to be donor-derived^[29]. Intravenous injection of adult bone marrow cells (c-kit^{high}Thy^{low}Lin^{low}Sca-1⁺) in the FAH^{-/-} mouse, an animal model of tyrosinemia type I, rescued the mouse and restored the biochemical function of its liver^[30]. Crosby *et al.*^[11] reported that there were c-kit⁺ cells in the periportal tract surrounding bile ducts, which coexpressed CK19. After cultured in biliary cell growth media, the isolated c-kit positive cells could form colony with the properties of cholangiocytes^[11]. We also found that oval cells in the periportal area in 2-AAF/PH expressed c-kit, but hepatocytes and liver in control animal were stained negative. The evidence of a cell lineage relationship between the hematopoietic system and the liver supports the extrahepatic origin of hepatic progenitors.

Suzuki *et al.* recently reported that CD49f^{low}c-Kit⁺CD45⁻TER119⁻ cell subpopulation in ED13.5 mouse fetal liver could form large colonies designated as 'hepatic colony-forming-unit in culture' (H-CFU-C), and expression of *c-kit*, *CD34* and *thy-1* became detectable in some of these colonies on d 21^[26]. These data may suggest that not only exogenous hepatic stem/progenitor cells derived from circulating bone marrow express hematopoietic stem cell markers, but endogenous tissue-determined stem/progenitor cells express such markers.

C-kit stem cell receptor tyrosine kinase (KIT) and its ligand, stem cell factor (SCF) system play a crucial role in the development of oval cells. If the c-kit kinase activity was severely impaired, the number of oval cells on d 7, 9, and 13 after PH was significantly reduced to 15%, 18%, and 27% of those in control normal rats in the AAF/PH model, respectively^[10]. So we chose c-kit as a surface marker to purify oval cells. After depletion of CD45⁺ cells and rat erythroid cells from nonparenchymal fractions, oval cells were further enriched by MACS using c-kit antibody. The result showed that more than 90% sorted cells were OV6 positive. After cultured in our special medium the sorted oval cells could form large colonies. BrdU incorporation test was positive in most progenies of oval cells on d 7, indicating that the sorted oval cells have high growth potential. At wk 2, some of the progenies lost the c-kit marker of the sorted cells. Immunohistochemical staining showed that there were 3 types of cells in the colony after cultured for 2 wk *in vitro*, that marked albumine, only CK19, and both albumin and CK19. RT-PCR on the colony showed that expression of albumin, AFP and CK19 genes was detectable. All these data suggest that the sorted oval cells are facultative hepatic stem/progenitor cells with self-renewing capacity and can differentiate along hepatocyte and cholangiocyte lineages *in vitro*, and the progeny lost stem cell marker during differentiation. Crosby *et al.* purified c-kit positive cells from

cirrhotic tissue by MACS and the sorted cells could form colonies with 2 types of cells in morphology cultured *in vitro* on d 7. But the sorted c-kit⁺ or CD34⁺ cells by Crosby *et al.* could only differentiate along cholangiocyte lineage^[11]. The difference might be due to the fact that they used just biliary cell growth medium.

In conclusion, we successfully isolated and purified viable c-kit positive oval cells which had high growth potential and bilineage differentiation activity from the 2-AAF/PH rat liver. The properties of proliferation and differentiation *in vivo* are still to be studied by cell transplantation.

REFERENCES

- 1 **Fausto N.** Liver regeneration: from laboratory to clinic. *Liver Transpl* 2001; **7**: 835-844
- 2 **Michalopoulos GK, DeFrances MC.** Liver regeneration. *Science* 1997; **276**: 60-66
- 3 **Overturf K, Al-Dhalimy M, Ou CN, Finegold M, Grompe M.** Serial transplantation reveals the stem-cell-like regenerative potential of adult mouse hepatocytes. *Am J Pathol* 1997; **151**: 1273-1280
- 4 **Alison MR, Poulson R, Forbes SJ.** Update on hepatic stem cells. *Liver* 2001; **21**: 367-373
- 5 **Lowes KN, Croager EJ, Olynyk JK, Abraham LJ, Yeoh GC.** Oval cell-mediated liver regeneration: Role of cytokines and growth factors. *J Gastroenterol Hepatol* 2003; **18**: 4-12
- 6 **Fujikawa T, Hirose T, Fujii H, Oe S, Yasuchika K, Azuma H, Yamaoka Y.** Purification of adult hepatic progenitor cells using green fluorescent protein (GFP) - transgenic mice and fluorescence-activated cell sorting. *J Hepatol* 2003; **39**: 162-170
- 7 **Alison M, Golding M, El-Lalani N, Sarraf C.** Wound healing in the liver with particular reference to stem cells. *Philos Trans R Soc Lond B Biol Sci* 1998; **353**: 877-894
- 8 **Petersen BE, Goff JP, Greenberger JS, Michalopoulos GK.** Hepatic oval cells express the hematopoietic stem cell marker Thy-1 in the rat. *Hepatology* 1998; **27**: 433-445
- 9 **Omori N, Omori M, Everts RP, Teramoto T, Miller MJ, Hoang TN, Thorgeirsson SS.** Partial cloning of rat CD34 cDNA and expression during stem cell-dependent liver regeneration in the adult rat. *Hepatology* 1997; **26**: 720-727
- 10 **Matsusaka S, Tsujimura T, Toyosaka A, Nakasho K, Sugihara A, Okamoto E, Uematsu K, Terada N.** Role of c-kit receptor tyrosine kinase in development of oval cells in the rat 2-acetylaminofluorene/partial hepatectomy model. *Hepatology* 1999; **29**: 670-676
- 11 **Crosby HA, Kelly DA, Strain AJ.** Human hepatic stem-like cells isolated using c-kit or CD34 can differentiate into biliary epithelium. *Gastroenterology* 2001; **120**: 534-544
- 12 **Tatematsu M, Kaku T, Medline A, Farber E.** Intestinal metaplasia is a common option of oval cells in relation to cholangiofibrosis in liver of rats exposed to 2-acetylaminofluorene. *Lab Invest* 1985; **52**: 354-362
- 13 **Seglen PO.** Hepatocyte suspensions and cultures as tools in experimental carcinogenesis. *J Toxicol Environ Health* 1979; **5**: 551-560
- 14 **Yaswen P, Hayner NT, Fausto N.** Isolation of oval cells by centrifugal elutriation and comparison with other cell types purified from normal and preneoplastic livers. *Cancer Res* 1984; **44**: 324-331
- 15 **Strom SC, Chowdhury JR, Fox IJ.** Hepatocyte transplantation for the treatment of human disease. *Semin Liver Dis* 1999; **19**: 39-48
- 16 **Kinoshita T, Miyajima A.** Cytokine regulation of liver development. *Biochim Biophys Acta* 2002; **1592**: 303-312
- 17 **Sell S.** Liver stem cells. *Mod Pathol* 1994; **7**: 105-112
- 18 **Sell S.** Heterogeneity and plasticity of hepatocyte lineage cells. *Hepatology* 2001; **33**: 738-750
- 19 **Farber E.** Similarities in the sequence of early histologic changes induced in the liver of rat by ethionine, 2-acetylaminofluorene, and 3-methyl-4-dimethylaminobenzene. *Cancer Res* 1956; **16**: 142-148
- 20 **Akhurst B, Croager EJ, Farley-Roche CA, Ong JK, Dumble ML,**

- Knight B, Yeoh GC. A modified choline-deficient, ethionine-supplemented diet protocol effectively induces oval cells in mouse liver. *Hepatology* 2001; **34**: 519-522
- 21 **Dabeva MD**, Shafritz DA. Activation, proliferation and differentiation of progenitor cells into hepatocytes in the D-galactosamine model of liver regeneration. *Am J Pathol* 1993; **143**: 1606-1620
- 22 **Factor VM**, Radaeva SA, Thorgeirsson SS. Origin and fate of oval cells in dipin-induced hepatocarcinogenesis in the mouse. *Am J Pathol* 1994; **145**: 409-422
- 23 **Rosenberg E**, Faris RA, Spray DC, Monfils B, Abreu S, Danishefsky I, Reid LM. Correlation of expression of connexin mRNA isoforms with degree of cellular differentiation. *Cell Adhes Commun* 1996; **4**: 223-235
- 24 **Neveu MJ**, Hully JR, Babcock KL, Vaughan J, Hertzberg EL, Nicholson BJ, Paul DL, Pitot HC. Proliferation-associated differences in the spatial and temporal expression of gap junction genes in rat liver. *Hepatology* 1995; **22**: 202-212
- 25 **Paku S**, Schnur J, Nagy P, Thorgeirsson SS. Origin and structural evolution of the early proliferating oval cells in rat liver. *Am J Pathol* 2001; **158**: 1313-1323
- 26 **Suzuki A**, Zheng Yw YW, Kaneko S, Onodera M, Fukao K, Nakauchi H, Taniguchi H. Clonal identification and characterization of self-renewing pluripotent stem cells in the developing liver. *J Cell Biol* 2002; **156**: 173-184
- 27 **Suzuki A**, Zheng Y, Kondo R, Kusakabe M, Takada Y, Fukao K, Nakauchi H, Taniguchi H. Flow-cytometric separation and enrichment of hepatic progenitor cells in the developing mouse liver. *Hepatology* 2000; **32**: 1230-1239
- 28 **Chen JZ**, Hong H, Xiang J, Xue L, Zhao GQ. A selective tropism of transfused oval cells for liver. *World J Gastroenterol* 2003; **9**: 544-546
- 29 **Petersen BE**, Bowen WC, Patrene KD, Mars WM, Sullivan AK, Murase N, Boggs SS, Greenberger JS, Goff JP. Bone marrow as a potential source of hepatic oval cells. *Science* 1999; **284**: 1168-1170
- 30 **Lagasse E**, Connors H, Al-Dhalimy M, Reitsma M, Dohse M, Osborne L, Wang X, Finegold M, Weissman IL, Grompe M. Purified hematopoietic stem cells can differentiate into hepatocytes *in vivo*. *Nat Med* 2000; **6**: 1229-1234

Edited by Zhang JZ and Wang XL Proofread by Xu FM

Influence of serum collected from rat perfused with compound *Biejiaaruangan* drug on hepatic stellate cells

Shun-Gen Guo, Wei Zhang, Tao Jiang, Min Dai, Lu-Fen Zhang, Yi-Chun Meng, Li-Yun Zhao, Jian-Zhao Niu

Shun-Gen Guo, Wei Zhang, Min Dai, Li-Yun Zhao, Jian-Zhao Niu, Laboratory of Cell and Biochemistry, Beijing University of Traditional Chinese Medicine, Beijing 100029, China

Tao Jiang, Department of Histology and Embryology, Medical College of Chinese People's Armed Police Forces, Tianjin 300162, China

Lu-Fen Zhang, College of Acupuncture and Moxibustion, Beijing University of Traditional Chinese Medicine, Beijing 100029, China

Yi-Chun Meng, Central Experimental Laboratory, Beijing Military Medicine College, Beijing 100071, China

Supported by the National Natural Science Foundation of China for Key Project, No. 30130220

Correspondence to: Shun-Gen Guo, Laboratory of Cell and Biochemistry, Beijing University of Traditional Chinese Medicine, Beijing 100029, China. guoshungen@sina.com

Telephone: +86-10-64286926 **Fax:** +86-10-64286871

Received: 2003-08-05 **Accepted:** 2003-10-27

Abstract

AIM: To observe the effect of compound *Biejiaaruangan* decoction (CBJRGC) (composite prescription of Carapax trionycis for softening the liver) on proliferation, activation, excretion of collagen and cytokine of hepatic stellate cells (HSCs) and to find the mechanism of prevention and treatment of hepatic fibrosis by CBJRGC.

METHODS: Using MTT, immunohistochemistry and image analysis technology, the related indexes for proliferation, activation, excretion of collagen and cytokine of hepatic stellate cells were detected in 24 h, 48 h, and 72 h after administration of different dosages of CBJRGC.

RESULTS: Statistical analysis showed that serum collected from rat perfused with CBJRGC could restrain the proliferation of HSC in 48 h and 72 h especially in high and medium dosage groups, markedly decrease the expression of desmin, synapsin and platelet derived growth factor (PDGF) in HSC in 24 h, 48 h and 72 h, as well as the expression of α -SMA, collagen III, TIMP and TGF β 1 in 48 h and 72 h, decrease the excretion of collagen I in 72 h. CBJRGC serum had no significant effect on collagens I, III and TIMP in 24 h.

CONCLUSION: CBJRGC serum has a good curative effect on hepatic fibrosis. Its main mechanism may be related to the following factors. The drug serum can restrain the proliferation and activation of HSC, decrease the number of activated HSC and the total number of HSC, the excretion of collagens I, III, enhance the degradation of collagen and restore the balance of synthesis and degradation of collagen, inhibit the expression of transforming growth factor β 1 (TGF β 1) and platelet derived growth factor (PDGF) in HSC, block and delay the process of hepatic fibrosis. Synapsin is a new marker of activation of HSC, which provides a theoretical and testing basis for neural regulation in the developing process of hepatic fibrosis.

Guo SG, Zhang W, Jiang T, Dai M, Zhang LF, Meng YC, Zhao

LY, Niu JZ. Influence of serum collected from rat perfused with compound *Biejiaaruangan* drug on hepatic stellate cells. *World J Gastroenterol* 2004; 10(10): 1487-1494
<http://www.wjgnet.com/1007-9327/10/1487.asp>

INTRODUCTION

Hepatic fibrosis is an inevitable pathological process of chronic liver disease to hepatic cirrhosis. Hepatic fibrosis is caused by excessive deposition of extracellular matrix (ECM), which is the result of more synthesis and less degradation of ECM. A clinical and experimental study has found that liver cells, hepatic stellate cells (HSC), kupffer cells and sinus endothelial cells all take part in the formation of hepatic fibrosis, in which HSC plays a very important role^[1]. Activation of HSC is commonly regarded as the major link of hepatic fibrosis and the main resource of synthesis of ECM^[2]. The main characteristic of activation of HSC is excessive proliferation of HSC^[3]. In addition, desmin is regarded as a marking protein of HSC and α -SMA is regarded as a marker of activation of HSC^[4]. A foreign study has reported that in process of activation of HSC, the expression of synapsin can increase^[5]. Activation of HSC can lead to excessive synthesis of collagen. MMP and TIMP also jointly take part in the synthesis and degradation of collagen^[6]. Multiple cytokines including TGF β 1 and PDGF play a very important role in proliferation, activation of HSC and synthesis of ECM^[7]. Therefore, it may be a good strategy to restrain the amount of activated HSC, decrease the synthesis and excretion of collagens I, III and TIMPs, and promote the synthesis and excretion of MMPs. Aiming at HSC, it has become a control issue in anti-hepatic fibrosis to restrain its proliferation, decrease the synthesis of ECM and accelerate the degradation of ECM, and even inverse activated HSC to silent HSC. Traditional Chinese medicine has shown its own advantage in treating some difficult diseases. Approved by the government, compound *Biejiaaruangan* decoction (CBJRGC) has been used as the first traditional Chinese medicine for treating hepatic fibrosis (approval document number: 1999 2-102). Clinical observations in Beijing, Shanghai and Hubei Province proved that its effective rate was 78.9% in 121 patients by the first hepatic puncture and in 52 patients by the second hepatic puncture. However, further study of its detailed anti-hepatic fibrosis mechanism is still needed. On the basis of the above-mentioned theory and research developments, our study with the cell culture as technical platform, was to observe the influence of serum collected from rats perfused with CBJRGC on activation and proliferation of HSC *in vitro*, and using immunohistochemistry and image analysis technology to observe its influence on the expressions of desmin, α -SMA, synapsin, collagens I, III, TIMP, TGF β 1 and PDGF of HSC *in vitro*.

MATERIALS AND METHODS

Main reagents

RPMI1640 was produced by Gibco, fetal bovine serum was produced by Hyclone, and 96-well plates by Costa. Dimethyl sulfoxide (DMSO), ethylenediaminetetra-acetic acid (EDTA), 3-

(4,5-dimethyl-1-thiazol-2-yl), 2,5-diphenyl tetrazolium bromide (MTT), N-2-Hydroxyethylpiperazine-N'-2-ethane sulfonine acid (HEPES), and trypsin were all products of Sigma. Rat desmin monoclonal antibody and rat α -SMA monoclonal antibody were bought from DAKO, rat synapsin monoclonal antibody was bought from Santa Cruz. Rat collagen I and III monoclonal antibodies, rat TIMP and PDGF as well as TGF- β 1 monoclonal antibodies, ABC and DAB test kits were all bought from Beijing Zhongshan Biotechnology Inc.

SD rat HSC line

The HSC line was established in our laboratory and prepared after long-term generation.

Preparation of SD rat serum^[8]

Normal SD rat serum A normal rat weighting 350 g fasted for 12 h was injected with diethylether for anesthesia. Under the sterile condition, 10 mL blood was obtained from abdominal aorta, then held for 2 h at room temperature. Blood serum was made by centrifugation at 427 g for 10 min, inactivated at 56 °C for 60 min, and frozen at -60 °C.

Hepatic fibrosis model SD rat serum Adapted Hernandez-Munoz method was used to establish animal model of hepatic fibrosis^[9], 0.2 mL CCl₄ (Olive oil, 1:6 dilution) was injected into abdominal cavity, three times each week for 7 wk. Serum preparation and preservation were the same as those of the normal SD rat serum.

Drug serum With 3.5, 7 and 14 times of human body dosage as low, medium and high dosage groups respectively, CBJRGC was perfused into rat stomach 3 times at 12 h intervals. Rats were fasted for 12 h before the third perfusion and blood sampling was conducted from abdominal aorta 2 h after the third perfusion. Serum preparation and preservation were the same as those of the normal SD rat serum.

Cell culture and grouping

Rat HSCs were inoculated in RPMI1640 with 100 g/L fetal bovine serum, and cultivated at 37 °C in an incubator containing 50 mL/L CO₂ to logarithm growth time. After treatment with digestive fluid, HSCs were suspended by adding D-Hank's fluid, deposited by centrifugation at 190 g with 5 min, and then counted. Using RPMI1640 containing 100 g/L fetal bovine serum, HSCs were adjusted to a density of 5×10⁴/mL and added to a 24-well plate containing flying sheet, 0.2 mL each well. According to intervening factors, HSCs were divided into 5 groups, i.e. control group, model group, high dosage serum group, medium dosage serum group and low dosage serum group. Each group had 4 wells. Upper culture medium was removed after cultivated for 12 h. Control group serum, model group serum, high dosage group serum, medium dosage group serum and low dosage group serum were accordingly added. Flying sheets were taken out respectively at 24 h, 48 h and 72 h, fixed with cold acetone for 10 min, dried and preserved at -60 °C.

Using MTT method to detect effect of drug serum on proliferation of HSC

HSCs with a density of 5×10⁴/mL were added to a 96-well plate, 0.2 mL each well. Each group contained 8 wells. Upper medium was removed after cultivated for 12 h. Control group serum, model group serum, high dosage group, medium dosage group serum and low dosage group serum were accordingly added. 50 μ L cultivating fluid was taken out respectively at 24 h, 48 h and 72 h. A 50 μ L of MTT (50 μ g MTT) was then added and the culture continued for 4 h at 37 °C. After upper fluid was removed, 150 μ L DMSO was added to each well. After concussed and dissolved, Absorbency value with wave-length of 450 nm was detected by enzyme labeled instrument (BioRad 2250, Japan).

The test was repeated 5 times.

Immunohistochemical staining

α -SMA staining Preserved cell flying sheets were immersed with PBC for 5 min, blocked with 10 mL/L H₂O₂ for 10 min, washed 3 times with PBC, 5 min each time, and then incubated with 10% goat serum for 30 min. Rat α -SMA, desmin, synapsin collagens I and II, TIMP, TGF β 1 and PDGF antibodies were diluted at a concentration of 1:100 and added as the first antibodies, staying overnight at 4 °C. After washed 3 times with PBC, 5 min each time, biotin goat anti-rat IgM was added, staying overnight at 4 °C, washed with PBC 3 times, 5 min each time. Streptavidin was added for 30 min, stained with DAB. The first antibody was replaced with fetal bovine serum as negative control, α -SMA male staining Absorbency value and relative area occupied by α -SMA male cells in the reference system were detected with TN-8502 image analysis system (Tractor Northern Co, USA). Data were treated with SPSS for ANOVA test. Results were presented mean \pm SD. $P < 0.05$ was considered statistically significant.

RESULTS

Influence of each group serum on proliferation of HSC at different time points

HSC just after digesting phase showed a global form under contrast microscope. After cultivated for 12 h, HSCs were pasted to the wall, changing into the oblate form. There were obvious lipid droplets in cytoplasm. Few cells started to show the extension of cytoplasm. After cultivated for 24 h, most cells showed the extension of cytoplasm, and some cells showed multi-angle pseudopodium and typical star-like form. The influence on proliferation of HSC detected by MTT method is presented in Table 1.

Influence of each group serum on α -SMA, desmin, synapsin of HSC at different time points

Tables 2, 3, 4 and Figures 1, 2 show the influence of each group serum on α -SMA, desmin, synapsin of HSC at different time points, which were detected with TN-8502 image analysis system.

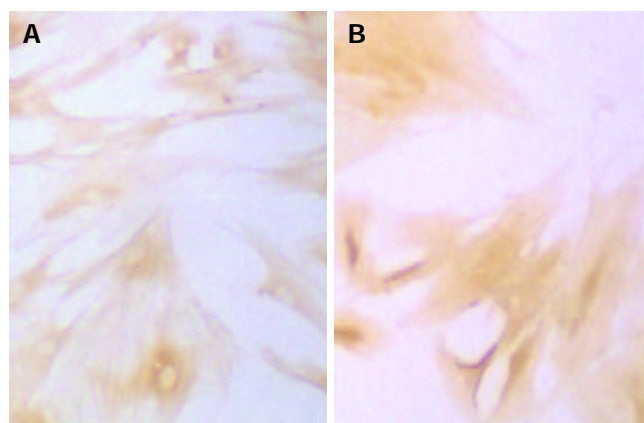


Figure 1 Immunohistochemical staining of α -SMA of SD rat HSC line in model group and medium dosage group ($\times 66$). A: Immunohistochemical staining of α -SMA of SD rat HSC line in model group, B: Immunohistochemical staining of α -SMA of SD rat HSC line in medium dosage group.

Influence of each group serum on collagen I, III and TIMP of HSC at different time points

The influence of each group serum detected with TN-8502 image analysis system on collagens I, III and TIMP of HSC at different time points is shown in Tables 5, 6, 7 and Figures 3, 4.

Table 1 Influence of each group serum on proliferation of HSC at different time points (A value: mean±SD)

	N	M	G	Z	D
24 h	0.40±0.06	0.40±0.03	0.38±0.03	0.391±0.02	0.38±0.03
48 h	0.52±0.03 ^c	0.66±0.05 ^a	0.47±0.02 ^{ac}	0.460±0.02 ^{ac}	0.51±0.03 ^c
72 h	0.75±0.09 ^c	0.96±0.05 ^a	0.55±0.07 ^{ac}	0.580±0.08 ^{ac}	0.69±0.07 ^c

N: control group; M: model group; G: high dosage group; Z: medium dosage group; D: low dosage group, ^a*P*<0.05 vs normal group; ^c*P*<0.05 vs model group.

Table 2 Influence of each group serum on α-SMA of HSC at different time points (A value: mean±SD)

	N		M		G		Z		D	
	A	Male cell area (%)	A	Male cell area (%)	A	Male cell area (%)	A	Male cell area (%)	A	Male cell area (%)
24 h	619.89±163.84 ^c	7.49±2.06 ^c	778.93±190.26 ^a	9.64±0.26 ^a	110.95±45.21 ^{ac}	0.90±0.22 ^{ac}	243.83±62.97 ^{ac}	2.72±1.48 ^{ac}	417.46±126.72 ^c	3.56±0.91 ^c
48 h	812.51±123.39 ^c	8.28±4.58 ^c	1032.69±106.64 ^a	10.56±1.83 ^a	333.71±57.9 ^{ac}	1.55±0.29 ^{ac}	345.08±51.85 ^{ac}	3.66±1.67 ^{ac}	675.35±202.20 ^c	5.45±2.50 ^c
72 h	989.77±166.32 ^c	9.36±2.39 ^c	1255.30±150.39 ^a	15.66±2.34 ^a	448.36±55.80 ^{ac}	3.25±0.56 ^{ac}	556.27±80.32 ^{ac}	4.66±1.24 ^{ac}	759.38±109.32 ^{ac}	6.99±1.58 ^{ac}

N: control group; M: model group; G: high dosage group; Z: medium dosage group; D: low dosage group, ^a*P*<0.05 vs normal group; ^c*P*<0.05 vs model group.

Table 3 Influence of each group serum on desmin of HSC at different time points (A value: mean±SD)

	N		M		G		Z		D	
	A	Male cell area (%)	A	Male cell area (%)	A	Male cell area (%)	A	Male cell area (%)	A	Male cell area (%)
24 h	78.93±18.56 ^c	17.49±2.06 ^c	119.69±23.84 ^a	20.64±2.26 ^a	58.95±5.21 ^{ac}	12.90±3.22 ^{ac}	63.83±12.97 ^{ac}	12.72±1.48 ^{ac}	75.46±26.72 ^c	13.56±0.91 ^c
48 h	103.78±36.64 ^c	10.28±4.58 ^c	182.51±28.43 ^a	14.56±1.83 ^a	63.71±7.94 ^{ac}	8.55±0.29 ^{ac}	65.08±18.85 ^{ac}	7.66±1.67 ^{ac}	79.35±22.28 ^c	9.35±2.50 ^c
72 h	125.30±40.39 ^c	9.36±2.39 ^c	1255.30±150.39 ^a	15.66±2.34 ^a	448.36±55.80 ^{ac}	3.25±0.56 ^{ac}	556.27±80.32 ^{ac}	4.66±1.24 ^{ac}	759.38±109.32 ^{ac}	6.99±1.58 ^{ac}

N: control group; M: model group; G: high dosage group; Z: medium dosage group; D: low dosage group, ^a*P*<0.05 vs normal group; ^c*P*<0.05 vs model group.

Table 4 Influence of each group serum on synapsin of HSC at different time points (A value: mean±SD)

	N		M		G		Z		D	
	A	Male cell area (%)	A	Male cell area (%)	A	Male cell area (%)	A	Male cell area (%)	A	Male cell area (%)
24 h	396.29±78.56 ^c	5.49±2.06 ^c	528.79±26.84 ^c	12.93±2.33 ^c	138.92±20.21 ^{ac}	2.64±0.22 ^{ac}	190.87±52.97 ^{ac}	3.69±1.24 ^{ac}	284.54±66.72 ^c	4.05±0.91 ^c
48 h	577.78±86.84 ^c	8.28±4.58 ^c	748.57±29.73 ^c	10.56±1.83 ^c	228.71±71.94 ^{ac}	1.55±0.29 ^{ac}	338.08±108.66 ^{ac}	3.66±1.67 ^{ac}	675.35±202.20 ^c	5.45±2.50 ^c
72 h	989.77±166.32 ^c	9.36±2.39 ^c	1255.30±150.39 ^c	15.66±2.34 ^c	448.36±55.80 ^{ac}	3.25±0.56 ^{ac}	556.27±80.32 ^{ac}	4.66±1.24 ^{ac}	759.38±109.32 ^{ac}	6.99±1.58 ^{ac}

N: control group; M: model group; G: high dosage group; Z: medium dosage group; D: low dosage group, ^a*P*<0.05 vs normal group; ^c*P*<0.05 vs model group.

Table 5 Influence of each group serum on collagen I of HSC at different time points (A value: mean±SD)

	N		M		G		Z		D	
	A	Male cell area (%)	A	Male cell area (%)	A	Male cell area (%)	A	Male cell area (%)	A	Male cell area (%)
24 h	50.87±9.84	5.49±2.06 ^c	60.63±9.26	4.64±0.26	46.95±5.21	2.90±0.22	44.83±6.97	3.72±0.48	49.46±7.36	3.89±0.79
48 h	270.51±13.56	5.28±0.58	456.78±106.64	5.56±1.83	107.79±17.9	4.45±0.29	115.28±51.85	4.66±1.67	129.35±22.20	4.45±0.50
72 h	507.77±66.38 ^c	11.36±2.39 ^c	800.30±150.39 ^a	15.66±2.34 ^a	300.23±25.80 ^{ac}	5.25±0.56 ^{ac}	329.37±45.98 ^{ac}	6.62±1.33 ^{ac}	425.38±19.32 ^c	7.99±1.25 ^c

N: control group; M: model group; G: high dosage group; Z: medium dosage group; D: low dosage group, ^a*P*<0.05 vs normal group; ^c*P*<0.05 vs model group.

Table 6 Influence of each group serum on collagen III of HSC at different time points (A value: mean±SD)

	N		M		G		Z		D	
	A	Male cell area (%)	A	Male cell area (%)	A	Male cell area (%)	A	Male cell area (%)	A	Male cell area (%)
24 h	60.93±18.56	12.49±3.16	65.69±23.84	13.64±2.36	40.95±5.21	8.90±3.82	45.83±12.97	9.72±1.47	52.46±26.72	10.56±0.56
48 h	203.78±36.64 ^c	25.28±4.27 ^c	282.51±28.43 ^a	31.56±3.69 ^a	63.71±7.94 ^{ac}	15.55±3.59 ^{ac}	65.08±18.85 ^{ac}	17.66±1.65 ^{ac}	79.35±22.28 ^{ac}	21.35±2.36 ^{ac}
72 h	325.30±40.39 ^c	30.36±2.50 ^c	501.77±56.42 ^a	40.66±4.82 ^a	178.36±5.82 ^{ac}	23.25±4.26 ^{ac}	182.27±20.32 ^{ac}	25.66±1.29 ^{ac}	220.38±19.32 ^c	29.70±1.72 ^c

N: control group; M: model group; G: high dosage group; Z: medium dosage group; D: low dosage group, ^a*P*<0.05 vs normal group; ^c*P*<0.05 vs model group.

Table 7 Influence of each group serum on TIMP of HSC at different time points (A value: mean±SD)

	N		M		G		Z		D	
	A	Male cell area (%)	A	Male cell area (%)	A	Male cell area (%)	A	Male cell area (%)	A	Male cell area (%)
24 h	60.93±18.56	12.49±3.16	65.69±23.84	13.64±2.36	40.95±5.21	8.90±3.82	45.83±12.97	9.72±1.47	52.46±26.72	10.56±0.56
48 h	203.78±36.64 ^c	25.28±4.27 ^c	282.51±28.43 ^a	31.56±3.69 ^a	63.71±7.94 ^{ac}	15.55±3.59 ^{ac}	65.08±18.85 ^{ac}	17.66±1.65 ^{ac}	79.35±22.28 ^{ac}	21.35±2.36 ^{ac}
72 h	325.30±40.39 ^c	30.36±2.50 ^c	501.77±56.42 ^a	40.66±4.82 ^a	178.36±5.82 ^{ac}	23.25±4.26 ^{ac}	182.27±20.32 ^{ac}	25.66±1.29 ^{ac}	220.38±19.32 ^c	29.70±1.72 ^c

N: control group; M: model group; G: high dosage group; Z: medium dosage group; D: low dosage group, ^a*P*<0.05 vs normal group; ^c*P*<0.05 vs model group.

Table 8 Influence of each group serum on TGFβ1 of HSC at different time points (A value: mean±SD)

	N		M		G		Z		D	
	A	Male cell area (%)	A	Male cell area (%)	A	Male cell area (%)	A	Male cell area (%)	A	Male cell area (%)
24 h	126.56±21.69	5.14±0.69	158.79±27.63	9.67±2.59	98.92±29.25	5.48±0.49	105.69±27.96	6.72±1.74	122.56±67.84	6.21±0.98
48 h	570.78±57.61 ^c	15.78±0.78 ^c	733.58±189.73 ^a	19.39±3.76 ^a	428.71±51.30 ^{ac}	7.36±0.87 ^{ac}	458.08±37.98 ^{ac}	9.87±1.98 ^{ac}	549.35±124.29 ^c	13.27±2.77 ^a
72 h	1 279.30±147.78 ^c	21.98±2.38 ^c	1 509.87±77.50 ^a	27.58±5.65 ^a	609.37±72.85 ^{ac}	9.25±0.67 ^{ac}	823.75±158.49 ^{ac}	12.35±1.75 ^{ac}	971.57±127.83 ^c	19.30±1.36 ^c

N: control group; M: model group; G: high dosage group; Z: medium dosage group; D: low dosage group, ^a*P*<0.05 vs normal group; ^c*P*<0.05 vs model group.

Table 9 Influence of each group serum on PDGF of HSC at different time points (A value: mean±SD)

	N		M		G		Z		D	
	A	Male cell area (%)	A	Male cell area (%)	A	Male cell area (%)	A	Male cell area (%)	A	Male cell area (%)
24 h	326.47±15.31 ^c	7.14±0.69	447.69±25.47 ^a	12.05±3.87	128.87±35.14 ^{ac}	4.21±0.29	187.39±36.67 ^{ac}	7.83±0.67	227.87±54.39 ^c	9.64±0.87
48 h	479.65±38.49 ^c	24.78±5.90 ^c	659.45±76.56 ^a	37.25±4.89 ^c	214.17±54.67 ^{ac}	9.28±0.70 ^{ac}	264.58±49.57 ^{ac}	14.02±2.06 ^{ac}	379.27±75.02 ^c	18.56±3.27 ^{ac}
72 h	805.30±121.04 ^c	32.98±5.49 ^c	1 208.02±132.21 ^a	45.94±5.37 ^c	427.21±39.72 ^{ac}	15.07±2.78 ^{ac}	560.41±132.02 ^{ac}	19.28±2.09 ^{ac}	720.34±102.07 ^c	27.19±3.29 ^{ac}

N: control group; M: model group; G: high dosage group; Z: medium dosage group; D: low dosage group, ^a*P*<0.05 vs normal group; ^c*P*<0.05 vs model group.

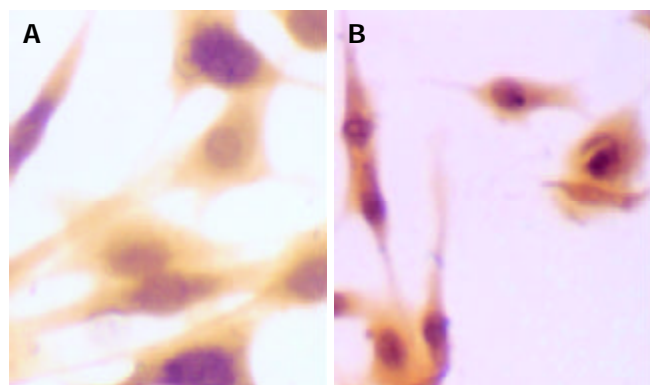


Figure 2 Immunohistochemical staining of synapsin of SD rat HSC line in model group and medium dosage group (×66). A: Immunohistochemical staining of synapsin of SD rat HSC line in model group, B: Immunohistochemical staining of synapsin of SD rat HSC line in medium dosage group.

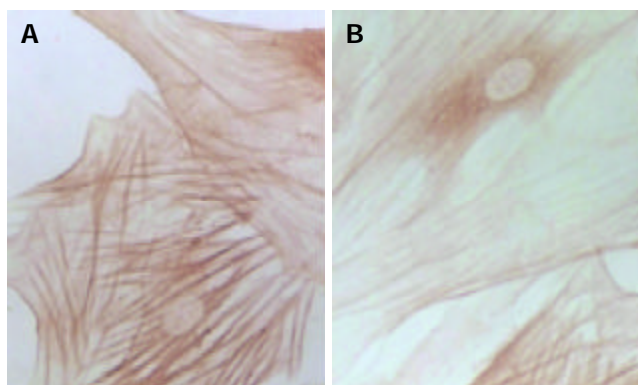


Figure 3 Immunohistochemical staining of type I collagen of SD rat HSC line in model group and medium dosage group (×132). A: Immunohistochemical staining of type I collagen of SD rat HSC line in model group, B: Immunohistochemical staining of type I collagen of SD rat HSC line in medium dosage group.

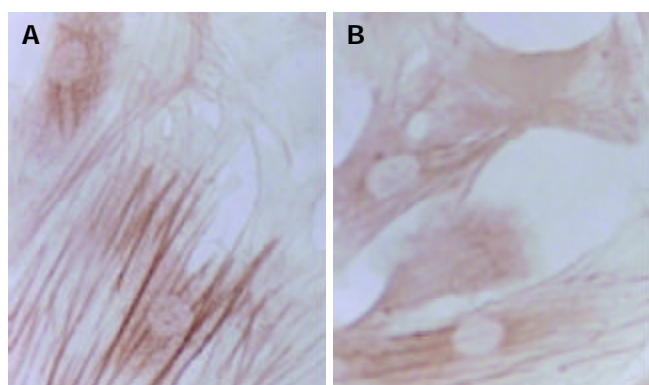


Figure 4 Immunohistochemical staining of type III collagen of SD rat HSC line in model group and medium dosage group ($\times 132$). A: Immunohistochemical staining of type III collagen of SD rat HSC line in model group, B: Immunohistochemical staining of type III collagen of SD rat HSC line in medium dosage group.

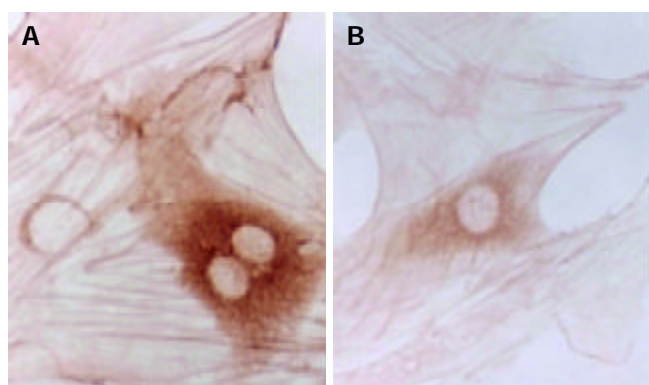


Figure 5 Immunohistochemical staining of TGF- $\beta 1$ of SD rat HSC line in model group and medium dosage group ($\times 132$). A: Immunohistochemical staining of TGF- $\beta 1$ of SD rat HSC line in model group, B: Immunohistochemical staining of TGF- $\beta 1$ of SD rat HSC line in medium dosage group.

Influence of each group serum on TGF $\beta 1$ and PDGF of HSC at different time points

The influence of each group serum detected with TN-8502 image analysis system on TGF $\beta 1$ and PDGF of HSC at different time points is shown in Tables 8, 9 and Figures 5, 6.

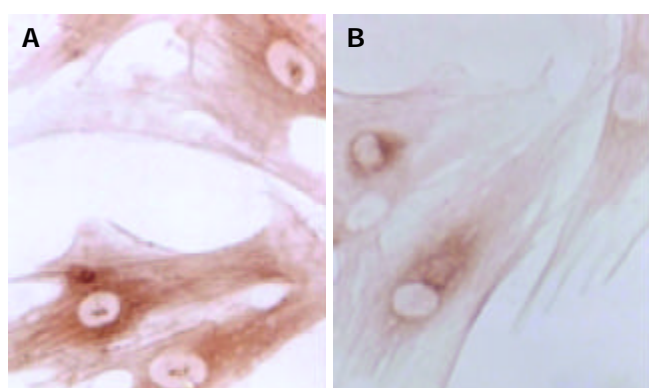


Figure 6 Immunohistochemical staining of PDGF of SD rat HSC line in model group and medium dosage group ($\times 132$). A: Immunohistochemical staining of PDGF of SD rat HSC line in model group, B: Immunohistochemical staining of PDGF of SD rat HSC line in medium dosage group.

DISCUSSION

In past studies about traditional Chinese medicine, the method of adding directly coarse extract of the medicine to environment of cells was adopted in most experiments *in vitro*. Because of the complicated components of traditional Chinese medicine, it could not effectively reflect its pharmacological role. Therefore, we adopted the blood serum pharmacological method in our experiment^[8]. After giving the drug to the animal orally, we took the drug serum as the drug source to add to the response system *in vitro*. This method could not only present the biotransformation *in vivo*, but also overcome confusion of other substances, aiding to make a pharmacokinetic study by finding the effective locus and the activity of components of traditional Chinese medicine. To avoid influence of different species animal sera on cells, animals were adopted in our experiment which were the same species with cultivated HSCs. Considering that the tested object of the drug was cells and the drug with biological reactivity in organism, we gave the drug to the animal orally with an equivalent dosage, to assure the maximum homeostasis concentration of the drug after bioconversion *in vivo*. The results of our experiment indicated that our experiment method was effective, stable and reliable.

A recent investigation has shown that proliferation and activation of HSCs are not only the central link of hepatic fibrosis, but also the cytological background of hepatic fibrosis^[10,11]. Therefore, inhibiting the proliferation and activation of HSC has important significance in prevention and treatment of chronic liver disease and anti-hepatic fibrosis. Cultivated in a non-coating plastic Petri dish, HSC could be automatically activated, thus possessing the biological characteristics of activation *in vivo*, and becoming an ideal anti-hepatic fibrosis cell model^[12]. Just as shown by the results of our experiment, with elongation of cultivating time, HSC showed multi-angle pseudopodium and typical star form. Cell proliferation and collagen synthesis were two important behaviors in activation of HSC. MTT chromatometry methods could be employed to detect cell ability of proliferation, which was based on the principle that succinic dehydrogenase in mitochondria of living cells could make ectogenical MTT recover to non-dissoluble blue and purple crystals and deposit in cells. DMSO could dissolve blue and purple crystals in cells. Adopting enzyme labeled instruments to detect the Absorbency value at some wave-length, the quantity of cells could be reflected indirectly.

The results of our experiment showed that there was no significant difference ($P > 0.05$) between all the groups 24 h after serum was added. It means that adding serum to cultivate for 24 h did not exert any effective influence and HSCs still proliferated at its original rate, suggesting that intervention in proliferation of HSCs needs a time process, which from accepting excitation of cell signal to changing proliferation quantity of HSC, is undoubtedly longer than 24 h. Thus, how to restrain the activation of HSC at earlier time to hold back quick proliferation of HSC, has undoubtedly important significance in prevention and cure of hepatic fibrosis. Our results showed that proliferation of HSC in model group in 48 h and 72 h had a significant difference compared with other groups, indicating that the model group might contain substances which could promote quick proliferation of HSC. The reason may be that after cultivated for 48 h and 72 h, the PDGF of HSC in the model group increased to the effective content, leading to excessive proliferation of HSC. But a 24 h cultivation was not enough for PDGF to increase to the effective content. This could explain our results that there was no significant proliferation of HSC in the model group after 24 h serum culture. The results of our experiment also showed that after cultivated for 48 h and 72 h, there were significant differences among the high, medium and low dosage drug serum groups and the model group ($P < 0.05$),

and between the high and medium dosage drug serum groups and the control group ($P < 0.05$), indicating that different dosage drug sera could inhibit the proliferation of HSC, and had an especially significant effect on the high and medium dosage groups. CBJRGC serum could significantly decrease and inhibit the proliferation of HSC. Its mechanism may be related to the inhibition of self-excretion or para-excretion of PDGF and TGF- β_1 ^[13], thus inhibiting the proliferation of HSC by decreasing the conversion from HSC to α -SMA.

Changes in form and function after HSC is activated could lead to production increase and degradation decrease of ECM, eventually resulting in deposition of hepatic collagens and hepatic fibrosis. Desmin could be regarded as a marker of HSC^[14], and α -SMA as the marker of activation of HSC^[15]. α -SMA is a kind of filament protein which is about 7 nm in diameter and mainly exists in smooth muscle cells as a portion of cytoplasm framework and a functional unit of cell contraction. Under normal conditions, this protein mainly exists in smooth muscle cells and myofibroblasts. There is a very small amount of this protein in HSCs of rats. In the animal model of liver diseases, HSC lost desmin expression and was changed to the expression of α -SMA in its activation process. So, α -SMA could be regarded as the marker of activation of HSC^[16]. In the process of inducing rat hepatic fibrosis by CCl₄^[17], the dynamic change of desmin male cells was a mono-cusp curve, increasing in number in the earlier period, reaching the peak in 12 wk and then gradually decreasing. A foreign study has found that increase of expression of synapsin could be regarded as another marker of activation of HSC^[18]. Our results showed that the dynamic changes in A value of male staining of α -SMA, desmin and synapsin and in the area occupied by α -SMA and synapsin male cells were almost synchronous. The area occupied by desmin male cells showed a tendency to decrease with elongation of cultivating time. This result was consistent with that reported by Li *et al.* that HSC lost the expression of desmin in its activation process^[19], suggesting that in the process of hepatic fibrosis, α -SMA, desmin and synapsin all can be regarded as the markers of activation of HSC, but each has its own characteristics. The expression of desmin in the earlier period of activation was significant, but weakened with elongation of activating time, while the expression of α -SMA and synapsin developed with elongation of activating time. It is estimated that activation and proliferation of HSC can synchronically occur. Our results also showed that after cultivated for 24 h, the expression of α -SMA had no significant difference among all groups, and after cultivated for 48 h, α -SMA male cell area was smaller than that of desmin, indicating that in the period of cultivation for 24 h and 48 h, proliferation was the main form of HSC growth, but with elongation of cultivating time, HSC began to be partly activated and changed to expression of α -SMA. Seventy-two h after cultivation, α -SMA male cell area was bigger than desmin male cell area, the amount of activated HSCs was more than that of silent HSCs and lots of HSCs altered in phenotype, further indicating that the activation of HSC could be synchronically expressed as proliferation and transformation of HSC. The results of our experiment showed that CBJRGC serum could inhibit the expressions of α -SMA, desmin and synapsin in HSC and inhibit the activation of HSC, whose drug effect was closely related to the concentration of drug serum.

Synapsin can be regarded as a new marker of activation of HSC. Its significance is to provide an important theoretic and testing basis for neuroregulation in the process of hepatic fibrosis. So far, no such study has been found in China. Our experiment firstly showed that after cultivated for 24 h, synapsin could express in HSC, and after cultivated for 48 h and 72 h, synapsin could continue to express. Expression of synapsin occurred before it was cultivated for 24 h and continued to

maintain a high level. CBJRGC serum could significantly inhibit expression of synapsin in HSC. Nevertheless, further studies such as the precise time of synapsin expression, the essential significance of the increase in its lasting expression, whether the nervous system involves regulation of stress condition of liver, and whether CBJRGC serum takes part in nervous regulation in hepatic fibrosis, are still needed.

Under normal conditions, liver contains collagen of types I, III, IV, V, and VI. Collagens I and III take the most proportion of collagen, accounting for about 60% of total collagen in liver. When hepatic fibrosis occurred, the proportion of collagens I and III might reach 95% of total collagen in liver^[20]. Thus, in hepatic fibrosis, deposited ECM mainly consists of collagens I and III.

Synthesis of collagen could reflect alternative ability of individual fiber hyperplasia of cells^[21]. Our experiment showed that after cultivated for 24 h, there was no significant difference of collagens I and III among all groups, indicating that within 24 h after acceptance of activating signal, HSC did not yet achieve enough time to excrete collagen. The outcome of our experiment showed that activated time should be longer than 24 h, so that activated HSC and transcription of collagen and cytokine could be altered. In further investigations we should observe and analyze changes in collagen-mRNA in this time process to test whether CBJRGC serum can influence collagen-mRNA. The results also suggested that to inhibit collagen in its transcriptional stage might have important significance in clinical treatment. In our experiment, collagen III began to markedly express after cultivated for 48 h, but collagen I started to markedly express after cultivated for 72 h, showing that expression of collagen III was earlier than that of collagen I, and that in the early time of hepatic fibrosis, collagen III expression took the most part of expression of collagen. Therefore collagen III can be the testing index of earlier hepatic fibrosis. The outcome of our experiment also showed that high and medium dosage groups could significantly inhibit the expression of collagen III in 48 h and 72 h and the expression of collagen I in 72 h. It means CBJRGC serum could play a role in anti-hepatic fibrosis at the earlier time when collagen was significantly expressed. It further suggested that CBJRGC serum could help quickly recover equilibration of synthesis and degradation of ECM in hepatic fibrosis, thus helping to cure hepatic fibrosis. Besides, low dosage group could only significantly inhibit the expression of collagen III in 48 h, but there was no significant difference compared with control group in 72 h. It is estimated that the effect of CBJRGC serum in inhibiting collagen III expression is related to the serum concentration of the drug.

MMP and TIMP mainly take part in regulation of equilibration in synthesis and degradation of collagen^[22]. Among numerous MMPs, MMP1 is the chief MMP, decomposing collagens I and III in liver^[23]. TIMP1 is an inhibiting factor of MMP, which plays its role by irreversibly binding to activated MMP1. Therefore, the imbalance of ratio of MMP/TIMP 1 plays a very important role in hepatic fibrosis. MMP can be inhibited by many specific or non-specific inhibitors, which at present, mainly include TIMP and α 2- macroglobulin. TIMP 1 is the most important inhibitor of MMP and is negatively correlated to the activity of MMP.

TIMP is a kind of coding protein of multigene family^[24]. It could irreversibly bind to activated MMP and inhibit the degradation of ECM^[25]. So far, there are four kinds of TIMP isolated from tissues and cloned^[26]. TIMP-1 is a kind of 28.5 ku glycoprotein, mainly inhibiting the activity of MMPs-1 and MMP-9. As the specific inhibitor of MMP, TIMP plays a very important role in hepatic fibrosis. TIMP could inhibit MMP, which is the important reason for specific descent of degradation of ECM^[27]. HSC is the main source cell of TIMP and MMP.

The results of our experiment showed that after cultivated for 24 h, there was no significant expression of TIMP in all groups, indicating that HSC did not have enough time to excrete excessive TIMP. The activated time should be longer than 24 h, and within this time, transcription of TIMP of activated HSC might be altered. In further studies, we should observe and analyze the change of TIMP-mRNA within this time, so as to find whether CBJRGC serum can influence TIMP-mRNA. It is also suggested that to inhibit TIMP in transcriptional stage might have important significance in clinical treatment. In this experiment, TIMP of the model group maintained high expression in 48 h and 72 h, indicating that there was some substance to promote high expression of TIMP in the model group. Further study on the precise characteristics of the substance is suggested.

Researches have found that HSC is the key cell in hepatic fibrosis. Under the stimulation of chronic injury and inflammation, HSC can be activated from normal silent behavior to MFB, and meanwhile can secrete and synthesize excessive ECM, forming the foundation of hepatic fibrosis. Previous studies have indicated that activation and phenotype conversion of HSC are closely related to TGF- β 1. TGF- β is a kind of polypeptide molecule of hormone activity, which is produced from kupffer cells by self-excretion and para-excretion and could take part in many pathological and physiological processes^[28]. TGF- β has at least 5 sub-types, but there are only TGF- β 1, TGF- β 2 and TGF- β 3 in human tissue cells. After binding to the recipient on the membrane, TGF- β could phosphorylate and activate its signal transduction molecule (SMAD protein) of intracytoplasmic downstream, which could subsequently enter the nucleus, regulating the transcription of related target gene^[29]. TGF- β 1 exhibits the significant biological activity of TGF- β and is the main cytokine inducing the production of collagen. Through the mechanism of para-excretion and self-excretion, TGF- β 1 could start and maintain the activation of HSC, regulating cell proliferation, accelerating transcription of collagen and proliferation of ECM^[30].

The results of our experiment showed that after cultivated for 24 h, there was no significant expression of TGF- β 1 among all groups. It showed that it was not enough for HSC to secrete TGF- β 1 24 h after it received the activated signal. It is suggested that in further studies we should observe and analyze the change in TGF- β 1-mRNA within this time, so as to find whether CBJRGC serum can influence TGF- β 1-mRNA. Our results also showed that after cultivated for 48 h and 72 h, TGF- β 1 in the model group maintained high expression, suggesting that it could continuously stimulate activated HSC to produce collagen and accelerate hepatic fibrosis. There might be some substance in the model group which could promote high expression of TGF- β 1. Study on the precise characteristics of this substance is still needed. The results also showed that the high and medium dosage groups could markedly inhibit the expression of TGF- β 1 in 48 h and 72 h, but the low dosage group did not obviously inhibit the expression of TGF- β 1 in 48 h and 72 h, suggesting that CBJRGC serum can inhibit the expression of TGF- β 1 and its effectiveness is related to the concentration of the drug serum.

PDGF is a kind of splitting agent and can promote activation and proliferation of HSC. It has been found PI3-K is the important pathway of intramembrane signal transduction^[31]. The outcome of our experiment showed that after cultivated for 24 h, the A value and male cell area of PDGF were not completely consistent. In 24 h, the A value of PDGF in the model group was significantly higher than that in the other groups, but the male cell area did not show any significant difference compared with the other groups. Although PDGF in the model group achieved significant expression, the PDGF might not entirely come from the excretion of HSC and might

include original PDGF existing in the model group. While PDGF bound to PDGF recipient of HSC and accelerated the proliferation of HSC, the absolute proportion of HSC in the situation of excretion of PDGF did not significantly increase. The outcome of our experiment showed that the high, medium and low dosage groups all could obviously inhibit the excretion of PDGF by HSC.

In summary, we suggest that further studies on the mechanism of anti-hepatic fibrosis of CBJRGC serum should focus on mRNA expression of TIMP1, collagens I, III and TGF- β 1 and signal transduction within the cell.

REFERENCES

- 1 **Burt AD.** Pathobiology of hepatic stellate cells. *J Gastroenterol* 1999; **34**: 299-304
- 2 **Cales P.** Apoptosis and liver fibrosis: antifibrotic strategies. *Biomed Pharmacother* 1998; **52**: 259-263
- 3 **Desmouliere A,** Xu G, Costa AM, Yousef IM, Gabbiani G, Tuchweber B. Effect of pentoxifylline on early proliferation and phenotypic modulation of fibrogenic cells in two rat models of liver fibrosis and on cultured hepatic stellate cells. *J Hepatol* 1999; **30**: 621-631
- 4 **Liu X,** Zhang Z, Yang L, Chen D, Wang Y. Inhibition of the activation and collagen production of cultured rat hepatic stellate cells by antisense oligonucleotides against transforming growth factor-beta 1 is enhanced by cationic liposome delivery. *Huaxi Yikedaxue Xuebao* 2000; **31**: 133-135
- 5 **Yu WP,** Brenner S, Venkatesh B. Duplication, degeneration and subfunctionalization of the nested synapsin-Timp genes in Fugu. *Trends Genet* 2003; **19**: 180-183
- 6 **Yoshiji H,** Kuriyama S, Yoshii J, Ikenaka Y, Noguchi R, Nakatani T, Tsujinoue H, Yanase K, Namisaki T, Imazu H, Fukui H. Tissue inhibitor of metalloproteinases-1 attenuates spontaneous liver fibrosis resolution in the transgenic mouse. *Hepatology* 2002; **36**: 850-860
- 7 **Tsukamoto H.** Cytokine regulation of hepatic stellate cells in liver fibrosis. *Alcohol Clin Exp Res* 1999; **23**: 911-916
- 8 **Liu C,** Liu P, Liu CH, Zhu XQ, Ji G. Effects of Fuzhenghuayu decoction on collagen synthesis of cultured hepatic stellate cells, hepatocytes and fibroblasts in rats. *World J Gastroenterol* 1998; **4**: 548-549
- 9 **Hernandez-Munoz R,** Diaz-Munoz M, Suarez-Cuenca JA, Trejo-Solis C, Lopez V, Sanchez-Sevilla L, Yanez L, De Sanchez VC. Adenosine reverses a preestablished CC14-induced micronodular cirrhosis through enhancing collagenolytic activity and stimulating hepatocyte cell proliferation in rats. *Hepatology* 2001; **34**: 677-687
- 10 **Woo SW,** Nan JX, Lee SH, Park EJ, Zhao YZ, Sohn DH. Aloe emodin suppresses myofibroblastic differentiation of rat hepatic stellate cells in primary culture. *Pharmacol Toxicol* 2002; **90**: 193-198
- 11 **Suzuki C,** Kayano K, Uchida K, Sakaida I, Okita K. Characteristics of the cell proliferation profile of activated rat hepatic stellate cells *in vitro* in contrast to their fibrogenesis activity. *J Gastroenterol* 2001; **36**: 322-329
- 12 **Levy MT,** McCaughan GW, Marinos G, Gorrell MD. Intrahepatic expression of the hepatic stellate cell marker fibroblast activation protein correlates with the degree of fibrosis in hepatitis C virus infection. *Liver* 2002; **22**: 93-101
- 13 **Yuan N,** Wang P, Wang X, Wang Z. Expression and significance of platelet derived growth factor and its receptor in liver tissues of patients with liver fibrosis. *Zhonghua Ganzhangbing Zazhi* 2002; **10**: 58-60
- 14 **Nitou M,** Ishikawa K, Shiojiri N. Immunohistochemical analysis of development of desmin-positive hepatic stellate cells in mouse liver. *J Anat* 2000; **197**(Pt 4): 635-646
- 15 **Guma FCR,** Mello TG, Mermelstein CS, Fortuna VA, Wofchuk ST, Gottfried C, Guaragna RM, Costa ML, Borojevic R. Intermediate filaments modulation in an *in vitro* model of the hepatic stellate cell activation or conversion into the lipocyte phenotype. *Biochem Cell Biol* 2001; **79**: 409-417
- 16 **Buniatian GH,** Gebhardt R, Mecke D, Traub P, Wiesinger H.

- Common myofibroblastic features of newborn rat astrocytes and cirrhotic rat liver stellate cells in early cultures and *in vivo*. *Neurochem Int* 1999; **35**: 317-327
- 17 **Zhou X**, Zhang Y, Zhang J, Zhu H, Zhou X, Du W, Zhang X, Chen Q. Expression of fibronectin receptor, integrin alpha 5 beta 1 of hepatic stellate cells in rat liver fibrosis. *Chin Med J* 2000; **113**: 272-276
- 18 **Cheetham JJ**, Hilfiker S, Benfenati F, Weber T, Greengard P, Czernik AJ. Identification of synapsin I peptides that insert into lipid membranes. *Biochem J* 2001; **354**: 57-66
- 19 **Li H**, Zhang J, Huang G, Zhang N, Chen Q, Zhang X. Effect of retinoid kappa receptor alpha (RXRalpha) transfection on the proliferation and phenotype of rat hepatic stellate cells *in vitro*. *Chin Med J* 2002; **115**: 928-932
- 20 **Zhang Q**, Wang J, Hu M. Effects of interferon-alpha on the mRNA expression of procollagen type I and III of hepatic stellate cells and on the deposition of collagen type I and III in fibrotic liver of rats. *Zhonghua Yixue Zazhi* 1999; **79**: 695-698
- 21 **Liu WB**, Yang CQ, Jiang W, Wang YQ, Guo JS, He BM, Wang JY. Inhibition on the production of collagen type I, III of activated hepatic stellate cells by antisense TIMP-1 recombinant plasmid. *World J Gastroenterol* 2003; **9**: 316-319
- 22 **Murphy FR**, Issa R, Zhou X, Ratnarajah S, Nagase H, Arthur MJ, Benyon C, Iredale JP. Inhibition of apoptosis of activated hepatic stellate cells by tissue inhibitor of metalloproteinase-1 is mediated via effects on matrix metalloproteinase inhibition: implications for reversibility of liver fibrosis. *J Biol Chem* 2002; **277**: 11069-11076
- 23 **Iredale JP**. Hepatic stellate cell behavior during resolution of liver injury. *Semin Liver Dis* 2001; **21**: 427-436
- 24 **Yoshiji H**, Kuriyama S, Miyamoto Y, Thorgeirsson UP, Gomez DE, Kawata M, Yoshii J, Ikenaka Y, Noguchi R, Tsujinoue H, Nakatani T, Thorgeirsson SS, Fukui H. Tissue inhibitor of metalloproteinases-1 promotes liver fibrosis development in a transgenic mouse model. *Hepatology* 2000; **32**: 1248-1254
- 25 **Yang C**, Zeisberg M, Mosterman B, Sudhakar A, Yerramalla U, Holthaus K, Xu L, Eng F, Afdhal N, Kalluri R. Liver fibrosis: insights into migration of hepatic stellate cells in response to extracellular matrix and growth factors. *Gastroenterology* 2003; **124**: 147-159
- 26 **Bennett RG**, Kharbanda KK, Tuma DJ. Inhibition of markers of hepatic stellate cell activation by the hormone relaxin. *Biochem Pharmacol* 2003; **66**: 867-874
- 27 **Lichtinghagen R**, Michels D, Haberkorn CI, Arndt B, Bahr M, Flemming P, Manns MP, Boeker KH. Matrix metalloproteinase (MMP)-2, MMP-7, and tissue inhibitor of metalloproteinase-1 are closely related to the fibroproliferative process in the liver during chronic hepatitis C. *J Hepatol* 2001; **34**: 239-247
- 28 **Bissell DM**. Chronic liver injury, TGF-beta, and cancer. *Exp Mol Med* 2001; **33**: 179-190
- 29 **Okuno M**, Akita K, Moriwaki H, Kawada N, Ikeda K, Kaneda K, Suzuki Y, Kojima S. Prevention of rat hepatic fibrosis by the protease inhibitor, camostat mesilate, via reduced generation of active TGF-beta. *Gastroenterology* 2001; **120**: 1784-1800
- 30 **Arias M**, Lahme B, Van de Leur E, Gressner AM, Weiskirchen R. Adenoviral delivery of an antisense RNA complementary to the 3' coding sequence of transforming growth factor-beta1 inhibits fibrogenic activities of hepatic stellate cells. *Cell Growth Differ* 2002; **13**: 265-273
- 31 **Kinnman N**, Francoz C, Barbu V, Wendum D, Rey C, Hultcrantz R, Poupon R, Housset C. The myofibroblastic conversion of peribiliary fibrogenic cells distinct from hepatic stellate cells is stimulated by platelet-derived growth factor during liver fibrogenesis. *Laboratory Invest* 2003; **83**: 163-173

Edited by Wang XL and Zhang JZ Proofread by Xu FM

Synthesis of ribozyme against vascular endothelial growth factor₁₆₅ and its biological activity *in vitro*

Zhong-Ping Gu, Yun-Jie Wang, Yu Wu, Jin-Ge Li, Nong-An Chen

Zhong-Ping Gu, Yun-Jie Wang, Yu Wu, Department of Thoracic Surgery, Tangdu Hospital, Fourth Military Medical University, Xi'an 710038, Shaanxi Province, China

Jin-Ge Li, Department of Infectious Disease, Tangdu Hospital, Fourth Military Medical University, Xi'an 710038, Shaanxi Province, China
Nong-An Chen, Shanghai Institute of Biochemistry, Academia Sinica, Shanghai 20020, China

Correspondence to: Dr. Zhong-ping Gu, Department of Thoracic Surgery, Tangdu Hospital, Fourth Military Medical University, Xi'an 710038, Shaanxi Province, China. zhongpg@xaonline.com.cn

Telephone: +86-29-3541718

Received: 2003-12-10 **Accepted:** 2004-02-01

Abstract

AIM: To investigate the designation, synthesis and biological activity of against vascular endothelial growth factor₁₆₅ (VEGF₁₆₅) ribozyme.

METHODS: The ribozyme against VEGF₁₆₅ was designed with computer. The transcriptional vector was constructed which included the anti-VEGF₁₆₅ ribozyme and 5', 3' self-splicing ribozymes. The hammerhead ribozyme and substrate VEGF₁₆₅ mRNA were synthesized through transcription *in vitro*. The cleavage activity of the ribozyme on target RNA was observed in a cell-free system.

RESULTS: The anti-VEGF₁₆₅ ribozyme was released properly from the transcription of pGEMRz212 cleaved by 5' and 3' self-splicing ribozymes which retained its catalytic activity, and the cleavage efficiency of ribozyme reached 90.7%.

CONCLUSION: The anti-VEGF₁₆₅ ribozyme designed with computer can cleave VEGF₁₆₅ mRNA effectively.

Gu ZP, Wang YJ, Wu Y, Li JG, Chen NA. Synthesis of ribozyme against vascular endothelial growth factor₁₆₅ and its biological activity *in vitro*. *World J Gastroenterol* 2004; 10(10): 1495-1498

<http://www.wjgnet.com/1007-9327/10/1495.asp>

INTRODUCTION

Ribozyme (Rz) is one kind of RNA with site-specific ligation and cleavage activities. Being sequence-specific binding and cleaving specific RNA of ribozyme, the target gene expression can be destructed by an artificially designed and synthesized ribozyme^[1-5]. A great attention has been attracted into the field of gene therapy for cancers with the hammerhead ribozyme, by the virtue of its simple structure, small molecule, easy designation, site-specific mRNA cleavage activity, and catalytic potential^[6-13]. Many studies have showed that the growth, metastasis and prognosis of solid tumors critically related to the angiogenesis. Tumor angiogenesis is a complex process. Among all of the known factors of tumor angiogenesis, vascular endothelial growth factor (VEGF) is a vascular endothelial cell-specific mitogen and the most important and direct one that can stimulate

tumor angiogenesis. VEGF₁₆₅ is the most effective angiogenic factor in the VEGF family^[14-22]. Conversely, inhibition of VEGF expression and tumor angiogenesis to inhibit tumor growth and metastasis become a new hot spot of tumor treatment^[23-34]. In this study, the ribozyme against VEGF₁₆₅ site 212 was designed with computer, the transcriptional vector including the anti-VEGF₁₆₅ ribozyme and self-splicing ribozymes were synthesized and constructed, and the cleavage effect of the ribozyme on target mRNA in cell-free system was observed.

MATERIALS AND METHODS

Vectors

The vector pGEM-3zf(+)VEGF (carrying full length amino acids cDNA of VEGF₁₆₅) was kindly provided by Dr. Abraham (Columbia University, USA). Vector pGEMRzHBV and bacterium JM 109 were gift from Dr. Li (Department of Infectious Disease, Tangdu Hospital, Fourth Military Medical University, China).

Ribozyme design

The cleavage sites of ribozyme anti-VEGF₁₆₅ were designed by computer analysis of the secondary structure of VEGF₁₆₅ mRNA with a computer program (Chen Nong-an, Shanghai Institute of Biochemistry, Academia Sinica). According to Symon's hammerhead ribozyme structural model, the sequences of the cleavage active core of ribozyme and the flanking sequences around the cleavage sites were designed.

Ribozyme synthesis

The hammerhead ribozyme was synthesized by 35 amplification cycles of PCR (TakaRa Biotechnology Co. Ltd. Dalian, China) with the following primer: 5' TGAAGATGCTGATGAGTCCGT GAGGACGAAACTCGAT 3' and purified by electrophoresis on a 100 g/L denaturing polyacrylamide gel.

Plasmid construction

In the down stream of T7 promoter, plasmid pGEMRzHBV included 5' cis-self-splicing ribozyme, RzHBV and 3' cis-self-splicing ribozyme in order. The pGEMRzHBV was digested with *Xba* I and *Aat* II, then the linear vector was purified by 10 g/L agarose gel electrophoresis by using plasmid purification kit (Gibco, USA) according to the manufacturer's instruction. The two complementary strands of designed ribozyme gene cDNA ends were prepared by adding linkers to create sticky ends (*Xba* I and *Aat* II). The double-stranded DNA was then subcloned into the multicloning site (at *Xba* I and *Aat* II) of pGEM by using T4 DNA ligase (Promega, USA) to create the self-splicing transcriptional plasmid pGEMRz212 (Figure 1). After being transformed competent JM109 cells with pGEMRz212 and blue-white screening, the plasmids were extracted from the positive colonies. The sequences of the VEGF₁₆₅ ribozyme and self-splicing ribozymes were confirmed by restriction enzyme and DNA sequencing.

Ribozyme transcription and cleavage activity *in vitro*

The pGEM-3zf(+)VEGF was cut by *Eco*R I, and pGEMRz212 by *Xba* I and *Aat* II. The ribozyme and substrate RNAs were

prepared from the cDNA templates with T7 RNA polymerase (Gibco-BRL, USA) with [α - 32 P]UTP (Yahui Co., Beijing) by *in vitro* transcription. Both the ribozyme and substrate mRNA were synthesized by using T7 *in vitro* transcriptional kit (Gibco-BRL, USA). Equal amounts of ribozyme and substrate were mixed in 10 μ L of reaction buffer (10 mmol/L MgCl₂ and pH 7.6, 75 mmol/L Tris-HCl) at 95 °C for one minute and cooled in ice immediately. The mixture was then reacted at 37 °C for 2 h. The reaction was quenched with EDTA. The cleavage products were detected by autoradiography after 60 g/L denaturing polyacrylamide gel electrophoresis.

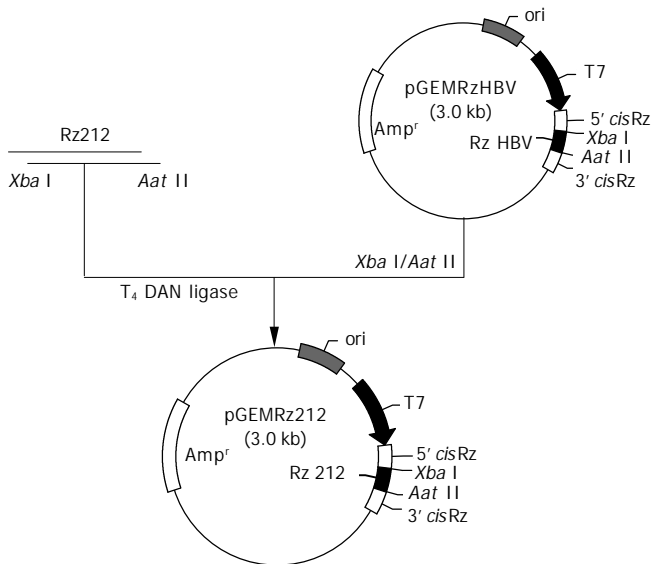


Figure 1 Diagram of construction of the vector pGEMRz212.

RESULTS

Ribozyme designation with computer

The topography of the substrate RNA could be simulated by analyzing the cleavage site and the region surrounding the cleavage site by using an RAN secondary structure folding program. In this way, it might be possible to determine whether or not the target site is buried within an obvious thermodynamically stable region of secondary structure. Among the VEGF₁₆₅ mRNA, there were four hammerhead ribozyme cleavage sites. The site 212 was selected as the optimal cleavage site due to its in single chain region of substrate RNA secondary structure and its both binding arms forming a loop structure to expose for ribozyme cleavage interaction as well as site 212 creating the ribozyme essential core (Figure 2). We called the ribozyme Rz212.

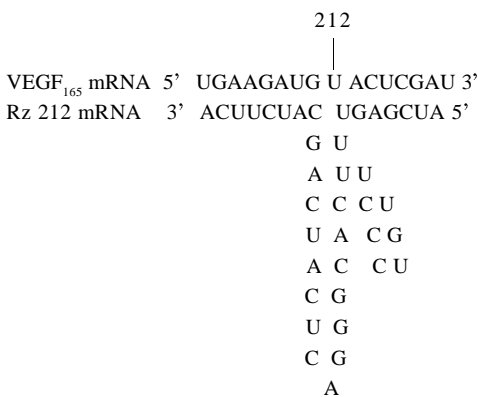


Figure 2 Sequencing of the Rz212 and the target mRNA of VEGF₁₆₅.

Synthesis and transcription Rz212

The synthesized ribozyme was confirmed by restriction enzyme and sequencing analysis. The ribozyme molecule was transcribed *in vitro*. Autoradiography showed three fragments after electrophoresis. The fragments were 5' *cis* ribozyme (64 nt), 3' *cis* ribozyme (54 nt) and Rz212 (47 nt), respectively (Figure 3). The results indicated synthesized ribozyme presenting self-cleavage and releasing the desired ribozyme.

Cleavage activity of Rz212

The cleavage reaction was carried out *in vitro* in a cell-free system. Rz212 cleaved the substrate VEGF₁₆₅ mRNA into 2 fragments (259 nt and 380 nt) (Figure 4) consistent with anticipation. After being cleaved by ribozyme, the density was analyzed by using laser density scanner and the substrate residue was just about 9.3%, indicating that the substrate was nearly cleaved completely by ribozyme.

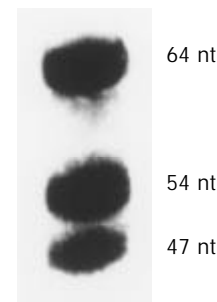


Figure 3 Transcription of pGEMRz212.

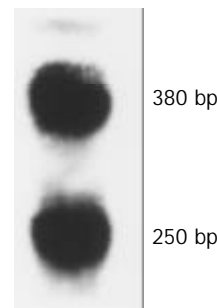


Figure 4 Cleavage activity of VEGF₁₆₅ mRNA with Rz212.

DISCUSSION

The cleavage site and both binding arms must be considered attentively while designing ribozyme. First of all, the cleavage site should be in the important functional region of the target gene assuring the corresponding protein function lost after being cleaved. In addition, the flanking sequences around the cleavage site should be as conserved as possible so that the ribozyme cleavage spectrum become broader. The ribozyme arms sequence context can also influence cleavage rate significantly. In a simple term, the longer the binding arms, the lower the turnover in cleavage of short substrate^[35]. Results from various studies have indicated that ribozyme activity is closely related to the arms length and this depends somewhat on the sequence context^[36,37]. The ribozyme design program we used was approved and improved continuously by experiments. It can resolve the cleavage site design and the sequence surrounding the cleavage site as well as the predicting of ribozyme secondary structure. In this study, we designed successfully the ribozyme target VEGF₁₆₅ mRNA site 212 using the program, synthesized Rz212 and constructed self-cleavage plasmid pGEMRz212. *In vitro* transcription and cleavage

experiment showed that the designed ribozyme was released and cut the target mRNA into two fragments.

Practically, ribozyme gene was constructed in the transcriptional and eukaryotic vector. The ribozyme molecule was transcribed in cells. But there are some long additional sequence in the both arms of ribozyme. The long additional sequence has a strong secondary structure and influenced ribozyme catalytic core, resulted in forming the incorrect secondary structure, even blocking ribozyme binding site. The long additional sequence also influenced ribozyme dissociation from the cleaved target mRNA and reduced cleavage rate^[38,39]. In order to cleave the long additional sequence, we designed and constructed the trimming plasmid pGEMRz212, which included 5' *cis*-self-splicing ribozyme, Rz212 and 3' *cis*-self-splicing ribozyme in order. The long additional sequence was cleaved while pGEMRz212 transcription *in vitro* and VEGF₁₆₅ mRNA specific ribozyme released without long additional sequence. The result showed 5' and 3' *cis* ribozyme neither cleaved the substrate and nor influenced Rz212 cleavage efficacy.

Compared with antisense RNA, ribozyme can not only block target mRNA but also cleave the target mRNA in a sequence-specific manner. Ribozyme has received much attention for their potential use due to their inherent simplicity, relatively small size, repetition use and the ability to be incorporated into a variety of flanking sequence motifs without changing site-specific cleavage capacities^[40-42]. In this experiment, the cleavage efficacy of ribozyme we designed and synthesized reached up to 90.7%. It can suppress effectively the expression of substrate. This research may facilitate the development of ribozyme anti-angiogenesis gene therapy for the treatment in the tumors. Further studies are required for therapeutic application of anti-angiogenesis in human cancer.

REFERENCES

- Doherty EA**, Doudna JA. Ribozyme structures and mechanisms. *Annu Rev Biophys Biomol Struct* 2001; **30**: 457-475
- Takagi Y**, Warashina M, Stec WJ, Yoshinari K, Taira K. Recent advances in the elucidation of the mechanisms of action of ribozymes. *Nucleic Acids Res* 2001; **29**: 1815-1834
- Aigner A**, Renneberg H, Bojunga J, Apel J, Nelson PS, Czubayko F. Ribozyme-targeting of a secreted FGF-binding protein (FGF-BP) inhibits proliferation of prostate cancer cells *in vitro* and *in vivo*. *Oncogene* 2002; **21**: 5733-5742
- Li JG**, Lian JQ, Jia ZS, Feng ZH, Nie QH, Wang JP, Huang CX, Bai XF. Effect of ribozymes on inhibiting expression of HBV mRNA in HepG2 cells. *Shijie Huaren Xiaohua Zazhi* 2003; **11**: 161-164
- Tekur S**, Ho SM. Ribozyme-mediated downregulation of human metallothionein II(a) induces apoptosis in human prostate and ovarian cancer cell lines. *Mol Carcinog* 2002; **33**: 44-55
- Lin JS**, Song YH, Kong XJ, Li B, Liu NZ, Wu XL, Jin YX. Preparation and identification of anti-transforming growth factor beta1 U1 small nuclear RNA chimeric ribozyme *in vitro*. *World J Gastroenterol* 2003; **9**: 572-577
- Zheng Y**, Zhang J, Qu L. Effects of anti-HPV16E6-ribozyme on phenotype and gene expression of a cervical cancer cell line. *Chin Med J* 2002; **115**: 1501-1506
- Jia ZS**, Chen L, Hao CQ, Feng ZH, Li JG, Wang JP, Cao YZ, Zhou YX. Intracellular immunization by hammerhead ribozyme against HCV. *Shijie Huaren Xiaohua Zazhi* 2003; **11**: 148-150
- Castanotto D**, Li JR, Michienzi A, Langlois MA, Lee NS, Puymirat J, Rossi JJ. Intracellular ribozyme applications. *Biochem Soc Trans* 2002; **30**(Pt 6): 1140-1145
- Liu XJ**, Wu QM, Liu CZ, Yu JP, Wang Q. Construction and assessment of eukaryotic expression plasmid pBBS212Rz containing ribozyme gene against hTR. *Shijie Huaren Xiaohua Zazhi* 2002; **10**: 1261-1263
- Tong Q**, Zhao J, Chen Z, Zeng F, Lu G. Effects of blocking androgen receptor expression with specific hammerhead ribozyme on *in vitro* growth of prostate cancer cell line. *Chin Med J* 2003; **116**: 1515-1518
- Goodchild J**. Hammerhead ribozymes for target validation. *Expert Opin Ther Targets* 2002; **6**: 235-247
- Goodchild J**. Hammerhead ribozymes: biochemical and chemical considerations. *Curr Opin Mol Ther* 2000; **2**: 272-281
- Carmeliet P**. Angiogenesis in health and disease. *Nat Med* 2003; **9**: 653-660
- Gu ZP**, Wang YJ, Li JG, Zhou YA. VEGF₁₆₅ antisense RNA suppresses oncogenic properties of human esophageal squamous cell carcinoma. *World J Gastroenterol* 2002; **8**: 44-48
- Hughes GC**, Biswas SS, Yin B, Coleman RE, DeGrado TR, Landolfo CK, Lowe JE, Annex BH, Landolfo KP. Therapeutic angiogenesis in chronically ischemic porcine myocardium: comparative effects of bFGF and VEGF. *Ann Thorac Surg* 2004; **77**: 812-818
- Fernandez M**, Vizzutti F, Garcia-Pagan JC, Rodes J, Bosch J. Anti-VEGF receptor-2 monoclonal antibody prevents portal-systemic collateral vessel formation in portal hypertensive mice. *Gastroenterology* 2004; **126**: 886-894
- Willett CG**, Boucher Y, di Tomaso E, Duda DG, Munn LL, Tong RT, Chung DC, Sahani DV, Kalva SP, Kozin SV, Mino M, Cohen KS, Scadden DT, Hartford AC, Fischman AJ, Clark JW, Ryan DP, Zhu AX, Blaszkowsky LS, Chen HX, Shellito PC, Lauwers GY, Jain RK. Direct evidence that the VEGF-specific antibody bevacizumab has antivasular effects in human rectal cancer. *Nat Med* 2004; **10**: 145-147
- Fondevila C**, Metges JP, Fuster J, Grau JJ, Palacin A, Castells A, Volant A, Pera M. p53 and VEGF expression are independent predictors of tumour recurrence and survival following curative resection of gastric cancer. *Br J Cancer* 2004; **90**: 206-215
- Van Trappen PO**, Steele D, Lowe DG, Baithun S, Beasley N, Thiele W, Weich H, Krishnan J, Shepherd JH, Pepper MS, Jackson DG, Sleeman JP, Jacobs JJ. Expression of vascular endothelial growth factor (VEGF)-C and VEGF-D, and their receptor VEGFR-3, during different stages of cervical carcinogenesis. *J Pathol* 2003; **201**: 544-554
- Buchler P**, Reber HA, Ullrich A, Shiroiki M, Roth M, Buchler MW, Lavey RS, Friess H, Hines OJ. Pancreatic cancer growth is inhibited by blockade of VEGF-RII. *Surgery* 2003; **134**: 772-782
- Belotti D**, Paganoni P, Manenti L, Garofalo A, Marchini S, Tarabozetti G, Giavazzi R. Matrix metalloproteinases (MMP9 and MMP2) induce the release of vascular endothelial growth factor (VEGF) by ovarian carcinoma cells: implications for ascites formation. *Cancer Res* 2003; **63**: 5224-5229
- Li Q**, Dong X, Gu W, Qiu X, Wang E. Clinical significance of co-expression of VEGF-C and VEGFR-3 in non-small cell lung cancer. *Chin Med J* 2003; **116**: 727-730
- Qi JH**, Ebrahem Q, Moore N, Murphy G, Claesson-Welsh L, Bond M, Baker A, Anand-Apte B. A novel function for tissue inhibitor of metalloproteinases-3 (TIMP3): inhibition of angiogenesis by blockage of VEGF binding to VEGF receptor-2. *Nat Med* 2003; **9**: 407-415
- LeCouter J**, Lin R, Ferrara N. Endocrine gland-derived VEGF and the emerging hypothesis of organ-specific regulation of angiogenesis. *Nat Med* 2002; **8**: 913-917
- Riedel F**, Gotte K, Li M, Hormann K, Grandis JR. Abrogation of VEGF expression in human head and neck squamous cell carcinoma decreases angiogenic activity *in vitro* and *in vivo*. *Int J Oncol* 2003; **23**: 577-583
- Ferrara N**. Role of vascular endothelial growth factor in physiologic and pathologic angiogenesis: therapeutic implications. *Semin Oncol* 2002; **29**(6 Suppl 16): 10-14
- Bikfalvi A**, Bicknell R. Recent advances in angiogenesis, anti-angiogenesis and vascular targeting. *Trends Pharmacol Sci* 2002; **23**: 576-582
- Dvorak HF**. Vascular permeability factor/vascular endothelial growth factor: a critical cytokine in tumor angiogenesis and a potential target for diagnosis and therapy. *J Clin Oncol* 2002; **20**: 4368-4380
- Ferrara N**. VEGF and the quest for tumour angiogenesis factors. *Nat Rev Cancer* 2002; **2**: 795-803
- Hasan J**, Byers R, Jayson GC. Intra-tumoural microvessel den-

- sity in human solid tumours. *Br J Cancer* 2002; **86**: 1566-1577
- 32 **Chiarug V**, Ruggiero M, Magnelli L. Angiogenesis and the unique nature of tumor matrix. *Mol Biotechnol* 2002; **21**: 85-90
- 33 **Carmeliet P**, Jain RK. Angiogenesis in cancer and other diseases. *Nature* 2000; **407**: 249-257
- 34 **Yancopoulos GD**, Davis S, Gale NW, Rudge JS, Wiegand SJ, Holash J. Vascular-specific growth factors and blood vessel formation. *Nature* 2000; **407**: 242-248
- 35 **Sun LQ**, Cairns MJ, Saravolac EG, Baker A, Gerlach WL. Catalytic nucleic acids: from lab to applications. *Pharmacol Rev* 2000; **52**: 325-347
- 36 **Takagi Y**, Suyama E, Kawasaki H, Miyagishi M, Taira K. Mechanism of action of hammerhead ribozymes and their applications *in vivo*: rapid identification of functional genes in the post-genome era by novel hybrid ribozyme libraries. *Biochem Soc Trans* 2002; **30**(Pt 6): 1145-1149
- 37 **Blount KF**, Uhlenbeck OC. The hammerhead ribozyme. *Biochem Soc Trans* 2002; **30**(Pt 6): 1119-1122
- 38 **Amarzguioui M**, Prydz H. Hammerhead ribozyme design and application. *Cell Mol Life Sci* 1998; **54**: 1175-1202
- 39 **Pennati M**, Binda M, Colella G, Zoppe' M, Folini M, Vignati S, Valentini A, Citti L, De Cesare M, Pratesi G, Giacca M, Daidone MG, Zaffaroni N. Ribozyme-mediated inhibition of survivin expression increases spontaneous and drug-induced apoptosis and decreases the tumorigenic potential of human prostate cancer cells. *Oncogene* 2004; **23**: 386-394
- 40 **Weng DE**, Usman N. Angiozyme: a novel angiogenesis inhibitor. *Curr Oncol Rep* 2001; **3**: 141-146
- 41 **Brattstrom D**, Bergqvist M, Hesselius P, Larsson A, Wagenius G, Brodin O. Serum VEGF and bFGF adds prognostic information in patients with normal platelet counts when sampled before, during and after treatment for locally advanced non-small cell lung cancer. *Lung Cancer* 2004; **43**: 55-62
- 42 **Im SA**, Kim JS, Gomez-Manzano C, Fueyo J, Liu TJ, Cho MS, Seong CM, Lee SN, Hong YK, Yung WK. Inhibition of breast cancer growth *in vivo* by antiangiogenesis gene therapy with adenovirus-mediated antisense-VEGF. *Br J Cancer* 2001; **84**: 1252-1257

Edited by Kumar M Proofread by Xu FM

Auxiliary *en-bloc* liver-small bowel transplantation with partial pancreas preservation in pigs

Zhen-Yu Yin, Xiao-Dong Ni, Feng Jiang, Ning Li, You-Sheng Li, Xiao-Ming Wang, Jie-Shou Li

Zhen-Yu Yin, Xiao-Dong Ni, Feng Jiang, Ning Li, You-Sheng Li, Jie-Shou Li, Research Institute of General Surgery, School of Medicine, Nanjing University, Nanjing 210093, Jiangsu Province, China

Zhen-Yu Yin, Xiao-Ming Wang, Department of General Surgery, Zhongshan Hospital, Xiamen 361004, Fujian Province, China

Correspondence to: Zhen-Yu Yin, Department of General Surgery, Zhongshan Hospital, Xiamen 361004, Fujian Province, China. davidmd@sohu.com

Telephone: +86-592-2292045 **Fax:** +86-592-2212328

Received: 2003-8-30 **Accepted:** 2003-10-07

Abstract

AIM: The aim of this study was to describe an auxiliary combined liver-small bowel transplantation model with the preservation of duodenum, head of pancreas and hepatic biliary system in pigs. The technique, feasibility, security and immunosuppression were commented.

METHODS: Forty outbred long-white pigs were randomized into two groups, and the auxiliary composite liver/small bowel allotransplantations were undertaken in 10 long-white pigs in each group with the recipient liver preserved. Group A was not treated with immunosuppressive drugs while group B was treated with cyclosporine A and methylprednisolone after operation. The hemodynamic changes and amylase of body fluid (including blood, urine and abdominal drain) were analyzed.

RESULTS: The average survival time of the animals was 10 ± 1.929 d (6 to 25 d) in group A while more than 30 d in group B. The pigs could tolerate the hemodynamic fluctuation during operation and the hemodynamic parameters recovered to normal 2 h after blood reperfusion. The transient high amylase level was decreased to normal one week after operation and autopsy showed no pancreatitis.

CONCLUSION: Auxiliary *en-bloc* liver-small bowel transplantation with partial pancreas preservation is a feasible and safe model with simplified surgical techniques for composite liver/small bowel transplantation. This model may be used as a preclinical training model for clinical transplantation method, clinical liver-small bowel transplantation related complication research, basic research including immunosuppressive treatment, organ preservation, acute rejection, chronic rejection, immuno-tolerance and xenotransplantation.

Yin ZY, Ni XD, Jiang F, Li N, Li YS, Wang XM, Li JS. Auxiliary *en-bloc* liver-small bowel transplantation with partial pancreas preservation in pigs. *World J Gastroenterol* 2004; 10(10): 1499-1503

<http://www.wjgnet.com/1007-9327/10/1499.asp>

INTRODUCTION

Combined liver and small bowel transplantation (LSBT) is a

life-saving procedure in patients especially in children with intestinal failure and parenteral nutrition-related end-stage liver diseases^[1]. Recently, due to success in clinical technology and improvement of the operative modality, the American Health Care Financing Administration (HCFA) has granted combined liver-intestinal transplantation as the standard therapeutic modality for patients with irreversible intestinal failure^[2]. Patients undergoing composite liver-small bowel transplantation are mostly children. As conventional LSBT requires a loop of defunctionalized (Roux) allograft small bowel for biliary drainage^[3], its posttransplant biliary complications including anastomotic leaks and obstruction in 12% of cases, were significantly related with morbidity and mortality^[4]. In addition, the conventional composite transplantation needs more vascular anastomoses which would lead not only to more complications including vascular thrombosis but also more difficulties of the surgical techniques. In the present study, we described an auxiliary transplantation technique for LSBT by preserving duodenum, partial head of pancreas and hepatobiliary system in pigs. Experience with this technique and the immunosuppressive treatment for LSBT in pig has not been reported in the literature.

MATERIALS AND METHODS

Forty outbred long-white pigs weighing 20 - 40 kg were divided into 2 groups with random sex, and 10 LSBTs were undertaken in each group. The weight of the donor was generally lower than that of the corresponding recipient. Group A was not treated with immunosuppressive drugs while group B was treated by immunosuppressive therapy consisting of cyclosporine A and methylprednisolone after operation.

The animals were not allowed to eat for 24 h and to drink for 4 h before operation respectively. Gut decontamination was attempted in all donors with an oral antibiotic preparation 3 d before surgery.

After anesthesia with 25 mg/kg of intravenous pentobarbital sodium, the animals were intubated and mechanically ventilated with a mixture of oxygen, nitrous oxide and isoflurane. In addition, standard intravenous antibiotic prophylaxis was instituted with cefotaxime at the time of surgery.

Initial exposure and isolation of abdominal organs

The procurement varied in details but followed the standard techniques for human multiorgan retrieval and our previous report^[5-8].

Briefly, the proximal 3 to 4 m of jejunum (the total length of porcine small bowel is about 15 m) together with the liver was procured as the graft. After the redundant small bowel and the dissociative colon were removed from the operative field, the duodenum, proximal jejunum and aorta could be well exposed. An extensive Kocher maneuver allowed visualization of the inferior vena cava and its branch. The subhepatic vena cava was dissected and encircled. The left and right renal veins were ligated respectively. The superior mesenteric and celiac arteries were identified after extending dissection of the aorta. The right and left renal arteries were then isolated and ligated. The subrenal aorta was isolated and encircled distally for the

eventual insertion of an infusion cannula. The abdominal aorta was also encircled above the celiac axis for later crossclamping when cold fluid was infused through the distal aortic cannula^[9]. The splenic vein was then freed and prepared for portal perfusion cannulation after division of the splenic artery. The splenic vein should be well protected when dividing the splenic artery^[10].

In situ cooling and removal of organs

After completion of the preliminary dissection and collection of the donor's blood, the liver and small bowel connected by the portal vein and aortic segment were lavaged *in situ* with UW solution (Figure 1). The donor was fully heparinized and the previously encircled proximal aorta was crossclamped, and the distal donor aorta was cannulated with infusion of cold UW solution. For simultaneous portal venous infusion, a venous cannula was placed into the splenic vein and infused with the UW solution. The intrapericardial inferior vena cava and subhepatic vena cava were transected to decompress the infused solution as in other reports^[11,12]. The amount of infusion was variable (50-100 mL/kg). After infusion, the graft containing liver, hepatic hilus, pancreatic-duodeno complex, spleen together with splenic vein, and small bowel was achieved with preservation of a segment of aorta containing the superior mesenteric artery and celiac trunk in continuity. The intestine was entrapped by stapling its two ends and carried with the specimen throughout the preservation. Thus the graft was *en bloc* removed and stored in UW solution at 0 to 4 °C.

Back table procedure was performed in the cold UW solution. It included suturing the orifice of suprahepatic vena cava and the proximal end of the aorta. The spleen was removed. The body and tail of the pancreas along the portal vein were isolated and transected, leaving partial pancreatic head attached to the allograft duodenum. This preserved the superior and inferior pancreatic duodenal arcades. The stump of the pancreas was stapled and then oversewn with a running suture using 4-0 polypropylene.

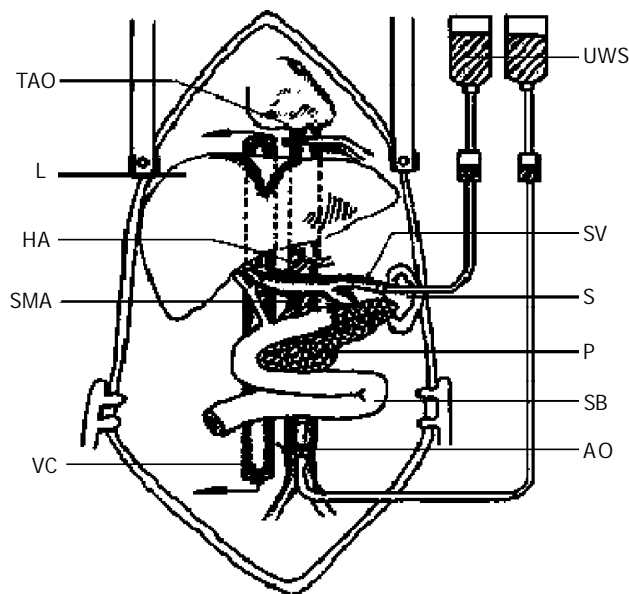


Figure 1 Infusion of grafts, (UWS=UW solution, SV=splenic vein, S=spleen, P=pancreas, SB=small bowel, AO=abdominal aorta, TAO=thoracic aorta, L=liver, HA=hepatic artery, SMA=supermesenteric artery, VC=vena cava).

Recipient operation

After anesthesia, a monitor was placed on the recipient. Two venous catheters (with one Swan-Ganz catheter) were inserted

for transfusion and hemodynamic parameters including central venous pressure (CVP), right ventricle pressure (VP), cardiac output (CO), pulmonary artery wedge pressure (PAWP) at the time of preoperation, the time just before blood reperfusion, 5 min, 30 min, 1 h and 2 h after blood reperfusion. The arterial blood pressure was monitored through a femoral artery catheter. The amylase levels of the blood, urine and abdominal drainage postoperative d 1, 3, 5, 7 were collected (determined by Somogyi method).

When the recipient's abdomen was opened, the dissociative colon and its mesentery were dissected and removed to ensure enough celiac space for the composite graft. Then, the end of the ascending colon and the end of the ileum were anastomosed directly to maintain the gastroenterologic continuity of the recipient.

The subrenal aorta was exposed and encircled 2 cm under the renal artery. Small arterial and lymphatic vessels along the aorta were ligated to avoid later bleeding or lymphorrhea. Subhepatic vena cava was also dissected and encircled. The subrenal vena cava was used for the donor out-flow anastomosis.

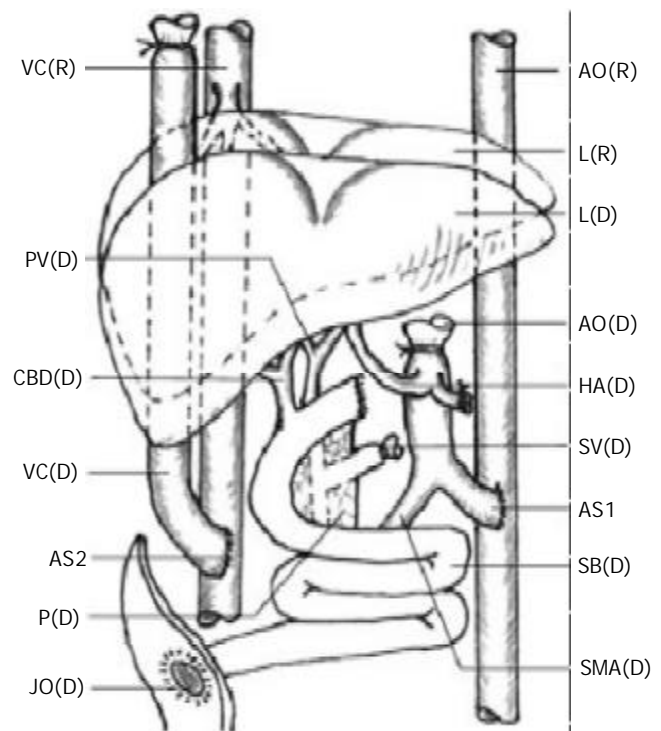


Figure 2 Auxiliary en-bloc liver-small bowel transplantation, (D=donor, R=recipient, AO=aorta, L=liver, HA=hepatic artery, SV= splenic vein, SB=small bowel, SMA=supermesenteric artery, VC= vena cava, PV=portal vein, CBD=common bile duct, P=pancreas, JO=jejunum ostomy, AS1=aorta-aorta anastomosis, AS2=vena cava- vena cava anastomosis).

Graft implantation and revascularization

The transplantation methods varied in details but followed the principles as described previously^[6,8] (Figure 2).

The arterial inflow was created via an end-to-side anastomosis of the graft aorta to the subrenal native aorta with a running polypropylene suture. Donor and recipient vena cava were anastomosed end to side. The venous outflow was the anastomosis of the end of the graft subhepatic vena cava to the side of the native subhepatic vena cava.

Before reperfusion, unclamping and perfusion of the allograft liver were achieved after a lavage of 300 to 500 mL donor blood or Ringer's solution through the splenic vein. The end of the spleen vein was ligated after the lavage.

The proximal duodenum was closed. A jejunostomy was

made at the end of donor distal intestine for early decompression and surveillance endoscopy as described in some clinical reports^[13,14].

After operation, the animals were returned to the monitor room, where hemodynamic monitoring and mechanical ventilation were performed as needed 24 h after operation. Due to the high rate of inflammatory complications, broad-spectrum antibacterial prophylaxis was administered for 5 d. Lactated Ringer's solution and parenteral nutrition were given daily for 2 d after operation.

Immunosuppressive drugs were used in the pigs of group B. Cyclosporine A was started at 15 mg/kg·d by venous injection in the first week, then reduced to 5 mg/kg·d from the second week as maintenance treatment. Methylprednisolone, used for induction and maintenance, was started with 500 mg at the first 24 h postoperation, reduced by 50% to about 2 mg/kg·d for the first week, then reduced by 50% on d 8 and again on day 15.

The survived animals were sacrificed for autopsy 30 d after operation.

RESULTS

After reperfusion, the liver was soft and pink with bile production, evidenced by jejunostomy drainage. If the liver was harder than normal, the outflow of the liver might be obstructed and the vena cava anastomosis needed to be checked. The small bowel should be perfused well, with good mesenteric arterial inflow and venous outflow. The peristalsis and intraluminal mucus production were evident within 15 min after reperfusion.

During the first three days, the intestinal graft stoma appeared healthy, and the mucosa was pink, moist, and well vascularized. No intestinal edema was found in most cases with output of bile-stained stool.

Histopathologic studies of the grafts showed no significant preservation injury. None of the biopsies obtained in the first postoperative week had histological evidence of submucosal bacterial invasion. The frequent cause of death of the pigs in group A was postoperative rejection evidenced by graft pathological examinations when the animal was dead.

Animals died 24 h after reperfusion were ruled out from the statistic series. One pig died because of operative techniques in group A, and all other animals in groups A and B lived for more than 24 h. The average survival time was 10.33±1.929 d (6 to 25 d) in group A while more than 30 d in group B. The difference was significant by Student's *t* test (*P*<0.01).

The hemodynamic changes are shown in Table 1. The results suggested that all hemodynamic parameters including CVP, CO, VP and PAWP were decreased during operation, but recovered very quickly after blood reperfusion, and returned to normal 2 h after blood reperfusion as shown in Figure 3.

Neither the duodenal allografts had signs of ischemia or stump leakage, nor any biliary complication. Blood, urine and abdominal drains were monitored serially for amylase level. Chemical pancreatitis was observed during the early postoperative period with amylase-rich fluid drainage.

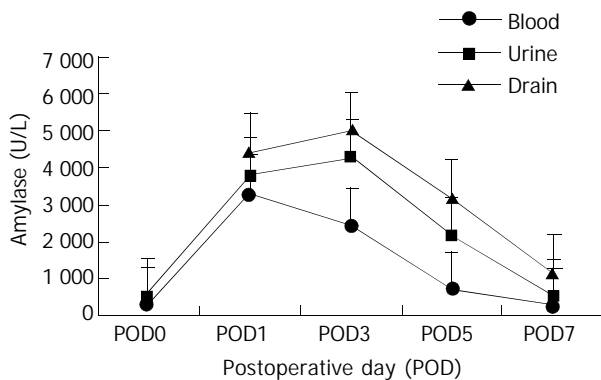


Figure 3 Postoperative amylase changes.

Table 1 Postoperative amylase in body fluid (U/L)

POD	0	1	3	5	7
Blood	329.60±28.31	3 314.70±415.29	2 448.60±413.53	718.70±103.61	327.70±27.58
Urine	514.80±55.67	3 404.80±335.96	4 307.40±429.16	2 187.00±148.43	491.40±48.80
Drain	---	4 444.80±545.67	5 023.80±472.64	3 217.20±213.91	1 177.10±98.12

POD=postoperative day.

Table 2 Hemodynamics changes

Time	N	preRP	RP5	RP30	RP60	RP120
CVP (cmH ₂ O)	14.80±0.42	13.00±0.49	10.20±1.07	9.50±0.27	9.90±0.37	14.00±0.36
VP (cmH ₂ O)	33.70±2.09	31.70±2.64	27.70±1.93	24.60±1.65	27.30±1.71	32.60±1.92
PAWP (cmH ₂ O)	16.70±0.59	13.40±0.40	16.30±0.52	14.10±0.41	15.90±0.46	17.20±0.44
CO (L/min)	4.48±0.15	3.36±0.22	4.27±0.15	3.98±0.15	4.23±0.15	4.59±0.16

CVP=central venous pressure, VP=ventricle pressure, PAWP=pulmonary artery wedge pressure, CO=cardiac output, N=normal, preRP=pre-reperfusion, RP5=5 min after reperfusion, RP30=30 min after reperfusion, RP60=60 min after reperfusion, RP120=120 min after reperfusion.

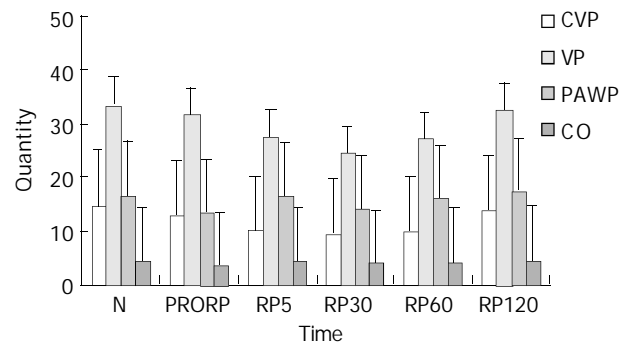


Figure 4 Hemodynamic changes.

and returned to preoperative level after one week as shown in Figure 4. Postoperative biopsy showed no sign of pancreatitis and also autopsy did not show any evidence of severe pancreatitis or calcification. Autopsy of the pigs in group B showed no evidence of graft rejection.

DISCUSSION

Total parenteral nutrition (TPN) for short bowel syndrome would induce end-stage liver diseases. In considering intestinal transplantation for treatment, 60% to 70% them required simultaneous liver allografts^[4,7]. Although many clinical liver/small bowel transplantations (LSBT) were reported from different medical centers^[15-17], it remains an experimental procedure^[18]. Although large animals that share physiological and anatomical similarities with humans, comparing to the widely used rat LSBT model^[19,20], large animal models such as LSBT in pigs and its related research were rarely reported.

Feasibility and benefits of auxiliary composite liver-small bowel transplantation model

As compared to the five anastomoses in conventional composite liver-small bowel transplantation including suprahepatic vena cava anastomosis, subhepatic vena cava anastomosis, hepatic artery anastomosis, portal vein anastomosis and bile duct anastomosis, only two anastomoses including aorta-aorta anastomosis and subhepatic vena cava anastomosis were needed in the auxiliary composite liver-small bowel transplantation model. This model could not only decrease possible complications related to the anastomoses such as bleeding, vascular obstruction, postoperative thromboses and bile leakage, but also simplify the surgical techniques. In this model, the vena cava anastomosis was modified by replacing the major hepatic vein (or suprahepatic vena cava) anastomosis in classical Piggy-back transplantation by the subhepatic vena cava anastomosis. This modification has at least two advantages in porcine LSBT. One is that subhepatic vena cava anastomosis can be easily performed, the other is that subhepatic vena cava anastomosis can adjust a flexible anastomotic interval to ensure the aorta-aorta anastomosis easier.

In clinical practice, Abu-Elmagd suggested that LSBT with preservation of pancreatic head and duodenum had some advantages including avoidance of biliary complications and simplification of the operative procedure^[20]. These possible advantages were also shown in animal LSBT.

The LSBT transplant procedure is a much more arduous surgical endeavor. The technique of retaining duodenum and the head of pancreas would simplify the back table preparation and avoid risks associated with dissection of the donor hepatic hilus.

Retrieval for composite grafts using the standard technique involved an obligatory reconstruction of the biliary system with a defunctionalized loop of proximal allograft jejunum^[3]. In this porcine LSBT model, no biliary reconstruction was required, so that the source of complications such as bile leakage, biliary tract stricture or even death of recipient could be avoided. Liver transplantation related biliary complication rate was about 12%, which would result in about 19% of mortality^[21,22]. LSBT with preservation of partial pancreas and duodenum would remarkably decrease such complications.

The potential benefits of any intestinal segment which was kept in direct continuity with alimentary tract freeing the pig for TPN would be enhanced without donor or recipient bowel for Roux-en-Y biliary reconstruction. The advantage of the composite technique was to maintain the hepatic hilus. The use of liver artery and superior mesenteric artery with a large arterial conduit would minimize the risk of hepatic artery thrombosis compared to isolated graft^[13,23].

Safety of porcine auxiliary LSBT with pancreatic head and duodenum

The porcine retrohepatic vena cava is passing through the liver parenchyma with numerous small hepatic veins in this segment besides the major hepatic veins. It is dangerous to remove the liver parenchyma by dissecting the retrohepatic vena cava with high risk of fetal blood loss. This is the reason why the classic piggyback liver transplantation is not suitable in pig. Typical orthotopic liver transplantation in combined LSBT needs not only blood shunt during operation but also a segment of additional artery to prolong the aorta to ensure the arterial anastomosis in pigs. Auxiliary LSBT could avoid the disadvantages of these transplantations.

In conventional composite liver-small bowel transplantation, blood shunt was always needed in the process of vascular exclusion. In pigs, this was much more important because the blood passing through portal vein was accounted for more than 60% of the total porcine blood. The vascular exclusion would lead to sudden cardiac failure and death of the pigs. Auxiliary composite liver-small bowel transplantation model with partial vascular exclusion during the vascular anastomosis did not lead to irreversible hemodynamic changes that would occur without blood shunt. This method would also avoid other possible hemodynamic damages such as kidney injuries, postoperative thrombosis and ischemia of the lower limb.

Inclusion of duodenum and pancreatic head to maintain continuity of the biliary system was associated with early postoperative allograft pancreatitis, but no significant mortality was reported^[24]. This complication was also found in our study. It could be detected by measuring amylase and lipase in peritoneal fluid from abdominal drains, blood and urine^[25]. In our study, chemical pancreatitis as shown in the experiment was always transient. The elevated amylase level would return to normal within one week and autopsy showed no signs of severe pancreatitis. At present, the following measures could be considered to protect the allografted pancreas from postoperative pancreatitis, namely to limit the amount and pressure of the cold solution used in perfusion^[3], to procure the pancreas *en-bloc* with the graft and avoid over-dissection of the tissue and vessels around duodenum and pancreas^[26], to ligate the pancreatic duct and suture the pancreatic interface efficiently and definitely.

Immunosuppressive treatment of auxiliary LSBT pigs

The optimal immunosuppressive treatment was not determined in big organ transplantations. Triple drugs (cyclosporine or FK506, azathioprine and prednisolone) and quadruple drugs (ATG, cyclosporine or FK506, azathioprine and prednisolone) treatment in pig transplantation were reported in the literature^[27-29]. But the optimal dose of immunosuppressive drugs was ascertained in previous reports. The suggested dose of cyclosporine was from 3 mg/kg·d to 25 mg/kg·d by IV or SB injection^[27,28,30,31]. Some reports indicated that pigs required a higher dose of cyclosporine than humans to prevent allograft rejection in thymus transplantation^[32]. Other authors suggested that immunosuppressive protocols that were successful in preventing allograft rejection in humans had no long-term effect on allografted pigs and the dose of most immunosuppressive agents administered to control rejection in pigs should be higher than that used in humans^[33]. This might be due to differences of absorption, binding, metabolism and excretion of the drugs in pigs. So we used the maintenance dose of CsA 5 mg/kg·d after a loading dose of 15 mg/kg·d, and the composite transplanted liver small bowel graft with preservation of pancreas head could be protected by CsA and methylprednisolone against acute rejection.

Some reports suggested that LSBT with preservation of duodenum and pancreatic head would neither increase the possibility of rejection nor require more immunosuppressive

treatment than standard LSBT without preservation of pancreas and duodenum^[13,23]. The presence of allograft pancreas in multivisceral allografts was not an important risk factor for mortality, and the incidence of rejection of pancreatic was only 12% in some report^[13]. So the technique with preservation of the pancreas should be considered safe in composite LSBT.

In summary, auxiliary en-bloc liver-small bowel transplantation with partial pancreas preservation is a feasible and safe model with simplified surgical techniques for composite liver/small bowel transplantation in pigs. This model might be used as a preclinical training model for clinical transplantation method, clinical liver-small bowel transplantation related complication research, basic research including immunosuppressive treatment, organ preservation, acute rejection, chronic rejection, immuno-tolerance and xenotransplantation research.

REFERENCES

- 1 **Lacaille F**, Canioni D, Fournet JC, Revillon Y, Cezard JP, Goulet O. Centrilobular necrosis in children after combined liver and small bowel transplantation. *Transplantation* 2002; **73**: 252-257
- 2 **Abu-Elmagd K**, Bond G. The current status and future outlook of intestinal transplantation. *Minerva Chir* 2002; **57**: 543-560
- 3 **Furukawa H**, K Abu-Elmagd K, Reyes JL. Technical aspects of intestinal transplantation, in: Braverman MH, Tawas RL, (eds): Surgical Technology International II, San Francisco CA. *TF Laszlo* 1994: 165-170
- 4 **Reyes J**, Bueno J, Kocoshis S, Green M, Abu-Elmagd K, Furukawa H, Barksdale EM, Strom S, Fung JJ, Todo S, Irish W, Starzl TE. Current status of intestinal transplantation in children. *J Pediatr Surg* 1998; **33**: 243-254
- 5 **Starzl TE**, Todo S, Tzakis A, Alessiani M, Casavilla A, Abu-Elmagd K, Fung JJ. The many faces of multivisceral transplantation. *Surg Gynecol Obstet* 1991; **172**: 335-344
- 6 **Casavilla A**, Selby R, Abu-Elmagd K, Tzakis A, Todo S, Reyes J, Fung J, Starzl TE. Logistics and technique for combined hepatic-intestinal retrieval. *Ann Surg* 1992; **216**: 605-609
- 7 **Williams JW**, Sankary HN, Foster PF. Technique for splanchnic transplantation. *J Pediatr Surg* 1991; **26**: 79-81
- 8 **Yin ZY**, Ni XD, Jiang F, Li N, Li YS, Li JS. Modified technique for combined liver-small bowel transplantation in pigs. *World J Gastroenterol* 2003; **9**: 1625-1628
- 9 **Abu-Elmagd K**, Fung J, Bueno J, Martin D, Madariaga JR, Mazariegos G, Bond G, Molmenti E, Corry RJ, Starzl TE, Reyes J. Logistics and technique for procurement of intestinal, pancreatic, and hepatic grafts from the same donor. *Ann Surg* 2000; **232**: 680-687
- 10 **de Ville de Goyet J**, Mitchell A, Mayer AD, Beath SV, McKiernan PJ, Kelly DA, Mirza D, Buckles JA. En block combined reduced-liver and small bowel transplants: from large donors to small children. *Transplantation* 2000; **69**: 555-559
- 11 **Starzl TE**, Hakala TR, Shaw BW Jr, Hardesty RL, Rosenthal TJ, Griffith BP, Iwatsuki S, Bahnson HT. A flexible procedure for multiple cadaveric organ procurement. *Surg Gynecol Obstet* 1984; **158**: 223-230
- 12 **Starzl TE**, Miller C, Bronznick B, Makowka L. An improved technique for multiple organ harvesting. *Surg Gynecol Obstet* 1987; **165**: 343-348
- 13 **Reyes J**, Fishbein J, Bueno J, Mazariegos G, Abu-Elmagd K. Reduced-size orthotopic composite liver-intestinal allograft. *Transplantation* 1998; **66**: 489-492
- 14 **Todo S**, Tzakis AG, Abu-Elmagd K, Reyes J, Fung JJ, Casavilla A, Nakamura K, Yagihashi A, Jain A, Murase N. Cadaveric small bowel and small bowel-liver transplantation in humans. *Transplantation* 1992; **53**: 369-376
- 15 **Grant D**. London health sciences centre, ontario, canada. Intestinal transplantation: 1997 report of the international registry. Intestinal transplant registry. *Transplantation* 1999; **67**: 1061-1064
- 16 **Todo S**, Reyes J, Furukawa H, Abu-Elmagd K, Lee RG, Tzakis A, Rao AS, Starzl TE. Outcome analysis of 71 clinical intestinal transplantations. *Ann Surg* 1995; **222**: 270-280
- 17 **Goulet O**, Jan D, Sarnacki S, Brousse N, Colomb V, Salomon R, Cuenod B, Piloquet H, Ricour C, Revillon Y. Isolated and combined liver-small bowel transplantation in Paris: 1987-1995. *Transplant Proc* 1996; **28**: 2750
- 18 **Muiesan P**, Dhawan A, Novelli M, Mieli-Vergani G, Rela M, Heaton ND. Isolated liver transplant and sequential small bowel transplantation for intestinal failure and related liver disease in children. *Transplantation* 2000; **11**: 2323-2326
- 19 **Zhong R**, He G, Sakai Y, Zhang Z, Garcia B, Li XC, Jevnikar A, Grant D. The effect of donor-recipient strain combination on rejection and graft-versus-host disease after small bowel/liver transplantation in the rat. *Transplantation* 1993; **56**: 381-385
- 20 **Li XC**, Zhong R, He G, Sakai Y, Garcia B, Jevnikar A, Grant D. Host immune suppression after small bowel/liver transplantation in rats. *Transpl Int* 1994; **7**: 131-135
- 21 **Lopez RR**, Benner KG, Ivancev K, Keeffe EB, Deveney CW, Pinson CW. Management of biliary complications after liver transplantation. *Am J Surg* 1992; **163**: 519-524
- 22 **Greif F**, Bronsther OL, Van Thiel DH, Casavilla A, Iwatsuki S, Tzakis A, Todo S, Fung JJ, Starzl TE. The incidence, timing, and management of biliary tract complications after orthotopic liver transplantation. *Ann Surg* 1994; **219**: 40-45
- 23 **Bueno J**, Abu-Elmagd K, Mazariegos G, Madariaga J, Fung J, Reyes J. Composite liver-small bowel allografts with preservation of donor duodenum and hepatic biliary system in children. *J Pediatr Surg* 2000; **35**: 291-296
- 24 **Casavilla A**, Selby R, Abu-Elmagd K, Tzakis A, Todo S, Starzl TE. Donor selection and surgical technique for en bloc liver-small bowel graft procurement. *Transplant Proc* 1993; **25**: 2622-2623
- 25 **Abu-Elmagd K**, Reyes J, Todo S, Rao A, Lee R, Irish W, Furukawa H, Bueno J, McMichael J, Fawzy AT, Murase N, Demetris J, Rakela J, Fung JJ, Starzl TE. Clinical intestinal transplantation: new perspectives and immunologic considerations. *J Am Coll Surg* 1998; **186**: 512-527
- 26 **Kato T**, Romero R, Verزارo R, Misiakos E, Khan FA, Pinna AD, Nery JR, Ruiz P, Tzakis AG. Inclusion of entire pancreas in the composite liver and intestinal graft in pediatric intestinal transplantation. *Pediatr Transplant* 1999; **3**: 210-214
- 27 **Gruessner RW**, Fasola C, Fryer J, Nakhleh RE, Kim S, Gruessner AC, Beebe D, Moon C, Troppmann C, Najarian JS. Quadruple Immunosuppression in a pig model of small bowel transplantation. *J Surg Res* 1996; **61**: 260-266
- 28 **McCurry KR**, Parker W, Cotterell AH, Weidner BC, Lin SS, Daniels LJ, Holzkecht ZE, Byrne GW, Diamond LE, Logan JS, Platt JL. Humoral responses to pig-to-baboon cardiac transplantation: implications for the pathogenesis and treatment of acute rejection and for accommodation. *Hum Immunol* 1997; **58**: 91-105
- 29 **Wennberg L**, Groth CG, Tibell A, Zhu S, Liu J, Rafael E, Soderlund J, Biggerfeld P, Morris RE, Karlsson-Parra A, Korsgren O. Triple drug treatment with cyclosporine, leflunomide and mycophenolate mofetil prevents rejection of pig islets transplanted into rats and primates. *Transplant Proc* 1997; **29**: 2498
- 30 **Alvira LG**, Herrera N, Salas C, Pereira F, Herrera J, Sua' rez-Massa MD, Castillo-Olivares JL. Influence of cyclosporine on graft regeneration and function after liver transplantation: trial in pigs. *Trans Proc* 2002; **34**: 315-316
- 31 **Biffi R**, Privitera G, Matinato C, Pozzi S, Marzona L, De Ral P, Andreoni B, Tiberio G, Frezza E, Van Thiel DH. Parenteral antibiotics and selective intestinal decontamination do not prevent enteric bacterial overgrowth or translocation observed in a swine model of small bowel transplantation. *J Surg Res* 1995; **58**: 391-394
- 32 **Tuch BE**, Wright DC, Martin TE, Keogh GW, Deol HS, Simpson AM, Roach W, Pinto AN. Differentiation of fetal pig endocrine cells after allografting into the thymus gland. *Transplantation* 1999; **67**: 1184-1187
- 33 **Wright DC**, Deol HS, Tuch BE. A comparison of the sensitivity of pig and human peripheral blood mononuclear cells to the antiproliferative effects of traditional and newer immunosuppressive agents. *Transpl Immunol* 1999; **7**: 141-147

Biochemical and radiological predictors of malignant biliary strictures

Ibrahim A. Al-Mofleh, Abdulrahman M. Aljebreen, Saleh M. Al-Amri, Rashed S. Al-Rashed, Faleh Z. Al-Faleh, Hussein M. Al-Freih, Ayman A. Abdo, Arthur C. Isnani

Ibrahim A. Al-Mofleh, Abdulrahman M. Aljebreen, Saleh M. Al-Amri, Rashed S. Al-Rashed, Faleh Z. Al-Faleh, Hussein M. Al-Freih, Ayman A. Abdo, Gastroenterology Division, department of Medicine (38), King Khalid University Hospital, Riyadh, Kingdom of Saudi Arabia
Arthur C. Isnani, King Khalid University Hospital, College of Medicine and Research Center (74), PO Box 2925, Riyadh 11461, Kingdom of Saudi Arabia

Correspondence to: Professor Ibrahim A. Al-Mofleh, Gastroenterology Division, Department of Medicine (38), King Khalid University Hospital, PO Box 2925, Riyadh 11461, Kingdom of Saudi Arabia

Telephone: +966-467-1215 **Fax:** +966-467-1217

Received: 2003-11-22 **Accepted:** 2004-01-09

Abstract

AIM: Differentiation of benign biliary strictures (BBS) from malignant biliary strictures (MBS) remains difficult despite improvement in imaging and endoscopic techniques. The aim of this study was to identify the clinical, biochemical and or radiological predictors of malignant biliary strictures.

METHODS: We retrospectively reviewed all charts of patients who had biliary strictures (BS) on endoscopic retrograde cholangiopancreatography (ERCP) or percutaneous cholangiography (PTC) in case of unsuccessful ERCP from March 1998 to August 2002. Patient characteristics, clinical features, biochemical, radiological and biopsy results were all recorded. Stricture etiology was determined based on cytology, biopsy or clinical follow-up. A receiver operator characteristic (ROC) curve was constructed to determine the optimal laboratory diagnostic criterion threshold in predicting MBS.

RESULTS: One hundred twenty six patients with biliary strictures were enrolled, of which 72 were malignant. The mean age for BBS was 53 years compared to 62.4 years for MBS ($P=0.0006$). Distal bile duct stricture was mainly due to a malignant process 48.6% vs 9% ($P=0.001$). Alkaline phosphates and AST levels were more significantly elevated in MBS ($P=0.0002$). ROC curve showed that a bilirubin level of 84 $\mu\text{mol/L}$ or more was the most predictive of MBS with a sensitivity of 98.6%, specificity of 59.3% and a positive likelihood ratio of 2.42 (95% CI=0.649-0.810). Proximal biliary dilatation was more frequently encountered in MBS compared to BBS, 73.8% vs 39.5% ($P=0.0001$). Majority of BBS (87%) and MBS (78%) were managed endoscopically.

CONCLUSION: A serum bilirubin level of 84 $\mu\text{mol/L}$ or greater is the best predictor of MBS. Older age, proximal biliary dilatation, higher levels of bilirubin, alkaline phosphatase, ALT and AST are all associated with MBS. ERCP is necessary to diagnose and treat benign and malignant biliary strictures.

Al-Mofleh IA, Aljebreen AM, Al-Amri SM, Al-Rashed RS, Al-Faleh FZ, Al-Freih HM, Abdo AA, Isnani AC. Biochemical and radiological predictors of malignant biliary strictures. *World J Gastroenterol* 2004; 10(10): 1504-1507

<http://www.wjgnet.com/1007-9327/10/1504.asp>

INTRODUCTION

Biliary stricture (BS) may result from an intra or extra-luminal benign or malignant process. Although history, laboratory investigations and imaging techniques may help to differentiate benign from malignant biliary strictures, it remains a clinical challenge. Endoscopic retrograde cholangiopancreatography (ERCP) has been considered the method of choice for the diagnosis of BS as a result of its accuracy in establishing the site and cholangiographic features of stricture^[1]. Cytology specimens can be obtained, which has a sensitivity rate of only 35% but a specificity rate approaching 100% for the diagnosis of malignancy^[2].

Recently, new imaging techniques with increased diagnostic yield have emerged. For instance, magnetic resonance cholangiopancreatography (MRCP) as a non-invasive method has similar or even better diagnostic yield with the advantage of avoiding complications of ERCP^[1,3,4]. Also, with the advent of multislice CT (MS-CT), it has been possible to detect minute biliary and pancreatic tumours as well as small lymph nodes and vessels^[5]. MS-CT cholangiography has become valuable in pre-operative evaluation and determining unresectability^[6]. Therefore, CT has maintained as the method of choice for pancreatic and biliary tumours imaging^[7,8]. Furthermore, intraductal ultrasonography (IDUS) has been valuable in the differentiation of MBS from BBS. It has increased the accuracy of ERC-tissue sampling, but it has not been suitable for staging lymphadenopathy-associated MBS^[8].

The aim of this study was to identify the clinical, biochemical and or radiological predictors of malignant biliary strictures.

MATERIALS AND METHODS

All patients with biliary strictures from March 1998 to August 2002 who had ERCP or PTC in case of unsuccessful ERCP were included. Demographic characteristics, presenting features, laboratory data, imaging technique findings and management modalities were analyzed.

Definition of biliary strictures was suggested by cholangiographic features and it was supported by brush cytology, fine needle aspiration (FNA), the presence of mass or metastases by imaging and or clinical follow-up.

ERCP was performed by three experienced gastroenterologists using 4.2 mm channel duodenoscopes (Pentax or Olympus). All patients received diazepam and demerol as premedication. In addition, patients with biliary dilatation received cefuroxime prophylaxis. Endoscopic and cholangiographic findings were recorded.

Biopsy and brushing materials were obtained when feasible, strictures dilated with balloon or Soehendra dilator and large 10-12 F stent inserted.

Data collected were entered into the computer using Microsoft Excel. After all data were checked for completeness, statistical analysis was performed using Stat Pac gold analysis software and Microsoft Excel programs. Two-tailed P values of less than 0.05 were considered statistically significant. A receiver operator characteristic (ROC) curve was constructed

to determine the optimal laboratory diagnostic criterion threshold (*i.e.* total bilirubin, ALT, AST and alkaline phosphatase) in predicting a malignant biliary stricture. A ROC curve displayed the false positive rate on the x axis (specificity), and the true positive rate on the y axis (sensitivity) for varying test thresholds, thus plotting the performance of a diagnostic test^[10]. The ideal cut-off criteria for the laboratory results were chosen by determining the point lying geometrically closest to an ideal test with 100% specificity and sensitivity^[11].

RESULTS

One hundred twenty six patients were included, 54 of those had a BBS while 72 had a MBS. The main causes of BBS were related to stone disease (choledocholithiasis, Mirizzi syndrome or postcholecystectomy). In 22 patients the cause could not be identified. Cholangiocarcinoma and pancreatic head carcinoma were the most common causes of MBS. Other causes of BS are shown in Table 1.

The mean age of patients with MBS (62.4±11.7 years) was significantly higher than that of patients with BBS (53±18 years) ($P=0.0006$). Fifty percent of BBS were proximal ($P=0.01$) and approximately 50% of MBS were distal ($P<0.001$). There were no significant gender differences (Table 2). Jaundice was found in more than 80% of patients with BBS and MBS, and right upper quadrant (RUQ) pain in 50% of patients. Anorexia, weight loss and fever were less common and no significant differences were observed when both groups were compared (Table 3).

Table 1 Causes of biliary strictures ($n=126$)

Benign	<i>n</i>	%	Malignant	<i>n</i>	%
Choledocholithiasis	12	22	Cholangiocarcinoma	31	43
Mirizzi syndrome	7	13	Pancreatic head CA	23	32
Postcholecystectomy	6	11	Ampullary CA	5	7
Sclerosing cholangitis	3	5.5	Gallbladder CA	5	7
Choledochal cyst	2	3.7	Metastatic CA	4	5.5
Chronic pancreatitis	1	1.9	Hepatocellular CA	2	2.7
Juxtapapillary diverticulum	1	1.9	Lymphoma	2	2.7
Non-specified	22	40.7			
TOTAL	54		TOTAL	72	

Table 2 Demographic data of patients with biliary strictures ($n=126$)

	Benign	Malignant	<i>P</i> value
Number of patients	54 (%)	72 (%)	
Mean age	53±18	62.4±11.7	0.0006
Males	25 (46)	41 (56.9)	0.2255
Females	29 (54)	31 (43.1)	0.2255
Sites of biliary stricture			
Proximal	27 (50)	20 (27.7)	0.0107
Middle	22 (41)	17 (23.6)	0.0394
Distal	5 (9)	35 (48.6)	<0.001

Table 3 Presenting symptoms of patients with biliary strictures ($n=126$)

	Benign <i>n</i> =54 (%)	Malignant <i>n</i> =72 (%)	<i>P</i> value
Jaundice	44 (81)	61 (84.7)	0.5884
RUQ pain	27 (50)	38 (52.8)	0.7561
Weight loss	4 (7)	11 (15.3)	0.1326
Fever	3 (5)	7 (9.7)	0.3066
Anorexia	4 (7)	7 (9.7)	0.5843

Mean serum values of bilirubin, alkaline phosphatase, ALT and AST were significantly higher in patients with MBS. However GGT levels were not significantly different in both groups (Table 4).

As shown in Table 5 and Figure 1, ROC analysis identified total bilirubin of 84 $\mu\text{mol/L}$ as the best cut-off value for predicting a malignant biliary stricture with a sensitivity of 98.6%, a specificity of 59.3% and a positive likelihood ratio of 2.42 (area under the curve=0.735, SE=0.044, 95% CI=0.649-0.810). On the other hand, ROC analysis showed that other laboratory tests including ALT, AST and alkaline phosphates to have a poor sensitivity and specificity.

Proximal biliary dilatation was more frequently encountered in MBS compared to BBS, 73.8% vs 39.5% ($P=0.0001$). Majority of patients, 87% of BBS and 78% of MBS were treated endoscopically.

Table 4 Laboratory data of patients with biliary strictures ($n=126$)

	Benign <i>n</i> =54	Malignant <i>n</i> =72	<i>P</i> value
Total bilirubin ($\mu\text{mol/L}$)	142.6±98.4	184.61±120.8	0.0389
Direct bilirubin ($\mu\text{mol/L}$)	102.4±95.3	138.10±98.5	0.0433
Alkaline phosphatase (IU/L)	108.5±48.5	145.50±57.5	0.0002
GGT (IU/L)	397.0±496.5	436.50±325.1	0.591
ALT (IU/L)	52.7±38.3	66.94±35.6	0.0339
AST (IU/L)	76.5±43.2	107.80±45.7	0.0002

Table 5 Receiver operator characteristic (ROC) test results in predicting malignant biliary strictures

Parameter	Cut-off value	Sensitivity (%)	Specificity (%)	+LR	-LR
Total bilirubin ($\mu\text{mol/L}$)	84	98.6	59.3	2.42	0.02
Direct bilirubin ($\mu\text{mol/L}$)	63	91.7	61.1	2.36	0.14
Alkaline phosphatase (IU/L)	136	59.7	83.3	3.58	0.48
GGT (IU/L)	246	80.6	53.7	1.74	0.36
ALT (IU/L)	68	45.8	81.5	2.47	0.66
AST (IU/L)	85	76.4	74.1	2.95	0.32

+LR=positive likelihood ratio; -LR=negative likelihood ratio.

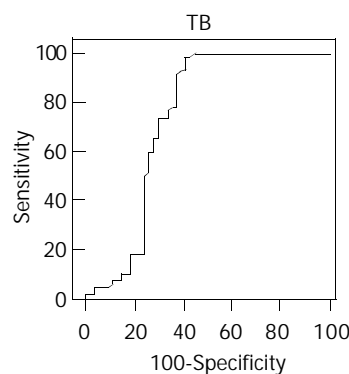


Figure 1 ROC analysis of total bilirubin.

DISCUSSION

The differentiation between benign and malignant biliary strictures can be difficult but is of obvious importance in regard to prognosis and planning optimal therapy.

In our study, majority of patients with BS presented with obstructive jaundice and half had right upper quadrant pain. Other less frequent symptoms included anorexia, weight loss and fever. In contrast to Tandon *et al*^[12], who have encountered more anorexia and weight loss in MBS, we found no significant difference between MBS and BBS. This could be due to the early stage at presentation in our patients.

In our study, although statistically significant differences were found in most biochemical parameters, bilirubin was the best predictor of malignant biliary stricture. A serum bilirubin level of 84 $\mu\text{mol/L}$ or greater was highly predictive of malignant biliary stricture with a sensitivity of 98.6%, a specificity of 59.3% and a positive likelihood ratio of 2.42. Furthermore, proximal biliary dilatation was more frequently encountered in MBS compared to BBS, 73.8% vs 39.5% ($P=0.0001$). Similarly, in a prospective study of 29 patients, Bain *et al.* have shown that a bilirubin of level of 75 $\mu\text{mol/L}$ or greater or a stricture length of greater than 14 mm was highly predictive of malignant biliary stricture. In the same study, intrahepatic duct dilatation was present in 93% of malignant strictures versus 36% of BBS ($P=0.002$)^[13].

In our study, we found that distal bile duct strictures were mainly due to a malignant process, 48.6% vs 9% in BBS ($P<0.001$), which is contrary to other studies. This is probably because we have rarely encountered BBS secondary to chronic pancreatitis which is commonly present with distal benign BS (we had only one patient).

ERCP remains to be an important imaging technique in the diagnosis and treatment of obstructive jaundice^[14]. The yield of ERCP in differentiating MBS from BBS can be further improved with tissue sampling. Sensitivity of biliary fluid and brushing cytology is unsatisfactorily low. It can be improved by combining fine needle aspiration biopsy with intraductal forceps biopsy. This method has been known as triple tissue sampling^[15,16]. Despite the triple tissue sampling, the sensitivity and negative predictive value have not exceeded 62% and 39%, respectively^[16]. Furthermore, brushing cytology yield could be improved by stricture brushing after a 10 F dilatation of malignant stricture^[17]. Similar observation on improvement of bile cytology has been reported earlier by Mohandas *et al*^[18]. Evaluation of cytology specimens for aneuploidy and tumour markers, CA 19-9 and CEA might also increase the diagnostic yield^[19].

Recently, intraductal ultrasonography (IDUS) has been evaluated in the differential diagnosis of MBS from BBS with conflicting results. While Gress *et al.* have not found reliable differentiation criteria^[20], Inui *et al.* and Tamada *et al.*, who used special biliary and pancreatic probes, have provided encouraging results^[21,22]. However, its accuracy is still not exceeding 80%. IDUS has been reported to be superior to conventional endoscopic ultrasonography in terms of diagnostic accuracy, and prediction of tumour respectability^[23].

Treatment of BS depends on the etiology, benign or malignant, magnitude of damage in post-surgical injuries and prediction of respectability of MBS. Endoscopic management of BBS has been considered the primary method before the decision of surgical intervention^[24]. Major bile duct injuries require surgical construction. After initial evaluation of anatomy by direct cholangiogram and inserting a biliary drain, surgical reconstruction with Roux-en-Y hepaticojejunostomy has been associated with an overall success rate exceeding 90%^[25]. It has been considered as the best treatment modality of BBS^[26]. On the other hand Born *et al.* have considered endoscopic or percutaneous management as an adequate short and long-term alternative to surgery^[27].

The decision of therapeutic modality for biliary or pancreatic tumours depends on the evaluation of respectability. It is important to determine preoperatively the spread of MBS. These events may help decide the appropriate treatment for

each condition. Surgery has to be considered for the management of resectable tumours. However, at the time when the diagnosis of MBS has been established, it is often late for curable resection^[28]. Therefore, endoscopic approach remains the method of choice for palliation. Majority of our patients (78%) had endoscopic palliation.

In a large series with 505 patients, Costamagna *et al.* strongly suggested ERCP in the diagnosis and palliation of all patients with suspected MBS^[29]. ERCP has been considered as the optimal technique for diagnosis and palliation of MBS^[30].

In conclusion, a serum bilirubin level of 84 $\mu\text{mol/L}$ or greater is the best predictor of MBS. Older age, proximal biliary dilatation, higher levels of bilirubin, alkaline phosphates, ALT and AST are all associated with MBS. ERCP is the best imaging technique in demonstrating stricture and biliary dilatation, and remains the method of choice in managing BBS and MBS.

REFERENCES

- 1 **Hawes RH.** Diagnostic and therapeutic uses of ERCP in pancreatic and biliary tract malignancies. *Gastrointest Endosc* 2002; **56**(6 Suppl): S201-205
- 2 **Scudera PL,** Koizumi J. Brush Cytology evaluation of lesions encountered during ERCP. *Gastrointest Endosc* 1990; **36**: 281-284
- 3 **Hall-Craggs MA,** Allen CM, Owens CM, Theis BA, Donald JJ, Paley M, Wilkinson ID, Chong WK, Hatfield AR, Lees WR. MR Cholangiography: Clinicalevaluation in 40 cases. *Radiology* 1993; **189**: 423-427
- 4 **Soto JA,** Barish MA, Yucel ED, Steinberg D, Ferucci JT, Chuttani R. Magnetic resonance cholangiography: Comparison with endoscopic retrograde cholangiography. *Gastroenterology* 1996; **110**: 589-597
- 5 **Kim HJ,** Kim MH, Lee SK, Yoo KS, Seo DW, Min YI. Tumour vessel: a valuable cholangioscopic clue of malignant biliary stricture. *Gastrointest Endosc* 2000; **52**: 635-638
- 6 **O' Malley ME,** Boland GW, Wood BJ, Fernandez-del-Castillo C, Warshaw AL, Meuller PR. Adenocarcinoma of the head of the pancreas: determination of surgical unresectability with thin section pancreatic-phase helical CT. *Am J Roentgenol* 1999; **173**: 1513-1518
- 7 **Cha JH,** Han JK, Kim TK, Kim AY, Park SJ, Choi BI, Suh KS, Kim SW, Han MC. Preoperative evaluation of Klatskin tumour: Accuracy of spiral CT in determining vascular invasion as a sign of unresectability. *Abdom Imaging* 2000; **25**: 500-507
- 8 **Mortele KJ,** Ji H, Ros PR. CT and magnetic resonance imaging in pancreatic and biliary tract malignancies. *Gastrointest Endosc* 2002; **56**(6 Suppl): S206-212
- 9 **Farell RJ,** Agarwal B, Brandwein SL, Underhill J, Chuttani R, Pleskow DK. Intraductal US is useful adjunct to ERCP for distinguishing malignant from benign biliary strictures. *Gastrointest Endosc* 2002; **56**: 681-687
- 10 **McNeil BJ,** Keller E, Adelstein SJ. Primer on certain elements of medical decision making. *N Engl J Med* 1975; **293**: 211-215
- 11 **Hanley JA,** McNeil BJ. A method of comparing the areas under receiver operating characteristic curves derived from the same cases. *Radiology* 1983; **148**: 839-843
- 12 **Tandon RK,** Mehrotra R, Arora A, Acharya SK, Vashisht S. Biliary strictures on ERCP: A study in Northern India. *J Assoc Physicians India* 1994; **42**: 865-870
- 13 **Bain VG,** Abraham N, Jhangri GS, Alexander TW, Henning RC, Hoskinson ME, Maguire CG, Lalor EA, Sadowski DC. Prospective study of biliary strictures to determine the predictors of malignancy. *Can J Gastroenterol* 2000; **14**: 397-402
- 14 **Khurram M,** Durrani AA, Hasan Z, Butt AA, Ashfaq S. Endoscopic retrograde cholangiopancreatographic evaluation of patients with obstructive jaundice. *J Coll Physicians Surg Pak* 2003; **13**: 325-328
- 15 **Fogel EL,** Sherman S. How to improve the accuracy of diagnosis of malignant biliary strictures. *Endoscopy* 1999; **31**: 758-760
- 16 **Jailwala J,** Fogel EL, Sherman S, Gottlieb K, Fluekiger J, Bucksot LG, Lehman GA. Triple tissue sampling at ERCP in malignant biliary obstruction. *Gastrointest Endosc* 2000; **51**(4 Pt 1): 383-390
- 17 **Parasher VK,** Huibregtse K. Endoscopic retrograde wire-guided

- cytology of malignant biliary strictures using a novel scraping brush. *Gastrointest Endosc* 1998; **48**: 288-290
- 18 **Mohandas KM**, Swaroop VS, Gullar SU, Dave UR, Jagannath P, DeSouza LJ. Diagnosis of malignant obstructive jaundice by bile cytology: results improved by dilating the bile duct strictures. *Gastrointest Endosc* 1994; **40**(2 Pt 1): 150-154
- 19 **Ryan ME**, Baldauf MC. Comparison of flow cytometry for DNA content and brush cytology for detection of malignancy in pancreatobiliary strictures. *Gastrointest Endosc* 1994; **40**(2 Pt 1): 133-139
- 20 **Gress F**, Chen YK, Sherman S, Savides T, Zaidi S, Jaffe P, Lehman G, Wonn MJ, Hawes R. Experience with a catheter-based ultrasound probe in the bile duct and pancreas. *Endoscopy* 1995; **27**: 178-184
- 21 **Inui K**, Nakazawa S, Yoshino J, Wakabayashi T, Okushima K, Nakamura Y, Hattori T, Miyoshi H. Ultrasound probes of biliary lesions. *Endoscopy* 1998; **30** (Suppl 1): A 120-123
- 22 **Tamada K**, Hagai H, Yasuda Y, Tomiyama T, Ohashi A, Wada S, Kanai N, Satoh Y, Ido K, Sugano K. Transpapillary intraductal US prior to biliary drainage in the assessment of longitudinal spread of extrahepatic bile duct carcinoma. *Gastrointest Endosc* 2001; **53**: 300-307
- 23 **Menzel J**, Poremba C, Dietl KH, Domschke W. Preoperative diagnosis of bile duct strictures. Comparison of intraductal ultrasonography with conventional endosonography. *Scand J Gastroenterol* 2000; **35**: 77-82
- 24 **Al-Karawi MA**, Mohamed AELS. Endoscopic management of benign biliary strictures. *Saudi Med J* 1994; **15**: 56-60
- 25 **Lillemoe KD**, Melton GB, Cameron JL, Pitt HA, Campbell KA, Talomini MA, Sauter PA, Coleman J, Yeo CJ. Postoperative bile duct strictures: Management and outcome in the 1990s. *Ann Surg* 2000; **232**: 430-441
- 26 **Tocchi A**, Mazzoni G, Liotta G, Costa G, Lepre L, Miccini M, DeMasi E, Lamazza MA, Fiori E. Management of benign biliary strictures: biliary enteric anastomosis vs endoscopic stenting. *Arch Surg* 2000; **135**: 153-157
- 27 **Born P**, Rosch T, Bruhl K, Sandschin W, Allescher HD, Frimberger E, Classen M. Long-term results of endoscopic and percutaneous transhepatic treatment of benign biliary strictures. *Endoscopy* 1999; **31**: 725-731
- 28 **Sugiyama M**, Atomi Y, Kuroda A, Muto T. Bile duct carcinoma without jaundice: Clues to early diagnosis. *Hepatogastroenterology* 1997; **44**: 1477-1483
- 29 **Costamagna G**, Gabrielli A, Mutignani M, Perri V, Bunonato M, Crucitti F. Endoscopic diagnosis and treatment of malignant biliary strictures: review of 505 patients. *Acta Gastroenterol Belg* 1993; **56**: 201-206
- 30 **Al-Mofleh IA**, Rashed RS, Al-Amri SM, Al-Ghamdi AS, Al-Faleh FZ, Al-Freihi HM, Isnani ACL. Malignant biliary strictures: Diagnosis and management. *Saudi Med J* 2003; **24**: 1360-1363

Edited by Wang XL Proofread by Xu FM

Polymorphisms at cholesterol 7 α -hydroxylase, apolipoproteins B and E and low density lipoprotein receptor genes in patients with gallbladder stone disease

Zhao-Yan Jiang, Tian-Quan Han, Guang-Jun Suo, Dian-Xu Feng, Sheng Chen, Xing-Xing Cai, Zhi-Hong Jiang, Jun Shang, Yi Zhang, Yu Jiang, Sheng-Dao Zhang

Zhao-Yan Jiang, Tian-Quan Han, Guang-Jun Suo, Dian-Xu Feng, Sheng Chen, Xing-Xing Cai, Zhi-Hong Jiang, Jun Shang, Yi Zhang, Yu Jiang, Sheng-Dao Zhang, Department of Surgery, Ruijin Hospital, Shanghai Second Medical University, Shanghai Institute of Digestive Surgery, Shanghai 200025, China
Supported by a grant from Shanghai Science and Technology Committee in China, No. 954119027

Correspondence to: Tian-Quan Han, M.D., Ph.D., Department of Surgery, Ruijin Hospital, Shanghai Second Medical University, Shanghai 200025, China. digsurgrj@yahoo.com.cn

Telephone: +86-21-64373909 **Fax:** +86-21-64373909

Received: 2003-04-08 **Accepted:** 2003-05-19

Abstract

AIM: To investigate the relationship between gallbladder stone disease (GSD) and single nucleotide polymorphisms of cholesterol 7 α -hydroxylase (*CYP7A*) gene promoter, apolipoprotein (*APO*) B gene exon 26, *APOE* gene exon 4 or microsatellite polymorphism of low density lipoprotein receptor (*LDLR*) gene exon 18.

METHODS: Genotypes of *CYP7A*, *APOB*, *APOE* and *LDLR* genes were determined in 105 patients with GSD diagnosed by B-mode ultrasonography and 274 control subjects. Serum lipids were analyzed with HITACHI 7060 automatic biochemical analyzer.

RESULTS: Body mass index (BMI) was significantly higher in patients with GSD (24.47 \pm 3.09) than in controls (23.50 \pm 2.16). Plasma total cholesterol was lower in patients with GSD (4.66 \pm 0.92 mmol/L) than in controls (4.91 \pm 0.96 mmol/L), $P < 0.01$ after adjusted for age, sex and BMI. The significantly higher frequency of A allele of *CYP7A* gene polymorphism and X+ allele of *APOB* gene polymorphism was seen in GSD patients. Percentages of A allele in patients and controls were 62.86% and 54.38% ($P < 0.05$) and those of X+ allele 8.57% and 4.01% ($P < 0.01$). Subjects with A allele had significantly lower plasma total cholesterol and LDL cholesterol than subjects with CC homozygote. In a multiple variable logistic regression model, the BMI (OR=1.13, 95% CI: 1.05-1.22), A allele (OR=1.48, 95% CI: 1.05-2.09) and X+ allele (OR=2.28, 95% CI: 1.14-4.59) were positively associated with GSD ($P < 0.05$). Plasma total cholesterol (OR=0.69, 95% CI: 0.64-0.74) was negatively related to GSD ($P < 0.05$).

CONCLUSION: With an association analysis, it was determined that A allele of *CYP7A* gene and X+ allele of *APOB* gene might be considered as risk genes for GSD. These alleles are related with differences of serum lipids among subjects. Multiple-variable logistic regression model analysis showed that besides BMI, GSD was affected by polygenetic factors. But the mechanism for these two alleles responsible for GSD requires further investigations.

Jiang ZY, Han TQ, Suo GJ, Feng DX, Chen S, Cai XX, Jiang ZH, Shang J, Zhang Y, Jiang Y, Zhang SD. Polymorphisms at cholesterol 7 α -hydroxylase, apolipoproteins B and E and low density lipoprotein receptor genes in patients with gallbladder stone disease. *World J Gastroenterol* 2004; 10(10): 1508-1512 <http://www.wjgnet.com/1007-9327/10/1508.asp>

INTRODUCTION

Gallbladder stone disease (GSD) is prevalent in China with a gradually increasing incidence. Studies on the pathogenesis of GSD have demonstrated that supersaturation of biliary cholesterol caused by excessive biliary cholesterol and/or decreased bile acid is the requisite for the formation of gallstones^[1]. Both the cholesterol secreted into bile and the bile acids converted from cholesterol in the liver are involved in regulating cholesterol homeostasis. It was shown in studies^[2-4] that genetic variations might affect gallstone formation. In 1995, Khajuana *et al.* reported a murine lithogenic gene, *Lith 1*, as a possible regulator of hepatic cholesterol synthesis^[4]. The primary *Lith* phenotype was considered to induce secondary events characterized by multiple enzyme alterations which increase available cholesterol and supply the sterol to hepatocytes for hypersecretion into bile^[5]. Additional quantitative traits linkage analysis^[6] maps other *Lith* genes on murine chromosomes 6, 7, 8, 10, 19 and X to confirm the polygenic mode of inheritance. A few studies^[7-10] have focused on the relationship between human GSD and certain genetic factors contributing to cholesterol metabolism.

Cholesterol 7 α -hydroxylase (*CYP7A*, EC 1.14.13.17), a cytochrome P-450 enzyme, is the rate limiting enzyme of hepatic bile acid synthesis, with its activity regulated by bile acids, cholesterol and hormones^[11]. Although the amino acid sequence of *CYP7A* between species is highly homologous (80-90% sequence identity), species respond differently to diet cholesterol^[12]. As compared with control subjects, the activity of *CYP7A* varied in patients with gallstones^[13-15], and diminished or elevated patterns were observed. The heterogeneity of activities of *CYP7A* in patients with GSD may be related to *CYP7A* polymorphisms. A linkage of A-204C single nucleotide polymorphism of the *CYP7A* gene promoter with plasma low density lipoprotein (*LDL*) cholesterol was found in recent studies of nuclear families^[16] and within the general population^[17]. However, the polymorphism for patients with GSD has never been studied. Apolipoprotein (*APO*) E^[18] is an extremely efficient ligand for the *LDLR* and is the determinant for receptor-mediated catabolism of all *APOE* containing lipoproteins. The polymorphism of *APOE* is controlled by three alleles in exon 4, namely $\epsilon 2$, $\epsilon 3$ and $\epsilon 4$. The physiological importance of *APOE* exhibits in disorders of lipoprotein metabolism such as atherosclerosis^[19] as well as in Alzheimer's disease which is not obviously related to lipoprotein metabolism^[20]. The role of *APOE* has also been examined in relation to GSD^[7,9]. The *APOE4* allele is associated with high cholesterol content in gallstones^[7,9], faster crystallization^[7] and frequent stone recurrence after lithotripsy^[21].

Table 1 PCR condition and restriction enzymes

Genes	Primers	Annealing temp	RE
CYP7A ^[16, 17]	5' TGGTAGGTAAATTATTAATAGATGT 3' 5' AAATTAATGGATGAATCAAAGAGC3'	61 °C	Bsa I
apo B ^[10]	5' GGA GAC TAT TCA GAA GCT AA 3' 5' GAA GAG CCT GAA GAC TGA CT 3'	60 °C	Xba I
apo E ^[24]	5' ACAGAATTCGCCCGGCTGGTACAC 3' 5' TAAGCTTGGCACGGCTGTCCAAGGA 3'	60 °C	Hha I
LDL receptor ^[25]	5' CACTTTGTATATTGGTTGAAACTGT 3' 5' CACTGAACAAATACAGCAACCAGGG 3'	62 °C	

The *LDLR* on the surface of hepatocytes plays an important role in cholesterol homeostasis in humans^[22]. The receptor can recognize *APOB* or *APOE* containing lipoproteins such as LDL and high-density lipoprotein (HDL) with different affinities mediating the absorption of plasma lipoproteins. There are many polymorphic sites on this gene and some of those are related to plasma cholesterol metabolism^[23].

In the present study, we analyzed the polymorphism of A-204C of *CYP7A* gene promoter, *APOE* exon 4 and microsatellite polymorphism of *LDLR* gene exon 18. Their relationships with asymptomatic GSD on the Chinese Han population were examined. The association of Xba I polymorphism on *APOB* gene exon 26 with GSD, shown in our previous study^[10], was also evaluated using multiple regression analysis.

MATERIALS AND METHODS

Patients

A total of 379 subjects were recruited for this study from February to May 1998. Patients in this study consisted of 78 males and 27 females with stones and/or cholesterol crystals in their gallbladder. None of the patients had previous onset of cholecystitis defined as colic, fever with chills or jaundice. Two hundred and seventy-four healthy subjects (184 males and 90 females) with normal liver, kidney and endocrine function were included as controls. The mean ages of patients and controls were 47.53 and 47.94 years, respectively. After a 12-h fast, the participants received B-mode ultrasonography with Aloka 500/SSD equipped with a transducer of 3.5 MHz. A total of 10 mL venous blood was extracted and half of it was immediately mixed with ACD anti-coagulants containing citric acid, sodium citric acid and glucose for DNA extraction. The other half of this sample was prepared for biochemical analysis. Body mass index (BMI) was calculated by weight/height² (kg/m²). All subjects gave informed consent to participate in this study which was approved by the Ethical Committee of Ruijin Hospital, Shanghai Second Medical University.

Analysis of plasma lipids and lipoproteins

Plasma total cholesterol, triglyceride, HDL cholesterol, LDL cholesterol, APO AI and APO B were assayed by commercially available kits (Boehringer Mannheim GmbH, Mannheim, Germany) on an automatic analyzer (HITACHI 7060, Hitachi Koki Co. Ltd., Hitachinaka City, Japan).

Genotyping

Genomic DNA was extracted from leukocytes using a method provided by GIBCO-BRL DNA extraction kit (Cat: #28350-015, GIBCO-BRL, Gaithersburg, MD, USA). The fragments containing target polymorphic sequences of *CYP7A*, *APOB*, *APOE* and *LDLR* genes were amplified using polymerase chain reaction (PCR) on PTC-200 Peltier Thermal Cycler (MJ Research Inc, MA, USA). Primers and the conditions of PCR are listed in Table 1. For the single nucleotide polymorphisms of *CYP7A*,

APOB and *APOE*, the products of PCR were each digested by restriction enzymes (New England Biolabs Inc., Beverly, MA, USA). The enzymes are indicated in Table 1. The digested PCR products were electrophoresed in agarose gel; then stained with ethidium bromide and visualized under ultraviolet light. A 968-bp fragment containing A-204C polymorphism of *CYP7A* gene was digested with restrictive enzyme *Bsa I* (New England Biolabs Inc., Beverly, MA, USA) and electrophoresed on 10 g/L agarose gel and stained with ethidium bromide. The band with a cutting site was designated as C allele and that without as A allele. A 244-bp fragment containing *APOE* exon 4 gene was digested with *Hha I* followed by electrophoresis on 100 g/L polyacrylamide gel and then stained with silver. The genotypes were determined from the pattern of restrictive fragments on the gel as described in detail by Hixson and Vernier^[24]. The bands representing the genotype of microsatellite polymorphism of *LDLR* gene exon 18 were obtained from direct electrophoresis on 100 g/L PAGE (100 v, 2.5 h) and stained with silver. The genotype of *LDLR* gene was determined for the bands with 106-bp as A allele (7 repeats of TA), 108-bp as B allele (8 repeats of TA) or 112-bp as C allele (10 repeats of TA)^[25]. Genotyping of *APOB* gene was performed as previously described by Han *et al.*^[10].

Statistics

The results were expressed as means±SD. The differences in concentrations of lipids between patients and controls and those among genotypes were calculated using Student's *t* test. Statistical analysis was performed using the statistical software package SAS 6.12 for Windows (SAS Institute Inc., Cary, NC, USA). SAS GLM procedure was used to compare the concentrations of lipids between patients and controls after adjustment for sex, age and BMI. Frequencies of alleles between patients and controls were evaluated for statistical significance using Chi-square test. A multivariate model was used to predict the relative odds of GSD with all the variables by multiple logistic regressions. Logistic regression coefficients and standard errors were calculated to determine the estimates of odds ratio (OR) and 95% confidence intervals (CI) for significant factors.

RESULTS

Demographic and biochemical characteristics

Gallbladder stones and/or cholesterol crystals were detected in 105 cases by B-mode ultrasonography. The demographic characteristics and biochemistry are shown in Table 2. BMI was significantly higher in the patients than in the controls (24.47±3.09 vs 23.50±2.16, *P*<0.01). Concentrations of plasma total cholesterol and APO AI were significantly lower in patients than in controls. Although the concentrations of HDL cholesterol and LDL cholesterol were slightly lower in patients than in controls, the differences were not significant. Plasma lipid levels varied with sex, age and BMI. We compared the plasma lipids between patients and controls using the analysis of covariance. After

adjustment for sex, age and BMI, the plasma total cholesterol and LDL cholesterol as well as APO B were found significantly lower in patients than in controls as shown in Table 2.

Table 2 Demographic characteristics and biochemistry for patients and controls

	Patients	Controls	P value	P value ¹
No. (male/female)	105 (78/27)	274 (184/90)		
Age (yr)	47.53±10.98	47.94±12.21		
BMI (kg/m ²)	24.47±3.09	23.50±2.16	<0.01	
Triglycerine (mmol/L)	1.32±1.15	1.19±0.82		
Cholesterol (mmol/L)	4.66±0.92	4.91±0.96	<0.05	<0.01
HDL (mmol/L)	1.33±0.36	1.40±0.34		
LDL (mmol/L)	2.56±0.67	2.69±0.73		<0.05
apo A I (g/L)	1.34±0.21	1.39±0.18	<0.05	
apo B (g/L)	1.00±0.22	1.03±0.24		<0.05

¹After adjustment for sex, age and BMI.

Distribution of genotypes and association of polymorphisms with GSD

Figure 1 indicates the genotypes of *CYP7A*, *APOB*, *APOE* and *LDLR* gene polymorphisms. The distributions of genotypes for patients and controls are listed in Table 3. Using Chi-square test, there was a significantly higher frequency of A allele of *CYP7A* gene and X+ allele of *APOB* gene observed in patients compared with controls (A allele: 62.86% vs 54.38%, $P<0.05$; X+ allele: 8.57% vs 4.01%, $P<0.01$, Table 4). There were no significant differences between patients and controls in the polymorphisms of *APOE* gene and *LDLR* gene.

Association between gene polymorphism and plasma lipid concentrations

Table 5 indicates that plasma total cholesterol, LDL cholesterol and APOB were lower in subjects with A allele (AA homozygote or AC heterozygote) than in those without A allele (CC homozygote). The difference was significant only within the control group or within the group combining patients and controls, but not in the patients only group. Within each genotype, the difference of lipid concentration was incongruent between

patients and controls. In subjects with A allele, the LDL cholesterol was significantly higher in patients than in controls, while in subjects without A allele, patients had significantly lower concentrations of HDL cholesterol and APOAI.

Table 3 Distribution of genotypes for patients and controls

Genes	Genotypes	Patients (%)	Controls (%)
CYP7A	AA	44 (41.90)	79 (28.83)
	AC	44 (41.90)	140 (51.10)
	CC	17 (16.20)	55 (20.07)
Apo B	X+/+	1 (0.95)	0 (0)
	X+/-	16 (15.24)	22 (8.03)
	X-/-	88 (83.81)	252 (91.97)
Apo E	ε2/2	0 (0)	1 (0.36)
	ε2/3	15 (14.29)	45 (16.42)
	ε2/4	5 (4.76)	6 (2.19)
	ε3/3	73 (69.52)	183 (66.80)
	ε3/4	11 (10.48)	37 (13.50)
	ε4/4	1 (0.95)	2 (0.73)
LDL receptor	AA	41 (39.05)	90 (32.85)
	AB	2 (1.90)	13 (4.74)
	AC	32 (30.48)	104 (37.96)
	BB	3 (2.85)	4 (1.46)
	BC	8 (7.62)	22 (8.03)
	CC	19 (18.60)	41 (14.96)

Table 4 Frequency of alleles for patients and controls (%)

Genes	Alleles	Patients	Control
CYP7A	A	62.86 ^a	54.38
	C	37.14	45.62
Apo B	X+	8.57 ^b	4.01
	X-	91.43	95.99
Apo E	ε2	9.52	9.67
	ε3	81.90	81.75
	ε4	8.57	8.57
LDL receptor	A	55.24	54.20
	B	7.62	7.84
	C	37.14	37.96

^a $\chi^2=4.44$, $P<0.05$; ^b $\chi^2=6.31$, $P<0.01$.

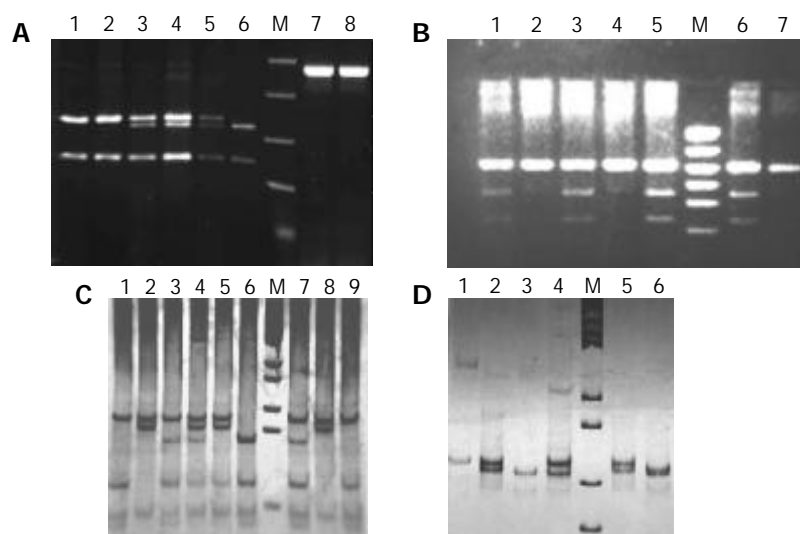


Figure 1 Genotypes of *CYP7A*, apolipoproteins B, E and *LDLR* gene. A: *CYP7A* gene, M: DNA Marker: 1 000, 750, 500, 300, 150 bp (Cat. G3161, Promega, Madison, WI, USA); lanes 1, 2: AA type; lanes 3-5: AC type; lane 6: CC type; lanes 7, 8: PCR products, B: Apolipoprotein B gene, M: DNA Marker: 1 543, 994, 695, 515, 377, 237 bp (Cat. MG0781, SABC, Shanghai, China), lane 1, 3, 5, 6: X+/- type; 2, 4, 7: X-/- type. C: Apo E gene, M: pGEM 7zf(+)/Hae III DNA Marker (Cat. MG0861, SABC, Shanghai, China), from lanes 1-9: ε3/3, ε2/2, ε3/4, ε2/4, ε2/3, ε4/4, ε3/4, ε2/2, ε3/3 types. D: *LDLR* gene, M: pGEM 7zf(+)/Hae III DNA Marker, from lanes 1-6: CC, BC, AA, AC, BC and AB types.

Table 5 Association of CYP7A gene polymorphism with plasma lipids

	Patients		Controls		All	
	AA/AC	CC	AA/AC	CC	AA/AC	CC
No.	88	17	219	55	307	72
Triglyceride (mmol/L)	1.25±0.99	1.70±7.77	1.15±0.82	1.36±0.81	1.18±0.87	1.44±1.11
Cholesterol (mmol/L)	4.64±0.95	4.78±0.79	4.84±0.94 ^c	5.16±0.99 ^c	4.78±0.95 ^g	5.07±0.95 ^g
HDL (mmol/L)	1.32±0.37 ^a	1.35±0.32	1.42±0.34 ^a	1.33±0.72	1.39±0.35	1.33±0.32
LDL (mmol/L)	2.56±0.70	2.59±0.45 ^e	2.63±0.72 ^c	2.91±0.72 ^{e, c}	2.61±0.71 ^g	2.83±0.67 ^g
Apo AI (g/L)	1.34±0.22 ^a	1.36±0.15	1.39±0.18 ^a	1.36±0.20	1.38±0.19	1.36±0.18
Apo B (g/L)	1.00±0.23	1.02±0.15	1.01±0.24 ^c	1.10±0.23 ^c	1.01±0.23 ^g	1.08±0.22 ^g

^a $P<0.05$, patients vs controls with AA/AC genotype, ^c $P<0.05$, AA/AC vs CC within control group, ^e $P<0.05$, patients vs controls with CC genotype, ^g $P<0.05$, AA/AC vs CC in all the subjects.

Logistic regression analysis

A multiple variable logistic regression analysis was performed to compare the effects of both genetic factors and other quantitative variables. In Table 6, only *CYP7A* (OR=1.48, $P<0.05$) and *APOB* (OR=2.28, $P<0.05$) gene polymorphism, plasma cholesterol (OR=0.69, $P<0.01$) and BMI (OR=1.13, $P<0.05$) were correlated with GSD (Table 6).

Table 6 Stepwise logistic regression of multiple variables

Variables	OR	95% CI
A allele ^a	1.48	1.05-2.09
X+ allele ^a	2.28	1.14-4.59
Cholesterol ^b	0.69	0.64-0.74
BMI ^a	1.13	1.05-1.22

^a $P<0.05$; ^b $P<0.01$.

DISCUSSION

Epidemiological studies have stressed the relationship between plasma lipid concentration and GSD. The present study indicated that patients with GSD had lower plasma cholesterol, even after adjustment for sex, age and BMI. Our results were consistent with those of Juvonen^[7], Scragg^[26] and Attili^[27], although there were unchanged results^[28] or only lowered plasma cholesterol levels in women^[29] reported by other authors. The plasma lipid concentrations varied in populations due to diet habits, genetic factors, ethnicity, etc. This explains why previous studies remain controversial. Whether changes in plasma lipid concentration are major factors inducing GSD or represent the end stage of gallstone formation is still questionable. The mechanism for the change in plasma lipid concentrations that increases the risk for GSD is also unclear. However, epidemiological studies indicate that genetic predisposition has been confirmed to have a close relation with GSD. Our present study on the Chinese Han population verified that GSD was genetically controlled by polygenic factors. A-204C polymorphism at *CYP7A* gene promoter and Xba I polymorphism at *APOB* gene may be susceptible genes linked to GSD.

Our previous study on the *APOB* gene Xba I polymorphism revealed that X+ allele was associated with a higher incidence of GSD^[10]. The relationship between GSD and the other three polymorphic sites, A-204C polymorphism of *CYP7A*, Hha I polymorphism of *APOE* and a dinucleotide repeat microsatellite polymorphism of *LDLR*, was also studied by our group. Only did *CYP7A* gene polymorphism seem to be related to GSD. We found a significantly higher frequency of A allele in patients than in controls (0.62 vs 0.54, $P<0.05$). The A-204C polymorphism located 204 bp upstream of the transcription start site of *CYP7A*^[17]. This single nucleotide polymorphism^[16],

at which site C replaced A, created a cutting site for the Bsa I restrictive enzyme. The frequency of A allele of *CYP7A* gene was 0.58^[16] in the Caucasian population and 0.60 in Framingham families^[17] which was slightly higher than that in the Chinese Han population. Analysis of plasma lipid levels revealed that plasma LDL cholesterol concentrations were associated with A-204C polymorphism, similar to the results of Wang *et al.* and Couture^[16,17]. Individuals with A allele tended to have lower LDL cholesterol concentrations. This difference was significant in controls, but not in patients in this study. No studies have assayed the activity of hepatic *CYP7A* among different genotypes up to this time. The mechanism and rationale for A allele to induce low LDL cholesterol are still unknown.

Contrary to our expectation, there was no association between *APOE* gene and GSD or between *LDLR* gene and GSD. Since *APOE* isoforms had different affinities to receptors^[22] affecting lipid metabolism, there was a demonstrated relationship between *APOE* gene polymorphism and various plasma lipids. Its polymorphism was well documented in atherosclerosis^[19] and Alzheimer's disease^[20] as well as cholesterol gallstone disease^[7,9]. Juvonen^[7] studied for the first time the relationship between *APOE* polymorphism and gallstones. Patients with $\epsilon 4$ allele had higher cholesterol content in stones, rapid cholesterol crystallization and shorter median nucleation time in the Finnish population^[7] while Bertomeu^[9] found significantly higher $\epsilon 4$ allele frequency in Spanish patients with gallstones. But other studies^[9,30,31] had contradictory results. There were reports that median nucleation time^[9] was similar in patients between the genotypes and that the cholesterol saturation index^[30] was lower in patients with $\epsilon 4$ allele. Our study concluded that there was no significant difference in the frequency of $\epsilon 4$ allele between patients and controls. A similar result on Chinese patients with GSD was reported previously in a study from Sichuan, China^[32].

LDLR was important for the absorption of APOB and APOE containing lipoproteins^[22]. Herein, we studied a dinucleotide repeat polymorphism. The frequency of these alleles did not differ between the patient and control groups. But we could not exclude the possibility of existence of other polymorphic sites to account for the differences in hepatic LDLR activities that, in turn, would lead to high absorption of plasma cholesterol for biliary secretion.

We analyzed all our variables using a logistic regression model to evaluate the role of genetic factors and quantitative variables. Higher cholesterol concentration in serum may provide a protective factor for GSD since it is negatively related with GSD (OR<1). The cause of gallstone formation might be due to hepatic overabsorption of cholesterol via receptors such as SRB1^[33] or LDLR^[22] leading to hypersaturation of biliary cholesterol. Besides BMI and cholesterol, GSD may be controlled by multiple genetic factors such as the *APOB* gene or *CYP7A* gene. The OR of the *APOB* gene polymorphism

was 2.28, and *CYP7A* was 1.48 with $P < 0.05$. This implies that subjects with A allele of *CYP7A* gene or X+ allele of *APOB* gene can easily form gallstones.

The present study determined the relationship between *CYP7A* or *APOB* gene polymorphism and GSD. However, the relationship should be investigated further in family pedigrees with GSD. Since gene polymorphisms are heterogeneous among ethnic groups, GSD may be caused by different risk genes among different population. The main cause for GSD is hypersaturation of biliary cholesterol. So all genes (known or yet to be determined) involved in hepatic cholesterol metabolism remain the focus for future studies to discover the primary risk genes for GSD. Once a human genomic map for GSD, similar to murine^[34], is completed, it can be useful for early predictive and preventive measures for subjects susceptible to GSD. The genomic map will provide the necessary link in the discovery of effective pharmaceutical agents for treatment.

REFERENCES

- 1 **Apstein MD**, Carey MC. Pathogenesis of cholesterol gallstones: a parsimonious hypothesis. *Eur J Clin Invest* 1996; **26**: 343-352
- 2 **Miquel JF**, Covarrubias C, Villaroel L, Mingrone G, Greco AV, Puglielli L, Carvallo P, Marshall G, Del Pino G, Nervi F. Genetic epidemiology of cholesterol cholelithiasis among Chilean Hispanics, Amerindians, and Maoris. *Gastroenterology* 1998; **115**: 937-946
- 3 **Duggirala R**, Mitchell BD, Blangero J, Stern MP. Genetic determinants of variation in gallbladder disease in the Mexican-American population. *Genet Epidemiol* 1999; **16**: 191-204
- 4 **Khanuja B**, Cheah YC, Hunt M, Nishina PM, Wang DQH, Chen HW, Billheimer JT, Carey MC, Paigen B. *Lith1*, a major gene affecting cholesterol gallstone formation among inbred strains of mice. *Proc Natl Acad Sci U S A* 1995; **92**: 7729-7733
- 5 **Lammert F**, Wang DQH, Paigen B, Carey MC. Phenotypic characterization of *Lith* genes that determine susceptibility to cholesterol cholelithiasis in inbred mice: integrated activities of hepatic lipid regulatory enzymes. *J Lipid Res* 1999; **40**: 2080-2090
- 6 **Paigen B**, Schork NJ, Svenson KL, Cheah YC, Mu JL, Lammert F, Wang DQH, Bouchard G, Carey MC. Quantitative trait loci mapping for cholesterol gallstones in AKR/J and C57L/J strains of mice. *Physiol Genomics* 2000; **4**: 59-65
- 7 **Juononen T**, Kervinen K, Kairaluoma MI, Lajunen LHJ, Kesäniemi YA. Gallstone cholesterol content is related to apolipoprotein E polymorphism. *Gastroenterology* 1993; **104**: 1806-1813
- 8 **Juononen T**, Savolainen MJ, Kairaluoma MI, Lajunen LHJ, Humphries SE, Kesäniemi YA. Polymorphisms at the apoB, apoA-I, and cholesteryl ester transfer protein gene loci in patients with gallbladder disease. *J Lipid Res* 1995; **36**: 804-812
- 9 **Bertomeu A**, Ros E, Zambón D, Vela M, Pérez-Ayuso RM, Targarona E, Trías M, Sanllehy C, Casals E, Ribó JM. Apolipoprotein E polymorphism and gallstones. *Gastroenterology* 1996; **111**: 1603-1610
- 10 **Han T**, Jiang Z, Suo G, Zhang S. Apolipoprotein B-100 gene *Xba* I polymorphism and cholesterol gallstone diseases. *Clin Genet* 2000; **57**: 304-308
- 11 **Einarsson C**, Ellis E, Abrahamsson A, Ericzon BG, Björkhem I, Axelson M. Bile acid formation in primary human hepatocytes. *World J Gastroenterol* 2000; **6**: 522-525
- 12 **Xu G**, Shneider BL, Shefer S, Nguyen LB, Batta AK, Tint GS, Arrese M, Thevananther S, Ma L, Stengelin S, Kramer W, Greenblatt D, Pcolinsky M, Salen G. Ileal bile acid transport regulates bile acid pool, synthesis, and plasma cholesterol levels differently in cholesterol-fed rats and rabbits. *J Lipid Res* 2000; **41**: 298-304
- 13 **Ito T**, Kawata S, Imai Y, Kakimoto H, Trzaskos JM, Matsuzawa Y. Hepatic cholesterol metabolism in patients with cholesterol gallstones: enhanced intracellular transport of cholesterol. *Gastroenterology* 1996; **110**: 1619-1627
- 14 **Reihner E**, Angelin B, Björkhem I, Einarsson K. Hepatic cholesterol metabolism in cholesterol gallstone disease. *J Lipid Res* 1991; **32**: 469-475
- 15 **Shoda J**, He BF, Tanaka N, Matsuzaki Y, Osuga T, Yamamori S, Miyazaki H, Sjövall J. Increase of deoxycholate in supersaturated bile of patients with cholesterol gallstone disease and its correlation with de novo syntheses of cholesterol and bile acids in liver, gallbladder emptying, and small intestinal transit. *Hepatology* 1995; **21**: 1291-1302
- 16 **Wang J**, Freeman DJ, Grundy SM, Levine DM, Guerra R, Cohen JC. Linkage between cholesterol 7 α -hydroxylase and high plasma low-density lipoprotein cholesterol concentrations. *J Clin Invest* 1998; **101**: 1283-1291
- 17 **Couture P**, Otvos JD, Cupples LA, Wilson PWF, Schaefer EJ, Ordovas JM. Association of the A-204C polymorphism in the cholesterol 7 α -hydroxylase gene with variations in plasma low density lipoprotein cholesterol levels in the Framingham offspring study. *J Lipid Res* 1999; **40**: 1883-1889
- 18 **Mahley RW**. Apolipoprotein E: cholesterol transport protein with expanding role in the cell biology. *Science* 1988; **240**: 622-630
- 19 **Curtiss LK**, Boisvert WA. Apolipoprotein E and atherosclerosis. *Curr Opin Lipidol* 2000; **11**: 243-251
- 20 **Strittmatter WJ**, Saunders AM, Schmechel D, Pericak-Vance M, Enghild J, Salvesen GS, Roses AD. Apolipoprotein E: high-avidity binding to β -amyloid and increased frequency of type 4 allele in late-onset familial Alzheimer disease. *Proc Natl Acad Sci U S A* 1993; **90**: 1977-1981
- 21 **Portincasa P**, van Erpecum KJ, van de Meeberg PC, Dallinga-Thie GM, de Bruin TWA, van Berge-Henegouwen GP. Apolipoprotein E4 genotype and gallbladder motility influence speed of gallstone clearance and risk of recurrence after extracorporeal shock-wave lithotripsy. *Hepatology* 1996; **24**: 580-587
- 22 **Brown MS**, Goldstein JL. A receptor-mediated pathway for cholesterol homeostasis. *Science* 1986; **232**: 34-47
- 23 **Pedersen JC**, Berg K. Normal DNA polymorphism at the low density lipoprotein receptor (LDLR) locus associated with serum cholesterol level. *Clin Genet* 1988; **34**: 306-312
- 24 **Hixson JE**, Vernier DT. Restriction isotyping of human apolipoprotein E by gene amplification and cleavage with Hha I. *J Lipid Res* 1990; **31**: 545-548
- 25 **Zuliani G**, Hobbs HH. Dinucleotide repeat polymorphism at the 3' end of the LDL receptor gene. *Nucleic Acid Res* 1990; **18**: 4300
- 26 **Scragg RKR**, Calvert GD, Oliver JR. Plasma lipids and insulin in gall stone disease: a case-control study. *Br Med J* 1984; **289**: 521-525
- 27 **Attili AF**, Capocaccia R, Carulli N, Festi D, Roda E, Barbara L, Capocaccia L, Menotti A, Okolicsanyi L, Ricci G, Lalloni L, Mariotti S, Sama C, Scafato E. Factors associated with gallstone disease in the MICOL experience. *Hepatology* 1997; **26**: 809-818
- 28 **Barbara L**, Sama C, Labate AMM, Taroni F, Rusticali AG, Festi D, Sapio C, Roda E, Banterle C, Puci A, Formentini F, Colasanti S, Nardin F. A population study on the prevalence of gallstone disease: the Sirmione study. *Hepatology* 1987; **7**: 913-917
- 29 **GREPCO**. The epidemiology of gallstone disease in Rome, Italy. Part II. Factors associated with the disease. *Hepatology* 1988; **8**: 907-913
- 30 **van Erpecum KJ**, van Berge-Henegouwen GP, Eckhardt ERM, Portincasa P, van de Heijning BJM, Dallinga-Thie GM, Groen AK. Cholesterol crystallization in human gallbladder bile: relation to gallstone number, bile composition, and apolipoprotein E4 isoform. *Hepatology* 1998; **27**: 1508-1516
- 31 **Ko CW**, Beresford SAA, Alderman B, Jarvik GP, Schulte SJ, Calhoun B, Tsuchida AM, Koepsell TD, Lee SP. Apolipoprotein E genotype and the risk of gallbladder disease in pregnancy. *Hepatology* 2000; **31**: 18-23
- 32 **Liu QY**, Xiao LJ, Chen NS, Li N, Fu MD, Yan LN. A prospective study on the serum lipids in different apo E genotype patients with gallstones. *Zhonghua Yixue Yichuanxue Zazhi* 1997; **14**: 223-226
- 33 **Ji Y**, Wang N, Ramakrishnan R, Sehayek E, Huszar D, Breslow JL, Tall AR. Hepatic scavenger receptor BI promotes rapid clearance of high density lipoprotein free cholesterol and its transport into bile. *J Biol Chem* 1999; **274**: 33398-33402
- 34 **Lammert F**, Carey MC, Paigen B. Chromosomal organization of candidate genes involved in cholesterol gallstone formation: a murine gallstone map. *Gastroenterology* 2001; **120**: 221-238

Different therapy for different types of ulcerative colitis in China

Xue-Liang Jiang, Hui-Fei Cui

Xue-Liang Jiang, Department of Gastroenterology, Chinese PLA General Hospital of Jinan Military Command, Jinan 250031, Shandong Province, China

Hui-Fei Cui, College of Pharmaceutical Science, Shandong University, Jinan 250012, Shandong Province, China

Supported by Youth Research Foundation of the Public Health Bureau of Shandong Province, No. 2001CA2EFB2

Correspondence to: Dr. Xue-Liang Jiang, Department of Gastroenterology, Chinese PLA General Hospital of Jinan Military Command, 25 Shifanlu, Jinan 250031, Shandong Province, China. jiangxueliang678@126.com

Telephone: 13585909956

Received: 2003-08-08 **Accepted:** 2003-10-07

Abstract

AIM: To study the different therapy for different types of ulcerative colitis (UC) in China.

METHODS: Among 102 UC patients, 42 chronic relapse type UC patients were randomly divided into olsalazine sodium treatment group ($n=21$) and SASP group ($n=21$). Clinical effects and safety were observed in the 2 groups. Forty-two first episode type UC patients were randomly divided into Heartleaf houttuynia herb treatment group ($n=21$) and SASP group ($n=21$). Clinical effects were observed in the 2 groups while ultrastructure of colonic mucosa, ICAM-1 and the pressure of distant colon were studied in Heartleaf houttuynia herb group. Eighteen patients (8 males, 10 females) with refractory UC and unresponsive to high-dose prednisolone and sulfasalazine therapy more than one month were treated with Kangshuanling (7 200 U/d). Prednisolone was gradually stopped and sulfasalazine was maintained. Stool frequency, rectal bleeding, colonoscopy, general well-being, histology were observed and CD62p, CD63, CD54, Pgp-170 (flow cytometry), TXA2 (RIA), blood platelet aggregation rate and thrombosis length *in vitro* were assessed.

RESULTS: In the 42 chronic relapse type UC patients, the overall clinical effects of olsalazine sodium group (complete remission in 16, improvement in 4, inefficiency in 1) were better than those of SASP group (complete remission in 10, improvement in 4, inefficiency in 7, $P<0.05$). Symptomatic remission of olsalazine sodium group (complete remission in 15, partial remission in 5, inefficiency in 1) was better than that of SASP group (complete remission in 10, partial remission in 5, inefficiency in 6, $P<0.05$). The colonoscopic remission of olsalazine sodium group (complete remission in 11, partial remission in 9, inefficiency in 1) was better than that of SASP group (complete remission in 7, partial remission in 8, inefficiency in 6, $P<0.05$). The histologic remission of olsalazine sodium group (complete remission in 13, partial remission in 7, inefficiency in 1) was better than that of SASP group (complete remission in 6, partial remission in 10, inefficiency in 5, $P<0.05$). The side effects of gastrointestinal tract in olsalazine sodium group were less than those of SASP group except for frequency of watery diarrhea. No other side effects were observed in

olsalazine sodium group while ALT increase, WBC decrease and skin eruption were observed in SASP group. Two patients relapsed in olsalazine sodium group while 8 cases relapsed in SASP group during the flow-up period (from six months to one year). In the 42 first episode type UC patients, the clinical effect of Heartleaf houttuynia herb group (complete remission in 20, 95.2%; improvement in 1, 4.8%) was better than that of SASP group (complete remission in 15, 72.4%, improvement in 5, 23.8%; inefficiency in 1, 3.8%, $P<0.01$). The time of stool frequency recovering to normal (5.6 ± 3.3 d), and blood stool disappearance (6.7 ± 3.8 d) and abdominal pain disappearance (6.1 ± 3.5 d) in Heartleaf houttuynia herb group was all shorter than that in SASP group (9.5 ± 4.9 d, 11.7 ± 6.1 d, 10.6 ± 5.3 d, $P<0.01$). Heartleaf houttuynia herb could inhibit the epithelial cell apoptosis of colonic mucous membrane and the expression of ICAM-1 ($45.8\pm 5.7\%$ vs $30.7\pm 4.1\%$, $P<0.05$). Compared with normal persons, the mean promotive speed of contraction wave stepped up (4.6 ± 1.6 cm/min vs 3.2 ± 1.8 cm/min, $P<0.05$) and the mean amplitude of the wave decreased (14.2 ± 9.3 kPa vs 18.4 ± 8.0 kPa, $P<0.05$) in active UC patients. After treatment with Heartleaf houttuynia herb, these 2 indexes improved significantly (17.3 ± 8.3 kPa, 3.7 ± 1.7 cm/min, $P<0.05$). In normal persons, the postprandial pressure of sigmoid (2.9 ± 0.9 kPa) was higher than that of descending colon (2.0 ± 0.7 kPa) and splenic flexure (1.7 ± 0.6 kPa), while the colonic pressure (1.5 ± 0.5 kPa, 1.4 ± 0.6 kPa, 1.3 ± 0.6 kPa) decreased significantly ($P<0.05$) in active UC patients. After treatment with Heartleaf houttuynia herb, the colonic pressure (2.6 ± 0.8 kPa, 1.8 ± 0.6 kPa, 1.6 ± 0.5 kPa) recovered to normal. The pain threshold of distant colon (67.3 ± 18.9 mL) in active UC patients decreased significantly compared with that of normal persons (216.2 ± 40.8 mL, $P<0.05$) and recovered to normal after treatment with Heartleaf houttuynia herb (187.4 ± 27.2 mL, $P<0.05$). In the 18 refractory UC patients with platelet activation, after more than 4 wk of combined Kangshuanling and sulfasalazine therapy, 16 patients achieved clinical remission, with a highly significant statistical difference ($P<0.01$) between pre- and post-treatment mean scores for all disease parameters: stool frequency (8.2/d vs 1.6/d), rectal bleeding (score 2.7 vs 0.3), colonoscopy (score 2.6 vs 1.1), histology (score 12.0 vs 5.0), general well being (score 4.0 vs 0.6) and CD62p ($8.0\pm 3.1\%$ vs $4.1\pm 1.8\%$), CD63 ($6.3\pm 2.1\%$ vs $3.2\pm 1.6\%$), TXA2 (548 ± 85 ng/L vs 390 ± 67 ng/L), platelet aggregation rate ($43.2\pm 10.7\%$ vs $34.8\pm 8.1\%$), thrombosis length *in vitro* (2.3 ± 0.6 cm vs 1.8 ± 0.3 cm), CD54 in blood ($26.9\pm 6.9\%$ vs $14.4\pm 5.1\%$), CD54 in tissues ($51.1\pm 6.2\%$ vs $23.1\pm 4.1\%$), Pgp-170 in blood ($18.9\pm 3.9\%$ vs $10.4\pm 2.7\%$), Pgp-170 in tissues ($16.5\pm 3.2\%$ vs $10.2\pm 2.3\%$, $P<0.01$ or 0.05).

CONCLUSION: Based on the characteristics of UC cases in China, different therapy should be given to different types of UC with expected satisfactory results.

Jiang XL, Cui HF. Different therapy for different types of ulcerative colitis in China. *World J Gastroenterol* 2004; 10(10): 1513-1520

<http://www.wjgnet.com/1007-9327/10/1513.asp>

INTRODUCTION

Ulcerative colitis (UC) is a common digestive disease in Western countries. It was believed that the occurrence of UC was rare in China. But recent reports reveal that UC cases have increased remarkably^[1,2]. According to our study, UC cases from 1991 to 2000 have increased 2.7 times compared with those from 1981 to 1990^[3-5]. Due to the fact that the etiology and mechanism of UC are still not quite clear, and there is no specific treatment available, the disease usually becomes chronic with repeated relapses, thus seriously endangering patient's health^[6-25]. SASP and corticosteroid, despite their widespread use in the treatment of UC, do not offer an ideal cure because of its long course of treatment, various adverse reactions as well as tendency to relapse when medication stops. The emphasis laid on the study of UC, therefore, is to find an effective drug with fewer adverse reactions in accord with the characteristics of UC cases in China. The diagnosis and treatment of UC still remain a challenge to clinicians^[26-34]. Respecting treatment and improvement of curative effect in refractory cases, lower of relapse rate and reduction of side effects of aminosalicylic acid and corticosteroids are questions to be encountered. Based upon the characteristics of UC cases in China, we adopted the method of giving different therapy to different types of UC, hoping to get better therapeutic results.

MATERIALS AND METHODS

Total cases

A total of 102 UC patients (42 chronic relapse type, 42 first episode type, 18 refractory type) were studied, their diagnoses conformed to the criteria of Lennard-Jones^[28].

Chronic relapse type

Among the 42 chronic relapse type cases, 19 were males and 23 females with an average age of 32.6 years. They had a UC history of 6 mo to 5 years and bloody diarrhea, abdominal pain of varying degrees. Pathological changes above the sigmoid were found in 12 and 30 patients by colonoscopic examinations, respectively. Lesions were characterized by ulcerations, crypt abscesses, non-specific inflammation and atypical hyperplasia, etc. They were randomly divided into treatment group which received olsalazine sodium capsules (Tianjin Lisheng Pharmaceutical Co., Ltd. 250 mg) were used twice a day (1.0 g/d) for 8 wk, and comparison group received sulfasalazine (1.0) 4 times a day for 8 wk. There was no significant difference in the severity of symptoms between olsalazine group (11 mild, 8 moderate, 2 severe) and SASP group (13 mild, 7 moderate, 1 severe, Ridit analysis, $P > 0.05$). For patients who could not tolerate diarrhea of 2-3 times a day, 1-2 bills of imodium were given daily, but not more than 10 d. Patients were seen before and after 1, 2, 4, 6, 8 wk of treatment. Symptoms and physical signs were recorded. Colonoscopy was done 3 d before treatment and within 3 d after completion of treatment. A total of 7 items were observed and recorded. Purulent secretion and pseudopolyp were classified into 2 grades. Ulcer, erosion, mucous bleeding, hyperemic edema and vascular blurring were classified into grades 0, 1, 2, 3, 4 based upon the severity (0=nil, 1=mild, 2=moderate, 3=relative severe, 4=severe). Routine blood and stool tests were performed before and after 1, 2, 4, 6 and 8 wk of treatment. Coagulation time and erythrocyte sedimentation rate were examined before and after 4 and 8 wk of treatment. Blood serum potassium, sodium, chloride, anhydride, urea nitrogen, ALT and total bilirubin were examined before and after 8 wk of treatment. Histological examination with grading of its changes was performed on colonoscopic biopsy specimens before and after treatment (grade 0: no polymorphonuclear cell, grade 1: some polymorphonuclear cells in lamina

propria, grade 2: obvious polymorphonuclear cells infiltration in lamina propria involving more than 50% of recesses, grade 3: massive polymorphonuclear cells with recess abscess, grade 4: obvious acute inflammation with ulcer). Criteria of therapeutic efficacy were adopted that proposed by Chinese Society of Gastroenterology^[35] (complete remission: subsidence of clinical symptoms with relative normal mucous membrane in colonoscopy, effective: basically without symptoms and mild mucous inflammatory reaction or pseudopolyp formation upon colonoscopy, ineffective: no improvement in clinical symptoms, colonoscopic and pathologic examinations). Complete clinical remission: after 8 wk treatment, defecation 0-2 times a day, with no gross blood or microscopic red cells in stool; partial remission: after 8 wk of treatment, defecation 3-4 times a day, with no gross blood in stool but less than 10 RBC per high power microscopic field; no improvement: defecation 5 times or more per day with gross bloody stool. Colonoscopic remission: complete remission (among the 7 items, 5 or more lowered by a grade after treatment), partial remission (3-4 items lowered by a grade after treatment), no remission (0-2 items lowered by a grade after treatment). Histological remission: complete remission (pathological grade lowered after treatment, being grades 0-1), partial remission (pathological grade lowered after treatment, but still >1), no remission (no change before and after treatment). Adverse reactions record: nausea, diarrhea, insomnia, abdominal pain, dizziness, rash, lumbar soreness, edema, etc. Their time of occurrence, severity, duration and measures taken for treatment were recorded.

First episode type

Among the 42 cases of first episode type, 16 were males and 26 females with average age of 31.4 years. They had a UC history of 1 mo to a year, and all had bloody diarrhea, abdominal pain of different degrees. Lesions above the sigmoid were found in 2 patients by colonoscopic examination, while pathological changes were found below the sigmoid in 40 patients. Lesions were characterized by ulceration, crypt abscesses, non-specific inflammation and atypical hyperplasia, etc. They were randomly divided into treatment group that received treatment of heartleaf houttuynia (2 kg/L, pH 4.0-6.0, Nanfang pharmaceutical Co., Ltd.) enema (20 mL diluted with NS 100 mL, once every evening before sleep for 1-2 mo), and SASP group that administered 1 g of SASP four times a day for 1-2 mo. Clinical observations included frequency of defecation, bloody stool, and general condition. Therapeutic effects^[28]: complete remission (complete disappearance of symptoms with mucous membrane returned to normal in colonoscopy), partial remission (abatement of symptoms with conditions of mucous membrane improved, only a small amount of red blood cells and leucocytes found in routine stool test), no remission (no obvious changes both in symptoms and in colonoscopy). Ultrastructure^[7] Microvilli, mitochondria and apoptosis were observed under electronic microscopy. Content of CD54 (ICAM-1, Immunotech) in colonic mucous membrane was examined according to our methods^[15].

PC Polygraph HR (CTD-SYNECTICS, Sweden) was used to examine colonic motility. Distances between the 8 tracts (outer diameter 8 mm and side hole diameter 1 mm) of manometric tube were 5 cm, medication that would affect gastrointestinal motility was suspended at least for 3 d before the examination. Intestinal tract was cleaned in the afternoon prior to the examination and food intake was suspended during the day of examination. Manometric tube was inserted to colonic splenic flexure as guided by colonoscopy. Colonic motility of each patient was recorded one hour before meal and two hours after meal, the result was then analyzed by Polygram and Windows Polygram. Contractions above 6.67 kPa and spreading

to side holes 10 cm away were regarded as propulsive contractions, while contractions below 1.33 kPa were not considered so as to minimize the effect of respiration. Baseline was automatically set up by computer, which calculated the mean oscillation amplitude every 30 min before and after meals. Hand injectors were used to fill air of 20 mL each time to the self-made rubber air pocket with the maximum capacity of 120 mL at 30 s intervals. Patients' feeling of expansion of air pocket was recorded (cognitive, defecation and pain threshold values).

Refractory UC patients with platelet activation

Among the 18 refractory UC patients, there were 8 males and 10 females aged 20 to 52 years (mean 32.4 years), including 10 cases of severe UC, and 8 moderately severe UC. Duration of diseases ranged from 7 mo to 10 years (mean 4.3 years). Rectal bleeding, diarrhea, mucus stool, abdominal pain were the main symptoms. Three patients were associated with thromboembolic diseases. All patients were treated with high-dose corticosteroid and sulfasalazine for more than 4 wk without effect, sulfasalazine was maintained in combination with Kangshuanling sublingual tablet (low molecular heparin, produced by Shandong Songling Pharmaceutical Factory, 2 tablets, 3 times daily (7 200U/d) for 15 d, then 1 tablet, 3 times daily (3 600 U/d) for more than 4 wk). Prednisolone was tapered and stopped.

Pre- and post-treatment scores were calculated for the following disease parameters^[36]: (1) Stool frequency (average number per day for the past week); (2) Rectal bleeding (0: absent, 1: streak of blood on stools occasionally, 2: obvious blood on stool frequently, 3: complete bloody stools); (3) Colonoscopic appearance 0: normal vascular pattern, 1: mild lesion (loss of vascular pattern, mucosal edema, no bleeding), 2: moderate lesion (granularity and friability of the mucosa), 3: severe lesion (discrete ulceration and spontaneous bleeding); (4) Histological grading: serial biopsies from rectum and colon were taken. Five histological changes seen in UC (cellular infiltrate in lamina propria, cryptitis, crypt abscess formation, goblet cell depletion, and regenerative hyperplasia of epithelium). Each was scored from 0 (absent) to 3 (severe). A total UC score of 5 or less indicated mild disease; 5-10, moderate; and 10-15, severe disease. (5) General health status (0: excellent, 1: good, 2: poor, 3: poorer, 4: very poor, 5: poorest).

To assess platelet activation and aggregability^[22,37], we used a sensitive flow cytometric technic designed to render minimize sample handling and render fixation unnecessary to quantify platelet activation. Blood samples were incubated 10 min before venesection with fluorescein isothiocyanate (FITC) conjugated antibodies to the platelet surface antigens, P-selectin (CD62P) and CD63 (Immunotech, Marseilles, France). Analysis was made 15 min before venesection using a BD (Becton Dickinson Immunocytometry Systems) FAC scan. TXA-2 (Suzhou Medical College) was measured using RIA method, samples were taken without tourniquet into chilled tubes containing 1:9 anticoagulant/ antiaggregant solution (trisodium citrate 3.8%), centrifuged for 15-30 min, later at 4 °C for 30 min to minimize *in vitro* activation, supernatant was decanted off and stored at -20 °C for assay within 3 mo. Platelet aggregation rates (PAR) and thrombosis length (TL) *in vitro* were assessed by XSN-RII instrument according to the manufacturer's instructions. CD54 and Pgp-170 in blood and tissues were measured using flow cytometric technique according to our previous report^[15] and literature^[38,39].

Statistical analysis

T test and Ridit analysis were adopted. Student's *t* test and Friedman test were used to assess the significance of differences between mean pre- and post-treatment parameters.

RESULTS

Chronic relapse type UC

In the 42 chronic relapse type UC patients, the total clinical effect of olsalazine sodium group (completely remission in 16 cases, improvement in 4 patients, inefficiency in one case) was better than that of SASP group (completely remission in 10 cases, improvement in 4, inefficiency in 7, $P < 0.05$). The clinical symptomatic remission of olsalazine sodium group (complete remission in 15 cases, partial in 5, inefficiency in one) was better than that of SASP group (complete remission in 10 cases, partial in 5, inefficiency in 6, $P < 0.05$). The colonoscopic remission of olsalazine sodium group (complete remission in 11 cases, partial in 9, inefficiency in 1) was better than that of SASP group (complete remission in 7 cases, partial in 8, inefficiency in 6, $P < 0.05$). The colonoscopic images of pre and post treatment with olsalazine are shown in Figure 1. The histologic remission of olsalazine sodium group (complete remission in 13 cases, partial in 7, inefficiency in 1) was better than that of SASP group (complete remission in 6 cases, partial in 10, inefficiency in 5, $P < 0.05$). The side effects of gastrointestinal tract in olsalazine sodium group were less than those of SASP group (abdominal discomfort: 3 vs 15, heartburn 1 vs 7, nausea 2 vs 5) except for frequency of watery diarrhea (5 vs 1). No other side effects were observed in olsalazine sodium group while increased ALT (1 case), decreased WBC (1 case) and skin eruption (2 cases) were observed in SASP group. Two patients relapsed in olsalazine sodium group while 8 cases relapsed in SASP group during the flow-up period (from 6 mo to 1 year).

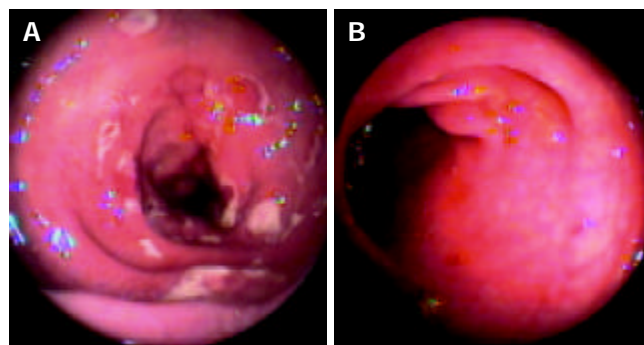


Figure 1 Colonoscopic image before and after treatment of olsalazine. A: Colonoscopic image before treatment of olsalazine; B: Colonoscopic image after treatment of olsalazine for 4 wk.

First episode type UC

In the 42 first episode type UC patients, the clinical effect of Heartleaf houttuynia herb group (complete remission in 20 cases, 95.2%; improvement in 1 case, 4.8%) was better than that of SASP group (complete remission in 15 cases, 72.4%; improvement in 5 cases, 23.8%; inefficiency in 1 case, 3.8%, $P < 0.01$). The time of stool frequency recovering to normal (5.6 ± 3.3 d), blood stool disappearance time (6.7 ± 3.8 d) and abdominal pain disappearance time (6.1 ± 3.5 d) in Heartleaf houttuynia herb group were all shorter than those in SASP group (9.5 ± 4.9 d, 11.7 ± 6.1 d, 10.6 ± 5.3 d, $P < 0.01$). Pathological changes of ultrastructure, such as swollen mitochondria with depleted ridge, shortened microvilli, maldevelopment of goblet cells and increased epithelial cell apoptosis (Figure 2) could be found on the surface of mucous membrane and recess prior to Heartleaf houttuynia herb injection treatment, which recovered to normal gradually after treatment (Figure 3).

Heartleaf houttuynia herb could inhibit the expression of CD54 (ICAM-1) of colonic mucous membrane (45.8 ± 5.7 vs $30.7 \pm 4.1\%$, $P < 0.05$, Figure 4).

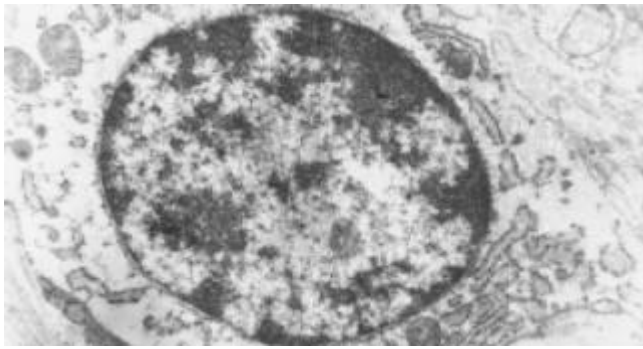


Figure 2 Epithelial cell apoptosis and swollen mitochondria with depleted ridge in UC patients.

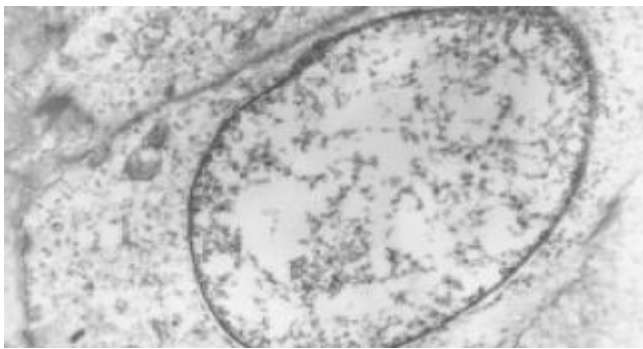


Figure 3 Gradual recovery of epithelial cells to normal after treatment with Heartleaf houttuynia herb injection.

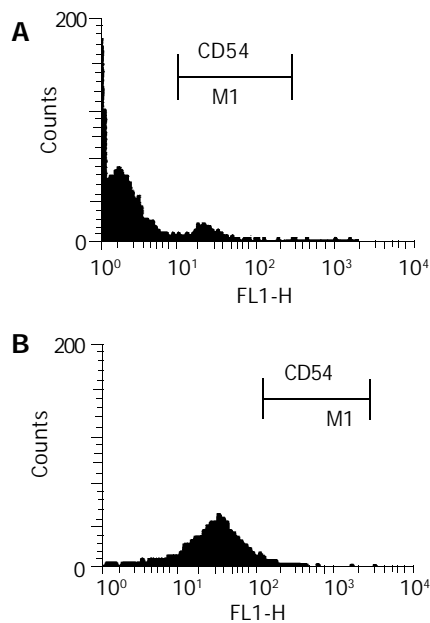


Figure 4 Expression of CD54 (ICAM-1) in colonic mucous membrane of UC patients before and after treatment of Heartleaf houttuynia herb. A: Increased expression of CD54 in colonic mucous membrane of UC patients before treatment of Heartleaf houttuynia herb; B: Decreased expression of CD54 in colonic mucous membrane of UC patients after treatment of Heartleaf houttuynia herb.

Compared with normal persons, the mean promotive speed of contraction wave stepped up (4.6 ± 1.6 cm/min vs 3.2 ± 1.8 cm/min, $P < 0.05$) and the mean amplitude of wave decreased (14.2 ± 9.3 kPa vs 18.4 ± 8.0 kPa, $P < 0.05$) in active UC patients. After treatment of Heartleaf houttuynia herb, these 2 indexes improved significantly (17.3 ± 8.3 kPa, 3.7 ± 1.7 cm/min, $P < 0.05$). In normal persons, the

post-meal pressure of sigmoid (2.9 ± 0.9 kPa) was higher than that of descending colon (2.0 ± 0.7 kPa) and splenic flexure (1.7 ± 0.6 kPa), while the respective colonic pressures (1.5 ± 0.5 kPa, 1.4 ± 0.6 kPa, 1.3 ± 0.6 kPa) were significantly decreased ($P < 0.05$) in active UC patients. After treatment of Heartleaf houttuynia herb, the colonic pressures (2.6 ± 0.8 kPa, 1.8 ± 0.6 kPa, 1.6 ± 0.5 kPa) recovered to normal.

The pain threshold of distant colon (67.3 ± 18.9 mL) in active UC patients decreased significantly compared with that in normal persons (216.2 ± 40.8 mL, $P < 0.05$) and recovered to normal after treatment of Heartleaf houttuynia herb (187.4 ± 27.2 mL, $P < 0.05$). There were no adverse reactions in Heartleaf houttuynia herb therapy, while SASP therapy had adverse reactions such as heartburn (5 cases), increased ALT (1 case), decreased WBC (1 case) and rash (2 cases).

Refractory UC patients with platelet activation

Sixteen patients achieved clinical remission (normal stool frequency and no rectal bleeding) after combined treatment of Kangshuanling sublingual tablets with sulfasalazine. Two patients had reduced rectal bleeding only. The average time of marked improvement and remission was 3 wk (1-5 wk), and 6 wk (1-12 wk), respectively. Rectal bleeding ceased in 16 patients (4 patients within 7-14 d, the others within 2-6 wk). Sixteen patients improved in general health condition earlier than bowel symptoms. There was highly significant improvement in mean scores for all disease parameters (Table 1).

Blood contents of CD62p, CD63, TXA2, platelet aggregation rate (PAR) and thrombosis length (TL) in vitro

All the indexes in refractory UC patients increased significantly as compared with the normal controls ($P < 0.01$). After treatment with Kangshuanling sublingual tablets, all the parameters of UC patients decreased ($P < 0.05$, but CD62P and CD63 remained higher than normal ($P < 0.05$, Table 2, Figure 5).

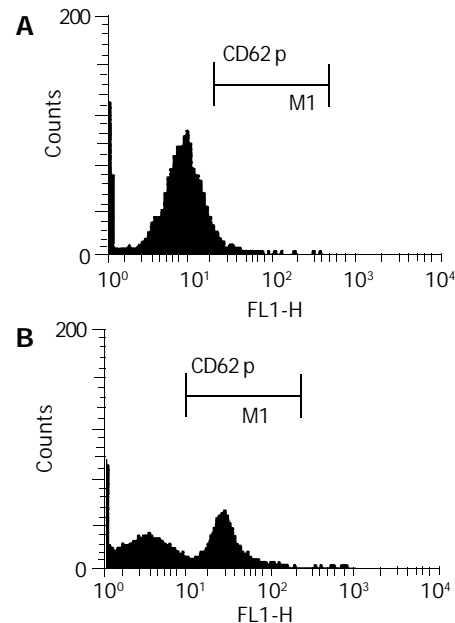


Figure 5 CD62p in blood of normal persons and active UC patients. A: CD62p in blood of normal persons; B: Significant increase of CD62p in blood of active UC patients.

CD54 and products of MDR expression (Pgp-170) in blood and tissues

Compared with normal persons (Figure 6A), CD54 elevated in both blood and tissues in refractory UC patients ($P < 0.01$), CD54 in tissues was higher than in blood (Figure 6B). After treatment

Table 1 Therapeutic effects of Kangshuanling sublingual tablets on refractory UC patients

Group	Stool frequency (times/d)	Rectal bleeding (score)	Colonoscopy (score)	Histology (score)	Well-being (score)
Pre-treatment	8.2	2.7	2.6	12.0	3.9
Post-treatment	1.6 ^b	0.3 ^b	1.1 ^b	5.0 ^b	0.7 ^b

^b*P*<0.01 vs pretreatment.

Table 2 Effects of Kangshuanling sublingual tablet on CD62P and CD63, TXA2, platelet aggregation rate (PAR) and thrombosis length (TL) *in vitro* in UC patients (mean±SD)

Group	CD62p (%)	CD63 (%)	TXA2 (ng/L)	PAR (%)	TL (cm)
UC patients					
Pre-treatment	8.0±3.1 ^b	6.3±2.1 ^b	548.2±84.9 ^b	43.2±10.1 ^b	2.3±0.6 ^b
Post-treatment	4.1±1.8 ^{a,d}	3.2±1.6 ^{a,d}	390.1±67.0 ^d	34.8±8.1 ^d	1.8±0.3 ^d
Normal controls	1.9±0.4	1.6±0.8	340.2±40.4	34.1±9.1	1.7±0.4

^a*P*<0.05, ^b*P*<0.01 vs normal controls; ^d*P*<0.01 vs pretreatment.

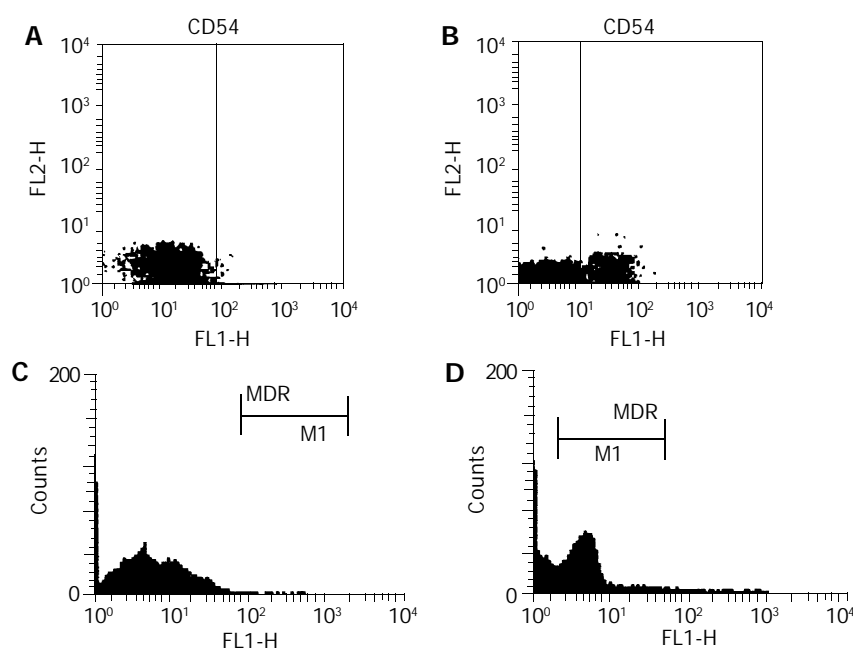


Figure 6 CD54 and MDR in tissues of normal persons and refractory UC patients. A: CD54 in tissues of normal persons; B: Significant increase of CD54 in tissues of refractory UC patients; C: MDR in tissues of normal persons; D: Significant increase of MDR in tissues of refractory UC patients.

with Kangshuanling sublingual tablets, CD54 was significantly decreased in both blood and tissues (*P*<0.01), but still higher than that in normal controls (*P*<0.05), (Table 3). Compared with normal persons (Figure 6C), Pgp-170 elevated in both blood and tissues in refractory UC patients (*P*<0.01, Figure 6D), there was no difference between Pgp-170 in tissues and blood. After treatment with Kangshuanling sublingual tablets, Pgp-170 was significantly decreased in both blood and tissues (*P*<0.05), but still higher than that of normal controls (*P*<0.05), (Table 3).

Table 3 Effects of Kangshuanling sublingual tablets on CD54 in UC patients (mean±SD,%)

Group	Blood CD54	Tissue CD54	Blood Pgp-170	Tissue Pgp-170
UC patients				
Pre-treatment	26.9±6.9 ^b	51.1±6.2 ^b	18.9±3.9 ^b	16.5±3.2 ^b
Post-treatment	14.4±5.1 ^{a,d}	23.1±4.1 ^{a,d}	10.4±2.7 ^{a,c}	10.2±2.3 ^{a,c}
Normal controls	6.2±3.7	8.8±3.2	6.2±2.2	6.8±3.1

^a*P*<0.05, ^b*P*<0.01 vs normal controls; ^c*P*<0.05 vs pre-treatment, ^d*P*<0.01 vs pre-treatment.

Complications

No complications were found during the treatment with Kangshuanling sublingual tablets.

DISCUSSION

SASP is still widely used in the treatment of chronic relapse type ulcerative colitis, with advantages such as quick effect and high clinical remission rate. However, its effect is not satisfactory in some chronic cases and has various adverse reactions. In addition, UC usually relapses when medication is stopped. Therefore, we should place emphasis in the study of UC on more effective drugs with less adverse reactions^[2,27-31]. At present, the cause and pathogenesis of UC are unclear^[1-15], nonspecific anti-inflammatory drugs, in a relatively long period, will still remain as the main drugs for treating UC. While the curative effect of traditional aminosalicylic acid has been affirmed, its side reactions are too many. Main approaches today centered on enhancing the curative effect and reducing side reactions by developing new preparations and changing routes of administration^[1]. SASP, when taken orally, is cleaved by bacteria in the colon into 5-ASA and Sulfapyridine. The

former is the effective component of SASP, and the latter is the carrier of 5-ASA, which may cause such side reactions as sulfanilamide allergy, gastrointestinal upset, hepatorenal impairment, thus affecting its clinical application. In the present study, the above mentioned side reactions in various degrees were also seen in the SASP group. Therefore, to achieve a satisfactory curative effect but without toxicity, the best therapy for UC is to administer 5-ASA that does not contain sulfapyridine and to make it working on diseased areas directly. 5-ASA, however, is usually absorbed rapidly, hence unable to reach inflamed mucous membrane. So, the question posed for the development of new drugs for UC, is how to make 5-ASA reaching and working on the diseased area. Olsalazine sodium gives an answer to this problem, for it is the prodrug of 5-ASA, formed by 2-molecules of 5-ASA jointed by diazo bond. When it is taken orally, only a very small amount is absorbed before reaching colon (absorbing rate <5%). It does not decompose and its biological utilization rate in the body is extremely low. When it reaches the colon, bacterial enzymes in the colon split the diazo bond, liberating the two-molecules of 5-ASA. It has no side effects of SASA, while maintaining the same curative effects. Olsalazine sodium has been on market for more than 10 years and its curative effect on UC and safety have been widely accepted. Domestic olsalazine sodium is a fourth grade new drug jointly developed by Tianjin Lisheng Pharmaceutical Co., Ltd. and Tianjing Medical Research Institute. The fourth grade new drug with the trade name "Changmei", in capsule form was put into market in 2000. This study centered on the clinical effects and safety of olsalazine sodium in patients with chronic UC. Our results indicated that olsalazine sodium was superior to SASP in overall clinical response rate, amelioration of clinical symptoms, colonoscopic examination and histology test. In addition, it has fewer side effects on digestive tract and is unharmed to liver function, WBC and skin. The cause of the increased watery stool frequencies may be related with sodium salt, which inhibits intestinal absorption of water. It mainly occurs at the beginning of medication or during increase of dosage. This side effect, however, does not affect the continuing medication. Patients' worries may be eliminated when the cause is explained. To increase medication frequencies or to take medicine after meal may ameliorate or eliminate this symptom. Imodium may also be given temporarily to some patients to maintain curative effect. In China, the chronic relapse type accounted for 52.6% of all UC cases^[3], maintenance treatment may lower relapse rate. In summary, this study shows that the curative effect and safety of domestic olsalazine sodium is superior to SASP in the treatment of chronic UC. It boosts remission rate, lowers relapse rate and causes fewer side effect, especially applicable to patients who are irresponsive or allergic to SASP therapy.

According to our statistics, the first episode type accounted for 34.8% of all ulcerative colitis cases in China^[3]. The disease mostly starts in rectum and sigmoid colon. When Heartleaf houttuynia enema is used, it can work on diseased areas directly. In this way, it not only can avoid the effects of pH and enzyme on the medicine, but also can make the herb absorbed completely and prolong the time of drug action. Then, colonic mucous membrane will recover gradually to normal with healing of the ulcers. Volatile oil extract of fresh Heartleaf houttuynia is used to produce Heartleaf houttuynia injection. Its utility components (Houttuynin, luraldehyde, quercitrin, isoquercitrin, etc.) are higher than that of Heartleaf houttuynia herb with widespread pharmacological actions. For instance, relaxation of intestinal smooth muscle could relieve enterospasm, prolong the retention time of intestinal contents, alleviate and eliminate the symptoms of diarrhea and abdominal pain^[8,24,25]. Quercitrin and isoquercitrin can ameliorate capillary fragility for haemostasis, which lead to the stoppage of bloody stool. Pathological changes, such

as swollen mitochondria with depleted ridge, shortened microvilli, maldevelopment of goblet cells and increased epithelial cell apoptosis could be found on the surface of mucous membrane and recess prior to Heartleaf houttuynia herb injection treatment. All these results in malabsorption of water with symptoms of diarrhea, while the increase of epithelial cell apoptosis can lead to the formation of ulcer due to damage of the colonic mucous membrane barrier. The expression of CD54 can further promote the inflammatory reaction. After treatment with Heartleaf houttuynia herb injection, epithelial cell apoptosis^[11], swollen mitochondria, shortened microvilli and the expression of CD54 could recover to normal gradually, which led to plerosis of colonic mucous membrane and healing of ulcer, the effect was superior to that of SASP. Heartleaf houttuynia herb is not only a medicine, but also a safe edible plant. The pH and osmotic pressure of the injection are close to those of intrinsic human environment, so there are no adverse reactions in Heartleaf houttuynia herb therapy, while SASP therapy may have side effects such as the heartburn, increased ALT, decrease WBC and rash.

UC patients often have symptoms of diarrhea, abdominal pain and tenesmus. Are these symptoms related to colonic motility disturbance? In this study, compared with the normal persons, the mean promotive speed of contraction wave stepped up and the mean amplitude of wave decreased in active UC patients, which led to diarrhea. The gastrocolic hyperreflex resulted in awareness of defecation and abdominal pain after eating that could be relieved after defecation. These two indexes improved significantly after treatment with Heartleaf houttuynia herb ($P < 0.05$). In normal persons, the postprandial pressure of sigmoid was higher than that of descending colon and splenic flexure, the pressure gradient and segmental construction made the colonic contents mixed and milled to expose to the colonic mucous membrane fully. Reabsorption of water and electrolytes were thus promoted. In active UC patients, the colonic pressure was significantly decreased ($P < 0.05$), and there was no pressure gradient in different colonic loci which could lead to disturbance of reabsorption of water and electrolytes. Diarrhea occurred due to the decrease of segmental construction and also inflammation of colonic mucosa occurred. The pain threshold of distant colon in active UC patients decreased significantly compared with that of normal persons, indicating that the distant colonic sensibility was increased. So, a small amount of intestinal contents could stimulate defecation reflex, leading to symptoms of diarrhea^[23], abdominal pain and tenesmus. After treatment with Heartleaf houttuynia herb, the colonic pressure and pain threshold recovered to normal due to the following reasons. Heartleaf houttuynia caused relaxation of intestinal smooth muscle which could relieve the enterospasm, prolong the retention time of intestinal contents, alleviate and eliminate the symptoms of diarrhea and abdominal pain. Our prophase study proved that Heartleaf houttuynia herb could improve the colonic motility disturbance of UC rats. In this study, the remission of diarrhea and abdominal pain might be partly related to this. Heartleaf houttuynia herb also has anti-inflammatory actions as we have proven in our previous animal study, which led to the remission of symptoms.

The main component of Kangshuangling sublingual tablets is low molecular mass (molecular mass ranged from 5-15 ku, peak ranged from 5-8 ku) heparin substance. Each tablet contains 1 200IU LMWH, which can be absorbed by the sublingual mucosa, so it not only has no first-pass effects by the liver compared with oral LMWH used in our previous study^[29], but also has no inconvenience of injection. Heparin, a group of sulphated glycosaminoglycans, in addition to its physiological effects and anticoagulant, antithromboembolic, antiallergic, antiviral, antiendotoxic and immunoregulative biological activities, has been found with a wide range of potentially anti-

inflammatory effects, including inhibition of neutrophil elastase and inactivation of chemokines^[40]. Compared with heparin, LMWH has higher antithromboembolic effects, longer half life period, less bleeding tendency, higher bioavailability, easier absorption by sublingual administration, as well as anti-inflammatory effects^[29,41]. Previous reports^[29] on improvement of UC patients treated with heparin prompted us to perform a pilot study of Kangshuangling sublingual tablets to find a more convenient and effective drug for patients with refractory UC. The observed response to Kangshuangling sublingual tablets was paradoxical. Sixteen of 18 patients with refractory UC unresponsive to high-dose prednisolone and sulfasalazine therapy for more than 4 wk achieved clinical remission and became asymptomatic after treatment of Kangshuangling sublingual tablets in combination with sulfasalazine. Contrary to the traditional idea that heparin could enhance bleeding, rectal bleeding was the first symptom to be improved by Kangshuangling sublingual tablets. The results were similar to other reports of heparin treatment^[42,43].

If Kangshuangling sublingual tablets have a therapeutic effect on UC, their mechanism of action should shed some lights on the elusive pathogenesis of this disease. Several thrombophilic features of UC that suggest the effect of Kangshuangling sublingual tablets on colitic symptoms may be attributable to their anticoagulant and antithrombotic properties. Evidences of a thrombotic process in UC included: reports of a hypercoagulable state^[20,22], an increased incidence of thromboembolic event^[44], and ischemic complications such as toxic megacolon and pyoderma gangrenosum. In this study, the membrane marks of platelet activity CD62p and CD63 were increased significantly, and the derivative of active platelet TXA2 was also elevated, suggesting that blood platelet TXA2 was in an active state, which not only led to a hypercoagulable state and an increased incidence of thromboembolic events, but also enhanced inflammatory reaction^[20,22]. Activated hyperaggregable platelets in the mesenteric circulation could amplify the inflammatory cascade by promoting neutrophil recruitment and chemotaxis. P-selectin has an established action as the adhesion molecule for neutrophils, and circulating platelet aggregates may contribute to ischemic damage and infarction by occluding the intestinal microvasculature. Platelets derived thromboxane A₂ may also contribute to ischemia by inducing local vasoconstriction. After treatment with Kangshuangling sublingual tablets, all these parameters dropped markedly, suggesting that the therapeutic effect of LMWH was partly related to inhibition of platelet activity, and improvement of hypercoagulable state, leading to the remission of clinical symptoms. But the membrane marks of platelet CD62p and CD63 were still higher than those of the normal controls. Whether it has predictive value for recurrence or prognosis should be further studied.

CD54 antigen could react with 85-110 ku integral membrane glycoprotein, and it is also known as an intercellular adhesion molecule-1 (ICAM-1) expressed on endothelial cells and both resting (weak) and activated (moderate) lymphocytes and monocytes^[15]. CD54 is ligand for the leukocyte function antigen-1 (CD11a). Its expression was up-regulated upon stimulation by inflammatory mediators such as cytokines and LPS, and it was involved in B cell-T cell co-stimulatory interactions. In this study, CD54 elevated significantly in blood and tissues of UC patients, being higher in tissues than in blood. Therefore, it could reflect the inflammation of intestinal mucosa. After treatment with Kangshuangling sublingual tablets, CD54 dropped significantly in both blood and tissues, indicating that Kangshuangling sublingual tablets could relieve the inflammatory activity in refractory UC patients who received high-dose prednisolone and sulfasalazine therapy for a long period (more than 4 wk) without significant improvement and

were regarded as corticosteroid-resistant refractory cases of UC. It was reported that heparin could also inhibit c-reactive protein (CRP), tumor necrosis factor (TNF) and L-selectin of UC patients. The detailed mechanisms by which anti-inflammatory properties of oral L MWH are mediated in UC remain to be elucidated further.

The multidrug resistance (MDR) gene coding for a drug efflux pump P-glycoprotein 170(Pgp-170) expressed on the surface of lymphocytes and intestinal epithelial cells^[38,39]. In this study, Pgp-170 was elevated significantly in blood and tissues of refractory UC patients. Poor response to medical therapy of certain UC patients might be related to MDR expression because glucocorticoids are known Pgp-170 substrates. There was no difference of Pgp-170 in tissues and blood, indicating that peripheral blood lymphocyte (PBL) MDR remained stable over time and was not influenced by disease activity or glucocorticoid therapy, both PBL and mucosal MDR expression appeared independent of disease activity, and there was a significant correlation between PBL and MDR expression and intestinal epithelial lymphocyte and epithelial cell expression^[38,39]. After treatment with Kangshuangling sublingual tablets, Pgp-170 dropped significantly in both blood and tissues, indicating that Kangshuangling sublingual tablet could inhibit the expression of MDR, but Pgp-170 was still higher than that of the normal controls, indicating that PBL and mucosal MDR may play an important role in determining the response of refractory UC patients to glucocorticoid therapy. From these results, we conclude that Kangshuanling sublingual tablets may play a role in treating refractory UC with activated platelets, the mechanism is partly related to the inhibition of platelet activity, hypercoagulable state, MDR expression, and its anti-inflammatory effects. No complications are found to be associated with the use of Kangshuanling sublingual tablets. It is still the focus of study in treating refractory UC with the Chinese features^[3].

REFERENCES

- 1 **Jiang XL**, Wang ZK, Qin CY. Current research and strategy on ulcerative colitis in China. *Shijie Huaren Xiaohua Zazhi* 2000; **8**: 610-613
- 2 **Jiang XL**, Quan QZ, Liu T, Dong XC. Recent advances in research of ulcerative colitis. *Shijie Huaren Xiaohua Zazhi* 2000; **8**: 216-218
- 3 **Jiang XL**, Cui HF. An analysis of 10218 ulcerative colitis cases in China. *World J Gastroenterol* 2002; **8**: 158-161
- 4 **Jiang XL**, Cui HF. Features of ulcerative colitis cases in China: An analysis of 10218 cases. *Shijie Huaren Xiaohua Zazhi* 2001; **9**: 869-873
- 5 **Jiang XL**. Strength the analysis of digestive diseases. *Shijie Huaren Xiaohua Zazhi* 2001; **9**: 864-868
- 6 **Jiang XL**, Cui HF. A new chronic ulcerative colitis model produced by combined methods in rats. *World J Gastroenterol* 2000; **6**: 742-746
- 7 **Jiang XL**, Quan QZ, Wang D, Sun ZQ, Wang YJ. A new ulcerative colitis model induced by compound method and the change of immune and ultrastructure. *Shijie Huaren Xiaohua Zazhi* 1999; **7**: 381
- 8 **Jiang XL**, Quan QZ, Wang D, Sun ZQ, Wang YJ, Qi F. Experimental study of heartleaf houttuynia herb on ulcerative colitis. *Shijie Huaren Xiaohua Zazhi* 1999; **7**: 786
- 9 **Jiang XL**, Quan QZ, Sun ZQ, Wang YJ, Qi F, Wang D, Zhang XL. Expression of lymphocyte apoptosis in patients with ulcerative colitis. *Shijie Huaren Xiaohua Zazhi* 1999; **7**: 903-904
- 10 **Jiang XL**, Quan QZ, Cheng GR, Sun ZQ, Wang YJ, Wang YP. Expression of apoptosis on biopsy tissue in patients with ulcerative colitis. *Shijie Huaren Xiaohua Zazhi* 2000; **8**: 107-108
- 11 **Jiang XL**, Pan BR, Ma JY, Ji ZH, Ma LS. Review for the 20th century and prospect for the 21st century of digestology. *Shijie Huaren Xiaohua Zazhi* 2000; **8**: 1161-1176
- 12 **Xu NZ**. Expression of adhesion molecules in tissues and pe-

- ripheral lymphocyte of patients with ulcerative colitis. *Huaren Xiaohua Zazhi* 1998; **6**(Suppl 7): 54-55
- 13 **Jiang XL**, Quan QZ, Sun ZQ, Wang YJ, Qi F, Wang D, Zhang XL. Detection of soluble CD44v6 in patients with inflammatory bowel disease. *Shijie Huaren Xiaohua Zazhi* 1999; **7**: 1028
 - 14 **Jiang XL**, Quan QZ, Chen GR, Sun ZQ, Wang YJ, Qi F, Wang D. Detection of CD44v6 on biopsy tissue can't differ ulcerative colitis from Chron's disease. *Zhonghua Xiaohua Beijing Zazhi* 2000; **19**: 298-299
 - 15 **Jiang XL**, Quan QZ, Chen GR, Yin GP, Sun ZQ, Wang YJ. Detection of CD54, CD44 on biopsy tissues in patients with ulcerative colitis. *Zhonghua Xiaohua Beijing Zazhi* 1998; **15**: 292-294
 - 16 **Jiang XL**, Quan QZ, Sun ZQ, Wang YJ, Qi F, Yin GP, Sun XM. Detection of adhesion molecules in tissues and peripheral blood of patients with ulcerative colitis. *Zhonghua Weishengwu He Mianyixue Zazhi* 1998; **18**: 156
 - 17 **Jiang XL**, Quan QZ, Sun ZQ, Wang YJ, Qi F. Effect of glucocorticoid on lymphocyte adhesion molecule phenotype expression in patients with ulcerative colitis. *Zhongguo Weizhongbing Jijiu Yixu* 1998; **10**: 366-368
 - 18 **Jiang XL**, Quan QZ, Sun ZQ, Wang YJ, Qi F, Chen GR, Gao TS, Pan X. Detection of P-selectin and CD63 in peripheral blood of patients with ulcerative colitis. *Zhongguo Weizhongbing Jijiu Yixue* 1998; **10**: 174-175
 - 19 **Jiang XL**, Quan QZ, Sun ZQ, Wang YJ. Detection of P-selectin and CD63 in patients with ulcerative colitis. *Shanghai Mianyixue Zazhi* 1998; **18**: 230
 - 20 **Jiang XL**, Quan QZ, Liu TT, Wang YJ, Sun ZQ, Qi F, Ren HB, Zhang WL, Zhang L. Detection of blood platelet activation in patients with ulcerative colitis. *Xin Xiaohuabingxue Zazhi* 1997; **5**: 736
 - 21 **Jiang XL**, Quan QZ, Wang D, Sun ZQ, Wang YJ. One case report of ulcerative colitis accompanied with acute myocardial infarction. *Shijie Huaren Xiaohua Zazhi* 1999; **7**: 963
 - 22 **Jiang XL**, Quan QZ, Sun ZQ, Wang YJ, Qi F. Relationship between syndrome-typing of ulcerative colitis and activation of platelet. *Zhongyi Zazhi* 1997; **38**: 730-731
 - 23 **Jiang XL**, Quan QZ, Wang YJ, Sun ZQ, Wang D, Qi F. Measurement of rectual and annual motility in patients with ulcerative colitis. *Zhonghua Xiaohua Beijing Zazhi* 2000; **17**: 170-171
 - 24 **Jiang XL**, Quan QZ, Dong XC, Liu T. Effects of houttuynia herb on rectual and annual motility in patients with ulcerative colitis. *Zhongyiyao Xubao* 2000; **4**: 43-44
 - 25 **Jiang XL**, Quan QZ, Wang D, Sun ZQ, Wang YJ, Qi F. Effect of heartleaf houttuynia herb on colonic pressure in rats with ulcerative colitis. *Shijie Huaren Xiaohua Zazhi* 1999; **7**: 639
 - 26 **Zhang ZD**, Chen J, Zhong YW, Zhang ST. Strength the diagnosis and treatment of ulcerative colitis. *Shijie Huaren Xiaohua Zazhi* 2003; **11**: 1027-1028
 - 27 **Jiang XL**. Diagnosis and treatment of ulcerative colitis. *Shijie Huaren Xiaohua Zazhi* 2000; **8**: 332
 - 28 **Jiang XL**, Quan QZ, Wang ZK. Diagnosis, typing and effect criteria of ulcerative colitis. *Shijie Huaren Xiaohua Zazhi* 2000; **8**: 332-334
 - 29 **Cui HF**, Jiang XL. Treatment of corticosteroid resistant ulcerative colitis with oral low molecular weight heparin. *World J Gastroenterol* 1999; **5**: 448-450
 - 30 **Jiang XL**, Qin CY, Li GQ. Special treatment for ulcerative colitis. *Shijie Huaren Xiaohua Zazhi* 2000; **8**: 341-342
 - 31 **Jiang XL**, Liu T. Treatment of refractory ulcerative colitis with heparin. *Shijie Huaren Xiaohua Zazhi* 1999; **7**: 694
 - 32 **Jiang XL**, Quan QZ, Sun ZQ, Wang YJ, Shang RL, Qi F. Clinical study on ulcerative colitis treated with Heartleaf houttuynia herb injection. *Shijie Huaren Xiaohua Zazhi* 2003; **11**: 1207-1210
 - 33 **Jiang XL**, Quan QZ, Sun ZQ, Wang YJ, Shang RL, Qi F. A control study on ulcerative colitis treated with olsalazine sodium. *Shijie Huaren Xiaohua Zazhi* 2003; **11**: 1211-1213
 - 34 **Jiang XL**, Quan QZ, Sun ZQ, Wang YJ, Shang RL, Qi F. Treatment of refractory ulcerative colitis with Kangshuangling. *Shijie Huaren Xiaohua Zazhi* 2003; **11**: 1214-1218
 - 35 **Chinese Society of Gastroenterology**. Suggestion on the diagnosis and treatment of inflammatory bowel diseases. *Zhonghua Neike Zazhi* 2001; **40**: 138-141
 - 36 **Gaffney PR**, Doyle CT, Gaffney A, Hogen J, Hayes DP, Annis P. Paradoxical response to heparin in 10 patients with ulcerative colitis. *Am J Gastroenterol* 1995; **90**: 220-223
 - 37 **Collins CE**, Cahill MR, Newland AC, Rampton DS. Platelets circulate in an activated state in inflammatory bowel disease. *Gastroenterology* 1994; **106**: 840-845
 - 38 **Farrell RJ**, Murphy A, Long A, Donnelly S, Cherikuri A, O' Toole D, Mahumd N, Keeling PW, Weir DG, Kelleher D. High multidrug resistance (P-glycoprotein 170) expression in inflammatory bowel disease patients who fail medical therapy. *Gastroenterology* 2000; **118**: 279-288
 - 39 **Yacyshyn B**, Maksymowych W, Bowen-Yacyshyn MB. Differences in P-glycoprotein -170 expression and activity between Crohn's disease and ulcerative colitis. *Hum Immunol* 1999; **60**: 677-687
 - 40 **Tyrrell DJ**, Kilfeather S, Page CP. Therapeutic uses of heparin beyond its traditional role as an anticoagulant. *Trends Pharmacol Sci* 1995; **16**: 198-204
 - 41 **Jiang XL**, Cui HF, Wang YJ, Quan QZ, Sun ZQ. Effects of oral low molecular weight heparin on hemorrheology of rabbit liver damaged by D-galuctosamine. *Xin Xiaohuabingxue Zazhi* 1997; **5**: 355-356
 - 42 **Folwaczny C**, Frike H, Endres S, Hartmann G, Jochum M, Loeschke K. Anti-inflammatory properties of unfractionated heparin in patients with highly active ulcerative colitis: a pilot study. *Am J Gastroenterol* 1997; **92**: 911-912
 - 43 **Evans RC**, Wong VS, Morris AI, Rhodes JM. Treatment of corticosteroid-resistant ulcerative colitis with heparin: a report of 16 cases. *Aliment Pharmacol Ther* 1997; **11**: 1037-1040
 - 44 **Koenigs KP**, Mcphedran P, Spiro HM. Thrombosis in inflammatory bowel disease. *J Clin Gastroenterol* 1987; **9**: 627-631

Edited by Wang XL Proofread by Xu FM

Effects of probiotic on intestinal mucosa of patients with ulcerative colitis

Hai-Hong Cui, Cun-Long Chen, Ji-De Wang, Yu-Jie Yang, Yong Cun, Jin-Bao Wu, Yu-Hu Liu, Han-Lei Dan, Yan-Ting Jian, Xue-Qing Chen

Hai-Hong Cui, Cun-Long Chen, Ji-De Wang, Yu-Jie Yang, Yong Cun, Jin-Bao Wu, Yu-Hu Liu, Han-Lei Dan, Yan-Ting Jian, Xue-Qing Chen, Chinese PLA Institute of Digestive Medicine, First Military Medical University, Guangzhou 510515, Guangdong Province, China

Correspondence to: Dr. Cun-Long Chen, Department of Gastroenterology, Chinese PLA Institute of Digestion Medicine, First Military Medical University, Guangzhou 510515, Guangdong Province, China. cunlong@fimmu.edu.cn

Telephone: +86-20-61641544 **Fax:** +86-20-61641530

Received: 2003-05-11 **Accepted:** 2003-06-27

Abstract

AIM: To investigate the effects of probiotic on intestinal mucosae of patients with ulcerative colitis (UC), and to evaluate the role of probiotic in preventing the relapse of UC.

METHODS: Thirty patients received treatment with sulphasalazine (SASP) and glucocorticoid and then were randomly administered bifid triple viable capsule (BIFICO) (1.26 g/d), or an identical placebo (starch) for 8 wk. Fecal samples were collected for stool culture 2 wk before and after the randomized treatments. The patients were evaluated clinically, endoscopically and histologically after 2 mo of treatment or in case of relapse of UC. p65 and I κ B expressions were determined by Western blot analysis. DNA-binding activity of NF- κ B in colonic nuclear extracts was detected by electrophoretic mobility shift assay (EMSA). mRNA expressions of cytokines were identified by semi-quantitative assay, reverse transcriptase-polymerase chain reaction (RT-PCR).

RESULTS: Three patients (20%) in the BIFICO group had relapses during 2-mo follow-up period, compared with 14 (93.3%) in placebo group ($P < 0.01$). The concentration of fecal lactobacilli, bifidobacteria was significantly increased in BIFICO-treated group only ($P < 0.01$). The expressions of NF- κ B p65 and DNA binding activity of NF- κ B were significantly attenuated in the treatment group than that in control ($P < 0.05$). The mRNA expression of anti-inflammatory cytokines was elevated in comparison with the control group.

CONCLUSION: The probiotic could impede the activation of NF- κ B, decrease the expressions of TNF- α and IL-1 β and elevate the expression of IL-10. These results suggest that oral administration of this new probiotic preparation is effective in preventing flare-ups of chronic UC. It may become a prophylactic drug to decrease the relapse of UC.

Cui HH, Chen CL, Wang JD, Yang YJ, Cun Y, Wu JB, Liu YH, Dan HL, Jian YT, Chen XQ. Effects of probiotic on intestinal mucosa of patients with ulcerative colitis. *World J Gastroenterol* 2004; 10(10): 1521-1525

<http://www.wjgnet.com/1007-9327/10/1521.asp>

INTRODUCTION

Ulcerative colitis (UC) is a chronic disease and easy to relapse, its etiology and pathogenesis have not been definitively elaborated^[1]. Primary therapy for UC is usually a combination of sulfasalazine and glucocorticoids. Sulfasalazine can be given alone or in combination with other drugs. However, a large number of patients are resistant or intolerant to sulfasalazine. Glucocorticoids suppress active inflammation very effectively, but its long-term use is associated with high rates of relapse and unacceptable toxicities. Recently, probiotic has been recommended to ameliorate the milieu of intestine and prolong the time of relapse^[2-14]. This study intended to evaluate the role of bifidobacteria in remission of UC.

MATERIALS AND METHODS

Sample collection and processing

Thirty active UC patients were recruited for this study from 2001 to 2002 at Nanfang Hospital. Severity of the disease in colon and rectum was assessed by one gastroenterologist with an endoscope. These patients on sulphasalazine (SASP) and glucocorticoid had clinical and endoscopic remission and were randomized to receive either bifid triple viable capsule (BIFICO) (1.26 g/d), or an identical placebo (starch) for 8 wk. Biopsy specimens were obtained with standard biopsy forceps to include the most macroscopically inflamed site with UC and immediately frozen in liquid nitrogen and stored at -80 °C for RNA and protein extraction. Meanwhile, fecal samples were collected for stool culture before and after 2 wk of treatments. Patients were assessed clinically, endoscopically and histologically after a 2-mo period of treatment or in case of relapse of UC.

Fecal analysis

Fecal samples were collected for microbiological examinations. We prepared the selective medium to incubate ten strains of luminal resident bacteria in large intestine. *Enterobacteria* (EMB), *Enterococcus* (EC), *Staphylococcus* (SP) and *Saccharomyces* (yeast) (SB) are aerobes. *Bacteroides* (BD), *Bifidobacterium* (BL), *Lactobacillus* (LC), *Peptococcus* (PS), *Eubacterium* (ES) and *Clostridium* (CD) are anaerobes. 0.5 g feces in a small bottle containing 4.5 mL diluted solution and 4-5 beads were concussed 1 min on a vortex agitator, 1.8 mL diluted solution was added to each of other 7 bottles. The solution was diluted in series as 10⁻², 10⁻³, ..10⁻⁸, respectively. Aerobes and anaerobes were observed 24 h and 72 h after incubation at 37 °C.

Preparation of cytoplasmic and nuclear extracts

Nuclear extracts from biopsy tissues were prepared by the method of Deryckere and Gannon^[15]. Frozen tissue was ground with a mortar in liquid nitrogen and transferred to a tissue homogenizer. Protease inhibitor cocktail (Sigma) was added and centrifuged at 2 000 r/min for 30 s. Supernatant was incubated on ice for 5 min and then centrifuged at 5 000 r/min for 5 min. The final supernatant containing cytoplasmic extracts was collected and stored at -80 °C. Pelleted nuclei were then resuspended in 50-100 μ L of buffer G and incubated on ice for 20 min.

The lysed nuclei were then transferred to a microcentrifuge tube, centrifuged at 12 000 r/min for 10 min, and the supernatant containing the nuclear extracts was collected and stored at -80°C . Protein concentration was determined with BCA-protein estimation kit.

Western blot analysis

For each sample, an equal amount (50 μg) of protein lysates was analyzed on 100 g/L or 120 g/L sodium dodecyl sulfate-polyacrylamide gel. Proteins were electroblotted onto Immobilon PVDF membranes (Millipore, Bedford, MA), blocked in 50 g/L dry skim milk for 1 h, and then incubated with the indicated antibodies. The antibodies used were 1:700 rabbit polyclonal anti-NF- κB and I κB antibodies, the secondary antibodies used were provided in an enhanced chemiluminescence detection kit (Santa Cruz, CA). Exposure time (5-60 s) varied with the antibodies used.

Electrophoretic mobility shift assays

DNA-binding activity of NF- κB in colon nuclear extracts was determined by electrophoretic mobility shift assay (EMSA). The sequence of NF- κB probe was 5' -AGT TGA GGG GAC TTT CCC AGG C-3' [16], 10 μg of nuclear protein was incubated at room temperature for 20 min with radiolabeled [γ - ^{32}P] ATP using T4 polynucleotide kinase. A 20 μL reaction buffer contained 2 μg poly dI-dC (Sigma), 10 mmol/L tris-HCl (pH7.5), 100 mmol/L NaCl, 10 mmol/L EDTA, 20 mmol/L MgCl₂, 10 mmol/L DTT, 3 μL of 250 mL/L glycerol and 1 μL of labeled probe. For competition assays, 100-fold molar excess of unlabeled oligonucleotide was added to the binding reaction. Nucleoprotein- oligonucleotide complexes were resolved by electrophoresis on a 50 g/L non-denaturing polyacrylamide gel (PAGE; acrylamide/bisacrylamide at 30:1) in 0.1 \times TBE buffer at 150 V for 2 h at 4°C . The gel was dried and autoradiographed with intensifying screen at -80°C for 72 h. The radioactivity of appropriate bands was counted using a BAS2000 phosphorimage analyzer (Fuji Film, Minamiashigara, Japan).

Proinflammatory and inhibitive factor mRNA detected by RT-PCR

Total RNA was isolated from biopsies using TRIzol reagent (Life Technologies). cDNA was generated from 1 μg of total RNA in a reaction volume of 20 μL , using M-MLV reverse transcriptase (MBI). PCR was performed in the linear range of amplification (determined for each primer pair-cDNA combination). Standard PCR reactions were performed with 1 μL of the cDNA solution, 50 $\mu\text{mol/L}$ of each primer solution, 10 mmol/L of each Dntp, 25 mmol/L MgCl₂, 10 \times Goldstar DNA polymerase reaction buffer, and 0.5 units of Goldstar DNA polymerase (Eurogentec, Seraing, Belgium). Each PCR cycle was performed at 94°C for 1 min, at 56°C for 1 min, and at 72°C for 1 min, respectively. Following sense / antisense primers were designed to amplify cDNA fragments [17,18]: glyceraldehydes-3-phosphate dehydrogenase (G3PDH): sense primer: 5' -ACCACAGTCCATGCCATCAC-3', antisense: 5' -TCCACCACCTGTGCTGTA-3' (452 bp); TNF- α : sense primer: 5' -CTGTA GCCATGTTGTAGC-3', antisense: 5' -CAATGATCCC AAAGTAGACCT-3' (467 bp); IL-1 β : sense primer: 5' -CAGCCATGGCAGAAGTACCT-3', antisense: 5' -GGCCACAACAACCTGACGC-3' (223 bp); IL-10: sense primer: 5' -CTGAGGCGCTGTCATCGATT-3', antisense: 5' -AGGTCCTGGAGTCCAGCAGA-3' (328 bp). The PCR products were then visualized on a 10 g/L agarose gel by ethidium bromide (5 $\mu\text{g/mL}$) staining.

Statistical analysis

All results were expressed as mean \pm SD. Statistical differences between means were determined using independent-sample *t* test and paired-sample *t* test by SPSS 10.0 statistical software.

A *P* value ≤ 0.05 was considered statistically significant.

RESULTS

Fecal analysis

The number of fecal bacteria before treatment in these 2 groups had no significant difference. After treatment, the fecal specimens of the patients on BIFICO were obviously different from the patients on placebo. The number of Gram-positive Bacilli and Enterococci was significantly higher than that in control group. The number of *Enterococci*, *Bacteroides* and *Bifidobacteria* was obviously less than that in control group ($P < 0.05$). In control group, the number of *Bifidobacteria* (6.44 ± 0.25 , $P < 0.01$) and Lactobacilli (6.67 ± 0.43 , $P < 0.05$) was less than that in treatment group (Table 1).

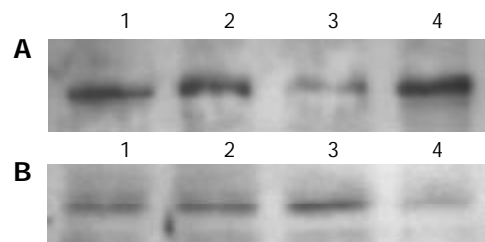


Figure 1 Expressions of NF- κB p65 and I κB in nuclei and cytoplasm. A: Expression of NF- κB p65 in nuclei, B: Expression of I κB in cytoplasm, Lanes 1-2: expression before treatment, Lanes 3: expression after probiotics treatment, Lanes 4: expression in control.

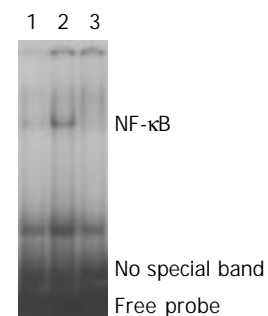


Figure 2 Inhibition of NF- κB binding DNA by BIFICO. 1, Cool probe; 2, Activation NF- κB before treatment; 3, Probiotic significantly inhibited activation of NF- κB .

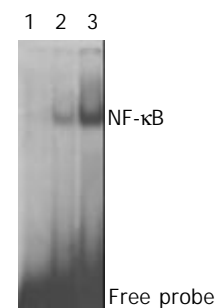


Figure 3 Activation of NF- κB in. Placebo group 1, Cool probe; 2, Activation of NF- κB before treatment; 3, Placebo did not obviously inhibit the activation of NF- κB .

NF- κB and I κB examination

The degradation of I κB in cytoplasm was obviously inhibited by BIFICO and NF- κB in nuclei was less expressed after treatment ($P < 0.05$) (Figures 1, Table 2).

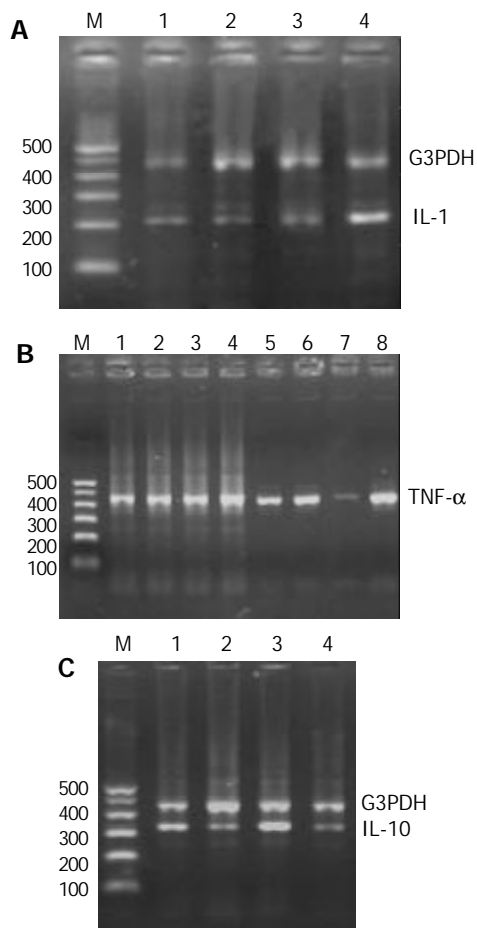


Figure 4 Expressions of IL-1 mRNA, TNF- α mRNA and IL-10 mRNA. A: Expression of IL-1 mRNA, Lanes 1,2: IL-1 mRNA expression before treatment; lane 3: BIFICO inhibited IL-1 mRNA expression; lane 4: IL-1 mRNA expression in placebo group. B: Expression of TNF- α mRNA, Lanes 1,2,3,4 G3PDH; lanes 5,6: TNF- α mRNA expression before treatment; Lane 7: BIFICO inhibited significantly mRNA expression of TNF- α ; lane 8: TNF- α mRNA expression in placebo group. C: Expression of IL-10 mRNA, Lanes 1,2: IL-10 mRNA before treatment; lane 3: BIFICO enhanced IL-10 mRNA expression; lane 4: IL-10 mRNA in placebo group.

Table 1 Flora analysis (mean \pm SD, Lg10ⁿ/g)

Index	BIFICO group		Placebo group	
	Pretreatment (n=15)	Post-treatment (n=15)	Pretreatment (n=15)	Post-treatment (n=15)
EMB	8.21 \pm 0.69	8.11 \pm 0.29	8.23 \pm 0.42	8.93 \pm 0.62 ^{ac}
EC	6.63 \pm 0.21	7.20 \pm 0.31 ^a	6.71 \pm 0.39	6.67 \pm 0.48 ^c
SP	3.55 \pm 0.96	3.61 \pm 0.19	3.65 \pm 0.41	3.72 \pm 0.30
SB	3.45 \pm 0.83	3.09 \pm 0.25 ^a	3.36 \pm 0.35	3.47 \pm 0.96
BD	6.79 \pm 0.29	7.26 \pm 0.03 ^a	6.77 \pm 0.88	6.81 \pm 0.35
BL	6.92 \pm 0.34	7.69 \pm 0.34 ^b	7.03 \pm 0.34	6.44 \pm 0.25 ^{bd}
PS	7.26 \pm 0.61	7.32 \pm 0.74	6.78 \pm 0.59	6.93 \pm 0.52
LC	6.95 \pm 0.52	7.39 \pm 0.72 ^a	7.07 \pm 0.97	6.67 \pm 0.43 ^c
ES	5.91 \pm 0.92	5.45 \pm 0.25	5.45 \pm 0.67	5.68 \pm 0.80
CD	6.18 \pm 0.78	6.13 \pm 0.66	6.19 \pm 0.72	6.37 \pm 0.96

^a P <0.05, ^b P <0.01 vs post-treatment; ^c P <0.05, ^d P <0.01 vs control. EMB: *Enterobacter*; EC: *Enterococcus*; SP: *Staphylococcus*; SB: *Saccharomyces* (yeast); BD: *Bacteroides*; BL: *Bifidobacterium*; LC: *Lactobacillus*; PS: *Peptococcus*; ES: *Eubacterium*; CD: *Clostridium*.

Activation of NF- κ B in nuclei

The results of EMSA showed that activation of NF- κ B was

elevated in patients who did not take BIFICO in comparison with pretreatment, more NF- κ B was combined with special recognition sites of DNA (P <0.05, Figures 2,3).

Table 2 Expression of NF- κ B (nucleus) and I κ B (cytoplasm) before and after therapy (mean \pm SD)

Index	BIFICO group		Placebo group	
	Pretreatment	Post-treatment	Pretreatment	Post-treatment
I κ B (cytoplasm)	0.99 \pm 0.11	0.97 \pm 0.07	0.89 \pm 0.08	0.43 \pm 0.15 ^{bd}
NF- κ B (nucleus)	0.82 \pm 0.05	0.31 \pm 0.05 ^b	0.79 \pm 0.14	0.97 \pm 0.09 ^d

^a P <0.05, ^b P <0.01 vs post-treatment; ^c P <0.05, ^d P <0.01 vs control.

Expression of IL-1- β , TNF- α , IL-10 mRNA

IL-1- β , TNF- α , IL-10 mRNAs in both groups were determined with RT-PCR. In control group, the level of IL-1- β , TNF- α mRNA at intestinal epithelial mucosa did not significantly decrease. (P <0.05, Figures 4, Table 3).

Table 3 mRNA expression of cytokines before and after therapy (OD value, mean \pm SD)

Index	BIFICO group		Placebo group	
	Pretreatment	Post-treatment	Pretreatment	Post-treatment
IL-1	0.41 \pm 0.09	0.53 \pm 0.11	0.38 \pm 0.12	1.20 \pm 0.08 ^d
TNF- α	0.79 \pm 0.06	0.35 \pm 0.12 ^b	0.86 \pm 0.05	1.40 \pm 0.18 ^d
IL-10	0.76 \pm 0.32	1.11 \pm 0.21 ^b	0.54 \pm 0.26	0.45 \pm 0.04 ^d

^a P <0.05, ^b P <0.01 vs post-treatment; ^c P <0.05, ^d P <0.01 vs control.

DISCUSSION

The pathogenesis of UC remains unknown. Genetic and environmental factors are obviously contributory. Luminal bacteria could play a major role in the initiation and perpetuation of chronic UC^[14,19-21]. Thousand of endogenous bacteria live in the large intestine and may be an essential factor in certain pathological disorders. Animal models of UC showed that colitis did not occur in a germ-free environment. In human UC, inflammation is present in parts of the gut housing the highest concentration of bacteria. Moreover, terminal ileum, caecum and rectum are relatively static, providing prolonged mucosal contact with luminal contents. Enhanced mucosal permeability may play a pivotal role in maintaining a chronic inflammatory state due to a genetic predisposition or direct contact with bacteria or their products. So far, no specific micro-organism has been directly associated with the pathogenesis of UC. Analysis of the luminal enteric flora, however, has revealed differences in the composition of this flora to healthy controls. In UC, concentrations of *Bacteroides*, *Eubacteria*, *Peptostreptococci* and facultative anaerobic bacteria are increased, whereas the number of *Bifidobacteria* is significantly reduced. Over the past few years, use of probiotics in IBD and other intestinal disorders has gained attention. Manipulation of the colonic bacteria with antibiotics and probiotics proved to be more effective and tolerable than immunosuppressants^[11,22]. Probiotics and prebiotics have a role in prevention or treatment of some diseases. The mechanisms through which dysregulation may play a central role in initiation and perpetuation of inflammatory bowel disease were discussed^[23]. BIFICO probiotic capsule was used for *Enterococci*, *Bifidobacteria*, *Lactobacilli* triple viable bacteria, probiotics such as VSL#3 could also be used to maintain clinical remission and prevent relapse in patients with

relapsing or chronic pouchitis. Therapy with anti-inflammatory agents and immunomodulators were often required for patients with chronic pouchitis resistant to antibiotics^[24,25]. Probiotic *Lactobacillus rhamnosus* GG (LGG) has proved to be beneficial to the treatment of viral- and antibiotic-associated diarrhea. Nitric oxide (NO) is involved in the protective mechanisms in the gastrointestinal tract and may contribute to some of the beneficial effects of probiotics. LGG induces NO production in J774 macrophages and in human T84 colon epithelial cells through induction of iNOS by a mechanism involving activation of transcription factor NF- κ B. Induction of iNOS and low-level synthesis of NO might be involved in the protective actions of LGG in the gastrointestinal tract^[26]. Recent results supported the concept that intestinal bacteria could induce endogenous signals that play a pathogenic role in hepatic insulin resistance and NAFLD and suggest novel therapies for these common conditions^[27,28]. We discovered that the high concentration of Gram-positive bacteria in luminal flora could effectively prolong the time of relapse of ulcerative colitis.

It is well known that transcriptional factor NF- κ B plays a pivotal role in expression of LPS-induced inflammatory factors. Because NF- κ B activation could lead to enhanced expression of proinflammatory cytokines, chemokines, inflammatory enzymes such as inducible NO synthase (iNOS) and cyclooxygenase (COX-2), adhesion molecules and inflammatory receptors^[29], modulation of NF- κ B activation might provide a direct way to inhibit inflammatory mediators^[30]. Activation of NF- κ B is triggered by phosphorylation of an inhibitory subunit, I κ B. In unstimulated cells, NF- κ B is sequestered in the cytoplasm through interaction with I κ B a and I κ Ba inhibitory proteins. In response to proinflammatory stimuli, I κ B is first phosphorylated in its N-terminal domain by a large multi-kinase complex, then polyubiquitinated, and finally degraded by the proteasome. The released NF- κ B complex could translocate into the nuclei where it initiates gene transcription upon binding to its cognate DNA motifs in regulatory segments of TNF- α gene and other target genes involved in inflammatory and immune process^[31]. At the same time, we also detected the effect of probiotics on the initiation and perpetuation of inflammation. The expressions of I κ B in cytoplasm and NF- κ B in nuclei were detected by Western blot. The result manifested that probiotics efficaciously inhibited the degradation of I κ B protein. Less NF- κ B translocation into nuclei could be detected by Western blot in treatment group. Activation of NF- κ B was analyzed by EMSA, the result likewise manifested that much more NF- κ B proteins were significantly activated in control group than in probiotics group.

Recent data have demonstrated that mucosal immune response is involved in patients with IBD. The nuclear transcription factor NF- κ B is a key regulator of inducible expressions of many genes involved in immune and inflammatory responses in the gut. Stimuli like oxidative stress, cytokines (IL-1, IL-6, TNF- α), bacteria and viruses can release NF- κ B from their inactive cytoplasmatic form to the nuclei. Inhibitory cytokines can prevent the activation of NF- κ B. More potent and selective treatment strategies with anti-sense p65, proteasome inhibitors and viral I kappa B alpha expression vectors have been aimed to prevent NF- κ B activation in mucosal macrophages and T lymphocytes. However, NF- κ B regulated genes are also involved in survival responses of epithelial cells. Selective inhibition of NF- κ B activation in inflammatory cells could be an option in management of IBD^[32-35]. In our study, the expression of proinflammatory cytokines such as TNF- α , IL-1 β influenced by the activation of NF- κ B obviously were inhibited by probiotics and mRNA expression of anti-inflammatory cytokine IL-10 was elevated by the effect of probiotics.

In conclusion, supplementation with probiotics is helpful in maintaining remission and preventing the relapse of UC.

REFERENCES

- 1 **Rampton DS**. Management of difficult inflammatory bowel disease: where are we now? *World J Gastroenterol* 2000; **6** (Suppl 3): 8
- 2 **Mitsuyama K**, Toyonaga A, Sata M. Intestinal microflora as a therapeutic target in inflammatory bowel disease. *J Gastroenterol* 2002; **37**(Suppl 14): 73-77
- 3 **Schultz M**, Sartor RB. Probiotics and inflammatory bowel diseases. *Am J Gastroenterol* 2000; **95**(1 Suppl): S19-21
- 4 **Shanahan F**. Probiotics and inflammatory bowel disease: is there a scientific rationale? *Inflamm Bowel Dis* 2000; **6**: 107-115
- 5 **Gionchetti P**, Rizzello F, Venturi A, Brigidi P, Matteuzzi D, Bazzocchi G, Poggioli G, Miglioli M, Campieri M. Oral bacteriotherapy as maintenance treatment in patients with chronic pouchitis: a double-blind, placebo-controlled trial. *Gastroenterology* 2000; **119**: 305-309
- 6 **Baert FJ**, Rutgeerts PJ. Medical therapies for ulcerative colitis and crohn's disease. *Curr Gastroenterol Rep* 2000; **2**: 446-450
- 7 **Gionchetti P**, Amadini C, Rizzello F, Venturi A, Palmonari V, Morselli C, Romagnoli R, Campieri M. Probiotics-role in inflammatory bowel disease. *Dig Liver Dis* 2002; **34**(Suppl 2): S58-62
- 8 **Fooks LJ**, Gibson GR. Probiotics as modulators of the gut flora. *Br J Nutr* 2002; **88**(Suppl 1): S39-49
- 9 **Hanauer SB**. Update on medical management of inflammatory bowel disease: ulcerative colitis. *Rev Gastroenterol Disord* 2001; **1**: 169-176
- 10 **Madsen KL**. The use of probiotics in gastrointestinal disease. *Can J Gastroenterol* 2001; **15**: 817-822
- 11 **Linskens RK**, Huijsdens XW, Savelkoul PH, Vandenbroucke-Grauls CM, Meuwissen SG. The bacterial flora in inflammatory bowel disease: current insights in pathogenesis and the influence of antibiotics and probiotics. *Scand J Gastroenterol Suppl* 2001; **234**: 29-40
- 12 **Steidler L**. Microbiological and immunological strategies for treatment of inflammatory bowel disease. *Microbes Infect* 2001; **3**: 1157-1166
- 13 **Madsen K**, Cornish A, Soper P, McKaigney C, Jijon H, Yachimec C, Doyle J, Jewell L, De Simone C. Probiotic bacteria enhance murine and human intestinal epithelial barrier function. *Gastroenterology* 2001; **121**: 580-591
- 14 **Campieri M**, Gionchetti P. Bacteria as the cause of ulcerative colitis. *Gut* 2001; **48**: 132-135
- 15 **Deryckere F**, Gannon F. A one-hour minipreparation technique for extraction of DNA-binding proteins from animal tissues. *Biotechniques* 1994; **16**: 405
- 16 **Xu L**, Fidler IJ. Acidic pH-induced elevation in interleukin 8 expression by human ovarian carcinoma cells. *Cancer Res* 2000; **60**: 4610-4616
- 17 **Haller D**, Bode C, Hammes WP, Pfeifer AM, Schiffrin EJ, Blum S. Non-pathogenic bacteria elicit a differential cytokine response by intestinal epithelial cell/leucocyte co-cultures. *Gut* 2000; **47**: 79-87
- 18 **Todt J**, Sonstein J, Polak T, Seitzman GD, Hu B, Curtis JL. Repeated intratracheal challenge with particulate antigen modulates murine lung cytokines. *J Immunol* 2000; **164**: 4037-4047
- 19 **Karban A**, Eliakim R, Brant SR. Genetics of inflammatory bowel disease. *Isr Med Assoc J* 2002; **4**: 798-802
- 20 **Duerr RH**. The genetics of inflammatory bowel disease. *Gastroenterol Clin North Am* 2002; **31**: 63-76
- 21 **Hendrickson BA**, Gokhale R, Cho JH. Clinical aspects and pathophysiology of inflammatory bowel disease. *Clin Microbiol Rev* 2002; **15**: 79-94
- 22 **Guarner F**, Malagelada JR. Gut flora in health and disease. *Lancet* 2003; **361**: 512-519
- 23 **Kanai T**, Iiyama R, Ishikura T, Uraushihara K, Totsuka T, Yamazaki M, Nakamura T, Watanabe M. Role of the innate immune system in the development of chronic colitis. *J Gastroenterol* 2002; **37**(Suppl 14): 38-42
- 24 **Shen B**. Diagnosis and treatment of patients with pouchitis. *Drugs* 2003; **63**: 453-461
- 25 **Gionchetti P**, Amadini C, Rizzello F, Venturi A, Campieri M. Review article: treatment of mild to moderate ulcerative coli-

- tis and pouchitis. *Aliment Pharmacol Ther* 2002; **16**(Suppl 4): 13-19
- 26 **Korhonen R**, Korpela R, Saxelin M, Maki M, Kankaanranta H, Moilanen E. Induction of nitric oxide synthesis by probiotic *Lactobacillus rhamnosus* GG in J774 macrophages and human T84 intestinal epithelial cells. *Inflammation* 2001; **25**: 223-232
- 27 **Li Z**, Yang S, Lin H, Huang J, Watkins PA, Moser AB, Desimone C, Song XY, Diehl AM. Probiotics and antibodies to TNF inhibit inflammatory activity and improve nonalcoholic fatty liver disease. *Hepatology* 2003; **37**: 343-350
- 28 **Folwaczny C**. Anti-inflammatory effects of a pathogenic salmonella: relevance for therapy with probiotics? *Z Gastroenterol* 2001; **39**: 329-332
- 29 **Christman JW**, Lancaster LH, Blackwell TS. Nuclear factor kappa B: a pivotal role in the systemic inflammatory response syndrome and new target for therapy. *Intensive Care Med* 1998; **24**: 1131-1138
- 30 **Naik S**, Kelly EJ, Meijer L, Pettersson S, Sanderson IR. Absence of Toll-like receptor 4 explains endotoxin hyporesponsiveness in human intestinal epithelium. *J Pediatr Gastroenterol Nutr* 2001; **32**: 449-453
- 31 **Cong B**, Li SJ, Yao YX, Zhu GJ, Ling YL. Effect of cholecystokinin octapeptide on tumor necrosis factor alpha transcription and nuclear factor-kappaB activity induced by lipopolysaccharide in rat pulmonary interstitial macrophages. *World J Gastroenterol* 2002; **8**: 718-723
- 32 **Dijkstra G**, Moshage H, Jansen PL. Blockade of NF- κ B activation and donation of nitric oxide: new treatment options in inflammatory bowel disease? *Scand J Gastroenterol Suppl* 2002; **236**: 37-41
- 33 **Hanada T**, Yoshimura A. Regulation of cytokine signaling and inflammation. *Cytokine Growth Factor Rev* 2002; **13**: 413-421
- 34 **Haddad JJ**. Recombinant TNF-alpha mediated regulation of the I kappa B-alpha/NF-kappa B signaling pathway: evidence for the enhancement of pro- and anti-inflammatory cytokines in alveolar epithelial cells. *Cytokine* 2002; **17**: 301-310
- 35 **Iwadou H**, Morimoto Y, Iwagaki H, Sinoura S, Chouda Y, Kodama M, Yoshioka T, Saito S, Yagi T, Tanaka N. Differential cytokine response in host defence mechanisms triggered by gram-negative and gram-positive bacteria, and the roles of gabexate mesilate, a synthetic protease inhibitor. *J Int Med Res* 2002; **30**: 99-108

Edited by Ren SY and Wang XL **Proofread by** Xu FM

Rat liver transplantation without preservation of “phrenic ring” using double cuff method

Yong Jiang, Yu-Dong Qiu, Xiao-Ping Gu, Xin-Hua Zhu, Yi-Tao Ding

Yong Jiang, Yu-Dong Qiu, Xiao-Ping Gu, Xin-Hua Zhu, Yi-Tao Ding, Department of Hepatobiliary Surgery, Gulou Hospital, Medical Department of Nanjing University, Nanjing, 210008, Jiangsu Province, China

Yong Jiang, Department of Hepatobiliary Surgery, Changzhou 1st People's Hospital, Changzhou, 213003, Jiangsu Province, China

Supported by the Medical Administration Bureau of Jiangsu Province, No. SZ9902

Correspondence to: Dr. Yong Jiang, Department of Hepatobiliary Surgery, Changzhou 1st People's Hospital, Changzhou, 213003, Jiangsu Province, China. yyjiang8888@hotmail.com

Telephone: +86-519-6102280 **Fax:** +86-519-6621235

Received: 2003-09-06 **Accepted:** 2003-10-07

Abstract

AIM: To develop a double cuff method for rat liver transplantation without preservation of “phrenic ring” to shorten the portal vein clamping time.

METHODS: “Phrenic ring” was completely excluded from the donor liver, and end to end anastomosis of suprahepatic inferior vena cava was performed.

RESULTS: The portal vein clamping time was shortened to 10.6 min, the successful rate was 83.1%.

CONCLUSION: This method can simplify the operation and shorten the portal vein clamping time.

Jiang Y, Qiu XD, Gu XP, Zhu XH, Ding YT. Rat liver transplantation without preservation of “phrenic ring” using double cuff method. *World J Gastroenterol* 2004; 10(10): 1526-1527

<http://www.wjgnet.com/1007-9327/10/1526.asp>

INTRODUCTION

The orthotopic rat liver transplantation (ORLT) model was first described by Lee *et al.* in 1973^[1], and subsequently modified by Kamada and Calne in 1979^[2]. This model has been widely accepted and used in current scientific researches^[3-13]. In order to study the ischemia/reperfusion injury after liver transplantation, we modified the ORLT model established by Jiang *et al.*^[14]. We constructed a double cuff ORLT model without preservation of “phrenic ring”. This model can simplify the operation and shorten the portal vein clamping time.

MATERIALS AND METHODS

Animals

Male Sprague Dawley rats weighing 200-250 g were used as donors and recipients respectively. The body mass of donors was generally lower than that of corresponding recipients. The rats were housed in pathogen-free conditions with a 12 h light-dark cycle and had free access to water and were fasted for 14 h before operation. All experiments were performed in compliance with the standards for animal use and care set by Institutional Animal Care Committee.

Surgical procedures

All surgical procedures were performed under the naked eye. On the basis of the procedures described by Kamada *et al.*^[2], we made the following modifications. (1) The harvested liver from the donor was placed in a 4 °C saline bath measuring 6 cm in diameter and 3 cm in depth. The whole “phrenic ring” was removed from the suprahepatic inferior vena cava (IVC), leaving the vessel wall of suprahepatic IVC. After the double-cuff preparation was finished, the liver was perfused with cold lactated Ringer's solution through the portal vein and infrahepatic IVC. The liver was preserved in 4 °C University of Wisconsin (UW) solution for 24 h (in order to study cold preservation/reperfusion injury). (2) Instead of anastomosis of the donor “phrenic ring” with the receptor's suprahepatic IVC, the donor suprahepatic IVC was anastomosed end-to-end with the receptor suprahepatic IVC using a 7/0 continuous nylon suture.

RESULTS

Seventy-two ORLTs were performed without preservation of “phrenic ring” in rats. Of which, 59 were successful (success rate 83.1%). The rats survived over 24 h. One rat had survived more than 2 mo. One-week survival rate was not obtained because specimens were taken for study. Our criteria for operative success were as follows. After ORLT, the receptor rat could turn over, and run about actively. The rats were agile to the surrounding and could drink water. The portal vein clamping time (PVCT) was shortened (10.6±1.36 min), and the shortest PVCT reached 8 min. The cause of death included a number of contributing factors: anesthesia too deep and respiratory failure (4/13); thrombosis of the portal vein (1/13); wound bleeding of the right adrenal gland area (1/13); failure of the portal vein anastomosis (2/13); stenosis or obstruction of suprahepatic IVC (4/13); and failure of the infrahepatic IVC anastomosis (1/13). Failure to control ether anesthesia and narrowing or obstruction of the outflow tract was the main cause of operative failure. In the latter case, most of them occurred at the initial stage.

DISCUSSION

Original intention of establishing the model

The author has been engaged in the research of ischemia/reperfusion injury of liver transplantation. In this process, PVCT needs to be shortened in order to reduce the interference with a too long period of splanchnic congestion. PVCT should be shortened to less than 14 min, otherwise a lethal endotoxin like syndrome induced by splanchnic congestion might play the central role which might bring about a noted systemic error in research^[15]. In the beginning by following Kamada's method, we found that the repair of “phrenic ring” and eversion anastomosis were the “bottleneck” of PVCT. Thus we established the double cuff method for ORLT without preservation of “phrenic ring”. In the early stage, suprahepatic IVC was sometimes lacerated. But on the basis of improved microsurgery and vascular anastomosis technique, this method can not only avoid laceration of the suprahepatic IVC, but also shorten PVCT. A more scientific model is thus provided for

the research of ischemia-reperfusion and rejection-tolerance in liver transplantation.

Good exposure is the key point of a successful operation

As other surgical operations, good exposure is also the key point of liver transplantation. As “phrenic ring” is not preserved, anastomosis of suprahepatic IVC becomes more important. Good exposure was achieved in the following ways. Full-length median incision on the abdomen was dragged to both sides and fixed, xiphoid process was dragged cephalad with our designed apparatus, a small pillow underlied the rat chest to raise the suprahepatic IVC stoma. By this method, no suprahepatic IVC was lacerated, PVCT was shortened to nearly 10 min. Not only the disturbance of respiratory and circulation was reduced, but also splanchnic congestion induced endotoxin like syndrome was reduced, which was hard to be attained by “triple-cuff” or conventional “double-cuff” liver transplantation.

Other relevant experiences concerning anaesthesia of donor and receptor rats

Donor livers were anaesthetized by ketamine. Kamada *et al.* recommended a dosage of 100 mg/5 Kg body mass^[2], but actually 40 to 50 mg ketamine was administered to rats weighing 180-230 g. Receptor rats were maintained by ether inhalation anaesthesia. Steadiness of this anaesthesia is also crucial to a successful ORLT. The shallow anaesthesia would result in difficulty of operation and even bleeding, but too deep anaesthesia would lead to depression of breath and difficulty in postoperative recovery or even death. Out of control of the depth of ether anaesthesia was the main reason of postoperative respiratory failure, and also one of the main causes of death of the receptor rats (30.8%, 4/13). Our experience is “deep induction, shallow maintenance”. In the induction period, a bigger dosage of ether was given, but a low density of ether in mask was maintained during operation.

Turning over of the donor liver during its harvest

We adopted the methods recommended by Wang *et al.*^[16]. After a midline abdominal incision was made, the liver was freed from surrounding ligaments, the left infraphrenic vein and para-oesophagus vein were ligated and divided. Then the right renal vein and right adrenal vein were ligated. The suprahepatic vein was freed. Hepatoportal structure was dissected and freed. The common duct was cannulated. The donor liver was thus harvested. It was turned over only once. So this method can not only protect the donor liver, but also shorten the heat ischemic time.

REFERENCES

- 1 **Lee S**, Charters AC, Chandler JG, Orloff MJ. A technique for orthotopic liver transplantation in the rat. *Transplantation* 1973; **16**: 664-669
- 2 **Kamada N**, Calne RY. Orthotopic liver transplantation in the rat. Technique using cuff for portal vein anastomosis and biliary drainage. *Transplantation* 1979; **28**: 47-50
- 3 **Zhu XH**, Qiu YD, Shen H, Shi MK, Ding YT. Effect of matriline on Kupffer cell activation in cold ischemia reperfusion injury of rat liver. *World J Gastroenterol* 2002; **8**: 1112-1116
- 4 **Xu MQ**, Yao ZX. Functional changes of dendritic cells derived from allogeneic partial liver graft undergoing acute rejection in rats. *World J Gastroenterol* 2003; **9**: 141-147
- 5 **Svensson G**, Fjalling M, Gretarsdottir J, Jacobsson L, Holmberg SB. Kupffer cell and hepatocyte function in rat transplanted liver. *Transpl Int* 1992; **5**(Suppl 1): S417-419
- 6 **Tashiro H**, Fudaba Y, Itoh H, Mizunuma K, Ohdan H, Itamoto T, Asahara T. Hepatocyte growth factor prevents chronic allograft dysfunction in liver-transplanted rats. *Transplantation* 2003; **76**: 761-765
- 7 **Kataoka M**, Margenthaler JA, Ku G, Eilers M, Flye MW. “Infectious tolerance” develops after the spontaneous acceptance of Lewis-to-Dark Agouti rat liver transplants. *Surgery* 2003; **134**: 227-234
- 8 **Fujino M**, Adachi K, Kawasaki M, Kitazawa Y, Funeshima N, Okuyama T, Kimura H, Li XK. Prolonged survival of rat liver allograft with adenoviral gene transfection of human immunodeficiency virus type 1 nef. *Liver Transpl* 2003; **9**: 805-813
- 9 **Kato Y**, Shimazu M, Kondo M, Uchida K, Kumamoto Y, Wakabayashi G, Kitajima M, Suematsu M. Bilirubin rinse: A simple protectant against the rat liver graft injury mimicking heme oxygenase-1 preconditioning. *Hepatology* 2003; **38**: 364-373
- 10 **Fernandez L**, Heredia N, Peralta C, Xaus C, Rosello-Catafau J, Rimola A, Marco A, Serafin A, Deulofeu R, Gelpi E, Grande L. Role of ischemic preconditioning and the portosystemic shunt in the prevention of liver and lung damage after rat liver transplantation. *Transplantation* 2003; **76**: 282-289
- 11 **Li XL**, Man K, Liu YF, Lee TK, Tsui SH, Lau CK, Lo CM, Fan ST. Insulin in University of Wisconsin solution exacerbates the ischemic injury and decreases the graft survival rate in rat liver transplantation. *Transplantation* 2003; **76**: 44-49
- 12 **Lehmann TG**, Wheeler MD, Froh M, Schwabe RF, Bunzendahl H, Samulski RJ, Lemasters JJ, Brenner DA, Thurman RG. Effects of three superoxide dismutase genes delivered with an adenovirus on graft function after transplantation of fatty livers in the rat. *Transplantation* 2003; **76**: 28-37
- 13 **Sun Z**, Klein AS, Radaeva S, Hong F, El-Assal O, Pan HN, Jaruga B, Batkai S, Hoshino S, Tian Z, Kunos G, Diehl AM, Gao B. *In vitro* interleukin-6 treatment prevents mortality associated with fatty liver transplants in rats. *Gastroenterology* 2003; **125**: 202-215
- 14 **Jiang Y**, Gu XP, Qiu XD, Sun XM, Chen LL, Zhang LH, Ding YT. Ischemic preconditioning decreases C-X-C chemokine expression and neutrophil accumulation early after liver transplantation in rats. *World J Gastroenterol* 2003; **9**: 2025-2029
- 15 **Urata K**, Nguyen B, Brault A, Lavoie J, Rocheleau B, Huet PM. Decreased survival in rat liver transplantation with extended cold preservation: role of portal vein clamping time. *Hepatology* 1998; **28**: 366-373
- 16 **Wang X**, Yang JM, Yan YQ, Yao XP, Wu MC. Studies on the ways of orthotopic liver transplantation in rats. *Zhonghua Qiguan Yizhi Zazhi* 1998; **19**: 76-78

Edited by Xu JY and Wang XL Proofread by Xu FM

mRNA expression profiling reveals a role of *Helicobacter pylori* vacuolating toxin in escaping host defense

Jian-Ping Yuan, Tao Li, Zhen-Hong Li, Gui-Zhen Yang, Bao-Yu Hu, Xiao-Dong Shi, Tie-Liu Shi, Shan-Qing Tong, Xiao-Kui Guo

Jian-Ping Yuan, Tao Li (equal contributor), Zhen-Hong Li, Gui-Zhen Yang, Bao-Yu Hu, Xiao-Dong Shi, Shan-Qing Tong, Xiao-Kui Guo, Department of Medical Microbiology and Parasitology, Shanghai Second Medical University, Shanghai 200025, China
Tie-Liu Shi, Shanghai Institutes for Biological Sciences, Chinese Academy of Sciences, Shanghai 200025, China

Supported by the State Ministry of Education Research Foundation for Returned Overseas Chinese Scholars Abroad (2001) 498

Correspondence to: Xiao-Kui Guo, Department of Microbiology and Parasitology, Shanghai Second Medical University, 280 Chongqingnan Road, Shanghai 200025, China. xkguo@shsmu.edu.cn

Telephone: +86-21-64671226 **Fax:** +86-21-64671226

Received: 2003-10-31 **Accepted:** 2004-02-01

Abstract

AIM: To study the immune response of host to *Helicobacter pylori* VacA.

METHODS: The monocyte/macrophage-like U937 cells were infected with *Helicobacter pylori* vacA-positive strain NCTC 11638 or isogenic vacA-negative mutant. Differentially expressed genes were identified at 2, 6, 10, and 24 h post-infection by cDNA microarray. Differential expressions of some genes were confirmed by Northern blot.

RESULTS: More than 100 genes altered their mRNA expression at different time points respectively, many of which were identified to be related to immune evasion.

CONCLUSION: VacA is a crucial element for *H pylori* to escape from host immune defense by means of differentially regulating the expression of some related genes. These genes, previously known or unknown to be involved in the mechanism of immune evasion, deserve further investigation to unearth much more information complicated in the immune response.

Yuan JP, Li T, Li ZH, Yang GZ, Hu BY, Shi XD, Shi TL, Tong SQ, Guo XK. mRNA expression profiling reveals a role of *Helicobacter pylori* vacuolating toxin in escaping host defense. *World J Gastroenterol* 2004; 10(10): 1528-1532

<http://www.wjgnet.com/1007-9327/10/1528.asp>

INTRODUCTION

Helicobacter pylori infects about half of the world's population. Despite the induction of an immunological reaction, the infection of *H pylori* is commonly life-long, suggesting that this pathogen has evolved mechanisms to evade protective immune responses to achieve the state of host-microbial equilibrium^[1]. Some products of *H pylori* have been determined to have immunosuppressive effects for prolonging the infection. A 100 ku *H pylori* protein inhibits proliferation of T-cell and macrophage^[2], and VacA, a cytotoxin that has been found to cause massive vacuolation in several mammalian cell lines and in the gastric epithelia of patients with active chronic

gastritis associated with *H pylori* infection^[3], may perform targeted action to disable T cells. VacA interferes with proteolytic processing of tetanus toxin and toxoid and specifically inhibits the Ii-dependent pathway of antigen presentation mediated by newly synthesized major histocompatibility complex (MHC) class II, suggesting that VacA may contribute to the persistence of *H pylori* by interfering with protective immunity^[4]. However, to the author's knowledge, the exact mechanism of such an immunosuppression effect has not been fully studied. Hence, in this study, we performed a large scale measurement of gene expression alteration in host cells using gene microarray technology, which provided the crucial information for interpreting the mechanisms of immunosuppression.

MATERIALS AND METHODS

Bacterial strains and growth conditions

H pylori NCTC 11638 strain positive for vacA was given as a gift by Dr. Shi (Shanghai Institute of Gastroenterology). Isogenic vacA-negative mutant 11638-Δ vacA was constructed by substitution of a kanamycin resistant gene for a short fragment of vacA through homologous recombination, as described previously^[5]. *H pylori* strains were cultured routinely on brain heart infusion (BHI) agar plates with 5% sheep blood in mixed air containing 100 ml/L CO₂, 50 mL/L O₂, and 850 mL/L N₂ at 37 °C.

H pylori infection of monocyte/macrophage-like cell line U937

The U937 cells were maintained in RPMI 1640 medium (Gibco BRL, USA) with 2 mmol/L L-glutamine, 1.5 g/L sodium bicarbonate, 4.5 g/L glucose, 10 mmol/L HEPES, 1.0 mmol/L sodium pyruvate and 100 ml/L fetal bovine serum. The day before *H pylori* infection, fresh medium with 20 mL/L fetal calf serum was substituted. Eighteen hours later, the cells grown to 90% confluency were cocultured with *H pylori* isogenic strains at a multiplicity of infection of 10 in culture medium for 2, 6, 10, and 24 h.

Total RNA Isolation

U937 cells cocultured with NCTC 11638 and 11638-Δ vacA were collected at 2, 6, 10, and 24 h after the infection for mRNA extraction. Total RNA was isolated using TRIZOL reagent (Invitrogen, USA) according to the manufacturer's instruction.

cDNA microarrays

The cDNA microarrays were designed by Shanghai BioStar Genechip Inc. In this study, microarrays with 8 464 human cDNAs were used, including full-length and partial complementary DNAs representing novel, known, and control genes.

Preparation and hybridization of fluorescent-labeled cDNA

Aliquots of 30 μg of total RNA were fluorescently labeled with Cy5- or Cy3-dCTP (Amersham Pharmacia, Sweden) by reverse transcription in the presence of 5 μg of oligo(dT) and 1 μL of SuperScriptII (Gibco-BRL, USA). The labeled cDNAs were purified using MicroSpin S-200 columns (Amersham

Pharmacia, Sweden) and lyophilized. The probes were resuspended in 20 μ L hybridization solution containing 8 μ g of poly(dA), 2 μ g of yeast tRNA, 10 μ g of human *Cot* I DNA (Gibco-BRL, USA). After heated to 95 °C for 2 min and then cooled to room temperature, the mixture was applied to the slides and covered by a coverslip. The slides were incubated in a humid cabinet of an incubator for 16-18 h at 42 °C. Then the slides were washed at 60 °C for 10 min in solutions of 2 \times SSC with 2 g/L SDS, 0.1 \times SSC with 2 g/L SDS, and 0.1 \times SSC sequentially, and then dried at room temperature.

Array scanning and data processing

Each slide was scanned at 10 μ m resolution on a GenePix 4000B scanner (Axon Instruments, Inc., Foster City, CA) at variable PMT voltage to obtain maximal signal intensities with no more than 1% probe saturation. The images were processed with GenePix Pro 3.0. Ratios were normalized by a linear regression between ln(Cy5) and ln(Cy3) of all the genes' background-corrected signal intensities on the microarray. Genes exhibited a 2-fold or greater change in expression level and exceeded 200 in signal intensity were considered true outliers.

Preparation of ³²P-labeled probes

The plasmids containing cDNA clone used for preparing probes were provided by Shanghai BioStar Genechip Inc. A total amount of 200 ng plasmids were used as templates for PCR amplification. PCR products were purified using QIAquick Gel Extraction Kit (Qiagen, Germany). The probes were labeled using random primed Strip-EZ DNA Kit (Ambion, Austin, TX). A total amount of 25 ng purified DNA diluted in 9 μ L TE (10 mmol/L Tris-HCl, pH8, 1 mmol/L EDTA) was denatured at 95 °C for 5 min and then immediately frozen in liquid nitrogen, thawed, microfuged, and placed on ice. Afterwards, the following reaction was assembled as follows and mixed gently: A 9.0 μ L of denatured DNA, 2.5 μ L of 10 \times Decamer solution, 5.0 μ L of 5 \times buffer-dATP/-dCTP, 2.5 μ L of 10 \times dCTP, 5.0 μ L of [α -³²P]dATP (3 000 Ci/mmol,

10 mCi/mL), 1.0 μ L of exonuclease-free Klenow, and nuclease-free water to 25 μ L. After 20 min incubation at 37 °C, 1 μ L of 0.5 mol/L EDTA was added to stop the reaction.

Northern blot analysis

A 10 μ g sample of total RNA per lane was subjected to electrophoresis on 12 g/L agarose gels containing 2.2 mol/L formaldehyde. RNAs were transferred onto Zeta-probe blotting membranes (Bio-Rad Laboratories, Hercules, CA) using Vacuum Blotter (model 785, Bio-Rad Laboratories) and baked under vacuum at 80 °C for 2 h. Membranes were hybridized for 16 h at 60 °C with ULTRArray hybridization solution (Ambion, Austin, TX) containing cDNA probes labeled with [α -³²P] dCTP by random priming (Strip-EZ DNA labeling system, Ambion). The hybridized membranes were serially washed at 55 °C using 2 \times SSC with 1 g/L SDS solution, then exposed to a phosphorimager. Blots were scanned and quantified by a phosphorimager in combination with Optiquant software v. 2.50 (Cyclone Storage Phosphor System, Packard Instruments).

RESULTS

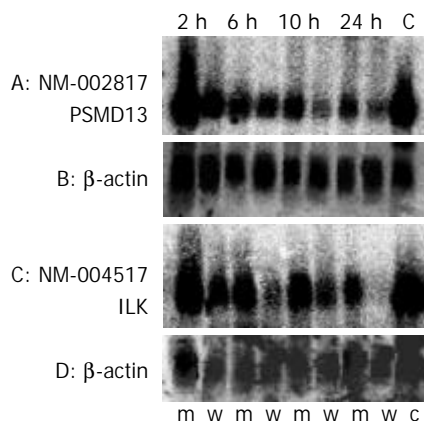
The mRNA expression in U937 cells was compared at 2, 6, 10, and 24 h after the infection with NCTC 11638 or 11638- Δ vacA. More than 100 genes altered their mRNA expression at different time points respectively, among which, the genes related to immune evasion were selected (Table 1). To confirm the differential expression profiling of the cDNA microarrays, two genes: *PSMD13* and *ILK* were chosen for northern blot analysis. As shown in Figure 1, the expression levels of these 2 genes were lower in the cells treated with *H pylori* NCTC11638 than those treated with 11638- Δ vacA. In addition, in both cases, the fold ratio changes detected by the microarray were confirmed by Northern blot (Table 2). The level of β -actin transcript was present at approximately the same level in both samples, providing an assessment of RNA content in each sample used for Northern blot analysis.

Table 1 Differentially expressed genes related to immune evasion

GeneBank_ID	Definition	Fold change			
		2 h	6 h	10 h	24 h
NM_004517	Integrin-linked kinase (ILK)	0.717	0.218	0.245	0.454
NM_001964	Early growth response 1 (EGR1)	3.184	1.149	—	—
NM_022555	Major histocompatibility complex, class II, DR beta 3 (HLA-DRB3)	1.000	0.448	0.518	0.621
NM_002116	Major histocompatibility complex, class I, A (HLA-A)	0.584	0.322	0.336	—
NM_002124	Major histocompatibility complex, class II, DR beta 1 (HLA-DRB1)	—	0.661	0.485	0.567
NM_002817	Proteasome (prosome, macropain) 26S subunit, non-ATPase, 13 (PSMD13)	0.445	0.122	0.333	0.402
NM_004159	Proteasome (prosome, macropain) subunit, beta type, 8 (large multifunctional protease 7) (PSMB8)	0.573	0.150	0.304	0.254
NM_000616	CD4 antigen (p55) (CD4)	0.855	0.560	0.317	0.831
NM_015953	eNOS interacting protein (NOSIP),	0.857	0.517	0.450	0.463
NM_020998	Macrophage stimulating 1 (hepatocyte growth factor-like) (MST1)	0.690	0.562	0.353	—
NM_005944	Antigen identified by monoclonal antibody MRC OX-2 (MOX2)	1.514	1.027	2.042	—
NM_021138	TNF receptor-associated factor 2 (TRAF2)	0.817	0.773	0.713	0.465
NM_004001	Fc fragment of IgG, low affinity IIb, receptor for (CD32) (FCGR2B)	0.581	0.569	0.467	—
NM_001100	Actin, alpha 1, skeletal muscle (ACTA1)	0.368	0.266	0.139	—
NM_001615	Actin, gamma 2, smooth muscle, enteric (ACTG2)	0.419	0.229	0.191	—
NM_005718	Actin related protein 2/3 complex, subunit 4 (20 ku) (ARPC4)	0.461	0.362	0.370	0.611
NM_020040	Tubulin, beta polypeptide 4, member Q (TUBB4Q)	0.462	0.345	0.335	0.573
NM_006009	Tubulin, alpha 3 (TUBA3)	1.062	0.710	0.484	0.885
NM_001665	ras homolog gene family, member G (<i>rho G</i>) (ARHG)	0.590	0.445	0.524	0.590
AB055890	<i>c-lbc</i> mRNA for guanine nucleotide exchange factor Lbc	1.065	0.315	0.701	0.433
NM_006400	Dynactin 2 (p50) (DCTN2)	0.865	0.361	0.334	—
NM_005428	vav 1 oncogene (VAV1)	0.510	0.421	0.387	—
NM_005993	Tubulin-specific chaperone d (TBGD)	0.770	0.485	0.524	—
NM_001747	Capping protein (actin filament), gelsolin-like (CAPG)	0.512	0.213	0.191	0.323

Table 2 Ratio of expression values obtained in U937 cells cocultured with *H pylori* NCTC11638 versus those cocultured with 11638- Δ vacA as assessed by microarray analysis and Northern blot

GeneBank ID	Gene product	Microarray ratio				Northern blot ratio			
		2 h	6 h	10 h	24 h	2 h	6 h	10 h	24 h
NM_002817	PSMD13	0.445	0.122	0.333	0.402	0.07	0.71	0.25	0.33
NM_004517	ILK	0.717	0.218	0.245	0.454	0.57	0.19	0.43	0.15

**Figure 1** Northern blot analysis result. RNA from U937 cells cocultured with *H pylori* NCTC11638 (wild type, w) or 11638- Δ vacA (mutant type, m) or RNA from normal cells (c) were separated by agarose electrophoresis, transferred onto nylon membranes, and probed with the human cDNAs as follows: NM_002817 (PSMD13), and NM_004517 (ILK). Control blots with human β -actin were provided.

DISCUSSION

Helicobacter pylori has found its own way to thrive within host cells, despite the presence of a well-functioning immune system. In the present study, differential expression of macrophage upon stimulation of VacA gives clear evidence that this vacuolating cytotoxin has evolved with various tricks to escape from the innate and adaptive immunity of the host.

Recognition of pathogen-infected host cells by effector T lymphocytes requires intracellular processing of microbial antigens and their presentation on the surface of the antigen-presenting cells (APCs) in association with MHC molecules. To avoid immune recognition, many kinds of microorganisms have evolved mechanisms which interfere with antigen presentation pathways. These mechanisms may be pivotal, especially for those pathogens causing persistent infections. The present differential expressions provide clear evidence that VacA downregulates the expression of MHC class I and class II molecules in macrophage. Thus, specific T lymphocytes may not be activated, resulting in the evasion of *H pylori* from the host's immune response and colonization of the bacteria in gastric mucosa persistently, remaining "invisible" to both CD8⁺ and CD4⁺ T cells. Interference with the class II antigen presentation pathway by *Listeria monocytogenes* has been shown to result in a reduced proliferation of CD4⁺ T lymphocytes in response to heterologous antigens^[6]. Interactions between MHC class I and human immunodeficiency virus (HIV) resulted in down-regulation of MHC-I surface expression, contributing to pathogenesis by suppressing the host's immune response^[7]. The role of MHC class I and class II-restricted functions in *H pylori* infection and immunity upon oral immunization has also been examined *in vivo*. It was found that experimental challenge with *H pylori* resulted in significantly greater colonization in MHC class I and class II mutant mice than in wild-type mice^[8]. MHC class II-deficient mice were unable to respond to oral antigenic stimulation and

remained persistently infected with *H pylori*^[8].

Nitric oxide (NO) is an important mediator of biological processes including inflammatory response. It is synthesized from L-arginine by a family of nitric oxide synthases (NOS), in which, endothelial NOS (eNOS) is a constitutively expressed isoform present in vascular endothelial cells, cardiac myocytes, and blood platelets^[9]. eNOS interacting protein (NOSIP) is a 34 ku protein specifically binds to the carboxylterminal region of the human eNOS oxygenase domain, overexpression of which in eNOS-expressing cells has been demonstrated to inhibit NO synthase activity^[10]. Thus, down-regulation of this protein upon stimulation of VacA may relieve such inhibition, leading to more NO production. The original concept that the small quantities of NO generated in a pulsatile fashion by constitutive eNOS mainly fulfil regulatory functions required for normal homeostatic function of the vasculature, while the high amount of NO produced by inducible NOS (iNOS) exerts antimicrobial and cytotoxic effects in the immune system, has recently been modified^[11]. The expression of eNOS is not restricted to endothelial cells, as it has been found to be present in monocytes/macrophages and in B and T lymphocytes^[12]. eNOS can also assume typical immunological functions previously assigned to iNOS, such as the induction of apoptotic cell death and the control of viruses^[11]. NO endows macrophages with cytostatic or cytotoxic activity against microbes and tumor cells^[13]. Nevertheless, more and more evidences have demonstrated a role for NO in the induction of immunosuppression by inhibiting T-cell proliferation during G1/S transition^[14-16]. In mouse models of T-cell-mediated autoimmunity, such as myelin antigen-induced EAE, the disease was exacerbated by genetic deletion of iNOS, indicating that NO suppressed T-cell-mediated immunity *in vivo*^[17]. In addition, NO induces apoptosis, which, the ubiquitin/proteasome and NF- κ B pathway have been determined to be involved in^[18].

In eukaryotic cells, degradation of many proteins involves their initial modification by conjugation of ubiquitin (Ub). Ubiquitinated proteins are rapidly degraded by the 26S proteasome^[19]. NO can inhibit the activities of the 20S and 26S proteasomes, providing a likely mechanism for the accumulation of NO-induced pro-apoptotic proteins p53 and Bax, the substrates of the ubiquitin/proteasome system^[18]. Apart from the indirect effect via NO functioning, the mRNA expression of proteasomes shows a significant downregulation as the result of being directly stimulated by VacA. Ub/proteasome pathway can catalyze the proteolytic processing of inactive 105 ku NF- κ B precursor into 50 ku subunit. p50 is then maintained in the cytosol conjugated with the p65 subunit in an inactive complex bound to I κ B. In addition, Ub/proteasome is involved in proteolytic digestion of I κ B, which is required for NF- κ B activation^[19]. Therefore, decreased proteasome activity should inhibit the proteolysis of NF- κ B precursor and inhibit I κ B degradation, thus blocking NF- κ B activation. Another involved protein, integrin-linked kinase (ILK), which has been determined to upregulate NF- κ B activity^[20], also shows decreased expression in this study. It might be the result of VacA induction, and moreover, ILK mRNA expression was found to be downregulated by NO^[21], corresponding to the above speculation that more NO may be produced due to downregulation of NOSIP. NF- κ B is known to be important

to cell survival. Fibroblasts and macrophages from Rel A (p65 subunit of NF- κ B) (-/-) mice were sensitive to TNF- α -induced cell death, and reintroduction of Rel A enhanced cell survival^[22]. Activation of NF- κ B is required for inflammatory cytokine release by macrophages during infection^[23]. Consequently, inhibition of NF- κ B activation may be responsible for decreased cytokine release from macrophages and the resulting immunosuppression. Additionally, because ILK is an apoptosis suppressor^[24], decreased production of this protein in macrophage may accelerate apoptosis of the cell that plays important roles in innate host defense and antigen presentation, leading to the evasion from host immunity against *H pylori*.

The capability of degrading proteins by the proteasome accounts for another important function to generate peptides presented on MHC-class I molecules to circulating lymphocytes. The presentation of these peptides enables the immune system to screen for and destroy cells expressing unusual polypeptides^[19]. Selective proteasome inhibitors were determined to prevent MHC-class I presentation of the antigenic peptide^[25]. Moreover, LMP2 and LMP7, two subunits of the proteasome, were found to be encoded in the major histocompatibility complex (MHC)^[26-28]. The experiment using specific antibodies against LMP2 and LMP7 showed that they were co-expressed with MHC-class I molecules^[29]. The levels of MHC-class I expression were shown to coincide perfectly with the LMP levels in different tissues, corresponding to the result in the present study, which shows simultaneous downregulation of MHC-class I and LMP7.

MSP, also known as HGF-like protein, is a serum protein belonging to the plasminogen-related growth factor family. It was originally discovered by Leonard and Skeel as a serum protein that stimulates shape change, movement, chemotaxis and phagocytosis of mouse peritoneal resident macrophages^[30,31]. The other important effect of MSP on macrophages was to inhibit endotoxin- or cytokine-stimulated NO production^[32]. Thereby, the decreased expression of MSP may contribute to deactivating macrophage and producing more NO, which, as described above, functions as an immunosuppressor.

The early growth response 1 (EGR1), a zinc-finger transcription factor that was shown to be significantly upregulated by 2 h postinfection in the present study, has been determined to induce downregulation of copper-zinc superoxide dismutase and manganese superoxide dismutase and stimulate the generation of reactive oxygen species (ROS) via the NADH/NADPH-oxidase system^[33]. In addition to NO, ROS produced by NADPH oxidase also have the ability to inhibit the proliferation of lymphocytes by a mechanism that suppressor macrophages impair the proliferative response of T lymphocytes to antigens or mitogens^[11]. Otsuji *et al.*^[34] demonstrated that the oxidative stress from tumor-derived macrophages mediated the decrease of CD3 ζ chain within T cells, which suppressed the antigen-specific T-cell responses. Pre-treatment of CTL or NK cells with nontoxic concentrations of H₂O₂ severely reduced their cytotoxic activity, leading to the speculation that macrophage-derived reactive oxygen metabolites contribute directly to alterations in signal transducing molecules of T cells and NK cells and to the mechanism of immunosuppression^[35]. Furthermore, the defective expression of CD3 ζ on lymphocytes has been related to some kind of carcinoma, including gastric adenocarcinoma^[36,37].

From Table 1, we may find up-regulation of MRC OX-2 (the antigen identified by monoclonal antibody, MOX2), a broadly expressed membrane glycoprotein, which has been shown to be important for regulation of the macrophage lineage. In the OX-2-deficient spleens, the number of macrophages was nearly twice the number of those in normal spleens^[38], implying a role of OX-2 in suppressing the activation of macrophage. The immunosuppression effects of OX-2 could be further

determined by many other studies. For example, several studies reported that increased expression of OX-2 in mice receiving renal allografts was associated with immunosuppression leading to increased graft survival, along with the polarization of cytokine production to type 2 cytokines in lymphocytes harvested from the transplanted animals^[39-41]. Furthermore, infusion of a mAb to OX-2 blocks both the increased graft survival and the altered cytokine production^[42]. All these data make clear that upregulation of OX-2 does favor to the immune evasion of *H pylori*.

Table 1 also demonstrates significant downregulation of many cytoskeleton-related gene expression. For example, RhoG is a member of the Rho family of GTPases, which signals to actin assembly during phagocytosis^[43]. Vav1 serves as a guanine nucleotide exchange factor (GEF) for Rho proteins, and establishes an essential and direct link between receptors with intrinsic or associated tyrosine kinase activity and the mitogenic and cytoskeletal pathways regulated by Rho proteins^[44]. Cytoskeleton has been known to be an important structural basis for phagocytosis since cytochalasin B, a toxin that blocks actin polymerization, was shown to inhibit uptake of IgG-coated erythrocytes by mouse macrophages^[45]. Phagocytosis is a process by which macrophages and leukocytes could ingest microbial pathogens to accomplish two essential immune functions, *i.e.*, to initiate the microbial death pathway, and to direct antigens to both MHC I and MHC II compartments. That is to say, phagocytosis serves not only as an innate immune effector but as a bridge between the innate and acquired immune responses^[1]. Thus, to destruct cytoskeleton may be another trick of VacA to evade host immune response.

In conclusion, we have shown that *H pylori* VacA induces the alteration of a series of genes related to immune evasion in macrophage, which ultimately establishes a state of host-microbial equilibrium. Some of these genes are for the first time made an association with VacA stimulation. Further investigations of the previously uncharacterized genes should be made to help us see through the underlying mechanisms utilized by *H pylori* to escape host immunity.

REFERENCES

- 1 **Ibraghimov A**, Pappo J. The immune response against *Helicobacter pylori*—a direct linkage to the development of gastroduodenal disease. *Microbes Infect* 2000; **2**: 1073-1077
- 2 **Knipp U**, Birkholz S, Kaup W, Opferkuch W. Partial characterization of a cell proliferation-inhibiting protein produced by *Helicobacter pylori*. *Infect Immun* 1996; **64**: 3491-3496
- 3 **Telford JL**, Ghiara P, Dell'Orco M, Comanducci M, Burroni D, Bugnoli M, Tecce MF, Censini S, Covacci A, Xiang Z. Gene structure of the *Helicobacter pylori* cytotoxin and evidence of its key role in gastric disease. *J Exp Med* 1994; **179**: 1653-1658
- 4 **Molinari M**, Salio M, Galli C, Norais N, Rappuoli R, Lanzavecchia A, Montecucco C. Selective inhibition of Ii-dependent antigen presentation by *Helicobacter pylori* toxin VacA. *J Exp Med* 1998; **187**: 135-140
- 5 **Yuan JP**, Li T, Shi XD, Hu BY, Yang GZ, Tong SQ, Guo XK. Deletion of *Helicobacter pylori* vacuolating cytotoxin gene by introduction of directed mutagenesis. *World J Gastroenterol* 2003; **9**: 2251-2257
- 6 **Leyva-Cobian F**, Unanue ER. Intracellular interference with antigen presentation. *J Immunol* 1988; **141**: 1445-1450
- 7 **Kamp W**, Breij EC, Nottet HS, Berk MB. Interactions between major histocompatibility complex class II surface expression and HIV: implications for pathogenesis. *Eur J Clin Invest* 2001; **31**: 984-991
- 8 **Pappo J**, Torrey D, Castriotta L, Savinainen A, Kabok Z, Ibraghimov A. *Helicobacter pylori* infection in immunized mice lacking major histocompatibility complex class I and class II functions. *Infect Immun* 1999; **67**: 337-341
- 9 **Michel T**, Feron O. Nitric oxide synthases: which, where, how, and why? *J Clin Invest* 1997; **100**: 2146-2152

- 10 **Dedio J**, Konig P, Wohlfart P, Schroeder C, Kummer W, Muller-Esterl W. NOSIP, a novel modulator of endothelial nitric oxide synthase activity. *FASEB J* 2001; **15**: 79-89
- 11 **Bogdan C**, Rollinghoff M, Diefenbach A. Reactive oxygen and reactive nitrogen intermediates in innate and specific immunity. *Curr Opin Immunol* 2000; **12**: 64-76
- 12 **Reiling N**, Kroncke R, Ulmer AJ, Gerdes J, Flad HD, Hauschildt S. Nitric oxide synthase: expression of the endothelial, Ca²⁺/calmodulin-dependent isoform in human B and T lymphocytes. *Eur J Immunol* 1996; **26**: 511-516
- 13 **MacMicking J**, Xie QW, Nathan C. Nitric oxide and macrophage function. *Annu Rev Immunol* 1997; **15**: 323-350
- 14 **Albina JE**, Abate JA, Henry WL Jr. Nitric oxide production is required for murine resident peritoneal macrophages to suppress mitogen-stimulated T cell proliferation. Role of IFN-gamma in the induction of the nitric oxide-synthesizing pathway. *J Immunol* 1991; **147**: 144-148
- 15 **Eisenstein TK**, Huang D, Meissler JJ Jr, al-Ramadi B. Macrophage nitric oxide mediates immunosuppression in infectious inflammation. *Immunobiology* 1994; **191**: 493-502
- 16 **Liew FY**. Regulation of lymphocyte functions by nitric oxide. *Curr Opin Immunol* 1995; **7**: 396-399
- 17 **van der Veen RC**. Nitric oxide and T helper cell immunity. *Int Immunopharmacol* 2001; **1**: 1491-1500
- 18 **Glockzin S**, von Knethen A, Scheffner M, Brune B. Activation of the cell death program by nitric oxide involves inhibition of the proteasome. *J Biol Chem* 1999; **274**: 19581-19586
- 19 **Coux O**, Tanaka K, Goldberg AL. Structure and functions of the 20S and 26S proteasomes. *Annu Rev Biochem* 1996; **65**: 801-847
- 20 **Tan C**, Mui A, Dedhar S. Integrin-linked kinase regulates inducible nitric oxide synthase and cyclooxygenase-2 expression in an NF- κ B-dependent manner. *J Biol Chem* 2002; **277**: 3109-3116
- 21 **Beck KF**, Walpen S, Eberhardt W, Pfeilschifter J. Downregulation of integrin-linked kinase mRNA expression by nitric oxide in rat glomerular mesangial cells. *Life Sci* 2001; **69**: 2945-2955
- 22 **Beg AA**, Baltimore D. An essential role for NF-kappaB in preventing TNF-alpha-induced cell death. *Science* 1996; **274**: 782-784
- 23 **Baeuerle PA**, Henkel T. Function and activation of NF-kappa B in the immune system. *Annu Rev Immunol* 1994; **12**: 141-179
- 24 **Attwell S**, Roskelley C, Dedhar S. The integrin-linked kinase (ILK) suppresses anoikis. *Oncogene* 2000; **19**: 3811-3815
- 25 **Rock KL**, Gramm C, Rothstein L, Clark K, Stein R, Dick L, Hwang D, Goldberg AL. Inhibitors of the proteasome block the degradation of most cell proteins and the generation of peptides presented on MHC class I molecules. *Cell* 1994; **78**: 761-771
- 26 **Brown MG**, Driscoll J, Monaco JJ. Structural and serological similarity of MHC-linked LMP and proteasome (multicatalytic proteinase) complexes. *Nature* 1991; **353**: 355-357
- 27 **Martinez CK**, Monaco JJ. Homology of proteasome subunits to a major histocompatibility complex-linked LMP gene. *Nature* 1991; **353**: 664-667
- 28 **Yang Y**, Waters JB, Fruh K, Peterson PA. Proteasomes are regulated by interferon gamma: implications for antigen processing. *Proc Natl Acad Sci U S A* 1992; **89**: 4928-4932
- 29 **Fruh K**, Yang Y, Arnold D, Chambers J, Wu L, Waters JB, Spies T, Peterson PA. Alternative exon usage and processing of the major histocompatibility complex-encoded proteasome subunits. *J Biol Chem* 1992; **267**: 22131-22140
- 30 **Leonard EJ**, Skeel A. A serum protein that stimulates macrophage movement, chemotaxis and spreading. *Exp Cell Res* 1976; **102**: 434-438
- 31 **Leonard EJ**, Skeel AH. Isolation of macrophage stimulating protein (MSP) from human serum. *Exp Cell Res* 1978; **114**: 117-126
- 32 **Wang MH**, Cox GW, Yoshimura T, Sheffler LA, Skeel A, Leonard EJ. Macrophage-stimulating protein inhibits induction of nitric oxide production by endotoxin- or cytokine-stimulated mouse macrophages. *J Biol Chem* 1994; **269**: 14027-14031
- 33 **Bek MJ**, Reinhardt HC, Fischer KG, Hirsch JR, Hupfer C, Dayal E, Pavenstadt H. Up-regulation of early growth response gene-1 via the CXCR3 receptor induces reactive oxygen species and inhibits Na⁺/K⁺-ATPase activity in an immortalized human proximal tubule cell line. *J Immunol* 2003; **170**: 931-940
- 34 **Otsuji M**, Kimura Y, Aoe T, Okamoto Y, Saito T. Oxidative stress by tumor-derived macrophages suppresses the expression of CD3 zeta chain of T-cell receptor complex and antigen-specific T-cell responses. *Proc Natl Acad Sci U S A* 1996; **93**: 13119-13124
- 35 **Kono K**, Salazar-Onfray F, Petersson M, Hansson J, Masucci G, Wasserman K, Nakazawa T, Anderson P, Kiessling R. Hydrogen peroxide secreted by tumor-derived macrophages down-modulates signal-transducing zeta molecules and inhibits tumor-specific T cell and natural killer cell-mediated cytotoxicity. *Eur J Immunol* 1996; **26**: 1308-1313
- 36 **Kono K**, Ichihara F, Iizuka H, Sekikawa T, Matsumoto Y. Expression of signal transducing T-cell receptor zeta molecules after adoptive immunotherapy in patients with gastric and colon cancer. *Int J Cancer* 1998; **78**: 301-305
- 37 **Takahashi A**, Kono K, Amemiya H, Iizuka H, Fujii H, Matsumoto Y. Elevated caspase-3 activity in peripheral blood T cells coexists with increased degree of T-cell apoptosis and down-regulation of TCR zeta molecules in patients with gastric cancer. *Clin Cancer Res* 2001; **7**: 74-80
- 38 **Hoek RM**, Ruuls SR, Murphy CA, Wright GJ, Goddard R, Zurawski SM, Blom B, Homola ME, Streit WJ, Brown MH, Barclay AN, Sedgwick JD. Down-regulation of the macrophage lineage through interaction with OX2 (CD200). *Science* 2000; **290**: 1768-1771
- 39 **Gorczynski L**, Chen Z, Hu J, Kai Y, Lei J, Ramakrishna V, Gorczynski RM. Evidence that an OX-2-positive cell can inhibit the stimulation of type 1 cytokine production by bone marrow-derived B7-1 (and B7-2)-positive dendritic cells. *J Immunol* 1999; **162**: 774-781
- 40 **Gorczynski RM**, Yu K, Clark D. Receptor engagement on cells expressing a ligand for the tolerance-inducing molecule OX2 induces an immunoregulatory population that inhibits alloreactivity *in vitro* and *in vivo*. *J Immunol* 2000; **165**: 4854-4860
- 41 **Gorczynski RM**, Chen Z, Hu J, Kai Y, Lei J. Evidence of a role for CD200 in regulation of immune rejection of leukaemic tumour cells in C57BL/6 mice. *Clin Exp Immunol* 2001; **126**: 220-229
- 42 **Gorczynski RM**, Cattral MS, Chen Z, Hu J, Lei J, Min WP, Yu G, Ni J. An immunoadhesin incorporating the molecule OX-2 is a potent immunosuppressant that prolongs allo- and xenograft survival. *J Immunol* 1999; **163**: 1654-1660
- 43 **Vigorito E**, Billadeu DD, Savoy D, McAdam S, Doody G, Fort P, Turner M. RhoG regulates gene expression and the actin cytoskeleton in lymphocytes. *Oncogene* 2003; **22**: 330-342
- 44 **Bustelo XR**. Regulatory and signaling properties of the Vav family. *Mol Cell Biol* 2000; **20**: 1461-1477
- 45 **Kaplan G**. Differences in the mode of phagocytosis with Fc and C3 receptors in macrophages. *Scand J Immunol* 1977; **6**: 797-807

Effect of *c-myc*, Ki-67, MMP-2 and VEGF expression on prognosis of hepatocellular carcinoma patients undergoing tumor resection

Jun Cui, Bao-Wei Dong, Ping Liang, Xiao-Ling Yu, De-Jiang Yu

Jun Cui, Bao-Wei Dong, Ping Liang, Xiao-Ling Yu, De-Jiang Yu,
Department of Ultrasound, Chinese PLA General Hospital, Beijing
100853, China

Supported by the Medical and Health Science Foundation of PLA
during the 10th Five-year plan period, No.01Z038

Correspondence to: Dr. Jun Cui, Department of Gastroenterology,
Yu Huang Ding Hospital, Yantai, 264000, Shandong Province,
China. cuijun89@hotmail.com

Telephone: +86-535-7062606

Received: 2003-11-27 **Accepted:** 2003-12-16

Abstract

AIM: To explore the effect of *c-myc*, Ki-67, MMP-2 and VEGF expression on prognosis of hepatocellular carcinoma (HCC) patients undergoing tumor resection.

METHODS: Primary HCC patients underwent tumor resection were retrospectively analysed. The maximum size of the tumor was less than 5 cm, there was only one nodule in each patient. No chemoembolization was performed before resection. They were followed up after resection, and the time of recurrence was recorded. They were divided into 2 groups: group A (15 cases): tumor recurrence within 1 year after tumor resection, and group B (15 cases): with or without tumor recurrence 2 years after tumor resection. Pathological slices were made with tumor wax-sample. Immunohistochemistry staining was performed with *c-myc*, Ki-67, MMP-2 and VEGF monoclonal antibodies. Staining intensity was quantitatively analysed with a pathological diagram-writing analyzing system. The expressing intensity differences of stained molecules in cancer tissue and para-cancer were analysed.

RESULTS: *c-myc*, Ki-67, MMP-2 and VEGF expressing intensities in cancer tissue in group A were higher than those in group B (*P* values were 0.010, 0.030, 0.022 and 0.004, respectively), but they were not significantly different in para-cancer tissue in groups A and B (*P* values were 0.334, 0.343, 0.334 and 0.334, respectively).

CONCLUSION: The expression of *c-myc*, Ki-67, MMP-2 and VEGF in cancer tissue is related to the recurrence of HCC after tumor resection.

Cui J, Dong BW, Liang P, Yu XL, Yu DJ. Effect of *c-myc*, Ki-67, MMP-2 and VEGF expression on prognosis of hepatocellular carcinoma patients undergoing tumor resection. *World J Gastroenterol* 2004; 10(10): 1533-1536
<http://www.wjgnet.com/1007-9327/10/1533.asp>

INTRODUCTION

Recurrence is the main factor influencing prognosis of hepatocellular carcinoma (HCC) after tumor resection. The therapeutic measures for patients before and after operation are similar, but their prognosis after operation differs largely.

Some patients had tumor recurrence within 1 year after operation, while others had or did not have tumor recurrence 2 years after operation. The reason why there is such a difference is not clear. Researches on molecular biology have demonstrated that the prognosis of HCC is related to the activation of proto-oncogene, inactivation of tumor suppressor gene, abnormal expression of growth factors and/or their receptors^[1]. Four kinds of molecules related to biologic characteristics of HCC were studied in this experiment to clarify their relationship with recurrence of HCC after resection.

MATERIALS AND METHODS

Patients

Thirty primary HCC patients undergoing resection at Department of Hepatobiliary Surgery in General Hospital of PLA (301 Hospital) were retrospectively analysed. All resected samples were proved as HCC with pathologic examination. The selecting standards were as follows: solitary nodule with its maximum size less than 5 cm, no transarterial chemoembolization (TACE) or local thermal therapy (such as microwave coagulation or radiofrequency) before resection, no other specific treatment after resection. There were 28 males and 2 females. Their mean age was 51.5 (range, 27-75) years. The mean size of tumors was 3.0 cm. The patients were divided into two groups according to follow-up results: group A, which had tumor recurrence within 1 year after resection, group B, had or did not have tumor recurrence 2 years after resection. 15 cases were in group A (14 males and 1 female) and 15 cases in group B (14 males and 1 female). The differences of clinical data (sex, age, tumor size, liver function, serum AFP, transaminase, HBV infection) were not significant (Table 1).

Table 1 Clinical data of patients in groups A and B

Item	Group A (n=15)	Group B (n=15)
Sex	14 males, 1 female	14 males, 1 female
Age (yr)	54.7±14.3	48.2±8.4
Mean diameter (cm)	3.2±1.0	2.9±1.1
Tumor volume (cm ³)	22.0±21.4	18.2±17.6
Liver function	grade A	grade A
Serum AFP ^a (grade)	0.9±1.0	0.6±1.0
ALT (U/L)	58.0±54.1	64.9±56.6
AST (U/L)	49.9±46.8	42.0±37.7
HBV infection rate	87% (13/15)	100 (15/15)

^aserum AFP was graded as follows: 0: 0-200 µg/L, 1: 201-400 µg/L, 2: >400 µg/L.

Instrument and reagent

HPIAS-1000 high acuity color pathologic diagram-writing analyzing system (produced by Wuhan Champion Image Technology Corporation Limited). SP and DAB kit, monoclonal antibodies of *c-myc*, Ki-67, MMP-2 and VEGF were all purchased from Beijing Zhongshan Biological Technology Corporation Limited. The characteristics of antibodies are listed in Table 2.

Table 2 Characteristics of antibodies used in this study

Name of antibody	Specificity	Dilution	Secondary antibody
c-myc	Monoclonal Mouse anti human	1:50	Goat anti mouse
Ki-67	Monoclonal Mouse anti human	1:50	Goat anti mouse
MMP-2	Monoclonal Mouse anti human	1:50	Goat anti mouse
VEGF	Monoclonal Mouse anti human	1:50	Goat anti mouse

Immunohistochemistry staining

Serial 4 μ m thick sections were made with wax sample of resected tumors. Immunohistochemistry staining was performed with SP three-step method using the monoclonal antibodies listed in Table 2.

Quantitative analysis of positive cells

Quantitative analysis of the examined molecules was performed with HPIAS-1000 high acuity color pathologic diagram-writing analyzing system. Molecules in cancer and para-cancer tissues were analysed. Three fields of view (FOV) were randomly selected in cancer and para-cancer tissues to quantitatively analyse the expressing intensity. One hundred cells were observed in each FOV, positively stained cells were calculated, finally the average positively stained cells in 100 observed cells were determined. The cells were determined as positive-staining only if they were stained without considering their staining intensity. The medium optical density (MOD) of plasma or nuclei in positively stained cells was calculated with a pathologic diagram-writing analyzing system. The product of multiplication of average positively stained cells and MOD was calculated, which was considered as the expressing intensity of positively stained molecules.

Comparison of staining

The difference of expressing intensity of examined molecules in cancer and para-cancer tissues was compared in the same group (group A or B), the difference of expressing intensity in groups A and B was compared in the same tissue (cancer tissue or para-cancer tissue).

Statistical analysis

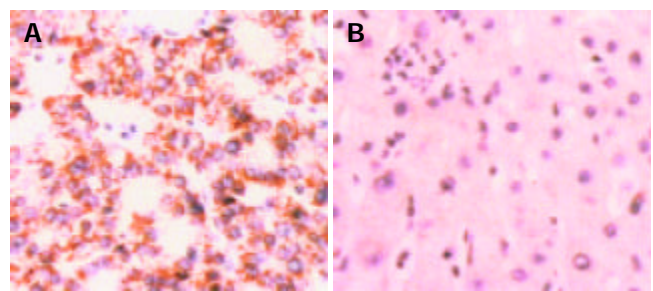
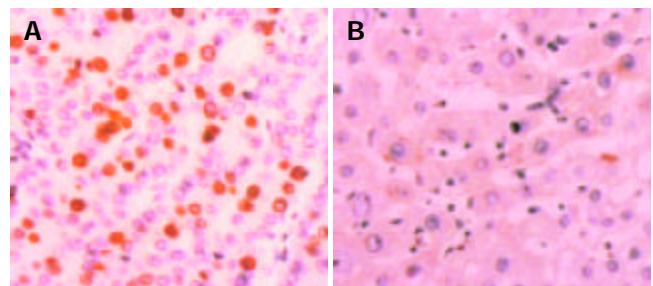
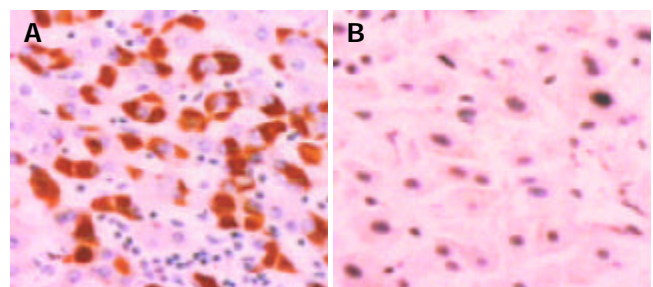
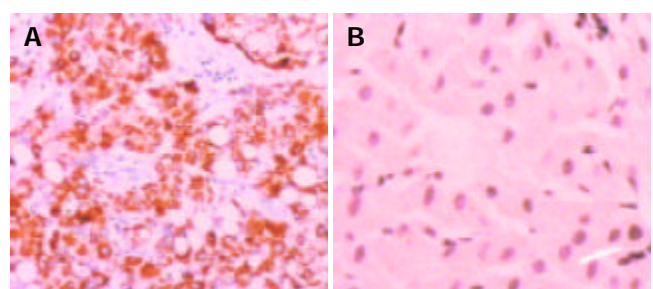
Data were presented as mean \pm SD. Paired-sample *t* test was used to compare the difference, the statistic software SPSS 10.0 was used. $P < 0.05$ was considered statistically significant.

RESULTS

Expressing rate and intensity of examined molecules in cancer and para-cancer tissues in group A (Table 3)

Table 3 Expressing rate(%) and intensity of examined molecules in cancer and para-cancer tissues in group A

Item	Cancer tissue	Para-cancer tissue
c-myc	80 (12/15) ^b ; 3.95 \pm 2.81 ^b	0 (0/15); 0.00 \pm 0.00
Ki-67	60 (9/15) ^b ; 1.57 \pm 2.20	7 (1/15); 0.57 \pm 2.21
MMP-24	7 (7/15) ^a ; 3.70 \pm 4.13 ^a	7 (1/15); 0.80 \pm 3.10
VEGF	67 (10/15) ^b ; 5.44 \pm 4.20 ^b	7 (1/15); 0.04 \pm 0.15

^a $P < 0.05$, ^b $P < 0.01$ vs Para-cancer tissue.**Figure 1** Positive and negative c-myc, A: Positive c-myc; B: Negative c-myc.**Figure 2** Positive and negative Ki67, A: Positive Ki67; B: Negative Ki67.**Figure 3** Positive and negative MMP-2, A: Positive MMP-2; B: Negative MMP-2.**Figure 4** Positive and negative VEGF, A: Positive VEGF; B: Negative VEGF.

Expressing rate and intensity of examined molecules in cancer and para-cancer tissues in group B (Table 4)

Table 4 Expressing rate (%) and intensity of examined molecules in cancer and para-cancer tissues in group B

Item	Cancer tissue	Para-cancer tissue
c-myc	40 (6/15); 1.34 \pm 2.74	7 (1/15); 0.26 \pm 1.00
Ki-67	40 (6/15); 0.18 \pm 0.38	7 (1/15); 0.01 \pm 0.04
MMP-2	20 (3/15); 0.61 \pm 1.70	0 (0/15); 0.00 \pm 0.00
VEGF	27 (4/15); 1.04 \pm 3.38	0 (0/15); 0.00 \pm 0.00

Expressing rate and intensity of examined molecules in cancer tissues in groups A and B (Table 5)

Table 5 Expressing rate (%) and intensity of examined molecules in cancer tissues in groups A and B

Item	Group A	Group B
<i>c-myc</i>	80 (12/15); 3.95±2.81 ^b	40 (6/15); 1.34±2.74
Ki-67	60 (9/15); 1.57±2.20 ^a	40 (6/15); 0.18±0.38
MMP-2	47 (7/15); 3.70±4.13 ^a	20 (3/15); 0.61±1.70
VEGF	67 (10/15); 5.44±4.20 ^b	27 (4/15); 1.04±3.38

^a*P*<0.05, ^b*P*<0.01 vs Group B.

Expressing rate and intensity of examined molecules in para-cancer tissues in groups A and B (Table 6)

Table 6 Expressing rate (%) and intensity of examined molecules in para-cancer tissues in groups A and B

Item	Group A	Group B
<i>c-myc</i>	0 (0/15); 0.00±0.00	7 (1/15); 0.26±1.00
Ki-67	7 (1/15); 0.57±2.21	7 (1/15); 0.01±0.04
MMP-2	7 (1/15); 0.80±3.10	0 (0/15); 0.00±0.00
VEGF	7 (1/15); 0.04±0.15	0 (0/15); 0.00±0.00

Micrographs of *c-myc*, Ki-67, MMP-2 and VEGF

The micrographs of *c-myc*, Ki-67, MMP-2 and VEGF positive and negative expression were listed in figures 1-4.

DISCUSSION

Relationship of *c-myc* expression with prognosis of HCC

Activation of *c-myc* oncogene plays important role in cancer occurrence, gene location on chromosome of 8q24. *c-myc* oncogene can be activated through two ways. One is that it is confluenced by light chain sequence of immunoglobulin through chromosomal translocation, the other is through DNA amplification. The protein coded by *c-myc* oncogene contains 439 amino acids, and can be combined specifically with intranuclear DNA to play transcription regulating function. *c-myc* oncogene is not expressed in the resting phase of cells, while it is rapidly expressed under the induction of mitoses, then it promotes cell proliferation and infiltration. It was reported in literature^[2] that HBV interpolation could promote amplification and over-expression of *c-myc* oncogene, then normal cellular genetic regulation was disturbed. Genetic mutation related with cancer occurrence could be induced through this mechanism, it was related with occurrence of HCC. *c-myc* oncogene codes phosphoric acid protein whose molecular weight is 62 KD. The protein is located in the nuclei of normal hepatocytes and HCC cells, as well as in plasm of some cells. It was demonstrated *in vitro* that the blockage of *c-myc* expression could suppress the growth of HCC cells^[3-5]. Some researchers demonstrated that the expression of *c-myc* in HCC tissue was related with the prognosis of HCC patients^[6]. Wang *et al.*^[7] reported that amplification of *c-myc* oncogene was correlated with a poor prognosis of HCC. Niu *et al.*^[8] reported that the positive expressing rate of *c-myc* in HCC was correlated with the histological differentiation, and was significantly higher in the poorly differentiated samples than in well differentiated samples. Zhang *et al.*^[9] reported that *c-myc* gene amplification was closely related to the development and progression of HCC. This study showed that *c-myc* expressing rate and intensity in cancer tissue in patients of group A were higher than those in para-cancer tissue, while the *c-myc* expressing rate and intensity in cancer tissue in patients of group B were not significantly

different from those in para-cancer tissue. *c-myc* expressing intensity in cancer tissue in patients of group A was higher than that in patients of group B. It demonstrated that the expression of *c-myc* in cancer tissue could reflect the malignancy of HCC. HCC with high *c-myc* expression in cancer tissue had a high recurrence rate. *c-myc* expressing rates in cancer tissue in the two groups of patients were significantly different, suggesting that *c-myc* over-expression occurs in HCC, its expressing intensity is related to the prognosis of HCC.

Relationship of Ki-67 expression with prognosis of HCC

Tumor cells consist of proliferating cells (S, G₂, M, G₁ stage), temporarily non-proliferating cells (G₀) and non-proliferating cells. Ki-67 can label proliferating cells in any stage except those in stage G₀, while it is not expressed in cells in silent stage. Ki-67 is rapidly degraded or its antigenic determinant is disappeared after mitosis. So Ki-67 is considered as a kind of objective marker reflecting proliferating activity of cells. Ki-67 is located in cell nuclei, and always in particle shape in immunohistochemistry staining. Ki-67 labelling index has been considered as a marker of cellular proliferative activity, the higher the Ki-67 labelling index, the lower the cellular differentiation and the poorer the prognosis of HCC^[10-16]. It was demonstrated in this study that Ki-67 expressing rate in cancer tissue in group A was higher than that in para-cancer tissue, while the expressing intensity was not significantly different. Ki-67 expressing rate and intensity in cancer tissue in group B were not significantly different from those in para-cancer tissue. Ki-67 expressing intensity in cancer tissue in group A was much higher than that in group B, suggesting that Ki-67 expression could reflex malignancy of HCC. HCC with a high Ki-67 expression had a high recurrence rate. Ki-67 expressing rate in cancer tissue of the two groups was not significantly different, suggesting that Ki-67 is abnormally expressed in HCC, its expressing intensity is related to the prognosis of HCC.

Relationship of MMP-2 expression with prognosis of HCC

A main step of invasion and metastasis of malignant tumor is to degrade extracellular matrix (ECM) and basement membrane. There are much collagen IV in ECM and basement membrane, collagen IV is very important for maintaining the integrity of ECM and basement membrane. Collagenase IV could degrade collagen IV and destroy the integrity of basement membrane. Matrix metalloproteinase II (MMP-2) is a kind of collagenase IV, its expression is related to tumor recurrence and metastasis. Positive particles of MMP-2 are located in cell plasm. Some researchers reported that MMP-2 expression in cancer tissue was related with prognosis of HCC, HCC with high MMP-2 expression had high malignancy, easy recurrence and metastasis^[17-23]. This study showed that MMP-2 expressing rate and intensity in cancer tissue in group A were higher than those in para-cancer tissue, MMP-2 expressing rate and intensity in cancer tissue in group B were not significantly different from those in para-cancer tissue. MMP-2 expressing intensity in cancer tissue in group A was much higher than that in group B, suggesting that MMP-2 expression could reflex malignancy of HCC. HCC with a high MMP-2 expression had a high recurrence rate. MMP-2 expressing rate in cancer tissue of the two groups was not significantly different, suggesting that MMP-2 is abnormally expressed in HCC, its expressing intensity is related to the prognosis of HCC.

Relationship of VEGF expression with prognosis of HCC

Vascularization is an important link in tumor growth, invasion and metastasis. Tumor blood vessels not only provide nutrition needed for tumor growth, but also provide pathways for spreading tumor cells. Vascular endothelial growth factor (VEGF) could promote cell proliferation and vascularization, and is

closely related to growth, invasion and metastasis of HCC. Expression of VEGF in HCC tissue is positively correlated with growth and metastasis of HCC, it could be a marker for determining the prognosis of HCC. Positive particles of VEGF are located in plasma of tumor cells. Some researchers reported that HCC patients with high VEGF expression had poor prognosis^[24-28]. This study showed that VEGF expressing rate and intensity in cancer tissue in group A were higher than those in para-cancer tissue, VEGF expressing rate and intensity in cancer tissue in group B were not significantly different from those in para-cancer tissue. VEGF expressing intensity in cancer tissue in group A was much higher than that in group B, suggesting that VEGF expression could reflex malignancy of HCC. HCC with a high VEGF expression had a high recurrence rate. VEGF expressing rate in cancer tissue of the two groups was not significantly different, suggesting that VEGF is abnormally expressed in HCC, its expressing intensity is related to the prognosis of HCC.

Clinical value of this study

Ultrasound guided biopsy becomes a kind of mature diagnostic technique for HCC. It was shown in this study that characters of HCC with recurrence within 1 year after tumor resection were *c-myc*, Ki-67, MMP-2 and VEGF high expression in cancer tissue. If prognosis of HCC patients could be determined through quantitative analysis of biopsied tissue stained with immunohistochemistry before treatment, then theoretical fundamentals for HCC patients to select therapy method could be provided.

REFERENCES

- 1 **Qin LX**, Tang ZY. The prognostic molecular markers in hepatocellular carcinoma. *World J Gastroenterol* 2002; **8**: 385-392
- 2 **Wu CG**, Salvay DM, Forgues M, Valerie K, Farnsworth J, Markin RS, Wang XW. Distinctive gene expression profiles associated with Hepatitis B virus x protein. *Oncogene* 2001; **20**: 3674-3682
- 3 **Cheng J**, Luo J, Zhang X, Hu J, Hui H, Wang C, Stern A. Inhibition of cell proliferation in HCC-9204 hepatoma cells by a *c-myc* specific ribozyme. *Cancer Gene Ther* 2000; **7**: 407-412
- 4 **Zhang H**, Lin C, Shao Y. Experimental therapy of adenovirus-transferred antisense *c-myc* on hepatocellular cancer cell. *Zhonghua Yixue Gongchengxue Zazhi* 2001; **81**: 673-676
- 5 **Ebinuma H**, Saito H, Kosuga M, Wakabayashi K, Saito Y, Takagi T, Nakamoto N, Okuyama T, Ishii H. Reduction of *c-myc* expression by an antisense approach under Cre/loxP switching induces apoptosis in human liver cancer cells. *J Cell Physiol* 2001; **188**: 56-66
- 6 **Fang Y**, Huang B, Liang Q, Li H, Huang C. Clinical significance of *c-myc* oncogene amplification in primary hepatocellular carcinoma by interphase fluorescence *in situ* hybridization. *Zhonghua Binglixue Zazhi* 2001; **30**: 180-182
- 7 **Wang Y**, Wu MC, Sham JS, Zhang W, Wu WQ, Guan XY. Prognostic significance of *c-myc* and AIB1 amplification in hepatocellular carcinoma. A broad survey using high-throughput tissue microarray. *Cancer* 2002; **95**: 2346-2352
- 8 **Niu ZS**, Li BK, Wang M. Expression of p53 and *C-myc* genes and its clinical relevance in the hepatocellular carcinomatous and pericarcinomatous tissues. *World J Gastroenterol* 2002; **8**: 822-826
- 9 **Zhang J**, Wang K, Cong S, Qiu F, Wang X, Wang P. Correlation of *c-myc* gene amplification, MTS1/p16 gene alternation, and HBV infection in human hepatocellular carcinoma. *Zhonghua Ganzhangbing Zazhi* 2001; **9**: 294-296
- 10 **Schmitt-Graff A**, Ertelt V, Allgaier HP, Koelble K, Olschewski M, Nitschke R, Bochaton-Piallat ML, Gabbiani G, Blum HE. Cellular retinol-binding protein-1 in hepatocellular carcinoma correlates with beta-catenin, Ki-67 index, and patient survival. *Hepatology* 2003; **38**: 470-480
- 11 **Aoki T**, Inoue S, Imamura H, Fukushima J, Takahashi S, Urano T, Hasegawa K, Ogushi T, Ouchi Y, Makuuchi M. EBAG9/RCAS1 expression in hepatocellular carcinoma: correlation with tumour dedifferentiation and proliferation. *Eur J Cancer* 2003; **39**: 1552-1561
- 12 **Daveau M**, Scotte M, Francois A, Coulouarn C, Ros G, Tallet Y, Hiron M, Hellot MF, Salier JP. Hepatocyte growth factor, transforming growth factor alpha, and their receptors as combined markers of prognosis in hepatocellular carcinoma. *Mol Carcinog* 2003; **36**: 130-141
- 13 **Shirahashi H**, Sakaida I, Terai S, Hironaka K, Kusano N, Okita K. Ubiquitin is a possible new predictive marker for the recurrence of human hepatocellular carcinoma. *Liver* 2002; **22**: 413-418
- 14 **Tamano M**, Sugaya H, Oguma M, Iijima M, Yoneda M, Murohisa T, Kojima K, Kuniyoshi T, Majima Y, Hashimoto T, Terano A. Serum and tissue PIVKA-II expression reflect the biological malignant potential of small hepatocellular carcinoma. *Hepatol Res* 2002; **22**: 261-269
- 15 **Inagawa S**, Itabashi M, Adachi S, Kawamoto T, Hori M, Shimazaki J, Yoshimi F, Fukao K. Expression and prognostic roles of beta-catenin in hepatocellular carcinoma: correlation with tumor progression and postoperative survival. *Clin Cancer Res* 2002; **8**: 450-456
- 16 **Ito Y**, Takeda T, Sakon M, Monden M, Tsujimoto M, Matsuura N. Expression and prognostic role of cyclin-dependent kinase 1 (*cdc2*) in hepatocellular carcinoma. *Oncology* 2000; **59**: 68-74
- 17 **Ishii Y**, Nakasato Y, Kobayashi S, Yamazaki Y, Aoki T. A study on angiogenesis-related matrix metalloproteinase networks in primary hepatocellular carcinoma. *J Exp Clin Cancer Res* 2003; **22**: 461-470
- 18 **Liu Z**, Yan L, Xiang T, Jiang L, Yang B. Expression of vascular endothelial growth factor and matrix metalloproteinase-2 correlates with the invasion and metastasis of hepatocellular carcinoma. *Shengwu Yixue Gongchengxue Zazhi* 2003; **20**: 249-250
- 19 **McKenna GJ**, Chen Y, Smith RM, Meneghetti A, Ong C, McMaster R, Scudamore CH, Chung SW. A role for matrix metalloproteinases and tumor host interaction in hepatocellular carcinomas. *Am J Surg* 2002; **183**: 588-594
- 20 **Giannelli G**, Bergamini C, Marinosci F, Fransvea E, Quaranta M, Lupo L, Schiraldi O, Antonaci S. Clinical role of MMP-2/TIMP-2 imbalance in hepatocellular carcinoma. *Int J Cancer* 2002; **97**: 425-431
- 21 **Niu Q**, Tang Z, Ma Z, Qin L, Bao W, Zhang L. Relationship between serum matrix metalloproteinase-2 and metastasis and recurrence following radical hepatic resection in hepatocellular carcinoma. *Zhonghua Ganzhangbing Zazhi* 2001; **9**(Suppl): 58-60
- 22 **Sawada S**, Murakami K, Murata J, Tsukada K, Saiki I. Accumulation of extracellular matrix in the liver induces high metastatic potential of hepatocellular carcinoma to the lung. *Int J Oncol* 2001; **19**: 65-70
- 23 **Maatta M**, Soini Y, Liakka A, Autio-Harmainen H. Differential expression of matrix metalloproteinase (MMP)-2, MMP-9, and membrane type 1-MMP in hepatocellular and pancreatic adenocarcinoma: implications for tumor progression and clinical prognosis. *Clin Cancer Res* 2000; **6**: 2726-2734
- 24 **Xiong ZP**, Yang SR, Xiao EH, Zhou SK, Zhang ZS, Liang ZY. Relation between vascular endothelial growth factor and reoccurrence-metastasis after transcatheter arterial chemoembolization in hepatocellular carcinoma. *Zhonghua Zhongliu Zazhi* 2003; **25**: 562-565
- 25 **Zhao ZC**, Zheng SS, Wan YL, Jia CK, Xie HY. The molecular mechanism underlying angiogenesis in hepatocellular carcinoma: the imbalance activation of signaling pathways. *Hepatobiliary Pancreat Dis Int* 2003; **2**: 529-536
- 26 **Zhao J**, Hu J, Cai J, Yang X, Yang Z. Vascular endothelial growth factor expression in serum of patients with hepatocellular carcinoma. *Chin Med J* 2003; **116**: 772-776
- 27 **Moon WS**, Rhyu KH, Kang MJ, Lee DG, Yu HC, Yeum JH, Koh GY, Tarnawski AS. Overexpression of VEGF and angiopoietin 2: a key to high vascularity of hepatocellular carcinoma? *Mod Pathol* 2003; **16**: 552-557
- 28 **Chao Y**, Li CP, Chau GY, Chen CP, King KL, Lui WY, Yen SH, Chang FY, Chan WK, Lee SD. Prognostic significance of vascular endothelial growth factor, basic fibroblast growth factor, and angiogenin in patients with resectable hepatocellular carcinoma after surgery. *Ann Surg Oncol* 2003; **10**: 355-362

Effects of bile reflux and intragastric microflora changes on lesions of remnant gastric mucosa after gastric operation

Chao Zhang, Zhan-Kui Liu, Pei-Wu Yu

Chao Zhang, Zhan-Kui Liu, Pei-Wu Yu, Department of General Surgery, Southwest Hospital, Third Military Medical University, Gaotan Yan, Chongqing 400038, China

Correspondence to: Professor, Dr. Chao Zhang, M.D., Department of General Surgery, Southwest Hospital, Third Military Medical University, Gaotan Yan, Chongqing 400038, China. meizhang6688@yahoo.com
Telephone: +86-23-68773074

Received: 2003-06-06 **Accepted:** 2003-10-22

Abstract

AIM: To investigate the effects of bile reflux and intragastric microflora changes on lesions of remnant gastric mucosa after gastric operation.

METHODS: Concentration of bile acid and total bacterial counts (TBC) in gastric juice were measured in 49 patients with peptic ulcer before and after gastrectomy. One year after the operation, sample of gastric mucosa taken from all the patients were used for histological examination.

RESULTS: The concentration of gastric bile acid was significantly increased in group B-I, or B-II and SV+A than that in group HSV ($P < 0.05-0.01$). The abnormal histological changes in the remnant gastric mucosa were more common in the first 2 groups than in the last group.

CONCLUSION: The type of gastrectomy can affect bile reflux. The abnormal histological changes in the remnant gastric mucosa are closely related to the elevation of bile acid concentration and increase of TBC in gastric juice. HSV can effectively prevent bile reflux and keep the gastric physiological functions stable.

Zhang C, Liu ZK, Yu PW. Effects of bile reflux and intragastric microflora changes on lesions of remnant gastric mucosa after gastric operation. *World J Gastroenterol* 2004; 10 (10): 1537-1539

<http://www.wjgnet.com/1007-9327/10/1537.asp>

INTRODUCTION

Bile reflux was usually found after routine operation in the treatment of peptic ulcer, and for some patients, it could be found very serious complications, such as epigastric causalgia, obstinate bilious vomiting, body mass descent and so on, its incidence is 5-35%^[1-4]. Forty-nine patients with gastric resection in treating peptic ulcer were observed in order to investigate the effects of bile reflux and intragastric microflora changes on lesions of remnant gastric mucosa after gastrectomy gastric resection.

MATERIALS AND METHODS

A total of 49 patients with peptic ulcer (32 male, 17 female, average age 44.3 years) including 14 patients with gastric ulcer, 28 patients with duodenal ulcer and 7 patients with compound

ulcer were investigated in a retrospective manner. These patients were divided into 4 groups according to the operation kind: 10 patients with Billroth I (B-I), 14 patients with Billroth II (B-II), 12 patients with selected vagotomy plus antrectomy (SV+A), 13 patients with High selected vagotomy (HSV).

Gastric juice on an empty stomach was been extracted at 3-5 d pre-operation, 7 d post-operation, 3 wk and 1 year post-operation, the bile acid concentration was measured by radio-immunity analysis (RIA), obtained from Wuzhou Institute of Isotope.

A 0.5 mL gastric juice plus 5 mL broth was put into sterilization test tube and cultured at 37 °C for 24-48 h, it was defined sterile growth if it had no bacteria growth through observation of 48 h, if bacteria were found, it were separated and evaluated by means of platinum loop.

For pro-operation annual patients, 2 samples of gastric mucosa were fixed by formaldehyde solution, then were observed through light microscope. Diagnosis of gastric ulcer was based on the detection standard of gastric mucosal disease formulated by gastric cancer co-operation group in 1981. The result was indicated by count scores as follow: the normal gastric mucosa was equal to 0; slight-degree, medium-degree, and sever-degree superficial gastritis were 1, 2, and 3; slight -degree, medium-degree, and sever-degree atrophic gastritis were 4, 5, and 6; if gastritis plused slight-degree, medium-degree and severe-degree intestinal metaplasia, the scores would be plus 1, 2, 3.

RESULTS

Bile acid concentration at post-operation 3 wk and 1 year was significantly increased than that at pre-operation in group B-II ($P < 0.05$), and is the same in group B-I ($P < 0.05$) and in group SV+V ($P < 0.05$); Bile acid concentration at post-operation was slight increased ($P > 0.05$). From post-operation 3 wk, bile acid concentration in B-II, B-I and group SV+V were significantly increased than that in group HSV, especially in group B-II (Table 1).

After operation, total bacterial count of gastric juice in group B-II, B-I and group SV+V were significantly increased than that in group HSV ($P < 0.05-0.01$). In this study, 204 samples of gastric juice were cultivated, 88 samples were found bacteria growing in 92 samples that pH was > 4.0 and the count of bacteria will be more along the higher of pH ($r = 0.784$, $P < 0.01$). Gram-Negative bacillus were always found after operation, and associated with the level of bile reflux. The rate of finding Gram-Negative bacillus was 64.1% in group B-II, 25.81% in group B-I, 29.62% in SV+A, and 10.25% in group HSV and significantly lower than that in 3 groups ($P < 0.01$, $P < 0.05$, $P < 0.05$). *Escherichia coli* and *Bacillus proteus* were common in group B-II, B-I and group SV+V, but, *Streptococcus* and *Lactobacillus* were common in group HSV.

During 1 year after operation, the incidence of atrophic gastritis was 35.7% in group B-II, 30% in group B-I, 33.3% in SV+A, 15.4% in group HSV. The incidence of Intestinal metaplasia was 28.6% in group B-II, 20% in group B-I, 25% in SV+A, 7.8% in group HSV. It was found by statistics analysis that the degree of change of gastric remnant

Table 1 Changes of bile acid concentration of gastric juice in different group($C_B/nmol \cdot mL^{-1}$, mean \pm SD)

Group	n	Pre-operation	Post-operation		
			1 wk	3 wk	1 yr
B-I	14	21.15 \pm 9.36	36.50 \pm 25.27	76.60 \pm 48.38 ^b	59.75 \pm 29.80 ^b
B-I	10	22.17 \pm 7.74	45.13 \pm 19.08 ^a	52.98 \pm 25.04 ^a	43.79 \pm 9.89 ^b
SV+A	12	22.43 \pm 10.15	39.04 \pm 18.72	54.84 \pm 27.49 ^a	46.33 \pm 14.52 ^b
HSV	13	23.54 \pm 11.56	30.12 \pm 17.24	28.02 \pm 16.18	27.68 \pm 15.44

^a $P < 0.05$, ^b $P < 0.01$ vs HSV.

Table 2 Changes of total bacterial count of gastric juice in different groups (log₁₀/mL, mean \pm SD)

Group	n	Pre-operation	Post-operation		
			1 wk	3 wk	1 yr
B-II	14	1.27 \pm 2.14	3.83 \pm 2.09 ^a	4.86 \pm 0.38 ^b	3.97 \pm 1.97 ^b
B-I	10	1.77 \pm 2.35	4.30 \pm 1.64 ^a	4.33 \pm 1.55 ^a	3.82 \pm 1.99 ^b
SV+A	12	1.84 \pm 2.27	3.90 \pm 1.79 ^a	4.13 \pm 1.68 ^a	3.85 \pm 2.04 ^b
HSV	13	1.26 \pm 2.07	2.41 \pm 2.35	2.59 \pm 2.78	1.56 \pm 2.13

^a $P < 0.05$, ^b $P < 0.01$ vs HSV.

Table 3 Results of histological examination of remnant gastric mucosa 1 year after operation

Group	n	Normal	Superficial gastric	Atrophic gastritis			Intestinal metaplasia		
				Slight	Medium	Severe	Slight	Medium	Severe
B-II	14	0	9	2	2	1	1	1	2
B-I	10	0	7	2	1	0	1	0	1
SV+A	12	0	8	1	1	1	1	1	1
HSV	13	0	10	1	1	0	1	0	0

histological abnormality alteration in group B-II, B-I and group SV+V was significantly higher than that in group HSV (t values separately were 2.047, 2.025, 2.029, $P < 0.05$), and the change of gastric remnant histological abnormality alteration associated with increasing of concentration of gastric juice cholalic acid.

DISCUSSION

Bile reflux was common in gastric post-operation and the mod of operation could affect the degree of bile reflux, generally speaking, it was slight after high selected vogotomy, it was severe after gastrectomy, and it was very common in Billroth II^[1]. In our study, the concentration of gastric juice cholalic acid was significantly increased in group B-II, it was higher in group B-I and group SV+V than that in group HSV, There was no significant difference between pre-operation and post-operation in group HSV although it was slight higher after operation, so it suggested that HSV could reduce bile reflux. Traditional gastrectomy and SV+A destructed the normal gastric dissection and deleted the function of Pyloric and innervation, these factors resulted in gastric emptying disorder and dodecadactylon increased reversed peristalsis, so bile reflux was increased and it could lead to the lesion of gastric mucosa. HSV remained the Pyloric dissection and innervation, it maintained the usual diet passage, and the function of Pyloric is normal, so it could prevent intestines and stomach reflux^[2].

Alkaline reflux gastritis was a complex complication after gastric operation, and its mechanism is not yet fully understood. We think when mod of operation was selected, we should excerpt the mod in coincidence to normal physiology function and based on the patient's specific situation in order to reduce the complication.

The effect of bile reflux on total bacterial count and the

changes of remnant gastric mucosa histological Current concepts suggest that gastric acid posses strongly germicidal effect, the count of bacteria of gastric acid was only $10^5/mL$, and the denomination of bacteria was similar to that in buccal cavity. Oxyntic cell was deleted or its innervation was broken after gastric operation, so the ability of stomach excreting acid was decreased, the data of pH were creasing, if the small intestinal juice including bile reflux to stomach, the data of pH would be more increased. These factors are advantageous to bacteria growth and breeding, resulted in intragastric bacterial over-growth (IBO), the flora in Lower digestive tract (especially Gram-Negative bacillus and Anaerobe) could reflux to stomach and reproduced here^[5-10]. Because of these bacteria, the conjugate cholalic acid changed to freeing cholalic acid which has a strongly toxic effect, and the following could damaged the integrity of gastric mucosa, certain cationic permeability could increased, such as H⁺ could contra-direction diffuse, and these changes can resulted in Mast cell releasing histamine and 5-serotonin, so it could be found capillary telangiectasia, mucosa hyperemia, edema, bleeding, and superficial Ulceration^[11,12].

In our study, the concentration of cholalic acid in gastric juice was higher, the bacterial count of gastric juice was more, and the denomination of flora in intestinal tract was more. Pathological examination found that flaming cell infiltration, atrophic gastritis, and intestinal metaplasia, all these could indicate that the abnormal histological changes of gastric mucosa associated with the increasing concentration of cholalic acid in gastric juice and increasing total bacterial count of gastric juice.

The role of dodecadactylon regurgitation resulting in gastric mucosa precancerous lesion and gastric cancer was though highly, Houghton *et al.* found that follicle cell and DNA count was increased if rat was raised by carcinogens (MNNG) and

at the same time reinforced regurgitation from dodecadactylon to stomach, so the ratio of gastric carcinoma was significantly increased. Freeing cholalic acid was confirmed as carcinogen, it could result in stomach carcinoma if it was higher in a long term^[13-17]. For patients with higher concentration of cholalic acid in gastric juice, intragastric bacterial over-growth (IBO), and pathological examination finding abnormal changes, should be thought highly of the occurrence of stomach carcinoma.

REFERENCES

- 1 **Madura JA**. Primary bile reflux gastritis: which treatment is better, Roux-en-Y or biliary diversion? *Am Surg* 2000; **66**: 417-423
- 2 **Barrett MW**, Myers JC, Watson DI, Jamieson GG. Detection of bile reflux: *in vivo* validation of the Bilitec fibreoptic system. *Dis Esophagus* 2000; **13**: 44-50
- 3 **Menges M**, Muller M, Zeitz M. Increased acid and bile reflux in Barrett's esophagus compared to reflux esophagitis, and effect of proton pump inhibitor therapy. *Am J Gastroenterol* 2001; **96**: 331-337
- 4 **Dixon MF**, Neville PM, Mapstone NP, Moayyedi P, Axon AT. Bile reflux gastritis and Barrett's oesophagus: further evidence of a role for duodenogastro-oesophageal reflux? *Gut* 2001; **49**: 359-363
- 5 **Johnnesson KA**, Hammar E, Stael von Holstein C. Mucosal changes in the gastric remnant: long-term effects of bile reflux diversion and *Helicobacter pylori* infection. *Eur J Gastroenterol Hepatol* 2003; **15**: 35-40
- 6 **Sundbom M**, Hedenstrom H, Gustavsson S. Duodenogastric bile reflux after gastric bypass: a cholescintigraphic study. *Dig Dis Sci* 2002; **47**: 1891-1896
- 7 **Dixon MF**, Mapstone NP, Neville PM, Moayyedi P, Axon AT. Bile reflux gastritis and intestinal metaplasia at the cardia. *Gut* 2002; **51**: 351-355
- 8 **Talley NJ**, Abeygunasekera S. Bile reflux and Barrett's oesophagus: innocent bystander or sinister companion? *Dig Liver Dis* 2002; **34**: 246-248
- 9 **Konturek PC**, Brzozowski T, Kania J, Konturek SJ, Hahn EG. Nitric oxide-releasing aspirin protects gastric mucosa against ethanol damage in rats with functional ablation of sensory nerves. *Inflamm Res* 2003; **52**: 359-365
- 10 **Zhou L**, Sung JJ, Lin S, Jin Z, Ding S, Huang X, Xia Z, Guo H, Liu J, Chao W. A five-year follow-up study on the pathological changes of gastric mucosa after *H pylori* eradication. *Chin Med J* 2003; **116**: 11-14
- 11 **Penagini R**. Bile reflux and oesophagitis. *Eur J Gastroenterol Hepatol* 2001; **13**: 1-3
- 12 **Blackstone M**. Pancreatitis from bile reflux-again? *Gastroenterology* 2003; **124**: 863-864
- 13 **Shi X**, Zhao F, Dai X, Dong X, Fang J, Yang H. Effects of san qi on gastric secretion and protective factors of gastric mucosa in the rat with precancerous lesion of stomach. *J Tradit Chin Med* 2003; **23**: 220-224
- 14 **Qiu GB**, Gong LG, Hao DM, Zhen ZH, Sun KL. Expression of MTLC gene in gastric carcinoma. *World J Gastroenterol* 2003; **9**: 2160-2163
- 15 **Chen BQ**, Yang YM, Gao YH, Liu JR, Xue YB, Wang XL, Zheng YM, Zhang JS, Liu RH. Inhibitory effects of c9, t11-conjugated linoleic acid on invasion of human gastric carcinoma cell line SGC-7901. *World J Gastroenterol* 2003; **9**: 1909-1914
- 16 **Du JJ**, Dou KF, Peng SY, Xiao HS, Wang WZ, Guan WX, Wang ZH, Gao ZQ, Liu YB. cDNA suppression subtraction library for screening down-regulated genes in gastric carcinoma. *World J Gastroenterol* 2003; **9**: 1439-1443
- 17 **Zhu XD**, Lin GJ, Qian LP, Chen ZQ. Expression of survivin in human gastric carcinoma and gastric carcinoma model of rats. *World J Gastroenterol* 2003; **9**: 1435-1438

Edited by Chen WW and Wang XL Proofread by Xu FM

Blossoming of gastroenterology during the twentieth century

Joseph B. Kirsner

Joseph B. Kirsner, The Louis Block Distinguished Service Professor of Medicine, Department of Medicine - Section of Gastroenterology, The University of Chicago, IL 60637, USA
Based in part on Kirsner, J.B. "100 Years of American Gastroenterology (1900-2000). *Medscape Gastroenterology*. (Available on the world wide web at: http://www.medscape.com/viewarticle/407942_4) and Kirsner, J.B. "The Scientification of Gastroenterology During the Twentieth Century." Foreword in *Colonic Diseases*. Koch, T.R., (Ed.) (With Permission)

Correspondence to: Joseph B Kirsner, M.D., Louis Block Distinguished Service, Professor of Medicine, The University of Chicago, 5841 South Maryland, MC 4076, Chicago, IL 60637,

USA. jkirsner@medicine.bsd.uchicago.edu

Telephone: +1-773-702-6101 **Fax:** +1-773-752-4876

Received: 2004-03-20 **Accepted:** 2004-04-10

Kirsner JB. Blossoming of gastroenterology during the twentieth century. *World J Gastroenterol* 2004; 10(11): 1541-1542

<http://www.wjgnet.com/1007-9327/10/1541.asp>

INTRODUCTION

Awareness of the digestive system began with the dawn of civilization, when man observing the feeding habits of animals in the surrounding environment, experimented with foods, edible and inedible. Identity came with discoveries of the digestive organs during the 16th and 17th centuries. Function was revealed by physiologic studies of digestion, absorption and secretion, metabolism, and motility during the 18th and 19th centuries. Diagnostic access improved with the technological advances of the 20th century. Understanding of gastrointestinal (GI) disease followed growth of the basic sciences and gastroenterology's increased involvement in scientific research during the 20th century.

The scientification of medicine and gastroenterology began during the latter part of the 19th century when the discovery of bacterial causes of disease revealed the potential of research in the discovery of new knowledge, and when the dogma of the past began to yield to clinical and basic investigation. Additional impetus came from A. Flexner's 1910 report on medical education, documenting the importance of a scientific foundation in medicine. Funds for gastroenterologic investigation were small, but research was in progress in the physiology laboratories of academic medical centers. Early in the 20th century, gastroenterology was yet an incompletely defined activity; but during the 1920s, outstanding clinicians established gastroenterology programs at university academic centers and major clinics. The entry of scientifically trained young physicians into gastroenterology during the 1930s and 1940s increased research interest.

Specialization in medicine was underway and, in the United States in 1940, gastroenterology was certified as an academic specialty, important to the attraction of students and support for education and research. Similar recognition occurred elsewhere, but further progress was interrupted by World War II (1939-1945).

Post-World War II was a highly productive period for the basic and biomedical sciences. Wartime discoveries had documented the remarkable success of research and had motivated public and governmental support of basic investigation.

This trend accelerated in the United States, when the office of Scientific Research and Development (U.S. War Department) transferred 44 research contracts with universities and with industry to the then fledging National Institutes of Health (NIH) at the end of World War II. The General Medicine Study Section of the National Institute of Arthritis and Metabolic Diseases (NIH) became a major support of GI research and training. During the 1960s, 1970s and 1980s, academic medical center faculties enlarged and research training programs increased, creating new technologies and new disciplines. Important advances occasionally developed from insightful clinical observations. A classic example concerns the "epidemic" of pellagra, considered an infection early in the 20th century and accounting annually for 250 000 cases and 7 000 deaths in 15 Southern cotton-growing U.S. states. In 1914, at age 40, Dr. Joseph G. Goldberger of the Public Health Service, through shrewd clinical observations of patients, hospital staff, and patient diets, implicated a dietary deficiency (confirmed later as a nicotinic acid deficiency) as the cause of pellagra. However, scientific activity was associated with much prestige, and gastroenterology sought to become more "scientific".

Gastroenterology essentially incorporates basic concepts and technology, from multiple scientific disciplines, into its own investigation. The early 1900s' view of swallowing, as the forceful "bolting" of food from the throat directly into the stomach, was replaced by the recognition of pharyngeal and esophageal neuromuscular function, facilitating the physiological management of swallowing disorders. Histologic and microbiologic examination of endoscopically obtained gastric biopsies replaced the subjective diagnosis of "chronic gastritis". Not until the 1980s, however, was the role of *Helicobacter pylori* in gastritis and peptic ulcer identified. Multidisciplinary research clarified the process of gastric secretion and led to the development of H₂ blockers and proton pump inhibitors. Metabolic studies identified the specific L-glutamine requirement for the intestinal epithelium and the short-chain fatty acid, n-butyrate, for the colonic epithelium. Research into the nature of inflammation led to more effective strategies for the treatment of inflammatory bowel disease. Cellular biology identified the intracellular heat shock proteins, trefoil peptides, and stem cell growth factors, with therapeutic potential. The important role of genetic influence, in the development of colorectal cancer, celiac disease, and inflammatory bowel disease, was extended to other GI diseases.

Gastroenterology's 20th-century technological progress was equally impressive. The study of esophageal motility progressed from balloon kymography to intraluminal catheter manometry, transducers, and neuropharmacologic methodology. Fiberoptic endoscopy expanded diagnostic access to virtually all areas of the gastrointestinal tract. Safer polyethylene tubing eased transintestinal intubation and perfusion studies, and with small bowel biopsy and radioimmuno-assays, clarified intestinal absorption mechanisms. Microbiological and chromatographic technologies, including hydrogen and carbon-14 breath tests, increased knowledge of the enteric flora, enabling the diagnosis of bacterial overgrowth responsive to antibacterial therapy. Needle biopsy of the liver established the morphological basis of hepatic disease and provided guidelines for the treatment of hepatitis and the monitoring of

liver transplantation. Discovery of the Australia antigen stimulated research, identifying seven types of hepatitis viruses (A, B, C, D, E, F, G), a major impetus in the growth of knowledge of liver disease. Biochemical and chromatographic technology determined the composition of bile and the process of formation, as well as the chemical dissolution of cholesterol gallstones. Enzyme and protein chemistry established the synthesis and trafficking of intracellular proteins and intracellular enzyme activation as the cause of acute pancreatitis. Transmission, electron microscopy and laser-scanning confocal microscopy facilitated the study of intestinal epithelial cells, intracellular protein processing, and epithelial barrier function. Molecular biological techniques made possible the cloning of genes for cystic fibrosis, sodium, calcium, glucose, and amino acid transport. Advances in radiologic image intensification, ultrasonography, computed x-ray tomography of the abdomen, and magnetic resonance imaging among other achievements, increased access to the gastrointestinal tract.

Neuro-humoral and neuro-immune interactions of the GI tract, mediating colonic motility and visceral sensitivity, replaced psychogenic hypotheses of the irritable bowel. Studies of gastrointestinal immunology, including the gut mucosal immune system and the molecular mechanisms of inflammation, generated new pathogenic concepts and therapeutic resources in inflammatory bowel disease (IBD). Measurements of gastrointestinal blood flow, including laser Doppler velocimetry, facilitated recognition of abdominal vascular impairment. Neurogastroenterology introduced methods of electrophysiology and cellular neurophysiology, identified the enteric nervous system as a "minibrain with intelligent circuits", and provided new understanding of "physiologic" GI disorders. Transgenic methodology created innovative animal models, enabling multidisciplinary studies of intestinal inflammation.

Expanded access to the gastrointestinal tract, including fiberoptic endoscopy, biopsies of the esophagus, stomach, small intestine, and colon, X-ray (CT scan)-guided biopsy of the liver and the pancreas, tests of hepatic and pancreatic functions, breath tests, quality X-rays, ultrasonography, computerized abdominal tomography, magnetic resonance imaging, and assessment of gastrointestinal motility improved the diagnosis of digestive disorders. Gastrointestinal therapy advanced with the discovery of sulfonamides, antibiotics, adrenocortical steroids, immune modifiers, H₂ receptor blockers, proton pump inhibitors, anti-inflammatory compounds, nutritional supports, vaccines, cancer chemotherapy, organ transplantation, and increasingly skilled abdominal surgery.

Many favorable circumstances converged to bring gastroenterology into the mainstream of advancing scientific thought, including an enlarging body of scientific knowledge, technological innovations permitting safer, more precise human studies, increased support of research and training, controlled clinical studies, establishment of research and scientific training programs, by the NIH and private philanthropy, and the enlarging global scientific communication network (journals, databases, electronic and computer systems).

The major accomplishment of gastroenterology during the 20th century has been the successful application of new scientific knowledge and technology to the investigation of gastrointestinal disorders. Digestive diseases involving multiple disciplines and innovative technology today are recognized as exciting and challenging problems. Now that gastroenterologic research frontiers are at the cutting edge of modern science, including such "new" sciences as biotechnology, structural biology, and pharmacogenetics, together with the ongoing molecular disciplines (microbiology, immunology, genetics). They will establish the 21st century as the gastroenterologic century.

Edited by Xu XQ and Wang XL **Proofread by** Xu FM

Survival of patients with stomach cancer in Changle city of China

Jun Tian, Xiao-Dong Wang, Zhen-Chun Chen

Jun Tian, Department of Epidemiology and Health Statistics, Fujian Medical University, Fuzhou 350004, Fujian Province, China

Xiao-Dong Wang, College of Mathematics and Computer science, Fuzhou University, Fuzhou 350002, Fujian Province, China

Zhen-Chun Chen, Fujian Cancer Hospital, Fuzhou 350014, Fujian Province, China

Supported by the Natural Science Foundation of Fujian, No. A0210012

Correspondence to: Jun Tian, Department of Epidemiology and Health Statistics, Fujian Medical University, Fuzhou 350004, Fujian Province, China. tianjun@mail.fjmu.edu.cn

Telephone: +86-591-3569264

Received: 2004-02-02 **Accepted:** 2004-02-21

Abstract

AIM: The survival rate of patients with stomach cancer is used to evaluate the effects of treatments. The short- and mid-term survival of patients on the present level of treatments can be described by calculating 1- to 5-year survival rates. The aims of this study were to document patterns of survival after treatments for stomach cancer in Changle city and analyze whether the stage of cancer and the way of treatment impacted on survival of patients or not.

METHODS: A total number of 745 patients with stomach cancer reported in the Changle Cancer Registry from 1993 to 1998 were investigated with respect to the disease condition, the way of treatment and survival time. 1- to 5-year survival rates were estimated by using life-table method.

RESULTS: The 1- to 5-year survival rates in the patients with stomach cancer in Changle city were 54.23%, 41.77%, 37.95%, 33.98% and 30.47%, respectively. The 1- to 5-year survival rates in stagel or II group were 3, 6.1, 7.4, 8.9 and 9.8 times as high as those in stage III or IV group, respectively. The 1- to 5-year survival rates in operation group were 3.5, 8.7, 11.2, 11.7 and 19 times as high as those in no operation group, respectively. For the patients with stage III or IV stomach cancer the 1-year survival rate in operation group was 3 times as high as that in no operation group and 2-year survival rate in operation group was 11.9 times as high as that in no operation group. For the patients with stage III or IV stomach cancer, the differences of the survival rates average survival times between total gastrectomy and partial gastrectomy were not significant and the median survival times in these 2 groups were 8 mo and 9 mo, respectively.

CONCLUSION: Mid-term survival rates of patients with stomach cancer in Changle city are low. Stage of cancer is an important factor influencing survival of patients with stomach cancer. Surgery is an effective treatment for the patients with stage IV cancer and can raise short- and mid-term survival rates. Total gastrectomy should not be encouraged for the patients with late stage of cancer.

Tian J, Wang XD, Chen ZC. Survival of patients with stomach cancer in Changle city of China. *World J Gastroenterol* 2004; 10(11): 1543-1546

<http://www.wjgnet.com/1007-9327/10/1543.asp>

INTRODUCTION

The survival time is used to evaluate the effects of treatments for stomach cancer. The survival rates are calculated in the analysis for the survival time^[1]. Many studies have been conducted on the survival analysis of stomach cancer in recent several decades^[2-8]. The survival of patients with stomach cancer was influenced by the stage of cancer and the way of treatment^[8,9]. Since stomach cancer often was not detected until an advanced state, survival rate was rather low. Only a few patients diagnosed with stomach cancer survive five years or more after diagnosis. There is a higher incidence rate of stomach cancer in Changle city of Fujian Province. To study the survival rates of the patients with stomach cancer and the prognostic factors in Changle city, we investigated the survival time of the patients with stomach cancer diagnosed from 1993 to 1998 and registered in the Changle Cancer Registry. The contents of our research were: (1) to estimate the survival rates of the patients with different stages of cancer and to compare these survival rates; (2) to estimate the survival rates of the patients with different ways of treatments and to compare these survival rates; (3) to analyze the survival benefit of the operation on the patients with stage IV stomach cancer; and (4) To make a comparison of survival between the patients with total gastrectomy and partial gastrectomy of stage IV stomach cancer.

MATERIALS AND METHODS

Materials

There were 747 patients with stomach cancer reported in Changle Cancer Registry from 1993 to 1998. Since two patients had no information of survival, the study sample consisted of 745 patients aged from 28 to 85 at registration. There were 593 male with age (60.1±10.1) years and 152 female with age (62.1±11.4) years in our sample. There were 473 dead patients and 272 patients were still alive during the term of investigation with the age (58.4±9.9).

Methods

The survival times of the 745 patients were obtained by visiting their home. After informed consent was obtained from each patient's family, the stage of cancer at diagnosis and way of treatment for the patient were obtained from the patient's medical record. The cause of death for each dead patient with stomach cancer was identified in the Hospital of Changle. The survival times of the patients who were not died of gastric cancer were not included in the data.

The proportion of stomach cancer patients surviving for one, two, three and five years can be a measure of the effect of treatments. The total survival rates by the stage of cancer and surgery were calculated and analyzed by Chi-square (χ^2 test) statistics. Survival analyses were performed by the life-table method^[1]. The data were analyzed using the SAS 8.2 software.

RESULTS

The 1-, 2-, 3-, 4- and 5-year survival rates and their 95% confidence intervals (CI) were estimated using life-table method (Table 1). Table 1 shows that the 1-year survival rate is 54.2% and the 5-year survival rate is 30.5%.

Table 1 Survival rates using life-table method

Time(yr)	Survival rate	95% confidence interval
1	0.542	0.506-0.578
2	0.418	0.382-0.454
3	0.379	0.343-0.416
4	0.340	0.302-0.377
5	0.305	0.265-0.345

The survival rates by the stage of cancer

The stages of cancer and survival status of 745 patients are shown in Table 2. The patients with stage III or IV cancer had 66.67% total survival rate. There were significance differences between these four total survival rates ($\chi^2=353.76, P<0.0001$).

A total number of 745 patients were grouped according to their stages of cancer. One group consisted of the patients with stage I or stage II stomach cancer and the other group consisted of the patients with stage III or stage IV stomach cancer. The survival rates using life-table method in two groups are shown in Table 3. The 1-, 2-, 3-, 4- and 5-year survival rates in stage I or stage II group were 3, 6.1, 7.4, 8.9 and 9.8 times higher than those in stage III or IV group, respectively. The difference of the distributions of survival times between the two groups was significant since the two 95% confidence intervals at each year did not overlap.

Table 2 Total survival rates by stage of cancer

Stage of cancer	Number of patients	Patients alive (n)	Death patients (n)	Total survival rate(%)
I	120	115	5	95.83
II	120	80	40	66.67
III	121	42	79	34.71
IV	384	35	349	9.11

Table 3 Survival rates using life-table method by stage of cancer

Time (yr)	Stage I or II		Stage III or IV	
	Survival rate	95% confidence interval	Survival rate	95% confidence interval
1	1.000	-	0.324	0.283-0.365
2	0.955	0.929-0.982	0.156	0.124-0.189
3	0.899	0.857-0.940	0.122	0.090-0.154
4	0.820	0.763-0.877	0.092	0.057-0.127
5	0.739	0.665-0.813	0.075	0.034-0.117

Table 4 Survival rates of surgical and non-surgical patients using life-table method by surgery

Time (yr)	Operation		No operation	
	Survival rate	95% confidence interval	Survival rate	95% confidence interval
1	0.753	0.713-0.793	0.217	0.170-0.265
2	0.639	0.594-0.684	0.074	0.043-0.105
3	0.589	0.541-0.636	0.053	0.024-0.081
4	0.528	0.477-0.580	0.045	0.017-0.073
5	0.478	0.420-0.535	0.025	0.013-0.051

The survival rates of patients with and without surgery

A total number of 745 patients were divided into 2 groups according to the way of treatments. One group consisted of 453 patients who underwent operation with total survival rate 55.63% (252/453) and the other group consisted of 292 patients who had no operation with total survival rate 6.85% (20/292). The

difference of the total survival rates between the two groups was significant ($\chi^2=182.26, P<0.0001$). The survival rates using life-table method in 2 groups are shown in Table 4. The 1-, 2-, 3-, 4- and 5-year survival rates in operation group were 3.5, 8.7, 11.2, 11.7 and 19 times as high as those in no operation group, respectively. The difference of the distributions of survival times between these two groups was significant.

The survival of the patients with late stage of cancer with and without surgery

A total number of 505 patients with stage III or IV stomach cancer were divided into two groups according to the way of treatments. One group consisted of 230 patients who underwent the gastrectomy operations and the other group consisted of 275 patients who had no operation. The survival rates using life-table method in the two groups are shown in Table 5. The 1-year and 2-year survival rates in operation group were 3 times and 11.9 times as high as those in no operation group, respectively. It was obvious that the survival times of the patients undergone the operation were longer than those of the patients not operated.

A total number of 145 (37.76%) patients with stage IV stomach cancer had gastric resection and 239 (62.24%) were not subjected to surgery. The 1-year survival rates in the 2 groups of patients with stage IV stomach cancer were 0.244 (95% CI 0.173-0.315) and 0.063 (95% CI 0.032-0.094), respectively. The averages of survival times in the two groups of the patients were 13.3 mo (95% CI 11.03-15.57) and 6.1 mo (95% CI 5.64-6.56), respectively. Median survival times in these 2 groups of the patients were 8 mo and 6 mo, respectively. The 1- and 2-year survival rates were significantly higher in operated patients than no operated patients. However, the average of survival time in operated patients prolonged only for 7.2 mo.

Table 5 Survival rates of surgical and non-surgical patients with stage III or IV stomach cancer using life-table method by surgery for patients

Time(yr)	Operation		No Operation	
	Survival rate	95% confidence interval	Survival rate	95% confidence interval
1	0.511	0.446-0.576	0.168	0.124-0.213
2	0.314	0.251-0.376	0.026	0.007-0.046
3	0.252	0.189-0.315	0.000	-
4	0.202	0.130-0.274	0.000	-
5	0.165	0.078-0.253	0.000	-

The survival of the patients with late stage of cancer by way of operation

Of 230 operated patients with late stage of cancer, 85 (36.96%) patients were with stage III cancer. There were 106 (46.09%) patients had total gastrectomy, 89 (38.70%) had partial gastrectomy and 20 (8.70%) had nonresectional surgery. The survival rates using life-table method in both total gastrectomy and partial gastrectomy are shown in Table 6. The averages of survival times and their 95% confidence intervals are shown in Table 7.

Table 6 Survival rates using life-table method by the way of operation for patients with stage III or IV stomach cancer

Time(yr)	Total gastrectomy		Partial gastrectomy	
	Survival rate	95% CI	Survival rate	95% CI
1	0.536	0.451-0.627	0.571	0.466-0.677
2	0.289	0.207-0.370	0.416	0.306-0.526

The 95% confidence interval for both the 1-year survival rate and 2-year survival rate in total gastrectomy group and those in partial gastrectomy group overlapped. These indicated that all the differences of the survival rates (both 1- and 2-year survival rates) between total gastrectomy group and partial gastrectomy group were not significant. Also, the 95% confidence interval for average of survival time in total gastrectomy group and that in partial gastrectomy group overlapped. This indicated that the difference of survival times between total gastrectomy group and partial gastrectomy group was not significant.

Table 7 Average of survival time by the way of operation in the patients with stage III or IV stomach cancer

Way of operation	Number of patients	Average of survival time (mo)	95% confidence interval
Total Gastrectomy	106	19.56	16.408-22.712
Partial Gastrectomy	89	16.42	14.300-18.540
Nonresectional Surgery	20	5.22	3.84-6.60

Of 145 operated patients with stage IV stomach cancer, 89(61.38%) were subjected to total gastrectomy and 41(28.28%) had partial gastrectomy. The 1-year survival rates in total gastrectomy and in partial gastrectomy were 0.1846(95% *CI* 0.0903-0.2789) and 0.2911(95% *CI* 0.1478-0.4344), respectively. The averages of survival times in total gastrectomy and in partial gastrectomy were 12.36 mo (95% *CI* 9.37-15.350) and 9.28 mo (95% *CI* 8.10-10.46), respectively. Median survival times in total gastrectomy and in partial gastrectomy were 8 mo and 9 mo, respectively. The result showed that prognosis of the patients with total gastrectomy was not better than that with partial gastrectomy.

DISCUSSION

Compared to other tumors, stomach cancer has a dismal prognosis and a low 5-year survival rate. In our research, 5-year survival rate of patients with stomach cancer in Changle city is 30.47%, which close to the results of some previous researches^[7,8,14].

The stage of cancer is the most important independent prognostic factor^[5,8-11]. The results using COX model in some researches showed that the death hazard of the patients with stage III cancer was 2.82 time as high as that of the patients with stage II cancer, and that with stage IV was 3.29 times as high as that with stage II cancer^[5]. The 1- and 2-year survival rates in stage IV stomach cancer were 1.65 and 10 times as high as those in stage III cancer respectively^[12]. The 5-year survival rate in stage I-stage IV were 81.2%, 50.4%, 24.4% and 5.2%, respectively^[7]. Our research also showed that stage of cancer might make a notable impact on survival rate of stomach cancer and 1- to 5- year survival rates in stage I or II of cancer were higher than those in stage III or IV. Among the patients in our study, 94% of the patients visited the doctors after they had had the symptoms of stomach cancer, so 51.54% of the patients had late stage of cancer (stage IV). Only 1.6% of the patients were discovered tumor by the general check up, and they had long survival times since they were diagnosed at early stage. So, researching on how to discover stomach cancer at early stage must play an important role in preventing and curing of tumors.

Surgery provides the only possibility of cure in stomach cancer patients. The 1- and 2-year survival rates of operated patients were much higher than those of not operated patients^[12-16]. Our results also confirmed this. However, whether resection should be performed in patients with the stage IV stomach cancer is still a question^[12,17,18]. Some researchers suggested that surgery could raise 3-year survival rate of patients

with stage IV cancer only if tumors were not diffusely infiltrative type, while short-term survival rates could not be raised even though resections were conducted for the patients with diffusely infiltrative type of cancer^[19]. However, surgery did not prolong survival time in patients with peritoneal dissemination, hepatic metastasis, lymph node involvement and invasion to adjacent organs or with 3 of these 4 factors^[12,20]. Some other researchers suggested that short-term improvement in survival for resected patients with distant metastases could be obtained and resectional surgery should be undertaken whenever possible in patients with stage IV stomach cancer as both short-term and long-term survival advantages had been demonstrated^[12,21-23]. We suggest that surgery not only can raise 1-year survival rate for the patients with stage IV cancer, but also can make them have the possibility of survival for more than 2 years, however, the average of survival time in operated patients with stage IV cancer does not prolong much.

Some researchers suggested that total gastrectomy had a lower relapsing rate than partial gastrectomy, so it could raise long-term survival^[12,14,24]. To improve long-term therapeutic effects, total gastrectomy should be recommended for stage III patients with cancer of the cardia and stomach fundus when tumor size is bigger than 3.0 cm or lymph node metastasis occur^[22]. Some researches also showed that subtotal and total gastrectomies had a similar postoperative complication rate and surgical outcome, and total gastrectomies had benefits of survival prolongation and symptomatic palliation^[23,25,26]. However, other researchers suggested that total gastrectomy could not get a higher survival rate than partial gastrectomy, but carried a higher postoperative complications rate and poorer quality of life than partial resections^[8,27-33]. We suggest that although surgery can raise 1-year survival rate of patients with stage IV cancer, total gastrectomy does not get a better survival than partial gastrectomy for the patients with stage IV stomach cancer. Besides, result obtained from earlier stage research also showed that the quality of life in the patients with total gastrectomy was worse than those with partial gastrectomy.

In summary, our data obtained by epidemiological survey have shown that mid-term survival rates of patients with stomach cancer in Changle city are low. Stage of cancer is an important factor influencing survival of patients with stomach cancer. Surgery is an effective treatment for the patients with stage IV cancer and can raise short- and mid-term survival rates. Total gastrectomy should not be encouraged for the patients with late stage of cancer.

REFERENCES

- 1 **Lee ET.** Statistical Methods For Survival Data Analysis. Second Edition. New York: *John Wiley Sons Inc* 1992: 9-117
- 2 **Jimeno-Aranda A,** Sainz Samitier R, Aragues GM. Gastric cancer in the province of Zaragoza: a survival study. *Neoplasma* 1996; **43**: 199-203
- 3 **Janer G,** Sala M, Kogevinas M. Health promotion trials at worksites and risk factors for cancer. *Scand J Work Environ Health* 2002; **28**: 141-157
- 4 **Lundegardh G,** Adami HO, Malmer B. Gastric cancer survival in Sweden: lack of improvement in 19 years. *Ann Surg* 1986; **204**: 546-551
- 5 **Barchielli A,** Amorosi A, Balzi D, Crocetti E, Nesi G. Long-term prognosis of gastric cancer in a European country: a population-based study in Florence. 10-year survival of cases diagnosed in 1985-1987. *Eur J Cancer* 2001; **37**: 1674-1680
- 6 **Pinheiro PS,** van der Heijden LH, Coebergh JW. Unchanged survival of gastric cancer in the southeastern Netherlands since 1982: result of differential trends in incidence according to Lauren type and subsite. *Int J Cancer* 1999; **84**: 28-32
- 7 **Msika S,** Benhamiche AM, Jouve JL, Rat P, Faivre J. Prognostic factors after curative resection for gastric cancer. A population-based study. *Eur J Cancer* 2000; **36**: 390-396

- 8 **Msika S**, Benhamiche AM, Rat P, Faivre J. Long-term prognosis of gastric cancer in the population of Cote-d'Or. *Gastroenterol Clin Biol* 2000; **24**: 649-655
- 9 **Monnet E**, Faivre J, Raymond L, Garau I. Influence of stage at diagnosis on survival differences for rectal cancer in three European populations. *Br J Cancer* 1999; **81**: 463-468
- 10 **Casariago Vales E**, Pita Fernandez S, Rigueiro Veloso MT, Pertega Diaz S, Rabunal Rey R, Garcia-Rodeja ME, Alvarez Cervela L. Survival and prognostic factors for gastric cancer. Analysis of 2334 patients. *Med Clin* 2001; **117**: 361-365
- 11 **Faivre J**, Forman D, Esteve J, Gatta G. Survival of patients with oesophageal and gastric cancers in Europe. EUROCARE Working Group. *Eur J Cancer* 1998; **34**: 2167-2175
- 12 **Haugstvedt T**, Viste A, Eide GE, Soreide O. The survival benefit of resection in patients with advanced stomach cancer: the norwegian multicenter experience. Norwegian stomach cancer Trial. *World J Surg* 1989; **13**: 617-621
- 13 **Pointner R**, Wetscher GJ, Gadenstatter M, Bodner E, Hinder RA. Gastric remnant cancer has a better prognosis than primary gastric cancer. *Arch Surg* 1994; **129**: 615-619
- 14 **Doglietto GB**, Pacelli F, Caprino P, Sgadari A, Crucitti F. Surgery: independent prognostic factor in curable and far advanced gastric cancer. *World J Surg* 2000; **24**: 459-464
- 15 **Tuech JJ**, Cervi C, Pessaux P, Villapadierna F, Bergamaschi R, Ronceray J, Arnaud JP. Early gastric cancer: univariate and multivariate analysis for survival. *Hepatogastroenterology* 1999; **46**: 3276-3280
- 16 **Maetani S**, Tobe T, Hirakawa A, Kashiwara S, Kuramoto S. Parametric survival analysis of gastric cancer patients. *Cancer* 1980; **46**: 2709-2716
- 17 **Valen B**, Viste A, Haugstvedt T, Eide GE, Soreide O. Treatment of stomach cancer. A national experience. *Br J Surg* 1988; **75**: 708-714
- 18 **Bonenkamp JJ**, Sasako M, Hermans J, van de Velde CJ. Tumor load and surgical palliation in gastric cancer. *Hepatogastroenterology* 2001; **48**: 1219-1221
- 19 **Murata S**, Terata N, Eguchi Y, Tani T, Shibata J, Kodama M. Prognosis of patients with resection of stage IV gastric cancer. *Int Surg* 1998; **83**: 283-286
- 20 **Maekawa S**, Saku M, Maehara Y, Sadanaga N, Ikejiri K, Anai H, Kuwano H, Sugimachi K. Surgical treatment for advanced gastric cancer. *Hepatogastroenterology* 1996; **43**: 178-186
- 21 **Kunisaki C**, Shimada H, Akiyama H, Nomura M, Matsuda G, Ono H. Survival benefit of palliative gastrectomy in advanced incurable gastric cancer. *Anticancer Res* 2003; **23**: 1853-1858
- 22 **Huang CM**, Zhang XF, Lu HS, Zhang JZ, Wu XY, Guan GX, Wang C. Long-term therapeutic effects of total gastrectomy in cancer of the cardia and stomach fundus. *Zhonghua Waike Zazhi* 2003; **41**: 729-732
- 23 **Wan YL**, Liu YC, Tang JQ, Wang X, Wu T, Pan YS, Huang SJ, Huang YT. Clinical analysis of combined resection for T4 gastric cancer: report of 69 cases. *Zhonghua Waike Zazhi* 2003; **41**: 594-596
- 24 **Wang CS**, Chao TC, Jan YY, Jeng LB, Hwang TL, Chen MF. Benefits of palliative surgery for far-advanced gastric cancer. *Chang Gung Med J* 2002; **25**: 792-802
- 25 **Bozzetti F**, Marubini E, Bonfanti G, Miceli R, Piano C, Crose N, Gennari L. Total versus subtotal gastrectomy: surgical morbidity and mortality rates in a multicenter Italian randomized trial. The Italian Gastrointestinal Tumor Study Group. *Ann Surg* 1997; **226**: 613-620
- 26 **Meriggi F**, Forni E. Radical surgical treatment of gastric cancer. Personal experience. *G Chir* 2002; **23**: 361-367
- 27 **Sjostedt S**, Pieper R. Gastric cancer. Factors influencing longterm survival and postoperative mortality. *Acta Chir Scand Suppl* 1986; **530**: 25-29
- 28 **Viste A**, Haugstvedt T, Eide GE, Soreide O. Postoperative complications and mortality after surgery for gastric cancer. *Ann Surg* 1988; **207**: 7-13
- 29 **Hansson LE**, Sparen P, Nyren O. Survival in stomach cancer is improving: results of a nationwide population-based Swedish study. *Ann Surg* 1999; **230**: 162-169
- 30 **Harrison LE**, Karpeh MS, Brennan MF. Total gastrectomy is not necessary for proximal gastric cancer. *Surgery* 1998; **123**: 127-130
- 31 **Bozzetti F**, Marubini E, Bonfanti G, Miceli R, Piano C, Gennari L. Subtotal versus total gastrectomy for gastric cancer: five-year survival rates in a multicenter randomized Italian trial. Italian Gastrointestinal Tumor Study Group. *Ann Surg* 1999; **230**: 170-178
- 32 **De Manzoni G**, Verlato G, Roviello F, Di Leo A, Marrelli D, Morgagni P, Pasini F, Saragoni L, Tomezzoli A. Italian Research Group for Gastric Cancer. Subtotal versus total gastrectomy for T3 adenocarcinoma of the antrum. *Gastric Cancer* 2003; **6**: 237-242
- 33 **Yamamoto M**, Baba H, Kakeji Y, Endo K, Ikeda Y, Toh Y, Kohnoe S, Okamura T, Maehara Y. Postoperative morbidity/mortality and survival rates after total gastrectomy, with splenectomy/pancreaticosplenectomy for patients with advanced gastric cancer. *Hepatogastroenterology* 2004; **51**: 298-302

Edited by Kumar M Proofread by Xu FM

Gender difference in clinicopathologic features and survival of patients with hepatocellular carcinoma

Pisit Tangkijvanich, Varocha Mahachai, Pongspeera Suwangool, Yong Poovorawan

Pisit Tangkijvanich, Department of Biochemistry, Faculty of Medicine, Chulalongkorn University, Bangkok 10330, Thailand

Varocha Mahachai, Department of Medicine, Faculty of Medicine, Chulalongkorn University, Bangkok 10330, Thailand

Pongspeera Suwangool, Department of Pathology, Faculty of Medicine, Chulalongkorn University, Bangkok 10330, Thailand

Yong Poovorawan, Viral Hepatitis Research Unit, Department of Pediatrics, Faculty of Medicine, Chulalongkorn University, Bangkok 10330, Thailand

Correspondence to: Professor Yong Poovorawan, Viral Hepatitis Research Unit, Department of Pediatrics, Faculty of Medicine, Chulalongkorn University, Bangkok 10330, Thailand. yong.p@chula.ac.th

Telephone: +662-256-4909 **Fax:** +662-256-4929

Received: 2003-11-18 **Accepted:** 2004-01-29

Abstract

AIM: To determine the influence of gender on the clinicopathologic characteristics and survival of patients with hepatocellular carcinoma (HCC).

METHODS: A retrospective analysis of medical records was performed in 299 patients with HCC and their clinicopathologic features and survival were compared in relation to gender.

RESULTS: There were 260 male (87%) and 39 female patients (13%), with a male-to-female ratio of 6.7:1. Female patients had lower mean serum bilirubin levels ($P=0.03$), lower proportion of alcohol abuse ($P=0.002$), smaller mean tumor size ($P=0.02$), more frequent nodular type but less frequent massive and diffuse types of HCC ($P=0.01$), were less advanced in Okuda's staging ($P=0.04$), and less frequently associated with venous invasion ($P=0.03$). The median survivals in females (14 mo) were significantly longer than that of male patients (4 mo) ($P=0.004$, log-rank test). Multivariate analysis demonstrated that high serum alpha-fetoprotein levels, venous invasion, extrahepatic metastasis and lack of therapy were independent factors related to unfavorable prognosis. However, gender did not constitute a predictive variable associated with patient survival.

CONCLUSION: Female patients tend to have higher survival rates than males. These differences were probably due to more favorable pathologic features of HCC at initial diagnosis and greater likelihood to undergo curative therapy in female patients.

Tangkijvanich P, Mahachai V, Suwangool P, Poovorawan Y. Gender difference in clinicopathologic features and survival of patients with hepatocellular carcinoma. *World J Gastroenterol* 2004; 10(11): 1547-1550

<http://www.wjgnet.com/1007-9327/10/1547.asp>

INTRODUCTION

Hepatocellular carcinoma (HCC) is one of the most common cancers worldwide with a particularly high incidence in areas where chronic hepatitis B virus (HBV) and hepatitis C virus

(HCV) are common^[1,2]. These regions include sub-Saharan Africa, Far East and Southeast Asia where the annual rate is more than 30 cases per 100 000 persons. In contrast, in low-incidence areas such as Europe and North America, the annual rate is less than 5 cases per 100 000 persons^[3]. In Thailand, where chronic HBV is endemic, it is estimated that more than 10 000 new cases of HCC are diagnosed each year. Indeed, HCC represents the most common malignancy in Thai males and the third most common malignancy in females^[4].

Previously, we demonstrated that HCC in Thailand had an indisputable male predominance, with a male-to-female ratio of approximately 6:1^[5]. In fact, HCC is notably more prevalent in males worldwide, with reported male-to-female ratios ranging from 2:1 to 8:1 in most series. Until now, however, only a few studies have specifically compared the clinicopathologic characteristics of patients with HCC in relation to gender. In addition, the contribution of sex difference to patient survival and prognosis is controversial^[6-13]. The aim of the present study was, therefore, to determine the influence of gender on clinicopathologic features and patient survival. In this respect, we analyzed the medical records on individuals in whom HCC was diagnosed during a four-year period at King Chulalongkorn Memorial Hospital (Bangkok, Thailand).

MATERIALS AND METHODS

A total of 299 patients with HCC who were admitted to King Chulalongkorn Memorial Hospital between January 1996 and September 1999 were retrospectively analyzed and included in this study. All patients were diagnosed based on liver tumor characteristics detected by ultrasound/CT scan and confirmed by histology or serum alpha-fetoprotein (AFP) levels above 400 IU/mL. Of those, there were 260 male (87%) and 39 female patients (13%), making a male-to-female ratio of 6.7:1. We compared the difference and the clinicopathologic features, including age, biochemical liver function test, presence or absence of associated cirrhosis, etiologic factors predisposing towards HCC (alcohol abuse, hepatitis B or C), degree of tumor differentiation, gross pathology of tumor, tumor size, presence of vascular invasion, stage of HCC according to Okuda's criteria, evidence of distant metastasis and modalities of therapy of HCC. In addition, the patients' survival time for each group was also calculated, starting with the time of cancer diagnosis (including any incidence of perioperative mortality).

Gross pathology, tumor size, and localization of HCC as well as presence of portal or hepatic venous involvement, were obtained by abdominal ultrasound or computerized tomography (CT). In this study, the gross pathologic types of HCC were categorized according to Trevisani *et al.*^[14] as follows: nodular, multinodular, infiltrative, diffuse (the mass was not clearly defined and the boundary was indistinct) or massive type (a huge mass >10 cm with the boundary not well defined).

Biochemical liver function tests were determined by automated chemical analyzer (Hitachi 911) at the central laboratory of Chulalongkorn Hospital. The normal levels obtained with healthy adults are within the range of 0-38 IU/L for serum aspartate aminotransferase (AST) and alanine aminotransferase (ALT) and 98-279 IU/L for serum alkaline

phosphatase (AP). Enzyme-linked immunosorbent assays (ELISA) were used for the detection of HBsAg (Auszyme II, Abbott Laboratories, North Chicago, IL), anti-HCV (ELISA II; Ortho Diagnostic Systems, Chiron Corp., Emeryville, CA) and AFP (Cobus[®]Core, Roche Diagnostics, Basel, Switzerland).

Statistical analysis

Data were presented as percentage, mean and standard deviation. The Chi-square test and unpaired *t* test were used to assess the statistical significance of the difference between groups as appropriate. Survival curves were established using the Kaplan-Meier method and differences between curves were demonstrated using the log-rank test. The Cox regression analysis was performed to identify which independent factors have a significant influence on the overall survival. *P* values below 0.05 were considered statistically significant.

RESULTS

As shown in Table 1, the mean age of female patients (56.4±15.2 years) was slightly higher, but not significantly different from that of male patients (52.6±13.2 years). There was a significantly lower proportion of heavy alcohol consumption among females than males (*P*=0.002). However, there were no significant differences in positive rates of serum HBsAg and anti-HCV, nor in the frequency of associated liver cirrhosis between the two groups. Similarly, no significant differences between groups were observed regarding mean serum AFP levels and biochemical abnormalities, with the exception that female patients had significantly lower serum bilirubin levels than male patients (*P*=0.03).

Table 1 Demographic and clinical data of female and male patients with HCC at initial diagnosis

Characteristics	Female (n=39)	Male (n=260)	<i>P</i>
Age (yr)	56.4±15.2	52.6±13.2	NS
Underlying cirrhosis (+/-)	36:3	251:9	NS
Viral hepatitis marker			
HBsAg (+/-)	18:21	147:113	NS
Anti-HCV (+/-)	5:34	23:237	NS
Heavy alcohol consumption (+/-)	3:36	83:177	0.002
Mean AFP (IU/mL)	48 435.4±105 231.6	40 221.9±89 147.9	NS
Biochemical liver function tests			
Total bilirubin (mg/dL)	1.5±1.2	3.1±2.3	0.03
Alkaline phosphatase (IU/L)	451.6±277.3	529.3±375.0	NS
AST (IU/L)	128.4±133.2	154.3±135.2	NS
ALT (IU/L)	62.7±52.6	87.6±97.5	NS
Albumin (g/dL)	3.6±0.7	3.4±0.7	NS
Prothrombin time (sec)	14.5±2.8	15.1±9.3	NS

Quantitative variables were expressed as mean±SD; (+/-) indicates positive:negative. NS=not significant.

Table 2 demonstrates the clinicopathologic data of the patients at the time of the diagnosis of HCC. Female patients in this study tended to have less aggressive tumor characteristics than male patients. For instance, the mean tumor size in females (8.6 cm) was significantly smaller than that of male patients (11.6 cm) (*P*=0.02). In addition, the nodular type of HCC appeared to be more frequently found among female patients, whereas the massive and diffuse types were more common among males (*P*=0.01). Furthermore, the tumors in the female group tended to be of a less advanced stage according to Okuda's criteria (*P*=0.04) and less frequently associated with portal or hepatic vein invasion (*P*=0.03). Nonetheless, no significant differences between groups were observed as to the degree of tumor differentiation, the prevalence of extrahepatic metastasis or ruptured HCC.

Table 2 Clinicopathologic data of female and male patients with HCC at initial diagnosis

Characteristics	Female (n=39)	Male (n=260)	<i>P</i>
Mean tumor size (cm)	8.1±3.9	11.6±4.5	0.02
Tumor size			
≤5 cm:>5cm	9:30	30:230	0.04
Gross appearance of HCC			
Nodular:Multinodular:	12:10:14:3	30:52:115:63	0.01
Massive:Diffuse			
Tumor cell differentiation			
Well:Moderately:Poorly	3:5:4	11:66:32	NS
Okuda's staging (I:II:III)	13:23:3	43:180:37	0.04
Portal or hepatic vein invasion (+/-)	6:33	84:176	0.03
Extrahepatic metastasis (+/-)	5:34	37:223	NS
Ruptured HCC (+/-)	1:38	29:231	NS
Therapy for HCC (+/-)	22:17	105:155	NS
Modality of therapy			
Surgical resection (+/-)	9:30	27:233	0.02
Chemoembolization (+/-)	13:26	43:217	0.01
Systemic chemotherapy (+/-)	0:39	31:229	0.02

Quantitative variables were expressed as mean±SD; (+/-) indicates positive:negative.

Likewise, there was no statistically significant difference between groups in terms of the number of patients treated with specific therapeutic modalities. However, female patients were more likely than male patients to undergo surgical resection, which included segmental and lobar resection, or treated with transcatheter arterial chemoembolization (TACE) (*P*=0.02 and 0.01, respectively). In contrast, a significantly higher proportion of male patients were treated with systemic chemotherapy than females (*P*=0.02).

The median survival time of all patients in this study, regardless of their gender, was 5 mo. The Kaplan-Meier survival curves demonstrated that the overall median survival for female and male patients were 14 and 4 mo, respectively (*P*=0.004, using log-rank test) (Figure 1). For patients who were treated with any specific therapeutic modality, the median survival for the female and male group were 17 and 7 mo, respectively (*P*=0.025). In the untreated cases, the median survival of the female group was longer than that of the male group (9 and 3 mo, respectively), however, this difference did not achieve statistical significance (*P*=0.24).

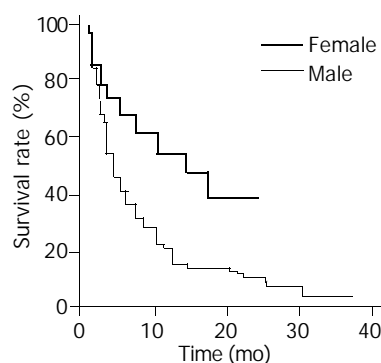


Figure 1 Overall survival of male and female patients with HCC.

Univariate analysis of the main variables was performed to determine significant risk factors associated with the overall survival. In addition to male sex, serum AFP levels >400 IU/mL, Okuda's stage II and III HCC, massive or diffuse types of tumors, tumor mass size over 5 cm in diameter, venous invasion and

extrahepatic metastasis, and an unfavorable prognosis were observed in patients who did not receive any specific therapy for HCC. Stepwise Cox regression multivariate analysis revealed that high serum AFP levels, venous invasion, extrahepatic metastasis and absence of specific therapy were significantly and independently predictive for unfavorable prognosis (Table 3). Nonetheless, gender was not selected in the final analysis as an independent predictor of survival.

Table 3 Independent predictors influencing survival in HCC

Variables	Regression coefficient (95% CI)	P value ¹
AFP (>400 IU/mL)	1.67 (1.03-2.71)	0.037
Portal or hepatic vein invasion	1.73 (1.04-2.89)	0.035
Extrahepatic metastasis	2.37 (1.30-4.37)	0.005
No therapy	2.87 (1.63-5.04)	0.0002

95% CI: 95% confidence interval; ¹P value based on multivariate Cox regression analysis

DISCUSSION

Various types of cancer occur more frequently in male than in female patients. Such is also the case with HCC. In fact, marked male predominance in HCC incidence is observed in both high- and low-risk areas, regardless of ethnic and geographic diversity^[15]. Despite this, the exact reasons for sex difference in the incidence of HCC are unclear. It has been reported that DNA synthetic activities are higher in male than in female cirrhotics and this might be one of the possible explanations for the gender discrepancy in HCC^[16]. However, in patients who had already developed HCC, a significant difference in tumor cellular proliferation between male and female patients was not detected^[11]. It has also been suggested that the effect of sex hormones may contribute, at least in part, to the greater incidence of HCC observed in male patients. Although the mechanism remains to be elucidated, studies from animal models has implicated that the hormonal effect may be related to testosterone's ability in enhancing transforming growth factor (TGF) alpha related hepatocarcinogenesis and hepatocyte proliferation^[17].

Beside this, other possible factors contributing to the male predominance in HCC include the association with HBV infection, the higher proportion of male cirrhotics and differences in life-style habits, such as heavy alcohol consumption and smoking^[6,10]. However, in this study, no significant difference was found between groups in the prevalence of associated cirrhosis. Likewise, although HBsAg carriers were slightly more common in males, this discrepancy did not reach statistical significance. Notably, this was also the case with the prevalence of chronic HCV infection in our study. In contrast, the prevalence of heavy alcohol consumption was significantly different, being higher in male than in female patients. Indeed, alcoholic cirrhosis has long been recognized as a risk factor for developing HCC, although its role in direct hepatocarcinogenesis is uncertain^[18]. Nonetheless, it is reasonable to speculate that chronic alcohol abuse might accelerate cancer development in some cases with HBV- or HCV-associated cirrhosis and this may be partially responsible for the male preponderance of HCC in our series.

In addition, to confirm the marked male predominance, our study has demonstrated that male patients with HCC had a less favorable prognosis than females after initial diagnosis. Specifically, better survival in females was observed in those who had undergone surgical resection or treated with TACE. For untreated cases, the influence of gender on prognosis seemed to be limited since significant difference in survival between groups was not achieved, although there was a trend for females to survive longer. These results were consistent

with previous reports in which a better prognosis was observed in females following hepatic resection^[9-13]. For instance, according to the study in Japan by Nagasue *et al.*, significantly better survival rates were found in females after 4 years of hepatic surgery^[9]. A previous report on Chinese patients by Cong *et al.* also demonstrated that the survival rates after surgery were approximately 50% and 25% in females and males, respectively^[10]. Likewise, a study in Hong Kong by Ng *et al.*, indicated that females had a lower incidence of tumor recurrence following the surgical operations, with a median disease free survival of 19.5 mo compared with 4.5 mo for males^[11]. Recently, Lee *et al.* reported that female cirrhotics with HCC had 5-year disease survival rates after hepatic resection, which was higher than males (approximately 65% and 30%, respectively)^[12]. Conversely, such favorable prognosis in females was not consistently observed among patients with inoperable tumors^[6-8].

Thus, it could be speculated that the prognosis of HCC is not directly influenced by the sex of the patients. This is confirmed in our study that gender was not selected as an independent predictor of survival from the multivariate analysis. In fact, a better prognosis in females was probably attributed to a less advanced stage of HCC at initial diagnosis and, as a result, a higher proportion of cases was likely to undergo surgical resection or treated with TACE. In this study, for example, approximately 25% and 35% of female patients were treated with hepatic resection or TACE, respectively, while only approximately 10% and 15% of males were treated with such modalities. It has been generally recognized that hepatic resection is one of the most effective therapeutic modalities offering a hope of cure for patients with HCC^[19,20]. Moreover, a non-surgical approach such as TACE appears to be beneficial in prolonging survival for some patients with unresectable tumors^[21-22].

In addition to therapeutic factors, some pathobiologic features indicative of tumor invasiveness, such as venous involvement, appear to be significant factors influencing the survival of HCC^[23]. It has also been demonstrated that the presence of venous invasion is associated with a higher intrahepatic recurrence rate after the resection of the tumor^[24]. Although HCC is characterized by its propensity for vascular invasion, it is interesting that female patients with HCC had a much lower prevalence of venous involvement than males. It seems, therefore, that this is probably one of the main factors contributing to different survival rates between the two sexes in our study. Similarly, yet to be addressed, are the effects of other tumor pathologic features, such as tumor encapsulation during the disease-free period after surgical resection of HCC^[25]. Previous data have demonstrated that females have a significantly higher prevalence of tumor encapsulation than males (80% and 45%, respectively). Furthermore, the tumors in females were frequently less invasive in terms of lower prevalence of tumor microsatellites and positive histological margin^[11].

In conclusion, our data indicated that female patients with HCC had certain clinicopathologic features different from those in male patients. Moreover, females with HCC appeared to have better survival rates than males. This better prognosis in females was related to more favorable tumor characteristics such as a lower prevalence of hepatic or portal venous invasion and less advanced stages at initial diagnosis. As a result, female patients were more likely than male patients to undergo hepatic resection or to be treated with TACE.

ACKNOWLEDGEMENT

We would like to express our gratitude to the Thailand Research Fund, Senior Research Scholar and the Molecular Biology Project, Chulalongkorn University for supporting the study.

We also would like to thank Ms. Pisanee Saiklin for editing the manuscript.

REFERENCES

- 1 **Chen CJ**, Yu MW, Liaw YF. Epidemiological characteristics and risks factors of hepatocellular carcinoma. *J Gastroenterol Hepatol* 1997; **12**: S290-308
- 2 **Tang ZY**. Hepatocellular carcinoma-cause, treatment and metastasis. *World J Gastroenterol* 2001; **7**: 445-454
- 3 **McGlynn KA**, Tsao L, Hsing AW, Devesa SS, Fraumeni JF Jr. International trends and patterns of primary liver cancer. *Int J Cancer* 2001; **94**: 225-236
- 4 **Srivatanakul P**. Epidemiology of liver cancer in Thailand. *Asian Pac J Cancer Prev* 2001; **2**: 117-121
- 5 **Tangkijvanich P**, Hirsch P, Theamboonlers A, Nuchprayoon I, Poovorawan Y. Association of hepatitis viruses to hepatocellular carcinoma in Thailand. *J Gastroenterol* 1999; **34**: 227-233
- 6 **Lai CL**, Gregory PB, Wu PC, Lok AS, Wong KP, Ng MM. Hepatocellular carcinoma in Chinese males and females. Possible causes for the male predominance. *Cancer* 1987; **60**: 1107-1110
- 7 **Calvet X**, Bruix J, Gines P, Bru C, Sole M, Vilana R, Rodes J. Prognostic factors of hepatocellular carcinoma in the west: a multivariate analysis in 206 patients. *Hepatology* 1990; **12**: 753-760
- 8 **Falkson G**, Cnaan A, Schutt AJ, Ryan LM, Falkson HC. Prognostic factors for survival in hepatocellular carcinoma. *Cancer Res* 1988; **48**: 7314-7318
- 9 **Nagasue N**, Galizia G, Yukaya H, Kohno H, Chang YC, Hayashi T, Nakamura T. Better survival in women than in men after radical resection of hepatocellular carcinoma. *Hepatogastroenterology* 1989; **36**: 379-383
- 10 **Cong WM**, Wu MC, Zhang XH, Chen H, Yuan JY. Primary hepatocellular carcinoma in women of Mainland China. A clinicopathologic analysis of 104 patients. *Cancer* 1993; **71**: 2941-2945
- 11 **Ng IO**, Ng MM, Lai EC, Fan ST. Better survival in female patients with hepatocellular carcinoma. Possible causes from a pathologic approach. *Cancer* 1995; **75**: 18-22
- 12 **Lee CC**, Chau GY, Lui WY, Tsay SH, King KL, Loong CC, Hshia CY, Wu CW. Better post-resectional survival in female cirrhotic patients with hepatocellular carcinoma. *Hepatogastroenterology* 2000; **47**: 466-469
- 13 **Dohmen K**, Shigematsu H, Irie K, Ishibashi H. Longer survival in female than in male with hepatocellular carcinoma. *J Gastroenterol Hepatol* 2003; **18**: 267-272
- 14 **Trevisani F**, Caraceni P, Bernardi M, D'Intino PE, Arienti V, Amorati P, Stefanin GF, Grazi G, Mazziotti A, Fornale L. Gross pathological types of hepatocellular carcinoma in Italian patients. Relationship with demographic, environmental and clinical factors. *Cancer* 1993; **72**: 1557-1563
- 15 **El-Serag HB**. Hepatocellular carcinoma: an epidemiologic view. *J Clin Gastroenterol* 2002; **35**(5 Suppl 2): S72-78
- 16 **Tarao K**, Ohkawa S, Shimizu A, Harada M, Nakamura Y, Ito T, Tamai S, Hoshino H, Okamoto N, Iimori K. The male preponderance in incidence of hepatocellular carcinoma in cirrhotic patients may depend on the higher DNA synthetic activity of cirrhotic tissue in men. *Cancer* 1993; **72**: 369-374
- 17 **Matsumoto T**, Takagi H, Mori M. Androgen dependency of hepatocarcinogenesis in TGF alpha transgenic mice. *Liver* 2000; **20**: 228-233
- 18 **Adami HO**, Hsing AW, McLaughlin JK, Trichopoulos D, Hacker D, Ekblom A, Perrson I. Alcoholism and liver cirrhosis in the etiology of primary liver cancer. *Int J Cancer* 1992; **51**: 898-902
- 19 **Befeler AS**, Di Bisceglie AM. Hepatocellular carcinoma: diagnosis and treatment. *Gastroenterology* 2002; **122**: 1609-1619
- 20 **Qian J**, Feng GS, Vogl T. Combined interventional therapies of hepatocellular carcinoma. *World J Gastroenterol* 2003; **9**: 1885-1891
- 21 **Pawarode A**, Tangkijvanich P, Voravud N. Outcome of primary hepatocellular carcinoma treatment: an 8-year experience with 368 patients in Thailand. *J Gastroenterol Hepatol* 2000; **15**: 860-864
- 22 **Lo CM**, Ngan H, Tso WK, Liu CL, Lam CM, Poon RT, Fan ST, Wong J. Randomized controlled trial of transarterial lipiodol chemoembolization for unresectable hepatocellular carcinoma. *Hepatology* 2002; **35**: 1164-1171
- 23 **Ringe B**, Pichlmayr R, Wittekind C, Tusch G. Surgical treatment of hepatocellular carcinoma: Experience with liver resection and transplantation in 198 patients. *World J Surg* 1991; **15**: 270-285
- 24 **Nagasue N**, Uchida M, Makino Y, Takemoto Y, Yamanoi A, Hayashi T, Chang YC, Kohno H, Nakamura T, Yukaya H. Incidence and factors associated with intrahepatic recurrence following resection of hepatocellular carcinoma. *Gastroenterology* 1993; **105**: 488-494
- 25 **Ng IO**, Lai EC, Ng MM, Fan ST. Tumor encapsulation in hepatocellular carcinoma. A pathologic study of 189 cases. *Cancer* 1992; **70**: 690-693

Edited by Ma JY Proofread by Xu FM

Effect of phosphorus-32 glass microspheres on human hepatocellular carcinoma in nude mice

Dong-Sheng Zhang, Lu Liu, Li-Qiang Jin, Mei-Ling Wan, Qun-Hui Li

Dong-Sheng Zhang, Li-Qiang Jin, Mei-Ling Wan, Qun-Hui Li, School of Basic Medical Sciences, Southeast University, Nanjing 210009, Jiangsu Province, China

Lu Liu, Experimental Center of Modern Medical Sciences, Southeast University, Nanjing 210009, Jiangsu Province, China

Supported by the Science and Technology Commission of Jiangsu Province, No. BJ93007 and Natural Science Foundation of Jiangsu Province, No. BK2001003

Correspondence to: Professor Dong-Sheng Zhang, School of Basic Medical Sciences, Southeast University, 87 Ding Jia Qiao Road, Nanjing 210009, Jiangsu Province, China. b7712900@jlonline.com

Telephone: +86-25-83272502 **Fax:** +86-25-57712900

Received: 2003-11-21 **Accepted:** 2003-12-29

Abstract

AIM: To study the effects of phosphorus-32 glass microspheres (^{32}P -GMS) on human hepatocellular carcinoma in nude mice.

METHODS: Human liver cancer cell line was implanted into the dorsal subcutaneous tissue of 40 BALB/c nude mice. Then the 40 tumor-bearing BALB/c nude mice were allocated into treatment group ($n=32$) and control group ($n=8$). In the former group different doses of ^{32}P -GMS were injected into the tumor mass, while in the latter nonradioactive ^{31}P -GMS was injected into the tumor mass. The experimental animals were sacrificed on the 14th day. The ultrastructural changes of tumor in both treatment group and control group were studied with transmission electron microscopy (TEM) and stereology.

RESULTS: In treatment group, a lot of tumor cells were killed and the death rate of tumor cells was much higher (35-70%). Ultrastructurally, severe nuclear damage was observed in the death cells. The characteristics of apoptosis such as margination of heterochromatin was also found in some tumor cells. Besides, well differentiated tumor cells, degenerative tumor cells and some lymphocytes were seen. The skin and muscle adjacent to the tumor were normal. In control group, the tumor consisted of poorly differentiated tumor cells, in which there were only a few of dead cells (5%). Stereological analysis of ultrastructural morphology showed that Vv of nuclei (53.31 ± 3.46) and Vv of nucleoli (20.40 ± 1.84) in the control group were larger than those (30.21 ± 3.52 and 10.96 ± 2.52) in the treatment group respectively ($P<0.01$), and Vv of RER (3.21 ± 0.54) and Vv of mitochondria (4.53 ± 0.89) in the control group were smaller than those (8.67 ± 1.25 and 7.12 ± 0.95) in the treatment group respectively ($P<0.01$, 0.05). Sv of the membrane of microvilli and canaliculi ($27.12\text{ }\mu\text{m}^2/100\text{ }\mu\text{m}^3\pm 11.84\text{ }\mu\text{m}^2/100\text{ }\mu\text{m}^3$) in the control group was smaller than that ($78.81\text{ }\mu\text{m}^2/100\text{ }\mu\text{m}^3\pm 19.69\text{ }\mu\text{m}^2/100\text{ }\mu\text{m}^3$) in the treatment group ($P<0.01$). But Vv of lipid particles (3.71 ± 1.97) and Vv of vacuoles (5.72 ± 1.58) were much larger than those (0.30 ± 0.16 and 0.35 ± 0.15) in the treatment group respectively ($P<0.05$, $P<0.01$).

CONCLUSION: The experimental results indicate that local administration of ^{32}P -GMS can produce obvious effect on

liver cancer cells and the anticancer effect of ^{32}P -GMS is directly proportional to the dose administered. Ultrastructural stereology can also show the effect of ^{32}P -GMS on the normalization of tumor cells, which is beneficial to the prognosis and treatment of patients. Moreover, local administration of ^{32}P -GMS is also safe.

Zhang DS, Liu L, Jin LQ, Wan ML, Li QH. Effect of phosphorus-32 glass microspheres on human hepatocellular carcinoma in nude mice. *World J Gastroenterol* 2004; 10(11): 1551-1554
<http://www.wjgnet.com/1007-9327/10/1551.asp>

INTRODUCTION

In recent years, nuclide labeled nontoxic and undegradable micro-carriers such as phosphorus-32 glass microsphere (^{32}P -GMS)^[1,2] and yttrium-90 glass microsphere^[3-5] have been successfully developed and gained much attention as a new radioactive medicine for treating malignant liver neoplasms. Experimental researches using micro-carriers such as microsphere, microcapsule, nano-microsphere (nano-sphere), liposome and nano-liposome in treating malignant tumors have been carried out for more than a decade and gained much interesting development. Microspheres conjugated with anticancer drugs including traditional Chinese medicine could release drugs slowly into the cancer tissues, thus keeping their anti-cancer effect for a long time^[6-9]. However, there are only a few reports about the researches of cytotoxic effect of local internal irradiation of ^{32}P -GMS on tumor cells. The ultrastructural stereology study of human liver cancer cell treated by ^{32}P -GMS has not been reported^[10,11]. So the authors used a human liver tumor-bearing nude mouse model to explore the anticancer effect of ^{32}P -GMS and the ultrastructural stereology changes in the tumor with TEM.

MATERIALS AND METHODS

Materials

^{32}P -GMS By activating of standardized glass microspheres through nuclear-chemical reaction, nonradioactive ^{31}P (^{31}P -GMS, cold sphere) was transformed into radioactive ^{32}P glass microsphere (provided by Nuclear Power Research Institute of China). It had the following properties. The diameter of glass sphere was 46-76 μm , ^{32}P physical half-life was 14.28 d, average β ray energy per disintegration was 0.695 MeV, and soft tissue penetration distance was max. 8.0 mm, averaging 3.2 mm. ^{32}P -GMS suspension was prepared by mixing ^{32}P -GMS with super-liquidized iodized oil or 500 g/L glucose solution to the concentrations of 370 MBq.mL/L and 37 MBq.mL/L on an oscillator.

Animal experiment Human liver cancer cell line subset (H-CS) with higher oncogenicity and liability of metastasis was implanted into the dorsal subcutaneous tissue of 40 BALB/c nu/nu nude mice (male, mean body mass 19.2 g, aged 4 wk, derived from Shanghai Experimental Animal Center, Chinese Academy of Sciences) at the dosage of 0.1-0.2 mL (1×10^7 tumor cells for each animal).

Forty tumor-bearing nude mice with the tumor mass diameter of 0.7-1.0 cm, different doses (7 320 Gy, 3 660 Gy, 1 830 Gy, 366 Gy and 183 Gy) of ^{32}P -GMS were injected to the mass center of 32 nude mice (subgroup A: $n=6$, B: $n=6$, C: $n=8$, D: $n=6$, E: $n=6$) in the treatment group and non-radioactive ^{31}P -GMS to the mass center of 8 nude mice as the control group. The experimental animals were sacrificed on the 14th day.

Preparation of electron microscopical sections Biopsy specimens from all the tumors and their adjacent tissues were immediately placed in 40 g/L glutaraldehyde and allowed to stand for 2 h at room temperature. Then the tissue was washed 3 times and postfixed for 1 h in 10 g/L osmium tetroxide. After rinsed in distilled water and dehydrated in acetone, the tissue specimens were embedded in Epon 812, polymerized for 48 h, ultrathin sectioned and stained. The electron microscopical sections were viewed in a H600 transmission electron microscope. At the same time, all specimens from tumors and their adjacent tissues were subjected to gross inspection, light microscopy to observe the morphological changes, and compared with the ultrastructural changes, and then the death rate of tumor cells was calculated. Death rate = the number of death cells / the number of total cells.

Method of stereological study Test grid method was used^[12]. The areas of test web was 120 mm×90 mm, and the length of each small grid was 5 mm. There were 432 tested dots in test web. The TEM pictures were magnified to 30 000-fold, and 30 pictures were taken in each group. When the picture was tested, the test web was put on the picture to test the constructure observed. Stereological parameters (volume density V_v ; surface density S_v) were used to test the cell organallae such as nucleus, nucleolus, RER and mitochondrion, lysosome, lipid, vesicles and membrane of microvilli and canaliculi. The point counting method was used. The standard deviation and standard error of stereological parameters in each group were calculated. The statistical method used was t test.

The formula of volume density V_v is

$$V_v = \frac{\sum_{i=1}^n P_{xi}}{\sum_{i=1}^n P_{ri}}$$

(n : the number of pictures, i : the ordinal number of pictures, P_{xi} : the number of test points within the scope of some constructs in i picture, P_{ri} : the number of test points within the section scope of the frames of reference in the same picture as above).

The formula of surface density S_v is

$$S_v = \frac{2 \sum_{i=1}^n I_{xi}}{z \sum_{i=1}^n P_{ri}}$$

(n : the number of pictures, i : the ordinal number of pictures, I_{xi} : the number of the points of transversal intersection of some membranes and test line in i picture, P_{ri} : the number of test points within the section scope of the frames of reference in the same picture as above, $2/z$ is coefficient).

RESULTS

Ultrastructure observation

In the treatment group, the tumor cells of subgroup A revealed necrotic injury and a lot of tumor cells were killed (Figure 1A). In the severely injured cells the nuclei lysed, cell membrane disrupted and numerous debris were found. The injured tumor cells showed condensation of nuclear chromatin, peripheral aggregation of heterochromatin in pieces, damaged organellae in cytoplasm, disappearance of mitochondrial cristae and ribosomes, appearance of a few of vacuoles and lipid particles. The death rate of tumor cells in the subgroup A was much higher (70%). In subgroup B, many tumor cells presented histological structures similar to those in subgroup A (the death rate: 65%), but with many lysosomes. Some were differentiated

tumor cells with the characteristics of round nuclei with small nucleoli, evenly distributed chromatin, mainly euchromatin, lots of mitochondria and rough endoplasmic reticula in the cytoplasm, formation of plenty of microvilli at the interface of tumor cells (Figure 1B). The capillaries between the moderately differentiated tumor cells had thickened or loosened basal membranes with local defects. Abundant fibroblasts and collagen fibers could be found in the matrix. There was a tendency to form bile canaliculi somewhere between tumor cells (Figure 1C). Under light microscope, the tumor tissues both in subgroups A and B showed scattered focal necrosis. The tumor cells in subgroup C (the death rate: 50%) showed different morphologic appearances, some damaged mildly and others severely, but some were moderately differentiated with plenty of cytoplasmic free polyribosomes. Plasma cells were scattered among the tumor cells, and some lymphocytes protruded the pseudopodia when they were contacted with the tumor cells. There were residual tumor cells showing active proliferation. In subgroups D and E (the death rate: 35%), the histological structure was manifested in various complicated forms, and active multiplication of tumor cells was readily seen. Under light microscope, the histological characteristics in subgroups C, D and E were the arrangement of tumor cells transformed from dense to loose with scattered spot necrosis. No abnormality was found in the muscle and dermal cells of adjacent skin nearby the tumor.

In the control group, most tumor cells were poorly differentiated and rapidly multiplied (Figure 1D), with characteristics of irregular large nuclei with deep indentations and plenty of chromatins, several peripherally aggregated large and prominent nucleoli. In cytoplasm, a lot of free polyribosomes, vacuoles and lipid particles were presented, while mitochondria, glycogen and rough endoplasmic reticulum were scant. Only a few of dead cells (5%) were found in this group. In the nearby interstitial tissue infiltrated tumor cells, degenerative lymphocytes, damaged fibroblasts, loose collagen fibers were found.

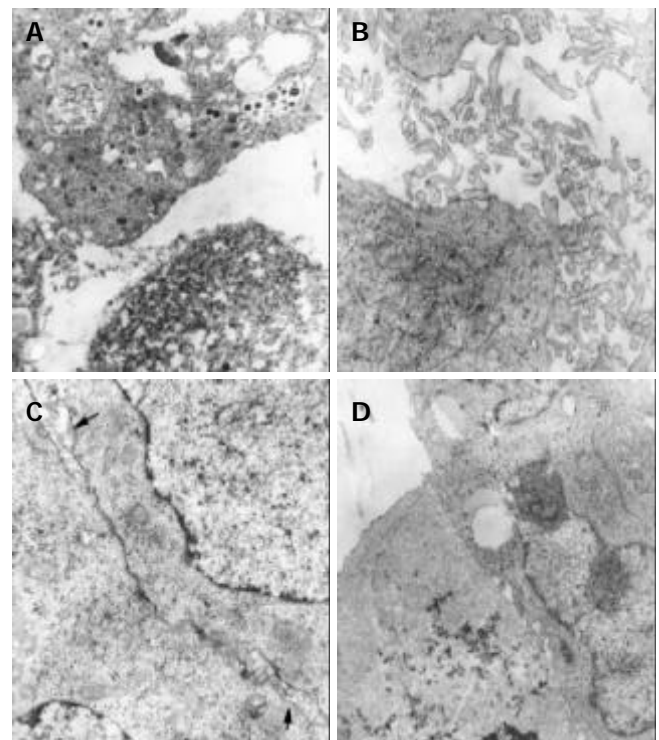


Figure 1 Ultrastructural characteristics of effect of ^{32}P -GMS on human hepatocellular carcinoma. A: Necrosed tumor cells ($\times 12\ 000$). B: Microvilli on the surface of tumor cells and mitochondria in cytoplasm ($\times 18\ 000$). C: Formation of bile duct-like structure in tumor cells (arrow, $\times 18\ 000$). D: Heteromorphic tumor cells with cleavage of nuclei and scanty microvilli on surface ($\times 12\ 000$).

Stereological study

The results of stereological analysis of ultrastructural morphology are summarized in Tables 1, 2 and 3.

Table 1 Comparison of liver cancer cell Vv in control group and treatment group

Constructure	Liver cancer cell Vv(mean±SD)×100%	
	Control group	Treatment group
Nuclei	53.31±3.46 ^b	30.21±3.52 ^b
Cytoplasm	46.79±3.46	69.79±3.52
Mitochondria	4.53±0.89 ^a	7.12±0.95 ^a
Lysosomes	2.07±0.22	1.94±1.12
RER	3.21±0.54 ^d	8.67±1.25 ^d
Lipid particles	3.71±1.97 ^c	0.30±0.16 ^c
Vacuoles	5.72±1.58 ^f	0.35±0.15 ^f

Nuclei Vv in control group was larger than that in treatment group, ^a $P<0.05$. Vv of RER in control group was smaller than that in treatment group, ^b $P<0.01$. Vv of mitochondria in control group was smaller than that in treatment group, ^d $P<0.01$. Vv of lipid particles was larger in control group than that in treatment group, ^c $P<0.05$. Vv of vacuoles was larger in control group than that in treatment group, ^f $P<0.01$.

Table 2 Comparison of nucleoli Vv of liver cancer cells in control group and treatment group

Constructure	Nucleoli Vv liver cancer cell Vv(mean±SD)×100%	
	Control group	Treatment group
Nucleoli	20.40±1.84 ^b	10.96±2.52 ^b
Nuclei	79.60±1.84	89.04±2.52

Nucleoli Vv in control group was larger than that in treatment group, ^b $P<0.01$.

Table 3 Comparison of Sv in membranes of microvilli and canaliculi of liver cancer cells in control group and treatment group

Constructure	Sv of liver cancer cell (mean±SD)×100%	
	Control group	Treatment group
Membrane of microvilli and canaliculi	27.12 $\mu\text{m}^2/100 \mu\text{m}^3$ ±11.84 $\mu\text{m}^2/100 \mu\text{m}^3$ ^b	78.81 $\mu\text{m}^2/100 \mu\text{m}^3$ ±19.69 $\mu\text{m}^2/100 \mu\text{m}^3$ ^b

Sv of the membranes of microvilli and canaliculi of liver cancer cells in control group was smaller than that in treatment group, ^b $P<0.01$.

DISCUSSION

Anticancer effect and mechanism of ³²P-GMS

On the 14th day of local injection of ³²P-GMS to the tumor, the tumor cell death rate was 35-70% in different treatment groups, and was 5% in control group. The results showed that local internal irradiation of ³²P-GMS had cytotoxic effects on tumor cells and the anticancer effect of ³²P-GMS was directly proportional to the dose administrated.

Anticancer mechanism of ³²P-GMS mainly includes two parts. The first is that β -ray energy of ³²P-GMS could directly destroy or injury DNA of tumor cells to induce cell death because of the breakage, disaggregation and synthetic obstruction of DNA. The second is that β -ray irradiation conducted ionization and irradiation of the water molecules in intracellular environment to produce several kinds of free radicals and superoxides which indirectly killed the tumor cells by injuring the biological macromolecules^[13,14]. Besides, researches also

showed that β -ray could induce cell-death related gene expressions to accelerate the apoptosis of tumor cells^[15]. Because ³²P-GMS internal irradiation is one kind of continued low linear energy transfer(LET) irradiation, its indirect effect on tumor cells might be much more important^[16].

Ultrastructure characteristics and significance of effect of ³²P-GMS on tumor

In specimens of different treatment groups, the tumor cells might exhibit as survived, degenerative or necrosed (in early or typical changes). It seems that this reflected the whole course of tumor cell progression from degeneration to death after irradiation. The ultrastructural changes demonstrated that under the effect of high-dose irradiation, the tumor tissues received a lethal radiation energy in a short period, resulting in nonexistence of tumor cells which had a high ability to synthesize endogenous proteins. Under the appropriate dose of irradiation, besides the necrosis of most tumor cells, the tendency to derive to nearly normal histological pictures appeared, such as microvilli on the cell surface, formation of bile canaliculi-like structure. These demonstrated that ³²P-GMS had the ability to kill actively proliferative tumor cells and to promote their normalization. On the other hand, proliferation of connective tissue after irradiation could lead to disorganization, which could destroy the survived tumor cells. This was consistent with what was reported^[13]. At the lower dose of irradiation, plasma cells and some lymphocytes were scattered among tumor cells, but this was rarely seen in the high-dose subgroup. Whether the immune function during treatment can be enhanced to some extent is still unknown. The irradiation injured some interstitial tissues such as thickened or loosened basal membrane of capillaries with local defects and damaged collagen fibers. But acute irradiative inflammation was not found and the tissue adjacent the tumor was normal, indicating that local administration of ³²P-GMS is safe.

Stereological ultrastructure analysis of effect of ³²P-GMS on tumor

Stereological analysis is a kind of image analysis technology widely used in pathomorphological researches. Researches discovered that image analysis was of importance to explore the criteria for pathological diagnosis, grading and morphogenesis of human hepatocellular carcinoma^[17-19]. Compared with qualitative analysis, stereological analysis was much more objective.

Differentiated malignant tumor cells have some characteristics under electron microscope. The general characteristics of poorly differentiated and rapidly multiplied tumor cells included irregular large nuclei, peripherally aggregated large and prominent nucleoli, lots of free polyribosomes in cytoplasm, scanty mitochondria and rough endoplasmic reticulum^[20,21]. The characteristics of differentiated tumor cells are different, including round nuclei with small nucleoli, mitochondria and rough endoplasmic reticula in the cytoplasm, formation of microvilli at the interface of tumor cells. There was a tendency to form bile canaliculi somewhere between liver tumor cells. Stereological results showed that Vv of nuclei (53.31±3.46) and Vv of nucleoli (20.40±1.84) in the control group were larger than those (30.21±3.52 and 10.96±2.52) in the treatment group respectively ($P<0.01$) and Vv of RER (3.21±0.54) and Vv of mitochondria (4.53±0.89) in the control group were smaller than those (8.67±1.25 and 7.12±0.95) in the treatment group respectively ($P<0.01$, 0.05). Sv of the membrane of microvilli and canaliculi (27.12 $\mu\text{m}^2/100 \mu\text{m}^3$ ±11.84 $\mu\text{m}^2/100 \mu\text{m}^3$) in the control group was smaller than that (78.81 $\mu\text{m}^2/100 \mu\text{m}^3$ ±19.69 $\mu\text{m}^2/100 \mu\text{m}^3$) in the treatment group ($P<0.01$). The results indicated that local administration of ³²P-GMS could produce obvious anticancer effects, besides, it played a role in

making poorly differentiated tumor cells become well differentiated ones, which was obviously beneficial to the prognosis and treatment of patient. Stereological study also showed that Vv of lipid particles (3.71 ± 1.97) and Vv of vacuoles (5.72 ± 1.58) in control group were much larger than those (0.30 ± 0.16 , and 0.35 ± 0.15) in treatment group ($P<0.05$, $P<0.01$). There is a possibility that the cells with lipid particles and vacuoles were degenerative cells which were much easier to be killed by β -ray energy of ^{32}P -GMS, so the Vv of lipid particles and vacuoles in treatment group was smaller than that in control group.

In conclusion, local administration of ^{32}P -GMS has obvious anticancer effects on liver cancer cells, which is directly proportional to the dose administrated. Ultrastructural stereology can also show the role of ^{32}P -GMS in promoting the normalization of tumor cells. Moreover, local administration of ^{32}P -GMS is safe.

REFERENCES

- 1 **Liu L**, Sun WH, Wu FP, Han DQ, Teng GJ, Fan J. An experimental study of treatment of liver cancer by locally administration with phosphate-32 glass microspheres & estimation of tissue-absorbed dose. *Nanjing Tiedao Yixueyuan Xuebao* 1997; **16**: 223-226
- 2 **Liu L**, Fan J, Zhang J, Du MH, Wu FP, Teng GJ. Experimental treatment of carcinoma in a mouse model by local injection of phosphorus-32 glass microspheres. *J Vasc Interv Rad* 1998; **9**: 166
- 3 **Herba MJ**, Illescas FF, Thirlwell MP, Boos GJ, Rosenthal L, Atri M, Bret PM. Hepatic malignancies: improved treatment with intraarterial Y-90. *Radiology* 1988; **169**: 311-314
- 4 **Wollner I**, Knutsen C, Smith P, Prieskorn D, Chrisp C, Andrews J, Juni J, Warber S, Klevering J, Crudup J, Ensminger W. Effects of hepatic arterial yttrium 90 glass microspheres in dogs. *Cancer* 1988; **61**: 1336-1344
- 5 **Andrews JC**, Walker SC, Ackermann RJ, Cotton LA, Ensminger WD, Shapiro B. Hepatic radioembolization with yttrium-90 containing glass microspheres: preliminary results and clinical follow-up. *J Nucl Med* 1994; **35**: 1637-1644
- 6 **Zhang DS**, Jia XP, Fan XS, Jin LQ, Wan ML, Li QH, Zheng J, Gu N. Preparation and characterization of magnetic nanomicrospheres containing arsenic trioxide. *Dianzi Xianwei Xuebao* 2002; **21**: 507-508
- 7 **Zhang DS**, Fan XS, Jia XP, Zheng J, Gu N, Ding AW, Jin LQ, Wan ML, Li QH. Effects of Nano-magnetoliposomes containing arsenic trioxide on heLa cells. *Zhonghua Zhongxiyi Zazhi* 2003; **4**: 1289-1292
- 8 **Fan XS**. The use of magnetic liposomes in cancer therapy. *Guowai Yixue Zhongliuxue Fence* 2003; **30**: 147-149
- 9 **Lu XL**. Advances of nanotechnology in breast cancer treatment. *Guowai Yixue Zhongliuxue Fence* 2003; **30**: 201-204
- 10 **Zhang DS**, Liu L, Wan ML, Li QH, Hong DR. Phosphorus-32 glass microspheres to treat human hepatocellular carcinoma in nude mice. *Zhonghua Shiyian Waike Zazhi* 1999; **16**: 327-328
- 11 **Liu L**, Teng GJ, Zhang DS, Song JZ, He SC, Guo JH, Fang W. Toxicology of intrahepatic arterial administration of interventional phosphorous-32 glass microspheres to domestic pigs. *Chin Med J* 1999; **112**: 632-636
- 12 **Han ZB**. Cai WQ. Application of electron microscopy in clinical medicine. *Chong Qing: Chong Qing Publishing House* 1988: 74-82
- 13 **Editorial board of practical oncology**. Practical Oncology. Vol. 1. *Beijing: People's Health Publishing House* 1977: 406-413
- 14 **Liu L**, Jiang Z, Teng GJ, Song JZ, Zhang DS, Guo QM, Fang W, He SC, Guo JH. Clinical and experimental study on regional administration of phosphorus-32 glass microspheres in treating hepatic carcinoma. *World J Gastroenterol* 1999; **5**: 492-505
- 15 **Zheng DX**. Advance in apoptosis research. *Zhonghua Binglixue Zazhi* 1996; **25**: 50-53
- 16 **Wang YY**, Wang DZ, Zheng GY, Mao ZY. Apoptosis induced by interstitial irradiation with ^{32}P glass microspheres combination with hyperthermia in mous solid tumor S180. *Huaxi Kouqiang Yixue Zazhi* 2001; **19**: 118-119
- 17 **Shen LJ**, Zhang ZJ, Ou YM, Zhang HX, Huang R, He Y, Wang MJ, Xu GS. Computed morphometric analysis and expression of alpha fetoprotein in hepatocellular carcinoma and its related lesion. *World J Gastroenterol* 2000; **6**: 415-416
- 18 **Zhang ZJ**, Shen LJ, Ou YM, Huang R, Zhang HX, He Y, Xu GS. Image analysis on the pathological morphogenesis and forecasting diagnosis of human hepatocarcinoma. *Zhongguo Tishixue Tuxiang Fenxi* 2000; **5**: 230-234
- 19 **Zhang ZJ**, Shen LJ, Huang R, Zhang HX, Ou YM, He Y, Xu GS, Wang MJ. Morphometric application to grading of human hepatocellular carcinoma. *Zhonghua Xiaohua Zazhi* 1995; **15**: 327-329
- 20 **Bo AH**, Shun SX, Li JL. Medical electron microscopy. *Beijing: People's Health Publishing House* 2000: 69-94
- 21 **Wu ZB**. Basis of Ultrastructural Pathology. *Beijing: People's Health Publishing House* 1990: 20-99

Edited by Wang XL and Xu FM

Structure analysis and expressions of a novel tetra-transmembrane protein, lysosoma-associated protein transmembrane 4 b associated with hepatocellular carcinoma

Xin-Rong Liu, Rou-Li Zhou, Qing-Yun Zhang, Ye Zhang, Yue-Ying Jin, Ming Lin, Jing-An Rui, Da-Xiong Ye

Xin-Rong Liu, Rou-Li Zhou, Ye Zhang, Yue-Ying Jin, Ming Lin, Department of Cell Biology and Genetics, School of Basic Medical Sciences, Peking University, Beijing 100083, China

Qing-Yun Zhang, Department of Clinical Laboratory, School of Oncology, Peking University, Beijing 100037, China

Jing-An Rui, Da-Xiong Ye, Department of General Surgery/Pathology, Peking Union Medical College Hospital, Beijing 100032, China

Supported by the 248 Major R&D Program of Beijing, No. H020220020310 and Special Fund for Promotion of Education, Ministry of Education, China

Correspondence to: Dr. Rou-Li Zhou, Department of Cell Biology and Genetics, School of Basic Medical Sciences, Peking University, Beijing 100083, China. rlzhou@bjmu.edu.cn

Telephone: +86-10-82801034 **Fax:** +86-10-62358270

Received: 2003-07-12 **Accepted:** 2003-07-30

Abstract

AIM: To analyze the structure and expressions of the protein encoded by an HCC-associated novel gene, lysosome-associated protein transmembrane 4 β (*LAPTM4B*).

METHODS: Primary structure and fundamental characteristics of *LAPTM4B* protein were analysed with bioinformatics. Expressions of *LAPTM4B* in HCC tissues and various cell lines were detected using polyclonal antibodies and Western blot.

RESULTS: *LAPTM4B* encoded two isoforms of proteins with molecular masses 35-ku and 24-ku, respectively. The expression level of *LAPTM4B*-35 protein in HCC tissues was dramatically upregulated and related to the differentiation status of HCC tissues, and it was also high in some cancer cell lines. Computer analysis showed *LAPTM4B* was an integral membrane protein with four transmembrane domains. *LAPTM4B* showed relatively high homology to *LAPTM4A* and *LAPTM5* in various species.

CONCLUSION: *LAPTM4B* gene encoded two isoforms of tetra-transmembrane proteins, *LAPTM4B*-35 and *LAPTM4B*-24. The expression of *LAPTM4B*-35 protein is upregulated and associated with poor differentiation in human HCC tissues, and also at high levels in some cancer cell lines. *LAPTM4B* is an original and conserved protein.

Liu XR, Zhou RL, Zhang QY, Zhang Y, Jin YY, Lin M, Rui JA, Ye DX. Structure analysis and expressions of a novel tetra-transmembrane protein, lysosoma-associated protein transmembrane 4 β associated with hepatocellular carcinoma. *World J Gastroenterol* 2004; 10(11): 1555-1559
<http://www.wjgnet.com/1007-9327/10/1555.asp>

INTRODUCTION

We have previously reported the cloning and identification of a novel gene, which was designated by the International

Nomenclature Committee as lysosomal associated protein transmembrane 4 β (*LAPTM4B*)^[1-4]. *LAPTM4B* was overexpressed in 87.3% human hepatocellular carcinomas (HCC) at mRNA level performed by Northern blot^[2]. BLAST program analysis showed that the *LAPTM4B* gene was mapped to chromosome 8 q22.1, spanning approximately at least 50 kb. It is composed of seven exons separated by six introns. The cloned full-length cDNA sequence (GenBank accession number: AY057051) of *LAPTM4B* is 2.2 kb and contains two ATGs at the 5' end with an interval of 273 bp and two polyadenylation signals: aataaa and aataaa^[2].

In this study, primary structures of proteins encoded by *LAPTM4B* gene were analyzed using bioinformatics. Specific polyclonal antibodies directing against two epitopes of the 10-peptides localized at the N-terminus (28-37aa) and in between the 3rd and 4th transmembrane domains (232-241aa) of *LAPTM4B*, respectively, were prepared. The expressions of *LAPTM4B* proteins in HCC, paired noncancerous liver (PNL), normal liver (NL) tissues and various cancer cell lines were detected by Western blot. The functions of *LAPTM4B* protein was discussed.

MATERIALS AND METHODS

Specimens

Fresh HCC and paired noncancerous liver specimens were obtained during operations on patients with HCC, normal liver tissues were obtained during operations on patients with hepatohemangioma.

Cell lines and culture

Human hepatoma cell lines BEL-7402, QGY-7701, SMMC-7721, HLE and human hepatic cell line L-02, human cervical cancer cell line HeLa, human prostate carcinoma cell lines PC3M and PC3, human pulmonary giant cell carcinoma cell lines BE1 and LH7, and human melanoma cell lines WM451 and WM983A were maintained in RPMI 1640 (GIBCO BRL) medium supplemented with 100 mL/L fetal bovine serum.

Protein extraction^[5-7]

The tissues stored at -80 °C or living cells were homogenized and extracted with lysis buffer (pH7.6) containing 10 mmol/L Tris, 150 mmol/L NaCl, 1 mmol/L EDTA, 5 g/L NP40, 1 mmol/L PMSF, 1 μ g/mL aprotinin, 1 μ g/mL pepstatin A. After centrifugation at 12 000 g for 10 min at 4 °C, the supernatants were collected and the proteins were quantitated by Bradford microassay.

Peptide synthesis and antibody preparation^[8-10]

Two KLH-conjugated 10 peptides (KLH-Ala-Lys-Gly-Thr-Asp-Pro-Ala-Glu-Ala-Arg and KLH-Pro-Tyr-Arg-Asp-Asp-Val-Met-Ser-Val-Asn) were synthesized by Invitrogen Company. Rabbits were immunized subcutaneously with 1 mg of KLH-peptide conjugates emulsified in Freund's complete adjuvant (GIBCO BRL). The immunization was repeated with the antigens in Freund's incomplete adjuvant (GIBCO BRL) 4 wk after the first

injection and 2 wk after the second injection. The anti-sera were designated as LAPT_{M4B}-N28-37-pAb and LAPT_{M4B}-EC2-pAb, respectively. The titers of these two sera were both above 1×10⁵ detected by ELISA with peptide-coated plates. The pre-immune sera did not show any reactivity to the peptides.

Western blotting

Proteins in cell lysates were fractionated by 100 g/L SDS-PAGE and then electrotransferred onto a nitrocellulose filter (Bio-Rad). The filters were blocked at 4 °C overnight with blocking buffer (pH7.6) containing 50 g/L fat free dry milk. Then the filters were incubated with indicated antibody for 2 h at room temperature. After washed with TBST (pH6.0), the filters were incubated at room temperature for 1 h with horseradish peroxidase conjugated goat anti-rabbit IgG at 1:2 000 dilution in TBS-5 g/L fat free dry milk. Immunoreactive bands were visualized using ECL detection reagents (Santa Cruz).

Bioinformatics analysis tool

The Bioinformatics analysis tool included BLAST and FASTA for basic local alignment of sequences, PCGENE software for predicting primary structure and fundamental characteristics of the protein, Kyte&Doolittle hydrophobicity index for calculating

hydrophobicity value, ClustalW software for multiple sequence alignment and DNAMAN software for displaying phylogenic tree.

RESULTS

Bioinformatics analysis of primary structure of LAPT_{M4B} protein

The primary structure of LAPT_{M4B} is shown in Figure 1. The LAPT_{M4B} cDNA may encode two putative proteins with 35 ku (317 aa) and 24 ku (226 aa). Computer analysis (PCGENE) showed that LAPT_{M4B} was an integral membrane protein with four highly conserved hydrophobic transmembrane domains, forming two extracellular loops (EC1 and EC2), a cytoplasmic loop and intracellular amino- and carboxyl tails. The transmembrane regions were located at 117-133, 163-179, 200-216, and 243-259 aa, respectively. The full amino acid sequence contained one N-glycosylation site, eight phosphorylation sites, and four N-myristoylation sites. A tyrosine phosphorylation site was predicted at 285 aa at C-terminal region, which depending on phosphorylation might form a binding site for specific SH2 domain in some signaling proteins. It was also predicted that LAPT_{M4B} containing proline-rich motif (PXXP) at N-terminal region would be a SH3 domain binding protein. Moreover, LAPT_{M4B} contained typical lysosomal targeting signals (3 YXX Φ motifs)^[11] at C-terminal region. Human LAPT_{M4B}

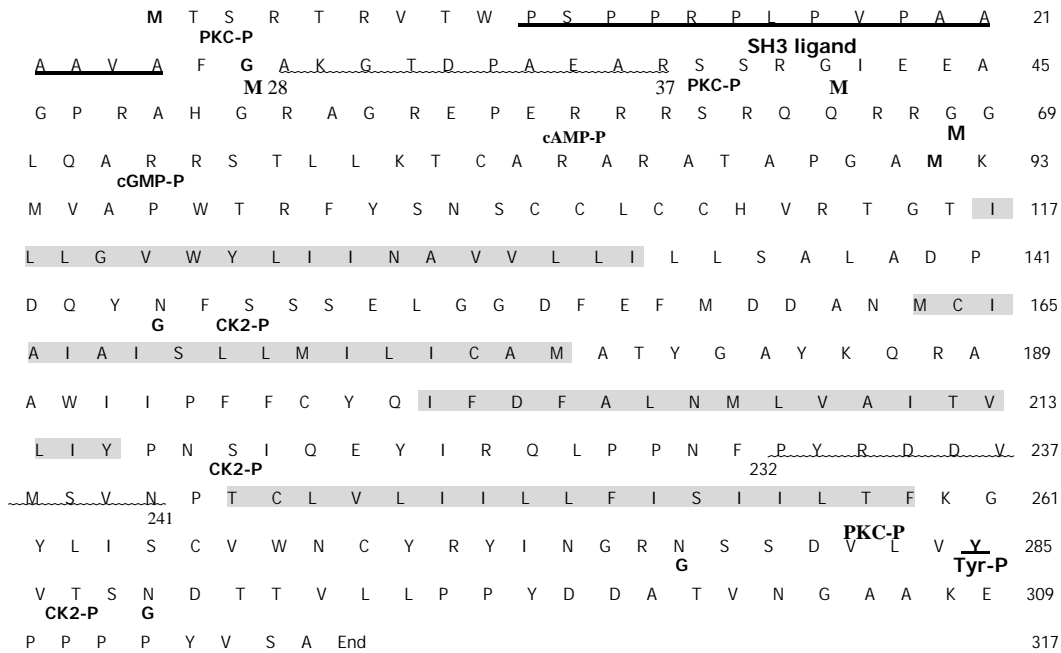


Figure 1 Putative amino-acid sequence of LAPT_{M4B}. The four transmembrane domains are shadowed with gray color. Two translation initiation sites are thick black. Putative SH3 ligand is indicated by thick underlining. The sequence containing 10 amino acid residues (28aa-37aa or 232aa-241 aa) and used as immunogen is wavy underlined. PKC-P, cAMP-P, cGMP-P, CK2-P, Tyr-P: various phosphorylation sites; G: N-glycosylation site; M: myristylation site.

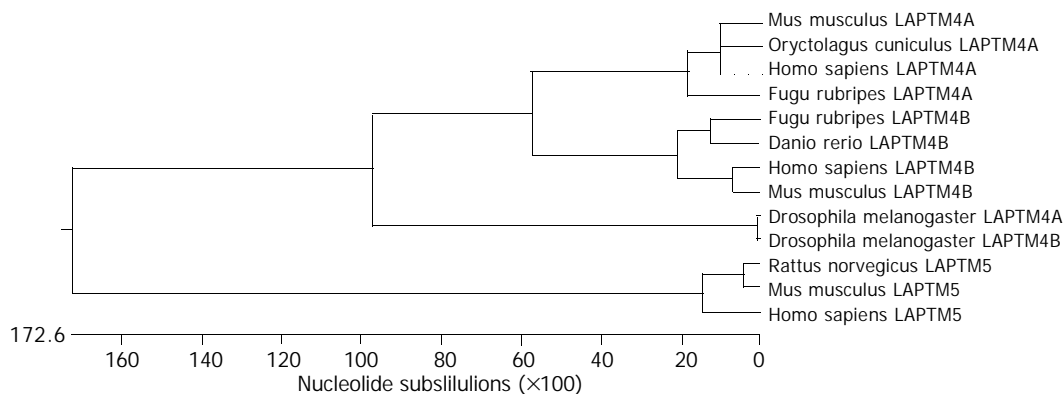


Figure 2 Phylogenetic tree of LAPT_{M4B}.

shared 92% homology with mouse LAPTM4B (GenBank accession number: AAH1912)^[12] at amino acid level, suggesting that LAPTM4B was highly conserved within vertebrate species. The region from 140 aa to 317 aa of LAPTM4B was highly conserved compared with mouse LAPTM4B. But the N-terminal region from 1 aa to 91 aa (between the first ATG and the second ATG) of LAPTM4B-35 was highly specific and no homological sequence was found using BLAST in nr database. LAPTM4B also showed 46% homology to a lysosomal tetra-transmembrane protein, LAPTM4A, at amino acid level. The ortholog of LAPTM4A in murine was a nucleoside transporter in intracellular membrane-bound compartments, and mediated a multidrug resistance phenotype in drug-sensitive strains of *S. cerevisiae*^[12-14].

The phylogenetic tree (Figure 2) was constructed according to multiple sequence alignment results. It showed that LAPTM4B, LAPTM4A and LAPTM5 proteins were distributed in clusters. Human LAPTM4B showed the most close homology to *Mus musculus* and also had certain homology to *Danio rerio* and *Fugu rubripes*, as well as *Drosophila melanogaster*, but was far-away from Yeast. In addition, LAPTM4B showed relatively high homology to LAPTM4A and LAPTM5 in various species to a certain extent, and LAPTM4B was closer to LAPTM4A than LAPTM5. These results indicated that LAPTM4B was an original and conserved protein.

Expression of LAPTM4B protein in HCC tissues

As shown in Figure 3, 2 proteins with molecular masses 35-ku and 24-ku both reacted with LAPTM4B-EC2-pAb were identified by Western blot in HCC, PNL and NL tissues, and designated as LAPTM4B-35 and LAPTM4B-24, respectively. Nevertheless, only one band at the 35 ku position appeared when LAPTM4B-N28-37-pAb was used for Western blot in HCC tissues, indicating that LAPTM4B-35 was translated from the whole ORF and initiated from the first ATG, whereas LAPTM4B-24 was translated from the second ATG. Furthermore, LAPTM4B proteins were significantly overexpressed in HCC tissues than in PNL and NL tissues. Notably, the expression levels of LAPTM4B-35 were significantly related to the differentiation status of HCC tissues, they were higher in poorly differentiated HCCs than in moderately and well differentiated HCCs (Figure 4)^[4]. In addition, the ratio of LAPTM4B-35 to LAPTM4B-24 was remarkably higher in HCC than in PNL and NL (Table 1). However, the ratio of LAPTM4B-35 to LAPTM4B-24 in PNL was kept at the same level as in NL, even though LAPTM4B-35 and LAPTM4B-24 were both slightly increased. Thus the development of HCC might be associated with the raised ratio of LAPTM4B-35 to LAPTM4B-24.

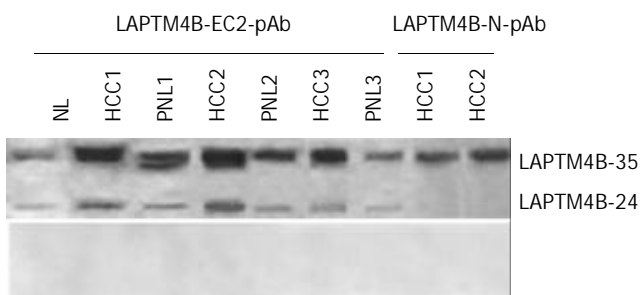


Figure 3 Expressions of LAPTM4B proteins in HCC tissues identified by Western blot with various antibodies. Top: Western Blot profiles performed with anti serum. LAPTM4B-EC2-pAb: polyclonal antibody directing against the epitope localized at the EC2 domain between the 3rd and 4th transmembrane regions of LAPTM4B. LAPTM4B-N28-37-pAb: polyclonal antibody directing against the epitope localized at the N-terminal region of LAPTM4B. Bottom: Western blot profiles performed with pre-immune serum.

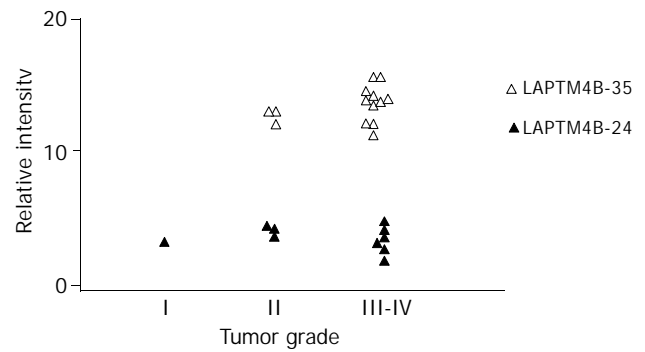


Figure 4 Correlation between LAPTM4B-35 protein expression and pathological grade of HCC.

Table 1 Relative intensity of LAPTM4B-35 and LAPTM4B-24 (mean±SD)

	HCC	PNL	NL
LAPTM4B-35	13.32±1.98 ^b	4.58±1.31	2.78±0.11
LAPTM4B-24	3.59±1.78 ^b	1.76±1.24	1.00±0.02
LAPTM4B-35/LAPTM4B-24 (ratio)	3.71	2.60	2.78

^bP<0.01 vs PNL and NL.

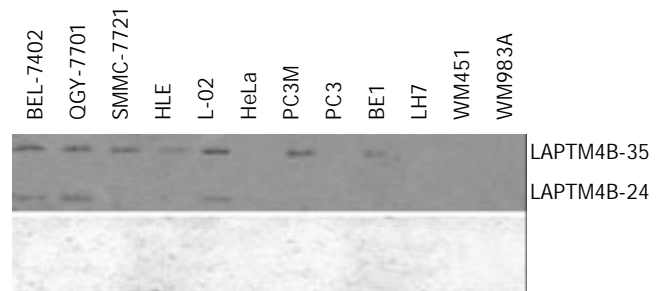


Figure 5 Expression of LAPTM4B proteins in various cell lines shown via Western blot with LAPTM4B-EC2-pAb. Top: Western blot profiles performed with LAPTM4B-EC2-pAb. Bottom: Western blot profiles performed with pre-immune serum.

Table 2 Relative intensity of LAPTM4B-35 and LAPTM4B-24 in various cell lines

Cell line	LAPTM4B-35	LAPTM4B-24	LAPTM4B-35/-24 (ratio)
BEL-7402	3.98	2.09	1.91
QGY-7701	3.21	2.20	1.45
SMMC-7721	2.98	-	-
HLE	2.24	-	-
L-02	3.32	2.56	1.29
HeLa	-	-	-
PC3M	2.96	-	-
PC3	-	-	-
BE1	1.47	-	-
LH7	-	-	-
WM451	-	-	-
WM983A	-	-	-

Expression of LAPTM4B proteins in various cell lines

LAPTM4B proteins in 12 cell lines were detected by Western blot with LAPTM4B-EC2-pAb (Figure 5). With exception of HLE cells, LAPTM4B proteins were remarkably expressed in

all of HCC-derived cell lines including BEL-7402, QGY-7701 and SMMC-7721, and human hepatic cell line L-02 cells. The ratio of LAPTM4B-35 to LAPTM4B-24 was higher in HCC cell lines than in immortal hepatic cell line L-02 (Table 2), suggesting that disturbance of LAPTM4B-35 to LAPTM4B-24 equilibrium in expressions might cause the malignant transformation in hepatocarcinogenesis. Moreover, the expressions of LAPTM4B-35 were also higher in highly metastatic cell lines^[15-17], including prostate carcinoma PC-3M and pulmonary giant cell carcinoma BE1 cell lines than in the syngenic low metastatic cell lines, including PC-3 and LH7 cell lines. Therefore, the overexpression of LAPTM4B-35 was likely related to cancer cell invasion and metastasis. However, LAPTM4B was not detected in human cervical carcinoma cell line HeLa and human melanoma cell lines WM451 and WM983A^[15], indicating that overexpression of LAPTM4B-35 was somehow specific for some carcinomas.

DISCUSSION

HCC is one of the most common cancers world-wide, and is the major cause of malignant deaths in Asia and Africa^[18-20]. The pathogenesis of HCC is particularly complex. The current model for HCC carcinogenesis postulated a multistage progression involving an accumulation of genetic alterations^[21,22], including activation of oncogenes N-ras, H-ras, K-ras, c-erbA, c-met, and c-myc etc.^[23,24], repression or mutation of tumor suppressor genes^[25], besides the transcriptional activation of c-jun and nuclear factor NF- κ B by HBV and HCV^[26,27]. But the roles of these genes in cell proliferation, differentiation, and premalignant status in liver malignancy are far from elucidated.

We previously reported^[2] that *LAPTM4B* was a novel gene associated with HCC, and significantly overexpressed in HCC as shown via Northern blot and *in situ* hybridization. *LAPTM4B* is also widely expressed in human tissues with a relatively high level in the testis, heart and skeletal muscles, and moderately in the ovary, kidney and pancreas, and poorly in the liver, spleen, and thymus, and lowest in the lung and peripheral leukocytes. It was remarkably overexpressed in 87.3% (48/55 cases) HCC tissues when compared with PNL and NL tissues. Furthermore, the *LAPTM4B* mRNA expression levels were significantly related to the differentiation status of HCC tissues. They were highest in poorly differentiated HCCs, higher in moderately differentiated HCCs, and relatively low in well differentiated HCCs.

Here we report the expressions of LAPTM4B proteins in HCC, PNL, NL and a number of cell lines via Western blot analysis using two antibodies, LAPTM4B-N28-37-pAb or LAPTM4B-EC2-pAb, which were prepared by immunization with two KLH-conjugated 10-peptides whose sequences are localized at either the second extracellular loop (EC2) between the third and fourth transmembrane regions or the N-terminal region in the cytoplasm. These two 10-peptides used as immunogens were highly specific, i.e. having very low homology compared to known proteins of Homo sapiens. By using PCGENE software, the 10-peptides should have characteristics of high hydrophilicity and no residues of putative glycosylation and phosphorylation. KLH was conjugated with the N-termini of 10-peptides in order to increase immunogenicity. Two isoforms of LAPTM4B, LAPTM4B-35 and LAPTM4B-24, whose mass was coincident with the predicted products translated from the first and second ATG in ORF, were identified. Expressions of LAPTM4B-35 proteins were highly upregulated in HCC with poor differentiation. This result was coincident with expression of *LAPTM4B* mRNA in HCC tissues. LAPTM4B expressions were also high in human HCC cell lines and some other cancer cell lines. Transient transfection of murine BHK cells was performed with two plasmids, *pcDNA3/LAPTM4B-AE*

containing a full-length cDNA of *LAPTM4B* ORF and *pcDNA3/LAPTM4B-BE* containing the same ORF sequence but with 273 nucleotides deleted at 5' end, respectively. The transfectants in AE-series expressed mainly LAPTM4B-35 and slightly LAPTM4B-24, and proliferated very rapidly and formed colonies powerfully. However, the transfectants in BE-series expressed only LAPTM4B-24, and lost potentials of long term survival and growth. Therefore, it is suggested that LAPTM4B-24 may play an antagonistic role in cell survival and proliferation, and the equilibrium of LAPTM4B-35 and LAPTM4B-24 in expression is involved in controlling cell survival/proliferation and differentiation. The disequilibrium in expressions of LAPTM4B-35 and LAPTM4B-24 may be involved in malignant transformation of hepatocytes and carcinogenesis.

REFERENCES

- 1 **Liu J**, Zhou R, Zhang N, Rui J, Jin C. Biological function of a novel gene overexpressed in human hepatocellular carcinoma. *Chin Med J* 2000; **113**: 881-885
- 2 **Shao GZ**, Zhou RL, Zhang QY, Zhang Y, Liu JJ, Rui JA, Wei X, Ye DX. Molecular cloning and characterization of LAPTM4B, a novel gene upregulated in hepatocellular carcinoma. *Oncogene* 2003; **22**: 5060-5069
- 3 **He J**, Shao G, Zhou R. Effects of the novel gene, LAPTM4B, highly expression in hepatocellular carcinoma on cell proliferation and tumorigenesis of NIH3T3 cells. *Beijing Daxue Xuebao* 2003; **35**: 348-352
- 4 **Liu X**, Zhou R, Zhang Q, Zhang Y, Shao G, Jin Y, Zhang S, Lin M, Rui J, Ye D. Identification and characterization of LAPTM4B encoded by a human hepatocellular carcinoma-associated novel gene. *Beijing Daxue Xuebao* 2003; **35**: 340-347
- 5 **Schuck S**, Honscho M, Ekroos K, Shevchenko A, Simons K. Resistance of cell membranes to different detergents. *Proc Natl Acad Sci U S A* 2003; **100**: 5795-5800
- 6 **Jones MN**. Surfactants in membrane solubilisation. *Int J Pharm* 1999; **177**: 137-159
- 7 **Shetty J**, Diekman AB, Jayes FC, Sherman NE, Naaby-Hansen S, Flickinger CJ, Herr JC. Differential extraction and enrichment of human sperm surface proteins in a proteome: identification of immunocontraceptive candidates. *Electrophoresis* 2001; **22**: 3053-3066
- 8 **Shen L**, Guo ZY, Chen Y, Liu LY, Feng YM. Expression, purification, characterization of amphioxus insulin-like peptide and preparation of polyclonal antibody to it. *Shengwu Huaxue Yu Shengwu Wuli Xuebao* 2001; **33**: 629-633
- 9 **Hadidi S**, Yu K, Chen Z, Gorczynski RM. Preparation and functional properties of polyclonal and monoclonal antibodies to murine MD-1. *Immunol Lett* 2001; **77**: 97-103
- 10 **Missbichler A**, Hawa G, Schmal N, Woloszczuk W. Sandwich ELISA for proANP 1-98 facilitates investigation of left ventricular dysfunction. *Eur J Med Res* 2001; **6**: 105-111
- 11 **Hogue DL**, Nash C, Ling V, Hobman TC. Lysosome-associated protein transmembrane 4 alpha (LAPTM4 alpha) requires two tandemly arranged tyrosine-based signals for sorting to lysosomes. *Biochem J* 2002; **365**(Pt 3): 721-730
- 12 **Hogue DL**, Ellison MJ, Young JD, Cass CE. Identification of a novel membrane transporter associated with intracellular membranes by phenotypic complementation in the yeast *Saccharomyces cerevisiae*. *J Biol Chem* 1996; **271**: 9801-9808
- 13 **Cabrita MA**, Hobman TC, Hogue DL, King KM, Cass CE. Mouse transporter protein, a membrane protein that regulates cellular multidrug resistance, is localized to lysosomes. *Cancer Res* 1999; **59**: 4890-4897
- 14 **Hogue DL**, Kerby L, Ling V. A mammalian lysosomal membrane protein confers multidrug resistance upon expression in *Saccharomyces cerevisiae*. *J Biol Chem* 1999; **274**: 12877-12882
- 15 **Li S**, Fang W, Zhong H. Expression of tumor metastasis suppressor gene KAI1/CD82 in human cancer cell lines with different metastasis potential. *Zhonghua Yixue Zazhi* 1999; **79**: 708-710

- 16 **Kim IY**, Kim BC, Seong do H, Lee DK, Seo JM, Hong YJ, Kim HT, Morton RA, Kim SJ. Raloxifene, a mixed estrogen agonist/antagonist, induces apoptosis in androgen-independent human prostate cancer cell lines. *Cancer Res* 2002; **62**: 5365-5369
- 17 **Liu Y**, Zheng J, Fang W, You J, Wang J, Cui X, Wu B. Identification of metastasis associated gene G3BP by differential display in human cancer cell sublines with different metastatic potentials G3BP as highly expressed in non-metastatic. *Chin Med J* 2001; **114**: 35-38
- 18 **Liu YH**, Zhou RL, Rui JA. Detection of hepatoma cells in peripheral blood of HCC patients by nested RT-PCR. *World J Gastroenterol* 1998; **4**: 106-108
- 19 **Bosch FX**, Ribes J, Borrás J. Epidemiology of primary liver cancer. *Semin Liver Dis* 1999; **19**: 271-285
- 20 **Rui JA**, Wang SB, Chen SG, Zhou R. Right trisectionectomy for primary liver cancer. *World J Gastroenterol* 2003; **9**: 706-709
- 21 **Kondoh N**, Wakatsuki T, Ryo A, Hada A, Aihara T, Horiuchi S, Goseki N, Matsubara O, Takenaka K, Shichita M, Tanaka K, Shuda M, Yamamoto M. Identification and characterization of genes associated with human hepatocellular carcinogenesis. *Cancer Res* 1999; **59**: 4990-4996
- 22 **Qin LX**, Tang ZY. The prognostic molecular markers in hepatocellular carcinoma. *World J Gastroenterol* 2002; **8**: 385-392
- 23 **Luo D**, Liu QF, Gove C, Naomov N, Su JJ, Williams R. Analysis of N-ras gene mutation and p53 gene expression in human hepatocellular carcinomas. *World J Gastroenterol* 1998; **4**: 97-99
- 24 **Ueki T**, Fujimoto J, Suzuki T, Yamamoto H, Okamoto E. Expression of hepatocyte growth factor and its receptor c-met proto-oncogene in hepatocellular carcinoma. *Hepatology* 1997; **25**: 862-866
- 25 **Zhu AX**. Hepatocellular carcinoma: are we making progress? *Cancer Invest* 2003; **21**: 418-428
- 26 **Henkler F**, Waseem N, Golding MH, Alison MR, Koshy R. Mutant p53 but not hepatitis B virus X protein is present in hepatitis B virus-related human hepatocellular carcinoma. *Cancer Res* 1995; **55**: 6084-6091
- 27 **Sansonno D**, Cornacchiulo V, Racanelli V, Dammacco F. *In situ* simultaneous detection of hepatitis C virus RNA and hepatitis C virus-related antigens in hepatocellular carcinoma. *Cancer* 1997; **80**: 22-33

Edited by Zhu LH and Wang XL **Proofread by** Xu FM

Quantitative detection of *common deletion* of mitochondrial DNA in hepatocellular carcinoma and hepatocellular nodular hyperplasia

Jian-Yong Shao, Hong-Yi Gao, Yu-Hong Li, Yu Zhang, You-Yong Lu, Yi-Xin Zeng

Jian-Yong Shao, Hong-Yi Gao, Yu-Hong Li, Yu Zhang, Yi-Xin Zeng, Cancer Center, Sun Yat-Sen University, Guangzhou 510060, Guangdong Province, China

You-Yong Lu, Beijing Institute for Cancer Research, Beijing Laboratory of Molecular Oncology, School of Oncology, Peking University, Beijing 100034, China

Supported by the National Key Basic Science Research Program, Contract No: G1998051201; The Foundation of Guangdong Science and Technology Committee, Contract No: 2003A3080202; and The Foundation of Guangzhou Science and Technology Committee, Contract No: 2003I-E0341

Correspondence to: Jian-Yong Shao, M.D., Ph.D., Department of Pathology, Cancer Center, Sun Yat-Sen University, 651 Dong Feng Road East, Guangzhou 510060, Guangdong Province, China. jyshao@gzsums.edu.cn

Telephone: +86-20-87343391 **Fax:** +86-20-87343391

Received: 2003-08-23 **Accepted:** 2003-10-12

Abstract

AIM: To study the deletion of mitochondrial DNA in hepatocellular carcinoma and hepatocellular nodular hyperplasia and its significance in the development of cancer.

METHODS: Deleted mtDNA (CD-mtDNA) and wild type mtDNA (WT-mtDNA) were quantitatively analyzed by using real-time PCR in 27 hepatocellular carcinomas (HCC) and corresponding noncancerous liver tissues and 27 hepatocellular nodular hyperplasiae (HNH).

RESULTS: A novel CD (4 981 bp) was detected in 85% (23/27) and 83% (22/27) of HCC and HNH tumor tissues, respectively, which were significantly higher than that in paired noncancerous liver tissues (57%, 15/27) ($P < 0.05$). The CD/WT-mtDNA ratio in HCC tumors was 0.00092 (median, interquartile range, 0.0001202-0.00105), which was significantly higher than that in paired noncancerous liver tissues (median, 0.000, quartile range, 0-0) ($P = 0.002$, Mann-Whitney Test), and was 25 of times of that in HNH tissues (median, 0.0000374, quartile range, 0-0.0004225) ($P = 0.002$, Mann-Whitney test).

CONCLUSION: CD-mtDNA mutation plays an important role in the development and progression of HCC.

Shao JY, Gao HY, Li YH, Zhang Y, Lu YY, Zeng YX. Quantitative detection of *common deletion* of mitochondrial DNA in hepatocellular carcinoma and hepatocellular nodular hyperplasia. *World J Gastroenterol* 2004; 10(11): 1560-1564 <http://www.wjgnet.com/1007-9327/10/1560.asp>

INTRODUCTION

Hepatocellular carcinoma (HCC) is one of the common malignancies worldwide, and has been ranked the 2nd cancer killer in China. Hepatitis B and C viruses (HBV and HCV) and dietary aflatoxin intake remain the major causative factors of HCC^[1]. Previous

studies also revealed that frequent genetic aberrations were involved in hepatocarcinogenesis^[2,3]. However, the molecular mechanisms of hepatocarcinogenesis remain unclear. Recently, morphological features of the tumor, both gross and histological, have been found to be significantly associated with tumor recurrence and patient survival.

Nuclear gene alterations are correlated to invasion, metastasis, recurrence of HCC, which are regarded as biomarkers for the malignant phenotype of HCC, and related to the prognosis and therapeutic outcomes. These biomarkers include p53 gene mutation^[4], VEGF overexpression^[5,6], apoptosis related genes, cell adhesion and extracellular matrix related genes such as E-cadherin, β -catenins, CD44s, MMPs and their inhibitor TIMPs^[7-13].

Human mitochondrial DNA (mtDNA) is located in cytoplasm, is becoming the study hotspot for its alteration in correlation with its tumorigenesis. Mitochondria are involved in apoptosis^[14], and probably also tumorigenesis^[15], which has led researchers to examination the potential roles of mtDNA alterations in the development and maintenance of cancers.

The most abundant change in mtDNA is called common deletion (4 977 bp, CD). CD-containing mitochondrial DNA (CD-mtDNA) was first observed in patients with mitochondrial myopathies, and was also found to accumulate in patients with heteroplasmic mtDNA mutations and in normal individuals during aging, particularly in postmitotic tissues such as muscle and brain^[16]. The CD-mtDNA mutation has been detected in several types of human tumors including thyroid Hürthle cell tumor^[17], gastric cancer^[18], and hepatocellular carcinoma^[19]. However, knowledge about the common deletion of mtDNA in HCC in China is poor. This is the first report of a high incidence (70%) of a novel CD-mtDNA (4 981 bp) in tumor tissues of HCC and hepatocellular nodular hyperplasia (HNH) from southern China, and the first analysis correlating CD-mtDNA level to clinicopathological parameters and age.

MATERIALS AND METHODS

Clinical data and histopathologic analysis of tumor samples

Patients with histologically proved HCC and HNH at the Cancer Center, Sun Yat-Sen University (Guangzhou, China) were recruited with informed consent from January 1999 to January 2003. Samples consisted of 27 surgically resected HCC and 27 HNH specimens. In HCC specimens, the tumor tissue and paired adjacent noncancerous liver tissue were obtained independently for mtDNA analysis. In serum, hepatitis B viral surface antigen and HCV antibody titer were detected by enzyme-linked immunosorbent assay and radio-immunoassay. Grading of differentiation was performed according to the method of Edmondson and Steiner. Tumors were classified into well differentiated group (grades 1 and 2) and poorly differentiated group (grades 3 and 4). The tumor size was classified into small (tumor mass < 3 cm in greatest diameter) and large (tumor mass size > 3 cm in greatest diameter). There were 24 males and 3 females aged from 40 to 79 years, with an average age of 58 years.

DNA extraction

Total (nuclear and mitochondria) DNA was extracted from

Table 1 TaqMan primers and probes for detection of WT-mtDNA and CD-mtDNA

Target	Amplicon	Oligonucleotide sequence (5' -3')
Wild Type mtDNA	101 bp	WT1 forward primer (7 878-7 897): 5' -AATCAATTGGCGACCAATGG-3' WT2 reverse primer (7 979-7 958): 5' -CGCCTGGTTCTAGGAATAATGG-3' WT probe (7 899-7 917): 5' FAM-ACTGAACCTACGAGTACAC-MGB-3'
Common Deletion mtDNA	132 bp	CD1 forward primer (8 448-8 472): 5' -TATTAACACAAACTACCACCTACC-3' CD2 reverse primer (13 560-13 539): 5' -GGCTCAGGCGTTTGTGTATGAT-3' CD probe: (13 456-13 471): 5' FAM- ACC ATTGGC AGC CTA G -MGB 3'

paraffin-embedded tissues of HNH, HCC and adjacent noncancerous liver tissues using the QIAamp DNeasy Tissue Kit (Qiagen, Hilden, Germany). Prior to DNA extraction, a microdissection technique was used in certain cases when tumor tissues and non-tumor tissues were mixed in one sample to enrich tumor cells^[20]. Five 10- μ m thick sections were cut and placed into a 1.5 mL Eppendorff tube. The sections were deparaffinized twice with xylene and alcohol.

Conventional PCR detection of CD-mtDNA

In this investigation, we developed a real-time PCR protocol that reliably quantified mtDNA through amplification of different regions of the mitochondrial genomes: one just outside the CD region in cytochrome c oxidase II (MTCO2) coding region (IS), and one overlapping the CD itself (Figure 1). PCR primers for detection of CD-mtDNA were designed according to MITOMAP Human mtDNA Cambridge Sequence data (www.mitomap.org). Real-time PCR primers and fluorogenic probes for regions of WT-mtDNA (forward primer, L7878-7897; reverse primer, H7979-7958; probe, L7899-7917) and CD-mtDNA (forward primer, L8448-8472; reverse primer, H13560-13539; probe, L13456-13471) were designed with the Primer Express software (Table 1).

Conventional PCR was performed in 20 μ L volume consisting of 2 μ L 10 \times PCR buffer, 25 μ mol/L of each dNTP, 2.5 U Taq polymerase, 15 pmol/L of each primer and 50 ng of DNA template. The reaction was performed in a PE2700 thermocycler (Applied Biosystem Inc., USA). PCR reaction included at 95 $^{\circ}$ C for 10 min, 40 cycles at 94 $^{\circ}$ C for 30 s, at 60 $^{\circ}$ C for 30 s and at 72 $^{\circ}$ C for 30 s. The PCR products were separated on 20 g/L agarose gels at 80 V for 60 min, visualized by ethidium bromide staining and UV light, and photographed. The results of amplification of CD-mtDNA by conventional PCR in HCC and HNH tissues are shown in Figure 2A.

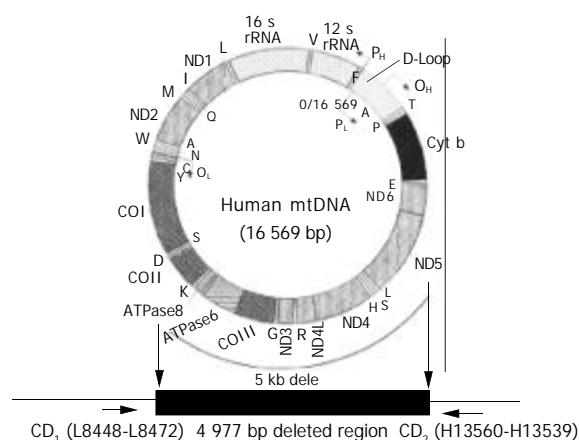


Figure 1 Human mitochondrial DNA showing the 4 997-bp deletion. The genes disrupted by the 4 997 bp deletion between nucleotide positions 8 469 and 13 447 encode four polypeptides for complex I (ND3, ND4, ND4L and ND5), one for complex IV (CO III) and two for complex V (ATP8 and ATP6), and five tRNA genes for the amino acids G, R, H, S and L. CD represent the PCR primers position that flank the common deletion region.

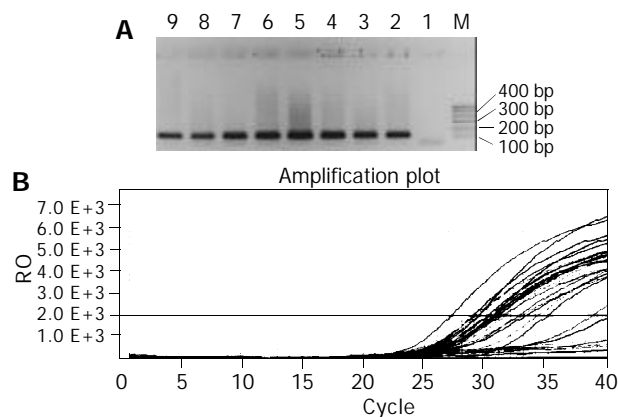


Figure 2 Detection results of CD-mtDNA in HCC. A: Conventional PCR results: Lane M, marker, Lane 1, negative control, Lane 2, positive control, Lane 3-4, nasopharyngitis samples, and Lane 5-8, NPC samples; B: Real-time PCR result shows the amplification plot of fluorescence intensity against the PCR cycle. Each plot corresponds to a HCC sample. The X axis denotes the cycle number of a quantitative PCR reaction. The Y axis denotes the Rn, which is the fluorescence intensity over the background. The correlation coefficient is 0.994.

TaqMan-PCR

The principles of real-time PCR and methods for absolutely quantification of target DNA were described^[18]. The quantitative TaqMan-PCR method could provide real-time measurement of target input.

Triplicate amplification reactions were performed in a 96-well microplate. Total WT-mtDNA and CD-mtDNA reactions (25 μ L) each containing 100 ng DNA, 1 \times TaqMan Universal PCR Master Mix, 300 mmol/L of each dNTP and 300 mmol/L of each IS or CD primer were performed. The reactions were completed by adding 100 nmol/L of the specific WT or CD probe. PCR and fluorescence analysis were performed using the ABI GeneAmp 7900HT sequence detection system (Applied Biosystems Inc., USA). Amplification conditions included at 50 $^{\circ}$ C for 2 min (for optimal AmpErase UNG activity), at 95 $^{\circ}$ C for 10 min (for deactivation of AmpErase UNG and activation of AmpliTaq Gold), then 40 cycles at 95 $^{\circ}$ C 15 s and at 60 $^{\circ}$ C for 1 min (for probe/primer hybridization and DNA synthesis).

Analysis of the reactions was carried out in an ABI PRISM 7900HT sequence detector equipped with the sequence detection software version 2.0 (PE Applied Biosystems, Foster City, USA). Absolute DNA quantification was performed using the standard curve method. Reactions were carried out with different concentrations (10¹⁰, 10⁹, 10⁸, 10⁷, 10⁶, 10⁵, 10⁴ copies/mL) of two standard plasmids in parallel with test reactions. The standard plasmids, one carrying sequences flanking the common deletion and one carrying a unique mtDNA sequence independent of the CD, allowed the generation of two standard curves showing the number of copies of total WT-mtDNA or CD-mtDNA versus the measured CT. The CT values of samples were then converted to the number of DNA copies by comparing the sample CT to that of a known concentration of plasmid DNA.

The amount of mutation corresponded to the concentration ratio of CD-mtDNA to WT-mtDNA within each sample. If DNA was not detected within 40 cycles (CT=40), it was considered absent from a particular sample. The amplification plot CD-mtDNA detected by TaqMan PCR in HCC tissues is presented in Figure 2B.

The CD-mtDNA PCR products were sequenced using the ABI PRISM BigDye termination cycle sequencing ready reaction kit on an ABI PRISM377 sequencer (Applied Biosystem Inc., USA). Blast sequencing analysis confirmed that PCR products of the CD-mtDNA were homologous to the Cambridge version of the mtDNA sequence.

Statistical analysis

The levels of CD/MT-mtDNA ratio in different groups were compared using the Mann-Whitney rank-sum test. The chi-square test and Fisher's exact test were used to assess the difference in different groups. A *P* value less than 0.05 was considered statistically significant.

RESULTS

The 132 bp PCR fragment amplified from CD-mtDNA was cloned and sequenced to confirm the deletion junction created by the CD, which was characterized by the presence of one of the two 13 bp repeats that normally flanked wild-type mtDNA. Sequence comparison (Human mtDNA Cambridge Sequence data, www.mitomap.org) revealed that the common deletion region in our HCC samples was a 4 981 bp fragment extending from position 8 470 bp to 13 450 bp (Figure 3). This was a novel mtDNA deletion belonging to the 4 977 bp deletion subtype that was first reported in liver diseases.

Incidence of CD-mtDNA by conventional PCR detection

CD-mtDNA was detected by conventional PCR in 70% (19/27), 63% (17/27) and 44% (12/27) in HCC tumors, HNH tissues and HCC adjacent liver tissues, respectively. The detected rate of CD-mtDNA in HCC and HNH tumors by conventional PCR was significantly higher than that in adjacent liver tissues ($P < 0.05$, chi-square test). There was no significant difference in CD-mtDNA detected rate between HCC and HNH ($P > 0.05$, chi-square test).

By quantitative TaqMan-PCR, the detection rate of CD-mtDNA in HCC tumors, HNH tissues and adjacent liver tissues was 70% (19/27), 63% (17/27) and 44% (12/27), respectively. When these results were combined with those of conventional PCR, CD-mtDNA was detected in 85% (23/27) of HCC, 83% (22/27) of HNH, and 57% (15/27) of HCC paired adjacent liver tissues. The detected CD-mtDNA rate in HCC and HNH tumors was significantly higher than that in paired noncancerous liver tissues ($P < 0.05$, chi-square test). (Figure 4).

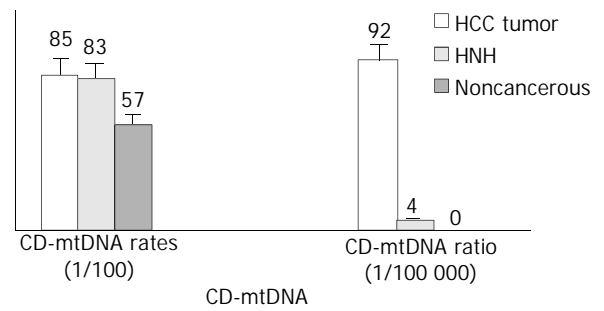


Figure 4 Correlations of CD-mtDNA with HCC and HNH. The CD-mtDNA rate in HCC and HNH lesions was significantly higher than that in paired noncancerous tissues; the CD/WT-mtDNA ratio in HCC was significant higher than that in paired noncancerous liver tissues ($P = 0.02$), and was about 25 times that in HNH lesions ($P = 0.02$).

CD/WT-mtDNA ratio in HCC and HNH lesions

We evaluated the relative level of CD-mtDNA by calculating the ratio of CD-mtDNA to WT-mtDNA in each sample. In this study, the CD/WT-mtDNA ratio was 0.00092 (median, interquartile range, 0.0001202-0.00105) in HCC tumor, 0.000 (median, quartile range, 0-0) in paired noncancerous liver tissues, and 0.0000374 (median, quartile range, 0-0.0004225) in HNH tissues. The CD/WT-mtDNA ratio in HCC tumor was significantly higher than that in paired noncancerous liver tissues ($P = 0.002$, Mann-Whitney test), and was 25 times of that in HNH tissues ($P = 0.002$, Mann-Whitney test, Figure 4). No correlation of the detected rate and the ratio of CD-mtDNA with ageing, staging, tumor size, HBV infection and differentiation of patients with HCC were found.

DISCUSSION

It has been found that human mitochondrial DNA (mtDNA) has a double-stranded circular molecule of 16 569 bp that encodes 37 genes: 2 rRNAs, 22 tRNAs and 13 polypeptides^[21]. The mtDNA was present in high copy levels (10^3 - 10^4 copies per cell) in virtually all cells, and the vast majority of an individual's copies were identical at birth^[22]. It has been generally accepted that high mutation rates of mtDNA are caused by a lack of protective histones, inefficient DNA repair systems, and continuous exposure to mutagenic effects of oxygen radicals generated by oxidative phosphorylation^[23,24]. The deletion was thought to be the product of an intragenomic recombination event between two 13 bp direct repeats (positions 8 470-8 482 and 13 447-13 459) after a single-strand break caused by ultraviolet A (UVA) or ROS^[25].

Recently, somatic mutations in mitochondrial DNA (mtDNA)

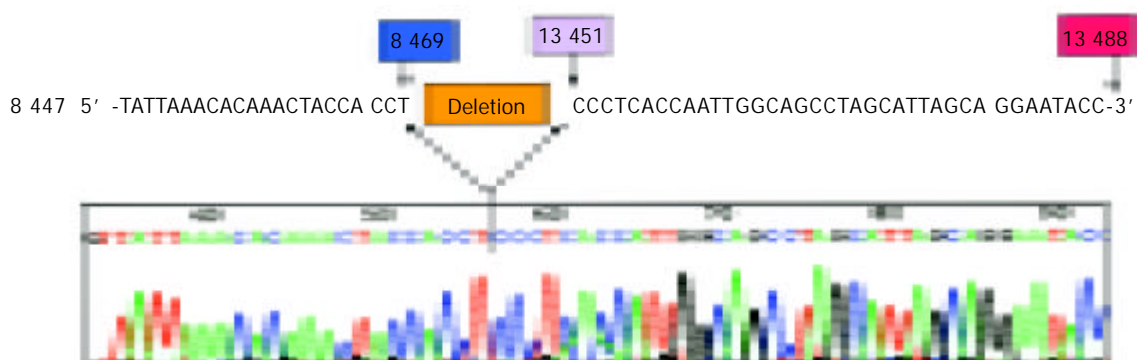


Figure 3 Sequencing result of the amplified CD-mtDNA from HCC. Comparison with the MITOMAP Human mtDNA Cambridge Sequence data (www.mitomap.org), the deletion region (red bar region) is a 4981 bp deletion from position 8 470 to 13 450 of the mtDNA.

have been detected in various cancers including HCC. Mutations in the D-loop were frequent events and could be used as a molecular tool to determine clonality of HCC^[26]. There are controversial reports of CD-mtDNA mutation in HCC. CD-mtDNA was reported to be detected in HCC tumors and noncancerous liver tissues, whereas lower level even no CD-mtDNA was detected in HCC tumors^[27,28]. In this investigation, we detected a novel CD-mtDNA mutation (4 981 bp) in 85% HCC, which was higher than that in gastric cancer (50%)^[18], but less than that in thyroid Hürthle cell tumors (100%)^[17]. Moreover, we found that both the detected CD-mtDNA rate and CD/WT-mtDNA ratio in HCC were higher than those in paired noncancerous liver tissues of individuals with HCC. This result was different from previous studies. The different risk factors and different genetic background in HCC tumorigenesis between Chinese and Japanese might explain the disparity of the results. Further studies are required to determine if CD-mtDNA mutation is correlated with malignant transformation.

However, the biological impact of mtDNA deletion on HCC tumors is not entirely clear. Defects in mitochondrial function have long been suspected to contribute to the development and progression of cancer. These mutations could contribute to neoplastic transformation by changing cellular energy capacities, increasing mitochondrial oxidative stress, and/or modulating apoptosis^[25]. Diaz *et al.*^[29] reported that mtDNA with large deletions, but not with pathogenic point mutations, repopulated organelles significantly faster than wild-type genomes in the same cell. Under proliferating conditions, cells harboring relatively high levels of deleted mtDNAs showed a slight reduction in the mutated fraction. This was consistent with the observation that patients with mitochondrial diseases had relatively low percentages of mutated mtDNA in proliferating peripheral blood cells and fibroblasts^[30]. This situation paralleled the accumulation of large-scale mtDNA deletions in postmitotic tissues, where selection based on cellular growth or survival did not take place, and abnormal organelle proliferation would lead to an increase in mtDNA replication rates^[31,32]. Amuthan^[33] showed that damage to mtDNA and the mitochondrial membrane might change nuclear gene expression, leading to overexpression of genes including cathepsin L, transforming growth factor (TGF β), and mouse melanoma antigen (MMA), which are well known markers for tumor progression. Singh^[34] showed that mtDNA played an important role in cellular sensitivity to cancer therapeutic agents. Since each cell contains many mitochondria with multiple copies of mtDNAs, it is possible that wild-type and mutant mtDNA can co-exist in a state called heteroplasmy. Thus, the biological impact of a given mutation may vary, depending on the proportion of mutant mtDNAs carried by individuals.

It has been shown that mtDNA deletions accumulate with age in many tissues. However, in tumors, the CD has been associated with external factors such as radiation and cigarette smoking^[35-37]. In this investigation, we found that although there was no significant difference in detected CD-mtDNA rate between HCC and paired adjacent liver tissues as well as HNH, the CD-mtDNA ratio in HCC was significantly higher than that in HNH (25-fold) and paired noncancerous liver tissues. These results suggest that CD-mtDNA mutation may be accumulated during the hepatocyte transformation. No correlation of CD-mtDNA with ageing, staging and HBV infection of the individuals with HCC and HNH was found. In this investigation, the high detected rate and high ratio of CD-mtDNA in HCC and HNH suggested that this rapid and quantitative assay of CD-mtDNA and WT-mtDNA copy number was potentially useful in a variety of molecular and evolutionary fields of HCC.

In conclusion, this is the first quantitative study of frequent occurrence of CD-mtDNA mutations in patients with HCC. This study provides further evidence that CD-mtDNA mutation

might play an important role in the development and progression of HCC. Studies evaluating the CD-mtDNA mutations as a biomarker may be potentially useful for early diagnosis of HCC.

REFERENCES

- 1 **Tang ZY.** Hepatocellular carcinoma-cause, treatment and metastasis. *World J Gastroenterol* 2001; **7**: 445-454
- 2 **Shao J, Li Y, Li H, Wu Q, Hou J, Liew C.** Deletion of chromosomes 9p and 17 associated with abnormal expression of p53, p16/MTS1 and p15/MTS2 gene protein in hepatocellular carcinomas. *Chin Med J* 2000; **113**: 817-822
- 3 **Fujimoto Y, Hampton LL, Wirth PJ, Wang NJ, Xie JP, Thorgeirsson SS.** Alterations of tumor suppressor genes and allelic losses in human hepatocellular carcinomas in China. *Cancer Res* 1994; **54**: 281-285
- 4 **Shiota G, Kishimoto Y, Suyama A, Okubo M, Katayama S, Harada K, Ishida M, Hori K, Suou T, Kawasaki H.** Prognostic significance of serum anti-p53 antibody in patients with hepatocellular carcinoma. *J Hepatol* 1997; **27**: 661-668
- 5 **Poon RT, Ng IO, Lau C, Zhu LX, Yu WC, Lo CM, Fan ST, Wong J.** Serum vascular endothelial growth factor predicts venous invasion in hepatocellular carcinoma: a prospective study. *Ann Surg* 2001; **233**: 227-235
- 6 **Niu Q, Tang ZY, Ma ZC, Qin LX, Zhang LH.** Serum vascular endothelial growth factor is a potential biomarker of metastatic recurrence after curative resection of hepatocellular carcinoma. *World J Gastroenterol* 2000; **6**: 565-568
- 7 **Wei Y, Van Nhieu JT, Prigent S, Srivatanakul P, Tiollais P, Buendia MA.** Altered expression of E-cadherin in hepatocellular carcinoma: correlations with genetic alterations, beta-catenin expression, and clinical features. *Hepatology* 2002; **36**: 692-701
- 8 **Endo K, Ueda T, Ueyama J, Ohta T, Terada T.** Immunoreactive E-cadherin, alpha-catenin, beta-catenin, and gamma-catenin proteins in hepatocellular carcinoma: relationships with tumor grade, clinicopathologic parameters, and patients' survival. *Hum Pathol* 2000; **31**: 558-565
- 9 **Cui J, Zhou XD, Liu YK, Tang ZY, Zile MH.** Abnormal β -catenin gene expression with invasiveness of primary hepatocellular carcinoma in China. *World J Gastroenterol* 2001; **7**: 542-546
- 10 **Endo K, Terada T.** Protein expression of CD44 (standard and variant isoforms) in hepatocellular carcinoma: relationships with tumor grade, clinicopathologic parameters, p53 expression, and patient survival. *J Hepatol* 2000; **32**: 78-84
- 11 **Jiang YF, Yang ZH, Hu JQ.** Recurrence or metastasis of HCC: predictors, early detection and experimental antiangiogenic therapy. *World J Gastroenterol* 2000; **6**: 61-65
- 12 **Bu W, Huang X, Tang Z.** The role of MMP-2 in the invasion and metastasis of hepatocellular carcinoma (HCC) Article in Chinese. *Zhonghua Yixue Zazhi* 1997; **77**: 661-664
- 13 **Fox SB, Taylor M, Grondahl-Hansen J, Kakolyris S, Gatter KC, Harris AL.** Plasminogen activator inhibitor-1 as a measure of vascular remodeling in breast cancer. *J Pathol* 2001; **195**: 236-243
- 14 **Green DR, Reed JC.** Mitochondria and apoptosis. *Science* 1998; **281**: 1309-1312
- 15 **Cavalli LR, Liang BC.** Mutagenesis, tumorigenicity, and apoptosis: are the mitochondria involved? *Mutat Res* 1998; **398**: 19-26
- 16 **Corral-Debrinski M, Horton T, Lott MT, Shoffner JM, Beal MF, Wallace DC.** Mitochondrial DNA deletions in human brain: regional variability and increase with advanced age. *Nat Genet* 1992; **2**: 324-329
- 17 **Maximo V, Soares P, Lima J, Cameselle-Teijeiro J, Sobrinho-Simoes M.** Mitochondrial DNA somatic mutations (point mutations and large deletions) and mitochondrial DNA variants in human thyroid pathology: a study with emphasis on Hurthle cell tumors. *Am J Pathol* 2002; **160**: 1857-1865
- 18 **Maximo V, Soares P, Seruca R, Rocha AS, Castro P, Sobrinho-Simoes M.** Microsatellite instability, mitochondrial DNA large deletions, and mitochondrial DNA mutations in gastric carcinoma. *Genes Chromosomes Cancer* 2001; **32**: 136-143
- 19 **Fukushima S, Honda K, Awane M, Yamamoto E, Takeda R, Kaneko I, Tanaka A, Morimoto T, Tanaka K, Yamaoka Y.** The frequency of 4977 base pair deletion of mitochondrial DNA in

- various types of liver disease and in normal liver. *Hepatology* 1995; **21**: 1547-1551
- 20 **Moskaluk CA**, Kern SE. Microdissection and polymerase chain reaction amplification of genomic DNA from histologic tissue sections. *Am J Pathol* 1997; **150**: 1547-1552
- 21 **Anderson S**, Bankier AT, Barrell BG, de Bruijn MH, Coulson AR, Drouin J, Eperon IC, Nierlich DP, Roe BA, Sanger F, Schreier PH, Smith AJ, Staden R, Young IG. Sequence and organization of the human mitochondrial genome. *Nature* 1981; **290**: 457-465
- 22 **Lightowlers RN**, Chinnery PF, Thunball DM, Howell N. Mammalian mitochondrial genetics: heredity, heteroplasmy and disease. *Trends Genet* 1997; **13**: 450-455
- 23 **Wallace DC**. Diseases of the mitochondrial DNA. *Annu Rev Biochem* 1992; **61**: 1175-1212
- 24 **Wallace DC**. Mitochondrial genetics: a paradigm for aging and degenerative diseases? *Science* 1992; **256**: 628-632
- 25 **Shoffner JM**, Lott MT, Voljavec AS, Soueidan SA, Costigan DA, Wallace DC. Spontaneous Kearns-Sayre/chronic external ophthalmoplegia plus syndrome associated with a mitochondrial DNA deletion: a slip-replication model and metabolic therapy. *Proc Natl Acad Sci U S A* 1989; **86**: 7952-7956
- 26 **Nomoto S**, Yamashita K, Koshikawa K, Nakao A, Sidransky D. Mitochondrial D-loop mutations as clonal markers in multicentric hepatocellular carcinoma and plasma. *Clin Cancer Res* 2002; **8**: 481-487
- 27 **Nishikawa M**, Nishiguchi S, Shiomi S, Tamori A, Koh N, Takeda T, Kubo S, Hirohashi K, Kinoshita H, Sato E, Inoue M. Somatic mutation of mitochondrial DNA in cancerous and noncancerous liver tissue in individuals with hepatocellular carcinoma. *Cancer Res* 2001; **61**: 1843-1845
- 28 **Yamamoto H**, Tanaka M, Katayama M, Obayashi T, Nimura Y, Ozawa T. Significant existence of deleted mitochondrial DNA in cirrhotic liver surrounding hepatic tumor. *Biochem Biophys Res Commun* 1992; **182**: 913-920
- 29 **Diaz F**, Bayona-Bafaluy MP, Rana M, Mora M, Hao H, Moraes CT. Human mitochondrial DNA with large deletions repopulates organelles faster than full-length genomes under relaxed copy number control. *Nucleic Acids Res* 2002; **30**: 4626-4633
- 30 **Moraes CT**, DiMauro S, Zeviani M, Lombes A, Shanske S, Miranda AF, Nakase H, Bonilla E, Werneck LC, Servidei S. Mitochondrial DNA deletions in progressive external ophthalmoplegia and Kearns-Sayre syndrome. *N Engl J Med* 1989; **320**: 1293-1299
- 31 **Johnston W**, Karpate G, Carpenter S, Arnold D, Shoubridge EA. Late-onset mitochondrial myopathy. *Ann Neurol* 1995; **37**: 16-23
- 32 **Moslemi AR**, Melberg A, Holme E, Oldfors A. Clonal expansion of mitochondrial DNA with multiple deletions in autosomal dominant progressive external ophthalmoplegia. *Ann Neurol* 1996; **40**: 707-713
- 33 **Amuthan G**, Biswas G, Zhang SY, Klein-Szanto A, Vijayasarathy C, Avadhani NG. Mitochondria-to-nucleus stress signaling induces phenotypic changes, tumor progression and cell invasion. *EMBO J* 2001; **20**: 1910-1920
- 34 **Singh KK**, Russell J, Sigala B, Zhang Y, Williams J, Keshav KF. Mitochondrial DNA determines the cellular response to cancer therapeutic agents. *Oncogene* 1999; **18**: 6641-6646
- 35 **Kotake K**, Nonami T, Kurokawa T, Nakao A, Murakami T, Shimomura Y. Human livers with cirrhosis and hepatocellular carcinoma have less mitochondrial DNA deletion than normal human livers. *Life Sci* 1999; **64**: 1785-1791
- 36 **Rogounovitch TI**, Saenko VA, Shimizu-Yoshida Y, Abrosimov AY, Lushnikov EF, Roumiantsev PO, Ohtsuru A, Namba H, Tsyb AF, Yamashita S. Large deletions in mitochondrial DNA in radiation-associated human thyroid tumors. *Cancer Res* 2002; **62**: 7031-7041
- 37 **Ballinger SW**, Boudier TG, Davis GS, Judice SA, Nicklas JA, Albertini RJ. Mitochondrial genome damage associated with cigarette smoking. *Cancer Res* 1996; **56**: 5692-5697

Edited by Ren SY and Wang XL Proofread by Xu FM

Expression of *cytochrome P4502E1* gene in hepatocellular carcinoma

Xiao-Bo Man, Liang Tang, Xiu-Hua Qiu, Li-Qun Yang, Hui-Fang Cao, Meng-Chao Wu, Hong-Yang Wang

Xiao-Bo Man, Liang Tang, Xiu-Hua Qiu, Hui-Fang Cao, Hong-Yang Wang, International Co-operation Laboratory on Signal Transduction, Eastern Hepatobiliary Surgery Hospital, 225 Changhai Road, Shanghai 200438, China

Li-Qun Yang, Department of Anesthesiology, Eastern Hepatobiliary Surgery Hospital, 225 Changhai Road, Shanghai 200438, China

Meng-Chao Wu, Department of Clinical Surgery, Eastern Hepatobiliary Surgery Hospital, 225 Changhai Road, Shanghai 200438, China

Correspondence to: Dr. Hong-Yang Wang, International Co-operation Laboratory on Signal Transduction, Eastern Hepatobiliary Surgery Hospital, 225 Changhai Road, Shanghai 200438, China. hywangk@online.sh.cn

Telephone: +86-21-25070856 **Fax:** +86-21-65566851

Received: 2003-06-10 **Accepted:** 2003-08-16

Abstract

AIM: To investigate *cytochrome P4502E1* (*CYP2E1*) gene expression in occurrence and progression of hepatocellular carcinoma (HCC).

METHODS: The human liver arrayed library was spotted onto the nylon membranes to make cDNA array. Hybridization of cDNA array was performed with labeled probes synthesized from RNA isolated from HCC and adjacent liver tissues. Sprague-Dawley rats were administered diethylnitrosamine (DNA) to induce HCC. *CYP2E1* expression was detected by the method of RT-PCR and Northern blot analysis.

RESULTS: *CYP2E1* was found by cDNA array hybridization to express differently between HCC and liver tissues. *CYP2E1* only expressed in liver, but did not express in HCC tissues and expressed lowly in cirrhotic tissues. In the progression of cirrhosis and HCC, the expression level of *CYP2E1* was gradually decreased and hardly detected until the late stage of HCC.

CONCLUSION: Using arrayed library to make cDNA arrays is an effective method to find differential expression genes. *CYP2E1* is a unique gene expressing in liver but did not express in HCC. *CYP2E1* expression descended along with the initiation and progression of HCC, which is noteworthy further investigations in its significance in the development of HCC.

Man XB, Tang L, Qiu XH, Yang LQ, Cao HF, Wu MC, Wang HY. Expression of *cytochrome P4502E1* gene in hepatocellular carcinoma. *World J Gastroenterol* 2004; 10(11): 1565-1568
<http://www.wjgnet.com/1007-9327/10/1565.asp>

INTRODUCTION

Hepatocellular carcinoma (HCC) is one of the most common cancers in China and the world^[1,2]. Although the wide use of diagnostic technology and the improvement in curative treatment may evolve to a better scenario, it still represents more than 5% of all cancers^[3]. To investigate HCC associated

genes is very helpful to elucidating the molecular mechanism of proliferation, differentiation and transformation of hepatocytes in the occurrence and development of HCC^[4,5]. cDNA microarray analysis is a powerful technique in the investigation of cancer associated gene identification and function^[6]. The gene expression can be simultaneously monitored in a large scale with cDNA microarray^[7]. The potential analysis of the expression of thousands of genes in one experiment provided new insights into the molecular study of the occurrence and development of HCC^[8-10].

In the present study, a method of making cDNA array from the arrayed library was developed to identify the differentially expressed genes. *CYP2E1*, the gene encoding cytochrome P450 2E1 (*CYP2E1*), a member of cytochrome P450s present in prokaryotes and through the eukaryotes^[11], was identified to express in normal liver or cirrhotic tissues adjacent to tumors but not express in HCC tissues. *CYP2E1* is one of the important members of cytochrome P450 superfamily, with functions ranging from catalysis of the conversion of ethanol to acetaldehyde and from acetate to metabolization of many exotic drugs and procarcinogens^[12]. A rat HCC model was then induced to study *CYP2E1* expression in the procession of HCC. The results showed that *CYP2E1* expression descended along with the initiation, promotion and progression of HCC. It is suggested that *CYP2E1* is correlated to HCC and noteworthy further investigations for its significance in the development of HCC.

MATERIALS AND METHODS

Arrayed library preparation

The human liver cDNA library (Invitrogen, USA) was cultured on the agar plate and were picked into 96-well microplates with 200 μ L culture medium. After an overnight culture, 1 μ L of the bacterial medium in each well was diluted into 20 μ L from which 1 μ L was transferred to the corresponding 96-well PCR microplates and the remaining was added to 50 μ L glycerol and stored at -80 $^{\circ}$ C.

PCR amplification of plasmids

PCR reaction was carried out with oligonucleotide T7 (5' gga aga agg gaa ctg att cag 3') and oligonucleotide BGHR (5' cac atc cag atc ata tgc cag 3') as forward primer and reverse primer. The procedure of PCR was made with denaturing at 94 $^{\circ}$ C for 4 min followed by 35 cycles of reaction including denaturing at 94 $^{\circ}$ C for 50 s, annealing at 58 $^{\circ}$ C for 50 s and elongation at 72 $^{\circ}$ C for 90 s, and a final bonus extension elongation at 72 $^{\circ}$ C for 7 min. The amplified products were randomly selected for electrophoresis to validate PCR efficiency.

DNA arrays preparation

The PCR products in the microplates were spotted with TAS (BioRobotics, UK) onto the 8 cm \times 12 cm nylon membrane to form 2 \times 2 \times 96 array in each membrane. The 0.7 mm diameter 96-pin spotting setting was used. Each product from a well was spotted onto the same position 3 times. The membranes were denatured immediately in the denature buffer (1.5 mol/L

NaCl, 0.5 mol/L NaOH) for 5 min and then equalized in the equalizing buffer (0.9 mol/L NaCl, 0.5 mol/L Tris, pH7.5) for 5 min followed by baking at 80 °C.

DENA-induced HCC in rats

DENA (Sigma, USA) was diluted into 1×10^{-4} concentration in drinkable water. Male Sprague-Dawley rats were obtained from the Experimental Animal Center of Chinese Academy of Sciences, Shanghai. The rats in HCC group were administrated DENA via drinking DENA-diluted water while the rats in control group drank clean water. Three HCC-induced rats and one control rat were sacrificed by decollation under pentobarbital anesthesia every week. The liver tissue was immediately stored in liquid nitrogen for RNA isolation and fixed for histological analysis.

Total RNA and mRNA isolation

Total RNA was isolated from 0.1 g frozen tissues in 1 mL Trizol™ reagent (Invitrogen, USA) according to the manufacturer's instructions. Isolation of mRNA was carried out with the Oligotex™ mRNA Mini kit (Qiagen, Germany) from 250 µg total RNA.

Labeling of cDNA from mRNA of HCC tissues

Probes for the array hybridization were labeled with Atlas™ SpotLight™ labeling kit (Clontech, USA) according to the user's manual. A 2 µg mRNA respectively from paired HCC tumor and adjacent normal or cirrhotic tissues was added with 2.5 µL CDS Primer Mix and incubated at 70 °C for 10 min. Reaction buffer (5×) 5 µL, Labeling Mix (10×) 2.5 µL, DTT (100 mmol/L) 1.25 µL were added and incubated at 48 °C for 5 min. PowerScript reverse transcriptase (1.25 µL) per reaction and 10 mL of Master Mix were added and incubated at 48 °C for an additional 45 min. The reaction was stopped by adding 0.5 mL of 0.5 mol/L EDTA (pH8.0) and then purified routinely.

Hybridization of DNA array

DNA array hybridization and detection were preceded with SpotLight™ chemiluminescent hybridization & detection kit (Clontech, USA). The array membranes were wetted and pre-hybridized while a biotinylated array probe was denatured. Cot-1 and the biotinylated probe were added to pre-hybridization solution to incubate overnight. The membranes were washed and blocked, and added with enough stabilized Streptavidin-HRP conjugate. After equilibrated, the membranes were covered with the luminol/peroxide working solution and incubated at room temperature for 5 min and exposed the membrane to film for an appropriate time to obtain desired signals.

RT-PCR of CYP2E1 in rats

First strand cDNA was reversibly transcribed from total RNA with SuperScript™ reverse transcriptase (Invitrogen, USA). The procedure of RT-PCR of *CYP2E1* was carried out in normal rat tissues with the oligonucleotide (5' act tct acc tgc tga gca c 3') and oligonucleotide (5' ttc agg tct cat gaa cgg g 3') as forward and reverse primer respectively and with denaturing at 94 °C for 4 min followed by 33 cycles of reaction including denaturing at 94 °C for 50 s, annealing at 55 °C for 50 s and extension at 72 °C for 1 min, and a final bonus extension for 7 min. An 874-bp sequence product was amplified.

Cloning of rat CYP2E1

The PCR product was purified using the QIAquick PCR purification kit (Qiagen, Germany) and cloned into the T-vector (Promega, USA) directly and transfected into DH5- α bacteria. The plasmid was purified to be sequenced and confirmed according to the GenBank sequence.

Northern blot analysis

The plasmid was digested and electrophoresed. The template fragment was purified from agarose gel using the gel extracting kit (Qiagen, Germany). The probe was labeled from 25 ng template DNA by the random primer method using DNA polymerase I large (Klenow) fragment (Promega, USA) with α -³²P-dCTP followed by purification using the QIAquick purification kit (Qiagen, Germany). Total RNA (40 µg) justified by 28 s and 18 s intensity of each sample, was loaded. Electrophoresis was carried out under denaturing conditions and RNA was transferred onto nitrocellulose membrane and cross-linked by baking at 80 °C for 2 h. The filters were then prehybridized, hybridized, and washed under high stringency conditions. All blots were screened by Fuji BAS2000 and analyzed by LABwork software and then exposed at -80 °C to Kodak X-ray film for 2 wk.

RESULTS

Identification of CYP2E1 as an HCC-silent gene with cDNA array gene expression profile analysis

The arrayed library clones were spotted onto each nylon membrane to $2 \times 2 \times 96$ array from 4 microplates. There were 96 subarrays in one membrane. The arrayed membranes were denatured, fixed and preserved under dry condition. The mRNA from HCC tissues and corresponding adjacent liver tissues was labeled to hybridize to the above arrayed membranes. A spot then identified low signals in HCC tissues but high signals in corresponding adjacent liver tissues (Figure 1). It was suggested that the gene was a liver-expressing gene that was downregulated in HCC tissues. According to the position of the spot in membrane, the clones in microplates of arrayed library was recruited and sequenced as *CYP2E1*.

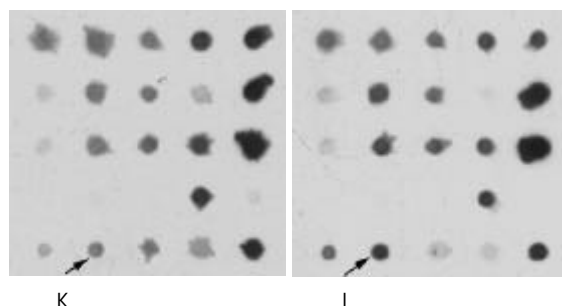


Figure 1 Differential expression profile of cDNA array hybridization result. Part of the membrane is displayed. The clones the arrows point represent *CYP2E1*. K: HCC tissue, L: adjacent liver tissue.

HCC model of DENA-induced rats

The liver tissue from DENA-induced rats that were killed after 3 wk appeared almost normal as the control rats. The pathological examination indicated the liver lesion in these rats. The livers of rats after the 4th wk were smaller than those of control rats and the color of the liver surface was much dingy. Cirrhotic nodi could be seen on the liver surface of rats killed in the 7th wk and cirrhosis could be detected as early as in the 5th wk by pathological examination. There were few liver cancer nodi in 1 rat detected in the 9th wk. So the 9th wk might be the boundary between cirrhosis and HCC in the present study. In the 10th wk, HCC could be detected in all rats and HCC nodi could be seen by naked eyes after the 10th wk. After the 16th wk, HCC nodi were spread almost all over the rat liver.

CYP2E1 expression in normal tissues

Twelve types of human normal tissues except liver were used

for Northern blot analysis of *CYP2E1* expression. *CYP2E1* did not express at all in the 12 normal human tissues. To represent the expression level of *CYP2E1* in these organs, the RNA sample of heart, brain, lung, intestine and liver were selected with 2 cases of HCC tissues and 1 case of kidney cancer tissue to be transferred onto one membrane for Northern blot analysis. The hybridization result showed that *CYP2E1* indeed only expressed in non-tumor liver tissues (Figure 2). The expression pattern of *CYP2E1* in rats was the same as in human. By RT-PCR analysis, it was indicated that *CYP2E1* was only amplified from normal liver tissues and did not express in other tissues (Figure 3).

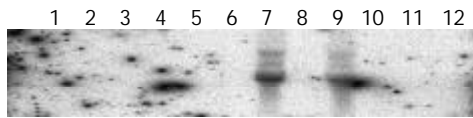


Figure 2 *CYP2E1* expression in normal human organs and HCC tissues detected by Northern blot analysis. 1: heart, 2: brain, 3: muscle, 4: intestine, 5: stomach, 6: lung, 7: liver tissues adjacent to HCC, 8: HCC, 9: liver tissues adjacent to HCC, 10: HCC, 11: renal tissues adjacent to carcinoma, 12: renal carcinoma.

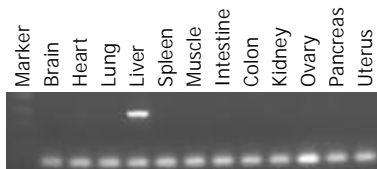


Figure 3 *CYP2E1* expression in normal organs of rat detected by RT-PCR analysis.

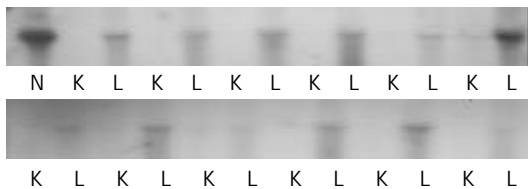


Figure 4 *CYP2E1* expression in human HCC tissues detected by Northern blot analysis. N: normal liver, K: HCC, L: liver tissue adjacent to HCC.

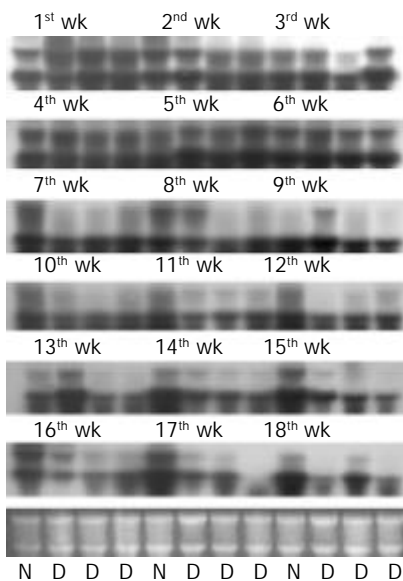


Figure 5 *CYP2E1* expression in occurrence and development of rat HCC detected by Northern blot analysis. There were 12

lanes in one membrane including specimen of 3 wk. Ribosomal RNA of 28 s and 18 s as control was in the bottom. N: normal control group, D: DENA-induced group.

***CYP2E1* expression in HCC**

Northern blot analysis showed that *CYP2E1* expressed in normal liver tissues and adjacent tissues with cirrhosis. There was no hybridization signal in HCC tissues from all 14 cases. *CYP2E1* was significantly downregulated in HCC (Figure 4). The rat HCC model simulated the progression of HCC. The change of expression was analyzed also by Northern blot (Figure 5). In the early liver lesion stage of the DENA-induced rats after 1-3 wk, *CYP2E1* expression was slightly upregulated compared with normal livers. But after 4 wk, the gene was down-regulated and when cirrhosis occurred after 5 wk, the expression level was almost the same in the liver between the 2 groups. It was obvious that the cirrhotic tissues of the rats expressed at lower level than the normal livers after 7 wk. When the DENA-induced rats progressed to the stage of tumor from the 10th wk, *CYP2E1* expressed at much lower level than normal livers and liver of cirrhotic stages. Until the very later stage of HCC, the expression level was very low and the hybridization signal was hardly detected.

DISCUSSION

An ideal support allowed effective immobilization of probe onto its surface, and robust hybridization of target with the probe^[13]. Nylon membrane, as a standard support used for making microarrays^[14,15] could hold more DNA. The hybridization and detection of membranes arrays cost much less. Here we used the nylon membranes as the matrix of cDNA arrays. The DNA on the membranes was denatured before cross-linking to the matrix by baking the array at 80 °C. In many cases, the cDNA targets were chosen directly from cDNAs library of interest for DNA microarray manufacturing^[16]. The collection should include an aggregation of gene clones as many as possible. On the other hand, for certain purpose of an investigation, most genes on a large content array might not be necessary. The method to make cDNA microarray in this study arose from the concept of arrayed library. The cDNA plasmid library was transferred to the microplates to be the arrayed library, which was copied to the nylon membranes to make the DNA arrays after PCR amplification. Because most genes on the arrays did not differently express between samples, the tumor and normal tissues, for example, the sequencing expense of these genes could be saved. It was after the array hybridization, the genes that were detected to express differently would be selected from the arrayed library and were sequenced for further studies. In this study, most genes showed no differential expression between HCC and adjacent liver tissues. Only the differently expressed genes were sequenced for further investigations. *CYP2E1* was identified as a liver profound but HCC silent gene.

P450 enzymes were found in almost all eukaryotes and prokaryotes^[17]. *CYP2E1* enzyme had a molecular weight of 57 KD and the encoding gene was located on chromosome 10 spanning 11 413 base pairs^[18,19]. *CYP2E1* was found to play an important role in its polymorphism during tumor occurrence. The significance of this polymorphism currently unclear^[20,21]. To date, the results in possible associations between *CYP2E1* genetic polymorphisms and alcoholic liver disease susceptibility have been varied and often contradictory^[22]. Because hepatic *CYP2E1* has been shown to activate various carcinogens, there has been interest in whether certain *CYP2E1* polymorphisms might predispose to liver cancer^[23,24]. It was demonstrated that possession of the less common *Rsa* I/*Pst* I allele was associated with increased susceptibility to HCC^[25].

Although CYP2E1 was said to be located in most tissues with the largest concentration in the liver, it was constitutively expressed in the liver and only induced to express in other tissues by treatment with acetone, ethanol, isoniazid and other compounds, many of which are substrates for the enzyme^[26-28]. This study showed that *CYP2E1* expressed only in the liver but did not express in the other normal organs in human and rats. So it could be concluded that *CYP2E1* is the liver-specific functional gene. Furthermore, *CYP2E1* was found to loose expression in HCC. Northern blot analysis was performed to validate the result of chip experiment. *CYP2E1* expressed at a high level in normal or cirrhotic tissues but was silent in HCC tissues from 14 cases of HCC. So *CYP2E1* did not express in HCC. To further understand the expression of *CYP2E1* in the initiation, promotion and progression of HCC, the DENA-induced rat HCC model was made to study the role of *CYP2E1* in the process of HCC. The development of rat HCC underwent the progression of liver lesion and cirrhosis until the tumor occurrence. The results showed that at the early stage of the rat model the expression level of *CYP2E1* in the liver lesion tissues was slightly higher than that in normal rat liver in the first to third week. Because CYP2E1 was involved in the metabolism of nitrosamines, DENA might induce *CYP2E1* expression. But along with the aggravation of liver lesion and development of cirrhosis, the expression level of *CYP2E1* was gradually descended. After the progressing stage of HCC, *CYP2E1* did not express as in human HCC. There were very low signals because at the late stages of HCC the tumor were grown sporadically and the samples were intermixed with cirrhotic tissues where *CYP2E1* still expressed. The expression pattern of *CYP2E1* in the HCC was worth of further studies. It is suggested that these differential expression might help further understand the molecular genetic and gene regulation mechanism of HCC progression. Because *CYP2E1* does not express in HCC cells, there might be a guided biological treatment for HCC with its potential substrate.

REFERENCES

- 1 **Qin LX**, Tang ZY. The prognostic significance of clinical and pathological features in hepatocellular carcinoma. *World J Gastroenterol* 2002; **8**: 193-199
- 2 **Ince N**, Wands JR. The increasing incidence of hepatocellular carcinoma. *N Engl J Med* 1999; **340**: 798-799
- 3 **Llovet JM**, Beaugrand M. Hepatocellular carcinoma: present status and future prospects. *J Hepatol* 2003; **38**(Suppl 1): S136-S149
- 4 **Thorgeirsson SS**, Grisham JW. Molecular pathogenesis of human hepatocellular carcinoma. *Nat Genet* 2002; **31**: 339-346
- 5 **Tannapfel A**, Wittekind C. Genes involved in hepatocellular carcinoma: deregulation in cell cycling and apoptosis. *Virchows Arch* 2002; **440**: 345-352
- 6 **Berns A**. Gene expression in diagnosis. *Nature* 2000; **403**: 491-492
- 7 **Young RA**. Biomedical discovery with DNA arrays. *Cell* 2000; **102**: 9-15
- 8 **Chen X**, Cheung ST, So S, Fan ST, Barry C, Higgins J, Lai KM, Ji J, Dudoit S, Ng IO, Van De Rijn M, Botstein D, Brown PO. Gene expression patterns in human liver cancers. *Mol Biol Cell* 2002; **13**: 1929-1939
- 9 **Delpuech O**, Trabut JB, Carnot F, Feuillard J, Brechot C, Kremsdorf DR. Identification, using cDNA macroarray analysis, of distinct gene expression profiles associated with pathological and virological features of hepatocellular carcinoma. *Oncogene* 2002; **21**: 2926-2937
- 10 **Lee JS**, Thorgeirsson SS. Functional and genomic implications of global gene expression profiles in cell lines from human hepatocellular cancer. *Hepatology* 2002; **35**: 1134-1143
- 11 **Peterson JA**, Graham SE. A close family resemblance: the importance of structure in understanding cytochromes P450. *Structure* 1998; **6**: 1079-1085
- 12 **Tanaka E**, Terada M, Misawa S. Cytochrome P450 2E1: its clinical and toxicological role. *J Clin Pharm Ther* 2000; **25**: 165-175
- 13 **Southern E**, Mir K, Shchepinov M. Molecular interactions on microarrays. *Nat Genet* 1999; **21**(Suppl): 5-9
- 14 **Schlaak JF**, Hilkens CM, Costa-Pereira AP, Strobl B, Aberger F, Frischauf AM, Kerr IM. Cell-type and donor-specific transcriptional responses to interferon-alpha. Use of customized gene arrays. *J Biol Chem* 2002; **277**: 49428-49437
- 15 **Mochii M**, Yoshida S, Morita K, Kohara Y, Ueno N. Identification of transforming growth factor-beta- regulated genes in caenorhabditis elegans by differential hybridization of arrayed cDNAs. *Proc Natl Acad Sci U S A* 1999; **96**: 15020-15025
- 16 **Cheung VG**, Morley M, Aguilar F, Massimi A, Kucherlapati R, Childs G. Making and reading microarrays. *Nat Genet* 1999; **21**(1 Suppl): 15-19
- 17 **Nelson DR**, Koymans L, Kamataki T, Stegeman JJ, Feyereisen R, Waxman DJ, Waterman MR, Gotoh O, Coon MJ, Estabrook RW, Gunsalus IC, Nebert DW. P450 superfamily: update on new sequences, gene mapping, accession numbers and nomenclature. *Pharmacogenetics* 1996; **6**: 1-42
- 18 **Umeno M**, McBride OW, Yang CS, Gelboin HV, Gonzalez FJ. Human ethanol-inducible P450IIE1: complete gene sequence, promoter characterization, chromosome mapping, and cDNA-directed expression. *Biochemistry* 1988; **27**: 9006-9013
- 19 **Umeno M**, Song BJ, Kozak C, Gelboin HV, Gonzalez FJ. The rat P450IIE1 gene: complete intron and exon sequence, chromosome mapping, and correlation of developmental expression with specific 5' cytosine demethylation. *J Biol Chem* 1988; **263**: 4956-4962
- 20 **Tsutsumi M**, Takada A, Wang JS. Genetic polymorphisms of cytochrome P4502E1 related to the development of alcoholic liver disease. *Gastroenterology* 1994; **107**: 1430-1435
- 21 **Ueshima Y**, Tsutsumi M, Takase S, Matsuda Y, Kawahara H. Acetaminophen metabolism in patients with different cytochrome P-4502E1 genotypes. *Alcohol Clin Exp Res* 1996; **20**(1 Suppl): 25A-28A
- 22 **Wong NA**, Rae F, Simpson KJ, Murray GD, Harrison DJ. Genetic polymorphisms of cytochrome p4502E1 and susceptibility to alcoholic liver disease and hepatocellular carcinoma in a white population: a study and literature review, including meta-analysis. *Mol Pathol* 2000; **53**: 88-93
- 23 **Chen CJ**, Yu MW, Liaw YF. Epidemiological characteristics and risk factors of hepatocellular carcinoma. *J Gastroenterol Hepatol* 1997; **12**: S294-308
- 24 **Yu MW**, Gladek-Yarborough A, Chiamprasert S, Santella RM, Liaw YF, Chen CJ. Cytochrome p4502E1 and glutathione S-transferase M1 polymorphisms and susceptibility to hepatocellular carcinoma. *Gastroenterology* 1995; **109**: 1266-1273
- 25 **Ladero JM**, Agundez JA, Rodriguez-Lescure A, Diaz-Rubio M, Benitez J. RsaI polymorphism at the cytochrome P4502E1 locus and risk of hepatocellular carcinoma. *Gut* 1996; **39**: 330-333
- 26 **Rumack BH**. Acetaminophen hepatotoxicity: the first 35 years. *J Toxicol Clin Toxicol* 2002; **40**: 3-20
- 27 **Johansson I**, Eliasson E, Norsten C, Ingelman-Sundberg M. Hydroxylation of acetone by ethanol-and acetone-inducible cytochrome P-450 in liver microsomes and reconstituted membranes. *FEBS Lett* 1986; **196**: 59-64
- 28 **Nakajima T**, Elovaara E, Park SS, Gelboin HV, Hietanen E, Vainio H. Immunochemical characterization of cytochrome P-450 isozymes responsible for benzene oxidation in the rat liver. *Carcinogenesis* 1989; **10**: 1713-1717

Constitutive activation of Stat3 signaling pathway in human colorectal carcinoma

Xiang-Tao Ma, Shan Wang, Ying-Jiang Ye, Ru-Yu Du, Zhi-Rong Cui, Ma Somsouk

Xiang-Tao Ma, Shan Wang, Ying-Jiang Ye, Ru-Yu Du, Department of Surgery, Peking University People's Hospital, Beijing 100044, China

Zhi-Rong Cui, Division of Surgical Oncology, Peking University People's Hospital, Beijing 100044, China

Ma Somsouk, Gastrointestinal Unit, Department of Medicine, Massachusetts General Hospital, Harvard Medical School, 32 Fruit Street, Boston, MA 02114, USA

Supported by the National Natural Science Foundation of China, No. 30271269

Correspondence to: Dr. Shan Wang, Department of Surgery, Peking University People's Hospital, Beijing 100044, China. shwang60@sina.com

Telephone: +86-10-68792772 **Fax:** +86-10-68318386

Received: 2003-10-24 **Accepted:** 2003-12-08

Abstract

AIM: Signal transducers and activators of transcription (STATs) are a family of transcription factors activated in response to cytokines and growth factors. Constitutive activation of Stat3 has been observed in a growing number of tumor-derived cell lines, as well as tumor specimens from human cancers. The purpose of this study was to investigate the expression of p-Stat3, activated form of Stat3, and its downstream mediators including cyclin D1 and Bcl-x_L in colorectal carcinoma (CRC), and to explore the possible mechanism of Stat3 signaling pathway in the tumorigenesis of colorectal carcinoma.

METHODS: Tissue samples from 45 patients of primary colorectal carcinoma were selected for studying Stat3 signaling pathway protein expression. Western blot analysis was used to measure the expression of p-Stat3, cyclin D1, and Bcl-x_L proteins in colorectal carcinomas. Furthermore, the expression patterns of these proteins were analyzed for their distribution at the cellular level by immunohistochemical staining of the tissues.

RESULTS: Protein levels of p-Stat3, cyclin D1, and Bcl-x_L were increased in colorectal carcinomas compared with adjacent normal mucosae ($P < 0.05$). Elevated levels of p-Stat3 were correlated with the nodal metastasis and the stage ($P < 0.05$). Overexpression of cyclin D1 was associated with the nodal metastasis ($P < 0.05$). There was also a significant correlation between the expressions of p-Stat3 and cyclin D1 ($r = 0.382$, $P < 0.05$).

CONCLUSION: Constitutive activation of Stat3 may play an important role in the tumorigenesis of colorectal carcinoma, and the detailed mechanism of Stat3 signaling pathway in CRC deserves further investigation.

Ma XT, Wang S, Ye YJ, Du RY, Cui ZR, Somsouk M. Constitutive activation of Stat3 signaling pathway in human colorectal carcinoma. *World J Gastroenterol* 2004; 10(11): 1569-1573

<http://www.wjgnet.com/1007-9327/10/1569.asp>

INTRODUCTION

Colorectal carcinoma (CRC) is a very common malignancy in developed countries and the incidence of CRC has been increasing rapidly in the latter part of the twentieth century in urban China^[1,2]. Although there have been advances in surgical and cytotoxic treatments of colorectal carcinoma, the overall survival percentage has not changed in recent years. While significant progresses have been achieved in identifying oncogenes and tumor suppressor genes involved in the tumorigenesis of colorectal carcinoma, the molecular mechanisms in colorectal carcinoma are still poorly understood. Recently, with the delineation of important signal transduction cascades, it has become clear that the signal transducers and activators of transcription (STATs) signaling pathway may play an important role in the malignant transformation of a number of human malignancies^[3].

STATs are transcription factors activated in response to cytokines and growth factors. At present, seven STATs have been identified in mammals: Stat1, Stat2, Stat3, Stat4, Stat5a, Stat5 b, and Stat6. Stat5 a and Stat5 b are encoded by distinct genes whereas Stat1 and Stat3 exhibit two isoforms, each resulting from alternative splicing^[4]. These proteins have a conserved structural organization and range in size from 750 to 900 amino acids. Activated STATs rapidly translocate into nuclei, bind to recognition sequences in the promoter region of target genes, and regulate their transcription. Recent studies have demonstrated the essential roles of STATs proteins in modulating the process of cell proliferation, differentiation, and apoptosis^[5-7].

Constitutively activated STAT proteins have been observed in a wide variety of human tumor cell lines and primary tumors including leukemia, multiple myeloma, breast cancer, prostate cancer, and other cancers^[8-13]. Further investigation demonstrated that activation of Stat3 was associated with the transformation by v-Src and other viral oncoproteins^[13-15]. Stat3 has been classified as an oncogene because constitutively activated Stat3 was found to mediate oncogenic transformation in cultured cells and tumor formation in nude mice^[16,17]. Stat3 activation may not only provide a growth advantage, but also confer resistance to conventional therapies that rely on the mechanism of apoptosis to eliminate tumor cells^[18]. The events downstream from constitutive activation of Stat3 that promote tumorigenesis are unclear but could include deregulation of cell cycle progression and/or providing protection against apoptosis. Recent studies showed that constitutive activation of Stat3 correlated with cyclin D1 expression and might provide a prognostic marker in head and neck cancer^[19], and activated Stat3 contributed to the process of apoptosis in ovarian cancer cells by regulating the expression of Bcl-x_L^[20]. These findings suggest that constitutive activation of Stat3 participates in the development of different human malignancies. However, the expression and activation of Stat3 protein in human colorectal carcinomas have not been studied. It is important to know whether or not constitutive activation of Stat3 signaling pathway plays a central role in human colorectal carcinomas.

In the present study, we examined the expression of p-Stat3, the activated form of Stat3, cyclin D1, and Bcl-x_L in 45 primary

tumor samples obtained from patients with CRC. Our results demonstrate that constitutive activation of Stat3 signaling pathway may play an important role in the tumorigenesis of colorectal carcinoma. Furthermore, activation of Stat3 is correlated with the overexpression of cyclin D1 in colorectal carcinoma.

MATERIALS AND METHODS

Materials

PVDF membranes for Western blot analysis were purchased from Millipore (Bedford, MA), and x-ray film was from Eastman Kodak (Rochester, NY). All antibodies were from Santa Cruz Biotechnology (Santa Cruz, CA). Prestained molecular mass markers were from GIBCO/BRL (Grand Island, NY). The enhanced chemiluminescence (ECL) system for Western blot analysis was from Amersham (Arlington Heights, IL). Concentrated protein assay dye reagents were from Bio-Rad Laboratories (Hercules, CA). All other reagents were of molecular biology grade and were purchased from either Sigma (St. Louis, MO) or Amresco (Solon, OH).

Patients and tissue samples

Primary colorectal adenocarcinomas and adjacent normal mucosae distant from the tumor (5-10 cm away) were obtained from 45 patients undergoing colorectal cancer resection at the Department of Surgery, Peking University People's Hospital from February, 1999 to February, 2000. No patient had received chemotherapy or radiation therapy before surgery. The samples were collected after informed consent was obtained from the patients at the time of surgery. Malignant tissues and adjacent normal mucosae were immediately snap-frozen in liquid nitrogen within 15-20 min after surgical removal to ensure preservation of Stat3 activities. Detailed clinicopathological parameters including gender, age, site of primary tumor, stage, and degree of differentiation are shown in Table 1. Staging of the tumors was conducted according to the American Joint Committee on Cancer (AJCC)/International Union Against Cancer (UICC) TNM Classification after brief histological studies.

Table 1 Clinicopathological parameters of 45 patients with colorectal carcinoma

Clinicopathological parameters		Numbers (%)
Gender	Male	24 (53.3)
	Female	21 (46.7)
Age (yr)	Range	35-81
	Mean	61.7
	Median	66.0
Primary site	Colon	25 (55.6)
	Rectum	20 (44.4)
	I	1 (0.22)
	II	24 (53.3)
	III	14 (31.1)
Depth of invasion and Lymph node involvement	IV	6 (13.3)
	T1-T2 N0	7 (15.6)
	T3-T4 N0	18 (40.0)
	T1-T2 N1-2N2	12 (26.7)
Distant Metastasis	T3-T4 N1-N2	8 (17.8)
	M0	39 (86.7)
	M1	6 (13.3)
Histological grade	G1	12 (26.7)
	G2	22 (48.9)
	G3	11 (24.4)
Tumor size	>5 cm	22 (48.9)
	≤5 cm	23 (51.1)

T1: tumor invades the submucosa; T2: tumor invades the mus-

cularis propria; T3: tumor invades through the muscularis propria into the subserosa or perirectal tissues; T4: tumor directly invades other organs or structures and/or perforates visceral peritoneum; N0: no regional lymph node metastasis; N1: metastasis in one to three regional lymph nodes; N2: metastasis in four or more regional lymph nodes; M0: no distant metastasis; M1: distant metastasis; G1: well differentiated tumor; G2: moderately differentiated tumor; G3: poorly differentiated tumor.

Western blot analysis

Tissues were lysed with lysis buffer (150 mmol/L NaCl, 10 g/L sodium deoxycholate, 10 g/L Triton X-100, 1 g/L SDS, 10 mmol/L Tris, pH 7.2, 1 mmol/L Na₃VO₄, 1 mmol/L phenylmethylsulfonyl fluoride, 1 mmol/L NaF, 0.1 mmol/L aprotinin, and 1 mmol/L leupeptin). After centrifugation at 13 000 g for 30 min at 4 °C, the protein concentrations in the cell lysates were determined by the Bradford assay. For Western blot analysis, whole cell extracts were mixed with 2×sodium dodecyl sulfate (SDS) sample buffer (125 mmol/L Tris·HCl, pH 6.8, 40 g/L SDS, 200 mL/L glycerol, 100 mL/L 2-mercaptoethanol) at 1:1 ratio and were heated for 5 min at 100 °C. Proteins (50 µg/lane) were separated by electrophoresis on 7.5-10% gradient SDS-polyacrylamide gel and transferred onto a PVDF membrane. Prestained molecular weight markers were included in each gel. Membranes were blocked for 30 min in Tris-buffered saline (TBS: 10 mmol/L Tris·HCl, pH 7.5 and 150 mmol/L NaCl) with 5 g/L Tween-20 (TBST) and 50 g/L BSA. After blocking, membranes were incubated at 4 °C overnight with Stat3 (C-20) phospho-independent, phospho-specific (Tyr-705) p-Stat3 (B-7); cyclin D1 (M-20), and Bcl-x_L (H-62) antibody in TBST and 10 g/L BSA respectively. Additionally, anti-glyceraldehydes-3-phosphate dehydrogenase (GAPDH) antibody was used to determine the amount of endogenous GAPDH protein to serve as an internal control. After the membranes were washed three times with TBST (5 min each), they were incubated with horseradish peroxidase-conjugated secondary antibody in TBST and 10 g/L BSA for 30 min. Subsequently, membranes were washed three times with TBST and developed by using the enhanced chemiluminescence (ECL) detection system. The optical density (OD) was measured by densitometry using a Storm PhosphoImager (Molecular Dynamics, Sunnyvale, CA) and the result was shown as relative expression for tumor (T) versus normal mucosae (N).

Immunohistochemical staining

Tissue samples were fixed in 40 g/L buffered formaldehyde, and embedded in paraffin. Five-micrometer sections of normal mucosa and colorectal carcinoma were cut and mounted onto poly-L-lysine-coated glass slides, air-dried, and heated for 2 h at 60 °C in an oven. The sections were dewaxed in xylene, rehydrated in descending alcohols, and endogenous peroxidase activity was blocked using 3 mL/L H₂O₂-methanol solution. These sections were then subjected to an antigen retrieval procedure; slides were heated in citrate buffer 10 mmol/L (pH 6.0) for 10 min. The sections were then cooled and washed in phosphate-buffered saline (pH 7.4) and nonspecific binding sites were blocked by incubating with 50 mL/L goat serum for 30 min in a humidified chamber at room temperature. The slides were incubated at 4 °C overnight with appropriate primary antibody [Stat3 (C-20), dilution 1:75; p-Stat3 (B-7), dilution 1:150; cyclin D1 (M-20), dilution 1:100; Bcl-x_L (H-62), dilution 1:100]. Immunologic reaction was developed using 3-3'-diaminobenzidine in TBS containing 0.2 mL/L hydrogen peroxide. The slides were counterstained with hematoxylin. Negative controls were performed by substituting the primary antibody with Tris-buffered saline.

Statistical analysis

Statistical analysis was performed with SPSS software version 10.0 (SPSS Inc., Chicago, IL). Data were presented as mean±SD.

The relationship between levels of p-Stat3, cyclin D1 or Bcl-x_L and various clinicopathological parameters was determined by Student's *t* test or one-way ANOVA. The association between p-Stat3, cyclin D1 and Bcl-x_L expression was analyzed by Pearson's correlation coefficient. $P < 0.05$ was considered statistically significant.

RESULTS

Activated Stat3 was constitutively expressed in colorectal carcinoma

One objective was to determine whether Stat3 was constitutively activated in human colorectal carcinoma and whether activation of Stat3 correlated with various clinicopathological parameters in patients with CRC. To determine whether Stat3 was activated in CRC, we performed Western blot analysis using antibody to p-Stat3, activated form of Stat3. Representative cases are shown in Figure 1. Of the 45 CRC samples examined, 57.8% (26 of 45) of the samples showed strong p-Stat3 expression. Quantitative evaluation of the relative expression (tumor versus normal mucosae) of these experiments demonstrated an average 2.6-fold increase in the level of p-Stat3 protein in cancers compared with adjacent normal mucosae ($P = 0.002$, Table 2). Both cytoplasmic and nuclear localizations of the Stat3 (p-Stat3) were detected in CRC primary tumors (Figure 2). When we examined possible correlations with various clinicopathological parameters, we found that increased levels of p-Stat3 were significantly correlated with the existence of nodal metastasis ($P = 0.018$). We also found that the levels of p-Stat3 were increased in stages III and IV, whereas its levels were decreased in stages I and II ($P = 0.026$). No statistically significant correlation was observed between p-Stat3 expression and gender, age, primary site, size, and grade of tumors (Table 3).

Expression of downstream mediators of Stat3 in colorectal carcinoma

We next investigated the expression of cyclin D1 and Bcl-x_L, which could be potential downstream mediators of Stat3 in

CRC. We found that cyclin D1 and Bcl-x_L were overexpressed in CRC tissues ($P < 0.05$, Table 2). When we examined possible correlations with various clinicopathological parameters, we found that increased expression of cyclin D1 correlated with the nodal metastasis ($P = 0.041$), whereas increased expression of Bcl-x_L did not significantly correlate with any of these parameters (Figure 1, Table 3). The expression pattern of cyclin D1 and Bcl-x_L was also checked with immunohistochemistry. Representative examples of immunohistochemical staining are shown in Figure 2. Furthermore, we studied the possible correlations between expression of p-Stat3 and downstream mediators. When these data were analyzed by Pearson's correlation coefficient, we found a significant association between expressions of p-Stat3 and cyclin D1 ($r = 0.382$, $P < 0.05$). No statistically significant correlation was observed between p-Stat3 and Bcl-x_L expressions ($r = 0.162$, $P > 0.05$).

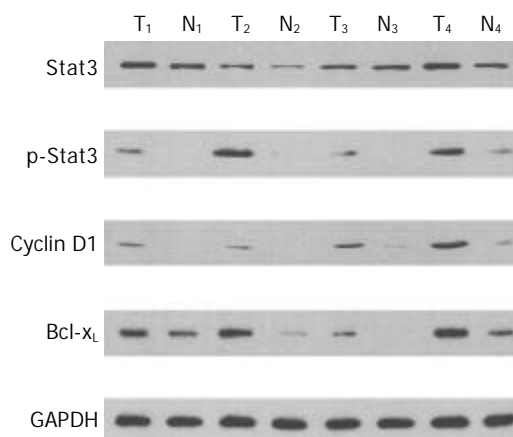


Figure 1 Expressions of Stat3, p-Stat3, cyclin D1, and Bcl-x_L in colorectal carcinoma. Lysates were made as described under Materials and Methods. GAPDH represents the internal protein control. Elevated levels of Stat3, p-Stat3 (Tyr-705), cyclin D1, and Bcl-x_L in tumor (T) tissues were compared to adjacent normal mucosae (N).

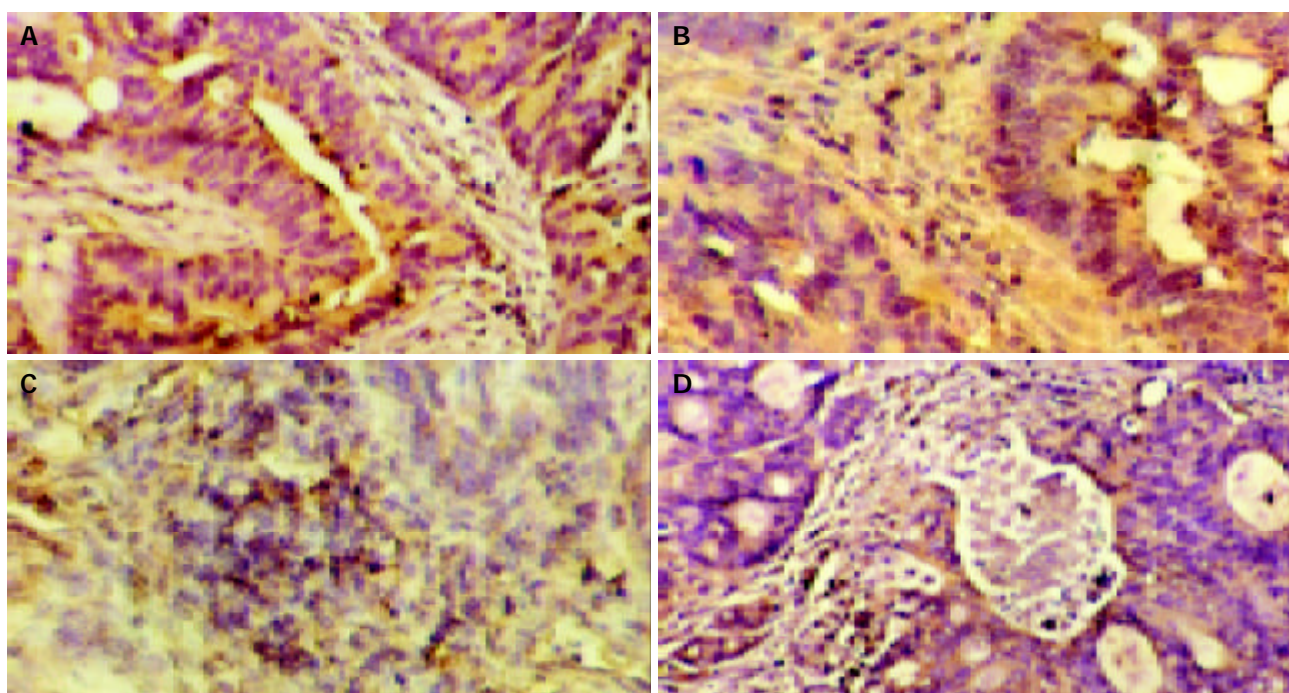


Figure 2 Expressions of Stat3, p-Stat3, cyclin D1, and Bcl-x_L in colorectal carcinoma. A: Cytoplasmic staining of Stat3 in CRC (original magnification $\times 200$); B: Nuclear staining of p-Stat3 in CRC (original magnification $\times 200$); C: Nuclear staining of cyclin D1 in CRC (original magnification $\times 200$); D: Cytoplasmic staining of Bcl-x_L (original magnification $\times 200$).

Table 2 Expressions of p-Stat3, cyclin D1, and Bcl-x_L in colorectal carcinoma (mean±SD)

Items	n	Percentage (%)	A Value		t	P
			Tumor	Normal		
p-Stat3	45	57.8 (26/45)	114 263±53 598	55 971±28 762	3.573	0.002
cyclin D1	45	64.4 (29/45)	58 321±24 872	22 563±11 160	5.191	0.0001
Bcl-x _L	45	68.9 (31/45)	71 032±43 425	37 281±14 622	4.627	0.0001

Table 3 Correlations between p-Stat3, cyclin D1, Bcl-x_L and clinicopathological parameters in colorectal carcinoma (mean±SD)

Item	n	p-Stat3	P	cyclin D1	P	Bcl-x _L	P
Gender							
Male	24	2.7±0.6	0.846	4.1±1.6	0.913	3.7±1.2	0.746
Female	21	2.5±0.5		4.3±1.8		3.3±1.1	
Age (yr)							
≥65	22	2.8±0.7	0.736	4.8±2.1	0.825	3.4±1.5	0.870
<65	23	2.4±0.4		3.6±1.3		3.6±0.8	
Stage							
III+IV	20	3.6±0.6	0.026	5.2±1.9	0.065	4.2±1.3	0.235
I+II	25	1.8±0.5		3.4±1.5		3.1±1.0	
Histological							
Grade							
G1	12	2.3±0.5	0.778	4.7±1.8	0.732	3.9±1.3	0.894
G2	22	2.4±0.6	0.645	4.2±1.4	0.627	3.3±1.0	0.771
G3	11	3.4±0.6	0.530	3.6±2.2	0.565	3.6±1.2	0.832
Node							
Metastasis							
Positive	27	3.8±0.8	0.018	5.5±1.9	0.041	4.4±1.4	0.162
Negative	18	1.6±0.4		3.3±1.5		2.9±1.0	
Distant							
Metastasis							
M1	6	3.6±0.8	0.638	5.4±2.2	0.612	5.2±1.6	0.324
M0	39	2.5±0.5		4.0±1.6		3.3±1.1	
Tumor Size							
≥5 cm	22	3.0±0.7	0.582	4.5±1.8	0.776	3.8±1.3	0.735
<5 cm	23	2.2±0.4		3.9±1.6		3.2±1.0	

G1: well differentiated tumor, G2: moderately differentiated tumor, G3: poorly differentiated tumor, M0: no distant metastasis, M1: distant metastasis.

DISCUSSION

Though significant progresses have been achieved in delineating the molecular mechanisms of colorectal carcinoma tumorigenesis, specific signal transduction pathways involved in CRC have not been fully characterized^[21]. Increasing reports suggested that Stat3 signaling pathway played a critical role in malignant transformation and tumor progression^[3]. Constitutive activation of Stat3 has been detected in a wide variety of human primary tumors and tumor cell lines including blood malignancies, breast cancer, and other cancers^[8-13]. In the current study, we provided evidences that constitutive activation of Stat3 signaling might play an important role in human colorectal carcinoma.

Western blot analysis with p-Stat3 antibody showed that the activated form of Stat3 was elevated in the majority (57.8%) of CRC samples. Both cytoplasmic and nuclear localizations of Stat3 (p-Stat3) were also detected in CRC primary tumors. Nagpal *et al.*^[22] reported in their work on head and neck carcinomas that 58.9% (53/90) of HNSCC tumors showed very high Stat3 protein accumulation, and none of the normal epithelium samples showed Stat3 absence. Campbell *et al.*^[23] found that in 51 human primary tissues from normal prostate, benign prostatic hyperplasia, and prostate cancer, p-Stat3 was observed more

prominently in the nuclei of cells residing in malignant glands compared to those in nonmalignant samples. As previously discussed, there were a growing number of evidences associating constitutive or aberrant activation of Stat3 with human cancers. The presence of p-Stat3 and its up-regulation in colorectal carcinoma could have important implications in colorectal cancer biology.

Because the above results provided evidence that Stat3 was constitutively activated in colorectal carcinomas, it was of interest to determine whether activation of stat3 correlated with various clinicopathological parameters in patients with CRC. When we examined possible correlations with various parameters, we found that increased levels of p-Stat3 significantly correlated with the existence of nodal metastasis and its stage but not with other parameters. Masuda *et al.*^[19] indicated in their work on HNSCC, that elevated levels of the activated form of Stat3 had a significant association with the clinical stage of HNSCC. Ni *et al.*^[24,25] demonstrated that Stat3 DNA binding activity was correlated with malignant potential in both human prostate cancer cell lines and a large series of rat Dunning prostate cancer cell lines. The most aggressive cell lines were found to have the highest Stat3 DNA binding activities. Blockade of activated Stat3 by dominant-negative Stat3 constructs significantly suppressed their growth *in vitro* and tumorigenicity *in vivo*. This specific activation of Stat3 in the tumorigenesis of colorectal carcinoma could qualify it as a potential diagnostic marker.

Tumor progression could be facilitated by activation of genes that regulate proliferation and/or apoptosis. However, the downstream events from constitutively activated Stat3 are not fully understood. Cyclin D1, an important cell cycle regulator, was overexpressed and associated with the poor prognosis in colorectal carcinoma^[26]. We investigated the expression of cyclin D1 in CRC tissues. When we examined possible correlations with various parameters, we found that increased levels of cyclin D1 correlated with the nodal metastasis, and there was a significant correlation between overexpressions of p-Stat3 and cyclin D1. However, the precise mechanism underlying the overexpression of cyclin D1 in CRC is unclear. In the majority of the cases of CRC, cyclin D1 gene was not amplified, suggesting that the increased expression of cyclin D1 was due to defects at the level of gene transcription^[27]. The similar discrepancy between cyclin D1 overexpression and gene amplification was also reported in breast and HNSCC cancers^[28,29]. Constitutive activation of Stat3 constructs has been shown to activate the cyclin D1 promoter in rodent fibroblast cell lines^[16], and overexpression of cyclin D1 was associated with increased activation of Stat3 in ovarian carcinoma and HNSCC^[20,30]. Therefore, frequent overexpression of cyclin D1 in CRC might be attributable, at least in part, to increased levels of p-Stat3.

Another important downstream mediator is Bcl-x_L. Bcl-x_L is a member of Bcl-2 family that could play a critical role in apoptosis^[31]. Previous studies showed that Bcl-x_L was overexpressed in colorectal carcinomas, and Bcl-x_L might be a useful prognostic marker in CRC^[32,33]. We also found that Bcl-x_L was overexpressed in CRC tissues, but the increased protein level did not significantly correlate with the clinicopathological parameters in CRC. No statistically significant correlation was observed between p-Stat3 and Bcl-x_L expressions. Bromberg *et al.*^[16] observed that Stat3 could transcriptionally up-regulate the expression of Bcl-x_L in Stat3 transformed cell lines. Evidence suggested that blocking of the activated Stat3 in multiple myeloma cells and ovarian cancer cells could down-regulate the expression of Bcl-x_L and enhance the apoptosis, and the cells regained the sensitivity to chemotherapy^[9,20]. The precise mechanism by which activation of Stat3 enhances the transcription of Bcl-x_L in CRC remains to be determined.

Our results demonstrated that in comparison with normal

mucosae, p-Stat3 protein was overexpressed in human colorectal carcinomas. Expression of p-Stat3 was associated with the presence of nodal metastasis and its stage. Our clinical data also provides evidence that there is a strong association of p-Stat3 and cyclin D1 overexpression in CRC. These results suggest that constitutive activation of Stat3 signaling pathway may play an important role in the tumorigenesis of colorectal carcinoma, and the detailed mechanism of Stat3 signaling pathway in CRC deserves further investigation.

ACKNOWLEDGEMENTS

We appreciate the technical assistance of Dr. Li-Mei Ma at Cornell University Weill Medical College and Dr. Cong-Rong Yu at Columbia University.

REFERENCES

- Jemal A**, Thomas A, Murray T, Thun M. Cancer statistics, 2002. *CA Cancer J Clin* 2002; **52**: 23-47
- Jin F**, Devesa SS, Chow WH, Zheng W, Ji BT, Fraumeni JF Jr, Gao YT. Cancer incidence trends in urban shanghai, 1972-1994: an update. *Int J Cancer* 1999; **83**: 435-440
- Bromberg J**. Stat proteins and oncogenesis. *J Clin Invest* 2002; **109**: 1139-1142
- Darnell JE Jr**. STATs and gene regulation. *Science* 1997; **277**: 1630-1635
- Levy DE**, Darnell JE Jr. Stats: transcriptional control and biological impact. *Nat Rev Mol Cell Biol* 2002; **3**: 651-662
- Smithgall TE**, Briggs SD, Schreiner S, Lerner EC, Cheng H, Wilson MB. Control of myeloid differentiation and survival by Stats. *Oncogene* 2000; **19**: 2612-2618
- Mora LB**, Buettner R, Seigne J, Diaz J, Ahmad N, Garcia R, Bowman T, Falcone R, Fairclough R, Cantor A, Muro-Cacho C, Livingston S, Karras J, Pow-Sang J, Jove R. Constitutive activation of Stat3 in human prostate tumors and cell lines: direct inhibition of Stat3 signaling induces apoptosis of prostate cancer cells. *Cancer Res* 2002; **62**: 6659-6666
- Spiekermann K**, Biethahn S, Wilde S, Hiddemann W, Alves F. Constitutive activation of STAT transcription factors in acute myelogenous leukemia. *Eur J Haematol* 2001; **67**: 63-71
- Catlett-Falcone R**, Landowski TH, Oshiro MM, Turkson J, Levitzki A, Savino R, Ciliberto G, Moscinski L, Fernandez-Luna JL, Nunez G, Dalton WS, Jove R. Constitutive activation of Stat3 signaling confers resistance to apoptosis in human U266 myeloma cells. *Immunity* 1999; **10**: 105-115
- Garcia R**, Bowman TL, Niu G, Yu H, Minton S, Muro-Cacho CA, Cox CE, Falcone R, Fairclough R, Parsons S, Laudano A, Gazit A, Levitzki A, Kraker A, Jove R. Constitutive activation of Stat3 by the Src and JAK tyrosine kinases participates in growth regulation of human breast carcinoma cells. *Oncogene* 2001; **20**: 2499-2513
- Dhir R**, Ni Z, Lou W, DeMiguel F, Grandis JR, Gao AC. Stat3 activation in prostatic carcinomas. *Prostate* 2002; **51**: 241-246
- Grandis JR**, Drenning SD, Zeng Q, Watkins SC, Melhem MF, Endo S, Johnson DE, Huang L, He Y, Kim JD. Constitutive activation of Stat3 signaling abrogates apoptosis in squamous cell carcinogenesis *in vivo*. *Proc Natl Acad Sci U S A* 2000; **97**: 4227-4232
- Feng DY**, Zheng H, Tan Y, Cheng RX. Effect of phosphorylation of MAPK and Stat3 and expression of c-fos and c-jun proteins on hepatocarcinogenesis and their clinical significance. *World J Gastroenterol* 2001; **7**: 33-36
- Bromberg JF**, Horvath CM, Besser D, Lathem WW, Darnell JE Jr. Stat3 activation is required for cellular transformation by v-src. *Mol Cell Biol* 1998; **18**: 2553-2558
- Bowman T**, Broome MA, Sinibaldi D, Wharton W, Pledger WJ, Sedivy JM, Irby R, Yeatman T, Courtneidge SA, Jove R. Stat3-mediated Myc expression is required for Src transformation and PDGF-induced mitogenesis. *Proc Natl Acad Sci U S A* 2001; **98**: 7319-7324
- Bromberg JF**, Wrzeszczynska MH, Devgan G, Zhao Y, Pestell RG, Albanese C, Darnell JE Jr. Stat3 as an oncogene. *Cell* 1999; **98**: 295-303
- Bowman T**, Garcia R, Turkson J, Jove R. STATs in oncogenesis. *Oncogene* 2000; **19**: 2474-2488
- Real PJ**, Sierra A, De Juan A, Segovia JC, Lopez-Vega JM, Fernandez-Luna JL. Resistance to chemotherapy via Stat3-dependent overexpression of Bcl-2 in metastatic breast cancer cells. *Oncogene* 2002; **21**: 7611-7618
- Masuda M**, Suzui M, Yasumatu R, Nakashima T, Kuratomi Y, Azuma K, Tomita K, Komiyama S, Weinstein IB. Constitutive activation of signal transducers and activators of transcription 3 correlates with cyclin D1 overexpression and may provide a novel prognostic marker in head and neck squamous cell carcinoma. *Cancer Res* 2002; **62**: 3351-3355
- Huang M**, Page C, Reynolds RK, Lin J. Constitutive activation of stat 3 oncogene product in human ovarian carcinoma cells. *Gynecol Oncol* 2000; **79**: 67-73
- Oving IM**, Clevers HC. Molecular causes of colon cancer. *Eur J Clin Invest* 2002; **32**: 448-457
- Nagpal JK**, Mishra R, Das BR. Activation of Stat-3 as one of the early events in tobacco chewing-mediated oral carcinogenesis. *Cancer* 2002; **94**: 2393-2400
- Campbell CL**, Jiang Z, Savarese DM, Savarese TM. Increased expression of the interleukin-11 receptor and evidence of STAT3 activation in prostate carcinoma. *Am J Pathol* 2001; **158**: 25-32
- Ni Z**, Lou W, Lee SO, Dhir R, DeMiguel F, Grandis JR, Gao AC. Selective activation of members of the signal transducers and activators of transcription family in prostate carcinoma. *J Urol* 2002; **167**: 1859-1862
- Ni Z**, Lou W, Leman ES, Gao AC. Inhibition of constitutively activated Stat3 signaling pathway suppresses growth of prostate cancer cells. *Cancer Res* 2000; **60**: 1225-1228
- Maeda K**, Chung Y, Kang S, Ogawa M, Onoda N, Nishiguchi Y, Ikehara T, Nakata B, Okuno M, Sowa M. Cyclin D1 overexpression and prognosis in colorectal adenocarcinoma. *Oncology* 1998; **55**: 145-151
- Tetsu O**, McCormick F. Beta-catenin regulates expression of cyclin D1 in colon carcinoma cells. *Nature* 1999; **398**: 422-426
- Lin SY**, Xia W, Wang JC, Kwong KY, Spohn B, Wen Y, Pestell RG, Hung MC. Beta-catenin, a novel prognostic marker for breast cancer: its roles in cyclin D1 expression and cancer progression. *Proc Natl Acad Sci U S A* 2000; **97**: 4262-4266
- Quon H**, Liu FF, Cummings BJ. Potential molecular prognostic markers in head and neck squamous cell carcinomas. *Head Neck* 2001; **23**: 147-159
- Kijima T**, Niwa H, Steinman RA, Drenning SD, Gooding WE, Wentzel AL, Xi S, Grandis JR. STAT3 activation abrogates growth factor dependence and contributes to head and neck squamous cell carcinoma tumor growth *in vivo*. *Cell Growth Differ* 2002; **13**: 355-362
- Tsujimoto Y**, Shimizu S. Bcl-2 family: life-or-death switch. *FEBS Lett* 2000; **466**: 6-10
- Krajewska M**, Moss SF, Krajewski S, Song K, Holt PR, Reed JC. Elevated expression of Bcl-X and reduced Bak in primary colorectal adenocarcinomas. *Cancer Res* 1996; **56**: 2422-2427
- Biroccio A**, Benassi B, D' Agnano I, D' Angelo C, Buglioni S, Mottolese M, Ricciotti A, Citro G, Cosimelli M, Ramsay RG, Calabretta B, Zupi G. c-Myb and Bcl-x overexpression predicts poor prognosis in colorectal cancer: clinical and experimental findings. *Am J Pathol* 2001; **58**: 1289-1299

Postprocessing techniques of CT colonography in detection of colorectal carcinoma

Ming-Yue Luo, Hong Shan, Li-Qing Yao, Kang-Rong Zhou, Wen-Wei Liang

Ming-Yue Luo, Hong Shan, Wen-Wei Liang, Department of Radiology, the Third Affiliated Hospital, Sun Yat-Sen University, Guangzhou 510630, Guangdong Province, China

Li-Qing Yao, Endoscopy Center, Zhongshan Hospital, Fudan University Medical School, Shanghai 200032, China

Kang-Rong Zhou, Department of Radiology, Zhongshan Hospital, Fudan University Medical School, Shanghai 200032, China

Correspondence to: Dr. Ming-Yue Luo, Department of Radiology, the Third Affiliated Hospital, Sun Yat-Sen University, Guangzhou 510630, Guangdong Province, China. myluo@yahoo.com.cn

Telephone: +86-20-85516867 **Fax:** +86-20-87536401

Received: 2003-06-04 **Accepted:** 2003-09-18

Abstract

AIM: To evaluate the value of postprocessing techniques of CT colonography, including multiplanar reformation (MPR), virtual colonoscopy (VC), shaded surface display (SSD) and Raysum, in detection of colorectal carcinomas.

METHODS: Sixty-four patients with colorectal carcinoma underwent volume scanning with spiral CT. MPR, VC, SSD and Raysum images were obtained by using four kinds of postprocessing techniques in workstation. The results were comparatively analyzed according to circumferential extent, lesion length and pathology pattern of colorectal carcinomas. All diagnoses were proved pathologically and surgically.

RESULTS: The accuracy of circumferential extent of colorectal carcinoma determined by MPR, VC, SSD and Raysum was 100.0%, 82.8%, 79.7% and 79.7%, respectively. There was a significant statistical difference between MPR and VC. The consistent rate of lesion length was 89.1%, 76.6%, 95.3% and 100.0%, respectively. There was a statistical difference between VC and SSD. The accuracy of discriminating pathology pattern was 81.3%, 92.2%, 71.9% and 71.9%, respectively. There was a statistical difference between VC and SSD. MPR could determine accurately the circumference of colorectal carcinoma, Raysum could determine the length of lesion more precisely than SSD, VC was helpful in discriminating pathology patterns.

CONCLUSION: MPR, VC, SSD and Raysum have advantage and disadvantage in detection of colorectal carcinoma, use of these methods in combination can disclose the lesion more accurately.

Luo MY, Shan H, Yao LQ, Zhou KR, Liang WW. Postprocessing techniques of CT colonography in detection of colorectal carcinoma. *World J Gastroenterol* 2004; 10(11): 1574-1577 <http://www.wjgnet.com/1007-9327/10/1574.asp>

INTRODUCTION

Multiplanar reformation (MPR), virtual colonoscopy (VC), shaded surface display (SSD) and Raysum images could be obtained after source data of CT colonography are processed

in workstation. Numerous literatures on CT colonography are based on examination of colon polyp^[1-17]. No research report on the diagnosis of colorectal carcinoma with postprocessing techniques of MPR, VC, SSD and Raysum is available. The aim of this study was to investigate the clinical value of four postprocessing techniques in detection of colorectal carcinomas by comparing the results of 64 colorectal carcinomas.

MATERIALS AND METHODS

Clinical data

Sixty-four patients (39 men, 25 women, aged 20-78 years, mean age 55.6 years) with colorectal carcinomas were studied. All cases were diagnosed surgically and pathologically.

Examination protocol

The whole procedure of CT colonography included patient preparation, volume scanning and image postprocessing^[18-20].

Patient preparation

A liquid diet for 48 h was used and 500 mL of 200 g/L mannite mixed with 1 000 mL of 50 g/L glycol saline solution was administered orally in the evening prior to examination.

Anisodamine hydrochloride injection (654-2) (10 mg) was administered intramuscularly 10 min before CT scanning to alleviate colon spasm, minimize peristalsis and allow optimal colonic distention. The patient lay on right lateral decubitus position on CT table after dwelling a rectal enema tube. Then, the patient lay on supine, and room air was gently insufflated into the colorectum to distend the colon as long as the patient was tolerable.

Volume scanning

A HighSpeed advantage helical CT scanner (General Electric Medical System) was used to acquire a standard scout view image of the abdomen and pelvis to assess the degree of colorectal distension, room air was further insufflated if required. Images were acquired by using 3.0 mm collimation with a pitch of 2.0, 100-120 mA, 120 kV, and a 512×512 matrix. The range of scanning encompassed the entire colon from the rectum to cecum.

Image postprocessing

Image reconstruction data were transferred to a workstation (Sun Sparc 20 workstation, GE Advantage Windows 2.0 image analysis software) via picture archive and communication system, after retro-reconstructing the initial image data of scanning with 1.5 mm thickness, 0.5 mm interval. MPR, VC, SSD and Raysum images were obtained with postprocessing techniques in workstation.

MPR image: axial, coronal, sagittal and oblique images were acquired with the center on colorectal carcinoma segment by using CT software to display wall, lumen and adjacent structure of the lesion.

VC image: intraluminal image was obtained by applying Navigator software with about - 700 HU threshold from the rectum to cecum. Lesions were observed with Fly-through program along the longitudinal lumen^[21].

SSD image: image reconstruction of colorectal area was performed with SSD software, then the interested colorectal segment were obtained by trimming off unnecessary part with Scalpel program, magnification and rotation were done to demonstrate colorectal carcinoma.

Raysum image: transparent image of interested colorectum was acquired by using Raysum software on the basis of SSD image to display the situation of endolumen and wall.

Statistical analysis

The following 3 aspects were comparatively analyzed according to surgery and pathology results. According to the invasive extent of colorectal carcinoma along the wall, tumors were divided into <1/2, 1/2-3/4 and >3/4 circumference. According to the longitudinal length of the lesion, it was classified into categories of 2.0-3.0 cm, 3.1-5.0 cm and 5.1-11.0 cm, respectively. The pathology pattern was classified into massive, ulcerous, infiltrative, ulcerous and infiltrative types.

Results of 4 kinds of postprocessing techniques were compared with surgical observation and pathology results. Accuracy of diagnosis with 4 kinds of postprocessing techniques was compared by using *U* test.

RESULTS

Examination results of circumferential extents, lesion lengths and pathology patterns in 64 colorectal carcinomas with 4 kinds of postprocessing techniques (Table 1)

Diagnostic accordance of 64 colorectal carcinomas with 4 kinds of postprocessing techniques (Table 2)

DISCUSSION

MPR, VC, SSD and Raysum images obtained by postprocessing technique displayed colorectal carcinoma in different manners with different clinical values.

Circumferential extent

The accuracy of circumferential extent of colorectal carcinoma determined with MPR, VC, SSD and Raysum was 100.0%, 82.8%,

79.7% and 79.7%, respectively (Tables 1, 2). Significant statistical difference between MPR and VC, MPR and SSD, MPR and Raysum were obtained, respectively.

Table 2 Diagnosis accordance of 64 colorectal carcinomas with postprocessing techniques

Postprocessing technique	Circumferential extent		Lesion length		Pathological pattern	
	Case (n)	%	Case (n)	%	Case (n)	%
MPR	64	100.0	57	89.1	52	81.2
VC	53	82.8	49	76.6	59	92.2
SSD	51	79.7	61	95.3	46	71.9
Raysum	51	79.7	64	100.0	46	71.9
χ^2 value		14.748 ^b		22.430 ^b		10.909 ^a

^a $P < 0.05$ vs pathological pattern, ^b $P < 0.01$ vs circumferential extent and lesion length.

MPR had two dimensional axial, coronal, sagittal and oblique reconstruction images in series, on the center of colorectal carcinoma segments. MPR might reflect different density tissues by using different attenuation scales with high density resolution and it has no obvious artifact. It could clearly display intraluminal lesion and range invaded by carcinoma along its wall and adjacent structure, and accurately determine the circumferential extent of colorectal carcinoma^[22].

VC, SSD and Raysum images could be obtained by using appropriate CT threshold values with transparency of the part beyond them, could make use of only certain information without favorable disclosure of lesions in detail. Sometimes, they had difficulty in showing directly the condition of colorectal wall when thickening was not obvious. Therefore, the determination of circumferential extent of colorectal carcinoma was not so accurate as MPR (Figure 1A-C).

Length of tumors

The correction rate of lesion lengths determined with MPR, VC, SSD and Raysum was 89.1%, 76.6%, 95.3% and 100.0%, respectively (Tables 1, 2).

Table 1 Circumferential extents, lesion lengths and pathology patterns in 64 colorectal carcinomas determined with postprocessing techniques

Item	S&p c	Diagnostic accordance (n)				Accurate diagnosis (%)			
		MPR	VC	SSD	Raysum	MPR	VC	SSD	Raysum
Circumf extent	64	64	53	51	51	100.0	82.8	79.7	79.7
<1/2 circum	7	7	6	6	6	100.0	85.7	85.7	85.7
1/2-3/4 circum	14	14	12	11	11	100.0	85.7	78.6	78.6
>3/4 circum	43	43	35	34	34	100.0	81.4	79.1	79.1
Lesion length (cm)	64	57	49	61	64	89.1	76.6	95.3	100.0
2.0-3.0	6	6	6	6	6	100.0	100.0	100.0	100.0
3.1-5.0	33	31	26	32	33	93.9	78.8	97.0	100.0
5.1-11.0	25	20	17	23	25	80.0	68.0	92.0	100.0
Pathology pattern	64	52	59	46	46	81.2	92.2	71.9	71.9
Massive type	38	32	38	27	27	84.2	100.0	71.1	71.1
Ulcerous type	5	4	4	3	4	80.0	80.0	60.0	80.0
Infiltrative type	13	11	12	11	12	84.6	92.3	84.6	92.3
Ulc and inf type	8	5	5	5	3	62.5	62.5	62.5	37.5

S & p c=Surgery and pathology case, Circumf=Circumferential, circum=circumference, Ulc and inf=Ulcerous and infiltrative. For circumferential extent, comparison between MPR and VC, $U=3.472$, $P < 0.001$; comparison between VC and SSD, $U=0.449$, $P > 0.05$; comparison between SSD and Raysum, $U=0.000$, $P > 0.05$. For Lesion length, comparison between MPR and VC, $U=1.875$, $P > 0.05$; comparison between VC and SSD, $U=3.034$, $P < 0.05$; comparison between SSD and Raysum $U=1.759$, $P > 0.05$. For pathologic pattern, comparison between MPR and VC, $U=1.817$, $P > 0.05$; comparison between VC and SSD, $U=2.991$, $P < 0.05$; comparison between SSD and Raysum, $U=0.000$, $P > 0.05$.



Figure 1 Massive rectal carcinoma in a 74 years old man. VC, SSD displayed an irregular mass, but unable to determine circumferential extent (A, B). MPR showed the mass with 1/4 circumference around rectal wall (C).

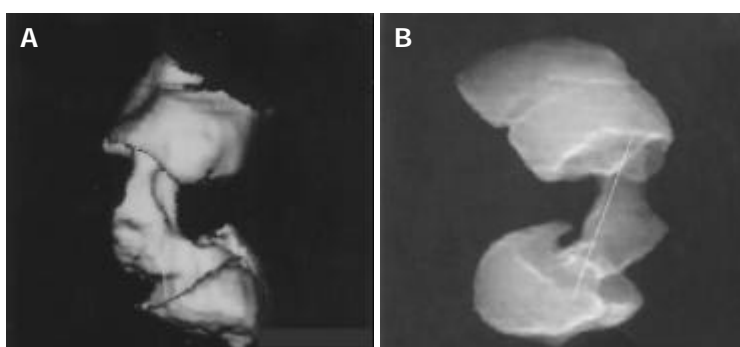


Figure 2 Infiltrative rectal carcinoma in a 46 years old man. SSD disclosed the two ends of carcinoma and measured its length (A). Raysum manifested the two ends of carcinoma more clearly and measured its length more accurately than SSD (B).

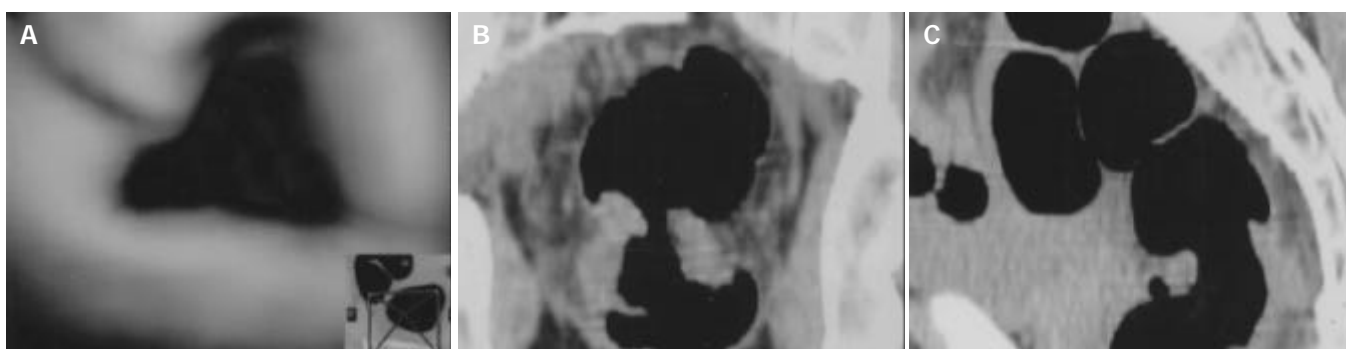


Figure 3 Infiltrative rectal carcinoma in a 48 years old man. VC demonstrated the carcinoma around rectal wall (A). Combination of coronal and sagittal images of MPR revealed an infiltrative carcinoma, but was not so obvious as VC (B, C).

SSD image displayed the surface of colorectal lumen from outside to inside, being similar to the image of filling phase in double contrast barium enema. It could be locally magnified and rotated polygonally to demonstrate colorectal carcinoma as clear as possible and show lesion lengths and morphology of two ends. But it utilized only certain information and did not reveal the lesion in detail due to the appropriate CT threshold value and transparency of the part beyond it. Moreover, because of partial covering of lesions by the colorectum, sometimes its manifestation was not quite precise^[23]. Its correction rate of lesion lengths was 95.3 % in our series.

Raysum was obtained on the basis of SSD image similar to the image of mucosa phase in double contrast barium enema. It could display the situation of endolumen and wall by transparency and avoid the disadvantages of partial overlapping of lesions by colorectum with SSD, hence clearly revealing lesion lengths and morphology at two ends and accurately manifesting the lesion lengths^[24] (Figure 2A, B).

MPR was a two dimensional image formed by reconstruction. But the colorectum was tortuous in structure, moreover, it was

complicated by the presence of colorectal carcinoma. Therefore, measurement of the lesion length with MPR was not accurate^[25]. In our study its accuracy was 89.1%.

VC could obtain virtual cubic images from colorectal endolumen. Its image was similar to that of fiberoptic colonoscopy. It could directly show the surface morphology of colorectal carcinoma, and its distal and proximal situations. But its manifestation of lesion lengths had a comparatively great error^[3,4,14,18,26-28]. The correct rate was only 76.6% in our series.

Pathological patterns

The accuracy of pathology patterns determined by MPR, VC, SSD and Raysum was 81.3%, 92.2%, 71.9% and 71.9%, respectively (Tables 1, 2). Significant statistical differences between VC and SSD were noticed.

VC image could disclose the surface morphology of colorectal carcinoma and its distal and proximal situations directly with observations from endolumen, favoring the discrimination of pathology patterns. However, there was certain difficulty in revealing the detail of carcinoma. It had errors in discriminating

pathology patterns^[29-30]. The correction rate was 92.2% in our study.

MPR was a two-dimensional image formed by reconstruction, and was combined with axial, coronal, sagittal and oblique images. But it had no direct three dimensional manifestation with a relative great error in discriminating pathology patterns (Figure 3A-C).

SSD, Raysum images could display the surface of colorectal lumen from outside to inside, similar to the images of filling and mucosa phase in double contrast barium enema. But they could use certain information and could not show carcinoma details, and were fairly inaccurate in discriminating pathology patterns. Its correction rate was only 71.9% in our series.

In conclusion, MPR, VC, SSD and Raysum have both advantage and disadvantage in detection of colorectal carcinoma. MPR can accurately determine the circumferential extent, Raysum can fairly determine the length of lesions, and is more trustworthy than SSD, VC is helpful in discriminating pathology patterns. Their combination can disclose colorectal carcinomas more accurately.

ACKNOWLEDGEMENTS

The authors are grateful to Zhongshan Hospital, Fudan University Medical School, Shanghai 200032, China, for its help in accomplishing of the study.

REFERENCES

- Podolsky DK.** Going the distance--the case for true colorectal-cancer screening. *N Engl J Med* 2000; **343**: 207-208
- Fletcher RH.** The end of barium enemas? *N Engl J Med* 2000; **342**: 1823-1824
- Bond JH.** Virtual colonoscopy--promising, but not ready for widespread use. *N Engl J Med* 1999; **341**: 1540-1542
- Fenlon HM, Nunes DP, Schroy PC 3rd, Barish MA, Clarke PD, Ferrucci JT.** A comparison of virtual and conventional colonoscopy for the detection of colorectal polyps. *N Engl J Med* 1999; **341**: 1496-1503
- Zalis ME, Perumpillichira J, Del Frate C, Hahn PF.** CT colonography: digital subtraction bowel cleansing with mucosal reconstruction initial observation. *Radiology* 2003; **226**: 911-917
- Yee J, Kumar NN, Hung RK, Akerkar GA, Kumar PR, Wall SD.** Comparison of supine and prone scanning separately and in combination at CT colonography. *Radiology* 2003; **226**: 653-661
- Summers RM, Jerebko AK, Franaszek M, Malley JD, Johnson CD.** Colonic polyps: complementary role of computer-aided detection in CT colonography. *Radiology* 2002; **225**: 391-399
- McFarland EG, Pilgram TK, Brink JA, McDermott RA, Santillan CV, Brady PW, Heiken JP, Balfe DM, Weinstock LB, Thyssen EP, Littenberg B.** CT colonography: multiobserver diagnostic performance. *Radiology* 2002; **225**: 380-390
- Lefere PA, Gryspeerdt SS, Dewyspelaere J, Baekelandt M, Van Holsbeeck BG.** Dietary fecal tagging as a cleansing method before CT colonography: initial results polyp detection and patient acceptance. *Radiology* 2002; **224**: 393-403
- Yoshida H, Masutani Y, MacEneaney P, Rubin DT, Dachman AH.** Computerized detection of colonic polyps at CT colonography on the basis of volumetric features: pilot study. *Radiology* 2002; **222**: 327-336
- Yee J, Akerkar GA, Hung RK, Steinauer-Gebauer AM, Wall SD, McQuaid KR.** Colorectal neoplasia: performance characteristics of CT colonography for detection in 300 patients. *Radiology* 2001; **219**: 685-692
- Summers RM, Johnson CD, Pusanik LM, Malley JD, Youssef AM, Reed JE.** Automated polyp detection at CT colonography: feasibility assessment in a human population. *Radiology* 2001; **219**: 51-59
- Ferrucci JT.** Colon cancer screening with virtual colonoscopy: promise, polyps, politics. *Am J Roentgenol* 2001; **177**: 975-988
- Luo MY, Zhou KR, Yao LQ.** Experimental study of simulated polyp in pig colon: detection with CT virtual colonoscopy. *Zhongguo Yixue Yingxiang Jishu* 2000; **16**: 719-721
- Luo MY, Zhou KR, Yao LQ.** Comparative study on the detecting colorectal polyps with virtual colonoscopy or other postprocessing techniques. *Linchuang Fangshexue Zazhi* 2000; **19**: 699-702
- Summers RM, Beaulieu CF, Pusanik LM, Malley JD, Jeffrey RB Jr, Glazer DI, Napel S.** Automated polyp detector for CT colonography: feasibility study. *Radiology* 2000; **216**: 284-290
- Macari M, Milano A, Lavelle M, Berman P, Megibow AJ.** Comparison of time-efficient CT colonography with two- and three-dimensional colonic evaluation for detecting colorectal polyps. *Am J Roentgenol* 2000; **174**: 1543-1549
- Luo M, Shan H, Zhou K.** CT virtual colonoscopy in patients with incomplete conventional colonoscopy. *Chin Med J* 2002; **115**: 1023-1026
- Zalis ME, Hahn PF.** Digital subtraction bowel cleansing in CT colonography. *Am J Roentgenol* 2001; **176**: 646-648
- Fletcher JG, Johnson CD, Welch TJ, MacCarty RL, Ahlquist DA, Reed JE, Harmsen WS, Wilson LA.** Optimization of CT colonography technique: prospective trial in 180 patients. *Radiology* 2000; **216**: 704-711
- Neri E, Giusti P, Battolla L, Vaghi P, Boraschi P, Lencioni P, Caramella D, Bartolozzi C.** Colorectal cancer: role of CT colonography in preoperative evaluation after incomplete colonoscopy. *Radiology* 2002; **223**: 615-619
- McFarland EG, Brink JA, Pilgram TK, Heiken JP, Balfe DM, Hirselj DA, Weinstock L, Littenberg B.** Spiral CT colonography: reader agreement and diagnostic performance with two- and three-dimensional image-display techniques. *Radiology* 2001; **218**: 375-383
- Hopper KD, Iyriboz AT, Wise SW, Neuman JD, Mauger DT, Kasales CJ.** Mucosal detail at CT virtual reality: surface versus volume rendering. *Radiology* 2000; **214**: 517-522
- Glick S.** double-contrast barium enema for colorectal cancer screening: a review of the issues and a comparison with other screening alternatives. *Am J Roentgenol* 2000; **174**: 1529-1537
- Macari M, Megibow AJ.** Pitfalls of using three-dimensional CT colonography with two-dimensional imaging correlation. *Am J Roentgenol* 2001; **176**: 137-143
- Makin GB, Breen DJ, Monson JR.** The impact of new technology on surgery for colorectal cancer. *World J Gastroenterol* 2001; **7**: 612-621
- Spinzi G, Belloni G, Martegani A, Sangiovanni A, Del Favero C, Minoli G.** Computed tomographic colonography and conventional colonoscopy for colon diseases: a prospective, blinded study. *Am J Gastroenterol* 2001; **96**: 394-400
- Mendelson RM, Foster NM, Edwards JT, Wood CJ, Rosenberg MS, Forbes GM.** Virtual colonoscopy compared with conventional colonoscopy: a developing technology. *Med J Aust* 2000; **173**: 472-475
- Pescatore P, Glucker T, Delarive J, Meuli R, Pantoflickova D, Duvoisin B, Schnyder P, Blum AL, Dorta G.** Diagnostic accuracy and interobserver agreement of CT colonography (virtual colonoscopy). *Gut* 2000; **47**: 126-130
- Johnson CD, Ahlquist DA.** Computed tomography colonography (virtual colonoscopy): a new method for colorectal screening. *Gut* 1999; **44**: 301-305

Dendritic cells from chronic hepatitis B patients can induce HBV antigen-specific T cell responses

Ruo-Bing Li, Hong-Song Chen, Yao Xie, Ran Fei, Xu Cong, Dong Jiang, Song-Xia Wang, Lai Wei, Yu Wang

Rou-Bing Li, Hong-Song Chen, Ran Fei, Xu Cong, Dong Jiang, Song-Xia Wang, Lai Wei, Yu Wang, Hepatology Institute, People's Hospital, Peking University, Beijing 100044, China

Yao Xie, Ditan Hospital, Beijing 100011, China

Supported by "973" Program No. G1999054106, National Natural Science Foundation of China, No. 30170047 and "863" Program No. 2001AA217151 and No. 2002AA217071

Co-correspondents: Yu Wang

Correspondence to: Dr. Hong-Song Chen, Hepatology Institute, People's Hospital, Peking University, Beijing 100044, China. chen2999@sohu.com

Telephone: +86-10-68314422 Ext 5726 **Fax:** +86-10-68321900

Received: 2003-09-06 **Accepted:** 2003-09-25

Abstract

AIM: To determine whether dendritic cells (DCs) from chronic hepatitis B patients could induce HBV antigen-specific T cell responses or not.

METHODS: DCs were generated from peripheral blood mononuclear cells of patients with chronic hepatitis B (CHB) infection and healthy donors. We compared the phenotypes of these DCs and their ability to secrete cytokines and to participate in mixed lymphocyte reactions. In addition, autologous lymphocytes were cultured with DCs loaded with HBV core region peptide HBcAg8-27, an epitope recognized by cytotoxic T lymphocytes (CTL), and bearing human leucocyte antigen (HLA)-A2 for 10 d. Cytokine secretion and lytic activity against peptide-pulsed target cells were assessed.

RESULTS: DCs with typical morphology were generated successfully by culturing peripheral blood mononuclear cells (PBMCs) from CHB patients with AIM-V containing GM-CSF and IL-4. Compared with DCs from normal donors, the level of CD80 expressed in DCs from CHB patients was lower, and DCs from patients had lower capacity of stimulate T cell proliferation. When PBMCs isolated from patients with chronic or acute hepatitis B infection and from normal donors were cocultured with HBcAg18-27 peptide, the antigen-specific memory response of PBMCs from acute hepatitis B patients was stronger than that of PBMCs from chronic hepatitis B patients or normal donors. PBMCs cocultured with DCs treated with HBcAg18-27 CTL epitope peptide induced an antigen-specific T cell reaction, in which the level of secreted cytokines and lytic activity were higher than those produced by memory T cells.

CONCLUSION: DCs from patients with CHB can induce HBV antigen-specific T cell reactions, including secretion of cytokines essential for HBV clearance and for killing cells infected with HBV.

Li RB, Chen HS, Xie Y, Fei R, Cong X, Jiang D, Wang SX, Wei L, Wang Y. Dendritic cells from chronic hepatitis B patients can induce HBV antigen-specific T cell responses. *World J Gastroenterol* 2004; 10(11): 1578-1582
<http://www.wjgnet.com/1007-9327/10/1578.asp>

INTRODUCTION

In patients infected by hepatitis B virus (HBV), the virus may easily escape from immune surveillance, thus inducing tolerance and becoming a persistent infection. Persistently infected patients produce a weak or undetectable HBV-specific CTL response^[1]. Therefore, when treating chronically infected patients with HBV, the population of T cells recognizing HBV should be increased, thus producing an effective immune response.

Dendritic cells (DCs) are the most potent antigen presenting cells throughout the body. These cells express high levels of MHC class I and II antigens, as well as costimulatory molecules, and play essential roles in triggering primary immune responses^[2,3]. The use of DCs, as a type of natural adjuvant, has been applied to the immunotherapy of melanomas and prostate gland carcinomas^[4]. In addition, administration of DCs activated by cytokines to transgenic mice has been shown to break CTL immune tolerance and induce specific CTL reactions against HBV^[5]. The aim of this study was to compare the anti-HBV activity of DCs derived from patients infected with HBV with those from healthy donors. DCs derived from different individuals were cultured, reacted with a peptide specific to the HBV antigen, HBcAg18-27, and cocultured with autogeneic PBMCs to determine if this procedure could induce antigen-specific CTL, which could then be utilized to kill target cells loaded with HBV antigens or to secrete specific cytokines.

MATERIALS AND METHODS

Patients

Of the HBV patients, four were studied during an episode of acute hepatitis B, and 12 (8 males, 4 females; average age, 38.3 years) were chronically infected with HBV. In addition, 20 patients were HLA-A2 positive, and 4 patients were HLA-A2 negative. We also included eight uninfected healthy volunteers (4 males, 4 females; average age, 35.2 years) as normal controls, of them six were HLA-A2 positive and two were HLA-A2 negative.

The diagnosis of acute and chronic hepatitis B was based on standard diagnostic criteria, as formulated by the 5th China Infection Disease and Parasitology Conference in 2000. HBV-infected patients had no complications of other organs. Normal controls had no clinical history of HBV infection and were serologically negative for HBV markers. All patients and normal controls were serologically negative for antibodies to HIV and HCV.

Cytokines and reagents

Recombinant human GM-CSF was purchased from Leucomax Corp (Germany), and recombinant human IL-4 and TNF- α were purchased from Peprotech Corp (England). Ficoll-Hypaque fluid was from Dingguo Corporation, Beijing. Mouse anti-human HLA-A*02 monoclonal antibody (BB7.2 cell line) was a gift from Professor. Wei-Feng Chen, and T₂ cell line was a gift from Professor. Yan-Fang Sui. FITC-conjugated mouse monoclonal antibodies to human CD86, CD14, and CD3, and PE-labeled mouse monoclonal antibodies to human CD80, HLA-DR, CD54, CD11c, and CD19, were obtained from B-D Corp (USA). Mouse monoclonal antibodies to human CD83 and CD1a, FITC- and

PE-labeled goat anti-mouse Ig (H+L) antibodies, PE-labeled mouse anti-human IFN- γ , TNF- α , and IL-2 were all purchased from Pharmingen Corp (USA). CytoTox 96 non-radioactive cytotoxicity assay kits were from Promega Corp (USA). AIMV and RPMI 1 640 were from GIBCO Corp (USA), and IL-12 ELISA kit was from Endogen Corp (USA).

Synthetic peptide

HLA-A2 restricted HBcAg18-27 CTL epitope peptide, FLPSDFFPSV, was synthesized by Saibaisheng Biological Corporation (Beijing) and purified to >90% homogeneity by HPLC. The lyophilized peptide was dissolved in DMSO at a concentration of 2 mg/mL, and stored at -20 °C.

Isolation of PBMCs

Following informed consent obtained from each subject, 100 mL anticoagulated venous blood was obtained from each, and peripheral blood mononuclear cells (PBMCs) were isolated by Ficoll-Hypaque density gradient centrifugation (density, 1.077). Cells at the interface were transferred to RPMI 1 640 incomplete medium containing 100 U/mL penicillin and 100 U/mL streptomycin, and washed twice.

Generation of DCs from PBMCs

DCs were cultured as described previously^[6,7] with slight modifications. PBMCs were suspended in DC culture medium (AIMV), plated at a density of 2×10^7 cells/well in 6-well polystyrene culture plates, and cultured overnight at 37 °C in 950 mL air/50 mL CO₂. Nonadherent cells were removed by gently swirling the plate, and the adherent cells were cultured in AIMV containing 1 000 U/mL recombinant human GM-CSF and 500 U/mL recombinant human IL-4 at 37 °C in 950 mL air/50 mL CO₂ and refed daily with half volumes of fresh medium. Cells and culture supernatants were harvested on d 3, 5, 7, 9, 11, 13, and 15. Where indicated, TNF- α (20 ng/mL) was added on d 7, and the cells and supernatant were harvested on d 9.

Flow cytometric analysis

The phenotype of harvested DCs was analyzed by flow cytometry (Becton Dickinson, FACScalibur). Cells (5×10^5) were suspended in PBS, centrifuged at 313 r/min for 5 min at 4 °C, incubated for 30 min at 4 °C with fluorescent monoclonal antibody, and fixed in 4 g/L paraformaldehyde.

IL-12 detection

IL-12 concentration in cell supernatants was assayed by ELISA, using standard curves according to the manufacturer's instructions.

Allogeneic mixed lymphocyte reaction

To test T cell stimulatory function of DCs, DCs were irradiated with ⁶⁰Co (3 000 rad), suspended in AIMV and placed in 96-well flat bottom culture plates at densities of 0.5, 1.0, and 2.5×10^4 cells/well. Responder T cells were added to each well, at a density of 5×10^5 cells/well, and cultured for 120 h. The ratio of DC:T was 1:20, 1:50, and 1:100, and each assay was performed in triplicate. T cells plated without DCs were utilized as negative controls. During the last 16 h of incubation, 1 Ci/well of [³H] thymidine was added. On d 5, the cells were harvested, and the amounts of [³H] thymidine incorporated into responder cells were counted with a beta counter.

Isolation of CD8⁺ T cells

Purified populations of T cells were isolated from PBMCs using magnetic beads. Briefly, PBMCs were incubated with anti-CD8 MACS (Miltenyi Biotech, Germany) according to the manufacturer's protocol. Cells retained by MACS beads were regarded as CD8 positive cells, with purity greater than 90%.

Stimulation of PBMCs with synthetic peptide

PBMCs from patients and normal donors were plated in 24-well plates at densities of 2×10^6 cells/well, in 2 mL RPMI 1 640 containing IL-2 (50 mg/L). Synthetic peptides were added to the cell cultures at a final concentration of 20 mg/L. As a negative control, DMSO alone was added to the wells. After 1 h, 0.7 μ L Golgistop was added per mL culture medium, cells were collected 4 h later, and intracellular cytokine stain (ICCS) was applied.

Intracellular cytokine stain assay

Harvested cells were washed twice with PBS, 10 μ L FITC-labelled mouse anti-human CD8 Ab was added to each tube, and the tubes were incubated in the dark on ice for 30 min. To each tube 250 μ L FACS permeabilization solution was added, and the tubes were incubated for 20 min on ice in the dark. Cells were washed twice with 1 mL/tube FACS perm-wash and incubated with PE-conjugated mouse monoclonal antibody to human IFN- γ , IL-2, or TNF- α for 30 min on ice in the dark. The cells were washed with FACS perm-wash solution, PBS + 1 g/L BSA was added, and the cells were loaded onto a FACS calibur flow cytometer within 24 h, with data analysis performed using Cell Quest software (Becton Dickinson). A total of 400 000 events were measured in each analysis. PE-conjugated mouse Ab was used as isotype controls. A lymphocyte gate was set to exclude monocytes, debris and dead cells.

CTL generation

CD8⁺ responders for peptide-specific CTL were generated from nonadherent PBMCs. CD8⁺ T cells were stimulated with DCs loaded with peptide at a stimulator-to-responder (S:R) ratio of 1:30. These cells were cultured in RPMI containing 100 g/L fetal calf serum (FCS) and IL-2 (50 mg/L). Responders were restimulated every 5 d with DCs pulsed with peptide. As controls, CD8⁺ T cells were stimulated with unpulsed DC. Six h before harvesting, 0.7 μ L Golgistop was added to per mL culture medium. On d 10, CD8⁺ T cells were harvested, ICCS was applied, and CTL cytotoxicity assays were performed.

CTL cytotoxicity assay

HLA-A2 restricted antigen recognition by CTL was assessed by a standard cytotox 96 non-radioactive cytotoxicity assay. Recognition of HBcAg18-27 peptide by CTL was assessed using T2 cells preincubated for 4 h with 20 μ g/mL peptide. Target cells were resuspended at a density of 1×10^5 cells/mL, thus making the ratios of effectors to target cells 30:1, 10:1, and 3:1, with a triplicate set of wells prepared for each ratio and for the controls. The percent of lyses was calculated as:

$$\text{Percent of lysis (\%)} = \frac{100 \times A (\text{experimental-effector} - \text{spontaneous-target spontaneous})}{A (\text{target maximum-target spontaneous})}$$

Statistical analysis

Result were expressed as mean \pm SD and analyzed using the Student's *t* test. *P* < 0.05 was regarded as statistically significant.

RESULTS

Detection of DC surface markers

PBMCs were isolated from patients and healthy donors and cultured overnight. After removal of the nonadherent cells, the remaining adherent monocytes were cultured in AIMV containing GM-CSF and IL-4. Cell cultures were observed after 24 h, becoming larger after 48 h and exhibiting DC morphology with veiled processes and dendrites (Figure 1). The yields of DCs from hepatitis B patients and normal donors did not differ significantly.

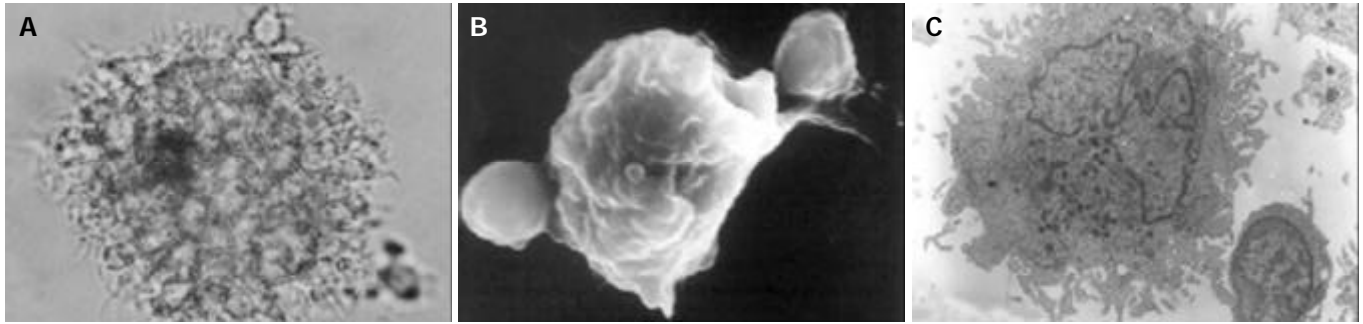


Figure 1 Morphology of dendritic cells after 7 and 9 d. A: Cluster of DCs after 9 d (light microscope, ×100); B: A DC on day 7 (scanning electron microscope, ×5 000); C: A DC on day 7 (transmitting electron microscope, ×5 000).

DCs were identified by their typical morphology and by CD86/HLA-DR double positive expression. These cells were harvested and counted, and surface markers were measured over time. The number of DCs peaked on d 9, decreasing gradually thereafter. The expression of DC-related cell markers was first detected on d 3. After cultured for 7 d with GM-CSF and IL-4, these DCs expressed costimulatory and MHC molecules, showing that cells derived from both patients and controls were morphologically compatible with DCs. Among the MHC and costimulatory molecules examined, we found that CD80 expression in patients with hepatitis B was weaker than that in normal donors (Table 1).

Table 1 Phenotype of DCs from HB patients and normal donors (n=10,%, mean±SD)

DC Antigen	Positive DCs of HB patients	Positive DCs of normal donors	P
CD86	89.89±1.14	91.17±3.41	0.633
CD80	36.86±2.30	59.87±6.31	0.021
CD1a	23.25±7.04	32.92±4.58	0.405
HLA-DR	97.29±1.09	97.11±1.14	0.852
CD83	23.25±7.34	33.18±11.12	0.265

Responses to TNF-α in DCs from HBV patients and healthy donors

Following addition of 20 μg/mL TNF-α to the culture medium on the 5th d of culture, the cells and culture supernatants were harvested 48 h later. When cell phenotypes were assayed by flow cytometry, we found that the expression of CD83 was weaker in cells cultured in the absence of TNF-α than in its presence. However, culture in the presence of TNF-α did not alter the expression of CD86, CD80 or HLA-DR. While production of IL-12 by cultured DCs from hepatitis B patients and healthy donors did not differ, the secretion of IL-12 was significantly increased in cells cultured with TNF-α (Figure 2).

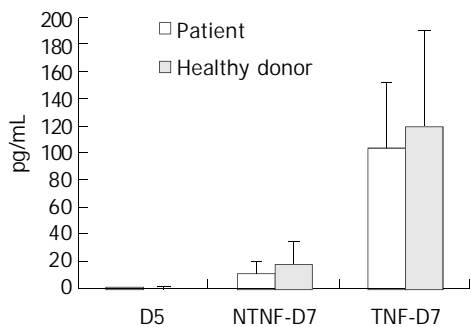


Figure 2 Effect of TNF-α on DC secretion of IL-12.

DCs from HB patients and healthy donors were cultured for 5 d, at which time TNF-α was added to some of the cultures

(TNF-D7) but not to others (NTNF-D7), and incubation was continued for an additional 2 d. IL-12 secretion was measured on d 5 and 7. Each bar represents mean±SD of DCs from 6 different individuals.

Immune stimulatory activity of DCs

When we tested T cell-stimulatory activity of DCs in allogeneic MLR, we found that patients with chronic hepatitis B tended to have decreased T cell-stimulatory activity compared with normal donors, but the difference did not attain statistical significance (Figure 3).

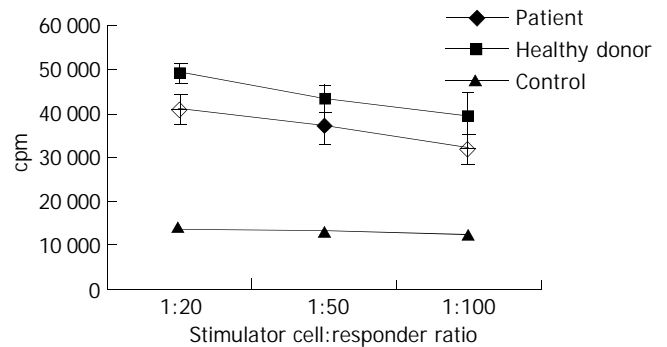


Figure 3 MLR of DCs against allogeneic T cells.

Each MLR was set up in triplicate in flat-bottom 96-well plates. The responder T cells were obtained from a healthy donor, while irradiated DCs were used as stimulators at different ratios to T cells. Each point represents the mean±SD. of measurements from 6 different individuals.

T cell memory response to HBcAg18-27 CTL epitope

PBMCs isolated from patients with chronic hepatitis B (CHB) and acute hepatitis B (AHB) and from normal donors were incubated with HBcAg 18-27 peptide for 6 h, and ICCS was used to determine the frequency of HBcAg 18-27 peptide reactive T cells secreting cytokines. We found that stimulated PBMCs from the AHB group produced significantly stronger T cell memory reactions than PBMCs from either of the other groups (P<0.05) (Table 2).

DCs from CHB patients induced specific immune responses of CD8⁺ T cells

DCs primed with HBcAg18-27 peptide were cultured with lymphocytes for 10 d to determine whether peptide-reactive T cells were able to secrete various cytokines, including IFN-γ, IL-2 and TNF-α. Using the ICCS assay, we found that DCs from CHB patients induced peptide-reactive T cells to secrete cytokines (Figure 4), to a significantly greater degree than that secreted by peptide-stimulated PBMCs (P<0.05). We also

observed significant differences between DCs and PBMCs of CHB patients (Table 3).

Table 2 Memory immune responses of PBMCs from patients with chronic hepatitis B (CHB), acute hepatitis B (AHB) and normal donors (mean±SD)

Group	n	Percent CD8 ⁺ T cells secreting cytokines		
		IFN- γ /CD8	IL-2/CD8	TNF- α /CD8
CHB	7	0.18±0.14	0.13±0.05	0.37±0.18
AHB	4	4.26±2.49	4.80±2.23	4.57±2.29
Donor	6	0.28±0.13	0.59±0.27	0.68±0.33
P value ^a		0.019	0.024	0.010
P value ^c		0.013	0.031	0.010

^aP<0.05 AHB vs CHB. ^cP<0.05 AHB vs Donor.

Table 3 CD8⁺T cell immune responses induced by peptide-pulsed DCs (mean±SD)

Group	n	Percent of CD8 ⁺ T cells secreting cytokines (%)		
		IFN- γ /CD8	IL-2/CD8	TNF- α /CD8
CHB ¹	7	0.28±0.15	0.46±0.13	0.68±0.15
CHB ²	4	0.59±0.39	0.74±0.16	1.52±0.38
P value ^a		0.043	0.049	0.028

1: T cells induced by unpulsed DCs; 2: T cells induced by peptide-pulsed DCs; a: comparison of CHB¹ and CHB².

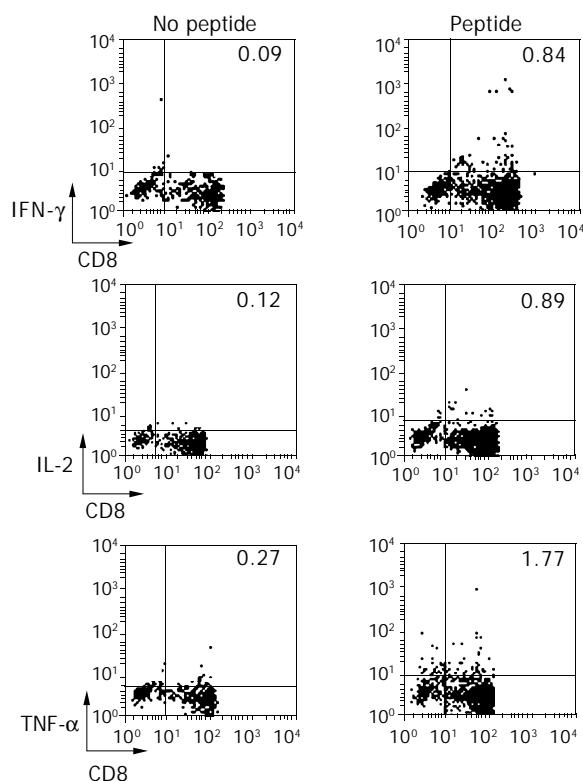


Figure 4 Cytokine secretion of peptide-reactive T cells induced by DCs from one CHB patient. T cells from one CHB patient was incubated with autologous DCs pulsed with the HBV-specific peptide HBcAg 18-27 (Peptide) or without peptide (No peptide), and T cell response was detected by flow cytometry by measuring cytokine secretion by the activated T cells. The dot-plots show levels of intracellular staining for IFN- γ , IL-2 and TNF- α (y-axis) and surface CD8 molecule (x-axis). The number in the upper-right quadrant indicates the percentage of CD8-positive T cells that secrete cytokines.

CTL cytotoxicity induced by DCs loaded with peptide

Target cells were divided into 2 groups, with one group incubated with peptide and the other group without. CTL cytotoxicity of the DCs from CHB patients against T cells incubated with peptide was (57.28±20.00)%, (47.54±20.70)%, and (21.38±12.86)% at effector to target cell ratios of 30:1, 10:1, and 3:1, respectively, while CTL cytotoxicity of these same DCs against T cells incubated without peptide was (30.38±10.00)%, (26.99±12.72)%, and (13.74±3.22)%, respectively (Figure 5).

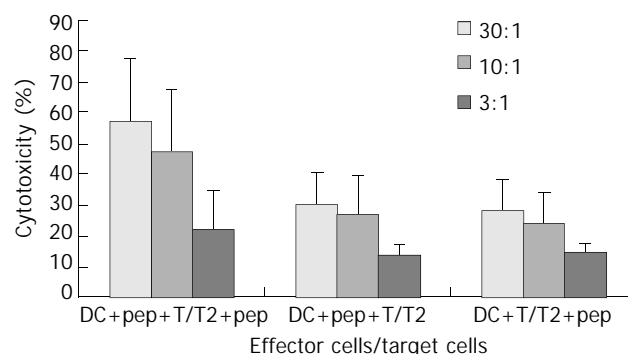


Figure 5 T cell cytotoxicity induced by DCs in CHB patients. DC+pep+T, T cells induced by DCs loaded with specific peptide; DC+T, T cells induced by DCs without peptide; T₂+pep, peptide-loaded target cells; T₂, target cells.

DISCUSSION

DCs are the most potent antigen presenting cells crucial for activating CD8⁺ killer T cells and CD4⁺ helper T cells. DCs release bioactive cytokine IL-12, which can stimulate NK cells, induce Th1 type cytokine production and foster the development of cytotoxic T lymphocytes. DCs may thus be a powerful natural adjuvant for the treatment of tumors and viral infections. It is now known that the function of DCs is not fixed, depending on alterations in the cellular environment. Alterations in DC function may result from the effects of anti-inflammatory cytokines, including IL-10 and TGF- β , and on the characteristics of pathogens.

It was observed that, the functional activity of DCs was decreased, as measured by the stimulation of allogeneic T cell proliferation. In patients with chronic hepatitis B, however, it was unclear if DCs could act as natural adjuvants. In HBV transgenic (Tg) mice, DC function was normal, and there were CTLs specific for HBsAg, which were functionally quiescent. When cytokine-activated DCs were administered to these Tg mice, tolerance was broken, and antiviral reactions were induced^[2]. In contrast, the expression of MHC II (I a) and CD86 and the ability of DCs to induce cell proliferation were lower in Tg than in normal mice^[8].

In this study, we isolated PBMCs from the peripheral blood of patients with chronic hepatitis B infection and from healthy donors and compared the functional activity of their DCs. We found that, while CD80 expression was lower on DCs from patients than on those from healthy donors, other surface markers including HLA and costimulatory molecules were expressed to an equal extent. Functionally, DCs from CHB patients were able to stimulate the proliferation of allogeneic T cells, but to a lower extent than observed with DCs from non-CHB donors.

T cell activation requires costimulatory molecules (*e.g.*, CD28-B7), which provide a second signal. The B7 family is comprised primarily of B7-1 (CD80) and B7-2 (CD86). Although their function is not fully known, several studies have shown that CD80 signals preferentially promote development of Th1 cells, whereas CD86 signals promote Th2 development. While

CD80 gene knockout mice have a normal immunoglobulin superfamily repertoire, a complete deficiency of CD86 would destroy humoral immunity. B7 receptors have two ligands. CD28 provides a costimulatory signal essential to T cell activation, whereas CTLA-4 blocks T cell proliferation. CTLA-4 bound with greater affinity to CD80 than to CD86, suggesting that the binding of CD80 tends to inhibit T cell proliferation^[9-11]. Our finding, that CD80 expression by DCs from patients with chronic hepatitis B was weaker than that from healthy donors, might be related to the inhibition of T cell activation seen in these patients and to the decreased function of DCs from these patients observed in our MLR assay. In addition, our results confirmed Akbar's study^[7], in that the decreased functional activity of patient DCs results in the inability of these cells to present antigens to T cells, thus leading to reduced induction of a specific cytotoxic reaction. This, in turn, resulted in a lower rate of killing of infected cells and a reduction in the suppression of viral replication, finally leading to a state of persistent infection.

When pathogens invade a host, a potent immune response is produced to eliminate the pathogens. At the end stage of this immune response, the majority of effector T and B cells gradually undergo apoptosis, while a smaller number differentiate into long-lived memory T or B cells. Memory T cells produce vigorous secondary responses to antigen and rapidly eliminate pathogens. For example, the infected cells were cytolysed by CTLs. On the other hand, the primary difference between memory and naïve T cells is that, when they are activated, the former had higher reactivity to antigens and secreted more cytokines^[12-14]. Thus, when an individual is infected with HBV, certain soluble products of the immune response, especially IFN- γ , IL-2, and TNF- α , can suppress HBV gene expression, as well as replication *in vivo*.

Hepatocellular HBV gene expression has been shown to be profoundly suppressed by non-cytolytic regulatory signals delivered by HBsAg-specific CTL through their secretion of IFN- γ and induction of TNF- α following antigen recognition. These effects were mediated by a posttranscriptional mechanism that selectively accelerates the degradation of cytoplasmic HBV mRNA^[15]. We therefore assayed the cytokines secreted by CD8⁺T cells to illuminate the immune response of individuals to viral infection. We found that PBMCs from patients with CHB and AHB and from normal donors could be stimulated by HBcAg18-27 peptide. However, stimulated PBMCs from patients with AHB produced stronger memory reactions than those from patients with CHB or healthy donors, suggesting that AHB PBMCs have potent memory immune reactions to this specific antigen, whereas CHB PBMCs are at least partially tolerant to this antigen. The mechanism of tolerance includes factors from the host and from the virus. New-born babies contaminated by HBV transmitted from their mothers were in a state of immune tolerance to HBV and about 90% carry HBV as a persistent infection.

T cells play an important role in the immune system. Not only do they have effector functions, but also they are the major regulators of immune function. T cell activation requires two signals, one from the T cell receptor that recognizes the complex of MHC and antigen on the surfaces of antigen presenting cells (APCs), and the other from costimulatory molecules such as CD28-B7. To determine whether the immune tolerance of DCs from CHB patients could be broken, we primed DCs with HBcAg18-27 and incubated them with lymphocytes, and we assayed CTL generation. Our finding, that an antigen-specific T cell reaction was induced when these peptide-primed DCs

were co-cultured with CD8⁺ T cells, and that the cytotoxic activity of CTLs against target cells cultured with peptide was higher than that against target cells cultured without peptide, suggested that DCs from patients with CHB could break immune tolerance and induce an HBV antigen-specific T cell reactions.

DCs have great potential in anti-viral therapy as antigen presenting cells. Our findings showed that, although the function of patient DCs was lower than that of control DCs, the former still expressed signals necessary for T cell activation, released of IL-12 and stimulation of allogeneic T cell proliferation. Moreover DCs from these patients could break immune tolerance to induce HBV antigen-specific T cell responses. IL-12 is a critical cytokine secreted by DCs, which can induce the production of specific T cells, suggesting that TNF- α is an important factor in immunotherapy. Thus, our findings suggest that DCs originating from cytokine activated PBMCs of CHB patients can be utilized in immunotherapy, which will be a potential treatment for hepatitis B.

REFERENCES

- 1 **Chisari FV.** Cytotoxic T cells and viral hepatitis. *J Clin Invest* 1997; **99**: 1472-1477
- 2 **Hart DN.** Dendritic cells: unique leukocyte population which control the primary immune response. *Blood* 1997; **90**: 3245-3287
- 3 **Steinman RM.** The dendritic cell system and its role in immunogenicity. *Annu Rev Immunol* 1991; **9**: 271-296
- 4 **Rescigno M, Granucci F, Ricciardi-Castagnoli P.** Dendritic cells at the end of the millennium. *Immunol Cell Biol* 1999; **77**: 404-410
- 5 **Shimizu Y, Guidotti LG, Fowler P, Chisari FV.** Dendritic cell immunization breaks cytotoxic T lymphocyte tolerance in hepatitis B virus transgenic mice. *J Immunol* 1998; **161**: 4520-4529
- 6 **Romani N, Reider D, Heuer M, Ebner S, Kampgen E, Eibl B, Niederwieser D, Schuler G.** Generation of mature dendritic cells from human blood. An improved method with special regard to clinical applicability. *J Immunol Methods* 1996; **196**: 137-151
- 7 **Romani N, Gruner S, Brang D, Kampgen E, Lenz A, Trockenbacher B, Konwalinka G, Fritsch PO, Steinman RM, Schuler G.** Proliferating dendritic cell progenitors in human blood. *J Exp Med* 1994; **180**: 83-93
- 8 **Akbar SM, Inaba K, Onji M.** Upregulation of MHC class II antigen on dendritic cells from hepatitis B virus transgenic mice by interferon- γ : abrogation of immune response defect to a T-cell-dependent antigen. *Immunology* 1996; **87**: 519-527
- 9 **Freeman GJ, Boussiotis VA, Anumanthan A, Bernstein GM, Ke XY, Rennert PD, Gray GS, Gribben JG, Nadler LM.** B7-1 and B7-2 do not deliver identical costimulatory signals, since B7-2 but not B7-1 preferentially costimulates the initial production of IL-4. *Immunity* 1995; **2**: 523-532
- 10 **Kuchroo VK, Das MP, Brown JA, Ranger AM, Zamvil SS, Sobel RA, Weiner HL, Nabavi N, Glimcher LH.** B7-1 and B7-2 costimulatory molecules activate differentially the Th1/Th2 developmental pathways: application to autoimmune disease therapy. *Cell* 1995; **80**: 707-718
- 11 **Coyle AJ, Gutierrez-Ramos JC.** The expanding B7 superfamily: increasing complexity in costimulatory signals regulating T cell function. *Nat Immunol* 2001; **2**: 203-209
- 12 **Ahmed R, Gray D.** Immunological memory and protective immunity: understanding their relation. *Science* 1996; **272**: 54-60
- 13 **Sprent J, Surh CD.** Generation and maintenance of memory T cells. *Curr Opin Immunol* 2001; **13**: 248-254
- 14 **Champagne P, Dumont AR, Sekaly RP.** Learning to remember: generation and maintenance of T-cell memory. *DNA Cell Biol* 2001; **20**: 745-760
- 15 **Chisari FV.** Viruses, immunity, and cancer: lessons from hepatitis B. *Am J Pathol* 2000; **156**: 1117-1132

Selection of a peptide mimicking neutralization epitope of hepatitis E virus with phage peptide display technology

Ying Gu, Jun Zhang, Ying-Bing Wang, Shao-Wei Li, Hai-Jie Yang, Wen-Xin Luo, Ning-Shao Xia

Ying Gu, Jun Zhang, Ying-Bing Wang, Shao-Wei Li, Hai-Jie Yang, Wen-Xin Luo, Ning-Shao Xia, The Key Laboratory of Ministry of Education for Cell Biology and Tumor Cell Engineering, Xiamen University, Xiamen 361005, Fujian Province, China

Supported by Grant from Science and Technology Projects of Fujian Province, China; No.2002 F013; Excellent Scholar Incubation Plan of the Ministry of Education, China

Correspondence to: Ning-Shao Xia, The Key Laboratory of Ministry of Education for Cell Biology and Tumor Cell Engineering, Xiamen University, Xiamen 361005, Fujian Province, China. nsxia@jingxian.xmu.edu.cn

Telephone: +86-592-2184110 **Fax:** +86-592-2184110

Received: 2003-10-27 **Accepted:** 2003-12-08

Abstract

AIM: To select the peptide mimicking the neutralization epitope of hepatitis E virus which bound to non-type-specific and conformational monoclonal antibodies (mAbs) 8C11 and 8H3 from a 7-peptide phage display library, and expressed the peptide recombinant with HBcAg in *E. coli*, and to observe whether the recombinant HBcAg could still form virus like particle (VLP) and to test the activation of the recombinant polyprotein and chemo-synthesized peptide that was selected by mAb 8H3.

METHODS: 8C11 and 8H3 were used to screen for binding peptides through a 7-peptide phage display library. After 4 rounds of panning, monoclonal phages were selected and sequenced. The obtained dominant peptide coding sequences was then synthesized and inserted into amino acid 78 to 83 of hepatitis B core antigen (HBcAg), and then expressed in *E. coli*. Activity of the recombinant proteins was detected by Western blotting, VLPs of the recombinant polyproteins were tested by transmission electron microscopy and binding activity of the chemo-synthesized peptide was confirmed by BIAcore biosensor.

RESULTS: Twenty-one positive monoclonal phages (10 for 8C11, and 11 for 8H3) were selected and the inserted fragments were sequenced. The DNA sequence coding for the obtained dominant peptides 8C11 (N'-His-Pro-Thr-Leu-Leu-Arg-Ile-C', named 8C11A) and 8H3 (N'-Ser-Ile-Leu-Pro-Tyr-Pro-Tyr-C', named 8H3A) were then synthesized and cloned to the HBcAg vector, then expressed in *E. coli*. The recombinant proteins aggregated into homodimer or polymer on SDS-PAGE, and could bind to mAb 8C11 and 8H3 in Western blotting. At the same time, the recombinant polyprotein could form virus like particles (VLPs), which could be visualized on electron micrograph. The dominant peptide 8H3A selected by mAb 8H3 was further chemo-synthesized, and its binding to mAb 8H3 could be detected by BIAcore biosensor.

CONCLUSION: These results implicate that conformational neutralizing epitope can be partially modeled by a short peptide, which provides a feasible route for subunit vaccine development.

Gu Y, Zhang J, Wang YB, Li SW, Yang HJ, Luo WX, Xia NS. Selection of a peptide mimicking neutralization epitope of hepatitis E virus with phage peptide display technology. *World J Gastroenterol* 2004; 10(11): 1583-1588

<http://www.wjgnet.com/1007-9327/10/1583.asp>

INTRODUCTION

Hepatitis E is an acute hepatitis caused by hepatitis E virus (HEV) in developing countries, where it occurs sporadically and in an epidemic form. The causative agent, HEV, is transmitted primarily by the fecal-oral route, and it accounts for about 15-20% sporadic cases of acute hepatitis in China^[1,2]. HEV is an icosahedron non-enveloped virus, and its genome is a single-stranded positive-sense, 3' polyadenylated RNA about 7.5 kb in length. It contains 3 open reading frames (ORFs). ORF1 codes for a polyprotein of 1 693 amino acids and contains domains homologous to a viral methyltransferase, a papainlike cysteine protease, an RNA helicase, and an RNA-dependent RNA polymerase, and the most hypervariable region of HEV genome. ORF2 codes for the viral capsid protein of 660 amino acids, while ORF3 codes for a 123-amino-acid-long polypeptide with unknown function.

It has been proved that the major viral capsid protein encoded by ORF2 contains the protective epitope^[3]. We recombined a fragment of HEV ORF2 and expressed the polypeptide named NE2 in *E. coli* recently^[4], and proved it to be a protective antigen^[5], which naturally forms homodimer by virtue of its interface domain^[6]. Three anti-NE2 neutralization mAbs, 8C11, 8H3 and 13D8 were selected, which could recognize 2 separated neutralization conformational surface epitopes of HEV, 8C11 and 13D8 against one and 8H3 against the other. The 3 mAbs can neutralize HEV *in vitro* and *in vivo* test of Rhesus monkey^[7-9].

8C11 and 8H3 were used to screen binding peptides from a heptapeptide phage display library, which could mimic the 2 neutralizing epitopes of HEV binding to 8C11 and 8H3 respectively. The obtained dominant peptides' DNA sequences were then synthesized and cloned into amino acid 78 to 83 of hepatitis B core antigen (HBcAg), then expressed in *E. coli*. While it has been proven that HBcAg could be expressed in eukaryocytes or prokaryocytes, and assembled into VLP automatically. The inserted sequence between amino acids 73 and 94 could be expressed on the HBcAg VLP surface^[10]. Because HBcAg is an immunodominant immunogen^[11], which results in the immunodominance of the insertion, we expressed the linear epitopes, which could conformationally mimic epitope on the surface of HBcAg, resulting in a VLP antigen, and prove its activity. This assay would not only mimic the neutralizing epitope of HEV but also provide insights into a novel route for subunit vaccine development.

MATERIALS AND METHODS

Monoclonal antibodies

8C11 and 8H3 mAbs, which could conformationally bind to neutralizing epitopes of HEV were prepared in our

laboratory^[7,9]. Affinity purified antibody phosphatase labeled goat anti-mouse IgG (H+L) was from Kirkegaard & Perry Laboratory (2 Cessua Court, Gaithersburg Maryland 20879, USA).

Affinity selection and amplification of peptide library

Heptapeptide phage display library and host strain *E.coli* ER2738 were purchased from New England BioLabs Company. Anti-HEV mAbs binding phages were isolated from the phage display library by successive cycles of selection and amplification. The biopanning procedure was essentially used as described in the phage display library user manual. Briefly, mAbs 8C11 and 8H3 (100 µg/mL) were coated on 96-well microtiter plates. After blocked with 20 g/L BSA, 100 µL diluted phage (10 uL of the original library) was piped onto the coated plate and shaken gently for 1 h at room temperature, the plates were washed for 10 times with PBST (10 g/L Tween 20). The bound phages were eluted with 100 µL 10 mmol/L Glycyl (pH 2.2), 1 mg/mL BSA, rocked gently for 10 min. The eluate was piped into a microcentrifuge tube and neutralized with 10 µL 1 mol/L Tris-HCl (pH 9.1). The eluate was added to 20 mL ER2738 culture and incubated at 37 °C with vigorous shaking for 4.5 h. The culture was transferred to a centrifuge tube and spun for 10 min at 10 000 g at 4 °C. The supernatant was collected and 1/6 volume of PEG/NaCl (200 g/L PEG8000, 2.5 mol/L NaCl) was added. The phage was allowed to precipitate at 4 °C overnight. PEG precipitation was spun for 15 min at 10 000 g at 4 °C. The pellet was re-suspended in 1 mL PBS, and re-precipitated with PEG/NaCl. Finally the pellet was suspended in 200 µL PBS, and stored at 4 °C. The amplified eluate was titered as general methods. The concentration of target mAbs was lowered to 50 µg/mL, at the same time the concentration of Tween-20 was risen to 50 g/L in the washing step, then was panned 3 more times by repeating the above steps. After 4 rounds panning, individual monoclonal antibodies were sequenced. The single-stranded DNA of M13 phages was purified by using the M13 mini kit purchased from Shanghai Huashun Biotech Ltd, and then sequenced by Shanghai Boya Ltd.

Construction of recombinant expression vector for peptide

The recombinant expression vector named pC149-mut was composed in our laboratory. The peptide of amino acids 1 to 149 of HBcAg expressed in *E.coli* formed viral like particles (VLPs). The amino acid residues 78 to 83 were exposed at the VLP's surface. According to this we cloned the HBcAg's genome of amino acid residues 1 to 149 into the expression vector pTO-T7^[12] of *E.coli*, and designed a linker to replace the immunodominant epitope located at 79 to 80aa of HBc and composed the mutant vector pC149-mut. After exogenous gene was inserted into the amino acid residues 78 to 83, recombinant C antigen was still able to form VLP and expose the exogenous epitope.

We designed the primer (Table 1) according to the dominant sequence of selected monoclonal phages, and the linker sequence of pC149-mut vector. Therefore, we could insert heptapeptide exogenome into the vector and co-express it with HBcAg using 8C11AFP or 8H3AFP as a former primer and

149 mutRP as a lower primer, and using the pC149-mut vector as a template. PCR was carried out after pre-denaturation at 94 °C for 5 min, 25 cycles of denaturation at 94 °C for 50 s, annealing at 56 °C for 50 s, and extension at 72 °C for 25 s, then extension at 72 °C for 10 min. The PCR fragment was cloned into pMD 18-T vector and formed positive clones containing the genome of peptide 8C11A (CATCCTACTC TTTTGCGTATT), which could bind to mAb 8C11 or the genome of peptide 8H3A (TCTATTCTGCCGTATCCTTAT), which could bind to mAb 8H3. Then they were digested with *Bam*H I and *Eco*R I, and the product fragment was linked into the pC149-mut vector to compose the expression vector named pC149-mut-8C11A or pC149-mut-8H3A (Figure 1).

Expression and purification of recombinant polyprotein

Host stain ER2566 was cultured and transformed with the recombinant vector pC149-mut-8C11A or pC149-mut-8H3A in LB culture medium at 37 °C in a shaker, till the A_{600} reached 0.8-1.0, then the culture was incubated with 0.2 mmol/L IPTG for 6 h at 37 °C. The cells were spun to be collected and were disintegrated by an ultrasonic disintegrator (Uilbra-Cell VGX500 of SONICS & MATERIALS Co.). The insoluble protein was spun and collected, then suspended and deposited 2 times into 10 g/L Triton X-200. The pellet was finally suspended into buffer A (4 mol/L Urea, 20 mmol/L Tris-HCl pH 8.5, 5 mmol/L EDTA, 100 mmol/L NaCl), dialysed in PBS overnight. The lysate was spun and collected.

Western blotting

Boiled supernatant of ultrasonic lysate and boiled deposition of ultrasonic lysate and control samples (the expression of pC149-mut could not react with mAbs, and the recombinant polyprotein NE2 was used to select mAbs including 8C11 and 8H3^[7,9]) were dissolved in 120 g/L SDS-PAGE, transferred to a nitrocellulose membrane. Each contained one lane of the protein molecular mass mark between 18.3 and 215 ku. The membrane containing proteins with 5 g/L non-fat dry milk as blocking solution was incubated for 90 min and reacted with the test mAb 8H3 or 8C11 diluted in 5 g/L non-fat dry milk. The immunocomplexes were detected by using Ap-labeled goat-anti-mouse IgG, BCIP and NBT as substrates.

Transmission electron microscopy of chimeric VLPs

After renatured by the methods described above, the particles were adsorbed to carbon-coated grids, stained with 2 g/L uranyl acetate, and examined by JEM-100CXII electron microscope at about ×100 000 magnification.

Active analysis of recombinant proteins by BIAcore biosensor

Heptapeptide named 8H3A (N'-Ser-Ile-Leu-Pro-Tyr-Pro-Tyr-C') was synthesized and purified by Xi'an Meilian Ltd (Xi'an, China). Then the biosensor chip was coupled with anti-mouse Fc, which was carried out according to the user manual. Briefly, the sensor chip CM5 with CM Dextran on its reaction-surface was activated with EDC and NHS, and then the flow cells were treated with a standard amine-coupling reagent (injecting 10 mmol/L NaOAc, pH4.8, instead of protein) or with amine-coupling reagents and anti-mouse Fc polyclonal antibody. The

Table 1 Primers for expression vector of mimic peptide

Primer ID	Primer sequence
8C11AFP	GGATCCCATCCTACTCTTTTGCGTATTGGTGGTGGAGGTTTCAGG
8H3AFP	GGATCCCTATTCTGCCGTATCCTTATGGTGGTGGAGGTTTCAGG
149 mutRP	GAATTCCTAAACAACAGTAGTTT

The underlined sequences are the insert genes coding the selected peptides.

coupling density of the antibody was 900 RU. Experiments were run at 25 °C. After mAb 8H3 was bound to anti-mouse Fc antibody, peptide 8H3A was injected. The data of association and dissociation indicating the reaction between mAb 8H3 and peptide 8H3A were collected. Biacore X biosensor, CM5 sensor chip and reagent of EDC & NHS were from Amersham Biosciences Company (Uppsala, Sweden).

RESULTS

Sequence characteristics of peptide binding to neutralizing mAb 8C11 or 8H3

After 4 rounds of biopanning, 21 monoclonal phages were

selected for sequencing (in which 10 phage could bind to mAb 8C11, and the other 11 could bind to mAb 8H3). According to the DNA sequence, the peptide sequence of the phage displayed was made out (Figure 2). Heptapeptide with amino acid sequence HPTLLRI was dominant (50%) in the 10 monoclonal bound to mAb 8C11. While in the 11 monoclonal bound to mAb 8H3, the preponderant amino acid sequence was SILPYPY (27.3%). Furthermore, in the heptapeptide binding to mAb 8H3, the amino acid sequence of S*LP, S*P, S*L or LP was also more frequent, indicating that S, L and P would be more important to form the domain binding to mAb 8H3. Likewise, amino acids P, T and L were found to be more important in the interaction between peptide and mAb 8C11.

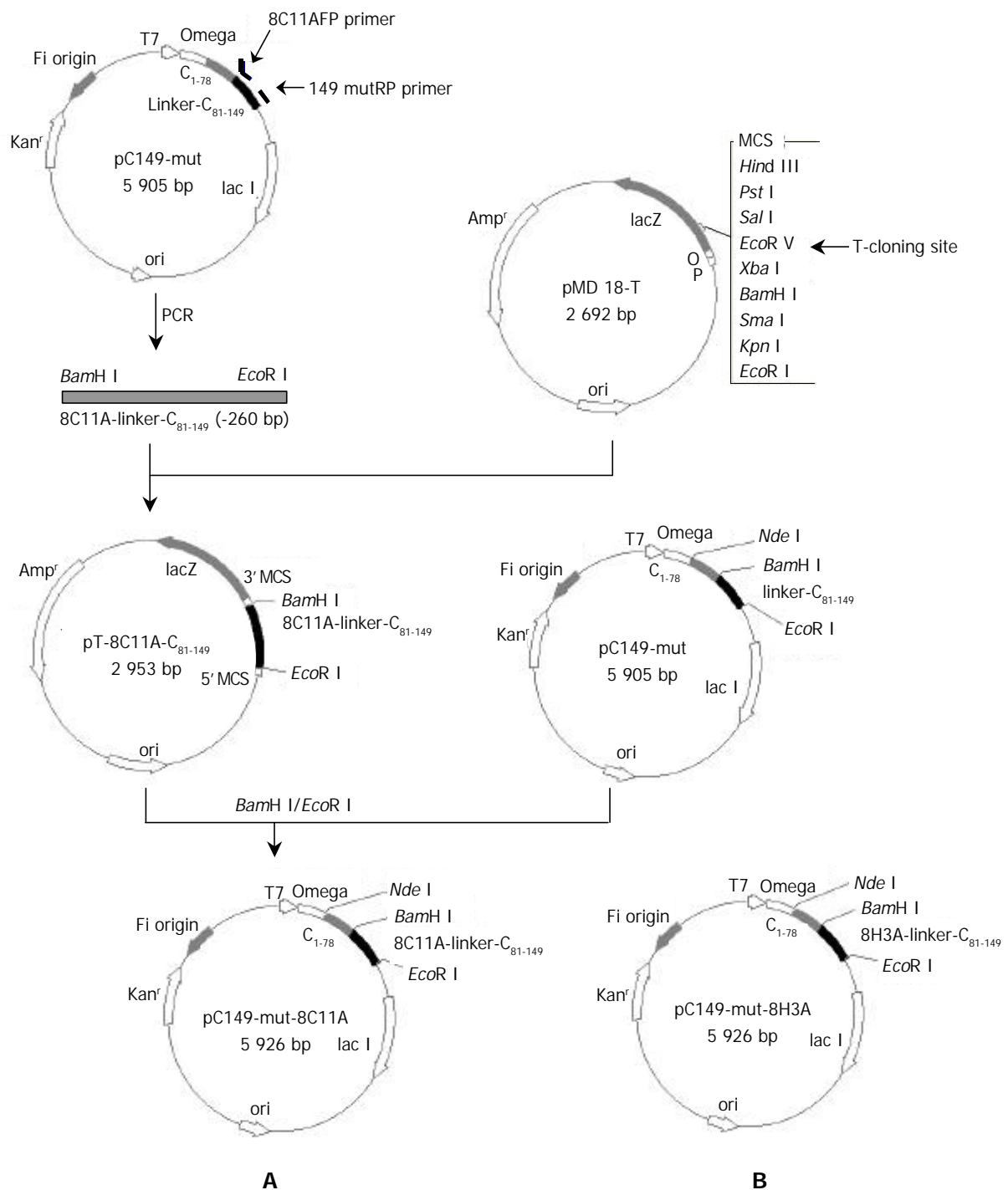


Figure 1 Expression vector construction of pC149-mut-8C11A and pC149-mut-8H3A. A: Construction of pC149-mut-8C11A, B: Map of pC149-mut-8H3A, which was constructed as pC149-mut-8C11A except using the primer 8H3AFP instead of 8C11AFP.

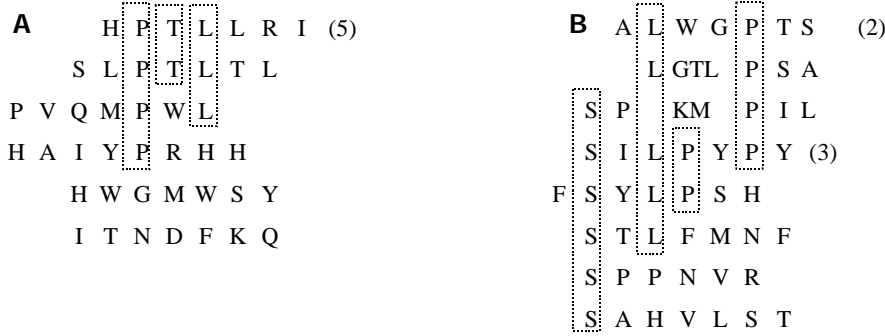


Figure 2 Sequences of peptides selected by monoclonal antibodies. A: Selected by mAb 8C11, B: Selected by mAb 8H3.

Expression and western blotting of peptide mimic neutralization epitope

Dominant peptides 8C11A (N' -His-Pro-Thr-Leu-Leu-Arg-Ile-C') and 8H3A (N' -Ser-Ile-Leu-Pro-Tyr-Pro-Tyr-C') were cloned into the vector pC149-mut named C8C11A and C8H3A respectively, and expressed. The result of expression was shown in Figure 3. Recombinant polyprotein C8C11A was found in the insoluble cell pellet, and formed dimer (about M_r 40 000 in mass) on the SDS-PAGE mainly while the monomer (about M_r 20 000) was hard to be seen. As to the Western blotting result, it was the dimer that could interact with mAb 8C11 in the same level as the monomer of NE2 protein (about M_r 29 000). C8H3A fusions were also found in the insoluble cell pellet. Beside the dimer, a monomer was in the majority, but only the $-M_r$ 40 000 dimer was able to bind to mAb 8H3 when tested by Western blotting.

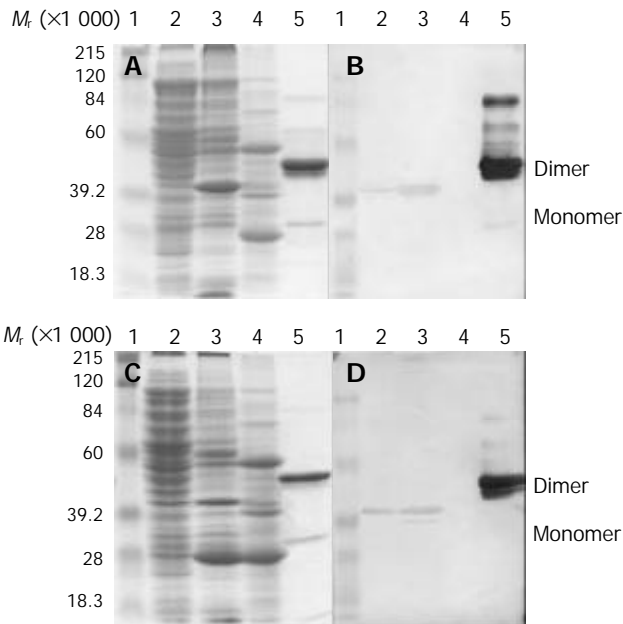


Figure 3 Expression and Western blotting of pC149-mut-8C11A and pC149-mut-8H3A. A, C: SDS-PAGE, B, D: Western blotting of mAbs 8C11 and 8H3 respectively, A, B: pC149-mut-8C11A, C, D: pC149-mut-8H3A. 1, Protein molecular weight marker; 2, Supernatant of ultrasonic lysate; 3, Deposition of ultrasonic lysate; 4, C149-mut control; 5, Purified NE2 antigen

Electron micrograph of VLP

The renatured recombinant polyprotein particles were adsorbed to carbon-coated grids, stained with 20 g/L uranyl acetate, and examined with TEM. The recombinant HBcAg with 8C11A or 8H3A on its surface and HBcAg could form VLPs and VLPs' diameter was about 20 nm (Figure 4).

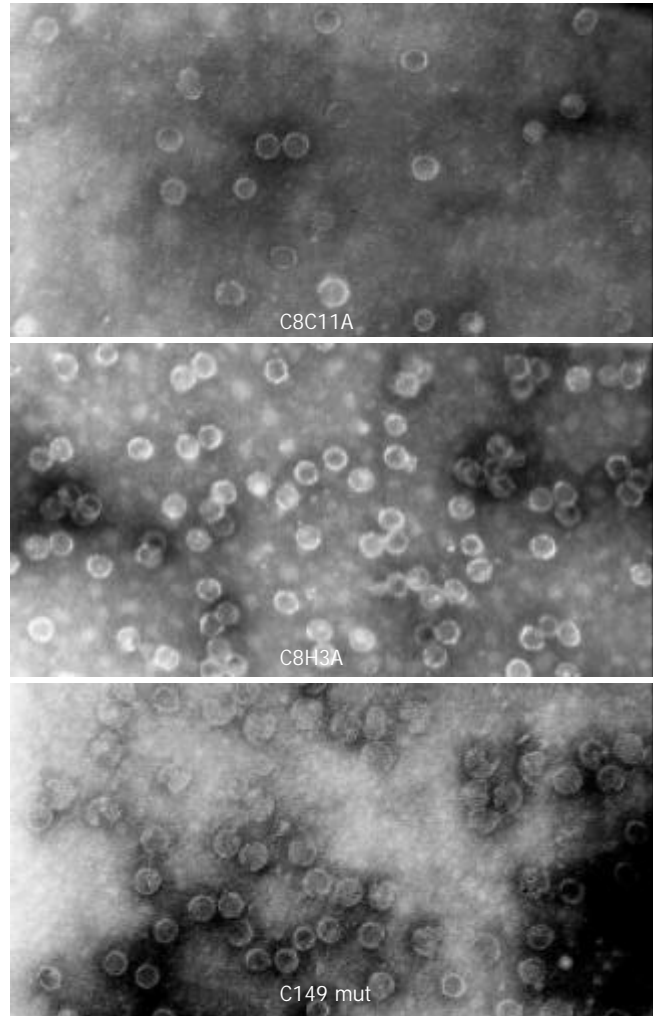


Figure 4 Virus like particles assembled by recombinant protein C8C11A, C8H3A or C149 mut (Negative staining electron microscopy, $\times 100\ 000$).

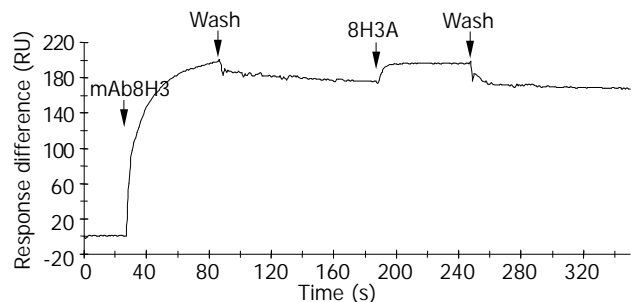


Figure 5 Binding curve of chemo-synthesized seven peptide 8H3A against monoclonal antibody 8H3 in BIAcore biosensor.

Interaction between chemo-synthesized heptapeptide 8H3A and mAb 8H3

The mAb 8H3 was bound to the anti-mouse Fc polyclonal antibody coupled on the cells of CM5 chip. After mAb 8H3 was bound to the anti-mouse Fc antibody, peptide 8H3A (1 mg/mL) was injected and the data of association and dissociation were collected. Chemo-synthesized heptapeptide 8H3A could bind to mAb 8H3, but not stably (Figure 5).

DISCUSSION

Phage display technique has been widely used in constructing antibody library or biopanning of random peptides according to their biological activities, and in many other fields or so^[13,14]. As a new technique, it makes use of the characteristics of the coat protein of the phage, that is, a peptide is expressed as a fusion with the phage coat protein pIII, resulting in the display of fused protein on the surface of virion. Phage display technique allows rapid identification and amplification of the peptide ligands for target molecules by the affinity of their specific-binding. Recently, random peptide libraries displayed on phage have been widely used in many fields, such as identification and analysis of a peptide mimic the epitope of HIV^[15] and HIV-1-infected cells^[16], identification of enzyme inhibitors^[17] and immunodepressants^[18], and many antigens etc.^[19-22]. Phage display technique is specially useful to mimic a variety of half-antigens and non-peptide target molecules' function, which is a very useful way to produce mimic peptide medication. Many reports have been available on the peptides mimicking epitope, which can neutralize *Neisseria meningitidis*^[23,24] and many other bacteria to produce bacterial vaccines.

There are still no cell models of HEV, or effective methods to produce HEV artificially. Different sections of HEV capsid protein were expressed, and the structures of the recombinant polyproteins were analysed, which can help us to speculate the crude structure of HEV capsid. We cloned a section of HEV ORF2 (named NE2) and expressed this recombinant protein in *E.coli*. It was found that NE2 formed polymer spontaneously, from dimer to hexamer concretely. This was very similar to the assemble process of HEV capsid protein^[4,25,26]. NE2 was used to immunize Rhesus monkey, and induce protective antibodies. The above findings indicate that polyprotein NE2 mimics the crude structure of HEV ORF2^[4]. Monoclonal antibodies were selected by immunizing BALB/c mice with NE2^[7,9], 3 of which named 8C11, 8H3 and 13D8 were identified to be mAbs which could recognize 2 different epitopes of HEV. These 3 mAbs were proved to be neutralizing mAb by *in vivo* neutralization test in rhesus. The 2 epitopes recognized by mAbs (1 bound to 8C11 and 13D8, and the other to 8H3) were tested to be conformational epitopes. We panned the random phage display heptapeptide library, which displayed the linear epitope constructed by heptapeptide, and the peptides could mimic the neutralizing epitope that could bind to the 2 mAbs (8C11 and 8H3). Furthermore, heptapeptides were recombined on HBcAg for expression in *E.coli*, and their activities were tested by Western blotting. The recombinant polyprotein expressed by plasmid pC149-mut-8C11A appeared to be the dimer of M_r 40 000 on SDS-PAGE, which could bind to mAb 8C11 similar to the monomer of NE2. While the production of plasmid pC149-mut-8H3A could form monomer (M_r 20 000) and dimer (M_r 40 000) on SDS-PAGE, and only the dimer could react with mAb on Western blotting. Maybe it is because that 7 amino acid peptide is too short, and to display it on the surface of recombinant HBcAg is in need of assistance of special conformation, HBcAg is a large protein while the monomer recombinant HBcAg can not display the exogenesis epitope of heptapeptide, so the activity of the monomer is not obvious.

The chemo-synthesized heptapeptide 8H3A could bind to mAb 8H3, but the binding was not stable. Comparing the dominant peptides' sequence with the primary structure of NE2, no same sequence was found, conforming that the epitopes recognized by mAbs 8C11 and 8H3 are not constructed by continuous amino acid of NE2, but the function of their spatial structure is similar to the mimic peptides.

The immunogenicity of HBcAg is the highest in all kinds of antigens of HBV. The design of vector pC149-mut was to insert foreign genes into amino acids 78 to 83^[10], the immunogenicity of that position was better. The inserted amino acid could replace the epitope that reacts with B cells easily, thus reducing their interference with the exogenous epitope in immune response. This feature made HBcAg to be a very useful vector for multi-epitope chimeric vaccine^[10,27], so did the pC149-mut vector, which was designed accordingly. In this study, heptapeptide was cloned into pC149-mut between the amino acids 78 to 83 of HBcAg, and the recombinant polyprotein could form VLP, which displayed the foreign heptapeptide on their surface and kept its immunogenicity. The known neutralizing epitopes of viruses are almost conformational epitopes, so the genetically engineered vaccine needs the recombinant protein to be in correct conformation, and be able to preserve the immunity. These 2 qualifications could result in a mass of genetically engineered screen. But if using the peptides which mimic the conformational neutralizing epitopes, using the plasmid pC149-mut as a vector to mimic peptide vaccine expression will get VLP antigens, which remain the activation of neutralizing epitopes, and ensure the immunity of the vaccine, at the same time result in protective immunity. On the one hand, this tactics makes it available to unite more than one kind of virus' s neutralizing epitopes on the VLP antigen. That is to say, it is a way to develop polyvalent vaccines, which shows new direction in the development of new vaccine^[28-31]. The preventer of polyvalent vaccine is that the neutralizing epitopes are almost conformational, if in term of the routine method the conformational epitope cannot be exactly formed. On the other hand, if the chemo-synthesized peptide is used, the immunity will be influenced because of the low molecular mass of peptide. In a word, using the recombinant vector to express the protein, which can form VLP, and using the linear functional mimic epitope, which is displayed on the surface of VLP antigen instead of the conformational neutralizing epitope, is a new feasible idea to settle the difficulties in polyvalent vaccines.

REFERENCES

- Zhuang H**, Cao XY, Liu CB, Wang GM. Epidemiology of hepatitis E in China. *Gastroenterol Jpn* 1991; **26** (Suppl 3): 135-138
- Huang RT**, Li XY, Xia XB, Yuan XT, Liu MX, Li DR. Antibody detection and sequence analysis of sporadic HEV in Xiamen region. *World J Gastroenterol* 1999; **5**: 270-272
- Purcell RH**, Emerson SU. Hepatitis E virus. In Knipe DM, Howley PM, Griffin DE, eds. *Fields virology*, 4th ed. vol2. Philadelphia: *Lippincott Raven Pub* 2001: 3051-3061
- Li SW**, Zhang J, He ZQ, Ge SX, Gu Y, Ling J, Liu RS, Xia NS. The study of aggregate of the ORF2 peptide of hepatitis E virus expressed in *Escherichia coli*. *Shengwu Gongcheng Xuebao* 2002; **18**: 463-467
- Ge SX**, Zhang J, Huang GY, Pang SQ, Zhou KJ, Xia NS. The Immuno-protect study of a hepatitis E virus ORF2 peptide expressed in *E.coli*. *Weishengwu Xuebao* 2003; **43**: 35-42
- Li SW**, He ZQ, Wang YB, Chen YX, Liu RS, Lin J, Gu Y, Zhang J, Xia NS. Interface domain of hepatitis E virus capsid protein homodimer. *Shengwu Gongcheng Xuebao* 2004; **20**: 90-98
- Gu Y**, Zhang J, Li SW, Ge SX, He ZQ, Zhu ZH, Xian YL, Li YM, Xia NS. Characterization of the anti-HEV ORF2 monoclonal antibodies by biosensor. *Xibao Yu Fenzi Mianyixue Zazhi* 2002; **18**: 617-620

- 8 **Ge SX**, Zhang J, Peng G, Huang GY, He ZQ, Gu Y, Zhu ZH, Ng MH, Xia NS. Development and evaluation of ELISAs for anti-hepatitis E virus IgM and IgG detection based on polymerized recombinant antigen. *Bingdu Xuebao* 2003; **19**: 78-86
- 9 **Gu Y**, Ge SX, Huang GY, Li SW, Zhu ZH, He ZQ, Chen YX, Wang YB, Zhang J, Xia NS. Identification of neutralizing monoclonal antibodies to the hepatitis E virus. *Bingdu Xuebao* 2003; **19**: 217-223
- 10 **Bottecher B**, Wynne SA, Crowther RA. Determination of the fold of the core protein of hepatitis B virus by electron cryomicroscopy. *Nature* 1997; **386**: 88-91
- 11 **Ding CL**, Yao K, Zhang TT, Zhou F, Xu L, Xu JY. Generation of cytotoxic T cell against HBcAg using retrovirally transduced dendritic cells. *World J Gastroenterol* 2003; **9**: 1512-1515
- 12 **Luo WX**, Zhang J, Yang HJ, Li SW, Xie XY, Pang SQ, Li SQ, Xia NS. Construction and application of an Escherichia coli high effective expression vector with an enhancer. *Shengwu Gongcheng Xuebao* 2000; **16**: 578-581
- 13 **Yu ZC**, Ding J, Nie YZ, Fan DM, Zhang XY. Preparation of single chain variable fragment of MG₇ mAb by phage display technology. *World J Gastroenterol* 2001; **7**: 510-514
- 14 **Wu BP**, Xiao B, Wan TM, Zhang YL, Zhang ZS, Zhou DY, Lai ZS, Gao CF. Construction and selection of the natural immune Fab antibody phage display library from patients with colorectal cancer. *World J Gastroenterol* 2001; **7**: 811-815
- 15 **Ferrer M**, Sullivan BJ, Godbout KL, Burke E, Stump HS, Godoy J, Golden A, Profy AT, van Schravendijk MR. Structural and functional characterization of an epitope in the conserved C-terminal region of HIV-1 gp120. *J Pept Res* 1999; **54**: 32-42
- 16 **MacDonald NJ**, Shivers WY, Narum DL, Plum SM, Wingard JN, Fuhrmann SR, Liang H, Holland-Linn J, Chen DH, Sim BK. Endostatin binds tropomyosin. A potential modulator of the antitumor activity of endostatin. *J Biol Chem* 2001; **276**: 25190-25196
- 17 **Kiczak L**, Kasztura M, Koscielska-kasprzak K, Dadlez M, Otlewski J. Selection of potent chymotrypsin and elastase inhibitors from M13 phage library of basic pancreatic trypsin inhibitor (BPTI). *Biochim Biophys Acta* 2001; **1550**: 153-163
- 18 **Aramburu J**, Yaffe MB, Lopez-Rodriguez C, Cantley LC, Hogan PG, Rao A. Affinity-driven peptide selection of an NFAT inhibitor more selective than cyclosporin A. *Science* 1999; **285**: 2129-2133
- 19 **Shchelkunov SN**, Nesterov AE, Ryazankin IA, Ignat'ev GM, Sandakhchiev LS. Development of a candidate polyvalent live vaccine against human immunodeficiency, hepatitis B, and orthopox viruses. *Dokl Biochem Biophys* 2003; **390**: 180-183
- 20 **Ragupathi G**, Livingston P. The case for polyvalent cancer vaccines that induce antibodies. *Expert Rev Vaccines* 2002; **1**: 193-206
- 21 **Cardo-Vila M**, Arap W, Pasqualini R. Alpha v beta 5 integrin-dependent programmed cell death triggered by a peptide mimic of annexin V. *Mol Cell* 2003; **11**: 1151-1162
- 22 **Xu L**, Jin BQ, Fan DM. Selection and identification of mimic epitopes for gastric cancer-associated antigen MG7 Ag. *Mol Cancer Ther* 2003; **2**: 301-306
- 23 **Grothaus MC**, Srivastava N, Smithson SL, Kieber-Emmons T, Williams DB, Carlone GM, Westerink MA. Selection of an immunogenic peptide mimic of the capsular polysaccharide of Neisseria meningitidis serogroup A using a peptide display library. *Vaccine* 2000; **18**: 1253-1263
- 24 **Prinz DM**, Smithson SL, Westerink MA. Two different methods result in the selection of peptides that induce a protective antibody response to Neisseria meningitidis serogroup C. *J Immunol Methods* 2004; **285**: 1-14
- 25 **Zhang JZ**, Ng MH, Xia NS, Lau SH, Che XY, Chau TN, Lai ST, Im SW. Conformational antigenic determinants generated by interactions between a bacterially expressed recombinant peptide of the hepatitis E virus structural protein. *J Med Virol* 2001; **64**: 125-132
- 26 **Im SW**, Zhang JZ, Zhuang H, Che XY, Zhu WF, Xu GM, Li K, Xia NS, Ng MH. A bacterially expressed peptide prevents experimental infection of primates by the hepatitis E virus. *Vaccine* 2001; **19**: 3726-3732
- 27 **Pumpens P**, Razanskas R, Pushko P, Renhof R, Gusars I, Skrastina D, Ose V, Borisova G, Sominskaya I, Petrovskis I, Jansons J, Sasnauskas K. Evaluation of HBs, HBc, and frCP virus-like particles for expression of human papillomavirus 16 E7 oncoprotein epitopes. *Intervirology* 2002; **45**: 24-32
- 28 **Sompuram SR**, Kodala V, Ramanathan H, Wescott C, Radcliffe G, Bogen SA. Synthetic peptides identified from phage-displayed combinatorial libraries as immunodiagnostic assay surrogate quality-control targets. *Clin Chem* 2002; **48**: 410-420
- 29 **Poloni F**, Puddu P, Moretti F, Flego M, Romagnoli G, Tombesi M, Capone I, Chersi A, Felici F, Cianfriglia M. Identification of a LFA-1 region involved in the HIV-1-induced syncytia formation through phage-display technology. *Eur J Immunol* 2001; **31**: 57-63
- 30 **Li BW**, Rush A, Zhang SR, Curtis KC, Weil GJ. Antibody responses to Brugia malayi antigens induced by DNA vaccination. *Filaria J* 2004; **3**: 1
- 31 **Combredet C**, Labrousse V, Mollet L, Lorin C, Delebecque F, Hurtrel B, McClure H, Feinberg MB, Brahic M, Tangy F. A molecularly cloned Schwarz strain of measles virus vaccine induces strong immune responses in macaques and transgenic mice. *J Virol* 2003; **77**: 11546-11554

Community-based survey of HCV and HIV coinfection in injection drug abusers in Sichuan Province of China

Yu-Hua Ruan, Kun-Xue Hong, Shi-Zhu Liu, Yi-Xin He, Feng Zhou, Guan-Ming Qin, Kang-Lin Chen, Hui Xing, Jian-Ping Chen, Yi-Ming Shao

Yu-Hua Ruan, Kun-Xue Hong, Shi-Zhu Liu, Yi-Xin He, Feng Zhou, Hui Xing, Jian-Ping Chen, Yi-Ming Shao, Center for AIDS/STD Control and Prevention, Chinese Center for Disease Control and Prevention, Beijing 100050, China

Guan-Qming Qin, Sichuan Provincial Center for Disease Control and Prevention, Chengdu 610031, Sichuan Province, China

Kang-Lin Chen, Xichang Center for STD and Leprosy Control, Xichang County 615000, Sichuan Province, China

Supported by the National Key Technologies Research and Development Program of China during Tenth Five-Year Plan Period, No. 2001BA705B02 and National Natural Science Foundation of China, No. 30170823

Correspondence to: Dr. Yi-Ming Shao, Division of Virology and Immunology, National Center for AIDS/STD Control and Prevention, Chinese Center for Disease Control and Prevention, 27 Nanwei Road, Xuanwu District, Beijing 100050, China. yshao@public3.bta.net.cn

Telephone: +86-10-63166184 **Fax:** +86-10-63154638

Received: 2003-10-10 **Accepted:** 2003-12-08

Abstract

AIM: To investigate the prevalence and risk factors of HCV/HIV coinfection in injection drug abusers (IDAs) in Lianshan Yi Autonomous Prefecture of Sichuan province, China.

METHODS: From November 8, 2002 to November 29, 2002, a community-based survey was conducted to investigate the demographic characteristics, patterns of shared injectors devices and sexual behaviors in IDAs. Blood samples were also collected to test HCV and HIV infection. A total of 379 subjects were recruited in the study through community outreach and peer recruiting methods.

RESULTS: Of the 379 IDAs, the HCV prevalence and HIV prevalence were 71.0% and 11.3%, respectively, and HCV/HIV coinfection was 11.3%. HCV infection was found in 100% and 67.3% of HIV-positive and HIV-negative IDAs, respectively. HIV prevalence was 16.0% in HCV positive IDAs while none of the HCV negative IDAs was positive for HIV. Ethnicity, shared needles or syringes and cotton in the past 3 mo and syphilis infection were associated with HCV/HIV coinfection shown by univariate analysis using chi-square test. Multivariate logistic regression analysis showed that shared needles or syringes in the past 3 mo (Odds ratio=3.121, 95% CI: 1.278-7.617, $P<0.05$) and syphilis infection (Odds ratio=2.914, 95% CI: 1.327-6.398, $P<0.01$) were significantly associated with HCV infection. No statistically significant association was found in univariate analysis between sexual behaviors and HCV/HIV coinfection.

CONCLUSION: Shared needles and syringes in the past 3 mo and syphilis infection were significantly associated with HCV infection. Further sero-epidemiological prospective cohort studies should be conducted to clarify the impact of syphilis and high risk sexual behaviors on HCV transmission through unprotected sexual intercourse.

Ruan YH, Hong KX, Liu SZ, He YX, Zhou F, Qin GM, Chen KL,

Xing H, Chen JP, Shao YM. Community-based survey of HCV and HIV coinfection in injection drug abusers in Sichuan Province of China. *World J Gastroenterol* 2004; 10(11): 1589-1593
<http://www.wjgnet.com/1007-9327/10/1589.asp>

INTRODUCTION

Since the first case in China of an injection drug abuser (IDA) with AIDS was reported in Yunnan Province along the border with Burma (Myanmar) in 1985^[1], China has experienced a rapid increase in the number of HIV/AIDS cases. The majority of HIV infections in China were currently found in rural residents in the western provinces. Furthermore, 71% of documented HIV cases were IDAs. The IDA population is at high risk for HIV infection and also has a high prevalence of HCV. The major mode of HCV and HIV transmission among IDAs is through shared drug injection devices^[2-9]. Because unprotected sexual intercourse is widespread among injection drug abusers, unsafe sexual intercourse is also a notable mode of HIV transmission in IDAs and general population. On the other hand, the association between HCV transmission and high-risk sexual behaviors needs to be clarified^[10-15]. Some studies have reported that HCV transmission through unsafe sexual intercourse can be enhanced in HIV positive patients due to HCV viremia and more active HCV infection with persistent viremia^[16,17]. Clinical progression is more rapid in patients with HCV/HIV coinfection than in patients with HIV only. The prognostic value of HCV infection for both clinical and immunological progression is significant at early stages of HIV infection^[18-24]. Furthermore, HIV coinfection in patients with HCV is associated with more rapid progression to liver failure and liver cancer. The HCV and HIV epidemics are a significant public health problem in China because of high HCV prevalence among HIV-positive IDAs. Studies have investigated HCV/HIV coinfection among IDAs recruited from detoxification centers or re-education centers in China. However, few community- or population-based studies have been performed on HCV/HIV coinfection among IDAs in China, especially in regard to the relationship between risk factors, such as shared injection devices and sexual behaviors, and HCV/HIV coinfection or HCV infection.

A community-based survey of HCV/HIV coinfection among IDAs was conducted in Xichang County, Sichuan Province, China, in November 2002. The aim of the cross-sectional study was to identify the specific risk factors for HCV/HIV coinfection among IDAs in Sichuan Province, China.

MATERIALS AND METHODS

Materials

Study participants were recruited through a community-based outreach method that involved the distribution of information materials regarding the study to the community. The outreach campaign was especially targeted to the known IDA groups. During the informed consent process, potential participants in our study were invited to be peer recruiters with the offer of financial incentives for recruiting other IDAs in the community.

After providing written informed consent, potential study participants underwent a screening interview designed to identify IDAs eligible for the study. All participants were at least 18 years of age, and injected drugs at least one time in the past 3 mo. Those who met the inclusion criteria then completed an HCV and HIV risk assessment interview, received HIV pre-test and risk reduction, underwent phlebotomy for HCV and HIV antibody testing, and received HIV post-testing counseling.

Sichuan Province is located in southwest China and the main drug transportation route from Yunnan and Guangxi to Xinjiang. Xichang County is located in Lianshan Yi Autonomous Prefecture of southwest Sichuan. The total population of Xichang County is 617 000. From November 8, 2002 to November 29, 2002, 379 IDAs based in the community of Xichang County were enrolled by the Xichang Center for STD and Leprosy Control to estimate the prevalence of HCV/HIV coinfection and to investigate the risk factors associated with HCV and HIV infection. The study protocol and informed consent were approved by the Institutional Review Board (IRB) of the Center for AIDS/STD Control and Prevention, Chinese Center for Disease Control and Prevention. Informed consent was obtained from all study participants before being interviewed.

Methods

Each study participant was assigned a unique and confidential identification number that was subsequently used to label questionnaire responses and serum specimens. An interviewer-administrated questionnaire was used to collect data on risk factors for HCV and HIV infection. Questions were concerned with demographic characteristics, drug use and drug injection behaviors, condom use and sexual behaviors. Demographic variables included age, gender, ethnicity, education, employment, marital status, and home ownership. Questions pertaining to drug use investigated the frequency of drug use and drug injection in the past 3 mo and the frequency of shared injection devices in the past 3 mo, including shared needles or syringes, cookers, cotton, rinse water, and use of front- or back-loading. Assessment of sexual behaviors included questions regarding sex behaviors with a steady partner or other partner(s) in the past 6 mo, condom use in the past month, exchange of money for sex partner in the past 6 mo, and the addition of any new sex partners in the past 6 mo. The interview, counseling and blood collection were performed at the site clinic of the Xichang Center for STD and Leprosy Control.

Each serum or plasma sample was collected from IDAs by venipuncture and tested for antibodies to HIV by enzyme-linked immunosorbent assay (ELISA; Beijing Wantai Biological Medicine Company, China). Positive results were confirmed by an HIV-1/HIV-2 Western immunoblot assay (HIV BLOT 2.2 WB; Genelabs, Singapore). Samples were considered as HIV-positive when both ELISA and Western immunoblot results were positive. Samples were tested for antibodies to HCV by ELISA (Beijing Jinhao Biological Production Company, China). The presence of antibodies to syphilis was tested by ELISA (Beijing Jinhao Biological Production Company, China), positivity was confirmed by passive particle agglutination test for detection of antibodies to *Treponema pallidum* (TPPA; Fujirebio, Inc., Japan).

EpiData software (EpiData 2.1 for Windows; The EpiData Association, Odense, Denmark) was used for data double entry and validation. Statistical analysis of chi-square test or Fisher's exact test was performed to screen behaviors and demographic characteristics associated with high risk for HCV and HIV infection. A multivariate logistic regression model was constructed to select independent risk factors of HCV infection and to control confoundings among various risk factors which provided both *P*-values and 95% confidence intervals for the Odds ratio (OR) point estimates. Data analyses were carried

out using the statistical analysis system (SAS 8.2 for Windows; SAS Institute Inc., North Carolina, USA).

RESULTS

Prevalence of HCV and HIV coinfection in IDAs

A total of 379 IDAs were investigated in this study. As shown in Table 1, HCV prevalence and HIV prevalence were 71.0% and 11.3%, respectively. HCV/HIV coinfection was 11.3%. HCV infection was found in 100% and 67.3% of HIV-positive and HIV-negative IDAs, respectively. HIV prevalence was 16.0% among HCV-positive IDAs and none of the HCV-negative IDAs was found to be HIV-positive.

Table 1 Prevalence of HCV/HIV coinfection in IDAs in Xichang County, Sichuan Province, China

HCV	HIV		Total
	Positive	Negative	
Positive	43	226	269
Negative	0	110	110
Total	43	336	379

Risk factors for HCV and HIV infection in IDAs

Table 2 presents the results of univariate analysis of demographics, risk variables of injection drug abusers in the past 3 mo, sexual behaviors in the past 6 mo, and syphilis infection. HCV/HIV coinfection showed a statistically significant association with ethnicity ($P < 0.01$), frequency of shared needles or syringes ($P < 0.05$) and cotton in the past 3 mo ($P < 0.05$) and syphilis infection ($P < 0.01$). The frequency of drug injection, shared rinse water and cooker in the past 3 mo all showed a strong but not statistically significant correlation with HCV/HIV coinfection, with *P* values near 0.05.

Stepwise multivariate logistic regression analyses were performed using risk factors of ethnicity; Frequency of drug injection, shared needles or syringes, rinse water, cooker and cotton in the past 3 mo and syphilis infection were included in the initial model to investigate the association with HCV infection. As shown in Table 3, shared needles or syringes in the past 3 mo ($P < 0.05$) and syphilis infection ($P < 0.01$) were independently associated with HCV infection.

DISCUSSION

Among male IDAs in preparatory cohorts for HIV vaccine trials in Thailand, the prevalence of HCV and HCV/HIV coinfection was 96.4% and 50.7%^[25]. In a study on IDAs from drug detoxification centers in Yunnan Province of China in 2000, the prevalence of HCV was 99.3% in HIV-positive IDAs^[26]. Lai *et al.*^[27] reported 15.4% HIV infection and 63.5% HCV infection in IDAs in Guangxi Zhuang Autonomous Region of China; HCV incidence was about 10 times more than HIV incidence. These studies showed that the prevalence of HCV and HIV was high in IDAs, and that HCV transmission was more rapid than HIV transmission.

In previous studies of HIV-positive populations in Xichang County in Sichuan Province, the prevalence of HCV was found to be approximately 60% in HIV-positive individuals^[28,29]. In this study, we found a relatively high prevalence (11.3%) of HCV/HIV coinfection in IDAs in Xichang County. Shared needles or syringes in the past 3 mo ($P < 0.05$) was significantly associated with HCV infection after demographic characteristics and other risk factors were controlled. However, multivariate analysis showed that shared devices were indirectly related to drug injection, such as cotton, rinse water, cookers, and front- or back-loading, while not significantly associated with HCV/HIV coinfection or with HCV infection. Univariate analysis showed

Table 2 Risk factors associated with HCV/HIV coinfection in IDAs in Xichang County, Sichuan Province, China

	Factor	Total <i>n</i>	HCV/HIV coinfection		HCV infection		χ^2	<i>P</i>
			<i>n</i>	Prevalence (%)	<i>n</i>	Prevalence (%)		
General								
Gender	Male	313	38	12.1	180	57.5	3.45	0.178
	Female	66	5	7.6	46	69.7		
Age(yr)	<29	208	25	12.0	123	59.1	0.21	0.901
	≥29	171	18	10.5	103	60.2		
Ethnicity	Han	243	20	8.2	142	58.4	10.29	0.006
	Other	136	23	16.9	84	61.8		
Years of education	≤6	158	22	13.9	94	59.5	2.93	0.231
	>6	221	21	9.5	130	58.8		
Marriage	Yes	113	16	14.2	66	58.4	1.30	0.521
	No	266	27	10.2	160	60.2		
Employed	Yes	167	20	12.0	91	54.5	3.52	0.172
	No	212	23	10.8	135	63.7		
Own home	Yes	132	20	15.2	76	57.6	2.94	0.23
	No	247	23	9.3	150	60.7		
Drug abuse and drug injection behaviors (past 3 mo)								
Frequency of Drug injection	<1 time/d	79	6	7.6	42	53.2	5.53	0.063
	≥1 time/d	300	37	12.3	184	61.3		
Frequency of shared Needles or syringes	<2 times/wk	332	35	10.5	193	58.1	7.42	0.025
	≥2 times/wk	47	8	17.0	33	70.2		
Frequency of Shared rinse water	<2 times/wk	336	36	10.7	196	58.3	5.67	0.059
	≥2 times/wk	43	7	16.3	30	69.8		
Frequency of Shared cooker	<2 times/wk	335	36	10.7	195	58.2	5.95	0.051
	≥2 times/wk	44	7	15.9	31	70.5		
Frequency of shared cotton	No	352	36	10.2	213	60.5	6.19	0.045
	Yes	27	7	25.9	13	48.1		
Front- or back-loading	No	364	40	11.0	220	60.4		0.180 ¹
	Yes	15	3	20.0	6	40.0		
Sexual behaviors (past 6 mo)								
Steady sex partner	No	209	25	12.0	124	59.3	0.18	0.914
	Yes	170	18	10.6	102	60.0		
Sex behavior with non-steady sex partner	No	241	25	10.4	144	59.8	0.72	0.698
	Yes	138	18	13.0	82	59.4		
Steady sex partner of IDU	No	308	35	11.4	182	59.1	0.24	0.889
	Yes	71	8	11.3	44	62.0		
Gave money for sex behavior	No	303	32	10.6	186	61.4	2.09	0.351
	Yes	76	11	14.5	40	52.6		
Received money for sex Behavior	No	334	39	11.7	195	58.4	1.82	0.403
	Yes	45	4	8.9	31	68.9		
Addition of new sex partner(s)	No	264	25	9.5	160	60.6	3.08	0.214
	Yes	115	18	15.7	66	57.4		
Presence of syphilis infection	No	321	30	9.3	189	58.9	13.07	0.001
	Yes	58	13	22.4	37	63.8		

Note:¹ χ^2 Fisher's exact test.

Table 3 Multivariate logistic regression analyses of risk factors associated with HCV prevalence in IDAs in Xichang County, Sichuan Province, China

Factor	β	SEM	<i>P</i> -value	Odds ratio	95% CI
Shared needle or syringe in the past 3 mo	1.1380	0.4553	0.0124	3.121	1.278-7.617
Syphilis infection	1.0695	0.4013	0.0077	2.914	1.327-6.398

that shared cotton in the past 3 mo was associated with HCV/HIV coinfection. Some studies reported that factors of indirectly shared injection devices, including cotton, rinse water, and cookers, posed significant risks for HIV infection in IDAs^[30-32].

The modes of HCV transmission have been a matter of important controversy in literature^[10-15]. Although a high prevalence of HCV was found in STD patients, female workers and homosexual partners might be suggestive of sexual transmission, drug injection might also play a significant role in HCV transmission^[14]. Furthermore, drug injection was the

main risk factor associated with HCV infection in homosexual and bisexual men, while the other risk factors after adjusting injection drug abuse included the number of sexual partners in the past year, anal sex and oral sex behaviors^[33]. Moreover, Alter *et al.*^[15] reported that unsafe heterosexual behavior, anal sex and oral sex behavior were associated with HCV infection, suggesting that both sex behavior and injection drug abuse may play significant roles in HCV transmission. Univariate and multivariate analysis showed that syphilis infection was associated with HCV/HIV coinfection and HCV infection.

However, univariate analysis showed that high risk sexual behaviors were not associated with HCV/HIV coinfection. Lai *et al.*^[27] reported that history of sexually transmitted diseases was independently associated with HIV infection in Guangxi Zhuang Autonomous Region. A study showed that the total number of past sexual partners was associated with HCV infection, but there was no relationship between HCV infection and the total number of sexual partners or sexual behaviors in the past several months^[34]. Two studies of STD individuals confirmed the important role that IDA played a role in HCV infection and sexual transmission played a minor role in HCV epidemiologies, such as homosexuality/bisexuality, syphilis seropositivity, and a history of syphilis^[35,36]. In our study, persistent use of condom (vaginal sex only) and non-use of condom in IDAs with steady sex partners, and non steady sex partners accounted for 7.6% (9/119) and 88.2% (105/119), 14.6% (13/89) and 68.5% (61/89) in the past month, respectively. This was the first evidence in our study that syphilis infection might contribute to HCV infection in IDAs in Sichuan Province, and syphilis infection is a significant indicator of past high risk sexual behaviors, which increase risk for HCV sexual transmission.

Further sero-epidemiological prospective cohort studies should be conducted to clarify the impact of syphilis and high risk sexual behaviors on HCV transmission through unprotected sexual intercourse.

ACKNOWLEDGEMENTS

The authors would like to thank Dr. Jon L. Yang, School of Medicine, University of California, San Francisco, for his comments.

REFERENCES

- 1 **Ma Y**, Li ZZ, Zhang KX, Yang WQ, Ren XH, Yang YF, Ning DM, Cun SZ, Wang BH, Liu SQ, Zhang JP, Zhao SD. Identification of HIV infection among drug users in China. *Zhonghua Liuxing Bingxue Zazhi* 1990; **11**: 184-185
- 2 **Yin N**, Mei S, Li L, Wei FL, Zhang LQ, Cao YZ. Study on the epidemiology and distribution of human immunodeficiency virus-1 and hepatitis C virus infection among intravenous drug users and illegal blood donors in China. *Zhonghua Liuxing Bingxue Zazhi* 2003; **24**: 962-965
- 3 **Zhong RX**, Luo HT, Zhang RX, Li GR, Lu L. Investigation on infection of hepatitis G virus in 105 cases of drug abusers. *World J Gastroenterol* 2000; **6**(Suppl 3): 63-63
- 4 **Hahn JA**, Page-Shafer K, Lum PJ, Ochoa K, Moss AR. Hepatitis C virus infection and needle exchange use among young injection drug users in San Francisco. *Hepatology* 2001; **34**: 180-187
- 5 **Maier I**, Wu GY. Hepatitis C and HIV co-infection: a review. *World J Gastroenterol* 2002; **8**: 577-579
- 6 **Murray JM**, Law MG, Gao Z, Kaldor JM. The impact of behavioural changes on the prevalence of human immunodeficiency virus and hepatitis C among injecting drug users. *Int J Epidemiol* 2003; **32**: 708-714
- 7 **Wu NP**, Li D, Zhu B, Zou W. Preliminary research on the co-infection of human immunodeficiency virus and hepatitis virus in intravenous drug users. *Chin Med J* 2003; **116**: 1318-1320
- 8 **Quaglio GL**, Lugoboni F, Pajusco B, Sarti M, Talamini G, Mezzelani P, Des Jarlais DC. Hepatitis C virus infection: prevalence, predictor variables and prevention opportunities among drug users in Italy. *J Viral Hepat* 2003; **10**: 394-400
- 9 **Taketa K**, Ikeda S, Suganuma N, Phornphutkul K, Peerakome S, Sitvacharanum K, Jittiwutikarn J. Differential seroprevalences of hepatitis C virus, hepatitis B virus and human immunodeficiency virus among intravenous drug users, commercial sex workers and patients with sexually transmitted diseases in Chiang Mai, Thailand. *Hepatol Res* 2003; **27**: 6-12
- 10 **Valdivia JA**, Rivera S, Ramirez D, De Los Rios R, Bussalleu A, Huerta-Mercado J, Pinto J, Piscocoy A. Hepatitis C virus infection in female sexual workers from northern lima. *Rev Gastroenterol Peru* 2003; **23**: 265-268
- 11 **Hammer GP**, Kellogg TA, McFarland WC, Wong E, Louie B, Williams I, Dille J, Page-Shafer K, Klausner JD. Low incidence and prevalence of hepatitis C virus infection among sexually active non-intravenous drug-using adults, San Francisco, 1997-2000. *Sex Transm Dis* 2003; **30**: 919-924
- 12 **Fletcher S**. Sexual transmission of hepatitis C and early intervention. *J Assoc Nurses Aids Care* 2003; **14**(Suppl 5): S87-S94
- 13 **Russi JC**, Serra M, Vinales J, Perez MT, Ruchansky D, Alonso G, Sanchez JL, Russell KL, Montano SM, Negrete M, Weissenbacher M. Sexual transmission of hepatitis B virus, hepatitis C virus, and human immunodeficiency virus type 1 infections among male transvestite commercial sex workers in Montevideo, Uruguay. *Am J Trop Med Hyg* 2003; **68**: 716-720
- 14 **Brettler DB**, Mannucci PM, Gringeri A, Rasko JE, Forsberg AD, Rumi MG, Garsia RJ, Rickard KA, Colombo M. The low risk of hepatitis C virus transmission among sexual partners of hepatitis C-infected hemophilic males: an international multicenter study. *Blood* 1992; **80**: 540-543
- 15 **Alter MJ**, Coleman PJ, Alexander WJ, Kramer E, Miller JK, Mandel E, Hadler SC, Margolis HS. Importance of heterosexual activity in the transmission of hepatitis B and non-A, non-B hepatitis. *JAMA* 1989; **262**: 1201-1205
- 16 **Mendes-Correa MC**, Barone AA, Guastini C. Hepatitis C virus seroprevalence and risk factors among patients with HIV infection. *Rev Inst Med Trop Sao Paulo* 2001; **43**: 15-19
- 17 **Lissen E**, Alter HJ, Abad MA, Torres Y, Perez-Romero M, Leal M, Pineda JA, Torronteras R, Sanchez-Quijano A. Hepatitis C virus infection among sexually promiscuous groups and the heterosexual partners of hepatitis C virus infected index cases. *Eur J Clin Microbiol Infect Dis* 1993; **12**: 827-831
- 18 **Romero M**, Perez-Olmeda M, Garcia-Samaniego J, Soriano V. Management of chronic hepatitis C in patients co-infected with HIV: Focus on safety considerations. *Drug Saf* 2004; **27**: 7-24
- 19 **Livry C**, Binquet C, Sgro C, Froidure M, Duong M, Buisson M, Grappin M, Quantin C, Portier H, Chavanet P, Piroth L. Acute liver enzyme elevations in HIV-1-infected patients. *HIV Clin Trials* 2003; **4**: 400-410
- 20 **Quintana M**, del Amo J, Barrasa A, Perez-Hoyos S, Ferreros I, Hernandez F, Villar A, Jimenez V, Bolumar F. Progression of HIV infection and mortality by hepatitis C infection in patients with haemophilia over 20 years. *Haemophilia* 2003; **9**: 605-612
- 21 **Hisada M**, Chatterjee N, Zhang M, Battjes RJ, Goedert JJ. Increased hepatitis C virus load among injection drug users infected with human immunodeficiency virus and human T lymphotropic virus type II. *J Infect Dis* 2003; **188**: 891-897
- 22 **Klein MB**, Lalonde RG, Suissa S. The impact of hepatitis C virus coinfection on HIV progression before and after highly active antiretroviral therapy. *J Acquir Immune Defic Syndr* 2003; **33**: 365-372
- 23 **Greub G**, Ledergerber B, Battegay M, Grob P, Perrin L, Furrer H, Burgisser P, Erb P, Boggian K, Piffaretti JC, Hirschel B, Janin P, Francioli P, Flepp M, Telent A. Clinical progression, survival, and immune recovery during antiretroviral therapy in patients with HIV-1 and hepatitis C virus coinfection: the Swiss HIV Cohort Study. *Lancet* 2000; **356**: 1800-1805
- 24 **Piroth L**, Duong M, Quantin C, Abrahamowicz M, Michardiere R, Aho LS, Grappin M, Buisson M, Waldner A, Portier H, Chavanet P. Does hepatitis C virus co-infection accelerate clinical and immunological evolution of HIV-infected patients? *AIDS* 1998; **12**: 381-388
- 25 **Paris R**, Sirisopana N, Benenson M, Amphaiphis R, Tuntichaivanich C, Myint KSA, Brown AE. The association between hepatitis C virus and HIV-1 in preparatory cohorts for HIV vaccine trials in Thailand. *AIDS* 2003; **17**: 1363-1367
- 26 **Zhang CY**, Yang RG, Xia XS, Qin SY, Dai JP, Zhang ZB, Peng ZZ, Wei T, Liu H, Pu DC, Luo JH, Takebe YT, Ben KL. High

- prevalence of HIV-1 and hepatitis C virus coinfection among injection drug users in the southeastern region of Yunnan, China. *JAIDS* 2002; **29**: 191-196
- 27 **Lai SH**, Liu W, Chen J, Yang JY, Li ZI, Li RJ, Liang FX, Liang SL, Zhu QY, Yu XF. Changes in HIV-1 incidence in Heroin Users in Guangxi province, China. *JAIDS* 2001; **26**: 365-370
- 28 **Yang TL**, Xu YC, Hu XH. The prevalence of HIV, HBC and HCV among drug users in Xichang county of Sichuan province. *Yufang Yixue Qingbao Zazhi* 2001; **17**: 170-171
- 29 **Wei DY**, Ma MJ, Gong WH, Han YH. The survey of HIV, HBV and HCV infection. *Yufang Yixue Qingbao Zazhi* 2000; **16**: 187
- 30 **Denis B**, Dedobbeleer M, Collet T, Petit J, Jamouille M, Hayani A, Brenard R. High prevalence of hepatitis C virus infection in belgian intravenous drug users and potential role of the "cotton-filter" in transmission: the GEMT study. *Acta Gastroenterol Belg* 2000; **63**: 147-153
- 31 **Hagan H**, Thiede H, Weiss NS, Hopkins SG, Duchin JS, Alexander ER. Sharing of drug preparation equipment as a risk factor for hepatitis C. *Am J Public Health* 2001; **91**: 42-46
- 32 **Thorpe L**, Ouellet L, Hershov R, Bailey S, Williams II, Monerrosso E. The multiperson use of non-syringe injection equipment and risk of hepatitis C infection in a cohort of young adult injection drug users, Chicago 1997-1999. *Ann Epidemiol* 2000; **10**: 472-473
- 33 **Osmoda DH**, Charlebois E, Sheppard HW, Page K, Winkelstein W, Moss AR, Reingold A. Comparison of risk factors for hepatitis C and hepatitis B virus infection in homosexual men. *J Infect Dis* 1993; **167**: 66-71
- 34 **Zhou PY**, Xu JH, Liao KH, Xu M, Wang JS. A survey of HCV prevalence and sexual behavior among STD patients in STD clinic. *Zhonghua Pifuke Zazhi* 1999; **32**: 403-404
- 35 **Fiscus SA**, Kelly WF, Battigelli DA, Weber DJ, Schoenbach VJ, Landis SE, Wilber JC, Van der Horst CM. Hepatitis C virus seroprevalence in clients of sexually transmitted disease clinics in North Carolina. *Sex Transm Dis* 1994; **21**: 155-160
- 36 **Bodsworth NJ**, Cunningham P, Kaldor J, Donovan B. Hepatitis C virus infection in a large cohort of homosexually active men: independent associations with HIV-1 infection and injecting drug use but not sexual behaviour. *Genitourin Med* 1996; **72**: 118-122

Edited by Wang XL and Xu FM

Modulation of human enteric epithelial barrier and ion transport function by Peyer's patch lymphocytes

Jie Chen, Lai-Ling Tsang, Lok-Sze Ho, Dewi K. Rowlands, Jie-Ying Gao, Chuen-Pei Ng, Yiu-Wa Chung, Hsiao-Chang Chan

Jie Chen, Lai-Ling Tsang, Lok-Sze Ho, Dewi K. Rowlands, Chuen-Pei Ng, Yiu-Wa Chung, Hsiao-Chang Chan, Epithelial Cells Biology Research Center, Department of Physiology, Faculty of Medicine, Chinese University of Hong Kong, Hong Kong, China

Jie-Ying Gao, Department of Immunology, Institute of Microbiology and Epidemiology, Academy of Military Medical Sciences, Beijing 100071, China

Jie Chen, Department of Biology, Faculty of Medicine, Shanxi Medical University, Taiyuan 030001, Shanxi Province, China

Supported by Strategic Program of Chinese University of Hong Kong, and Distinguished Yong Investigator Fund of the National Natural Science Foundation of China, 30029002

Correspondence to: Dr. Hsiao-Chang Chan, Department of Physiology, Chinese University of Hong Kong, Shatin, NT, Hong Kong, China. hsiaocchan@cuhk.edu.hk

Telephone: +852-2609-6839 **Fax:** +852-2603-5022

Received: 2003-12-28 **Accepted:** 2004-02-11

and ion transport function by Peyer's patch lymphocytes. *World J Gastroenterol* 2004; 10(11): 1594-1599
<http://www.wjgnet.com/1007-9327/10/1594.asp>

INTRODUCTION

The mucosal surface of the gastrointestinal tract is lined by a single layer of epithelial cells jointed together at their apical poles by tight junctions, forming a barrier that separates the luminal contents from the effector immune cells underneath. It has become increasingly clear that the intense immunological activities occurring at the enteric mucosal surface involve interactions between epithelial and immune cells^[1,2]. Accumulating evidence suggests that epithelial cells can produce cytokines and chemokines that attract and activate immune cells with potentially important effects on the immediate and long-term host defense functions. Effective immune surveillance of the mucosal surface requires transport of intact macromolecules and microorganisms across the epithelial barrier to the cells of mucosal immune system. Groups of organized mucosal lymphoid follicles, named Peyer's patches, lined along the gastrointestinal tract in a specialized overlying epithelium, are the sites for transporting, processing and presenting foreign antigens. In Peyer's patches, each follicle is separated from the overlying epithelium by a subepithelial "dome" region that is rich in lymphocytes and dendritic cells. It is apparent that the immune cells in the dome region interact intimately with the overlying epithelium, giving rise to mucosal immune response without the needs of systemic involvement^[3]. Although a mucosal lympho-epithelial internet has been proposed to mediate the interactions between epithelial and immune cells, details of the interactions are far from understood. The close contact between Peyer's patch lymphocytes and intestinal epithelial cells suggests that these lymphocytes may play a role in the modulation of epithelial barrier/transport functions in homeostasis as well as host defense. However, no evidence has been provided so far concerning the role of Peyer's patch lymphocytes in intestinal epithelial physiology.

In addition to their major defensive role as a passive barrier, the intestinal epithelial cells also play an active role in physiology and pathophysiology of the gut. While the absorptive properties of the epithelium are known to be of vital importance for the nutrition of the body, as well as the maintenance electrolytes and fluid balance, the secretory activities of the epithelium are also important for protective purpose. Luminally directed transport of Cl⁻ and HCO₃⁻ is the driving force for fluid secretion that flushes away noxious substances from the intestinal mucosal surface. Secretory diarrhea is often the consequence for increased water and electrolyte secretion upon invasion by microorganisms. *Escherichia*, *Salmonella* and *Shigella* are the most important bacterial causes of diarrhea worldwide^[4]. The pathogenesis of bacteria-induced diarrhea with regard to the involvement of Peyer's patch lymphocytes remains largely unknown although the barrier function and ion secretory responses of the intestinal epithelium have been shown to be affected by both proinflammatory and anti-inflammatory cytokines^[5-7].

Abstract

AIM: To investigate the role of Peyer's patch lymphocytes in the regulation of enteric epithelial barrier and ion transport function in homeostasis and host defense.

METHODS: Mouse Peyer's patch lymphocytes were co-cultured with human intestinal epithelial cell line Caco-2 either in the mixed or separated (isolated but permeable compartments) culture configuration. Barrier and transport functions of the Caco-2 epithelial monolayers were measured with short-circuit current (*I*_{sc}) technique. Release of cytokines was measured by enzyme-linked immunosorbent assay (ELISA) and cytokine mRNA expression was analyzed by semi-quantitative RT-PCR. Barrier and iontransport functions of both culture conditions following exposure to *Shigella* lipopolysaccharide (LPS) were also examined.

RESULTS: The transepithelial resistance (TER) of the epithelial monolayers co-cultured with Peyer's patch lymphocytes was maintained whereas that of the Caco-2 monolayers alone significantly decreased after eight days in culture. The forskolin-induced anion secretion, in either absence or presence of LPS, was significantly suppressed in the both co-cultures as compared with the Caco-2 cells alone. Furthermore, only the mixed co-culture condition induced the expression and release of mL-6 from Peyer's patch lymphocytes, which could be further enhanced by LPS. However, both co-culture conditions suppressed expression and release of epithelial hIL-8 under the unstimulated conditions, while the treatment with LPS stimulated their hIL-8 expression and release.

CONCLUSION: Peyer's patch lymphocytes may modulate intestinal epithelial barrier and ion transport function in homeostasis and host defense via cell-cell contact and cytokine signaling.

Chen J, Tsang LL, Ho LS, Rowlands DK, Gao JY, Ng CP, Chung YW, Chan HC. Modulation of human enteric epithelial barrier

The co-culture of characterized epithelial cells with defined immune cell populations and subsequent analysis of epithelial physiology have contributed significantly to our appreciation of the immune regulation of epithelial function^[8,9]. Kerneis *et al.*^[10] have successfully induced functional M cells by co-culturing Caco-2 cells, a human intestinal surface epithelial cell line, with murine Peyer's patch lymphocytes. This phenomenon indicates the profound influence of Peyer's patch lymphocytes on intestinal epithelial phenotypes^[11]. Thus, to investigate the role of Peyer's patch lymphocytes in intestinal epithelial barrier/transport function during infection, we adopted this co-culture system to build an infection model with *Shigella* LPS, one of the major virulence factors of Gram-negative bacteria that is responsible for eliciting a wide array of immune responses^[11,12]. The present study includes different co-culture configurations: One consisting of upper and lower compartments with a permeable filter separating the epithelial layer and lymphocytes, and the other mixing both epithelial cells and lymphocytes in the same compartment. Using these co-culture configurations, epithelial-immune interactions through cell-cell contact as well as cytokine signaling could be examined independently.

MATERIALS AND METHODS

Isolation of peyer's patch lymphocytes

BALB/c mice (SPF, female, 6-8 wk old) were obtained from the Animal House of Chinese University of Hong Kong. The lymphoid follicles of the Peyer's patch were carefully excised from the intestinal serosal side and placed in 10 mL phosphate buffered saline (PBS, pH 7.4, GIBCO 10010-31) supplemented with 20 mL/L FBS and 2% penicillin-streptomycin. The collected patches were triturated by pipetting up and down a few times and smashing through a metallic grid (mesh: 100). Individual lymphocytes were released in the liquid below the metallic grid. The lymphocytes were washed with PBS, the distribution of Peyer's patch T and B cell populations was consistent with previous data when they were checked by flow cytometry^[10], then diluted to the expected concentration.

Enteric epithelial cell culture

Human colonic cell line Caco-2, which is a villus cell-like colonic cell line^[13], was purchased from American Type Culture Collection (Rockville, MD). The cells were grown in Dulbecco Modified Eagle's minimal essential medium (DMEM, high glucose, GIBC-BRL) with 100 mL/L fetal bovine serum (FBS, GIBCO 16000-044), 2 mmol/L L-glutamine (GIBCO-BRL), 100 µmol/L non-essential amino acid (GIBCO-BRL), 200 units/mL penicillin and 200 µg/mL streptomycin (GIBCO-BRL) at 37 °C in a 50 mL/L CO₂ atmosphere. Caco-2 cells were seeded at a density of 3×10⁵ cells on a floating permeable support, which was made of a membrane filter (Millipore, 0.45 µm pore size) with a silicone rubber ring attached on top of it for confining the cells (0.45 cm² growth area).

Co-culture configurations

Three types of culture configurations were established in this study: (1) Caco-2 culture alone: Caco-2 cells (3×10⁵ cells) were grown as a homogenous polarized monolayer according to the epithelial cell culture method mentioned above and served as the control. (2) Separated co-culture: Epithelial cells (3×10⁵ cells) were plated on a permeable support (growth area of 0.45 cm² as described), which floated above 2 mL culture medium containing Peyer's patch lymphocytes (5×10⁶ cells) in a Petri dish (3.5-cm diameter). (3) Mixed co-culture: Caco-2 cells (3×10⁵ cells) were directly mixed with Peyer's patch lymphocytes (1×10⁶ cells), and then were seeded on the same permeable support described above and grown at 37 °C in a 50 mL/L CO₂ atmosphere.

Shigella F2a-12 LPS pretreatment

When the Caco-2 cells grown as polarized monolayers on the membrane filter reached confluence on the 4th d, *Shigella F2a-12* LPS (5 µg/mL, obtained from the Immunology Department of Institute of Microbiology & Epidemiology, Academy of Military Medical Sciences) was added to the apical side of the epithelial monolayers and treated for 8, 24 and 48 h at 37 °C in a 50 mL/L CO₂ atmosphere.

Short-circuit current measurements (Isc)

The *Isc* measurement has been described previously^[14]. In short, the confluent monolayers were clamped vertically between the two halves of an Ussing chamber. Monolayers were short circuited (transepithelial potential difference clamped at zero) using a voltage-clamp amplifier (DVC-1000; World Precision Instruments Inc., New Haven, CT, USA). The resulting *Isc* was displayed on-line on a pen recorder (Kipp and Zonen, Delft, The Netherlands). Transepithelial electrical resistance (TER) was determined based on Ohm's law by clamping the tissue intermittently at a value of 0.2 mV. For most measurements, the monolayers were bathed in normal Krebs-Henseleit solutions (NaCl, 117 mmol/L; KCl, 4.7 mmol/L; MgCl₂, 1.2 mmol/L; NaHCO₃, 24.8 mmol/L; KH₂PO₄, 1.2 mmol/L; CaCl₂, 2.56 mmol/L; Glucose, 11.1 mmol/L) with 950 mL/L O₂ and 50 mL/L CO₂.

Semi-quantitative RT-PCR

Caco-2 monolayers grown on the filters (Millipore, 0.22 µm pore size, cell growth area of 7.065 cm²) were harvested for RT-PCR after 8-h and 24-h *Shigella F2a-12* LPS pre-treatment. The specific primers for hIL-8^[15] were 5' tct ctt ggc agc ctt cct 3' (sense) and 5' gaa gtg tca ctg gca tct tca c 3' (antisense), corresponding to the nucleotides 98-427 with the expected cDNA size of 390 bp (Tm 58 °C, 30 cycle); mIL-6^[16] were 5' ctg caa gag act tcc atc cag 3' (sense) and 5' tcc agt ttg gta gca tcc atc 3' (antisense), corresponding to the nucleotides 45-340 with the expected cDNA size of 296 bp (Tm 55 °C, 35 cycle). Their expression was compared to the house-keeping gene GAPDH (forward: 5' tcc cat cac cat ctt cca g 3' and reverse: 5' tcc acc act gac acg ttg 3'). RT-PCR was performed using the PTC-200 Peltier Thermal Cycler (MJ Research Company) and software for analysis data is GraphPad Prism 3.02.

Enzyme-linked immunosorbent assay (ELISA)

After confluent Caco-2 monolayers on the Millipore filter was challenged by *Shigella F2a-12* LPS pretreatment for 8 and 24 h, the culture medium was collected and kept at -20 °C until evaluation hIL-8 and mIL-6 bioassay using ELISA kits (BIOSOURCE Company) according to manufacturer's instructions.

Statistical analysis

All data were expressed as mean±SE. The number of experiments represents independent measurements on separate monolayers. Comparisons between groups of data were made by one-way ANOVA. A "P" value of less than 0.05 was considered statistically significant.

RESULTS

Co-culture with Peyer's patch lymphocytes results in better maintenance of epithelial barrier function but LPS decreases it

Polarized monolayers of Caco-2 were tested for transepithelial resistance (TER) at various times (the 4th, 6th and 8th d after co-culture) (Figure 1). A significant decrease in TER was observed in Caco-2 alone after eight days in culture, whereas high TER could still be maintained for either mixed or separated co-cultures for the same period of time (Figure 1). However, after treatment with *Shigella* LPS (5 µg/mL) for 48 h, TER measured on the

6th d of co-culture, decreased significantly in both co-culture groups but not in Caco-2 alone (Figure 2).

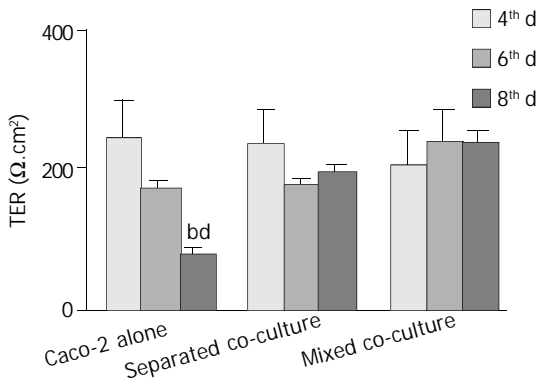


Figure 1 Comparison of time-dependent changes in transepithelial resistance (TER) of different culture groups. Data in all panels are mean±SE for 4 experiments, significant differences relative to its own 4-d of culture in Caco-2 alone (^b*P*<0.01), and to its own 6th day culture of Caco-2 alone (^d*P*<0.001) are indicated.

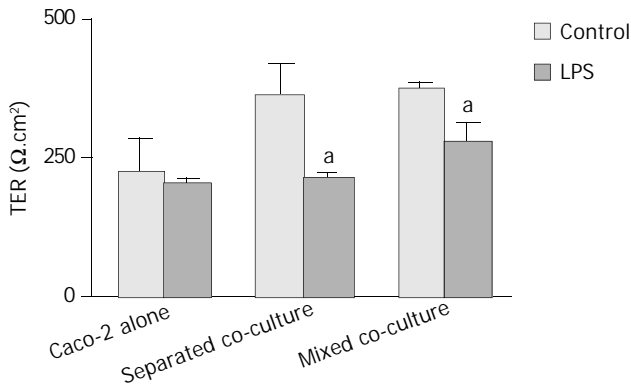


Figure 2 Effect of *Shigella* F2a-12 LPS on transepithelial resistance (TER) of different culture groups. Cultured monolayers were exposed to LPS 48-h prior to TER measurement on the 6 d of culture. Comparison of TER in the absence or presence of *Shigella* F2a-12 LPS among the three culture groups. The values indicate mean±SE; *n*=5; ^a*P*<0.05 (compared to its own control).

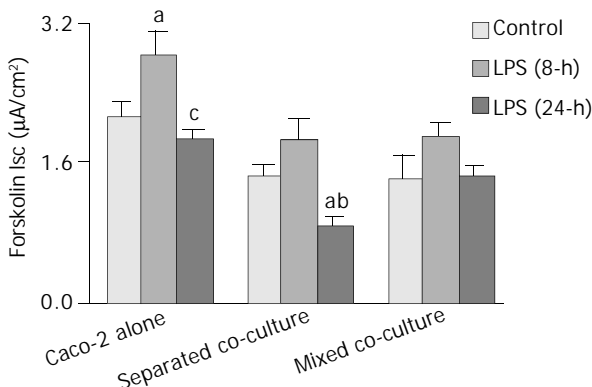


Figure 3 Effect of *Shigella* F2a-12 LPS on the Forskolin-induced *Isc*. Comparison of the Forskolin (4 μg/mL, basoateral addition)-induced *Isc* in the absence or presence of LPS for 8-h and 24-h under different culture conditions. The values indicate mean±SE; *n*=12; ^a*P*<0.05 (compared to its own control); ^c*P*<0.05 and ^b*P*<0.001 (compared to its own LPS treatment for 8-h).

Co-culture with Peyer’s patch lymphocytes alters anion secretory responses

The *Isc* responses of the co-cultures and Caco-2 alone to the

challenge of an adenylate cyclase activator, forskolin, were characterized. As shown in Figure 3, significantly lower *Isc* response was observed in both co-cultures than that of the Caco-2 alone control in the absence of LPS. Increased responses in all groups were observed after 8-h LPS treatment. Significantly more upregulated *Isc* response was observed in Caco-2 alone group (Figure 3). After 24 h of LPS treatment, the *Isc* responses of the separated co-culture and Caco-2 alone groups decreased significantly as compared with that of 8-h LPS treatment but not the mixed co-culture (Figure 3). No significant differences in the basal *Isc* among the groups were observed, nor did it change significantly upon treatment with LPS (data not shown).

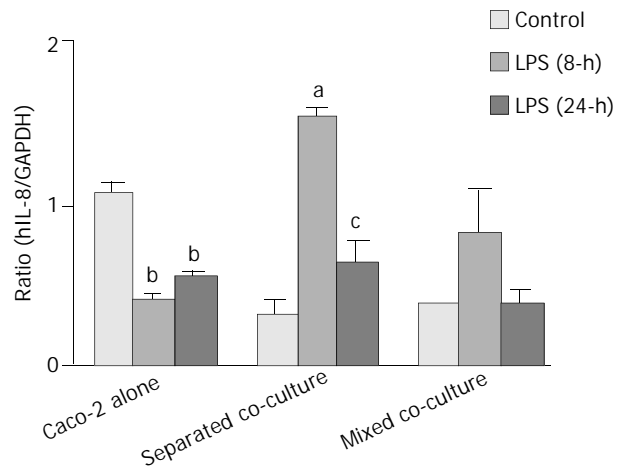
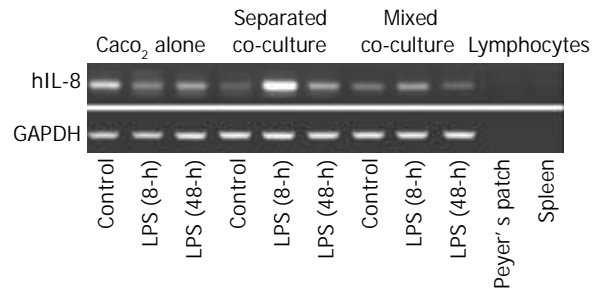


Figure 4 Induction of hIL-8 expression in Caco-2 cells by *Shigella* F2a-12 LPS in different culture groups. Comparison of hIL-8 expression in Caco-2 cells in the absence or presence of LPS for 8-h and 24-h between three culture groups by semi-quantitative RT-PCR with Peyer’s patch lymphocytes as negative control. The values indicate mean±SE; ^a*P*<0.05, ^b*P*<0.01 (compared to its own control); ^c*P*<0.05 (compared to separated co-culture LPS pre-treatment for 8-h).

Separated co-culture results in enhanced expression and release of hIL-8 from Caco-2 cells

To examine the mRNA expression of hIL-8, primers specific for hIL-8 were used in RT-PCR experiments, and the RNA from mouse Peyer’s patch lymphocytes was used as negative control to detect any potential. The results are shown in Figure 4. The highest level of hIL-8 expression was observed in the Caco-2 alone as compared to the other two co-cultures when they were cultured in the absence of LPS. However, after treatment with LPS for 8 h, lower hIL-8 expression was observed in the Caco-2 culture alone while increased hIL-8 expression was evident in both co-cultures. The increase in the hIL-8 expression was particularly more enhanced in the separated co-culture. After 24 h, the expression of hIL-8 in the co-cultures returned closer to their basal levels but the expression in the Caco-2 alone remained low as compared with its own control. The expression of hIL-8 was not detected in mouse Peyer’s patch lymphocytes confirming that the above expression profile of hIL-8 was associated with human intestinal epithelial cells.

ELISA using a human kit was conducted to confirm the release of hIL-8 from different cultures with mouse Peyer's patch lymphocytes as a control for cross-reactivity. The results showed that the levels of hIL-8 released from the Caco-2 alone culture under the unstimulated condition and 8-h LPS treatment were significantly greater than that from both co-cultures (Figure 5). However, following the 24-h LPS treatment, levels of hIL-8 in both co-culture groups increased considerably while a decrease was observed in Caco-2 alone (Figure 5). A detectable amount of hIL-8 was also observed from mouse Peyer's patch lymphocytes (1×10^6 cells), indicating the presence of condition cross-reactivity of human IL-8 antibody to mouse IL-8 (Figure 5).

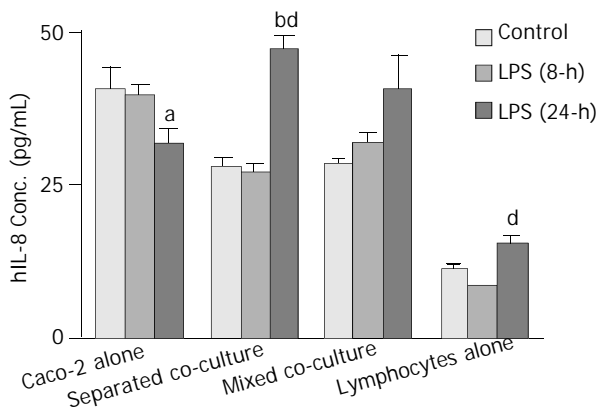


Figure 5 Comparison of *Shigella* F2a-12 LPS-induced hIL-8 release from different culture groups by ELISA. Culture groups and Peyer's patch lymphocytes alone (control, 1×10^6 cells) were treated with LPS for 8-h and 24-h. The presented values indicate mean \pm SE; $n=8$; ^b $P < 0.001$ (compared to its own control); ^a $P < 0.05$ and ^d $P < 0.001$ (compared to its own LPS treatment for 8-h).

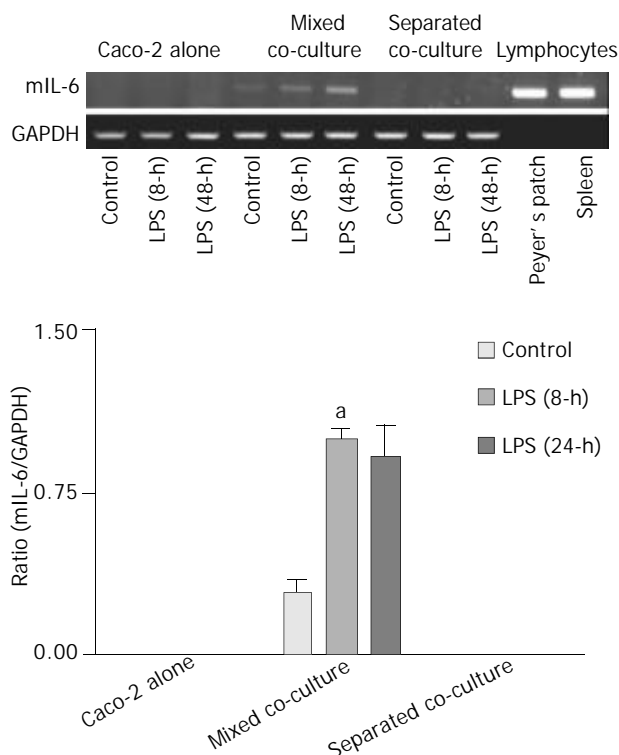


Figure 6 Induction of mIL-6 expression by *Shigella* F2a-12 LPS in different culture groups. Comparison of mIL-6 expression in the absence or presence of LPS for 8-h and 24-h among the culture groups by semi-quantitative RT-PCR with mouse Peyer's patch lymphocytes as positive control. The values indicate mean \pm SE ^a $P < 0.01$ (compared to the mixed control).

The mixed co-culture condition triggers expression and release of mIL-6 from Peyer's patch lymphocytes

Using primers specific for mIL-6, the expected RT-PCR product of mIL-6 was detected in the mixed co-culture and mouse lymphocytes but not in the Caco-2 culture alone or separated co-culture, where only the epithelial cells in the upper compartment were subjected to RT-PCR, thus excluding detection of IL-6 from the Peyer's patch lymphocytes in the medium. The expression of mIL-6 in the mixed co-culture further increased after 8 and 24 h of treatment with LPS (Figure 6).

The release of mIL-6 from different cultures, as well as mouse Peyer's patch lymphocytes (1×10^6 cells), was measured using a mouse ELISA kit. The results showed that no groups except the mixed co-culture had detectable mIL-6 release either in the absence or presence of LPS treatment (Figure 7). The level of mIL-6 measured in the mixed co-culture group significantly increased after 24-h LPS treatment (Figure 7).

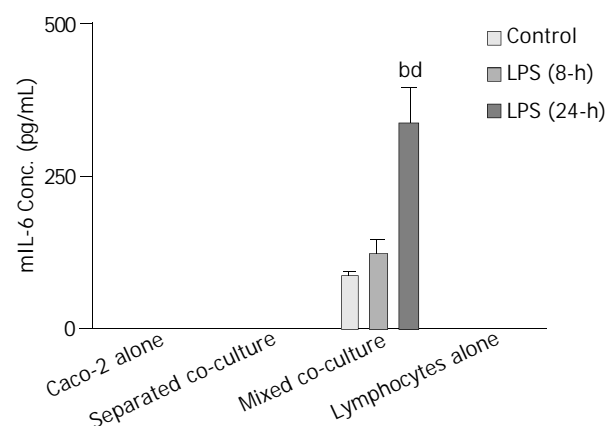


Figure 7 Comparison of *Shigella* F2a-12 LPS-induced mIL-6 release from different culture groups by ELISA. Culture groups and Peyer's patch lymphocytes (1×10^6 cells) were treated with LPS for 8-h and 24-h. The values indicate mean \pm SE; $n=5$; ^b $P < 0.01$ (compared to mixed co-culture control) and ^d $P < 0.01$ (compared to the mixed LPS treatment for 8-h).

DISCUSSION

The present study has demonstrated for the first time the role of Peyer's patch lymphocytes in intestinal epithelial physiology in homeostasis as well as host defense. Both epithelial barrier function and anion secretory activities, under normal or infected conditions, were affected by the presence of Peyer's patch lymphocytes to various extent depending on the co-culture configurations. TER has been used as an index of epithelial barrier integrity, which is sometimes compromised in certain infections, possibly as a direct result of modulation by immune cells^[17]. Previous studies in co-cultures of epithelial cells and immune cells, including lamina propria mononuclear cells (LPMC)^[18] and intraepithelial lymphocytes^[19], invariably resulted in disruption of epithelial barrier function as indicated by a decrease in TER. However, the present study did not observe significant reduction in the TER in the Caco-2 co-cultures with Peyer's patch lymphocytes, either in the separated or mixed configuration, as compared with the Caco-2 culture alone. On the contrary, the TER in both co-cultures could be maintained up to eight days whereas that in Caco-2 control decreased drastically. These results suggest that unlike other types of immune cells previously studied, Peyer's patch immune cells, which consist mostly of lymphocyte (99%)^[10], play a distinct homeostatic regulatory role in maintaining the barrier function of the epithelial monolayers. However, TER of both co-cultures decreased substantially after treatment with *Shigella* LPS for

48 h, indicating that *Shigella* LPS may have direct effect on epithelial barrier function without the modulation of Peyer's patch lymphocytes. This notion is also supported by the observed mRNA expression of tight junction-associated protein ZO-1 in both co-cultures with Peyer's patch lymphocytes (data not shown). It has been shown that LPS accounts for a large part of the transepithelial signaling caused by apical *Shigella* bacteria that induces adherence and transmigration of basal polymorphonuclear leukocytes (PMNs), which disrupt the monolayer permeability and facilitate bacterial invasion^[20].

Similar to the barrier function, the epithelial secretory activities, in both homeostasis and infection, were also affected by the presence of Peyer's patch lymphocytes, depending on the configuration of the co-cultures. In normal conditions (or in the absence of LPS), reduced forskolin-induced *Isc* was observed when Peyer's patch lymphocytes were co-cultured with Caco-2 and the *Isc* response in the Caco-2 alone group was significantly increased after LPS challenge up to eight hours. These results suggest that the forskolin-induced *Isc* response could be suppressed by Peyer's patch lymphocytes. However, down-regulation of forskolin-induced anion secretion could be seen in all groups 24 h after LPS challenge, suggesting that cytokine signaling also plays a role at later stages of infection, perhaps affecting the expression of ion channels. Interestingly, the *Isc* response of anion secretion in the mixed co-culture showed no significant change in the absence or presence of LPS, suggesting that cell-cell contact is important for modulation of epithelial anion secretion by Peyer's patch lymphocytes. In contrast to many previous results obtained from *in vitro* epithelial model cells showing anion secretion stimulated by bacteria^[21] or immune and inflammatory modulators produced by inflammatory cells^[22], the present results show no change in the forskolin-induced anion secretion in the mixed co-cultures in the absence or presence of LPS. Reduced secretory responsiveness has also been observed in the epithelial cell models that are co-cultured with a number of different immune cells^[7]. This is also consistent with the observation that colonic mucosa from patients with chronic inflammatory bowel disease respond poorly to secretagogues^[23]. Thus, it appears that the epithelial secretory response in homeostasis and infection is modulated by immune cells including Peyer's patch lymphocytes. The present results showed that Peyer's patch lymphocytes suppressed epithelial secretory activity, especially upon LPS challenge, suggesting that the secretory diarrhea caused by bacterial infection may not be solely due to enhanced water and electrolyte secretion. Recent studies have suggested that the inhibition of Na⁺-K⁺-ATPase by interferon γ that leads to the reduction of Na⁺ absorption may be a major cause of inflammation-associated diarrhea^[24]. The inhibition of Na⁺-K⁺-ATPase induced by interferon γ may also account for the presently observed Peyer's patch lymphocyte-suppressed anion secretion since secondary active anion secretion depends on the Na⁺ gradient generated by the Na⁺-K⁺-ATPase. Further studies examining the expression of various ion channels and transporters including Na⁺-K⁺-ATPase and CFTR in response to LPS challenge are currently undertaken in our laboratory.

The present results suggest that the modulation of epithelial physiology by Peyer's patch lymphocytes involves both cell-cell contact and cytokine signaling. The mouse-human hybrid co-cultures in different configurations, mixed and separated, not only allow the distinction of contact-dependent and independent signaling mechanisms but also the identification of the source of cytokines, although homology between human and mouse cytokine may result in cross-reactivity as seen in the ELISA results showing detectable hIL-8 measured from mouse Peyer's patch lymphocytes using a human kit. Further experiment with RT-PCR using species-specific primers could also be conducted to confirm the source of cytokines. In fact,

the ELISA results were closely correlated with the RT-PCR results with a time lag in the response to LPS. This observation is consistent with the fact that the transcriptional changes occur prior to the translational changes^[25].

The more prominent effects on forskolin-induced anion secretion observed in the mixed co-culture as compared to that in the separated co-culture indicate the importance of cell-cell contact in addition to cytokine communication. In fact, cell-cell contact appears to be absolutely required for the enhancement of the expression and release of mIL-6 from Peyer's patch lymphocytes under both normal condition and LPS challenge. This observation is of physiological significance considering the close contact between Peyer's patch lymphocytes and intestinal epithelial cells in the Peyer's patches. IL-6 is known to be produced by a number of cell types including antigen-presenting cells and B cells and it is involved in the acute phase response, B cell maturation and macrophage differentiation^[26]. IL-6 has also been reported to activate transcription of a variety of molecules including cytokines and receptors^[27]. Therefore, cell-cell contact-induced IL-6 release from Peyer's patch lymphocytes may affect the expression of epithelial ion channels and transporters and lead to modulation of epithelial function. On the other hand, more enhanced expression and release of hIL-8 from Caco-2 cells was observed in the separated co-culture than the mixed co-culture. This is consistent with the properties of IL-8 as a chemokine for attracting immune cells to the site of inflammation since the separation of Peyer's patch lymphocytes from Caco-2 cells in the separated co-culture presents a need for IL-8 to signal the recruitment of lymphocytes. However, there is no need for production of IL-8 if the lymphocytes are present next to the epithelial cells as in the mixed co-culture. Epithelial hIL-8 production has been implicated in the disruption of the epithelial barrier function by *Shigella*^[28] as well as other enteroinvasive bacteria^[29]. Bacterial invasion turns the infected epithelial cells to become strongly proinflammatory with subsequent IL-8 production that attracts polymorphonuclear leukocytes (PMNs), ultimately leading to the disruption of the epithelium. This study only investigated the mIL-6 and hIL-8 expression and release from lymphocytes and epithelial cell to illustrate possible interactions through soluble factors between epithelial and immune cells. Other cytokines may also play a role in the regulation of epithelial physiology by Peyer's patch lymphocytes. The observed expression and release of mIL-6 and hIL-8, constitutively and in response to the LPS challenge, suggest that they may be involved in mediating the modulatory effects of Peyer's patch lymphocytes on epithelial barrier and ion transport function in homeostasis and host defense. Further studies are required to identify their specific roles as well as the involvement of other immune mediators in the modulation of epithelial physiology.

In summary, being the sensory arm of the intestinal mucosa, Peyer's patches are not only involved in transporting, processing and presentation of antigens/pathogens that are essential to eliciting mucosal immune response, but also play an important role in modulating epithelial physiology. This function is distinct from other types of lymphocytes previously studied. Our results indicated that lymphocytes in Peyer's patches receive information from mucosal surface epithelial cells, via both cell-cell contact and cytokine signaling, and in return modulate epithelial barrier and ion transport function in both homeostasis and host defense. Since immune modulation determines the epithelial responsiveness to infection, the co-cultures of epithelial cells with Peyer's patch lymphocytes may provide useful models in studying the initiation process involved in the pathogenesis of inflammation-associated diarrhea.

REFERENCES

- 1 Berin MC, McKay DM, Perdue MH. Immune-epithelial inter-

- actions in host defense. *Am J Trop Med Hyg* 1999; **60**: 16-25
- 2 **Hamzaoui N**, Pringault E. Interaction of microorganisms, epithelium, and lymphoid cells of the mucosa-associated lymphoid tissue. *Ann N Y Acad Sci* 1998; **859**: 65-74
 - 3 **Neutra MR**, Mantis NJ, Kraehenbuhl JP. Collaboration of epithelial cells with organized mucosal lymphoid tissues. *Nat Immunol* 2001; **2**: 1004-1009
 - 4 **Farthing MJ**. Novel targets for the pharmacotherapy of diarrhoea: a view for the millennium. *J Gastroenterol Hepatol* 2000; **15**(Suppl): G38-G45
 - 5 **Beltinger J**, McKaig BC, Makh S, Stack WA, Hawkey CJ, Mahida YR. Human colonic subepithelial myofibroblasts modulate transepithelial resistance and secretory response. *Am J Physiol* 1999; **277**: C271-C279
 - 6 **Lu J**, Philpott DJ, Saunders PR, Perdue MH, Yang PC, McKay DM. Epithelial ion transport and barrier abnormalities evoked by superantigen-activated immune cells are inhibited by interleukin-10 but not interleukin-4. *J Pharmacol Exp Ther* 1998; **287**: 128-136
 - 7 **McKay DM**, Singh PK. Superantigen activation of immune cells evokes epithelial (T84) transport and barrier abnormalities via IFN-gamma and TNF alpha: inhibition of increased permeability, but not diminished secretory responses by TGF-beta2. *J Immunol* 1997; **159**: 2382-2390
 - 8 **McKay DM**, Croitoru K, Perdue MH. T cell-monocyte interactions regulate epithelial physiology in a coculture model of inflammation. *Am J Physiol* 1996; **270**: C418-C428
 - 9 **Kanzato H**, Manabe M, Shimizu M. An *in vitro* approach to the evaluation of the cross talk between intestinal epithelium and macrophages. *Biosci Biotechnol Biochem* 2001; **65**: 449-451
 - 10 **Kerneis S**, Bogdanova A, Kraehenbuhl JP, Pringault E. Conversion by Peyer's patch lymphocytes of human enterocytes into M cells that transport bacteria. *Science* 1997; **277**: 949-952
 - 11 **Kerneis S**, Caliot E, Stubbe H, Bogdanova A, Kraehenbuhl J, Pringault E. Molecular studies of the intestinal mucosal barrier physiopathology using cocultures of epithelial and immune cells: a technical update. *Microbes Infect* 2000; **2**: 1119-1124
 - 12 **Heumann D**, Roger T. Initial responses to endotoxins and Gram-negative bacteria. *Clin Chim Acta* 2002; **323**: 59-72
 - 13 **Takahashi A**, Iida T, Naim R, Naykaya Y, Honda T. Chloride secretion induced by thermostable direct haemolysin of vibrio parahaemolyticus depends on colonic cell maturation. *J Med Microbiol* 2001; **50**: 870-878
 - 14 **Cuthbert AW**, George AM, MacVinish L. Kinin effects on electrogenic ion transport in primary cultures of pig renal papillary collecting tubule cells. *Am J Physiol* 1985; **249**: F439-F447
 - 15 **Rodriguez BL**, Rojas A, Campos J, Ledon T, Valle E, Toledo W, Fando R. Differential interleukin-8 response of intestinal epithelial cell line to reactogenic and nonreactogenic candidate vaccine strains of vibrio cholerae. *Infect Immun* 2001; **69**: 613-616
 - 16 **Faruqi TR**, Gomez D, Bustelo XR, Bar-Sagi D, Reich NC. Rac1 mediates STAT3 activation by autocrine IL-6. *Proc Natl Acad Sci U S A* 2001; **98**: 9014-9019
 - 17 **Rescigno M**, Rotta G, Valzasina B, Ricciardi-Castagnoli P. Dendritic cells shuttle microbes across gut epithelial monolayers. *Immunobiology* 2001; **204**: 572-581
 - 18 **Willemsen LE**, Schreurs CC, Kroes H, Spillenaar Bilgen EJ, Van Deventer SJ, Van Tol EA. A coculture model mimicking the intestinal mucosa reveals a regulatory role for myofibroblasts in immune-mediated barrier disruption. *Dig Dis Sci* 2002; **47**: 2316-2324
 - 19 **Taylor CT**, Murphy A, Kelleher D, Baird AW. Changes in barrier function of a model intestinal epithelium by intraepithelial lymphocytes require new protein synthesis by epithelial cells. *Gut* 1997; **40**: 634-640
 - 20 **Sansonetti PJ**. Molecular and cellular mechanisms of invasion of the intestinal barrier by enteric pathogens. The paradigm of Shigella. *Folia Microbiol* 1998; **43**: 239-246
 - 21 **Resta-Lenert S**, Barrett KE. Enteroinvasive bacteria alter barrier and transport properties of human intestinal epithelium: role of iNOS and COX-2. *Gastroenterology* 2002; **122**: 1070-1087
 - 22 **O'Loughlin EV**, Pang GP, Noltorp R, Koina C, Batey R, Clancy R. Interleukin 2 modulates ion secretion and cell proliferation in cultured human small intestinal enterocytes. *Gut* 2001; **49**: 636-643
 - 23 **Sandle GI**, Higgs N, Crowe P, Marsh MN, Venkatesan S, Peters TJ. Cellular basis for defective electrolyte transport in inflamed human colon. *Gastroenterology* 1990; **99**: 97-105
 - 24 **Sugi K**, Musch MW, Field M, Chang EB. Inhibition of Na⁺,K⁺-ATPase by interferon gamma down-regulates intestinal epithelial transport and barrier function. *Gastroenterology* 2001; **120**: 1393-1403
 - 25 **Pedron T**, Thibault C, Sansonetti PJ. The invasive phenotype of Shigella flexneri directs a distinct gene expression pattern in the human intestinal epithelial cell line Caco-2. *J Biol Chem* 2003; **278**: 33878-33886
 - 26 **Diehl S**, Rincon M. The two faces of IL-6 on Th1/Th2 differentiation. *Mol Immunol* 2002; **39**: 531-536
 - 27 **Sitaraman SV**, Merlin D, Wang L, Wong M, Gewirtz AT, Si-Tahar M, Madara JL. Neutrophil-epithelial crosstalk at the intestinal luminal surface mediated by reciprocal secretion of adenosine and IL-6. *J Clin Invest* 2001; **107**: 861-869
 - 28 **Sansonetti PJ**. Microbes and microbial toxins: paradigms for microbial-mucosal interactions III. Shigellosis: from symptoms to molecular pathogenesis. *Am J Physiol Gastrointest Liver Physiol* 2001; **280**: G319-G323
 - 29 **Fleckenstein JM**, Kopecko DJ. Breaching the mucosal barrier by stealth: an emerging pathogenic mechanism for enteroadherent bacterial pathogens. *J Clin Invest* 2001; **107**: 27-30

Edited by Ma JY and Xu FM

Association of differentially expressed genes with activation of mouse hepatic stellate cells by high-density cDNA microarray

Xiao-Jing Liu, Li Yang, Feng-Ming Luo, Hong-Bin Wu, Qu-Qiang

Xiao-Jing Liu, Hong-Bin Wu, Qu Qiang, Laboratory of Department of Internal Medicine, West China Hospital, Sichuan University, Chengdu 610041, Sichuan Province, China

Li Yang, Department of Gastroenterology of West China Hospital, Sichuan University, Chengdu 610041, Sichuan Province, China

Feng-Ming Luo, Department of Internal Medicine of West China Hospital, Sichuan University, Chengdu 610041, Sichuan Province, China

Supported by the National Natural Science Foundation of China, No.39800054 and No.39700068

Correspondence to: Xiao-Jing Liu, Department of Internal Medicine, West China Hospital, Sichuan University, 37 Wainan Guoxuexiang, Chengdu 610041, Sichuan Province, China. xiaojingliu67@yahoo.com

Telephone: +86-28-85422388

Received: 2003-10-08 **Accepted:** 2003-12-08

Abstract

AIM: To characterize the gene expression profiles associated with activation of mouse hepatic stellate cell (HSC) and provide novel insights into the pathogenesis of hepatic fibrosis.

METHODS: Mice HSCs were isolated from BALB/c mice by *in situ* perfusion of collagenase and pronase and single-step density Nycodenz gradient. Total RNA and mRNA of quiescent HSC and culture-activated HSC were extracted, quantified and reversely transcribed into cDNA. cDNAs from activated HSC were labeled with Cy5 and cDNAs from the quiescent HSC were labeled with Cy3, which were mixed with equal quantity, then hybridized with cDNA chips containing 4 000 genes. Chips were washed, scanned and analyzed. Increased expression of 4 genes and decreased expression of one gene in activated HSC were confirmed by reverse transcription- polymerase chain reaction (RT-PCR).

RESULTS: A total of 835 differentially expressed genes were identified by cDNA chip between activated and quiescent HSC, and 465 genes were highly expressed in activated HSC. The differentially expressed genes included those involved in protein synthesis, cell-cycle regulation, apoptosis, and DNA damage response.

CONCLUSION: Many genes implicated in intrahepatic inflammation, fibrosis and proliferation were up-regulated in activated HSC. cDNA microarray is an effective technique in screening for differentially expressed genes between two different situations of the HSC. Further analysis of the obtained genes will help understand the molecular mechanism of activation of HSC and hepatic fibrosis.

Liu XJ, Yang L, Luo FM, Wu HB, Qiang Q. Association of differentially expressed genes with activation of mouse hepatic stellate cells by high-density cDNA microarray. *World J Gastroenterol* 2004; 10(11): 1600-1607

<http://www.wjgnet.com/1007-9327/10/1600.asp>

INTRODUCTION

Liver fibrosis is a common consequence of chronic liver injury

and is characterized by the progressive accumulation of extracellular matrix (ECM) proteins, particularly type I and III collagens. Hepatic stellate cells (HSC) are the major source of ECM in hepatic fibrosis and HSC is one of the sinusoid-constituent cells that plays multiple roles in the liver pathophysiology. After hepatic injury, HSC undergoes an activation process, characterized by loss of vitamin A, trans-differentiation to a smooth muscle α -actin (α -SMA)-positive myofibroblast like cell type, increased proliferation and increased production of ECM proteins^[1,2]. Activation and transformation of HSC from the vitamin A-storing phenotype (also called "quiescent" phenotype) to the "myofibroblastic" one has been identified as a critical step in hepatic fibrogenesis and is regulated by several factors including cytokines and oxidative stress^[3-5]. However, the molecular mechanism for HSC activation is not well understood. The activation of HSC involves many genes from multiple pathogenic pathways.

cDNA microarray analysis is a powerful descriptive method of examining the expression profile of hundreds to thousands of genes in unison. It has become an increasingly popular tool to investigate the function of genes, especially those genes involved in tumor generation and growth^[6]. Recently, cDNA array has been used to identify differentially expressed genes in HCV-associated cirrhosis and achieve new insights into HCV liver injury^[7].

Further advances in our knowledge about HSC activation requires more genes to be identified. Microarray technology provides us with a genomic approach to explore the genetic markers and molecular mechanisms leading to hepatic fibrosis. To this end, we have used cDNA microarray analysis to detect genes whose mRNA expression changes in the cultured activated HSC. RT-PCR analysis confirmed up-regulation of 4 previously unreported transcripts and down-regulation of one gene transcript in the activated HSC. The identification of these genes provides new insight into the understanding of HSC activation and hepatic fibrogenesis. Culturing HSC on plastic surface converts them from a quiescent phenotype to an activated phenotype similar to *in vivo* activation and this cultured-induced activation has been extensively studied as a model of the activation secondary to liver fibrogenesis^[8,9]. Therefore, we used the *in vitro* model in which the activation of HSC was induced by growth on plastic dishes to study the differentially expressed genes associated with the activation of HSC.

MATERIALS AND METHODS

Materials

Male BALB/c mice were obtained from Experimental Animal Center of West China Medical School, Sichuan University (Chengdu, Sichuan). All animals were treated humanely according to the national guideline for the care of animals.

Pronase, DNase I and Collagenase B were from Roche Molecular Biochemicals (Mannheim, Germany). Nycodenz was from Sigma (St. Louis, USA). Dulbecco's modified medium (DMEM), trypsin-EDTA and new-born calf serum were from Invitrogen Corp (Grand Island, USA). Monoclonal antibodies against desmin, α -smooth muscle actin (α -SMA) were obtained from Dako (Glostrup, Denmark). Gene chips (MGEC-40s) were

purchased from BioStar Genechip Inc. (Shanghai, P.R.China), and each chip contains 4 000 mouse cDNAs, including 1 500 cDNAs of known sequence and function, and 2 500 novel cDNAs whose function has not been known in the public database.

Methods

HSC isolation and culture HSC was isolated from male Balb/c mice by *in situ* pronase, collagenase perfusion and single-step Nycodenz gradient according to our previous report. The purity of primary HSC after 3 d in culture was approximately 95% as estimated by vitamin A auto-fluorescence and immunocytochemistry with antibody against desmin. Therefore, HSC cultured in uncoated plastic dishes spontaneously acquired an activated phenotype, characterized by expression of α -SMA and by loss of vitamin A droplets. After reaching confluence (about 10–14 d after plating), activated HSC was detached by trypsin, and split in a 1:2 ratio. Experiments were performed on primary cells cultured for 3 d and activated HSC of the third passages using 3 independent cell lines, and the purity of activated HSC exceeded 98%.

Preparation of RNA and cDNA microarray Total RNA was isolated from primary mouse HSC and sub-confluent culture-activated mouse HSC (passage 3), using Trizol reagent (Invitrogen Life Technologies Inc, USA) according to the manufacturer's protocol. Poly (A) mRNA was isolated from total RNA using Oligotex mRNA Midi Kit (Qiagen, USA) according to the manufacturer's protocol.

All microarray procedures were performed by BioStar Genechip Inc. (Shanghai, P.R.China). Equal quantities of mRNA from each cell phenotype were used to prepare probes, hybridized to gene chips (MGEC-40 s, Biostar Genechip Inc.), and analyzed for the quantity of mRNA encoded by 4 000 mouse genes. The preparation of Cy5 and Cy3 probes from mRNA samples and the hybridization were conducted by the BioStar Genechip Inc.

RT-PCR assays To validate the expression pattern identified on the expression arrays, 4 genes (MIF, Annexin VI, N-Cadherin, DAD1) from the up-regulated genes and one gene (BHMT) from the down-regulated genes in activated HSC were picked and semi-quantitative RT-PCR was performed to confirm their changed expression with cDNA templates from activated and quiescent HSC. The total RNA was isolated from HSC using Trizol reagent, precipitated in ethanol and resuspended in sterile RNAase-free water and stored at -70°C , as described previously. One-step reverse transcription-polymerase chain reaction (RT-PCR) was performed according to the method of the supplier (TaKaRa Biotechnology Co., Ltd, Dalian). Primers were designed using the Primer 3 program from Whitehead Institute for

Biomedical Research (Cambridge, MA, USA)^[10], synthesized and purified by PAGE in Genebase BRL Custom Primers (Genebase Biotechnology Co., Shanghai). Primer sequences are shown in Table 1. The PCR products was analyzed by 20 g/L agarose gel electrophoresis with TAE buffer at 80 V for 40 min, visualized with ethidium bromide and photographed under UV light by Gel Documentation system (Gel Doc 2000TM, Bio-Rad, USA). The semi-quantitative analysis was performed using the volume analysis in the Quantity One Software (Bio-Rad, USA). Each detected gene/GAPDH quotient is the indication of the detected gene. Experiments were performed for at least five times with similar results.

Statistical analysis

RT-PCR results were expressed as mean \pm SD. Differences between means were analyzed with Student *t* test for paired samples. A value of $P < 0.05$ was considered statistically significant.

RESULTS

Expression pattern of genes in activated HSC

Differences in gene expression patterns between mouse activated HSC and quiescent HSC were assessed using microarray analysis. This array allows a quantitative measurement of 4 000 known genes and expressed sequence tags. Genes that differed in intensity by at least 2-fold were considered to be differentially regulated. Figure 1 shows that the cDNA array images along with color charts indicating up-regulated genes with red, down-regulated ones with green and non-changed with yellow. Of the 4 000 genes analyzed by microarray, a total of 835 genes (20.8%) revealed differential expression in the activated HSC when compared with the quiescent HSC (Tables 2–4). Of the 835 genes with altered expression in the activated HSC, 462 genes (including 204 known function genes) revealed elevated expression whereas 373 genes (including 132 known function genes) revealed reduced expression. Array analysis identified many differentially expressed genes that are important in inflammation, fibrosis, proliferation, signaling, apoptosis and oxidative stress.

Validation of array data with RT-PCR

To further investigate the reliability of our array data, we picked 5 differential expressed genes and measured the expression of the genes in the activated and quiescent HSC. Figures 2 and 3 and Table 5 show that the different expression pattern of each of the five genes as determined by RT-PCR were similar to those observed with cDNA array, confirming the reliability of our array data.

Table 1 Primer sequences for RT-PCR

Gene name	Primer sequence	Expected product size
Betaine homocysteine methyltransferase (BHMT)	Left 5' -GCC TAT AGC GGC TAC CAT GT-3' Right 5' -CTC TGC AAT GGC CCT GAT GT-3'	399 bp
Defender against cell death protein 1 (DAD1)	Left 5' -TTC GGC TAC TGT CTC CTC GT -3' Right 5' -ACG AGG TGC AGG ATA GTG CT-3'	197 bp
Annexin VI	Left 5' -TAC CCC GGA GTA TTT TGC TG-3' Right 5' -GTC CCC TCC ACA TAG CTT CA-3'	220 bp
Neural cadherin (N-Cadherin)	Left 5' -ATA CAG TGT CAC TGG GCC AG- 3' Right 5' -CGT AAG TGG GAT TGC CTT CC- 3'	499 bp
Macrophage migration inhibitory factor (MIF)	Left 5' -TTT TAG TGG CAC GAG CGA CC-3' Right 5' -AAG CGA AGG TGG AAC CGT TC- 3'	199 bp
GAPDH	Left 5' -ACC ACA GTC CAT GCC ATC AC-3' Right 5' -TCC ACC ACC CTG TTG CTG TA-3'	452 bp

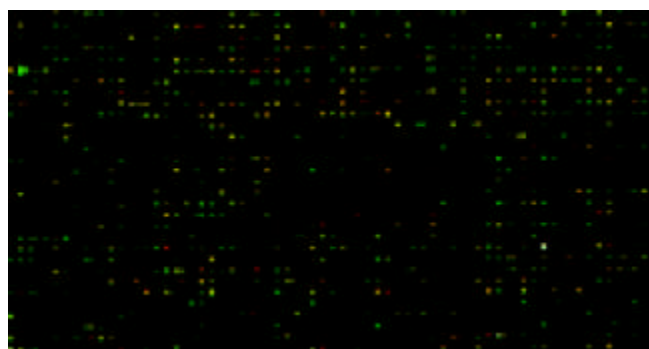


Figure 1 cDNA microarray scanning result of gene expression profile between quiescent HSC and activated HSC.

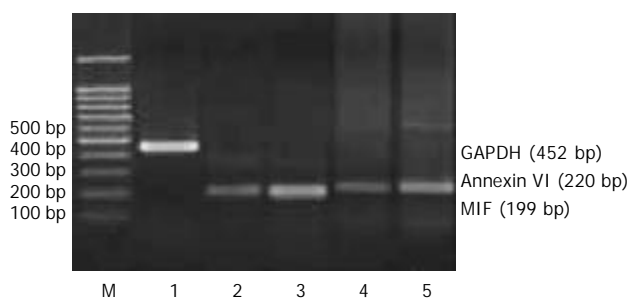


Figure 2 Electrophoresis analysis of RT-PCR products. Lane M: 100 bp DNA ladder; Lane 1: GAPDH; Lane 2, 3: MIF amplified from quiescent HSC and activated HSC mRNA respectively; Lane 3 shows increased expression of MIF in activated HSC compared with lane 2 in quiescent HSC. Lane 4, 5: Annexin VI amplified from quiescent HSC and activated HSC mRNA respectively; Lane 5 shows increased expression of Annexin VI in activated HSC compared with lane 4 in quiescent HSC.

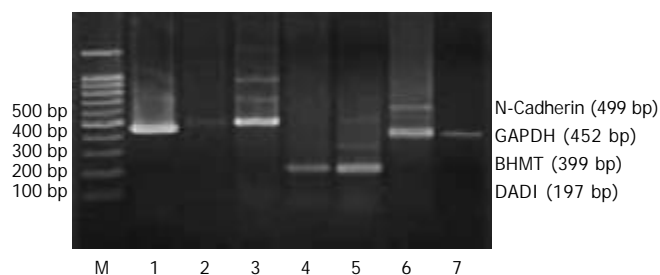


Figure 3 Electrophoresis analysis of RT-PCR products. Lane M: 100 bp DNA ladder; Lane 1: GAPDH; Lane 2, 3: N-Cadherin amplified from quiescent HSC and activated HSC mRNA respectively; Lane 3 shows increased expression of N-Cadherin in activated HSC compared with lane 2 in quiescent HSC. Lane 4, 5: DAD1 amplified from quiescent HSC and activated HSC mRNA respectively; Lane 5 shows increased expression of Annexin VI in activated HSC compared with lane 4 in quiescent HSC. Lane 6, 7: BHMT amplified from quiescent HSC and activated HSC mRNA respectively; Lane 7 shows decreased expression of BHMT in activated HSC compared with lane 6 in quiescent HSC.

DISCUSSION

Genome-wide expression profiling by microarray of cDNA or oligonucleotide probes on a glass or nylon substrate is an exceptionally powerful tool for the study of gene regulation. This methodology has been used to investigate the phenomena particularly appropriate for the analysis of expressed liver genes^[7]. cDNA microarrays were used to profile changes in gene expression in activated HSC. Scatter plot analysis showed that approximately 20.8% of all mouse genes examined on the 4 000 gene microarrays exhibited altered expression, with 11.5% showing up-regulation and 9.3% showing down-regulation. These genes will be future studied.

Table 2 Part of the previously reported up-regulated genes in activation of HSC

GenBank accession number	Gene name	Ratio (Cy5/Cy3)	Potential gene function
M73741	Alpha-B2-crystallin, complete cds	155.619	Small heat shock protein gene, an early marker for HSC activation
X52046	Procollagen, type III, alpha 1	119.092	Extracellular matrix (ECM), over- expressed in hepatic fibrosis
M18194	Fibronectin mRNA	29.958	ECM, over expressed in hepatic fibrosis
J02870	Laminin receptor mRNA	6.62	ECM receptor (integrin), cell adhesion
L08115	CD9 antigen	6.094	Cell membrane glycoprotein, involved in cell activation and adhesion
U16163	Prolyl 4-hydroxylase alpha (II)-subunit mRNA, complete cds	4.555	An enzyme which is essential for the collagen synthesis in HSC
X62622	TIMP-2 mRNA for tissue inhibitor of metalloproteinase, type 2	3.732	Inhibition for ECM degradation
X04017	mRNA for cysteine-rich glycoprotein SPARC	3.435	Regulation of cell shape, adhesion, migration and proliferation
AF070470	SPARC-related protein (SRG) mRNA, complete cds	3.181	Regulation of cell shape, adhesion, migration and proliferation
M21495	Cytoskeletal gamma-actin mRNA,	3.092	Relate skeleton structure of cell
AF188297	TGF-beta receptor binding protein (Trip1) mRNA, complete cds	2.976	TGF-beta mediated signaling pathway
AJ245923	alpha-tubulin 8 (Tuba 8 gene) mRNA	2.901	Relate skeleton structure of cell
AF053454	Tetraspan TM4SF (Tspan-6) mRNA, complete cds	2.896	Cell development, differentiation, motility
AF013262	Lumican gene, complete cds	2.862	Small, leucine-rich proteoglycan which involves in the regulation of collagen fibril assembly
L02526	Protein kinase (MEK) mRNA	2.714	Signaling molecule in MAPK family
Y00769	mRNA for integrin beta subunit	2.521	Signaling molecular in cell adhesion, proliferation and migration

Table 3 A portion of up-regulated genes in activated HSC

GenBank accession number	Gene name	Ratio (Cy5/Cy3)	Potential gene function
AF061017	UDP-glucose dehydrogenase, mRNA complete cds	15.56	Glycosaminoglycan , hyaluronan and heparan sulfate biosynthesis
X65553	mRNA for poly (A) binding protein	7.405	A regulator of translation initiation
AF029844	Elongation factor 1-beta homology mRNA, complete cds	6.305	Translation factor and has multi-functions
NM_010798	Macrophage migration inhibitory factor (Mif), mRNA	5.847	Proinflammatory peptide and a mediator of growth factor dependent ERK MAP kinase activation and cell cycle progression
M31131	Neural cadherin (N-cadherin) mRNA	5.559	Cell adhesion molecule
AB029930	mRNA for caveolin-1 beta isoform	4.945	Inhibit the eNOS activity
D12618	mRNA for nucleosome assembly protein-1, complete cds	4.528	Histone H2A-H2B shutting protein that promotes histone deposition, and is important for maintaining chromatin structure
M22432	Protein synthesis elongation factor Tu (eEF-Yu, eEf-1-1alpha) mRNA, complete cds	4.344	Translation factor involved in the protein biosynthesis
D31717	mRNA for ribophorin	4.319	Glycoprotein synthesis
NM_012052	Ribosomal protein S3 (Rps3), mRNA	4.297	Protein biosynthesis
X72711	mRNA for replication factor C (140 Kda), long subunit	4.245	DNA synthesis and repair, and a regulator of NF-kappa B
X13460	Annexin VI, p68 (Mouse mRNA for p68 protein of the lipocortin family)	4.218	Calcium binding protein
NM_011290	Ribosomal protein L6 (Rp16), mRNA	4.089	Protein biosynthesis
U12273	Apurinic/aprimidinic endonuclease (APEX) gene, complete cds	3.488	A DNA repair enzyme and an activator of several transcription factors
D42048	mRNA for squalene epoxidase	3.298	Rate-limiting enzyme of cholesterol biosynthesis
AJ250491	mRNA for receptor activity modifying protein 3 (Ramp3) gene	3.255	Complex with the calcitonin receptor-like receptor, establishing a functional receptor for adrenomedullin
L04280	Ribosomal protein (RPL12) mRNA	3.172	Protein biosynthesis
K02927	Ribonucleotide reductase subunit M1 mRNA, complete cds	3.156	Rate-limiting enzyme in DNA synthesis and repair
AF087568	Palmitoyl-protein thioesterase precursor mRNA, complete cds	3.059	Cell survival signaling
AF020039	NADP-dependent isocitrate dehydrogenase (Idh) mRNA, complete cds	3.038	A key enzyme of the tricarboxylic acid cycle
X57960	Ribosomal protein L7	2.962	Protein biosynthesis
U09816	GM2 activator protein (Gm2a) mRNA	2.888	Enzymatic hydrolysis of GM2
AB018575	Cdc 7 mRNA, complete cds	2.816	Essential for G1/S transition
AF041054	E1B19K/Bcl-2 binding protein homology (Nip3) mRNA, nuclear gene encoding mitochondria protein, complete cds	2.813	Nips is a pro-apoptotic mitochondria protein
L04128	Ribosomal protein L18 (rpL18) mRNA	2.751	Protein biosynthesis
Z31554	(129/SV) Cctd mRNA for CCT (chaperonin containing TCP-1) delta subunit	2.743	Stabilize the cytoskeletal protein actin and tubulin
D63784	mRNA for MIDA1, complete cds	2.703	Regulate cell growth
AF026481	eIF-1A (eIF-1A) mRNA, complete cds	2.682	Translation initiation factor
U35249	CDK-activating kinase assembly factor p36/MAT1, complete cds	2.645	An assembly factor and a targeting subunit of cyclin-dependent kinase-activating kinase that is involved in cell cycle control, transcription and DNA repair
M76131	Elongation factor (ef-2) mRNA, 3' end	2.614	Protein biosynthesis
X64713	mRNA for cyclin B1	2.576	Cell cycle regulatory protein
D26091	mRNA for mCDC47, complete cds	2.570	A member of the minichromosome maintenance (Mcm) family involve in the DNA replication licensing system
U78085	Ribosomal protein S5 mRNA	2.507	Protein synthesis
AF141322	Caveolin-2 mRNA, complete cds	2.458	Inhibit the eNOS activity
M33934	IMP dehydrogenase mRNA, complete cds	2.429	An enzyme involved in de novo synthesis of guanine nucleotides
U83628	Defender against cell death protein 1 (DAD1) mRNA, complete cds	2.372	Apoptotic suppressor gene

Table 4 Part of down-regulated genes in the activated HSC

GenBank accession number	Gene name	Ratio (Cy5/Cy3)	Potential gene function
D49949	mRNA for IGIF precursor poly-peptide in (Interleukin 18), complete cds	0.065	In the development of Th1 cells and tissue injury inflammatory reaction
U63146	Retinal binding protein (RBP) mRNA	0.125	Retinoid storage and metabolism
AF035644	Potentially prenylated protein tyrosine phosphatase mPRL-2 mRNA, complete cds	0.226	Cellular regulation
X58287	mR-PTPu gene for protein tyrosine phosphatase, receptor-type M	0.280	Cellular regulation
AF033381	Betaine homocysteine methyl transferase (BHMT) mRNA, complete cds	0.299	A key liver enzyme that is important for homocysteine homeostasis
M75720	Alpha-1 serine protease inhibitor 3 mRNA, complete cds	0.308	Anti-inflammatory effect
U20497	P19 protein mRNA, complete cds	0.324	CDK4&CDK6 inhibitor, cell cycle inhibitor
D85596	AMP deaminase H-type, complete cds	0.339	Involved in the biosynthesis, inter-conversion and degradation of purine compounds
Y10138	Gene encoding prostaglandin D synthase	0.361	A PGD producing enzyme and a retinoid transporter
NM_013498	CAMP response element modulator (CREM) mRNA	0.366	Down-regulator of CAMP-induced transcription
U67187	G protein signaling regulator RGS2 (rgs2) mRNA, complete cds	0.369	Negatively regulate G-coupled receptor function
AF023919	PK-120 precursor (itih-4) mRNA, complete cds	0.421	Inter-alpha-trypsin-inhibitor H4, is a potential regulator for ECM proteins
AF077950	Protein inhibitor of activated STAT protein PIAS 1 mRNA, complete cds	0.433	Inhibition of STAT-1-mediated gene activation
M75718	Alpha-1 protease inhibitor 4 mRNA, complete cds	0.437	Anti-inflammatory activity
D38046	mRNA for type II DNA topoisomerase beta isoform, complete cds	0.445	An essential enzyme that alters DNA topology which is important for cell survive and apoptosis
AF073996	myotubularin (Mtm1) mRNA complete cds	0.464	Subfamily of protein tyrosine phosphatases

Table 5 Semi-quantitative analysis of RT-PCR results

Groups	Mean±SD (quotient of the detected gene/GAPDH)	N	p value
MIF from quiescent HSC	0.269±0.016	5	
MIF from activated HSC	0.759±0.046	5	<0.05
N-Cadherin from quiescent HSC	0.177±0.063	5	
N-Cadherin from activated HSC	0.776±0.087	5	<0.05
Annexin VI from quiescent HSC	0.137±0.04	5	
Annexin VI from activated HSC	0.478±0.025	5	<0.05
DAD1 from quiescent HSC	0.174±0.016	5	
DAD1 from activated HSC	0.593±0.047	5	<0.05
BHMT from quiescent HSC	0.602±0.083	5	
BHMT from activated HSC	0.134±0.059	5	<0.05

In the up-regulated genes associated with the activation of HSC, some genes have already been reported (Table 2). Alpha B-crystallin was first reported by Lang *et al*^[11] recently as an early marker for HSC activation. In our experiment, the ratio of Cy5 to Cy3 for its mRNA was the highest in all the genes in the gene-chip, suggesting that mRNA expression of alpha B-crystallin in activated HSC up-regulated mostly comparing with the quiescent HSC. The mRNA expression for procollagen type III^[12], fibronectin^[13], laminin receptor, prolyl 4-hydroxylase^[14], TIMP-2, TGF-beta and its receptor binding protein^[15], MEK^[16] and integrin beta^[17] was increased in activated HSC. Tetraspanins (TM4SF) super family which includes CD9, CD53, CD81 and CD151 were highly expressed in the activated human HSC and have been implicated in HSC migration, a key event in liver

tissue wound healing and fibrogenesis^[18]. Secreted protein, acidic and rich in cysteine (SPARC), which functions in tissue remodeling, was expressed by activated HSC in chronic hepatitis, suggesting the involvement of SPARC in hepatic fibrogenesis after chronic injuries^[19]. Lumican is a small leucine-rich proteoglycan, which contributes to cell migration, proliferation, tissue hydration and collagen fibrillogenesis, and its expression is increased in HSC in diseased liver during the process of fibrogenesis^[20]. Although we employed different methods, animal models or different sources of HSC, our experimental data was consistent with the results observed by others, demonstrating that the technique of cDNA microarray has a higher reliability. In addition, the expression of those that were not previously linked to the activation of HSC was also

found to be changed. These include genes involved in the control of HSC morphology, growth, differentiation, migration and apoptosis.

Analysis of the genes showed elevated expression in the activated HSC clustered into distinct functional groups. Genes showing elevated expression included many genes involved in the formation and remodeling of the extracellular matrix (ECM) and in the regulation of cellular response (including cell adhesion, proliferation and migration) to the ECM, such as procollagen type III, fibronectin, TIMP-2, TGF beta, UDP-glucose dehydrogenase (AF061017), N-cadherin (M131131) and lumican (AF013262).

The enzyme UDP-glucose dehydrogenase (Udpgh) (EC 1.1.1.22) converts UDP-glucose to UDP-glucuronate, a critical component of the glycosaminoglycans, hyaluronan, chondroitin sulfate and heparan sulfate^[21]. It is known that heparan sulfate proteoglycans are essential cofactors in cell-matrix adhesion processes, in cell-cell recognition system, and in receptor-growth factor interactions. Cultured human HSC can synthesize all four cyndecans and the increased expression of glycosaminoglycans and hyaluronic acid may be important in the deposition of matrix components and activation of growth factors accompanying fibrogenesis. Our results suggested that the increased expression of heparan sulfate proteoglycans in activated HSC might be partially caused by the elevated expression of the enzyme UDP-glucose dehydrogenase.

Neural cadherin (N-cadherin) is an adhesion molecule of the cadherin family, whose expression was up regulated in response of smooth muscle cells to arterial injury^[22]. Annexin VI is a 68-Kda protein of the annexin family, a group of structural similar, calcium-dependent, phospholipid-binding proteins^[23]. Our cDNA microarray data along with the RT-PCR results showed increased expression of N-cadherin and annexin VI in activated HSC, suggesting their regulations might be important for the hepatic fibrogenesis.

In all cells, protein synthesis is coordinated by the ribosome, and the large ribonucleoprotein is composed of at least 50 distinct molecules and several large RNA molecules. Genes showing elevated expression included many genes that encode ribosomal proteins and proteins involved in the translation and protein synthesis, such as mRNA for poly A-binding protein (X65553), elongation factor 1-beta homology mRNA (AF029844), elongation factor Tu (M22432), ribosomal protein S3 (NM_012052), S5 (U78085), L6 (NM_011290), L12 (L04280), L18 (L04128) and eukaryotic initiation factor 1A (eIF1A) (AF026481). HSC proliferated during the process of activation, so it is not surprising that many genes involved in the protein synthesis up-regulated in the activated HSC.

Our work has identified some previously unreported genes involved in DNA synthesis and repair showing elevated expression in the activated HSC, such as replication factor C gene (X72711), apurinic/apyrimidinic endonuclease (APEX) gene (U12273), ribonucleotide reductase subunit M1 (M1-RR) mRNA (K02917), and IMP dehydrogenase mRNA (M33934), an enzyme involved in *de novo* synthesis of guanine nucleotides.

Replication factor C (RFC) is a clamp loader, catalyzes assembly of circular proliferating cell nuclear antigen clamps around primed DNA, enabling processive synthesis by DNA polymerase during DNA replication and repair. The Rel A (p65) subunit of NF-kappa B is an important regulator of inflammation, proliferation and apoptosis, but the large subunit of RFC can function as a regulator of Rel A. In addition to its previously described function in DNA replication and repair, RFC plays an important role as a regulator of transcription factor NF-kappa B activity^[24].

APEX nuclease is a mammalian DNA repair enzyme having apurinic/apyrimidinic endonuclease, 3' -5' -exonuclease, DNA 3' repair diesterase and DNA 3' -phosphatase activities. It is also a redox factor (Ref-1), stimulating DNA binding activity of

AP-1 binding proteins such as Fos and Jun^[25]. Ribonucleotide reductase (RR) is a cytoplasmatic enzyme catalyzing the reduction of all four ribonucleotides to their corresponding deoxyribonucleotides, so it is a rate-limiting enzyme in the DNA synthesis and repair. Its activity strongly correlates to the rate of DNA synthesis, and the expression of M1-RR antigen was found to correlate positively with the expression of Ki-67 and PCNA, the cell cycle markers of proliferating cells^[26]. We conclude that mechanisms for DNA synthesis and repair are activated during the process of HSC activation.

Elevated expression was also observed for a number of genes involved in the control of cell growth, survival, differentiation and apoptosis. Palmitoyl-protein thioesterase (PPT) is a newly described lysosomal enzyme that hydrolyzes long chain fatty acids from lipid-modified cysteine residues in proteins, and its precursor mRNA (AF087568) was up-regulated in activated HSC. It was reported that inhibition of PPT increased the susceptibility of neurons to apoptotic cell death^[27]. Id, a helix-loop-helix protein not only regulates cell differentiation negatively, but also promote growth and apoptosis, and an Id-associate protein, MIDA1 (Mouse Id associate1), regulated cell growth positively. MIDA1 is a novel sequence-specific DNA binding protein with some different properties from the usual transcription factors and may act as a mediator of Id-mediated growth-promoting function through its DNA binding activity^[28], and its gene expression was increased in the activated HSC.

The cyclin-dependent kinase (CDK)-activating kinase (CAK) is involved in cell cycle control, transcription, and DNA repair, and MAT1 gene (U35249), an assembly factor and a targeting subunit of CAK, was also up regulated in the activated HSC. It was reported that abrogation of MAT1 expression by retrovirus-mediated gene transfer of antisense MAT1 RNA in cultured rat aortic smooth muscle cells (SMC) retarded SMC proliferation and inhibits cell activation from a nonproliferation state, and this effect was due to G1 phase arrest and apoptotic cell death^[29].

Up-regulation of the DAD1 (U83628), a putative anti-apoptosis gene identified in several distantly related organisms^[28], was observed as well as the Nip3 (AF041054), a proapoptotic member of the Bcl-2 family of cell death factors^[29] in the activated HSC. CDC7, an evolutionarily conserved serine-threonine kinase, plays a pivotal role in linking cell cycle regulation to genome duplication, being essential for the firing of DNA replication origins^[30]. Our microarray experiments also identified elevated expression for CDC7 gene (AB018575) and cyclin B₁ (X64713) in the activated HSC. The strategy for terminating the proliferation of activated HSC by apoptosis might be an exciting therapy for patients with chronic liver injury and fibrosis^[10,31], therefore, our experimental data about the differentially expressed genes involved in apoptosis will give some new ideas on induce apoptosis in HSC.

Macrophage migration inhibitory factor (MIF) (NM_010798), a pro-inflammatory peptide and a mediator of growth factor-dependent ERK MAP kinase activation and cell cycle progression^[32], was up-regulated by the process of HSC activation. MIF has been shown to contribute significantly to the development of immuno-pathology in several models of inflammatory, such as glomerulonephritis^[33]. Our RT-PCR results confirmed the increased expression of MIF mRNA in the activated HSC. This is the first study to demonstrate that activated HSC can produce MIF *in vitro*, and its up-regulation in activated HSC might suggest a role for MIF in the hepatic fibrogenesis *in vivo*. It is necessary to carry further more research to understand how MIF regulates proliferation in activated HSC.

Down-regulation was observed for genes encoding interleukin 18 (D49949) and retinal binding protein (RBP) (U63146) in the activated HSC. IL-18 has an anti-fibrotic effect and it was reported that intrasplenic transplantation of IL-18

gene modified hepatocytes could be a candidate for therapeutic intervention in hepatic fibrosis through induction of a dominant Th1 response^[34]. HSCs are the body's major cellular storage sites for retinoid, but the immortalized rat HSC cell line HSC-T6 failed to express RBP^[35]. Our cDNA microarray results were consistent with the previous reports.

In the activated HSC, reduced expression was observed for genes involved in general cellular regulation including a family of protein-tyrosine phosphatase (PTPases) and some negative regulators of cell growth signaling, such as P19 protein (U20497), CAMP response element modulator (Crem)(NM_013498), G protein signaling regulator RGS2 (U67187), and protein inhibitor of activated STAT protein - PIAS1 (AF077950). The PTPases included the potentially prenylated protein tyrosine phosphatase mPRL-2 (AF035644)^[36], myotubularin (Mtm1)(AF071996)^[37] and mR-PTPu gene for protein tyrosine phosphatase, receptor type M. Protein tyrosine kinase and phosphatase play diverse roles in involving energy metabolism, cell proliferation and stimulation of MHC class I molecule pathway. Down-regulation was also observed for the alpha-1 serine protease inhibitor 3 (M75720), alpha-1 protease inhibitor 4 (M75718) and PK-120 precursor (itih-4)(AF023919), a serine protease inhibitor.

P19 is a tumor suppressing protein and belongs to a family of cyclin D-dependent kinase inhibitors of CDK4 and CDK6, which play a key role in human cell cycle control^[38]. Addition of p19 protein can lead to inhibition of the CDK's activity and may cause the cells to arrest at G1 phase. Transcriptional factors binding to camp-response elements (CREs) in the promoters of various genes belong to the basic domain-leucine zipper super family and are composed of three genes in mammals, CREB, CREM, and ATF-1. Activation is classically brought about by signaling-dependent phosphorylation of a key acceptor site (Ser133 in CREB) by a number of possible kinases, including PKA, CamKIV and RSK-2. Repression may involve dynamic dephosphorylation of the activators and decreased association with CREB-binding protein (CBP). Another pathway of transcriptional repression on CRE sites implicates the inducible repressor ICER (inducible camp early repressor), a product of the CREM gene. Being an inducible repressor, ICER is involved in auto-regulatory feedback loops of transcription that govern the down-regulation of early response genes, such as the proto-oncogene c-fos^[39]. It is known that CREB is one of the transcription factors whose expression is increased in the activated HSC during the liver injury^[40], but the important role of CREM in the pathophysiology of liver fibrogenesis has not been studied. Similarly, Jak-Stat signaling is one of the signaling pathways in the HSC proliferation and activation^[41], but the role of a negative regulator in this cytokine signaling, protein inhibitor of activated STAT-1 (PIAS-1), has not been understood. Thus, our microarray data might provide novel potential approaches to the treatment of hepatic fibrogenesis in patients with chronic liver diseases.

Reduced mRNA expression was also found for betaine-homocysteine methyl transferase (BHMT). BHMT is a key liver enzyme for homocysteine (Hcy) homeostasis. It catalyzes the synthesis of methionine from betaine and homocysteine, utilizing a zinc ion to activate Hcy. Elevated plasma levels of Hcy have been shown to interfere with normal cell function in a variety of tissues and organs, such as the vascular wall and the liver. It is known that Hcy is able to induce the expression and synthesis of the TIMP-1 in variety of cell types ranging from vascular smooth muscle cells to hepatocytes, HepG2 cells and HSCs. In HSCs, Hcy also stimulates alpha₁(I) procollagen mRNA expression, promotes activating protein-1 (AP-1) binding activity^[42]. Hcy is a key metabolite in methionine metabolism, which takes place mainly in the liver. Hyperhomocysteinemia may develop as a consequence of defects in Hcy-metabolizing genes (such as BHMT); nutritional conditions leading to vitamin

B (6), B (12), or folate deficiencies; or chronic alcohol consumption. We postulated that hyperhomocysteinemia in the hepatic fibrosis was partly due to the reduced expression of BHMT gene in the activated HSC.

We used cDNA array analysis to detect genes whose mRNA expression changes in the activated mouse HSC after culture on the plastic dishes. RT-PCR analysis confirmed the up-regulation of four previously unreported transcripts and down-regulation of one gene in activated HSC. The identity of these genes provides new insights into the understanding of activation of HSC during the liver injury and hepatic fibrogenesis.

REFERENCES

- 1 **Reeves HL**, Friedman SL. Activation of hepatic stellate cells—a key issue in liver fibrosis. *Front Biosci* 2002; **7**: d808-826
- 2 **Dai WJ**, Jiang HC. Advances in gene therapy of liver cirrhosis: a review. *World J Gastroenterol* 2001; **7**: 1-8
- 3 **Mann DA**, Smart DE. Transcriptional regulation of hepatic stellate cell activation. *Gut* 2002; **50**: 891-896
- 4 **Pinzani M**, Marra F. Cytokine receptors and signaling in hepatic stellate cells. *Semin Liver Dis* 2001; **21**: 397-416
- 5 **Liu XJ**, Yang L, Mao YQ, Wang Q, Huang MH, Wang YP, Wu HB. Effects of the tyrosine protein kinase inhibitor genistein on the proliferation, activation of cultured rat hepatic stellate cells. *World J Gastroenterol* 2002; **8**: 739-745
- 6 **Tan ZJ**, Hu XG, Cao GS, Tang Y. Analysis of gene expression profile of pancreatic carcinoma using cDNA microarray. *World J Gastroenterol* 2003; **9**: 818-823
- 7 **Shackel NA**, McGuinness PH, Abbott CA, Gorrell MD, McCaughan GW. Insights into the pathobiology of hepatitis C virus-associated cirrhosis: analysis of intrahepatic differential gene expression. *Am J Pathol* 2002; **160**: 641-654
- 8 **Liu C**, Gaca MD, Swenson ES, Vellucci VF, Reiss M, Wells RG. Smads 2 and 3 are differentially activated by transforming growth factor-beta (TGF-beta) in quiescent and activated hepatic stellate cells. Constitutive nuclear localization of Smads in activated cells is TGF-beta-independent. *J Biol Chem* 2003; **278**: 11721-11728
- 9 **Galli A**, Crabb DW, Ceni E, Salzano R, Mello T, Svegliati-Baroni G, Ridolfi F, Trozzi L, Surrenti C, Casini A. Antidiabetic thiazolidinediones inhibit collagen synthesis and hepatic stellate cell activation *in vivo* and *in vitro*. *Gastroenterology* 2002; **122**: 1924-1940
- 10 **Rozen S**, Skaletsky H. Primer 3 on the WWW for general users and for biologist programmers. *Methods Mol Biol* 2000; **132**: 365-386
- 11 **Lang A**, Schrum LW, Schoonhoven R, Tuvia S, Solis-Herruzo JA, Tsukamoto H, Brenner DA, Rippe RA. Expression of small heat shock protein alpha B-crystallin is induced after hepatic stellate cell activation. *Am J Physiol Gastrointest Liver Physiol* 2000; **279**: G1333-1342
- 12 **Wei HS**, Li DG, Lu HM, Zhan YT, Wang ZR, Huang X, Zhang J, Cheng JL, Xu QF. Effects of AT1 receptor antagonist, losartan, on rat hepatic fibrosis induced by CCl₄. *World J Gastroenterol* 2000; **6**: 540-545
- 13 **Svegliati-Baroni G**, Ridolfi F, Di Sario A, Saccomanno S, Bendia E, Benedetti A, Greenwel P. Intracellular signaling pathways involved in acetaldehyde-induced collagen and fibronectin gene expression in human hepatic stellate cells. *Hepatology* 2001; **33**: 1130-1140
- 14 **Aoyagi M**, Sakaida I, Suzuki C, Segawa M, Fukumoto Y, Okita K. Prolyl 4-hydroxylase inhibitor is more effective for the inhibition of proliferation than for inhibition of collagen synthesis of rat hepatic stellate cells. *Hepatology* 2002; **23**: 1-6
- 15 **Tahashi Y**, Matsuzaki K, Date M, Yoshida K, Furukawa F, Sugano Y, Matsushita M, Himeno Y, Inagaki Y, Inoue K. Differential regulation of TGF-beta signal in hepatic stellate cells between acute and chronic rat liver injury. *Hepatology* 2002; **35**: 49-61
- 16 **Kim KY**, Rhim T, Choi I, Kim SS. N-acetylcysteine induces cell cycle arrest in hepatic stellate cells through its reducing activity. *J Biol Chem* 2001; **276**: 40591-40598

- 17 **Yang C**, Zeisberg M, Mosterman B, Sudhakar A, Yerramalla U, Holthaus K, Xu L, Eng F, Afdhal N, Kalluri R. Liver fibrosis: insights into migration of hepatic stellate cells in response to extracellular matrix and growth factors. *Gastroenterology* 2003; **124**: 147-159
- 18 **Mazzocca A**, Carloni V, Sciammetta S, Cordella C, Pantaleo P, Caldini A, Gentilini P, Pinzani M. Expression of transmembrane 4 superfamily (TM4SF) proteins and their role in hepatic stellate cell motility and wound healing migration. *J Hepatol* 2002; **37**: 322-330
- 19 **Nakatani K**, Seki S, Kawada N, Kitada T, Yamada T, Sakaguchi H, Kadoya H, Ikeda K, Kaneda K. Expression of SPARC by activated hepatic stellate cells and its correlation with the stages of fibrogenesis in human chronic hepatitis. *Virchows Arch* 2002; **441**: 466-474
- 20 **Gressner AM**, Krull N, Bachem MG. Regulation of proteoglycan expression in fibrotic liver and cultured fat-storing cells. *Pathol Res Pract* 1994; **190**: 864-882
- 21 **Ge X**, Penney LC, van de Rijn I, Tanner ME. Active site residues and mechanism of UDP-glucose dehydrogenase. *Eur J Biochem* 2004; **271**: 14-22
- 22 **Jones M**, Sabatini PJ, Lee FS, Bendeck MP, Langille BL. N-cadherin upregulation and function in response of smooth muscle cells to arterial injury. *Arterioscler Thromb Vasc Biol* 2002; **22**: 1972-1977
- 23 de Diego I, Schwartz F, Siegfried H, Dauterstedt P, Heeren J, Beisiegel U, Entich C, Grewal T. Cholesterol modulates the membrane binding and intracellular distribution of annexin 6. *J Biol Chem* 2002; **277**: 32187-32194
- 24 **Anderson LA**, Perkins ND. Regulation of RelA (p65) function by the large subunit of replication factor C. *Mol Cell Biol* 2003; **23**: 721-732
- 25 **Ranalli TA**, Tom S, Bambara RA. AP endonuclease 1 coordinates flap endonuclease 1 and DNA ligase I activity in long patch base excision repair. *J Biol Chem* 2002; **277**: 41715-41724
- 26 **Chen S**, Zhou B, He F, Yen Y. Inhibition of human cancer cell growth by inducible expression of human ribonucleotide reductase antisense cDNA. *Antisense Nucleic Acid Drug Dev* 2000; **10**: 111-116
- 27 **Dawson G**, Dawson SA, Marini C, Dawson PE. Anti-tumor promoting effects of palmitoyl: protein thioesterase inhibitors against a human neurotumor cell line. *Cancer Lett* 2002; **187**: 163-168
- 28 **Inoue T**, Shoji W, Obinata M. MIDA1 is a sequence specific DNA binding protein with novel DNA binding properties. *Genes Cells* 2000; **5**: 699-709
- 29 **Wu L**, Chen P, Shum CH, Chen C, Barsky LW, Weinberg KI, Jong A, Triche TJ. MAT1-modulated CAK activity regulates cell cycle G (1) exit. *Mol Cell Biol* 2001; **21**: 260-270
- 30 **Kim JM**, Nakao K, Nakamura K, Saito I, Katsuki M, Arai K, Masai H. Inactivation of Cdc7 kinase in mouse ES cells results in S-phase arrest and p53-dependent cell death. *EMBO J* 2002; **21**: 2168-2179
- 31 **Abriss B**, Hollweg G, Gressner AM, Weiskirchen R. Adenoviral-mediated transfer of p53 or retinoblastoma protein blocks cell proliferation and induces apoptosis in culture-activated hepatic stellate cells. *J Hepatol* 2003; **38**: 169-178
- 32 **Liao H**, Bucala R, Mitchell RA. Adhesion-dependent signaling by macrophage migration inhibitory factor (MIF). *J Biol Chem* 2003; **278**: 76-81
- 33 **Fingerle-Rowson G**, Koch P, Bikoff R, Lin X, Metz CN, Dhabhar FS, Meinhardt A, Bucala R. Regulation of macrophage migration inhibitory factor expression by glucocorticoids *in vivo*. *Am J Pathol* 2003; **162**: 47-56
- 34 **Zhang LH**, Pan JP, Yao HP, Sun WJ, Xia DJ, Wang QQ, He L, Wang J, Cao X. Intrasplenic transplantation of IL-18 gene-modified hepatocytes: an effective approach to reverse hepatic fibrosis in schistosomiasis through induction of dominant Th1 response. *Gene Ther* 2001; **8**: 1333-1342
- 35 **Vogel S**, Piantedosi R, Frank J, Lalazar A, Rockey DC, Friendman SL, Blaner WS. An immortalized rat liver stellate cell line (HSC-T6): a new cell model for the study of retinoid metabolism *in vitro*. *J Lipid Res* 2000; **41**: 882-893
- 36 **Si X**, Zeng Q, Ng CH, Hong W, Pallen CJ. Interaction of farnesylated PRL-2, a protein-tyrosine phosphatase, with the beta-subunit of geranylgeranyltransferase II. *J Biol Chem* 2001; **276**: 32875-32882
- 37 **Maehama T**, Taylor GS, Dixon JE. PTEN and myotubularin: novel phosphoinositide phosphatases. *Annu Rev Biochem* 2001; **70**: 247-279
- 38 **Zeeb M**, Rosner H, Zeslawski W, Canet D, Holak TA, Balbach J. Protein folding and stability of human CDK inhibitor p19 (INK4d). *J Mol Biol* 2002; **315**: 447-457
- 39 **Servillo G**, Della Fazio MA, Sassone-Corsi P. Coupling cAMP signaling to transcription in the liver: pivotal role of CREB and CREM. *Exp Cell Res* 2002; **275**: 143-154
- 40 **Eng FJ**, Friedman SL. Transcriptional regulation in hepatic stellate cells. *Semin Liver Dis* 2001; **21**: 385-395
- 41 **Saxena NK**, Ikeda K, Rockey DC, Friedman SL, Anania FA. Leptin in hepatic fibrosis: evidence for increased collagen production in stellate cells and lean littermates of ob/ob mice. *Hepatology* 2002; **35**: 762-771
- 42 **Garcia-Tevijano ER**, Berasain C, Rodriguez JA, Corrales FJ, Arias R, Martin-Duce A, Caballeria J, Mato JM, Avila MA. Hyperhomocysteinemia in liver cirrhosis: mechanism and role in vascular and hepatic fibrosis. *Hypertension* 2001; **38**: 1217-1221

Edited by Ma JY Proofread by Xu FM

Leflunomide attenuates hepatocyte injury by inhibiting Kupffer cells

Hong-Wei Yao, Jun Li, Ji-Qiang Chen, Shu-Yun Xu

Hong-Wei Yao, Ji-Qiang Chen, Zhejiang Respiratory Drugs Research Laboratory of State Drugs Administration of China, School of Medicine, Zhejiang University, Hangzhou 310031, Zhejiang Province, China

Jun Li, Shu-Yun Xu, Institute of Clinical Pharmacology, Anhui Medical University, Hefei, 230032, Anhui Province, China

Supported by Natural Science Foundation of Anhui Province, No. 98446733

Correspondence to: Professor Jun Li, Institute of Clinical Pharmacology, Anhui Medical University, Hefei, 230032, Anhui Province, China. amuicplj@mail.hf.ah.cn

Telephone: +86-551-5161040 **Fax:** +86-551-5161040

Received: 2003-11-13 **Accepted:** 2003-12-29

Abstract

AIM: To investigate the importance of direct contact between Kupffer cells (KCs) and hepatocytes (HCs) during hepatic inflammatory responses, and the effect of leflunomide's active metabolite, A₇₇₁₇₂₆, on cytokines in KCs, HCs and KC cocultures (DC cocultures).

METHODS: KCs and HCs in liver were isolated by digestion with pronase and collagenase. Lipopolysaccharide (LPS)-induced inflammatory response in monocultures of rat HCs and KCs was compared with that in DC cocultures. Tumor necrosis factor- α (TNF- α) and interleukin-1 (IL-1) concentrations in different culture supernatants were measured with ELISA. TNF- α mRNA in KCs of inflammatory liver injury was analyzed with reverse transcriptase polymerase chain reaction (RT-PCR).

RESULTS: DC cocultures strongly exhibited the production of TNF- α and IL-1 compared with other cultures, and these cytokines were mainly produced by KCs, especially by activated KCs. Time course studies revealed an increased production of TNF- α preceding the IL-1 production, suggesting that increased TNF- α levels could be involved in the increase of IL-1 production. Leflunomide's active metabolite, A₇₇₁₇₂₆, had significantly inhibitory effect on TNF- α and IL-1 at protein and transcription levels, and the reduced production of IL-1 by A₇₇₁₇₂₆ was associated with the inhibitory action of A₇₇₁₇₂₆ on TNF- α .

CONCLUSION: Leflunomide can inhibit hepatocyte damage by inhibiting proinflammatory cytokine release from KCs.

Yao HW, Li J, Chen JQ, Xu SY. Leflunomide attenuates hepatocyte injury by inhibiting Kupffer cells. *World J Gastroenterol* 2004; 10(11): 1608-1611

<http://www.wjgnet.com/1007-9327/10/1608.asp>

INTRODUCTION

Tissue inflammation plays a critical role in liver pathology via induction of cellular injury. In fact, infiltration of mononuclear phagocytes into the liver correlates with the severity of liver

injury. Moreover, proinflammatory cytokines such as tumor necrosis factor- α (TNF- α) and interleukin-1 (IL-1) have been linked to the promotion of liver injury^[1-3], and the anti-inflammatory cytokine interleukin-10 (IL-10) was believed to inhibit liver injury^[4,5]. Kupffer cells (KCs) are among the first cells that respond to endotoxins, including lipopolysaccharides (LPS), and are considered to be the primary macrophages involved in the clearance of gut-derived bacteria or bacterial toxins. High portal level of LPS could lead to a pronounced secretion of proinflammatory mediators by KCs and ultimately to endotoxin-induced liver injury^[6,7]. KCs are located in hepatic sinusoids and lie in between or on top of endothelial cells. However, they do have direct cell contacts with parenchymatous hepatocytes (HCs) through their cytoplasmic extensions. Cellular communication between KCs and HCs has been thought to occur mainly by production of cytokines and excretion of inflammatory mediators such as eicosanoids, nitric oxide (NO), and/or reactive oxygen species (ROS)^[8,9]. Proinflammatory cytokines, TNF- α and IL-1 in particular, have been shown to be early and important mediators of HC injury^[8,10].

Leflunomide, an isoxazole derivative and a unique immunomodulatory agent, is capable of treating rheumatoid arthritis, allograft and xenograft rejection, systemic lupus erythematosus, Crohn's disease, and prostate cancer^[11-16]. Leflunomide is a prodrug that could be rapidly converted in the cell to an active metabolite, A₇₇₁₇₂₆^[17-19]. Our investigations demonstrated that leflunomide had therapeutic actions on acute and chronic liver diseases^[20-22]. In order to study the mechanisms of leflunomide on liver injury, the interaction between KCs and HCs *in vitro*, and the effect of leflunomide's active metabolite, A₇₇₁₇₂₆, on TNF- α and IL-1 were investigated.

MATERIALS AND METHODS

Animals and reagents

Male Sprague-Dawley rats weighing 200-250 g were purchased from Animal Center of Anhui Medical University. Rats were allowed to take food and tap water *ad libitum*. *Bacillus Calmette-Guérin* (BCG) was purchased from Institute of Shanghai Biological company. Collagenase, Nycodenz, LPS from *Escherichia coli* O111:B4, 3-(4,5-dimethylthiazol-2-yl)-2, 5-diphenyltetrazolium bromide (MTT), and ELISA kits of TNF- α and IL-1 were obtained from Sigma Chemical (St. Louis, Mo). Powdered 1640 medium was obtained from GIBCO Co., USA. Leflunomide and its active metabolite, A₇₇₁₇₂₆, were kindly donated by Cinkate Co., USA.

Preparation of inflammatory liver injury

Each rat was injected with 15 mg BCG in 0.2 mL saline via tail vein, and 14 d later with 10 μ g LPS in 0.2 mL saline^[23]. At 16 h post-injection of LPS, rats were anesthetized and KCs were isolated.

Preparation of HCs

The procedure for isolation of rat HCs was based on Seglen's method^[24], with some modifications. The obtained cell suspension was diluted in modified Hanks' buffered salt solution

(pH 7.65, 4 °C, 9.2 mmol/L HEPES, 9.91 g/L Hanks' buffered salt solution without Ca²⁺ and Mg²⁺) and centrifuged at 200 g for 5 min. The supernatant was discarded, and cells were resuspended with PBS (pH 7.4) to a final volume of 100 mL and centrifuged for 2 min at 50 g. The supernatant, containing mainly nonparenchymal cells, was collected for isolation of KCs (see Preparation of KCs). Pellets containing mainly HCs were resuspended in RPMI 1640 medium and washed 4 times for 2 min at 50 g. After the final wash step, cells were counted and diluted with RPMI 1640 medium supplemented with 50 mL/L FBS, glutamine (2 mmol/L), and gentamicin (50 µg/mL) to a final concentration of 1×10⁶ cells/mL. Viability of cultures was ≥95% as assessed by trypan blue dye exclusion. Light microscopic observations revealed a purity of 90-95% HCs for HC cultures.

Preparation of KCs

The procedure for KCs isolation was based on the method of Smedsrod *et al.*^[25], with slight modifications. Supernatants (see Preparation of HC cultures) containing mainly nonparenchymal cells were transferred to four 50 mL Falcon tubes followed by centrifugation at 50 g in a swing-out rotor at 4 °C for 2 min. This procedure was repeated twice to discard the remaining HCs. After the final step, supernatants were centrifuged at 200 g in a swing-out rotor at 4 °C for 10 min, and discarded. The resulting pellets were resuspended in PBS to a final volume of 40 mL. The nonparenchymal cell suspension was prepared by centrifugation on a double-layered (17.2%/11.5%) Nycodenz solution. After centrifugation at 1400 g for 20 min (4 °C), KCs and endothelial cells were present at the boundary between the upper and lower layers. The cell suspension containing both KCs and endothelial cells, was collected and centrifuged at 200 g for 10 min, and the resulting pellets were diluted with RPMI 1640 medium (without serum) and washed again. Hereafter, the pellets consisting of 50% KCs and 50% endothelial cells were diluted in RPMI 1640 medium (without serum) to a final concentration of 2×10⁶ cells/mL. To separate KCs from endothelial cells, cells were plated on tissue culture plates at 37 °C and 50 mL/L CO₂ for 30 min followed by a single wash step discarding the nonadherent endothelial cells. Viability of KCs was ≥95% as determined by trypan blue dye exclusion assay. Immunohistochemistry and fluoroscopy revealed a purity of ≥85% KCs for KC cultures.

Cell cultures

HCs were cultured at a density of 0.5×10⁶ cells/well in 24-well culture dishes using RPMI 1640 medium, supplemented with 50 mL/L FBS, glutamine (2 mmol/L), and gentamicin (50 µg/mL). KCs were cultured in RPMI 1640 medium containing 100 mL/L FBS, 2 mmol/L glutamine, and 50 µg/mL gentamicin at a density of 0.5×10⁶ cells/well in 24-well culture dishes. DC cocultures consisted of 0.5×10⁶ attached KCs in 24-well tissue culture plates with the addition of 0.5×10⁶ HCs in direct contact. RPMI 1640 medium supplemented with 50 mL/L FBS, glutamine (2 mmol/L), and gentamicin (50 µg/mL) was used. After an attachment period of 4 h, the medium was replaced by a fresh medium in all culture types.

Experimental design

After a recovery period of 24 h at 37 °C and 50 mL/L CO₂, the medium was replaced by a medium containing 0, 1, 5, or 10 µg/mL LPS. Because HCs are known to produce various important serum compounds such as LPS-binding protein, medium of KC cultures still contained 50 mL/L FBS. After 2, 4, 8, and 24 h of incubation, tissue culture supernatants were collected for analysis of cytokines. To study the effect of A₇₇₁₇₂₆ on excretion of TNF-α and IL-1 in DC coculture supernatants, A₇₇₁₇₂₆ was dissolved with RPMI 1640 medium and added to DC cocultures

from 0 h to 4 h (0-4 h), to 24 h (0-24 h) and from 4 h to 24 h (4-24 h) after incubation with LPS, respectively.

Measurement of TNF-α and IL-1

TNF-α and IL-1 concentrations in cell culture supernatants were measured using commercial ELISA kits with recombinant rat TNF-α and IL-1 as standard. Measurements were performed in duplicate.

Semiquantitative RT-PCR assay for TNF-α mRNA in KCs of inflammatory liver tissue

After incubation with or without A₇₇₁₇₂₆ (0.001-10 µmol/L), KCs of inflammatory liver tissue were harvested and kept at -70 °C until RNA extraction. Total cellular RNA was extracted using RNA easy kits (Invitrogen, USA). To test the efficacy of reverse transcriptase, RT-PCR was performed for GAPDH mRNA. Briefly, the first strain of cDNA was synthesized by reverse transcriptase and pooled. The resulting cDNA samples were adjusted to PCR buffer conditions and run for PCR simultaneously. The primers for TNF-α were 5' -CGAGTGACAAGCCCGTAGCC and 5' -GGATGAACACGCCAGTCGCC. The primers for GAPDH were 5' -CCACCCATGGCAAATTCATGGCA and 5' -TCTAGACGGCAGGTCAGGTCCACC^[26]. The amplification of TNF-α and GAPDH genes was expected to generate 753 bp and 600 bp fragments, respectively. Amplification was performed for 35 cycles, each consisting of denaturation at 94 °C for 1 min, annealing at 51 °C for 1 min, and extension at 72 °C for 2 min. Ten µL of reaction mixture was loaded to 10 g/L agarose gel containing 0.5 µg/mL ethidium bromide for electrophoresis, the gel was then placed under ultraviolet ray for semi-quantitation detection.

Statistics

Unless stated otherwise, data were expressed as mean±SD and evaluated using two-way ANOVA followed by Student's *t* test for comparison between 2 groups. *P*<0.05 was considered statistically significant.

RESULTS

Proinflammatory cytokine production after stimulation with LPS

The production of TNF-α and IL-1 was measured after incubation of HC and KC cultures, and DC cocultures in medium with or without LPS. A time course study showed that maximal cytokine levels in KC cultures and DC cocultures were observed after 4 h incubation for TNF-α and 24 h incubation for IL-1 respectively (Figure 1). Moreover, TNF-α and IL-1 levels in culture supernatants were positive correlated with the concentration of LPS (Figure 2). TNF-α and IL-1 levels at 2, 4, 8, 24 h in DC cocultures were significantly higher than those in KC or HC cultures (Figure 1). However, two cytokines levels in HC cultures showed no statistically significant changes throughout the experiments (Figures 1-2).

Effect of A₇₇₁₇₂₆ on TNF-α and IL-1 production in DC cocultures after stimulation with LPS

Based on the results as above, we selected DC cocultures stimulated with 10 µg/mL LPS as targets, and A₇₇₁₇₂₆ was added to DC cocultures with different time course. After 4 h incubation (0-4 h), TNF-α and IL-1 production in DC cocultures stimulated with LPS (10 µg/mL) was significantly inhibited in A₇₇₁₇₂₆ (0.1, 10 µmol/L) and dexamethasone (2×10⁻⁵ µmol/L) group (Figure 3A). Likewise, TNF-α and IL-1 production in DC cocultures was also significantly inhibited after 24 h incubation (0-24 h) in A₇₇₁₇₂₆ (10 µmol/L) group (Figure 3B). Because the concentration of TNF-α reached its maximal level after 4 h incubation, we designed a protocol that A₇₇₁₇₂₆ was added to DC cocultures from 4 h to 24 h after incubation (4-24 h). The results showed

that the concentration of TNF- α and IL-1 in DC cocultures supernatants was not inhibited in A₇₇₁₇₂₆ (10 μ mol/L, 4-24 h) group (Figure 3B). Furthermore, TNF- α and IL-1 levels in A₇₇₁₇₂₆ (10 μ mol/L, 0-24 h) group were significantly lower than those in A₇₇₁₇₂₆ (10 μ mol/L, 4-24 h) group.

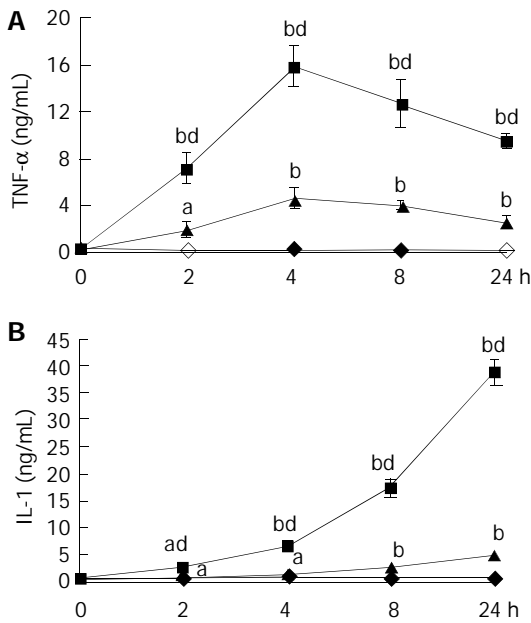


Figure 1 Changes of TNF- α and IL-1 levels in different type culture supernatants with LPS (10 μ g/mL) ($n=3$, mean \pm SD). DC, solid line; KC, dot line; HC, dashed line. ^a $P < 0.05$, ^b $P < 0.01$ for IL-1 levels in DC, KC, and HC vs. control. ^d $P < 0.01$, vs KC and HC. A: Changes of TNF- α levels in different type culture supernatants with LPS. B: Changes of IL-1 levels in different type culture supernatants with LPS.

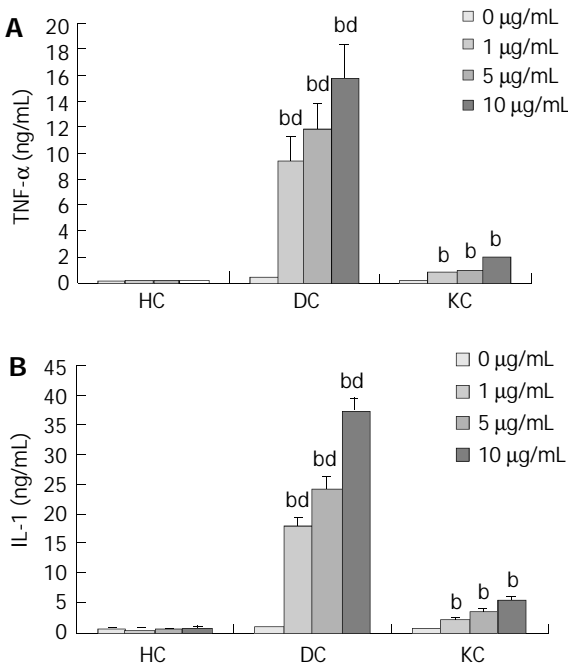


Figure 2 Changes of TNF- α and IL-1 levels in culture supernatants of HC, DC, KC after 4 h and 24 h incubation with various concentrations of LPS ($n=3$, mean \pm SD). ^b $P < 0.01$ for TNF- α and IL-1 levels in DC, KC vs control; ^d $P < 0.01$ for DC coculture vs other cultures after 0, 1, 5, and 10 μ g/mL LPS. A: Changes of TNF- α levels in culture supernatants of HC, DC, KC after 4 h incubation with various concentrations of LPS. B: Changes of IL-1 levels in culture supernatants of HC, DC, KC after 24 h incubation with various concentrations of LPS.

Effect of A₇₇₁₇₂₆ on TNF- α mRNA in KCs of inflammatory liver tissue
 A₇₇₁₇₂₆ had significantly inhibitory actions on the production of TNF- α in supernatants of DC cocultures. To gain insights into the potentially inhibitory action of A₇₇₁₇₂₆ on TNF- α via transcriptional level, TNF- α mRNA was analyzed by RT-PCR in KCs during liver inflammation induced by injection with BCG and LPS. Gel electrophoresis and semiquantitation analysis showed that A₇₇₁₇₂₆ significantly reduced the expression of TNF- α mRNA in KCs of inflammatory liver tissue induced by BCG and LPS (Figure 4, Table 1).

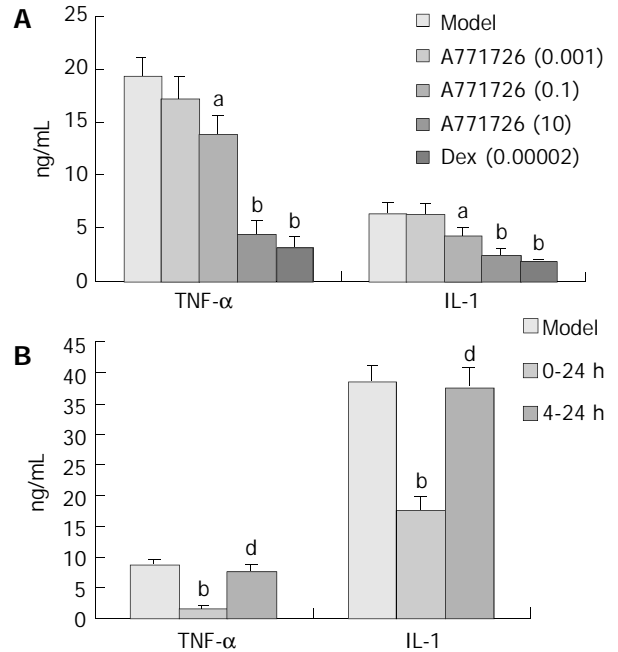


Figure 3 Effect of A₇₇₁₇₂₆ on TNF- α and IL-1 levels in culture supernatants of DC stimulated by LPS (10 μ g) with different administration time ($n=3$, mean \pm SD). ^a $P < 0.05$, ^b $P < 0.01$, vs model; ^d $P < 0.01$, vs 0-24 h group.

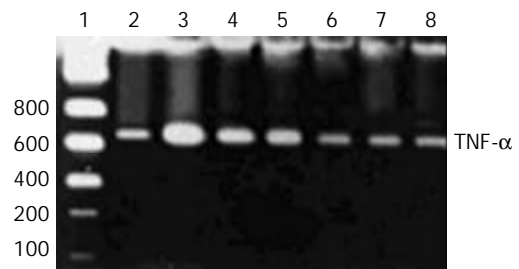


Figure 4 Effect of A₇₇₁₇₂₆ on TNF- α mRNA of KCs in immunological liver injury rats. 1: DNA marker; 3: model; 2: Dexamethasone; 4-8: A₇₇₁₇₂₆ at concentration of 1×10^{-3} , 1×10^{-2} , 1×10^{-1} , 1×10^0 , 1×10^1 μ mol/L.

Table 1 Effect of A₇₇₁₇₂₆ on TNF- α mRNA in KCs of inflammatory liver injury rats ($n=3$, mean \pm SD)

Group	Dose (μ mol/L)	TNF- α
Model	-	2.669 \pm 0.252
A ₇₇₁₇₂₆	1×10^{-3}	2.507 \pm 0.051
	1×10^{-2}	2.213 \pm 0.044 ^a
	1×10^{-1}	1.955 \pm 0.080 ^b
	1×10^0	1.432 \pm 0.067 ^b
	1×10^1	0.987 \pm 0.048 ^b
Dexamethasone	2×10^{-5}	1.021 \pm 0.110 ^b

^a $P < 0.05$, ^b $P < 0.01$, vs Model.

DISCUSSION

In the intact liver, HCs are in direct contact with KCs. The present experiments were designed to assess whether direct contact between HCs and KCs was of influence on the LPS-induced inflammatory response. When compared the production of TNF- α and IL-1 in the different culture types, direct cell-to-cell contact between KCs and HCs seemed to be essential, because an 4- or 7-fold increase of TNF- α and IL-1, could be observed in DC cocultures. Although the cytokine levels in KC cultures were markedly lower than those observed in DC cocultures, incubation of KC cultures with LPS still resulted in an abundant cytokine response. LPS-induced cytokine expression in DC cocultures or KC cultures has been extensively studied, but in this study we showed that direct contact between KCs and HCs significantly increased TNF- α and IL-1 production by rat KCs. However, the levels of two cytokines in HC cultures showed no statistically significant changes throughout the experiments. The results indicated proinflammatory mediators such as TNF- α and IL-1 in culture supernatants were mainly produced by KCs, especially activated KCs. Time course studies performed with these cultures revealed an increased production of TNF- α preceding the IL-1 production, suggesting that increased TNF- α levels could be involved in IL-1 production. The results were consistent with Shito's report^[1] that TNF- α could be a cause of liver injury and might help regulate the expression of IL-1.

Leflunomide was mainly used to inhibit the activity of dihydroorotate dehydrogenase (DHODH) involved in *de novo* pyrimidine biosynthesis. But at a high concentration, it mainly inhibited protein tyrosine kinases initiating signaling, and therefore reduced the cell response to mitogens and cytokines. Recent evidences suggested the anti-inflammatory and immunoregulatory effects of leflunomide were related with its ability to suppress TNF- α and IL-1 selectively over their inhibitors in T lymphocyte/monocyte activation, and the activation of nuclear factor kappa B, a potent mediator of inflammation when stimulated by inflammatory stimuli. We found that TNF- α and IL-1 levels in supernatants of DC cocultures were apparently inhibited by A₇₇₁₇₂₆ (0.1, 10 μ mol/L, 0-4 h) and A₇₇₁₇₂₆ (10 μ mol/L, 0-24 h). However, TNF- α and IL-1 levels in supernatants of DC cocultures were not affected in A₇₇₁₇₂₆ (10 μ mol/L, 4-24 h) group, and the levels of the two cytokines in A₇₇₁₇₂₆ (10 μ mol/L, 0-24 h) group were significantly lower than those in A₇₇₁₇₂₆ (10 μ mol/L, 4-24 h) group. The results indicated that the inhibitory action of A₇₇₁₇₂₆ on TNF- α and IL-1 levels was generated mainly from 0-4 h incubation, and reduced production of IL-1 by A₇₇₁₇₂₆ was associated with the inhibitory action of A₇₇₁₇₂₆ on TNF- α . Furthermore, RT-PCR analysis showed that A₇₇₁₇₂₆ significantly reduced the expression of TNF- α mRNA in KCs of inflammatory liver tissue induced by BCG+LPS. The results showed A₇₇₁₇₂₆ had significantly inhibitory effects on production of TNF- α in KCs at transcriptional level.

Although further work is required to demonstrate whether A₇₇₁₇₂₆ has other targets in inflammatory liver injury, A₇₇₁₇₂₆ can inhibit hepatocyte damage by inhibiting proinflammatory cytokine release from KCs.

REFERENCES

- 1 Shito M, Balis UJ, Tompkins RG, Yarmush ML, Toner M. A fulminant hepatic failure model in the rat: involvement of interleukin-1 β and tumor necrosis factor- α . *Dig Dis Sci* 2001; **46**: 1700-1708
- 2 Bradham CA, Plumpe J, Manns MP, Brenner DA, Trautwein C. Mechanisms of hepatic toxicity. I. TNF-induced liver injury. *Am J Physiol* 1998; **275**: G387-392
- 3 Nishioji K, Okanoue T, Mori T, Sakamoto S, Itoh Y. Experimental liver injury induced by *Propionibacterium acnes* and lipopolysaccharide in macrophage colony stimulating factor-deficient osteopetrotic (op/op) mice. *Dig Dis Sci* 1999; **44**: 1975-1984
- 4 Sermon F, Le Moine O, Gustot T, Quertinmont E, Louis H, Nagy N, Degraef C, Deviere J. Chronic alcohol exposure sensitizes mice to galactosamine-induced liver injury through enhanced keratinocyte chemoattractant and defective IL-10 production. *J Hepatol* 2003; **39**: 68-76
- 5 Louis H, Le Moine O, Goldman M, Deviere J. Modulation of liver injury by interleukin-10. *Acta Gastroenterol Belg* 2003; **66**: 7-14
- 6 Enomoto N, Ikejima K, Yamashina S, Hirose M, Shimizu H, Kitamura T, Takei Y, Sato And N, Thurman RG. Kupffer cell sensitization by alcohol involves increased permeability to gut-derived endotoxin. *Alcohol Clin Exp Res* 2001; **25**(6 Suppl): 51S-54S
- 7 Lukkari TA, Jarvelainen HA, Oinonen T, Kettunen E, Lindros KO. Short-term ethanol exposure increases the expression of Kupffer cell CD14 receptor and lipopolysaccharide binding protein in rat liver. *Alcohol Alcohol* 1999; **34**: 311-319
- 8 Wang JH, Redmond HP, Wu QD, Bouchier-Hayes D. Nitric oxide mediates hepatocyte injury. *Am J Physiol* 1998; **275**: G1117-1126
- 9 Kmiec Z. Cooperation of liver cells in health and disease. *Adv Anat Embryol Cell Biol* 2001; **161**: 1-151
- 10 Hoek JB, Pastorino JG. Ethanol, oxidative stress, and cytokine-induced liver cell injury. *Alcohol* 2002; **27**: 63-68
- 11 Sanders S, Harisdangkul V. Leflunomide for the treatment of rheumatoid arthritis and autoimmunity. *Am J Med Sci* 2002; **323**: 190-193
- 12 Osiri M, Shea B, Robinson V, Suarez-Almazor M, Strand V, Tugwell P, Wells G. Leflunomide for the treatment of rheumatoid arthritis: a systematic review and metaanalysis. *J Rheumatol* 2003; **30**: 1182-1190
- 13 Williams JW, Mital D, Chong A, Kottayil A, Millis M, Longstreth J, Huang W, Brady L, Jensik S. Experiences with leflunomide in solid organ transplantation. *Transplantation* 2002; **73**: 358-366
- 14 Kessel A, Toubi E. Leflunomide in systemic lupus erythematosus. *Harefuah* 2002; **141**: 355-357
- 15 Prajapati DN, Knox JF, Emmons J, Saeian K, Csuka ME, Binion DG. Leflunomide treatment of Crohn's disease patients intolerant to standard immunomodulator therapy. *J Clin Gastroenterol* 2003; **37**: 125-128
- 16 Ko YJ, Small EJ, Kabbinnavar F, Chachoua A, Taneja S, Reese D, DePaoli A, Hannah A, Balk SP, Bublely GJ. A multi-institutional phase ii study of SU101, a platelet-derived growth factor receptor inhibitor, for patients with hormone-refractory prostate cancer. *Clin Cancer Res* 2001; **7**: 800-805
- 17 Lucient J, Dias VC, LeGatt DF, Yatscoff RW. Blood distribution and single-dose pharmacokinetics of leflunomide. *Ther Drug Monit* 1995; **17**: 454-459
- 18 Li J, Yao HW, Jin Y, Zhang YF, Li CY, Xu SY. Pharmacokinetics of leflunomide in Chinese healthy volunteers. *Acta Pharmacol Sin* 2002; **23**: 551-555
- 19 Rozman B. Clinical pharmacokinetics of leflunomide. *Clin Pharmacokinet* 2002; **41**: 421-430
- 20 Yao HW, Li J, Jin Y, Zhang YF, Li CY, Xu SY. Effect of leflunomide on immunological injury in mice. *World J Gastroenterol* 2003; **9**: 320-323
- 21 Yao HW, Jin Y, Li J, Zhang YF, Li CY, Xu SY. Effect of leflunomide on immunological injury. *Yaoxue Xuebao* 2001; **36**: 727-730
- 22 Yao HW, Jin Y, Li J, Zhang YF, Li CY, Xu SY. Effect of leflunomide on the acute chemical injury. *Anhui Yiyao* 2001; **5**: 7-9
- 23 Zhang GL, Lin ZB, Zhang B. Effects of selective inducible nitric oxide synthase inhibitor on immunological hepatic injury in rat. *Zhonghua Yixue Zazhi* 1998; **78**: 540-543
- 24 Seglen PO. Preparation of isolated rat liver cells. *Methods Cell Biol* 1976; **13**: 29-83
- 25 Smedsrod B, Pertoft H, Eggertsen G, Sundstrom C. Functional and morphological characterization of cultures of Kupffer cells and liver endothelial cells prepared by means of density separation in Percoll, and selective substrate adherence. *Cell Tissue Res* 1985; **241**: 639-649
- 26 Yin F, Yang YJ, Yu PL, Mao DA, Tao YG. Tumor necrosis factor- α in brain tissues of rats with pertussis bacilli induced brain edema. *Chin J Contemp Pediatr* 2000; **2**: 82-85

A rapid and efficient method to express target genes in mammalian cells by baculovirus

Tong Cheng, Chen-Yu Xu, Ying-Bin Wang, Min Chen, Ting Wu, Jun Zhang, Ning-Shao Xia

Tong Cheng, Chen-Yu Xu, Ying-Bin Wang, Min Chen, Ting Wu, Jun Zhang, Ning-Shao Xia, Key Laboratory of Cell Biology and Tumor Cell Engineering of Ministry of Education, Xiamen University, Xiamen 361005, Fujian Province, China

Supported by the grant from 863 Program, No.2001AA628120

Correspondence to: Professor Ning-Shao Xia, Key Laboratory of Cell Biology and Tumor Cell Engineering of Ministry of Education, Xiamen University, Xiamen 361005, Fujian Province, China. nsxia@jingxian.xmu.edu.cn

Telephone: +86-592-2184110 **Fax:** +86-592-2184110

Received: 2003-10-27 **Accepted:** 2003-12-08

Abstract

AIM: To investigate the modification of baculovirus vector and the feasibility of delivering exogenous genes into mammalian cells with the culture supernatant of *Spodoptera frugiperda* (Sf9) cells infected by recombinant baculoviruses.

METHODS: Two recombinant baculoviruses (BacV-CMV-EGFP, BacV-CMV-EGFPB) containing CMV-EGFP expression cassette were constructed. HepG2 cells were directly incubated with the culture supernatant of Sf9 cells infected by recombinant baculoviruses, and reporter gene transfer and expression efficiencies were analyzed by flow cytometry (FCM). The optimal transduction conditions were investigated by FCM assay in HepG2 cells. Gene-transfer and expression efficiencies in HepG2 or CV1 cells by baculovirus vectors were compared with lipofectAMINE, recombinant retrovirus and vaccinia virus expression systems. Twenty different mammalian cell lines were used to investigate the feasibility of delivering exogenous genes into different mammalian cells with the culture supernatant of infected Sf9 cells.

RESULTS: CMV promoter could directly express reporter genes in Sf9 cells with a relatively low efficiency. Target cells incubated with the 1:1 diluted culture supernatant (moi=50) for 12 h at 37 °C could achieve the highest transduction and expression efficiencies with least impairment to cell viability. Under similar conditions the baculovirus vector could achieve the highest gene-transfer and expression efficiency than lipofectAMINE, recombinant retrovirus and vaccinia virus expression systems. Most mammalian cell lines could be transduced with recombinant baculovirus. In primate adherent culture cells the recombinant baculovirus could arrive the highest infection and expression efficiencies, but it was not very satisfactory in the cell lines from mice and suspended culture cells.

CONCLUSION: Mammalian cells incubated with the culture supernatant of infected Sf9 cells could serve as a very convenient way for rapid and efficient expression of foreign genes in mammalian cells, but it might be more suitable for primate adherent culture cells.

Cheng T, Xu CY, Wang YB, Chen M, Wu T, Zhang J, Xia NS. A rapid and efficient method to express target genes in mammalian cells by baculovirus. *World J Gastroenterol* 2004; 10(11): 1612-1618
<http://www.wjgnet.com/1007-9327/10/1612.asp>

INTRODUCTION

The baculovirus (*Autographa californica* multiple nuclear polyhedrosis virus, AcMNPV) insect cell expression system has been extensively developed and widely used for the production of numerous recombinant proteins in insect cells^[1-5]. As the previous reports described, baculovirus had a strict host range, which was only limited to lepidopteran insects. However, researchers have reported that baculoviruses can be taken up by some mammalian cells^[6,7], but are incapable of replicating in these mammalian cells^[8,9]. A modified AcMNPV containing promoters that are active in mammalian cells, such as Rous sarcoma virus (RSV) promoter and cytomegalovirus immediate early (CMV-IE) promoter, can express exogenous genes in mammalian cells^[10-14]. So a new way could be chosen by researchers for experiments of delivering target genes into mammalian cells, besides the conventional lipid transfection and mammalian viral vector expression systems, such as retrovirus expression system, adenovirus expression system. Previous reports have described that recombinant baculoviruses used in gene-transfer experiments were often concentrated by ultracentrifugation. Although this way can markedly increase the virus titer, but it needs to culture a large number of cells to obtain sufficient viruses, and the manipulation is complex and burdensome. So it is inconvenient in some daily common experiments.

Bac-to-Bac system is the most often used baculovirus-based expression system for the production of recombinant proteins in insect cells. In our research, based on the Bac-to-Bac system recombinant baculoviruses were constructed, which contain the enhanced green fluorescent protein (eGFP) gene driven by CMV promoter, to investigate the modification of baculovirus vector and the feasibility of delivering exogenous genes into mammalian cells with the culture supernatant of Sf9 cells infected by recombinant baculoviruses. Compared with lipid transfection, retrovirus and vaccinia virus expression system, efficiencies of gene transfer and expression in mammalian cells by the culture supernatant of infected Sf9 cells were superior to the traditional ways. Since direct application of the culture supernatant could simplify the procedures of delivering foreign genes into mammalian cells by baculovirus vectors, it could serve as a valuable tool for some daily common experiments.

MATERIALS AND METHODS

Cell lines

Spodoptera frugiperda (Sf9) cell line was purchased from Invitrogen (California, USA). CV1, 293, 143B, HepG2, PLC/PRF/5, BNL 1ME A.7R.1, WI-38, DMS-114, JC, L-929, P815, PT67 cell lines were obtained from the American Type Culture Collection. HeLa, CHO, NIH3T3, Raji, CNE, MCF-7, BGC-223 cell lines were stored in our laboratory. LCL-cm and pT67-EGFP cell lines were constructed in our laboratory.

Bacteria and plasmids

E.coli DH5 α was stored in our laboratory. *E.coli* DH10Bac was purchased from Invitrogen (California, USA). pcDNA3.1

(+) was purchased from Invitrogen (California, USA). pEGFP was purchased from Clontech (California, USA). pMD18-EF1A, pCDNA3.1-EGFP was constructed in our laboratory.

Construction of shuttle vectors

Plasmid pEGFP was digested with *Bam*HI and *Eco*RI, a 760 bp fragment containing EGFP gene was retrieved and inserted into the pFastBacI backbone that was digested with *Bam*HI and *Eco*RI to form pFB-EGFP. EGFP gene was moved from pEGFP to pCDNA3.1(+) as an *Eco*RI-*Bam*HI fragment to construct pN31-EGFP. An 1.6 kb *Bgl*III-*Eco*RI fragment from pN31-EGFP, containing CMV-IE promoter/enhancer and EGFP gene, was inserted into the pFastBacI backbone which was digested with *Bam*HI and *Eco*RI to obtain pFB-CMV-EGFPA. A *Bgl*III-*Bam*HI fragment containing the polyadenylation signal was inserted into the *Bam*HI site of pFastBacI to construct pFB-EF1A. An 1.6 kb *Sal*I-*Eco*RI fragment from pN31-EGFP was inserted into pFB-EF1A which was digested with *Xho*I and *Eco*RI to construct pFB-CMV-EGFPB (Figure 1).

Construction of recombinant baculoviruses^[15]

Shuttle vectors pFB-EGFP, pFB-CMV-EGFPA, pFB-CMV-EGFPB were transformed into *E. coli* DH10Bac cells, which were incubated on LB agar plates containing 100 µg/mL Bluogal, 40 µg/mL IPTG, 7 µg/mL gentamicin, 50 µg/mL kanamycin, 10 µg/mL tetracycline for 24-48 h at 37 °C. White colonies were inoculated into LB medium containing the same antibiotics and bacmid DNA was isolated according to the standard manual (Invitrogen).

pUC/M13 amplification primers were directed at sequences on either side of the *miniatt*Tn7 site within the *lacZ*α-complementation region of bacmid. If transposition occurred, the PCR product produced by these primers (at 94 °C for 50 s, at 55 °C for 50 s, at 72 °C for 5 min, 30 cycles, at 72 °C for 10 min) was 2 300 bp plus the size of the insert. The PCR product of bacmid alone was about 300 bp, bacmid transposed with pFB-EGFP was 3 060 bp, bacmid transposed with pFB-CMV-EGFPA was 3 978 bp, and bacmid transposed with pFB-CMV-EGFPB was 4 633 bp.

Sf9 cells were cultured in Grace's supplemented insect medium containing 100 mL/L fetal bovine serum (HyClone). Recombinant baculoviruses were generated by Bac-to-Bac system according to the standard manual (Invitrogen). Viruses were amplified to a high titer by propagation in Sf9 cells. Virus titers were measured by plaque assay on Sf9 cells.

Transduction of mammalian cells by recombinant baculoviruses

Mammalian cells were seeded in 24-well culture dishes about 50 000 cells per well and incubated in a 37 °C CO₂ incubator for 12 h. Culture medium was removed, replaced with the collected culture supernatant (500 µL), and incubated for 1-24 h at 37 °C. After removal of viruses, fresh medium was added

and cultures were incubated at 37 °C. Cells that grew in suspension were pelleted by centrifugation before addition of virus inoculums. Forty-eight h post transduction, cultures were examined for eGFP expression using fluorescence microscopy and FCM.

Fluorescence microscopy

The cells transduced with recombinant baculoviruses were observed by Nikon ECLIPSE TE200 inverted microscope, and fluorescence photos were collected by the digital camera Nikon coolpix990.

Flow cytometry

After 48 h, transduction cultures were harvested with trypsin and washed with Dulbecco's PBS. Dispersive cells were pelleted by centrifugation (1 500 r/min, 5 min) and resuspended in Dulbecco's PBS with 50 mL/L fetal bovine serum and filtered by a nylon filter. Data collection was performed on a flow cytometer (FCM, Beckman Coulter EPICS XL), the exciting spectrum was 488 nm, and the detection spectrum was 525 nm. About 20 000 signals were collected per specimen. The negative control was the cells without treatment with the viruses, the eGFP positive domain (B domain) was set and the percentage of cell numbers in B domain of the negative control sample did not exceed 2%. The transfer efficiency of reporter genes was obtained by subtracting the percentage of cell numbers in B domain of the negative control from the percentage of cell numbers in B domain of the target sample. The reporter gene expression efficiency was reflected by mean fluorescence intensity of positive cells in the B domain.

Mammalian cells transfected by LipofectAMINE

Cells were seeded in 24-well culture dishes about 50 000 cells per well and incubated in a 37 °C CO₂ incubator for 12 h. One µg of target DNA was diluted into 50 µL free-serum culture medium (solution A), 2 µL LipofectAMINE reagent was diluted into 50 µL free-serum culture medium (solution B), the two solutions were mixed gently and incubated for 45 min at room temperature. The cells were washed twice with 1 mL free-serum culture medium. Five hundred µL free-serum culture medium and transfection mixture was added, cells were incubated for 6 h in a 37 °C incubator. The transfection mixture was removed and 500 µL supplemented culture media containing 100 mL/L fetal bovine serum was added. After 48 h transfection cultures were examined for GFP expression by FCM.

Mammalian cells infected by retrovirus

pT67-EGFP cell line constructed in our laboratory could produce recombinant retroviruses containing the EGFP expression cassette. Mammalian cells were seeded in 24-well culture dishes about 50 000 cells per well and incubated in a 37 °C CO₂ incubator for 12 h. The culture medium was removed

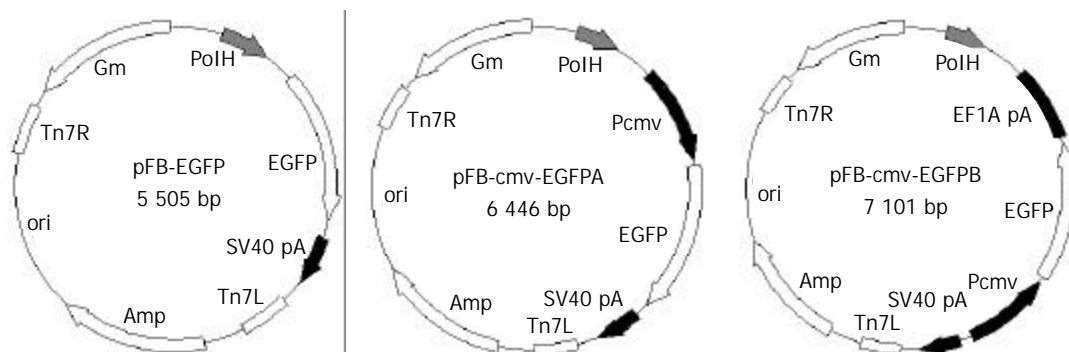


Figure 1 Plasmids pFB-EGFP, pFB-CMV-EGFPA and pFB-CMV-EGFPB.

and replaced with the collected culture supernatant of pT67-EGFP (500 μ L), and incubated at 37 $^{\circ}$ C for 12 h. After removal of the viruses, fresh medium was added and cultures were incubated at 37 $^{\circ}$ C. After 48 h, infection cultures were examined for GFP expression by FCM.

Mammalian cells infected by vaccinia virus

The recombinant vaccinia viruses containing the EGFP expression cassette were constructed in our laboratory. Mammalian cells were seeded in 24-well culture dishes about 50 000 cells per well and incubated in a 37 $^{\circ}$ C CO₂ incubator for 12 h. The culture medium was removed and replaced with the collected vaccinia viruses diluted by PBS (500 μ L), and incubated at 37 $^{\circ}$ C for 1 h. After removal of the viruses, fresh medium was added and cultures were incubated at 37 $^{\circ}$ C. After 24 h, infection cultures were examined for GFP expression by FCM.

RESULTS

EGFP expression in Sf9 cells driven by different promoters

The recombinant baculoviruses (BacV-EGFP, BacV-CMV-EGFPA, BacV-CMV-EGFPB) were constructed with the reporter gene coding for eGFP under the control of either the PH promoter of baculovirus or the immediate early promoter of CMV. Sf9 cells were infected by the recombinant baculoviruses at a moi of 10. After 72 h, cells were observed by inverted

fluorescence microscope (Figure 2). High level of eGFP expression was observed in Sf9 cells infected by BacV-EGFP, whereas low levels of eGFP expression were found in Sf9 cells infected by BacV-CMV-EGFPA or BacV-CMV-EGFPB, showing that CMV promoter was utilized weakly in insect cells, resulting in low expression of eGFP in these cultures.

EGFP expression in HepG2 cells transduced with different recombinant baculoviruses

The culture supernatants of Sf9 cells infected by recombinant baculoviruses (BacV-EGFP, BacV-CMV-EGFPA, and BacV-CMV-EGFPB) for 4 d were collected and virus titers were determined by plaque assay. All the collected culture supernatants were diluted with fresh Grace's culture medium to make the virus titers 1.0×10^7 pfu/mL. HepG2 cells were incubated with the collected supernatants (moi=100) for 8 h at 37 $^{\circ}$ C. Twenty-four h post transduction, gene transfer and expression efficiencies were analyzed by inverted microscopy and FCM (Figure 3). High levels of eGFP expression could be detected in HepG2 cells transduced with BacV-CMV-EGFPA or BacV-CMV-EGFPB, and the gene transfer and expression efficiencies were similar. In contrast, no eGFP expression was found in HepG2 cells transduced with BacV-EGFP, showing that the PH promoter of baculoviruses was inactive in HepG2 cells. During the experiment, the morphological characteristics and growth of HepG2 cells were normal.

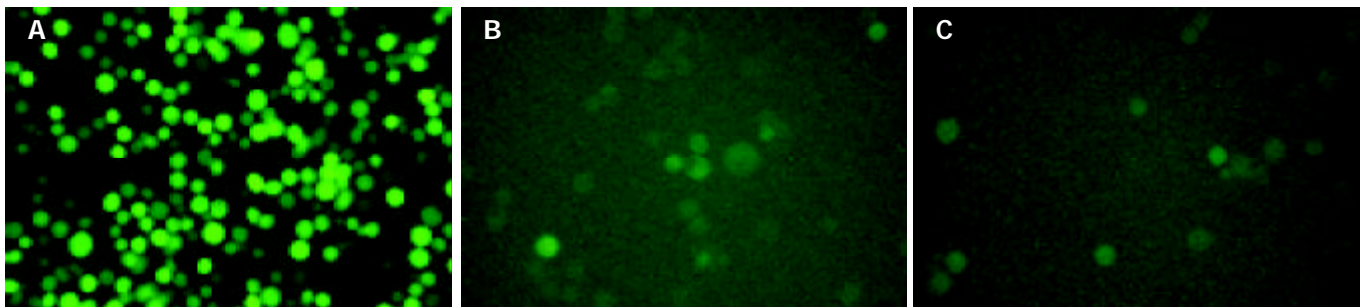


Figure 2 Fluorescence photos of Sf9 cells infected with recombinant baculoviruses. A: BacV-EGFP; B: BacV-CMV-EGFPA; C: BacV-CMV-EGFPB.

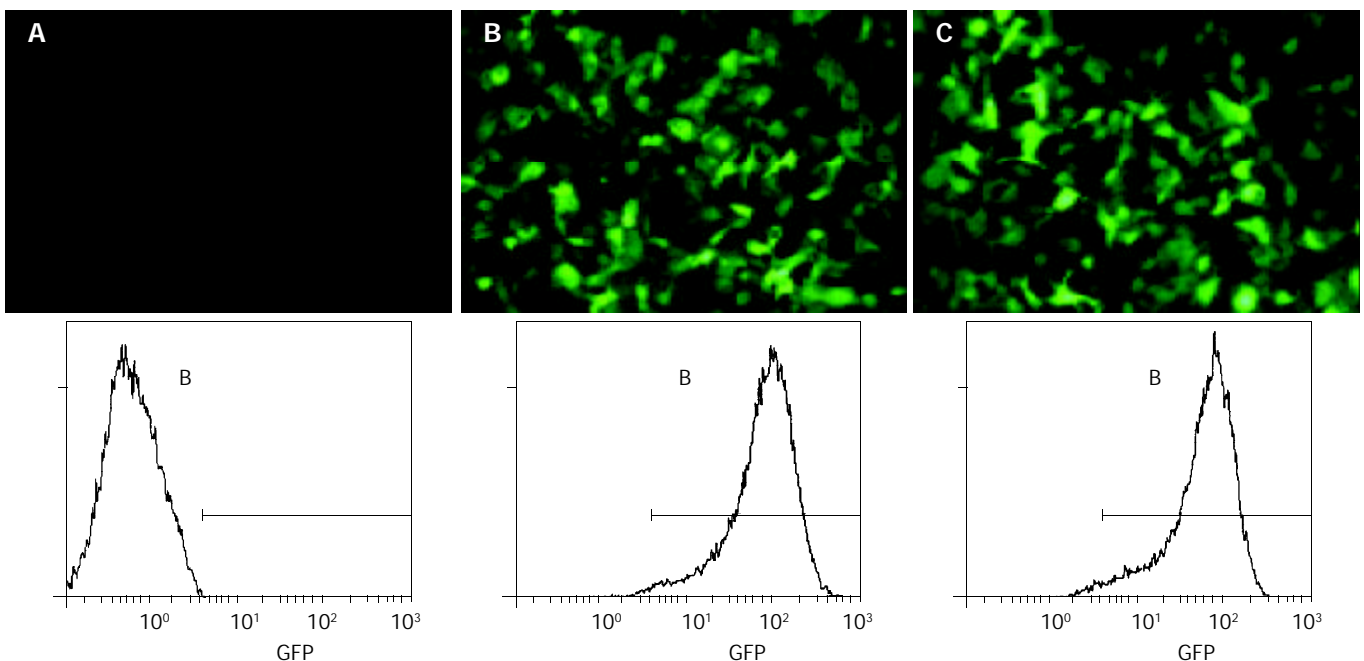


Figure 3 Fluorescence photos (up) and FCM analysis (down) of HepG2 cells transduced with recombinant baculoviruses. A: BacV-EGFP; B: BacV-CMV-EGFPA; C: BacV-CMV-EGFPB.

Effects of different dilution ratio and incubation time on efficiencies of gene transfer and expression

To optimize the way of delivering exogenous genes into mammalian cells with the culture supernatant of Sf9 cells infected by recombinant baculoviruses, HepG2 cells were incubated with the collected culture supernatant serially diluted by DMEM culture medium containing 100 mL/L fetal bovine serum and the transduction time ranged from 1 h to 24 h. After 24 h, the reporter gene transfer and expression efficiencies were analyzed by FCM (Figure 4). With increase of incubation time and moi, the efficiencies of gene transfer and expression in target cells increased.

Continuous expression of eGFP in HepG2 cells by baculovirus vector

HepG2 cells seeded in 24-well culture dishes were incubated with the culture supernatant of Sf9 cells infected by BacV-CMV-EGFPA (moi=50). Culture medium was changed every two days. The cells were harvested at various times and quantitatively assayed for eGFP expression by FCM. As shown in Figure 5, the expression of EGFP could be detected during a long time post transduction and peaked 24-48 h after transduction, which implied that the target gene could be continuously expressed in mammalian cells by recombinant baculovirus vectors.

Comparison of different gene delivery methods

pcDNA3.1(+)-EGFP was transfected into HepG2 and CV1 cells by LipofectAMINE. After 48 h, the reporter gene transfer and expression efficiencies were analyzed by FCM. pT67-EGFP cell line was constructed in our laboratory, which could produce the recombinant retroviruses containing the EGFP expression cassette. HepG2 and CV1 cells were incubated with the collected culture supernatant of pT67-EGFP for 12 h at 37 °C. After 48 h, the reporter gene transfer and expression efficiencies were analyzed by FCM. HepG2 and CV1 cells

were incubated with the culture supernatant of Sf9 cells infected by BacV-CMV-EGFPA for 12 h at 37 °C (moi=50). After 48 h, the reporter gene transfer and expression efficiencies were analyzed by FCM. The recombinant vaccinia viruses containing the EGFP expression cassette were constructed in our laboratory. HepG2 and CV1 cells were incubated with the collected vaccinia viruses diluted by PBS at 37 °C for 1 h. After 24 h, infection cultures were examined for GFP expression by FCM.

As shown in Table 1, under the similar conditions recombinant baculoviruses and vaccinia viruses could achieve higher gene-transfer and expression efficiencies than lipofectAMINE and recombinant retrovirus system. But obvious cytopathic effects could be observed at 24-32 h on HepG2 or CV1 cells infected by vaccinia viruses, while in mammalian cells transduced with recombinant baculoviruses, no cytopathic effect could be observed during the experiment.

Table 1 Comparison of gene-transfer and expression efficiency in HepG2 and CV1 cells among different gene-transfer systems

	Gene-transfer rate (%)		Mean fluorescence intensity	
	HepG2	CV1	HepG2	CV1
LipofectAMINE	29.6	34.2	138.1	103.4
Retro-EGFP	13.5	18.2	95.8	76.6
Vaccinia-EGFP	93.5 ^a	94.2 ^a	172.5 ^a	148.4 [†]
BacV-CMV-EGFPA	92.5	95.6	294.5	232.1

[†]Cytopathic effects could be observed within 24 h post infection and most cells were lysed within 48 h.

Baculovirus-mediated gene delivery to various mammalian cell lines

To investigate the feasibility of delivering the reporter gene into various mammalian cells with the culture supernatant of

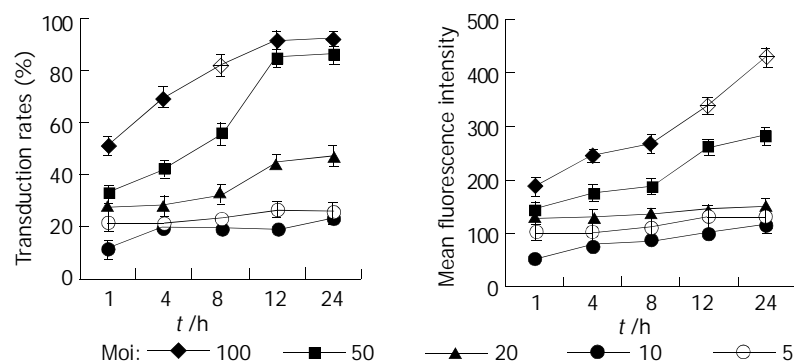


Figure 4 Effect of different moi and incubation time on gene transfer and expression efficiencies in HepG2 cells transduced with BacV-CMV-EGFPA.

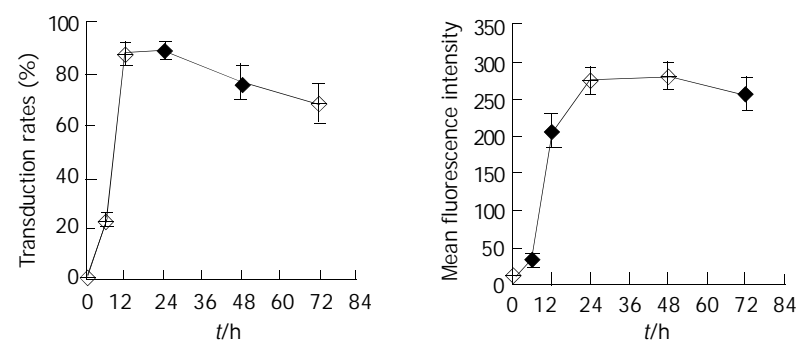


Figure 5 Reporter gene transfer and expression efficiencies at different times in HepG2 cells transduced with BacV-CMV-EGFPA.

infected Sf9 cells, twenty different mammalian cell lines were used, including twelve human cell lines (WI-38, HeLa, HepG2, 293, PLC/PRF/5, 143B, MCF-7, BGC-223, DMS 114, CNE, Raji, LCL-cm), seven mice cell lines (BNL 1ME A.7R.1, CHO-K1, L-929, JC, PT67, NIH3T3, P815), and one monkey cell line (CV1). These cells were incubated with the infected Sf9 cell culture supernatant diluted with complete culture medium for the corresponding mammalian cells at ratio 1:1 (vol:vol) for 12 h (BacV-CMV-EGFP, moi=50). After 48 h, the reporter gene transfer and expression efficiencies were analyzed by FCM (Table 2). Results showed that most mammalian cell lines could be transduced with recombinant baculoviruses by this way.

Activity of CMV promoter in different mammalian cell lines

In our research the susceptibility of mammalian cells lines to recombinant baculoviruses was determined by the expression of reporter gene in different cells. So the results might be affected by different expression efficiencies of reporter gene

in different cell lines. The reporter gene used in these experiments was the EGFP gene, which was one of the most widely used reporter genes and had many advantages such as no cytotoxicity to host cells, easy detectable, more sensitive^[16,17]. The CMV promoter was usually used in experiments, which had the ability to give strong expression of target genes in a variety of mammalian cell types^[18].

We investigated the activity of CMV promoter in different mammalian cell lines used in our experiments by FCM. Plasmid pcDNA3.1-EGFP containing an expression cassette of EGFP reporter gene under control of CMV promoter, was transfected by LipofectAMINE into some mammalian cells especially those difficult for baculoviruses to enter. After 48 h, reporter gene transfer and expression efficiencies were analyzed by FCM (Table 3). Results showed that CMV promoter could effectively direct the expression of reporter gene in these mammalian cells. Although the expression efficiencies differed in various cell lines, all the expressions could be detected by FCM. So the gene transfer efficiencies to mammalian cells by

Table 2 Comparison of gene-transfer and expression efficiencies in different mammalian cell lines transduced with BacV-CMV-EGFP

Organism	Tissue	Growth properties	Transduction efficiency(%)	Mean fluorescence intensity
Human				
WI-38	Lung fibroblast	Adherent	~85	~220
HeLa	Adenocarcinoma	Adherent	~85	~180
HepG2	Hepatocellular carcinoma	Adherent	~85	~200
293	Kidney	Adherent	~85	~150
PLC/PRF/5	Hepatoma	Adherent	~85	~150
143B	Osteosarcoma	Adherent	~85	~150
MCF-7	Gastric carcinoma	Adherent	~85	~150
BGC-223	Breast carcinoma	Adherent	~85	~150
DMS 114	Small cell lung cancer	Adherent	~85	~180
CNE	Nasopharyngeal carconoma	Suspension	~5	~50
Raji	Burkitt' s lymphoma	Suspension	~5	~50
LCL-cm	B lymphocyte	Suspension	~5	~50
Mouse				
BNL 1ME A.7R.1	Liver	Adherent	~45	~150
CHO-K1	Ovary	Adherent	~35	~120
L-929	Subcutaneous connective tissue	Adherent	~35	~150
JC	Adenocarcinoma	Adherent	~15	~100
PT67	Embryo fibroblast	Adherent	~10	~80
NIH3T3	Embryo fibroblast	Adherent	~10	~80
P815	Mastocytoma	Suspension	~5	~50
Monkey				
CV1	Normal kidney	Adherent	~85	~220

Table 3 Comparison of gene-transfer and expression efficiencies in different mammalian cell lines transfected with pcDNA3.1-EGFP

Organism	Tissue	Growth properties	Transfection efficiency(%)	Mean fluorescence intensity
Human				
WI-38	Lung fibroblast	Adherent	24.53	58.3
HepG2	Hepatocellular carcinoma	Adherent	18.60	79.4
HeLa	Adenocarcinoma	Adherent	19.82	42.7
293	Kidney	Adherent	61.45	86.6
Raji	Burkitt' s lymphoma	Suspension	5.56	14.6
LCL-cm	B lymphocyte	Suspension	7.62	17.4
Mouse				
BNL 1ME A.7R.1	Liver	Adherent	13.09	19.1
CHO-K1	Ovary	Adherent	47.36	48.6
JC	Adenocarcinoma	Adherent	12.54	22.8
PT67	Embryo fibroblast	Adherent	22.63	31.6
NIH3T3	Embryo fibroblast	Adherent	25.31	35.3
P815	Mastocytoma	Suspension	12.78	16.8

recombinant baculoviruses containing CMV-EGFP expression cassette could basically show the ability of baculoviruses to enter different mammalian cell lines.

Efficiencies of gene transfer into suspended or adherent culture cells by recombinant baculoviruses

The cells used in our experiments were derived from primate or mice. We compared the transfer efficiencies of reporter gene in adherent or suspended culture cells of these two cell types (Table 4). The result showed that in primate cell lines the efficiencies of gene transfer into adherent culture cells were markedly higher than those of gene transfer into the suspended culture cells ($t=20.6484$, $P<0.05$). In mice cell lines, only one suspended culture cell line was used in our experiment, its gene transfer efficiency by baculovirus vector was also markedly lower than the adherent culture cell line from the same organism. Furthermore we also noticed that, the efficiencies of gene transfer into the primate adherent culture cells were markedly higher than those of gene transfer into the adherent culture cells from mice ($t=7.9674$, $P<0.05$), and the efficiencies of reporter gene transfer to the suspended culture cells from primate and mice were both low, the difference between them was not distinct. In primate adherent culture cells recombinant baculoviruses could arrive the highest infection and expression efficiencies, but they were not very satisfactory in the cell lines from mice and suspended culture cells.

Table 4 Comparison of transduction efficiencies in adherent and suspended culture cells of different species transduced with BacV-CMV-EGFP

		Adherent culture	Suspended culture
Primate	Total	10	3
	Mean transduction efficiency(%)	77.25±11.37	1.12±0.53
Mice	Total	6	1
	Mean transduction efficiency(%)	21.84±15.85	0.61

DISCUSSION

It has been proved that recombinant baculoviruses could serve as a powerful tool for delivering foreign genes into mammalian cells^[19]. Previous reports have described that recombinant baculoviruses used in gene-transfer experiments were often concentrated by ultracentrifugation. This could yield a large number of recombinant viruses with high purity, but it needed to culture a large number of cells to obtain sufficient viruses, and the manipulation was complex and burdensome. We investigated the feasibility of delivering exogenous genes into mammalian cells directly with the culture supernatant of Sf9 cells infected by recombinant baculoviruses. The results showed that when the incubation time was identical, with the increase of dilution ratio and the decrease of moi, the reporter gene transfer and expression efficiencies were decreased; when the dilution ratio and moi were identical, with the prolongation of incubation time, the gene transfer and expression efficiencies were increased too, suggesting that virus titers and incubation time were the most important factors that affected the efficiencies of the gene transfer and expression, and the virus titer was the crucial factor. In direct morphological observation in the transduced cells, we found that the growth of target cells was affected when undiluted culture supernatant was used or the incubation time was long. The morphological characteristics of some cells were abnormal, and the number of dead cells increased. So according to the observed results of the morphology and growth of transduced cells, we thought that incubating

target mammalian cells with the culture supernatant of infected Sf9 cells ($\geq 1.0 \times 10^7$ pfu/mL) 1:1 (vol:vol) diluted by the mammalian cell complete culture medium for 12 h in a 37 °C CO₂ incubator (moi=50) could achieve the highest efficiency of gene transfer and expression, together with the least impairment to cell viability.

In our research twenty mammalian cell lines were used to investigate the feasibility of delivering reporter genes into various mammalian cells with the culture supernatant of infected Sf9 cells. The results showed that the reporter gene could be effectively transferred into the majority of mammalian cell lines by recombinant baculovirus vectors. The gene transfer efficiencies in adherent culture cells from human or monkey by baculovirus vectors were markedly higher than those from mice, indicating that the susceptibility of mammalian adherent culture cell lines to baculoviruses might be different between different species. Furthermore, baculoviruses could be hardly taken up by suspended culture cells. A total of four suspended culture cell lines were used in our experiment, three from human, and one from mice. Their efficiencies of gene transfer by baculovirus vectors were not more than 2%, markedly lower than those of the adherent culture cell lines from the same species respectively. Similar results were also observed by Condreay *et al*^[20].

Numerous methods have been developed for introducing target genes into mammalian cells including chemical-based procedures, electroporation, and mammalian viral vector-based systems. Lipid transfection, retrovirus expression system and vaccinia virus expression system were most often used in experiments among these methods. The advantages of lipid transfection were short time-used, wide host range, but in common cases the transfection efficiencies were low, and was not suitable for some experiments that needed high transfection efficiencies^[21]. Retroviruses could infect many mammalian cell lines, and were able to integrate with host cell genomes stably. But retroviruses could only be taken up by the cells in mitosis phase, and the infection efficiencies in the non dividing cells were very low^[22,23]. The successful application of the retrovirus expression system needs high virus titers. If the culture supernatants of retrovirus package cell line were directly used in the gene transfer experiment, the virus titers were usually difficult to meet our need. So increasing the virus titer of recombinant retroviruses has become an important research content in the application of retrovirus expression system, and this was also an important factor that restricted the wide application of the retrovirus expression system^[24,25]. A package cell line that can stably generate high titer recombinant viruses would also take a long time for cloning. The vaccinia virus expression systems have been widely used for *in vitro* production and functional characterization of proteins and live vaccines in vaccine research^[26,27]. The life cycle of poxviruses occurs exclusively within the cytoplasm of infected cells and can lead to the lysis of infected cells within 12-24 h^[28]. So the vaccinia virus expression system is unsuitable for continuous expression of foreign genes in target cells. Similar problems also occur in application of other mammalian viral vector-based systems. The cost and time-used in application of these expression systems were too expensive and burdensome for some daily common experiments.

As described in our report, the culture supernatant of Sf9 cells infected by recombinant baculoviruses could be directly used for delivery of foreign genes into mammalian cells. Their virus titer was sufficient for efficient gene transfer experiments. So under common circumstances without special requirements, there is no need for concentration and purification of the virus, which can markedly decrease our workloads, and improve our work. In comparison to lipid transfection system, retrovirus expression system and vaccinia virus expression system, we

could find that under similar conditions recombinant baculoviruses could achieve the highest gene-transfer and expression efficiencies in mammalian cells. Baculoviruses are inherently unable to replicate in mammalian cells, have few or no microscopically observable cytopathic effects on target cells. These modified recombinant baculoviruses containing mammalian cell-active expression cassettes could be used more widely in a variety of gene transfer. We also noticed that the gene transfer and expression efficiencies in mice cells and suspended culture cells by recombinant baculoviruses containing CMV promoter were not satisfactory, suggesting that although recombinant baculoviruses could serve as a very convenient tool for gene transfer in mammalian cells, but they also have limitations and might not be suitable for all cell lines.

REFERENCES

- 1 **Miller LK**. Baculoviruses for foreign gene expression in insect cells. *Biotechnology* 1988; **10**: 457-465
- 2 **Luckow VL**, Summers MD. Signals important for high-level expression of foreign genes in *Autographa californica* nuclear polyhedrosis virus expression vectors. *Virology* 1988; **167**: 56-71
- 3 **Ren H**, Zhu FL, Zhu SY, Song YB, Qi ZT. Immunogenicity of HGV NS5 protein expressed from Sf9 insect cells. *World J Gastroenterol* 2001; **7**: 98-101
- 4 **Li B**, Wu HY, Qian XP, Li Y, Chen WF. Expression, purification and serological analysis of hepatocellular carcinoma associated antigen HCA587 in insect cells. *World J Gastroenterol* 2003; **9**: 678-682
- 5 **Hou LH**, Du GX, Guan RB, Tong YG, Wang HT. *In vitro* assay for HCV serine proteinase expressed in insect cells. *World J Gastroenterol* 2003; **9**: 1629-1632
- 6 **Groner A**, Granados RR, Burand JP. Interaction of *Autographa californica* nuclear polyhedrosis virus with two nonpermissive cell lines. *Intervirology* 1984; **21**: 203-209
- 7 **Carbonell LF**, Miller LK. Baculovirus interaction with nontarget organisms: a virus-borne reporter gene is not expressed in two mammalian cell lines. *Appl Environ Microbiol* 1987; **53**: 1412-1417
- 8 **Tjia ST**, zu Altenschildesche GM, Doerfler W. *Autographa californica* nuclear polyhedrosis virus (AcNPV) DNA does not persist in mass cultures of mammalian cells. *Virology* 1983; **125**: 107-117
- 9 **Carbonell LF**, Klowden MJ, Miller LK. Baculovirus-mediated expression of bacterial genes in dipteran and mammalian cells. *J Virol* 1985; **56**: 153-160
- 10 **Hofmann C**, Sandig V, Jennings G, Rudolph M, Schlag P, Strauss M. Efficient gene transfer into human hepatocytes by baculovirus vectors. *Proc Natl Acad Sci U S A* 1995; **92**: 10099-10103
- 11 **Boyce FM**, Bucher NLR. Baculovirus-mediated gene transfer into mammalian cells. *Proc Natl Acad Sci U S A* 1996; **93**: 2348-2352
- 12 **Shoji I**, Aizaki H, Tani H, Ishii K, Chiba T, Saito I, Miyamura T, Matsuura Y. Efficient gene transfer into various mammalian cells, including non-hepatic cells, by baculovirus vectors. *J Gen Virol* 1997; **78**(Pt 10): 2657-2664
- 13 **Delaney WE**, Isom HC. Hepatitis B virus replication in human HepG2 cells mediated by hepatitis B virus recombinant baculovirus. *Hepatology* 1998; **28**: 1134-1146
- 14 **Duisit G**, Saleun S, Douthe S, Barsoum J, Chadeuf G, Moullier P. Baculovirus vector requires electrostatic interactions including heparan sulfate for efficient gene transfer in mammalian cells. *J Gene Med* 1999; **1**: 93-102
- 15 Bac-to-Bac baculovirus expression systems instruction manual. Invitrogen life technologies 2002
- 16 **Chalfie M**, Tu Y, Euskirchen G, Ward WW, Prasher DC. Green fluorescent protein as a marker for gene expression. *Science* 1994; **263**: 802-805
- 17 **Kain SR**, Adams M, Kondepudi A, Yang TT, Ward WW, Kitts P. Green fluorescent protein as a reporter of gene expression and protein localization. *Biotechniques* 1995; **19**: 650-655
- 18 **Davis MG**, Huang ES. Transfer and expression of plasmids containing human cytomegalovirus immediate-early gene 1 promoter-enhancer sequences in eukaryotic and prokaryotic cells. *Biotechnol Appl Biochem* 1988; **10**: 6-12
- 19 **Kost TA**, Condreay JP. Recombinant baculoviruses as mammalian cell gene-delivery vectors. *Trends Biotechnol* 2002; **20**: 173-180
- 20 **Condreay JP**, Witherspoon SM, Clay WC, Kost TA. Transient and stable gene expression in mammalian cells transduced with a recombinant baculovirus vector. *Proc Natl Acad Sci U S A* 1999; **96**: 127-132
- 21 **Bebok Z**, Abai AM, Dong JY, King SA, Kirk KL, Berta G, Hughes BW, Kraft AS, Burgess SW, Shaw W, Felgner PL, Sorscher EJ. Efficiency of plasmid delivery and expression after lipid-mediated gene transfer to human cells *in vitro*. *J Pharmacol Exp Ther* 1996; **279**: 1462-1469
- 22 **Chuck AS**, Clarke MF, Palsson BO. Retroviral infection is limited by Brownian motion. *Hum Gene Ther* 1996; **7**: 1527-1534
- 23 **Miller DG**, Adam MA, Miller AD. Gene transfer by retrovirus vectors occurs only in cells that are actively replicating at the time of infection. *Mol Cell Biol* 1990; **10**: 4239-4242
- 24 **Chuck AS**, Palsson BO. Consistent and high rates of gene transfer can be obtained using flow-through transduction over a wide range of retroviral titers. *Hum Gene Ther* 1996; **7**: 743-750
- 25 **Bowles NE**, Eisensmith RC, Mohuiddin R, Pyron M, Woo SL. A simple and efficient method for the concentration and purification of recombinant retrovirus for increased hepatocyte transduction *in vivo*. *Hum Gene Ther* 1996; **7**: 1735-1742
- 26 **Mackett M**, Smith GL, Moss B. Vaccinia virus: a selectable eukaryotic cloning and expression vector. *Biotechnology* 1992; **24**: 495-499
- 27 **Whitman ED**, Tsung K, Paxson J, Norton JA. *In vitro* and *in vivo* kinetics of recombinant vaccinia virus cancer-gene therapy. *Surgery* 1994; **116**: 183-188
- 28 **Moss B**. Genetically engineered poxviruses for recombinant gene expression, vaccination and safety. *Proc Natl Acad Sci U S A* 1996; **93**: 11341-11348

Edited by Wang XL and Xu CT Proofread by Xu FM

Risk factors of development of gut-derived bacterial translocation in thermally injured rats

Zhong-Tang Wang, Yong-Ming Yao, Guang-Xia Xiao, Zhi-Yong Sheng

Zhong-Tang Wang, Yong-Ming Yao, Zhi-Yong Sheng, Department of Microbiology and Immunology, Burns Institute, 304th Hospital of PLA, Beijing 100037, China

Guang-Xia Xiao, Institute of Burn Research, Southwestern Hospital, Third Military Medical University, Chongqing 400038, China

Supported by the National Key Program for Fundamental Research and Development, No.G1999054203; the National Science Fund for Outstanding Young Scholars, No.30125020; the "10th Five-Year Plan" Scientific Research Foundation of Chinese PLA, No.01MA207

Correspondence to: Yong-Ming Yao, M.D., Department of Microbiology and Immunology, Burns Institute, 304th Hospital of PLA, 51 Fu-Cheng Road, Beijing 100037, China. c_ff@sina.com

Telephone: +86-10-66867394 **Fax:** +86-10-68429998

Received: 2003-09-23 **Accepted:** 2003-12-29

Abstract

AIM: Studies have demonstrated that gut-derived bacterial translocation (BT) might play a role in the occurrence of sepsis and multiple organ dysfunction syndrome (MODS). Yet, no convincing overall analysis of risk factors for BT has been reported. The purpose of this study was to evaluate the related factors for the development of BT in burned rats.

METHODS: Wistar rats were subjected to 30% third-degree burns. Then samples were taken on postburn d 1, 3, and 5. Incidence of BT and counts of mucosal bifidobacteria, fungi and *E. coli*, mucus sIgA, degree of injury to ileal mucosa, and plasma interleukin-6 were observed. Univariate analysis and multivariate logistic regression analysis were performed.

RESULTS: The overall BT rate was 53.9% (69 in 128). The result of univariate analysis showed that the levels of plasma endotoxin and interleukin-6, the counts of mucosal fungi and *E. coli*, and the scores of ileum lesion were markedly increased in animals with BT compared with those without ($P=0.000-0.005$), while the levels of mucus sIgA and the counts of mucosal bifidobacteria were significantly reduced in animals with translocation compared with those without ($P=0.000$). There was a significant positive correlation between mucus sIgA and the counts of mucosal bifidobacteria ($r=0.74$, $P=0.001$). Moreover, there were strong negative correlations between scores of ileum-lesion and counts of bifidobacteria ($r=-0.67$, $P=0.001$). Multivariate logistic regression revealed that ileum lesion score (odds ratio [OR] 45.52, 95% confidence interval [CI] 5.25-394.80), and counts of mucosal bifidobacteria (OR 0.039, 95% CI 0.0032-0.48) were independent predictors of BT secondary to severe burns.

CONCLUSION: Ileal lesion score and counts of mucosal bifidobacteria can be chosen as independent prognosis factors of the development of BT. Specific interventions targeting these high-risk factors might be implemented to attenuate BT, including strategies for repair of damaged intestinal mucosae and restoration of the balance of gastrointestinal flora.

Wang ZT, Yao YM, Xiao GX, Sheng ZY. Risk factors of development

of gut-derived bacterial translocation in thermally injured rats. *World J Gastroenterol* 2004; 10(11): 1619-1624
<http://www.wjgnet.com/1007-9327/10/1619.asp>

INTRODUCTION

Sepsis and multiple organ dysfunction syndrome (MODS) remain the leading causes of death 72 h after a severe burn and other traumas. Early MODS after a severe injury is usually due to an excessive and overwhelming malignant systemic inflammatory response and massive hemorrhagic shock as a result of the initial insults. On account of the finding that as many as 30% patients died of early sepsis and MODS with no identifiable septic foci^[1], some investigators postulated that systemic infections might be originated from the gut.

At present, many animal and a few clinical studies have demonstrated that gut-derived bacterial translocation does play a role in the occurrence of early sepsis and MODS^[2-5]. Because most of the pathogens come from the gut, the gastrointestinal tract is even termed as an "undrained abscess" under certain circumstances such as trauma, endotoxemia, hemorrhage, and thermal injury. A generally accepted theory is that translocation of luminal bacteria and toxins is mechanically linked to the following factors, namely disruption of the normal balance in indigenous microflora with subsequent overgrowth of potentially pathogenic bacteria, impaired intestinal immunologic barrier of the host, and disruption of the mucosal physical barrier of the gut^[1]. However, to our knowledge, what role these three factors play in the incidence of bacterial translocation under some conditions has not been fully elucidated.

In the past decade, literature on the mechanisms and methods of treatment and prevention of bacterial translocation has been substantial. However, to date no convincing overall analysis of risk factors for bacterial translocation has been reported.

The purpose of our study was to clarify the individual role of intestinal mucosa, mucosal flora, and gut sIgA in producing bacterial translocation in scalded rats, in an attempt to propose a formula for predicting the probability of incidence of bacterial translocation by using univariate analysis and multivariate logistic regression.

MATERIALS AND METHODS

Animals

Wistar rats, weighing 180 to 220 g, male and female in equal number, were purchased from the Experiment Animal Center of Third Military Medical University in Chongqing, China. Animals were housed in separate steel cages in a temperature-controlled room with a 12-h light-dark cycle, and acclimatized for at least seven days prior to use. Animals had free access to an irradiated commercial rodent diet and autoclaved water *ad lib*. All experimental manipulations were undertaken in accordance with the NIH Guide for the Care and Use of Laboratory Animals, with the approval of the Scientific Investigation Board of the Institute of Burn Research, Southwestern Hospital, Third Military Medical University, Chongqing, China.

Burn injury

After an overnight fast, rats were weighed, numbered, and anesthetized with sodium pentobarbital (40 mg/kg body mass, i.p.), with the dorsal hair shaved, and then subjected to 30% total body surface area skin full-thickness thermal injury, which was produced by exposure to 94 °C water bath for 18 s using a wood template with an aluminium wand for fixing rat abdomen. Rats were quickly dried and resuscitated with Ringer's lactate (40 mL/kg, i.p.) immediately after injury. Animals were then allowed to fully recover from anesthesia before being returned to their cages, and had free access to radiated commercial rodent chow and autoclaved water *ad lib*. Sulphadiazine silver suspension (20 g in 100 mL water) was applied to the wounds once a day to prevent infection. Samples were taken on post-burn d 1, 3, and 5. Fifty animals were included at each time point except for sham burned group with ten.

Microbiologic analysis

Techniques for culturing and bacterial translocation studies were performed with a modification of the methodology described by Tadros *et al*^[6]. After the animals were anesthetized (50 mg/kg body mass, i.p.), their abdomens were shaved, sterilized with tincture of iodine and 750 mL/L alcohol, and opened through a midline incision with sterile scissors. Under aseptic conditions, blood was obtained from portal vein and vena cava under direct visualization, and a swab culture was taken from the exposed belly cavity. Then mesenteric lymph nodes (MLN), spleen, liver, and kidney were obtained and weighed. Each organ was homogenized in brain heart infusion broth. Two hundred µL homogenates from tissues, as well as 200 µL blood, were inoculated on both Gram-negative bacteria-specific MacConkey's agar and blood agar. A duplicate culture was made for each specimen. All specimens were incubated at 37 °C for 24 h. Positive specimens were sub-cultured, and the bacteria were identified by standard bacteriologic techniques. Cultures were considered positive when more than 100 colonies per gram of tissue were found. No culture for obligate anaerobics was made, because they had a low tendency to translocate to extra-intestinal sites.

Following removal of the aforementioned organs, the terminal ileal loop was excised, opened longitudinally, then its content was wiped off lightly with sterile cotton swabs, rinsed three times with 10 mL sterile 0.01 mol/L phosphate-buffered saline (PBS). The residual liquid was dried with sterile filter paper. The specimen was then put into a CO₂ filled bottle immediately. The samples were weighed, homogenized with a sterile blender, and diluted by 10-fold with brain heart infusion broth. One hundred µL desired diluted specimen was poured separately onto the *E. coli*-specific MacConkey's agar, bifidobacteria-specific BLB agar, and fungi-specific medium (modified by including Imipenium 30 µg/mL). The cultures were all duplicated. Plates were incubated for 24 h for aerobic bacterial culture, and 72 h for anaerobic and fungus cultures, at 37 °C, respectively. Then colonies of bacteria or fungi were counted, and the suspiciousness was identified using standard microbiologic technique. All plates and brain-heart infusion were purchased from Shanghai Med&Chem Institute, Shanghai, China.

Quantitative culture results were expressed as the number of log₁₀ colony-forming units (CFU) per gram tissue. The terminal ileal loop was used because bacterial translocation correlated with colonization of the ileum rather than that of the colon^[6]. The limit detection of the assay was 10 bacteria.

Plasma endotoxin measurement

Portal blood was collected and put into pyrogen-free polypropylene tubes containing 2 µL of sterile heparin. Platelet-

rich plasma was obtained by centrifugation at 4 °C, 260 r/min for 10 min, and then aliquots of which were prepared and transferred to sterile pyrogen-free tubes under laminar air flow, and stored at -35 °C until use. Plasma endotoxin concentration was measured by the chromogenic limulus amoebocyte lysate (LAL) method. The procedure followed was based on the protocol provided with the kit (Shanghai Med&Chem Institute, Shanghai, China). Briefly, in order to avoid activation and inhibitory effects of plasma on LAL test, 0.1 mL serum specimen was diluted (1:10) in apyrogenic sterile water 0.2 mL and Tris-HCl buffer 0.2 mL, boiled for 10 min, and then supernatant obtained by centrifugation at 4 °C, 5 000 r/min for 10 min was used for detection. The supernatants were coincubated for 25 min at 37 °C with LAL, and 3 min after chromogenic substrate was added, reaction was stopped with an aqueous solution of 0.5 g/L naphthyl ethylenediamine. Absorbance was read in a spectrophotometer at 545 nm. The absorbance of a control was subtracted from these absorbances in order to adjust the samples' intrinsic color development. The endotoxin concentration was corrected for dilution and calculated from a standard curve derived from assay of standard (*Escherichia coli* 0111:B4, 1EU [endotoxin units]=100 pg) supplied by the company. This method was sensitive to 0.03 EU/mL of endotoxin. Depyrogen of detection material was approved by ⁶⁰Co exposure.

Measurement of intestinal mucus sIgA

Duodenum, jejunum and ileum were excised, cut into 3 segments, opened longitudinally. Intestinal contents were wiped off with bamboo sticks. Intestinal mucus was collected by scraping with glass slides, and dissolved in 1 mL 0.01 mol/L PBS [including 1 mmol/L dithiothreitol (DTT), 100 µg/mL phenylmethyl sulfonyl fluoride (PMSF), 10 µg/mL Leupeptin, 10 µg/mL soybean trypsin inhibitor, and 2 µg/mL aprotinin]. The solution was centrifuged at 30 000 g at 4 °C for 10 min. The supernatant was aspirated and frozen until use.

The supernatants were diluted to 1:400 with 0.01 mol/L PBS for measurement of sIgA concentrations by radioimmunoassay (RIA), based on the protocol supplied with the kit (Biotinge-Tech. Co., Beijing, China). In short, samples were added into glass tubes, incubated with polystyrene-balls which were coated with mouse anti-rat sIgA mAb (Sigma chemical co., St Louis, MO), at 37 °C for 2 h, washed 4 times with deionized water, then ¹²⁵I conjugated goat anti-rat IgA antibody was added. They were kept at room temperature over night. After washed four times, the balls were transferred into another tube for detection. Additionally, a rat myeloma IgA (Zymed, San Francisco, CA) diluted into 15.6 ng/mL, 31.3 ng/mL, 62.5 ng/mL, 125 ng/mL, 250 ng/mL, 500 ng/mL, 1 000 ng/mL, and 2 000 ng/mL, was serially measured for a standard curve. Radionuclide counts were determined in term of disintegrations per minute (dpm) using a gama counter and calibrated by subtracting the background count. Interassay and intraassay coefficients of variation were < 10%. The assay had a sensitivity of 20 pg/mL. Total protein in supernatants was estimated using the Lowry method, simultaneously. Therefore, the concentrations of sIgA from gut mucus were expressed as µg per mg of protein (sIgA µg/mg protein).

Microscopic evaluation

Ileum specimens were dehydrated in progressive concentrations of ethanol, cleared in xylene, and embedded in paraffin. Deparaffinized 4-µm thick sections were stained with hematoxylin-eosin. Glass slides were coded to allow two experienced histopathologists to examine the tissue sections blindly. The degree of intestinal tissue injuries was evaluated using a grading scale from 0 to 8^[7]. Grade 0 was defined as

normal mucosa. Pathognomonic for grades 1 to 3 was an increasing subepithelial space of the villi. In grade 4, the villi were denuded, and grade 5 was characterized by loss of the villi. In grade 6, the intestinal crypt layer was also injured, and in grade 7, the entire intestinal mucosa was necrotic. Grade 8 represented transmural infarction.

ELISA for IL-6

Caval blood was collected, centrifuged at 260 r/min for 10 min. Samples were serially diluted with 0.01 mol/L PBS, and IL-6 was determined by sandwich ELISA. The following procedure was based on the protocol supplied with the kit (Bioting-Tech. Co., Beijing, China). Briefly, 96-well plates (Corning Costar, Cambridge, MA) were coated with 100 μ L anti-IL-6 mAb diluted in 0.1 mL bicarbonate buffer (pH 8.2) and incubated at 4 °C for 48 h. The wells were blocked with PBS containing 10 g/L BSA at room temperature for 1 h. Serial 2-fold dilutions of plasma were added to duplicate wells over night at 4 °C. Then the wells were incubated with biotinylated anti-IL-6 Ab, at 37 °C for 1 h, and then with peroxidase-labeled anti-biotin Ab for 1 h, and developed with ABTS reagent (Sigma). Similarly, a standard curve ranging from 0 to 2 000 pg/mL was plotted using recombinant human IL-6. Absorbance was then read at 410 nm, and the amount of IL-6 in each sample was computed from the standard curve. Interassay and intraassay coefficients of variation were <10%. The assay had a sensitivity of 100 pg/mL.

Statistical analysis

The software package Stata for Windows (Version 6.0) was used for analysis. Results were expressed as mean \pm SD, except for data of the grading of mucosal injury, which were expressed as median and range. Continuous variables were compared by

Student's *t* test or Wilcoxon-Mann-Whitney rank sum test, whereas the Chi-square test (χ^2 test) was used for comparing proportions. Correlation analysis, univariate and stepwise multivariate logistic regression analysis, with bacterial translocation as the dependent variable, were used to identify factors associated with bacterial translocation to develop a model to predict the probability of incidence. A *P* value of 0.05 or less was considered to statistically significance.

RESULTS

Incidence of bacterial translocation

The overall mortality was 14.7% (22 in 150) during the experiment. The incidence of bacterial translocation was 53.9% (69 in 128) after burn. There were 17 positively cultured strains from abdominal cavity swabs, which were coincident with those strains cultured in organs. The rate of bacterial translocation was 84%, 59%, and 28% on post-burn d 1, 3, and 5, respectively (84% vs 59%, *P*=0.02; 84% vs 28%, *P*=0.000; 59% vs 28%, *P*=0.04), while it was 10% in shame-burn animals.

Univariate analysis

Univariate analysis showed that the levels of plasma endotoxin and interleukin-6, the counts of mucosal fungi and *E. coli*, and the scores of ileum lesion were markedly increased in animals with bacterial translocation compared with those without (*P*=0.000-0.005), while mucus sIgA and the counts of mucosal bifidobacteria were significantly reduced in animals with bacterial translocation compared with those without (*P*=0.000). Moreover, the ratio of bifidobacteria to *E. coli* was decreased significantly from 2 000:1 in animals without bacterial translocation to 10:1 in animals with translocation (Table 1).

Table 1 Univariate analysis of suspected factors for development of bacterial translocation

	BT ¹ (n=69)	Non-BT ² (n=59)	<i>t</i> - or <i>z</i> -value	<i>P</i> -value
Endotoxin (EU/mL)	0.158 \pm 0.0447	0.110 \pm 0.0348	6.443	0.000
Microbe flora ³				
Fungi	3.80 \pm 0.8	3.2 \pm 0.7	2.859	0.005
<i>E. coli</i>	4.90 \pm 1.0	4.0 \pm 1.0	5.076	0.000
Bifidobacteria	6.10 \pm 0.6	7.3 \pm 0.5	6.967	0.000
SigA (μ g/mg protein)	55.78 \pm 9.81	87.51 \pm 10.69	16.857	0.000
Ileo-lesion score	4(2-6)	2(0-4)	9.178	0.000
IL-6 (pg/mL)	871 \pm 588	499 \pm 308	4.125	0.0001

¹Animals with bacterial translocation; ²Animals without bacterial translocation; ³Mucosal micro-flora (log₁₀ CFU/g tissue).

Table 2 Correlation analysis of data associated with bacterial translocation

	X1	X2	X3	X4	X5	X6	X7
X1	1.0000						
X2	0.7166	1.0000					
X3	0.4586	0.3847	1.0000				
X4	-0.5135	-0.4029	-0.5516	1.0000			
X5	-0.5434	-0.4416	-0.4795	0.7363	1.0000		
X6	0.4834	0.3369	0.3663	-0.6676	-0.7312	1.0000	
X7	0.4807	0.3679	0.2550	-0.3772	-0.3772	0.3549	1.0000

X1: endotoxin levels (EU/mL), X2: counts of fungi (log₁₀ CFU/g tissue), X3: counts of *E. coli* (log₁₀ CFU/g tissue), X4: counts of bifidobacteria (log₁₀ CFU/g tissue), X5: mucous sIgA levels (μ g/mg protein), X6: ileal lesion score, X7: IL-6 levels (pg/mL).

Table 3 Independent predictors of bacterial translocation evaluated by multivariate analysis

	Coefficient	Odds ratio (95% CI) ¹	<i>z</i> -value	<i>P</i> -value
X6 ²	3.8182 \pm 1.1022	45.52(5.25-394.80)	3.464	0.001
X4 ³	-3.2424 \pm 1.2757	0.039(0.003-0.48)	-2.542	0.011
Constant	9.9220 \pm 8.7435		1.135	0.256

¹Confidence interval; ²Ileal lesion score; ³Counts of bifidobacteria (log₁₀ CFU/g tissue).

Correlations among experimental findings

As shown at Table 2, there was a significant positive correlation between levels of endotoxin and counts of mucosal fungi and *E. coli*, scores of ileum lesion, and levels of interleukin-6 ($r=0.72, 0.46, 0.48, 0.48$, respectively. $P<0.001$), and between mucus sIgA and counts of mucosal bifidobacteria ($r=0.74, P<0.001$). Moreover, there were strong negative correlations between scores of ileum lesion and counts of bifidobacteria and concentrations of sIgA ($r=-0.67, -0.73$, respectively. $P<0.001$), as well as significant negative correlations between counts of mucosal bifidobacteria and levels of endotoxin, and counts of fungi and *E. coli* ($r=-0.51, -0.40, -0.55$, respectively, $P<0.01$). Figures 1 and 2 respectively showed the correlation between levels of mucus sIgA and counts of mucosal bifidobacteria, and between counts of mucosal bifidobacteria and scores of ileum lesion.

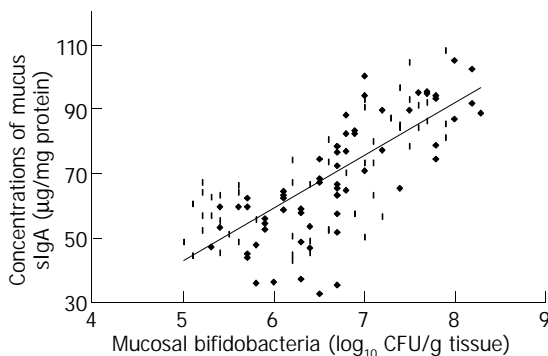


Figure 1 Correlation between counts of mucosal bifidobacteria and intestinal mucous sIgA ($r=0.74, P=0.000$).

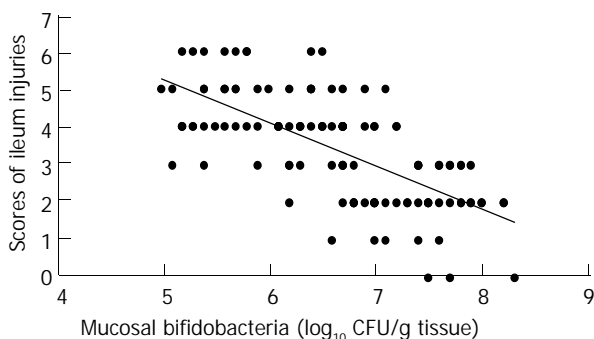


Figure 2 Correlation between counts of mucosal bifidobacteria and scores of ileum injury ($r=-0.67, P=0.000$).

Multivariate analysis

In multivariate analysis, as shown in Table 3, only two variables in seven parameters remained independent prognosis factors of the development of bacterial translocation associated with postburn injuries. Ileal lesion score was considered as the auxo-action factor, and the counts of mucosal bifidobacteria as the prevention factor. This model was described by the following formula: $P(\text{bacterial translocation}) = e^{\text{logit}} / (1 + e^{\text{logit}})$ { $\text{logit} = 9.9220 - 3.2424 [\log_{10}(\text{count of bifidobacteria/g tissue})] + 3.8182 (\text{ileal-lesion score})$ }, with likelihood ratio $\chi^2=141.28$, and the accuracy of the formula for burn rats was $(50+67)/128=91\%$ when ileal-lesion score was no less than 4, and the counts of bifidobacteria was no more than 10^6 CFU/g tissue.

DISCUSSION

Intestinal mucosa is a key barrier to prevent the invasion and spread of microorganisms that normally reside within the gut lumen. Under certain conditions, however, bacteria and their

products such as endotoxin, can cross this barrier and get access to visceral organs via lymph or blood stream, a process that has been referred to as bacterial translocation. Factors that could promote bacterial translocation included overgrowth of Gram-negative enteric bacilli, impaired host immune defenses, and injury to the intestinal mucosa resulting in increased intestinal permeability^[1]. These mechanisms could act in concert to promote synergistically the systemic spread of indigenous translocating bacteria to cause lethal sepsis. Many pathological conditions could evoke bacterial translocation, such as ionization radiation, endotoxemia, dystrophia, peritonitis, renal failure, intestinal obstruction, lesion of mucosa, hemorrhagic shock, long-term fasting, deficiency in secretory IgA, total parenteral nutrition, severe trauma, massive operation, and extensive burn. Recently, some measures were taken to prevent and treat bacterial translocation secondary to trauma with bactericidal/permeability increasing protein, glucagons-like peptide, growth hormone, insulin-like growth factor I, inhibitor of angiotensin II, C1 inhibitor, bombesin, inhibitors of NO synthase, glutamine, lactulose, interleukin-1alpha, probiotics and selective digestive tract decontamination^[6,8-17], and their effects on the incidence of bacterial translocation were found to be resulted from ameliorating indigenous flora, strengthening the mucosal barrier, and promoting host systemic or intestinal immunity. However, what role does each of the above mentioned factors play in inciting bacterial translocation is yet to be clarified.

At the early stage of severe burns, there was a considerable change in gut mucosal flora, while only mild alternations occurred in intestinal luminal flora. It is noteworthy that bacterial translocation correlated with the state of colonization in ileum rather than in colon^[16]. With these facts in mind, in the present study, we paid more attention to the changes in mucosal microorganisms of the terminal ileal loop. Bifidobacterium, which was the most common species in feces of human^[18,19], *E. coli*, which was known to be the most commonly translocated microorganism^[4,20,21], as well as fungi, which commonly constituted the pathogens of nosocomial infection in an intensive care unit (ICU), were chosen as representatives of intestinal microflora. Concomitantly, the main pathological changes were located in mucosa of the terminal ileum^[22], the scores of lesion in ileum, reflecting the status of mucosa barrier^[7], and the levels of mucus sIgA, showing the function of intestinal immunity^[23], were determined. The levels of plasma endotoxin and IL-6 were used to evaluate the systemic inflammatory reactions^[24,25]. Furthermore, univariate analysis was used to identify the relationship between different variables with occurrence of bacterial translocation, correlation analysis was used for the compliance with the examined variables, and then logistic regression analysis was used to determine the independent predicting factors associated with bacterial translocation.

Bacterial translocation might result from a breach of the intestinal mucosa, as a result of ischemia, atrophy, mechanical injury, etc. Repair of injured mucosa depended on the improvement of local microcirculation^[26]. During burn shock, with re-distribution of blood circulation, the gastrointestinal suffered a prolonged ischemia, even when systemic hemodynamic parameters were normalized. This condition is known as compensatory covert shock. Our data showed that this hypoxic condition produced injuries to the mucosa of terminal ileum, followed by a significantly increased incidence of bacterial translocation at the early postburn stage. Moreover, the scores of ileal lesion had a significantly positive correlation with serum endotoxin levels. It has been documented that translocated endotoxin could trigger systemic inflammatory response through LBP/CD14 sensibility-increasing system^[27], and resulted in an over-release of inflammatory factors such as TNF- α , IL-6, which might further damage intestinal

mucosae^[25,27].

There was a marked negative correlation between scores of ileal lesion and mucosal bifidobacteria counts or mucus sIgA. The injury to intestinal mucosa predisposed bacteria to escape from the intestinal wall, while mucosal bifidobacteria and mucus sIgA might be protective against it^[15,23,28].

Katouli and colleagues demonstrated that the composition and diversity of gut flora were associated with bacterial translocation, and the proportion and quantity of *E. coli* might influence the incidence of bacterial translocation secondary to hemorrhagic shock^[20]. Our results showed that the counts of bifidobacteria decreased by 16-fold, and the counts of *E. coli* and fungi increased respectively by 8- and 4-fold in animals in which bacterial translocation was found. Moreover, the ratio of bifidobacteria to *E. coli* was decreased from 2 000:1 in animals without translocation to 16:1 in animals with translocation. This result might imply that the number of bifidobacteria, especially the ratio of bifidobacteria to *E. coli*, might be of more significance as a marker of bacterial translocation than the quantity and proportion of *E. coli*. Multivariate analysis showed that only the count of mucosal bifidobacteria was the independent predictor for the incidence of bacterial translocation, indicating that bifidobacteria, the predominant anaerobes in the gut, might play a key role in maintaining the biological barrier. The work of others showed that bifidobacteria as a mucosal flora could prevent other intestinal bacteria from adhering to intestinal epithelia through a competitive mechanism, and by producing lactic acid and acetate to create a harmful environment of lowered pH for the growth of *E. coli*, Salmonella, and methicillin-resistant *Staphylococcus aureus*^[28-35]. Our data supported these assertions that administration of bifidobacteria could restore the disrupted gut micro-ecology, which was favorable to the host. As a result, endotoxin release was lessened, and the incidence of bacterial translocation was lowered.

Local immunological defense of the gut was mainly provided by the gut-associated lymphoid tissue (GALT), principally in the form of secretory IgA. sIgA, the predominant immunoglobulin present in mucosal secretions, was the first line of defense on the intestinal mucosal surface^[23]. The importance of the mucosal immune system has been extensively recognized, for it relates to the potential pathogenic role of gut flora. Failure of the barrier function of the gut challenged by stress of severe trauma could lead to the translocation of viable enteric bacteria and endotoxin^[1]. Our results showed that mucous sIgA was reduced by 56% in animals with bacterial translocation as compared to animals without translocation. However, the concentration of intestinal mucous sIgA was excluded as an independent predictor when examined by multivariate statistical analysis. This might be partially due to the significant positive correlation between the level of sIgA and the count of bifidobacteria. Moreover, the synthesis and excretion of sIgA depended mainly on healthy and stable commensal bacteria^[23,30,34]. Overgrowth of Gram-negative bacteria after hemorrhagic shock might also suppress intestinal immunological function and sIgA secretion, augmenting bacterial translocation^[36,37]. On the contrary, selective decontamination of the digestive tract (SDD) or supplement of exogenous bifidobacteria could attenuate the incidence of bacterial translocation accompanied by improved intestinal and systemic immunity^[15,17,23].

In summary, the development of bacterial translocation was closely associated with overgrowth of pathogens such as fungi and *E. coli*, lowering of intestinal immunologic barrier function, breaching of gut mucosal barrier, and systemic inflammatory reaction subsequent to severe burns. The independent factors related to bacterial translocation were ileal injury score and the counts of gut bifidobacteria. Among them, the score of ileal injury was considered as the augmentative

factor, and the counts of mucosal bifidobacteria as the protective factor. Thus specific interventions targeting the high-risk factors, including repair of damaged intestinal mucosa by improving gut microcirculation and improvement of gastrointestinal micro-ecology by increasing the quantity and proportion of bifidobacteria, might be beneficial to the attenuation of bacterial translocation. Moreover, determination of the quantity of bifidobacteria and the ratio of bifidobacteria to *E. coli* in feces might be used to predict the occurrence of bacterial translocation.

ACKNOWLEDGEMENT

The authors thank Wang ZQ, He GY and Chen XW for their technical assistance, Bai XD and Chen J (Southwestern Hospital, Third Military Medical University) for their microscopic evaluation.

REFERENCES

- 1 **Swank GM**, Deitch EA. Role of the gut in multiple organ failure: bacterial translocation and permeability changes. *World J Surg* 1996; **20**: 411-417
- 2 **Sheng ZY**, Dong YL, Wang XH. Bacterial translocation and multiple system organ failure in bowel ischemia and reperfusion. *J Trauma* 1992; **32**: 148-153
- 3 **Yeh DC**, Wu CC, Ho WM, Cheng SB, Lu IY, Liu TJ, Peng FK. Bacterial translocation after cirrhotic liver resection: a clinical investigation of 181 patients. *J Surg Res* 2003; **111**: 209-214
- 4 **MacFie J**, O'Boyle C, Mitchell CJ, Buckley PM, Johnstone D, Sudworth P. Gut origin of sepsis: a prospective study investigating associations between bacterial translocation, gastric microflora, and septic morbidity. *Gut* 1999; **45**: 223-228
- 5 **Steinberg SM**. Bacterial translocation: what it is and what it is not. *Am J Surg* 2003; **186**: 301-305
- 6 **Tadros T**, Traber DL, Hegggers JP, Herndon DN. Angiotensin II inhibitor DuP753 attenuates burn- and endotoxin-induced gut ischemia, lipid peroxidation, mucosal permeability, and bacterial translocation. *Ann Surg* 2000; **231**: 566-576
- 7 **Park PO**, Haglund U. Regeneration of small bowel mucosa after intestinal ischemia. *Crit Care Med* 1992; **20**: 135-139
- 8 **Ding LA**, Li JS. Effects of glutamine on intestinal permeability and bacterial translocation in TPN-rats with endotoxemia. *World J Gastroenterol* 2003; **9**: 1327-1332
- 9 **Koutelidakis I**, Papaziogas B, Giamarellos-Bourboulis EJ, Makris J, Pavlidis T, Giamarellou H, Papaziogas T. Systemic endotoxaemia following obstructive jaundice: the role of lactulose. *J Surg Res* 2003; **113**: 243-247
- 10 **Ulusoy H**, Usul H, Aydin S, Kaklikkaya N, Cobanoglu U, Reis A, Akyol A, Ozen I. Effects of immunonutrition on intestinal mucosal apoptosis, mucosal atrophy, and bacterial translocation in head injured rats. *J Clin Neurosci* 2003; **10**: 596-601
- 11 **Fujino Y**, Suzuki Y, Kakinoki K, Tanioka Y, Ku Y, Kuroda Y. Protection against experimental small intestinal ischaemia-reperfusion injury with oxygenated perfluorochemical. *Br J Surg* 2003; **90**: 1015-1020
- 12 **Li JY**, Lu Y, Hu S, Sun D, Yao YM. Preventive effect of glutamine on intestinal barrier dysfunction induced by severe trauma. *World J Gastroenterol* 2002; **8**: 168-171
- 13 **Cevikel MH**, Ozgun H, Boylu S, Demirkiran AE, Sakarya S, Culhaci N. Nitric oxide regulates bacterial translocation in experimental acute edematous pancreatitis. *Pancreatology* 2003; **3**: 329-335
- 14 **Tadros T**, Traber DL, Hegggers JP, Herndon DN. Effects of interleukin-1alpha administration on intestinal ischemia and reperfusion injury, mucosal permeability, and bacterial translocation in burn and sepsis. *Ann Surg* 2003; **237**: 101-109
- 15 **Wang ZT**, Yao YM, Xiao GX, Cao WH, Sheng ZY. Bifidobacterial supplement enhances the expression and excretion of intestinal sIgA in severely burned rats. *Zhonghua Waikexue* 2003; **41**: 385-388
- 16 **Wang ZT**, Yao YM, Xiao GX, Sheng ZY. Improvement of bifidobacterial supplement on the barrier function of intestinal mucosa and microbe flora induced by thermal injury in rats. *Zhongguo Weizhongbing Jijiu Yixue* 2003; **15**: 154-158

- 17 **Yao YM**, Lu LR, Yu Y, Liang HP, Chen JS, Shi ZG, Zhou BT, Sheng ZY. Influence of selective decontamination of the digestive tract on cell-mediated immune function and bacteria/endotoxin translocation in thermally injured rats. *J Trauma* 1997; **42**: 1073-1079
- 18 **Locascio M**, Holgado AP, Perdigon G, Oliver G. Enteric bifidobacteria: isolation from human infants and challenge studies in mice. *Can J Microbiol* 2001; **47**: 1048-1052
- 19 **Satokari RM**, Vaughan EE, Akkermans AD, Saarela M, de Vos WM. Bifidobacterial diversity in human feces detected by genus-specific PCR and denaturing gradient gel electrophoresis. *Appl Environ Microbiol* 2001; **67**: 504-513
- 20 **Nettelbladt CG**, Katouli M, Bark T, Svenberg T, Mollby R, Ljungqvist O. Orally inoculated *Escherichia coli* strains colonize the gut and increase bacterial translocation after stress in rats. *Shock* 2003; **20**: 251-256
- 21 **Eaves-Pyles T**, Alexander JW. Comparison of translocation of different types of microorganisms from the intestinal tract of burned mice. *Shock* 2001; **16**: 148-152
- 22 **Mosenthal AC**, Xu D, Deitch EA. Elemental and intravenous total parenteral nutrition diet-induced gut barrier failure is intestinal site specific and can be prevented by feeding nonfermentable fiber. *Crit Care Med* 2002; **30**: 396-402
- 23 **Macpherson AJ**, Gatto D, Sainsbury E, Harriman GR, Hengartner H, Zinkernagel RM. A primitive T cell-independent mechanism of intestinal mucosal IgA responses to commensal bacteria. *Science* 2000; **288**: 2222-2226
- 24 **Gong JP**, Wu CX, Liu CA, Li SW, Shi YJ, Yang K, Li Y, Li XH. Intestinal damage mediated by Kupffer cells in rats with endotoxemia. *World J Gastroenterol* 2002; **8**: 923-927
- 25 **Yao YM**, Bahrami S, Redl H, Fuerst S, Schlag G. IL-6 release after intestinal ischemia/reperfusion in rats is under partial control of TNF. *J Surg Res* 1997; **70**: 21-26
- 26 **Akin ML**, Gulluoglu BM, Erenoglu K, Terzi K, Erdemoglu A, Celenk T. Hyperbaric oxygen prevents bacterial translocation in thermally injured rats. *J Invest Surg* 2002; **15**: 303-310
- 27 **Fang WH**, Yao YM, Shi ZG, Yu Y, Wu Y, Lu LR, Sheng ZY. Effect of recombinant bactericidal/permeability-increasing protein on endotoxin translocation and lipopolysaccharide-binding protein/CD14 expression in rats after thermal injury. *Crit Care Med* 2001; **29**: 1452-1459
- 28 **Caplan MS**, Miller-Catchpole R, Kaup S, Russell T, Lickerman M, Amer M, Xiao Y, Thomson R Jr. Bifidobacterial supplementation reduces the incidence of necrotizing enterocolitis in a neonatal rat model. *Gastroenterology* 1999; **117**: 577-583
- 29 **Urao M**, Fujimoto T, Lane GJ, Seo G, Miyano T. Does probiotics administration decrease serum endotoxin levels in infants? *J Pediatr Surg* 1999; **34**: 273-276
- 30 **Hooper LV**, Gordon JI. Commensal host-bacterial relationships in the gut. *Science* 2001; **292**: 1115-1118
- 31 **He F**, Ouwehand AC, Hashimoto H, Isolauri E, Benno Y, Salminen S. Adhesion of *Bifidobacterium spp.* to human intestinal mucus. *Microbiol Immunol* 2001; **45**: 259-262
- 32 **Eizaguirre I**, Urkia NG, Asensio AB, Zubillaga I, Zubillaga P, Vidales C, Garcia-Arenzana JM, Aldazabal P. Probiotic supplementation reduces the risk of bacterial translocation in experimental short bowel syndrome. *J Pediatr Surg* 2002; **37**: 699-702
- 33 **Wang ZT**, Xiao GX, Xiao J, Wang HJ, Peng YZ, Luo QZ. Effects of bifidobacteria preparation on restoring the disorder of intestinal flora induced by Meropenium in severely burned patients. *Zhonghua Shaoshang Zazhi* 2002; **18**: 111-112
- 34 **Guarner F**, Malagelada JR. Gut flora in health and disease. *Lancet* 2003; **361**: 512-519
- 35 **Gilmore MS**, Ferretti JJ. Microbiology. The thin line between gut commensal and pathogen. *Science* 2003; **299**: 1999-2002
- 36 **Gordon DM**, Diebel LN, Liberati DM, Myers TA. The effects of bacterial overgrowth and hemorrhagic shock on mucosal immunity. *Am Surg* 1998; **64**: 718-721
- 37 **Choudhry MA**, Fazal N, Goto M, Gamelli RL, Sayeed MM. Gut-associated lymphoid T cell suppression enhances bacterial translocation in alcohol and burn injury. *Am J Physiol Gastrointest Liver Physiol* 2002; **282**: G937-947

Edited by Wang XL and Xu FM

Gene expression profiles of hepatocytes treated with $\text{La}(\text{NO}_3)_3$ of rare earth in rats

Hui Zhao, Wei-Dong Hao, Hou-En Xu, Lan-Qin Shang, You-Yong Lu

Hui Zhao, Wei-Dong Hao, Hou-En Xu, Lan-Qin Shang, Department of Toxicology, Peking University Health Science Center, Beijing 100083, China

You-Yong Lu, School of Oncology, Beijing Institute for Cancer Research, Peking University, Beijing 100034, China

Supported by grant of Key Project of National Natural Science Foundation of China, No. 29890280-3

Correspondence to: Wei-Dong Hao, Department of Toxicology, Peking University Health Science Center, No 38 Xue Yuan Road, Beijing 100083, China. whao@bjmu.edu.cn

Telephone: +86-10-82802352 **Fax:** +86-10-62015583

Received: 2002-08-01 **Accepted:** 2002-08-31

Abstract

AIM: To compare the gene expression between $\text{La}(\text{NO}_3)_3$ -exposed and control rats *in vivo*.

METHODS: Rats were fed $\text{La}(\text{NO}_3)_3$ once daily at a dose of 20 mg/kg for one month by gavage. Gene expression of hepatocytes was detected using mRNA differential display (DD) technique and cDNA microarray and compared between treated and control groups.

RESULTS: Six differentially expressed sequence tags were cloned by DD, of which five were up regulated and one was down regulated in treated rats. Two sequences were determined. One band was novel. The other shared 100% sequence homology with AU080263 Sugano mouse brain mncb Mus musculus cDNA clone MNCb-5435 5'. With DNA microarray, 136 differentially expressed genes were identified including 131 over-expressed genes and 5 under-expressed genes. Most of these differentially expressed genes were cell signal and transmission genes, genes associated with metabolism, protein translation and synthesis.

CONCLUSION: $\text{La}(\text{NO}_3)_3$ could change the expression levels of some kinds of genes. Further analysis of the differentially expressed genes would be helpful for understanding the wide biological effect spectrum of rare earth elements.

Zhao H, Hao WD, Xu HE, Shang LQ, Lu YY. Gene expression profiles of hepatocytes treated with $\text{La}(\text{NO}_3)_3$ of rare earth in rats. *World J Gastroenterol* 2004; 10(11): 1625-1629
<http://www.wjgnet.com/1007-9327/10/1625.asp>

INTRODUCTION

Rare earth (RE) includes 17 elements. According to the physical and chemical nature, 16 elements except for scandium (Sc) are categorized into two groups. One is called light RE, which is represented by cerium, including lanthanum (La), cerium (Ce), praseodymium (Pr), neodymium (Nd), promethium (Pm), samarium (Sm) and europium (Eu). The other is called heavy RE, which is represented by yttrium, including gadolinium (Gd), terbium (Tb), dysprosium (Dy), holmium (Ho), erbium (Er), thulium (Tm), ytterbium (Yb), lutetium (Lu) and yttrium (Y).

Recently, RE has become one of the common xenobiotics in our surroundings as it is widely used in industry, stockbreeding and medicine, especially as trace fertilizers in agriculture, and they can be concentrated by food chain. Therefore, understanding the effects of RE on health has become more and more important.

Studies on RE toxicology have lasted for a long time. However, deeper exploration of its mechanism is highly needed. It is well known the biological effect spectrum of RE is wide and the dose-response relationship is complicated. For example, RE elements could induce chromosome damage of blood lymphocytes^[1] and liver damage^[2-4], depress learning and memory^[5], increase or suppress cell-mediated immunity of the spleen^[6], inhibit gap junctional intercellular communication^[7], etc. However, safety evaluation of RE is not easy, and the research of biomarkers by molecular biology is in its infancy. It is necessary to find more sensitive biomarkers by new techniques and methods, and to acquire a deeper understanding of the mechanism.

In this paper, the molecular mechanism of RE toxicity was explored by DD and cDNA microarray. $\text{La}(\text{NO}_3)_3$, which is the major component in RE trace fertilizers, was selected as the study material.

MATERIALS AND METHODS

La(NO₃)₃ treatment of rats

In the study of DD, 86-week-old Wistar rats were chosen. One half of them were male, and the others were female. To guarantee the treated rats and control had similar heredity backgrounds, the rule of same-breeding and same-sex control was applied. A $\text{La}(\text{NO}_3)_3$ -treated rat and its control were called a pair of test animals. There were two pairs of male rats and female rats, respectively. Treated rats were fed $\text{La}(\text{NO}_3)_3$ once daily at a dose of 20 mg/kg for one month by gavage. Control rats were fed distilled water. One pair of female rats was chosen in the study of cDNA microarray. Parts of isolated rat livers were used to observe morphology of hepatocytes by light microscopy and electron microscopy. Others were snap frozen in liquid nitrogen and then stored at -80 °C until RNA extraction.

Preparation of total RNA

Total RNA was prepared with single-step method by acid guanidinium isothiocyanate-phenol-chloroform according to Chomczynski and Sacchi^[8]. In brief, 0.5 g liver was homogenized with 2.5 mL solution D, then 0.25 mL 0.2 mol/L NaAc/0.1 mmol/L ATA, 2.75 mL phenol, 0.55 mL chloroform/isoamyl alcohol (24:1) were added and shaken in order. It was cooled on ice for 15 min and centrifuged at 10 000 g at 4 °C for 20 min. The supernatant was removed put into new tubes and 2.75 mL isopropanol was added to precipitate at -20 °C. It was then centrifuged at 10 000 g at 4 °C for 20 min. The supernatant was discarded and the pellet was dissolved in RNA denature buffer, then 15 µL 3 mol/L NaAc and 330 µL 1 000 mL/L ethanol were added to precipitate at -20 °C for 1 h. Contaminated chromosomal DNA was digested with DNase I (Promega).

Differential Display (DD)

For reverse transcription, RNA (in 1.0 µL DEPC treated water) was mixed with 2.0 µL API (Beckman) and incubated at 70 °C

for 5 min, then cooled on ice immediately. The solution was mixed with 8.8 μ L DEPC treated water, 4.0 μ L 5 \times reverse transcript buffer, 2.0 μ L dNTP (250 μ mol/L), 2.0 μ L DTT (100 mmol/L) and 0.2 μ L MMLV reverse transcriptase (200 U/ μ L, GIBCO). Reverse transcription was performed at 42 $^{\circ}$ C for 5 min, then at 50 $^{\circ}$ C for 50 min, and finally at 70 $^{\circ}$ C for 15 min.

For amplification of cDNA, AP1 was chosen as anchor 3' primer and ARP1-ARP4 were selected as arbitrary 5' primers. A 2 μ L cDNA was mixed with 8.2 μ L DEPC treated water, 2.0 μ L 10 \times PCR buffer (Promega), 2.0 μ L MgCl₂ (25 mmol/L, Promega), 1.6 μ L dNTP (2.5 mmol/L), 2.0 μ L ARP (2 μ mol/L), 2.0 μ L AP (2 μ mol/L) and 0.2 μ L TaqE (2.0 U/ μ L, Promega). The PCR amplification program was at 95 $^{\circ}$ C for 2 min, then 4 cycles at 92 $^{\circ}$ C for 15 s, at 50 $^{\circ}$ C for 30 s, and at 72 $^{\circ}$ C for 2 min, followed by 30 cycles at 92 $^{\circ}$ C for 15 s, at 60 $^{\circ}$ C for 30 s, at 72 $^{\circ}$ C for 2 min, and finally at 72 $^{\circ}$ C for 7 min.

A 7 μ L PCR mixture was redissolved in 4 μ L loading dye, heated at 95 $^{\circ}$ C for 2 min, then run on 80 g/L polyacrylamide-urea gels at 9 mA. DNA fragments on gels were displayed by silver stain method. Bands representing cDNA, which appeared to be differentially expressed, were excised and reamplified under the same conditions as above except the primers. In this procedure, T7 promoter and M13 reverse (-48) were used.

DNA sequence analysis

DNA sequence analysis was carried out with dye-terminator method in ABI DNA sequencer. DNA sequences were identified by comparison to those in GenBank BLASTn on Internet.

cDNA microarray

cDNA probes were prepared through reverse transcription and then purified. The probes from normal rats were labeled with Cy3-dUTP, and the probes from La(NO₃)₃-treated rats were labeled with Cy5-dUTP. The chips were scanned using ScanArray3000 laser scanner (General Scanning, Inc) at two wavelengths to detect emissions from both Cy3 and Cy5. The acquired images were analysed using ImaGene3.0 software (BioDiscovery, Inc.). The intensity of each spot at the two wavelengths represented the quantity of Cy3-dUTP and Cy5-dUTP, respectively. Each ratio of Cy3 and Cy5 was computed. Overall intensities were normalized by a coefficient according to the ratios of the located 40 housekeeping genes. To minimize artifacts arising from low expression values, only the genes with raw intensity values larger than 800 counts for one or both of Cy3 and Cy5 were chosen for differential analysis.

RESULTS

Effects of La(NO₃)₃ on morphology of rat hepatocytes

La(NO₃)₃ had no significant effects on histopathology by light microscopy. Swollen or cavitated mitochondria were observed in hepatocytes by electron microscopy (Figure 1).

Differential expression of La(NO₃)₃-induced genes of rat hepatocytes

Six differentially expressed bands in two pairs of rats, were obtained (Figure 2). Among them, five were up regulated and one was down regulated in treated rats. Two bands were sequenced. The results were as follows. LaFT1-4-1: The expression level of EST in treated rats was higher than that in control. Its length was about 160 bp (Figure 3A). EST was compared with known ESTs in GeneBank BLASTn. The homology was low (\leq 15%). LaFT1-4-1 was novel. Its sequence was as follow: 5'-AGCGGATAACA ATTCACACAGGAGTAGCAGACCCCTGCCCCAGGAAA TAACACACTAAACTCTCAAAAAAAAAAGCCCTATA GTGAGTCGTATTACACCCTATAGTGAGTCGTATTAGC GGATAACAATTCACACAGGACGCCCTATAGTGAGTA-3'.

LaMT1-4-1: The expression level of EST in treated rats was higher than that in control. Its length was about 144 bp (Figure 3B). The EST was compared with known ESTs in GenBank BLASTn and it shared 100% sequence homology with AU080263 Sugano mouse brain mncb Mus musculus cDNA clone MNCb-5435 5'. Its sequence was as follow: 5'-ACTCAAAGGCGGTAATACGG TTATCCACAGAATCAGGGGATAACGCAGGAAAGAA CATGTGAGCAAAAAGGCCAGCAAAAAGGCCAGGAAC CGTAAAAAGCCCGCGTTGCTGGCGTTTTTCCATAGG CTCCGCCCCCTGACGAGC-3'.

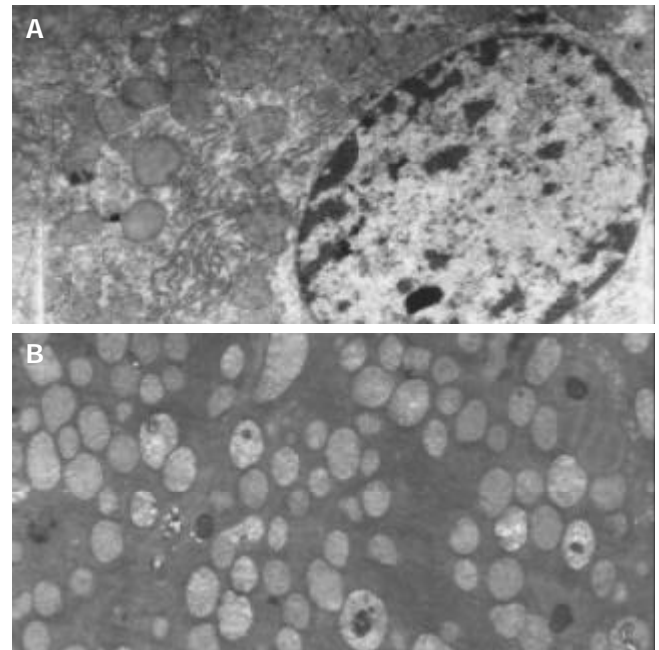


Figure 1 Electron microscopic images of hepatocytes. A: Normal mitochondria in control hepatocytes (TEM \times 6 700), B: Swollen or cavitated mitochondria in treated hepatocytes (TEM \times 5 800).

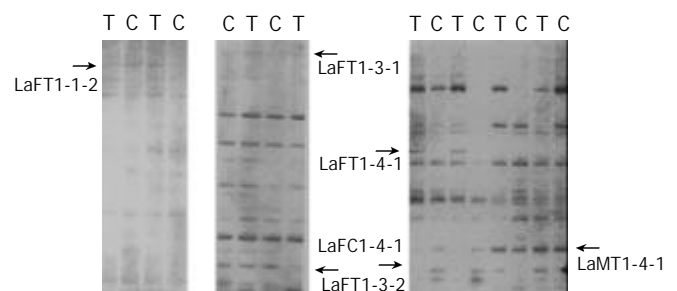


Figure 2 Polyacrylamide-urea gel of DNA fragments. Six differentially expressed bands in two pairs of rats were obtained. "T" above the bands and in name represents treated group, while "C" represents control group, "M" represents male, and "F" represents female. Among the bands, the expression levels of LaFT1-1-2, LaFT1-3-1, LaFT1-3-2, LaFT1-4-1 and LaMT1-4-1 were increased in treated rats. However, the level of LaFC1-4-1 was decreased.

Profile of gene expression in La(NO₃)₃-treated rat liver

HGEC-40D expression profile microarray, which consisted of 4 096 human cDNAs containing 60 control genes and 4 036 target genes, was provided by United Gene Holdings, Ltd. For every gene, there were two parallels in microarray. Target genes were divided into 15 types: oncogenes and tumor suppressor genes, ionic passage and transportation protein genes, cell cycle protein genes, stress reaction protein genes, cell skeleton

and movement protein genes, genes related to cell apoptosis, DNA synthesis, repair and recombination genes, DNA binding, transcription and transcription factor genes, cell receptor genes, immunity related genes, cell signal and transmission genes, metabolism related genes, protein translation and synthesis genes, growth related genes, and others.

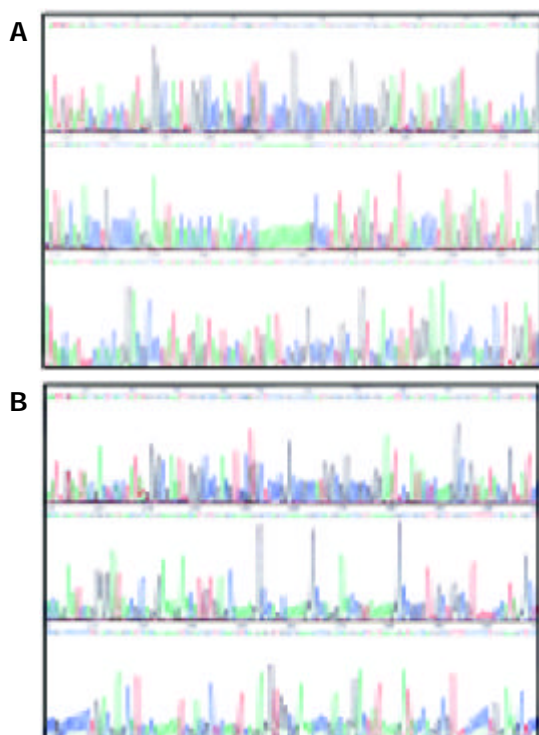


Figure 3 Sequences of cDNA. A: Sequence of LaFT1-4-1. Its length was about 160 bp. The primers used were AP1 and ARP4. B: Sequence of LaMT1-4-1. Its length was about 144 bp. The primers used were AP1 and ARP4.

In order to monitor the preparation and hybridization of DNA microarray, positive and negative controls were arranged. Forty housekeeping genes were used as positive controls. 821 gene (8 spots) and 1×spot solution (8 spots) were used as negative control spots. Positive control spots showed high intensity of signals and negative control spots showed low intensity, which proved the reliability of the data.

Cy3 fluorescent signal (labeled control) and Cy5 fluorescent signal (labeled treated group) were represented with red and green respectively. For overlying two signals of one spot, the spot showed green if the intensity of Cy3 signal was stronger (indicating down-regulation tendency), the spot showed red if the intensity of Cy5 signal was stronger (indicating up-regulation tendency), the spot showed yellow if the intensities of Cy3 and Cy5 signals were similar. In this study, the result of microarray is shown in Figure 4.

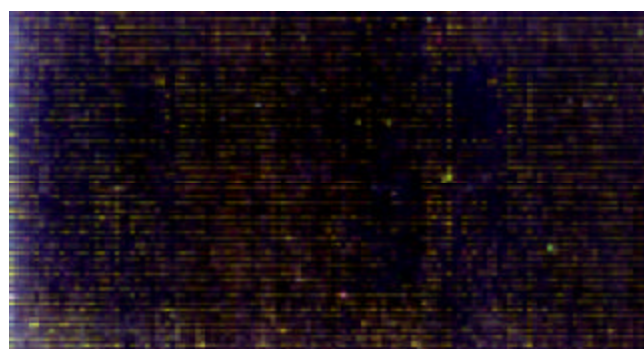


Figure 4 Two overlying fluorescent signals.

We screened out 136 differentially expressed genes according to the following rules. The ratio of Cy3 and Cy5 signal was larger than 2 or smaller than 0.5, the raw intensity value of one or both of Cy3 and Cy5 was larger than 800, the trend of up-regulation or down-regulation in parallels was the same. Of the

Table 1 Profile of gene expression in La(NO₃)₃-treated rat liver

Trend	GenBank-ID	Definition	Average ratio
up	ab023148	Homo sapiens mRNA for KIAA0931 protein, partial cds.	23.4
	hsu38545	Human ARF-activated phosphatidylcholine-specific phospholipase D1a (hPLD1) mRNA, complete cds.	10.1
	hstrke	H.sapiens TRK E mRNA.	8.7
	humrp17a	Human ribosomal protein L7a (surf 3) large subunit mRNA, complete cds.	7.8
	humcda24a	Homo sapiens CD24 signal transducer mRNA, complete cds.	6.9
	hsu76111	Human translation repressor NAT1 mRNA, complete cds.	6.4
	af125042	Homo sapiens bisphosphate 3'-nucleotidase mRNA, complete cds.	6.1
	hsu43701	Human ribosomal protein L23a mRNA, complete cds.	6.0
	hsu85946	Homo sapiens brain secretory protein hSec10p (HSEC10) mRNA, complete cds.	5.7
	ae000136	Escherichia coli K-12 MG1655 section 26 of 400 of the complete genome.	5.6
	af077951	Homo sapiens protein inhibitor of activated STAT protein PIAS1 mRNA, complete cds.	5.3
	af044671	Homo sapiens MM46 mRNA, complete cds.	5.1
	hsu35048	Human TSC-22 protein mRNA, complete cds.	5.1
	af068302	Homo sapiens choline/ethanolamine phosphotransferase (CEPT1) mRNA, complete cds.	5.1
	hsy17392	Homo sapiens mRNA for prefoldin subunit 1.	5.0
	af131820	Homo sapiens clone 25077 mRNA sequence, complete cds.	4.8
	af094481	Homo sapiens trinucleotide repeat DNA binding protein p20-CGGBP (CGGBP) gene, complete cds.	4.8
	ab020636	Homo sapiens mRNA for KIAA0829 protein, partial cds.	4.4
	ab020697	Homo sapiens mRNA for KIAA0890 protein, complete cds.	4.4
	down	ab011098	Homo sapiens mRNA for KIAA0526 protein, complete cds.
hsifi56r		Human mRNA for 56-ku protein induced by interferon.	0.437
hssgk		Homo sapiens sgk gene.	0.405
hsu87967		Human ATP diphosphohydrolase mRNA, complete cds.	0.364
humkuant		Human Ku autoimmune antigen gene, complete cds.	0.352

136 genes with altered expression, 131 genes had an elevated expression and 5 genes had a reduced expression. Most of the differentially expressed genes were cell signal and transmission genes, genes related to metabolism, protein translation and synthesis genes. Five down-regulated and 19 up-regulated genes with their differential expression levels more than 4-fold and having similar trends, are described in Table 1.

DISCUSSION

Studies on toxicities of RE elements by different intake pathways showed that the liver was the target organ of RE element toxicity^[9-15], and 20 mg/kg was believed to be the effective dose in oral administration^[15]. So, rats treated with La(NO₃)₃ at a dose of 20 mg/kg by gavage were chosen in our study.

mRNA differential display could provide a unique and powerful experimental system to study differential gene expression. In this study, six differentially expressed tags were obtained. Of the 2 bands sequenced, one (LaFT1-4-1) was novel.

The technique of DNA microarray could allow expression monitoring of thousands of genes in parallel^[16]. This technique promotes the identification of differentially expressed genes and investigation of the function of genes. In this study, human cDNA microarray was used. The genomes of human and rodent were very similar^[17,18], the homology of human genes and rat genes was over 70%. So it is of significance to analyse rat samples by a HGEC-40D expression profile microarray. One hundred and thirty-six differentially expressed genes were found by DNA microarray, which included mainly cell signal and transmission genes, genes related to metabolism, protein translation and synthesis genes. These genes accounted for 15%, 14% and 13%, respectively. Analysis on capital genes was described as follows.

Some genes encoding mitochondrial proteins were up regulated. The levels of homo sapiens NADH-ubiquinone oxidoreductase B22 subunit mRNA, ND2 gene, NDUFA5 gene and NDUFS8 gene were elevated 2.543, 3.540, 3.645 and 3.767 fold respectively, which were possibly associated with the damage of mitochondria.

Twelve differentially expressed KIAA genes were found in the study. Eleven were up regulated and one was down regulated. The expression level of KIAA0931 was elevated 23.4-fold. A family of KIAA includes new genes published by Kazusa DNA Research Institute in Japan. The functions of KIAA genes were supposed to be related to cell signal transmission, cell structure and cell movement based on the sequence studies^[19-21].

Phosphatidylcholine-specific phospholipase D1a (hPLD), is an important member of cell signal transducers. Active hPLD could produce biological effects by the following mechanisms. Phosphatidic acid (PA), diacyl-glycerol (DG) and lysophosphatidic acid (LPA), which are the direct and indirect products of hPLD, are important second messengers. Hydrolysis of phosphatidyl choline (PC) by hPLD could change local components of the membranes, consequently the characteristics of the membranes^[22]. It has been revealed that the process of hydrolysis of PC is related to many physiological activities including metabolism, cell cleavage, secretion, immunity, inflammatory reaction^[23]. In this study the expression level of hPLD gene was elevated by 10.1-fold, suggesting that activated hPLD which affects cell signal transmission is an important pathway of La(NO₃)₃ toxicity.

Signal transducer and activator of transcription (STAT) proteins play an important role in cell proliferation and differentiation induced by cytokines. STAT1 protein is believed to be the transcription factor of IFN reactivity. In addition, the mice with Stat1 gene picked out were found to be lacking of congenital immunity to viruses and bacteria^[24]. Protein inhibitor of activated STAT1 (PIAS1) could depress the activity of STAT1

by blocking STAT1 binding to specific DNA^[25]. PIAS1 gene was up regulated 5.3-fold in the study. It was suggested that La(NO₃)₃ might affect congenital immunity and the reactivity to IFN.

There were 7 differentially expressed genes related to immunity, of which 6 genes were up regulated and 1 was down regulated. In the up-regulated genes, H12.3 protein gene could regulate lymphocyte proliferation^[26]. CD9 antigen gene^[27], β -globulin gene, immuno-globulin light chain gene, CD24 signal transducer gene were related to humoral immunity. Calnexin protein gene played a role in cellular immunity and humoral immunity^[28]. The results suggested that La(NO₃)₃ had effects on both cellular immunity and humoral immunity. This was in good agreement with the results obtained by other researchers^[29-31].

In conclusion, the expression profiles of certain genes of La(NO₃)₃ treated rats differed markedly from those of control rats. This is consistent with the wide biological effect spectrum of RE elements. Multiple genes may join together to play a same role. Further analysis of the differentially expressed genes would be helpful for understanding the wide biological effect spectrum of RE elements. It would be interesting to explore further if the differentially expressed genes could be used as more sensitive biomarkers.

REFERENCES

- Xu HE**, Gao GH, Jia FL, Wang XY, Xie Q, Liu HS, Wang NF. Effect of mixed rare earth Changle on the micronuclei formation of blood lymphocytes in rats. *Zhonghua Yufang Yixue Zazhi* 2000; **34**(Suppl): 5-7
- Nakamura Y**, Tsumura Y, Tonogai Y, Shibata T, Ito Y. Differences in behavior among the chlorides of seven rare earth elements administered intravenously to rats. *Fundam Appl Toxicol* 1997; **37**: 106-116
- Tuchweber B**, Trost R, Salas M, Sieck W. Effect of praseodymium nitrate on hepatocytes and Kupffer cells in the rat. *Can J Physiol Pharmacol* 1976; **54**: 898-906
- Salas M**, Tuchweber B, Kovacs K, Garg BD. Effect of cerium on the rat liver: an ultrastructural and biochemical study. *Beitr Pathol* 1976; **157**: 23-44
- Li XQ**, Jiang JJ, Yang L, Liu M, Yang LY. Effect of low level mixed rare earth Changle on learning and memory, locomotor activity and NMDA-and M-receptors activity and morphology of divisions of hippocampal cortex in rats. *Zhonghua Yufang Yixue Zazhi* 2000; **34**(Suppl): 20-23
- Liu JM**, Chen D, Wang XM, Nie YX, Li Y, Li J. Long-term effect of Changle and La(NO₃)₃ on level of IL-2 and γ -IFN of splenic lymphocytes in rats. *Zhonghua Yufang Yixue Zazhi* 2000; **34**(Suppl):49-51
- Guo XB**, Gao ZH, Luo LZ, Yao BY. Effects of rare earth compounds on metabolic cooperation between Chinese hamster V79 cells. *Zhonghua Yufang Yixue Zazhi* 2000; **34**(Suppl): 17-19
- Chomczynski P**, Sacchi N. Single-step method of RNA isolation by acid guanidinium thiocyanate-phenol-chloroform extraction. *Anal Biochem* 1987; **162**: 156-159
- Godin DV**, Frohlich J. Erythrocyte alterations in praseodymium-induced lecithin: cholesterol acyltransferase(LCAT) deficiency in the rat: comparison with familial LCAT deficiency in man. *Res Commun Chem Pathol Pharmacol* 1981; **31**: 555-566
- Langer GA**, Frank JS. Lanthanum in heart cell culture. Effect on calcium exchange correlated with its localization. *J Cell Biol* 1972; **54**: 441-455
- Arvela P**, Kraul H, Stenback F, Pelkonen O. The cerium-induced liver injury and oxidative drug metabolism in DBA/2 and C57BL/6 mice. *Toxicology* 1991; **69**: 1-9
- Spencer A**, Wilson S, Harpur E. Gadolinium chloride toxicity in the mouse. *Hum Exp Toxicol* 1998; **17**: 633-637
- Hirano S**, Kodama N, Shibata K, Suzuki KT. Metabolism and toxicity of intravenously injected yttrium chloride in rats. *Toxicol Appl Pharmacol* 1993; **121**: 224-232
- Shinohara A**, Chiba M, Inaba Y. Distribution of terbium and increase of calcium concentration in the organs of mice i.v.-

- administered with terbium chloride. *Biomed Environ Sci* 1997; **10**: 73-84
- 15 **Chen AJ**, Chen D, Liu Y, Liu P, Wang XM, Nie YX, Wang X, Sun SY. The long term effect of low dose of Changle on the structure and function of liver in rats. *Zhonghua Yufang Yixue Zazhi* 2000; **34**(Suppl): 46-48
- 16 **Schena M**, Shalon D, Davis RW, Brown PO. Quantitative monitoring of gene expression patterns with a complementary DNA microarray. *Science* 1995; **270**: 467-470
- 17 **Pennisi E**. Genomics. Sequence tells mouse, human genome secrets. *Science* 2002; **298**: 1863-1865
- 18 **Pennisi E**. Genomics. Charting a genome's hills and valleys. *Science* 2002; **296**: 1601-1603
- 19 **Nagase T**, Ishikawa K, Miyajima N, Tanaka A, Kotani H, Nomura N, Ohara O. Prediction of the coding sequences of unidentified human genes. IX. The complete sequences of 100 new cDNA clones from brain which can code for large proteins *in vitro*. *DNA Res* 1998; **5**: 31-39
- 20 **Nagase T**, Ishikawa K, Suyama M, Kikuno R, Hirose M, Miyajima N, Tanaka A, Kotani H, Nomura N, Ohara O. Prediction of the coding sequences of unidentified human genes. XII. The complete sequences of 100 new cDNA clones from brain which code for large proteins *in vitro*. *DNA Res* 1998; **5**: 355-364
- 21 **Nagase T**, Ishikawa K, Suyama M, Kikuno R, Hirose M, Miyajima N, Tanaka A, Kotani H, Nomura N, Ohara O. Prediction of the coding sequences of unidentified human genes. XIII. The complete sequences of 100 new cDNA clones from brain which code for large proteins *in vitro*. *DNA Res* 1999; **6**: 63-70
- 22 **Exton JH**. Phospholipase D: Enzymology, mechanisms of regulation, and function. *Physiol Rev* 1997; **77**: 303-320
- 23 **Morris AJ**, Engebrecht J, Frohman MA. Structure and regulation of phospholipase D. *Trends Pharmacol Sci* 1996; **17**: 182-185
- 24 **Coffman RL**, Leberman DA, Rothman P. Mechanism and regulation of immunoglobulin isotype switching. *Adv Immunol* 1993; **54**: 229-270
- 25 **Liu B**, Liao J, Rao X, Kushner SA, Chung CD, Chang DD, Shuai K. Inhibition of Stat1-mediated gene activation by PIAS1. *Proc Natl Acad Sci U S A* 1998; **95**: 10626-10631
- 26 **Guillemot F**, Billault A, Auffray C. Physical linkage of a guanine nucleotide-binding protein-related gene to the chicken major histocompatibility complex. *Proc Natl Acad Sci U S A* 1989; **86**: 4594-4598
- 27 **Boucheix C**, Benoit P, Frachet P, Billard M, Worthington RE, Gagnon J, Uzan G. Molecular cloning of the CD9 antigen. A new family of cell surface proteins. *J Biol Chem* 1991; **266**: 117-122
- 28 **Hochstenbach F**, David V, Watkins S, Brenner MB. Endoplasmic reticulum resident protein of 90 kilodaltons associates with the T- and B-cell antigen receptors and major histocompatibility complex antigens during their assembly. *Proc Natl Acad Sci U S A* 1992; **89**: 4734-4738
- 29 **Wang YZ**, Li ZX, Li F, Li M, Shi Y. Effects of RE elements on workers' immune function. *Zhiye Yixue* 1995; **22**: 7-8
- 30 **Zhang ZS**, Xue B, Chen XA. Effects of RE nitrate on the function of T- lymphocytes, B- lymphocytes and macrophage. *Weisheng Dulixue Zazhi* 1993; **7**: 157-158
- 31 **Wei XT**, Ma N, Lei ZM, Xue B, Xu HE. Effects of La(NO₃)₃ on the immune function and cell apoptosis of splenic lymphocytes and thymocytes. *Zhonghua Yufang Yixue Zazhi* 2000; **34** (Suppl): 42-45

Edited by Zhu LH and Wang XL Proofread by Xu FM

Competitive inhibition of adherence of enterotoxigenic *Escherichia coli*, enteropathogenic *Escherichia coli* and *Clostridium difficile* to intestinal epithelial cell line Lovo by purified adhesin of *Bifidobacterium adolescentis* 1027

Shi-Shun Zhong, Zhen-Shu Zhang, Ji-De Wang, Zhuo-Sheng Lai, Qun-Ying Wang, Ling-Jia Pan, Yue-Xin Ren

Shi-Shun Zhong, Zhen-Shu Zhang, Ji-De Wang, Zhuo-Sheng Lai, Qun-Ying Wang, Ling-Jia Pan, Yue-Xin Ren, Chinese PLA Institute of Digestive Diseases, Nanfang Hospital, First military Medical University, Guangzhou 510515, Guangdong Province, China
Supported by Natural Science Foundation of Guangdong Province, No.010621

Correspondence to: Dr. Shi-Shun Zhong, Chinese PLA Institute of Digestive Disease, Nanfang Hospital, First military Medical University, Guangzhou 510515, Guangdong Province, China. zdoctor@sohu.com
Telephone: +86-20-61641530

Received: 2004-01-10 **Accepted:** 2004-02-18

Abstract

AIM: To observe competitive inhibition of adherence of enterotoxigenic *Escherichia coli* (EPEC), enteropathogenic *Escherichia coli* (EPEC) and *Clostridium difficile* (*C. difficile*) to intestinal epithelial cell line Lovo by purified adhesin of *Bifidobacterium adolescentis* 1027 (*B. ado* 1027).

METHODS: The binding of bacteria to intestinal epithelial cell line Lovo was counted by adhesion assay. The inhibition of adherence of EPEC, EPEC and *C. difficile* to intestinal epithelial cell line Lovo by purified adhesin of *B. ado* 1027 was evaluated quantitatively by flow cytometry.

RESULTS: The purified adhesin at the concentration of 10 µg/mL, 20 µg/mL and 30 µg/mL except at 1 µg/mL and 5 µg/mL could inhibit significantly the adhesion of EPEC, EPEC and *C. difficile* to intestinal epithelial cell line Lovo. Moreover, we observed that a reduction in bacterial adhesion was occurred with increase in the concentration of adhesin, and MFI (Mean fluorescent intensity) was decreased with increase in the concentration of adhesin.

CONCLUSION: The purified adhesin of *B. ado* 1027 can inhibit the adhesion of EPEC, EPEC and *C. difficile* to intestinal epithelial cell line Lovo in a dose-dependent manner.

Zhong SS, Zhang ZS, Wang JD, Lai ZS, Wang QY, Pan LJ, Ren YX. Competitive inhibition of adherence of enterotoxigenic *Escherichia coli*, enteropathogenic *Escherichia coli* and *Clostridium difficile* to intestinal epithelial cell line Lovo by purified adhesin of *Bifidobacterium adolescentis* 1027. *World J Gastroenterol* 2004; 10(11): 1630-1633
<http://www.wjgnet.com/1007-9327/10/1630.asp>

INTRODUCTION

It is well known that enterotoxigenic *Escherichia coli* (EPEC) and enteropathogenic *Escherichia coli* (EPEC) are major cause of diarrhoea in neonates and travelers. The gastrointestinal tract appears to be a reservoir for *E. coli* which are able to translocate across the intestinal mucosa. *Clostridium difficile* (*C. difficile*),

a gram-positive spore-forming anaerobic bacillus, is the most common cause of infectious diarrhoea in hospitalized patients^[1]. Adherence of bacteria to intestinal epithelium is known to be a prerequisite for colonization and infection of the gastrointestinal tract by many gastrointestinal pathogens^[2-4]. The intestinal epithelium is the primary site of contact for pathogens with host cells and plays an important role in the cross-talk between epithelial cells, luminal micro-organisms and immune cells. Therefore, inhibition of bacterial adhesion to the intestinal surface may prevent enteropathogens from translocating across the intestinal mucosa.

Bifidobacterium is known to be a predominant constituent of the human intestinal microflora^[5]. The presence of bifidobacteria in the human intestine has been reported to contribute to human health and well being^[6,7]. Adherence of bifidobacteria to intestinal mucus is regarded as one of the prerequisites for successful colonization^[8], antagonistic activity against enteropathogens^[9,10], modulation of the immune system^[11]. In addition, mucosal adhesion has been proposed as one of the main selection criteria for probiotic strains^[12-14]. Recently, studies have focused on its anti-infectious effects, particularly the inhibition activity against enteropathogens for protecting human^[15-17]. As the production and preservation of live bifidobacterium are difficult, so its application is restricted. Bernet *et al.*^[18] observed that the occurrence of bifidobacteria adhering to the human intestinal cells by a mechanism of adhesion which involved a proteinaceous component. Fujiwara *et al.*^[19,20] clarified that bifidobacterium longum SBT2928 produced a proteinaceous factor which prevented the binding of EPEC to the binding receptor ganglioside GM1. Zheng *et al.*^[21] extracted and purified a protein with a molecular weight of 16 ku from spent culture supernatant of *Bifidobacterium adolescentis* 1027 (*B. ado* 1027). In the present study, competitive inhibition of adherence of EPEC, EPEC and *Clostridium difficile* to intestinal epithelial cells by purified adhesin of *B. ado* 1027 was observed by adhesion assay and flow cytometry assay.

MATERIALS AND METHODS

Bacterial strains

B. ado 1027 was isolated from healthy infants feces and identified by API-20A and TAB system (British). *B. ado* 1027 was cultured in sulfglycolic acid salt broth at 37 °C for 48 h under anaerobic conditions. EPEC and EPEC were obtained from Department of Epidemiology, First Military Medical University. EPEC and EPEC were cultured in agitation, nutrient broth at 37 °C for 48 h. A toxin-producing *C. difficile* strain (VPI10463) was obtained from Lanzhou Institute of Biological Products (China). *C. difficile* strain was grown in brain-heart infusion broth at 37 °C for 48 h under anaerobic conditions. All bacteria were harvested from the broth culture by centrifugation at 2 500 r/min for 10 min, followed by resuspension of the pellet in phosphate buffered saline (PBS, pH 7.4) to a concentration of 1×10⁸ colony forming units (cfu)/mL.

Cell line

Human intestinal epithelial cell line Lovo was obtained from American type culture collection (ATCC) and was maintained in RPMI-1 640 (Gibco) supplemented with 2 mmol/L *L*-glutamine and 100 mL/L FCS at 37 °C in a humidified atmosphere containing 50 mL/L CO₂. For the adhesion assay, monolayer of Lovo cell was prepared on glass coverslips which were placed in six-well tissue culture plates (Corning Glass Works, Corning, N.Y.).

Extraction and purification of adhesin

The adhesin of bifidobacterium was extracted and purified as reported earlier by Zheng *et al.*^[21]. In short, the adhesin of bifidobacterium was isolated and purified by Superdex 75 gel filtration and Q-Sepharose FF ion exchange chromatography, and the adhesin was analyzed by SDS-PAGE. It was a protein with a molecular weight of 16 Ku, stored at -20 °C.

In vitro adhesion assay

The adherence of bacteria strains to Lovo cells was examined as described previously^[22-24]. Briefly, the Lovo monolayer prepared on glass coverslips which were placed in six-well tissue culture plates, was washed twice with PBS. The adhesin (1 µg/mL, 5 µg/mL, 10 µg/mL, 20 µg/mL, and 30 µg/mL) of bifidobacterium was added to each well of the tissue culture plate, and the plate was incubated at 37 °C in a humidified atmosphere containing 50 mL/L CO₂. After 30 min of incubation, the monolayer was washed one time with PBS. The suspensions of bacteria (1 mL) were added to each well, respectively. After 3 h of incubation at 37 °C atmosphere, the monolayer was washed twice with

sterile PBS, fixed with methanol, stained with Gram stain, and examined microscopically. For each monolayer on a glass coverslip, the number of adherent bacteria was evaluated in 30 random microscopic areas. Adherence was evaluated by two different technicians to eliminate bias. Bifidobacterium+bacteria and alone bacteria group were used as controls of adhesion.

Mean fluorescent intensity (MFI) of human intestinal epithelial cell with adherent bacteria were detected by flow cytometer

The fluorochrome FITC (Fluorescein isothiocyanate) was used in this study. All bacteria were washed 2 times in bicarbonate buffer (0.1 mol/L, pH 9.2), and labelled with fluorochrome FITC (1.5 mg/mL) by incubating 1×10⁸ bacteria/mL at 4 °C for 1 h. Excess fluorochrome was removed by washing 5 times with PBS at 1 500 g. All bacteria were resuspended in PBS which contained B. ado 1027 (1×10⁸/mL), adhesin of different concentrations and non-adhesin. Fluorescently labelled bacteria (1×10⁸) were incubated with 1×10⁵ epithelial cells for 2 h at 37 °C. After incubation, cells were washed three times with PBS to remove non-adherent bacteria. MFI (wave-length of excitation: 488 nm, wave-length of emission: 575 nm) of human intestinal epithelial cells with adherent bacteria was measured in a FACS-420 flow cytometer (Coulter, U.S). A total of 10 000 cells was acquired and the data were analysed with the Cell Quest software program from Coulter.

Statistical analysis

Values were expressed as mean±SD. Statistical comparisons between the means were made with students *t* test by SPSS 10.0 version. A *P* value of <0.05 was assumed for statistical significance.

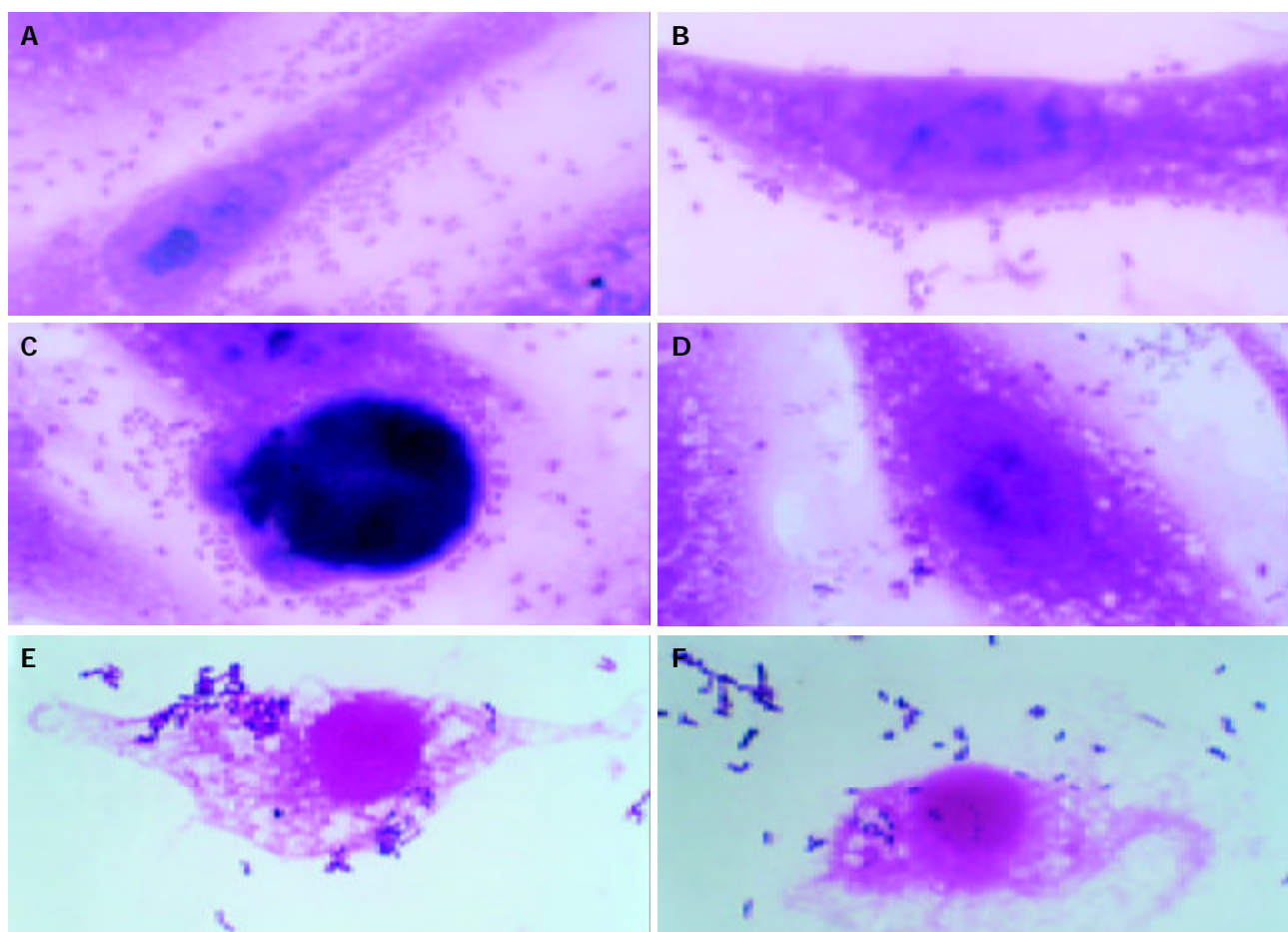


Figure 1 Gram staining of ETEC, EPEC and *Clostridium difficile* (×1000). Competitive inhibition of adherence of ETEC, EPEC and *Clostridium difficile* to intestinal epithelial cells by purified adhesin of *B. ado* 1027 was observed by adhesion assay. A: adherence of EPEC to intestinal epithelial cells without adhesin; B: adherence of EPEC to intestinal epithelial cells with adhesin; C: adherence of ETEC to intestinal epithelial cells without adhesin; D: adherence of ETEC to intestinal epithelial cells with adhesin; E: adherence of *C. difficile* to intestinal epithelial cells without adhesin; and F: adherence of *C. difficile* to intestinal epithelial cells with adhesin.

RESULTS

Effect of purified adhesin of *B. ado 1027* on adherence of ETEC, EPEC and *C. difficile* to intestinal epithelial cells

The adhesion assay was performed after Lovo cell and different concentrations adhesin were incubated at 37 °C for 30 min. As shown in Table 1, the purified adhesin at the concentration of 10 µg/mL, 20 µg/mL and 30 µg/mL except at 1 µg/mL and 5 µg/mL could significantly inhibit the adhesion of ETEC, EPEC and clostridium difficile to intestinal epithelial cell line Lovo. Adhesion of ETEC, EPEC or *Clostridium difficile* to intestinal epithelial cell was significantly decreased when the concentration of purified adhesin was 10 µg/mL, 20 µg/mL or 30 µg/mL ($P < 0.05$, $P < 0.01$). Moreover, we observed that the ability of inhibition was enhanced with increase in the concentration of adhesin. These results indicated that purified adhesin of *B. ado 1027* was involved in the adhesion of bacteria. The adhesion of ETEC and EPEC to intestinal epithelial cell was linear (Figures 1A, B, C and D). The adhesion of *C. difficile* to intestinal epithelial cell was like cluster (Figures 1E and F). The number of adherence of ETEC, EPEC and clostridium difficile to intestinal epithelial cells with adhesin was less than that of without adhesin. Inhibition of adherence of ETEC, EPEC and *Clostridium difficile* to intestinal epithelial cell by purified adhesin of *B. ado 1027* was not significantly different between adhesin (30 µg/mL) and bacteria+ *B. ado 1027* group (1×10^8 /mL).

Table 1 Effect of purified adhesin of *B. ado 1027* on adhesion of ETEC, EPEC and *C. difficile* to intestinal epithelial cell line Lovo

Group	Bacteria/cell		
	ETEC	EPEC	<i>C.difficile</i>
Adhesin (0 µg/mL)	108.83±16.34	110.27±13.12	110.00±16.91
Adhesin (1 µg/mL)	106.00±14.46	107.77±13.28	108.07±14.54
Adhesin (5 µg/mL)	102.97±7.65	104.20±10.82	104.23±9.62
Adhesin (10 µg/mL)	81.37±7.18 ^b	81.73±9.01 ^b	78.83±6.23 ^b
Adhesin (20 µg/mL)	41.23±7.13 ^b	42.37±7.54 ^b	38.77±7.82 ^b
Adhesin (30 µg/mL)	11.97±4.42 ^b	11.33±4.35 ^b	11.40±4.20 ^b
<i>B. ado 1027</i>	10.87±3.22	10.07±3.32	11.73±3.66

^b $P < 0.01$ vs adhesin (0 µg/mL).

Table 2 Mean fluorescent intensity (MFI) of human intestinal epithelial cell with adherent ETEC, EPEC and *C. difficile*

Group	MFI		
	ETEC	EPEC	<i>C.difficile</i>
Adhesin (0 µg/mL)	5.76±0.43	5.26±0.29	5.14±0.21
Adhesin (1 µg/mL)	5.55±0.44	5.06±0.32	5.06±0.14
Adhesin (5 µg/mL)	5.10±0.24	4.83±0.28	4.84±0.15
Adhesin (10 µg/mL)	3.91±0.20 ^b	3.67±0.35 ^b	3.25±0.32 ^b
Adhesin (20 µg/mL)	2.23±0.43 ^b	2.21±0.32 ^b	2.19±0.26 ^b
Adhesin (30 µg/mL)	1.41±0.23 ^b	1.25±0.18 ^b	0.89±0.14 ^b
<i>B. ado 1027</i>	1.25±0.23	0.98±0.13	0.79±0.19

^b $P < 0.01$ vs adhesin (0 µg/mL) group

Flow cytometric analysis of bacteria adherence to intestinal epithelial cell

ETEC, EPEC and a toxin-producing *C. difficile* strain (VPI10463) were assessed for their ability to adhere to human intestinal epithelial cell line Lovo (Table.2). There was no significant difference in MFI of ETEC, EPEC or *C. difficile* when the concentrations of adhesin were 1 µg/mL and 5 µg/mL. However, MFI was significantly decreased when the concentrations of adhesin were 10 µg/mL, 20 µg/mL and 30 µg/mL ($P < 0.05$, $P < 0.01$).

MFI was decreased with increase in the concentration of adhesin. There was no significant difference in MFI between adhesin (30 µg/mL) and bacteria+ *B. ado 1027* group (1×10^8 /mL).

DISCUSSION

Adherence of pathogenic to the intestinal mucus is regarded a prerequisite for prolonged transient colonization and infection of the gastrointestinal tract, and plays an important role in invasion and in yielding and secretion of virulence factor^[25]. Bifidobacteria, the predominant bacteria in the human intestinal microflora, are considered to be microorganisms with a great influence on human health^[26]. There have been many studies demonstrating that strains of bifidobacteria have anti-infectious properties against enteropathogenic bacteria^[18,27-29]. However, there existed a few flaws when live bifidobacteria agents was used in gut barrier dysfunction: live bifidobacteria was difficult to produce and preserve, and also difficult to breed sufficiently due to lack of local gas and growth substrate. Bernet *et al.*^[18] and Zheng *et al.*^[30] reported the occurrence of bifidobacteria adhering to the human intestinal cells by a mechanism of adhesion which involves a proteinaceous component. Fujiwara *et al.*^[31] reported that SBT2928 produced a proteinaceous factor, binding inhibitory factor (BIF), which prevented the binding of the ETEC to GA1 *in vitro*, and the binding of ETEC to the human intestinal epithelial cell line HCT-8 was reduced by BIF treatment in a dose-dependent manner. These results showed there was adhesin component in bifidobacteria.

Adherence assay which can Gram stain and microscopically examine bacteria to human intestinal epithelial has been accepted widely for quantitative and direct visual. However, light microscopic methods, while useful, are tedious and time-consuming and may be prone to observer error. Flow cytometry allows analysis of cell populations by virtue of their physical characteristics and has been used previously to assess the adherence of *Helicobacter pylori*^[32]. With this approach, it is possible to distinguish differences in cell populations based on changes in fluorescent intensities for test and control populations. When compared with conventional microscopy, it is also possible to examine much larger numbers of cells in a shorter time period^[33]. The present study used Gram stain and flow cytometry to demonstrate competitive inhibition of adherence of ETEC, EPEC and *C. difficile* to intestinal epithelial cell line Lovo by purified adhesin of *B. ado 1027*. Our study showed that the purified adhesin at the concentration of 10 µg/mL, 20 µg/mL and 30 µg/mL except at 1 µg/mL and 5 µg/mL could significantly inhibit the adhesion of ETEC, EPEC and *C. difficile* to intestinal epithelial cell line Lovo. Moreover, we observed that the ETEC, EPEC and *C. difficile* adhesion were reduced by adhesin treatment in a dose-dependent manner. Inhibition of the binding of ETEC, EPEC and *C. difficile* to intestinal epithelial cell was not significantly different between adhesin (30 µg/mL) and bacteria+ *B. ado 1027* group. The results of flow cytometry analysis of bacteria adherence to intestinal epithelial cell also confirmed it. MFI was decreased with increase in the concentration of adhesin. These results indicated that purified adhesin of *B. ado 1027* was involved in the adhesion of bacteria. Two basic factors, receptor and adhesin, are required for classical adhesion. One of the mechanisms by which probiotic bacteria can protect epithelial is receptor competition^[34]. Our results suggest that adhesin functions by blocking the binding site of ETEC, EPEC and *C. difficile* to intestinal epithelial cell. Adhesin produced by bifidobacterial may play an important role in protecting the host. Future studies need to carry out a survey of the resistance of adhesin against the activities of digestive enzymes in the gastrointestinal tract of human. In addition, it is important to determine whether all strains or all species of bifidobacteria produce adhesin or a similar protein(s)

which prevents the binding of pathogens to receptor in intestinal epithelial surfaces.

We also observed that the adhesive behaviors of bacteria to intestinal epithelial cell line Lovo were different. The adhesion of ETEC and EPEC to intestinal epithelial cell was linear, whereas the adhesion of *C. difficile* to intestinal epithelial cell was like cluster. This suggests that different bacteria may have different distribution of receptor on cell surface.

In conclusion, the purified adhesin of *B. ado* 1027 can effectively inhibit adherence of ETEC, EPEC and *C. difficile* to intestinal epithelial cell *in vitro*. However, whether adhesin could prevent diseases related with ETEC, EPEC and *C. difficile*, still needs to be proved *in vivo* by human clinical studies.

REFERENCES

- Kelly CP, LaMont JT. Clostridium difficile infection. *Annu Rev Med* 1998; **49**: 375-390
- Kagnoff MF, Eckmann L. Epithelial cells as sensors for microbial infection. *J Clin Invest* 1997; **100**: 6-10
- Raupach B, Meccas J, Heczko U, Falkow S, Finlay BB. Bacterial epithelial cell cross talk. *Curr Top Microbiol Immunol* 1999; **236**: 137-161
- Eckmann L, Kagnoff MF, Fierer J. Intestinal epithelial cells as watchdogs for the natural immune system. *Trends Microbiol* 1995; **3**: 118-120
- Finegold SM, Sutter VL, Sugihara PT, Elder HA, Lehman SM, Phillips RL. Fecal microbial flora in Seventh Day Adventist populations and control subjects. *Am J Clin Nutr* 1977; **30**: 1781-1792
- Bezkorovainy A. Probiotics: determinants of survival and growth in the gut. *Am J Clin Nutr* 2001; **73**(2 Suppl): 399S-405S
- Isolauri E. Probiotics in human disease. *Am J Clin Nutr* 2001; **73**: 1142S-1146S
- Alander M, Satokari R, Korpela R, Saxelin M, Vilpponen-Salmela T, Mattila-Sandholm T, von Wright A. Persistence of colonization of human colonic mucus by a probiotic strain, *Lactobacillus rhamnosus* GG after oral consumption. *Appl Environ Microbiol* 1999; **65**: 351-354
- Coconnier MH, Bernet MF, Chauviere G, Servin AL. Adhering heat-killed human *Lactobacillus acidophilus* strain LB, inhibits the process of pathogenically of diarrhoeagenic bacteria in culture human intestinal cells. *J Diarrhoeal Dis Res* 1993; **11**: 235-242
- Coconnier MH, Bernet MF, Kernis S, Chauviere G, Fourniat J, Servin AL. Inhibition of adhesion of enteroinvasive pathogens to human intestinal Caco-2 cells by *Lactobacillus acidophilus* strain LB decrease bacterial invasion. *FEMS Microbiol Lett* 1993; **110**: 299-305
- Schiffirin EJ, Brassart D, Servin AL, Rochat F, Donnet-Hughes A. Immune modulation of blood leukocytes in human by lactic acid bacteria: criteria for strain selection. *Am J Clin Nutr* 1997; **66**: 515S-520S
- Del Re B, Sgorbati B, Miglioli M, Palenzona D. Adhesion, autoaggregation and hydrophobicity of 13 strains of *Bifidobacterium longum*. *Lett Appl Microbiol* 2000; **31**: 438-442
- Kirjavainen PV, Ouwehand AC, Isolauri E, Salminen SJ. The ability of probiotic bacteria to bind to human intestinal mucus. *FEMS Microbiol Lett* 1998; **167**: 185-189
- He F, Ouwehand AC, Isolauri E, Hashimoto H, Benno Y, Salminen S. Comparison of mucosal adhesion of *Bifidobacteria* isolated from healthy and allergic infants. *FEMS Immunol Med Microbiol* 2001; **30**: 43-47
- Matsumoto M, Tani H, Ono H, Ohishi H, Benno Y. Adhesive property of *bifidobacterium lactis* LKM512 and predominant bacteria of intestinal microflora to human intestinal mucin. *Curr Microbiol* 2002; **44**: 212-215
- Lee YJ, Yu WK, Heo TR. Identification and screening for antimicrobial activity against *Clostridium difficile* of *Bifidobacterium* and *Lactobacillus* species isolated from healthy infant faeces. *Int J Antimicrob Agents* 2003; **21**: 340-346
- Setoyama H, Imaoka A, Ishikawa H, Umesaki Y. Prevention of gut inflammation by *Bifidobacterium* in dextran sulfate-treated gnotobiotic mice associated with *Bacteroides* strains isolated from ulcerative colitis patients. *Microbes Infect* 2003; **5**: 115-122
- Bernet MF, Brassart D, Neeser JR, Servin AL. Adhesion of human bifidobacterial strains to cultured human intestinal epithelial cells and inhibition of enteropathogen-cell interactions. *Appl Environ Microbiol* 1993; **59**: 4121-4128
- Fujiwara S, Hashiba H, Hirota T, Forstner JF. Proteinaceous factor(s) in culture supernatant fluids of bifidobacteria which prevents the binding of enterotoxigenic *Escherichia coli* to gangliosylceramide. *Appl Environ Microbiol* 1997; **63**: 506-512
- Fujiwara S, Hashiba H, Hirota T, Forstner JF. Purification and characterization of a novel protein produced by *Bifidobacterium longum* SBT2928 that inhibits the binding of enterotoxigenic *Escherichia coli* Pb176 (CFA/II) to gangliosylceramide. *J Appl Microbiol* 1999; **86**: 615-621
- Zheng YJ, Pan LJ, Wang LS, Zhou DY, Guo LA, Yan Z. Purified of bifidobacterium adhesin. *Chin J Microbiol Immunol* 1999; **19**: 196
- Zheng YJ, Pan LJ, Ye GA, Zhou DY. Competitive inhibition of adherence of EPEC and ETEC to intestinal epithelial by human Bifidobacterial strains. *Chin J Microbiol* 1999; **11**: 329-331
- Tuomola EM, Ouwehand AC, Salminen SJ. The effect of probiotic bacteria on the adhesion of pathogens to human intestinal mucus. *FEMS Immunol Med Microbiol* 1999; **26**: 137-142
- Coconnier MH, Klaenhammer TR, Kerneis S, Bernet MF, Servin AL. Protein-mediated adhesion of *Lactobacillus acidophilus* BG2FO4 on human enterocyte and mucus-secreting cell lines in culture. *Appl Environ Microbiol* 1992; **58**: 2034-2039
- Cotter PA, Miller JF. Triggering bacterial virulence. *Science* 1996; **273**: 1183-1184
- Rycroft CE, Fooks LJ, Gibson GR. Methods for assessing the potential of prebiotics and probiotics. *Curr Opin Clin Nutr Metab Care* 1999; **2**: 481-484
- Shu Q, Gill HS. A dietary probiotic (*Bifidobacterium lactis* HNO19) reduces the severity of *Escherichia coli* O157: H7 infection in mice. *Med Microbiol Immunol* 2001; **189**: 147-152
- Madsen KL. The use of probiotics in gastrointestinal disease. *Can J Gastroenterol* 2001; **15**: 817-822
- Bai AP, Ouyang Q, Zhang W, Wang CH, Li SF. Probiotics inhibit TNF- α -induced interleukin-8 secretion of HT29 cells. *World J Gastroenterol* 2004; **10**: 455-457
- Zheng YJ, Pan LJ, Ye GA, Zhou DY. Study on the adherence of human Bifidobacteria to cultured human intestinal epithelial cells. *Chin J Microbiol Immunol* 1997; **17**: 85-87
- Fujiwara S, Hashiba H, Hirota T, Forstner JF. Inhibition of the binding of enterotoxigenic *Escherichia coli* Pb176 to human intestinal epithelial cell line HCT-8 by an extracellular protein fraction containing BIF of *Bifidobacterium longum* SBT2928: suggestive evidence of blocking of the binding receptor gangliosylceramide on the cell surface. *Int J Food Microbiol* 2001; **67**: 97-106
- Clyne M, Drumm B. Adherence of *Helicobacter pylori* to the gastric mucosa. *Can J Gastroenterol* 1997; **11**: 243-248
- Drudy D, O'Donoghue DP, Baird A, Fenelon L, O'Farrelly C. Flow cytometric analysis of *Clostridium difficile* adherence to human intestinal epithelial cells. *J Med Microbiol* 2001; **50**: 526-534
- Madsen K, Cornish A, Soper P, Mckaigney C, Jijon H, Yachimec C, Doyle J, Jewell L, De Simone C. Probiotic bacteria enhance murine and human intestinal epithelial barrier function. *Gastroenterology* 2001; **121**: 580-591

Blockage of transforming growth factor β receptors prevents progression of pig serum-induced rat liver fibrosis

Wei Jiang, Chang-Qing Yang, Wen-Bin Liu, Yi-Qing Wang, Bo-Ming He, Ji-Yao Wang

Wei Jiang, Chang-Qing Yang, Wen-Bin Liu, Yi-Qing Wang, Bo-Ming He, Ji-Yao Wang, Department of Gastroenterology, Zhongshan Hospital, Fudan University, Shanghai 200032, China

Correspondence to: Professor Ji-Yao Wang, Department of Gastroenterology, Zhongshan Hospital, Fudan University, Shanghai 200032, China. jiyao_wang@hotmail.com

Telephone: +86-21-64041990 Ext 2420 **Fax:** +86-21-34160980

Received: 2003-08-26 **Accepted:** 2003-10-29

CONCLUSION: Antisense T β R I and T β R II recombinant plasmids have certain reverse effects on liver fibrosis and can be used as possible candidates for gene therapy.

Jiang W, Yang CQ, Liu WB, Wang YQ, He BM, Wang JY. Blockage of transforming growth factor β receptors prevents progression of pig serum-induced rat liver fibrosis. *World J Gastroenterol* 2004; 10(11): 1634-1638

<http://www.wjgnet.com/1007-9327/10/1634.asp>

Abstract

AIM: To test the hypothesis that introduction of antisense T β R I and T β R II eukaryotic expressing plasmids into a rat model of immunologically induced liver fibrosis might block the action of TGF- β_1 and halt the progression of liver fibrosis.

METHODS: RT-Nest-PCR and gene recombination techniques were used to construct rat antisense T β R I and T β R II recombinant plasmids which could be expressed in eukaryotic cells. The recombinant plasmids and empty vector (pcDNA3) were encapsulated by glycosyl-poly-L-lysine and then transduced into rats of pig serum-induced liver fibrosis model. Expression of exogenously transfected gene was assessed by Northern blot, and hepatic expressions of T β R I and T β R II were evaluated by RT-PCR and Western blot. We also performed ELISA for serum TGF- β_1 , hydroxyproline of hepatic tissues, immunohistochemistry for collagen types I and III, and VG staining for pathological study of the liver tissues.

RESULTS: The exogenous antisense T β R I and T β R II plasmids could be well expressed *in vivo*, and block mRNA and protein expression of T β R I and T β R II in the fibrotic liver at the level of mRNA respectively. These exogenous plasmid expressions reduced the level of TGF- β_1 (antisense T β R I group 23.998 \pm 3.045 ng/mL, antisense T β R II group 23.156 \pm 3.131 ng/mL, disease control group 32.960 \pm 3.789 ng/mL; $F=38.19, 36.73, P<0.01$). Compared with disease control group, the contents of hepatic hydroxyproline (antisense T β R I group 0.169 \pm 0.015 mg/g liver, antisense T β R II group 0.167 \pm 0.009 mg/g liver, disease control group 0.296 \pm 0.026 mg/g liver; $F=14.39, 15.48, P<0.01$) and the deposition of collagen types I and III decreased in the two antisense treatment groups (antisense T β R I group, collagen type I 669.90 \pm 50.67, collagen type III 657.29 \pm 49.48; antisense T β R II group, collagen type I 650.26 \pm 51.51, collagen type III 661.58 \pm 55.28; disease control group, collagen type I 1209.44 \pm 116.60, collagen type III 1175.14 \pm 121.44; $F=15.48$ to $74.89, P<0.01$). Their expression also improved the pathologic classification of liver fibrosis models (compared with disease control group, $\chi^2=17.14, 17.24, P<0.01$). No difference was found in the level of TGF- β_1 , the contents of hepatic hydroxyproline and collagen types I and III and pathologic grade between pcDNA3 control group and disease control group or between the two antisense treatment groups ($F=0.11$ to $1.06, \chi^2=0.13$ to $0.16, P>0.05$).

INTRODUCTION

Liver fibrosis is a common sequel to diverse liver injuries. In the formation of liver fibrosis and cirrhosis, synthesis of collagen increases and its degradation decreases. It has been thought that liver fibrosis can be reversed and liver cirrhosis is irreversible^[1-5]. Profound studies have been conducted on the treatment of liver fibrosis. However, this disease is still lack of efficient therapy^[6-11]. Searching for a new therapy seems very important.

In the formation of liver fibrosis and cirrhosis, many cytokines produce marked effects through autocrine and paracrine^[1,2,5]. Molecular mechanisms involved in fibrogenesis reveal that transforming growth factor β (TGF- β), especially TGF- β_1 , plays a pivotal role^[12-16]. Signaling by TGF- β occurs through a family of transmembranes and ser/thr kinase receptors. Both components of the receptor complex, known as receptor I (T β R I) and receptor II (T β R II) are essential for signal transduction^[17,18]. So in theory, blockage of TGF- β signal transduction by inhibiting the expression of T β R I and/or T β R II may have therapeutic effects on liver fibrosis.

At present, gene therapy for liver fibrosis targeting TGF- β mainly includes inhibiting the expression of TGF- β_1 (for instance, antisense TGF- β_1 RNA) and using deficient T β R II^[19-21]. But therapeutic researches which target T β R I or use antisense T β R II as a therapeutic tool have not been reported. In the present experiments, we constructed antisense T β R I and T β R II eukaryotic expressing plasmids and performed *in vivo* transfection. We aimed to test the hypothesis that introduction of these two exogenous plasmids into a rat model of immunologically induced liver fibrosis might block the action of TGF- β_1 and halt the progression of liver fibrosis.

MATERIALS AND METHODS

Construction of recombinant plasmid

Nested primers were designed and synthesized according to rat T β R I and T β R II cDNA sequences (GenBank)^[22,23]. The length of amplified PCR products was anticipated to be 470 bp, 606 bp (Table 1). Total RNA was extracted from normal rat liver with Trizol reagent (GIBCO, USA) according to the manufacturer's directions. RT-Nest-PCR was used to construct T β R I and T β R II cDNA fragments. Samples were heated at 94 °C for 7 min and subjected to 32 PCR cycles of denaturation at 94 °C for 1 min, annealing at 55 °C for 1 min, extension at 72 °C for 1 min, followed by a final extension at 72 °C for 5 min. After separation, reclaim and purification, the PCR products of T β R I and T β R II were

connected with T vector (Promega, USA) and then transferred into JM-109 strain. PT/ T β R I and PT/ T β R II were successfully constructed after IPTG/X-gal screening. The target fragments were cut and inserted reversely into eukaryotic expressing plasmid pcDNA3 (Invitrogen, CA), and then transferred into JM-109 strain again. By using enzyme-cutting identification (T β R I: *EcoRI* and *XhoI*; T β R II: *EcoRI* and *BamHI*) and DNA autosequencing (PE377 Auto sequencer, USA), the successful constructions of antisense T β R I and T β R II eukaryotic expressing plasmids were proved (Figure 1).

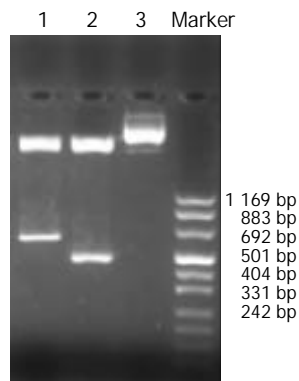


Figure 1 Enzyme-cutting identification of the recombinant plasmids, Lane 1: pANTI-RII, Lane 2: pANTI-RI, Lane 3: pcDNA3.

Table 1 Primer pairs for PCR reactions

RI 1: 5' ACAGGCGCAAACAGTGGCAG 3' (18-33)
RI 2: 5' AGTCTCGTAGACAATGGTCC 3' (643-661)
RI 3: 5' TTCACCTCGAGAGTGGCAGCGGGACC 3' (25-39)
<i>Xho I</i>
RI 4: 5' CTACCGAATTCTGGACCATCAGCATAAG 3' (456-470)
<i>Eco R I</i>
RII 1: 5' TTCATAGGCTCGGTTCCGGG 3' (199-213)
RII 2: 5' GCAGTTGTCGCTGAAATCCA 3' (882-901)
RII 3: 5' AACATGAATTCGGTCTATGACGAGCG 3' (227-241)
<i>Eco R I</i>
RII 4: 5' ACAATGGATCCGAAGATGGCAATGACAG 3' (795-811)
<i>BamH I</i>

Experimental protocols

Forty-six male Sprague-Dawley rats (weighing 100 to 120 g) provided by Experimental Animal Center, Zhongshan Hospital, Fudan University, were randomly divided into the following 5 groups: 10 in experimental liver fibrosis model induced by pig-serum as disease control group (M), 10 in antisense T β R I plasmid transfection as treatment group (A), 10 in antisense T β R II plasmid transfection as treatment group (B), 10 in pcDNA3 transfection as pcDNA3 control group (C) and 6 in normal control group (N). Animals in the normal control group received 0.5 mL of NS twice weekly by intraperitoneal injection for 8 wk. Rats in the other 4 groups received 0.5 mL of pig-serum twice weekly by intraperitoneal injection for 8 wk^[24]. Among groups A, B and C, the recombinant antisense T β R I and T β R II plasmids and empty vector (pcDNA3) of 100 μ g each time were encapsulated by glycosyl-poly-L-lysine (G-PLL) and then transduced into rats of liver fibrosis model via caudal vein every 2 wk respectively. The molecular ratio of galactose and poly-L-lysine was 15:28 and the average molecular weight of G-PLL was 8.5 ku. All experimental rats were sacrificed at the end of the 8th wk. The middle lobes of the livers were removed and specimens were fixed in Carnoy's fixative (glacial acetic acid, chloroform, and ethanol at a volume ratio of 1:3:6) and

then embedded in paraffin for histological analysis. The remaining tissue was quickly partitioned and immediately stored in liquid nitrogen and then frozen below -70 °C. After that the rats were humanely killed.

RNA isolation and Northern blot analysis for exogenous gene and hepatic T β R I and T β R II expression

For Northern blot analysis, 30 μ g of total tissue RNAs was separated by electrophoresis on a 1% denaturing agarose gel, transferred to a Hybond-N membrane (Amersham, UK) and fixed by baking for 2 h at 80 °C. The probe for pcDNA3 according to its special T7 promoter sequence (the oligonucleotide fragment: 5'-CAGAGGGATATCACTCAGCATAAT-3'), which was to detect exogenous gene expression, was labeled with [α -³²P]dATP using DNA tailing kit (Roche, Germany). T β R I and T β R II cDNA probes were labeled with [α -³²P]dCTP using a high prime DNA labeling kit (Roche, Germany) to detect rat T β R I and T β R II expression. Blots were pre-hybridized for at least 3 h at 42 °C, and then hybridized for 20 h at 42 °C. Auto radiographs were exposed for indicated times to Kodak films at -70 °C for 7 d. As an internal standard (loading control) the blots were re-hybridized with [α -³²P] β -actin.

RT-PCR analysis for T β R I and T β R II mRNA expression

Total RNA of 1 μ g from each sample was reversely transcribed and amplified using an RT-PCR kit (ShengNeng-BoCai Biotechnology Co. Shanghai, China). The RT-PCR reaction contained 12.5 pmol each primer (T β R I: sense sequence 5' - TCACTAGATCGCCCTTTCAT-3' ; antisense sequence 5' - GATAATCCGACACCAACCAC-3' , a product of 355 bp; T β R II: sense sequence 5' -CCACGACCCCAAGTTCACCT-3' , antisense sequence 5' -TGGGCAGCAGTTCGGTATTG-3' , a product of 428 bp) for detecting the T β R I and T β R II mRNA expression in rat liver tissues. Additionally primer pairs (sense sequence 5' - TGGGACGATATGGAGAAGAT -3' ; antisense sequence 5' - ATTGCCGATAGTGATGACCT -3') were used for amplifying the expression of β -actin (a product of 521 bp) as internal control. Samples were placed in a thermocycler with the incubation program at 37 °C for 60 min, at 90 °C for 5 min, then 30 cycles at 94 °C for 45 s, at 54 °C for 45 s, and at 72 °C for 1 min, and a final extension at 72 °C for 5 min. Products of RT-PCR were electrophoresed on a 20 g/L agarose gel to show the amplified bands. The areas under curve of the bands were calculated by Photo-Treater (Tanon GIS-1000, China). The ratio of the objective band and β -actin (control) represented the relative value of expression of the objective band.

Western blot for hepatic T β R I and T β R II expression

Lysates from 50 mg rat liver tissues were prepared with RIPA buffer [1 \times PBS, 10 g/L NP40, 5 g/L sodium deoxycholate, 1 g/L SDS, 10 mmol/L PMSF (in isopropanol), 36 μ g/mL aprotinin and 1mmol/L sodium orthovanadate]. Tissue lysates were centrifuged at 3000 r/min for 10 min at 4 °C, and protein concentrations were determined by BCA protein assay (Pierce, IL). Protein samples (100 μ g) were heated for 5 min at 100 °C and separated on 120 g/L SDS-PAGE and then transferred to PVDF membranes (Schleicher&Schuell, Germany) in Tris-glycine buffer (pH 8.5) plus 200 mL/L methanol. The membranes were blocked overnight in 50 mL/L non-fat dried milk in Tris-buffer containing 1 g/L Tween-20 and then washed with Tris-buffer. The blots were incubated overnight at 4 °C with rabbit T β R I, T β R II and β -actin polyclonal IgG (Santa Cruz, USA) diluted 1:200 in Tris-buffer. The blots were washed and then incubated with AP-conjugated secondary antibodies (Santa Cruz, USA) at 1:500 dilution for 2 h at room temperature. The protein bands were visualized with BCIP/NBT (DAKO, USA) system.

ELISA assay of serum TGF- β_1

Assay of serum TGF- β_1 content was performed with double antibody ABC-ELISA method according to the previous reports of Ueno *et al.*^[21] and Roth *et al.*^[25].

Hepatic hydroxyproline (OH-Pro) content

Hydroxyproline content was determined by the previous method with some modification^[26]. A total of 500 mg of liver tissues was hydrolyzed in 6 mol/L HCl solution at 120 °C for 24 h. The hydroxyproline content of the liver was expressed as micrograms per gram of wet weight.

Immunohistochemistry of hepatic collagen types I and II

After dewaxed with xylene and rehydrated through a graded alcohol series, sections were digested with 4 g/L trypsin. The sections were incubated with rabbit polyclonal antibodies against types I or II collagen (diluted 1:100) at 37 °C for 60 min and then overnight at 4 °C. Then the sections were incubated with Envision™ secondary antibodies of biotinylated sheep anti-rabbit IgG (DAKO, USA) at 37 °C for 30 min and then with the substrate solution (3,3'-diaminobenzidine tetrahydrochloride in H₂O₂ in Tris buffer pH 7.4) for 10 min, followed by counterstaining with hematoxylin. The sections were washed 3 times with 0.01 mol/L PBS (pH 7.4) after each step. For control staining, PBS was used instead of the primary antibody. The slides were then analyzed with an image analyzing system (LeiCA-Q500IW System, Germany) to obtain the integral light density and the average area of positive staining. The multiplication of both parameters represented the relative contents of hepatic collagen types I and II.

Histology

Sections from paraffin-embedded blocks were dewaxed and stained with Van Gieson method. Fibrosis was scored according to the classification which graded liver fibrosis into seven degrees (0-VI).

Statistical analysis

All values were expressed as mean±SD. Differences between groups were analyzed by one-way ANOVA (SPSS10.0 software) and the pathological grading of fibrosis of each group was analyzed by trend analysis and chi-square test (EPI5.0 software). $P < 0.05$ was considered statistically significant.

RESULTS

General situation of animals

No animal died during the experimental period. No significant difference was found in the levels of ALT (51±9 U/L vs 53±8 U/L) and Cr (91±13 μmol/L vs 92±14 μmol/L) between pcDNA3 control group and disease control group ($P > 0.05$). No significant difference was found in the height or weight of rats among antisense TβR I, antisense TβR II and pcDNA3 control groups ($P > 0.05$).

Expression of exogenous gene and TβR I, TβR II gene in liver tissues by Northern blot

The exogenous gene expression could be detected in transfection groups (antisense TβR I, antisense TβR II and pcDNA3 control groups) by Northern blot, but not in disease control group (Figure 1). The expression of TβR I mRNA was much higher in pcDNA3 control group and disease control group than in antisense TβR I group. The expression of TβR II was also much higher in pcDNA3 control group and disease control group than in antisense TβR II group at mRNA level (Figure 2).

Hepatic TβR I and TβR II mRNA expression by RT-PCR

The expression of antisense TβR I RNA induced a decreased mRNA level of TβR I in antisense TβR I group (1.039±0.110)

compared with pcDNA3 control group (1.453±0.112) and disease control group (1.472±0.099) ($P < 0.01$). The expression of antisense TβR II RNA also induced a decreased mRNA level of TβR II in antisense TβR II group (0.805±0.105) compared with pcDNA3 control group (1.743±0.151) and disease control group (1.798±0.139) ($P < 0.01$). No difference was found in the level of TβR I and TβR II mRNA between pcDNA3 control and disease control groups ($P > 0.05$).

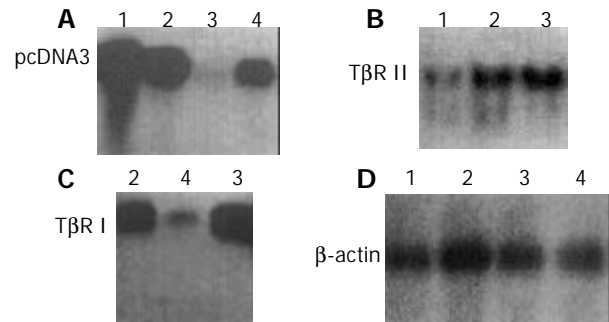


Figure 2 Expression of exogenous transfected gene assessed by Northern blot, A: Hybridization using ³²P labeled oligonucleotide probe which targets T7 promoter; B: Hybridization by using ³²P labeled TβR II cDNA probe; C: Hybridization by using ³²P labeled TβR I cDNA probe; D: β-actin probe used as control. Lane 1: Antisense TβR II group; Lane 2: pcDNA3 control group; Lane 3: Disease control group; Lane 4: Antisense TβR I group.

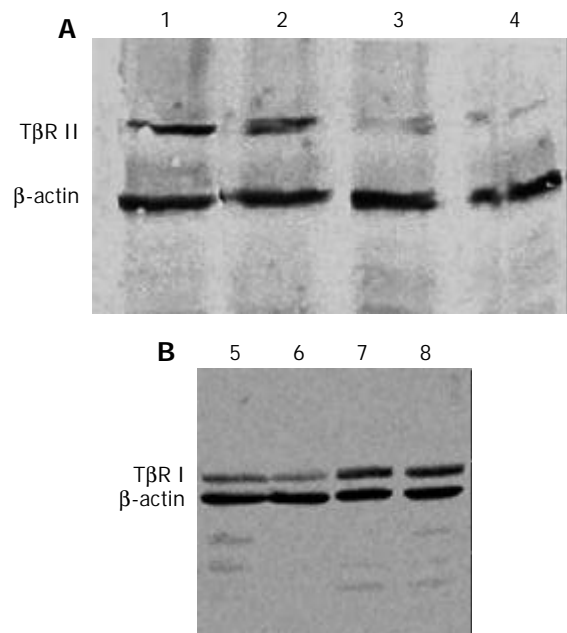


Figure 3 Hepatic protein expression of TβR I, TβR II assessed by Western blot, A: Hepatic protein expression of TβR II; B: Hepatic protein expression of TβR I; Lanes 1,8: Disease control group; Lanes 2,7: pcDNA3 control group; Lane 3: Antisense TβR II group; Lanes 4,6: Normal control group; Lane 5: Antisense TβR I group.

Hepatic TβR I and TβR II protein expression by Western blot

The expression of TβR I protein was decreased in antisense TβR I group and the expression of TβR II protein was also decreased in antisense TβR II group when compared with pcDNA3 control group and disease control group, but they were still slightly higher than those in normal control group. The expressions of TβR I and TβR II protein in pcDNA3 control group were similar to those in disease control group (Figure 3).

Table 2 Effects of transfected plasmid on the content of hepatic hydroxyproline and deposition of collagen types I and III (mean \pm SD)

Group	Number	Hydroxyproline (mg/g liver)	Collagen I	Collagen III
Disease control group	10	0.296 \pm 0.026 ^d	1 209.44 \pm 116.60 ^d	1 175.14 \pm 121.44 ^d
Antisense T β R II group	10	0.167 \pm 0.009 ^{bd}	650.26 \pm 51.51 ^{bd}	661.58 \pm 55.28 ^{bd}
Antisense T β R I group	10	0.169 \pm 0.015 ^d	669.90 \pm 50.67 ^d	657.29 \pm 49.48 ^d
pcDNA3 control group	10	0.284 \pm 0.025 ^d	1 205.70 \pm 110.11 ^d	1 149.89 \pm 91.61 ^d
Normal control group	6	0.128 \pm 0.004	449.33 \pm 35.95	421.15 \pm 20.15

^b*P*<0.01 vs disease control group and pcDNA3 control group, ^d*P*<0.01 vs normal control group.

Table 3 Pathological grade of liver fibrosis at the 8th week

Group	Grade						Total	
	0	I	II	III	IV	V		VI
Disease control group ^d	0	0	0	1	4	4	1	10
Antisense T β R II group ^{db}	1	7	2	0	0	0	0	10
Antisense T β R I group ^{db}	1	6	3	0	0	0	0	10
pcDNA3 control group ^d	0	0	0	1	5	3	1	10
Normal control group	6	0	0	0	0	0	0	6

^b*P*<0.01 vs disease control group and pcDNA3 control group, ^d*P*<0.01 vs normal control group.

ELISA assay of serum TGF- β_1

The level of serum TGF- β_1 was reduced in antisense T β R I group (23.998 \pm 3.045 ng/mL) and antisense T β R II group (23.156 \pm 3.131 ng/mL) compared with pcDNA3 control group (32.275 \pm 1.884 ng/mL) and disease control group (32.960 \pm 3.789 ng/mL), but was still higher than that in normal control group (14.338 \pm 2.421 ng/mL) (*P*<0.01). No significant difference was found between antisense T β R I and antisense T β R II groups (*P*>0.05).

Effects of antisense T β R I and T β R II plasmid transfection on hepatic hydroxyproline and collagen types I and II content

The hepatic hydroxyproline content and the accumulation of hepatic collagen types I and III in antisense T β R I and antisense T β R II groups were significantly decreased compared with disease control and pcDNA3 control groups (*P*<0.01). No statistical difference was found between pcDNA3 control and disease control groups or between antisense T β R I and antisense T β R II groups (*P*>0.05). Hepatic hydroxyproline content and accumulation of collagen in these four groups were significantly higher than those in normal control group (*P*<0.01) (Table 2).

Effects of transfected plasmid on patho-histology

The fibrosis grade of antisense T β R I and antisense T β R II groups alleviated significantly compared with disease control and pcDNA3 control groups (*P*<0.01). All these four groups had significantly higher fibrosis grades when compared to normal control group (*P*<0.01). No significant difference was found between disease control and pcDNA3 control groups or between antisense T β R I and antisense T β R II groups (*P*>0.05) (Table 3).

DISCUSSION

Pig serum-induced rat hepatic fibrosis is a model that shows an intense immune response to the administration of heterologous serum. Histologically, the changes were characterized by mononuclear cell infiltration and fibrotic response in the periportal area, followed by the septum formation connecting portal tract with central veins without hepatocyte injury^[24].

In the formation of liver fibrosis and cirrhosis, a number of cytokines could produce marked effects through autocrine and

paracrine^[25,26]. Molecular mechanisms involved in fibrogenesis revealed that transforming growth factor β (TGF- β), especially TGF- β_1 , played a pivotal role in the regulation of the production, degradation and accumulation of extracellular matrix (ECM)^[1,21,27]. Secreted as a latent precursor, TGF- β is activated at sites of injury. Active TGF- β binds to specific, high-affinity receptors present on most cells, initiating a signaling cascade that results in biological effects. Signaling by TGF- β occurs through a family of transmembranes and ser/thr kinase receptors. Both components of the receptor complex, known as receptor I (T β R I) and receptor II (T β R II) are essential for signal transduction. Signaling is initiated by binding of TGF- β to the T β R II. Once bound, the TGF- β / T β R II complex then recruits T β R I into a heteromeric complex. Within the heteromeric complex, the kinase domain of type II receptor could transphosphorylate and activate type I receptor kinase, which then functioned to propagate the signal to downstream targets^[21-23]. At present, gene therapy for liver fibrosis targeting TGF- β receptor mainly used adenoviral vectors expressing a dominant-negative type II TGF- β receptor or an adenovirus expressing an entire ectodomain of human TGF- β type II receptor fused to Fc portion of human IgG to block the TGF- β signal transduction^[19,21].

Antisense technique has been used to inhibit the target genes and proteins expressed in experimental rat hepatic fibrosis^[7]. We used RT-Nest-PCR and gene recombination techniques to construct rat antisense T β R I and T β R II recombinant plasmids successfully which could be expressed in eucaryotic cells. We transduced the exogenous plasmid into the fibrotic liver based on our previous research on gene target therapy. The exogenous antisense T β R I and T β R II recombinant plasmids were well expressed *in vivo*, and could block the mRNA and protein expression of T β R I and T β R II in the fibrotic liver induced by pig serum.

In our study, serum TGF- β_1 analysis showed the expression of TGF- β_1 was decreased after the expression of T β R I and T β R II was blocked. Our results were similar to the previous report that used deficient T β R II in treating experimental liver fibrosis. It was indicated that the production of active TGF- β_1 was inhibited after the expression of TGF- β receptors was blocked and the signal transduction of TGF- β was also inhibited.

Collagen types I and III constitute the main components of increased ECM in liver fibrosis. It has been proposed that degradation of collagen types I and III is very important in the

reversion of liver fibrosis^[5,28,29]. In our study, the recombinant plasmid could be delivered to liver by G-PLL and expressed in the tissue of liver. In addition, there was a significant decrease of collagen deposition after the recombinant antisense T β R I and T β R II plasmids was transduced into fibrotic liver through measuring the hepatic hydroxyproline content and immunohistochemistry of collagen types I and III. This suggested that the recombinant plasmids could increase the degrading capacity of collagen types I and III, decrease the deposition of ECM, and probably reverse hepatic fibrosis. In the data analysis, there was a significant difference in fibrosis grades between the disease control group and the recombinant plasmid transfected group. It showed that the antisense T β R I and T β R II plasmids had significant ameliorative effects on liver fibrosis.

No difference was found in the level of TGF- β ₁, the contents of hepatic hydroxyproline and collagen types I and III and the pathologic grade between empty plasmid control and disease control groups or between the two antisense treatment groups. It indicated that the signal transduction of TGF- β could be inhibited by blocking the expression of either T β R I or T β R II and the effects of antisense T β R I and antisense T β R II plasmids on experimental liver fibrosis were similar. Both T β R I and T β R II were essential for signal transduction.

In summary, our results demonstrate that TGF- β ₁ plays an important role in liver fibrosis development especially in degradation of collagens. Antisense T β R I and antisense T β R II recombinant plasmids have certain reverse effects on liver fibrosis and could be used as possible candidates for gene therapy. As a new therapeutic means, gene therapy has a long way to go, especially in transductive efficiency, gene targeting, stability and adverse effects.

REFERENCES

- 1 **Alcolado R**, Arthur MJ, Iredale JP. Pathogenesis of liver fibrosis. *Clin Sci* 1997; **92**: 103-112
- 2 **Olaso E**, Friedman SL. Molecular regulation of hepatic fibrogenesis. *J Hepatol* 1998; **29**: 836-847
- 3 **Huang ZG**, Zhai WR, Zhang YE, Zhang XR. Study of heteroserum-induced rat liver fibrosis model and its mechanism. *World J Gastroenterol* 1998; **4**: 206-209
- 4 **Benyon RC**, Iredale JP. Is liver fibrosis reversible? *Gut* 2000; **46**: 443-446
- 5 **Neubauer K**, Saile B, Ramadori G. Liver fibrosis and altered matrix synthesis. *Can J Gastroenterol* 2001; **15**: 187-193
- 6 **Lieber CS**. Prevention and treatment of liver fibrosis based on pathogenesis. *Alcohol Clin Exp Res* 1999; **23**: 944-949
- 7 **Rockey DC**. Gene therapy for hepatic fibrosis-bringing treatment into the new millennium. *Hepatology* 1999; **30**: 816-818
- 8 **Cheng ML**, Wu YY, Huang KF, Luo TY, Ding YS, Lu YY, Liu RC, Wu J. Clinical study on the treatment of liver fibrosis due to hepatitis B by IFN-alpha1 and traditional medicine preparation. *World J Gastroenterol* 1999; **5**: 267-269
- 9 **Wang LT**, Zhang B, Chen JJ. Effect of anti-fibrosis compound on collagen expression of hepatic cells in experimental liver fibrosis of rats. *World J Gastroenterol* 2000; **6**: 877-880
- 10 **Du B**, You S. Present situation in preventing and treating liver fibrosis with TCM drugs. *J Tradit Chin Med* 2001; **21**: 147-152
- 11 **Murphy F**, Arthur M, Iredale J. Developing strategies for liver fibrosis treatment. *Expert Opin Investig Drugs* 2002; **11**: 1575-1585
- 12 **Bachem MG**, Meyer D, Melchior R, Sell KM, Gressner AM. Activation of rat liver perisinusoidal lipocytes by transforming growth factors derived from myofibroblastlike cells. A potential mechanism of self perpetuation in liver fibrogenesis. *J Clin Invest* 1992; **89**: 19-27
- 13 **Okuno M**, Moriwaki H, Imai S, Muto Y, Kawada N, Suzuki Y, Kojima S. Retinoids exacerbate rat liver fibrosis by inducing the activation of latent TGF-beta in liver stellate cells. *Hepatology* 1997; **26**: 913-921
- 14 **Pinzani M**, Marra F, Carloni V. Signal transduction in hepatic stellate cells. *Liver* 1998; **18**: 2-13
- 15 **Friedman SL**. Molecular regulation of hepatic fibrosis, an integrated cellular response to tissue injury. *J Biol Chem* 2000; **275**: 2247-2250
- 16 **Bissell DM**, Roulot D, George J. Transforming growth factor β and the liver. *Hepatology* 2001; **34**: 859-867
- 17 **Wrana JL**, Attisano L, Wieser R, Ventura F, Massague J. Mechanism of activation of the TGF-beta receptor. *Nature* 1994; **370**: 341-347
- 18 **Willis SA**, Zimmerman CM, Li LI, Mathews LS. Formation and activation by phosphorylation of activin receptor complexes. *Mol Endocrinol* 1996; **10**: 367-379
- 19 **Qi Z**, Atsuchi N, Ooshima A, Takeshita A, Ueno H. Blockade of type beta transforming growth factor signaling prevents liver fibrosis and dysfunction in the rat. *Proc Natl Acad Sci U S A* 1999; **96**: 2345-2349
- 20 **Lin JS**, Song YH, Kong XJ, Li B, Liu NZ, Wu XL, Jin YX. Preparation and identification of anti-transforming growth factor beta1 U1 smallnuclear RNA chimeric ribozyme *in vitro*. *World J Gastroenterol* 2003; **9**: 572-577
- 21 **Ueno H**, Sakamoto T, Nakamura T, Qi Z, Atsuchi N, Takeshita A, Shimizu K, Ohashi H. A soluble transforming growth factor beta receptor expressed in muscle prevents liver fibrogenesis and dysfunction in rats. *Hum Gene Ther* 2000; **11**: 33-42
- 22 **Choi ME**, Kim EG, Huang Q, Ballermann BJ. Rat mesangial cell hypertrophy in response to transforming growth factor-beta 1. *Kidney Int* 1993; **44**: 948-958
- 23 **Bassing CH**, Yingling JM, Howe DJ, Wang T, He WW, Gustafson ML, Shah P, Donahoe PK, Wang XF. A transforming growth factor beta type I receptor that signals to activate gene expression. *Science* 1994; **263**: 87-89
- 24 **Tsukamoto H**, Matsuoka M, French SW. Experimental models of hepatic fibrosis: a review. *Semin Liver Dis* 1990; **10**: 56-65
- 25 **Roth S**, Schurek J, Gressner AM. Expression and release of the latent transforming growth factor β binding protein by hepatocytes from rat liver. *Hepatology* 1997; **25**: 1398-1405
- 26 **Sakaida I**, Hironaka K, Uchida K, Suzuki C, Kayano K, Okita K. Fibrosis accelerates the development of enzyme-altered lesions in the rat liver. *Hepatology* 1998; **28**: 1247-1252
- 27 **Takiya S**, Tagaya T, Takahashi K, Kawashima H, Kamiya M, Fukuzawa Y, Kobayashi S, Fukatsu A, Katoh K, Kakumu S. Role of transforming growth factor β ₁ on hepatic regeneration and apoptosis in liver diseases. *J Clin Pathol* 1995; **48**: 1093-1097
- 28 **Branch AD**. A hitchhiker's guide to antisense and nonantisense biochemical pathways. *Hepatology* 1996; **24**: 1517-1529
- 29 **Brenner DA**, Waterboer T, Choi SK, Lindquist JN, Stefanovic B, Burchardt E, Yamauchi M, Gillan A, Rippe RA. New aspects of hepatic fibrosis. *Hepatology* 2000; **32**(1 Suppl): 32-38

Edited by Zhu LH and Wang XL Proofread by Xu FM

Imaging diagnosis of 12 patients with hepatic tuberculosis

Ri-Sheng Yu, Shi-Zheng Zhang, Jian-Jun Wu, Rong-Fen Li

Ri-Sheng Yu, Jian-Jun Wu, Rong-Fen Li, Department of Radiology, Second Affiliated Hospital, Zhejiang University School of Medicine, Hangzhou 310009, Zhejiang Province, China

Shi-Zheng Zhang, Department of Radiology, Sir Run Run Shaw Hospital, Zhejiang University School of Medicine, Hangzhou 310009, Zhejiang Province, China

Correspondence to: Dr. Ri-Sheng Yu, Department of Radiology, the Second Affiliated Hospital, Zhejiang University School of Medicine, Hangzhou 310009, Zhejiang Province, China. yurisheng2003@yahoo.com.cn

Telephone: +86-571-87783860 **Fax:** +86-571-87783804

Received: 2003-08-30 **Accepted:** 2003-10-22

Abstract

AIM: To assess CT, MR manifestations and their diagnostic value in hepatic tuberculosis.

METHODS: CT findings in 12 cases and MR findings in 4 cases of hepatic tuberculosis proved by surgery or biopsy were retrospectively analyzed.

RESULTS: (1) CT findings: One case of serohepatic type of hepatic tuberculosis had multiple-nodular lesions in the subcapsule of liver. Parenchymal type was found in 10 cases, including multiple, miliary, micronodular and low-density lesions with miliary calcifications in 2 cases; singular, low-density mass with multiple flecked calcifications in 3 cases; multiple cystic lesions in 1 case; multiple micronodular and low-density lesions fusing into multiloculated cystic mass or "cluser" sign in 3 cases; and singular, macronodular and low-density lesion with multiple miliary calcifications in 1 case. One case of tuberculous cholangitis showed marked dilated intrahepatic ducts with multiple flecked calcifications in the porta hepatis. (2) MR findings in 4 cases were hypointense on both T1-weighted imagings and T2-weighted imagings in one case, hypointense on T1-weighted imagings and hyperintense on T2-weighted imagings in 3 cases. Enhanced MR in 3 cases was slightly shown peripheral enhancement or with multilocular enhancement.

CONCLUSION: Various types of hepatic tuberculosis have different imaging findings, and typical CT and MR findings can suggest the diagnosis.

Yu RS, Zhang SZ, Wu JJ, Li RF. Imaging diagnosis of 12 patients with hepatic tuberculosis. *World J Gastroenterol* 2004; 10 (11): 1639-1642

<http://www.wjgnet.com/1007-9327/10/1639.asp>

INTRODUCTION

During the second half of the twentieth century, as a result of improved nutrition, reduced crowding, public health measures, and effective chemotherapy, a dramatic decrease in the incidence of tuberculosis was seen in the world^[1]. But in recent years, increased incidence of tuberculosis has been attributed to several causes, including AIDS epidemic, iv drug abuse and

increase in the number of immunocompromised patients^[2,3]. Hepatic tuberculosis is the most common manifestation of upper abdominal parenchymatous organ tuberculosis and its incidence has also been increasing.

Imaging features of hepatic tuberculosis have been described by several researchers at computed tomography (CT) and magnetic resonance imaging (MRI), the imaging appearance of these lesions is considered as nonspecific and, a histopathological or bacteriological confirmation is often required^[4-7].

The CT and MRI features of 12 patients with pathologically proven hepatic tuberculosis examined between 1984 and 1999 were analyzed retrospectively to improve the imaging diagnostic accuracy and differentiation of hepatic tuberculosis.

MATERIALS AND METHODS

Subjects

Of the 12 hepatic tuberculosis patients, 7 were male and 5 female, aged from 18 to 69 years (mean, 38.2 years). The diagnosis was proved by surgery (8 cases), liver biopsy (3 cases) and abdominoscopy (1 case). The duration of symptoms ranged from 1 to 18 mo. The most frequent clinical symptoms and signs were right upper abdominal pain ($n=10$), upper abdominal tenderness ($n=8$), low-grade fever ($n=8$), night sweat ($n=6$), weight-loss and fatigue ($n=5$), abdominal mass ($n=1$), hepatomegaly ($n=4$) and jaundice ($n=2$). Among the 12 cases, 4 were accompanied by extra-hepatic tuberculosis. Laboratory test showed anemia ($n=10$), raised erythrocyte sedimentation rate ($n=9$) and abnormal liver function ($n=7$). Tuberculin test was positive in 4 out of 5 patients tested. Eight patients were examined with ultrasound, but only 2 were correctly diagnosed. All the 12 patients had chest x-ray, and evidences of pulmonary tuberculosis were found in 2.

CT scanning

CT was performed with Siemens Somatom DR3 and HiQ units for the patients in routine fasting state. Some patients were given 500 mL of diluted iodinated contrast medium (10 g/L meglumine diatrizoate) orally 30 min before scanning. Scan scope ranged from the dome of diaphragm to the last plane of liver. All patients were examined with plain scanning at first and then using 600 g/L meglumine diatrizoate 60-80 mL for enhanced scanning with section thickness of 8-10 mm and interval of 10 mm.

MR scanning

MR was performed with a superconducting unit (Impact; Siemens, Germany) operating at a field strength of 1.0 T by using a body coil. The matrix size for data acquisition was 256×128, and a 6-10-mm section thickness with a section gap of 0-4-mm. Conventional fast spin-echo (TSE) included T1-weighted images (700/12 ms, TR/TE) and T2-weighted images (2 600-5 000/128-165 ms, TR/TE). If necessary, FLASH T1-weighted images with transverse angle of 70-75° were added. Post-contrast MRI was obtained on FLASH T1-weighted images and TSE T1-weighted images after 0.2 mmol/kg GD-DTPA. Some patients were examined by using T1-weighted imaging fat suppression.

RESULTS

CT findings of hepatic tuberculosis based on its pathologic classification

Serohepatic type One case of serohepatic type of hepatic tuberculosis had multiple-nodular hypodense lesions with slightly peripheral enhancement in the subcapsule of liver and thickened subcapsule of quadratus lobe on CT (Figure 1).

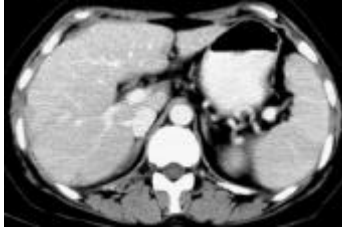


Figure 1 Serohepatic type: multiple-nodular hypodense lesions in the subcapsule of liver and thickened subcapsule of quadratus lobe on CT.

Parenchymal type Ten cases of parenchymal type of hepatic tuberculosis were divided into 3 subtypes: (1) Miliary tuberculosis ($n=2$): CT showed multiple, miliary, micronodular and low-density lesions with size ranging from 0.6 cm to 1.8 cm and no marked enhancement (Figure 2). Multiple miliary calcifications were found in 1 case. (2) Nodular tuberculosis ($n=7$): Nodule was more than 2.0 cm in diameter. Singular, slightly low-density (ranging from 34-42 Hu) lesions in liver were seen in 3 cases with multiple flecked calcifications in 2 cases (Figure 3), and with slightly peripheral enhancement in 2 cases, no marked enhancement in 1 case. Multi-nodular lesions were in 4 cases. One case of scattered multi-nodular lesions was two isolated cystic masses, with 23 Hu and 29 Hu respectively, and had no marked enhancement (Figure 4). Gathered multiple masses were found in the other 3 cases. CT revealed multiple micronodular and low-density lesions fusing into multiloculated cystic mass or "cluser" sign with multiloculated enhancement. (3) Mixed tuberculosis ($n=1$): CT demonstrated singular, macronodular and low-density lesion with slightly enhanced rim and multiple miliary calcifications (Figure 5).



Figure 2 Miliary tuberculosis: scattered distribution of multiple, miliary, micronodular and low-density lesions in liver.



Figure 3 Nodular tuberculosis: singular low-density mass with multiple flecked calcifications in the right lobe of liver and tuberculous lymphadenopathy encroaching on head of pancreas.

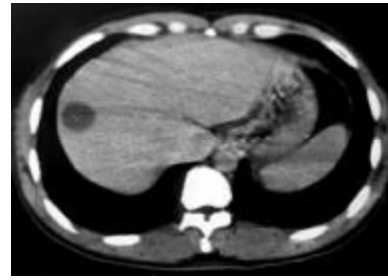


Figure 4 Nodular tuberculosis: cystic mass with 23 Hu in the right lobe of liver.

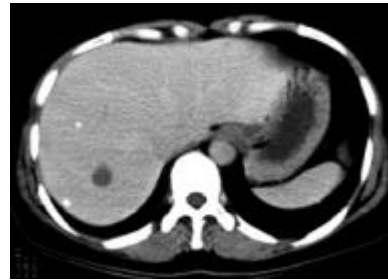


Figure 5 Mixed tuberculosis: singular, round-like and low-density lesion and multiple miliary calcifications in the right lobe of liver.

Tuberculous cholangitis One case of tuberculous cholangitis showed slightly diffuse hepatomegaly, marked dilated intrahepatic ducts, multiple calcificated lymph nodes in the porta hepatis and other regional distribution of lymph nodes in abdomen, and a large amount of hyperdense ascites. It was proved by surgery and pathology that tuberculosis of common hepatic duct involved left and right intrahepatic ducts and secondary marked dilated distant ducts. Lymph node tuberculosis and tuberculous peritonitis were also diagnosed pathologically.

MR findings

MR was performed in 4 patients. One case of serohepatic type of hepatic tuberculosis diagnosed on CT was reexamined with MR after therapy, showing multiple-nodular lesions with hypointense on T1-weighted images and hyperintense on T2-weighted images in the subcapsule of liver. The lesions had slightly peripheral enhancement after contrast administration. The other 3 cases were classified as parenchymal type of hepatic tuberculosis on CT, including miliary tuberculosis, mixed tuberculosis and nodular tuberculosis. Miliary tuberculosis showed multiple, miliary, micronodular lesions with hypointense on T1-weighted images and hyperintense on T2-weighted images. Mixed tuberculosis showed singular, macronodular lesion presented as a hypointense mass on both T1-weighted images and T2-weighted images (Figure 6) with peripheral enhancement. In this case, the lesion presented round-like on axial plane but irregular strip with multilocular enhancement on coronary and sagittal planes (Figure 7). Nodular tuberculosis revealed multiple micronodular lesions fusing into multiloculated cystic mass, which was hypointense on T1-weighted images and marked hyperintense on T2-weighted images, with multiloculated enhancement (Figure 8).

Abdominal extra-hepatic tuberculosis

Among the 12 cases, 4 had lymph node tuberculosis, showing enlarged lymph nodes, with ringed peripheral enhancement or calcifications in 2 cases respectively (Figure 3). Pancreatic tuberculosis, adrenal tuberculosis and tuberculous peritonitis were found in 1 case.



Figure 6 MR T2-weighted images showing singular, round-like hypointense lesion.

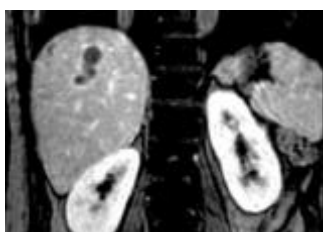


Figure 7 MRI showing irregular strip lesion with multilocular enhancement on coronary plane.

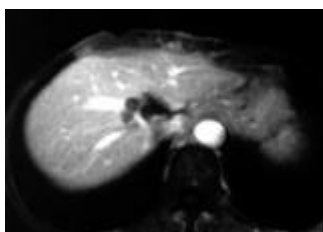


Figure 8 Enhanced MRI showing multiple micronodular lesions fusing into multiloculated cystic mass near the second porta hepatis.

DISCUSSION

Hepatic tuberculosis is considered to be a rare clinical entity. Unless there was a high index of suspicion, the diagnosis was often overlooked^[1,4]. Hepatic tuberculosis can be manifested by relatively nonspecific clinical presentation. The most frequent clinical symptoms and signs were right upper abdominal pain, upper abdominal tenderness, low-grade fever, night sweat, weight-loss and fatigue, abdominal mass, hepatomegaly and jaundice^[4,8,9]. Anemia, raised ESR, abnormal hepatic function and positive tuberculin test could be found in laboratory examinations.

Classification

Classification of hepatic tuberculosis has remained in dispute by now^[8-10]. The authors of this article considered it comprehensive and reasonable to classify hepatic tuberculosis into serohepatic type, parenchyma type and tuberculous cholangitis. In a sense, we do not agree that tuberculous cholangitis belonged to parenchymal type of hepatic tuberculosis^[8]. The parenchymal type is the most common one among the 3 types, which can be further divided into 3 subtypes, *i.e.* miliary tuberculosis, nodular tuberculosis and mixed tuberculosis.

CT findings of various types of hepatic tuberculosis

Parenchyma type Miliary tuberculosis: This subtype is the most common form of hepatic tuberculosis and was found in 80-100% of autopsied patients with disseminated pulmonary tuberculosis^[11]. It is depicted as multiple or diffuse miliary micronodular lesions (≤ 2.0 cm in diameter on CT), often as a

part of tuberculosis in the whole body. So clinically it was not difficult to diagnose correctly^[9,12]. Radiographic examination could detect hepatomegaly and micronodular lesions, but it was extremely difficult to find noncalcificated lesions with less than 0.5 cm in diameter with CT^[12-17]. In this series, CT revealed multiple, miliary, micronodular, hypodense lesions (>0.5 cm in diameter) scattered in liver in 2 cases with miliary calcifications in one case.

Nodular tuberculosis: The lesion, with a diameter >2 cm, is less common and has been found to be fused by miliary lesions or micronodular lesions^[4]. Because nodular lesion is apt to be found by CT and MRI, most reported hepatic tuberculosis belongs to nodular tuberculosis^[10,12-15,17-28]. Pathological features of this subtype are more complex than those of other subtypes. If tuberculous granuloma had no evident caseating necrosis or had a large amount of fibrous tissue existed, CT revealed a hypodense mass with slightly peripheral enhancement and no features on imaging findings could be found, it was difficult to diagnose it correctly^[13]. In tuberculous granuloma, when calcium deposited calcificans punctata or even “powdery” calcificans, it might appear in the hypodense lesion that could be detected on CT and is therefore helpful to the diagnosis^[6,13,24-26]. Two cases in this study were found to have calcificans punctata in the lesion center. When marked caseation or liquefaction necrosis emerged in the center of tuberculous granuloma, it means tuberculous abscess was formed and CT manifestation would be a cystic lesion with slightly or no enhanced rim^[12,17,18]. In this study there were two isolated cystic masses with no marked enhancement. Compared with liver cyst, the CT findings of the isolated cystic masses were higher than those of liver cyst and the wall of isolated cystic was more blurring. When multiple micronodular lesions fused into macronodular mass, CT present as a “clunter” sign or a multilobulated cystic mass with multilobulated enhancement^[13,19], which could be considered as a special CT feature but small pyogenic hepatic abscesses needed to be ruled out firstly^[29]. Such manifestation was characterized by a less marked enhancement and a shorter duration, being different from bacterial hepatic abscess. Three cases in this study were found.

Mixed tuberculosis (or miliary macronodular tuberculosis): One case showed multiple miliary calcifications with singular hypodense lesion. We considered that one of the typical CT features of hepatic tuberculosis might be multiple, various-dense lesions, indicating that there are lesions developed in different pathologic stage coexisting in hepatic tuberculosis, including tuberculous granuloma, liquefaction necrosis, fibrosis or calcification.

Tuberculous cholangitis Tuberculous cholangitis is rare and occurs mainly in children. Obstructive jaundice is the most common in clinic. Pathology revealed regional or diffuse duct dilation with duct wall thickening and stiffening^[8]. Imaging findings showed irregular dilated intrahepatic ducts or diffuse miliary calcifications along the course of the bile ducts. The latter was considered as a typical feature of tuberculous cholangitis^[13,30]. In our case, CT demonstrated mild diffuse hepatomegaly, marked dilated intrahepatic ducts and multiple flecked calcifications in the porta hepatis, complicated with tuberculous peritonitis.

Serohepatic type Serohepatic type of hepatic tuberculosis is the most uncommon one in the 3 types and was depicted as miliary tuberculous lesions in the subcapsule of liver or “frosted liver”, formed by thickened subcapsule^[8]. To our knowledge, the imaging findings of this type have not been reported. In our case, CT revealed multi-nodular hypodense lesions in the subcapsule of liver and thickened subcapsule of quadratus lobe. On MRI, multi-nodular lesions appeared as hypointense areas on T1-weighted imagings and as hyperintense areas on T2-weighted imagings, with slightly peripheral enhancement

after contrast administration. The features of CT and MRI were consistent with pathological features.

MR findings

MRI of hepatic tuberculosis showed a hypointense nodule with a hypointense rim on T1-weighted imagings, and hypointense, isointense or hyperintense with a less intense rim on T2-weighted imagings, and peripheral enhancement or internal septal enhancement on post-contrast MRI^[20,21,24,31]. MR findings were related to different pathological stages of tuberculosis^[20,24,31]. At the early and medium stages of granuloma with or without caseation or liquefaction necrosis, the lesion showed a low signal intensity on T1-weighted imagings and a high signal intensity on T2-weighted imagings. Similar lesions with hypointense on T1-weighted imaging and hypo- and isointense on T2-weighted imagings were corresponding to fibrous stage of tuberculosis and may have slightly or no peripheral enhancement. Tuberculous granuloma at early or medium stage and fibro-proliferous lesions all depicted as a low-density area on CT but as various signal intensities on T2-weighted imaging, which is the main advantage of MRI in the diagnosis of hepatic tuberculosis. In addition, 3D-MR imaging is helpful to distinguish the pattern of lesions and diagnose the disease. But MRI is limited to detect calcification. MR findings in 4 cases of this study were hypointense on T1-weighted imaging, hypointense in one case and hyperintense on T2-weighted imaging in 3 cases. Calcificated lesions on CT showed no signal intensity on MRI. In 2 cases in our study, lesions with hyperintense on T2-weighted imaging were pathologically proved by surgery to be a caseation necrosis in tuberculous granuloma and hypointense, and were proved to be a complete fibrosis. In short, CT and MRI have some characteristic manifestations valuable for the qualitative diagnosis of hepatic tuberculosis.

REFERENCES

- Hassan I**, Brilakis ES, Thompson RL, Que FG. Surgical management of abdominal tuberculosis. *J Gastrointest Surg* 2002; **6**: 862-867
- Yilmaz T**, Sever A, Gur S, Killi RM, Elmas N. CT findings of abdominal tuberculosis in 12 patients. *Comput Med Imaging Graph* 2002; **26**: 321-325
- Yang ZG**, Min PQ, Sone S, He ZY, Liao ZY, Zhou XP, Yang GQ, Silverman PM. Tuberculosis versus lymphomas in the abdominal lymph nodes: evaluation with contrast-enhanced CT. *Am J Roentgenol* 1999; **172**: 619-623
- Fang SG**, Yang JZ. Diagnosis of hepatic tuberculosis. *Shijie Huaren Xiaohua Zazhi* 1999; **7**: 412-413
- Suri R**, Gupta S, Gupta SK, Singh K, Suri S. Ultrasound guided fine needle aspiration cytology in abdominal tuberculosis. *Br J Radiol* 1998; **71**: 723-727
- Tan TC**, Cheung AY, Wan WY, Chen TC. Tuberculoma of the liver presenting as a hyperechoic mass on ultrasound. *Br J Radiol* 1997; **70**: 1293-1295
- Xing X**, Xia S. Diagnosis and treatment of hepatic tuberculoma. *Chin J Tuberc Respir Dis* 1997; **20**: 169-171
- Wu JP**, Qiu FZ. Huang Jiashi Surgery. 5th ed. *Beijing: People's hygiene publisher* 1992: 1324-1325
- Li YH**, Chi J. Clinical and pathological features of hepatospleic tuberculosis. *J Chin Med Univ* 1996; **25**: 193-194
- Levine C**. Primary macronodular hepatic tuberculosis: US and CT appearances. *Gastrointest Radiol* 1990; **15**: 307-309
- Thoeni RF**, Margulis AR. Gastrointestinal tuberculosis. *Semin Roentgenol* 1979; **14**: 283-294
- Xie R**, Zhou X, Chen J. CT diagnosis of tuberculosis of liver and spleen. *Chin J Tuberc Respir Dis* 1999; **22**: 237-238
- Hou MH**, Xue YS, Gen SQ, Liu QW, Huang H, Wang J, Gou LX, Jian ZJ, Ju CQ. CT manifestation of hepatic tuberculosis. *Chin J Radiol* 1996; **30**: 151-154
- Suri S**, Gupta S, Suri R. Computed tomography in abdominal tuberculosis. *Br J Radiol* 1999; **72**: 92-98
- Leder RA**, Low VH. Tuberculosis of the abdomen. *Radiol Clin North Am* 1995; **33**: 691-705
- Jadvar H**, Mindelzun RE, Olcott EW, Levitt DB. Still the great mimicker: abdominal tuberculosis. *Am J Roentgenol* 1997; **168**: 1455-1460
- Oto A**, Akhan O, Ozmen M. Focal inflammatory diseases of the liver. *Eur J Radiol* 1999; **32**: 61-75
- Reed DH**, Nash AF, Valabhji P. Radiological diagnosis and management of a solitary tuberculous hepatic abscess. *Br J Radiol* 1990; **63**: 902-904
- Malde HM**, Chadha D. The "cluster" sign in macronodular hepatic tuberculosis: CT features. *J Comput Assist Tomogr* 1993; **17**: 159-161
- Kawamori Y**, Matsui O, Kitagawa K, Kadoya M, Takashima T, Yamahana T. Macronodular tuberculoma of the liver: CT and MR findings. *Am J Roentgenol* 1992; **158**: 311-313
- Fan ZM**, Zeng QY, Huo JW, Bai L, Liu ZS, Luo LF, Yang JC, Zhou XH. Macronodular multi-organs tuberculoma: CT and MR appearances. *J Gastroenterol* 1998; **33**: 285-288
- Varela M**, Fernandez J, Navasa M, Bruix J. Pseudotumoral hepatic tuberculosis. *J Hepatol* 2003; **39**: 654
- Lupatkin H**, Brau N, Flomenberg P, Simberkoff MS. Tuberculous abscesses in patients with AIDS. *Clin Infect Dis* 1992; **14**: 1040-1044
- Maeda N**, Tanaka S, Andachi H, Osaki M, Horie Y, Suou T, Kawasaki H. Solitary hepatic tuberculoma with chronic hepatitis C diagnosed by polymerase chain reaction using paraffin-embedded resected specimen. *Hepatol Res* 1999; **15**: 80-89
- Kok KY**, Yapp SK. Isolated hepatic tuberculosis: report of five cases and review of the literature. *J Hepatobiliary Pancreat Surg* 1999; **6**: 195-198
- Stoupis C**, Taylor HM, Paley MR, Buetow PC, Marre S, Baer HU, Vock P, Ros PR. The Rocky liver: radiologic-pathologic correlation of calcified hepatic masses. *Radiographics* 1998; **18**: 675-685
- Hickey N**, McNulty JG, Osborne H, Finucane J. Acute hepatobiliary tuberculosis: a report of two cases and review of the literature. *Eur Radiol* 1999; **9**: 886-889
- Andronikou S**, Welman CJ, Kader E. The CT features of abdominal tuberculosis in children. *Pediatr Radiol* 2002; **32**: 75-81
- Jeffrey RB Jr**, Tolentino CS, Chang FC, Federle MP. CT of small pyogenic hepatic abscesses: the cluster sign. *Am J Roentgenol* 1988; **151**: 487-489
- Abascal J**, Martin F, Abreu L, Pereira F, Herrera J, Ratia T, Menendez J. Atypical hepatic tuberculosis presenting as obstructive jaundice. *Am J Gastroenterol* 1988; **83**: 1183-1186
- Yan FH**, Zeng MS, Cheng WZ, Liu R, Zhou KR, Fang J, Ji Y. MRI findings of hepatic tuberculosis. *Linchuang Fangshexue Zazhi* 2002; **21**: 439-442

Edited by Xu CT and Wang XL Proofread by Pan BR and Xu FM

Tumor type M₂ pyruvate kinase expression in gastric cancer, colorectal cancer and controls

Bo Zhang, Jian-Ying Chen, Dao-Da Chen, Guo-Bin Wang, Ping Shen

Bo Zhang, Jian-Ying Chen, Dao-Da Chen, Guo-Bin Wang, Department of General Surgery, Affiliated Xiehe Hospital of Huazhong University of Science and Technology, Wuhan 430022, Hubei Province, China
Ping Shen, Department of Biology, Wuhan University, Wuhan 430074, Hubei Province, China

Co-correspondents: Ping Shen

Correspondence to: Bo Zhang, Department of General Surgery, Affiliated Xiehe Hospital of Huazhong University of Science and Technology, Wuhan 430022, Hubei Province, China. wvestor@whu.edu.cn

Telephone: +86-27-87648533

Received: 2003-09-18 **Accepted:** 2003-10-07

Abstract

AIM: Tumor formation is generally linked to an expansion of glycolytic phosphometabolite pools and aerobic glycolytic flux rates. To achieve this, tumor cells generally overexpress a special glycolytic isoenzyme, termed pyruvate kinase type M₂. The present study was designed to evaluate the use of a new tumor marker, tumor M₂-PK, in discriminating gastrointestinal cancer patients from healthy controls, and to compare with the reference tumor markers CEA and CA72-4.

METHODS: The concentration of tumor M₂-PK in body fluids could be quantitatively determined by a commercially available enzyme-linked immunosorbent assay (ELISA)-kit (ScheBo® Tech, Giessen, Germany). By using this kit, the tumor M₂-PK concentration was measured in EDTA-plasma of 108 patients. For the healthy blood donors a cut-off value of 15 U/mL was evaluated, which corresponded to 90% specificity. Overall 108 patients were included in this study, 54 patients had a histological confirmed gastric cancer, 54 patients colorectal cancer, and 20 healthy volunteers served as controls.

RESULTS: The cut-off value to discriminate patients from controls was established at 15 U/mL for tumor M₂-PK. The mean tumor M₂-PK concentration of gastric cancer was 26.937 U/mL. According to the TNM stage system, the mean tumor M₂-PK concentration of stage I was 16.324 U/mL, of stage II 15.290 U/mL, of stage III 30.289 U/mL, of stage IV 127.31 U/mL, of non-metastasis 12.854 U/mL and of metastasis 35.711 U/mL. The mean Tumor M₂-PK concentration of colorectal cancer was 30.588 U/mL. According to the Dukes stage system, the mean tumor M₂-PK concentration of Dukes A was 16.638 U/mL, of Dukes B 22.070 U/mL, and of Dukes C 48.024 U/mL, of non-metastasis 19.501 U/mL, of metastasis 49.437 U/mL. The mean tumor M₂-PK concentration allowed a significant discrimination of colorectal cancers (30.588 U/mL) from controls (10.965 U/mL) ($P < 0.01$), and gastric cancer (26.937 U/mL) from controls (10.965 U/mL) ($P < 0.05$). The overall sensitivity of tumor M₂-PK for colorectal cancer was 68.52%, while that of CEA was 43.12%. In gastric cancer, tumor M₂-PK showed a high sensitivity of 50.47%, while CA72-4 showed a sensitivity of 35.37%.

CONCLUSION: Tumor M₂-PK has a higher sensitivity than markers CEA and CA72-4, and is a valuable tumor marker for the detection of gastrointestinal cancer.

Zhang B, Chen JY, Chen DD, Wang GB, Shen P. Tumor type M₂ pyruvate kinase expression in gastric cancer, colorectal cancer and controls. *World J Gastroenterol* 2004; 10(11): 1643-1646
<http://www.wjgnet.com/1007-9327/10/1643.asp>

INTRODUCTION

Pyruvate kinase plays a key role in the glycolytic pathway. One of its functions is to control nucleotide triphosphate generation^[1-3]. Different isoforms of this enzyme exist (pyruvate kinases L, R, M₁, M₂, Tumor M₂), which are tissue-specifically expressed in various organisms. All isoforms are known to be homotetramers in their active state. In tumor cells, however, tetrameric pyruvate kinase M₂ isoenzyme is disrupted and predominant in a dimeric form. It has been suggested that at least a part of the mechanisms is to disrupt the tetrameric form of pyruvate kinase M₂ phosphorylated by receptor tyrosine kinases. The concentration of dimeric pyruvate kinase M₂ isoenzyme is dramatically increased in a metabolic state characteristic for tumor cells. It is thus called tumor M₂-PK^[4,5]. Tumor M₂-PK is also present in body fluids, most likely released from tumor cells by tumor necrosis and cell turnover. It can be detected by a sandwich-ELISA based on two monoclonal antibodies. Furthermore, it has been demonstrated that tumor M₂-PK determination should be carried out in EDTA-plasma for its stability^[6-9].

Circulating tumor markers are an established index of monitoring systemic therapies in a number of solid tumors. In the diagnosis of gastrointestinal cancer, CA19-9, CA72-4 and CEA are the major tumor markers. Since the diagnosis of gastrointestinal cancer was dependent on endoscopies and cytology more than these tumor markers, the present study was designed to evaluate the use of a new tumor marker tumor M₂-PK in discriminating gastrointestinal cancer patients from healthy donors in order to increase the sensitivity of the diagnosis for gastrointestinal cancer^[10-13].

It was previously shown for renal and pancreatic carcinoma that tumor M₂-PK determination in circulation could provide a good discrimination of benign disease from malignant one and might correlate with stage of disease^[14-18]. Only limited data are available on tumor M₂-PK in gastrointestinal cancer. Thus, we investigated this new marker in patients with gastrointestinal cancer focusing on whether tumor M₂-PK plasma levels increased in gastrointestinal cancer patients in comparison to healthy controls, whether tumor M₂-PK was correlated with the classical tumor marker CEA, whether tumor M₂-PK gave any predictive information on response to therapy.

MATERIALS AND METHODS

Patients

A total of 108 consecutive patients with histological confirmed primary gastrointestinal cancer were included in the study. The

mean age was 47.9 years (ranging from 32 to 66 years). There were 76 men and 32 women. Among them, 54 were gastric cancer patients (25 non metastasized, 29 metastasized), 54 were colorectal cancer patients (20 non-metastasized, 34 metastasized). According to TNM stage system, 5 gastric cancer patients were classified as stage I, 24 as stage II, 23 as stage III, 2 as stage IV. According to Dukes stage system, 14 colorectal cancer patients were classified as Dukes A, 19 as Dukes B, 21 as Dukes C. Twenty healthy donors served as a control group.

Methods

The test kit (ScheBo· Tu M₂-PK, ScheBo@Tech GmbH, Giessen, Germany) required 10 µL EDTA-plasma per sample and was performed according to the manufacturer's instructions. Samples were collected as EDTA-blood, followed by centrifugation (2 000 r/min, 10 min) and removal of the supernatant plasma. Tumor M₂-PK concentration in EDTA-plasma was determined immunologically using a sandwich enzyme-linked immunosorbent assay (ELISA) based on two monoclonal antibodies (clones I and II) specific for tumor M₂-PK. The antibodies did not cross-react with other isoforms of pyruvate kinase.

The ELISA plate was coated with a monoclonal antibody that only recognized tumor M₂-PK. Tumor M₂-PK from EDTA plasma samples and standards bound to the antibody and thus were immobilized on the plate. EDTA plasma samples were diluted (1:100) with sample/washing buffer, 50 µL of diluted sample and ready-to-use standard were transferred into wells, incubated for 60 min at room temperature. Then the wells were emptied of the sample and each well was washed 3 times with sample/washing buffer (250 µL/well). The plate was inverted and tapped on a clean paper towel to remove any remaining liquid. Fifty µL/well of the 1:100 biotin-conjugated second monoclonal antibody was added and incubated for 30 min at room temperature. After washing, 50 µL/well of ready-to-use POD-streptavidin was added and incubated for 30 min in dark at room temperature. After washing, 100 µL of ready-to-use substrate solution was added to each well, and incubated for 30 min in dark at room temperature. The substrate reaction was stopped by adding 100 µL of stop solution per well. The contents were mixed well by agitating the plate. The optical density was read at 405 nm wavelengths with a micro titer plate reader between 5 and 30 min after addition of the stop solution. The contents were mixed well before measuring. The 492 nm was used as a reference wavelength.

For determination of CEA and CA72-4, serum samples (25 µL, undiluted) were measured using the fully automatic, competitive chemiluminescent immunoassay with a diagnosis kit.

Statistical analysis

Data were statistically analyzed with origin 6.1 for windows. All *P* values were resulted from a two-sided test. *P* value less than 0.05 was considered statistically significant.

RESULTS

The mean tumor M₂-PK concentration of gastric cancer was 26.937 U/mL. According to the TNM stage system, the mean tumor M₂-PK concentration of stage I was 16.324 U/mL, of stage II 15.290 U/mL, of stage III 30.289 U/mL, of stage IV 127.31 U/mL, of non-metastasis 12.854 U/mL and of metastasis 35.711 U/mL (Table 1).

The mean tumor M₂-PK concentration of colorectal cancer was 30.588 U/mL. According to the Dukes stage system, the mean tumor M₂-PK concentration of Dukes A was 16.638 U/mL, of Dukes B 22.070 U/mL, of Dukes C 48.024 U/mL, of non-metastasis 19.501 U/mL, and of metastasis 49.437 U/mL (Table 2).

The mean tumor M₂-PK concentration allowed a significant discrimination of colorectal cancers (30.588 U/mL) from controls (10.965 U/mL) ($t=3.173$, $P=0.0022$, $P<0.01$), gastric cancer (26.937 U/mL) from controls (10.965 U/mL) ($t=2.314$, $P=0.024$, $P<0.05$) (Table 3 and Figure 1).

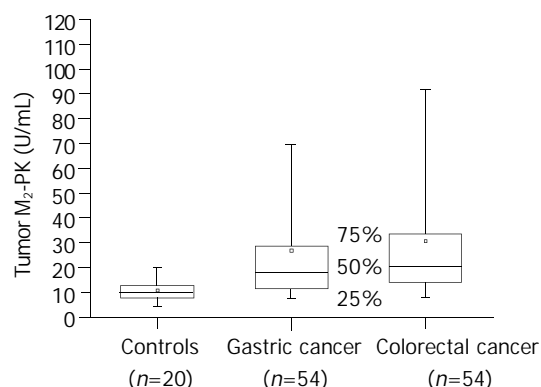


Figure 1 Concentrations of tumor M₂-PK in patients with gastrointestinal tumors and controls.

Table 1 Concentration of tumor M₂-PK and common clinical status in 54 patients with gastric cancer

No.	Tumor M ₂ -PK (U/mL)	TNM stage	Metastasis	No.	Tumor M ₂ -PK (U/mL)	TNM stage	Metastasis
1	9.26	II	N	28	24.52	IIIB	M
2	36.5	IIIA	N	29	16.6	II	M
3	23.08	II	N	30	9.26	II	N
4	23.08	IIIB	M	31	37.85	IA	N
5	165.3	IIIA	M	32	17.06	II	N
6	18.06	II	N	33	34.81	IIIA	M
7	8.81	II	N	34	14.81	II	N
8	17.34	II	N	35	23.49	II	M
9	6.87	IB	M	36	28.25	IIIA	M
10	17.91	IIIB	M	37	12.87	II	N
11	24.07	IIIB	M	38	10.62	II	M
12	12.67	II	N	39	118.02	IV	M
13	28.4	IIIB	M	40	28.75	IIIA	N
14	56.76	IIIA	N	41	14.31	II	M
15	6.42	IIIA	M	42	32.4	II	M
16	28.7	IIIB	M	43	7.61	II	N
17	7.47	IA	N	44	12.23	IA	N
18	13.9	IIIA	M	45	18.1	II	M
19	14.5	II	M	46	25.17	IIIA	M
20	69.24	IIIB	M	47	10.63	II	N
21	12.33	IIIA	M	48	8.84	II	N
22	28.66	IIIB	M	49	19.35	IIIA	N
23	136.6	IV	M	50	41.11	II	M
24	11.36	II	N	51	11.38	IIIA	N
25	7.62	II	N	52	21.75	IIIA	M
26	17.2	IB	N	53	30.03	IIIB	M
27	11.36	IIIA	M	54	11.3	II	N

N=non metastasis, M=metastasis.

The sensitivity of tumor M₂-PK for a cutoff point of 15 U/mL was compared to the established tumor markers CEA (cutoff point of 3.0 µg/µL) and CA72-4 (cut-off point of 4 KU/L). The overall sensitivity of tumor M₂-PK to colorectal cancer was 68.52%, while that of CEA was 43.12%. In gastric cancer, tumor M₂-PK showed a higher sensitivity of 50.47%, while CA72-4

showed a sensitivity of 35.37% (Figure 2).

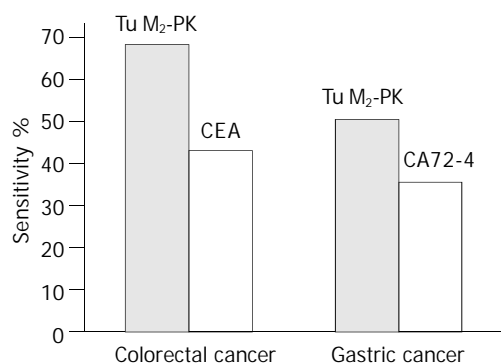


Figure 2 Comparison of sensitivities of tumor M₂-PK, CEA, CA72-4 in different gastrointestinal tumors.

Table 2 Concentration of tumor M₂-PK and common clinical status in 54 patients with colorectal cancer

No.	Tumor M ₂ -PK (U/mL)	Dukes stage	Metastasis	No.	Tumor M ₂ -PK (U/mL)	Dukes stage	Metastasis
1	16.14	A	N	28	11.35	A	N
2	14.35	A	N	29	37.86	A	M
3	21.96	A	N	30	41.3	A	M
4	9.86	B	N	31	21.5	B	N
5	28.71	B	N	32	13.6	B	N
6	16.29	A	N	33	6.42	A	N
7	29.75	C1	M	34	10.76	C1	N
8	20.93	A	N	35	15.78	A	N
9	18.83	C1	M	36	12.4	C1	N
10	14.8	C1	M	37	56.4	C1	M
11	20.93	A	N	38	76.32	A	M
12	15.09	C1	M	39	14.85	C1	N
13	113.8	C1	M	40	8.76	C1	N
14	18.55	B	N	41	22.35	B	M
15	67.02	C1	M	42	28.13	C1	M
16	20.05	B	N	43	33.46	B	M
17	20.05	A	N	44	25.78	A	N
18	17.95	C1	M	45	7.93	C1	N
19	91.7	C1	M	46	13.44	C1	N
20	20.2	B	N	47	48.66	B	M
21	29.75	C1	M	48	106.3	C1	M
22	86.16	C1	M	49	14.78	C1	N
23	53.11	C1	M	50	10.66	C1	N
24	108.75	B	N	51	23.35	B	N
25	42.19	A	N	52	30.16	A	N
26	7.72	A	N	53	6.11	A	N
27	19.26	B	N	54	9.45	B	N

N=non metastasis, M=metastasis.

Table 3 Detection of tumor M₂-PK in patients with gastrointestinal cancer and healthy donors

	n	Min (U/mL)	Max (U/mL)	Mean (U/mL)	Median (U/mL)	SD
Controls	20	4.62	20.73	10.965	9.43	4.774
Gastric cancer	54	6.42	165.3	26.937	17.34	30.604
Colorectal cancer	54	6.11	113.8	30.588	20.05	27.385

DISCUSSION

The metabolic state of tumor cells is different from that of normally proliferating cells. Tumor cells exhibit an increased glycolysis to lactate initiated by multiple steps, including a switch of isoenzyme pattern and activity. Pyruvate kinase is a key enzyme of glycolysis. Different isoforms of this enzyme exist (pyruvate kinases L, R, M₁, M₂, tumor M₂) and are tissue-specifically expressed in various organisms. The L-type is found in the liver and proximal tubules of normal kidneys, erythrocytes express the R-type, the M₁-type predominates in skeletal muscle, heart and brain, and the M₂-type is expressed in the lung, distal tubules of normal kidney, fetal and undifferentiated or proliferating tissues. All isoforms are known to be homotetramers in their active state.

In tumor cells, pyruvate kinase isoenzyme M₂ is strongly overexpressed and shifted into the dimeric state. The tetrameric form has a high affinity to phosphoenolpyruvate (PEP), whereas the dimeric form has a considerably lower PEP affinity, which consequently leads to an increase of phosphometabolite pool. The concentration of the dimeric pyruvate kinase M₂ isoenzyme is dramatically increased in a metabolic state characteristic of tumor cells. It is thus called tumor type M₂ pyruvate kinase (tumor M₂-PK) by means of specific monoclonal antibodies against tumor M₂-PK, which does not cross-react with the pyruvate kinase M₂ tetramer and other pyruvate kinase isoforms. A sensitive immunoassay (ELISA) was employed to measure tumor M₂-PK in body fluids.

It was previously shown that tumor M₂-PK determination in the circulation provided a good discrimination of benign disease from a malignant one and might correlate with stage of disease^[19-22]. Only limited data are available on tumor M₂-PK in gastrointestinal cancer. In the present study, tumor M₂-PK in the diagnosis of gastrointestinal cancer was evaluated.

Since proliferating cells had an altered metabolism with an over-expression of the dimeric form of the tumor-specific pyruvate kinase isoenzyme tumor M₂-PK, the present study was initiated to evaluate tumor M₂-PK in diagnosis of gastrointestinal cancer, in comparison with the established tumor markers CEA and CA72-4. Significant discrimination of tumor patients from healthy controls was observed^[23-28]. In the diagnosis of colorectal cancer, the sensitivity of tumor M₂-PK was higher than that of CEA. But the sensitivity of tumor M₂-PK in the diagnosis of gastric cancer was lower than that in the diagnosis of colorectal cancer, whereas it was higher than that of CA72-4.

From the presented data, it is concluded that tumor M₂-PK can be used as a valuable diagnostic marker for gastrointestinal cancer. Further studies should focus on disease monitoring, therapy evaluation and the combination of tumor M₂-PK with other tumor markers^[29-32].

REFERENCES

- Mazurek S**, Grimm H, Boschek CB, Vaupel P, Eigenbrodt E. Pyruvate kinase type M2: a crossroad in the tumor metabolome. *Br J Nutr* 2002; **87**(Suppl 1): S23-29
- Mazurek S**, Eigenbrodt E. The tumor metabolome. *Anticancer Res* 2003; **23**: 1149-1154
- Mazurek S**, Zwerschke W, Jansen-Durr P, Eigenbrodt E. Effects of the human papilloma virus HPV-16 E7 oncoprotein on glycolysis and glutaminolysis: role of pyruvate kinase type M2 and the glycolytic-enzyme complex. *Biochem J* 2001; **356**(Pt 1): 247-256
- Mazurek S**, Grimm H, Oehmke M, Weisse G, Teigelkamp S, Eigenbrodt E. Tumor M2-PK and glutaminolytic enzymes in the metabolic shift of tumor cells. *Anticancer Res* 2000; **20**: 5151-5154
- Oremek GM**, Gerstmeier F, Sauer-Eppel H, Sapoutzis N, Wechsel HW. Pre-analytical problems in the measurement of tumor type pyruvate kinase (tumor M2-PK). *Anticancer Res*

- 2003; **23**(2A): 1127-1130
- 6 **Hugo F**, Fischer G, Eigenbrodt E. Quantitative detection of tumor M2-PK in serum and plasma. *Anticancer Res* 1999; **19**(4A): 2753-2757
- 7 **Zwerschke W**, Mazurek S, Massimi P, Banks L, Eigenbrodt E, Jansen-Durr P. Modulation of type M2 pyruvate kinase activity by the human papillomavirus type 16 E7 oncoprotein. *Proc Natl Acad Sci U S A* 1999; **96**: 1291-1296
- 8 **Schneider J**, Morr H, Velcovsky HG, Weisse G, Eigenbrodt E. Quantitative detection of tumor M2-pyruvate kinase in plasma of patients with lung cancer in comparison to other lung diseases. *Cancer Detect Prev* 2000; **24**: 531-535
- 9 **Roigas J**, Schulze G, Raytarowski S, Jung K, Schnorr D, Loening SA. Tumor M2 pyruvate kinase in plasma of patients with urological tumors. *Tumour Biol* 2001; **22**: 282-285
- 10 **Hardt PD**, Ngoumou BK, Rupp J, Schnell-Kretschmer H, Kloer HU. Tumor M2-pyruvate kinase: a promising tumor marker in the diagnosis of gastro-intestinal cancer. *Anticancer Res* 2000; **20**: 4965-4968
- 11 **Schulze G**. The tumor marker tumor M2-PK: an application in the diagnosis of gastrointestinal cancer. *Anticancer Res* 2000; **20**: 4961-4964
- 12 **Hardt PD**, Toepler M, Ngoumou B, Rupp J, Kloer HU. Fecal pyruvate kinase concentrations (ELISA based on a combination of clone 1 and clone 3 antibodies) for gastric cancer screening. *Anticancer Res* 2003; **23**(2A): 855-857
- 13 **Hardt PD**, Toepler M, Ngoumou B, Rupp J, Kloer HU. Measurement of fecal pyruvate kinase type M2 (tumor M2-PK) concentrations in patients with gastric cancer, colorectal cancer, colorectal adenomas and controls. *Anticancer Res* 2003; **23**(2A): 851-853
- 14 **Oremek GM**, Teigelkamp S, Kramer W, Eigenbrodt E, Usadel KH. The pyruvate kinase isoenzyme tumor M2 (Tu M2-PK) as a tumor marker for renal carcinoma. *Anticancer Res* 1999; **19**: 2599-2601
- 15 **Wechsel HW**, Petri E, Bichler KH, Feil G. Marker for renal cell carcinoma (RCC): the dimeric form of pyruvate kinase type M2 (Tu M2-PK). *Anticancer Res* 1999; **19**(4A): 2583-2590
- 16 **Oremek GM**, Sapoutzis N, Kramer W, Bickeboller R, Jonas D. Value of tumor M2 (Tu M2-PK) in patients with renal carcinoma. *Anticancer Res* 2000; **20**: 5095-5098
- 17 **Roigas J**, Deger S, Schroeder J, Wille A, Turk I, Brux B, Jung K, Schnorr D, Loening SA. Tumor type M2 pyruvate kinase expression in metastatic renal cell carcinoma. *Urol Res* 2003; **26**
- 18 **Roigas J**, Schulze G, Raytarowski S, Jung K, Schnorr D, Loening SA. Tumor M2 pyruvate kinase in renal cell carcinoma. Studies of plasma in patients. *Urologe A* 2000; **39**: 554-556
- 19 **Schneider J**, Velcovsky HG, Morr H, Katz N, Neu K, Eigenbrodt E. Comparison of the tumor markers tumor M2-PK, CEA, CYFRA 21-1, NSE and SCC in the diagnosis of lung cancer. *Anticancer Res* 2000; **20**: 5053-5058
- 20 **Schneider J**, Neu K, Grimm H, Velcovsky HG, Weisse G, Eigenbrodt E. Tumor M2-pyruvate kinase in lung cancer patients: immunohistochemical detection and disease monitoring. *Anticancer Res* 2002; **22**(1A): 311-318
- 21 **Schneider J**, Peltri G, Bitterlich N, Neu K, Velcovsky HG, Morr H, Katz N, Eigenbrodt E. Fuzzy logic-based tumor marker profiles including a new marker tumor M2-PK improved sensitivity to the detection of progression in lung cancer patients. *Anticancer Res* 2003; **23**(2A): 899-906
- 22 **Schneider J**, Peltri G, Bitterlich N, Philipp M, Velcovsky HG, Morr H, Katz N, Eigenbrodt E. Fuzzy logic-based tumor marker profiles improved sensitivity of the detection of progression in small-cell lung cancer patients. *Clin Exp Med* 2003; **2**: 185-191
- 23 **Pottek T**, Muller M, Blum T, Hartmann M. Tu-M2-PK in the blood of testicular and cubital veins in men with testicular cancer. *Anticancer Res* 2000; **20**: 5029-5033
- 24 **Luftner D**, Mesterharm J, Akrivakis C, Geppert R, Petrides PE, Wernecke KD, Possinger K. Tumor type M2 pyruvate kinase expression in advanced breast cancer. *Anticancer Res* 2000; **20**: 5077-5082
- 25 **Hoopmann M**, Warm M, Mallmann P, Thomas A, Gohring UI, Schondorf T. Tumor M2 pyruvate kinase-determination in breast cancer patients receiving trastuzumab therapy. *Cancer Lett* 2002; **187**: 223-228
- 26 **Schneider J**, Neu K, Velcovsky HG, Morr H, Eigenbrodt E. Tumor M2-pyruvate kinase in the follow-up of inoperable lung cancer patients: a pilot study. *Cancer Lett* 2003; **193**: 91-98
- 27 **Oremek GM**, Rox S, Mitrou P, Sapoutzis N, Sauer-Eppel H. Tumor M2-PK levels in haematological malignancies. *Anticancer Res* 2003; **23**(2A): 1135-1138
- 28 **Oremek GM**, Muller R, Sapoutzis N, Wigand R. Pyruvate kinase type tumor M2 plasma levels in patients afflicted with rheumatic diseases. *Anticancer Res* 2003; **23**: 1131-1134
- 29 **Aisaki K**, Kanno H, Oyaizu N, Hara Y, Miwa S, Ikawa Y. Apoptotic changes precede mitochondrial dysfunction in red cell-type pyruvate kinase mutant mouse erythroleukemia cell lines. *Jpn J Cancer Res* 1999; **90**: 171-179
- 30 **Steinberg P**, Klingelhoffer A, Schafer A, Wust G, Weisse G, Oesch F, Eigenbrodt E. Expression of pyruvate kinase M2 in preneoplastic hepatic foci of N-nitrosomorpholine-treated rats. *Virchows Arch* 1999; **434**: 213-220
- 31 **Oremek GM**, Rutner F, Sapoutzis N, Sauer-Eppel H. Tumor marker pyruvate kinase type tumor M2 in patients suffering from diabetic nephropathy. *Anticancer Res* 2003; **23**(2A): 1155-1158
- 32 **Pezzilli R**, Migliori M, Morselli-Labate AM, Campana D, Ventrucci M, Tomassetti P, Corinaldesi R. Diagnostic value of tumor M2-pyruvate kinase in neuroendocrine tumors. A comparative study with chromogranin A. *Anticancer Res* 2003; **23**: 2969-2972

Edited by Wang XL and Zhu LH Proofread by Xu FM

• CLINICAL RESEARCH •

Epidemiology of gastroesophageal reflux disease: A general population-based study in Xi'an of Northwest China

Jin-Hai Wang, Jin-Yan Luo, Lei Dong, Jun Gong, Ming Tong

Jin-Hai Wang, Jin-Yan Luo, Lei Dong, Jun Gong, Department of Gastroenterology, Second Hospital of Xi'an Jiaotong University, Xi'an 710004, Shaanxi Province, China

Ming Tong, Department of Preventive Medicine, Medical College of Xi'an Jiaotong University, Xi'an 710061, Shaanxi Province, China

Correspondence to: Dr. Jin-Hai Wang, Department of Gastroenterology, Second Hospital of Xi'an Jiaotong University, Xi'an 710004, Shaanxi Province, China. jinhaiwang@hotmail.com

Telephone: +86-29-7679290 **Fax:** +86-29-7231758

Received: 2003-11-21 **Accepted:** 2003-12-16

Abstract

AIM: Gastroesophageal reflux disease (GERD) is a common disorder in the Western population, but detailed population-based data in China are limited. The aim of this study was to understand the epidemiology of symptomatic gastroesophageal reflux (SGER) in adults of Xi'an, a northwestern city of China, and to explore the potential risk factors of GERD.

METHODS: Symptoms suggestive of GERD, functional dyspepsia (FD), irritable bowel syndrome (IBS), upper respiratory diseases and some potential risk factors were investigated in a face-to-face manner in a region-stratified random samples of 2 789 residents aged 18-70 years in Xi'an by using a standardized questionnaire.

RESULTS: With a response rate of 91.8%, the prevalence of SGER was 16.98% (95% CI, 14.2-18.92) in Xi'an adults, and no gender-related difference was observed ($P>0.05$). SGER was more common among subjects aged 30-70 years than in those aged 18-29 years ($P<0.05$). The prevalence of SGER in rural, urban and suburban subjects was 21.07%, 17.44% and 12.12%, respectively, and there was a significant difference between rural, urban and suburban regions ($P<0.05$). Compared with subjects without SGER, the prevalence of symptoms suggestive of FD and IBS, pneumonia, asthma, bronchitis, laryngitis, pharyngitis, chronic cough, wheeze, globus sensation, oral ulcer and snore was significantly increased in subjects with SGER ($P<0.01$). Heavy smoking (OR=4.94; CI, 3.70-6.61), heavy alcohol use (OR=2.85; CI, 1.67-4.49), peptic ulcer (OR=5.76; CI, 3.99-8.32), cerebral palsy (OR=3.97; CI, 1.97-8.00), abdominal operation (OR=2.69; CI, 1.75-4.13), obesity (OR=2.16; CI, 1.47-3.16), excessive food intake (OR=1.43; CI, 1.17-1.75), sweet food (OR=1.23; CI, 0.89-1.54), and consumption of coffee (OR=1.23; CI, 0.76-2.00) were independently associated with SGER. The episodes of GERD were commonly precipitated by dietary factors (66.05%), followed by body posture (26.54%), ill temper (23.72%), fatigue (22.32%) and stress (10.93%).

CONCLUSION: GERD is common in Xi'an's adult population with a mild or moderate degree. The etiology and pathogenesis of GERD are probably associated with FD, IBS, and some respiratory, laryngopharyngeal and odontostological diseases or symptoms. Some lifestyles, diseases and dietary factors are the risk factors of GERD.

Wang JH, Luo JY, Dong L, Gong J, Tong M. Epidemiology of gastroesophageal reflux disease: A general population-based study in Xi'an of Northwest China. *World J Gastroenterol* 2004; 10(11): 1647-1651

<http://www.wjgnet.com/1007-9327/10/1647.asp>

INTRODUCTION

Gastroesophageal reflux disease (GERD) is a common disorder, and approximately 17-38% of adults in the Western population experienced heartburn and/or acid regurgitation, the main symptoms of GERD, at least once per week; with 4-9% having daily symptoms^[1-3]. Some patients with GERD would develop Barrett's esophagus, intestinal metaplasia of esophageal mucosa that predisposes to adenocarcinoma of the esophagus^[4-8], which has increased rapidly since 1970s^[9,10]. Patients with esophageal carcinoma have been proved to have a low 5-year survival rate^[11,12]. In addition to the risk of cancer, GERD is well recognized to be associated with some upper respiratory diseases, having an adverse impact on the quality of life, and the cost of long-term medical therapy is substantial. Therefore, it is of much importance to understand the prevalence of GERD and to identify the potential risk factors to prevent GERD and GERD-related diseases. As detailed population-based data on GERD in China are currently limited, we aimed in this study to estimate the prevalence of SGER in Xi'an adults, to determine the relationship between GERD and FD, IBS, and upper respiratory diseases, and to explore the risk factors of GERD.

MATERIALS AND METHODS

Subjects

Xi'an is a northwestern city of China, consisting of 7 administrative districts and 3 counties. Of the administrative districts 4 are in the urban region and 3 in the suburban region, and the counties are all in the rural region. Each district includes numerous neighboring communities including multiple residential areas, and each of the county covers several townships governing a number of villages. Based on the 1997 census data obtained from the local government and the proportion of population within the regions, we randomly selected one or more residential areas or villages in the urban, suburban and rural regions, respectively. Finally, a total of 2 789 subjects entered this survey, including 911 subjects from the urban region, 853 from the suburban region, and 1 025 from the rural region. The proportion of subjects in different regions was similar to that of Xi'an population ($P>0.05$), and the selected samples were matched for age and gender with Xi'an population ($P>0.05$).

Questionnaire

The questionnaire was designed on the basis of previous works from two university hospitals^[13], but modified to suit the local conditions. The modified version contained 8 fractions covering a total of 130 relative questions (items), of which 15 were specifically concerned with the frequency and severity of symptoms suggestive of GERD in the past years. Other questions included those concerning general condition of the subject (self-reported

height and weight), the symptoms suggestive of functional dyspepsia (FD) and irritable bowel syndrome (IBS) in the past year, symptoms or history of respiratory, laryngopharyngeal, and odontostological diseases in the past year; history of illness and operation, personal habits (smoking, alcohol), and dietary habits.

Definitions

The following definitions for symptom categories and diseases were used. Only symptoms occurring in the past year before the interview were considered. (1) Heartburn: a burning pain or burning sensation behind the sternum in the chest. (2) Acid regurgitation: a bitter or sour-tasting fluid reflux into the throat or mouth. (3) Food regurgitation: eaten food reflux into the mouth. Heartburn, acid regurgitation, and food regurgitation were considered to be the main symptoms of GERD. Each of the typical symptoms was estimated according to its severity and frequency, which measured on a 4-score scale. The severity was assessed as follows: 0, none; 1, mild (could be ignored); 2, moderate (could not be ignored but did not affect lifestyle); 3, severe (affected lifestyle). The score of symptom frequency was estimated as follows: 0, none or less than one occasion per month on average; 1, several occasions (1 to 3) a month; 2, several occasions (1 to 6) a week; 3, one or more than one occasions daily. Based on the scores of the severity and frequency of the main GERD symptoms, a total score (range, 0 to 18) of each subject was calculated. (4) SGER: subjects with a total score (St) no less than 3. (5) Chest pain: any pain or discomfort felt inside the chest more than once per month on average but not including any pain caused by diagnosed heart disease. (6) Dysphagia: a feeling that food stuck in the throat or chest more than one per month. (7) Symptoms suggestive of FD and IBS and symptoms of respiratory, laryngopharyngeal, and odontostological diseases: any of these symptoms presented more than once a week on average in the past year. (8) History of diseases or operations: any disease or operation diagnosed or performed in a hospital before the interview. (9) Alcohol use: taking 300 g of alcohol per month. (10) Heavy alcohol use: taking 210 g or more of alcohol per week. (11) Smoking status: defined as current smoking, current non-smoking, and heavy smoking (more than one pack a day). (12) Obesity: a body mass index ≥ 30 kg/m². (13) Coffee and special beverages: drinking more than one cup per day on average. (14) Dietary habits: taking special food more than one servings per day on average.

Training of interviewers

The team of interviewers was constituted mainly by medical students studying preventive medicine in our university, who were trained by the same two professors, one was a physician of gastroenterology and understood well the relative definitions, and the other was a specialist in preventive medicine and had rich experience in survey.

Assessment of feasibility

Before the actual study, a pilot study was conducted among 100 unselected outpatients attending our gastroenterological clinic, to test the appropriateness of the questionnaire and to familiarize the interviewers with the survey procedure and the definitions. The problems that the interviewers encountered during the pilot study were discussed and their solutions were provided accordingly.

Survey design and response rate

According to the list of selected subjects and guiding by the members of residents or village's committee, all subjects were interviewed face to face at their home by the interviewers. The completed questionnaires were checked and kept by same physician. The absent subjects were registered and two reminder

interviews were conducted at weekly intervals. Finally, the survey was closed after 16 wk. Among the 2 789 selected subjects, 74 had moved away, 58 could not be interviewed due to their absence during the survey period, 6 died, and 91 explicitly refused to participate in the study. A total of 2 560 subjects were successfully interviewed within a period of 4 mo, resulting in a response rate of 91.8%. There was no difference between the responders and non-responders with respect to their age and gender ($P>0.05$), and the constitution of the non-responder in different regions was reasonably similar ($P>0.05$). Twenty-eight individuals were subsequently excluded from the analysis because of inadequately questionnaires. Data from 2 532 questionnaires were entered in a computer.

Statistical analysis

The questionnaires were coded for analysis, and the data were entered in a computer and analyzed by using DBASE software. The prevalence was derived with 95% confidence intervals (95%CI). Comparison of the data was performed using EP15.0 χ^2 test. The odds ratios (OR) and 95% CI for each significant variable in the final model were calculated from the coefficients estimated in the logistic regression model. All P values were two-tailed, with the level of statistical significance specified at 0.05.

RESULTS

Main symptoms of GERD

The prevalence of heartburn for at least once monthly, weekly and daily episodes was 10.98% (278/2 532), 4.07% (103/2 532) and 1.66% (42/2 532), respectively. That for acid regurgitation monthly was 21.01% (532/2 532), weekly 7.78% (197/2 532), and daily 3.53% (89/2 532). For food regurgitation, the prevalence was 8.57% (217/2 532), 3.28% (83/2 532), and 1.42% (36/2 532) for at least one occasion monthly, weekly, and daily, respectively.

Symptomatic gastroesophageal reflux

The distribution of the total score of main GERD symptoms in the responders is shown in Table 1. The prevalence of SGER was 16.98% (95%CI, 14.20-18.92), of which, 13.11%, 2.92%, and 0.95% were considered as mild, moderate, and severe, respectively. Responders with SGER were more likely to be a mild or moderate degree.

Table 1 The distribution of total score of main GERD symptoms of responders ($n=2 532$)

Total score (St)	Responders (n)	Rate (%)
≥ 3	2 102	83.02
≥ 3 (SGER)	430	16.98
3-7 (mild)	332	13.11
8-12 (moderate)	74	2.92
13-18 (severe)	24	0.95

Relationship between SGER and gender, age, and region

There was no statistically significant difference between men and women in the prevalence of GERD (61.71% vs 17.25%, $P>0.05$), and the ratio of male/female was 1:1.03. The prevalence of SGER was relatively constant across each of 10-year age interval (Table 2, χ^2 for trend; $P=0.075$), but by cutting χ^2 apart, we found that the prevalence of GERD was significantly higher in the responders aged 30-70 years than in those aged 18-29 years ($\chi^2=4.40$, $P<0.05$), and the group aged 50-59 years had the highest prevalence of SGER (21.39%). The responders in the urban and rural regions were more likely than the responders in suburban regions to have SGER (21.07% and 17.44% vs 12.12%, $P<0.05$). However, SGER was similarly prevalent in the urban and rural regions ($P>0.05$).

Table 2 The prevalence of SGER in each age group

Age group (yr)	Responders (n)	Responders with SGER (n)	Prevalence of SGER (%)
<20	64	9	14.06
20-29	517	73	14.12
30-39	621	106	17.07
40-49	584	100	17.12
50-59	360	77	21.39
60-69	354	60	16.95
70	32	5	15.63
18-70	2 532	430	16.98

Association between SGER and respiratory, laryngopharyngeal, and odontostological diseases

Table 3 summarized the prevalence of some respiratory, laryngopharyngeal, and odontostological diseases or symptoms in responders with and without SGER. The responders with SGER reported a higher prevalence of pneumonia, asthma, bronchitis, pharyngitis, laryngitis, chronic cough, wheeze, globus sensation, oral ulcer, and snore than the responders without SGER.

Table 3 The prevalence of respiratory, laryngopharyngeal, and odontostological diseases or symptoms in responders with and without SGER

Disease or symptom	Responders with SGER (n=430)		Responders without SGER (n=2 102)		P value
	n	Rate (%)	n	Rate (%)	
Pneumonia	12	2.79	15	0.73	<0.01
Asthma	28	6.51	46	2.19	<0.01
Bronchitis	66	15.35	187	8.90	<0.01
Pharyngitis	35	8.14	82	3.90	<0.01
Laryngitis	102	23.73	248	11.80	<0.01
Chronic cough	92	21.40	232	11.04	<0.01
Wheeze	33	7.67	80	3.80	<0.01
Globus sensation	102	23.72	104	4.95	<0.01
Oral ulcer	77	17.91	162	7.71	<0.01
Snore	121	28.14	362	12.27	<0.01

Relationship between SGER and other common gastrointestinal symptoms

The prevalence rate of pain behind the sternum, dysphagia,

retching, nausea, vomiting, epigastric discomfort, epigastric fullness, epigastric pain, diarrhoea, and constipation in responders with SGER was significantly higher than that in the responders without SGER ($P<0.01$, Table 4).

Table 4 Other common gastrointestinal symptoms in responders with and without GERD

Symptom	Responders with SGER (n=430)		Responders without SGER (n=2 102)		P value
	n	Rate (%)	n	Rate (%)	
Pain behind breastbone	100	23.25	84	4.14	<0.01
Dysphagia	24	5.58	20	0.95	<0.01
Retching	164	38.14	228	10.85	<0.01
Nausea	137	31.86	148	7.04	<0.01
Vomiting	78	18.14	71	3.38	<0.01
Epigastric discomfort	161	37.44	216	10.28	<0.01
Epigastric fullness	201	46.74	303	14.41	<0.01
Epigastric pain	122	28.37	147	6.99	<0.01
Diarrhoea	59	13.72	102	5.07	<0.01
Constipation	93	21.63	199	9.47	<0.01

The potential risk factors

The data obtained from Table 5 showed that heavy smoking (OR=4.94; CI, 3.70-6.61), heavy alcohol use (OR=2.85; CI, 1.67-4.49), peptic ulcer (OR=5.76; CI, 3.99-8.32), abdominal operation (OR=2.69; CI, 1.75-4.13) were strongly associated with SGER; obesity (OR=2.16; CI, 1.47-3.16) was moderately associated. The association between SGER and current smoking (OR=1.27; CI, 1.17-1.38), excessive food intake (OR=1.43; CI, 1.17-1.75), sweet food (OR=1.23; CI, 0.98-1.54), and coffee (OR=1.23; CI, 0.76-2.00) still existed, but it was mild. The prevalence of SGER was not influenced by tea (OR=1.13; CI, 0.91-1.44), pepper food (OR=1.07; CI, 0.86-1.32), and fat intake (OR=1.00; CI, 0.81-1.23).

Precipitating factors for SGER

Of 430 responders with SGER, 79.07% (340/432) reported the episodes of SGER with specially precipitating factors. Some dietary factors (sweet foods, peppery foods, fat or oil foods, and sour beverage) were the most common precipitating factors (66.05%), followed by body posture (26.54%), ill temper (23.72%), fatigue (22.32%), and stress (10.93%).

Table 5 The Association Between SGER and Selected Risk Factors

Selected risk factors	Factor exposure			Non-factor exposure			P value	OR ¹ (95%CI)
	Responders n	Responders with SGER n	Rate (%)	Responders n	Responders with SGER n	Rate (%)		
Current smoking	992	189	19.05	1 540	241	15.65	<0.05	1.27(1.17-1.38)
Heavy smoking	219	99	45.21	2 313	320	13.84	<0.01	4.94(3.70-6.61)
Heavy alcohol use	74	26	35.14	2 458	404	16.44	<0.01	2.85(1.67-4.49)
Peptic ulcer	59	31	52.54	2 473	399	16.13	<0.01	5.76(3.99-8.32)
Abdominal operation	99	34	34.34	2 433	396	16.28	<0.01	2.69(1.75-4.13)
Erebral palsy	18	8	44.44	2 514	422	16.78	<0.01	3.97(1.97-8.00)
Obesity	139	41	29.50	2 392	389	16.26	<0.01	2.16(1.47-3.16)
Over intake	614	129	21.01	1 918	301	15.69	<0.01	1.43(1.17-1.75)
Sweet food	695	133	19.14	1 837	297	16.17	>0.05	1.23(0.98-1.54)
Coffee	85	17	20.00	2 447	413	16.88	>0.05	1.23 0.76-2.00)
Tea	798	145	18.17	1 734	285	16.44	>0.05	1.13(0.91-1.44)
Pepper food	1 533	266	17.35	999	164	16.42	>0.05	1.07(0.86-1.32)
Fat intake	1 065	181	17.00	1 467	249	16.97	>0.05	1.00(0.81-1.23)

¹OR ~ RR2.6: a strong association; OR=1.7-2.5: a moderate association; OR=1.2-1.6: a mild association; OR=0.9-1.1: no association.

DISCUSSION

Population-based research well suits the purpose of investigating the epidemiology of gastroesophageal reflux disease, which is a common disorder in the community. The diagnosis could be made on the basis of its specific symptoms of heartburn and acid regurgitation without further diagnostic test^[14]. Thus, the methodology utilizing a self-reported questionnaire has become popular in population-based study of GERD^[1-3]. However, this kind of research can be limited by the varied ability of the interviewees to comprehend the definitions used and also by the relatively low response rates. Our research was conducted face to face in subjects' home with the guidance by the members of local community, therefore a high response rate (91.8%) was insured, significant responder bias was avoided, and the definitions were understood accurately assisted by the explanation provided by the trained interviewers, making possible a semi-quantitative diagnosis of SGER which was made by quantifying not only the frequency, but also the severity of main GERD symptoms so as to exclude those subjects with trivial symptoms. The prevalence of heartburn for at least weekly episodes in our study was 4.07%, similar to the prevalence rates reported in other two studies in Asia^[15,16], but was lower than those of Western population, such as the rate of 17.8% in Americans^[2], 14.7% in Australians^[17], 15% in Finlanders^[18] and 11.76% in Belgians^[19].

In the past few years, there has been an increase in the frequency of GERD in Asia, but the related information remains scarce^[20]. The prevalence of GERD in Western adult population varied between 17% and 38%, depending on the definitions and methodology used^[1,2,3]. A community-based study showed that the ethnic-adjusted prevalence of GERD was 1.6% in Singapore, in which GERD was defined as the presence of heartburn and/or acid regurgitation at least once a month^[15]. The prevalence of SGER was 16.98% in the present study. Although these studies are not comparable because of differences in methodologies and definitions used, the different prevalence of GERD may suggest that the prevalence of GERD actually varies between these populations. These differences were probably caused by genetic factors, environmental factors, dietary habits, and health habits. In our study, the variation of the prevalence of SGER in different regions was more likely to be explained by these factors. We found that the prevalence rate of SGER did not differ between men and women, which agreed with many studies^[1,2,15]. Our data also suggested that elder subjects were more likely to have SGER. The reasons are mainly that old people had a poor esophageal acid clearance and decreased defense mechanisms against reflux of acid gastric contents on the esophageal mucosa^[21,22].

The association between GERD and atypical reflux symptoms^[2], FD^[1,15,17,1], and IBS^[23-26] was assessed in some studies, but no related studies were conducted in China. The high prevalence of atypical reflux symptoms (pain behind the sternum and dysphagia) and symptoms suggestive of FD (retching, nausea, vomiting, epigastric discomfort, epigastric fullness, *etc.*), and IBS (epigastric pain, diarrhoea, and constipation.) in the responders with SGER in this population-based study confirmed the association among these symptoms. Subjects with aggravated dysphagia and pain behind the sternum caused by heart or coronary diseases were excluded in the analysis, so to some extent, the high prevalence of non-obstructive dysphagia and non-cardiac chest pain in subjects with SGER suggested that these two symptoms might be a late sequela of GERD. The considerable overlap among symptoms suggestive of GERD, FD and IBS may imply the same etiology and pathogenesis in these diseases. This conclusion, however, needs to be tested by further clinical and experimental studies.

Clinical studies have shown a cause-effect relationship between GERD and some respiratory, laryngopharyngeal, and odontostological diseases or symptoms^[27-32]. This association was further confirmed by our population-based research. Therefore, when a general medical therapy failed to improve the patients' conditions, a 24-h pH monitoring was necessary to detect pathological reflux, and a medical antireflux treatment would be more effective to relieve these conditions with pathological reflux^[28].

Laboratory studies demonstrated a correlation between both weight and body mass index with gastroesophageal reflux^[33,34]. This correlation was still held in our population-based study. Cigarette smoking could reduce lower esophageal sphincter pressure and predispose strain-induced reflux^[35,36]. Our research confirmed the association between smoking and SGER, and the association was weaker when cigarette consumption was decreased. We also observed a more than twofold increase in the prevalence of SGER in heavy alcohol users (42.9%) as compared with non-drinkers (15.7%). Although weight loss, smoking and drinking cessation have been recommended for patients with GERD, some patients reported improvement in their symptoms by doing so^[37], a multicentre-randomized clinical trial is still needed to certify the efficacy of these therapies for GERD.

We also found that GERD was strongly associated with peptic ulcer, post abdominal operation conditions (cholecystectomy and gastrectomy), and cerebral palsy (intellectually disabled and sequela of apoplexy) which were not reported by the other population-based studies. High gastric acid output and abnormal gastric empty are responsible for the increased prevalence of GERD in patients with peptic ulcer. Abdominal operations change the normal anatomic structure of upper gastrointestinal tract and commonly cause alkaline reflux. The main reasons for the high prevalence of SGER in individuals with cerebral palsy were the abnormal motility of esophagus or gastric tract of these patients and a number of common medications used (calcium channel blockers and tricyclic antidepressants) which promote GER by relaxing the lower esophageal sphincter^[38,39].

Consumption of special foods such as fat, chocolate, mints, coffee, onion, citrus fruit and tomato products and eating habits have been shown to be associated with temporary GER or relaxed LES in laboratory settings^[40-42]. However, our population-based study demonstrated that excessive food intake, sweet foods, and coffee were only weakly associated with SGER and no positive association was observed between SGER and fat intake, tea, and peppery foods. Our results were partly similar to the observation by Paul and his colleagues, whose nationwide population-based case-control study showed that GER symptoms and the risk of adenocarcinoma of esophagus or gastric cardia were not associated with dietary factors^[43]. The main explanation is that the quantity of these special foods was difficult to be accurately assessed in population-based study other than in a laboratory experiment. Another conceivable explanation is that the consumption of these foods might not be enough in quantity and/or frequency to cause GERD symptoms. The finding that episodes of SGER were commonly precipitated by dietary factors in our study also supports the above explanations.

In summary, GERD is common in Xi'an adult population, and a significant health problem in the community. The etiology and pathogenesis of GERD are probably associated with FD, IBS, and some respiratory, laryngopharyngeal and odontostological diseases or symptoms. Some life habits, diseases and dietary factors are the risk factors for GERD, and avoidance of these risk factors should be recommended as a primary prevention therapy of GERD.

REFERENCES

- 1 **Kennedy T**, Jones R. The prevalence of gastro-oesophageal reflux symptoms in a UK population and the consultation behaviour of patients with these symptoms. *Aliment Pharmacol Ther* 2000; **14**: 1589-1594
- 2 **Locke GR 3rd**, Talley NJ, Fett SL, Zinsmeister AR, Melton LJ 3rd. Prevalence and clinical spectrum of gastroesophageal reflux: a population-based study in Olmsted County. *Gastroenterology* 1997; **112**: 1448-1456
- 3 **Talley NJ**, Zinsmeister AR, Schleck CD, Melton LJ 3rd. Dyspepsia and dyspepsia subgroups: a population-based study. *Gastroenterology* 1992; **102**: 1259-1268
- 4 **Bytzer P**, Christensen PB, Damkier P, Vinding K, Seersholm N. Adenocarcinoma of the esophagus and Barrett's esophagus: a population-based study. *Am J Gastroenterol* 1999; **94**: 86-91
- 5 **Falk GW**. Barrett's esophagus. *Gastroenterology* 2002; **122**: 1569-1591
- 6 **Buttar NS**, Wang KK, Leontovich O, Westcott JY, Pacifico RJ, Anderson MA, Krishnadath KK, Lutzke LS, Burgart LJ. Chemoprevention of esophageal adenocarcinoma by COX-2 inhibitors in an animal model of Barrett's esophagus. *Gastroenterology* 2002; **122**: 1101-1112
- 7 **Shirvani VN**, Ouatu-Lascar R, Kaur BS, Omary MB, Triadafilopoulos G. Cyclooxygenase 2 expression in Barrett's esophagus and adenocarcinoma: Ex vivo induction by bile salts and acid exposure. *Gastroenterology* 2000; **118**: 487-496
- 8 **Sampliner RE**. Practice guidelines on the diagnosis, surveillance, and therapy of Barrett's esophagus. *Am J Gastroenterol* 1998; **93**: 1028-1033
- 9 **Devesa SS**, Blot WJ, Fraumeni JF Jr. Changing patterns in the incidence of esophageal and gastric carcinoma in the united states. *Cancer* 1998; **83**: 2049-2053
- 10 **Cameron AJ**, Lomboy CT. Barrett's esophagus: age, prevalence and extent of columnar epithelium. *Gastroenterology* 1992; **103**: 1241-1245
- 11 **Sampliner RE**. Effect of up to 3 years of high-dose lansoprazole on Barrett's esophagus. *Am J Gastroenterol* 1994; **89**: 1844-1848
- 12 **Sharma P**, Sampliner RE, Camargo E. Normalization of esophageal pH with high-dose proton pump inhibitors therapy dose not result in regression of Barrett's esophagus. *Am J Gastroenterol* 1997; **92**: 582-585
- 13 **Pan GZ**, Xu GM, Ke MY, Han SM, Guo HP, Li ZS, Fang XC, Zou DW, Lu SC, Liu J. Epidemiological study on symptomatic gastroesophageal reflux disease in China: Beijing and Shanghai. *Chin J Dig Dis* 2000; **1**: 2-8
- 14 **Hollenz M**, Stolten M, Labenz J. Prevalence of gastro-oesophageal reflux disease in general practice. *Dtsch Med Wochenschr* 2002; **127**: 1007-1012
- 15 **Ho KY**, Kang JY, Seow A. Prevalence of gastrointestinal symptoms in a multiracial Asian population, with particular reference to reflux-type symptoms. *Am J Gastroenterol* 1998; **93**: 1816-1822
- 16 **Ho KY**. Gastroesophageal reflux disease is uncommon in Asia: evidence and possible explanations. *World J Gastroenterol* 1999; **5**: 4-6
- 17 **Talley NJ**, Boyce P, Jones M. Identification of distinct upper and lower gastrointestinal symptom groupings in an urban population. *Gut* 1998; **42**: 690-695
- 18 **Isolauri J**, Laippala P. Prevalence of symptoms suggestive of gastro-oesophageal reflux disease in an adult population. *Ann Med* 1995; **27**: 67-70
- 19 **Louis E**, DeLooze D, Deprez P, Hiele M, Urbain D, Pelckmans P, Deviere J, Deltenre M. Heartburn in Belgium: prevalence, impact on daily life, and utilization of medical resources. *Eur J Gastroenterol Hepatol* 2002; **14**: 279-284
- 20 **Lim LG**, Ho KY. Gastroesophageal reflux disease at the turn of millennium. *World J Gastroenterol* 2003; **9**: 2135-2136
- 21 **Huang X**, Zhu HM, Deng CZ, Porro GB, Sangaletti O, Pace F. Gastroesophageal reflux: the features in elderly patients. *World J Gastroenterol* 1999; **5**: 421-423
- 22 **Ter RB**, Johnston BT, Castell DO. Influence of age and gender on gastroesophageal reflux in symptomatic patients. *Dis Esophagus* 1998; **11**: 106-108
- 23 **Pimentel M**, Rossi F, Chow EJ, Ofman J, Fullerton S, Hassared P, Lin HC. Increased prevalence of irritable bowel syndrome in patients with gastroesophageal reflux. *J Clin Gastroenterol* 2002; **34**: 221-224
- 24 **Holtmann G**, Goebell H, Talley NJ. Functional dyspepsia and irritable bowel syndrome: is there a common pathophysiological basis? *Am J Gastroenterol* 1997; **92**: 954-959
- 25 **Stanghellini V**, Tosetti C, Paternico A, De Giorgio R, Barbara G, Salvioli B, Corinaldesi R. Predominant symptoms identify different subgroups in functional dyspepsia. *Am J Gastroenterol* 1999; **94**: 2080-2085
- 26 **Kennedy TM**, Jones RH, Hungin APS, O'flanagan H, Kelly P. Irritable bowel syndrome, gastro-oesophageal reflux, and bronchial hyper-responsiveness in the general population. *Gut* 1998; **43**: 770-774
- 27 **Tomonaga T**, Awad ZT, Filipi CJ, Hinder RA, Selima M, Tercero F, Marsh RE, Shiino Y, Welch R. Symptom predictability of reflux-induced respiratory disease. *Dig Dis Sci* 2002; **47**: 9-14
- 28 **Tauber S**, Gross M, Issing WJ. Association of laryngopharyngeal symptoms with gastroesophageal reflux disease. *Laryngoscope* 2002; **112**: 879-886
- 29 **Jiang SP**, Liang RY, Zeng ZY, Liu QL, Liang YK, Li JG. Effects of antireflux treatment on bronchial hyper-responsiveness and lung function in asthmatic patients with gastroesophageal reflux disease. *World J Gastroenterol* 2003; **9**: 1123-1125
- 30 **Giacchi RJ**, Sullivan D, Rothstein SG. Compliance with anti-reflux therapy in patients with otolaryngologic manifestation of gastroesophageal reflux disease. *Laryngoscope* 2000; **110**: 19-22
- 31 **Branski RC**, Bhattacharyya N, Shapiro J. The reliability of the assessment of endoscopic laryngeal findings associated with laryngopharyngeal reflux disease. *Laryngoscope* 2002; **112**: 1019-1024
- 32 **Garcia-Compean D**, Gonzalez MV, Galindo G, Mar DA, Trevino JL, Martinez R, Bosques F, Maldonado H. Prevalence of gastroesophageal reflux disease in patients with extraesophageal symptoms referred from otolaryngology, allergy, and cardiology practices: a prospective study. *Dig Dis* 2000; **18**: 178-182
- 33 **Fisher BL**, Pennathur A, Mutnick JLM, Little AG. Obesity correlates with gastroesophageal reflux. *Dig Dis Sci* 1999; **44**: 2290-2294
- 34 **Locke GR 3rd**, Talley NJ, Fett SL, Zinsmeister AR, Melton LJ 3rd. The factors associated with symptoms of gastroesophageal reflux. *Am J Med* 1999; **106**: 642-649
- 35 **Pandolfino JE**, Kahrilas PJ. Smoking and gastro-oesophageal reflux disease. *Eur J Gastroenterol Hepatol* 2000; **12**: 837-842
- 36 **Kadakia SC**, De La Baume HR, Shaffer RT. Effects of transdermal nicotine on lower esophageal sphincter and esophageal motility. *Dig Dis Sci* 1996; **41**: 2130-2134
- 37 **Häuser W**, Grandt D. Tobacco associated gastrointestinal disorders: smoking cessation therapy – a task for gastroenterologists. *Z Gastroenterol* 2002; **40**: 815-821
- 38 **Bohmer CJ**, Klinkenberg-knol EC, Niezen-de Boer RC, Meuwissen SG. The prevalence of gastro-oesophageal reflux disease based on non-specific symptoms in institutionalized, intellectually disabled individuals. *Eur J Gastroenterol Hepatol* 1997; **9**: 187-190
- 39 **Böhmer CJM**, Klinkenberg-Knol EC, Niezen-de Boer MC, Meuwissen SGM. Gastroesophageal reflux disease in intellectually disabled individuals: how often, how serious, how manageable? *Am J Gastroenterol* 2000; **95**: 1868-1872
- 40 **Cranley JP**, Achkar E, Fleshler B. Abnormal lower esophageal sphincter pressure responses in patients with orange juice-induced heartburn. *Am J Gastroenterol* 1986; **81**: 104-106
- 41 **Allen ML**, Mellow MH, Robinson MG, Orr WC. The effect of raw onions on acid reflux and reflux symptoms. *Am J Gastroenterol* 1990; **85**: 377-380
- 42 **Cohen S**, Booth GH Jr. Gastric acid secretion and low-esophageal-sphincter pressure in response to coffee and caffeine. *N Engl J Med* 1975; **293**: 897-899
- 43 **Terry P**, Lagergren J, Wolk A, Nyren O. Reflux-inducing dietary factors and risk of adenocarcinoma of the esophagus and gastric cardia. *Nutrition Cancer* 2000; **38**: 186-191

Serum hepatic enzyme manifestations in patients with severe acute respiratory syndrome: Retrospective analysis

Hui-Juan Cui, Xiao-Lin Tong, Ping Li, Ying-Xu Hao, Xiao-Guang Chen, Ai-Guo Li, Zhi-Yuan Zhang, Jun Duan, Min Zhen, Bin Zhang, Chuan-Jin Hua, Yue-Wen Gong

Hui-Juan Cui, Xiao-Lin Tong, Ping Li, Ying-Xu Hao, Xiao-Guang Chen, Ai-Guo Li, Zhi-Yuan Zhang, Jun Duan, Min Zhen, Bin Zhang, Chuan-Jin Hua, Chinese-Japanese Friendship Hospital, Beijing 100029, China

Yue-Wen Gong, Faculty of Pharmacy, University of Manitoba, Canada

Co-correspondents: Dr. Ping Li

Correspondence to: Dr. Hui-Juan Cui, Chinese-Japanese Friendship Hospital, Yinghua Dong Lu, Hepingli Chaoyang District, Beijing 100029, China. cuihj1963@sina.com

Telephone: 13911835018 **Fax:** +86-10-64206643

Received: 2003-09-15 **Accepted:** 2003-10-22

Abstract

AIM: To evaluate the hepatic function in patients with severe acute respiratory syndrome (SARS) and possible causes of hepatic disorder in these patients.

METHODS: One hundred and eighty-two patients with SARS were employed in a retrospective study that investigated hepatic dysfunction. Liver alanine aminotransferase (ALT), aspartate aminotransferase (AST) and lactic dehydrogenase (LDH) were analyzed in these patients. Patients with different hospital treatments were further investigated.

RESULTS: Of the 182 patients, 128(70.3%) had abnormal ALT activity, 57(31.3%) had abnormal AST activity and 87 (47.8%) had abnormal LDH activity. The peak of elevated hepatic enzyme activities occurred between the sixth day and the tenth day after the first day of reported fever. Of the 182 patients, 160(87.9%) had been treated with antibiotics, 137(75.2%) with Ribavirin, and 115(63.2%) with methylprednisolone. There was no statistically significant correlation between the duration of Ribavirin treatment and hepatic dysfunction.

CONCLUSION: Abnormal liver functions were common in patients with SARS and could be associated with virus replication in the liver.

Cui HJ, Tong XL, Li P, Hao YX, Chen XG, Li AG, Zhang ZY, Duan J, Zhen M, Zhang B, Hua CJ, Gong YW. Serum hepatic enzyme manifestations in patients with severe acute respiratory syndrome: Retrospective analysis. *World J Gastroenterol* 2004; 10(11): 1652-1655

<http://www.wjgnet.com/1007-9327/10/1652.asp>

INTRODUCTION

Severe acute respiratory syndrome (SARS) or so-called atypical pneumonia with unknown etiology started to appear in Guangdong Province, China in November 2002 and quickly spread to other parts of China and around the world^[1,2-4]. A novel coronavirus has been identified as the etiological agent of the syndrome^[5-8]. Most coronaviruses may cause either a respiratory or an enteric change. During the outbreak of SARS,

abnormal hepatic enzyme activity was reported in patients of Toronto area, Canada^[9]. The present study summarized the hepatic enzyme activities in patients with SARS who were treated at the China-Japan Friendship Hospital, Beijing, which started to receive patients with SARS in mid-March 2003, and was designated as one of the three hospitals in Beijing to treat patients with SARS in April 2003.

MATERIALS AND METHODS

Patients

Our study included all patients who received a diagnosis of SARS with no pre-existing live diseases and were treated at the China-Japan Friendship Hospital between March 10 and May 31, 2003, and excluded such patients with a history of liver disorders. According to the criteria for SARS that have been established by the Ministry of Health, China-Clinical Diagnostic Criteria for Severe Acute Respiratory Syndrome^[10], our case definition was a fever (temperature >38 °C), a chest radiograph of the thorax showing evidence of consolidation with or without respiratory symptoms and a history of close contact with a person to whom SARS had been diagnosed. The diagnosis was confirmed by an indirect immunofluorescence assay with fetal rhesus kidney cells that were infected with coronavirus and fixed in acetone to detect a serological response to the virus^[3] or by a positive viral culture. Patients in the study included 103 male and 79 female with age ranging from 11 to 86. The age distribution is shown in Table 1.

Table 1 Age distribution of the patient

Age range (yr)	Case number (n)	%
Under 20	18	9.89
21-30	45	24.73
31-40	35	19.23
41-50	29	15.93
51-60	18	9.89
Above 60	37	20.33

Laboratory examination

Hepatic functions included alanine aminopeptidase (ALT), aspartate aminotransferase (AST) and lactic dehydrogenase (LDH). We studied these variables from the first day of admission to May 31, 2003. The normal values of these enzymes were 0-40 U/L for ALT, 0-42 U/L for AST and 100-250 U/L for LDH.

Data collection

We retrospectively analyzed data from 3 aspects. First, total incidence rate of abnormal liver enzyme activities were analyzed from 182 patients with SARS. Second, the time course of abnormal liver enzyme activities was dissected in 57 patients because these patients were admitted to China-Japan Friendship Hospital from beginning of the illness. The other large proportion of patients with SARS was transferred to China-Japan Friendship Hospital after the hospital was designated

specifically to treat patients with SARS on April 28, 2003. Third, analysis of ribavirin treatment for patients with SARS was performed in 84 cases, as well as their abnormal liver enzyme activities after ribavirin treatment.

Statistical analysis

We used univariate analysis to compare patients with normal and abnormal serum hepatic enzyme activities, and an unpaired Student's *t* test, χ^2 test, or Fisher's exact test, as appropriate. We then performed multiple logistic regression analysis with stepwise analysis to identify independent predictors of the abnormality^[3]. A *P* value of less than 0.05 was considered to indicate statistical significance. All probabilities are two tailed. Statistical analysis software StatView 5.0 for Macintosh OS was employed and data were reported as mean \pm SD unless otherwise indicated.

RESULTS

Between March 10, and May 31, 2003, more than 100 of patients with SARS were admitted to the China-Japan Friendship Hospital; especially on May 8 a large number of patients with SARS were transferred to our hospital at severe stage and some patients were at convalescent stage. Serum samples were collected immediately after the patients were admitted to the hospital. The study included 103 male and 79 female patients from all ethnic background. The mean age was 40.42 years (range 15-78 years).

Incidence rate of abnormal liver enzyme activities in 182 patients

Transiently elevated ALT was observed in 128 (70.3%) patients with SARS. Of the 182 patients with SARS, 57 (31.3%) had elevated AST while 87 (47.8%) had abnormal LDH as indicated in Table 2.

Table 2 Incidence rate of abnormal-liver-function outcomes

	ALT	AST	LDH
Total cases (<i>n</i>)	182	182	139
Abnormal cases (<i>n</i>)	128	57	87
Ratio (%)	70.3	31.3	62.6

Time course of abnormal liver enzyme activities

The time course of abnormal liver enzyme activities was obtained from 57 patients with SARS who were admitted to our hospital at the beginning of illness. The earliest day of abnormal liver enzyme activities was the first day of illness. The peak of abnormal liver enzyme activities was between the sixth and the tenth d of illness. Liver function started to recover 15 d after onset. However, for some patients, abnormal liver enzyme activities could last for almost a month (Figure 1).

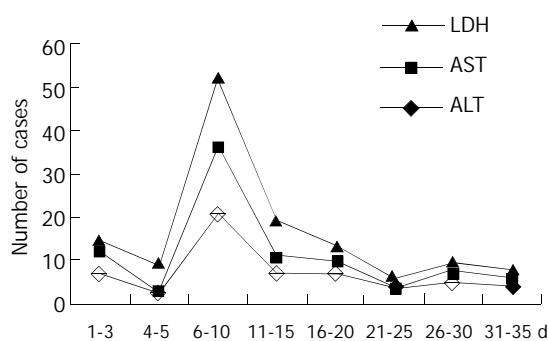


Figure 1 Abnormal-liver-function outcomes at different days.

Comparison of liver enzyme activities before and after hospital treatment

To explore whether hospital treatment could lead to abnormal liver enzyme activities in patients with SARS, we analyzed data of all patients who had normal or abnormal liver enzyme activities before and after hospital treatment. The deadline for entering analysis was June 15, 2003. Patients with hospital treatment less than 15 d were excluded from the study. As shown in Table 3, statistically significant difference was observed in AST and LDH ($P < 0.01$) while no significant difference was obtained in ALT.

Table 3 Abnormal-liver-function outcomes before treatment vs after treatment

Cases (<i>n</i>)	ALT		AST		LDH	
	Before	After	Before	After	Before	After
Total	182	166	182	164	122	105
Normal	93	85	133	145	46	81
Abnormal	89	81	49	19	76	24

Hospital treatment in 182 patients with SARS

Most patients with SARS in our hospital received empirical treatment with antibiotics or ribavirin 400-500 mg, twice daily, or intravenous methylprednisolone at high dosage. As listed in Table 4, of the 182 patients with SARS, 160 (87.9%) received antibiotics, 137 (75.2%) received ribavirin and 115 (63.2%) received methylprednisolone. Since Ribavirin is a drug that inhibits viral replication, it has been widely used in patients with SARS after it was confirmed that coronavirus is etiological factor of SARS. We further analyzed the duration of Ribavirin treatment and its relation to abnormal liver enzyme activities in patients with SARS.

Table 4 Therapeutic drugs in 182 SARS patients

	Antibiotics	Ribavirin	Methylprednisolone
Cases (<i>n</i>)	160	137	115
Rate of usage (%)	87.9	75.2	63.2

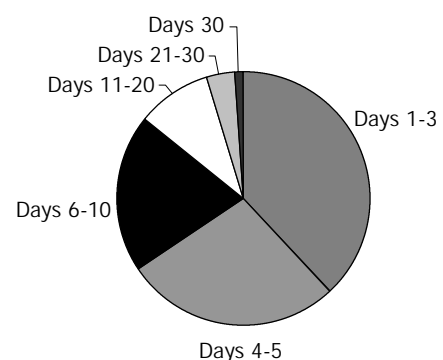


Figure 2 The distribution of of ribavirin treatment in 84 SARS patients.

Distribution of ribavirin treatment in 84 patients with SARS

Although 137 patients with SARS were recorded of ribavirin treatment, only 84 patients were employed for analysis of ribavirin treatment. The reason for choosing these patients was that these patients had detailed record of receiving ribavirin in our hospital and the other 53 patients had already received ribavirin treatment before admitting to our hospital. As shown in Figure 2, 32 (38.1%) patients with SARS received ribavirin treatment at d 1 to 3 after diagnosis of SARS, 23 (27.4%) patients received ribavirin treatment at d 4 to 5, 17 (20.2%)

patients received ribavirin treatment at days 6 to 10. A total of 55(65.5%) patients with SARS received ribavirin treatment within 5 d of the illness while a total of 72(85.7%) patients received ribavirin treatment within 10 d of the illness.

Correlation of ribavirin treatment and abnormal liver enzyme activities

Correlation of ribavirin treatment and abnormal liver enzyme activities was analyzed in 84 patients with SARS. The duration of ribavirin treatment was different among these patients. Twenty-six (29.8%) patients with SARS received ribavirin treatment for 1 to 7 d, 32(35.7%) patients for 8 to 14 d, 20(22.6%) patients for 15 to 21 d and 10(11.9%) patients for more than 22 d. However, as shown in Table 5, there was small increase in liver enzyme activities in patients with longer Ribavirin treatment, but it did not reach statistically significant.

Table 5 The distribution of ribavirin treatment in 84 SARS patients

Treatment	Days 1-3	Days 4-5	Days 6-10	Days 11-20	Days 21-30	Days 30
Cases number	32	23	17	8	3	1
%	38.1%	27.4%	20.2%	9.5%	3.6%	1.2%

DISCUSSION

Abnormal serum liver enzyme activities have been reported by different hospitals with inconsistent incident rates. It was reported that there were 44.7% patients with SARS having abnormal liver enzyme activities in Guangzhou Southern Hospital^[11], And 53.3% was reported in the First Hospital of Beijing University^[12]. Moreover, 40% patients with SARS having abnormal liver enzyme activities were reported in hospitals around great Toronto area^[9]. In our study, we have found that 70% patients with SARS suffered from abnormal liver enzyme activities. The higher percentage of liver damage in our patients might be related to the fact that large number of patients with severe illness were transferred to our hospital.

The difference between these reports may also be associated with different treatment strategies between these areas, especially in the use of ribavirin. Ribavirin (1-b-D-ribofuranosyl-1,2,4-triazole), a broad spectrum antiviral nucleoside, is one of the first antiviral drugs ever discovered. It was first approved in the United States in an aerosol form for the treatment of a severe lung infection in infants^[13]. Recently, it has been employed as an anti-HIV treatment^[14-17] and in combination with interferon for the treatment of hepatitis A, B, and C^[18-21]. Compared with hospitals around great Toronto area (88%), the usage of ribavirin in our hospital (75%) was less. However there were a larger proportion of patients (70%) with abnormal liver enzyme activities in our hospital than that (40%) in hospital around Toronto area. This indicated that ribavirin could not be a contributing factor for abnormal liver enzyme activities observed in patients with SARS. Although there was an increased trend of elevated liver enzyme activities with duration of ribavirin treatment, there was no statistic significant correlation between abnormal liver enzyme activities and duration of ribavirin treatment.

Abnormal liver enzyme activities could also be caused by coronavirus induced liver damage. Although liver biopsy was not feasible in these patients, pathological evaluation of the fatal cases revealed that hepatocytes underwent fatty degeneration, cloudy swelling, focal hemorrhage, apoptosis and dot necrosis, Kupffer cell proliferation, portal infiltration of lymphocytes and dispersive eosinophilic body in the liver^[22, 23]. There was an enlargement of the liver in 23 patients with SARS in our study observed by B-ultrasonic examination

(data reported in another study). Because of difficulty in clinical practice, it was not documented whether pathological impairments of liver function and structure were present in the early stage of the disease. However, we have used herbal medicines and liver protective drugs in these patients. These treatments did not alter the outcome of abnormal liver enzyme activities. Therefore, it is unlikely that hospital treatment contributes to the outcome of abnormal liver enzyme activities in patients with SARS.

Our conclusions are that abnormal liver enzyme activities are common in patients with SARS and coronaviruses that cause severe acute respiratory syndrome might affect the liver and induce liver damage in the course of infection.

REFERENCES

- Luo D.** SARS treatment: experience from a team in Guangdong, China. *Chin Med J* 2003; **116**: 838-839
- Chan YM, Yu WC.** Outbreak of severe acute respiratory syndrome in Hong Kong Special Administrative Region: case report. *Bmj* 2003; **326**: 850-852
- Lee N, Hui D, Wu A, Chan P, Cameron P, Joynt GM, Ahuja A, Yung MY, Leung CB, To KF, Lui SF, Szeto CC, Chung S, Sung JJ.** A major outbreak of severe acute respiratory syndrome in Hong Kong. *N Engl J Med* 2003; **348**: 1986-1994
- Poutanen SM, Low DE, Henry B, Finkelstein S, Rose D, Green K, Tellier R, Draker R, Adachi D, Ayers M, Chan AK, Skowronski DM, Salit I, Simor AE, Slutsky AS, Doyle PW, Krajden M, Petric M, Brunham RC, McGeer AJ.** Identification of severe acute respiratory syndrome in Canada. *N Engl J Med* 2003; **348**: 1995-2005
- Drosten C, Gunther S, Preiser W, van der Werf S, Brodt HR, Becker S, Rabenau H, Panning M, Kolesnikova L, Fouchier RA, Berger A, Burguiere AM, Cinatl J, Eickmann M, Escriou N, Grywna K, Kramme S, Manuguerra JC, Muller S, Rickerts V, Sturmer M, Vieth S, Klenk HD, Osterhaus AD, Schmitz H, Doerr HW.** Identification of a novel coronavirus in patients with severe acute respiratory syndrome. *N Engl J Med* 2003; **348**: 1967-1976
- Ksiazek TG, Erdman D, Goldsmith CS, Zaki SR, Peret T, Emery S, Tong S, Urbani C, Comer JA, Lim W, Rollin PE, Dowell SF, Ling AE, Humphrey CD, Shieh WJ, Guarner J, Paddock CD, Rota P, Fields B, DeRisi J, Yang JY, Cox N, Hughes JM, LeDuc JW, Bellini WJ, Anderson LJ.** A novel coronavirus associated with severe acute respiratory syndrome. *N Engl J Med* 2003; **348**: 1953-1966
- Peiris JS, Lai ST, Poon LL, Guan Y, Yam LY, Lim W, Nicholls J, Yee WK, Yan WW, Cheung MT, Cheng VC, Chan KH, Tsang DN, Yung RW, Ng TK, Yuen KY.** Coronavirus as a possible cause of severe acute respiratory syndrome. *Lancet* 2003; **361**: 1319-1325
- Kuiken T, Fouchier RA, Schutten M, Rimmelzwaan GF, van Amerongen G, van Riel D, Laman JD, de Jong T, van Doornum G, Lim W, Ling AE, Chan PK, Tam JS, Zambon MC, Gopal R, Drosten C, van der Werf S, Escriou N, Manuguerra JC, Stohr K, Peiris JS, Osterhaus AD.** Newly discovered coronavirus as the primary cause of severe acute respiratory syndrome. *Lancet* 2003; **362**: 263-270
- Booth CM, Matukas LM, Tomlinson GA, Rachlis AR, Rose DB, Dwosh HA, Walmsley SL, Mazzulli T, Avendano M, Derkach P, Ephtimos IE, Kitai I, Mederski BD, Shadowitz SB, Gold WL, Hawryluck LA, Rea E, Chenkin JS, Cescon DW, Poutanen SM, Detsky AS.** Clinical features and short-term outcomes of 144 patients with SARS in the greater Toronto area. *JAMA* 2003; **289**: 2801-2809
- Ministry of Health, PR China.** Clinical diagnostic criteria for Severe Acute Respiratory Syndrome (SARS) (On Trial). <http://www.ChinacdcNetcn/56/kong56-2htm#/May 3, 2003>
- Peng J, Hou JL, Guo YB, Feng YK, Cheng JJ, Liu DL, Zhu YY, Jiang RL, Chen YP.** Clinical features of severe acute respiratory syndrome in the Guangzhou area. *Zhonghua Chuanranbing* 2003; **21**: 89
- Huo N, Lu HY, Xu XY, Wang GF, Li HC, Wang GQ, Li JP, Wang J, Nie LG, Gao XM, Zhao ZH, Li J, Li YH, Zhuang H.** The clinical characteristics and outcome of 45 early patients with SARS. *Beijing Daxue Xuebao* 2003; **35**(S1): 19-22

- 13 **Hall CB**, McBride JT, Walsh EE, Bell DM, Gala CL, Hildreth S, Ten Eyck LG, Hall WJ. Aerosolized Ribavirin treatment of infants with respiratory syncytial viral infection. A randomized double-blind study. *N Engl J Med* 1983; **308**: 1443-1447
- 14 **Japour AJ**, Lertora JJ, Meehan PM, Erice A, Connor JD, Griffith BP, Clax PA, Holden-Wiltse J, Hussey S, Walesky M, Cooney E, Pollard R, Timpone J, McLaren C, Johanneson N, Wood K, Booth D, Bassiakos Y, Crumpacker CS. A phase-I study of the safety, pharmacokinetics, and antiviral activity of combination didanosine and Ribavirin in patients with HIV-1 disease. AIDS Clinical Trials Group 231 Protocol Team. *J Acquir Immune Defic Syndr Hum Retrovirol* 1996; **13**: 235-246
- 15 **Vogt MW**, Hartshorn KL, Furman PA, Chou TC, Fyfe JA, Coleman LA, Crumpacker C, Schooley RT, Hirsch MS. Ribavirin antagonizes the effect of azidothymidine on HIV replication. *Science* 1987; **235**: 1376-1379
- 16 **Crotty S**, Andino R. Implications of high RNA virus mutation rates: lethal mutagenesis and the antiviral drug Ribavirin. *Microbes Infect* 2002; **4**: 1301-1307
- 17 **Meier V**, Burger E, Mihm S, Saile B, Ramadori G. Ribavirin inhibits DNA, RNA, and protein synthesis in PHA-stimulated human peripheral blood mononuclear cells: possible explanation for therapeutic efficacy in patients with chronic HCV infection. *J Med Virol* 2003; **69**: 50-58
- 18 **Saito Y**, Escuret V, Durantel D, Zoulim F, Schinazi RF, Agrofoglio LA. Synthesis of 1, 2, 3-triazolo-carbanucleoside analogues of Ribavirin targeting an HCV in replicon. *Bioorg Med Chem* 2003; **11**: 3633-3639
- 19 **Liu CJ**, Chen PJ, Lai MY, Kao JH, Jeng YM, Chen DS. Ribavirin and interferon is effective for hepatitis C virus clearance in hepatitis B and C dually infected patients. *Hepatology* 2003; **37**: 568-576
- 20 **Rakov NE**. Peginterferon alfa-2a plus Ribavirin for chronic hepatitis C. *N Engl J Med* 2003; **348**: 259-260
- 21 **Zhang H**, Yang G, Yang X. Prospective study of combination of interferon-alpha with Ribavirin for treatment of chronic hepatitis C in children. *Zhonghua Shiyan Helin Chuangbing Duxue Zazhi* 2001; **15**: 81-82
- 22 **Wang CE**, Qin ED, Gan YH, Li YC, Wu XH, Cao JT, Yu M, Si BY, Yan G, Li JF, Zhu QY. Pathological observation on sucking mice and Vero E6 cells inoculated with SARS samples. *Jifangjun Yuxue Zazhi* 2003; **28**: 383-384
- 23 **Hong T**, Wang JW, Sun YL, Duan SM, Chen LB, Qu JG, Ni AP, Liang GD, Ren LL, Yang RQ, Guo L, Zhou WM, Chen J, Li DX, Xu WB, Xu H, Guo YJ, Dai SL, Bi SL, Dong XP, Ruan L. Chlamydia-like and coronavirus-like agents found in dead cases of atypical pneumonia by electron microscopy. *Zhonghuan Yixue Zazhi* 2003; **83**: 632-636

Edited by Zhu LH Proofread by Xu FM

Maastricht II treatment scheme and efficacy of different proton pump inhibitors in eradicating *Helicobacter pylori*

Engin Altintas, Orhan Sezgin, Oguz Ulu, Ozlem Aydin, Handan Camdeviren

Engin Altintas, Orhan Sezgin, Department of Gastroenterology, Mersin University, Faculty of Medicine, Mersin, Turkey

Oguz Ulu, Department of Internal Medicine, Mersin University, Faculty of Medicine, Mersin, Turkey

Ozlem Aydin, Department of Pathology, Mersin University, Faculty of Medicine, Mersin, Turkey

Handan Camdeviren, Department of Biostatistics, Mersin University, Faculty of Medicine, Mersin, Turkey

Correspondence to: Engin Altintas, MD, Asst. Professor Mersin Universitesi Tip Fakultesi Hastanesi, İç Hastalıkları A.D. Zeytinlibahçe Caddesi, Eski Otogar Yani 33079 Mersin, Turkey. enginaltintas@mersin.edu.tr

Telephone: +90-324-3374300 **Fax:** +90-324-3367117

Received: 2003-12-28 **Accepted:** 2004-01-09

Altintas E, Sezgin O, Ulu O, Aydin O, Camdeviren H. Maastricht II treatment scheme and efficacy of different proton pump inhibitors in eradicating *Helicobacter pylori*. *World J Gastroenterol* 2004; 10(11): 1656-1658

<http://www.wjgnet.com/1007-9327/10/1656.asp>

Abstract

AIM: The Maastricht II criteria suggest the use of amoxicillin and clarithromycin in addition to a proton pump inhibitor over 7-10 d as a first line therapy in the eradication of *Helicobacter pylori* (*H. pylori*). For each proton pump inhibitor, various rates of eradication have been reported. The present study was to compare the efficacy of different proton pump inhibitors like omeprazole, lansoprazole and pantoprazole in combination with amoxicillin and clarithromycin in the first line eradication of *H. pylori* and to investigate the success of *H. pylori* eradication in our district.

METHODS: A total of 139 patients were included having a *Helicobacter pylori* (+) gastroduodenal disorders diagnosed by means of histology and urease test. Besides amoxicillin (1 000 mg twice a day) and clarithromycin (500 mg twice a day), they were randomized to take omeprazole (20 mg twice a day), or lansoprazole (30 mg twice a day), or pantoprazole (40 mg twice a day) for 14 d. Four weeks after the therapy, the eradication was assessed by means of histology and urease test. It was evaluated as eradicated if the *H. pylori* was found negative in both. The complaints (pain in epigastrium, nocturnal pain, pyrosis and bloating) were graded in accordance with the Licert scale. The compliance of the patients was recorded.

RESULTS: The eradication was found to be 40.8% in the omeprazole group, 43.5% in the lansoprazole group and 47.4% in the pantoprazole group. Sixty-three out of 139 patients (45%) had eradication. No statistically significant difference was observed between the groups. Significant improvements were seen in terms of the impact on the symptom scores in each group.

CONCLUSION: There was no difference between omeprazole, lansoprazole and pantoprazole in *H. pylori* eradication, and the rate of eradication was as low as 45%. Symptoms were improved independent of the eradication in each treatment group. The low eradication rates suggest that the antibiotic resistance or the genetic differences of the microorganism might be in effect. Further studies are required to verify these suggestions.

INTRODUCTION

So far, no ideal treatment exists although there have been plenty of treatment schemes in the eradication of *Helicobacter pylori* (*Hp*). Therefore, research on this subject has substantially increased. In order to achieve the optimal treatment regimen various combinations including antibiotics and antisecretory agents have been tested^[1]. In 2000, use of amoxicillin and clarithromycin for a period of at least 1 wk in combination with a proton pump inhibitor (PPI) was suggested^[2]. Diverse eradication rates have been reported with this specific treatment scheme^[3-6]. Up to date, five diverse PPIs have been launched in our country. The outcomes obtained from studies related with those inhibitors have resulted in confusing eradication rates.

The present study aimed to investigate the efficacy of three different PPIs given in combination with antibiotics, which have been accepted to be standard in the eradication of *Hp* and the success of *Hp* eradication by this standard treatment.

MATERIALS AND METHODS

Between September 2001 and July 2002, 139 patients with gastritis, gastric ulcer and duodenal ulcer were enrolled in this study. All patients were positive in urease test and histopathological examination for *Hp*. Patients with a concomitant serious illness and a history of gastric surgery, pregnancy, patients taking antibiotics, H-2 receptor blockers or on PPI treatment within the last two months, being allergic to macrolides and having a previous eradication treatment were excluded. Their written informed consent was received. They were randomized to take omeprazole 2×20 mg/d (OAC), lansoprazole 2×30 mg/d (LAC) or pantoprazole 2×40 mg/d (PAC) plus amoxicillin 2×1 000 mg/d and clarithromycin 2×500 mg/d for 14 d. All of the eligible patients had standard laboratory tests, and their history, physical examination and concomitant treatment regimens were recorded. Their complaints (epigastric pain, bloating, nocturnal pain and pyrosis) were graded in accordance to the Licert scale (0=none, 1=mild, 2=moderate, 3=severe, 4=very severe). Two biopsies were taken from the antrum and corpus for pathology, and a biopsy from the antrum for urease test. The pathological assessment was based on the Sidney classification for gastritis. 4 wk after the therapy the side effects and alterations were re-evaluated, and a blinded gastroenterologist repeated the endoscopical examination. Negative *Hp* in both urease test and biopsy was accepted as eradication.

To understand the compliance, the patients were asked to report how many prescribed drugs they used (100%-forgotten for 0 d, 80-99%-forgotten only for 1 d, 60-79%-forgotten for 2 d and below 59%-forgotten more than 2 d). The side effects were recorded.

Statistical analysis

The definitive statistics were calculated (mean±SD, numbers and % values). For age comparison in three groups, simple analysis of variance was used while gender, smoking, NSAID use, alcohol consumption, eradication status and relationship between the three groups were determined by Pearson chi-square test, which was also used to determine the relation between the eradication status and antral gastritis and pangastritis plus smoking and histological activity in the antrum prior to eradication. The differences in the symptom score between the eradicated and non-eradicated were investigated by Wilcoxon test before and after the eradication. Furthermore, t-test was applied to compare the improvement rates in the separate symptom score between the eradicated and non-eradicated in relation to the difference between the rates in 3 groups.

RESULTS

Table 1 gives the demographical characteristics of the patients in the three groups. Of the patients, 73(58.3%) were women, and 66(41.7%) were men, and the average age was 47.9±11.8 years. The patient compliance was 95%. Two patients from each group discontinued the therapy for 8 d due to side effects (nausea, vomiting, and diarrhea). The endoscopic lesions are shown in Table 2. The eradication was found in 22 out of 49 patients (40.8%) in the omeprazole group, 20 out of 46 patients (43.5%) in the lansoprazole group, and 21 out of 44 patients (47.4%) in the pantoprazole group. There was no any differences between three groups ($P>0.05$). The overall eradication rate was 45%. Twenty-two out of 62 patients (37%) with antral gastritis had eradication while 19 out of 34 patients (55%) with pangastritis had eradication ($P<0.05$). No correlation was found between eradication and smoking and histological activity in the antrum prior to eradication ($P>0.05$). Significant improvements were observed in the symptom score between the eradicated and non-eradicated compared to pre-eradication status ($P<0.05$), but no significant differences were found between the groups.

Table 1 Demographic features of study population

	OAC	LAC	PAC	P
Patient number	49	46	44	NS
Female/Male	26/23	23/23	24/20	NS
Year				
Mean	47.5±13.4	45.7±12.5	44.5±13.5	NS
Range	20-75	21-73	20-70	NS
Smoking	7 (14.2%)	6 (13%)	6 (13.6%)	NS
NSAID	9 (18.3%)	8 (17.3%)	8 (17.1%)	NS
Alcohol	(22.4%)	9 (19.5%)	10 (22.7%)	NS

Table 2 Endoscopic findings

Finding	Patient n, (%)
Antral gastritis	62 (44.5)
Pangastritis	34 (24.5)
Bulbitis	14 (10)
Bile reflux gastritis	12 (8.6)
Duodenal ulcer	7 (5.3)
Atrophic gastritis	6 (4.3)
Gastric ulcer	4 (2.8)

DISCUSSION

Recently, triple therapies including a PPI and two antibiotics have been found to be the most effective eradication regimens

in the treatment of *Hp* eradication^[7,8]. The most common antibiotics used in the triple therapies were amoxicillin, clarithromycin and metronidazole^[7,8]. Treatment regimens including PPIs are now used at all stages of the *Hp* eradication. The highest eradication rates for *Hp* (80-95%) have been achieved by using antibiotics at least for one week^[9]. However, even the highest doses of omeprazole or an increased treatment duration for 2 wk did not provide 100% eradication^[10-13]. In the European consensus meeting, it suggested that PPI treatment for one week including amoxicillin and clarithromycin was the first line therapy^[10].

Our study showed that triple therapy for 2 wk was safe and well tolerated. The patient compliance was 95%. However, the eradication rate was 45%. Similarly in a study from Adana (Southern Anatolia), a two-week usage of lansoprazole, amoxicillin and clarithromycin resulted in 59% eradication^[14]. In Istanbul (North Western Anatolia) and Nigde (Central Anatolia) the eradication rates were found below 50% in two different studies^[15,16].

Similarly, in Iran, the eradication rates with omeprazole, amoxicillin and clarithromycin were found to be below 70%^[17]. Also, some European studies reported similar rates of eradication^[12,13,18-20,22,23]. Rinaldi^[21] studied 278 patients by using a treatment regimen similar to ours (omeprazole, lansoprazole and pantoprazole in combination with amoxicillin and clarithromycin for one week). The eradication rates were found to be 86%, 74% and 76% respectively, which were higher than our results, yet far beyond the acceptance levels^[21].

Different eradication results obtained by similar treatment regimens suggest that resistance to antibiotics, virulent factors of *Hp* or type of gastroduodenal disorders of patients might have played a role in the outcomes. In some of the studies resulted in lower eradication rates, the resistance to clarithromycin was as high as 10%^[24]. In a study carried out in Ankara (Central Anatolia), the resistance to clarithromycin was 11.4%^[25]. An Italian study found the primary resistance to clarithromycin was 3.2%^[26]. The primary resistance to macrolides was between 3-12% in Europe and 2-10% in the United States^[27,28]. We did not investigate the resistance to antibiotics in the present study. However, we believe that the resistance to antibiotics might have played an important role in our results. Also the majority of the events were from the non-ulcer dyspepsia group, therefore this might have an effect on the result because a lower rate of eradication was reported in patients with non-ulcer dyspepsia compared to those with peptic ulcer^[24,29]. Our results showed that patients with pangastritis had a better eradication than those with antral gastritis ($P<0.05$). This was in compliance with the correlation between the severity of gastritis and the rate of eradication^[30,31].

In conclusion, our findings from Mersin (Southern Anatolia) with lower eradication rates obtained by similar treatment regimens compared to other districts in Turkey and in the World demonstrate that it is necessary to find out a treatment scheme specific to the district. The findings prove that standard treatment regimens might not be suitable and therefore establishment of a new treatment protocol in accordance with the results obtained locally is inevitable. We believe that the lower rates of eradication might have resulted from the resistance to antibiotics.

REFERENCES

- 1 **Fennerty MB.** What are the treatment goals for helicobacter pylori infection? *Gastroenterology* 1997; **113** (Suppl): S120-125
- 2 **Malfertheiner P,** Megraud F, O' Morain C, Hungin AP, Jones R, Axon A, Graham DY, Tytgat G. European *Helicobacter pylori* Study Group (EHPSG). Current concepts in the management of helicobacter pylori infection-The Maastricht 2-2 000 Consen-

- sus report. *Aliment Pharmacol Ther* 2002; **16**: 167-180
- 3 **Herrerias JM**, Bujanda L, Pena D. Efficacy and cost study in Portugal and Spain of three different 7 day eradication regimens of *Helicobacter pylori*. *Gastroenterology* 1999; **116**: A186
 - 4 **Spinzi GC**, Bortoli A, Corbellini A. One week therapy with omeprazole (PPY) or ranitidine bismuth citrate (RBC) and two antibiotics for the eradication of *Helicobacter pylori* in duodenal ulcer: a preliminary report. *Gastroenterology* 1998; **116**: A294
 - 5 **Sung JY**, Leung WK, Ling TK, Yung MY, Chan FK, Lee YT, Cheng AF, Chung SC. One week use of ranitidine bismuth citrate, amoxicillin and claritromycin for the treatment of *Helicobacter pylori* related duodenal ulcer. *Aliment Pharmacol Ther* 1998; **12**: 723-730
 - 6 **Susi D**. The best treatment for *Helicobacter pylori* infection among for different 7 day triple therapies. *Gut* 1998; **43** (Suppl 2): A80
 - 7 **Peura DA**. The report of the digestive health initiative international update conference on *Helicobacter pylori*. *Gastroenterology* 1997; **113**: 4-8
 - 8 **Chey WD**. Treating *Helicobacter pylori*: candidate and regimen selection. *Contemp* 1997; **9**: 52-61
 - 9 **Pounder RE**. New developments in *H pylori* eradication therapy. *Scand J Gastroenterol* 1997; **32** (suppl): 43-45
 - 10 **The European Helicobacter Pylori Study Group**. Current European concepts in the management of *Helicobacter pylori* infection. The Maastricht Consensus Report. *Gut* 1997; **41**: 8-13
 - 11 **Forne M**, Viver JM, Esteve M, Fernandez-Banares F, Lite J, Quintana S, Salas A, Garau J. Randomized clinical trial comparing two one week triple therapy regimens for the eradication of *Helicobacter pylori* infection and duodenal ulcer healing. *Am J Gastroenterol* 1998; **93**: 35-38
 - 12 **Delchier JC**, Elamine I, Goldfain D, Chaussade S, Barthelemy P, Idstrom JP. Omeprazole-amoxicillin versus omeprazole-amoxicillin-clarithromycin in the eradication of *Helicobacter pylori*. *Aliment Pharmacol Ther* 1995; **10**: 263-268
 - 13 **Scwartz H**, Krause R, Sahba B, Haber M, Weissfeld A, Rose P, Siepman N, Freston J. Triple versus dual therapy eradication of *Helicobacter pylori* and preventing ulcer recurrence: a randomized, double-blind, multicenter study of lansoprazole, clarithromycin, and/or amoxicillin in different dosing regimens. *Am J Gastroenterol* 1998; **93**: 584-590
 - 14 **Ergün Y**, Abaylı B, Öksüz M. Helikobakter pilori pozitif kronik aktif gastritli hastalarda değişik iki tedavi protokolünün etkinliği. *Turk J Gastroenterol* 2002; **13**(Suppl 1): 86
 - 15 **Bölükbaşı F**, Kılıç H, Bölükbaşı C. *Helikobakter pilori* eradikasyonu sonrası reflü özefajit sıklığı. *Turk J Gastroenterol* 2001; **12**(Suppl 1): 87
 - 16 **Bölükbaşı F**, Kılıç H, Bölükbaşı C. *Helikobakter pilori* eradikasyon tedavisinde eradikasyon oranları ve tedavi süresinin bu oranlara etkisi. *Turk J Gastroenterol* 2001; **12**(Suppl 1): 88
 - 17 **Sotoudehmanesh R**, Malekzadeh R, Vahedi H, Dariani NE, Asgari AA, Massarrat S. Second-line *Helicobacter pylori* eradication with a furazolidon-based regimen in patients who have failed a metranidazole-based regimen. *Digestion* 2001; **64**: 222-225
 - 18 **Tursi A**, Cammarato G, Montalto M, Papa A, Veneto G, Cuoco L, Trua F, Branca G, Fedeli G, Gasbarrini G. Low-dose omeprazole plus clarithromycin and either tinidazole or amoxicillin for *Helicobacter pylori* infection. *Aliment Pharmacol Ther* 1996; **10**: 285-288
 - 19 **Spinzi GC**, Bierty L, Bortoli A, Colombo E, Fertitta AM, Lanzi GL, Venturelli R, Minoli G. Comparison of omeprazole and lansoprazole in short term triple therapy for *Helicobacter pylori* infection. *Aliment Pharmacol Ther* 1998; **12**: 433-438
 - 20 **Catalano F**, Catanzaro R, Bentivegna C, Brogna A, Condorelli G, Cipolla R. Ranitidine bismuth citrate versus omeprazole triple therapy for *Helicobacter pylori* infection. *Aliment Pharmacol Ther* 1998; **12**: 59-62
 - 21 **Rinaldi V**, Zullu A, De Francesco V, Hassan C, Winn S, Stoppino V, Faleo D, Attili AF. *H pylori* eradication with proton pump inhibitor based triple therapies and re-treatment with ranitidine bismuth citrate based triple therapy. *Aliment Pharmacol Ther* 1999; **13**: 163-168
 - 22 **Deltenre M**, Jonas C, van Gossum M, Buset M, Otero J, De Koster E. Omeprazole-based antimicrobial therapies: results in 198 *H pylori* positive patients. *Eur J Gastroenterol Hepatol* 1995; **7**(Suppl 1): 39-44
 - 23 **Labenz J**, Stolte M, Peitz U, Tillenburg B, Becker T, Borsch G. One-week triple therapy with omeprazole, amoxicillin and clarithromycin or metranidazole for cure of *Helicobacter pylori* infection. *Aliment Pharmacol Ther* 1996; **10**: 207-210
 - 24 **Biggard MA**, Delchier JC, Riachi G, Thibault P, Barthelemy P. One week triple therapy using omeprazole, amoxicillin and clarithromycin for the eradication of *Helicobacter pylori* infection in patients with non-ulcer dyspepsia: influence of dosage of amoxicillin and clarithromycin. *Aliment Pharmacol Ther* 1998; **12**: 383-388
 - 25 **Özaslan E**, Balaban G, Tatar H. *Helikobakter pilori* eradikasyonunda en yaygın kullanılan LAK protokolünün başarısı azalıyor mu? *Turk J Gastroenterol* 2001; **12**(Suppl 1):93
 - 26 **Bazzoli F**, Zagari M, Pozzato P, Varoli O, Fossi S, Ricciardiello L, Alampi G, Nicolini G, Sottili S, Simoni P, Roda A, Roda E. Evaluation of short term low dose triple therapy for the eradication of *Helicobacter pylori* by factorial design in a randomized, double-blind, controlled study. *Aliment Pharmacol Ther* 1998; **12**: 439-445
 - 27 **Huang JQ**, Hunt RH. Treatment failure: the problem of non-responders. *Gut* 1999; **45**(Suppl): 140-144
 - 28 **Tankowic J**, Lamarque D, Lascols C, Soussy CJ, Delchier JC. The impact of *Helicobacter pylori* resistance to clarithromycin on the efficacy of the omeprazole-amoxicillin-clarithromycin therapy. *Aliment Pharmacol Ther* 2001; **15**: 707-713
 - 29 **Schimd CH**, Ross SD, Witing GW. Omeprazole plus antibiotics in the eradication of *Helicobacter pylori* infection: a meta regression. *Gut* 1996; **39**(Suppl 2): A37
 - 30 **Kamada T**, Haruma K, Komoto K, Mihara M, Chen X, Yoshihara M, Sumii K, Kajiyama G, Tahara K, Kawamura Y. Effect of smoking and histological gastritis severity on the rate of *Helicobacter pylori* eradication with omeprazole, amoxicillin and clarithromycin. *Helicobacter* 1999; **4**: 204-210
 - 31 **Georgopoulos SD**, Ladas SD, Karatapanis S, Mentis A, Spiliadi C, Artikis V, Raptis SA. Factors that may affect treatment outcome of triple *Helicobacter pylori* eradication therapy with omeprazole, amoxicillin, and clarithromycin. *Dig Dis Sci* 2000; **45**: 63-67

Liver regional continuous chemotherapy: Use of femoral or subclavian artery for percutaneous implantation of catheter-port systems

An-Long Zhu, Lian-Xin Liu, Da-Xun Piao, Ya-Xin Lin, Jin-Peng Zhao, Hong-Chi Jiang

An-Long Zhu, Lian-Xin Liu, Da-Xun Piao, Jin-Peng Zhao, Hong-Chi Jiang, Department of General Surgery, First Clinical College, Harbin Medical University, Harbin, 150001, Heilongjiang Province, China

Ya-Xin Lin, Department of Neurology, Heilongjiang Province Hospital, Harbin 150036, Heilongjiang Province, China

Supported by National Natural Science Foundation of China, No. 30300339

Correspondence to: Lian-Xin Liu, Department of General surgery, First Clinical College, Harbin Medical University, Harbin, 150001, Heilongjiang Province, China. liulianxin@sohu.com

Telephone: +86-451-53658828 **Fax:** +86-451-53670428

Received: 2004-02-06 **Accepted:** 2004-02-18

Abstract

AIM: To evaluate the feasibility and safety of the intraarterial chemotherapy of the liver cancer by an interventional method, catheter-port system.

METHODS: Thirty-two catheter-port systems were implanted percutaneously via the femoral artery or subclavian artery. Chemotherapies were performed 0-5 d after the implantation of the catheter-port systems. The mean interval between two sequent chemotherapies was 4 wk. The occurrence of side effects of the implantation was examined clinically.

RESULTS: Implantation of the catheter-port was successful in all patients. Mean patency period was 210 d. One occlusion (3.1%) of the catheter was observed. Displacement of the catheter was observed in one case (3.1%). One patient rated a hematoma in the chest wall as important. Mild hematoma was reported in 8 cases (25%). In 3 of 32 cases (9.4%), mild pain was reported initially, and dysesthesia was reported in seven (21.9%). No patient rated overall discomfort as mild, severe, or important.

CONCLUSION: Percutaneous placement is feasible and safe for liver regional continuous chemotherapy. Compared with surgical placement, the overall complication rate is comparable or less.

Zhu AL, Liu LX, Piao DX, Lin YX, Zhao JP, Jiang HC. Liver regional continuous chemotherapy: Use of femoral or subclavian artery for percutaneous implantation of catheter-port systems. *World J Gastroenterol* 2004; 10(11): 1659-1662
<http://www.wjgnet.com/1007-9327/10/1659.asp>

INTRODUCTION

Systemic chemotherapy in cases of liver cancer and liver metastases of colorectal cancer has nearly been abandoned due to the high non-response rates. Regional continuously intraarterial chemotherapy has demonstrated better response rates than systemic chemotherapy^[1-4]. Percutaneously

implantable catheter-port systems have been developed for long-term use to facilitate the long-term administration of chemotherapeutic agents. These systems allow easy and repetitive puncture in infusion therapy without doing much harm to the vessels, and their use is comfortable for the patient. So far, the implantation of permanent intraarterial catheter systems in the gastroduodenal artery^[1,5-9] or via the subclavian, axillary, or brachial arteries into the common hepatic artery^[10-12] has been performed surgically with considerable complication rates. Moreover, the repair and replacement of malfunctioning port systems previously required surgery^[9,13,15,16]. Thus far, percutaneous implantation of catheter-port systems for intraarterial use in various target organs, particularly in regional chemotherapy of the liver, has been successfully performed by radiologists^[14,17-20].

MATERIALS AND METHODS

Patients

From December 1999 to July 2003, 32 percutaneously implantable catheter-port systems (B|BRAUN, Germany) were placed in 32 patients (23 men and 9 women; age range, 26-65 years; mean age, 56 years) with primary malignancies of the liver (26 cases) and metastasizes (6 cases). Three patients had Cholangioma within the 25 primary malignancies. In all patients, the catheter-port system implanted percutaneously with radiologic guidance was the first method used to administer intraarterial chemotherapy. One patient had been performed intervention for 2 times because the catheter-port systems failed to be implanted through the femoral arteries in the first performance of intervention. The catheter-ports were implanted percutaneously through subclavian arteries in the second time. We obtained informed consent from each patient prior to the procedure.

Catheter-port system

The standard catheter-port device consisted of a polysulphone port reservoir with a silicone septum at the puncture site and a lateral stem to slip the silicone catheter over. The connection between the silicone catheter and the polyurethane catheter was reinforced with a small plastic cannula. The port reservoir, polyurethane catheter, cannula, and suture material were commercially available as part of the standard catheter-port system.

Technical procedure

The angiographic catheter was advanced into the respective target vessel such as the common or proper hepatic artery with fluoroscopic guidance after the common femoral or subclavian artery was punctured with use of the Seldinger technique, and visceral arteriography was performed to assess variant arterial supply. The final position of the catheter tip, and thereby the region of perfusion, was chosen according to the anatomy of each patient and the location of the lesion at digital subtraction angiography. The catheter tip was placed into the right hepatic artery ($n=9$), the proper hepatic artery ($n=21$), and the common hepatic artery ($n=1$). The latter position was used in one patient

with variant common hepatic artery without the proper hepatic artery (Figure 1). In this patient, the gastroduodenal artery was occluded because of the variant arterial supplies (Figure 2). The correct position of the catheter was verified with digital subtraction angiography.

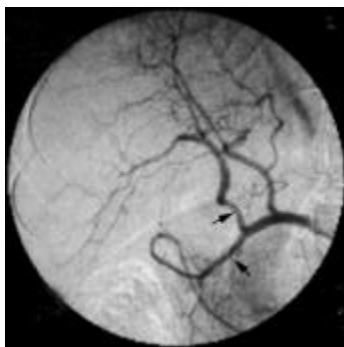


Figure 1 The gastroduodenal artery is the end of the branch of the common hepatic artery. The proper hepatic artery was absent. Gastroduodenal artery (white arrow), right hepatic artery (black arrow).



Figure 2 The gastroduodenal artery has been occluded by a fibred platinum coil (arrow).

The catheter-port systems were implanted percutaneously in inpatients. The antibiotic agent was given 20 min before operation and no conscious sedation treatment was administered.

To insert the catheter-port system, an incision approximately 3 cm long was made in the skin distally to the right groin at the anterior surface of the thigh or at the anterior surface of the left or right chest wall, starting from 3 cm distally to the cutaneous puncture site and leading downward along the femoral triangle or leading parallel to the dermatoglyph. A subcutaneous pocket was then formed wherein the port reservoir was to be placed. The end of the catheter was cut off distally to the puncture site, and then was connected tightly to the port reservoir.

Tunneling was made from the puncture site to the incision and the port reservoir was not fixed to the subcutaneous tissue with an extra suture (Figure 3). Final port angiography helped verify the integrity of the system and correct position of the catheter. When necessary, malposition or dysfunction was corrected before the subcutaneous pocket was closed. A compression bandage was applied in each patient for 24 h.

The patients were mobilized 24 h after the intervention. There were no restrictions on patient activity 24 h after the device was in place. Bed rest was not necessary. By choice, most patients stayed in hospital until the onset of chemotherapy, which was 0-5 d after implantation (mean, 2 d) because of the healing of the incisions or the amelioration of liver function. We regularly flushed the catheter system with 10 mL of heparin sodium (25 eIU/mL heparin) at the end of each chemotherapeutic cycle, and before final withdrawal of the port needle, but not

between two chemotherapeutic cycles. Patients did not receive any anticoagulation therapy systemically or via the catheter system. At the end of the study, no patients were lost to follow-up. Correct functioning of each catheter-port system was verified with digital subtraction angiography prior to each chemotherapeutic treatment cycle. At each angiographic study, patients were examined clinically for the occurrence of negative side effects, such as peripheral embolization, occlusion. They were also asked to complete a questionnaire regarding their satisfaction with the percutaneously implanted catheter-port system and the presence of local complications, such as hematoma, infection, pain, restriction of motion, dysesthesia, and long-term discomfort. The patients rated these complications as absent, mild, or important. Mild hematoma was defined as discoloration of the skin without subcutaneous swelling or induration for a maximum of 1 wk. Important hematoma was defined as subcutaneous induration with palpable liquid collection around the device of more than 2 cm in diameter.



Figure 3 Fluoroscopic image depicts a catheter-port system in the right side of the groin in a 36-year-old male patient with hepatic carcinoma catheter (arrowheads), stem (large open arrow), and port reservoir (thin black arrow).

RESULTS

Implantation of the catheter-port was successful in all patients. Only 2 patients were performed for 2 times because of the failures of implantation through femoral arteries in the first operation. We changed to the subclavian artery and the implantation was successful in the second time. All implantation procedures were performed in the interventional radiology suite with a mean procedure time of 51 min (range, 30-145 min). No peri-interventional complications were noticed. The mean follow-up of the systems was 210 d (range, 36-680 d).

Complications occurred in 2(6.25%) of 32 cases. One occlusion (1 of 32 cases, 3%) of the catheter was observed on d 36. The occlusion was a result of misuse of heparin solution after the chemotherapy with a subsequent reflux of blood into the catheter. Because lytic therapy with 10 000 IU of urokinase in 2 mL of water solution was not successful in this patient, the catheter-port system was disused.

Displacement of the catheter was observed in one case (1 of 32 cases, 3%) at the third angiographic follow-up study. The catheter tip was dislocated into the abdominal artery and could be repositioned into the common hepatic artery by using an interventional maneuver. Since the patient did not want to continue chemotherapy, the port system was entirely disused, but was not removed by operation.

The overall disused rate was 6% (2 of 32 cases). All disused catheter-ports were not removed.

After implantation of a catheter-port system, one patient rated a hematoma in the chest wall as important, but this could not be verified at any clinical follow-up examination, and it did

not require surgical intervention. Immediately after implantation, mild hematoma was reported in 8 of 32 cases (25%), but no hemorrhage at the implantation or puncture site was found at the first follow-up examination in any of these cases. In 3 of 32 cases (9%), mild pain was reported initially, and dysesthesia was reported in 7 (22%). No patient rated overall discomfort as mild, severe, or important.

Till July 2003, 145 port angiographic studies were performed as follow-up examinations at a mean interval of 4 wk between each study. The patients were examined clinically for the occurrence of side effects at the time of each angiographic examination. No patients showed signs of peripheral arterial embolization, occlusion, or embolic effects. At all follow-up examinations, we did not find infection, leakage, kinking, or disconnection of any catheter-port system. According to the patient questionnaires, all patients were entirely satisfied with the system. No patient reported restriction of motion or discomfort owing to the port reservoir in the groin or chest wall.

DISCUSSION

Continuous chemotherapeutic infusion has proved to be prior to the systemic chemotherapy in liver cancer. Permanent percutaneously implanted catheter-port systems are widely used method for it with the advantage for repeated external arterial or central venous access for regional or systemic chemotherapy and prolonged parenteral nutrition^[2,6,16]. The majority of catheter-port devices developed for intraarterial regional chemotherapy have necessitated surgical implantation before the interventional method was applied clinically^[7,11,21-23]. The common sites of surgical implantation are gastroduodenal, common or proper hepatic arteries for regional intraarterial chemotherapy of the liver.

It has been reported the implantation of an intraarterial catheter-port with fluoroscopic guidance in the interventional radiology suite without laparotomy^[8]. The femoral arteries were used for minimally invasive catheter placement. Radiologic implantation is also associated with various complications, such as catheter dislocation, occlusion, and infection. Dislocation and occlusion of catheter are the severest complications, which lead to the termination of chemotherapy or another traumatic implantation procedure^[10,12,16,23].

Thrombotic complications such as catheter occlusion and occlusion of the hepatic artery are also commonly associated with both surgically and radiologically implanted catheter-port systems^[1,7,9,10,12,23]. Catheter placement via the brachial artery can also be accompanied by thrombosis or occlusion of the brachial artery^[12,13]. In our patient group, one case of catheter occlusion was caused by blood reflux into the 4-F catheter. Catheters with small diameters have higher occlusion rates. Niederhuber *et al.*^[20] also found that small-bore catheters had an inferior patency rate and drug infusion might be difficult owing to the higher resistance of small catheters. Some infusion pumps might stop at pressure levels that are too high. Therefore, on the basis of results in our study and the literature, we do not recommend the use of catheter below 4-F for permanent implantation in this context.

With regard to prevent catheter thrombosis, different authors have various ideas. Two methods have been recommended: administration of warfarin sodium and continuous catheter perfusion with heparin^[18]. We believe that keeping blood from the lumen of catheter and perfusion with the end of each chemotherapy are the efficient methods. We do not consider systemic or other type of anticoagulation therapy necessary. Lytic therapy with tissue plasminogen activator, urokinase, or streptokinase has been reported to be useful in cases of catheter occlusion, but this method is successful only in a few cases^[9,16]. In our study, lytic therapy was not effective.

But the permanent existence of the disused catheter-port system has no harm to the patient if there is no septic episode.

The frequency of dislocation appeared to be particularly high when the axillary or brachial artery was used^[10,12]. It could be due to the too soft and flexible catheter material and the mobility of the upper limb. In our study, displacement occurred in one of our cases (3.1%), in which the port reservoir was implanted in the chest wall through right subclavian artery, into the abdominal artery. Retrospectively, we believe this displacement into the abdominal artery was probably due to too much tension on the indwelling catheter and the mobility of upper limb. Therefore, optimal catheter configuration and the approach are crucial. We recommend that the right femoral artery should be the best approach.

Infection is another complication in permanently implanted catheter systems that often makes removal of the device necessary^[18,19,24,29,30]. Infection rates ranged from 0%^[25-28] to 7.6%^[11,17,23,24]. Infection and sepsis during chemotherapy can be caused by the use of inappropriate hygienic measures and can be treated successfully with antibiotic therapy. It has been noticed that after an infected catheter-port system was removed and replaced with a new one, however, infection recurred in some patients^[14]. In our study patients, antibiotic agents were administered 20 min before operation for the aim of prophylaxis of infection, and infection was not observed. Infection rates after radiologic implantation are lower than those after surgical implantation. Therefore, interventional radiology suites and the antibiotic agent seem to provide sufficient hygienic conditions for this type of intervention.

The relatively low complication rate and pain increase patient acceptance of this procedure. Placement of the catheter-port system on the anterior surface of the thigh below the groin or chest wall seems to be well accepted, even in very active patients. Its superficial placement allows easy palpation and puncture, and provides little risk for dislocation or disconnection of the port needle from the reservoir during chemotherapy. But careful palpations are required in obese patients.

Radiologic implantation of catheter-port systems is a quick and simple procedure that does not require general anesthesia compared with surgical implantation. Patency rates are equal to or higher than those for surgically implanted systems. Radiologic placement is also possible in patients with anatomic vascular variations. In contrast to the surgical method, catheter-port systems placed radiologically cause less morbidity in the case of dysfunction, because the systems can be removed or repositioned more easily. Complicated surgical revisions or corrections requiring laparotomy can be avoided as proposed by Doughty *et al.*^[31]. Radiologic placement does not allow performance of preventive cholecystectomy to avoid cholecystitis, but this does not seem to be a crucial problem.

Our results indicate that percutaneous implantation of a catheter-port system via the femoral artery or subclavian artery is easy to perform, simplifies intraarterial chemotherapy of the liver with equal patency rates, and has fewer complications as compared with surgical placement, and is well accepted by patients.

REFERENCES

- 1 **de Takats PG**, Kerr DJ, Poole CJ, Warren HW, McArdle CS. Hepatic arterial chemotherapy for metastatic colorectal carcinoma. *Br J Cancer* 1994; **69**: 372-378
- 2 **Sterchi JM**. Hepatic artery infusion for metastatic neoplastic disease. *Surg Gynecol Obstet* 1985; **160**: 477-489
- 3 **Hohn DC**, Stagg RJ, Friedman MA, Hannigan JF Jr, Rayner A, Ignoffo RJ, Acord P, Lewis BJ. A randomized trial of continuous intravenous versus hepatic intraarterial floxuridine in patients with colorectal cancer metastatic to the liver: the Northern California Oncology Group trial. *J Clin Oncol* 1989; **7**: 1646-1654
- 4 **Chang AE**, Schneider PD, Sugarbaker PH, Simpson C, Culnane

- M, Steinberg SM. A prospective randomized trial of regional versus systemic continuous 5-fluorodeoxyuridine chemotherapy in the treatment of colorectal liver metastases. *Ann Surg* 1987; **206**: 685-693
- 5 **Kemeny N**, Seiter K, Conti JA, Cohen A, Bertino JR, Sigurdson ER, Botet J, Chapman D, Mazumdar M, Budd AJ. Hepatic arterial floxuridine and leucovorin for unresectable liver metastases from colorectal carcinoma. New dose schedules and survival update. *Cancer* 1994; **73**: 1134-1142
- 6 **Link KH**, Sunelaitis E, Kornmann M, Schatz M, Gansauge F, Leder G, Formentini A, Staib L, Pillasch J, Beger HG. Regional chemotherapy of nonresectable colorectal liver metastases with mitoxantrone, 5-fluorouracil, folinic acid, and mitomycin C may prolong survival. *Cancer* 2001; **92**: 2746-2753
- 7 **Strecker EP**, Ostheim-Dzerowycz W, Boos IB. Intraarterial infusion therapy via a subcutaneous port for limb-threatening ischemia: a pilot study. *Cardiovasc Intervent Radiol* 1998; **21**: 109-115
- 8 **Oberfield RA**, McCaffrey JA, Polio J, Clouse ME, Hamilton T. Prolonged and continuous percutaneous intra-arterial hepatic infusion chemotherapy in advanced metastatic liver adenocarcinoma from colorectal primary. *Cancer* 1979; **44**: 414-423
- 9 **Ekberg H**, Tranberg KG, Lundstedt C, Hanff G, Ranstam J, Jeppsson B, Bengmark S. Determinants of survival after intraarterial infusion of 5-fluorouracil for liver metastases from colorectal cancer: a multivariate analysis. *J Surg Oncol* 1986; **31**: 246-254
- 10 **Okuyama K**, Tohnosu N, Koide Y, Awano T, Matsubara H, Sano T, Nakaichi H, Funami Y, Matsushita K, Kikuchi T. Complications and their management in intraarterial infusion chemotherapy. *Gan To Kagaku Ryoho* 1992; **19**: 1007-1013
- 11 **Allen-Mersh TG**, Earlam S, Fordy C, Abrams K, Houghton J. Quality of life and survival with continuous hepatic-artery floxuridine infusion for colorectal liver metastases. *Lancet* 1994; **344**: 1255-1260
- 12 **Laffer U**, Durig M, Bloch HR, Zuber M, Stoll HR. Implantable catheter systems. Experience with 205 patients. *Dtsch Med Wochenschr* 1989; **114**: 655-658
- 13 **Germer CT**, Boese-Landgraf J, Albrecht D, Wagner A, Wolf KJ, Buhr HJ. The fully implantable minimally invasive hepatic artery catheter for locoregional chemotherapy of nonresectable liver metastases in defective conventional implanted therapy catheters. *Chirurg* 1996; **67**: 458-462
- 14 **Kuroiwa T**, Honda H, Yoshimitsu K, Irie H, Aibe H, Shinozaki K, Nishie A, Nakayama T, Masuda K. A safe and simple method of percutaneous transfemoral implantation of a port-catheter access system for hepatic artery chemotherapy infusion. *Gan To Kagaku Ryoho* 2001; **28**: 1573-1577
- 15 **Pullyblank AM**, Carey PD, Pearce SZ, Tanner AG, Guillou PJ, Monson JR. Comparison between peripherally implanted ports and externally sited catheters for long-term venous access. *Ann R Coll Surg Engl* 1994; **76**: 33-38
- 16 **Harvey WH**, Pick TE, Reed K, Solenberger RI. A prospective evaluation of the Port-A-Cath implantable venous access system in chronically ill adults and children. *Surg Gynecol Obstet* 1989; **169**: 495-500
- 17 **Civalleri D**, Cafiero F, Cosimelli M, Craus W, Doci R, Repetto M, Simoni G. Regional arterial chemotherapy of liver tumours. I. Performance comparison between a totally implantable pump and a conventional access system. *Eur J Surg Oncol* 1986; **12**: 277-282
- 18 **Huk I**, Entschaff P, Prager M, Schulz F, Polterauer P, Funovics J. Patency rate of implantable devices during long-term intraarterial chemotherapy. *Angiology* 1990; **41**: 936-941
- 19 **Ross MN**, Haase GM, Poole MA, Burrington JD, Odom LF. Comparison of totally implanted reservoirs with external catheters as venous access devices in pediatric oncologic patients. *Surg Gynecol Obstet* 1988; **167**: 141-144
- 20 **Niederhuber JE**, Ensminger W, Gyves JW, Liepman M, Doan K, Cozzi E. Totally implanted venous and arterial access system to replace external catheters in cancer treatment. *Surgery* 1982; **92**: 706-712
- 21 **Wopfner F**. Treatment of inoperable liver metastases: preliminary results with intrahepatic chemotherapy via a new type of indwelling catheter (author's transl). *Dtsch Med Wochenschr* 1981; **106**: 1099-1102
- 22 **Balch CM**, Urist MM, McGregor ML. Continuous regional chemotherapy for metastatic colorectal cancer using a totally implantable infusion pump. A feasibility study in 50 patients. *Am J Surg* 1983; **145**: 285-290
- 23 **Buchwald H**, Grage TB, Vassilopoulos PP, Rohde TD, Varco RL, Blackshear PJ. Intraarterial infusion chemotherapy for hepatic carcinoma using a totally implantable infusion pump. *Cancer* 1980; **45**: 866-869
- 24 **Dresing K**, Lottner C, Stock W. Port-catheter perforation into the duodenum and other early complications after port implantation before intra-arterial infusion therapy of the liver with chemotherapeutic drugs. *Med Klin* 1991; **86**: 245-250
- 25 **al-Hathal M**, Malmfors G, Garwicz S, Bekassy AN. Port-A-Cath in children during long-term chemotherapy: complications and outcome. *Pediatr Hematol Oncol* 1989; **6**: 17-22
- 26 **Hohn DC**, Rayner AA, Economou JS, Ignoffo RJ, Lewis BJ, Stagg RJ. Toxicities and complications of implanted pump hepatic arterial and intravenous floxuridine infusion. *Cancer* 1986; **57**: 465-470
- 27 **Strecker EP**, Boos IB, Ostheim-Dzerowycz W, Heber R, Vetter SC. Percutaneously implantable catheter-port system: preliminary technical results. *Radiology* 1997; **202**: 574-577
- 28 **Fuchs R**, Leimer L, Koch G, Westerhausen M. Clinical experience with bacterial contamination of Port-A-Cath systems in tumor patients. *Dtsch Med Wochenschr* 1987; **112**: 1615-1618
- 29 **Zanon C**, Grosso M, Zanon E, Veltri A, Alabiso O, Bazzan M, Chiappino I, Mussa A. Transaxillary access to perform hepatic artery infusion (HAI) for secondary or primitive hepatic tumors. *Minerva Chir* 1996; **51**: 755-758
- 30 **Bern MM**, Lokich JJ, Wallach SR, Bothe A Jr, Benotti PN, Arkin CF, Greco FA, Huberman M, Moore C. Very low doses of warfarin can prevent thrombosis in central venous catheters. A randomized prospective trial. *Ann Intern Med* 1990; **112**: 423-428
- 31 **Doughty JC**, Keogh G, McArdle CS. Methods of replacing blocked hepatic artery catheters. *Br J Surg* 1997; **84**: 618-619

Expression of subtypes of somatostatin receptors in hepatic stellate cells

Sheng-Han Song, Xi-Sheng Leng, Tao Li, Zhi-Zhong Qin, Ji-Run Peng, Li Zhao, Yu-Hua Wei, Xin Yu

Sheng-Han Song, Xi-Sheng Leng, Tao Li, Zhi-Zhong Qin, Ji-Run Peng, Li Zhao, Yu-Hua Wei, Xin Yu, Department of Hepatobiliary Surgery, Peking University People's Hospital, Beijing 100044, China

Supported by National Nature Science Foundation of China, No. 30271270

Correspondence to: Xi-Sheng Leng, Professor, Department of Hepatobiliary Surgery, Peking University People's Hospital, Beijing 100044, China. lengxs2003@yahoo.com.cn

Telephone: +86-10-6868792703

Received: 2003-12-19 **Accepted:** 2004-02-01

Abstract

AIM: To elucidate the mechanism by which somatostatin and its analogue exert the influence on liver fibrosis, and to investigate the mRNA expression of somatostatin receptors subtypes (SSTRs) and the distribution of somatostatin analogue octreotide in rat hepatic stellate cells (HSCs).

METHODS: HSCs were isolated from Sprague Dawley (SD) rats by *in situ* perfusion and density gradient centrifugation. After several passages, the mRNA expression of 5 subtypes of SSTRs were assessed by reverse transcription-polymerase chain reaction (RT-PCR). HSCs were planted on coverslip and co-cultured with octreotide tagged by FITC. Then the distribution of FITC fluorescence was observed under laser scanning confocal microscope (LSCM) in 12-24 h.

RESULTS: There were mRNA expression of SSTR2, SSTR3 and SSTR5 but not SSTR1 and SSTR4 in SD rat HSCs. The mRNA expression level of SSTR2 was significantly higher than that of other subtypes ($P < 0.01$). FITC fluorescence of octreotide was clearly observed on the surface and in the cytoplasm, but not in the nuclei of HSCs under LSCM.

CONCLUSION: The effect exerted by somatostatin and its analogues on HSCs may mainly depend on the expression of SSTR2, SSTR3 and SSTR5. Octreotide can perfectly combine with HSCs, and thereby exerts its biological activity on regulating the characters of active HSCs. This provides a potential prevention and management against liver fibrosis.

Song SH, Leng XH, Li T, Qin ZZ, Peng JR, Zhao L, Wei YH, Yu X. Expression of subtypes of somatostatin receptors in hepatic stellate cells. *World J Gastroenterol* 2004; 10(11): 1663-1665 <http://www.wjgnet.com/1007-9327/10/1663.asp>

INTRODUCTION

In recent years, it has become clear that HSCs play an important role during occurrence and progress of hepatic fibrosis and portal hypertension^[1,2]. HSCs are located in a perisinusoidal orientation within the sinusoid and encircle vascular endothelial cells. They can also contract or relax in response to various vasoactive mediators. All of these suggest that these cells may

have the capacity to modulate intrahepatic vascular resistance and blood flow at the sinusoidal level^[3]. When HSCs are activated and proliferated abundantly, they can excrete many kinds of cytokine related to fibrosis to promote synthesis and deposition of extracellular matrix (ECM)^[4,5]. Therefore, how to reduce and inhibit activation and proliferation of HSCs has become a hot spot in the area of liver fibrosis research^[6].

Somatostatin and its analogues have comprehensive inhibitory actions on proliferation of many kinds of cells and the capacity to induce apoptosis, so they have been applied in cancer biotherapy at the present time^[7,8]. The biological base by which somatostatin exerts its actions is the existence of somatostatin receptors (SSTRs). SSTRs belong to G-protein-coupled receptors family and are located on cell membrane. Only after somatostatin combines with SSTRs, could it exert the actions of anti-proliferation. Up to date, five different SSTR subtypes, termed SSTR1 to SSTR5, have been cloned and characterized^[9].

In this research, we studied the mRNA expression and distribution of somatostatin receptors in hepatic stellate cells (HSCs) of rats to elucidate the mechanism by which somatostatin and its analogue exert the influence on liver fibrosis.

MATERIALS AND METHODS

Materials

Male Sprague Dawley rats, weighing (450±50) g, were purchased from Experimental Animal Center of the Chinese Academy of Medical Science, Beijing, China. Nycodenz, fluorescein isothiocyanate (FITC) and collagenase IV were purchased from Sigma Co., U.S.A. Fetal bovine serum (FBS), Dulbecco MEM (DMEM) culture medium, Trizol and superscript II reverse transcriptase were produced by Gibco Co., U.S.A. Taq DNA polymerase, dNTPs, Oligo (dT) and RNasin were products of Promega Co. Octreotide (0.1 g/mL) was provided by Novartis Co. Mouse anti-human desmin antibody and rabbit anti-cow glial fibrillary acidic protein (GFAP) antibody were purchased from Genetech Co. Primers were synthesized by Shanghai Sangon Co.

Isolation and culture of hepatic stellate cells (HSC)

Adult male Sprague Dawley rats (450±50 g) were treated in accordance with the institution's guidelines for the care and use of laboratory animals in research. All procedures were performed with animals under ether anesthesia. According to the method of Geerts and Weng *et al*^[10,11], HSCs were isolated by *in situ* perfusion and density gradient centrifugation with nycodenz. Firstly, the trocar was inserted into the rat's portal vein and the liver was perfused with pre-perfusion liquid. Then the liver was removed from the body and continuously perfused with perfusion liquid containing collagenase IV to digest the extracellular matrix. After centrifugation with 150 g/L nycodenz, the cells located in the interface were extracted and cultured in DMEM containing 200 mL/L FBS. HSC were fully stick to the wall within 48 h. Then the culture medium was exchanged in every 2-3 d. The identification of HSC was performed by observation of ultraviolet-excited fluorescence of vitamin A

lipid droplet in HSC and immunocytochemical stain for desmin and GFAP.

Isolation of total RNA and semiquantitative RT-PCR

Total RNA was isolated from HSC with Trizol by phenol-chloroform extraction and isopropanol precipitation following manufacturer's instructions. Reverse transcription of total RNA was carried out according to the instructions of the RT kit. Design of specific primers against rat SSTRs sequences was referred to the references^[12] and verified in NCBI Blast. They are shown in Table 1. The PCR system (total 25 μ L) contained 40 pmol/L primers of SSTRs or β -actin, 0.5 μ L of 10 mmol/L dNTPs, 1.5 μ L of 50 mmol/L MgCl₂, 2 μ L of cDNA, 2.5 μ L of 10 \times PCR buffer, 2.5 μ L of Taq DNA polymerase. The PCR conditions included an initial denaturation for 5 min at 94 $^{\circ}$ C; 40 amplification cycles consisting of denaturation at 94 $^{\circ}$ C for 1 min, primer annealing at 60 $^{\circ}$ C for 1 min and elongation at 72 $^{\circ}$ C for 1 min; and a final extension at 72 $^{\circ}$ C for 7 min. The PCR products or DNA marker mixed with 2 μ L of loading buffer were electrophoresed on a 15 g/L agarose gel and visualized under ultraviolet light excitation. Then the images were taken and analyzed by Kodak digital camera and science software (Kodak, EDAS290, U.S.A). The expression of SSTRs was calculated by determining the ratio of SSTRs relative to β -actin.

Table 1 Primer sequence and expected PCR product length

Primer designation	Sequence	Product length
SSTR1	upstream 5' -CAC GCA CCG CAG CCA ACA-3'	390 bp
	downstream 5' -GGA AGC CGT AGA GTA TGG GGT T-3'	
SSTR2	upstream 5' -CCG GAG CAA CCA GTG GGG-3'	390 bp
	downstream 5' -GCG TAC AGG ATG GGG TTG GC-3'	
SSTR3	upstream 5' -CCC GGG GCA TGA GCA CGT-3'	415 bp
	downstream 5' -AAG CCG TAG AGG ATG GGG TTT GC-3'	
SSTR4	upstream 5' -TCG TGG GGG TGA GGC AGT AG-3'	365 bp
	downstream 5' -CAT AGA GAA TCG GGT TGG CAC AG-3'	
SSTR5	upstream 5' -ATG GAG CCC CTC TCT CTG G-3'	250 bp
	downstream 5' -CGT CAG CCA CGG CCA GGTT-3'	
β -actin	upstream 5' -TGG GAC GAT ATG GAG AAG AT-3'	522 bp
	downstream 5' -ATT GCC GAT AGT GAT GAC CT-3'	

The observation of combination of octreotide with HSC and distribution in HSC

After 3-4 passages, HSCs were planted on coverslip and culture medium was exchanged after sticking to the walls. Then octreotide tagged by FITC was added into the culture medium (10 μ g/mL). After 24 h, the culture medium was removed and the coverslips were rinsed three times with PBS, whereafter the distribution of FITC fluorescence in live HSCs was observed by laser scanning confocal microscope (LSCM).

Statistical methods

The results of electrophoresis of PCR products were expressed as mean \pm SD and analyzed by *t*-test and analysis of variance.

RESULTS

Expression of mRNA of somatostatin receptor subtypes

The mRNA expression of SSTR2, SSTR3 and SSTR5 were observed, whereas those of SSTR1 and SSTR4 were not observed in rat HSCs. Moreover the mRNA expression level of SSTR2 was significantly higher than those of other subtypes (4 and 5.64 times higher than that of SSTR3 and SSTR5, respectively, $P < 0.01$). There was no significant difference between the mRNA expression of SSTR3 and SSTR5 (Figures 1, 2, and 3, Table 2).

Table 2 Expression of SSTRs mRNA in quantity (mean \pm SD)

Subtypes	<i>n</i>	Expression of mRNA
SSTR2	3	0.8213 \pm 0.1210
SSTR3	3	0.2041 \pm 0.1662 ^b
SSTR5	3	0.1457 \pm 0.1981 ^d

^b $P < 0.01$ vs SSTR2, ^d $P < 0.01$ vs SSTR2.

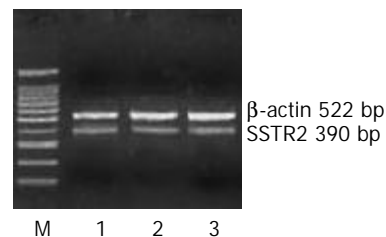


Figure 1 Expression of SSTR2 mRNA. M: 100 bp Marker; Lanes 1-3: three groups of samples.

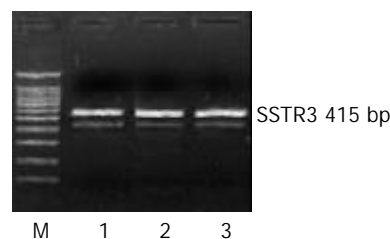


Figure 2 Expression of SSTR3 mRNA. M: 100 bp Marker; Lanes 1-3: three groups of samples.

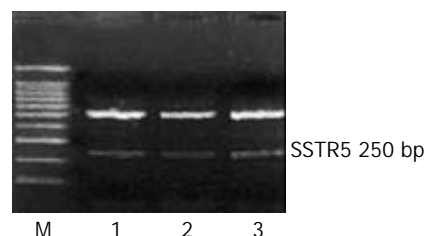


Figure 3 Expression of SSTR5 mRNA. M: 100 bp Marker; Lanes 1-3: three groups of samples.

Distribution of octreotide in HSCs

The green fluorescence of FITC had an extensive distribution on the surface of HSCs and also in cytoplasm, but not in nucleus (Figure 4).

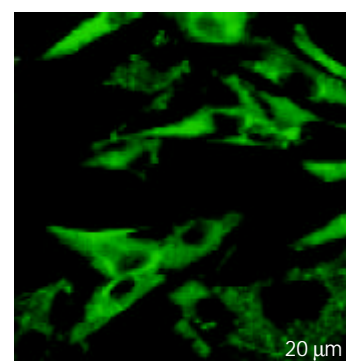


Figure 4 Distribution of the green fluorescence of octreotide tagged by FITC in live HSCs. FITC fluorescence of octreotide was clearly observed on the surface and in the cytoplasm, but not in the nuclei of HSCs under LSCM.

DISCUSSION

Several studies have demonstrated that somatostatin could restrain and decrease the process of hepatic fibrosis of rat liver cirrhosis models^[14-16]. In addition, researchers studied the anti-fibrosis mechanisms of somatostatin. Reynaert *et al.*^[13] proved that somatostatin could suppress rat hepatic stellate cell contraction induced by endothelin-1. Chatterjee *et al.*^[17] found that in rat liver cirrhosis models of schistosomiasis, somatostatin might have the direct anti-fibrosis effects through modulating the synthesis and expression of collagen I, III and smooth muscle actin (SMA) of rat HSCs. All of these findings suggest that there are SSTRs on the surface of HSCs, thereby somatostatin could exert its actions on HSCs.

Whether SSTRs exist and what kind of SSTRs subtypes are expressed in rat HSCs? We observed mRNA expression of SSTR2, SSTR3 and SSTR5, but not of SSTR1 and SSTR4 in Sprague Dawley rat HSCs. Our results slightly differed from Reynaert *et al.*^[13] that SSTR1, SSTR2 and SSTR3 were expressed, but not SSTR4 and SSTR5 in Wistar rat HSCs. Besides, we found that the mRNA level of SSTR2 was significantly higher than those of other subtypes in quantity. These results suggest that theoretically, somatostatin may be available to exert its inhibitive and pre-apoptosis actions on active HSCs by means of SSTRs (especially SSTR2) and consequently has the ability of anti-fibrotic action. Therefore, if the proper somatostatin analogues that have strong affinity to SSTR2, 3 and 5 are chosen, they will be able to exert better effect on active HSCs.

Taking advantage of the strong appetency by which somatostatin could combine with SSTRs, some researchers have applied the somatostatin analogues tagged by radioactive isotope to study the expression and distribution of SSTRs in cancer tissues and consequently the locational diagnosis of cancers. This kind of method has been proved to be satisfactory. Since our results showed that SSTR2, 3 and 5 were expressed and other studies reported that octreotide had the special affinity to SSTR2 and SSTR5^[7,9], we treated HSCs with octreotide tagged by FITC. By means of the characteristics that hormones can specially bind to its receptors, we observed the green fluorescence on the surface of live HSCs, which reflected the distribution of SSTRs. This proves that octreotide has strong affinity with HSCs and thus the existence of SSTRs is supported. Meanwhile, we also observed the distribution of octreotide in the cytoplasm, but not in the nuclei of HSCs. In general, octreotide contains 8 peptides, so it can't pass through the cell membrane without other pathways were introduced. Thereby, we presume that the endocytosis conducted by the receptors may works. But whether octreotide in cytoplasm is able to exert its biological actions by a certain mechanism independent of SSTRs remains to be confirmed in the future.

In conclusion, we demonstrates that SSTR2, 3 and 5 are obviously expressed in SD rat HSCs. In addition, octreotide, a somatostatin analogue, is able to combine perfectly with HSCs

and thereby exerts its biological actions on liver fibrosis in clinical practice.

REFERENCES

- 1 **Wu J**, Zern MA. Hepatic stellate cells: a target for the treatment of liver fibrosis. *J Gastroenterol* 2000; **35**: 665-672
- 2 **Pinzani M**, Gentilini P. Biology of hepatic stellate cells and their possible relevance in the pathogenesis of portal hypertension in cirrhosis. *Semin Liver Dis* 1999; **19**: 397-410
- 3 **Rockey DC**. Hepatic blood flow regulation by stellate cells in normal and injured liver. *Semin Liver Dis* 2001; **21**: 337-349
- 4 **Shen H**, Huang GJ, Gong YW. Effect of transforming growth factor beta and bone morphogenetic proteins on rat hepatic stellate cell proliferation and trans-differentiation. *World J Gastroenterol* 2003; **9**: 784-787
- 5 **Pinzani M**, Marra F. Cytokine receptors and signaling in hepatic stellate cells. *Semin Liver Dis* 2001; **21**: 397-416
- 6 **Liu XJ**, Yang L, Mao YQ, Wang Q, Huang MH, Wang YP, Wu HB. Effects of the tyrosine protein kinase inhibitor genistein on the proliferation, activation of cultured rat hepatic stellate cells. *World J Gastroenterol* 2002; **8**: 739-745
- 7 **Pawlikowski M**, Melen-Mucha G. Perspectives of new potential therapeutic applications of somatostatin analogs. *Neuroendocrinol Lett* 2003; **24**: 21-27
- 8 **Wang CH**, Tang CW, Liu CL, Tang LP. Inhibitory effect of octreotide on gastric cancer growth via MAPK pathway. *World J Gastroenterol* 2003; **9**: 1904-1908
- 9 **Patel YC**. Somatostatin and its receptor family. *Fron Neuroendocrinol* 1999; **20**: 157-198
- 10 **Geerts A**, Niki T, Hellemans K, De Crarmer D, Van Den Berg K, Lazou JM, Stange G, Van De Winkel M, De Bleser P. Purification of rat hepatic stellate cells by side scatter-activated cell sorting. *Hepatology* 1998; **27**: 590-598
- 11 **Weng SG**, Leng XS, Wei YH, Peng JR, Zheng ET, Cheng JH, Zham YB, Lu JF, Du RY. An improved method of isolating and identifying rat hepatic stellate cells. *Beijing Daxue Xuebao* 2001; **1**: 83-86
- 12 **Zhong ZH**, Zhu JY, Leng XS, Du RY. Study on mRNA expression of subtypes of somatostatin receptors in the liver tissue of liver cirrhosis rats. *Zhonghua Shiyian Waike Zazhi* 2000; **5**: 439-441
- 13 **Reynaert H**, Vaeyens F, Qin H, Hellemans K, Chatterjee N, Winand D, Quartier E, Schuit F, Urbain D, Kumar U, Patel YC, Geerts A. Somatostatin suppresses Endothelin1-induced rat hepatic stellate cell contraction via somatostatin receptor subtype 1. *Gastroenterology* 2001; **121**: 915-930
- 14 **Karalis K**, Mastorakos G, Chrousos GP, Tolis G. Somatostatin analogues suppress the inflammatory reaction *in vivo*. *J Clin Invest* 1994; **93**: 2000-2006
- 15 **Fort J**, Oberti F, Pilette C, Veal N, Gallois Y, Douay O, Rousselet MC, Rosenbaum J, Cales P. Antifibrotic and hemodynamic effects of the early and chronic administration of octreotide in two models of liver fibrosis in rats. *Hepatology* 1998; **28**: 1525-1531
- 16 **Wang J**, Gong H, Wang Y. Experimental study on the preventive effect of octreotide on liver fibrosis. *Zhonghua Gandan Waike Zazhi* 2003; **2**: 100-102
- 17 **Chatterjee S**, Van Marck E. The role of somatostatin in schistosomiasis: a basis for immunomodulation in host-parasite interactions? *Trop Med Int Health* 2001; **6**: 578-581

Edited by Kumar M and Xu FM

Filamentous-actins in human hepatocarcinoma cells with CLSM

Xia Huo, Xi-Jin Xu, Yao-Wen Chen, Hai-Wei Yang, Zhong-Xian Piao

Xia Huo, Xi-Jin Xu, Yao-Wen Chen, Hai-Wei Yang, Zhong-Xian Piao, Central Laboratory, Shantou University Medical College, Shantou 515031, Guangdong Province, China

Supported by the Medical Research Fund of Guangdong Province, No. 2000004

Correspondence to: Dr. Xia Huo, Central Laboratory, Shantou University Medical College, 22 Xinlin Road, Shantou 515031, Guangdong Province, China. xhuo@stu.edu.cn

Telephone: +86-754-8900307 **Fax:** +86-754-8557562

Received: 2002-12-30 **Accepted:** 2003-02-17

Abstract

AIM: To establish a method for optical sections of HepG2 human hepatoblastoma cells with confocal laser scanning microscope (CLSM) and to study the spatial structure of filamentous actin (F-actin) in HepG2 cells.

METHODS: HepG2 cells were stained with FITC-phalloidin that specifically binds F-actin, with propidium iodide (PI) to the nucleus, and scanned with a CLSM to generate optically sectioned images. A series of optical sections taken successively at different focal levels in steps of 0.7 μm were reconstructed with the CLSM reconstruction program.

RESULTS: CLSM images showed that the FITC-stained F-actin was abundant microfilament bundles parallel or netted through the whole cell and its processes. Most F-actin microfilaments extended through the cell from one part toward the other or run through the process. Some microfilaments were attached to the plasma membrane, or formed a structural bridge connecting to the neighboring cells.

CONCLUSION: A method for double labeling HepG2 human hepatoblastoma cells and CLSM imaging F-actin microfilaments and nuclei by image thin optical sections and spatial structure was developed. It provides a very useful way to study the spatial structure of F-actin.

Huo X, Xu XJ, Chen YW, Yang HW, Piao ZX. Filamentous-actins in human hepatocarcinoma cells with CLSM. *World J Gastroenterol* 2004; 10(11): 1666-1668

<http://www.wjgnet.com/1007-9327/10/1666.asp>

INTRODUCTION

Cytoskeleton, consisting of proteins, is the structural network in cells. It closely relates to the functions of cells, such as cell movement, cell morphology and transmembrane signal conduction, etc. Observation and analysis of cell F-actin with CLSM are a precise, rapid, and simple method. This paper aimed at using CLSM in combination with double label for the observation and analysing of the three-dimensional structure of cytoskeleton system in HepG2 hepatocarcinoma cells.

MATERIALS AND METHODS

Cell culture

HepG2 cells were inoculated in improved Petri dish (normal

Petri dishes with a center hole bottomed by quartz glass), with 100 mL/L BAS/RPMI-1640 as culture medium for 24-48 h in an incubator at 37 °C with a 950 mL/L air/50 mL/L CO₂ atmosphere. After the dish glass was covered fully with cells, the culture medium was poured out. The cells were rinsed with PBS twice, and then fixed in 40 g/L paraformaldehyde for 30 min at 4 °C.

Specimen preparation

The above-mentioned specimens were rinsed with PBS twice, then permeabilized for 10 min in 2 g/L Triton X-100 at room temperature, and nonspecific background was blocked using 5 g/L BSA for a while. Specimens were then stained with 5 mg/L FITC-phalloidin (Sigma) at room temperature for 30 min. After that, the specimens were rinsed with PBS twice and stained with 5 mg/L PI (Sigma), and finally rinsed twice with PBS and a little PBS in dishes was reserved for observation. All procedures must be performed from light.

CLSM observation and examination

Specimens were examined with an ACAS Ultima 312 CLSM (Meridian Instruments, USA) equipped with an argon ion laser providing simultaneous excitation at 514.5 nm, 488 nm and 351-364 nm, an output power of 50 mW for the UV and 200 mW for the combined visible wavelengths, a high-precision mechanical scanning stage (0.1 μm in the X-Y plane and 0.1 μm in the Z axis), and an inverted microscope (Olympus), three photomultiplier tubes (PMT). The availability of a variety of excitation wavelengths on a single microscope setup offers the power and convenience of using combinations of fluorescent probes in a single specimen. In this experiment, the parameters were as follows: Objective: 100 \times 1.30 oil, Pinhole: 255 μm , X points: 270, Y point: 290, Z step: 0.7 μm , Data model: Z image, Scan Type: Mirror, Step Size: 0.20 μm , Speed: 20 mm/s, Samples/pt: 15, Laser Power: 612 mw, Scan stress: 100%, PMT 1: 40%, PMT 2: 40%, Z point: 15. According to the above parameters, a series of images were collected sequentially from single optical sections at 0.7 μm intervals (15 planes per series) using the 488, 530 nm laser lines to excite FITC and PI, respectively. Randomly selected regions of specimens were scanned to image using Z-series program of CLSM. With the program the specimens could be scanned cross-sectionally along the X, Y, and Z axes, and serial optical sections of different layers could be obtained without injury. Firstly, the cell top was confirmed by prescanning, and then the specimen from top to bottom was scanned according to Z-step to obtain optical sections layer by layer, and each image was recorded. The images were electronically colored. The optical sections were reconstructed to stereoscopic images with CLSM reconstruction program.

RESULTS

The HepG2 cells stained with FITC-phalloidin and PI were successfully labeled. There were six serial optical sections of HepG2 cells as shown in Figure 1. The interval between two sections was fixed at 0.7 μm . The images shown on Figure 2-Figure 4 were all three-dimensional images obtained from sequential optical sections, which were reconstructed with the reconstruction program of CLSM. The HepG2 cells, having many primary and secondary processes, were irregular in shape. The FITC-stained F-actin filaments appeared in bundles,

which ran in parallel to the main cell axis or through cell processes. Some microfilaments were attached to the plasma membrane, or formed a structural bridge connecting to the neighboring cells. When detector 1 of CLSM for 488 nm line was on, only F-actin marked with FITC-phalloidin could be shown (Figure 1). When both of the two detectors of CLSM were turned on, F-actin marked with FITC-phalloidin and the nuclei marked with PI could be shown simultaneously (Figure 2). F-actin appeared green, the distinct nuclei appeared red, and the region around the nuclei was overlapped by green F-actin and red nuclei appeared yellow.

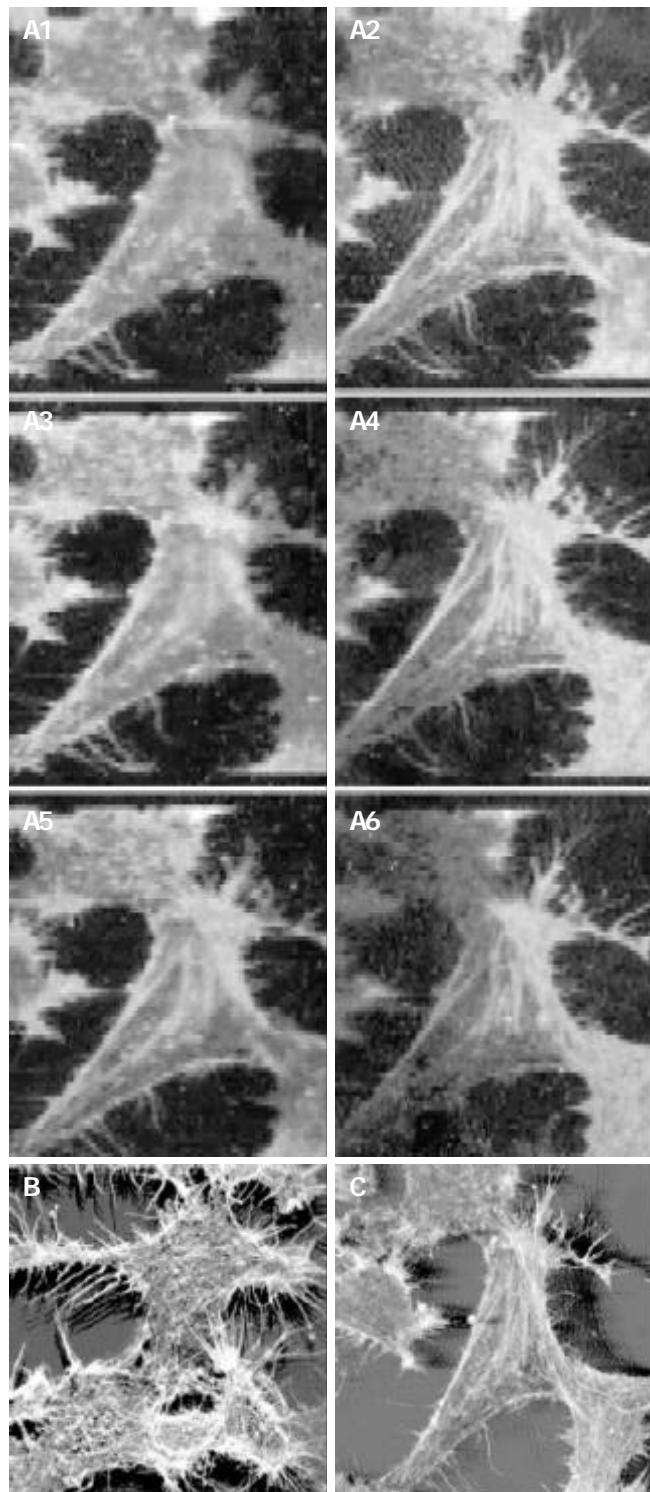


Figure 1 CLSM images of HepG2 cells stained with FITC-phalloidin. (A: Serial optical sections (1-6) B: Three-dimensional images of Figure 1 serial optical sections. C: Three-dimensional images of HepG2 cells).

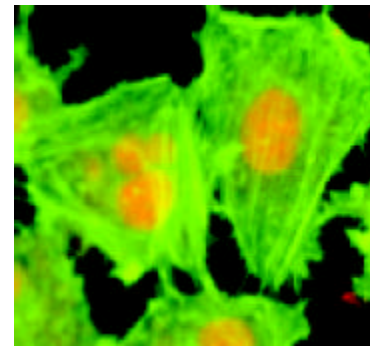


Figure 2 CLSM three-dimensional images of HepG2 cells by double labeling.

DISCUSSION

Cytoskeleton, composed largely of actin filaments, is the internal framework of a cell. It includes micro-tubes, microfilaments and middling fibers, and is the base structure for cell movement, cell morphology and transmembrane signal conduction. Microfilament mainly consists of actin participating in keeping cell pattern and tight junction between cells. It is also related to the adhesion of the ground substance outside the cells. Microfilament exists in the form of G-actin when it is dissociated or exists in the form of F-actin when it is polymerized. The change and balance of microfilament dissociation and polymerization in normal cells are the important regulatory factors for the movement, adhesion and fission cycle of cells^[1,2]. Cell mutation involves cytoskeletal rearrangement and morphological alterations. As a sensitive norm in examining the development of tumor cells at the early stage, F-actin has been used in human mammary gland cancer and T-lymphocyte cancer^[3-5]. Our result showed that F-actin microfilaments of HepG2 cells existed in the form of bunches of fibers that were thick, long and dense. F-actin filaments formed bundles running through the main cell axis or cellular processes. The relationship between the change of microfilament morphology and cancer occurrence in cells is still unknown. But when microfilament's component and distribution change, cells cannot receive normal regulation. And it leads to the loss of control of cell growth and propagation and to cancer occurrence. According to some researches, the change of microfilaments might reduce the gap junction in number and function, and the communication function of cells, which is the main reason why propagation ability of carcinoma cells rose up and the ability of adherence lowered, and easily fell off^[6-9]. The mechanism underlying the morphological changes of microfilaments in the process of cancer cells is unclear.

In this experiment, F-actin was marked with FITC-phalloidin and the nuclei with PI, so the cytoskeleton and nuclei could be observed. This provides a very useful way to study the relationship between cytoskeleton and nucleus. Compared with other methods, such as immunohistochemistry, light microscopy or electrical microscopy^[10-12], CLSM has several advantages^[13-17]: Firstly, resolution obtained with a CLSM is better than that of conventional microscopy because of the combination of laser illuminator and detection pinhole. With conventional light microscopy, the fluorescence of the entire specimen interferes with the resolution, while CLSM allows examining the organization of fluorescent labeled cells and tissues by eliminating the "out-of-focus" flare of the specimen, thus providing sharp, high-contrast images of cells and subcellular structures within thick samples. Since images are obtained by scanning, excessive illumination of the specimen and quick decrease of the fluorescent signal are avoided. And light bleaching is minimized because exposure to light is restricted

to the area of the preparation being examined. Secondly, this method of embedding and sectioning specimens, which are a time-consuming and a destructive procedure, can now be avoided. So it is quick and simple to make samples using CLSM. Under conventional microscopy, structures present in the tissues can be observed only after sectioning (microtome sections). With the CLSM it is possible to obtain a number of serial optical sections of quite thick specimens without physical sectioning. Furthermore, serial optical sections can be collected and displayed as digitalized images, and by using a computer, the digitalized images obtained may be reconstructed as a 3-dimensional structure. In addition, the procedure is not destructive for a living cell or tissue. In this experiment using CLSM, the images of the cytoskeleton marked by the double label technique and the stereoscopy of three-dimensional images were very clear. As the sectioning with CLSM is not done physically but optically, the procedure is not destructive for an intact cell, and the process of sectioning turns simpler and quicker and more reliable, and it can notably keep the normal morphology and function of the cell.

In summary, our results showed that in HepG2 cells F-actin microfilaments existed in the form of bunches of fibers that were thick, long and dense, and ran through the main cell axis or cellular processes. It is suggested that F-actin may play an important role in HepG2 cells.

REFERENCES

- 1 **Yang YL**. Polymerization of actins. *Biology* 1995; **18**: 13-14
- 2 **Shumilina EV**, Negulyaev YA, Morachevskaya EA, Hinssen H, Khaitlina SY. Regulation of sodium channel activity by capping of actin filaments. *Mol Biol Cell* 2003; **14**: 1709-1716
- 3 **Sugiura T**, Nakane S, Kishimoto S, Waku K, Yoshioka Y, Tokumura A. Lysophosphatidic acid, a growth factor-like lipid, in the saliva. *J Lipid Res* 2002; **43**: 2049-2055
- 4 **Shestakova EA**, Wyckoff J, Jones J, Singer RH, Condeelis J. Correlation of beta-actin messenger RNA localization with metastatic potential in rat adenocarcinoma cell lines. *Cancer Res* 1999; **59**: 1202-1205
- 5 **Williams JI**, Weitman S, Gonzalez CM, Jundt CH, Marty J, Str SD, Holroyd KJ, Mclane MP, Chen Q, Zasloff M, Von Hoff DD. Squalamine treatment of human tumors in nu/nu mice enhances platinum-based chemotherapies. *Clin Cancer Res* 2001; **7**: 724-733
- 6 **Autieri MV**, Carbone C, Mu A. Expression of allograft inflammatory factor-1 is a marker of activated human vascular smooth muscle cells and arterial injury. *Arterioscler Thromb Vasc Biol* 2000; **20**: 1737-1744
- 7 **Yamakita Y**, Oosawa F, Yamashiro S, Matsumura F. Caldesmon inhibits Arp2/3-mediated actin nucleation. *J Cell Biol* 2003; **278**: 17937-17944
- 8 **Yan H**, Rivkees SA. Hepatocyte growth factor stimulates the proliferation and migration of oligodendrocyte precursor cells. *J Neurosci Res* 2002; **69**: 597-606
- 9 **Fischer R**, Fritz-Six KL, Fowler VM. Pointed-end capping by tropomodulin3 negatively regulates endothelial cell motility. *J Cell Biol* 2003; **161**: 371-380
- 10 **Uchida M**, Hanai S, Uematsu N, Sawamoto K, Okano H, Miwa M, Uchida K. Overexpression of poly (ADP-ribose) polymerase disrupts organization of cytoskeletal F-actin and tissue polarity in *Drosophila*. *J Biol Chem* 2002; **277**: 6696-6702
- 11 **Lin H**, Bhatia R, Lal R. Amyloid beta protein forms ion channels: implications for Alzheimer's disease pathophysiology. *FASEB J* 2001; **15**: 2433-2444
- 12 **Fischer RS**, Lee A, Fowler VM. Tropomodulin and tropomyosin mediate lens cell actin cytoskeleton reorganization *in vitro*. *Invest Ophthalmol Vis Sci* 2000; **41**: 166-174
- 13 **Masuda T**, Fujimaki N, Ozawa E, Ishikawa H. Confocal laser microscopy of dystrophin localization in guinea pig skeletal muscle fibers. *J Cell Biol* 1992; **119**: 543-548
- 14 **Huo X**, Lu JX, Yang RD, Li ZZ, Wei WX, Zheng XH, Tu WX, Xiao ZX, Zhang FL. Comparison of laser scanning confocal microscope with light microscope. *Jiguang Shengwu Xuebao* 2001; **10**: 76-79
- 15 **Dailey M**, Marrs G, Satz J, Waite M. Concepts in imaging and microscopy. Exploring biological structure and function with confocal microscopy. *Biol Bull* 1999; **197**: 115-122
- 16 **Li J**, Jester JV, Cavanagh HD, Black TD, Petroll WM. On-line 3-Dimensional confocal imaging *in vivo*. *Invest Ophthalmol Vis Sci* 2000; **41**: 2945-2953
- 17 **Benbow U**, Orndorff KA, Brinckerhoff CE, Givan AL. Confocal assay for invasion: use of propidium iodide fluorescence and laser reflectance to quantify the rate of migration of cells through a matrix. *Cytometry* 2000; **40**: 253-259

Edited by Ma JY and Wang XL Proofread by Xu FM

Effect of intraoperative radiotherapy combined with external beam radiotherapy following internal drainage for advanced pancreatic carcinoma

Hong-Bing Ma, Zheng-Li Di, Xi-Jing Wang, Hua-Fen Kang, Huai-Ci Deng, Ming-Hua Bai

Hong-Bing Ma, Zheng-Li Di, Xi-Jing Wang, Hua-Fen Kang, Ming-Hua Bai, Department of Oncology, the Second Hospital of Xi'an Jiaotong University, Xi'an 710004, Shaanxi Province, China
Huai-Ci Deng, Department of Radiation Oncology, the First Hospital of Xi'an Jiaotong University, Xi'an 710068, Shaanxi Province, China
Supported by the Technology Project Entry Foundation of Shaanxi Province, No. 2002K10-G3

Correspondence to: Dr. Hong-Bing Ma, Department of Oncology, the Second Hospital of Xi'an Jiaotong University, Xi'an 710004, Shaanxi Province, China. m68d69@pub.xaonline.com

Telephone: +86-29-7679789

Received: 2003-07-04 **Accepted:** 2003-09-18

Abstract

AIM: To determine the survival of advanced pancreatic cancer patients treated with intraoperative radiotherapy (IORT) combined with external beam radiation therapy (EBRT) following internal drainage (cholecystojejunostomy or choledochojejunostomy).

METHODS: Eighty-one patients with advanced pancreatic cancer who received IORT combined with EBRT following internal drainage (ID) between 1996 and 2001 were retrospectively analyzed. Among the 81 patients, 18 underwent ID+IORT, 25 ID+IORT+EBRT (meanwhile, given 5-Fu 300 mg/m² iv drip, 2f/w), 16 EBRT, 22 had undergone simple internal drainage. The IORT dose was 15-25Gy in a single fraction. The usual EBRT dose was 30-40Gy with a daily fraction of 1.8-2.0 Gy.

RESULTS: The complete remission rate, partial remission rate of patients with backache and abdominal pain treated with ID+IORT were 55.5%, 33.3% respectively. Alleviation of pain was observed 2 or 3 wk after IORT. The median survival time (MST) of ID+IORT group was 10.7 mo. The pain remission rate of patients treated with ID+IORT+EBRT was 92%, and their MST was 12.2 mo. The MST of patients treated with EBRT and simple internal drainage was 5.1 mo and 7.0 mo, respectively. The survival curve of ID+IORT group and ID+IORT+EBRT group was significantly better than that of EBRT group ($P<0.05$). The difference between the ID+IORT+EBRT group and ID group was significant ($P<0.05$).

CONCLUSION: IORT combined with EBRT following internal drainage can alleviate pain, improve quality of life and prolong survival time of patients with advanced pancreatic cancer.

Ma HB, Di ZL, Wang XJ, Kang HF, Deng HC, Bai MH. Effect of intraoperative radiotherapy combined with external beam radiotherapy following internal drainage for advanced pancreatic carcinoma. *World J Gastroenterol* 2004; 10 (11): 1669-1771

<http://www.wjgnet.com/1007-9327/10/1669.asp>

INTRODUCTION

During the past two decades, the incidence rate of pancreatic cancer has been increasing. Pancreatic cancer is extremely difficult to diagnose at early stage, and the prognosis is very poor. In spite of the developments in surgical and anesthetic techniques, the median survival time (MST) remains in the range of 7-11 mo, and only 3% of the patients were alive 5 years after diagnosis^[1-6].

The local recurrence rate is extremely high even after curative resection. Evans *et al.*^[7] reported that more than 50% of patients with post-operative relapse were due to local recurrence. Local recurrence is the most uncomfortable event for patients, and often produces various complications, and decreases the patients' quality of life. Thus, local control is an important issue for pancreatic cancer. IORT is one of the most potent local interventions. Saeki *et al.*^[8] reported that IORT could reduce pain and improve quality of life in patients with unresectable pancreatic cancer. In the present study, we investigated the survival time of advanced pancreatic cancer patients treated with intraoperative radiotherapy (IORT) combined with external beam radiation therapy (EBRT) following internal drainage.

MATERIALS AND METHODS

Patient selection

From 1996 to 2001, 81 patients with advanced pancreatic cancer were treated at our hospital. The patients aged from 43 to 72 years with a median of 57 years. Fifty-nine patients were male and 22 were female. All the tumors had no interspace between the superior mesenteric vein and portal vein, and the blood vessel was wrapped by the tumor. All patients had jaundice, the blood total bilirubin ranged from 156 μmol/L to 402 μmol/L with a median of 304 μmol/L. Sixty-one (75.3%) 81 of the patients were given AP-237 or pethidine to relieve pain, and other 20 (24.7%) patients took oral acesodyne intermittently. No ascitic fluid and liver metastasis were noted. Among the 81 patients, 18 received ID+IORT, 25 received ID+IORT+EBRT (meanwhile, given 5-Fu 300 mg/m² iv drip, 2 f/w), 16 received simple EBRT and 22 received simple internal drainage.

Surgery

Under continuous epidural anesthesia, all patients underwent laparotomy and their tumors were found unresectable. Cholecystojejunostomy and choledochojejunostomy were performed for patients whose cystic ducts were obstructed and unobstructed after IORT.

IORT

IORT was administered using high-energy electron beams from a Varian Clinac linear accelerator for patients without distant metastases and severe cardiac and lung diseases. A cylinder of 5 cm×5 cm to 8 cm×8 cm, 5 to 8 cm in diameter, or an ellipse with an inclination angle of 10-30° degree was introduced into the patients to encompass the tumor bed and paraaortic lymph

node area. The IORT dose was 15-25 Gy with a median dose of 20 Gy in a single fraction.

EBRT

EBRT was administered mainly postoperatively by 6- or 15-MV photons from a linear accelerator, mostly using two portal veins from the anterior, left, right and/or posterior in directions. In the irradiated field, the paraaortic lymph node area and tumor or tumor bed were completely included with a margin of 3 cm. The usual median EBRT dose was 42 Gy (range, 30-45 Gy) with a daily fraction of 1.8-2.0 Gy, 5F/w. The patients, meanwhile, were given 5-Fu 300 mg/m², iv drip, 2f/w.

Statistic analysis

The cause-specific survival rate was calculated and plotted from the day of operation using the Kaplan-Meier method with significance compared by log-rank test.

RESULTS

Relief of pain and survival condition

The causes of death were local relapse and extensive metastasis. The MST of patients treated with ID+IORT, ID+IORT+EBRT, EBRT, ID, was 10.7, 12.2, 5.1 and 7 mo, respectively, which was significantly longer than the patients treated with EBRT ($\chi^2=10.5835$, $P<0.05$; $\chi^2=17.8972$, $P<0.05$). The difference of MST between ID+IORT+EBRT and ID was significant ($\chi^2=8.1361$, $P<0.05$), and it was not significant while between ID+IORT and ID+IORT+EBRT, ($P>0.05$) (Figure 1). No significant differences in remission of pain and tumor were detected among ID+IORT, ID+IORT+EBRT, and EBRT ($P>0.05$) groups (Table 1).

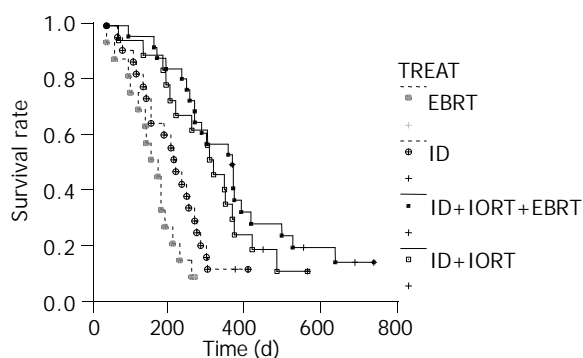


Figure 1 Survival curves for pancreatic cancer according to radiation modalities.

Complications

Three patients had the delayed gastric emptying after ID+IORT, and they recovered after given parenteral nutritional support for 4-5 wk. One patient died of liver and renal failure in the ID+IORT group. Intestinal perforation and digestive tract bleeding

were unrelated to ID+IORT. Nausea, decreased appetite and frequent defecation were found early after ID+IORT+EBRT. One patient died of liver and renal failure after simple internal drainage, and 2 patients had delayed gastric emptying and 1 wound infection. No significant difference in the occurrence rate of complications was observed among different treatment methods ($P>0.05$).

DISCUSSION

The goal of IORT is used to enhance regional tumor control, and have been IORT is used in most modern protocol studies as a radiation boost component of multidisciplinary treatment approaches. More recently, clinical experiences have shown that IORT could improve local control and disease-free survival time, especially when it was used in adjuvant setting, combined with external beam irradiation in some neoplasms such as cancer of the stomach, pancreas, colorectum, and soft tissue sarcoma^[9].

The use of IORT for unresectable pancreatic cancer has been reported by several groups. Many reports failed to prove its survival benefit^[9,10]. Miyamatsu demonstrated that the MST to IORT group was 7.6 mo, compared to 3 mo for palliative therapy group, with no statistical significance^[10]. Ouchi proposed that IORT was not beneficial to either survival or quality of life^[11]. Shibamoto reported that among non-stage IV patients, the median survival of the EBRT+IORT group (8.5 mo) and the EBRT group (8 mo) was similar, while in stage IV patients, the prognosis was not influenced by the type of radiotherapy^[12]. In contrast to these results, survival advantage with IORT was reported by several groups. Literature data suggested the use of schedules with IORT had a better local control and perhaps a better survival than surgery alone or the palliative treatment^[13]. Tanada demonstrated a significant difference in the survival rate between IORT cases and no treatment cases (median survival of 212 d and 109 d, respectively)^[14]. Dobelbower reported that the median survival time of patients treated with radical surgery alone was 6.5 mo. The median survival time for the surgery plus IORT group was 9 mo, and 33.3% (2 of 6) of these patients survived longer than 5 years. This survival pattern was significantly better than that for the surgery alone group. The surgery plus EBRT and the surgery plus IORT and EBRT groups had a median survival time of 14.5 and 17.5 mo, respectively. These were significantly better than that of the surgery alone group. The addition of radiation therapy did not increase the treatment complication rate^[15].

Patients with advanced pancreatic cancer usually have symptoms such as obstructive jaundice, poor appetite, fatigue and weight loss. Therefore, relief of symptoms, especially relief of obstructive jaundice and improvement of liver function, is clinically beneficial to these patients. In the colligation treatment, internal drainage has been used for the extinction of obstructive jaundice, enhancement of appetite and improvement of liver

Table 1 Patient characteristics after treated with ID+IORT, ID+IORT+EBRT, ID, and EBRT

	IORT+ID		IORT+ERBT+ID		ID		ERBT	
	n	%	n	%	n	%	n	%
Pain								
Complete remission	10	55.5	15	60.0	/		5	31.3
Partial remission	6	33.3	8	32.0	/		7	43.7
Tumor								
Light diminution	4	22.2	8	32.0	/		2	12.5
Unchanged	14	77.7	17	68.0	22	100.0	14	87.5
Jaundice	extinction		extinction		extinction		extinction	

function, which was also beneficial to IORT and EBRT^[16,17]. IORT has also been used in an attempt to increase the radiotherapy dose on the target without damaging surrounding normal tissues. A higher radiation dose could be given to the target tumor by combining IORT with EBRT^[11,18]. Our studies showed that colligation treatment (ID+IORT+EBRT) could relieve jaundice, pain, improve quality of life, diminish tumor and prolong survival time in patients with unresectable pancreatic cancer.

Among the groups of ID+IORT, surgery, ID+IORT+EBRT, jaundice was improved quickly. However, it was not obviously improved in EBRT group. Pain was not relieved in surgery group, but obviously relieved in 75-92% of the patients in the other groups. So radiotherapy had a good and a long-term pain relieving effect. IORT relieved pain quickly and could kill the remnant tumor, better than drugs. The tumor was not reduced in size in surgery group, while in the other groups, the tumor size was decreased in varying degrees, with no statistical significance ($P>0.05$).

In the present study, the MST was 5.1 mo for EBRT group, 7 mo for ID group, 10.7 mo for ID+IORT group and 12.2 mo for ID+IORT+EBRT group. The survival curves of the ID+IORT group and ID+IORT+EBRT group were significantly better than that of the EBRT group ($P<0.05$). The difference between the ID+IORT+EBRT and the ID groups was significant ($P<0.05$). Thus, ID+IORT+EBRT could relieve the pain and jaundice, improve survival and quality of life.

Complications resulting from surgery and radiotherapy occurred in 9.3% of patients (4/43) in both ID+IORT and ID+IORT+EBRT groups. No major side effects were noted during the course of treatment. Schwarz reported IORT was not related to a significantly increased risk of complications, hospital stay, or survival hazard^[19]. Though a very small amount of normal tissues was exposed in IORT, complications often occurred if radiotherapy dose was too big. The safety level of a radiation dose for IORT alone is limited to 30 Gy^[20]. The dose in IORT ranging from 20 Gy to 25 Gy combined with the dose in EBRT ranging from 40 Gy to 50 Gy was considered to contribute to the improvement of prognosis without causing serious side effects^[21].

In conclusion, multimodal therapy can relieve jaundice, pain, improve quality of life, reduce tumor mass and prolong survival time of patients with advanced pancreatic cancer.

REFERENCES

- 1 **Reni M**, Panucci MG, Ferreri AJ, Balzano G, Passoni P, Cattaneo GM, Cordio S, Scaglietti U, Zerbi A, Ceresoli GL, Fiorino C, Calandrino R, Staudacher C, Villa E, Di Carlo V. Effect on local control and survival of electron beam intraoperative irradiation for resectable pancreatic adenocarcinoma. *Int J Radiat Oncol Biol Phys* 2001; **50**: 651-658
- 2 **Kokubo M**, Nishimura Y, Shibamoto Y, Sasai K, Kanamori S, Hosotani R, Imamura M, Hiraoka M. Analysis of the clinical benefit of intraoperative radiotherapy in patients undergoing macroscopically curative resection for pancreatic cancer. *Int J Radiat Oncol Biol Phys* 2000; **48**: 1081-1087
- 3 **Wang L**, Yang GH, Lu XH, Huang ZJ, Li H. Pancreatic cancer mortality in China (1991-2000). *World J Gastroenterol* 2003; **9**: 1819-1823
- 4 **Shankar A**, Russell RC. Recent advances in the surgical treatment of pancreatic cancer. *World J Gastroenterol* 2001; **7**: 622-626
- 5 **Liu MP**, Ma JY, Pan BR, Ma LS. Study of Chinese pancreatic cancer. *Shijie Huaren Xiaohua Zazhi* 2001; **9**: 1103-1109
- 6 **Wang ZQ**, Li JS, Lu GM, Zhang XH, Chen ZQ, Meng K. Correlation of CT enhancement, tumor angiogenesis and pathologic grading of pancreatic carcinoma. *World J Gastroenterol* 2003; **9**: 2100-2104
- 7 **Evans DB**, Abbruzzese JL, Rich TA. Cancer of the pancreas. In: Devita VT, Hellmann S, Rosenberg SA, eds. *Cancer, principles and practice of oncology*. 6th ed. Philadelphia:Lippincott 2001: 1126-1161
- 8 **Saeki H**, Sugimasa Y, Yamada R, Akaike M, Takemiya S, Masaki T, Miyagawa K, Okawa S. Intraoperative radiotherapy (IORT) for unresectable stage IVb pancreatic cancer. *Gan To Kagaku Ryoho* 2002; **29**: 2221-2223
- 9 **Valentini V**, Balducci M, Tortoreto F, Morganti AG, De Giorgi U, Fiorentini G. Intraoperative radiotherapy: current thinking. *Eur J Surg Oncol* 2002; **28**: 180-185
- 10 **Miyamatsu A**, Morinaga S, Yukawa N, Akaike M, Sugimasa Y, Takemiya S. Intraoperative radiation therapy (IORT) for locally unresectable pancreatic cancer. *Gan To Kagaku Ryoho* 1999; **26**: 1846-1848
- 11 **Ouchi K**, Sugawara T, Ono H, Fujiya T, Kamiyama Y, Kakugawa Y, Mikuni J, Yamanami H. Palliative operation for cancer of the head of the pancreas: significance of pancreaticoduodenectomy and intraoperative radiation therapy for survival and quality of life. *World J Surg* 1998; **22**: 413-416
- 12 **Shibamoto Y**, Manabe T, Ohshio G, Sasai K, Nishimura Y, Imamura M, Takahashi M, Abe M. High-dose intraoperative radiotherapy for unresectable pancreatic cancer. *Int J Radiat Oncol Biol Phys* 1996; **34**: 57-63
- 13 **Fellin G**, Pani G, Tomio L, Tirone G, Eccher C. Intraoperative radiotherapy in the combined treatment of pancreatic cancers. *Tumori* 1999; **85**(1 Suppl): S33-S35
- 14 **Tanada M**, Takashima S, Endoh H, Hyoudou I, Jinno K, Kataoka M. Multimodal treatment including intraoperative irradiation for advanced pancreatic cancer with extended metastasis. *Gan To Kagaku Ryoho* 2001; **28**: 1681-1683
- 15 **Dobelbower RR**, Merrick HW, Khuder S, Battle JA, Herron LM, Pawlicki T. Adjuvant radiation therapy for pancreatic cancer: a 15-year experience. *Int J Radiat Oncol Biol Phys* 1997; **39**: 31-37
- 16 **Zhou ZH**, Song MZ. Current therapy of pancreatic carcinoma. *Shijie Huanren Xiaohua Zazhi* 2000; **8**: 214-215
- 17 **Ghaneh P**, Slavin J, Sutton R, Hartley M, Neoptolemos JP. Adjuvant therapy in pancreatic cancer. *World J Gastroenterol* 2001; **7**: 482-489
- 18 **Shibamoto Y**, Nishimura U, Abe M. Intraoperative radiotherapy and hyperthermia for unresectable pancreatic cancer. *Hepatogastroenterology* 1996; **43**: 326-332
- 19 **Schwarz RE**, Smith DD, Keny H, Ikle DN, Shibata SI, Chu DZ, Pezner RD. Impact of intraoperative radiation on postoperative and disease-specific outcome after pancreatoduodenectomy for adenocarcinoma: a propensity score analysis. *Am J Clin Oncol* 2003; **26**: 16-21
- 20 **Egawa S**, Tsukiyama I, Akine Y, Kajiura Y, Ogino T, Ozaki H, Kinoshita T, Kosuge T. Control of aftereffects due to intraoperative radiotherapy. *Gan No Rinsho* 1990; **36**: 815-820
- 21 **Tanaka Y**, Takeshita N, Niwa K, Matsuda T. Studies on treatment results and prognostic factors of intraoperative radiotherapy in pancreatic carcinoma. *Nippon Igaku Hoshasen Gakkai Zasshi* 1989; **49**: 614-621

Effects of *mu* and *kappa* opioid receptor agonists and antagonists on contraction of isolated colon strips of rats with cathartic colon

Bao-Hua Liu, Ping Mo, Sheng-Ben Zhang

Bao-Hua Liu, Ping Mo, Sheng-Ben Zhang, Department of General Surgery, Daping Hospital, Third Military Medical University, Chongqing 400042, China

Correspondence to: Dr. Bao-Hua Liu, Department of General Surgery, Daping Hospital, Third Military Medical University, Chongqing 400042, China. lbh57268@163.com

Telephone: +86-23-68757248

Received: 2003-07-12 **Accepted:** 2003-08-18

Abstract

AIM: To study the effects of *mu* and *kappa* opioid receptor agonists and antagonists on the isolated colon strips of rats with cathartic colon.

METHODS: Cathartic colon model was established by feeding rats with contact laxatives, and effects of *mu* and *kappa* opioid receptor agonists and antagonists on electricity-stimulated contraction of isolated colon strips of rats with cathartic colon were observed.

RESULTS: Compared with control group, exogenous *mu* and *kappa* agonists inhibited significantly electricity-stimulated contraction of strips of cathartic colon (8.50±0.89 mm, 6.24±0.91 mm, 3.35±0.6 mm vs 11.40±0.21 mm $P<0.01$; 8.98±0.69 mm, 6.89±0.71 mm, 4.43±0.99 mm vs 11.40±0.21 mm, $P<0.01$). In contrast, the exogenous *mu* antagonist significantly enhanced electricity-stimulated contraction of isolated colon strips (13.18±0.93 mm, 15.87±0.98 mm, 19.46±1.79 mm vs 11.40±0.21 mm, $P<0.01$), but *kappa* antagonist had no effect on the isolated colon strips of rats with cathartic colon.

CONCLUSION: *Mu* and *kappa* opioid receptors are involved in the regulation of colon motility of rats with cathartic colon.

Liu BH, Mo P, Zhang SB. Effects of *mu* and *kappa* opioid receptor agonists and antagonists on contraction of isolated colon strips of rats with cathartic colon. *World J Gastroenterol* 2004; 10 (11): 1672-1674

<http://www.wjgnet.com/1007-9327/10/1672.asp>

INTRODUCTION

The cause and pathogenesis of slow-transit constipation (STC) still remain unknown now^[1]. To study the mechanism of STC, more and more attention has been recently paid on the function of numerous neurotransmitters involved in the onset of STC^[2-8]. With a rat model of cathartic colon^[9,10], we investigated the effects of opioids, inhibitory neurotransmitters, on the electricity-stimulated contraction of isolated cathartic colon strips.

MATERIALS AND METHODS

Materials

Rhubarb and phenolphthalein powders were provided by

Chongqing Traditional Chinese Medicine Pharmaceutical Factory and Chongqing Dongfeng Reagent Factory, respectively. *Mu* and *kappa* opioid receptor antagonists (Naloxone, Norbni) and agonists (Damgo, U50488H) were purchased from Sigma Co USA.

Fifty Wistar rats of either sex, weighing 230±70 g, were divided randomly into control group ($n=10$) and cathartic colon group treated with rhubarb ($n=20$) and phenolphthalein ($n=20$). Because both rhubarb and phenolphthalein belong to the same kind of contact cathartics, the two groups were considered as one cathartic colon group.

Rats were housed in cage, one per cage under standard laboratory conditions (room temperature, 18-28 °C, relative humidity, 40-80%). Control rats were given soft chows, while the rats in rhubarb group were given chows premixed with rhubarb powder. The initial rhubarb dosage was 200 mg/kg.d, and another 200 mg/kg was added every day until it reached 1000 mg/kg.d for several days until loose stool disappeared. Then, rhubarb was added 200 mg/kg.d again until 2 400 mg/kg.d for 3 mo. The rats in phenolphthalein group were fed chows premixed with an initial dosage of phenolphthalein 200 mg/kg. Its 50% for dosage diarrhea was 1 400 mg/kg.d and its final dosage was 3 200 mg/kg.d.

Method

Rats were killed by head-strike, the abdominal cavity was opened through a median incision, and a 5 cm colon in length far from the ileocecum was then quickly dissected and transferred to Krebs solution and rinsed. The Krebs solution contained NaCl, 112.8 mmol; KCl, 5.90 mmol; CaCl₂, 1.97; MgCl₂, 1.18 mmol; NaHPO₄, 1.22 mmol; NaHCO₃, 25.0 mmol; Glu, 11.49 mmol (pH 7.2-7.4). Rinsed colon was scratched off serous membrane and cut into 2 cm×2 cm strips. One end of the strip was fixed on a supporting rod, and the another was fixed to the tension transducer. Each muscle strip was vertically placed in an organ bath filled with 10 mL Krebs solution maintained at 37 °C and gased with (950 mL/LO₂)/(50 mL/LCO₂). Muscle contraction was activated by electrical field stimulation with a pair of external platinum ring electrodes connected to a square wave stimulator. The electrodes were parallelly placed on each end of the strip, on which continuous electrical stimulations (4 ms in duration, 10 Hz and 70 V in electric pressure) were conducted. The strips were given 1 g initial tensions and equilibrated for 60 min. Isometric contraction was measured with a tension transducer connected to a physiological recorder, and the contraction amplitude was printed on standard chart paper. The direct effects of opioid receptor agonists and antagonists on the contractility of isolated muscle strips were studied by addition of opioid receptor agonists and antagonists to organ bath to make a required solution. The recorded data were depicted into concentration-response curves. To evaluate the response of muscle strips to electrical stimulation, the contraction amplitude was calculated and the average of amplitude was accounted.

Statistical Analysis

Results were expressed as mean±SE. Differences were

analyzed by Student t test. $P < 0.05$ was considered statistically significant.

RESULTS

Electricity-stimulated contractile response of isolated colon strips

The contractile response of most colon strips (about 70%) showed a typical sinusoid curve, while about 30% strips demonstrated wild and irregular waves. In the cathartic colon group, the decrease of contraction amplitude was about 27.43% of that in control group.

Effect of mu opioid receptor agonists on electricity-stimulated contractile response of cathartic colon strips

The mu opioid receptor, agonist Damgo, caused a concentration-dependent inhibition of electricity-stimulated contraction of cathartic colon strips. Damgo solutions (0.05 $\mu\text{mol/L}$, 0.10 $\mu\text{mol/L}$, 1.00 $\mu\text{mol/L}$) could induce a significant inhibition of the contractile response, which showed that the amplitude of muscle strip contraction was significantly reduced ($P < 0.01$) in the presence of Damgo (Table 1).

Table 1 Effect of Damgo on electricity-stimulated contractile response of cathartic colon strips (mean \pm SD)

Concentration ($\mu\text{mol/L}$)	Basic contraction amplitude without Damgo (mm)	Contraction amplitude with Damgo (mm)
0.05	11.40 \pm 0.21	8.50 \pm 0.89 ^b
0.10	11.40 \pm 0.21	6.24 \pm 0.91 ^{ab}
1.00	11.40 \pm 0.21	3.35 \pm 0.64 ^{bd}

^a $P < 0.05$ vs 0.05 $\mu\text{mol/L}$, ^b $P < 0.01$ vs without Damgo, ^d $P < 0.01$ vs 0.05 $\mu\text{mol/L}$.

Effect of mu opioid receptor antagonists on electricity-stimulated contractile response of cathartic colon strips

The mu opioid receptor antagonist, naloxone, could induce a concentration-dependent elevation of electricity-stimulated contraction amplitude of cathartic colon strips. Each naloxone concentration (0.05 $\mu\text{mol/L}$, 0.10 $\mu\text{mol/L}$, 1.00 $\mu\text{mol/L}$) induced a significant elevation of the contractile response, which showed the contraction amplitude was significantly elevated ($P < 0.01$) in the presence of naloxone (Table 2).

Table 2 Effect of naloxone on electricity-stimulated contractile response of cathartic colon strips (mean \pm SD)

Concentration ($\mu\text{mol/L}$)	Basic contraction amplitude without naloxone (mm)	Contraction amplitude with naloxone (mm)
0.05	11.40 \pm 0.21	13.18 \pm 0.93 ^b
0.10	11.40 \pm 0.21	15.87 \pm 0.98 ^{ab}
1.00	11.40 \pm 0.21	19.46 \pm 1.79 ^{bd}

^a $P < 0.05$ vs 0.05 $\mu\text{mol/L}$, ^b $P < 0.01$ vs without Naloxone, ^d $P < 0.01$ vs 0.05 $\mu\text{mol/L}$.

Table 3 Effects of U50488H on electricity-stimulated contractile response of cathartic colon strips (mean \pm SD)

Concentration ($\mu\text{mol/L}$)	Basic contraction amplitude before administration (mm)	Contraction amplitude after administration (mm)
0.05	11.40 \pm 0.21	8.98 \pm 0.69 ^b
0.10	11.40 \pm 0.21	6.89 \pm 0.71 ^{ab}
1.00	11.40 \pm 0.21	4.43 \pm 0.99 ^{bd}

^a $P < 0.05$ vs 0.05 $\mu\text{mol/L}$, ^b $P < 0.01$ vs before administration, ^d $P < 0.01$ vs 0.05 $\mu\text{mol/L}$.

Effect of kappa opioid receptor agonists on electricity-stimulated contractile response of cathartic colon strips

U50488H, a highly-selective kappa opioid receptor agonist, could cause an evident suppression of the electricity stimulated contraction of colon strips of rats with cathartic colon. Each U50488H concentration (0.05 $\mu\text{mol/L}$, 0.10 $\mu\text{mol/L}$, 1.00 $\mu\text{mol/L}$) induced a significant inhibition of the contractile response ($P < 0.01$) (Table 3).

Effect of kappa opioid receptor antagonists on electricity-stimulated contractile response of cathartic colon strips

Norbin is a highly-selective kappa opioid receptor antagonist, which did not show any evident effect on the electricity stimulated contraction of colon strips of rats with cathartic colon. No concentration of Norbin in our experiment could induce any effect on the contraction amplitude of muscle strips, even at the maximal concentration of Norbin (data not shown).

DISCUSSION

Opioids have extensive distributions and potent effects on the gastrointestinal tract^[11,12]. Contractility studies also indicated that opioids, in combination with mu, kappa and delta opioid receptor agonists, could inhibit motor activity of the gastrointestinal tract by suppression of excitatory neurotransmitter release^[13-15]. Our study manifested that exogenously added opioid receptor agonists (*mu*, *kappa*) inhibited the contractility of colon strips of rats with cathartic colon, which showed a significant reduction of contraction amplitude as compared to the basic contraction with no agonists. The inhibitory effects were negatively correlated with concentrations. In contrast, mu receptor antagonists elevated electricity stimulated contraction of cathartic colon in rats. However, kappa receptor antagonists had no effect. The results suggested that mu and kappa opioid receptor might play an important role in the regulation of gastrointestinal motility in rats. It also further approved that opioids could slow down the propulsive peristalsis performed by nerves and muscles in colon and played a very important role in the onset and pathologic process of STC.

Kreek hypothesized that the changes of opioids activity were the important etiological factor, and STC patients could be successfully treated with naloxone, a mu opioid receptor antagonists. The present study was designed to investigate the effects of opioid agonists and antagonists on isolated cathartic colon muscle strips, it provided a new fundamental theory on the STC treatment with opioid receptor antagonists. It also indicated that the studies on the subtype and binding site of opioid receptors, as well as the overall research in clinic, would provide new methods for STC therapies, and also benefit the clarification of the pathogenesis of STC. In conclusion, mu and kappa opioid receptors are involved in the regulation of colon motility of rats with cathartic colon.

REFERENCES

- 1 Liu BH, Mo P, Tong WT, Gong SG, Fu T, Fang SW. Diagnosis and Therapy of Constipation. *Beijing: Military Medical Science Publishing House* 2002: P174-182
- 2 Hruby VJ, Agnes RS. Conformation-activity relationships of opioid peptides with selective activities at opioid receptors. *Biopolymers* 1999; **51**: 391-410
- 3 Sora I. Opioid receptor knockout mice. *Nihon Shinkei Seishin Yakurigaku Zasshi* 1999; **19**: 239-249
- 4 Camilleri M. Management of the irritable bowel syndrome. *Gastroenterology* 2001; **120**: 652-668
- 5 Callahan MJ. Irritable bowel syndrome neuropharmacology. A review of approved and investigational compounds. *J Clin Gastroenterol* 2002; **35**(1 Suppl): S58-67

- 6 **Tong WD**, Zhang SB, Zhang LY, Cai WQ, Du WH, Mu JH. Identification of interstitial cells of cajal in the myenteric plexus of colon of rats. *Chinese J Anatomy* 1999; **22**: 316-318
- 7 **Tong WD**, Zhang SB, Liu BH, Zhang LY, Huang XK, Gao F. Effect of long term application of rhubarb on colonic motility and enteric nervous system in rats. *World Chinese J Digestol* 2003; **11**: 665-667
- 8 **Tong WD**, Liu BH, Zhang SB, Zhang LY, Huang XK, Gao F. Abdominal colectomy as a treatment of obstinate slow transit constipation: clinical results and aetiological analysis. *Formos J Surg* 2003; **36**: 112-119
- 9 **Tong WD**, Zhang SB, Liu BH, Zhang LY, Huang XK. Effects of phenolphthalein on colonic motility and enteric nervous system in rats. *Chin J Dig Dis* 2003; **23**: 723-726
- 10 **Liu BH**, Zhang SB, Mo P. Effect of agonists, antagonists of mu, kappa receptors in mouse intestine transmission function. *J Coloproctol Surg* 2002; **8**: 14-16
- 11 **Tan-No K**, Nijima F, Nakagawasai O, Sato T, Satoh S, Tadano T. Development of tolerance to the inhibitory effect of loperamide on gastrointestinal transit in mice. *Eur J Pharm Sci* 2003; **20**: 357-363
- 12 **Sengupta JN**, Snider A, Su X, Gebhart GF. Effects of kappa opioids in the inflamed rat colon. *Pain* 1999; **79**: 175-185
- 13 **Bagnol D**, Henry M, Cupo A, Jule Y. Distribution of enkephalin-like immunoreactivity in the cat digestive tract. *J Auton Nerv Syst* 1997; **64**: 1-11
- 14 **Kaufman PN**, Krevsky B, Malmud LS, Maurer AH, Somers MB, Siegel JA, Fiaher RS. Role of opiate receptors in the regulation of colonic transit. *Gastroenterology* 1988; **94**: 1351-1356
- 15 **Liu M**, Wittbrodt E. Low-dose oral naloxone reverses opioid-induced constipation and analgesia. *J Pain Symptom Manage* 2002; **23**: 48-53

Edited by Ren SY and Wang XL **Proofread by** Xu FM

Serum level of TSGF, CA242 and CA19-9 in pancreatic cancer

Jing-Ting Jiang, Chang-Ping Wu, Hai-Feng Deng, Ming-Yang Lu, Jun Wu, Hong-Yu Zhang, Wen-Hui Sun, Mei Ji

Jing-Ting Jiang, Chang-Ping Wu, Hai-Feng Deng, Ming-Yang Lu, Jun Wu, Hong-Yu Zhang, Wen-Hui Sun, Mei Ji, Department of Tumor Biological Treatment, the Third Affiliated Hospital of Suzhou University, Changzhou 213003, Jiangsu Province, China

Correspondence to: Dr. Jing-Ting Jiang, Department of Tumor Biological Treatment, the Third Affiliated Hospital of Suzhou University, Changzhou 213003, Jiangsu Province, China. jitnew@163.com

Telephone: +86-519-6180978 **Fax:** +86-519-6621235

Received: 2003-12-19 **Accepted:** 2004-02-01

Abstract

AIM: To establish a method to detect the expression of the tumor specific growth factor TSGF, CA242 and CA19-9 in serum and evaluate their value in diagnosis of pancreatic cancer.

METHODS: ELISA and Biochemical colorimetric assay were used to detect the serum content of TSGF, CA242 and CA19-9 in 200 normal cases, 52 pancreatitis patients and 96 pancreatic cancer patients.

RESULTS: The positive likelihood ratios of TSGF, CA242 and CA19-9 were 5.4, 12.6 and 6.3, respectively, and their negative likelihood ratios were 0.10, 0.19 and 0.17, respectively. With single tumor marker diagnosed pancreatic cancer, the highest sensitivity and specificity of TSGF were 91.6% and 93.5%. In combined test with 3 markers, when all of them were positive, the sensitivity changed to 77.0% and the specificity and the positive predictive value were 100%. The levels of TSGF and CA242 were significantly higher in the patients with pancreatic cancer of head than those in the patients with pancreatic cancer of body, tail and whole pancreas, but the expression of CA19-9 had no correlation with the positions of the pancreatic cancer. The sensitivity of TSGF, CA242 and CA19-9 was increased with the progress in stages of pancreatic cancer. In stage I, the sensitivity of TSGF was markedly higher than CA242 and CA19-9.

CONCLUSION: The combined use of TSGF, CA242 and CA19-9 expressions can elevate the specificity for pancreatic cancer diagnosis. And it shows that it plays an important role to differentiate positions and tissue typing. It is a forepart diagnosis for the pancreatic cancer by combination checking. There is very important correlation between the three markers and the pancreatic cancer.

Jiang JT, Wu CP, Deng HF, Lu MY, Wu J, Zhang HY, Sun WH, Ji M. Serum level of TSGF, CA242 and CA19-9 in pancreatic cancer. *World J Gastroenterol* 2004; 10(11): 1675-1677

<http://www.wjgnet.com/1007-9327/10/1675.asp>

INTRODUCTION

Early period of pancreatic cancer lacked the typical clinic performances^[1,2], was high malignant and had a low survival time in five years^[3-6]. And it was difficult to be diagnosed and made the patients lose the chances of radical cures. So it was very important to diagnose pancreatic cancer early^[7-9]. But the sensitivity and specificity were not ideal in examining pancreatic

cancer with a single method. We assayed the content of TSGF, CA242 and CA19-9 in serum of pancreatic cancer suffers and analyzed their expression in different positions and tissue typing in order to improve the level of early period of the pancreatic cancer diagnosis.

MATERIALS AND METHODS

Materials

To collect 200 normal people who had medical check-up in the hospital as normal group, including 112 males and 88 females with a mean age of 55.0 ± 1.2 (range, 22-68 years). To collect 52 pancreatitis suffers as pancreatitis group, including 29 males and 23 females with an average age of 66.0 ± 8.0 (range, 60-74 years). To collect 96 pancreatic cancer suffers as pancreatic cancer group, including 61 males and 35 females with an average age of 67.6 ± 6.7 (range, 60-88 years). There were 64 heads of pancreatic cancer, 18 body of pancreatic cancer and 10 tail of pancreatic cancer, which were all proved by pathology.

Methods

TSGF was assayed by colorimetric of biochemistry from Fujian New Continent Biochemical Technology Limited Company. CA242 and CA19-9 were assayed by ELISA from Sweden CanAg Company. All operations were followed by manuals. All data were showed as mean \pm SD and calculated by *t* test, and positive ratios were calculated by χ^2 test.

RESULTS

TSGF, CA242 and CA19-9 assay of three groups

Statistical significance of the contents of the three markers was found when pancreatic cancer group was compared with normal group and pancreatitis group ($P < 0.01$). No statistical significance was found between normal group and pancreatitis group ($P > 0.05$, Table 1).

Table 1 Laboratory parameters of the 3 tumor markers in pancreatic cancer group, pancreatitis group and normal group (mean \pm SD, $\times 10^3$ U/L)

Group	No. of cases	TSGF	CA242	CA19-9
Critical value		>71	>20	>37
Pancreatic cancer	96	80.7 ± 7.6^b	90.2 ± 10.9^b	643.5 ± 203.6^b
Pancreatitis	52	61.4 ± 6.7	21.1 ± 10.5	30.9 ± 5.9
Normal				
22-59 yr	113	54.3 ± 5.1	17.5 ± 8.3	14.5 ± 5.0
60-68 yr	87	56.6 ± 5.8	19.2 ± 9.6	17.2 ± 5.9

^b $P < 0.01$ vs normal group.

Evaluate the value of diagnosis in pancreatic cancer by a single tumormarker

When diagnosing pancreatic cancer by a single tumor marker, TSGF had the highest sensitivity of 91.6%, CA242 had the highest specificity of 93.5%; TSGF and CA19-9 had the exactly validity. The positive likelihood ratio of TSGF, CA242 and CA19-9 were 5.4, 12.6 and 6.3, and the negative likelihood ratio were 0.10, 0.19 and 0.17 (Table 2).

Table 2 Evaluation of the value of diagnosis in pancreatic cancer by a single tumor marker of 96 cases

Value of diagnosis	Sensitivity (%)	Specificity (%)	Positive likelihood ratio	Negative likelihood ratio
TSGF	91.6 (88) ^a	83.0	5.4	0.10
CA242	82.3 (79)	93.5 ^b	12.6	0.19
CA19-9	85.4 (82)	86.5	6.3	0.17

(), No. of cases; ^a $P < 0.05$, ^b $P < 0.01$ vs the other two indexes. sensitivity=true positive/patients $\times 100\%$ =TP/(TP+FN) $\times 100\%$, specificity=true negative/normal $\times 100\%$ =TN/(TN+FP) $\times 100\%$ positive likelihood ratio=true positive/false positive=sensitivity/(1-specificity) negative likelihood ratio=(1-true positive)/(1-false positive)=(1-sensitivity)/specificity.

The different combinations of the 3 markers to the diagnosis in pancreatic cancer

When diagnosing pancreatic cancer by any of the 3 markers was over the critical value, the sensitivity, specificity and positive predictive value were 93.8%, 79.0% and 68.2%. When two of the 3 markers were over the critical value, the sensitivity, specificity and positive predictive value were 89.5%, 95.5% and 90.5%. When the 3 markers were all over the critical value, the sensitivity was 77.0% and the specificity and positive predictive value were both 100%. Therefore, the combination diagnosis in pancreatic cancer could increase the specificity of the diagnosis (Table 3).

Table 3 Analyses of The different combinations of the 3 markers to the diagnosis in pancreatic cancer (No. of cases)

Group	No. of cases	1 Item (+)	2 Item (+)	3 Item (+)
Pancreatic cancer	96	90 (93.8)	86 (89.5)	74 (77.0)
Normal	200	42 (21.0)	9 (4.5)	0 (100)
Positive likelihood rate (%)		68.2	90.5	100

(), sensitivity (%).

The correlation between the different positions of pancreatic cancer and the levels of the 3 markers

International Union Against Cancer (UICC) divided pancreatic cancer into head, body, tail and whole of pancreatic cancer. Statistical significance was found that the levels of TSGF and CA242 in head of pancreatic cancer were extra better than those in the other three kinds of pancreatic cancer ($P < 0.01$). But no statistical significance was found in the levels of the 3 markers in the other three kinds of pancreatic cancer ($P > 0.05$). The levels of CA19-9 had no correlation with the positions of the pancreatic cancer ($P > 0.05$). (Table 4).

Table 4 The content of the 3 markers in the different positions of pancreatic cancer (mean \pm SD, $\times 10^3$ U/L)

Position of pancreatic cancer	No. of cases	TSGF	CA242	CA19-9
Head	64	88.5 \pm 9.0 ^b	106.4 \pm 12.6 ^b	653.7 \pm 217.8
Body	18	78.2 \pm 6.7	82.5 \pm 10.4	633.9 \pm 192.4
Tail	10	77.1 \pm 5.7	81.6 \pm 8.2	659.4 \pm 211.0
Whole	4	74.5 \pm 3.1	83.0 \pm 9.5	615.3 \pm 187.1

^b $P < 0.001$ vs body, tail and whole of pancreatic cancer.

To compare the sensitivity of the 3 tumor markers in different stages of pancreatic cancer

We analyzed the sensitivity of the 3 tumor markers in serum in different stages of pancreatic cancer (Table 5). The results showed that the sensitivity gradually strengthened by the progress of clinical stages. Statistical significance was found

between stage II, III, IV, and stage I ($P < 0.01$). The sensitivity of CA19-9 was higher than that of CA242, but there was no statistical significance ($P > 0.05$). The sensitivity of TSGF in stage I was significant better than that of CA242 and CA19-9 ($P < 0.01$). So TSGF could be regarded as a tumor marker to filtrate pancreatic cancer in early stage.

Table 5 Analyses of the sensitivity of the 3 tumor markers in different stages of pancreatic cancer (No. of cases)

Clinical stages	No. of cases	TSGF	CA242	CA19-9
I	10	6 (60.0) ^{bd}	3 (30.0) ^d	4 (40.0) ^d
II	12	9 (75.0)	6 (50.0)	7 (58.3)
III	25	22 (88.0)	20 (80.0)	21 (84.0)
IV	49	46 (93.8)	40 (81.6)	42 (85.7)

Note: (), sensitivity (%); ^d $P < 0.01$ vs the sensitivity of stage II, III, IV; ^b $P < 0.01$ vs the sensitivity of CA242, CA19-9.

DISCUSSION

The incidence of pancreatic cancer is rising^[10,11]. We want to diagnose pancreatic cancer in early stage by tumor markers^[12]. First, we should find one tumor marker of good specificity^[13,14]. TSGF was a gene that could promote the growth of tumor blood vessels. It could greatly hyperplasy in the tumor tissues and capillary vessels around. No correlation was found in the hyperplasia of non-tumor blood vessels. TSGF had good sensitivity to malignant tumors. CA19-9 belonged to the ramification of lactotetraose and was a kind of the ganglioside lipoprotein protein^[15-17]. It was mucoprotein when in serum and its epipositions was pentaglucose determinant. Despite advances in preoperative radiologic imaging, a significant fraction of potentially resectable pancreatic cancers are found to be unresectable at laparotomy^[18]. CA242 was a kind of sialic acid mucoprotein tumor associated antigen linked Mucin pyrenoid by -O-. It existed in the same molecule with CA19-9. But it belonged to the different antigen determinant with CA19-9. Therefore, there was no correlation between CA19-9 and CA242^[19]. But they were complementary. They had good sensitivity in pancreatic cancer diagnosis. This result was exactly similar with the report of Ichihara *et al*^[20]. This research also showed that 3 tumor markers in pancreatic cancer group were remarkably higher than that of normal group. And the levels of the 3 tumor markers in pancreatitis group were not high.

The research showed that the positive likelihood ratio of TSGF, CA242 and CA19-9 were 5.4, 12.6 and 6.3, and the negative likelihood ratio were 0.1, 0.19 and 0.17. So the three indexes were very important in clinical pancreatic cancer diagnosis. TSGF had good sensitivity in pancreatic cancer diagnosis as 91.6%. CA19-9 was very important to evaluate the curative effect of chemotherapy and to judge the survival time^[21-26]. CA242 had good specificity as 93.5%. When diagnosing with the combination assay of the 3 indexes, the sensitivity was 77.0% and the specificity and positive predictive value were both 100%. Therefore, combination diagnosis should be used in pancreatic cancer diagnosis in order to improve the specificity^[27-29].

The research of Metsuyama *et al*. proved that there was significant correlation in malignant tumors between the creation of blood vessels and blood transfer^[30]. TSGF and CA242 had high levels. It was related to the rich blood supply of the head of pancreas. Pancreas had the priority and step artery pancreaticoduodenalis superior and the forward and back branches down pancereaticoduodenales inferiors. The arteries were connected by anastomosis at the head of pancreas to be arcuate arterial. The arcuate arterial gave out branches to supply the forward and back parts of the head of pancreas and duodenum. It accelerated the head of pancreas circulation. So

it made the carbohydrate antigen excreted by tumors to be a high level in serum. But there was no correlation between the expression of CA19-9 and the position of tumor. This needs further researches. TSGF was a new tumor marker related to the blood vessel hyperplasia of malignant tumors. It was also a result of the hyperplasia of the malignant tumors and the capillary vessels around. It was released to blood with the acceleration of blood circulation. In the different stage of pancreatic cancer, the sensitivity of the tumor markers TSGF, CA242 and CA19-9 increased with the progress in different stages. Statistical significance was found in the sensitivity of stage II, III, IV and stage I. This result disagreed that Frebourg *et al* reported that there was no correlation between the level of CA19-9 in serum and the stage of pancreatic cancer^[31]. The sensitivity of CA19-9 was a little higher than that of CA242, but there was no statistical significance. In the stage I of pancreatic cancer, the sensitivity of TSGF was remarkably higher than that of CA242 and CA19-9. Therefore, TSGF can be regarded as a tumor marker to filtrate pancreatic cancer in early stage.

The research shows that there is very important correlation between the levels of TSGF, CA242 and CA19-9 and pancreatic cancer. The combined assay of the 3 indexes does help to diagnose pancreatic cancer in early stage. At the same time they are very important in analyzing the position of pancreatic cancer and the pathology typings. Therefore, the 3 indexes can be regarded as the tumor markers of pancreatic cancer diagnosis in early stage.

REFERENCES

- 1 **Barbe L**, Ponsot P, Vilgrain V, Terris B, Flejou JF, Sauvanet A, Belghiti J, Hammel P, Ruszniewski P, Bernades P. Intraductal papillary mucinous tumors of the pancreas. Clinical and morphological aspects in 30 patients. *Gastroenterol Clin Biol* 1997; **21**: 278-286
- 2 **Love L**, Fizzotti G, Damascelli B, Ceglia E, Garbagnati F, Milella M. Pancreatic tumor imaging by III generation CT, gray-scale ultrasound and improved angiography. *Tumori* 1980; **66**: 357-372
- 3 **Sahmoun AE**, D'Agostino RA Jr, Bell RA, Schwenke DC. International variation in pancreatic cancer mortality for the period 1955-1998. *Eur J Epidemiol* 2003; **18**: 801-816
- 4 **Burcharth F**, Trillingsgaard J, Olsen SD, Moesgaard F, Federspiel B, Struckmann JR. Resection of cancer of the body and tail of the pancreas. *Hepatogastroenterology* 2003; **50**: 563-566
- 5 **Soga J**. Primary endocrinomas (carcinoids and variant neoplasms) of the gallbladder. A statistical evaluation of 138 reported cases. *J Exp Clin Cancer Res* 2003; **22**: 5-15
- 6 **Pingpank JF Jr**, Hoffman JP, Sigurdson ER, Ross E, Sasson AR, Eisenberg BL. Pancreatic resection for locally advanced primary and metastatic nonpancreatic neoplasms. *Am Surg* 2002; **68**: 337-340
- 7 **Birk D**, Schoenberg MH, Gansauge F, Formentini A, Fortnagel G, Beger HG. Carcinoma of the head of the pancreas arising from the uncinate process. *Br J Surg* 1998; **85**: 498-501
- 8 **Standop J**, Schneider MB, Ulrich A, Pour PM. Experimental animal models in pancreatic carcinogenesis: lessons for human pancreatic cancer. *Dig Dis* 2001; **19**: 24-31
- 9 **Berberat P**, Friess H, Kashiwagi M, Beger HG, Buchler MW. Diagnosis and staging of pancreatic cancer by positron emission tomography. *World J Surg* 1999; **23**: 882-887
- 10 **Zalatnai A**. Pancreatic cancer - a continuing challenge in oncology. *Pathol Oncol Res* 2003; **9**: 252-263
- 11 **Shore S**, Raraty MG, Ghaneh P, Neoptolemos JP. Review article: chemotherapy for pancreatic cancer. *Aliment Pharmacol Ther* 2003; **18**: 1049-1069
- 12 **Otsuki M**. Chronic pancreatitis in Japan: epidemiology, prognosis, diagnostic criteria, and future problems. *J Gastroenterol* 2003; **38**: 315-326
- 13 **Laurent-Puig P**, Lubin R, Semhoun-Ducloux S, Pelletier G, Fourre C, Ducreux M, Briantais MJ, Buffet C, Soussi T. Antibodies against p53 protein in serum of patients with benign or malignant pancreatic and biliary diseases. *Gut* 1995; **36**: 455-458
- 14 **Abrams RA**, Grochow LB, Chakravarthy A, Sohn TA, Zahurak ML, Haulk TL, Ord S, Hruban RH, Lillemoe KD, Pitt HA, Cameron JL, Yeo CJ. Intensified adjuvant therapy for pancreatic and periampullary adenocarcinoma: survival results and observations regarding patterns of failure, radiotherapy dose and CA19-9 levels. *Int J Radiat Oncol Biol Phys* 1999; **44**: 1039-1046
- 15 **Vestergaard EM**, Wolf H, Orntoft TF. Increased concentrations of genotype-interpreted Ca 19-9 in urine of bladder cancer patients mark diffuse atypia of the urothelium. *Clin Chem* 1998; **44**: 197-204
- 16 **Ugorski M**, Laskowska A. Sialyl Lewis^x: a tumor-associated carbohydrate antigen involved in adhesion and metastatic potential of cancer cells. *Acta Biochim Pol* 2002; **49**: 303-311
- 17 **Magnani JL**, Steplewski Z, Koprowski H, Ginsburg V. Identification of the gastrointestinal and pancreatic cancer-associated antigen detected by monoclonal antibody 19-9 in the sera of patients as a mucin. *Cancer Res* 1983; **43**: 5489-5492
- 18 **Schlieman MG**, Ho HS, Bold RJ. Utility of tumor markers in determining resectability of pancreatic cancer. *Arch Surg* 2003; **138**: 951-956
- 19 **Banfi G**, Zerbi A, Pastori S, Parolini D, Di Carlo V, Bonini P. Behavior of tumor markers CA19.9, CA195, CAM43, CA242 and TPS in the diagnosis and follow-up of pancreatic cancer. *Clin Chem* 1993; **39**: 420-423
- 20 **Ichihara T**, Nomoto S, Takeda S, Nagura H, Sakamoto J, Kondo K, Horisawa M, Nakao A. Clinical usefulness of the immunostaining of the tumor markers in pancreatic cancer. *Hepatogastroenterology* 2001; **48**: 939-943
- 21 **Frebourg T**, Bercoff E, Manchon N, Senant J, Basuyau JP, Breton P, Janvresse A, Brunelle P, Bourreille J. The evaluation of CA19-9 antigen level in the early detection of pancreatic cancer. A prospective study of 866 patients. *Cancer* 1988; **62**: 2287-2290
- 22 **Ziske C**, Schlie C, Gorschluter M, Glasmacher A, Mey U, Strehl J, Sauerbruch T, Schmidt-Wolf IG. Prognostic value of CA 19-9 levels in patients with inoperable adenocarcinoma of the pancreas treated with gemcitabine. *Br J Cancer* 2003; **89**: 1413-1417
- 23 **Halm U**, Schumann T, Schiefke I, Witzigmann H, Mossner J, Keim V. Decrease of CA 19-9 during chemotherapy with gemcitabine predicts survival time in patients with advanced pancreatic cancer. *Br J Cancer* 2000; **82**: 1013-1016
- 24 **Masaki T**, Ohkawa S, Hirokawa S, Miyakawa K, Tamai S, Tarao K. A case of advanced pancreatic cancer showing remarkable response to gemcitabine treatment. *Gan To Kagaku Ryoho* 2003; **30**: 1333-1336
- 25 **Kamisawa T**, Tu Y, Egawa N, Ishiwata J, Tsuruta K, Okamoto A, Hayashi Y, Koike M, Yamaguchi T. Ductal and acinar differentiation in pancreatic endocrine tumors. *Dig Dis Sci* 2002; **47**: 2254-2261
- 26 **Koopmann J**, Zhang Z, White N, Rosenzweig J, Fedarko N, Jagannath S, Canto MI, Yeo CJ, Chan DW, Goggins M. Serum diagnosis of pancreatic adenocarcinoma using surface-enhanced laser desorption and ionization mass spectrometry. *Clin Cancer Res* 2004; **10**: 860-868
- 27 **Schlieman MG**, Ho HS, Bold RJ. Utility of tumor markers in determining resectability of pancreatic cancer. *Arch Surg* 2003; **138**: 951-956
- 28 **Dianxu F**, Shengdao Z, Tianquan H, Yu J, Ruoqing L, Zurong Y, Xuezhi W. A prospective study of detection of pancreatic carcinoma by combined plasma K-ras mutations and serum CA19-9 analysis. *Pancreas* 2002; **25**: 336-341
- 29 **Mu DQ**, Wang GF, Peng SY. p53 protein expression and CA19.9 values in differential cytological diagnosis of pancreatic cancer complicated with chronic pancreatitis and chronic pancreatitis. *World J Gastroenterol* 2003; **9**: 1815-1818
- 30 **Metsuyama K**, Chiba Y, Sasaki M, Tanaka H, Muraoka R, Tanigawa N. Tumor angiogenesis as a prognostic marker in operable non-small cell lung cancer. *Ann Thorac Surg* 1998; **65**: 1405-1409
- 31 **Frebourg T**, Bercoff E, Mouchon N, Senant J, Basuyau JP, Breton P, Janvresse A, Brunelle P, Bourreille J. The evaluation of CA19-9 antigen level in the early detection of pancreatic cancer. *Cancer* 1988; **62**: 2287-2290

Liver biopsy in evaluation of complications following liver transplantation

Ying-Yan Yu, Jun Ji, Guang-Wen Zhou, Bai-Yong Shen, Hao Chen, Ji-Qi Yan, Cheng-Hong Peng, Hong-Wei Li

Ying-Yan Yu, Jun Ji, Guang-Wen Zhou, Bai-Yong Shen, Hao Chen, Ji-Qi Yan, Cheng-Hong Peng, Hong-Wei Li, Transplantation Center and Institute of Digestive Surgery, Ruijin Hospital, Shanghai Second Medical University, Shanghai 200025, China

Correspondence to: Ying-Yan Yu, Transplantation Center and Institute of Digestive Surgery, Ruijin Hospital, Shanghai Second Medical University, Shanghai 200025, China. yingyan3y@yahoo.com.cn

Telephone: +86-21-64370045-611018 **Fax:** +86-21-64370045

Received: 2003-10-10 **Accepted:** 2003-11-06

Abstract

AIM: To analyze the role of liver biopsies in differential diagnosis after liver transplantation.

METHODS: A total of 50 biopsies from 27 patients with liver dysfunction out of 52 liver transplantation cases were included. Biopsies were obtained 0-330 d after operation, in which, 44 were fine needle biopsies, another 6 were wedge biopsies during surgery. All tissues were stained with haematoxylin-eosin. Histochemical or immunohistochemical stain was done.

RESULTS: The rate of acute rejection in detected cases and total transplantation cases was 48.2% and 25.0%, chronic rejection rate in detected cases and total transplantation cases was 14.8% and 7.7%, preservation-reperfusion injury in detected cases and total transplantation cases was 25.9% and 13.5%, hepatic artery thrombosis rate in detected cases and total transplantation cases was 11.1% and 5.8%, intrahepatic biliary injury rate in detected cases and total transplantation cases was 7.4 % and 3.8%, CMV infection rate in detected cases and total transplantation cases was 3.7% and 1.9%, hepatitis B recurrence rate in detected cases and total transplantation cases was 3.7% and 1.9%, the ratio of suspicious drug-induced hepatic injury in detected cases and total transplantation cases was 11.1% and 5.8%.

CONCLUSION: Acute rejection and preservation-reperfusion injury are the major factors in early liver dysfunction after liver transplantation. Hepatic artery thrombosis and prolonged cold preservation may result in intrahepatic biliary injury. Acute rejection and viral infection may involve in the pathogenesis of chronic rejection. Since there are no specific lesions in drug-induced hepatic injury, the diagnosis must closely combine clinical history and rule out other possible complications.

Yu YY, Ji J, Zhou GW, Shen BY, Chen H, Yan JQ, Peng CH, Li HW. Liver biopsy in evaluation of complications following liver transplantation. *World J Gastroenterol* 2004; 10(11): 1678-1681 <http://www.wjgnet.com/1007-9327/10/1678.asp>

INTRODUCTION

Liver transplantation has been accepted as an effective therapeutic option for patients with acute or chronic end-stage

liver diseases. However, the postoperative course of liver transplant recipients will face to rejection for alloantigens and a number of complications. Among which, hepatic artery thrombosis, intrahepatic biliary injury, preservation-reperfusion injury, opportunistic infection as well as immunosuppressive drug-induced hepatic injury are critically for allograft liver poor function. Clinically, the complications are short of specific symptoms and signs, although the supervision for blood biochemistry, Doppler-ultrasound and radiologic image has some value to the evaluation of graft liver dysfunction, the final diagnosis still relies on liver biopsy evaluation. Here is a pathological study on fifty allograft liver biopsies which have been collected in our transplantation center since June 2002. These biopsies covered a number of complications following liver transplantation.

MATERIALS AND METHODS

Collection of allograft liver biopsies

From June 2002 to September 2003, a total of 52 orthotopic liver transplantations (OLTs) were performed in Transplantation Center, Ruijin Hospital of Shanghai. Fifty liver biopsies were obtained from 27 patients with liver dysfunction 0-330 d after operation. In which, 44 were fine needle biopsies, another 6 were wedge biopsies during surgery. All tissues were fixed in 40 g/L buffered formaldehyde and embedded in paraffin.

Histopathologic evaluation of liver biopsies

Serial 3 μ m thick sections were cut on all biopsies. One section was stained with hemotoxylin-eosin. Others were stained by histochemical or immunohistochemical methods whenever it was needed. For example, if cytomegalovirus (CMV) infection was suspicious, CMV antigen immunohistochemistry would be done. If chronic rejection was suspicious, CK19 or CA19-9 immunohistochemistry for bile duct detection would be done. Criteria for evaluating acute rejection were based on Banff Schema published in 1997^[1,2]. Criteria for evaluating chronic rejection were based on Banff Schema published in 2000^[3]. Acute rejection was characterized by predominant portal-based lesions, including a classical triad of mixed inflammatory cell infiltrates, venous endothelial inflammation and inflammatory infiltration of bile ducts. Chronic rejection was characterized by ductopenia and obliterative arteriopathy.

Evaluation of preservation-reperfusion injury was based on the criteria proposed by Starzl Transplantation Institute of Pittsburgh University as well as University of Birmingham^[4]. The histological features included: sinusoidal neutrophilic infiltration without portal mixed inflammatory cell infiltration, hepatocyte ballooning, cholestasis, hepatocyte apoptosis and regenerative change. Macrovesicular steatosis was graded as follows: mild, fat present in less than 30% of hepatocyte; moderate, fat infiltration of 30-60%; and severe, fat infiltration greater than 60% of hepatocytes.

This clinical study was performed on archival pathological files, which were obtained as part of routine clinical practice.

RESULTS

In this group, the earliest biopsy was got at 5 h following the

re-vascularization during transplantation procedure, the latest biopsy was got 330 d after transplantation. Twenty-seven cases out of 52 liver transplantation patients with poor allograft function accepted 1 to 6 liver biopsy detections according to clinical requirement. The lesions revealed in biopsy tissues are summarized in Table 1.

Table 1 Classification of lesions in 50 allograft liver biopsies

Lesions	n	Rate in detected cases (%) (n=27)	Ratio in total transplantation cases(%) (n=52)
Acute rejection	13	48.2	25.0
Chronic rejection	4	14.8	7.7
CMV infection	1	3.7	1.9
Hepatic artery thrombosis	3	11.1	5.8
Intrahepatic biliary injury	2	7.4	3.8
Drug-induced hepatic injury	3	11.1	5.8
Preservation-reperfusion injury	7	25.9	13.5
Recurrent hepatitis	1	3.7	1.9

The occurring time of different complications was different. Preservation-reperfusion injury and hepatic artery thrombosis mainly occurred within 2 wk following operation. Acute rejection could happen at any time from 1 wk to 310 d, but often took place at the end of 1 wk to 30 d following operation. The poor graft liver function that occurred 60-90 d postoperation was closely related to intrahepatic biliary injury. Early chronic rejection could happen as early as 45 d after transplantation but mainly occurred from 90 to 330 d post-transplantation. Only one recurrent hepatitis B happened in this group, 300 d after transplantation. The occurring time features of different complications are shown in Figure 1.

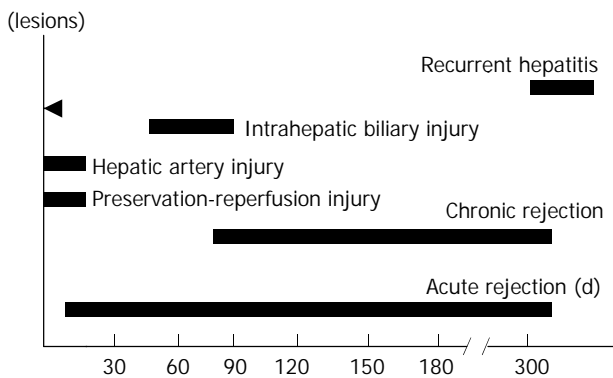


Figure 1 Time features of different complications in allograft liver biopsy.

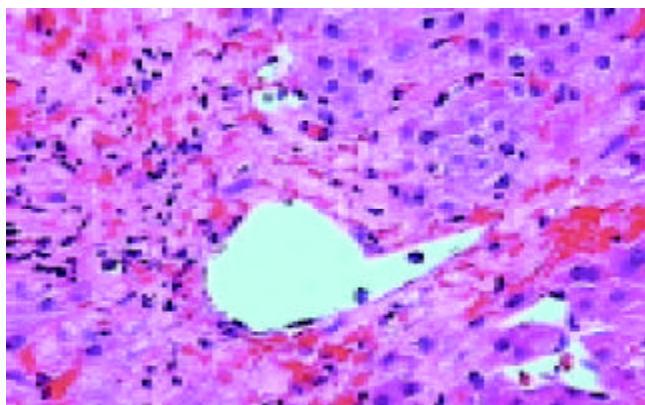


Figure 2 Hepatocytes necrosis and bleeding surrounding central vein caused by HAT 12 d after transplantation, HE ×200.

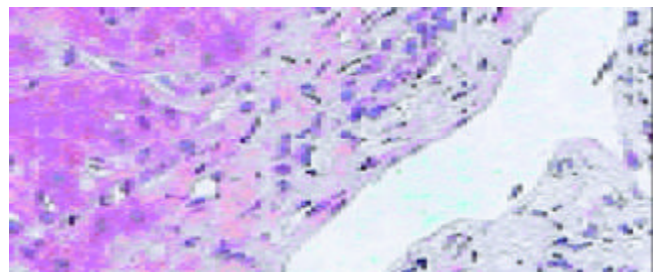


Figure 3 Bile duct damage with inflammation 80 d after transplantation. HE ×200.

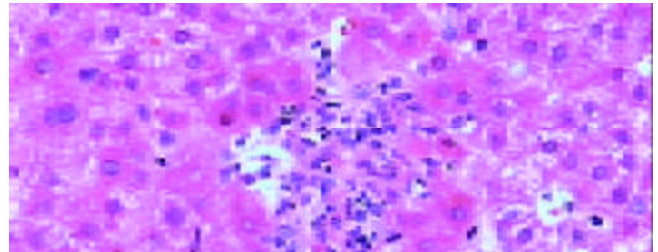


Figure 4 CMV infection in peripheral blood and micro-abscess without inclusion bodies in liver cells 1 mo after transplantation. HE ×200.

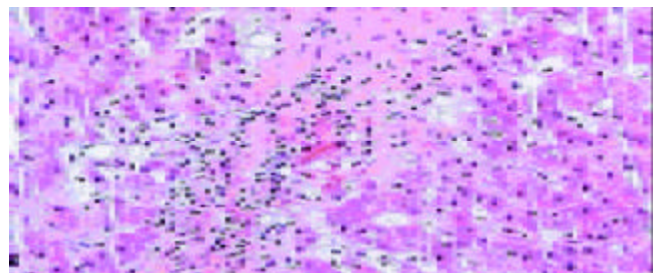


Figure 5 Bile duct loss in portal tract compatible with early chronic rejection 3 mo after transplantation. HE×200.

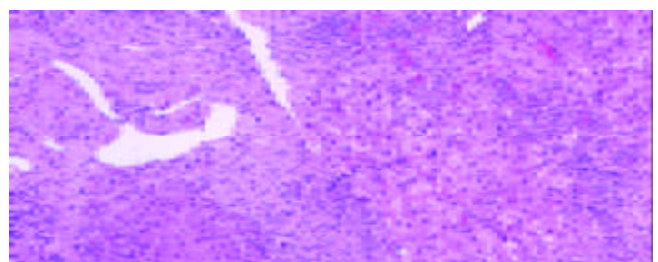


Figure 6 Fibrosis in portal area with lymphocyte infiltration and interface hepatitis in patient with recurrent hepatitis B 300 d post-transplantation, HE ×100.

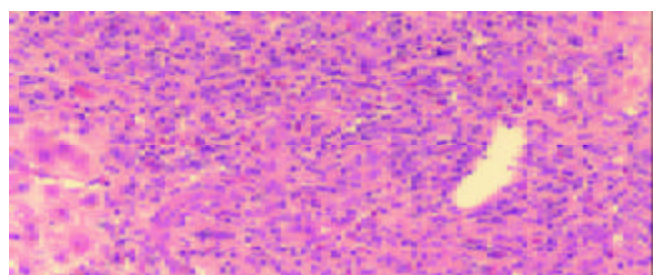


Figure 7 Acute rejection and mixed inflammatory cells in portal area with bile duct infiltration and venous endothelial inflammation 7 d post-transplantation. HE ×100.

The pathological examination on different biopsies from the same patient showed that one patient with hepatic artery thrombosis (HAT) 12 d postoperation (Figure 2) developed to intrahepatic biliary injury (IBI) 80 d following transplantation (Figure 3). Two cases in our group occurred IBI 2-3 mo after operation. One of which was secondary to HAT (the donor liver with warm ischemia for 5 min, cold storage time was 9 h), there was warm ischemia after 7 min, and cold storage time was 8 h for donor liver in another case with IBI. One case was diagnosed as chronic rejection (Figure 4) at 3 mo postoperation and disclosed persistent cytomegalovirus (CMV) infection at early stage following transplantation (Figure 5). Chronic rejection was occurred in another case due to recurrence of hepatitis B (Figure 6). Chronic rejection occurred in one case due to acute rejection (Figure 7), early chronic rejection occurred in one case at onset. If poor allograft liver function was persistent, liver biopsy showed hepatocyte ballooning, macrovesicular steatosis, cholestasis, and above-mentioned complications could not be confirmed, drug-induced hepatic injury was suspected.

DISCUSSION

In liver transplantation, liver biopsy is currently used to confirm the clinical diagnosis, to assess the degree of necroinflammatory injury or fibrosis, to evaluate a space-occupying lesion, and to evaluate the changes following therapeutic intervention. Since liver biopsy plays an important role in the diagnosis and management, a representative tissue sampling is needed. Ideally, a good biopsy sample should include at least 4 portal tracts. The subcapsular hepatic parenchyma is avoided in interpretation, as it often contains fibrous extensions from the capsule and has some injuries during peri-operative period^[5].

The experience for evaluation of allograft liver biopsy in our transplantation center revealed that although acute rejection was still the major factor of liver dysfunction at the first few weeks following operation, there was referable international consensus evaluating criteria for acute rejection. All the cases with acute rejection were promptly diagnosed and cured by the close cooperation between the clinician and pathologist^[2]. Chronic rejection is also called ductopenic allograft rejection and characterized by the presence of ductopenia and foamy cell arteriopathy. The overall occurrence rate of chronic rejection was 2-20%. The pathogenesis of chronic rejection was more complex than that in acute rejection. It involved in several factors such as cellular immunology, humoral immunology, ischemia and infection^[6]. In our group, the chronic rejection rate in detected cases and total transplantation cases was 14.8% and 7.7% respectively, similar to those reported by other transplantation center. Chronic rejection occurred due to CMV infection and hepatitis B recurrence in two cases, due to acute rejection in one case, early chronic rejection occurred in one case 45 d post-transplantation. Therefore, the mechanisms of chronic rejection are multiple and complex. The above data confirmed that viral infection was the inducing factor of chronic rejection.

Preservation-reperfusion injury (PRI) refers to any injury during donor liver harvesting, cold storage as well as liver implantation. It is a major contributing factor to primary allograft failure after orthotopic liver transplantation. Clinically, it is characterized by high serum aspartate transaminase (AST) levels in the early postoperative period without technique problem, hepatic artery thrombosis and hyperacute rejection. To date, the pathogenesis of PRI is not very clear and there are no consistent histological evaluation criteria for PRI. A number of histological features have been observed in our group. For example, the predominant features of reperfusion especially at the first several hours after re-vascularization were sinusoidal endothelial cell impairment with neutrophilic cells infiltration;

hepatocyte injuries such as ballooning change, centrilobular cholestasis and apoptosis become predominance at late course of reperfusion. It is suggested that sinusoidal endothelial cells are more susceptible to PRI than hepatocytes themselves. Busquets *et al.*^[7] found that there were 17% PRI out of 162 postreperfusion liver biopsy specimens in their retrospective analysis. They also disclosed that if cold storage time longer than 12 h, intrahepatic biliary complications resulted from PRI were increased. Another report revealed that storage time exceed 10 to 12 h, late posttransplantation biliary strictures occurred in more than 25% of liver transplant recipients, 30% of patients with graft dysfunction needed retransplantation within the first 3 mo after transplantation^[8].

Hepatic artery thrombosis (HAT) occurred in 2-9% of adult transplantation recipients. It is the most frequent arterial complication in liver transplantation. Surgical technique, hemodynamic, immunologic factors, PRI and hypercoagulation have been suggested as the causes for HAT^[9]. In Humboldt University Transplantation Center, among 1 192 liver transplantation cases, 30 HAT were observed, resulting in an incidence of 2.5%. Re-transplantation was necessary in 46.7% of patients with HAT in that group^[10]. The histological features in HAT showed severe midzonal hepatocyte necrosis and bleeding, especially in centrolobular of allograft.

Intrahepatic biliary injury (IBI) is characterized by non anastomotic biliary strictures and is a relatively late complication, usually diagnosed between 1 and 4 mo after liver transplantation. The incidence of IBI was 2-10% of transplantation recipients. Clinically, there were repeated episodes of cholangitis and the necessity for re-transplantation was about 30-50%. Accumulating evidence has shown that IBI is associated with ischemia, secondary to HAT, ABO incompatible blood group donors, and chronic ductopenic rejection as well as prolonged warm ischemic time or cold ischemic time prior to implantation^[11-14]. IBI occurred in 2 cases of our group 2-3 mo after operation. One of which was secondary to HAT (the donor liver with warm ischemia was 5 min, cold storage time was 9 h), another case of IBI showed warm ischemia for 7 min, cold storage time was 8 h for donor liver. It is suggested that improved hepatic artery supplying and the lowest total ischemia time may reduce the incidence of IBI.

Drug-induced hepatic injury (DIHI) is the "hot" but also troublesome problem in hepatic diseases. Therapeutic drugs such as corticosteroids, azathioprine and cyclosporine A in transplantation recipients could cause liver damage^[15]. However, the report about DIHI after liver transplantation is rare. Recently, an introductory review about drug-induced hepatotoxicity progress was published in *The New England Journal of Medicine*^[16]. The most frequent hepatotoxic drug reactions could lead to moderate to severe injuries to hepatocytes with a clinical symptom that resembles viral hepatitis, characterized by a rapid onset of jaundice in association with elevated aminotransferase levels. Acute liver failure may develop after weeks of onset, particularly if the patient has continued the drug. The histological characteristics of DIHI include ballooning degeneration or steatosis of hepatocytes with cholestasis, centrolobular or midzonal hepatocyte dropout or necrosis, portal tracts with severe bile duct damage surrounded by lymphocytes, plasma cells and eosinophils with or without granulomas, and lobular disarray with acidophilic bodies and sinusoidal chronic inflammation. Since many pathological changes in DIHI overlapped with the features observed at acute or chronic rejection, PRI or viral hepatitis recurrence, the diagnosis of DIHI in transplantation population is more difficult than in non-transplant population.

REFERENCES

- 1 **An International Panel.** Banff schema for grading liver allograft

- rejection: an international consensus document. *Hepatology* 1997; **25**: 658-663
- 2 **Yu YY**, Shen BY, Zhou GW, Chen H, Yan JQ, Peng CH, Li HW. Application of Banff schema in grading acute rejection following transplantation. *Zhonghua Qiguan Yizhi Zazhi* 2003; **24**: 76-77
 - 3 **Demetris A**, Adams D, Bellamy C, Blakolmer K, Clouston A, Dhillon AP, Fung J, Gouw A, Gustafsson B, Haga H, Harrison D, Hart J, Hubscher S, Jaffe R, Khettry U, Lassman C, Lewin K, Martinez O, Nakazawa Y, Neil D, Pappo O, Parizhakaya M, Randhawa P, Rasoul-Rockenschaub S, Reinholt F, Reynes M, Robert M, Tsamandas A, Wanless I, Wiesner R, Wernerson A, Wrba F, Wyatt J, Yamabe H. Update of the international Banff schema for liver allograft rejection: working recommendations for the histopathologic staging and reporting of chronic rejection. *Hepatology* 2000; **31**: 792-799
 - 4 **Neil DA**, Hubscher SG. Are parenchymal changes in early post-transplant biopsies related to preservation-reperfusion injury or rejection? *Transplantation* 2001; **71**: 1566-1572
 - 5 **Brunt EM**. Liver biopsy interpretation for the gastroenterologist. *Curr Gastroenterol Rep* 2000; **2**: 27-32
 - 6 **Quaglia AF**, Del Vecchio Blanco G, Greaves R, Burroughs AK, Dhillon AP. Development of ductopenic liver allograft rejection includes a "hepatic" phase prior to duct loss. *J Hepatol* 2000; **33**: 773-780
 - 7 **Busquets J**, Figueras J, Serrano T, Torras J, Ramos E, Rafecas A, Fabregat J, Lama C, Xiol X, Baliellas C, Jaurrieta E. Postreperfusion biopsies are useful in predicting complications after liver transplantation. *Liver Transpl* 2001; **7**: 432-435
 - 8 **Kukan M**, Haddad PS. Role of hepatocytes and bile duct cells in preservation-reperfusion injury of liver grafts. *Liver Transpl* 2001; **7**: 381-400
 - 9 **Bramhall SR**, Minford E, Gunson B, Buckels JAC. Liver transplantation in the UK. *World J Gastroenterol* 2001; **7**: 602-611
 - 10 **Stange BJ**, Glanemann M, Nuessler NC, Settmacher U, Steinmuller T, Neuhaus P. Hepatic artery thrombosis adult liver transplantation. *Liver Transpl* 2003; **9**: 612-620
 - 11 **Rull R**, Garcia Valdecasas JC, Grande L, Fuster J, Lacy AM, Gonzalez FX, Rimola A, Navasa M, Iglesias C, Visa J. Intrahepatic biliary lesions after orthotopic liver transplantation. *Transpl Int* 2001; **14**: 129-134
 - 12 **Huang XQ**, Huang ZQ, Duan WD, Zhou NX, Feng YQ. Severe biliary complications after hepatic artery embolization. *World J Gastroenterol* 2002; **8**: 119-123
 - 13 **Abt P**, Crawford M, Desai N, Markmann J, Olthoff K, Shaked A. Liver transplantation from controlled non-heart-beating donors: an increased incidence of biliary complications. *Transplantation* 2003; **75**: 1659-1663
 - 14 **Jagannath S**, Kalloo AN. Biliary Complications after liver transplantation. *Curr Treat Options Gastroenterol* 2002; **5**: 101-112
 - 15 **Farrell GC**. Drugs and steatohepatitis. *Semin Liver Dis* 2002; **22**: 185-194
 - 16 **Lee WM**. Drug-induced hepatotoxicity. *N Engl J Med* 2003; **349**: 474-485

Edited by Wang XL and Xu CT Proofread by Xu FM

CDw75 is a significant histopathological marker for gastric carcinoma

Lei Shen, Hai-Xia Li, He-Sheng Luo, Zhi-Xiang Shen, Shi-Yun Tan, Jie Guo, Jun Sun

Lei Shen, Hai-Xia Li, He-Sheng Luo, Zhi-Xiang Shen, Shi-Yun Tan, Jie Guo, Jun Sun, Department of Gastroenterology, Renmin Hospital, Wuhan University, 238 Jie-fang Road, Wuhan 430060, Hubei Province, China

Correspondence to: Lei Shen, Department of Gastroenterology, Renmin Hospital, Wuhan University, 238 Jie-fang Road, Wuhan 430060, Hubei Province, China. mssquall@263.net

Telephone: +86-27-88041911-8571

Received: 2003-08-06 **Accepted:** 2003-09-18

Abstract

AIM: To study the expression of CDw75 in patients with gastric carcinoma and to correlate CDw75 expression with progression of the tumor.

METHODS: Immunohistochemical method was used to examine the expression of CDw75 in 72 cases of the gastric carcinoma and adjacent normal gastric mucosa, and the percentage of the cells positively stained with CDw75 was calculated using a computer-aided microscopic image analysis system.

RESULTS: CDw75 was not expressed in normal gastric mucosa but detected in 37 of the 72 neoplastic gastric lesions. The expression of CDw75 was associated with the tumor progression as indicated by its close correlation with the depth of the tumor infiltration ($\chi^2=18.415$, $P<0.01$), TNM stage ($\chi^2=10.419$, $P<0.05$) and lymph node metastasis ($\chi^2=6.675$, $P<0.01$). The overall survival rate of the patients with positive CDw75 expression (32.4%) was significantly lower than that of the patients without CDw75 expression (71.4%) ($P<0.01$). There was no significant correlation between the expression of CDw75 and the sex and age and histological type of patients ($P>0.05$).

CONCLUSION: These findings suggest that the expression of CDw75 is a significant histopathological marker for more advanced stage of gastric carcinoma and indicates a poor prognosis for the patients.

Shen L, Li HX, Luo HS, Shen ZX, Tan SY, Guo J, Sun J. CDw75 is a significant histopathological marker for gastric carcinoma. *World J Gastroenterol* 2004; 10(11): 1682-1685
<http://www.wjgnet.com/1007-9327/10/1682.asp>

INTRODUCTION

Invasiveness and metastasis are the most important characteristics of malignant tumor and mortality factors. Clinicopathological parameters are usually used for diagnosis and prognosis. Recent studies have shown that the expression of sialylated glycoconjugates is closely associated with the aggressiveness and metastatic potential of malignant cells. CDw75 epitope is a sialylated carbohydrate determinant generated by the β -galactosyl α -2,6-sialyltransferase, and it has been reported to be associated with the progression of gastric cancer^[1]. Gastric cancer is one of the most common tumors of alimentary tract in China, and its mortality is high. In this study, we examined the

expression of CDw75 in 72 cases of gastric carcinoma and adjacent normal gastric mucosa using immunohistochemical method to determine whether CDw75 is correlated with the invasiveness and metastasis of gastric carcinoma.

MATERIALS AND METHODS

Materials

Seventy-two patients with gastric cancer, who were diagnosed and treated at the Departments of Pathology and General Surgery, Renmin Hospital of Wuhan University, from 1995 to 1999, were randomly selected for this study. The patients had undergone subtotal or total gastrectomy combined with lymph node resection. Sections from the surgical specimens were fixed in 40 g/L formaldehyde and embedded in paraffin. The mean age of the patients was 59 years with a range from 35 to 74 years and a male-to-female ratio of 1.48. The patients were followed to determine clinical outcome and the median follow-up time at the end of the study was 45 mo (range, 3-64 mo). The other clinicopathological characteristics are listed in Table 1. The histological type of the tumor was defined by World Health Organization classification (tubular, papillary, mucinous, or signet ring^[2]), the degree of differentiation (well, moderate, or poor) was recorded on haematoxylin and eosin (H & E) stained tissues, and tumor stage was graded according to new PTNM criterion which was published by International Union Against Cancer (IUCC)^[2].

Immunohistochemistry

Streptavidin-peroxidase (S-P) method was used to detect the expression of CDw75. The mouse monoclonal antibody against human CDw75 (LN1) was purchased from NeoMarkers Company, Wuhan, China, immunostaining S-P kit and DAB reagent were purchased from Fuzhou Maxim Biotechnical Company, Fuzhou, China. Sections from each primary tumor and adjacent mucosa were deparaffinized and heated in a microwave oven for 15 min to retrieve antigens. Endogenous peroxidase was blocked with 3 mL/L hydrogen peroxide methanol for 10 min at room temperature. After washing with phosphate-buffered saline (0.01 g/L, pH 7.4) for 3×5 min, the tumor sections were incubated with normal non-immune serum from bull for 15 min at room temperature to eliminate nonspecific staining. The sections were then incubated with the primary antibody against CDw75 (dilution 1/100) for 60 min at room temperature, washed with PBS for 3×5 min, and incubated with the secondary biotinylated antibody for 15 min followed by avidin-biotin-peroxidase for 15 min at room temperature. Finally, the slides were washed for 3×15 min with PBS, visualized with DAB reagent and counterstained with haematoxylin. Negative and positive controls were used simultaneously to ensure specificity and reliability of the staining process. The negative controls were performed by substituting the primary antibody with PBS, and a positive section supplied by manufacturer of the staining kit was taken as positive control.

Positive staining with CDw75 was defined as brown staining of cell membrane or cytoplasm. The degree of the CDw75 staining was calculated semiquantitatively with computer-aided analysis of four non-overlapping high power microscopic fields and classified as follows: -, negative staining; +, less than 25% tumor cells were CDw75 positive; ++, between 25% and 50% of

tumor cells were CDw75 positive; +++, between 51% and 75% of tumor cells were CDw75 positive; and +, more than 75% of tumor cells were CDw75 positive.

Statistical analysis

CDw75 expression in all patients with gastric carcinoma was analyzed against clinicopathological parameters. The correlation between CDw75 expression and selected clinicopathological parameters was analyzed with the Wilcoxon rank sum test and χ^2 test. Kaplan-meier curve was constructed to assess the survival. *P* value of less than 0.05 was considered to be statistically significant.

RESULTS

Immunohistochemical staining of CDw75

Normal gastric mucosa was consistently negative for CDw75 staining (Figure 1), while positive staining was observed in 37 of 72 (51.4%) gastric cancers. The staining intensity was as follows: -, 35 cases (48.6%); +, 9 cases (12.5%); ++, 13 cases (18.1%); +++, 9 cases (12.5%); +, 6 cases (8.3%). The positive staining of CDw75 was localized predominantly in gastric cancer cells, and all the positive cases showed diffuse membrane staining, or cytoplasmic staining in some cases (Figure 2). The immunoreactive cells were either distributed unevenly throughout the tumor tissue or aggregated in focal clusters. In addition, positive staining was occasionally detected in lymphocytes or other inflammatory cells infiltrating the cancer nests (Figure 3).

Table 1 xClinicopathological parameters of gastric carcinoma and their association with CD75w expression.

	Expressing levels of CDw75			<i>P</i>	<i>P</i>
	Negative	Positive	Positive rate (%)		
Sex					
Male	43	24	19	44.19	2.217
Female	29	11	18	62.07	
Age (yr)					
<50	17	9	8	47.06	0.167
≥50	55	26	29	52.73	
Histologic type					
WD	12	8	4	33.33	3.445
MD	16	9	7	43.75	
PD	35	15	20	57.14	
Mucinous	5	2	3	60.00	
Signet ring	4	1	3	75.00	
Depth of invasion					
T1	8	7	1	12.50	18.415 ^b
T2	17	13	4	23.53	
T3	32	13	19	59.38	
T4	15	2	13	86.67	
TNM stage					
I	24	17	7	29.17	10.419 ^a
II	8	5	3	37.50	
III	20	8	12	60.00	
IV	20	5	15	75.00	
Lymph node metastasis					
Negative	32	21	11	34.38	6.675 ^b
Positive	40	14	26	65.00	
Distant metastasis					
M0	56	30	26	46.43	2.482
M1	16	5	11	68.75	

^a*P*<0.05, ^b*P*<0.01; WD: Well differentiation, MD: Moderate differentiation, PD: Poor differentiation.

Table 2 Survival time of patients with gastric carcinoma

CDw75 expression	Death/survival	Median survival time
Negative (n=35)	10/25	53
Positive (n=37)	25/12	37

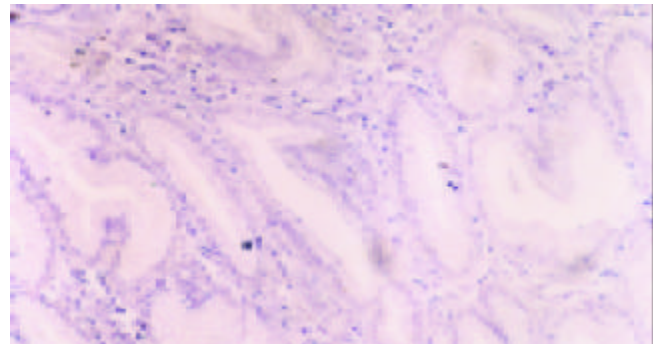


Figure 1 Expression of CDw75 in normal gastric mucosa. No gastric mucosa cell were brown-stained either on membrane or in cytoplasm. (SP×400).

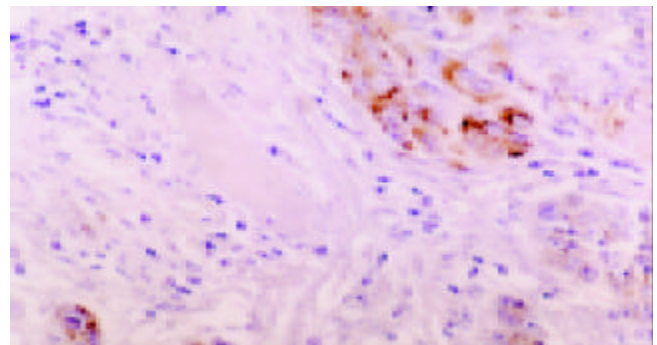


Figure 2 Weak staining of CDw75 in gastric cancer cells. There were a few gastric cancer cells brown-stained on membrane or in cytoplasm (SP×200).

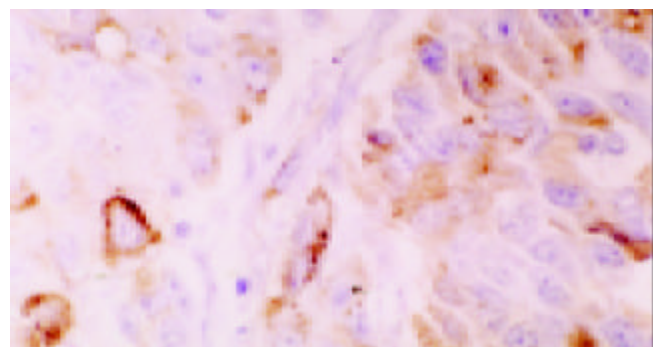


Figure 3 Strong staining of CDw75 in gastric cancer cells. There were many gastric cancer cells brown-stained on membrane or in cytoplasm (SP×200).

Correlation between CDw75 and the invasiveness or the metastasis of gastric carcinoma

The CDw75 expression in tumor tissues was related significantly to clinicopathologic factors, such as the depth of tumor invasion, TNM stage and lymph node metastasis (Table 1). The percentage of CDw75 expression in tumors which invaded serosal or deeper layers (T3 or T4) was significantly higher than that in tumors which were restricted within mucosa or muscular layers (T1 or T2) (*P*<0.01). When tumors were accompanied by lymph node metastasis, CDw75 expression was elevated significantly

compared with those without metastasis ($P < 0.05$). The cases were also categorized by TNM staging. To compensate the error due to shortage of cases, stage I and stage II cases were combined into one group. CDw75 expression was found in 10 of 32 (31.3%) stage I+II cases, 12 of 20 (60.0%) stage III cases and 15 of 20 (75.0%) stage IV cases. The percentage of positive CDw75 staining in stage III and IV cases was significantly higher than that in stage I+II ($P < 0.05$ and $P < 0.01$, respectively), while there was no significant difference in those between stage III and stage IV ($P > 0.05$).

No significant correlation was found between the expression of CDw75 antigen and the distant metastasis or the histological type of gastric cancer. Similarly, no significant difference was found between the cases with positive and negative CDw75 expression regarding the sex and age of patients.

Correlation between CDw75 expression and the survival of the patients with gastric carcinoma

At the end of the follow-up period, 37 of 72 patients (51.4%) were alive. The survival of patients with positive CDw75 expression was significantly shorter than those with negative CDw75 expression (Table 2). As shown by the Kaplan-Meier curve, the overall survival rate of patients with CDw75 expression (32.4%) was significantly lower than that of patients without CDw75 expression (71.4%) ($P < 0.01$, Figure 4).

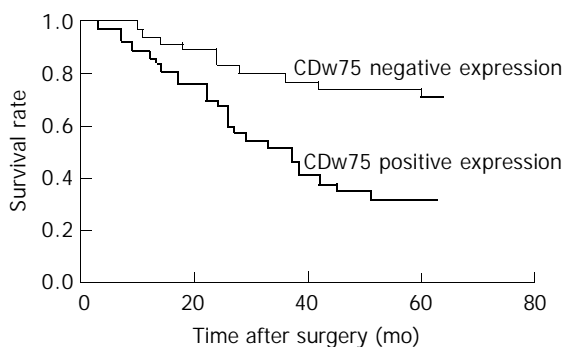


Figure 4 A Kaplan-Meier plot shows the survival rates after curative resection for gastric carcinoma patients with or without CDw75 expression.

DISCUSSION

The infiltration and metastasis of gastric carcinoma is a multi-stage, complicated process, which could be influenced by many factors, such as the formation of neoplastic vessels, degradation of tissue membrane and matrix, mobility of tumor cells and quantity and activity of infiltrating leucocyte inside the tumor tissues. Recently, many tumor makers have been identified which are used not only for diagnosis but also for assessment of aggressiveness and prognosis of tumors^[3-8]. Tumor markers are antigens or other biological products generated by tumor cells, which are present few or none in normal and non-neoplastic tissues. They usually indicate the change of genes associated with development of tumor and can be detected in tumor tissues or body humour or excretions of the patients^[9,10]. CDw75 antigen is one plausible tumor marker that has been shown recently to be associated with the progression and metastasis of gastric carcinoma^[1]. Consistent with previous finding^[1], the present work demonstrated that CDw75 expression was constantly negative in normal gastric mucosa but positive in 37 of 72 (51.4%) gastric cancers.

CDw75 antigen is a cluster of differentiation antigen of human leucocyte designated at the fourth World Leucocyte-Type Conference in 1989^[1]. It is a sialylated carbohydrate determinant generated by Sia-T1^[11] and has many different

isomers, which are specifically expressed in different tissues and can be recognized by corresponding monoclonal antibodies. There have been 4 monoclonal antibodies raised to react with CDw75 antigen, including EBU-141, OKB4, HH2 and LN1, *etc.*^[1]. These CDw75 monoclonal antibodies are likely to identify spatially related structures since binding inhibition studies have shown that binding of each CDw75 monoclonal antibody blocks the binding of the other CDw75 monoclonal antibody. The epitopes recognized by HH2, LN1 and EBU-141 are completely destroyed when cells are treated with neuraminidase, suggesting that sialic acid is a part of these CDw75 determinants^[1,12]. In contrast, when the epitope reacts with neuraminidase, the binding of OKB4 with CDw75 epitope is increased, indicating that the OKB4 epitope may be masked by sialic acid and can appear after treatment with the neuraminidase^[1,12]. These results suggest that sialic acid may have determinant impact on the character of CDw75 antigen.

Furthermore, studies have shown that cell-surface glycoconjugates play an important role in cell proliferation, adhesion, metastasis and immunogenicity. Only the subclone of primary tumor cells that express specific glycoconjugates has metastatic ability^[1,12]. The composition and structure of cell surface glycoproteins change frequently during the neoplastic transformation, and most of these changes are the extensive sialylation of cell surface glycoproteins. Moreover, tumor-associated expression of sialylated glycoconjugates has been found to be closely associated with aggressive activity and increased metastatic potential of malignant cells^[3]. There are several plausible mechanisms underlining such a correlation: sialic acid reduces the attachment of tumor cells to collagen type IV and fibronectin, masks antigen determinants, inhibits the action of natural killer cells, and induces immunologic tolerance through an increase of the serum half-life of glycoconjugates, *etc.*^[1,12]. In gastric carcinoma, various sialylated glycoconjugates, such as Lewis X (Le^x), Lewis A (CA-19-9) and sialosyl-Tn, etc, have become clinically important in the detection of aggressive behavior of tumor cells and prediction of disease prognosis^[13-16].

CDw75, a Sia-T1-dependent sialylated glycoconjugate, is associated with the biological behaviors of tumors^[12,17]. In patients with gastric carcinoma, David and Elpek *et al.*^[1] found that there was no CDw75 expression in normal gastric mucosa (except a few isolated parietal cells in the body of the stomach), foveolar hyperplasia, intestinal metaplasia and the adjacent tissues to carcinoma. In contrast, the expression of CDw75 in primary tumor and the metastatic focus of gastric carcinoma was significantly increased. The CDw75 antigen could, therefore, be used as a marker of malignant transformation of gastric epithelium. Our study agreed with their findings. In addition, we found that the expression of CDw75 antigen is closely associated with the depth of the tumor invasion. Patients with serosal or deeper layer invasion of the tumor (T3 or T4) showed significantly higher expression of CDw75 than those with the tumor restricted within mucosa or muscular layers (T1 or T2), indicating that the gastric cancer cells with CDw75 high expression might have increased potential to invade into adjacent tissues. The most important feature of gastric carcinoma is its infiltrative growth and the earliest metastasis path is lymph node metastasis. We found that the positive expression rate of CDw75 (65%) in gastric cancer tissues with lymph node metastasis was significantly higher than that without lymph node metastasis (34%). With regard to TNM stage, CDw75 expression in stage I or stage II tumor tissues was not much higher than normal mucosa, but significantly higher in stage III and stage IV tumor tissues. These findings suggested that CDw75 plays an important role in the progression of gastric cancer from localized lesion to metastasized neoplasia. As a result, overall survival rate of patients with CDw75

expression (32.4%) was lower than that of patients without CDw75 expression (71.4%), and the survival curve of patients with CDw75 expression was significantly poorer than that of patients without CDw75 expression by Kaplan Meier analysis. In conclusion, CDw75 was not detected in normal gastric mucosa but expressed in gastric cancer tissues and the higher expression rate was seen in patients with deeper tumor invasion, higher TNM stage and in patients with lymph node metastasis. The survival time of patients with CDw75 expression was less than that of patients without CDw75 expression. Therefore, CDw75 appears to be a useful marker indicating more advanced stage of the malignancy and poor prognosis in patients with gastric carcinoma.

REFERENCES

- 1 **Elpek GO**, Gelen T, Karpuzoglu G, Karpuzoglu T, Keles N. Clinicopathologic evaluation of CDw75 antigen expression in patients with gastric carcinoma. *J Pathol* 2001; **193**: 169-174
- 2 **Luk GD**. Tumors of the stomach In: Mark Feldman, Brwe F. Gastrointestinal and Liver Disease. Volume I, 6th, Edition. Science Press, 2001, Beijing
- 3 **Zheng CX**, Zhan WH, Zhao JZ, Zheng D, Wang DP, He YL, Zheng ZQ. The prognostic value of preoperative serum levels of CEA, CA19-9 and CA72-4 in patients with colorectal cancer. *World J Gastroenterol* 2001; **7**: 431-434
- 4 **Duraker N**, Celik AN. The prognostic significance of preoperative serum CA 19-9 in patients with resectable gastric carcinoma: comparison with CEA. *J Surg Oncol* 2001; **76**: 266-271
- 5 **Marrelli D**, Roviello F, De Stefano A, Farnetani M, Garosi L, Messano A, Pinto E. Prognostic significance of CEA, CA 19-9 and CA 72-4 preoperative serum levels in gastric carcinoma. *Oncology* 1999; **57**: 55-62
- 6 **American Society of Clinical Oncology**. 1997 update of recommendations for the use of tumor markers in breast and colorectal cancer. *J Clin Oncol* 1998; **16**: 793-795
- 7 **Gartner F**, David L, Seruca R, Machado JC, Sobrinho-Simoes M. Establishment and characterization of two cell lines derived from human diffuse gastric carcinomas xenografted in nude mice. *Virchows Arch* 1996; **428**: 91-98
- 8 **Hammer RD**, Vnencak-Jones CL, Manning SS, Glick AD, Kinney MC. Microvillous lymphomas are B-cell neoplasms that frequently express CD56. *Mod Pathol* 1998; **11**: 239-246
- 9 **Huang CW**, Bai L. Clinical value of carbohydrate antigen 50 and carbohydrate antigen 242 in the diagnosis of colorectal carcinoma. *Diyi Junyi Daxue Xuebao* 2002; **22**: 1116-1118
- 10 **Zhang S**, Ma Y, Yang X. The diagnostic values of CA242 combining other tumor markers for lung cancer. *Zhonghua Jiehe Hehexi Zazhi* 1999; **22**: 271-273
- 11 **Dall'Olivo F**, Chiricolo M, Mariani E, Facchini A. Biosynthesis of the cancer-related sialyl-alpha 2,6-lactosaminyl epitope in colon cancer cell lines expressing beta-galactoside alpha 2,6-sialyltransferase under a constitutive promoter. *Eur J Biochem* 2001; **268**: 5876-5884
- 12 **Elpek GO**, Gelen T, Karpuzoglu G, Karpuzoglu T, Aksoy NH, Keles N. Clinicopathologic evaluation of CDw75 antigen expression in colorectal adenocarcinomas. *Pathol Oncol Res* 2002; **8**: 175-182
- 13 **Nakagoe T**, Sawai T, Tsuji T, Jibiki MA, Nanashima A, Yamaguchi H, Yasutake T, Ayabe H, Arisawa K, Ishikawa H. Difference in prognostic value between sialyl Lewis(a) and sialyl Lewis(x) antigen levels in the preoperative serum of gastric cancer patients. *J Clin Gastroenterol* 2002; **34**: 408-415
- 14 **Futamura N**, Nakamura S, Tatematsu M, Yamamura Y, Kannagi R, Hirose H. Clinicopathologic significance of sialyl Le (x) expression in advanced gastric carcinoma. *Br J Cancer* 2000; **83**: 1681-1687
- 15 **Nakagoe T**, Fukushima K, Sawai T, Tsuji T, Jibiki M, Nanashima A, Tanaka K, Yamaguchi H, Yasutake T, Ayabe H, Ishikawa H. Increased expression of sialyl Lewis(x) antigen in penetrating growth type A early gastric cancer. *J Exp Clin Cancer Res* 2002; **21**: 363-369
- 16 **Nakagoe T**, Sawai T, Tsuji T, Jibiki M, Nanashima A, Yamaguchi H, Yasutake T, Ayabe H, Arisawa K, Ishikawa H. Pre-operative serum levels of sialyl Tn antigen predict liver metastasis and poor prognosis in patients with gastric cancer. *Eur J Surg Oncol* 2001; **27**: 731-739
- 17 **Dunphy CH**, Polski JM, Lance Evans H, Gardner LJ. Paraffin immunoreactivity of CD10, CDw75, and Bcl-6 in follicle center cell lymphoma. *Leuk Lymphoma* 2001; **41**: 585-592

Edited by Liu HX and Xu FM

Fatal liver failure due to reactivation of lamivudine-resistant HBV mutant

Tatehiro Kagawa, Norihito Watanabe, Hisashi Kanouda, Ichiro Takayama, Tadahiko Shiba, Takashi Kanai, Kazuya Kawazoe, Shinji Takashimizu, Nobue Kumaki, Kazuo Shimamura, Shohei Matsuzaki, Tetsuya Mine

Tatehiro Kagawa, Norihito Watanabe, Hisashi Kanouda, Ichiro Takayama, Tadahiko Shiba, Takashi Kanai, Kazuya Kawazoe, Shinji Takashimizu, Shohei Matsuzaki, Tetsuya Mine, Department of Internal Medicine, Tokai University School of Medicine, Boseidai, Isehara, Kanagawa 259-1193, Japan

Nobue Kumaki, Kazuo Shimamura, Department of Pathology, Tokai University School of Medicine, Boseidai, Isehara, Kanagawa 259-1193, Japan

Correspondence to: Dr. Tatehiro Kagawa, Department of Internal Medicine, Tokai University School of Medicine, Boseidai, Isehara, Kanagawa 259-1193, Japan. kagawa@is.icc.u-tokai.ac.jp

Telephone: +81-463-931121

Received: 2003-11-17 **Accepted:** 2004-02-11

Abstract

We report a case of fatal liver failure due to reactivation of lamivudine-resistant HBV. A 53-year-old man was followed since 1998 for HBV-related chronic hepatitis. Serum HBV-DNA was 150 MEq/mL (branched DNA signal amplification assay) and ALT levels fluctuated between 50-200 IU/L with no clinical signs of liver cirrhosis. Lamivudine (100 mg/d) was started in May 2001 and serum HBV-DNA subsequently decreased below undetectable levels. In May 2002, serum HBV-DNA had increased to 410 MEq/mL, along with ALT flare (226 IU/L). The YMDD motif in the DNA polymerase gene had been replaced by YIDD. Lamivudine was continued and ALT spontaneously decreased to the former levels. On Oct 3 the patient presenting with general fatigue, nausea and jaundice was admitted to our hospital. The laboratory data revealed HBV reactivation and liver failure (ALT: 1828 IU/L, total bilirubin: 10 mg/dL, and prothrombin INR: 3.24). For religious reasons, the patient and his family refused blood transfusion, plasma exchange and liver transplantation. The patient died 10 d after admission. The autopsy revealed remarkable liver atrophy.

Kagawa T, Watanabe N, Kanouda H, Takayama I, Shiba T,

Kanai T, Kawazoe K, Takashimizu S, Kumaki N, Shimamura K, Matsuzaki S, Mine T. Fatal liver failure due to reactivation of lamivudine-resistant HBV mutant. *World J Gastroenterol* 2004; 10(11): 1686-1687

<http://www.wjgnet.com/1007-9327/10/1686.asp>

INTRODUCTION

The emergence of lamivudine-resistant hepatitis B virus (HBV) mutant is relatively frequent after long-term lamivudine treatment. Liaw *et al.* reported acute exacerbation in 41% of lamivudine-treated patients who developed YMDD mutation, recovering mostly with HBeAg seroconversion^[1]. Conversely, evolution toward acute liver failure is rare but possibly fatal as published in 2001 by Kim *et al.*^[2]. We report here a new case of fatal liver failure consecutive to the emergence of a lamivudine-resistant mutant HBV.

CASE REPORT

This 53-year-old man had been followed since 1998 for HBV-related chronic hepatitis. He was positive for HBs and HBe antigens. Serum HBV-DNA was 150 MEq/mL (branched DNA signal amplification assay)^[3]. Alanine aminotransferase (ALT) fluctuated between 50-200 IU/L with no clinical signs of liver cirrhosis. Serum albumin and prothrombin time were normal. Lamivudine (100 mg/d) was started in May 2001 (Figure 1). Subsequently, serum HBV-DNA decreased below undetectable level (October 2001). In May 2002, serum HBV-DNA had increased to 410 MEq/mL, along with ALT flare (226 IU/L). Mini-sequencing^[4] showed that the YMDD motif in the DNA polymerase gene had been replaced by YIDD, supporting reactivation was due to the emergence of a lamivudine-resistant HBV mutant. Lamivudine was continued and ALT spontaneously decreased to the former levels. To improve a pre-existing non-insulin dependent diabetes mellitus (serum HgA1c: 6.5-7.6%) acarbose (300 mg/d) was initiated on Aug 20, 2002, but

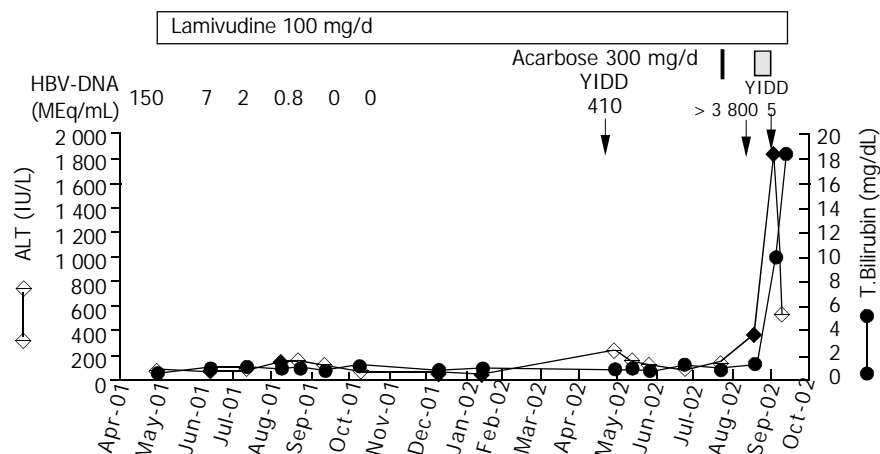


Figure 1 Serum ALT, total bilirubin and HBV-DNA levels.

discontinued after only 3 d due to flatulence. At the next outpatient clinic visit (Sept 17), the patient presented no clinical sign of liver disorder, so acarbose was restarted. In fact, laboratory investigations performed prior to restarting acarbose revealed that HBV-DNA had dramatically increased to 3 800 MEq/mL while ALT was 9 times that of the upper limit of normal (357 IU/L). On Oct 3, the patient presenting with general fatigue, nausea and jaundice was admitted to the hospital. ALT was 1 828 IU/L, total and direct bilirubin, 10 and 5.8 mg/dL, respectively, and prothrombin INR 3.24. Antinuclear and antismooth muscle antibodies as well as HIV tests were negative. Despite discontinuation of acarbose, liver failure developed and hepatic encephalopathy appeared. For religious reasons, the patient and his family refused blood transfusion, plasma exchange and liver transplantation. The patient died 10 d after admission. The autopsy revealed liver atrophy (620 g) and panlobular necrosis surrounded by extensive fibrosis consisting of immature collagen (Figure 2). Lymphoid cell infiltration was observed in the fibrosis.



Figure 2 Histological findings of liver autopsy specimens. Irregularly shaped parenchymal islands are surrounded by extensive fibrosis consisting of immature collagen. 75 x EVG staining.

DISCUSSION

The reactivation of HBV prior to any clinical sign and administration of acarbose supports that the liver failure reported here is consecutive to the rapid proliferation of lamivudine-resistant HBV (YIDD). Although rare, acute liver failure associated with lamivudine-resistant HBV is reported in the literature, including one successfully treated with liver transplant^[5], one co-infected with HIV^[6], two with advanced cirrhosis^[7] and one immunocompetent patient^[2]. The last case was a Korean male, who developed fatal liver failure after 20 mo of lamivudine therapy. The background is similar to our patient, indicating that Asian males might be susceptible to this type of mutants. Lamivudine-resistant HBV is sensitive to adefovir dipivoxil^[8], a nucleotide analogue, shown to be effective for chronic HBV infection^[9]. Adefovir dipivoxil, unavailable in Japan, could not be used in our case.

Acarbose is a pseudotetrasaccharide acting by competitive inhibition of intestinal alpha-glucosidases, indicated for the

treatment of type II diabetes mellitus. The incidence of acarbose-related liver injury is low although a few severe cases were reported^[10,11]. It is unclear whether acarbose might have aggravated the liver injury consecutive to the mutation-related relapse of viral activity. In any case, as stressed in the Summary of Product Characteristics for acarbose "*Glucobay is contraindicated in patients with hepatic impairment*". The above medical history supports closely monitoring patients with lamivudine-resistant HBV even in immunocompetent patients and, once reactivation occurs, adefovir dipivoxil should be administered.

ACKNOWLEDGEMENTS

We thank Dr. Jean C. Delumeau for his help with preparation of manuscript.

REFERENCES

- 1 **Liaw YF**, Chien RN, Yeh CT, Tsai SL, Chu CM. Acute exacerbation and hepatitis B virus clearance after emergence of YMDD motif mutation during lamivudine therapy. *Hepatology* 1999; **30**: 567-572
- 2 **Kim JW**, Lee HS, Woo GH, Yoon JH, Jang JJ, Chi JG, Kim CY. Fatal submassive hepatic necrosis associated with tyrosine-methionine-aspartate-aspartate-motif mutation of hepatitis B virus after long-term lamivudine therapy. *Clin Infect Dis* 2001; **33**: 403-405
- 3 **Hendricks DA**, Stowe BJ, Hoo BS, Kolberg J, Irvine BD, Neuwald PD, Urdea MS, Perrillo RP. Quantitation of HBV DNA in human serum using a branched DNA (bdNA) signal amplification assay. *Am J Clin Pathol* 1995; **104**: 537-546
- 4 **Kobayashi S**, Shimada K, Suzuki H, Tanikawa K, Sata M. Development of a new method for detecting a mutation in the gene encoding hepatitis B virus reverse transcriptase active site (YMDD motif). *Hepatology* 2000; **17**: 31-42
- 5 **de Man RA**, Bartholomeusz AI, Niesters HG, Zondervan PE, Locarnini SA. The sequential occurrence of viral mutations in a liver transplant recipient re-infected with hepatitis B: hepatitis B immune globulin escape, famciclovir non-response, followed by lamivudine resistance resulting in graft loss. *J Hepatol* 1998; **29**: 669-675
- 6 **Bonacini M**, Kurz A, Locarnini S, Ayres A, Gibbs C. Fulminant hepatitis B due to a lamivudine-resistant mutant of HBV in a patient coinfecting with HIV. *Gastroenterology* 2002; **122**: 244-245
- 7 **Malik AH**, Lee WM. Hepatitis B therapy: the plot thickens. *Hepatology* 1999; **30**: 579-581
- 8 **Perrillo R**, Schiff E, Yoshida E, Statler A, Hirsch K, Wright T, Gutfreund K, Lamy P, Murray A. Adefovir dipivoxil for the treatment of lamivudine-resistant hepatitis B mutants. *Hepatology* 2000; **32**: 129-134
- 9 **Marcellin P**, Chang TT, Lim SG, Tong MJ, Sievert W, Shiffman ML, Jeffers L, Goodman Z, Wulfsohn MS, Xiong S, Fry J, Brosgart CL. Adefovir dipivoxil for the treatment of hepatitis B e antigen-positive chronic hepatitis B. *N Engl J Med* 2003; **348**: 808-816
- 10 **Fujimoto Y**, Ohhira M, Miyokawa N, Kitamori S, Kohgo Y. Acarbose-induced hepatic injury. *Lancet* 1998; **351**: 340
- 11 **Carrascosa M**, Pascual F, Aresti S. Acarbose-induced acute severe hepatotoxicity. *Lancet* 1997; **349**: 698-699

Edited by Ma JY and Xu FM

Brain metastasis of hepatocellular carcinoma: A case report and review of the literature

Bilge Tunc, Levent Filik, Irsel Tezer-Filik, Burhan Sahin

Bilge Tunc, Levent Filik, Burhan Sahin, Türkiye Yüksek İhtisas Hospital, Gastroenterology Clinic, Ankara 06520, Turkey

Irsel Tezer-Filik, Hacettepe University, Department of Neurology, Ankara 06520, Turkey

Correspondence to: Dr. Levent Filik, Cemal Gursel Cad. Erk Apt: 52/2, Kurtulus, Ankara 06520, Turkey. leventfilik@yahoo.co.uk

Telephone: +90-536-4881179

Received: 2003-12-28 **Accepted:** 2004-02-11

Tunc B, Filik L, Tezer-Filik I, Sahin B. Brain metastasis of hepatocellular carcinoma: A case report and review of the literature. *World J Gastroenterol* 2004; 10(11): 1688-1689 <http://www.wjgnet.com/1007-9327/10/1688.asp>

INTRODUCTION

Hepatocellular carcinoma (HCC) is one of the most frequent malignancies in the world. It is more common in far eastern countries and relatively rare in the United States and western European countries where at autopsy it accounts for only 1-2% of malignant tumors. The disease is usually manifested in the 6th and 7th decade of life. HCC is one of the highly malignant neoplasms. Extrahepatic metastases are seen in 64% of patients with HCC. The lungs, regional lymph nodes, kidney, bone marrow and adrenals are common sites of HCC metastasis^[1-3]. But, metastasis to brain and skull is extremely rare. Table 1 shows some of the reported cases of HCC with brain metastasis. These case reports reaffirms the complex and multidisciplinary care of these patients^[4-15].

The interval between diagnosis of primary cancer and detection of brain metastasis ranged from 2 to 54 mo. The mean survival period was only 3 mo after diagnosis of brain metastasis. The patients with HCC metastasized to brain died of neurologic causes rather than hepatic failure. Although no treatment is clearly defined to increase survival in patients with unresectable tumors, early diagnosis could improve the chance of curative surgical resection^[9-12].

We describe a case of HCC presenting with the initial manifestations of an intracranial mass lesion without any symptoms or signs suggestive of the primary hepatic site of the tumor. The diagnosis could not be made until he was admitted to hospital with unilateral weakness and numbness.

CASE REPORT

The patient was a 55-year-old man admitted to our hospital due to numbness and weakness on his right side. The patient's medical history was significant for chronic HBV-related hepatitis and insulin dependent-diabetes mellitus. The patient was oriented and did not have pathologic reflexes. His initial laboratory examination revealed Hb: 12.6 g/dL, Hct: 36.8, white blood cell count 3 560/ μ L, plt: 54 000/ μ L, prothrombin time (INR): 1.9, erythrocyte sedimentation rate: 28 mm/h, blood glucose: 196 mg/dL, urea: 39 mg/dL, creatinine: 0.8 mg/dL, AST: 160 U/L, ALT: 88 U/L, GGT: 55 U/L, alkalene phosphatase: 288 mg/dL, albumin: 2.59, globulin: 3.7, total bilirubin: 1.6 mg/dL. Serum electrolyte levels, urinalysis were within normal range.

Computed tomography (CT) of the patient's head revealed multiple intracranial masses and homogenous enhancement by post-contrast CT (Figure 1).



Figure 1 CT image of the lesion in the liver.

Abdominal sonography revealed findings consistent with chronic hepatitis. Thorax-abdomen-pelvic CT scan showed a hypodense mass lesion with irregular margins and 2.8 cm in diameter in the left lobe of the liver (Figure 2). Serum alpha-feto-protein level was higher than 400 U/L. Fine needle biopsy from the mass in the liver was performed. Pathological examination was consistent with the HCC.

He was given glucocorticoid therapy and referred to radiation oncology division for cranial radiotherapy.

Table 1 Some of the previous case presentations with HCC and brain metastasis in the literature

Author	Distinctive presentation
Moriya <i>et al.</i>	Brain metastasis seen in 1 year interval after hepatectomy for HCC
Endo <i>et al.</i>	Subgaleal and epidural metastasis presenting as epidural hemorrhage and died from hepatic failure
Peres <i>et al.</i>	Cerebral metastasis presenting as initial finding of HCC
Tanabe <i>et al.</i>	15-year-old boy and the other case presenting as headache
Loo <i>et al.</i>	Two cases with cerebral metastasis presenting as initial finding of HCC
Salvati <i>et al.</i>	Cerebral metastasis with stroke-like presentation
Asahara <i>et al.</i>	Brain metastasis seen after hepatectomy for HCC in 5 cases
Kim <i>et al.</i>	Seven patients with brain metastasis
Yen <i>et al.</i>	Eighteen cases with brain metastasis
Shuangshoti <i>et al.</i>	Nine cases with brain metastasis
Friedman <i>et al.</i>	A rare case with no identifiable risk factor for primary liver cancer

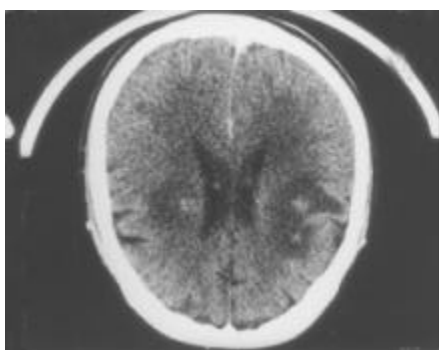


Figure 2 CT image of the metastatic lesions in brain.

DISCUSSION

Although brain metastasis may arise from primary sites in various organs and tissues, they are frequently seen with bronchogenic, breast, and prostate cancers. HCC commonly metastasizes to the lung, regional lymph nodes, peritoneum, and adrenal glands, but rarely to brain. Shuangshoti *et al.* reported that the secondary intracranial hepatic carcinomas were 1.3-2.9% among intracranial metastatic tumors^[14].

Most extrahepatic HCC occurs in patients at advanced intrahepatic tumor stage. Incidental extrahepatic lesions found at CT in patients having HCC of intrahepatic stage I or II are unlikely to represent metastatic HCC^[2]. Our case had single nodule 2.8 cm in diameter. His bilirubin level was near normal. He did not have ascites. He had neither ascites nor history of hepatic encephalopathy. He had liver cirrhosis in Child A stage. If he had not had brain metastasis, he could have been candidate for curative hepatectomy. We believe that brain metastasis from HCC is relatively early in the disease progression.

Yen *et al.* reported a well documented group of 33 patients. Eighteen had brain parenchymal metastasis without skull involvement, the other 15 cases disclosed skull metastasis with brain invasion. The underlying HCC are mainly of expanding 39.4% and multifocal 39.4% types, and 54.5% had mental changes not related to hypoglycemia or hepatic encephalopathy. Nevertheless, our case had unifocal HCC^[16].

Yen *et al.* reported that 90% of 15 cases had hyperdense mass lesion by non-contrast computed tomography scan and 17 cases showed homogenous enhancement (77.3%) by post-contrast CT images. In the non-skull involved group, 41.7% disclosed ring-shape enhancement and 87.5% had perifocal edema, and 24.2% presented as intracerebral hemorrhage. Our patient had perifocal edema in the brain but without hemorrhage^[16].

Because no effective treatment for brain metastasis from HCC is available, further study is needed. Yen *et al.* reported 36.4% death of brain herniation^[16].

Most of non-skull involved cases had simultaneous lung metastasis without bony metastasis, while the skull involved group (66.7%) disclosed extracranial bony metastasis without lung metastasis^[15,16]. However, no other simultaneous metastasis site was found of our patient. HCC with intracranial metastasis is symptomatic and life threatening. Half the cases may come from pulmonary metastasis and the other half may be from bony metastasis even though our patient had neither of them. Surgery of the brain or skull metastasis is of no particular technical problem as long as they are located in accessible areas. Brain irradiation or surgery can prolong the survival. Radiotherapy seems to improve the quality and quantity of residual life, although the number of patients describes in the literature is not large enough

to draw any definite conclusion.

Loo *et al.* reported that light microscopic examination of the metastatic tumor from HCC revealed a trabecular HCC with focal hemorrhage and necrosis. Their immunohistochemical profile was identical to that described in primary HCC^[12].

Salvati *et al.* suggested that the stroke-like presentation of the cerebral localization of the disease can be explained by both the important vascularization of the tumor and the frequent hemocoagulative alterations caused by the cirrhosis^[9].

In conclusion, the rarity of this type of case gives the clinician the suspicion of such associations when confronted with a patient with liver dysfunction and neurologic findings.

REFERENCES

- 1 **Katyal S**, Oliver JH 3rd, Peterson MS, Ferris JV, Carr BS, Baron RL. Extrahepatic metastasis of hepatocellular carcinoma. *Radiology* 2000; **216**: 698-703
- 2 **Tang ZY**. Hepatocellular carcinoma- cause, treatment and metastasis. *World J Gastroenterol* 2001; **7**: 445-454
- 3 **Sithinamsuwan P**, Piratvisuth T, Tanomkiat W, Apakupakul N, Tongyoo S. Review of 336 patients with hepatocellular carcinoma at Songklanagarind Hospital. *World J Gastroenterol* 2000; **6**: 339-343
- 4 **Moriya H**, Ohtani Y, Tsukui M, Tanaka Y, Tajima T, Makuuchi H, Tanaka Y, Itou K. A case report: tumorectomy for brain metastasis of hepatocellular carcinoma. *Tokai J Exp Clin Med* 1999; **24**: 105-110
- 5 **Fрати A**, Salvati M, Giarnieri E, Santoro A, Rocchi G, Frati L. Brain metastasis from hepatocellular carcinoma associated with hepatitis B virus. *J Exp Clin Cancer Res* 2002; **21**: 321-327
- 6 **Endo M**, Hamano M, Watanebe K, Wakai S. Combined chronic subdural and acute epidural hematoma secondary to metastatic hepatocellular cancer: case report. *No Shinkei Geka* 1999; **27**: 331-334
- 7 **Peres MF**, Forones NM, Malheiros SM, Ferraz HB, Stavale JN, Gabbai AA. Hemorrhagic cerebral metastasis as a first manifestation of a hepatocellular carcinoma. Case report. *Arg Neuropsiquiatr* 1998; **56**: 658-660
- 8 **Kim M**, Na DL, Park SH, Jeon BS, Roh JK. Nervous system involvement by metastatic hepatocellular carcinoma. *J Neurooncol* 1998; **36**: 85-90
- 9 **Salvati M**, Cimatti M, Frati A, Santoro A, Gagliardi FM. Brain metastasis from hepatocellular carcinoma. A case report. *J Neurosurg Sci* 2002; **462**: 77-80
- 10 **Asahara T**, Yano M, Fukuda S, Fukuda T, Nakahara H, Katayama K, Itamoto T, Dohi K, Nakanishi T, Kitamoto M, Azuma K, Ito K, Moriwaki K, Yuge O, Shimamoto F. Brain metastasis from hepatocellular carcinoma after radical hepatectomy. *Hiroshima J Med Sci* 1999; **48**: 91-94
- 11 **Tanabe H**, Kondo A, Kinuta Y, Matsuura N, Hasegawa K, Chin M, Saiki M. Unusual presentation of brain metastasis from hepatocellular carcinoma-two case reports. *Neurol Med Chir* 1994; **34**: 748-753
- 12 **Loo KT**, Tsui WM, Chung KH, Ho LC, Tang SK, Tse CH. Hepatocellular carcinoma metastasizing to the brain and orbit: report of three cases. *Pathology* 1994; **26**: 119-122
- 13 **Friedman HD**. Hepatocellular carcinoma with central nervous system metastasis: a case report and literature review. *Med Pediatr Oncol* 1991; **19**: 139-144
- 14 **Shuangshoti S**, Rungruxsivorn S, Panyathanya R. Intracranial metastasis of hepatic carcinomas: a study of 9 cases within 28 years. *J Med Assoc Thai* 1989; **72**: 307-313
- 15 **Lee JP**, Lee ST. Hepatocellular carcinoma presenting as intracranial metastasis. *Surg Neurol* 1988; **30**: 316-320
- 16 **Yen FS**, Wu JC, Lai CR, Sheng WY, Kuo BI, Chen TZ, Tsay SH, Lee SD. Clinical and radiological pictures of hepatocellular carcinoma with intracranial metastasis. *J Gastroenterol Hepatol* 1995; **10**: 413-418

Milling of wheat, maize and rice: Effects on fibre and lipid content and health

FI Tovey, M Hobsley

FI Tovey, Hon. Research Fellow, M Hobsley, Professor Emeritus, Dept. of Surgery, UCL, UK

Correspondence to: FI Tovey, 5 Crossborough Hill, Basingstoke RG21 4AG, UK. frank@tovey.fsnet.co.uk

Telephone: +44-01256-461521

Received: 2004-04-20 **Accepted:** 2004-05-06

Tovey FI, Hobsley M. Milling of wheat, maize and rice: Effects on fibre and lipid content and health. *World J Gastroenterol* 2004; 10(12): 1695-1696

<http://www.wjgnet.com/1007-9327/10/1695.asp>

During the last thirty years the main interest in the medical consequences of milling of staple carbohydrate foods, particularly wheat and maize, has been in its effect on the fibre content as a result of the milling. The late nineteenth and early twentieth centuries in the West saw great changes in milling processes, from stone milling using water or wind power, to increasingly sophisticated roller milling, with an increasing loss of fibre in the process. In the 1970s and onwards there was an enhanced interest in possible diseases which could be related to the loss of fibre in the diet. At one time the list included diverticulitis, appendicitis, varicose veins, deep vein thrombosis, carcinoma of the colon, Crohn's disease, ulcerative colitis, irritable bowel syndrome, peptic ulcer, gall stones, hiatus hernia and gastro-oesophageal reflux, disorders of lipid metabolism and coronary heart disease! Over the course of time medical evidence has narrowed this list down to a much smaller number, of which the most important are diverticular disease and carcinoma of the colon.

The effect of fibre on peptic ulcer disease was attributed to its buffering effect on acid secretion. There seemed to be a relationship between the fibre content of staple diet and the geographical prevalence of duodenal ulceration. The prevalence was lower in populations using unrefined wheat, millets or maize with a high fibre content and higher in populations using refined wheat or maize flour or milled rice with low fibre contents^[1-4]. There were, however, abnormalities which did not fit in with this pattern, such as the high prevalence of duodenal ulcer in the Highlands of Ethiopia, where the staple food was unrefined teff (*Eragrostis abyssinica*) with a high fibre content^[4]. A possible explanation of this abnormality may lie in the lipid content of teff (see next paragraph). However, in addition, acid secretion studies showed that, whilst fibre had an initial buffering effect on gastric acidity, the resulting antral stimulation led to a higher acid output^[5].

A further effect of milling was on the lipid content of staple carbohydrate foods. Experiments on animal peptic ulcer models showed that the lipids present in the unrefined staple foods in areas with low prevalence of duodenal ulcer had a gastroprotective effect against ulceration and also promoted ulcer healing. These were not present in the refined staple foods of the areas with high duodenal ulcer prevalence^[6-9].

Lipids are found in both the bran and the germ of staple carbohydrate foods. In wheat and rice more lipids are found in the bran, but in maize the bulk lies in the predominantly large germ. Lipases are also present principally in the germ.

Milling has different effects on the bran and germ. In the case of wheat the two come apart separately. They can be separated by sieving and are stable for a period of time without further treatment. In the case of maize and rice the bran and germ come away together and the resultant bruising releases the lipases which interact with the oil content leading, if left untreated, to early rancidity of the combined germ and bran. Thus wholemeal wheat flour has a stable shelf life for a variable period of time, but the only satisfactory way to eat whole maize is either on the cob or home-pounded and cooked on the same day. Rice can only be eaten in the unrefined state as brown or unmilled rice. Milled rice undergoes changes during storage. During the milling of rice some of the lipase present in the bran enters the endosperm and as the rice is stored it reacts with a small amount of oil present in the rice grain. Some say that this results in an improvement in taste. The resulting lipolysis results in the formation of free fatty acids followed by a process of peroxidation that produces ketoaldehydes. Experiments on animal peptic ulcer models have shown that the latter are ulcerogenic. Similar experiments have shown that freshly milled rice bran is protective, but that it rapidly becomes ulcerogenic^[10,11]. Thus milled rice is not only deprived of gastroprotective lipids but also, on storage, becomes ulcerogenic, which is a possible factor in the high prevalence of duodenal ulceration in milled rice-eating countries.

With the discovery of *Helicobacter pylori* there has been much emphasis on its being the prime cause of duodenal ulceration. However, evidence is increasing to suggest that it may be a secondary infection affecting chronicity^[12,13]. Moreover, it should be remembered that many other factors have been shown to be associated with duodenal ulceration. These include familial tendency, acute anxiety as in the Second World War, cigarette smoking and the introduction of roller milling. Of these factors, the latter two greatly increased at the beginning of the twentieth century, which is the time when the epidemic of duodenal ulceration began. A suggestive feature about smoking is that it results in an increase in the parietal cell mass and therefore in an increase in the maximal ability of the stomach to secrete acid^[14], which itself is so strongly associated with duodenal ulceration^[15]. Which of these factors are truly aetiological and which are confounding factors that happened to be increasing at the same time remain unknown. It is important to keep an open mind.

The results of experiments on animal peptic ulcer models, however, strongly support the possibility that the loss of certain protective lipids, resulting from the milling of staple carbohydrate foods, may be an important factor. More needs to be known about the nature and action of these lipids.

REFERENCES

- 1 **Tovey FI**. Peptic ulcer in India and Bangladesh. *Gut* 1979; **20**: 329-347
- 2 **Tovey FI**, Tunstall M. Duodenal ulcer in black populations in Africa south of the Sahara. *Gut* 1975; **16**: 564-576
- 3 **Tovey FI**. Duodenal ulcer in China. *J Gastroenterol Hepatol* 1992; **7**: 427-431
- 4 **Tovey FI**. Diet and duodenal ulcer. *J Gastroenterol Hepatol* 1994;

- 9: 177-185
- 5 **Tovey FI.** Aetiology of duodenal ulcer: an investigation into the buffering action and effect on pepsin of bran and unrefined carbohydrate foods. *Postgrad Med J* 1974; **50**: 683-688
- 6 **Jayaraj AP,** Tovey FI, Clark CG. Possible dietary factors in relation to the distribution of duodenal ulcer in India and Bangladesh. *Gut* 1980; **21**: 1068-1076
- 7 **Jayaraj AP,** Tovey FI, Lewin MR, Clark CG. Duodenal ulcer prevalence: Experimental evidence for the possible role of dietary lipids. *J Gastroenterol Hepatol* 2000; **15**: 610-616
- 8 **Jayaraj AP,** Tovey FI, Clark CG, Hobsley M. Dietary factors in relation to the distribution of duodenal ulcer in India as assessed by studies in rats. *J Gastroenterol Hepatol* 2001; **16**: 501-505
- 9 **Jayaraj AP,** Tovey FI, Hobsley M. Duodenal ulcer prevalence: Research into the nature of possible protective dietary lipids. *Phytother Res* 2003; **17**: 391-398
- 10 **Jayaraj AP,** Tovey FI, Clark CG, Rees KR, White JS, Lewin MR. The ulcerogenic and protective action of rice and rice fractions in experimental peptic ulceration. *Clin Sci* 1987; **72**: 463-466
- 11 **Jayaraj AP,** Rees KR, Tovey FI, White JS. A molecular basis for peptic ulceration due to diet. *Br J exp Path* 1986; **67**: 149-155
- 12 **Tovey FI,** Hobsley M. Is *Helicobacter pylori* the primary cause of duodenal ulceration? *J Gastroenterol Hepatol* 1999; **14**: 1053-1056
- 13 **Hobsley M,** Tovey FI. *Helicobacter pylori*: the primary cause of duodenal ulceration or a secondary infection? *World J Gastroenterol* 2001; **7**: 149-151
- 14 **Whitfield PF,** Hobsley M. Comparison of maximal gastric secretion in smokers and non-smokers with and without duodenal ulcer. *Gut* 1987; **28**: 557-560
- 15 **Hobsley M,** Whitfield PF. The likelihood of a disease in relation to the magnitude of a risk factor. The example of duodenal ulcer. *Theor Surg* 1987; **2**: 106-109

Edited by Xu XQ and Wang XL **Proofread by** Xu FM

Surgery for pancreatic necrosis: "Whom, when and what"

S Connor, JP Neoptolemos

S Connor, JP Neoptolemos, Department of Surgery, Royal Liverpool University Hospital, Daulby Street, Liverpool, L69 3GA, UK

Correspondence to: Professor JP Neoptolemos, Department of Surgery, Royal Liverpool University Hospital, 5th floor UCD, Daulby Street, Liverpool, L69 3GA, United Kingdom. j.p.neoptolemos@liv.ac.uk

Telephone: +44-151-7064177 **Fax:** +44-151-7065826

Received: 2004-01-14 **Accepted:** 2004-02-26

Connor S, Neoptolemos JP. Surgery for pancreatic necrosis: "Whom, when and what". *World J Gastroenterol* 2004; 10 (12): 1697-1698

<http://www.wjgnet.com/1007-9327/10/1697.asp>

Acute pancreatitis is a common condition in which 70% of patients will recover with simple medical management. For patients who develop extensive or infected pancreatic necrosis the outcome is significantly different with a high morbidity and mortality^[1]. Surgery is the mainstay of treatment for these patients but several unresolved issues remain including *who requires surgery, when is the optimal time to intervene and what technique should be used*.

Infected necrosis is generally accepted as a strong indication for surgery^[2]. This has developed not from randomised data but observational studies over time that seemed to show a reduction in the previously reported mortality^[3-5]. A small number of recent reports^[6-8] have attempted to cast doubt on whether all patients with infected pancreatic necrosis should undergo surgery. So should a randomised controlled trial be undertaken? On the available evidence most surgeons and gastroenterologists would lack the "equipoise" required to perform such a trial. The number of patients successfully responding to conservative treatment remains small compared to the overall population with infected pancreatic necrosis. Further identification of factors associated with spontaneous resolution of infected necrosis needs to be identified before conservative treatment can be recommended as an acceptable alternative.

With the main indication for surgery being infected necrosis, the absence of infection is not an absolute contraindication. Over 90% of patients with sterile necrosis can be successfully treated without surgical intervention^[9,10], but a small subset with extensive necrosis warrants surgery. Indications in this setting include deteriorating organ failure despite maximal support^[10,11] or persisting symptoms which preclude hospital discharge despite several weeks of optimum conservative treatment^[9,12].

The timing of surgery is an important determinant of outcome with early surgery (within the first week) associated with a high mortality^[13,14]. The development of infected necrosis is time dependant, increasing to a peak in weeks 2-4^[15]. Some studies have suggested that antibiotics may reduce the incidence of infected necrosis^[16-22] but other recent large randomized controlled trials now reject this notion^[23,24]. Moreover whether prophylactic antibiotics can delay the onset of infected necrosis or the need for intervention is unknown. Another unknown factor is whether those patients who develop infected necrosis within the first 14 d of their illness should continue to be managed conservatively to allow the necrotic tissue to demarcate the reduction of complications associated with early debridement. Infected necrosis is almost universally associated with the progressive escalation of organ failure^[17].

Increasing pre-operative organ dysfunction scores have been associated with an increase in mortality^[25,26] and thus any delay in surgery following the diagnosis of infected necrosis is likely to be detrimental.

The aim of intervention in those with pancreatic necrosis is to remove the necrotic tissue and to provide adequate drainage for the remaining debris while preserving viable pancreatic tissue with minimal morbidity and mortality. It is generally accepted that debridement is preferable to resection^[2] and the approaches to the pancreatic necrosis include trans-peritoneal, retro-peritoneal, minimally invasive and percutaneous techniques^[4,12,14,25-32]. Post operative management includes laparostomy, packing, closed retroperitoneal lavage and repeat debridement^[4,12,14,25-32]. There is no standardised optimal technique as there are no randomised trials that compared surgical techniques. In the largest reported series^[17] the mortality was 39% but it has been reported as low as 6-8%^[12,28], which was the same as that for the overall mortality associated with pancreatitis in the United Kingdom^[33]. The reason for this wide inter-study variation is likely to be due to a number of factors. Firstly, there was an inter-study heterogeneity in both the reporting and the frequency of adverse patient prognostic factors. Secondly, intervention rates varied 10-fold^[34,35], suggesting that the indications for intervention provided by guidelines are not uniformly interpreted. Thirdly, many studies were relatively small, retrospective or based over long time periods during which there was often a change in management.

The Regional Pancreas Centre at the Royal Liverpool University Hospital has adopted a minimally invasive approach in preference to an open approach because it was associated with a very high mortality despite expert surgery and intensive care^[26,27]. Minimally, invasive retroperitoneal pancreatic necrosectomy has the dual advantages of removal of the solid necrotic material under direct vision through a wide bore tract^[27,31,32] and the use of high volume post-operative lavage through the wide tract^[27]. Moreover minimally invasive retroperitoneal pancreatic necrosectomy can be performed under local anaesthesia and reduces the need for post-operative intensive care, by avoiding an escalation in organ dysfunction which is usually seen after open surgery^[26,31]. The disadvantages of minimally invasive retroperitoneal pancreatic necrosectomy include an increase in the number of procedures and possible increase in hospital stay^[26,27]. Minimally invasive retroperitoneal pancreatic necrosectomy has not yet been shown to significantly reduce mortality although the trend is strong in this direction. Further experience with this technique and possible multi-centre randomised trials are needed.

Future studies on the outcome from intervention for pancreatic necrosis should incorporate standardised reporting of the precise profile of patients to allow for more valid comparisons between the different surgical techniques. In particular, there should be a clear description of the indications for intervention, the overall sample size from which the patients are selected, key prognostic indicators including age, organ dysfunction scores, extent of necrosis and the incidence of primary infection of the necrosis. It is notable that most studies failed to provide these critical factors and did not distinguish primary from secondary infection. Improving the reporting of studies will lead to the identification of the optimal patient at the optimal time undergoing the optimal procedure.

REFERENCES

- 1 **Neoptolemos JP**, Raraty M, Finch M, Sutton R. Acute pancreatitis: the substantial human and financial costs. *Gut* 1998; **42**: 886-891
- 2 **Uhl W**, Warshaw A, Imrie C, Bassi C, McKay CJ, Lankisch PG, Carter R, Di Magno E, Banks PA, Whitcomb DC, Dervenis C, Ulrich CD, Satake K, Ghaneh P, Hartwig W, Werner J, McEntee G, Neoptolemos JP, Buchler MW. International Association of Pancreatologists. IAP Guidelines for the surgical management of acute pancreatitis. *Pancreatology* 2002; **2**: 565-573
- 3 **Altemeier WA**, Alexander JW. Pancreatic abscess. *Arch Surg* 1963; **87**: 80-85
- 4 **Bradley EL**. Management of infected pancreatic necrosis by open drainage. *Ann Surg* 1987; **204**: 542-549
- 5 **Sarr M**. Invited Commentary. *Dig Surg* 2003; **20**: 300
- 6 **Dubner H**, Steinberg W, Hill M, Bassi C, Chardavoigne R, Bank S. Infected pancreatic necrosis and peripancreatic fluid collections: Serendipitous response to antibiotic and medical therapy in three patients. *Pancreas* 1996; **12**: 298-302
- 7 **Salas CJ**, Gallego RFJ, Sanchez SJC, Diez GF. Medical treatment of infected pancreatic necrosis. *Gastroenterol Hepatol* 2001; **24**: 268-269
- 8 **Ramesh H**, Prakash K, Lekha V, Jacob G, Venugopal A. Are some cases of infected pancreatic necrosis treatable without intervention. *Dig Surg* 2003; **20**: 296
- 9 **Ashley SW**, Perez A, Pierce EA, Brooks DC, Moore FD Jr, Whang EE, Banks PA, Zinner MJ. Necrotising pancreatitis. *Ann Surg* 2001; **234**: 572-580
- 10 **Buchler MW**, Gloor B, Muller CA, Friess H, Seiler CA, Uhl W. Acute necrotising pancreatitis: treatment strategy according to status of infection. *Ann Surg* 2000; **232**: 619-626
- 11 **Beger HG**, Isenmann R. Acute pancreatitis: Who needs an operation? *J Hepatobiliary Pancreat Surg* 2002; **9**: 436-442
- 12 **Fernandez-del Castillo C**, Rattner DW, Makary MA, Mostafavi A, McGrath D, Warshaw A. Debridement and closed packing for the treatment of necrotising pancreatitis. *Ann Surg* 2000; **228**: 676-684
- 13 **Mier J**, Leon EL, Castillo A, Robledo F, Blanco R. Early versus late necrosectomy in severe pancreatitis. *Am J Surg* 1997; **173**: 71-75
- 14 **Gotzinger P**, Wamser P, Exner R, Schwanzner E, Jakesz R, Fugger R, Sautner T. Surgical treatment of severe acute pancreatitis: timing of operation is crucial for survival. *Surg Infect* 2003; **4**: 205-211
- 15 **Beger HG**, Bittner R, Block S, Buchler M. Bacterial contamination of pancreatic necrosis. A prospective clinical study. *Gastroenterology* 1986; **91**: 433-438
- 16 **Pederzoli P**, Bassi C, Vesentini S, Campedelli A. A randomised multicentre clinical trial of antibiotic prophylaxis of septic complications in acute necrotising pancreatitis with imipenem. *Surg Gynecol Obstet* 1993; **176**: 480-483
- 17 **Gotzinger P**, Sautner T, Kriwanek S, Beckerhinn P, Barlan M, Armbruster C, Wamser P, Fugger R. Surgical treatment for severe acute pancreatitis: Extent and surgical control of necrosis determine outcome. *World J Surg* 2002; **26**: 474-478
- 18 **Pederzoli P**, Bassi C, Vesentini S, Girelli R, Cavallini G, Falconi M, Nifosi F, Riela A, Dagradi A. A randomised multi-centre clinical trial of antibiotic prophylaxis of septic complications in acute necrotising pancreatitis with imipenem. *Surg Gynecol Obstet* 1993; **176**: 480-483
- 19 **Sainio V**, Kempainen E, Puolakkainen P, Taavitsainen M, Kivisaari L, Valtonen V, Haapiainen R, Schroder T, Kivilaakso E. Early antibiotic treatment in acute necrotising pancreatitis. *Lancet* 1995; **346**: 663-667
- 20 **Delcenserie R**, Yzet T, Ducroix JP. Prophylactic antibiotics in treatment of severe acute alcoholic pancreatitis. *Pancreas* 1996; **13**: 198-201
- 21 **Schwarz M**, Isenmann R, Meyer H, Beger HG. Antibiotic use in necrotizing pancreatitis. Results of a controlled study. *Dtsch Med Wochenschr* 1997; **122**: 356-361
- 22 **Nordback I**, Sand J, Saaristo R, Paajanen H. Early treatment with antibiotics reduces the need for surgery in acute necrotizing pancreatitis-a single-center randomized study. *J Gastrointest Surg* 2001; **5**: 113-118
- 23 **Isenmann R**, Runzi M, Kron M, Kahl S, Kraus D, Jung N, Maier L, Malfertheiner P, Goebell H, Beger HG. Prophylactic antibiotic treatment in patients with predicted severe acute pancreatitis: A placebo-controlled, double-blind trial. *Gastroenterology* 2004; **126**: 997-1004
- 24 **Spicak J**, Hejtmanekova S, Cech P, Hoskovec D, Kostka R, Leffler J, Kasalicky M, Svoboda P, Bartova J. Antibiotic prophylaxis in severe acute pancreatitis: randomized multicenter prospective trial with meropenem. *Pancreatology* 2003; **3**: 220
- 25 **Beattie GC**, Mason J, Swan D, Madhavan KK, Siriwardena AK. Outcome of necrosectomy in acute pancreatitis. *Scand J Gastroenterol* 2002; **12**: 1450-1453
- 26 **Connor S**, Ghaneh P, Raraty M, Rosso E, Hartley MN, Garvey C, Hughes M, McWilliams R, Evans J, Rowlands P, Sutton R, Neoptolemos JP. Increasing age and APACHE II scores are the main determinants of outcome from pancreatic necrosectomy. *Br J Surg* 2003; **90**: 1542-1548
- 27 **Connor S**, Ghaneh P, Raraty M, Sutton R, Rosso E, Garvey CJ, Hughes ML, Evans JC, Rowlands P, Neoptolemos JP. Minimally invasive retroperitoneal pancreatic necrosectomy. *Dig Surg* 2003; **20**: 270-277
- 28 **Beger HG**, Buchler M, Bittner R, Block S, Nevalainen T, Roscher R. Necrosectomy and post-operative local lavage in necrotising pancreatitis. *Br J Surg* 1988; **75**: 207-212
- 29 **Lasko DS**, Habib FA, Sleeman D, Levi J, Shatz D, Livingstone A. Percutaneous lavage for infected pancreatic necrosis. *J Gastrointest Surg* 2003; **7**: 288-289
- 30 **Tzovaras G**, Parks RW, Diamond T, Rowlands BJ. Early and long term results of surgery for severe necrotising pancreatitis. *Dig Surg* 2004; **21**: 41-47
- 31 **Carter RC**, McKay CJ, Imrie CW. Percutaneous necrosectomy and sinus tract endoscopy in the management of infected pancreatic necrosis: An initial experience. *Ann Surg* 2000; **232**: 175-180
- 32 **Gambiez LP**, Denimal FA, Porte HL, Saudemont A, Chambon JP, Quandalle PA. Retroperitoneal approach and endoscopic management of peripancreatic necrosis collections. *Arch Surg* 1998; **133**: 66-72
- 33 **Winslet M**, Hall C, London NJ, Neoptolemos JP. Relation serum amylase levels to aetiology and severity of acute pancreatitis. *Gut* 1992; **33**: 982-986
- 34 **Oleynikov D**, Cook C, Sellers B, Mone MC, Barton R. Decreased mortality from necrotising pancreatitis. *Am J Surg* 1998; **176**: 648-653
- 35 **Branum G**, Galloway J, Hirchowit W, Fendley M, Hunter J. Pancreatic necrosis: results of necrosectomy, packing and ultimate closure over drains. *Ann Surg* 1998; **227**: 870-877

Edited by Xu XQ and Wang XL Proofread by Xu FM

Hyperhomocysteinemia, endoplasmic reticulum stress, and alcoholic liver injury

Cheng Ji, Neil Kaplowitz

Cheng Ji, Neil Kaplowitz, Gastroenterology/Liver Division, Keck School of Medicine, University of Southern California, Los Angeles, CA 90033, USA

Supported by the U.S. National Institute of Alcohol Abuse and Alcoholism, R01 AA014428 and by the Robert E. and May R. Wright Foundation, No. 263

Correspondence to: Cheng Ji, Ph.D., Faculty of Medicine, Gastroenterology/Liver Division, Keck School of Medicine, University of Southern California, HMR-101, 2011 Zonal Avenue, Los Angeles, CA 90033, USA. chengji@usc.edu

Telephone: +1-323-442-3452 **Fax:** +1-323-442-5425

Received: 2004-04-20 **Accepted:** 2004-05-06

Abstract

Deficiencies in vitamins or other factors (B6, B12, folic acid, betaine) and genetic disorders for the metabolism of the non-protein amino acid-homocysteine (Hcy) lead to hyperhomocysteinemia (HHcy). HHcy is an integral component of several disorders including cardiovascular disease, neurodegeneration, diabetes and alcoholic liver disease. HHcy unleashes mediators of inflammation such as NF κ B, IL-1 β , IL-6, and IL-8, increases production of intracellular superoxide anion causing oxidative stress and reducing intracellular level of nitric oxide (NO), and induces endoplasmic reticulum (ER) stress which can explain many processes of Hcy-promoted cell injury such as apoptosis, fat accumulation, and inflammation. Animal models have played an important role in determining the biological effects of HHcy. ER stress may also be involved in other liver diseases such as α_1 -antitrypsin (α_1 -AT) deficiency and hepatitis C and/or B virus infection. Future research should evaluate the possible potentiative effects of alcohol and hepatic virus infection on ER stress-induced liver injury, study potentially beneficial effects of lowering Hcy and preventing ER stress in alcoholic humans, and examine polymorphism of Hcy metabolizing enzymes as potential risk-factors for the development of HHcy and liver disease.

Ji C, Kaplowitz N. Hyperhomocysteinemia, endoplasmic reticulum stress, and alcoholic liver injury. *World J Gastroenterol* 2004; 10(12): 1699-1708

<http://www.wjgnet.com/1007-9327/10/1699.asp>

INTRODUCTION

Homocysteine (Hcy) is a toxic non-protein sulfur containing amino acids in humans. It is formed exclusively upon demethylation of the essential amino acid- methionine. Hcy is metabolized either through remethylation or transsulfuration pathways and is nutritionally regulated. Normal concentrations of total homocysteine in plasma are in the range of 5 to 16 μ mol/L and the desired upper limit for Hcy concentration should be 10 μ mol/L. An elevated plasma Hcy level is denoted hyperhomocysteinemia (HHcy). Three ranges of HHcy are defined: moderate (16 to 30 μ mol/L), intermediate (31 to 100 μ mol/L), and severe (>100 μ mol/L). Individuals who

consume a large amount of food rich in animal protein may ingest two to three grams of methionine, resulting in postprandial Hcy concentrations greater than 20 μ mol/L. Clinical HHcy was first described more than 40 years ago in children with learning difficulties^[1-3], and it has since been estimated that moderate HHcy occurs in 5-7% of the general population. Evidence now indicates that moderate HHcy is an important and independent risk factor for several disorders, including atherosclerosis, diabetes, fatty liver, immune activation, and neurodegenerations such as Alzheimer's and Parkinson's diseases^[3-9].

Readers are referred to recent reviews on HHcy and functions of Hcy^[10,11]. The main goal of this article is to provide information on major causes of HHcy, potential mechanisms of Hcy toxicity, with emphasis on endoplasmic reticulum (ER) stress mechanism, and animal models for the study of biological effects of HHcy. We would also summarize our ongoing work on ethanol-induced HHcy and liver injury in an intragastric ethanol fed murine model.

HCY METABOLISM AND HHCY

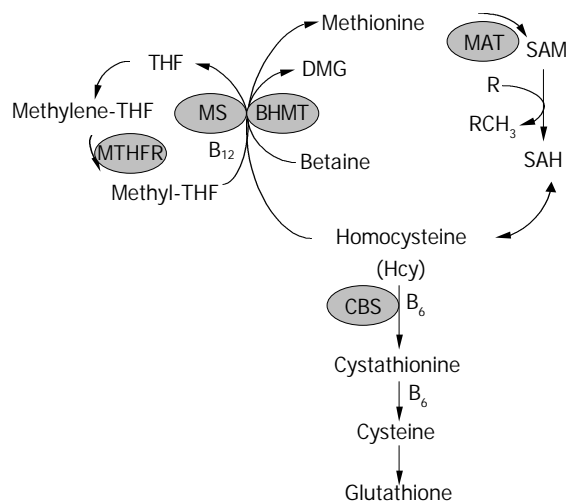


Figure 1 Homocysteine metabolism. Homocysteine has three main metabolic fates: to be remethylated to methionine, to enter the cysteine biosynthetic pathway, and to be released into the extracellular medium. CBS, cystathionine -synthase; MS, methionine synthase; THF, tetrahydrofolate; MTHFR, 5, 10-methylenetetrahydrofolate reductase; BHMT, betaine-homocysteine methyltransferase; DMG, dimethylglycine; MAT, methionine adenosyltransferase; SAM, S-adenosylmethionine; SAH, S-adenosylhomocysteine.

Hcy was formed from methionine after removal of the methyl group on S-adenosylmethionine (SAM) (Figure 1). Hcy metabolism involves reversible formation of S-adenosylhomocysteine (SAH), remethylation to methionine by betaine-homocysteine methyltransferase (BHMT) (liver and kidney restricted), which is vitamin-independent, and by the ubiquitous methionine synthase (MS), which is dependent on vitamin B12 and

methylenetetrahydrofolate (MTHF) production *via* 5, 10-methylenetetrahydrofolate reductase (MTHFR). Hcy can also be converted through transsulfuration to cystathionine for the formation of cysteine and glutathione (GSH). The transsulfuration is catalyzed by cystathionine- β -synthase (CBS) and is dependent on vitamin B6. In addition, Hcy can be converted to Hcy-tRNA. Although it was not incorporated into protein due to editing mechanisms, nitroso-Hcy-tRNA is stable and might play a role in Hcy-induced protein misfolding along with the formation of Hcy-protein-SH mixed disulfides and Hcy thiolactone covalent binding to lysine amino groups^[11]. Hcy-t-RNA is edited through the action of methionyl-t-RNA synthetase (ATP consuming) by formation of a thioester thiolactone which could covalently bind to protein amino groups. Thus, homocysteinylation of proteins depends on the formation of thiolactone^[12,13].

Tight regulation of Hcy metabolism depends on different affinities of MS, BHMT, and CBS for Hcy. MS and BHMT show low Km values for Hcy (<0.1 mmol/L), and CBS has high Km values for Hcy (>1 mmol/L). At low Hcy concentrations, methionine conservation was favored; and at high Hcy concentrations, immediate and long-term drainage of Hcy via the transsulfuration pathway was ensured^[14]. SAM could play a key regulatory role by allosterically inhibiting MTHFR and BHMT and activating CBS^[15-18]. Thus, SAM may be a regulatory switch in Hcy metabolism: low SAM favors remethylation and conservation of Hcy for methionine synthesis, whereas high levels favor transsulfuration. High Hcy levels can decrease the SAM/SAH ratio, since most methyltransferases bind to SAH with higher affinity than SAM, elevated SAH inhibits methylation. *In vitro*, under "physiological" conditions of concentrated 27 000 g postmitochondrial supernatant with 8 mmol/L GSH, 0.3 mmol/L serine, 2 mmol/L betaine, 60 μ mol/L methionine, 50 μ mol/L methyl THF, 60 μ mol/L SAM and 10 μ mol/L SAH, transsulfuration accounted for 46% of Hcy metabolism and the remainder was equally contributed to by MS and BHMT. The need to conserve methionine (*e.g.* low protein diet) resulted in decreased cystathionine production and increased Hcy remethylation. Conversely, in the presence of excess methionine, SAM activated the cystathionine pathway.

HHcy results from increased levels of intracellular Hcy that is readily released into the extracellular medium: plasma or body fluid. Kidney might be a major site for the removal and metabolism of Hcy primarily through the transsulfuration pathway^[19]. Renal impairment often causes HHcy, reflecting a role of kidney in Hcy clearance from plasma. This fact might contribute to the high incidence of vascular complications in patients with chronic renal failure^[20]. Genetic abnormalities, age, sex and various nutritional and hormonal determinants contribute to HHcy. However, genetic and nutritional disorders are the major factors. Genetic disorders involve polymorphism in the genes coding for MTHFR and CBS. The most common genetic defect associated with mild HHcy is a point mutation, namely, a C to T substitution at nucleotide 677 (C677 \rightarrow T) in the open reading frame of the gene for MTHFR. This point mutation could cause a substitution of valine for alanine in the functional enzyme^[21], resulting in a thermolabile variant of the enzyme with decreased total activity. This is an autosomal recessive mutation, and the frequency of the C677 \rightarrow T polymorphism varied among racial and ethnic groups, with 13% of T/T homozygous and 50% C/T heterozygous among Caucasian and Asian populations, and very low incidence among African-Americans^[21-27]. Premature atherosclerosis and thrombotic disease were observed in MTHFR deficiency^[23-28]. The most common genetic cause associated with severe HHcy is homozygous CBS deficiency, which resulted in plasma Hcy concentrations of up to 400 μ mol/L, compared to normal

plasma levels of 10 μ mol/L^[28-30]. Homozygous CBS deficiency, T833 \rightarrow C and G919 \rightarrow A mutations, were inherited as an autosomal recessive disorder with pleiotropic clinical manifestations, including mental retardation, ectopia lentis, osteoporosis, skeletal abnormalities and hepatic steatosis^[28-30]. Patients were usually at higher risk for premature atherosclerosis and thrombotic disease, which is the major cause of death^[31-33]. CBS deficiency has a worldwide incidence of 1:344 000 live births, ranging from 1:58 000 to 1:1 000 000 in countries that perform newborn screening^[31]. While homozygous CBS deficiency is rare, heterozygous CBS deficiency occurs in approximately 1% of the general population and is associated with premature atherosclerosis and thrombotic disease in phenotypically normal individuals^[31-33].

Nutritional disorders that potentially lead to HHcy include deficiencies in vitamin B12, folate and vitamin B6, as the *de novo* synthesis of methionine methyl groups requires both vitamin B12 and folate cofactors whereas the synthesis of cystathionine requires pyridoxal 5-phosphate (vitamin B6). Although it has been shown that deficiencies of vitamin B12 and folate are related to increased plasma Hcy concentrations^[32-35], the relationship of Hcy levels to vitamin B6 status is less clear^[36,37]. In addition, excess dietary methionine in normal mice has been shown to induce HHcy^[38]. Under normal conditions, several methylation reactions in the liver contribute to the bulk (90%) of SAM utilization and Hcy production via SAH. For example, phosphatidylethanolamine to phosphatidylcholine is mediated by phosphatidylethanolamine N-methyltransferase (PEMT). PEMT $^{-/-}$ mice had 50% decreased plasma Hcy despite being choline and betaine deficient^[39]. PEMT null mice exhibited fatty liver and apoptosis but this was not prevented by betaine administration, impaired lipoprotein secretion rather than methyl donor deficiency appeared to be the dominant effect of choline deficiency^[40]. The other major source of Hcy is the activity of hepatic guanidinoacetate (GAA) N-methyltransferase (NMT). GAA is produced in the kidney by L-arginine:glycine amidinotransferase. GAA is then converted to creatine in the liver by GAA-NMT, utilizing SAM and generating SAH. Creatine is exported to muscle and also represses the kidney enzyme which produces GAA. GAA supplementation could induce HHcy and creatine feeding lowers Hcy^[41].

HCY TOXICITY

Possible cellular mechanisms by which elevated Hcy promotes liver disease are oxidative stress, endoplasmic reticulum (ER) stress and the activation of pro-inflammatory factors (Figure 2). Hcy enhances the production of several pro-inflammatory cytokines. Expression of monocyte chemoattractant protein 1 (MCP-1) was increased in cultured human vascular endothelial cells, smooth muscle cells and monocytes treated with Hcy^[42-44]. Hcy has also been shown to increase expression of IL-8^[42], a T-lymphocyte and neutrophil chemoattractant, in cultured endothelial cells. Hcy-induced expression of MCP-1 and IL-8 in monocytes and endothelial cells has been shown to occur through activation of NF- κ B, a transcription factor involved in mediating downstream inflammatory processes^[44,45]. Active NF- κ B could stimulate production of cytokines, chemokines, interferons, leukocyte adhesion molecules, hemopoietic growth factors and major histocompatibility (MHC) class I molecules—all of which are thought to influence inflammation^[45,46].

Hcy can generate a procoagulant state, which may be related to its proclivity to auto-oxidize, generating H₂O₂. Various *in vitro* studies using vascular tissues have implicated Hcy in causing abnormal vascular relaxation responses by enhancing the intracellular production of superoxide anion (O₂⁻)^[47-54]. O₂⁻ is believed to react with and decrease the availability of endothelial nitric oxide (NO) and yield peroxynitrite, thereby

limiting normal vasodilation responses^[55,56]. Decreased GSH peroxidase transcription (reduction of peroxides protects NO) may play a role in this process^[49,57], since overexpression of GSH peroxidase could restore the NO response^[57]. O₂⁻ and peroxynitrite are also known to contribute to the oxidative modification of tissues, resulting in the formation of lipid peroxides and nitrosated end products such as 3-nitrotyrosine. The observations that Hcy decreased the expression of a wide range of antioxidant enzymes^[57-59] and impaired endothelial NO bioavailability by inhibiting glutathione peroxidase activity raise the possibility that Hcy sensitizes cells to the cytotoxic effects of agents or conditions known to generate ROS. Decreased NO bioavailability has also been shown *in vitro* to increase the expression of MCP-1, which may enhance intravascular monocyte recruitment and lead to accelerated lesion formation^[60].

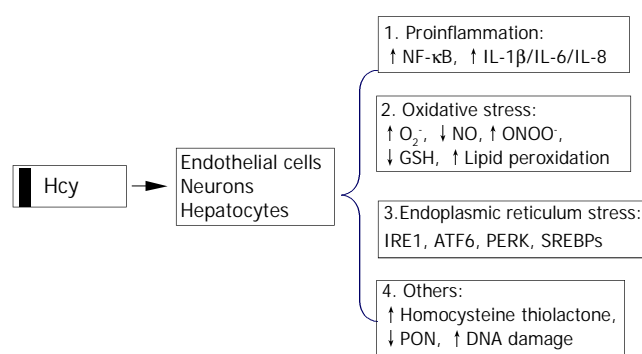


Figure 2 Cellular mechanisms by which homocysteine promotes cell injury. Homocysteine causes activation of necrosis factor- κ B (NF- κ B) and enhances production of cytokines (IL-1 β , IL-6, and IL-8) resulting in inflammatory reactions, increases intracellular levels of superoxide anion causing oxidative stress, and induces endoplasmic reticulum (ER) stress by causing misfolding of proteins traversing the ER. Homocysteinyl-tRNA increases production of highly reactive derivative homocysteine thiolactone which damages enzymes and DNA. IRE1, type 1 ER transmembrane protein kinase; ATF6, the activating transcription factor 6; PERK, the PKR like ER kinase; SREBP, sterol regulatory element binding protein, PON, paraoxonase.

Intracellular Hcy can be converted by methionyl tRNA synthase into an Hcy-AMP complex, which is subsequently catabolised to Hcy thiolactone, thereby preventing the incorporation of Hcy into nascent polypeptide chains. Hcy thiolactone has unique reactive properties that can lead to the homocysteinylation of lysine residues and free amine groups on numerous cellular proteins, thereby resulting in decreased biological activity and premature degradation^[61]. In addition, Hcy thiolactone secreted into the circulation may induce widespread modifications of plasma proteins that could potentially contribute to the development of liver and cardiovascular diseases. Recent studies have demonstrated that Hcy thiolactone decreases paraoxonase activity associated with HDL, thereby rendering HDL less protective against oxidative damage or against toxicity of Hcy thiolactone^[62].

HCY-INDUCED ER STRESS

ER is a principal site for protein synthesis and folding, calcium storage and calcium signaling. It also serves as a site of biosynthesis for steroids, cholesterol and other lipids. The physiological roles of the ER include regulation of protein synthesis, folding and targeting and maintenance of cellular calcium homeostasis. The ER has a high concentration of numerous resident chaperone proteins such as glucose

regulated protein-78 (GRP78) and GRP94, a high level of calcium and an oxidative environment to carry out these functions efficiently. Proteins that were translocated into the ER lumen underwent post-translational modifications and the folding required for optimal function. Properly folded proteins were allowed to reach their destiny via the secretory pathway, whereas unfolded and misfolded proteins were exported or dislocated from the ER and degraded by cytoplasmic proteasomes^[63-68]. ER stress is a condition under which unfolded and misfolded proteins accumulate (Figure 3). ER stress triggers the unfolded protein response (UPR), which is an intracellular signaling pathway and is mediated via three ER-resident sensors in mammalian cells: a type-I ER transmembrane protein kinase (IRE-1), the activating transcription factor 6 (ATF-6) and the PKR like ER kinase (PERK). Activation of these three pathways is mediated by GRP78, which is associated with each sensor in the absence of ER stress. As unfolded proteins accumulated in the ER, GRP78 dissociated from and thereby activating IRE-1, ATF-6 and PERK^[68-70]. Activation of both IRE-1 and ATF-6 increases the expression of ER-resident chaperones. IRE-1 is a stress-activated transmembrane protein kinase having endoribonuclease activity. Following ER stress, IRE-1 dimerized and was autophosphorylated, thereby allowing IRE-1 to act as an endoribonuclease in the alternative splicing of XBP-1 mRNA. The removal of a 26 base pair intron resulted in a translation frameshift that permits XBP-1 to act as a transcriptional activator of genes containing upstream ER stress response elements (ERSE). Upon ER stress, ATF-6 was transported to the Golgi where the cytosolic transactivation domain of ATF-6 is cleaved from the membrane by specific proteases (S1P and S2P) that also recognize, cleave and activate sterol regulatory element-binding proteins (SREBPs) leading to increased lipids needed for ER membrane synthesis. Following release, the transactivation domain of ATF-6 localized to the nucleus where it interacts with ERSE, thereby activating transcription of numerous UPR-responsive genes, including GRP78, GADD153 (CHOP), XBP-1, ERp72, and Hcy-induced ER protein (Herp). ER stress could also lead to a rapid attenuation in protein synthesis, a cellular process mediated by the transmembrane protein kinase, PERK. Activation of PERK could cause phosphorylation of eukaryotic initiation factor-2 α (eIF-2 α), which blocks mRNA translation initiation to help relieve the unfolded protein burden on the ER. Recent studies have also demonstrated that PERK-dependent eIF-2 α phosphorylation is required for transcriptional activation of a wide range of UPR-responsive genes^[71,72]. The early UPR co-coordinately enhances cell survival by ensuring that the adverse effects of ER stress are dealt with in a timely and efficient manner. However, prolonged UPR following ER stress has severe consequences. It can lead to activation of the tumor necrosis factor receptor associated factor 2 (TRAF2), which activates caspases (e.g. caspase-12 in mice) and JNK resulting in programmed cell death. Overexpression of CHOP, a basic region leucine zipper transcription factor, could also promote cell death^[71]. Overproduction of lipids by SREBP can lead to fat accumulation. In addition, ER stress is associated with release of ER Ca²⁺ stores which can trigger oxidative stress *via* effects on mitochondria and NF- κ B activation leading to inflammatory reactions^[73]. NF- κ B activation could be blocked by calcium chelators and antioxidants^[19]. Increased cytosol calcium also activates calpains which proteolytically cleave Bcl-X_L (inactivation) and caspase 12 (activation). ER stress could contribute to the pathogenesis of a number of human diseases, including diabetes, Alzheimer's disease, Parkinson's disease and cancer^[72].

Hcy induced ER stress response has recently received much attention^[6,74-79]. Hcy causes ER stress by disrupting disulphide bond formation and causing misfolding of proteins traversing

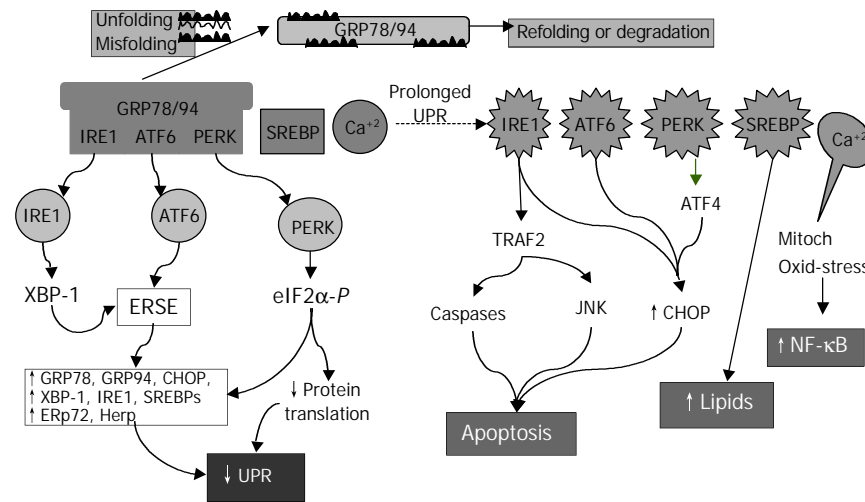


Figure 3 Consequences of endoplasmic reticulum (ER) stress response. In the early phase, unfolded proteins cause dissociation of chaperones such as Bip/GRP78 from ER resident kinases-IRE1 and PERK and transcription factor-ATF6. Activated PERK phosphorylates eIF2 resulting in translational attenuation. Activated IRE1 and ATF6 up-regulate genes encoding ER chaperone proteins such as GRP78/94 leading to increased protein-folding capacity. Overall, the unfolded protein response (UPR) goes down. In the late phase, IRE1 interacts with TRAF2 (tumor necrosis factor receptor associated factor 2) which activates caspases and JNK (cJUN NH2-terminal kinase) leads to apoptosis. ATF6 and PERK upregulate CHOP (C/EBP homologous protein) promoting cell death. SREBP upregulates lipid synthesis. Prolonged UPR leads to Ca²⁺ release from ER causing production of reactive oxygen intermediates which may lead to activation of NF-κB.

the ER. Elevated levels of intracellular Hcy could increase the expression of several ER stress response genes, including GRP78, GRP94, Herp and RTP^[6,58,74,77,78,80-82]. Hcy could induce expression of GADD153^[58,78,79] involved in ER stress-induced cell death^[83]. Hcy-induced ER stress could cause dysregulation of lipid biosynthesis by activating the SREBPs^[6,76-79], ER resident transcription factors are responsible for the induction of genes in the cholesterol/triglyceride biosynthesis and uptake pathways^[6]. Hcy-induced cell death was mimicked by other ER stress agents and was dependent on IRE-1 signaling. Activation of IRE-1 by Hcy could lead to a rapid and sustained activation of JNK protein kinases^[84,85], a result consistent with the finding that activation of JNK by ER stress involved binding of IRE-1 to TRAF2^[86]. Because persistent activation of JNK correlated with cell death^[87], these studies could provide further support for a mechanism involving Hcy-induced programmed cell death.

APPROACHES FOR STUDY OF HHcy

Cell and animal models with altered plasma Hcy are among the most useful approaches in determining the biological effects of HHcy. However, cell and transgenic animal models expressing Hcy metabolism-related genes/enzymes are not available. Nevertheless, diet- and, especially, genetic-induced animal models of HHcy have been developed. The gene knockout animals have significantly enhanced the status of Hcy as an independent risk factor for several disorders.

Homozygous and heterozygous CBS-deficient mice were generated in 1995^[88]. Homozygous mutants completely lacking CBS were born at the expected frequency from mating of heterozygotes, but they suffered from severe growth retardation and a majority of them died within 5 wk after birth. Histological examination showed that the hepatocytes of homozygotes were enlarged, multinucleated, and filled with microvesicular lipid droplets. Plasma Hcy levels of the homozygotes (203.6±65.3 μmol/L) were 33 times higher than normal (6.1±0.8 μmol/L). The homozygous CBS deficient mice represented a model for severe HHcy. Heterozygous CBS deficient mice had 50% reduction in CBS mRNA and enzyme activity in the liver and had twice normal plasma Hcy levels (13.5±3.2 μmol/L). The CBS knockouts significantly help elucidate the *in vivo* role of

elevated levels of Hcy in the etiology of several HHcy-related disorders and in the cellular mechanisms by which Hcy promote cell injury. The CBS-deficient mice were predisposed to HHcy during dietary folate deficiency, and moderate HHcy was associated with marked impairment of endothelial function in mice^[89]. Results from a subsequent study indicated that endothelial dysfunction occurred in HHcy mice even in the absence of folate deficiency^[90]. Endothelial dysfunction in CBS (+/-) mice was associated with increased tissue levels of SAH, which suggests that altered SAM-dependent methylation may contribute to vascular dysfunction in HHcy^[91]. Further studies with the CBS deficient mice revealed the importance of intracellular redox balance for nitric oxide bioactivity and endothelial function, and the importance of ER stress in abnormal hepatic accumulation of lipid^[92,93]. Expression of several genes analyzed by DNA microarray was found to be reproducibly abnormal in the livers of heterozygous and homozygous CBS-deficient mice^[94]. These genes encode ribosomal protein S3a and methylthioadenosine phosphorylase, suggesting cellular growth and proliferation perturbations may occur in homozygous CBS-deficient mice liver.

MTHFR-deficient mice have been recently developed to examine the effects of HHcy resulting from genetic deficiencies in the remethylation pathway^[95]. MTHFR-deficient mice shared basic phenotypic similarities with CBS-deficient mice. However, they were unique in that they developed mild HHcy and atherosclerosis. Recent study has demonstrated the importance of choline metabolism in HHcy in this model^[96]. Comparison study by administering the alternate choline-derived methyl donor, betaine, to wild-type mice and MTHFR deficient mice revealed that plasma Hcy and liver choline metabolite levels were strongly dependent on the MTHFR genotype. Betaine supplementation decreased Hcy in all three genotypes, restored liver betaine and phosphocholine pools, and prevented severe steatosis in MTHFR-deficient mice. Since there was a significant negative correlation between plasma betaine and Hcy concentrations in humans with cardiovascular disease, the results emphasize the strong interrelationship between Hcy, folate, and choline metabolism. MTHFR-compromised mice with HHcy appeared to be much more sensitive to changes of choline/betaine intake than wild-type

animals. HHcy, in the range of that associated with folate deficiency or with homozygosity for the 677T MTHFR variant, may be associated with disturbed choline metabolism.

MS could directly catalyze the remethylation pathway and inactivation of this gene has been attempted recently^[97]. Heterozygous MS knockout mice from an outbred background had slightly elevated plasma Hcy (6.1 mol/L) and methionine compared to wild-type mice (4.1 μ mol/L) but seemed to be otherwise indistinguishable. Homozygous knockout embryos survived through implantation but died soon thereafter. Nutritional supplementation during pregnancy was unable to rescue embryos that were completely deficient in MS. This study indicated that MS activity was essential for early embryonic development of mice. Although the MS knockout mouse has not provided an immediately obvious animal model of human disease, heterozygotes with 50% reduction of MS activity may be useful. It is likely that MS heterozygote knockouts are more susceptible to dietary deficiencies than wild type mice and thus having merits as a model in which interactions between genetic status and nutritional status can be studied.

The animal models are valuable *in vivo* tools to further examine potential therapeutic approaches in lowering plasma Hcy while decreasing the prevalence of HHcy-induced disorders. However, the animal models neither have tissue or organ specificity nor exclude potential compensatory pathways of Hcy metabolism. Conditional disruption of Hcy metabolism-related genes and crossing between animal models that are deficient in different genes should be the future directions in the effort of creating animal models for study of HHcy.

ETHANOL-INDUCED HHCY AND LIVER INJURY

The pathogenesis of the pathologic features of alcoholic liver injury, namely steatosis, apoptosis, necrosis, inflammation and fibrosis, is an area of intense interest. Although much progress has been made over the past decade, we still do not have a complete understanding of this process^[98]. We recently found that in a murine model of intragastric ethanol there was an upregulation of genes associated with endoplasmic reticulum (ER) stress response, including GRP78 and 94, CHOP and SREBP. The expression of these genes was associated with protein misfolding as well as apoptosis and lipid synthesis^[78,79]. Since alcoholism and alcohol-related diseases constitute a severe health problem in the world and ER stress has been linked to Hcy in the pathogenesis of several disorders such as atherosclerosis, Alzheimer's disease, and liver steatosis, we would direct the readers' attention to ethanol-induced alterations in Hcy metabolism.

Alcoholic patients have been shown to have elevated plasma Hcy (average two-fold) which ranged from 10-120 mol/L (normal 5-15 mol/L)^[99-101]. Total folate, B₁₂ and B₆ levels were normal. However, Hcy levels correlated with folate levels and blood alcohol levels. Well nourished alcoholics exhibited markedly lower levels of serum pyridoxal-phosphate (PLP) and mildly lower red cell folate^[102]. Even "social" drinking (30 g/d \times 6 wk) caused 20% increased Hcy and decreased folate^[99,103]. Heavy alcohol consumption is a risk factor for stroke and brain atrophy^[103-105]. Rats fed ethanol exhibited a doubling of plasma Hcy despite normal levels of folate, PLP and B₁₂^[106]. We have observed a 7 fold increase of plasma Hcy levels (22.3 \pm 2.8 μ mol/L *vs* pair-fed control 3.0 \pm 0.9 μ mol/L) in mice fed ethanol intragastrically for 4 wk^[78].

With alcohol feeding of rats intragastrically for 9 wk liver specific MAT1A protein expression did not change, whereas MAT2A increased in conjunction with -40% decreased hepatic levels of methionine and SAM^[107]. However, shorter exposure of rats and minipigs to ethanol was not associated with a decrease in methionine or SAM in most studies. Depending

on route, ethanol dose and duration, variable changes in SAM and SAH have been described^[107-110].

Ethanol feeding has been known to lower MS^[111], leading to increased accumulation of 5-methyl THF and to increased BHMT leading to utilization-induced decreased betaine levels^[111]. These effects depended on increased blood ethanol. Golden Syrian hamsters with high ADH fed a 360 mL/L ethanol diet did not develop increased blood ethanol levels or changes in Hcy metabolism unless ADH was inhibited^[112]. Of note, the SAM levels were maintained by the utilization of betaine. However prolonged ethanol feeding eventually could lead to depletion of SAM. Chronic alcohol could increase choline uptake^[113] and mitochondrial oxidation to betaine^[114] suggesting compensation for increased demand for betaine. Feeding betaine (0.5%) raised SAM levels which was accentuated in alcohol fed animals (minimal to begin with) and prevented fatty liver^[78,108,111]. Raised SAM was initially assumed to contribute to betaine's ameliorative effect on fatty liver. It may be equally important that the protective role of betaine was due to lowering Hcy directly through BHMT and indirectly by raised SAM leading to activation of CBS.

The mechanism of the ethanol induced decrease in MS is not well understood. Kenyon *et al.*^[110] showed that the enzyme was inhibited by high concentrations of acetaldehyde, whereas we have found decreased mRNA. Increase in BHMT activity appeared to be a compensatory phenomenon to maintain methionine and was seen after 2 wk in ethanol fed rats and after 4 wk in ethanol fed mice.

In the chronic (12 mo) ethanol fed micropigs with adequate folate, MS activity decreased by 20% which was associated with slightly decreased serum methionine, 20% increased serum Hcy, and increased hepatic SAH but no change in SAM. These small changes due to ethanol were not associated with increased ALT or fatty liver but were associated with increased scattered apoptosis^[115]. Interestingly addition of folate deficient diet to ethanol feeding of the castrated minipig accentuated plasma Hcy and liver injury^[116] although ER stress was not considered in this study.

Betaine lowered Hcy and prevented ER stress and alcoholic liver injury in alcohol fed mice^[78]. However, we need to be cognizant of other actions of betaine. Feeding rats betaine in drinking water (1.5 g/kg) blunted the TNF response to LPS and decreased concomitant liver injury^[117]. Importantly, however, taurine was equally effective. Earlier work has suggested an indirect protective role of choline supplementation, suggesting choline oxidation to betaine could protect against Kupffer cell activation^[118-120]. It has been suggested that betaine and taurine serve as organic osmolytes which are critical in regulating Kupffer cell function^[121]. Hyperosmotic conditions induce Na⁺ betaine transporter mRNA while hypoosmotic conditions do the opposite, this occurred in Kupffer cells but not hepatocytes. Betaine or taurine protects the liver against warm ischemia-reperfusion. Recently, betaine pretreatment was shown to protect the hepatocyte from bile acid induced apoptosis. The mechanism is not certain and high concentrations of betaine (mmol/L) were required^[122,123]. We observed that increased gene expression of TNF and CD 14 was indicative of the alcohol-induced Kupffer cell activation^[78]. However, betaine treatment did not significantly attenuate these changes, suggesting that betaine either acts downstream of alcohol-induced Kupffer cell activation or acts via an independent pathway.

The effect of SAM feeding is of interest since it was reported to decrease fatty liver and mitochondrial abnormalities^[115]. SAM might be expected to inhibit re-methylation and promote transsulfuration of Hcy. It is unclear as to what the overall effect on Hcy would be. Severe SAM deficiency in MAT1A knockout did not alter Hcy but was associated with increased expression of BHMT and CBS^[124]. SAM could transcriptionally

activate MAT1A and suppress MAT2A^[125].

Overall chronic ethanol exposure seemed to cause a modest decrease in SAM and increase in SAH along with early-decreased MS and late-increased BHMT. All these changes were accompanied with increased Hcy which occurs despite adequate dietary folate, B₁₂, B₆ and choline. Thus there are possible contributions of decreased MS, unknown effects on CBS, and decreased SAM (decreased activation of CBS) leading to HHcy. The decrease in SAM levels was accompanied with increased SAH levels. Since both SAM and SAH activated CBS, it is doubtful that changes in levels of these metabolites exerted a significant regulatory role on transsulfuration^[11,16]. The increase in BHMT appeared insufficient to lower Hcy due to limitation on the availability of betaine and already-impaired cell function. Although high dietary choline might generate sufficient betaine in rodents, the choline oxidase pathway is normally low in primates. Thus, providing excess dietary betaine rather than choline would seem to be an approach more applicable to the human situation. Since betaine corrects hyperhomocysteinemia, fatty liver injury and ER stress, and homocysteine is known to cause all these changes, it is reasonable to state that an important mechanism by which betaine protects against alcoholic liver disease is the correction of hyperhomocysteinemia and proof of this hypothesis requires further work.

POSSIBLE ROLE OF ER STRESS IN OTHER LIVER DISEASES

ER stress may also be involved in liver injury caused by α_1 -antitrypsin (α_1 -AT) deficiency and hepatitis C virus (HCV) or hepatitis B virus (HBV) infection. α_1 -antitrypsin (α_1 -AT) deficiency was caused by a point mutation encoding a substitution of lysine for glutamate-342^[126]. Aggregated mutant α_1 -AT was retained in ER rather than secreted in the blood and body fluids where its function is to inhibit neutrophil proteases. Individuals with this deficiency had a markedly increased risk of developing emphysema by a loss of function mechanism by which reduced levels of α_1 -AT in the lung inhibit connective tissue breakdown by neutrophil elastase, cathepsin G, and proteinase 3. Some individuals with α_1 -AT deficiency developed liver injury and hepatocellular carcinoma by a gain of function mechanism, i.e., accumulation of aggregated mutant α_1 -AT within the ER which is toxic to liver cells. However, the exact mechanism by which ER retention of this aggregated mutant protein leads to cellular injury is still unknown. Recent studies have demonstrated that ER retention of mutant α_1 -AT induces a marked autophagic response in cell culture and transgenic mouse models of α_1 -AT deficiency as well as in the liver of patients with α_1 -AT deficiency^[127]. The autophagic response is a general mechanism whereby cytosol and intracellular organelles, such as ER, are first sequestered from the rest of the cytoplasm within unique vacuoles and then degraded by fusion with lysosomes to clear the cells of senescent constituents. Under a fasting condition, a marked increase in fat accumulation was observed in α_1 -AT-containing globules in the liver of α_1 -AT deficient mice^[128], suggesting a malfunction of ER caused by accumulation of mutant α_1 -AT. Investigations of ER stress markers such as GRP78, CHOP, SREBP, XBP1, and ATF6 are needed to assess the direct involvement of ER stress in α_1 -AT deficiency-induced liver injury.

Evidence of ER stress in HBV or HCV infection is emerging. HBV codes for three forms of surface protein. The minor and large forms are translated from transcripts specified by the preS1 promoter, while the middle and small forms are translated from transcripts specified by the downstream S promoter. Overexpression of the large surface protein of HBV could lead to a 10-fold activation of the S promoter but not of an unrelated promoter^[129]. The large surface protein could also activate the cellular grp78 and grp94 promoters. Neither the

middle nor the small surface protein, nor a secretable form of the large surface protein, could activate the S promoter, but agents that induced endoplasmic reticulum (ER) stress had an effect similar to that of the large surface protein, suggesting that HBV may evolve a feedback mechanism, such that ER stress induced by accumulation of the large surface protein increases the synthesis of the middle and small surface proteins, which in combination with the large surface protein can form mixed, secretable particles. HCV-induced ER stress was more evident. HCV replicates from a ribonucleoprotein (RNP) complex that is associated with ER membrane. The replication activities of the HCV subgenomic replicon have been shown to induce ER stress^[130]. HCV replicons induce the UPR which is paralleled by the proteolytic cleavage of ATF6. The HCV non-structural protein 5A (NS5A) can bind to and inactivate the cellular double-stranded RNA-activated protein kinase, PKR. NS5A has recently been demonstrated to engage ER-nucleus signal transduction pathway^[131]. Expression of NS5A in the ER could induce an ER stress leading to the activation of STAT-3 and NF- κ B, which is sensitive to inhibitors of Ca²⁺ uptake. The NS5A-induced ER stress signaling has also been shown in the context of an HCV subgenomic replicon^[131]. Another HCV component, the HCV envelope protein E2, is an ER-bound protein that contains a region of sequence homology with the PKR and its substrate, the eIF2 α . E2 could modulate global translation by inhibition of the interferon-induced PKR through its PKR-eIF2 α phosphorylation site homology domain (PePHD)^[132]. E2 could also bind to and inhibit PERK^[132]. At low expression levels, E2 induced ER stress, but at high expression levels, E2 inhibited PERK kinase activity *in vitro*. Mammalian cells that stably expressed E2 were refractory to the translation-inhibitory effects of ER stress inducers, and E2 relieved general translation inhibition induced by PERK. The PePHD of E2 was required for the rescue of translation that was inhibited by activated PERK. These findings may explain why the virus promotes persistent infection by overcoming the cellular ER stress response. In addition, HCV-induced ER stress resulted in a decline in protein glycosylation. Decreasing protein glycosylation could disrupt the proper protein folding of MHC class I molecules, preventing the assembly of MHC class I molecules. Cells expressing HCV subgenomic replicons had a lower MHC class I cell surface expression^[133]. HCV-infected cells may thus be undetectable in the immune system by suppressing MHC class I antigen presentation to cytotoxic T lymphocytes. Therefore, the persistence and pathogenesis of HCV may depend upon the ER stress-mediated interference of MHC class I assembly and cell surface expression. Finally, HCV infection may suppress the degradation of misfolded proteins while stimulating the synthesis of its viral proteins in the ER. In the ER, IRE1-XBP1 pathway directs both protein refolding and degradation in response to ER stress. It was demonstrated that XBP1 expression was elevated in cells carrying HCV subgenomic replicons, but XBP1 transactivating activity was repressed^[134]. This prevents the IRE1-XBP1 transcriptional induction of EDEM (ER degradation-enhancing -mannosidase-like protein), which is required for the degradation of misfolded proteins. Consequently, misfolded proteins are stable in cells expressing HCV replicons. Study with a cell line with a defective IRE1-XBP1 pathway showed elevated levels of HCV internal ribosome entry site-mediated translation^[134]. This study indicated that the HCV suppression of misfolded protein degradation in the ER not only promoted HCV expression but also contributed to the persistence of the virus in infected hepatocytes.

HCV infection is common in alcoholic patients presenting with liver disease. Heavy alcohol intake would worsen the outcome of HCV infection^[135-137], which has directed much attention to the interaction between alcohol and HCV infection.

Alcohol plays an important role in HCV infection resulting in increased viral replication, enhanced HCV quasispecies complexity, increased liver-cell death, suppression of immune responses, and iron overload^[138]. However, the pathogenic mechanisms underlying the alcohol-HCV interactions are not fully understood. Based on the above evidence that both HCV and homocysteine could induce endoplasmic reticulum (ER) stress response^[6,78,130] and that there was a link between alcohol-induced significant elevation of homocysteine level, ER stress, and the pathogenesis of liver injury^[78], it is reasonable to hypothesize that a locus of the potentiative interaction between alcohol and HCV in accelerating the progression of liver disease is at the level of ER stress. In the case of both HBV and HCV infection, it is widely recognized that severely immunosuppressed patients may develop a paradoxically severe and rapidly progressive liver disease. This has been seen in the post-OLT setting and in patient with AIDS. Therefore, the loss of immune detection of viral-infected hepatocytes may lead to an unopposed massive overload of hepatocytes with viral proteins triggering ER stress. Future studies should examine the contribution of ER stress to these pathologic conditions.

CONCLUSION

HHcy is an integral component of several disorders including cardiovascular and cerebrovascular diseases, neurodegeneration, liver steatosis, diabetes, and cancer. HHcy can result from deficiencies of vitamin cofactors (B6, B12, folic acid) required for Hcy metabolism and/or from genetic disorders of its metabolism. Hcy unleashes inflammation mediators such as NF κ B, IL-1 β , IL-6, and IL-8. Hcy increases production of intracellular superoxide anion causing oxidative stress. Hcy-induced misfolding or malfunctioning of numerous intracellular proteins are increasingly important and attract much attention because the Hcy-induced ER stress mechanism can explain many processes of cell injury. Animal model creation and integral investigation of available animal models will certainly play important role in determining precisely the biological effects of HHcy. Our observations with the murine intragastric ethanol fed model have suggested a link between Hcy metabolism, ER stress, and the pathogenesis of alcohol induced liver injury. Figure 4 demonstrates our hypothesis in which ethanol feeding causes HHcy which then induces the ER stress response in parenchymal and nonparenchymal cells in the liver leading to fatty liver, apoptosis and possibly inflammation. The potential beneficial effects of lowering Hcy and preventing ER stress in alcoholic humans needs to be studied. In addition, since a minority of alcoholics develop liver disease and a wide range of Hcy levels are seen in alcoholics, it will be important to examine polymorphism of Hcy metabolizing enzymes as potential risk-factors for the development of HHcy and liver disease.

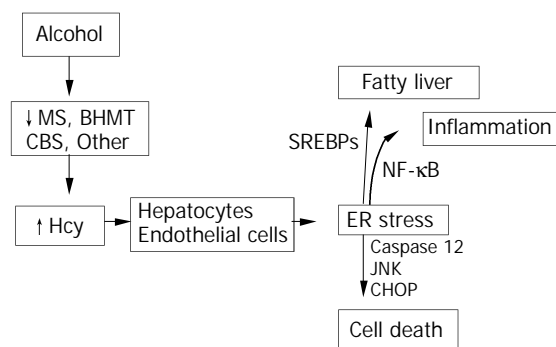


Figure 4 Hypothesis for the role of ethanol-induced HHcy in the pathogenesis of alcoholic liver disease.

REFERENCES

- Carson NAJ**, Neil DW. Metabolic abnormalities detected in a survey of mentally backward individuals in Northern Ireland. *Arch Dis Child* 1962; **37**: 505-513
- Gerritsen T**, Vaughn JG, Weisman HA. The identification of homocysteine in the urine. *Biochem Biophys Res Commun* 1962; **9**: 593-596
- Mudd SH**, Finkelstein JD, Irreverre F, Laster L. Homocystinuria: An Enzymatic Defect. *Science* 1964; **27**: 1443-1445
- Clarke R**, Daly L, Robinson K, Naughten E, Cahalane S, Fowler B, Graham I. Hyperhomocysteinemia: an independent risk factor for vascular disease. *N Engl J Med* 1991; **324**: 1149-1155
- Audelin MC**, Genest J Jr. Homocysteine and cardiovascular disease in diabetes mellitus. *Atherosclerosis* 2001; **159**: 497-511
- Werstuck GH**, Lentz SR, Dayal S, Hossain GS, Sood SK, Shi YY, Zhou J, Maeda N, Krisans SK, Malinow MR, Austin RC. Homocysteine-induced endoplasmic reticulum stress causes dysregulation of the cholesterol and triglyceride biosynthetic pathways. *J Clin Invest* 2001; **107**: 1263-1273
- Schrocksadel K**, Frick B, Wirlleitner B, Winkler C, Schennach H, Fuchs D. Moderate hyperhomocysteinemia and immune activation. *Curr Pharm Biotechnol* 2004; **5**: 107-118
- Herrmann W**, Knapp JP. Hyperhomocysteinemia: a new risk factor for degenerative diseases. *Clin Lab* 2002; **48**: 471-481
- Polidori MC**, Marvardi M, Cherubini A, Senin U, Mecocci P. Heart disease and vascular risk factors in the cognitively impaired elderly: implications for Alzheimer's dementia. *Aging* 2001; **13**: 231-239
- Lawrence de Koning AB**, Werstuck GH, Zhou J, Austin RC. Hyperhomocysteinemia and its role in the development of atherosclerosis. *Clin Biochem* 2003; **36**: 431-441
- Medina M**, Urdiales JL, Amores-Sanchez MI. Roles of homocysteine in cell metabolism: old and new functions. *Eur J Biochem* 2001; **268**: 3871-3882
- Jakubowski H**. Molecular basis of homocysteine toxicity in humans. *Cell Mol Life Sci* 2004; **61**: 470-487
- Jakubowski H**, Zhang L, Bardeguet A, Aviv A. Homocysteine thiolactone and protein homocysteinylation in human endothelial cells: implications for atherosclerosis. *Circulation Research* 2000; **87**: 45-51
- Finkelstein JD**, Martin JJ, Harris BJ. Methionine metabolism in mammals. The methionine-sparing effect of cysteine. *J Biol Chem* 1988; **263**: 11750-11754
- Finkelstein JD**. Pathways and regulation of homocysteine metabolism in mammals. *Semin Thromb Hemost* 2000; **26**: 219-225
- Finkelstein JD**. Homocysteine: a history in progress. *Nutr Rev* 2000; **58**: 193-204
- Finkelstein JD**, Martin JJ. Methionine metabolism in mammals. Distribution of homocysteine between competing pathways. *J Biol Chem* 1984; **259**: 9508-9513
- Mato JM**, Corrales FJ, Lu SC, Avila MA. S-Adenosylmethionine: a control switch that regulates liver function. *Faseb J* 2002; **16**: 15-26
- Bostom AG**, Lathrop L. Hyperhomocysteinemia in end-stage renal disease: prevalence, etiology, and potential relationship to arteriosclerotic outcomes. *Kidney Int* 1997; **52**: 10-20
- van Guldener C**, Stehouwer CD. Homocysteine metabolism in renal disease. *Clin Chem Lab Med* 2003; **41**: 1412-1417
- Mudd SH**, Lev HL, Skovby F. Disorders of transsulfuration. In Scriver CR, Beaudet AL, Sly WS, Valle D. (eds), *The Metabolic Basis of Inherited Disease*. New York: McGraw-Hill 1995: 1279-1327
- Rosenblatt DS**. Inherited disorders of folate transport and metabolism. In Scriver CR, Beaudet AL, Sly WS, Valle D. (eds), *The Metabolic Basis of Inherited Disease*. New York: McGraw-Hill 1995: 3111-3128
- Frosst P**, Blom HJ, Milos R, Goyette P, Sheppard CA, Matthews RG, Boers GJH, den Heijer M, Kluijtmans LAJ, van den Heuvel LP, Rozen RA. A candidate genetic risk factor for vascular disease: a common mutation in methylenetetrahydrofolate reductase. *Nature Genet* 1995; **10**: 111-113
- Ma J**, Stampfer MJ, Hennekens CH, Frosst P, Selhub J, Horsford J, Malinow MR, Willett WC, Rozen R. Methylenetetrahydrofolate reductase polymorphism, plasma folate, homocysteine, and risk of myocardial infarction in US physicians. *Circulation* 1996; **94**: 2410-2416

- 25 **Jacques PF**, Bostom AG, Williams RR, Ellison RC, Eckfeldt JH, Rosenberg IH, Selhub J, Rozen R. Relation between folate status, a common mutation in methylenetetrahydrofolate reductase, and plasma homocysteine concentrations. *Circulation* 1996; **93**: 7-9
- 26 **Jeng YL**, Wu MH, Huang HB, Lin WY, You SL, Chu TY, Chen CJ, Sun CA. The methylenetetrahydrofolate reductase 677C->T polymorphism and lung cancer risk in a Chinese population. *Anticancer Res* 2003; **23**: 5149-5152
- 27 **Woo KS**, Qiao M, Chook P, Poon PY, Chan AK, Lau JT, Fung KP, Woo JL. Homocysteine, endothelial dysfunction, and coronary artery disease: emerging strategy for secondary prevention. *J Card Surg* 2002; **17**: 432-435
- 28 **Mudd SH**, Levy HL, Skovby F. Disorders of transsulfation. In: Scriver CR, Beaudet AL, Sly WS, Valle D, editors. *The Metabolic Basis for Inherited Disease*. New York: McGraw-Hill 1989: 693
- 29 **Kalra DK**. Homocysteine and cardiovascular disease. *Curr Atheroscler Rep* 2004; **6**: 101-106
- 30 **Wilcken DEL**, Dudman NPB. Homocystinuria and atherosclerosis. In: Lusis AJ, Rotter JI, Sparkes RS, editors. *Molecular genetics of coronary artery disease; candidate genes and process in atherosclerosis*. *Monographs in human genetics*. New York: Karger 1992: 311
- 31 **Mudd SH**, Levy HL, Kraus JP. Disorders of transsulfuration. In: Scriver CR, Beaudet AL, Sly WS, Eds. *The Metabolic and Molecular Bases of Inherited Disease*. New York: McGraw-Hill 2001: 2007-2056
- 32 **Ueland PM**, Refsum H. Plasma homocysteine, a risk factor for vascular disease: plasma levels in health, disease, and drug therapy. *J Lab Clin Med* 1989; **114**: 473-501
- 33 **Moat SJ**, Bao L, Fowler B, Bonham JR, Walter JH, Kraus JP. The molecular basis of cystathionine beta-synthase (CBS) deficiency in UK and US patients with homocystinuria. *Hum Mutat* 2004; **23**: 206
- 34 **Haynes WG**. Hyperhomocysteinemia, vascular function and atherosclerosis: effects of vitamins. *Cardiovasc Drugs Ther* 2002; **16**: 391-399
- 35 **Billion S**, Tribut B, Cadet E, Queindec C, Rochette J, Wheatley P, Bataille P. Hyperhomocysteinemia, folate and vitamin B12 in unsupplemented haemodialysis patients: effect of oral therapy with folic acid and vitamin B12. *Nephrol Dial Transplant* 2002; **17**: 455-461
- 36 **Lakshmi AV**, Maniprabha C, Krishna TP. Plasma homocysteine level in relation to folate and vitamin B6 status in apparently normal men. *Asia Pac J Clin Nutr* 2001; **10**: 194-196
- 37 **Cravo ML**, Camilo ME. Hyperhomocysteinemia in chronic alcoholism: relations to folic acid and vitamins B(6) and B(12) status. *Nutrition* 2000; **16**: 296-302
- 38 **Troen AM**, Lutgens E, Smith DE, Rosenberg IH, Selhub J. The atherogenic effect of excess methionine intake. *Proc Natl Acad Sci U S A* 2003; **100**: 15089-15094
- 39 **Noga AA**, Stead LM, Zhao Y, Brosnan ME, Brosnan JT, Vance DE. Plasma homocysteine is regulated by phospholipid methylation. *J Biol Chem* 2003; **278**: 5952-5955
- 40 **Shin OH**, Mar MH, Albright CD, Citarella MT, da Costa KA, Zeisel SH. Methyl-group donors cannot prevent apoptotic death of rat hepatocytes induced by choline-deficiency. *J Cell Biochem* 1997; **64**: 196-208
- 41 **Stead LM**, Au KP, Jacobs RL, Brosnan ME, Brosnan JT. Methylation demand and homocysteine metabolism: effects of dietary provision of creatine and guanidinoacetate. *Am J Physiol Endocrinol Metab* 2001; **281**: E1095-1100
- 42 **Poddar R**, Sivasubramanian N, Dibello PM, Robinson K, Jacobsen D. Homocysteine induces expression and secretion of monocyte chemoattractant protein-1 and interleukin-8 in human aortic endothelial cells: implications for vascular disease. *Circulation* 2001; **103**: 2717-2723
- 43 **Wang G**. Homocysteine stimulates the expression of monocyte chemoattractant protein-1 receptor (CCR2) in human monocytes: possible involvement of oxygen free radicals. *Biochem J* 2001; **357**: 233-240
- 44 **Wang G**, Siow YL. Homocysteine induces monocyte chemoattractant protein-1 expression by activating NF-kappa B in THP-1 macrophages. *Am J Physiol Heart Circ Physiol* 2001; **280**: H2840-2847
- 45 **Collins T**, Cybulsky MI. NF-kappaB: pivotal mediator or innocent bystander in atherogenesis? *J Clin Invest* 2001; **107**: 255-264
- 46 **Hofmann MA**, Lalla E, Lu Y, Gleason MR, Wolf BM, Tanji N, Ferran LJ Jr, Kohl B, Rao V, Kiesel W, Stern DM, Schmidt AM. Hyperhomocysteinemia enhances vascular inflammation and accelerates atherosclerosis in a murine model. *J Clin Invest* 2001; **107**: 675-683
- 47 **Loscalzo J**. The oxidant stress of hyperhomocyst(e)inemia. *J Clin Invest* 1996; **98**: 5-7
- 48 **Tawakol A**, Omland T, Gerhard M, Wu JT, Creager MA. Hyperhomocyst(e)inemia is associated with impaired endothelium-dependent vasodilation in humans. *Circulation* 1997; **95**: 1119-1121
- 49 **Weiss N**, Heydrick S, Zhang YY, Bierl C, Cap A, Loscalzo J. Cellular redox state and endothelial dysfunction in mildly hyperhomocysteinemic cystathionine beta-synthase-deficient mice. *Arterioscler Thromb Vasc Biol* 2002; **22**: 34-41
- 50 **Lang D**, Kredan MB, Moat SJ, Hussain SA, Powell CA, Bellamy MF, Powers HJ, Lewis MJ. Homocysteine-induced inhibition of endothelium-dependent relaxation in rabbit aorta: role for superoxide anions. *Arterioscler Thromb Vasc Biol* 2000; **20**: 422-427
- 51 **Chambers JC**, McGregor A, Jean-Marie J, Mbeid OA, Kooner JS. Demonstration of rapid onset vascular endothelial dysfunction after hyperhomocysteinemia: an effect reversible with vitamin C therapy. *Circulation* 1999; **99**: 1156-1160
- 52 **Stanger O**, Weger M. Interactions of homocysteine, nitric oxide, folate and radicals in the progressively damaged endothelium. *Clin Chem Lab Med* 2003; **41**: 1444-1454
- 53 **Franken DG**, Boers GHJ, Blom HJ, Trijbels FJM, Kloppenborg PW. Treatment of mild hyperhomocysteinemia in vascular disease patients. *Arterioscler Thromb* 1994; **14**: 465-470
- 54 **Mosharov E**, Cranford MR, Banerjee R. The quantitatively important relationship between homocysteine metabolism and glutathione synthesis by the transsulfuration pathway and its regulation by redox changes. *Biochemistry* 2000; **39**: 13005-13011
- 55 **Gryglewski RJ**, Palmer RM, Moncada S. Superoxide anion is involved in the breakdown of endothelium-derived vascular relaxing factor. *Nature* 1986; **320**: 454-456
- 56 **Heinecke JW**, Rosen H, Suzuki LA, Chait A. The role of sulfurcontaining amino acids in superoxide production and modification of low density lipoprotein by arterial smooth muscle cells. *J Biol Chem* 1987; **262**: 10098-10103
- 57 **Upchurch GR**, Welch GN, Fabian AJ, Freedman JE, Johnson JL, Keaney JF Jr, Loscalzo J. Homocyst(e)ine decreases bioavailable nitric oxide by a mechanism involving glutathione peroxidase. *J Biol Chem* 1997; **272**: 17012-17017
- 58 **Outinen PA**, Sood SK, Liaw PC, Sarge KD, Maeda N, Hirsh J, Ribau J, Podor TJ, Weitz JI, Austin RC. Characterization of the stress-inducing effects of homocysteine. *Biochem J* 1998; **332**: 213-221
- 59 **Dayal S**, Brown KL, Weydert CJ, Oberley LW, Arning E, Bottiglieri T, Faraci FM, Lentz SR. Deficiency of glutathione peroxidase-1 sensitizes hyperhomocysteinemic mice to endothelial dysfunction. *Arterioscler Thromb Vasc Biol* 2002; **22**: 1996-2002
- 60 **Yla-Herttuala S**, Palinski W, Rosenfeld ME, Parthasarathy S, Carew TE, Butler S, Witztum JL, Steinberg D. Evidence for the presence of oxidatively modified low density lipoprotein in atherosclerotic lesions of rabbit and man. *J Clin Invest* 1989; **84**: 1086-1095
- 61 **Jakubowski H**. Protein homocysteinylation: possible mechanism underlying pathological consequences of elevated homocysteine levels. *FASEB J* 1999; **13**: 2277-2283
- 62 **Ferretti G**, Bacchetti T, Marotti E, Curatola G. Effect of homocysteinylation on human high-density lipoproteins: a correlation with paraoxonase activity. *Metabolism* 2003; **52**: 146-151
- 63 **Kaufman RJ**. Stress signaling from the lumen of the endoplasmic reticulum: coordination of gene transcriptional and translational controls. *Genes Dev* 1999; **13**: 1211-1233
- 64 **Welihinda AA**, Tirasophon W, Kaufman RJ. The cellular response to protein misfolding in the endoplasmic reticulum. *Gene Expr* 1999; **7**: 293-300
- 65 **Kaufman RJ**, Scheuner D, Schroder M, Shen X, Lee K, Liu CY, Arnold SM. The unfolded protein response in nutrient sensing and differentiation. *Nat Rev Mol Cell Biol* 2002; **3**: 411-421
- 66 **Kaufman RJ**. Orchestrating the unfolded protein response in health and disease. *J Clin Invest* 2002; **110**: 1389-1398
- 67 **Ma Y**, Hendershot LM. The mammalian endoplasmic reticu-

- lum as a sensor for cellular stress. *Cell Stress Chaperones* 2002; **7**: 222-229
- 68 **Shen J**, Chen X, Hendershot L, Prywes R. ER stress regulation of ATF6 localization by dissociation of BiP/GRP78 binding and unmasking of golgi localization signals. *Dev Cell* 2002; **3**: 99-111
- 69 **Liu CY**, Schroder M, Kaufman RJ. Ligand-independent dimerization activates the stress response kinases IRE1 and PERK in the lumen of the endoplasmic reticulum. *J Biol Chem* 2000; **275**: 24881-24885
- 70 **Liu CY**, Wong HN, Schauer JA, Kaufman RJ. The protein kinase/endoribonuclease IRE1a that signals the unfolded protein response has a luminal amino-terminal ligand-independent dimerization domain. *J Biol Chem* 2002; **277**: 18346-18356
- 71 **Rao RV**, Ellerby HM, Bredesen DE. Coupling endoplasmic reticulum stress to the cell death program. *Cell Death Differ* 2004; **11**: 372-380
- 72 **Kaufman RJ**. Regulation of mRNA translation by protein folding in the endoplasmic reticulum. *Trends Biochem Sci* 2004; **29**: 152-158
- 73 **Pahl HL**, Baeuerle PA. The ER-overload response: activation of NF-kappa B. *Trends Biochem Sci* 1997; **22**: 63-67
- 74 **Outinen PA**, Sood SK, Pfeifer SI, Pamidi S, Podor TJ, Li J, Weitz JL, Austin RC. Homocysteine-induced endoplasmic reticulum stress and growth arrest leads to specific changes in gene expression in human vascular endothelial cells. *Blood* 1999; **94**: 959-967
- 75 **Althausen S**, Paschen W. Homocysteine-induced changes in mRNA levels of genes coding for cytoplasmic- and endoplasmic reticulum-resident stress proteins in neuronal cell cultures. *Brain Res Mol Brain Res* 2000; **84**: 32-40
- 76 **Roybal CN**, Yang S, Sun CW, Hurtado D, Vander Jagt DL, Townes TM, Abcouwer SF. Homocysteine increases the expression of VEGF by a mechanism involving endoplasmic reticulum stress and transcription factor ATF4. *J Biol Chem* 2004; **279**: 14844-14852
- 77 **Zhang C**, Cai Y, Adachi MT, Oshiro S, Aso T, Kaufman RJ, Kitajima S. Homocysteine induces programmed cell death in human vascular endothelial cells through activation of the unfolded protein response. *J Biol Chem* 2001; **276**: 35867-35874
- 78 **Ji C**, Kaplowitz N. Betaine decreases hyperhomocysteinemia, endoplasmic reticulum stress, and liver injury in alcohol-fed mice. *Gastroenterology* 2003; **124**: 1488-1499
- 79 **Lluis JM**, Colell A, Garcia-Ruiz C, Kaplowitz N, Fernandez-Checa JC. Acetaldehyde impairs mitochondrial glutathione transport in HepG2 cells through endoplasmic reticulum stress. *Gastroenterology* 2003; **124**: 708-724
- 80 **Agarwala KL**, Kokame K, Kato H, Miyata T. Phosphorylation of RTP, an ER stress-responsive cytoplasmic protein. *Biochem Biophys Res Commun* 2000; **272**: 641-647
- 81 **Kokame K**, Agarwala KL, Kato H, Miyata T. Herp, a new ubiquitin-like membrane protein induced by endoplasmic reticulum stress. *J Biol Chem* 2000; **275**: 32846-32853
- 82 **Dimitrova KR**, DeGroot K, Myers AK, Kim YD. Estrogen and homocysteine. *Cardiovasc Res* 2002; **53**: 577-588
- 83 **Wang XZ**, Lawson B, Brewer JW, Zinszner H, Sanjay A, Mi LJ, Boorstein R, Kreibich G, Hendershot LM, Ron D. Signals from the stressed endoplasmic reticulum induce C/EBP-homologous protein(CHOP/GADD153). *Mol Cell Biol* 1996; **16**: 4273-4280
- 84 **Cai Y**, Zhang C, Nawa T, Aso T, Tanaka M, Oshiro S, Ichijo H, Kitajima S. Homocysteine-responsive ATF3 gene expression in human vascular endothelial cells: activation of c-Jun NH(2)-terminal kinase and promoter response element. *Blood* 2000; **96**: 2140-2148
- 85 **Zhang C**, Kawauchi J, Adachi MT, Hashimoto Y, Oshiro S, Aso T, Kitajima S. Activation of JNK and transcriptional repressor ATF3/LRF1 through the IRE1/TRAF2 pathway is implicated in human vascular endothelial cell death by homocysteine. *Biochem Biophys Res Commun* 2001; **289**: 718-724
- 86 **Urano F**, Wang X, Bertolotti A, Zhang Y, Chung P, Harding HP, Ron D. Coupling of stress in the ER to activation of JNK protein kinases by transmembrane protein kinase IRE1. *Science* 2000; **287**: 664-666
- 87 **Chen YR**, Meyer CF, Tan TH. Persistent activation of c-Jun N-terminal kinase 1 (JNK1) in gamma radiation-induced apoptosis. *J Biol Chem* 1996; **271**: 631-634
- 88 **Watanabe M**, Osada J, Aratani Y, Kluckman K, Reddick R, Malinow MR, Maeda N. Mice deficient in cystathionine beta-synthase: animal models for mild and severe homocyst(e)inemia. *Proc Natl Acad Sci U S A* 1995; **92**: 1585-1589
- 89 **Lentz SR**, Erger RA, Dayal S, Maeda N, Malinow MR, Heistad DD, Faraci FM. Folate dependence of hyperhomocysteinemia and vascular dysfunction in cystathionine beta-synthase-deficient mice. *Am J Physiol Heart Circ Physiol* 2000; **279**: H970-975
- 90 **Lentz SR**, Piegors DJ, Malinow RM, Heistad DD. Supplementation of atherogenic diet with B vitamins does not prevent atherosclerosis or vascular dysfunction in monkeys. *Circulation* 2001; **103**: 1006-1011
- 91 **Dayal S**, Bottiglieri T, Arning E, Maeda N, Malinow MR, Sigmund CD, Heistad DD, Faraci FM, Lentz SR. Endothelial dysfunction and elevation of S-adenosylhomocysteine in cystathionine beta-synthase-deficient mice. *Circ Res* 2001; **88**: 1203-1209
- 92 **Eberhardt RT**, Forgione MA, Cap A, Leopold JA, Rudd MA, Trolliet M, Heydrick S, Stark R, Klings ES, Moldovan NI, Yaghoubi M, Goldschmidt-Clermont PJ, Farber HW, Cohen R, Loscalzo J. Endothelial dysfunction in a murine model of mild hyperhomocyst(e)inemia. *J Clin Invest* 2000; **106**: 483-491
- 93 **Weiss N**, Heydrick S, Zhang YY, Bierl C, Cap A, Loscalzo J. Cellular redox state and endothelial dysfunction in mildly hyperhomocysteinemic cystathionine beta-synthase-deficient mice. *Arterioscler Thromb Vasc Biol* 2002; **22**: 34-41
- 94 **Robert K**, Chasse JF, Santiard-Baron D, Vayssettes C, Chabli A, Aupetit J, Maeda N, Kamoun P, London J, Janel N. Altered gene expression in liver from a murine model of hyperhomocysteinemia. *J Biol Chem* 2003; **278**: 31504-31511
- 95 **Chen Z**, Karaplis AC, Ackerman SL, Pogribny IP, Melnyk S, Lussier-Cacan S, Chen MF, Pai A, John SW, Smith RS, Bottiglieri T, Bagley P, Selhub J, Rudnicki MA, James SJ, Rozen R. Mice deficient in methylenetetrahydrofolate reductase exhibit hyperhomocysteinemia and decreased methylation capacity, with neuropathology and aortic lipid deposition. *Hum Mol Genet* 2001; **10**: 433-443
- 96 **Schwahn BC**, Chen Z, Laryea MD, Wendel U, Lussier-Cacan S, Genest J Jr, Mar MH, Zeisel SH, Castro C, Garrow T, Rozen R. Homocysteine-betaine interactions in a murine model of 5,10-methylenetetrahydrofolate reductase deficiency. *FASEB J* 2003; **17**: 512-514
- 97 **Swanson DA**, Liu ML, Baker PJ, Garrett L, Stitzel M, Wu J, Harris M, Banerjee R, Shane B, Brody LC. Targeted disruption of the methionine synthase gene in mice. *Mol Cell Biol* 2001; **21**: 1058-1065
- 98 **Tsukamoto H**, Lu SC. Current concepts in the pathogenesis of alcoholic liver injury. *FASEB J* 2001; **15**: 1335-1349
- 99 **Bleich S**, Bleich K, Kropp S, Bittermann HJ, Degner D, Sperling W, Ruther E, Kornhuber J. Moderate alcohol consumption in social drinkers raises plasma homocysteine levels: a contradiction to the 'French Paradox'? *Alcohol Alcohol* 2001; **36**: 189-192
- 100 **Stickel F**, Choi SW, Kim YI, Bagley PJ, Seitz HK, Russell RM, Selhub J, Mason JB. Effect of chronic alcohol consumption on total plasma homocysteine level in rats. *Alcohol Clin Exp Res* 2000; **24**: 259-264
- 101 **Carmel R**, James SJ. Alcohol abuse: an important cause of severe hyperhomocysteinemia. *Nutr Rev* 2002; **60**: 215-221
- 102 **Cravo ML**, Camilo ME. Hyperhomocysteinemia in chronic alcoholism: relations to folic acid and vitamins B(6) and B(12) status. *Nutrition* 2000; **16**: 296-302
- 103 **Bleich S**, Bandelow B, Javaheripour K, Muller A, Degner D, Wilhelm J, Havemann-Reinecke U, Sperling W, Ruther E, Kornhuber J. Hyperhomocysteinemia as a new risk factor for brain shrinkage in patients with alcoholism. *Neurosci Lett* 2003; **335**: 179-182
- 104 **Reynolds K**, Lewis B, Nolen JD, Kinney GL, Sathya B, He J. Alcohol consumption and risk of stroke: a meta-analysis. *JAMA* 2003; **289**: 579-588
- 105 **Bleich S**, Kornhuber J. Relationship between plasma homocysteine levels and brain atrophy in healthy elderly individuals. *Neurology* 2003; **60**: 1220
- 106 **Stickel F**, Choi SW, Kim YI, Bagley PJ, Seitz HK, Russell RM, Selhub J, Mason JB. Effect of chronic alcohol consumption on total plasma homocysteine level in rats. *Alcohol Clin Exp Res* 2000; **24**: 259-264

- 107 **Lu SC**, Huang ZZ, Yang H, Mato JM, Avila MA, Tsukamoto H. Changes in methionine adenosyltransferase and S-adenosylmethionine homeostasis in alcoholic rat liver. *Am J Physiol Gastrointest Liver Physiol* 2000; **279**: G178-185
- 108 **Barak AJ**, Beckenhauer HC, Junnila M, Tuma DJ. Dietary betaine promotes generation of hepatic S-adenosylmethionine and protects the liver from ethanol-induced fatty infiltration. *Alcohol Clin Exp Res* 1993; **17**: 552-555
- 109 **Trimble KC**, Molloy AM, Scott JM, Weir DG. The effect of ethanol on one-carbon metabolism: increased methionine catabolism and lipotrope methyl-group wastage. *Hepatology* 1993; **18**: 984-989
- 110 **Kenyon SH**, Nicolaou A, Gibbons WA. The effect of ethanol and its metabolites upon methionine synthase activity *in vitro*. *Alcohol* 1998; **15**: 305-309
- 111 **Barak AJ**, Beckenhauer HC, Tuma DJ. Betaine, ethanol, and the liver: a review. *Alcohol* 1996; **13**: 395-398
- 112 **Barak AJ**, Beckenhauer HC, Tuma DJ. Hepatic transmethylation and blood alcohol levels. *Alcohol Alcohol* 1991; **26**: 125-128
- 113 **Tuma DJ**, Keefer RC, Beckenhauer HC, Barak AJ. Effect of ethanol on uptake of choline by the isolated perfused rat liver. *Biochim Biophys Acta* 1970; **218**: 141-147
- 114 **Thompson JA**, Reitz RC. Studies of the acute and chronic effects of ethanol ingestion on choline oxidation. *Ann N Y Acad Sci* 1976; **273**: 194-204
- 115 **Halsted CH**, Villanueva J, Chandler CJ, Stabler SP, Allen RH, Muskhelishvili L, James SJ, Poirier L. Ethanol feeding of micropigs alters methionine metabolism and increases hepatocellular apoptosis and proliferation. *Hepatology* 1996; **23**: 497-505
- 116 **Halsted CH**, Villanueva JA, Devlin AM, Niemela O, Parkkila S, Garrow TA, Wallock LM, Shigenaga MK, Melnyk S, James SJ. Folate deficiency disturbs hepatic methionine metabolism and promotes liver injury in the ethanol-fed micropig. *Proc Natl Acad Sci U S A* 2002; **99**: 10072-10077
- 117 **Kim SK**, Kim YC. Attenuation of bacterial lipopolysaccharide-induced hepatotoxicity by betaine or taurine in rats. *Food Chem Toxicol* 2002; **40**: 545-549
- 118 **Rose ML**, Rivera CA, Bradford BU, Graves LM, Cattley RC, Schoonhoven R, Swenberg JA, Thurman RG. Kupffer cell oxidant production is central to the mechanism of peroxisome proliferators. *Carcinogenesis* 1999; **20**: 27-33
- 119 **Rivera CA**, Bradford BU, Seabra V, Thurman RG. Role of endotoxin in the hypermetabolic state after acute ethanol exposure. *Am J Physiol* 1998; **275**: G1252-1258
- 120 **Rivera CA**, Wheeler MD, Enomoto N, Thurman RG. A choline-rich diet improves survival in a rat model of endotoxin shock. *Am J Physiol* 1998; **275**: G862-867
- 121 **Zhang F**, Warskulat U, Wettstein M, Haussinger D. Identification of betaine as an osmolyte in rat liver macrophages (Kupffer cells). *Gastroenterology* 1996; **110**: 1543-1552
- 122 **Graf D**, Kurz AK, Reinehr R, Flischer R, Kircheis G, Haussinger D. Prevention of bile acid-induced apoptosis by betaine in rat liver. *Hepatology* 2002; **36**: 829-839
- 123 **Lieber CS**, Casini A, DeCarli LM, Kim CI, Lowe N, Sasaki R, Leo MA. S-adenosyl-L-methionine attenuates alcohol-induced liver injury in the baboon. *Hepatology* 1990; **11**: 165-172
- 124 **Lu SC**, Alvarez L, Huang ZZ, Chen L, An W, Corrales FJ, Avila MA, Kanel G, Mato JM. Methionine adenosyltransferase 1A knockout mice are predisposed to liver injury and exhibit increased expression of genes involved in proliferation. *Proc Natl Acad Sci U S A* 2001; **98**: 5560-5565
- 125 **Garcia-Trevijano ER**, Latasa MU, Carretero MV, Berasain C, Mato JM, Avila MA. S-adenosylmethionine regulates MAT1A and MAT2A gene expression in cultured rat hepatocytes: a new role for S-adenosylmethionine in the maintenance of the differentiated status of the liver. *Faseb J* 2000; **14**: 2511-2518
- 126 **Teckman JH**, Qu D, Perlmutter DH. Molecular pathogenesis of liver disease in alpha1-antitrypsin deficiency. *Hepatology* 1996; **24**: 1504-1516
- 127 **Perlmutter DH**. Liver injury in alpha1-antitrypsin deficiency: an aggregated protein induces mitochondrial injury. *J Clin Invest* 2002; **110**: 1579-1583
- 128 **Teckman JH**, An JK, Loethen S, Perlmutter DH. Fasting in alpha1-antitrypsin deficient liver: constitutive activation of autophagy. *Am J Physiol Gastrointest Liver Physiol* 2002; **283**: G1156-1165
- 129 **Xu Z**, Jensen G, Yen TS. Activation of hepatitis B virus S promoter by the viral large surface protein via induction of stress in the endoplasmic reticulum. *J Virol* 1997; **71**: 7387-7392
- 130 **Tardif KD**, Mori K, Siddiqui A. Hepatitis C virus subgenomic replicons induce endoplasmic reticulum stress activating an intracellular signaling pathway. *J Virol* 2002; **76**: 7453-7459
- 131 **Waris G**, Tardif KD, Siddiqui A. Endoplasmic reticulum (ER) stress: hepatitis C virus induces an ER-nucleus signal transduction pathway and activates NF-kappaB and STAT-3. *Biochem Pharmacol* 2002; **64**: 1425-1430
- 132 **Pavio N**, Romano PR, Graczyk TM, Feinstone SM, Taylor DR. Protein synthesis and endoplasmic reticulum stress can be modulated by the hepatitis C virus envelope protein E2 through the eukaryotic initiation factor 2alpha kinase PERK. *J Virol* 2003; **77**: 3578-3585
- 133 **Tardif KD**, Siddiqui A. Cell surface expression of major histocompatibility complex class I molecules is reduced in hepatitis C virus subgenomic replicon-expressing cells. *J Virol* 2003; **77**: 11644-11650
- 134 **Tardif KD**, Mori K, Kaufman RJ, Siddiqui A. Hepatitis C virus suppresses the IRE1-XBP1 pathway of the unfolded protein response. *J Biol Chem* 2004; **279**: 17158-17164
- 135 **Lieber CS**. Hepatitis C and alcohol. *J Clin Gastroenterol* 2003; **36**: 100-102
- 136 **Szabo G**. Pathogenic interactions between alcohol and hepatitis C. *Curr Gastroenterol Rep* 2003; **5**: 86-92
- 137 **Peters MG**, Terrault NA. Alcohol use and hepatitis C. *Hepatology* 2002; **36**: S220-225
- 138 **Bhattacharya R**, Shuhart MC. Hepatitis C and Alcohol. *J Clin Gastroenterol* 2003; **36**: 242-252

Edited by Wang XL and Xu XQ Proofread by Xu FM

Review of cytokine profiles in patients with hepatitis

Qiao-Ling Sun, Wei Ran

Qiao-Ling Sun, The Department of Biotechnological Pharmaceutics, Taishan Medical University, Tai'an 271000, Shangdong Province, China

Wei Ran, Basic Medical Research Institute, Taishan Medical University, Tai'an 271000, Shangdong Province, China

Correspondence to: Qiao-Ling Sun, The Department of Biotechnological Pharmaceutics, Taishan Medical University, Tai'an 271000, Shangdong Province, China. sunsunpublic@sina.com

Telephone: +86-538-6222435

Received: 2003-09-18 **Accepted:** 2003-10-12

Abstract

The development of T helper 1 versus T helper 2 cells is a major branch point in the immune response and is an important determinant of the body's response to an infectious pathogen, leading to protection of the host or dissemination of the disease. Recent studies have shown that there exist macrophage activation states in parallel to the T helper cell type 1/2 paradigm, and the T helper 1 development process is governed to a great degree by cytokine IL-12 provided mainly by antigen presenting cells such as macrophages and dendritic cells. A model in patients with hepatitis is proposed that links the pathogen, macrophage activation and T helper cell polarization.

Sun QL, Ran W. Review of cytokine profiles in patients with hepatitis. *World J Gastroenterol* 2004; 10(12): 1709-1715
<http://www.wjgnet.com/1007-9327/10/1709.asp>

INTRODUCTION

The immune response that occurs during infectious disease is characterized by plasticity in both its nature and its magnitude. This feature provides an important advantage that permits the immune system to tailor its defense strategy to particular groups of infectious pathogens. Interactions between CD4+ T helper (Th) lymphocytes and antigen-presenting-macrophage cells in liver shape and amplify the subsequent immune response. The Th precursors differentiate into 2 subsets of effector Th cells with different functions^[1,2]. Th1 cells produce IFN- γ , IL-2 and Th2 cells produce IL-4, IL-10 and IL-13. The ensuing Th1- and Th2-type immune responses include both potent humoral and cell-mediated components. Th1-derived IFN- γ suppresses Th2 response and Th2-derived IL-10 inhibits the development of Th1 populations^[3]. In addition, the effector cells and antibody isotypes involved are quite distinct^[4]. Th1 cells are responsible for activation of macrophages to a microbicidal state, induction of IgG2a Abs that mediate phagocytosis, and support of CD8+ antiviral effector T cells. By contrast, Th2 cells stimulate the growth and differentiation of mast cells and eosinophils, as well as the production of Ab isotypes, including IgE and IgG4, which can mediate the activation of these cells. IL-12, a cytokine elaborated mainly by macrophages/monocytes, induces the maturation of Th1 cells. An imbalance of Th1 and Th2 appears to be important in the pathogenesis of chronic viral and nonviral infections in humans, such as infection with human immunodeficiency virus, leprosy, leishmaniasis^[5-7], and viral hepatitis^[8].

Recent studies have shown macrophage activation states in parallel to the Th cell type 1/2 paradigm. IFN- γ has long been known as the classical macrophage activating factor inducing cytokine secretion by macrophages to support Th1-driven immune responses. IL-4 which was historically regarded as macrophage deactivators is now thought to induce alternative immunological activation of macrophages^[9], in that it enhances of the capacity of macrophages for endocytosis and antigen presentation by the induction of mannose receptor expression^[10]. In normal immunological process, classical and alternative macrophage activation maintains the balance of macrophage.

IMBALANCE OF Th1/Th2

Th1 and Th2 type cytokines in patients with hepatitis

Chronic hepatitis is characterized by incomplete clearance of virus and damage hepatocytes. Since hepatitis B virus (HBV) is known to have no cytopathic effect on the infected hepatocytes, cell-mediated immunity is thought to play an important role in the pathogenesis of hepatocellular damage and HBV clearance^[11]. Although immune evading mechanisms used by HBV are largely unknown, defects in T cell response have been suspected as a major factor involved in the pathogenesis of chronic hepatitis^[11-15]. Different from acute self-limited hepatitis in which protective immunity develops after elimination of HBV, immune response fails to remove HBV-infected hepatocytes in chronic hepatitis B. Th1 type pattern of secreted immunity can be considered as an appropriate response of the immune system to inhibit viral replication and HBV eradication. Mechanisms by which IFN- γ favors the elimination of HBV may include enhancement of cytotoxic T lymphocyte (CTL) activation, direct anti-viral activity, increased expression of major histocompatibility complex class I molecules on infected cells, and activation of macrophages^[16-18]. It has been shown in a transgenic mouse model that adoptive transfer of CTLs producing IFN- γ could inhibit HBV replication without cytolysis^[19].

Studies have shown^[18] that predominant Th1 (IFN- γ) cytokine profile of hepatitis B core Ag (HbcAg)-specific and hepatitis B surface Ag (HbsAg)-reactive T cells is associated with acute self-limited hepatitis B. In most patients with acute hepatitis, CTL responses to epitopes of HBsAg, while there are no such responses in patients with chronic hepatitis^[20]. Thus, Th1 might be insufficient for complete removal of HBV in chronic hepatitis and positively correlated with hepatic inflammatory activity.

Meanwhile, Barnaba *et al.* cloned CD4+ HBV envelope antigen (HbeAg)-reactive T cells and showed signs of cytotoxicity only when they produced IFN- γ ^[21]. This is in agreement with findings that production of IFN- γ ^[22] by peripheral blood mononuclear cells (PBMCs) upon HBsAg stimulation was associated with higher level of hepatocyte damage. The dissociation between the mechanisms responsible for the immune-mediated hepatocytolysis, and for viral clearance in HBV infection was proposed^[23]. It has been demonstrated that the interaction between Ag-specific CTL and target hepatocytes results in spotty necrosis which is limited to a very few hepatocytes^[24]. Instead, the antiviral effect is mediated by IFN- γ , IL-2, and TNF- α released by HBV-specific CTLs or by antigen nonspecific macrophages, and these

cytokines profoundly suppress HBV gene expression in infected hepatocytes by noncytolytic mechanisms^[25] through eliminating HBV nucleocapsid particles and destabilizing the viral RNA^[26]. Thus, after recognition of HBV antigens on the surface of infected hepatocytes, CTLs perform two distinct functions; they kill a small fraction of infected hepatocytes and secrete IFN- γ and TNF- α , which exert antiviral effects without destruction of hepatocytes. Effective clearance of duck HBV and woodchuck hepatitis virus has also been shown to occur without massive hepatocellular necrosis^[27].

In addition, a cytokine balance favoring Th2 type cytokine production such as IL-4 and IL-10 has been associated with progressive virus infections. Co-activation of Th3 cells with Th2 cells can negatively regulate immune responses and may be associated with the immune tolerant state of chronic HBV infection^[28]. The shift from Th1 to Th2 or Th0 profiles was observed in acquired immune deficiency syndrome^[29]. Result also indicates the existence of a Th2 type response to HBsAg in chronic hepatitis B patients with more severe liver damage^[30]. Th2 cells may be associated with the persistence of HBV infection^[31]. Probably the virus can mutate effectively and evade T-cell immune defense mechanisms. Persistent infection upsets the balance between immunostimulatory and inhibitory cytokines which can prolong inflammation and lead to necrosis, fibrosis, and chronic liver disease^[32].

In chronic hepatitis C virus (HCV) infection, Fan *et al.* observed that the elevated levels of Th2 cytokines were greater than Th1 cytokines measured by ELISA^[33]. This result is in agreement with Kobayashi *et al.* who showed a significant increase in number of IL-4-producing Th2 cells and a significant decrease in number of IFN- γ -producing Th1 cells (PBMC stimulated by anti-CD3 antibody)^[34]. They^[34] suggested that, theoretically, stimulation with anti-CD3 antibody results in the expansion of T lymphocytes, whereas stimulation with HCV core protein results in the expansion of T lymphocytes responsive to HCV core antigen. The stimulation of PBMC with anti-CD3 antibody could reflect the patient's real situation better than that with HCV core protein. In addition, they measured the IFN- γ after the depletion of CD8+ T cells—one of the major sources of IFN- γ production. This could explain that the increased production of IFN- γ (Th1) shown in others studies were due to IFN- γ secretion by CD8+ T lymphocytes.

However, Iwata *et al.* found that in patients with chronic hepatitis C there was the increasing production of IFN- γ (Th1) by PBMC after stimulation with HCV core protein^[35]. Bergamini *et al.* obtained the similar result that the percentage of Th1 cells was significantly increased in CD4+, CD8+, 'naive' - CD45RA+ and 'memory' - CD45RO+ T-cell subsets (PBMC by mitogen-stimulation) from patients versus controls^[36], and Sobue *et al.*^[37] also found that a shift to Th1 cytokine profile correlated with the progress of liver damage, which could be related to the higher proportion of CD4+ T cells. Although in chronic hepatitis C infection, the levels of mononuclear cells derived from peripheral blood reflected the level of mononuclear cells derived from liver, the profile of Th1/Th2 in liver tissue and in peripheral blood was different^[37]. In liver tissue, a predominance of Th1-type cytokines was seen in CD4+ T cells^[38], while a predominance of Th1 type cytokines was observed in CD8+ cells in peripheral blood. Thus, the elevated cytokine production may also have been caused by a higher proportion of CD4+ T cells in the liver tissue of patients with chronic HCV infection compared with that in healthy controls, and intrahepatic CD4+ T cells may be more important than CD8+ T cells in the pathogenesis of liver damage in chronic hepatitis C infection. In addition, the percentage of CD4+ T cells in liver correlated with the histological activity of hepatitis^[38,39]. These results may indicate a preferential compartmentalization of Th1 cytokine-producing CD4+ T cells in the liver^[40], suggesting that

some liver-derived CD4+ T cells had a direct cytotoxic effect^[41,21]. Meanwhile cytokines produced may inhibit viral replication, such as IFN- γ and TNF- α ^[26].

The probable mechanism of Th1 predominance in HCV infection is that in order to eliminate HCV and inhibit viral replication, the compartmentalized CD4+ T cells may shift to a Th1 profile and induce nonspecific immune responses to activate nonspecific immune cells and effector molecules, resulting in liver cell damage. Nevertheless, further studies are needed to investigate the significance of CD4+ T cells in liver tissue.

But the different result was observed regarding Th1 or Th2 predominance in patients with chronic hepatitis C, which was probably due to the administration of PBMC and the measurement for Th1 cytokines from CD4+ T, or both CD4+ and CD8+ T cells. It is also possible that the HCV-related antigen influences T helper cells to produce a different cytokine profile from that in healthy subjects. For example, in transgenic mice with HBeAg, the T cell response against peptide 120-31 of HBeAg was predominantly Th1, whereas the response against peptide 129-40 was predominantly Th2-like^[42]. Moreover, escaping variants of HCV epitope attenuate or fail to stimulate T-cell proliferation, which is accompanied by a shift in cytokine secretion patterns from one characteristic of a Th1 antiviral responses to a Th2 form^[43]. Recent evidence suggests that the polymorphic nature of the MHC binding sites and differences in the T-cell repertoire among persons lead to highly variable binding affinity for the immunodominant HBV peptides, which in turn determines the outcome after acute HBV infection^[44,45].

The role of IL-12 in hepatitis disease

IL-12, a heterodimer composed of 2 subunits of p40 and p35 and secreted mainly by antigen-presenting cells (APC) such as activated macrophages and dendritic cells (DCs), is a crucial mediator between innate and adaptive immune responses. The transcriptional factor T-bet, which can induce transcription of an IFN- γ reporter gene and is specifically expressed in Th1 cells generated in the presence of IL-12^[46], suppresses the expression of genes encoding IL-4, IL-5 and induces the synthesis of IFN- γ . These studies suggest that Th1 development process is governed by cytokine IL-12 to a great degree.

IL-12 is a key cytokine not only promoting Th1-synergizing with IL-2, IL-12 induces rapid and efficient production of IFN- γ ^[47] by stimulation of the TCR-CD3 complex and activation of the CD28 receptor, but also maintaining Th1 responses^[48] (Figure 1), in that Th-cell differentiation is determined most probably early after infection by the balance between IL-12 and IL-10, IL-4, which favour Th1- and Th2-cell development, respectively. In addition, IL-12 correlates with virus clearance. In HBV-infected patients, a significant increase in IL-12 production was observed only in patients who cleared the virus. The peak of serum IL-12 associated with Th1 cytokines (IFN- γ) occurred after the ALT flare and preceded or coincided with the time of HBe seroconversion^[8]. Thus, the findings in patients with chronic HBV infection support a proposed combination strategy for therapy with IL-12 plus vaccination^[49,50]. After the ALT flare, the occurrence of IL-12 peak would be the reason that hepatocellular necrosis induced by CTL leads to the recruitment of macrophages and noncommitted T helper cells in the liver. Then the native particles of HBeAg are released from damaged hepatocytes and provide potent antigenic stimulation for these cells. In patients who are able to respond with an increase in IL-12 production, this will promote Th1 cell development and stimulate the production of IFN- γ and TNF- α , which will exert their noncytolytic antiviral effects.

IL-12 may be instrumental in the defense mechanism against HBV infection, and the elevation of its level can be indicative of hepatitis recovery^[51]. The enhancing effect of IL-12 on IFN- γ production of PBMC in patients with chronic hepatitis B virus

infection is increased during IFN- α treatment. Therefore, IFN- α and IL-12 may enhance the efficacy for the treatment of chronic HBV infection^[52], and HCV-related cellular immune defect in patients with hepatitis C can be restored in most patients by IL-12^[53]. However, Quiroga *et al.*^[54] found that HCV-infected patients with greater necro-inflammatory activity of liver showed greater IL-12 production by PBMC than those with minimal or mild activity and normal donors. Massive induction of the proinflammatory cytokines IL-12 and IFN- γ in liver specimens is apparently not counterbalanced by the anti-inflammatory cytokine IL-10, which may play an important role in promoting inflammatory reactions leading to massive liver damage in murine models of fulminant hepatitis B^[55].

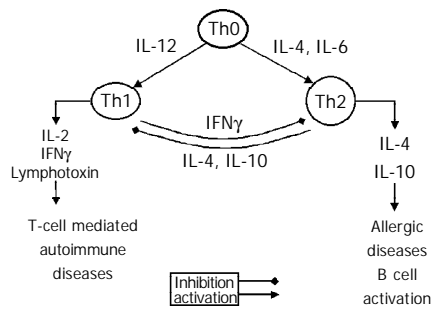


Figure 1 Development of Th1/Th2 From Marc and Weeber.

BLANCE OF MACROPHAGE IN PATIENTS WITH HEPATITIS

Macrophage and macrophage activation

Macrophages can be segregated into two broad groups: resident tissue macrophages and inflammatory macrophages. Tissue macrophages are heterogeneous, and those isolated from different anatomical sites differ in function presumably because of adaptive responses to the local micro-environment^[56]. Inflammatory macrophages are derived largely from circulating monocytes, which infiltrate damaged tissue, but some arise by local cell division^[57]. There is now increasing evidence for the heterogeneity of macrophages that have infiltrated inflamed or otherwise damaged tissue, depending on the type and severity of injury, the stage of its evolution and the localization of the macrophages within the tissue^[58].

One major function of macrophages is to provide a defense line against microbial invasion and to recognize and kill tumor cells. Macrophages can accomplish this in a direct manner, involving the release of products such as oxygen radicals and tumor necrosis factor that are harmful to microorganisms or cancer cells. On the other hand, they play an indirect role in these anti-microbial or anti-tumor activities by secretion of cytokines or by antigen processing and presentation, thereby regulating the immune system^[59].

The macrophage presents HBV-derived proteins which activates CD4+T cells. The effects of stimulation on macrophages include increased cytokine production (TNF- α , IFN- γ , IL-1), expression of inducible nitric oxide synthase, nitric oxide secretion, and up-regulation of adhesion molecules. All these processes can lead, directly or indirectly, to increased cytotoxicity of the macrophages. We also found the higher expression level of granulate and activation-linked surface antigen CD69 by CD14 macrophage from peripheral blood in patients with chronic hepatitis than in controls^[60]. This activity was associated with high level transcription of IL-1, IL-6 and TNF- α (unpublished data). Probably, plasma HBV antigens activate macrophages from peripheral blood. Subsequently, such cytokines are produced. In addition, the increasing number of macrophage functions and heterogeneity *in vitro* and *in vivo* has led to the definition of macrophage activation states

in parallel to the Th 1/2 paradigm. IFN- γ has long been known as the classical macrophage activating factor inducing cytokine secretion by macrophages supporting Th1-driven immune responses. IL-4 which was historically regarded as macrophage deactivators is now thought to induce alternative immunological activation of macrophages^[9], in that it enhances of the capacity of macrophages for endocytosis and antigen presentation by the induction of mannose receptor expression^[10]. In normal immunological process, classical and alternative macrophage activation maintains the balance of macrophage.

Balanced macrophage activation hypothesis

Figure 2 shows a macrophage activation cycle wherein multiple steps occur during various forms of activation and recycling of macrophage function so as to achieve balanced macrophage activation (Steps 1-5)^[61]. When hepatitis virus invades the body, tissue-resident macrophages undergo local activation and engulf the virus or antigen and enhanced recruitment of monocytes and precursors from bone-marrow pools results in the accumulation of tissue macrophages that have enhanced turnover and an altered phenotype^[62]. After the antigen presentation, Th cells are activated through MHC class II. Th1 (stand for active Th) cell produces IL-2 and IFN- γ and Th2 (stand for inhibitor T) cell secretes IL-4 and IL-10, which is involved in B cell activation as well as providing signals for balanced macrophage activation. Production of IL-4 is known to activate the alternative macrophage activation pathway^[10] (step 5). Although IL-4 induces mannose receptor expression and enhance the capacity of macrophages for endocytosis and antigen presentation^[62], alternative pathway activated macrophages *in vitro* actively inhibit mitogen-induced proliferation of peripheral blood lymphocytes^[63] and CD4+T cells^[64-66]. These findings convincingly confirm that alternative activation generates immunosuppressive macrophage populations. In fact, co-induction of IL-10 with IL-4 secreted by Th2 cells, mainly contributes to the inhibition effect. The net result of excess IL-10 production shuts off the Th1 activation pathway^[61]. Therefore, the balance of macrophage and these cytokines are closely related to viral infectious diseases such as AIDS and viral hepatitis.

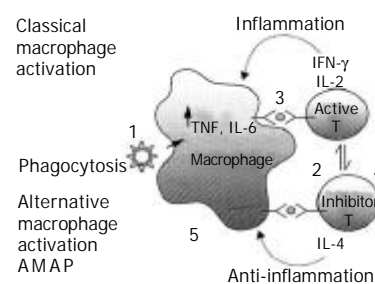


Figure 2 Blanced macrophage activation cycles From Michael^[61].

Macrophages may contribute either directly or indirectly to the hepatonecrosis with fulminant virus infection^[67] through classical macrophage pathway. Macrophages in the liver called Kupffer cells activate Th1 (IFN- γ), IFN- γ will activate Kupffer cells^[68,69]. This results in Kupffer overactivation, which in turn promotes cytokines production (TNF- α , IFN- γ), expression of inducible NOS (iNOS), nitric oxide (NO) secretion. All these processes can lead, directly or indirectly, to increased cytotoxicity of the macrophages-this is the classical macrophage activation pathway.

IL-12 is a cytokine secreted by APCs such as activated macrophages and DCs^[70]. It has an important role against intracellular pathogens by promoting Th1 cell development, cell mediated cytotoxicity and IFN- γ production^[71,72]. For

example, a significant increase in IL-12 production was observed only in patients with chronic hepatitis C who cleared the virus^[73]. On the one hand, IFN- γ , activating macrophage and TNF- α secreted by macrophage, exert their noncytolytic antiviral effects. On the other hand, macrophage kills small fraction of infected hepatocytes. As mentioned above, the increase of serum IL-12 and Th1 cytokines always followed the ALT flare^[73], confirming the function of IL-12 in promoting Th1 cell development, and binary function of macrophage. This also explains that HCV-infected patients with greater necro-inflammatory activity of liver showed greater IL-12 production by PBMC than those with minimal or mild activity in normal donors, and why Th1 predominance in HCV infection was correlated with the direct cytotoxic effect^[41,21] and the inhibition of viral replication.

The greater production of IL-12 associated with greater necro-inflammatory activity of liver in HCV-infected patients^[54] and response of IFN- γ to HCV core protein with chronic liver disease suggest a cellular immune response to the onset of the necroinflammatory process of hepatitis^[35]. In murine model of fulminant hepatitis B, massive liver damage was associated with the massive induction of IL-12 and IFN- γ in liver specimens. Probably, the proinflammatory cytokines are apparently not counterbalanced by the anti-inflammatory cytokine IL-10. Thus IL-12 may play an important role in promoting inflammatory reactions^[55]. These cases suggest that the macrophages are in the hyperactive situation, probably due to the imbalance of Th1/Th2 and failing to establish the alternative macrophage activation, which results in the imbalance of macrophage. Thus massive hepatocytes are killed by macrophages or overactivated CTLs.

The steps 2 and 3 in Figure 2 are continually stimulated when foreign virus can not be cleared by successful immune response for Lack of optimal T-cell reactivity that would reestablish balanced macrophage activation. The immunologic overstimulation would predictably lead to pathologic sequelae such as cirrhosis and hepatoma in chronic hepatitis B and C infections^[74]

After long periods of time during which steps 2 and 3 are overemphasized, there would be a predicted shortage of cells to accomplish steps 5 and 1. There would also be an initial overdrive of Th1 cell population. Patients with HIV also have been observed to have a dramatic Th1 to Th2 shift as described in step 4 and patients with chronic hepatitis B appeared to be Th2 predominant^[30]. The balanced macrophage activation theory predicts that this shift is compensatory in nature with the T cells attempting to regulate balanced macrophage activation through production of IL-4 which induces step 5. Th2 predominance would be suffered by patients with chronic viral disease, which would cause secondary immunopathogenic changes, such as HCV-related liver cirrhosis (HCC)^[75], while patients with histology of inflammation showed a significantly higher CD4+Th1 response to the HCV core antigen as compared to patients with histology of fibrosis/cirrhosis^[76]. These findings suggest that Th1/Th2 imbalance in HCV-related cirrhosis would decrease the antitumor immunity and its improvement might present the protective effect from HCC^[75]. At the same time, there exists the exhaustion of cells in steps 5 and 1. This would decrease the rate of phagocytosis.

Alternative macrophage pathway (step 4) has the following features: (1) the production of angiogenic factors, (2) inhibition of T cell responses, (3) associated downregulation of inflammatory-mediator production characteristic of classical activated macrophages, and (4) with the alternative macrophage activation chemokine-1 (AMAC-1)^[77], also known as macrophage inflammatory protein-4 (MIP-4). But few studies were performed in aspect of macrophage, and little is known about the mechanism of the balanced macrophage theory in chronic virus liver infection.

CONCLUSION

Recent data have made a major shift in the role of macrophages in HIV^[78] and inflammatory kidney disease. They can no longer be regarded solely as causing injury but rather as cells that can also promote resolution^[79,80]. This means that strategies to prevent macrophage influx may be beneficial to patients with hepatitis. Future experiments will need to define methods for determining the functional attributes of macrophages in clinical liver biopsies, and effective ways to manipulate the function of inflammatory macrophages *in vivo*.

Given the diverse range of functions macrophages can assume, it becomes possible to modulate disease by altering macrophage activity. The classic view would be that the overall inflammatory environment is a balance between pro- and anti-inflammatory cytokines, determining infiltrating and resident cell function. An increase of pro-inflammatory cytokines from macrophages such as TNF- α or IL-1 β thus worsens inflammation, whereas antagonists of these molecules such as IL-1 receptor antagonist (IL-1ra), IL-1 type II decoy receptor (IL-1RII) and soluble TNF receptor result in reduced injury^[81]. A number of cytokines are described as anti-inflammatory, including the Th2 cytokines IL-4, IL-10 and IL-13, IL-6 and TGF- β . rIL-10 treatment of patients with advanced fibrosis who had failed antiviral therapy appeared to decrease disease activity^[82]. TGF- β 2 significantly suppressed IFN- γ production at the single-cell level, indicating that the enhanced down-regulation of Th1 by TGF- β 2 in patients with HCV-related liver cirrhosis might be effective against hepatoma^[83]. But not all anti-inflammatory cytokines are equal in their ability to modulate macrophage function *in vivo*. In contrast to the results with the Th2 cytokines, IL-4 and IL-10, infusions of TGF- β do not modulate inflammatory macrophage function in glomerulonephritis. For example, Infusion of TGF- β 3 in rats with NTN (nephrotoxic nephritis RANTES) before the onset of disease did not alter the degree of proteinuria, although the number of infiltrating macrophages was reduced^[84]. The study about TGF- β treatment of animal models and patients with hepatitis is still unknown.

Advanced clinical studies of WF10 (completely blocked antigen activation of T cells responsiveness -in step 2) are currently underway in the USA for treatment of patients with HIV disease. The patients who received two cycles of WF10 showed chronic immunological changes by downregulating inflammatory macrophages and reestablished alternative macrophage activation, which was consistent with induction of balanced macrophage activation^[85]. Similarly, it is possible to modify inflammatory virus liver disease using a range of cytokines (Th1/Th2 types) with well-defined effects on macrophage activation. For example, defects in T cell response have been suspected as a major factor involved in the pathogenesis of chronic hepatitis B^[11-15], and favoring Th2 type cytokine may lead to chronic infections with HBV. Recent study has shown that activation of Th1 immunity accompanied by enhancement of CTL activity during therapy is a common immune mechanism for the successful treatment of hepatitis B and C^[86]. Using HBV core gene transduced DCs as APCs, HBcAg specific CTLs and Th1 type immune responses could be generated in the mice, which would be a new way to deal with the viral hepatitis^[87]. Thus, treatment with IL-12 to drive T cell reactivity^[88], and usage of IL-4 receptor antagonist are probably the practicable way to clear virus and remove HBV-infected hepatocytes. Although IL-12 as monotherapy in patients with HCV did not alter the production of regulatory cytokines produced by Th1/2 cells^[89] and had low efficacy^[90,91], IL-12 combining with IFN- α may enhance the efficacy for the treatment of chronic hepatitis B virus infection^[92] and may be a predisposition for elimination of HBeAg and successful treatment of hepatitis B^[93].

REFERENCES

- 1 **Mosmann TR**, Cherwinski H, Bond MW, Giedlin MA, Coffman RL. Two types of murine helper T cell clones. I. Definition according to profiles of lymphokine activities and secreted proteins. *J Immunol* 1986; **136**: 2348-2357
- 2 **Romagnani S**, Parronchi P, D'Elia MM, Romagnani P, Annunziato F, Piccinni MP, Manetti R, Sampognaro S, Mavilia C, De Carli M, Maggi E, Del Prete GF. An update on human Th1 and Th2 cells. *Int Arch Allergy Immunol* 1997; **113**: 153-156
- 3 **Racke MK**, Bonomo A, Scott DE, Cannella B, Levine A, Raine CS, Shevach EM, Rocken M. Cytokine-induced immune deviation as therapy for inflammatory autoimmune disease. *J Exp Med* 1994; **180**: 1961-1966
- 4 **Abbas AK**, Murphy KM, Sher A. Functional diversity of helper T lymphocytes. *Nature* 1996; **383**: 787-793
- 5 **Clerici M**, Shearer GM. The Th1-Th2 hypothesis of HIV infection: new insights. *Immunol Today* 1994; **15**: 575-581
- 6 **Yamamura M**, Uyemura K, Deans RJ, Weinberg K, Rea TH, Bloom BR, Modlin RL. Defining protective responses to pathogens: cytokine profiles in leprosy lesions. *Science* 1991; **254**: 277-279
- 7 **Sher A**, Coffman RL. Regulation of immunity to parasites by T cells and T cell-derived cytokines. *Annu Rev Immunol* 1992; **10**: 385-409
- 8 **Rossol S**, Marinos G, Carucci P, Singer MV, Williams R, Naoumov NV. Interleukin-12 induction of Th1 cytokines is important for viral clearance in chronic hepatitis B. *J Clin Invest* 1997; **99**: 3025-3033
- 9 **Birk RW**, Gratchev A, Hakiy N, Politz O, Schledzewski K, Guillot P, Orfanos CE, Goerdts S. Alternative activation of antigen-presenting cells: concepts and clinical relevance. *Hautarzt* 2001; **52**: 193-200
- 10 **Montaner LJ**, da Silva RP, Sun J, Sutterwala S, Hollinshead M, Vaux D, Gordon S. Type 1 and type 2 cytokine regulation of macrophages endocytosis: differential activation by IL-4/IL-13 as opposed to IFN- γ or IL-10. *J Immunol* 1999; **162**: 4606-4613
- 11 **Chisari FV**, Ferrari C. Hepatitis B virus immunopathogenesis. *Springer Semin Immunopathol* 1995; **13**: 29-60
- 12 **Ishikawa T**, Kakumu S, Yoshika K, Wakita T, Takayanagi M, Orido E. Immune response of peripheral blood mononuclear cells to antigenic determinants within hepatitis B core antigen in HB virus-infected man. *Liver* 1992; **12**: 100-105
- 13 **Marinos G**, Torre F, Chokshi S, Hussain M, Clarke BE, Rowlands DJ, Eddleston AL, Naoumov NV, Williams R. Induction of T-helper cell response to hepatitis B core antigen in chronic hepatitis B: a major factor in activation of the host immune response to the hepatitis B virus. *Hepatology* 1995; **22** (4 Pt 1): 1040-1049
- 14 **Ferrari C**, Penna A, Bertolotti A, Valli A, Antoni AD, Giuberti T, Cavalli A, Petit MA, Fiaccadori F. Cellular immune response to hepatitis B virus-encoded antigens in acute and chronic hepatitis B virus infection. *J Immunol* 1990; **145**: 3442-3449
- 15 **Lohr HF**, Weber W, Schlaak J, Goergen B, Meyer zum Buschenfelde KH, Gerken G. Proliferative response of CD4-T cells and hepatitis B virus clearance in chronic hepatitis with or without hepatitis B minus hepatitis B virus mutants. *Hepatology* 1995; **22**: 61-68
- 16 **Toyonaga T**, Hino O, Sugai S, Wakasugi S, Abe K, Shichiri M, Yamamura K. Chronic active hepatitis in transgenic mice expression interferon- γ in the liver. *Proc Natl Acad Sci U S A* 1994; **91**: 614-618
- 17 **Peters M**. Actions of cytokines on the immune response and viral interactions: an overview. *Hepatology* 1996; **23**: 909-916
- 18 **Ando K**, Moriyama T, Guidotti LG, Wirth S, Schreiber RD, Schlicht HJ, Huang SN, Chisari FV. Mechanisms of class I restricted immunopathology. A transgenic mouse model of fulminant hepatitis. *J Exp Med* 1993; **178**: 1541-1554
- 19 **Guidotti LG**, Ando K, Hobbs MV, Ishikawa T, Runkel L, Schreiber RD, Chisari FV. Cytotoxic T lymphocytes inhibit hepatitis B virus gene expression by a noncytolytic mechanism in transgenic mice. *Proc Natl Acad Sci U S A* 1994; **91**: 3764-3768
- 20 **Nayersina R**, Fowler P, Guillhot S, Missale G, Cerny A, Schlicht HJ, Vitiello A, Chesnut R, Person JL, Redeker AG. HLA A2 restricted cytotoxic T lymphocyte responses to multiple hepatitis B surface antigen epitopes during hepatitis B infection. *J Immunol* 1993; **150**: 4659-4671
- 21 **Barnaba V**, Franco A, Paroli M, Benvenuto R, De Petrillo G, Burgio VL, Santilio I, Balsano C, Bonavita MS, Cappelli G. Selective expansion of cytotoxic T lymphocytes with a CD4+CD56+ surface phenotype and a T helper type 1 profile of cytokine secretion in the liver of patients chronically infected with Hepatitis B virus. *J Immunol* 1994; **152**: 3074-3087
- 22 **Clerici M**, Hakim FT, Venzon DJ, Blatt S, Hendrix CW, Wynn TA, Shearer GM. Changes in interleukin-2 and interleukin-4 production in asymptomatic, human immunodeficiency virus-seropositive individuals. *J Clin Invest* 1993; **91**: 759-765
- 23 **Chisari FV**. Hepatitis B virus transgenic mice: insights into the virus and the disease. *Hepatology* 1995; **22**(4 Pt 1): 1316-1325
- 24 **Ando K**, Guidotti LG, Wirth S, Ishikawa T, Missale G, Moriyama T, Schreiber RD, Schlicht HJ, Huang SN, Chisari FV. Class I-restricted cytotoxic T lymphocytes are directly cytopathic for their target cells *in vivo*. *J Immunol* 1994; **152**: 3245-3253
- 25 **Gilles PN**, Fey G, Chisari FV. Tumor necrosis factor alpha negatively regulates hepatitis B virus gene expression in transgenic mice. *J Virol* 1992; **66**: 3955-3960
- 26 **Guidotti LG**, Ishikawa T, Hobbs MV, Matzke B, Schreiber R, Chisari FV. Intracellular inactivation of the hepatitis B virus by cytotoxic T lymphocytes. *Immunity* 1996; **4**: 25-36
- 27 **Jilbert AR**, Wu TT, England JM, Hall PM, Carp NZ, O'Connell AP, Mason WS. Rapid resolution of duck hepatitis B virus infections occurs after massive hepatocellular involvement. *J Virol* 1992; **66**: 1377-1388
- 28 **Jiang R**, Lu Q, Hou J. Polarized populations of T helper cells in patients with chronic hepatitis B virus infection. *Zhonghua Yixue Zazhi* 2000; **80**: 741-744
- 29 **Maggi E**, Mazzetti M, Ravina A, Annunziato F, de Carli M, Piccinni MP, Manetti R, Carbonari M, Pesce AM, del Prete G. Ability of HIV to promote a TH1 to TH0 shift and to replicate preferentially in TH2 and TH0 cells. *Science* 1994; **265**: 244-248
- 30 **Lee M**, Lee SK, Son M, Cho SW, Park S, Kim HI. Expression of Th1 and Th2 type cytokines responding to HbsAg and HBxAg in chronic hepatitis B patients. *J Korean Med Sci* 1999; **14**: 175-181
- 31 **Jiang R**, Feng X, Guo Y, Lu Q, Hou J, Luo K, Fu N. T helper cells in patients with chronic hepatitis B virus infection. *Chin Med J* 2002; **115**: 422-424
- 32 **Jacobson Brown PM**, Neuman MG. Immunopathogenesis of hepatitis C viral infection: Th1/Th2 responses and the role of cytokines. *Clin Biochem* 2001; **34**: 167-171
- 33 **Fan XG**, Liu WE, Li CZ, Wang ZC, Luo LX, Tan DM, Hu GL, Zhang Z. Circulating Th1 and Th2 cytokines in patients with hepatitis C virus infection. *Mediators Inflamm* 1998; **7**: 295-297
- 34 **Kobayashi K**, Ishii M, Igarashi T, Satoh T, Miyazaki Y, Yajima Y, Ukai K, Suzuki H, Kanno A, Ueno Y, Miura T, Toyota T. Profiles of cytokines produced by CD4-positive T-lymphocytes stimulated by anti-CD3 antibody in patients with chronic hepatitis C. *J Gastroenterol* 1998; **33**: 500-507
- 35 **Iwata K**, Wakita T, Okumura A, Yoshioka K, Takayanagi M, Wands JR, Kakumu S. Interferon gamma production by peripheral blood lymphocytes to hepatitis C virus core protein in chronic hepatitis C infection. *Hepatology* 1995; **22**(4 Pt 1): 1057-1064
- 36 **Bergamini A**, Bolacchi F, Cerasari G, Carvelli C, Faggioli E, Cepparulo M, Demin F, Uccella I, Bongiovanni B, Niutta P, Capozzi M, Lupi M, Piscitelli E, Rocchi G, Angelico M. Lack of evidence for the Th2 predominance in patients with chronic hepatitis C. *Clin Exp Immunol* 2001; **123**: 451-458
- 37 **Sobue S**, Nomura T, Ishikawa T, Ito S, Saso K, Ohara H, Joh T, Itoh M, Kakumu S. Th1/Th2 cytokine profiles and their relationship to clinical features in patients with chronic hepatitis C virus infection. *J Gastroenterol* 2001; **36**: 544-551
- 38 **Tran A**, Yang G, Doglio A, Ticchioni M, Laffont C, Durant J, Bernard JL, Gugenheim J, Saint-Paul MC, Bernard A, Rampal P, Benzaken S. Phenotyping of intrahepatic and peripheral blood lymphocytes in patients with chronic hepatitis C. *Dig Dis Sci* 1997; **42**: 2495-2500
- 39 **Khakoo SI**, Soni PN, Savage K, Brown D, Dhillon AP, Poulter LW, Dusheiko GM. Lymphocyte and macrophage phenotypes

- in chronic hepatitis C infection Correlation with disease activity. *Am J Pathol* 1997; **150**: 963-970
- 40 **Pickler LJ**, Singh MK, Zdraveski Z, Treer JR, Waldrop SL, Bergstresser PR, Maino VC. Direct demonstration of cytokine synthesis heterogeneity among human memory/effector T cells by flow cytometry. *Blood* 1995; **86**: 1408-1419
- 41 **Minutello MA**, Pileri P, Unutmaz D, Censini S, Kuo G, Houghton M, Brunetto MR, Bonino F, Abrignani S. Compartmentalization of T lymphocytes to the site of disease: intrahepatic CD4+T cells specific for the protein NS4 of hepatitis C virus in patients with chronic hepatitis C. *J Exp Med* 1993; **178**: 17-25
- 42 **Milich DR**, Schodel F, Peterson DL, Jones JE, Hughes JL. Characterization of self-reactive T cells that evade tolerance in hepatitis Be antigen transgenic mice. *Eur J Immunol* 1995; **25**: 1663-1672
- 43 **Wang JH**, Layden TJ, Eckels DD. Modulation of the peripheral T-Cell response by CD4 mutants of hepatitis C virus: transition from a Th1 to a Th2 response. *Hum Immunol* 2003; **64**: 662-673
- 44 **Ferrari C**, Bertolotti A, Penna A, Cavalli A, Valli A, Missale G, Pilli M, Fowler P, Giuberti T, Chisari FV. Identification of immunodominant T cell epitopes of the hepatitis B virus nucleocapsid antigen. *J Clin Invest* 1991; **88**: 214-222
- 45 **Thursz MR**, Kwiatkowski D, Allsopp CE, Greenwood BM, Thomas HC, Hill AV. Association between an MHC class II allele and clearance of hepatitis B virus in the Gambia. *N Engl J Med* 1995; **332**: 1065-1069
- 46 **Szabo SJ**, Kim ST, Costa GL, Zhang X, Fathman CG, Glimcher LH. A novel transcription factor, T-bet, directs Th1 lineage commitment. *Cell* 2000; **100**: 655-669
- 47 **Chan SH**, Kobayashi M, Santoli D, Perussia B, Trinchieri G. Mechanisms of IFN- γ induction by natural killer) cell stimulatory factor (NKSF/IL-12): role of transcription and mRNA stability in the synergistic interaction between NKSF and IL-2. *J Immunol* 1992; **148**: 92-98
- 48 **Trinchieri G**. Interleukin-12 and the regulation of innate resistance and adaptive immunity. *Nat Rev Immunol* 2003; **3**: 133-146
- 49 **Milich DR**, Wolf SF, Hughes JL, Jones JE. Interleukin 12 suppresses autoantibody production by reversing helper T-cell phenotype in hepatitis B e antigen transgenic mice. *Proc Natl Acad Sci U S A* 1995; **92**: 6847-6851
- 50 **Gherardi MM**, Ramirez JC, Esteban M. Towards a new generation of vaccines: the cytokine IL-12 as an adjuvant to enhance cellular immune responses to pathogens during prime-booster vaccination regimens. *Histol Histopathol* 2001; **16**: 655-667
- 51 **Liu Q**, Feng GX, Lin YL, Peng YZ, Mo BQ. Detection of interleukin-6 and -12 in hepatitis B patients and its clinical significance. *Diyi Junyi Daxue Xuebao* 2001; **21**: 858-859
- 52 **Wang S**, Lin Y, Ma W, Zhang B, Qi S, Lan F. Effect of IL-12 on IFN-gamma and IL-10 produced by peripheral blood mononuclear cells in patients with chronic hepatitis B virus infection during IFN-alpha treatment. *Zhonghua Ganzangbing Zazhi* 2002; **10**: 116-119
- 53 **Schlaak JF**, Pitz T, Lohr HF, Meyer zum Buschenfelde KH, Gerken G. Interleukin 12 enhances deficient HCV-antigen-induced Th1-type immune response of peripheral blood mononuclear cells. *J Med Virol* 1998; **56**: 112-117
- 54 **Quiroga JA**, Martin J, Navas S, Carreno V. Induction of interleukin-12 production in chronic hepatitis C virus infection correlates with the hepatocellular damage. *J Infect Dis* 1998; **178**: 247-251
- 55 **Leifeld L**, Cheng S, Ramakers J, Dumoulin FL, Trautwein C, Sauerbruch T, Spengler U. Imbalanced intrahepatic expression of interleukin 12, interferon gamma, and interleukin-10 in fulminant hepatitis B. *Hepatology* 2002; **36**(4 Pt 1): 1001-1008
- 56 **Henson PM**, Riches DW. Modulation of macrophage maturation by cytokines and lipid mediators: a potential role in resolution of pulmonary inflammation. *Ann N Y Acad Sci* 1994; **725**: 298-308
- 57 **Yang N**, Wu LL, Nikolic-Paterson DJ, Ng YY, Yang WC, Mu W, Gilbert RE, Cooper ME, Atkins RC, Lan HY. Local macrophage and myofibroblast proliferation in progressive renal injury in the rat remnant kidney. *Kidney Int* 1998; **54**: 143-151
- 58 **Segeer S**, MacK M, Regele H, Kerjaschki D, Schlondorff D. Expression of the C-C chemokine receptor 5 in human kidney diseases. *Kidney Int* 1999; **56**: 52-64
- 59 **Klimp AH**, de Vries EG, Scherphof GL, Daemen T. A potential role of macrophage activation in the treatment of cancer. *Crit Rev Oncol Hematol* 2002; **44**: 143-161
- 60 **Wel R**, Chen B, Gan TF, Zhou XM, Zhang YQ, Ren DL. Application of flow cytometry to analyzing the activation states of peripheral blood mononuclear cells CD14 macrophage. *Chin J Lab Med* 2003; **26**: 1-4
- 61 **Mcgrath MS**, Kodelja V. Balanced macrophage activation hypothesis: a biological model for development of drugs targeted at macrophage functional states. *Pathobiology* 1999; **67**: 277-281
- 62 **Gordon S**. Alternative activation of macrophages. *Nat Rev Immunol* 2003; **3**: 23-35
- 63 **Wand J**, Crawford K, Yuan M, Wang H, Gorry PR, Gabuzda D. Regulation of CC chemokine receptor 5 and CD4 expression and human immunodeficiency virus type 1 replication in human macrophages and microglia by T helper type 2 cytokines. *J Infect Dis* 2002; **185**: 885-897
- 64 **Kodellia V**, Muller C, Schebesch C, Orfanos CE, Tenorio S, Goerdts S. Differences in angiogenic potential of classically vs alternatively activated macrophages. *Immunobiology* 1997; **197**: 478-493
- 65 **Saha B**, Das G, Vohra H, Ganguly NK, Mishra GC. Macrophage-T cell interaction in experimental mycobacterial infection. Selective regulation of co-stimulatory molecules on mycobacterium-infected macrophages and its implication in the suppression of cell-mediated immune response. *Eur J Immunol* 1994; **24**: 2618-2624
- 66 **Kirschmann DA**, He X, Murasko DM. Inhibition of macrophage-induced, antigen-specific T-cell proliferation by poly I : C role of suppressor macrophages. *Immunology* 1994; **82**: 238-243
- 67 **Liu M**, Chan CW, Mcgilvray I, Ning Q, Levy GA. Fulminant viral hepatitis: molecular and cellular basis, and clinical implications. *Expert Rev Mol Med* 2001; **28**: 1-9
- 68 **Shiratori Y**, Takikawa H, Kawase T, Sugimoto T. Superoxide anion generating capacity and lysosomal enzyme activities of Kupffer cells in galactosamine induced hepatitis. *Gastroenterol Jpn* 1986; **21**: 135-144
- 69 **Andus T**, Bauer J, Gerok W. Effects of cytokines on the liver. *Hepatology* 1991; **13**: 364-375
- 70 **D' Andrea A**, Rengaraju M, Valiante NM, Chehimi J, Kubin M, Aste M, Chan SH, Kobayashi M, Young D, Nickbarg E. Production of natural killer cell stimulatory factor (interleukin 12) by peripheral-blood mononuclear cells. *J Exp Med* 1992; **176**: 1387-1398
- 71 **Park AY**, Hondowicz BD, Scott P. IL-12 is required to maintain a Th1 response during Leishmania major infection. *J Immunol* 2000; **165**: 896-902
- 72 **Yap G**, Pesin M, Sher A. Cutting edge: IL-12 is required for the maintenance of IFN-gamma production in T cells mediating chronic resistance to the intracellular pathogen, Toxoplasma gondii. *J Immunol* 2000; **165**: 628-631
- 73 **Rossol S**, Marinos G, Carucci P, Singer MV, Williams R, Naoumov NV. Interleukin-12 induction of Th1 cytokines is important for viral clearance in chronic hepatitis B. *J Clin Invest* 1997; **99**: 3025-3033
- 74 **Chen YP**, Feng XR, Dai L, Ding HB, Zhang L. Screening and evaluation of non-invasive diagnosis markers for compensated liver cirrhosis in patients with chronic hepatitis B. *Zhonghua Ganzangbing Zazhi* 2003; **11**: 225-227
- 75 **Sakaguchi E**, Kayano K, Segawa M, Aoyagi M, Sakaida I, Okita K. Th1/Th2 imbalance in HCV-related liver cirrhosis. *Nippon Rinsho* 2001; **59**: 1259-1263
- 76 **Sreenarasimhaiah J**, Jaramillo A, Crippin J, Lisker-Melman M, Chapman WC, Mohanakumar T. Lack of optimal T-cell reactivity against the hepatitis C virus is associated with the development of fibrosis/cirrhosis during chronic hepatitis. *Hum Immunol* 2003; **64**: 224-230
- 77 **Kitching AR**, Tipping PG, Mutch DA, Huang XR, Holdsworth SR. Interleukin-4 deficiency enhances Th1 responses and crescentic glomerulonephritis in mice. *Kidney Int* 1998; **53**: 112-118
- 78 **Raffanti SP**, Schaffner W, Federspiel CF, Blackwell RB, Ching OA, Kuhre FW. Randomized, double-blind placebo-controlled

- trial of the immune modulator WF10 in patients with advanced AIDS. *Infection* 1998; **26**: 202-207
- 79 **Rovin BH**. Chemokine blockade as a therapy for renal disease. *Curr Opin Nephrol Hypertens* 2000; **9**: 225-232
- 80 **Erwig LP**, Stewart K, Rees AJ. Macrophages from inflamed but not normal glomeruli are unresponsive to anti-inflammatory cytokines. *Am J Pathol* 2000; **156**: 295-301
- 81 **Kluth DC**, Rees AJ. New approaches to modify glomerular inflammation. *J Nephrol* 1999; **12**: 66-75
- 82 **Nelson DR**, Tu Z, Soldevila-Pico C, Abdelmalek M, Zhu H, Xu YL, Cabrera R, Liu C, Davis GL. Long-term interleukin 10 therapy in chronic hepatitis C patients has a proviral and anti-inflammatory effect. *Hepatology* 2003; **38**: 859-868
- 83 **Sakaguchi E**, Kayano K, Segawa M, Okamoto M, Sakaida I, Okita K. Th1 down-regulation at the single-lymphocyte level in HCV-related liver cirrhosis and the effect of TGF-beta on Th1 response: possible implications for the development of hepatoma. *Hepatol Res* 2002; **24**: 282
- 84 **Wilson HM**, Minto AW, Brown PA, Erwig LP, Rees AJ. Transforming growth factor-beta isoforms and glomerular injury in nephrotoxic nephritis. *Kidney Int* 2000; **57**: 2434-2444
- 85 **McGrath MS**, Benike C, Kuchne FW, Engleman E. Effect of WF10 (TCDO) on antigen presentation. *Transplant Proc* 1998; **30**: 4200-4204
- 86 **Tsai SL**, Sheen IS, Chien RN, Chu CM, Huang HC, Chuang YL, Lee TH, Liao SK, Lin CL, Kuo GC, Liaw YF. Activation of Th1 immunity is a common immune mechanism for the successful treatment of hepatitis B and C: tetramer assay and therapeutic implications. *J Biomed Sci* 2003; **10**: 120-135
- 87 **Ding CL**, Yao K, Zhang TT, Zhou F, Xu L, Xu JY. Generation of cytotoxic T cell against HBcAg using retrovirally transduced dendritic cells. *World J Gastroenterol* 2003; **9**: 1512-1515
- 88 **Teuber G**, Rossol S, Lee JH, Dietrich CF, Zeuzem S. TH1/TH2 serum cytokine profiles and soluble TNF-receptor response in patients with chronic hepatitis C during recombinant human interleukin-12 (rHuIL-12) treatment. *Z Gastroenterol* 2002; **40**: 487-495
- 89 **Barth H**, Klein R, Berg PA, Wiedenmann B, Hopf U, Berg T. Analysis of the effect of IL-12 therapy on immunoregulatory T-cell subsets in patients with chronic hepatitis C infection. *Hepatogastroenterology* 2003; **50**: 201-206
- 90 **Pockros PJ**, Patel K, O'Brien C, Tong M, Smith C, Rustgi V, Carithers RL, McHutchison JG, Olek E, DeBruin MF. A multicenter study of recombinant human interleukin 12 for the treatment of chronic hepatitis C virus infection in patients nonresponsive to previous therapy. *Hepatology* 2003; **37**: 1368-1374
- 91 **Zeuzem S**, Carreno V. Interleukin-12 in the treatment of chronic hepatitis B and C. *Antiviral Res* 2001; **52**: 181-188
- 92 **Wang S**, Lin Y, Ma W, Zhang B, Qi S, Lan F. Effect of IL-12 on IFN-gamma and IL-10 produced by peripheral blood mononuclear cells in patients with chronic hepatitis B virus infection during IFN-alpha treatment. *Zhonghua Ganzangbing Zazhi* 2002; **10**: 116-119
- 93 **Barth H**, Klein R, Berg PA, Wiedenmann B, Hopf U, Berg T. Induction of T helper cell type 1 response and elimination of HBcAg during treatment with IL-12 in a patient with therapy-refractory chronic hepatitis B. *Hepatogastroenterology* 2001; **48**: 553-555

Edited by Liu HX and Xu FM

Differential gene expression between squamous cell carcinoma of esophageus and its normal epithelium; altered pattern of mal, akr1c2, and rab11a expression

Sakineh Kazemi-Noureini, Sergio Colonna-Romano, Abed-Ali Ziaee, Mohammad-Ali Malboobi, Mansour Yazdanbod, Parviz Setayeshgar, Bruno Maresca

Sakineh Kazemi-Noureini, Abed-Ali Ziaee, Institute of Biochemistry and Biophysics, University of Tehran, Tehran, Iran; PO Box: 13145-1384

Sergio Colonna-Romano, International Institute of Genetics and Biophysics, National Research Council, Via Marconi 12, 80125 Naples, Italy

Mohammad-Ali Malboobi, National Research Center for Genetic Engineering and Biotechnology (NRCGEB), Tehran, Iran

Mansour Yazdanbod, Shariati Hospital, Department of Surgery, Medical University of Tehran, Tehran, Iran

Parviz Setayeshgar, Pathology department, Madaen Hospital, Tehran, Iran

Bruno Maresca, International Institute of Genetics and Biophysics, National Research Council, Via Marconi 12, 80125 Naples, Italy; and University of Salerno, School of Pharmacy, Dept. Pharmaceutical Sciences, Fisciano, Salerno, Italy

Correspondence to: Associate Professor Abed-Ali Ziaee (Ph.D.), Institute of Biochemistry and Biophysics, University of Tehran, PO Box: 13145-1384, Tehran, Iran. aa_ziaee@yahoo.uk.co

Telephone: +98-21-6956975 **Fax:** +98-21-6404680

Received: 2003-08-23 **Accepted:** 2003-12-01

Abstract

AIM: To identify the altered gene expression patterns in squamous cell carcinoma of esophagus (ESCC) in relation to adjacent normal esophageal epithelium.

METHODS: Total RNA was extracted using SV total RNA isolation kit from snap frozen tissues of ESCC samples and normal esophageal epithelium far from the tumor. Radio-labeled cDNA were synthesized from equal quantities of total RNAs of tumor and normal tissues using combinations of 24 arbitrary 13-mer primers and three different anchoring oligo-dT primers and separated on sequencing gels. cDNA with considerable different amounts of signals in tumor and normal tissue were reamplified and cloned. Using southern blot, the clones of each band were controlled for false positive results caused by probable heterogeneity of cDNA population with the same size. Clones that confirmed differential expression by slot blot selected for sequencing and northern analysis. Corresponding full-length gene sequences was predicted using human genome project data, related transcripts were translated and used for various protein/motif searches to speculate their probable functions.

RESULTS: The 97 genes showed different levels of cDNA in tumor and normal tissues of esophagus. The expression of mal gene was remarkably down regulated in all 10 surveyed tumor tissues. Akr1c2, a member of the aldo-keto reductase 1C family, which is involved in metabolism of sex hormones and xenobiotics, was up-regulated in 8 out of 10 inspected ESCC samples. Rab11a, RPL7, and RPL28 showed moderate levels of differential expression.

Many other cDNAs remained to further studies.

CONCLUSION: The mal gene which is switched-off in all ESCC samples can be considered as a tumor suppressor gene that more studies in its regulation may lead to valuable explanations in ESCC development. Akr1c2 which is up-regulated in ESCC probably plays an important role in tumor development of esophagus and may be proposed as a potential molecular target in ESCC treatments. Differential display technique in spite of many disadvantages is still a valuable technique in gene function exploration studies to find new candidates for improved ones like gene chips.

Kazemi-Noureini S, Colonna-Romano S, Ziaee AA, Malboobi MA, Yazdanbod M, Setayeshgar P, Maresca B. Differential gene expression between squamous cell carcinoma of esophageus and its normal epithelium; altered pattern of mal, akr1c2, and rab11a expression. *World J Gastroenterol* 2004; 10(12): 1716-1721

<http://www.wjgnet.com/1007-9327/10/1716.asp>

INTRODUCTION

Esophageal squamous cell carcinoma (ESCC) is a predominant kind of cancer in the developing world as well as the north and northeast of Iran, which show age-standardized incidence rate of about 150 per 100 000 person-years for both sexes^[1]. The exposure of esophageal cells to both exogenous agents such as food, alcohol, smoke and endogenous causes such as genetic and inflammation of esophagus tissue as well as the race and cultural habits have been accounted for high incidence in certain geographical regions^[2]. Many genes including several oncogenes and tumor suppressor genes are deregulated in esophageal carcinoma^[3, 4]. Some new publications reported gene expression profiles of normal and ESCC tissues recently^[5-8].

Two-dimensional gel electrophoresis has been already studied in Institute of Biochemistry and Biophysics, University of Tehran, Tehran, Iran to compare the protein populations of normal esophagus and ESCC tissues^[9]. A predominant transition of C to T at CpG dinucleotides has been reported for p53 gene as well as over expression of cox-2 gene and accumulation of nitrotyrosine was detected in ESCC tumors of Iranian patients^[10] confirming the concept of chronic inflammatory stress and sensitivity of esophageal cells to exogenous risk factors are involved in ESCC development in Iranian patients.

In order to find new molecular markers suitable for diagnosis and to identify probable potent molecular targets for drug design we started to screen genes with different levels of expression in normal and ESCC tissues of patients that were operated in 2 000 in Madaen Hospital. Using differential display methodology on fresh normal and cancer tissues in this propose we scanned expression of almost 6 000 genes. Using this

technique we tried to screen out all real mRNA population of transcribed genes in tumor and normal tissues in order to include the probable unknown genes too. Among them 97 cDNAs were found with lower or higher expression levels in comparing normal and tumor tissues. 47 cDNAs with remarkable different levels of expression between normal and tumor states were cloned. Six genes that confirmed to have different expression in normal and ESCC tumor tissues are reported here.

MATERIALS AND METHODS

Tissue collection and sample preparation

Tumor tissues of ESCC patients and normal adjacent parts were surgically removed and snap frozen in liquid nitrogen and stored at -80 °C until use. By histopathological examinations tumors were classified into three major groups of well, moderately, and poorly differentiated squamous cell carcinoma according to WHO classification by a pathologist. A brief pathological and clinical data of the patients were shown in Table 1^[12]. Histological normal adjacent epithelium from the same patient was used as the normal pair. A pair of tumor and normal tissues both from the same patient (RP; as reference patient) was chosen randomly for differential display. According to the clinical date this patient is a 47-year-old woman carried moderately differentiated tumor with reactive lymph nodes, which is an indicative of non-metastatic tumor. For a survey of gene expression in other ECSS patients, northern blotting was conducted for RP and nine other ESCC patients at different stages of tumor development. Patients were middle- to old-age all living in north of Iran.

Table 1 Sex, age and histopathological status of the inspected ESCC patients

No	Sex	Age	Differentiation degree of ESCC tumor	Metastatic lymphnodes
1	F	47	Moderately differentiated	None
2	M	53	Well differentiated	3 out of 8
3	F	47	Well differentiated	2 out of 10
4	F	50	Moderately differentiated	1 out of 1
5	M	69	Moderately differentiated	3 out of 9
6	F	60	Moderately differentiated	1 out of 6
7	M	66	Moderately differentiated	All five
8	M	76	Moderately differentiated	None
9	F	55	Poorly differentiated	No evidence
10	F	70	Well differentiated	All three

RNA purification

Using SV Total RNA extraction Kit (Promega), total RNA was purified from ESCC tumor and normal tissue pairs of the same patient in parallel. After DNase-I treatment, DNA-free RNA was recovered in a solution of 0.01 mol/L dithiothriitol (DTT), 10 U/L RNasin (Promega) in diethyl pyrocarbonate-treated water. The quality of RNAs and quantifications were done by spectrophotometry of Absorbency at 260 nm and gel electrophoresis.

Differential display reverse transcriptase-PCR

After 5 min of incubation of 0.2 g of RNA samples at 65 °C, reverse transcriptions were done in 20 L reactions RT buffer containing 50 mmol/L Tris-HCl (pH 8.3), 125 mmol/L KCl, 5 mmol/L MgCl₂, 0.01 mol/L DDT, 0.2 mol/L of a anchored oligo-dT 11M (where M is A, C or G), 20 mol/L dNTPs and 200 U SuperScript™ RNase-H Reverse Transcriptase (Gibco BRL), for 60 min at 37 °C. For amplification 2.0 µL of each reverse transcribed RNA was added into a 20 l reaction containing 1.25 mmol/L MgCl₂, 2.0 µmol/L dNTPs, 0.2 µmol/L of the respective oligo-dT 11 mol/L, 0.2 mol/L of one 13-mer arbitrary primer, 1 µL [³⁵S]dATP [4.44×10⁴ GBq/mmol

(1 200 Ci/mmol), Amersham] and 1.0 U of Ampli-Taq (Perkin Elmer). PCR cycles/parameters were: a denaturation step at 94 °C for 5 min followed by 3 cycles at 94 °C for 30 s, 42 °C for 2 min, 72 °C for 30 s, and 37 cycles at 94 °C for 30 s, 45 °C for 2 min, 72 °C 30 s and a final extension at 72 °C for 5 min.

Identification and cloning of differentially expressed cDNA bands

The amplified products of DDRT-PCR were fractionated on standard 60 g/L poly-acrylamide/urea gel, and then transferred to 3 mm filter paper (Amersham) without methanol/acetic acid fixing, dried and exposed to X-ray film overnight. The putative differentially displayed bands that showed the same pattern of expression in repeated DDRT gels were eluted and re-amplified by the same primers used in related first amplification sets. Molecular mass and quality of re-amplified cDNA fragments were checked by gel electrophoresis before cloning into the cloning vector pCR2.1 (Invitrogen Co, CA). Escherichia coli TOP10 harboring recombinant plasmids of pCR2.1 were selected on agar plates containing ampicillin and X-gal. Since probable heterogeneity in cDNA populations of the same size existing in each band can leads to false positive results, for each cloned band six single well grown colonies were subjected to Southern blot. Radio-labeled probe was prepared from the inserted fragment of one of these six colonies.

Slot and northern blots analysis

For slot blots preparation, 2.0 g of RNA samples were vacuum-dried and resuspended in 50 L of DEPC-dd H₂O. Fifty microliters of formaldehyde/20SSC solution (1:1 vol/vol) was added and incubated for 15 min at 60 °C before loading on nylon filters (Hybond, Amersham, UK). For northern blots, 30 g of N and T total RNAs were run on denaturing 1.2 g/L agarose gel and blotted onto Hybond membrane dried at 37 °C and fixed using UV cross-linking. As probes, gel purified cDNA fragments of interest were radio-labeled using High Prim™ DNA labeling system (Boehringer) and 4 of [³²P]-dCTP [1.11×10⁵ GBq/mmol (3 000 Ci/mmol), Amersham]. Blots were hybridized with respective probes in hybridization solution containing 0.5 mol/L phosphate buffer pH 7.2, 10 mmol/L EDTA and 50 g/L SDS at 60 °C overnight. Filters were washed twice at 55 °C in 0.1 hybridization solution for 15 min and scanned with a phosphor imager SF (Molecular Dynamics) following 4 h exposure at room temperature. Differentially expressed cDNA clones were sequenced using Sequenase kit Version 2.0 (USB) and fractionated on standard sequencing gels^[13].

Analysis of the sequences

Data entry, sequence management, sequence alignment and protein sequence analysis were performed by Lasergene software package^[12]. Sequence similarity search and several structural features were predicted by the use of online databases and related software including BLAST N, X and P (www.ncbi.nlm.nih.gov/BLAST/)^[13,14], Pfam (www.sanger.ac.uk/Software/Pfam/search.shtml)^[15], PRINTS (www.bioinf.man.ac.uk/dbbrowser/PRINTS/)^[16,17], Blocks (condor.urbb.jussieu.fr/logiciels/Protein_Blocks/Structural_Words/motif_PB_m.html)^[18], SMART (www.bork.embl-heidelberg.de/NAIL/RSmart)^[19,20], PROSITE (www.expasy.org/prosite/)^[21] and PSORT (psort.nibb.ac.jp/form.html)^[22].

RESULTS

Isolation of differentially expressed genes

The expression pattern of about 6 000 genes was scanned using combinations of 24 arbitrary 13-mer primers and three different anchoring oligo-dT primers in differential display reverse transcription-PCR reactions. We identified 97 genes with

different levels of cDNA in tumor and normal tissues of esophagus. 47 bands with considerable differential level of cDNA signals in tumor and normal tissues (Figure 1 panel A; Table 2) were reamplified and cloned. The clones that confirmed differential expression by slot blot (Figure 1 panel B) were selected for sequencing and northern analysis on other tumor samples. To annotate the isolated cDNA fragments, corresponding full-length gene sequences was predicted by the use of human genome project data (Table 2). The generated transcripts were translated and used for various protein motif searches.

Down regulation of mal gene

A 360-bp cDNA fragment, ESC1 clone, was found down regulated in ESCC tumor cells (Figure 1). ESC1 sequence was localized to 2cen-q13 locus of chromosome 2 that encompass

mal gene, a T-cell differentiation antigen. The amino acid sequence encoded by ESC1 aligned with the last 34 amino acids at the C-terminal of human MAL protein family members (Table 2). The available data shows that mal gene encodes four transcript variants as a result of alternative splicing. The detected band with estimated mRNA size of almost 1.1 kb by northern blot, strongly suggests that Mal-a variant is the only form expressed in normal esophagus. The expression of this gene was found to be down regulated in all 10 surveyed patients carrying tumors at different stages of ESCC (Figure 2).

Induced expression of a member of ras oncogene family

Another under-represented gene was found as a 273-bp cDNA fragment named ESC2 (Figure 1). The expression level of the related gene to ESC2, with approximate length of 1.0 kb mRNA,

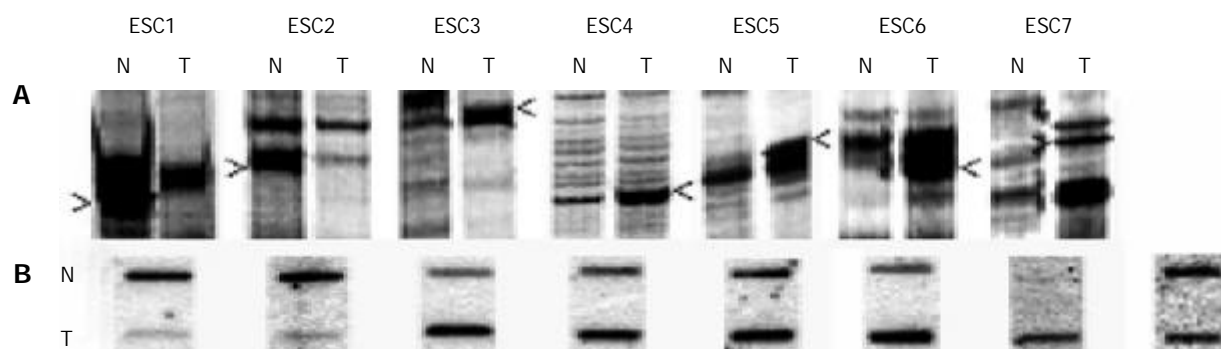


Figure 1 Parts of DDRT gels including cDNA fragments that show transcriptional alteration in comparing normal esophageal and ESCC tissues (have been pointed with arrows (panel A)), and the results of slot blots containing two microgram RNAs of normal (N) and tumor (T) tissues of esophagus in hybridization with radio-labeled related cDNAs (panel B). All of the slots have been prepared simultaneously and from the same RNA stocks of T and N. One piece of the slots has been hybridized with radio-labeled GADPH probe as shown in the right most side in panel B.

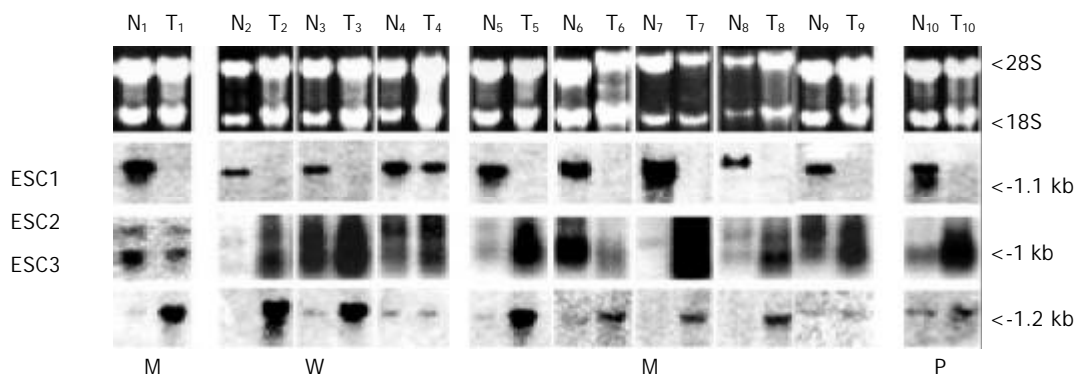


Figure 2 Northern results of patient 1 (RP) and other patients in hybridization with radio-labeled probes of ESC1, ESC2 and ESC3. Each northern membrane contains about 30 micrograms RNA of normal (N) and tumor (T) tissues of esophagus. The differentiation status of each tumor has been shown as W: Well differentiated tumor; M: Moderately differentiated tumor; P: poorly differentiated tumor. The estimated sizes of each bands has been shown on the right side and the ethidium bromide stained gel on top shows the relative amounts of RNAs loaded in each lane.

Table 2 The cDNAs, primers have been used in RT reactions and their related genes with different expression level in normal esophageal and ESCC tissues

cDNA name	cDNA' s length (bp)	3' end primer (5'→3')	5' end primer (5'→3')	GeneBank accession number
ESC1	360	AAG CTT TTT TTT TTT G	AAG CTT TAC GTA C	BC000458
ESC2	273	AAG CTT TTT TTT TTT A	AAG CTT CTC AGA C	BC013348
ESC3	300	AAG CTT TTT TTT TTT C	AAG CTT CTC AGA C	BC007024
ESC4	325	AAG CTT TTT TTT TTT C	AAG CTT AAC GAGG	BC006095
ESC5	442	AAG CTT TTT TTT TTT G	AAG CTT GAT TCG C	BC000072
ESC6	271	AAG CTT TTT TTT TTT C	AAG CTT GCG ATG T	AF_061732
ESC7	273	AAG CTT TTT TTT TTT C	AAG CTT TGG TCA G	NM001759

in RP and patient no. 6 was consistent with that observation. However it showed increased level of expression in five tumors (no. 2, 5, 7, 9, 10) out of eight other patients (Figure 2). The sequence of ESC2 was identical to a sequence localized at chromosome 15q21 of human genome corresponding to the 3' region of human *rab11a* gene. The expression of this gene was down regulated in RP and patient no.6 while over-expressed in 5 other surveyed patients and unchanged in three others. No clear correlation was detected between the *rab11a* expression and pathological parameters and/or patients prognosis.

Up-regulation of an aldo-keto reductase encoding gene

A 300 bp of cDNA fragment, ESC3 clone, was clearly up regulated in ESCC tumor (Figure 1). ESC3 sequence identified a locus on chromosome 10 p15 encoding AKR1C1, 2 and 3 three members of aldo-keto reductase protein family 1C. The nucleotide sequence of ESC3 is identical to 3' end of AKR1C2. The corresponding protein sequence encompasses all six conserved blocks of the family. This gene is highly expressed in 8 out of 10 tumors of different stages of ESCC (Figure 2). Low abundance of its transcripts was detected in the other two patients. Again, no clear correlation was found between the expression level and histopathological classification of tumor samples (Figure 2) (Table 2).

Other differentially expressed genes

The expression of two cDNA fragments ESC4 and 5 with the length of 325 bp and 442 bp, respectively, were found to be induced in tumor tissues (Figure 1). They are localized on locus 5q32, the location of ribosomal protein L7 (RpL7), which is a member of RPL30 gene family, and on chromosome 19q13.4 that juxtaexpose the location of ribosomal protein 28 (RpL28) encoding gene respectively. Both of these ribosomal proteins are the components of 60S subunit of ribosome. Northern blots showed increase expression of RpL7 (ESC4) in three tumor samples of ESCC (pair no.1; 4 and 5 if RNA shown in the first panel is normalized), while there is no substantial alterations for its expression in other pairs (Figure 3). The over-expression of RpL28 (ESC5) was confirmed on at least 4 out of 6 ESCC tumor samples by northern (Figure 3, pair samples No: 1, 3, 5 and 8). ESC6 clone carries a 271 bp cDNA fragment that contains a sequence identical to 100-amino acid hypothetical protein, which is moderately over expressed in tumor tissues of RP. A longer transcript of this sequence is also seen in related counting constructed from ESTs in TIGR and GeneBank (Table 2). This contig for ESC6 locates on 19p13.2 as shown by BLAST searches in Map Viewer. This aligned with a fetus brain protein called My029. The motif searches in BLOCKS, Pfam, CD, TIGR

fam failed to identify any conserved motif, while there are two bipartite nuclear targeting sequence (RRqpslrglksrrkprc), three protein kinase C phosphorylation sites as showed by PSORT seraches. Northern analysis shows a moderate over expression of this gene in at least 4 out of 6 samples of well and moderately differentiated ESCC tumors (Figure 3).

The sequence of a 273 bp cDNA fragment, ESC7, localized in 12p13 that code for cyclin D2. Northern analysis on normal and tumor RNA of RP indicates the over expression of this gene in ESCC (Figure 1). No further work was done on this clone.

DISCUSSION

The expression level of two genes encoding MAL, and AKR1C2 have been enormously altered, so that they may be mentioned as switched off and on genes respectively, while the other genes as ribosomal proteins L7 and L28 and a hypothetical protein showed moderate differences of expression between normal and tumor tissues. Except for *mal* gene^[23], differential expression of the other genes in ESCC is reported for the first time in this study.

ESC1 and 2 are the related clones for genes encode for two membrane proteins MAL and Rab11a respectively. A clear suppression of *mal* gene is seen in all ten ESCC samples (Figure 2). *Mal* gene has been already shown to express in four alternatively spliced forms of transcripts during intermediate and late stages of T-cell differentiation^[24], also in differentiating epithelial cells^[25]. The possible roles for MAL⁺ Cglycosphingolipid complexes in cell signaling, differentiation and apical sorting have been suggested^[25]. Here, we report down-regulation of this gene in all surveyed Iranian ESCC patients with different stages of tumor development, which is in good agreement by similar observations from China^[23] and Japan^[26]. As *mal* gene is up-regulated during the late stages of T-cell^[24] and urothelial cells^[25] differentiation, the switching-off of this gene in ESCC may suggest its involvement in a determining event in developing esophageal cancer. Although further studies are needed to clarify the role of MAL in normal esophageal cells and regulation of its expression, in a recent study the ectopic expression of MAL in carcinoma TE3 cells led to repressed formation of tumor induced by TE3 cells in nude mice, inhibition of cell motility and production of apoptosis by Fas pathway^[26]. These observations suggest MAL protein as a potential candidate for ESCC diagnosis/treatment and we expect it to be a tumor suppressor protein as it has been reported just recently^[26].

Rab11a, a non-oncogene member of small GTPase Ras oncogene family, involves in secretory pathways, vesicle trafficking and apical recycling system in epithelial cells^[27]. The most important role of Rab11a might be to facilitate cell migration

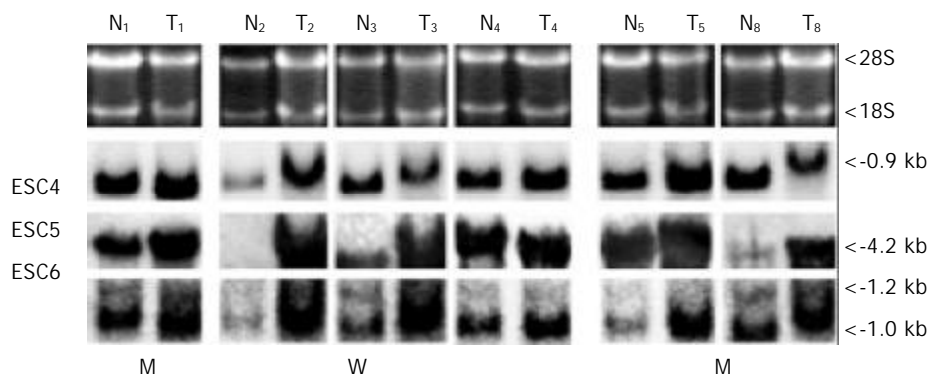


Figure 3 Northern results of patient 1 (RP) and other patients in hybridization with radio-labeled probes of ESC4, ESC5 and ESC6. Each northern membrane contains about 20 μ g RNA of normal (N) and tumor (T) tissues of esophagus. The differentiation status of each tumor has been shown as W: Well differentiated tumor; M: Moderately differentiated tumor. The estimated sizes of each bands has been shown on the right side and the ethidium bromide stained gel on top shows the relative amounts of RNAs loaded in each lane.

by internalizing integrins at the rear of cell and transporting them forward at the leading edge to form new contacts with the extra cellular matrix^[28]. To our knowledge, this is the first report of alterations of Rab11a expression in ESCC cancer. Similarly, massive synthesis of mRNA and protein of Rab11 was observed in cell line of esophagus adenocarcinoma and in low-grade dysplastic cells during esophageal adenocarcinoma development^[29]. Roles rab11a can play in ESCC is to be studied.

One of the most important results of this study was demonstration of the up regulation of gene encoding AKR1C2 that catalyzes the interconversion of aldehydes and ketones to their corresponding alcohol compounds in sex hormones and similar substrates. Such reactions lead to the production of reactive oxygen species (ROS) and consequent DNA damage as carcinogenesis progresses^[30]. Akr1c2 is also over expressed in lung carcinoma cell line^[31], in non-small cell lung cancer^[32], and in ovarian carcinoma cells^[33]. The pertinent enzyme activity, dehydration dehydrogenase type 2 (DDH2), (EC 1.1.1.213) plays a critical role in metabolism of steroid hormone^[34], drugs^[35] and polycyclic aromatic hydrocarbons (PAH)^[36]. As the esophagus tissue is not directly involved in steroid hormone metabolism the most probable substrate for this enzyme can be polycyclic aromatic hydrocarbons (PAH), some drugs and so on^[35]. During metabolic pathway of these xenobiotic compounds, the resulting o-quinones lead to stable depurination of DNA adducts^[36] that in turn can establish futile redox cycles and amplify ROS. These by-products are potent causative agents for establishing G to T transversion commonly found in ras and p53 genes^[37,38] as shown to occur in ESCC tumors too^[10]. Indeed oxidative stress has been considered as a major pathogenic factor in esophageal carcinoma^[39].

Furthermore oxidative stress leads to 4-hydroxy-2-nonenal (HNE) formation during lipid peroxidation, which diffuses through the cell membranes and with a longer half-life, it is even more destructive than ROS^[40]. On the other hand HNE specifically induces the expression of AKR1C1 isoform^[40]. Since AKR1C2 and AKR1C1 differ for only seven amino acids, it is indistinguishable if AKR1C1 is also being over-expressed in ESCC. As these two enzymes differ just slightly in their untranslated 3' end regions, at least some portions of the signal in northern can belong to akr1c1 transcripts so that both enzymes may be up-regulated in ESCC.

A clear up-regulation of akr1c2 in 8 out of 10 tumor samples of Iranian ESCC patients with different degrees of tumor development was shown in Figure 2. This enzyme is suggested to be involved in esophageal carcinogenesis at least indirectly, and this speculation is in a good agreement with the hypothesis of PAH exposure association with carcinogenesis of this tissue^[41]. However AKR1C2 is of special interest in cancer biology and drug design for prostate cancer^[42] and may be considered also as a potent molecular target in ESCC treatments.

The expression of RpL7 is higher in tumor tissues of all three samples of ESCC, wherein the amount of normal and tumor RNA can be normalized, considering the signals showed in Figure 2 for ESC4. The up-regulation of RpL7 has been reported recently in prostate cancer too^[43]. Several ribosomal proteins are suggested to be involved in cell proliferation, apoptosis, DNA repair, regulation of development and malignancies as their second function^[44], however the possible role of this protein in cancer cells remains to be clear. ESC5 cDNA fragment, that identified as RpL28 shows a higher expression in tumor tissues of ESCC. RpL28 seems to have a regulatory role as it is strongly ubiquitinated during S phase in *Saccharomyces cerevisiae*, while the levels of RpL28 ubiquitination is reduced in G1. As the human ortholog of RpL28 is also ubiquitinated, this modification is highly conserved in evolution, and a probable regulatory role for multiubiquitin of RpL28 has been speculated not necessarily as a target for degradation^[45].

We have seen also the over expression of cyclin D2 using Northern blot on RNA samples of RP, but no more experiments have done on other patients because of low amounts of available RNA. Although the over expression of Cyclin D2 in different kinds of squamous carcinoma cell lines has been shown to modulate proliferation after induced quiescence and enhance *in vivo* aggressive growth behavior^[46], however the RP sample has no metastasis in pathology report of tumor.

It is obviously anticipated that many genes are involved in carcinogenesis of esophagus, although differential expression of these genes could be the consequence rather than a cause. Many complicated events like cell to cell/matrix interactions, cell communications and transportations, normal regulation of protein synthesis, translation and cell cycle regulation as well as metabolic enzymes are affected by cancer development of esophagus.

ACKNOWLEDGEMENTS

We would like to thank Alfredo Franco Romano for his technical assists. This work has been done in collaboration between Molecular Biology Lab, Institute of Biochemistry and Biophysics, University of Tehran and Cell Stress Lab, International Institute of Biophysics and Genetics, Naples as a part of Ph.D. thesis of Sakineh Kazemi-Noureini.

REFERENCES

- 1 **Saidi F**, Sepehr A, Fahimi S, Farahvash MJ, Salehian P, Esmailzadeh A, Keshoofy M, Pirmoazen N, Yazdanbod M, Roshan MK. Oesophageal cancer among the Turkomans of northeast Iran. *Br J Cancer* 2000; **83**: 1249-1254
- 2 **Munoz N**. Epidemiological aspects of oesophageal cancer. *Endoscopy* 1993; **23**: 609-612
- 3 **Lam AK**. Molecular biology of oesophageal squamous cell carcinoma. *Crit Rev Oncol Hematol* 2000; **33**: 71-90
- 4 **Mandard AM**, Hainaut P, Hollstein M. Genetic steps in the development of squamous cell carcinoma of the esophagus. *Mutat Res* 2000; **462**: 335-342
- 5 **Graber MW**, Schweinfest CW, Reed CE, Papas TS, Baron PL. Isolation of differentially expressed genes in carcinoma of the esophagus. *Ann Surg Oncol* 1996; **3**: 192-197
- 6 **Xu Z**, Wang MR, Xu X, Cai Y, Han YL, Wu KM, Wang J, Chen BS, Wang XQ, Wu M. Novel human esophagus-specific gene C1orf10: cDNA cloning, gene structure, and frequent loss of expression in oesophageal cancer. *Genomics* 2000; **69**: 322-330
- 7 **Hu YC**, Lam KY, Law S, Wong J, Srivastava G. Identification of differentially expressed genes in esophageal squamous cell carcinoma (ESCC) by cDNA expression array: overexpression of Fra-1, Neogenin, Id-1 and CDC25B genes in ESCC. *Clin Cancer Res* 2001; **7**: 2213-2221
- 8 **Zhou J**, Zhao LQ, Xiong MM, Wang XQ, Yang GR, Qiu ZL, Wu M, Liu ZH. Gene expression profiles at different stages of human esophageal squamous cell carcinoma. *World J Gastroenterol* 2003; **9**: 9-15
- 9 **Rastegar-Jazii F**, Ziaee AA, Yazdanbod M. Application of two-dimensional electrophoresis and HIH 3T3 cell transfection assay in the study of tumor-associated proteins and genomic DNA tumorigenicity in malignant human oesophageal specimens. *J Sciences IRI* 1998; **9**: 216-225
- 10 **Sepehr A**, Taniere P, Martel-Planche G, Ziaee AA, Rastegar-Jazi F, Yazdanbod M, Etemad-Moghadam G, Kamangar F, Saidi F, Hainaut P. Distinct pattern of TP53 mutations in squamous cell carcinoma of the esophagus in Iran. *Oncogene* 2001; **20**: 7368-7374
- 11 **Watanabe H**, Jass JR, Sobin LH. Histological typing of oesophageal and gastric tumors. In: International Histological Classification of Tumors, Ed. 2. Berlin: Springer-Verlag 1990
- 12 **Burland TG**. DNASTAR's Lasergene sequence analysis software. *Methods Mol Biol* 2000; **132**: 71-91
- 13 **Gish W**, States DJ. Identification of protein coding regions by database similarity search. *Nat Genet* 1993; **3**: 266-272

- 14 **Pertsemlidis A**, Fondon JW 3rd. Having a BLAST with bioinformatics (and avoiding BLASTphemy). *Genome Biol* 2001; **2**: REVIEWS 2002
- 15 **Bateman A**, Birney E, Durbin R, Eddy SR, Howe KL, Sonnhammer ELL. The Pfam protein families database. *Nucleic Acid Res* 2000; **28**: 263-266
- 16 **Attwood TK**, Croning MD, Flower DR, Lewis AP, Mabey JE, Scordis P, Selley NL, Wright W. PRINTS-S: the database formerly known as PRINTS. *Nucleic Acid Res* 2000; **28**: 225-227
- 17 **Attwood TK**, Blythe MJ, Flower DR, Gaulton A, Mabey JE, Maudling N, McGregor L, Mitchell AL, Moulton G, Paine K, Scordis P. PRINTS and PRINTS-S shed light on protein ancestry. *Nucleic Acids Res* 2002; **30**: 239-241
- 18 **Pietrovski S**. Searching databases of conserved sequence regions by aligning protein multiple-alignments. *Nucleic Acids Res* 1996; **24**: 3836-3845
- 19 **Schultz J**, Copley RR, Doerks T, Ponting CP, Bork P. A web-based tool for the study of genetically mobile domains. *Nucleic Acid Res* 2000; **28**: 231-234
- 20 **Letunic I**, Goodstadt L, Dickens NJ, Doerks T, Schultz J, Mott R, Ciccarelli F, Copley RR, Ponting CP, Bork P. Recent improvements to the SMART domain-based sequence annotation resource. *Nucleic Acids Res* 2002; **30**: 242-244
- 21 **Falquet L**, Pagni M, Bucher P, Hulo N, Sigrist CJ, Hofmann K, Bairoch A. The PROSITE database, its status in 2002. *Nucleic Acids Res* 2002; **30**: 235-238
- 22 **Nakai K**, Horton P. PSORT: a program for detecting sorting signals in proteins and predicting their subcellular localization. *Trends Biochem Sci* 1999; **24**: 34-36
- 23 **Wang Z**, Wang M, Xu X, Xu Z, Han Y, Cai Y, Sun Y, Wu M. Studies of MAL gene in human oesophageal cancer by RNA in situ hybridization. *Zhonghua Yixue Yichuanxue Zazhi* 2000; **17**: 329-331
- 24 **Alonso MA**, Weissman SM. cDNA cloning and sequence of MAL, a hydrophobic protein associated with human T-cell differentiation. *Proc Natl Acad Sci U S A* 1987; **84**: 1997-2001
- 25 **Liebert M**, Hubbel A, Chung M, Wedemeyer G, Lomax MI, Hegeman A, Yuan TY, Brozovich M, Wheelock MJ, Grossman HB. Expression of mal is associated with urothelial differentiation *in vitro*: identification by differential display reverse-transcriptase polymerase chain reaction. *Differentiation* 1997; **61**: 177-185
- 26 **Mimori K**, Shiraishi T, Mashino K, Sonoda H, Yamashita K, Yoshinaga K, Masuda T, Utsunomiya T, Alonso MA, Inoue H, Mori M. MAL gene expression in esophageal cancer suppresses motility, invasion and tumorigenicity and enhances apoptosis through the Fas pathway. *Oncogene* 2003; **22**: 3463-3471
- 27 **Somsel Rodman J**, Wandinger-Ness A. Rab GTPases coordinate endocytosis. *J Cell Sci* 2000; **113**(Pt 2): 183-192
- 28 **Kamei T**, Matozaki T, Takai Y. Mechanisms of cell adhesion and migration. *Gan To Kagaku Ryoho* 1999; **26**: 1359-1366
- 29 **Goldenring JR**, Ray GS, Lee JR. Rab11 in dysplasia of Barrett's epithelia. *Yale J Biol Med* 1999; **72**: 113-120
- 30 **Burczynski ME**, Lin HK, Penning TM. Isoform-specific induction of a human aldo-keto reductase by polycyclic aromatic hydrocarbons (PAHs), electrophiles, and oxidative stress: implications for the alternative pathway of PAH activation catalyzed by human dihydrodiol dehydrogenase. *Cancer Res* 1999; **59**: 607-614
- 31 **Palackal NT**, Lee SH, Harvey RG, Blair IA, Penning TM. Activation of polycyclic aromatic hydrocarbon trans-dihydrodiol proximate carcinogens by human aldo-keto reductase (AKR1C) enzymes and their functional overexpression in human lung carcinoma (A549) cells. *J Biol Chem* 2002; **277**: 24799-24808
- 32 **Hsu NY**, Ho HC, Chow KC, Lin TY, Shih CS, Wang LS, Tsai CM. Overexpression of dihydrodiol dehydrogenase as a prognostic marker of non-small cell lung cancer. *Cancer Res* 2001; **61**: 2727-2731
- 33 **Deng HB**, Parekh HK, Chow KC, Simpkins H. Increased expression of dihydrodiol dehydrogenase induces resistance to cisplatin in human ovarian carcinoma cells. *J Biol Chem* 2002; **277**: 15035-15043
- 34 **Penning TM**, Burczynski ME, Jez JM, Hung CF, Lin HK, Ma H, Moore M, Palackal N, Ratnam K. Human 3 α -hydroxysteroid dehydrogenase isoforms (AKR1C1-AKR1C4) of the aldo-keto reductase superfamily: functional plasticity and tissue distribution reveals roles in the inactivation and formation of male and female sex hormones. *Biochem J* 2000; **351**(Pt 1): 67-77
- 35 **Breyer-Pfaff U**, Nill K. High-affinity stereoselective reduction of the enantiomers of ketotifen and ketonic nortriptyline metabolites by aldo-keto reductases from human liver. *Biochem Pharmacol* 1999; **59**: 249-260
- 36 **Shou M**, Harvey RG, Penning TM. Reactivity of benzo[a]pyrene-7,8-dione with DNA. Evidence for the formation of deoxyguanosine adducts. *Carcinogenesis* 1993; **14**: 475-482
- 37 **Esterbauer H**, Schaur RJ, Zollner H. forming propano-dGuo adducts which can lead to a pre-mutagenic lesion. *Free Radic Biol Med* 1991; **11**: 81-128
- 38 **Penning MT**, Burczynski ME, Hung CF, McCoull KD, Palackal NT, Tsuruda LS. Dihydrodiol dehydrogenase and polycyclic aromatic hydrocarbon activation: generation of reactive and redox active o-quinones. *Chem Res Toxicol* 1999; **12**: 1-18
- 39 **Lee JS**, Oh TY, Abn BO, Cho H, Kim WB, Kim YB, Surh YJ, Kim HJ, Hahm KB. Involvement of oxidative stress in experimentally induced reflux esophagitis and Barrett's esophagus: clue for the chemoprevention of esophageal carcinoma by antioxidants. *Mutat Res* 2001; **480-481**: 189-200
- 40 **Burczynski ME**, Sridhar GR, Palackal NT, Penning TM. The reactive oxygen species- and Michael acceptor-inducible human aldo-keto reductase AKR1C1 reduces the α,β -unsaturated aldehyde 4-hydroxy-2-nonenal to 1,4-dihydroxy-2-nonenal. *J Biol Chem* 2001; **276**: 2890-2897
- 41 **Nadon L**, Siemiatycki J, Dewar R, Krewski D, Gerin M. Cancer risk due to occupation exposure to polycyclic aromatic hydrocarbons. *Am J Ind Med* 1995; **28**: 303-324
- 42 **Lin HK**, Jez JM, Overby AM, Burczynski ME, Peehl DM, Penning TM. Type 3 3-hydroxysteroid dehydrogenase (3-HSD) accumulate 5-DHT and activates the androgen receptor in human prostate cancer PC3 cell. *Proc Am Assoc Cancer Res* 2000; **41**: 1510
- 43 **Wang Q**, Holmes DI, Powell SM, Lu QL, Waxman J. Analysis of stromal-epithelial interactions in prostate cancer identifies PTPCAAX2 as a potential oncogene. *Cancer Lett* 2002; **175**: 63-69
- 44 **Cehn FW**, Ioannou YA. Ribosomal proteins in cell proliferation and apoptosis. *Int Rev Immunol* 1999; **18**: 429-448
- 45 **Spence J**, Gali RR, Dittmar G, Sherman F, Karin M, Finley D. Cell cycle-regulated modification of the ribosome by a variant multiubiquitin chain. *Cell* 2000; **102**: 67-76
- 46 **Liu SC**, Bassi DE, Zhang SY, Holoran D, Conti CJ, Klein-Szanto AJ. Overexpression of cyclin D2 is associated with increased *in vivo* invasiveness of human squamous carcinoma cells. *Mol Carcinog* 2002; **34**: 131-139

Reversal of multidrug resistance in drug-resistant human gastric cancer cell line SGC7901/VCR by antiprogestin drug mifepristone

Da-Qiang Li, Zhi-Biao Wang, Jin Bai, Jie Zhao, Yuan Wang, Kai Hu, Yong-Hong Du

Da-Qiang Li, Zhi-Biao Wang, Jin Bai, Jie Zhao, Yuan Wang, Kai Hu, Yong-Hong Du, State Key Laboratory of Ultrasound Engineering in Medicine, Chongqing Medical University, Chongqing 400016, China
Supported by the National Key Research Project Foundation of China, No. 96-905-02-01, and the National Natural Science Foundation of China, No. 39630340

Correspondence to: Dr. Da-Qiang Li, State Key Laboratory of Ultrasound Engineering in Medicine, Chongqing Medical University, PO Box 153, Chongqing 400016, China. lidaqiang1974@sohu.com
Telephone: +86-23-68485022 **Fax:** +86-23-68485023
Received: 2003-07-04 **Accepted:** 2003-08-16

Abstract

AIM: To explore the reversal effect of mifepristone on multidrug resistance (MDR) in drug-resistant human gastric cancer cell line SGC7901/VCR and its mechanisms.

METHODS: Expression of multidrug resistance-associated protein(MRP) was detected using reverse transcription-polymerase chain reaction(RT-PCR). Flow cytometry was used to assay the expression of P-glycoprotein(P-gp), Bcl-2, Bax, and the mean fluorescent intensity of intracellular rhodamine 123 in the cells. Meanwhile, the protein levels of Bcl-2 and Bax were also detected by Western blotting analysis. The sensitivity of cells to the anticancer agent, vincrimycin(VCR), and the intracellular [³H]VCR accumulation were determined by tetrazolium blue (MTT) assay and a liquid scintillation counter, respectively.

RESULTS: Expression of MRP and P-gp in SGC7901/VCR cells was 6.04- and 8.37-fold higher as compared with its parental SGC7901 cells, respectively. After treatment with 1, 5, 10, and 20 μmol/L mifepristone, SGC7901/VCR cells showed a 1.34-, 2.29-, 3.11-, and 3.71-fold increase in the accumulation of intracellular VCR, a known substrate of MRP, and a 1.03-, 2.04-, 3.08-, and 3.68-fold increase in the retention of rhodamine 123, an indicator of P-gp function, respectively. MTT assay revealed that the resistance of SGC7901/VCR cells to VCR was 11.96-fold higher than that of its parental cells. The chemosensitivity of SGC7901/VCR cells to VCR was enhanced by 1.02-, 7.19-, 12.84-, and 21.17-fold after treatment with mifepristone at above-mentioned dose. After 96 h of incubation with mifepristone 10 μmol/L, a concentration close to plasma concentrations achievable in human, the expression of Bcl-2 protein was decreased to (9.21±0.65)% from (25.32±1.44)%, whereas the expression of Bax protein was increased to (19.69±1.13)% from (1.24±0.78)% (*P*<0.01). Additionally, the effects of mifepristone on the expression of Bcl-2 and Bax proteins in SGC7901/VCR cells were further demonstrated by Western blotting analysis.

CONCLUSION: Mifepristone has potent reversal effect on MDR in SGC7901/VCR via inhibiting the function of MRP and P-gp, modulating the expression of Bcl-2 and Bax proteins, and enhancing the sensitivity to anticancer agent VCR.

Li DQ, Wang ZB, Bai J, Zhao J, Wang Y, Hu K, Du YH. Reversal

of multidrug resistance in drug-resistant human gastric cancer cell line SGC7901/VCR by antiprogestin drug mifepristone. *World J Gastroenterol* 2004; 10(12): 1722-1725
<http://www.wjgnet.com/1007-9327/10/1722.asp>

INTRODUCTION

Gastric cancer is still the second most common cancer and the second most cause of cancer-related mortality^[1-2]. Surgery is effective for the majority of cases but chemotherapy plays an important role in the management of the patients with advanced gastric cancer^[3-4]. However, intrinsic or acquired resistance of gastric cancer cells to a broad spectrum of structurally and functionally unrelated anticancer agents, termed multidrug resistance(MDR), is a major obstacle to effective chemotherapy^[5-7]. Thus, there is an urgent need to identify effective reversal agents against the tumor.

The accumulating evidence^[8-12] showed that the mechanisms responsible for the MDR of gastric cancer involve, at least in part, overexpression of two ATP-dependent drug transporter proteins, P-glycoprotein(P-gp) and multidrug resistance-associated protein(MRP), as well as maladjustment of apoptosis-related genes Bcl-2 and Bax. Recent studies^[13-15] proved that mifepristone, as a potent antiprogestin agent, effectively reversed P-gp- and MRP-mediated MDR in mouse S7CD-5 thymoma cells and human GLC4/sb30 lung cancer cells, and induced apoptosis in human LNCaP prostate cancer cells by regulating the expression of Bcl-2 and Bax. However, the effects of mifepristone on MDR in human gastric cancer cells remain unknown. The present study was therefore undertaken to explore the reversal effect of mifepristone on the MDR in drug-resistant human gastric cancer cell line SGC7901/VCR and its mechanisms.

MATERIALS AND METHODS

Cell culture and treatment

Human gastric cancer cell line SGC7901, and its drug-resistant counterpart SGC7901/VCR selected by stepwise exposure of parental SGC7901 cells to increasing concentrations of vincristine (VCR), were purchased from Wuhan University Type Culture Collection (Wuhan, China). Both cell lines were maintained in RPMI1640 medium (Gibco BRL, Grand Island, NY) supplemented with 100 mL/L heat-inactivated fetal bovine serum(Hyclone, Logan, UT), 10⁵ U/L penicillin and 100 mg/L streptomycin in a incubator containing 50 mL/L CO₂ at 37 °C. When cells were grown to approximately 50% confluence, the medium was then replaced with serum-free RPMI1640. After 24 h, fresh media containing 1, 5, 10, and 20 μmol/L mifepristone (Sigma Chemical Co., St Louis, MO) was added, respectively. Control cells were treated with the same volume of vehicle (ethanol). Unless otherwise indicated, the cells were harvested after 96 h of incubation.

RT-PCR for MRP

Total RNA was extracted from the cultured cells using Trizol reagent (Gibco BRL) according to the manufacturer's instructions. Two milligrams of total RNA was used for reverse transcription in a total volume of 20 μL with the SuperScript

preamplification system (Gibco BRL). Aliquots of 2 μ L cDNA were then amplified using a PCR kit (Promega, USA) following conditions recommended by the manufacturer. The sense and antisense primers for MRP, designed according to the sequences published previously^[16], were 5' -AGGAGAGAT-CATCATCGATGG-3' and 5' -GCCTCCTGCACATTCATGG-3', respectively. The sense and anti-sense primers for β -actin were 5' -ATCTG-GCACCACACCTTCTACAATGAGCTGC-G-3' and 5' -CGTCATACTCCTGCTTGCTGATCCACATCTGC-3', respectively. The cycling conditions were 95 °C for 1 min, followed by 30 cycles of 94 °C for 60 s, 58 °C for 45 s, and 72 °C for 1 min and a final extension of 72 °C for 8 min. PCR products were separated on a 20 g/L agarose gel and visualized by ethidium bromide staining. The density of each band was measured on a densitometer, and the relative level of MRP mRNA expression in cells was calculated according to the ratio of MRP gene to β -actin.

Detection of P-gp, Bcl-2, Bax by flow cytometry

The harvested cells were fixed with 40 g/L paraformaldehyde for 10 min, followed by treatment with 2 g/L Triton X-100 for 10 min. After incubation with normal rabbit serum for 10 min to block non-specific binding, the cells were incubated for 1 h at 4 °C with mouse anti-human monoclonal antibodies against P-gp, Bcl-2, Bax (Santa Cruz Biotechnology, Inc., USA) respectively, followed by treatment with FITC-conjugated goat anti-mouse IgG for 30 min at 4 °C. The percentage of positive cells were determined using the FACS Calibur flow cytometry (Becton & Dickinson) with an excitation wavelength of 488 nm.

Western blotting analysis of Bcl-2 and Bax

Western blotting analysis was made to detect Bcl-2 and Bax protein levels according to the published method with some modifications^[17]. Briefly, proteins were extracted from the harvested cells using a lysis buffer containing 50 mmol/L HEPES, pH7.2, 100 mmol/L NaCl, 200 mL/L glycerol, 0.1 mmol/L EDTA, pH8.0, 2 g/L Triton X-100, 2 mmol/L phenylmethylsulfonyl fluoride (PMSF) and 1 mmol/L dithiothreitol (DTT), and then quantitated using the Bio-Rad Detergent Compatible Protein Assay kit (Bio-Rad, Hercules, CA). Equal amounts of protein (10-20 μ g) were resolved on a 100 g/L minigel by SDS-polyacrylamide gel electrophoresis. Proteins were transferred to a PVDF membrane (Millipore, Bedford, MA) using the Multiphor Novoblot electrophoresis transfer system, followed by immunoblotting using a monoclonal mouse anti-human antibody against Bcl-2 and Bax (Santa Cruz Biotechnology, Inc., USA), respectively. A horseradish peroxidase-conjugated secondary antibody (goat anti-mouse HRP, Amersham, Arlington Heights, IL) was used at a dilution of 1:3 000. The membranes were subsequently developed using Enhanced Chemiluminescence (ECL, Amersham) and exposed to film.

Intracellular [³H]VCR accumulation

Cells were incubated with 20 nmol/L [³H]VCR (specific activity

5.8 Ci/mmol, Amersham Pharmacia Biotech Co.) at 37 °C for 90 min in the absence or presence of various concentrations of mifepristone. Cells were then washed three times with ice-cold PBS and lysed in distilled water by ultrasonication. Radioactivity of [³H]VCR in the cell extract was then determined with a liquid scintillation counter (Beckman LS1801, USA) and normalized to cellular protein content.

Rhodamine 123 retention assay

Retention of rhodamine 123 (Sigma) was determined by flow cytometry as a functional index of P-gp activity. Cells (2×10^5) were treated with various concentrations of mifepristone for 24 h prior to the addition of 10 g/L rhodamine 123. After incubation at 37 °C for 1 h, cells were harvested and centrifuged at 300 g for 10 min. Cell pellets were resuspended with 500 μ L of PBS and immediately used for flow cytometric analysis of rhodamine 123 retention.

Drug-sensitivity assay

The sensitivity of cells to VCR was determined using the MTT assay as described previously^[18]. The drug concentration producing 50% inhibition of growth (IC_{50}) was determined graphically for VCR using the relative survival curves. The reversal effects of mifepristone were determined as the IC_{50} value in the absence of mifepristone to that in the presence of mifepristone. Assays were performed in quadruplicate for at least three times.

Statistical analysis

Data were expressed as mean \pm SD. Statistical analysis of the data was performed using the Student's *t* test and the Chi-square test. $P < 0.05$ was considered statistically significant.

RESULTS

Expression of MRP mRNA and P-gp protein

To examine the relationship between the levels of MRP and P-gp expression in SGC7901/VCR and SGC7901 cells and the changes in drug resistance, RT-PCR and flow cytometry were used to detect the expression of MRP mRNA and P-gp protein. As indicated in Figure.1, a 6.04-fold overexpression of MRP mRNA was found in SGC7901/VCR cells as compared with the parental line. The relative level of MRP mRNA expression in drug-resistant cells and drug-sensitive cells was 1.45 ± 0.23 and 0.24 ± 0.17 , respectively. Similarly, the expression of P-gp was significantly increased in the SGC7901/VCR cells in comparison with the parental cells ($57.64 \pm 8.56\%$ vs $6.89 \pm 1.25\%$, 8.37-fold, $P < 0.005$).

Intracellular [³H]VCR accumulation and rhodamine 123 retention

Intracellular accumulation of [³H]VCR, a known substrate of MRP, was measured in the presence or the absence of various concentrations of mifepristone in both cell lines. After treatment with 1, 5, 10, and 20 μ mol/L mifepristone for 90 min, the

Table 1 Effects of mifepristone on intracellular VCR accumulation and rhodamine 123 retention in drug-resistant human gastric cancer cell line SGC7901/VCR and its parental counterpart SGC7901

Mifepristone (μ mol/L)	Intracellular [³ H]VCR accumulation (pmol/mg protein)		Fluorescent intensity of intracellular rhodamine 123	
	SGC7901	SGC7901/VCR	SGC7901	SGC7901/VCR
0 (control)	3.36 \pm 0.54	0.98 \pm 0.20	82.36 \pm 4.23	22.32 \pm 3.14
1	3.41 \pm 0.49	1.31 \pm 0.29 ^a	83.21 \pm 5.50	28.89 \pm 4.25 ^a
5	3.54 \pm 0.68	2.24 \pm 0.62 ^b	85.12 \pm 4.89	45.63 \pm 6.34 ^b
10	3.65 \pm 0.87	3.05 \pm 0.75 ^b	86.01 \pm 6.12	68.69 \pm 7.40 ^b
20	3.84 \pm 0.79	3.64 \pm 0.84 ^b	88.20 \pm 6.45	82.10 \pm 9.21 ^b

^a $P < 0.05$, ^b $P < 0.01$ vs control group.

accumulation of intracellular VCR in SGC7901/VCR cells was enhanced by 1.34-, 2.29-, 3.11-, and 3.71-fold as compared with medium control, respectively (Table 1). It had been documented that the efflux of rhodamine 123 correlated with well P-gp expression. By this rational, we used rhodamine 123 to evaluate the function of P-gp. As shown in Table 1, after treatment with various concentrations of mifepristone for 24 h, the retention of rhodamine 123 in SGC7901/VCR cells was increased by 1.03-, 2.04-, 3.08-, and 3.68-fold as compared with the medium control. In contrast, no significant increase in the intracellular rhodamine 123 retention and VCR accumulation was observed in mifepristone-treated SGC7901 cells.

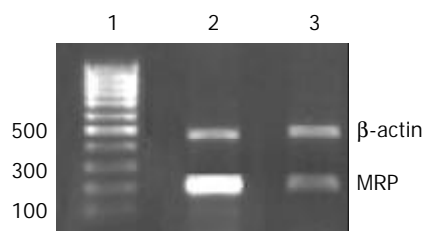


Figure 1 RT-PCR analysis of MRP mRNA expression in human gastric cancer cell line SGC7901 and its drug-resistant counterpart SGC7901/VCR. Lane 1-3: marker(bp), SGC7901/VCR, SGC7901, respectively.

Expression of Bcl-2 and Bax

Flow cytometric assay revealed that the expression of Bcl-2 protein was significantly increased, whereas the expression of Bax was decreased in SGC-7901/VCR cells as compared with drug-sensitive SGC7901 cells (Table 2). Mifepristone when used at 10 $\mu\text{mol/L}$, a concentration close to plasma concentrations achievable in human, markedly up-regulated the expression of Bax and simultaneously down-regulated the expression of Bcl-2 in SGC7901/VCR cells (Table 3). Additionally, the results were further demonstrated by Western blotting analysis (Figure 2). Western blotting revealed that mifepristone dose-dependently modulated the expression of Bcl-2 and Bax proteins, which was especially remarkable at the 20 $\mu\text{mol/L}$ concentration.

Table 2 Flow cytometric analysis of Bcl-2 and Bax expression in human gastric cancer cell line SGC7901 and its drug-resistant counterpart SGC7901/VCR

Cell line	Bcl-2(%)	Bax(%)
SGC7901	17.23 \pm 0.86	5.85 \pm 0.56
SGC7901/VCR	25.32 \pm 1.44 ^a	1.24 \pm 0.78 ^a

^a $P < 0.05$ vs SGC7901 cell line.

Table 3 Effect of mifepristone on Bcl-2 and Bax expression in SGC7901/VCR cells

Mifepristone ($\mu\text{mol/L}$)	Bcl-2(%)	Bax(%)
0 (control)	25.32 \pm 1.44	1.24 \pm 0.78
10	9.21 \pm 0.65 ^a	19.69 \pm 1.13 ^a

^a $P < 0.05$ vs control group.

Drug sensitivity assay

The sensitivity of SGC7901/VCR cells and its parental cells to VCR is shown in Table 4. Our results showed that the resistance of the SGC7901/VCR cells to VCR was 11.96-fold higher than that of its parental counterparts in terms of IC_{50} value. After incubation with 1, 5, 10, and 20 $\mu\text{mol/L}$ mifepristone for 96 h, the sensitivity of SGC7901/VCR cells to VCR was enhanced by 1.02, 7.19, 12.84, and 21.17 times, respectively. In contrast, mifepristone did not obviously alter the sensitivity to VCR in parental SGC-7901 cells.

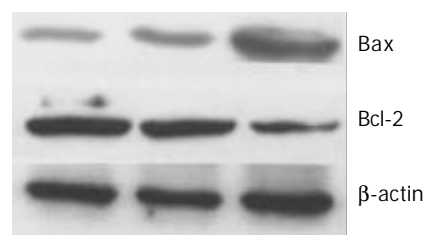


Figure 2 Western blotting analysis of Bcl-2 and Bax proteins in cellular extracts of SGC7901/VCR cells cultured for 96 h in the absence or the presence of mifepristone. Lane 1-3: control, 1 $\mu\text{mol/L}$ and 10 $\mu\text{mol/L}$ mifepristone, respectively.

Table 4 Effects of mifepristone on the sensitivity of SGC7901 cells and its drug-resistant counterpart SGC7901/VCR to VCR

Mifepristone ($\mu\text{mol/L}$)	SGC7901		SGC7901/VCR	
	IC_{50}	Reversal fold	IC_{50}	Reversal fold
0 (control)	4.23 \pm 1.02		46.36 \pm 5.14	
1	4.19 \pm 1.00	1.01	45.23 \pm 4.21	1.02
5	4.05 \pm 0.94	1.04	6.45 \pm 1.23 ^b	7.19
10	3.81 \pm 0.89	1.11	3.61 \pm 0.87 ^b	12.84
20	3.49 \pm 0.74	1.21	2.19 \pm 0.54 ^a	21.17

Data represent IC_{50} values of VCR (nmol/L) expressed as mean \pm SD of 3 independent experiments. ^a $P < 0.005$, ^b $P < 0.01$, vs control group.

DISCUSSION

Mifepristone is a potent antiprogesterin agent that has been widely used as the first-line drug for the termination of early pregnancy^[19,20]. Interestingly, recent studies^[21-25] have proved that mifepristone exerts markedly anticancer effects and reversal effects on MDR in some cancer cells with no serious side-effects. Thus, there is an increasing interest in exploring the reversal effect of mifepristone on MDR in human gastric cancer cells. In the present study, we reported for the first time that mifepristone effectively reversed MDR in SGC7901/VCR via multiple mechanisms.

Previous studies^[26-28] have proved that MDR in gastric cancer cells is closely related to overexpression of two ATP-dependent transporter proteins, P-gp encoded by MDR1 gene and MRP identified by Cole *et al.*^[16] from adriamycin-selected MDR lung cancer cell line H69/ADR. Both proteins belong to the ATP-binding cassette(ABC) protein superfamily, and efflux anticancer agents out of cells and therefore decrease their intracellular accumulation. Thus, we firstly determined the relationship between the levels of P-gp and MRP expression in SGC7901/VCR and its parental cells and the changes of drug resistance. Results showed that the expression of P-gp and MRP in SGC7901/VCR cells was 8.37- and 6.04-fold higher as compared with its parental counterparts. The data indicate that the overexpression P-gp and MRP confers, at least in part, the MDR phenotype of VCR-selected SGC7901/VCR cells.

To determine the effects of mifepristone on the function of P-gp and MRP, we further investigated the accumulation of intracellular VCR, a substrate of MRP, and the retention of rhodamine 123, an indicator of P-gp function, in both cell lines. Results revealed that mifepristone dose-dependently enhanced the intracellular VCR accumulation and rhodamine 123 retention in SGC7901/VCR cells. In contrast, mifepristone had no significant effects on the drug-sensitive SGC7901 cells. The results were further proved by the drug sensitivity assay. We found that, after incubation with 1, 5, 10, and 20 $\mu\text{mol/L}$ mifepristone for 96 h, the sensitivity of SGC7901/VCR cells to VCR was enhanced by 1.02, 7.19, 12.84, and 21.17 times, whereas

no significant changes in the sensitivity to VCR were observed in mifepristone-treated SGC901 cells. The findings are in agreement with those of previous studies on other cancer cell lines *in vitro*^[13,14]. Taken together, it seems reasonable to conclude that mifepristone can inhibit the function of P-gp and MRP and therefore enhance the sensitivity of cells to anticancer agent VCR.

Although overexpression of the P-gp and MRP plays an important role in the MDR of gastric cancer, this does not explain all of the MDR^[29]. Recent studies have shown that overexpression of anti-apoptotic proteins, such as Bcl-2, Bcl-X_L and Mcl-1, induces cancer cells resistance to chemotherapeutic agents in cancer cells that act by apoptosis, whereas high levels of pro-apoptotic proteins, Bcl-Xs and Bax, contribute to sensitize MCF-7 breast cancer cells to etoposide (VP16), taxol and epirubicin. These data were also proved by the work of Zhao *et al.*^[10], who reported that the Bax gene-transfected SGC7901/VCR cells were more sensitive to adriamycin and VCR than mock vector transfected cells. In a word, Bcl-2/Bax pathway may be an alternative mechanism of drug resistance in gastric cancer. In this study, we proved that mifepristone when used at 10 μmol/L, a concentration close to plasma concentrations achievable in human, significantly up-regulated the expression of Bcl-2 and simultaneously down-regulated the expression of Bax in SGC7901/VCR cells. In addition, the modulating effects of mifepristone on the expression of Bcl-2 and Bax proteins in SGC7901/VCR cells were further demonstrated by Western blotting analysis. These results may partly explain the reversal effects of mifepristone on SGC7901/VCR.

In conclusion, mifepristone exerts potent reversal effect on MDR in SGC7901/VCR via inhibiting MRP- and P-gp-mediated drug transporter, modulating the expression of apoptosis-related genes Bcl-2 and Bax, and enhancing the sensitivity of cells to anticancer agents such as VCR. These results indicate that mifepristone may be a promising chemosensitizer likely allowing to reverse the MDR of human gastric cancer cells although further studies are clearly needed to prove the possibility.

REFERENCES

- 1 **Albert C.** Clinical aspects of gastric cancer. In: Rustgi AK, eds. *Gastrointestinal cancer: biology, diagnosis and therapy*. Philadelphia: Lippincott Raven 1995; 197-216
- 2 **Lu JB,** Sun XB, Dai DX, Zhu SK, Chang QL, Liu SZ, Duan WJ. Epidemiology of gastroenterologic cancer in Henan Province, China. *World J Gastroenterol* 2003; **9**: 2400-2403
- 3 **Sasako M.** Principles of surgical treatment for curable gastric cancer. *J Clin Oncol* 2003; **21**: 274s-275s
- 4 **Roth AD.** Chemotherapy in gastric cancer: a never ending saga. *Ann Oncol* 2003; **14**: 175-177
- 5 **Choi JH,** Lim HY, Joo HJ, Kim HS, Yi JW, Kim HC, Cho YK, Kim MW, Lee KB. Expression of multidrug resistance-associated protein1, P-glycoprotein, and thymidylate synthase in gastric cancer patients treated with 5-fluorouracil and doxorubicin-based adjuvant chemotherapy after curative resection. *Br J Cancer* 2002; **86**: 1578-1585
- 6 **Ludwig A,** Dietel M, Lage H. Identification of differentially expressed genes in classical and atypical multidrug-resistant gastric carcinoma cells. *Anticancer Res* 2002; **22**: 3213- 3221
- 7 **Kowalski P,** Stein U, Scheffer GL, Lage H. Modulation of the atypical multidrug-resistant phenotype by a hammerhead ribozyme directed against the ABC transporter BCRP/MXR / ABCG2. *Cancer Gene Ther* 2002; **9**: 579-586
- 8 **Endo K,** Maehara Y, Kusumoto T, Ichiyoshi Y, Kuwano M, Sugimachi K. Expression of multidrug-resistance-associated protein (MRP) and chemosensitivity in human gastric cancer. *Int J Cancer* 1996; **68**: 372-377
- 9 **Fan K,** Fan D, Cheng LF, Li C. Expression of multidrug resistance-related markers in gastric cancer. *Anticancer Res* 2000; **20**: 4809-4814
- 10 **Zhao Y,** Xiao B, Chen B, Qiao T, Fan D. Upregulation of drug sensitivity of multidrug-resistant SGC7901/VCR human gastric cancer cells by bax gene transduction. *Chin J Med* 2000; **113**: 977-980
- 11 **Ramesh S,** Shanthi P, Krishnan KB, Shanthi AV, Taralakshmi VV, Subulakshmi S. Multidrug resistance 1 gene expression in Indian patients with gastric carcinoma. *Indian J Gastroenterol* 2003; **22**: 19-21
- 12 **Pohl A,** Lage H, Muller P, Pomorski T, Herrmann A. Transport of phosphatidylserine via MDR1 (multidrug resistance 1) P-glycoprotein in a human gastric carcinoma cell line. *Biochem J* 2002; **365**: 259-268
- 13 **Payen L,** Delugin L, Courtois A, Trinquart Y, Guillouzo A, Fardel O. Reversal of MRP-mediated multidrug resistance in human lung cancer cells by the antiprogesterin drug RU486. *Biochem Biophys Res Commun* 1999; **258**: 513-518
- 14 **Gurol DJ,** Zee MC, Trotter J, Bourgeois S. Reversal of multidrug resistance by RU486. *Cancer Res* 1994; **54**: 3088-3091
- 15 **El Etreby MF,** Liang Y, Lewis RW. Induction of apoptosis by mifepristone and tamoxifen in human LNCaP prostate cancer cells in culture. *Prostate* 2000; **43**: 31-42
- 16 **Cole SP,** Bhardwaj G, Gerlach H, Mackie JE, Grant CE, Almquist KC, Stewart AJ, Kurz EU, Duncan AM, Deeley RG. Overexpression of a transporter gene in multidrug-resistant human lung cancer cell line. *Science* 1992; **258**: 1650-1654
- 17 **Kamradt MC,** Mohideen N, Vaughan ATM. RU486 increases radiosensitivity and restores apoptosis through modulation of HPV E6/E7 in dexamethasone-treated cervical carcinoma cells. *Gynecol Oncol* 2000; **77**: 177-182
- 18 **Hotta T,** Tanimura H, Iwahashi M, Tani M, Tsunoda T, Noguchi K, Mizobata S, Arii K, Terasawa H, Nakamori M, Yamaue H. P-glycoprotein-expressing tumor cells are resistant to anticancer drugs in human gastrointestinal cancer. *Surg Today* 1999; **29**: 591- 596
- 19 **Mahajan DK,** London SN. Mifepristone(RU486): a review. *Fertil Steril* 1997; **68**: 967-976
- 20 **Basu R,** Gundlach T, Tasker M. Mifepristone and misoprostol for medical termination of pregnancy: the effectiveness of a flexible regimen. *J Fam Plann Reprod Health Care* 2003; **29**: 139-141
- 21 **Rocereto TF,** Saul HM, Aikins JA Jr, Paulson J. Phase II study of mifepristone(RU486) in refractory ovarian cancer. *Gynecol Oncol* 2000; **77**: 429-432
- 22 **Hyder SM,** Chiappetta C, Stancel GM. Pharmacological and endogenous progestins induce vascular endothelial growth factor expression in human breast cancer cells. *Int J Cancer* 2001; **92**: 469-473
- 23 **Peters MG,** Vanzulli S, Elizalde PV, Charreau EH, Goin MM. Effects of antiprogesterins RU486 and ZK98299 on the expression of cell cycle proteins of a medroxyprogesterone acetate (MPA)-induced murine mammary tumor. *Oncol Rep* 2001; **8**: 445-449
- 24 **Yokoyama Y,** Shinohara A, Takahashi Y, Wan X, Takahashi S, Niwa K, Tamaya T. Synergistic effects of danazol and mifepristone on the cytotoxicity of UCN-01 in hormone-responsive breast cancer cells. *Anticancer Res* 2000; **20**: 3131-3135
- 25 **Liang Y,** Hou M, Kallab AM, Barrett JT, El Etreby F, Schoenlein PV. Induction of antiproliferation and apoptosis in estrogen receptor negative MDA-231 human breast cancer cells by mifepristone and 4-hydroxytamoxifen combination therapy: a role for TGFβ1. *Int J Oncol* 2003; **23**: 369-380
- 26 **Stein U,** Lage H, Jordan A, Walther W, Bates SE, Litman T, Hohenberger P, Dietel M. Impact of BCRP/MXR, MRP1 and MDR1/P-Glycoprotein on thermoresistant variants of atypical and classical multidrug resistant cancer cells. *Int J Cancer* 2002; **97**: 751-760
- 27 **Lin HL,** Liu TY, Wu CW, Chi CW. Berberine modulates expression of mdr1 gene product and the responses of digestive track cancer cells to Paclitaxel. *Br J Cancer* 1999; **81**: 416- 422
- 28 **Alexander D,** Yamamoto T, Kato S, Kasai S. Histopathological assessment of multidrug resistance in gastric cancer: expression of P-glycoprotein, multidrug resistance-associated protein, and lung-resistance protein. *Surg Today* 1999; **29**: 401-406
- 29 **Kim R,** Ohi Y, Inoue H, Aogi K, Toge T. Introduction of gadd153 gene into gastric cancer cells can modulate sensitivity to anticancer agents in association with apoptosis. *Anticancer Res* 1999; **19**: 1779-1783

Effects of mifepristone on invasive and metastatic potential of human gastric adenocarcinoma cell line MKN-45 *in vitro* and *in vivo*

Da-Qiang Li, Zhi-Biao Wang, Jin Bai, Jie Zhao, Yuan Wang, Kai Hu, Yong-Hong Du

Da-Qiang Li, Zhi-Biao Wang, Jin Bai, Jie Zhao, Yuan Wang, Kai Hu, Yong-Hong Du, State Key Laboratory of Ultrasound Engineering in Medicine, Chongqing Medical University, Chongqing 400016, China

Supported by the National Key Research Project Foundation of China, No.96-905-02-01, and the National Natural Science Foundation of China, No. 39630340

Correspondence to: Dr. Zhi-Biao Wang, State Key Laboratory of Ultrasound Engineering in Medicine, Chongqing Medical University (PO Box 153), Chongqing 400016, China. wangzhibiao@netease.com

Telephone: +86-23-68485022 **Fax:** +86-23-68485023

Received: 2003-08-23 **Accepted:** 2003-12-06

Abstract

AIM: To investigate the effects of mifepristone on the invasive and metastatic potential of human gastric adenocarcinoma cell line MKN-45 and its mechanisms.

METHODS: After incubation with various concentrations of mifepristone (5, 10, 20 $\mu\text{mol/L}$), the adhesion to artificial basement membrane, Matrigel, and the migration of MKN-45 cells were assayed using MTT assay and Transwell cell culture chambers, respectively. Enzyme-linked immunoabsorbent assay (ELISA) and flow cytometry were used to determine the expression of vascular endothelial growth factor (VEGF) and integrin $\beta 3$ in the cells. After subcutaneous transplantation of MKN-45 cells in nude mice, mifepristone (50 mg/kg·d) was administered subcutaneously for 8 wk to assess its effects on tumor metastasis. Immunohistochemical analysis was used to detect the expression of VEGF and microvascular density (MVD) in xenografted tumors.

RESULTS: Mifepristone dose-dependently inhibited the heterotypic adhesion to Matrigel of MKN-45 cells. The inhibition was accompanied by a significant down-regulation of integrin $\beta 3$ expression in the cells. After incubation with 5, 10, 20 $\mu\text{mol/L}$ mifepristone, the number of migrated MKN-45 cells was 72 ± 8 , 50 ± 6 , 41 ± 5 in experiment group, and 94 ± 16 in control group ($P < 0.01$). Meanwhile, secreted VEGF protein of MKN-45 cells in mifepristone-treated group (14.2 ± 2.9 , 8.9 ± 3.1 , 5.4 ± 2.1 ng/g per liter) was significantly lower than that in control group (22.7 ± 4.3 ng/g per liter, $P < 0.01$). *In vivo*, mifepristone decreased the number of metastatic foci in lungs of nude mice and down-regulated the expression of VEGF and MVD in the xenografted tumors.

CONCLUSION: Mifepristone can effectively inhibit the invasive and metastatic potential of human gastric adenocarcinoma cell line MKN-45 *in vitro* and *in vivo* through inhibition of heterotypic adhesion to basement membrane, cell migration and angiogenesis.

Li DQ, Wang ZB, Bai J, Zhao J, Wang Y, Hu K, Du YH. Effects of mifepristone on invasive and metastatic potential of human gastric adenocarcinoma cell line MKN-45 *in vitro* and *in vivo*. *World J Gastroenterol* 2004; 10(12): 1726-1729

<http://www.wjgnet.com/1007-9327/10/1726.asp>

INTRODUCTION

Mifepristone is a progesterone receptor (PR) antagonist that has been widely used as the first-line drug for the termination of early pregnancy^[1]. Recently, considerable studies^[2,3] have proved that mifepristone exerts markedly anti-tumor effects on PR-positive tumor cells, such as breast cancer and ovarian cancer, without obvious side-effects and drug resistance. Its similar effect on PR-positive human gastric adenocarcinoma cell line MKN-45 was also demonstrated in our laboratory.

More interestingly, accumulating evidences show that embryo implantation and tumor metastasis share striking similarities in biological behaviors, such as cell adhesion^[4], immune escape^[5], angiogenesis^[6], invasion^[7] and tumor metastasis-related gene expression^[8]. By this rational, there is an increasing interest in addressing the role of mifepristone, an agent against embryo implantation, in anti-tumor invasion and metastasis. Therefore, the present study was undertaken to further investigate the effects of mifepristone on the invasive and metastatic potential of MKN-45 cells *in vitro* and *in vivo* and its possible mechanisms.

MATERIALS AND METHODS

Cell culture and treatment

Human gastric adenocarcinoma cell line MKN-45 was obtained from Wuhan University Type Culture Collection (Wuhan, China), and maintained in phenol red-free RPMI1640 (Gibco BRL, Grand Island, NY) supplemented with 100 mL/L¹ fetal bovine serum (Hyclone, Logan, UT), 10^5 U/L penicillin and 100 mg/L streptomycin at 37 °C in a humidified atmosphere containing 50 mL/L CO₂ in air. When cells were grown to approximately 50% confluence, the medium was then replaced with serum-free RPMI1640. After 24 h, fresh media containing 5, 10, 20 $\mu\text{mol/L}$ mifepristone (Sigma Chemical Co., St Louis, MO) were added, respectively. Control cells were treated with the same volumes of vehicle (ethanol). Unless otherwise stated, the cells were harvested after 96 h of incubation.

Adhesion assay

Each well in 96-well tissue culture plates was coated with 2 μg of Matrigel (Collaborative Research Inc., Bedford, MA) and allowed to dry in a laminar flow cabinet overnight at room temperature. After washed three times with PBS to remove excess and unbound Matrigel, the wells were blocked with 20 μL of a 20 mg/L bovine serum albumin (BSA, Sigma) solution in RPMI1640 medium for 1 h at 37 °C. Aliquots of 8×10^4 cells, in 100 μL of serum-free RPMI1640 medium containing various concentrations of mifepristone, were added to each well and the cells were allowed to adhere for 1 h at 37 °C. When the incubation was completed, the wells were washed three times with PBS to remove unbound cells. Then, the remaining cells were continuously incubated with MTT solutions (40 $\mu\text{g}/\text{well}$) for 4 h at 37 °C, followed by treatment with 200 μL of dimethyl sulfoxide (DMSO) for 10 min. Finally, $A_{570\text{nm}}$ of each well was measured using an ELISA plate reader (Bio-Rad, USA). Results were expressed as the adhesive rate (%) that was calculated according to the

following formula: $(A_{570nm} \text{ of the adhered cells} / A_{570nm} \text{ of total cells}) \times 100\%$.

Detection of integrin $\beta 3$ by flow cytometry

The harvested cells were fixed with 40 mg/L paraformaldehyde for 10 min, followed by treatment with 2 mg/L Triton X-100 for 10 min. After treatment with normal rabbit serum for 10 min to block non-specific binding, the cells were incubated for 1 h at 4 °C with mouse anti-human monoclonal antibody against $\beta 3$ (Santa Cruz, USA), followed by treatment with FITC-conjugated goat anti-mouse IgG (Vector, Burlingame, CA) for 30 min at 4 °C. The percentage of positive cells was determined using the FACS Calibur flow cytometry (Becton & Dickinson) with an excitation wavelength of 488 nm.

Migration assay

Migration of MKN-45 cells was assayed in Transwell cell culture chambers with 6.5-mm-diameter polycarbonate membrane filters containing 8- μm -pore size (Becton Dickinson Labware, Bedford, MA). Fibroblast-conditioned medium, obtained from confluent NIH 3T3 cell cultures in serum-free RPMI 1640, was used as the chemoattractant and added to the lower wells of the chambers. Aliquots of 2×10^4 cells in 300 μL fresh medium containing various concentrations of mifepristone were seeded into the upper wells of the cell inserts. After 24 h of incubation at 37 °C, the non-migrating cells were removed from the upper surface of the membrane with a cotton swab. The cells on the lower surface of the membrane were fixed with ice-cold methanol and then stained with haematoxylin and eosin. The number of migrated cells was counted under a light microscope. Five random microscopic fields ($\times 400$) were counted per well and the mean was determined.

Measurement of VEGF by ELISA

The media were collected after 48 h for VEGF ELISA determinations as described below. The cells were taken through three freeze-thaw cycles, centrifuged and supernatant was collected for determination of protein concentration as described previously. VEGF levels in the cell culture media were measured using a Quantikine kit from R & D Diagnostics (Minneapolis, MN) using the procedure provided by the supplier. Human recombinant VEGF included in the kit was used to construct a standard curve and obtain absolute values of VEGF protein content. The values were then normalized to the total protein concentration in each dish.

Xenografts of MKN-45 cells in nude mice

Two $\times 10^7$ MKN-45 cells were subcutaneously xenografted in the right flank of 8-wk-old male BALB/c-*nu/nu* mice (Shanghai Experimental Animal Center, Chinese Academy of Sciences, China). When tumors reached a mean volume of 100 mm^3 , mice were randomly divided into two groups (8 mice in per group) and treated as the following. Mice in experiment group were administrated subcutaneously with mifepristone at the dose of 50 mg/kg·d, whereas mice in control were subcutaneously injected with saline every day. After 8 wk of treatment, lungs were harvested, and the weights of lungs were determined. The number of metastatic foci in lungs fixed with Bouin's solution for 24 h was counted under a stereomicroscope. Meanwhile, the tumors were resected, fixed with 40 g/L formaldehyde in PBS, embedded in paraffin and sliced into 4- μm -thick sections for immunohistochemical analysis.

Immunohistochemical staining for VEGF and MVD

The expression of VEGF and MVD in harvested tumors was determined immunohistochemically using an avidin-biotin-peroxidase complex (ABC) kit (Vector Laboratories, USA).

Unless otherwise stated, all steps were performed at room temperature. Briefly, after removal of wax, tissue sections were treated with 30 mL/L hydrogen peroxidase for 30 min to block endogenous peroxidase activity, and microwaved in 10 mmol/L citrate buffer for 10 min to retrieve antigens. After blocked with normal goat serum, rabbit anti-human polyclonal antibody against VEGF and factor VIII-related antigen (Santa Cruz Biotechnology, USA) at a 100-fold dilution were separately applied to sections and incubated overnight at 4 °C. This was followed by treatment with biotin-labeled goat anti-rabbit IgG for 60 min. The ABC complex was added and allowed to stand for 30 min. Sites of immunoreaction were visualized with 3, 3'-diaminobenzidine (DAB), followed by counterstaining with Mayer's haematoxylin, if necessary. Between each step, the sections were washed three times with 100 mmol/L Tris-HCl buffer containing 0.1 mg/L Triton X-100. For a positive control, breast cancer tissue was used and the primary antibody was replaced by normal rabbit serum as a negative control.

Statistical analysis

Data were expressed as mean \pm SD. Statistical analysis was performed using the Student's *t* test and chi-square test. $P < 0.05$ was considered statistically significant.

RESULTS

Adhesion assay and expression of integrin $\beta 3$

MTT assay revealed that mifepristone dose-dependently inhibited the cell adhesion to artificial basement membrane, Matrigel. The adhesive rate of MKN-45 cells was $78.2 \pm 5.0\%$, $65.4 \pm 4.7\%$, $49.8 \pm 4.2\%$ in mifepristone-treated group, and $85.6 \pm 6.3\%$ in control group ($P < 0.05$). To further explore whether the change of cell adhesion molecule expression in MKN-45 cells contributed to the inhibition, flow cytometry was used to detect the expression of integrin $\beta 3$ in the cells. Results showed that the expression of integrin $\beta 3$ in MKN-45 cells treated with 5, 10, 20 $\mu\text{mol/L}$ mifepristone was significantly lower than that in control group ($25.4 \pm 3.6\%$, $19.6 \pm 2.9\%$, $15.8 \pm 2.2\%$ vs $31.8 \pm 4.1\%$, $P < 0.05$).

Migration assay

The effect of mifepristone on the migration of MKN-45 cells was evaluated in the Transwell cell culture chambers. As shown in Figure 1, there was a significant decrease in the number of migrated MKN-45 cells in mifepristone-treated group (72 ± 8 , 50 ± 6 , 41 ± 5) as compared with that in control group (94 ± 16 , $P < 0.01$).

Expression of VEGF protein

After treatment with 5, 10, 20 $\mu\text{mol/L}$ mifepristone for 48 h, secreted VEGF protein in the cell culture media measured by ELISA assay, was 14.2 ± 2.9 , 8.9 ± 3.1 and 5.4 ± 2.1 ng/g per liter, respectively. There was a significant difference in VEGF expression as compared with that in the control cells (22.7 ± 4.3 ng/g per liter, $P < 0.01$).

Xenografts of MKN-45 cells in nude mice

During necropsy, lung metastasis of gastric cancer was found in 6 mice of the control group, and in 4 mice of mifepristone group (Figure 2). As far as the number of metastatic foci in lungs was concerned, there was a significant difference in mifepristone-treated group as compared with control group (8 ± 2 vs 18 ± 7 , $P < 0.05$). In addition, the weights of xenografted tumors in nude mice treated with mifepristone (201 ± 36 mg) were significantly lower than those in control group (298 ± 54 mg, $P < 0.05$). To evaluate the effects of mifepristone on MVD and VEGF expression in xenografted tumors, immunohistochemical

staining was performed using ABC method. Results revealed that VEGF was highly expressed in xenografted gastric cancer in nude mice (Figure 3A). After treatment with mifepristone for 8 wk, the expression of VEGF was markedly down-regulated in the tumors (Figure 3B). In addition, MVD of xenografted tumors was $(11.2 \pm 2.5)/400 \times$ visual field in mifepristone-treated group, and $(29.8 \pm 7.6)/400 \times$ in the control group ($P < 0.01$).

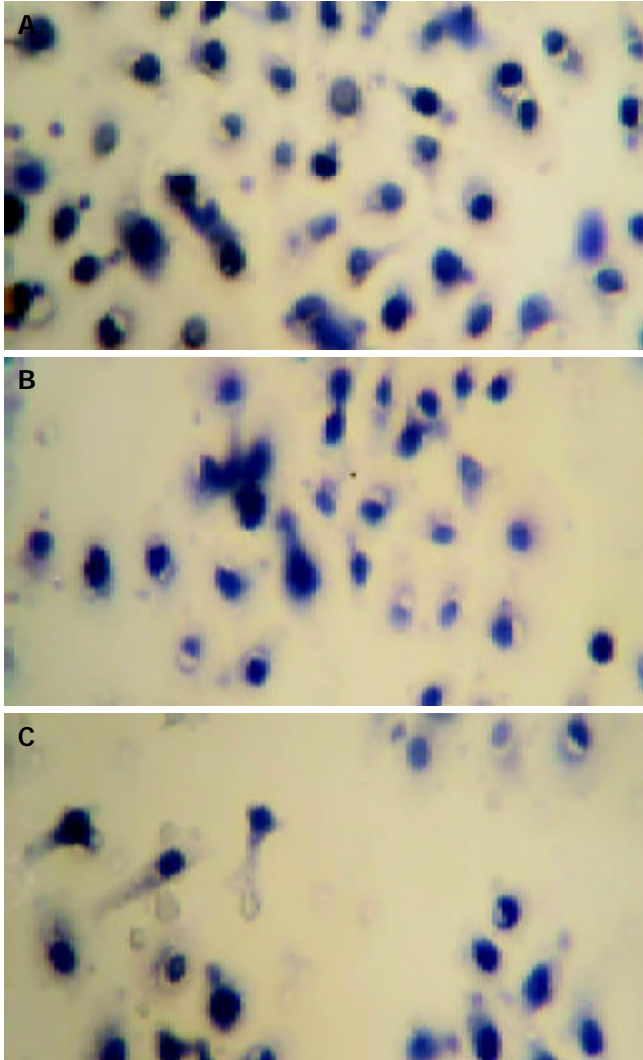


Figure 1 Effect of mifepristone on migration of MKN-45 cells incubated in Transwell cell culture chambers for 24 h in the absence (A) or presence of 10 $\mu\text{mol/L}$ (B) and 20 $\mu\text{mol/L}$ (C) mifepristone (H.E, $\times 200$).



Figure 2 Metastatic foci in lungs of nude mice (arrow). After 24 h of fixation with Bouin's solution, lung tissues exhibited yellow, whereas the tumors exhibited white.

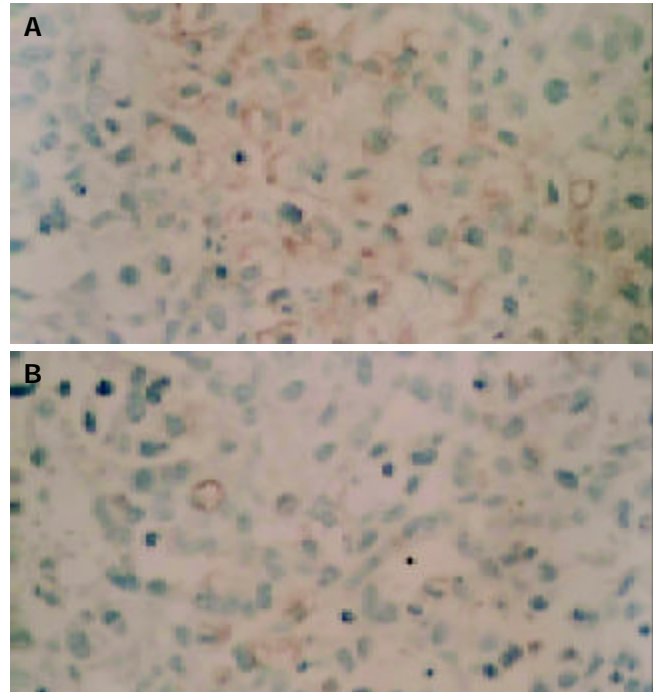


Figure 3 Immunohistochemical detection of VEGF expression in xenografted gastric cancer tissues of nude mice treated for 8 wk without (A) or with (B) 50 mg/kg·d mifepristone (ABC, $\times 100$).

DISCUSSION

Although considerable evidence^[9,10], both clinical and experimental, has demonstrated that mifepristone exerts markedly anti-proliferative effects on PR-positive malignant tumor cells, the role of mifepristone in anti-tumor invasion and metastasis, especially on gastric cancer, is poorly understood. In the present study, we demonstrated that mifepristone effectively inhibited the invasive and metastatic potential of human gastric adenocarcinoma cell line MKN-45 *in vitro* and *in vivo* through multiple mechanisms.

For tumor cells, increase of heterotypic adhesion to basement membrane and decrease of homotypic adhesion to the same cells have been defined as the critical event of tumor invasion that signals the initiation of metastatic cascade^[11,12]. In the present study, heterotypic adhesion of MKN-45 cells to artificial basement membrane, Matrigel, was examined with MTT dye assay to stain the adhered cells. Results showed that mifepristone dose-dependently decreased the adhesive rate of MKN-45 cells. Moreover, the findings were further proved by the down-regulation of integrin $\beta 3$ expression in the cells treated with mifepristone.

Integrin $\beta 3$, one member of integrins superfamily, plays a fundamental role in tumor cell heterotypic adhesion to extracellular matrix and basement membrane, which has been found to be mediated through a specific arginine-glycine-aspartic acid (RGD) amino acid sequence^[13]. Brakebusch *et al.*^[14] reported that high expression of integrin $\beta 3$ directly correlated with tumorigenicity and tumor progression. To further explore whether the change of integrin $\beta 3$ expression in MKN-45 cells contributed to the inhibitory effect of mifepristone on cell adhesion, flow cytometry was performed. We found that mifepristone down-regulated the expression of integrin $\beta 3$ in MKN-45 cells in a dose-dependent manner. The results were also demonstrated by the work of Li *et al.*^[15], who reported that mifepristone significantly down-regulated the expression of integrin $\beta 3$ in decidua and chorionic villi of early pregnancy, and the effect might be related with the anti-pregnancy mechanism of mifepristone. Taken together, the inhibitory

effect of mifepristone on heterotypic adhesion of MKN-45 cells may be associated with the down-regulation of integrin $\beta 3$. Moreover, integrin $\beta 3$ has been found to function not only as a cell adhesion molecule, but also as a signaling molecule for regulation of angiogenesis^[16]. Therefore, down-regulation of integrin $\beta 3$ expression in MKN-45 cells may be partially responsible for the inhibition of angiogenesis in the cells by mifepristone.

Continuous growth, invasion and metastasis of malignant tumors including human gastric cancer are dependent on angiogenesis factors regulated by peptide growth factors, of which VEGF is one of the most selective and potent^[17]. Hyder *et al.*^[18] reported that progestins could induce the expression of VEGF mRNA and protein in human breast cancer cell line T47D, and this effect was blocked by the antiprogestin agent mifepristone. The finding suggests that mifepristone may be useful to inhibit proliferation and metastasis in some tumors by blocking VEGF production. Thus, there is a great interest in exploring the effect of mifepristone on the expression of VEGF in MKN-45 cells. After exposure of MKN-45 cells to various concentrations of mifepristone for 48 h, a dose-dependent decrease in the media levels of VEGF was observed. Furthermore, the results were further supported by animal experiments. Immunohistochemical analysis showed that mifepristone significantly down-regulated the expression of VEGF and MVD in xenografted gastric cancer in nude mice. Summarily, it seems reasonable to conclude that the inhibitory effect of mifepristone on the invasive and metastatic potential of MKN-45 cells is mediated partially via blocking VEGF production.

On the other hand, tumor cell migration was necessary at the initiation of metastatic cascade, when the tumor cells left the primary site and gained access to the circulation and also at the end of invasion, when they were entering the secondary site^[19]. Theoretically, the decrease of tumor cell migration would contribute to the inhibition of tumor invasion and metastasis. In the study, the effect of mifepristone on the migration of MKN-45 cells was estimated in Transwell cell culture chambers. Results showed that a significant decrease in the number of migrated MKN-45 cells was observed in mifepristone-treated group as compared with control group.

In summary, mifepristone effectively inhibited the invasive and metastatic potential of human MKN-45 gastric adenocarcinoma cells through inhibition of the heterotypic adhesion to basement membrane, cell migration and angiogenesis. These findings, linked to its anti-proliferative effects, indicate that mifepristone may be a beneficial agent for additional and complementary use in the management of gastric cancer.

REFERENCES

- 1 **Mahajan DK**, London SN. Mifepristone(RU486): a review. *Fertil Steril* 1997; **68**: 967- 976
- 2 **Rocereto TF**, Saul HM, Aikins JA Jr, Paulson J. Phase II study of

- mifepristone (RU486) in refractory ovarian cancer. *Gynecol Oncol* 2000; **77**: 429-432
- 3 **Thomas M**, Monet JD. Combined effects of RU486 and tamoxifen on the growth and cell cycle phases of the MCF-7 cell line. *J Clin Endocrinol Metab* 1992; **75**: 865-870
- 4 **Lash GE**, Fitzpatrick TE, Graham CH. Effect of hypoxia on cellular adhesion to vitronectin and fibronectin. *Biochem Biophys Res Commun* 2001; **287**: 622-629
- 5 **Arck PC**, Hertwig K, Hagen E, Hildebrandt M, Klapp BF. Pregnancy as a model of controlled invasion might be attributed to the ratio of CD3/CD8 to CD56. *Am J Reprod Immunol* 2000; **44**: 1-8
- 6 **Murray MJ**, Lessey BA. Embryo implantation and tumor metastasis: common pathways of invasion and angiogenesis. *Semin Reprod Endocrinol* 1999; **17**: 275-290
- 7 **Fitzpatrick TE**, Lash GE, Yanaihara A, Charnock-Jones DS, Macdonald-Goodfellow SK, Graham CH. Inhibition of breast carcinoma and trophoblast cell invasiveness by vascular endothelial growth factor. *Exp Cell Res* 2003; **283**: 247-255
- 8 **Janneau JL**, Maldonado-Estrada J, Tachdjian G, Miran I, Motte N, Saulnier P, Sabourin JC, Cote JF, Simon B, Frydman R, Chaouat G, Bellet D. Transcriptional expression of genes involved in cell invasion and migration by normal and tumoral trophoblast cells. *J Clin Endocrinol Metab* 2002; **87**: 5336-5339
- 9 **Yokoyama Y**, Shinohara A, Takahashi Y, Wan X, Takahashi S, Niwa K, Tamaya T. Synergistic effects of danazol and mifepristone on the cytotoxicity of UCN-01 in hormone-responsive breast cancer cells. *Anticancer Res* 2000; **20**: 3131-3135
- 10 **El Etreby MF**, Liang Y, Lewis RW. Induction of apoptosis by mifepristone and tamoxifen in human LNCaP prostate cancer cells in culture. *Prostate* 2000; **43**: 31-42
- 11 **Stetler-Stevenson WG**, Kleiner DE. Molecular biology of cancer: invasion and metastases. In: Devita VT, Hellman S, Rosenberg SA, eds. *Cancer principles and practice of oncology*. 6th ed. Philadelphia: Lippincott Williams Wilkins 2001: 123-136
- 12 **Hanahan D**, Weinberg RA. The hallmarks of cancer. *Cell* 2000; **100**: 57-70
- 13 **Liotta LA**, Kohn EC. Invasion and metastases. In: Frin H, eds. *Cancer medicine*. 5th ed. Baltimore: Williams Wilkins 2001: 121-131
- 14 **Brakebusch C**, Bouvard D, Stanchi F, Sakai T, Fassler R. Integrins in invasive growth. *J Clin Invest* 2002; **109**: 999-1006
- 15 **Li RZ**, Wang ZH, Wu RF, Lu SY, Shi B. Expression of integrin $\beta 3$ and extracellular matrix: fibronectin and laminin in deciduas and chorionic villi of medical abortion for early pregnancy. *J Reprod Med* 1999; **8**: 214-216
- 16 **Kohn EC**, Liotta LA. Metastasis and angiogenesis: molecular dissection and novel applications. In: Mendelsohn J, Howley PM, Israel MA, Liotta LA. eds. *The molecular basis of cancer*. 2nd ed. Philadelphia: W.B Saunders Company 2001: 163-172
- 17 **Folkman J**. Tumor angiogenesis. In: Abeloff MD, Armitage JO, Lichter AS, Niederhuber JE, eds. *Clinical oncology*. 2nd ed. Orlando: Harcourt Publishers Limited 2001: 132-151
- 18 **Hyder SM**, Chiappetta C, Stancel GM. Pharmacological and endogenous progestins induce vascular endothelial growth factor expression in human breast cancer cells. *Int J Cancer* 2001; **92**: 469-473
- 19 **Fidler IJ**. Cancer biology: invasion and metastasis. In: Abeloff MD, Armitage JO, Lichter AS, Niederhuber JE, eds. *Clinical oncology*. 2nd ed. Orlando: Harcourt Publishers Limited 2001: 29-53

Edited by Xu FM and Wang XL

Microvessel density of malignant and benign hepatic lesions and MRI evaluation

Jian-Ping Lu, Jian Wang, Tao Wang, Yi Wang, Wei-Qing Wu, Li Gao

Jian-Ping Lu, Jian Wang, Department of Radiology, Changhai Hospital, Second Military Medical University, Shanghai 200433, China

Tao Wang, Yi Wang, Wei-Qing Wu, Eastern Hepatobiliary Surgery Institute, Second Military Medical University, Shanghai 200433, China
Li Gao, Department of Pathology, Changhai Hospital, Second Military Medical University, Shanghai 200433, China

Supported by the National Natural Science Foundation of China, No. 39970728

Correspondence to: Dr. Jian-Ping Lu, Department of Radiology, Changhai Hospital, Second Military Medical University, Shanghai 200433, China

Telephone: +86-21-25072133

Received: 2003-08-23 **Accepted:** 2003-10-12

Abstract

AIM: To study the difference of microvessel density (MVD) between malignant and benign hepatic lesions and study the relationship between MVD and dynamic enhanced magnetic resonance imaging (MRI) for evaluation of microvessels within malignant and benign hepatic lesions.

METHODS: A total of 265 specimens of hepatocellular carcinoma (HCC), 122 cirrhosis tissues and 22 hepatic benign lesions were enrolled for MVD by immunohistochemistry on tissue microarray, of which 49 underwent MRI examination before surgery, then contrast-to-noise ratios (CNR) and enhancement index (EI) in all the phases were calculated. Pearson correlation was performed for correlation analysis between CNR, EI and MVD.

RESULTS: MVD of HCC was 22.7 ± 15.8 (mean \pm SD), which was obviously higher than that of cirrhosis tissue (8.3 ± 7.6 , $P < 0.01$), but was not statistically different from that of benign lesions (31.3 ± 22.7 , $P > 0.05$). Among HCC, MVD of grades I-II was 29.9 ± 18.6 , which was much higher than those of grade III (22.2 ± 18.2 , $P < 0.01$) and grade IV (22.9 ± 19.0 , $P < 0.01$). MVD of HCC ($P = 0.018$) and of benign lesions ($P = 0.014$) were both correlative with CNR in arterial phase.

CONCLUSION: Neoangiogenesis is an important feature for malignant tumor, and MVD may act as a biological marker in differentiating malignant from benign hepatic lesions. Dynamic enhanced MRI, especially image in arterial phase, may act as an MVD evaluation criterion for malignant and benign hepatic lesions.

Lu JP, Wang J, Wang T, Wang Y, Wu WQ, Gao L. Microvessel density of malignant and benign hepatic lesions and MRI evaluation. *World J Gastroenterol* 2004; 10(12): 1730-1734
<http://www.wjgnet.com/1007-9327/10/1730.asp>

INTRODUCTION

It is well known that hepatocellular carcinoma (HCC) is a type of hypervascular lesion^[1], but there were seldom reports on

difference of microvessel density (MVD) between HCC and benign hepatic lesions. The tissue microarray, which has been developed recently as a high-throughput technique for rapid scanning hundreds or thousands of samples at the same time, can be applied in analyzing expression of some DNA, RNA or protein^[2]. In this research, differences of MVD of a large number of hepatic malignant and benign lesions were studied with tissue microarray, which further demonstrated some biological features of HCC.

Recent advances in magnetic resonance imaging (MRI) have led to the establishment of fast scan techniques, which, combined with bolus injection of contrast material, allows the acquisition of dynamic enhanced MRI for higher confident detection of HCC^[3-5]. There have been reports on correlation among digital subtraction angiography (DSA), ultrasound angiography (USAG), computed tomography during arterial portography (CTAP) and immunohistochemical findings^[6], but the relationship between MVD and dynamic MRI has been seldom reported. In this research, correlation between MVD and dynamic enhanced MRI of hepatic malignant and benign lesions was studied in order to establish a theoretical foundation for microvessels evaluation within these lesions with MRI images, which will give more references to clinical diagnosis or HCC therapy.

MATERIALS AND METHODS

Tissue specimens

Tissue specimens were obtained at surgery from Eastern Hepatobiliary Surgery Institute, including 265 of HCC, 122 of cirrhosis tissue adjacent to carcinoma, 5 of hepatocellular adenoma and 17 of focal nodular hyperplasia (FNH). The 265 specimens of HCC included 45 of small HCC (tumor diameter ≤ 3 cm). All the case of HCC were graded by Edmondson-Steiner's pathological criteria into 3 groups: grades I-II (37 cases), grade III (218 cases) and grade IV (10 cases). All the specimens were fixed in 10% formalin and embedded in paraffin. All the pathologic diagnoses were confirmed by two the pathologists.

Constructing tissue microarray

For tissue microarray construction, a hematoxylin and eosin (H&E)-stained section was made from each block to define representative regions. With a tissue-microarray-constructor (Beecher Instruments, Silver Spring, MD), a hole (diameter=6 mm) was punched into a recipient paraffin block, and then a cylindrical core sample (diameter=6 mm), which had been punched from the donor tissue block, was deposited into the hole. This process was repeated till all the samples were deposited into the recipient block. After finishing the recipient block, multiple sections were cut from the block with a microtome.

Immunohistochemical staining and evaluation criteria

Avidin-biotin-peroxidase complex (ABC) method was used for immunohistochemical staining with monoclonal antibody CD-34 (Antibody Dignostic Inc., U.S.A.). After staining, the tubular, sinusoidal, cystiform or vacuolar structures shaped by endothelial cells or immature endothelial cells, which were stained yellow

or brown by CD34, were considered as positive microvessels. In high power microscopic views, all the positive microvessels were counted for MVD.

MRI technique

Forty-eight patients with 49 of the lesions underwent MRI examination before surgery, including 33 HCC (only one belonged to grade IV, and the others belonged to grade III and all diameters were ≤ 3 cm) and 16 benign lesions. MRI was performed with a 1.5 T system (Symphony, Siemens) and a phased array coil was used. All the patients underwent axial T1 weighted (fast low angle shot, FLASH, TR=123 ms, TE=4.8 ms), T2 weighted (half-fourier acquisition single-shot turbo spin echo, HASTE, TR=1 200 ms, TE=57 ms) and multiphase dynamic gadolinium-DTPA enhanced (the same sequence as T1 weighted) imaging. The section thickness was 8 mm, with an intersection gap of 0.5-2 mm. The contrast material dose was 0.2 mmol/kg b.w. and was administered as a rapid bolus. Arterial phase images were obtained in 15-20 s after the start of bolus administration. Portal venous and equilibrium phase images were obtained in the 45 s and 90 s, respectively.

Image analyses

In all the images, signal intensities of lesions (SI_l), liver parenchyma (SI_p) and background noise (SI_n) were evaluated, respectively. Signal-to-noise ratios (SNR) of lesions and parenchyma were both calculated as $SNR = SI_l / SI_n$. Contrast-to-noise ratios (CNR) in all the phases were calculated as $CNR = SNR_l - SNR_p$. Enhancement indexes (EI) of lesions in all the phases were calculated as $EI = (SNR_{\text{contrasted}} - SNR_{\text{uncontrasted}}) / SNR_{\text{uncontrasted}}$.

Statistical analyses

All data were analyzed by SPSS 9.0. Analysis of variance was used to determine significant differences of MVD among HCC, cirrhosis and benign lesion, of MVD of HCC among different pathological grades and tumor diameters, and of CNR between HCC and benign lesion among nonenhanced, arterial, portal venous and equilibrium phases. Pearson correlation was performed for correlation analysis among CNRs, EIs and MVD in arterial, portal venous and equilibrium phases of HCC or

benign lesion, respectively.

RESULTS

Outcome of tissue microarray constructing, immunohistochemical staining and MRI

Overview of a piece of tissue microarray is shown in Figure 1. Microvessel density stained by immunohistochemistry and dynamic MR images of HCC, hepatocellular adenoma and FNH are shown in Figures 2, 3 and 4, respectively.

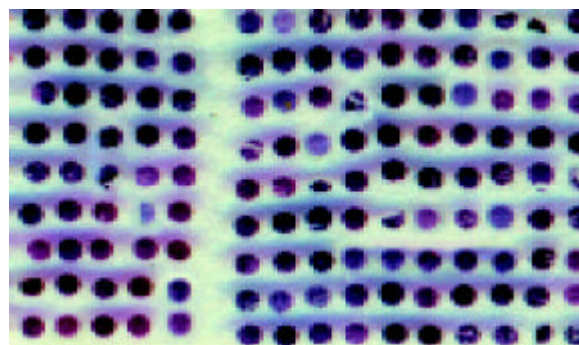


Figure 1 Overview of a piece of tissue microarray including 234 samples (HE staining).

Table 1 MVD of malignant and benign liver lesions

	Number	MVD (mean \pm SD)
HCC	265	22.7 \pm 15.8 ^b
Cirrhosis	122	8.3 \pm 7.6
Benign lesion	22	31.3 \pm 22.7

^b $P < 0.01$ vs cirrhosis.

MVD of hepatic benign and malignant lesions

MVD of HCC was significantly higher than that of cirrhosis, but there was no significant difference between those of HCC and of benign lesions (Table 1).

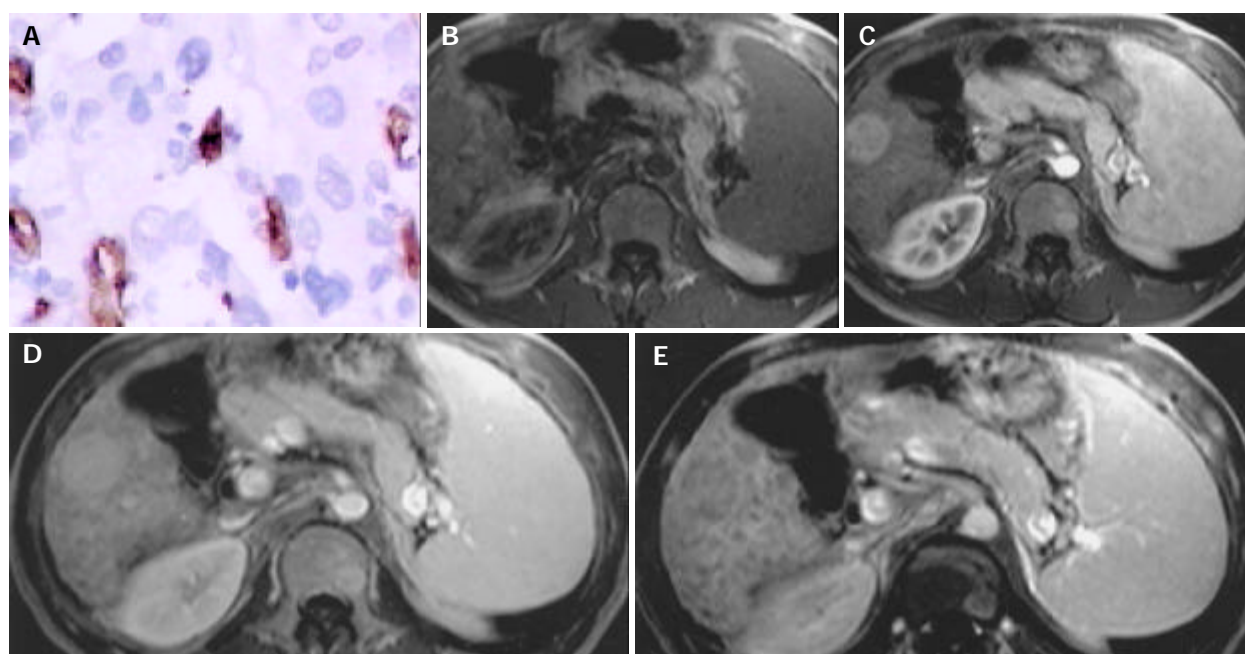


Figure 2 HCC in right lobar of liver. A: Microvessel density, stained by CD34 (Original magnification: $\times 200$); B: MR image, T1 weighted, nonenhanced, CNR=-1.50; C: MR image, arterial phase, CNR=11.00; D: MR image, portal venous phase, CNR=10.50; E: MR image, equilibrium phase, CNR=-6.00.

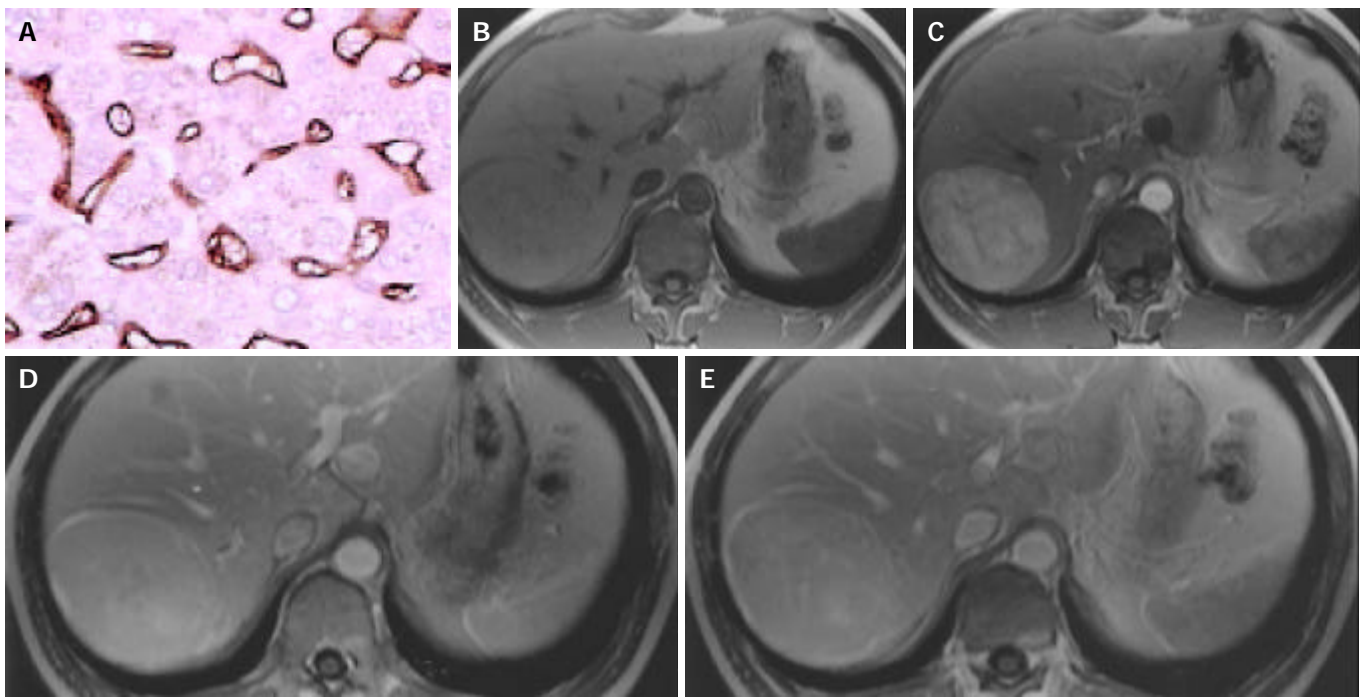


Figure 3 Hepatocellular adenoma in right lobar of liver. A: Microvessel density, stained by CD34 (Original magnification: $\times 200$); B: MR image, T1 weighted, nonenhanced, $\text{CNR} = -0.10$; C: MR image, arterial phase, $\text{CNR} = 16.93$; D: MR image, portal venous phase, $\text{CNR} = 9.42$; E: MR image, equilibrium phase, $\text{CNR} = 6.42$.

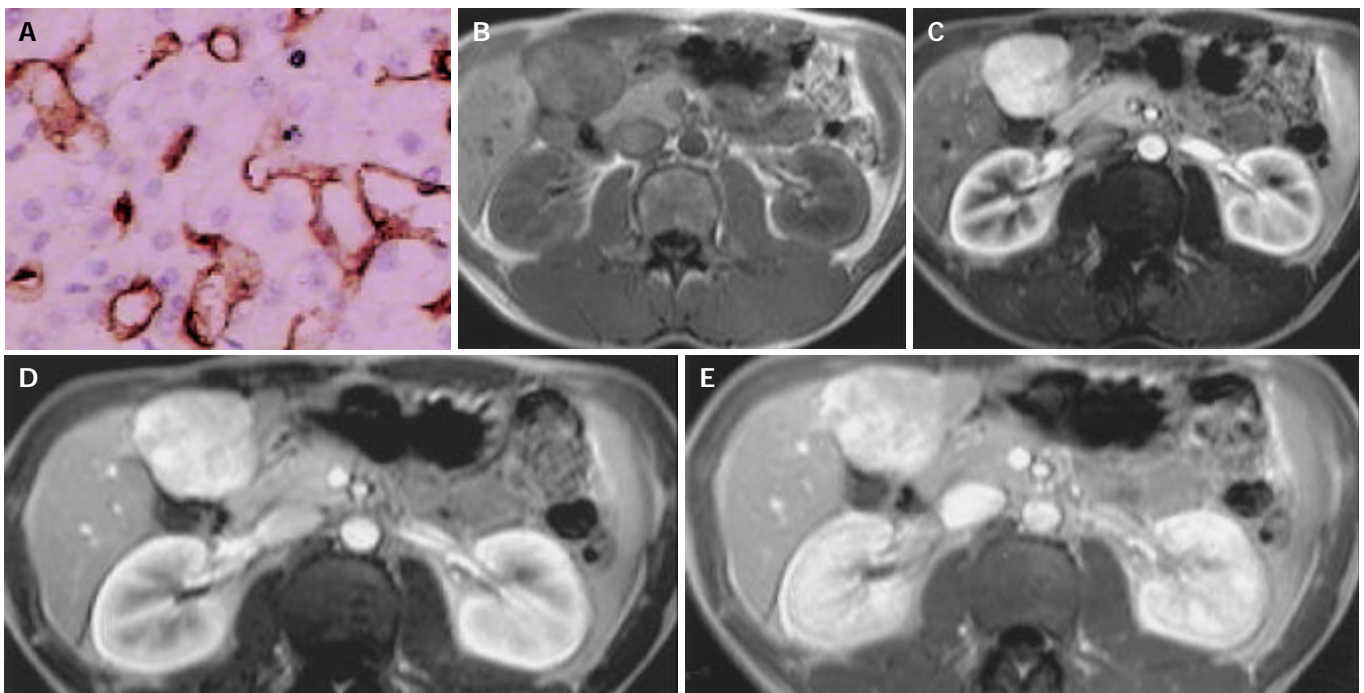


Figure 4 FNH in left inner lobar of liver. A: Microvessel density, stained by CD34 (Original magnification: $\times 200$); B: MR image, T1 weighted, nonenhanced, $\text{CNR} = -3.48$; C: MR image, arterial phase, $\text{CNR} = 15.43$; D: MR image, portal venous phase, $\text{CNR} = 5.81$; E: MR image, equilibrium phase, $\text{CNR} = 2.97$.

MVD of HCC among different pathological grades and tumor sizes

MVD of grades I-II was 29.9 ± 18.6 (mean \pm SD), which was much higher than those of grade III (22.2 ± 18.2 , $P < 0.01$) and grade IV (22.9 ± 19.0 , $P < 0.01$). There was no significant difference in MVD between small HCC (26.1 ± 15.3) and those HCC whose diameters were more than 3 cm (22.1 ± 15.8).

CNR of HCC and benign lesion in all the phases

CNRs of HCC and benign lesion in T1 weighted nonenhanced, arterial, portal venous and equilibrium phases are shown in

Table 2. There was significant difference among all the phases ($F = 9.761$, $P < 0.001$), but no significant difference among nonenhanced, portal venous and equilibrium phases ($P = 0.279$) or between HCC and benign lesion ($F = 0.380$, $P = 0.539$).

Correlation between MVD and CNRs

Forty-eight patients with 49 of the lesions underwent MRI examination before surgery, including 33 HCC (only one belonged to grade IV, and the others belonged to grade III and all the diameters were ≤ 3 cm) and 16 benign lesions. Pearson

Correlation coefficients among MVD and CNRs of HCC in arterial, portal venous and equilibrium phases were 0.409 ($P=0.018$), 0.264 ($P=0.138$) and 0.212 ($P=0.236$), respectively, while Pearson Correlation coefficients between MVD and CNRs of benign lesions in arterial, portal venous and equilibrium phases were 0.599 ($P=0.014$), 0.581 ($P=0.018$) and 0.540 ($P=0.031$), respectively.

Table 2 CNR of HCC and benign lesion (mean \pm SD)

	Nonenhanced	Arterial phase	Portal venous phase	Equilibrium phases
HCC ($n=33$)	-2.86 \pm 2.94	3.88 \pm 5.63	-1.43 \pm 8.39	-1.08 \pm 2.80
Benign lesion ($n=16$)	-2.91 \pm 2.79	2.12 \pm 9.08	-2.05 \pm 8.56	-0.92 \pm 6.59

Correlation between MVD and EIs

Pearson Correlation coefficients between MVD and EIs of the 33 specimens of HCC in arterial, portal venous and equilibrium phases were 0.155 ($P=0.389$), 0.072 ($P=0.692$) and -0.122 ($P=0.497$), respectively, while Pearson Correlation coefficients between MVD and EIs of the 16 specimens of benign lesions in arterial, portal venous and equilibrium phases were 0.077 ($P=0.776$), 0.180 ($P=0.506$) and -0.062 ($P=0.821$), respectively.

DISCUSSION

Utilization of tissue microarray technique in detecting nucleic acid and protein has recently made great progress in basic research of tumor. A large number of samples in one section of tissue microarray can be stained under the same pre-treatment condition, the same antibody titer and the same detection systems. And reproducibility of the staining reaction, as well as the speed and reliability of the interpretation, is improved, since all the samples are on the same slide^[7,8]. Then, quickly and efficiently scanning a great number of specimens with tissue microarray can reduce mistakes not only from sample selecting and statistical analysis but also from tumor heterogeneity. In MVD counting, utilization of tissue microarray can standardize sample areas and overcome manual deviation. In this research, tissue microarray technique, combined with immunohistochemistry, was used to study difference of MVD between malignant and benign hepatic lesions in order to further demonstrate some biological features of these lesions.

CD34, which is expressed in blood stem cells and neovessel endothelial cells, is the most distinctive marker for demonstrating vessel endothelial cells^[9,10], especially for demonstrating sinusoid-like vessels in tumor tissues^[11,12]. Angiogenesis is very common within normal and pathologic tissues and is regulated by many factors, such as hypoxia-inducible factor 1 α (HIF-1 α), vascular endothelial growth factor (VEGF), human macrophage metalloelastase (HME), basic fibroblast growth factor (bFGF) and so on^[13-16]. Vessels, as an important part of tumor interstitial tissue, interact with tumor cells to construct microenvironment of tumor. Researches showed that angiogenesis plays an important role in tumor invasion^[17], MVD is a novel prognostic marker in patients after resection of small HCC^[11,18-20], and high expression of CD34-positive sinusoidal endothelial cells is a risk factor for HCC in patients with chronic liver diseases^[21]. Sun *et al.*^[18] reported that MVD level was not related to tumor size, capsule status, Edmondson-Steiner's grade, alpha-fetoprotein (AFP) level, associated cirrhosis, gamma-glutamyltransferase and serum HBsAg status. Yamamoto *et al.*^[22] demonstrated that sinusoidal capillarization occurring in well-differentiated HCC is related to dedifferentiation of parenchymal tumor cells, but not to tumor size. But some reports showed that tumor size, poor differentiation and portal invasion are significantly related to MVD^[11,23]. In this research,

MVD of HCC was significantly higher than that of cirrhosis, but there was no significant difference between those of HCC and of benign lesion, which probably means that microvessels play an important role not only in occurrence and development of HCC, but also in some other benign lesions, thus may be helpful to identify malignant lesions or precancerous lesions (for example, high-grade dysplastic nodule) from regenerative nodules or low-grade dysplastic nodules^[24,25]. MVD in grades I-II was higher than those in grade III and grade IV, suggesting that angiogenesis is more active during the beginning of hepatocarcinogenesis.

DSA and CTAP have been used for assessing angiogenesis of HCC^[6], but these examinations are all invasive and expensive with dangerousnesses of ionized radiation and allergy induced by iodine contrast material. Shimizu *et al.*^[26] used xenon-enhanced CT to quantitatively measure tissue blood flow in HCC, but xenon is a kind of scarce gas. Compared with DSA, CTAP and xenon-enhanced CT, MRI is uninvase, safe, rapid, and cheap. Gadolinium has a strong hydrogen-proton spin-lattice relaxation effect, which will increase the signal intensity of adjacent tissue on T1 weighted images. The MRI contrast agent, gadolinium-DTPA, does not penetrate cell membrane and only diffuses into vascular space and interstitial space, which may reveal that the signal intensity of tissue on enhanced T1 weighted image is correlated with the vascularity. There have been reports on correlation of dynamic contrast enhancement MRI with MVD in prostate cancer and in breast cancer^[27,28]. With development of fast scan technique, rapid MRI is available to image the whole liver during the arterial phase^[29]. In this research, CNR in arterial phase, regardless of malignant or benign lesions, was correlative with MVD. Since MVD of HCC is much higher than that of cirrhosis, arterial phase images of MRI could be a useful method to distinguish HCC from regenerative nodules. Some reports have confirmed this view^[30,31]. In this research, CNR of HCC in portal venous or equilibrium phase was not correlated with MVD. This phenomenon probably demonstrates that CNR is regulated by many factors besides MVD. Reports have shown that with small HCC increasing in size and becoming increasingly dedifferentiated, the number of portal tracts apparently decreases and intratumoral arteriole develops^[22,23]. Because of portal tracts' decreasing and intratumoral arterioles' developing, there was no unified blood supply in HCC nodules, which would not demonstrate unified relationship between MVD and CNR in portal venous or equilibrium phase. There was no change of blood supply in benign nodules, so unified relationship between MVD and CNR in portal venous or equilibrium phase was demonstrated. CNR in arterial phase is mostly regulated by MVD, while in portal venous or equilibrium phase, blood supply plays a more important role. This hypothesis should be tested by advanced research.

In conclusion, angiogenesis is secondary to occurrence and development of benign and malignant tumors. Since dynamic MRI could evaluate microvessel of lesions, it is a very useful method to demonstrate HCC.

REFERENCES

- 1 **El-Assal ON**, Yamanoi A, Soda Y, Yamaguchi M, Igarashi M, Yamamoto A, Nabika T, Nagasue N. Clinical significance of microvessel density and vascular endothelial growth factor expression in hepatocellular carcinoma and surrounding liver: possible involvement of vascular endothelial growth factor in the angiogenesis of cirrhotic liver. *Hepatology* 1998; **27**: 1554-1562
- 2 **Kallioniemi OP**, Wagner U, Kononen J, Sauter G. Tissue microarray technology for high-throughput molecular profiling of cancer. *Hum Mol Genet* 2001; **10**: 657-662
- 3 **Tomemori T**, Yamakado K, Nakatsuka A, Sakuma H, Matsumura K, Takeda K. Fast 3D dynamic MR imaging of the liver with MR SmartPrep: comparison with helical CT in de-

- etecting hypervascular hepatocellular carcinoma. *Clin Imaging* 2001; **25**: 355-361
- 4 **Shinozaki K**, Honda H, Yoshimitsu K, Taguchi K, Kuroiwa T, Irie H, Aibe H, Nishie A, Nakayama T, Shimada M, Masuda K. Optimal multi-phase three-dimensional fast imaging with steady-state free precession dynamic MRI and its clinical application to the diagnosis of hepatocellular carcinoma. *Radiat Med* 2002; **20**: 111-119
 - 5 **Noguchi Y**, Murakami T, Kim T, Hori M, Osuga K, Kawata S, Okada A, Sugiura T, Tomoda K, Narumi Y, Nakamura H. Detection of hypervascular hepatocellular carcinoma by dynamic magnetic resonance imaging with double-echo chemical shift in-phase and opposed-phase gradient echo technique: comparison with dynamic helical computed tomography imaging with double arterial phase. *J Comput Assist Tomogr* 2002; **26**: 981-987
 - 6 **Toyoda H**, Fukuda Y, Hayakawa T, Kumada T, Nakano S. Changes in blood supply in small hepatocellular carcinoma: correlation of angiographic images and immunohistochemical findings. *J Hepatol* 1997; **27**: 654-660
 - 7 **Bubendorf L**, Kononen J, Koivisto P, Schraml P, Moch H, Gasser TC, Willi N, Mihatsch MJ, Sauter G, Kallioniemi OP. Survey of gene amplifications during prostate cancer progression by high-throughout fluorescence *in situ* hybridization on tissue microarrays. *Cancer Res* 1999; **59**: 803-806
 - 8 **Richter J**, Wagner U, Kononen J, Fijan A, Bruderer J, Schmid U, Ackermann D, Maurer R, Alund G, Knönagel H, Rist M, Wilber K, Anabitarte M, Hering F, Hardmeier T, Schönsberger A, Flury R, Jager P, Fehr JL, Schraml P, Moch H, Mihatsch MJ, Gasser T, Källioniemi OP, Sauter G. High-throughput tissue microarray analysis of cyclin E gene amplification and overexpression in urinary bladder cancer. *Am J Pathol* 2000; **157**: 787-794
 - 9 **Kimura H**, Nakajima T, Kagawa K, Deguchi T, Kakusui M, Katagishi T, Okanou T, Kashima K, Ashihara T. Angiogenesis in hepatocellular carcinoma as evaluated by CD34 immunohistochemistry. *Liver* 1998; **18**: 14-19
 - 10 **Frachon S**, Gouysse G, Dumortier J, Couvelard A, Nejjar M, Mion F, Berger F, Paliard P, Boillot O, Scoazec JY. Endothelial cell marker expression in dysplastic lesions of the liver: an immunohistochemical study. *J Hepatol* 2001; **34**: 850-857
 - 11 **Tanigawa N**, Lu C, Mitsui T, Miura S. Quantitation of sinusoid-like vessels in hepatocellular carcinoma: its clinical and prognostic significance. *Hepatology* 1997; **26**: 1216-1223
 - 12 **Gottschalk-Sabag S**, Ron N, Glick T. Use of CD34 and factor VIII to diagnose hepatocellular carcinoma on fine needle aspirates. *Acta Cytol* 1998; **42**: 691-696
 - 13 **Ravi R**, Mookerjee B, Bhujwala ZM, Sutter CH, Artemov D, Zeng Q, Dillehay LE, Madan A, Semenza GL, Bedi A. Regulation of tumor angiogenesis by p53-induced degradation of hypoxia-inducible factor 1alpha. *Genes Dev* 2000; **14**: 34-44
 - 14 **Gorrin-Rivas MJ**, Arie S, Mori A, Takeda Y, Mizumoto M, Furutani M, Imamura M. Implications of human macrophage metalloelastase and vascular endothelial growth factor gene expression in angiogenesis of hepatocellular carcinoma. *Ann Surg* 2000; **231**: 67-73
 - 15 **Yoshiji H**, Kuriyama S, Yoshii J, Ikenaka Y, Noguchi R, Hicklin DJ, Huber J, Nakatani T, Tsujinoue H, Yanase K, Imazu H, Fukui H. Synergistic effect of basic fibroblast growth factor and vascular endothelial growth factor in murine hepatocellular carcinoma. *Hepatology* 2002; **35**: 834-842
 - 16 **Park YN**, Kim YB, Yang KM, Park C. Increased expression of vascular endothelial growth factor and angiogenesis in the early stage of multistep hepatocarcinogenesis. *Arch Pathol Lab Med* 2000; **124**: 1061-1065
 - 17 **Ker CG**, Chen HY, Juan CC, Lo HW, Shen YY, Chen JS, Lee KT, Sheen PC. Role of angiogenesis in hepatitis and hepatocellular carcinoma. *Hepatogastroenterology* 1999; **46**: 646-650
 - 18 **Sun HC**, Tang ZY, Li XM, Zhou YN, Sun BR, Ma ZC. Microvessel density of hepatocellular carcinoma: its relationship with prognosis. *J Cancer Res Clin Oncol* 1999; **125**: 419-426
 - 19 **Salizzoni M**, Romagnoli R, Lupo F, David E, Mirabella S, Cerutti E, Ottobrelli A. Microscopic vascular invasion detected by anti-CD34 immunohistochemistry as a predictor of recurrence of hepatocellular carcinoma after liver transplantation. *Transplantation* 2003; **76**: 844-848
 - 20 **Poon RT**, Ng IO, Lau C, Yu WC, Yang ZF, Fan ST, Wong J. Tumor microvessel density as a predictor of recurrence after resection of hepatocellular carcinoma: a prospective study. *J Clin Oncol* 2002; **20**: 1775-1785
 - 21 **Ohmori S**, Shiraki K, Sugimoto K, Sakai T, Fujikawa K, Wagayama H, Takase K, Nakano T. High expression of CD34-positive sinusoidal endothelial cells is a risk factor for hepatocellular carcinoma in patients with HCV-associated chronic liver diseases. *Hum Pathol* 2001; **32**: 1363-1370
 - 22 **Yamamoto T**, Hirohashi K, Kaneda K, Ikebe T, Mikami S, Uenishi T, Kanazawa A, Takemura S, Shuto T, Tanaka H, Kubo S, Sakurai M, Kinoshita H. Relationship of the microvascular type to the tumor size, arterIALIZATION and dedifferentiation of human hepatocellular carcinoma. *Jap J Cancer Res* 2001; **92**: 1207-1213
 - 23 **Nakashima Y**, Nakashima O, Hsia CC, Kojiro M, Tabor E. Vascularization of small hepatocellular carcinomas: correlation with differentiation. *Liver* 1999; **19**: 12-18
 - 24 **Roncalli M**, Roz E, Coggi G, Di Rocco MG, Bossi P, Minola E, Gambacorta M, Borzio M. The vascular profile of regenerative and dysplastic nodules of the cirrhotic liver: implications for diagnosis and classification. *Hepatology* 1999; **30**: 1174-1178
 - 25 **de Boer WB**, Segal A, Frost FA, Sterrett GF. Can CD34 discriminate between benign and malignant hepatocytic lesions in fine-needle aspirates and thin core biopsies? *Cancer* 2000; **90**: 273-278
 - 26 **Shimizu J**, Oka H, Dono K, Sakon M, Takamura M, Murakami T, Hayashi S, Nagano H, Nakamori S, Umeshita K, Sase S, Gotoh M, Wakasa K, Nakamura H, Monden M. Noninvasive quantitative measurement of tissue blood flow in hepatocellular carcinoma using xenon-enhanced computed tomography. *Dig Dis Sci* 2003; **48**: 1510-1516
 - 27 **Schlemmer HP**, Merkle J, Grobholz R, Jaeger T, Michel MS, Werner A, Rabe J, van Kaick G. Can pre-operative contrast-enhanced dynamic MR imaging for prostate cancer predict microvessel density in prostatectomy specimens? *Eur Radiol* 2004; **14**: 309-317
 - 28 **Su MY**, Cheung YC, Fruehauf JP, Yu H, Nalcioğlu O, Mechetner E, Kyshtoobayeva A, Chen SC, Hsueh S, McLaren CE, Wan YL. Correlation of dynamic contrast enhancement MRI parameters with microvessel density and VEGF for assessment of angiogenesis in breast cancer. *J Magn Reson Imaging* 2003; **18**: 467-477
 - 29 **Van Beers BE**, Materne R, Lacrosse M, Jamart J, Smith AM, Horsmans Y, Gigot JF, Gilon R, Pringot J. MR imaging of hypervascular liver tumors: timing optimization during the arterial phase. *J Magn Reson Imaging* 1999; **9**: 562-567
 - 30 **Yoshimitsu K**, Honda H, Jimi M, Kuroiwa T, Irie H, Aibe H, Shinozaki K, Asayama Y, Shimada M, Masuda K. Correlation of three-dimensional gradient echo dynamic MR imaging with CT during hepatic arteriography in patients with hypervascular hepatocellular carcinomas: preliminary clinical experience. *J Magn Reson Imaging* 2001; **13**: 258-262
 - 31 **Noguchi Y**, Murakami T, Kim T, Hori M, Osuga K, Kawata S, Kumano S, Okada A, Sugiura T, Nakamura H. Detection of hepatocellular carcinoma: comparison of dynamic MR imaging with dynamic double arterial phase helical CT. *Am J Roentgenol* 2003; **180**: 455-460

Cloning and identification of *NS5ATP2* gene and its spliced variant transactivated by hepatitis C virus non-structural protein 5A

Qian Yang, Jun Cheng, Yan Liu, Yuan Hong, Jian-Jun Wang, Shu-Lin Zhang

Qian Yang, Shu-Lin Zhang, Department of Infectious Disease, First Hospital of Xi'an Jiaotong University, Xi'an 710061, Shaanxi Province, China

Jun Cheng, Yan Liu, Yuan Hong, Jian-Jun Wang, Gene Therapy Research Center, Institute of Infectious Diseases, 302 Hospital of PLA, 100 Xisihuanzhong Road, Beijing 100039, China

Supported by the National Natural Science Foundation of China, No. C03011402, No. C30070690 and the 9th Five-year Plan Period Research and Development Foundation of PLA, No. 98D063 and the Start-up for Students Studying Overseas of PLA, No. 98H038 and the 10th Five-year period Youth Research and Technology Foundation of PLA, No. 01Q138 and the 10th Five-year period Research and Technology Foundation of PLA, No. 01MB135

Correspondence to: Dr. Jun Cheng, Gene Therapy Research Center, Institute of Infectious Diseases, 302 Hospital of PLA, 100 Xisihuanzhong Road, Beijing 100039, China. cj@genetherapy.com.cn

Telephone: +86-10-66933391 **Fax:** +86-10-63801283

Received: 2003-11-21 **Accepted:** 2003-12-29

Abstract

AIM: To clone, identify and study new *NS5ATP2* gene and its spliced variant transactivated by hepatitis C virus non-structural protein 5A.

METHODS: On the basis of subtractive cDNA library of genes transactivated by NS5A protein of hepatitis C virus, the coding sequence of new gene and its spliced variant were obtained by bioinformatics method. Polymerase chain reaction (PCR) was conducted to amplify *NS5ATP2* gene.

RESULTS: The coding sequence of a new gene and its spliced variant were cloned and identified successfully.

CONCLUSION: A new gene has been recognized as the new target transactivated by HCV NS5A protein. These results brought some new clues for studying the biological functions of new genes and pathogenesis of the viral proteins.

Yang Q, Cheng J, Liu Y, Hong Y, Wang JJ, Zhang SL. Cloning and identification of *NS5ATP2* gene and its spliced variant transactivated by hepatitis C virus non-structural protein 5A. *World J Gastroenterol* 2004; 10(12): 1735-1739
<http://www.wjgnet.com/1007-9327/10/1735.asp>

INTRODUCTION

Hepatitis C virus (HCV) is the major causative agent of non-A, non-B hepatitis worldwide, which often leads to cirrhosis and an increased risk of hepatocellular carcinoma. The single-stranded RNA genome of HCV is a 9.6 kb-long positive-sense molecule, belonging to the *Flaviviridae* family. The viral genome encodes a single polyprotein precursor of approximately 3 010 amino acids, which is cleaved by both host and viral proteases to generate putative structural proteins (core, E1, and E2/p7) and the nonstructural proteins (NS2, NS3, NS4A, NS4B, NS5A, and NS5B)^[1-3]. The nonstructural protein 5A (NS5A) is a phosphoprotein consisting of 447 amino acid residues. NS5A exists in two

forms of polypeptide p56 and p58, which are phosphorylated mainly at serine residues both *in vitro* and *in vivo*^[4,5].

It was previously shown that NS5A could function as a transcriptional trans-activator. Although these reports implicate a functional role of NS5A in transcription, the exact nature of its role or the mechanism (s) involved in regulating the cellular transcription has not been investigated. NS5A is localized to the endocytosolic reticulum (ER), whereas transcriptional trans-activation traditionally requires the protein to be in the nucleus. The NS5A protein must participate in signal transduction pathways that are initiated in the cytoplasm where it resides^[6,7]. However, some studies show NS5A protein possesses a nuclear localization-like signal sequence and is present in the nuclear periplasmic membrane fraction related to transcription or translation^[8]. The present study shows NS5A protein has transactivating effect on SV40 early promoter.

MATERIALS AND METHODS

Plasmid construction

The HCV-NS5A sequences were generated by PCR amplification of HCV plasmid (HCV strain 1b). The plasmid contains coding sequences for all of the nonstructural proteins. The PCR conditions were as follows: 94 °C for 40 s. 10 ng of PCR product was cloned with pEGM-T vector (Promega). The primary structure of insert was confirmed by direct sequencing. To create pcDNA3.1 (-)-NS5A, the fragments of encoding NS5A were released from the pEGM-T-NS5A by digestion with *Eco*R I and *Kpn* I, and ligated to pcDNA3.1 (-)^[9].

Cell culture and transfection

The hepatoblastoma cell line HepG2 was propagated in DMEM supplemented with 10% FBS, 200 μmol/L L-glutamine, penicillin, and streptomycin. The HepG2 cells were plated at a density of 1×10⁶/well in 35-mm dishes. About 60-70% confluent HepG2 cells were cotransfected with plasmids pcDNA3.1 (-)-NS5A and pCAT3-promoter, transfected with pcDNA3.1 (-)-NS5A, pcDNA3.1 (-) with FuGENE 6(Roche).

Confirmation of protein expression of HCV-NS5A

Expression plasmid pcDNA3.1 (-)-NS5A was transfected using FuGENE 6 into HepG2 cells. The proteins expressed in these cells were analyzed on an immunoblot using the NS5A-specific antibody. The proteins were resolved by electrophoresis on a sodium dodecyl sulfate 125 g/L polyacrylamide gel. The lysate of cells transfected with expression vector pcDNA3.1 (-) served as negative control^[10].

CAT assay

Cells were then harvested after 48 h for CAT assay. Lysates of transfected cells were analyzed for CAT density using a commercial enzyme-linked immunosorbent assay (Roche Molecular Biochemicals). The absorbance of the samples was measured at 405 nm^[11].

RNA extraction and SSH

mRNAs from HepG2 cells transfected with plasmids pcDNA3.1

(-)-NS5A and pcDNA3.1(-) were extracted by using QuickPrep micro mRNA Purification Kit (Amersham Pharmacia). The amount of mRNA from two samples was 3-4 µg.

SSH was performed with the cDNA Subtraction Kit (Clontech) according to the manufacturer's protocol. cDNA was synthesized from 2 µg of poly A+RNA from two samples being compared. The cDNA from pcDNA3.1 (-)-NS5A acted as the tester, the cDNA from pcDNA3.1 (-) as the driver. The tester and driver cDNAs were digested with *Rsa* I, which yielded blunt ends. Two different PCR adaptors that could join only 5' ends DNA were ligated to different aliquots of tester DNA. These ligated DNAs were denatured, mixed with an excess of driver DNA (that had no adaptors), and allowed to anneal. The two DNA pools were then mixed together, and more denatured driver DNAs were added to further bind tester that was also present in the driver. Remaining complementary single strands of tester DNA were allowed to anneal, and the adaptor sequences were copied into their 3' ends. PCR was then performed to obtain exponential amplification of tester DNAs with different adaptors at each end. PCR amplifications products were directly purified by using Wizard PCR Preps DNA Purification System (Promega), and subcloned into pEGM-T easy vectors (Promega) to set up the subtractive library^[12,13].

New gene cloned

On the basis of subtractive cDNA library of genes transactivated by NS5A protein of hepatitis C virus, the coding sequence of a new gene, named NS5ATP2, was obtained by bioinformatics methods. The standard PCR cloning technique was used to amplify NS5ATP2 gene. Cytoplasmic RNA was isolated from HepG2 cells. RNA was used for RT-PCR as described previously, primers were: sense 5' -GGA TTC ATG GCT TCG GTC TCC TCT GC-3', antisense 5' -GGT ACC TCA GGA GTG TGG CTC ACT GG -3' (HepG2 cDNA). The PCR condition was as follows: at 94 °C for 60 s, at 60 °C for 60 s, at 72 °C for 60 s, for 30 cycles. The PCR product was cloned with pGEM-T vector (Promega). The primary structure of insert was confirmed by direct sequencing.

RESULTS

NS5A protein expressed in HepG2 cells

NS5A protein expressed in cells was analyzed by Western blot. The lysates of cells transfected with plasmid pcDNA3.1 (-)-NS5A were specifically detected by NS5A specific antibody (Figure 1).

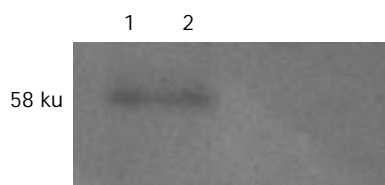


Figure 1 Western blotting of NS5A protein expression in HepG2 cells. Lane 1: Expression plasmid pcDNA3.1 (-)-NS5A; Lane 2: Plasmid pcDNA3.1 (-)-vector.

Transactivating effect of NS5A on SV40 early promoter

To determine whether NS5A protein has transactivating effect, we constructed plasmid pcDNA3.1 (-)-NS5A, and HCV NS5A protein expressed in Hep G2 cells was detected by reverse transcription PCR (RT-PCR) and Western blotting. HepG2 cells were transiently cotransfected with pcDNA3.1 (-)-NS5A/pCAT3-promoter, pcDNA3.1(-)/pCAT3-promoter. Chloramphenicol acetyltransferase (CAT) activity in cells

that were cotransfected with pcDNA3.1 (-)-NS5A/pCAT3-promoter is shown in Figure 2.

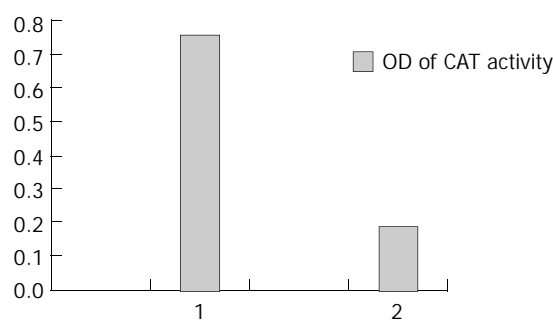


Figure 2 Transactivation on SV40 promoter by NS5A. 1: Plasmid pcDNA3.1 (-)-NS5A was cotransfected with pCAT3-promoter in HepG2 cells. 2: Plasmid pcDNA3.1 (-) was cotransfected with pCAT3-promoter in HepG2 cells.

Construction of subtractive cDNA library

Our studies showed NS5A protein had transactivation effect on SV40 promoter. In order to investigate influence of NS5A protein on cells gene expression, Suppression subtraction hybridization (SSH) was introduced to establish subtractive cDNA library of HepG2 transfected with plasmid pcDNA3.1 (-)-NS5A. We performed the PCR experiment to analyse the ligation efficiency. The result showed that at least 25% of the cDNA had adaptors at both ends. The efficiency of subtraction was estimated by PCR experiment. The test was done by comparison of the abundance of G3PDH before and after subtraction. G3PDH primers were provided by the kit (Figure 3).



Figure 3 Reduction of G3PDH amount by PCR-selective subtraction. PCR was performed on unsubtracted (Lanes 1-4) and subtracted (Lanes 5-8) secondary PCR products with the G3PDH 5' and 3' primers. Lanes 1, 5: 18 cycles; Lanes 2,6: 23 cycles; Lanes 3,7: 28 cycles.

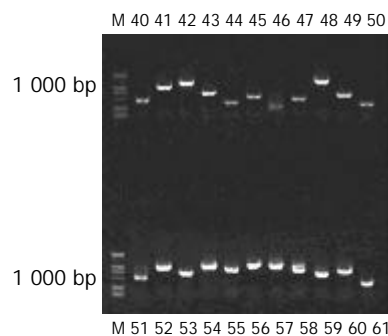


Figure 4 Map of colony PCR on 9 g/L agarose/EtBr gel.

After tester cDNA was hybridized with driver cDNA twice and underwent nested PCR twice, they were then subcloned into pGEM-T easy vectors to set up the subtractive library. Amplification of the library was carried out with *E. coli* strain JM109. The amplified library contained 121 positive clones.

Colony PCR showed that 115 clones contained 200-1 000 bp inserts (Figure 4). The nucleotide sequences of 90 clones from this cDNA library was analyzed, the full length sequences were obtained with Vector NTI 6 and BLAST database homology search (<http://www.ncbi.nlm.nih.gov/>). Altogether 44 kinds of coding sequences were obtained, consisting of 29 known and 15 unknown ones. Some genes code for proteins involved in cell cycle regulation, cell apoptosis, signal transduction pathway and tumour (Table 1).

Table 1 Sequence analysis of 46 clones isolated from subtractive cDNA library

Known genes	Number of clones	Homology (%)
Ribosomal protein	15	99
Eukaryotic translation initiation factor	4	99
HCV NS5A protein	4	98
Sentrin	4	99
Pro-oncosis receptor inducing membrane injury (Porimin)	3	100
Importin	3	98
Serine/threonine kinase	3	100
Cadherin-associated protein	2	100
Mitogen-activated protein kinase phosphatase	2	99
Adenylyl cyclase-associated protein	2	100
Serum response element	2	100
Rho GTPase activating protein	2	100
Fibronectin	3	99
Laminin	3	99
Lysophospholipase A2	2	100
Lysophospholipase B	2	100
Dual specificity phosphatase 6	1	99
Putative homeodomain transcription factor	2	92
Transcription factor B2	2	100
NF-E2-like basic leucine zipper	2	98
Transcriptional activator	2	100
Transcriptional elongation factor (TFIIS)	1	100
MHC-I binding protein	1	99
C response protein binding protein (CRPBP)	1	99
Integrin	2	99
Iron-regulated transporter (IREG)	1	99
Tumor associated protein L6	2	100
WW domain-containing protein 1 (WWP1)	1	100
Nascent polypeptide-associate complex α (NACA)	1	99
Thioredoxin reductase	1	99

Confirmation of new gene expression by RT-PCR

We found the spliced variant of NS5A-TP2 (Figures 5, 6). After EST database homology search (<http://www.ncbi.nlm.nih.gov/>), the locations of NS5A-TP2 and its spliced variant were detected on chromosome 6q22. 1-23. 3. The exons and introns of two new genes were compared (Figure 7). The direct sequencing showed we acquired the ORF of NS5A-TP2 (Figure 8).

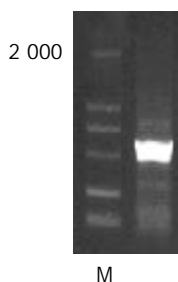


Figure 5 NS5A-TP2 fragment amplified by RT-PCR. M: Marker.

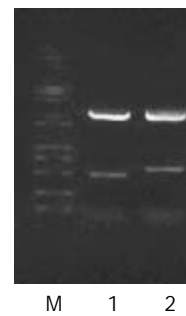


Figure 6 pEGM-T-NS5A-TP2 cut by EcoR I/Kpn I. M: Marker; Lane 1: A 512-bp fragment; Lane 2: A 615-bp fragment.



Figure 7 Comparison of exons and introns of NS5A-TP2 (615) and (512) gene.

```

615 ATG GCT TCG GTC TCC TCT GCG ACC TTC TCG
512 ATG GCT TCG GTC TCC TCT GCG ACC TTC TCG

615 GGC CAC GGG GCT CGG TCC CTA CTG CAG TTC
512 GGC CAC GGG GCT CGG TCC CTA CTG CAG TTC

615 CTG CGG CTG GTA GGG CAG CTC AAG AGA GTC
512 CTG CGG CTG GTA GGG CAG CTC AAG AGA GTC

615 CCA CGA ACT GGC TGG GTA TAC AGA AAT GTC
512 CCA CGA ACT GGC TGG GTA TAC AGA AAT GTC

615 CAG AGG CCG GAG AGC GTT TCA GAT CAC ATG
512 CAG AGG CCG GAG AGC GTT TCA GAT CAC ATG

615 TAC CGG ATG GCA GTT ATG GCT ATG GTG ATC
513 TAC CGG ATG GCA GTT ATG GCT ATG GTG ATC

615 AAA GAT GAC CGT CTT AAC AAA GAC CGA TGT
512 AAA GAT GAC CGT CTT AAC AAA GAC C-- ---

615 GTA CGC CTA GCC CTG GTT CAT GAT ATG GCA
512 --- --- --- --- --- --- --- --- ---

615 GAA TGC ATC GTT GGG GAC ATA GCA CCA GCA
512 --- --- --- --- --- --- --- --- ---

615 GAT AAC ATC CCC AAA GAA GAA AAA CAT AGG
512 --- --- --- --- --- --- --- --- ---

615 CGA GAA GAG GAA GCT ATG AAG CAG ATA ACC
512 --- --- --- G GAA GCT ATG AAG CAG ATA ACC

615 CAG CTC CTA CCA GAG GAC CTC AGA AAG GAG
512 CAG CTC CTA CCA GAG GAC CTC AGA AAG GAG

615 CTC TAT GAA CTT TGG GAA GAG TAC GAG ACC
512 CTC TAT GAA CTT TGG GAA GAG TAC GAG ACC

615 CAA TCT AGT GCA GAA GCC AAA TTT GTG AAG
512 CAA TCT AGT GCA GAA GCC AAA TTT GTG AAG

615 CAG CTA GAC CAA TGT GAA ATG ATT CTT CAA
512 CAG CTA GAC CAA TGT GAA ATG ATT CTT CAA

615 GCA TCT GAA TAT GAA GAC CTT GAA CAC AAA
512 GCA TCT GAA TAT GAA GAC CTT GAA CAC AAA

615 CCT GGG AGA CTG CAA GAC TTC TAT GAT TCC
512 CCT GGG AGA CTG CAA GAC TTC TAT GAT TCC

615 ACA GCA GGA AAA TTC AAT CAC CCT GAG ATA
512 ACA GCA GGA AAA TTC AAT CAC CCT GAG ATA

615 GTC CAG CTT GTT TCT GAA CTT GAG GCA GAA
512 GTC CAG CTT GTT TCT GAA CTT GAG GCA GAA

615 AGA AGC ACT AAC ATA GCT GCA GCT GCC AGT
512 AGA AGC ACT AAC ATA GCT GCA GCT GCC AGT

615 GAG CCA CAC TCC TGA
512 GAG CCA CAC TCC TGA
    
```

Figure 8 ORF comparison of NS5A-TP2 (615) and (512).

DISCUSSION

Hepatitis C virus often causes persistent infection with a significant risk of end-stage cirrhosis and hepatocellular carcinoma. HCV may benefit by regulation of cellular genes leading to the disruption of normal cell growth. Viral genes can override cellular control mechanisms, which in untransformed cells regulate cell cycle progression in response to various antiproliferative signals. In HCV persistently infected cells, the continued presence of viral gene products is likely to be detrimental for host cells. Many studies demonstrated NS5A protein of HCV transcriptionally modulates cellular genes and promotes murine fibroblast cell growth into a tumorigenic phenotype. It may be possible that the NS5A protein plays a role in hepatocarcinogenesis, since many other viral proteins that play a role in carcinogenesis often function as transcriptional activators^[14-17]. However, the precise mechanism is still unknown.

In the present study, we investigated the possible mechanism by which NS5A protein transactivated gene expression and its role in hepatocarcinogenesis. NS5A protein in Hep G2 cells was detected by RT-PCR and Western blotting. HepG2 cells were transiently cotransfected with pcDNA3.1 (-)-NS5A/pCAT3-promoter. CAT activity was evidently higher in the cotransfected cells than in control. It is suggested that NS5A protein has transactivating effect on SV40 early promoter. We predicted that NS5A protein transcriptionally regulated gene expression through regulating promoter activity, either directly or through signal transduction pathways.

On the basis of this study, we constructed subtractive cDNA library by SSH. After sequencing analysis, we obtained coding sequences of 46 genes, which consisted of 26 kinds of known and 15 kinds of unknown ones. Some genes code for proteins involved in cell cycle regulation, cell apoptosis, and tumor angiogenesis. Sentrin is a 101-amino acid ubiquitin-like protein that interacts with the death domains of Fas and TNFR1, with PML, a tumor suppressor implicated in the pathogenesis of promyelocytic leukemia, with Rad51 and Rad52, proteins that are involved in repairing double-stranded DNA breaks, and with RanGAP1, a GTPase-activating protein that is critically involved in nuclear protein transport^[18-20]. Overexpression of sentrin in mammalian cells protects them against anti-Fas or tumor necrosis factor-induced cell death^[21]. Porimin is a highly glycosylated protein that can be classified as a member of the cell membrane-associated mucin family^[22]. Porimin is a membrane mucin that mediates cell death. Although mucins mainly affect cell adhesion and ligand binding, several membrane mucins have also been documented to trigger cell death or inhibit cell proliferation, such as CD43 (leukosialin, sialophorin), CD162 (PSGL-1), and CD164 (MGC-24v)^[23]. Likewise, serine/threonine kinase, cadherin-associated protein, adenylyl cyclase-associated protein, mitogen-activated protein kinase phosphatase involving in cell cycle regulation, and cell growth may be correlated with hepatocarcinogenesis of NS5A protein^[24-28].

Alternative pre-mRNA splicing is a fundamental mechanism for differential gene expression that has been reported to regulate the tissue distribution, the intracellular localization, and the activity of different protein kinases. In the process of our study on new genes, we accidentally acquired the spliced variant of NS5A-TP2 and confirmed the ORF of NS5A-TP2 (516) and its location on chromosome. Both of NS5A-TP2 (615) and its spliced variant- NS5A-TP2 (516) locate on 6q22.1-23.3, but they have different exons and introns^[29-31].

The result of this study shows that the NS5A protein is a potent transcriptional activator and transactivates some genes involved in cell cycle regulation, cell apoptosis, and tumor angiogenesis. The study on new genes NS5A-TP2 (516), and

NS5A-TP2 (615) brings some new clues to the biological functions of novel genes and pathogenesis of the viral proteins.

REFERENCES

- 1 **Pawlotsky JM**. Hepatitis C virus (HCV) NS5A protein: role in HCV replication and resistance to interferon-alpha. *J Viral Hepat* 1999; **6**(Suppl 1): 47-48
- 2 **Kumar U**, Tuthill T, Thomas HC, Monjardino J. Sequence, expression and reconstitution of an HCV genome from a British isolate derived from a single blood donation. *J Viral Hepat* 2000; **7**: 459-465
- 3 **Sandres K**, Dubois M, Pasquier C, Payen JL, Alric L, Duffaut M, Vinel JP, Pascal JP, Puel J, Izopet J. Genetic heterogeneity of hypervariable region 1 of the hepatitis C virus (HCV) genome and sensitivity of HCV to alpha interferon therapy. *J Virol* 2000; **74**: 661-668
- 4 **Neddemann P**, Clementi A, De Francesco R. Hyperphosphorylation of the hepatitis C virus NS5A protein requires an active NS3 protease, NS4A, NS4B, and NS5A encoded on the same polyprotein. *J Virol* 1999; **73**: 9984-9991
- 5 **Reed KE**, Rice CM. Identification of the major phosphorylation site of the hepatitis C virus H strain NS5A protein as serine 2321. *J Biol Chem* 1999; **274**: 28011-28018
- 6 **Ghosh AK**, Steele R, Meyer K, Ray R, Ray RB. Hepatitis C virus NS5A protein modulates cell cycle regulatory genes and promotes cell growth. *J Gen Virol* 1999; **80**(Pt 5): 1179-1183
- 7 **Ghosh AK**, Majumder M, Steele R, Yaciuk P, Chrivia J, Ray R, Ray RB. Hepatitis C virus NS5A protein modulates transcription through a novel cellular transcription factor SRCAP. *J Biol Chem* 2000; **275**: 7184-7188
- 8 **Song J**, Nagano-Fujii M, Wang F, Florese R, Fujita T, Ishido S, Hotta H. Nuclear localization and intramolecular cleavage of N-terminally deleted NS5A protein of hepatitis C virus. *Virus Res* 2000; **69**: 109-117
- 9 **Liu Y**, Cheng J, Lu YY. Cloning of genes transactivated by hepatitis B virus X protein. *Zhonghua Ganzangbing Zazhi* 2003; **11**: 5-7
- 10 **Wang L**, Li K, Cheng J, Chen TY, Hong Y, Liu Y, Wang G, Zhong YW. Screening of gene encoding of hepatic protein interacting with Hcsp6 via yeast two hybridization. *Shijie Huanren Xiaohua Zazhi* 2003; **11**: 385-388
- 11 **Liu Y**, Dong J, Cheng J, Lu YY. The study of transactivating effect of HBV X protein on SV40 early promoter. *Jiefangjun Yixue Zazhi* 2001; **26**: 404-406
- 12 **Shridhar V**, Sen A, Chien J, Staub J, Avula R, Kovats S, Lee J, Lillie J, Smith DI. Identification of underexpressed genes in early- and late-stage primary ovarian tumors by suppression subtraction hybridization. *Cancer Res* 2002; **62**: 262-270
- 13 **Diatchenko L**, Lau YF, Campbell AP, Chenchik A, Moqadam F, Huang B, Lukyanov S, Lukyanov K, Gurskaya N, Sverdlov ED, Siebert PD. Suppression subtractive hybridization: a method for generating differentially regulated or tissue-specific cDNA probes and libraries. *Proc Natl Acad Sci U S A* 1996; **93**: 6025-6030
- 14 **Majumder M**, Ghosh AK, Steele R, Ray R, Ray RB. Hepatitis C virus NS5A physically associates with p53 and regulates p21/waf1 gene expression in a p53-dependent manner. *J Virol* 2001; **75**: 1401-1407
- 15 **De Mitri MS**, Morsica G, Cassini R, Bagaglio S, Zoli M, Alberti A, Bernardi M. Prevalence of wild-type in NS5A-PKR protein kinase binding domain in HCV-related hepatocellular carcinoma. *J Hepatol* 2002; **36**: 116-122
- 16 **Park KJ**, Choi SH, Choi DH, Park JM, Yie SW, Lee SY, Hwang SB. 1Hepatitis C virus NS5A protein modulates c-Jun N-terminal kinase through interaction with tumor necrosis factor receptor-associated factor 2. *J Biol Chem* 2003; **278**: 30711-30718
- 17 **Reyes GR**. The nonstructural NS5A protein of hepatitis C virus: an expanding, multifunctional role in enhancing hepatitis C virus pathogenesis. *J Biomed Sci* 2002; **9**: 187-197
- 18 **Ryu SW**, Chae SK, Kim E. Interaction of Daxx, a Fas binding protein, with sentrin and Ubc9. *Biochem Biophys Res Commun* 2000; **279**: 6-10
- 19 **Okura T**, Gong L, Kamitani T, Wada T, Okura I, Wei CF, Chang

- HM, Yeh ET. Protection against Fas/APO-1- and tumor necrosis factor-mediated cell death by a novel protein, sentrin. *J Immunol* 1996; **157**: 4277-42781
- 20 **Kretz-Remy C**, Tanguay RM. SUMO/sentrin: protein modifiers regulating important cellular functions. *Biochem Cell Biol* 1999; **77**: 299-309
- 21 **Kamitani T**, Kito K, Nguyen HP, Fukuda-Kamitani T, Yeh ET. Characterization of a second member of the sentrin family of ubiquitin-like proteins. *J Biol Chem* 1998; **273**: 11349-11353
- 22 **Ma F**, Zhang C, Prasad KV, Freeman GJ, Schlossman SF. Molecular cloning of Porimin, a novel cell surface receptor mediating oncotic cell death. *Proc Natl Acad Sci U S A* 2001; **98**: 9778-9783
- 23 **Zhang C**, Xu Y, Gu J, Schlossman SF. A cell surface receptor defined by a mAb mediates a unique type of cell death similar to oncosis. *Proc Natl Acad Sci U S A* 1998; **95**: 6290-6295
- 24 **Tamari M**, Daigo Y, Nakamura Y. Isolation and characterization of a novel serine threonine kinase gene on chromosome 3p22-21.3. *J Hum Genet* 1999; **44**: 116-120
- 25 **Ohteki T**, Parsons M, Zakarian A, Jones RG, Nguyen LT, Woodgett JR, Ohashi PS. Negative regulation of T cell proliferation and interleukin 2 production by the serine threonine kinase GSK-3. *J Exp Med* 2000; **192**: 99-104
- 26 **Ratcliffe MJ**, Rubin LL, Staddon JM. Dephosphorylation of the cadherin-associated p100/p120 proteins in response to activation of protein kinase C in epithelial cells. *J Biol Chem* 1997; **272**: 31894-31901
- 27 **Nagafuchi A**, Takeichi M, Tsukita S. The 102 kd cadherin-associated protein: similarity to vinculin and posttranscriptional regulation of expression. *Cell* 1991; **65**: 849-857
- 28 **Zelicof A**, Gatica J, Gerst JE. Molecular cloning and characterization of a rat homolog of CAP, the adenylyl cyclase-associated protein from *Saccharomyces cerevisiae*. *J Biol Chem* 1993; **268**: 13448-13453
- 29 **Shima F**, Yamawaki-Kataoka Y, Yanagihara C, Tamada M, Okada T, Kariya K, Kataoka T. Effect of association with adenylyl cyclase-associated protein on the interaction of yeast adenylyl cyclase with Ras protein. *Mol Cell Biol* 1997; **17**: 1057-1064
- 30 **Chen P**, Li J, Barnes J, Kokkonen GC, Lee JC, Liu Y. Restraint of proinflammatory cytokine biosynthesis by mitogen-activated protein kinase phosphatase-1 in lipopolysaccharide-stimulated macrophages. *J Immunol* 2002; **169**: 6408-6416
- 31 **Cheng J**, Li K, Lu YY, Wang L, Liu Y. Bioinformatics analysis of human hepatitis C virus core protein-binding protein 6 gene and protein. *Shijie Huanren Xiaohua Zazhi* 2003; **11**: 378-384

Edited by Zhu LH and Chen WW **Proofread by** Xu FM

Gene expression profiles in an hepatitis B virus transfected hepatoblastoma cell line and differentially regulated gene expression by interferon- α

Xun Wang, Zheng-Hong Yuan, Ling-Jie Zheng, Feng Yu, Wei Xiong, Jiang-Xia Liu, Gen-Xi Hu, Yao Li

Xun Wang, Zheng-Hong Yuan, Ling-Jie Zheng, Wei Xiong, Jiang-Xia Liu, Department of Molecular Virology, Shanghai Medical College, Fudan University, Shanghai 200032, China

Feng Yu, Gen-Xi Hu, Institute of Biochemistry and Cell Biology, CAS, Shanghai 200031, China

Yao Li, State Key Laboratory of Genetics, Fudan University School of Life Science, Shanghai 200433, China

Supported by the Chinese State Basic Science Foundation, No. 1999054105 and Med-X Foundation of Fudan University

Correspondence to: Zheng-Hong Yuan, Department of Molecular Virology, Shanghai Medical College, Fudan University Fudan, 138 Yi Xue Yuan Road, Shanghai 200032, China. zhyuan@shmu.edu.cn

Telephone: +86-21-64161928 **Fax:** +86-21-64227201

Received: 2003-10-15 **Accepted:** 2003-12-22

Abstract

AIM: To study interactions between hepatitis B virus (HBV) and interferon- α in liver-derived cells.

METHODS: mRNAs were separately isolated from an HBV-transfected cell line (HepG₂.2.2.15) and its parental cell line (HepG₂) pre- and post-interferon- α (IFN- α) treatment at 6, 24 and 48 h, followed by hybridization with a cDNA microarray filter dotted with 14 000 human genes. After hybridization and scanning of the arrays, the data were analyzed using ArrayGauge software. The microarray data were further verified by Northern blot analysis.

RESULTS: Compared to HepG₂ cells, 14 genes with known functions were down-regulated 3 to 12- magnitudes, while 7 genes were up-regulated 3-13 magnitudes in HepG₂.2.2.15 cells prior to IFN- α treatment. After interferon- α treatment, the expression of four genes (vascular endothelial growth factor, tyrosine phosphate 1E, serine protein with IGF-binding motif and one gene of clathrin light chain) in HepG₂.2.2.15 were up-regulated, while one gene encoding a GTP-binding protein, two genes of interferon-induced kinases and two proto-oncogenes were further down-regulated. Interestingly, under IFN- α treatment, a number of differentially regulated genes were new ESTs or genes with unknown functions.

CONCLUSION: The up-regulated genes in HepG₂.2.2.15 cell line suggested that under IFN- α treatment, these repressed cellular genes in HBV infected hepatocytes could be partially restored, while the down-regulated genes were most likely the cellular genes which could not be restored under interferon treatment. These down-regulated genes identified by microarray analysis could serve as new targets for anti-HBV drug development or for novel therapies.

Wang X, Yuan ZH, Zheng LJ, Yu F, Xiong W, Liu JX, Hu GX, Li Y. Gene expression profiles in an hepatitis B virus transfected hepatoblastoma cell line and differentially regulated gene expression by interferon- α . *World J Gastroenterol* 2004; 10 (12): 1740-1745

<http://www.wjgnet.com/1007-9327/10/1740.asp>

INTRODUCTION

Viral hepatitis B continues to be a significant global problem. It is estimated that there are approximately 350 million chronic hepatitis B virus (HBV) carriers world-wide. Furthermore, chronic hepatitis B patients are at high risk of developing liver cirrhosis and hepatocellular carcinoma with high mortality rates.

In the past two decades, interferon- α (IFN- α) has proven effective in the treatment of chronic hepatitis B patients. However, sustained responses were observed in only one-third of chronic hepatitis B patients^[1-3]. In the normal physiological state, interferon- α is expressed at a low level and is induced to high levels by viral or bacterial infections and the exposure to double-stranded RNA^[4]. In contrast to other types of viral infections, IFN- α was either non-detectable or present in extremely low levels in HBV chronically infected patients^[5,6]. Additionally, decreased synthesis of 2' -5' A synthetase, belonging to a family of enzymes induced by IFNs, has been reported in chronic hepatitis B patients^[7,8]. To date, mechanisms underlying defective production of IFN or defective responses to IFN in chronic hepatitis B patients have not been fully elucidated.

Development of microarray technology has provided a powerful tool for study of the complicated biological process in cells which results in altered global gene expression. cDNA microarray has been used to analyze virus-host cell interactions in Human Immunodeficiency Virus (HIV), Human Cytomegalovirus (HCMV), Herpes Simplex Virus (HSV) and Influenza Virus infected cell cultures^[9-13]. By comparing virus infected cell cultures with non-infected cell cultures, a number of differentially expressed genes were identified. For HBV, although several studies have been undertaken to clarify the effects of HBV infection on hepatocytes^[14-16], the global effects of all HBV proteins or HBV replication on host cells, especially the interaction between HBV and interferon remain unclear. Therefore, in this study, cDNA microarray filters dotted with 14 000 human genes were used to analyze transcriptional changes between an HBV DNA-transfected cell line (HepG₂.2.2.15)^[17,18] and its parental cell line (HepG₂) pre- and post- IFN treatment. Based on analysis of altered mRNA expression, several IFN-differentially regulated genes including new ESTs or genes with unknown functions were further investigated for their potential antiviral activity.

MATERIALS AND METHODS

Cell culture

The HBV DNA transfected hepatoblastoma cell line HepG₂.2.2.15, that has been confirmed to produce infectious virus^[18,19], and its parental cell line HepG₂ were maintained in Dulbecco's modified Eagle's medium supplemented with 10 mL/L fetal calf serum and antibiotics. The cells were incubated at 37 °C in 50 mL/LCO₂. Cell viability was estimated by the trypan blue dye exclusion method.

Preparation of cell samples for cDNA microarray

The cells were separately seeded into T-75 flasks at 40%

confluence (4×10^4 cells/cm²) one day prior to the experiment. After overnight culture, two flasks of cells for each cell line were harvested before treatment with IFN- α for RNA preparation and were regarded as 0 h cells for IFN- α treatment. The other cells were exposed to 5×10^3 IU/mL of IFN- α (Calbiochem, San Diego, CA, USA) and harvested 6, 24 and 48 h after IFN- α treatment. The culture media were removed and stored at -70°C . For each flask of cells, 5 mL of TRIzol Reagent (Gibco BRL) was added directly into the flask.

RNA extraction

Total RNA was extracted using standard TRIzol RNA isolation protocol (Gibco BRL). The isolated total RNA was divided into two aliquots, one for RNA slot analysis and the other for mRNA preparation.

Generation of microarray

Generation of microarrays and microarray analysis were carried out by the Institute of Biochemistry and Cell Biology, CAS as described previously^[20]. Human cDNA clones were derived from liver, hepatocarcinoma cell lines and hypothalamus-pituitary-adrenal libraries^[21] or purchased from Research Genetics (Huntsville, AL, USA). A cDNA array was assembled with 14 000 cDNA clones representing the same number of independent cDNA clusters, of which 7 565 clusters were homologous to that in the UniGene Database. All cDNA fragments were amplified and verified by gel electrophoresis and sequencing. The average length of the cDNA fragments was ~ 1 kb. PCR products were precipitated in isopropanol, redissolved in 10 μL of denaturing buffer (1.5 mol/L NaCl, 0.5 mol/L NaOH) and spotted onto 8×12 cm Hybond-N nylon membranes (Amersham Pharmacia, Buckinghamshire, UK) using an arrayer (BioRobotics, Cambridge, UK). Each spot carried ~ 100 nL in volume and was 0.4 mm in diameter; each cDNA fragment was spotted as two different spots (double-offset). Lambda phage and pUC18 vector DNA were spotted as negative controls.

Eight housekeeping genes encoding ribosomal protein S9 (RPS9), β -actin (ACTB), glyceraldehydes-3-phosphate dehydrogenase, hypoxanthine phosphoribosyltransferase 1, M_r 23 000 highly basic protein (RPL13A), ubiquitin C, phospholipase A2, and ubiquitin thiolesterase (UCHL1) were each evenly distributed in 12 spots on each 8×12 cm array as an intramembrane control. Hybridization data were considered invalid if the intensity of the darkest spot exceeded 1.5 times that of the weakest spot among the 12 spots representing the same gene.

mRNA isolation and probe preparation

The poly (A)⁺ mRNA was isolated from the total RNA using a poly (dT) resin (Qiagen, Hilden, Germany). Approximately 1–2 μg of mRNA were labeled in a reverse transcription reaction in the presence of 200 μCi [$\alpha^{32}\text{P}$] deoxyadenosine 5' -triphosphate (DuPont NEN, Boston, MA, USA) using Moloney murine leukemia virus reverse transcriptase as recommended by the manufacturer (Promega Corp., Madison, WI, USA).

Hybridization and Image Procession

Prehybridization was carried out in 20 mL of prehybridization

solution (6 \times SSC, 5 g/L SDS, 5 \times Denhardt's and 100 $\mu\text{g}/\text{mL}$ denatured salmon sperm DNA) at 68°C for 3 h. Overnight hybridization with the ^{32}P -labeled cDNA in 6 mL of hybridization solution (6 \times SSC, 5 g/L SDS, and 100 $\mu\text{g}/\text{mL}$ denatured salmon sperm DNA) was followed by stringent washing (0.1 \times SSC, 5 g/L SDS, at 65°C for 1 h). Membranes were exposed to Phosphor Screen overnight and scanned with an FLA-3 000A Plate/Fluorescent Image Analyzer (Fuji Photo Film, Tokyo, Japan). Radioactive intensity of each spot was linearly digitalized to 65 536 gray-grade in a pixel size of 50 μm in the Image Reader and recorded using the Array Gauge software (Fuji Photo Film, Tokyo, Japan). After subtraction of background (3 ± 3) chosen from an area where no cDNA was spotted, genes with intensities >10 were considered as positive signals to ensure that they were distinguished from background with statistical significance $>99.9\%$. Normalization among arrays was based on the sum of background-subtracted signals from all genes on the membrane^[22].

RNA slot analysis

Total cellular RNA, 10 $\mu\text{g}/\text{sample}$ was mixed with 7 μL formaldehyde, 20 μL formamide and 2 μL 20 \times SSC (1 \times SSC=0.15 mol/L NaCl plus 0.015 mol/L sodium citrate). After being denatured at 65°C for 15 min and immediately cooled in an ice bath, the RNA sample was applied to the nylon membrane (Boehringer Mannheim, Germany) with Minifold I (Schleicher & Schuell). After fixation at 120°C for 30 min, the membrane was pre-hybridized in 20 mL of prehybridization solution (6 \times SSC, 5 g/L SDS, 5 \times Denhardt's and 100 $\mu\text{g}/\text{mL}$ denatured salmon sperm DNA) at 42°C for 6 h, and followed by hybridization with 20 mL hybridization solution (6 \times SSC, 5 g/L SDS, 5 \times Denhardt's and 100 $\mu\text{g}/\text{mL}$ denatured salmon sperm DNA) including [$\alpha^{32}\text{P}$]dCTP labeled cDNA probes (Random labeling kit, Boehringer Mannheim, Germany) at 42°C for 16 h. The cDNA probes represented the unique sequence of IFN related P27, KIAA0919, beta3gal-T5 and FLJ12673. After stringent membrane washing process (0.1 \times SSC, 5 g/L SDS at 68°C for 30 min, thrice), autoradiographs were exposed to X-ray film (Fijifilm, Japan) overnight at -70°C . Quantitative analysis was undertaken by scanning the intensity of the membranes. In order to normalize the total RNA quantity in each blot, an [$\alpha^{32}\text{P}$]dCTP labeled β -actin probe was hybridized to the membrane again after the first probe was removed. The change of regulated gene expression between different cell samples could be detected by comparing the intensity ratio of specific gene and β -actin.

RESULTS

Validation of microarray results

Similar to previous study, results from the reproducible analysis confirmed that the replicated experiments were in concordance with an R^2 (square of Pearson correlation coefficient, measuring similarity in gene expression pattern) of 0.97–0.98 on scatterplot^[20].

To confirm the altered expression level, 4 genes (interferon related genes P27, KIAA0919, β -3-gal-T5 gene and FLJ12673 human cDNA clone) were selected and tested by RNA slot

Table 1 Comparison of microarray and RNA slot analyses on 4 selected genes

Accession ID	X67325		AB023136		AA622328		NM_018300	
	Ratio of arrays	Ratio of slot	Ratio of arrays	Ratio of slot	Ratio of arrays	Ratio of slot	Ratio of arrays	Ratio of slot
6 h/0 h	3.6	Undetectable	3.4	1.3	2.0	0.5	1.1	2.9
24 h/0 h	5.9	>31	7.2	3.5	3.9	1.6	4.9	3.4
48 h/0 h	6.1	>33	8.4	6.2	3.8	5.7	1.0	1.3
Description	IFN-inducible P27		Sec15B(vesicle traffic protein)		beta3gal-T5 gene		cDNA FLJ12673	

analysis (Figure 1). The ratios of the signal intensity of specific genes and β -actin and their comparison with microarray result are listed in Table 1. It is observed that the results of RNA slot analysis are aligned with those from the microarray analyses (Figure 1 and Table 1).

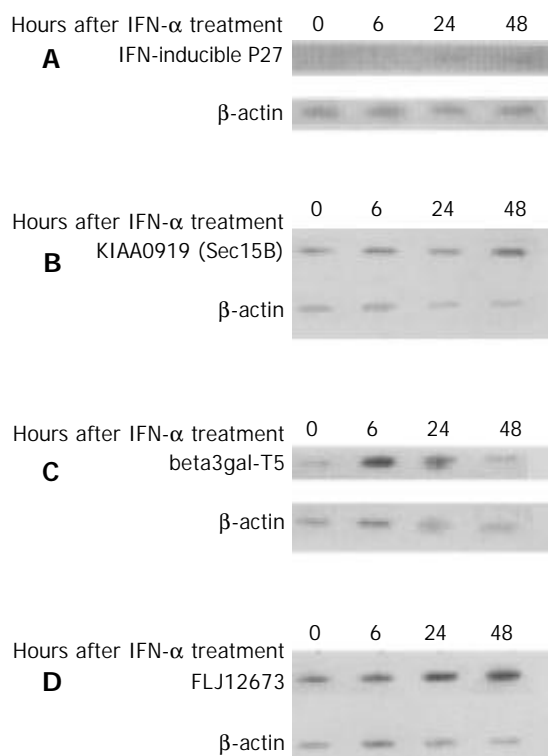


Figure 1 RNA slot analyses of IFN-inducible P27, KIAA0919 (Sec15B), beta3gal-T5 and FLJ12673 genes in HepG₂.2.2.15 before and after IFN treatment. Four genes (interferon related genes P27, KIAA0919, β -3-gal-T5 gene and FLJ12673 human cDNA clone) were selected and tested by RNA slot analysis to confirm the altered expression level indicated by the results of the microarrays. 10 μ g/sample total cellular RNA was blotted to the nylon membrane. The membrane was then hybridized with [α -³²P]dCTP labeled cDNA probes. Autoradiographs were exposed to X-ray film overnight at -70 °C. The β -actin gene was used as the control to normalize the total RNA quantity.

Differentially expressed genes in HepG₂.2.2.15 cell line and HepG₂ cell line prior to IFN- α treatment

To study the basic differentially expressed genes between HepG₂.2.2.15 cell line and its parental cell line HepG₂, systematic comparison of gene expression profiles from both cell lines before treatment with IFN- α was done at 0 h. Totally 89 genes were either up- or down-regulated three-fold (Table 2). In these 89 genes, 22 genes have defined functional activities (Table 3) while 67 genes were new ESTs with unknown functions. Fifteen of the 22 known genes were down-regulated by three- to twelve-fold, while 7 genes were up-regulated by three- to thirteen-fold. 4 genes could be catalogued in four classes, such as cell cycle (Y13467), ligands and receptors (AF022375), phosphatase (U12128), and transcription factors (D87258).

Table 2 Gene expression profiling in the microarray analysis

Ratio	Gene differences in HepG ₂ .2.2.15			Gene differences in HepG ₂			Gene differences in HepG ₂ .2.2.15/HepG ₂			
	6 h/0 h	24 h/0 h	48 h/0 h	6 h/0 h	24 h/0 h	48 h/0 h	0 h	6 h	24 h	48 h
3	34	48	45	83	103	48	89	40	33	36
5	10	18	12	37	37	23	27	12	8	11

Differentially regulated genes in HepG₂.2.2.15 cell line and HepG₂ after IFN- α treatment

Six hours after treatment with interferon- α , significant changes in mRNA expression were observed in both HepG₂ and HepG₂.2.2.15 cells, with 83 and 34 genes up- or down-regulated by at least three-fold (Table 2). A moderate increase in changes of cellular gene expression was detected at 24 h, at which time, 103 and 48 genes were up- or down-regulated respectively by at least three-fold (Table 2). Approximately half of these genes could be classified in functional categories, including interferon responsive proteins, signal transducing genes such as kinase, phosphatase and ligand as well as receptors (Table 4). It is interesting to note that the number of differentially expressed cellular genes in HepG₂ and HepG₂.2.2.15 cell lines could be decreased by interferon- α treatment from 89 to 40, 33 and 36 genes at 6, 24, 48 h post treatment (Table 2). The differentially regulated gene expressed profile in HepG₂.2.2.15 and HepG₂ cell lines after IFN- α treatment are available at http://www.mvlab-fudan.cn/microarray_databases.

Kinetics of IFN-treated gene expression profile in 23 genes from HepG₂ and HepG₂.2.2.15 cell lines

Twenty three selected genes, belonging catalogues of interferon induced proteins kinase/phosphatase, ligands and receptors, phosphatase, protein degradation, viral and clathrin receptors, protooncogenes and transcription factors respectively, were further compared between HepG₂.2.2.15 and its parental cell line HepG₂ to study the effect of interferon- α treatment on HBV and cellular gene expressions (Table 5). From this table, it is noted that most of these selected genes with known functions have two- three-fold expression regulated in both HepG₂ cell line and HepG₂.2.2.15 cell post interferon treatment. However, five genes (U02680, U07358, U52969, U50529 and U70321), were up-regulated only in HepG₂ cell line, while down-regulated in HepG₂.2.2.15 cells.

DISCUSSION

DNA microarray is an important and powerful tool for surveying changes in cellular gene expression on a large scale. Several groups have used this approach to analyze virus-host cell interactions in HBV infection. Rho *et al.* constructed a HepG₂ cell line stably expressing HBx (HepG₂-HBx), and performed cDNA microarray analysis on 588 cellular cDNAs to study the effect of HBx on the transcriptional regulation in the human liver cell^[15]. To gain more information on how HBV proteins regulate host cellular gene expression, Otsuka *et al.* examined the differences in the gene expression profiles of HepG₂.2.2.15 and HepG₂ cells, using an in-house cDNA microarray dotted with 2 304 cellular genes^[16]. To identify hepatocellular genes whose transcriptional regulation is tightly linked with IFN- γ and IFN- α / β -mediated inhibition of HBV replication, Chisari *et al.* used DNA microarrays and a high-throughput cDNA differential display method (total gene expression analysis (TOGA) to examine the gene expression profiles of HBV transgenic mouse livers before and after the intrahepatic induction of IFN- α / β and IFN- γ ^[23]. To further understand molecular mechanisms underlying HBV pathogenesis and identify novel cellular genes as new targets for anti-HBV drug development or for novel

Table 3 Differently expressed known genes in HepG₂ 2.2.15 and HepG₂ cell lines before IFN- α treatment

Accession ID	HepG ₂	HepG ₂ 2.2.15	Ratio	Description	Unigene
Cell cycle					
Y13467	101.95	29.54	-3.45	RB18A	Hs.15589
Ligands and receptors					
AF022375	16.17	5.19	-3.12	vascular endothelial growth factor	Hs.73793
Phosphatase					
U12128	152.03	27.26	-5.58	tyrosine phosphatase 1E (PTP1E)	Hs.211595
Transcription factors					
D87258	156.76	37.78	-4.15	serin protease with IGF-binding motif	Hs.75111
Miscellaneous					
X69962	242.93	73.77	-3.29	FMR-1	Hs.89764
X56597	1.64	21.98	13.40	humFib mRNA for fibrillar	Hs.99853
U76713	403.90	123.59	-3.27	apobec-1 binding protein 1	Hs.81361
U50410	189.94	27.03	-7.03	heparan sulphate proteoglycan (OCI5)	Hs.119651
U23070	5.35	16.82	3.14	putative transmembrane protein (nma)	Hs.78776
S68805	4.12	12.74	3.09	L-arginine:glycine amidinotransferase	Hs.75335
M22430	13.63	50.17	3.68	RASF-A PLA2	Hs.76422
M16961	221.65	61.50	-3.60	alpha-2-HS-glycoprotein alpha and beta chain	Hs.75430
M13928	21.15	163.32	7.72	delta-aminolevulinatase dehydratase	Hs.1227
L40157	14.58	92.98	6.38	endosome-associated protein (EEA1)	Hs.2864
L24123	1 309.05	430.92	-3.04	NRF1 protein (NRF1)	Hs.83469
D00096	7.61	31.28	4.11	Prealbumin	Hs.194366
AJ006835	150.29	49.21	-3.05	U17 small nucleolar RNA host gene	Hs.196769
AF073308	237.11	78.45	-3.02	nonsyndromic hearing impairment protein (DFNA5)	Hs.13530
AF050127	823.97	71.21	-11.57	hypoxia inducible factor (aHIF)	Hs.197540
AC002045	237.87	67.71	-3.51	Chromosome 16 BAC clone CIT987SK-A-589H1	Hs.253182
AB027013	15.62	2.31	-6.76	Nucleosome Assembly Protein 1-like 2	Hs.66180
AB023136	544.25	44.18	-12.32	KIAA0919	Hs.44175

Table 4 Functional catalogues of 3 fold regulated genes in HepG₂ and HepG₂ 2.2.15 cell lines post IFN- α treatment

Catalogue	3-fold regulated gene number in HepG ₂ 2.2.15			3-fold regulated gene number in HepG ₂		
	6 h/0 h	24 h/0 h	48 h/0 h	6 h/0 h	24 h/0 h	48 h/0 h
Cell cycle	-	1	1	-	-	-
Coagulation	-	1	1	-	1	-
Cytokine/receptors	1	2	2	1	1	-
Extracellular matrix and cell adhesion	-	-	1	-	1	-
GTP binding proteins and signal transduction	2	-	1	-	1	1
Interferon	8	6	3	6	5	5
Kinase and phosphatase	-	-	1	-	2	-
Ligands and receptors	-	1	2	-	-	-
Mitochondrial	-	1	1	-	2	-
Phosphatase and phosphodiesterase	2	2	2	1	2	1
Protooncogenes	-	1	-	1	-	-
Transcription factors	-	-	-	1	1	1
Viral and clathrin receptors	-	1	1	-	1	-
Miscellaneous	7	8	8	14	18	13
New ESTs	14	24	21	59	68	27
Total	34	48	45	83	103	48

therapies, we used cDNA microarray filters dotted with 14 000 human genes to analyze transcriptional changes between an HBV DNA-transfected cell line (HepG₂ 2.2.15) and its parental cell line (HepG₂) pre- and post-IFN treatment. The HepG₂ 2.2.15 cell line, that has four copies of HBV genome integrated in the cellular chromosome and can persistently secrete HBV virions, was used for HBV infected liver-derived cells^[17,18]. The parental hepatoblastoma cell line, HepG₂, from which HepG₂ 2.2.15 cell line was generated, was used as the uninfected cell control. In this study, the differentially expressed cellular genes detected between these two cell lines could be due to the integration of

HBV DNA, the replication of HBV or the expression of HBV proteins. In chronic HBV infections, the virus usually persists in hepatocytes similar to the status of HBV in HepG₂ 2.2.15 cell line; the differentially expressed cellular genes in HepG₂ 2.2.15 cell line could reveal similar changes in the hepatocytes of HBV chronically infected patients.

Prior to interferon- α treatment, compared to HepG₂ cells, 15 known genes were more than three-fold down-regulated, while 7 genes were more than 3-fold up-regulated (Table 3) in HepG₂ 2.2.15 cells. To concentrate on the down-regulated genes, 4 genes belonging to the categories of cell cycle, ligands and receptors,

Table 5 Kinetics of IFN-treated gene expression profiles in 23 selected genes from HepG₂ and HepG₂.2.15 cells

Accession ID	HepG ₂ .2.15 cell lines			HepG ₂ cell lines			Description
	6 h/0 h	24 h/0 h	48 h/0 h	6 h/0 h	24 h/0 h	48 h/0 h	
Interferon							
X57352	3.8	3.1	2.5	6.5	8.1	6.4	1-8U gene from interferon-inducible gene family
X57351	3.4	2.2	2.2	4.3	4.4	4.4	1-8U gene from interferon-inducible gene family
M87503	2.3	1.7	1.7	3.2	2.4	2.6	IFN-responsive transcription factor subunit
M33882	2.4	1.6	1.5	2.5	2.1	1.6	p78 protein
M11810	9.1	5.7	4.4	8.4	7.7	3.9	(2' -5') oligo A synthetase E gene
L07633	2.0	1.3	1.5	2.0	2.7	1.3	(clone 1950.2) interferon-gamma IEF SSP 5111
J04164	6.7	5.0	2.9	6.4	7.0	6.5	Interferon-inducible protein 9-27
D28137	3.0	3.3	2.8	2.7	2.6	1.8	BST-2
AJ225089	3.9	1.3	1.1	1.9	2.1	1.2	2' -5' oligoadenylate synthetase 59 kDa isoform
Kinase/Phosphate							
U07358	-1.3	-1.3	-2.5	1.1	2.4	1.4	Protein kinase (zpk)
U02680	-1.1	1.4	-2.5	1.5	7.1	1.6	Protein tyrosine kinase
AF032437	-1.1	-2.5	-1.7	-1.3	-3.3	-2.0	Mitogen activated protein kinase activated protein kinase
Ligands and receptors							
D86096	2.3	4.6	3.5	1.9	1.8	2.3	Prostaglandin E receptor EP3 subtype
AF022375	1.8	1.8	3.2	-1.2	-1.1	1.1	Vascular endothelial growth factor
Phosphatase							
U12128	3.0	4.8	4.7	-1.2	-1.1	-1.2	Protein tyrosine phosphatase 1E (PTP1E)
Protein degradation							
Z14977	2.2	1.2	1.4	2.7	1.3	1.6	Major histocompatibility complex encoded proteasome subunit LMP2
AF061736	2.6	1.5	1.4	2.3	2.3	2.0	Ubiquitin-conjugating enzyme RIG-B
Protooncogenes							
U52969	1.1	-2.0	-1.3	2.2	1.6	2.1	PEP19 (PCP4)
U50529	-2.5	-5.0	-2.5	1.7	1.5	2.2	BRCA2 region, mRNA sequence CG016
Transcription factors							
D87258	1.6	2.3	2.5	1.0	-1.1	-1.5	Serin protease with IGF-binding motif
Viral and clathrin receptors							
X81636	1.1	5.5	5.2	-1.1	6.4	-1.7	Clathrin light chain a
U70321	-1.3	-2.0	1.1	2.0	1.2	1.6	Herpesvirus entry mediator
AF079221	1.0	1.2	2.9	1.7	2.2	1.9	BCL2/adenovirus E1B 19kDa-interacting protein 3 a

phosphatase and transcription factors were down-regulated more than three-fold in HepG₂.2.15 cells (Table 3). In a microarray study on HCMV-host cell interactions compared to non-infected human fibroblasts, down-regulated genes belonging to these categories were also reported in HCMV infected cells^[10]. Though identical down-regulated genes from these categories were not found in the HCMV infected and HBV transfected cells, changes in the expression of cellular genes in these categories could reflect the common adverse effects of virus infections on host cells. In future studies, when more microarray analyses on virus-host interactions will be performed, it may be possible to identify significant changes of cellular gene expression due to HBV-hepatocyte interactions.

The effects of IFN- α on the global gene expression of HepG₂ and HepG₂.2.15 cells revealed interesting differences (data available at http://www.mvlab-fudan.cn/microarray_databases). In HepG₂ cells, compared with the expression of cellular genes at 0 h, no known gene was three-fold down-regulated 48 hr after IFN- α treatment. In contrast, 21 genes were up-regulated three-fold or more, and among these, five were IFN-induced genes, one belonging to the GTP-binding protein and signal transduction category, and one belonging to the phosphatase and phosphodiesterase category associated with the IFN-induced cascade. In HepG₂.2.15 cells, after being treated with IFN- α for 48 h, eight genes remained down-regulated three-fold or more. In comparison to the known functional genes, one gene was predicted as encoding the regulatory G protein

beta subunit, one was predicted as encoding an antigen of B cell differentiation, one encoding the thymosin beta 4Y isoform, one encoding a LDL-receptor related protein, which was also reported as encoding a human IFN- γ receptor, and one was an exon encoding a protein of the phosphatase and phosphodiesterase category, and the other 3 genes belonged to coagulation, mitochondrial and miscellaneous categories, respectively. These genes remained down-regulated and thus seemed refractory to the treatment of IFN- α . Since 2 of these genes are associated with thymosin and IFN- γ , microarray studies of HepG₂.2.15 cells treated with IFN- γ and/or cytokines may be able to elucidate whether these defects in cellular functions could be reversed. In HepG₂.2.15 cells, a number of IFN induced genes were up-regulated post IFN- α treatment; among these, genes p27 and 2' -5' A synthetase E were the top two up-regulated genes, being 6.1 and 9.1 respectively. Compared to the increases in these two genes up-regulated in HepG₂ (being 7.1 and 8.4 respectively), IFN- α was as effective in inducing these two genes in HBV infected cells as that in the uninfected hepatocytes.

To analyze whether there were HBV specific down-regulated cellular genes, which could be restored by IFN- α treatment, 23 matched genes from HepG₂ and HepG₂.2.15 cell lines were compared post IFN- α treatment. As shown in Table 5, the three genes which were found down-regulated in HepG₂.2.15 prior to IFN- α treatment (Table 3), namely described as encoding vascular endothelial growth factor, tyrosine phosphatase 1E,

serine protease with IGF-binding motif were all up-regulated by IFN- α treatment. In addition, a gene described as coding for clathrin light chain, which belongs to the viral and clathrin receptor category was also up-regulated 5.2 times. However, even after IFN- α treatment, the down-regulated protein kinase zpk and protein tyrosine kinase genes could not be restored (Table 5), which suggested a possible defective link in the IFN- α induced cascade. Measures for restoring the functions of the kinases could help to improve the therapeutic efficacy of IFN- α . The clinical implications of non-restorable down-regulated protooncogenes in HepG₂2.2.15 cell lines merit further study.

Analysis of gene expression profiles in HBV-hepatocyte interaction by microarray is an interesting field. The information gathered in this study, though preliminary in scope, provides an important basis for further study. The differentially expressed genes detected in this study should be further evaluated by cell transfection or by *in vivo* studies and should provide new insight into the molecular mechanisms of HBV infection. In addition, there were approximately 200 unknown genes or ESTs being up- or down-regulated in HepG₂2.2.15 cells. Preliminary transiently co-transfected functional assay has already shown that some of cellular genes significantly regulated by HBV infection and IFN are associated with the inhibition of HBV gene replication and expression (data not shown). It is predicted that other IFN-inducible proteins could be discovered and new mechanisms of this cytokine may be revealed.

ACKNOWLEDGMENTS

This work was supported by the Chinese State Basic Science Foundation (No.1999054105) and Med-X Foundation of Fudan University. Xun Wang and Wei Xiong are Ph.D. students supported by the Chinese Ministry of Education.

REFERENCES

- 1 **Hoofnagle JH**. Alpha-interferon therapy of chronic hepatitis B: Current status and recommendations. *J Hepatol* 1990; **11** (Suppl 1): S100-107
- 2 **Korenman JB**, Baker B, Waggoner J, Everhart JE, Di Bisceglie AM, Hoofnagle JH. Long-term remission of chronic hepatitis B after alpha-interferon therapy. *Ann Intern Med* 1991; **114**: 629-634
- 3 **Caselmann WH**, Eisenburg J, Hofschneider PH, Koshy R. Beta- and gamma-interferon in chronic active hepatitis B. A pilot trial of short-term combination therapy. *Gastroenterology* 1989; **96**(2 Pt 1): 449-455
- 4 **Samuel CE**. Antiviral actions of interferons. *Clin Microbiol Rev* 2001; **14**: 778-809
- 5 **Wen YM**, Qian LS, Lou HZ, Gao JQ, Wu XH, Yang PZ. Studies on production of interferon I by peripheral blood mononuclear cells in chronic hepatitis B patients. *Chin Med J* 1980; **60**: 239-241
- 6 **Wen YM**, Luo HZ, Qian LS, Duan SC, Zhu QR, Wu XH. Serial study on production of interferon by leucocytes in viral hepatitis B. *Chin J Microb Immunol* 1981; **1**: 342-345
- 7 **Wen YM**, Yu CZ, Huang YX, Wu XH, Zheng HD, Liu XY. Studies on 2' -5' oligo-isoadenylate synthetase and virus replication in hepatitis B. *Chin J Inf Dis* 1985; **3**: 106-109
- 8 **Fujisawa K**, Yamazaki K, Kawase H, Kitahara T, Kimura K, Ogura K, Kameda H. Interferon therapy for chronic viral hepatitis and the use of peripheral lymphocytic 2' -5' -oligoadenylate synthetase In: Zuckerman AJ, eds. *Viral hepatitis and liver disease. New York: Alan R Liss Inc* 1988: 834-839
- 9 **Geiss GK**, Bumgarner RE, An MC, Agy MB, van't Wout AB, Hammersmark E, Carter VS, Upchurch D, Mullins JI, Katze MG. Large-scale monitoring of host cell gene expression during HIV-1 infection using cDNA microarrays. *Virology* 2000; **266**: 8-16
- 10 **Zhu H**, Cong JP, Mamtora G, Gingeras T, Shenk T. Cellular gene expression altered by human cytomegalovirus: global monitoring with oligonucleotide arrays. *Proc Natl Acad Sci U S A* 1998; **95**: 14470-14475
- 11 **Browne EP**, Wing B, Coleman D, Shenk T. Altered cellular mRNA levels in human cytomegalovirus-infected fibroblasts: viral block to the accumulation of antiviral mRNAs. *J Virol* 2001; **75**: 12319-12330
- 12 **Stingley SW**, Ramirez JJ, Aguilar SA, Simmen K, Sandri-Goldin RM, Ghazal P, Wagner EK. Global analysis of herpes simplex virus type 1 transcription using an oligonucleotide-based DNA microarray. *J Virol* 2000; **74**: 9916-9927
- 13 **Geiss GK**, An MC, Bumgarner RE, Hammersmark E, Cunningham D, Katze MG. Global impact of influenza virus on cellular pathways is mediated by both replication-dependent and -independent events. *J Virol* 2001; **75**: 4321-4331
- 14 **Lara-Pezzi E**, Majano PL, Gomez-Gonzalo M, Garcia-Monzon C, Moreno-Otero R, Levrero M, Lopez-Cabrera M. The hepatitis B virus X protein up-regulates tumor necrosis factor α gene expression in hepatocytes. *Hepatology* 1998; **28**: 1013-1021
- 15 **Han J**, Yoo HY, Choi BH, Rho HM. Selective transcriptional regulations in the human liver cell by hepatitis B viral X protein. *Biochem Biophys Res Commun* 2000; **272**: 525-530
- 16 **Otsuka M**, Aizaki H, Kato N, Suzuki T, Miyamura T, Omata M, Seki N. Differential cellular gene expression induced by hepatitis B and C viruses. *Biochem Biophys Res Commun* 2003; **300**: 443-447
- 17 **Knowles BB**, Howe CC, Aden DP. Human cell lines secrete the major plasma proteins and hepatitis B surface antigen. *Science* 1980; **209**: 497-499
- 18 **Sells MA**, Chen ML, Acs G. Production of hepatitis B virus particles in Hep G₂ cells transfected with cloned hepatitis B virus DNA. *Proc Natl Acad Sci U S A* 1987; **84**: 1005-1009
- 19 **Gerber MA**, Sells MA, Chen ML, Thung SN, Tabibzadeh SS, Hood A, Acs G. Morphologic immunohistochemical and ultrastructural studies of the production of hepatitis B virus *in vitro*. *Lab Invest* 1988; **59**: 173-180
- 20 **Xu L**, Hui L, Wang S, Gong J, Jin Y, Wang Y, Ji Y, Wu X, Han Z, Hu G. Expression profiling suggested a regulatory role of liver-enriched transcription factors in human hepatocellular carcinoma. *Cancer Res* 2001; **61**: 3176-3181
- 21 **Hu RM**, Han ZG, Song HD, Peng YD, Huang QH, Ren SX, Gu YJ, Huang CH, Li YB, Jiang CL, Fu G, Zhang QH, Gu BW, Dai M, Mao YF, Gao GF, Rong R, Ye M, Zhou J, Xu SH, Gu J, Shi JX, Jin WR, Zhang CK, Wu TM, Huang GY, Chen Z, Chen MD, Chen JL. Gene expression profiling in the human hypothalamus-pituitary-adrenal axis and full-length cDNA cloning. *Proc Natl Acad Sci U S A* 2000; **97**: 9543-9548
- 22 **Rhee CH**, Hess K, Jabbur J, Ruiz M, Yang Y, Chen S, Chenchik A, Fuller GN, Zhang W. cDNA expression array reveals heterogeneous gene expression profiles in three glioblastoma cell lines. *Oncogene* 1999; **18**: 2711-2717
- 23 **Wieland SF**, Vega RG, Muller R, Evans CF, Hilbush B, Guidotti LG, Sutcliffe JG, Schultz PG, Chisari FV. Searching for interferon-induced genes that inhibit hepatitis B virus replication in transgenic mouse hepatocytes. *J Virol* 2003; **77**: 1227-1236

Edited by Xu FM and Wang XL

Transactivating effect of hepatitis C virus core protein: A suppression subtractive hybridization study

Min Liu, Yan Liu, Jun Cheng, Shu-Lin Zhang, Lin Wang, Qing Shao, Jian Zhang, Qian Yang

Min Liu, Shu-Lin Zhang, Qian Yang, Department of Infectious Diseases, The First Hospital of Xi'an Jiaotong University, Xi'an 710061, Shaanxi Province, China

Yan Liu, Jun Cheng, Lin Wang, Qing Shao, Jian Zhang, Gene Therapy Research Center, Institute of Infectious Diseases, 302 Hospital of PLA, Beijing 100039, China

Supported by the National Natural Science Foundation of China, No.39970674

Correspondence to: Dr. Jun Cheng, Gene Therapy Research Center, Institute of Infectious Diseases, 302 Hospital of PLA, 100 Xisihuanzhong Road, Beijing 100039, China. cj@genetherapy.com.cn

Telephone: +86-10-66933392 **Fax:** +86-10-63801283

Received: 2003-11-21 **Accepted:** 2003-12-29

Abstract

AIM: To investigate the transactivating effect of hepatitis C virus (HCV) core protein and to screen genes transactivated by HCV core protein.

METHODS: pcDNA3.1(-)-core containing full-length HCV core gene was constructed by insertion of HCV core gene into *EcoRI/BamHI* site. HepG2 cells were cotransfected with pcDNA3.1(-)-core and pSV-lacZ. After 48 h, cells were collected and detected for the expression of β -gal by an enzyme-linked immunosorbent assay (ELISA) kit. HepG2 cells were transiently transfected with pcDNA3.1(-)-core using Lipofectamine reagent. Cells were collected and total mRNA was isolated. A subtracted cDNA library was generated and constructed into a pGEM-Teasy vector. The library was amplified with *E. coli* strain JM109. The cDNAs were sequenced and analyzed in GenBank with BLAST search after polymerase chain reaction (PCR).

RESULTS: The core mRNA and protein could be detected in HepG2 cell lysate which was transfected by the pcDNA3.1(-)-core. The activity of β -galactosidase in HepG2 cells transfected by the pcDNA3.1(-)-core was 5.4 times higher than that of HepG2 cells transfected by control plasmid. The subtractive library of genes transactivated by HCV core protein was constructed successfully. The amplified library contained 233 positive clones. Colony PCR showed that 213 clones contained 100-1 000 bp inserts. Sequence analysis was performed in 63 clones. Six of the sequences were unknown genes. The full length sequences were obtained with bioinformatics method, accepted by GenBank. It was suggested that six novel cDNA sequences might be target genes transactivated by HCV core protein.

CONCLUSION: The core protein of HCV has transactivating effects on SV40 early promoter/enhancer. A total of 63 clones from cDNA library were randomly chosen and sequenced. Using the BLAST program at the National Center for Biotechnology Information, six of the sequences were unknown genes. The other 57 sequences were highly similar to known genes.

Liu M, Liu Y, Cheng J, Zhang SL, Wang L, Shao Q, Zhang J,

Yang Q. Transactivating effect of hepatitis C virus core protein: A suppression subtractive hybridization study. *World J Gastroenterol* 2004; 10(12): 1746-1749

<http://www.wjgnet.com/1007-9327/10/1746.asp>

INTRODUCTION

Hepatitis C virus (HCV) is a major causative agent of chronic liver diseases including chronic hepatitis, liver cirrhosis, and hepatocellular carcinoma worldwide^[1-4]. The majority of individuals infected with HCV cannot resolve their infection and suffer from persistent chronic hepatitis. The molecular mechanism of HCV persistence and pathogenesis is not well understood. HCV contains a single-stranded positive-sense RNA genome which encodes a precursor polypeptide of approximately 3 000 amino acids. After translation, a capsid protein (core), envelope glycoproteins (E1 and E2), and nonstructural proteins (NS2, NS3a, NS3b, NS4A, NS4B, NS5A, and NS5B) are processed from the polyprotein by cellular and viral proteases^[5-10].

HCV core gene contains the most conserved sequences in the coding region of most HCV genotypes, which implies an important biological function. Since suitable viral culture systems are not generally available^[10-13], analysis of HCV genome organization and viral-product function is important to understand the viral life cycle and the pathogenesis of HCV infection. In order to understand the pathogenesis of HCV infection, we investigated the transactivating effect of HCV core protein.

MATERIALS AND METHODS

Construction and identification of expression vectors

pcDNA3.1(-)-core containing full-length HCV core gene was constructed by insertion of HCV core gene into *EcoRI/BamHI* site, which could directly express core protein. pcDNA3.1(-) was obtained from Invitrogen. The gene was identified by PCR and digested by *EcoR* I, *BamH* I, and *Hind* III (Takara). PCR primers were: up primer, 5' -GAA TTC AAT GAG CAC GAA TCC TAA-3'; down primer, 5' -GGA TCC AGG CTG AAG CGG GCA CA-3' (Shanghai BioAsia Biotechnology Co., Ltd).

Cotransfection with reporter vectors pSV-lacZ

HepG2 cells were transfected by various concentrations of pSV-lacZ (0.1-1.8 μ g) (Promega). Expression of β -gal was detected by using β -gal assay kit (Promega). The best concentration of pSV-lacZ was selected, HepG2 cells with pcDNA3.1(-)-core and pSV-lacZ were cotransfected. At the same time, HepG2 cells were cotransfected with empty pcDNA3.1(-) and pSV-lacZ as control. After 48 h, cells were collected and the expression of β -gal was detected.

Expression of pcDNA3.1(-)-core in HepG2 cells

HepG2 cells were transiently transfected with pcDNA3.1(-)-core using Lipofectamine. At the same time, empty vectors were also transfected into cells as control. HepG2 cells were

plated at a density of 1×10^6 on a 35 mm plate in RPMI1640 containing 100 U/mL of penicillin, 100 μ g/mL of streptomycin, and 100 mL/L heat-inactivated FBS. After 24 h of growth to 40-50% confluence, the cells were transfected with plasmids by using Lipofectamine according to the manufacturer's protocol (Gibco Co.).

mRNA and cDNA isolation

Total cellular RNA was isolated using TRIzol (Invitrogen) according to the manufacturer's instructions. cDNAs were reversely-transcribed from total RNA. The result was identified by PCR. Cells were collected and mRNA was isolated by using a micro mRNA purification kit (Amersham Biosciences).

Generation of a subtracted cDNA library

Genome comparisons were performed by suppression subtraction hybridization according to the manufacturer's instructions of PCR-selectTM cDNA subtraction kit (Clontech). In brief, 2 μ g aliquots each of poly(A)⁺ mRNA from the tester and the pooled driver were subjected to cDNA synthesis. Tester and driver cDNAs were digested with *Rsa*I. The tester cDNA was subdivided into two portions, and each was ligated with a different cDNA adapter. In the first hybridization reaction, an excess of driver was added to each sample of tester. The samples were heat denatured and allowed to be annealed. Because of the second-order kinetics of hybridization, the concentration of high- and low-abundance sequences was equalized among the single-stranded tester molecules. At the same time single-stranded tester molecules were significantly enriched for differentially expressed sequences. During the second hybridization, the two primary hybridization samples were mixed without denaturation. Only the remaining equalized and subtracted single-stranded tester cDNAs could reassociate, forming double-stranded tester molecules with different ends. After the ends were filled with DNA polymerase, the entire population of molecules was subjected to nested PCR with two adapter-specific primer pairs.

Cloning subtracted library into pGEM-Teasy vector

Products of these amplified A overhangs containing a subtracted cDNA library (3 μ L) were ligated into a pGEM-Teasy plasmid (Promega). Subsequently, the plasmid was introduced into *Escherichia coli* strain JM109. Bacteria were transferred into 800 μ L of SOC medium and allowed to be incubated for 45 min at 37 °C and centrifuged at 225 rpm. Then they were plated onto agar plates containing ampicillin (50 μ g/mL), 5-bromo-4-chloro-3-indolyl- β -D-galactoside (X-Gal; 20 μ g/cm²), and isopropyl- β -D-thiogalactoside (IPTG; 12.1 μ g/cm²) and incubated overnight at 37 °C. White colonies were picked and identified by PCR. Primers were T7/SP6 primer of pGEM-Teasy plasmid. After the positive colonies (Shanghai BioAsia Biotechnology Co., Ltd) were sequenced, nucleic acid homology searches were performed using the BLAST (basic local alignment search tool) server at the National Center for Biotechnology Information.

RESULTS

Identification of expression vector

Figure 1 shows pcDNA3.1(-)-core of the PCR assay for plasmid and digestion of restriction enzyme analysis. Restriction enzyme analysis of pcDNA3.1(-)-core plasmid with *Eco*RI/*Bam*HI yielded two bands: 4 900 bp empty pcDNA3.1 (-) and 573 bp HCV core. Cleavage with *Hind*III produced only one 5 500 bp band (4 900 bp+573 bp). The products of plasmid were amplified by PCR. Analysis of the PCR reaction

products by agarose gel electrophoresis showed a clear band with the expected size (573 bp). Sequence of the PCR product was correct.

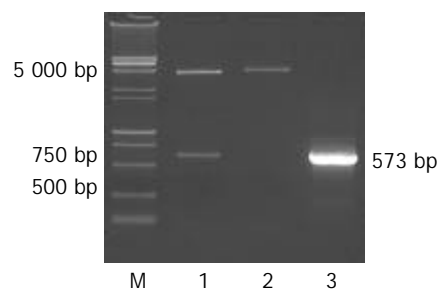


Figure 1 Products of pcDNA3.1(-)-core PCR and restriction enzyme cleavage were electrophoresed in 1% agarose gel. Lane 1: *Eco*RI/*Bam*HI cleaved; lane 2: *Hind*III cleaved; lane 3: products of plasmid PCR; M: DNA marker, (15 000 bp+ 2 000 bp).

Identification of HCV core transient expression

The total mRNA was reversely-transcribed by three different Oligo dT, identification of cDNA by PCR yielded a common 573 bp band (Figure 2). Table 1 shows co-transfected pcDNA3.1 (-)-core and pSV-lacZ into HepG2 cells, transient expression of HCV core was positive. On the contrary, empty pcDNA3.1 (-) co-transfected HepG2 cells were negative.

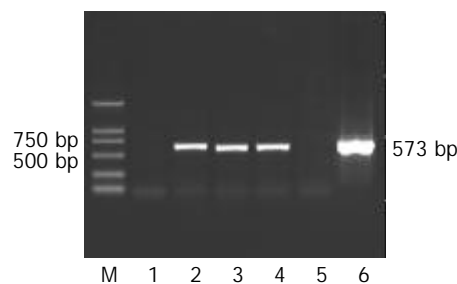


Figure 2 RT-PCR products were electrophoresed in 1% agarose gel. Lane 1: negative control; lanes 2-4: total RNA was isolated from pcDNA3.1(-)-core and RT-PCR was performed by three different Oligo dT; lane 5: blank control; lane 6: positive control; M: DNA marker (2 000 bp).

Table 1 Transient expression of pcDNA3.1(-)-core in HepG2 cells

Group	Coat Ag	P	P/N (n=0.05)	Results (+/-)
pcDNA3.1(-)-core	pcDNA3.1(-)-core lysate	0.219	4.38	+
Blank plasmid	pcDNA3.1(-) lysate	0.034	0.68	-
Positive control	HCV core Ag	1.299	24.60	+
Negative control	PBS	0.012	0.24	-

Result of pcDNA3.1(-)-core and pSV-lacZ cotransfection

Selection of 0.3 μ g pSV-lacZ served as the best concentration by analysis. After cotransfection of pcDNA3.1(-)-core and pSV-lacZ, the A value of expression of β -gal was 0.219. In contrast, the A value of expression of β -gal by cotransfected empty pcDNA3.1(-) and pSV-lacZ was 0.034. Expression of β -gal was 5.4-fold higher in cotransfected pcDNA3.1(-)-core and pSV-lacZ than in cotransfected empty pcDNA3.1(-) and pSV-lacZ (Figure 3). The significant increase of expression of β -gal was attributed to the transactivating effect of HCV core on early promoter of SV40, leading to the increased expression of downstream gene lacZ.

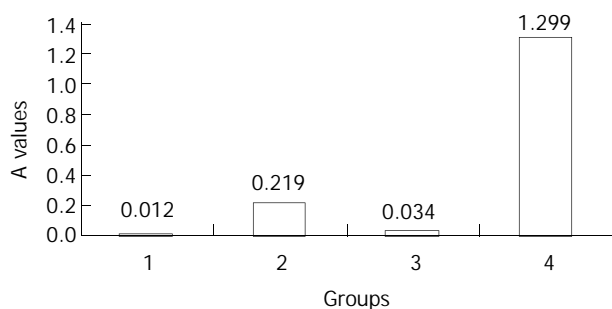


Figure 3 Comparison of A values among transfection groups. 1. Negative control (PBS); 2. pcDNA3.1(-)-core; 3. Blank plasmid; 4. Positive control.

Analysis of subtraction library

Using suppression subtractive hybridization technique (SSH), we obtained a total of 233 positive clones. These clones were prescreened by using PCR amplification to make sure that only clones with different inserts were subjected to sequencing (Figure 4). Two hundred and thirteen clones contained 100-1 000 bp inserts. A total of 63 clones from cDNA library were randomly chosen and sequenced. Using the BLAST program at the National Center for Biotechnology Information, six of the sequences were unknown genes. The full length sequences accepted by GenBank were obtained with bioinformatics method. The other 57 sequences had a high similarity to known genes. Twenty-one of the sequences were 100% identical in nucleotide sequence to previously described sequences. Summary of the data is presented in Table 2.

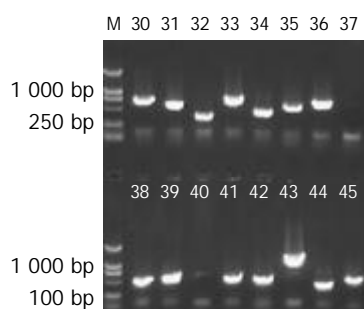


Figure 4 Agarose gel electrophoresis of PCR products of some clones (30-45). M: DNA marker (2 000 bp).

Table 2 Comparison between positive clones and similar sequences in GenBank

High similarity to known genes	Number of similar clones
Ribosomal protein	21
Eukaryotic translation elongation factor	6
Eukaryotic translation initiation factor	5
Heat shock factor binding protein (HSBP)	5
Apolipoprotein	5
NADH dehydrogenase	3
Heterogeneous nuclear ribonucleoprotein	3
D-like (HNRPDL), transcript variant	
Alpha-2-macroglobulin (A2M)	2
Bile acid-binding protein (BABP)	2
Cathepsin C (CTSC)	1
Fibronectin (FN precursor)	1
Magnesium-dependent protein phosphatase	1
Thioredoxin-related transmembrane protein	1
WEE1 gene for protein kinase	1

DISCUSSION

The diverse functional activities of HCV putative core protein have already been noted by a number of investigators. These include nucleocytoplasmic localization^[14], regulation of cellular and unrelated viral promoters in *in vitro* studies^[15-18], inhibition of apoptosis under certain conditions^[19], physical association with apolipoprotein II^[20] and cytoplasmic tail of the lymphotoxin β -receptor^[21,22], promotion of normal cells to a transformed phenotype^[23], and transactivation of suppression of cell growth^[12,24].

We cotransfected HepG2 cells with pcDNA3.1(-)-core and pSV-lacZ and demonstrated that the HCV core was successfully expressed in transfected HepG2 cells. Expression of β -gal was 5.4-fold higher in cotransfected pcDNA3.1(-)-core and pSV-lacZ than in cotransfected empty pcDNA3.1(-) and pSV-lacZ. HCV core had significant transactivating effects on the early promoter of SV40, through increasing the expression of downstream gene lacZ. This result indicates that the HCV core protein expressed in HepG2 cells retains its biological activity in terms of transcriptional activation, which was inconsistent with the previous report^[23].

The nucleocapsid core protein of HCV has been shown to trans-act on several viral or cellular promoters^[15,16,25,26]. To get insight into the trans-action mechanism of HCV core protein, an SSH was used for identification of relatively transactivated target genes of HCV core protein. HCV core protein relatively transactivated gene subtractive library was set up successfully. Sequence analysis was performed in 63 clones. Five of the sequences matched strongly (>97% nucleotide identity) with the apolipoprotein (Apo) sequence. Two of those sequences matched strongly (>97% nucleotide identity) with the bile acid-binding protein (BABP).

Several lines of evidence suggest that HCV core protein may modulate cellular transduction signals and alter lipid metabolism. A characteristic of HCV infection is the presence of liver steatosis. It is plausible that this steatosis could arise, at least in part, from direct effects of HCV proteins on lipid metabolism. The levels of apoAI and high density lipoprotein are independent predictive factors response to treatment^[27]. Apo, a protein that bind to lipids and renders them water soluble in the form of lipoproteins, could be a good candidate for an interaction with the core protein. HCV has been described as a lipid-containing virus and in plasma of patients shows a heterogeneous density distribution partially due to its binding to low density lipoprotein, very low density lipoprotein, IgG, and to a minor degree of IgM and high density lipoprotein^[28]. Barba *et al.*^[20] by double immunofluorescence and confocal analysis of the core and apo revealed colocalization of apoAII and the HCV core protein in the globular structures. Sabile *et al.*^[29] investigated the binding of HCV core protein to cellular proteins expressed in HepG2 cells by combining 2 yeast hybrid, confocal and surface plasmon resonance assays. The results showed the direct binding of the viral protein to apolipoprotein AII (apoAII) and mapped the interaction domain to the C-terminal of HCV core protein. Taking advantage of the well-established increase in apoAII expression caused by fibers in HepG2 cells, they identified that apoAII was one of the cellular targets for HCV core protein and the intervention of fenofibric acid in cellular lipid metabolism directly affected the expression pattern of HCV core protein.

It has been discovered that bile acids are the natural ligand for a nuclear receptor termed farnesoid X receptor (FXR; NR1H4)^[30-32]. Therefore, bile acids may be important regulators of gene expression in the liver and intestines. To date, the genes that have been shown to be responsive to regulation by FXR encoded proteins are involved in the biosynthesis and transport of bile acids^[33]. Bile acids have been shown to modulate a variety of other cellular functions, such as secretion of lipoproteins

from hepatocytes^[34,35] and translocation of bile acid transporters to the hepatocyte canalicular membrane^[36]. Our results indicate that HCV core protein interacts with bile acid-binding proteins. Maybe it is a way that HCV core protein affects cellular lipid metabolism.

Our results revealed a number of novel and known genes that responded to HCV core. The 6 unknown nucleotide sequences of SSH fragments are deposited in GenBank under accession numbers of AY038359, AY038361, AY039041, AY039042, AY039043, and AY039044.

REFERENCES

- Choo QL**, Kuo G, Weiner AJ, Overby LR, Bradley DW, Houghton M. Isolation of a cDNA clone derived from a blood-borne non-A, non-B viral hepatitis genome. *Science* 1989; **244**: 359-362
- Di Bisceglie AM**. Hepatitis C and hepatocellular carcinoma. *Hepatology* 1997; **26**(3 Suppl 1): 34S-38S
- Hasan F**, Jeffers LJ, De Medina M, Reddy KR, Parker T, Schiff ER, Houghton M, Choo QL, Kuo G. Hepatitis C-associated hepatocellular carcinoma. *Hepatology* 1990; **12**(3 Pt 1): 589-591
- Ito T**, Mukaigawa J, Zuo J, Hirabayashi Y, Mitamura K, Yasui K. Cultivation of hepatitis C virus in primary hepatocyte culture from patients with chronic hepatitis C results in release of high titre infectious virus. *J Gen Virol* 1996; **77**(Pt 5): 1043-1054
- Clarke B**. Molecular virology of hepatitis C virus. *J Gen Virol* 1997; **78**(Pt 10): 2397-2410
- Bukh J**, Purcell RH, Miller RH. Sequence analysis of the 5' noncoding region of hepatitis C virus. *Proc Natl Acad Sci U S A* 1992; **89**: 4942-4946
- Grakoui A**, McCourt DW, Wychowski C, Feinstone SM, Rice CM. Characterization of the hepatitis C virus-encoded serine proteinase: determination of proteinase-dependent polyprotein cleavage sites. *J Virol* 1993; **67**: 2832-2843
- Takamizawa A**, Mori C, Fuke I, Manabe S, Murakami S, Fujita J, Onishi E, Andoh T, Yoshida I, Okayama H. Structure and organization of the hepatitis C virus genome isolated from human carriers. *J Virol* 1991; **65**: 1105-1113
- Grakoui A**, Wychowski C, Lin C, Feinstone SM, Rice CM. Expression and identification of hepatitis C virus polyprotein cleavage products. *J Virol* 1993; **67**: 1385-1395
- Hijikata M**, Kato N, Ootsuyama Y, Nakagawa M, Shimotohno K. Gene mapping of the putative structural region of the hepatitis C virus genome by *in vitro* processing analysis. *Proc Natl Acad Sci U S A* 1991; **88**: 5547-5551
- Kato N**, Nakazawa T, Mizutani T, Shimotohno K. Susceptibility of human T-lymphotropic virus type I infected cell line MT-2 to hepatitis C virus infection. *Biochem Biophys Res Commun* 1995; **206**: 863-869
- Lanford RE**, Sureau C, Jacob JR, White R, Fuerst TR. Demonstration of *in vitro* infection of chimpanzee hepatocytes with hepatitis C virus using strand-specific RT/PCR. *Virology* 1994; **202**: 606-614
- Shimizu YK**, Purcell RH, Yoshikura H. Correlation between the infectivity of hepatitis C virus *in vivo* and its infectivity *in vitro*. *Proc Natl Acad Sci U S A* 1993; **90**: 6037-6041
- Yasui K**, Wakita T, Tsukiyama-Kohara K, Funahashi SI, Ichikawa M, Kajita T, Moradpour D, Wands JR, Kohara M. The native form and maturation process of hepatitis C virus core protein. *J Virol* 1998; **72**: 6048-6055
- Ray RB**, Lagging LM, Meyer K, Steele R, Ray R. Transcriptional regulation of cellular and viral promoters by the hepatitis C virus core protein. *Virus Res* 1995; **37**: 209-220
- Ray RB**, Steele R, Meyer K, Ray R. Transcriptional repression of p53 promoter by hepatitis C virus core protein. *J Biol Chem* 1997; **272**: 10983-10986
- Ray RB**, Steele R, Meyer K, Ray R. Hepatitis C virus core protein represses p21WAF1/Cip1/Sid1 promoter activity. *Gene* 1998; **208**: 331-336
- Shih CM**, Lo SJ, Miyamura T, Chen SY, Lee YH. Suppression of hepatitis B virus expression and replication by hepatitis C virus core protein in HuH-7 cells. *J Virol* 1993; **67**: 5823-5832
- Ray RB**, Meyer K, Ray R. Suppression of apoptotic cell death by hepatitis C virus core protein. *Virology* 1996; **226**: 176-182
- Barba G**, Harper F, Harada T, Kohara M, Goulinet S, Matsuura Y, Eder G, Schaff Z, Chapman MJ, Miyamura T, Brechot C. Hepatitis C virus core protein shows a cytoplasmic localization and associates to cellular lipid storage droplets. *Proc Natl Acad Sci U S A* 1997; **94**: 1200-1205
- Chen CM**, You LR, Hwang LH, Lee YH. Direct interaction of hepatitis C virus core protein with the cellular lymphotoxin-beta receptor modulates the signal pathway of the lymphotoxin-beta receptor. *J Virol* 1997; **71**: 9417-9426
- Matsumoto M**, Hsieh TY, Zhu N, VanArsdale T, Hwang SB, Jeng KS, Gorbalenya AE, Lo SY, Ou JH, Ware CF, Lai MM. Hepatitis C virus core protein interacts with the cytoplasmic tail of lymphotoxin-beta receptor. *J Virol* 1997; **71**: 1301-1309
- Chang J**, Yang SH, Cho YG, Hwang SB, Hahn YS, Sung YC. Hepatitis C virus core from two different genotypes has an oncogenic potential but is not sufficient for transforming primary rat embryo fibroblasts in cooperation with the H-ras oncogene. *J Virol* 1998; **72**: 3060-3065
- Ray RB**, Lagging LM, Meyer K, Ray R. Hepatitis C virus core protein cooperates with ras and transforms primary rat embryo fibroblasts to tumorigenic phenotype. *J Virol* 1996; **70**: 4438-4443
- Kim DW**, Suzuki R, Harada T, Saito I, Miyamura T. Trans-suppression of gene expression by hepatitis C viral core protein. *Jpn J Med Sci Biol* 1994; **47**: 211-220
- Shih CM**, Lo SJ, Miyamura T, Chen SY, Lee YH. Suppression of hepatitis B virus expression and replication by hepatitis C virus core protein in HuH-7 cells. *J Virol* 1993; **67**: 5823-5832
- Soardo G**, Pirisi M, Fonda M, Fabris C, Falletti E, Toniutto P, Vitulli D, Cattin L, Gonano F, Bartoli E. Changes in blood lipid composition and response to interferon treatment in chronic hepatitis C. *J Interferon Cytokine Res* 1995; **15**: 705-712
- Thomssen R**, Bonk S, Thiele A. Density heterogeneities of hepatitis C virus in human sera due to the binding of beta-lipoproteins and immunoglobulins. *Med Microbiol Immunol* 1993; **182**: 329-334
- Sabile A**, Perlemuter G, Bono F, Kohara K, Demaugre F, Kohara M, Matsuura Y, Miyamura T, Brechot C, Barba G. Hepatitis C virus core protein binds to apolipoprotein AII and its secretion is modulated by fibrates. *Hepatology* 1999; **30**: 1064-1076
- Makishima M**, Okamoto AY, Repa JJ, Tu H, Learned RM, Luk A, Hull MV, Lustig KD, Mangelsdorf DJ, Shan B. Identification of a nuclear receptor for bile acids. *Science* 1999; **284**: 1362-1365
- Parks DJ**, Blanchard SG, Bledsoe RK, Chandra G, Consler TG, Kliewer SA, Stimmel JB, Willson TM, Zavacki AM, Moore DD, Lehmann JM. Bile acids: natural ligands for an orphan nuclear receptor. *Science* 1999; **284**: 1365-1368
- Wang H**, Chen J, Hollister K, Sowers LC, Forman BM. Endogenous bile acids are ligands for the nuclear receptor FXR/BAR. *Mol Cell* 1999; **3**: 543-553
- Russell DW**. Nuclear orphan receptors control cholesterol catabolism. *Cell* 1999; **97**: 539-542
- Lin Y**, Havinga R, Schippers IJ, Verkade HJ, Vonk RJ, Kuipers F. Characterization of the inhibitory effects of bile acids on very-low-density lipoprotein secretion by rat hepatocytes in primary culture. *Biochem J* 1996; **316**(Pt 2): 531-538
- Lin Y**, Havinga R, Verkade HJ, Moshage H, Slooff MJ, Vonk RJ, Kuipers F. Bile acids suppress the secretion of very-low-density lipoprotein by human hepatocytes in primary culture. *Hepatology* 1996; **23**: 218-228
- Misra S**, Ujhazy P, Gatmaitan Z, Varticovski L, Arias IM. The role of phosphoinositide 3-kinase in taurocholate-induced trafficking of ATP-dependent canalicular transporters in rat liver. *J Biol Chem* 1998; **273**: 26638-26644

Effects of *Helicobacter pylori* infection on gastric emptying rate in patients with non-ulcer dyspepsia

Grigoris I Leontiadis, George I Minopoulos, Efstratios Maltezos, Stamatia Kotsiou, Konstantinos I Manolas, Konstantinos Simopoulos, Dimitrios Hatseras

Grigoris I Leontiadis, Efstratios Maltezos, 2nd Department of Internal Medicine, Democritus University of Thrace, Alexandroupolis, Greece
George I Minopoulos, Department of Endoscopic Surgery, Democritus University of Thrace, Alexandroupolis, Greece
Stamatia Kotsiou, 1st Department of Internal Medicine, Democritus University of Thrace, Alexandroupolis, Greece
Konstantinos I Manolas, 1st Department Surgery, Democritus University of Thrace, Alexandroupolis, Greece
Konstantinos Simopoulos, 2nd Department of Surgery, Democritus University of Thrace, Alexandroupolis, Greece
Dimitrios Hatseras, Department of Cardiology, Democritus University of Thrace, Alexandroupolis, Greece
Correspondence to: Dr. Grigoris I Leontiadis, 4 Karailia Street, Thessaloniki 546 44, Greece. grleo@yahoo.com
Telephone: +30-2310-323535 **Fax:** +30-2310-323535
Received: 2003-12-11 **Accepted:** 2004-01-30

Abstract

AIM: The pathogenesis of delayed gastric emptying in patients with non-ulcer dyspepsia (NUD) remains unclear. We aimed to examine whether gastric emptying rate in NUD patients was associated with *Helicobacter pylori* (*H pylori*) infection and whether it was affected by eradication of the infection.

METHODS: Gastric emptying rate of a mixed solid-liquid meal was assessed by the paracetamol absorption method in NUD patients and asymptomatic controls ($n=17$). *H pylori* status was assessed by serology and biopsy urease test. *H pylori*-positive NUD patients ($n=23$) received 10-day triple eradication therapy. *H pylori* status was re-assessed by biopsy urease test four weeks later, and if eradication was confirmed, gastric emptying rate was re-evaluated.

RESULTS: Thirty-three NUD patients and 17 controls were evaluated. NUD patients had significantly delayed gastric emptying compared with controls. The mean maximum plasma paracetamol concentration divided by body mass (Cmax/BM) was 0.173 and 0.224 mg/L·kg respectively ($P=0.02$), the mean area under plasma paracetamol concentration-time curve divided by body mass (AUC/BM) was 18.42 and 24.39 mg·min/L·kg respectively ($P=0.01$). Gastric emptying rate did not differ significantly between *H pylori*-positive and *H pylori*-negative NUD patients. The mean Cmax/BM was 0.172 and 0.177 mg/L·kg respectively ($P=0.58$), the mean AUC/BM was 18.43 and 18.38 mg·min/L·kg respectively ($P=0.91$). Among 14 NUD patients who were initially *H pylori*-positive, confirmed eradication of the infection did not significantly alter gastric emptying rate. The mean Cmax/BM was 0.171 and 0.160 mg/L·kg before and after *Hp* eradication, respectively ($P=0.64$), the mean AUC/BM was 17.41 and 18.02 mg·min/L·kg before and after eradication, respectively ($P=0.93$).

CONCLUSION: Although gastric emptying is delayed in NUD

patients compared with controls, gastric emptying rate is not associated with *H pylori* status nor it is affected by eradication of the infection.

Leontiadis GI, Minopoulos GI, Maltezos E, Kotsiou S, Manolas KI, Simopoulos K, Hatseras D. Effects of *Helicobacter pylori* infection on gastric emptying rate in patients with non-ulcer dyspepsia. *World J Gastroenterol* 2004; 10(12): 1750-1754
<http://www.wjgnet.com/1007-9327/10/1750.asp>

INTRODUCTION

Dyspepsia is defined as pain or discomfort centered in the upper abdomen, according to the Rome II criteria^[1]. Discomfort refers to a subjective, unpleasant feeling that the patient does not interpret as pain and which can include any of the following: upper abdominal fullness, early satiety, bloating, or nausea. Functional or non-ulcer dyspepsia (NUD) is defined as persistent or recurrent dyspepsia for at least 12 wk, which need not to be consecutive, within the preceding 12 mo of persistent or recurrent dyspepsia, with no evidence of organic disease that is likely to explain the symptoms, and no evidence that symptoms are exclusively relieved by defecation or associated with the onset of a change in stool frequency or stool form (*i.e.*, not irritable bowel syndrome)^[1].

NUD is a common healthcare problem: The estimated annual prevalence in Western countries is 15%^[2]. Despite a great deal of scientific attention, little is known about the pathogenesis of NUD. *Helicobacter pylori* (*H pylori*) infection and delayed gastric emptying have both been documented to have higher prevalence in patients with NUD compared with asymptomatic controls^[3,4]. However, it is unknown if *H pylori* infection and/or delayed gastric emptying are involved in the pathogenesis of NUD. Furthermore, it is still unclear whether there is a causal association between these two factors in patients with NUD.

Therefore, we designed this study to investigate whether gastric emptying rate in patients with NUD was associated with the presence of *H pylori* infection, and whether the eradication of the infection affected the gastric emptying rate in these patients. We also sought to confirm in our population the well-known finding of delayed gastric emptying in patients with NUD compared with asymptomatic controls.

MATERIALS AND METHODS

Subjects

Consecutive patients with dyspeptic symptoms who attended the self-referred out-patient clinic of the 2nd Department of Internal Medicine, General Regional Hospital of Alexandroupolis were candidates for inclusion in the study. Inclusion criteria were: (1) age between 18 and 65 years; (2) presence of dyspeptic symptoms, defined as upper abdominal pain, upper abdominal discomfort, upper abdominal fullness, early satiety, or nausea/vomiting, continuously or intermittently for at least three mo; (3) no relevant findings revealed by physical examination other

than epigastric tenderness; (4) normal gastroscopy except mild erythema of gastric or duodenal mucosa; (5) normal abdominal ultrasound scan; (6) normal full blood count, liver function tests, fasting glucose, urea, creatinine, electrolytes, amylase and thyroid function tests. Exclusion criteria were: (1) presence of any organic or psychiatric disease that could affect the evaluation, treatment or compliance of the patient; (2) heartburn as the predominant symptom; (3) predominant symptoms being compatible with the diagnosis of irritable bowel syndrome or functional constipation as defined by Rome I criteria^[5]; (4) pregnancy or breast feeding; (5) chronic alcoholism or drug abuse; (6) past medical history of peptic ulcer disease, oesophagitis, pancreatitis, abdominal trauma, or abdominal surgery other than uncomplicated appendectomy; (7) intake of antibiotics 4 wk prior to inclusion; (8) regular intake of non steroidal anti-inflammatory drugs, including aspirin, or other medications that could cause dyspepsia during the 3 mo prior to inclusion.

The asymptomatic controls were recruited from the employees of General Regional Hospital of Alexandroupolis. Eligibility criteria were: (1) age between 18 and 65 years; (2) absence of dyspeptic symptoms; (3) absence of any organic or psychiatric disease that could affect the evaluation, treatment or compliance of the participant; (4) intake of antibiotics 4 wk prior to inclusion.

Proton pump inhibitors and H₂-receptor antagonists were withheld from all participants for 7 d before gastroscopy or gastric emptying testing. Paracetamol and all medications with any known potential effect on gastrointestinal motility were withheld for, respectively, two and three days before gastric emptying testing.

Study protocol

Study procedures were timed as follows: NUD patients underwent gastroscopy and two biopsy specimens were collected, one from the antrum and one from the corpus, for urease testing for *H pylori* (CLOtest[®], Delta West Ltd, Australia). The presence of *H pylori* IgG antibodies in serum was assessed by ELISA (*H pylori* GVE 573II IgG, PLK, Italy). On the following day, gastric emptying rate was assessed by the paracetamol absorption method as described below. *H pylori* -positive NUD patients received 10 d of *H pylori* eradication therapy consisting of omeprazole 20 mg twice daily, amoxicillin 1 000 mg twice daily and clarithromycin 500 mg twice daily. Four weeks later, *H pylori* status was re-assessed by biopsy urease test. If eradication of *H pylori* infection was confirmed, gastric emptying rate was re-evaluated. Asymptomatic controls were tested for *H pylori* infection by serology (*H pylori* IgG ELISA) and had gastric emptying rate assessed by the paracetamol absorption method.

The study protocol conformed to the World Medical Association Helsinki Declaration in 1964 as amended in 1996 and was approved by the regional Ethics Committee. Informed consent was obtained from all study subjects. This work was not financially supported by any outside agency or pharmaceutical company.

Assessment of gastric emptying rate

Gastric emptying rate was assessed by the paracetamol absorption method, which was conceived by Heading *et al*^[6,7] and recently re-evaluated^[8,9]. The test meal was administered following overnight fasting and consisted of: (1) three cream crackers (total mass is 35 g); (2) a 200-mL carton of Fortimel[®] (Nutricia Clinical, Holland; liquid nutritional supplement; 410 mOsm/L; 4.184×10³ kJ/L; containing 19.4 g of protein, 4.2 g of fat and 20.8 g of carbohydrates per carton); (3) 1 g of paracetamol as two tablets 500 mg Depon[®], Bristol-Myers Squibb; (4) 100 mL of tap water. Peripheral venous blood samples were obtained *via* a heparinised cannula immediately after the

ingestion of paracetamol (time 0) and at 30 min intervals over a 3-h period (7 samples in total). During the 3-h test period, the subjects were free to sit, stand or walk; they were not allowed to eat, drink or smoke.

Paracetamol plasma concentration was determined with the TDxFLx[®] System (Abbott, IL, USA) by using fluorescence polarization immunoassay technology. The following parameters were calculated: time to detect paracetamol in plasma (lag phase), maximum plasma paracetamol concentration divided by body mass (C_{max}/BM); time to reach maximum plasma paracetamol concentration (T_{max}), area under the plasma paracetamol concentration – time curve divided by body weight (AUC/BM).

Primary outcomes were the absolute difference in gastric emptying rate as assessed by C_{max}/BW and AUC/BW in *H pylori*-positive and *H pylori*-negative NUD patients, and in *H pylori*-positive NUD patients before and after eradication.

Secondary outcomes were the absolute difference in gastric emptying rate as assessed by C_{max}/BM and AUC/BM in NUD patients compared to asymptomatic controls. We also assessed gastric emptying lag phase and T_{max} in all study groups.

Sample size calculation

Sample size was calculated *a priori* with the Altman nomogram^[10]. A pilot study of five *H pylori*-positive NUD patients provided an estimate of mean C_{max}/BM (19.0 mg·min/L·kg) and standard deviation (5.0 mg·min/L·kg). We calculated that at least 10 subjects were required in each study group (*H pylori*-negative NUD patients, *H pylori*-positive NUD patients, post-eradication NUD patients, asymptomatic controls) in order to detect a clinically important relative difference (*a priori* set as ≥25%) between two study groups or within person comparison before and after *H pylori* eradication (1-β=0.8, α=0.05, two tailed significance).

Statistic analysis

Statistical analysis was carried out according to a pre-established analysis plan. Proportions were compared by χ² test with Fisher's exact test when appropriate. Regarding continuous outcomes, study groups were compared by the Mann-Whitney *U* test, while differences before and after *H pylori* eradication were assessed by Wilcoxon matched pairs signed rank test. Two sided significance tests were used throughout. The software used was Statistical Package for the Social Sciences 10.0.1 for Windows (release 1999, SPSS Inc., Chicago, IL). Confidence intervals were calculated with Confidence Interval Analysis software 2.0.0 (release 2000, T. Bryant, Univ. of Southampton).

RESULTS

Thirty-three patients with NUD and 17 asymptomatic volunteers were included in the study during two recruitment periods (January to March 1997 and March to April 1998). All participants were Caucasian. Twenty-three of the NUD patients (70%) had both a positive serum anti-*H pylori* IgG and biopsy urease test and were considered *H pylori*-positive. The remaining 10 NUD patients had both tests negative and were considered *H pylori*-negative. The baseline characteristics of the study groups are displayed in Table 1. The only significant difference found was a difference in age between control group and NUD group (*P*=0.02). Nevertheless multiple regression (ANOVA) revealed that age had no effect on any of the study outcomes. There was, therefore, no need for adjustment for age.

All study subjects underwent evaluation of gastric emptying. There was no significant difference in gastric emptying rate between *H pylori*-positive and *H pylori*-negative NUD patients as assessed by the primary study parameters C_{max}/BM and

AUC/BM (Table 2). NUD patients had significantly delayed gastric emptying compared with asymptomatic controls as assessed by C_{\max} /BM and AUC/BM (Table 3). Gastric emptying lag phase and T_{\max} did not differ significantly in any comparison (data not shown).

All 23 *H. pylori*-positive NUD patients received eradication therapy. Of those, 18 completed the 10-d course and 4 wk later underwent repeat gastroscopy and biopsy urease test, eradication was confirmed in 14 patients (per protocol eradication rate 77.8%). Of the remaining five patients who received eradication therapy, 4 did not consent to repeat gastroscopy and 1 discontinued the course on the third day due to severe diarrhea (*C. difficile* toxin negative). No other side effects of the eradication regimen were reported on direct questioning.

All 14 NUD patients with confirmed *H. pylori* eradication underwent repeat assessment of gastric emptying. No significant difference was found in the gastric emptying parameters C_{\max} /BM and AUC/BM compared with the values prior to eradication (intra-individual comparisons) as shown in Table 4. Neither gastric emptying lag phase nor T_{\max} differed significantly compared with the values prior to eradication (data not shown).

DISCUSSION

This study confirmed that gastric emptying is significantly delayed in patients with NUD compared to asymptomatic controls (Table 3). This has been well established for years^[3, 11].

In fact, our results showed that the 95% confidence interval (CI) for the absolute difference between the medians of gastric emptying parameters, C_{\max} /BW and AUC/BW, was compatible with a relative difference encompassing the predefined limit of clinical importance (*i.e.* 25%). Consequently, our results need to be interpreted as evidence of a statistically significant difference in gastric emptying rate between patients with NUD and asymptomatic controls, which however is unclear if it is clinically relevant. The above comparison was not the primary outcome of our; Nonetheless the fact that these results are in agreement with the current medical literature corroborates the methodological validity of our study and the credibility of the main outcomes.

The pathophysiology of delayed gastric emptying in patients with NUD, as well as its clinical implications, remains unknown. *H. pylori* gastritis - which was also more prevalent in patients with NUD^[3] - has been suggested as a causal factor for the gastric motility disorders found in these patients. There is no solid evidence supporting this hypothesis although there is some biological plausibility since a mucosal inflammatory reaction could affect the function of enteric nerves and smooth muscle^[12].

In our attempt to investigate the potential role of *H. pylori* in the above mentioned motility disorders, we found that the gastric emptying rate in patients with NUD did not differ significantly between *H. pylori*-positive and *H. pylori*-negative patients (Table 2). Furthermore, eradication of *H. pylori* infection in patients with NUD did not induce any significant modification

Table 1 Baseline characteristics of patients with non-ulcer dyspepsia (NUD)

Characteristics	Controls (n=17)	All NUD pts (n=33)	Hp positive NUD pts (n=23)	Hp negative NUD pts (n=10)
Sex (Male:Female)	9:8	20:13	13:10	7:3
Age (yr) (mean±SD)	27.7±6.7	37.3±14.5	39.3±14.2	35.2±18.4
Body mass (kg) (mean±SD)	66.6±13.8	74.3±10.0	75.6±9.8	71.2±10.1
Hp(+) (%)	9 (52.9)	23 (69.7)	23 (100)	0 (0)
Smokers (%)	8 (47.1)	10 (30.3)	7 (30.4)	3 (30)

Table 2 Gastric emptying: *H. pylori*-positive NUD patients vs *H. pylori*-negative NUD patients

parameters (mean±SD, M)	Hp positive NUD pts (n=23)	Hp negative NUD pts (n=10)	Mann-Whitney U test	95% CI for difference between medians (Hp pos. -Hp neg.)
C_{\max} /BM(mg/L·kg)	0.172±0.070 (0.153)	0.177±0.050 (0.176)	P=0.58	-0.050 to 0.037
AUC/BM(mg·min/L·kg)	18.43±6.93 (18.53)	18.38±5.94 (19.42)	P=0.91	-5.36 to 4.62

C_{\max} /BM: maximum plasma paracetamol concentration divided by body mass; AUC/BW: area under the plasma paracetamol concentration-time curve divided by body mass. M: median.

Table 3 Gastric emptying: NUD patients vs asymptomatic controls

Parameters (mean±SD, M)	NUD pts (n=33)	Controls (n=17)	Mann-Whitney U test	95% CI for difference between medians (NUD pts-Controls)
C_{\max} /BM (mg/L·kg)	0.173±0.064 (0.163)	0.224±0.076 (0.221)	P=0.02	-0.012 to -0.095
AUC/BM (mg·min/L·kg)	18.42±6.56 (18.53)	24.34±8.06 (25.53)	P=0.01	-2.11 to -10.93

C_{\max} /BM: maximum plasma paracetamol concentration divided by body mass; AUC/BM: area under the plasma paracetamol concentration-time curve divided by body mass. M: median.

Table 4 Gastric emptying: *H. pylori*-positive NUD patients before and after eradication (intra-individual comparisons)

Parameters (mean±SD, M)	Initially Hp positive NUD pts (n=14)		Wilcoxon matched pairs test	95%CI for the median difference (after - before)
	Before eradication	After eradication		
C_{\max} /BM (mg/L·kg)	0.171±0.074 (0.167)	0.160±0.064 (0.146)	P=0.64	-0.047 to 0.278
AUC/BM (mg·min/L·kg)	17.41±5.25 (18.95)	18.02±7.25 (16.88)	P=0.93	-3.04 to 4.38

C_{\max} /BM: maximum plasma paracetamol concentration divided by body mass. AUC/BM: area under the plasma paracetamol concentration-time curve divided by body mass. M: median.

of the gastric emptying rate (Table 4). However, for both comparisons, the 95% CI for the absolute difference between the medians of gastric emptying parameters was marginally compatible with the pre-defined level of a clinically important relative difference of 25%. This should be interpreted, therefore, as insufficient evidence to confirm or exclude a clinically important difference in gastric emptying rate between *H pylori*-positive and *H pylori*-negative patients with NUD. The same conclusion applies to the changes of gastric emptying rate following eradication of *H pylori* infection in patients with NUD.

Our results are in agreement with most previous publications, which did not detect any influence of *H pylori* status on gastric emptying rate in patients with NUD^[13-23]. However, it is possible that some of these studies were not adequately powered to detect the targeted difference. Some investigators were able to demonstrate significant differences, but their conclusions differed. For example, Fock *et al.*^[24] found that gastric emptying was slower in *H pylori*-positive NUD patients compared to *H pylori*-negative NUD patients, while Tucci *et al.*^[25] found the opposite. No meta-analysis has yet addressed this issue.

Regarding the effect of the eradication of *H pylori* infection on gastric emptying rate in NUD patients, our results are in line with three other trials, which were unable to detect any changes in gastric emptying rate after a follow up period of one^[26], six^[27] and 12 mo^[28]. Nonetheless, other investigators found that eradication of the infection significantly increased gastric emptying rate after a follow-up of 1 mo^[29] or "normalised" previously abnormal (*i.e.* rapid or delayed) gastric emptying after a 2-mo follow up^[30]. There was considerable methodological heterogeneity among these trials, which complicates any attempts to draw a conclusive answer.

Further larger trials would be helpful. These would be facilitated by using safe and non-invasive methods of gastric emptying assessment, such as the paracetamol absorption method, ultrasonography^[31], or ¹³C octanoic acid breath test. Utilization of urea breath testing for confirmation of *H pylori* eradication^[32], which was not available to us at the time of the research, might improve the compliance of participants and could allow investigators to lengthen the post-eradication follow-up time without a significant dropout rate. Future studies should also explore whether specific *H pylori* characteristics, such as CagA phenotype^[19], or differences in host response are implicated in the pathogenesis of gastric emptying disorders in patients with NUD.

In conclusion, gastric emptying is delayed in patients with NUD but is unrelated to *H pylori* status. Eradication of *H pylori* infection in *H pylori*-positive patients with NUD does not significantly alter the gastric emptying rate. Although our results are not definitive, they will contribute to a better understanding of the pathogenesis of NUD - especially when quantitatively synthesised with analogous data in future meta-analyses.

ACKNOWLEDGMENTS

The authors thank Professor Nikolaos Gotsis for his help in the design of the study, Professor Colin Howden for helpful discussions, Associate Professor Areti Hitoglou-Makedou for performing the *H pylori* serology and expert technical advice and Ms. Vasiliki Katsilaki for her excellent technical assistance.

REFERENCES

- 1 Talley NJ, Stanghellini V, Heading RC, Koch KL, Malagelada JR, Tytgat GNJ. Functional gastroduodenal disorders. *Gut* 1999; **45**(Suppl 2): 37-42
- 2 Talley NJ, Silverstein MD, Agreus L, Nyren O, Sonnenberg A, Holtmann G. AGA Technical Review: Evaluation of dyspepsia. *Gastroenterology* 1998; **114**: 582-595
- 3 Jaakkimainen RL, Boyle E, Tudiver F. Is *Helicobacter pylori* associated with non-ulcer dyspepsia and will eradication improve symptoms? A meta-analysis. *BMJ* 1999; **319**: 1040-1044
- 4 Quatero AO, de Wit NJ, Lodder AC, Numans ME, Smout AJ, Hoes AW. Disturbed solid-phase gastric emptying in functional dyspepsia: a meta-analysis. *Dig Dis Sci* 1998; **43**: 2028-2033
- 5 Thompson WG, Creed F, Drossman DA, Heaton KW, Mazzacca G. Functional bowel disease and functional abdominal pain. *Gastroenterol Int* 1992; **5**: 75-91
- 6 Heading RC, Nimmo J, Prescott LF, Tothill P. The dependence of paracetamol absorption on the rate of gastric emptying. *Br J Pharmacol* 1973; **47**: 415-421
- 7 Clements JA, Heading RC, Nimmo WS, Prescott LF. Kinetics of acetaminophen absorption and gastric emptying in man. *Clin Pharmacol Ther* 1978; **24**: 420-431
- 8 Medhus AW, Sandstad O, Bredesen J, Husebye E. Delay of gastric emptying by duodenal intubation: sensitive measurement of gastric emptying by the paracetamol absorption test. *Aliment Pharmacol Ther* 1999; **13**: 609-620
- 9 Medhus AW, Lofthus CM, Bredesen J, Husebye E. The validity of a novel paracetamol absorption test for gastric emptying. *Gastroenterology* 2000; **118**(Suppl 2): A142
- 10 Altman D. Practical statistics for medical research. London: Chapman & Hall 1991: 455-459
- 11 Malagelada JR. Functional dyspepsia. Insights on mechanisms and management strategies. *Gastroenterol Clin North Am* 1996; **25**: 103-112
- 12 Olbe L, Malfertheiner P. Gastric pathophysiology - emphasis on acid secretion and gastrointestinal motility. *Curr Opin Gastroenterol* 1996; **12**(Suppl 1): 16-20
- 13 Caballero-Plasencia AM, Muros-Navarro MC, Martin-Ruiz JL, Valenzuela-Barranco M, de los Reyes-Garcia MC, Casado-Caballero FJ, Rodriguez-Tellez M, Lopez-Manas JG. Dyspeptic symptoms and gastric emptying of solids in patients with functional dyspepsia. Role of *Helicobacter pylori* infection. *Scand J Gastroenterol* 1995; **30**: 745-751
- 14 Chang CS, Chen GH, Kao CH, Wang SJ, Peng SN, Huang CK. The effect of *H pylori* infection on gastric emptying of digestible and indigestible solids in patients with nonulcer dyspepsia. *Am J Gastroenterol* 1996; **91**: 474-479
- 15 Perri F, Clemente R, Festa V, Annese V, Quitadamo M, Rutgeerts P, Andriulli A. Patterns of symptoms in functional dyspepsia: role of *H pylori* infection and delayed gastric emptying. *Am J Gastroenterol* 1998; **93**: 2082-2088
- 16 Wegener M, Borsch G, Schaffstein J, Schulz-Flake C, Mai U, Leverkus F. Are dyspeptic symptoms in patients with *Campylobacter pylori*-associated type B gastritis linked to delayed gastric emptying? *Am J Gastroenterol* 1988; **83**: 737-740
- 17 Dumitrascu DL, Pascu O, Drăghini A, Andreica A, Nagy Z. *Helicobacter pylori* infection does not influence the gastric emptying of a semisolid meal. *Rom J Gastroenterol* 1996; **5**: 167-174
- 18 Marzio L, Falcucci M, Ciccaglione AF, Malatesta MG, Lapenna D, Ballone E, Antonelli C, Grossi L. Relationship between gastric and gallbladder emptying and refilling in normal subjects and patients with *H pylori*-positive and -negative idiopathic dyspepsia and correlation with symptoms. *Dig Dis Sci* 1996; **41**: 26-31
- 19 Parente F, Imbesi V, Maconi G, Cucino C, Sangaletti O, Vago L, Bianchi Porro G. Influence of bacterial CagA status on gastritis, gastric function indices, and pattern of symptoms in *H pylori*-positive dyspeptic patients. *Am J Gastroenterol* 1998; **93**: 1073-1079
- 20 Minocha A, Mokshagundam S, Gallo SH, Rahal PS. Alterations in upper gastrointestinal motility in *Helicobacter pylori*-positive nonulcer dyspepsia. *Am J Gastroenterol* 1994; **89**: 1797-1800
- 21 Koskenpato J, Kairemo K, Korppi-Tommola T, Farkkila M. Role of gastric emptying in functional dyspepsia: a scintigraphic study of 94 subjects. *Dig Dis Sci* 1998; **43**: 1154-1158
- 22 Rhee PI, Kim YH, Son HJ, Kim JJ, Koh KC, Paik SW, Rhee JC, Choi KW. Lack of association of *Helicobacter pylori* infection with gastric hypersensitivity or delayed gastric emptying in functional dyspepsia. *Am J Gastroenterol* 1999; **94**: 3165-3169

- 23 **Scott AM**, Kellow JE, Shuter B, Cowan H, Corbett AM, Riley JW, Lunzer MR, Eckstein RP, Hoschl R, Lam SK, Jones MP. Intra-gastric distribution and gastric emptying of solids and liquids in functional dyspepsia. Lack of influence of symptom subgroups and *H pylori*-associated gastritis. *Dig Dis Sci* 1993; **38**: 2247-2254
- 24 **Fock KM**, Khoo TK, Chia KS, Sim CS. *Helicobacter pylori* infection and gastric emptying of indigestible solids in patients with dysmotility-like dyspepsia. *Scand J Gastroenterol* 1997; **32**: 676-680
- 25 **Tucci A**, Corinaldesi R, Stanghellini V, Tosetti C, Di Febo G, Paparo GF, Varoli O, Paganelli GM, Labate AM, Masci C, Zoccoli G, Monetti N, Barbara L. *Helicobacter pylori* infection and gastric function in patients with chronic idiopathic dyspepsia. *Gastroenterology* 1992; **103**: 768-774
- 26 **Goh KL**, Paramsothy M, Azian M, Parasakthi N, Peh SC, Bux S, Lo YL, Ong KK. Does *H pylori* infection affect gastric emptying in patients with functional dyspepsia? *J Gastroenterol Hepatol* 1997; **12**: 790-794
- 27 **Parente F**, Imbesi V, Maconi G, Cucino C, Manzionna G, Vago L, Bianchi Porro G. Effects of *Helicobacter pylori* eradication on gastric function indices in functional dyspepsia. *Scand J Gastroenterol* 1998; **33**: 461-467
- 28 **Koskenpato J**, Korppi-Tommola T, Kairemo K, Farkkila M. Long-term follow-up study of gastric emptying and *Helicobacter pylori* eradication among patients with functional dyspepsia. *Dig Dis Sci* 2000; **45**: 1763-1768
- 29 **Murakami K**, Fujioka T, Shiota K, Ito A, Fujiyama K, Kodama R, Kawasaki Y, Kubota T, Nasu M. Influence of *Helicobacter pylori* infection and the effects of its eradication on gastric emptying in non-ulcerative dyspepsia. *Eur J Gastroenterol Hepatol* 1995; **7**(Suppl 1): 93-97
- 30 **Miyaji H**, Azuma T, Ito S, Abe Y, Ono H, Suto H, Ito Y, Yamazaki Y, Kohli Y, Kuriyama M. The effect of *Helicobacter pylori* eradication therapy on gastric antral myoelectrical activity and gastric emptying in patients with non-ulcer dyspepsia. *Aliment Pharmacol Ther* 1999; **13**: 1473-1480
- 31 **Gilja OH**, Hausken T, Degaard S, Berstad A. Gastric emptying measured by ultrasonography. *World J Gastroenterol* 1999; **5**: 93-94
- 32 **Howden CW**, Hunt RH. Guidelines for the management of *Helicobacter pylori* infection. *Am J Gastroenterol* 1998; **93**: 2330-2338

Edited by Xu CT and Wang XL Proofread by Pan BR and Xu FM

Effects of lactose as an inducer on expression of *Helicobacter pylori* rUreB and rHpaA, and *Escherichia coli* rLTKA63 and rLTB

Jie Yan, Shou-Feng Zhao, Ya-Fei Mao, Yi-Hui Luo

Jie Yan, Shou-Feng Zhao, Ya-Fei Mao, Yi-Hui Luo, Department of Medical Microbiology and Parasitology, College of Medical Science, Zhejiang University, Hangzhou 310031, Zhejiang Province, China
Supported by the Excellent Young Teacher Fund of Ministry of Education of China and the General Science and Technology Research Plan of Zhejiang Province, No. 001110438

Correspondence to: Jie Yan, Department of Medical Microbiology and Parasitology, College of Medical Science, Zhejiang University, 353 Yan An Road, Hangzhou 310031, Zhejiang Province, China. yanchen@mail.hz.zj.cn

Telephone: +86-571-87217385 **Fax:** +86-571-87217044

Received: 2003-10-15 **Accepted:** 2003-12-16

Abstract

AIM: To demonstrate the effect of lactose as an inducer on expression of the recombinant proteins encoded by *Helicobacter pylori* ureB and hpaA, and *Escherichia coli* LTb and LTKA63 genes and to determine the optimal expression parameters.

METHODS: By using SDS-PAGE and BIO-RAD gel image analysis system, the outputs of the target recombinant proteins expressed by *pET32a-ureB-E.coliBL21*, *pET32a-hpaA-E.coliBL21*, *pET32a-LTKA63-E.coliBL21* and *pET32a-LTB-E.coliBL21* were measured when using lactose as inducer at different dosages, original bacterial concentrations, various inducing temperatures and times. The results of the target protein expression induced by lactose were compared to those by isopropyl- β -D-thiogalactoside (IPTG). The proteins were expressed in *E.coli*.

RESULTS: Lactose showed higher efficiency of inducing the expression of rHpaA, rUreB, rLTb and rLTKA63 than IPTG. The expression outputs of the target recombinant proteins induced at 37 °C were remarkably higher than those at 28 °C. Other optimal expression parameters for the original bacterial concentrations, dosages of lactose and inducing time were 0.8, 50 g/L and 4 h for rHpaA; 0.8, 100 g/L and 4 h for rLTKA63; 1.2, 100 g/L and 5 h for both rUreB and rLTb, respectively.

CONCLUSION: Lactose, a sugar with non-toxicity and low cost, is able to induce the recombinant genes to express the target proteins with higher efficiency than IPTG. The results in this study establish a beneficial foundation for industrial production of *H pylori* genetic engineering vaccine.

Yan J, Zhao SF, Mao YF, Luo YH. Effects of lactose as an inducer on expression of *Helicobacter pylori* rUreB and rHpaA, and *Escherichia coli* rLTKA63 and rLTb. *World J Gastroenterol* 2004; 10(12): 1755-1758

<http://www.wjgnet.com/1007-9327/10/1755.asp>

INTRODUCTION

In China, chronic gastritis and peptic ulcer are two most common

gastric diseases^[1], and gastric cancer is one of the malignant tumors with high mortalities and morbidities.

Helicobacter pylori (*H pylori*), a microaerophilic, spiral and Gram-negative bacterium, is recognized as a human-specific gastric pathogen that colonizes the stomachs of at least half of the world's populations. Most infected individuals are asymptomatic. However, in some subjects, *H pylori* infection causes acute, chronic gastritis and peptic ulceration^[2-4], and acts as a high risk factor on development of gastric adenocarcinoma^[5-10], and mucosa-associated lymphoid tissue (MALT) lymphoma^[10-13].

It is generally considered inoculation of *H pylori* vaccine is a most efficient measure for prevention and control of *H pylori* infection^[14]. However, high nutrition requirements, poor growth for a long time, easy contamination during the cultivation and difficulty of bacterial strain conservation make whole cell vaccine of *H pylori* impracticable. Genetic engineering vaccine seems to be a possible pathway for developing *H pylori* vaccine.

Isopropyl- β -D-thiogalactoside (IPTG), a highly stable and effective inducer on T7lac promoter for target recombinant protein expression, is widely used in laboratories. However, IPTG is a reagent with potential toxicity and high cost^[15], which limited it as a practical inducer for industrial production of genetic engineering vaccines. It was reported that lactose, a common disaccharide, is also able to induce T7lac promoter after it is transformed into allolactose^[16]. The low-cost and non-toxicity make lactose a practical potential for engineering products. In comparison with IPTG, the parameters of lactose inducing different recombinant protein expression vary greatly and its optimal working conditions are established usually by a large number of laboratory tests^[17]. In our previous studies, urease subunit B (UreB) and *H pylori* adhesin (HpaA) were demonstrated as fine candidates in *H pylori* engineering vaccine^[18,19]. For improving immunogenicity of the vaccine, heat-labile enterotoxin subunit A mutant at the 63rd position (LTKA63) and subunit B (LTb) of *Escherichia coli* were selected as adjuvants^[20]. In this study, 4 constructed prokaryotic expression systems of ureB, hpaA, LTKA63 and LTb were used as the target genes to determine the inducing effects with different lactose dosages, temperatures and times, and original bacterial concentrations on expression of the recombinant proteins.

MATERIALS AND METHODS

Materials

Four prokaryotic expression systems of *pET32a-ureB-E.coliBL21*, *pET32a-hpaA-E.coli BL21*, *pET32a-LTKA63-E.coliBL21* and *pET32a-LTB-E.coliBL21* were constructed and offered by our laboratory. Tryptone, yeast extract for LB medium were purchased from OXOID (Basingstoke, Hampshire, England). IPTG and lactose used for inducement, and SDS, glycine and DTT were offered by BBST (Shanghai, China). Acrylamide, N, N'-methylene-bis-acrylamid and TEMED were obtained from Serva (Heidelberg, Germany).

Methods

Determination of optimal inducing concentrations of lactose

and temperatures A colony of each the four engineering bacteria in LB agar plates was inoculated into 5 mL of LB liquid medium and then incubated on rotator with 200 r/min at 37 °C for 12 h. The values at A_{600} measured by spectrophotometry were used to indicate the bacterial concentrations. Lactose at the final concentrations of 5, 10, 50 and 100 g/L were added into the cultures of the 4 strains with the A_{600} values of 1.2, respectively, and then incubated on 200 r/min shaking at 28 °C or 37 °C for 4 h. The bacteria in the medium were collected by centrifugation. By using SDS-PAGE, the expression and outputs of the target recombinant proteins (rUreB, rHpaA, rLTKA63 and rLTB) were examined and estimated, respectively. BIO-RAD gel image analysis system was applied to measure the outputs of target protein fragments by their area percentages in the total bacterial proteins. 0.5 mmol/L IPTG was simultaneously used as an inducer control, which inducing effects for the four recombinant proteins had been confirmed in our previous studies^[18-20].

Determination of optimal original bacterium concentrations for inducement Four engineering bacterial strains were inoculated with proportion of 1:100 (V/V) into LB liquid medium and then incubated on 200 r/min shaking at 37 °C. According to the results obtained above, lactose at the final concentrations of 100, 50, 100 and 100 g/L for inducement of rUreB, rHpaA, rLTKA63 and rLTB expression was added into the cultures with the A_{600} values of 0.2, 0.4, 0.8, 1.2, 1.6, 2.0 and 2.4, respectively. The lactose added cultures were continuously incubated on 200 r/min shaking at 37 °C for 4 h. The outputs of rUreB, rHpaA, rLTKA63 and rLTB were examined by SDS-PAGE and BIO-RAD gel image analysis system.

Effects of the target protein expression by using different inducing time According to the results obtained above, the optimal original bacterial concentration for inducement was 1.2 (A_{600}). The four different bacterial cultures ($A_{600}=1.2$), which expressing rUreB, rHpaA, rLTKA63 or rLTB, were added with lactose at the final concentrations of 100, 50, 100, 100 g/L, respectively. The cultures were continuously incubated on 200 r/min shaker at 37 °C for 1, 2, 3, 4, 5, 6 and 7 h, respectively. The outputs of rUreB, rHpaA, rLTKA63 and rLTB were examined by SDS-PAGE and BIO-RAD gel image analysis system.

SDS-PAGE A vertical discontinuous plate polyacrylamide gel electrophoresis was applied^[21]. The isolation gels with 8%, 10%, 12% and 15% concentrations (W/V) were used to detect the expressed rUreB, rLTKA63, rHpaA and rLTB, respectively, based on their different molecular weights. The start voltage was 8 V/cm and then changed to 15 V/cm while the samples went into isolation gels. The gels after electrophoresis were stained by Coomassie brilliant blue and then decolorized with methanol-acetic acid solution.

RESULTS

Optimal inducing concentrations and temperatures of lactose

Lactose with multiple appropriate concentrations could

effectively induce expression of 4 target recombinant proteins (Figure 1). Beginning with the original bacterial concentrations of 1.2 A_{600} values, the outputs of rUreB, rHpaA, rLTKA63 and rLTB at the inducing temperature of 37 °C were 27.3-53.9%, 7.4-30.9%, 0.8-79.8% and 12.7-119.1% increased as compared with those of 28 °C, respectively (Table 1). When the concentrations of lactose were 100, 50, 100 and 100 g/L inducing at 37 °C for 4 h, outputs of the 4 recombinant proteins reached the highest (Table 1). In comparison with the inducing expression effects of 0.5 mmol/L IPTG, the highest outputs of rUreB, rHpaA, rLTKA63 and rLTB induced by lactose were 203.2%, 98.4%, 114.0% and 245.1% increased, respectively (Table 1).

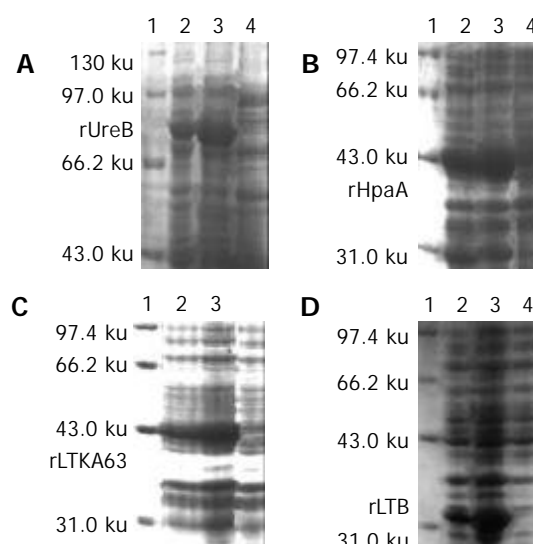


Figure 1 Effects of lactose on inducing expression of target recombinant proteins compared to IPTG. A: rUreB; Lane 1: Marker; Lane 2: Induced with 0.5 mmol/L IPTG; Lane 3: Induced with 100 g/L lactose; Lane 4: Non-induced. B: rHpaA; Lane 1: Marker; Lane 2: Induced with 0.5 mmol/L IPTG; Lane 3: Induced with 50 g/L lactose; Lane 4: Non-induced. C: rLTKA63 expression; Lane 1: Marker; Lane 2: Induced with 0.5 mmol/L IPTG; Lane 3: Induced with 100 g/L lactose. Lane 4: Non-induced; D: rLTB; Lane 1: Marker; Lane 2: Induced with 0.5 mmol/L IPTG; Lane 3: Induced with 100 g/L lactose; Lane 4: Non-induced.

Effects of the target protein expression of original bacteria with different A_{600} values under inducement by lactose

By using the inducing concentrations of lactose with 100, 50, 100 and 100 g/L inducing at 37 °C for 4 h, the expression outputs of the 4 recombinant proteins with the different original bacterial concentrations (0.2-2.4 A_{600} values) are showed in Figure 2. The results indicated that a better expression effect for any of the 4 recombinant proteins was present when the original bacterial concentration used was higher ($A_{600}=0.8-1.2$).

Table 1 Expression outputs of rUreB, rHpaA, rLTKA63 and rLTB proteins induced by different concentrations of lactose and temperatures

Concentrations of lactose(g/L) and IPTG(mmol/L)	Expression outputs (% of total bacterial proteins)							
	rUreB		rHpaA		rLTKA63		rLTB	
	(37 °C)	(28 °C)	(37 °C)	(28 °C)	(37 °C)	(28 °C)	(37 °C)	(28 °C)
Lactose (50)	40.59	26.38	50.35	44.72	23.36	22.41	39.55	21.91
(10)	50.52	39.70	57.61	44.86	35.84	27.09	42.66	26.17
(5)	30.51	22.17	60.80	46.42	35.64	22.09	26.99	23.94
(1)	27.33	18.92	54.00	50.29	21.91	21.73	23.33	10.65
(0.5)	20.78	13.63	42.29	36.05	22.01	12.24	14.72	10.31
IPTG (0.5)	16.66	14.72	30.65	22.61	16.75	14.48	12.36	10.06

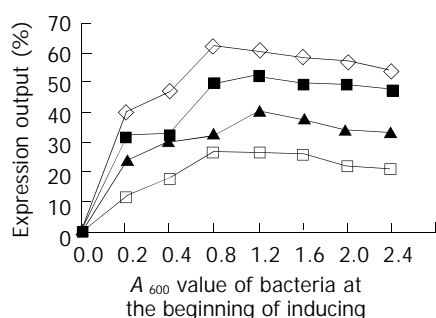


Figure 2 Expression of target recombinant proteins of original bacteria with different A_{600} values under inducement by lactose. \diamond : rHpaA; \blacksquare : rUreB; \blacktriangle : rLTB; \square : rLTKA63.

Effects of the target protein expression using different inducing time

When the original bacterial concentrations as A_{600} values of 1.2 and the lactose concentrations of 100, 50, 100 and 100 g/L, the outputs of rUreB, rHpaA, rLTKA63 and rLTB were shown in Figure 3. The results indicated that a higher output for any of the 4 recombinant proteins was present when the inducing time was 4-5 h.

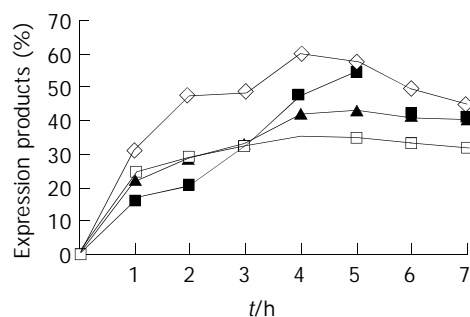


Figure 3 Expression outputs of the target proteins by using different inducing time. \diamond : rHpaA; \blacksquare : rUreB; \blacktriangle : rLTB; \square : rLTKA63.

DISCUSSION

H pylori causes a local superficial infection in human stomach and duodenum^[22]. So orally inoculating of *H pylori* vaccine has a good protective effect^[23]. So far, no commercial *H pylori* engineering vaccine has been available. An engineering vaccine has many advantages but its immunoprotective effect is usually poor because of the unitarity for antigen components. Using adjuvant is an efficient measure to improve immune effect of engineering vaccines^[24]. UreB and HpaA were demonstrated to be excellent antigen candidates as their stable and high expression, strong antigenicity, universal distribution in different *H pylori* isolates and exposure on the surface of the bacterium^[25,26]. *E. coli* LTKA63 and LTB were recently found and were generally considered as the most efficient adjuvants for mucosal immunization so far^[27,28]. So we planned to use the rUreB and rHpaA as antigens and LTB or LTKA63 as adjuvants to develop an oral-taken double-valence genetic engineering vaccine of *H pylori*.

Almost of all the recombinant proteins show a very low expression or non-expression without inducement. IPTG is a routinely laboratory used inducer with high efficiency on recombinant protein expression in *E. coli* but it must be removed by complicated methods from the induced products because of its toxicity. When at the efficient inducing dosages, the cost of IPTG is approximate hundredfold of lactose. Therefore, lactose as an inducer has industrially remarkable advantages. Lactose, differs from IPTG, is unable to enter the bacterial body. It must

be helped by a special enzyme called as primase to be transported into host bacterium. The lactose in bacterial cell must be transferred into allolactose by β -galactosidase and the latter is able to start T7 Lac promoter. In the process inducing expression of recombinant protein, lactose is much more complex than IPTG. So lactose, if used it as an efficient inducer, must be clarified its inducing parameters such as dosage, temperature, time and original bacterial concentration.

It was proved by our study that lactose at the multiple tested concentrations could efficiently induce the expression of rUreB, rHpaA, rLTKA63 and rLTB. The effects of lactose on inducing expression of the 4 recombinant proteins were much stronger than that by IPTG, which demonstrated by 98.4-245.1% increased outputs (Table 1). Furthermore, it was reported that lactose is a carbon source for bacteria to promote growth and increase number of bacteria in culture, which results in the increase of output of the target recombinant protein.

The results of this study indicated that at 37 °C for 4 h inducement the lactose concentration to obtain the highest expression outputs of rUreB, rHpaA, rLTKA63 and rLTB were 100, 50, 100 and 100 g/L, respectively. It was found in the study that inducing temperatures can obviously affect the expression of the recombinant proteins. For example, with the original bacterial concentration of 1.2 A_{600} value for 4 h inducement, using 37 °C as the inducing temperature could increase the expression outputs of rUreB, rHpaA, rLTKA63 and rLTB with 27.3-53.9%, 7.4-30.9%, 0.8-79.8% and 12.7-119.1% of those induced by 28 °C. The original bacterial concentrations when lactose addition was found to affect the outputs of the recombinant proteins. There were preferable expression effects of the recombinant proteins to add lactose when the original bacterial concentrations with the A_{600} values of 0.8-1.2. With the original bacterial concentration of 1.2 A_{600} values and at temperature 37 °C, the outputs of the recombinant proteins for 4-5 h inducement by the optimal concentrations of lactose were relatively higher.

Summarily, using lactose as an inducer on the expression of *pET32a-ureB-E.coliBL21*, *pET32a-hpaA-E.coli BL21*, *pET32a-LTKA63-E.coliBL21* and *pET32a-LTB-E.coliBL21*, the optimal temperature was 37 °C. The rest optimal parameters for the original bacterial concentrations, dosages of lactose and inducing time were 0.8, 50 g/L and 4 h for rHpaA; 0.8, 100 g/L and 4 h for rLTKA63; 1.2, 100 g/L and 5 h for both rUreB and rLTB, respectively. The results from this study established a beneficial foundation for industrial production of *H pylori* genetic engineering vaccines.

REFERENCES

- 1 Niu WX, Qin XY, Liu H, Wang CP. Clinicopathological analysis of patients with gastric. *World J Gastroenterol* 2001; **7**: 281-284
- 2 Peng ZS, Liang ZC, Liu MC, Ouyang NT. Studies on gastric epithelial cell proliferation and apoptosis in *Hp* associated gastric ulcer. *Shijie Huaren Xiaohua Zazhi* 1999; **7**: 218-219
- 3 Kate V, Ananthakrishnan N, Badrinath S. Effect of *Helicobacter pylori* eradication on the ulcer recurrence rate after simple closure of perforated duodenal ulcer: retrospective and prospective randomized controlled studies. *Br J Surg* 2001; **88**: 1054-1058
- 4 Yao YL, Zhang WD. Relation between *Helicobacter pylori* and gastric cancer. *Shijie Huaren Xiaohua Zazhi* 2001; **9**: 1045-1049
- 5 Lu SY, Pan XZ, Peng XW, Shi ZL. Effect of *Hp* infection on gastric epithelial cell kinetics in stomach diseases. *Shijie Huaren Xiaohua Zazhi* 1999; **7**: 760-762
- 6 Liu HF, Liu WW, Fang DC. Study of the relationship between apoptosis and proliferation in gastric carcinoma and its precancerous lesion. *Shijie Huaren Xiaohua Zazhi* 1999; **7**: 649-651
- 7 Zhu ZH, Xia ZS, He SG. The effects of ATRA and 5-Fu on telomerase activity and cell growth of gastric cancer cells *in vitro*. *Shijie Huaren Xiaohua Zazhi* 2000; **8**: 669-673
- 8 Cai L, Yu SZ. A molecular epidemiology study on gastric

- cancer in Changde, Fujian Province. *Shijie Huaren Xiaohua Zazhi* 1999; **7**: 652-655
- 9 **Suganuma M**, Kurusu M, Okabe S, Sueoka N, Yoshida M, Wakatsuki Y, Fujiki H. *Helicobacter pylori* membrane protein 1: a new carcinogenic factor of *Helicobacter pylori*. *Cancer Res* 2001; **61**: 6356-6359
- 10 **Uemura N**, Okamoto S, Yamamoto S, Matsumura N, Yamaguchi S, Yamakido M, Taniyama K, Sasaki N, Schlemper RJ. *Helicobacter pylori* infection and the development of gastric cancer. *N Engl J Med* 2001; **345**: 8298-8332
- 11 **Hiyama T**, Haruma K, Kitadai Y, Miyamoto M, Tanaka S, Yoshihara M, Sumii K, Shimamoto F, Kajiyama G. B-cell monoclonality in *Helicobacter pylori*-associated chronic atrophic gastritis. *Virchows Arch* 2001; **483**: 232-237
- 12 **Nakamura S**, Matsumoto T, Suekane H, Takeshita M, Hizawa K, Kawasaki M, Yao T, Tsuneyoshi M, Iida M, Fujishima M. Predictive value of endoscopic ultrasonography for regression of gastric low grade and high grade MALT lymphomas after eradication of *Helicobacter pylori*. *Gut* 2001; **48**: 454-460
- 13 **Morgner A**, Miehlke S, Fischbach W, Schmitt W, Muller-Hermelink H, Greiner A, Thiede C, Schetelig J, Neubauer A, Stolte M, Ehninger G, Bayerdorffer E. Complete remission of primary high-grade B-cell gastric lymphoma after cure of *Helicobacter pylori* infection. *J Clin Oncol* 2001; **19**: 2041-2048
- 14 **Houben MH**, van de Beek D, Hensen EF, Craen AJ, Rauws EA, Tytgat GN. A systematic review of *Helicobacter pylori* eradication therapy- the impact of antimicrobial resistance on eradication rates. *Aliment Pharmacol Ther* 1999; **13**: 1047-1055
- 15 **Donovan RS**, Robinson CW, Glick BR. Review: optimizing inducer and culture conditions for expression of foreign proteins under the control of the lac promoter. *J Ind Microbiol* 1996; **16**: 145-154
- 16 **Yildirim N**, Mackey MC. Feedback regulation in the lactose operon: a mathematical modeling study and comparison with experimental data. *Biophys J* 2003; **84**: 2841-2851
- 17 **Menzella HG**, Ceccarelli EA, Gramajo HC. Novel *Escherichia coli* strain allows efficient recombinant protein production using lactose as inducer. *Biotechnol Bioeng* 2003; **82**: 809-817
- 18 **Mao YF**, Yan J, LI LW. Cloning, expression and identification of hpaA gene from a clinical isolate of *Helicobacter pylori*. *Zhejiang Daxue Xuebao* 2003; **32**: 9-12
- 19 **Chen Z**, Yan J, Mao YF. Construction of prokaryotic expression system of ureB gene from a clinical isolate of *Helicobacter pylori* and identification of immunogenicity of the fusion protein. *Zhejiang Daxue Xuebao* 2003; **32**: 4-8
- 20 **Xia XP**, Yan J, Zhao SF. Cloning, expression and identification of *Escherichia coli* LTB gene and *Vibrio cholerae* CTB gene. *Zhejiang Daxue Xuebao* 2003; **32**: 17-20
- 21 **Sambrook J**, Fritsch EF, Maniatis T. Molecular Cloning. Cold Spring Harbor Laboratory Press 1989: pp 18.47-18.61
- 22 **Recavarren Ascencios R**, Recavarren Arce S. Chronic atrophic gastritis: pathogenic mechanisms due to cellular hypersensitivity. *Rev Gastroenterol Peru* 2002; **22**: 199-205
- 23 **Crabtree JE**. Eradication of chronic *Helicobacter pylori* infection by therapeutic vaccination. *Gut* 1998; **43**: 7-8
- 24 **Yuki Y**, Kiyono H. New generation of mucosal adjuvants for the induction of protective immunity. *Rev Med Virol* 2003; **13**: 293-310
- 25 **Corthesy-Theulaz I**, Porta N, Glauser M, Saraga E, Vaney AC, Haas R, Kraehenbuhl JP, Blum AL, Michetti P. Oral immunization with *Helicobacter pylori* urease B subunit as a treatment against *Helicobacter pylori* infection in mice. *Gastroenterology* 1995; **109**: 115-121
- 26 **Opazo P**, Muller I, Rollan A, Valenzuela P, Yudelevich A, Garcia-de la Guarda R, Urrea S, Venegas A. Serological response to *Helicobacter pylori* recombinant antigens in Chilean infected patients with duodenal ulcer, non-ulcer dyspepsia and gastric cancer. *Apmis* 1999; **107**: 1069-1078
- 27 **Verweij WR**, de Haan L, Holtrop M, Agsteribbe E, Brands R, van Scharrenburg GJ, Wilschut J. Mucosal immunoadjuvant activity of recombinant *Escherichia coli* heat-labile enterotoxin and its B subunit: induction of systemic IgG and secretory IgA responses in mice by intranasal immunization with influenza virus surface antigen. *Vaccine* 1998; **16**: 2069-2076
- 28 **Baudner BC**, Giuliani MM, Verhoef JC, Rappuoli R, Junginger HE, Giudice GD. The concomitant use of the LTK63 mucosal adjuvant and of chitosan-based delivery system enhances the immunogenicity and efficacy of intranasally administered vaccines. *Vaccine* 2003; **21**: 3837-3844

Edited by Zhang JZ Proofread by Chen WW and Xu FM

Coordinate increase of telomerase activity and c-Myc expression in *Helicobacter pylori*-associated gastric diseases

Guo-Xin Zhang, Yan-Hong Gu, Zhi-Quan Zhao, Shun-Fu Xu, Hong-Ji Zhang, Hong-Di Wang, Bo Hao

Guo-Xin Zhang, Yan-Hong Gu, Zhi-Quan Zhao, Shun-Fu Xu, Hong-Ji Zhang, Hong-Di Wang, Bo Hao, Department of Gastroenterology, the First Affiliated Hospital of Nanjing Medical University, Nanjing 210029, Jiangsu Province, China

Supported by the Ministry of Health of China, No. 8-1-323

Correspondence to: Dr. Guo-Xin Zhang, Department of Gastroenterology, the First Affiliated Hospital of Nanjing Medical University, 300 Guangzhou Road, Nanjing 210029, Jiangsu Province, China. guoxinz2002@yahoo.com

Telephone: +86-25-3718836-6973 **Fax:** +86-25-3724440

Received: 2003-08-06 **Accepted:** 2003-10-07

Abstract

AIM: To detect the telomerase activity and c-Myc expression in gastric diseases and to examine the relation between these values and *Helicobacter pylori* (*H pylori*) as a risk factor for gastric cancer.

METHODS: One hundred and seventy-one gastric samples were studied to detect telomerase activity using a telomerase polymerase chain reaction enzyme linked immunosorbent assay (PCR-ELISA), and c-Myc expression using immunohistochemistry.

RESULTS: The telomerase activity and c-Myc expression were higher in cancers (87.69% and 61.54%) than in noncancerous tissues. They were higher in chronic atrophic gastritis with severe intestinal metaplasia (52.38% and 47.62%) than in chronic atrophic gastritis with mild intestinal metaplasia (13.33% and 16.67%). In chronic atrophic gastritis with severe intestinal metaplasia, the telomerase activity and c-Myc expression were higher in cases with *H pylori* infection (67.86% and 67.86%) than in those without infection (21.43% and 7.14%). c-Myc expression was higher in gastric cancer with *H pylori* infection (77.27%) than in that without infection (28.57%). The telomerase activity and c-Myc expression were coordinately up-regulated in *H pylori* infected gastric cancer and chronic atrophic gastritis with severe intestinal metaplasia.

CONCLUSION: *H pylori* infection may influence both telomerase activity and c-Myc expression in gastric diseases, especially in chronic atrophic gastritis.

Zhang GX, Gu YH, Zhao ZQ, Xu SF, Zhang HJ, Wang HD, Hao B. Coordinate increase of telomerase activity and c-Myc expression in *Helicobacter pylori*-associated gastric diseases. *World J Gastroenterol* 2004; 10(12): 1759-1762
<http://www.wjgnet.com/1007-9327/10/1759.asp>

INTRODUCTION

Gastric cancer is one of the most common malignant tumors in the world. Gastric carcinogenesis is a multi-step process progressing from chronic gastritis to glandular atrophy, metaplasia, and dysplasia^[1-3]. Genetic analyses of gastric

cancers suggest alterations are involved in the structures and functions of several oncogenes and tumor suppressor genes as well as genetic instability^[3,4]. However, in addition to these genetic changes, cell immortality is important for the sustained growth properties of gastric cancer cells^[4,5]. The ribonucleoprotein enzyme telomerase that synthesizes the G-rich strand of telomeric DNA in germline tissues and in immortal tumor cells plays a critical role in the maintenance of telomeres^[6]. By using a highly sensitive PCR-based TRAP assay, telomerase activity has been observed in a wide range of human cancers, including cancers of breast, bladder, stomach, colon, prostate, and liver, so telomerase may be regarded as a molecular marker for cancer diagnosis and therapeutic strategies^[7-13]. Telomerase activity is also positive in gastric preneoplastic lesions^[14]. Therefore it is thought that reactivation of telomerase may occur at an early stage of carcinogenesis^[14].

Myc network proteins are known to be oncoproteins, which are involved in the control of cell proliferation, differentiation and apoptosis^[15,16]. The c-Myc oncogene is implicated in the transformation and progression of mutated cells^[17-19]. Deregulation of Myc genes is usually caused by chromosomal translocation involving the c-myc gene as well as by gene amplification. Overexpression of Myc is frequently observed in a wide variety of tumor types, and affects both the development and progression of hyperproliferations^[20,21].

It is well known that *Helicobacter pylori* (*H pylori*), the main cause of chronic gastritis, is a class I gastric carcinogen^[22]. It contributes to the induction of chronic gastritis to cancer through precursor lesions, such as atrophy, metaplasia and dysplasia^[23]. Precancerous phenotypic expression is generally associated with acquired genomic instability and activation of telomerase activity^[24]. *H pylori* inoculation into Mongolian gerbils has been reported to induce chronic gastritis and intestinal metaplasia. Chronic infection with *H pylori* induces activations of telomerase in gastric mucosa exhibiting intestinal metaplasia^[25]. In patients with intestinal-type gastric cancer, telomerase activity was higher in intestinal metaplasia with *H pylori* infection than in that without infection^[25,26]. These data indicate that *H pylori* infection may contribute to the precancerous stage through induction of telomerase activity, and that telomerase activation in intestinal metaplasia with *H pylori* infection may be correlated with oncogenesis, though the mechanism remains to be defined. To our knowledge, little is known about whether *H pylori* infection induces both genetic alterations and cell immortality in gastric mucosa. Recent evidence suggested that Myc protein was implicated in the regulation of hTERT^[27-29]. Therefore we measured telomerase activity and c-Myc expression in *H pylori* infected gastric cancer, chronic atrophic gastritis and chronic superficial gastritis. The results indicate that *H pylori* infection may induce telomerase activity and c-Myc protein expression in the process of carcinogenesis.

MATERIALS AND METHODS

Tissue samples

Samples were obtained from upper gastrointestinal endoscopy or surgical operation during the period of September 2000 to May 2001. It included 20 of chronic superficial gastritis(CSG),

30 of chronic atrophic gastritis(CAG) with mild intestinal metaplasia(IM), 42 of chronic atrophic gastritis with severe intestinal metaplasia, 14 of dysplasia(Dys) and 65 of gastric cancer(GC). Haematoxylin and eosin stains were used for the histopathological diagnosis. Degree of inflammatory reaction and glandular atrophy, intestinal metaplasia, and cellular dysplasia were evaluated according to the criteria of the updated Sydney system. The diagnosis of each sample was based on agreement between two pathologists.

H pylori infection

H pylori infection was detected by rapid urease test and bacteria culture. Infection was defined as positive when *H pylori* was detected and/or urease test was positive.

Immunohistochemistry

For each case, 4- μ m thick serial sections were cut from paraffin wax blocks, mounted on acid-cleaned glass slides, and heated at 55 °C for 60 min. Slides were dewaxed and rehydrated, then endogenous peroxidase activity was inhibited by incubation with 30 mL/L H₂O₂ in methanol for 20 min at room temperature. To reduce non-specific background staining, slides were incubated with 50 mL/L goat serum for 15 min at room temperature. To enhance immunostaining, sections were treated with an antigen retrieval solution (10 mmol/L citric acid monohydrate, pH 6.0, adjusted with 2 mol/L NaOH) and heated three times in a microwave oven at high power for five min. Finally, slides were incubated with appropriate primary antiserum in a moist chamber overnight at 4 °C. The monoclonal primary antibody, anti-c-Myc, was purchased from Maxim Biotech, Inc. (USA). S-P kit was purchased from Fujian Maixin Ltd (China). Samples were detected according to manufacturer's instructions. The degree of immunopositivity was evaluated semi-quantitatively. A total of 300 cells were counted in random fields from representative areas of the lesions, and the immunoreactive cells were roughly assessed and expressed as percentages. The scoring system for the antibody tested was: 0-5%(negative), 5-25%(low positivity), 25-50%(moderate positivity), >50%(high positivity).

Telomerase assay

Telomerase activity was measured by a modified version of the standard TRAP method, using PCR-ELISA detection kit (Roche Molecular Biochemicals), according to its manufacturer's instructions. Five 10- μ m thick cryostat sections of were transferred into a sterile reaction tube containing 200 μ L ice-cold lysis reagent. The lysates were homogenized and incubated on ice for 30 min. After centrifuged at 16 000 g for twenty minutes at 4 °C, 175 μ L of the supernatant was collected and transferred to a fresh tube. Three micro-litter of tissue extract was incubated with 25 μ L of reaction mixture including a biotin labeled P1-TS primer and P2 primer, telomerase substrate, and Taq polymerase for 20 min at 25 °C. After further incubation at 94 °C for 5 min for telomerase inactivation, the resulting mixture

was subjected to PCR for 30 cycles at 94 °C for 30 s, at 50 °C for 30 s, and at 72 °C for 90 s, the reaction was held at 72 °C for 10 min.

PCR products were denatured and hybridized with a digoxigenin labeled, telomeric repeat specific detection probe. The resulting product was immobilized through the biotin labeled TS primer to a streptavidin coated microtitre plate and detected with antidigoxigenin antibody conjugated with peroxidase. Absorbance values were measured using a microtitre (ELISA) reader at 450 nm with a reference wavelength of approximately 690 nm within 30 min after addition of the stop reagent. Heat-treatment of the cell extract for 10 min at 65 °C prior to the TRAP reaction was used to inactivate telomerase protein for producing negative controls. Positive controls were the 293 cells that expressed the telomerase activity. Samples were regarded as telomerase-positive if the difference in absorbance (ΔA) was higher than 0.2 (A 450 nm-A 690 nm units).

Statistical analyses

The correlations between qualitative data were studied with the χ^2 and Fisher tests. A probability *P* value <0.05 was considered statistically significant.

RESULTS

H pylori infection

One hundred and twelve of 171 cases were *H pylori* positive. The *H pylori* infection rate was 65%(13/20) in CSG, 63.89%(46/72) in CAG, 64.29%(9/14) in Dys, and 67.69%(44/65) in GC. It had no significant difference among these groups.

Telomerase activity

Telomerase activity was measured by a telomerase polymerase chain reaction (PCR) enzyme linked immunosorbent assay, which does not require radioactive PCR amplification and yields a semiquantitative measurement. Telomerase activity was detected in 57(87.69%) of 65 gastric carcinomas examined, 46(63.89%) of 72 CAG and 9(64.29%) of 14 Dys. No telomerase activity was detected in all the 20 CSG. The mean telomerase activity was higher in gastric cancer than in CAG, CSG and Dys (*P*<0.01 or *P*<0.05). Based on intestinal metaplasia, CAG was classified into two groups, severe IM and mild IM. The telomerase activity was higher in CAG with severe IM than that in mild IM (*P*<0.01).

Twenty-nine gastric cancers with complete clinical data were classified by histologic parameters such as gender, tumor location, tumor size and microscopic morphology. The telomerase activity among these groups had no significant difference (data not shown).

H pylori infection and telomerase activity in patients with gastric cancer and CAG are shown in Table 1. The mean telomerase activity was higher in CAG with severe intestinal metaplasia and *H pylori* infection than in that without infection (*P*<0.05), but there was no significant difference between those with and without *H pylori* infection in gastric cancer and CAG with mild intestinal metaplasia.

Table 1 Telomerase activity and c-Myc expression in *H pylori* infected gastric diseases

Diagnosis	Samples number	<i>H pylori</i> infection	Telomerase activity + (%)	<i>P</i>	c-Myc expression + (%)	<i>P</i>
GC	65	+(44)	38 (86.36)	>0.05	34 (77.27)	<0.05 ^a
		-(21)	19 (90.48)		6 (28.57)	
CAG with MM	30	+(18)	3 (16.67)	>0.05	4 (22.22)	>0.05
		-(12)	1 (8.33)		1 (8.33)	
CAG with SM	42	+(28)	19 (67.86)	<0.01 ^b	19 (67.86)	<0.01 ^d
		-(14)	3 (21.43)		1 (7.14)	

χ^2 test and Fisher's exact test. ^a*P*<0.05 vs c-Myc expression from samples without *H pylori* infection. ^b*P*<0.01 vs telomerase activity from samples without *H pylori* infection. ^d*P*<0.01 vs c-Myc expression from samples without *H pylori* infection. MM, mild intestinal metaplasia SM, severe intestinal metaplasia.



Figure 1 c-Myc protein expression in chronic superficial gastritis, chronic atrophic gastritis and gastric adenocarcinoma. A: c-Myc protein expression in chronic superficial gastritis. B: c-Myc protein expression in chronic atrophic gastritis. C: c-Myc protein expression in gastric adenocarcinoma.

c-Myc expression

c-Myc was expressed in 40 of 65 (61.5%) gastric cancers, 20 of 42 (47.62%) CAG with severe IM, 5 of 30 (16.67%) CAG with mild IM, 8 of 14 (57.14%) Dys and 1 of 20 (5%) CSG. The expression of c-Myc was highest in gastric cancer, and c-Myc expression in CAG with severe IM was significantly higher than that in CAG with mild IM. The c-Myc immunoreactivity was localized in both cytoplasm and nucleus (Figure 1).

H pylori infection and c-Myc expression in patients with gastric cancer and CAG are shown in Table 1. The expression of c-Myc was higher in *H pylori* infected gastric cancer and CAG with severe IM than in those without infection ($P < 0.01$), but there was no significant difference between those with and without *H pylori* infection in CAG with mild IM.

Coordinate up-regulation of telomerase activity and c-Myc expression in *H pylori* infected gastric cancer and CAG with severe intestinal metaplasia

The telomerase activity and c-Myc expression were coordinately increased in *H pylori* infected gastric cancer and CAG with severe IM (Figure 2). The rate of co-expression was 89.47% (34/38) and 100% (19/19), respectively.

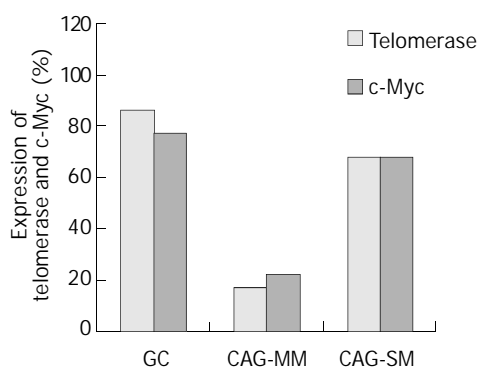


Figure 2 Coordinate increase of telomerase activity and c-Myc expression in *H pylori* infected gastric cancer and CAG with severe intestinal metaplasia. The rate of co-expression was 89.47% (34/38) and 100% (19/19), respectively. (CAG-MM: chronic atrophic gastritis with mild metaplasia; CAG-SM: chronic atrophic gastritis with severe metaplasia.)

DISCUSSION

In the present study, we demonstrated that most gastric tumors displayed telomerase activity, regardless of histological types. Telomerase activity was highest in cancer tissue, followed by chronic atrophic gastritis with complete intestinal metaplasia, dysplasia, chronic atrophic gastritis with mild intestinal metaplasia and chronic superficial gastritis. Telomerase activity was higher in CAG with severe metaplasia and *H pylori* infection than in that

without *H pylori* infection ($P < 0.01$). Our results indicate that telomerase activity is one of the most common and fundamental events of gastric cancers. What is more important is that telomerase was activated in precursor lesions, such as chronic atrophic gastritis with intestinal metaplasia and dysplasia. It suggested that there were a certain number of immortal cells existing in these lesions. In addition, *H pylori* infection might induce telomerase activity in chronic atrophic gastritis with intestinal metaplasia.

Recently, it was reported that *H pylori* infection played a role in activation of telomerase. Chronic infection with *H pylori* induced the activation of telomerase in gastric mucosa exhibiting intestinal metaplasia^[25]. In patients with intestinal-type gastric cancer, telomerase activity was higher in intestinal metaplasia with *H pylori* infection than in that without infection^[26]. We found that telomerase was activated in *H pylori* infected precursor lesions, such as chronic atrophic gastritis and dysplasia, and telomerase activity rose higher during the progression of the lesions. These data indicate that *H pylori* infection may contribute to gastric tumorigenesis through induction of telomerase activity, and that telomerase activation in *H pylori* infected chronic atrophic gastritis with intestinal metaplasia and dysplasia may be correlated with oncogenesis. It remains to be defined how *H pylori* infection activates telomerase. *H pylori* infection might influence the negative regulator of telomerase activity during early stages of stomach carcinogenesis^[26]. In addition, inflammatory gastric mucosa caused by *H pylori* infection could produce free radicals and cytokines that may induce telomerase activity^[30].

Frequent genetic alterations, such as c-myc proto-oncogene have been found in gastric pre-malignant lesions^[31,32]. Amplified c-Myc, which controls cell growth and cellular differentiation^[33,34], has been reported in small percent of gastric carcinomas^[35,36]. Expression of c-Myc was proved to be more frequent in poorly differentiated gastric cancer cells, and more frequent in gastric adenocarcinoma than in adenoma and has also been proposed as an aid to differentiate between the two conditions^[37,38]. In the present study, c-Myc was expressed in 61.54% (40/65) of gastric cancers, 47.62% (20/42) of chronic atrophic gastritis with severe IM, 16.67% (5/30) of CAG with mild IM, and 5% (1/20) of chronic superficial gastritis patients. The expression of c-Myc was highest in gastric cancers, and c-Myc expression in CAG with severe intestinal metaplasia was significantly higher than that in CAG with mild intestinal metaplasia. The expression of c-Myc was higher in *H pylori* infected gastric cancer and CAG with severe intestinal metaplasia than in that without infection ($P < 0.01$). We found that c-Myc expression in both gastric cancer and chronic atrophic gastritis with severe intestinal metaplasia is correlated with *H pylori* status. Previously, a study by Nardone *et al* showed that *H pylori* infection affected the expression of c-Myc in chronic gastritis, but the positive rate was very low (15%). The expression of c-Myc was very high in *H pylori* infected CAG in our study because we classified chronic gastritis as CSG

and CAG, the latter was further classified as CAG with mild intestinal metaplasia and with severe intestinal metaplasia.

Recent evidence suggested that the Myc protein could bind to the promotor of human telomerase reverse transcriptase (hTERT), the catalytic subunit of telomerase^[27-29]. It has been shown that hTERT is the determinant of telomerase activity control. A study by Hiyama *et al.* demonstrated a close association between a high level of telomerase activity and amplification of the myc locus in neuroblastomas. Thus, up-regulation of Myc due to gene alterations leading to subsequent activation of hTERT expression, may be one cause for telomerase activation in tumors. Interestingly, we found that telomerase activity and c-Myc were co-expressed in *H pylori* infected chronic atrophic gastritis. The correlation was not significant in patients without *H pylori* infection or in patients with *H pylori* infection but without gastric atrophy. Therefore, it is suggested that the presence of both gastric atrophy and chronic *H pylori* infection is essential for cell immortality and genomic instability.

REFERENCES

- 1 **Correa P.** *Helicobacter pylori* and gastric carcinogenesis. *Am J Surg Pathol* 1995; **19**(Suppl 1): S37-43
- 2 **Correa P,** Chen VW. Gastric cancer. *Cancer Surv* 1994; **19-20**: 55-76
- 3 **Rugge M,** Cassaro M, Leandro G, Baffa R, Avellini C, Bufo P, Stracca V, Battaglia G, Fabiano A, Guerini A, Di Mario F. *Helicobacter pylori* in promotion of gastric carcinogenesis. *Dig Dis Sci* 1996; **41**: 950-955
- 4 **Wright PA,** Williams GT. Molecular biology and gastric carcinoma. *Gut* 1993; **34**: 145-147
- 5 **Harley CB,** Kim NW, Prowse KR, Weinreich SL, Hirsch KS, West MD, Bacchetti S, Hirte HW, Counter CM, Greider CW, Wright WE, Shay JW. Telomerase, cell immortality, and cancer. *Cold Spring Harb Symp Quant Biol* 1994; **59**: 307-315
- 6 **Avilion AA,** Piatyszek MA, Gupta J, Shay JW, Bacchetti S, Greider CW. Human telomerase RNA and telomerase activity in immortal cell lines and tumor tissues. *Cancer Res* 1996; **56**: 645-650
- 7 **Kim NW,** Piatyszek MA, Prowse KR, Harley CB, West MD, Ho PL, Coviello GM, Wright WE, Weinrich SL, Shay JW. Specific association of human telomerase activity with immortal cells and cancer. *Science* 1994; **226**: 2011-2015
- 8 **Hiyama E,** Gollahon L, Kataoka T, Kuroi K, Yokohama T, Gazdar AF, Hiyama K, Piatyszek MA, Shay JW. Telomerase activity in human breast tumors. *J Natl Cancer Inst* 1996; **88**: 116-122
- 9 **Hiyama E,** Yokoyama T, Tatsumoto N, Hiyama K, Jmamura Y, Murakami Y, Kodama T, Piatyszek MA, Shay JW, Matsuura Y. Telomerase activity in gastric cancer. *Cancer Res* 1995; **55**: 3258-3262
- 10 **Shay JW,** Bacchetti S. A survey of telomerase activity in human cancer. *Eur J Cancer* 1997; **33**: 787-791
- 11 **Lin Y,** Miyamoto H, Fujinami K, Uemura H, Hosaka M, Iwasaki Y, Kubota Y. Telomerase activity in human bladder cancer. *Clin Cancer Res* 1996; **2**: 929-932
- 12 **Sommerfeld HJ,** Meeker AK, Piatyszek MA, Bova GS, Shay JW, Coffey DS. Telomerase activity: a prevalent marker of malignant human prostate tissue. *Cancer Res* 1996; **56**: 218-222
- 13 **Kojima H,** Yokosuka O, Imazeki F, Saisho H, Omata M. Telomerase activity and telomere length in hepatocellular carcinoma and chronic liver disease. *Gastroenterology* 1997; **112**: 493-500
- 14 **Tahara H,** Kuniyasu H, Yokozaki H, Yasui W, Shay JW, Ide T, Tahara E. Telomerase activity in preneoplastic and neoplastic gastric and colorectal lesions. *Clin Cancer Res* 1995; **1**: 1245-1251
- 15 **Henriksson M,** Lüscher B. Proteins of the Myc network: essential regulators of cell growth and differentiation. *Adv Cancer Res* 1996; **68**: 109-182
- 16 **Hurlin PJ,** Foley KP, Ayer DE, Eisenman RN, Hanahan D, Arbeit JM. Regulation of c-Myc and Mad during epidermal differentiation and HPV-associated tumorigenesis. *Oncogene* 1995; **11**: 2487-2501
- 17 **Xu D,** Popov N, Hou M, Wang Q, Bjorkholm M, Gruber A, Menkel AR, Henriksson M. Switch from Myc/Max to Mad1/Max binding and decrease in histone acetylation at the telomerase reverse transcriptase promoter during differentiation of HL60 cells. *Proc Natl Acad Sci U S A* 2001; **98**: 3826-3831
- 18 **Kuschak TI,** Taylor C, McMillan Ward E, Israels S, Henderson DW, Mushinski JF, Wright JA, Mai S. The ribonucleotide reductase R2 gene is a non-transcribed target of c-Myc-induced genomic instability. *Gene* 1999; **238**: 351-365
- 19 **Vaux DL,** Cory S, Adamas JM. Bcl-2 gene promotes haemopoietic cell survival and cooperates with c-Myc to immortalize pre-B cells. *Nature* 1988; **335**: 440-442
- 20 **Bissonnette RP,** Echeverri F, Mahboubi A, Green DR. Apoptotic cell death induced by c-Myc is inhibited by bcl-2. *Nature* 1992; **359**: 552-554
- 21 **Fanidi A,** Harrington EA, Evan GI. Cooperative interaction between c-Myc and bcl-2 proto-oncogenes. *Nature* 1992; **359**: 554-556
- 22 **Correa P,** Miller MJ. *Helicobacter pylori* and gastric atrophy-cancer paradoxes. *J Natl Cancer Inst* 1995; **87**: 1731-1732
- 23 **Kuipers EJ,** Uytendiele AM, Pena AS, Roosendaal R, Pals G, Nelis GF, Festen HP, Meuwissen SG. Long-term sequelae of *Helicobacter pylori* gastritis. *Lancet* 1995; **345**: 1525-1528
- 24 **Craanen ME,** Dekker W, Blok P, Ferwerda J, Tytgat GN. Intestinal metaplasia and *Helicobacter pylori*: an endoscopic bioptic study of the gastric antrum. *Gut* 1992; **33**: 16-20
- 25 **Kameshima H,** Yagihashi A, Yajima T, Watanabe N, Ikeda Y. *Helicobacter pylori* infection induces telomerase activity in premalignant lesions. *Am J Gastroenterol* 1999; **94**: 547-548
- 26 **Kameshima H,** Yagihashi A, Yajima T, Kobayashi D, Denno R, Hirata K, Watanabe N. *Helicobacter pylori* infection: augmentation of telomerase activity in cancer and noncancerous tissues. *World J Surg* 2000; **24**: 1243-1249
- 27 **Horikawa I,** Cable PL, Mazur SJ, Appella E, Afshari CA, Barrett JC. Downstream E-box-mediated regulation of the human telomerase reverse transcriptase (hTERT) gene transcription: evidence for an endogenous mechanism of transcriptional repression. *Mol Biol Cell* 2002; **13**: 2585-2597
- 28 **Cong YS,** Wen J, Bacchetti S. The human telomerase catalytic subunit hTERT: organization of the gene and characterization of the promoter. *Hum Mol Genet* 1999; **8**: 137-142
- 29 **Gunes C,** Lichtsteiner S, Vasserot AP, Englert C. Expression of the hTERT gene is regulated at the level of transcriptional initiation and repressed by Mad1. *Cancer Res* 2000; **60**: 2116-2121
- 30 **Tahara E.** Molecular mechanism of human stomach carcinogenesis implicated in *Helicobacter pylori* infection. *Exp Toxicol Pathol* 1998; **50**: 375-378
- 31 **Fest T,** Mougey V, Dalstein V, Hagerty M, Milete D, Silva S, Mai S. C-Myc overexpression in Ba/F3 cells simultaneously elicits genomic instability and apoptosis. *Oncogene* 2002; **21**: 2981-2990
- 32 **Wang J,** Chi D, Kalin G, Sosinski C, Miller LE, Burja I, Thomas E. *Helicobacter pylori* infection and oncogene expressions in gastric carcinoma and its precursor lesions. *Dig Dis Sci* 2002; **47**: 107-113
- 33 **Peng H,** Diss T, Isaacson PG, Pan L. C-myc gene abnormalities in mucosa-associated lymphoid tissue (MALT) lymphomas. *J Pathol* 1997; **181**: 381-386
- 34 **O'Leary JJ,** Landers RJ, Crowley M, Healy I, Kealy WF, Hogan J, Doyle CT. Alterations in exon 1 of c-myc and expression of p62 c-myc in cervical squamous cell carcinoma. *J Clin Pathol* 1997; **50**: 896-903
- 35 **Hajdu J,** Kozma L, Kiss I, Szentkereszty Z, Szakall S, Ember I. Is the presence of distant metastasis associated with c-myc amplification in gastric cancer? *Acta Chir Hung* 1997; **36**: 119-121
- 36 **Amadori D,** Maltoni M, Volpi A, Nanni O, Scarpì E, Renault B, Pellgata NS, Gaudio M, Magni E, Ranzani GN. Gene amplification and proliferative kinetics in relation to prognosis of patients with gastric carcinoma. *Cancer* 1997; **79**: 226-232
- 37 **Han S,** Kim HY, Park K, Cho HJ, Lee MS, Kim HJ, Kim YD. c-myc expression is related with cell proliferation and associated with poor clinical outcome in human gastric cancer. *J Korean Med Sci* 1999; **14**: 526-530
- 38 **Lee LA,** Dolde C, Barrett J, Wu CS, Dang CV. A link between c-Myc-mediated transcriptional repression and neoplastic transformation. *J Clin Invest* 1996; **97**: 1687-1695

Differential Cl^- and HCO_3^- mediated anion secretion by different colonic cell types in response to tetromethylpyrazine

Jin-Xia Zhu, Ning Yang, Qiong He, Lai-Ling Tsang, Wen-Chao Zhao, Yiu-Wa Chung, Hsiao-Chang Chan

Jin-Xia Zhu, Lai-Ling Tsang, Yiu-Wa Chung, Hsiao-Chang Chan, Epithelial Cell Biology Research Center, Department of Physiology, Faculty of Medicine, The Chinese University of Hong Kong, Shatin, Hong Kong

Jin-Xia Zhu, Ning Yang, Qiong He, Wen-Chao Zhao, Department of Physiology, Medical School, Zhengzhou University, Zhengzhou, 450052, Henan Province, China

Supported by the Innovation and Technology Commission of Hong Kong SAR, and Strategic program of The Chinese University of Hong Kong

Correspondence to: Professor Hsiao-Chang Chan, Epithelial Cell Biology Research Center, Department of Physiology, Faculty of Medicine, The Chinese University of Hong Kong, Shatin, NT, Hong Kong, China. hsiaocchan@cuhk.edu.hk

Telephone: +852-26096839 **Fax:** +852-26035022

Received: 2003-10-20 **Accepted:** 2004-01-31

Abstract

AIM: Colonic epithelium is known to secrete both Cl^- and HCO_3^- , but the secretory mechanisms of different colonic cell types are not fully understood. The present study aimed to investigate the differential activation of Cl^- and HCO_3^- secretion by tetramethylpyrazine (TMP) in human crypt-like cell line, T84, and villus-like cell line, Caco-2, in comparison to the TMP-induced secretory response in freshly isolated rat colonic mucosa.

METHODS: Colonic epithelial anion secretion was studied by using the short circuit current (I_{sc}) technique. RT-PCR was used to examine the expression of $\text{Na}^+-\text{HCO}_3^-$ -cotransporter in different epithelial cell types.

RESULTS: TMP produced a concentration-dependent I_{sc} which was increase in both T84 and Caco-2 cells. When extracellular Cl^- was removed, TMP-induced I_{sc} was abolished by 76.6% in T84 cells, but not in Caco-2 cells. However, after both Cl^- and HCO_3^- were removed, TMP-induced I_{sc} in Caco-2 cells was reduced to 10%. Bumetanide, an inhibitor of $\text{Na}^+-\text{K}^+-\text{Cl}^-$ -cotransporter, inhibited the TMP-induced I_{sc} by 96.7% in T84 cells, but only 47.9% in Caco-2 cells. In the presence of bumetanide and 4, 4'-diisothiocyanostilbene-2, 2'-disulfonic acid, an inhibitor of $\text{Na}^+-\text{HCO}_3^-$ cotransporter, inhibited the TMP-induced current in Caco-2 cells by 93.3%. In freshly isolated rat colonic mucosa, TMP stimulated distinct I_{sc} responses similar to that observed in T84 and Caco-2 cells depending on the concentration used. RT-PCR revealed that the expression of $\text{Na}^+-\text{HCO}_3^-$ cotransporter in Caco-2 cells was 4-fold more greater than that in T84 cells.

CONCLUSION: TMP exerts concentration-dependent differential effects on different colonic cell types with stimulation of predominant Cl^- secretion by crypt cells at a lower concentration, but predominant HCO_3^- secretion by villus cells at a higher concentration, suggesting different roles of these cells in colonic Cl^- and HCO_3^- secretion.

Zhu JX, Yang N, He Q, Tsang LL, Zhao WC, Chung YW, Chan

HC. Differential Cl^- and HCO_3^- mediated anion secretion by different colonic cell types in response to tetromethylpyrazine. *World J Gastroenterol* 2004; 10(12): 1763-1768
<http://www.wjgnet.com/1007-9327/10/1763.asp>

INTRODUCTION

Colonic epithelium, which lines the surface of both crypts and villi, plays an important role in the maintenance of water and electrolyte balance. While it is well established that colonic fluid secretion is driven by electrogenic colonic Cl^- secretion^[1], HCO_3^- secretion has also been shown to be important in the human colon. In many diarrhea disorders, a high concentration of HCO_3^- was frequently found in stool water and patients with severe diarrhea often suffered from metabolic acidosis due to sustained HCO_3^- losses in the stool^[2]. However, the contribution of crypts and villus epithelia to colonic Cl^- and HCO_3^- secretion is not known. Although it has been generally believed that colonic villus (or surface) epithelium is mainly involved in NaCl and water absorption while crypt epithelium is involved in secretion^[1,3]. There is now clear evidence that electrolyte secretion is located in both^[1,4]. The cystic fibrosis transmembrane conductance regulator (CFTR), a cAMP-dependent Cl^- channel known to mediate both Cl^- ^[5] and HCO_3^- secretion^[6,7], has been shown to be present in both crypt and villus epithelial cells although higher expression level of CFTR was found in crypts than in villi^[8,9]. Human colonic cell lines have been derived to provide useful models in studying electrolyte transport properties of colonic crypts and villus epithelial cells. T84 cell line is a well-characterized colonic epithelial model that maintains a secretory phenotype similar to crypt base cells, and has been widely used to examine the regulation of intestinal Cl^- secretion since CFTR and $\text{Na}^+-\text{K}^+-\text{Cl}^-$ cotransporter (NKCC) are highly expressed in this cell line^[1,10,11]. The properties of human colonic Caco-2 cells are mostly close to those of mature absorptive villus/surface cells but they possess a certain CFTR characteristic of secretory cells^[1,12,13]. However, few studies have been conducted to compare the secretory properties of these cell lines.

Tetramethylpyrazine (TMP, also named ligustrazine), a compound purified from *Ligustium Wollichii Francha*, is a widely used active ingredient in Chinese herbal medicine for the treatment of cardiovascular diseases due to its vasodilatory actions and antiplatelet activity^[14-16]. TMP has been proposed to act as an inhibitor of phosphodiesterase (PDE) and thereby it increases intracellular cAMP^[15]. We have recently demonstrated a stimulatory effect of a TMP-containing herbal formula on the anion secretion in human colonic^[17] and pancreatic duct cell lines^[18], indicating the involvement of cAMP and activation of CFTR. The present study aimed to compare the stimulatory effects of TMP on colonic anion secretion in different colonic cell types, T84 and Caco-2, as well as freshly isolated rat colonic mucosa, in an attempt to assess the different contribution of these two cell types to colonic anion secretion.

MATERIALS AND METHODS

Chemicals and solutions

Tetramethylpyrazine was purchased from Beijing Fourth

Pharmacy (Beijing, China). Diphenylamine-2, 2'-dicarboxylic acid (DPC) was obtained from Riedel-de Haen Chemicals (Hannover, Germany). Amilorode hydrochloride was obtained from Sigma Chemical Company (St. Louis, MO). Calbiochem (San Diego, CA) was the source for 4, 4'-diisothiocyanostilbene-2, 2'-disulfonic acid (DIDS), bumetanide, tetrodotoxin (TTX), indomethacin and glybenclamide. Dulbecco's modified Eagle's medium (DMEM)/F12, Hanks' balanced salt solution (HBSS) and fetal bovine serum were from Gibco Laboratory (New York, NY). Krebs-Henseleit solution (K-HS) had the following compositions (mmol/L): NaCl, 117; KCl, 4.5; CaCl₂, 2.5; MgCl₂, 1.2; NaHCO₃, 24.8; KH₂PO₄, 1.2; glucose, 11.1. The solution was gassed with 950 mL/L O₂ and 50 mL/L CO₂, and kept the pH at 7.4. In some experiments gluconate was used to replace anions Cl⁻ or Cl⁻/HCO₃⁻ for making a Cl⁻ free or Cl⁻/HCO₃⁻ free K-HS. For Cl⁻/HCO₃⁻-free K-HS, HEPES and Tris were used and the solution was gassed with absolute O₂.

Cell culture

Human colonic T84 and Caco-2 cells were purchased from American Type Culture Collection (Rockville, MD). The cells were routinely maintained in DMEM/F12 for T84 or in DMEM for Caco-2 with 100 mL/L fetal bovine serum, 100 kU/L penicillin and 100 mg/L streptomycin. The cells were fed 3 times a week, and (2-3)×10⁵ cells were plated on to the floating permeable support, which was made of a Millipore filter with a silicone rubber ring attached on top of it for confining the cells (0.45 cm²). Cultures were incubated at 37 °C in 950 mL/L O₂-50 mL/L CO₂ for 4-5 d before experiments.

Colonic mucosa preparation

Adult male Sprague-Dawley rats (Laboratory Animal Services Center, the Chinese University of Hong Kong) ranging in age from 8 to 12 wk had free access to standard rodent laboratory food and water until the day of the experiments. The animals were killed by exposure to absolute CO₂. Segments of distal colon about 8 cm proximal to the anus were quickly removed, cut along the mesenteric border into flat sheets and flushed with ice-cold K-HS bubbled with 950 mL/L O₂-50 mL/L CO₂. The tissues were pinned flat with the mucosal side down in a Sylgard-lined petri dish containing ice-cold oxygenated solution. The serosa, submucosa, and muscular layer were stripped away with fine forceps to obtain a mucosa preparation which was pretreated with indomethacin (10 μmol/L), a synthesis inhibitor of prostaglandins (PG), and 1 μmol/L of tetrodotoxin (TTX), a blocker of neuron sodium channel, 30 min before treatment with TMP. Three or four of these stripped mucosal preparations were obtained from each animal.

Short-circuit current measurements

The measurement of I_{SC} was described previously^[19]. Between the two halves of the Ussing chamber, in which the total cross-sectional area was 0.45 cm², monolayers of cell lines grown on permeable supports were clamped and flat sheets of rat stripped colonic mucosa were mounted, which were bathed in both sides with K-HS and maintained at 37 °C by a water jacket enclosing the reservoir. K-HS was bubbled with 950 mL/L O₂-50 mL/L CO₂ to maintain the pH of the solution at 7.4. Drugs could be added directly to apical or basolateral side of the epithelium. Transepithelial potential difference for every monolayer or colonic mucosa was measured by the Ag/AgCl reference electrodes (World Precision Instrument, USA) connected to a preamplifier that was in turn connected to a voltage-clamp amplifier DVC-1000 (World Precision Instrument, USA). In most of the experiments, the change in I_{SC} was defined as the maximal rise in I_{SC} following agonist stimulation and it was normalized to current change per unit area of the epithelial monolayer

(μA/cm²). The total charge transported for 15 min (the area under the curve of the agonist-induced I_{SC} response) was also used to describe the agonist-induced response (μC/cm²). Experiments were normally repeated in different batches of culture to ensure that the data were reproducible.

Reverse transcription PCR (RT-PCR) analysis

Total RNA (15 μg) was extracted from T84, Caco-2 cells and rat colonic mucosa. Human pancreatic duct epithelial cells, CAPAN-1, were used as a positive control. Expression of NBC was analyzed by competitive RT-PCR. The specific oligo nucleotide primers for NBC were CCT CAG CTC TTC ACG GAA CT for sense and AGC ATG ACA GCC TGC TGT AG for antisense corresponding to nucleotides 333-949 with expected cDNA of 616 bp^[20]. Internal marker, GAPDH was used for semi-quantitative analysis of NBC expression in Caco-2 and T84 cells. The specific oligo nucleotide primers for GAPDH were TCC CAT CAC CAT CTT CCA G for sense and TCC ACC ACT GAC ACG TTG for antisense corresponding to nucleotides 249-764 bp with expected cDNA of 515 bp^[20].

Statistical analysis

Results were expressed as mean±SE. The number of experiments represented independent measurements on separate monolayers. Comparisons between groups of data were made by either the Student's *t*-test (2-group comparison) or one-way ANOVA with Newman-Keuls *post-hoc* test (3-group comparison). A *P* value less than 0.05 was considered statistically significant. EC₅₀ values were determined by nonlinear regression using GraphPad Prism software.

RESULTS

TMP-induced I_{SC} responses in T84 and Caco-2 cells

TMP stimulation increased I_{SC} in both T₈₄ and Caco-2 cells when the drug was added to either the apical or basolateral membrane. However, greater responses were achieved when TMP was added to apical membrane of T84 and basolateral membrane of Caco-2. The TMP-induced responses were concentration-dependent with an apparent EC₅₀ at 0.5 and 5.1 mmol/L for T84 and Caco-2 cells respectively (Figure 1A). The TMP-induced changes in I_{SC} were calculated as the total charge transported for 15 min (the area under the curve of the TMP-induced I_{SC} response for the given time period) since the current kinetics was different in the two cell types. TMP produced a fast and sustained increase of I_{SC} in T84 cells with averaged total charge of 6100±451 μC/cm² (*n*=8, Figure 1B) transported over 15 min in response to TMP at a concentration close to corresponding EC₅₀ (1 mmol/L). However, TMP produced a I_{SC} response in Caco-2 cells with a fast transient peak followed by a lower but sustained plateau with averaged total charge of 2293±214.7 μC/cm² (*n*=7) in response to TMP at corresponding EC₅₀ (5 mmol/L, Figure 1C). Similar TMP-induced I_{SC} characteristics were observed in the same cell type at all concentrations of TMP used.

Involvement of Cl⁻ and HCO₃⁻ in TMP-induced I_{SC} responses in colonic cell lines

Removal of Cl⁻ from the bathing solution inhibited TMP-induced I_{SC} increase by 76%, from 6100±451 μC/cm² to 1375±103 μC/cm² in T84 cells (*n*=7, *P*<0.001, Figure 2). In Caco-2 cells the TMP-induced current in Cl⁻-free solution was not reduced, but rather increased to 3700±388 μC/cm² (*n*=6, *P*<0.001, Figure 3). However, the TMP-induced I_{SC} in Caco-2 was reduced by 90%, to 228.9±27.6 μC/cm² (*n*=6, *P*<0.001) when both extracellular Cl⁻ and HCO₃⁻ were removed (Figure 3). Apical addition of Cl⁻ channel blockers, DPC (2 mmol/L) or

glibenclamide (1 mmol/L), could completely abolish the TMP-induced response in T84 (Figure 2A,B) and Caco-2 cells (Figure 3A,B). Basolateral addition of Na⁺-K⁺-2Cl⁻ cotransporter (NKCC) inhibitor, bumetanide (100 μmol/L), inhibited TMP-induced I_{SC} in T84 cells by 96.7%, from 6 100±451 μC/cm² (*n*=8) to 200±71 μC/cm² (*n*=5, *P*<0.001, Figure 4A), but only 47.9% in Caco-2 cells, from 2 720±144 μC/cm² (*n*=6) to 1 304±200 μC/cm² (*n*=5, *P*<0.001, Figure 4B). However, when an inhibitor of NBC, DIDS (200 μmol/L), was combined with bumetanide, it reduced TMP-induced current in Caco-2 cells to 181±41 μC/cm² by 93.3% (*n*=5, *P*<0.001, Figure 4B). Pretreatment with epithelial Na⁺ channel (ENaC) blocker, amiloride (10 μmol/L) (*n*=5, *P*>0.05) or removal of Na⁺ from apical solution (*n*=4, *P*>0.05) did not significantly affect the TMP-induced I_{SC} (data not shown), indicating that TMP-produced responses were mediated by Cl⁻/HCO₃⁻ secretion, but not Na⁺ absorption.

TMP-induced I_{SC} response in colonic mucosa

In freshly isolated rat colonic mucosa, TMP induced different I_{SC} responses depending on the concentration used. One mmol/L of TMP evoked a sustained I_{SC} increase (Figure 5A) similar to that observed in T84 cells, with averaged total charge of 5 133±465 μC/cm² (Figure 5C, *n*=11). However, at the concentration greater than 5 mmol/L, TMP induced a I_{SC} response similar to that observed in Caco-2 cells, a transient peak followed by a more sustained phase (Figure 5B), with averaged total charge of 18 945±2 023 μC/cm² (Figure 5C, *n*=11). Removal of extracellular Cl⁻ inhibited 65.5% of the I_{SC} induced by 1 mmol/L TMP (Figure 5C, *n*=10, *P*<0.001). However, the I_{SC} induced by 5 mmol/L of TMP was not significantly reduced by Cl⁻ removal (*n*=6, *P*>0.05) but was reduced by 71.6% in Cl⁻ and HCO₃⁻-free solution (Figure 5, *n*=5), indicating a greater extent of the involvement of HCO₃⁻ in the response to 5 mmol/L TMP as compared to the response

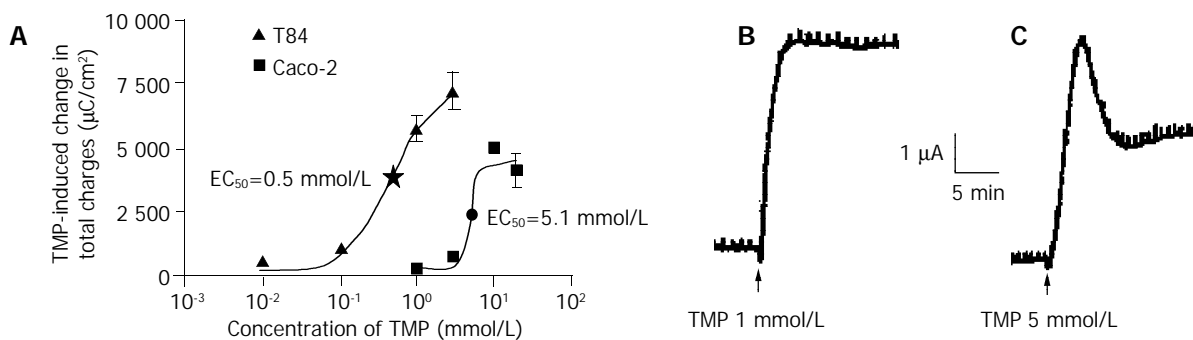


Figure 1 TMP-induced I_{SC} response in T84 and Caco-2 cell lines. The concentration-response curve for TMP-induced response in T84 and Caco-2 cells, and each datum was obtained from at least 4 individual experiments. A: Values are mean±SE of maximal I_{SC} increase; B: Representative I_{SC} recordings in response to apical addition of TMP (1 mmol/L) in T84 cells; C: Basolateral application of TMP (5 mmol/L) in Caco-2 cells.

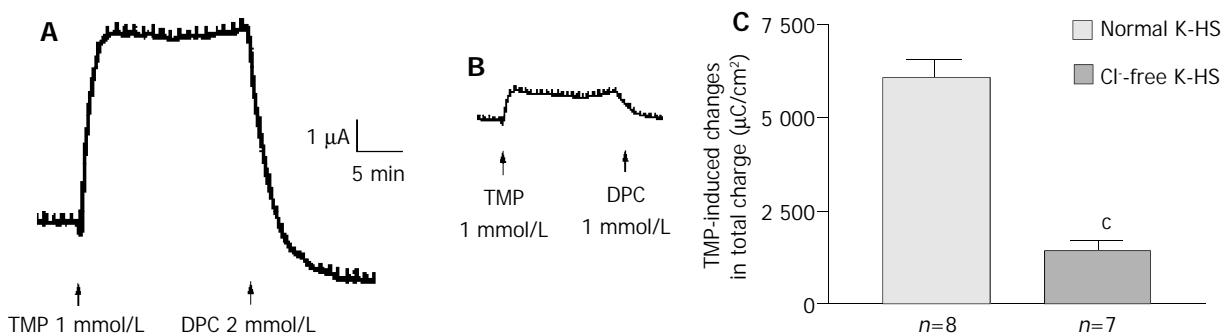


Figure 2 Cl⁻ dependence of TMP-induced I_{SC} increase in T84 cells. Representative I_{SC} recording with arrows indicating TMP (1 mmol/L) added apically, which was blocked by apical adding DPC. Values are mean±SE; ^c*P*<0.001. A: Normal; B: Cl-free; C: K-HS, comparison of TMP-induced total charge transferred in normal and Cl-free K-HS.

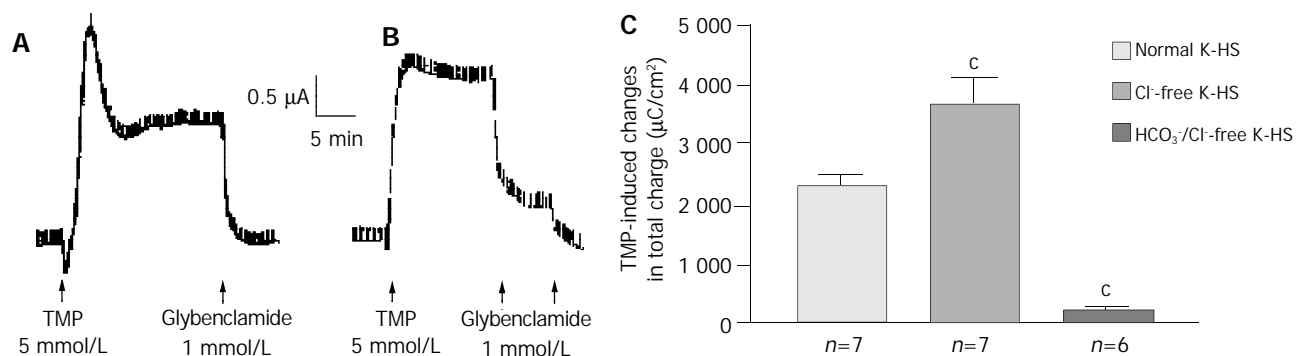


Figure 3 HCO₃⁻ dependence of TMP-induced I_{SC} increase in Caco-2 cells. Representative I_{SC} recording with arrows indicating TMP (5 mmol/L) added basolaterally, which was abolished by apical application of glibenclamide. Values are mean±SE; ^a*P*<0.05, ^b*P*<0.01 and ^c*P*<0.001. A: Normal; B: Cl-free; C: K-HS, comparison of TMP-induced total charges transferred in normal and Cl-free K-HS.

to 1 mmol/L TMP. Basolateral addition of bumetanide (100 μmol/L) blocked 80.9% responses induced by 1 mmol/L TMP, from 5 133±465 μC/cm² to 978±357 μC/cm² (n=9, P<0.001, Figure 5D), but only blocked 43.2% of the responses induced by 5 mmol/L of TMP, from 18 945±2 023 μC/cm² to 1 0762±2 513 μC/cm² (n=7, P<0.05). Basolateral addition of

DIDS (100 μmol/L) had no significant effect on the response induced by 1 mmol/L of TMP (n=7, P>0.05), but inhibited 66.5% of the responses induced by 5 mmol/L of TMP, from 17 143±2 408 μC/cm² to 8 248±2 328 μC/cm² (n=7, P<0.001), indicating possible involvement of NBC in the 5 mmol/L TMP-induced response.

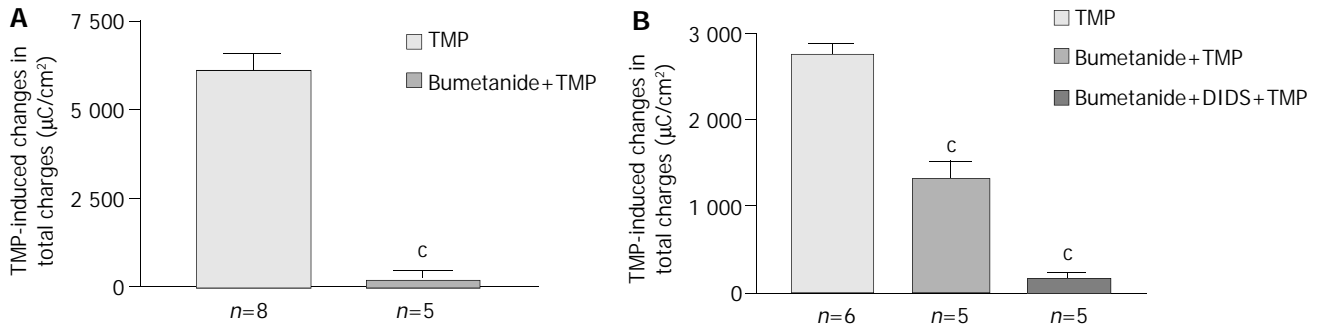


Figure 4 Effect of inhibitors of basolateral anion transporters on TMP-induced I_{SC} responses. Values are mean±SE; ^cP<0.001. A: Comparison of TMP (1 mmol/L)-induced I_{SC} responses in T84 cells in the absence and presence of basolateral addition of bumetanide (100 μmol/L); B: Comparison of TMP (5 mmol/L) -induced I_{SC} responses in Caco-2 cells in the absence and presence of basolateral addition of inhibitors indicated.

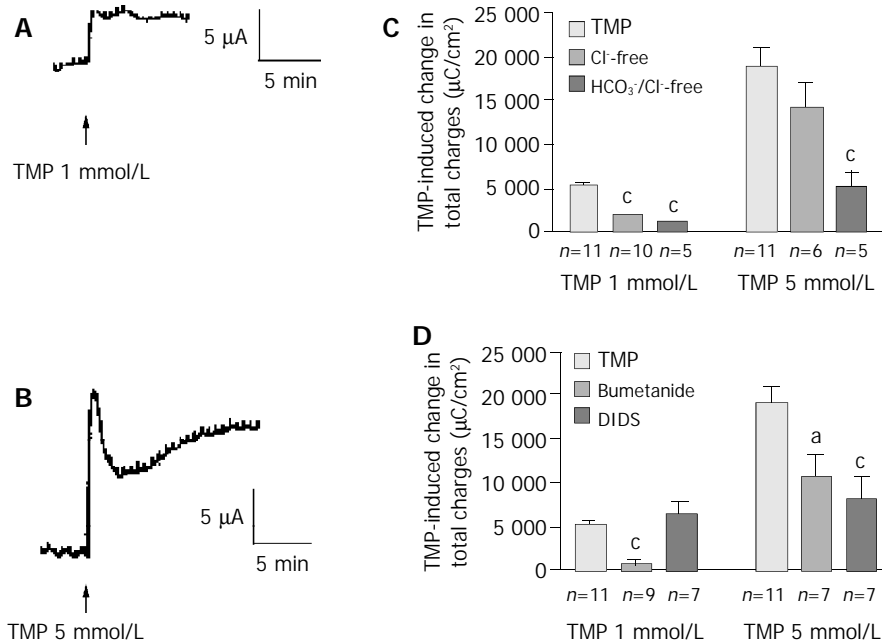


Figure 5 TMP-induced anion secretions in rat colonic mucosa. Representative I_{SC} recording values are mean±SE; ^aP<0.05, ^bP<0.01, ^cP<0.001. A: 1 mmol/L; B: 5 mmol/L of TMP added basolaterally in normal K-HS; C: Comparison of TMP (1 and 5 mmol/L)-induced I_{SC} obtained in normal and Cl-free as well as both of Cl and HCO₃⁻-free solutions; D: Comparison of TMP (1 and 5 mmol/L)-induced I_{SC} obtained in basolateral pretreatment of colonic mucosa with bumetanide (100 μmol/L) and DIDS (100 μmol/L).

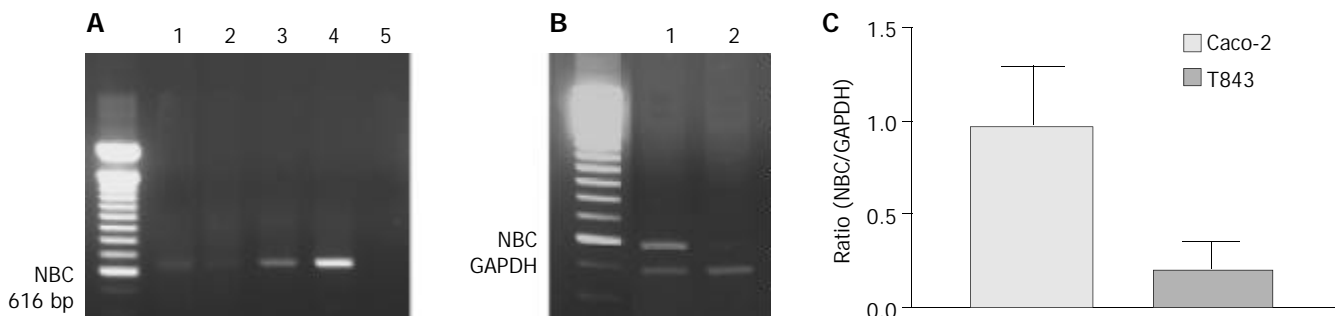


Figure 6 RT-PCR analysis of mRNA expression of Na⁺-HCO₃⁻ cotransporter (NBC) in colonic cells. A: RT-PCR results with products as expected of NBC found in rat colon (1), T84 (2) and Caco-2 (3) with positive control (4) using pancreatic duct cells (CAPAN-1) and negative control (5) where cDNA was omitted. B: Semi-quantitative analysis of NBC expression in Caco-2 (1) ; C: T84 (2) cells with NBC to GAPDH (internal marker) ratio shown.

RT-PCR analysis of NBC expression in T84, Caco-2 cells and colonic mucosa

NBC was expressed in all cells and tissues examined by RT-PCR (Figure 6A). However, semi-quantitative analysis showed that the nucleotide expression level in Caco-2 cells was 4.8-fold over that of T84 (Figure 6B). The NBC nucleotide fragment was confirmed by nucleotide sequencing (Figure 6C).

DISCUSSION

The present study has demonstrated for the first time the effects of TMP on the colonic anion secretion and revealed that the different doses of TMP could induce differential Cl^- and HCO_3^- mediated anion secretion by different colonic cell types. The differential effects of TMP on T84 and Caco-2 cells were not only reflected by the differences in the concentration-dependent I_{SC} responses and the I_{SC} kinetics, but also in the extents to which Cl^- and HCO_3^- were involved in mediating the TMP responses. This was supported by the observation that the TMP-induced response in T84 was sensitive to extracellular Cl^- replacement or an inhibitor of basolateral NKCC, bumetanide, while the response in Caco-2 cells was relatively insensitive to these treatments, at least to a much less extent. Instead, the response in Caco-2 cells was sensitive to the removal of extracellular HCO_3^- and an inhibitor of basolateral NBC, which has been shown to mediate HCO_3^- entry into the cells in a number of tissues including the pancreas^[21,22], intestine^[23], kidney^[24] and endometrium^[25]. Although DIDS is also known to inhibit $\text{Cl}^-/\text{HCO}_3^-$ exchanger (AE), the involvement of AE in this case was unlikely since it was not electrogenic. The high expression of NBC in Caco-2 cells but not T84 cells was also consistent with the DIDS sensitivity profiles in the two cell types, suggesting the involvement of NBC in mediating basolateral HCO_3^- transport in Caco-2 cells. The observed predominant Cl^- secretion elicited by TMP in T84 cells was consistent with the Cl^- -secreting characteristics of this colonic crypt-like cell model. Although secretory properties were less well characterized in Caco-2 cells, a previous study^[26] has demonstrated I_{SC} increases in response to cAMP-evoking agents including PDE inhibitor, 3-isobutyl-1-methylxanthine (IBMX), in Caco-2 cells with biphasic current kinetics and DIDS sensitivity similar to that of the TMP-induced I_{SC} response observed in the present study. Interestingly, in the same study alkalization of the apical solution could be induced which was also inhibited by basolateral addition of DIDS. Similar HCO_3^- -dependent and DIDS-sensitive I_{SC} was also observed in the intestine^[27-29]. Together with the presently demonstrated NBC expression in Caco-2 cells, these results strongly indicate a role of villus-like Caco-2 cells in HCO_3^- -potentiated secretion. Thus, it appears that colonic Cl^- and HCO_3^- -potentiated secretion may be differentially mediated by different colonic cell types.

The observed difference between T84 and Caco-2 cells in their I_{SC} responses to different concentrations of TMP suggested that colonic Cl^- and HCO_3^- mediated secretions might be differentially elicited by the same agent depending on the concentrations used, probably due to differential expression of receptors, cotransporters, exchangers and ion channels^[10-13] leading to differential responses to TMP. This notion is supported by the observation that TMP at different concentrations could elicit different I_{SC} responses from freshly isolated rat colon mucosa with distinct current characteristics. Interestingly, the colonic mucosal I_{SC} response elicited by 1 mmol/L of TMP had characteristics similar to the TMP-induced response in T84 cells (e.g. sensitive to Cl^- removal and bumetanide but insensitive to DIDS), indicating predominant Cl^- secretion, whereas the colonic mucosal I_{SC} response elicited by TMP at

concentrations greater than 5 mmol/L resembled the response observed in Caco-2 cells (e.g., more sensitive to DIDS than to Cl^- removal and bumetanide), indicating predominant HCO_3^- -potentiated secretion at this concentration range. The fact that distinct TMP-induced I_{SC} responses with characteristics similar to those observed in human colonic T84 and Caco-2 cells could be observed in intact rat colonic mucosa suggests that the secretory activities of T84 and Caco-2 cells may reflect the secretory properties of the colon, which may be similar in rats and humans. The present findings suggest that by having different sensitivities to stimulation in distinct colonic cell types, the colon in rats or humans, may be able to secrete either Cl^- -rich fluid or HCO_3^- -rich fluid. In other words, colonic Cl^- and HCO_3^- -mediated secretions may be differentially regulated by the same physiological regulator depending on its local concentration. Possible candidates of physiological regulators may include prostaglandins, VIP and secretin, all of which are known to be present in the colon and able to increase intracellular cAMP^[30-32]. In fact, secretin has been shown to stimulate Cl^- secretion in the colon^[33] and HCO_3^- secretion in Caco-2 cells^[26]. It should be noted that TMP has been shown to be a cAMP-evoking agent having an action similar to PDE inhibitor in antiplatelet activity^[15]. The further study is required to identify the signaling pathway in mediating TMP effects on colonic cells.

The present finding of predominant HCO_3^- -mediated secretion by villus-like Caco-2 cells is of physiological interest. Although a constant pH microclimate at the luminal surface has been considered to have a decisive influence on the reabsorption of Cl^- and absorption of weak electrolytes such as short-chain fatty acids^[34], the mechanisms involved in the maintenance and regulation of the pH microclimate are poorly understood. A recent study has demonstrated that HCO_3^- is the most important factor in maintaining a constant pH microclimate at the luminal surface^[35]. However, the origin of HCO_3^- responsible for this was not demonstrated although a continuous secretion of HCO_3^- at the luminal surface of the colonic epithelium has been observed^[36]. The present study suggested that the villus/surface-like epithelial cells were capable of secreting HCO_3^- upon stimulation, and thus, they are likely to contribute to the maintenance and regulation of the pH microclimate observed at the luminal surface of the colon. Being situated at the luminal surface, villus epithelial cells have the advantage over crypt cells in that they can sense the small variations in the pH microclimate at the luminal surface and secrete HCO_3^- directly adjusting the luminal microclimate. This suggests that the secretory role of villus/surface epithelium is distinct from that of crypts which are mainly responsible for Cl^- secretion on which colonic fluid secretion depends. The differential expression of NBC, the major basolateral transport mechanism for HCO_3^- entry^[23], in the two human colonic cells lines also supports this contention.

The mechanism(s) by which Cl^- and HCO_3^- exit through the apical membrane remains to be elucidated. The fact that both Cl^- and HCO_3^- secretions could be completely blocked by DPC and glibenclamide, both of which are known to inhibit CFTR, suggest that a common mechanism may be involved. CFTR appears to be a possible candidate since its involvement in Cl^- and HCO_3^- secretion has been demonstrated^[5-7]. The investigation of detail mechanism involved in mediating the TMP-stimulated anion secretions is currently undertaken in our laboratory.

It should be noted that while TMP has been used clinically to treat cardiovascular disorders^[14], no study has been reported, at the time of writing, on its effect on colonic secretion. The present results suggest that potential application of TMP as an alternative treatment of GI disorders may be further explored, considering its natural origin and differential effects on colonic Cl^- and HCO_3^- secretion.

REFERENCES

- 1 **Kunzelmann K**, Mall M. Electrolyte transport in the mammalian colon: mechanisms and implications for disease. *Physiol Rev* 2002; **82**: 245-289
- 2 **Fordtran JS**. Speculations on the pathogenesis of diarrhea. *Fed Proc* 1967; **26**: 1405-1414
- 3 **Welsh MJ**, Smith PL, Fromm M, Frizzell RA. Crypts are the site of intestinal fluid and electrolyte secretion. *Science* 1982; **218**: 1219-1221
- 4 **Stewart CP**, Turnberg LA. A microelectrode study of responses to secretagogues by epithelial cells on villus and crypt of rat small intestine. *Am J Physiol* 1989; **257**(3 Pt 1): G334-343
- 5 **O'Grady SM**, Jiang X, Maniak PJ, Birmachou W, Scribner LR, Bulbulian B, Gullikson GW. Cyclic AMP-dependent Cl secretion is regulated by multiple phosphodiesterase subtypes in human colonic epithelial cells. *J Membr Biol* 2002; **185**: 137-144
- 6 **Clarke LL**, Harline MC. Dual role of CFTR in cAMP-stimulated HCO₃⁻ secretion across murine duodenum. *Am J Physiol* 1998; **274** (4 Pt 1): G718-726
- 7 **Seidler U**, Blumenstein I, Kretz A, Viellard-Baron D, Rossmann H, Colledge WH, Evans M, Ratcliff R, Gregor M. A functional CFTR protein is required for mouse intestinal cAMP-, cGMP- and Ca(2+)-dependent HCO₃⁻-secretion. *J Physiol* 1997; **505**(Pt 2): 411-423
- 8 **Sood R**, Bear C, Auerbach W, Reyes E, Jensen T, Kartner N, Riordan JR, Buchwald M. Regulation of CFTR expression and function during differentiation of intestinal epithelial cells. *EMBO J* 1992; **11**: 2487-2494
- 9 **Strong TV**, Boehm K, Collins FS. Localization of cystic fibrosis transmembrane conductance regulator mRNA in the human gastrointestinal tract by *in situ* hybridization. *J Clin Invest* 1994; **93**: 347-354
- 10 **Merlin D**, Jiang L, Strohmeier GR, Nusrat A, Alper SL, Lencer WI, Madara JL. Distinct Ca²⁺- and cAMP-dependent anion conductances in the apical membrane of polarized T84 cells. *Am J Physiol* 1998; **275**(2 Pt 1): C484-495
- 11 **Barrett KE**. Positive and negative regulation of chloride secretion in T84 cells. *Am J Physiol* 1993; **265**(4 Pt 1): C859-868
- 12 **Grasset E**, Bernabeu J, Pinto M. Epithelial properties of human colonic carcinoma cell line Caco-2: effect of secretagogues. *Am J Physiol* 1985; **248**(5 Pt 1): C410-418
- 13 **Osyptiw JC**, Gleeson D, Loble RW, Pemberton PW, McMahon RF. Acid-base transport systems in a polarized human intestinal cell monolayer: Caco-2. *Exp Physiol* 1994; **79**: 723-739
- 14 **Liao F**. Herbs of activating blood circulation to remove blood stasis. *Clin Hemorheol Microcirc* 2000; **23**: 127-131
- 15 **Liu SY**, Sylvester DM. Antiplatelet activity of tetramethylpyrazine. *Thromb Res* 1994; **75**: 51-62
- 16 **Kwan CY**. Plant-derived drugs acting on cellular Ca²⁺ mobilization in vascular smooth muscle: tetramethylpyrazine and tetrandrine. *Stem Cells* 1994; **12**: 64-67
- 17 **Zhu JX**, Chan YM, Tsang LL, Chan LN, Zhou Q, Zhou CX, Chan HC. Cellular signaling mechanisms underlying pharmacological action of Bak Foong Pills on gastrointestinal secretion. *Jpn J Physiol* 2002; **52**: 129-134
- 18 **Zhu JX**, Lo PS, Zhao WC, Tang N, Zhou Q, Rowlands DK, Gou YL, Chung YW, Chan HC. Bak Foong Pills stimulate anion secretion across normal and cystic fibrosis pancreatic duct epithelia. *Cell Biol Int* 2002; **26**: 1011-1018
- 19 **Ussing HH**, Zerahn K. Active transport of sodium as the source of electric current in the short-circuited isolated frog skin. *J Am Soc Nephrol* 1999; **10**: 2056-2065
- 20 **Usui T**, Hara M, Satoh H, Moriyama N, Kagaya H, Amano S, Oshika T, Ishii Y, Ibaraki N, Hara C, Kunimi M, Noiri E, Tsukamoto K, Inatomi J, Kawakami H, Endou H, Igarashi T, Goto A, Fujita T, Araie M, Seki G. Molecular basis of ocular abnormalities associated with proximal renal tubular acidosis. *J Clin Invest* 2001; **108**: 107-115
- 21 **Marino CR**, Jeanes V, Boron WF, Schmitt BM. Expression and distribution of the Na⁺-HCO₃⁻ cotransporter in human pancreas. *Am J Physiol* 1999; **277**(2 Pt 1): G487-494
- 22 **Satoh H**, Moriyama N, Hara C, Yamada H, Horita S, Kunimi M, Tsukamoto K, Iso-O N, Inatomi J, Kawakami H, Kudo A, Endou H, Igarashi T, Goto A, Fujita T, Seki G. Localization of Na⁺-HCO₃⁻ cotransporter (NBC-1) variants in rat and human pancreas. *Am J Physiol Cell Physiol* 2003; **284**: C729-737
- 23 **Bachmann O**, Rossmann H, Berger UV, Colledge WH, Ratcliff R, Evans MJ, Gregor M, Seidler U. cAMP-mediated regulation of murine intestinal/pancreatic Na⁺-HCO₃⁻ cotransporter subtype pNBC1. *Am J Physiol Gastrointest Liver Physiol* 2003; **284**: G37-45
- 24 **Romero MF**, Hediger MA, Boulpaep EL, Boron WF. Expression cloning and characterization of a renal electrogenic Na⁺-/HCO₃⁻ cotransporter. *Nature* 1997; **387**: 409-413
- 25 **Wang XF**, Yu MK, Leung KM, Yip CY, Ko WH, Liu CQ, Chan HC. Involvement of Na⁺ HCO₃⁻ cotransporter in mediating cyclic adenosine 3', 5'-monophosphate-dependent HCO₃⁻ secretion by mouse endometrial epithelium. *Biol Reprod* 2002; **66**: 1846-1852
- 26 **Fukuda M**, Ohara A, Bamba T, Saek Y. Activation of transepithelial ion transport by secretin in human intestinal Caco-2 cells. *Jpn J Physiol* 2000; **50**: 215-225
- 27 **Taylor J**, Hamilton KL, Butt AG. HCO₃⁻ potentiates the cAMP-dependent secretory response of the human distal colon through a DIDS-sensitive pathway. *Pflugers Arch* 2001; **442**: 256-262
- 28 **Schultheiss G**, Horger S, Diener M. The bumetanide-resistant part of forskolin-induced anion secretion in rat colon. *Acta Physiol Scand* 1998; **164**: 219-228
- 29 **Joo NS**, London RM, Kim HD, Forte LR, Clarke LL. Regulation of intestinal Cl⁻ and HCO₃⁻ secretion by uroguanylin. *Am J Physiol* 1998; **274**(4 Pt 1): G633-644
- 30 **Simon B**, Kather H, Kommerell B. Colonic mucosal adenylate cyclase by prostaglandins. *Adv Prostaglandin Thromboxane Res* 1980; **8**: 1617-1620
- 31 **Dupont C**, Laburthe M, Broyart JP, Bataille D, Rosselin G. Cyclic AMP production in isolated colonic epithelial crypts: a highly sensitive model for the evaluation of vasoactive intestinal peptide action in human intestine. *Eur J Clin Invest* 1980; **10**: 67-76
- 32 **Chow BK**. Molecular cloning and functional characterization of a human secretin receptor. *Biochem Biophys Res Commun* 1995; **212**: 204-211
- 33 **Eto B**, Boisset M, Griesmar B, Desjeux JF. Effect of sorbin on electrolyte transport in rat and human intestine. *Am J Physiol* 1999; **276**(1 Pt 1): G107-114
- 34 **Rechkemmer G**, Wahl M, Kuschinsky W, von Engelhardt W. pH-microclimate at the luminal surface of the intestinal mucosa of guinea pig and rat. *Pflugers Arch* 1986; **407**: 33-40
- 35 **Genz AK**, v Engelhardt W, Busche R. Maintenance and regulation of the pH microclimate at the luminal surface of the distal colon of guinea-pig. *J Physiol* 1999; **517**(Pt 2): 507-519
- 36 **Feldman GM**, Berman SF, Stephenson RL. Bicarbonate secretion in rat distal colon *in vitro*: a measurement technique. *Am J Physiol* 1988; **254**(3 Pt 1): C383-390

Edited by Wang XL and Xu CT Proofread by Pan BR and Xu FM

Time- and pH-dependent colon-specific drug delivery for orally administered diclofenac sodium and 5-aminosalicylic acid

Gang Cheng, Feng An, Mei-Juan Zou, Jin Sun, Xiu-Hua Hao, Yun-Xia He

Gang Cheng, Feng An, Mei-Juan Zou, Jin Sun, Yun-Xia He, Department of Biopharmaceutics, School of Pharmacy, Shenyang Pharmaceutical University, Shenyang 110016, Liaoning Province, China
Xiu-Hua Hao, School of Pharmacy, Jilin University, Changchun 130021, Jilin Province, China

Supported by the Foundation of Ministry of Education of China for distinguished Teachers, No. 903 and the Natural Science Foundation of Liaoning Province, No. 9910500504

Correspondence to: Gang Cheng, Department of Biopharmaceutics, School of Pharmacy, Shenyang Pharmaceutical University, PO Box 32, 103 Wenhua Road, Shenyang 110016, Liaoning Province, China. chenggang63@hotmail.com

Telephone: +86-24-23843711-3536 **Fax:** +86-24-23953047

Received: 2004-01-09 **Accepted:** 2004-02-21

Abstract

AIM: To investigate Time- and pH-dependent colon-specific drug delivery systems (CDDS) for orally administered diclofenac sodium (DS) and 5-aminosalicylic acid (5-ASA), respectively.

METHODS: DS tablets and 5-ASA pellets were coated by ethylcellulose (EC) and methacrylic acid copolymers (Eudragit® L100 and S100), respectively. The *in vitro* release behavior of the DS coated tablets and 5-ASA coated pellets were examined, and then *in vivo* absorption kinetics of DS coated tablets in dogs were further studied.

RESULTS: Release profile of time-dependent DS coated tablets was not influenced by pH of the dissolution medium, but the lag time of DS release was primarily controlled by the thickness of the coating layer. The thicker the coating layer, the longer the lag time of DS release is. On the contrary, in view of the pH-dependent 5-ASA coated pellets, 5-ASA release was significantly governed by pH. Moreover, the 5-ASA release features from the coated pellets depended upon both the combination ratio of the Eudragit® L100 and S100 pH-sensitive copolymers in the coating formulation and the thickness of the coating layer. The absorption kinetic studies of the DS coated tablets in dogs demonstrated that *in vivo* lag time of absorption was in a good agreement with *in vitro* lag time of release.

CONCLUSION: Two types of CDDS, prepared herein by means of the regular coating technique, are able to achieve site-specific drug delivery targeting at colon following oral administration, and provide a promising strategy to control drug release targeting the desired lower gastrointestinal region.

Cheng G, An F, Zou MJ, Sun J, Hao XH, He YX. Time- and pH-dependent colon-specific drug delivery for orally administered diclofenac sodium and 5-aminosalicylic acid. *World J Gastroenterol* 2004; 10(12): 1769-1774

<http://www.wjgnet.com/1007-9327/10/1769.asp>

INTRODUCTION

Currently, a novel oral colon-specific drug delivery system

(CDDS) has been developing as one of the site-specific drug delivery systems. This delivery system, by means of combination of one or more controlled release mechanisms, hardly releases drug in the upper part of the gastrointestinal (GI) tract, but rapidly releases drug in the colon following oral administration. The necessity and advantage of CDDS have been well recognized and reviewed recently^[1-3]. In view of CDDS specifically delivering drug to the colon, a lot of benefits would be acquired in terms of improving safety and reducing toxicity when treating local or systemic chronic diseases. First, as for treating localized colonic diseases, i.e. ulcerative colitis, Crohn's disease and constipation *etc.*, the optimal drug delivery system, such as CDDS, should selectively deliver drug to the colon, but not to the upper GI tract^[1]. For this reason, the drug concentration was significantly lessened in the upper GI tract, while increased considerably in the colon, resulting in alleviated GI side effects. Second, the colon is referred to as the optimal absorption site for protein and polypeptide after oral administration, because of the existence of relatively low proteolytic enzyme activities and quite long transit time in the colon^[2,3]. To our knowledge, CDDS could provide reliable protection against GI enzymatic degradation by releasing the polypeptide and protein nearly unchanged and fully efficacious in the preferred colon, thereafter resulting in remarkably increased bioavailability for protein and polypeptide. Finally, CDDS would be advantageous when a delay in absorption is desirable from a therapeutic point of view, as for the treatment of diseases that have peak symptoms in the early morning and that exhibit circadian rhythms, such as nocturnal asthma, angina and rheumatoid arthritis^[1,4,5].

There were currently a few strategies to achieve colonic specificity, such as bacterially triggered and pressure-controlled CDDS^[6]. The aim of this study was to explore the feasibility of the time- and pH-dependent CDDS, diclofenac sodium (DS) and 5-aminosalicylic acid (5-ASA) being selected as model drugs, respectively. Besides, we were intended to exploit the typical pharmaceutical coating technology to attain the time- and pH-dependent colon-specific drug delivery. Time-dependent colon-specific DS coated tablets consisted of a tablet core and a coating layer composed of a water-insoluble ethylcellulose (EC) and a water-soluble channeling agent. pH-dependent colon-specific 5-ASA coated pellets consisted of a pellet core and a coating layer of the pH-sensitive methacrylic acid copolymers (Eudragit® L100 and S100).

DS was frequently used for treating rheumatoid arthritis^[2], which had apparent circadian rhythms and peak symptoms in the early morning. When orally administering DS conventional formulation, it was difficult to achieve the desired clinical effect, because it elicited patients' in compliance of administration in the early morning to coordinate the rhythm of rheumatoid arthritis, due to rapid absorption of the conventional formulation. However, colon-specific DS delivery was not only effective, but also more convenient for administration than the conventional formulation. On the other hand, 5-ASA was usually used to effectively treat ulcerative colitis and Crohn's disease in clinical practice^[7]. It was unstable in the stomach, and readily absorbed in the small intestine, eliciting the undesirable adverse effect. Thereby, 5-ASA was prepared as

the CDDS in this study, which protected 5-ASA from the upper GI conditions^[1] and allowed for 5-ASA rapid release in the designated colonic region.

MATERIALS AND METHODS

Preparation of time-dependent colon-specific DS coated tablets and in vitro/in vivo tests

Preparation of DS core tablets Core tablets consisted of 40% (w/w) diclofenac sodium (Yanzhou Pharm., China), 40% (w/w) sodium carboxymethyl starch sodium, 8% (w/w) sodium chloride, 2% (w/w) other excipients. Drug and excipients were blended and sieved (mesh 80); the mixtures were granulated with adhesives and dried 1 h at 55 °C. Core tablets with average weight of 100 mg were prepared using a single punch tablet machine (Type-TDP, 1st Pharm Machine Manu. Co., Shanghai, China). The diameter of core tablets was 6 mm.

Tablet coating The core tablets were coated in a conventional rotating pan. For the coating process, the rotation speed was adjusted to 36 r/min with the coating pan set at an angle of 45°, nozzle port size 0.8 mm; inlet air temperature was 35 °C; tablet bed temperature was 25 °C; the coating solution was sprayed onto the tablets at a flow rate of 0.8 mL/min. The coating solution was 30 g/L EC (Colorcon Co., China) in ethanol solution which contained diethyl phthalate (20% of EC, w/w) as plasticizer, and PEG 400 (15% of EC, w/w, Pharm. Med. Supply Ltd. Co., China) as channeling agent.

Dissolution test Dissolution studies were carried out with paddle method at a rotation speed of 100 r/min and 900 mL distilled water as medium at 37 °C ($n=6$). Samples were collected at predetermined time points, analyzed for DS contents using a UV-spectrophotometer (UV-9100, Ruili Co., China) at 276±1 nm and calculated cumulative release amounts of DS over the sampling times.

Absorption kinetics of time-dependent colon-specific DS coated tablets

Experimental protocol Six male dogs (weight 20±2.5 kg) were randomly assigned to one of two crossover experiments with a 7-d washout period. Dogs were fasted overnight for 12 h before administration and free access to water was allowed. Each dog was orally administered either reference formulation (four enteric coated tablets, Liaodong Pharm. Ltd. Co., batch: 010910, tablet containing 25 mg of DS) or test formulation (four EC coated tablets, each tablet containing 25 mg of DS with 7.5% coating level), respectively. Blood samples were collected at predetermined times for each protocol, respectively: (1) 1, 2, 2.5, 3, 3.5, 4, 4.5, 5, 6, 7, 8, 10, and 24 h for the reference; (2) 1, 3, 4, 5, 5.5, 6, 6.5, 7, 7.5, 8, 9, 10, 12, and 24 h for the test. Plasma was immediately obtained by centrifuging the blood samples at 3 000 r/min for 10 min. The plasma samples were maintained in a freezer at -20 °C until analysis.

Chromatographic conditions The quantitative determination was performed on a high-performance liquid chromatograph equipped with a PU-1580 pump (Jasco, Japan) and 970/975 UV detector (Jasco, Japan). The column was a Hypersil ODS C-18 (250 mm×4.6 mm, 5 μm). The mobile phase consisted of methanol: water: triethylamine: glacial acetic acid (68:22:0.044:0.044, v/v)^[8]. The eluate was monitored at 274 nm, with a sensitivity of 0.001 AUFS. A flow rate was 1.0 mL/min, and the column temperature was maintained at 35 °C.

Sample preparation A 0.5 mL plasma sample was mixed with 20 μL of 4.8 mmol/L inuprofen (internal standard) and 0.6 mL of 1.0 mol/L phosphate buffer in a glass centrifuge tube. The solution was mixed on a vortex mixer for 2 min, and then added 3 mL of a solution of hexane and isopropyl alcohol (4:1, v/v). The mixture was mixed on a vortex mixer for 2 min

again and centrifuged at 3 000 r/min for 5 min. The organic layer was transferred into a clean tube and evaporated to dryness under nitrogen at 35 °C. The residue was dissolved in 100 μL of mobile phase and 20 μL of the solution were injected into the HPLC system.

Data analysis C_{max} represents the maximum drug concentration, t_{max} the time to reach peak concentration, and t_{lag} the lag time of drug. These values were obtained as directly measured values. The elimination rate constant (K_e) was calculated from the slope of the logarithm plasma concentration to time at the end four points. The areas under the plasma concentration-time curve (AUC_{0-t_n}) were calculated by the trapezoidal method. The relative bioavailability ($F\%$) was calculated by the equation: $F(\%) = (AUC_{Test\ formulation} \cdot Dose_{Reference\ formulation}) / (AUC_{Reference\ formulation} \cdot Dose_{Test\ formulation})$. The percentages of absorption *in vivo* were calculated by the Wagner-Nelson method.

Preparation of pH-dependent colon-specific 5-ASA coated pellets

Preparation of 5-ASA pellets Pellets (1.0-1.2 mm in diameter) consisted of 5-aminosalicylic acid (5-ASA, Genlou Chem. Ltd. Co., China), microcrystalline cellulose (MCC, Avicel PH101, Asahi Chem. Ind. Ltd. Co., Japan) and lactose. Drug and excipients were blended and sieved (mesh 80); the mixtures were prepared as wet mass with adhesives. Pellets were prepared by extruder and spheronizer (Institute of Machinery for Chemical Industry East China University of Science and Technology, Shanghai, China). The speed of the extrusion was 30 r/min. The speed of the spheronization was 1 200 r/min and the time of the spheronization was 5 min^[9,10].

Pellet coating The pellets were coated in a fluidized-bed coating apparatus (Shenyang Pharm. Univer., China). For the coating process, nozzle port size was 0.8 mm; inlet air temperature 45 °C; atomizing pressure 1.2 kg/cm²; coating solution was sprayed onto the pellets at a flow rate of 0.8 mL/min. The coating solution was aqueous dispersions of various proportions of Eudragit® L100 and Eudragit® S100 (Röhm Pharma GmbH, Germany). The plasticizer TEC was added directly to the polymer dispersions^[11].

Dissolution test Dissolution studies were carried out with a basket method at a 100 r/min rotation speed and 37 °C, 900 mL dissolution medium according to ChP 2000. The dissolution tests were performed in HCl pH 1.2, phosphate buffer solution pH 6.0, 6.8, 7.2 or 7.5, respectively. Samples were collected at predetermined time points, analyzed for 5-ASA content using a UV-spectrophotometer (UV-9100, Ruili Co., China) at 302 nm and 330 nm for 5-ASA assay in 0.1 mol/L HCl and the phosphate buffer solutions, respectively.

In order to simulate the pH changes along the GI tract, three dissolution media with pH 1.2, pH 6.0, and pH 7.2, were sequentially used, referred to as the sequential pH change method (Table 1). pH 6.0, and pH 7.2 media were 0.05 mol/L phosphate buffer solution. When performing release experiments, the pH 1.2 medium was first used for 2 h, then removed, and the fresh pH 6.0 dissolution medium was added. After 1 h, the medium was removed again, and fresh pH 7.2 dissolution medium added. The UV readings were taken at 302 nm and 330 nm for 5-ASA measurement in 0.1 mol/L HCl and the buffer media, respectively^[12,13]. And then the 5-ASA cumulative release percentage was calculated over the sampling times.

Table 1 Dissolution conditions of 5-ASA coated pellets

pH	λ_{max} (nm)	Time (h)	Simulated GI region
1.2	302	2	Stomach
6.0	330	1	Duodenum
7.2	330	5	Lower small intestine and colon

RESULTS

Time-dependent colon-specific DS coated tablets

The DS core tablets were coated by the coating formulation, consisting of 30 g/L EC, diethyl phthalate (20% of EC, w/w) as a plasticizer and PEG 400 (15% of EC, w/w) as a channeling agent in ethanol solution. The *in vitro* release behavior of the DS coated tablets with different coating levels (3%, 5%, 7%, 9%, and 11%, w/w), was studied. As shown in Figure 1, the coating level exercised a significant effect on the lag time of DS release from the coated tablets. Manifestly, the greater the coating level, the longer the lag time of DS release from the coated tablets. However, once the coating layer was broken up, DS then was rapidly released from the coated tablets (Figure 1). The effects of dissolution medium pH on the release profiles of the DS coated tablets at 7.5% coating level are shown in Figure 2. To be evident, the pH values of media did not exert a significant effect on the DS release pattern from the coated tablets. The *in vitro* release profile of test DS coated tablets at 7.5% coating level was compared with the marketed DS enteric tablets, as shown in Figure 3.

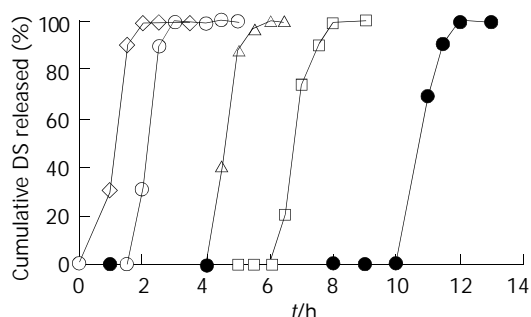


Figure 1 Effect of different coating levels on the DS release from the coated tablets in distilled water. The tablets were coated at five levels of 3% (◇), 5% (○), 7% (△), 9% (□) and 11% (×) (w/w, total solid applied) ($n=6$).

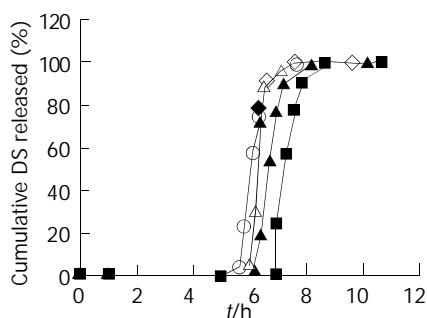


Figure 2 Effect of pH of the dissolution medium on DS release from the coated tablets. The tablets were coated at 7.5% (w/w, total solid applied) level ($n=6$). pH1.0 (◇), pH2.0 (■), pH5.0 (▲), pH6.8 (○), pH7.6 (△) of the dissolution media.

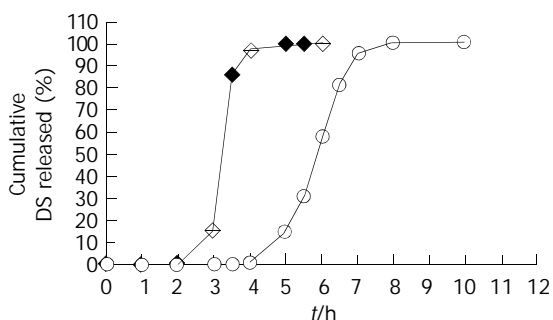


Figure 3 DS dissolution profiles of test coated tablets (○) and the reference enteric coated tablets (◆) ($n=6$).

The reference enteric tablets started DS release at 2 h, while the test DS coated tablets began to release DS at 4 h, after being put in the dissolution medium. The lag time of DS release from the test tablets was significantly longer than that of reference enteric tablets. Moreover, the cumulative DS release percentage of test tablet was nearly 100% within 7 h.

pH-dependent colon-specific 5-ASA coated pellets

The 5-ASA pellets were coated with combination of Eudragit® L100-Eudragit® S100 methacrylic acid pH-sensitive copolymers, and their release characteristics were examined by three sequential dissolution media with different pH values in order to mimic pH changes along GI tract. We investigated the effect of combination ratios of Eudragit® L100-Eudragit® S100 in the coating formulation on the release profiles of 5-ASA coated pellets, as shown in Figure 4.

The combination ratios of Eudragit® L100-Eudragit® S100 in the coating formulation played a significant role in regulating the release behavior of 5-ASA coated pellets. When employing 1:4 (w/w) combination ratio of Eudragit® L100-Eudragit® S100 as the coating formulation, 5-ASA was released less than 1.0% in pH 1.2 dissolution medium (simulated gastric fluid) until 2 h, and less than 3.0% in pH 6.0 (simulated duodenum fluid) at 1 h after changed to fresh medium, and more than 80% in pH 7.2 (simulated lower small intestinal and colonic fluid) at 1.5 h after changed to fresh medium. When the pellets were coated with Eudragit® L100-Eudragit® S100 combination (w/w) ratios of 1:0, 4:1, and 1:1, the cumulative release percentage of 5-ASA was 1.0-3.6% in pH 1.2 until 2 h, 11-37% in pH 6.0 at 1 h, and more than 80% in pH 7.2 at 1.5 h, the results indicating that the earlier measurable release occurred. Pellets coated with Eudragit® S100 alone displayed the slowest release rate, the cumulative release percentage of 5-ASA was less than 0.5% in pH 1.2 up to 2 h, was less than 1.0% in pH 6.0 at 1 h, and was not more than 10% in pH 7.2 at 1.5 h.

The effects of the coating level on the release properties of 5-ASA coated pellets were also examined, with the coating level ranging from 0% to 25% and the combination ratio of Eudragit® L100-Eudragit® S100 set at 1:4 (w/w), as shown in Figure 5. As the coating level and thickness of coating layer increased, the acid-resistant property of coating layer was enhanced. The coating level being 25% (w/w), almost none of the 5-ASA was released from coated pellets in pH 1.2 and pH 6.0 dissolution media. By contrast, the cumulative release percentage of 5-ASA was more than 80% in pH 7.2 at 1.5 h, regardless of the coating levels. Accordingly, this formulation, with the combination ratio Eudragit® L100-Eudragit® S100 being 1:4 (w/w) and the coating level being 25%, would be a promising candidate for designed DS pH-dependent CDDS.

Moreover, we examined the influences of medium pH values on the release characteristics of the 5-ASA coated pellets, utilizing 1:4 (w/w) combination ratio Eudragit® L100-Eudragit® S100 as the coating formulation and setting the coating level at 25%. Five pH values (1.2, 6.0, 6.8, 7.2 and 7.5) of dissolution media were utilized. As shown in Figure 6, pH values of medium notably affected 5-ASA release profiles from the pH-dependent coated pellets. When pH increased from 1.2 to 7.5, the release rate of 5-ASA from the coated pellets was outstandingly enhanced.

In vivo absorption kinetics of time-dependent colon-specific DS coated tablets

Either DS reference formulation (four 25 mg enteric coated tablets) or DS test formulation (four 25 mg EC coated tablets) was orally administered in the two crossover experimental design in dogs at a dose of 100 mg/body, respectively. The concentration-time curve of DS in plasma is illustrated in Figure 7. The pharmacokinetic parameters are calculated and listed in Table 2. The mean lag time of DS absorption from the test

formulation was as long as 5.80 h, while that for the reference formulation was 2.80 h after oral administration. This result was well consistent with the mean *in vitro* lag time of DS release from two formulations, the test tablets being 4 h versus reference enteric tablets being 2 h. In addition, C_{max} of the test and the reference formulations was 8.17 mg/L and 10.05 mg/L, respectively. The relative bioavailability of test formulation versus reference formulation was 86.38%.

Absorption percentage *in vivo* of DS for test formulation was assessed by the Wagner-Nelson method. Both absorption percentage *in vivo* of DS ($F(t)$) and the cumulative release percentage *in vitro* of DS ($f(t)$) versus time profiles, demonstrate a similar contour curve in Figure 8. Furthermore, there existed a significant correlation between $F(t)$ and $f(t)$ ($r=0.95$) for test formulation, indicative of the good relationship between *in vitro* release and *in vivo* absorption processes.

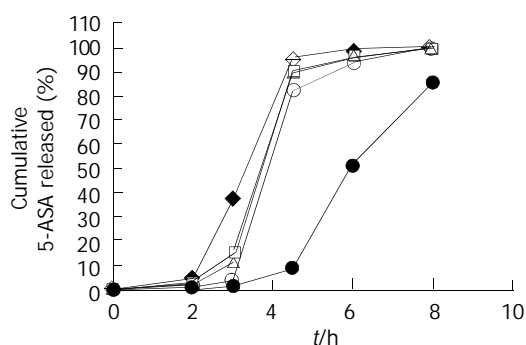


Figure 4 5-ASA release profile of pellets coated at 25% level with various Eudragit[®] L100-Eudragit[®] S100 combination ratios of 1:0 (◆), 4:1 (□), 1:1 (△), 1:4 (○) and 0:1 (●) (w/w), using the sequential pH change method ($n=6$).

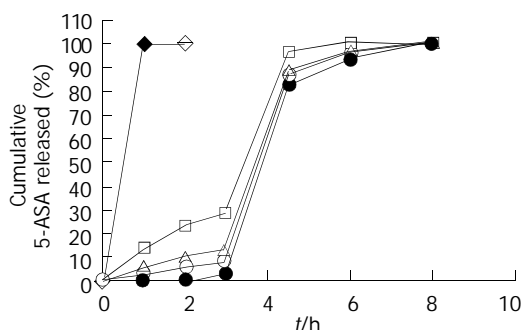


Figure 5 5-ASA release profile of pellets coated at 5 levels of uncoated (◆), 5% (□), 10% (△), 15% (○), 25% (●) (w/w, total solid applied) with Eudragit[®] L100-Eudragit[®] S100 combinations of 1:4 (w/w), using the sequential pH change method ($n=6$).

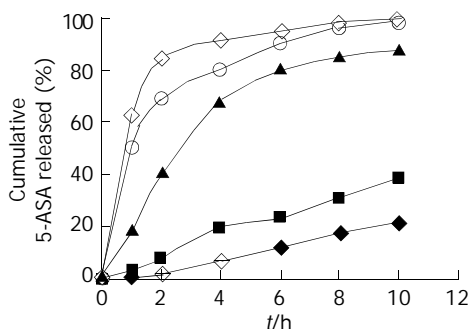


Figure 6 Effect of pH of the dissolution medium on 5-ASA release of coated pellets coated at 25% level with Eudragit[®] L100-Eudragit[®] S100 combination ratios of 1:4 (w/w) ($n=6$). PH 1.2 (◆), pH 6.0 (■), pH 6.8 (▲), pH 7.2 (○), pH 7.5 (◇) of the dissolution media.

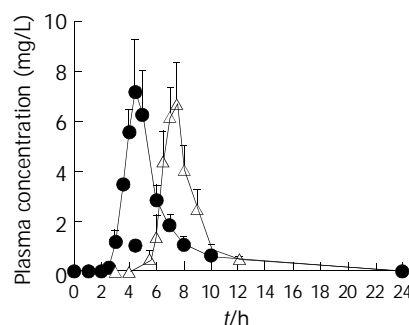


Figure 7 DS plasma concentration-time profiles after oral administration of coated formulation (△) and reference enteric formulation (●) in dogs at a dose of 100 mg/body. Each value represents mean±SE ($n=6$).

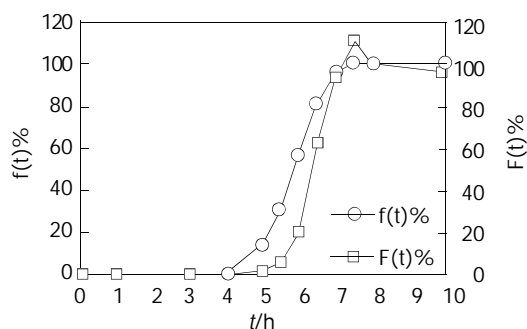


Figure 8 Comparison between the cumulative DS release percentage *in vitro* $f(t)$ and the absorption percentage *in vivo* $F(t)$ of coated formulation ($n=6$).

Table 2 Pharmacokinetic parameters after oral administration of DS coated formulation and reference enteric formulation in dogs at a dose of 100 mg/body ($n=6$, mean±SE)

Parameter	Test formulation	Reference formulation
C_{max} (mg/L)	8.17±1.35	10.05±1.66
t_{max} (h)	7.40±0.35	4.50±0.20
K_e (L/h)	0.56±0.06	0.44±0.11
t_{lag} (h)	5.80±0.42	2.80±0.21
AUC_{0-t_n} (mg·h/L)	17.21±2.09	19.91±2.83
F (%)	86.38±10.51	—

DISCUSSION

It has been well found that gastric emptying of a preparation was variable and depended primarily upon whether subjects were fed or not, and upon the properties of the preparation. On the contrary, the transit time in small intestine for the preparation was surprisingly constant at 3 ± 1 h and appeared to be independent of the types of the preparations and whether subjects were fed or not^[14]. On the basis of the above understandings, we designed the time-dependent colon-specific drug delivery to achieve no measurable drug release in the upper part of GI tract and a considerable drug release after arrival at colon.

The time-dependent DS coated tablets were prepared by means of the coating technology, with the coating formulation consisting of the water-insoluble EC, the water-soluble channeling agent PEG 400 and the membrane plasticizer diethyl phthalate. Generally, the coating layer of EC was mainly hydrophobic and was moderately impermeable to water molecules. And the water-soluble channeling agent was rapidly dissolved in water, resulting in the formation of numerous micro-channels across the coating layer. Then, water molecules

could penetrate into the tablet core via these channels to cross the hydrophobic EC membrane. Water uptake caused the expansion of the disintegrating agent within the tablet core, resulting in a gradual build-up of pressure within the coated tablets. Once the inside pressure exceeded the critical disrupted value that the coating layer resisted most, the coating layer would be ruptured and release drug in a manner of burst, thus forming the delay effect of drug release from the coated tablets. Taken together, the formation of micro-channels was the first crucial step, and the critical disrupted pressure governed by the coating layer and the expansibility of the disintegrating agent were the key factors for time-dependent controlled release^[15].

The release profiles of the DS coated tablets at 7.5% coating level were not affected by the pH values of media (Figure 2). This was reasonably expected, since the channeling agent PEG 400 was pH-insensitive and formation of the micro-channels was not affected by pH. The effects of the coating level on the lag time of DS release from the coated tablets were tested, indicating that the coating level played a significant role in controlling the lag time of release. To increase the coating level would extend the lag time of DS release from the coated tablets (Figure 1). There were two possible mechanisms contributing to this phenomenon. For one thing, since the hydrophobic EC membrane was relatively impermeable to water molecules, substantial effect on the rate of the water molecules diffusion and water uptake, was exerted by the number, size, length and tortuosity of the aqueous micro-channels in the coating layer. The coating level and thickness of the coating layer certainly determined the rate of water uptake, by controlling the formation rate and physical characteristics of the aqueous channels. To be evident, the increase of the coating level would elicit the longer and more tortuous aqueous micro-channels, severely impairing the rate of water uptake. Alternatively, the thicker coating layer developed the higher critical resistant pressure to be surpassed for disrupting the coating membrane, required the greater water uptake to gradually build up inside pressure by the disintegrating agent's expansion and prolonged the lag time of drug release from the coated tablets^[16].

The mean *in vivo* lag time of the DS absorption from coated tablets was significantly longer than that from enteric tablets, being 5.80 h vs 2.80 h (Figure 7 and Table 2). The results were in accordance with the *in vitro* lag time of DS release from two formulations, and the lag time of DS release from test tablets was nearly 2 h longer than that from the enteric tablets (Figure 3). Furthermore, the *in vivo* absorption kinetics of the time-dependent DS coated tablets was assessed by the typical Wagner-Nelson method. The absorption percentage *in vivo* versus time profile was analogous to the cumulative release percentage *in vitro* versus time profile, which validated the *in vitro* dissolution conditions and verified the utility of the time-dependent CDDS (Figure 8). The good correlation coefficient ($r=0.95$) between *in vivo* absorption and *in vitro* release percentages, further confirmed this conclusion.

To our knowledge, there exists a pH gradient along the GI tract, a fact that pH in the stomach is approximately 1.5 in the fasted state, ranges roughly from 5.0 to 7.0 in the small intestine, and from 6.0 to 7.2 in the colon^[1]. The pH values at the end of ileum and in the colon are notably higher than the upper GI tract, therefore providing the rationale for developing pH-dependent CDDS. In addition, a novel dosage form, pellets, is the multiple units' drug delivery system, and it is superior to the conventional preparation, such as tablets, for the following reasons. The pellets appear to be less influenced by the physiologic factors, such as the gastric emptying, intestinal transit, than tablets. Moreover, the pellets could be widely and evenly distributed in the GI tract surfaces, which increase the drug-tract contact surface and thus improve bioavailability.

Finally, the release failure of the individual unit hardly affects the total release behavior due to the multiple units, whereas tablets do not^[17].

Eudragit® L100 and S100 were methacrylic acid pH-sensitive copolymers and began to be dissolved from pH 6.0 and pH 7.0, respectively. The combination utilization of L100 and S100 would be capable of designing the suitable copolymers intended to begin being dissolved from the desired pH environment in the lower GI tract (pH variation range of 6.0-7.0). Clearly, the combination ratio of L100 and S100 exerted a great effect on the 5-ASA release characteristic from the coated pellets. The combination ratios (1:0, 4:1, 1:1, and 1:4, 0:1) of L100 and S100 hardly released drug in pH 1.2 until 2 h, indicating the acid-resistant properties of the coated polymers (Figure 4). After changing to pH 6.0 fresh medium, L100 could be dissolved and the channels were then quickly created in the coating membrane; conversely, S100 did not. Therefore, the higher the proportion of L100 in the coating formulation, the more channels formed, thus allowing for the higher 5-ASA release^[12]. After converting into the pH 7.2 fresh medium, both L100 and S100 could be dissolved; by contrast, the dissolution rate of L100 was faster than S100. Thus the higher amount of L100 in the coating formulation, the faster dissolution and disappearance of the coating layer, leading to rapid release of 5-ASA (Figure 4). The dissolution profile for the 0:1 coating formulation at pH 7.2 demonstrated that the dissolving process of the coating layer of S100 alone was rather slow, resulting in very slow drug release.

Fixing the combination ratio of Eudragit® L100 and S100 at 1:4, the coating level remarkably influenced the 5-ASA release from coated pellets (Figure 5). When the coating level was less than 25%, a measurable 5-ASA release was observed in pH 1.2 and 6.0 media. The coated pellets at 25% coating level scarcely released 5-ASA in pH 1.2 and 6.0 media, and rapidly released in pH 7.2 medium. This coating level of pellets (25%) was significantly higher than that of tablets (10%) in this study, because of the ratio of surface area of pellets considerably greater than tablets. The lower coating level for pellets would form an incomplete closed membrane around pellets, and elicited a measurable drug release in pH 1.2 and 6.0 media (Figure 5). The coating level of pellets 25%, however, could form uninterrupted and homogenous coating layer, swiftly released 5-ASA in pH 7.2, but not in pH 1.2 and 6.0 media. On the other hand, the higher coating level would require the longer processing time, escalation of cost and further 5-ASA was incapable of being rapidly released from pellets in pH 7.2 medium (the coating level $\geq 35\%$, unpublished data). Since the coating copolymers were pH-sensitive, 5-ASA release from the coated pellets was expected to be influenced by the dissolution medium pH, as confirmed in Figure 6.

In summary, two controlled release mechanisms, i.e. time- and pH-dependent, could achieve colonic-specific drug delivery following oral administration. In addition, both CDDS were relatively inexpensive and easy to be manufactured using conventional pharmaceutical coating technique, and provided the promising candidates for specifically delivering drug to the targeted colon region, in particular for DS and 5-ASA in this study, respectively.

REFERENCES

- 1 Kinget R, Kalala W, Vervoort L, van den Mooter G. Colonic drug targeting. *J Drug Target* 1998; **6**: 129-149
- 2 Watts PJ, Illum L. Colonic drug delivery. *Drug Dev Ind Pharm* 1997; **23**: 893-913
- 3 Yang L, Chu JS, Fix JA. Colon-specific drug delivery: new approaches and *in vitro/in vivo* evaluation. *Int J Pharm* 2002; **235**: 1-15

- 4 **Halsas M**, Penttinen T, Veski P, Jurjenson H, Marvola M. Time-controlled release pseudoephedrine tablets: bioavailability and *in vitro/in vivo* correlations. *Pharmazie* 2001; **56**: 718-723
- 5 **Halsas M**, Hietala J, Veski P, Jurjenson H, Marvola M. Morning versus evening dosing of ibuprofen using conventional and time-controlled release formulations. *Int J Pharm* 1999; **189**: 179-185
- 6 **Zou MJ**, Cheng G. The oral colon-specific drug delivery system. *Shenyang Yaoke Daxue Xuebao* 2001; **18**: 376-380
- 7 **Ardizzone S**, Porro GB. A practical guide to the management of distal ulcerative colitis. *Drugs* 1998; **55**: 519-542
- 8 **Miller RB**. High-performance liquid chromatographic determination of diclofenac in human plasma using automated column switching. *J Chromatogr* 1993; **616**: 283-290
- 9 **Pinto JF**, Buckton G, Newton JM. The influence of four selected processing and formulation factors on the production of spheres by extrusion and spheronisation. *Int J Pharm* 1992; **83**: 187-196
- 10 **Krogars K**, Heinamaki J, Vesalahti J, Marvola M, Antikainen O, Yliruusi J. Extrusion-spheronization of pH-sensitive polymeric matrix pellete for possible colonic drug delivery. *Int J Pharm* 2000; **199**: 187-194
- 11 **Khan MZ**, Prebeg Z, Kurjakovic N. A pH-dependent colon targeted oral drug delivery system using methacrylic acid copolymers I. Manipulation of drug release using Eudragit L100-55 and Eudragit S100 combinations. *J Control Release* 1999; **58**: 215-222
- 12 **Khan MZ**, Stedul HP, Kurjakovic N. A pH-dependent colon-targeted oral drug delivery system using methacrylic acid copolymers. II. Manipulation of drug release using Eudragit L100 and Eudragit S100 combinations. *Drug Dev Ind Pharm* 2000; **26**: 549-554
- 13 **Ashford M**, Fell JT, Attwood D, Woodhead PJ. An *in vitro* investigation into the suitability of pH-dependent polymers for colonic targeting. *Int J Pharm* 1993; **91**: 241-245
- 14 **Rouge N**, Buri P, Doelker E. Drug absorption sites in the gastrointestinal tract and dosage forms for site-specific delivery. *Int J Pharm* 1996; **136**: 117-139
- 15 **Xiao YC**, Cheng G, Zou MJ. Studies on coated theophylline tablets for colon-specific delivery using Eudragit NE 30D. *Shenyang Yaoke Daxue Xuebao* 2001; **18**(Suppl): 5-7
- 16 **Fan TY**, Wei SL, Yan WW, Chen DB, Li J. An investigation of pulsatile release tablets with ethylcellulose and Eudragit L as film coating materials and cross-linked polyvinylpyrrolidone in the core tablets. *J Control Release* 2001; **77**: 245-251
- 17 **Lu B**, Wang PY, Deng YJ, Zhou Q, Ni D, Xu HN, Xu HL, Liang WQ, Pei YY, Wei SL. New techniques and new dosage forms of drug. 1th ed. *Beijing: People's Medical Publishing House* 1998: 289-305

Edited by Zhang JZ and Chen WW Proofread by Xu FM

Inhibition of Fas/FasL mRNA expression and TNF- α release in concanavalin A-induced liver injury in mice by bicyclol

Min Li, Geng-Tao Liu

Min Li, Geng-Tao Liu, Department of Pharmacology, Institute of Materia Medica and Peking Union Medical College and Chinese Academy of Medical Sciences, Beijing 100050, China

Supported by the Grant from Ministry of Science and Technology of China, No. 94-ZD-02

Correspondence to: Professor Geng-Tao Liu, Department of Pharmacology, Institute of Materia Medica and Peking Union Medical College and Chinese Academy of Medical Sciences, Beijing 100050, China. gtliau2002@yahoo.com

Telephone: +86-10-63165178 **Fax:** +86-10-63017757

Received: 2004-01-02 **Accepted:** 2004-01-16

Abstract

AIM: Bicyclol, 4,4'-dimethoxy-5,6,5',6'-dimethylene-dioxy-2-hydroxymethyl-2'-carbonyl biphenyl, is a new anti-hepatitis drug. The aim of the present study was to investigate the protective effect of bicyclol on concanavalin A (Con A)-induced immunological liver injury in mice and its mechanism.

METHODS: Liver injury was induced by injection of Con A via tail vein of mice and assessed biochemically and histologically. Serum transaminase and tumor necrosis factor alpha (TNF- α) were determined. Liver lesions were observed by light microscope. Expressions of TNF- α , interferon gamma (IFN- γ), Fas and Fas ligand (FasL) mRNA in the livers were measured by RT-PCR.

RESULTS: Serum transaminase level and liver lesions in Con A-induced mice were markedly reduced by oral administration of 100, 200 mg/kg of bicyclol. TNF- α level in serum was also reduced by bicyclol. Con A injection induced up-regulation of TNF- α , IFN- γ , Fas and FasL mRNA expression in liver tissues. Bicyclol significantly down-regulated the expression of IFN- γ , Fas and FasL mRNA, but only slightly affected TNF- α mRNA expression in liver tissues.

CONCLUSION: Bicyclol protects against Con A-induced liver injury mainly through inhibition of Fas/FasL mRNA expression in liver tissues and TNF- α release in mice.

Li M, Liu GT. Inhibition of Fas/FasL mRNA expression and TNF- α release in concanavalin A-induced liver injury in mice by bicyclol. *World J Gastroenterol* 2004; 10(12): 1775-1779

<http://www.wjgnet.com/1007-9327/10/1775.asp>

INTRODUCTION

Viral hepatitis is a serious health problem worldwide, as more than two billion people alive today have been infected by hepatitis B virus, and 170 million people have been infected by hepatitis C virus^[1]. Although a number of drugs such as interferon- 2α and lamivudine have been used in the treatment of viral hepatitis, the efficacy of these drugs is still limited and some side effect are severe^[2,3]. Therefore, it is necessary to develop new anti-hepatitis drugs. Bicyclol is new synthesized anti-hepatitis drug, chemically named 4, 4' -dimethoxy-5, 6,

5' , 6' -dimethylene-dioxy-2-hydroxymethyl- 2' -carbonyl biphenyl. Our previous studies demonstrated that bicyclol has anti-liver injury, anti-liver fibrosis and anti-hepatitis virus activities^[4]. Clinical trials indicated that bicyclol markedly normalized the elevated level of serum transaminase in patient with viral hepatitis B, and also inhibited HBV-DNA replication^[5]. It is known that the liver injury induced by CCl₄, acetaminophen and D-galactosamine is mainly caused by free radicals and oxidative stress^[6,7]. The protection of bicyclol against CCl₄, acetaminophen-induced liver injury, is closely related to its elimination of free radicals and inhibition of oxidative stress. However, the pathogenesis of human viral hepatitis is different from hepatotoxicants induced liver injury. Human viral hepatitis is a disease resulting from destruction of virus-infected hepatocytes through immune-mediated mechanism^[8,9]. Thus, it is necessary to further investigate if there are other mechanisms involved in the protective effect of bicyclol against liver injury in addition to its anti-oxidative activity. Recently, a model of immune-mediated liver injury in mice was established by injection of T cell mitogen Con A, which is an available animal model relevant to human hepatitis and hepatocellular damage^[10]. Previous studies demonstrated that activated T cell-mediated cellular immunity is responsible for the liver damages in Con A model. TNF- α released from activated T lymphocytes and Kupffer cells plays a critical role in the process of liver damage and hepatocyte apoptosis^[11-13]. In addition, Fas and Fas ligand (FasL) pathway is involved in the pathogenesis of hepatocytes apoptosis and necrosis^[14]. Therefore, the present study was to investigate the effect of bicyclol on Con A induced immune-mediated liver injury and its mechanisms. Figure 1 shows the chemical structure of bicyclol.

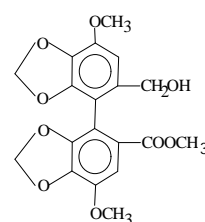


Figure 1 Chemical structure of bicyclol.

MATERIALS AND METHODS

Animals

Male C57BL/6 mice weighing 21-25 g were obtained from the Animal Center of Chinese Academy of Medical Sciences. They were fed standard maintenance diet and water throughout the experiments. All animals received care in compliance with the guidelines of China Ministry of Health.

Reagents

Bicyclol was kindly provided by Professor Zhang CZ in the Department of Pharmaceutical Chemistry of our institute. The purity of bicyclol was over 99% and not dissolved in water. Type IV Con A was purchased from Sigma Chemical Co. (St. Louis, MO, USA). ALT kit was purchased from BHKT Chemical Reagent Co., Ltd (Beijing, China). ELISA kit for

TNF- α determination was provided by Jingmei Biotechnology Co, Ltd (Beijing, China).

Con A-induced hepatitis in mice and drug administration

Control mice were injected pyrogen-free phosphate-buffered saline (PBS). A dose of 23 mg/kg of Con A was injected via tail vein. Bicyclol was suspended in 5 g/L sodium carboxymethylcellulose (Na-CMC) just before use. The 200 mg/kg and 100 mg/kg of bicyclol were administered orally three times, 24, 12, 1 h before Con A injection.

Assay for serum ALT activity and TNF- α levels

Serum from individual mouse was obtained at various intervals after Con A injection. Alanine aminotransferase (ALT) level was determined by a biochemical kit according to the manufacturer's instruction. The assay of serum TNF- α level was performed with specific ELISA kit.

Histopathological examination of liver tissue

Liver samples from individual mouse were fixed in 40 g/L neutral formaldehyde solution, embedded in paraffin, sliced into sections 5- μ m of thickness and stained with hematoxylin and eosin for histological examination. The degrees of liver injury were graded based on a score of 0-3^[15] and expressed as the mean of 10 different fields of each slide.

Detection of Fas, Fas ligand (FasL), TNF- α , and IFN- γ expression by semiquantitative RT-PCR

Total RNA from mouse liver was extracted by TRIzol reagent (Gibco USA)^[16]. RT-PCR was conducted to detect Fas, FasL, TNF- α and IFN- γ gene expression. The primers for Fas were as follows: 5' -TGCACAGAAGGGAAGGAGTA-3' and 5' -ATG GTTTCACGACTGGAGGT-3'; for FasL: 5' -GACAGCAGTG CCACTTCATC-3' and 5' -TTAAGGCTTTGGTTG GTGAA-3'; for IFN- γ : 5' -CTCAAGTGGCATAGATGTGG-3' and 5' -ACT CCTTTCCGCTTCCTGA-3'; for TNF- α : 5' -GGCGGTGCCT ATGCTCAG-3' and 5' -GGGCAGCCTTGTC CCTTGA-3'; and for Cu/Zn SOD: 5' -TCTGCGTGCTGAAG GGCGAC-3' and 5' -CTCCTGAGAGTGAGATCACA-3'. mRNA was reversely transcribed with AMV reverse transcriptase and then amplified using *Tfl* DNA polymerase for 35 cycles as follows: at 94 °C for 30 s (dissociation), at 60 °C for 60 s (annealing), and at 72 °C for 90 s (primer extension). PCR amplification products were visualized in 2% agarose gels after staining with ethidium bromide. The density of the PCR products was compared with Cu/Zn SOD, which was used as an internal control. Briefly, the spot density of each band in the gel was measured with the Kodak digital imaging system (Kodak DC120, Digital science 1D system, USA). The percentage of gene expression was calculated by the following equation: (density of cytokine product/density of SOD product) \times 100.

Statistical analysis

All data are expressed as mean \pm SD and analyzed by Student's *t*-test.

RESULTS

Effect of bicyclol on Con A-induced aminotransferase elevation in serum

Injection of Con A to mice caused a time dependent increase in serum ALT levels (Figure 2). ALT levels increased significantly and reached a maximum at 6 h and maintained at plateau for 16 h after Con A injection. Administration of 200 mg/kg and 100 mg/kg of bicyclol to mice for three times significantly reduced the elevated serum ALT levels at 12 h and 16 h after Con A administration (Table 1).

Effect of bicyclol on liver histology

Twelve hours after Con A injection, histological analysis of the liver sections of Con A-treated mice showed widespread areas of necrosis and inflammation within the liver lobules and around the central veins and portal tracts (Figure 3A,B). Extensive lesions were characterized by massive hepatocytes coagulative necrosis, and cytoplasmic swelling of most living hepatocytes and nuclear chromatin condensation were found frequently, which indicated hepatocytes apoptosis. A moderate infiltration of lymphocytes and mononuclear cells in the portal area and around the central vein were also observed. As shown in Figure 3C, bicyclol reduced the areas of lesions and the extent of liver injury induced by Con A. The extent of lymphocyte infiltration in bicyclol treated mice also reduced significantly. The extent of liver necrosis was classified using a four degree score as shown in the footnote of Table 2.

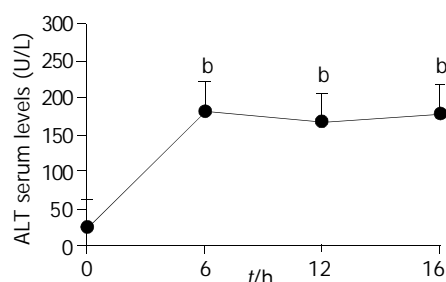


Figure 2 Time-course of Con A-induced liver serum ALT elevation in mice. ^b*P* < 0.01 vs other time.

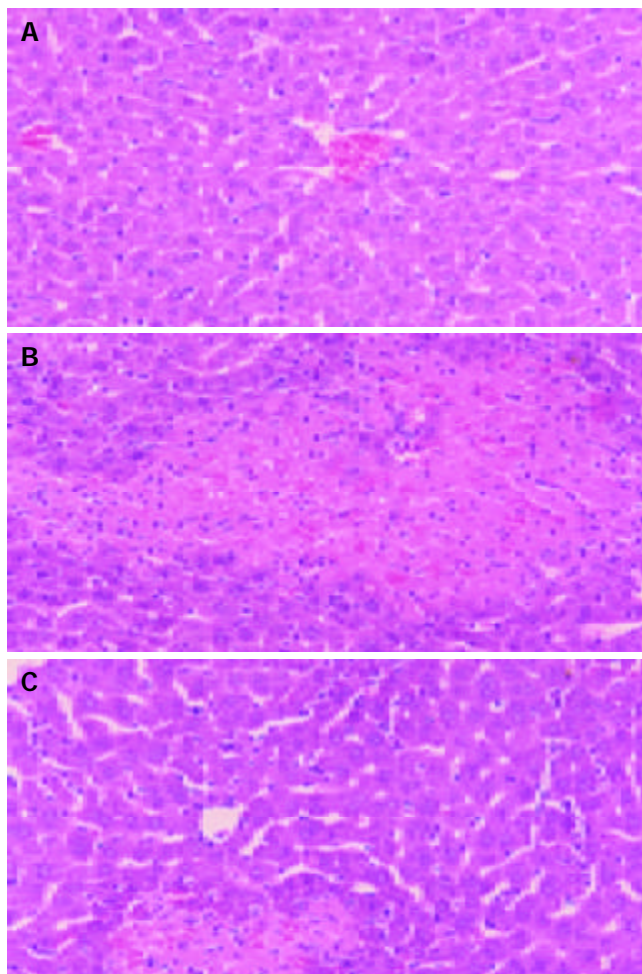


Figure 3 Light micrographs of livers from mice treated with Con A alone or in combination with bicyclol. Original magnification \times 200. A: normal control mouse; B: Con A injected mouse; C, mouse treated with bicyclol 200 mg/kg.

Table 1 Protection of bicyclol against Con A induced liver injury in mice as determined by ALT(U/L)

Time	Con A alone	Con A+bicyclol 200 mg/kg	Con A+bicyclol 100 mg/kg
12 h	161.5±63.11	27.1±10.8 ^b	50.1±15.9 ^a
16 h	165.8±8.76	10.6±12.8 ^b	30.7±27.4 ^b

Data are mean±SD of 8 mice per group. ^a $P<0.05$, ^b $P<0.01$. vs Con A alone. Serum ALT levels were measured 12 h and 16 h after Con A injection, respectively.

Table 2 Effect of bicyclol on liver histology by evaluation the degree of liver injury 12 h after Con A injection

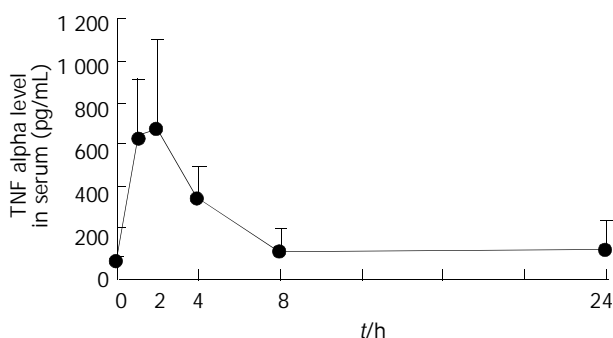
Group	Grade of liver injury			
	0	1	2	3
Normal (n=7)	7	0	0	0
Con A alone (n=7)	0	0	0	7
ConA+bicyclol 200 mg/kg (n=8)	3	2	1	2
ConA+bicyclol 100 mg/kg (n=7)	1	2	3	1

Histological degree of liver injury is classified according to the area of coagulative necrosis in hepatic lobules as follows: grade 0, no coagulative necrosis; grade 1, coagulative necrosis area <10%; grade 2, coagulative necrosis area between 10% and 25%; grade 3, coagulative necrosis area >25%.

Lowering effect of bicyclol on serum TNF- α level in Con A-injected mice

Mice were killed at the indicated time points after injection of 23 mg/kg Con A. As shown in Figure 4, serum TNF- α level increased significantly 1-2 h after Con A injection, and then showed a marked decline at 4 h. At 24 h, the level of TNF- α level was still slightly higher than the normal mice but not significantly (Figure 4).

The treatments of mice with bicyclol 200 mg/kg caused a decrease of the elevated TNF- α level by about 50% two hours after Con A injection ($P<0.05$). Bicyclol 100 mg/kg also decreased serum TNF- α concentration about 25% but not significantly statistically (Figure 5).

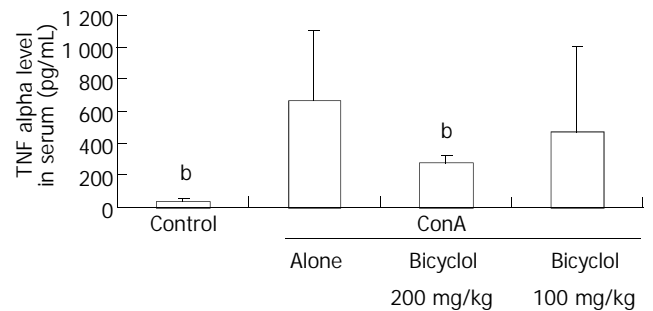
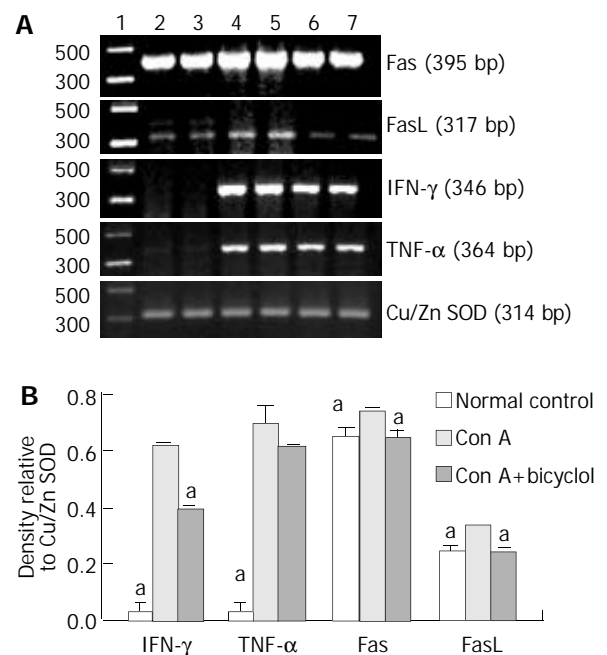
**Figure 4** Dynamic changes of serum TNF- α level after Con A injection in mice. Each point represents mean±SD of six mice.

Effect of bicyclol on expressions of liver TNF- α , IFN- γ , Fas and FasL mRNA in Con A-treated mice

One hour after the last administration of bicyclol, mice were injected 23 mg/kg of Con A. The livers were removed 2 h later. Total liver RNA was isolated, reversely transcribed, and amplified by PCR using primers for TNF- α , IFN- γ , Fas and FasL, respectively. Cu/Zn SOD was used as an internal control. As shown in Figure 6, TNF- α and IFN- γ mRNA were undetectable in livers from normal control mice, while the mice injected with Con A showed TNF- α and IFN- γ mRNA expression

apparently. Prior administration of bicyclol 200 mg/kg reduced about 40% IFN- γ mRNA expression induced by Con A, but had slight influence on up-regulation of TNF- α mRNA in Con A injected mice.

Although Fas and FasL mRNA levels were detectable in normal control mice, significant increase of both Fas and FasL mRNA levels was demonstrated in Con A challenged mice. Mouse liver Fas mRNA level was more than that of FasL both in normal control and Con A injected groups. Administration of bicyclol down-regulated Fas and FasL mRNA expression to approximately normal level.

**Figure 5** Lowering effect of bicyclol on the elevated serum TNF- α Level induced by Con A injection in mice. Each bar represents mean±SD of 6 mice per group ^b $P<0.01$ vs Con A alone.**Figure 6** Effect of bicyclol on Con A induced TNF- α , IFN- γ , Fas and FasL mRNA expression determined by RT-PCR. A: Photograph of ethidium bromide-stained amplification products. Lane 1, molecular mass markers; lane 2 and lane 3, control liver; lane 4 and lane 5, liver 2 h after Con A administration alone; lane 6 and lane 7, liver 2 h after injection of Con A in combination with 200 mg/kg bicyclol. B: Relative band intensity of amplification products compared with Cu/Zn SOD mRNA. Data represent the mean of two lanes. Each lane corresponds to the pooled livers from two mice. ^a $P<0.05$ vs Con A alone.

DISCUSSION

The immune cell-mediated liver injury is a critical event in the pathogenesis of human viral hepatitis^[17-19]. Cell immunity is involved in the immune clearance of virus-infected hepatocytes and at the same time damage virus-infected hepatocytes. This conclusion came from the findings that infiltrating T cells were

observed in the liver tissue of hepatitis patients^[20,21]. Con A induced liver injury is a T-cell-dependent hepatitis model, which situation is relevant to human liver injury^[22]. In Con A induced hepatitis, T cell activation plays a crucial role in the process of liver injury, because lymphocytes depleted mice or severe combined immunodeficiency disease (SCID) mice can not develop liver injury after Con A injection, and pretreatment of mice with a monoclonal antibody which *in vivo* destroys Thy1.2 antigen-bearing T cells abrogated the susceptibility of these animals toward the hepatotoxicity induced by Con A^[10]. In the present study lymphocyte infiltration was observed in the portal area and around the central vein of damaged liver tissue. Biochemical and histological data showed that prior administration of bicyclol, a new anti-hepatitis drug has protective effect against Con A induced liver injury in mice. In order to elucidate how bicyclol exerts its protective effect against Con A induced liver injury, mice were pretreated with bicyclol. The results showed that bicyclol markedly decreased lymphocyte accumulation into liver.

Cytotoxic T lymphocytes play an important role in the pathogenesis of viral hepatitis by inducing hepatocyte apoptosis^[23,8]. In the study of Moriyama *et al.*^[24] transfer of HBV-specific cytotoxic T lymphocytes can mediate liver cell necrosis in the HBV transgenic murine. As viral hepatitis, hepatocytes apoptosis is a dominant feature of Con A induced hepatitis as measured by DNA fragmentation and morphological observation. The apoptosis cascade can be initiated by a ligand, which binds to its receptors on the cell surface. Ligands such as FasL and TNF- α play an important role in Con A induced hepatitis. Interaction of Fas and FasL is an important pathway that mediates the target cytolysis by cytotoxic T lymphocytes^[25]. In *gld/gld* mice, in which FasL is defective, the development of the disease is completely suppressed and in *lpr/lpr* mice, the suppression of Fas mRNA is incomplete, the hepatitis is partially suppressed. Antibody against Fas can block the development of hepatitis^[14]. When FasL binds to Fas, the receptor molecules trimerize, leading to clustering of death domains, activation of a series of caspases and the final apoptosis of liver cells^[26]. In chronic hepatitis B (CHB), the intensity of FasL mRNA showed a positive correlation with the histological activity and serum alanine aminotransferase level^[27]. Immunohistochemical study suggested that Fas antigen expression plays an important role in inflammation in the hepatitis C virus-infected liver^[28]. In our previous study, we found that bicyclol inhibited Con A induced DNA fragmentation^[29]. To further investigate the mechanism of bicyclol in protection against liver injury, we measured the expression of Fas/FasL in Con A-induced liver injury.

In our study, we found that both FasL and Fas mRNA expressions were up-regulated significantly after Con A injection. Bicyclol down-regulated the expression of FasL and Fas close to normal level. The results explained why bicyclol could inhibit apoptosis of hepatocytes in Con A hepatitis model in our previous experiment^[29]. It is known that Fas expression can be activated by IFN- γ to enhance apoptosis. Fas mRNA expression was reduced by 50% in the liver of IFN- $\gamma^{-/-}$ mice compared with that in IFN- $\gamma^{+/+}$ mice^[30]. Because IFN- γ can affect the expression of Fas, we further investigated the effect of bicyclol on IFN- γ mRNA expression. Our results indicated that bicyclol reduced the expression of IFN- γ mRNA by about 40% in the livers of Con A treated mice, which was associated with the inhibition of Fas.

TNF- α is another important ligand to induce hepatocyte apoptosis. Activated lymphocytes stimulated the macrophages to release TNF- α and the activated lymphocyte itself is the potential source of TNF- α ^[31]. This proinflammatory cytokine can produce a direct cytotoxic effect to transcription-inhibited hepatocytes *in vitro* when bound to TNF-R^[32]. In addition to

the effect on Fas/FasL pathway, bicyclol significantly inhibited the release of TNF- α . Con A significantly increased the release of serum TNF- α and mRNA expression in liver tissue. Bicyclol reduced the serum level of TNF- α by about 50%. It, however, showed a slight effect (10%) on the mRNA expression in liver. It seems that bicyclol inhibited TNF- α release mostly at posttranscriptional level, which needs further investigation.

In conclusion, bicyclol protects mice against Con A-induced liver injury through at least two mechanisms: down-regulation of the expression of Fas/FasL mRNA, and prevention of proinflammatory cytokine TNF- α release.

ACKNOWLEDGEMENTS

We thank Ms. Yong-Rong Zhang and Ms. Yan Liu from the Department of Pathology of our institute for their support in the examination of liver morphology by light microscopy. We also thank Ling-Hong Yu for her helpful advice and excellent technical assistance.

REFERENCES

- 1 **Liu J**, McIntosh H, Lin H. Chinese medicinal herbs for chronic hepatitis B: a systematic review. *Liver* 2001; **21**: 280-286
- 2 **Haria M**, Benfield P. Interferon-alpha-2a. A review of its pharmacological properties and therapeutic use in the management of viral hepatitis. *Drugs* 1995; **50**: 873-896
- 3 **Heathcote J**. Treatment of HBe antigen-positive chronic hepatitis B. *Semin Liver Dis* 2003; **23**: 69-80
- 4 **Liu GT**. The anti-virus and hepatoprotective effect of bicyclol and its mechanism of action. *Chin J New Drug Clin* 2001; **10**: 325-327
- 5 **Yao GB**, Ji YY, Wang QH, Zhou XQ, Xu DZ, Chen XY. A randomized double-blind controlled trial of bicyclol in treatment of chronic hepatitis B. *Chin J New Drug Clin* 2002; **21**: 457-461
- 6 **Suematsu T**, Matsumura T, Sato N, Miyamoto T, Ooka T, Kamada T, Abe H. Lipid peroxidation in alcoholic liver disease in humans. *Alcohol Clin Exp Res* 1981; **5**: 427-430
- 7 **Slater TF**. Necrogenic action of carbon tetrachloride in the rat: a speculative mechanism based on activation. *Nature* 1966; **209**: 36-40
- 8 **Chisari FV**. Cytotoxic T cells and viral hepatitis. *J Clin Invest* 1997; **99**: 1472-1477
- 9 **Jacobson Brown PM**, Neuman MG. Immunopathogenesis of hepatitis C viral infection: Th1/Th2 responses and the role of cytokines. *Clin Biochem* 2001; **34**: 167-171
- 10 **Tiegs G**, Hentschel J, Wendel A. A T cell-dependent experimental liver injury in mice. *J Clin Invest* 1992; **90**: 196-203
- 11 **Gantner F**, Leist M, Lohse AW, Germann PG, Tiegs G. Concanavalin A induced T-cell mediated hepatic injury in mice: the role of tumor necrosis factor. *Hepatology* 1995; **21**: 190-198
- 12 **Ksontini R**, Colagiovanni DB, Josephs MD, Edwards CK 3rd, Tannahill CL, Solorzano CC, Norman J, Denham W, Clare-Salzler M, MacKay SL, Moldawer LL. Disparate roles for TNF-alpha and Fas ligand in concanavalin A-induced hepatitis. *J Immunol* 1998; **160**: 4082-4089
- 13 **Zang GQ**, Zhou XQ, Yu H, Xie Q, Zhao GM, Wang B, Guo Q, Xiang YQ, Liao D. Effect of hepatocyte apoptosis induced by TNF-alpha on acute severe hepatitis in mouse models. *World J Gastroenterol* 2000; **6**: 688-692
- 14 **Tagawa Y**, Kakuta S, Iwakura Y. Involvement of Fas/Fas ligand system-mediated apoptosis in the development of concanavalin A-induced hepatitis. *Eur J Immunol* 1998; **28**: 4105-4113
- 15 **Mochida S**, Ohno A, Arai M, Tamatani T, Miyasaka M, Fujiwara K. Role of adhesion molecules in the development of massive hepatic necrosis in rats. *Hepatology* 1996; **23**: 320-328
- 16 **Chomczynski P**, Sacchi N. Single-step method of RNA isolation by acid guanidinium thiocyanate-phenol-chloroform extraction. *Anal Biochem* 1987; **162**: 156-159
- 17 **Koziel MJ**. The immunopathogenesis of HBV infection. *Antivir Ther* 1998; **3**: 13-24
- 18 **Chisari FV**, Ferrari C. Hepatitis B virus immunopathogenesis.

- Annu Rev Immunol* 1995; **13**: 29-60
- 19 **Koziel MJ**. Cytokines in viral hepatitis. *Semin Liver Dis* 1999; **19**: 157-169
- 20 **Dienes HP**, Hutteroth T, Hess G, Meuer SC. Immunoelectron microscopic observations on the inflammatory infiltrates and HLA antigens in hepatitis B and non-A, non-B. *Hepatology* 1987; **7**: 1317-1325
- 21 **Volpes R**, van den Oord JJ, Desmet VJ. Memory T cells represent the predominant lymphocyte subset in acute and chronic liver inflammation. *Hepatology* 1991; **13**: 826-829
- 22 **Tiegs G**, Gantner F. Immunotoxicology of T cell-dependent experimental liver injury. *Exp Toxicol Pathol* 1996; **48**: 471-476
- 23 **Koziel MJ**, Dudley D, Wong JT, Dienstag J, Houghton M, Ralston R, Walker BD. Intrahepatic cytotoxic T lymphocytes specific for hepatitis C virus in persons with chronic hepatitis. *J Immunol* 1992; **149**: 3339-3344
- 24 **Moriyama T**, Guilhot S, Klopchin K, Moss B, Pinkert CA, Palmiter RD, Brinster RL, Kanagawa O, Chisari FV. Immunobiology and pathogenesis of hepatocellular injury in hepatitis B virus transgenic mice. *Science* 1990; **248**: 361-364
- 25 **Kagi D**, Vignaux F, Ledermann B, Burki K, Depraetere V, Nagata S, Hengartner H, Golstein P. Fas and perforin pathways as major mechanisms of T cell-mediated cytotoxicity. *Science* 1994; **265**: 528-530
- 26 **Kaplowitz N**. Mechanisms of liver cell injury. *J Hepatol* 2000; **32**: 39-47
- 27 **Seino K**, Kayagaki N, Takeda K, Fukao K, Okumura K, Yagita H. Contribution of Fas ligand to T cell-mediated hepatic injury in mice. *Gastroenterology* 1997; **113**: 1315-1322
- 28 **Hiramatsu N**, Hayashi N, Katayama K, Mochizuki K, Kawanishi Y, Kasahara A, Fusamoto H, Kamada T. Immunohistochemical detection of Fas antigen in liver tissue of patients with chronic hepatitis C. *Hepatology* 1994; **19**: 1354-1359
- 29 **Zhao DM**, Liu GT. Protective effect of bicyclol on concanavalinA-induced liver nuclear DNA injury in mice. *Natl Med J China* 2001; **81**: 844-848
- 30 **Tagawa Y**, Sekikawa K, Iwakura Y. Suppression of concanavalin A-induced hepatitis in IFN- γ (-/-) mice, but not in TNF- α (-/-) mice: role for IFN- γ in activating apoptosis of hepatocytes. *J Immunol* 1997; **159**: 1418-1428
- 31 **Gantner F**, Leist M, Kusters S, Vogt K, Volk HD, Tiegs G. T cell stimulus-induced crosstalk between lymphocytes and liver macrophages results in augmented cytokine release. *Exp Cell Res* 1996; **229**: 137-146
- 32 **Leist M**, Gantner F, Jilg S, Wendel A. Activation of the 55 kDa TNF receptor is necessary and sufficient for TNF-induced liver failure, hepatocyte apoptosis, and nitrite release. *J Immunol* 1995; **154**: 1307-1316

Edited by Zhu LH and Wang XL Proofread by Xu FM

Expression of gonadotropin-releasing hormone receptor and effect of gonadotropin-releasing hormone analogue on proliferation of cultured gastric smooth muscle cells of rats

Lei Chen, Hong-Xuan He, Xu-De Sun, Jing Zhao, Li-Hong Liu, Wei-Quan Huang, Rong-Qing Zhang

Lei Chen, Hong-Xuan He, Rong-Qing Zhang, Department of Biological Science and Biotechnology, Tsinghua University, Beijing, 100084, China

Xu-De Sun, Department of Anaesthesiology, Tangdu Hospital, the Fourth Military Medical University, Xi'an, 710038, Shaanxi Province, China
Lei Chen, Jing Zhao, Li-Hong Liu, Wei-Quan Huang, Faculty of Basic Medicine, the Fourth Military Medical University, Xi'an, 710032, Shaanxi Province, China

Supported by the Natural Science Foundation of China, No. 39770388

Co-correspondents: Wei-Quan Huang

Correspondence to: Professor Rong-Qing Zhang, Institute of Marine Biotechnology, Department of Biological Science and Biotechnology, Tsinghua University, Beijing, 100084, China. rqzhang@mail.tsinghua.edu.cn

Telephone: +86-10-62772899 **Fax:** +86-10-62772899

Received: 2003-12-19 **Accepted:** 2004-02-01

Abstract

AIM: To investigate the expression of gonadotropin-releasing hormone (GnRH) receptor and the effects of GnRH analog (alarelin) on proliferation of cultured gastric smooth muscle cells (GSMC) of rats.

METHODS: Immunohistochemical ABC methods and *in situ* hybridization methods were used to detect protein and mRNA expression of GnRH receptor in GSMC, respectively. Techniques of cell culture, OD value of MTT test, measure of ³H-TdR incorporation, average fluorescent values of proliferating cell nuclear antigen (PCNA) and flow cytometric DNA analysis were used in the experiment.

RESULTS: The cultured GSMC of rats showed immunoreactivity for GnRH receptor; positive staining was located in cytoplasm. GnRH receptor mRNA hybridized signals were also detected in cytoplasm. When alarelin (10^{-9} , 10^{-7} , 10^{-5} mol/L) was administered into the medium and incubated for 24 h, OD value of MTT, ³H-TdR incorporation and average fluorescent values of PCNA all decreased significantly as compared with the control group ($P < 0.05$). The maximum inhibitory effect on cell proliferation was achieved a concentration of 10^{-5} mol/L and it acted in a dose-dependent manner. Flow cytometric DNA analysis revealed that alarelin could significantly enhance ratio of G₁ phase and decrease ratio of S phase of GSMC of rats ($P < 0.05$). The maximum inhibitory effect on ratio of S phase was at the concentration of 10^{-5} mol/L and also acted in a dose-dependent manner.

CONCLUSION: Our data suggest that GnRH receptor can be expressed by GSMC of rats. GnRH analogue can directly inhibit proliferation and DNA synthesis of rat GSMC through GnRH receptors.

Chen L, He HX, Sun XD, Zhao J, Liu LH, Huang WQ, Zhang RQ. Expression of gonadotropin-releasing hormone receptor and effect of gonadotropin-releasing hormone analogue on proliferation

of cultured gastric smooth muscle cells of rats. *World J Gastroenterol* 2004; 10(12): 1780-1784

<http://www.wjgnet.com/1007-9327/10/1780.asp>

INTRODUCTION

Gonadotropin releasing hormone (GnRH), a decapeptide synthesized by the neuroendocrine cells in the pro-optic area of brain, plays an important role in regulation of reproductive function. After released from the hypothalamus, GnRH binds to a specific receptor on the plasma membrane of the pituitary gonadotroph, resulting in stimulation of FSH and LH biosynthesis and release. There is evidence that GnRH and its receptors are expressed in numerous extrapituitary tissues, such as syncytiotrophoblast cells^[1], human granulosa-Luteal cells^[2], human peripheral lymphocytes^[3,4] and so on. They are not only expressed in normal tissues, but also widely exist in various carcinoma that derived from reproductive (ovary cancer^[5] and prostate cancer^[6]) or non-reproductive tissues (breast cancer^[7], lung cancer^[8], pancreas cancer^[9] and hepatocellular carcinoma^[10], *et al*). Our previous studies have shown the presence of GnRH and its receptor in rat digestive tract^[11], submaxillary gland^[12], thyroid gland^[13] and pancreas^[14] and proposed that GnRH could be classified as a kind of brain-gut hormone. Presently, we first investigated the expression of GnRH receptor in cultured rat gastric smooth muscle cells (GSMC) and investigate the effect of GnRH analogue (alarelin) on the proliferation of cultured GSMC of rats.

MATERIALS AND METHODS

Materials

GnRH anti-idiotypic antibody was prepared by our department^[15]. ABC kit was the product of Vector Company (Vector Laboratories Burlingame, CA, U.S.A.). MTT (3-(4, 5-dimethylthiazol-2-yl)-2, 5-diphenyltetrazolium), collagenase I, PPO (2, 5-diphenyloxazole) and POPOP (1, 4-bis (5-phenyloxazol-2-yl) benzene) were purchased from Sigma Company (Staint Louis, Missouri, U.S.A.). DMEM and Trypsin were the products of Gibco Company (Carlsbad, California, U.S.A.). Alarelin was purchased from Shanghai Lizhu Biochemical and Pharmaceutical Company, Shanghai, China. PCNA (Proliferating cell nuclear antigen) antibody and immunofluorescent kit were purchased from Boster Company (Wuhan, China). ³H-TdR was purchased from Academy of Atomic Energy Sciences of China (Shanghai, China). The 1-3-day-old male Sprague-Dawley rats were purchased from the Center of Laboratory Animal Medicine, the Fourth Military Medical University, (Xi'an, China).

Preparation and culture of GSMC of rats

The culture of GSMC of rats was performed as described previously with modifications^[16,17]. 1-3-day-old immature male Sprague-Dawley rats were sterilized by 750 mL/L alcohol; removed the stomachs and put them into cool Hanks solution (mmol/L: CaCl₂ 1.3, KCl 5.4, KH₂PO₄ 0.4, MgCl₂·6H₂O 0.4, MgSO₄·7H₂O 0.4, NaCl 137, glucose 5.6) immediately. The mucosas were

removed by scrapping with razorblade. The gastric smooth muscle tissues were minced into 1.0 mm³ pieces with tissue chopper, then put them into DMEM containing 1 mg/L collagenase I at 37 °C for 30-60 min, and the GSMCs were collected at an interval of 20 min. The cell suspension was centrifuged at 500 r/min for 5 min, washed 2 times in DMEM, then cultured in DMEM containing 100 mL/L calf serum, 100 U/mL penicillin G and 100 U/mL streptomycin under a humidified atmosphere of 50 mL/L CO₂ in air. To obtain pure GSMC and remove the fibroblasts, the cells were preattached in flasks with 10% calf serum under DMEM in a humidified atmosphere of 5% CO₂ or 90 min at 37 °C. Afterwards, the cells were maintained in fresh DMEM containing 100 mL/L calf serum and removed it per 3 d and subsequently subcultured per 4-5 d by treatment with trypsin (2.5 g/L). The GSMC were identified by "valley and hill appearance"^[17] and showed α -actin immunoreactivity, which was located in cytoplasm. The experiments were performed with monolayer of cells from passage 3-5.

Immunocytochemical procedure

The GSMCs (1×10⁵/mL) were seeded in a six-well plate containing the coverglasses inside. The cells of passage 3-5 were fixed in 4% paraformaldehyde solution for 30 min at room temperature. The coverglasses were washed 3 times with phosphate-buffered saline (PBS, pH 7.2), and put into methanol-H₂O₂ for 30 min to remove endogenous peroxidase activity. Then they were stained using immunohistochemical ABC method. They were incubated with first antibody, rabbit GnRH anti-idiotypic antibody (1:200 dilution) at 4 °C for 18-24 h. Then they were incubated with second antibody, biotin labeled goat anti-rabbit IgG antibody (1:400 dilution), at room temperature for 2 h, followed by incubation with ABC complex (1:400 dilution), at room temperature for 1 h. Finally, DAB (diaminobenzidine) was used for color developed, and then the slides were washed in distilled water to stop the reaction, dehydrated in alcohol, hyalinized in xylene, and mounted on Canada balsam. The first antibody was replaced by normal and diluted rabbit serum for the negative control.

In situ hybridization

The probe was produced according to the cDNA sequence of the rat's pituitary GnRH receptor^[12,18]. The sequence was: 5' - ATGTATGCCCCAGCCTTCATGATGGTGATTAGCC TGGATC-3'. The digoxigenin was labeled at 5' -end by the TaKaRa Biotechnology Company, (Dalian, China). The *in situ* hybridization was carried out on the coverglasses after the cells were fixed in 40 g/L paraformaldehyde containing 1 g/L DEPC (Diethyl pyrocarbonate) for 30 min. Then they were processed as follows: The coverglasses were rinsed in 0.01 mol/L PBS (pH 7.2) for 5 min×3, in Proteinase K (1 μ g/mL) for 2 min at 37 °C. They were post-fixed in 40 g/L paraformaldehyde for 5 min, washed in distilled water for 5 min×3. After being dried in the air, each coverglass was applied with the hybridization buffer containing GnRH receptor oligonucleotide probe (2.0 μ g/mL), and hybridization was carried out in sealed humid box at 42 °C for 20 h. After that the slides were washed with 2×SSC at 37 °C for 5 min×3, 0.1×SSC at 37 °C for 10 min×2, they were incubated with mouse-anti-dig antibody at room temperature for 2 h. Thereafter, the slides were washed with 0.5 mol/L TBS for 5 min×3, followed by incubation with biotin-labeled goat-anti-mouse IgG antibody for 1 h at 37 °C. The slides were washed with 0.5 mol/L TBS for 5 min×3 and incubated with SABC-AP for 30 min at 37 °C. The sections were rinsed in 0.5 mol/L TBS for 5 min×4, and the alkaline phosphatase reaction was conducted by incubation with complex solution of NBT (Nitro-blue tetrazolium) and BCIP (5-bromo-4-chloro -3-indo-lyl phosphate) for 20-30 min.

Finally, the slides were washed in distilled water to stop the reaction, and then dehydrated in alcohol, hyalinized in xylene, and mounted on Canada balsam. The slides were incubated with normal mouse serum instead of the mouse-anti-dig antibody in absence of the labeled probe for the negative controls.

MTT assay

The cells were trypsinized in a solution of 2.5 g/L trypsin and seeded in a 96-well plate at a density of 10⁴ cells/(0.1 mL/well). After the cells were grown for 24 h to approximately 800 g/L subconfluent state, 0.1 mL medium containing 2.5% calf serum and various concentrations (10⁻⁹, 10⁻⁷, 10⁻⁵ mol/L) of alarelin was added to each well, respectively, and incubated for 24 h in a CO₂ incubator. Each concentration was tested in at least 12 wells. The MTT assay was performed as described previously with modifications^[19]. Briefly, 15 μ L of MTT solution (5 g/L, PBS, pH 7.2) was added to each well and incubated for 4 h. Then, the medium and MTT were removed and 150 μ L of DMSO was added to each well and shaken for 10 min to dissolve the crystal. The OD was determined at 490 nm using an ELISA reader.

³H-TdR incorporation

To observe the role of GnRH analogue in growth regulation of GSMC, a ³H-TdR incorporation assay was performed as previously described^[20]. The cells were plated into a 96-well plate at a density of 10⁴ cells/(0.1 mL/well). After the cells were grown for 24 h, 0.1 mL medium containing 2.5% calf serum and various concentrations (10⁻⁹, 10⁻⁷, 10⁻⁵ mol/L) of alarelin was added to each well, respectively, and incubated for 16 h in a CO₂ incubator. Then the ³H-TdR (2 μ Ci/mL) was added to each well and continuously incubated for 8 h. Incubation was stopped by adding 1 vol of cold 100 mL/L trichloroacetic acid (TCA) which disrupted cells and precipitated the macromolecules. After being washed with a methanol, the precipitate was collected in 9999 fiberglass filter paper, respectively. When the filter paper was dried, 0.5 mL scintillant liquid were mixed and the radioactivity was estimated with a scintillation counter (Backman LS5801). Each concentration was tested in at least 6 wells.

Fluorescent immunocytochemical reaction of PCNA in GSMC

The cells were seeded in six-well plate containing the coverglasses inside. After the cells were grown for 24 h to approximately 800 g/L subconfluent state, 2 mL medium containing 25 mL/L calf serum and various concentrations (10⁻⁹, 10⁻⁷, 10⁻⁵ mol/L) of alarelin was added to each well, respectively, and incubated for another 24 h in a CO₂ incubator. Then the monolayers were fixed in 40 g/L paraformaldehyde solution for 30 min. The cell coverglasses were washed 3 times with PBS (pH 7.2), and then put into methanol-H₂O₂ for 30 min to remove endogenous peroxidase activity. Then PCNA immunofluorescence reaction was carried out according to the manufacturer's instructions. The coverglasses were incubated with the first antibody (mouse antibody, 1:200 dilution) at 4 °C overnight, followed by incubation with the second antibody, biotin labeled goat anti-rabbit IgG antibody (1:200 dilution), at room temperature for 2 h. Then the coverglasses were incubated with SABC-fluo Cy3 (1:100 dilution) at room temperature for 1 h. At last, the cells were detected by using the laser confocal microscopy, and scanned the average fluorescent values of PCNA of GSMC. For the negative controls, the first antibody was replaced by normal rabbit serum.

Cell-cycle analysis by flow cytometry

The cells were seeded in 12-well plate at a density of 10⁷ cells/(1.5 mL/well). After the cells were grown for 24 h to approximately 800 g/L subconfluent state, 2 mL medium containing 25 mL/L calf serum and various concentrations (10⁻⁹-10⁻⁵ mol/L) of alarelin was added to each well, respectively,

and incubated for another 48 h in a CO₂ incubator. Then the cells were trypsinized in a solution of 2.5 g/L trypsin, fixed in 700 mL/L ethanol and stained by PI (propidium iodide) for DNA analysis. The flow cytometric analyses were performed using EPICS Profile II. DNA content was measured and ratio of each DNA period of cell proliferation was analyzed.

Data analysis

In the proliferation study, the data were expressed as mean±SD. The data were analyzed by SPLM statistical software. $P<0.05$ was considered statistically significant.

RESULTS

Expression and localization of GnRH receptor

Immunocytochemical reaction showed a dark-brown staining in cytoplasm for GnRH receptor immunoreactivity; background was light yellow or no staining; positive cells were identified easily. The two negative controls showed no staining for GnRH receptor. All cultured GSMCs showed immunoreactivity for GnRH receptor in the cytoplasm, but with variations in degrees of intensity of the immunoreactivity (Figure 1).

In situ hybridization showed GnRH receptor mRNA hybridized signal was blue, and the background was not stained. The GnRH receptor mRNA hybridization signals could be detected in all cultured GSMCs, but with variation in signal strength between them. The signals were only distributed in the cytoplasm with hybridization negative nuclei (Figure 2). The two negative controls did not show GnRH receptor mRNA hybridized signal.

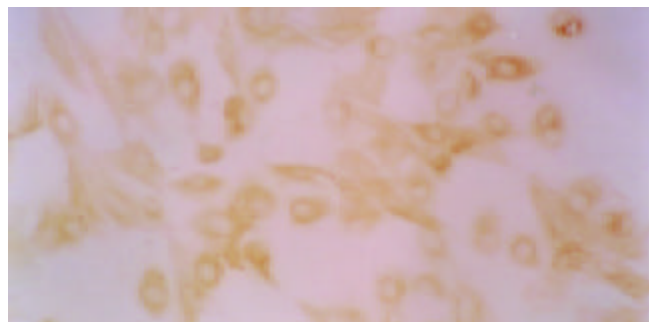


Figure 1 Gastric smooth muscle cells showed GnRH receptor immunoreactivity in cytoplasm. (×200).

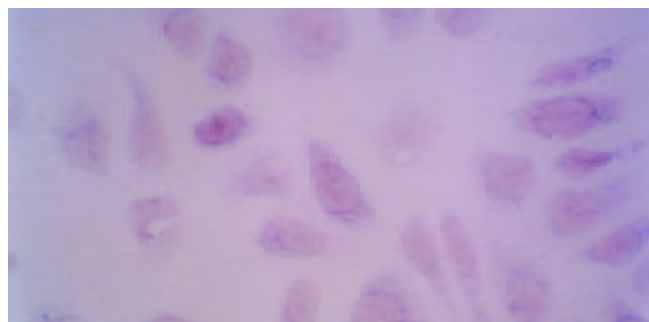


Figure 2 Gastric smooth muscle cells showed GnRH receptor mRNA hybridized signal in cytoplasm. (×400).

Effect of alarelin on GSMC viability

The influence of alarelin on GSMC viability was assessed using the MTT assay. The cell viability in the presence of alarelin was significantly lower than that in the absence of alarelin ($F=59.083$, $P<0.01$). The maximum stimulatory effect on cell viability was achieved at a concentration of 10⁻⁵ mol/L and it acted in a dose-dependent manner (Table 1).

Table 1 Effects of alarelin on A value of MTT of rat GSMC

Group	MTT/A value (n=12)
Control	0.728±0.100
10 ⁻⁹ mol/L alarelin	0.533±0.073
10 ⁻⁷ mol/L alarelin	0.368±0.029
10 ⁻⁵ mol/L alarelin	0.243±0.042

³H-TdR Incorporation assay

To evaluate the functional role of GnRH in GSMC, the cells were treated with different concentrations of alarelin and incubated for 16 h, and then ³H-TdR (2 μCi/mL) was added. After 8 h, ³H-TdR incorporation assays were performed. As shown in Table 2, alarelin inhibited the growth of GSMC in a dose-dependent manner. A significant inhibition of proliferation was detected in the different groups, and the antiproliferative effect was the most evident when the concentration of alarelin at 10⁻⁵ mol/L ($F=22.33$, $P<0.05$).

Table 2 Effects of alarelin on ³H-TdR Incorporation of rat GSMC

Group	³ H-TdR Incorporation (n=6)
Control	1 936.50±440.99
10 ⁻⁹ mol/L alarelin	1 448.17±327.72
10 ⁻⁷ mol/L alarelin	945.83±374.32
10 ⁻⁵ mol/L alarelin	385.83±184.66

The average fluorescent values of PCNA assay

The cells were treated with different concentrations of alarelin (10⁻⁹, 10⁻⁷, 10⁻⁵ mol/L) and incubated for another 24 h, and the average fluorescent values of PCNA assays were performed. As shown in Table 3, alarelin significantly inhibited the average fluorescent value in a dose-dependent manner compared with the control group ($F=15.86$, $P<0.01$).

Table 3 Effects of alarelin on average fluorescent values of PCNA in GSMC

Group	Average fluorescent values of PCNA (n=5)
Control	13.48±1.31
10 ⁻⁹ mol/L alarelin	11.37±1.99
10 ⁻⁷ mol/L alarelin	9.35±1.38
10 ⁻⁵ mol/L alarelin	7.37±1.06

Effects of alarelin on GSMC cell cycles

Table 4 showed the ratio of G₁ phase and S phase of DNA period of cell proliferation of each group. The ratio of G₁ phase of DNA in group II- VI were markedly higher than that of the control, but did not increase in a dose-dependent manner ($F=74.94$, $P<0.05$). Moreover, the ratio of S phase of DNA was significantly lower in group II-VI than that in the control and acted in a dose-dependent manner ($F=32.5$, $P<0.05$, except the Group III, V compared with their border groups).

Table 4 Effects of alarelin on GSMC cell cycles (n=4)

Group	Concentration of alarelin	G ₁ phase (%)	S phase (%)
Group I	Control	70.80±11.30	17.50±3.40
Group II	10 ⁻⁹ mol/L alarelin	80.00±9.42	9.93±1.73
Group III	10 ⁻⁸ mol/L alarelin	76.60±8.99	7.10±1.05
Group IV	10 ⁻⁷ mol/L alarelin	79.60±7.43	6.60±1.54
Group V	10 ⁻⁶ mol/L alarelin	78.50±10.66	5.10±1.01
Group VI	10 ⁻⁵ mol/L alarelin	80.20±10.03	3.20±1.20

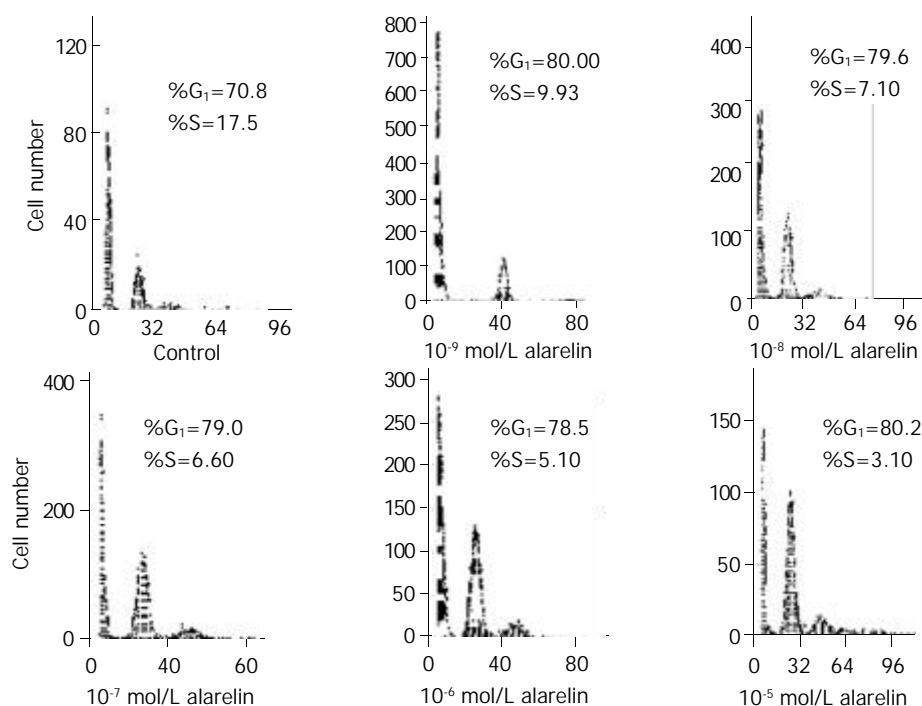


Figure 3 Effects of alarelin on DNA content of GSMCs cell cycles.

DISCUSSION

GnRH anti-idiotypic antibody has been widely applied in immunohistochemical studies of GnRH receptors^[11,12,21]. GnRH and its receptor mainly exist in hypothalamus-pituitary axis, and also expressed in extra-hypothalamically, and has extra-pituitary activity. Studies have reported that pancreatic islets have GnRH immunoreactivity^[14]. Jan *et al.*^[22] reported that GnRH was a possible transmitter in sympathetic ganglion in frog, and our previous studies^[4,5] revealed that both GnRH and GnRH receptor were all existed in digestive tract. Our present study revealed, for the first time, that GnRH receptor mRNA was expressed in cultured GSMC of rats. These findings have raised intriguing questions which concern the physiological function of GnRH and its receptor.

GnRH has been suggested to regulate cell growth and proliferation through its receptor in ex-pituitary tissues. GnRH analogues not only have been used and proven to be efficient in treating GnRH receptor-bearing tumors, including carcinomas of the ovary, breast, and endometrium^[23-25], but also inhibited the growth and proliferation of normal cell, such as granulosa cells and myometrial smooth muscle cells^[26,27]. MTT assays and ³H-TdR assays are considered to be the most reliable techniques for measurement of the cell population. Using MTT assays and ³H-TdR assays, we demonstrated that GnRH analogue inhibited growth of normal GSMC of rats in a dose-dependent manner. This inhibitory effect is consistent with the results of Minaretzis *et al.*^[26] in granulosa-lutein cells and Chegini *et al.*^[27] in myometrial smooth muscle cells. This inhibitory effect of GnRH analogue appears to be receptor-mediated and its exact mechanism of growth inhibitory effect at the receptor level is unclear.

To examine whether GnRH receptor (GnRHR) mediates direct antiproliferative effects, we attempted to assess the effects of alarelin on average fluorescent values of PCNA and cell cycle of GSMC. PCNA, a protein which functions as a cofactor to DNA polymerase delta, has many characteristics which make it an effective marker for evaluating cell proliferation, particularly in S phase^[28]. PCNA is a stable cell-cycle regulated nuclear protein, expressed differentially during the cell cycle^[29,30], and it is believed to reflect the different

stages of the cell cycles, which begins to increase in terminus of G₁, reaches at peak in S phase, and decreases in G₂ and M phases, and this is corresponded with the change of DNA content^[28]. In the present study, we found that alarelin inhibited the average fluorescent values of PCNA, and acted in a dose-dependent manner. These might cause by the binding of GnRH analogue with its receptor, which induced the activation of phosphatidylinositol kinase activity, known to stimulate mitogenic response in plasma membranes^[31]. By flow cytometry, we demonstrated the GnRH analogue improved the ratios of G₁/G₀ which did not act in a dose-dependent manner, and inhibited the ratios of S phase which acted in a dose-dependent manner. So, the reason of growth inhibition might be that GnRH analogue arrested at G₁/S phase, which inhibits DNA synthesis. These results are consistent with the results of MTT assay, ³H-TdR incorporation and fluorescent value of PCNA.

In summary, we have demonstrated for the first time that GnRH receptor is expressed in GSMC and GnRH analogue has a direct growth inhibitory effect on GSMC of rats that is mediated through GnRH receptor. Our findings strongly suggest that GnRH play an important role in digestive tract.

REFERENCES

- 1 **Currie WD**, Setoyama T, Lee PS, Baimbridge KG, Church J, Yuen BH, Leung PC. Cytosolic free Ca²⁺ in human syncytiotrophoblast cells increased by gonadotropin-releasing hormone. *Endocrinology* 1993; **133**: 2220-2226
- 2 **Nathwani PS**, Kang SK, Cheng KW, Choi KC, Leung PC. Regulation of gonadotropin-releasing hormone and its receptor gene expression by 17beta-estradiol in cultured human granulosa-Luteal cells. *Endocrinology* 2000; **141**: 1754-1763
- 3 **Azad N**, La Paglia N, Jurgens KA, Kirsteins L, Emanuele NV, Kelley MR, Lawrence AM, Mohaghehpour N. Immunoactivation enhances the concentration of luteinizing hormone-releasing hormone peptide and its gene expression in human peripheral T-lymphocytes. *Endocrinology* 1993; **133**: 215-223
- 4 **Weesner GD**, Becker BA, Matteri RL. Expression of luteinizing hormone-releasing hormone and its receptor in porcine immune tissues. *Life Sci* 1997; **61**: 1643-1649
- 5 **Furui T**, Imai A, Tamaya T. Intratumoral level of gonadotropin-releasing hormone in ovarian and endometrial cancers. *Oncol Rep*

- 2002; **9**: 349-352
- 6 **Leuschner C**, Enright FM, Gawronska-Kozak B, Hansel W. Human prostate cancer cells and xenografts are targeted and destroyed through luteinizing hormone releasing hormone receptors. *Prostate* 2003; **56**: 239-249
- 7 **Chen A**, Kaganovsky E, Rahimipour S, Ben-Aroya N, Okon E, Koch Y. Two forms of gonadotropin-releasing hormone (GnRH) are expressed in human breast tissue and overexpressed in breast cancer: a putative mechanism for the antiproliferative effect of GnRH by down-regulation of acidic ribosomal phosphoproteins P1 and P2. *Cancer Res* 2002; **62**: 1036-1044
- 8 **Nechushtan A**, Yarkoni S, Marianovsky I, Lorberboum-Galski H. Adenocarcinoma cells are targeted by the new GnRH-PE66 chimeric toxin through specific gonadotropin-releasing hormone binding sites. *J Biol Chem* 1997; **272**: 11597-11603
- 9 **Wang L**, Xie LP, Zhang RQ. Gene expression of gonadotropin-releasing hormone and its receptor in rat pancreatic cancer cell lines. *Endocrine* 2001; **14**: 325-328
- 10 **Yin H**, Cheng KW, Hwa HL, Peng C, Auersperg N, Leung PC. Expression of the messenger RNA for gonadotropin-releasing hormone and its receptor in human cancer cell lines. *Life Sci* 1998; **62**: 2015-2023
- 11 **Huang W**, Yao B, Sun L, Pu R, Wang L, Zhang R. Immunohistochemical and *in situ* hybridization studies of gonadotropin releasing hormone (GnRH) and its receptor in rat digestive tract. *Life Sci* 2001; **68**: 1727-1734
- 12 **Yao B**, Huang W, Huang Y, Chui Y, Wang Y, Li H, Pu R, Wan L, Zhang R. A study on the localization and distribution of GnRH and its receptor in rat submaxillary glands by immunohistochemical, *in situ* hybridization and RT-PCR. *Life Sci* 2003; **72**: 2895-2904
- 13 **Zhou J**, Huang WQ, Ji QH. The expression of gonadotropin-releasing hormone and its receptor in human thyroid gland. *Acta Anatomica Sinica* 2002; **33**: 511-515
- 14 **Wang L**, Xie LP, Huang WQ, Yao B, Pu RL, Zhang RQ. Presence of gonadotropin-releasing hormone (GnRH) and its mRNA in rat pancreas. *Mol Cell Endocrinol* 2001; **172**: 185-191
- 15 **Huang WQ**, Sun L, Zhong CL. Preparation and identification of GnRH anti-idiotypic antibody. *Chin J Anatom* 1994; **17**(Suppl): 353-356
- 16 **Fatigati V**, Murphy RA. Actin and tropomyosin variants in smooth muscles. Dependence on tissue type. *J Biol Chem* 1984; **259**: 14383-14388
- 17 **Chamley-Campbell J**, Campbell GR, Ross R. The smooth muscle cell in culture. *Physiol Rev* 1979; **59**: 1-61
- 18 **Kaiser UB**, Zhao D, Cardona GR, Chin WW. Isolation and characterization of cDNAs encoding the rat pituitary gonadotropin-releasing hormone receptor. *Biochem Biophys Res Commun* 1992; **189**: 1645-1652
- 19 **Chiba K**, Kawakami K, Tohyama K. Simultaneous evaluation of cell viability by neutral red, MTT and crystal violet staining assays of the same cells. *Toxicol In Vitro* 1998; **12**: 251-258
- 20 **Kang SK**, Choi KC, Cheng KW, Nathwani PS, Auersperg N, Leung PC. Role of gonadotropin-releasing hormone as an autocrine growth factor in human ovarian surface epithelium. *Endocrinology* 2000; **141**: 72-80
- 21 **Ji QH**, Huang WQ, Sun L, Zhao BQ. Double-labeling immunohistochemical location of glucagon, gonadorelin (GnRH) and GnRH receptor within pancreas of the guinea pig. *J Fourth Milit Med Univ* 1998; **19**: 34-36
- 22 **Jan YN**, Jan LY, Kuffler SW. A peptide as a possible transmitter in sympathetic ganglia of the frog. *Proc Natl Acad Sci U S A* 1979; **76**: 1501-1505
- 23 **Grundker C**, Emons G. Role of gonadotropin-releasing hormone (GnRH) in ovarian cancer. *Reprod Biol Endocrinol* 2003; **1**: 65
- 24 **Sayer HG**, Hoffken K. Hormone therapy, chemotherapy and immunotherapy in breast carcinoma. The best strategy for your patient. *MMW Fortschr Med* 2003; **145**: 40-42
- 25 **Krauss T**, Huschmand H, Hinney B, Viereck V, Emons G. Hormonal therapy and chemotherapy of endometrial cancer. *Zentralbl Gynakol* 2002; **124**: 45-50
- 26 **Minaretzis D**, Jakubowski M, Mortola JF, Pavlou SN. Gonadotropin-releasing hormone receptor gene expression in human ovary and granulosa-lutein cells. *J Clin Endocrinol Metab* 1995; **80**: 430-434
- 27 **Chegini N**, Rong H, Dou Q, Kipersztok S, Williams RS. Gonadotropin-releasing hormone (GnRH) and GnRH receptor gene expression in human myometrium and leiomyomata and the direct action of GnRH analogs on myometrial smooth muscle cells and interaction with ovarian steroids *in vitro*. *J Clin Endocrinol Metab* 1996; **81**: 3215-3221
- 28 **Galand P**, Del Bino G, Morret M, Capel P, Degraef C, Fokan D, Feremans W. PCNA immunopositivity index as a substitute to 3H-thymidine pulse-labeling index (TLI) in methanol-fixed human lymphocytes. *Leukemia* 1995; **9**: 1075-1084
- 29 **Kurki P**, Vanderlaan M, Dolbeare F, Gray J, Tan EM. Expression of proliferating cell nuclear antigen (PCNA)/ cyclin during the cell cycle. *Exp Cell Res* 1986; **166**: 209-219
- 30 **Mathews MB**, Bernstein RM, Franza BR Jr, Garrels JL. Identity of the proliferating cell nuclear antigen and cyclin. *Nature* 1984; **309**: 374-376
- 31 **Takagi H**, Imai A, Furui T, Horibe S, Fuseya T, Tamaya T. Evidence for tight coupling of gonadotropin-releasing hormone receptors to phosphatidylinositol kinase in plasma membrane from ovarian carcinomas. *Gynecol Oncol* 1995; **58**: 110-115

Evaluation of the viability and energy metabolism of canine pancreas graft subjected to significant warm ischemia damage during preservation by UW solution cold storage method

Chun-Hui Yuan, Gui-Chen Li, He Zhang, Ying Cheng, Ning Zhao, Yong-Feng Liu

Chun-Hui Yuan, Gui-Chen Li, He Zhang, Ying Cheng, Ning Zhao, Yong-Feng Liu, Department of Organ Transplantation, The First Affiliated Hospital of China Medical University, Shenyang 110001, Liaoning Province, China

Supported by a fund of Liaoning Province key Project, No.0025001
Correspondence to: Dr. Chun-Hui Yuan, Department of Organ Transplantation, The First Affiliated Hospital of China Medical University, Shenyang 110001, Liaoning Province, China. ychdoctor@hotmail.com

Telephone: +86-24-23256666 **Fax:** +86-24-23265284

Received: 2003-06-05 **Accepted:** 2003-11-06

Abstract

AIM: To evaluate the viability and energy metabolism of long warm ischemically damaged pancreas during preservation by the UW solution cold storage method.

METHODS: The pancreas grafts subjected to 30-120 min warm ischemia were preserved by the UW solution cold storage method for 24 h. The tissue concentrations of adenine nucleotides (AN) and adenosine triphosphate (ATP) and total adenine nucleotides (TAN) were determined by using high performance liquid chromatography (HPLC) and the viability of the pancreas graft was tested in the canine model of segmental pancreas autotransplantation.

RESULTS: The functional success rates of pancreas grafts of groups after 30 min, 60 min, 90 min, 120 min of warm ischemia were 100%, 100%, 67.7%, 0%, respectively. There was an excellent correlation between the posttransplant viability and tissue concentration of ATP and TAN at the end of preservation.

CONCLUSION: The UW solution cold storage method was effective for functional recovery of the pancreas suffering 60-min warm ischemia. The tissue concentration of ATP and TAN at the end of 24 h preservation by the UW solution cold storage method would predict the posttransplant outcome of pancreas graft subjected to significant warm ischemia.

Yuan CH, Li GC, Zhang H, Cheng Y, Zhao N, Liu YF. Evaluation of the viability and energy metabolism of canine pancreas graft subjected to significant warm ischemia damage during preservation by UW solution cold storage method. *World J Gastroenterol* 2004; 10(12): 1785-1788
<http://www.wjgnet.com/1007-9327/10/1785.asp>

INTRODUCTION

Preservation is necessary if organs for transplantation are removed from donors prior to preparation of the recipient^[1-3]. The methods used for preservation of pancreas grafts for experimental transplantation have produced variable results^[4,5].

As warm ischemic injury of pancreas graft before and during procurement strongly influences the results of pancreas transplantation, it is important to predict the viability of the ischemically damaged pancreas graft before transplantation^[6,7]. Recently we preserved the segmental pancreas in the UW solution after 30-120 min, and our experimental model was heterotopic segmental (left limb) pancreas autotransplantation in totally pancreatectomized dogs, and demonstrated that the UW solution cold storage method was effective for functional recovery of the pancreas suffering 60-min warm ischemia^[8]. There are some qualitative differences between warm and cold ischemic injuries^[9-12]. In this study we examined the viability and energy metabolism of the pancreas graft after significant warm ischemia and cold storage, and found tissue concentrations of ATP and TAN after preservation by the UW solution cold storage method were excellent markers to predict the posttransplant outcome^[13,14].

MATERIALS AND METHODS

Animals

Mongrel dogs of both sexes, weighing 10-15 kg were used for the experiments. UW solution was from China Pharmaceutical Corporation Guangzhou Branch. Chemicals were from Sigma Co.Ltd.

Operative procedures are as follows. Anesthesia was induced and maintained with sodium pentobarbiturate (25 mg/kg). The pancreas was exposed through a midline abdominal incision, and the left limb (tail) was removed with the splenic vessels in preparation for grafting, followed by splenectomy. The segmental pancreas graft was unflushed and left *in situ* for 30-120 min. After warm ischemia the pancreas was flushed with 30-50 mL heparinized cold UW solution (10 000 units/L heparin) and preserved in 50 mL heparinized cold UW solution for 24 h. A splenectomy was performed. The remainder of the pancreas was excised at the time of transplantation. The pancreatic tail was autotransplanted heterotopically, immediately or after preservation, with anastomosis of the splenic vessels to iliac vessels. A proper delicate tube was inserted into the pancreatic duct to drain the pancreatic juice. After operation, the dogs received saline with 100 g/L glucose (30 mL/kg) and 3.2 Mu penicillin for 3-5 days, then standard kennel diets were given.

Experimental protocol

There were two groups of control dogs: group 1, sham-operated group, abdomen was only opened and closed; group 2, no warm ischemia, pancreatic tail was flushed and preserved immediately after being harvested. The experimental group (group 3) was divided into 4 subgroups according to the warm ischemia time: group 3a, 30 min warm ischemia; group 3b, 60 min warm ischemia; group 3c, 90 min warm ischemia; group 3d, 120 min warm ischemia.

Functional studies

Blood glucose concentration was determined daily during the first postoperative week after autotransplantation. An

intravenous glucose tolerance test (IVGTT) was performed one week after transplantation. Glucose, 0.5 g/kg, was administered as a bolus and blood samples were collected serially over a 2-h period for plasma glucose. IVGTT K values were calculated from the plasma glucose levels at the end of 5 to 60 min^[15]. Maintenance of normoglycemia for at least five days after transplantation or a key value of IVGTT more than 1.0 one week after transplantation was considered a functional success of pancreas graft. The plasma insulin levels in splenic and peripheral vein one hour after transplantation were examined. The pancreatic juice was collected every day and amylase in the pancreatic juice of the first and the seventh days were determined.

Tissue extraction method for adenine nucleotides: After preservation, a part of pancreas was rapidly frozen in liquid nitrogen, lyophilized overnight, and kept at -80 °C until analysis. The dry tissue powder was weighed (200 mg) and homogenized in 3 mL of ice cold 0.5 mol/L perchloric acid. The precipitated protein was removed by centrifugation, and 500 µL of supernatant was neutralized by the additions of 50 µL 1 mol/L KOH and 50 µL Tris. Following centrifugation, 10 µL of supernatant was injected into HPLC for analysis.

Measurement of adenine nucleotides

High-performance liquid chromatography (HPLC, Waters, 510 Pump, 486 Detector) was performed on a reverse-phase column of Shim-pack, CLC-ODS (15 cm×3.96 mm, 4 µm) which was equilibrated with 100 mmol/L sodium phosphate buffer (pH 6.0) according to the method of Wynants *et al.*

TAN was calculated as the sum of ATP, adenosine diphosphate (ADP) and adenosine monophosphate (AMP).

Histological studies

Biopsies of the pancreas grafts were taken after cold preservation and one hour after transplantation. For light microscopy, the tissues were fixed in 100 ml/L formalin and stained with hematoxylin and eosin. For electron microscopic studies the tissues were prefixed in 25 g/L glutaraldehyde, postfixated in 25 g/L osmium tetroxide, sectioned at 1 µm, and stained with uranyl acetate and lead citrate.

Statistical analysis

All data were expressed as mean±SD. *F* test was used to compare values of different groups, χ^2 test for comparison of viability. A value of *P*<0.05 was considered statistically significant.

RESULTS

Graft function

Pancreatic graft endocrine function Plasma glucose and IVGTT K values in groups 1, 2, 3a and 3b recovered to normal 2-3 days after transplantation, while groups 3c and 3d did not one week after transplantation (Table 1). The plasma insulin levels in splenic and peripheral veins in groups 1, 2, 3a, and 3b were much higher than those in groups 3c, and 3d (*P*<0.05, Table 2).

Pancreatic graft exocrine function The pancreatic juice flow over the pancreatic duct 30 min after transplantation increased gradually and came to a climax on the fourth day after transplantation, and then declined gradually. The daily amounts of pancreatic juice of groups 1, 2, 3a and 3b were much more than those of groups 3c and 3d (*P*<0.05). The amylase activities in the pancreatic juice of the first and seventh days in groups 1, 2, 3a and 3b were much more than those in groups 3c and 3d (*P*<0.05, Tables 2, 3)

Tissue ATP, ADP, AMP and TAN after preservation The tissue concentrations of ATP, ADP, AMP and TAN after 24-hour preservation in groups 1, 2, 3a and 3b were much higher than those in groups 3c and 3d (*P*<0.05, Table 4).

Viability of canine pancreas autografts after preservation After significant warm and cold preservation, the functional success rates of groups 2, 3a, 3b, 3c and 3d were 5/5(100%), 6/6(100%), 6/6(100%), 4/6(66.7%) and 0/4(0%), respectively (Table 3). The UW cold preservation method was effective for functional recovery of the pancreas after 30 to 60-min warm ischemia (Table 3).

Relationship between posttransplantation viability and tissue ATP and TAN There was no overlap between the lowest ATP in the viable grafts and highest ATP in the nonviable grafts. If ATP level of 4.0 µmol/g dry weight was determined as a critical

Table 1 Plasma glucose and IVGTT K value at the first week after transplantation and plasma insulin level in splenic and peripheral vein one hour after transplantation (mean±SD)

Group	<i>n</i>	Plasma glucose (mol/L)	IVGTT K value	In splenic vein (mmol/L)	In peripheral vein (mmol/L)
1	3	5.6±0.9 ¹⁵	1.78±0.17 ²⁵	53.4±7.1 ³⁵	8.6±1.3 ⁴⁵
2	5	6.6±0.9	1.58±0.15	51.3±8.2	8.1±1.2
3a	6	6.7±1.1	1.45±0.12	50.6±7.6	7.5±1.1
3b	6	6.8±0.8	1.42±0.18	47.8±7.6	7.5±0.8
3c	6	11.9±1.3	0.87±0.16	35.0±5.2	3.2±0.7
3d	4	12.9±1.8	0.60±0.13	31.4±8.1	2.7±0.5

¹*F*=36.9, *P*<0.05; ²*F*=32.9, *P*<0.05; ³*F*=7.38, *P*<0.05; ⁴*F*=38.2, *P*<0.05; ⁵SNK test: between group 1, 2, 3a, 3b, *P*>0.05; between group 3c, 3d, *P*>0.05.

Table 2 Pancreatic juice flow during the first week after transplantation (mean±SD, mL)

Group	<i>n</i>	Pancreatic juice flow/d						
		1	2	3	4	5	6	7
2	5	27±7 ¹⁸	70±11 ²⁸	221±17 ³⁹	294±37 ⁴⁹	136±26 ⁵⁹	81±21 ⁶⁹	48±14 ⁷⁹
3a	6	24±7	74±17	216±36	285±36	138±24	91±19	53±15
3b	6	24±8	63±15	204±33	287±43	142±4	87±22	41±8
3c	6	12±4	20±6	68±19	69±19	83±18	54±12	30±7
3d	4	7±3	15±8	12±6	16±6	8±3	12±5	10±4

¹*F*=9.87, *P*<0.05; ²*F*=25.9, *P*<0.05; ³*F*=67.4, *P*<0.05; ⁴*F*=88.2, *P*<0.05; ⁵*F*=45.2, *P*<0.05; ⁶*F*=15.9, *P*<0.01; ⁷*F*=13.2, *P*<0.01; ⁸SNK test: between group 2, 3a, 3b, *P*>0.05; between group 3c, 3d, *P*>0.05; ⁹SNK test: between group 2, 3a, 3b, *P*>0.05.

value for the viability following transplantation, the specificity, sensitivity, predictive value and efficacy were all 100%. And there was also no overlap between the lowest TAN in the viable grafts and highest TAN in the nonviable grafts. If TAN level of 7.0 $\mu\text{mol/g}$ dry weight was determined as a critical value for the viability following transplantation, specificity, sensitivity, predictive value and efficacy were all 100%. Both ATP and TAN were reliable markers for determining the transplantation.

Table 3 Amylase in pancreatic juice of the first and the seventh day and viability after significant warm and cold preservation (mean \pm SD)

Group	n	Amylase ($\mu\text{kat/L}$)		Functioning grafts/rate(%)
		The first day	The seventh day	
2	5	182 \pm 45 ¹³	359 \pm 27 ²⁴	5/(100)
3a	6	183 \pm 48	355 \pm 37	6/(100)
3b	6	180 \pm 42	327 \pm 37	6/100)
3c	6	83 \pm 24	29 \pm 11	4/(66.7) ⁵
3d	4	77 \pm 30	28 \pm 10	0/(0) ⁵

¹F=10.3, $P<0.05$; ²F=205.5, $P<0.05$; ³SNK test: between group 2, 3a, 3b, $P>0.05$; ⁴SNK test: between group 2, 3a, 3b, $P>0.05$; between group 3c, 3d, $P>0.05$. ⁵compare with Group 2, $P<0.05$.

Table 4 Tissue concentration of ATP, ADP, AMP and TAN (mean \pm SD, $\mu\text{mol/L}$)

	ATP	ADP	AMP	TAN
Group 1 (n=3)	7.26 \pm 0.55 ¹³	3.33 \pm 0.20	1.49 \pm 0.34	11.43 \pm 1.37 ²³
Group 2 (n=5)	5.86 \pm 0.52	1.01 \pm 0.21	1.51 \pm 0.26	7.93 \pm 1.30
Group 3a (n=6)	5.28 \pm 0.37	1.31 \pm 0.35	1.55 \pm 0.35	8.02 \pm 0.78
Group 3b (n=6)	4.74 \pm 0.41	2.01 \pm 0.31	1.04 \pm 0.24	7.36 \pm 0.78
Group 3c (n=6)	2.18 \pm 0.21	0.83 \pm 0.19	0.81 \pm 0.23	4.04 \pm 0.51
Group 3d (n=4)	2.11 \pm 0.17	0.86 \pm 0.21	1.04 \pm 0.25	3.33 \pm 0.27

¹F=17.0, $P<0.05$; ²F=23.9, $P<0.05$; ³SNK test: between group 2, 3a, 3b, $P>0.05$.

Histologic studies

Under light microscope, the pancreas in groups 1 and 2 stored for 24 h showed normal architecture. After 24 h, preservation vacuolization of the acinar cells and interstitial edema were seen in grafts of groups 3a and 3b, and only mild edema of the islets was evident. Grafts of groups 3c and 3d showed severe edema, and after revascularization there was hemorrhage in the interstitial space.

Under electron microscope, the pancreas in groups 1 and 2 stored for 24 h showed well preserved cells. In grafts of groups 3a and 3b, acinar cells showed no nuclear changes, but rough endoplasmic reticulum (RER) cisternae were dilated. In grafts of groups 3c and 3d, irreversible cell damage was seen in most, but not all, specimens.

DISCUSSION

Pancreas graft injury due to warm ischemia strongly affects the posttransplant outcome^{16,17}. Therefore, resuscitation of an ischemically damaged pancreas is essential to enlarge the donor pool using the pancreas graft from the cardiac arrest donor¹⁸. We have demonstrated that canine pancreases subjected to 60 min of warm ischemia can be resuscitated during preservation by the UW solution preservation method at 4 °C for 24 h.

Restoration of cellular function of the pancreas graft subjected to significant warm ischemia by the UW solution cold preservation method will make it possible to use pancreas

grafts from cadaver with cardiac arrest^{19,20}, wait safely for the excision of the pancreas and enlarge the donor pool. Cerra^{21,22} reported that the canine pancreatic allografts tolerated warm ischemia up to one hour. Florack *et al.*^{23,24} demonstrated that the canine pancreatic autografts tolerated warm ischemia up to 60 min.

On the other hand, the assessment of a pancreas graft viability before transplantation is very important to prevent transplantation of a nonfunctioning allograft especially after significant warm ischemia because there is progressive depletion of ANs during warm ischemia²⁵, ultimately leading to ischemic damage. But the relationship between the tissue concentration of ANs before transplantation and organ viability after transplantation is controversial^{26,27}. In human liver preservation, Lanir *et al.*^{28,29} demonstrated a direct correlation between a high ATP concentration and good posttransplant outcome. On the contrary, correlation between the ATP level at the end of cold preservation and viability following transplantation was not proved in the rat liver^{30,31}.

We have also demonstrated that correlation between high ATP tissue concentration, which is necessary to maintain cellular integrity, and good posttransplant outcome of a canine pancreas graft after preservation by the UW solution cold preservation method^{32,33}. It is suggested that tissue concentration of ATP and TAN at the end of 24-h preservation by the UW solution cold preservation method will predict the posttransplant outcome of pancreas graft subjected to significant warm ischemia^{34,35}. But the mechanism responsible for the effectiveness of the UW solution cold preservation method in restoration of function of the pancreas graft subjected to significant warm ischemia remains unclear and is under investigation³⁵⁻³⁸.

We conclude that the tissue concentration of ATP and TAN at the end of 24-h preservation by the UW solution cold storage method will predict the posttransplant outcome of pancreas graft subjected to significant warm ischemia.

REFERENCES

- 1 **Pi F**, Badosa F, Sola A, Rosello Catafau J, Xaus C, Prats N, Gelpi E, Hotter G. Effects of adenosine on ischaemia-reperfusion injury associated with rat pancreas transplantation. *Br J Surg* 2001; **88**: 1366-1375
- 2 **Uhlmann D**, Armann B, Ludwig S, Escher E, Pietsch UC, Tannapfel A, Teupser D, Hauss J, Witzigmann H. Comparison of Celsior and UW solution in experimental pancreas preservation. *J Surg Res* 2002; **105**: 173-180
- 3 **Wakai A**. Effect of adenosine on ischaemia-reperfusion injury associated with rat pancreas transplantation. *Br J Surg* 2002; **89**: 494
- 4 **Thayer SP**, Fernandez-del Castillo C, Balcom JH, Warshaw AL. Complete dorsal pancreatectomy with preservation of the ventral pancreas: a new surgical technique. *Surgery* 2002; **131**: 577-580
- 5 **Fujita H**, Kuroda Y, Saitoh Y. The mechanism of action of the two-layer cold storage method in canine pancreas preservation—protection of pancreatic microvascular endothelium. *Kobe J Med Sci* 1995; **41**: 47-61
- 6 **Matsumoto S**, Kandaswamy R, Sutherland DE, Hassoun AA, Hiraoka K, Sageshima J, Shibata S, Tanioka Y, Kuroda Y. Clinical application of the two-layer (University of Wisconsin solution/perfluorochemical plus O₂) method of pancreas preservation before transplantation. *Transplantation* 2000; **70**: 771-774
- 7 **Sun B**, Jiang HC, Piao DX, Qiao HQ, Zhang L. Effects of cold preservation and warm reperfusion on rat fatty liver. *World J Gastroenterol* 2000; **6**: 271-274
- 8 **Kuroda Y**, Tanioka Y, Matsumoto S, Hiraoka K, Morita A, Fujino Y, Suzuki Y, Ku Y, Saitoh Y. Difference in energy metabolism between fresh and warm ischemic canine pancreases during preservation by the two-layer method. *Transpl Int* 1994; **7**(Suppl 1): S441-445

- 9 **Randhawa P**. Allograft biopsies in management of pancreas transplant recipients. *J Postgrad Med* 2002; **48**: 56-63
- 10 **Kim Y**, Kuroda Y, Tanioka Y, Matsumoto S, Fujita H, Sakai T, Hamano M, Suzuki Y, Ku Y, Saitoh Y. Recovery of pancreatic tissue perfusion and ATP tissue level after reperfusion in canine pancreas grafts preserved by the two-layer method. *Pancreas* 1997; **14**: 285-289
- 11 **Matsumoto S**, Kuroda Y, Fujita H, Tanioka Y, Sakai T, Hamano M, Kim Y, Suzuki Y, Ku Y, Saitoh Y. Extending the margin of safety of preservation period for resuscitation of ischemically damaged pancreas during preservation using the two-layer (University of Wisconsin solution/perfluorochemical) method at 20 degrees C with thromboxane A2 synthesis inhibitor OKY046. *Transplantation* 1996; **62**: 879-883
- 12 **Obermaier R**, Benz S, Kortmann B, Benthues A, Ansoerge N, Hopt UT. Ischemia/reperfusion-induced pancreatitis in rats: a new model of complete normothermic *in situ* ischemia of a pancreatic tail-segment. *Clin Exp Med* 2001; **1**: 51-59
- 13 **Matsumoto S**, Kuroda Y, Fujita H, Tanioka Y, Kim Y, Sakai T, Hamano M, Suzuki Y, Ku Y, Saitoh Y. Resuscitation of ischemically damaged pancreas by the two-layer (University of Wisconsin solution/perfluorochemical) mild hypothermic storage method. *World J Surg* 1996; **20**: 1030-1034
- 14 **Tanioka Y**, Kuroda Y, Kim Y, Matsumoto S, Suzuki Y, Ku Y, Fujita H, Saitoh Y. The effect of ouabain (inhibitor of an ATP-dependent Na⁺/K⁺ pump) on the pancreas graft during preservation by the two-layer method. *Transplantation* 1996; **62**: 1730-1734
- 15 **Moorhouse JA**, Granhame GR, Rosen NJ. Relationship between intravenous glucose tolerance and the fasting blood glucose level in healthy and diabetic subjects. *J Clin Endocrinol Metab* 1964; **24**: 145-159
- 16 **Troisi R**, Meester D, Regaert B, van den Broecke C, Cuvelier C, Hesse UJ. Tolerance of the porcine pancreas to warm and cold ischemia: comparison between University of Wisconsin and histidine-tryptophan-ketoglutarate solution. *Transplant Proc* 2002; **34**: 820-822
- 17 **Fujino Y**, Suzuki Y, Tsujimura T, Takahashi T, Tanioka Y, Tominaga M, Ku Y, Kuroda Y. Possible role of heat shock protein 60 in reducing ischemic-reperfusion injury in canine pancreas grafts after preservation by the two-layer method. *Pancreas* 2001; **23**: 393-398
- 18 **Ludwig S**, Armann B, Escher E, Gabel G, Teupser D, Tannapfel A, Pietsch UC, Hauss J, Witzigmann H, Uhlmann D. Pathomorphologic and microcirculatory changes and endothelin-1 expression in UW-and Celsior-preserved pancreata in experimental pancreas transplantation. *Transplant Proc* 2002; **34**: 2364-2365
- 19 **Lakey JR**, Kneteman NM, Rajotte RV, Wu DC, Bigam D, Shapiro AM. Effect of core pancreas temperature during cadaveric procurement on human islet isolation and functional viability. *Transplantation* 2002; **73**: 1106-1110
- 20 **Nagami H**, Tamura K, Kin S, Teramoto M, Ishida T. Beneficial effect of thromboxane A2 synthetase inhibitor (OKY-046) on 24-hr simple hypothermic preservation of the canine pancreas graft. *Int Surg* 1995; **80**: 274-277
- 21 **Cerra FB**, Adams JR, Eggert DE, Eilert JB, Bergan JJ. Pancreatic function after normothermic ischemia. II. Cadaveric transplantation. *Am J Surg* 1970; **120**: 693-696
- 22 **Tsiotos GG**, Sarr MG. Pancreas-preserving total duodenectomy. *Dig Surg* 1998; **15**: 398-403
- 23 **Florack G**, Sutherland DE, Ascherl R, Heil J, Erhardt W, Najarian JS. Definition of normothermic ischemia limits for kidney and pancreas grafts. *J Surg Res* 1986; **40**: 550-563
- 24 **Tanioka Y**, Sutherland DE, Kuroda Y, Suzuki Y, Matsumoto I, Deai T. Preservation of dog pancreas before islet isolation with the two-layer method. *Transplant Proc* 1998; **30**: 3419-3420
- 25 **Iwanaga Y**, Suzuki Y, Okada Y, Mori H, Matsumoto I, Mitsutsuji M, Tanioka Y, Fujino Y, Tominaga M, Ku Y, Kuroda Y. Ultrastructural analyses of pancreatic grafts preserved by the two-layer cold-storage method and by simple cold storage in University of Wisconsin solution. *Transpl Int* 2002; **15**: 425-430
- 26 **Belzer FO**, Southard JH. Principles of solid-organ preservation by cold storage. *Transplantation* 1988; **45**: 673-676
- 27 **Kim Y**, Kuroda Y, Tanioka Y, Matsumoto S, Fujita H, Sakai T, Hamano M, Suzuki Y, Ku Y, Saitoh Y. Recovery of adenosine triphosphate tissue levels of grafts preserved by the two-layer method after reperfusion. *Artif Organs* 1996; **20**: 1120-1124
- 28 **Lanir A**, Jenkins RL, Caldwell C, Lee RG, Khettry U, Clouse ME. Hepatic transplantation survival: correlation with adenine nucleotide level in donor liver. *Hepatology* 1988; **8**: 471-475
- 29 **Tsujimura T**, Suzuki Y, Takahashi T, Yoshida I, Fujino Y, Tanioka Y, Li S, Ku Y, Kuroda Y. Successful 24-h preservation of canine small bowel using the cavitory two-layer (University of Wisconsin solution/perfluorochemical) cold storage method. *Am J Transplant* 2002; **2**: 420-424
- 30 **Orii T**, Ohkohchi N, Satomi S, Taguchi Y, Mori S, Miura I. Assessment of liver graft function after cold preservation using 31P and 23Na magnetic resonance spectroscopy. *Transplantation* 1992; **53**: 730-734
- 31 **Uhlmann D**, Armann B, Ludwig S, Escher E, Pietsch UC, Tannapfel A, Teupser D, Hauss J, Witzigmann H. Comparison of Celsior and UW solution in experimental pancreas preservation. *J Surg Res* 2002; **105**: 173-180
- 32 **Lakey JR**, Rajotte RV, Warnock GL, Kneteman NM. Cold ischemic tolerance of human pancreas: assessment of islet recovery and *in vitro* function. *Transplant Proc* 1994; **26**: 3416
- 33 **Shi LJ**, Liu JF, Zhang ZQ, Lu YQ, Shu YG, Chen GL, Xin ZH, Xu JY. Alterations of ATPase activity and erythrocyte oxygen consumption in patients with liver-blood deficiency syndrome. *China Nati J New Gastroenterol* 1997; **3**: 180-181
- 34 **Humar A**, Kandaswamy R, Drangstveit MB, Parr E, Gruessner AG, Sutherland DE. Prolonged preservation increases surgical complications after pancreas transplants. *Surgery* 2000; **127**: 545-551
- 35 **Bottino R**, Balamurugan AN, Bertera S, Pietropaolo M, Trucco M, Piganelli JD. Preservation of human islet cell functional mass by anti-oxidative action of a novel SOD mimic compound. *Diabetes* 2002; **51**: 2561-2567
- 36 **Kim Y**, Kuroda Y, Tanioka Y, Matsumoto S, Fujita H, Sakai T, Hamano M, Suzuki Y, Ku Y, Saitoh Y. Recovery of pancreatic tissue perfusion and ATP tissue level after reperfusion in canine pancreas grafts preserved by the two-layer method. *Pancreas* 1997; **14**: 285-289
- 37 **Pi F**, Hotter G, Closa D, Prats N, Fernandez-Cruz L, Badosa F, Gelpi E, Rosello-Catafau J. Differential effect of nitric oxide inhibition as a function of preservation period in pancreas transplantation. *Dig Dis Sci* 1997; **42**: 962-971
- 38 **Matsumoto I**, Suzuki Y, Fujino Y, Tanioka Y, Deai T, Iwanaga Y, Mitsutsuji M, Iwasaki T, Tominaga M, Ku Y, Kuroda Y. Superiority of mild hypothermic (20 degrees C) preservation for pancreatic microvasculature using the two-layer storage method. *Pancreas* 2000; **21**: 305-309

Heme oxygenase-1 in cholecystokinin-octapeptide attenuated injury of pulmonary artery smooth muscle cells induced by lipopolysaccharide and its signal transduction mechanism

Xin-Li Huang, Yi-Ling Ling, Yi-Qun Ling, Jun-Lin Zhou, Yan Liu, Qiu-Hong Wang

Xin-Li Huang, Yi-Ling Ling, Qiu-Hong Wang, Department of Pathophysiology, Hebei Medical University, Shijiazhuang 050017, Hebei province, China

Yi-Qun Ling, Department of Universal Surgery of Second Hospital, Hebei Medical University, Shijiazhuang 050017, Hebei Province, China

Jun-Lin Zhou, Department of hand Surgery of third Hospital, Hebei Medical University, Shijiazhuang 050017, Hebei province, China

Yan Liu, Department of histogy and embryology, Hebei Medical University, Shijiazhuang 050017, Hebei province, China

Correspondence to: Professor Yi-Ling Ling, Department of Pathophysiology, Hebei Medical University, Shijiazhuang 050017, Hebei province, China. lingyl20@sina.com.cn

Telephone: +86-311-6052263

Received: 2003-07-17 **Accepted:** 2003-07-30

Abstract

AIM: To study the effect of cholecystokinin-octapeptide (CCK-8) on lipopolysaccharide (LPS) -induced pulmonary artery smooth muscle cell (PASMCS) injury and the role of heme oxygenase-1 (HO-1), and to explore the regulation mechanism of c-Jun N-terminal kinase (JNK) and activator protein-1 (AP-1) signal transduction pathway in inducing HO-1 expression further.

METHODS: Cultured PASMCS were randomly divided into 4 or 6 groups: normal culture group, LPS (10 mg/L), CCK-8 (10^{-6} mol/L) plus LPS (10 mg/L) group, CCK-8 (10^{-6} mol/L) group, zinc protoporphyrin 9 (ZnPPiX) (10^{-6} mol/L) plus LPS (10 mg/L) group, CCK-8 (10^{-6} mol/L) plus ZnPPiX and LPS (10 mg/L) group. Seven hours after LPS administration, ultrastructural changes and content of malondialdehyde (MDA) of PASMCS in each group were investigated by electron microscopy and biochemical assay respectively. HO-1 mRNA and protein of PASMCS in the former 4 groups were examined by reverse transcriptase polymerase chain reaction (RT-PCR) and immunocytochemistry staining. Changes of c-fos expression and activation of JNK of PASMCS in the former 4 groups were detected with immunocytochemistry staining and Western blot 30 min after LPS administration.

RESULTS: The injuries of PASMCS and the increases of MDA content induced by LPS were alleviated and significantly reduced by CCK-8 ($P < 0.05$). The specific HO-1 inhibitor-ZnPPiX could worsen LPS-induced injuries and weaken the protective effect of CCK-8. The expressions of c-fos, p-JNK protein and HO-1 mRNA and protein were all slightly increased in LPS group, and significantly enhanced by CCK-8 further ($P < 0.05$).

CONCLUSION: HO-1 may be a key factor in CCK-8 attenuated injuries of PASMCS induced by LPS, and HO-1 expression may be related to the activation of JNK and activator protein (AP-1).

Huang XL, Ling YL, Ling YQ, Zhou JL, Liu Y, Wang QH. Heme oxygenase-1 in cholecystokinin-octapeptide attenuated injury of pulmonary artery smooth muscle cells induced by lipopolysaccharide and its signal transduction mechanism. *World J Gastroenterol* 2004; 10(12): 1789-1794

<http://www.wjgnet.com/1007-9327/10/1789.asp>

INTRODUCTION

Lipopolysaccharide (LPS), a main component of Gram-negative bacterial endotoxin, is the main factor to induce endotoxic shock (ES). ES is a common and serious syndrome in clinic and its mortality is very high. The lung is one of the target organs easily insulted in ES. It was demonstrated that lung injury in ES was associated with oxygen free radicals (OFR)^[1,2] and the content of cholecystokinin (CCK) in serum was increased when ES occurred. Our previous *in vivo* and *in vitro* studies demonstrated that CCK-8 could protect animals from LPS-induced ES and lung injury, which may be related to its effect on reducing the production of OFR^[3-7].

There is a rapid increase in those substances that provide protection against oxidative stress. Among them one is heme oxygenase (HO)-1, which has generated much interest as a novel stress protein that is highly induced by many factors which induce oxidative injury and protect against oxidative stress^[8-12]. However, the regulation mechanism of HO-1 expression was still unclear and there were no reports about the relationship between HO-1 and the protection of CCK-8 in LPS-induced ES and lung injury. One of the earliest responses to LPS and CCK-8 is the activation of mitogen-activated protein kinases (MAPKs), including p38, p42/p44 extracellular signal-regulated kinase (ERK) and c-Jun N-terminal kinase (JNK)^[13,14]. A slightly later cellular response is the activation of activator protein (AP)-1. AP-1 is a dimeric protein complex containing 2 members of the real family of transcription factors, c-fos and c-Jun. Recent studies showed that, one or more members of AP-1 were likely involved in HO-1 gene transcription^[15-18]. The relationship between the activation of these signaling molecules and downstream HO-1 expression represents an active line of investigation. This can provide experimental evidences to elucidate whether the protective mechanism of CCK-8 is associated with HO-1.

Pulmonary artery hypertension (PAH) is the typical pathological change in the early phase of ES. It was reported that the degree and duration of PAH were the important factors of ES accompanied by acute lung injury, and pulmonary artery smooth muscle cells (PASMCS) played an important role in maintaining the tone of pulmonary artery. In the present study, the effect of CCK-8 pretreatment on the injuries of PASMCS induced by LPS was observed, and further investigated the role of HO-1 and the regulation mechanism of c-Jun N-terminal kinase (JNK) and AP-1 signal transduction pathway in inducing HO-1 expression were further investigated.

MATERIALS AND METHODS

Materials

CCK-8 (sulfated), LPS (*E. coli* LPS, serotype 0111:B4), ZnPPIX and Triton X-100 were all purchased from Sigma. Mouse anti-rat phosphorylate JNK(p-JNK) monoclonal antibody, rabbit anti-rat c-fos and HO-1 polyclonal antibody were all purchased from Santa Cruz. DMEM and fetal calf serum (FCS) were purchased from GibcoBRL. Total RNA isolation system and access RT-PCR system were purchased from Promega (USA). SABC kit was purchased from Boshide (China). All other reagents used were of analytic grade.

Methods

Cell isolation and culture Rat PSMCs were prepared as previously described^[19]. Briefly, male healthy Sprague-Dawley rats (100-150 g BM, Experimental Animal Center of Hebei Province) were anesthetized with intraperitoneal administration of pentobarbital sodium (35 mg/kg), and pulmonary arteries were obtained. The isolated pulmonary arteries were cleaned of connective tissues, and aseptically opened longitudinally. The adventitia was carefully removed and the luminal surface was scraped with forceps to remove endothelial cells and then minced into 1 mm² pieces and plated on culture flasks at 37 °C in humidified air containing 50 mL/L CO₂ for 2-3 h, and then cultured in Dulbecco modified Eagle medium (DMEM) supplemented with heat-inactivated 10 mL/L FCS and antibiotics (100 U penicillin, 100 µg/mL streptomycin) and grew until confluence. The medium was changed every 3-4 d, and confluent cells were passaged with 1.25 g/L trypsin solution every 5-7 d, and experiments were performed in an 80% confluent state on the sixth- to eighth-passages from primary culture. Cells were made quiescent by incubation in each medium without FCS for 24 h before LPS or CCK-8 addition. PSMCs in culture were elongated and spindle shaped, grown with the typical hill-and-valley appearance, and characterized by immunocytochemical assay with anti- α -actin monoclonal antibody, demonstrating positive staining in >95% of cells. The cultured PSMCs were randomly divided into 4 or 6 groups: normal culture (control) group, LPS (10 mg/L) group, CCK-8 (10⁻⁶ mol/L) group, CCK-8 (10⁻⁶ mol/L) plus LPS (10 mg/L) group, ZnPPIX (10⁻⁶ mol/L) plus LPS (10 mg/L) group, and CCK-8 (10⁻⁶ mol/L) plus ZnPPIX (10⁻⁶ mol/L) and LPS (10 mg/L) group.

Observation of ultrastructural changes with transmission electron microscopy After treated with LPS, CCK-8 or ZnPPIX, the cells were washed rapidly with PBS and harvested, then fixed with 40 g/L paraformaldehyde/5 g/L glutaraldehyde and postfixed with 40 g/L OsO₄/potassium hexacyanoferrate. After embedded in Epon, thin sections were cut, contrasted with uranyl acetate (20 g/L)/lead citrate (27 g/L) and examined with an EM10 electron microscope as described previously^[20].

Assessments of PSMCs malondialdehyde (MDA) content The cells were harvested after treated with LPS or CCK-8 or ZnPPIX and washed rapidly with PBS, then immediately homogenized on ice in 9 volumes of saline. The homogenates were centrifuged at 4 000 r/min at 4 °C for 10 min. The MDA content in the supernatants was measured using a MDA assay kit (Nanjing Jiancheng Corp. China).

Analysis of c-fos and HO-1 protein expression by immunocytochemistry Confluent cells were passaged with 2.5 g/L trypsin solution onto 20 mm×20 mm glass sheets in a 6-well plate. After treatment with LPS, CCK-8 or both LPS and CCK-8 for 30 min or 7 h, the cells were treated with 3 mL/L H₂O₂ in methanol to block endogenous peroxidase activity. Immunocytochemical staining was performed using rabbit polyclonal antibody against c-fos and HO-1 by an indirect streptavidin/peroxidase technique. Experiments were performed

following the manufacturer's recommendations. The cells were incubated with polyclonal anti-rat c-fos and HO-1 antibody for 12 h at 4 °C after antigen repair. Biotinylated IgG was added as the second antibody. Horseradish peroxidase labeled streptomycin-avidin complex was used to detect the second antibody. Slides were stained with DAB and examined under a light microscope. The brown or dark brown stained cytoplasm or cell nucleus was considered as positive. Phosphate-buffered saline (PBS) solution was used as negative control. The result of immunocytochemistry was analysed by using the CMIAS-8 image analysis system.

Analysis of HO-1 mRNA by RT-PCR After treatment with LPS, CCK-8 or both LPS and CCK-8 for 7 h, total RNA was extracted from PSMCs. The concentration of RNA was determined from absorbent at 260 nm. The primers for HO-1 and β -actin were as follows: HO-1 (309 bp), 5' -CTT TCA GAA GGGTCA GGTGTCCA-3' , 5' -CTGAGAGGT CACCCAGGT AGCGG-3' ; β -actin (224 bp), 5' -CGTGGG CCGCCCTAGGCA CCA-3' , 5' -CGG TTG CCT TAG GGT TCA GAG GGG-3' . Polymerase chain reactions (PCR) were performed in a 50 µL reaction volume. Reverse transcriptase polymerase chain reaction (RT-PCR) was run in the following procedures: at 42 °C for 45 min, 1 circle; at 95 °C for 3 min, at 60 °C for 30 s, at 72 °C for 30 s, 1 circle; at 94 °C for 30 s, at 60 °C for 30 s, at 72 °C for 30 s, 30 circles; at 94 °C for 30 s, at 60 °C for 30 s, at 72 °C for 6 min, 1 circle. A 10 µL PCR product was placed on to 15 g/L agarose gel and observed by EB staining using a Gel-Pro analyzer.

Western blot analysis of p-JNK protein in PSMCs After treatment with LPS or CCK-8 or both LPS and CCK-8 for 30 min, the cells were harvested and then lysed with ice-cold lysis buffer [50 mmol/L Tris (pH 7.5), 150 mmol/L NaCl, 10 g/L Triton X-100, 5 g/L deoxycholic acid, 1 g/L sodium dodecyl sulfate, 1 mmol/L phenylmethylsulfonyl (PMSF), 10 mmol/L NaF, 1 mmol/L sodium vanadate, 5 mmol/L EDTA (pH 8.0) and a 40 µg/mL protease inhibitor cocktail] as described previously for 1 h and then centrifuged at 12 000 g at 4 °C for 10 min. After precipitated unsolubilized fraction was discarded, protein concentration in the supernatant was determined by Coomassie blue dye-binding assay (Nanjing Jiancheng Corp. China). The supernatant containing 30 µg protein was treated with 2×Laemmli buffer, then subjected to SDS-PAGE using 100 g/L running gel for 3 h at 100 V. Protein was transferred to nitrocellulose membrane, and immunoblot analysis was performed as described previously. Briefly, the membrane was incubated successively with 3 mL/L milk in TPBS at room temperature for 1 h, with 1:1 000 diluted mouse anti-rat specific antibody of p-JNK at 37 °C for 2 h, and then with horseradish peroxidase-labeled secondary antibody at 37 °C for 30 min. After each incubation, the membrane was washed extensively with TPBS and the immunoreactive band was stained with diaminobenzidine (DAB). The brown or dark brown stained strap was considered as positive.

Statistical analysis

Data were reported as mean±SD. Statistical differences between values from different groups were determined by one way ANOVA and Newman-Keuls *q* test. Significance was set at *P*<0.05.

RESULTS

CCK-8 alleviated PSMC injury induced by LPS

PSMCs were harvested at 7 h. There were significantly ultrastructural injuries in LPS group such as seriously swollen mitochondria and mitochondria without or partly without cristallins. CCK-8 could significantly alleviate the above-mentioned changes. While the ultrastructural injuries induced

by LPS were aggravated and the protective effect of CCK-8 on cells was weakened by ZnPPiX. There was no significant difference between CCK-8 group and control group (Figure 1).

CCK-8 inhibited MDA production

The MDA content of PSMCs was significantly increased in LPS group when compared with control group ($P<0.05$). Compared with the LPS group, the MDA content was further increased in LPS+ZnPPiX group but markedly decreased in CCK-8+LPS group, however the protective effect of CCK-8 was weakened by ZnPPiX. There was no significant difference between CCK-8 group and control group ($P<0.05$) (Table 1).

Table 1 Change of MDA content in PSMCs (mean \pm SD, $n=8$)

Group	MDA content (nmol/mL)
Control	4.02 \pm 2.18
LPS	23.44 \pm 1.25 ^a
LPS+CCK-8	14.66 \pm 1.66 ^c
CCK-8	3.00 \pm 2.18
LPS+ZnPP	34.97 \pm 1.54 ^{ae}
LPS+CCK-8+ZnPP	29.68 \pm 2.18 ^{ec}

^a $P<0.05$ vs Control group, ^c $P<0.05$ vs LPS+CCK-8 group, ^e $P<0.05$ vs LPS group.

Change of c-fos and HO-1 protein expression

The expressions of c-fos and HO-1 protein in PSMCs were demonstrated by immunocytochemical staining. The results showed that in control group, no brown deposits were present in PSMCs. In contrast, LPS slightly increased the expressions of c-fos and HO-1 protein, some strong positive signals were observed in PSMCs from LPS group. CCK-8 could further enhance the increased expressions of c-fos and HO-1. The dimension and intensity of positive signals were increased also in CCK-8 group (Figure 2).

Table 2 Changes of HO-1 and c-fos protein expression by immunocytochemistry in PSMCs (mean \pm SD, $n=6$)

Group	Area (%)		(A)	
	HO-1	c-fos	HO-1	c-fos
Control	2.10 \pm 0.01	1.18 \pm 0.02	0.02 \pm 0.009	0.03 \pm 0.021
LPS	20.18 \pm 0.08 ^a	18.95 \pm 0.07 ^a	0.19 \pm 0.07 ^a	0.20 \pm 0.01 ^a
LPS+CCK-8	28.91 \pm 0.36 ^c	29.87 \pm 0.33 ^c	0.47 \pm 0.04 ^c	0.45 \pm 0.02 ^c
CCK-8	21.27 \pm 1.05	20.16 \pm 0.98	0.31 \pm 0.02	0.33 \pm 0.01

^a $P<0.05$ vs Control group, ^c $P<0.05$ vs LPS group.

RT-PCR detection of HO-1 mRNA

HO-1 mRNA in PSMCs was detected by RT-PCR analysis. The results showed that the PSMCs of rats 7 h after LPS administration expressed the gene coding for HO-1, because RT-PCR generated a DNA fragment corresponding to the predicted length, 309 bp, of the HO-1 amplification product. The expression of HO-1 increased significantly in LPS and CCK-8 groups compared with control group. The rate of β -actin was (11 \pm 2) % in control group, while it increased to (30 \pm 6) % and (47 \pm 7) % respectively in LPS and CCK-8 groups. The expression of HO-1 increased further in LPS+CCK-8 group compared with LPS group, it increased to (80 \pm 8) % in LPS+CCK-8 group. In each cell sample, all β -actin amplification products were 224 bp in length and there was no significant difference in β -actin expression (Figure 3).

Western blot analysis of p-JNK protein

There were a few of activated JNK proteins in control group. JNK could be activated by LPS, significant phosphorylation of JNK was observed in PSMCs 30 min after LPS administration. CCK-8 could significantly enhance LPS-induced phosphorylation of JNK. Phosphorylation of JNK was also observed in cells receiving CCK-8 (Figure 4).

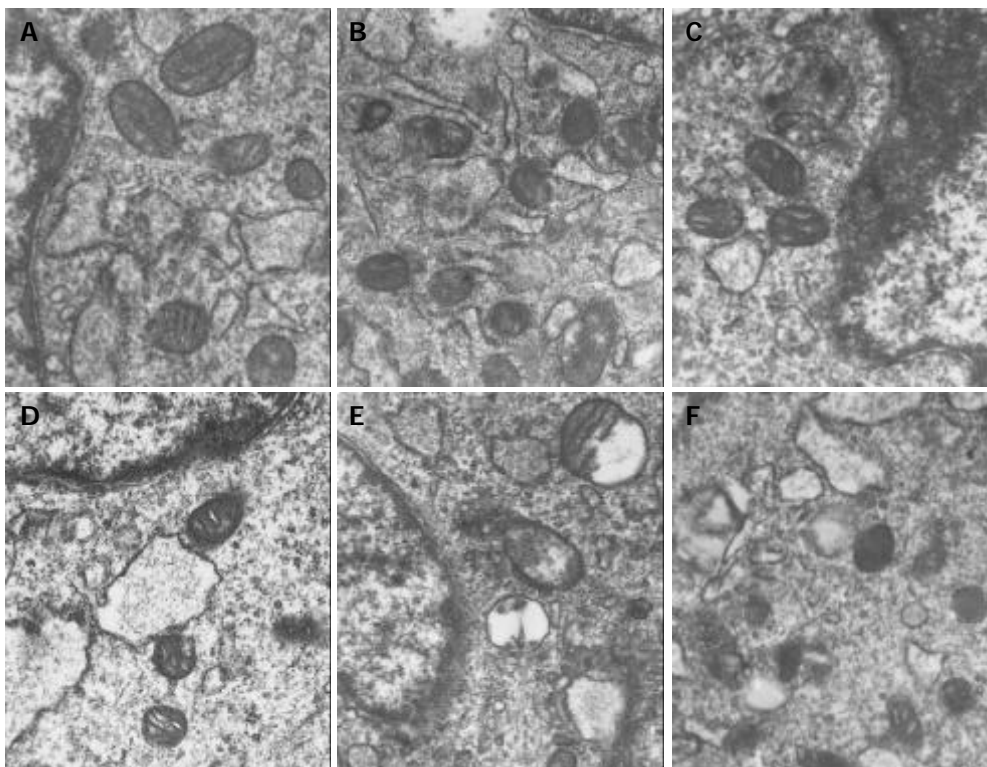


Figure 1 Mitochondria ultrastructural changes shown in EM photograph of PSMCs ($\times 25\,000$). A: Control group, B: LPS group, C: CCK-8+LPS group, D: CCK-8 group, E: LPS+ZnPP group, F: CCK-8+LPS+ZnPP group.

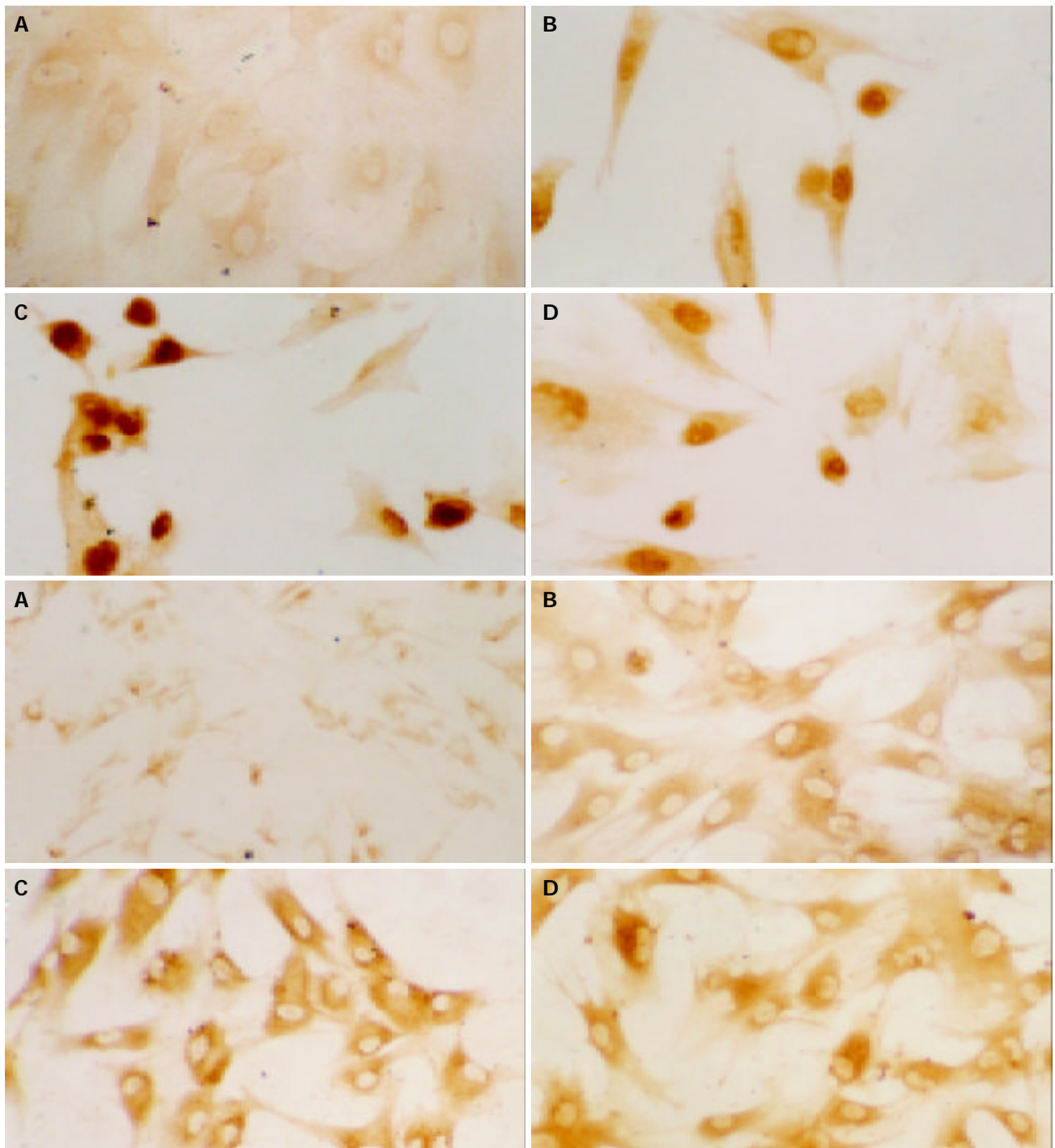


Figure 2 Effect of CCK-8 on LPS-induced c-fos (upper, $\times 400$) and HO-1 (lower, $\times 200$) protein expression in PASMCS. A: Control group, B: LPS group, C: CCK-8+LPS group, D: CCK-8 group.

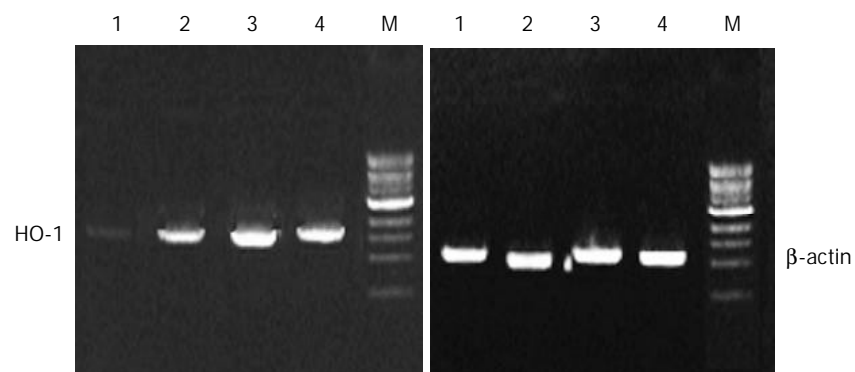


Figure 3 RT-PCR product gel electrophoresis. M: DNA marker, 1: Control, 2: LPS, 3: CCK-8 + LPS, 4: CCK-8.

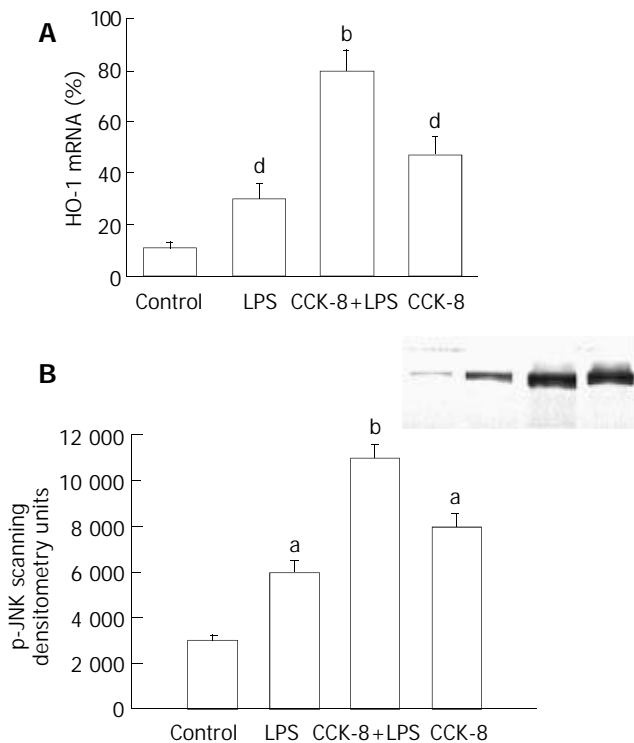


Figure 4 Effect of CCK-8 on LPS-induced HO-1 mRNA expression and JNK activation in PSMCs. **A:** Effect of CCK-8 on LPS-induced HO-1 mRNA expression in PSMCs. $n=3$. $^dP<0.01$ vs Control; $^bP<0.01$ vs LPS. **B:** CCK-8 increases JNK activation induced by LPS in PSMCs. $n=3$. $^aP<0.05$ vs Control; $^bP<0.01$ vs LPS.

DISCUSSION

CCK is a member of the gastrin-CCK family, first isolated from hog intestine, and shows a widespread distribution in different organs and tissues. The sulfated carboxy-terminal octapeptide (CCK-8), isolated from the central nervous system and digestive tract, is the predominant active form. Our previous *in vivo* and *in vitro* studies demonstrated that CCK-8 could protect animals from LPS-induced ES. Treatment of ES rats and rabbits with CCK-8 could lead to an increase in decreasing mean arterial pressure and a reduction in increasing pulmonary artery pressure. Pathological changes of lung could be ameliorated when CCK-8 was via vessel in advance. CCK-8 could protect pulmonary artery endothelia against detrimental effects and then reverse the inhibition of endothelia-dependent relaxation of pulmonary artery induced by LPS, which might be associated with the above-mentioned protective effect of CCK-8^[5-10]. Despite convincing data indicating the protective function of CCK-8 to the organisms in endotoxic shock or to the cells exposed to LPS, the precise mechanism remains unclear.

During stress state induced by administration of LPS, inflammation or therapeutic doses of inhaled oxygen, the bodies would evolve a complex, and redundant network of antioxidants. It has been found that an important arm of the antioxidant response consists of antioxidant enzymes and stress-response proteins^[21-23]. One such stress-response protein is HO-1, the rate-limiting enzyme in the oxidative degradation of heme into bilirubin, carbon monoxide (CO) and free iron. HO exists in three isoforms, whereas HO-2 and HO-3 are primarily constitutive. HO-1 also known as heat shock protein 32, has been found to be the only inducible HO isoform^[24-27]. There is a strong evidence to support the emerging paradigm that HO-1 is essential in maintaining cellular and tissue homeostasis in various *in vitro* and *in vivo* models of oxidant-induced injury. Recent analyses of HO-1 null mice as well as the first reported

HO-1-deficient human have strengthened the emerging paradigm that HO-1 is indeed an important molecule in the host's defense against oxidant stresses such as hypoxia, hyperthermia, and inflammation. It has been considered as one of the most sensitive indicators of cellular injury^[28-31]. Recent studies showed that HO-1 was an important regulator of the vascular response to injury. In this experiment we used the specific HO-1 inhibitor-ZnPPiX to study the relationship between induced HO-1 and injuries of PSMCs. The results showed that HO-1 mRNA and protein expression increased after LPS administration and ZnPPiX could worsen LPS-induced injuries, indicating that overexpression of HO-1 in PSMCs can attenuate their injuries induced by LPS. It is undoubtedly one of the adaptive and self-protective responses to the injury.

Given the overall consistency of data that show HO-1 expression is generally a protective response, it is necessary to study the relationship between HO-1 expression and the protection of CCK-8. We found that CCK-8 could ameliorate the ultrastructural injuries of PSMCs induced by LPS. However, the protective effect of CCK-8 was impaired by ZnPPiX. To further demonstrate the role of HO-1 in CCK-8 attenuated injury of PSMCs induced by LPS, the HO-1 expression and signal pathway of HO-1 induction in PSMCs were studied. The candidate upstream signaling pathways for HO-1 regulation were MAPKs, a group of protein kinases that could mediate the nuclear responses of cells to a wide variety of extracellular stresses such as inflammatory cytokines, growth factors, ultraviolet light, and osmotic stress^[32-34]. The "classical" MAPKs are the p44 and p42 isoforms. Recently, two novel MAPK-related enzymes have been identified, one is JNK and the other is p38^[35]. Although three distinct subfamilies have been described, there is a significant cross talk between the pathway and common downstream target^[36]. In our experiment, we found that CCK-8 significantly enhanced LPS-induced overexpression of HO-1 mRNA and protein. We also observed that LPS could also activate c-fos (one of the two members of the real family of AP-1) and JNK in PSMCs, while CCK-8 could further enhance the activation of c-fos and JNK induced by LPS. From all above, the role of MAPKs was potential in HO-1 signal pathway after LPS and CCK-8 administration to PSMCs, HO-1 might be the key for CCK-8 to exert its protective effect.

In summary, administration of CCK-8 can prevent injuries of PSMCs induced by LPS through overexpression of HO-1 mRNA and protein, which may involve c-fos and JNK.

REFERENCES

- Liaudet L**, Szabo C, Evgenov OV, Murthy KG, Pacher P, Virag L, Mabley JG, Marton A, Soriano FG, Kirov MY, Bjertnaes LJ, Salzman AL. Flagellin from gram-negative bacteria is a potent mediator of acute pulmonary inflammation in sepsis. *Shock* 2003; **19**: 131-137
- Molina PE**, Abunrad NN. Differential effects of hemorrhage and LPS on tissue TNF- α , IL-1 and associate neuro-hormonal and opioid alterations. *Life Sci* 2000; **66**: 399-409
- Bertolini A**, Guarini S, Ferrari W, Rompianesi E. Caerulein and cholecystokinin reverse experimental hemorrhagic shock. *Neuropeptides* 1986; **8**: 25-31
- Guarini S**, Bazzani C, Leo L, Bertolini A. Haematological changes induced by the intravenous injection of CCK-8 in rats subjected to haemorrhagic shock. *Neuropeptides* 1988; **11**: 69-72
- Ling YL**, Huang SS, Wang LF, Zhang JL, Wan M, Hao RL. Cholecystokinin-octapeptide (CCK-8) reverses experimental endotoxin shock. *Shengli Xuebao* 1996; **48**: 390-394
- Meng AH**, Ling YL, Wang DH, Gu ZY, Li SJ, Zhu TN. Cholecystokinin-octapeptide alleviates tumor necrosis factor- α induced changes in rabbit pulmonary arterial reactivity and injuries of endothelium *in vitro*. *Shengli Xuebao* 2000; **52**: 502-506
- Ling YL**, Meng AH, Zhao XY, Shan BE, Zhang JL, Zhang XP. Effect of cholecystokinin on cytokines during endotoxin shock

- in rats. *World J Gastroenterol* 2001; **7**: 667-671
- 8 **Otani K**, Shimizu S, Chijiwa K, Morisaki T, Yamaguchi T, Yamaguchi K, Kuroki S, Tanaka M. Administration of bacterial lipopolysaccharide to rats induces heme oxygenase-1 and formation of antioxidant bilirubin in the intestinal mucosa. *Dig Dis Sci* 2000; **45**: 2313-2319
- 9 **Zampetaki A**, Minamino T, Mitsialis SA, Kourembanas S. Effect of heme oxygenase-1 overexpression in two models of lung inflammation. *Exp Biol Med* 2003; **228**: 442-446
- 10 **Henningsson R**, Alm P, Lundquist I. Evaluation of islet heme oxygenase-CO and nitric oxide synthase-NO pathways during acute endotoxemia. *Am J Physiol Cell Physiol* 2001; **280**: C1242-1254
- 11 **Otterbein LE**, Choi AM. Heme oxygenase: colors and defense against cellular stress. *Am J Physiol Lung Cell Mol Physiol* 2000; **279**: L1029-1037
- 12 **Gonzalez A**, Schmid A, Salido GM, Camello PJ, Pariente JA. XOD-catalyzed ROS generation mobilizes calcium from intracellular stores in mouse pancreatic acinar cells. *Cell Signal* 2002; **14**: 153-159
- 13 **Jarvis BW**, Harris TH, Qureshi N, Splitter GA. Rough lipopolysaccharide from *Brucella abortus* and *Escherichia coli* differentially activates the same mitogen-activated protein kinase signaling pathways for tumor necrosis factor alpha in RAW 264.7 macrophage-like cells. *Infect Immun* 2002; **70**: 7165-7168
- 14 **Zieger M**, Oehrl W, Wetzker R, Henklein P, Nowak G, Kaufmann R. Different signaling pathways are involved in CCK (B) receptor-mediated MAP kinase activation in COS-7 cells. *Biol Chem* 2000; **381**: 763-768
- 15 **Yuksel M**, Okajima K, Uchiba M, Okabe H. Gabexate mesilate, a synthetic protease inhibitor, inhibits lipopolysaccharide-induced tumor necrosis factor-alpha production by inhibiting activation of both nuclear factor-kappaB and activator protein-1 in human monocytes. *J Pharmacol Exp Ther* 2003; **305**: 298-305
- 16 **Camhi SL**, Alam J, Wiegand GW, Chin BY, Choi AM. Transcriptional activation of the HO-1 gene by lipopolysaccharide is mediated by 5' distal enhancers: role of reactive oxygen intermediates and AP-1. *Am J Respir Cell Mol Biol* 1998; **18**: 226-234
- 17 **Lee PJ**, Camhi SL, Chin BY, Alam J, Choi AM. AP-1 and STAT mediate hyperoxia-induced gene transcription of heme oxygenase-1. *Am J Physiol Lung Cell Mol Physiol* 2000; **279**: L175-182
- 18 **Ryter SW**, Xi S, Hartsfield CL, Choi AM. Mitogen activated protein kinase (MAPK) pathway regulates heme oxygenase-1 gene expression by hypoxia in vascular cells. *Antioxid Redox Signal* 2002; **4**: 587-592
- 19 **Nelson MT**, Quayle JM. Physiological roles and properties of potassium channels in arterial smooth muscle. *Am J Physiol* 1995; **268**(4 Pt 1): C799-822
- 20 **Wang YX**, Zheng YM, Abdullaev I, Kotlikoff MI. Metabolic inhibition with cyanide induces calcium release in pulmonary artery myocytes and *Xenopus* oocytes. *Am J Physiol Cell Physiol* 2003; **284**: C378-388
- 21 **Haddad JJ**. Glutathione depletion is associated with augmenting a proinflammatory signal: evidence for an antioxidant/pro-oxidant mechanism regulating cytokines in the alveolar epithelium. *Cytokines Cell Mol Ther* 2000; **6**: 177-187
- 22 **Haddad JJ**, Land SC. Redox signaling-mediated regulation of lipopolysaccharide-induced proinflammatory cytokine biosynthesis in alveolar epithelial cells. *Antioxid Redox Signal* 2002; **4**: 179-193
- 23 **Wiesel P**, Foster LC, Pellacani A, Layne MD, Hsieh CM, Huggins GS, Strauss P, Yet SF, Perrella MA. Thioredoxin facilitates the induction of heme oxygenase-1 in response to inflammatory mediators. *J Biol Chem* 2000; **275**: 24840-24846
- 24 **Tenhunen R**, Marver HS, Schmid R. The enzymatic conversion of heme to bilirubin by microsomal heme oxygenase. *Proc Natl Acad Sci U S A* 1968; **61**: 748-755
- 25 **McCoubrey WK Jr**, Huang TJ, Maines MD. Isolation and characterization of a cDNA from the rat brain that encodes hemoprotein heme oxygenase-3. *Eur J Biochem* 1997; **247**: 725-732
- 26 **Maines MD**. Heme oxygenase: function, multiplicity, regulatory mechanism, and clinical applications. *FASEB J* 1988; **2**: 2557-2568
- 27 **Fujiwara T**, Takahashi T, Suzuki T, Yamasaki A, Hirakawa M, Akagi R. Differential induction of brain heme oxygenase-1 and heat shock protein 70 mRNA in sepsis. *Res Commun Mol Pathol Pharmacol* 1999; **105**: 55-66
- 28 **Agarwal A**, Nick HS. Renal response to tissue injury: lessons from heme oxygenase-1 gene GeneA blation and expression. *J Am Soc Nephrol* 2000; **11**: 965-973
- 29 **Yachie A**, Niida Y, Wada T, Igarashi N, Kaneda H, Toma T, Ohta K, Kasahara Y, Koizumi S. Oxidative stress causes enhanced endothelial cell injury in human heme oxygenase-1 deficiency. *J Clin Invest* 1999; **103**: 129-135
- 30 **Lee TS**, Chau LY. Heme oxygenase-1 mediates the anti-inflammatory effect of interleukin-10 in mice. *Nat Med* 2002; **8**: 240-246
- 31 **Inoue S**, Suzuki M, Nagashima Y, Suzuki S, Hashiba T, Tsuburai T, Ikehara K, Matsuse T, Ishigatsubo Y. Transfer of heme oxygenase 1 cDNA by a replication-deficient adenovirus enhances interleukin 10 production from alveolar macrophages that attenuates lipopolysaccharide-induced acute lung injury in mice. *Hum Gene Ther* 2001; **12**: 967-979
- 32 **Chan ED**, Riches DW, White CW. Redox paradox: effect of N-acetylcysteine and serum on oxidation reduction-sensitive mitogen-activated protein kinase signaling pathways. *Am J Respir Cell Mol Biol* 2001; **24**: 627-632
- 33 **Haddad JJ**, Land SC. Redox/ROS regulation of lipopolysaccharide-induced mitogen-activated protein kinase (MAPK) activation and MAPK-mediated TNF-alpha biosynthesis. *Br J Pharmacol* 2002; **135**: 520-536
- 34 **Tournier C**, Hess P, Yang DD, Xu J, Turner TK, Nimnual A, Bar-Sagi D, Jones SN, Flavell RA, Davis RJ. Requirement of JNK for stress-induced activation of the cytochrome c-mediated death pathway. *Science* 2000; **288**: 870-874
- 35 **Widmann C**, Gibson S, Jarpe MB, Johnson GL. Mitogen activated protein kinase: conversation of a three-kinase module from yeast to human. *Physiol Rev* 1999; **79**: 143-180
- 36 **Whitmarsh AJ**, Shore P, Sharrocks AD, Davis RJ. Integration of MAP kinase signal transduction pathway at the serum response element. *Science* 1995; **269**: 403-407

Investigation of regurgitation and other symptoms of gastroesophageal reflux in Indonesian infants

Badriul Hegar, Aswitha Boediarso, Agus Firmansyah, Yvan Vandenplas

Badriul Hegar, Aswitha Boediarso, Agus Firmansyah, Department of Pediatrics, Cipto Mangunkusumo Hospital, University of Indonesia, Jakarta, Indonesia

Yvan Vandenplas, Department of Pediatrics, Academisch Ziekenhuis Vrije Universiteit Brussel, Brussels, Belgium

Correspondence to: Yvan Vandenplas, Department of Pediatrics, Academic Children's Hospital, VUB, Laarbeeklaan 101, 1090 Brussels, Belgium. yvan.vandenplas@az.vub.ac.be

Telephone: +32-24775780 **Fax:** +32-24775783

Received: 2003-09-09 **Accepted:** 2003-12-01

Abstract

AIM: To evaluate the incidence of regurgitation and other symptoms of gastroesophageal reflux in Indonesian infants.

METHODS: In a cross-sectional study at the University Outpatient Clinic for vaccination in Jakarta, 138 mothers of healthy infants less than 12-mo old were prospectively asked to report the frequency of regurgitation.

RESULTS: Whatever the age was, some infants did not regurgitate (from 10% during the first month of life to 67% in 1-year-old infants). Regurgitation of at least once a day was reported in 77% of infants younger than 3 mo. Daily regurgitation decreased to 12% in the 9-12 mo old group. Reported peak prevalence was 81%(26/32) during the first month of life. Regurgitation decreased sharply between the 4-6 and 7-9 mo old groups (from 44% to 9%). The longer the regurgitation persisted, the more frequently the mother perceived regurgitation as a problem. Volume and frequency of regurgitation, back arching, irritability, crying and refusal of feeding were the symptoms causing maternal anxiety. The longer the regurgitation persisted, the more frequently the mothers viewed it as a health problem.

CONCLUSION: Regurgitation occurs frequently in Indonesian infants, and is a frequent cause of concern to mothers.

Hegar B, Boediarso A, Firmansyah A, Vandenplas Y. Investigation of regurgitation and other symptoms of gastroesophageal reflux in Indonesian infants. *World J Gastroenterol* 2004; 10(12): 1795-1797

<http://www.wjgnet.com/1007-9327/10/1795.asp>

INTRODUCTION

Regurgitation is the effortless return of gastric contents into the mouth, and the most common symptom of infantile gastroesophageal reflux (GER). Few attempts have been made to determine the prevalence of regurgitation and its natural course in infants. In the Western world, evaluation of the natural progression of symptoms of GER at any age has become virtually impossible because of widespread self-treatment and a lack of medical referral. It is not clear how important genetic, racial and ethnic factors may be in the clinical presentation, the prevalence and the natural history of GER disease. In the Eastern

part of the world, it is commonly thought that regurgitation is less frequent than in the United States and Europe. For these reasons, determining the prevalence of GER in Indonesian infants is of interest.

MATERIALS AND METHODS

Data were collected from mothers bringing their healthy infants to the Outpatient Clinic of the Cipto Mangunkusumo Hospital, Jakarta, for routine immunization. All infants were born at term and in good general health with adequate nutritional status (P50-97 NCHS). Most of the mothers were from the middle-low socioeconomic class and worked as housewives. The data were obtained by prospectively interviewing mothers using a standard questionnaire about the prevalence of regurgitation during the previous two wk and other descriptive information.

The same author (BH) interviewed 138 consecutive mothers, presenting to the outpatient clinic of one of the local authors. Each interview lasted for 15 to 20 min. All mothers agreed to participate in the study. Age distribution of the infants is listed in Table 1. There were 75 male and 63 female infants. Mothers were asked the number of episodes of regurgitation per day, and whether they considered regurgitation as a health problem, whether the frequency or volume of emesis was a health problem and whether the infant had such symptoms as crying, back arching, irritability, or refusal to feed, as well as whether the symptoms had an adverse impact on the baby's quality of life.

The two-tailed unpaired *t*-test was used, statistical significance was set at $P < 0.05$.

Table 1 Age distribution of studied infants

Age (mo)	Infants (n)
0-3	74
4-6	34
7-9	21
10-12	9
Total	138

RESULTS

Table 2 summarizes the prevalence and frequency of regurgitation in the infants by month of age. Up to the age of 3 mo, about half of the infants regurgitated more than two times a day, the number was slightly higher in the first mo of life and smaller at 3 mo. In the group regurgitating 1 to 4 times a day, there was a sharp decrease in the number of episodes of regurgitation to almost zero by the age of 7 to 8 mo. Twenty-five percent of the infants regurgitated more than 4 times a day during the first month of life, but from the age of 6 mo all infants regurgitated less than 4 times a day. Table 3 shows the number of mothers who were concerned about regurgitation. The evolution of concern was inversely related to the persistence of regurgitation. During the first month of life, many infants regurgitated, and few mothers expressed their concerns. However, the mothers of older infants with persistent vomiting became concerned about the symptom. Among infants regurgitating more than once a day, about 40% of the mothers asked for medical advice about

the symptom. The reasons for maternal concern are listed in Table 4, and included the excessive volume and frequency of regurgitation, and symptoms suggesting a decreased quality of life of the infants such as food refusal, crying, back arching and irritability. The volume of regurgitation was less frequently considered as a problem than the frequency of regurgitation (9% vs 66%). Crying and irritability were the second most frequent reasons for concern among the mothers (57%). Food refusal and back arching were reported as reasons for concern in 26% and 20%, respectively. Mothers of regurgitating infants estimated their infants had an impaired quality of life (75 vs 15 %, $P<0.05$). Infants of unconcerned mothers had much less frequent symptoms than infants of concerned mother ($P<0.05$).

Table 2 Daily frequency of regurgitation in 138 healthy infants

Age (mo)	Infants	Daily frequency of regurgitation (%)			
		0	<1	1-4	>4
1	32	3 (10)	3 (10)	18 (55)	8 (25)
2	25	3 (12)	2 (8)	13 (15)	7 (28)
3	17	5 (29)	1 (6)	8 (47)	3 (18)
4	10	6 (60)	1 (10)	3 (30)	0 (0)
5	14	3 (21)	2 (15)	6 (43)	3 (21)
6	10	6 (60)	1 (10)	3 (30)	0 (0)
7	10	6 (60)	2 (20)	2 (20)	0 (0)
8	3	1 (33)	2 (67)	0 (0)	0 (0)
9	8	8 (10)	0 (0)	0 (0)	0 (0)
10	5	4 (80)	0 (0)	1 (20)	0 (0)
11	1	1 (100)	0 (0)	0 (0)	0 (0)
12	3	2 (67)	1 (33)	0 (0)	0 (0)
	138	48(35)	15 (11)	54 (39%)	21 (15%)

Table 3 Number of mothers considering regurgitation as a health problem

	Daily regurgitation frequency (%)			
	<1	1-4	>4	
With concern	3	24	8	35 (25)
Without concern	60	30	13	103 (75)

Table 4 Symptoms of gastroesophageal reflux and number of mothers showing concern

Symptom	n (%)
Crying and irritability	20 (57)
Food refusal	9 (26)
Back arching	7 (20)
Excessive frequency of regurgitation	23 (66)
Excessive volume of regurgitation	3 (9)

DISCUSSION

Recent studies have suggested that GER may in part be genetically determined. Thus, its prevalence and severity might be expected to vary according to racial or ethnic background. Radiology is not recommended in the diagnosis of GER. The radiological method of GER evaluation showed a specificity of 50% and a sensitivity of 29%, as compared to 24-h pH monitoring^[1]. A genetic influence on the prevalence of GER was supported by the finding that GER symptoms are more frequently encountered in the relatives of GER disease patients^[2]. Moreover, the concordance for GER is higher in monozygotic than dizygotic twins^[3]. A locus on chromosome 13q, between microsatellite D13S171 and D13S263, has been linked with severe GER in 5 families with multigenerational histories^[4], but the

same abnormal locus was not found in 5 other families, possibly due to the genetic heterogeneity of GER and different clinical presentations among patients studied^[5]. The incidence of hiatal hernia was reported to be much lower in Korea (1.4%) than in Western world (2.3-50%)^[6]. Several studies have confirmed the familial segregation of hiatal hernia, Barrett's esophagus, esophageal carcinoma and GER.

There are only a few studies that have attempted to describe the natural history of GER in children. In some of these studies, infantile GER was excluded^[7]. Orenstein developed a questionnaire to identify infants with GER^[8]. At least regurgitation occurred once a day in half of 0- to 3-mo-old white non-Hispanic infants, and increased up to two thirds at 4 mo and decreased to 5% at 10-12 mo of age^[9]. Daily regurgitation was present in 50% of infants younger than 3 mo, in more than 66% at 4 mo, but only in 5% at 1 year of age^[8-10]. Nelson and coworkers documented the prevalence of regurgitation in a white non-Hispanic infant population in USA^[9]. However, as the authors stated, their findings could not be generalized and investigations of different racial/ethnic and socioeconomic groups are needed to determine differences in prevalence of symptoms in other populations. Also in Japanese infants, regurgitation was common and decreased with age^[11].

Our questionnaire intended to report the incidence of regurgitation, not of symptoms suggesting gastro-esophageal reflux (disease). Regurgitation occurred frequently in our small sample size of Indonesian infants. The sample size was relatively small for an epidemiological survey. In fact, the prevalence of regurgitation in our population was the highest ever reported. In the study by Nelson and coworkers, the prevalence of regurgitation peaked at 4 mo of age^[9], whereas in our population the prevalence was highest during the first month of life. In a study from northern India, the prevalence of regurgitation in 1-6-mo-old infants was 55%^[12]. In our study, 75% of 0-6-mo-old infants regurgitated at least once a day.

Complete resolution of regurgitation was the most common outcome in infant reflux, with a resolution by 10 mo of age in 55%, by 18 mo of age in 60-80% and by 2 years of age in 98%^[13,14]. In the study by Nelson and coworkers, and in our study, regurgitation was almost completely disappeared by 7 mo^[9]. In 6-12-mo old infants, the prevalence of regurgitation was 15% in North India^[12], which was similar to the findings in our population if all infants regurgitating at least once per day were considered. If the infants regurgitating less than once a day were included, then the prevalence of regurgitation among 6-12-mo old Indonesian infants was as high as 30%. In all studies evaluating the natural evolution of infant regurgitation, there was a sharp decline around 6-7 mo towards a disappearance at the age of 12 mo^[9,12,15].

According to epidemiological data from France, Australia and the United States, excessive regurgitation was a cause of concern and medical consult in about 25% of parents^[8-10]. Spilling in infancy was very common, but the majority of children settled by 13 to 14 mo of age. However, those with frequent spilling (>90 d) were more likely to have GER symptoms at 9 years of age^[16]. Esophagitis occurred in one quarter of infants with persistent distress^[17]. There was a subgroup of otherwise healthy infants, presenting with wheeze and/or stridor, who had isolated swallowing dysfunction and silent aspiration as the cause of their respiratory symptoms^[18]. Our findings were similar, 30% of the mothers showed concern over regurgitation. Symptoms causing parental perception that regurgitation might be a problem were comparable in both studies, and included the volume and frequency of regurgitation and symptoms suggesting decreased quality of life such as crying, back-arching and irritability^[9]. Parental reports about reflux-related behaviors were similar in Nelson's study and in ours^[9]. Despite the concern of parents, pediatricians generally stated

that intervention was not needed^[19]. Although a prospective follow-up of 63 regurgitating infants reported a complete disappearance of regurgitation by 12 mo of age, it is interesting that these same infants were reported on a long-term follow-up to have a significant increase in feeding refusal, prolonged eating time, parental distress about feeding and impaired quality of life when compared to non-regurgitating controls^[15].

In conclusion, the severity and incidence of GOR were significantly higher in symptomatic than asymptomatic infants^[20]. Food allergy might be common in regurgitating infants^[21,22]. Recommendations for a diagnostic workup have been published^[23,24]. Hydrolysates might treat regurgitation by improving gastric emptying^[25]. GER frequently caused apnea in infants^[26,27]. GER and regurgitation decreased the quality of life^[28] in infants, and increases hospital stay and cost^[29,30]. Worldwide, racial differences in the prevalence and persistence of infantile regurgitation seem minimal. Regurgitation in Indonesian infants tends to be very frequent, with more than 75% of 0-3-mo-old infants regurgitating at least once a day. Symptoms viewed as being related to GER and causing maternal concern are also similar. For one in three mothers worldwide, the symptom of regurgitation is a cause for concern. Mothers in Indonesia are no exception.

REFERENCES

- Akslaede K**, Pedersen JB, Lange A, Funch-Jensen P, Thommesen P. Gastro-oesophageal reflux demonstrated by radiography in infants less than 1 year of age. Comparison with pH monitoring. *Acta Radiol* 2003; **44**: 136-138
- Trudgill NJ**, Kapur KC, Riley SA. Familial clustering of reflux symptoms. *Am J Gastroenterol* 1999; **94**: 1172-1178
- Cameron AJ**, Lagergren J, Henriksson C. Gastroesophageal reflux disease in monozygotic and dizygotic twins. *Gastroenterology* 2002; **122**: 55-59
- Hu FZ**, Preston RA, Post JC, White GJ, Kikuchi LW, Wang X, Leal SM, Levenstien MA, Ott J, Self TW, Allen G, Stiffler RS, McGraw C, Pulsifer-Anderson EA, Ehrlich GD. Mapping of a gene for severe pediatric gastroesophageal reflux to chromosome 13q14. *JAMA* 2000; **284**: 325-334
- Orenstein SR**, Shalaby TM, Barmada MM, Whitcomb DC. Genetics of gastroesophageal reflux disease: a review. *J Pediatr Gastroenterol Nutr* 2002; **34**: 506-510
- Kim E**. Hiatus hernia and diverticulum of the colon: their low incidence in Korea. *N Engl J Med* 1964; **271**: 764-768
- Ashorn M**, Ruuska T, Karikoski R, Laippala P. The natural course of Gastroesophageal reflux disease in children. *Scand J Gastroenterol* 2002; **37**: 638-641
- Orenstein SR**, Shalaby TM, Cohn J. Reflux symptoms in 100 normal infants: diagnostic validity of the infant Gastroesophageal reflux questionnaire. *Clin Pediatr* 1996; **35**: 607-614
- Nelson SP**, Chen EH, Syniar GM, Christoffel KK. Prevalence of symptoms of gastroesophageal reflux during infancy. A pediatric-based survey. Pediatric Research Group. *Arch Pediatr Adolesc Med* 1997; **151**: 569-572
- Chouhou D**, Rossignol C, Bernard Fl. Le reflux gastrooesophagien dans le centres de bilan de sante de l' enfant de moins de 4 ans. *Arch Fr Pediatr* 1992; **49**: 843-845
- Miyazawa R**, Tomomasa T, Kaneko H, Tachibana A, Ogawa T, Morikawa A. Prevalence of gastro-oesophageal reflux-related symptoms in Japanese infants. *Pediatr Int* 2002; **44**: 513-516
- De S**, Rajeshwari K, Kalra KK, Gondal R, Malhotra V, Mittal SK. Gastroesophageal reflux in infants and children in north India. *Trop Gastroenterol* 2001; **22**: 99-102
- Carré I**. The natural history of the partial thoracic stomach ("hiatal hernia") in children. *Arch Dis Child* 1959; **34**: 344-353
- Shepherd RW**, Wren J, Evans S, Lander M, Ong TH. Gastroesophageal reflux in children. Clinical profile, course and outcome with active therapy in 126 cases. *Clin Pediatr* 1987; **26**: 55-60
- Nelson SP**, Chen EH, Syniar GM, Christoffel KK. One-year follow-up of symptoms of gastroesophageal reflux during infancy. Pediatric Research Group. *Pediatrics* 1998; **102**: E67
- Martin AJ**, Pratt N, Kennedy JD, Ryan P, Ruffin RE, Miles H, Marley J. Natural history and familial relationships of infant spilling to 9 years of age. *Pediatrics* 2002; **109**: 1061-1067
- Heine RG**, Cameron DJ, Chow CW, Hill DJ, Catto-Smith AG. Esophagitis in distressed infants: poor diagnostic agreement between esophageal pH monitoring and histopathologic findings. *J Pediatr* 2002; **140**: 14-19
- Sheikh S**, Allen E, Shell R, Hruschak J, Iram D, Castile R, McCoy K. Chronic aspiration without gastroesophageal reflux as a cause of chronic respiratory symptoms in neurologically normal infants. *Chest* 2001; **120**: 1190-1195
- Aggett PJ**, Agostoni C, Goulet O, Hermell O, Koletzko B, Lafeber HL, Michaelsen KF, Milla P, Rigo J, Weaver LT. Antireflux or antiregurgitation milk products for infants and young children: a commentary by the ESPGHAN Committee on Nutrition. *J Pediatr Gastroenterol Nutr* 2002; **34**: 496-498
- Thomas EJ**, Kumar R, Dasan JB, Chandrashekar N, Agarwala S, Tripathi M, Bal CS. Radionuclide scintigraphy in the evaluation of gastro-oesophageal reflux in post-operative oesophageal atresia and tracheo-oesophageal fistula patients. *Nucl Med Commun* 2003; **24**: 317-320
- Hill DJ**, Hosking CS, Heine RG. Clinical spectrum of food allergy in children in Australia and South-East Asia: identification and targets for treatment. *Ann Med* 1999; **31**: 272-281
- Salvatore S**, Vandenplas Y. Gastroesophageal reflux and cow milk allergy: is there a link? *Pediatrics* 2002; **110**: 972-984
- Vandenplas Y**. Diagnosis and treatment of gastroesophageal reflux disease in infants and children. *World J Gastroenterol* 1999; **5**: 375-382
- Gold BD**. Epidemiology and management of gastro-oesophageal reflux in children. *Aliment Pharmacol Ther* 2004; **19**(Suppl 1): 22-27
- Garzi A**, Messina M, Frati F, Carfagna L, Zagordo L, Belcastro M, Parmiani S, Sensi L, Marcucci F. An extensively hydrolysed cow's milk formula improves clinical symptoms of gastroesophageal reflux and reduces the gastric emptying time in infants. *Allergol Immunopathol* 2002; **30**: 36-41
- Sheikh S**, Stephen TC, Sisson B. Prevalence of gastroesophageal reflux in infants with recurrent brief apneic episodes. *Can Respir J* 1999; **6**: 401-404
- Wenzl TG**, Silny J, Schenke S, Peschgens T, Heimann G, Skopnik H. Gastroesophageal reflux and respiratory phenomena in infants: status of the intraluminal impedance technique. *J Pediatr Gastroenterol Nutr* 1999; **28**: 423-428
- Khalaf MN**, Porat R, Brodsky NL, Bhandari V. Clinical correlations in infants in the neonatal intensive care unit with varying severity of gastroesophageal reflux. *J Pediatr Gastroenterol Nutr* 2001; **32**: 45-49
- Ferlauto JJ**, Walker MW, Martin MS. Clinically significant gastroesophageal reflux in the at-risk premature neonate: relation to cognitive scores, days in the NICU, and total hospital charges. *J Perinatol* 1998; **18**: 455-459
- Frakaloss G**, Burke G, Sanders MR. Impact of gastroesophageal reflux on growth and hospital stay in premature infants. *J Pediatr Gastroenterol Nutr* 1998; **26**: 146-150

Severity of gastroesophageal reflux disease influences daytime somnolence: A clinical study of 134 patients underwent upper panendoscopy

Pál Demeter, Katalin Várdi Visy, Nóra Gyulai, Róbert Sike, Tamás G Tóth, János Novák, Pál Magyar

Pál Demeter, Róbert Sike, Tamás G Tóth, Outpatient Clinic of Gastroenterology, St. John's Hospital, Budapest, Hungary
Katalin Várdi Visy, Nóra Gyulai, Pál Magyar, Department of Pulmonology, Semmelweis Medical University, Budapest, Hungary
János Novák, Dept. of Internal Medicine and Gastroenterology, Pandy Hospital, Gyula, Békés County, Hungary
Correspondence to: Dr. Pál Demeter, St. John's Hospital, Outpatient Clinic of Gastroenterology, Szőlőskertút 7, Budakeszi 2092, Hungary. pauldemeter@axelero.hu
Telephone: +36-30-9222985 **Fax:** +36-23-457656
Received: 2003-12-10 **Accepted:** 2004-01-16

Abstract

AIM: To assess the relationship between severity of gastroesophageal reflux disease and Epworth sleepiness scale as an indicator of daytime somnolence.

METHODS: One hundred and thirty-four patients underwent an upper panendoscopy as indicated by the typical reflux symptoms and were also investigated with regard to somnolence. Sleepiness was evaluated by Epworth Sleepiness Scale, which was compared to the severity of endoscopic findings (Savary-Miller/modified by Siewert). Patients with psychiatric disorders or being on sedato-hypnotics as well as shift workers were excluded from the study. The relationship between the severity of the reflux disease and daytime somnolence was analyzed with the help of multivariate regression analysis.

RESULTS: A positive tendency was found between the severity of the reflux disease and the corresponding Epworth Sleepiness Scale. In the case of the more severe type - Savary-Miller III - at least a mild hypersomnia was found. For this group daytime somnolence was significantly higher than in the case of the non-erosive type of Gastroesophageal Reflux Disease representing the mildest stage of reflux disease.

CONCLUSION: The severity of Gastroesophageal Reflux Disease influences daytime somnolence.

Demeter P, Visy KV, Gyulai N, Sike R, Tóth TG, Novák J, Magyar P. Severity of gastroesophageal reflux disease influences daytime somnolence: A clinical study of 134 patients underwent upper panendoscopy. *World J Gastroenterol* 2004; 10(12): 1798-1801 <http://www.wjgnet.com/1007-9327/10/1798.asp>

INTRODUCTION

Sleep is potentially conducive to the gastro-esophageal reflux events. The physiological antireflux mechanisms – swallowing rate, salivation, the pressure of the upper and the lower esophageal sphincter, gastric emptying - are reduced as well as the “heartburn-signal” is depressed during the state of sleep^[1-6]. Moreover, the typical lying position facilitates the

flow of the gastric content towards the esophagus due to the forces of gravitation^[2]. Studies of parallel 24 h pH-metry and polysomnography amongst obstructive sleep apneic patients showed that some reflux events coincide with arousals^[3]. At the same time, it was also found that some apneic periods contribute to considerable reflux events, while others not. On the other hand, earlier investigations focusing on the relationship between sleep related breathing disorders and Gastroesophageal Reflux Disease (GERD) have indicated the adverse effect of nocturnal reflux events on the sleep structure^[4,5]. In this respect some epidemiological studies have suggested a relationship between GERD and daytime sleepiness^[6-9]. In 2003 the ProGERD study has established that the effective treatment of GERD reduces sleep disturbances^[10]. The results of a Gallup Telephone Survey – conducted on behalf of the American Gastroenterological Association – have shown that the nocturnal heartburn and the regurgitation of gastric content caused frequent awakenings and sleep disturbances, which could affect daytime performance and the quality of life^[11]. Therefore it appears that the nighttime reflux could have a considerable impact on the quality of sleep and it can also play a significant role in the developing of restless sleep experienced widely by the patients.

The influence of GERD on daytime cognitive functions has not been analyzed yet. In this study we focused on one of the important cognitive functions, on daytime sleepiness and its relation to the severity of GERD. The aim of the study was to describe the association between the severity of GERD and daytime somnolence.

MATERIALS AND METHODS

The database

The study was conducted by a gastroenterologist in two centers. The patients were referred for upper panendoscopy with the typical symptoms of GERD untreated. Psychiatric patients or those who took sedato-hypnotics and shift workers were excluded. The classification of GERD was based on endoscopic findings and the severity of the esophagitis^[12]. We used the conventional Savary-Miller classification of the disease modified by Siewert. The Epworth Sleepiness Scale (ESS) was used as an indicator of daytime somnolence, which is a simple questionnaire measure to assess daytime somnolence amongst patients suffering of sleep-awake disorders^[13-15]. The patient data were collated on an Excel 9.0 worksheet, including the severity grades of GERD (0-IV), the Epworth scale (0-24), age, gender and Body Mass Index (BMI).

Statistical methods

The extent and statistical strength of the potential relationship between GERD severity and daytime somnolence was captured by estimating the impact of diagnosed GERD categories on the indicators of sleepiness relative to the two endpoints of the reflux disease severity scale. We relied on the conventional $P < 0.05$ critical values regarding the statistical tests of the results. At the same time, we also took into account a somewhat weaker, 10% significance level when evaluating the observed

associations, given the relatively small size of the available sample. We used the *SPSS 9*-software package for the statistical procedures.

RESULTS

Basic descriptions of the study population

The total available population covered 134 patients the descriptive statistics are given in Table 1. This population was characterized by an average age of 52.9 years (std. dev. 16.7), a male/female ratio of 65: 69, and an average BMI of 26.4 (std. dev. 5.1). Using the Savary-Miller definitions as modified by Sievert, our patients displayed the following distribution alongside the endoscopic categorization of reflux disease: 24 (18.9%) GERD 0 subjects, 29(21.6%) GERD I subjects, 56 (41.8%) GERD II subjects, 13(9.7%) GERD III subjects, and 12 (8.9%) GERD IV subjects. Note that we included only the sample of GERD cases with 122 patients into the detailed statistical analysis. The exclusion of GERD IV group was justified on the basis of the consideration that this set of patients is inherently heterogeneous regarding the anatomic abnormalities as well as the severity of the reflux disease itself. Obviously, this could be a confounding factor in relation to the effect on our analyzed dependent variable, the daytime sleepiness.

Table 1 Descriptive statistics of the total study population

Variable	Minimum	Maximum	Mean	SD
Age (yr)	17.00	83.00	52.940	16.752
Male	0	1	0.485	-
BMI	17.54	43.94	26.420	5.133
GERD 0	0	1	0.179	-
GERD I	0	1	0.216	-
GERD II	0	1	0.418	-
GERD III	0	1	0.097	-
GERD IV	0	1	0.089	-
EPWORTH	1.00	24.00	7.440	4.226

n=134

Note: The mean values of the dichotomous variables (with cases taking values 0 or 1) refer to frequencies and thus the standard deviation is not an applicable measure for them.

The population means of the Epworth sleepiness scale used as a direct measure of somnolence here was 7.4 (SD. 4.2) (while slightly higher -7.6 (SD4.3) – for the sample covering the GERD 0 and GERD I-IV patients). We created a further dependent variable, "abnormal Epworth", for the observations with an index value greater than 8 taking into account that at least a mild form of hypersomnia could be diagnosed above this level. Since our sample was not primarily directed at patients suffering from sleep disorders, it did not seem to be reasonable to select a higher limit. Nevertheless, the detectable tendencies did not differ qualitatively for the critical Epworth value of 10 from the one, which is presented here. The "abnormal Epworth" took the frequency of 44.8% (and 44.3% after dropping the GERD IV group).

Table 2 shows the patterns for the two above described dependent variables by GERD diagnosis. It is evident that the means for the Epworth indices exhibited increasing values alongside the severity of GERD taking the sub-groups of GERD 0 and GERD I-III together. Whereas GERD I exceeded by 0.5 (6.2% of the population average) and GERD II by 0.7(9.2% of the population average) the 6.7 mean value of our GERD 0 cluster, this difference was already 4.1(54.5% of the population average) in the case of the GERD III group. This increasing tendency reflecting the severity of GERD appeared to be even

more characteristic with respect to the frequencies of "abnormal Epworth". Compared with the 29.1% ratio calculated for GERD 0, the observed percentage increments in the presence of hypersomnia were: 8.8% (19.7% of the population average) for GERD I, 17.3%(38.7% of the population average) for GERD II, and 47.8%(106.9% of the population average) for the GERD III group. For information, the table gives our observations for the GERD IV patients as well: we found the lowest group mean value with respect the Epworth index, but the occurrence of hypersomnia went above the population average. This seems to provide a further aspect regarding the heterogeneity of patients diagnosed with GERD IV.

Table 2 Measures of daytime somnolence by GERD groups

GERD	<i>n</i>	EPWORTH index Mean (Std. dev.)	"Abnormal" EPWORTH >8 Frequency
GERD 0	24	6.708 (4.639)	0.291
GERD I	29	7.172 (4.036)	0.379
GERD II	56	7.393 (3.706)	0.464
GERD III	13	10.769 (5.890)	0.769
GERD IV	12	6.166 (2.588)	0.500
Total sample	134	7.440 (4.226)	0.447

Notes: 1. The equality of the mean values for the Epworth indices could be rejected at 5% significance level on the basis of the Student *t*-tests for the following pairs of GERD groups: GERD III vs GERD II, GERD III vs GERD I, GERD III vs GERD 0, and GERD III vs GERD IV. 2. The Pearson chi-square tests for the frequencies of "abnormal" Epworth indices indicated significant differences at 5% critical value in the case of the following 2x2 tables : GERD III vs GERD II, GERD III vs GERD I, GERD III vs GERD 0.

Statistical analysis and results

To evaluate our observations indicating a positive association between severity of GERD and somnolence more precisely, we performed linear regressions for the variation of the Epworth index and logistic regressions for the probability of "abnormal Epworth" over the sample comprising the GERD 0 and GERD I-III cases. Apart from the categorical variables constructed for the reflux disease classifications, we also included the BMI values, and the observations for gender and age as explanatory variables. Since our estimated models typically gave a better overall fit when measuring age above 50 rather than the number of years directly, we present our result with the former control variable below.

Table 3 summarizes our linear regression analysis. The first two blocks of the table present the results with the inclusion of the additional control variables. Although the sign of the regression coefficient (B) obtained for BMI was positive as expected, the contribution of the variable did not emerge to be statistically significant. At the same time, the higher age was found to reduce the expected value of the Epworth index at $P<0.05$ critical values. As far as the estimates for the GERD categories were concerned, the multivariate regression seemed to support the direct observation that reflux disease severity incurs a positive effect on the extent of the Epworth index. When choosing GERD 0 as the reference category (that is the indicator for this group was excluded), the coefficients for the sub-groups of GERD I-III took positive and increasing values as it is shown by the figures of the first model. These coefficients reached a critical magnitude at the GERD III group, which already proved to be significant at 5% level. In numeric terms, this implied that after filtering out the joint effect of the control variables the Epworth index was estimated to be lifted up by 47.5% of the population mean relative to GERD 0 in the case of the third sub-group of GERD I-III. The negatively

Table 3 Linear regression and dependent variable: Epworth index

	Reference: GERD 0 & control variables			Reference: GERD III & control variables			Reference: GERD 0			Reference: GERD III		
	B	t-stat	Signif	B	t-stat	Signif	B	t-stat	Signif	B	t-stat	Signif
Constant	5.210	2.370	0.019	8.743	3.653	0.000	6.708	7.748	0.000	10.769	9.155	0.000
GERD 0				-3.534	-2.410	0.018				-4.061	-2.780	0.006
GERD I	0.503	0.433	0.666	-3.031	-2.125	0.036	0.464	0.397	0.692	-3.597	-2.541	0.012
GERD II	0.635	0.610	0.543	-2.899	-2.178	0.031	0.685	0.662	0.510	-3.376	-2.586	0.011
GERD III	3.534	2.410	0.018				4.061	2.780	0.006			
BMI	0.092	1.254	0.212	0.092	1.254	0.212						
NEM	-0.002	-0.003	0.998	-0.002	-0.003	0.998						
AGE50	-1.557	-1.999	0.048	-1.557	-1.999	0.048						

n=122

Table 4 Logistic regression, dependent variable: "abnormal" EPWORTH

	Reference: GERD 0 & control variables				Reference: GERD III & control variables				Reference: GERD 0				Reference: GERD III			
	B	Wald-stat	Signif	Odds ratio	B	Wald-stat	Signif	Odds ratio	B	Wald-stat	Signif	Odds ratio	B	Wald-stat	Signif	Odds ratio
Constant	-0.399	0.153	0.695		-0.399	0.153	0.695		-0.079	0.119	0.729		-0.079	0.119	0.729	
GERD		6.547	0.087			6.547	0.087			7.452	0.058			7.452	0.058	
GERD 0					-1.996	6.126	0.013	0.136					-2.091	6.887	0.008	0.124
GERD I	0.404	0.461	0.497	1.498	-1.592	4.234	0.039	0.204	0.394	0.447	0.503	1.484	-1.696	4.963	0.025	0.183
GERD II	0.704	1.748	0.186	2.023	-1.292	3.118	0.077	0.275	0.744	2.025	0.154	2.104	-1.347	3.592	0.058	0.260
GERD III	1.996	6.126	0.013	7.361					2.091	6.887	0.008	8.095				
BMI	0.023	0.406	0.523	1.023	0.023	0.406	0.523	1.023								
NEM	-0.166	0.174	0.675	0.847	-0.166	0.174	0.675	0.847								
AGE50	-0.408	1.112	0.291	0.664	-0.408	1.112	0.291	0.664								

n=122

signed coefficients with decreasing absolute values that were estimated relative to GERD III directly mirrored the results of the first model, but this regression exercise gave an opportunity for further statistical tests (see the second block). Thus, the coefficients obtained for GERD 0 as well as for GERD I, II were significantly ($P < 0.05$) different from zero, and consequently indicated statistically relevant deviations from the expected Epworth value at GERD III serving as the baseline. These two estimations above were repeated without the additional control variables as well (see the third and fourth blocks of Table 3). The coefficients in this case were of course equivalent with the differences of the Epworth means grouped in Table 2. At the same time, the corresponding t -values confirmed our previous results indicating that GERD III was associated with a significantly greater sleepiness scale relative to GERD 0, while GERD 0, GERD I and GERD II were associated with a significantly smaller one relative to the GERD III group.

We could reach essentially similar conclusions on the basis of the logistic regressions investigating the occurrences of the "abnormal Epworth" as it is presented in Table 4. The sign of the coefficients (B) obtained for the additional control variables was the same as in the case of the linear regression, but we could not identify a separate significant effect in this case on the basis of the Wald-tests. At the same time, the Wald-statistic referring to the joint effect of the GERD categories (i.e. the "GERD" row of the table) already displayed a weakly significant ($P < 0.1$) value. The estimates relative to GERD 0 gave again increasing coefficients with odds ratios greater than one (see the parameters of the first model). The odds ratio computed for GERD III was different from one at $P < 0.05$. Correspondingly, we found in absolute terms that the estimated ratio of hypersomnia to the normal cases *ceteris paribus* increased by 7.4 times in the GERD III group compared with

the least severe reflux disease cluster. At the same time, the increasing odds ratios with values lower than one derived from the logistic regression using GERD III as the reference category showed statistically significant differences in the case all less severe reflux disease groups (the second block of the table). (In this respect, GERD II could be regarded as a "transitory" category between GERD III and the milder disease classes as far as this difference appeared to be only weakly significant.) The regressions re-run without the control variables produced the odds ratios that could be directly calculated from the frequencies of Table 2 (see the third and fourth models of Table 4). The Wald-tests performed on these coefficients indicated again that the probability of hypersomnia to occur was significantly higher for GERD III relative to GERD 0, and significantly lower for GERD 0, GERD I and GERD II relative to GERD III.

DISCUSSION

We raised the question whether the well-known nocturnal symptoms of patients suffering from GERD results in the deterioration of daytime cognitive functions. Daytime sleepiness was chosen to relate the severity of GERD assessed by panendoscopy to the measure of ESS. Our results indicate that the more severe GERD groups categorized by the Savary-Miller classification exhibit a gradually increasing, more "somnolent" result by the ESS. Moreover, while in the group GERD 0 only 29% of patients reaches the mild somnolence value of 8 on ESS, in GERD I this rate grows up to 39% and in GERD II it reaches 46%. In the group of GERD III more than 77% of the subjects suffered of significant somnolence. This relationship was confirmed by the multivariate regression analysis when estimating the ESS result directly as well as

when examining the probability of at least mild hypersomnia, especially with regard to significantly higher somnolence observed in the most severe GERD population.

Our findings seem to imply that there is a significant fragmentation in the sleep structure in the case of severe GERD. Previous investigations already indicated that arousals, which play a major role in the fragmentation of the sleep structure, could be generated by some reflux events^[4,16]. The higher positioned and longer than 5 min reflux events are more likely to cause arousals. If the reflux content leaves the esophagus and migrates into the upper respiratory tract, it could irritate the acid sensitive receptors, which are located in the mucus layer^[17]. This irritation would lead to the change in muscle tone as a manifestation of arousal producing a motoric restless sleep. In addition, the regurgitation of the acidic gastric fluid may cause discomfort, choking, aspiration, and disturbed sleep with multiple awakenings. The motoric restless sleep is more likely to happen even independently of the pH value of the gastric content, if the refluxate reaches the sensitive pharyngeal level. We, however only assessed patients with the classical self-reported GERD. In fact, patients with extra esophageal symptoms may develop daytime somnolence even earlier and without visible esophagitis.

Finally, it should be noted that GERD is not the dysfunction of acid production but the insufficiency of the LES. So it is important to explore daytime somnolence in the cases of severe and therapy refractory GERD^[18]. These cases can be caused by sleep-related breathing disorders, which can augment the symptoms of GERD and cause daytime sleepiness as well.

REFERENCES

- 1 **Pasricha PJ.** Effect of sleep on gastroesophageal physiology and airway protective mechanisms. *Am J Med* 2003; **115**(Suppl 3A): 114S-118S
- 2 **Khoury RM,** Camacho-Lobato L, Katz PO, Mohiuddin MA, Castell DO. Influence of spontaneous sleep positions on nighttime recumbent reflux in patients with gastroesophageal reflux disease. *Am J Gastroenterol* 1999; **94**: 2069-2073
- 3 **Penzel T,** Becker HF, Brandenburg U, Labunski T, Pankow W, Peter JH. Arousal in patients with gastro-oesophageal reflux and sleep apnoea. *Eur Respir J* 1999; **14**: 1266-1270
- 4 **Ing AJ,** Ngu MC, Breslin AB. Obstructive sleep apnea and gastroesophageal reflux. *Am J Med* 200; **108**(Suppl 4A): 120S-125S
- 5 **Orr WC.** Sleep-related breathing disorders. Is it all about apnea? *Chest* 2002; **121**: 8-11
- 6 **Janson C,** Gislason T, De Backer W, Plaschke P, Bjornsson E, Hetta J, Kristbjarnason H, Vermeire P, Boman G. Daytime sleepiness, snoring and gastro-oesophageal reflux amongst young adults in three European countries. *J Intern Med* 1995; **237**: 277-285
- 7 **Gislason T,** Janson C, Vermeire P, Plaschke P, Bjornsson E, Gislason D, Boman G. Respiratory symptoms and nocturnal gastroesophageal reflux: a population-based study of young adults in three European countries. *Chest* 2002; **121**: 158-163
- 8 **Janson C,** Gislason T, De Backer W, Plaschke P, Bjornsson E, Hetta Kristbjarnason H, Vermeire P, Boman G. Prevalence of sleep disturbances among young adults in three European countries. *Sleep* 1995; **18**: 589-597
- 9 **Suganuma N,** Shigedo Y, Adachi H, Watanabe T, Kumano-Go T, Terashima K, Mikami A, Sugita Y, Takeda M. Association of gastroesophageal reflux disease with weight gain and apnea, and their disturbance on sleep. *Psychiatry Clin Neurosci* 2001; **55**: 255-256
- 10 **Leodolter A,** Kulig M, Nocon M, Vieth M, Lindner D, Labenz J. Esomeprazole therapy improves sleep disorders in patients with gastroesophageal reflux disease (GERD): A report from the ProGERD study. *Gastroenterology* 2003; **124**(Suppl 1): A-226
- 11 **Shaker R,** Castell DO, Schoenfeld PS, Spechler SJ. Nighttime heartburn is an under-appreciated clinical problem that impacts sleep and daytime function: the results of a Gallup survey conducted on behalf of the American Gastroenterological Association. *Am J Gastroenterol* 2003; **98**: 1487-1493
- 12 **Savary M,** Miller G. The esophagus: handbook and atlas of endoscopy. *Solothurn, Switzerland: Verlag Gassman* 1978: 135-142
- 13 **Johns MW.** A new method for measuring daytime sleepiness: the epworth sleepiness scale. *Sleep* 1991; **14**: 540-545
- 14 **Johns MW.** Sleep propensity varies with behaviour and the situation in which it is measured: the concept of somnificity. *J Sleep Res* 2002; **11**: 61-67
- 15 **Roth T,** Roehrs TA. Etiologies and sequelae of excessive daytime sleepiness. *Clin Ther* 1996; **18**: 562-576
- 16 **Orr WC,** Robinson MG, Johnson LF. The effect of esophageal acid volume on arousals from sleep and acid clearance. *Chest* 1991; **99**: 351-354
- 17 **Thach BT.** Maturation and transformation on reflexes that protect the laryngeal airway from liquid aspiration from fetal to adult life. *Am J Med* 2001; **111**(Suppl 8A): 69S-77S
- 18 **Wolf S,** Furman Y. Sleep apnea and gastroesophageal reflux disease. *Ann Intern Med* 2002; **136**: 490-491

Edited by Wang XL Proofread by Xu FM

Intestinal microecology and quality of life in irritable bowel syndrome patients

Jian-Min Si, Ying-Cong Yu, Yu-Jing Fan, Shu-Jie Chen

Jian-Min Si, Yu-Jing Fan, Shu-Jie Chen, Department of Gastroenterology, Sir Run Run Shaw Affiliated Hospital of Zhejiang University, Hangzhou 310016, Zhejiang Province, China

Ying-Cong Yu, Third People's Hospital of Wenzhou, Wenzhou 325000, Zhejiang Province, China

Supported by Shanghai Sine Pharmaceutical Co., Ltd. and Wenzhou Science and Technology Bureau, Zhejiang Province, China

Correspondence to: Professor Jian-Min Si, Department of Gastroenterology, Sir Run Run Shaw Affiliated Hospital of Zhejiang University, Hangzhou 310016, Zhejiang Province, China. sijm@163.net

Telephone: +86-571-86090073-2005

Received: 2003-08-02 **Accepted:** 2003-11-19

Abstract

AIM: It has been noticed that gastroenteritis or dysentery plays a role in pathogenesis of irritable bowel syndrome (IBS), and antibiotics can increase functional abdominal symptoms, both of which may be partly due to intestinal flora disorders. This study was to determine the change of gut flora of IBS, a cluster of abdominal symptoms. Because of the chronic course and frequent occurrence of the disease, IBS patients suffered much from it. So the quality of life (QoL) of IBS patients was also evaluated in this study.

METHODS: Twenty-five Rome II criteria-positive IBS patients were recruited, and 25 age and gender-matched healthy volunteers were accepted as control. The fecal flora, including *Lactobacillus*, *Bifidobacterium*, *Bacteroides*, *C. perfringens*, *Enterobacteriaceae* and *Enterococcus*, were analyzed quantitatively and qualitatively. We also calculated the ratio of *Bifidobacterium* to *Enterobacteriaceae* (B/E ratio) in both IBS patients and controls. In both groups, the data were further analyzed based on age difference, and comparisons were made between the younger and elder subgroups. We also evaluated the quality of life (QoL) of IBS patients and the control group using the Chinese version of SF-36 health questionnaire.

RESULTS: In IBS patients, the number of fecal *Bifidobacterium* was significantly decreased and that of *Enterobacteriaceae* was significantly increased compared with that in healthy controls (both $P < 0.05$). The mean microbial colonization resistance (CR) of the bowel in IBS patients was smaller than 1, making a significant difference compared with that in control which was more than 1 ($P < 0.01$). There was no significant difference in gut flora between two subgroups. While in control, the elder subgroup presented more *Enterobacteriaceae* than the younger one ($P < 0.05$). Compared with the control group, IBS patients had significantly lower scores on all SF-36 scales, with the exception of physical functioning. However, there was no significant correlation between quality of life and enteric symptoms in IBS patients.

CONCLUSION: There are intestinal flora disorders in IBS patients, which may be involved in triggering the IBS-like symptoms. IBS patients experience significant impairment

in QoL, however, the impairment is not caused directly by enteric symptoms.

Si JM, Yu YC, Fan YJ, Chen SJ. Intestinal microecology and quality of life in irritable bowel syndrome patients. *World J Gastroenterol* 2004; 10(12): 1802-1805

<http://www.wjgnet.com/1007-9327/10/1802.asp>

INTRODUCTION

Many patients with typical irritable bowel syndrome (IBS) blamed all their bowel symptoms for acute gastroenteritis or dysentery, and it has been shown that intestinal infection does play an important role in the pathogenesis of IBS^[1,2]. Although the mechanisms underlying postinfectious IBS are not clear, microbiological environmental alterations may be partly responsible for the pathogenesis. There is even evidence showing that antibiotics can increase functional abdominal symptoms^[3]. In some cases, this is due to the colonization of pathogenic bacteria such as *Clostridium difficile*. In others it may be due to changes in bowel flora, which have been shown to persist for many months after a single antibiotic course.

In this study, the changes of intestinal microecology were investigated. Since age or sex may influence the composition of gut flora^[4,5], age and sex-matched controls were recruited and the gut flora was also studied. Furthermore, the impact of IBS on quality of life (QoL) was evaluated using SF-36 health questionnaire (Chinese Version). Finally, the correlation between enteric symptoms scores and QoL in IBS patients was analyzed.

MATERIALS AND METHODS

Subjects

From September 2002 to March 2003, 25 Rome II criteria-positive^[6] IBS patients diagnosed at the Department of Gastroenterology, Sir Run Run Shaw Affiliated Hospital of Zhejiang University were recruited (8 males, 17 females, mean age 45.40 ± 10.56 years, ranging from 26 to 64 years). Subjects were excluded if they had any organic disease and those who had taken antibiotics or microecological modulators within 2 weeks before study were also ruled out. Twenty-five healthy volunteers (age and gender-matched) were accepted as control. All procedures were approved by the Ethical Committee of Medical College of Zhejiang University.

Bacteriological analysis of intestinal flora

Selective culture medium for *Lactobacillus* (LBS), *Bifidobacterium* (Bs), *Bacteroides* (NBGT), *Enterococcus* (EC) and *Enterobacteriaceae* (EMB) was prepared by the Institute of Infectious Diseases, the First Affiliated Hospital of Zhejiang University. The culture medium for *C. perfringens* (TSN) was bought from Biomerieux (French). Glove box (Forma Scientific, Lnc., USA) was also needed.

Bacteriological analysis of intestinal flora was performed using the method that was essentially the same as that established by Okusa *et al*^[7]. In brief, 10 g fresh stool was collected and sent to laboratory within 30 min in an anaerobic

jar. After 1 g fresh stool was aseptically quantified and homogenized, then diluted with an anaerobic solution in an anaerobic chamber (decimal dilutions up to 10^{-7} were prepared). Fifty μL of serial dilution volume (10^{-1} , 10^{-3} , 10^{-5} , 10^{-7}) of the specimens was spread over the above agar media with a L-shape stick. Aerobic bacteria were cultivated at 37°C in an incubator for 48 h and anaerobic bacteria were cultivated in glove box (800 mL/L nitrogen, 100 mL/L hydrogen, and 100 mL/L carbon dioxide) at 37°C for 48-72 h. After incubation, morphologically distinct colonies were described, calculated, isolated, and identified by morphology, Gram reaction and API fermentation tests, *etc.* The results were expressed as \log_{10} of the number of bacteria per gram wet weight of feces (colony forming units/g, CFU/g). In our study, 2×10^2 (CFU) were set as the lowest detection limit. The incidence of each bacterial group recorded as the percentage of each bacterial group relative to the total bacteria was calculated. Furthermore, the ratio of *Bifidobacterium* to *Enterobacteriaceae* (B/E ratio) was calculated as the microbial colonization resistance (CR) of the bowel according to literature^[8].

Evaluation of enteric symptoms

IBS patients were evaluated by enteric symptom questionnaire^[9] which included 6 scales concerning abdominal pain, mucous stool and distention, *etc.* (Table 1). Each scale was scored as "0" to "3" according to the severity and frequency of symptoms, whereas a higher score meant a more severe and frequent occurrence. The sum of each score was regarded as the general assessment of enteric symptoms.

Assessment of quality of life

The quality of life (QoL) of IBS patients and controls was evaluated with the Chinese version of short form 36 (SF-36) established by Wang *et al.*^[10], which included 8 multiple dimensions as physical functioning (PF), role physical (RP), bodily pain (BP), general health (GH), vitality (VT), social functioning (SF), role emotional (RE) and mental health (MH). Scores were calculated according to corresponding formula and rules. Each dimension was scored from 0 to 100, with higher scores indicating better QoL.

Statistical analysis

Quantitative data were compared using different *t* test according to different situations, with the results expressed as mean \pm SD. The detection frequency was analyzed by Chi-squares test. The correlation between enteric symptom scores and QoL in IBS patients was detected by Pearson's correlation analysis. A *P* value less than 0.05 was considered statistically significant. All analysis was conducted using SPSS10.0 statistical passage.

RESULTS

Gut flora and microbial colonization resistance and detection frequency

Compared with the control group, IBS patients showed a significant decrease in *Bifidobacterium* but an increase in

Enterobacteriaceae (both $P < 0.05$). The mean microbial colonization resistance (CR) of the bowel in IBS patients was smaller than 1, which was significantly different from that in control ($P < 0.01$). There were no significant differences in *Lactobacillus*, *Bacteroides*, *Enterococcus* between two groups. The detection frequency of *C. perfringens* in IBS group was much lower than that in the control group ($P < 0.01$, Table 2).

Table 2 Number of bacteria and B/E value in two groups (mean \pm SD, LgN/g stool)

Bacteria (%)	IBS patients (n=25)	Controls(n=25)
<i>Lactobacillus</i>	6.79 \pm 1.73 (92)	6.79 \pm 1.94 (84)
<i>Bifidobacteria</i> ^a	8.14 \pm 2.14 (96)	9.32 \pm 1.22 (100)
<i>Bacteroides</i>	10.49 \pm 0.56 (100)	10.62 \pm 0.79 (100)
<i>C. perfringens</i> ^d	7.32 \pm 2.12 (40)	6.66 \pm 1.68 (80)
<i>Enterococcus</i>	7.96 \pm 1.53 (100)	7.49 \pm 1.29 (100)
<i>Enterobacteriaceae</i> ^a	9.02 \pm 1.04 (100)	8.44 \pm 0.95 (100)
B/E value ^b	0.91 \pm 0.27 (96)	1.12 \pm 0.23 (100)

The data in the bracket mean positive rate (This is applicable for the following tables including flora.). ^a $P < 0.05$ flora vs control, ^b $P < 0.01$ B/E value vs control, ^d $P < 0.01$ detection frequency vs control.

The data were further analyzed based on age difference. Both groups were sorted on ascending order, the first 12 persons were chosen as younger subgroup (mean age 36.25 \pm 5.17) and the rest 13 (mean age 53.85 \pm 6.14) as elder one. We found that in IBS group, there was no significant difference in gut flora between two subgroups, but CR was smaller than 1 in both subgroups. While in control, the elder subgroup presented more *Enterobacteriaceae* than the younger subgroup ($P < 0.05$), but smaller CR (Tables 3, 4).

Table 3 Number of bacteria and B/E value in younger subgroup and elder subgroup in IBS group (mean \pm SD, LgN/g stool)

Bacteria (%)	Younger subgroup (n=12)	Elder subgroup (n=13)
<i>Lactobacillus</i>	6.63 \pm 1.83 (100)	6.98 \pm 1.70 (84)
<i>Bifidobacteria</i>	7.60 \pm 2.65 (100)	8.68 \pm 1.38 (92)
<i>Bacteroides</i>	10.52 \pm 0.42 (100)	10.47 \pm 0.72 (100)
<i>C. perfringens</i>	8.84 \pm 1.07 (25)	6.89 \pm 2.20 (54)
<i>Enterococcus</i>	8.26 \pm 1.58 (100)	7.69 \pm 1.50 (100)
<i>Enterobacteriaceae</i>	9.16 \pm 1.22 (100)	8.90 \pm 0.88 (100)
B/E value	0.85 \pm 0.33 (100)	0.98 \pm 0.19 (92)

QoL of IBS patients

IBS patients experienced significant impairment in QoL (Table 5). Compared with control group, IBS patients had significantly lower scores on all SF-36 scales, with the exception of physical functioning. Decrements in QoL were most pronounced in general health (GH, mean score 41.40), role physical (RP, mean score 52.00) and vitality (VT, mean score 53.40). Others like mental health (MH), role emotional (RE), bodily pain (BP) and social functioning (SF) were also impaired.

Table 1 Enteric symptom scales

Symptoms	0	1	2	3
Duration of abdominal pain (h/d)	None	<1	2-8	>8
Frequency of abdominal pain (d/wk)	None	1-2	3-5	6-7
Ratio of abnormal shape of stool	None	<1/4	1/4-3/4	>3/4
Ratio of abnormal passage of defecation	None	<1/4	1/4-3/4	>3/4
Ratio of mucous stool	None	<1/4	1/4-3/4	>3/4
Distention or gastrectasia when defecation	None	<1/4	1/4-3/4	>3/4

Table 4 Number of bacteria and B/E value in younger subgroup and elder subgroup of control group. (mean±SD, LgN/g stool)

Bacteria (%)	Younger subgroup (n=12)	Elder subgroup (n=13)
<i>Lactobacillus</i>	6.18±2.07 (75)	7.20±1.83 (92)
<i>Bifidobacteria</i>	9.32±1.08 (100)	9.32±1.38 (100)
<i>Bacteroides</i>	10.49±0.71 (100)	10.75±0.89 (100)
<i>C.perfringens</i>	6.45±1.82 (83)	6.89±1.59 (77)
<i>Enterococcus</i>	7.09±1.49 (100)	7.86±1.00 (100)
<i>Enterobacteriaceae^a</i>	8.05±1.14 (100)	8.81±0.57 (100)
B/E value	1.19±0.28 (100)	1.06±0.14(100)

^aP<0.05 flora vs control.

Table 5 QoL of IBS patients and normal control (mean±SD)

QoL scale	IBS patients (n =25)	Controls (n =25)
PF	74.40±26.78	85.40±15.53
RP ^a	52.00±44.44	77.00±37.44
BP ^b	73.33±17.57	84.89±16.00
GH ^b	41.40±15.04	73.40±13.52
VT ^b	53.40±16.94	69.60±17.38
SF ^b	75.00±12.50	84.50±12.12
RE ^b	61.33±41.59	96.00±11.06
MH ^b	58.24±16.21	80.00±13.52

^aP<0.05, ^bP<0.01 vs healthy control.

Correlation between QoL and enteric symptoms in IBS patients

Although IBS patients presented a negative correlation between bodily pain (BP) and enteric symptoms (correlation coefficient: 0.347), the difference was not significant ($P>0.05$). While vitality (VT), role emotional (RE), general health (GH) and physical functioning (PF), showed no significant difference with QoL in IBS patients (Table 6).

Table 6 Correlation between enteric symptoms and QoL in IBS (mean±SD)

	Score of QoL	Score of enteric symptoms	Correlation coefficient (r)
PF	74.40 (26.78)	7.56 (2.31)	-0.062
RP	52.00 (44.44)	7.56 (2.31)	0.060
BP	73.33 (17.57)	7.56 (2.31)	-0.347
GH	41.40 (15.04)	7.56 (2.31)	-0.137
VT	53.40 (16.94)	7.56 (2.31)	-0.280
SF	75.00 (12.50)	7.56 (2.31)	0.018
RE	61.33 (41.59)	7.56 (2.31)	-0.257
MH	58.24 (16.21)	7.56 (2.31)	0.001

DISCUSSION

The etiology of IBS is still unclear and the pathogenetic mechanisms are only partly understood. Intestinal motility alteration, visceral hypersensitivity, disturbed intestinal reflexes, psychological disorders, food intolerance and gastrointestinal infection and imbalance of gut flora were involved in the pathogenesis of IBS^[11]. IBS patients presented various intestinal motility alterations, which were recognized as the basic pathophysiological factor. Evidences have shown that there were gastroparesis and small bowel dysmotility in IBS^[12]. The motility index (MI), mean number and peak amplitude of high amplitude propagating contractions (HAPCs) in IBS patients were significantly greater than those in controls. These abnormalities might be related to shortened colonic transit time^[13]. The migrating motor complex (MMC) was found to be an

important mechanism controlling bacterial growth in the upper small bowel. Its disruption could promote duodenal bacterial overgrowth and bacterial translocation^[14].

Food-related microbial alteration of the bowel might be partly responsible for the occurrence of IBS, since many IBS symptoms might be triggered or aggravated by food intake^[15]. King and his colleagues found that colonic-gas production, particularly hydrogen, was greater in IBS patients, and both symptoms and gas production were reduced by an exclusion diet. This reduction might be associated with alterations in the activity of hydrogen-consuming bacteria^[16]. It has been shown that IBS patients have abnormal lactulose breath test (LBT), suggesting the presence of small intestinal bacterial overgrowth (SIBO) or an increased number of enteric organisms. Normalization of LBT could lead to a significant reduction in IBS symptoms^[17]. On the other hand, some studies reported that the incidence of IBS was increased after acute gastroenteritis or dysentery. Under the circumstance of infection, an alterant microbiological environment might influence the number of lymphocytes, mast cells and enteroendocrine cells in the mucosa, rapid transit and a tendency to a secretory state was often found^[1].

In this study, we found that IBS patients had a decrease of beneficial *Bifidobacteria* and overgrowth of potentially pathogenic *Enterobacteriaceae*. The ratio of B/E was smaller than 1, suggesting impairment of microbial colonization resistance (CR) of the bowel in IBS. Once CR was destroyed by antibiotics or other reasons, bacterial infection or dysbacteriosis might emerge^[18].

Intestinal dysbacteriosis may be related to the occurrence of symptoms of IBS, since *Bifidobacteria* are considered to be beneficial to health. It involves in the production of essential mucous nutrients, such as short-chain fatty acids (SCFAs) and lactic acid, by lactose fermentation. They have been shown to eliminate toxins and unnecessary substances, such as hydroxybenzene, ammonia and steroids. They may also participate in the regulation of intestinal functions, such as nutrient synthesis and absorption. *Bifidobacteria* could prevent the overgrowth of potentially pathogenic organisms by bacterial barrier or by producing antibiotics^[5,19]. *Enterobacteriaceae*, the main cause of endotoxin, may produce toxins such as ammonia, sulfured hydrogen^[5]. Endotoxin could temporarily impair canine gut absorptive function both in colon and in jejunum, with decreased absorption of water, glucose and electrolytes, including sodium, chloride, and potassium^[20]. When endotoxin of Gram-negative bacteria was administered intravenously in rats, the migrating myoelectric complex was replaced by spike bursts accompanied by rapid transit^[21]. These effects may contribute to the occurrence of diarrhea. Microecological modulators could prominently relieve IBS-like enteric symptoms, suggesting the close relationship between gut flora and IBS^[22,23].

Ageing may affect the flora residing in the gut and outside of it^[5]. In our study, we found that the intestinal microecology showed an overgrowth of *Enterobacteriaceae* with age in normal control, implying that age may interact with the gut flora. The overgrowth of *Enterobacteriaceae* may also account for the susceptibility to intestinal infection and endotoxemia in elderly people. *Bifidobacteria* have been shown to have a close relationship with human longevity^[5]. While in IBS group, age had no influence on gut flora, since there was intestinal dysbacteriosis in both younger and elder subgroups.

There was a high detection frequency of *C. perfringens* in normal control, without any apparent pathogenic effect. It was supposed that changes of gut flora in IBS might result in a relatively high detection frequency of *C. perfringens*. Therefore, further studies are needed to elucidate this phenomenon.

Anyway, microbial metabolic processes have been going on like in a black box^[24]. Although almost all organic compounds and nutrients, fiber, digestive secretions and desquamated

epithelial cells of the host can enter into microorganismic metabolic chains and processes, little is known about this metabolic chain and process. Further studies are still needed. However, there was dysbacteriosis in IBS patients. Whether it is the effect or just cause of IBS remains unclear.

The purpose of focusing on health-related quality of life (HRQL) is to go beyond the presence and severity of symptoms of disease and to examine how patients perceive and experience these manifestations in their daily lives^[25]. Briefly, HRQL concerns more about the physical, psychological and social functioning.

IBS is not a life-threatening disease. Its impacts include costs associated with diagnosis and treatment, production losses due to morbidity and pain and diarrhea, *etc.*^[26]. With a questionnaire, Silk^[27] found that IBS impacted significantly on personal relationships and working practices. Some even complained that IBS prevented them from applying for promotion or a new job. IBS patients had impaired quality of life in general health, vitality, social functioning, *etc.*^[9,28]. According to the research of Gralnek *et al.*^[29], IBS patients experienced significantly worse HRQL in some aspects than those with gastroesophageal reflux disease (GERD) or diabetes mellitus (DM). IBS patients had even worse bodily pain, fatigue, and social functioning when compared with dialysis-dependent end-stage renal disease patients.

In our study, we also found that IBS patients had significantly lower scores on all SF-36 scales with the exception of physical functioning, when compared with the age and sex-matched control group. Decrements in QoL were most pronounced in general health, role physical and vitality. However, there was no significant correlation between QoL and enteric symptoms, which might be due to the frequent presence of anxiety, depression, fatigue and anorexia in IBS patients^[11,30]. Compared with the control, neuroticism, hypochondriasis and depression were significantly more prevalent in IBS patients attending a clinic, which would have a prominently negative influence on QoL. Hypnotherapy was effective in treating IBS, suggesting that psychological factors may play an important role in IBS. Thus the general impacts of IBS may go far beyond those of enteric symptoms, implicating that IBS is a psychosomatic disease.

ACKNOWLEDGMENTS

The authors thank Professor Lan-Juan Li, Directors Yun-Song Yu, Yun-Bo Chen, Zhong-Wen Wu, Dang-Sheng Xiao at Department of Infectious Diseases, First Affiliated Hospital of Zhejiang University for their technical supports.

REFERENCES

- 1 **Robin CS**. Estimating the importance of infection in IBS. *Am J Gastroenterol* 2003; **98**: 238-241
- 2 **Wang LH**, Fang XC, Pan GZ. Intestinal infection and irritable bowel syndrome. *Zhonghua Neike Zazhi* 2002; **41**: 90-93
- 3 **Maxwell PR**, Rink E, Kumar D, Mendall MA. Antibiotics increase functional abdominal symptoms. *Am J Gastroenterol* 2002; **97**: 104-108
- 4 **Ran L**, Chen ZF, Fu P, Yang BL, Li ZG, Yao JH, Zhao X. A survey on gut flora of 184 cases of healthy populations in Beijing area. *Zhongguo Weishengtaixue Zazhi* 1999; **11**: 10-12
- 5 **Zhang DR**. Xiao Hua Xi Jibing Yu Weishengtai. The 1st edition. Shanghai: *Shanghai Science Technol Press* 2001: 58-61
- 6 **Thompson WG**, Longstreth GF, Drossman DA, Heaton KW, Irvine EJ, Muller-Lissner SA. Functional bowel disorder and functional abdominal pain. *Gut* 1999; **45**: 43-47
- 7 **Okusa T**, Ozaki Y, Sato C, Mikuni K, Ikeda H. Long-term ingestion of lactosucrose increases Bifidobacterium sp. In human fecal flora. *Digestion* 1995; **56**: 415-420

- 8 **Wu ZW**, Li LJ, Ma WH, Yu YS, Chen YG. A new index for microbial colonization resistance of the bowel-the ratio of B/E. *Zhejiang Yufang Yixue* 2000; **7**: 4-5
- 9 **Si JM**, Chen SJ, Sun LM. An epidemiological and quality of life study of irritable bowel syndrome in Zhejiang province. *Zhonghua Neike Zazhi* 2003; **42**: 34-37
- 10 **Wang HM**, Li L, Shen Y. A study on quality of life of inhabitants in Hangzhou area using Chinese version of SF-36. *Zhonghua Yufang Yixue Zazhi* 2001; **35**: 428-430
- 11 **Xu GM**. Strengthen the study on etiology of irritable bowel syndrome. *Zhonghua Neike Zazhi* 2003; **42**: 73-74
- 12 **Evans PR**, Bak YT, Shuter B, Hoschl R, Kellow JE. Gastroparesis and small bowel dysmotility in irritable bowel syndrome. *Dig Dis Sci* 1997; **42**: 2087-2093
- 13 **Chey WY**, Jin HO, Lee MH, Sun SW, Lee KY. Colonic motility abnormality in patients with irritable bowel syndrome exhibiting abdominal pain and diarrhea. *Am J Gastroenterol* 2001; **96**: 1499-1506
- 14 **Nieuwenhuijs VB**, Verheem A, van-Duijvenbode-Beumer H, Visser MR, Verhoef J, Gooszen HG, Akkermans LM. The role of interdigestive small bowel motility in the regulation of gut microflora, bacterial overgrowth, and bacterial translocation in rats. *Ann Surg* 1998; **228**: 188-193
- 15 **Simren M**, Mansson A, Langkilde AM, Svedlund J, Abrahamsson H, Bengtsson U, Bjornsson ES. Food-related gastrointestinal symptoms in the irritable bowel syndrome. *Digestion* 2001; **63**: 108-115
- 16 **King TS**, Elia M, Hunter JO. Abnormal colonic fermentation in irritable bowel syndrome. *Lancet* 1998; **352**: 1187-1189
- 17 **Mark P**, Evelyn JC, Henry CL. Normalization of lactulose breath testing correlates with symptom improvement in irritable bowel syndrome: a double-blind, randomized, placebo-controlled study. *Am J Gastroenterol* 2003; **98**: 412-419
- 18 **Van der Waaij D**. History of recognition and measurement of colonization resistance of the digestive tract as an introduction to selective gastrointestinal decontamination. *Epidemiol Infect* 1992; **109**: 315-326
- 19 **Jiang T**, Savaiano DA. Modification of colonic fermentation by Bifidobacteria and pH *in vitro*. Impact on lactose metabolism, short-chain fatty acid, and lactate production. *Dig Dis Sci* 1997; **42**: 2370-2377
- 20 **Cullen JJ**, Spates ST, Ephgrave KS, Hinkhouse MM. Endotoxin temporarily impairs canine colonic absorption of water and sodium. *J Surg Res* 1998; **74**: 34-38
- 21 **Hellstrom PM**, al-Saffar A, Ljung T, Theodorsson E. Endotoxin actions on myoelectric activity, transit, and neuropeptides in the gut. Role of nitric oxide. *Dig Dis Sci* 1997; **42**: 1640-1651
- 22 **Zhang DR**, Dong XX, Bao YF. Intestinal floral changes in patients with irritable bowel syndrome after ingestion of clostridium butyrium preparation. *Zhongguo Weishengtaixue Zazhi* 1999; **11**: 164-166
- 23 **Zhang J**, Jin F, Le QL, Zhang ZJ. The effect of Jinshuangqi on irritable bowel syndrome. *Zhongguo Weishengtaixue Zazhi* 2002; **14**: 289-291
- 24 **Porter J**, Pickup RW. Nucleic acid-based fluorescent probes in microbial ecology: application of flow cytometry. *J Microbiol Methods* 2000; **42**: 75-79
- 25 **Glise H**, Wiklund I. Health-related quality of life and gastrointestinal disease. *J Gastroenterol Hepatol* 2002; **17**(Suppl): S73-85
- 26 **Boivin M**. Socioeconomic impact of irritable bowel syndrome in Canada. *Can J Gastroenterol* 2001; **15**(SupplB): 8B-11B
- 27 **Silk DB**. Impact of irritable bowel syndrome on personal relationships and working practices. *Eur J Gastroenterol Hepatol* 2001; **13**: 1327-1332
- 28 **Hahn BA**, Yan S, Strassels S. Impact of irritable bowel syndrome on quality of life and resource use in the united states and united kingdom. *Digestion* 1999; **60**: 77-81
- 29 **Gralnek IM**, Hays RD, Kilbournem A, Naliboff B, Mayer EA. The impact of irritable bowel syndrome on health-related quality of life. *Gastroenterology* 2000; **119**: 654-660
- 30 **Lydiard RB**, Falsetti SA. Experience with anxiety and depression treatment studies: implications for designing irritable bowel syndrome clinical trials. *Am J Med* 1999; **107**: 65S-73S

Management of nonfunctioning islet cell tumors

Han Liang, Pu Wang, Xiao-Na Wang, Jia-Cang Wang, Xi-Shan Hao

Han Liang, Pu Wang, Xiao-Na Wang, Jia-Cang Wang, Xi-Shan Hao, Department of Gastrointestinal Oncological Surgery, Tianjin Cancer Hospital, Tianjin Medical University, Hexi District, Tianjin 300060, China

Correspondence to: Professor Han Liang, Department of Gastrointestinal Oncological Surgery, Tianjin Cancer Hospital, Tianjin Medical University, Hexi District, Tianjin 300060, China. hanliang86@yahoo.com

Telephone: +86-22-23340123

Received: 2002-08-26 **Accepted:** 2002-10-12

Abstract

AIM: To more clearly define the clinical and pathological characteristics and appropriate diagnosis and treatment of nonfunctioning (NFICTs) islet cell tumors, and to review our institutional experience over the last 30 years.

METHODS: The records of 43 patients confirmed to have nonfunctioning islet cell tumors of pancreas were retrospectively reviewed. Survival was estimated by the Kaplan-Meier methods and potential risk factors for survival were compared with the log-rank tests.

RESULTS: The mean age was 31.63 years (range, 8 to 67 years). There were 7 men and 36 women. Twenty-eight patients had a confirmed diagnosis of nonfunctioning islet cell carcinoma (NFICC) and benign islet cell tumors were found in 15 patients. The most common symptoms in patients with NFICTs were abdominal pain (55.8%), nausea and/or vomiting (32.6%), fatigue (25.6%) and abdominal mass (23.3%). Preoperative ultrasonic and computed tomography localized the tumors in all patients. Forty-three NFICTs were distributed throughout the pancreas, with 21 located to the right of the superior mesenteric vessels, 10 in the body of the pancreas, 6 in the tail of the pancreas, and multiple tumors were found in one patient. Thirty-nine of 43 patients (91%) underwent surgical resection. Surgical treatment was curative in 30 patients (70%) and palliative in 9(21%). The resectability and curative resection rate in patients with NFICC of pancreas were 89% and 61%, respectively. The overall cumulative 5- and 10-year survival rates for patients with NFICC were 58.05% and 29.03%, respectively. Radical operation and diameter of cancer small than 10 cm were positive prognostic factors in females younger than 30 years old. Multivariate Cox regression analysis indicated that radical operation was the only independent prognostic factor, $P=0.007$.

CONCLUSION: Nonfunctioning islet cell tumors of pancreas are found mainly in young women. The long-term results for patients undergone surgery, especially curative resection are good.

Liang H, Wang P, Wang XN, Wang JC, Hao XS. Management of nonfunctioning islet cell tumors. *World J Gastroenterol* 2004; 10(12): 1806-1809
<http://www.wjgnet.com/1007-9327/10/1806.asp>

INTRODUCTION

Tumors arising from the pancreatic islet cell are rare and represent a heterogeneous group of benign or malignant lesions. Most tumors present with well characterized syndromes, whereas others appear to be nonfunctioning. Functioning tumors, such as gastrinomas, insulinomas, and vasoactive intestinal peptide-secreting tumour (VIPomas), are characterized by extensive production of single polypeptide hormones which lead to specific clinical syndromes. Nonfunctioning tumors, which account for 15% and 52% of tumors, are not associated with clinical syndromes, as they do not produce an excess of any active polypeptide hormones^[1,2]. These Lesions tend to occur later and have a different clinical course from their functioning counterparts.

The purpose of this study was to analyze the clinical presentations, diagnosis, management, and prognosis of a large group of patients with nonfunctioning islet cell tumors (NFICTs) of pancreas managed at a single cancer center to determine the natural history and optimum management of such lesions.

MATERIALS AND METHODS

Patients

A total of 43 patients with NFICTs were treated between 1972-2002. The diagnosis of islet cell tumors of pancreas was established by histopathologic examination. Tumors were considered nonfunctional if no clinical symptoms of excess hormone were present.

The disease was considered regional if no evidence of metastases in the liver or elsewhere was found either during surgery or by imaging techniques. Metastases in the liver or elsewhere were considered distant.

Methods

Clinical records were reviewed with regard to patient demographics, clinical features, diagnostic procedures, pathologic findings, operative details, medical treatment, and long-term survival. All patients were followed up by return visits, letters from the follow-up department, correspondence with primary surgeons, or telephone contact within the last months from the conclusion of this study. Survival rate was estimated by the Kaplan-Meier methods, and potential risk factors for survival were compared with the log-rank tests and Cox methods. Ninety-five percent confidence intervals were calculated for specific estimates of survival.

RESULTS

Clinical characteristics

There were 36 females and 7 males with a mean age of 31.63 years and a range of 8 to 67 years and the details are shown in Figure 1. At the time of diagnosis, the median age of male and female patients was 33.57 and 31.25 years, respectively ($P>0.05$). The clinical presentations are illustrated in Table 1. The predominant presentations were abdominal pain, nausea and/or vomiting, fatigue and abdominal pain. None of the patients displayed the clinical features of an endocrine disorder. The duration from the onset of symptoms to diagnosis for all patients ranged from 3 d to 10 years (median 6 mo). Only three patients were asymptomatic, with the tumor found incidentally.

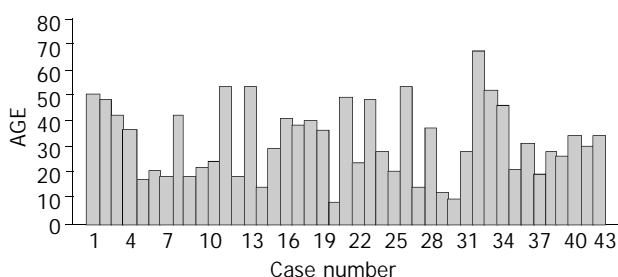


Figure 1 Age distribution in 43 NFICTs patients.

Abdominal ultrasonography (US) and spiral CT were the most commonly employed to detect the primary tumor in all but the patient with emergency operation. Correct prediction of an islet cell tumors based on CT and US results was achieved only in 6(20%) patients. The common diagnosis of CT was carcinoma of pancreas (in 20 patients). Endoscopic retrograde cholangiopancreatography(ERCP) was performed in 6 patients to determine the cause of obstructive jaundice. Magnetic resonance imaging (MRI) and endoscopic ultrasonography (EUS) localized the tumor and the local extension correctly in 5 and 4 patients, respectively.

Table 1 Clinical presentations

Symptoms	Patients(n=43)	(%)
Abdominal pain	24	55.8
Nausea and/or vomiting	14	32.6
Fatigue	11	25.6
Abdominal mass	10	23.3
Back pain	9	21.0
Jaundice	8	18.6
Weight loss	5	11.6
No symptoms	3	7.0
Acute abdomen	1	2.3

Pathological findings

Confirmation of malignancy was mainly based on the demonstration of local invasion, microscopic vascular or perineural invasion, lymph node metastases, hepatic metastasis or distant metastases. Twenty-eight patients were histopathologically diagnosed as nonfunctioning islet cell carcinoma (NFICC) of pancreas.

The size of islet malignant and benign tumors ranged from 2.5 cm to 15 cm (mean 10 cm) and from 4 cm to 30 cm (mean 9.9 cm), respectively ($P>0.05$). Metastases were presented in 6 patients at the time of operation. There were 21 tumors located in the head of the pancreas, 10 in tail, 6 in the body, 5 in body and tail (Table 2). Multiple tumors were presented only in one patient.

Table 4 Primary operative procedures

Procedure	Malignant (n=28)	(%)	Benign (n=15)	(%)
Pancreatoduodenectomy	8	28.5	2	13.3
Pylorus-preserving pancreatoduodenectomy	0	0	1	6.7
Distal pancreatectomy + splenectomy	7	25.0	5	33.3
Subtotal pancreatectomy + splenectomy	4	14.3	2	13.3
Distal pancreatectomy	2	7.1	0	0
Enucleation	1	3.6	4	26.7
Double bypass	1	3.6	0	0
Biliary bypass	3	10.7	1	6.7
Gastric bypass	1	3.6	0	0
Biopsy only	1	3.6	0	0

Table 2 Location of the tumors

Location	Malignant (n=28)	Benign (n=15)
Head	13	8
Tail	8	2
Body	2	4
Body+Tail	4	1
Multiple	1	0

Operative detail and outcome

We performed 30(70%) potentially curative resections, 9(21%) palliative resections, and 4(9.3%) bypass procedures, resulting in a resection rate of 91%. Of the 28 patients with islet cell carcinoma of pancreas, potentially curative resection, palliative resection, palliative bypass and biopsy were performed in 17(61%), 8(28.6%), 3(10.7%) and 1(3.6%), respectively (Table 3). The potentially curative resection was performed in 87% of patients with benign islet cell tumors compared to only 61% of those with NFICC ($P<0.05$). Table 4 shows the type of operative procedures for patients with benign and malignant islet cell tumors. There was no 30-day mortality.

Table 3 Nature operative procedures

Nature	Malignant (n=28)	(%)	Benign (n=15)	(%)
Curative resection	17	61.0	13	87.0
Palliative resection	8	28.6	1	6.7
Palliative bypass	2	5.1	1	6.7
Biopsy only	1	3.6	0	0

Other treatment modalities

A total of 13 cases of NFICC received adjuvant therapy after curative operation, of them 9 patients with NFICC underwent chemotherapy (5 of them with the regimen of FAM and 4 others with 5-FU only) after a curative operation. One of them developed liver metastasis one year later, the another patient died 23 mo postoperatively. The remaining 7 patients were alive with no evidence of disease for a median 45.5 mo (range 15-96 mo). Another 4 patients with malignant tumors underwent radiation plus chemotherapy (three with FAM, and one with 5-FU). All these 4 patients were alive with no evidence of disease for 55.6 mo in average (range 14-124 mo).

Among the patients with NFICC who underwent palliative resection, 4(50%) were given chemotherapy with 5-FU and CF, one developed multiple liver metastasis 13 mo later.

Survival

The cumulative 5- and 10-year survival rates for all patients with NFICC were 58.05% and 29.03%, respectively (Figure 2). Table 5 demonstrates the survival in detail. The median survival of female patients was 120 mo, which was better than the survival for male patients (45 mo, $P=0.312$, Figure 3). Patients who were

younger than 30 years had a better long-term survival than those elder than 30 years, but the difference was not statistical significant (Figure 4, $P=0.758$). Figure 5 compares survival curves for the curative operations and noncurative groups. Survivals at 5- and 10-years were significant better for patients who underwent PD and STRP than those who underwent palliative operation, $P=0.007$. As demonstrated in Figure 6, survivals were better for patients with smaller tumors than those with larger ones, but the difference was not statistically significant, $P=0.1169$.

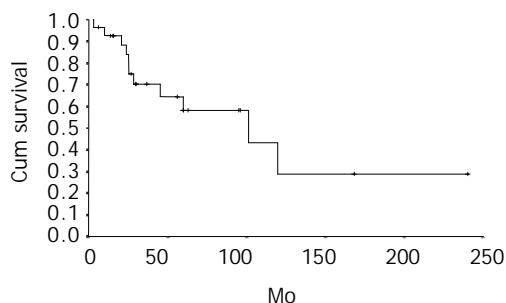


Figure 2 Actual survival for all patients with NFICC ($n=28$).

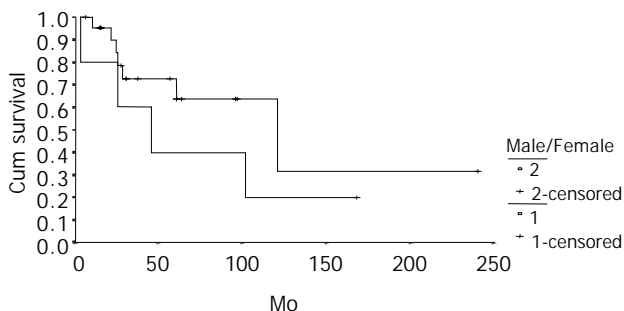


Figure 3 Survival comparison between male ($n=5$) and female ($n=23$) patients with NFICC ($P=0.312$).

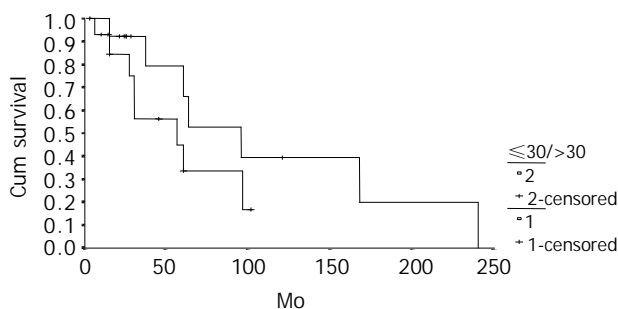


Figure 4 Survival comparison between younger (≤ 30 years, $n=14$) and elder (>30 years, $n=14$) patients with NFICC $P=0.7582$).

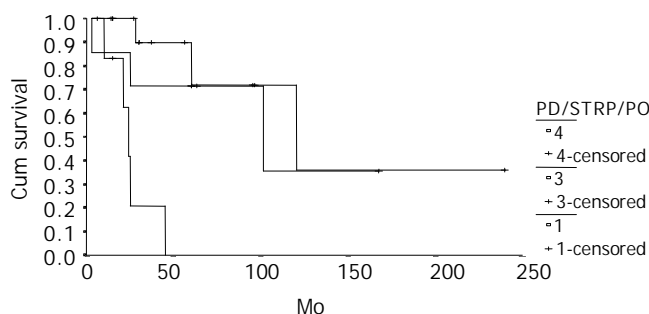


Figure 5 Survival comparison between patients who underwent different operations (PD, $n=7$; Subtotal resection of pancreas, $n=14$, palliative operation, $n=7$, $P=0.0005$).

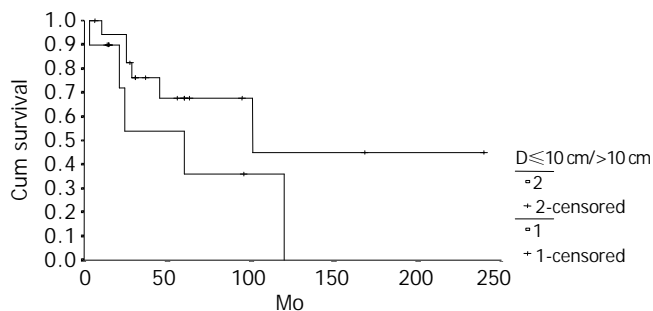


Figure 6 Survival comparison between patients with cancer of different diameters ($D\leq 10$ cm, $n=18$; $D>10$ cm, $n=10$, $P=0.1169$).

Table 5 Survival of patients with NFICC

Patients	n	5-yr survival (%)	10-yr survival (%)	Median survival (mo)
ALL cases	28	58.05	29.03	60±4.35
Male	5	40.00	20.00	45±21.92
Female	23	63.49	31.75	120±44.05
≤ 30 yr	14	54.17	36.11	120±64.02
>30 yr	14	57.69	0	101
$D^1\leq 10$ cm	18	67.57	49.05	101
$D^1>10$ cm	10	36.00	0	60±21.75
PD ²	7	71.43	35.71	101±56.73
STRP ³	14	72.00	36.00	120±44.94
PO ⁴	7	0	0	24±3.19

¹Diameter of the cancer, ²Pancreatoduodenectomy, ³Subtotal resection of pancreas, ⁴palliative operation.

Table 6 Multivariate Cox regression analysis

Factors	Standard Error	Degree of freedom	P value
Sex	2.190	1	0.679
Age	1.292	1	0.821
Location	35.889	1	0.917
Operation	1.528	1	0.007
Tumor Size	117.237	1	0.903
Radial/palliative	117.261	1	0.884

DISCUSSION

NFICTs are developmentally and histologically identical to functioning tumors but differ in their clinical course and outcome. In this group, the mean age at diagnosis (31.63 years) was 20 years younger than those reported by other researchers^[3-5], but it was similar to some domestic reports^[6-8]. The mean age of the females was 31.25 years, a little bit younger than that of males (33.57 years). It was considered that more male than female patients suffered from islet cell tumors. The ratio of males: females was 1.29:1^[9-12]. In contrast to other reports, we found there were more females than males with this disease (F:M=36:7). It was similar to domestic reports^[6-8]. The reason is unknown. The difference races may be responsible for this phenomenon.

The clinical presentations of NFICTs were mainly due to mass effects. When tumors were smaller than 5 cm in diameter, most patients were asymptomatic^[16]. The symptoms or signs at the time of diagnosis were abdominal pain, weight loss, nausea/vomiting, jaundice and abdominal mass^[5-7,10].

Abdominal US and contrast-enhanced spiral CT were used. In this series, abdominal US and CT were used to detect the primary tumor in all but the patients with emergency operation. Correct prediction of a NFICT based on CT and US results was

achieved only in 6(20%) patients. It is believed that the following features appear to be characteristic for NFICTs: a well defined pancreatic mass with a unusually large size, moderate to strong mass hyperdense in the arterial contrastographic phase of either the primary or the hepatic metastases, and no infiltration of vessels of the celiac axis or the proximal superior mesenteric artery^[4,13]. A recent report showed that in patients with NFICT, a hypoechoic mass with an irregular central echogenic area on EUS or complete obstruction of the main pancreatic duct on ERCP suggested a malignancy^[14].

EUS and laparoscopy could provide accurate preoperative and intraoperative localization to enhance laparoscopic or open operation^[15]. Magnetic resonance imaging, angiography, transabdominal sonography and portal venous sampling could yield an additional accuracy for the diagnosis.

NFICTs of pancreas were believed to be malignant in the presence of distant metastases, or histologic evidence of vascular, lymphatic, or perineural invasion^[3,10]. However, because all NFICTs had a similar histologic appearance, the absence of lymphovascular or perineural invasion could not exclude the potential for malignant behavior. Patients who had locally advanced nonmetastatic diseases at diagnosis subsequently died of complications of the primary tumor^[11]. It was believed that neither vascular or perineural invasion nor electron microscopy and any other histologic criteria could accurately predict whether tumor behavior was benign or malignant^[5]. Most previous reports have suggested that NFICTs are biologically very aggressive, with a malignancy rate ranging from 82% to 100%^[1,11]. However, our findings do not support these previous observations, as we found that the evidence of malignancy based upon evidence of local invasion or presence of metastases could accurately predict the clinical outcome. We believe that the diagnosis of malignancy in NFICTs should be mainly based upon gross findings of local tumor invasion or the presence of metastases. Some reports showed that patients with benign islet tumors were alive at the follow-up time point^[16]. The 5 year survival rate of patients with benign tumors in our group was 100%.

Despite of advances in the multidisciplinary management of NFICC of pancreas in recent decades, surgery plays still an important role in providing potentially curative resections, relieving symptoms, and improving long-term survival. The resectable rate of this disease was 24% to 100%^[3,4,17] and curative resection was performed only in 61% patients^[5]. In current series, the resectable rate was 91%, the curative resection rate for the patients was 61%, which was comparable to that in literature reports. Radical operation could yield a best survival for patients with NFICC, palliative debulking could reduce the mass of tumor, enhance other treatment modalities, it might also prevent other complications such as recurrent pancreatitis, intestinal obstruction, and gastrointestinal bleeding due to direct tumor invasion or varices secondary to splenic vein obstruction^[7]. For this reason, noncurative debulking of tumors might improve survival. Repeated resections for respectable recurrences or metastases might be indicated to improve survival also^[8].

Tumor size is not included in the diagnostic criteria, but when NFICC is definitely diagnosed, it is helpful to predict the survival. When the diameter was larger than 10 cm, the long-term survival would be poor. On the other hand, female and younger (≤ 30 years) patients would have a better survival.

One third of our patients received adjuvant chemotherapy after radical resection of the primary tumors. Obviously, this was too small a number to make any meaningful observations

regarding the efficacy of any specific chemotherapy regimen. Moertel and colleagues^[18] reported a large prospective, randomized multi-institutional trial of two regimens using 162 patients with advanced islet cell carcinomas. They concluded that the combination of streptozotocin and 5-fluorouracil could produce a response rate of 63%, which was significantly higher than 34% seen with streptozotocin alone.

REFERENCES

- 1 **Kent RB 3rd**, van Heerden JA, Weiland LH. Nonfunctioning islet cell tumors. *Ann Surg* 1981; **193**: 185-190
- 2 **Broughan TA**, Leslie JD, Soto JM, Hermann RE. Pancreatic islet cell tumors. *Surgery* 1986; **99**: 671-678
- 3 **Eriksson B**, Skogseid B, Lundqvist G, Wide I, Wilander E, Oberg K. Medical treatment and long-term survival in a prospective study of 84 patients with endocrine pancreatic tumors. *Cancer* 1990; **65**: 1883-1890
- 4 **Bartsch DK**, Schilling T, Ramaswamy A, Gerdes B, Celik I, Wagner HJ, Simon B, Rothmund M. Management of nonfunctioning islet cell carcinomas. *World J Surg* 2000; **24**: 1418-1424
- 5 **White TJ**, Edney JA, Thompson JS, Karrer FW, Moor BJ. Is there a prognostic difference between functional and nonfunctional islet cell tumors? *Am J Surg* 1994; **168**: 627-629
- 6 **Zheng X**, Guo K, Tian Y, Li J, Guo R, Zhan Y, Song M, Shen K. Cellular composition and anatomic distribution in nonfunctioning pancreatic endocrine tumors: immunohistochemical study of 30 cases. *Chin Med J* 1998; **111**: 373-376
- 7 **Lo CY**, van Heerden JA, Thompson GB, Grant CS, Soreide JA, Harmsen WS. Islet cell carcinoma of the pancreas. *World J Surg* 1996; **20**: 878-883
- 8 **Jiang XS**, Shou NH, Li ZY. Diagnosis and treatment of non-functional islet cell tumors. *Zhongguo Putong Waikē Zazhi* 1998; **7**: 87-89
- 9 **Cheslyn-Curtis S**, Sitaram V, Williamson RC. Management of non-functioning neuroendocrine tumours of the pancreas. *Br J Surg* 1993; **80**: 625-627
- 10 **Legaspi A**, Brennan MF. Management of islet cell carcinoma. *Surgery* 1988; **104**: 1018-1023
- 11 **Evans DB**, Skibber JM, Lee JE, Cleary KR, Ajani JA, Gagel RF, Sellin RV, Fenoglio CJ, Merrell RG, Hickey RC. Nonfunctioning islet cell carcinoma of the pancreas. *Surgery* 1993; **114**: 1175-1182
- 12 **Furukawa H**, Mukai K, Kosuge T, Kanai Y, Shimada K, Yamamoto J, Mizuguchi Y, Ushio K. Nonfunctioning islet cell tumors of the pancreas: clinical, imaging and pathological aspects in 16 patients. *Jpn J Clin Oncol* 1998; **28**: 255-261
- 13 **Procacci C**, Carbognin G, Accordini S, Biasiutti C, Bicego E, Romano L, Guarise A, Minniti S, Pagnotta N, Falconi M. Nonfunctioning endocrine tumors of the pancreas: possibilities of spiral CT characterization. *Eur Radiol* 2001; **11**: 1175-1183
- 14 **Sugiyama M**, Abe N, Izumisato Y, Yamaguchi Y, Yamato T, Tokuhara M, Masaki T, Mori T, Atomi Y. Differential diagnosis of benign versus malignant nonfunctioning islet cell tumors of the pancreas: the roles of EUS and ERCP. *Gastrointest Endosc* 2002; **55**: 115-119
- 15 **Spitz JD**, Lilly MC, Tetik C, Arregui ME. Ultrasound-guided laparoscopic resection of pancreatic islet cell tumors. *Surg Laparosc Endosc Percutan Tech* 2000; **10**: 168-173
- 16 **Yeo CJ**, Wang BH, Anthone GJ, Cameron JL. Surgical experience with pancreatic islet-cell tumors. *Arch Surg* 1993; **128**: 1143-1148
- 17 **Thompson GB**, van Heerden JA, Grant CS, Carney JA, Ilstrup DM. Islet cell carcinomas of the pancreas: a twenty-year experience. *Surgery* 1988; **104**: 1011-1017
- 18 **Moertel CG**, Hanley JA, Johnson LA. Streptozotocin alone compared with streptozotocin plus fluorouracil in the treatment of advanced islet-cell carcinoma. *N Eng J Med* 1980; **303**: 1189-1194

Association of -238G/A polymorphism of tumor necrosis factor-alpha gene promoter region with outcomes of hepatitis B virus infection in Chinese Han population

Liang-Ping Lu, Xing-Wang Li, Ying Liu, Guo-Chang Sun, Xue-Ping Wang, Xi-Lin Zhu, Quan-You Hu, Hui Li

Liang-Ping Lu, Hui Li, Department of Epidemiology, Institute of Basic Medical Sciences, Chinese Academy of Medical Sciences; School of Basic Medicine, Peking Union Medical College, Beijing 100005, China

Xing-Wang Li, Department of Internal Medicine, Ditan Hospital, Beijing 100011, China

Xue-Ping Wang, Department of Clinical Laboratory, Ditan Hospital, Beijing 100011, China

Ying Liu, Xi-Lin Zhu, National Laboratory of Medical Molecular Biology, Institute of Basic Medical Sciences, Chinese Academy of Medical Sciences; School of Basic Medicine, Peking Union Medical College, Beijing 100005, China

Guo-Chang Sun, Quan-You Hu, Department of Clinical Laboratory, Shunyi District Hospital, Beijing 101300, China

Supported by the Research Fund for the Doctoral Training Program from the Ministry of Education, No.2000002340 and Beijing Municipal Government Commission for Science & Technology, No. H020920020590

Correspondence to: Hui Li, Department of Epidemiology, Institute of Basic Medical Sciences, Chinese Academy of Medical Sciences; School of Basic Medicine, Peking Union Medical College, 5 Dongdan 3 Tiao, Beijing 100005, China. lihui99360@sohu.com

Telephone: +86-10-65296971 **Fax:** +86-10-65225752

Received: 2003-11-22 **Accepted:** 2003-12-16

Abstract

AIM: To clarify whether -238G/A polymorphism of tumor necrosis factor- α (TNF- α) gene promoter region was associated with outcomes of hepatitis B virus (HBV) infection in Han population of northern China, and to analyze the gene-environment interaction between -238G/A polymorphism and cigarette smoking or alcohol consumption.

METHODS: A case-control study was conducted to analyze the association of TNF- α gene promoter polymorphism with HBV infection outcomes. A total of 207 patients with chronic hepatitis B (HB) and 148 cases of self-limited HBV infection from Ditan Hospital and Shunyi District Hospital in Beijing, respectively were recruited. History of smoking and alcohol drinking was inquired by a questionnaire. The -238G/A polymorphism of TNF- α gene promoter was genotyped by polymerase chain reaction-restricted fragment length polymorphism (PCR-RFLP).

RESULTS: The frequencies of GG and GA genotypes were 98.07% and 1.93% in chronic HB patients and 93.24% and 6.76% in self-limited HBV infection individuals, respectively ($\chi^2=5.30$, $P=0.02$). The frequency of G allele was significantly higher in patients with chronic HB than in individuals with self-limited HBV infection (99.03% vs 96.62%, $\chi^2=5.20$, $P=0.02$). Only modestly increased risk of onset of chronic HB was found in smokers ($OR=1.40$, 95% CI : 0.87-2.28, $P=0.14$) and drinkers ($OR=1.26$, 95% CI : 0.78-2.05, $P=0.32$). There was a positive interaction between genotype GG and cigarette smoking with an interaction index (II) of 2.95, or alcohol consumption with an II of 1.64.

CONCLUSION: The -238G/A polymorphism of TNF- α gene promoter region is independently associated with different outcomes of HBV infection.

Lu LP, Li XW, Liu Y, Sun GC, Wang XP, Zhu XL, Hu QY, Li H. Association of -238G/A polymorphism of tumor necrosis factor-alpha gene promoter region with outcomes of hepatitis B virus infection in Chinese Han population. *World J Gastroenterol* 2004; 10(12): 1810-1814

<http://www.wjgnet.com/1007-9327/10/1810.asp>

INTRODUCTION

Human beings are susceptible to HBV. HBV infection in adults is usually clinically inapparent, and the virus is cleared after infection. Only about 5-10% of them become persistently infected and develop chronic liver disease with varied severity^[1], which could not be explained completely by the virus itself and environmental factors. Progress of HBV infection might be affected by host genetic susceptibility^[2].

Since HBV is not cytolytic for hepatocytes, and hepatocellular injuries caused by HBV infection are predominantly immune-mediated^[3-6]. Immune attacks by host against HBV are mainly mediated by a cellular reaction. Cytokines produced by immune cells, such as TNF- α , might play a role in immune pathogenesis of HBV infection.

TNF- α is secreted by macrophages, monocytes, neutrophils, T-cells and NK-cells following the stimulus by bacterial lipopolysaccharides and shows a broad spectrum of biological activities, causing cytolysis and cytostasis in many tumor cell lines *in vitro*. Several lines of evidence suggest the importance of TNF- α in HBV. Patients with acute and chronic hepatitis B have an elevated plasma concentration of TNF- α ^[7,8]. Some individual differences in cytokine production may be related to genetic components, and certain polymorphism alleles may be associated with higher or lower levels of TNF- α production, which has been ascribed to polymorphisms within the regulatory regions of cytokine genes^[9-14].

There were some studies about the association of TNF- α gene promoter polymorphism with progress of the disease^[13,15], but ethnic difference could lead to different results. The aim of the present study was to investigate whether the TNF- α promoter polymorphism at position -238 was associated with outcomes of HBV infection in Han people of northern China.

MATERIALS AND METHODS

Study design

Case-control study was used to analyze the association between the polymorphism at position -238 of TNF- α gene promoter and outcomes of HBV infection, as well as the interaction between the gene and smoking or alcohol drinking.

Subjects

The clinical diagnosis for all subjects in this study was based

on references^[16,17]. Two hundred and seven patients with chronic HB from Ditan Hospital in Beijing, China during November 2001 to August 2002 were recruited, with inclusion criteria as follows: hepatitis B surface antigen (HBsAg) seropositive, anti-HBs antibodies (anti-HBs) seronegative, abnormally elevated serum alanine aminotransferase level, and duration of chronic HB ≥ 2 years. One hundred and forty-eight subjects with self-limited HBV infection were from Shunyi District Hospital in Beijing, China during the same period, with inclusion criteria as positive for both anti-HBs and anti-HBc antibodies only, definitely negative for HBsAg, normal liver function tests, and no history of HBV vaccination. All subjects were Chinese Han people and they were recruited with their informed consent for genetic analysis. Venous blood was drawn from all subjects after an overnight fasting. Serum was separated immediately to detect ALT and blood corpuscles were stored at -70 °C to extract DNA and analyze genotypes.

Serological tests

Enzyme-linked immunosorbent assay (ELISA) was used for detection of serum HBsAg, anti-HBs, and anti-HBc (IMX; Abbott Diagnostics, North Chicago, IL).

Analysis of TNF- α gene promoter polymorphism

Genomic DNAs were obtained from peripheral blood leukocytes by standard phenol-chloroform extraction^[18]. The -238G/A polymorphism in the promoter region of TNF- α gene was detected by PCR-RFLP as described by Miyazoe *et al.*^[19]. A 152-bp fragment was amplified using primers (5' : 5' AGAAG ACCCCCCTCGGAACC3' and 3' : 5' ATCTGGAGGAAGCG GTAGTG3'). Amplification was performed in a Perkin Elmer thermocycler (2700; Applied Biosystems, Foster City, CA) with 50 ng of genomic DNA, 20 pmol/L of each primer, 200 μ mol/L each dNTP, 1.5 mmol/L MgCl₂, standard polymerase chain reaction (PCR) buffer and 1U Taq polymerase (Shanghai Biocolor) to 25 μ L reaction system. PCR procedure was as follows: predenaturation at 94 °C for 2 min, followed by 30 cycles of denaturation at 94 °C for 1 min, annealing at 59 °C for 1 min and extension at 72 °C for 1 min, with a final extension at 72 °C for 5 min to terminate the reaction. After amplification, 10 μ L PCR product was digested with restriction endonuclease (Msp-I 3U, Takara Bio Cor Dalian) at 37 °C for 5 h after addition of appropriate incubation buffer and ddH₂O to 20 μ L. The digestion products were separated on 3% agarose gel and visualized directly under UV light with ethidium bromide staining. One base-exchange substitution from A to G position at position -238 created the Msp-I restriction site, resulting in 20- and 132-bp fragments with Msp-I digestion, where -238A allele could not create the Msp-I restriction site, which resulted in an 152-bp fragment.

Cigarette smoking and alcohol consumption

Cigarette smoking and alcohol consumption of the subjects were assessed by their self-report in a questionnaire.

Evaluation of the interaction

The gene-environment interaction was defined according to Rothman *et al.*^[20], with a formula to estimate interaction index (II)=OR₁₁/OR₀₁ \times OR₁₀. II>1 was defined as positive, and II<1 as negative.

Statistical analysis

The frequencies of TNF- α promoter region alleles and genotypes were estimated. The Hardy-Weinberg equilibrium and frequencies of the alleles and genotypes between two groups were compared by χ^2 tests with two-tailed *P* values^[21].

Odds ratios and their 95% confidence intervals were also calculated as measures of association of the polymorphism with outcomes of HBV infection. All the statistical procedures were performed with SAS version 6.12.

RESULTS

Characteristics of subjects

The main characteristics of study subjects are summarized in Table 1. The average age of the patients with chronic HB and subjects with self-limited HBV infection was 40.06(40.06 \pm 14.55) and 37.75(37.75 \pm 13.35) years, respectively, without significant difference ($t=1.53$, $P=0.40$). The number of men was more in the group of patients with chronic HB than in the group of subjects with self-limited HBV infection ($\chi^2=36.54$, $P<0.01$). The proportion of married subjects was also different between the two groups ($\chi^2=6.29$, $P=0.01$), whereas their education level was not statistically different ($\chi^2=5.66$, $P=0.06$).

Table 1 Main characteristics of study groups

Variable	Chronic HB <i>n</i> =207(%)	Self-limited HBV infection <i>n</i> =148 (%)	<i>P</i>
Age (mean \pm SD)	40.06 \pm 14.55	37.75 \pm 13.35	0.40
Male/Female	162/45	70/78	<0.01
Marital status			0.01
Married	162 (78.26)	131 (88.51)	
Unmarried	45 (21.74)	17 (11.49)	
Education level			0.06
Lower than high school	13 (6.28)	18 (12.16)	
High school	126 (60.87)	94 (63.51)	
Above high school	68 (32.85)	36 (24.32)	

Association of -238G/A polymorphism of TNF- α promoter and behavior factors with outcomes of HBV infection

The distribution of genotype frequencies in patients with chronic HB and subjects with self-limited HBV infection was coincident with Hardy-Weinberg equilibrium ($\chi^2=0.02$, $P=0.89$; $\chi^2=0.02$, $P=0.89$).

The genotype distribution and allele frequencies of the -238 polymorphism in both groups are shown in Table 2. The homozygous AA genotype was not found in the study. Two hundred and three (98.07%) patients with chronic HB had GG genotype, significantly increased as compared with subjects with self-limited HBV infection ($\chi^2=5.30$, $P=0.02$). The frequency of G allele in patients with chronic HB was significantly higher than that in subjects with self-limited HBV infection (99.03% vs 96.62%, $\chi^2=5.20$, $P=0.02$).

The frequency of exposure to cigarette smoking or alcohol consumption in patients with chronic HB was significantly higher than that in subjects with self-limited HBV infection ($OR>1$), but there was no significant difference between the two groups ($\chi^2=2.13$, $P=0.14$ and $\chi^2=0.99$, $P=0.32$).

Multivariate unconditional logistic regression model was used to analyze the association of outcomes of HBV infection with age, sex, cigarette smoking, alcohol consumption and genotypes. It indicated that genotype GG was independently associated with chronic HB after the other factors were controlled (Table 4).

Gene-environmental interaction

As GG genotype was defined as positive exposure in this study, the results of gene-environmental interaction analysis between GG genotype and smoking or alcohol drinking are shown in Tables 5, 6. The odds ratios for smoking exposure alone and GG genotype alone were 0.50 ($P=1.00$) and 2.60 ($P=0.19$), respectively, whereas the odds ratio for combination of smoking and GG genotype was 3.84 ($P=0.07$) in a synergic pattern

Table 2 Genotype and allele frequencies in subjects with chronic HB and self-limited HBV infection

Group	n	Genotype (%) ¹			Allele (%) ²	
		A/A	A/G	G/G	A	G
Chronic HB	207	0 (0.0)	4 (1.93)	203 (98.07)	4 (0.97)	410 (99.03)
Self-limited HBV infection	148	0 (0.0)	10 (6.76)	138 (93.24)	10 (3.38)	286 (96.62)

¹ $\chi^2=5.30$, $P=0.02$, ² $\chi^2=5.20$, $P=0.02$.

Table 3 Association of behavior factors with risk of chronic HB

Characteristics	Chronic HB (%)	Self-limited HBV infection (%)	OR (95%CI)	P
Cigarette smoking			1.40 (0.87, 2.28)	0.14
Yes	74 (35.75)	42 (28.38)		
No	133 (64.25)	106 (71.62)		
Alcohol consumption			1.26 (0.78, 2.05)	0.32
Yes	69 (33.33)	42 (28.38)		
No	138 (66.67)	106 (71.62)		

Table 4 Multivariate logistic regression analysis for determinants of chronic HB

Variable	β	χ^2	P	OR	95%CI
Intercept	-0.5076	7.2203	0.0072	—	—
Sex (Male=1, Female=0)	1.4088	35.1138	<0.0001	4.091	2.567-6.519
-238G/A (GG=1, GA=0)	1.4183	5.1467	0.0233	4.132	1.212-14.085

($II=3.84/0.50 \times 2.60=2.95$). The odds ratio was 0.78 ($P=1.00$) for alcohol consumption alone and 3.18 ($P=0.11$) for GG genotype alone, respectively, and their combined odds ratio was 4.07 ($P=0.05$), indicating an effect of interaction between them ($II=4.07/0.78 \times 3.18=1.64$).

Table 5 Case-control analysis for interaction between cigarette smoking and GG genotype

Cigarette smoking	GG genotype	Case ¹	Control ²	OR (95%CI)	P
-	-	3	6	1	—
-	+	130	100	2.60 (0.56-13.49)	0.19
+	-	1	4	0.50 (0.01-10.45)	1.00
+	+	73	38	3.84 (0.79-20.73)	0.07

¹Chronic HB patients, ²self-limited HBV infection individuals.

Table 6 Case-control analysis for interaction between alcohol consumption and GG genotype

Alcohol consumption	GG genotype	Case ¹	Control ²	OR (95%CI)	P
-	-	3	7	1	—
-	+	135	99	3.18 (0.72-15.96)	0.11
+	-	1	3	0.78 (0.02-18.21)	1.00
+	+	68	39	4.07 (0.08-21.25)	0.05

¹Chronic HB patients, ²self-limited HBV infection individuals.

DISCUSSION

It is estimated that HBV is present in about 130 million chronic carriers, accounting for 10% of Chinese population^[22]. HBV infection can result in acute hepatitis, HBV carriage, chronic hepatitis, liver cirrhosis, even primary hepatocellular carcinoma. One reason of broad spectrum of HBV infection could be attributed to the interaction of genetic and environmental factors. The majority of human genetic studies on HBV

infection focused on human leucocyte antigen (HLA) in recent years^[23-27]. Several pro-inflammatory cytokines such as interleukin-2 and interferon- γ and TNF- α , have been identified to participate in the process of viral clearance and host immune response to HBV^[28,29]. In addition, TNF- α /TNF- α receptor system has an important role in the pathogenesis of liver damage and viral clearance^[30].

TNF- α is a principal mediator of inflammation and cellular immune response regulated both transcriptionally and posttranscriptionally^[31]. In the past years -238G/A polymorphism in a putative regulation box of the TNF- α gene promoter region has been identified. Genetic polymorphisms in the regulatory regions of various cytokine genes could influence the amount of cytokines produced in response to inflammatory stimuli.

In our study, chronic HB patients and self-limited HBV infection individuals (the same as the patients recovered from HB in other studies) were recruited to examine the TNF- α promoter polymorphism at position -238. The results demonstrated that 98.07% of the patients carried genotype GG, significantly higher than the frequency in those with self-limited infection, suggesting that genotype GG could increase the risk of chronic HB and was different from the report of Hohler^[32]. Fifty-three (75%) of 71 subjects with chronic HB were homozygous in TNF- α G/G, lower than the frequency of those with self-limited HBV infection (94%). Ethnic difference could play a certain role in these conflicting results, because the results from several studies suggested that the distribution of TNF promoter polymorphisms in the study subjects was different from those with other racial origins^[7,32,33].

The difference in genotype and allele frequency between patients with chronic HB and subjects with self-limited HB infection in our study suggested that GG genotype might have no advantage to antigen presenting, but further study would be needed to demonstrate its significance as a susceptible gene. This difference may be due to the fact that the TNF- α promoter polymorphism at position -238, likely serving as a marker, was in linkage disequilibrium with neighboring genes encoding HLA or other undefined genes, thus possibly influencing the

outcomes of diseases.

Some studies suggested that the TNFA-A allele falling within a putative Y regulation box of the TNF- α promoter, was associated with increased TNF- α expression^[34-36], which was inconsistent with other studies^[37-40]. It is necessary to carry out the experimental study to confirm the causality between the -238G/A polymorphism of TNF- α promoter gene and the outcome of HBV infection, based on the population study.

The gene of TNF- α is located in the HLA class III region in the short arm of chromosome 6. Some single nucleotide polymorphism (SNP) loci have been found in the promoter region of TNF- α gene. It is speculated that these loci would be in linkage disequilibrium with other unknown mutations or HLA genes. It is important to further demonstrate the association of their constructed haplotypes with outcomes of HBV infection.

Epidemiological findings indicated that alcohol consumption and viral hepatitis could act synergistically to promote the development and progression of liver disease. Patients with viral hepatitis and alcohol consumption accelerated their liver injury with a higher risk of liver cirrhosis and primary hepatocellular carcinoma than those with viral hepatitis alone or alcohol consumption alone^[41,42]. Wang^[43] reported cigarette smoking and alcohol consumption were independently associated with elevated ALT levels among anti-HCV-seropositive individuals. Our study showed cigarette smoking and alcohol consumption might be risk factors of chronic HB (OR>1), but further study is needed due to lack of evidence that could reveal statistically significant differences between groups of chronic HB and self-limited HBV infection.

The analysis of gene-environmental interaction in this study showed there was a synergic effect between GG genotype and cigarette smoking or alcohol consumption. The very wide confidence interval was due to only one subject who smoked or drank without GG genotype in patient group, which needs a larger sample size to be confirmed.

In summary, different outcomes of HBV infection are independently associated with TNF- α promoter polymorphism at position -238, and there might be a synergic effect between TNF- α promoter gene and cigarette smoking or alcohol consumption in the development of chronic HB.

ACKNOWLEDGMENT

The authors thank Drs. Yi-Fan Chen, Xiu-Yun Ma, Min-Ying Mu, Hao-Dong Cai, Yun-Zhong Wu, Qing-Hua Dong, Zhi-Hai Cheng, Jie Xu from Ditan Hospital and Drs. Guo-Hua Yan, Xiu-Ling Wang, Yi-Liu from Shunyi District Hospital for data and sample collection.

REFERENCES

- 1 **Chisari FV**, Ferrari C. Hepatitis B virus immunopathogenesis. *Annu Rev Immunol* 1995; **13**: 29-60
- 2 **Wang FS**. Current status and prospects of studies on human genetic alleles associated with hepatitis B virus infection. *World J Gastroenterol* 2003; **9**: 641-644
- 3 **Chisari FV**. Rous-Whipple Award lecture. Viruses, immunity, and cancer: lessons from hepatitis B. *Am J Pathol* 2000; **156**: 1117-1132
- 4 **Jung MC**, Pape GR. Immunology of hepatitis B infection. *Lancet Infect Dis* 2002; **2**: 43-50
- 5 **Chisari FV**. Cytotoxic T cells and viral hepatitis. *J Clin Invest* 1997; **99**: 1472-1477
- 6 **Rehermann B**. Immune responses in hepatitis B virus infection. *Seminars Liver Disease* 2003; **23**: 21-37
- 7 **Bozkaya H**, Bozdayi M, Turkyilmaz R, Sarioglu M, Cetinkaya H, Cinar K, Kose K, Yurdaydin C, Uzunlimoglu O. Circulating IL-2, IL-10 and TNF-alpha in chronic hepatitis B: their relations to HBeAg status and the activity of liver disease. *Hepato Gastroenterol* 2000; **47**: 1675-1679

- 8 **Tokushige K**, Yamaguchi N, Ikeda I, Hashimoto E, Yamauchi K, Hayashi N. Significance of soluble TNF receptor-I in acute-type fulminant hepatitis. *Am J Gastroenterol* 2000; **95**: 2040-2046
- 9 **Westendorp RGJ**, Langermans JAM, Huizinga TWJ, Elouali AH, Verweij CL, Boomsma DI, Vandenbrouke JP. Genetic influence on cytokine production and fatal meningococcal disease. *Lancet* 1997; **349**: 170-173
- 10 **Wilson AG**, Symons JA, McDowell TL, McDevitt HO, Duff GW. Effects of a polymorphism in the human tumor necrosis factor alpha promoter on transcriptional activation. *Proc Natl Acad Sci U S A* 1997; **94**: 3195-3199
- 11 **Winchester EC**, Millwood IY, Rand L, Penny MA, Kessling AM. Association of the TNF-alpha-308 (G-A) polymorphism with self-reported history of childhood asthma. *Hum Genet* 2000; **107**: 591-596
- 12 **Sleijffers A**, Yucesoy B, Kashon M, Garssen J, De Gruijl FR, Boland GJ, Van Hattum J, Luster MI, Van Loveren H. Cytokine polymorphisms play a role in susceptibility to ultraviolet B-induced modulation of immune responses after hepatitis B vaccination. *J Immunol* 2003; **170**: 3423-3428
- 13 **Jazrawi SF**, Zaman A, Muhammad Z, Rabkin JM, Corless CL, Olyaei A, Biggs A, Ham J, Chou S, Rosen HR. Tumor necrosis factor-alpha promoter polymorphisms and the risk of rejection after liver transplantation: a case control analysis of 210 donor-recipient pairs. *Liver Transpl* 2003; **9**: 377-382
- 14 **McCusker SM**, Curran MD, Dynan KB, McCullagh CD, Urquhart DD, Middleton D, Patterson CC, McIlroy SP, Passmore AP. Association between polymorphism in regulatory region of gene encoding tumour necrosis factor α and risk of Alzheimer's disease and vascular dementia: a case-control study. *Lancet* 2001; **357**: 436-439
- 15 **Shibue T**, Tsuchiya N, Komata T, Matsushita M, Shiota M, Ohashi J, Wakui M, Matsuta K, Tokunaga K. Tumor necrosis factor α 5' - flanking region, tumor necrosis factor receptor II, and HLA-DRB1 polymorphisms in Japanese patients with rheumatoid arthritis. *Arthritis Rheumatoid* 2000; **43**: 753-757
- 16 **Lok AS**, Heathcote EJ, Hoofnagle JH. Management of hepatitis B: 2000-summary of a workshop. *Gastroenterology* 2001; **120**: 1828-1853
- 17 The branch of infectious diseases, parasitology and hepatology of Chinese Medical Association. The strategy of prevention and cure in viral hepatitis. *Zhonghua Chuanranbing Zazhi* 2001; **19**: 56-62
- 18 **Sambrook J**, Russell DW. ed. Molecular Cloning: A Laboratory Manual. 2nd ed. Beijing: Science Publishing House 1992: 465-467
- 19 **Miyazoe S**, Hamasaki K, Nakata K, Kajiyama Y, Kitajima K, Nakao K, Daikoku M, Yatsushashi H, Koga M, Yano M, Eguchi K. Influence of interleukin-10 gene promoter polymorphisms on disease progression in patients chronically infected with hepatitis B virus. *Am J Gastroenterol* 2002; **97**: 2086-2092
- 20 **Rothman KJ**, Greenland S. ed. Interactions between Causes. Modern Epidemiology, 2nd ed, Boston: Lippincott Williams Wilkins 1998: 311-326
- 21 **Jiang SD**, Lv BZ. ed. Mathematical and Statistical Methods in Medical Genetics. 1st ed. Beijing: Science Publishing House 1998: 10-11
- 22 **Luo KX**. ed. Hepatitis B: Basic Biology and Clinical Science. 2nd ed. Beijing: People's Medical Publishing House 2001: 1-6
- 23 **Almari A**, Batchelor JR. HLA and hepatitis B infection. *Lancet* 1994; **344**: 1194-1195
- 24 **Thursz MR**, Kwiatkowski D, Allsopp CE, Greenwood BM, Thomas HC, Hill AV. Association between an MHC class II allele and clearance of hepatitis B virus in the Gambia. *N Engl J Med* 1995; **332**: 1065-1069
- 25 **Thursz MR**. Host genetic factors influencing the outcome of hepatitis. *J Viral Hepat* 1997; **4**: 215-220
- 26 **Thio CL**, Carrington M, Marti D, O'Brien SJ, Vlahov D, Nelson KE, Astemborski J, Thomas DL. Class II HLA alleles and hepatitis B virus persistence in African Americans. *J Infect Dis* 1999; **179**: 1004-1006
- 27 **Diepolder HM**, Jung MC, Keller E, Schraut W, Gerlach JT, Gruner N, Zachoval R, Hoffmann RM, Schirren CA, Scholz S, Pape GR. A vigorous virus-specific CD4+ T cell response may contribute to the association of HLA-DR13 with viral clearance in hepatitis B. *Clin Exp Immunol* 1998; **113**: 244-251

- 28 **Romero R**, Lavine JE. Cytokine inhibition of the hepatitis B virus core promoter. *Hepatology* 1996; **23**: 17-23
- 29 **Gonzalez-Amaro R**, Garcia-Monzon C, Garcia-Buey L, Moreno-Otero R, Alonso JL, Yague E, Pivel JP, Lopez-Cabrera M, Fernandez-Ruiz E, Sanchez-Madrid F. Induction of tumor necrosis factor alpha production by human hepatocytes in chronic viral hepatitis. *J Exp Med* 1994; **179**: 841-848
- 30 **Marinos G**, Naoumov NV, Rossol S, Torre F, Wong PY, Gallati H, Portmann B, Williams R. Tumor necrosis factor receptors in patients with chronic hepatitis B virus infection. *Gastroenterology* 1995; **108**: 1453-1463
- 31 **Ba DN**. ed. Contemporary Immunological Technology and Application. Beijing: *Peking Medical University and Peking Union Medical College Publishing House* 1998: 52-54
- 32 **Hohler T**, Kruger A, Gerken G, Schneider PM, Meyer zum Buschenfelde KH, Rittner C. A tumor necrosis factor-alpha (TNF-alpha) promoter polymorphism is associated with chronic hepatitis B infection. *Clin Exp Immunol* 1998; **111**: 579-582
- 33 **Higuchi T**, Seki N, Kamizono S, Yamada A, Kimura A, Kato H, Itoh K. Polymorphism of the 5' -flanking region of the human tumor necrosis factor (TNF)-alpha gene in Japanese. *Tissue Antigens* 1998; **51**: 605-612
- 34 **Grove J**, Daly AK, Bassendine MF, Day CP. Association of a tumor necrosis factor promoter polymorphism with susceptibility to alcoholic steatohepatitis. *Hepatology* 1997; **26**: 143-146
- 35 **Drouet C**, Shakov AN, Jongeneel CV. Enhancers and transcription factors controlling the inducibility of the tumor necrosis factor-alpha promoter in primary macrophages. *J Immunol* 1991; **147**: 1694-1700
- 36 **Soga Y**, Nishimura F, Ohyama H, Maeda H, Takashiba S, Murayama Y. Tumornecrosis factor-alpha gene (TNF-alpha) -1031/-863, -857 single-nucleotide polymorphisms (SNPs) are associated with severe adult periodontitis in Japanese. *J Clin Periodontol* 2003; **30**: 524-531
- 37 **Pociot F**, D' Alfonso S, Compasso S, Scorza R, Richiardi PM. Functional analysis of a new polymorphism in the human TNF alpha gene promoter. *Scand J Immunol* 1995; **42**: 501-504
- 38 **Kaijzel EL**, van Krugten MV, Brinkman BM, Huizinga TW, van der Straaten T, Hazes JM, Ziegler-Heitbrock HW, Nedospasov SA, Breedveld FC, Verweij CL. Functional analysis of a human tumor necrosis factor alpha (TNF-alpha) promoter polymorphism related to joint damage in rheumatoid arthritis. *Mol Med* 1998; **4**: 724-733
- 39 **Huizinga TW**, Westendorp RG, Bollen EL, Keijsers V, Brinkman BM, Langermans JA, Breedveld FC, Verweij CL, van de Gaer L, Dams L, Crusius JB, Garcia-Gonzalez A, van Oosten BW, Polman CH, Peña AS. TNF-alpha promoter polymorphisms, production and susceptibility to multiple sclerosis in different groups of patients. *J Neuroimmunol* 1997; **72**: 149-153
- 40 **Ugialoro AM**, Turbay D, Pesavento PA, Delgado JC, McKenzie FE, Gribben JG, Hartl D, Yunis EJ, Goldfeld AE. Identification of three new single nucleotide polymorphisms in the human tumor necrosis factor-alpha gene promoter. *Tissue Antigens* 1998; **52**: 359-367
- 41 **Khan KN**, Yatsushashi H. Effect of alcohol consumption on the progression of hepatitis C virus infection and risk of hepatocellular carcinoma in Japanese patients. *Alcohol Alcohol* 2000; **35**: 286-295
- 42 **Gao B**. Interaction of alcohol and hepatitis viral proteins: implication in synergistic effect of alcohol drinking and viral hepatitis on liver injury. *Alcohol* 2002; **26**: 69-72
- 43 **Wang CS**, Wang ST, Chang TT, Yao WJ, Chou P. Smoking and alanine aminotransferase levels in hepatitis C virus infection: implications for prevention of hepatitis C virus progression. *Arch Intern Med* 2002; **162**: 811-815

Edited by Zhang JZ and Wang XL Proofread by Xu FM

Hypermethylation of Syk gene in promoter region associated with oncogenesis and metastasis of gastric carcinoma

Shui Wang, Yong-Bin Ding, Guo-Yu Chen, Jian-Guo Xia, Zhen-Yan Wu

Shui Wang, Yong-Bin Ding, Guo-Yu Chen, Jian-Guo Xia, Zhen-Yan Wu, Department of General Surgery, First Affiliated Hospital of Nanjing Medical University, Nanjing 210029, Jiangsu Province, China
Supported by the Science Fund of Department of Science and Technology of Jiangsu Province. 03KJD320138

Correspondence to: Yong-Bin Ding, Department of General Surgery, First Affiliated Hospital of Nanjing Medical University, Nanjing 210029, Jiangsu Province, China. njdyb@sina.com

Telephone: +86-25-86563750 **Fax:** +86-25-86563750

Received: 2003-10-24 **Accepted:** 2003-12-08

Abstract

AIM: To investigate the relationship between methylation of Syk (spleen tyrosine kinase) gene in promoter region and oncogenesis, metastasis of gastric carcinoma. The relation between silencing of the Syk gene and methylation of Syk promoter region was also studied.

METHODS: By using methylation-specific PCR (MSP) technique, the methylation of Syk promoter region in specimens from 61 gastric cancer patients (tumor tissues and adjacent normal tissues) was detected. Meanwhile, RT-PCR was used to analyse syk expression exclusively.

RESULTS: The expression of the Syk gene was detected in all normal gastric tissues. Syk expression in gastric carcinoma was lower in 14 out of 61 gastric cancer samples than in adjacent normal tissues ($\chi^2=72.3$, $P<0.05$). No methylation of Syk promoter was found in adjacent normal tissues. hypermethylation of Syk gene in promoter was detected 21 cases in 61 gastric carcinoma patients. The rate of methylation of Syk promoter in gastric carcinoma was higher than that in adjacent normal tissues ($\chi^2=25.1$, $P<0.05$). In 31 patients with lymph node metastasis, 17 were found with Syk promoter methylation. A significant difference was noted between two groups ($\chi^2=11.4$, $P<0.05$).

CONCLUSION: Hypermethylation leads to silencing of the Syk gene in human gastric carcinoma. Methylation of Syk promoter is correlated to oncogenesis and metastasis of gastric carcinoma. Syk is considered to be a potential tumor suppressor and anti-metastasis gene in human gastric cancer.

Wang S, Ding YB, Chen GY, Xia JG, Wu ZY. Hypermethylation of Syk gene in promoter region associated with oncogenesis and metastasis of gastric carcinoma. *World J Gastroenterol* 2004; 10(12): 1815-1818

<http://www.wjgnet.com/1007-9327/10/1815.asp>

INTRODUCTION

Gastric cancer development and progression are thought to occur through a complex, multistep process, including oncogene activation and mutation or loss of tumor suppressor genes. Determining the function of genetic alterations in gastric carcinoma tumorigenesis and metastasis has been the focus of

intensive research efforts for several decades. One group of proteins that play a critical role in gastric cancer cell signaling pathways is tyrosine kinases. The decrease or loss of spleen tyrosine kinase (Syk) expression seems to be associated with increased motility and invasion of malignant phenotype^[1-5].

Syk, a non-receptor type of protein-tyrosine kinase that is widely expressed in hematopoietic cells, is one of the two members of the Syk family (Syk and ZAP-70). Syk is activated upon the binding to its tandem Src homology 2 (SH2) domains to immunoreceptor tyrosine-based activation motif (ITAM) and plays an essential role in lymphocyte development and activation of immune cells. Emerging evidence indicates that Syk may be a potent modulator of epithelial cell growth and a potential tumor suppressor in human breast carcinoma^[6,7]. But the role of Syk in gastric carcinoma remains unclear, so we examined Syk mRNA expression in human gastric cancer and the adjacent non-cancerous tissues, and explored whether methylation of Syk promoter region was associated with the loss of Syk expression in gastric cancer and the relationship between Syk mRNA expression in gastric cancer tissue and clinicopathological factors in the present study.

MATERIALS AND METHODS

Tissues

Gastric cancer and matched adjacent non-cancerous tissues were obtained during surgical excision from 61 patients with gastric cancer in our department between March 2001 and October 2002. The age of 38 male and 23 female patients was rang from 26 to 78 (mean, 58.1) years. All samples were placed in liquid nitrogen immediately after resection and stored at -70 °C until RNA extraction. No patient had received chemotherapy or radiation therapy prior to surgery. All patients were confirmed to have gastric carcinoma by pathologic test.

RNA extraction and semi-quantitative reverse transcription (RT)-polymerase chain reaction (PCR)

Total RNA was isolated from each specimen by Trizol reagent according to the manufacturer's recommendations. Samples were ground into a fine powder using a mortar and pestle, incubated in Trizol solution (100 g/L) for 15 min, and then 1/5 volume of choloform was added. After vigorous agitation for 5 min, the inorganic phase was separated by centrifugation at 12 000 g for 20 min at 4 °C, RNA was then precipitated in the presence of 1 volume of isopropanol and centrifuged at 10 000 g for 15 min at 4 °C. RNA pellets were washed with 700 ml/L ice-cold ethanol and then dissolved in diethyl pyrocarbonate (DEPC) - treated H₂O. Total RNA concentration and quantity were assessed by absorbency at 260 nm by using a nucleic acid and protein. Semi-quantitative RT-PCR of 40 pairs of gastric cancer tissues and 15 pair of benign fibroadenoma tissues was performed for intergrin beta1 displaying expression alterations. Five micrograms of total RNA in each hybridization sample was used to synthesize the first strand cDNA with SuperScript preamplification system for first strand cDNA synthesis kit. Then 1 mL product was used as the template to amplify specific fragments in 25 mL reaction mixture under the following conditions:

denaturation at 94 °C (3 min); 40 cycles at 94 °C (45 s), at 60 °C (45 s) and at 72 °C (60 s), then extensions at 72 °C (3 min). The PCR primers of Syk were as follow: Syk forward, 5' -CATGTCAAGGATAAGAACATCATAGA-3'; reverse: 5' -AGTTCACCACGTCATAGTAGTAATT-3'. A 514 bp nucleotide fragment of the human Syk cDNA was amplified. In each PCR reaction, primers for the human glyceraldehyde-3-phosphate dehydrogenase (*GAPDH*) gene were used as an internal control. *GAPDH* primer sequences were as forward: primer 5' -AGAAGGCTGGGGCTCATTTCAGGG-3' reverse primer 5' -GTCACCTGGCGTCTTACCACCATG-3'. Ten mL RT-PCR reaction product was analyzed by electrophoresis on a 15 g/L agarose gel. The electrophoresis images were scanned by Fluor-S MultiImager and the original intensity of each specific band was quantitated with the software Multi-Analyst. The data were compared after normalized by the intensity of *GAPDH*. After normalization, the adjusted intensities were calculated for the amplified gene products, and the ratios were calculated. The sequences of PCR primer pairs of intergrin beta1 and *GAPDH* were designed using Primer3 Internet software program. Their specificity was confirmed by a BLAST Internet software assisted search for a nonredundant nucleotide sequence database.

DNA extraction, purification, bisulfite modification and Sequencing

Genomic DNA from cell lines or frozen gastric tissues was extracted by using a Dneasy kit. Genomic DNA was treated with sodium bisulfite. DNA (20 mg/L) was denatured by NaOH (concentration 0.2 mol/L) for 10 min at 37 °C. Thirty μ L of 10 nmol/L hydroquinone and 520 μ L of 3 mol/L sodium bisulfate were added, followed by incubation at 50 °C for 16 h. The modified DNA was purified using Wizard DNA purification columns. The purified DNA was treated again with NaOH and precipitated. DNA was resuspended in 30 μ L of TE buffer (3 mmol/L Tris (P8.0/0.2 mmol/L EDTA) and subjected to PCR amplification using a primer set (forward 5' -GATTAA GATATATTTAGGGAATATG-3; reverse 5' -CACCTATA TTTTATTCACATAATTTC-3) that spanned the Syk CpG island. Fifteen μ L reaction containing 30 ng of bisulfite-treated DNA and 1xRDA buffer (67 mmol/L Tris (pH8.8)/16 mmol/L (NH₄)₂SO₄, 100 mmol/L 2-mercaptoethanol, 1 g/L BSA) was processed in 30 thermal cycles at 94 °C for 45 s, at 58 °C for 45 s, and at 72 °C for 45 s. One aliquot (2 μ L) of diluted PCR Product (40-fold) was subjected to PCR amplification in a 15- μ L volume.

Methylation-specific PCR (MSP)

Methylation-specific primers were designed to cover 9 CPG dinucleotides numbered 17-21 (forward) 47-50 (reverse). Similarly, unmethylation-specific primers were designed cover 8 CPG dinucleotides numbered 18-22 b, (forward) and 35-37 (reverse). Primers specific for methylation DNA (forward) 5' -CGATTCGCGGGTTTCGTTC-3; (reverse) 5' -AAAACGAACGCAACGCGAAAC-3; and unmethylation DNA (forward) 5' -ATTTTGTGGGTTTGTGGTG-3, reverse 5' -ACTTCCTTAACACACCCAAAC-3 were added to the same reaction and PCR products were subjected to electrophoresis on a 10 g/L agarose gel. The m-specific primer set yielded a band at 243 bp and the u primer set yielded a band at 140 bp. PCR conditions were 24 cycles at 94 °C for 30 s, at 67 °C for 30 s, and at 72 °C for 30 s.

Statistical analysis

t-test was used to compare the Syk mRNA expression levels with primary gastric cancer, the adjacent non-cancerous tissues. χ^2 test was also used to estimate the relationship between the silencing of Syk mRNA and methylation of Syk promoter region.

Values of $P < 0.05$ were considered statistically significant.

RESULTS

Expression of Syk in gastric cancer and adjacent non-cancerous tissues

The expression of Syk was found in 14 out of 61 gastric cancer tissues, Syk mRNA expression was detected in all adjacent normal gastric tissue (Figure 1). The rate of expression of Syk in gastric cancer tissue was significantly lower than that in adjacent non-cancerous normal gastric tissues ($\chi^2=72.3$, $P < 0.05$).

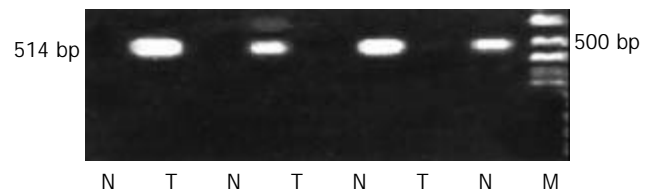


Figure 1 Syk mRNA expression in human gastric cancer and adjacent non-cancerous tissue (RT-PCR detection of Syk mRNA). T: tumor tissue; N: adjacent non-cancerous normal gastric tissue; M: marker.

Syk mRNA expressions were found in 11 out of the 30 gastric cancer patients without lymph node metastasis, but in 3 out of the 31 gastric cancer patients with lymph node metastasis. Expression of Syk mRNA in patients having lymph node metastasis was significantly lower than that in those having no lymph node metastasis ($\chi^2=4.85$, $P < 0.05$). Meanwhile no significant difference was found between Syk mRNA expression in the gastric cancer patients and age, tumor size, clinicopathological stage, histological type (data not shown).

Semi-quantitative RT-PCR

A total of 10 μ L RT-PCR products were electrophoresed on 15 g/L agarose gel contacting ethidium bromide. The level of *GAPDH* was used as internal control (Figure 2). The relative expression levels of Syk normalized to the expression level of *GAPDH*, in the primary gastric cancer tissues and adjacent mammary tissues were, 1.71 ± 1.28 and 3.19 ± 0.59 (mean \pm SD). A significant difference was found between the level of Syk mRNA expression in the primary gastric cancer tissues and adjacent mammary tissues ($t=2.1$, $P < 0.05$). Furthermore, the level of Syk mRNA in patients having lymph node metastasis was significantly lower than that in patients having no lymph node metastasis (1.18 ± 1.13 vs 2.14 ± 1.27 , $t=3.4$, $P < 0.05$).

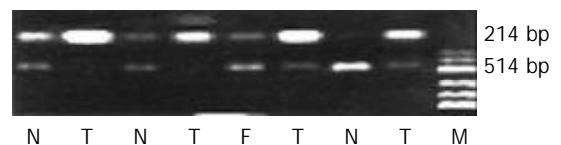


Figure 2 Partial semi-quantitative RT-PCR results in 40 gastric cancer tissues and adjacent non-cancerous tissues. T: tumor tissue; N: adjacent non-cancerous normal gastric tissue; M: marker.

Correlation between methylation of Syk gene in promoter region and oncogenesis, metastasis of gastric carcinoma

MSP was used to analyze the Syk methylation status of gastric carcinoma and its matched normal gastric tissues. Forty nonselective gastric cancers were screened. Among the 61 carcinomas examined, 21 exhibited strong Syk methylation. Representative examples are shown in Figure 3. In contrast to their corresponding carcinomas, the Syk gene of the 61 matched neighboring normal gastric tissues remained unmethylated. The

rate of methylation of Syk promoter in gastric carcinoma was higher than that of adjacent normal tissues ($\chi^2=25.1, P<0.05$).

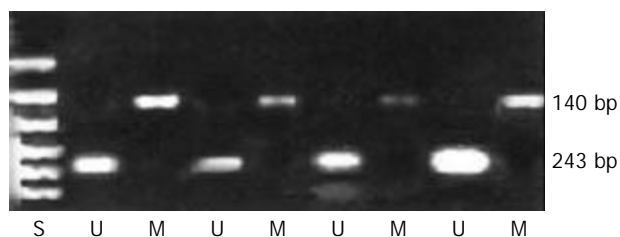


Figure 3 Representative examples of Syk methylation (neighboring normal gastric tissues unmethylated).

As shown in Table 1, of the 31 cases of lymph node metastasis, 17 were found with Syk promoter methylation. Syk promoter methylations in 4 out of 30 without lymph node metastasis were detected. A significant difference was noted between two groups ($\chi^2=11.4, P<0.05$). Correlation between methylation of Syk promoter region and clinicopathologic factors was shown in Table 1.

Table 1 Correlation between methylation of Syk promoter region and clinicopathologic factors (*n*)

Factor	Frequency of Syk promoter region methylation	<i>P</i>
Gender		
Male	14/38	
Female	7/23	0.26
Tumor size		
<3cm	8/26	
3	13/35	0.61
Depth of invasion		
Mucosa and submucosa	2/9	
Muscle and subserosa	7/29	
Serosa	12/23	0.075
Lymph node metastasis		
Present	17/31	
Absent	4/30	0.0016
Stage		
I-II	6/25	
III-IV	15/36	0.24
Tumor location		
Lower third	6/15	
Middle third	11/35	
Upper third	4/11	0.83

Relationship between Syk promoter region hypermethylation and loss of its expression in gastric carcinoma

Syk promoter methylation was found in 21 of 61 gastric tumors. They did not show any detectable Syk. In 40 cases without Syk promoter methylation, Syk mRNA expression was found in 13 cases. Syk promoter methylation was significantly related with loss of Syk expression in gastric carcinoma ($\chi^2=4.2, P<0.05$).

DISCUSSION

Syk is ubiquitously expressed in hematopoietic cells and has been extensively studied as effectors of B cell receptor (BCR) signaling^[8-10]. It has been found to be involved in coupling activated immunoreceptors to downstream signaling events that mediate diverse cellular responses including proliferation, differentiation and phagocytosis^[11-16]. Some reports are of opinions that Syk is a candidate suppressor gene.

In this paper, we explored expression of Syk mRNA in gastric

cancer and its adjacent non-cancerous tissues. Our results showed that the level and rate of Syk mRNA expression in gastric cancer tissues were significantly lower than those in adjacent non-cancerous tissues, especially invasive gastric cancer tissues did not show any detectable Syk mRNA expression, indicating that loss of Syk mRNA expression may be correlated to gastric carcinogenesis. Our findings were in agreement with the results of Goodman *et al.*^[17,18].

Furthermore, we observed that only four gastric cancer tissues from 31 patients with lymph node metastasis had Syk mRNA expression which was negatively correlated to lymph node metastasis. In B cells, Syk activity was a key regulator of Akt kinase activity after BCR engagement, because Syk induced PI3-K-dependent Akt activation and inhibition of apoptosis^[18]. Numerous studies have demonstrated deregulated Akt activity in gastric cancer cells. It is tempting to speculate that Syk may also regulate Akt activity in gastric cells. Syk mRNA expression was reduced during human gastric cancer progression, and then it was unlikely that Syk-dependent signaling contributed to the increased Akt activity observed in gastric cancer cells^[19-21]. Findings by Okamura *et al.*^[23] suggest that Syk mRNA expression was positively correlated to p53 expression. They found that Syk gene expression was repressed in a p53-dependent manner in human colon carcinoma cells, indicating that loss of p53 function during tumorigenesis could lead to deregulated Syk activity^[7,22]. Study by Mahabeshwar *et al.*^[19] suggested Syk suppressed cell motility and inhibited PI-3 kinase activity and uPA secretion by blocking NF- κ B activity through tyrosine phosphorylation of I κ B α . So loss of Syk expression might contribute to gastric oncogenesis and metastasis^[18,23].

However, the mechanism of Syk expression loss remains unclear. A number of cancer-associated genes have been shown to be inactivated by hypermethylation of CpG islands during gastric tumorigenesis. About 50% of human genes have clusters of CPG dinucleotides (CPG islands) in their 5' -regulatory sequences. Gene silencing through methylation of these sites has been observed in early developmental stages and aging. Aberrant methylation may lead to deregulation of gene expression. Most notably, tumor suppressor genes, mismatched repair genes, and others such as estrogen receptor, E-cadherin, death-associated protein kinase, and thrombospondin-1, were repressed by CPG island hypermethylation in cancer tissues, inhibition of the transcription of these genes could provide an epigenetic mechanism of clonal selection during tumorigenesis^[24,25].

In this study, the 5' CpG island methylation status of the Syk gene in gastric cancer tissues was examined. We found Syk 5' CpG hypermethylation in 35% (21/60) of unselected gastric tumors, whereas all of the matched neighboring normal gastric tissues exhibited unmethylated DNA. We found that the rate of methylation of Syk promoter in gastric carcinoma was significantly higher than that in adjacent normal tissues, suggesting that hypermethylation of Syk promoter region may be associated with oncogenesis of gastric cancer. In addition, the rate of Syk promoter region methylation in the patients with lymph node metastasis is significantly higher than that in the patients without lymph node metastasis, indicating that methylation of Syk promoter methylation is related to lymph node metastasis of gastric cancer. The absence of Syk protein was reflected by the loss of its mRNA expression in gastric cancers, suggesting that the loss of Syk mRNA expression occurs at the transcriptional level. 5' CpG hypermethylation of Syk was reported to be associated with loss or reduction of Syk gene expression, which may provide a new way to treat gastric cancer^[26,27].

However, we did not observe any significant correlation between Syk methylation and tumor grade. This may be attributable to a relatively small sample size and the complexity of unselected patient population. Additional detailed studies

using patient cohort should be done needed to examine the value of Syk methylation as a diagnostic or prognostic marker^[28,29].

The recent identification of Syk as a potent modulator of gastric epithelial cell growth has generated a need for further exploration of the role of nonreceptor tyrosine kinases in gastric cancer progression and metastasis^[28-30]. These initial results offer the promise that novel molecular targets may be identified both for the prevention of gastric cancer development and for inhibition of metastatic gastric cancer spread. The continual elucidation of novel targets such as Syk is a critical part of the endeavor to eradicate gastric cancer. These findings may provide promise molecular targets for the prevention of gastric cancer development^[31-33].

ACKNOWLEDGEMENTS

We are grateful for the technical assistance from Mrs. Yu Yue, Laboratory of General Surgery Department, the First Affiliated Hospital of Nanjing Medical University.

REFERENCES

- 1 **Kim JP**. Surgical results in gastric cancer. *Semin surg oncol* 1999; **17**:132-138
- 2 **Ding YB**, Chen GY, Xia JG, Zang XW, Yang HY, Yang L. Overexpression of VCAM-1 is associated with oncogenesis, tumor angiogenesis and metastasis of gastric carcinoma. *World J Gastroenterol* 2003; **9**: 1409-1414
- 3 **Sada K**, Takano T, Yanagi S, Yamamura H. Structure and function of Syk protein-tyrosine kinase. *J Biochem* 2001; **130**: 177-186
- 4 **Toyama T**, Iwase H, Yamashita H, Hara Y, Omoto Y, Sugiura H, Zhang Z, Fujii Y. Reduced expression of the Syk gene is correlated with poor prognosis in human breast cancer. *Cancer Lett* 2003; **189**: 97-102
- 5 **Li L**, Shaw PE. Autocrine-mediated activation of STAT3 correlates with cell proliferation in breast carcinoma lines. *J Biol Chem* 2002; **277**: 17397-17405
- 6 **Coopman PJ**, Do MT, Barth M, Bowden ET, Hayes AJ, Basyuk E, Blancato JK, Vezza PR, McLeskey SW, Mangeat PH, Mueller SC. The Syk tyrosine kinase suppresses malignant growth of human breast cancer cells. *Nature* 2000; **406**: 742-747
- 7 **Stewart Z**, Pietenpol J. Syk: a new player in the field of breast cancer. *Breast Cancer Res* 2001; **3**: 5-7
- 8 **Stupack DG**, Li E, Silletti SA, Kehler JA, Geahlen RL, Hahn K, Nemerow GR, Chersesh DA. Matrix valency regulates integrin-mediated lymphoid adhesion via Syk kinase. *J Cell Biol* 1999; **144**: 777-788
- 9 **Danam RP**, Qian XC, Howell R, Brent TP. Methylation of selected CpGs in the human O⁶-methylguanine-DNA methyltransferase promoter region as a marker of gene silencing. *Mol Carcinogenesis* 1999; **24**: 85-89
- 10 **Zhang J**, Siraganian RP. CD45 is essential for Fc epsilon RI signaling by ZAP70, but not Syk, in Syk-negative mast cells. *J Immunol* 1999; **163**: 2508-2516
- 11 **Zhu DM**, Tibbles HE, Vassilev AO, Uckun FM. SYK and LYN mediate B-cell receptor-independent calcium-induced apoptosis in DT-40 lymphoma B-cells. *Leuk Lymphoma* 2002; **43**: 2165-2170
- 12 **Chen L**, Widhopf G, Huynh L, Rassenti L, Rai KR, Weiss A, Kipps TJ. Expression of ZAP-70 is associated with increased B-cell receptor signaling in chronic lymphocytic leukemia. *Blood* 2002; **100**: 4609-4614
- 13 **Palmieri G**, Tullio V, Zingoni A, Piccoli M, Frati L, Lopez-Botet M, Santoni A. CD94/NKG2-A inhibitory complex blocks CD16-triggered Syk and extracellular regulated kinase activation, leading to cytotoxic function of human NK cells. *J Immunol* 1999; **162**: 7181-7188
- 14 **Chu DH**, Morita CT, Weiss A. The Syk family of protein tyrosine kinases in T-cell activation and development. *Immunol Rev* 1998; **165**: 167-180
- 15 **Murphy M**, Schnall R, Venter DJ, Barnett L, Bertoncetto I, Thien CB, Langdon WY, Dowtell DD. Tissue hyperplasia and enhanced T-cell signalling via ZAP-70 in c-Cbl-deficient mice. *Mol Cell Biol* 1998; **18**: 4872-4882
- 16 **Zompi S**, Hamerman JA, Ogasawara K, Schweighoffer E, Tybulewicz VL, Di Santo JP, Lanier LL, Colucci F. NKG2D triggers cytotoxicity in mouse NK cells lacking DAP12 or Syk family kinases. *Nat Immunol* 2003; **4**: 565-472
- 17 **Goodman PA**, Jurana B, Wood CM, Uckun F. Genomic studies of the spleen protein tyrosine kinase locus reveal a complex promoter structure and several genetic variants. *Leuk Lymphoma* 2002; **43**: 1627-1635
- 18 **Goodman PA**, Wood CM, Vassilev A, Mao C, Uckun FM. Spleen tyrosine kinase (Syk) deficiency in childhood pro-B cell acute lymphoblastic leukemia. *Oncogene* 2001; **20**: 3969-3978
- 19 **Mahabeleshwar GH**, Kundu GC. Syk, a protein tyrosine kinase suppresses the cell motility and nuclear factor kB mediated secretion of urokinase type plasminogen activator by inhibiting the phosphatidylinositol 3'-kinase activity in breast cancer cells. *J Biol Chem* 2003; **278**: 6209-6221
- 20 **Paolini R**, Molfetta R, Beitz LO, Zhang J, Scharenberg AM, Piccoli M, Frati L, Siraganian R, Santoni A. Activation of Syk tyrosine kinase is required for c-Cbl-mediated ubiquitination of Fc epsilon RI and Syk in RBL cells. *J Biol Chem* 2002; **277**: 36940-36947
- 21 **Carter W**, Hoying JB, Boswell C, Williams SK. HER2/neu over-expression induces endothelial cell retraction. *Int J Cancer* 2001; **91**: 295-299
- 22 **Qiu Y**, Kung HJ. Signaling network of the Btk family kinase. *Oncogene* 2000; **19**: 5651-5661
- 23 **Okamura S**, Ng C, Koyama K, Takei Y, Arakawa H, Monden M, Nakamura Y. Identification of seven genes regulated by wild-type p53 in a colon cancer cell line carrying a well-controlled wild-type p53 expression system. *Oncol Res* 1999; **11**: 281-285
- 24 **Dong G**, Loukinova E, Chen Z, Gangi L, Chanturita TI, Liu ET, Van Waes C. Molecular profiling of transformed and metastatic murine squamous carcinoma cells by differential display and cDNA microarray reveals altered expression of multiple genes related to growth, apoptosis, angiogenesis, and the NF-kappaB signal pathway. *Cancer Res* 2001; **61**: 4797-4808
- 25 **Yuan Y**, Mendez R, Sahin A, Dai JL. Hypermethylation leads to silencing of the SYK gene in human breast cancer. *Cancer Res* 2001; **61**: 5558-5561
- 26 **Ding YB**, Chen GY, Xia JG, Zang XW, Yang HY, Yang L. Correlation of tumor-positive ratio and number of perigastric lymph nodes with prognosis of gastric carcinoma in surgically treated patients. *World J Gastroenterol* 2004; **10**: 182-185
- 27 **Buchholz TA**, Wazer DE. Molecular biology and genetics of breast cancer development: a clinical perspective. *Semin Radiat Oncol* 2002; **12**: 285-295
- 28 **Arber N**, Shapira I, Katan J, Stern B, Fabian I, Halpern Z. Activation of c-k ras mutations in human gastrointestinal tumors. *Gastroenterology* 2000; **118**: 1045-1050
- 29 **Balaian L**, Zhong RK, Ball ED. The inhibitory effect of anti-CD33 monoclonal antibodies on AML cell growth correlates with Syk and/or ZAP-70 expression. *Exp Hematol* 2003; **31**: 363-371
- 30 **Djeu JY**, Jiang K, Wei S. A view to a kill: signals triggering cytotoxicity. *Clin Cancer Res* 2002; **8**: 636-640
- 31 **Uckun FM**, Sudbeck EA, Mao C, Ghosh S, Liu XP, Vassilev AO, Navara CS, Narla RK. Structure-based design of novel anticancer agents. *Curr Cancer Drug Targets* 2001; **1**: 59-71
- 32 **Xu R**, Seger R, Pecht I. Cutting edge: extracellular signal-regulated kinase activates syk: a new potential feedback regulation of Fc epsilon receptor signaling. *J Immunol* 1999; **163**: 1110-1114
- 33 **Wang L**, Duke L, Zhang PS, Arlinghaus RB, Symmans WF, Sahin A, Mendez R, Dai JL. Alternative splicing disrupts a nuclear localization signal in spleen tyrosine that is require for invasion suppression in breast cancer. *Cancer Res* 2003; **63**: 4724-4730

Comparison of nuclear matrix proteins between gastric cancer and normal gastric tissue

Qin-Xian Zhang, Yi Ding, Zhuo Li, Xiao-Ping Le, Wei Zhang, Ling Sun, Hui-Rong Shi

Qin-Xian Zhang, Yi Ding, Xiao-Ping Le, Wei Zhang, Molecular Cell Biology Research Center, Medical College of Zhengzhou University, Zhengzhou 450052, Henan Province, China
Zhuo Li, Ling Sun, Hui-Rong Shi, Henan Key Laboratory of Molecular Medicine, Zhengzhou 450052, Henan Province, China
Supported by the National Natural Science Foundation of China, No. 39170440

Correspondence to: Professor. Qin-Xian Zhang, Molecular Cell Biology Research Center, Medical College of Zhengzhou University, 40 Daxue Lu, Zhengzhou 450052, Henan Province, China. qxz53@zzu.edu.cn

Telephone: +86-371-6977002

Received: 2003-08-05 **Accepted:** 2003-10-22

Abstract

AIM: To study the alteration of nuclear matrix proteins (NMPs) in gastric cancer.

METHODS: The NMPs extracted from 22 cases of gastric cancer and normal gastric tissues were investigated by SDS-PAGE technique and the data were analyzed using Genetools analysis software.

RESULTS: Compared with normal gastric tissue, the expression of 30 ku and 28 ku NMPs in gastric cancer decreased significantly ($P=0.002$, $P=0.001$, $P<0.05$). No significant difference was found in the expression of the two NMPs between the various differentiated grades ($P=0.947$, $P=0.356$) and clinical stages of gastric cancer ($P=0.920$, $P=0.243$, $P>0.05$).

CONCLUSION: The results suggested that the alteration of NMPs in gastric cancer occurred at the early stage of gastric cancer development.

Zhang QX, Ding Y, Li Z, Le XP, Zhang W, Sun L, Shi HR. Comparison of nuclear matrix proteins between gastric cancer and normal gastric tissue. *World J Gastroenterol* 2004; 10 (12): 1819-1821

<http://www.wjgnet.com/1007-9327/10/1819.asp>

INTRODUCTION

Nuclear matrix (NM) is the structural framework of the nucleus comprising the peripheral lamins and pore complexes, an internal ribonucleic protein outside nucleoli^[1]. Nuclear matrix proteins (NMPs) are important for a variety of cell functions, including nuclear assembly, replication, transcription, and nuclear integrity^[2]. Specific changes of NMPs are associated with many cancers^[3-6]. However, the alteration of NMPs in gastric cancer has not been reported. In this paper, the NMPs in gastric cancer and normal gastric tissue were studied by SDS-PAGE and Genetools quantitative analysis software.

MATERIALS AND METHODS

Materials

Twenty-two cases of gastric cancer specimens (with no history

of radio- or chemotherapy preoperatively) and normal gastric mucosa were collected from the First Affiliated Hospital of Medical College of Zhengzhou University and the People's Hospital of Henan Province. All the specimens were diagnosed pathologically (well and moderately differentiated cancers in 10 cases, poorly differentiated cancers in 12 cases). According to the PTNM of International Alliance of Anticancer in 1987, the specimens were divided into 4 clinical stages, Nine were at stage I and II, and 13 at stage III and IV.

Preparation of nuclei

The gastric cancers and normal gastric tissues were minced and mixed with STM (0.25 mol/L sucrose, 10 mmol/L Tris-HCl pH 7.4, 5 mmol/L MgCl₂) and homogenized with a homogenizer. Nuclei were initially separated by low speed centrifugation at 750 r/min for 10 min. The pellet was suspended with STM containing 5 g/L Triton X-100 for 10 min and centrifuged at 750 r/min for 10 min. The crude nuclei were resuspended with 2 mol/L sucrose and centrifuged at 12 000 g for 10 min. The pellet containing purified nuclei was washed with STM.

Extraction of NMPs

The purified nuclei were digested with DNase I (200 U/mL) at room temperature for 45 min prior to low salt (LS) buffer (10 mmol/L Tris-HCl pH 7.4, 0.2 mmol/L MgCl₂) extraction and centrifuged at 1 000 r/min for 15 min. The pellet was extracted twice with high salt (HS) buffer (10 mmol/L Tris-HCl pH 7.4, 2 mol/L NaCl, 0.2 mmol/L MgCl₂) and centrifuged at 6 000 r/min for 15 min. Washed with LS buffer, the pellet was resuspended with 2×loading buffer and detected for the concentration of proteins in the sample.

SDS-PAGE

A 100 µg proteins were loaded in each well of 100 g/L SDS-polyacrylamide gel. The proteins were electrophoresed at constant voltage of 200 V. The gel was stained with Coomassie brilliant blue R-250 over 4 h. The protein bands were photoed with gel photography system and quantitatively analyzed with Genetools software.

Statistic analysis

Data were analyzed using nonparametric statistics with SPSS 10.0 statistic software and $P<0.05$ was considered statistically significant.

RESULTS

On the gel stained with Coomassie brilliant blue R-250, many bands were exhibited in both gastric cancer and normal gastric tissue, which suggested that NMPs were abundant in these tissues. The bands of 30 ku and 28 ku NMPs in the gastric cancer were stained more lightly than those in the normal gastric tissue (Figure 1). Analyzed with Genetools quantitative software, the expression of 30 ku and 28 ku NMPs in normal gastric tissues was significantly higher than those in gastric cancer ($P<0.05$). The difference of the expression of 30 ku and 28 ku NMPs between well and moderately differentiated and

poorly differentiated gastric cancers was not significant ($P>0.05$). There was no significant difference in the expression of the two NMPs between stage I, II and stage III, IV ($P>0.05$) (Table 1).



Figure 1 SDS-PAGE of nuclear matrix 1 gastric carcinoma tissue; 2 adjacent cancer tissue; 3 normal tissue; 4 marker.

Table 1 Comparison of the 30 ku, 28 ku bands between gastric cancer tissues and normal tissues

Group	30 ku			28 ku	
	n	T	Z	T	Z
Normal tissue group ^a	22	7.25	-3.165	4.33	-3.263
Gastric cancer group	22	12.44		14.19	
Well and moderately differentiated	10	11.60	-0.066	12.90	-0.923
Poorly differentiated	12	11.42		10.33	
Stage I, II	9	11.33	-0.100	13.44	-1.169
Stage III, IV	13	11.62		10.15	

T: mean of rank sum, Z: z value ^a $P<0.05$ vs gastric cancer.

DISCUSSION

NM is the structural framework of the nucleus^[7], and is involved in a variety of cell functions, including DNA replication^[8], RNA transcription^[9], architecture of chromatin^[10], carcinogenesis^[11] and apoptosis^[12]. The study on the relationship between NMPs and carcinogenesis has been carried out for a few years. In the experiment of Spencer *et al.*^[13], specific changes in NMPs of breast cell line were identified by two-dimensional gel electrophoresis. NMP66 was evaluated as a potential biomarker for early breast cancer in large-scale clinical trials^[11]. The extent of chromosomal rearrangements correlates positively with the level of expression of the nuclear matrix high mobility group (HMG) proteins HMG I (Y) when tested in three human prostate cancer cell lines (PC-3>DU145>LNCaP)^[14]. Using both one-dimensional and high-resolution two-dimensional immunoblot analyses, Leman *et al.*^[15] found that, in the transgenic adenocarcinoma of mouse prostate (TRAMP) model, HMG I (Y) was an NMP expressed as two protein bands with a molecular mass of 22-24 ku and HMG I (Y) expression was correlated with neoplastic and malignant properties in late stage of prostate tumor TRAMP model. In 26 pairs of human prostate cancer and normal tissue, Ishiguro *et al.*^[16] identified a specific upregulated gene encoding a 55 ku nuclear matrix protein (nmt55) by RT-PCR and real time quantitative PCR. nmt55 gene expression in human prostate cancer tissue was higher (20/26) than that in normal prostate tissue.

NMP22 has been identified as a tumor marker for transitional cell carcinoma of urinary tract^[17] and bladder cancer^[18-21]. Eissa *et al.*^[22] evaluated the diagnostic efficacy of NMP22, fibronectin and urinary bladder cancer antigen (UBC) in comparison with voided urine cytology on the detection of bladder cancer. They

found that NMP22 and fibronectin had superior sensitivities compared to UBC and voided urine cytology, while NMP22 and voided urine cytology had the highest specificities. Xu^[23] reported that the examination of NMP22 in urine was a rapid and effective way to detect the recurrence of bladder cancer. The urinary NMP22 levels were significantly higher in the renal cell carcinoma group than in the control group. The urinary NMP22 might be used in the evaluation of patients at risk of renal cell carcinoma^[24]. Konety *et al.*^[25] reported that the BLCA-4 was a very sensitive and specific marker for bladder cancer.

NMPs alterations were also associated with the cancer of digestive tract. Chen *et al.*^[26] found that the interaction between HPV-16 E6 and nuclear matrix might contribute to virus induced carcinogenesis in esophageal carcinoma. Brunagel *et al.*^[27] analyzed the NMPs expression by high-resolution two-dimensional gel electrophoresis, and found that the NMP composition was able to differentiate liver metastases from normal liver tissue and normal hepatocytes. In 2003, they identified an NMP, calreticulin, which was expressed much more strongly in colon cancer compared to adjacent and normal colon tissue^[28]. In our study, we found that the expression of 30 ku, 28 ku NMPs was significantly reduced in gastric cancer when compared with that in the normal gastric tissue ($P<0.05$). There were no significant differences in the expression of these two proteins between the various differentiation grades and clinical stages of the gastric cancer. The results suggested that the changes of NMPs in gastric cancer might occur at early stage of the tumor development.

Matrix attachment regions (MARs) are postulated to anchor chromatin onto the NM, thereby organizing genomic DNA into topologically distinct loop domains that are important in replication and transcription^[29]. The p300-SAF-A interactions at MAR elements of nontranscribed genes might poise these genes for transcription^[30]. NM was a key locus for CK2 signaling in the nucleus^[31]. Expression of p16 gene was significantly reduced in gastric cancer. The down-regulated expression of 30 ku, 28 ku NMPs in gastric cancer might be related to the down-regulated expression of p16 gene. In our previous study, we found the hypermethylation, mutation and microsatellite instability of p16 gene in gastric cancer. The binding of NMPs to the upstream of p16 gene and its relation to the down regulated expression of p16 gene in gastric cancer will be studied further.

REFERENCES

- Leman ES, Getzenberg RH. Nuclear matrix proteins as biomarkers in prostate cancer. *J Cell Biochem* 2002; **86**: 213-223
- Holaska JM, Wilson KL, Mansharamani M. The nuclear envelope, lamins and nuclear assembly. *Curr Opin Cell Biol* 2002; **14**: 357-364
- Pavao M, Huang YH, Hafer LJ, Moreland RB, Traish AM. Immunodetection of nmt55/p54nrb isoforms in human breast cancer. *BMC Cancer* 2001; **1**: 15
- Ishii T, Okadome A, Takeuchi F, Hiratsuka Y. Urinary levels of nuclear matrix protein 22 in patients with urinary diversion. *Urology* 2001; **58**: 940-942
- Brunzel G, Vietmeier BN, Bauer AJ, Schoen RE, Gerzenberg RH. Identification of nuclear matrix protein alterations associated with human colon cancer. *Cancer Res* 2002; **62**: 2437-2442
- Leman ES, Arlotti JA, Dhir R, Greenberg N, Getzenberg RH. Characterization of the nuclear matrix proteins in a transgenic mouse model for prostate cancer. *J Cell Biochem* 2002; **86**: 203-212
- Philimonenko VV, Flechon JE, Hozak P. The nucleoskeleton: a permanent structure of cell nuclei regardless of their transcriptional activity. *Exp Cell Res* 2001; **264**: 201-210
- Djeliova V, Russev G, Anachkova B. Dynamics of association of origins of DNA replication with the nuclear matrix during the cell cycle. *Nucleic Acids Res* 2001; **29**: 3181-3187
- Blencowe BJ, Bauren G, Eldridge AG, Issner R, Nickerson JA,

- Rosenina E, Sharp PA. The SRm160/300 splicing coactivator subunits. *RNA* 2000; **6**: 111-120
- 10 **Cremer T**, Kreth G, Koester H, Fink RH, Heintzmann R, Cremer M, Solovei I, Zink D, Cremer C. Chromosome territories, interchromatin domain compartment, and nuclear matrix: an integrated view of the functional nuclear architecture. *Crit Rev Eukaryot Gene Expr* 2000; **10**: 179-212
- 11 **Luftner D**, Possinger K. Nuclear matrix proteins as biomarkers for breast cancer. *Expert Rev Mol Diagn* 2002; **2**: 23-31
- 12 **Wang ZH**, Yu D, Li HK, Chow VW, Ng CC, Chan HB, Cheng SB, Chew EC. Alteration of nuclear matrix protein composition of neuroblastoma cells after arsenic trioxide treatment. *Anticancer Res* 2001; **21**: 493-498
- 13 **Spencer VA**, Samuel SK, Davie JR. Altered profiles in nuclear matrix proteins associated with DNA *in situ* during progression of breast cancer cells. *Cancer Res* 2001; **61**: 1362-1366
- 14 **Takaha N**, Hawkins AL, Griffin CA, Issaacs WB, Coffey DS. High mobility group protein I (Y): a candidate architectural protein for chromosomal rearrangements in prostate cancer cells. *Cancer Res* 2002; **62**: 647-651
- 15 **Leman ES**, Madigan MC, Brunagel G, Takaha N, Coffey DS, Getzenberg RH. Nuclear matrix localization of high mobility group protein I (Y) in a transgenic mouse model for prostate cancer. *J Cell Biochem* 2003; **88**: 599-608
- 16 **Ishiguro H**, Uemura H, Fujinami K, Ikeda N, Ohta S, Kubota Y. 55 kDa nuclear matrix protein (nmt55) mRNA is expressed in human prostate cancer tissue and is associated with the androgen receptor. *Int J Cancer* 2003; **105**: 26-32
- 17 **Shao Y**, Zhuang J, Xu SX, Liu DY. Significance of urinary nuclear matrix protein 22 in diagnosis of transitional cell carcinoma of urinary tract. *Aizheng* 2002; **21**: 1005-1007
- 18 **Friedrich MC**, Hellstern A, Hautmann SH, Graefen M, Conrad S, Huland E, Huland H. Clinical use of urinary markers for the detection and prognosis of bladder carcinoma: a comparison of immunocytology with monoclonal antibodies against Lewis X and 486p3/12 with the BTA STAT and NMP22 tests. *J Urol* 2002; **168**: 470-474
- 19 **Parekattil SJ**, Fisher HA, Kogan BA. Neural network using combined urine nuclear matrix protein-22 monocyte chemoattractant protein-1 and urinary intercellular adhesion molecule-1 to detect bladder cancer. *J Urol* 2003; **169**: 917-920
- 20 **Mahnert B**, Tauber S, Kriegmair M, Nagel D, Holdenrieder S, Hofmann K, Reiter W, Schmeller N, Stieber P. Measurements of complement factor H-related protein (BAT-TRAK) assay and nuclear matrix protein (NMP22 assay)-useful diagnostic tools in the diagnosis of urinary bladder cancer? *Clin Chem Lab Med* 2003; **41**: 104-110
- 21 **Bhuiyan J**, Akhter J, O' Kane DJ. Performance characteristics of multiple urinary tumor markers and sample collection techniques in the detection of transitional cell carcinoma of the bladder. *Clin Chim Acta* 2003; **331**: 69-77
- 22 **Eissa S**, Swellam M, Sadek M, Mourad MS, Ahmady OE, Khalifa A. Comparative evaluation of the nuclear matrix protein, fibronectin, urinary bladder cancer antigen and voided urine cytology in the detection of bladder tumors. *J Urol* 2002; **168**: 465-469
- 23 **Xu K**, Tam PC, Hou S, Wang X, Bai W. The role of nuclear matrix protein 22 combined with bladder tumor antigen stat test in surveillance of recurring bladder cancer. *Chin Med J* 2002; **115**: 1736-1738
- 24 **Ozer G**, Altinel M, Kocak B, Yazicioglu A, Gonenc F. Value of urinary NMP-22 in patients with renal cell carcinoma. *Urology* 2002; **60**: 593-597
- 25 **Konety BR**, Nguyen TS, Dhir R, Day RS, Becich MJ, Stadler WM, Getzenberg RH. Detection of bladder cancer using a novel nuclear matrix protein, BLCA-4. *Clin Cancer Res* 2000; **6**: 2618-2625
- 26 **Chen HB**, Chen L, Zhang JK, Shen ZY, Su ZJ, Cheng SB, Chew EC. Human papillomavirus 16 E6 is associated the nuclear matrix of esophageal carcinoma cells. *World J Gastroenterol* 2001; **7**: 788-791
- 27 **Brunagel G**, Schoen RE, Bauer AJ, Vietmeier BN, Getzenberg RH. Nuclear matrix protein alterations associated with colon cancer metastasis to the liver. *Clin Cancer Res* 2002; **8**: 3039-3045
- 28 **Brunagel G**, Shah U, Schoen RE, Getzenberg RH. Identification of calreticulin as a nuclear matrix protein associated with human colon cancer. *J Cell Biochem* 2003; **89**: 238-243
- 29 **Galande S**. Chromatin (dis) organization and cancer: BUR-binding proteins as biomarkers for cancer. *Curr Cancer Drug Targets* 2002; **2**: 157-190
- 30 **Martens JH**, Verlann M, Kalkhoven E, Dorsman JC, Zantema A. Scaffold/matrix attachment region elements interact with a p300-scaffold attachment factor A complex and are bound by acetylated nucleosomes. *Mol Cell Biol* 2002; **22**: 2598-2606
- 31 **Wang H**, Yu S, Davis AT, Ahmed K. Cell cycle dependent regulation of protein kinase CK2 signaling to the nuclear matrix. *J Cell Biochem* 2003; **88**: 812-822

Edited by Zhu LH and Xu FM

Apoptosis of human primary gastric carcinoma cells induced by genistein

Hai-Bo Zhou, Juan-Juan Chen, Wen-Xia Wang, Jian-Ting Cai, Qin Du

Hai-Bo Zhou, Juan-Juan Chen, Wen-Xia Wang, Jian-Ting Cai, Qin Du, Department of Gastroenterology, Second Affiliated Hospital of Zhejiang University, Hangzhou 310009, Zhejiang Province, China
Correspondence to: Dr. Hai-Bo Zhou, Department of Gastroenterology, Second Affiliated Hospital of Zhejiang University, Hangzhou 310009, Zhejiang Province, China. zhouhaibohz@163.com
Telephone: +86-571-87783564

Received: 2003-10-27 **Accepted:** 2004-01-15

Abstract

AIM: To investigate the apoptosis in primary gastric cancer cells induced by genistein, and the relationship between this apoptosis and expression of *bcl-2* and *bax*.

METHODS: MTT assay was used to determine the cell growth inhibitory rate *in vitro*. Transmission electron microscope and TUNEL staining were used to quantitatively and qualitatively detect the apoptosis of primary gastric cancer cells before and after genistein treatment. Immunohistochemical staining and RT-PCR were used to detect the expression of apoptosis-associated genes *bcl-2* and *bax*.

RESULTS: Genistein inhibited the growth of primary gastric cancer cells in dose- and time-dependent manner. Genistein induced primary gastric cancer cells to undergo apoptosis with typically apoptotic characteristics. TUNEL assay showed that after the treatment of primary gastric cancer cells with genistein for 24 to 96 h, the apoptotic rates of primary gastric cancer cells increased time-dependently. Immunohistochemical staining showed that after the treatment of primary gastric cancer cells with genistein for 24 to 96 h, the positivity rates of Bcl-2 proteins were apparently reduced with time and the positivity rates of Bax proteins were apparently increased with time. After exposed to genistein at 20 $\mu\text{mol/L}$ for 24, 48, 72 and 96 respectively, the density of *bcl-2* mRNA decreased progressively and the density of *bax* mRNA increased progressively with elongation of time.

CONCLUSION: Genistein is able to induce the apoptosis in primary gastric cancer cells. This apoptosis may be mediated by down-regulating the apoptosis-associated *bcl-2* gene and up-regulating the expression of apoptosis-associated *bax* gene.

Zhou HB, Chen JJ, Wang WX, Cai JT, Du Q. Apoptosis of human primary gastric carcinoma cells induced by genistein. *World J Gastroenterol* 2004; 10(12): 1822-1825
<http://www.wjgnet.com/1007-9327/10/1822.asp>

INTRODUCTION

Genistein is a planar molecule with an aromatic A-ring, has a second oxygen atom 11.5 Å from the one in the A ring, a molecular weight similar to those of the steroidal estrogens. It has estrogenic properties in receptor binding assays^[1,2], cell culture^[3,4], and uterine weight assays^[5-7]. Genistein inhibits

topoisomerase II^[8], platelet-activating factor- and epidermal growth factor-induced expression of *c-fos*^[9], diacylglycerol synthesis^[10], and tyrosine kinases^[11]. It also inhibits microsomal lipid peroxidation^[12] and angiogenesis^[13]. Genistein exhibits antioxidant properties^[14-16] and was reported to induce differentiation of numerous cell types^[17-19]. Moreover, a recent report shows that genistein is a potent cancer chemopreventive agent^[20-22]. The anti-tumor activity of genistein might be related to induce the apoptosis of tumor cells but the precise mechanism of antitumor activity is not well understood.

The Bcl-2 family plays a crucial role in the control of apoptosis. The family includes a number of proteins which have homologous amino acid sequences, including anti-apoptotic members such as Bcl-2 and Bcl-x_L, as well as pro-apoptotic members like Bax and Bad^[23-26]. Overexpression of Bax has the effect of promoting cell death^[27-31]. Conversely, overexpression of antiapoptotic proteins such as Bcl-2 will repress the function of Bax^[32-36]. Thus, the ratio of Bcl-2/Bax appears to be a critical determinant of cell apoptosis^[37].

In this study, MTT assay was used to determine the cell growth inhibitory rate. Transmission electron microscope and TUNEL staining method were used to quantitatively and qualitatively detect the apoptosis status of primary gastric cancer cells before and after the genistein treatment. Immunohistochemical staining and RT-PCR were used to detect the expression of apoptosis-associated genes *bcl-2* and *bax*.

MATERIALS AND METHODS

Materials

Genistein and MTT were obtained from Sigma Chemical Co, Ltd. *In situ* cell detection kit, anti-Bcl-2 monoclonal antibody and anti-Bax monoclonal antibody were purchased from Beijing Zhongshan Biotechnology Co, Ltd. Stock solution of genistein was made in dimethylsulfoxide (DMSO) at a concentration of 40 $\mu\text{mol/L}$. Working dilutions were directly made in the cell culture medium.

Methods

Cell culture Fresh sample from a patient with gastric cancer was obtained in operating room. A single-cell suspension of tumor cells with the concentration of $5 \times 10^5/\text{mL}$ was prepared for seeding. Primary gastric cancer cells were purified after culture.

MTT assay Cells $1 \times 10^5/\text{well}$ in a 96-well plate after incubation for 24 h were treated with different concentrations of genistein (5, 10, 20, 40 $\mu\text{mol/L}$) for 24, 48 and 72 h respectively. A 10 μL of 5 g/L of MTT was added to the medium triplicate at each dose and incubated for 4 h at 37 °C. Culture media were discarded followed by addition of 0.2 mL DMSO and vibration for 10 min. The absorbance (A) was measured at 570 nm using a microplate reader. The cell growth inhibitory rate was calculated as follows: $\{(A \text{ of control group} - A \text{ of experimental group}) / (A \text{ of control group} - A \text{ of blank group})\} \times 100\%$.

Transmission electron microscopy Cells treated with 20 $\mu\text{mol/L}$ genistein were harvested after incubation for 24 h. Subsequently

the cells were fixed in 40 g/L glutaral and immersed with Epon 821, imbedded for 72 h at 60 °C. After that the cells were prepared into ultrathin section (60 nm) and stained with uranyl acetate and lead citrate. Cell morphology was observed by transmission electron microscopy.

TUNEL assay Apoptosis of primary gastric cancer cells was evaluated by using an *in situ* cell detection kit. The cells were treated in the presence or absence of 20 µmol/L genistein for 24 to 96 h and fixed in ice-cold 800 mL/L ethanol for up to 24 h, treated with proteinase K and then 3 mL/L H₂O₂, and labeled with fluorescein dUTP in a humid box for 1 h at 37 °C. Cells were then combined with POD-horseradish peroxidase, colored with DAB and counterstained with methyl green. Controls received the same treatment except the labeling of omission of fluorescein dUTP. Cells were visualized under light microscope. The apoptotic index (AI) was calculated as follows: AI=(Number of apoptotic cells/Total number)×100%.

Immunohistochemical staining Immunohistochemical staining was done by an avidinbiotin technique. Primary gastric cancer cells treated in the presence or absence of 20 µmol/L genistein for 24 to 96 h were grown on six-well glass plates and were fixed by acetone. After washed in PBS, the cells were incubated in 3 mL/L H₂O₂ solution at room temperature for 5 min. The cells were then incubated with anti-Bcl-2 or anti-Bax monoclonal antibody at a 1:300 dilution at 4 °C overnight. After wash of cells in PBS, the second antibody, biotinylated antirat IgG was added and the cells were incubated at room temperature for 1 h. After wash of cells in PBS, ABC compound was added and the cells were then incubated at room temperature for 10 min. DAB was used as the chromagen. After 10 min, the brown color signifying the presence of antigen bound to antibodies was detected by light microscopy and photographed at ×200. Controls were treated the same as the experimental group except the incubation of the primary antibody instead of second antibody. The positive rate (PR) was calculated as follows: PR=(Number of positive cells/Total number)×100%.

RT-PCR The primary gastric cancer cells were treated in the presence or absence of 20 µmol/L genistein for 24 to 96 h and total RNA was extracted. The concentration of RNA was determined by absorption at 260 nm. The primers for Bcl-2, Bax and β-actin were as follows: β-actin (500 bp): 5' GTGGG GCGCCCCAGGCACCA 3', 5' CTCCTTAATGTCACG CACGATTC 3'; bcl-2 (716 bp): 5' GAAATATGGCGC ACGCT 3', 5' TCACTTGTGGCCAGAT 3'; bax (508 bp): 5' CCAGCTCTGAGCAGATCAT 3', 5' TATCAGCCCA TCTTCTCC 3'. Polymerase chain reactions were performed in a 25 µL reaction volume. PCR for Bcl-2 and β-actin was run in the following procedures: at 94 °C for 7 min, 1 circle; at 94 °C for 1 min, at 72 °C for 1 min, 30 cycles; at 72 °C for 7 min, 1 circle. PCR for Bax was run in the following procedure: 94 °C for 1 min, 60 °C for 45 s, 72 °C for 45 s, 35 cycles. Ten µL PCR product was placed onto 15 g/L agarose gel and observed by EB staining using Gel-Pro analyzer.

Statistical analysis

Data were analyzed by the paired two-tailed Student's *t* test, and significance was considered when $P < 0.05$.

RESULTS

MTT assay

Primary gastric cancer cells were exposed to increasing concentrations (5 µmol/L to 40 µmol/L) of genistein for 24 to 72 h, respectively. Primary gastric cancer cells showed death in a dose- and time-dependent manner. The data are summarized in Table 1.

Table 1 A value of primary gastric cancer cells treated with different concentrations of genistein

	24 h	48 h	72 h
Control	0.400±0.008	0.406±0.007	0.404±0.008
5 µmol/L genistein	0.361±0.002 ^a	0.334±0.012 ^b	0.305±0.004 ^b
10 µmol/L genistein	0.325±0.004 ^d	0.313±0.003 ^b	0.248±0.004 ^d
20 µmol/L genistein	0.308±0.003 ^d	0.249±0.002 ^d	0.206±0.003 ^d
40 µmol/L genistein	0.265±0.004 ^d	0.215±0.004 ^d	0.159±0.002 ^d

^a $P < 0.05$; ^b $P < 0.01$; ^d $P < 0.001$ vs control group.

Morphological changes

After treatment of primary gastric cancer cells with genistein (20 µmol/L) for 24 h, some cells presented apoptotic characteristics including chromatin condensation, appearance of chromatin crescent, nuclear fragmentation that could be seen by transmission electron microscope (Figure 1).

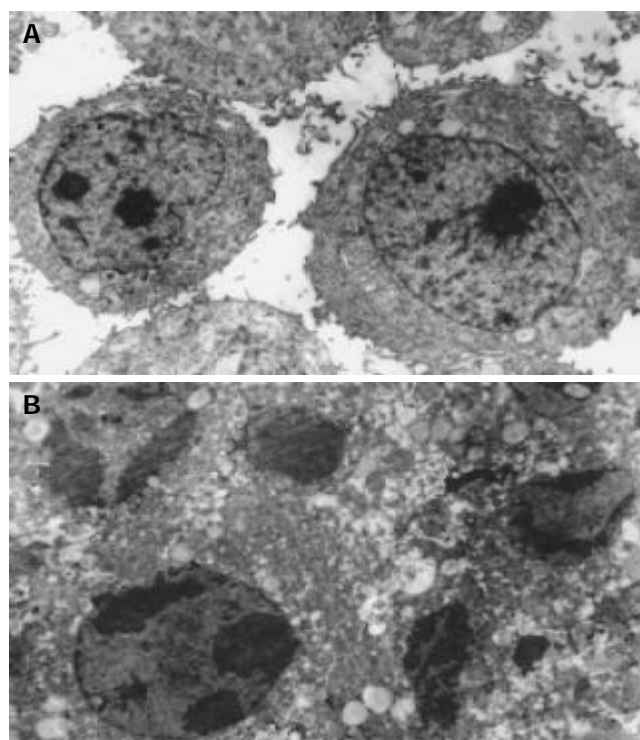


Figure 1 Ultra-microscopic structure of gastric cancer cells induced by genistein. A: Primary gastric cancer cells; B: apoptotic gastric cancer cells (Original magnification: ×4 800).

TUNEL assay

Apoptotic cells were determined by TUNEL assay according to the manufacture's instructions. Positive staining located in the nucleus. After treatment with genistein (20 µmol/L) for 24 to 96 h, Apoptotic index of the cells was apparently increased with the increase of treatment time ($P < 0.05$) (Table 2).

Expression of Bcl-2 proteins

Positive staining located in the cytoplasm. After treatment with genistein (20 µmol/L) for 24 to 96 h, Positivity rate of the cells of Bcl-2 proteins was apparently reduced with the increase of treatment periods ($P < 0.05$) (Table 3). This suggested that genistein could down-regulate the expression of Bcl-2.

Expression of Bax proteins

Positive staining located in the cytoplasm. After treatment with genistein (20 µmol/L) for 24 to 96 h, PRs of Bax proteins were apparently increased with increase of treated time ($P < 0.05$).

(Table 4). This suggested that genistein could up-regulate the expression of Bax.

Table 2 Apoptotic index (AI) of primary gastric cancer cells treated by genistein

	Control	24 h	48 h	72 h	96 h
AI (%)	1.25±0.30	4.97±0.80	18.44±1.92	35.18±0.35	43.93±1.11
<i>t</i>		-6.13	-13.82	-180.16	-52.80
<i>P</i>		<i>P</i> <0.05	<i>P</i> <0.05	<i>P</i> <0.05	<i>P</i> <0.05

P<0.05 vs control group; AI: Apoptotic index.

Table 3 Positivity rate (PR) of Bcl-2 in primary gastric cancer cells treated by genistein

	Control	24 h	48 h	72 h	96 h
PR(%)	36.34±0.72	21.62±0.08	10.60±0.49	7.21±0.45	4.54±0.36
<i>t</i>		31.93	44.67	73.80	59.32
<i>P</i>		<i>P</i> <0.01	<i>P</i> <0.01	<i>P</i> <0.01	<i>P</i> <0.01

P<0.01 vs control group; PR: Positivity rate.

Table 4 Positivity rate (PR) of Bax in primary gastric cancer cells treated by genistein

	Control	24 h	48 h	72 h	96 h
PR(%)	10.73±0.57	20.63±0.86	34.3±0.81	45.96±0.42	58.61±1.46
<i>t</i>		-57.49	-41.23	-69.53	-51.31
<i>P</i>		<i>P</i> <0.001	<i>P</i> <0.001	<i>P</i> <0.001	<i>P</i> <0.001

P<0.01 vs control group; PR: Positivity rate.

RT-PCR

After exposed to 20 μmol/L genistein for 24, 48, 72 and 96 h respectively, the density of bcl-2 mRNA decreased progressively and the density of bax mRNA increased progressively with elongation of time by RT-PCR. It suggested that genistein could down-regulate the expression of Bcl-2 and up-regulate the expression of Bax.

DISCUSSION

Populations who consume a diet high in soy are reported to have a lower incidence of breast and prostate cancer. The activity of the soy-derived phytoestrogen, genistein, is thought to account for a portion of the chemopreventative properties of soy; these include an inhibitory effect on tyrosine kinases^[11], DNA topoisomerases I and II^[8], and ribosomal S6 kinase, antiestrogenicity, antioxidant activity, anti-angiogenesis activity^[12], suppression of cell proliferation, induction of differentiation^[17-19], and modulation of apoptosis^[20-22].

In this study, we found that primary gastric cancer cells showed death in a dose- and time-dependent manner in MTT assay. This suggested genistein was able to restrain the growth of primary gastric cancer cells. It was found that genistein was able to induce the apoptosis of primary gastric cancer cells by transmission electron microscope assay and TUNEL assay. After treatment with 20 μmol/L genistein for 24 to 96 h, PRs of Bcl-2 proteins were apparently reduced and PRs of Bax proteins were apparently increased with increase of treated time by Immunohistochemical staining. After exposed to 20 μmol/L genistein for 24, 48, 72 and 96 h respectively, the density of bcl-2 mRNA decreased progressively and the density of bax mRNA increased progressively with elongation of time by RT-PCR.

Genistein could reduce Bcl-2 expression and enhance bax

expression. The ratio of Bcl-2/Bax was decreased when primary gastric cancer cells were treated with genistein, which could trigger the apoptosis of primary gastric cancer cells.

The present study demonstrated that genistein was able to induce the apoptosis in primary gastric cancer. This apoptosis may be mediated by down-regulating the expression of apoptosis-associated gene *bcl-2* and up-regulating the expression of apoptosis-associated gene *bax*. Genistein may be used as a potential chemotherapeutic drug in the anti-gastric carcinoma chemotherapy.

REFERENCES

- 1 **Shutt DA**, Cox RI. Steroid and phyto-oestrogen binding to sheep uterine receptors *in vitro*. *J Endocrinol* 1972; **52**: 299-310
- 2 **Mathieson RA**, Kitts WD. Binding of phytoestrogen and estradiol-17beta by cytoplasmic receptors in the pituitary gland and hypothalamus of the ewe. *J Endocrinol* 1980; **85**: 317-325
- 3 **Martin PM**, Horowitz KB, Ryan DS, McGuire WL. Phytoestrogen interaction with estrogen receptors in human breast cancer cells. *Endocrinology* 1978; **103**: 1860-1867
- 4 **Makela S**, Davis VL, Tally WC, Korkman J, Salo L, Vihko R, Santti R, Korach KS. Dietary estrogens act through estrogen receptor-mediated processes and show no antiestrogenicity in cultured breast cancer cells. *Environ Health Perspect* 1994; **102**: 572-578
- 5 **Thigpen JE**, Haseman JK, Saunders H, Locklear J, Caviness G, Grant M, Forsythe D. Dietary factors affecting uterine weights of immature CD-1 mice used in uterotrophic bioassays. *Cancer Detect Prev* 2002; **26**: 381-393
- 6 **Folman Y**, Pope GS. The interaction in the immature mouse of potent oestrogens with coumestrol, genistein and other uterovaginitrophic compounds of low potency. *J Endocrinol* 1966; **34**: 215-225
- 7 **Polkowski K**, Mazurek AP. Biological properties of genistein. A review of *in vitro* and *in vivo* data. *Acta Pol Pharm* 2000; **57**: 135-155
- 8 **Okura A**, Arakawa H, Oka H, Yoshinari T, Monden Y. Effect of genistein on topoisomerase activity and on the growth of [Val12] Ha-ras-transformed NIH 3T3 cells. *Biochem Biophys Res Commun* 1988; **157**: 183-189
- 9 **Tripathi YB**, Lim RW, Fernandez-Gallardo S, Kandala JC, Guntaka RV, Shukla SD. Involvement of tyrosine kinase and protein kinase C in platelet-activating-factor-induced c-fos gene expression in A-421 cells. *Biochem J* 1992; **286**(Pt 2): 527-533
- 10 **Akiyama T**, Ishida J, Nakagawa S, Ogawara H, Watanabe S, Itho N, Shibuya M, Fukami Y. Genistein, a specific inhibitor of tyrosine-specific protein kinases. *J Biol Chem* 1987; **262**: 5592-5595
- 11 **Dean NM**, Kanemitsu M, Boynton AL. Effects of the tyrosine-kinase inhibitor genistein on DNA synthesis and phospholipid-derived second messenger generation in mouse 10T1/2 fibroblasts and rat liver T51B cells. *Biochem Biophys Res Commun* 1989; **165**: 705-801
- 12 **Jha HC**, von Recklinghausen G, Zilliken F. Inhibition of *in vitro* microsomal lipid peroxidation by isoflavonoids. *Biochem Pharmacol* 1985; **34**: 1367-1369
- 13 **Fotsis T**, Pepper M, Adlercreutz H, Fleischman G, Hase T, Montesano R, Schweigerer L. Genistein, a dietary-derived inhibitor of *in vitro* angiogenesis. *Proc Natl Acad Sci U S A* 1993; **90**: 2690-2694
- 14 **Mitchell JH**, Gardner PT, McPhail DB, Morrice PC, Collins AR, Duthie GG. Antioxidant efficacy of phytoestrogens in chemical and biological model systems. *Arch Biochem Biophys* 1998; **360**: 142-148
- 15 **Tikkanen MJ**, Adlercreutz H. Dietary soy-derived isoflavone phytoestrogens. Could they have a role in coronary heart disease prevention? *Biochem Pharmacol* 2000; **60**: 1-5
- 16 **Wei H**, Bowen R, Cai Q, Barnes S, Wang Y. Antioxidant and antipromotional effects of the soybean isoflavone genistein. *Proc Soc Exp Biol Med* 1995; **208**: 124-130
- 17 **Watanabe T**, Kondo K, Oishi M. Induction of *in vitro* differentiation of mouse erythroleukemia cells by genistein, an inhibitor of tyrosine protein kinases. *Cancer Res* 1991; **51**: 764-768
- 18 **Miller DR**, Lee GM, Maness PF. Increased neurite outgrowth induced by inhibition of protein tyrosine kinase activity in PC12

- pheochromocytoma cells. *J Neurochem* 1993; **60**: 2134-2144
- 19 **Simon HU**, Yousefi S, Blaser K. Tyrosine phosphorylation regulates activation and inhibition of apoptosis in human eosinophils and neutrophils. *Int Arch Allergy Immunol* 1995; **107**: 338-339
- 20 **Huang P**, Robertson LE, Wright S, Plunkett W. High molecular weight DNA fragmentation: a critical event in nucleoside analogue-induced apoptosis in leukemia cells. *Clin Cancer Res* 1995; **1**: 1005-1013
- 21 **Xu LH**, Owens LV, Sturge GC, Yang X, Liu ET, Craven RJ, Cance WG. Attenuation of the expression of the focal adhesion kinase induces apoptosis in tumor cells. *Cell Growth Differ* 1996; **7**: 413-418
- 22 **Davis JN**, Singh B, Bhuiyan M, Sarkar FH. Genistein-induced upregulation of p21^{WAF1}, downregulation of cyclin B, and induction of apoptosis in prostate cancer cells. *Nutr Cancer* 1998; **32**: 123-131
- 23 **Konopleva M**, Konoplev S, Hu W, Zaritskey AY, Afanasiev BV, Andreeff M. Stromal cells prevent apoptosis of AML cells by up-regulation of anti-apoptotic proteins. *Leukemia* 2002; **16**: 1713-1724
- 24 **van der Woude CJ**, Jansen PL, Tiebosch AT, Beuving A, Homan M, Kleibeuker JH, Moshage H. Expression of apoptosis-related proteins in Barrett's metaplasia-dysplasia-carcinoma sequence: a switch to a more resistant phenotype. *Hum Pathol* 2002; **33**: 686-692
- 25 **Panaretakis T**, Pokrovskaja K, Shoshan MC, Grandt D. Activation of Bak, Bax and BH3-only proteins in the apoptotic response to doxorubicin. *J Biol Chem* 2002; **277**: 44317-44326
- 26 **Bellosillo B**, Villamor N, Lopez-Guillermo A, Marce S, Bosch F, Campo E, Montserrat E, Colomer D. Spontaneous and drug-induced apoptosis is mediated by conformational changes of Bax and Bak in B-cell chronic lymphocytic leukemia. *Blood* 2002; **100**: 1810-1816
- 27 **Matter-Reissmann UB**, Forte P, Schneider MK, Filgueira L, Groscurth P, Seebach JD. Xenogeneic human NK cytotoxicity against porcine endothelial cells is perforin/granzyme B dependent and not inhibited by Bcl-2 overexpression. *Xenotransplantation* 2002; **9**: 325-337
- 28 **Lanzi C**, Cassinelli G, Cuccuru G, Supino R, Zuco V, Ferlini C, Scambia G, Zunino F. Cell cycle checkpoint efficiency and cellular response to paclitaxel in prostate cancer cells. *Prostate* 2001; **48**: 254-264
- 29 **Mertens HJ**, Heineman MJ, Evers JL. The expression of apoptosis-related proteins Bcl-2 and Ki67 in endometrium of ovulatory menstrual cycles. *Gynecol Obstet Invest* 2002; **53**: 224-230
- 30 **Mehta U**, Kang BP, Bansal G, Bansal MP. Studies of apoptosis and bcl-2 in experimental atherosclerosis in rabbit and influence of selenium supplementation. *Gen Physiol Biophys* 2002; **21**: 15-29
- 31 **Chang WK**, Yang KD, Chuang H, Jan JT, Shiao MF. Glutamine protects activated human T cells from apoptosis by up-regulating glutathione and bcl-2 levels. *Clin Immunol* 2002; **104**: 151-160
- 32 **Chen GG**, Lai PB, Hu X, Lam IK, Chak EC, Chun YS, Lau WY. Negative correlation between the ratio of Bax to Bcl-2 and the size of tumor treated by culture supernatants from Kupffer cells. *Clin Exp Metastasis* 2002; **19**: 457-464
- 33 **Usuda J**, Chiu SM, Azizuddin K, Xue LY, Lam M, Nieminen AL, Oleinick NL. Promotion of photodynamic therapy-induced apoptosis by the mitochondrial protein Smac/DIABLO: dependence on Bax. *Photochem Photobiol* 2002; **76**: 217-223
- 34 **Sun F**, Akazawa S, Sugahara K, Kamihira S, Kawasaki E, Eguchi K, Koji T. Apoptosis in normal rat embryo tissues during early organogenesis: the possible involvement of Bax and Bcl-2. *Arch Histol Cytol* 2002; **65**: 145-157
- 35 **Jang MH**, Shin MC, Shin HS, Kim KH, Park HJ, Kim EH, Kim CJ. Alcohol induces apoptosis in TM3 mouse Leydig cells via bax-dependent caspase-3 activation. *Eur J Pharmacol* 2002; **449**: 39-45
- 36 **Tilli CM**, Stavast-Koey AJ, Ramaekers FC, Neumann HA. Bax expression and growth behavior of basal cell carcinomas. *J Cutan Pathol* 2002; **29**: 79-87
- 37 **Pettersson F**, Dalgleish AG, Bissonnette RP, Colston KW. Retinoids cause apoptosis in pancreatic cancer cells via activation of RAR-gamma and altered expression of Bcl-2/Bax. *Br J Cancer* 2002; **87**: 555-561

Edited by Zhu LH and Chen WW Proofread by Xu FM

Polymorphisms of interleukin-1B and interleukin-1 receptor antagonist genes in patients with chronic hepatitis B

Ping-An Zhang, Yan Li, Pu Xu, Jian-Min Wu

Ping-An Zhang, Yan Li, Pu Xu, Department of Laboratory Science, Renmin Hospital of Wuhan University, Wuhan 430060, Hubei Province, China

Jian-Min Wu, Department of Laboratory Science, Affiliated Union Hospital of Tongji Medical College, Huazhong University of Science and Technology, Wuhan 430030, Hubei Province, China

Correspondence to: Ping-An Zhang, Department of Laboratory Science, Renmin Hospital of Wuhan University, Wuhan 430060, Hubei Province, China. cydyjyk@public.wh.hb.com

Telephone: +86-27-88041911-8258

Received: 2003-10-10 **Accepted:** 2003-12-16

Abstract

AIM: To investigate the relationships between polymorphisms of interleukin-1B (IL-1B) promoter region -511C/T and interleukin-1 receptor antagonist gene (IL-1RN) and susceptibility to chronic hepatitis B in Chinese population.

METHODS: Genomic DNA was extracted from the peripheral blood of 190 patients with chronic hepatitis B and 249 normal controls and then subjected to polymerase chain reaction (PCR) amplification. The PCR products were digested by restriction endonuclease *Ava*I. The products of digestion were subjected to 20 g/L gel electrophoresis and ethidium bromide staining.

RESULTS: The frequencies of IL-1B (-511) genotypes CC, CT and TT in patients with chronic hepatitis B were 23.7%, 49.5% and 26.8%, while 26.1%, 47.4% and 26.5% respectively in controls. The results showed that there was no significant difference in the frequencies of alleles or genotypes in IL-1B between patients with chronic hepatitis B and controls. The distributions of IL-1B (-511) genotype CC were significantly different between the two subgroups (HBV-DNA $\leq 1 \times 10^3$ copies/mL as subgroup I, HBV-DNA $> 1 \times 10^3$ copies/mL as subgroup II) of chronic hepatitis B ($P=0.029$). Only four of the five kinds of polymorphism (1/1, 1/2, 2/2 and 1/4) were found in this study. The frequencies of IL-1RN genotypes 1/1, 1/2, 2/2 and 1/4 were 88.9%, 9.0%, 0.5% and 1.6% in patients with chronic hepatitis B respectively, while were 81.1%, 16.9%, 0.4% and 1.6% respectively in controls. The frequencies of genotype 1/2 and IL-1RN allele 2 in patients with chronic hepatitis B were lower than those in controls ($P=0.016$ and $P=0.029$, respectively).

CONCLUSION: There is an association between polymorphisms of the promoter region -511C/T of IL-1B and IL-1RN intron 2 and chronic hepatitis B virus infection. Subjects with IL-1RN allele 2 may be resistant to HBV infection, and IL-1B(-511) genotype CC is closely related with HBV-DNA replication, which gives some new clues to the study of pathogenesis of chronic hepatitis B.

Zhang PA, Li Y, Xu P, Wu JM. Polymorphisms of interleukin-1B and interleukin-1 receptor antagonist genes in patients with chronic hepatitis B. *World J Gastroenterol* 2004; 10(12): 1826-1829
<http://www.wjgnet.com/1007-9327/10/1826.asp>

INTRODUCTION

Hepatitis B virus (HBV) infection is one of the most important chronic viral diseases in the world. An estimated 400 million people worldwide are carriers of HBV, and approximately 250 000 deaths occur each year as a consequence of fulminant hepatic failure, cirrhosis, and hepatocellular carcinoma^[1]. When HBV is acquired in adulthood, the majority of infections are cleared, with chronic infection occurring in 5% to 10% of cases. However, the dynamic interaction of the host inflammatory response with HBV, and the subsequent impact of this interaction on the clinical outcome of HBV infection, are not yet fully understood, nor are the underlying mechanisms for persistence of the virus.

Cytokines play an important role in defense against viral infection, indirectly through determination of the predominant pattern of the host response, and directly through inhibition of viral replication^[2]. Interleukin(IL)-1 is one of the most proinflammatory agents, and has a central role in inflammation and destruction^[3]. The most important members of the IL-1 family are the IL-1 α , IL-1 β and IL-1 receptor antagonists (ra). IL-1ra is an IL-1 natural competitive inhibitor, acting by occupancy of cell surface receptor without triggering signal transduction^[4]. IL-1ra plays a role as an important regulator of inflammation and is currently evaluated in clinical trials. Genes encoding IL-1 are located on the 430 kb region of chromosome 2q13-21, consisting of three homologous genes: IL-1A, IL-1B and IL-1ra (IL-1RN)^[5]. Biallelic polymorphisms at positions IL-1A -889, IL-1B -511, and +3 953 have been described, all representing a C/T single nucleotide polymorphism (SNP). IL-1RN contains an 86 bp variable number tandem repeat (VNTR) polymorphism in intron 2^[6]. These polymorphisms are located within the regulatory regions of the genes and have potential functional importance by modulating IL-1 protein production, and are related with the development of some diseases^[7].

This research was to discuss the relationship between polymorphisms of IL-1 gene and susceptibility to HBV in the Chinese population, and tried to reveal the correlation between the genotype and phenotype distributions, in order to provide a certain scientific basis for prevention and treatment of chronic hepatitis B.

MATERIALS AND METHODS

Subjects

A total of 190 patients with chronic hepatitis B (130 males, 60 females) aged 11-68 years were recruited in Remin Hospital of Wuhan University. The diagnosis of all the patients was confirmed according to the criteria for chronic hepatitis B, and the patients did not have other viral hepatitis. Two hundred and forty-nine control subjects (150 males, 99 females) aged 18-82 years were selected in Wuhan area (HBsAg negative, anti-HBe negative, and anti-HBc negative), and liver, renal, endocrine and cardiovascular disorders were excluded.

PCR preparation

Two microliter peripheral venous blood was collected in an EDTA tube. Genomic DNA was extracted from peripheral

blood leukocytes and frozen at -20°C . Each PCR was carried out in 25 μL reaction mixture containing 100-200 ng genomic DNA, 100 $\mu\text{mol/L}$ dNTP, 25 mmol/L MgCl_2 , 20 pmol/L primers and 1U TaqDNA polymerase (Promega).

IL-1B and IL-1RN polymorphisms

SNP at position -511 in the promoter region (-702-398) of IL-1B was analyzed by the PCR-restriction fragment length polymorphism (RFLP) method^[8]. A 304 bp PCR fragment of the IL-1B promoter region was amplified using the following primers: 5' -TGGCATTGATCTGGTTCATC-3' and 5' -GTTTAGGATCTTCCCACTT-3'. PCR conditions were as follows: denaturation at 95°C for 5 min, then 35 cycles at 94°C for 30 s, at 55°C for 30 s, at 72°C for 1 min, and final extension at 72°C for 5 min. twenty μL of PCR products was digested with 5 U of *AvaI* (TaKaRa, shiga, Japan) at 37°C for 3 h and run on a 20 g/L agarose gel stained with ethidium bromide.

IL-1RN intron 2 contained a VNTR of an 86 bp length of DNA. Oligonucleotides 5' -CTCAGCAACTCTCTAT-3' and 5' -TCCTGGTCTGCAGGTAA-3' flanking this region were used as primers^[8]. Amplification conditions were same as the above. The PCR products were analyzed by electrophoresis on a 20 g/L agarose gel stained with ethidium bromide.

HBV-DNA measurement

Serum HBV-DNA level in patients with chronic hepatitis B was detected with the real-time fluorescent quantitative PCR method (reagents supplied by Shanghai Fosun Co. Ltd.) using a Lightcycler PCR system. Results were considered abnormal when HBV-DNA $>1 \times 10^3$ copies/mL.

Statistical analysis

IL-1B(-511) and IL-1RN(intron 2) allelic and genotype frequencies were calculated in patients with chronic hepatitis B and control subjects. Comparison of allelic and genotypes between groups, and association of IL-1B and IL-1RN polymorphisms with HBV-DNA replication were examined

for statistical significance with chi-square test. Analysis was completed with SPSS 9.0, and $P < 0.05$ was considered statistically significant.

RESULTS

Genotypes of IL-1B and IL-1RN

C/T transition polymorphism of IL-1B(-511) was analyzed by PCR-RFLP. *AvaI* digestion of the PCR products of IL-1B resulted in three genotypes, consisting of TT (intact, 304 bp), CT (three fragments of 304, 190 and 114 bp) and CC (two fragments of 190 and 114 bp), (Figure 1). The intron 2 of IL-1RN polymorphism contained VNTR of 86 bp. There were five alleles in humans, including allele 1 (four repeats, 410 bp), allele 2 (two repeats, 240 bp), allele 3 (five repeats, 500 bp), allele 4 (three repeats, 325 bp) and allele 5 (six repeats, 595 bp). Only four of the five kinds of polymorphism of IL-1RN(1/1, 1/2, 2/2, and 1/4) were found in this study (Figure 2).

Frequencies of IL-1B and IL-1RN genotypes in both groups

The genotype and allele frequencies of IL-1B and IL-1RN in patients with chronic hepatitis B and control subjects were determined, and explored with 2×2 χ^2 test under the Hardy-Weinberg law and shown to represent all population (Tables 1, 2). The frequencies of IL-1B genotypes CC, CT and TT in patients with chronic hepatitis B were 23.7% (45/190), 49.5% (94/190) and 26.8% (51/190), while those in controls were 26.1% (65/249), 47.4% (118/249), and 26.5% (66/249) respectively. The results showed that there was no significant difference in the frequencies of alleles ($\chi^2=0.16$, $P=0.69$) or genotypes ($\chi^2=0.35$, $P=0.84$) in IL-1B between patients with chronic hepatitis B and control subjects.

Only four of the five kinds of polymorphism of IL-1RN (1/1, 1/2, 2/2 and 1/4) were found in this study. The frequencies of 1/1, 1/2, 2/2 and 1/4 were 88.9%, 9.0%, 0.5% and 1.6% in chronic hepatitis B patients, while those in controls were 81.1%, 16.9%, 0.4% and 1.6% respectively. IL-1 RN allele 1 was

Table 1 Comparison of IL-1B(-511) polymorphism between patients with chronic hepatitis B and controls

Group	n	Frequency of genotypes (%)			Frequency of alleles (%)	
		CC	CT	TT	C	T
Patients	190	45 (23.7)	94 (49.5)	51 (26.8)	184 (48.4)	196 (51.6)
Controls	249	65 (26.1)	118 (47.4)	66 (26.5)	248 (49.8)	250 (50.2)

Patients vs controls, $\chi^2=0.35$, $P=0.84$; $\chi^2=0.16$, $P=0.69$.

Table 2 Comparison of IL-1RN intron 2 polymorphism between patients with chronic hepatitis B and controls

Group	n	Frequency of genotypes(%)				Frequency of alleles(%)		
		1/1 ^a	1/2 ^b	2/2	1/4	1	2 ^c	4
Patients	190	169 (88.9)	17 (9.0)	1 (0.5)	3 (1.6)	358 (94.2)	19 (5.0)	3 (0.8)
Controls	249	202 (81.1)	42 (16.9)	1 (0.4)	4 (1.6)	450 (90.4)	44 (8.8)	4 (0.8)

Patients vs controls, ^a $\chi^2=5.03$, $P=0.025$; ^b $\chi^2=5.81$, $P=0.016$; ^c $\chi^2=4.76$, $P=0.029$.

Table 3 Association between IL-1B, IL-1RN genotypes and HBV copies in chronic hepatitis B patients

Subgroup	n	IL-1B genotype (%)			IL-1RN genotype (%)			
		CC ^a	CT	TT	1/1	1/2	2/2	1/4
I	104	31 (29.8)	49 (47.1)	24 (23.1)	93 (89.4)	9 (8.7)	0	2(1.9)
II	86	14 (16.3)	45 (52.3)	27 (31.4)	76 (88.3)	8 (9.3)	1 (1.2)	1(1.2)

HBV-DNA $\leq 1 \times 10^3$ copies/mL as I, HBV-DNA $> 1 \times 10^3$ copies/mL as II, ^asubgroup I vs subgroup II, $\chi^2=4.77$, $P=0.029$.

detected in 94.2% of chronic hepatitis B patients and 90.4% of controls, while IL-1RN allele 2 was detected in 5.0% of the patients and 8.8% of controls, The frequencies of genotype 1/2 and IL-1RN allele 2 in patients with chronic hepatitis B were lower than those in controls ($\chi^2=5.81$, $P=0.016$ and $\chi^2=4.76$, $P=0.029$ respectively).

Association of IL-1B and IL-1RN polymorphism with HBV-DNA replication

For further analysis of the relationship between IL-1B, IL-1RN polymorphisms and HBV-DNA replication in patients with chronic hepatitis B, the patients were divided into two subgroups (HBV-DNA $\leq 1 \times 10^3$ copies/mL as subgroup I, HBV-DNA $> 1 \times 10^3$ copies/mL as subgroup II). As shown in Table 3, the distributions of IL-1B(-511) genotype CC were of significant difference between the two subgroups ($\chi^2=4.77$, $P=0.029$).

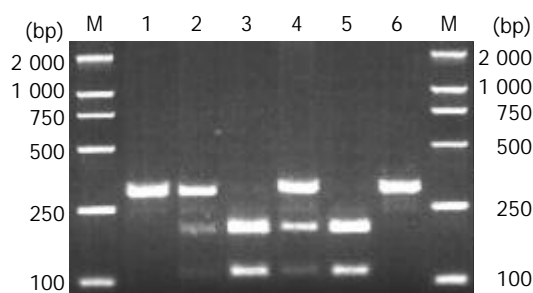


Figure 1 Results of IL-1B(-511) gene typing. Lane M: DNA molecular mass marker; Lanes 1, 6: TT; Lanes 2, 4: CT; Lanes 3, 5: CC.

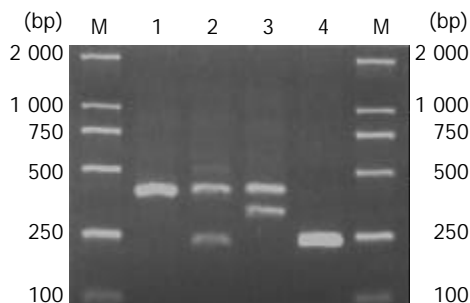


Figure 2 Results of IL-1RN intron 2 VNTR. Lane M: DNA molecular mass marker; Lane 1: 1/1; Lane 2: 1/2; Lane 3: 1/4; Lane 4: 2/2.

DISCUSSION

HBV infection is a major global health problem with an estimated 300 million people chronically infected worldwide^[9,10]. Individuals with an inadequate primary immune response to HBV are at increased risk of developing chronic hepatitis B. Age is the strongest host feature associated with chronic infection with 90% infants and 5-10% of adults developing chronic hepatitis B after exposure. In addition, people with the same age, sex and ethnical group were exposed to the same HBV strain, which could cause a broad spectrum ranging from no infection to different clinical outcomes^[11]. These data suggest that host genetic factors are responsible for the clinical outcomes of HBV infection. Clearance of HBV requires a coordinated innate and adaptive humoral and cell-mediated immune response. Cytokines are soluble polypeptide molecules that mediate cell-to-cell communication and regulate the intensity and duration of the immune response. Previous studies have shown that the maximal capacity of cytokine production

varies among individuals and correlates with SNP in the promoter region of various cytokine genes^[12,13]. Furthermore, cytokine gene polymorphisms were associated with liver disease severity in patients with viral hepatitis^[14]. In the present study we compared the distributions of IL-1B(-511) and IL-1RN intron 2 VNTR polymorphisms between patients with chronic B and control subjects.

IL-1B is one of the IL-1 gene family members, and located in the proximal region of chromosome 2q13-21. Different polymorphisms have been described in IL-1B, and at least two of them could influence the protein production. One is located in the promoter region at position -511, and the other in exon 5. Pociot *et al.*^[15] reported that IL-1B polymorphisms were correlated with IL-1 β expression. IL-1B allele T carrier had higher productions of IL-1 β than IL-1B allele C carrier. In the study, genotype distributions and allelic frequencies for IL-1B(-511) promoter polymorphisms in patients with chronic hepatitis B and control subjects were not statistically different. Further analysis of the relationship between IL-1B polymorphism and HBV-DNA replication in patients with chronic hepatitis B showed that IL-1B(-511) genotype CC was associated with HBV-DNA replication.

IL-1ra is a naturally occurring anti-inflammatory protein, competitively blocks the binding of IL-1 α and IL-1 β type I and type II IL-1 receptors, but exerts no agonist activity, despite sharing 30% amino acid sequence homology with IL-1 β , and 19% with IL-1 α . IL-1ra has been shown to inhibit the effects of IL-1 both *in vitro* and *in vivo*^[16]. Increasing evidence showed that IL-1RN polymorphisms were related with susceptibility to individual diseases, including psoriasis, systemic lupus erythematosus, and inflammatory bowel disease^[4]. By the study of IL-1RN intron 2 polymorphisms, our results suggested that the distributions of IL-1RN 1/2 genotype and IL-1RN allele 2 in patients with chronic hepatitis B were significantly lower than those in control subjects. A possible explanation of this result could be provided by the fact that carriage of IL-1RN allele 2 of each of these polymorphisms was related with high production of IL-1 β ^[17], which may augment the production of other cytokines, such as IL-2, IL-6 and TNF- α , and trigger the complex immunological processes to eliminate the virus and its complex.

In summary, the findings of this study and others may provide further evidence that genetic factors are important in the pathogenesis of HBV infection. Our results suggest that the carriage of IL-1RN allele 2 may play a protective role in the development of HBV infection and IL-1B CC genotype may be associated with HBV-DNA replication. However, the real roles of IL-1 polymorphisms in the pathogenesis of developing chronic hepatitis B should be further investigated by large population-based studies.

REFERENCES

- 1 **Perrillo RP.** How will we use the new antiviral agents for hepatitis B? *Curr Gastroenterol Rep* 2002; **4**: 63-71
- 2 **Koziel MJ.** Cytokines in viral hepatitis. *Semin Liver Dis* 1999; **19**: 157-169
- 3 **Hutyrova B,** Pantelidis P, Drabek J, Zurkova M, Kolek V, Lenhart K, Welsh KL, Du Bois RM, Petrek M. Interleukin-1 gene cluster polymorphisms in sarcoidosis and idiopathic pulmonary fibrosis. *Am J Respir Crit Care Med* 2002; **165**: 148-151
- 4 **Ma P,** Chen D, Pan J, Du B. Genomic polymorphism within interleukin-1 family cytokines influences the outcome of septic patients. *Crit Care Med* 2002; **30**: 1046-1050
- 5 **Nemetz A,** Nosti-Escanilla MP, Molnar T, Kope A, Kovacs A, Feher J, Tulassay Z, Nagy F, Garcia-Gonzalez MA, Pena AS. IL-1B gene polymorphisms influence the course and severity of inflammatory bowel disease. *Immunogenetics* 1999; **49**: 527-531
- 6 **Garcia-Gonzalez MA,** Lanas A, Santolaria S, Crusius JB, Serrano

- MT, Pena AS. The polymorphic IL-1B and IL-1RN genes in the aetiopathogenesis of peptic ulcer. *Clin Exp Immunol* 2001; **125**: 368-375
- 7 **Moos V**, Rudwaleit M, Herzog V, Hohlig K, Sieper J, Muller B. Association of genotypes affecting the expression of interleukin-1beta or interleukin-1 receptor antagonist with osteoarthritis. *Arthritis Rheum* 2000; **43**: 2417-2422
- 8 **Kanemoto K**, Kawasaki J, Mjyamoto T, Obayashi H, Nishimura M. Interleukin (IL)-1 β , IL-1 α , and IL-1 receptor antagonist gene polymorphisms in patients with temporal lobe epilepsy. *Ann Neurol* 2000; **47**: 571-574
- 9 **Wang FS**. Current status and prospects of studies on human genetic alleles associated with hepatitis B virus infection. *World J Gastroenterol* 2003; **9**: 641-644
- 10 **Cacciola I**, Cerenzia G, Pollicino T, Squadrito G, Castellana S, Zanetti AR, Mieli-Vergani G, Raimondo G. Genomic heterogeneity of hepatitis B virus (HBV) and outcome of perinatal HBV infection. *J Hepatol* 2002; **36**: 426-432
- 11 **Rapicetta M**, Ferrari C, Levrero M. Viral determinants and host immune responses in the pathogenesis of HBV infection. *J Med Virol* 2002; **67**: 454-457
- 12 **Giedraitis V**, He B, Huang WX, Hillert J. Cloning and mutation analysis of the human IL-18 promoter: a possible role of polymorphisms in expression regulation. *J Neuroimmunol* 2001; **112**: 146-152
- 13 **Ben-Ari Z**, Mor E, Papo O, Kfir B, Sulkes J, Tambur AR, Turkaspa R, Klein T. Cytokine gene polymorphisms in patients infected with hepatitis B virus. *Am J Gastroenterol* 2003; **98**: 144-150
- 14 **Miyazoe S**, Hamasaki K, Nakata K, Kajiya Y, Kitajima K, Nakao K, Daikoku M, Yatsushashi H, Koga M, Yano M, Eguchi K. Influence of interleukin-10 gene promoter polymorphisms on disease progression in patients chronically infected with hepatitis B virus. *Am J Gastroenterol* 2002; **97**: 2086-2092
- 15 **Pociot F**, Molvig J, Wogensen L, Worsaae H, Nerup J. A Taq I polymorphism in the human interleukin-1 beta (IL-1 beta) gene correlates with IL-1 beta secretion *in vitro*. *Eur J Clin Invest* 1992; **22**: 396-402
- 16 **Gabay C**, Smith MF, Eidlen D, Arend WP. Interleukin 1 receptor antagonist(IL-1Ra) is an acute- phase protein. *J Clin Invest* 1997; **99**: 2930-2940
- 17 **Santtila S**, Savinainen K, Hurme M. Presence of the IL-1RA allele 2 (ILRN*2) is associated with enhanced IL-1 beta production *in vitro*. *Scand J Immunol* 1998; **47**: 195-198

Edited by Zhang JZ and Wang XL **Proofread by** Xu FM

Effects of tegaserod on Fos, substance P and calcitonin gene-related peptide expression induced by colon inflammation in lumbar sacral spinal cord

Yi-Ning Sun, Jin-Yan Luo

Yi-Ning Sun, Jin-Yan Luo, Department of Gastroenterology, Second Hospital of Xi'an Jiaotong University, Xi'an 710004, Shaanxi Province, China

Correspondence to: Professor Jin-Yan Luo, Department of Gastroenterology, Second Hospital of Xi'an Jiaotong University, Xi'an 710004, Shaanxi Province, China

Telephone: +86-29-87678758

Received: 2003-09-06 **Accepted:** 2003-10-22

Abstract

AIM: To investigate the mechanisms of tegaserod, a partial 5-HT₄ agonist, in reducing visceral sensitivity by observing Fos, substance P (SP) and calcitonin gene-related peptide (CGRP) expression in the lumbar sacral spinal cord induced by colonic inflammation in rats.

METHODS: Twenty-four male rats with colonic inflammation induced by intraluminal instillation of trinitrobenzenesulfonic acid (TNBS) were divided into 3 groups. Treatment group 1: intra-gastric administration of tegaserod, 2 mg/kg·d; Treatment group 2: intra-gastric administration of tegaserod, 1 mg/kg·d; Control group: intra-gastric administration of saline, 2.0 mL/d. After 7 d of intra-gastric administration, lumbar sacral spinal cord was removed and processed for Fos, SP and CGRP immunohistochemistry.

RESULTS: In rats of the control group, the majority of Fos labeled neurons was localized in deeper laminae of the lumbar sacral spinal cord (L₅-S₁). SP and CGRP were primarily expressed in the superficial laminae of the spinal cord after TNBS injection. Intra-gastric administration of tegaserod (2 mg/kg·d) resulted in a significant decrease of Fos labeled neurons (22.0±7.7) and SP density (12.5±1.4) in the dorsal horn in the lumbar sacral spinal cord compared to those of the control group (62.2±18.9, 35.9±8.9, *P*<0.05). However, CGRP content in dorsal horn did not significantly reduce in rats of treatment group 1 (1.2±1.1) compared to that of the control group (2.8±2.4, *P*>0.05). Neither Fos expression nor SP or CGRP density in the dorsal horn significantly declined in rats of treatment group 2 compared to those of the control group (*P*>0.05).

CONCLUSION: Tegaserod can significantly reduce Fos labeled neurons in the lumbar sacral spinal cord induced by colonic inflammation. Tegaserod may reduce visceral sensitivity by inhibiting SP expression in the dorsal horn of spinal cord.

Sun YN, Luo JY. Effects of tegaserod on Fos, substance P and calcitonin gene-related peptide expression induced by colon inflammation in lumbar sacral spinal cord. *World J Gastroenterol* 2004; 10(12): 1830-1833

<http://www.wjgnet.com/1007-9327/10/1830.asp>

INTRODUCTION

Irritable bowel syndrome (IBS) is a common functional gastrointestinal disorder. Its typical feature is recurrent abdominal discomfort or pain associated with disordered defecation. Studies have shown that visceral sensitivity plays an important role in the pathophysiology of IBS^[1]. Tegaserod, a partial 5-HT₄ agonist, acts selectively on 5-HT₄ receptors in the gut. Tegaserod can relieve symptoms in IBS patients with abdominal discomfort or pain and significantly decrease visceral sensitivity^[2]. The objectives of the present study were to identify regions of the Fos protein, substance P (SP) and calcitonin gene-related peptide (CGRP) expression in the lumbar sacral spinal cord in response to colonic inflammation induced by intraluminal instillation of TNBS, and to compare the effects of tegaserod on the spinal Fos, SP and CGRP expression induced in the same animal model.

MATERIALS AND METHODS

Animals

Twenty-four adult male Sprague-Dawley rats (The Fourth Military Medical University) weighing 220-250 g were used in this study. The animals were housed in a quiet room with a constant ambient temperature of 20 °C with free access to rat chow and water.

Experimental protocol

After 24 h fast, TNBS (100 mg/kg in 300 mL/L ethanol) was administered intrarectally through a silicone rubber catheter introduced 7 cm into the anus under light diethyl-ether anesthesia. To keep TNBS in the colon for a longer time and to avoid leakage, the catheter was slowly withdrawn and the tail of the rat was kept elevating for 8-10 min.

Tegaserod (20 mg, Beijing Novartis Pharmacy Company) was dissolved in 100 mL distilled water. After one day of TNBS instillation, the rats were randomly divided into 3 groups. Each group had eight rats. Treatment group 1: intra-gastric administration of tegaserod 2 mg/kg; Treatment group 2: intra-gastric administration of tegaserod 1 mg/kg; Control group: intra-gastric administration of saline 2.0 mL. Tegaserod or saline was administered once daily (10:00AM) for consecutive 7 d after TNBS instillation.

Fos, SP and CGRP immunohistochemistry

One day after the last time of tegaserod or saline administration, the rats were deeply anesthetized with pentobarbital Na (80 mg/kg, i.p.) and perfused with 100 mL saline followed by 500 mL fixative of 40 g/L paraformaldehyde in 0.1 mol/L phosphate buffer (PH 7.4). L₃-S₂ segments of the spinal cord were removed, post-fixed in the same fixative at 4 °C for 2-4 h and then cryoprotected in 200 g/L sucrose overnight. Serial frozen sections of 40-μm thickness cut on a Leitz cryocut. Sections were collected in 0.01 mol/L PBS for immunohistochemistry.

The spinal cord sections were stained for Fos, SP and CGRP using avidin-biotin-peroxidase complex (ABC) method. Free

floating tissue sections were treated in 800 mL/L methanol containing 30 mL/L H₂O₂ to block endogenous peroxidase activity for 30 min at room temperature. They were treated with 0.01 mol/L PBS containing 1 g/L Triton ×100 for 20 min at room temperature. The sections were then incubated with a polyclonal rabbit anti-Fos serum (1:3 000, Santa Cruz), polyclonal rabbit anti-SP serum (1:500, Boster) and polyclonal rabbit anti-CGRP serum (1:500, Boster) respectively for 48 h at 4 °C. After the step, the sections were incubated with biotinylated goat anti-rabbit IgG (1:500, Sigma), and subsequently with the ABC complex (1:500, Sigma) at room temperature for 2 h each. The antigen-antibody reaction sites were visualized by incubation with glucose oxidase-DAB-nickel method for 15-30 min at room temperature. The sections were rinsed in 0.01 mol/L PBS for 3×10 min between transition of these steps. Finally, the sections were mounted onto gelatin-coated slides, dried, dehydrated, cleared and coverslipped.

Fos immunoreactive neuronal counts and measurement of the density of dorsal horn SP and CGRP staining

The number of neuronal nuclear profiles expressing Fos was analyzed with computer assisted QUIC menu system. Precise regional localization was done by outlining specific regions and then particles (stained nuclei) were counted in the outlined regions. The number of profiles counted in five sections was averaged for each animal, and comparisons were made between the groups^[3].

The density of SP and CGRP staining in the dorsal horn of spinal cord was also measured in specific outlined regions using computer assisted QUIC menu system. The ratio of the area of stained SP or CGRP to the area of the outlined regions was presented as the density of SP or CGRP. The averages were obtained for density measurements from five randomly selected spinal cord sections for each animal, and comparisons were

made between treatment and control groups^[3].

Statistical analysis

Pictures were taken under BX-60 microscopy with the support of IM50 software. All results are expressed as mean±SD. An unpaired *t*-test was used to compare Fos-IR (immunoreactive) cell count data, SP and CGRP density between the groups. A difference was accepted as significant if the probability was less than 5% ($P<0.05$).

RESULTS

Effect of tegaserod on Fos expression in spinal cord

In animals of the control group, Fos protein was expressed bilaterally in the nuclei of cells of the dorsal horn in L₅, L₆ and S₁ of lumbarsacral spinal cord. The nuclei of Fos-IR neurons were black and there was no cytoplasmic staining. Among 62.2±18.9 neurons exhibited Fos-IR, most of them were distributed in the deeper laminae (III-IV, V-VI) of the dorsal horn. Only few Fos-IR neurons were sparsely distributed in the superficial laminae (I-II) of the dorsal horn (Figure 1A).

After intra-gastric administration of tegaserod 1 mg/kg·d for 7 d, Fos-IR cells in the dorsal horn decreased to 42.6±7.5, but was not significantly different with that of the control group (62.2±18.9, $P>0.05$). After intra-gastric administration of tegaserod 2 mg/kg·d for seven days, Fos-IR neurons in the dorsal horn decreased to 22.0±7.7, a significant difference ($P<0.05$) (Table 1, Figure 2A).

Effect of tegaserod on SP and CGRP expression in spinal cord

In rats of the control group, SP was expressed bilaterally in the superficial laminae (I-II) in the dorsal horn. The density of SP



Figure 1 Sections from the control rats. ×10. A: Fos-IR neurons induced by TNBS administration were observed as black spots in the dorsal horn. Note that most Fos-IR neurons were distributed in the deeper laminae of the dorsal horn. B: SP was mainly distributed in the superficial laminae of the dorsal horn. C: CGRP was primarily localized in the superficial laminae of the dorsal horn.



Figure 2 Sections from rats treated with tegaserod 2 mg/kg·d. ×10. A: After treatment with tegaserod, the number of Fos-IR cells was decreased significantly compared with that of the control group. B: Note that the density of SP in rats treated with tegaserod was decreased significantly compared with that of the control rats. C: The density of CGRP was not different between the treatment group and the control group.

was 35.9 ± 8.9 . After 7 d of intra-gastric injection of tegaserod $1 \text{ mg/kg} \cdot \text{d}$, the density of SP in the superficial laminae did not significantly reduce (33.3 ± 3.4 , $P > 0.05$). However, after intra-gastric administration of tegaserod $2 \text{ mg/kg} \cdot \text{d}$ for 7 d, the density of SP decreased to 12.5 ± 1.4 , a significant difference compared to that of the control group ($P < 0.05$) (Table 1, Figures 1B, 2B).

In animals of the control group, most CGRP were expressed in the superficial laminae of the dorsal horn. A few CGRP were distributed in the deeper laminae. The density of CGRP in rats of the control group was 2.8 ± 2.4 . The density of CGRP did not significantly decrease in rats treated with tegaserod $1 \text{ mg/kg} \cdot \text{d}$ for 7 d (2.2 ± 2.3 , $P > 0.05$). After treatment with tegaserod $2 \text{ mg/kg} \cdot \text{d}$ for 7 d, the density of CGRP decreased 56.7% compared to that of the control group (1.2 ± 1.1), but there was no significant difference ($P > 0.05$) (Table 1, Figures 1C, 2C).

Table 1 Number of Fos-IR neurons and density of SP, CGRP (%) in dorsal horn of rats in various groups

	Fos	SP	CGRP
Treatment group 1 ($2 \text{ mg/kg} \cdot \text{d}$)	22.0 ± 7.7^a	12.5 ± 1.4^a	1.2 ± 1.1
Treatment group 1 ($1 \text{ mg/kg} \cdot \text{d}$)	42.6 ± 7.5	33.3 ± 3.4	2.2 ± 2.3
Control group	62.2 ± 18.9	35.9 ± 8.9	2.8 ± 2.4

^a $P < 0.05$, vs the control.

DISCUSSION

Irritable bowel syndrome is a common functional gastrointestinal disorder. Its typical feature is recurrent abdominal discomfort or pain associated with disordered defecation or a change in bowel habit. Routine investigation revealed no evidence of structural or biochemical abnormality. There is evidence that patients with IBS showed a lower threshold for discomfort and/or pain, increased sensitivity to stimuli, or altered viscerosomatic referral^[4]. Therefore, visceral hypersensitivity could play an important role in the pathophysiology of IBS^[1].

Tegaserod is a partial 5-HT₄ agonist. The absence of blood-brain barrier permeation makes it selectively bind to 5-HT₄ receptors in the gastrointestinal tract. Tegaserod has been shown to modulate both gastrointestinal motility and visceral sensitivity^[2]. Studies demonstrated that tegaserod produced rapid and sustained improvements of the abdominal pain/discomfort and constipation in IBS patients, especially in female IBS patients^[5,6]. These improvements were seen within the first week, and maintained throughout the treatment period. A randomized, double-blind, placebo-controlled study showed that tegaserod reduced the sensitivity to rectal distension in healthy subjects^[7].

Fos, one of the inducible transcription factors, serves as a quantifiable marker to identify neuronal populations activated by noxious somatic and visceral stimulations. Noxious stimulation of hollow viscera induced a specific pattern of Fos expression in rat spinal cord that reflected the intensity of the stimulation^[8]. Recently, the anti-nociceptive effects of some drugs have been studied in animal models of persistent visceral pain using Fos expression as an independent measure. Lu reported that baclofen, a selective GABA_B receptor agonist, specifically reduced Fos expression in the superficial dorsal horn of spinal cord induced by mustard oil irritation of the colon^[3]. A recent study has demonstrated that opiate receptor agonists, especially morphine, attenuate pain related behavior and Fos expression in rat spinal cord neurons following noxious visceral stimulation^[9]. Thus, localization of Fos expression can be a useful tool to examine the effectiveness of different analgesic drugs after nociceptive stimulation.

In rats of the control group, Fos protein expression became bilaterally evident as nuclear staining in cells in L₅, L₆ and S₁ of

lumbar-sacral spinal cord. In the rats, the descending colon was innervated by sensory afferent fibers in the pelvic nerve projecting bilaterally to the lumbar-sacral (L₆-S₂) spinal cord^[10]. The result was consistent with the viscerotopic organization of the afferent fibers that innervate the descending colon. Most of the Fos-IR neurons were distributed in the deeper laminae (III-IV, V-VI) of the dorsal horn. Few Fos expressed in the superficial laminae (I-II) of the dorsal horn. Imbe demonstrated that Fos-IR cells had the tendency to spread from the superficial laminae to the deeper laminae when deep tissue inflammation became persistent^[11]. From the segment and laminae distribution of Fos-IR neurons, we conclude that neurons in the dorsal horn of lumbar-sacral spinal cord are activated via sensory afferent fibers in the pelvic nerve by noxious stimulation induced by persistent colonic inflammation. Therefore, tegaserod can dose-dependently prevent sensory neurons in the dorsal horn from being activated by colonic inflammation.

Substance P was released from primary sensory nociceptive neurons in response to noxious stimuli. Up to 80% of dorsal root ganglion (DRG) neurons supplying viscera contained SP, suggesting the importance of SP in transmission of signals from the viscera to the spinal cord^[12]. Study of Kishimoto demonstrated that high concentrations of SP were significantly related to abdominal pain^[13]. SP could play a pivotal role at the spinal cord level in postsynaptic sensitization, particularly during and after gut inflammation^[14]. In the spinal cord, SP releasing from the primary afferents could activate the dorsal horn neurons by inducing an influx of Ca²⁺ throughout voltage-gated Ca²⁺ channels^[15]. The results of this study showed that the density of SP in the dorsal horn decreased significantly compared to the control group after treatment with tegaserod $2 \text{ mg/kg} \cdot \text{d}$ for 7 d. Therefore, tegaserod can inhibit SP expression in the dorsal horn of the spinal cord.

CGRP is one of the major neuropeptides expressed in the spinal cord sensory processing region and is widely distributed in the nervous system, particularly in sensory neurons. CGRP, which is generally colocalized with SP in the primary afferent nociceptors, is likely to be involved in pain transmission. CGRP may produce a direct nociceptive effect. CGRP might also enhance SP-induced nociceptive sensation by facilitating the release of SP in the spinal dorsal horn^[16]. Compared with that of the control group, the density of CGRP decreased 21.4% in treatment group 1 and 57.1% in treatment group 2, showing an insignificant difference ($P > 0.05$). The results suggest that tegaserod may not act on CGRP expression to reduce visceral nociceptive transmission. However, whether a much larger dose of tegaserod can significant decrease CGRP expression in the spinal cord still needs more studies.

The results of the present study showed that tegaserod could significantly decrease Fos and SP expression in the dorsal horn of the spinal cord. Tegaserod can exert antinociceptive effect. This effect is related to SP expression inhibition in the spinal cord. The study of Schikowski showed that in decerebrated cats the static discharge rate of the afferents evoked by rectal distension decreased significantly after intravenous administration of tegaserod. They proposed that 5-HT₄ receptor activation had an inhibitory effect on intramural mechanoreceptors in cat rectum^[17]. Today there is considerable evidence that serotonin influences nociceptive reflexes at different anatomic levels. For example, intrathecal and iontophoretic applications of serotonin to the dorsal horn produced pain relief, and serotonin antagonists produced hyperalgesia^[18]. Ghelardini found that BIMU1 and BIMU8, two 5-HT₄ agonists, exerted an antinociceptive effect by centrally potentiating endogenous cholinergic activity^[19]. Since there are serotonin-SP and serotonin-Ach neurotransmitter links, we conclude that tegaserod, acting on 5-HT₄ receptors in the gut, produces an antinociceptive effect by inhibiting the expression of SP in spinal dorsal horn.

REFERENCES

- 1 **Bueno L**, Fioramonti J, Delvaux M, Frexinos J. Mediators and pharmacology of visceral sensitivity: from basic to clinical investigations. *Gastroenterology* 1997; **112**: 1714-1743
- 2 **Lacy BE**, Yu S. Tegaserod: a new 5-HT₄ agonist. *J Clin Gastroenterol* 2002; **34**: 27-33
- 3 **Lu Y**, Westlund KN. Effects of baclofen on colon inflammation-induced Fos, CGRP and SP expression in spinal cord and brainstem. *Brain Res* 2001; **889**: 118-130
- 4 **Mertz H**, Naliboff B, Munakata J, Niazi N, Mayer EA. Altered rectal perception is a biological marker of patients with irritable bowel syndrome. *Gastroenterology* 1995; **109**: 40-52
- 5 **Muller-Lissner SA**, Fumagalli I, Bardhan KD, Pace F, Pecher E, Nault B, Ruegg P. Tegaserod, a 5-HT₄ receptor partial agonist, relieves symptoms in irritable bowel syndrome patients with abdominal pain, bloating and constipation. *Aliment Pharmacol Ther* 2001; **15**: 1655-1666
- 6 **Novick J**, Miner P, Krause R, Glebas K, Bliesath H, Ligozio G, Ruegg P, Lefkowitz M. A randomized double-blind, placebo-controlled trial of tegaserod in female patients suffering from irritable bowel syndrome with constipation. *Aliment Pharmacol Ther* 2002; **16**: 1877-1888
- 7 **Coffin B**, Farmachidi JP, Rueegg P, Bastie A, Bouhasira D. Tegaserod, a 5-HT₄ receptor partial agonist, decreases sensitivity to rectal distension in healthy subjects. *Aliment Pharmacol Ther* 2003; **17**: 577-585
- 8 **Traub RJ**, Pechman P, Iadarola MJ, Gebhart GF. Fos-like proteins in the lumbosacral spinal cord following noxious and non-noxious colorectal distention in the rat. *Pain* 1992; **49**: 393-403
- 9 **Traub RJ**, Stitt S, Gebhart GF. Attenuation of c-Fos expression in the rat lumbosacral spinal cord by morphine or tramadol following noxious colorectal distention. *Brain Res* 1995; **701**: 175-182
- 10 **Traub RJ**, Murphy A. Colonic inflammation induces fos expression in the thoracolumbar spinal cord increasing activity in the spinoparabrachial pathway. *Pain* 2002; **95**: 93-102
- 11 **Imbe H**, Iwata K, Zhou QQ, Zuo S, Dubner R, Ren K. Orofacial deep and cutaneous tissue inflammation and trigeminal neuronal activation. Implications for persistent temporomandibular pain. *Cells Tissues Organs* 2001; **169**: 238-247
- 12 **Palecek J**, Paleckova V, Willis WD. Postsynaptic dorsal column neurons express NK1 receptors following colon inflammation. *Neuroscience* 2003; **116**: 565-572
- 13 **Kishimoto S**, Kobayash H, Machino H. High concentrations of substance P as a possible transmission of abdominal pain in rats with chemical induced ulcerative colitis. *Biomed Res* 1994; **15**: 133-140
- 14 **Bueno L**, Fioramonti J. Effects of inflammatory mediators on gut sensitivity. *Can J Gastroenterol* 1999; **13**(Suppl A): 42A-46A
- 15 **Coderre TJ**, Katz J, Vaccarino AL, Melzack R. Contribution of central neuroplasticity to pathological pain: review of clinical and experimental evidence. *Pain* 1993; **52**: 259-285
- 16 **Friese N**, Diop L, Chevalier E, Angel F, Riviere PJ, Dahl SG. Involvement of prostaglandins and CGRP-dependent sensory afferents in peritoneal irritation-induced visceral pain. *Regul Pept* 1997; **70**: 1-7
- 17 **Schikowski A**, Thewissen M, Mathis C, Ross HG, Enck P. Serotonin type-4 receptors modulate the sensitivity of intramural mechanoreceptive afferents of the cat rectum. *Neurogastroenterol Motil* 2002; **14**: 221-227
- 18 **Gyermek L**. Pharmacology of serotonin as related to anesthesia. *J Clin Anesth* 1996; **8**: 402-425
- 19 **Ghelardini C**, Galeotti N, Casamenti F, Malmberg-Aiello P, Pepeu G, Gualtieri F, Bartolini A. Central cholinergic antinociception induced by 5-HT₄ agonists: BIMU1 and BIMU8. *Life Sci* 1996; **58**: 2297-2309

Edited by Zhao M and Wang XL Proofread by Xu FM

Epidemiological investigation of esophageal carcinoma

Hong Zhang, Shao-Hua Chen, You-Ming Li

Hong Zhang, Shao-Hua Chen, You-Ming Li, Digestive department, the First Affiliated Hospital, Medical College of Zhejiang University, Hangzhou 310003, Zhejiang Province, China

Correspondence to: Professor You-Ming Li, Digestive Department, the First Affiliated Hospital, Medical College, Zhejiang University, No.79 Qingchun Road, Hangzhou, 310003, Zhejiang, China. liyouming@dna.net.cn

Telephone: +86-571-87236603 **Fax:** +86-571-87236611

Received: 2003-11-21 **Accepted:** 2004-01-08

Abstract

AIM: To review the characteristics of esophageal carcinoma in recent 30 years in the epidemiological investigation.

METHODS: A total of 1 520 cases of esophageal carcinoma in the First Affiliated Hospital of Zhejiang University Medical College admitted from 1970 until now were reviewed. Their age, gender, position of carcinoma and histological type were analyzed.

RESULTS: The morbidity of esophageal carcinoma was increasing during the observation period. Compared with the 1970s (9.5%), the ratio of adenocarcinoma significantly increased after the 1980s (19.1%). The difference was significant ($P \leq 0.05$).

CONCLUSION: The morbidity of esophageal adenocarcinoma was increasing and advanced clinical study should be strengthened.

Zhang H, Chen SH, Li YM. Epidemiological investigation of esophageal carcinoma. *World J Gastroenterol* 2004; 10(12): 1834-1835

<http://www.wjgnet.com/1007-9327/10/1834.asp>

INTRODUCTION

Carcinoma of esophagus is one of the most common cancers with a high mortality. Squamous cell carcinoma and adenocarcinoma account for more than 95% of esophageal tumors^[1]. The incidence rate of squamous cell carcinoma of the esophagus in the pathological feature is more frequent compared with adenocarcinoma. Increasing prevalence of adenocarcinoma of the esophagus has been reported from western countries in recent years and its incidence since the 1970s in China is unknown. Our study aimed to make an epidemiological investigation of carcinoma of esophagus and compare the incidence rate of adenocarcinoma and squamous cell carcinoma of the esophagus.

MATERIALS AND METHODS

Medical records of all patients ($n=1\ 520$) with adenocarcinoma or squamous cell carcinoma of the esophagus seen at the the First Affiliated Hospital of Zhejiang University Medical College between 1970 and 2001 were reviewed. The following data were retrieved: age, gender, tumor location, history of surgery and pathological features. The patients were divided into 3 groups:

group A (211 patients) were patients seen from 1970 to 1979, group B (451 patients) were patients from 1980 to 1989 and group C (858 patients) were from 1990 to 2001.

RESULTS

The data of the 1520 patients with adenocarcinoma or squamous cell carcinoma were analyzed. Among them, 236 (15.5%) were female and 1 284 (84.5%) were male. In group A there were 184 (87.2%) male patients and 27 (12.8%) female patients, in group B there were 380 (84.3%) male and 71 (15.7%) female, in group C there were 720 (83.9%) male and 138 (16.1%) female. No differences were found between the groups in gender. Among 240 cases of adenocarcinoma of esophagus, 195 (81.3%) were male and 45 (18.7%) were female. And among 1280 cases of squamous cell carcinoma of the esophagus, 1 089 (85.1%) were male and 191 (14.9%) were female. No significant difference of sex ratios were found in patients with adenocarcinoma of esophagus and squamous cell carcinoma of the esophagus.

The age distribution of the patients is shown in Table 1. Patients in their 50s are at highest risk for carcinoma of the esophagus in the 1970s. And patients in their 60s are at highest risk for carcinoma of the esophagus since 1980s.

From clinical pathological data, 20, 80, 134 cases with adenocarcinoma and 191, 365, 724 cases with squamous cell carcinoma were found in groups A, B, C, respectively. The proportion of esophageal adenocarcinoma of all groups were 9.5% (20/211), 19.1% (86/451) and 15.6% (134/858), respectively. The difference was significant between groups A and B ($P=0.002$) and also between groups A and C ($P=0.023$). And there was no significant difference between groups B and C ($P=0.113$).

We investigated the location of adenocarcinoma of esophagus (193 cases), whose pathological findings showed the definite location. Two (1.0%) cases were located at the upper esophagus, 15 (7.8%) at the middle and 176 (91.2%) located at the lower esophagus.

Table 1 Age distribution of all patients with carcinoma of esophagus: n (%)

Age (yr)	A	B	C
≤ 30	3 (1.4)	2 (0.4)	5 (0.6)
30-	15 (7.1)	20 (4.3)	26 (3.0)
40-	47 (22.3)	72 (16.0)	162 (18.9)
50-	103 (48.8)	160 (35.5)	250 (29.1)
>60	43 (20.4)	197 (43.7)	415 (48.4)

DISCUSSION

Esophageal cancer is one of the most deadly forms of gastrointestinal cancer in China and death rate from carcinoma of esophagus ranked the third annually. Epidemiological data defined a certain geographical distribution^[2]. In high mortality areas of China, Iran and Africa, the incidence of esophageal tumors is approximately equal in men and women^[3]. By comparison, in low-incidence regions such as the United States and parts of Europe, there is a significant predilection for males^[4]. It was reported that the incidence rate in male is higher than that of female, and the sex ratios (male/female) was 5-10:1. In our study, the male to female

ratio was 5.5:1 and the difference was not significant among groups.

Although squamous cell carcinoma was traditionally considered synonymous with esophageal cancer, the incidence of adenocarcinoma of the esophagus is increasing in most Western industrialized nations in recent years^[5,6]. The incidence of esophageal adenocarcinoma increased from 1.5 to 7.0 per 100 000 men and from 0.4 to 1.5 per 100 000 women between 1971 and 1998 in England and Wales^[7]. The proportion of adenocarcinomas has increased, probably in connection with the increasing incidence of Barrett's esophagus. But the risk of Barrett's esophageal mucosa advancing to esophageal adenocarcinoma is not well established^[8]. Even though the incidence of esophageal adenocarcinoma has been rising in Western populations over the past two decades and squamous cell carcinoma has been declining^[9,10], esophageal squamous cell carcinoma remains the predominant type of esophageal malignancy in the remainder of the world.

The mechanism of increased incidence of adenocarcinoma remained to be unclear. Gastroesophageal reflux disease (GERD), Barrett's esophagus, smoking, alcohol drinking and dysfunction of esophageal motility may be associated with the increase of incidence of adenocarcinoma. Adenocarcinoma is an uncommon cause of mortality in patients with Barrett's esophagus. Forty-four patients were confirmed to have Barrett's esophagus and were followed up for 209 patient-years. Only 2 patients developed esophageal adenocarcinoma, resulting in an incidence of one case in 209 patient-years, a 55-fold risk compared with age- and sex-matched population in Scotland^[11]. Gastric juice that refluxes into the esophagus can injure esophageal squamous epithelium. When the injury heals through a metaplastic process in which an abnormal columnar epithelium replaces the injured squamous one, the resulting condition is called Barrett's esophagus^[12]. Barrett's esophagus is the major risk factor for the development of esophageal adenocarcinoma, which is increasing in incidence faster than any other cancer in the Western world. Barrett's adenocarcinomas are increasing in epidemic proportions for as yet unknown reasons, approximately 0.5-1% of patients with Barrett's will develop adenocarcinoma^[13,14]. Although GERD symptoms precede the development of adenocarcinoma of esophagus in many patients, fewer than 50% of patients have pathologic evidence of esophagitis or Barrett's epithelium at presentation.

There are clear racial, gender and site predilections for esophageal adenocarcinoma^[15,16]. Our study demonstrated that 176 cases (91.2%) of adenocarcinoma of esophagus were located at the lower esophagus, being different from squamous cell carcinoma of the esophagus which were located mainly at the middle of the esophagus. Adenocarcinoma of esophagus shared with the same location with Barrett's esophagus.

Further study is required to determine the risk factors such

as food^[17] for the development of esophageal cancer and epidemiological investigation will prove important developing methods of detection and therapeutic intervention of this disease.

REFERENCES

- 1 **Klimstra DS.** Pathologic prognostic factors in esophageal carcinoma. *Semin Oncol* 1994; **21**: 425-430
- 2 **Stathopoulos GP,** Tsiaras N. Epidemiology and pathogenesis of esophageal cancer management and its controversial results (review). *Oncol Rep* 2003; **10**: 449-454
- 3 **Lu JB,** Sun XB, Dai DX, Zhu SK, Chang QL, Liu SZ, Duan WJ. Epidemiology of gastroenterologic cancer in Henan Province, China. *World J Gastroenterol* 2003; **9**: 2400-2403
- 4 **Blot WJ.** Esophageal cancer trends and risk factors. *Semin Oncol* 1994; **21**: 403-410
- 5 **Wei JT,** Shaheen N. The changing epidemiology of esophageal adenocarcinoma. *Semin Gastrointest Dis* 2003; **14**: 112-127
- 6 **Lukanich JM.** Section I: epidemiological review. *Semin Thorac Cardiovasc Surg* 2003; **15**: 158-166
- 7 **Newnham A,** Quinn MJ, Babb P, Kang JY, Majeed A. Trends in the subsite and morphology of oesophageal gastric cancer in English and Wales 1971-1998. *Aliment Pharmacol Ther* 2003; **17**: 665-676
- 8 **Zaninotto G,** Costantini M, Molena D, Rizzetto C, Ekser B, Ancona E. Barrett's esophagus. Prevalence, risk of adenocarcinoma, role of endoscopic surveillance. *Minerva Chir* 2002; **57**: 819-836
- 9 **Powell J,** McConkey CC, Gillison EW, Spychal RT. Continuing rising trend in oesophageal adenocarcinoma. *Int J Cancer* 2002; **102**: 422-427
- 10 **Younes M,** Henson DE, Ertan A, Miller CC. Incidence and survival trends of esophageal carcinoma in the United States: racial and gender differences by histological type. *Scand J Gastroenterol* 2002; **37**: 1359-1365
- 11 **Rana PS,** Johnston DA. Incidence of adenocarcinoma and mortality in patients with Barrett's oesophagus diagnosed between 1976 and 1986: implications for endoscopic surveillance. *Dis Esophagus* 2000; **13**: 28-31
- 12 **Spechler SJ.** Barrett's esophagus and esophageal adenocarcinoma: pathogenesis, diagnosis, and therapy. *Med Clin North Am* 2002; **86**: 1423-1445
- 13 **Reynolds JC,** Rahimi P, Hirschl D. Barrett's esophagus: clinical characteristics. *Gastroenterol Clin North Am* 2002; **31**: 441-460
- 14 **Cossentino MJ,** Wong RK. Barrett's esophagus and risk of esophageal adenocarcinoma. *Semin Gastrointest Dis* 2003; **14**: 128-135
- 15 **Younes M,** Henson DE, Ertan A, Miller CC. Incidence and survival trends of esophageal carcinoma in the United States: racial and gender differences between histological type. *Scand J Gastroenterol* 2002; **37**: 1359-1365
- 16 **Vega KJ,** Jamal MM. Changing pattern of esophageal cancer incidence in New Mexico. *Am J Gastroenterol* 2000; **95**: 2352-2356
- 17 **Li K,** Yu P. Food groups and risk of esophageal cancer in Chaoshan region of China: a high-risk area of esophageal cancer. *Cancer Invest* 2003; **21**: 237-240

Edited by Ma JY Proofread by Xu FM

Fathal pulmonary hypertension after distal splenorenal shunt in schistosomal portal hypertension

Roberto de Cleve, Paulo Herman, Vincenzo Pugliese, Bruno Zilberstein, William Abrão Saad, Joaquim José Gama-Rodrigues

Roberto de Cleve, Gastroenterology Department, Hospital Das Clinicas-University of Sao Paulo Medical School

Paulo Herman, Vincenzo Pugliese, Digestive Tract Surgery Division, Hospital Das Clinicas-University of Sao Paulo Medical School

Bruno Zilberstein, Digestive Tract Surgery Division, Hospital Das Clinicas-University of Sao Paulo Medical School

William Abrão Saad, Digestive Tract Surgery Division, Hospital Das Clinicas-University of Sao Paulo Medical School

Joaquim José Gama-Rodrigues, Digestive Tract Surgery Division, Hospital Das Clinicas-University of Sao Paulo Medical School

Correspondence to: Roberto de Cleve, Hospital Das Clinicas-Department of Gastroenterology, University of Sao Paulo Medical School, Rua Cel. Artur Godoy, 125 Apto 152. São Paulo-SP-Brazil. CEP 04018-050. roberto.cleve@hcnet.usp.br

Telephone: +55-11-30828000 **Fax:** +55-11-30828000

Received: 2003-09-15 **Accepted:** 2004-01-12

de Cleve R, Herman P, Pugliese V, Zilberstein B, Saad WA, Gama-Rodrigues JJ. Fathal pulmonary hypertension after distal splenorenal shunt in schistosomal portal hypertension. *World J Gastroenterol* 2004; 10(12): 1836-1837
<http://www.wjgnet.com/1007-9327/10/1836.asp>

INTRODUCTION

Mansonic schistosomiasis is the main cause of portal hypertension in Brazil. Hepatosplenic (HS) form is manifested by hepatomegaly mainly on the left hepatic lobe associated with large splenomegaly and bleeding due to esophageal varices with high mortality rates^[1,2].

Pulmonary hypertension in the HS form of mansonic schistosomiasis is described in association with both the acute and chronic forms of the disease, with a prevalence of 5% and may be a serious complication in the evolution of the disease. It can also be the triggering factor for serious complications associated with any form of surgical approach^[3,4].

Surgical treatment is indicated for patients with a history of bleeding due to esophageal varix rupture based on world previous experience with endoscopic treatment results^[5]. At present, techniques vary in azigo-portal disconnection and splenectomy (APDS) and distal splenorenal shunt (DSRS) for surgical treatment of such patients. All patients submitted to DSRA were carefully evaluated pre-operatively with eletrocardiography, chest X-ray and transthoracic echocardiography to rule out pulmonary hypertension. We report two fatal cases of pulmonary hypertension arising after DSRS.

Case Reports

Case 1 A 33-year-old man was admitted to the Liver and Portal Hypertension Surgical Unit, Hospital das Clínicas, University of São Paulo Medical School for surgical treatment of portal hypertension due to hepatosplenic mansonic schistosomiasis after previous episode of bleeding esophageal varices. Ultrasound scan of the abdomen revealed discrete hepatomegaly, mainly on the left hepatic lobe associated with splenomegaly. Esophagogastroduodenoscopy revealed four large variceal vessels. The results found in routine laboratory

tests were alanine amino transferase (ALT) of 29 U/L (normal: 10-30), aspartate amino transferase (AST) of 20 U/L (normal: 10-36), bilirubin of 0.8 mg/dL (normal: 0.2-1.0), gamma-glutamyl transferase of 86 U/L (normal: 7-32), and alkaline phosphatase of 241 U/L (normal: 32-104). The electrocardiogram, chest X-ray and echocardiography were within normal limits. The patient was submitted to DSRS. On the 4th postoperative day he developed progressive dyspnea and dyed 3 h later. The necropsy showed severe pulmonary hypertension, right ventricular dilatation and secondary myocardial infarction. The shunt was pervious.

Case 2 A 25-year-old woman was admitted to the Liver and Portal Hypertension Surgical Unit, Hospital das Clínicas, University of São Paulo Medical School for surgical treatment of portal hypertension due to hepatosplenic mansonic schistosomiasis after an episode of bleeding esophageal varices. Ultrasound scan of the abdomen revealed discrete hepatomegaly, mainly on the left hepatic lobe associated with splenomegaly. Esophagogastroduodenoscopy revealed two large variceal vessels. The results found in routine laboratory tests were alanine amino transferase (ALT) of 25 U/L (normal 7-45), aspartate amino transferase (AST) of 38 U/L (normal 7-45), bilirubin of 1.0 mg/dL (normal 0.2-1.0), gamma-glutamyl transferase of 31 U/L (normal 7-32), and alkaline phosphatase of 96 U/L (normal 32-104). The electrocardiogram, chest X-ray and echocardiography were within normal limits. The patient was submitted to DSRA. One the 7th postoperative day he developed progressive dyspnea and cardiogenic shock. A pulmonary artery catheter was inserted and showed high pulmonary mean artery pressure (64 mmHg) and a reduced cardiac index (CI = 1,2 L/min/m²). The patient died before the shunt could be occluded. The necropsy showed severe pulmonary hypertension, right ventricular dilatation and secondary myocardial infarction. The shunt was pervious.

DISCUSSION

The treatment of portal hypertension in hepatosplenic schistosomiasis is very different in cirrhotic patients mostly because hepatic function is well preserved in Manson's disease. The surgical treatment has been considered the best alternative for schistosomotic patients with a history of bleeding from esophageal varix rupture because these patients had normal liver function and the only severe complication of the disease was digestive bleeding^[2-6].

The two modalities of elective surgical treatment are selective shunt surgery (Warren procedure) or an esophagogastric devascularization procedure with splenectomy (EGDS). Shunt surgeries have been found to be effective for bleeding control, but were associated with postoperative encephalopathy and higher operative mortality rates when compared to devascularization procedures^[2,5,6].

Although recognizable as a complication of shunt procedures, acute and fatal pulmonary hypertension have never been previously reported since Warren procedure for treatment of portal hypertension in mansonic schistosomiasis. Some groups in Brazil performed thousands of shunt surgeries for schistosomal portal hypertension, but have never described this important

complication^[7-11]. Our group routinely performed a transthoracic echocardiography in order to evaluate pulmonary hypertension. The two patients had a normal pre-operative evaluation and were submitted to DSRS. The necropsy revealed typical findings of acute pulmonary hypertension, suggesting that sub-clinical elevated pulmonary artery pressure be present before surgery. The hyperflow determined by shunt surgery aggravated a previously unsuspected pulmonary hypertension, leading to death. This observation suggests that shunt surgeries should be employed very cautiously in young patients with portal hypertension due to hepatosplenic mansonic schistosomiasis and should be performed only after measurement of pulmonary artery pressure, if indicated.

REFERENCES

- 1 **Kelner S**, Silveira M. História natural das varizes do esôfago na esquistossomose mansônica hepatoesplênica . In: Kelner S, Silveira M(eds). Varizes de esôfago na esquistossomose mansônica hepatoesplênica. Recife: *Universitária da UFPE* 1997: 55-61
- 2 **Ferraz AAB**, Bacelar TS, Silveira MJC, Coelho ARB, Câmara Neto RD, Araújo JR JGC, Ferraz EM. Surgical treatment of schistosomal portal hypertension. *Int Surg* 2001; **86**: 1-8
- 3 **Ezzat FA**, Abu-Elmagd K, Aly MA, Fathy OM, Ghawly NA, EL Fiky AM. Selective shunt versus non-shunt surgery for management of both schistosomal and non-schistosomal. *Ann Surg* 1990; **212**: 97-108
- 4 **Ezzat FA**, Aly MA, Bahgat OO. Distal splenorenal shunt for management of variceal bleeding in patients with schistosomal hepatic fibrosis. *Ann Surg* 1986; **204**: 566-574
- 5 **Sakai P**, Boaventura S, Capacci ML, Macedo TM, Ishioka SZ. Endoscopic sclerotherapy of bleeding esophageal varices. A comparative study of results in patients with schistosomiasis and cirrhosis. *Endoscopy* 1988; **20**: 134-136
- 6 **Raia S**, Silva LC, Gayotto LCC, Forster SC, Fukushima J, Strauss E. Portal hypertension in schistosomiasis: a long-term follow-up of a randomized trial comparing three types of surgery. *Hepatology* 1994; **20**: 398-403
- 7 **Clevo R**, Pugliese V, Zilberstein B, Saad WA, Pinotti HW, Laudanna AA. Hyperdynamic circulation in Manson's hepatosplenic schistosomiasis. *Rev Hosp Clin Fac Med São Paulo* 1998; **53**: 6-10
- 8 **Clevo R**, Pugliese V, Zilberstein B, Saad WA, Pinotti HW, Laudanna AA. Systemic hemodynamic changes in mansonic schistosomiasis with portal hypertension treated by azygoportal disconnection and splenectomy. *Am J Gastroenterol* 1999; **94**: 1632-1637
- 9 **Abrantes WL**, Drumond DAF. Anastomose espleno-renal distal em esquistossomóticos - Revisão de 200 pacientes operados há 11 a 22 anos. *Clin Bras Cir* 1995; **2**: 243-254
- 10 **Pitanga LC**. Selective splenorenal anastomosis: technical details and results of 340 patients subjected in 15 years. *Dig Dis Sci* 1986; **31**: 398 S
- 11 **Pitanga LC**, Pereira WLM. Anastomose espleno-renal distal na urgência em esquistossomóticos. In: Clínica Brasileira de Cirurgia, Colégio Brasileiro de Cirurgias-Hipertensão portal. *Estado atual Ed Robe vol 2* 1995

Edited by Wang XL Proofread by Xu FM

Gastric ulcer penetrating to liver diagnosed by endoscopic biopsy

Ertugrul Kayacetin, Serra Kayacetin

Ertugrul Kayacetin, Department of Gastroenterology, Selcuk University, Meram Medical Faculty, Konya, Turkey

Serra Kayacetin, Department of Pathology, Selcuk University, Meram Medical Faculty, Konya, Turkey

Correspondence to: Dr. Ertugrul Kayacetin, Selcuk Universitesi Meram Tip Fakultesi, Ic Hastaliklari AD, Gastroenteroloji BD, Konya/Turkey. ekayacetin@mynet.com

Fax: +90-332-3236063

Received: 2003-11-12 **Accepted:** 2003-12-24

Abstract

Liver penetration is a rare but serious complication of peptic ulcer disease. Usually the diagnosis is made by operation or autopsy. Clinical and laboratory data were non-specific. A 64-year-old man was admitted with upper gastrointestinal bleeding. Hepatic penetration was diagnosed as the cause of bleeding. Endoscopy showed a large gastric ulcer with a pseudotumoral mass protruding from the ulcer bed. Definitive diagnosis was established by endoscopic biopsies of the ulcer base.

Kayacetin E, Kayacetin S. Gastric ulcer penetrating to liver diagnosed by endoscopic biopsy. *World J Gastroenterol* 2004; 10(12): 1838-1840

<http://www.wjgnet.com/1007-9327/10/1838.asp>

INTRODUCTION

Penetration into the liver is a rare complication of peptic ulcer disease and may lead to unusual complications such as abscess formation or upper gastrointestinal hemorrhage^[1,2]. The absolute frequency of this complication in patient with peptic ulcers is not known.

We reported on a patient who presented with upper gastrointestinal bleeding due to a gastric ulcer penetrating into the liver. Diagnosis was based on histologic examination of endoscopic biopsy materials. We also reviewed 13 other reported cases of endoscopically and histologically diagnosed peptic ulcer penetration into the liver^[2-13].

CASE REPORT

A 64-year-old man was admitted because of a 2-wk history of weakness, dizziness, and melena. One week before his admission, the patient noted intermittent mild mid-epigastric pain and nausea after meals. He had undergone a highly selective vagotomy and primer suture 13 years before for peptic ulcer perforation.

Physical examination demonstrated that he was afebrile with a regular heart rate at 88 beats/min and a blood pressure of 110/60 mm Hg. The abdomen was soft, nontender, nondistended, and without organomegaly or masses. Bowel sounds were hyperactive. Rectal examination revealed no masses and the stool was melanic. A nasogastric tube was passed in emergency room, "coffee grounds" material were aspirated from the stomach. Initial laboratory evaluation showed mild leukocytosis (white blood cell counts, 15 800/mm³; normal, 4-10 10³/mm³) and severe anemia (hemoglobin, 4.7 g/dL; normal hemoglobin, 14.1-17.2 g/dL; hematocrit, 13.8%; normal hematocrit, 36.1-50.3%; mean red cell

volume, 68.2 fL; normal red cell volume, 82.2-99 fL). The stool was positive for occult blood. Coagulation parameters and liver function tests were within normal limits. The patient had no gastrointestinal symptoms and was not receiving aspirin or nonsteroidal antiinflammatory drugs (NSAIDs). Emergency endoscopy showed a large (4.5 cm) ulcer on the anterior wall of the gastric antrum, with malignant appearance (Figure 1). The ulcer base was covered with fibrin, and the margins were irregular. No active bleeding was present at the time of investigation, but stigmata of recent hemorrhage were detected. Sonographic examination demonstrated the "target" sign of the gastric antral area with suggestion of eccentric "tumour" extension into liver (Figure 2). The center of the target was echogenic. Multiple biopsies were taken separately from the ulcer margins and the pseudotumoral mass. Histologic examination of the specimens showed gastric mucosa with granulation tissue and also normal-appearing hepatocytes (Figure 3).

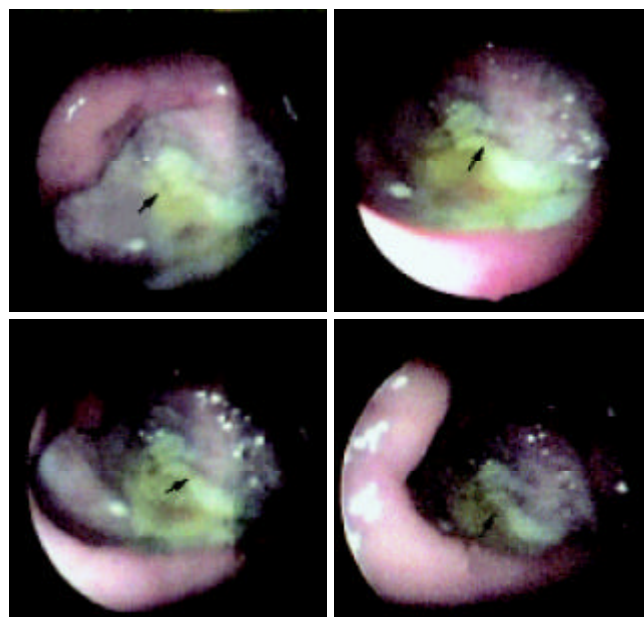


Figure 1 Endoscopic photograph showing a giant deep ulcer (about 4.5 cm in diameter) with malignant appearance (arrow).



Figure 2 Longitudinal ultrasound scan showing the target like appearance (arrows) representing the giant ulcer seen on gastroscopy.

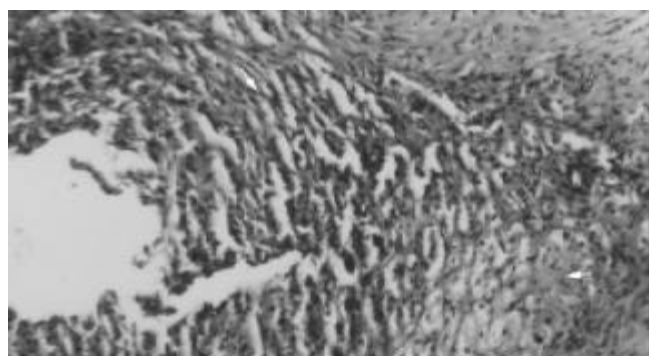


Figure 3 Endoscopic biopsy showing granulation tissue (arrowhead) adjacent to normal-appearance hepatocytes (arrow) (HE x20).

Urease (CLO test) for *Helicobacter pylori* was negative. Treatment was started with 40 mg of omeprazole twice per day. He received 4 units of packed red blood cells by transfusion. The symptoms improved. The surgery service was then consulted for potential resection, however the patient and family refused surgical intervention. On the 17th d of hospitalization, he died of gastrointestinal bleeding.

DISCUSSION

We reported a very rare case of an endoscopically and histologically proven liver penetration by a gastric ulcer in an older man. In general, penetration into the liver by a peptic

ulcer is not a frequent event. We have found only a few reports of liver penetration by gastric ulcer diagnosed by endoscopy . None of them was clinically or radiologically recognised prior to endoscopy. There were thirteen previous case reports of liver penetration in patients with peptic ulcer disease. Four of these cases were for duodenal ulcer and nine were for gastric ulcer. Three of these cases could be diagnosed at the time of surgery, but the other cases were diagnosed on the basis of histologic finding of hepatic tissue on endoscopic biopsies. All of the patients, including ours, showed severe gastrointestinal bleeding. Abdominal pain was described in only 4 patients^[7,8,11,13], thus in our case, abdominal pain did not seem to be a common finding. These case reports, including the present one, are summarized in Table1.

Endoscopically, 3 of the patients had a large ulcer crater with a pseudotumoral mass protruding from the ulcer bed, however no histologic signs of malignancy were seen^[2,6,7]. Another patient had only a mass without any ulcer^[5]. The rest of them had ulcers ranging from 2.5 cm to 9 cm×3 cm in diameter.

The correct diagnosis was established in all the cases by the presence of liver tissue in the histologic examination of endoscopic biopsies. In contrast to the cases, described by Guerrieri and Waxman^[9], the liver tissue in this case did not show severe inflammation or inflammatory atypia. The hepatic histological changes found in our case were consistent with those reported by others. All reported cases except two^[6,9] had normal liver function tests. This may reflect that local hepatic injury does not cause abnormalities in liver functions. The diagnostic value of liver function tests in cases of ulcer penetration into the liver is very limited.

Table 1 Comparison of published reports of liver penetration by peptic ulcer

Source	Age/Gender	Epigastric Pain/tenderness	Main clinical feature	Location	Endoscopic appearance	NSAIDs	Treatment
Martinez-onsurbe (10)	91/Female	-	GI bleeding	Anterior wall of antrum	ulcer	?	?
Guerrieri (9)	53/Male	-	GI bleeding	Lesser curve of antrum	ulcer	?	Antiacids,Op (BII)
Goldman (6)	65/Male	Tenderness	Nausea,anemia	Lesser curve of stomach	ulcer with mass	?	Op (BII)
Park (4)	52/Male	-	GI bleeding	Lesser curve of antrum	giant ulcer	?	H ₂ RA
Sperber (3)	69/Male	Tenderness	GI bleeding	Lesser curve of corpus	ulcer	?	?
Jimenez-Perez(2)	61/Male	Tenderness	GI bleeding	Lesser curve of corpus	ulcer with mass	?	Op
Castellano (11)	77/Male	-	GI bleeding	posterior wall of duodenal bulb	ulcer	+	Op (BII)
Castellano (11)	70/ Male	Epigastric pain	GI bleeding	posterior wall of antrum	ulcer	?	Op (BII)
Matsuoka (12)	53/Male	Tenderness	GI bleeding	Lesser curve of corpus	Giant ulcer	?	H ₂ RA,Op
Novacek(8)	33/Female	Epigastric pain	GI bleeding	Posterior wall of duodenal bulb	ulcer	+	PPI,Op
PaddaS (5)	78/Male	-	GI bleeding	Anterior wall of duodenal bulb	Mass without ulcer	+	H ₂ RA,Op
Brullet (7)	89/Female	Epigastric Pain	GI bleeding	Anterior wall of gastric antrum	ulcer with mass	?	Op (BII)
Mostbeck(13)	53/Male	Epigastric pain	-	Anterior wall of duodenal bulb	ulcer	?	?
Present case	61/ Male	-	GI bleeding	Anterior wall of gastric antrum	giant ulcer	-	PPI

GI Bleeding: gastrointestinal bleeding; Op (BII): subtotal gastrectomy with Billroth II reconstruction; H₂RA: histamine H₂- receptor antagonist; PPI: proton pump inhibitor.

Larger lesions of the upper gastrointestinal tract have some characteristic sonographic patterns. These have been described variously as ring sign, pseudo-kidney, target-like and bull's-eye^[13,14]. Ultrasonographic examination of the present case showed a 'target' lesion with echogenic centre in the gastric antral area with suggestion of exogastric extension into the liver, leading to the suspicion of hepatic penetration by a gastric tumor as described by Sperber^[3]. The center of the ulcer appeared as cavity lesions (hypoechoic area) which were considered secondary to fluid secretions within the cavity of the giant ulcer. Endoscopic ultrasonography is useful for the diagnosis and treatment of a variety of gastrointestinal diseases. We could not perform endoscopic ultrasonography because of its absence in our unit. Endoscopic ultrasonography may be helpful for the diagnosis of gastric ulcer complications such as penetration into an adjacent structure^[15]. Only one of the patients was treated successfully with a histamine H₂-receptor antagonist^[4], but an operation was necessary for all other patients. A subtotal gastrectomy with Billroth II reconstruction was performed in 5 cases^[6,7,9,11]. In the present case, the patient did not require an emergency operation and was initially treated with a proton pump inhibitor. All patients had uneventful postoperative courses except for 2 patients, of them one died of a sepsis^[7], and the other died of pulmonary embolism^[11]. The outcome was not given in 3 cases^[3,10,13]. These reports indicate that penetration as a serious complication of peptic ulcer disease often required operative treatment. Results of a recent study have not shown a decrease in severe ulcer complications despite the use of histamine- H₂ receptor antagonists^[16]. This was likely due to the increase, mean population age in developed countries and the high prevalence of nonsteroidal anti-inflammatory drug use. Lanás *et al.* found that NSAID use was the most important independent risk factor for upper and lower gastrointestinal perforation^[17]. Endoscopic studies have shown an increase in the prevalence of peptic ulcers and gastrointestinal perforation in patients who took NSAIDs regularly^[18]. Only three of these cases were regularly using NSAIDs^[5,8,11]. Nonsteroidal antiinflammatory drugs, therefore, seem to be the most important risk factor for ulcer penetration into the liver.

Finally, as in other reported cases, results of the liver function tests in our patient were unremarkable and so did not focalise our attention on the probability of liver process. Endoscopic view of the lesion did not make us suspect penetrating peptic ulcer disease. However, ultrasound was the first procedure to raise suspicion of hepatic penetration by a gastric ulcer. This diagnosis was subsequently confirmed by endoscopic biopsy. A high index of suspicion to make the diagnosis is necessary.

REFERENCES

- 1 **Isenberg JJ**, McQuaid KR, Laine L, Rubin W. Acid peptic disorders In: Yamada T, eds. Text book of gastroenterology. Philadelphia: J.B Lippincott company 1991: 1241-1340
- 2 **Jimenez-Perez FJ**, Munoz-Navas MA. Endoscopic diagnosis of gastric peptic ulcer penetrating into the liver. *Endoscopy* 1991; **23**: 98-99
- 3 **Sperber AD**, Fenyves D, Barky Y, Yanai-Inbar I, Levy Y. Penetration of gastric ulcers. *Dig Dis Sci* 1991; **36**: 700-702
- 4 **Park RH**, Russell RI. Liver penetration by peptic ulcer. *Am J Gastroenterol* 1988; **83**: 793
- 5 **Padda SS**, Morales TG, Earnest DL. Liver penetration by a duodenal ulcer. *Am J Gastroenterol* 1997; **92**: 352-354
- 6 **Goldman IS**. Endoscopic diagnosis of hepatic penetration into a gastric ulcer. *Am J Gastroenterol* 1988; **83**: 589-590
- 7 **Bullet E**, Campo R, Calvet X, Gimenez A. Gastric ulcer penetrating to the liver: endoscopic diagnosis. *Am J Gastroenterol* 1993; **88**: 794-795
- 8 **Novacek G**, Geppert A, Kramer L, Wrba F, Herbst F, Schima W, Gangl A, Potzi R. Liver penetration by a duodenal ulcer in a young woman. *J Clin Gastroenterol* 2001; **33**: 56-60
- 9 **Guerrieri C**, Waxman M. Hepatic tissue in gastroscopic biopsy: evidence of hepatic penetration by peptic ulcer. *Am J Gastroenterol* 1987; **82**: 890-893
- 10 **Martinez-Onsurbe P**, Ruiz-Villaespesa A, Gonzales-Estecha A, Butron-Vila M, de la Iglesia-Ramos M. Cytodiagnosis of gastric ulcer penetration of the liver by examination of endoscopic brushings. *Acta Cytol* 1991; **35**: 464-466
- 11 **Castellano G**, Galvao A, Vargas J, Canga F, Moreno D, Sanchez F, Solis Herruzo JA. The diagnosis of peptic ulcer penetration in to the liver by endoscopic biopsy. A report of 2 cases and a review of the literature. *Rev Esp Enferm Dig* 1992; **82**: 235-238
- 12 **Matsuoka T**, Nagai Y, Muguruma K, Yoshikawa K, Higuchi K, Seki S, Satake K. Liver penetration and gastrobronchial fistula: unusual complication of a peptic ulcer. *Am Surg* 1995; **61**: 492-494
- 13 **Mostbeck G**, Mallek R, Gebauer A, Tscholakoff D. Hepatic penetration by duodenal ulcer: sonographic diagnosis. *J Clin Ultrasound* 1990; **18**: 726-729
- 14 **Morgan CL**, Trought WS, Oddson TA, Clark WM, Rice RP. Ultrasound patterns of disorders affecting the gastrointestinal tract. *Radiology* 1980; **135**: 129-135
- 15 **Nakazawa S**. Recent advances in endoscopic ultrasonography. *J Gastroenterol* 2000; **35**: 257-260
- 16 **Petersen H**. Over the counter sales of histamine-2 receptor antagonists. *Scand J Gastroenterol Suppl* 1988; **155**: 20-22
- 17 **Lanas A**, Serrano P, Bajador E, Esteva F, Benito R, Sainz R. Evidence of aspirin use in both upper and lower gastrointestinal perforation. *Gastroenterology* 1997; **112**: 683-689
- 18 **Higham J**, Kang JY, Majeed A. Recent trends in admissions and mortality due to peptic ulcer in England: increasing frequency of haemorrhage among older subjects. *Gut* 2002; **50**: 460-464

Edited by Wang XL and Xu FM

Inflammatory pseudotumor of the liver in association with a gastrointestinal stromal tumor: A case report

Oswens S. Lo, Ronnie T. Poon, Chi Ming Lam, Sheung Tat Fan

Oswens S. Lo, Ronnie T. Poon, Chi Ming Lam, Sheung Tat Fan, Centre for the Study of Liver Disease and Department of Surgery, The University of Hong Kong, Pokfulam, Hong Kong, China
Correspondence to: Dr. Ronnie T. Poon, Department of Surgery, University of Hong Kong Medical Centre, Queen Mary Hospital, 102 Pokfulam Road, Hong Kong, China. poontp@hkucc.hku.hk
Telephone: +852-28553641 **Fax:** +852-28175475
Received: 2003-10-20 **Accepted:** 2003-12-30

Abstract

Inflammatory pseudotumor of the liver is a rare benign lesion that can mimic a malignant liver neoplasm. A case of inflammatory pseudotumor of the liver found in association with a malignant gastrointestinal stromal tumor (GIST) of the small bowel was reported. The inflammatory pseudotumor was misdiagnosed as a metastasis from the GIST by frozen section. A correct diagnosis was made only after histopathological examination of the paraffin section of the resected specimen. This case is particularly interesting because of the association of the two rare pathological entities and the diagnostic dilemma that arose from the similarity of their histological appearances. To our knowledge, this association has not been reported in the literature.

Lo OS, Poon RT, Lam CM, Fan ST. Inflammatory pseudotumor of the liver in association with a gastrointestinal stromal tumor: A case report. *World J Gastroenterol* 2004; 10(12): 1841-1843
<http://www.wjgnet.com/1007-9327/10/1841.asp>

INTRODUCTION

Inflammatory pseudotumors of the liver are rare benign lesions characterized by proliferating fibrovascular tissue mixed with inflammatory cells. They are associated with fever, pain and a mass effect, and are commonly mistaken for malignant tumors or liver abscesses. Usually the radiological or cytological examinations fail to differentiate hepatic pseudotumors from liver neoplasms. We report a patient with an inflammatory tumor of the liver who was found to have a malignant gastrointestinal stromal tumor (GIST) of the small bowel at the same time, with special emphasis on their possible etiological association and the diagnostic dilemma.

CASE REPORT

A 46-year-old housewife was admitted to our hospital in January 1998 with right upper quadrant abdominal pain and low grade fever for one week. Blood tests showed leukocytosis ($16.7 \times 10^9/L$) and raised erythrocyte sedimentation rate (ESR) (92 mm/h). Serum alkaline phosphatase (138 IU/L) was slightly increased but hepatic parenchymal enzymes were normal. The levels of serum alpha-fetoprotein (AFP) and carcinoembryonic antigen (CEA) were within normal ranges. Hepatitis B and C

viral serology tests were negative. Repeated blood culture did not reveal any bacterial growth.

In view of the mildly deranged liver function, an abdominal ultrasonography was performed which showed a space-occupying lesion in the right hepatic lobe. No dilated intrahepatic or common bile ducts were noted. Helical computer tomography (CT) scan showed a heterogeneous lesion of 10 cm in size in the right lobe of the liver (Figure 1). The right portal vein was displaced anteriorly. Radiologist commented that it could be a large multi-septated liver abscess, but the possibility of a liver tumor could not be excluded.

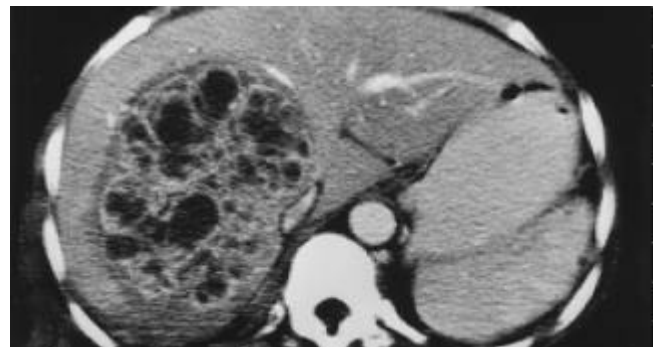


Figure 1 Contrast CT scan showing heterogeneous contrast enhancement in the lesion with a multi-septated appearance.

The patient was treated initially with intravenous cefotaxime and metronidazole, and the fever subsided after 1 wk of antibiotics treatment. However, due to the large size of the lesion and the worry about possible malignancy, surgical exploration was decided. Intraoperatively, in addition to the liver mass, a 10 cm soft tissue tumor was found in the ileum at 15 cm from the ileocecal valve. The tumor and a segment of the small bowel were resected and frozen section examination showed a spindle cell tumor. Trucut biopsy of the liver mass and frozen section suggested a metastatic spindle cell tumor. In view of an isolated hepatic metastasis without lymph node involvement or other evidence of metastasis, an extended right hepatectomy with a 1 cm resection margin from the tumor was performed (Figure 2).



Figure 2 Yellowish firming well-circumscribed mass in the right hepatectomy specimen.

Histopathological examination of the paraffin section of the small bowel tumor confirmed the diagnosis of a malignant GIST. Microscopic examination of the paraffin section of the liver "tumor" showed that it was composed of fascicles of spindle fibroblasts and myofibroblasts admixed with chronic inflammatory cells, which were mainly lymphocytes and plasma cells. The overall pathological features were those of an inflammatory pseudotumor of the liver.

The patient recovered well after the operation and was discharged without complication. The patient had regular follow-up in our outpatient clinic with yearly CT scan. After 4 years of follow-up, the patient was in good health and there was no evidence of tumor recurrence or further liver lesion.

DISCUSSION

Inflammatory pseudotumor of the liver is a rare clinical and pathological entity. Pack and Baker first described it in a patient after right hepatic lobectomy in 1953^[1]. To date, there have been fewer than 80 cases reported in the literature^[2-7]. These "tumors" were so named because of the difficulty in distinguishing them from malignant lesions preoperatively, as in the case of our patient. Histologically, these tumors are composed of densely hyalinized collagenous tissue infiltrated by a variety of cells, mainly plasma cells and the enigmatic plump spindle cells, although monocytes and lymphocytes have also been found^[3]. The pathogenesis and etiology of inflammatory pseudotumors of the liver are uncertain. Some authors suggested that they might be attributed to a septic origin from aberrant inflammatory reaction to migrating microorganisms from large bowel^[2]. Though bacterial culture growths, such as *Escherichia coli* and *Klebsiella pneumoniae*, have been reported in a few cases^[8], no definite microorganism could be isolated from the specimens in most cases. Other authors suggested that Epstein Barr viral infection might play a role in the pathogenesis of inflammatory pseudotumors^[9], but this still needs to be verified by further studies.

In the reported cases, patients with an inflammatory pseudotumor of the liver usually complained of non-specific symptoms at first presentation, such as abdominal pain, fever, weight loss and malaise. Elevated ESR, leukocytosis and mildly elevated hepatic transaminases and bilirubin were typical. Inflammatory pseudotumor has been reported in children as young as 3 mo of age and in adults up to 83 years of age^[4,5], with male preponderance. Schmid reported that more patients with inflammatory pseudotumors were observed in Southeast Asians (54.7%) when compared with other Western counterparts^[4]. As hepatitis B infection is common in Southeast Asia, hepatocellular carcinoma is the most common liver tumor encountered in this area. However, inflammatory pseudotumor should be included in the differential diagnosis of a hepatic mass, especially in those patients with normal hepatitis B screening and AFP level.

The recommended therapeutic approach for inflammatory pseudotumors of the liver is still controversial, though surgical resection is generally considered as an overtreatment^[8,10]. Spontaneous regression of the lesion was reported in some cases, and cases that regressed with the use of antibiotics^[11] or nonsteroidal anti-inflammatory drugs^[12] have also been reported. When the inflammatory pseudotumors caused major complications, such as biliary obstruction^[13] and portal hypertension^[14], the patients might need surgical resection or even liver transplantation^[15]. Although most authors believed that inflammatory pseudotumors had a benign behavior, there have been some reports of invasive course and mortality^[2].

To our knowledge, this is the first patient reported to have an inflammatory pseudotumor in association with a small bowel

GIST. The exact etiological link between the two is uncertain. However, the presence of an ileal GIST could potentially enhance entry of enteric bacteria into the portal circulation, which could then result in an inflammatory pseudotumor if the hypothesis of an infective etiology is true. In our patient, frozen section examination of the hepatic mass suggested that it was a metastasis from the malignant small bowel GIST, but we proceeded with hepatic resection in view of the absence of other obvious extrahepatic metastasis. In the past, patients with hepatic metastases from malignant GIST or leiomyosarcoma were considered to have poor prognosis even after surgical resection^[16,17]. Hence, hepatic resection was usually not offered to patients with liver metastasis from gastrointestinal leiomyosarcoma. However, recently some authors advocated that aggressive surgical resection for liver metastasis might provide survival benefit to the patients^[18,19]. In a recent report from a single institution, a median survival of 40 mo and a 5-year survival rate of 33% were observed after hepatic resection for hepatic metastases from leiomyosarcoma^[17]. We adopted a similar approach and performed a major hepatectomy. The final pathology of the liver lesion turned out to be an inflammatory pseudotumor, and the patient had survived without any disease recurrence for four years by the time of writing the manuscript. Our case illustrated the difficulty in differentiating an inflammatory pseudotumor from a malignancy not only in the preoperative imaging but also even by frozen section examination. The histological appearance of an inflammatory pseudotumor and a GIST is particularly difficult to differentiate. The surgeons should be aware of their possible association as illustrated in this case. A favorable long-term outcome may be expected with resection of the GIST together with hepatic resection for the inflammatory pseudotumor in the liver.

REFERENCES

- 1 **Pack G**, Backer H. Total right hepatic lobectomy. Report of a case. *Ann Surg* 1953; **138**: 253-258
- 2 **Horiuchi R**, Uchida T, Kojima T, Shikata T. Inflammatory pseudotumor of the liver. Clinicopathologic study and review of the literature. *Cancer* 1990; **65**: 1583-1590
- 3 **Shek TW**, Ng IO, Chan KW. Inflammatory pseudotumor of the liver. Report of four cases and review of the literature. *Am J Surg Pathol* 1993; **17**: 231-238
- 4 **Schmid A**, Janig D, Bohuszlavizki A, Henne-Bruns D. Inflammatory pseudotumor of the liver presenting as incidentaloma: report of a case and review of the literature. *Hepatogastroenterology* 1996; **43**: 1009-1014
- 5 **Lee SL**, DuBois JJ. Hepatic inflammatory pseudotumor: case report, review of the literature, and a proposal for morphologic classification. *Pediatr Surg Int* 2001; **17**: 555-559
- 6 **Ciftci AO**, Tanyel FC. Inflammatory pseudotumor of the liver. *J Pediatr Surg* 2001; **36**: 1737-1738
- 7 **Sakai M**, Ikeda H, Suzuki N, Takahashi A, Kuroiwa M, Hirato J, Hatakeyama SI, Tsuchida Y. Inflammatory pseudotumor of the liver: case report and review of the literature. *J Pediatr Surg* 2001; **36**: 663-666
- 8 **Torzilli G**, Inoue K, Midorikawa Y, Hui AM, Takayama T, Makuuchi M. Inflammatory pseudotumors of the liver: prevalence and clinical impact in surgical patients. *Hepatogastroenterology* 2001; **48**: 1118-1123
- 9 **Arber DA**, Weiss LM, Chang KL. Detection of Epstein-Barr Virus in inflammatory pseudotumor. *Semin Diagn Pathol* 1998; **15**: 155-160
- 10 **Gluszek S**, Kot M, Czerwaty M. Inflammatory pseudotumor of the liver treated surgically. *Hepatogastroenterology* 1999; **46**: 2959-2960
- 11 **Jais P**, Berger JF, Vissuzaine C, Paramelle O, Clays-Schouman E, Potet F, Mignon M. Regression of inflammatory pseudotumor of the liver under conservative therapy. *Dig Dis Sci* 1995; **40**:

- 752-756
- 12 **Hakozaki Y**, Katou M, Nakagawa K, Shirahama T, Matsumoto T. Improvement of inflammatory pseudotumor of the liver after nonsteroidal anti-inflammatory agent therapy. *Am J Gastroenterol* 1993; **88**: 1121-1122
 - 13 **Pokorny CS**, Painter DM, Waugh RC, McCaughan GW, Gallagher ND, Tattersall MH. Inflammatory pseudotumor of the liver causing biliary obstruction. Treatment by biliary stenting with 5-year follow-up. *J Clin Gastroenterol* 1991; **13**: 338-341
 - 14 **Heneghan MA**, Kaplan CG, Priebe CJ Jr, Partin JS. Inflammatory pseudotumor of the liver: a rare cause of obstructive jaundice and portal hypertension in a child. *Pediatr Radiol* 1984; **14**: 433-435
 - 15 **Kim HB**, Maller E, Redd D, Hebra A, Davidoff A, Buzby M, Hoffman MA. Orthotopic liver transplantation for inflammatory myofibroblastic tumor of the liver hilum. *J Pediatr Surg* 1996; **31**: 840-842
 - 16 **DeMatteo RP**, Lewis JJ, Leung D, Mudan SS, Woodruff JM, Brennan MF. Two hundred gastrointestinal stromal tumors: recurrence patterns and prognostic factors for survival. *Ann Surg* 2000; **231**: 51-58
 - 17 **Lang H**, Nussbaum KT, Kaudel P, Fruhauf N, Flemming P, Raab R. Hepatic metastases from leiomyosarcoma: A single-center experience with 34 liver resections during a 15-year period. *Ann Surg* 2000; **231**: 500-505
 - 18 **Chen H**, Pruitt A, Nicol TL, Gorgulu S, Choti MA. Complete hepatic resection of metastases from leiomyosarcoma prolongs survival. *J Gastrointest Surg* 1998; **2**: 151-155
 - 19 **DeMatteo RP**, Shah A, Fong Y, Jarnagin WR, Blumgart LH, Brennan MF. Results of hepatic resection for sarcoma metastatic to liver. *Ann Surg* 2001; **234**: 540-547

Edited by Wang XL **Proofread by** Xu FM

Human cyclosporiosis in Turkey

Süleyman Yazar, Saban Yalçın, Yzzet Sahin

Süleyman Yazar, Saban Yalçın, Yzzet Sahin, Department of Parasitology, Medical Faculty, Erciyes University, 38039, Kayseri-Turkey

Correspondence to: Süleyman Yazar, Department of Parasitology, Medical Faculty, Erciyes University, 38039, Kayseri, Turkey. syazar@erciyes.edu.tr

Telephone: +90-352-4374937 **Fax:** +90-352-4375285

Received: 2003-10-08 **Accepted:** 2004-01-09

Abstract

Six patients infected with *Cyclospora cayetanensis* who sought medical care at three different hospitals in Turkey are herein presented. Four patients were male and the others were female and their ages ranged from 7 to 62 years. The first patient was HIV-positive and presented with watery diarrhea with a frequency of up to 18 times a day for more than ten months and diagnosed as cyclosporiosis in Kayseri, 1996. The second patient was also HIV positive and diagnosed as cyclosporiosis in Kayseri, 2000. The third patient was an acute myeloblastic leukemia (AML) patient and diagnosed in Istanbul, 2000. The fourth patient was idiopathic hepatic cirrhosis complaining of diarrhea and weakness and diagnosed in Kayseri, 2001. The fifth and sixth patients were immunocompetent patients complaining of diarrhea and diagnosed in Izmir and Kayseri, 2002. Diarrhea occurring from one to ten times a day continued for 7 to 70 d in the last 5 patients. Treatment with a trimethoprim/sulfamethoxazole compound was done for all patients. Both symptomatic and parasitologic improvements were quickly observed. In summary, *C. cayetanensis* infection is rare in Turkey and most patients infected with this pathogen tend to be immunosuppressive individuals at present.

Yazar S, Yalçın S, Sahin Y. Human cyclosporiosis in Turkey. *World J Gastroenterol* 2004; 10(12): 1844-1847
<http://www.wjgnet.com/1007-9327/10/1844.asp>

INTRODUCTION

The genus *Cyclospora* is in the subclass Coccidia, phylum Apicomplexa. This genus is taxonomically related to coccidian genera in humans. This organism is a unilocular parasite previously known as cyanobacterium-like or coccidian-like body (CLB) and, in recent years, a new coccidian pathogen, *Cyclospora*, has been putatively identified^[1,2]. The organisms are seen as nonrefractile spheres and are acid-fast variable with the modified Kinyoun's acid-fast stains, those are unstained appear as glassy, wrinkled spheres. Modified acid-fast stains stain the oocysts from light pink to deep red, some of which may contain granules or have a bubbly appearance. The oocysts autofluoresce (strong green or intense blue) under UV epifluorescence^[3]. The first known human cases of illness caused by *Cyclospora* infection (i.e., cyclosporiosis) were reported in the medical literature in 1979^[4]. Our aim in this study was to present cases of human cyclosporiosis in Turkey and to review the literature.

MATERIALS AND METHODS

We evaluated all of the human cases in our country

retrospectively which were belongs to Kayseri (three cases), Istanbul (one case) and Izmir (one case) regions between 1996 and 2002^[5-9]. Following these, we determined a new case with *C. cayetanensis* in December 2002. In this study, we discuss all of the six cases with cyclosporiosis in Turkey.

RESULTS

Case 1^[5]

A 50 year-old woman with acquired immune deficiency syndrome (AIDS) was admitted in December 1996 for chronic diarrhea, vomiting, and fever to the Erciyes University Medical Faculty Hospital. There was preceding history of episodic watery diarrhea, vomiting, and weight loss along with intermittent fever over a period of one year. She was cachectic, with mild abdominal tenderness and alert, thrush and palpable small cervical lymph nodes. She had anemia (Hb 8.4 g/L). Enzyme immunoassays for HIV antibodies were positive and the T4/T8 ratio was 0.6 in serum. *E. coli* and *Proteus* spp. were found at 10⁴ cfu/mL from urine specimens. Microscopical analysis of the stool revealed numerous spherical double walled microorganisms 8-9 µm in diameter, some with internal granulation. After Kinyoun's acid fast staining of the stool, the organisms appeared faint pink to red in colors, some cysts not taking up the stain and appearing as "ghosts". Empty cysts varied in shape but had generally collapsed into crescents. The organisms were identified as *Cyclospora* sp. The patient was treated with TMP/SMZ (160/800 mg) bid for three weeks. Following treatment, re-examination of a stool sample revealed no more organisms and diarrhea stopped. This case was the first report of *Cyclospora* infection in Turkey.

Case 2^[6]

A 40-year old man with AIDS was evaluated parasitologically for the etiologic agent of his persistent diarrhea for two months in Erciyes University Medical Faculty Hospital in 2000. Stool samples were examined by conventional coprological methods such as fresh preparation, iodine stain, and flotation. Suspicious organisms (8-10 µm in diameter) were seen in stool, which were stained with Kinyoun's acid-fast stain and identified as *C. cayetanensis*. He was treated with TMP/SMZ (160/800 mg) bid for two weeks. We could not find the organism in the stool samples after the treatment and diarrhea stopped.

Case 3^[7]

In 2000, at the Istanbul University Medical Faculty Hospital there was another 7 year-old male patient with acute myeloblastic leukemia (AML). A sudden diarrhea developed while bone marrow transplantation was being planned. The patient's stool samples were examined with respect to pathogen bacteria and fungi and rotavirus. None of them was determined, isolated and/or seen. Two stool specimens, which were taken in one-week interval, also were examined with modified trichrome, acid fast and safranin staining methods. In microscopic examinations, *C. cayetanensis* oocysts were seen with all three staining methods. After four weeks of therapy with trimethoprim-sulphamethoxazole (15 mg/kg.d) diarrhea stopped and in the new stool specimens, *C. cayetanensis* oocysts were not encountered.

Case 4^[8]

A 52 year-old male patient with idiopathic hepatic cirrhosis

complaining of diarrhea and weakness was accepted to the gastroenterology clinic of Erciyes University Medical Faculty Hospital in 2001. In the patient's history, there were watery, bad smelling, bloodless episodes of diarrhea, fever, cold, sweating, and a 10 kg lost of weight which all began three weeks prior to hospitalization. The patient had never traveled to a foreign country. Physical examination did not reveal any abnormalities except subicteric conjunctivas and a hyperemic tongue. The patient was afebrile. In laboratory examination, blood values were found as Hb: 14.2 g/dL, white blood cells: 4 900/mm³, platelets: 69 000/mm³. Biochemical values were as follows: K: 2.9 mmol/L (↑), P: 1.7 mg/dL (↑), Ca: 7.6 mg/dL (↑), Mg: 0.9 mg/dL (↑), uric acid: 9.3 mg/dL (↑), total bilirubin: 4.2 mg/dL (↑), AST: 165 U/L (↑), ALT: 76 U/L (↑), CK-MB: 120 U/L (↑), albumin: 2.8 gr/dL (↑), acetone, protein and bilirubin were (+) in urine. Anti-HBs Ag and Anti-HAV were positive and other hepatitis markers were negative. Anti-HIV antibodies were found to be negative by ELISA test. In abdominal USG, liver with lobule contour was smaller than normal size, and its echo was increased. Widespread intraperitoneal exudate was seen.

In order to find out the causative etiologic agent of diarrhea, stool samples were examined by different methods and stained using modified Kinyoun's acid-fast stain. Following examination, acid-fast variable wrinkled spheres approximately 9 µm in diameter, were seen and diagnosed as *C. cayetanensis*. Confirmation of the diagnosis was established by fluorescent microscope (380 to 420 nm excitation filter), which showed bright green to intense blue autofluorescent oocysts.

Consequently, this organism was diagnosed as *C. cayetanensis*. The patient was treated with TMP/SMZ (160/800 mg) bid for 7 d. Following treatment, re-examination of a stool sample, however, did not reveal the presence of any organisms.

Case 5^{9]}

A 30 year-old female patient complaining of diarrhea and weakness was admitted to the gastroenterology clinic of Atatürk State Hospital in Izmir, 2002. In the patient's history, there were watery diarrhea, fever, nausea which all began one week prior to admission to hospital. Stool samples were examined by conventional coprological methods such as fresh preparation, iodine stain, flotation, modified Ritchie's method and modified Kinyoun's acid-fast stain. Acid-fast variable wrinkled spheres were seen and diagnosed as oocysts of *C. cayetanensis*. Confirmation of the diagnosis was established by fluorescent microscope. After one-week therapy with trimethoprim-sulphamethoxazole for 7 d, diarrhea stopped and in the new stool specimens, *C. cayetanensis* oocysts were not seen. This patient was different from the other four cases in Turkey because there were no abnormalities in immunologic tests of the patient. That is, she was an immunocompetent patient.

Case 6

A 62-year-old male patient complaining of diarrhea was admitted to the Erciyes University Medical Faculty Hospital in October 2002. This case was not reported anywhere. In the patient's history, there were watery, bad smelling diarrhea, fever, sweating, which all began one week before admission to hospital. Stool samples were examined by conventional coprological methods. Acid-fast variable oocysts were seen and diagnosed as oocysts of *C. cayetanensis* (Figure 1).

After one-week therapy with trimethoprim-sulphamethoxazole (160/800 mg) bid for 7 d diarrhea stopped and in the new stool specimens, *C. cayetanensis* oocysts were not encountered and all the symptoms disappeared. This patient was also immunocompetent similar to case 5. There were no abnormalities in immunologic tests of the patient.

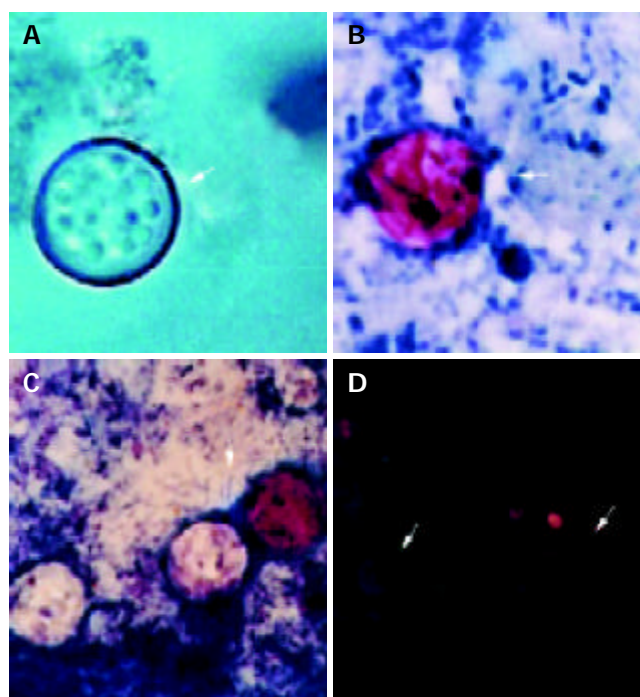


Figure 1 *Cyclospora* oocysts in stool smear preparations. A: *Cyclospora* oocysts in native preparation (original magnification. ×1 000). B: Acid-fast stained *Cyclospora* oocysts (Modified Kinyoun's acid-fast stain: original magnification. ×1 000). C: Acid-fast stained and unstained *Cyclospora* oocysts (Modified Kinyoun's acid-fast stain: original magnification. ×1 000). D: *Cyclospora* oocysts' autofluorescence in wet preparation with fluorescent microscope of 380-420 nm wavelength. (×400).

DISCUSSION

Cyclospora organisms were first reported in the intestines of moles in 1870 by Eimer, and Schneider introduced the genus *Cyclospora* in 1881. The first report of human *Cyclospora* infection came from Papua New Guinea in 1979^[4].

Cyclospora oocysts in freshly excreted stool are non-infectious. The oocysts are thought to require days to weeks outside the host under favorable environmental conditions to sporulate and thus to become infectious. Direct person-to-person transmission by fecal exposure is unlikely, because excreted oocysts must sporulate to become infective^[10].

C. cayetanensis constitutes a significant cause of chronic and intermittent diarrhea in immunocompromised patients especially those with AIDS. A study in Haiti has documented the occurrence of chronic diarrhea in most patients with AIDS^[11]. *Cyclospora* infection has also been reported in patients with severe AIDS in other areas^[12,13]. Lontie *et al.*^[14] reported 2 cases of intestinal *Cyclospora* infection in immunocompetent Belgians. In Turkey, there were 6 cases between 1996 and 2002, 2 of them were AIDS patients^[5,6], 1 of them was an AML patient^[7], 1 of them was idiopathic hepatic cirrhosis^[8] and the last two patients were immunocompetent individuals^[9,10].

Both epidemiological and environmental data suggested that the organism be waterborne^[1]. The transmissibility of *Cyclospora* through water depends on the probability that the water source of interest could become contaminated and that the water treatment would kill or remove oocysts. *Cyclospora* oocysts, like *Cryptosporidium* oocysts, probably are highly chlorine resistant, but they could be more easily removed by conventional filtration because they are about twice as big as *Cryptosporidium* oocysts^[10].

In 1994, an outbreak of *Cyclospora* occurred among British soldiers and dependents stationed in a small military base detachment in Pokhara, Nepal. That outbreak was epidemiologically

Table 1 Similarities and differences between *Cryptosporidium parvum* and *Cyclospora cayetanensis*^[10]

Similarities	<i>C. cayetanensis</i>	<i>C. parvum</i>
Acid-fast staining of oocysts	Variable acid-fast	Acid-fast
Number of infective units (sporozoites) per sporulated oocyst	4	4
Completion of life cycle within humans	Yes, except for sporulation	Yes
Multiplication outside the host (e.g. in water or food)	No	No
Differences		
Size of oocysts	8-10 µm in diameter (intermediate in size between <i>Cryptosporidium parvum</i> and <i>Isoospora belli</i>)	Average width of 4.5 µm and average length of 5 µm
Number of organisms in stools of symptomatic nonimmune hosts	Typically excreted in low to moderate number	Often excreted in somewhat higher numbers
Autofluorescence of oocyst wall	Yes	No
Internal morphology of sporulated oocysts	Each oocyst has 2 internal sporocysts, each contains 2 sporozoites	The 4 sporozoites are naked within the oocyst
Infectivity of oocysts in freshly excreted stool	Must sporulate outside host to become infectious	Fully sporulated and infectious when excreted (sporozoites can be visualised when oocysts are excreted)
Zoonotic potential	Host range unknown	Infects virtually all commonly known wild and domestic mammals
Location in enterocytes of small bowel	Intracytoplasmic within a parasitophorous vacuole in apical supranuclear region	Intracellular, extracytoplasmic, within a parasitophorous vacuole at luminal surface of enterocyte
Susceptibility to antimicrobial agents	Treatment with TMP-SMZ leads to both clinical and parasitologic cure	Some antimicrobial agents (e.g. paromomycin) may cause clinical improvement, but no agents has been consistently demonstrated to provide parasitologic cure

linked to drinking water, because the organism was identified in the water source^[15].

In the 1990s, at least 11 definite and probable food born outbreaks of cyclosporiasis, affecting at least about 3 600 people, were documented, all of which occurred in North America^[10]. The outbreak that brought cyclosporiasis to prominence in North America and definitively established that *Cyclospora* was transmissible through food, occurred in 1996 in the United States and Canada and was linked to a third country, Guatemala, which was the source of implicated fresh raspberries^[16].

The symptoms presenting in one patient (watery diarrhea, nausea, weight loss, and abdominal pain) were similar to those classically *Cyclospora* infection^[11,13,17]. Since the oocysts of *Cyclospora* are acid-fast like those of *Cryptosporidium*, we recommend that all laboratories screening for the latter parasite include precise measurements of oocysts. *Cyclospora* oocysts are 8-10 µm in diameter (intermediate size between *Cryptosporidium parvum* and *Isoospora belli*). *Cryptosporidium parvum* oocysts have an average width and length of 4.5 µm 5 µm, respectively. It is possible that many cases of diarrhea reported to be due to *Cryptosporidium* might actually be due to *Cyclospora* because size discriminations are not often made. *Cyclospora* organisms have now been isolated in chronic diarrhea and this infection should be carefully distinguished from cryptosporidiosis^[11,11,18]. A list of some of the similarities and differences between these two organisms is shown in Table 1.

The treatment for *Cyclospora* infections cotrimoxazole (TMP-SMZ) was given for 7-10 d (longer, if symptoms persist)^[19]. The adult dosage was 160 mg TMP plus 800 mg SMZ orally twice daily. In a double blind, placebo controlled trial among Peruvian children, a three-day course of TMP (5 mg/kg.d) plus SMZ (25 mg/kg.d) decreased the duration of oocyst

excretion, but few symptomatic children were treated to address the effect on duration of diarrhea^[20]. Alternative treatments have not yet been identified. Limited data suggest that the following drugs are ineffective: albendazole, azithromycin, nalidixic acid, norfloxacin, tinidazole, metronidazole, quinacrine, tetracycline, and diloxanide furoate. Approaches to alternative treatment of patients who could not tolerate TMP-SMZ therapy include observation and symptomatic treatment^[21-25]. In a small, randomized, controlled-trial comparing oral TMP-SMZ and ciprofloxacin for treatment of and secondary prophylaxis for *Cyclospora* infection in HIV infected Haitians, ciprofloxacin (500 mg twice daily for 7 d as therapy and thrice weekly for 10 wk as secondary prophylaxis) was moderately effective, though it was less active than TMP-SMZ^[26]. These results suggest that ciprofloxacin might be an alternative for patients who cannot tolerate TMP-SMZ. However, these results should be confirmed in a large number of patients as well as in non-HIV population.

Sporadic cases of infection may be part of widespread outbreaks and should in any case be reported to public health officials. Public health personals and clinicians should also be aware that stool examination for *Cyclospora* should be specifically required in case of clinical suspicion of *Cyclospora* infection (protracted or relapsing diarrheal episode)^[10]. In conclusion, this organism should be considered in the differential diagnosis of unexplained diarrhea in both immunosuppressive and immunocompetent patients. However, further studies are needed to confirm the causative association with other diseases and to determine the incidence and epidemiological features of this organism.

REFERENCES

- 1 Long EG, Ebrahimzadeh A, White EH, Swisher B, Callaway

- CS. Alga associated with diarrhea in patient with acquired immunodeficiency syndrome and in travelers. *J Clin Microbiol* 1990; **28**: 1101-1104
- 2 **Ortega YR**, Sterling CR, Gilman RH, Cama VA, Diaz F. Cyclospora species a new protozoan pathogen of humans. *N Engl J Med* 1993; **328**: 1308-1312
- 3 **Garcia SL**, Bruckner AD. Intestinal protozoa: Coccidia and Microsporidia in Diagnostic medical parasitology. Washington, D.C: *American Society Microbiol* 1997: 54-89
- 4 **Ashford RW**. Occurrence of an undescribed coccidian in man in Papua New Guinea. *Am Trop Med Parasit* 1979; **73**: 497-500
- 5 **Koc AN**, Aygen B, Sahin Y, Kayabas Ü. Cyclospora sp. associated with diarrhea in a patient with AIDS in Turkey. *Tr J Med Scien* 1998; **28**: 557-558
- 6 **Yazar S**, Aygen B, Koc AN, Altunoluk B, Alp E, Sahin I. A diarrheal case caused by Cyclospora cayetanensis: Case report. *Erciyes Med J* 2000; **22**: 48-51
- 7 **Büget E**, Büyükbaba BÖ, Kirkoyun UH, Ağırbaşlı H, Yalman N, Anak S, Can E, Gedikoglu G. Türkiye' de ilk kez belirlenen Cyclospora cayetanensis etkenli diyare olgusu. *J Turks Mic Soc* 2000; **30**: 162-165
- 8 **Yazar S**, Yaman O, Demirtas F, Yalcın S, Yücesoy M, Sahin Y. Cyclospora cayetanensis associated with diarrhea in a patient with idiopathic compensated hepatic cirrhosis. *Acta Gastro-Enterol Belg* 2002; **65**: 241-244
- 9 **Turk M**, Turker M, Ak M, Karaayak B, Kaya T. Cyclosporiasis associated with diarrhoea in an immunocompetent patient in Turkey. *J Med Microbiol* 2004; **53**: 255-257
- 10 **Herwaldt BL**. Cyclospora cayetanensis: A review, focusing on the outbreaks of cyclosporiasis in the 1990s. *Clin Inf Dis* 2000; **31**: 1040-1057
- 11 **Pape JW**, Verdier RI, Boncy M, Boncy J, Johnson WD Jr. Cyclospora infection in adults infected with HIV clinical manifestations, treatment and prophylaxis. *Ann Intern Med* 1994; **121**: 654-657
- 12 **Madico G**, Gilman RH, Miranda E, Cabrera L, Sterling CR. Treatment of Cyclospora infection with co-trimoxazole. *Lancet* 1993; **342**: 122-123
- 13 **Hart AS**, Ridinger MT, Soundarajan R, Peters CS, Swiatlo AL, Kocka FE. Novel organisms associated with chronic diarrhea in AIDS. *Lancet* 1990; **335**: 169-170
- 14 **Lontie M**, Degroote K, Michiels J, Bellers J, Mangelschots E, Vandepitte J. Cyclospora sp.: a coccidian that causes diarrhea in travellers. *Acta Clin Belg* 1995; **50**: 288-290
- 15 **Rabold JG**, Hoge CW, Shlim DR, Kefford C, Rajah R, Echeverria P. Cyclospora outbreak associated with chlorinated drinking water. *Lancet* 1994; **344**: 1360-1361
- 16 **Herwaldt BL**, Ackers ML. Cyclospora working group. An outbreak in 1996 of cyclosporiasis associated with imported raspberries. *N Engl J Med* 1997; **336**: 1548-1556
- 17 **Albert MJ**, Kabir I, Azim T, Hossain A, Ansaruzzaman M, Unicomb L. Diarrhea associated with Cyclospora Sp. in Bangladesh. *Diagn Microbiol Infect Dis* 1994; **19**: 47-49
- 18 **Soave R**. Cyclospora: An overview. *Clin Infect Dis* 1996; **23**: 429-437
- 19 **Hoge CW**, Shlim DR, Ghimire M, Rabold JG, Pandey P, Walch A, Rajah R, Gaudio P, Echeverria P. Placebo-controlled trial of cotrimoxazole for Cyclospora infections among travellers and foreign residents in Nepal. *Lancet* 1995; **345**: 691-693
- 20 **Madico G**, McDonald J, Gilman RH, Cabrera L, Sterling CR. Epidemiology and treatment of Cyclospora cayetanensis infection in Peruvian children. *Clin Infect Dis* 1997; **24**: 977-981
- 21 **Soave R**, Herwaldt BL, Relman DA. Cyclospora. *Infect Clin Dis North Am* 1998; **12**: 1-12
- 22 **Shlim DR**, Cohen MT, Eaton M, Rajah R, Long EG, Ungar BL. An alga-like organism associated with an outbreak of prolonged diarrhea among foreigners in Nepal. *Am J Trop Med Hyg* 1991; **45**: 383-389
- 23 **Shlim DR**, Pandey P, Rabold JG, Walch A, Rajah R. An open trial of trimethoprim along against Cyclospora infection. *J Travel Med* 1997; **4**: 44-45
- 24 **Connor BA**, Shlim DR, Scholes JV, Rayburn JL, Reidy J, Rajah R. Pathologic changes in the small bowel in nine patients with diarrhea associated with a coccidian-like body. *Ann Intern Med* 1993; **119**: 377-382
- 25 **Wurtz R**. Cyclospora: a newly identified intestinal pathogen of humans. *Clin Infect Dis* 1994; **18**: 620-623
- 26 **Verdier RI**, Fitzgerald DW, Johnson WD Jr, Pape JW. Trimethoprim-sulfamethoxazole compared with ciprofloxacin for treatment and prophylaxis of *Isospora belli* and *Cyclospora cayetanensis* infection in HIV infected patients. *Ann Intern Med* 2000; **132**: 885-888

Edited by Wang XL and Xu FM

Biological functions of melanoma-associated antigens

Jiang Xiao, Hong-Song Chen

Jiang Xiao, Hong-Song Chen, Hepatology Institute, People's Hospital, Peking University, Beijing 100044, China

Supported by National Natural Science Foundation, No. 30170047, the State "863" Program, No. 2001AA217151 and No. 2002AA217071 and "211" project of Peking University

Correspondence to: Dr. Hong-Song Chen, Hepatology Institute, People's Hospital, Peking University, Beijing 100044, China. chen2999@sohu.com

Telephone: +86-10-68314422 Ext. 5726 **Fax:** +86-10-68321900

Received: 2003-12-17 **Accepted:** 2004-01-08

Abstract

To date, dozens of melanoma-associated antigens (MAGEs) have been identified and classified into 2 subgroups, I and II. Subgroup I consists of antigens which expression is generally restricted to tumor or germ cells, also named as cancer/testis (CT) antigen. Proteins and peptides derived from some of these antigens have been utilized in promising clinical trials of immunotherapies for gastrointestinal carcinoma, esophageal carcinoma, pulmonary carcinoma and so on. Various MAGE family members play important physiological and pathological roles during embryogenesis, germ cell genesis, apoptosis, etc. However, little is known regarding the role of MAGE family members in cell activities. It is reasonable to speculate that the genes for subgroup I MAGEs, which play important roles during embryogenesis, could be later deactivated by a genetic mechanism such as methylation. In the case of tumor formation, these genes are reactivated and the resultant proteins may be recognized and attacked by the immune system. Thus, the subgroup I MAGEs may play important roles in the immune surveillance of certain tumor types. Here, we review the classifications of MAGE family genes and what is known of their biological functions.

Xiao J, Chen HS. Biological functions of melanoma-associated antigens. *World J Gastroenterol* 2004; 10(13): 1849-1853
<http://www.wjgnet.com/1007-9327/10/1849.asp>

INTRODUCTION

In 1991, researchers first isolated a melanoma-associated antigen (MAGE) gene, MAGE-A1^[1]. This antigen, isolated from an MZ-2 human melanoma cell line, could be recognized by cytotoxic T lymphocytes (CTLs). In the following years, dozens of new MAGE gene were identified. MAGE proteins act as anti-tumoral immune targets, making these antigens a popular focus of immunotherapy researches on gastrointestinal carcinoma and other cancers^[2]. Although much work has investigated the expression of MAGE genes and HLA-restricted epitopes, relatively little is known about the functions of the MAGE proteins. In this paper, we review the classifications of MAGE family genes and what is known of their biological functions.

CLASSIFICATIONS OF THE HUMAN MAGE PROTEIN FAMILY

In 1991, Terry Boon's laboratory established a method for identifying tumor antigens based on tumor-specific CTLs recognition^[1]. Using this method, the group identified a new tumor antigen which they called MAGE-1. Subsequently, this

and other screening methods were used to identify a large number of tumor-specific and tumor-related antigens, including dozens of MAGEs (Table 1)^[3-7]. The MAGE family proteins share certain homologous regions, including the MAGE homology domain (MHD). Sequence comparison and analysis revealed 3 subgroups of acidic MAGEs, termed A, B, and C, and one basic subgroup, MAGE-D, which includes Nectin, Restin and others^[8]. Based on expression patterns, the MAGEs were further classified as belonging to either subgroup I or II. Members of subgroup I, including MAGE-A, -B, and -C, are expressed in malignant tumors and testis, but not in other normal tissues. These members are also named as cancer/testis (CT) antigen and tumor-specific antigen. In contrast, subgroup II MAGEs are expressed in various normal adult human tissues^[4,9]. Interestingly, testis germ cells do not express MHC I/II molecules and cannot present the MAGE proteins, so testis tissue is generally immune-exempt. Based on this, tumor-expressed MAGE-A, -B, and -C proteins have become important targets for cancer immunotherapy, and some clinical trials are ongoing for treating gastrointestinal carcinoma, esophageal carcinoma, pulmonary carcinoma and so on. Now researchers are continuing to identify additional MAGE genes in the hope of identifying better therapeutic targets.

CELLULAR FUNCTIONS OF MAGE PROTEINS

Regulation of subgroup I MAGE gene expression in normal somatic cells

In normal mature somatic cells, subgroup I MAGE genes are static. When cells become neoplastic, MAGE genes are activated and the corresponding proteins are expressed. Interestingly, some non-MAGE-A1-expressing tumor cells have been found to contain transcription factors capable of activating the MAGE-A1 promoter^[10]. This suggests that the presence of the relevant transcription factor is not sufficient to trigger expression, indicating that alternative regulatory mechanisms may exist in terms of MAGE-1 gene activation.

Recent studies have shown that MAGE gene activation may be related to promoter demethylation^[11]. The promoter of the MAGE-A1 gene contains several cis-regulatory sequences located from nt -792 to +47. Among them, the B and B' domains are critical for MAGE-1 gene expression. Both domains contain Ets transcription factor binding sites, including a critical CpG bi-nucleotide site. When this CpG is methylated, the Ets transcription factor cannot bind to the B and B' domains, and expression of MAGE-1 is inhibited. Therefore, promoter methylation inhibits the expression of MAGE-1^[10]. Indeed, when non-MAGE-A1-expressing tumor cells were treated with the demethylating reagent, 5-aza-2-deoxycytidine (5DC), MAGE-A1 expression was induced^[11]. When normally non-MAGE-expressing cells (i.e. fibroblasts) were treated with 5DC, some cells expressed MAGE genes^[11], while others did not^[12]. In explanation of this, the authors proposed that most normal cells possess strong methylating actions, and that demethylating reagents such as 5DC are insufficient to demethylate MAGE promoters to a degree that would allow for MAGE gene expression. Taken together, these studies suggest that both normal and tumor cells contain the transcription factors that activate subgroup I MAGEs, and that expression of these genes is regulated by promoter demethylation.

Table 1 The MAGE family genes

Subtype	Gene name	Access number	Expression status	Length of amino acids
MAGE-A	MAGE-A1	JC2358 ^[27-29]	T	280
	MAGE-A2	AAH13098 ^[30]	T	314
	MAGE-A3	AAH00340 ^[30]	T	314
	MAGE-A4	BAA06841 ^[31]	T	317
	MAGE-A5	NP_064402 ^[32]	T	320
	MAGE-A6	AAA68875 ^[5]	T	314
	MAGE-A7	NP_064677 ^[33]	P	80
	MAGE-A8	AAH02455 ^[30]	T	318
	MAGE-A9	P43362 ^[5]	T	315
	MAGE-A10	AAA68869 ^[5]	T	369
	MAGE-A11	P43364 ^[5]	T	319
	MAGE-A12	AAF44789 ^[34]	T	314
	MAGE-A13	U71148	P	-
	MAGE-A14	NT_011534.1	P	-
	MAGE-A15	NT_025309.1	P	-
MAGE-B	MAGE-B1	AAC23616 ^[35]	T	347
	MAGE-B2	AAC23617 ^[35]	T	319
	MAGE-B3	AAC23618 ^[35]	T	346
	MAGE-B4	AAC23619 ^[35]	T	346
	MAGE-B5	Q9BZ81 ^[36]	T	111
	MAGE-B6	Q8N7X4 ^[37]	T	407
	MAGE-B7	AC005297.1	P	-
	MAGE-B8	AC005297.1	P	-
	MAGE-B9	AC005297.1	P	-
	MAGE-B10	AC011693.5	T	348
	MAGE-B11	AC011693.5	P	-
	MAGE-B12	AC011693.5	P	-
	MAGE-B13	AC011693.5	P	-
	MAGE-B14	NT_025279.3	P	-
	MAGE-B15	NT_011752.1	P	-
MAGE-C	MAGE-B16	NT_025279.3	T	320
	MAGE-B17	NT_011766.3	T	203
	MAGE-C1	NP_005453 ^[38-40]	T	1 142
	MAGE-C2	NP_057333 ^[41-42]	T	373
	MAGE-C3	AAK00358 ^[36]	T	346
	MAGE-C4	AL023279.1	T	115
	MAGE-C5	NT_025337.2	P	-
	MAGE-C6	NT_025337.2	P	-
MAGE-D	MAGE-C7	NT_025337.2	P	-
	MAGE-D1	AAG09704 ^[25,43]	N	778
	MAGE-D2	CAB10841 ^[44-46]	N	606
	MAGE-D3	Q12816 ^[47,48]	N	1 387
MAGE-E	MAGE-D4	Q96JG8 ^[49-52]	N	741
	MAGE-E1	Q96JG8 ^[49-52]	N	741
MAGE-F	MAGE-E2	-	N	-
	MAGE-E3	NP_032879 ^[53-55]	N	424
	MAGE-F1	NP_071432 ^[56]	N	307
MAGE-G	MAGE-G1	AAG38607 ^[57]	N	100
MAGE-H	MAGE-H1	AAG38608 ^[58]	N	219
MAGE-I	MAGE-I1	NT_011638.3	P	-
	MAGE-I2	NT_011638.3	P	-
MAGE-J	MAGE-J1	NT_011577	P	-
MAGE-K	MAGE-K1	Z81311	P	-
MAGE-L2	MAGE-L2	NP_061939 ^[59,60]	N	529
Necdin	Necdin	XM_007686 ^[61-65]	N	321
Restin	Restin (Apr-1)	NP_054780 ^[66-70]	N	219

T: Only expressed in tumor cells or germ cells. P: Pseudogene; N: Expressed in normal cells. -: Unknown.

The functions of MAGE genes in germ cells

Most MAGE genes are expressed in germ cells under physiological conditions, but their functions remain unclear. Early work has focused on the functions of the mouse MAGE-b4 gene during embryonic development^[13]. The mouse MAGE-b4 gene is expressed in adult and fetal reproductive gland cells and shares high homology with members of the human MAGE-B sub-

type. The MAGE-b4 protein is located in the cytoplasm but not in the nucleus. In male testes, germ cells (gonocytes) continuously proliferate until they arrest at the G0/G1 stage, differentiate into foot cells and form the spermatogenic cords. After birth, the gonocytes differentiate into spermatogonia, which in turn undergo meiosis during adolescence and differentiate into sperm cells. The MAGE-b4 gene is highly expressed in germ cells suspended in G0/G1; in contrast, the gene is barely expressed in meiotic spermatogonia. Thus, MAGE-b4 likely plays an important role in male germ cells, perhaps by maintaining gonocytes in a non-proliferative state.

In female germ cells, MAGE-b4 is expressed prior to meiosis, and also during the pachytene and telophase portions of meiosis. Other cell cycle proteins have shown similar differences in expression in the two sexes. For instance, cyclin A1 deficiency in male germ cells inhibits meiosis but does not affect that in female germ cells^[14]. Similarly, deficiencies of Hsp70-2 or A-myb suppress the development of male germ cells and male fertility but do not affect female development^[15]. Therefore, we speculate that MAGE-b4 may similarly play an important role in the control of the cycle of male germ cells, while playing a less dramatic role in female germ cells.

Another member of the MAGE family Magphinin plays an important role in germ cell development. Mouse Trophinin is a membrane protein that plays an adhesive role in the process of zygotic implantation into the uterine endometrium; an alternative transcript of the Trophinin gene encodes Magphinin^[16]. Although the Trophinin protein is not homologous with the MAGE family members, the mouse Magphinin protein shares high homology with Necdin, Dlxin and NRAGE. Of these, Necdin can bind transcription factor E2F-1, which is responsible for inducing the expression of cyclin and promoting cell cycle progression from G1 to S. Thus, it is possible that the Necdin homolog, Magphinin, acts similarly to bind E2F-1 and inhibit cell proliferation. Magphinin has three alternatively spliced forms: magphinin- α , β and γ . Northern blot analysis reveals that Magphinin protein is expressed in mouse brain, ovary, testis, and epididymis. Western blot analysis indicates that in mouse ovary and epididymis, Magphinin is derived from alternative translation of the Trophinin transcript beginning at the second start codon (AUG). The Magphinin protein sequence contains a nuclear localization signal that allows it to enter the nucleus and inhibit cell proliferation. Immunohistochemical studies suggest that the localization of Magphinin protein varies between male and female germ cells at various stages of the cell cycle. Before meiosis, Magphinin- β is mainly distributed in the cytoplasm of male germ cells. After the first meiosis, when primary spermatocytes differentiate into secondary spermatocytes, Magphinin is localized in both the cytoplasm and the nucleus, and after this nuclear translocation, cell division terminates. Based on this, we speculate that Magphinin regulates the cell cycle during the formation of male spermatocytes. In the female germ cell, the distribution of Magphinin is somewhat different. When the oocyte has only single- or double-layer vesicles, intracellular Magphinin (especially Magphinin- γ) is strictly cytoplasmic. When the oocyte has divided into multi-layer vesicles, the protein is only located in nucleus. In this case, meiosis terminates at stage G2, suggesting that Magphinin also controls the formation of the female ovum.

May these expression patterns and functional roles be generalized to other members of the MAGE family? This remains to be shown. Indeed, at present, little is known about the functions of MAGE family proteins inside germ cells. Further studies will show whether human MAGE proteins control the cell cycle in manners similar to the actions of MAGE-b4 and Magphinin.

Below, we will discuss several specific examples of MAGEs and what is known of their cellular functions.

MAGE-A4

In terms of cancer biology, yeast two-hybrid studies identified binding between the MAGE-A4 protein and a cancer protein: the gann ankyrin repeat protein (also called Gankyrin, PSMD10 or p28). This MAGE-A4-specific binding is mediated by its C-terminus^[17]. Gankyrin, which consists of six gann ankyrin repeats and a 38 amino acid N-terminus, can bind the cancer-suppressing protein Rb, the S6 ATP enzyme subunit of the 26S protein, and cell cycle-dependent kinase 4 (Cdk4). Gankyrin expression is increased in the livers of hepatocellular carcinoma patients; this increase is seen at the earliest stages of tumor genesis^[18,19]. Overexpression of Gankyrin can increase the phosphorylation and degradation of Rb, as well as immortalization of NIH/3T3 cells. In addition, the binding of Gankyrin to Cdk4 counteracts the cancer-inhibiting functions of p16^{INK4A} and p18^{INK4C}^[20]. Therefore, Gankyrin plays an important role in controlling cell cycle during liver cancer tumorigenesis. Studies have shown that exogenous MAGE-A4 can partly inhibit the adhesion-independent growth of Gankyrin-overexpressing cells *in vitro* and suppress the formation of migrated tumors from these cells in nude mice. This inhibition is dependent upon binding between MAGE-A4 and Gankyrin, suggesting that interactions between Gankyrin and MAGE-A4 inhibit Gankyrin-mediated carcinogenesis^[17].

Necdin

Necdin, first identified in 1991, is the best-characterized member of the MAGE protein family. The gene was isolated from P19 neural cells; the encoded protein consists of 325 amino acids and shares about 30% homology with other MAGE proteins^[21]. Studies have shown that overexpression of Necdin may induce cell cycle arrest in NIH3T3 and SAOS2 cell lines, suggesting that Necdin functions in cell cycle arrest and maintenance of cell stability. *In vivo*, Necdin can interact with cell cycle promoting proteins such as the SV40 big-T protein, adenovirus E1A and transcription factor E2F-1, which acts as a cell cycle regulator by trans-activating the relevant genes in an Rb-regulated pathway. The latter binds to E2F-1 protein during G1 stage and inhibits the binding ability of E2F-1, leading to inhibition of gene activation. Similarly, Necdin can bind to E2F-1 and initiate conformational changes to decrease E2F-1 binding and inhibit cell growth^[22]. In addition, Necdin can bind to and inhibit p53, which normally induces cell cycle arrest and cell death^[23]. Thus, Necdin plays important roles in inhibiting cell growth and apoptosis through its interactions with E2F-1 and p53.

The human Necdin gene is localized at 15q¹¹⁻¹³, an area genetically associated with the neurological behavior disorder, Prader-willi Syndrome (PWS). Newborn PWS patients generally suffer respiratory failure and myasthenia, and adolescent PWS patients show psychonosema, sexual dysfunction and obesity. The PWS chromosomal region contains several genes, including Necdin and MAGE-L2. Indeed, knockouts of the mouse Necdin homolog show symptoms similar to human PWS^[24], suggesting that Necdin plays a role in proper development, and that lack of Necdin may be involved in the pathogenesis of PWS.

MAGE-D1

The MAGE-D1, also named as NRAGE or Dlxin, plays important roles in mediating apoptosis and transcription. NRAGE interacts with p75^{NTR}, a TNF receptor responsible for binding the Trk receptor and forming a complex that facilitates binding of neurotrophin, which in turn activates the Trk receptor. p75^{NTR} is also capable of mediating cell death. NRAGE-p75^{NTR} binding, identified by yeast two-hybrid screening, occurs through an 80 amino acid intracellular segment of p75^{NTR} located near the plasma membrane.

Overexpression of NRAGE inhibited the interaction between p75^{NTR} and the Trk receptor and induced cell apoptosis. In contrast, overexpression of the Trk receptor increased binding between Trk and p75^{NTR}, leading to inhibition of NRAGE-p75^{NTR} complex-induced cell death. This indicates that NRAGE-p75^{NTR} and Trk receptor-p75^{NTR} binding are mutually exclusive.

Another NRAGE-binding protein, XIAP, can inhibit apoptosis by binding to activated Caspases. The NRAGE-XIAP complex accelerates the decomposition of XIAP, suggesting that NRAGE accelerates cell death by degrading XIAP and activating Caspases^[4].

Indeed, members of the MAGE-D1 subgroup can bind to several proteins that control apoptosis and cell cycle^[4]. The MAGE-D1 repeat regions can directly interact with Msx2, Dlx7 and Dlx5. Msx generally acts as a transcription inhibitor, whereas Dlx acts as a transcriptional activator. In addition, Msx1 and Msx2 play roles in the control of cell cycle, and Msx2 can promote cell death. The effect of MAGE-D1 on Msx remains unknown, but MAGE-D1 is necessary for Dlx5 to promote transcription.

CONCLUSION

Although subgroup I and II MAGE genes are expressed in different tissue-specific patterns, all family members contain the MAGE homology domain (MHD), suggesting some functional conservation. Biochemical analyses of these two subgroups have provided some insights into the physiological effects of the MAGE genes. Embryonic cells have much less CpG methylation at the MAGE genes than do somatic cells^[25,26]. Similarly, MAGE genes in tumor cells are hypomethylated; indeed, the entire tumor genome is generally hypomethylated^[10]. Thus, it is likely that MAGE gene expression in tumor tissues is the result of tumor genesis, not a cause. It is reasonable to speculate that this family of proteins functions during embryonic development, and that the genes are subsequently deactivated, perhaps by methylation. During neoplastic transformation, these genes are re-activated, expressed, and may become antigenic targets that are recognized and attacked by the immune system^[8]. Therefore, MAGE genes take part in the immune process by targeting some early tumor cells for immune destruction. Consequently, these genes should be studied further in terms of their various functions as they relate to the pathogenic mechanism of tumors, immunotherapy, and other important fields.

REFERENCES

- 1 **van der Bruggen P**, Traversari C, Chomez P, Lurquin C, De Plaen E, Van den Eynde B, Knuth A, Boon T. A gene encoding an antigen recognized by cytolytic T lymphocytes on a human melanoma. *Science* 1991; **254**: 1643-1647
- 2 **Sadanaga N**, Nagashima H, Mashino K, Tahara K, Yamaguchi H, Ohta M, Fujie T, Tanaka F, Inoue H, Takesako K, Akiyoshi T, Mori M. Dendritic cell vaccination with MAGE peptide is a novel therapeutic approach for gastrointestinal carcinomas. *Clin Cancer Res* 2001; **7**: 2277-2284
- 3 **Chen YT**, Scanlan MJ, Sahin U, Tureci O, Gure AO, Tsang S, Williamson B, Stockert E, Pfreundschuh M, Old LJ. A testicular antigen aberrantly expressed in human cancers detected by autologous antibody screening. *Proc Natl Acad Sci USA* 1997; **94**: 1914-1918
- 4 **Barker PA**, Salehi A. The MAGE proteins: emerging roles in cell cycle progression, apoptosis, and neurogenetic disease. *J Neurosci Res* 2002; **67**: 705-712
- 5 **Chomez P**, De Backer O, Bertrand M, De Plaen E, Boon T, Lucas S. An overview of the MAGE gene family with the identification of all human members of the family. *Cancer Res* 2001; **61**: 5544-5551
- 6 **De Plaen E**, Arden K, Traversari C, Gaforio JJ, Szikora JP, De Smet C, Brasseur F, van der Bruggen P, Lethe B. Structure, chromosomal localization and expression of 12 genes of the MAGE family. *Immunogenetics* 1994; **40**: 360-369

- 7 <http://www.ncbi.nlm.nih.gov/Genbank>
- 8 **Zhao ZL**, Lu F, Zhu F, Yang H, Chai YB, Chen SM. Cloning and biological comparison of Restin, a novel member of Mage superfamily. *Sci China* 2002; **45**: 412-420
- 9 **Chiba T**, Yokosuka O, Kanda T, Fukai K, Imazeki F, Saisho H, Nishimura M, Saito Y. Hepatic graft-versus-host disease resembling acute hepatitis: additional treatment with ursodeoxycholic acid. *Liver* 2002; **22**: 514-527
- 10 **De Smet C**, Lurquin C, Lethe B, Martelange V, Boon T. DNA methylation is the primary silencing mechanism for a set of germ line- and tumor-specific genes with a CpG-rich promoter. *Mol Cell Biol* 1999; **19**: 7327-7335
- 11 **De Smet C**, De Backer O, Faraoni I, Lurquin C, Brasseur F, Boon T. The activation of human gene MAGE-1 in tumor cells is correlated with genome-wide demethylation. *Proc Natl Acad Sci U S A* 1996; **93**: 7149-7153
- 12 **Weber J**, Salgaller M, Samid D, Johnson B, Herlyn M, Lassam N, Treisman J, Rosenberg SA. Expression of the MAGE-1 tumor antigen is up-regulated by the demethylating agent 5-aza-2'-deoxycytidine. *Cancer Res* 1994; **54**: 1766-1771
- 13 **Osterlund C**, Tohonen V, Forslund KO, Nordqvist K. Mage-b4, a novel melanoma antigen (MAGE) gene specifically expressed during germ cell differentiation. *Cancer Res* 2000; **60**: 1054-1061
- 14 **Liu D**, Matzuk MM, Sung WK, Guo Q, Wang P, Wolgemuth DJ. Cyclin A1 is required for meiosis in the male mouse. *Nat Genet* 1998; **20**: 377-380
- 15 **Toscani A**, Mettus RV, Coupland R, Simpkins H, Litvin J, Orth J, Hatton KS, Reddy EP. Arrest of spermatogenesis and defective breast development in mice lacking A-myb. *Nature* 1997; **386**: 713-717
- 16 **Saburi S**, Nadano D, Akama TO, Hiram K, Yamanouchi K, Naito K, Tojo H, Tachi C, Fukuda MN. The trophinin gene encodes a novel group of MAGE proteins, magphinins, and regulates cell proliferation during gametogenesis in the mouse. *J Biol Chem* 2001; **276**: 49378-49389
- 17 **Meier S**, Haussinger D, Jensen P, Rogowski M, Grzesiek S. High-accuracy residual 1HN-13C and 1HN-1HN dipolar couplings in perdeuterated proteins. *J Am Chem Soc* 2003; **125**: 44-45
- 18 **Higashitsuji H**, Itoh K, Nagao T, Dawson S, Nonoguchi K, Kido T, Mayer RJ, Arai S, Fujita J. Reduced stability of retinoblastoma protein by gankyrin, an oncogenic ankyrin-repeat protein overexpressed in hepatomas. *Nat Med* 2000; **6**: 96-99
- 19 **Park TJ**, Kim HS, Byun KH, Jang JJ, Lee YS, Lim IK. Sequential changes in hepatocarcinogenesis induced by diethylnitrosamine plus thioacetamide in Fischer 344 rats: induction of gankyrin expression in liver fibrosis, pRB degradation in cirrhosis, and methylation of p16(INK4A) exon 1 in hepatocellular carcinoma. *Mol Carcinog* 2001; **30**: 138-150
- 20 **Li J**, Tsai MD. Novel insights into the INK4-CDK4/6-Rb pathway: counter action of gankyrin against INK4 proteins regulates the CDK4-mediated phosphorylation of Rb. *Biochemistry* 2002; **41**: 3977-3983
- 21 **Maruyama K**, Usami M, Aizawa T, Yoshikawa K. A novel brain-specific mRNA encoding nuclear protein (necdin) expressed in neurally differentiated embryonal carcinoma cells. *Biochem Biophys Res Commun* 1991; **178**: 291-296
- 22 **Taniura H**, Taniguchi N, Hara M, Yoshikawa K. Necdin, a postmitotic neuron-specific growth suppressor, interacts with viral transforming proteins and cellular transcription factor E2F1. *J Biol Chem* 1998; **273**: 720-728
- 23 **Taniura H**, Matsumoto K, Yoshikawa K. Physical and functional interactions of neuronal growth suppressor necdin with p53. *J Biol Chem* 1999; **274**: 16242-16248
- 24 **Nakada Y**, Taniura H, Uetsuki T, Inazawa J, Yoshikawa K. The human chromosomal gene for necdin, a neuronal growth suppressor, in the Prader-Willi syndrome deletion region. *Gene* 1998; **213**: 65-72
- 25 **Salehi AH**, Roux PP, Kubu CJ, Zeindler C, Bhakar A, Tannis LL, Verdi JM, Barker PA. NRAGE, a novel MAGE protein, interacts with the p75 neurotrophin receptor and facilitates nerve growth factor-dependent apoptosis. *Neuron* 2000; **27**: 279-288
- 26 **Reik W**, Dean W, Walter J. Epigenetic reprogramming in mammalian development. *Science* 2001; **293**: 1089-1093
- 27 **Ding M**, Beck RJ, Keller CJ, Fenton RG. Cloning and analysis of MAGE-1-related genes. *Biochem Biophys Res Commun* 1994; **202**: 549-555
- 28 **Suyama T**, Ohashi H, Nagai H, Hatano S, Asano H, Murate T, Saito H, Kinoshita T. The MAGE-A1 gene expression is not determined solely by methylation status of the promoter region in hematological malignancies. *Leuk Res* 2002; **26**: 1113-1118
- 29 **Chen YT**, Stockert E, Chen Y, Garin-Chesa P, Rettig WJ, van der Bruggen P, Boon T, Old LJ. Identification of the MAGE-1 gene product by monoclonal and polyclonal antibodies. *Proc Natl Acad Sci U S A* 1994; **91**: 1004-1008
- 30 **Strausberg RL**, Feingold EA, Grouse LH, Derge JG, Klausner RD, Collins FS, Wagner L, Shenmen CM, Schuler GD, Altschul SF, Zeeberg B, Buetow KH, Schaefer CF, Bhat NK, Hopkins RF, Jordan H, Moore T, Max SI, Wang J, Hsieh F, Diatchenko L, Marusina K, Farmer AA, Rubin GM, Hong L, Stapleton M, Soares MB, Bonaldo MF, Casavant TL, Scheetz TE, Brownstein MJ, Usdin TB, Toshiyuki S, Carninci P, Prange C, Raha SS, Loquellano NA, Peters GJ, Abramson RD, Mullahy SJ, Bosak SA, McEwan PJ, McKernan KJ, Malek JA, Gunaratne PH, Richards S, Worley KC, Hale S, Garcia AM, Gay LJ, Hulyk SW, Villalón DK, Muzny DM, Sodergren EJ, Lu X, Gibbs RA, Fahey J, Helton E, Ketteman M, Madan A, Rodrigues S, Sanchez A, Whiting M, Madan A, Young AC, Shevchenko Y, Bouffard GG, Blakesley RW, Touchman JW, Green ED, Dickson MC, Rodriguez AC, Grimwood J, Schmutz J, Myers RM, Butterfield YS, Krzywicki MI, Skalska J, Smailus DE, Schnerch A, Schein JE, Jones SJ, Marra MA. Mammalian Gene Collection Program Team. Generation and initial analysis of more than 15,000 full-length human and mouse cDNA sequences. *Proc Natl Acad Sci U S A* 2002; **99**: 16899-16903
- 31 **Imai Y**, Shichijo S, Yamada A, Katayama T, Yano H, Itoh K. Sequence analysis of the MAGE gene family encoding human tumor-rejection antigens. *Gene* 1995; **160**: 287-290
- 32 **Wang PJ**, McCarrey JR, Yang F, Page DC. An abundance of X-linked genes expressed in spermatogonia. *Nat Genet* 2001; **27**: 422-426
- 33 **De Plaen E**, De Backer O, Arnaud D, Bonjean B, Chomez P, Martelange V, Avner P, Baldacci P, Babinet C, Hwang SY, Knowles B, Boon T. A new family of mouse genes homologous to the human MAGE genes. *Genomics* 1999; **55**: 176-184
- 34 **Mallon AM**, Platzer M, Bate R, Gloeckner G, Botcherby MR, Nordsiek G, Strivens MA, Kioschis P, Dangel A, Cunningham D, Straw RN, Weston P, Gilbert M, Fernando S, Goodall K, Hunter G, Greystrom JS, Clarke D, Kimberley C, Goerdes M, Blechschmidt K, Rump A, Hinzmann B, Mundy CR, Miller W, Poustka A, Herman GE, Rhodes M, Denny P, Rosenthal A, Brown SD. Comparative genome sequence analysis of the Bpa/Str region in mouse and Man. *Genome Res* 2000; **10**: 758-775
- 35 **Lurquin C**, De Smet C, Brasseur F, Muscatelli F, Martelange V, De Plaen E, Brasseur R, Monaco AP, Boon T. Two members of the human MAGEB gene family located in Xp21.3 are expressed in tumors of various histological origins. *Genomics* 1997; **46**: 397-408
- 36 **Lucas S**, De Plaen E, Boon T. MAGE-B5, MAGE-B6, MAGE-C2, and MAGE-C3: four new members of the MAGE family with tumor-specific expression. *Int J Cancer* 2000; **87**: 55-60
- 37 **Ota T**, Suzuki Y, Nishikawa T, Otsuki T, Sugiyama T, Irie R, Wakamatsu A, Hayashi K, Sato H, Nagai K, Kimura K, Makita H, Sekine M, Obayashi M, Nishi T, Shibahara T, Tanaka T, Ishii S, Yamamoto J, Saito K, Kawai Y, Isono Y, Nakamura Y, Nagahari K, Murakami K, Yasuda T, Iwayanagi T, Wagatsuma M, Shiratori A, Sudo H, Hosoiri T, Kaku Y, Kodaira H, Kondo H, Sugawara M, Takahashi M, Kanda K, Yokoi T, Furuya T, Kikkawa E, Omura Y, Abe K, Kamihara K, Katsuta N, Sato K, Tanikawa M, Yamazaki M, Ninomiya K, Ishibashi T, Yamashita H, Murakawa K, Fujimori K, Tanai H, Kimata M, Watanabe M, Hiraoka S, Chiba Y, Ishida S, Ono Y, Takiguchi S, Watanabe S, Yosida M, Hotuta T, Kusano J, Kanehori K, Takahashi-Fujii A, Hara H, Tanase TO, Nomura Y, Togiya S, Komai F, Hara R, Takeuchi K, Arita M, Imose N, Musashino K, Yuuki H, Oshima A, Sasaki N, Aotsuka S, Yoshikawa Y, Matsunawa H, Ichihara T, Shiohata N, Sano S, Moriya S, Momiyama H, Satoh N, Takami S, Terashima Y, Suzuki O, Nakagawa S, Senoh A, Mizoguchi H, Goto Y, Shimizu F, Wakebe H, Hishigaki H, Watanabe T, Sugiyama A, Takemoto M, Kawakami B, Yamazaki M, Watanabe K, Kumagai A, Itakura S, Fukuzumi Y, Fujimori Y, Komiyama M, Tashiro H, Tanigami A, Fujiwara T, Ono T, Yamada K, Fujii Y, Ozaki K, Hirao M, Ohmori Y, Kawabata A, Hikiji T, Kobatake N, Inagaki H, Ikema Y, Okamoto S, Okitani R, Kawakami T, Noguchi S, Itoh T, Shigeta

- K, Senba T, Matsumura K, Nakajima Y, Mizuno T, Morinaga M, Sasaki M, Togashi T, Oyama M, Hata H, Watanabe M, Komatsu T, Mizushima-Sugano J, Satoh T, Shirai Y, Takahashi Y, Nakagawa K, Okumura K, Nagase T, Nomura N, Kikuchi H, Masuo Y, Yamashita R, Nakai K, Yada T, Nakamura Y, Ohara O, Isogai T, Sugano S. Complete sequencing and characterization of 21,243 full-length human cDNAs. *Nat Genet* 2004; **36**: 40-45
- 38 **Jungbluth AA**, Chen YT, Busam KJ, Coplan K, Kolb D, Iversen K, Williamson B, Van Landeghem FK, Stockert E, Old LJ. CT7 (MAGE-C1) antigen expression in normal and neoplastic tissues. *Int J Cancer* 2002; **99**: 839-845
- 39 **Lim SH**, Bumm K, Chiriva-Intemati M, Xue Y, Wang Z. MAGE-C1 (CT7) gene expression in multiple myeloma: relationship to sperm protein 17. *Eur J Haematol* 2001; **67**: 332-334
- 40 **Chen YT**, Gure AO, Tsang S, Stockert E, Jager E, Knuth A, Old LJ. Identification of multiple cancer/testis antigens by allogeneic antibody screening of a melanoma cell line library. *Proc Natl Acad Sci U S A* 1998; **95**: 6919-6923
- 41 **Lucas S**, De Smet C, Arden KC, Viars CS, Lethe B, Lurquin C, Boon T. Identification of a new MAGE gene with tumor-specific expression by representational difference analysis. *Cancer Res* 1998; **58**: 743-752
- 42 **Gure AO**, Stockert E, Arden KC, Boyer AD, Viars CS, Scanlan MJ, Old LJ, Chen YT. CT10: a new cancer-testis (CT) antigen homologous to CT7 and the MAGE family, identified by representational-difference analysis. *Int J Cancer* 2000; **85**: 726-732
- 43 **Hennuy B**, Reiter E, Cornet A, Bruyninx M, Daukandt M, Houssa P, N' Guyen VH, Closset J, Hennen G. A novel messenger ribonucleic acid homologous to human MAGE-D is strongly expressed in rat Sertoli cells and weakly in Leydig cells and is regulated by follitropin, lutropin, and prolactin. *Endocrinology* 2000; **141**: 3821-3831
- 44 **Kurt RA**, Urba WJ, Schoof DD. Isolation of genes overexpressed in freshly isolated breast cancer specimens. *Breast Cancer Res Treat* 2000; **59**: 41-48
- 45 **Langnaese K**, Kloos DU, Wehnert M, Seidel B, Wieacker P. Expression pattern and further characterization of human MAGED2 and identification of rodent orthologues. *Cytogenet Cell Genet* 2001; **94**: 233-240
- 46 **Lucas S**, Brasseur F, Boon T. A new MAGE gene with ubiquitous expression does not code for known MAGE antigens recognized by T cells. *Cancer Res* 1999; **59**: 4100-4103
- 47 **Kikuno R**, Nagase T, Ishikawa K, Hirosawa M, Miyajima N, Tanaka A, Kotani H, Nomura N, Ohara O. Prediction of the coding sequences of unidentified human genes. XIV. The complete sequences of 100 new cDNA clones from brain which code for large proteins *in vitro*. *DNA Res* 1999; **6**: 197-205
- 48 **Fukuda MN**, Sato T, Nakayama J, Klier G, Mikami M, Aoki D, Nozawa S. Trophinin and tastin, a novel cell adhesion molecule complex with potential involvement in embryo implantation. *Genes Dev* 1995; **9**: 1199-1210
- 49 **Sasaki M**, Nakahira K, Kawano Y, Katakura H, Yoshimine T, Shimizu K, Kim SU, Ikenaka K. MAGE-E1, a new member of the melanoma-associated antigen gene family and its expression in human glioma. *Cancer Res* 2001; **61**: 4809-4814
- 50 **Kawano Y**, Sasaki M, Nakahira K, Yoshimine T, Shimizu K, Wada H, Ikenaka K. Structural characterization and chromosomal localization of the MAGE-E1 gene. *Gene* 2001; **277**: 129-137
- 51 **Wiemann S**, Weil B, Wellenreuther R, Gassenhuber J, Glassl S, Ansorge W, Bocher M, Blocker H, Bauersachs S, Blum H, Lauber J, Dusterhoft A, Beyer A, Kohrer K, Strack N, Mewes HW, Ottenwalder B, Obermaier B, Tampe J, Heubner D, Wambutt R, Korn B, Klein M, Poustka A. Toward a catalog of human genes and proteins: sequencing and analysis of 500 novel complete protein coding human cDNAs. *Genome Res* 2001; **11**: 422-435
- 52 **Nagase T**, Nakayama M, Nakajima D, Kikuno R, Ohara O. Prediction of the coding sequences of unidentified human genes. XX. The complete sequences of 100 new cDNA clones from brain which code for large proteins *in vitro*. *DNA Res* 2001; **8**: 85-95
- 53 **Sasaki A**, Masuda Y, Iwai K, Ikeda K, Watanabe K. A RING finger protein Praja1 regulates Dlx5-dependent transcription through its ubiquitin ligase activity for the Dlx/Msx-interacting MAGE/Necdin family protein, Dlxin-1. *J Biol Chem* 2002; **277**: 22541-22546
- 54 **Stork O**, Stork S, Pape HC, Obata K. Identification of genes expressed in the amygdala during the formation of fear memory. *Learn Mem* 2001; **8**: 209-219
- 55 **Mishra L**, Tully RE, Monga SP, Yu P, Cai T, Makalowski W, Mezey E, Pavan WJ, Mishra B. Praja1, a novel gene encoding a RING-H2 motif in mouse development. *Oncogene* 1997; **15**: 2361-2368
- 56 **Stone B**, Schummer M, Paley PJ, Crawford M, Ford M, Urban N, Nelson BH. MAGE-F1, a novel ubiquitously expressed member of the MAGE superfamily. *Gene* 2001; **267**: 173-182
- 57 **Kuwako K**, Taniura H, Yoshikawa K. Necdin-related MAGE proteins differentially interact with the E2F1 transcription factor and the p75 neurotrophin receptor. *J Biol Chem* 2004; **279**: 1703-1712
- 58 **Tcherpakov M**, Bronfman FC, Conticello SG, Vaskovsky A, Levy Z, Niinobe M, Yoshikawa K, Arenas E, Fainzilber M. The p75 neurotrophin receptor interacts with multiple MAGE proteins. *J Biol Chem* 2002; **277**: 49101-49104
- 59 **Lee S**, Kozlov S, Hernandez L, Chamberlain SJ, Brannan CI, Stewart CL, Wevrick R. Expression and imprinting of MAGEL2 suggest a role in Prader-willi syndrome and the homologous murine imprinting phenotype. *Hum Mol Genet* 2000; **9**: 1813-1819
- 60 **Boccaccio I**, Glatt-Deeley H, Watrin F, Roeckel N, Lalande M, Muscatelli F. The human MAGEL2 gene and its mouse homologue are paternally expressed and mapped to the Prader-Willi region. *Hum Mol Genet* 1999; **8**: 2497-2505
- 61 **Andrieu D**, Watrin F, Niinobe M, Yoshikawa K, Muscatelli F, Fernandez PA. Expression of the Prader-Willi gene Necdin during mouse nervous system development correlates with neuronal differentiation and p75NTR expression. *Gene Expr Patterns* 2003; **3**: 761-765
- 62 **Hu B**, Wang S, Zhang Y, Feghali CA, Dingman JR, Wright TM. A nuclear target for interleukin-1alpha: interaction with the growth suppressor necdin modulates proliferation and collagen expression. *Proc Natl Acad Sci U S A* 2003; **100**: 10008-10013
- 63 **Matsuda T**, Suzuki H, Oishi I, Kani S, Kuroda Y, Komori T, Sasaki A, Watanabe K, Minami Y. The receptor tyrosine kinase Ror2 associates with the melanoma-associated antigen (MAGE) family protein Dlxin-1 and regulates its intracellular distribution. *J Biol Chem* 2003; **278**: 29057-29064
- 64 **Ren J**, Lee S, Pagliardini S, Gerard M, Stewart CL, Greer JJ, Wevrick R. Absence of Ndn, encoding the Prader-Willi syndrome-deleted gene necdin, results in congenital deficiency of central respiratory drive in neonatal mice. *J Neurosci* 2003; **23**: 1569-1573
- 65 **Takazaki R**, Nishimura I, Yoshikawa K. Necdin is required for terminal differentiation and survival of primary dorsal root ganglion neurons. *Exp Cell Res* 2002; **277**: 220-232
- 66 **Zhu F**, Yan W, Zhao ZL, Chai YB, Lu F, Wang Q, Peng WD, Yang AG, Wang CJ. Improved PCR-based subtractive hybridization strategy for cloning differentially expressed genes. *Biotechniques* 2000; **29**: 310-313
- 67 **Sahin U**, Neumann F, Tureci O, Schmits R, Perez F, Pfreundschuh M. Hodgkin and Reed-Sternberg cell-associated autoantigen CLIP-170/restin is a marker for dendritic cells and is involved in the trafficking of macropinosomes to the cytoskeleton, supporting a function-based concept of Hodgkin and Reed-Sternberg cells. *Blood* 2002; **100**: 4139-4145
- 68 **Ramchandran R**, Dhanabal M, Volk R, Waterman MJ, Segal M, Lu H, Knebelmann B, Sukhatme VP. Antiangiogenic activity of restin, NC10 domain of human collagen XV: comparison to endostatin. *Biochem Biophys Res Commun* 1999; **255**: 735-739
- 69 **Gripovic L**, Keller TC. Identification and expression of two novel CLIP-170/Restin isoforms expressed predominantly in muscle. *Biochim Biophys Acta* 1998; **1405**: 35-46
- 70 **Delabie J**, Bilbe G, Bruggen J, Van Leuven F, De Wolf-Peeters C. Restin in Hodgkin's disease and anaplastic large cell lymphoma. *Leuk Lymphoma* 1993; **12**: 21-26

Theory of traditional Chinese medicine and therapeutic method of diseases

Ai-Ping Lu, Hong-Wei Jia, Cheng Xiao, Qing-Ping Lu

Ai-Ping Lu, Hong-Wei Jia, Cheng Xiao, Institute of Basic Theory, China Academy of Traditional Chinese Medicine, Beijing 100700, China

Qing-Ping Lu, National Pharmaceutical Engineering Research Center, Nanchang 330077, Jiangxi Province, China

Supported by the Key Grant Program in National Administration of Traditional Chinese Medicine, No.2000-J-Z-02 and the Key Program in National Natural Science Foundation of China, No. 90209002

Correspondence to: Dr. Ai-Ping Lu, Institute of Basic Theory, China Academy of Traditional Chinese Medicine, Beijing 100700, China. catcm@public.bta.net.cn

Telephone: +86-10-64067611 **Fax:** +86-10-64013896

Received: 2003-11-18 **Accepted:** 2004-02-01

Abstract

Traditional Chinese medicine, including herbal medicine and acupuncture, as one of the most important parts in complementary and alternative medicine (CAM), plays the key role in the formation of integrative medicine. Why do not the modern drugs targeting the specificity of diseases produce theoretical effects in clinical observation? Why does not the traditional Chinese medicine targeting the Zheng (syndrome) produce theoretical effects in clinic? There should have some reasons to combine Western medicine with Chinese herbal medicine so as to form the integrative medicine. During the integration, how to clarify the impact of CAM theory on Western medicine has become an emergent topic. This paper focuses on the exploration of the impact of theory of traditional Chinese medicine on the therapy of diseases in Western medicine.

Lu AP, Jia HW, Xiao C, Lu QP. Theory of traditional Chinese medicine and therapeutic method of diseases. *World J Gastroenterol* 2004; 10(13): 1854-1856

<http://www.wjgnet.com/1007-9327/10/1854.asp>

INTRODUCTION

More than one third of patients in the United States use complementary and alternative medicine (CAM)^[1], and more and more scientists are interested in integrative medicine research in USA. Recent research showed that integrative medicine (also complementary and alternative medicine) could contribute to primary health care^[2,3]. Traditional Chinese medicine (TAM), including herbal medicine and acupuncture, as one of the most important parts in CAM, should play the key role in the formation of integrative medicine. During the integration, how to clarify the impact of CAM theory on Western medicine has become the emergent topic.

TCM was formed two thousand years ago, and developed in the following centuries. TCM recognizes human body by system discrimination and cybernetic way. TCM can be characterized as holistic with emphasis on the integrity of the human body and the close relationship between human and its social and natural environment. TCM focuses on health maintenance and in the treatment of disease emphasizes on

enhancing the body's resistance to diseases. For improving health, TCM applies multiple natural therapeutic methods.

Zheng (syndrome) is the basic unit and key term in TCM theory. Zheng is an outcome after analyzing all symptoms and signs. All therapeutic methods in TCM come from the differentiation of Zheng. The methods have been used for thousands of years, which proves that TCM therapeutic approach is effective. From this point of view, Zheng should play an important role in determining the effect. Combined with modern medicine, Zheng should have an impact on disease pathogenesis that directly influences the therapeutic effect.

HISTORICAL BACKGROUND

At the time when TCM formed, there was nothing modernized in medical and biological fields, but there was something developed in Chinese philosophy, astronomy and literature. Also at that time, people got a great amount of experiences on how to deal with the disorders by natural methods, such as puncture, Qigong (mind controlling), taking plants. Some talents in China began to summarize those phenomena and sublimated to theory based on their philosophical and social knowledge at that time. The theory is the original TCM. Thus TCM handles human physiology and pathology following old Chinese philosophical thinking. In the following centuries, accumulation of experiences and addition of relative knowledge (such as clinical observation data and less anatomical experience) made TCM developed. The terminology TCM is partially originated from Chinese philosophy. Other terms in TCM, even same as those in modern medicine, have completely different meanings. It is believed that to understand the physiology of TCM, to some extent, should have some knowledge about Chinese philosophy.

PHYSIOLOGY AND PATHOLOGY IN TCM

During the formation and development of TCM, there are two ideological ideas that fully penetrate into the whole process. The first is the homeostasis idea that focuses on the integrity of human body, and emphasizes the close relationship between human body and its social and natural environment (integrity between human and cosmos). The second is the dynamic balance idea that takes emphasis on the movement in the integrity. Physiologically TCM recognizes human body by system discrimination and cybernetic way. In system discrimination approach, the intrinsic activities of human body can be clarified by analyzing the audio-visual information. The human body, a complicated system, could be identified as different closely related systems that form a network (integrity). The external information should reflect something intrinsic because of the integrity between human body and its social and natural environment. For example, the heart as a center, together with blood, vessel, mind, tongue, small intestine, consists of the heart system in TCM. Any information from any parts in the system can demonstrate the system's activity even the structure of the part is unclear. In cybernetic approach, TCM takes human body as a self-controlled system network. The network is connected by the meridian that exists in whole body. Blood

and vital energy flow also contributes to the connection. The Five elements theory in TCM, named as wood, fire, earth, metal and water, divides human body into five systems. Each system has its own specific features that can be inferred by analyzing those natural materials. The movement and interchange among the five elements are used to explain human body's physiology.

Since TCM has its unique physiology in understanding human body, it has its special understanding on human body's disorders. Pathologically, TCM focuses on the pathogenicity of social and natural factors. The factors have a close relationship with humans to consist of the integrity. Mostly they are non-direct and non-specific factors if we say bacteria or viruses are direct and specific ones. TCM is not completely to seek the specific pathogen, and pathological changes in a specific organ, while it is to seek the disturbances among the self-controlled systems by analyzing all symptoms and signs. In the heart system, any disturbance in any part of the system is useful to clarify the pathology. At the same time, comparison of the disturbance happened in different period is also important in pathological analyses. TCM takes emphasis on the dynamic changes in any parts and any connections in the self-controlled system.

THERAPEUTIC MECHANISM IN TCM

Physiology in TCM is featured with self-controlled system discrimination and its pathology is featured with dynamic changes in the system (whether direct or indirect, specific or non-specific). The therapeutic mechanism in TCM focuses on enhancing human body's resistance to diseases and prevention by improving the inter-connections among self-controlled systems. To reach the approach, TCM uses different therapeutic methods, such as mind-spiritual methods (such as Qigong, Taiji boxing), natural methods (acupuncture, moxibustion, herbal medicine). These therapeutic methods are characterized by fewer side effects since they are natural. TCM evaluates the therapeutic results by comparing the symptoms before and after the treatment. The treatment is based on the differentiation of symptoms to clarify what is wrong in the self-controlled system. TCM seeks the therapeutic mechanism from the integrity. The integrity includes the human itself as integrity, and the integrity between human and its social and natural environment. The therapeutic mechanism can be achieved by activating systems, improving system connection and enhancing human resistance. The mechanism in TCM is not like modern medicine that seeks the mechanism from cellular or molecular level (such as killing bacteria and virus, antagonistic method). If someone lives well (no symptoms), she is healthy in TCM, whether she has some signs in cellular and molecular level such as high blood pressure.

KEY TERM IN TCM THERAPEUTIC APPROACH: DIFFERENTIATION OF ZHENG

Zheng (syndrome), a basic unit in TCM, decides the therapeutic methods. Zheng is the outcome after a careful analysis of all symptoms and signs (tongue appearance and pulse feeling included). Zheng outcome might change since the symptoms and signs might change. There are many Zhengs in TCM, either simple Zheng or combined ones.

Zheng, as the key term and basic unit in TCM therapeutic theory, develops following the progress in disease theory progress. Tens of years ago, Zheng did not include any signs from modern diagnostic instruments, and nowadays, Zheng is combined with or referred to disease diagnosis during the therapeutic process to some content.

The process of how to get the outcome is called differentiation

of Zheng, which is based on the physiology and pathology of TCM.

IMPACT OF ZHENG ON DISEASE TREATMENT

Disease's key units usually contain etiology, pathology and disease location. Modern medicine is trying to get the specificity of the cause, pathology and location, and as a result, the therapeutic approach is targeting on the specificity. New drugs in modern medicine are developed from strictly designed scientific pharmacological tests that are targeting on the specificity. Pharmacological tests show better effect than the effect shown in clinic.

In differentiation of Zheng, clinical effect should be better if the theory of differentiation of Zheng and physiology of TCM are followed. Unfortunately the effect in practice, even completely following the differentiation of Zheng, is not as good as the theoretical one. There should have some reasons to explain the difference between theoretical and clinical effects in TCM practice.

As summarized, there are two questions about the therapeutic problem in medical science. One is why is there difference between the pharmacological and clinical effects in modern medicine? The other is why is there difference between the theoretical and clinical effects in traditional Chinese medicine?

The questions refer to that there are some shortages of therapeutic approach both in modern medicine and in traditional Chinese medicine.

Any disease (morbidity) could contain two parts of appearance. One is the so-called specificity to the realities of morbidity, such as the pathological change. The other is the non-specificity that refers to the reactions caused by interactions between personal physique and environments, such as heterogeneous manifestations. Modern medicine is aimed to explore the specificity of morbidity, while traditional Chinese medicine is mainly aimed to explore the reality of the morbidity by checking the external appearance (that is the differentiation of Zheng). It is believed that the non-specificity sometimes could influence or change the process of morbidity, and only targeting the specificity is not enough to stop the progress of morbidity^[4].

Disease mainly refers to the specificity of cause and pathology with less emphasis on the non-specificity. Non-specificity includes all symptoms and signs not directly induced by the specific cause and pathology. Usually the specificity decides the process of diseases. Drugs in modern medicine are targeting the specific cause and pathology, and it usually gives good effect even though the effect is not as good as the pharmacological effect. Since the specific cause and pathology cannot be found in all diseases, the effect of modern drugs depends on whether the cause and pathology are clear or not. In reality, modern drugs are good at curing those diseases with clarified cause and pathology, and not good at curing those diseases due to multiple factors in the pathogenesis, which have become more common in medical science.

However, whenever the non-specificity influences on the specificity, drugs targeting the specificity have no good effect. That is the main reason why modern drugs sometimes are not effective in some cases in the treatment of a disease with a clarified cause and pathology.

Zheng mainly refers to the non-specificity and part of specificity that is only obtained from symptoms and signs by asking, watching and feeling since there are no modern diagnostic instruments. Chinese herbal medicine, based on the Zheng which is taken as an outcome of differentiation of symptoms and signs, targets to the non-specificity and part of the specificity. The effect of herbal medicine is not so good in curing a disease with specific signs, which can be only obtained

by modern diagnostic instruments since Zheng does not refer to those signs. However, the effect of herbal medicine is better in treating some cases when the non-specificity decides the process of a disease. Thus, the reason why there is a difference between the theoretical effect based on Zheng differentiation and the clinical effect is that Zheng differentiation can not exactly differentiate the specificity of a disease.

COMBINING ZHENG WITH DISEASE: NEW STRATEGY IN THERAPEUTIC APPROACH

Following TCM Zheng theory, different diseases may be treated by a same therapeutic approach if they show same Zhengs. One herbal preparation can be used to treat different diseases, a common phenomenon in TCM. Similarly, the same disease may be treated by different therapeutic approaches if the disease shows different Zhengs. It is common in TCM that one kind of disease is treated with different therapies. As mentioned above, Zheng is the outcome of differentiation of symptoms and primary signs obtained by getting from watching (tongue watching) and feeling (pulse feeling), and definitely Zheng is not so accurate. The following example can be used to explain the shortage of Zheng information. Gastritis and stomach cancer could show similar symptoms and primary signs, suggesting that they could be differentiated as the same Zheng in TCM, and could be treated by the same TCM approach. The effect, there is no doubt, should be different since stomach cancer is difficult to be cured by herbal medicine. Thus, the differentiation of Zheng would not give any good effect when the specificity is not clarified resulting from the decisive factor in the evaluation of effects.

It was reported that the effects of two herbal preparations that targeted on coronary heart disease with different Zhengs were at least partially dependent on the Zhengs. The results showed that for coronary heart disease cases with Qi deficiency, Zheng could be alleviated by herbal medicine to reinforce Qi deficiency at effective rate of 89%, while the cases could be alleviated by herbal medicine targeting coronary heart disease and nourishing Yin at effective rate of 60%. For the coronary heart disease cases with Yin deficiency, Zheng could be alleviated by herbal medicine to nourish Yin at the effective rate of 87%, while the cases could be alleviated by herbal medicine to reinforce Qi at effective rate of 65%. Thus, the differentiation of Zheng plays an important role in the therapeutic process and affects the therapeutic result of a specific disease.

Following the disease theory there should have a specific therapy targeting the specific cause, pathology and location. If the specificity is clarified, the disease would be cured. Actually, there might not be so good effect in alleviating some diseases or symptoms even the specificity is clarified. The reason is that the non-specificity influences the specificity. Thus, targeting the specificity of a disease may not result in a good effect or give no effect at all when the non-specificity is decisive in the effect evaluation. The example about drugs in lowering blood pressure would be helpful to explain the reason. In patients with hypertension, there are some good drugs in decreasing blood pressure, and the real thing is that there always have some cases showing any effect after taking drugs. The partial reason is that, in some cases of hypertension, the non-specific appearance could play a key role in influencing the effect of

drugs. At this point, new anti-hypertension drugs for the cases in which the non-specificity is a decisive factor need to be developed.

Combining the differentiation of Zheng with diagnosis of disease, which is combining herbal medicine mainly targeting non-specificity with modern drugs targeting the specificity, would achieve the best therapeutic effect.

Many clinical studies have shown that combining modern drugs with herbal medicine would dominantly increase the effect. For example, the effect rate in treating coronary heart disease with modern drugs (routine therapy) was 45.5%, while combining with herbal medicine it was up to 87.3%^[5]. The importance is to explore how to combine the two therapies.

More double-blinded clinical trials need to be conducted, both for modern drugs and herbal medicine. All specific and non-specific information needs to be collected for further analysis.

Any new drug, even targeting the exact specific pathology, does not act on all cases of diseases since the effect of non-specificity may affect the process of pathogenesis. Any herbal medicine originating from the exact differentiation of Zheng does not act on all cases with Zheng since lack of enough specificity may lose the decisive factor in the treatment.

After the information about new drug classification is obtained, the best effect could be achieved by either combination of drugs targeting the specificity with herbal medicine targeting the non-specificity, or by complex new drug development focusing both on specificity and non-specificity.

TCM focuses on the integrity of human body and the close relationship with its social and natural environments. It recognizes human physiology by analyzing external information by system discrimination and cybernetic approach, and regards that any disorders are caused by the disturbance in any part of the self-controlled system in the integrity. In therapeutics, TCM targets the non-specificity and part of specificity by natural ways.

Why modern drugs cannot achieve the effect as the pharmacological study and the same effect in a same disease is that Zheng in TCM contributes to the progress of a disease. It is important to clarify that in what situation drugs targeting the disease specificity would be effective and how to make the drug become more effective.

REFERENCES

- 1 **Eisenberg DM**, Davis RB, Ettner SL, Appel S, Wilkey S, Van Rompay M, Kessler RC. Trends in alternative medicine use in the United States, 1990-1997: results of a follow-up national survey. *JAMA* 1998; **280**: 1569-1575
- 2 **Bell IR**, Caspi O, Schwartz GE, Grant KL, Gaudet TW, Rychener D, Maizes V, Weil A. Integrative medicine and systemic outcomes research: issues in the emergence of a new model for primary health care. *Arch Intern Med* 2002; **162**: 133-140
- 3 **Corbin Winslow L**, Shapiro H. Physicians want education about complementary and alternative medicine to enhance communication with their patients. *Arch Intern Med* 2002; **162**: 1176-1181
- 4 **Tsokos GC**, Nepom GT. Gene therapy in the treatment of autoimmune diseases. *J Clin Invest* 2000; **106**: 181-183
- 5 **Wang X**, Chen K, Wang W. Clinical study of purified Xuefu capsule in the treatment of angina pectoris. *Zhongguo Zhongxiyi Jiehe Zazhi* 1998; **18**: 399-401

Edited by Wang XL Proofread by Chen WW and Xu FM

Cytomegalovirus and chronic allograft rejection in liver transplantation

Liang-Hui Gao, Shu-Sen Zheng

Liang-Hui Gao, Shu-Sen Zheng, Department of Hapatobiliary and Pancreatic Surgery, First Affiliated Hospital, Zhejiang University, Hangzhou 310003, Zhejiang Province, China

Supported by the National Natural Science Foundation of China, No. 30170899

Correspondence to: Liang-Hui Gao, PO Box 4193, Hubin Campus, 353 Yan' an Road, Hangzhou 310031, Zhejiang Province, China. gaoh@zju.edu.cn

Telephone: +86-571-87230531 **Fax:** +86-571-87072577

Received: 2004-02-20 **Accepted:** 2004-03-12

Abstract

Cytomegalovirus (CMV) remains one of the most frequent viral infections and the most common cause of death after liver transplantation (LT). Chronic allograft liver rejection remains the major obstacle to long-term allograft survival and CMV infection is one of the suggested risk factors for chronic allograft rejection. The precise relationship between cytomegalovirus and chronic rejection remains uncertain. This review addresses the morbidity of cytomegalovirus infection and the risk factors associated with it, the relationship between cytomegalovirus and chronic allograft liver rejection and the potential mechanisms of it.

Gao LH, Zheng SS. Cytomegalovirus and chronic allograft rejection in liver transplantation. *World J Gastroenterol* 2004; 10(13): 1857-1861

<http://www.wjgnet.com/1007-9327/10/1857.asp>

INTRODUCTION

Chronic allograft liver transplantation, also termed vanishing bile duct syndrome (VBDS), develops slowly over a period of months or years and is a main cause of late graft loss. In fact, the onset is usually within several months after transplantation. Diagnostic criteria for chronic rejection are (1) the presence of bile duct atrophy/pyknosis, affecting the majority of bile ducts, with or without bile duct loss; (2) convincing foam cell obliterative arteriopathy; or (3) bile duct loss affecting greater than 50% of the portal tracts^[1]; (4) total fibrous obliteration of main portal vein and portal foam cell venopathy^[2]. Risk factors for chronic liver rejection include transplantation for primary sclerosing cholangitis (PSC)^[3], primary biliary cirrhosis (PBC)^[4], certain patterns of HLA match between donor and recipient^[5-7], positive lymphocyte cross-match^[8], cytomegalovirus infection, transplantation between donor and recipient of different ethnic origins^[9], sex mismatch^[10], and absence of azathioprine from the immunosuppressive regimen^[11]. Not all these risk factors have subsequently been confirmed. Cytomegalovirus infection is one of the suggested risk factors for chronic allograft liver rejection. Some results showed there was no direct correlation between them, others demonstrated CMV infection somehow implicated in mechanisms of chronic rejection and played a key role in the pathological changes of atrophy of bile duct and generation of graft arteriosclerosis, characteristic of chronic rejection.

The review addresses several questions. First, CMV infection and risk factors associated with it in liver transplantation. Second, CMV infection and cytokines. Third, relation between CMV infection and chronic liver rejection, potential etiological mechanism of CMV infection in chronic liver transplantation. Is the actual incidence of CMV infection a cause of VBDS?

CMV INFECTION AND RISK FACTORS

Human cytomegalovirus (HCMV) infection occurred in 30-65% of liver transplantation recipients, of which 18-40% were symptomatic infection and mostly developed 1 to 3 mo after transplantation. HCMV infection has two pathways: primary infection and infection activated by latent infection. Many factors are involved in HCMV infection. A prospective study of 218 LT recipients by Paya CV showed that 55% of patients developed CMV infection during the 1st year post-transplantation^[12]. Symptomatic CMV infection developed in 25% of all patients, being a major cause of death (21% of all deaths). Of the 62 episodes of documented organ invasion, liver was the major site (38 episodes), followed by lung, gastrointestinal tract and retina. Multivariate statistical analysis of risk factors indicated that the R-/D+ group was the main risk factor for CMV infection and symptomatic infection. Use of antilymphocyte preparations, retransplantation, donor CMV seropositivity, use of antilymphocyte preparations, and retransplantation were risk factors for the development of CMV diseases following liver transplantation^[13]. A higher incidence of cytomegalovirus infection was seen in the liver recipients of alcoholic sclerosis^[14]. Intraoperative hypothermia during liver transplantation increased the risk of CMV infection in the 1st month postoperation and active warming seemed to reduce this risk^[15]. Early application of OKT-3 was the risk factor for development of spreading HCMV diseases; FK506 could reverse rejection effectively, but increased the incidence of HCMV diseases^[16]. Others found that immunosuppressant FK506 after liver transplantation augmented inducible NK cell activity and alleviated CMV infection^[17]. Among immunosuppressive drugs, only anti-interleukin-2Rab was proved to significantly reduce the incidence of CMV^[18]. The role of antirejection therapy may be particularly important, since it could suppress CMV specific cytotoxic T-cell responses and result in prolonged viraemia, which in turn could cause a prolonged alloreactive cytotoxic response. HCMV infection is associated with human herpesviruses (HHV) 6 and 7. Lautenschlager *et al.*^[19] analyzed it in consecutive 34 adult liver allograft recipients, CMV disease was diagnosed in 12 patients, in which 10 patients had concurrent HHV-6 infection and 9 had HHV-7 infection. A prolonged prothrombin time, acute fulminant hepatitis diagnosed as the underlying liver disease and hepatic artery thrombosis were found to be significant risk factors for CMV infection^[20]. Total number of units of blood transfusion and transfusion of seropositive CMV blood had no effect on primary CMV infection after liver transplantation, though it had an influence on the severity of CMV infection and seropositive CMV recipients. The study about the effect of cytomegalovirus infection status on the first-year mortality among orthotopic liver transplantation recipients showed^[21]:

seronegative donors and recipients (11%), seronegative donors and seropositive recipients (22%), seropositive donors and recipients (30%), and seropositive donors and seronegative recipients (44%). Multivariate analysis showed that retransplantation, total number of units of blood products administered during transplantation, CMV infection and bacteremia were associated with higher mortality rates. Thus donor and recipient CMV serologic status is a significant pretransplantation determinant for death in liver transplant recipients.

HCMV INFECTION AND CYTOKINES

The significance of some cytokines highly expressed in grafts and blood serum after liver transplantation with HCMV infection remains unknown. Vascular adhesion molecules and their ligands are important both in leukocyte-endothelial cell interactions and in T-cell activation of rejection cascade. A significant induction of intercellular adhesion molecule-1 and vascular cell adhesion molecule-1 was seen in vascular and sinusoidal endothelium associated with both CMV and rejection, and induction of endothelial leukocyte adhesion molecule-1 in vascular endothelium was seen in rejection only. In both cases, the number of leukocytes expressing leukocyte function antigen-1 was significantly increased, but very late antigen-4-positive cells were more characteristic for CMV^[22]. IL2-receptor (IL2R) positivity was practically seen in rejection only, but both IL2R and CD8 were increased in cytomegalovirus hepatitis. Simultaneously increased IL2R and CD8 may mean the development of cytomegalovirus hepatitis on the basis of acute rejection. Vascular adhesion protein-1 (VAP-1), an adhesion molecule involved in lymphocyte adhesion, was up-regulated in acute liver rejection of sinusoids, hepatocytes in bile duct and this up-regulation was prolonged by RCMV infection^[23]. Thus the severity of acute rejection was intensified. Tumor necrosis factor-alpha (TNF- α) plays a key role in regulating reactivation of CMV infection. TNF- α could activate CMV-IE enhancer and result in high CMV-IE antigen expression in peripheral blood mononuclear cells particularly in monocytes. Increased tumor necrosis factor- α (TNF- α) could lead to occurrence of cachexy after CMV infection and mediate development of vanishing bile duct syndrome. Inhibition of TNF- α release or action might be an alternative strategy for preventing CMV-associated morbidity in allograft recipients^[24].

CMV-IE protein could activate transforming growth factor- β 1 (TGF- β 1) promoter during CMV infection and result in early high expression of TGF- β 1 mRNA^[25]. In chronic human allograft rejection, increased infiltrated macrophages and up-regulated platelet-derived growth factor (PDGF), fibroblast growth factor (FGF) could lead to transformation of lipocytes to myofibroblast-like cells, which would lead to increase secretion of extracellular matrix and were engaged in hepatic fibrosis^[26]. TGF- β 1 increased levels of FGF and FGF receptor mRNAs in myofibroblast cells and expression levels of PDGF mRNA^[27]. Thereafter CMV infection may implicate in chronic rejection by secretion of chronic fibroblast factors. Whether by regulating some of the cytokines which were thought to be involved in chronic rejection, skewing of immunity towards Th2 cytokines (TGF- β , IL-4, IL-10) and humoral response, expression of adhesive molecules and antigens can be induced in graft, to mediate occurrence of chronic rejection, needs further research.

HCMV INFECTION AND CHRONIC REJECTION IN TRANSPLANT LIVER

Many studies have demonstrated a close relationship between HCMV infection and chronic liver rejection. Analysis of ten

liver transplants whose graft was lost due to histologically confirmed chronic rejection showed^[28] that there was at least one episode or many times of rejection early after transplantation. All patients had a history of CMV infection usually following acute rejection. Persistent CMV-DNA was found in all of those grafts examined by DNA-hybridization *in situ*, CMV-DNA was strongly expressed in the remaining bile ducts and moderately expressed in endothelial cells of the vascular structures. Persistent CMV genome was found in those structures that were the major targets of chronic rejection process in the liver. These findings support the suggestion that CMV infection is one of the risk factors for chronic allograft rejection. Arnold *et al.*^[29] found that CMV-DNA was identified in hepatocytes in 10 of 12 patients with VBDS, of whom 1 had no serological evidence of CMV infection, 9 developed cytomegalovirus infection at 1 wk until death or retransplantation. Cytomegalovirus DNA was identified in hepatocytes and never identified in either biliary or endothelial tissue. CMV-DNA was identified in all 18 patients with HCMV infection but no bile duct was injured. However in those with uncomplicated cytomegalovirus, infection occurred earlier but was eliminated more quickly, and the number of infected hepatocytes was greater when compared with those with vanishing bile duct syndrome. The data indicated that vanishing bile duct syndrome was associated with persistent cytomegalovirus replication within hepatocytes. Further study showed^[30] that interferon-alpha (IFN- α) was identified more frequently and patients developed VBDS after a longer period in the bile duct cytoplasm compared with those with acute HCMV infection without evidence of VBDS. These indicate that persistent CMV infection of bile duct cells resulting in increased IFN- α is likely a co-factor linked to progression to VBDS. Martelius *et al.*^[31] performed liver transplantations in a rat strain combination with PVG (RT1c) \rightarrow BN (RT1n). One group of animals was infected with RCMV intraperitoneally. They found in liver allografts undergoing acute rejection, CMV significantly increased portal inflammation and caused more severe bile duct damage linked to the induction of VCAM-1 in endothelial cells. The ongoing infection was found to vary over time in different structures of liver grafts. These results support an association between CMV infection and the immunological mechanisms of rejection, as well as the role of CMV in the development of bile duct damage in liver allografts. In the same rat strain combination, Martelius *et al.*^[32] examined CMV infection of the graft at various time points and found that rat cytomegalovirus (RCMV) caused an active infection in the graft from 5 d to 2 wk after transplantation. Thereafter the cultures were negative. RCMV antigens and DNA were found in hepatocytes, endothelial, inflammatory, and bile duct cells during the active infection. At 4 wk, RCMV DNA positive cells decreased. IE-1 mRNA expression was, however, only detected during the active infection, but not at 4 wk postinfection. They concluded the CMV-induced graft damage did not require the continued expression of IE-1. Halme *et al.*^[33] demonstrated that CMV infection was a risk factor for development of biliary complication after liver transplantation.

A variety of risk factors for VBDS have been postulated, but they are controversial. O'Grady *et al.*^[34] confirmed A 1-2 antigen matched for HLA DR antigens, a zero matched for HLA A/B antigens, and active CMV infection were independently associated with an increased risk of VBDS. Hoffmann *et al.*^[35] examined 120 liver transplants retrospectively and analyzed the risk factors for VBDS. Ten patients (8.3%) developed VBDS. Seventeen patients had hepatitis C virus infections after liver transplantation. In this group, the incidence of VBDS was the highest (4 of 17, or 23.5%) and reached statistical significance. They found hepatitis C infection predisposed one to the development of VBDS after OLT.

The potential mechanisms of CMV cause VBDS. (1) Virus itself directly destroys or liquefies the infected structure. (2) Cytotoxic T lymphocyte plays a role in inducing VBDS. CMV infection may trigger an immune response by inducing MHC antigens and adhesion molecules on the bile ductal cell surface and make the ductal cells a target for immunological attack. For example, a cross-reaction between the viral protein and MHC molecules is possible because CMV has been shown to code a protein homologous to MHC class I antigen^[36], and a CMV IE₂ protein has been found to share an epitope with the HLA-DR β chain^[37]. CMV is known to increase expression of class II human leukocyte antigens on bile duct epithelial cells. After immune recognition of these foreign antigens by host antigen-presenting cells, CD₄⁺T would release cytokines and stimulate differentiation and proliferation of cytotoxic T cells (CD₈⁺T). The activated CD₈⁺T then plays a immune killing role. CMV has been shown to induce proinflammatory cytokines, such as IFN- γ and TNF- α , which could lead to other immunological events. (3) Dystrophy and ischemic sequelae caused by obliterative arteriopathy. Although CMV-DNA can not be detected on some bile duct epithelial cells in VBDS, CMV might play a pathogenetic role in the development of VBDS^[38]. The sequelae of clearing infection, host immune response would selectively kill these bile duct epithelial cells with CMV infection. CMV infection of hepatocytes would in some way up-regulate the expression of HLA antigens on biliary epithelial cells. CMV viral antigens are present and bound to HLAs on the surface of bile duct cells. So even though CMV was cleared *in vivo*, they could exhibit their episode role.

Few studies about the relation of CMV infection and angiopathy are available. Greffe *et al.*^[39] demonstrated that in patients with active CMV infection, distinctive large cells were present in peripheral blood. Moreover, these cells were shown to express CMV antigens and to have endothelial origin with immunologic staining, indicating an association between CMV infection and widespread occult vascular damage. CMV-induced endothelial damage may be a potent antigenic stimulus, leading to the production of anti-endothelial cells autoantibodies. Anti-endothelial cell autoantibodies may represent not only a marker of cell injury but also contribute to the progression of inflammatory response leading to the exposure of tissue-privileged self-antigens and induction of other autoantibodies such as SMA. These would further aggravate pathological damages. Analysis of autoantibody was carried out in sequential sera from 40 liver transplantation patients by Varani *et al.*^[40]. Ten out of 23 antigenemia-positive and none of antigenemia-negative patients developed serum autoantibodies. Anti-endothelial cell autoantibodies were found in 9 cases and SMA in 4 patients. Antinuclear antibodies were detected in 1 autoantibody-negative patient. All but 1 case of autoantibody positivity were observed in the high antigenemia group and detected in blood during the antigenemia phase and in most cases in coincidence with or after the antigenemia peak.

In the arteries of an allografted organ, endothelial injury may arise from immune injury, ischemia/reperfusion injury, and injuries due to dyslipidemia, hypertension, or infectious agents. The injured endothelial cells can elaborate small molecules and cytokines that can activate macrophages and smooth muscle cells to express functions that may contribute to arterial lesion formation. The precise immunological mechanisms underlying chronic vascular rejection are unknown. Three potential effector mechanisms have been implicated in allograft rejection^[41]: alloreactive CD₄⁺ cytokine-producing "helper" T (TH) lymphocytes, alloreactive CD₈⁺ cytolytic T lymphocytes (CTL), and alloreactive antibodies (produced by B lymphocytes). Chronic delayed-type hypersensitivity mediated by host CD₄⁺ T cells activated by graft alloantigens presented directly by graft endothelial and

dendritic cells or indirectly by host dendritic cells, is likely a candidate. All of which contribute to atherosclerotic vascular disease, and chronic vascular rejection.

CMV infection might directly increase MHC antigens on the surface of graft cells through the induction of release of mediators such as interferon and may activate cytotoxic T cells, which can trigger acute rejection in association with concurrent alloantigen stimulation. Acute rejection results in a generalized inflammatory response. Kas-Deelen and colleagues have postulated that the occurrence of acute rejection at the allograft site could sensitize the endothelial surface of the host to CMV-induced damage^[42]. These endothelial cells then became a target for alloreactive T cells. According to these *in vitro* studies, even a few CMV-infected endothelial cells in a transplanted organ might trigger autoreactivity^[43]. CMV infection enhances several steps, with ensuing chronic rejection. Endothelial adhesion molecule expression, in particular, could provoke influx of inflammatory cells and smooth muscle cell proliferation. In addition, CMV infection could induce vascular wall changes resembling fatty streaks reported in the early stages of classic atherosclerosis^[44].

There is still a controversy concerning the relationship between CMV infection and chronic allograft rejection. Paya *et al.*^[45] studied 81 liver transplant recipients and found that cytomegalovirus infection developed in 46 recipients (57%), and VBDS occurred in 9 recipients (11%). CMV infection developed in only 5 of the 9 patients with VBDS. Univariate analysis of pretransplantation recipient/donor CMV serological tests and human leukocyte antigen typing showed they were not significant risk factors for the development of VBDS. The data indicated no association was found between CMV infection alone or in relation to class I or II human leukocyte antigen match and the subsequent development of VBDS. van den Berg *et al.*^[46] in a retrospective study confirmed there was no association among CMV infection, HLA-DR and VBDS. Wright TL in an editorial postulated that CMV was indeed an innocent bystander rather than a culprit. In the pathogenesis of VBDS, it is the immune responsiveness of the patient that is important. It is quite possible that patients with VBDS have an inherent defect in immune response that allows persistence of CMV infection, and CMV is unrelated to destruction of bile ducts. On the other hand, if CMV infection is really an etiological factor for VBDS, antiviral therapy would be effective in decreasing incidence of the chronic rejection. Unfortunately, many studies about antiviral therapy for CMV failed to show an association between the development of CMV disease and the occurrence of rejection^[47].

CONCLUSION

Many studies have demonstrated a close association between CMV infection and chronic allograft liver transplantation, but it did not prove an etiological role for the virus in this syndrome. CMV infection may be one of the risk factors for development of VBDS. A better understanding of the etiologic role of CMV in VBDS, is important for designing effective therapeutic strategies to ameliorate this process.

ACKNOWLEDGMENTS

We thank Dr. Ran Tao, Department of Starzl Transplantation Center, University of Pittsburgh, for critically reading this paper and discussion.

REFERENCES

- 1 **Demetris A**, Adams D, Bellamy C, Blakolmer K, Clouston A, Dhillon AP, Fung J, Gouw A, Gustafsson B, Haga H, Harrison D, Hart J, Hubscher S, Jaffe R, Khettry U, Lassman C, Lewin

- K, Martinez O, Nakazawa Y, Neil D, Pappo O, Parizhskaya M, Randhawa P, Rasoul-Rockenschaub S, Reinholt F, Reynes M, Robert M, Tsamandas A, Wanless I, Wiesner R, Wernerson A, Wrba F, Wyatt J, Yamabe H. Update of the international banff schema for liver allograft rejection: working recommendations for the histopathologic staging and reporting of chronic rejection. *Hepatology* 2000; **31**: 792-799
- 2 **Jain D**, Robert ME, Navarro V, Friedman AL, Crawford JM. Total fibrous obliteration of main portal vein and portal foam cell venopathy in chronic hepatic allograft rejection. *Arch Pathol Lab Med* 2004; **128**: 64-67
 - 3 **Wiesner RH**, Ludwig J, van Hoek B, Krom RA. Current concepts in cell-mediated hepatic allograft rejection leading to ductopenia and liver failure. *Hepatology* 1991; **14**(4 Pt 1): 721-729
 - 4 **Demetris AJ**, Markus BH, Esquivel C, Van Thiel DH, Saidman S, Gordon R, Makowka L, Sysyn GD, Starzl TE. Pathologic analysis of liver transplantation for primary biliary cirrhosis. *Hepatology* 1988; **8**: 939-947
 - 5 **Gubernatis G**, Kemnitz J, Tusch G, Pichlmayr R. HLA compatibility and different features of liver allograft rejection. *Transpl Int* 1988; **1**: 155-160
 - 6 **Manez R**, White LT, Linden P, Kusne S, Martin M, Kramer D, Demetris AJ, Van Thiel DH, Starzl TE, Duquesnoy RJ. The influence of HLA matching on cytomegalovirus hepatitis and chronic rejection after liver transplantation. *Transplantation* 1993; **55**: 1067-1071
 - 7 **Bismuth A**, Ducot B, Samuel D, Arulnaden JL, Gugenheim J, Debat P, Azoulay D, Farrokhi P, Pillier-Loriette C, Bourdon G. Liver transplantation and the major histocompatibility complex. *Rev Fr Transfus Hemobiol* 1991; **34**: 449-457
 - 8 **Batts KP**, Moore SB, Perkins JD, Wiesner RH, Grambsch PM, Krom RA. Influence of positive lymphocyte crossmatch and HLA mismatching on vanishing bile duct syndrome in human liver allografts. *Transplantation* 1988; **45**: 376-379
 - 9 **Devlin JJ**, O' Grady JG, Tan KC, Calne RY, Williams R. Ethnic variations in patient and graft survival after liver transplantation. Identification of a new risk factor for chronic allograft rejection. *Transplantation* 1993; **56**: 1381-1384
 - 10 **Candinas D**, Gunson BK, Nightingale P, Hubscher S, McMaster P, Neuberger JM. Sex mismatch as a risk factor for chronic rejection of liver allografts. *Lancet* 1995; **346**: 1117-1121
 - 11 **Van Hoek B**, Wiesner RH, Ludwig J, Gores GJ, Moore B, Krom RA. Combination immunosuppression with azathioprine reduces the incidence of ductopenic rejection and vanishing bile duct syndrome after liver transplantation. *Transplant Proc* 1991; **23** (1 Pt 2): 1403-1405
 - 12 **Paya CV**, Marin E, Keating M, Dickson R, Porayko M, Wiesner R. Solid organ transplantation: results and implications of acyclovir use in liver transplants. *J Med Virol* 1993; **1**(Suppl): 123-127
 - 13 **Wiesner RH**, Marin E, Porayko MK, Steers JL, Krom RA, Paya CV. Advances in the diagnosis, treatment, and prevention of cytomegalovirus infections after liver transplantation. *Gastroenterol Clin North Am* 1993; **22**: 351-366
 - 14 **Stefanini GF**, Biselli M, Grazi GL, Iovine E, Moscatello MR, Marsigli L, Foschi FG, Caputo F, Mazziotti A, Bernardi M, Gasbarrini G, Cavallari A. Orthotopic liver transplantation for alcoholic liver disease: rates of survival, complications and relapse. *Hepatogastroenterology* 1997; **44**: 1356-1359
 - 15 **Paterson DL**, Staplefeldt WH, Wagener MM, Gayowski T, Marino IR, Singh N. Intraoperative hypothermia is an independent risk factor for early cytomegalovirus infection in liver transplant recipients. *Transplantation* 1999; **67**: 1151-1155
 - 16 **Woodle ES**, Perdrizet GA, So S, Jendrisak MD, White HM, Marsh JW. FK 506 rescue therapy: the rapidity of rejection reversal is related to the subsequent development of CMV disease. *Transplant Proc* 1993; **25**: 1992-1993
 - 17 **Kageyama S**, Matsui S, Hasegawa T, Yoshida Y, Sato H, Yamamura J, Kurokawa M, Yamamoto H, Shiraki K. Augmentation of natural killer cell activity induced by cytomegalovirus infection in mice treated with FK506. *Acta Virol* 1997; **41**: 215-220
 - 18 **Oldakowska-Jedynak U**, Niewczas M, Ziolkowski J, Mucha K, Fronciewicz B, Bartlomiejczyk I, Senatorski G, Wyzgal J, Krawczyk M, Zieniewicz K, Nyckowski P, Paczek L. Cytomegalovirus infection as a common complication following liver transplantation. *Transplant Proc* 2003; **35**: 2295-2297
 - 19 **Lautenschlager I**, Lappalainen M, Linnavuori K, Suni J, Hockerstedt K. CMV infection is usually associated with concurrent HHV-6 and HHV-7 antigenemia in liver transplant patients. *J Clin Virol* 2002; **25**(Suppl 2): S57-S61
 - 20 **Paya CV**, Wiesner RH, Hermans PE, Larson-Keller JJ, Ilstrup DM, Krom RA, Rettke S, Smith TF. Risk factors for cytomegalovirus and severe bacterial infections following liver transplantation: a prospective multivariate time-dependent analysis. *J Hepatol* 1993; **18**: 185-195
 - 21 **Falagas ME**, Snyderman DR, Griffith J, Ruthazer R, Werner BG. Effect of cytomegalovirus infection status on first-year mortality rates among orthotopic liver transplant recipients. The Boston Center for Liver Transplantation CMVIG Study Group. *Ann Intern Med* 1997; **126**: 275-279
 - 22 **Lautenschlager I**, Hockerstedt K, Taskinen E, von Willebrand E. Expression of adhesion molecules and their ligands in liver allografts during cytomegalovirus (CMV) infection and acute rejection. *Transpl Int* 1996; **9**(Suppl 1): S213-215
 - 23 **Martelius T**, Salmi M, Wu H, Bruggeman C, Hockerstedt K, Jalkanen S, Lautenschlager I. Induction of vascular adhesion protein-1 during liver allograft rejection and concomitant cytomegalovirus infection in rats. *Am J Pathol* 2000; **157**: 1229-1237
 - 24 **Fietze E**, Prosch S, Reinke P, Stein J, Docke WD, Staffa G, Loning S, Devaux S, Emmrich F, von Baehr R. Cytomegalovirus infection in transplant recipients. The role of tumor necrosis factor. *Transplantation* 1994; **58**: 675-680
 - 25 **Michelson S**, Alcamí J, Kim SJ, Danielpour D, Bachelier F, Picard L, Bessia C, Paya C, Virelizier JL. Human cytomegalovirus infection induces transcription and secretion of transforming growth factor beta 1. *J Virol* 1994; **68**: 5730-5737
 - 26 **Hoshino K**, Demirci G, Schlitt HJ, Wonigeit K, Pichlmayr R, Nashan B. Evidence for transformation of lipocytes to myofibroblast-like cells as source of transplant fibrosis in chronic human allograft rejection. *Transplant Proc* 1995; **27**: 1144-1145
 - 27 **Rosenbaum J**, Blazejewski S, Preaux AM, Mallat A, Dhumeaux D, Mavrier P. Fibroblast growth factor 2 and transforming growth factor beta 1 interactions in human liver myofibroblasts. *Gastroenterology* 1995; **109**: 1986-1996
 - 28 **Lautenschlager I**, Hockerstedt K, Jalanko H, Loginov R, Salmela K, Taskinen E, Ahonen J. Persistent cytomegalovirus in liver allografts with chronic rejection. *Hepatology* 1997; **25**: 190-194
 - 29 **Arnold JC**, Portmann BC, O' Grady JG, Naoumov NV, Alexander GJ, Williams R. Cytomegalovirus infection persists in the liver graft in the vanishing bile duct syndrome. *Hepatology* 1992; **16**: 285-292
 - 30 **Arnold JC**, Nouri-Aria KT, O' Grady JG, Portmann BC, Alexander GJ, Williams R. Hepatic alpha-interferon expression in cytomegalovirus-infected liver allograft recipients with and without vanishing bile duct syndrome. *Clin Invest* 1993; **71**: 191-196
 - 31 **Martelius T**, Krogerus L, Hockerstedt K, Bruggeman C, Lautenschlager I. Cytomegalovirus infection is associated with increased inflammation and severe bile duct damage in rat liver allografts. *Hepatology* 1998; **27**: 996-1002
 - 32 **Martelius TJ**, Blok MJ, Inkinen KA, Loginov RJ, Hockerstedt KA, Bruggeman CA, Lautenschlager IT. Cytomegalovirus infection, viral DNA, and immediate early-1 gene expression in rejecting rat liver allografts. *Transplantation* 2001; **71**: 1257-1261
 - 33 **Halme L**, Hockerstedt K, Lautenschlager I. Cytomegalovirus infection and development of biliary complications after liver transplantation. *Transplantation* 2003; **75**: 1853-1858
 - 34 **O' Grady JG**, Alexander GJ, Sutherland S, Donaldson PT, Harvey F, Portmann B, Calne RY, Williams R. Cytomegalovirus infection and donor/recipient HLA antigens: interdependent co-factors in pathogenesis of vanishing bile-duct syndrome after liver transplantation. *Lancet* 1988; **2**: 302-305
 - 35 **Hoffmann RM**, Gunther C, Diepolder HM, Zachoval R, Eissner HJ, Forst H, Anthuber M, Paumgartner G, Pape GR. Hepatitis C virus infection as a possible risk factor for ductopenic rejection (vanishing bile duct syndrome) after liver transplantation. *Transpl Int* 1995; **8**: 353-359
 - 36 **Beck S**, Barrell BG. Human cytomegalovirus encodes a glycoprotein homologous to MHC class I antigens. *Nature* 1988; **331**:

- 269-272
- 37 **Fujinami RS**, Nelson JA, Walker L, Oldstone MB. Sequence homology and immunologic-cross-reactivity of human cytomegalovirus with HLA-DR beta chain: a means for graft rejection and immunosuppression. *J Virol* 1988; **62**: 100-105
- 38 **Wright TL**. Cytomegalovirus infection and vanishing bile duct syndrome: culprit or innocent bystander? *Hepatology* 1992; **16**: 494-496
- 39 **Grefte A**, van der Giessen M, van Son W, The TH. Circulating cytomegalovirus (CMV)-infected endothelial cells in patients with an active CMV infection. *J Infect Dis* 1993; **167**: 270-277
- 40 **Varani S**, Muratori L, De Ruvo N, Vivarelli M, Lazzarotto T, Gabrielli L, Bianchi FB, Bellusci R, Landini MP. Autoantibody appearance in cytomegalovirus-infected liver transplant recipients: correlation with antigenemia. *J Med Virol* 2002; **66**: 56-62
- 41 **Libby P**, Pober JS. Chronic rejection. *Immunity* 2001; **14**: 387-397
- 42 **Kas-Deelen AM**, Harmsen MC, de Maar EF, Oost-Kort WW, Tervert JW, van der Meer J, van Son WJ, The TH. Acute rejection before cytomegalovirus infection enhances von Willebrand factor and soluble VCAM-1 in blood. *Kidney Int* 2000; **58**: 2533-2542
- 43 **Waldman WJ**, Adams PW, Knight DA, Sedmak DD. CMV as an exacerbating agent in transplant vascular sclerosis: potential immune-mediated mechanisms modelled *in vitro*. *Transplant Proc* 1997; **29**: 1545-1546
- 44 **Span AH**, Grauls G, Bosman F, Van Boven CP, Bruggeman CA. Cytomegalovirus infection induces vascular injury in the rat. *Arteriosclerosis* 1992; **93**: 41-52
- 45 **Paya CV**, Wiesner RH, Hermans PE, Larson-Keller JJ, Ilstrup DM, Krom RA, Moore SB, Ludwig J, Smith TF. Lack of association between cytomegalovirus infection, HLA matching and the vanishing bile duct syndrome after liver transplantation. *Hepatology* 1992; **16**: 66-70
- 46 **van den Berg AP**, Klompemaker IJ, Hepkema BG, Gouw AS, Haagsma EB, Lems SP, The TH, Slooff MJ. Cytomegalovirus infection does not increase the risk of vanishing bile duct syndrome after liver transplantation. *Transpl Int* 1996; **9**(Suppl 1): S171-173
- 47 **Shibolet O**, Ilan Y, Kalish Y, Safadi R, Ashur Y, Eid A, Shouval D, Wolf D. Late cytomegalovirus disease following liver transplantation. *Transpl Int* 2003; **16**: 861-865

Edited by Wang XL **Proofread by** Chen WW and Xu FM

Expression of COX-2, iNOS, p53 and Ki-67 in gastric mucosa-associated lymphoid tissue lymphoma

Hong-Ling Li, Bing-Zhong Sun, Fu-Cheng Ma

Hong-Ling Li, Bing-Zhong Sun, Department of Hematology, Xijing Hospital, Fourth Military Medical University, Xi'an 710032, Shaanxi Province, China

Fu-Cheng Ma, Department of Pathology, Xijing Hospital, Fourth Military Medical University, Xi'an 710032, Shaanxi Province, China

Correspondence to: Dr. Hong-Ling Li, Department of Hematology, Xijing Hospital, Fourth Military Medical University, 127 Changle West Road, Xi'an 710032, Shaanxi Province, China. lhl882002@hotmail.com

Telephone: +86-29-3375579

Received: 2003-11-12 **Accepted:** 2004-01-15

Abstract

AIM: To assess the expression of cyclooxygenase-2 (COX-2), nitric oxide synthase (iNOS), p53 and Ki-67 in gastric mucosa-associated lymphoid tissue (MALT) lymphoma and clarify the relationship between COX-2 expression and iNOS or p53 expression in these patients.

METHODS: The expressions of COX-2, iNOS, p53 and Ki-67 were detected in 32 gastric MALT lymphoma specimens and 10 adjacent mucosal specimens by immunohistochemical Envision method.

RESULTS: COX-2 and iNOS expressions were significantly higher in gastric MALT lymphoma tissues than those in adjacent normal tissues. The expression of COX-2 was observed in 22 of 32 cases of MALT lymphoma tissues (68.8%). A positive cytoplasmic immunoreactivity for iNOS was detected in 17 of 31 cases (53.1%). COX-2 expression in gastric MALT lymphoma tissues was positively correlated with iNOS expression ($r=0.448$, $P=0.010$) and cell proliferative activity analyzed by Ki-67 labeling index ($r=0.410$, $P=0.020$). The expression of COX-2 protein did not correlate with age, sex, stage of disease, lymph node metastasis or differentiation. The accumulation of p53 nuclear phosphoprotein was detected in 19 (59.4%) of tumors. p53 protein was expressed in 11 of 23 assessed LG tumors and in 8 of 9 assessed HG tumors. The difference of p53 positivity was found statistically significant between LG and HG cases ($P=0.0302$). The p53 accumulation correlated with advanced clinical stage (stage III+IV vs stage I+II, $P=0.017$). There was a significant positive correlation between COX-2 expression and p53 accumulation status ($r=0.403$, $P=0.022$). The mean PI of Ki-67 in each grade group were $36.0\pm 7.73\%$ in HG and $27.4\pm 9.21\%$ in LG. High-proliferation rate correlated with HG tumors ($r=0.419$, $P=0.017$). The correlation coefficient showed a significant positive correlation between PI and COX-2 expression in MALT lymphoma patients ($r=0.410$, $P=0.020$).

CONCLUSION: COX-2 expresses in the majority of gastric MALT lymphoma tissues and correlates with cellular proliferation and iNOS expression. COX-2 overexpression is closely associated with p53 accumulation status. iNOS and COX-2 may play a synergistic role in the pathogenesis of gastric MALT lymphoma.

Li HL, Sun BZ, Ma FC. Expression of COX-2, iNOS, p53 and Ki-67 in gastric mucosa-associated lymphoid tissue lymphoma. *World J Gastroenterol* 2004; 10(13): 1862-1866

<http://www.wjgnet.com/1007-9327/10/1862.asp>

INTRODUCTION

Lymphomas of mucosa-associated lymphoid tissue (MALT) are a distinct subgroup of extranodal B-cell non-Hodgkin's lymphomas. Gastric MALT lymphomas are the majority of the cases and account for 1-10% of all gastric malignant neoplasms^[1]. Epidemiological and clinical studies demonstrated a link between gastric MALT lymphoma and chronic infection with *Helicobacter pylori* (*H pylori*)^[2,3]. Cyclooxygenase-2 (COX-2) and nitric oxide synthase (iNOS) are important enzymes that mediate inflammatory processes. In recent years, it has been demonstrated that both COX-2 and iNOS play important roles in various tumors, including gastric MALT lymphoma^[4,5]. COX-2, a key isoenzyme in conversion of arachidonic acid to prostaglandins, is inducible by various agents such as growth factors and tumor promoters, and is frequently overexpressed in various tumors^[6,7]. iNOS are isoenzymes that catalyze the synthesis of nitric oxide (NO). Overexpression of iNOS has been demonstrated in various human neoplasms, such as breast cancer^[8], colorectal cancer^[9], and gastric cancer^[10]. The p53 tumor suppressor protein is a critical mediator of apoptosis and tumorigenesis. Although studies have suggested interactions between COX-2 and iNOS or p53 in different tumors, the relationship between COX-2 expression and a variety of other molecular markers of tumor progression has not been reported for gastric MALT lymphomas. In the present study, we conducted to determine the expressions of COX-2, iNOS and p53 expression as well as cell proliferative index (Ki-67) in 32 gastric MALT lymphomas by using immunohistochemistry.

MATERIALS AND METHODS

Specimens

Thirty-two gastric MALT lymphoma specimens and 10 adjacent specimens were obtained from surgical resection. The patients underwent surgery at Xijing Hospital of the Fourth Military Medical University (Xi'an, China) between January 1996 and September 2002. The tumor specimens were retrieved from the archives of the Department of Pathology, Xijing Hospital. The mean age of the gastric MALT lymphoma group was 52.8 years (range 29-70 years), and there were 22 males and 10 females. All cases were of B-cell origin as immunohistochemistry showed CD20 expression in all MALT cases. The cases were categorized in two basic groups, according to (REAL) Classification^[11] and the WHO Classification^[12] for MALT lymphomas: low-grade lymphoma of MALT (composed of centrocyte-like cells, lymphoid follicles and plasma cell differentiation) and high-grade lymphoma of MALT (diffuse large B cell lymphoma (DLBCL) with or without low grade MALT +lymphoma component). Of the 32 patients, 23 were low grade MALT lymphoma (LG) and 9 high grade MALT lymphoma (HG). Patients were staged according to the Ann Arbor system. All specimens

were fixed in 40 g/L buffered formaldehyde, and embedded in paraffin wax.

Immunohistochemical assay for expression of COX-2, iNOS, p53 and Ki-67

The expression of COX-2, iNOS, p53 and Ki-67 was studied by immunohistochemical Envision method according to the manufacturer's instructions. H-62 (COX-2) is a rabbit polyclonal antibody raised against a recombinant protein corresponding to amino acids 50-111 mapping near the amino terminus of COX-2 of human origin (sc-7951, Santa Cruz Biotechnology, dilution 1:50). M-19 (iNOS) was provided as a rabbit affinity-purified polyclonal antibody raised against a peptide mapping at the carboxyl terminus of iNOS of mouse origin (sc-650, Santa Cruz Biotechnology, dilution 1:50). The Ki-67 antibody recognizes the Ki-67 antigen of paraffin-embedded tissues. To detect the p53 protein, a mouse monoclonal antibody (sc-126, Santa Cruz Biotechnology, dilution 1:50) was used which recognizes an epitope in the N-terminus of the human p53 protein. Staining for Ki-67 was performed by using an anti-Ki-67 monoclonal mouse antibody (ZM-0166, Zhongshan Biotechnology, dilution 1:50). Briefly, 5- μ m sections cut from formalin-fixed, paraffin-embedded specimens were deparaffinized in xylene and rehydrated in graded alcohol. For antigen retrieval, the deparaffinized slides were microwaved in 0.01 mol/L sodium citrate buffer (pH 6.0) for 10 min. Endogenous peroxidase activity was then blocked by incubating the sections with 30 mL/L H₂O₂ in 0.05 mol/L phosphate buffer (pH 7.4), containing 0.45 mol/L NaCl for 15 min. Non-specific antibody binding was blocked by pretreatment with PBS containing 5 g/L bovine serum albumin. The sections were then incubated with the primary antibodies diluted as described above. After incubation, these sections were washed with 0.02 mol/L sodium phosphate buffer. The slides were then incubated with a secondary antibody for 30 min. Diaminobenzidine was used as chromogen and the sections were counterstained with hematoxylin. Negative controls were established by replacing the primary antibody with PBS.

Assessment of immunohistochemical results

The slides were evaluated independently by two observers who were unknown to the histological status. At the cellular level, COX-2 and iNOS staining was cytoplasmic in most cases, however, p53 and Ki-67 staining was nuclear. COX-2 is cytoplasmic enzyme detectable in tumor cells, epithelial cells, endothelial cells, smooth muscle cells and inflammatory cells. For final analysis, the expression of COX-2 was scored in the tumor cells. Staining for COX-2 and iNOS was considered positive only when more than 10% of the tumor cells in the entire tumor area were judged to be positive. The level of p53 was calculated by expressing the number of p53-positive cancer cells as a percentage of the total number of cancer cells in a high-power field. For analysis, tumors were classified as p53-negative (less than 10% positive nuclei) or p53-positive (more than 10% positive nuclei). The Ki-67 labeling index (proliferation index, PI) was determined by counting the percentage of positive cells among 1 000 tumor cells in 10 random regions in 400-fold fields.

Statistical analysis

Statistical comparisons for significance were made with the Student's *t* test and Chi-square test. Spearman correlation test was used for the correlation between positive rates. A *P* value <0.05 was considered statistically significant.

RESULTS

Expression of COX-2 and iNOS in gastric MALT lymphoma

The expression of COX-2 was observed in 22 of 32 cases of MALT lymphoma tissues (68.8%). Immunohistochemically, COX-2 was stained diffusely in cytoplasm of the tumor cells (Figure 1A). In contrast, no or very faint signal was found in neighboring normal tissues. A positive cytoplasmic immunoreactivity for iNOS was detected in 17 of 31 cases (53.1%, Figure 1B). However, no staining could be observed in neighboring normal tissues.

There was a significant correlation between COX-2 and iNOS expression ($r = 0.448$, $P = 0.010$). The positive expression

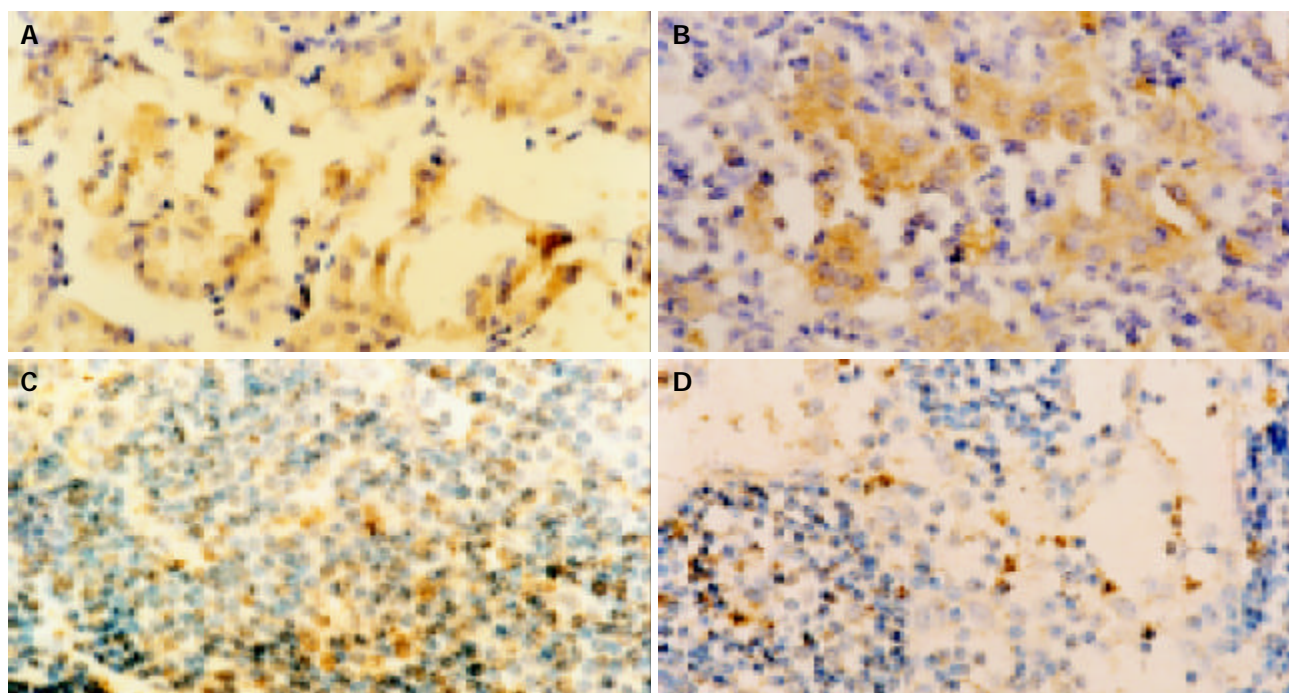


Figure 1 Results of immunohistochemical staining (Original magnification: $\times 400$). A: Expression of COX-2 in gastric MALT lymphoma; B: Expression of iNOS in gastric MALT lymphoma; C: Expression of p53 in gastric MALT lymphoma; D: Expression of Ki-67 in gastric MALT lymphoma.

rate of iNOS (88.2%) in the COX-2 positive group was significantly higher than that in the COX-2-negative group (46.7%, $P=0.011$).

Correlation between COX-2 expression and clinicopathological factors

The correlation between COX-2 expression and the clinicopathologic findings was analyzed by Spearman correlation test. All the parameters analyzed in COX-2 positive cases, including age, gender, stage of disease, lymph node metastasis and differentiation degree of the tumor, did not reached statistical significance ($P>0.05$, Table 1).

Expression of p53 in gastric MALT lymphoma

The accumulation of p53 nuclear phosphoprotein was detected in 19(59.4%) of tumors (Table 1, Figure 1C), whereas the p53 accumulation was undetectable in normal gastric tissues. A relationship between p53 status and several clinicopathological characteristics was investigated. p53 protein was expressed in 11 of 23 assessed LG tumors and in 8 of 9 assessed HG tumors. The difference of p53 positivity was found statistically significant between LG and HG cases ($P=0.033$). The p53 accumulation correlated with advanced clinical stage (stage III+IV vs stage I+II, $P=0.017$). The other parameters, such as age, gender and lymph node metastasis did not show any significant relation to the expression of p53.

There was a significant positive correlation between COX-2 expression and p53 accumulation status ($r=0.403$, $P=0.022$). Tumors that overexpressed p53 had higher expression levels of COX-2 than those without p53 overexpression ($P=0.022$, Table 1).

Expression of Ki-67 in gastric MALT lymphoma

Ki-67 staining was nuclear (Figure 1D). Very few cells were positive for Ki-67 in non-neoplastic gastric tissues. The mean PI of Ki-67 in the tumors was $29.81\pm 9.54\%$ (mean \pm SD). Mean values in each grade group were $36.0\pm 7.73\%$ in HG and $27.4\pm 9.21\%$ in LG. A significant correlation was observed between the high-proliferation rate and HG tumors ($r=0.419$, $P=0.017$).

The PI in COX-2 positive group was significantly higher than that in COX-2 negative group ($P=0.031$). The correlation coefficient showed a significant positive correlation between PI and COX-2 expression in MALT lymphoma patients ($r=0.410$, $P=0.020$). However, no significant correlation between PI and iNOS expression was found ($r=-0.037$, $P=0.839$).

Table 1 Correlation between expression of COX-2 and iNOS/p53 and clinicopathological factors in gastric MALT lymphoma (n, %)

Variable	Total	COX-2 positive	COX-2 negative	P value	
Gender	Male	22	15(68.2)	7(31.8)	0.918
	Female	10	7(70.0)	3(30.0)	
Age (yr)	≤ 50	9	6(66.7)	3(33.3)	0.874
	>50	23	16(69.6)	7(30.4)	
Lymph node	+	10	8(80.0)	2(20.0)	0.355
Metastasis	-	22	14(63.6)	8(36.4)	
Histological	Low	23	14(60.7)	9(39.1)	0.124
Grade	High	9	8(88.9)	1(11.1)	
Histological	I+II	22	16(72.7)	6(27.3)	0.472
Stage	III+IV	10	6(60.0)	4(40.0)	
INOS	+	17	15(88.2)	2(11.8)	0.011
	-	15	7(46.7)	8(53.3)	
p53	+	19	16(84.2)	3(15.8)	0.022
	-	13	6(46.2)	7(53.8)	

DISCUSSION

Gastric MALT lymphoma is a unique disease. Normal human gastric mucosa is devoid of MALT. MALT accumulates within gastric mucosa as a result of long-standing *H pylori* infection in a subset of infected patients, and from this acquired MALT, low-grade B cell MALT lymphoma may eventually develop^[13]. *H pylori* can be demonstrated in the gastric mucosa of the majority of cases of gastric MALT lymphoma^[14,15]. Additionally, eradication of *H pylori* was reported to result in the complete regression of the majority of these tumors^[16,17]. However, the exact mechanism responsible for the development of MALT lymphoma still remains obscure.

The contribution of COX-2 to carcinogenesis and the malignant phenotype of tumor cells have been thought to be related to its abilities: (1) increase production of prostaglandins^[18]; (2) convert procarcinogens to carcinogens^[19]; (3) inhibit apoptosis^[20]; (4) promote angiogenesis^[21]; (5) modulate inflammation and immune function^[22,23]; (6) increase tumor cell invasiveness^[24,25]. Like COX-2, iNOS is also involved in the process of carcinogenesis. Sustained induction of iNOS in chronic inflammation may be mutagenic through NO-mediated DNA damage or hindrance to DNA repair, and thus potentially carcinogenic. In addition, NO can favour tumor growth and development by stimulating angiogenesis^[10,26-28] and causing immunosuppression^[29].

In the current study, we demonstrated that a high positive immunostaining rate for COX-2 and iNOS was observed in gastric MALT lymphoma. Our results agree with the findings of previous investigations^[4,5,14,17]. The present results indicated that the increased expression of COX-2 and iNOS might be important molecular events that contribute to gastric MALT lymphoma carcinogenesis. We speculate that *H pylori* infection might induce gastric carcinogenesis via overexpression of COX-2. These processes may be completed by the expression of COX-2 as an inflammation enzyme to release excessive amounts of prostaglandins, leading to further proliferation, reduction in apoptosis, angiogenesis and tumor growth.

It has been reported that COX-2 overexpression in tumors significantly correlates with iNOS overexpression^[4,5]. In the current study, we also discovered that COX-2 expression was positively correlated with iNOS expression, suggesting a link between the COX-2 and iNOS pathways. In addition, iNOS and COX-2 may play a synergistic role in the pathogenesis of gastric MALT lymphoma. Because the product of iNOS catalysis, NO, is an important regulator of COX-2 activity and expression^[30,31], and the products of COX-2 (diverse prostaglandins) may also influence iNOS expression^[32]. Furthermore, prostaglandins and NO have been proposed to be involved in angiogenesis *in vivo*^[33]. The inhibition of NO production by COX-2 inhibitors suggests NO-COX cross-talk between COX-2 and iNOS pathways^[34].

Our results demonstrated that COX-2 expression in MALT lymphoma tissues was positively correlated with cell proliferative activity analyzed by Ki-67 labeling index. Ki-67 is expressed in cells that undergo active proliferation and have left the G₀ phase of the cell cycle^[35]. These results suggest that COX-2 expression may be actively associated with the modulation of cellular proliferation and transformation during the evolution of *H pylori*-associated gastritis to MALT lymphoma.

So far, there have been some ambiguous points with regard to relationships between COX-2 overexpression and clinicopathological characteristics of tumors. Several reports have demonstrated that COX-2 expression in various tumors influences tumor cell differentiation, invasiveness, size, and survival^[36]. However, we found no significant relation between COX-2 expression and clinicopathological characteristics in our study, which was compatible with previous reports on other organs^[37].

Low-grade MALT lymphoma can transform into high-grade lymphoma and is associated with other genetic events such as p53 inactivation^[38,39]. In the current study, p53 positivity increased significantly as the histological grade advanced. The results of our study support the concept that the expression of p53 in gastric lymphomas may be associated with transformation from low-grade to high-grade disease. In addition, there have been many workers reporting that high-proliferation rate is associated with the presence of a large cell component of MALT lymphoma^[40,41]. The results of our experiments showed that high proliferation rate expressed by Ki-67 was correlated with HG tumors. These suggested that high proliferation index in MALT lymphoma may help in identifying a population of patients with an increased risk of developing MALT lymphoma.

Consistent with the findings of others^[40], we found that COX-2 overexpression was closely associated with p53 accumulation status. With regard to the negative regulation of COX-2, it has recently been shown that wild-type p53 suppresses promoter activities of COX-2 and the expression of COX-2 protein. Wild-type p53 was shown to suppress COX-2 promoter activity by competing with TATA-binding proteins^[41]. Han *et al.*^[42] identified that COX-2 expression was inducible by wild-type p53 and DNA damage. They also found that p53-induced COX-2 expression resulted from p53-mediated activation of the Ras/Raf/MAPK cascade, as demonstrated by suppression of COX-2 induction in response to p53 by dominant-negative Ras or Raf1 mutants. Furthermore, heparin-binding epidermal growth factor-like growth factor (HB-EGF), a p53 downstream target gene, induced COX-2 expression, implying that COX-2 is an ultimate effector in the p53→HB-EGF→Ras/Raf/MAPK→COX-2 pathway.

In conclusion, COX-2 is expressed in the majority of gastric MALT lymphoma tissues and correlates with cellular proliferation and iNOS expression. iNOS and COX-2 may play a synergistic role in the pathogenesis of gastric MALT lymphoma. COX-2 overexpression is closely associated with p53 accumulation status. The molecular basis for the expression of COX-2 and iNOS and their roles in the evolution of *H pylori*-associated gastritis to gastric MALT lymphoma requires to be carefully investigated in follow-up studies.

REFERENCES

- Nakamura S**, Akazawa K, Yao T, Tsuneyoshi M. A clinicopathologic study of 233 cases with special reference to evaluation with the MIB-1 index. *Cancer* 1995; **76**: 1313-1324
- Konturek PC**, Konturek SJ, Starzyska T, Marlicz K, Bielanski W, Pierzchalski P, Karczewska E, Hartwich A, Rembiasz K, Lawniczak M, Ziemniak W, Hahn EC. *Helicobacter pylori*-gastrin link in MALT lymphoma. *Aliment Pharmacol Ther* 2000; **14**: 1311-1318
- Fu S**, Ramanujam KS, Wong A, Fantry GT, Drachenberg CB, James SP, Meltzer SJ, Wilson KT. Increased expression and cellular localization of inducible nitric oxide synthase and cyclooxygenase 2 in *Helicobacter pylori* gastritis. *Gastroenterology* 1999; **116**: 1319-1329
- Kong G**, Kim EK, Kim WS, Lee KT, Lee YW, Lee JK, Paik SW, Rhee JC. Role of cyclooxygenase-2 and inducible nitric oxide synthase in pancreatic cancer. *J Gastroenterol Hepatol* 2002; **17**: 914-921
- Nose F**, Ichikawa T, Fujiwara M, Okayasu I. Up-regulation of cyclooxygenase-2 expression in lymphocytic thyroiditis and thyroid tumors: significant correlation with inducible nitric oxide synthase. *Am J Clin Pathol* 2002; **117**: 546-551
- Denkert C**, Winzer KJ, Muller BM, Weichert W, Pest S, Kobel M, Kristiansen G, Reles A, Siegert A, Guski H, Hauptmann S. Elevated expression of cyclooxygenase-2 is a negative prognostic factor for disease free survival and overall survival in patients with breast carcinoma. *Cancer* 2003; **97**: 2978-2987
- Liu JW**, Li KZ, Dou KF. Expression of cyclooxygenase-2 in pancreatic cancer and its correlation with p53. *Shijie Huaren Xiaohua Zazhi* 2003; **11**: 229-232
- Bing RJ**, Miyataka M, Rich KA, Hanson N, Wang X, Slosser HD, Shi SR. Nitric oxide, prostanoids, cyclooxygenase, and angiogenesis in colon and breast cancer. *Clin Cancer Res* 2001; **7**: 3385-3392
- Xu MH**, Deng CS, Zhu YQ, Lin J. Role of inducible nitric oxide synthase expression in aberrant crypt foci-adenoma-carcinoma sequence. *World J Gastroenterol* 2003; **9**: 1246-1250
- Song ZJ**, Gong P, Wu YE. Relationship between the expression of iNOS, VEGF, tumor angiogenesis and gastric cancer. *World J Gastroenterol* 2002; **8**: 591-595
- Harris NL**, Jaffe ES, Stein H, Banks PM, Chan JK, Cleary ML, Delsol G, De Wolf-Peeters C, Falini B, Gatter KC. A revised European-American classification of lymphoid neoplasms: a proposal from the International Lymphoma Study Group. *Blood* 1994; **84**: 1361-1392
- Harris NL**, Jaffe ES, Diebold J, Flandrin G, Muller-Hermelink HK, Vardiman J, Lister TA, Bloomfield CD. World Health Organization classification of neoplastic diseases of the hematopoietic and lymphoid tissues: report of the clinical advisory committee meeting-airline house, virginia, november 1997. *J Clin Oncol* 1999; **17**: 3835-3849
- Du MQ**, Isaacson PG. Recent advances in our understanding of the biology and pathogenesis of gastric mucosa-associated lymphoid tissue (malt) lymphoma. *Forum* 1998; **8**: 162-173
- Konturek PC**, Konturek SJ, Pierzchalski P, Bielanski W, Duda A, Marlicz K, Starzyska T, Hahn EG. Cancerogenesis in *Helicobacter pylori* infected stomach-role of growth factors, apoptosis and cyclooxygenases. *Med Sci Monit* 2001; **7**: 1092-1107
- Konturek SJ**, Konturek PC, Hartwich A, Hahn EG. *Helicobacter pylori* infection and gastrin and cyclooxygenase expression in gastric and colorectal malignancies. *Regul Pept* 2000; **93**: 13-19
- Ohashi S**, Segawa K, Okamura S, Urano H, Kanamori S, Ishikawa H, Hara K, Hikutomi A, Shirai K, Maeda M. A clinicopathologic study of gastric mucosa-associated lymphoid tissue lymphoma. *Cancer* 2000; **88**: 2210-2219
- Konturek PC**, Konturek SJ, Pierzchalski P, Starzyska T, Marlicz K, Hartwich A, Zuchowicz M, Darasz Z, Papiez D, Hahn EG. Gastric MALT-lymphoma, gastrin and cyclooxygenases. *Acta Gastroenterol Belg* 2002; **65**: 17-23
- Zweifel BS**, Davis TW, Ornberg RL, Masferrer JL. Direct evidence for a role of cyclooxygenase 2-derived prostaglandin E2 in human head and neck xenograft tumors. *Cancer Res* 2002; **62**: 6706-6711
- Hosomi Y**, Yokose T, Hirose Y, Nakajima R, Nagai K, Nishiwaki Y, Ochiai A. Increased cyclooxygenase 2 (COX-2) expression occurs frequently in precursor lesions of human adenocarcinoma of the lung. *Lung Cancer* 2000; **30**: 73-81
- Miyata Y**, Koga S, Kanda S, Nishikido M, Hayashi T, Kanetake H. Expression of cyclooxygenase-2 in renal cell carcinoma: correlation with tumor cell proliferation, apoptosis, angiogenesis, expression of matrix metalloproteinase-2, and survival. *Clin Cancer Res* 2003; **9**: 1741-1749
- Kim MH**, Seo SS, Song YS, Kang DH, Park IA, Kang SB, Lee HP. Expression of cyclooxygenase-1 and -2 associated with expression of VEGF in primary cervical cancer and at metastatic lymph nodes. *Gynecol Oncol* 2003; **90**: 83-90
- Ermert L**, Dierkes C, Ermert M. Immunohistochemical expression of cyclooxygenase isoenzymes and downstream enzymes in human lung tumors. *Clin Cancer Res* 2003; **9**: 1604-1610
- Sharma S**, Stolina M, Yang SC, Baratelli F, Lin JF, Atianzar K, Luo J, Zhu L, Lin Y, Huang M, Dohadwala M, Batra RK, Dubinett SM. Tumor Cyclooxygenase 2-dependent suppression of dendritic cell function. *Clin Cancer Res* 2003; **9**: 961-968
- Zhang H**, Sun XF. Overexpression of cyclooxygenase-2 correlates with advanced stages of colorectal cancer. *Am J Gastroenterol* 2002; **97**: 1037-1041
- Wu QM**, Li SB, Wang Q, Wang DH, Li XB, Liu CZ. The expression of COX-2 in esophageal carcinoma and its relation to clinicopathologic characteristics. *Shijie Huaren Xiaohua Zazhi* 2001; **9**: 11-14
- Cianchi F**, Cortesini C, Fantappie O, Messerini L, Schiavone N, Vannacci A, Nistri S, Sardi I, Baroni G, Marzocca C, Perna F, Mazzanti R, Bechi P, Masini E. Inducible nitric oxide synthase

- expression in human colorectal cancer: correlation with tumor angiogenesis. *Am J Pathol* 2003; **162**: 793-801
- 27 **Tao WH**, Deng CS, Zhu YQ. Expression of inducible nitric oxide synthase and angiogenesis in gastric cancer. *Shijie Huaren Xiaohua Zazhi* 2003; **11**: 33-35
- 28 **Franchi A**, Gallo O, Paglierani M, Sardi I, Magnelli L, Masini E, Santucci M. Inducible nitric oxide synthase expression in laryngeal neoplasia: correlation with angiogenesis. *Head Neck* 2002; **24**: 16-23
- 29 **Kojima M**, Morisaki T, Tsukahara Y, Uchiyama A, Matsunari Y, Mibu R, Tanaka M. Nitric oxide synthase expression and nitric oxide production in human colon carcinoma tissue. *J Surg Oncol* 1999; **70**: 222-229
- 30 **Liu Q**, Chan ST, Mahendran R. Nitric oxide induces cyclooxygenase expression and inhibits cell growth in colon cancer cell lines. *Carcinogenesis* 2003; **24**: 637-642
- 31 **Perez-Sala D**, Lamas S. Regulation of cyclooxygenase-2 expression by nitric oxide in cells. *Antioxid Redox Signal* 2001; **3**: 231-248
- 32 **Kobayashi O**, Miwa H, Watanabe S, Tsujii M, Dubois RN, Sato N. Cyclooxygenase-2 downregulates inducible nitric oxide synthase in rat intestinal epithelial cells. *Am J Physiol Gastrointest Liver Physiol* 2001; **281**: G688-G696
- 33 **Davel L**, D'Agostino A, Espanol A, Jasnis MA, Lauria de Cidre L, de Lustig ES, Sales ME. Nitric oxide synthase-cyclooxygenase interactions are involved in tumor cell angiogenesis and migration. *J Biol Regul Homeost Agents* 2002; **16**: 181-189
- 34 **Fantappie O**, Masini E, Sardi I, Raimondi L, Bani D, Solazzo M, Vannacci A, Mazzanti R. The MDR phenotype is associated with the expression of COX-2 and iNOS in a human hepatocellular carcinoma cell line. *Hepatology* 2002; **35**: 843-852
- 35 **Scholzen T**, Gerdes J. The Ki-67 protein: from the known and the unknown. *J Cell Physiol* 2000; **182**: 311-322
- 36 **Rajnakova A**, Mochhala S, Goh PM, Ngoi S. Expression of nitric oxide synthase, cyclooxygenase, and p53 in different stages of human gastric cancer. *Cancer Lett* 2001; **172**: 177-185
- 37 **Kokawa A**, Kondo H, Gotoda T, Ono H, Saito D, Nakadaira S, Kosuge T, Yoshida S. Increased expression of cyclooxygenase-2 in human pancreatic neoplasms and potential for chemoprevention by cyclooxygenase inhibitors. *Cancer* 2001; **91**: 333-338
- 38 **Insabato L**, Di Vizio D, Tornillo L, D'Armiento FP, Siciliano A, Milo M, Palmieri G, Pettinato G, Terracciano LM. Clinicopathologic and immunohistochemical study of surgically treated primary gastric MALT lymphoma. *J Surg Oncol* 2003; **83**: 106-111
- 39 **Pozzi B**, Hotz AM, Feltri M, Cornaggia M, Campiotti L, Bonato M, Pinotti G, Capella C. Primary gastric lymphomas. Clinicopathological study and evaluation of prognostic factors in 65 cases treated surgically. *Pathologica* 2000; **92**: 503-515
- 40 **Niki T**, Kohno T, Iba S, Moriya Y, Takahashi Y, Saito M, Maeshima A, Yamada T, Matsuno Y, Fukayama M, Yokota J, Hirohashi S. Frequent co-localization of Cox-2 and laminin-5 gamma2 chain at the invasive front of early-stage lung adenocarcinomas. *Am J Pathol* 2002; **160**: 1129-1141
- 41 **Subbaramaiah K**, Altorki N, Chung WJ, Mestre JR, Sampat A, Dannenberg AJ. Inhibition of cyclooxygenase-2 gene expression by p53. *J Biol Chem* 1999; **274**: 10911-10915
- 42 **Han JA**, Kim JI, Ongusaha PP, Hwang DH, Ballou LR, Mahale A, Aaronson SA, Lee SW. P53-mediated induction of Cox-2 counteracts p53- or genotoxic stress-induced apoptosis. *EMBO J* 2002; **21**: 5635-5644

Edited by Kumar M Proofread by Chen WW and Xu FM

Endostatin gene therapy for liver cancer by a recombinant adenovirus delivery

Li Li, Jia-Ling Huang, Qi-Cai Liu, Pei-Hong Wu, Ran-Yi Liu, Yi-Xin Zeng, Wen-Lin Huang

Li Li, Jia-Ling Huang, Ran-Yi Liu, Pei-Hong Wu, Yi-Xin Zeng, Wen-Lin Huang, Cancer Center, Sun Yat-sen University, 651 Dongfeng Road East, Guangzhou 510060, Guangdong Province, China
Qi-Cai Liu, Experimental Medical Research Center, Guangzhou Medical College, 195 Dongfeng Road West, Guangzhou 510182, Guangdong Province, China

Supported by the National High Technology Research and Development Program of China (863 Program), No. 2003AA216061 and CMB-SUMS Scholar Program, No. 98-677 and Guangdong Provincial Science and Technology Program, No. 2003A10902

Co-first-authors: Jia-Ling Huang and Qi-Cai Liu

Correspondence to: Dr. Wen-Lin Huang, Cancer Center, Sun Yat-sen University, 651 Dongfeng Road East, Guangzhou 510060, Guangdong Province, China. wl_huang@hotmail.com

Telephone: +86-20-87343146 **Fax:** +86-20-87343392

Received: 2004-01-15 **Accepted:** 2004-02-21

Abstract

AIM: To investigate the expression of adenovirus-mediated human endostatin (Ad/hEndo) gene transfer and its effect on the growth of hepatocellular carcinoma (HCC) BEL-7402 xenografted tumors.

METHODS: Immunohistochemistry analysis with an anti-endostatin antibody was performed to detect endostatin protein expression in HCC BEL-7402 cells infected with Ad/hEndo. MTT assay was used to investigate the effects of Ad/hEndo on proliferation of human umbilical vein endothelial cells (HUVEC). Intra-tumoral injections of 1×10^9 pfu Ad/hEndo was given to treat BEL-7402 xenografted tumors in nude mice once weekly for 6 wk. Mice received injections of Ad/LacZ and DMEM were regarded as control groups. After intra-tumoral administration with Ad/hEndo, the endostatin mRNA expression in tumor tissue was analyzed by Northern blotting, and plasma endostatin levels were determined using enzyme-linked immunosorbent assay (ELISA).

RESULTS: High level expression of endostatin gene was detected in the infected HCC BEL-7402 cells. Ad/hEndo significantly inhibited HUVEC cell proliferation by 57.2% at a multiplicity of infection (MOI) of 20. After 6-week treatment with Ad/hEndo, the growth of treated tumors was inhibited by 46.50% compared to the Ad/LacZ control group ($t=2.729$, $P<0.05$) and by 48.56% compared to the DMEM control group ($t=2.485$, $P<0.05$). The ratio of mean tumor volume in treated animals to mean tumor volume in the control animals (T:C ratio) was less than 50% after 24 d of treatment. Endostatin mRNA in tumor tissue was clearly demonstrated as a band of approximately 1.2 kb, which was the expected size of intact and functional endostatin. Plasma endostatin levels peaked at 87.52 ± 8.34 ng/mL at d 3 after Ad/hEndo injection, which was significantly higher than the basal level (12.23 ± 2.54 ng/mL). By d 7, plasma levels dropped to nearly half the peak level (40.34 ± 4.80 ng/mL).

CONCLUSION: Adenovirus-mediated human endostatin

gene can successfully express endogenous endostatin *in vitro* and *in vivo*, and significantly inhibit the growth of BEL-7402 xenografted liver tumors in nude mice.

Li L, Huang JL, Liu QC, Wu PH, Liu RY, Zeng YX, Huang WL. Endostatin gene therapy for liver cancer by a recombinant adenovirus delivery. *World J Gastroenterol* 2004; 10(13): 1867-1871

<http://www.wjgnet.com/1007-9327/10/1867.asp>

INTRODUCTION

Increasing evidence suggests that solid tumors and their metastasis are angiogenesis dependent^[1]. Angiogenesis, the formation of new microvessels generated by vascular endothelial cells, provides essential nutrition for rapid growth of malignant cells. Without angiogenesis, neoplasm might remain in dormancy^[2]. Anti-angiogenesis therapies, which block the blood supply of a growing tumor by inhibiting proliferation of endothelial cells, provide a new strategy for treatment of solid tumors^[3]. Vascular endothelial cells, the target of anti-angiogenic treatment are genetically stable. So it is unlikely that anti-angiogenic agents would induce the drug resistance^[4].

Transcatheter arterial embolization (TAE) has been widely practiced in the treatment of unresectable hepatocellular carcinoma (HCC)^[5]. However, the obstruction of hepatic artery induces extensive ischemic necrosis or hypoxia which are strongly correlated with increased expression of angiogenic factors, such as vascular endothelial growth factor (VEGF), basic fibroblast growth factor (bFGF)^[6]. The proliferative activity of vascular endothelial cells and tumour cells was increased in residual tumor following arterial embolization^[7]. Combination of antiangiogenesis and TAE therapy could inhibit increased proliferation of vascular endothelial cells and capillary vessel formation induced by arterial embolization, and improve the therapeutic effect^[5].

Endostatin, a carboxyl-terminal proteolytic fragment of collagen XVIII, was regarded as one of the most potent inhibitors of tumor angiogenesis^[8]. Several studies have shown that recombinant endostatin protein generated from *Escherichia coli* and *Pichia pastoris* yeast significantly inhibited growth and metastasis of xenografted tumor in different tumor models with no drug resistance and side effects^[9,10]. However, its widespread application has been hampered by difficulties in the large-scale production of high bioactive protein^[11,12].

In this study, we constructed a replication-defective recombinant adenoviral vector harboring a human endostatin gene (Ad/hEndo), and demonstrated efficient expression of endostatin gene *in vivo* and its antitumoral effect on BEL-7402 xenografted liver tumors in nude mice.

MATERIALS AND METHODS

Materials

Cells and adenoviruses BEL-7402 cells (Hepatocellular

carcinoma, HCC) and human umbilical vein endothelial cells (HUVEC) were maintained in RPMI 1640 supplemented with 100 mL/L fetal bovine serum (FBS). The culture medium contained 100 U/mL of penicillin and 100 µg/mL of streptomycin (GIBCO BRL, Gaithersburg, MD).

Recombinant adenovirus vectors carrying the human endostatin gene (Ad/hEndo) and *LacZ* gene (Ad/*LacZ*) were generated as described previously^[12,13]. All virus particles were amplified in 293 cells and purified by cesium chloride gradient centrifugation. Viruses were titered using a standard plaque-forming unit (pfu) assay.

Animals Four to 6-week-old male BALB/c nude mice (with body weight of 19 to 23 g) were purchased from Animal Experiment Center (Medial College, Sun Yat-sen University) and maintained in a specific pathogen-free (SPF) environment (certificate: 26-99S029).

Agents Human endostatin protein accucyte EIA (Oncogene Research Products, Boston, MA), rabbit anti-human endostatin polyclonal antibody (Chemicon International, Temecula, CA).

Methods

Immunohistochemistry for expression of endostatin protein *in vitro* BEL-7402 cells were infected with Ad/hEndo at a multiplicity of infection (MOI) of 10. At 2 h postinfection, the medium was replaced with Dulbecco's minimal essential medium (DMEM) containing 100 mL/L FBS. After 72-h incubation, cells were collected and plated on slides. The slides were washed, fixed and blocked for 20 min in Tris-buffered saline (TBS) containing 10 mL/L goat serum, then incubated with rabbit anti-human endostatin polyclonal antibody diluted 1:50 in PBS overnight. After washing 3 times, biotinylated goat anti-rabbit secondary antibody (Dako Corp., Carpinteria, CA) diluted 1:200 in PBS was added, and slides were incubated for an additional 30 min. Slides were then washed 3 times with PBS and stained with streptavidin-biotinylated horseradish peroxidase complex.

HUVEC cells proliferation assay Human umbilical vein endothelial cells (HUVEC) were seeded in a 96-well plate at a density of 1×10^4 /well and allowed to adhere overnight. Cells were then infected for 2 h with Ad/hEndo at MOIs of 0.05, 0.5, 1.0, 5.0, 10 and 20, and with Ad/*LacZ* at an MOI of 20. Cells were washed 3 times with PBS and incubated at 37 °C in fresh medium. Seventy-two hours later, 20 µL of 3-(4,5-dimethylthiazol-2-yl)-2,5-diphenyl-2H-tetrazolium bromide (MTT) (Fluka Biochemika, Buchs, Switzerland) was added to the wells and the plate was incubated for an additional 4 h at 37 °C. Then, 100 µL DMSO was added to the wells and the plate was incubated for 10 min at 37 °C. Absorbance was read using a Bio-Rad 550 microplate reader (Bio-Rad Laboratories, Hercules, CA) at 570 nm. The value of the treated cells was calculated as percent of the untreated control.

***In vivo* tumor growth inhibition** BEL-7402 cells were subcutaneously inoculated into the flanks of 6-week-old female BALB/c nude mice (5×10^6 cells in 200 µL). Ten days after tumor cell inoculation, intra-tumoral injections of virus (Ad/hEndo or Ad/*LacZ*; 1×10^9 pfu in 100 µL) was given once weekly for 6 wk. An additional 7 animals received injections of 100 µL of DMEM as a negative control. Tumors were measured with a caliper gauge twice a week over a 6-week period following the initial virus injections. Tumor volume was calculated according to the formula: volume = width² × length × 0.52^[10]. One week after the 6th injection of Ad/hEndo, the mice were sacrificed and the xenografted tumors were excised and weighed. The inhibition rates of growth of BEL-7402 xenografted tumors were calculated according to the formula: Inhibition rate (%) = (1 - mean Weight_(Ad/hEndo) / mean Weight_(control)) × 100.

Northern blotting for expression of endostatin mRNA *in vivo* On d 1, 4 and 8 after intra-tumoral administration with 100 µL

of 1×10^9 pfu Ad/hEndo, the mice were sacrificed. The xenografted tumors were excised and snap frozen in liquid nitrogen. Total RNA was isolated from tumor tissues using the Trizol reagent (Invitrogen) according to the manufacturer's instructions. RNA isolated from the tumors injected with DMEM was used as a negative control. Total RNA of 15 µg was resolved on a 10 g/L formaldehyde agarose gel, and transferred to nylon membrane. The RNA was fixed onto the membrane by UV cross-linking. The membrane was prehybridized in DIG Easy Hyb hybridization solution (Roche, Basel, Switzerland) at 68 °C for 30 min, then hybridized in DIG Easy Hyb hybridization solution containing digoxin (DIG)-labeled endostatin probe at 68 °C overnight. The membrane was incubated with anti-DIG antibody for 30 min and stained with NBT/BCIP for 10 min.

Plasma endostatin levels detected by ELISA Blood samples were harvested on d 0, 3 and 7 after intra-tumoral administration with 100 µL of 1×10^9 pfu Ad/hEndo. Samples were centrifuged, and plasma endostatin levels were determined using a human endostatin enzyme-linked immunosorbent assay (ELISA) kit (Oncogene Research Products, Boston, MA), according to the manufacturer's instructions.

Pathological observation One week after the 6th course of treatment, the animals were sacrificed. The major organs including heart, liver, spleen, kidney, lung and brain were extracted from the nude mice, fixed in 40 g/L buffered formaldehyde phosphate, cut into 4 µm thick for tissue section and stained with haematoxylin and eosin.

RESULTS

High level transgene expression in BEL-7402 cells infected with Ad/hEndo

Three days after transfection with Ad/hEndo at a MOI of 10, BEL-7402 cells were probed with rabbit anti-human endostatin antibody. Immunohistochemistry with an anti-endostatin antibody clearly demonstrated that endostatin protein was expressed in the transduced BEL-7402 cells. Extensive positive staining was observed in the cytoplasm of transduced cells (Figure 1). This indicated that human endostatin gene mediated by recombinant adenovirus was highly expressed in BEL-7402 cells and provided evidence for the feasibility of local gene therapy for HCC BEL-7402 xenografted tumors.

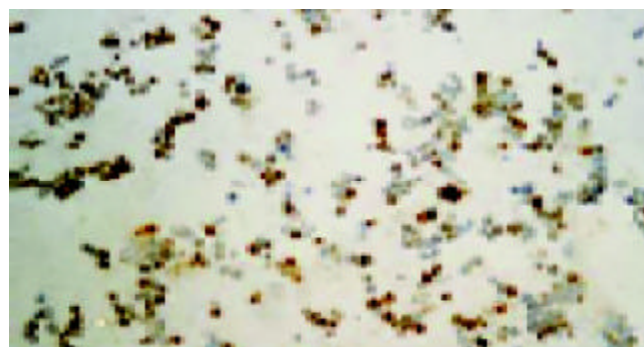


Figure 1 Immunohistochemistry analysis for endostatin protein *in vitro* (×100). Extensive positive staining was observed in the cytoplasm of transduced cells. This indicated that human endostatin gene mediated by recombinant adenovirus was highly expressed in BEL-7402 cells.

Inhibition of proliferation of HUVEC cells by Ad/hEndo

In order to investigate the effects of this secreted endostatin on proliferation of HUVEC cells, cell proliferation assays were performed by MTT assay. Ad/hEndo inhibited HUVEC cell proliferation by 7.61%, 12.61%, 24.8%, 29.86%, 38.78% and 57.2% at MOIs of 0.05, 0.5, 1.0, 5, 10 and 20, respectively. The

Ad/LacZ control group showed inhibition of cellular proliferation by 7.25% at a MOI of 20 (Figure 2). These results indicated that the endostatin protein secreted by the transduced cells was highly bioactive and inhibited the proliferation of vascular endothelial cells *in vitro* in a dose-dependent manner, while the viral vector alone did not.

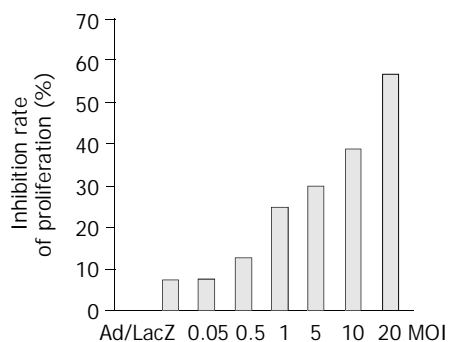


Figure 2 Effect of Ad/hEndo on the proliferation of HUVEC cells.

Inhibition of the growth of BEL-7402 xenograft tumors by Ad/hEndo

In order to observe the effect of Ad/hEndo on the growth of tumors, we established a BEL-7402 xenograft tumor model in BALB/c nude mice. After 6 wk of treatment, the growth of treated tumors was inhibited by 46.50% compared to the Ad/LacZ control group ($t=2.729$, $P<0.05$) and by 48.56% compared to the DMEM control group ($t=2.485$, $P<0.05$). The ratio of mean tumor volume in treated animals to that of the control animals (T:C ratio) was <50% after 24 d of treatment (Figure 3). These results showed that Ad/hEndo significantly inhibited the growth of BEL-7402 xenografted tumors.

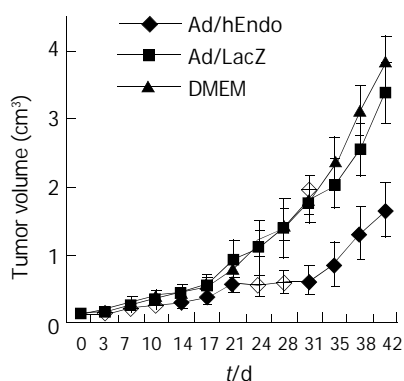


Figure 3 Effect of Ad/hEndo on growth of BEL-7402 xenografted liver tumors.

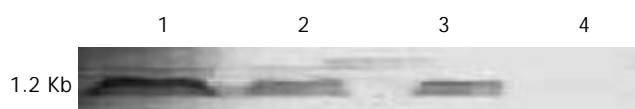


Figure 4 Northern blotting of endostatin mRNA *in vivo*. Lanes 1-3: RNA extracted from tumors on d 1, 4 and 8 after Ad/hEndo injection, respectively; Lane 4: RNA extracted from control tumors injected with DMEM.

Full-length expression of endostatin mRNA *in vivo*

Northern blotting was performed to test whether the *in vivo* expressed endostatin mRNA was of full-length. After hybridization, the membrane was stained with NBT/BCIP, and endostatin mRNA was clearly demonstrated as a band of

approximately 1.2 kb (Figure 4), which was the expected size of intact and functional endostatin. The highest level of endostatin mRNA *in vivo* was detected 1 d after intra-tumoral administration of Ad/hEndo. On d 4 and 8, endostatin mRNA levels significantly decreased. Therefore, Northern blotting showed that adenovirus-mediated human endostatin gene transfer resulted in expression of intact endostatin mRNA *in vivo*.

Plasma levels of endostatin protein

ELISA was used to measure the plasma endostatin levels. Plasma endostatin levels peaked at 87.52 ± 8.34 ng/mL on d 3 after Ad/hEndo injection, which was significantly higher than the basal level (12.23 ± 2.54 ng/mL). By d 7, plasma levels dropped to half the peak level (40.34 ± 4.80 ng/mL) (Figure 5). These results showed that intra-tumoral delivery of the endostatin gene resulted in high plasma endostatin concentrations.

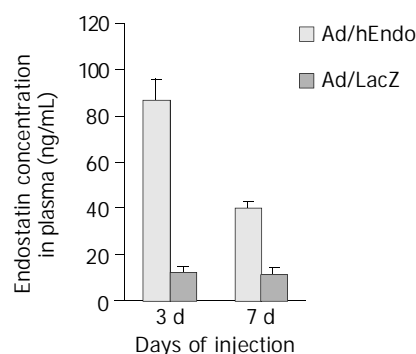


Figure 5 Detection of endostatin concentration in plasma by ELISA.

Pathological changes of main organs

All animals were survived and appeared to be physically normal. There were no histological changes in main organs of DMEM control animals. However, histological examination in several mice of the Ad/hEndo (3/8) and Ad/LacZ (3/8) groups revealed slight to modest hepatocyte fatty degeneration, cloudy swelling and occasional necrosis accompanied with infiltration of lymphocyte and inflammatory cells. (Figure 6) One mouse in Ad/hEndo group (1/8) and 1 in Ad/LacZ (1/8) group demonstrated slight cloudy swelling in some proximal renal tubule cells and distal renal tubule cells. No histological changes were found in spleen, lung, heart and brain of both these groups. There was no significant difference in histological changes between Ad/hEndo group and Ad/LacZ group. These results suggested that it was the recombinant adenoviruses, not endostatin protein that caused the liver and kidney toxicity.

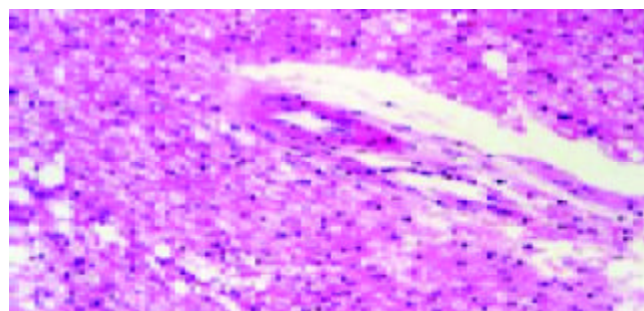


Figure 6 Pathological changes of liver 1 wk after 6 wk of treatment with Ad/hEndo (HE, original magnification: $\times 200$).

DISCUSSION

Animal experiments on angiogenesis have frequently been conducted on tumors recently implanted in mice. However, in

the human situation, tumors are often established for months or years and may possess mature vasculature that is less sensitive to anti-angiogenic therapy^[1,2]. Indeed, antiangiogenesis therapies, which inhibit the growth and metastasis of neoplasms by blocking the formation of new blood vessels from existing vessels, appear to require long-term administration of the angiogenic inhibitor to ensure tumor growth suppression^[3]. Endostatin protein derived from yeast (*Pichia pastoris*) had been introduced into clinical trials as a possible antiangiogenic tumor fighting drug^[15]. The clinical studies showed that the mean half-life of recombinant human endostatin was only 10.7±4.1 h in the human body, suggesting that this protein-based therapy was likely to require repeated daily or long-term administration of high-quality protein for optimal therapeutic benefits^[16].

It is hoped that these difficulties of protein-based therapy may be overcome by direct expression of therapeutic gene in the body^[17]. Endostatin gene therapy is a promising strategy for anti-angiogenic therapy, for a single transduction of endostatin gene could achieve a relatively long-term and high-quality protein expression *in vivo*^[17,18]. Adenoviral vectors are commonly used as carriers for gene transfer due to their high efficiency and high capacity^[19,20]. We cloned the human endostatin gene into an adenoviral shuttle plasmid and generated an adenoviral expressing system which resulted in highly efficient expression of endostatin gene and demonstrated high level of bioactivity by significantly inhibiting the proliferation of endothelial cells. In our studies, endostatin gene therapy using a recombinant adenovirus delivery significantly inhibited the growth of BEL-7402 xenografted liver tumors. Since d 24 of treatment with intra-tumoral injection with Ad/hEndo, the T:C ratio of mean tumor volume was less than 50%. After 6 courses of treatment, the growth of xenografted tumors treated with Ad/hEndo was markedly inhibited as compared with the control group.

Adenovirus can infect dividing and nondividing cells and obtain high efficiency of transgene expression^[21,22]. These properties of adenoviral vector provide the possibility of local treatment, such as intra-tumoral injection and transcatheter arterial infusion of recombinant adenovirus^[23]. In this study, we investigated the possibility of tumor-targeted endostatin gene therapy for liver cancer. First, we demonstrated high level transgene expression in BEL-7402 cells infected with Ad/hEndo. Then, intra-tumoral endostatin mRNA expression was clearly detected by Northern blotting on d 1 after injection with Ad/hEndo. Northern blotting indicated that the endostatin mRNA expressed inside tumor tissue was intact, thus the resultant endostatin protein could be biologically active *in vivo*. These positive results had provided solid evidence for local endostatin gene therapy for liver cancer.

The tumor-targeted gene therapy produced endostatin protein mostly inside the tumors^[23,24], however, some of the protein entered the circulation, resulting in the peak of plasma endostatin concentration of 87.52±8.34 ng/mL by d 3 post-administration. Although this plasma level was considerably lower than those reached by intravenous delivery of recombinant adenoviral vector for endostatin gene therapy^[19,20], it had been shown that circulating endostatin levels of 35–40 ng/mL was sufficient to exert an antiangiogenic effect *in vivo*^[24], suggesting that our delivery system was able to induce therapeutically relevant circulating endostatin levels.

The transient expression is a key problem for any therapeutic use^[23,25], while the reason for the transient *in vivo* transgene expression is unclear^[26,27]. Repetition of administration with therapeutic gene *in vivo* using a transgene vector was recommended to achieve better therapeutic effect^[23,28,29]. However, multiple injections of immunogenic transgene vector will get an immune response to the vector which not only make

expression even worse, but also cause systemic toxicity^[30,31]. Indeed, we observed slight liver and renal damage in mice after 6 courses of endostatin gene therapy using a recombinant adenovirus delivery. Histological examination in several mice administrated with adenoviral vector revealed slight to modest hepatocyte and renal tubule cell degeneration and some degree of inflammatory reaction. It was the recombinant adenovirus, not endostatin protein that caused the liver and kidney toxicity^[27,32]. Our results suggested that cautions should be taken for clinical repeated administration within a short time of the recombinant adenoviral vector carrying endostatin gene.

In conclusion, a recombinant adenoviral vector carrying human endostatin gene can be successfully constructed, with highly efficient expression of endostatin gene both *in vitro* and *in vivo*, thereby significantly inhibiting the growth of BEL-7402 xenografted liver tumors in nude mice.

REFERENCES

- 1 **Folkman J.** What is the evidence that tumors are angiogenesis-dependent? *J Natl Cancer Inst* 1990; **82**: 4-6
- 2 **Folkman J.** Seminars in medicine of the beth israel hospital, boston. Clinical applications of research on angiogenesis. *N Engl J Med* 1995; **333**: 1757-1763
- 3 **Bergers G, Javaherian K, Lo KM, Folkman J, Hanahan D.** Effects of angiogenesis inhibitors on multistage carcinogenesis in mice. *Science* 1999; **284**: 808-812
- 4 **Boehm T, Folkman J, Browder T, O' Reilly MS.** Antiangiogenic therapy of experimental cancer does not induce acquired drug resistance. *Nature* 1997; **390**: 404-407
- 5 **Qian J, Feng GS, Vogl T.** Combined interventional therapies of hepatocellular carcinoma. *World J Gastroenterol* 2003; **9**: 1885-1891
- 6 **Li X, Feng GS, Zheng CS, Zhuo CK, Liu X.** Influence of transarterial chemoembolization on angiogenesis and expression of vascular endothelial growth factor and basic fibroblast growth factor in rat with Walker-256 transplanted hepatoma: An experimental study. *World J Gastroenterol* 2003; **9**: 2445-2449
- 7 **Kim YB, Park YN, Park C.** Increased proliferation activities of vascular endothelial cells and tumour cells in residual hepatocellular carcinoma following transcatheter arterial embolization. *Histopathology* 2001; **38**: 160-166
- 8 **O' Reilly MS, Boehm T, Shing Y, Fukai N, Vasios G, Lane WS, Flynn E, Birkhead JR, Olsen BR, Folkman J.** Endostatin: an endogenous inhibitor of angiogenesis and tumor growth. *Cell* 1997; **88**: 277-285
- 9 **Dhanabal M, Ramchandran R, Volk R, Stillman IE, Lombardo M, Iruela-Arispe ML, Simons M, Sukhatme VP.** Endostatin: yeast production, mutants, and antitumor effect in renal cell carcinoma. *Cancer Res* 1999; **59**: 189-197
- 10 **Huang X, Wong MK, Zhao Q, Zhu Z, Wang KZ, Huang N, Ye C, Gorelik E, Li M.** Soluble recombinant endostatin purified from *Escherichia coli*: antiangiogenic activity and antitumor effect. *Cancer Res* 2001; **61**: 478-481
- 11 **Chen QR, Kumar D, Stass SA, Mixson AJ.** Liposomes complexed to plasmids encoding angiostatin and endostatin inhibit breast cancer in nude mice. *Cancer Res* 1999; **59**: 3308-3312
- 12 **Ding I, Sun JZ, Fenton B, Liu WM, Kimsely P, Okunieff P, Min W.** Intratumoral administration of endostatin plasmid inhibits vascular growth and perfusion in MCa-4 murine mammary carcinomas. *Cancer Res* 2001; **61**: 526-531
- 13 **Huang W, Flint SJ.** The tripartite leader sequence of subgroup C adenovirus major late mRNAs can increase the efficiency of mRNA export. *J Virol* 1998; **72**: 225-235
- 14 **Huang W, Flint SJ.** Unusual properties of adenovirus E2E transcription by RNA polymerase III. *J Virol* 2003; **77**: 4015-4024
- 15 **Mundhenke C, Thomas JP, Wilding G, Lee FT, Kelzc F, Chappell R, Neider R, Sebree LA, Friedl A.** Tissue examination to monitor antiangiogenic therapy: a phase I clinical trial with endostatin. *Clin Cancer Res* 2001; **7**: 3366-3374
- 16 **Herbst RS, Hess KR, Tran HT, Tseng JE, Mullani NA, Charnsangavej C, Madden T, Davis DW, McConkey DJ, O' Reilly MS, Ellis LM, Pluda J, Hong WK, Abbruzzese JL.** Phase I study of recombinant human endostatin in patients

- with advanced solid tumors. *J Clin Oncol* 2002; **20**: 3792-3803
- 17 **Folkman J.** Antiangiogenic gene therapy. *Proc Natl Acad Sci U S A* 1998; **95**: 9064-9066
- 18 **Szary J, Szala S.** Intra-tumoral administration of naked plasmid DNA encoding mouse endostatin inhibits renal carcinoma growth. *Int J Cancer* 2001; **91**: 835-839
- 19 **Sauter BV, Martinet O, Zhang WJ, Mandeli J, Woo SL.** Adenovirus-mediated gene transfer of endostatin *in vivo* results in high level of transgene expression and inhibition of tumor growth and metastases. *Proc Natl Acad Sci U S A* 2000; **97**: 4802-4807
- 20 **Feldman AL, Restifo NP, Alexander HR, Bartlett DL, Hwu P, Seth P, Libutti SK.** Antiangiogenic gene therapy of cancer utilizing a recombinant adenovirus to elevate systemic endostatin levels in mice. *Cancer Res* 2000; **60**: 1503-1506
- 21 **St George JA.** Gene therapy progress and prospects: adenoviral vectors. *Gene Ther* 2003; **10**: 1135-1141
- 22 **Chen CT, Lin J, Li Q, Phipps SS, Jakubczak JL, Stewart DA, Skripchenko Y, Forry-Schaudies S, Wood J, Schnell C, Hallenbeck PL.** Antiangiogenic gene therapy for cancer via systemic administration of adenoviral vectors expressing secreted endostatin. *Hum Gene Ther* 2000; **11**: 1983-1996
- 23 **Kianmanesh A, Hackett NR, Lee JM, Kikuchi T, Korst RJ, Crystal RG.** Intratumoral administration of low doses of an adenovirus vector encoding tumor necrosis factor alpha together with naive dendritic cells elicits significant suppression of tumor growth without toxicity. *Hum Gene Ther* 2001; **12**: 2035-2049
- 24 **Shi W, Teschendorf C, Muzyczka N, Siemann DW.** Adenovirus-mediated gene transfer of endostatin inhibits angiogenesis and tumor growth *in vivo*. *Cancer Gene Ther* 2002; **9**: 513-521
- 25 **Reid T, Warren R, Kirn D.** Intravascular adenoviral agents in cancer patients: lessons from clinical trials. *Cancer Gene Ther* 2002; **9**: 979-986
- 26 **Molinier-Frenkel V, Le Boulaire C, Le Gal FA, Gahery-Segard H, Tursz T, Guillet JG, Farace F.** Longitudinal follow-up of cellular and humoral immunity induced by recombinant adenovirus-mediated gene therapy in cancer patients. *Hum Gene Ther* 2000; **11**: 1911-1920
- 27 **Wen XY, Bai Y, Stewart AK.** Adenovirus-mediated human endostatin gene delivery demonstrates strain-specific antitumor activity and acute dose-dependent toxicity in mice. *Hum Gene Ther* 2001; **12**: 347-358
- 28 **Liu Q, Muruve DA.** Molecular basis of the inflammatory response to adenovirus vectors. *Gene Ther* 2003; **10**: 935-940
- 29 **Geutskens SB, van der Eb MM, Plomp AC, Jonges LE, Cramer SJ, Ensink NG, Kuppen PJ, Hoeben RC.** Recombinant adenoviral vectors have adjuvant activity and stimulate T cell responses against tumor cells. *Gene Ther* 2000; **7**: 1410-1416
- 30 **Chen P, Kovesdi I, Bruder JT.** Effective repeat administration with adenovirus vectors to the muscle. *Gene Ther* 2000; **7**: 587-595
- 31 **Pagliari LC, Keyhani A, Williams D, Woods D, Liu B, Perrotte P, Slaton JW, Merritt JA, Grossman HB, Dinney CP.** Repeated intravesical instillations of an adenoviral vector in patients with locally advanced bladder cancer: a phase I study of p53 gene therapy. *J Clin Oncol* 2003; **21**: 2247-2253
- 32 **Reid T, Galanis E, Abbruzzese J, Sze D, Wein LM, Andrews J, Randlev B, Heise C, Uprichard M, Hatfield M, Rome L, Rubin J, Kirn D.** Hepatic arterial infusion of a replication-selective oncolytic adenovirus (dl1520): phase II viral, immunologic, and clinical endpoints. *Cancer Res* 2002; **62**: 6070-6079

Edited by Kumar M Proofread by Chen WW and Xu FM

Primary targeting of recombinant Fv-immunotoxin hscFv₂₅-mTNF α against hepatocellular carcinoma

Jing Zhang, Yan-Fang Liu, Shou-Jing Yang, Qing Qiao, Hong Cheng, Chuan-Shan Zhang, Fu-Cheng Ma, Hua-Zhang Guo

Jing Zhang, Yan-Fang Liu, Shou-Jing Yang, Hong Cheng, Chuan-Shan Zhang, Fu-Cheng Ma, Hua-Zhang Guo, Department of Pathology, Xijing Hospital, Fourth Military Medical University, Xi'an 710033, Shaanxi Province, China

Qing Qiao, Department of General Surgery, Tangdu Hospital, Fourth Military Medical University, Xi'an 710038, Shaanxi Province, China
Supported by Military 95 Major Supplementary Project, No.98M098

Correspondence to: Jing Zhang, Department of Pathology, Xijing Hospital, Fourth Military Medical University, Xi'an 710033, Shaanxi Province, China. jzhang@fmmu.edu.cn

Telephone: +86-29-83375497 **Fax:** +86-29-83375497

Received: 2003-12-28 **Accepted:** 2004-01-08

Abstract

AIM: To obtain human recombinant Fv-immunotoxin hscFv₂₅-mTNF α (mutant human TNF α fused to human scFv₂₅) against hepatocellular carcinoma (HCC).

METHODS: Two relevant sites of enzymatic digestion were added to mTNF α by PCR. mTNF α was linked to the 3' end of hscFv₂₅ in pGEX4T-1 vector. This anti-HCC recombinant Fv-immunotoxin hscFv₂₅-mTNF α was expressed in *Escherichia coli* and purified from inclusions. After purified by glutathione-S-transferase affinity chromatography and thrombin digestion, it was identified by electrophoresis and Western blot. And then, the purified recombinant Fv-immunotoxin was injected into nude mice with HCC xenografts through their tail veins. mTNF α protein and PBS were used as control at the same time. After treated for two weeks, nude mice were executed. The bulk and weight of tumors were observed. The tumor tissues were stained by immunohistochemical method with TNF α antibody.

RESULTS: The expression ratio of recombinant Fv-immunotoxin hscFv₂₅-mTNF α was 12% of bacterial protein. The result of tumor restraining trials of hscFv₂₅-mTNF α showed 2/5 complete remission and 3/5 partial remission. mTNF α restraining trials showed 5/5 partial remission. The therapeutic result of hscFv₂₅-mTNF α was better than that of mTNF α ($F=8.70$, $P<0.05$). The hscFv₂₅-mTNF α remedial tumor tissues were positive for TNF α by immunohistochemical staining. The positive granules mainly existed in the cytoplasm of tumor cell.

CONCLUSION: Recombinant Fv-immunotoxin hscFv₂₅-mTNF α has better therapeutic effect than mTNF α . It can inhibit the cellular growth of HCC and has some potential of clinical application.

Zhang J, Liu YF, Yang SJ, Qiao Q, Cheng H, Zhang CS, Ma FC, Guo HZ. Primary targeting of recombinant Fv-immunotoxin hscFv₂₅-mTNF α against hepatocellular carcinoma. *World J Gastroenterol* 2004; 10(13): 1872-1875

<http://www.wjgnet.com/1007-9327/10/1872.asp>

INTRODUCTION

Hepatocellular carcinoma (HCC) is a common malignant tumor

in China with poor prognosis^[1,2]. Its diagnosis and therapy are still major challenges^[3,4]. The single chain Fv (scFv) is consisted of heavy-chain and light-chain variable region of the antibody, linked with a peptide chain. They have shown a various application value in tumor therapy^[5-7]. Our laboratory, through collaboration with the Academy of Military Medical Science, constructed human scFv₂₅ against HCC (hscFv₂₅) several years ago^[8]. In this study, we fused human mutant tumor necrosis factor-alpha (mTNF α) to hscFv₂₅ and constructed prokaryotic expressing vector pGEX4T-1/hscFv₂₅-mTNF α . After recombinant Fv-immunotoxin hscFv₂₅-mTNF α was expressed, purified and identified, we used it in tumor restraining trials of the HCC (SMMC-7721) xenografts in nude mice.

MATERIALS AND METHODS

Main materials

Isopropyl-1-thio-D-galactopyranoside (IPTG), PCR marker, T4 ligase and thrombin were purchased from Promega. Glutathione-S-transferase affinity chromatogram and low molecular weight marker were purchased from Pharmacia. The plasmid extracting reagent kit was purchased from Huashun Biologic Co. (Shanghai, China). EnVision™ System was purchased from Dako. The mTNF α protein produce was offered by Biologic Center of the Fourth Military Medical University. The mouse anti-human TNF α monoclonal antibody was purchased from Santa Cruz, USA.

Vector construction

According to cDNA of mTNF α , *Sal* I site was added to its 5' -end and *Xho* I site to its 3' -end. The 5' primer was: ACTCTCGAG TCAGAAGGCAATGATCCCAAAGTA; and the 3' primer was: ACGCGTCGACCGCAAACGTAAGCCTGTA.

The primers were synthesized by Sangon (Shanghai, China). After digested by *Sal* I and *Xho* I restriction enzymes, mTNF α PCR products were linked to 3' -end of pGEX4T-1/hscFv₂₅, which was digested by the same restriction enzymes. And then, pGEX4T-1/hscFv₂₅-mTNF α was transformed into *E. coli* JM109. *E. coli* were cultivated in the Amp^r/LB medium at 37 °C for 16-22 h. The positive clones were selected and identified by *Eco*R I and *Sal* I, *Eco*R I and *Xho* I, *Sal* I and *Xho* I restriction enzymes analysis and 10 g/L agarose gel electrophoresis.

Recombinant Fv-immunotoxin expression and purification

E. coli were cultivated at 37 °C in LB medium containing 50 g/L ampicillin. When their density reached $A_{650}=1.0$, bacteria were induced by 1.0 mmol/L IPTG for 3-4 h. And then they were harvested by centrifugation and their inclusions were isolated, purified, denatured and re-natured. After purified by glutathione-S-transferase affinity chromatography, glutathione-S-transferase (GST) was removed by thrombin digestion. The immunotoxin was analyzed by 120 g/L SDS-PAGE.

Western blot

When 120 g/L SDS-PAGE electrophoresis was completed, stacking gel was removed and equilibrated in transfer buffer

(25 mmol/L Tris, 190 mmol/L glycocine, 200 mL/L methanol). The expressing proteins were transferred from gel to NC membrane by electrophoresis. The membrane in heat-sealable plastic bag was blocked with buffer (TBS with 30 g/L bovine serum albumin, BSA) overnight at 4 °C. After the blocking buffer was removed, the solution with TNF α antibody was added, which was diluted with TBS (containing 10 g/L BSA). And then the membrane was incubated for 1h at 37 °C. After washed 3 times with TBS, the membrane was transferred to fresh plastic bag containing goat anti-mouse IgG antibody for one hour at 37 °C and stained with DAB for 10-20 min.

Tumor therapy

The SMMC-7721 cells were cultivated in RPMI 1640 containing 100 mL/L fetal bovine serum, which was obtained from Gibco BRL. Fifteen immunodeficient nude mice BALB/nu, purchased from our Experiment Animal Center and Shanghai Cellular and Biologic Center, were implanted s.c. 2×10^6 SMMC-7721 cells (PBS suspended) at right rear flank respectively. When tumors grew to a palpable size about 2 mm subcutaneously, fifteen mice were divided into three groups randomly. Each group had five mice. PBS was injected to the first group of mice. Twelve μ g mTNF α was injected to each mouse in the second group and 16 μ g hscFv₂₅-mTNF α was injected to each mouse in the third group. All mice were injected through their tail veins. Fourteen days were one course of therapy. At the end of the second week, the mice were dissected. Their tumors were weighed and examined for morphological evidence of damage, along with lungs and livers. The paraffin sections were prepared for histological examination and immunohistochemical staining.

Immunohistochemical staining

The sections were stained by immunohistochemical method. Those in the control groups were stained according to the same method, with the first antibody substituted by PBS, normal mouse serum and an irrelevant antibody IB₃ respectively. All paraffin embedded samples were deparaffined and rehydrated, pretreated for 20 min at 95 °C in a microwave oven. After being treated with 3 mL/L H₂O₂ for 30 min to block the endogenous peroxidase, the sections were incubated with 20 mL/L fetal calf serum for 30 min to reduce nonspecific binding, and then the primary TNF α antibody was applied to sections at 4 °C overnight. The sections were subsequently incubated with horseradish peroxidase (HR)-labeled goat anti-mouse immunoglobulin at 37 °C for 1 h, and stained with DAB-H₂O₂ for 5-10 min and counterstained with hematoxylin.

Statistical methods

The *F* test was used for statistical analysis of tumor bulk and weight among three groups. The criterion of significance was set at *P*<0.05.

RESULTS

Vector construction and verification

One ladder was observed at 450 bp, with the same size as mTNF α . After PCR products were digested by *Sal* I, *Xho* I and linked to 3' -end of pGEX4T-1/hscFv₂₅, which was digested by the same restriction enzymes, the prokaryotic expressing vector pGEX4T-1/hscFv₂₅-mTNF α was constructed. Then it was transformed to *E. coli* JM109. The bacteria were cultivated in the Amp^r/LB medium at 37 °C for 16-22 h. Six clones were selected at random. Three clones had one ladder about 450 bp digested by *Sal* I and *Xho* I restriction enzymes. After subsequently digested by *Eco*R I and *Xho* I, *Eco*R I and *Sal* I, 1 180 bp and 730 bp ladders were observed,

corresponding well with the size of hscFv₂₅-mTNF α and hscFv₂₅ (Figure 1).

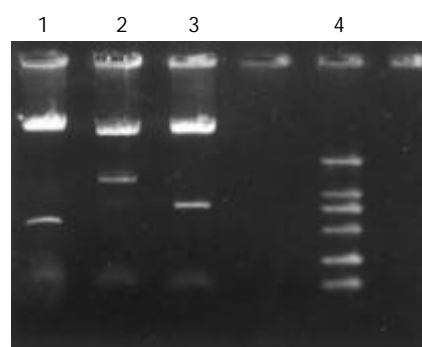


Figure 1 The result of enzyme digested pGEX4T-1/hscFv₂₅-mTNF α . Lane1: mTNF α ; Lane 2: hscFv₂₅; Line 3: hscFv₂₅-mTNF α ; Lane 4: DNA ladder (100, 250, 500, 750, 1 000, 2 000 bp).

Fv-immunotoxin expression, purification and identification

The bacteria containing pGEX4T-1/hscFv₂₅-mTNF α were induced by IPTG. Compared with the same bacteria without induction by IPTG, there was a new transcript of *M_r* 68 000, corresponding well with the size of fusion protein GST-hscFv₂₅-mTNF α (GST *M_r* 26 000, hscFv₂₅ *M_r* 26 000, mTNF α *M_r* 16 000). The result of absorbance scanning showed that the expressing amount of GST-hscFv₂₅-mTNF α was 12% bacterial protein. The fusion protein existed in the form of infusibility inclusions. After the inclusions were denatured, renatured, purified by affinity chromatography, only 2 mg preliminarily purified GST-hscFv₂₅-mTNF α was obtained from 100 mL bacteria. Digested by thrombin subsequently and purified by GST affinity chromatography again, hscFv₂₅-mTNF α protein was obtained. The result of SDS-PAGE showed that proteins were accorded to electrophoresis purification (Figure 2). The GST-hscFv₂₅-mTNF α studied by Western blot was seen as a new transcript of *M_r* 68 000, the same as the fusion protein GST-hscFv₂₅-mTNF α .

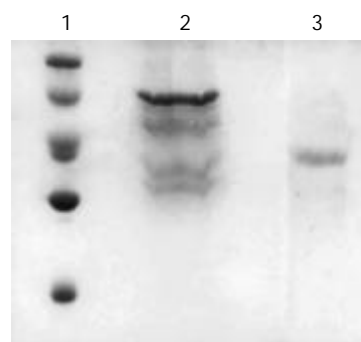


Figure 2 GST-hscFv₂₅-mTNF α and hscFv₂₅-mTNF α SDS-PAGE Lane 1: Low molecular mass marker (20.1, 31.0, 43.0, 66.2, 97.4 KD); Lane 2: Preliminarily purified GST-hscFv₂₅-mTNF α ; Lane 3: Purified hscFv₂₅-mTNF α .

hscFv₂₅-mTNF α targeting therapy

Fifteen nude mice, weighing 16-24 g, were implanted s.c. 2×10^6 SMMC-7721 cells at their right rear flanks and received drug treatment on the tenth day. The tumor of bulk and weight of 15 nude mice were shown in Table 1. The tumor restraining trials of hscFv₂₅-mTNF α to HCC xenografts showed 2/5 complete remission (CR) and 3/5 partial remission (PR). The therapeutic result of mTNF α showed 5/5 PR. The therapeutic effectiveness of mTNF α was less than that of hscFv₂₅-mTNF α (*F*=8.70, *P*<0.05). In the PBS group, tumors showed no remission

Table 1 Targeting therapy of hscFv₂₅-mTNF α for HCC xenografts

		Tumor bulk (mm×mm)	Tumor weight (mg)	Regression rate of tumor bulk (%)	Regression rate of tumor weight (%)	Curative effect
PBS	1	9×5	119	0	0	NR
	2	7×7	87	0	0	NR
	3	9×4	51	0	0	NR
	4	5×3	26	0	0	NR
	5	5×4	30	0	0	NR
hscFv ₂₅ -mTNF α	1	0.8×0.5	2	99.2	96.8	PR
	2	2×3	10	81.8	84.0	PR
	3	2×3	15	81.8	76.0	PR
	4	0	0	100	100	CR
	5	0	0	100	100	CR
mTNF α	1	2×2	11	87.9	82.4	PR
	2	3×3	22	72.7	64.9	PR
	3	2×4	5	75.8	76.0	PR
	4	2×3	10	81.8	84.0	PR
	5	2×3	10	81.8	84.0	PR

NR: non-remission; PR: partial remission; CR: complete remission.

(NR). After the liver and lung specimens were sliced up continuously and examined, no metastatic tumors and surviving tumor cells were seen in CR xenografts. The tissues of PR xenografts showed a large number of necrotic areas.

Immunohistochemical staining

The remnant tumor tissues treated by hscFv₂₅-mTNF α showed diffusely positive for TNF α . The positive granules mainly existed in the cytoplasm of tumor cells (Figure 3). Immunohistochemical staining with the irrelevant antibody IB₃, PBS and normal mouse serum was negative. The tumor tissues treated by PBS showed negative or weak positive for TNF α .

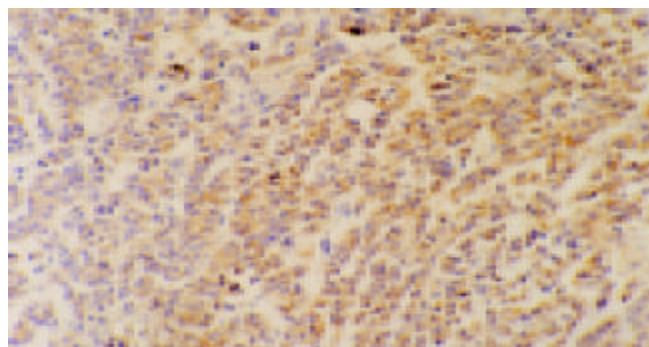


Figure 3 The remnant tumor tissues treated by hscFv₂₅-mTNF α were positive for TNF α . The positive granules mainly existed in the cytoplasm of tumor cells. EnVision™ ×200.

DISCUSSION

In the past 20 years, the antibody study has passed through 3 stages: polyclonal antibody, monoclonal antibody and genetic engineering antibody. Among them, the genetic engineering antibody was the most arresting focus of research because of its prominent advantage, such as lower molecular weight, better specificity and affinity^[9-12]. It had minimal antigenicity of human against mouse immunoglobulin antibody (HAMA)^[13]. Many scFvs against tumors have been used in the phase I-III clinical therapy trials^[14-16]. HAB₂₅ is a kind of the monoclonal antibody against HCC constructed by our laboratory. The hscFv₂₅ against HCC is constructed from HAB₂₅. Previous experiment showed that it had better targeting action compared to HAB₂₅^[17-19].

The recombinant Fv-immunotoxin was constructed if the

scFv C' end was linked to protein toxins, such as pseudomonas exotoxin (PE)^[20]. Once bound to the target cells, immunotoxins could kill the tumor cells. Due to PE being nonhuman, to produce effect, it must be internalized into endocytic vesicles where the catalytic protein of the toxin was processed and released into cytosol. Some results of clinical trials using such exotoxin were not satisfactory. Here, we have constructed the single chain recombinant Fv-immunotoxin hscFv₂₅-mTNF α . The mTNF α we used was a mutant from natural human TNF α .

The TNF α is one of the strongest active factors in organisms which can kill tumor cells directly. It has severe side effects and is often used in local therapy or targeting therapy by antitumor antibodies^[21,22]. Some studies found that the toxicity of TNF α could be reduced by genic fix point mutation or polymeric alteration^[23,24]. When natural TNF α 's N-end seven amino acids were cut out and Pro⁸Ser⁹Asp¹⁰ changed to ArgLysArg, and its C-end 157th amino acid of Leu changed to Phe, mTNF α was attained. Compared with natural TNF α , the toxicity of mTNF α was reduced evidently and its cytotoxicity was enhanced greatly^[25].

Our study showed the hscFv₂₅-mTNF α could kill tumor cells effectively. Compared with dosage of mTNF α and the former experimentation^[17], the dosage of hscFv₂₅-mTNF α was reduced markedly. Those results revealed that mTNF α could concentrate in tumor tissues and killed tumor cells by the targeting of hscFv₂₅. The anti-HCC recombinant Fv-immunotoxin with TNF α replaced by mTNF α could increase its cytotoxicity. Furthermore, we found tumor cells were positive for TNF α in immunohistochemical staining. It also indicated hscFv₂₅ had better targeting action.

All these showed the hscFv₂₅-mTNF α had better distributive ratio in HCC tissues. It could help local tumor cells to attain a high level of mTNF- α and reduce dose-limiting toxicity. The recombinant Fv-immunotoxin hscFv₂₅-mTNF α might have potentiality of clinical application. Due to few nude mice in our study, it maybe lacked rigorous statistical significance. The experimental results need be approved in the future.

REFERENCES

- 1 **Qian J**, Feng GS, Vogl T. Combined interventional therapies of hepatocellular carcinoma. *World J Gastroenterol* 2003; **9**: 1885-1891
- 2 **Zeng ZX**, Wang WL, Luo WJ, Wang ZL. Construction of differentially expressed cDNA library in human hepatocellular carcinoma apoptotic cells with suppression subtractive hybridization. *Shijie Huaren Xiaohua Zazhi* 2001; **9**: 1233-1237

- 3 **Qi YY**, Zhou LG, Wang WX, Chen WJ, Xiang KL, Zhao XY, Yang TH, Yi XZ. Dual-phase enhanced spiral CT in the diagnosis of hepatocellular carcinoma with tumor thrombus in portal vein. *Shijie Huaren Xiaohua Zazhi* 2002; **10**: 384-387
- 4 **Zhen JY**, Li KZ, Wang WZ. Impact of the expression of P^{27KIP1} on apoptosis and progression of hepatocellular carcinoma. *Shijie Huaren Xiaohua Zazhi* 2002; **10**: 883-886
- 5 **Rosenblum MG**, Cheung LH, Liu Y, Marks JW 3rd. Design, expression, purification, and characterization, *in vitro* and *in vivo*, of an antimelanoma single-chain Fv antibody fused to the toxin gelonin. *Cancer Res* 2003; **63**: 3995-4002
- 6 **Reinartz S**, Hombach A, Kohler S, Schlebusch H, Wallwiener D, Abken H, Wagner U. Interleukin-6 fused to an anti-idiotypic antibody in a vaccine increases the specific humoral immune response against CA125+ (MUC-16) ovarian cancer. *Cancer Res* 2003; **63**: 3234-3240
- 7 **Goel A**, Colcher D, Baranowska-Kortylewicz J, Augustine S, Booth BJ, Pavlinkova G, Batra SK. Genetically engineered tetravalent single-chain Fv of the pancarcinoma monoclonal antibody CC49: improved biodistribution and potential for therapeutic application. *Cancer Res* 2000; **60**: 6964-6971
- 8 **Yuan QA**, Yu WY, Huang CF. Construction and expression of a hepatocellular carcinoma specific rodent and its humanized single-chain Fv fragments in *Escherichia coli*. *Shengwu Gongcheng Xuebao* 2000; **16**: 86-90
- 9 **Niv R**, Assaraf YG, Segal D, Pirak E, Reiter Y. Targeting multidrug resistant tumor cells with a recombinant single-chain FV fragment directed to P-glycoprotein. *Int J Cancer* 2001; **94**: 864-872
- 10 **McCall AM**, Shahied L, Amoroso AR, Horak EM, Simmons HH, Nielson U, Adams GP, Schier R, Marks JD, Weiner LM. Increasing the affinity for tumor antigen enhances bispecific antibody cytotoxicity. *J Immunol* 2001; **166**: 6112-6117
- 11 **Cooke SP**, Boxer GM, Lawrence L, Pedley RB, Spencer DI, Begent RH, Chester KA. A strategy for antitumor vascular therapy by targeting the vascular endothelial growth factor: receptor complex. *Cancer Res* 2001; **61**: 3653-3659
- 12 **van der Poel HG**, Molenaar B, van Beusechem VW, Haisma HJ, Rodriguez R, Curiel DT, Gerritsen WR. Epidermal growth factor receptor targeting of replication competent adenovirus enhances cytotoxicity in bladder cancer. *J Urol* 2002; **168**: 266-272
- 13 **Whittington HA**, Hancock J, Kemshead JT. Generation of a humanized single chain Fv (scFv) derived from the monoclonal Eric-1 recognising the human neural cell adhesion molecule. *Med Pediatr Oncol* 2001; **36**: 243-246
- 14 **Turatti F**, Mezzanzanica D, Nardini E, Luisson E, Maffioli L, Bambiandieri E, de Lalla C, Canevari S, Figini M. Production and validation of the pharmacokinetics of a single-chain Fv fragment of the MGR6 antibody for targeting of tumors expressing HER-2. *Cancer Immunol Immunother* 2001; **49**: 679-686
- 15 **Mayer A**, Tsiompanou E, O' Malley D, Boxer GM, Bhatia J, Flynn AA, Chester KA, Davidson BR, Lewis AA, Winslet MC, Dhillon AP, Hilson AJ, Begent RH. Radioimmunoguided surgery in colorectal cancer using a genetically engineered anti-CEA single-chain Fv antibody. *Clin Cancer Res* 2000; **6**: 1711-1719
- 16 **Chester KA**, Bhatia J, Boxer G, Cooke SP, Flynn AA, Huhlov A, Mayer A, Pedley RB, Robson L, Sharma SK, Spencer DI, Begent RH. Clinical applications of phage-derived sFvs and sFv fusion proteins. *Dis Markers* 2000; **16**: 53-62
- 17 **Sun Z**, Liu Y, Yuan Q, Yu W, Huang C, Ma L, Yu J. Targeting studies of humanized scFv25 fusing to TNFalpha against hepatocellular carcinoma. *Zhonghua Ganzhangbing Zazhi* 2000; **8**: 352-354
- 18 **Cheng H**, Liu YF, Zhang HZ, Shen WN, Zhang J, Zhang J. *In vivo* antitumor activity of PBMCs via genetic modification of single-chain immunotoxin. *Shijie Huaren Xiaohua Zazhi* 2003; **11**: 708-711
- 19 **Cheng H**, Liu YF, Zhang HZ, Shen WN, Zhang J, Zhang J. *In vitro* cytotoxicity of PBMCs via genetic modification of single-chain immunotoxin. *Shijie Huaren Xiaohua Zazhi* 2003; **11**: 281-284
- 20 **Fan D**, Yano S, Shinohara H, Solorzano C, Van Arsdall M, Bucana CD, Pathak S, Kruzel E, Herbst RS, Onn A, Roach JS, Onda M, Wang QC, Pastan I, Fidler IJ. Targeted therapy against human lung cancer in nude mice by high-affinity recombinant antimesothelin single-chain Fv immunotoxin. *Mol Cancer Ther* 2002; **1**: 595-600
- 21 **Thomas PS**, Heywood G. Effects of inhaled tumour necrosis factor alpha in subjects with mild asthma. *Thorax* 2002; **57**: 774-778
- 22 **Cooke SP**, Pedley RB, Boden R, Begent RH, Chester KA. *In vivo* tumor delivery of a recombinant single chain Fv::tumor necrosis factor-alpha fusion protein. *Bioconjug Chem* 2002; **13**: 7-15
- 23 **Yamamoto M**, Oshiro S, Tsugu H, Hirakawa K, Ikeda K, Soma G, Fukushima T. Treatment of recurrent malignant supratentorial astrocytomas with carboplatin and etoposide combined with recombinant mutant human tumor necrosis factor-alpha. *Anti-cancer Res* 2002; **22**: 2447-2453
- 24 **Terlikowski SJ**. Local immunotherapy with rhTNF-alpha mutein induces strong antitumor activity without overt toxicity-a review. *Toxicology* 2002; **174**: 143-152
- 25 **Nakamura S**, Kato A, Masegi T, Fukuoka M, Kitai K, Ogawa H, Ichikawa Y, Maeda M, Watanabe N, Kohgo Y. A novel recombinant tumor necrosis factor-alpha mutant with increased anti-tumor activity and lower toxicity. *Int J Cancer* 1991; **48**: 744-748

Cell apoptosis and regeneration of hepatocellular carcinoma after transarterial chemoembolization

Zhen Li, Dao-Yu Hu, Qian Chu, Jian-Hong Wu, Chun Gao, Yu-Qing Zhang, Yan-Rong Huang

Zhen Li, Dao-Yu Hu, Yu-Qing Zhang, Yan-Rong Huang, Department of Radiology, Tongji Hospital, Tongji Medical College of Huazhong University of Science and Technology, Wuhan 430030, Hubei Province, China

Qian Chu, Department of Neurology, Tongji Hospital, Tongji Medical College of Huazhong University of Science and Technology, Wuhan 430030, Hubei Province, China

Jian-Hong Wu, Chun Gao, Department of Surgery, Tongji Hospital, Tongji Medical College of Huazhong University of Science and Technology, Wuhan 430030, Hubei Province, China

Supported by the Natural Science Foundation of Hubei Province, No. 2002AB130

Correspondence to: Dr. Zhen Li, Department of Radiology, Tongji Hospital, Tongji Medical College of Huazhong University of Science and Technology, Wuhan 430030, Hubei Province, China. doclizhen@hotmail.com

Telephone: +86-27-83663575 **Fax:** +86-27-83643059

Received: 2003-05-11 **Accepted:** 2003-06-02

Abstract

AIM: To evaluate whether cell apoptosis and regeneration were existed in normal liver cells adjacent to carcinoma after transarterial chemoembolization (TACE).

METHODS: Fifty rabbits with hepatic carcinoma were divided into 5 groups at random: group A (control group), groups B and C (TACE treatment groups), groups D and E (partial hepatectomy groups). There were 10 rabbits in each group. Rabbits in groups B-E were treated by transarterial chemoembolization (TACE) and partial hepatectomy (PH) respectively. The changes of S-phase cell fraction (SPF), proliferation index (PI) and cell apoptosis in the normal liver tissue were determined with flow cytometry (FCM) after operations on the first and third days. We determined the mitosis index (MI) with histo-pathological method and the apoptosis index (AI) with TUNEL method at the same time.

RESULTS: Twenty-four hours after operations, compared with control group, the rabbits in TACE group had much higher index of SPF, PI and MI (MI: $t=4.89$, $P<0.001$; SPF: $t=5.27$, $P<0.001$; PI: $t=4.87$, $P<0.001$). Moreover, the proliferation of liver cells in TACE group was much weaker than that of the cells treated by partial hepatectomy, and the differences were significant (MI: $t=7.02$, $P<0.001$; SPF: $t=4.06$, $P<0.001$; PI: $t=2.70$, $P<0.05$). Seventy-two h after operations, FCM showed a small sub-G1 peak in TACE group and PH group, compared with the control group, but there was no difference between them ($t=0.41$, $P>0.05$). TACE showed that AI in the treated rabbits was higher than that in control group ($t=3.07$, $P<0.05$), and there were no differences between TACE group and PH group, either ($t=0.93$, $P>0.05$).

CONCLUSION: Cell apoptosis and regeneration exist in rabbit liver tissues after TACE in some degree, which may be associated with the selective embolization of iodised oil, chemotherapeutic drug and free radical damage.

Li Z, Hu DY, Chu Q, Wu JH, Gao C, Zhang YQ, Huang YR. Cell apoptosis and regeneration of hepatocellular carcinoma after transarterial chemoembolization. *World J Gastroenterol* 2004; 10(13): 1876-1880

<http://www.wjgnet.com/1007-9327/10/1876.asp>

INTRODUCTION

The efficacy of transarterial chemoembolization (TACE) is greatly determined by the liver function reserve of liver cancer patients. More than 40% patients died of liver failure after TACE, in which most of them were accompanied by poor liver function and damage due to chemotherapy. Therefore, it is important to study the effects of TACE on non-neoplastic liver tissue to decrease the death rate. We have established the animal model of rabbit VX2 hepatic carcinoma. All the rabbits were treated by TACE to detect the effect on cell cycle of non-neoplastic liver tissues after operations^[1].

MATERIALS AND METHODS

Establishment of the animal model

Fifty Japanese alpine hares, weighing 2.5-3.3 kg, provided by the Experiment Animal Center of Tongji Medical College were used in this experiment. The rabbits were implanted hepatocellular carcinoma cell VX2, and observed for 3 wk before experiment^[2].

Treatment and radiological examination^[3,4]

Fifty rabbits with VX2 hepatic carcinoma were randomly divided into 5 groups: Group A (control group), groups B and C (TACE treatment groups), groups D and E (partial hepatectomy groups), 10 rabbits in each group. Three weeks later, at laparotomy of the rabbits, the feeding artery of liver carcinoma was punctured and arteriography was made^[5]. A 1 mL of physiological saline was administered to group A. Groups B and C were treated with 0.6-0.8 mL of a mixture of iodine oil (10 mL) and mitomycin (10 mg)^[6,7]. Groups D and E were treated by hepatectomy. Groups B and C were performed CT and MRI after TACE^[8,9].

Flow cytometry analysis

Rabbits in groups A, B and C were killed on the first day after the procedure, and those in groups D and E were killed on the third day after the procedure. As soon as the rabbits died, a piece of non-neoplastic liver tissue was cut from each rabbit and digested with enzymes. The cells were fixed by 800 mL/L ice ethanol, hatched by 40 μ L PC on ice for 30 min, and washed in 1 g/L PBS. At last, they were stained by at 100 μ L PI 10 mg/L and 50 μ L 1 g/L RNA enzyme for 20 min, then flow cytometry was performed. The cells were detected by FAC Sort FCM machine (Becton Dickson Co, USA). The fluorescence of cells was analyzed with Cellquest software and the cell cycle was studied. The other liver tissues were photographed, fixed with 40 g/L formaldehyde, and stained by HE^[10].

Groups B and C were performed CT after TACE, and accumulation of iodized oil was observed. General pathological changes of carcinoma were detected in all the rabbits. Under the microscope, we calculated the number of liver cells in the mitosis

phase per 1 000 liver cells, which was called mitosis index (MI).

FCM analysis

S phase cell fraction (SPF) was calculated according to the equation: $SPF = S / (S + G1 / G0 + G2 / M) \times 100\%$. Proliferation index (PI) was calculated according to the equation: $PI = (S + G2 / M) / (S + G1 / G0 + G2 / M) \times 100\%$. Apoptosis index (AI) was analyzed by TUNEL method^[11], the number of apoptotic cells was calculated under microscope^[12].

Statistic analysis

All the data were analyzed by *t* test.

RESULTS

General pathological and radiological findings

Three wk after tumor implantation, the size of VX2 liver carcinoma was 3.5 ± 1.6 cm on average, and appeared as white nodules near the liver surface. There were no definite margins between carcinomas and normal liver tissues. On DSA, there was increased and irregular angiogenesis of the tumor vessels, with tumor stained mainly at the periphery (Figure 1). On MR, the signal of cancer was slightly lower than that of normal liver tissue on T1WI and slightly higher on T2WI (Figure 2). The iodized oil deposited well after TACE on CT^[13] (Figure 3).

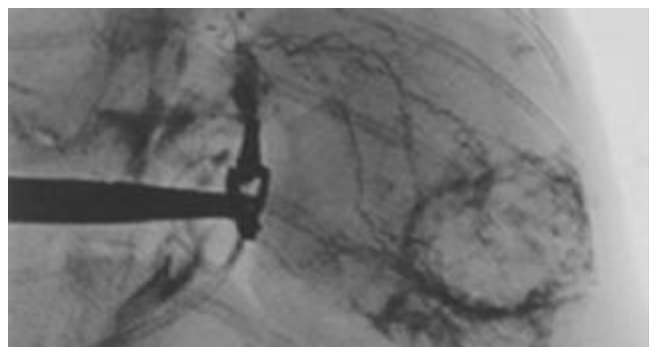


Figure 1 Hepatic arteriography of rabbits. There was increased angiogenesis with thickening and irregularity of the vessels. There was also tumor staining mainly in the periphery of the tumor.

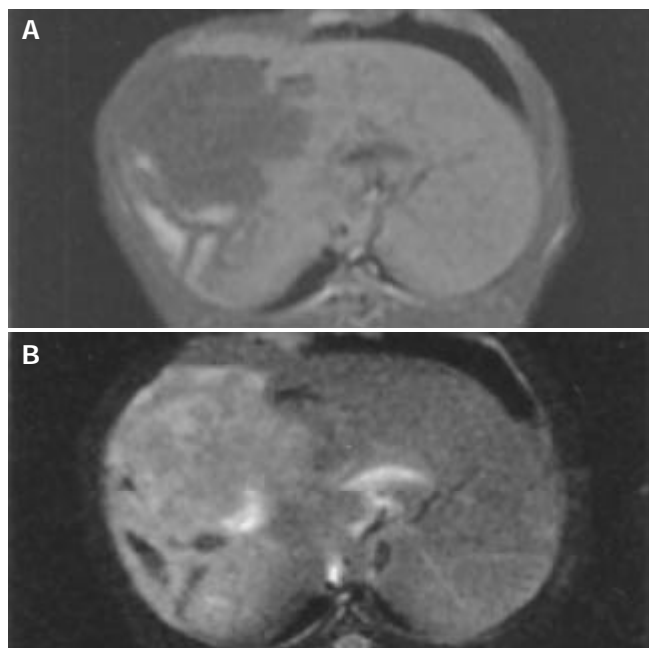


Figure 2 MRI of rabbit liver. The tumor appeared hypointense on T1WI (A) and hyperintense on T2WI (B).

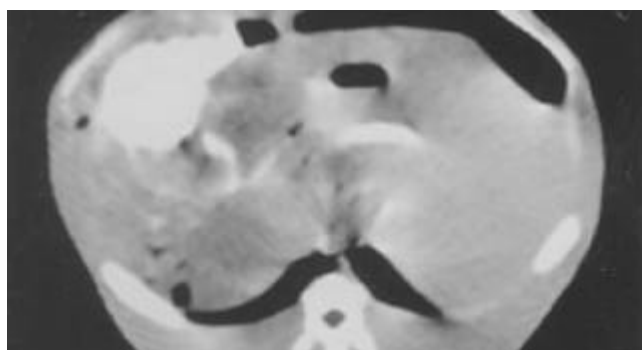


Figure 3 CT scan shows massive retention of iodized oil in tumor after TACE.

Cytological changes

Red fluorescent light could be seen in the cells under laser confocal microscope (Figure 4). Under light microscope (Olympus), we could find cell mitosis clearly, and mitosis index (MI) could be calculated. Flow cytometry showed that S phase and G2/M phase cells in TACE groups and partial hepatectomy groups increased much more on the first day after operations than that in the control group (Figure 5). On the third day after operations, the amount of S-phase and G2/M phase cells in TACE group and partial hepatectomy group was about the same as control group (Figure 6). In the cell apoptosis index (AI) determined by TUNEL method, no significant difference existed between TACE group (Figure 7) and partial hepatectomy group.

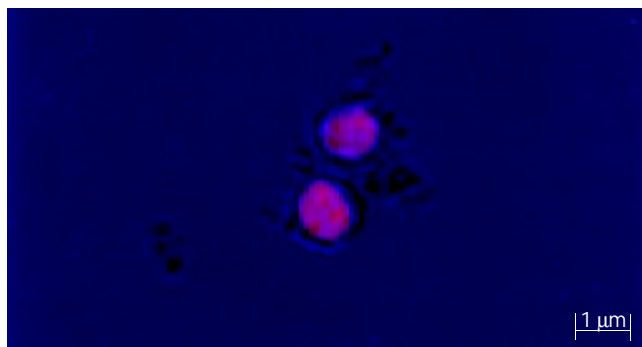


Figure 4 Cells giving out red fluorescent light under laser confocal microscope.

The *t* test values of MI, SPF and PI of TACE groups and control group are listed in Table 1. The *t* test values of MI, SPF and PI of TACE groups and partial hepatectomy groups are listed in Table 2.

Table 1 *t* test value of MI, SPF and PI of TACE groups and control group on the first day after operations

Index	TACE group	Control group	<i>t</i> value	<i>P</i> value
MI (%)	1.42±0.55	0.51±0.21	4.89	<i>P</i> <0.001
SPF (%)	12.46±4.18	4.90±1.76	5.27	<i>P</i> <0.001
PI (%)	23.38±8.31	9.93±2.68	4.87	<i>P</i> <0.001

Table 2 *t* test value of MI, SPF and PI of TACE groups and partial hepatectomy group on the first day after operations

Index	TACE group	Partial hepatectomy group	<i>t</i> value	<i>P</i> value
MI (%)	1.42±0.55	3.13±0.54	7.02	<i>P</i> <0.001
SPF (%)	12.46±4.18	21.76±5.92	4.06	<i>P</i> <0.001
PI (%)	23.38±8.31	32.51±6.75	2.70	<i>P</i> <0.05

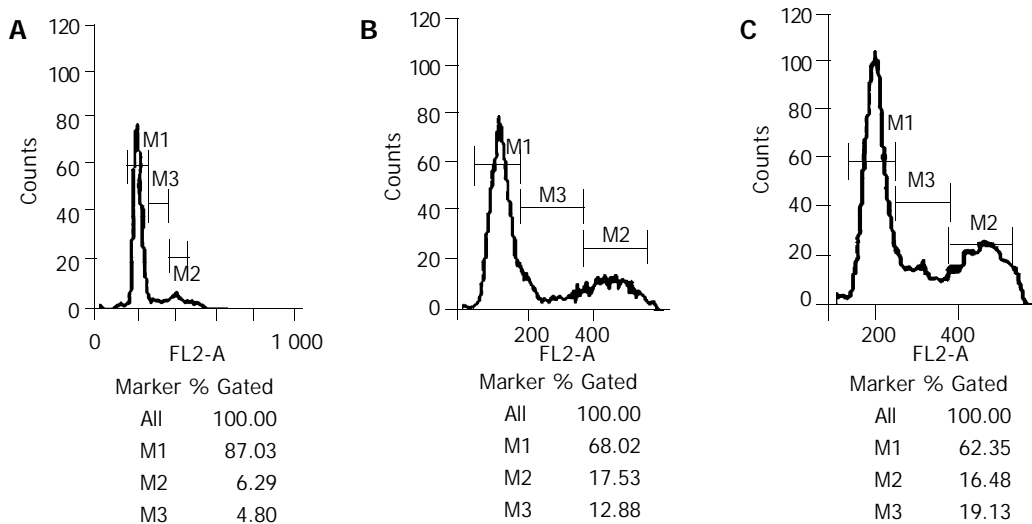


Figure 5 A: Shows the S phase and G2/M phase cells were small in proportion on the first day after operations (4.80%, 6.29%) in control group. B: Shows the S phase and G2/M phase cells grew much more on the first day after operations (17.53%, 12.88%) in TACE group. C: Shows the S phase and G2/M phase cells grew much more on the first day after operations (16.48%, 19.13%) in PH group. *M1 is G0/G1 phase cell ratio/M2 is G2/M phase cell ratio, M3 is S phase cell ratio.

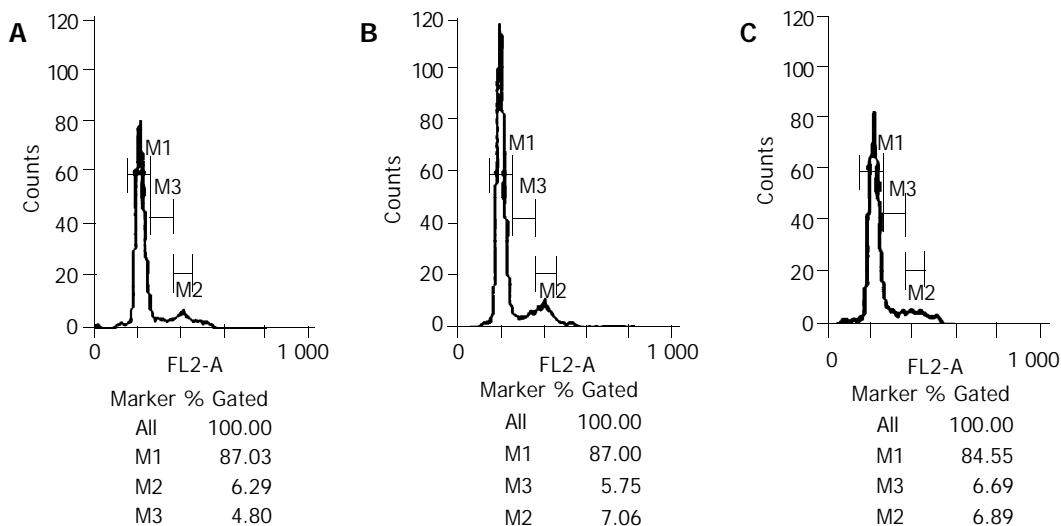


Figure 6 A: Shows the S phase and G2/M phase cells were small in proportion on the third day after operations (4.80%, 6.29%) in control group. B and C: Show the S phase and G2/M phase cells had slight changes on the third day after operations in TACE group and PH group.

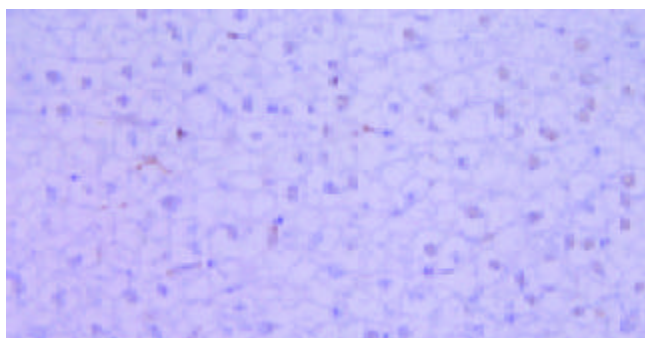


Figure 7 Analysis of apoptosis cells by TUNEL method in TACE group. The nuclei of apoptosis cells appeared brown while those of normal cells appeared blue. It was found that part of the cells were apoptotic cells.

The *t* test values of MI, SPF of TACE groups and control group are listed in Table 3. There was no significant difference between the two groups ($P > 0.05$). However, the *P* value of AI and sub-G1 was less than 0.05. The *t* test values of MI, SPF, AI and PI of TACE groups and partial hepatectomy groups are listed in Table 4.

Table 3 *t* test value of MI, SPF, AI, Sub-G1 and PI of TACE groups and control group on the third day after operations

Index	TACE group	Control group	<i>t</i> value	<i>P</i> value
MI (%)	0.62±0.33	0.51±0.21	0.88	$P > 0.05$
SPF (%)	5.70±1.93	4.90±1.76	0.95	$P > 0.05$
PI (%)	11.69±1.74	9.93±2.68	1.68	$P > 0.05$
Sub-G1 (%)	2.31±1.57	1.18±0.45	2.18	$P < 0.05$
AI (%)	20.33±2.36	13.68±1.97	3.07	$P < 0.05$

Table 4 *t* test value of MI, SPF, sub-G1 and PI of TACE groups and partial hepatectomy group on the third day after operations

Index	TACE group	Partial hepatectomy group	<i>t</i> value	<i>P</i> value
MI(%)	0.62±0.33	0.81±0.30	1.28	$P > 0.05$
SPF(%)	5.70±1.93	6.62±1.56	1.34	$P > 0.05$
PI(%)	11.69±1.74	11.85±2.00	0.17	$P > 0.05$
Sub-G1 (%)	2.31±1.57	2.05±1.07	0.41	$P > 0.05$
AI(%)	20.33±2.36	22.69±3.79	0.93	$P > 0.05$

DISCUSSION

Transarterial chemoembolization (TACE) has been one of the most important and commonly used methods for treatment of hepatocarcinoma^[14]. Because most patients died of liver failure after TACE^[15,16], it is important to study the condition of postoperative normal liver tissues^[17]. The most precise method to evaluate hepatocyte reproduction and apoptosis has been the study of cell cycle^[18]. In our research, normal hepatocytes were isolated, fixed and stained, flow cytometry (FCM) was performed and DNA was analyzed. Results showed SPF, PI and MI value of TACE group was much higher than that of control group ($P < 0.001$, Table 1). We could conclude that there existed liver regeneration after TACE. From Table 2 at the same time, we could find that hepatocyte regeneration in PH group was stronger than that in TACE group on the first day ($P < 0.05$). On the third day after TACE, the difference between TACE group and control group was not significant in all indexes. Furthermore, the difference between TACE group and PH group was not significant either on the third day. From these data, we could conclude that the regeneration process stopped, most of the cells entered the dormancy phase (G_0 phase). However, the value of hypodiploid peak (sub-G1) increased on the third day after TACE ($t = 2.18$, $P < 0.05$). The difference of sub-G1 between TACE group and PH group was obvious ($P > 0.05$, Tables 3, 4). The apoptosis index (AI) became greater on the third day after TACE.

Cell apoptosis (programmed cell death) means the maintenance of stability of internal environment, i.e. the process of autonomic programmed cell death has been controlled by gene^[19]. After partial hepatectomy, the hepatocytes would regenerate soon. At the peak of regeneration, cell apoptosis begins. Accompanying cell reproduction, cell apoptosis would eliminate the overgrown cells, and rebuilding of the tissue constitution is achieved. Some authors^[20] pointed out that the process was mitogen \rightarrow cell reproduction \rightarrow regeneration \rightarrow cell apoptosis. It was different from the necrosis caused by liver cytotoxic material, which was in the order of cytotoxic material \rightarrow necrosis \rightarrow compensatory hyperplasia \rightarrow cell regeneration. Liver tissue regeneration after PH has been studied comprehensively. When the liver is resected less than 70%, the regeneration is proportional to the volume of the resected portion. Mitosis reaches the peak in 24 h, and completes in 72 h. Liver tissue regeneration exists also after TACE, this is due to the effect of super-selective embolization with iodized oil. The liver regeneration in TACE group was weaker than that in PH group, the reason was that the extent of "medical hepatectomy" was much smaller^[21]. However, from Tables 3 and 4, we could find the apoptosis levels between TACE and hepatectomy groups. The apoptosis level following liver regeneration was directly proportional to the regeneration level. It is easy to draw the conclusion that there must exist a new mechanism, which promotes cell apoptosis after TACE. The mechanism might be that mitomycin depressed DNA synthesis and promoted cell apoptosis^[22]. Some authors^[23] pointed out that mitomycin (5 mg/mL) could cause cell apoptosis after 24 h. Almost all chemotherapeutic drugs could induce cell apoptosis by different ways^[24]. For example, vincristine (VCR) and colchicine could induce cell apoptosis by disturbance of microtubule function \rightarrow loss of hepatocyte function \rightarrow identification of the injury by hepatocytes \rightarrow decrease of protein synthesis \rightarrow increase of $[Ca^{2+}]$ activation of endonuclease and protein kinase \rightarrow DNA split \rightarrow cell apoptosis^[25]. On the other hand, there were ischemia and hypoxia of locally embolized tissue, and release of a large amount of free radicals and cell toxins^[26,27]. They could induce cell apoptosis^[28,29]. For example, free radicals could injure DNA which would lead to activation of polydiadenosine phosphate pibotransferase^[30] and accumulation of p53. A cell calcium ion would cause cell apoptosis. It could activate nucleus transcription factors such

as NF- κ B which would induce cell apoptosis^[31]. Normal hepatocyte apoptosis was mainly resulted from the effects of chemotherapeutic drugs and free radical injury rather than from normal tissue repair^[32,33].

The regeneration and apoptosis level of normal hepatocytes usually determine the patients' prognosis after transarterial chemoembolization. The obvious apoptosis after TACE was due to chemotherapeutic drugs and free radicals, which made the normal process of apoptosis more rapid. Therefore, excessive dosage of chemotherapeutic drugs may promote apoptosis and injury of normal hepatocytes in non-neoplastic area of the liver, and deteriorate the liver function of patients. We can draw the conclusion that it is important to use chemotherapeutic drugs, because they can protect the liver function of patients and improve their survival rate after treatment.

REFERENCES

- 1 **El Khaddari S**, Gaudin JL, Abidi H, Picaud G, Rode A, Souquet JC. Chemoembolization in hepatocellular carcinoma: multivariate analysis of survival prognostic factors after the first session. *Gastroenterol Clin Biol* 2002; **26**: 728-734
- 2 **Lin WY**, Chen J, Lin Y, Han K. Implantation of VX2 carcinoma into the liver of rabbits: a comparison of three direct-injection methods. *J Vet Med Sci* 2002; **64**: 649-652
- 3 **Li X**, Zheng CS, Feng GS, Zhuo CK, Zhao JG, Liu X. An implantable rat liver tumor model for experimental transarterial chemoembolization therapy and its imaging features. *World J Gastroenterol* 2002; **8**: 1035-1039
- 4 **Shiozawa S**, Tsuchiya A, Endo S, Kumazawa K, Ogawa K. Transradial approach for transcatheter arterial chemoembolization in patients with hepatocellular carcinoma. *Nippon Shokakibyo Gakkai Zasshi* 2002; **99**: 1450-1454
- 5 **Yi J**, Liao X, Yang Z, Li X. Study on the changes in microvessel density in hepatocellular carcinoma following transcatheter arterial chemoembolization. *J Tongji Med Univ* 2001; **21**: 321-331
- 6 **Chen M**, Li J, Zhang Y. Transarterial chemoembolization with high dose iodized oil for the treatment of large hepatocellular carcinoma. *Zhonghua Zhongliu Zazhi* 2001; **23**: 165-167
- 7 **Pacella CM**, Bizzarri G, Cecconi P, Caspani B, Magnolfi F, Bianchini A, Anelli V, Pacella S, Rossi Z. Hepatocellular carcinoma: long-term results of combined treatment with laser thermal ablation and transcatheter arterial chemoembolization. *Radiology* 2001; **219**: 669-678
- 8 **Liu H**, Li D, Yang S, Wu Y. Efficacy of TACE in treatment of intraportal tumor thrombi with double helical CT. *Hunan Yike Daxue Xuebao* 1999; **24**: 47-49
- 9 **Kim HC**, Kim AY, Han JK, Chung JW, Lee JY, Park JH, Choi BI. Hepatic arterial and portal venous phase helical CT in patients treated with transcatheter arterial chemoembolization for hepatocellular carcinoma: added value of unenhanced images. *Radiology* 2002; **225**: 773-780
- 10 **Jia HS**, Quan XY, Zeng S, Wen ZB. Dynamic evaluation of rabbit VX2 hepatic carcinoma with CT and MRI. *Diyi Junyi Daxue Xuebao* 2002; **22**: 141-144
- 11 **Xiao E**, Li D, Shen S, Zhou S, Tan L, Wang Y, Luo J, Wu Y, Tan C, Liu H, Zhu H. Effect of preoperative transcatheter arterial chemoembolization on apoptosis of hepatocellular carcinoma cells. *Chin Med J* 2003; **116**: 203-207
- 12 **Sano B**, Sugiyama Y, Kunieda K, Sano J, Saji S. Antitumor effects induced by the combination of TNP-470 as an angiogenesis inhibitor and lentinan as a biological response modifier in a rabbit spontaneous liver metastasis model. *Surg Today* 2002; **32**: 503-509
- 13 **Vogl TJ**, Eichler K, Zangos S, Mack M, Hammerstingl R. Hepatocellular carcinoma: Role of imaging diagnostics in detection, intervention and follow-up. *Rofo Fortschr Geb Rontgenstr Neuen Bildgeb Verfahr* 2002; **174**: 1358-1368
- 14 **Barone M**, Ettorre GC, Ladisa R, Schiavariello M, Santoro C, Francioso G, Vinciguerra V, Francavilla A. Transcatheter arterial chemoembolization (TACE) in treatment of hepatocellular carcinoma. *Hepatogastroenterology* 2003; **50**: 183-187
- 15 **Ramsey DE**, Kernagis LY, Soulen MC, Geschwind JF.

- Chemoembolization of hepatocellular carcinoma. *J Vasc Interv Radiol* 2002; **13**(9 Pt 2): S211-221
- 16 **Huang YS**, Chiang JH, Wu JC, Chang FY, Lee SD. Risk of hepatic failure after transcatheter arterial chemoembolization for hepatocellular carcinoma: predictive value of the monoethylglycineylidide test. *Am J Gastroenterol* 2002; **97**: 1223-1227
- 17 **Grieco A**, Marcocchia S, Miele L, Marmiroli L, Caminiti G, Ragazzoni E, Cotroneo AR, Cefaro GA, Rapaccini GL, Gasbarrini G. Transarterial chemoembolization (TACE) for unresectable hepatocellular carcinoma in cirrhotics: functional hepatic reserve and survival. *Hepatogastroenterology* 2003; **50**: 207-212
- 18 **Schuchmann M**, Galle PR. Apoptosis in liver disease. *Eur J Gastroenterol Hepatol* 2001; **13**: 785-790
- 19 **Wright MC**, Issa R, Smart DE, Trim N, Murray GI, Primrose JN, Arthur MJ, Iredale JP, Mann DA. Gliotoxin stimulates the apoptosis of human and rat hepatic stellate cells and enhances the resolution of liver fibrosis in rats. *Gastroenterology* 2001; **121**: 685-698
- 20 **Neuman MG**. Apoptosis in diseases of the liver. *Crit Rev Clin Lab Sci* 2001; **38**: 109-166
- 21 **Saccheri S**, Lovaria A, Sangiovanni A, Nicolini A, De Fazio C, Ronchi G, Fasani P, Del Ninno E, Colombo M. Segmental transcatheter arterial chemoembolization treatment in patients with cirrhosis and inoperable hepatocellular carcinomas. *J Vasc Interv Radiol* 2002; **13**: 995-999
- 22 **Durand RE**, LePard NE. Effects of mitomycin C on the oxygenation and radiosensitivity of murine and human tumours in mice. *Radiother Oncol* 2000; **56**: 245-252
- 23 **Castaneda F**, Kinne RK. Effects of doxorubicin, mitomycin C, and ethanol on Hep-G2 cells *in vitro*. *J Cancer Res Clin Oncol* 1999; **125**: 1-8
- 24 **Sato N**, Mizumoto K, Maehara N, Kusumoto M, Nishio S, Urashima T, Ogawa T, Tanaka M. Enhancement of drug-induced apoptosis by antisense oligodeoxynucleotides targeted against Mdm2 and p21WAF1/CIP1. *Anticancer Res* 2000; **20**: 837-842
- 25 **Crenesse D**, Gugenheim J, Hornoy J, Tornieri K, Laurens M, Cambien B, Lenegrade G, Cursio R, De Souza G, Auberger P, Heurteaux C, Rossi B, Schmid-Alliana A. Protein kinase activation by warm and cold hypoxia-reoxygenation in primary-cultured rat hepatocytes-JNK (1)/SAPK (1) involvement in apoptosis. *Hepatology* 2000; **32**: 1029-1036
- 26 **Ben-Ari Z**, Hochhauser E, Burstein I, Papo O, Kaganovsky E, Krasnov T, Vamichkim A, Vidne BA. Role of anti-tumor necrosis factor-alpha in ischemia/reperfusion injury in isolated rat liver in a blood-free environment. *Transplantation* 2002; **73**: 1875-1880
- 27 **Kobayashi T**, Sugawara Y, Ohkubo T, Imamura H, Makuuchi M. Effects of amrinone on hepatic ischemia-reperfusion injury in rats. *J Hepatol* 2002; **37**: 31-38
- 28 **Barros LF**, Stutzin A, Calixto A, Catalan M, Castro J, Hetz C, Hermosilla T. Nonselective cation channels as effectors of free radical-induced rat liver cell necrosis. *Hepatology* 2001; **33**: 114-122
- 29 **Karbowski M**, Kurono C, Wozniak M, Ostrowski M, Teranishi M, Nishizawa Y, Usukura J, Soji T, Wakabayashi T. Free radical-induced megamitochondria formation and apoptosis. *Free Radic Biol Med* 1999; **26**: 396-409
- 30 **Song BC**, Suh DJ, Yang SH, Lee HC, Chung YH, Sung KB, Lee YS. Lens culinaris agglutinin-reactive alpha-fetoprotein as a prognostic marker in patients with hepatocellular carcinoma undergoing transcatheter arterial chemoembolization. *J Clin Gastroenterol* 2002; **35**: 398-402
- 31 **Factor V**, Oliver AL, Panta GR, Thorgeirsson SS, Sonenshein GE, Arsura M. Roles of Akt/PKB and IKK complex in constitutive induction of NF-kappaB in hepatocellular carcinomas of transforming growth factor alpha/c-myc transgenic mice. *Hepatology* 2001; **34**: 32-41
- 32 **Won JY**, Lee do Y, Lee JT, Park SI, Kim MJ, Yoo HS, Suh SH, Park SJ. Supplemental transcatheter arterial chemoembolization through a collateral omental artery: treatment for hepatocellular carcinoma. *Cardiovasc Intervent Radiol* 2003; **26**: 136-140
- 33 **Zaragoza A**, Diez-Fernandez C, Alvarez AM, Andres D, Cascales M. Mitochondrial involvement in cocaine-treated rat hepatocytes: effect of N-acetylcysteine and deferoxamine. *Br J Pharmacol* 2001; **132**: 1063-1070

Edited by Wang XL and Zhu LH Proofread by Xu FM

Transjugular intrahepatic portosystemic shunt for palliative treatment of portal hypertension secondary to portal vein tumor thrombosis

Zai-Bo Jiang, Hong Shan, Xin-Ying Shen, Ming-Sheng Huang, Zheng-Ran Li, Kang-Shun Zhu, Shou-Hai Guan

Zai-Bo Jiang, Hong Shan, Xin-Ying Shen, Ming-Sheng Huang, Zheng-Ran Li, Kang-Shun Zhu, Shou-Hai Guan, Department of Radiology, the 3rd Affiliated Hospital of Sun Yat-Sen University, Guangzhou 510630, Guangdong Province, China

Correspondence to: Dr. Hong Shan, the 3rd Affiliated Hospital of Sun Yat-Sen University, Guangzhou 510630, Guangdong Province, China. jzb01@163.net

Telephone: +86-20-85516867 **Fax:** +86-20-87580725

Received: 2003-12-28 **Accepted:** 2004-01-08

Abstract

AIM: To evaluate the palliative therapeutic effects of transjugular intrahepatic portosystemic shunt (TIPS) in portal vein tumor thrombosis (PVTT) complicated by portal hypertension.

METHODS: We performed TIPS for 14 patients with PVTT due to hepatocellular carcinoma (HCC). Of the 14 patients, 8 patients had complete occlusion of the main portal vein, 6 patients had incomplete thrombosis, and 5 patients had portal vein cavernous transformation. Clinical characteristics and average survival time of 14 patients were analysed. Portal vein pressure, ascites, diarrhoea, and variceal bleeding and circumference of abdomen were assessed before and after TIPS.

RESULTS: TIPS was successful in 10 cases, and the successful rate was about 71%. The mean portal vein pressure was reduced from 37.2 mmHg to 18.2 mmHg. After TIPS, the ascites decreased, hemorrhage stopped and the clinical symptoms disappeared in the 10 cases. The average survival time was 132.3 d. The procedure failed in 4 cases because of cavernous transformation in portal vein and severe cirrhosis.

CONCLUSION: TIPS is an effective palliative treatment to control hemorrhage and ascites due to HCC complicated by PVTT.

Jiang ZB, Shan H, Shen XY, Huang MS, Li ZR, Zhu KS, Guan SH. Transjugular intrahepatic portosystemic shunt for palliative treatment of portal hypertension secondary to portal vein tumor thrombosis. *World J Gastroenterol* 2004; 10(13): 1881-1884 <http://www.wjgnet.com/1007-9327/10/1881.asp>

INTRODUCTION

TIPS is effective in treating patients with hemorrhage, intractable ascites and portal hypertensive gastropathy, and many favorable results and experiences have been obtained as well^[1-7]. TIPS has been widely used for portal hypertension with portal vein thrombosis (PVT), type-III Budd-Chiari syndrome, even bile duct occlusive diseases, and other portal hypertension^[8-17]. But how to treat primary hepatocarcinoma

with secondary portal hypertension is a challenge. In 1995, Zhang^[18] first reported the clinical experiences that TIPS procedure was applied to HCC patients with variceal hemorrhage, but the portal vein must be opened before TIPS. There were no reports about whether TIPS could be a palliative method for portal vein tumor thrombosis (PVTT). Since 1998 we have tried to study TIPS in the treatment of portal hypertension secondary to PVTT.

MATERIALS AND METHODS

Clinical data

There were 14 patients with end-stage HCC in our hospital from December 1998 to May 2001, 13 men and one woman. The patients aged from 28 to 75 years, and the average age was 56.3 years. Three patients did not receive any treatment before TIPS and the others were treated with transarterial chemoembolization (TACE) and other procedures. One patient survived for 6 years after 8 times of TACE, and 2 patients emerged ascites and hemorrhage after they were treated by radiofrequency ablation. Of the 14 patients, there were three patients with intractable ascites, one patient with simple hemorrhage and 10 patients with hemorrhage and ascites (Tables 1, 2). Their hepatic function was poor and assigned to Child-Pugh class C. The diagnosis of PVTT was based on contrast-enhanced CT and color Doppler sonography while the cavernous transformation in the portal vein was detected by color Doppler sonography, contrast-enhanced CT and angiography.

TIPS procedure

TIPS was performed by using the RTPS 100 (Cook, America) portal venous puncture set. After administration of local anesthetic (20 g/L lidocaine hydrochloride) the Colapinto needle (Cook, America) was advanced into the right hepatic vein, and then the right portal vein was punctured. A wire guide (hydrophilic coating wire guide, Terumo) was introduced through the needle. Because of stenosis, occlusion and cavernous transformation of portal vein trunk and its right and left branches, puncture was difficult. So small branches were also available. With a guiding wire the catheter was advanced into the portal vein trunk. After measurement of the portal venous pressure, the needle track was dilated with a balloon (10 mm-diameter, 40 mm-length). Then an expandable stent (8-10 mm-diameter, 6-8 cm-length) was placed. The number of stents was based on the length of the shunt tract to ensure the stents covering all along stenosis segments arising from tumor emboli. The portal venous pressure was also measured after shunt was established.

RESULTS

The portosystemic shunt was successful in 10 of 14 patients. Shunt tract was achieved with a single stent in four patients, two stents in four patients, and four stents in two patients. The mean portal pressure was 37.2 mmHg and 18.2 mmHg before

and after TIPS. The mean abdomen circumference was 86.3 cm and 77.65 cm before and after the procedure (Table 1). TIPS could be performed for four patients with incomplete occlusion of portal vein trunk as standard TIPS (Figure 1), while it could be performed for six patients with complete occlusion of portal vein trunk by introducing hydrophilic coating wire guide through the potential vascular lumen to superior mesenteric vein (Figure 2). The 4 patients with cavernous transformation in portal vein and severe cirrhosis failed to TIPS procedure, no portal vein trunk and branches but vascular plexus sign was displayed on angiogram. They had no improvement in clinical symptoms and their mean survival time was 34 days, shorter than the successful ones. The needles were punctured out of liver and into the peritoneum cavity in two patients, but they had no severe complications during and after the procedure. The needle tract was passed through the tumor in one patient, but no metastasis was found in 3 mo of follow-up. In all patients the mean content of serum bilirubin and aminotransferase increased transiently after TIPS procedure,

and improved after one week of treatment.

Table 1 Clinical characteristics of 14 patients assigned to treatment with transjugular intrahepatic portosystemic stent-shunt procedure

Characteristic	Value
Age (yr)	
Range	28-75
mean±SD	53.6±12.7
Sex (M/F)	13/1
Occlusion of portal vein	
Portal vein trunk (complete/ incomplete)	10/4
Right branch (complete/ incomplete)	10/1
Left branch (complete/ incomplete)	2/2
Tumor type (nodular/massive/diffuse)	2/6/6
With cavernous transformation of PV	5
Times of TACE (mean±SD)	3.7±1.8

Table 2 Portal pressure, ascites and clinical symptoms before and after TIPS procedure in 10 patients receiving stents (mean±SD)

	Before procedure	After procedure	(t/ χ^2 value)	P Value
Portal vein pressure (mmHg)	37.5±4.8	18.2±1.8	t:13.032	0.000
Circumference of abdomen (cm)	85.3±4.7	79.2±5.2	t:3.823	0.002
Ascites				
Mild	3	8		
Moderate	1	4		
Severe	10	2		
Diarrohea (times/d)	3.8±4.4	0±0	t:3.202	0.007
Hepatic encephalopathy				
0	9	9		
I	3	5		
II	2	0		
Variceal bleeding (times)	1.9±1.5	0±0	T:4.759	0.000

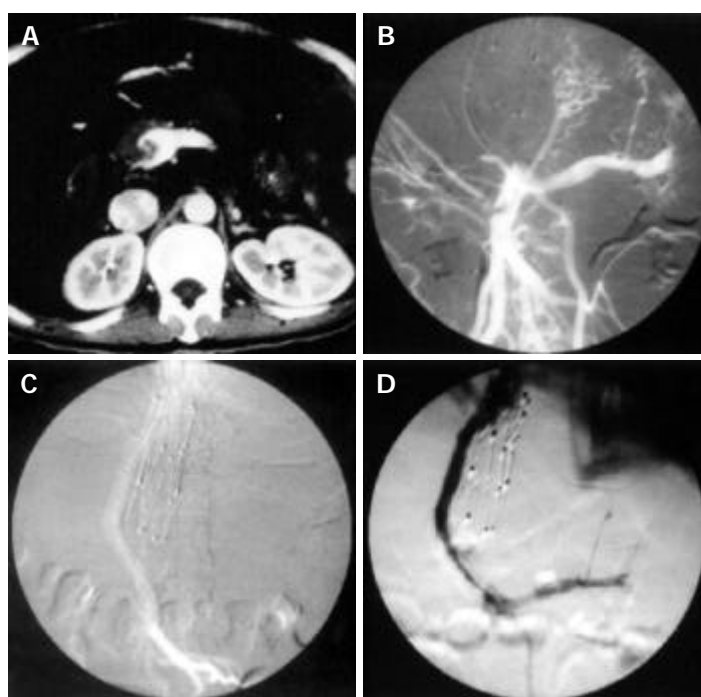


Figure 1 TIPS procedure in patient with incomplete occlusion of portal vein trunk. A: Main portal vein dilation with eccentric tumor thrombi shown on enhanced Ctgram. B: Superior mesenteric vein dilation with eccentric filling defect and main portal vein occlusion shown on superior mesenteric vein angiogram. C: Open shunt shown on superior mesenteric vein angiogram after stent implantation. D: Recurrence of symptoms of ascites and diarrhoea 30 d after TIPS and shunt stenosis as well as segmental filling defects shown on follow-up angiogram.

DISCUSSION

The incidence of PVTT in end-staged HCC was very high, about 20-30% in small hepatoma (2-3 cm in diameter) and 50-75% in those above 5 cm in diameter, and 86% of HCC patients with variceal bleeding had PVTT^[18]. The tumor emboli resulting in portal hypertension and high resistance made the patients tend to have variceal bleeding and ascites. Tumor thrombosis in main portal vein was more prone to variceal bleeding and more difficult to be treated than that in branches and hepatic vein. Therefore some conservative measures were taken to relieve the patients' ailments, such as endoscopic sclerotherapy and ligation. But these measures were less effective. Because of low efficacy and huge cost, many patients abandoned treatment.

Current status and application of TIPS in PVTT

TIPS procedure is an effective and safe treatment for patients with variceal hemorrhage and intractable ascites, but its use is limited due to its complications of encephalopathy and poor long-term efficacy^[19-25]. It was reported that the rate of stenosis of shunt was 33-66% within 1 year and that of encephalopathy was 10-30%^[1-2,19,22]. In recent years some scholars applied TIPS to portal hypertension secondary to portal thrombosis to ensure the patients to have time for further treatments including liver transplantation^[26-29]. But the thrombus must be newly happened because old emboli possibly led to cavernous transformation and made the TIPS and liver transplantation difficult. Some authorities applied TIPS to HCC patients with esophagogastric variceal bleeding, but they thought that patients must be with hepatic function class A or B (Child-Pugh classification), under-controlled or small nodular type hepatoma and without PVTT^[18,30-34].

Key skill points in TIPS procedure for PVTT

Of the 14 cases, 10 cases were technically successful and the ratio of success was consistent with that reported^[1-2]. It was very difficult to puncture the right main portal branch directly because of portal occlusion, stenosis and cavernous transformation. Even a small branch of portal vein was punctured with good blood regurgitation, and hydrophilic coating wire guide could be introduced into the superior mesenteric vein or splenic vein through the loose thrombus (Figure 2). The stent should cover all the thrombus to prevent tumor from growing into the shunt. The slower the blood flow passing the stent, the more easily the shunt is thrombosed. Esophagogastric vein should be embolized after TIPS procedure because low blood flow tended to form thrombosis in the shunt^[8,25]. The embolism of esophagogastric vein could also prevent variceal bleeding, keep high flow and reduce thrombosis in the stent. But esophagogastric vein was not displayed very well because of PVTT in most cases.

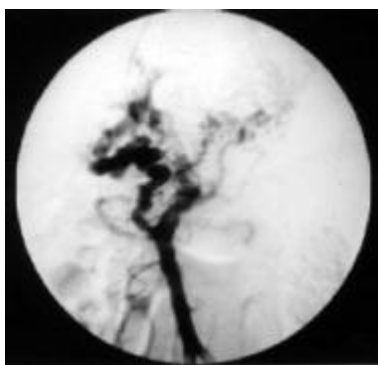


Figure 2 Occlusive portal vein, dilated superior mesenteric vein, portal vein cavernous transformation, and esophagogastric varices shown on portal vein angiogram after introducing a catheter into superior mesenteric vein.

Experiences and clinical effect

TIPS procedure is very effective for diarrhoea secondary to PVTT. A male patient with PVTT had mechanical diarrhoea 12-15 times a day and it lasted for a month with no abnormality in stool examination. Following the decrease of portal pressure after TIPS, ascites and diarrhoea decreased. The causes of diarrhoea were similar to those of ascites. Too high portal vein pressure could make fluid leak out of vessels not only into peritoneal cavity but also into intestinal tract as watery stool.

All patients who failed to TIPS procedure had cavernous transformation. Two patients with tumor thrombus in portal vein had no dilation in superior mesenteric vein and the pressure was not high as well (Figure 3). Considering that the effect was probably not very well in patients with little pressure gradient, we did not continue further procedure. In these portal hypertension patients there were areas with both a portal and a systemic venous drainage including esophagus, anal canal, retroperitoneum and umbilical region. Partial spleen artery embolization or gastric coronary vein embolization was not effective and variceal rebleeding was inevitable in the following months. In this study only one patient had a successful procedure in five patients with cavernous transformation, so it should be careful to carry out TIPS procedure in such cases.

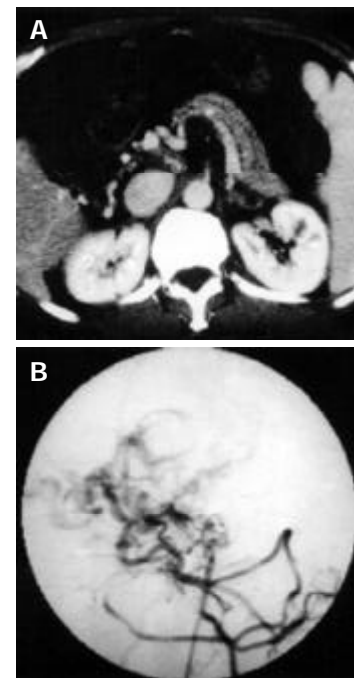


Figure 3 Main portal vein occlusion, hepatic arteric portal shunt and portal cavernous transformation in a 64-year-old patient with refractory ascites and hematemesis. A: Thin splenic and superior mesenteric vein shown on enhanced CT gram. B: Thin superior mesenteric vein and disordered drainage vein shown on angiogram.

A suitable size of stent is important to improve shunt flow, prevent esophagogastric variceal bleeding and decrease ascites^[23-34]. Too large a stent could lead to encephalopathy and we used stents of 10 mm in diameter. The shunt stenosed in one patient with a stent of 8 mm in diameter 15 days after TIPS and died of rebleeding after 20 d. Another patient was placed 4 stents because the shunt was too long. Stenosis of the shunt happened 30 d after the stents were placed and the angiogram displayed shunt rugged and segmental filling defects (Figure 1D). Treatment of the shunt stenosis was similar to that of standard TIPS. The rate of shunt stenosis was relatively low in these patients, partly because of short-term follow-up and abnormal coagulation. By actively preventing encephalopathy and closely

monitoring condition change, patients in this study did not have encephalopathy of stage II and only 5 patients had transitory encephalopathy of stage I. Although patients died of dyscrasia or liver failure, their quality of life was improved.

REFERENCES

- Papathodoridis GV**, Goulis J, Leandro G, Patch D, Burroughs AK. Transjugular intrahepatic portosystemic shunt compared with endoscopic treatment for prevention of variceal rebleeding: a meta-analysis. *Hepatology* 1999; **30**: 612-622
- Schepke M**, Sauerbruch T. Transjugular portosystemic stent shunt in treatment of liver diseases. *World J Gastroenterol* 2001; **7**: 170-174
- Xu K**, Zhang HG, He XF, Zhao ZC, Ren K, Jin CY, Han MJ, Wang CL. Preliminary report on portal hypertension in liver cirrhosis treated by transjugular intrahepatic portosystemic stent-shunt: analysis of 8 cases. *Zhonghua Fangshexue Zazhi* 1993; **27**: 294-297
- Zhang JS**, Wang MQ, Yang L. Transjugular intrahepatic portosystemic stent shunts. *Zhonghua Yixue Zazhi* 1994; **74**: 150-152
- Wang MQ**, Zhang JS, Gao YA. Transjugular intrahepatic portosystemic stent-shunt: an experimental study. *Zhonghua Fangshexue Zazhi* 1993; **28**: 324-327
- Trotter JF**, Suhocki PV, Rockey DC. Transjugular intrahepatic portosystemic shunt (TIPS) in patients with refractory ascites: effect on body weight and Child-Pugh score. *Am J Gastroenterol* 1998; **93**: 1891-1894
- Han SW**, Joo YE, Kim HS, Choi SK, Rew JS, Kim JK, Kim SJ. Clinical results of the transjugular intrahepatic portosystemic shunt (TIPS) for the treatment of variceal bleeding. *Korean J Intern Med* 2000; **15**: 179-186
- Walser EM**, McNees SW, DeLa Pena O, Crow WN, Morgan RA, Soloway R, Broughan T. Portal venous thrombosis percutaneous therapy and outcome. *J Vasc Interv Radiol* 1998; **9**(1 Pt 1): 119-127
- Cwikiel W**, Keussen I, Larsson L, Solvig J, Kullendorff CM. Interventional treatment of children with portal hypertension secondary to portal vein occlusion. *Eur J Pediatr Surg* 2003; **13**: 312-318
- Opitz T**, Buchwald AB, Lorf T, Awuah D, Ramadori G, Nolte W. The transjugular intrahepatic portosystemic stent-shunt (TIPS) as rescue therapy for complete Budd-Chiari syndrome and portal vein thrombosis. *Z Gastroenterol* 2003; **41**: 413-418
- Ganger DR**, Klapman JB, McDonald V, Matalon TA, Kaur S, Rosenblatt H, Kane R, Saker M, Jensen DM. Transjugular intrahepatic portosystemic shunt (TIPS) for Budd-Chiari syndrome or portal vein thrombosis: review of indications and problems. *Am J Gastroenterol* 1999; **94**: 603-608
- Sehgal M**, Haskal ZJ. Use of transjugular intrahepatic portosystemic shunts during lytic therapy of extensive portal splenic and mesenteric venous thrombosis: long-term follow-up. *J Vasc Interv Radiol* 2000; **11**: 61-65
- Yamagami T**, Nakamura T, Tanaka O, Akada W, Takayama T, Maeda T. Transjugular intrahepatic portosystemic shunts after complete obstruction of portal vein. *J Vasc Interv Radiol* 1999; **10**: 575-578
- Shibata D**, Brophy DP, Gordon FD, Anastopoulos HT, Sentovich SM, Bleday R. Transjugular intrahepatic portosystemic shunt for treatment of bleeding ectopic varices with portal hypertension. *Dis Colon Rectum* 1999; **42**: 1581-1585
- Azoulay D**, Castaing D, Lemoine A, Samuel D, Majno P, Reynes M, Charpentier B, Bismuth H. Successful treatment of severe azathioprine-induced hepatic veno-occlusive disease in a kidney-transplanted patient with transjugular intrahepatic portosystemic shunt. *Clin Nephrol* 1998; **50**: 118-122
- Nolte W**, Canelo R, Figulla HR, Kersten J, Sattler B, Munke H, Hartmann H, Ringe B, Ramadori G. Transjugular intrahepatic portosystemic stent-shunt after orthotopic liver transplantation in a patient with early recurrence of portal hypertension of unknown origin. *Z Gastroenterol* 1998; **36**: 159-164
- Benador N**, Grimm P, Lavine J, Rosenthal P, Reznik V, Lemire J. Transjugular intrahepatic portosystemic shunt prior to renal transplantation in a child with autosomal-recessive polycystic kidney disease and portal hypertension: A case report. *Pediatr Transplant* 2001; **5**: 210-214
- Zhang XT**, Xu K, Zhang HG, Zhang LC, Zhao ZC, Han MJ. Primary hepatocellular carcinoma with portal hypertension treated with TIPSS. *Linchuang Fangshexue Zazhi* 1995; **14**: 236-238
- Hausegger KA**, Sternthal HM, Klein GE, Karaic R, Stauber R, Zenker G. Transjugular intrahepatic portosystemic shunt: angiographic follow-up and secondary interventions. *Radiology* 1994; **191**: 177-181
- Willkomm P**, Schomburg A, Brensing KA, Reichmann K, Bangard M, Overbeck B, Sauerbruch T, Biersack HJ. Liver perfusion scintigraphy prior to and after transjugular intrahepatic portosystemic shunts (TIPS) in patients with portal hypertension. *Nuklearmedizin* 2000; **39**: 139-141
- Zuckerman DA**, Darcy MD, Bocchini TP, Hildebolt CF. Encephalopathy after transjugular intrahepatic portosystemic shunting: analysis of incidence and potential risk factors. *Am J Roentgenol* 1997; **169**: 1727-1731
- Sterling RK**, Sanyal AJ. Are TIPS tops in the treatment of portal hypertension? A review on the use and misuse of transjugular intrahepatic portosystemic shunts. *Can J Gastroenterol* 2000; **14**(Suppl D): 122D-128D
- Sanyal AJ**. The use and misuse of transjugular intrahepatic portosystemic shunts. *Papathodoridis G Curr Gastroenterol Rep* 2000; **2**: 61-71
- Younossi ZM**, McHutchison JG, Broussard C, Cloutier D, Sedghi-Vaziri A. Portal decompression by transjugular intrahepatic portosystemic shunt and changes in serum-ascites albumin gradient. *J Clin Gastroenterol* 1998; **27**: 149-151
- Latimer J**, Bawa SM, Rees CJ, Hudson M, Rose JD. Patency and reintervention rates during routine TIPSS surveillance. *Cardiovasc Intervent Radiol* 1998; **21**: 234-239
- Khan TT**, Reddy KS, Johnston TD, Lo FK, Shedlofsky S, Grubb S, Ranjan D. Transjugular intrahepatic portosystemic shunt migration in patients undergoing liver transplantation. *Int Surg* 2002; **87**: 279-281
- Hidajat N**, Vogl T, Stobbe H, Schmidt J, Wex C, Lenzen R, Berg T, Neuhaus P, Felix R. Transjugular intrahepatic portosystemic shunt. Experiences at a liver transplantation center. *Acta Radiol* 2000; **41**: 474-478
- Liatsos C**, Vlachogiannakos J, Patch D, Tibballs J, Watkinson A, Davidson B, Rolles K, Burroughs AK. Successful recanalization of portal vein thrombosis before liver transplantation using transjugular intrahepatic portosystemic shunt. *Liver Transpl* 2001; **7**: 453-460
- Menegaux F**, Keeffe EB, Baker E, Egawa H, Concepcion W, Russell TR, Esquivel CO. Comparison of transjugular and surgical portosystemic shunts on the outcome of liver transplantation. *Arch Surg* 1994; **129**: 1018-1023
- Nicolini A**, Saccheri S, Lovaria A, Maggi A, Cazzaniga M, Panzeri A, Salerno F. Prevention of variceal rebleeding and treatment of liver carcinoma by consecutive transjugular intrahepatic portosystemic shunt and hepatic artery chemoembolization. *Ital J Gastroenterol* 1996; **28**: 269-271
- Burger JA**, Ochs A, Wirth K, Berger DP, Mertelsmann R, Engelhardt R, Roessle M, Haag K. The transjugular stent implantation for the treatment of malignant portal and hepatic vein obstruction in cancer patients. *Ann Oncol* 1997; **8**: 200-202
- Serafini FM**, Zwiebel B, Black TJ, Carey LC, Rosemurgy AS 2nd. Transjugular intrahepatic portosystemic stent shunt in the treatment of variceal bleeding in hepatocellular cancer. *Dig Dis Sci* 1997; **42**: 59-65
- Tazawa J**, Sakai Y, Yamane M, Kakinuma S, Maeda M, Suzuki K, Miyasaka Y, Nagayama K, Kusano F, Sato C. Long-term observation after transjugular intrahepatic portosystemic stent-shunt in two patients with hepatocellular carcinoma. *J Clin Gastroenterol* 2000; **31**: 262-267
- Sakaguchi H**, Uchida H, Maeda M, Matsuo N, Kichikawa K, Ohishi H, Nishida H, Ueno K, Nishimine K, Rosch J. Combined transjugular intrahepatic portosystemic shunt and segmental Lipiodol hepatic artery embolization for the treatment of esophagogastric varices and hepatocellular carcinoma in patients with cirrhosis: Preliminary report. *Cardiovasc Intervent Radiol* 1995; **18**: 9-15

Angiogenesis in rabbit hepatic tumor after transcatheter arterial embolization

Xiao-Feng Liao, Ji-Lin Yi, Xing-Rui Li, Wei Deng, Zhi-Fang Yang, Geng Tian

Xiao-Feng Liao, Ji-Lin Yi, Xing-Rui Li, Wei Deng, Zhi-Fang Yang, Geng Tian, Department of General Surgery, Tongji Hospital, Tongji Medical College, Huazhong University of Science and Technology, Wuhan 430030, Hubei Province, China

Correspondence to: Xiao-Feng Liao, Department of General Surgery, Tongji Hospital, Tongji Medical College, Huazhong University of Science and Technology, Wuhan 430030, Hubei Province, China. liaoxiaofeng66@163.com

Telephone: +86-27-83660410

Received: 2003-11-17 **Accepted:** 2003-12-18

Abstract

AIM: To investigate the effect of transcatheter arterial embolization (TAE) on angiogenesis of hepatic tumor.

METHODS: Twenty New Zealand White rabbits were randomly divided into two groups of 10 each and VX2 carcinoma was implanted in the left medial lobes of the livers. Fourteen days later, a silicon catheter was inserted into the left hepatic artery of rabbit with VX2 hepatic tumor and infusion was performed via the hepatic artery using Lipiodol (the TAE group) or saline (the control group). Rabbits were sacrificed 7 d after treatment and tumor tissues were excised. Expression of vascular endothelial growth factor (VEGF) protein and microvessel density (MVD) of tumors were examined using immunohistochemistry. The staining intensity of VEGF was evaluated with a computer-assisted image-analyzer. Reverse transcription-polymerase chain reaction (RT-PCR) was used to detect the VEGF mRNA expression of tumors.

RESULTS: MVD was higher in the TAE group compared with the control group (28.6 ± 10.6 vs 16.3 ± 6.9 , $P < 0.01$). Expression of VEGF protein was enhanced after TAE. The staining intensity of VEGF in the TAE group was 0.162 ± 0.018 , significantly higher than in the control group (0.142 ± 0.01 , $P < 0.01$). At mRNA level, VEGF165 mRNA was significantly higher in the TAE group compared with the control group (2.58 ± 0.42 vs 1.99 ± 0.21 , $P < 0.001$). MVD was well correlated to VEGF expression in both the TAE group ($r = 0.69$, $P < 0.05$) and the control group ($r = 0.72$, $P < 0.05$).

CONCLUSION: TAE promotes the development of neovascularization of residual tumors through up-regulation of VEGF expression, possibly due to hypoxic insult.

Liao XF, Yi JL, Li XR, Deng W, Yang ZF, Tian G. Angiogenesis in rabbit hepatic tumor after transcatheter arterial embolization. *World J Gastroenterol* 2004; 10(13): 1885-1889
<http://www.wjgnet.com/1007-9327/10/1885.asp>

INTRODUCTION

Hepatocellular carcinoma (HCC) is one of the most common malignant tumors in Asia, including China. Surgical resection is still the treatment of first choice for patients with HCC

nowadays^[1]. However, because of tumor extension, poor hepatic functional reserve due to underlying liver cirrhosis, or both, only a small portion of patients are suitable candidates for surgery^[2-4]. Transcatheter arterial chemoembolization (TACE) is considered to be an effective treatment for patients with HCC who are not candidates for surgical resection^[5,6]. TACE could reduce tumor size^[7-8]. However, intrahepatic or extrahepatic metastasis after TACE is the major factor limiting its overall therapeutic effect^[9].

Angiogenesis, the process leading to the formation of new blood vessels from preexisting vessels, plays a central role in the survival of tumor cells, in local tumor growth, and in the development of distant metastasis^[10]. Microvessel density (MVD) has been the gold standard for the quantification of tumor angiogenesis, showing a good correlation with the prognosis in a variety of cancers including HCC^[11-15]. Among the known angiogenic factors produced by tumor cells, vascular endothelial growth factor (VEGF) is one of the most potent angiogenic factors involved in tumor development. VEGF is a specific mitogenic factor for vascular endothelial cells, which stimulates endothelial cells proliferation, promotes neovascularization and increases vascular permeability. Evidence from preclinical and clinical studies indicates VEGF is associated with formation of metastases and poor prognosis in various cancers^[16-18].

VEGF protein is produced by alternative splicing of the primary transcript leading to the production of at least four major isoforms of VEGF: 121, 165, 189, and 206^[19]. VEGF189 and VEGF206 contain heparin-binding domains and are highly concentrated in the extracellular matrix. VEGF165 and VEGF121 are diffusible and predominate in most tissues, lacking this particular domain. The presence or absence of these domains affects the properties, actions, and distribution of the isoform produced^[19].

Little is known of the changes of angiogenesis and VEGF expression in HCC after TACE. Thus, we established a rabbit model of transcatheter arterial embolization (TAE) with hepatic VX2 carcinoma, and examined MVD and VEGF expression in the hepatic tumors after TAE.

MATERIALS AND METHODS

Implantation procedure

The rabbit VX2 carcinoma was selected for implantation in the liver because of the similarities of its blood supply to that of human hepatomas^[20,21]. The VX2 strain (obtained from Dr. Li Xin of Department of Radiology, the Union Hospital, Tongji Medical College of Huazhong University of Science and Technology, Wuhan, China) was maintained by serial passage in rabbit hindlimbs. Twenty male New Zealand White rabbits (3.0 to 3.5 kg) were used for all experiments. Studies with these animals were approved by the Animal Care and Use Committee of Tongji Medical College of Huazhong University of Science and Technology and carried out according to their guidelines. Tumor implantation was performed as described previously^[22] with a slight modification. Briefly, rabbits were anesthetized by i.v. injection of sodium pentobarbital (30 mg/kg) via a marginal ear vein. The abdominal area was shaved and

sterilized, and a midline subxyphoid incision was made. The left medial lobe of rabbit liver was gently exposed, and one piece of the VX2 tumor tissue excised from the carrier rabbit and broken into fine pieces (1 mm×1 mm×1 mm in size per piece) in Hanks' solution was implanted into the subcapsule of the left medial hepatic lobe. The implanted site was closed with gelatin sponge to prevent the leakage of tumor cells into the peritoneal cavity. The hepatic lobe was then returned to the abdominal cavity. This method allows the growth of a single solitary, well-demarcated tumor in the liver of each recipient rabbit. The incision was closed in two layers. The tumors were allowed to grow for 2 wk, and studies were performed when the tumors reached 1 to 2 cm in diameter.

TAE procedure

Twenty rabbits were divided into two groups of 10 rabbits each randomly. The animals were relaparotomized through a midline abdominal incision under the general anesthesia as described above, and a silicone catheter (outer diameter 0.8 mm) with a tip in the shape of a hockey-stick was inserted retrogradely into the left hepatic artery via the gastroduodenal artery under the operating microscope (Zeiss OPMI 6-S, Aalen, Germany). The catheter was tightly secured and hepatic arterial infusion was made, with 0.5 mL/kg of lipiodol in TAE group or with the same volume of saline in control group. After the injection, the catheter was removed and the gastroduodenal artery was ligated. The incision was closed in two layers. CT scan was performed 2 d after TAE, and confirmed that the lipiodol had been retained in the tumors of all cases (Figure 1).

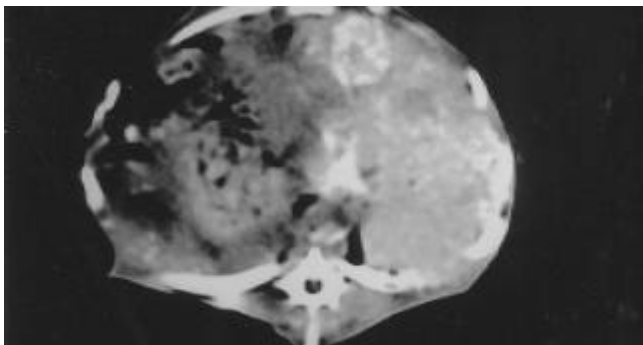


Figure 1 CT scan 2 d following lipiodol infusion.

Tissue preparation

The rabbits were sacrificed 7 d after treatment, and the tumor was removed. Part of the specimen was flash-frozen at -70°C for RT-PCR, and the rest was fixed in 40 g/L formaldehyde and embedded in paraffin for immunohistochemical study.

Immunohistochemistry

Consecutive 4- μm sections were cut and mounted on glass slides. Sections were stained with H&E. VEGF expression was examined immunohistochemically with an anti-VEGF mouse monoclonal antibody (JH121, Neomarkers, Inc., Fremont, CA) at a dilution of 1:80, and by using streptavidin-peroxidase technique with SPTm kit (Zymed Laboratories, Inc., USA). The JC/70 monoclonal antibody (Dako, Glostrup, Denmark) against CD31 was used for microvessel staining using the LSAB method (Dako LSAB kit; Glostrup, Denmark). Negative controls were prepared by PBS substitution for the primary antibodies staining, and known positive controls were included in each staining run.

Morphometric analyses

The positive expression cells of VEGF were ones with brown-

yellow granular patterns in the cytoplasm. In intensively positive staining area, three fields of vision were selected at $\times 400$ magnification. Staining intensity of VEGF was assessed morphometrically with a computer-assisted image-analyzer (HPIAS-1 000 high precision color-image measure system, Tongji Qiangping Image Engineer Company). The image analyzer is an integrated system of Windows-based software specially designed for immunohistochemical analysis.

Determination of MVD

MVD was evaluated according to the method described by Gasparini *et al.*^[23] The stained sections were screened at low power field ($\times 40$), and five areas with the most intense neovascularization (hot spots) were selected. Microvessel counts of these areas were performed at high power field ($\times 200$). Any brown-stained endothelial cell or endothelial cell cluster clearly separated from adjacent microvessels, tumor cells, and other connective-tissue elements was counted as one microvessel, irrespective of the presence of a vessel lumen. The mean microvessel count of the five richest vascular areas was taken as the MVD, which was expressed as the absolute number of microvessels per 0.74 mm^2 ($\times 200$).

RNA preparation and reverse transcription-polymerase chain reaction (RT-PCR)

Total RNA was extracted using TriZol reagent (Life Technologies, Grand Island, NY) according to the manufacturer's recommendations. Briefly, the tissue was homogenized with a Polytron homogenizer in 1 mL TriZol per 100 mg tissue. The suspension was left at room temperature for 10 min before being centrifuged at $12\,000\text{ g}$ at 4°C for 10 min. The aqueous supernatant containing the RNA was carefully removed and transferred to a fresh tube. Total RNA was precipitated by addition of isopropanol and centrifuged at $12\,000\text{ g}$ at 4°C for 10 min. The RNA pellet was washed with 750 mL/L ethanol and re-dissolved in DEPC-treated water. Before being used in RT-PCR these samples were phenol/chloroform extracted and phenol precipitated. The RNA concentration and quality were determined by UV spectrophotometer at absorbances of 260 and 280 nm.

cDNA was synthesized from total RNA with Avian Myeloblastosis Virus and oligo dT-Adaptor Primer (TaKaRa RNA PCR Kit, TaKaRa Bioteth., Dalian, CHN) according to the manufacturer's instructions. Amplification of cDNA was performed using published sense and antisense primers for rabbit β -actin and VEGF^[19,24,25]. The primer sequence for β -actin sense was 5' -CCT TCC TGC GCA TGG AGT CCT GG-3', and the primer sequence for β -actin antisense was 5' -GGA GCA ATG ATC TTG ATC TTC-3'. The sense primer sequence for VEGF was 5' -CAG TGA ATT CGA GAT GAG CTT CCT ACA GCA C-3', and the antisense primer sequence was 5' -CCT GGA ATT CTC ACC GCC TCG GCT TGT CAC-3'. The PCR cycle profile was at 94°C for 30 s, 59°C for 60 s and 72°C for 60 s, with 30 cycles.

After visualization of the PCR products by 20 g/L agarose gel electrophoresis with ethidium bromide staining gel, images were obtained and the densities of the products were quantified using a digital gel image analysis system (GDS8 000, UVP Co., UK). The PCR fragments were identified according to their molecular mass using a DNA marker (DL2 000 marker, TaKaRa Bioteth., Dalian, China). The relative expression levels were calculated as the density of the product of the respective target genes after normalization with the β -actin internal control.

Statistical analysis

All data are expressed as mean \pm SD. Differences in staining

intensity of VEGF, quantity of variant VEGF isoforms and MVD between the TAE group and the control group were compared with Student's *t* test. The correlation of VEGF and MVD was performed with linear regression analysis. $P < 0.05$ was considered statistically significant. Statistical analysis was done using SPSS 10.0 for Windows.

RESULTS

MVD and its pathologic features

Figure 2A shows microvessels were stained in brown color. Microvessels were heterogeneously distributed inside the tumor, and, in general, maximal density was observed near the margins of the invasive tumor or in the central regions of tumor where necrosis could be seen. The MVD was 28.6 ± 10.6 in the TAE group, and 16.3 ± 6.9 in the control group. The MVD was significantly higher in the TAE group than that of the control group ($P < 0.01$).

Expression of VEGF protein

Immunoreactive products of anti-VEGF antibody were positively detected in the cytoplasm of hepatoma cells and scarcely detected in endothelial cells. In general, hepatoma cells showed stronger VEGF immunoreactivity than endothelial cells. The intensity of immunoreactive products was heterogeneous (Figure 2B). The staining intensity of VEGF in the TAE group was 0.162 ± 0.018 , significantly higher compared to the control group (0.142 ± 0.01 , $P < 0.01$).

There was a significant correlation between MVD and VEGF protein expression in both the TAE group ($r = 0.69$, $P < 0.05$) and the control group ($r = 0.72$, $P < 0.05$).

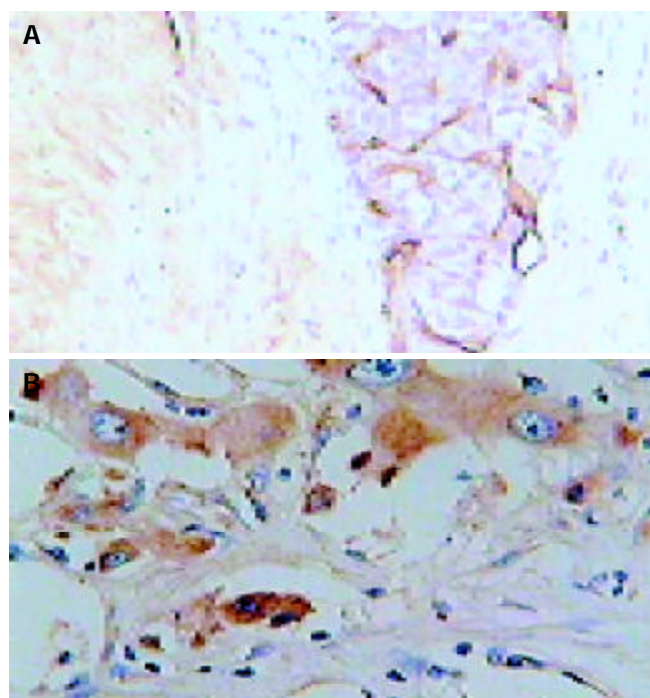


Figure 2 Immunohistochemical staining in hepatic tumor tissues obtained from a rabbit underwent TAE. A: CD31, original magnification $\times 200$; B: VEGF, original magnification $\times 400$.

Expression of VEGF mRNA

PCR amplification of cDNA prepared from frozen sections showed the expression of three bands of 110, 242 and 314 bp corresponding to VEGF121, VEGF165 and VEGF189, respectively (Figure 3A). The band corresponding to VEGF206 was not detected. In both the TAE group and the control group, VEGF165 was strongly detected (Figure 3B). The intensity of

VEGF165 mRNA was significantly higher in the TAE group (2.58 ± 0.42), as compared with the control group (1.99 ± 0.21 , $P < 0.001$). Although the signal of VEGF121 mRNA was slightly higher in the TAE group (1.14 ± 0.19) than that of the control group (0.99 ± 0.11), there was no statistical significance. No significant difference between VEGF189 mRNA in the TAE group (1.03 ± 0.14) and the control group (1.01 ± 0.11) was demonstrated (Figure 3B).

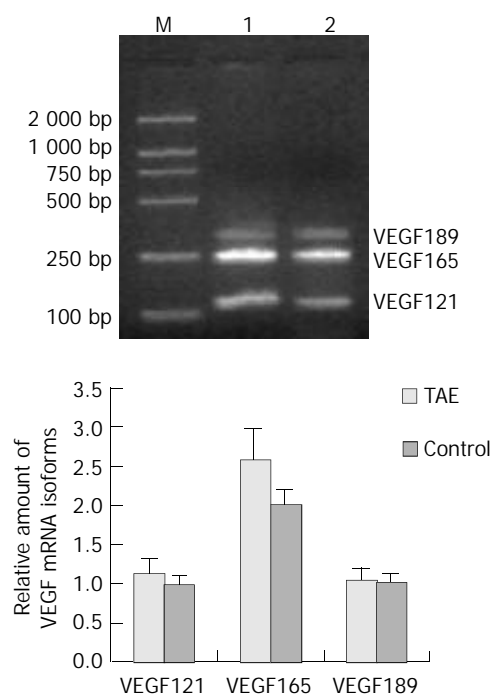


Figure 3 Expression of VEGF mRNA in hepatic tumor tissues. A: Results of RT-PCR of VEGF mRNA in TAE (lane 1), control (lane 2) and M (molecular mass marker); B: quantification of RT-PCR data.

DISCUSSION

TACE has been accepted as one of the most effective palliative treatments for patients with unresectable HCC on the basis of the characterization of its blood supply. Since the blood supply of HCC is derived almost exclusively from hepatic arteries, hepatoma cells undergo ischemic necrosis in TAE. The addition of chemotherapy aimed to enhance the antitumor effect of the ischemia. However, it was only a small proportion of HCC that occurred complete necrosis after TACE^[26]. We have occasionally noticed rapid growth and extensive metastasis after multiple TACE treatments. TACE prior to surgical resection may facilitate recurrence of HCC^[27]. The recurrence rate after 3 years of treatment is 30-60%^[28,29]. It is possible that in addition to the limited ability of chemoembolization to eliminate cancer cells, it may play a role in enhancing the malignant potential of the tumor and the ability of some cells to escape necrosis after treatment^[30]. Huang *et al.*^[26] and Kim *et al.*^[31] reported that the proliferative activity of tumor cells was increased after TACE.

In the present study, we investigated the change of angiogenesis in VX2 hepatic tumor that underwent TAE using immunohistochemical techniques. The results showed that MVD of the tumors markedly increased after TAE. MVD is currently considered the gold standard for histological assessment of the degree of angiogenesis within a tumor. It is an independent predictor for the growth, metastasis and prognosis of tumor. Increasing evidence suggests that there is a clear relationship between the MVD and HCC prognosis^[1,14,32,33]. These findings thus provide evidence that the development of neovascularization

in hepatic residual tumors after TAE may be one of the reasons why the majority of tumor nodes do not show complete necrosis and why tumors have an increased tendency to metastasize after TAE.

Until recently, VEGF was the only growth factor proven to be specific and critical for blood vessel formation^[34]. Many studies have indicated that VEGF is not only correlated with HCC angiogenesis, but also closely correlated with the invasion and metastasis of HCC. The levels of VEGF in tumor and peripheral blood of patients with HCC might be a useful indicator for both HCC metastasis and poor prognosis^[18,35-41]. In our study, the expression of VEGF protein was well correlated to MVD, and the level of VEGF expression in TAE group was increased significantly compared with the control. These findings show that VEGF plays a vital role in the process of angiogenesis in hepatic tumors after TAE.

It has been known that four alternatively spliced products can be generated from the single VEGF gene, yielding different protein products composed of 121, 165, 189 and 206 amino acids, designated as VEGF121, VEGF165, VEGF189 and VEGF206, respectively. Among them, only VEGF121 and VEGF165 are secreted and can induce mitogenesis of endothelial cells; VEGF189 and VEGF206 are membrane anchored and act as vascular permeability factors. To identify the changes of VEGF mRNA isoform expression in hepatic tumors after TAE, we performed RT-PCR. In our study three bands of 110, 242 and 314 bp were shown, corresponding to VEGF121, VEGF165 and VEGF189, respectively. The major VEGF isoform expressed in VX2 hepatic tumor was VEGF165. The significantly enhanced expression of VEGF165 mRNA in the TAE group was observed compared with the control group. Although VEGF121 mRNA was slightly higher in the TAE group than in the control group, there was no statistical significance. We detected no VEGF206 mRNA, consistent with the very restricted expression of this splice variant.

The possible reason for up-regulation of VEGF expression after embolization was anoxia and ischemia of tumor tissues. Hypoxia is known to be a very important stimulus for the new vessel formation seen in tumor angiogenesis by stimulating the expression of VEGF^[42,43]. Kim *et al.*^[44] reported that hypoxia might induce HCC cells to secrete more VEGF and IGF-II. Moreover, the combination of hypoxia and IGF-II brought an additional induction of VEGF. In the current study, it was found that more microvessel was observed in the tumor margins or areas around the necrotic tissues, which might be resulted from more severe local anoxia in these areas.

Song *et al.*^[45] reported that plasma IGF-II level was increased after TACE, which implied that expression of other angiogenic factors besides VEGF might also be changed after TACE.

In conclusion, these results indicate that TAE is involved in the development of neovascularization of hepatic residual tumors after TAE through up-regulation of VEGF expression, possibly due to hypoxic insult. Therefore, the combination of TAE and antiangiogenic therapy may be superior to TAE alone in the treatment of HCC.

REFERENCES

- 1 **Tang Z**, Zhou X, Lin Z, Yang B, Ma Z, Ye S, Wu Z, Fan J, Liu Y, Liu K, Qin L, Tian J, Sun H, He B, Xia J, Qiu S, Zhou J. Surgical treatment of hepatocellular carcinoma and related basic research with special reference to recurrence and metastasis. *Chin Med J* 1999; **112**: 887-891
- 2 **Yan FH**, Zhou KR, Cheng JM, Wang JH, Yan ZP, Da RR, Fan J, Ji Y. Role and limitation of FMPSPGR dynamic contrast scanning in the follow-up of patients with hepatocellular carcinoma treated by TACE. *World J Gastroenterol* 2002; **8**: 658-662
- 3 **Faivre J**, Forman D, Esteve J, Obradovic M, Sant M. Survival of patients with primary liver cancer, pancreatic cancer and biliary tract cancer in Europe. *Eur J Cancer* 1998; **34**: 2184-2190
- 4 **El-Serag HB**, Mason AC, Key C. Trends in survival of patients with hepatocellular carcinoma between 1977 and 1996 in the United States. *Hepatology* 2001; **33**: 62-65
- 5 **Acunas B**, Rozanes I. Hepatocellular carcinoma: treatment with transcatheter arterial chemoembolization. *Eur J Radiol* 1999; **32**: 86-89
- 6 **Tang ZY**. Hepatocellular carcinoma. *J Gastroenterol Hepatol* 2000; **15**(Suppl): G1-7
- 7 **Poon RT**, Ngan H, Lo CM, Liu CL, Fan ST, Wong J. Transarterial chemoembolization for inoperable hepatocellular carcinoma and postresection intrahepatic recurrence. *J Surg Oncol* 2000; **73**: 109-114
- 8 **Lo CM**, Ngan H, Tso WK, Liu CL, Lam CM, Poon RT, Fan ST, Wong J. Randomized controlled trial of transarterial lipiodol chemoembolization for unresectable hepatocellular carcinoma. *Hepatology* 2002; **35**: 1164-1171
- 9 **Liou TC**, Shih SC, Kao CR, Chou SY, Lin SC, Wang HY. Pulmonary metastasis of hepatocellular carcinoma associated with transarterial chemoembolization. *J Hepatol* 1995; **23**: 563-568
- 10 **Folkman J**. What is the evidence that tumors are angiogenesis dependent? *J Natl Cancer Inst* 1990; **82**: 4-6
- 11 **Zheng HC**, Sun JM, Li XH, Yang XF, Zhang YC, Xin Y. Role of PTEN and MMP-7 expression in growth, invasion, metastasis and angiogenesis of gastric carcinoma. *Pathol Int* 2003; **53**: 659-666
- 12 **Abramson LP**, Grundy PE, Rademaker AW, Helenowski I, Cornwell M, Katzenstein HM, Reynolds M, Arensman RM, Crawford SE. Increased microvascular density predicts relapse in Wilms' tumor. *J Pediatr Surg* 2003; **38**: 325-330
- 13 **Pruneri G**, Ponzoni M, Ferreri AJ, Decarli N, Tresoldi M, Raggi F, Baldessari C, Freschi M, Baldini L, Goldaniga M, Neri A, Carboni N, Bertolini F, Viale G. Microvessel density, a surrogate marker of angiogenesis, is significantly related to survival in multiple myeloma patients. *Br J Haematol* 2002; **118**: 817-820
- 14 **Poon RT**, Ng IO, Lau C, Yu WC, Yang ZF, Fan ST, Wong J. Tumor microvessel density as a predictor of recurrence after resection of hepatocellular carcinoma: a prospective study. *J Clin Oncol* 2002; **20**: 1775-1785
- 15 **Ng IO**, Poon RT, Lee JM, Fan ST, Ng M, Tso WK. Microvessel density, vascular endothelial growth factor and its receptors Flt-1 and Flk-1/KDR in hepatocellular carcinoma. *Am J Clin Pathol* 2001; **116**: 838-845
- 16 **Takahashi R**, Tanaka S, Kitadai Y, Sumii M, Yoshihara M, Haruma K, Chayama K. Expression of vascular endothelial growth factor and angiogenesis in gastrointestinal stromal tumor of the stomach. *Oncology* 2003; **64**: 266-274
- 17 **White JD**, Hewett PW, Kosuge D, McCulloch T, Enholm BC, Carmichael J, Murray JC. Vascular endothelial growth factor-D expression is an independent prognostic marker for survival in colorectal carcinoma. *Cancer Res* 2002; **62**: 1669-1675
- 18 **Torimura T**, Sata M, Ueno T, Kin M, Tsuji R, Suzaku K, Hashimoto O, Sugawara H, Tanikawa K. Increased expression of vascular endothelial growth factor is associated with tumor progression in hepatocellular carcinoma. *Hum Pathol* 1998; **29**: 986-991
- 19 **Watkins RH**, D'Angio CT, Ryan RM, Patel A, Maniscalco WM. Differential expression of VEGF mRNA splice variants in newborn and adult hyperoxic lung injury. *Am J Physiol* 1999; **276**: L858-867
- 20 **Geschwind JF**, Artemov D, Abraham S, Omdal D, Huncharek MS, McGee C, Arepally A, Lambert D, Venbrux AC, Lund GB. Chemoembolization of liver tumors in a rabbit model: assessment of tumor cell death with diffusion-weighted MR imaging and histologic analysis. *J Vasc Interv Radiol* 2000; **11**: 1245-1255
- 21 **Ko YH**, Pedersen PL, Geschwind JF. Glucose catabolism in the rabbit VX2 tumor model for liver cancer: characterization and targeting hexokinase. *Cancer Lett* 2001; **173**: 83-91
- 22 **Geschwind JF**, Ko YH, Torbenson MS, Magee C, Pedersen PL. Novel therapy for liver cancer: direct intraarterial injection of a potent inhibitor of ATP production. *Cancer Res* 2002; **62**: 3909-3913
- 23 **Gasparini G**, Harris AL. Clinical importance of the determination of tumor angiogenesis in breast carcinoma: much more than a new prognostic tool. *J Clin Oncol* 1995; **13**: 765-782
- 24 **Ozaki NK**, Beharry KD, Nishihara KC, Akmal Y, Ang JG, Sheikh R, Modanlou HD. Regulation of retinal vascular endothelial

- growth factor and receptors in rabbits exposed to hyperoxia. *Invest Ophthalmol Vis Sci* 2002; **43**: 1546-1557
- 25 **Houck KA**, Leung DW, Rowland AM, Winer J, Ferrara N. Dual regulation of vascular endothelial growth factor bioavailability by genetic and proteolytic mechanisms. *J Biol Chem* 1992; **267**: 26031-26037
- 26 **Huang J**, He X, Lin X, Zhang C, Li J. Effect of preoperative transcatheter arterial chemoembolization on tumor cell activity in hepatocellular carcinoma. *Chin Med J* 2000; **113**: 446-448
- 27 **Adachi E**, Matsumata T, Nishizaki T, Hashimoto H, Tsuneyoshi M, Sugimachi K. Effects of preoperative transcatheter hepatic arterial chemoembolization for hepatocellular carcinoma. The relationship between postoperative course and tumor necrosis. *Cancer* 1993; **72**: 3593-3598
- 28 **Matsui O**, Kadoya M, Yoshikawa J, Gabata T, Arai K, Demachi H, Miyayama S, Takashima T, Unoura M, Kogayashi K. Small hepatocellular carcinoma: treatment with subsegmental transcatheter arterial embolization. *Radiology* 1993; **188**: 79-83
- 29 **Ohnishi K**, Yoshioka H, Kosaka K, Toshima K, Nishiyama J, Kameda C, Ito S, Fujiwara K. Treatment of hypervascular small hepatocellular carcinoma with ultrasound-guided percutaneous acetic acid injection: comparison with segmental transcatheter arterial embolization. *Am J Gastroenterol* 1996; **91**: 2574-2579
- 30 **Seki T**, Tamai T, Ikeda K, Imamura M, Nishimura A, Yamashiki N, Nakagawa T, Inoue K. Rapid progression of hepatocellular carcinoma after transcatheter arterial chemoembolization and percutaneous radiofrequency ablation in the primary tumour region. *Eur J Gastroenterol Hepatol* 2001; **13**: 291-294
- 31 **Kim YB**, Park YN, Park C. Increased proliferation activities of vascular endothelial cells and tumour cells in residual hepatocellular carcinoma following transcatheter arterial embolization. *Histopathology* 2001; **38**: 160-166
- 32 **Sun HC**, Tang ZY, Li XM, Zhou YN, Sun BR, Ma ZC. Microvessel density of hepatocellular carcinoma: its relationship with prognosis. *J Cancer Res Clin Oncol* 1999; **125**: 419-426
- 33 **Tanigawa N**, Lu C, Mitsui T, Miura S. Quantitation of sinusoid-like vessels in hepatocellular carcinoma: its clinical and prognostic significance. *Hepatology* 1997; **26**: 1216-1223
- 34 **Yancopoulos GD**, Davis S, Gale NW, Rudge JS, Wiegand SJ, Holash J. Vascular-specific growth factors and blood vessel formation. *Nature* 2000; **407**: 242-248
- 35 **Jinno K**, Tanimizu M, Hyodo I, Nishikawa Y, Hosokawa Y, Doi T, Endo H, Yamashita T, Okada Y. Circulating vascular endothelial growth factor (VEGF) is a possible tumor marker for metastasis in human hepatocellular carcinoma. *J Gastroenterol* 1998; **33**: 376-382
- 36 **Zhou J**, Tang ZY, Fan J, Wu ZQ, Li XM, Liu YK, Liu F, Sun HC, Ye SL. Expression of platelet-derived endothelial cell growth factor and vascular endothelial growth factor in hepatocellular carcinoma and portal vein tumor thrombus. *J Cancer Res Clin Oncol* 2000; **126**: 57-61
- 37 **Iguchi H**, Yokota M, Fukutomi M, Uchimura K, Yonemasu H, Hachitanda Y, Nakao Y, Tanaka Y, Sumii T, Funakoshi A. A possible role of VEGF in osteolytic bone metastasis of hepatocellular carcinoma. *J Exp Clin Cancer Res* 2002; **21**: 309-313
- 38 **Yoshiji H**, Kuriyama S, Yoshii J, Ikenaka Y, Noguchi R, Hicklin DJ, Huber J, Nakatani T, Tsujinoue H, Yanase K, Imazu H, Fukui H. Synergistic effect of basic fibroblast growth factor and vascular endothelial growth factor in murine hepatocellular carcinoma. *Hepatology* 2002; **35**: 834-842
- 39 **Chao Y**, Li CP, Chau GY, Chen CP, King KL, Lui WY, Yen SH, Chang FY, Chan WK, Lee SD. Prognostic significance of vascular endothelial growth factor, basic fibroblast growth factor, and angiogenin in patients with resectable hepatocellular carcinoma after surgery. *Ann Surg Oncol* 2003; **10**: 355-362
- 40 **Poon RT**, Ng IO, Lau C, Zhu LX, Yu WC, Lo CM, Fan ST, Wong J. Serum vascular endothelial growth factor predicts venous invasion in hepatocellular carcinoma: a prospective study. *Ann Surg* 2001; **233**: 227-235
- 41 **Gorriñ-Rivas MJ**, Arii S, Mori A, Takeda Y, Mizumoto M, Furutani M, Imamura M. Implications of human macrophage metalloelastase and vascular endothelial growth factor gene expression in angiogenesis of hepatocellular carcinoma. *Ann Surg* 2000; **231**: 67-73
- 42 **von Marschall Z**, Cramer T, Hocker M, Finkenzeller G, Wiedenmann B, Rosewicz S. Dual mechanism of vascular endothelial growth factor upregulation by hypoxia in human hepatocellular carcinoma. *Gut* 2001; **48**: 87-96
- 43 **Shweiki D**, Itin A, Soffer D, Keshet E. Vascular endothelial growth factor induced by hypoxia may mediate hypoxia-initiated angiogenesis. *Nature* 1992; **359**: 843-845
- 44 **Kim KW**, Bae SK, Lee OH, Bae MH, Lee MJ, Park BC. Insulin-like growth factor II induced by hypoxia may contribute to angiogenesis of human hepatocellular carcinoma. *Cancer Res* 1998; **58**: 348-351
- 45 **Song BC**, Chung YH, Kim JA, Lee HC, Yoon HK, Sung KB, Yang SH, Yoo K, Lee YS, Suh DJ. Association between insulin-like growth factor-2 and metastases after transcatheter arterial chemoembolization in patients with hepatocellular carcinoma: a prospective study. *Cancer* 2001; **91**: 2386-2393

Relationship between serum calcium and CA 19-9 levels in colorectal cancer

Peter Fuszek, Peter Lakatos, Adam Tabak, Janos Papp, Zsolt Nagy, Istvan Takacs, Henrik Csaba Horvath, Peter Laszlo Lakatos, Gabor Speer

Peter Fuszek, Peter Lakatos, Adam Tabak, Janos Papp, Zsolt Nagy, Istvan Takacs, Henrik Csaba Horvath, Peter Laszlo Lakatos, Gabor Speer, 1st Department of Medicine, Faculty of Medicine, Semmelweis University, Budapest, Hungary
Correspondence to: Peter Fuszek MD, 1st Department of Medicine, Faculty of Medicine, Semmelweis University, 1083 Budapest, Korányi S. u. 2/a, Hungary. fuszpet@bell.sote.hu
Telephone: +36-20-9280-451
Received: 2004-02-20 **Accepted:** 2004-03-13

Abstract

AIM: To examine the calcium metabolism of colorectal cancer (CRC) in patients with colorectal cancer and control patients.

METHODS: Seventy newly diagnosed CRC patients were included. The healthy control group was age and gender matched ($n=32$). Particular attention was devoted to the relationship between serum calcium of patients, and levels of AFP, CEA, carbohydrate antigen 19-9 (CA 19-9) (that could be considered as prognostic factors). Furthermore, the Ca-sensing receptor (CaSR) gene A986S polymorphism was investigated in these patients, as well as the relationship between different CaSR genotypes and the data stated above.

RESULTS: A lower level of ionized calcium (also corrected for albumin) was found in the serum of CRC patients with normal 25(OH) vitamin D levels. The ionized calcium concentration was inversely correlated with the serum level of CA 19-9. There was no difference in the distribution of CaSR genotypes, between CRC patients and general population. The genotypes did not correlate with other data examined.

CONCLUSION: Based on these results, lower levels of serum calcium might be a pathogenic and prognostic factor in colorectal cancer.

Fuszek P, Lakatos P, Tabak A, Papp J, Nagy Z, Takacs I, Horvath HC, Lakatos PL, Speer G. Relationship between serum calcium and CA 19-9 levels in colorectal cancer. *World J Gastroenterol* 2004; 10(13): 1890-1892

<http://www.wjgnet.com/1007-9327/10/1890.asp>

INTRODUCTION

Mortality statistics of the developed countries show that colorectal cancer (CRC) is the second leading cause of death. Even though tumorigenesis is a complex process, epidemiological and experimental data indicate that beside the genetic factors, eating habits (and thus the calcium intake) also play a key role in the development of CRC^[1]. In the past few years, we have learned more and more about the process, but not every possible factor has been uncovered yet.

Several *in vitro* and *in vivo* studies have confirmed the chemopreventive role of calcium in CRC^[1-5]. The experimental

data showed that there was a definite connection between low calcium and vitamin D intake and the prevalence of CRC^[6,7]. Some researchers described a protective effect against the development of CRC, when the calcium intake was 1 200 mg daily^[8]. Alimentary calcium (among others) together with bile acids creating insoluble calcium-soaps inhibit the cytotoxic effect of fatty acids in the bowel, thus protecting the mucus membrane^[9-12].

According to twin studies, serum calcium level was mostly determined by genetic factors^[13]. One of the key factors of this determination is the calcium-sensing receptor (CaSR), which by sensing the concentration of calcium in target organs could respond to the changes of calcium level, thus regulating calcium homeostasis^[13]. Also, a connection has been found between the CaSR gene A986S genotypes (986 Ala/Ser) and serum calcium concentrations within the normal range in healthy adult population^[14].

In our work, we examined the calcium metabolism of 70 recently diagnosed CRC patients and analyzed its possible role in the pathogenesis of CRC, and also the relationship between serum levels of AFP, CEA, CA 19-9 (that could be considered as prognostic factors) and parameters of calcium metabolism. Furthermore, we examined the genotype frequencies (CASR A986S) of our patients and the relationship between genotypes and laboratory parameters of calcium homeostasis and tumor markers.

MATERIALS AND METHODS

Patients

Seventy newly diagnosed CRC patients were examined. All the subjects were in good general conditions. Colonoscopy was performed partly for screening purposes ($n=10$), partly due to symptoms ($n=60$), such as abdominal pain, discomfort and flatulence, anemia, hematochezia, changes in bowel habits, and partly to search for primary tumor (for example in cases of hepatic metastasis). In each selected case, the histological diagnosis was adenocarcinoma. Clinical stage was Dukes A: 20, B: 32, C: 18. Five patients had liver metastasis at presentation. The clinical data of the patients are presented in Table 1. An age and gender adjusted healthy control group ($n=32$) was selected for comparison of the laboratory data. The CASR genotype frequency was compared to the genotype frequency of our previously determined control group, consisting of 201 healthy adults. Written informed consent was obtained from all subjects. The study was approved by the Semmelweis University Regional and Institutional Committee of Science and Research Ethics (141/2003).

Laboratory parameters

To analyze the calcium metabolism of the subjects, serum calcium, phosphate and albumin levels were determined by photometric analysis (Roche, Mannheim, Germany). Ionized calcium levels were also measured in a similar way (Easy-Lite, Bedford, USA). The calcium levels were also corrected to the serum albumin levels (corrected calcium). HPLC (Biorad,

Hercules, USA) was used to measure the serum 25(OH) vitamin D levels, while serum levels of parathyroid hormone (PTH) were determined by chemiluminescence assay (Elecsys/Roche, Basel, Switzerland). To measure AFP, CEA and CA 19-9, immunoassays (Axxym/Abbott, North Chicago, USA) were utilized.

Sampling and histology

In each case, the diagnosis was established by colonoscopy (Fujinon, Japan), and tissue samples were taken for histological analysis.

Genotyping

The polymorphic region of *CaSR* gene was amplified by allele specific PCR technique. The following primers were used: primer M: 5' ACG GTC ACC TTC TCA CTG ACG TTT GAT GAG CCT CAG AAG TAC T 3' 43-mer; primer W: 5' GCT TTG ATG AGC CTC AGA AGA TCG ' 24-mer; and primer R: 5' CTC TTC AGG GTC CTC CAC CTC T 3' 22-mer (10 µmol/L final concentration). PCR reaction was carried out in 20 µL final volume containing: 2 µL 10× Mg free reaction buffer, 4 µL dNTP (1 mmol/L), 1.2 µL 25 mmol/L MgCl₂, 1 µL DNA (25 ng/mL), 3-2-1 µL (primer R, -W, -M), 0.1 µL (0.5 U/µL) Taq (Promega, Madison, USA) and 5.7 µL 2D PCR water. The PCR conditions were at 94 °C for 12 min, 35 cycles at 94 °C for 20 min, at 55 °C for 20 min, at 72 °C for 30 min and at 72 °C for 5 min. There were two types of *CaSR* alleles, the allele A and allele S, so the genotypes were AA, AS, SS. Electrophoretic separation was carried out in a 70 g/L Spreadex/acrilamide-bis (29:1) gel (Elchrom, Cham, Switzerland). For the PCR reaction; Hybaid express thermocycler (Teddington, Middlesex, UK) was used.

Statistics

As the first step, the distribution of continuous parameters was analyzed (Kolmogorov-Smirnov test). Logarithmic transformation was performed as needed. However, results were presented using the original units for easier understanding. The average values for CRC and the control population as well as difference between patients with different genotypes were compared using Student *t* test with separate variance estimates. χ^2 test was used to describe the relation between the allele frequency and tumor localization. Finally, we used parametric correlation (Pearson) to describe the relationship between tumor markers and the calcium homeostasis. A *P* value <0.05 was considered statistically significant. All the statistical analyses were performed using SPSS 9.0 for Windows.

RESULTS

By examining the calcium metabolism of CRC patients, we found that the serum calcium, ionized and corrected calcium levels of our patients were significantly lower, than those of controls. These calcium levels were at the lower limits of the normal range. Serum phosphate and albumin levels were also determined, which were in the lower end of the normal range (Table 1).

There was no difference in serum 25(OH)-vitamin D and PTH values between patients and controls (Table 1). When examining the correlation between calcium metabolism and CEA, AFP, CA 19-9 tumor markers, we found that the ionized calcium levels of our patients were inversely correlated with the serum level of CA 19-9 tumor marker (Table 2).

There was no significant difference in the *CaSR* A986S genotype frequency between healthy population and CRC patients [(CRC: AA=51/70(73%), AS=19/70(27%), SS=0/70(0%); control group: AA=145/201(72%), AS=54/201(27%), SS=2/201(1%)].

In case of the different *CaSR* A986S genotypes of CRC patients, no difference was observed in the examined biochemical parameters and tumor markers (Table 3). Different alleles or genotypes did not show any correlation with the localization of tumor.

Table 1 Laboratory data of CRC patients (mean±SE)

	CRC	Control	<i>P</i>	Normal value
Calcium (Ca)	2.26±0.17	2.45±0.09	0.0001	2.25-2.61 mmol/L
Corrected Ca	2.26±0.14	2.37±0.11	0.0001	2.25-2.61 mmol/L
Ionized calcium	1.07±0.07	1.2±0.05	0.0001	1.05-1.25 mmol/L
Phosphate	1.07±0.13	1.2±0.22	0.006	0.85-1.45 mmol/L
Albumin	39.5±4.61	43.87±4.37	0.0001	35-50 g/L
AFP	4.19±2.85	3.34±1.58	NS	0-15 ng/L
CEA	18.84±69	1.79±1.86	0.043	0-10 ng/L
CA 19-9	86.49±406	10.20±9.95	NS	0-37 ng/L
PTH	38.2±16.8	41.5±14.6	NS	10-65 pg/mL
25(OH) vit. D	44.7±73.8	46.84±13.7	NS	20-60 ng/L
Age (yr)	65.6±10.9	63.6±8.2	NS	-

NS=no significant difference.

Table 2 Correlation between tumor marker levels and parameters of calcium metabolism of CRC patients

	Ca	Corrected Ca	<i>P</i>	Ca ²⁺	Albumin	PTH	25 (OH) vit. D
AFP	0.67	0.33	0.53	0.40	0.80	0.87	0.30
CEA	0.21	0.79	0.80	0.23	0.15	0.94	0.95
Ca19-9	0.57	0.57	0.63	0.007	0.10	0.74	0.94

Table 3 Laboratory parameters associated with different *CaSR* A986S genotypes (mean±SE)

	AA	AS	<i>P</i>
Calcium	2.23±0.16	2.31±0.18	NS
Corrected Ca	2.24±0.12	2.30±0.14	NS
Phosphate	1.07±0.13	1.08±0.11	NS
Ionized calcium	1.07±0.08	1.09±0.07	NS
Albumin	39.61±4.40	39.20±5.30	NS
AFP	4.18±2.96	4.29±2.68	NS
CEA	9.2±23.8	45±125	NS
CA 19-9	68±379	143±492	NS
PTH	37.3±14.2	41.2±23.0	NS
25(OH) vit. D	51±85	27.3±11.4	NS
Age (yr)	66.18±10.96	64.8±11.2	NS

NS=no significant difference.

DISCUSSION

The results of our study support the role of low serum calcium in the pathogenesis of CRC. Contrasting to previous data of others, we found that beside normal vitamin D values the level of calcium and the concentration of serum phosphate were both lower than that of controls^[7], suggesting that in CRC the function of vitamin D receptor (VDR) might be damaged. Our previous study corroborates this hypothesis since we showed that oncogene (HER-2) expression correlated with VDR genotypes in CRC patients^[15].

Western style diet (low in calcium and vitamin D and high in fat) has been shown to induce hyperproliferation in colonic epithelial cells. This cell proliferation could be inhibited by calcium and vitamin D supplementation^[10,16,17]. By increasing calcium intake, the number of apoptotic cells in colon epithelium increased,

as well^[18]. Based on several human studies, high calcium and vitamin D intake might prevent CRC development^[1,3,5,6]. A prospective study claimed that the frequency of CRC was three times less in those patients whose serum vitamin D level was above 20 ng/mL^[7]. More than 3.75 µg daily vitamin D intake appeared to reduce 50% incidence of CRC, while 1 200 mg daily calcium intake decreased 75% of its incidence^[7,8].

Low calcium level may influence CRC pathogenesis in several ways. Calcium ion (Ca²⁺) is needed for cell proliferation and differentiation. On the other hand, Ca²⁺ could play an important role in intercellular connections and signal-transduction cascades^[19-24]. Furthermore, it has an influence on the cell-cycle regulatory genes (p53, K-ras, epidermal growth factor) that had a well-documented role in CRC pathogenesis^[25,26]. The functions mentioned above are mediated partly through CaSR. Similarly to other tissues, CaSR could be detected in normal colon epithelial cells as well. Besides, stimulation of the CaSR could increase the expression of E-cadherin and decrease that of beta-catenin. E-cadherin is the inducer of cell differentiation while beta-catenin is responsible for the genesis of malignant phenotype. The fundamental question is whether the low serum calcium level influencing CRC development is present during a life-long period or emerges only in a phase of the patient's life right before the appearance of cancer. Answering this question is crucial in deciding when to start chemoprevention.

A986S polymorphism of the CaSR gene has been suggested to have a role in the development of parathyroid adenoma. Others have demonstrated that healthy women with CaSR 986 AA homozygote had lower levels of serum calcium compared to women having AS heterozygote and SS homozygote CaSR 986 alleles^[14]. Earlier, we demonstrated that CaSR A986S allele frequencies in CRC patients were not different from those in healthy subjects. However, patients with homozygote AA genotype had a significantly higher UICC stage at the time of discovery compared to the heterozygote AS patients. We could not find an association between serum calcium concentrations and CaSR A986S genotypes in our CRC subjects. We also could not detect a correlation between CaSR polymorphism and CRC. The role of CaSR A986S polymorphism in CRC development requires further investigation.

A large array of evidence indicates that CA 19-9 tumor marker had a prognostic role in CRC. Elevated serum levels were associated with the recurrence of CRC or the presence of metastasis. In our patients, serum calcium levels inversely correlated with CA 19-9 concentration, which could support the significance of serum calcium not only as a pathogenic factor but also as a prognostic factor.

In conclusion, our results further strengthen the possibility that serum calcium might be a pathogenic and prognostic factor in the development of colorectal cancer. Our data draw attention to the possibility that by increasing calcium intake, the multi-leveled pathogenic process leading to tumorigenesis might be influenced. In order to prove this, further studies are necessary.

REFERENCES

- Pence BC.** Role of calcium in colon cancer prevention: experimental and clinical studies. *Mutat Res* 1993; **290**: 87-95
- Buras RR, Shabahang M, Davoodi F, Schumaker LM, Cullen KJ, Byers S, Nauta RJ, Evans SR.** The effect of extracellular calcium on colonocytes: evidence for differential responsive based upon degree of cell differentiation. *Cell Profil* 1995; **28**: 245-262
- Greenwald PJ.** Cancer risk factors for selecting cohorts for large-scale chemoprevention trials. *Cell Biochem Suppl* 1996; **25**: 29-36
- Lipkin M.** New rodent models for studies of chemopreventive agents. *J Cell Biochem Suppl* 1997; **28-29**: 144-147
- Lipkin M, Newmark H.** Calcium and the prevention of colon cancer. *J Cell Biochem Suppl* 1995; **22**: 65-73
- Bostick RM.** Human studies of calcium supplementation and colorectal epithelial cell proliferation. *Cancer Epidemiol Biomarkers Prev* 1997; **11**: 971-980
- Garland CF, Comstock GW, Garland FC, Helsing KJ, Shaw EK, Gorham ED.** Serum 25-hydroxyvitamin D and colon cancer: eight-year prospective study. *Lancet* 1989; **2**: 1176-1178
- Holt PR, Atillasoy EO, Gilman J, Guss J, Moss SF, Newmark H, Fan K, Yang K, Lipkin M.** Modulation of abnormal colonic epithelial cell proliferation and differentiation by low-fat dairy foods: a randomized controlled trial. *JAMA* 1998; **12**: 1074-1079
- Pence BC, Buddingh F.** Inhibition of dietary fat-promoted colon carcinogenesis in rats by supplemental calcium or vitamin D3. *Carcinogenesis* 1988; **1**: 187-190
- Xue L, Lipkin M, Newmark H, Wang J.** Influence of dietary calcium and vitamin D on diet-induced epithelial cell hyperproliferation in mice. *J Natl Cancer Inst* 1999; **2**: 176-181
- Van der Meer R, Kleibeuker JH, Lapre JA.** Calcium phosphate, bile acids and colorectal cancer. *Eur J Cancer Prev* 1991; **1**(Suppl 2): 55-62
- Van der Meer R, Lapre JA, Govers MJ, Kleibeuker JH.** Mechanisms of the intestinal effects of dietary fats and milk products on colon carcinogenesis. *Cancer Lett* 1997; **114**: 75-83
- Brown EM, Pollak M.** The extracellular calcium-sensing-receptor: Its Role in Health and Disease. *Annu Rev Med* 1998; **49**: 15-29
- Cole DE, Vieth R, Trang HM, Wong BY, Hendy GN, Rubin LA.** Association between total serum calcium and the A986S polymorphism of the calcium-sensing receptor gene. *Mol Genet Metab* 2001; **72**: 168-174
- Speer G, Dworak O, Cseh K, Bori Z, Salamon D, Torok I, Winkler G, Vargha P, Nagy Z, Takacs I, Kucsera M, Lakatos P.** Vitamin D receptor gene BsmI polymorphism correlates with erbB-2/HER-2 expression in human rectal cancer. *Oncology* 2000; **58**: 242-247
- Llor X, Jacoby RF, Teng BB, Davidson NO, Sitrin MD, Brasitus TA.** K-ras mutations in 1,2-dimethylhydrazine-induced colonic tumors: effects of supplemental dietary calcium and vitamin D deficiency. *Cancer Res* 1991; **51**: 4305-4309
- Nobre-Leitao C, Chaves P, Fidalgo P, Cravo M, Gouveia-Oliveira A, Ferra MA, Mira FC.** Calcium regulation of colonic crypt cell kinetics: evidence for a direct effect in mice. *Gastroenterology* 1995; **109**: 498-504
- Penman ID, Liang QL, Bode J, Eastwood MA, Arends MJ.** Dietary calcium supplementation increases apoptosis in the distal murine colonic epithelium. *J Clin Pathol* 2000; **53**: 302-307
- Buchan AM, Squires PE, Ring M, Meloche RM.** Mechanism of action of the calcium-sensing receptor in human antral gastrin cells. *Gastroenterology* 2001; **120**: 1279-1281
- Cerda SR, Bissonnette M, Scaglione-Sewell B, Lyons MR, Khare S, Mustafi R, Brasitus TA.** PKC-δ inhibits anchorage-dependent and -independent growth, enhances differentiation, and increases apoptosis in CaCo-2 cells. *Gastroenterology* 2001; **120**: 1700-1712
- Frey MR, Clark JA, Leontieva O, Uronis JM, Black AR, Black JD.** Protein kinase C signaling mediates a program of cell cycle withdrawal in the intestinal epithelium. *J Cell Biol* 2000; **151**: 763-778
- Osada S, Hashimoto Y, Nomura S, Kohno Y, Chida K, Tajima O, Kubo K, Akimoto K, Koizumi H, Kitamura Y.** Predominant expression of nPKC ε, a Ca(2+)-independent isoform of protein kinase C in epithelial tissues, in association with epithelial differentiation. *Cell Growth Differ* 1993; **4**: 167-175
- Rhee SG.** Regulation of phosphoinositide-specific phospholipase C. *Annu Rev Biochem* 2001; **70**: 281-312
- Todd C, Reynolds NJ.** Up-regulation of p21WAF1 by phorbol ester and calcium in human keratinocytes through a protein kinase C-dependent pathway. *Am J Pathol* 1998; **153**: 39-45
- Kawase T, Orikasa M, Oguro A, Burns DM.** Possible regulation of epidermal growth factor-receptor tyrosine autophosphorylation by calcium and G proteins in chemically permeabilized rat UMR106 cells. *Arch Oral Biol* 1999; **44**: 157-171
- Metcalfe S, Weeds A, Okorokov AL, Milner J, Cockman M, Pope B.** Wild-type p53 protein shows calcium-dependent binding to F-actin. *Oncogene* 1999; **18**: 2351-2355

SEN virus does not affect treatment response in hepatitis C virus coinfecting patients but SEN virus response depends on SEN virus DNA concentration

Abdurrahman Sagir, Ortwin Adams, Oliver Kirschberg, Andreas Erhardt, Tobias Heintges, Dieter Häussinger

Abdurrahman Sagir, Oliver Kirschberg, Andreas Erhardt, Tobias Heintges, Dieter Häussinger, Klinik für Gastroenterologie, Hepatologie und Infektiologie, Universitätsklinikum Düsseldorf, Moorenstr 5, 40225 Düsseldorf, Germany

Ortwin Adams, Institut für Virologie der Heinrich-Heine-Universität Düsseldorf, Moorenstr 5, 40225 Düsseldorf, Germany

Correspondence to: Dr. A. Sagir, Klinik für Gastroenterologie, Hepatologie und Infektiologie, Universitätsklinikum Düsseldorf, Moorenstr 5, 40225 Düsseldorf, Germany. sagir@med.uni-duesseldorf.de

Telephone: +49-211-8117820 **Fax:** +49-211-8118752

Received: 2003-10-16 **Accepted:** 2004-02-11

Abstract

AIM: To clarify the effect of SEN virus (SENV) infection on a combination therapy including interferon alfa (IFN- α) or pegylated-IFN with ribavirin in patients with chronic hepatitis and the effect of a combination therapy on SENV.

METHODS: SENV DNA was determined by polymerase chain reaction in serum samples from 95 patients with chronic hepatitis C. Quantitative analysis was done for SENV H DNA.

RESULTS: Twenty-one (22%) of 95 patients were positive for SENV DNA. There was no difference in clinical and biochemical parameters between patients with HCV infection alone and coinfecting patients. The sustained response rate for HCV clearance after combination therapy did not differ between patients with SENV (52%) and without SENV (50%, n.s.). SENV DNA was undetectable in 76% of the initially SENV positive patients at the end of follow-up. SENV H response to combination therapy was significantly correlated with SENV DNA level ($P=0.05$).

CONCLUSION: SENV infection had no influence on the HCV sustained response rate to the combination therapy. Response rate of SENV to the combination therapy depends on SENV DNA level.

Sagir A, Adams O, Kirschberg O, Erhardt A, Heintges T, Häussinger D. SEN virus does not affect treatment response in hepatitis C virus coinfecting patients but SEN virus response depends on SEN virus DNA concentration. *World J Gastroenterol* 2004; 10(13): 1893-1897

<http://www.wjgnet.com/1007-9327/10/1893.asp>

INTRODUCTION

Five hepatitis viruses (A-E) are responsible for more than 80% of cases of viral hepatitis. Recently, a new family of DNA viruses was discovered and designated as "SEN virus" (SENV)^[1]. SENV is a single-stranded circular virus of approximately 3 800 nucleotides. By phylogenetic analysis, 8 different strains of SENV have been identified. SENV is a member of the *Circoviridae* family, a group of small, single-stranded,

nonenveloped circular DNA virus that includes TT virus, TUS01, SANBAN, and YONBAN^[2].

Two strains of SENV (SENV D and SENV H) have been extensively studied and have been shown to be present in approximately 2% of blood donors in the United States, 2% in Italy and 10% in Japan and to be readily transmitted by blood transfusion and other common parenteral routes^[3]. Although SENV infection is cleared spontaneously in the majority of patients, approximately 45% develop persistent infection that exceeds 1 year and has been documented as long as 12 years. Hypervariable regions with mutation rates of 7.32×10^{-4} per site per year may be involved in the persistence^[4]. Although SENV D and SENV H infections were strongly associated with transfusion-associated non-A to non-E hepatitis in one study, this association does not establish causality and the vast majority of patients infected with SENV did not develop hepatitis at the time of transfusion^[3]. However, the clinical role of SENV infection is not yet clear.

HCV is a major cause of post-transfusion hepatitis and chronic liver disease^[5]. More than half of patients with HCV infection develop chronic hepatitis that leads to liver cirrhosis, and hepatocellular carcinoma (HCC)^[6]. The prevalence of SENV in patients with chronic hepatitis was reported to be between 24% and 40%^[3,7]. There is no evidence that SENV infection affects the progression of HCV infection, but the influence of SENV on HCV response to interferon alfa (IFN- α) is not clear^[3]. Three studies investigated the influence of SENV on the response to interferon therapy in HCV infected patients^[8-10]. Rigas *et al.* and Kao *et al.* investigated the patients with chronic hepatitis treated for 6 mo with 3 million units interferon (IFN) 2 alfa 3 times per week plus 1 000-1 200 mg ribavirin daily. The morning dose was reduced to 400 mg for those weighing less than 72 kg. Rigas *et al.* could demonstrate a negative effect of SENV coinfection on the outcome of therapy^[8]. Kao *et al.* showed that SENV infection has no effect on response to combination therapy^[10]. The third study investigated 104 patients who were treated with IFN at a dosage of 9 million units (MU) daily for 2 wk, followed by 9 MU 3 times a week for 22 wk (total dose, 720 MU). There was no effect of SENV coinfection on interferon response in this study^[9].

None of the studies represent the current therapy scheme. Therapy duration depends on HCV genotype. Patients with HCV genotype 2 or 3 are treated for 24 wk with IFN 3 MU 3 times a week plus ribavirin at a dosage of 1 200 mg or 1 000 mg daily. Patients with genotypes other than 2 or 3 are treated for 48 wk^[11,12].

The aim of this study was to determine the prevalence of SENV infection in chronic HCV infected patients, the influence on clinical and virological characteristics and the effect of SENV coinfection on HCV response to combination therapy including IFN and ribavirin.

MATERIALS AND METHODS

Subjects

Ninety-five patients with chronic hepatitis C virus infection

were seen at the outpatient department of the University of Düsseldorf. Diagnosis of chronic hepatitis C was based on the following criteria: (1) detectable HCV-RNA; (2) absence of detectable hepatitis B surface antigen; (3) exclusion of other liver diseases (autoimmune hepatitis, hemochromatosis, Wilson disease). All patients received combination therapy with IFN α or pegylated-interferon (PEG-IFN) α plus ribavirin, and treated for 24 or 48 wk with IFN α 2a (Intron) or 2b (Roferon)- or PEG-IFN α 2a (PEG-Intron) or 2b (Pegasys), and oral ribavirin (Rebetol, Schering Plough) at a dose of 1 000 mg (weight<75 kg) or 1 200 mg (weight>75 kg) daily. Patients infected with HCV genotype 1 or 4 were treated for 48 wk. Patients with HCV genotype 2 or 3 were treated for 24 wk. Blood samples were taken at baseline, at the end of treatment and six months after the treatment. HCV RNA was detected at baseline, 24, 48 and 24 wk after treatment.

Responders were defined as patients who had undetectable levels of HCV RNA in serum and normal ALT 6 mo after the treatment. Patients, who were positive for HCV-RNA at wk 24 discontinued the treatment and were defined as nonresponders. Patients who relapsed after end of treatment were defined as nonresponders. No patient had a history of or developed decompensated cirrhosis or HCC during the study period and all were negative for the antibody to human immunodeficiency virus.

Ninety-five patients entered the study between 1999 and 2002. Forty-nine patients were treated in combination with IFN and 46 patients in combination with PEG-IFN. Fifty-nine of them were men and 36 women with mean age of 42 \pm 12 years. Sixty-eight (71%) of them were infected with HCV genotype 1 or 4 and 26(27%) with genotype 2/3 and HCV genotype of 2(2%) patients were undetermined. Mean ALT was 72 \pm 73 U/l.

SENV-detection and quantification

The presence of SENV D and SENV H DNA was determined by PCR. Total DNA was extracted from 200 μ L serum with the QIAamp blood kit (QIAGEN) and resuspend in 200 μ L of elution buffer. The oligonucleotide primers were synthesized according to the published SENV sequences. The selection of the real-time PCR primers for SENV H-virus and SENV D was done with the support of the Primer Express Software (PE Applied Biosystems, Weiterstadt, Germany).

The primer for the SENV H were designated SENV H-F1 (GGTTAACCKSAGCTGACTTCA (K=G/T; S=G/C)) and SENV H-R1 (GGAAGGTGTAGCAAGGGTTGTC), the fluorogenic TaqMan[®]probe (5' FAM TTTCCGTTCTGCTCACCACAAA 3' TAMRA). A 69-base pair amplicon in a conserved region of the ORF 1 gene was amplified and detected. The primers for the SENV D were designated SENV D-F1 (CCAGACTTTRTGC AAAGTTCCTCTTG (R=A/G)) and SENV D-R1 (GTGGTGAG CAGAACGGATGTT), the fluorogenic TaqMan[®]probe (5' FAM AACTTTGCGGTC AACTGCCGCTG 3' TAMRA). A 76-base pair amplicon in a conserved region of the ORF 1 gene was amplified and detected. Each PCR contained 5 μ L sample DNA, 300 nmol/L forward and reverse primer, 200 nmol/L fluorogenic Taq-man probe, 200 μ mol/L (each) dATP, dCTP, and dGTP, 400 μ mol/L dUTP, 10 mmol/L Tris-HCl (pH 8.3), 5 mmol/L MgCl₂, 0.5 U uracyl-N-glycosylase (UNG) and 1.25 U Taq Gold polymerase in a final volume of 50 μ L. Following inactivation of the UNG (2 min, 50 °C) and activation of the AmpliTaq Gold for 10 min at 95 °C, 40 cycles (15 s at 95 °C and 1 min at 60 °C) were performed with an thermocycler 5 700 system (PE Applied Biosystems). As a DNA standard for the SENV H-PCR, a SENV H-coding plasmid (pSGSEN-H), encompassing the amplified region of the TaqMan[®]-PCR, was created by PCR-cloning and serially diluted. The sensitivity of the TaqMan PCR was

determined as <5 copies/assay. A standard graph of the C_T values obtained from serial dilutions of the standard was constructed by the software and the C_T values of the unknown samples were plotted on the standard curves and the number of SENV H genomes were calculated. For the SENV D-PCR no standard-plasmid was created and the results were only determined qualitatively.

Serologic testing of hepatitis B and C

The qualitative analysis of HCV-RNA was tested by a commercial PCR assay (Amplicor HCV Amplification 2.0, Roche Diagnostics, Indianapolis, IN). The quantitative analysis of HBV-DNA was made by a commercial assay (Digene Hybrid Capture System HBV DNA Assay). HBs-Ag as a serologic marker of HBV-infection was detected by a commercial immunoassay (AxSYM HBs-Ag, Abbott Laboratories, North Chicago, IL).

Genotyping of HCV

The genotype analysis of HCV was performed by a commercial hybridization assay (Inno-Lipa HCV II, Innogenetics, Ghent, Belgium) using HCV-positive amplification products from the PCR assay (Amplicor HCV Amplification 2.0, Roche Diagnostics, Indianapolis, IN).

Statistical analysis

Data were entered in SPSS (version 11.0, Inc., Munich, Germany). A χ^2 or Fisher's exact test (F-test) was used for the comparison of categorical variables, and a Mann-Whitney test was used for the comparison of continuous variables. The significance level was set at 0.05, and all P values were two tailed. All statistical analyses were performed using of SPSS.

ULTS

SENV was detected in 21 (22%) of 95 patients. Of the 21 patients, 16 were infected with SENV H, 4 with SENV D, and one with both strains. The mean SENV H DNA level in serum was 461 \pm 381 copies/mL. The mean age and the proportion of men and women were similar in the SENV positive and SENV negative group. There was no significant difference between both groups concerning serum levels of ALT, HCV genotype, number of patients who received PEG-IFN, and the proportion of pretreated patients (Table 1). Therefore, many confounding variables known to influence the outcome of the therapy were excluded. Sustained response rates did not differ significantly between the 21 SENV positive patients and 74 SENV negative patients. Eleven of the 21 SENV positive and 37 of the 74 SENV negative patients were responders (52% vs 50%, P=1.0).

Table 1 Characteristics of SENV positive and SENV negative patients

	SENV positive (n=21)	SENV negative (n=74)	P value
Median age (yr)	42 \pm 12	42 \pm 12	0.99 ¹
Male, m (%)	13 (62%)	46 (62%)	1.0 ²
Median baseline ALT (IU/L)	81 \pm 109	69 \pm 60	0.56 ¹
Pretreated, n (%)	3 (14%)	10 (14%)	1.0 ²
Hepatitis C genotype, n (%)			
1,4	16 (76%)	51 (69%)	0.6 ²
2,3	5 (24%)	21 (28%)	0.79 ²
Undetermined	0 (0%)	2 (3%)	
PEG-IFN	11 (52%)	35 (47%)	0.81 ²
Sustained HCV response to therapy	11 (52%)	37 (50%)	1.0 ²

¹Mann-Whitney test; ²Fisher's exact test.

Of the 95 patients receiving combination therapy, 48 were sustained responders, who lost detectable HCV RNA for more than 24 wk after completing the therapy (51%). Of these 48 patients, 30 were infected with HCV genotype 1 or 4 and 16 with HCV genotype 2 or 3 and in 2 patients HCV genotypes were undetermined. Sustained responders were found to be independent in relation to gender, ALT before treatment, HCV genotype, and SENV DNA positivity. Sustained HCV response rate to the combination therapy was correlated inversely with age of the patients ($P < 0.01$). A higher mean SENV H DNA level was observed in the nonresponder group, but the difference was not statistically significant (393 ± 297 vs 523 ± 452 , $P = 0.48$) (Table 2).

Table 2 Clinical, biochemical and viral characteristics in relation to HCV response to combination therapy

	Sustained response (n=48)	No sustained response (n=47)	P value
Male, n (%)	30 (63%)	29 (62%)	0.34 ¹
Age (yr)	39±11	45±11	<0.01 ²
ALT	70±78	74±68	0.54 ²
HCV genotype, n (%)			
1 or 4	30 (63%)	37(79%)	
2 or 3	16 (33%)	10 (21%)	0.16 ¹
Undetermined	2 (4%)		
SENV positive, n (%)	10 (21%)	11 (23%)	0.81 ¹
SENV H-DNA (copies/mL)	393±297	523±452	0.48 ²

¹Fisher's exact test; ²Mann-Whitney test.

We analysed the response of SENV to the combination therapy in 20 of the 21 SENV positive patients. The clinical and virological characteristics are shown in Table 3. Of the 21 patients with SENV DNA, 16 were infected with SENV-H, 3

Table 3 Clinical and virological characteristics of patients coinfecting with HCV and SENV

No	Age(yr)	SEX	ALT (U/L)	HCV genotype	SENV genotype	SENV H copies/mL	HCV response	SENV response
1	60	M	62	1	H	218	Yes	Yes
2	47	F	26	1	D/H	74	No	Yes
3	41	F	41	1	D	-	Yes	No
4	31	M	26	1	H	208	Yes	Yes
5	59	F	62	1	H	1304	No	No
6	47	F	169	2	H	1184	No	No
7	31	M	26	1	H	484	Yes	No
8	28	M	32	1	H	308	Yes	Yes
9	63	M	168	1	H	310	No	No
10	59	F	121	4	H	338	No	Yes
11	35	F	42	2	H	38	Yes	Yes
12	36	M	43	1	H	532	No	Yes
13	41	M	24	1	H	848	Yes	Yes
14	41	M	180	1	D	-	Yes	Yes
15	32	F	513	3	H	224	Yes	Yes
16	44	F	36	3	D	-	Yes	Yes
17	28	M	28	2	H	814	Yes	Yes
18	42	M	40	1	H	74	No	Yes
19	37	M	32	4	H	230	No	Yes
20	62	F	41	1	H	662	No	Yes

with SENV-D, and 1 with both. Fifteen (75%) of 20 patients had no detectable SENV DNA after treatment. Two (66%) of the 3 patients infected with SENV D responded to the combination therapy, 12 (75%) of the 16 patients infected with SENV H, and the patient who was infected with both strains responded to combination therapy. SENV response to the combination therapy did not correlate with sex, age, or ALT level (Table 4). SENV H response rates correlated with the SENV-DNA titer before treatment. SENV H-DNA level was significantly lower in patients who responded to the combination therapy (371 ± 276 copies/mL vs 820 ± 497 copies/mL, $P = 0.05$).

Of the five patients who failed to eradicate SENV, two lost HCV-RNA, one of these two patients did not have ALT normalized.

Table 4 Clinical and virological parameter of SENV response to combination therapy in 20 HCV/SENV-coinfecting patients

	SENV response (15)	SENV nonresponse (5)	P
Age (yr, mean)	41±12	48±13	0.23 ¹
Male	10 (63%)	3 (60%)	1.0 ²
ALT	85±61	80±123	0.35 ¹
SENV H-DNA (copies/mL)	371±276 (n=13)	820±497 (n=4)	0.05 ¹

¹Mann-Whitney test; ²Fisher's exact test.

DISCUSSION

SENV D or SENV H-DNA was detectable in 22% of the patients, which is comparable to recent reports^[13]. The observed frequency of HCV and SENV infection is not surprising because these agents are transmitted by similar routes. SENV has been shown to be associated with blood transfusion and intravenous drug abuse^[3,14]. Dual infection with HCV and other

hepatitis virus (HAV, HBV) has been reported to be associated with a more severe and rapidly progressing liver disease^[15-17]. In our study no clinical or biochemical difference was found between patients with HCV infection alone and those coinfecting with HCV and SENV. In this and previous studies, there was no evidence to suggest that SENV coinfection leads to increased severity or persistence of chronic hepatitis C^[7]. It was demonstrated that infection with SENV in patients with non-A to non-E liver disease has no effect on disease progression^[18].

Five independent factors could be identified which are significantly associated with response to antiviral therapy: genotype 2 or 3, viral load less than 2 million copies/mL, age 40 years or less, minimal fibrosis stage, and female sex^[11]. Of these five factors, we studied sex, age, ALT, and HCV genotype and found a significant correlation for response of age ($P=0.006$) but not of sex, ALT, or HCV genotype. This result may reflect the patient selection. We observed on an average, 1.3 times higher SENV DNA level in patients who failed to the therapy compared with patients with sustained response. Nevertheless, this difference was not statistically significant (393 ± 297 vs 523 ± 452 , $P=0.48$) and may be due to the small cohort studied.

Response rates to antiviral therapy in hepatitis C has increased after combination therapy consisting of IFN and ribavirin was used. Further increase was observed after introduction of PEG-IFN. Sustained response rates of up to 80% in HCV genotype 2/3 are described^[12]. Patients coinfecting with other hepatotropic viruses are still difficult to treat. Coinfection with hepatitis B virus impairs sustained rate^[15]. On the other hand, it could be demonstrated that coinfection with TT virus has no influence on response rates to IFN therapy in patients with chronic hepatitis C infection^[19,20]. Three studies tried to clarify the influence of SENV on chronic hepatitis C. Rigas *et al.* reported that coinfection with HCV and SENV adversely affected the HCV response to combination therapy with interferon and ribavirin^[8]. This cohort was treated for 6 mo with 3 million units IFN 2ab three times per week plus 1 000/1 200 mg ribavirin/day depending on body mass more or less than 72 kg. They did not take into account that antiviral therapy duration in hepatitis C depends on HCV genotype. In contrast, Umemura *et al.* found no influence of SENV coinfection on HCV therapy^[9]. They investigated the patients with chronic hepatitis C virus infection, who underwent an IFN-monotherapy. Kao *et al.* studied 100 patients with chronic hepatitis C who were treated with IFN and ribavirin. These patients were treated for 24 wk independent of HCV genotype. They showed that coinfection with SENV has no effect on response to the therapy. However, none of the studies represented the current standard in the therapy of HCV infection.

In our study, patients received combination therapy for a duration depending on HCV genotype. We found no significant difference in sustained response rates between patients with HCV and SENV coinfection and those who had HCV infection alone (52% vs 50%, $P=1.0$). Therefore, our data are in concordance with the results from Umemura *et al.* and Kao *et al.* Overall sustained response rates were higher in our study as compared with the study by Umemura. This results from the higher efficiency of combination therapy compared with IFN-monotherapy.

Sixteen of 20 coinfecting patients lost SENV DNA after treatment. There was no influence of the SENV strain on the response rates. SENV D and SENV H response to the combination therapy was not different (2/3 (66%) vs 12/16 (75%), $P=1.0$). This result is in contrast to the results published by Umemura *et al.* The authors reported a response rate of SENV D to a IFN- α therapy of 73% (11/15 patients) and 33% (1/3 patients) for SENV H. This discrepancy may be a result of our cohort. In contrast to their studies we detected more often SENV H than SENV D.

It is well known that virus load is a predictive factor for response to treatment in different virus infections. For example, sustained response rate of HCV therapy correlates with the virus load at initiation of therapy^[21]. Patients with high HBV-DNA levels fail more often to antiviral therapy than patients with low HBV-DNA levels^[22]. Similarly, a significant difference in SENV DNA levels between patients who lost SENV DNA and those who did not respond was found. SENV H-DNA levels were significantly lower in the group who lost SENV ($P=0.05$).

In conclusion, SENV infection is common in patients with HCV infection. SENV coinfection does not influence the clinical course of hepatitis C or the response rates of HCV to the combination therapy. SENV is sensitive to IFN- α , and additional medication with ribavirin does not improve response to IFN- α . The SENV response rate is correlated with the SENV DNA level prior to treatment. Higher levels influence response rate adversely.

REFERENCES

- 1 **Primi D**, Fiordalisi G, Mantero JL, Mattioli S, Sottini A, Bonelli F. Identifikation of SEN V genotypes. Worlds Intellectual Property Organisation. May 2000
- 2 **Tanaka Y**, Primi D, Wang RY, Umemura T, Yeo AE, Mizokami M, Alter HJ, Shih JW. Genomic and molecular evolutionary analysis of a newly identified infectious agent (SEN virus) and its relationship to the TT virus family. *J Infect Dis* 2001; **183**: 359-367
- 3 **Umemura T**, Yeo AE, Sottini A, Moratto D, Tanaka Y, Wang RY, Shih JW, Donahue P, Primi D, Alter HJ. SEN virus infection and its relationship to transfusion-associated hepatitis. *Hepatology* 2001; **33**: 303-311
- 4 **Umemura T**, Tanaka Y, Kiyosawa K, Alter HJ, Shih JW. Observation of positive selection within hypervariable regions of a newly identified DNA virus (SEN virus). *FEBS Lett* 2002; **510**: 171-174
- 5 **Alter HJ**, Purcell RH, Shih JW, Melpolder JC, Houghton M, Choo QL, Kuo G. Detection of antibody to hepatitis C virus in prospectively followed transfusion recipients with acute and chronic non-A, non-B hepatitis. *N Engl J Med* 1989; **321**: 1494-1500
- 6 **Alter HJ**, Seeff LB. Recovery, persistence, and sequelae in hepatitis C virus infection: a perspective on long-term outcome. *Semin Liver Dis* 2000; **20**: 17-35
- 7 **Umemura T**, Alter HJ, Tanaka E, Yeo AE, Shih JW, Orii K, Matsumoto A, Yoshizawa K, Kiyosawa K. Association between SEN virus infection and hepatitis C in Japan. *J Infect Dis* 2001; **184**: 1246-1251
- 8 **Rigas B**, Hasan I, Rehman R, Donahue P, Wittkowski KM, Lebovics E. Effect on treatment outcome of coinfection with SEN viruses in patients with hepatitis C. *Lancet* 2001; **358**: 1961-1962
- 9 **Umemura T**, Alter HJ, Tanaka E, Orii K, Yeo AE, Shih JW, Matsumoto A, Yoshizawa K, Kiyosawa K. SEN virus: response to interferon alfa and influence on the severity and treatment response of coexistent hepatitis C. *Hepatology* 2002; **35**: 953-959
- 10 **Kao JH**, Chen W, Chen PJ, Lai MY, Chen DS. SEN virus infection in patients with chronic hepatitis C: preferential coinfection with hepatitis C genotype 2a and no effect on response to therapy with interferon plus ribavirin. *J Infect Dis* 2003; **187**: 307-310
- 11 **Poynard T**, Marcellin P, Lee SS, Niederau C, Minuk GS, Ideo G, Bain V, Heathcote J, Zeuzem S, Trepo C, Albrecht J. Randomised trial of interferon alpha2b plus ribavirin for 48 weeks or for 24 weeks versus interferon alpha2b plus placebo for 48 weeks for treatment of chronic infection with hepatitis C virus. International hepatitis interventional therapy group (IHIT). *Lancet* 1998; **352**: 1426-1432
- 12 **Manns MP**, McHutchison JG, Gordon SC, Rustgi VK, Shiffman M, Reindollar R, Goodman ZD, Koury K, Ling M, Albrecht JK. Peginterferon alfa-2b plus ribavirin compared with interferon alfa-2b plus ribavirin for initial treatment of chronic hepatitis C:

- a randomised trial. *Lancet* 2001; **358**: 958-965
- 13 **Shibata M**, Wang RY, Yoshida M, Shih JW, Alter HJ, Mitamura K. The presence of a newly identified infectious agent (SEN virus) in patients with liver diseases and in blood donors in Japan. *J Infect Dis* 2001; **184**: 400-404
- 14 **Wilson LE**, Umemura T, Astemborski J, Ray SC, Alter HJ, Strathdee SA, Vlahov D, Thomas DL. Dynamics of SEN virus infection among injection drug users. *J Infect Dis* 2001; **184**: 1315-1319
- 15 **Zignego AL**, Fontana R, Puliti S, Barbagli S, Monti M, Careccia G, Giannelli F, Giannini C, Buzzelli G, Brunetto MR, Bonino F, Gentilini P. Impaired response to alpha interferon in patients with an inapparent hepatitis B and hepatitis C virus coinfection. *Arch Virol* 1997; **142**: 535-544
- 16 **Pontisso P**, Ruvoletto MG, Fattovich G, Chemello L, Gallorini A, Ruol A, Alberti A. Clinical and virological profiles in patients with multiple hepatitis virus infections. *Gastroenterology* 1993; **105**: 1529-1533
- 17 **Vento S**, Garofano T, Renzini C, Cainelli F, Casali F, Ghironzi G, Ferraro T, Concia E. Fulminant hepatitis associated with hepatitis A virus superinfection in patients with chronic hepatitis C. *N Engl J Med* 1998; **338**: 286-290
- 18 **Mikuni M**, Moriyama M, Tanaka N, Abe K, Arakawa Y. SEN virus infection does not affect the progression of non-A to -E liver disease. *J Med Virol* 2002; **67**: 624-629
- 19 **Nishizawa Y**, Tanaka E, Orii K, Rokuhara A, Ichijo T, Yoshizawa K, Kiyosawa K. Clinical impact of genotype 1 TT virus infection in patients with chronic hepatitis C and response of TT virus to alpha-interferon. *J Gastroenterol Hepatol* 2000; **15**: 1292-1297
- 20 **Kawanaka M**, Niiyama G, Mahmood S, Ifukube S, Yoshida N, Onishi H, Hanano S, Ito T, Yamada G. Effect of TT virus co-infection on interferon response in chronic hepatitis C patients. *Liver* 2002; **22**: 351-355
- 21 **Lindsay KL**, Trepo C, Heintges T, Shiffman ML, Gordon SC, Hoefs JC, Schiff ER, Goodman ZD, Laughlin M, Yao R, Albrecht JK. A randomized, double-blind trial comparing pegylated interferon alfa-2b to interferon alfa-2b as initial treatment for chronic hepatitis C. *Hepatology* 2001; **34**: 395-403
- 22 **Niedermaier C**, Heintges T, Lange S, Goldmann G, Niedermaier CM, Mohr L, Häussinger D. Long-term follow-up of HBeAg-positive patients treated with interferon alfa for chronic hepatitis B. *N Engl J Med* 1996; **334**: 1422-1427

Edited by Ma JY and Xu FM

Effect of vector-expressed siRNA on HBV replication in hepatoblastoma cells

Jun Liu, Ying Guo, Cai-Fang Xue, Ying-Hui Li, Yu-Xiao Huang, Jin Ding, Wei-Dong Gong, Ya Zhao

Jun Liu, Cai-Fang Xue, Ying-Hui Li, Yu-Xiao Huang, Jin Ding, Wei-Dong Gong, Ya Zhao, Department of Etiology, Fourth Military Medical University, Xi'an 710033, Shaanxi Province, China

Ying Guo, Department of Obstetrics and Gynecology, Second Hospital of Xi'an Jiaotong University, Xi'an 710001, Shaanxi Province, China

Supported by National Natural Science Foundation of China, No. 30100157; Medical Research Fund of Chinese PLA, No. 01MA184; and Innovation Project of FMMU, No. CX99005

Correspondence to: Dr. Jun Liu, Department of Etiology, Fourth Military Medical University, Xi'an 710033, Shaanxi Province, China. etiology@fmmu.edu.cn

Telephone: +86-29-83374536 **Fax:** +86-29-83374594

Received: 2003-12-12 **Accepted:** 2004-01-15

Abstract

AIM: To study the effect of siRNA expressed from DNA vector on HBV replication.

METHODS: Human U6 promoter was amplified from genomic DNA and cloned into plasmid pUC18 to construct a mammalian siRNA expression vector pUC18U6. Then oligonucleotides coding for a short hairpin RNA against HBV were cloned into pUC18U6 to form pUC18U6HBVsiRNA which was introduced into 2.2.15 cells by using liposome-mediated transfection. 2.2.15 cells transfected by pUC18U6 and pUC18U6GFPsiRNA which expressed siRNA against green fluorescent protein and mock-transfected 2.2.15 cells were used as controls. Concentration of HBsAg in the supernatant of the transfected cells was measured by using solid-phase radioimmunoassay.

RESULTS: A mammalian siRNA expression vector pUC18U6 was constructed successfully. Compared with controls, pUC18U6HBVsiRNA which expressed siRNA against HBV decreased concentration of HBsAg significantly by 44% ($P < 0.05$).

CONCLUSION: HBV replication in 2.2.15 cells is inhibited by siRNA expressed from the DNA vector.

Liu J, Guo Y, Xue CF, Li YH, Huang YX, Ding J, Gong WD, Zhao Y. Effect of vector-expressed siRNA on HBV replication in hepatoblastoma cells. *World J Gastroenterol* 2004; 10 (13): 1898-1901

<http://www.wjgnet.com/1007-9327/10/1898.asp>

INTRODUCTION

RNA interference (RNAi) is a potent gene silencing mechanism conserved in all eukaryotes, in which double-stranded RNAs suppress the expression of cognate genes inducing degradation of mRNAs or blocking mRNA translation^[1-3]. The physiological functions of RNAi are not very clear as yet, but it has been used successively as a potent method of gene knockdown in study of gene function and in experimental treatment of some diseases^[4-19]. In mammalian cells, double-stranded RNAs inducing RNAi must be short in length (<30 bp) so that they would not activate nonspecific interferon reactions. These short

interfering RNAs (siRNAs) can be produced by four different ways: chemical synthesis, *in vitro* transcription, enzymatic digestion of dsRNAs and transfection of DNA vectors encoding siRNAs. Among the four ways, transfection of DNA vectors has some advantages such as low cost, lasting expression of siRNA, easiness of preparation, which make it the preferential method when siRNAs are used in treatment of diseases.

Hepatitis B virus (HBV) is a small enveloped DNA virus which belongs to hepadnaviridae. Human beings are HBV's natural host, though some primates can be infected in laboratory. Liver is the primary target organ of infection and persistent infection of HBV usually leads to severe diseases, such as chronic hepatitis, cirrhosis and hepatocellular carcinoma. Current treatment regimens for chronic HBV infection, namely administration of interferon- γ , lamivudine, adefovir, or different combinations of these drugs have only limited long-term efficacy and many adverse effects or drug resistance^[20,21]. Considering the huge population infected by HBV (more than 350 million people are infected by HBV around the world), the exploration of novel treatment strategies is both necessary and urgent. Many ingenious treatment strategies have been tested for inhibition of HBV replication, such as antisense nucleotides, ribozymes, intracellular antibodies, and targeted ribonucleases^[22], and all of them have been demonstrated to inhibit HBV replication to various degrees.

To explore RNAi as a novel alternative strategy for treating HBV, we constructed a DNA vector which can express siRNAs in mammalian cells, and then the vector was used to express in 2.2.15 cells a siRNA against HBV to study its effect on HBV replication.

MATERIALS AND METHODS

Cell culture

Human hepatoblastoma Hep G2 cell line 2.2.15 cells stably transfected by HBV genome, were cultured in Dulbecco's modified Eagle's medium (DMEM, from Gibco Life Technologies, Grand Island, NY) supplemented with 100 mL/L fetal calf serum (Sijiqing Biotech Company, Hangzhou, China).

Construction of mammalian siRNA expression vector-pUC18U6

Human genomic DNA was extracted from HepG2 cells with DNeasyTM tissue kit (Qiagen, Germany) according to the manufacturer's protocol. Purified human genomic DNA was used as the template in PCR to obtain human U6 promoter. The sequences of the primers are as follows: Forward primer: 5' GCGATCTAGAAAGGTCGGGCAGGAAGAG3', reverse primer: 5' GCGAGGTACCGGTGTTTCGTCCTTCCACAAG3'.

The underlined bases in forward and reverse primers have recognition sites for *Xba* I and *Kpn* I, respectively. The condition of PCR was at 94 °C for 5 min, then 35 cycles at 94 °C for 30 s, at 60 °C for 30 s, and at 72 °C for 1.5 min followed by extension at 72 °C for 7 min. The PCR product was analyzed with 100 g/L agarose gel electrophoresis and then purified by PCR fragment recovery kit as recommended by the manufacturer (Takara, Dalian, China). The purified PCR product was digested by *Xba* I and *Kpn* I, ligated with pUC18,

and transformed into competent *E. coli*. The recombinant plasmid was then purified from transformed *E. coli*, and verified by *Xba* I/*Kpn* I digestion analysis and DNA sequencing.

Construction of HBV-siRNA expression vector-pUC18U6HBVsiRNA

Two oligodeoxyribonucleotides encoding shRNA against HBV were synthesized by Bioasia Company (Shanghai) and their sequences are as follows: Oligo 1:5' CAGGCTTTCACCTTCTCGCTCGAGCGAGAAAAGTCAAAGCCTGCTTTTTTGG3', Oligo 2:5' AATTCAAAAAGCAGGCTTTCACCTTTCCTCGCTCGAGCGAGAAAAGTCAAAGCCTG3'.

The underlined bases are spacer region and recognition site for *Xho* I. The target of shRNA was 1 086-1 103 nt of HBV genome. To clone the two oligodeoxyribonucleotides, downstream of U6 promoter into pUC18U6, 400 nmol/L for each of the two oligodeoxyribonucleotides was mixed, heated at 100 °C for 5 min, and cooled gradually to room temperature to anneal. pUC18U6 was digested with *Kpn* I, blunt-ended with T4 DNA polymerase, then digested with *Eco*R I, purified and ligated with the annealed oligodeoxyribonucleotides. The ligation mixture was transformed into competent *E. coli*. The recombinant plasmid was then purified from transformed *E. coli*, and verified by *Hind* III/*Xho* I digestion analysis. A control vector, pUC18U6GFPsiRNA, which expressed a siRNA against green fluorescent protein (GFP), was constructed with the same methods and the sequences of the two oligodeoxyribonucleotides encoding the siRNA were synthesized as previously described^[23]: Oligo1:5' GGCGATGCCACCTACGGCAAGCTCGAGCTTGCCGTAGGTGGCATCGCCCCCTTTTTTGG3', Oligo2:5' AATTCAAAAAGGGCGATGCCACCTACGGCAAGCTCGAGCTTGCCGTAGGTGGCATCGGCC3'.

The underlined bases are spacer region and recognition site for *Xho* I.

Transfection

Twenty-four hours before transfection, 2.2.15 cells were seeded

into the culture plate at a density of 2×10^8 /L. LipofectamineTM 2000 reagent (Gibco Life Technologies, Grand Island, NY) was used for the transfection of 2.2.15 cells by pUC18U6HBVsiRNA, pUC18U6, pUC18U6GFPsiRNA, or mock solution (DMEM plus LipofectamineTM 2000 reagent containing no plasmid) according to the manufacturer's protocol.

Quantification of HBsAg in supernatant of cell culture

Forty-eight hours after the transfection, the supernatant of the cell culture was collected, and HBsAg in the supernatant was quantified using the solid phase radio-immunoassay kit for quantification of HBsAg (Beimian Dongya Biotech Institute, Beijing) according to the manufacturer's protocol. Briefly, 200 μ L of the supernatant was incubated with a plastic tube coated by anti-HBs antibody at 45 °C for 1.5 h. After the tube was thoroughly washed with deionized water, 200 μ L of ¹²⁵I-labelled secondary antibody was added and incubated at 45 °C for 2 h. The tube was thoroughly washed, and cpm was measured. The concentration of HBsAg of each sample was calculated by comparing the cpm of each sample with a standard curve.

Statistical analysis

One-way ANOVA was used for data analysis. Differences were considered significant when $P < 0.05$.

RESULTS

Construction of pUC18U6 and pUC18U6HBVsiRNA

Agarose gel analysis showed that human U6 promoter was amplified from genomic DNA (Figure 1A). Restriction digestion analysis and DNA sequencing indicated a vector suitable for siRNAs expression in mammalian cells, pUC18U6, was successfully constructed (Figure 1B and Figure 2A). We then cloned into pUC18U6, downstream of U6 promoter, the annealed two oligodeoxyribonucleotides encoded a short-hairpin RNA (shRNA) against HBV. shRNAs could be

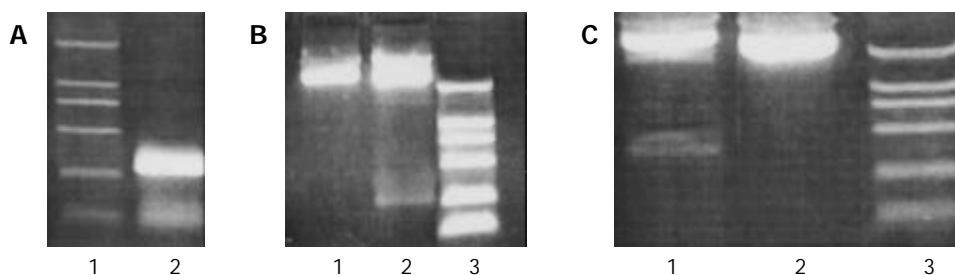


Figure 1 Construction of mammalian siRNA expression vector pUC18U6 and HBV-siRNA expression vector pUC18U6HBVsiRNA. A: Amplification of human U6 promoter by PCR. 1: DNA marker (2 000, 1 000, 750, 500, 250, 100 bp from top to bottom); 2: PCR product. B: Restriction digestion analysis of recombinant vector pUC18U6. 1: pUC18; 2: pUC18U6; 3: DNA marker (2 000, 1 000, 750, 500, 250, 100 bp from top to bottom). C: Restriction digestion analysis of recombinant vector pUC18U6HBVsiRNA. 1: pUC18U6HBVsiRNA; 2: pUC18; 3: DNA marker (2 000, 1 000, 750, 500, 250, 100 bp from top to bottom).

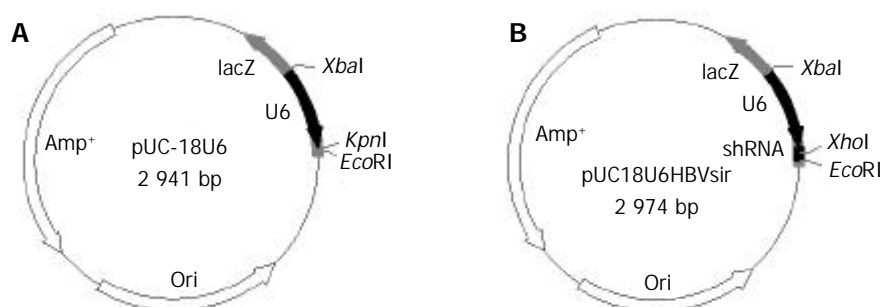


Figure 2 Maps of pUC18U6 and pUC18U6HBVsiRNA. A: pUC18U6. B: pUC18U6HBVsiRNA.

processed into siRNA in cells^[24,25]. Since there was no *Xho* I site in pUC18U6, we designed the spacer (CTCGAG) in shRNA recognized by *Xho* I. Therefore, the recombinant vector pUC18U6HBV_{si}r containing the shRNA coding sequence could yield a new 310 bp fragment compared with pUC18U6 after digested with *Xho* I and *Hind* III (Figure 2B), and this was verified by agarose gel analysis (Figure 1C). This indicated that pUC18U6HBV_{si}r which could express a siRNA against HBV, was successfully constructed (Figure 2B).

Effect of pUC18U6HBV_{si}r expressed siRNA on HBV replication

pUC18U6HBV_{si}r and its control plasmids were transfected into 2.2.15 cells by using liposome. Forty-eight hours after the transfection, the supernatant of the cell culture was collected, and HBsAg in the supernatant was quantified as described in Materials and Methods. As shown in Figure 3, transfection of pUC18U6HBV_{si}r reduced HBsAg significantly as compared with the controls ($P < 0.05$), suggesting that siRNA expressed by pUC18U6HBV_{si}r suppressed the replication of HBV, and this suppression was specific because transfection of pUC18U6GFP_{si}r, which expressed siRNA against GFP, had no effect on HBV replication.

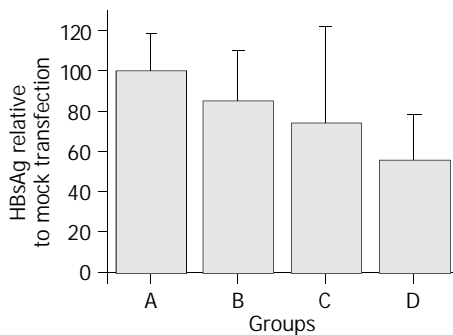


Figure 3 HBsAg concentrations in supernatants of transfected 2.2.15 cells. Groups A-D represent mock-transfected 2.2.15 cells or 2.2.15 cells transfected by pUC18U6, pUC18U6GFP_{si}r and pUC18U6HBV_{si}r, respectively. The concentration of HBsAg in the supernatant of 2.2.15 cells transfected by pUC18U6HBV_{si}r was decreased by 44% as compared with that of mock-transfected 2.2.15 cells.

DISCUSSION

The aim of the present study was to explore siRNAs as a novel strategy in the treatment of HBV infection. Firstly, we first constructed a vector which was suitable to express siRNAs in mammalian cells. siRNAs could be produced *in vitro* and *in vivo*. *In vitro*, siRNAs could be produced by chemical synthesis, *in vitro* transcription, or by enzymatic digestion of dsRNAs^[26-29]. siRNAs produced *in vitro* could be transfected directly into mammalian cells to knockdown gene expression. However, *in vitro* produced siRNAs have several shortcomings, such as transient effect, and high cost. To overcome these shortcomings, several groups have developed a couple of DNA-vectors which could express siRNAs *in vivo*^[11,23-25,27,28]. These vectors had different promoters and different backbones, and expressed siRNAs via two approaches: sense and antisense strands of siRNAs transcribed from tandem promoters and then combined to form siRNAs, or short hairpin RNAs transcribed from a single promoter and then processed by Dicer, a key enzyme in RNA interference, to yield siRNAs. The mammalian siRNAs expression vector constructed by us used human U6 promoter, a pol III promoter, to drive the expression of shRNAs. Compared with other reported vectors, our vector has some features which make the cloning of shRNA expression cassettes easy. The *Kpn* I and *Eco*R I sites downstream of the U6 promoter

were used for directional cloning of shRNA expression cassettes and the first nucleotide of the *Kpn* I site was guanosine, just the required nucleotide for the +1 position of the U6 promoter. Therefore, there was no need to consider this requirement when we designed shRNA sequences by using our vector. Additionally, our vector has no *Xho* I site. By incorporating *Xho* I site as the spacer in the shRNA sequences, it is easy to identify positive shRNA expression vectors containing shRNA expression cassettes by routine agarose gel analysis of *Xho* I/*Hind* III digestion products of the vectors. Positive vectors should reveal a new small fragment of about 300 bp which was absent from the negatives (Figures 1C and 2B). Some reported vectors also identify positive shRNA expression by double enzyme digestion. However, the double enzyme digestion sites in these vectors are just the sites used for cloning of shRNA expression cassettes. Therefore, for these vectors it is not easy to identify the positive shRNA expression vectors by routine agarose gel analysis, especially minigel analysis widely used in laboratories, since shRNA expression cassettes are generally 50-60 bp in length, almost the limit of resolving power of routine agarose gel analysis. The same constraint of routine agarose gel analysis also requires shRNA expression cassettes without double enzyme digestion sites, and limit siRNA target site selection. In contrast, there was no such limitation when using our vector to express siRNAs.

Several groups have reported using siRNAs to inhibit HBV replication in cell cultures and animal models^[12-19]. Although all of these reports showed that HBV replication was inhibited to various degrees by siRNAs, several factors must be taken into account before siRNAs are used to treat HBV infection. One is target selection. siRNAs target at different sites of the same gene can vary from strong to less inhibition of the gene expression. Up to now, little is known about the mechanism of this selection. Therefore, it is still an empirical matter to design the most effective siRNAs. In our study, we chose 1 086-1 103 nt of HBV genome as the target, different from other groups. Our results suggested that siRNA targeting this site specifically inhibited HBV replication. Considering that HBV genome is 3.2 kb and there are no general rules to predetermine the most effective siRNAs, a systematic comparison by experiments of the efficiency of siRNAs against different targets of HBV genome in inhibiting HBV replication should be done to pick out the most effective siRNAs for treating HBV infection. Another concern of using siRNAs for treatment of HBV infection is viral mutants. RNAi is so specific in gene silencing that even a single-base mismatch between siRNAs and cognate genes can significantly reduce the silencing effect. Since viruses evolve very rapidly, they can gain the resistance to once-effective siRNA molecules in short time. In fact, two recent studies reported HIV and poliovirus escape mutants after extended siRNAs treatment^[30,31]. To overcome this obstacle, multiple viral sequences must be targeted simultaneously. In this aspect, our study adds another target when designing multi-target siRNAs to inhibit HBV replication. Further studies are needed to determine the optimal combination of these targets.

REFERENCES

- Hannon GJ. RNA interference. *Nature* 2002; **418**: 244-251
- McManus MT, Sharp PA. Gene silencing in mammals by small interfering RNAs. *Nat Rev Gene* 2002; **3**: 737-747
- Dykxhoorn DM, Novina CD, Sharp PA. Killing the messenger: short RNAs that silence gene expression. *Nat Rev Mol Cell Biol* 2003; **4**: 457-467
- Ashrafi K, Chang FY, Watts JL, Fraser AG, Kamath RS, Ahringer J, Ruvkun G. Genome-wide RNAi analysis of *Caenorhabditis elegans* fat regulatory genes. *Nature* 2003; **421**: 268-272
- Kamath RS, Fraser AG, Dong Y, Poulin G, Durbin R, Gotta M, Kanapin A, Le Bot N, Moreno S, Sohrmann M, Welchman DP,

- Zipperlen P, Ahringer J. Systematic functional analysis of the *Caenorhabditis elegans* genome using RNAi. *Nature* 2003; **421**: 231-237
- 6 **Simmer F**, Moorman C, Van Der Linden AM, Kuijk E, Van Den Berghe PV, Kamath R, Fraser AG, Ahringer J, Plasterk RH. Genome-wide RNAi of *C. elegans* using the hypersensitive rrf-3 strain reveals novel gene functions. *PLoS Biol* 2003; **1**: E12
- 7 **Hingorani SR**, Jacobetz MA, Robertson GP, Herlyn M, Tuveson DA. Suppression of BRAF (V599E) in human melanoma abrogates transformation. *Cancer Res* 2003; **63**: 5198-5202
- 8 **Konnikova L**, Kotecki M, Kruger MM, Cochran BH. Knockdown of STAT3 expression by RNAi induces apoptosis in astrocytoma cells. *BMC Cancer* 2003; **3**: 23
- 9 **Butz K**, Ristriani T, Hengstermann A, Denk C, Scheffner M, Hoppe-Seyler F. siRNA targeting of the viral E6 oncogene efficiently kills human papillomavirus-positive cancer cells. *Oncogene* 2003; **22**: 5938-5945
- 10 **Jacque JM**, Triques K, Stevenson M. Modulation of HIV-1 replication by RNA interference. *Nature* 2002; **418**: 435-438
- 11 **Lee NS**, Dohjima T, Bauer G, Li H, Li MJ, Ehsani A, Salvaterra P, Rossi J. Expression of small interfering RNAs targeted against HIV-1 rev transcripts in human cells. *Nat Biotechnol* 2002; **20**: 500-505
- 12 **Giladi H**, Ketzinel-Gilad M, Rivkin L, Felig Y, Nussbaum O, Galun E. Small interfering RNA inhibits hepatitis B virus replication in mice. *Mol Ther* 2003; **8**: 769-776
- 13 **McCaffrey AP**, Nakai H, Pandey K, Huang Z, Salazar FH, Xu H, Wieland SF, Marion PL, Kay MA. Inhibition of hepatitis B virus in mice by RNA interference. *Nat Biotechnol* 2003; **21**: 639-644
- 14 **Shlomai A**, Shaul Y. Inhibition of hepatitis B virus expression and replication by RNA interference. *Hepatology* 2003; **37**: 764-770
- 15 **Hamasaki K**, Nakao K, Matsumoto K, Ichikawa T, Ishikawa H, Eguchi K. Short interfering RNA-directed inhibition of hepatitis B virus replication. *FEBS Lett* 2003; **543**: 51-54
- 16 **Ying C**, De Clercq E, Neyts J. Selective inhibition of hepatitis B virus replication by RNA interference. *Biochem Biophys Res Commun* 2003; **309**: 482-484
- 17 **Chen Y**, Du D, Wu J, Chan CP, Tan Y, Kung HF, He ML. Inhibition of hepatitis B virus replication by stably expressed shRNA. *Biochem Biophys Res Commun* 2003; **311**: 398-404
- 18 **Konishi M**, Wu CH, Wu GY. Inhibition of HBV replication by siRNA in a stable HBV-producing cell line. *Hepatology* 2003; **38**: 842-850
- 19 **Klein C**, Bock CT, Wedemeyer H, Wustefeld T, Locarnini S, Dienes HP, Kubicka S, Manns MP, Trautwein C. Inhibition of hepatitis B virus replication in vivo by nucleoside analogues and siRNA. *Gastroenterology* 2003; **125**: 9-18
- 20 **Conjeevaram HS**, Lok AS. Management of chronic hepatitis B. *J Hepatol* 2003; **38**(Suppl 1): S90-103
- 21 **Jaboli MF**, Fabbri C, Liva S, Azzaroli F, Nigro G, Giovanelli S, Ferrara F, Miracolo A, Marchetto S, Montagnani M, Colecchia A, Festi D, Reggiani LB, Roda E, Mazzella G. Long-term alpha interferon and lamivudine combination therapy in non-responder patients with anti-HBe-positive chronic hepatitis B: results of an open, controlled trial. *World J Gastroenterol* 2003; **9**: 1491-1495
- 22 **Beterams G**, Nassal M. Significant interference with hepatitis B virus replication by a core-nuclease fusion protein. *J Biol Chem* 2001; **276**: 8875-8883
- 23 **Sui G**, Soohoo C, Affar el B, Gay F, Forrester WC, Shi Y. A DNA vector-based RNAi technology to suppress gene expression in mammalian cells. *Proc Natl Acad Sci U S A* 2002; **99**: 5515-5520
- 24 **Brummelkamp TR**, Bernards R, Agami R. A system for stable expression of short interfering RNAs in mammalian cells. *Science* 2002; **296**: 550-553
- 25 **Paddison PJ**, Caudy AA, Bernstein E, Hannon GJ, Conklin DS. Short hairpin RNAs (shRNAs) induce sequence-specific silencing in mammalian cells. *Genes Dev* 2002; **16**: 948-958
- 26 **Elbashir SM**, Harborth J, Lendeckel W, Yalcin A, Weber K, Tuschl T. Duplexes of 21-nucleotide RNAs mediate RNA interference in cultured mammalian cells. *Nature* 2001; **411**: 494-498
- 27 **Yu JY**, DeRuiter SL, Turner DL. RNA interference by expression of short-interfering RNAs and hairpin RNAs in mammalian cells. *Proc Natl Acad Sci U S A* 2002; **99**: 6047-6052
- 28 **Calegari F**, Haubensak W, Yang D, Huttner WB, Buchholz F. Tissue-specific RNA interference in postimplantation mouse embryos with endoribonuclease-prepared short interfering RNA. *Proc Natl Acad Sci U S A* 2002; **99**: 14236-14240
- 29 **Miyagishi M**, Taira K. U6 promoter-driven siRNAs with four uridine 3' overhangs efficiently suppress targeted gene expression in mammalian cells. *Nat Biotechnol* 2002; **20**: 497-500
- 30 **Gitlin L**, Karelsky S, Andino R. Short interfering RNA confers intracellular antiviral immunity in human cells. *Nature* 2002; **418**: 430-434
- 31 **Boden D**, Pusch O, Lee F, Tucker L, Ramratnam B. Human immunodeficiency virus type 1 escape from RNA interference. *J Virol* 2003; **77**: 11531-11535

Edited by Zhang JZ and Wang XL Proofread by Xu FM

Therapeutic polypeptides based on HBV core 18-27 epitope can induce CD₈⁺ CTL-mediated cytotoxicity in HLA-A2⁺ human PBMCs

Tong-Dong Shi, Yu-Zhang Wu, Zheng-Cai Jia, Li-Yun Zou, Wei Zhou

Tong-Dong Shi, Yu-Zhang Wu, Zheng-Cai Jia, Li-Yun Zou, Wei Zhou, Institute of Immunology, Third Military Medical University, Chongqing 400038, China

Supported by the National Natural Science Foundation of China, No.30271189, and the National 973 Project, No.2001CB510001

Co-correspondents: Dr. Yu-Zhang Wu

Correspondence to: Dr. Tong-Dong Shi, Institute of Immunology, Third Military Medical University, 30 Gaotanyan Street, Chongqing 400038, China. tdshih@yahoo.com.cn

Telephone: +86-23-68752236-801 **Fax:** +86-23-68752789

Received: 2003-12-12 **Accepted:** 2004-01-12

Abstract

AIM: To explore how to improve the immunogenicity of HBcAg CTL epitope based polypeptides and to trigger an HBV-specific HLA I-restricted CD₈⁺ T cell response *in vitro*.

METHODS: A new panel of mimetic therapeutic peptides based on the immunodominant B cell epitope of HBV PreS2 18-24 region, the CTL epitope of HBcAg18-27 and the universal T helper epitope of tetanus toxoid (TT) 830-843 was designed using computerized molecular design method and synthesized by Merrifield's solid-phase peptide synthesis. Their immunological properties of stimulating activation and proliferation of lymphocytes, of inducing T_{H1} polarization, CD₈⁺ T cell magnification and HBV-specific CD₈⁺ CTL mediated cytotoxicity were investigated *in vitro* using HLA-A2⁺ human peripheral blood mononuclear cells (PBMCs) from healthy donors and chronic hepatitis B patients.

RESULTS: Results demonstrated that the therapeutic polypeptides based on immunodominant HBcAg18-27 CTL, PreS2 B- and universal T_H epitopes could stimulate the activation and proliferation of lymphocytes, induce specifically and effectively CD₈⁺ T cell expansion and vigorous HBV-specific CTL-mediated cytotoxicity in human PBMCs.

CONCLUSION: It indicated that the introduction of immunodominant T helper plus B-epitopes with short and flexible linkers could dramatically improve the immunogenicity of short CTL epitopes *in vitro*.

Shi TD, Wu YZ, Jia ZC, Zou LY, Zhou W. Therapeutic polypeptides based on HBV core 18-27 epitope can induce CD₈⁺ CTL-mediated cytotoxicity in HLA-A2⁺ human PBMCs. *World J Gastroenterol* 2004; 10(13): 1902-1906

<http://www.wjgnet.com/1007-9327/10/1902.asp>

INTRODUCTION

Despite the existence of effective vaccines against hepatitis B virus (HBV) for many years and massive prophylactic vaccination campaigns, HBV infection remains an important health problem worldwide. HBV can evade the immune defence system and present consistently in hepatocytes. Patients carrying the virus can develop chronic hepatitis, liver cirrhosis,

and ultimately hepatocellular carcinoma^[1-3]. Currently, the two approved therapies for chronic hepatitis with definite clinical beneficial effects are IFN- α and lamivudine. IFN- α therapy combines antiviral and immunostimulant properties and can result in sustained suppression of HBV replication in one-third of patients. Lamivudine leads to a rapid and almost absolute discontinuation of HBV replication as well as a rapid improvement of the necro-inflammatory activity of the liver disease and to a lesser extent of fibrosis. However, short-term treatment leads to a frequent relapse of HBV replication. On the other hand, long-term treatment has shown to result in virological breakthrough related to the selection of resistant viral variants with a yearly incidence of 15-25%. These outcomes emphasize the need for novel therapeutic approaches^[4]. And it is known that cytotoxic T lymphocytes (CTLs) recognize short peptides derived from the intracellular processing of viral antigens in association with HLA class I molecules on the surface of the infected cells, and HLA-I restricted T cell mediated responses, especially virus antigen specific CTL mediated cytotoxicity, play the key role in controlling HBV infection and in the clearance of infected cells^[5-7]. Since HBV does not efficiently infect human cells *in vitro*, the use of short synthetic peptides comprised of a set of immunodominant epitopes of virus antigens mimicking the processed antigen fragments can be a rational strategy to stimulate the HBV specific CTL response and break to some extent the immune tolerance to HBV antigens^[8-12]. Based on this concept, a new panel of short polypeptides (mimogens) representing the immunodominant CTL, B- and T helper epitopes of the HBcAg, pre-S2 and tetanus toxoid was designed and used for CTL-mediated response analysis. This issue was addressed *in vitro* with HLA-A2⁺ human peripheral blood lymphocytes (PBMCs) from healthy donors and chronic hepatitis B patients.

MATERIALS AND METHODS

Materials

HLA-A2⁺ human peripheral blood mononuclear cells (PBMCs) from 9 healthy donors and 9 chronic viral hepatitis B patients were kindly donated by Southwest Hospital, Chongqing municipality, China. Amino acids used for peptide synthesis were purchased from PE & ACT companies. Na₂⁵¹GrO₄ for target cell labeling in standard ⁵¹Gr release assay and ³H-TdR were both from New England Nuclear (NENTM), Boston, USA. Other materials used in this study were as the following: RPMI 1640 medium (Gibco), fetal calf serum (FCS) (HyClone), HLA-A*0201/FLPSDFFPSV tetramer kit (ProImmune, UK) and human IFN- γ ELISpot kit (DiaClone, France).

Methods

Mimetic polypeptides The immunodominant B- and CTL epitopes of HBV pre-S2 and HBcAg were identified on the basis of the HLA-A2.1 binding motifs^[13-15]. Peptide1 was chosen from the immunodominant HBcAg₁₈₋₂₇ CTL epitope (FLPSDFFPSV). The N-termini of peptide 1 linking to the universal T helper sequence of TT 830-843 through a linker of "-Gly-Gly-Gly-" was named as peptide 2 (QYIKANSKFIGITE GGG FLPSDFFPSV). The universal T helper epitope of tetanus

toxoid and the Pre-S_{2,18-24} B-epitope were linked to the N- and C-termini of the HBcAg₁₈₋₂₇ sequence respectively with the linker of "Ala-Ala-Ala-" and "-Gly-Gly-Gly-" as peptide 3 (QYIKANSKFIGITE AAA FLPSDFFPSV GGG DPRVRGLYFPA). Melanoma associated MART-1₂₇₋₃₅ CTL epitope peptide (AAGIGILTV) was used as irrelevant control. All mimogens were calculated and optimized using computerized molecular design theories and methods in O2 workstation(SGI).

The above peptides were synthesized with a Merrifield's solid-phase peptide synthesis method (PE431A synthesizer), purified by RP-HPLC (WATERS 600) and analyzed by MS/MS (API 2000). All peptides with a purity over 95% were solved in DMSO at the concentration of 10 mg/mL and preserved at -70 °C.

Lymphocytes proliferation assay

Human PBMCs were separated from peripheral blood by centrifugation on Ficoll-Hypaque gradients and used as fresh samples^[16]. PBMCs were plated at a concentration of 2×10^6 /mL in 96-well microplates in RPMI 1640 medium supplemented with 100 mL/L fetal bovine serum, 5×10^{-5} mol/L α -mercaptoethanol, and in the presence of 10 μ g/mL mimetic peptides respectively. Eighteen to 24 h later, 1 μ Ci/well of ³H-TdR was added into the medium. Four to 6 h later, lymphocytes were collected and counted using a β -counter. Non-stimulated PBMCs were used as negative control. Results of samples were considered positive if the stimulation index (SI) >2.1 .

T_{H1} polarization assay

For the assay of T_{H1} polarization induced by mimetic peptides, IFN- γ ELISPOT kit was used. Briefly^[16,17], 96-well PVDF membrane-bottomed plates were coated with capture anti-human IFN- γ mAb at 4 °C overnight. Fresh PBMCs were stimulated with 10 μ g/mL of mimetic peptide 1, 2 and 3 respectively, and then added to triplicated wells at 5×10^3 /well and the plates were incubated for 18 h at 37 °C in 50 mL/L CO₂. At the end of incubation, cells were washed off and a second biotinylated anti-IFN- γ mAb was added, followed by streptavidin-alkaline phosphatase conjugate and substrates. After the plates were washed with tap water and dried overnight, spots were counted under a stereomicroscope. The number of T_{H1} polarized cells (HBcAg₁₈₋₂₇-specific CD8⁺ T cells), expressed as IFN- γ secreting cells (ISCs) /10⁶ PBMCs, was calculated after subtracting negative control values (non-stimulated PBMCs). Results of samples were considered as positive if above the mean by three standard deviations and with a cut off of 50 ISCs /10⁶ PBMCs above mean background.

Cytotoxicity assay

Peptide-specific CTL lines were primed as follows: at d 0, fresh PBMCs were plated at a concentration of 2×10^5 /mL in 24-well microplates (2 mL /well) in RPMI 1640 medium supplemented with 100 mL/L fetal bovine serum and L-glutamine, and in the presence of 10 μ g/mL mimetic peptides respectively. Two days later, 30 IU/mL rhIL-2 was added to the medium. Lymphocytes were then re-stimulated weekly for 2 wk as follows: Cells were harvested, washed once, and replated in 24-well plates at the concentration of 2×10^5 /mL in the above medium, and restimulated respectively with 10 μ g/mL mimetic polypeptides. Twenty hours after last stimulation, cells were harvested, and used as fresh effectors.

CTL-mediated cytotoxicity was detected by standard 4 h ⁵¹Cr release assay^[17]. T2(HLA-A2) cells were used as targets and pre-incubated with 10 μ g/mL of HBcAg₁₈₋₂₇ peptide 2 h before use. The 1×10^6 target cells were labeled with 3.7×10^6 Bq Na₂⁵¹GrO₄ in 1.0 mL RPMI 1640 medium supplemented with 150 mL/L fetal bovine serum and in the presence of 10 μ g/mL of HBcAg₁₈₋₂₇ peptide for 60 min at 37 °C, and then

washed three times before the addition of effectors. Various concentrations of effector cells were mixed with 1×10^4 targets at effector/target (E/T) ratios of 12.5, 25, 50 and 100 in 200 μ L of culture medium in 96-well V-bottomed microplate in triplicate. The microplate was centrifuged for 3 min at 500 r/min, and then incubated for 4 h at 37 °C in 50 mL/L CO₂. After the incubation terminated, 100 μ L of supernatants was harvested and counted on a γ -counter. Percentage of target cell specific lysis was determined as:(average sample counts-average spontaneous counts/average maximum counts-average spontaneous counts) $\times 100\%$. Maximum and spontaneous counts were measured using supernatants from wells receiving 50 g/L SDS or culture medium alone, respectively. In all experiments, spontaneous counts should be less than 30% of maximum counts. CTL responses were considered positive if they exceeded the mean of specific lysis caused by irrelevant mimetic antigen by three standard deviations and by 10%.

HBcAg₁₈₋₂₇-specific CD8⁺ CTL quantitative detection

HLA class I^{PEP} tetramer-binding assay was used to quantify the HBcAg₁₈₋₂₇-specific CD8⁺ T cells from the fresh effectors produced^[18]. Briefly, fresh effectors were collected, washed twice with 0.02 mol/L, pH7.2 phosphate buffered saline (PBS), counted and separated equally into different tubes in 1.0 mL of PBS each. The effectors were stained with 2 μ L of R-PE-conjugated HLA-A*0201/FLPSDFFPSV and 20 μ L of Cy-Chrome-conjugated mouse anti-human CD8 mAb for 30 min at room temperature. R-PE-conjugated avidin and Cy-Chrome-conjugated mouse IgG_{1, κ} antibodies were used as isotype control, and non-stimulated PBMCs were used as negative controls. All samples were collected, washed twice, dissolved into 300 μ L of PBS and FACS-sorted on a FACstar (Beckton-Dickson) with Cell Quest software. Results were expressed as percentages of tetramer-binding cells in the CD8⁺ population. A total of 50 000 events were acquired in each analysis. Results were considered as positive for tetramer-binding cells when above negative controls and by 0.1% CD8⁺ T cells.

Statistical analysis

All data were expressed as mean \pm SD. Statistical analysis was performed using a two-tailed Student's *t* test.

RESULTS

Lymphocytes proliferation assay

Fresh PBMCs were stimulated respectively with three mimetic peptides we designed, and ³H-TdR was used to detect the proliferation of lymphocytes. Data demonstrated that peptide 3 pulsed the most vigorous activation and proliferation of lymphocytes, and with SI >4.1 by average in healthy PBMCs and >3.3 in PBMCs from chronic hepatitis patients. Peptide 2 could also induce weak lymphocytes proliferation, with the mean of SI >2.3 and 2.1 respectively in the PBMCs from healthy donors and chronic hepatitis patients. No activation and proliferation of lymphocytes were detected in peptide 1 stimulated PBMCs (Table 1).

T_{H1} polarization induced by mimetic peptides

HLA-A2⁺ human PBMCs were pulsed respectively with three mimetic peptides we initially designed and synthesized, and the T_{H1} polarization induced was detected using IFN- γ ELISPOT method. Spots of IFN- γ secreting cells can be observed in each of the mimetic peptide samples. Peptide 1 could induce peptide-specific CD8⁺ T cells magnification up to approximately $1\ 667 \pm 231$ ISCs /10⁶ PBMCs in PBMCs from healthy donors and $1\ 420 \pm 253$ ISCs /10⁶ PBMCs in PBMCs from chronic hepatitis B patients, which were dramatically weaker than those of Peptide 2 and 3, which induced

Table 1 Lymphocytes proliferation assay (mean±SD, n=27)

	³ H-TdR counts(cpm)			
	Peptide1	Peptide2	Peptide3 ^b	Negative controls
PBMCs from healthy donors	4 001.6±328.3	5 882.6±397.2	10 497.6±859.7	2 556.3±211.3
PBMCs from chronic hepatitis patients	3 967.5±285.9	4 912.3±421.1	7 696.2±781.8	2 327.6±169.2

^bP<0.01 vs negative control and peptide1 and 2 groups.

Table 2 Peptide-specific CD8⁺ T cells induced expressed as ISCs/10⁶ PBMCs (mean±SD, n=27)

	ISCs /10 ⁶ PBMCs				
	Peptide1 ^d	Peptide2 ^d	Peptide3 ^{db}	Irrelevant control	Negative controls
PBMCs from healthy donors	1 667.5±231.3	4 133.7±416.6	9 200.5±1638.1	1 315.5±321.3	233.3±208.6
PBMCs from chronic hepatitis patients	1 420.0±253.5	3 915.7±685.9	8 966.7±1435.3	1 230.0±355.2	245.1±223.3

^bP<0.01 vs peptide1 and 2 groups, ^dP<0.01 vs negative control.

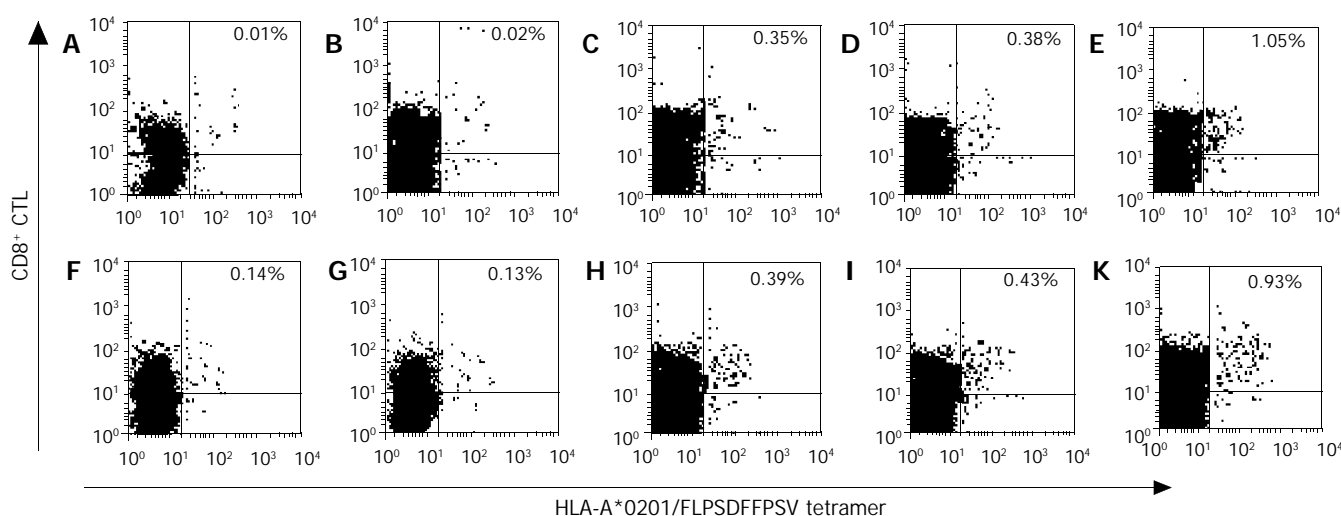


Figure 1 Detection of the HBcAg₁₈₋₂₇-specific CD8⁺ T cells produced with HLA-A*0201/FLPSDFFPSV tetramer-binding assay. A: Non-stimulated HLA-A2⁺ PBMCs from healthy donors; B: Irrelevant peptide pulsed HLA-A2⁺ PBMCs from healthy donors; C: Peptide1 pulsed HLA-A2⁺ PBMCs from healthy donors; D: Peptide2 pulsed HLA-A2⁺ PBMCs from healthy donors; E: Peptide3 pulsed HLA-A2⁺ PBMCs from healthy donors; F: Non-stimulated HLA-A2⁺ PBMCs from chronic hepatitis patients; G: Irrelevant peptide pulsed HLA-A2⁺ PBMCs from chronic hepatitis patients; H: Peptide1 pulsed HLA-A2⁺ PBMCs from chronic hepatitis patients; I: Peptide2 pulsed HLA-A2⁺ PBMCs from chronic hepatitis patients; K: Peptide3 pulsed HLA-A2⁺ PBMCs from chronic hepatitis patients.

approximately 4 133±416 and 9 200±1 638 ISCs/10⁶ PBMCs respectively in PBMCs from healthy donors, and 3 915±685 and 8 966±1 435 ISCs/10⁶ PBMCs in PBMCs from chronic hepatitis B patients. These results suggest that all the 3 peptides could pulse T_{H1} polarization of T cells, and peptide 3 was more vigorous than peptide 2 and 1 (P<0.01). It showed no difference between the PBMCs from healthy donors and chronic hepatitis patients (Table 2).

Cytotoxicity assay

HLA-A2⁺ human PBMCs were pulsed with the 3 mimetic peptides and the irrelevant control peptide respectively, and the CTL-mediated cytotoxicity induced was tested by standard 4 h ⁵¹Cr release assay against HBcAg₁₈₋₂₇ peptide pre-incubated T2 targets. The results demonstrated that all the 3 mimetic peptides could induce positive HBV-specific CTL response, among which peptide 3 induced the most vigorous CTL activity and as high as (68.4±15)% target cell lysis was observed at E/T=100. The percentages of target cells lysed between peptide 1 and 2 pulsing groups were of statistically no difference, and both were dramatically lower than that of peptide 3 (P<0.01). The targets lysis observed in both healthy donors and chronic hepatitis

patients showed no statistical difference (Tables 3 and 4).

HBcAg₁₈₋₂₇-specific CD8⁺ CTL detection

HLA-A2⁺ human PBMCs were pulsed respectively with the above three mimetic peptides and the irrelevant peptide MART-1₂₇₋₃₉, the HBcAg₁₈₋₂₇-specific CD8⁺ T cells induced were quantified using HLA-A*0201/FLPSDFFPSV tetramer-binding assay. No HBcAg₁₈₋₂₇-specific CD8⁺ T cells could be detected in the PBMCs pulsed with MART-1₂₇₋₃₅ peptide, and the tetramer staining was almost the same as control background (0.02% in PBMCs from healthy donors, and 0.04-0.14% in PBMCs from chronic hepatitis patients). In PBMCs stimulated with peptide 1, 2 and 3, the frequencies of HLA-A*0201/FLPSDFFPSV-CD8 double-positive T cells were on average 0.35% (3 500/10⁶ PBMCs), 0.38% (3 800/10⁶ PBMCs) and 1.05% (10 500/10⁶ PBMCs) respectively in the PBMCs from healthy donors, and 0.39% (3 900/10⁶ PBMCs), 0.43% (4 300/10⁶ PBMCs) and 0.93% (9 300/10⁶ PBMCs) respectively in the PBMCs from chronic patients. Data showed no statistical differences between the PBMCs from healthy donors and chronic hepatitis patients, and between the effects induced by peptide1 and peptide 2 (Figure 1).

Table 3 Percentages of specific targets lysis by HLA-A2⁺ effector CTLs induced by PBMCs from healthy donors with different peptide antigens (mean±SD, n=27)

E/T ratios	Percentage of specific cell lysis (%)				
	Peptide1 ^d	Peptide2 ^d	Peptide3 ^{db}	Irrelevant control ^a	Negative controls
12.5	22.7±5.3	21.7±6.1	36.1±7.7	3.7±0.7	3.5±0.7
25	29.3±6.5	28.6±6.3	41.4±9.1	5.7±0.7	3.7±0.7
50	33.5±7.1	33.9±8.2	52.3±12.5	7.3±0.9	6.4±0.9
100	37.2±11.2	36.8±10.9	68.4±14.7	7.4±1.1	8.7±1.3

^aP>0.05 vs negative control, ^bP<0.01 vs peptide1 and 2 groups, ^dP<0.01 vs negative control.

Table 4 Percentages of specific targets lysis by HLA-A2⁺ effector CTLs induced by PBMCs from chronic hepatitis B patients with different peptide antigens (mean±SD, n=27)

E/T ratios	Percentage of specific cell lysis (%)				
	Peptide1 ^d	Peptide2 ^d	Peptide3 ^{db}	Irrelevant control ^a	Negative controls
12.5	18.7±3.6	23.1±4.9	30.2±6.1	5.1±0.8	4.3±0.6
25	22.7±4.1	28.6±5.6	38.4±7.4	4.5±0.7	7.1±1.0
50	31.3±6.0	33.9±6.5	52.7±10.3	7.3±1.1	7.7±1.3
100	35.5±5.7	39.1±7.3	58.5±15.9	9.5±1.7	8.5±1.5

^aP>0.05 vs negative control, ^bP<0.01 vs peptide1 and 2 groups, ^dP<0.01 vs negative control.

DISCUSSION

HBV-specific CD8⁺ cytotoxic T cells play a critical role in viral clearance. Low HBV-specific CTL responses in chronic HBV infection may favor the persistence of virus, whereas stimulation and expansion of HBV-specific CTL activity may assist elimination of HBV infection^[1-3]. Natural HBV antigens generally contain inappropriate epitopes which could elicit T_{H1}/T_{H2} disequilibrium, immune deviation or immune deficiency, and the conserved amino acid sequences might interfere with intercellular communication and thus elicit immune subversion. Thereby some viruses may evade the immune defence system and present consistently in hepatocytes, and result in chronic hepatitis, liver cirrhosis, and even hepatocellular carcinoma. Thus new generations of therapeutic vaccines should induce CTL responses different from that induced by natural virus infection, and at the same time hold the specificity of HBV antigens^[19-22]. According to modern immune theories, effective protection relies on the appropriate match of a set of epitopes^[8,23]. Thus, natural antigens should be redesigned or modified using molecular design techniques on the basis of immunodominant epitopes.

Among the different CTL epitopes of HBV core, envelope, and polymerase so far identified, the sequence 18-27 of the HBV core antigen is immunodominant and subdominant in the different supertype of HLA-A2 molecules, and could induce HBV-specific CTL responses in patients of different HLA-A2 subtypes with indistinguishable frequency and magnitude, and represents the main component of a peptide-based therapeutic vaccine aiming at stimulating the antiviral CTL response in patients with chronic hepatitis B. Furthermore, this epitope was also found to stimulate HLA class II restricted T-cell responses. These data illustrate its potential usefulness for the development of therapeutic vaccines^[24-26].

As in other infections with noncytotoxic viruses, helper T cells control the intensity of CD8⁺ T-cell responses and helper T-cell responses might be compromised in chronic carriers of

HBV, and according to *in vivo* studies, administration of single CTL epitope vaccine could initiate CTL activity, but the magnitude was lower, and the low-level CTL activity was considered not associated with viral clearance^[26-30]. In this study, we chose the immunodominant B cell epitope of HBV PreS₂ region and the CTL epitope of HBcAg, and introduced the universal T_H epitope of tetanus toxoid to strengthen the T_H response. Three mimetic peptides based on the above epitopes were initially designed and synthesized, and their immunological properties of pulsing lymphocyte activation and proliferation, of inducing T_{H1} polarization and HBV-specific CD8⁺ CTL-mediated cytotoxicity were preliminarily investigated using human PBMCs from HLA-A2⁺ healthy donors and chronic hepatitis B patients.

After *in vitro* stimulation, a direct tetramer-binding assay was used to detect the frequencies of HBV-specific CD8⁺ T cells. The results varied according to the peptides used. The highest frequencies were from peptide3 pulsing group, about 1.05% (10 500/10⁶ PBMCs) and 0.93% (9 300/10⁶ PBMCs) HLA-A*0201/HbcAg₁₈₋₂₇-CD8⁺ CTLs produced in the PBMCs from healthy donors and chronic hepatitis patients respectively, remarkably higher than those of peptide 2 and peptide 1 (P<0.01). No HBcAg₁₈₋₂₇-specific CD8⁺ T cells could be detected in the PBMCs pulsed with irrelevant peptide, the tetramer staining was almost the same as control background. These data demonstrated the specificity of the therapeutic peptides we designed.

The tetramer-binding assay detects only the number of cells with an appropriate TCR but not their function^[31], so chromium release assay, IFN-γELISpot assay and lymphocyte proliferation assay were used to detect the function of the effectors pulsed. And a highly significant correlation was found between the frequencies of peptide-specific CD8⁺ T cells and the functions of responding T cells. All the three mimetic polypeptides designed were potent to induce *in vitro* cultured human PBMCs activation and proliferation, T_{H1} polarization, CD8⁺ T cell expansion and generation of cytotoxicity. Peptide 3 with the immunodominant B-, CTL and T helper epitope was the most potent. After introduction of T helper epitope into peptide 1, CTL frequency was not remarkably improved, and cytotoxic activity remained low suggesting that this conformation was not sufficient to drive proliferation of CTLs, and its differentiation into mature killer cells. The comparatively higher immunogenicity of peptide 3 was attributed to its molecular structure: the introduction of T helper and B-epitopes, and the design of short linkers “-A-A-A-” and “-G-G-G-”. The linker was designed and proved to be highly flexible and might act as “hinges”. We surmise that this peptide might be recognized by MHC-I/II restricted molecules, and be presented to CD4⁺ T cells and CD8⁺ T cells, and ultimately T helper and Tc cells should be activated and function interactively. The results demonstrate that the peptides designed are highly immunogenic and HBV-specific, and the introduction of short and flexible linker and immunodominant T_H plus B- epitopes into short CTL epitopes may dramatically improve the therapeutic peptides' immunogenicity and the possibility of being presented to antigen presenting cells (APCs).

According to reports as yet, the vast majority of polypeptides, especially short epitope peptides can not induce CTL responses vigorously by *in vivo* because of poor immunogenicity^[32-35]. Little knowledge is known so far on the molecular mechanisms leading to the difference between the peptides' *in vitro* and *in vivo* functions. In our opinion, *in vivo* induction of cytotoxic activity relies on the efficient presentation by APCs, and the crucial point is how to improve the antigenicity of short peptides and to meet the needs for efficient antigen presentation *in vivo*. In the present study, we redesigned and modified the structure of linear short peptides on the basis of immunodominant

epitopes, changed the molecular properties of the natural peptides, and triggered the direct recognition of the peptides by T_H and T_H cells, and the mimogens sieved were proved to be highly immunogenic *in vitro*. Whether this conformation can meet the needs for efficient antigen presentation *in vivo* needs to be addressed in HLA-A2 transformed HBV transgenic mice.

REFERENCES

- Uprichard SL**, Wieland SF, Althage A, Chisari FV. Transcriptional and posttranscriptional control of hepatitis B virus gene expression. *Proc Natl Acad Sci U S A* 2003; **100**: 1310-1315
- El-Serag HB**. Hepatocellular carcinoma: an epidemiologic view. *J Clin Gastroenterol* 2002; **35**(5 Suppl 2): S72-S78
- Rabe C**, Pilz T, Klostermann C, Berna M, Schild HH, Sauerbruch T, Caselmann WH. Clinical characteristics and outcome of a cohort of 101 patients with hepatocellular carcinoma. *World J Gastroenterol* 2001; **7**: 208-215
- Michel ML**. Towards immunotherapy for chronic hepatitis B virus infections. *Vaccine* 2002; **20**(Suppl 4): A83-A88
- Huang J**, Cai MY, Wei DP. HLA class I expression in primary hepatocellular carcinoma. *World J Gastroenterol* 2002; **8**: 654-657
- Thimme R**, Wieland S, Steiger C, Ghayeb J, Reimann KA, Purcell RH, Chisari FV. CD8⁺ T cells mediate viral clearance and disease pathogenesis during acute hepatitis B virus infection. *J Virol* 2003; **77**: 68-76
- Thimme R**, Bukh J, Spangenberg HC, Wieland S, Pemberton J, Steiger C, Govindarajan S, Purcell RH, Chisari FV. Viral and immunological determinants of hepatitis C virus clearance, persistence, and disease. *Proc Natl Acad Sci U S A* 2002; **99**: 15661-15668
- Chaiken IM**, Williams WV. Identifying structure-function relationships in four-helix bundle cytokines: towards de novo mimetics design. *Trends Biotechnol* 1996; **14**: 369-375
- Kessler JH**, Beekman NJ, Bres-Vloemans SA, Verdijk P, van Veelen PA, Kloosterman-Joosten AM, Vissers DC, ten Bosch GJ, Kester MG, Sijts A, Wouter Drijfhout J, Ossendorp F, Offringa R, Melief CJ. Efficient identification of novel HLA-A*0201-presented cytotoxic T lymphocyte epitopes in the widely expressed tumor antigen PRAME by proteasome-mediated digestion analysis. *J Exp Med* 2001; **193**: 73-88
- Kakimi K**, Isogawa M, Chung J, Sette A, Chisari FV. Immunogenicity and tolerogenicity of hepatitis B virus structural and nonstructural proteins: implications for immunotherapy of persistent viral infections. *J Virol* 2002; **76**: 8609-8620
- Engler OB**, Dai WJ, Sette A, Hunziker IP, Reichen J, Pichler WJ, Cerny A. Peptide vaccines against hepatitis B virus: from animal model to human studies. *Mol Immunol* 2001; **38**: 457-465
- Sette AD**, Oseroff C, Sidney J, Alexander J, Chesnut RW, Kakimi K, Guidotti LG, Chisari FV. Overcoming T cell tolerance to the hepatitis B virus surface antigen in hepatitis B virus-transgenic mice. *J Immunol* 2001; **166**: 1389-1397
- Preikschat P**, Kazaks A, Dishlers A, Pumpens P, Kruger DH, Meisel H. Interaction of wild-type and naturally occurring deleted variants of hepatitis B virus core polypeptides leads to formation of mosaic particles. *FEBS Lett* 2000; **478**: 127-132
- Livingston BD**, Crimi C, Fikes J, Chesnut RW, Sidney J, Sette A. Immunization with the HBV core 18-27 epitope elicits CTL responses in humans expressing different HLA-A2 supertype molecules. *Hum Immunol* 1999; **60**: 1013-1017
- Kazaks A**, Dishlers A, Pumpens P, Ulrich R, Kruger DH, Meisel H. Mosaic particles formed by wild-type hepatitis B virus core protein and its deletion variants consist of both homo- and heterodimers. *FEBS Lett* 2003; **549**: 157-162
- Guan XJ**, Wu YZ, Jia ZC, Shi TD, Tang Y. Construction and characterization of an experimental ISCOMS-based hepatitis B polypeptide vaccine. *World J Gastroenterol* 2002; **8**: 294-297
- Sun Y**, Iglesias E, Samri A, Kamkamidze G, Decoville T, Carcelain G, Autran B. A systematic comparison of methods to measure HIV-1 specific CD8 T cells. *J Immunol Methods* 2003; **272**: 23-34
- Kuzushima K**, Hayashi N, Kudoh A, Akatsuka Y, Tsujimura K, Morishima Y, Tsurumi T. Tetramer-assisted identification and characterization of epitopes recognized by HLA A*2402-restricted Epstein-Barr virus-specific CD8⁺ T cells. *Blood* 2003; **101**: 1460-1468
- Bocher WO**, Dekel B, Schwerin W, Geissler M, Hoffmann S, Rohrer A, Arditti F, Cooper A, Bernhard H, Berrebi A, Rose-John S, Shaul Y, Galle PR, Lohr HF, Reisner Y. Induction of strong hepatitis B virus (HBV) specific T helper cell and cytotoxic T lymphocyte responses by therapeutic vaccination in the trimera mouse model of chronic HBV infection. *Eur J Immunol* 2001; **31**: 2071-2079
- Blackman MA**, Rouse BT, Chisari FV, Woodland DL. Viral immunology: challenges associated with the progression from bench to clinic. *Trends Immunol* 2002; **23**: 565-567
- Kurts C**, Miller JF, Subramaniam RM, Carbone FR, Heath WR. Major histocompatibility complex class I-restricted cross-presentation is biased towards high dose antigens and those released during cellular destruction. *J Exp Med* 1998; **188**: 409-414
- Stober D**, Trobonjaca Z, Reimann J, Schirmbeck R. Dendritic cells pulsed with exogenous hepatitis B surface antigen particles efficiently present epitopes to MHC class I-restricted cytotoxic T cells. *Eur J Immunol* 2002; **32**: 1099-1108
- Wiesmuller KH**, Bessler WG, Jung G. Solid phase peptide synthesis of lipopeptide vaccines eliciting epitope-specific, B-, T-helper and T-killer cell response. *Int J Pept Protein Res* 1992; **40**: 255-260
- Bertoletti A**, Southwood S, Chesnut R, Sette A, Falco M, Ferrara GB, Penna A, Boni C, Fiaccadori F, Ferrari C. Molecular features of the hepatitis B virus nucleocapsid T-cell epitope 18-27: interaction with HLA and T-cell receptor. *Hepatology* 1997; **26**: 1027-1034
- Maini MK**, Boni C, Ogg GS, King AS, Reignat S, Lee CK, Larrubia JR, Webster GJ, McMichael AJ, Ferrari C, Williams R, Vergani D, Bertoletti A. Direct ex vivo analysis of hepatitis B virus-specific CD8(+) T cells associated with the control of infection. *Gastroenterology* 1999; **117**: 1386-1396
- Heathcote J**, McHutchison J, Lee S, Tong M, Benner K, Minuk G, Wright T, Fikes J, Livingston B, Sette A, Chestnut R. A pilot study of the CY-1899 T-cell vaccine in subjects chronically infected with hepatitis B virus. *Hepatology* 1999; **30**: 531-536
- Ciavarra RP**, Greene AR, Horeth DR, Buhner K, van-Rooijen N, Tedeschi B. Antigen processing of vesicular stomatitis virus *in situ*. Interdigitating dendritic cells present viral antigens independent of marginal dendritic cells but fail to prime CD4⁺ and CD8⁺ T cells. *Immunology* 2000; **101**: 512-520
- Carcelain G**, Tubiana R, Samri A, Calvez V, Delaugerre C, Agut H, Katlama C, Autran B. Transient mobilization of human immunodeficiency virus (HIV)-specific CD4 T-helper cells fails to control virus rebounds during intermittent antiretroviral therapy in chronic HIV type 1 infection. *J Virol* 2001; **75**: 234-241
- Zhu F**, Eckels DD. Functionally distinct helper T-cell epitopes of HCV and their role in modulation of NS3-specific, CD8⁺/tetramer positive CTL. *Hum Immunol* 2002; **63**: 710-718
- Livingston BD**, Alexander J, Crimi C, Oseroff C, Celis E, Daly K, Guidotti LG, Chisari FV, Fikes J, Chesnut RW, Sette A. Altered helper T lymphocyte function associated with chronic hepatitis B virus infection and its role in response to therapeutic vaccination in humans. *J Immunol* 1999; **162**: 3088-3095
- Cederbrant K**, Marcusson-Stahl M, Condevaux F, Descotes J. NK-cell activity in immunotoxicity drug evaluation. *Toxicology* 2003; **185**: 241-250
- Maini MK**, Boni C, Lee CK, Larrubia JR, Reignat S, Ogg GS, King AS, Herberg J, Gilson R, Alias A, Williams R, Vergani D, Naoumov NV, Ferrari C, Bertoletti A. The role of virus-specific CD8(+) cells in liver damage and viral control during persistent hepatitis B virus infection. *J Exp Med* 2000; **191**: 1269-1280
- Gripone P**, Rumin S, Urban S, Le Seyec J, Glaise D, Cannie J, Guyomard C, Lucas J, Trepo C, Guguen-Guillouzo C. Infection of a human hepatoma cell line by hepatitis B virus. *Proc Natl Acad Sci U S A* 2002; **99**: 15655-15660
- Stebbing J**, Patterson S, Gotch F. New insights into the immunology and evolution of HIV. *Cell Res* 2003; **13**: 1-7
- Li D**, Takyar ST, Lott WB, Gowans EJ. Amino acids 1-20 of the hepatitis C virus (HCV) core protein specifically inhibit HCV IRES-dependent translation in HepG2 cells, and inhibit both HCV IRES- and cap-dependent translation in HuH7 and CV-1 cells. *J Gen Virol* 2003; **84**: 815-825

Effect of biopsies on sensitivity and specificity of ultra-rapid urease test for detection of *Helicobacter pylori* infection: A prospective evaluation

Li Lin Lim, Khek Yu Ho, Bow Ho, Manuel Salto-Tellez

Li Lin Lim, Khek Yu Ho, Department of Medicine, National University Hospital, Singapore

Bow Ho, Department of Microbiology, National University Hospital, Singapore

Manuel Salto-Tellez, Department of Pathology, National University Hospital, Singapore

Correspondence to: Dr. Khek Yu Ho, Department of Medicine, National University Hospital, 5 Lower Kent Ridge Road, 119074, Singapore. mdchoky@nus.edu.sg

Fax: +65-67794112

Received: 2003-10-27 **Accepted:** 2004-02-09

Abstract

AIM: To prospectively assess the sensitivity, specificity and time to positivity of the Ultra-rapid urease test (URUT) for *Helicobacter pylori* (*H pylori*), and compare the results of one with those of two biopsies.

METHODS: Five antral biopsies were taken in consecutive patients undergoing upper endoscopy: one and two biopsies for URUT, and one each for *H pylori* culture and histology. URUT was read at 1, 5, 10, 20 and 30 min, 1, 2, 3 and 24 h after biopsy insertion into the reagent. A positive histology and/or culture was used as positive reference "gold standards".

RESULTS: URUT was more sensitive for detecting *H pylori* with two biopsies rather than one, at all time points up to 120 min. The sensitivity improved from 3.6% to 82.1% for one biopsy and 10.7% to 85.7% for two biopsies from 1 to 120 min. The sensitivity reached 96.4% at 24 h for both, but the specificity reduced from 100% to 96% and 92% for one and two biopsies, respectively.

CONCLUSION: Development of a positive URUT result is hastened by doubling the number of gastric biopsies. We recommend taking two instead of one biopsy to achieve an earlier positive URUT result so that *H pylori* eradication therapy can be initiated before patient is discharged from the endoscopy suite.

Lim LL, Ho KY, Ho B, Salto-Tellez M. Effect of biopsies on sensitivity and specificity of ultra-rapid urease test for detection of *Helicobacter pylori* infection: A prospective evaluation. *World J Gastroenterol* 2004; 10(13): 1907-1910
<http://www.wjgnet.com/1007-9327/10/1907.asp>

INTRODUCTION

The biopsy urease test was introduced as a simple and convenient method for diagnosing *Helicobacter pylori* (*H pylori*) infection. The biopsy urease test is based on the presence of large amounts of preformed urease enzymes in *H pylori*. The breakdown of urea by urease produces a high local concentration of ammonia, which raises the gastric pH. A phenol indicator that changes

the color from yellow at pH 6.8 to magenta at pH 8.4 can detect this pH alteration. The color change with the introduction of the gastric biopsy is an indication for the presence of *H pylori*.

Despite many advances on the study of *H pylori*, the use of the biopsy urease test still remains invaluable in the diagnosis and management of gastroduodenal disease^[1,2]. The rapid urease test is able to offer a sensitivity of 80-99% and a specificity of 92-100%^[3-5] in untreated patients when compared with histology as the gold standard in the diagnosis of *H pylori* infection.

Since McNulty and Wise first described the biopsy urease test in 1985^[6], several modifications of this test have been developed and validated. A test kit (CLOtest, Delta West Limited, W Australia) is commercially available but its costs and the time taken to positive results, which may be up to 24 h, limits its usefulness. The detection rate of *H pylori* at 20 min was 75% and 92% at 3 h and 98% at 24 h^[7]. The length of time it takes for CLOtest still poses a hindrance to those clinicians wishing to treat infected patients while they are still in the endoscopy room.

The ultra-rapid urease test (URUT), as described by Arvind^[8] is reported to overcome the latter shortcoming by enabling most positive tests to be apparent even before the end of the endoscopy^[8].

We had previously reported the sensitivity, specificity, and the time to positivity for the URUT^[9]. We found that better sensitivity could be obtained if the test continued to be read over a 24-h period although this was achieved at the expense of an increase in the number of false positive cases. We used only one antral biopsy for the URUT. In the CLOtest, the use of two biopsy specimens has been shown to hasten the time to a positive reaction^[10]. Taking two specimens also may theoretically improve the sensitivity and specificity of the test.

The aim of this study was to assess prospectively the sensitivity, specificity and time to positivity for the URUT and compare the results of one biopsy and those of two biopsies in patients undergoing upper endoscopy.

MATERIALS AND METHODS

Patients

From September 1999 to June 2000, 53 consecutive patients who were given routine diagnostic upper gastrointestinal endoscopic examinations by one of the authors (KYH) and who had not been exposed to antibiotics, proton pump inhibitor or bismuth compounds within the past four weeks, and in whom gastric antral biopsies were clinically indicated, were prospectively studied. Patients who had been previously treated for *H pylori* infection and those with an abnormal coagulation profile were excluded from the study.

After an overnight or six-hour fast, each patient underwent esophagogastroduodenoscopy, during which five antral biopsies were taken from within 2 cm of the pylorus using sterilised biopsy forceps (Olympus 16K; Olympus Corp., Tokyo, Japan). Three of the biopsies were used for URUT

wherein the tests were done using one and two of the biopsies, respectively. The remaining two biopsies were sent for culture and histologic examination for *H pylori*. Biopsy specimens for the urease test and culture were taken before those used for histologic examination to avoid contamination with formalin. All patients gave informed consent before endoscopy. The study was conducted in accordance with the provisions of the Declaration of Helsinki and was approved by the Hospital Research & Ethics Committee.

Ultra-rapid urease test

The ultra-rapid urease test kit is composed of a capped polypropylene tube containing 0.5 mL aliquot of 100 g/L unbuffered solution of urea in deionised water (pH 6.8). The solution contains two drops of 10 g/L phenol red, which acts as the indicator^[11]. The biopsy specimens for the URUT were removed from the biopsy forceps with a sterile toothpick and placed immediately into the polypropylene tube. Particular care was taken not to shake the tube after placing the biopsy into it so that a rapid positive result could be achieved^[12]. The reagent was prepared in large batches, frozen, and was ready for thawing just before use. A positive test result was indicated when there was a color change in the medium surrounding the biopsy from yellow to magenta. The test tube was left at room temperature and examined by experienced observers without knowing the clinical details at pre-determined intervals over 24 h. Convenient times chosen were 1, 5, 10, 20, 30 min and 1, 2, 3 and 24 h after insertion of the biopsy specimen into the urease test reagent.

Histologic assessment

The gastric biopsies for histologic assessment were fixed in 40 g/L neutral buffered formaldehyde paraffin processed and stained with haematoxylin and eosin (H&E) in the normal way. Experienced pathologists without knowledge of the clinical data and URUT results assessed the presence or absence of *H pylori* by examining 3 sets of tissue levels within 12 consecutive sections. Histologic diagnosis of *H pylori* infection with H&E stain was compared with the use of Giemsa^[13,14] and thus the Giemsa stain was used only when a few organisms were identified with H&E stain, always confirming the original diagnostic impression.

Culture assessment

For *H pylori* culture, gastric biopsies were smeared on pre-

reduced chocolate blood agar plates and incubated in a humidified carbon dioxide incubator at 37 °C with 50 mL/L carbon dioxide for 3-4 d. The identity of any colonies grown was confirmed using Gram's stain and biochemical tests. Experienced microbiologists without knowledge of the clinical data and URUT results assessed the presence or absence of *H pylori*^[15,16].

Statistical considerations

Only patients with both culture and histology results were analyzed. Results from the URUT were compared with those from culture and histology of biopsy specimens obtained from the same patient. *H pylori* was considered as positive if either culture or histology demonstrated *H pylori*, and negative if *H pylori* was not detected in both culture and histology. Based on these results, the sensitivity and specificity of the URUT at various time points were determined. For this study, sensitivity was defined as the frequency of a positive URUT in patients with either gastric histology or culture positive for *H pylori*. Specificity was the frequency of a negative test in patients with both negative histology and culture for *H pylori*.

RESULTS

Of the 53 patients included in this study, 39(74%) were Chinese, 7(13%) were Malays, 6(11%) were Indians and 1(2%) was of another race. There were 29(55%) males and 24(45%) females. Their ages ranged from 23 to 85 (median, 52) years. The indications for the endoscopy included abdominal pain in 33 patients (62.2%), anemia or drop in hemoglobin in 6(11.3%), atypical chest pain in 5(9.5%), gastric ulcer follow-up in 1(1.9%), and other symptoms in 8(15.1%). The findings during esophagogastroduodenoscopy were esophagitis in 15(28%), duodenal ulcers in 14(26%), gastric ulcers in 8(15%), gastritis in 8(15%), duodenitis in 3(6%), and others in 5(10%).

H pylori was positive in 28 of the 53 patients (53%), in whom either the histology or culture demonstrated the organism. Twenty-four patients were *H pylori* positive in histology and 28 patients were culture positive.

The results of sensitivity and specificity of URUT at various time points are shown in Table 1. URUT was more sensitive for detecting *H pylori* when two biopsies rather than one were used, at all time points up to 120 min. At 1 min, the sensitivity was 3.6% for one biopsy and 10.7% for two biopsies. At 5 min, the sensitivities improved to 32.1% and 50% respectively. At

Table 1 Ultra-rapid urease test results at various time intervals comparing one vs two antral biopsies in 53 patients

		1 m	5 m	10 m	20 m	30 m	60 m	2 h	3 h	24 h
True positive	1 Bx	1	9	13	18	20	23	23	24	24
	2 Bx	3	14	17	21	23	24	24	24	27
True negative	1 Bx	25	25	25	25	25	25	25	25	24p
	2 Bx	25	25	25	25	25	25	25	25	23
False positive	1 Bx	0	0	0	0	0	0	0	0	1
	2 Bx	0	0	0	0	0	0	0	0	2
False negative	1 Bx	27	19	15	10	8	5	5	4	1
	2 Bx	25	14	11	7	5	4	4	4	1
Sensitivity (%)	1 Bx	3.6	32.1	46.4	64.3	71.4	82.1	82.1	85.7	96.4
	2 Bx	10.7	50	60.7	75	82.1	85.7	85.7	85.7	96.4
Specificity (%)	1 Bx	100	100	100	100	100	100	100	100	96
	2 Bx	100	100	100	100	100	100	100	100	92
PPV (%)	1 Bx	100	100	100	100	100	100	100	100	96.4
	2 Bx	100	100	100	100	100	100	100	100	96.4
NPV (%)	1 Bx	48.1	55.6	62.5	71.4	75.8	83.3	83.3	86.2	96
	2 Bx	50	64.1	69.4	78.1	83.3	86.2	86.2	86.2	95.8

Bx=Biopsy, m=minutes, h=hours, PPV=positive predictive value, NPV=negative predictive value.

60 min, the sensitivity was 82.1% for one biopsy and 85.7% for two biopsies. Thereafter there was still some increase in sensitivity with either one or two biopsies, reaching 96.4% at 24 h in each case, but with a reduction in the specificity from 100% to 96% and 92%, for one and two biopsies respectively. Using the receiver operating characteristic curve (Figure 1), the optimal times to read the test appeared to be 1 h when two biopsies were used and 3 h when only a single biopsy was used, and at these time points, the optimal combination of sensitivity and specificity was obtained.

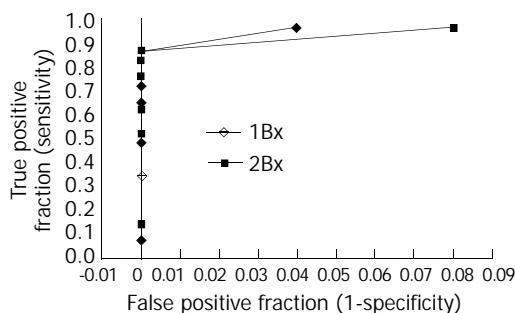


Figure 1 Receiver operating characteristic curve plot of urease test for detection of *H pylori* infection. Bx=Biopsy.

DISCUSSION

The ultra-rapid urease test, as described by Arvind^[8] is reported to overcome the shortcoming of the CLOtest which takes a while to become positive. Using this home-made URUT preparation, we had found the test to be highly specific but not very sensitive when interpreted at one minute^[9]. However, if the test continued to be read, the sensitivity improved to 87% at 24 h. This was however achieved at the expense of a longer reading time and a reduction in specificity to 90% at 24 h^[9]. The development of false positives with delayed reading of the urease tests has previously been noted and attributed to other urease-producing bacteria, or to relatively small numbers of *H pylori*, which are not identified histologically, i.e., false-negative histology^[17].

We previously used only one antral biopsy for the ultra-rapid urease test^[9]. We hypothesize that if more gastric tissue was sampled, a positive test result might appear earlier, thus improving the test sensitivity without compromising its specificity. The present study confirmed this hypothesis. The URUT was more sensitive in detecting *H pylori* when two biopsies instead of one, were used at all time points up to 60 min. In this study a receiver operating characteristic curve analysis was used to select the optimal time for reading the test. The 1-h reading was found to give the optimal sensitivity/specificity combination when two biopsies were used, this does not automatically ensure that it is the best time to read the test. In many centers in the Asia Pacific region, the URUT is used as an initial screening test, with an additional sample taken for histology, which is sent only if the URUT is negative and when there is a strong clinical suspicion of *H pylori* infection. This approach is of great benefit to avoid the additional cost of the histology. Despite the fact that the *H pylori* infection is a chronic disease, the necessity to treat it soon after endoscopy is desirable to minimize the cost as well as the inconvenience of a second clinic visit. If this is the practice, then the most appropriate time point at which to read the test is 30 min when there is maximal specificity (as false positives will not be checked by histology) and minimal gain in sensitivity by reading the test beyond this time. Most importantly, reading the test at 30 min allows the physician to prescribe *H pylori* eradication treatment to the patient before discharging him or

her from the endoscopy suite.

We are unable to explain the initial low sensitivity of the URUT test results found in this study when compared with the original study^[9]. One possible explanation is the reduced size of the biopsy specimens using smaller biopsy forceps as compared with the original study. However, the discrepancy is unlikely to be caused by the difference in the study populations, the incubation temperature of the biopsy specimens, and the volume and concentration of the phenol red used to make the test reagents since these parameters were similar to our previous study^[9]. The initially low test sensitivity might not be a major problem as test sensitivity difference between one and two biopsies, and not the initial test sensitivity was the primary concern of this study. The conclusions reached by this study therefore, should remain valid.

There may be additional yield in taking biopsy specimens from different sites of the stomach due to the differences in the geographical distribution of *H pylori*, for example from the gastric body, in addition to the antral biopsies. However, we do not believe the addition of these biopsies would add significantly to the sensitivity of the tests. As part of another protocol (personal communication, KYH), two antral and two body biopsies were taken from 115 consecutive patients, and the specimens stained with H&E to assess the presence or absence of *H pylori*. Of a total of 66 histology positives, only three (4.5%) were correctly identified by the body biopsies while negative in the antral biopsies. Thus body biopsies contributed to an increased yield of only 4.5% in identifying histology positives. Previous other studies to determine the topographic distribution and density of *H pylori* to provide the maximum yield and to reduce the fallacious results due to sampling error have also concluded that biopsies taken from the antrum was sufficient^[18-20].

Increasing the number of biopsies to more than two biopsies from the antrum, that is three or even four antral biopsy specimens, may increase the sensitivity given that this probably increases the *H pylori* load and therefore the amount of urease. However, this will prolong the endoscopy time and add inconvenience to the patient.

In our study, *H pylori* positivity was 53% based on either culture or histology result, which is in agreement with the local background *H pylori* colonization rate from our previously published data^[9,21]. There were 24 patients who were *H pylori* positive on histology and 28 patients who were culture positive. This difference may reflect the difference in *H pylori* density. In this case, culture appears more sensitive than histology in identifying *H pylori*.

In conclusion, this study showed that the development of a positive URUT result could be hastened by doubling the gastric tissue samples. We recommend to take two biopsies instead of one for the URUT to achieve an earlier positive test result so that appropriate *H pylori* eradication therapy can be prescribed before the patient is discharged from the endoscopy suite.

REFERENCES

- 1 **Basset C**, Holton J, Ricci C, Gatta L, Tampieri A, Perna F, Miglioli M, Vaira D. Review article: diagnosis and treatment of *Helicobacter*: a 2002 updated review. *Aliment Pharmacol Ther* 2003; **17**(Suppl 2): 89-97
- 2 **Versalovic J**. *Helicobacter pylori*. Pathology and diagnostic strategies. *Am J Clin Pathol* 2003; **119**: 403-412
- 3 **Wong BC**, Wong WM, Wang WH, Tang VS, Young J, Lai KC, Yuen ST, Leung SY, Hu WH, Chan CK, Hui WM, Lam SK. An evaluation of invasive and non-invasive tests for the diagnosis of *Helicobacter pylori* infection in Chinese. *Aliment Pharmacol Ther* 2001; **15**: 505-511
- 4 **Chen YK**, Godil A, Wat PJ. Comparison of two rapid urease tests for detection of *Helicobacter pylori* infection. *Dig Dis Sci* 1998; **43**:

- 1636-1640
- 5 **Viiala CH**, Windsor HM, Forbes GM, Chairman SO, Marshall BJ, Mollison LC. Evaluation of a new formulation CLOtest. *J Gastroenterol Hepatol* 2002; **17**: 127-130
 - 6 **McNulty CA**, Wise R. Rapid diagnosis of Campylobacter associated gastritis (Letter). *Lancet* 1985; **1**: 1443-1444
 - 7 **Marshall BJ**, Warren JR, Francis GJ, Langton SR, Goodwin CS, Blincow ED. Rapid urease test in the management of Campylobacter pyloridis-associated gastritis. *Am J Gastroenterol* 1987; **82**: 200-210
 - 8 **Arvind AS**, Cook RS, Tabaqchali S, Farthing MJG. One minute endoscopy room test for Campylobacter pylori (Letter). *Lancet* 1988; **1**: 704
 - 9 **Ho KY**, Kang JY, Lim TP, Yeoh KG, Wee A. The effect of test duration on the sensitivity and specificity of ultra-rapid urease test for the detection of Helicobacter pylori infection. *Aust NZ J Med* 1998; **28**: 615-619
 - 10 **Laine L**, Chun D, Stein C, El-Beblawi I, Sharma V, Chandrasoma P. The influence of size or number of biopsies on rapid urease test results: a prospective evaluation. *Gastrointest Endosc* 1996; **43**: 49-53
 - 11 **Thillainayagam AV**, Arvind AS, Cook RS, Harrison IG, Tabaqchali S, Farthing MJG. Diagnostic efficiency of an ultra-rapid endoscopy room test for Helicobacter pylori. *Gut* 1991; **32**: 467-469
 - 12 **Katellaris PH**, Lowe DG, Norbu P, Farthing MJG. Field evaluation of a rapid, simple and inexpensive urease test for the detection of Helicobacter pylori. *J Gastroenterol Hepatol* 1992; **7**: 569-571
 - 13 **Kang JY**, Wee A, Math MV, Guan R, Tay HH. Helicobacter pylori and gastritis in patients with peptic ulcer and non-ulcer dyspepsia: ethnic differences in Singapore. *Gut* 1990; **31**: 850-853
 - 14 **Kang JY**, Ho KY, Yeoh KG, Guan R, Wee A, Lee E, Lye WC, Leong SO, Tan CC. Peptic ulcer and gastritis in uraemia, with particular reference to the effect of Helicobacter pylori infection. *J Gastroenterol Hepatol* 1999; **14**: 771-778
 - 15 **Hua J**, Ng HC, Yeoh KG, Ho KY, Ho B. Characterization of clinical isolates of Helicobacter pylori in Singapore. *Microbios* 1998; **94**: 71-81
 - 16 **Hua JS**, Zheng PY, Fong TK, Mar KM, Bow H. Helicobacter pylori acquisition of metronidazole resistance by natural transformation in vitro. *World J Gastroenterol* 1998; **4**: 385-387
 - 17 **Laine L**, Estrada R, Lewin DN, Cohen H. The influence of warming on rapid urease test results: a prospective evaluation. *Gastrointest Endosc* 1996; **44**: 429-432
 - 18 **Misra V**, Misra S, Dwivedi M, Singh UP, Bhargava V, Gupta SC. A topographic study of Helicobacter pylori density, distribution and associated gastritis. *J Gastroenterol Hepatol* 2000; **15**: 737-743
 - 19 **Vassallo J**, Hale R, Ahluwalia NK. CLO vs histology: Optimal numbers and site of gastric biopsies to diagnose Helicobacter pylori. *Eur J Gastroenterol Hepatol* 2001; **13**: 387-390
 - 20 **Kalantar J**, Xia HHX, Ma Wyatt J, Rose D, Talley NJ. Determination of optimal biopsy sites for detection of H pylori in patients treated for not treated with antibiotic and anti-secretory drugs. *Gastroenterology* 1997; **112**: A165
 - 21 **Kang JY**, Yeoh KG, Ho KY, Guan R, Lim TP, Quak SH, Wee A, Teo D, Ong YW. Racial differences in Helicobacter pylori seroprevalence in Singapore. *J Gastroenterol Hepatol* 1997; **12**: 655-659

Edited by Ma JY Proofread by Xu FM

Effect of rat serum containing Biejiajian oral liquid on proliferation of rat hepatic stellate cells

Li Yao, Zhen-Min Yao, Heng Weng, Ge-Ping Zhao, Yue-Jun Zhou, Tao Yu

Li Yao, Department of Pharmacology, Zhejiang College of Traditional Chinese Medicine, Hangzhou 310053, Zhejiang Province, China

Zhen-Min Yao, Heng Weng, Yue-Jun Zhou, Tao Yu, Department of Basic Medicine, Zhejiang College of Traditional Chinese Medicine, Hangzhou 310053, Zhejiang Province, China

Ge-Ping Zhao, Institute of Molecular Medicine, Zhejiang College of Traditional Chinese Medicine, Hangzhou 310053, Zhejiang Province, China

Supported by the Natural Science Foundation of Zhejiang Province, No.398402

Correspondence to: Dr. Li Yao, Department of Pharmacology, Zhejiang College of Traditional Chinese Medicine, Hangzhou 310053, Zhejiang Province, China. ylyj@mail.hz.zj.cn

Received: 2003-08-08 **Accepted:** 2003-09-18

Abstract

AIM: Liver fibrosis is a common pathological process of chronic liver diseases. Activation of hepatic stellate cells (HSCs) is the key issue in the occurrence of liver fibrosis. In this study, we observed the inhibitory action of rat serum containing Biejiajian oral liquid (BOL), a decoction of turtle shell, on proliferation of rat HSCs, and to explore the anti-hepatofibrotic mechanisms of BOL.

METHODS: A rat model of hepatic fibrosis was induced by subcutaneous injection of CCl₄. Serum containing low, medium and high dosages of BOL was prepared respectively. Normal and fibrotic HSCs were isolated and cultured. The effect of sera containing BOL on proliferation of HSCs was determined by ³H-TdR incorporation.

RESULTS: The inhibitory rate of normal rat HSC proliferation caused by 100 mL/mL sera containing medium and high dosages of BOL showed a remarkable difference as compared with that caused by colchicine (medium dosage group: 34.56±4.21% vs 29.12±2.85%, *P*<0.01; high dosage group: 37.82±1.32% vs 29.12±2.85%, *P*<0.01). The inhibitory rate of fibrotic rat HSC proliferation caused by 100 mL/L serum containing medium and high dosages of BOL showed a remarkable difference as compared with that caused by colchicine (medium dosage group: 51.31±3.14% vs 38.32±2.65%, *P*<0.01; high dosage group: 60.15±5.36% vs 38.32±2.65%, *P*<0.01). The inhibitory rate of normal rat HSC proliferation caused by 100 mL/L and 200 mL/L sera containing a medium dosage of BOL showed a significant difference as compared with that caused by 50 mL/L (100 mL/L group: 69.02±9.96% vs 50.82±9.28%, *P*<0.05; 200 mL/L group: 81.78±8.92% vs 50.82±9.28%, *P*<0.01). The inhibitory rate of fibrotic rat HSC proliferation caused by 100 mL/L and 200 mL/L sera containing a medium dosage of BOL showed a significant difference as compared with that caused by 50 mL/L (100 mL/L group: 72.19±10.96% vs 61.38±7.16%, *P*<0.05; 200 mL/L group: 87.16±8.54% vs 61.38±7.16%, *P*<0.01).

CONCLUSION: Rat serum containing BOL can inhibit proliferation of rat HSCs, and the inhibition depends on the dosage and concentration of BOL. The inhibitory effect on

HSC proliferation is one of the main anti-hepatofibrotic mechanisms of BOL.

Yao L, Yao ZM, Weng H, Zhao GP, Zhou YJ, Yu T. Effect of rat serum containing Biejiajian oral liquid on proliferation of rat hepatic stellate cells. *World J Gastroenterol* 2004; 10(13): 1911-1913 <http://www.wjgnet.com/1007-9327/10/1911.asp>

INTRODUCTION

Liver fibrosis is a common pathological process of chronic liver diseases. Injury factors would cause an unbalance between synthesis and degradation of extracellular matrix (ECM), which results in excessive collagen deposition in the liver^[1]. Liver fibrosis could be reversed before developing into liver cirrhosis. Therefore, it is fundamental to prevent and treat cirrhosis to arrest its progression to liver cancer.

There are several steps in treating liver fibrosis in Western medicine, namely to inhibit activation of HSCs and proliferation of fibroblast-like HSCs and/or synthesis of matrix protein, to promote degradation of matrix protein, to impair activation of cytokines which lead to liver fibrosis, and to give gene therapy^[2,3]. At the same time, the wide application of Western drugs should be restricted due to their toxicity and side effects.

The anti-hepatofibrotic effect of Biejiajian oral liquid (BOL) has been confirmed in our previous studies^[4-6]. At present, we investigated the effect of rat serum containing BOL on the proliferation of rat hepatic stellate cells (HSCs) to further explore its anti-hepatofibrotic mechanisms.

MATERIALS AND METHODS

Materials

One hundred and forty male Wistar rats, weighing (360±20) g, were supplied by Animal Center of Academy of Medical Sciences of Zhejiang Province. Fodder was maize powder (Hangzhou Sijiqing Feed Factory). Lard (commercially available) and cholesterol were produced by Chemical Branch of Guangzhou Medicinal Company (batch number: 980503). Ethanol (A.R) was purchased from Changyuan Chemical Plant of Changshu City (batch number: 980630). BOL was prepared by the Pharmaceutical Laboratory, Zhejiang College of Traditional Chinese Medicine.

Methods

Animal model Except 30 rats for normal control, the rest of 60 Wistar rats received sc 5 mL/kg CCl₄ in the first day of experiment, followed by sc 400 mL/L CCl₄-liquid paraffin mixture 3 mL/kg daily for 3 d. The normal group received an equal amount of 9 g/L NaCl (NS) daily for 6 wk. Except the normal group, each rat was fed with mixed fodder (maize powder with 5 g/L cholesterol and 200 g/L lard) and drank 200 g/L ethanol only. The normal group was fed with general fodder and water. The time required to complete the induction of model was 6 wk^[7].

Serum containing BOL preparation Eighty Wistar rats were divided into NS group, colchicine (0.1 mg/kg) group, groups

receiving high (9.2 g/kg), medium (4.6 g/kg) and low dosages (2.3 g/kg) of BOL. Each group received the drug once a day for 7 d. Venous blood was collected from inferior vena cava under asepsis 1 h after the last ig, then serum was separated (3 000 r/min, 20 min, 4 °C), inactivated at 56 °C for 30 min, and stored at -70 °C for use.

HSC isolation and culture HSCs were isolated from the livers of normal rats and those with liver fibrosis. Isolation and culture were performed according to the modified Freidman method.

HSC proliferation determination Monolayer HSCs appeared in the 24-well culture plate after they were cultured in 1640 culture medium (Gibco BRC) with sera containing different dosages and concentration of BOL for 48 h. ³H-TdR (Shanghai Institute of Atomic Energy) was added on 92.5 μGBq/well. HSCs were collected after cultured again for 24 h. The HSCs were digested with 2.5 g/L trypsin-1.1 g/L EDTA (Sigma), fixed by 100 mL/L trichloroacetic acid, dehydrated by alcohol, and then oven dried. Dimethylbenzene solution containing 5 mL/L ppo (Amersham) and 0.2 mL/L PoPop was added to measure CPM value of every sample.

Statistical analysis

Statistical analysis was performed with ANOVA. Data were presented as mean±SD. Significant differences were determined by using ANOVA. Results were considered statistically significant when $P<0.05$.

RESULTS

Effect of BOL on rat HSC proliferation

We used 100 mL/L sera containing different dosages of BOL to culture HSCs from normal and hepatofibrotic rats. Results showed that ³H-TdR incorporated into rat HSCs was inhibited obviously by each dosage group, and the higher the dose, the better the effect (Tables 1, 2).

Table 1 Effect of different BOL dosage sera on ³H-TdR incorporation of normal rat HSCs (mean±SD)

Groups	n	Cpm/well	Inhibitory rate (%)
Control	6	2 846.31±218.92	
Colchicine	6	2 018.37±39.31 ^b	29.12±2.85
Low-dose	6	1 968.42±78.32 ^b	30.84±2.71
Intermediate-dose	6	1 870.21±109.45 ^b	34.56±4.21 ^{a,d}
High-dose	6	1 779.86±61.12 ^{a,d,f}	37.82±1.32 ^{d,f}

^a $P<0.05$ vs low-dose group, ^b $P<0.01$ vs control group, ^d $P<0.01$ vs colchicine group, ^f $P<0.01$ vs low-dose group.

Table 2 Effect of different BOL dosage sera on ³H-TdR incorporation of hepatofibrotic rat HSCs (mean±SD)

Groups	n	Cpm/well	Inhibitory rate (%)
Control	6	1 657.82±67.21	
Colchicine	6	1 022.54±12.18 ^b	38.32±2.65
Low-dose	6	994.69±37.86 ^b	40.15±5.36
Intermediate -dose	6	828.91±48.19 ^{b,d,f}	51.31±3.14 ^{d,f}
High-dose	6	662.59±17.87 ^{b,d,f}	60.15±5.36 ^{d,f}

^b $P<0.01$ vs control group, ^d $P<0.01$ vs colchicine group, ^f $P<0.01$ vs low-dose group.

Effect on rat HSC proliferation caused by different concentration sera containing medium dosage of BOL

We used 50 mL/L, 100 mL/L and 200 mL/L sera containing

an intermediate dosage of BOL to culture normal and hepatofibrotic rat HSCs, which were controlled with normal rat sera at the same concentration. We observed that ³H-TdR incorporation increased gradually as normal serum concentration increased. ³H-TdR incorporation decreased gradually as drug serum concentration increased. ³H-TdR incorporation in drug serum group at the same concentration was significantly lower than that in control group ($P<0.05$, Tables 3, 4).

Table 3 Effect of different concentration sera containing intermediate dosage of BOL on ³H-TdR incorporation of normal rat HSCs (mean±SD)

Concentration	n	Control group (cpm/well)	BOL group (cpm/well)	Inhibitory rate (%)
50 mL/L	6	1 479.79±171.01	701.19±134.25 ^a	50.82±9.28
100 mL/L	6	1 990.80±601.42	640.11±209.69 ^a	69.02±9.96 ^c
200 mL/L	6	2 699.89±789.10	479.59±257.30 ^a	81.78±8.92 ^b

^a $P<0.05$ vs control group, ^b $P<0.01$ vs 50 mL/L concentration, ^c $P<0.05$ vs 50 mL/L concentration.

Table 4 Effect of different concentration sera containing intermediate dosage of BOL on ³H-TdR incorporation of hepatofibrotic rat HSCs (mean±SD)

Concentration	n	Control group (cpm/well)	BOL group (cpm/well)	Inhibitory rate (%)
50 mL/L	6	987.73±154.02	563.07±124.38 ^a	61.38±7.16
100 mL/L	6	1 342.58±701.36	375.92±109.47 ^a	72.19±10.96 ^c
200 mL/L	6	2 306.39±652.14	299.83±123.51 ^a	87.16±8.54 ^b

^a $P<0.05$ vs control group, ^b $P<0.01$ vs 50 mL/L concentration, ^c $P<0.05$ vs 50 mL/L concentration.

DISCUSSION

Mechanism of liver fibrosis

The cells synthesizing extracellular matrix (ECM) in the liver were mainly active HSCs^[8]. HSCs are situated in the Disse's spaces. As liver cells were injured, HSCs would be activated and might increase, and then converted into myofibroblast-like cells (MFBLC), which could express cytokines, receptors, smooth muscle alpha-actin (alpha-SMA) and synthesize a great deal of ECM. Therefore, activation of HSCs is a key step in the pathogenesis of liver fibrosis^[9-13]. Activation of local renin-angiotensin system might relate to hepatic fibrosis. Active HSCs could synthesize angiotensin II, which could participate in tissue remodeling in human liver^[14]. It is the main source of collagen formation. HSC apoptosis could relieve experimental liver fibrosis in rats. Thus, it is an important pathway for preventing liver cirrhosis that inhibits HSC proliferation and collagen synthesis. Moreover, HSC proliferation is a key phase in liver fibrosis. Inhibiting proliferation of HSCs had an important sense for anti-hepatofibrosis^[15,16]. Basement membrane-like matrix could inhibit proliferation of HSCs, estrogen could relieve liver fibrosis, and lipid could induce HSC proliferation^[17,18].

Recognition of liver fibrosis in TCM

Researches on preventing and treating liver fibrosis in TCM have been increasing^[4-7]. According to the theory of TCM, liver fibrosis is manifested as weakened body resistance while pathogenic factors prevail, damp-heat and blood stasis coexist, and the liver is depressed due to deficiency of Qi and blood in the spleen and kidney. Liver depression and Qi stagnation can result in blood stasis, blood fails to nourish the liver, and the

key pathogenetic mechanism is blood stasis. At beginning, the pathogenetic mechanism is Qi stagnation and blood stasis. If treated improperly, the disease would evolve into blood stasis, so that body resistance is weakened and excessive superficiality is present. The therapy is to promote the circulation and relieve the stasis, and to strengthen the body resistance to eliminate pathogenic factors, to resolve and soften the hard masses.

Anti-hepatofibrotic mechanism of BOL

BOL is an improved preparation from Biejiajian Pill that was recorded in an ancient medical book (*Jinkui Yaolue*). Its ingredients include more than twenty herbs, they are Carapax trionycis, Blackberrylily rhizome, Baical skullcap root, Zingiberis, rhizoma, Radix et rhizoma rhei, Ramulus cinnamomi, Folium pyrososiae, Magnoliae cortex, Lilac pink herb, Lagerstroemia indica L, Colla corii asini, Radix bupleuri, Catharsius, Paeonia, Ppaonia suffruticosa, Pruni persicae, semen, Radix ginseng, Pinelliae tuber, Tansymustard seed, Nitrum, Beehive. The combination of ingredients has the effect on promoting circulation and relieving stasis, strengthening body resistance and eliminating pathogenic factors, as well as resolving and softening the hard masses, which is conformable with the principle of treating liver fibrosis. Our previous experiments indicated the mechanisms of anti-hepatofibrosis of BOL as follows. It can prevent hepatocytes from degeneration and necrosis, eliminate liver fibrosis, inhibit the synthesis and secretion of ECM, relieve the capillarization of hepatic sinusoids, and improve the microcirculation of liver. HSCs are sensitive to oxygen and hypoxia could enhance liver fibrosis^[19-22]. BOL could also regulate the immune function, and reduce the damage of liver cells^[4-6].

In conclusion, serum-containing BOL can inhibit HSC proliferation and the inhibition may be dependent with the dosage and concentration of BOL.

REFERENCES

- Bedossa P**, Paradis V. Liver extracellular matrix in health and disease. *J Pathol* 2003; **200**: 504-515
- Huang GC**, Zhang JS, Zhang YE. Effects of retinoic acid on proliferation, phenotype and expression of cyclin-dependent kinase inhibitors in TGF-beta1-stimulated rat hepatic stellate cells. *World J Gastroenterol* 2000; **6**: 819-823
- Albanis E**, Friedman SL. Hepatic fibrosis. Pathogenesis and principles of therapy. *Clin Liver Dis* 2001; **5**: 315-334
- Yao ZM**, Lu GY, Zhao ZY. Experimental study on anti-hepatofibrosis effect of Biejiajian Pill. *Zhejiang Zhongyi Xueyuan Xuebao* 1997; **21**: 45-46
- Yao ZM**, Xiong YK, Li JP. Experimental study on anti-hepatofibrosis effect of Biejiajian Oral Liquid (BOL). *Zhejiang Zhongyi Xueyuan Xuebao* 2000; **24**: 58-61
- Zhao ZY**, Yao ZM, Zhong QP, Zhu FY, Wu CZ, Lu GY, Wang GY. Clinical study on Chinese herb Biejiajian pill for treating hepatic fibrosis. *Zhongxiyi Jiehe Ganbing Zazhi* 2001; **11**: 136-138
- Han DW**, Ma XH, Zhao YC. Research on animal model of liver cirrhosis. *Shanxi Yiyao Zazhi* 1979; **4**: 1-5
- Schwabe RF**, Batailler R, Brenner DA. Human Hepatic Stellate cells express CCR5 and RANTES to induce proliferation and migration. *Am J Physiol Gastrointest Liver Physiol* 2003; **285**: G949-958
- Brenner DA**, Waterboer T, Choi SK, Lindquist JN, Stefanovic B, Burchardt E, Yamauchi M, Gillan A, Rippe RA. New aspects of hepatic fibrosis. *J Hepatol* 2000; **32**(1 Suppl): 32-38
- Benyon RC**, Iredale JP. Is liver fibrosis reversible. *Gut* 2000; **46**: 443-446
- Rockey DC**. The cell and molecular biology of hepatic fibrogenesis. Clinical and therapeutic implications. *Clin Liver Dis* 2000; **4**: 319-355
- Arthur MJ**. Fibrogenesis II. Metalloproteinases and their inhibitors in liver fibrosis. *Am J Physiol Gastrointest Liver Physiol* 2000; **279**: 245-249
- Batailler R**, Brenner DA. Hepatic stellate cells as a target for the treatment of liver fibrosis. *Semin Liver Dis* 2001; **21**: 437-451
- Batailler R**, Sancho-Bru P, Gines P, Lora JM, Al-Garawi A, Sole M, Colmenero J, Nicolas JM, Jimenez W, Weich N, Gutierrez-Ramos JC, Arroyo V, Rodes J. Activated human hepatic stellate cells express the renin-angiotensin system and synthesize angiotensin II. *Gastroenterology* 2003; **125**: 117-125
- Ikeda H**, Nagashima K, Yanase M, Tomiya T, Arai M, Inoue Y, Tejima K, Nishikawa T, Omata M, Kimura S, Fujiwara K. Involvement of Rho/Rho Kinase Pathway in regulation of apoptosis in rat hepatic stellate cells. *Am J Physiol Gastrointest Liver Physiol* 2003; **285**: G880-886
- Batailler R**, Brenner DA. Hepatic stellate cells as a target for the treatment of liver fibrosis. *Semin Liver Dis* 2001; **21**: 437-451
- Gaca MD**, Zhou X, Issa R, Kiriella K, Iredale JP, Benyon RC. Basement membrane-like matrix inhibits proliferation and collagen synthesis by activated rat hepatic stellate cells: evidence for matrix-dependent deactivation of stellate cells. *Matrix Biol* 2003; **22**: 229-239
- Zhou Y**, Shimizu I, Lu G, Itonaga M, Okamura Y, Shono M, Honda H, Inoue S, Muramatsu M, Ito S. Hepatic stellate cells contain the functional estrogen receptor beta but not the estrogen receptor alpha in male and female rats. *Biochem Biophys Res Commun* 2001; **286**: 1059-1065
- Zar HA**, Tanigawa K, Kim YM, Lancaster JR Jr. Rat liver postischemic lipid peroxidation and vasoconstriction depend on ischemia time. *Free Radic Biol Med* 1998; **25**: 255-264
- Ankoma-Sey V**, Wang Y, Dai Z. Hypoxic stimulation of vascular endothelial growth factor expression in activated rat hepatic stellate cells. *Hepatology* 2000; **31**: 141-148
- Nagatomi A**, Sakaida I, Matsumura Y, Okita K. Cytoprotection by glycine against hypoxia-induced injury in cultured hepatocytes. *Liver* 1997; **17**: 57-62
- Jungermann K**, Kietzmann T. Oxygen: modulator of metabolic zonation and disease of the liver. *Hepatology* 2000; **31**: 255-260

Edited by Wang XL and Xu FM

Effect of traditional Chinese medicinal enemas on ulcerative colitis of rats

Song-Ming Guo, Hong-Bin Tong, Lian-Song Bai, Wei Yang

Song-Ming Guo, Hong-Bin Tong, Department of Traditional Chinese Medicine, Tongji Hospital, Tongji University, Shanghai 200065, China

Lian-Song Bai, Wei Yang, Department of Traditional Chinese Medicine, Shuguang Hospital, Shanghai Traditional Chinese Medicine University, Shanghai 200032, China

Supported by the Science and Technology Development Fund of Shanghai, No. 98DB14586

Correspondence to: Song-Ming Guo, Department of Traditional Chinese Medicine, Tongji Hospital, Tongji University, Shanghai 200065, China. guosm@msn.com

Telephone: +86-21-56741593

Received: 2003-05-11 **Accepted:** 2003-06-02

Abstract

AIM: To investigate the effects of traditional Chinese medicinal enema (TCME) on inflammatory and immune response of colonic mucosa of rats with ulcerative colitis (UC), and to observe the pathogenic mechanism.

METHODS: Thirty UC rats, induced by intestinal enema together with 2,4-dinitrochlorobenzene (DNCB) and acetic acid, were randomly divided into 3 groups, i.e., GI, GII and GIII. Groups GI and GII were administered with TCME and salazosulfapyridine enema (SASPE), respectively. Group GIII was clystered with only normal saline (NSE), served as control. Group GIV was taken from normal rats as reference, once daily, from the 7th day after the establishment of UC for total 28 d. Interleukin-6 (IL-6) in the colonic mucosa was assayed by ³H-TdR incorporation assay. Colonic mucosal lymphocyte subpopulation adhesive molecules, CD₄⁺CD_{11a}⁺, CD₄⁺CD₁₈⁺, CD₈⁺CD_{11a}⁺, CD₈⁺CD₁₈⁺ (LSAM), tumor necrosis factor (TNF)- α , and interferon- γ (IFN- γ), were detected by enzyme linked immunosorbent assay (ELISA). Moreover, the expression of TNF- α mRNA and IFN- γ mRNA in colonic mucosa were detected by polymerase chain reaction (RT-PCR).

RESULTS: Before therapies, in model groups, GI, GII and GIII, levels of IL-6, TNF- α , IFN- γ , CD₈⁺CD_{11a}⁺ and CD₈⁺CD₁₈⁺ were significantly different (38.29 \pm 2.61 U/mL, 16.54 \pm 1.23 ng/L, 8.61 \pm 0.89 ng/L, 13.51 \pm 2.31% and 12.22 \pm 1.13%, respectively) compared to those in GIV group (31.56 \pm 2.47 U/mL, 12.81 \pm 1.38 ng/L, 5.28 \pm 0.56 ng/L, 16.68 \pm 1.41% and 16.79 \pm 1.11%, respectively). After therapeutic enemas, in GI group, the contents of IL-6 (32.48 \pm 2.53 U/mL), TNF- α (13.42 \pm 1.57 ng/L) and IFN- γ (5.87 \pm 0.84 ng/L) were reduced; then, the contents of CD₈⁺CD_{11a}⁺ (16.01 \pm 1.05%) and CD₈⁺CD₁₈⁺ (16.28 \pm 0.19%) were raised. There was no significant difference between groups GI and GIV, but the difference between groups GI and GII was quite obvious (P <0.05). The expressions of TNF- α mRNA and IFN- γ mRNA in group GIII were much higher than those of group GIV, but those in group GI were significantly suppressed by TCME therapy.

CONCLUSION: Ulcerative colitis is related to colonic regional mucosal inflammatory factors and immune imbalance. TCME

can effectively inhibit regional mucosal inflammatory factors and improve their disorder of immunity.

Guo SM, Tong HB, Bai LS, Yang W. Effect of traditional Chinese medicinal enemas on ulcerative colitis of rats. *World J Gastroenterol* 2004; 10(13): 1914-1917

<http://www.wjgnet.com/1007-9327/10/1914.asp>

INTRODUCTION

Ulcerative colitis (UC) is a refractory, chronic and non-specific disease. Its pathogenesis is probably related to the deficiency of autoimmunity and imbalance of immunoregulation^[1-5]. The relationship between pathogenesis and immunity of colonic mucosa remains a focus at present^[6-11]. In view of poor curative effect and high recurrence rate, traditional Chinese medicinal formulae were used to treat the disease in recent years, and the therapeutic effectiveness is quite satisfactory^[12]. In order to explore the mechanism of UC and pharmacological action of the traditional Chinese medicinal formulae, rat models were established to observe the effect of traditional Chinese medicinal enema on immunological and inflammatory factors in colonic mucosa of rats with UC.

MATERIALS AND METHODS

Materials

Six-week-old Wistar rats ($n=56$), half of male and half of female were purchased from Shanghai Laboratory Animal Center of Chinese Academy of sciences (SLAC. CAS), calf serum, ConA and PHA (Institute of Cell Research of CAS) and mRNA reagent kit and PCR reagent (Promega), IL-6, TNF- α , IFN- γ reagent kit and PE marked CD_{11a}⁺, CD₁₈⁺ monoclonal antibody (Sigma). ³H-TdR was from Shanghai Atomic Nuclear Institute of CAS. Cell factor primer-detector was purchased from Shanghai Biological Engineering Center of CAS. The formulae of traditional Chinese medicinal herbs for enema consisted of Huangqi (*astragalus*), Dahuang (*caulis fibraureae*), Huangbai (*cortex phellodendri*), Wubeizi (*galla chinensis*) and Baiji (*rhizoma bletillae*), mixed with 1g crude drug per milliliter by Medicament Section of Shanghai Tongji Hospital. Salazosulfapyridine (SASP, batch No.921101, Shanghai Sine Pharmaceutical Factory) was prepared as suspension (20 mg/mL) at the same section.

UC model establishment

The models were prepared in reference to literature^[13]. Fifty six Wistar rats weighing 200 \pm 20 g, were fed for 1 week before experiment. Then 38 rats were randomly taken as subjects for experiment. After depilation on back and neck, the rats were administered 0.3 mL of DNCB acetone liquid (DNCB 2.0 g: acetone 100 mL) solution on their bare backs and necks once daily for total 14 d. At the 15th day, 0.25 mL of 0.04 mmol/L DNCB ethanol (500 mL/L) solution was infused through a nylon hose inserted into the colon of rat 8 cm depth. At the 16th day, 2 mL of 80 mL/L-1 acetic acid solution was infused at the same depth. Then, the colon was rinsed with 5 mL normal

saline after 15 s of retention. The remaining 18 rats acted as controls after infusion of normal saline (NS) at 1 week since the preparation of the models, 8 rats were taken respectively from the group of model and group for reference to detect the levels of colonic mucosa lymphocytes: IL-6, TNF- α , IFN- γ and LSAM. The remaining 30 rats were randomly divided into 3 groups of 10 each: GI, GII and GIII were clusted daily with 2 mL of TCM, SASP and NS for 28 d respectively. Another group (GIV) of 10 rats, administered 2 mL of NS daily for 28 d, was taken as reference of normality. At the end of 4 wk experimental period, the lymphocytes were again detected and also the expressions of TNF- α mRNA and IFN- γ mRNA were examined.

Assay of cytokines and immunological factors

Separation and culture of intestinal theca mucosa cells

Mucosa cells were separated and routinely cultured to prepare monolayer culture cells suspension of colonic mucosa, and the suspension was adjusted to 5×10^9 /L in RPMI 1640 containing 100 mL/L calf serum. Then, 1.0 mL of suspension, was put in 24-well plate, then 1.0 mL of ConA (final density 5 mg/L) was added, and cultured at 37 °C for 24 h in a humidified atmosphere containing 50 mL/L CO₂. The supernatant of the culture was centrifuged at 3 000 r/min and preserved at -20 °C for detection of IL-6, TNF- α , IFN- γ and LSAM levels according to the manufacturer's instructions.

RNA extraction

Total RNA from colonic mucosa tissue of rats was extracted as previously described^[14-16]: using single-step method of RNA isolation (acid guanidinium thiocyanate-phenol-chloroform extraction). Formaldehyde denatured electrophoresis stained with ethidium bromide (EB) was used to examine infect RNA. Reverse transcription reaction was performed as previously described^[17-19]: a total amount of 1 μ g of RNA as template was mixed with RNasin (40 U/ μ L) 0.5 μ L, 25 μ mol/L oligo (dT) 1 μ L, 5 \times RT buffer 5 μ L, dNTP (10 mmol/L) 1 μ L and AMV (9 U/ μ L) 1 μ L to a total reaction volume of 25 μ L, followed by incubation at 37 °C for 1 h and at 94 °C for 5 min. PCR reaction was carried out as described previously^[20-22]: 10 μ L cDNA was added with 0.1 μ g of primer, 0.05 μ g of β -action primer and 2.5 U of *Taq* enzyme (5 U/ μ L). Total PCR reaction volume was 100 μ L. PCR condition was as follows: deraturation at 94 °C for 1 min; primer annealing at 54 °C for 40 s, and extension at 72 °C for 40 s, followed a further extension at 72 °C for 7 min. Other cycles were as follows: after 30 cycles of amplification, 20 μ L of PCR product was electrophoresed on 20 g/L agarose gel, then recorded with camera under ultraviolet for density scanning and calculated the relative expression of the gene.

Statistical analysis

Experimental results were expressed as mean \pm SD. $P < 0.05$ was considered statistically significant. All statistical calculations were performed using the SPSS for Windows version 9.0 software package.

RESULTS

Expression of colonic mucosal cytokines and adhesion molecules in rats of model group (MG) and control group (CG)

At 1 week after setting of models, the expression of cytokines in MG was found to be significantly higher than that in CG ($P < 0.01$, Table 1). The expressions of lymphocyte T subpopulation surface adhesive molecules, CD₈⁺CD_{11a}⁺ and CD₈⁺CD₁₈⁺, were remarkably lower in MG than those in CG ($P < 0.01$, Table 2).

Colonic mucosal TNF- α mRNA and IFN- γ mRNA

In group GI clusted with TCME, the levels of IL-6, TNF- α

and IFN- γ were obviously reduced. Levels of CD₈⁺CD_{11a}⁺ and CD₈⁺CD₁₈⁺ were remarkably raised, which were no obvious differences compared with those in GIV group (i.e., control group) ($P > 0.05$, Tables 3 and 4), but, there were significant differences between groups GI and GII ($P < 0.05$, Tables 3 and 4).

Table 1 Expression of colonic mucosal cytokines in MG and RG before therapy (mean \pm SD)

Group	n	IL-6 (U/mL)	TNF- α (ng/L)	IFN- γ (ng/L)
Model	8	38.29 \pm 2.61 ^b	16.54 \pm 1.23 ^b	8.61 \pm 0.89 ^b
Control	8	31.56 \pm 2.47	12.81 \pm 1.38	5.28 \pm 0.56

^b $P < 0.01$ vs control group.

Table 2 Comparison between expressions of colonic lymphocyte surface adhesive molecules (mean \pm SD, %)

Group	n	CD ₄ ⁺ CD _{11a} ⁺	CD ₄ ⁺ CD ₁₈ ⁺	CD ₈ ⁺ CD _{11a} ⁺	CD ₈ ⁺ CD ₁₈ ⁺
Model	8	29.81 \pm 1.17	26.24 \pm 1.12	13.51 \pm 2.31 ^a	12.22 \pm 1.13 ^a
Control	8	29.70 \pm 1.36	26.89 \pm 1.26	16.68 \pm 1.41	16.79 \pm 1.11

^a $P < 0.05$ vs control group.

Table 3 Changes of colonic mucosal cytokines after therapy (n=10, mean \pm SD)

Group	IL-6 (U/mL)	TNF- α (ng/L)	IFN- γ (ng/L)
GI	32.48 \pm 2.53 ^{ae}	13.42 \pm 1.57 ^{ae}	5.87 \pm 0.84 ^{ae}
GII	34.56 \pm 3.21 ^c	14.81 \pm 1.48 ^c	6.36 \pm 0.62 ^c
GIII	37.32 \pm 2.54	16.13 \pm 1.36	8.21 \pm 0.77
GIV	31.16 \pm 2.19	12.71 \pm 1.51	5.35 \pm 0.63

^a $P > 0.05$, ^c $P < 0.05$ vs GIV; ^e $P < 0.05$ vs GII.

Table 4 Expression of colonic mucosal lymphoid T surface adhesive molecules (n=10, mean \pm SD)

Group	CD ₄ ⁺ CD _{11a} ⁺ (%)	CD ₄ ⁺ CD ₁₈ ⁺ (%)	CD ₈ ⁺ CD _{11a} ⁺ (%)	CD ₈ ⁺ CD ₁₈ ⁺ (%)
GI	27.51 \pm 1.13	25.23 \pm 1.45	16.01 \pm 1.05 ^{ae}	16.28 \pm 0.19 ^{ae}
GII	27.35 \pm 1.23	25.54 \pm 1.50	13.16 \pm 1.34 ^c	13.27 \pm 1.44 ^c
GIII	27.42 \pm 1.56	25.51 \pm 1.28	11.52 \pm 1.29	11.34 \pm 1.61
GIV	27.61 \pm 1.43	25.45 \pm 1.26	16.45 \pm 1.23	16.56 \pm 1.13

^a $P > 0.05$, ^c $P < 0.05$ vs GIV; ^e $P < 0.05$ vs GII.

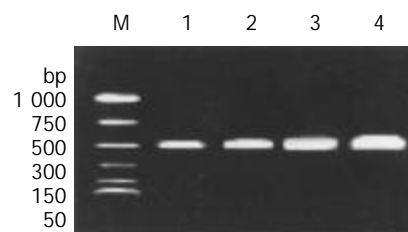


Figure 1 Analysis of TNF- α mRNA expression in UC mice after a 4-week treatment. A 550-bp fragment was amplified by PCR. M: Marker; Lane 1: Group GIV (control); Lane 2: Group GI (TCME); Lane 3: Group GII (SASPE); Lane 4: Group GIII (NSE). The primers used were: upstream, 5' -GGAGCTGCTCA GAGTAAATCAC-3'; and the downstream, 5' -GCACGAGTCA CTCTCGTTTC-3' [23].

Expression of TNF- α mRNA and IFN- γ mRNA in colonic mucosal tissue

The expression of TNF- α mRNA and IFN- γ mRNA in colonic mucosal tissue, was higher in GIII group than those in GIV group (Figures 1, 2). After treatment, TNF- α mRNA and IFN- γ

mRNA levels were obviously suppressed in groups GI and GII, especially in group GI.

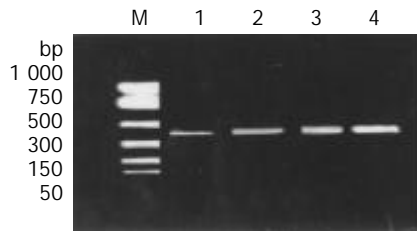


Figure 2 Analysis of IFN- γ mRNA expression in UC mice after a 4-week treatment. A 430-bp fragment was amplified by PCR. M: Marker; Lane 1: Group GIV (control); Lane 2: Group G I (TCME); Lane 3: Group GII (SASPE); Lane 4: Group GIII (NSE). The primers used were: upstream, 5' -TTTTGGGTCTCTTGGCT GTT-3'; and the downstream, 5' -CTCCTTTTCGCTCCCTGT-3' [23].

DISCUSSION

The pathogenesis of colonic colitis remains unclear up to now. It is believed that colonic colitis results from the interaction of many factors, such as environment, immunity and heredity, etc. Probably, susceptible population in heredity is affected by environmental factors, such as water, food and infection, which trigger excessive reaction of intestinal immunity. The reaction can cause an inflammatory stimulation to intestinal mucosa and damage it [24,25]. More and more attention has been paid to autoimmunity. An opinion suggests that there exists an inevitable correlation between the immunity system of intestinal mucosa and its integrity [26-28]. It has been reported that IL-6, a mononuclear macrophage, is a cytokine secreted by T and B cell. IL-6 can promote proliferation of T cell and enhance T cell reaction to cell toxicity. Our experimental result showed that IL-6 was high active in colonic mucosal tissue of UC models, the higher level of IL-6 can further aggravate the injury on colonic tissue by antigen-antibody reaction and complement activation [29,35]. More endogenous IFN- γ and TNF- α produced by colonic epithelia of UC models cause the changes in epithelia, which may lead directly to scatches of inflammatory epithelia [36,37]. Disorder of autoimmunity is closely related to the imbalance of Th₁ and Th₂ cells. For IFN- γ being on Th₁ cell, abnormal expressions of IFN- γ and IFN- γ mRNA cause inevitably the imbalance of Th₁/Th₂ and result in immune disorder [38-40]. CD_{11a}⁺/CD₁₈⁺ are cell surface adhesive albumin, also known as lymphocyte function antigen-1 (LFA-1), a representative of β_2 integrants. It possesses a series of functions, such as introduction of adhesion, chemotaxis of cell and homing of lymphocytes, etc. It expresses on surfaces of white cells, phagocytes and large granular lymphocytes, acting as a key channel in interaction and information between cells. A few of cellular factors, affected by them, such as IL-6, IFN- γ , TNF- α and endotoxin, can affect their expressions [41-43]. CD₈⁺CD_{11a}⁺ and CD₈⁺CD₁₈⁺ (on T_s cell) were found in suffers with moderate and severe ulcerative colitis, and significantly lower than those in normal control rats [44]. This is in conformity to our findings.

Our study showed that expressions of IL-6, TNF- α , TNF- α mRNA, IFN- γ , IFN- γ mRNA were found to be obviously higher and the levels of lymphocyte T surface adhesive molecules, CD₈⁺CD_{11a}⁺ and CD₈⁺CD₁₈⁺ were lower than those in normal rats in colonic mucosal tissue of UC models. The results were in agreement with the findings of others [45]. The results indicated that ulcerative colitis was correlated with disfunction and disorder of autoimmunity. The abnormal expressions of local inflammatory factors and adhesive albumin of cell surface in colonic tissue play a critical role in regulation of immunity. The mutual affects of these factors and

abnormality of regulation of immune system are regarded as the core of pathogenesis. The imbalance of regulation between pre-inflammation cytokines and anti-inflammation cytokines is considered an important mechanism of intestine inflammation, including ulcerative colitis.

At present, ulcerative colitis lacks more effective therapy for radical cure. Principally, steroid hormones and salicylic acid preparation are used to control and suppress the inflammation. In recent years, along with the development of immunology and molecular biology, the accumulation of knowledge about the disease and further understanding of the mechanism of drug action, new methods of treatment have come up into being one after another. But the ordinary UC sufferers can not afford remedies due to the exorbitant price of drugs, and the safety of the remedies needs to be further identified. Our study demonstrated that salazosulfapyridine (SASP) is still the principal remedy for ulcerative colitis. It can improve the conditions of patients in mild and moderate states. But the side-effect and high relapse rate after the remedy are unsatisfactory. Traditional Chinese medicine is popular in China. It is characteristic of TCM to treat intestinal diseases with TCM herbs enemas [12]. The study showed that the treatment of TCME was better on UC than SASPE. Our TCME could effectively inhibit the activity of granulocyte, macrophage and monocyte. Also it could reduce immune response and formation of inflammation in colonic mucosal tissue, which might be due to that our TCME could reduce the expressions of IL-6, TNF- α , IFN- γ and raise the levels of surface adhesive molecules (CD₈⁺CD_{11a}⁺ and CD₈⁺CD₁₈⁺), could also suppress the abnormal expressions of IFN- α and IFN- γ mRNA, improve the disorder of immunity in UC and the Baiji could protect colonic mucosa, Bahuang and Huangbai could promote cruur. SASP suspension has more side-effects than the formulae of TCM herbs, although it has a certain effect in treatment of ulcerative colitis clinically. Therefore, the retention enema prepared from TCM herbs may be an ideal choice to manage the disease.

REFERENCES

- 1 **Furrie E**, Macfarlane S, Cummings JH, Macfarlane GT. Systemic antibodies towards mucosal bacteria in ulcerative colitis and Crohn's disease differentially activate the innate immune response. *Gut* 2004; **53**: 91-98
- 2 **Ioachim E**, Michael M, Katsanos C, Demou A, Tsianos EV. The immunohistochemical expression of metallothionein in inflammatory bowel disease. Correlation with HLA-DR antigen expression, lymphocyte subpopulations and proliferation-associated indices. *Histol Histopathol* 2003; **18**: 75-82
- 3 **Ludwiczek O**, Kaser A, Tilg H. Plasma levels of soluble CD40 ligand are elevated in inflammatory bowel diseases. *Int J Colorectal Dis* 2003; **18**: 142-147
- 4 **Sawada-Hase N**, Kiyohara T, Miyagawa J, Ueyama H, Nishibayashi H, Murayama Y, Kashiwara T, Nakahara M, Miyazaki Y, Kanayama S, Nezu R, Shinomura Y, Matsuzawa Y. An increased number of CD40-high monocytes in patients with Crohn's disease. *Am J Gastroenterol* 2000; **95**: 1516-1523
- 5 **Candelli M**, Nista EC, Nestola M, Armuzzi A, Silveri NG, Gasbarrini G, Gasbarrini A. Saccharomyces cerevisiae-associated diarrhea in an immunocompetent patient with ulcerative colitis. *J Clin Gastroenterol* 2003; **36**: 39-40
- 6 **Ohman L**, Franzen L, Rudolph U, Harriman GR, Hultgren Hornquist E. Immune activation in the intestinal mucosa before the onset of colitis in Galp α 2-deficient mice. *Scand J Immunol* 2000; **52**: 80-90
- 7 **Fukushima K**, Yonezawa H, Focchi C. Inflammatory bowel disease-associated gene expression in intestinal epithelial cells by differential cDNA screening and mRNA display. *Inflamm Bowel Dis* 2003; **9**: 290-301
- 8 **Fahlgren A**, Hammarstrom S, Danielsson A, Hammarstrom ML. Increased expression of antimicrobial peptides and lysozyme in colonic epithelial cells of patients with ulcerative colitis. *Clin Exp*

- Immunol* 2003; **131**: 90-101
- 9 **Carvalho AT**, Elia CC, de Souza HS, Elias PR, Pontes EL, Lukashok HP, de Freitas FC, Lapae Silva JR. Immunohistochemical study of intestinal eosinophils in inflammatory bowel disease. *J Clin Gastroenterol* 2003; **36**: 120-125
- 10 **Carty E**, De Brabander M, Feakins RM, Rampton DS. Measurement of in vivo rectal mucosal cytokine and eicosanoid production in ulcerative colitis using filter paper. *Gut* 2000; **46**: 487-492
- 11 **McKaig BC**, McWilliams D, Watson SA, Mahida YR. Expression and regulation of tissue inhibitor of metalloproteinase-1 and matrix metalloproteinases by intestinal myofibroblasts in inflammatory bowel disease. *Am J Pathol* 2003; **162**: 1355-1360
- 12 **Jiang XL**, Cui HF. An analysis of 10 218 ulcerative colitis cases in China. *World J Gastroenterol* 2002; **8**: 158-161
- 13 **Padol I**, Huang JQ, Hogaboam CM, Hunt RH. Therapeutic effects of the endothelin receptor antagonist Ro 48-5695 in the TNBS/DNBS rat model of colitis. *Eur J Gastroenterol Hepatol* 2000; **12**: 257-265
- 14 **Tahara K**, Fujii K, Yamaguchi K, Suematsu T, Shiraishi N, Kitano S. Increased expression of P-cadherin mRNA in the mouse peritoneum after carbon dioxide insufflation. *Surg Endosc* 2001; **15**: 946-949
- 15 **Xiang X**, Qiu D, Hegele RD, Tan WC. Comparison of different methods of total RNA extraction for viral detection in sputum. *J Virol Methods* 2001; **94**: 129-135
- 16 **Yamada H**, Koizumi S. Lymphocyte metallothionein-mRNA as a sensitive biomarker of cadmium exposure. *Ind Health* 2001; **39**: 29-32
- 17 **Fasshauer M**, Kralisch S, Klier M, Lossner U, Bluher M, Chambaut-Guerin AM, Klein J, Paschke R. Interleukin-6 is a positive regulator of tumor necrosis factor alpha-induced adipose-related protein in 3T3-L1 adipocytes. *FEBS Lett* 2004; **27**: 153-157
- 18 **Barbier M**, Vidal H, Desreumaux P, Dubuquoy L, Bourreille A, Colombel JF, Cherbut C, Galmiche JP. Overexpression of leptin mRNA in mesenteric adipose tissue in inflammatory bowel diseases. *Gastroenterol Clin Biol* 2003; **27**: 987-991
- 19 **Ridyard AE**, Nuttall TJ, Else RW, Simpson JW, Miller HR. Evaluation of Th1, Th2 and immunosuppressive cytokine mRNA expression within the colonic mucosa of dogs with idiopathic lymphocytic-plasmacytic colitis. *Vet Immunol Immunopathol* 2002; **86**: 205-214
- 20 **Akazawa A**, Sakaida I, Higaki S, Kubo Y, Uchida K, Okita K. Increased expression of tumor necrosis factor-alpha messenger RNA in the intestinal mucosa of inflammatory bowel disease, particularly in patients with disease in the inactive phase. *J Gastroenterol* 2002; **37**: 345-353
- 21 **Ogawa A**, Andoh A, Araki Y, Bamba T, Fujiyama Y. Neutralization of interleukin-17 aggravates dextran sulfate sodium-induced colitis in mice. *Clin Immunol* 2004; **110**: 55-62
- 22 **Sawa Y**, Oshitani N, Adachi K, Higuchi K, Matsumoto T, Arakawa T. Comprehensive analysis of intestinal cytokine messenger RNA profile by real-time quantitative polymerase chain reaction in patients with inflammatory bowel disease. *Int J Mol Med* 2003; **11**: 175-179
- 23 **Egger B**, Bajaj-Elliott M, MacDonald TT, Inglin R, Eysselein VE, Buchler MW. Characterisation of acute murine dextran sodium sulphate colitis: cytokine profile and dose dependency. *Digestion* 2000; **62**: 240-248
- 24 **Elson CO**, Sartor RB, Targan SR, Sandborn WJ. Challenges in IBD Research: updating the scientific agendas. *Inflamm Bowel Dis* 2003; **9**: 137-153
- 25 **Mow WS**, Vasilias EA, Lin YC, Fleshner PR, Papadakis KA, Taylor KD, Landers CJ, Abreu-Martin MT, Rotter JJ, Yang H, Targan SR. Association of antibody responses to microbial antigens and complications of small bowel Crohn's disease. *Gastroenterology* 2004; **126**: 414-424
- 26 **Akazawa A**, Sakaida I, Higaki S, Kubo Y, Uchida K, Okita K. Increased expression of tumor necrosis factor-alpha messenger RNA in the intestinal mucosa of inflammatory bowel disease, particularly in patients with disease in the inactive phase. *J Gastroenterol* 2002; **37**: 345-353
- 27 **Rioux JD**, Silverberg MS, Daly MJ, Steinhart AH, McLeod RS, Griffiths AM, Green T, Brettin TS, Stone V, Bull SB, Bitton A, Williams CN, Greenberg GR, Cohen Z, Lander ES, Hudson TJ, Siminovitch KA. Genomewide search in Canadian families with inflammatory bowel disease reveals two novel susceptibility loci. *Am J Hum Genet* 2000; **66**: 1863-1870
- 28 **Obermeier F**, Schwarz H, Dunger N, Strauch UG, Grunwald N, Scholmerich J, Falk W. OX40/OX40L interaction induces the expression of CXCR5 and contributes to chronic colitis induced by dextran sulfate sodium in mice. *Eur J Immunol* 2003; **33**: 3265-3274
- 29 **Beil WJ**, McEuen AR, Schulz M, Wefelmeyer U, Kraml G, Walls AF, Jensen-Jarolim E, Pabst R, Pammer J. Selective alterations in mast cell subsets and eosinophil infiltration in two complementary types of intestinal inflammation: ascariasis and Crohn's disease. *Pathobiology* 2002-2003; **70**: 303-313
- 30 **Stuchi AF**, Shebani KO, Leeman SE, Wang CC, Reed KL, Fruin AB, Gower AC, McClung JP, Andry CD, O'Brien MJ, Pothoulakis C, Becker JM. A neurokinin 1 receptor antagonist reduces an ongoing ileal pouch inflammation and the response to a subsequent inflammatory stimulus. *Am J Physiol Gastrointest Liver Physiol* 2003; **285**: G1259-1267
- 31 **Drissler F**, Venstrom K, Sabat R, Asadullah K, Schottelius AJ. Molecular mechanisms of interleukin-10-mediated inhibition of NF-kappaB activity: a role for p50. *Clin Exp Immunol* 2004; **135**: 64-73
- 32 **Redwine L**, Hauger RL, Gillin JC, Irwin M. Effects of sleep and sleep deprivation on interleukin-6, growth hormone, cortisol, and melatonin levels in humans. *J Clin Endocrinol Metab* 2000; **85**: 3597-3603
- 33 **Papadakis KA**, Targan SR. Role of cytokines in the pathogenesis of inflammatory bowel disease. *Annu Rev Med* 2000; **51**: 289-298
- 34 **Sandborn WJ**. Evidence-based treatment algorithm for mild to moderate Crohn's disease. *Am J Gastroenterol* 2003; **98**(12 Suppl): S1-S5
- 35 **Gasche C**, Bakos S, Dejaco C, Tillinger W, Zakeri S, Reinisch W. IL-10 secretion and sensitivity in normal human intestine and inflammatory bowel disease. *J Clin Immunol* 2000; **20**: 362-370
- 36 **Abreu MT**, Taylor KD, Lin YC, Hang T, Gaiennie J, Landers CJ, Vasilias EA, Kam LY, Rojany M, Papadakis KA, Rotter JJ, Targan SR, Yang H. Mutations in NOD2 are associated with fibrostenosing disease in patients with Crohn's disease. *Gastroenterology* 2002; **123**: 679-688
- 37 **Suryaprasad AG**, Prindiville T. The biology of TNF blockade. *Autoimmun Rev* 2003; **2**: 346-357
- 38 **Loher F**, Bauer C, Landauer N, Schmall K, Siegmund B, Lehr HA, Dauer M, Schoenharting M, Endres S, Eigler A. The interleukin-1 beta-converting enzyme inhibitor pralnacasan reduces dextran sulfate sodium-induced murine colitis and T helper 1 T-cell activation. *J Pharmacol Exp Ther* 2004; **308**: 583-590
- 39 **Topilski I**, Harmelin A, Flavell RA, Levo Y, Shachar I. Preferential Th1 immune response in invariant chain-deficient mice. *J Immunol* 2002; **168**: 1610-1617
- 40 **Fuss IJ**, Boirivant M, Lacy B, Strober W. The interrelated roles of TGF-beta and IL-10 in the regulation of experimental colitis. *J Immunol* 2002; **168**: 900-908
- 41 **Noti JD**, Johnson AK, Dillon JD. Structural and functional characterization of the leukocyte integrin gene CD11d. Essential role of Sp1 and Sp3. *J Biol Chem* 2000; **275**: 8959-8969
- 42 **Schneeberger EE**, Vu Q, LeBlanc BW, Doerschuk CM. The accumulation of dendritic cells in the lung is impaired in CD18-/- but not in ICAM-1-/- mutant mice. *J Immunol* 2000; **164**: 2472-2478
- 43 **Tilg H**, Vogelsang H, Ludwiczek O, Lochs H, Kaser A, Colombel JF, Ulmer H, Rutgeerts P, Kruger S, Cortot A, D'Haens G, Harrer M, Gasche C, Wrba F, Kuhn I, Reinisch W. A randomised placebo controlled trial of pegylated interferon alpha in active ulcerative colitis. *Gut* 2003; **52**: 1728-1733
- 44 **Vainer B**, Brimnes J, Claesson MH, Nielsen OH. Impaired sensitivity to beta 2 integrin-blocking in ICAM-1-mediated neutrophil migration in ulcerative colitis. *Scand J Gastroenterol* 2001; **36**: 621-629
- 45 **Vainer B**, Sorensen S, Seidelin J, Nielsen OH, Horn T. Expression of ICAM-1 in colon epithelial cells: an ultrastructural study performed on *in vivo* and *in vitro* models. *Virchows Arch* 2003; **443**: 774-781

Expression of inducible nitric oxide synthase and cyclooxygenase-2 in pancreatic adenocarcinoma: Correlation with microvessel density

Hans U. Kasper, Hella Wolf, Uta Drebber, Helmut K. Wolf, Michael A. Kern

Hans U. Kasper, Michael A. Kern, Uta Drebber, Department of Pathology, University of Cologne, Germany

Hans U. Kasper, Michael A. Kern, Center of Molecular Medicine of the University of Cologne, Germany

Helmut K. Wolf, Department of Pathology, Johannes-Gutenberg, University of Mainz, Germany

Hella Wolf, Department of Pathology, University of Magdeburg, Germany

Correspondence to: Dr. Hans U. Kasper, Department of Pathology, University of Cologne, Joseph-Stelzmann-Str. 9, D-50931 Koeln, Germany. hans-udo.kasper@uni-koeln.de

Telephone: +49-221-4787223 **Fax:** +49-221-478-6360

Received: 2003-11-18 **Accepted:** 2004-01-17

Abstract

AIM: Cyclooxygenases (COX) are key enzymes for conversion of arachidonic acid to prostaglandins. Nitric oxide synthase (NOS) is the enzyme responsible for formation of nitric oxide. Both have constitutive and inducible isoforms. The inducible isoforms (iNOS and COX-2) are of great interest as regulators of tumor angiogenesis, tumorigenesis and inflammatory processes. This study was to clarify their role in pancreatic adenocarcinomas.

METHODS: We investigated the immunohistochemical iNOS and COX-2 expression in 40 pancreatic ductal adenocarcinomas of different grade and stage. The results were compared with microvessel density and clinicopathological data.

RESULTS: Twenty-one (52.5%) of the cases showed iNOS expression, 15 (37.5%) of the cases were positive for COX-2. The immunoreaction was heterogeneously distributed within the tumors. Staining intensity was different between the tumors. No correlation between iNOS and COX-2 expression was seen. There was no relationship with microvessel density. However, iNOS positive tumors developed more often distant metastases and the more malignant tumors showed a higher COX-2 expression. There was no correlation with other clinicopathological data.

CONCLUSION: Approximately half of the cases expressed iNOS and COX-2. These two enzymes do not seem to be the key step in angiogenesis or carcinogenesis of pancreatic adenocarcinomas. Due to a low prevalence of COX-2 expression, chemoprevention of pancreatic carcinomas by COX-2 inhibitors can only achieve a limited success.

Kasper HU, Wolf H, Drebber U, Wolf HK, Kern MA. Expression of inducible nitric oxide synthase and cyclooxygenase-2 in pancreatic adenocarcinoma: Correlation with microvessel density. *World J Gastroenterol* 2004; 10(13): 1918-1922
<http://www.wjgnet.com/1007-9327/10/1918.asp>

INTRODUCTION

Cancer of the pancreas is still one of the most dismal malignant

diseases with a death to incidence rate of 0.99^[1]. In Germany alone, more than 11 000 patients die of this disease per year^[2]. The only effective therapy is surgical excision^[3]. Adjuvant chemo- and radiotherapy provide only a minimal survival advantage without consistent improvement in outcome^[4]. Until now, the molecular biology of pancreatic cancer still is relatively unknown. A number of studies have focused on genetic changes^[3,5,6]. But also inflammation has been identified as a significant factor in the development of pancreatic cancer^[7]. Both hereditary and sporadic forms of chronic pancreatitis may be associated with increased cancer risk^[8]. Cytokines, reactive oxygen species and mediators of the inflammatory pathway have been identified to increase cell cycling, cause loss of tumor suppressor function and stimulate oncogene expression^[7]. These cytokines are also part of angiogenesis, being an important step for tumor development and could be a therapeutic target also for pancreatic adenocarcinomas.

Nitric oxide (NO) is a pleiotropic biomolecule with a short half time. It has part in the signal transduction in a great variety of mechanisms including neural transmission, vasodilatation, immunoregulation and defense mechanism as well as influencing cancerogenesis^[9]. NO is a product of the conversion of L-arginine to L-citrulline by nitric oxide synthase (NOS)^[10]. This enzyme exists in three isoforms, namely the constitutively expressed calcium-dependent endothelial (eNOS) and neuronal (nNOS) nitric oxide synthase and the calcium independent inducible or immunological (iNOS or NOS-2) isoforms^[11].

iNOS expression in human diseases has long been a matter of investigation. NO production by iNOS in tumor infiltrating macrophages may be part of their antitumoral cytotoxic potential^[12]. On the other hand, expression of iNOS in endothelial cells of tumor vessels and in cancer cells itself supports the assumption that the cancer uses this isoform to regulate the tumor vascularisation and blood flow^[13,14].

Cyclooxygenases (COX) are enzymes which are involved in the synthesis of prostaglandins (PGs) from arachidonic acid. They catalyze the insertion of molecular oxygen into arachidonic acid to form the unstable intermediate PG-G2 being rapidly converted to PGH₂. PGH₂ is the source of several biological active PGs, thromboxanes and prostacyclines which contribute to many physiological and pathological processes like hemostasis, kidney and gastric function, pain, inflammation and tumor defense and also tumorigenesis^[15].

The two isoforms of COX (COX-1 and COX-2) differ in many respects^[16]. COX-1 is constitutively expressed in most tissues and seems to be responsible for the baseline production of PG. COX-2 is not detected in most normal tissues but is highly inducible by inflammatory and mitogenic stimuli. COX-2 is strongly implicated in tumorigenesis and COX-2 inhibitors are discussed as the target for cancer prevention and therapy^[17].

Current knowledge regarding the rate of iNOS and COX-2 expressions and their relationship to MVD in pancreatic cancer is rather limited. We investigated therefore iNOS and COX-2 expression in pancreatic adenocarcinomas in comparison to microvessel density to clarify the influence of these mediators in pancreatic carcinomas.

MATERIALS AND METHODS

Tissue specimens

All tissues used in this study were surgical resection specimens obtained from the files of the Department of Pathology, Johannes Gutenberg- University, Mainz, Germany. All pancreatic adenocarcinomas were of ductal origin. Carcinomas from 18 women and 22 men with a mean age of 62.2 years (range 45- 81 years) were investigated. Thirty-three tumors were located in the head of the pancreas, 3 in the corpus and 5 in the tail of the pancreas. TNM- classification according to the TNM classification of malignant tumors was as follows: 5× T1, 27× T2, 7× T3, 1× T4. Twenty-three patients showed lymph node metastases and in 5 patients, distant metastases were known. There were 3 well differentiated, 15 moderately differentiated and 22 poorly differentiated pancreatic carcinomas.

Immunohistochemistry

Resected specimens were fixed overnight in 40 g/L buffered formaldehyde, embedded in paraffin and further processed.

For iNOS detection, 4- μ m thick sections were deparaffinized and rehydrated, washed in tap water and distilled water and finally in 0.05 mol/L Tris buffer (pH 7.6). After blocking of nonspecific binding sites (Protein blocking agent, Ultratech, Coulter-Immunotech, Marseille, France), sections were washed and incubated with the primary polyclonal rabbit antibody (Transduction Laboratories, Biomol, Hamburg, Germany) with a dilution of 1:1 200 overnight at 4 °C. This antibody is directed against the mouse iNOS C-terminal peptide (1 131-1 144) plus additional N-terminated Cys conjugated to KLH (CKKGSALLEEPKATRL). According to the manufacturer, the antibody could recognize the human, mouse and rat iNOS 130 kDa protein without cross reaction to eNOS or nNOS. A biotinylated goat anti-rabbit antibody (Vectastain, ABC-AP Elite Kit, Vector Laboratories, Burlingame, USA) served as secondary antibody. After incubation with the avidine-biotin-complex with alkaline phosphatase, as described by the manufacturer, Fast Red chromogen system (Coulter Immunotech) was used for visualization.

For COX-2 immunohistochemistry, antigen retrieval was achieved by microwave treatment 3 times for 5 min with 600 watt in 0.01 mol/L citrate buffer pH 6.0. The monoclonal antibody COX-2 (h-62 sc-7951; Santa Cruz, Santa Cruz, CA USA) was used as primary antibody in a dilution of 1:50. According to the producer, this antibody reacts with COX-2 of mouse, rat and human origin with no cross reaction with Cox-1. For visualization, the envision kit (DAKO, Glostrup, Denmark) was used.

The results of MVD were retrieved from a previous study [18]. In brief, it was determined using a monoclonal mouse anti-CD34 antibody (Biogenex, San Ramon, Calif, USA). After the endogenous peroxidase was blocked with 30 mL/L hydrogen peroxide the staining procedure was automated including detection with DAB (Ventana, Strassbourg, France).

Nuclear counterstaining was done in all sections with hematoxyline. For every staining procedure sections were incubated without the primary antibody as negative controls. Tissues from colorectal cancer were used as positive controls for all three antibodies.

Evaluation

Semiquantitative analysis of the immunostainings for iNOS and COX-2 was performed for the whole tissue sections considering staining intensity and percentage of positive tumor cells. Using a light microscope (Aristoplan, Leitz, Wetzlar, Germany), in ten randomly selected tumor areas the amount of positive tumor cells and the amount of all tumor cells were determined using an ocular grid at 400 \times . A case without

positive tumor cells was considered negative. A case with less than 10% positive tumor cells was scored 1, 10-50% was scored 2, 50-80% was scored 3 and more than 80% was scored 4. The staining intensity was divided in weak (I), moderate (II) and strong (III). An immunoreactive score was calculated by multiplication of staining intensity with the amount of positive cells (lowest end score 0, highest end score 12). This evaluation was performed according to Remmele [19]. Specimens with a grade of more than 1 were regarded as positive.

Intratumoral MVD was measured as previously described [18]. In brief, stained sections were screened at 50 \times magnification to identify the highest vascular area within the tumor. In these hot spots, individual microvessel count was evaluated at 200 \times magnification using an ocular grid. Every cluster of cells stained with CD34 was counted as a vessel. Branching structures were counted as single vessels. Vascular counts for each case were calculated.

Statistics

Statistical analysis was performed with the Statistical Program for Social Science (SPSS, Chicago, Ill., USA). The Pearson's chi-square test and Fischer's exact test were used to examine the association with the clinicopathological parameters. Nonparametric correlation with Spearman's rho correlation coefficient was used to compare iNOS and COX-2 expressions as well as MVD. A *P*-value <0.05 was considered statistically significant.

RESULTS

iNOS

Positive iNOS immunostaining was detected in 21 (52.5%) of all 40 cases of pancreatic carcinoma. Immunoreactive tumor cells were both diffusely and focally distributed throughout the tumor. The immunoreaction was seen in the cytoplasm with completely unstained nuclei (Figure 1). Nine cases (22.5%) showed a mild staining intensity (grade I), 8 cases (20%) a moderate staining intensity (grade II) and 4 cases (10%) a strong staining intensity (grade III). One case (2.5%) expressed iNOS only focally in less than 10% of tumor cells. Eight cases (20%) showed immunoreaction in 10- 50% of tumor cells, 11 cases (27.5%) in 50-80% of positive tumor cells. In one case (2.5%) more than 80% of tumor cells were stained (Table 1).

There was no correlation with tumor stage (*P*=0.971), histological grade (*P*=0.591), location within the pancreas (*P*=0.184), lymph node metastases (*P*=0.652), age (*P*=0.651) or sex (*P*=0.546) of the patients. A relationship between iNOS expression and distant metastases was seen, but the low amount of cases with distant metastases did not allow statistical evaluation.

In the surrounding tissue the islets of Langerhans showed positive reaction in several cells. The original acini were negative. In the negative controls, immunoreactivity was completely lacking while the positive controls displayed a clear cut immunopositivity.

COX-2

Positive COX-2 staining was seen in 15 out of the 41 (37.5%) pancreatic carcinomas. The immunoreactivity here was also focally distributed throughout the tumor with cytoplasmic reaction only. Nuclear staining was not observed (Figure 2). The staining intensity in the positive cases differed. Among them, 5 cases (12.5%) were slightly stained (grade I), 4 cases (10%) were moderately stained (grade II) and 6 cases (15%) were intensely stained (grade III). The amount of positive cells was as follows: 3 cases (7.5%) with less than 10% positive tumor cells, 7 cases (17.5%) with 10-50% positive tumor cells, 4 cases (10%) with 50-80% positive tumor cells and 1 case with more than 80% (2.5%) positive tumor cells (Table 1).

Table 1 Comparison between expression of iNOS and COX-2 and clinicopathological features in pancreatic adenocarcinomas (n=40)

Variables	No. of patients (%)	iNOS positive	iNOS negative	P value	COX-2 positive	COX-2 negative	P value
Tumor stage							
I	5 (12.5)	1	4	0.971	1	4	0.983
II	27 (67.5)	15	12		11	16	
III	7 (17.5)	4	3		3	4	
IV	1 (2.5)	1	0		0	1	
Nodal stage							
n=0	17 (42.5)	10	7	0.652	6	11	0.945
n=1	23 (57.5)	11	12		9	14	
Distant metastases							
M0	35 (87.5)	18	17	0.043	13	22	0.459
M1	5 (12.5)	3	2		2	3	
Grade							
G1	3 (7.5)	2	1	0.591	1	2	0.000
G2	15 (37.5)	10	5		6	9	
G3	22 (55)	9	13		8	14	
MVD		5.7 (+/-2.4)	6.4 (+/-2.9)		6.4 (+/-3)	5.8 (+/- 2.4)	

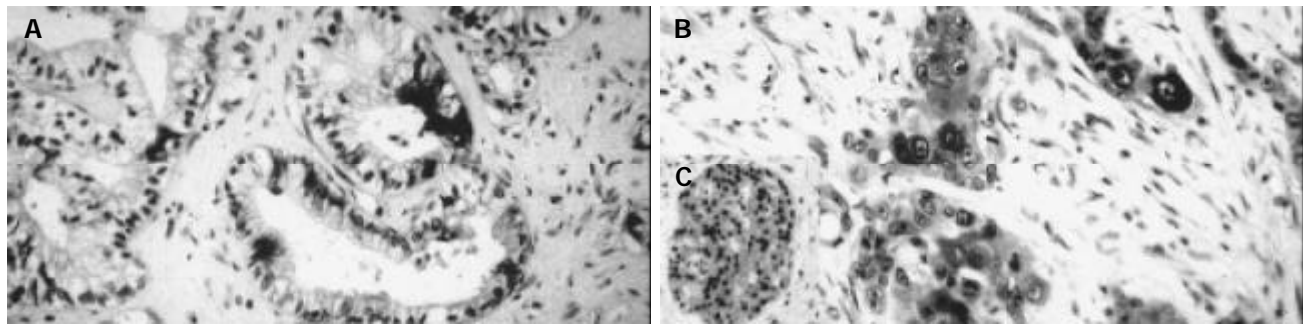


Figure 1 Immunohistochemical demonstration of iNOS expression in cases of pancreatic adenocarcinomas with moderate (A) and strong (B) staining intensity. There was a cytoplasmatic staining pattern with distribution within the tumor. No nuclear staining was observed. Cells of the islets of Langerhans were also positive (C). Original magnification $\times 200$, Hematoxylin counterstaining.

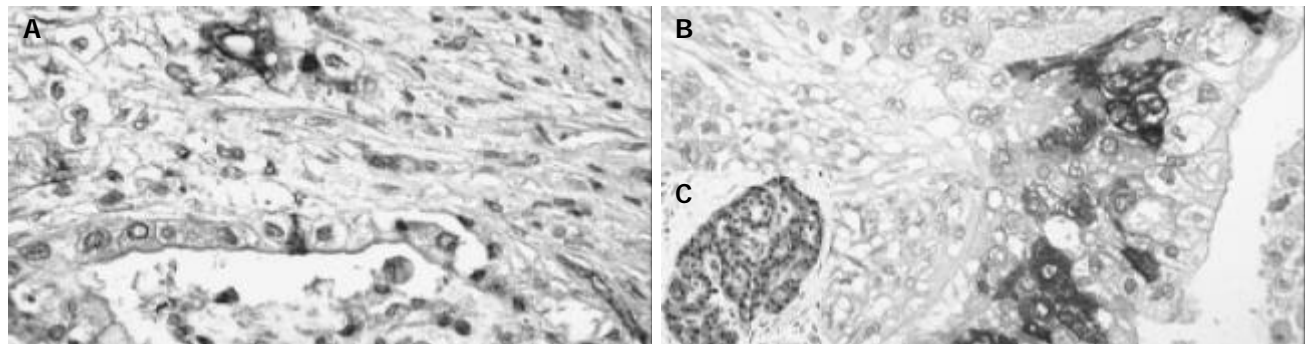


Figure 2 COX-2 immunohistochemistry in pancreatic adenocarcinomas shown in a case with (A) moderate and (B) strong staining intensity. Immunostaining was restricted to the cytoplasm. Even in the case with high staining only a portion of tumor cells expressed COX-2. Cells of the islets of Langerhans were also stained (C). Original magnification $\times 200$, Hematoxylin counterstaining.

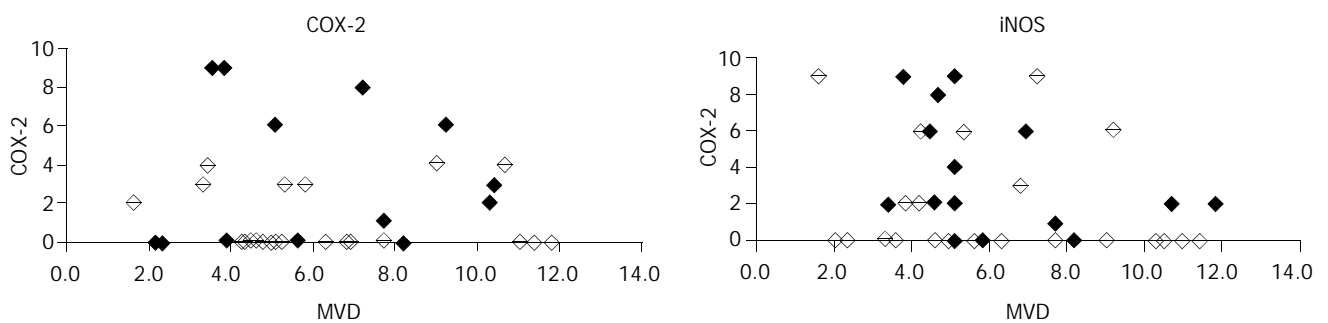


Figure 3 Comparison of iNOS or COX-2 expression with microvessel density. No statistically significant correlation could be noted.

Comparing the immunoreactive score of COX-2 expression with histological grade, a significant relationship could be seen. The more malignant tumors (grade 3) showed a higher COX-2 expression ($P=0.000$). This association depended stronger on the amount of positive cells ($P=0.000$). Considering staining intensity alone, no relationship was seen ($P=0.118$). The carcinomas in the head of the pancreas showed more often COX-2 expression than in other locations ($P=0.006$).

COX-2 did not correlate with tumor stage ($P=0.983$), lymph node ($P=0.945$) or distance metastases ($P=0.459$), age ($P=0.369$) or sex ($P=0.331$) of the patients.

In the surrounding tissue, the islets of Langerhans had positive reaction in several cells. The original acini were negative. In the negative control, immunoreactivity was completely lacking while the positive control displayed a clear cut immunopositivity.

MVD

The mean MVD in pancreatic carcinoma was 6.08 vessels per mm^2 (range 1.6 to 11.8 vessels per mm^2 , standard derivation of 2.67 vessels per mm^2 , median value of 5.25 vessels per mm^2).

MVD analysis demonstrated a significant relationship to the age groups (younger or older than 60 years) with higher MVD in the older patients ($P=0.024$). There was no statistically significant trend regarding the histological grade with more malignant carcinomas (grade 3) having higher MVD ($P=0.056$).

MVD had no association with tumor stage ($P=0.154$), location within the pancreas ($P=0.678$), lymph node ($P=0.325$) or distance metastases ($P=0.137$) or sex ($P=1.000$) of the patients.

Correlation between iNOS, COX-2 and MVD

There was no statistically significant correlation between INOS and COX-2 expression in pancreatic adenocarcinomas ($P=0.137$, Figure 3). MVD did neither depend on iNOS expression ($P=0.160$) nor COX-2 expression ($P=0.989$). Considering only COX-2 positive cases, no correlation of COX-2 with MVD could be found ($P=0.459$). Also, considering iNOS positive cases alone, there was no relationship between iNOS expression and MVD ($P=0.436$) noticeable.

DISCUSSION

Folkman *et al.* suggested that the step from prevascular to vascular phase was the prerequisite for the growth and spread of many solid tumors^[20]. Thus, angiogenesis contributes significantly to the progression of carcinomas. Intratumoral microvessel density is believed to reflect the overall degree of tumor angiogenesis. It has been accepted as an independent prognostic factor for several types of tumors like breast cancer, colon cancer or lung adenocarcinomas^[21-23]. For pancreatic carcinoma, we could not find a correlation with parameters linked to survival^[18].

Both COX-2 and iNOS, were play- markers of tumor angiogenesis^[24]. Hypoxia induces iNOS together with erythropoietin, the molecule leading to erythropoiesis and improvement of oxygen supply. COX-1 could regulate angiogenesis in endothelial cells, whereas COX-2 could regulate the production of nearly all angiogenetic factors in cancer cells^[24].

We could show that iNOS was inconstantly expressed in pancreatic adenocarcinomas. This is in concordance with other studies^[25,26]. INOS expression has been observed also in other carcinomas such as urothelial carcinomas^[27], gynecological cancers^[28], breast carcinomas^[29], colon cancers^[14], and lung tumors^[30].

The role of iNOS in cancerogenesis is still not clear. NO, the product of NOS, has several properties in addition to angiogenesis, which might enhance tumor growth. NO has been

found to be a mediator of angiogenesis and blood flow^[31]. Also, high concentrations of NO could lead to apoptosis, low concentrations might protect many cells from cell death^[32-34]. It could be shown that NO induces a G1-arrest followed by apoptosis in pancreatic carcinoma cell lines^[35].

Multiple lines of evidence suggest that COX-2 is important in carcinogenesis. For example, COX-2 was upregulated in various forms of cancers^[36]. A null mutation for COX-2 caused marked reduction in intestinal polyposis in a murine model of familial adenomatous polyposis^[37]. Newly developed selective inhibitors of COX-2 were reported to protect against gastrointestinal tumor formation.

We found COX-2 expression in 15 out of 40 cancer cases. This is slightly lower than that reported in the literature, which was up to 74% by using different methods including Northern and Western blot as well as immunohistochemistry^[38-40]. Okami reported a weak staining in most of the investigated carcinoma specimens^[41]. COX-2 staining in pancreatic carcinoma was very heterogeneous and there were great variations between specimens.

For pancreatic carcinoma, Koshiba *et al.* suggested that COX-2 might be associated with the degree of malignancy comparing intraductal papillary mucinous adenomas, intraductal papillary carcinomas and intraductal carcinomas^[42]. We and others could show that in the group of carcinomas the expression of COX-2 depended on the histological grading, and higher malignant tumors showed more enhanced COX-2 expression. A dependence of histological grade was also described by Nijijima^[43]. With a higher expression in more malignant tumors COX-2 seems to be a late or bystander effect. In our cohort, we could not prove a positive or negative correlation of COX-2 expression with MVD.

In chronic pancreatitis COX-2 overexpression was also recently observed^[44]. The enzyme was found in atrophic acinar cells, hyperplastic ductal cells and islets cells. As chronic pancreatitis is a risk factor for pancreatic cancer, this opens whether COX-2 is involved in the tumorigenesis via chronic inflammation. Apart from positive islets cells, we could not see any COX-2 expression in normal tissues, especially in the surrounding tissue of the tumor. If COX-2 is constantly expressed in chronic inflammation of pancreas one would expect enzyme induction also in the inflamed peritumoral region. Other reports mentioning the nonneoplastic tissue also found no COX-2 expression. It seems therefore unlikely that this enzyme is involved in early tumor development via inflammation.

In summary, approximately half of pancreatic adenocarcinomas express iNOS and COX-2. Both enzymes are heterogeneously distributed in the tumors without any correlation to each other nor to MVD. COX-2 is a phenomenon of higher malignant tumors. Both enzymes do not appear to be a key step in the angiogenesis of pancreatic adenocarcinomas.

ACKNOWLEDGMENTS

The excellent technical assistance by K. Petmecki, the help in editing the manuscript by Y. A. Weidemann and the statistical support by H. Christ are gratefully acknowledged.

REFERENCES

- 1 **Devesa SS**, Blot WJ, Miller BA, Tarone RE, Fraumeni JF Jr. Recent cancer trends in the united states. *J Natl Cancer Inst* 1995; **87**: 175-182
- 2 **Bundesamt S**. Statistical year book for the Federal Republic of Germany. *Metzler Poeschel Stuttgart* 1996: 430-433
- 3 **Yeo TP**, Hruban RH, Leach SD, Wilentz RE, Sohn TA, Kern SE, Iacobuzio-Donahue CA, Maitra A, Goggins M, Canto MI, Abrams RA, Laheru D, Jaffee EM, Hidalgo M, Yeo CJ. Pancreatic cancer.

- Curr Probl Cancer* 2002; **26**: 176-275
- 4 **Yeo CJ**, Abrams RA, Grochow LB, Sohn TA, Ord SE, Hruban RH, Zahurak ML, Dooley WC, Coleman J, Sauter PK, Pitt HA, Lillemoe KD, Cameron JL. Pancreaticoduodenectomy for pancreatic adenocarcinoma: Postoperative adjuvant chemoradiation improves survival. A prospective, single-institution experience. *Ann Surg* 1997; **225**: 621-633
 - 5 **Bardeesy N**, DePinho RA. Pancreatic cancer biology and genetics. *Nat Rev Cancer* 2002; **2**: 897-909
 - 6 **Sohn TA**. The molecular genetics of pancreatic ductal carcinoma. *Minerva Chir* 2002; **57**: 561-574
 - 7 **Farrow B**, Evers BM. Inflammation and the development of pancreatic cancer. *Surg Oncol* 2002; **10**: 153-169
 - 8 **Hall Pde L**, Wilentz RE, de Klerk W, Bornman PP. Premalignant conditions of the pancreas. *Pathology* 2002; **34**: 504-517
 - 9 **Knowles RG**, Moncada S. Nitric oxide synthases in mammals. *Biochem J* 1994; **298**(Pt2): 249-258
 - 10 **Moncada S**, Higgs A. The L-arginine-nitric oxide pathway. *N Engl J Med* 1993; **329**: 2002-2012
 - 11 **Forstermann U**, Kleinert H. Nitric oxide synthase: expression and expressional control of the three isoforms. *Naunyn Schmiedebergs Arch Pharmacol* 1995; **352**: 351-364
 - 12 **Kroncke KD**, Fehsel K, Kolb-Bachofen V. Nitric oxide: cytotoxicity versus cytoprotection—how, why, when, and where? *Nitric Oxide* 1997; **1**: 107-120
 - 13 **Amb S**, Ogunfusika MO, Merriam WG, Bennett WP, Billiar TR, Harris CC. Up-regulation of inducible nitric oxide synthase expression in cancer-prone p53 knockout mice. *Proc Natl Acad Sci U S A* 1998; **95**: 8823-8828
 - 14 **Amb S**, Merriam WG, Bennett WP, Felley-Bosco E, Ogunfusika MO, Oser SM, Klein S, Shields PG, Billiar TR, Harris CC. Frequent nitric oxide synthase-2 expression in human colon adenomas: implication for tumor angiogenesis and colon cancer progression. *Cancer Res* 1998; **58**: 334-341
 - 15 **Williams CS**, Mann M, DuBois RN. The role of cyclooxygenases in inflammation, cancer, and development. *Oncogene* 1999; **18**: 7908-7916
 - 16 **Smith WL**, Garavito RM, DeWitt DL. Prostaglandin endoperoxide H synthases (cyclooxygenases)-1 and -2. *J Biol Chem* 1996; **271**: 33157-33160
 - 17 **Lin DT**, Subbaramaiah K, Shah JP, Dannenberg AJ, Boyle JO. Cyclooxygenase-2: a novel molecular target for the prevention and treatment of head and neck cancer. *Head Neck* 2002; **24**: 792-799
 - 18 **Kasper HU**, Ebert M, Malfertheiner P, Roessner A, Kirkpatrick CJ, Wolf HK. Expression of thrombospondin-1 in pancreatic carcinoma: correlation with microvessel density. *Virchows Arch* 2001; **438**: 116-120
 - 19 **Remmele W**, Stegner HE. Recommendation for uniform definition of an immunoreactive score (IRS) for immunohistochemical estrogen receptor detection (ER-ICA) in breast cancer tissue. *Pathology* 1987; **8**: 138-140
 - 20 **Folkman J**. What is the evidence that tumors are angiogenesis dependent? *J Natl Cancer Inst* 1990; **82**: 4-6
 - 21 **Tarta C**, Teixeira CR, Tanaka S, Haruma K, Chiele-Neto C, da Silva VD. Angiogenesis in advanced colorectal adenocarcinoma with special reference to tumoral invasion. *Arq Gastroenterol* 2002; **39**: 32-38
 - 22 **Sauer G**, Deissler H. Angiogenesis: prognostic and therapeutic implications in gynecologic and breast malignancies. *Curr Opin Obstet Gynecol* 2003; **15**: 45-49
 - 23 **Meert AP**, Paesmans M, Martin B, Delmotte P, Berghmans T, Verdebout JM, Lafitte JJ, Mascaux C, Sculier JP. The role of microvessel density on the survival of patients with lung cancer: a systematic review of the literature with meta-analysis. *Br J Cancer* 2002; **87**: 694-701
 - 24 **Chiarugi V**, Magnelli L, Gallo O. Cox-2, iNOS and p53 as play-makers of tumor angiogenesis (review). *Int J Mol Med* 1998; **2**: 715-719
 - 25 **Kong G**, Kim E, Kim W, Lee Y, Lee J, Paik S, Rhee J, Choi K, Lee K. Inducible nitric oxide synthase (iNOS) immunoreactivity and its relationship to cell proliferation, apoptosis, angiogenesis, clinicopathologic characteristics, and patient survival in pancreatic cancer. *Int J Gastrointest Cancer* 2001; **29**: 133-140
 - 26 **Kong G**, Kim EK, Kim WS, Lee KT, Lee YW, Lee JK, Paik SW, Rhee JC. Role of cyclooxygenase-2 and inducible nitric oxide synthase in pancreatic cancer. *J Gastroenterol Hepatol* 2002; **17**: 914-921
 - 27 **Wolf H**, Haeckel C, Roessner A. Inducible nitric oxide synthase expression in human urinary bladder cancer. *Virchows Arch* 2000; **437**: 662-666
 - 28 **Thomsen LL**, Lawton FG, Knowles RG, Beesley JE, Riveros-Moreno V, Moncada S. Nitric oxide synthase activity in human gynecological cancer. *Cancer Res* 1994; **54**: 1352-1354
 - 29 **De Paepe B**, Verstraeten VM, De Potter CR, Bullock GR. Increased angiotensin II type-2 receptor density in hyperplasia, DCIS and invasive carcinoma of the breast is paralleled with increased iNOS expression. *Histochem Cell Biol* 2002; **117**: 13-19
 - 30 **Amb S**, Bennett WP, Merriam WG, Ogunfusika MO, Oser SM, Khan MA, Jones RT, Harris CC. Vascular endothelial growth factor and nitric oxide synthase expression in human lung cancer and the relation to p53. *Br J Cancer* 1998; **78**: 233-239
 - 31 **Jenkins DC**, Charles IG, Thomsen LL, Moss DW, Holmes LS, Baylis SA, Rhodes P, Westmore K, Emson PC, Moncada S. Roles of nitric oxide in tumor growth. *Proc Natl Acad Sci U S A* 1995; **92**: 4392-4396
 - 32 **Nicotera P**, Ankracrona M, Bonfoco E, Orrenius S, Lipton SA. Neuronal necrosis and apoptosis: two distinct events induced by exposure to glutamate or oxidative stress. *Adv Neurol* 1997; **72**: 95-101
 - 33 **Dimmeler S**, Rippmann V, Weiland U, Haendeler J, Zeiher AM. Angiotensin II induces apoptosis of human endothelial cells. Protective effect of nitric oxide. *Circ Res* 1997; **81**: 970-976
 - 34 **Tzeng E**, Kim YM, Pitt BR, Lizonova A, Kovsesi I, Billiar TR. Adenoviral transfer of the inducible nitric oxide synthase gene blocks endothelial cell apoptosis. *Surgery* 1997; **122**: 255-263
 - 35 **Gansauge S**, Nussler AK, Beger HG, Gansauge F. Nitric oxide-induced apoptosis in human pancreatic carcinoma cell lines is associated with a G1-arrest and an increase of the cyclin-dependent kinase inhibitor p21WAF1/CIP1. *Cell Growth Differ* 1998; **9**: 611-617
 - 36 **Ricchi P**, Zarrilli R, Di Palma A, Acquaviva AM. Nonsteroidal anti-inflammatory drugs in colorectal cancer: from prevention to therapy. *Br J Cancer* 2003; **88**: 803-807
 - 37 **Oshima M**, Dinchuk JE, Kargman SL, Oshima H, Hancock B, Kwong E, Trzaskos JM, Evans JF, Taketo MM. Suppression of intestinal polyposis in Apc delta716 knockout mice by inhibition of cyclooxygenase 2 (COX-2). *Cell* 1996; **87**: 803-809
 - 38 **Molina MA**, Sitja-Arnau M, Lemoine MG, Frazier ML, Sinicrope FA. Increased cyclooxygenase-2 expression in human pancreatic carcinomas and cell lines: growth inhibition by nonsteroidal anti-inflammatory drugs. *Cancer Res* 1999; **59**: 4356-4362
 - 39 **Yip-Schneider MT**, Barnard DS, Billings SD, Cheng L, Heilman DK, Lin A, Marshall SJ, Crowell PL, Marshall MS, Sweeney CJ. Cyclooxygenase-2 expression in human pancreatic adenocarcinomas. *Carcinogenesis* 2000; **21**: 139-146
 - 40 **Kokawa A**, Kondo H, Gotoda T, Ono H, Saito D, Nakadaira S, Kosuge T, Yoshida S. Increased expression of cyclooxygenase-2 in human pancreatic neoplasms and potential for chemoprevention by cyclooxygenase inhibitors. *Cancer* 2001; **91**: 333-338
 - 41 **Okami J**, Yamamoto H, Fujiwara Y, Tsujie M, Kondo M, Noura S, Oshima S, Nagano H, Dono K, Umeshita K, Ishikawa O, Sakon M, Matsuura N, Nakamori S, Monden M. Overexpression of cyclooxygenase-2 in carcinoma of the pancreas. *Clin Cancer Res* 1999; **5**: 2018-2024
 - 42 **Koshiha T**, Hosotani R, Miyamoto Y, Wada M, Lee JU, Fujimoto K, Tsuji S, Nakajima S, Doi R, Imamura M. Immunohistochemical analysis of cyclooxygenase-2 expression in pancreatic tumors. *Int J Pancreatol* 1999; **26**: 69-76
 - 43 **Niijima M**, Yamaguchi T, Ishihara T, Hara T, Kato K, Kondo F, Saisho H. Immunohistochemical analysis and in situ hybridization of cyclooxygenase-2 expression in intraductal papillary-mucinous tumors of the pancreas. *Cancer* 2002; **94**: 1565-1573
 - 44 **Schlosser W**, Schlosser S, Ramadani M, Gansauge F, Gansauge S, Beger HG. Cyclooxygenase-2 is overexpressed in chronic pancreatitis. *Pancreas* 2002; **25**: 26-30

Increased hepatic expression of nitric oxide synthase type II in cirrhotic rats

Hai Wang, Xiao-Ping Chen, Fa-Zu Qiu

Hai Wang, Xiao-Ping Chen, Fa-Zu Qiu, Liver Center of Tongji Hospital, Tongji Medical College, Huazhong University of Science and Technology, Wuhan 430030, Hubei Province, China

Supported by the Clinical Focal Point Subject Foundation of Ministry of Public Health, No. (2001)321

Correspondence to: Dr. Xiao-Ping Chen, Hepatic Surgery Center of Tongji Hospital, Tongji Medical College, Huazhong University of Science and Technology, Wuhan 430030, Hubei Province, China. chenxp53@sina.com

Telephone: +86-27-83662599 **Fax:** +86-27-83662851

Received: 2002-10-09 **Accepted:** 2002-12-30

Abstract

AIM: To determine the role and effect of nitric oxide synthase type II (NOSII) in cirrhotic rats.

METHODS: Expression of NOSII mRNA was detected by real time RT-PCR. The activity of nitric oxide synthase and serum levels of NO, systemic and portal hemodynamics and degrees of cirrhosis were measured with high sensitive methods. Chinese traditional medicine tetrandrine was used to treat cirrhotic rats and to evaluate the function of NO. Double-blind method was applied during the experiment.

RESULTS: The concentration of NO and the activity of NOS were increased markedly at all stages of cirrhosis, and iNOSmRNA was greatly expressed. Meanwhile the portal-venous-pressure (PVP), and portal-venous-flow (PVF) were significantly increased. NO, NOS and iNOSmRNA were positively correlated to the quantity of hepatic fibrosis. Tetrandrine significantly inhibited NO production and the expression of iNOSmRNA.

CONCLUSION: Increased hepatic expression of NOSII is one of the important causes of hepatic cirrhosis and portal hypertension.

Wang H, Chen XP, Qiu FZ. Increased hepatic expression of nitric oxide synthase type II in cirrhotic rats. *World J Gastroenterol* 2004; 10(13): 1923-1927

<http://www.wjgnet.com/1007-9327/10/1923.asp>

INTRODUCTION

Nitric oxide (NO) is a vasodilator formerly detected in vascular system, but is currently recognized as a multifunctional molecule widely distributed in many other tissues, such as immune and neuronal systems. NO is synthesized from L-arginine by the NO synthase isozyme family of which three different members have been characterized, namely NOSI, NOSII and NOSIII. NOSI and NOSIII are constitutive and Ca²⁺/calmodulin-independent. The first was initially discovered in neurons and the second in endothelial cells^[1-2]. NOSII is Ca²⁺-independent, and is located in macrophages and smooth muscle cells, and is induced by appropriate proinflammatory stimuli and bacterial lipopolysaccharides^[3]. Its activity can be competitively inhibited

by several L-arginine analogues such as N^w-nitro-L-arginine.

However, proinflammatory cytokines, endotoxins, and bacterial infections in various pathologic entities are associated with enhanced production of NO, hyporesponsiveness to vasoconstrictors, and development of a hyperdynamic state^[4-7]. Vallance and Moncada hypothesized that bacterial endotoxin might account for hemodynamic changes in severe cirrhosis by stimulating the expression of inducible NO synthase (iNOS) to produce NO^[8].

Recently, numerous studies have focused on NO as a possible major causative agent of the decreased vascular resistance in cirrhosis. In fact, most investigations are coincident in reporting an increased NO activity in the vasculature of patients and rats with cirrhosis^[9-12], a phenomenon in which both NOSII and NOSIII seem to be involved^[13]. There is, however, little information on the progress in liver diseases affecting the L-arginine/NO pathway in organs other than the systemic vasculature. This is particularly intriguing in the liver, as it largely affects the consequence of the derangement under pathologic conditions. Whereas most investigations consider NO as an important mediator of hemodynamic alterations in experimental cirrhosis^[14].

Chinese traditional medicine tetrandrine has the function of inhibiting calcium influx^[15,16], and effect in treatment of liver fibrosis^[17]. We postulated that if NO was a key mediator in cirrhosis and portal hypertension, Tetrandrine would affect the level of NO by inhibiting the expression of NOSmRNA and the activity of NOS. Therefore, in this study, mRNAs of NOSII and NOSIII were determined in liver tissue of rats with CCL₄-induced cirrhosis to assess the level of NO. In addition, the NOS activity of liver tissue and the serum levels of NO, hemodynamic changes of portal vein and pathologic changes at all stages of cirrhosis were also investigated.

MATERIALS AND METHODS

Induction of cirrhosis in rats

Hepatic injury and fibrosis were induced in male retired breeder Sprague-Dawley rats (450-550 g) by intragastric administration of carbon tetrachloride as described previously^[18]. CCL₄ (1.0 mL/kg) in a 1:1 mixture with corn oil was administered by gavage at 7-day intervals. After the second intragastric administration of carbon tetrachloride, Tetrandrine group inhaled the suspension of Tetrandrine (1 mL/0.1 kg). Animal weight was monitored, and the dosage of CCL₄ and Tetrandrine was adjusted accordingly. Portal hypertension (portal venous dilation with portal pressure >10 cm H₂O) was documented in all animals after 10 doses of CCL₄. Controls received corn oil on the same schedule as experimental animals.

In vivo effects of tetrandrine administration

There were 90 conscious rats in this study. Animals were anesthetized with ketamine (100 mg/kg.bm) and prepared with P-50 catheters in portal vein and inferior vena cava. The catheter was connected to a highly sensitive transducer and a multichannel recorder (MX4P and MT4, Lectromed Ltd, Jersey, Channels Islands, UK) and portal venous pressure and portal venous

flow were recorded. Then, a 2-mL blood sample was taken to measure NO. Blood was immediately centrifuged at 4 °C and serum was frozen at -20 °C until further analysis. Tissue specimens were obtained from the middle liver lobe in each animal. Liver specimens were fixed in 40 g/L buffered formaldehyde and stained with hematoxylin and eosin, reticulin, and Masson's trichrome for histological examination. Moreover, additional liver tissues were immediately frozen in dry ice and stored in liquid nitrogen until further analysis. Serum NO and liver NOS activity were determined.

Expression of inducible and constitutive NOS mRNA

mRNAs of NOSII and NOSIII were assessed in liver tissues of all groups. Under anesthesia with ketamine (100 mg/kg) animals were exsanguinated by cardiac puncture. Liver tissue was dissected, placed in a Petri dish containing a diethyl pyrocarbonate (0.01%) -treated PBS buffer solution, total RNA was extracted by the guanidine isothiocyanate method^[19].

NOSII and NOSIII mRNA expression was assessed by real-Time RT-PCR

Reverse transcription (RT) reaction was performed with cDNA synthesis kit (Promega, Madison, WI) and followed the attached protocol with reaction kit. The final volume of the reaction (20 µL) was completed with RNase free water. First strand cDNA synthesis was carried out at 42 °C for 30 min in a DNA thermal cycler (PTC-100, MJ Reserch Inc, Watertown, MA). Afterwards, the tubes were incubated at 99 °C for 5 min to terminate the reaction. Then each tube was kept at 4 °C until PCR was performed.

Real-time RT-PCR

Expression of the target genes (NOSII and NOSIII) was quantified. The primers were designed using the software Primer Express (Applied Biosystems) (Table 1).

RT-PCR was performed according to a TaqMan 2-step method using an ABI PRISM 7 700 sequence detection system (Applied Biosystems). PCR cycling conditions included an initial phase at 50 °C for 2 min, followed by at 95 °C for 10 min for AmpErase, 40 cycles at 95 °C for 15 s, and at 60 °C for 1 min. Quantification of the PCR products was based on the TaqMan 5' nuclease assay using the ABI PRISM 7 700 sequence detection system. The starting amount of a specific mRNA in an unknown sample was determined. The standard curve was generated on the basis of the linear relationship between the Ct value and logarithm of the starting quantity. Ct value was the cycle number at which a significant increase in the fluorescence signal was initially detected. The unknown samples were quantified by the software of the ABI PRISM 7 700 sequence detector system, which calculated the Ct value for each sample and then determined the initial amount of the target using the standard curve. The amount of the target was normalized to the reference.

Table 1 Oligonucleotides used for PCR

Gene	Quantification method	Primer sequence	cDNA
NOSII	Forward primer	5'-CCCTCCGAAGTTTCTGGCAGCAG-3'	2 793-2 817
	Reverse primer	5'-GGGCTCCTCCAAGGTGTTGCC-3'	3 424-3 446
	Probe	5'-(FAM)TCTTCGGTGCGGTCTTTTCCTATGGAGCAA(TAMRA)-3'	3 391-3 421
NOSIII	Forward primer	5'-CAAGACCGATTACACGACAT-3'	31-51
	Reverse primer	5'-GCTGGTTGCCATAGTGACAT-3'	300-321
	Probe	5'-(FAM)GAGTGTTGGACAAGTCCTCACCGCCTTTT-(TAMRA)-3'	158-188
GAPDH	Forward primer	5'-GAAGGTGAAGTCCGAGTCA-3'	
	Reverse primer	5'-GAAGATGGTGATGGGA-3'	
	Probe	5'-(JOE)CAAGCTTCCCGTCTCAGCC(TAMRA)-3'	

Statistical analysis

One-way ANOVA, Newman-Keuls's, and unpaired Student's *t* tests were used for statistical analysis. Data are expressed as mean±SE, *P* level at 0.05 or less was considered statistically significant.

RESULTS

The cirrhotic liver treated with CCL₄ had a finely granulated surface. Histological examination showed the distinct features of three-grade fibrosis. Tetrandrine group had slight fibrosis in the third grade of cirrhosis.

Pathologic examination

Pathologic examination indicated that tetrandrine had an obvious effect on preventing the necrosis of hepatic cells and delaying the development of hepatic fibrosis (Figure 1).

Serum NO and NOS activity of liver tissue

Serum NO and NOS activity in cirrhotic group were significantly higher than those in normal control, and had no difference between the normal and therapeutic groups (Tables 2, 3).

Table 2 Effects of tetrandrine and on serum NO in cirrhotic rats (µmol/L, mean±SD)

Grade	Tetrandrine (n=8)	Cirrhosis (n=8)	Negative control (n=8)
Earlier period	6.51±0.56 ^b	10.27±0.71	5.91±0.67
Metaphase	6.87±0.78 ^b	10.88±0.82	6.04±0.98
Late period	6.49±0.83 ^b	6.35±1.48 ^b	6.17±0.73

^b*P*<0.01 vs cirrhosis.

Table 3 Effects of Tetrandrine on NOS activity in cirrhotic rats (mol/min·g, mean±SD)

Grade	Tetrandrine (n=8)	Cirrhosis (n=8)	Negative control (n=8)
Earlier period	0.5165±1455 ^a	1.6916±0.8099	0.4275±0.2037
Metaphase	0.6901±0.2092 ^a	1.9756±0.7833	0.5639±0.4275
Late period	0.8483±0.2393 ^a	1.9789±0.7690	0.6723±0.5784

^a*P*<0.05 vs cirrhosis.

Hemodynamics

High hemodynamics was observed in cirrhotic rats. Portal-venous-pressure (PVP) and portal-venous-flow (PVF) were significantly increased. But PVP in tetrandrine groups was significantly decreased in all stages of cirrhosis. PVF was only decreased in the metaphase of cirrhosis (Table 4).

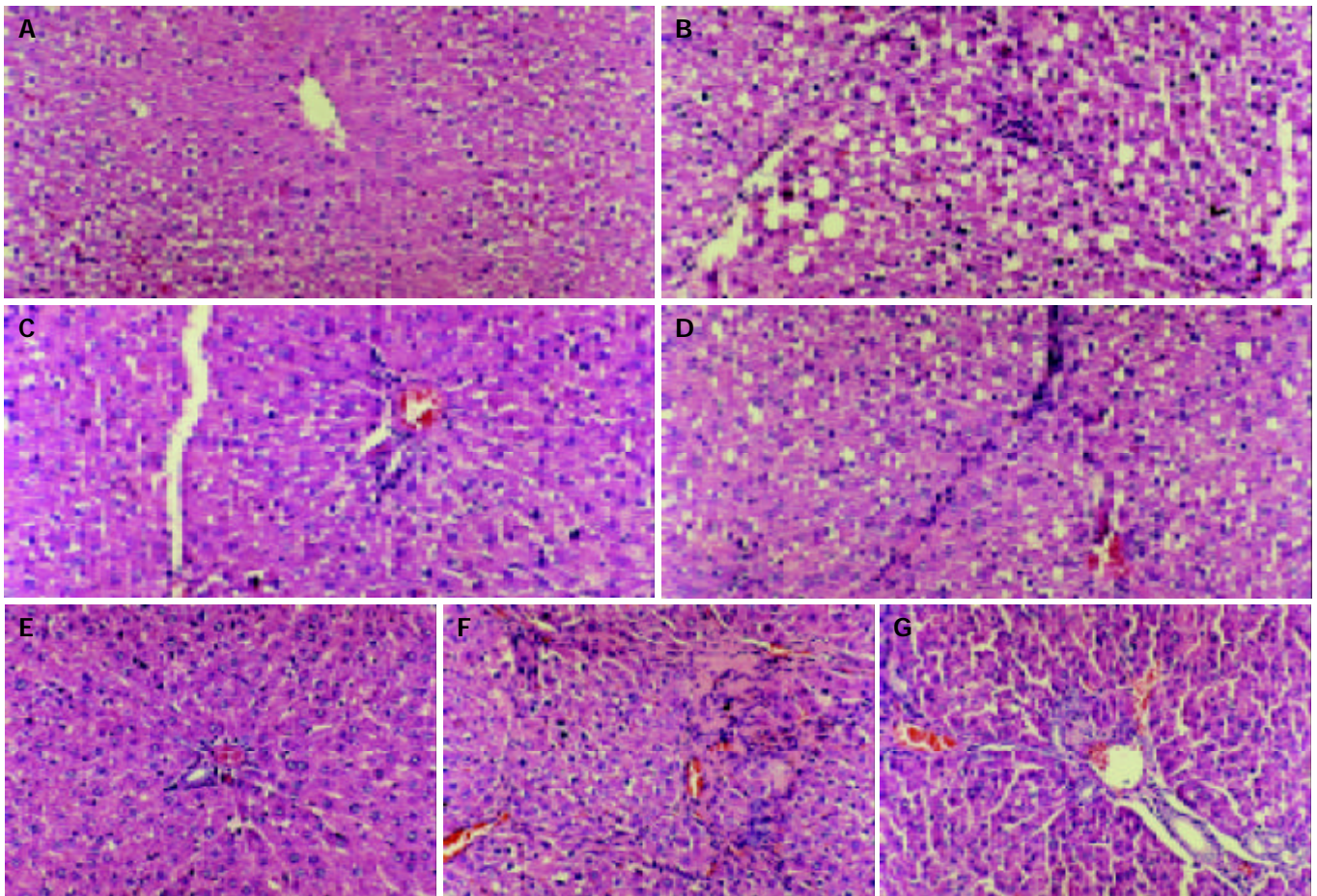


Figure 1 Histological images of three-grade fibrosis and tetrandrine treated group (200×). A: normal group, B: earlier cirrhosis group, C: earlier tetrandrine group, D: metaphase cirrhosis group, E: metaphase tetrandrine group, F: late cirrhosis group, G: late tetrandrine group.

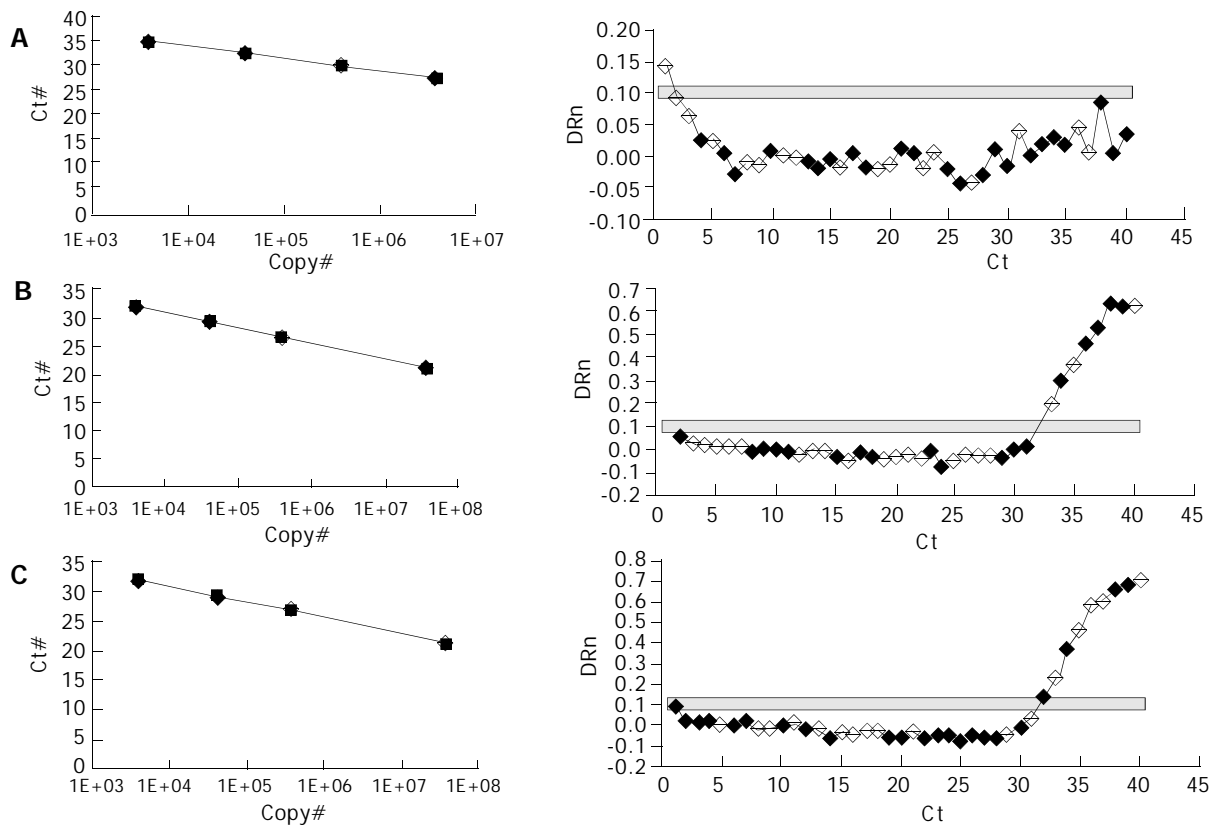


Figure 2 Real-time RT-PCR images: Expression of iNOS in normal hepatic tissue (A), Expression of iNOS in Tetrandrine therapeutic hepatic tissue (B), Expression of iNOS in cirrhotic tissue (C). NOSII was not expressed in normal rat tissue, but highly expressed in cirrhotic rat tissue and NOSII in therapeutic groups was significantly decreased than that in cirrhosis.

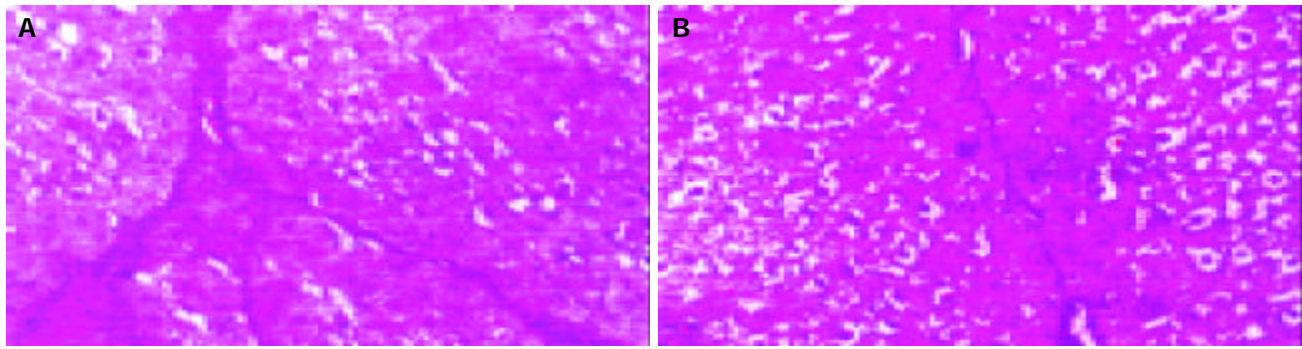


Figure 3 Quantification of cirrhosis: cirrhotic group (A), Tetrandrine group (B).

Table 4 Effects of tetrandrine on hemodynamics in cirrhotic rats (mean±SD)

Stage	Index	Tetrandrine (n=8)	Cirrhosis (n=8)	Negative control (n=8)
Earlier period	PVF	18.37±1.83	21.25±1.76	16.50±1.73
	PVP	1.35±0.25 ^b	1.67±0.21	1.18±0.13
	ICVP	0.31±0.04	0.32±0.04	0.31±0.04
	PVR	5.73±0.88	6.38±1.12	5.81±1.04
Metaphase	PVF	14.50±1.61 ^a	20.35±1.07	17.75±1.37
	PVP	1.44±0.13 ^b	1.72±0.69	1.30±0.21
	ICVP	0.32±0.04	0.31±0.04	0.32±0.04
	PVR	7.98±1.68	9.56±1.29	5.53±0.67
Late period	PVF	15.85±1.23	17.57±1.93	15.42±1.27
	PVP	1.45±0.24 ^b	1.67±0.23	1.37±0.10
	ICVP	0.31±0.04	0.32±0.04	0.32±0.04
	PVR	7.44±1.08	8.01±0.79	6.76±0.34

^a $P < 0.05$, ^b $P < 0.01$ vs cirrhosis.

Relationship between NO and hemodynamics

NO concentration correlated significantly with PVP ($r=0.69$, $P < 0.01$) and PVF ($r=0.72$, $P < 0.01$), but inversely with PVR ($r=-0.63$, $P < 0.01$).

Quantitative RT-PCR

Quantification of the PCR products showed that NOSII was highly expressed in cirrhotic rat tissue (Figure 2C), and NOSII in therapeutic groups was significantly decreased than cirrhosis (Figure 2B) ($P < 0.01$). NOSII was not found in normal rat tissue (Figure 2A). NOSIII expression was not different among all groups ($P > 0.05$) (Table 5).

Table 5 Quantification of PCR products

Stage	Index	Tetrandrine (n=8)	Cirrhosis (n=8)	Negative control (n=8)
Earlier period	NOSII	0.1723±0.0014	0.5635±0.0104	-
	NOSIII	0.2578±0.0076	0.2694±0.0043	0.2786±0.0107
Metaphase	NOSII	0.1679±0.0093	0.7521±0.0098	-
	NOSIII	0.3210±0.0084	0.3412±0.0113	0.2916±0.0089
Late period	NOSII	0.1876±0.0065	0.6987±0.0078	-
	NOSIII	0.2917±0.0102	0.3002±0.0091	0.2815±0.0098

Quantification of cirrhosis

Quantification of cirrhosis showed that cirrhosis significantly decreased in Tetrandrine group than in cirrhotic group (Figure 3).

DISCUSSION

The function of NO in human beings or experimental animals is

invariably associated with marked systemic and portal venous hemodynamic effects, including arterial hypotension, portal hypertension, increased portal venous perfusion. The intensity and full manifestation of this response depend on the expression of NOS and the NOS activity. To ascertain which isoforms of NOS displayed a differential effect on cirrhotic liver of rats, the expressions of NOSII and NOSIII were determined. The study showed that NOSII was markedly increased in cirrhotic rat liver tissues. However, we did not find the expression of NOSII in normal liver tissues. Because macrophages were of central importance in the initiation and regulation of nonspecific and specific immune responses^[20], it was considered that NO from these cells was implicated in the nonspecific defense against parasitic diseases and participated in the production of free radicals that are toxic to bacteria and parasites^[21]. Rodent macrophages were extremely sensitive to agents promoting NOSII expression^[22]. In this study, no difference in NOSIII expression between cirrhotic and normal rats was found. We postulated that NOSIII expression in cirrhotic liver had no effect on portal hypertension. But it might have a great function in cirrhosis due to its expression in big blood vessels^[23-25]. Intrahepatic endothelial NO mediated by shear stress-dependence seems impaired by shunt.

Chinese traditional medicine Tetrandrine had a good therapeutic effect for fibrosis^[16,17]. It is often used to treat hepatitis of HBV. In a recent study, it was tested to inhibit calcium influx. We therefore postulated that if NO played a role in the mechanism of cirrhosis and portal hypertension, Tetrandrine would have the effect on the inhibition of NO production. This study approved our hypothesis and showed NOSII mRNA was markedly expressed in cirrhotic liver tissues. NOSIII was mainly distributed in endothelial cells and its function was relied on calmodulin(CaM)^[26]. Tetrandrine affected NOSIII expression, however, had no effect on NOSIII expression. Thus, we reason the changes of NOSIII could be stimulated by shear stress. NOSII was mainly distributed in microphages and endothelial cells. NOSII did not express in normal physiological conditions. Amino acid sequence analysis showed that NOSII had the conjugated site of calmodulin, and rodent NOSII could be conjugated tightly with CaM without calcium^[27]. In this study, an important finding in cirrhotic liver exposed to Tetrandrine was an NO antagonist. Moreover, tetrandrine could also affect NOS enzymatic activity. The results of the present study indicated that portal-venous-pressure and portal-venous-flow decreased by tetrandrine were mediated by lower level NO and cirrhotic blood vessel.

In conclusion, NOSII is markedly expressed in cirrhotic liver, inducing a high hemodynamic change of portal vein and pathologic changes in all stages of cirrhosis. Tetrandrine inhibits NOSII expression, decreases NOS activity and reduces the NO production. The mechanism of fibrosis and portal hypertension is NO mediated, and tetrandrine is effective for improving portal hypertension by reducing NO in cirrhotic patients.

ACKNOWLEDGMENTS

The authors are acknowledged the skillful technical assistance of Dr. Bing-Quan Wu.

REFERENCES

- 1 **Bredt DS**, Hwang PM, Glatt CE, Lowenstein C, Reed RR, Snyder SH. Cloned and expressed nitric oxide synthase structurally resembles cytochrome P-450 reductase. *Nature* 1991; **351**: 714-718
- 2 **Lamas S**, Marsden PA, Li GK, Tempst P, Michel T. Endothelial nitric oxide synthase: molecular cloning and characterization of a distinct constitutive enzyme isoform. *Proc Natl Acad Sci U S A* 1992; **89**: 6348-6352
- 3 **Lowenstein CJ**, Glatt CS, Bredt DS, Snyder SH. Cloned and expressed macrophage nitric oxide synthase contrasts with the brain enzyme. *Proc Natl Acad Sci U S A* 1992; **89**: 6711-6715
- 4 **Guarner C**, Soriano G, Tomas A, Bulbena O, Novella MT, Balanzo J, Vilardell F, Mourelle M, Moncada S. Increased serum nitrite and nitrate levels in patients with cirrhosis: relationship to endotoxemia. *Hepatology* 1993; **18**: 1139-1143
- 5 **Lee FY**, Wang SS, Yang MC, Tsai YT, Wu SL, Lu RH, Chan CY, Lee SD. Role of endotoxaemia in hyperdynamic circulation in rats with extrahepatic or intrahepatic portal hypertension. *J Gastroenterol Hepatol* 1996; **11**: 152-158
- 6 **Lin RS**, Lee FY, Lee SD, Tsai YT, Lin HC, Lu RH, Hsu WC, Huang CC, Wang SS, Lo KJ. Endotoxemia in patients with chronic liver diseases: relationship to severity of liver diseases, presence of esophageal varices, and hyperdynamic circulation. *J Hepatol* 1995; **22**: 165-172
- 7 **Albillos A**, de la Hera A, Gonzalez M, Moya JL, Calleja JL, Monserrat J, Ruiz-del-Arbol L, Alvarez-Mon M. Increased lipopolysaccharide binding protein in cirrhotic patients with marked immune and hemodynamic derangement. *Hepatology* 2003; **37**: 208-217
- 8 **Vallance P**, Moncada S. Hyperdynamic circulation in cirrhosis: a role for nitric oxide? *Lancet* 1991; **337**: 776-778
- 9 **Claria J**, Jimenez W, Ros J, Asbert M, Castro A, Arroyo V, Rivera F, Rodes J. Pathogenesis of arterial hypotension in cirrhotic rats with ascites: role of endogenous nitric oxide. *Hepatology* 1992; **15**: 343-349
- 10 **Ros J**, Jimenez W, Lamas S, Claria J, Arroyo V, Rivera F, Rodes J. Nitric oxide production in arterial vessels of cirrhotic rats. *Hepatology* 1995; **21**: 554-560
- 11 **Sieber CC**, Lopez-Talavera JC, Groszmann RJ. Role of nitric oxide in the in vitro splanchnic vascular hyporeactivity in ascitic cirrhotic rats. *Gastroenterology* 1993; **104**: 1750-1754
- 12 **Morales-Ruiz M**, Jimenez W, Perez-Sala D, Ros J, Leivas A, Lamas S, Rivera F, Arroyo V. Increased nitric oxide synthase expression in arterial vessels of cirrhotic rats with ascites. *Hepatology* 1996; **24**: 1481-1486
- 13 **Martin PY**, Xu DL, Niederberger M, Weigert A, Tsai P, St John J, Gines P, Schrier RW. Upregulation of endothelial constitutive NOS: a major role in the increased NO production in cirrhotic rats. *Am J Physiol* 1996; **270**: F494-499
- 14 **Ros J**, Claria J, Jimenez W, Bosch-Marce M, Angeli P, Arroyo V, Rivera F, Rodes J. Role of nitric oxide and prostacyclin in the control of renal perfusion in experimental cirrhosis. *Hepatology* 1995; **22**: 915-920
- 15 **Liu YL**, Li DG, Lu HM, Xu QF. The control to 3T6 fibroblast from four calcium antagonist. *Beijing Yixue Zazhi* 1996; **18**: 26-29
- 16 **Wang BE**, Sun M, Bai N, Li XM, Yin WY, Wang TL. The therapeutic observation to experimental liver fibrosis of the active and decongestive Chinese Medicine. *Zhongcaoyao* 1990; **21**: 23
- 17 **Li DG**, Liu YL, Lu HM, Jiang ZM, Xu QF. The effects of tetrandrine to mitochondrion of cirrhotic rat. *Zhonghua Xiaohua Zazhi* 1994; **14**: 339-342
- 18 **Andiran F**, Kilinc K, Renda N, Ayhan A, Tanyel FC. Lipid peroxidation and extracellular matrix in normal and cirrhotic rat livers following 70% hepatectomy. *Hepatogastroenterology* 2003; **50**: 805-808
- 19 **Kimura B**, Kawasaki S, Nakano H, Fujii T. Rapid, quantitative PCR monitoring of growth of *Clostridium botulinum* type E in modified-atmosphere-packaged fish. *Appl Environ Microbiol* 2001; **67**: 206-216
- 20 **Kincaid EZ**, Ernst JD. Mycobacterium tuberculosis exerts gene-selective inhibition of transcriptional responses to IFN-gamma without inhibiting STAT1 function. *J Immunol* 2003; **171**: 2042-2049
- 21 **MacMicking J**, Xie QW, Nathan C. Nitric oxide and macrophage function. *Annu Rev Immunol* 1997; **15**: 323-350
- 22 **Lyons CR**, Orloff GJ, Cunningham JM. Molecular cloning and functional expression of an inducible nitric oxide synthase from a murine macrophage cell line. *J Biol Chem* 1992; **267**: 6370-6374
- 23 **Cahill PA**, Redmond EM, Hodges R, Zhang S, Sitzmann JV. Increased endothelial nitric oxide synthase activity in the hyperemic vessels of portal hypertensive rats. *J Hepatol* 1996; **25**: 370-378
- 24 **Gadano AC**, Sogni P, Yang S, Cailmail S, Moreau R, Nepveux P, Couturier D, Lebrec D. Endothelial calcium-calmodulin dependent nitric oxide synthase in the *in vitro* vascular hyporeactivity of portal hypertensive rats. *J Hepatol* 1997; **26**: 678-686
- 25 **Martin PY**, Xu DL, Niederberger M, Weigert A, Tsai P, St John J, Gines P, Schrier RW. Upregulation of endothelial constitutive NOS: a major role in the increased NO production in cirrhotic rats. *Am J Physiol* 1996; **270**(3 Pt 2): F494-F499
- 26 **Murthy KS**, Zhang KM, Jin JG, Grider JR, Makhlof GM. VIP-mediated G protein-coupled Ca²⁺ influx activates a constitutive NOS in dispersed gastric muscle cells. *Am J Physiol* 1993; **265**(4 Pt 1): G660-G671
- 27 **Cho HJ**, Xie QW, Calaycay J, Mumford RA, Swiderek KM, Lee TD, Nathan C. Calmodulin is a subunit of nitric oxide synthase from macrophages. *J Exp Med* 1992; **176**: 599-604

Edited by Ren SY and Wang XL Proofread by Xu FM

Isolation of murine hepatic lymphocytes using mechanical dissection for phenotypic and functional analysis of NK1.1⁺ cells

Zhong-Jun Dong, Hai-Ming Wei, Rui Sun, Bin Gao, Zhi-Gang Tian

Zhong-Jun Dong, Hai-Ming Wei, Rui Sun, Zhi-Gang Tian, Institution of Immunology, University of Science and Technology of China, Hefei 230027, Anhui Province, China

Zhi-Gang Tian, Rui Sun, Shandong Cancer Biotherapy Center, Shandong Academy of Medical Science, Jinan City, Jinan 250062, Shandong Province, China

Bin Gao, Section on Liver Biology, Laboratory of Physiologic Studies, National Institute on Alcohol Abuse and Alcoholism, National Institutes of Health, Bethesda, Maryland 20892, USA

Supported by the National Science Fund for Distinguished Young Scholars, No. 30125038 and the Key Project of National Natural Science Foundation of China, No. 30230340 and the National High Technology Research and Development Program of China (863 Program), No. 2002AA216151 and Chinese Academy of Sciences, No. KSCX2-2-08

Correspondence to: Dr. Zhi-Gang Tian, School of Life Sciences, University of Science and Technology of China, 443 Huangshan Road, Hefei 230027, Anhui Province, China. ustctzg@yahoo.com.cn

Telephone: +86-551-360-7379 **Fax:** +86-551-360-6783

Received: 2003-08-02 **Accepted:** 2003-10-07

Abstract

AIM: To choose an appropriate methods for the isolation of hepatic lymphocytes between the mechanical dissection and the enzymatic digestion and investigate the effects of two methods on phenotype and function of hepatic lymphocytes.

METHODS: Hepatic lymphocytes were isolated from untreated, poly (I:C)-stimulated or ConA-stimulated mice using the two methods, respectively. The cell yield per liver was evaluated by direct counting under microscope. Effects of digestive enzymes on the surface markers involved in hepatic lymphocytes were represented by relative change rate [(percentage of post-digestion - percentage of pre-digestion)/percentage of pre-digestion]. Phenotypic analyses of the subpopulations of hepatic lymphocytes and intracellular cytokines were detected by flow cytometry. The cytotoxicity of NK cells from wild C57BL/6 or poly (I:C)-stimulated C57BL/6 mice was analyzed with a 4-h ⁵¹Cr release assay.

RESULTS: NK1.1⁺ cell markers, NK1.1 and DX5, were significantly down-expressed after enzymatic digestion and their relative change rates were about 28% and 32%, respectively. Compared with the enzymatic digestion, the cell yield isolated from unstimulated, poly (I:C)-treated or ConA-treated mice by mechanical dissection was not significantly decreased. Hepatic lymphocytes isolated by the mechanical dissection comprised more innate immune cells like NK, NKT and $\gamma\delta$ cells in normal C57BL/6 mice. After poly (I:C) stimulation, hepatic NK cells rose to about 35%, while NKT cells simultaneously decreased. Following ConA injection, the number of hepatic NKT cells was remarkably reduced to 3.67%. Higher ratio of intracellular IFN- γ (68%) or TNF- α (15%) NK1.1⁺ cells from poly (I:C)-treated mice was obtained using mechanical dissection method than control mice. There was no difference in

viability between the mechanical dissection and the enzymatic digestion, and hepatic lymphocytes obtained with the two methods had similar cytotoxicity against YAC-1 cells.

CONCLUSION: There is no difference in the cell yield and viability of the hepatic lymphocyte isolated with the two methods. The mechanical dissection, but not the enzymatic digestion, may be suitable for the phenotypic analysis of hepatic NK1.1⁺ cell.

Dong ZJ, Wei HM, Sun R, Gao B, Tian ZG. Isolation of murine hepatic lymphocytes using mechanical dissection for phenotypic and functional analysis of NK1.1⁺ cells. *World J Gastroenterol* 2004; 10(13): 1928-1933

<http://www.wjgnet.com/1007-9327/10/1928.asp>

INTRODUCTION

In recent decades, isolated lymphocytes from human or murine liver were universally used to explore the immune mechanisms in the defense of pathogens such as hepatitis virus^[1,2] and in the pathogenesis of liver diseases, especially in the autoimmune hepatitis^[3] and liver transplantation^[4]. Several lymphocyte subpopulations reside in the normal adult human liver. These cells mainly include a large number of T cells, B cells, natural killer (NK) cells and natural killer T (NKT) cells, which are distinct from the peripheral blood lymphocytes (PBL)^[5-7]. Up to now, mechanical dissection and enzymatic digestion are two main techniques for isolation of hepatic lymphocytes. The former method started in the early of 1980 and has been used yet. Reportedly, the viability of lymphocyte with this method is poor, and this method also leads to low yield. The latter methods was through incubation with digestive enzymes, 0.5 g/L collagenase IV and 0.01 g/L DNAase I^[8] and was considered to have a relative low contamination of PBL. Because the manipulation of the method is difficult to handle for tenderfoots, the prevalent use is limited. Some investigators also discovered that two digestive enzymes used could influence and decrease the percentage of surface markers of human hepatic lymphocytes such as CD56 molecule^[9]. However, the effects of two digestive enzymes on the surface markers of murine hepatic lymphocytes especially NK1.1⁺ cells, remain obscure. Yet there was not any report exclusively focused on the difference between these two methods. To compare these two methods for suitably selecting an appropriate method to analyze the NK1.1⁺ cells in the liver, we used these methods to isolate the murine hepatic mononuclear cells for the phenotypic and functional analysis.

MATERIALS AND METHODS

Animal

Female C57BL/6 (H-2^b), 6 to 8 week-old, was purchased from Shanghai Experimental Animal Center, Chinese Academy of Sciences (Shanghai, China). All mice were maintained under controlled conditions (22 °C, 55% humidity, and 12-h day/night

rhythm) in compliance with the regulations of animal care of University of Science and Technology of China.

Reagent

Collagenase IV and DNase I were purchased from Sigma Chemical Co. (St. Louis, MO) and dissolved in the pyrogen-free RPMI 1640 at the concentration of 0.5 g/L and 0.01 g/L, respectively.

Poly (I:C) or ConA treatment

Polyinosinic-polycytidylic acid sodium [Poly (I:C)] and Concanavalin A (Con A) were purchased from Sigma Chemical Co. (St. Louis, MO) and dissolved in the pyrogen-free saline at the concentration of 1 mg/mL. For *in vivo* stimulation of NK cells, mice were intraperitoneally injected with Poly (I:C) (7.5 µg/g·b.m.) for 6 h. For *in vivo* stimulation of NKT cells, mice were intravenously injected with ConA (7.5 µg/g·b.m.) for 6 h.

Protocols for isolation of mononuclear cells (MNC) from liver

Under deep ether anesthesia, mice were euthanized by exsanguinations from the subclavian artery and vein. A needle was inserted into the portal vein. The liver was perfused with 20 mL pH 7.0 PBS, and then the liver was removed. Isolation of hepatic lymphocytes with the mechanical dissection was carried out as follows: step 1, the liver was thoroughly dissected and gently passed through a 200-gauge stainless steel mesh and then suspended in RPMI 1640 medium containing 100 mL/L fetal calf serum (FCS). Step 2, the above cell suspension was centrifuged at 1 500 r/min. The pellet was resuspended in 40% Percoll solution containing 100 U/mL heparin, and then loaded on the layer of 70% Percoll solution followed by centrifugation at 2 000 r/min for 20 min at room temperature. Step 3, the cells were aspirated from the Percoll interface and harvested by centrifugation and washed twice with Hanks' balanced salt solution (HBSS) containing 50 mL/L FCS before use. The procedures for the enzymatic digestions were as follows: step 1, the liver was dissected into 1 mm³ pieces and 5 mL digestive solution was added. The mixture was incubated at 37 °C for 1 h. The supernatant was collected and diluted 1/2 in complete RPMI 1640. Step 2 and 3 were similar to the mechanical dissection.

Assessment of yield and viability of hepatic lymphocytes

Isolated hepatic lymphocytes from different groups (4 mice per group) were diluted 1:20 with 20 mL/L acetic acid, and cell numbers were assessed by direct counting under microscope. Cell viability was assessed by staining with trypan blue, and the stained-positive cells were enumerated to dead cell, while negative cells to viable lymphocyte.

Effects of digestive enzymes on the surface markers

Effects of digestive enzymes, collagenase IV and DNase I, on the surface markers were determined by the percentage in the pre-digestion and post-digestion. It was represented as relative change rate (%). Relative change rate=[(percentage of post-digestion - percentage of pre-digestion)/percentage of pre-digestion].

Immunofluorescence

The phenotype of lymphocytes was analyzed using monoclonal antibody (mAb) in conjunction with two-color or three-color immunofluorescence. The mAb used in this study included fluorescein isothiocyanate (FITC)-, phycoerythrin (PE)-, or Cy5-conjugated gamma/delta T cell receptor (γδ TCR), anti-CD3e, anti-CD25, anti-CD69, anti-IFN-γ, anti-DX5, and anti-NK1.1 mAb (PharMingen, San Diego, CA). For Intracellular cytokine staining, liver mononuclear cells were incubated in the presence of brefeldin A (5 µg/mL; BD PharMingen) and phorbol myristate

acetate (PMA) (20 ng/mL; BD PharMingen) for 3 h, and then stained with FITC-conjugated anti-NK1.1 mAb and Cy-5 conjugated anti-CD3e mAb. After fixation with fixation solution and permeabilization with permeabilization solution (Bioscience, Camarillo, USA), intracellular cytokine staining was performed using PE-conjugated anti-IFN-γ or anti-TNF-α mAb. To prevent nonspecific binding, respective isotype antibodies were used as control. Stained cells were acquired by FACSCalibur and analyzed with WinMDI2.8.

Cytotoxicity assay

Target cells used in NK cytotoxicity assay were YAC-1 cells, which were propagated in RPMI 1640 medium supplemented with 100 mL/L heat-inactivated FCS, 2 mmol/L L-glutamine and 25 mmol/L NaHCO₃ in a humidified atmosphere containing 50 mL/L CO₂ at 37 °C. Cytotoxicity assay was carried out as described previously^[10]. Labeled target cells (10³/well) were incubated in a total volume of 200 µL with effector cells in RPMI 1640 containing 100 mL/L FCS in 96-well round-bottom microtiter plates at various cell densities in order to achieve effector-to-target (E/T) ratios. The plate was incubated for 4 h, and the supernatant was collected after centrifugation and then counted in a gamma counter. The cytotoxicity was calculated as the percentage of releasable counts after subtraction of spontaneous release. The spontaneous release was less than 15% of the maximum release.

Statistical analysis

Data were expressed as mean±SD. Statistical analysis was performed using *t* test. Difference between the groups was considered statistically significant when *P* value was less than 0.05.

RESULTS

Effects of enzymatic digestion on surface molecules of hepatic lymphocytes

To understand the effect of collagenase IV and DNase I on murine hepatic lymphocytes, we detected the percentage of lymphocyte-related markers, CD3, CD4, CD8e, CD25, CD69, NK1.1, DX5 and γδ TCR in the enzyme-treated and untreated hepatic lymphocytes. Surface markers, CD3, CD4, CD8e, CD25, CD69 and γδ-TCR, remained unchanged and two markers associated with NK and NKT cells, NK1.1 and DX5, were significantly decreased in the enzyme-treated group compared to untreated group and their relative change rates were about 28% and 32% in NK1.1 and DX5 groups respectively (Figure 1). The percentages of NK and NKT cells isolated with the mechanical dissection were higher than those in the enzymatic digestion (Table 1, *P*<0.05). This finding suggested that the enzymatic digestion might decrease the proportion of NK1.1⁺ cells in murine hepatic lymphocytes by decreasing the NK or NKT-related surface molecules, and should be avoided in the study of NK1.1⁺ in the liver.

Table 1 Subpopulations of hepatic lymphocytes isolated by two the methods (%)

Group	T cell	NK cell	NKT cell	γδ T cell
Mechanical dissection	38.56±5.63	13.35±4.61	20.42±4.65	13.6±3.15
Enzymatic digestion	36.96±4.68	8.35±2.69 ^a	13.48±4.25 ^a	12.6±2.74

^a*P*<0.05 vs dissection.

Cell yield of the two methods

In normal C57BL/6 mice, the total cell number obtained with the mechanical dissection was about 2.6×10⁶ per liver and that

obtained with the enzymatic digestion was 2.9×10^6 per liver, showing no significant difference (Figure 2A). To further investigate the cell yield in the stress condition, two stimuli, Poly (I:C) and ConA, were used to trigger hepatic lymphocytes, respectively. About 7×10^6 hepatic lymphocytes per liver were obtained in Poly (I:C)-stimulated or ConA-stimulated mice using either the mechanical dissection or the enzyme digestion, without any significant difference between the two isolation methods (Figures 2B,C). These results suggested that the mechanical dissection was as effective as the enzymatic digestion in the cell yield.

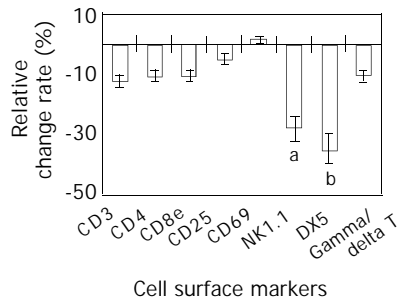


Figure 1 Effects of enzymatic digestion on surface molecules of hepatic lymphocytes. ^a $P < 0.05$, NK1.1 vs other groups except DX5; ^b $P < 0.01$, DX5 vs other groups except NK1.1.

Hepatic lymphocytes isolated with mechanical dissection were suitable for phenotypic analysis

Using mechanical dissection, we isolated the hepatic lymphocytes for analyzing the subpopulations of hepatic lymphocytes. Different from other immune organs, hepatic

lymphocytes of normal C57BL/6 mice comprised more innate immune cells like NK, NKT and $\gamma\delta$ cells, which accounted for 18.60%, 16.62% and 18.60% respectively (Figure 3A). Following Poly (I:C) stimulation, hepatic NK cells increased to about 35% and NKT cells simultaneously decreased, which was consistent with other reports^[11] (Figure 3B). Following ConA injection, hepatic NKT cells were remarkably reduced to 3.67%. In addition, after Poly (I:C) stimulation intracellular IFN- γ and TNF- α were significantly augmented to about 68% and 25% within NK (CD3⁺NK1.1⁺) cells, respectively (Figure 3C). Taken together, the results indicated that hepatic lymphocytes obtained with the mechanical dissection could be used for the antibody-based phenotypic analysis of NK1.1⁺ cells. On the other hand, the liver had the predominance of more innate immune cells.

Hepatic lymphocytes isolated with mechanical dissection were suitable for the functional analysis

In order to understand whether hepatic lymphocytes obtained with mechanical dissection were suitable for functional assays, cell viability was assessed through staining with trypan blue. The cell viability of hepatic lymphocytes from normal C57BL/6 mice accounted for 90% using mechanical dissection method, which was similar to enzyme digestion method (Figure 4A). Next, we examined NK cells cytotoxic function against an NK-sensitive cell line, YAC-1 cells, and found that there was no difference between the two methods (Figure 4B). In the absence of Poly (I:C) stimulation, the cytotoxicity of NK cells to YAC-1 cells was about 15% at the E:T ratio of 1:12.5. After Poly (I:C) stimulation, it increased to 35% at the same E:T ratio. These results indicated that the isolated lymphocytes with the two different methods had the similar viability and were suitable for functional analysis of hepatic lymphocytes prior to or after immune stimulation.

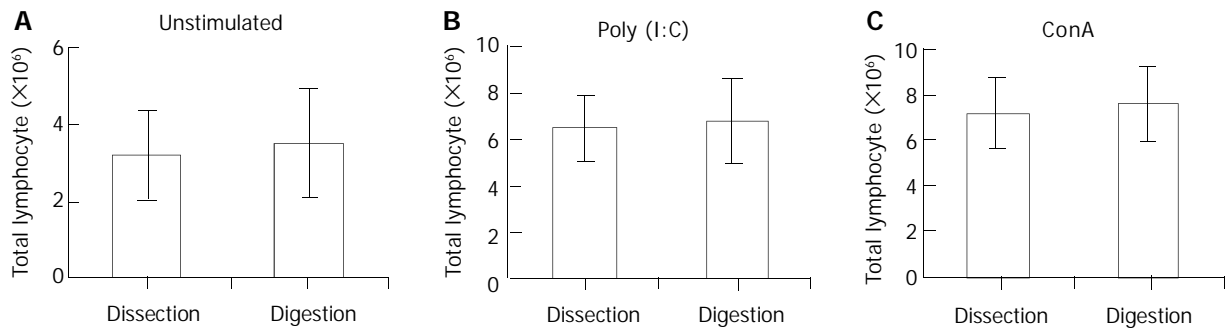


Figure 2 Cell yields between the two isolating methods. Hepatic lymphocytes were isolated using mechanical dissection method and the enzymatic digestion method, respectively, from normal C57BL/6 mice (A), Poly (I:C)-treated C57BL/6 mice (B) or ConA-treated C57BL/6 mice (C).

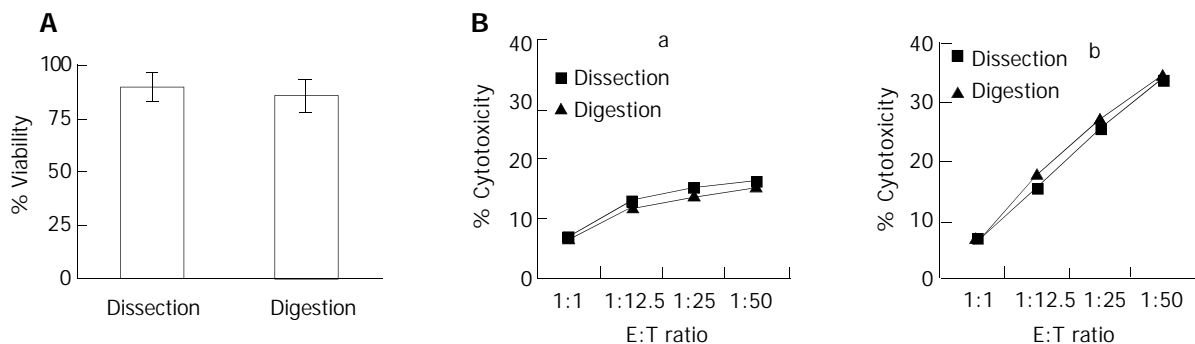


Figure 4 Hepatic lymphocytes isolated with mechanical dissection were suitable for the functional analysis of NK1.1⁺ cells. A: Viability of hepatic lymphocytes isolated with two methods; B: Cytotoxicity analysis of hepatic lymphocytes. Hepatic lymphocytes were isolated by two different methods, respectively, from control B6 mice (a) or Poly (I:C)-treated B6 mice (b). Their cytotoxicity against YAC-1 cells was tested at the (E/T) ratios.

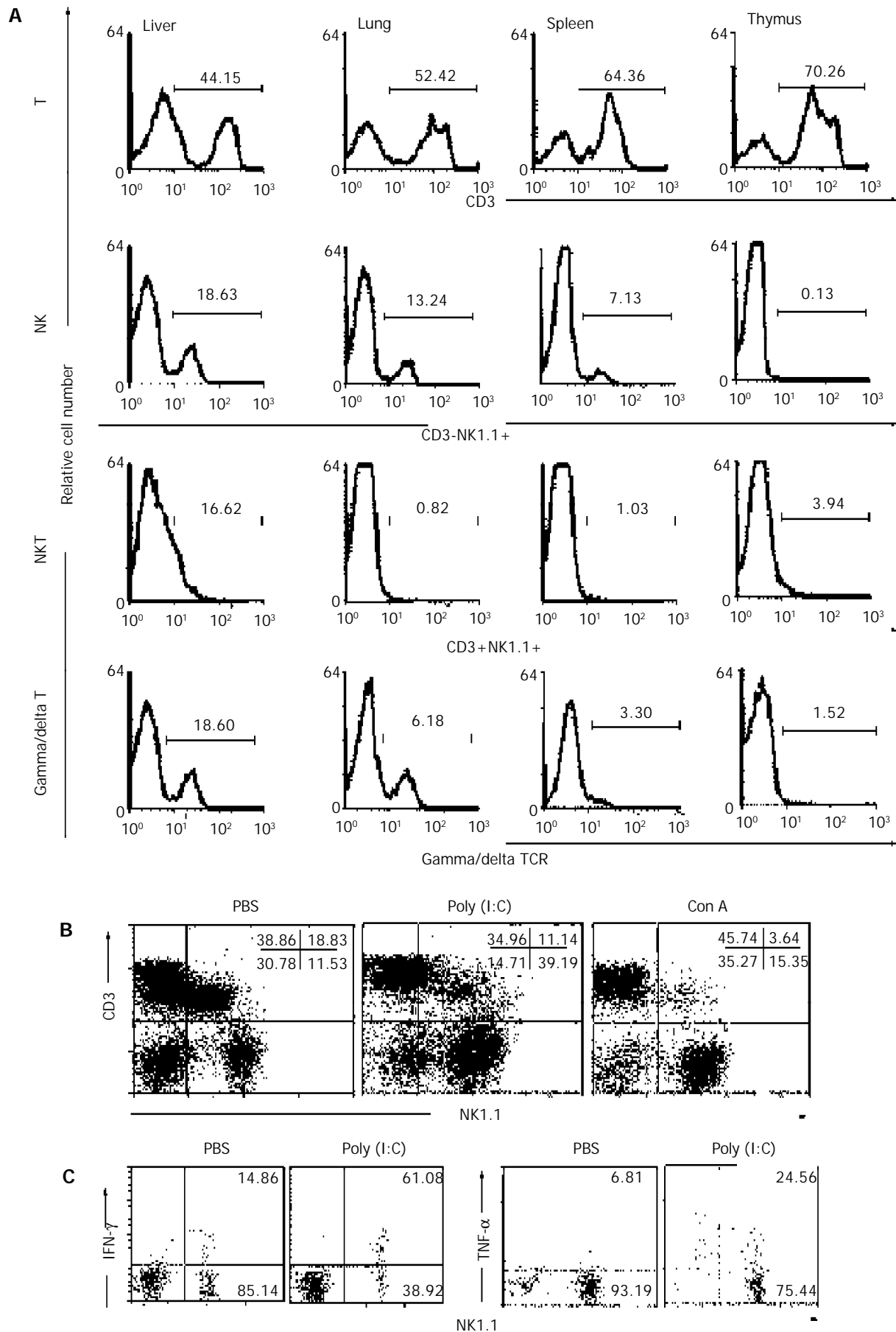


Figure 3 Hepatic lymphocytes isolated with mechanical dissection were suitable for phenotypic analysis of NK1.1⁺ cells. A: Lymphocytes from liver, lung, spleen and thymus of normal C57BL/6 mice were labeled with two-color immunofluorescence; B, C: C57BL/6 mice were injected with PBS, Poly (I:C) or ConA, respectively. Hepatic lymphocytes were isolated and labeled for phenotype (CD3 and NK1.1) and intracellular cytokine (IFN- γ and TNF- α) detection.

DISCUSSION

Liver has a unique dual blood supply with venous blood from the gut via the portal veins and arterial blood delivered via the hepatic arteries. In view of this distinct anatomy character, liver is thus constantly exposed to gut-derived antigens and infectious organisms in the portal blood. So many unidentified mechanisms have been involved to allow rapid and selective immune responses within this tissue^[12,13]. Structurally and functionally, qualification of liver as a lymphoid organ has been reflected by many studies^[14,15], and therefore a new term "hepatoinmunology" was emerged in 2002^[16]. Liver harbors many innate immune cells, such as NK, NKT and $\gamma\delta$ T cells. The predominance of these cells in the liver endows liver with the character of innate immune organ^[17], which was supported by the response of NK cells to the innate immune stimulus, Poly (I:C) in our study. However, the exact roles of these cells in the liver remain unclear. NK1.1 molecule is a member of NKR-P1 family, also named as CD161 in human^[18], and NK1.1⁺ cells often have DX5 molecule on their membrane in mice^[19]. Their remarkable distinction was that NK1.1 was only expressed by certain strain of mice, such as C57BL/6 and NZB, but not BALB/c^[20]. Conventionally, NK1.1⁺ cells mainly included NK cells and NKT cells. However, upon certain stimulation, activated cytotoxic T cell could also upregulate NK1.1 molecule. NK and NKT cells are two important subpopulations in the liver. They exerted their versatile roles in the defense of pathogens like murine cytomegalovirus (MCMV)^[21,22]. Several studies also reported that hepatic NK and NKT cell took part in the antimetastasis of tumor^[23-25]. NK1.1⁺ cells were reported to involve in the pathogenesis of many diseases, like human immunodeficiency virus (HIV) infection and liver disease^[26,27]. The demonstration that NK cell or NKT cell could give rise to liver injury had been confirmed by different groups, including our laboratory^[28-30]. Accurate assessment of these NK1.1⁺ cells in the liver required an appropriate technique to purify the hepatic lymphocytes. Various enzymatic or mechanical methods were proposed in the past to isolate lymphocytes from human or murine liver^[9]. The Enzymatic digestion was considered to be a satisfied method in the preparation of human organ-specific lymphocytes^[31]. In addition, this method has been used to isolate cells like hepatocytes^[32]. However, results from different studies appeared to be inconsistent. For example, Trobonjaca *et al.* reported that NKT cells accounted for 35.9% of the total hepatic lymphocytes in normal mice^[8], while Osman *et al.* reported that NKT cell accounted for only 16%^[33]. This difference may contribute to the different isolating methods taken by them. The roles of collagenase on surface makers of peripheral blood lymphocytes were investigated in 1996. They found collagenase could disrupt the surface markers, such as CD3, CD4, CD8, $\alpha\beta$ and $\gamma\delta$ TCR by about 20-40%^[34]. It was also reported that isolation of intestinal lymphocytes using collagenase released cytotoxic factors, which were found to suppress NK cell activity of isolated cell^[35]. Although the mechanical dissection for preparation of hepatic lymphocytes has been used for many years and still used yet, this technique has a defect in cell yield. To make sure the extent, in this study we found that there was no difference in cell yields and viability between the mechanical dissection method and the enzymatic digestion method. We did not observe any decrease in the surface molecules of hepatic lymphocytes in all cases except NK1.1 and DX5, suggesting that enzymatic digestion using collagenase IV and DNase is unsuitable for isolating hepatic lymphocytes for NK1.1⁺ cell analysis.

ACKNOWLEDGEMENT

We are thankful to Dr. Jing Wang and Dr. Yong-Yan Cheng for their continuous technical helping during this work.

REFERENCES

- Vigan I**, Jouvin-Marche E, Leroy V, Pernollet M, Tongiani-Dashan S, Borel E, Delachanal E, Colomb M, Zarski JP, Marche PN. T lymphocytes infiltrating the liver during chronic hepatitis C infection express a broad range of T-cell receptor beta chain diversity. *J Hepatol* 2003; **38**: 651-659
- Boisvert J**, Kunkel EJ, Campbell JJ, Keeffe EB, Butcher EC, Greenberg HB. Liver-infiltrating lymphocytes in end-stage hepatitis C virus: subsets, activation status, and chemokine receptor phenotypes. *J Hepatol* 2003; **38**: 67-75
- Kaneko Y**, Harada M, Kawano T, Yamashita M, Shibata Y, Gejyo F, Nakayama T, Taniguchi M. Augmentation of Valpha14 NKT cell-mediated cytotoxicity by interleukin 4 in an autocrine mechanism resulting in the development of concanavalin A-induced hepatitis. *J Exp Med* 2000; **191**: 105-114
- Otto C**, Kauczok J, Martens N, Steger U, Moller I, Meyer D, Timmermann W, Ulrichs K, Gassel HJ. Mechanisms of tolerance induction after rat liver transplantation: intrahepatic CD4 (+) T cells produce different cytokines during rejection and tolerance in response to stimulation. *J Gastrointest Surg* 2002; **6**: 455-463
- Norris S**, Collins C, Doherty DG, Smith F, McEntee G, Traynor O, Nolan N, Hegarty J, O'Farrelly C. Resident human hepatic lymphocytes are phenotypically different from circulating lymphocytes. *J Hepatol* 1998; **28**: 84-90
- Luo DZ**, Vermijlen D, Ahishali B, Triantis V, Plakoutsi G, Braet F, Vanderkerken K, Wisse E. On the cell biology of pit cells, the liver-specific NK cells. *World J Gastroenterol* 2000; **6**: 1-11
- Doherty DG**, Norris S, Madrigal-Estebas L, McEntee G, Traynor O, Hegarty JE, O'Farrelly C. The human liver contains multiple populations of NK cells, T cells, and CD3⁺CD56⁺ natural T cells with distinct cytotoxic activities and Th1, Th2, and Th0 cytokine secretion patterns. *J Immunol* 1999; **163**: 2314-2321
- Trobonjaca Z**, Kroger A, Stober D, Leithauser F, Moller P, Hauser H, Schirmbeck R, Reimann J. Activating immunity in the liver. II. IFN-beta attenuates NK cell-dependent liver injury triggered by liver NKT cell activation. *J Immunol* 2002; **168**: 3763-3770
- Curry MP**, Norris S, Golden-Mason L, Doherty DG, Deignan T, Collins C, Traynor O, McEntee GP, Hegarty JE, O'Farrelly C. Isolation of lymphocytes from normal adult human liver suitable for phenotypic and functional characterization. *J Immunol Methods* 2000; **242**: 21-31
- Luo DZ**, Vermijlen D, Ahishali B, Triantis V, Vanderkerken K, Kuppen PJ, Wisse E. Participation of CD45, NKR-P1A and ANK61 antigen in rat hepatic NK cell (pit cell) mediated target cell cytotoxicity. *World J Gastroenterol* 2000; **6**: 546-552
- Hobbs JA**, Cho S, Roberts TJ, Sriram V, Zhang J, Xu M, Brutkiewicz RR. Selective loss of natural killer T cells by apoptosis following infection with lymphocytic choriomeningitis virus. *J Virol* 2001; **75**: 10746-10754
- Seki S**, Habu Y, Kawamura T, Takeda K, Dobashi H, Ohkawa T, Hiraide H. The liver as a crucial organ in the first line of host defense: the roles of Kupffer cells, natural killer (NK) cells and NK1.1 Ag⁺ T cells in T helper 1 immune responses. *Immunol Rev* 2000; **174**: 35-46
- Knolle PA**, Gerken G. Local control of the immune response in the liver. *Immunol Rev* 2000; **174**: 21-34
- Mehal WZ**, Azzaroli F, Crispe IN. Immunology of the healthy liver: old questions and new insights. *Gastroenterology* 2001; **120**: 250-260
- Kita H**, Mackay IR, Van de Water J, Gershwin ME. The lymphoid liver: considerations on pathways to autoimmune injury. *Gastroenterology* 2001; **120**: 1485-1501
- Mackay IR**. Hepatoimmunology: a perspective. *Immunol Cell Biol* 2002; **80**: 36-44
- Doherty DG**, O'Farrelly C. Innate and adaptive lymphoid cells in the human liver. *Immunol Rev* 2000; **174**: 5-20
- Lanier LL**, Chang C, Phillips JH. Human NKR-P1A. A disulfide-linked homodimer of the C-type lectin superfamily expressed by a subset of NK and T lymphocytes. *J Immunol* 1994; **153**: 2417-2428
- Rosmaraki EE**, Douagi I, Roth C, Colucci F, Cumano A, Di Santo JP. Identification of committed NK cell progenitors in

- adult murine bone marrow. *Eur J Immunol* 2001; **31**: 1900-1909
- 20 **Arase H**, Saito T, Phillips JH, Lanier LL. Cutting edge: the mouse NK cell-associated antigen recognized by DX5 monoclonal antibody is CD49b (alpha 2 integrin, very late antigen-2). *J Immunol* 2001; **167**: 1141-1144
- 21 **Lodoen M**, Ogasawara K, Hamerman JA, Arase H, Houchins JP, Mocarski ES, Lanier LL. NKG2D-mediated natural killer cell protection against cytomegalovirus is impaired by viral gp40 modulation of retinoic acid early inducible 1 gene molecules. *J Exp Med* 2003; **197**: 1245-1253
- 22 **van Dommelen SL**, Tabarias HA, Smyth MJ, Degli-Esposti MA. Activation of natural killer (NK) T cells during murine cytomegalovirus infection enhances the antiviral response mediated by NK cells. *J Virol* 2003; **77**: 1877-1884
- 23 **Sun R**, Wei H, Zhang J, Li A, Zhang W, Tian Z. Recombinant human prolactin improves antitumor effects of murine natural killer cells *in vitro* and *in vivo*. *Neuroimmunomodulation* 2002; **10**: 169-176
- 24 **Joo SS**, Kim MS, Oh WS, Lee DI. Enhancement of NK cytotoxicity, antimetastasis and elongation effect of survival time in B16-F10 melanoma cells by oregonin. *Arch Pharm Res* 2002; **25**: 493-499
- 25 **Park SH**, Kyin T, Bendelac A, Carnaud C. The contribution of NKT cells, NK cells, and other gamma-chain-dependent non-T non-B cells to IL-12-mediated rejection of tumors. *J Immunol* 2003; **170**: 1197-1201
- 26 **Vergani D**, Choudhuri K, Bogdanos DP, Mieli-Vergani G. Pathogenesis of autoimmune hepatitis. *Clin Liver Dis* 2002; **6**: 439-449
- 27 **Fleuridor R**, Wilson B, Hou R, Landay A, Kessler H, Al-Harhi L. CD1d-restricted natural killer T cells are potent targets for human immunodeficiency virus infection. *Immunology* 2003; **108**: 3-9
- 28 **Takeda K**, Hayakawa Y, Van Kaer L, Matsuda H, Yagita H, Okumura K. Critical contribution of liver natural killer T cells to a murine model of hepatitis. *Proc Natl Acad Sci U S A* 2000; **97**: 5498-5503
- 29 **Abe T**, Kawamura H, Kawabe S, Watanabe H, Gejyo F, Abo T. Liver injury due to sequential activation of natural killer cells and natural killer T cells by carrageenan. *J Hepatol* 2002; **36**: 614-623
- 30 **Liu ZX**, Govindarajan S, Okamoto S, Dennert G. NK cells cause liver injury and facilitate the induction of T cell-mediated immunity to a viral liver infection. *J Immunol* 2000; **164**: 6480-6486
- 31 **Flynn L**, Carton J, Byrne B, Kelehan P, O'Herlihy C, O'Farrelly C. Optimisation of a technique for isolating lymphocyte subsets from human endometrium. *Immunol Invest* 1999; **28**: 235-246
- 32 **Mitry RR**, Hughes RD, Aw MM, Terry C, Mieli-Vergani G, Girlanda R, Muiesan P, Rela M, Heaton ND, Dhawan A. Human hepatocyte isolation and relationship of cell viability to early graft function. *Cell Transplant* 2003; **12**: 69-74
- 33 **Osman Y**, Kawamura T, Naito T, Takeda K, Van Kaer L, Okumura K, Abo T. Activation of hepatic NKT cells and subsequent liver injury following administration of alpha-galactosylceramide. *Eur J Immunol* 2000; **30**: 1919-1928
- 34 **Abuzakouk M**, Feighery C, O'Farrelly C. Collagenase and dispase enzymes disrupt lymphocyte surface molecules. *J Immunol Methods* 1996; **194**: 211-216
- 35 **Gibson PR**, Hermanowicz A, Verhaar HJ, Ferguson DJ, Bernal AL, Jewell DP. Isolation of intestinal mononuclear cells: factors released which lymphocyte viability and function. *Gut* 1985; **26**: 60-68

Edited by Kumar M **Proofread by** Chen WW and Xu FM

Role of mitochondria in cell apoptosis during hepatic ischemia-reperfusion injury and protective effect of ischemic postconditioning

Kai Sun, Zhi-Su Liu, Quan Sun

Kai Sun, Zhi-Su Liu, Quan Sun, Department of General Surgery, Zhongnan Hospital, Wuhan University, Wuhan 430071, Hubei Province, China

Correspondence to: Professor Zhi-Su Liu, Department of General Surgery, Zhongnan Hospital, Wuhan University, Wuhan 430071, Hubei Province, China. hyfr@mail.wh.cej.gov.cn

Telephone: +86-27-87331752 **Fax:** +86-27-87330795

Received: 2003-06-28 **Accepted:** 2003-10-12

Abstract

AIM: To investigate the role of mitochondria in cell apoptosis during hepatic ischemia-reperfusion injury and protective effect of ischemic postconditioning (IPC).

METHODS: A rat model of acute hepatic ischemia-reperfusion was established, 24 healthy male Wistar rats were randomly divided into sham-operated group, ischemia-reperfusion group (IR) and IPC group. IPC was achieved by several brief pre-reperfusion followed by a persistent reperfusion. Concentration of malondialdehyde (MDA) and activity of several antioxidant enzymes in hepatic tissue were measured respectively. Apoptotic cells were detected by TdT-mediated dUTP-biotin nick end labeling (TUNEL) and expression of Bcl-2 protein was measured by immunohistochemical techniques. Moreover, mitochondrial ultrastructure and parameters of morphology of the above groups were observed by electron microscope.

RESULTS: Compared with IR group, the concentration of MDA and the hepatocellular apoptotic index in IPC group was significantly reduced ($P < 0.05$), while the activity of antioxidant enzymes and OD value of Bcl-2 protein were markedly enhanced ($P < 0.05$). Moreover, the injury of mitochondrial ultrastructure in IPC group was also obviously relieved.

CONCLUSION: IPC can depress the synthesis of oxygen free radicals to protect the mitochondrial ultrastructure and increase the expression of Bcl-2 protein that lies across the mitochondrial membrane. Consequently, IPC can reduce hepatocellular apoptosis after reperfusion and has a protective effect on hepatic ischemia-reperfusion injury.

Sun K, Liu ZS, Sun Q. Role of mitochondria in cell apoptosis during hepatic ischemia-reperfusion injury and protective effect of ischemic postconditioning. *World J Gastroenterol* 2004; 10(13): 1934-1938

<http://www.wjgnet.com/1007-9327/10/1934.asp>

INTRODUCTION

Hepatic ischemia-reperfusion injury (IRI) is a common pathological process of traumatic surgical diseases in the liver, such as severe liver trauma, extensive hepatic lobus excision, liver transplantation, shock and infection. When hepatic IRI

happens, a series of metabolic and structural and functional disorder of hepatic tissue cells would occur, which directly influence the prognosis of patients^[1,2]. At present, the study about the mechanism and intervention method of hepatic IRI has been carried out extensively. It has been confirmed that apoptosis as a way of cell death is significant for maintaining normal cell development and stabilization, and is closely related to the initiation and development of many clinical diseases, and it also participates in IRI of tissues and organs^[3-6]. Mitochondria as one of the organelle of cells play an important role in providing energy, adjusting osmotic pressure, calcium balance, and pH value, and cell signaling. Mitochondria perform their function by production of ATP and reactive oxygen species (ROS) which are also known as signals regulating gene expression and triggering cell death^[7,8]. At present, mitochondria/ cytochrome C apoptotic pathway has attracted close attention of scholars. Many stimulators such as ROS, Ca^{2+} and cytokines could activate cysteine aspartate-specific proteases (Caspase) by inducing cytochrome C release^[9-12]. But the study on the changes of the structure and function of mitochondria in hepatic IRI and the adjusting function of mitochondria in hepatocellular apoptosis was rarely reported at home and abroad. We established a hepatic IRI model in liver of rats, and observed the influence of ischemic postconditioning (IPC) on cell apoptosis in hepatic IRI and the adjustment function of mitochondria. This experiment lays a theoretical foundation for adopting a more reasonable method to restore the blood flow after hepatic ischemia.

MATERIALS AND METHODS

Materials

Twenty-four healthy male Wistar rats, weighing 200-250 g, were supplied by the Experimental Animal Center of Wuhan University. Malondialdehyde (MDA), superoxide dismutase (SOD), catalase (CAT) and glutathione peroxidase (GSH-PX) assay kits were purchased from Nanjing Jiancheng Bioengineering Co.Ltd, China. Mouse anti-rat Bcl-2 monoclonal antibody and SP assay kit were provided by Beijing Zhongshan Biotechnology Co.Ltd, China. Terminal deoxynucleotidyl transferase (TdT) mediated dUTP nick end labeling (TUNEL) *in situ* cell death detection kit was the product of Boehringer Mannheim Co.Ltd, USA.

Animal model

The animals were fed standard laboratory chow. Before the day of experiment, the animals were fasted overnight, but allowed free access to water. They were anesthetized by sodium pentobarbital (30 mg/kg). Hepatoduodenal ligament was separated after entry into the belly, the first porta hepatis was exposed and a rat local hepatic IRI model was established with reference to the previous method^[13]. Blood flow of caudate and left lobe of the liver was blocked with non-trauma mini artery clamp, causing 70% liver ischemia. However, the blood flow of right lobe was not blocked to prevent blood clot in portal vein and gastrointestinal tract. Twenty-four rats were randomly divided into three groups (eight in each group) and

subjected to the following treatments. (1) Sham-operated group: only hepatoduodenal ligament was separated after entry into the belly, blood flow of porta hepatis was not blocked. (2) Ischemia-reperfusion group (IR): the livers were undergone ischemia for 60 min followed by reperfusion for 120 min. (3) Ischemic postconditioning group (IPC): the livers were subjected to porta hepatis occlusion for 60 min, then treated for 2 min, 3 min, 5 min, 7 min by brief reperfusion consecutively, each was separated with occlusion for 2 min, followed by a persistent reperfusion for 95 min, which made the total reperfusion time the same as the other two groups.

MDA and antioxidant enzyme measurement

Concentration of MDA and activity of SOD, CAT and GSH-PX in hepatic tissue were measured according to the commercial kit manual.

Immunohistochemical staining

Fresh hepatic tissues, cut from left lobe of the liver, were fixed in formalin for 12-24 h and then embedded in paraffin wax. A 4- μ m thick sections were cut and mounted onto slides. They were deparaffinized by passing through xylene and graded series of ethanol, followed by rinsing in tap water and 0.01 mmol/L phosphate buffered saline (PBS) respectively. Endogenous peroxidase activity was quenched by treating the sections with 30 mL/L hydrogen peroxide for 10 min. Nonspecific binding was blocked by incubating sections in PBS containing 10 g/L bovine albumin for 10 min. Then the sections were incubated for an hour in primary antibody (mouse anti-rat Bcl-2 monoclonal antibody). After rinsed in PBS, the sections were treated sequentially with biotin-conjugated second antibody for 10 min and then with streptavidin-peroxidase for another 10 min with PBS rinsing after each step. The sections were stained subsequently with freshly prepared DAB reagent for 3 min, terminated by rinsing in water, then immersed in hematoxylin for 3-5 min and 0.5 mmol/L HCl for 10 s. Finally, after passing through xylene and graded series of ethanol, the sections were covered with coverslips for light analysis. The sections were examined with HAIPS-2 000 image analysis and the Absorbency value was used to evaluate the content of Bcl-2 protein.

Hepatic TUNEL staining

In situ terminal deoxynucleotidyl transferase-mediated dUTP nick-end labeling (TUNEL) of fragmented DNA was performed on paraffin slices using the *in situ* cell death detection kit as described in the commercial kit manual. Positively labeled nuclei (brown color) were identified from negatively unstained nuclei (blue color). The number of positive nuclei was determined by counting (magnification \times 400) all the positively labeled nuclei present in five random visual fields under a microscope. The percentage of TUNEL positive nuclei to all nuclei counted was used as apoptotic index (AI). The

apoptotic cells had the following characteristics: single cells, no inflammation, curling of cell membrane, brown particulate or fragmented nuclei.

Morphopathological observation of ultrastructural organization

One mm³ fresh hepatic tissue, cut from left lobe of the liver, was pre-fixed with glutaraldehyde at the volume fraction of 2.5 % and post-fixed with 1 g/L osmic acid. Then the specimens were immersed in propylene oxide after dehydration with gradient ethanol, embedded with epoxy resin and made into ultrathin sections. The sections were stained subsequently with lead-uranium and the changes of ultrastructural organization were observed under H-600 transmission electron microscope. Finally, the sections were measured for cross-sectional area (A), cross-sectional perimeter (P) of mitochondria (using Image Pro Plus, USA), and computed specific surface of mitochondria following the formula: $\delta=4P/(\pi A)$.

Statistical analysis

All data were expressed as mean \pm SD. Comparisons between groups were analyzed with one-way ANOVA and Student-Newman-Keuls *q* test. *P* values less than 0.05 were considered statistically significant.

RESULTS

MDA concentration and antioxidant enzyme activity

The concentration of MDA in hepatic tissue was rapidly elevated after reperfusion in IR and IPC groups against sham group ($P<0.05$), while the activity of SOD, CAT and GSH-PX was significantly reduced ($P<0.05$). Compared with IR group, the concentration of MDA in IPC group was markedly reduced and activity of each antioxidant enzyme was significantly enhanced ($P<0.05$) (Table 1).

Table 1 Measurement of MDA concentration and antioxidant enzyme activity (mean \pm SD, *n*=8)

Group	MDA (nmol/mg)	SOD (U/mg prot)	CAT (U/mg prot)	GSH-PX (U/mg prot)
Sham	3.42 \pm 1.12	241.47 \pm 19.52	91.66 \pm 8.16	124.17 \pm 24.37
IR	17.56 \pm 4.80 ^a	132.99 \pm 22.11 ^a	40.24 \pm 7.73 ^a	51.75 \pm 16.43 ^a
IPC	10.18 \pm 3.56 ^{ab}	176.84 \pm 20.50 ^{ad}	64.81 \pm 7.19 ^{ad}	89.70 \pm 28.15 ^{ad}

^a $P<0.05$ vs sham, ^d $P<0.05$ vs IR.

Expression of Bcl-2 protein

The A value of Bcl-2 protein in IR group (0.067 \pm 0.011) was significantly lower than that in sham group (0.096 \pm 0.017) ($P<0.05$). After postconditioning, the expression of Bcl-2 protein was more eminent (A value 0.138 \pm 0.016) than that in IR group ($P<0.05$) (Figure 1A, B, C).

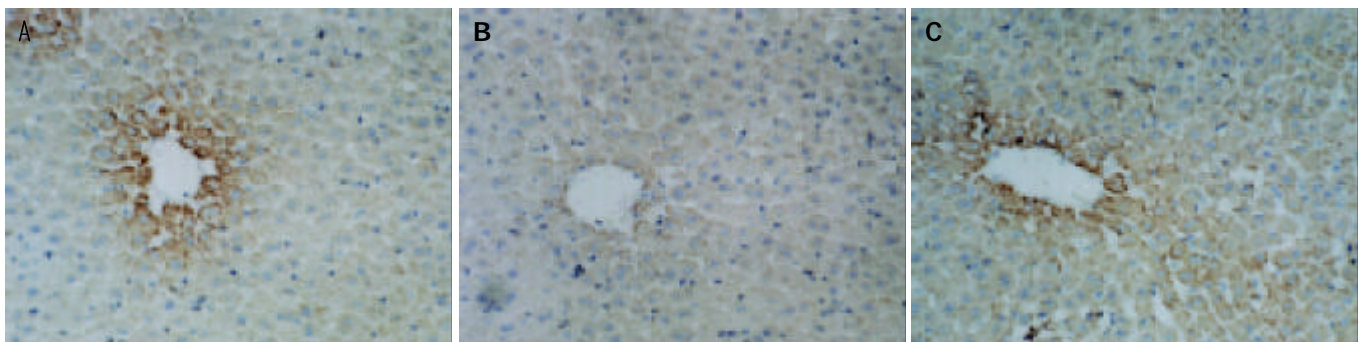


Figure 1 Bcl-2 expression in sham, IR and IPC groups (\times 200). A: Bcl-2 expression in sham group, B: Bcl-2 expression in IR group, C: Bcl-2 expression in IPC group.

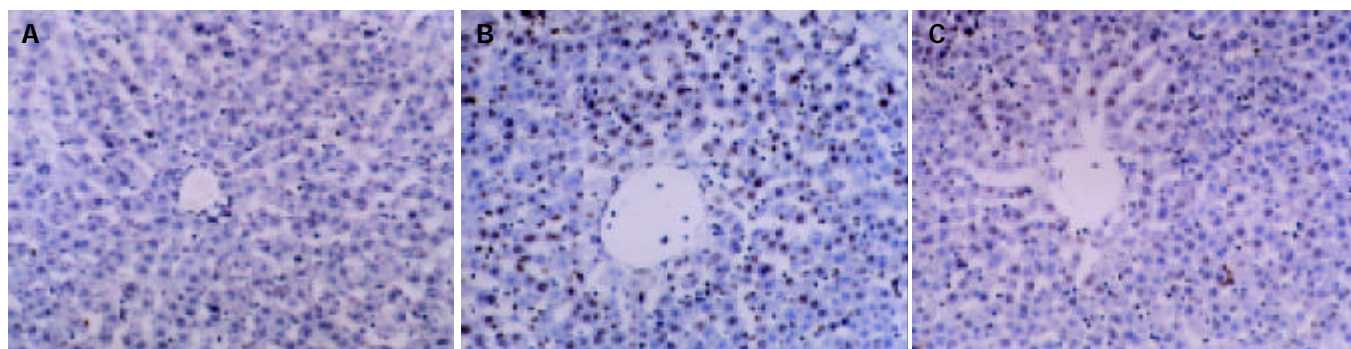


Figure 2 TUNEL staining in sham, IR and IPC groups ($\times 200$). A: TUNEL staining in sham group, B: TUNEL staining in IR group, C: TUNEL staining in IPC group.

Effect of IPC on hepatocellular apoptosis

Under light microscope, TUNEL staining indicated that cell injury occurred primarily in the form of apoptosis at the early stage of reperfusion and apoptotic cells were mainly around the central vein (Figure 2A, B, C). Under electron microscope, the early manifestations of apoptosis, such as swelling and rounding of cells, cell exfoliation, and aggregation of chromatin in the edge, as well as the typical manifestations of apoptosis, such as the concentration of cytoplasm and nucleus, and formation of apoptotic body, could be seen (Figure 3). The apoptotic index in IR group (46.53 ± 3.47) was significantly higher than that in sham group (2.05 ± 0.83) ($P < 0.05$). After postconditioning, the apoptotic index (23.16 ± 2.67) was significantly reduced compared with IR group ($P < 0.05$).

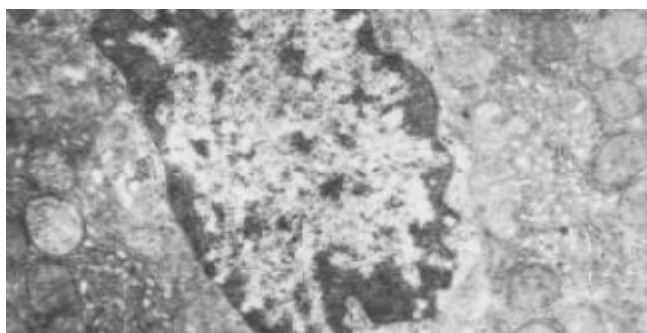


Figure 3 Morphological change of hepatocellular apoptosis in IR group (TEM $\times 15\ 000$).

Ultrastructural changes of mitochondria

In sham group, mitochondrial structure was normal. Mitochondria were orderly arranged in the form of round or ellipsoid without swelling. Mitochondrial membrane was intact and cristae were arranged in the form of concentric ring or vertical line,

congested and clear (Figure 4A). In IR group, mitochondria were swollen obviously. Mitochondrial membrane was vague or partly ruptured and cristae were obviously loose and dissolved, a lot of vacuoluses were formed (Figure 4B). In IPC group, mitochondrial structure was basically normal. Mitochondria were orderly arranged, mitochondrial membrane was basically intact, cristae were congested and there was no vacuolization (Figure 4C).

Quantitative analysis of mitochondrial morphology

The cross-sectional area and perimeter of mitochondria were markedly increased after reperfusion in IR and IPC groups against sham group ($P < 0.05$), while the specific surface of mitochondria was significantly reduced ($P < 0.05$). Compared with IR group, the cross-sectional area and perimeter of mitochondria in IPC group were markedly reduced and the specific surface was significantly increased ($P < 0.05$) (Table 2).

Table 2 Changes of parameters of mitochondrial morphology (mean \pm SD, $n=8$)

Group	Area (μm^2)	Perimeter (μm)	Surface (μm^{-1})
Sham	76.2 ± 8.1	22.7 ± 4.6	0.39 ± 0.04
IR	278.3 ± 22.2^a	60.9 ± 5.9^a	0.17 ± 0.05^a
IPC	150.9 ± 16.4^{ac}	42.1 ± 4.3^{ac}	0.26 ± 0.05^{ac}

^a $P < 0.05$ vs sham, ^c $P < 0.05$ vs IR.

DISCUSSION

Under the influence of many kinds of stress factors such as ROS, Ca^{2+} overloading, and toxin, mitochondrial ultrastructure and its function were easily damaged, then the active substance originally in mitochondria related to apoptosis including cytochrome C, was released into cytoplasm^[14-18]. Recent progress in studies on apoptosis has revealed that cytochrome

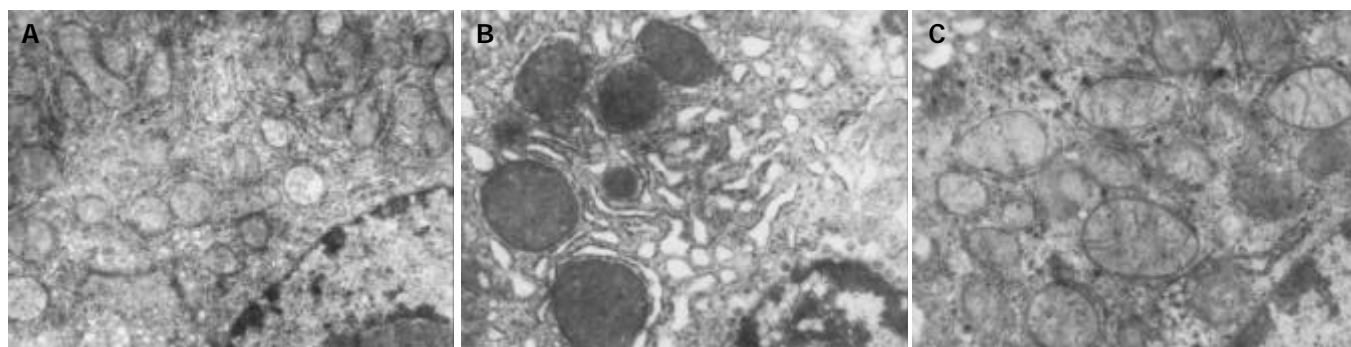


Figure 4 Mitochondrial ultrastructure in sham, IR and IPC groups (TEM $\times 15\ 000$). A: Mitochondrial ultrastructure in sham group, B: Mitochondrial ultrastructure in IR group, C: Mitochondrial ultrastructure in IPC group.

C is a pro-apoptotic factor. It is released at early stage of apoptosis and, by combining with some cytosolic proteins, could activate conversion of the latent apoptosis-promoting protease to its active form^[19]. Once cytochrome C was released, cells would die through two ways. One was through quick apoptotic mechanism. Released cytochrome C and apoptotic protease activating factor-1 (Apaf-1) and Caspase-9 were combined, and then CytC-Apaf-1-Caspase-9 compound was formed, which would lead to the activation of pro-Caspase-9, and subsequently, downstream Caspase-3 was activated, and apoptotic cascade reaction was promoted. At the same time, part of the unreleased cytochrome C was steadily combined with cytochrome b-c1 and C oxidase, and adequate ATP was produced to provide energy for apoptosis^[20-23]. The other was through necrotic process. Permeability transition pore (PTP) opened, mitochondrial matrix was swollen and ruptured due to hyperosmotic effect, the transmembrane potential ($\Delta \Psi_m$) of the original mitochondrial membrane quickly collapsed, cytochrome C was released in great amount, electron transferring respiratory chain was blocked, ATP content was radically reduced, effective supply of energy could not be realized and cell necrosed. Consequently, mitochondria could determine the cells to go into apoptosis or necrosis^[24]. This experiment proved that early injury of cells after reperfusion occurred mainly in the form of apoptosis. The end product MDA of lipid peroxidation in liver tissue increased after reperfusion, while SOD, CAT and GSH-PX as the major antioxidant enzyme and free radical scavenger were obviously decreased, indicating their capacity of preventing cells from the injury caused by ROS. Excessive oxygen free radicals could directly react with unsaturated fatty acid on the surface of mitochondrial membrane, which led to the destruction of its structure and function. Cytochrome C and other apoptosis-promoting substances were released in great amount, which triggered the apoptosis of cells.

The quantitative analysis of the stereo-form of mitochondria indicated that the major morphological change of mitochondrial injury was swelling. It was considered previously that the apoptotic cells manifested condensed chromatin but intact mitochondria. Now much more evidence revealed that significant changes of mitochondria such as swelling, megamitochondria, mitochondrial pyknosis and disrupted outer-membrane could take place in many apoptotic models^[25,26]. Specific surface is the ratio of average area of granular membrane to its volume. It is the objective index to reflect the swelling degree of mitochondria. Our study found that, after reperfusion, the cross-sectional area and perimeter of mitochondria were obviously increased, but specific surface was markedly smaller. The swelling of mitochondria was obvious, and this was in accordance with the changing tendency of mitochondrial ultrastructural organization observed under electron microscope. After postconditioning, the degree of mitochondrial swelling injury was obviously relieved and hepatocellular apoptotic index was also decreased, indicating that the structural and functional changes of mitochondria in apoptotic cells were correlated with the initiation and development of cell apoptosis, suggesting that mitochondrial dysfunction might be the key event in the development of cell apoptosis. Moreover, IPC had a protective effect on the mitochondrial ultrastructure and function.

The exact mechanisms underlying this postconditioning-produced protection remain unclear. It is most likely, though still speculative, that the IPC scheme (reiterative brief pre-reperfusion followed by continuous reperfusion) adopted in this experiment to some extent equaled a controlled slow intermittent reoxygenation, which might reduce the burst production of oxygen free radicals at the early stage of reperfusion and stimulate the release of antioxidant enzymes and free radical scavengers, thus producing protective effects. Compared with IR group, in IPC group MDA in the liver tissue

was decreased and every antioxidant enzyme was increased conspicuously, which reduced the injury to mitochondrial membrane lipid peroxidation by toxic oxygen radicals, protected the integrity of the structure and function of mitochondria, and prevented the apoptosis of liver parenchyma cells. Cave *et al.*^[27] reported that, in an isolated perfused heart model, compared with sudden reperfusion (remove artery snare occluder abruptly), controllable and slow reperfusion could decrease the occurrence of ventricular fibrillation. The postconditioning treatment in the present study was essentially comparable in some senses to those controlled and slow reoxygenation.

In addition, in order to know the function of mitochondria in apoptotic regulatory pathway, we also measured the change of the content of Bcl-2 protein in liver tissue. Bcl-2 protein as the major representative of apoptotic restraining proteins in Bcl-2 family, functioned through signal-anchor sequence of carboxyl terminal stretching cross mitochondrial membrane^[28-31]. Bcl-2 protein could regulate the permeability of PTP on the surface of mitochondrial membrane, or itself could participate in the formation of the specific pathway directly. This could maintain the stability of transmembrane potential and inhibit the release of cytochrome C and other apoptosis-promotion substances, and consequently inhibit the activation of Caspase in cytoplasm and block apoptotic cascade reaction^[32-35]. Our experiment confirmed that after postconditioning, the A value of Bcl-2 protein was obviously higher than that of IR group, and apoptotic index was obviously decreased. This showed that IPC could decrease apoptosis in liver IRI by up-regulating trans-mitochondrial membrane Bcl-2 protein expression. But the detailed mechanism needs to be further studied.

To sum up, in hepatic IRI, various stress factors can activate the apoptotic pathway mediated by mitochondria, which leads to the increase of apoptosis, and the decrease of the total number of parenchyma cells, and thus the hepatic tissue and liver function are severely damaged. Mitochondrial apoptotic pathway participates in hepatic IRI, and is a ring-point in this complicated mechanism. IPC can protect the mitochondrial ultrastructural organization and function through the inhibition of synthesis of excessive oxygen free radicals after reperfusion and increase trans-mitochondrial membrane Bcl-2 protein expression. Consequently, IPC can inhibit cell apoptosis and reduce hepatic IRI. IPC should carry out after operation and before comprehensive blood perfusion. It is easy to perform and the time is adequate. Undoubtedly, it has direct clinical application value.

REFERENCES

- 1 **Lei DX**, Peng CH, Peng SY, Jiang XC, Wu YL, Shen HW. Safe upper limit of intermittent hepatic inflow occlusion for liver resection in cirrhotic rats. *World J Gastroenterol* 2001; **7**: 713-717
- 2 **Kiemer AK**, Heinze SK, Gerwig T, Gerbes AL, Vollmar AM. Stimulation of p38 MAPK by hormonal preconditioning with atrial natriuretic peptide. *World J Gastroenterol* 2002; **8**: 707-711
- 3 **Oshiro T**, Shiraishi M, Muto Y. Adenovirus mediated gene transfer of antiapoptotic protein in hepatic ischemia-reperfusion injury: the paradoxical effect of Bcl-2 expression in the reperfused liver. *J Surg Res* 2002; **103**: 30-36
- 4 **Chen MF**, Chen JC, Chiu DF, Ng CJ, Shyr MH, Chen HM. Prostacyclin analogue (OP-2507) induces delayed ex vivo neutrophil apoptosis and attenuates reperfusion-induced hepatic microcirculatory derangement in rats. *Shock* 2001; **16**: 473-478
- 5 **Sileri P**, Schena S, Morini S, Rastellini C, Pham S, Benedetti E, Cicalese L. Pyruvate inhibits hepatic ischemia-reperfusion injury in rats. *Transplantation* 2001; **72**: 27-30
- 6 **Ikebe N**, Akaike T, Miyamoto Y, Hayashida K, Yoshitake J, Ogawa M, Maeda H. Protective effect of S-nitrosylated alpha (1)-protease inhibitor on hepatic ischemia-reperfusion injury. *J Pharmacol Exp Ther* 2000; **295**: 904-911
- 7 **Susin SA**, Zamzami N, Castedo M, Hirsch T, Marchetti P, Ma-

- cho A, Daugas E, Geuskens M, Kroemer G. Bcl-2 inhibits the mitochondrial release of an apoptogenic protease. *J Exp Med* 1996; **184**: 1331-1341
- 8 **Kluck RM**, Bossy-Wetzel E, Green DR, Newmeyer DD. The release of cytochrome c from mitochondria: a primary site for Bcl-2 regulation of apoptosis. *Science* 1997; **275**: 1132-1136
- 9 **Marchetti P**, Susin SA, Decaudin D, Gamen S, Castedo M, Hirsch T, Zamzami N, Naval J, Senik A, Kroemer G. Apoptosis-associated derangement of mitochondrial function in cells lacking mitochondrial DNA. *Cancer Res* 1996; **56**: 2033-2038
- 10 **Petit PX**, Susin SA, Zamzami N, Mignotte B, Kroemer G. Mitochondria and programmed cell death: back to the future. *FEBS Lett* 1996; **396**: 7-13
- 11 **Hengartner MO**. The biochemistry of apoptosis. *Nature* 2000; **407**: 770-776
- 12 **Desagher S**, Martinou JC. Mitochondria as the central control point of apoptosis. *Trends Cell Biol* 2000; **10**: 369-377
- 13 **Nauta RJ**, Tsimoyiannis E, Uribe M, Walsh DB, Miller D, Butterfield A. Oxygen-derived free radicals in hepatic ischemia and reperfusion injury in the rat. *Surg Gynecol Obstet* 1990; **171**: 120-125
- 14 **Liu X**, Kim CN, Yang J, Jemmerson R, Wang X. Induction of apoptotic program in cell-free extracts: requirement for dATP and cytochrome c. *Cell* 1996; **86**: 147-157
- 15 **Sola S**, Brito MA, Brites D, Moura JJ, Rodrigues CM. Membrane structural changes support the involvement of mitochondria in the bile salt-induced apoptosis of rat hepatocytes. *Clin Sci* 2002; **103**: 475-485
- 16 **Reichert AS**, Neupert W. Contact sites between the outer and inner membrane of mitochondria-role in protein transport. *Biochim Biophys Acta* 2002; **1592**: 41-49
- 17 **Xue L**, Borutaite V, Tolkovsky AM. Inhibition of mitochondrial permeability transition and release of cytochrome c by anti-apoptotic nucleoside analogues. *Biochem Pharmacol* 2002; **64**: 441-449
- 18 **Siskind LJ**, Kolesnick RN, Colombini M. Ceramide channels increase the permeability of the mitochondrial outer membrane to small proteins. *J Bio Chem* 2002; **277**: 26796-26803
- 19 **Skulachev VP**. Cytochrome c in the apoptotic and antioxidant cascades. *FEBS Lett* 1998; **423**: 275-280
- 20 **Marcocci L**, Marchi U, Salvi M, Milella ZG, Nocera S, Agostinelli E, Mondovi B, Toninello A. Tyramine and monoamine oxidase inhibitors as modulators of the mitochondrial membrane permeability transition. *J Membr Biol* 2002; **188**: 23-31
- 21 **Kim TS**, Jeong DW, Yun BY, Kim IY. Dysfunction of rat liver mitochondria by selenite: induction of mitochondrial permeability transition through thiol-oxidation. *Biochem Biophys Res Commun* 2002; **294**: 1130-1137
- 22 **Rodrigues T**, Santos AC, Pigoso AA, Mingatto FE, Uyemura SA, Curti C. Thioridazine interacts with the membrane of mitochondria acquiring antioxidant activity toward apoptosis-potentially implicated mechanisms. *Br J Pharmacol* 2002; **136**: 136-142
- 23 **Li P**, Nijhawan D, Budihardjo I, Srinivasula SM, Ahmad M, Alnemri ES, Wang X. Cytochrome c and dATP-dependent formation of Apaf-1/caspase-9 complex initiates an apoptotic protease cascade. *Cell* 1997; **91**: 479-489
- 24 **Green DR**, Reed JC. Mitochondria and apoptosis. *Science* 1998; **281**: 1309-1312
- 25 **Frey TG**, Mannella CA. The internal structure of mitochondria. *Trends Biochem Sci* 2000; **25**: 319-324
- 26 **Wakabayashi T**. Structural changes of mitochondria related to apoptosis: swelling and megamitochondria formation. *Acta Biochim Pol* 1999; **46**: 223-237
- 27 **Cave AC**, Collis CS, Downey JM, Hearse DJ. Improved functional recovery by ischaemic preconditioning is not mediated by adenosine in the globally ischaemic isolated rat heart. *Cardiovasc Res* 1993; **27**: 663-668
- 28 **Nguyen M**, Branton PE, Walton PA, Oltvai ZN, Korsmeyer SJ, Shore GC. Role of membrane anchor domain of Bcl-2 in suppression of apoptosis caused by E1B-defective adenovirus. *J Bio Chem* 1994; **269**: 16521-16524
- 29 **Decaudin D**, Geley S, Hirsch T, Castedo M, Marchetti P, Macho A, Kofler R, Kroemer G. Bcl-2 and Bcl-XL antagonize the mitochondrial dysfunction preceding nuclear apoptosis induced by chemotherapeutic agents. *Cancer Res* 1997; **57**: 62-67
- 30 **Castedo M**, Hirsch T, Susin SA, Zamzami N, Marchetti P, Macho A, Kroemer G. Sequential acquisition of mitochondrial and plasma membrane alterations during early lymphocyte apoptosis. *J Immunol* 1996; **157**: 512-521
- 31 **Zamzami N**, Susin SA, Marchetti P, Hirsch T, Gomez-Monterrey I, Castedo M, Kroemer G. Mitochondrial control of nuclear apoptosis. *J Exp Med* 1996; **183**: 1533-1544
- 32 **Marchetti P**, Castedo M, Susin SA, Zamzami N, Hirsch T, Macho A, Haeflner A, Hirsch F, Geuskens M, Kroemer G. Mitochondrial permeability transition is a central coordinating event of apoptosis. *J Exp Med* 1996; **184**: 1155-1160
- 33 **Zamzami N**, Marchetti P, Castedo M, Hirsch T, Susin SA, Masse B, Kroemer G. Inhibitors of permeability transition interfere with the disruption of the mitochondrial transmembrane potential during apoptosis. *FEBS Lett* 1996; **384**: 53-57
- 34 **Akao Y**, Maruyama W, Shimizu S, Yi H, Nakagawa Y, Shamoto-Nagai M, Youdim MB, Tsujimoto Y, Naoi M. Mitochondrial permeability transition mediates apoptosis induced by N-methyl(R) salsolinol, an endogenous neurotoxin, and is inhibited by Bcl-2 and rasagiline, N-propargyl-1(R)-aminoindan. *J Neurochem* 2002; **82**: 913-923
- 35 **Li S**, Zhao Y, He X, Kim TH, Kuharsky DK, Rabinowich H, Chen J, Du C, Yin XM. Relief of extrinsic pathway inhibition by the Bid-dependent mitochondrial release of Smac in Fas-mediated hepatocyte apoptosis. *J Bio Chem* 2002; **277**: 26912-26920

Edited by Zhu LH and Wang XL Proofread by Xu FM

Relationship between encephalopathy and portal vein-vena cava shunt: Value of computed tomography during arterial portography

Qian Chu, Zhen Li, Su-Ming Zhang, Dao-Yu Hu, Ming Xiao

Qian Chu, Su-Ming Zhang, Department of Neurology, Tongji Hospital, Tongji Medical College of Huazhong University of Science and Technology, Wuhan 430030, Hubei Province, China
Zhen Li, Dao-Yu Hu, Ming Xiao, Department of Radiology, Tongji Hospital, Tongji Medical College of Huazhong University of Science and Technology, Wuhan 430030, Hubei Province, China
Supported by the National Natural Science Foundation of China, No. 30070825

Correspondence to: Dr. Qian Chu, Department of Neurology, Tongji Hospital, Tongji Medical College of Huazhong University of Science and Technology, Wuhan 430030, Hubei Province, China. qianchu@163.com

Telephone: +86-27-83691562 **Fax:** +86-27-83612633

Received: 2003-07-17 **Accepted:** 2003-10-07

Abstract

AIM: To assess the value of computed tomography during arterial portography (CTAP) in portal vein-vena cava shunt, and analysis of the episode risk in encephalopathy.

METHODS: Twenty-nine patients with portal-systemic encephalopathy due to portal hypertension were classified by West Haven method into grade I(29 cases), grade II(16 cases), grade III(10 cases), grade IV(4 cases). All the patients were scanned by spiral-CT. Plane scans, artery phase and portal vein phase enhancement scans were performed, and the source images were thinly reconstructed to 1.25 mm. We reconstructed the celiac trunk, portal vein, inferior vena cava and their branches and subjected them to three-dimensional vessel analysis by volume rendering (VR) technique and multiplanar volume reconstruction (MPVR) technique. The blood vessel reconstruction technique was used to evaluate the scope and extent of portal vein-vena cava shunt, portal vein emboli and the fistula of hepatic artery- portal vein. The relationship between the episode risk of portal-systemic encephalopathy and the scope and extent of portal vein-vena cava shunt, portal vein emboli and fistula of hepatic artery- portal vein was studied.

RESULTS: The three-dimensional vessel reconstruction technique of spiral-CT could display celiac trunk, portal vein, inferior vena cava and their branches at any planes and angles and the scope and extent of portal vein-vena cava shunt, portal vein emboli and the fistula of hepatic artery- portal vein. In twenty-nine patients with portal-systemic encephalopathy, grade I accounted for 89.7% esophageal varices, 86.2% paragastric varices; grade II accounted for 68.75% cirsoomphalos, 56.25% paraesophageal varices, 62.5% retroperitoneal varices and 81.25% dilated azygos vein; grade III accounted for 80% cirsoomphalos, 60% paraesophageal varices, 70% retroperitoneal varices, 90% dilated azygos vein, and part of the patients in grades II and III had portal vein emboli and fistula of hepatic artery-portal vein; grade IV accounted for 75% dilated left renal vein, 50% paragallbladder varices, all the patients had fistula of hepatic artery- portal vein.

CONCLUSION: The three-dimensional vessel reconstruction technique of spiral-CT can clearly display celiac trunk, portal vein, inferior vena cava and their branches at any planes and angles and the scope and extent of portal vein-vena cava shunt. The technique is valuable for evaluating the episode risk in portal-systemic encephalopathy.

Chu Q, Li Z, Zhang SM, Hu DY, Xiao M. Relationship between encephalopathy and portal vein-vena cava shunt: Value of computed tomography during arterial portography. *World J Gastroenterol* 2004; 10(13): 1939-1942

<http://www.wjgnet.com/1007-9327/10/1939.asp>

INTRODUCTION

Portal-systemic encephalopathy is a kind of syndrome caused by portal hypertension and the construction of lateral branches, leading to a series of metabolic disorders, and is related to many neuron conduction mechanisms^[1]. The main clinical manifestation is coma or the alteration of consciousness and behaviors. The syndrome has a close relationship with the construction of portal vein lateral branches. The three-dimensional vessel reconstruction technique of spiral-CT is the best method to display the vascular system^[2]. Using this technique, we detected the scope and degree of portal vein-vena cava shunt, analyzed the risk of portal-systemic encephalopathy, and the relationship between them. This is of importance for doctors to make appropriate therapy plan and predict the disease's prognosis.

MATERIALS AND METHODS

Selection of clinical portal-systemic encephalopathy patients

From April to October 2003, 480 patients were performed spiral-CT because of liver or portal vein diseases. Among them, 59 patients had portal-systemic encephalopathy, including 44 males and 15 females. They aged from 34 to 69 years, averaging 48.9 years. All the patients were diagnosed by clinical symptoms, laboratory examination and radiologic findings. They were classified by West Haven method into grade I (29 cases), grade II (16 cases), grade III (10 cases), grade IV (4 cases).

Based on West Haven method, encephalopathy was divided into 4 grades^[3]. Grade I had absence of normal consciousness, euphoria or anxious, shortening of attention time, and other damage manifestations. Grade II had somnolence or indifference, mild disorder of time or space, mild change of personality, unsuitable behaviors, damage of subtraction. Grade III had lethargy, even half coma, reactions to word stimulation, confusion, obvious orientation disorder. Grade IV had coma (The patient had no reaction to word stimulation or harmful stimulation).

Scan technique of spiral-CT

Lightspeed spiral-CT (GE Corporation, U.S.A) performed high-speed scan. The parameters^[4] were 120 KV, 250 mA, slice thickness 10 mm, pitch 1.375:1, and matrix 512×512. We

performed plane scan at first, and then enhancement scan. The dosage of Ultravist 300 (62.3 mg/mL) was 2 mL/kg, and the injection speed was 3.5 mL/s. The injection was executed by a hyperbaric injection syringe in elbow vein by bolus injection. We performed the artery phase and portal vein phase enhancement scans after the injection^[5].

Three-dimensional vessel reconstruction technique of spiral-CT

Double-phase enhancement 10-mm thick images were reconstructed in CT^[6], and the reconstructed slices were 1.25-mm thick. Then the images were pushed to the workstation. The three-dimensional blood vessel reconstruction was performed by ADW4.0 software. The reconstructed celiac trunk, portal vein, inferior vena cava and their branches were subjected to three-dimensional vessel analysis by volume rendering (VR) technique^[7,8] and multiplanar volume reconstruction (MPVR) technique^[9]. The VR technique could utilize any axis as basic axis and carry out 360-degree rotation so that we could observe the vessels in any degree^[10]. The MPVR technique could perform any slice cross-sectional analysis^[11]. We evaluated the scope and degree of portal vein-vena cava shunt, portal vein emboli and the fistula of hepatic artery-portal vein with the aid of source images and reconstructed images^[12], and analyzed the relationship between the above-mentioned changes and the risk of portal-systemic encephalopathy^[13,14].

RESULTS

Display effects of three-dimensional vessel reconstruction technique of spiral-CT for portal vein and its branches

Referring to Ishikawa vessel classification method and considering the patients' condition, we classified the portal vein-vena cava shunt into nine types, normally cirrhosis, paragallbladder varices, lienorenal vein collateral branch opening, retroperitoneal varices, esophageal varices, paraesophageal varices, dilated azygos vein, paragastric varices and dilated left renal vein. At the same time, we observed whether there were portal vein emboli and fistula of hepatic artery-portal vein.

Assessment of hepatic artery-portal vein fistula

The VR technique could display the 3-dimensional vascular structures of celiac trunk, hepatic artery, superior mesenteric artery and their branches at any angle in artery phase. We could analyze the relationship between the arteries and portal vein. The VR technique could display artery-portal vein fistula very well. In the artery phase, the portal vein was visualized early, and the blood in portal vein was seen refluxed (Figure 1A). In portal vein phase, the portal vein was very slightly developed and portal vein-vena cava shunt emerged (Figure 1B).

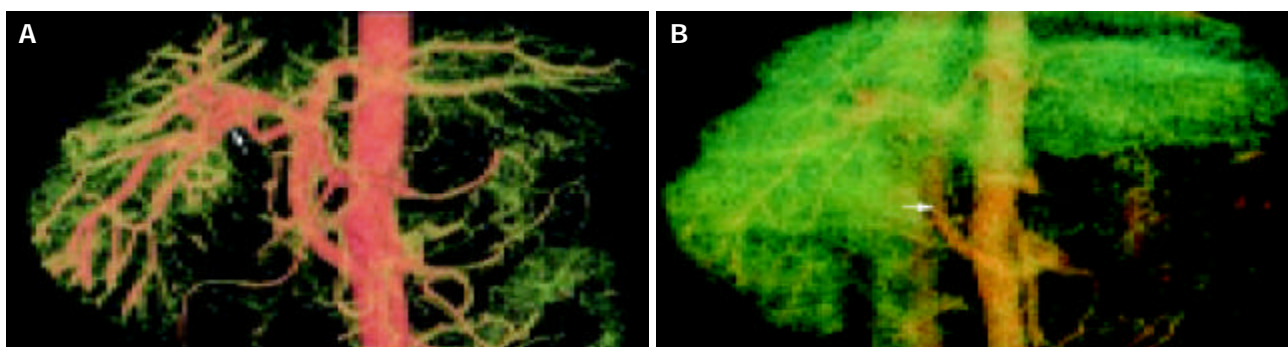


Figure 1 Portal vein in artery phase and in portal vein phase. A: Portal vein in artery phase. VR technique could display artery-portal vein fistula clearly in artery phase, the portal vein was visualized early, even portal vein blood up the stream. The arrow points the fistula aperture between the right hepatic artery and right portal vein. B: Portal vein in portal vein phase. The portal vein was very slightly developed and portal vein-vena cava shunt emerged in the portal vein phase.

Detection of portal vein emboli

In the portal vein phase, the VR technique could show the 3-dimensional vascular structures of portal vein and its branches at any angle. The enlarged portal vein and a non-flow region in the trunk could be seen (Figure 2). An image of portal vein was reconstructed by MPVR, and the emboli's scope and size could be displayed at many angles (Figure 3).

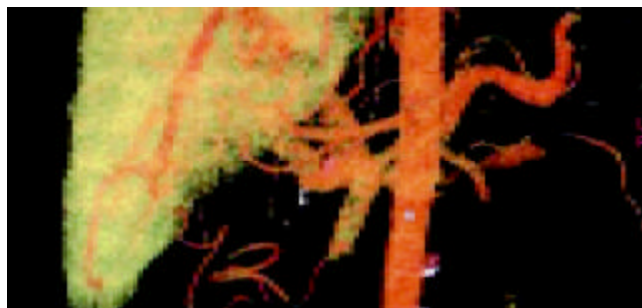


Figure 2 Enlarged portal vein and a non-flow region in the trunk (arrow).

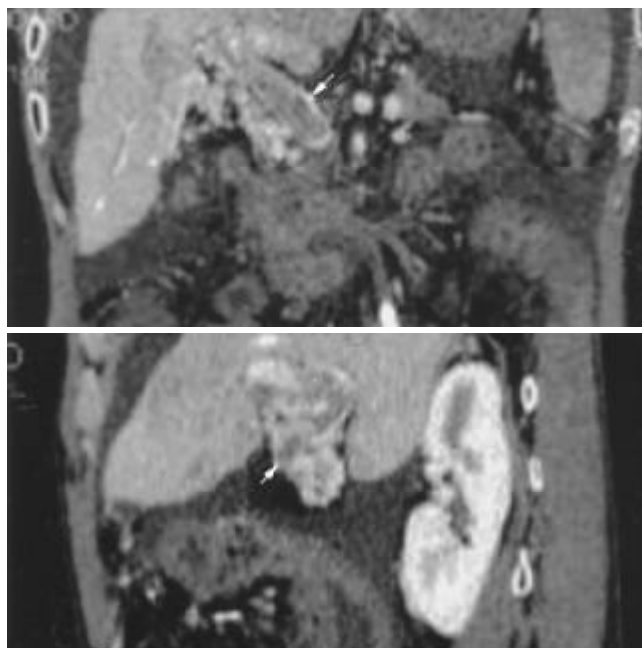


Figure 3 Image of portal vein reconstructed by MPVR. We could see the emboli's scopes and sizes at different planes (arrow).

Analysis of portal vein-vena cava shunt

The MPVR technique could perform any cross-section analysis. Combining the source images, we evaluated the scope and degree of portal vein-vena cava shunt, portal vein emboli and fistula of hepatic artery- portal vein on MPVR images (Figures 4A, B).

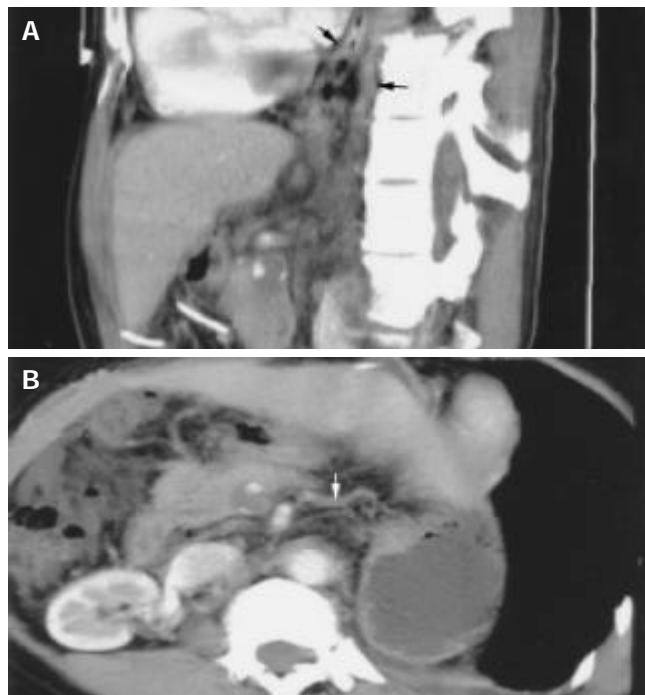


Figure 4 Portal vein-vena cava shunt, portal vein emboli and fistula of hepatic artery-portal vein on MPVR images. A: Paraesophageal varices and dilated azygos vein on MPVR image (arrow). B: Paragastric varices on MPVR image (arrow).

Assessment of portal vein-vena cava shunt in encephalopathy

Referring to Ishikawa vessel classification method, the patients were classified into 4 grades by West Haven method: grade I, 29 cases; grade II, 16 cases; grade III, 10 cases; grade IV, 4 cases. The main portal vein disorders are listed in Table 1.

Table 1 Assessment of portal vein-vena cava shunt in encephalopathy

	Grade I n(%)	Grade II n(%)	Grade III n(%)	Grade IV n(%)
Esophageal varices	26(89.7)	9(56.25)	8(80)	4 (100)
Paragastric varices	25(86.2)	11(68.75)	7(70)	3(75)
Cirsomphalos	12(41.3)	11(68.75)	8(80)	4(100)
Retroperitoneal varices	11(37.9)	9(56.25)	6(60)	4(100)
Paraesophageal varices	13(44.8)	10(62.5)	7(70)	3(75)
Dilated azygos vein	6(20.1)	13(81.25)	9(90)	2(50)
Dilated left renal vein	2(6.9)	1(6.25)	1(10)	3(75)
Paragallbladder varices	0(0)	1(6.25)	1(10)	2(50)
Hepatic artery- portal vein fistula	0(0)	3(18.75)	6(60)	4(100)
Portal vein emboli	2(6.9)	8(50)	7(70)	3(75)

As it shows in this table, esophageal varices and paragastric varices were common in grade I. Besides the varices in grade I patients, the patients in grades II and III had cirsomphalos, paraesophageal varices, retroperitoneal varices and dilated azygos vein, and some of them had portal vein emboli and hepatic artery- portal vein fistula. Among the patients in grade IV, dilated left renal vein and paragallbladder varices were usual, and all patients had hepatic artery- portal vein fistula.

DISCUSSION

Encephalopathy is a nervous system syndrome, originating from chronic liver disease and hepatic cirrhosis. It is associated with portal hypertension, hepatic artery- portal vein fistula, portal vein emboli, hyperammonemia and other metabolic disorders. It also has a close relationship with hypertension, portal vein-vena cava shunt and lateral branch formation. The three-dimensional vessel reconstruction technique of spiral-CT can display portal vein, its branches, the scope and degree of portal vein-vena cava shunt. The technique is valuable for evaluating the risk of encephalopathy.

Spiral-CT double-phase (artery phase, portal vein phase) scan and the reconstruction technique could display portal vein-vena cava shunt, hepatic artery- portal vein fistula and portal vein emboli^[15]. Computed tomography during arterial portography (CTAP) was one of the best ways to show portal vein disorders^[16]. Sixteen-slice spiral-CT had unique superiority for portal vein pictures^[17]. To evaluate hepatic artery- portal vein fistula, early visualization of portal vein, enlargement of portal vein and blood of portal vein reflux were the main characteristics^[18,19]. The double-phase images of volume rendering technique could not only display the position and size of fistulae, but also the diameter of portal vein and the extent of portal vein reflux. Reflux and fistulae would advance the portal hypertension, accelerate the portal vein-vena cava shunt, decrease the portal vein blood flow into the liver, and increase the opportunity for encephalopathy^[20]. There was no hepatic artery- portal vein fistula in grade I patients (n=29), only 18.75% patients had fistulae in grade II (Table 1). However, in grades III and IV patients, 60% and 100% patients had fistulae. We can draw a conclusion that hepatic artery- portal vein fistula increases the risk of encephalopathy, and fistulae would aggravate encephalopathy or indicate the risk of encephalopathy.

On the assessment of portal vein emboli, the VR images in portal vein phase could show the vein because the blood flow was hindered by emboli or the complete obstruction of the trunk. The portal vein embolus was possibly one of the markers that hint the deterioration of encephalopathy^[21,22]. Perhaps portal vein embolus could hinder blood flow into the liver^[23]. It was believed that encephalopathy would appear if the blood flow of portal vein was less than 692 mL/min^[24]. The portal vein embolus would accelerate portal hypertension and induce brain disorder at the same time.

Portal vein-vena cava shunts include^[25,26] esophageal varices, paragastric varices^[27], paraesophageal varices, cirsomphalos, paraumbilical veins^[28,29], retroperitoneal varices (Retzius venous plexus), dilated azygos vein, dilated spleno- renal vein and stomach- renal vein, even internal iliac vein communication^[30]. CT and barium meal had the same role in diagnosing esophageal varices and paragastric varices. But CT was more valuable than barium meal and esophagoscope in diagnosing other varices^[31,32]. Spiral-CT scan is a kind of volume scan, and its merits include high speed and short reconstruction time. An examination of a patient's liver can be finished in a breathholding. VR images could display large lateral branch circulation clearly, but the small branches unclearly. The multiplanar volume reconstruction (MPVR) technique could perform any slice cross-sectional analysis of the vessels and disclose their relationship with the surrounding tissues (Figures 2, 3), and esophageal varices, paragastric varices and azygos vein.

In a word, simple esophageal varices, paragastric varices and paraesophageal varices would not induce severe encephalopathy. However, the portal vein emboli, or hepatic artery- portal vein fistula, or wide portal vein-vena cava shunt, particularly the dilated left renal vein and paragallbladder varices, which may hint encephalopathy, would occur or deteriorate.

Not only would portal vein-vena cava shunt induce portal-systemic encephalopathy, but also the liver function of patients,

metabolic status^[33] and diseases outside the liver^[34] played a role. The relationship between them is still unclear. More work needs to be done. However, the three-dimensional vessel reconstruction technique of spiral-CT can display the celiac trunk, portal vein, inferior vena cava and their branches at any plane and from any angle, and show the scope and degree of portal vein-vena cava shunt. The technique is valuable for evaluating the episode risk in portal-systemic encephalopathy, and helpful for TIPSS.

REFERENCES

- Butterworth RF.** Hepatic encephalopathy: a neuropsychiatric disorder involving multiple neurotransmitter systems. *Curr Opin Neurol* 2000; **13**: 721-727
- Calculi L, Casadei R, Amore B, Albini Riccioli L, Minni F, Caputo M, Marrano D, Gavelli G.** The usefulness of spiral Computed Tomography and colour-Doppler ultrasonography to predict portal-mesenteric trunk involvement in pancreatic cancer. *Radiol Med* 2002; **104**: 307-315
- Ferenci P, Lockwood A, Mullen K, Tarter R, Weissenborn K, Blei AT.** Hepatic encephalopathy-definition, nomenclature, diagnosis, and quantification: final report of the working party at the 11th World Congresses of Gastroenterology, Vienna, 1998. *Hepatology* 2002; **35**: 716-721
- Francis IR, Cohan RH, McNulty NJ, Platt JF, Korobkin M, Gebremariam A, Ragupathi K.** Multidetector CT of the liver and hepatic neoplasms: effect of multiphasic imaging on tumor conspicuity and vascular enhancement. *Am J Roentgenol* 2003; **180**: 1217-1224
- Matoba M, Yokota H, Yabuno K, Kuga G, Tinami H, Yamamoto I.** Evaluation of two injection protocols by time-density curves for possible application to hepatic dynamic and upper abdominal CT angiography in MDCT: high concentration (350 mgI/ml) with conventional volume (100 ml) vs conventional concentration (300 mgI/ml) with larger volume (150 ml) and higher injection rate. *Nippon Igaku Hoshasen Gakkai Zasshi* 2003; **63**: 98-102
- Jayakrishnan VK, White PM, Aitken D, Crane P, McMahon AD, Teasdale EM.** Subtraction helical CT angiography of intra- and extracranial vessels: technical considerations and preliminary experience. *Am J Neuroradiol* 2003; **24**: 451-455
- Dudeck O, Hoffmann KT, Wieners G, Pech M, Knollmann F, Felix R.** Application of multislice detector spiral computed tomography to intracranial aneurysms: first clinical experience. *Radiologie* 2003; **43**: 310-318
- Byun JH, Kim TK, Lee SS, Lee JK, Ha HK, Kim AY, Kim PN, Lee MG, Lee SG.** Evaluation of the hepatic artery in potential donors for living donor liver transplantation by computed tomography angiography using multidetector-row computed tomography: comparison of volume rendering and maximum intensity projection techniques. *J Comput Assist Tomogr* 2003; **27**: 125-131
- Frohner S, Wagner M, Schmitt R, Brunn J, Muller M, Christopoulos G, Coblenz G, Kerber S, Urbanski P.** Multi-slice CT of aortocoronary venous bypasses and mammary artery bypasses: evaluation of bypasses and their anastomoses. *Rontgenpraxis* 2002; **54**: 163-173
- Fink C, Hallscheidt PJ, Hosch WP, Ott RC, Wiesel M, Kauffmann GW, Dux M.** Preoperative evaluation of living renal donors: value of contrast-enhanced 3D magnetic resonance angiography and comparison of three rendering algorithms. *Eur Radiol* 2003; **13**: 794-801
- Kuiper JW, Geleijns J, Matheijssen NA, Teeuwisse W, Pattynama PM.** Radiation exposure of multi-row detector spiral computed tomography of the pulmonary arteries: comparison with digital subtraction pulmonary angiography. *Eur Radiol* 2003; **13**: 1496-1500
- Van Straten M, Venema HW, Streekstra GJ, Reekers JA, den Heeten GJ, Grimbergen CA.** Removal of arterial wall calcifications in CT angiography by local subtraction. *Med Phys* 2003; **30**: 761-770
- Kobayashi Y, Nakazawa J, Sakata M.** Comparison of the depiction of pancreaticoduodenal arcades and dorsal pancreatic artery, using three-point scale with volume rendering (VR), maximum intensity projection (MIP), and shaded surface display (SSD). *Nippon Hoshasen Gijutsu Gakkai Zasshi* 2002; **58**: 297-300
- Piotin M, Gailloud P, Bidaut L, Mandai S, Muster M, Moret J, Rufenacht DA.** CT angiography, MR angiography and rotational digital subtraction angiography for volumetric assessment of intracranial aneurysms. An experimental study. *Neuroradiology* 2003; **45**: 404-409
- Nakayama Y, Imuta M, Funama Y, Kadota M, Utsunomiya D, Shiraishi S, Hayashida Y, Yamashita Y.** CT portography by multidetector helical CT: comparison of three rendering models. *Radiat Med* 2002; **20**: 273-279
- Kim HC, Kim TK, Sung KB, Yoon HK, Kim PN, Ha HK, Kim AY, Kim HJ, Lee MG.** CT during hepatic arteriography and portography: an illustrative review. *Radiographics* 2002; **22**: 1041-1051
- Calculi L, Casadei R, Amore B, Albini Riccioli L, Minni F, Caputo M, Marrano D, Gavelli G.** The usefulness of spiral Computed Tomography and colour-Doppler ultrasonography to predict portal-mesenteric trunk involvement in pancreatic cancer. *Radiol Med* 2002; **104**: 307-315
- Choi BI, Lee KH, Han JK, Lee JM.** Hepatic arteriportal shunts: dynamic CT and MR features. *Korean J Radiol* 2002; **3**: 1-15
- Lawler LP, Fishman EK.** Extrahepatic arteriportal venous fistula: multidetector CT and volume-rendered angiographic imaging. *Abdom Imaging* 2001; **26**: 616-618
- Haussinger D, Kircheis G.** Hepatic encephalopathy. *Schweiz Rundsch Med Prax* 2002; **91**: 957-963
- Federico P, Zochodne DW.** Reversible parkinsonism and hyperammonemia associated with portal vein thrombosis. *Acta Neurol Scand* 2001; **103**: 198-200
- Olson MM, Ilada PB, Apelgren KN.** Portal vein thrombosis. *Surg Endosc* 2003; **13**: 255-262
- Blei AT, Cordoba J.** Hepatic Encephalopathy. *Am J Gastroenterol* 2001; **96**: 1968-1976
- Del Piccolo F, Sacerdoti D, Amodio P, Bombonato G, Bolognesi M, Mapelli D, Gatta A.** Central nervous system alterations in liver cirrhosis: the role of portal-systemic shunt and portal hypoperfusion. *Metab Brain Dis* 2003; **18**: 51-62
- Watanabe A.** Portal-systemic encephalopathy in non-cirrhotic patients: classification of clinical types, diagnosis and treatment. *J Gastroenterol Hepatol* 2000; **15**: 969-979
- Luo JJ, Yan ZP, Zhou KR, Qian S.** Direct intrahepatic portacaval shunt: an experimental study. *World J Gastroenterol* 2003; **9**: 324-328
- Tsai HM, Lin XZ, Chang YC, Lin PW, Hsieh CC.** Hepatofugal flow on computed tomography of arterial portography: its correlation with esophageal varices bleeding. *Hepatogastroenterology* 2000; **47**: 1615-1618
- Gupta D, Chawla YK, Dhiman RK, Suri S, Dilawari JB.** Clinical significance of patent paraumbilical vein in patients with liver cirrhosis. *Dig Dis Sci* 2000; **45**: 1861-1864
- Lin J, Zhou KR, Chen ZW, Wang JH, Wu ZQ, Fan J.** Three-dimensional contrast-enhanced MR angiography in diagnosis of portal vein involvement by hepatic tumors. *World J Gastroenterol* 2003; **9**: 1114-1118
- Otake M, Kobayashi Y, Hashimoto D, Igarashi T, Takahashi M, Kumaoka H, Takagi M, Kawamura K, Koide S, Sasada Y, Kageyama F, Kawasaki T, Nakamura H.** An inferior mesenteric-caval shunt via the internal iliac vein with portosystemic encephalopathy. *Intern Med* 2001; **40**: 887-890
- Gulati MS, Paul SB, Arora NK, Berry M.** Evaluation of extrahepatic portal hypertension and surgical portal systemic shunts by intravenous CT portography. *Clin Imaging* 1999; **23**: 377-385
- Vignaux O, Gouya H, Augui J, Oudjit A, Coste J, Dousset B, Chaussade S, Legmann P.** Hepatofugal portal flow in advanced liver cirrhosis with spontaneous portosystemic shunts: effects on parenchymal hepatic enhancement at dual-phase helical CT. *Abdom Imaging* 2002; **27**: 536-540
- Haghighat N, McCandless DW, Geraminegad P.** The effect of ammonium chloride on metabolism of primary neurons and neuroblastoma cells *in vitro*. *Metab Brain Dis* 2000; **15**: 151-162
- Akhtar AJ, Alamy ME, Yoshikawa TT.** Extrahepatic conditions and hepatic encephalopathy in elderly patients. *Am J Med Sci* 2002; **324**: 1-4

Role of curved planar reformations using multidetector spiral CT in diagnosis of pancreatic and peripancreatic diseases

Jing-Shan Gong, Jian-Min Xu

Jing-Shan Gong, Jian-Min Xu, Department of Radiology, Shenzhen People's Hospital (Second Affiliated Hospital, School of Medicine, Jinan University), Shenzhen 518020, Guangdong Province, China
Supported by the Medical Research Fund of Guangdong Province, No. A2002634

Correspondence to: Dr. Jing-Shan Gong, Department of Radiology, Shenzhen People's Hospital (Second Affiliated Hospital, School of Medicine, Jinan University), Shenzhen 518020, Guangdong Province, China. jshgong@sina.com.cn

Telephone: +86-755-25533018 **Fax:** +86-755-25618655

Received: 2003-12-10 **Accepted:** 2004-01-12

Abstract

AIM: To investigate the role of curved planar reformations using multidetector spiral CT (MSCT) in diagnosis of pancreatic and peripancreatic diseases.

METHODS: From October 2001 to September 2003, 47 consecutive patients with pancreatic or peripancreatic diseases, which were confirmed by operation, endoscopic retrograde cholangiopancreatography and clinical follow-up, were enrolled in this study. CT scanning was performed at a MSCT with four rows of detector. A set of images with an effective thickness of 1.0-2.0 mm and a gap of 0.5-1.0 mm (50% overlap) were acquired in all patients for post-processing. Curved planar reformations were carried out by drawing a curved line on transverse source images, coronal or sagittal multiplanar reformations according to certain anatomic structures (such as cholangiopancreatic ducts or peripancreatic vessels) and the position of lesion.

RESULTS: With thin collimation, MSCT could acquire high-quality curved planar reformations to display the profile of the whole pancreas, to trace the cholangiopancreatic ducts and peripancreatic vessels, and to show the relationship of lesions with pancreas and peripancreatic anatomic structures in one curved plane, which facilitates diagnosis and rapid communication of diagnostic information with referring physicians.

CONCLUSION: MSCT with thin collimation could be used to create high-quality curved planar reformations in evaluating pancreatic and peripancreatic diseases with pertinent anatomic information and relative pathologic signs to facilitate the diagnosis and enhance communication with the referring physician. Curved planar reformations can serve as supplements for transverse images in diagnosis and management of pancreatic and peripancreatic diseases.

Gong JS, Xu JM. Role of curved planar reformations using multidetector spiral CT in diagnosis of pancreatic and peripancreatic diseases. *World J Gastroenterol* 2004; 10(13): 1943-1947
<http://www.wjgnet.com/1007-9327/10/1943.asp>

INTRODUCTION

Pancreas is located in the retroperitoneum with a tortuous

course, which is difficult for CT and MR to display the whole pancreas in one slice. There are abundant vessels around the pancreas. It is important to visualize these vessels and the cholangiopancreatic ducts for diagnosing and evaluating the local involvement of pancreatic and peripancreatic lesions. Curved planar reformations can delineate a curved path and display the whole course of pancreas in a single cross-section image according to a curved line drawn on the transverse source images, coronal or sagittal multiplanar reformations (MPR) from a three dimension (3-D) volumetric data set acquired by spiral CT^[1,2]. They have been widely used to display vessels and evaluate vascular abnormalities in conjunction with CT angiography^[1-7]. Recently the new techniques have been applied to evaluate the pancreas and bile duct system pathologically^[8-11]. This article focuses on the role of curved planar reformations using MSCT in the diagnosis of pancreatic and peripancreatic diseases.

MATERIALS AND METHODS

Patients

From October 2001 to September 2003, 47 consecutive patients (21 female and 26 male, age range: 13-72 years, mean age: 53 years) with pancreatic or peripancreatic diseases, which were confirmed by operation ($n=18$), endoscopic retrograde cholangiopancreatography (ERCP) ($n=6$) and clinical follow-up ($n=23$), were enrolled in this study. The diseases included pancreatic carcinoma ($n=9$), cystadenoma ($n=3$), neuroendocrine tumor ($n=4$), chronic pancreatitis with pseudocyst ($n=16$), real cyst of pancreas ($n=1$), choledochal cyst ($n=2$), ampullary carcinoma ($n=3$), choledocholithiasis ($n=5$), duodenal diverticulum ($n=1$), peripancreatic adenopathy ($n=3$) and splenic arterial aneurysm ($n=1$).

CT imaging

CT scans were performed with a MSCT scanner (Toshiba Aquilion, Tokyo, Japan). Seven patients underwent plain scanning, 38 patients underwent both plain and enhanced scanning, and the other two patients a drip infusion CT cholangiography. A scanning with parameters of 120 kVp, 300 mA, 4×1-2 mm collimation, rotation time of 0.5 s, and a pitch of 5.5 was included in all patients during a breathhold of 10-15 s. In patients who underwent both plain and enhanced scanning, this protocol was obtained at the pancreatic parenchyma phase (a delay of 40 s after the beginning of intravenous injection of nonionic contrast media with an iodine content of 300 mg/mL [Omnipaque, Nycomed-Amersham, Shanghai] at 3 mL/s using a power injector). The CT cholangiographic image was acquired 60 min after intravenous drip infusion of iodipamide methylglucamine. A set of images with an effective thickness of 1-2 mm and a gap of 0.5-1.0 mm (50% overlap) was reconstructed and transmitted to workstation for post-processing.

Curved planar reformations

Curved planar reformations were obtained using a cursor to draw a curved line along a special anatomic structure on a stack of axial, sagittal, coronal section at a SGI workstation

(Alatoview 1.21) by an experienced radiologist who was familiar with the pancreatic and peripancreatic anatomic structures and had carefully reviewed all transverse source images. The operator was asked to adjust the trace of the cursor interactively to create several curved planes to display essential anatomic structures, such as cholangiopancreatic ducts and peripancreatic vessels, and the relationship of the lesion with those structures according to diagnostic and clinical need (Figure 1). The section thickness of curved plane will never be larger than the effective section thickness or smaller than the transverse pixel dimensions.



Figure 1 Curve drawn on a transverse image along the pancreatic duct in a patient with pancreatic adenocarcinoma.

RESULTS

With thinner collimation and overlap image data sets, high quality curved planar reformations were obtained in all the 47 patients, displaying the whole pancreas and tracing cholangiopancreatic ducts or peripancreatic vessels in a single cross-section image without any misregistration and steps artifacts (Figures 2-12). For the 20 pancreatic local lesions (9 cases of pancreatic adenocarcinoma, 3 cystic adenomas, 4 neuroendocrine tumors, 3 intrapancreatic pseudocysts and 1 real cyst of pancreas), curved planar reformations demonstrated that the whole or major portions of the lesion was located in the pancreatic parenchyma clearly, which made it easier to determine lesion's location (Figures 2-5). Curved planar reformations, by tracing a certain vessel, such as the celiac artery, the superior mesenteric artery, the portal vein, could demonstrate changes in the caliber of the vessel and wall invasion, which was helpful for determining whether these vessels were involved and the length of involvement, as in the 9 patients with pancreatic adenocarcinoma and the 3 patients with ampullary carcinoma (Figures 6, 7). Combining with transverse images, curved planar reformations demonstrated 2 positivities and 1 false positivity in predicting respectability, 6 positivities in assessment of unresectability in 9 patients with pancreatic adenocarcinoma. The dilatation of cholangiopancreatic ducts in patients with chronic pancreatitis, pancreatic or ampullary carcinoma and peripancreas lymph nodes enlargement were well depicted on curved planar reformations (Figures 8,9). In 1 patient with pancreatic real cyst, the curved planar reformations after CT cholangiography revealed the beaded dilatation of pancreatic duct and the dilatation and stenosis of the common bile duct. The cyst lay beside the dilated common bile duct (Figure 4). In the 13 patients with pseudocyst beyond the pancreas and the 2 patients with choledochal cyst, curved planar reformations displayed the cystic lesion and the relationship of cysts with pancreas well. Stones' location and cholangiopancreatic ducts morphologic changes distal and proximal to obstruction were depicted on curved planar reformations in all patients with choledocholithiasis (Figure 10). The location and relationship with pancreas of peripancreatic

enlarged lymph nodes were easily identified on curved planar reformations, which made differential diagnosis from pancreatic mass more simple (Figure 11). In 1 case of splenic arterial aneurysm, the dilatation of the artery was detected on curved planar reformations but missed on transverse source images due to its small diameter and dilatation along the z axis of CT imaging (Figure 12).

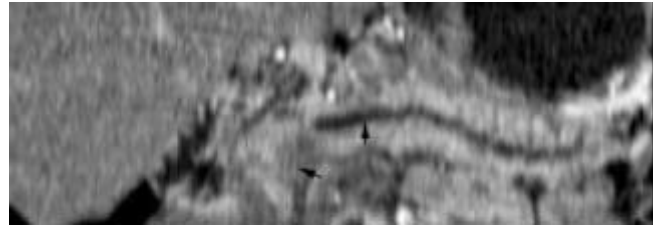


Figure 2 Curve obtained from the curved line on Figure 1 displayed the hypoattenuation tumor at the head of pancreas and the distal dilated pancreatic duct (arrow).

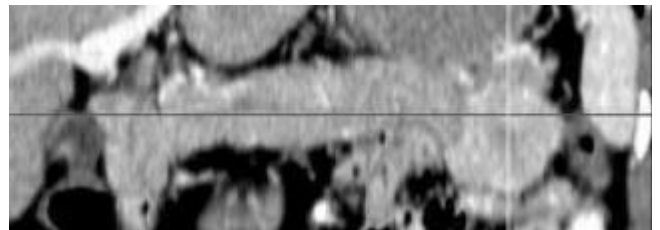


Figure 3 Neuroendocrine tumor of pancreas. Curved planar reformations during pancreatic parenchyma phase demonstrated the enhanced mass located in the tail of pancreas.

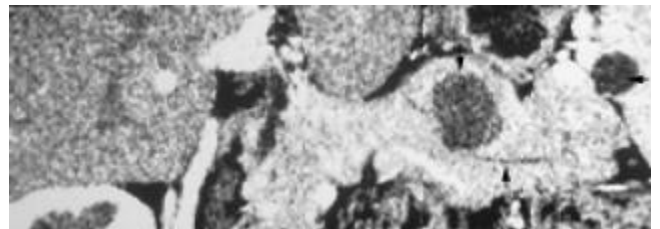


Figure 4 Neuroendocrine tumor of pancreas and peripancreatic pseudocyst. Curved plane showed a non-enhanced hypoattenuation mass located in the pancreatic parenchyma (arrow) and a pseudocyst at the port of spleen during the pancreatic parenchyma phase. The normal pancreatic duct was also well depicted (long arrow).

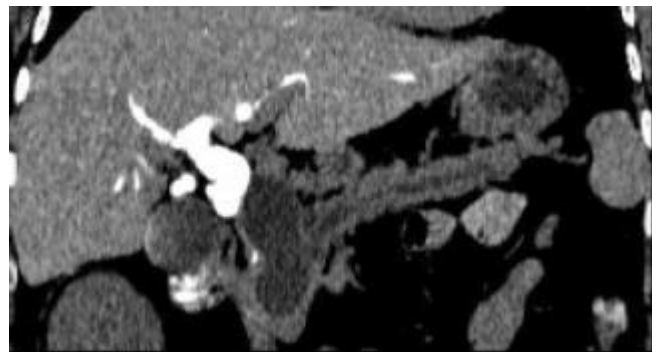


Figure 5 Real cyst of pancreas. Curved planar reformations obtained after CT cholangiography showed the dilatation and obstruction of bile duct system, and the beaded-like dilatation of pancreatic duct. The cyst located beside the common bile duct. There was no contrast media entrancing into cyst.

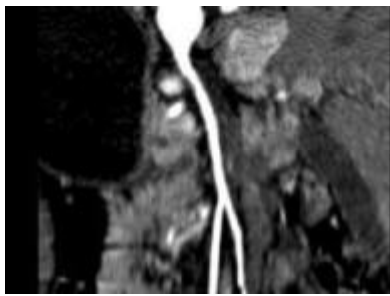


Figure 6 A curved plane tracing superior mesenteric artery of the same patient with Figure 1 and Figure 2 demonstrated the vessel was not involved. The tumor was confirmed to be resectable at operation.

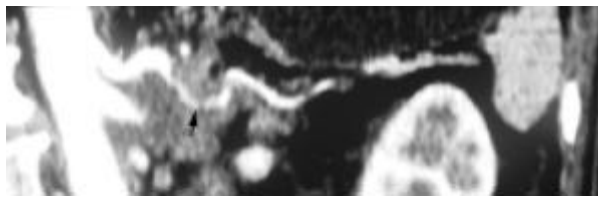


Figure 7 A curved plane tracing the celiac trunk and the splenic artery of a patient with pancreatic adenocarcinoma demonstrated the irregular stricture (arrow).



Figure 8 Ampullary carcinoma. Curved planar reformations depicted a low attenuation mass around the pancreatic head and the dilatation of both bile duct (arrow) and pancreatic duct (long arrow).



Figure 9 Gastric cancer with peripancreatic adenopathy. Curved planar reformations depicted the dilatation of the pancreatic duct.



Figure 10 Choledocholithiasis of common bile duct. Curved plane displayed the dilatation of the bile duct system and the pancreatic duct. The location of stones was depicted clearly.



Figure 11 Peripancreatic adenopathy. Curved planar reformations showed several enlarged lymph nodes located at the pancreatic head.



Figure 12 Splenic artery aneurysm. Curved planar reformations depicted the local dilatation of splenic artery (arrow).

DISCUSSION

Computed tomography (CT) is the most frequently used imaging modality for the evaluation of patients with suspected pancreatic and peripancreatic diseases, especially for diagnosing and staging pancreatic adenocarcinoma^[12-17]. In detection and staging of pancreatic ductal adenocarcinoma, CT had a sensitivity of more than 90% and a positive predictive value in the range of 96% to 100% for determining surgical unresectability^[9,12-14]. In determining resectability, the accuracy of CT remained low with positive predictive values ranging from 53% to 79% due to underestimation of vascular invasion and failure to detect small peritoneal and liver metastases^[9,12,14]. The introduction of MSCT and the development of three-dimensional (3D) imaging software have significantly improved the ability of CT to image the pancreas and evaluate a wide range of pancreatic and peripancreatic pathology^[8-11,17,18].

One major advantage of MSCT over single-detector spiral CT is substantial improvement in the speed of scan acquisition, which permits routine use of very thin collimation covering a large region during breath-hold to acquire volumetric data sets with high resolution along all three axes, especially along z axis, even with isotropic image^[9,10,18,19]. The improvement of resolution along the z axis is very helpful for generating high quality multiplanar reformations (MPR) and 3D images. Curved planar reformations are a special form of MPR; which depict the cross-section profile along any curved line the operator draws from the volumetric data sets to trace the course of an anatomic structure. The plane presents results in a 2D image that displays the entire course of the anatomic structure^[9]. Thus the techniques are very useful in displaying a complex anatomic structure with a tortuous course. They can delineate the curved vascular structure and display its whole course in one cross-section image. Therefore, curved planar reformations were used to display vessels and evaluate their abnormality^[2-7]. This provided a convenient and fast review method for radiologists and an effective format for communicating the pertinent findings to referring physicians. These techniques were especially useful in evaluating those vessels, such as the

carotid siphon, which has a tortuous course and is surrounded by complex bony structures and thus the maximal intensity projection (MIP) and 3D images were difficult to depict them^[5]. Recently, the application of curved planar reformations in the pancreatic and bile duct system showed that these techniques could provide helpful unique anatomic information, highlight critical anatomic and pathologic relationships, which were useful for surgical planning^[8-11]. The other advantage of curved planar reformations was that the referring physicians could review a few curved planes to acquire critical information instead of reviewing a large number of images in great detail, which enhanced rapid communication^[8].

In the present series, curved planar reformations using MSCT were performed in 47 patients with pancreatic and peripancreatic diseases. With thin collimation and overlap reconstruction, high quality curved planar reformations were obtained in all the patients displaying the whole tortuous pancreas in one cross-section image, tracing critical surrounding anatomic structures, such as cholangiopancreatic ducts and peripancreatic vessels, or highlighting relationships of the lesion with essential anatomic structures. All these were helpful for determining the lesion's location and evaluating its invasion to surrounding anatomic structures. The latter was important to determining the resectability of pancreatic ductal adenocarcinoma. In 9 patients with pancreatic carcinoma, curved planar reformations tracing critical peripancreatic vessels could not only demonstrate the vascular involvement of tumor, but also depict the length of the affected segment. Although one study showed that curved planar reformations were equivalent to transverse images in the detection of pancreatic tumors and determination of surgical resectability^[10], we did not assess the resectability according to curved planar reformations only due to their operator dependence, which would be discussed later. In this series, by combination of curved planar reformations with transverse images, 2 positivities and 1 false positivity in predicting resectability and 6 positivities in determining unresectability in 9 patients with pancreatic adenocarcinoma were obtained. Whether it would improve the accuracy of staging of pancreatic adenocarcinoma by combining curved planar reformation with transverse images was not carried out in this study due to the small sample size of pancreatic carcinoma, which was one limitation of this study. In one case of pancreatic real cyst, curved planar reformations after CT cholangiography demonstrated the beaded dilatation of pancreatic duct and the dilatation and obstruction of the bile duct system. The relationship of the cystic lesion with the pancreatic and bile duct system was depicted clearly. All these could provide guides for operation, although a correct diagnosis was not acquired before operation. For the peripancreatic lesions, such as peripancreatic adenopathy, ampullary carcinoma, duodenal diverticulum and pseudocysts, curved planar reformations depicted the changes of the bile duct system and pancreatic duct, and relationships of lesions with surrounding important anatomic structures, which were helpful for making diagnostic and treatment strategies. Direct display of morphologic changes of bile duct system and stones location in curved planar reformations would be very useful for surgical planning, especially for endoscopic management of choledocholithiasis. With their advantage in demonstrating vascular abnormality, curved planar reformations displayed the small splenic arterial aneurysm easily in this series although it was missed in transverse images. On the one hand, it needs the operator interactively to adjust the path of cursor and work intensively to generate proper curved planar reformations with highlight important diagnostic information. On the other hand, several curved planes may transfer the important information to referring physicians. This reduces

the referring physicians' burden to review all the transverse images for useful information.

One limitation of curved planar reformations is that they are exceedingly operator-dependent. Improper path of the cursor may generate spurious stenoses of cholangiopancreatic ducts and vessels, distort the anatomic structures or cause important lesion missed. Therefore, the operator should be familiar with the anatomy of pancreas and carefully review all transverse source images before beginning to draw the line. Although careful view of all transverse source images may be a time-consuming and tedious job, it is helpful to create proper curved planar reformations to highlight critical anatomic structures and pathologic signs. Due to this limitation, in this series a comparison with standard transverse images was not carried out. Curved planar reformations can serve as supplements in evaluating pancreatic and peripancreatic diseases while not a substitute. Recently, Raman *et al.*^[20] developed an automated method to generate curved planar reformations with reduced time and effort. With the development of post-processing software, a well-trained radiologic technologists may generate curved planar reformations routinely.

In summary, MSCT with thin collimation can be used to generate high quality curved planar reformations for evaluating pancreatic and peripancreatic diseases. Our preliminary study showed that curved planar reformations could clearly depict essential anatomic structures and highlight critical anatomic information and pathologic signs in several cross-section images, which enhanced the rapid communication with referring physicians. Curved planar reformations can serve as supplements for transverse images in diagnosis and management of pancreatic and peripancreatic diseases.

ACKNOWLEDGEMENTS

We are grateful to Mr. Xiang-Peng Zheng, Ph.D candidate for radiological biology at University of Texas Health Science Center, for language review.

REFERENCES

- 1 **Rubin GD**, Dake MD, Semba CP. Current status of three-dimensional spiral CT scanning for imaging the vasculature. *Radiol Clin North Am* 1995; **33**: 51-70
- 2 **Achenbach S**, Moshage W, Ropers D, Bachmann K. Curved multiplanar reconstructions for the evaluation of contrast-enhanced electron beam CT of the coronary arteries. *Am J Roentgenol* 1998; **170**: 895-899
- 3 **Portugaller HR**, Schoellnast H, Tauss J, Tiesenhausen K, Hausegger KA. Semitransparent volume-rendering CT angiography for lesion display in aortoiliac arteriosclerotic disease. *J Vasc Interv Radiol* 2003; **14**: 1023-1030
- 4 **Takase K**, Sawamura Y, Igarashi K, Chiba Y, Haga K, Saito H, Takahashi S. Demonstration of the artery of Adamkiewicz at multi-detector row helical CT. *Radiology* 2002; **223**: 39-45
- 5 **Teasdale E**. Curved planar reformatted CT angiography: utility for the evaluation of aneurysms at the carotid siphon. *Am J Neuroradiol* 2000; **21**: 985
- 6 **Ochi T**, Shimizu K, Yasuhara Y, Shigesawa T, Mochizuki T, Ikezoe J. Curved planar reformatted CT angiography: usefulness for the evaluation of aneurysms at the carotid siphon. *Am J Neuroradiol* 1999; **20**: 1025-1030
- 7 **Prokesch RW**, Coulam CH, Chow LC, Bammer R, Rubin GD. CT angiography of the subclavian artery: utility of curved planar reformations. *J Comput Assist Tomogr* 2002; **26**: 199-201
- 8 **Nino-Murcia M**, Jeffrey RB Jr, Beaulieu CF, Li KC, Rubin GD. Multidetector CT of the pancreas and bile duct system: value of curved planar reformations. *Am J Roentgenol* 2001; **176**: 689-693
- 9 **Nino-Murcia M**, Jeffrey RB Jr. Multidetector-row CT and volumetric imaging of pancreatic neoplasms. *Gastroenterol Clin North Am* 2002; **31**: 881-896
- 10 **Prokesch RW**, Chow LC, Beaulieu CF, Nino-Murcia M,

- Mindelzun RE, Bammer R, Huang J, Jeffrey RB Jr. Local staging of pancreatic carcinoma with multi-detector row CT: use of curved planar reformations initial experience. *Radiology* 2002; **225**: 759-765
- 11 **Nino-Murcia M**, Tamm EP, Charnsangavej C, Jeffrey RB Jr. Multidetector-row helical CT and advanced postprocessing techniques for the evaluation of pancreatic neoplasms. *Abdom Imaging* 2003; **28**: 366-377
- 12 **Tabuchi T**, Itoh K, Ohshio G, Kojima N, Maetani Y, Shibata T, Konishi J. Tumor staging of pancreatic adenocarcinoma using early- and late-phase helical CT. *Am J Roentgenol* 1999; **173**: 375-380
- 13 **Boland GW**, O' Malley ME, Saez M, Fernandez-del-Castillo C, Warshaw AL, Mueller PR. Pancreatic-phase versus portal vein-phase helical CT of the pancreas: optimal temporal window for evaluation of pancreatic adenocarcinoma. *Am J Roentgenol* 1999; **172**: 605-608
- 14 **O' Malley ME**, Boland GW, Wood BJ, Fernandez-del Castillo C, Warshaw AL, Mueller PR. Adenocarcinoma of the head of the pancreas: determination of surgical unresectability with thin-section pancreatic-phase helical CT. *Am J Roentgenol* 1999; **173**: 1513-1518
- 15 **Sheth S**, Hruban RK, Fishman EK. Helical CT of islet cell tumors of the pancreas: typical and atypical manifestations. *Am J Roentgenol* 2002; **179**: 725-730
- 16 **Demos TC**, Posniak HV, Harmath C, Olson MC, Aranha G. Cystic lesions of the pancreas. *Am J Roentgenol* 2002; **179**: 1375-1388
- 17 **McNulty NJ**, Francis IR, Platt JF, Cohan RH, Korobkin M, Gebremariam A. Multi-detector row helical CT of the pancreas: effect of contrast-enhanced multiphase imaging on enhancement of the pancreas, peripancreatic vasculature, and pancreatic adenocarcinoma. *Radiology* 2001; **220**: 97-102
- 18 **Rydberg J**, Liang Y, Teague SD. Fundamentals of multichannel CT. *Radiol Clin North Am* 2003; **41**: 465-474
- 19 **Hu H**, He HD, Foley WD, Fox SH. Four multidetector-row helical CT: image quality and volume coverage speed. *Radiology* 2002; **215**: 55-62
- 20 **Raman R**, Napel S, Beaulieu CF, Bain ES, Jeffrey RB Jr, Rubin GD. Automated generation of curved planar reformations from volume data: method and evaluation. *Radiology* 2002; **223**: 275-280

Edited by Zhu LH and Chen WW Proofread by Xu FM

Miniature ultrasonic probes for diagnosis and treatment of digestive tract diseases

Guo-Qiang Xu, Yong-Wei Li, Yong-Mei Han, You-Ming Li, Wei-Xing Chen, Feng Ji, Jing-Hua Li, Qing Gu

Guo-Qiang Xu, You-Ming Li, Wei-Xing Chen, Feng Ji, Jing-Hua Li, Qing Gu, Department of Gastroenterology, First Affiliated Hospital, Medical School of Zhejiang University, Hangzhou 310003, Zhejiang Province, China

Yong-Wei Li, Yong-Mei Han, Department of Rheumatology, First Affiliated Hospital, Medical School of Zhejiang University, Hangzhou 310003, Zhejiang Province, China

Supported by the Initiative Fund for Scientific Research of Zhejiang Personnel Department for Returned Overseas Scholars, No. (2001)275

Correspondence to: Guo-Qiang Xu, Department of Gastroenterology, First Affiliated Hospital, Medical School of Zhejiang University, Hangzhou 310003, Zhejiang Province, China. xuguoqi@mail.hz.zj.cn

Telephone: 13957121569 **Fax:** +86-571-87236611

Received: 2003-12-23 **Accepted:** 2004-01-12

Abstract

AIM: To investigate the clinical value of miniature ultrasonic probes (MUPs) for the diagnosis and treatment of digestive tract diseases.

METHODS: Endoscopic ultrasonography (EUS) was performed for patients with its indications with 7.5-20 MHz MUPs and double-cavity electronic endoscope. According to the diagnosis of MUPs, patients who had indications of treatment received endoscopic resection or surgical excision. Postoperative histological results were compared with the preoperative diagnosis of MUPs. A few patients without endoscopic resection or surgical excision were periodically followed up with MUPs.

RESULTS: A total of 537 patients were examined by MUPs, of them, 256 were diagnosed with gastrointestinal submucosal lesions, 146 with pseudo-submucosal lesions, 50 with digestive tract cancers, 17 with peptic ulcer, 11 with cholecystolithiasis, 8 with chronic pancreatitis, and 2 with achalasia and 47 were diagnosed as normal. After MUPs examinations, 220 patients received endoscopic resection or surgical excision, and the postoperative histological results of 211 patients were completely consistent with the preoperative diagnosis of MUPs. The diagnostic accuracy of MUPs was 95.9%. The result of follow-up with MUPs indicated that gastrointestinal leiomyoma, lipoma, phlebotomy and cyst were unchanged within 1-2 years. The patients who received endoscopic resection or centesis did not have any complications.

CONCLUSION: MUPs are of value in diagnosing gastrointestinal submucosal lesions, staging of digestive tract cancers and biliary-pancreatic diseases. They play a very important role in making therapeutic plans.

Xu GQ, Li YW, Han YM, Li YM, Chen WX, Ji F, Li JH, Gu Q. Miniature ultrasonic probes for diagnosis and treatment of digestive tract diseases. *World J Gastroenterol* 2004; 10(13): 1948-1953

<http://www.wjgnet.com/1007-9327/10/1948.asp>

INTRODUCTION

With the development of endoscopic ultrasonography (EUS) in clinical application, great progress has been made in diagnostic specificity and sensitivity of digestive tract diseases. EUS has usually been performed with a standard ultrasonic endoscope since the introduction of EUS with miniature ultrasonic probes (MUPs) in clinical diagnosis in the 1990s^[1]. In August 2000, MUPs series were adopted in the First Affiliated Hospital of Zhejiang University and since then EUS with MUPs have been performed in 537 patients with digestive tract diseases. In the present article, the clinical values of MUPs in the diagnosis of gastrointestinal submucosal lesions, digestive tract cancers, and biliary-pancreatic diseases were analyzed and reported.

MATERIALS AND METHODS

Patients

A total of 537 patients presenting EUS indications were examined by MUPs. Their mean age was 54 years, ranging from 16 to 89 years. There were 280 men and 257 women.

Instruments

Instruments of EUS with MUPs included Fujino EG-410D double-cavity electronic gastroscope, Olympus-100 electronic colonoscope and Fujino SP-70 high-frequency echoprobe system. The frequency spectrum of the probes is between 7.5-20 MHz.

Methods

The preparation before MUPs examinations was the same as that before gastroscopy and colonoscopy examinations. Intramuscular injection of atropine or scopolamine could also be made. According to the information of the location and size of the lesion in gastrointestinal gained by conventional endoscope examinations, microprobes of different frequencies were used. Patients who presented the indications of treatment accepted endoscopic resection or surgical excision according to the diagnosis by MUPs. Postoperative histological examination results of resected lesions were checked with the preoperative diagnosis by MUPs, and for patients with biliary-pancreatic diseases, diagnosis by MUPs was checked with that by ERCP and spiral CT examination. A few patients who did not receive endoscopic resection or surgical excision were periodically followed up with MUPs. The tolerance to EUS with MUPs and complications related to the examination in all these patients were investigated as well.

RESULTS

The results of MUPs examinations of the 537 suspected patients and the histopathologic diagnoses of some cases are summarized in Table 1. After examinations by MUPs, 256 patients were diagnosed with gastrointestinal submucosal lesions, 146 with pseudo-submucosal lesions, 50 with digestive tract cancer, with peptic ulcer, 11 with cholecystolithiasis, 8 with chronic pancreatitis, and 2 with achalasia and 47 were

diagnosed as normal. Among the 256 patients with gastrointestinal submucosal lesions, 162 (64.3%) were diagnosed with leiomyoma. Among the 162 patients with leiomyoma, 96 had esophageal leiomyoma. Of the 96 esophageal leiomyoma cases, 62 had lesions originating from muscularis mucosae and 34 had lesions originating from muscularis propria. Of the 57 gastric leiomyoma cases, 5 had lesions originating from muscularis mucosae and 52 had lesions originating from muscularis propria. Of the 5 duodenal leiomyoma cases, 1 was derived from muscularis mucosae and 4 from muscularis propria. All the 4 cases of colonic leiomyomas were derived from muscularis propria. After MUPs examinations, 122 patients with gastrointestinal true submucosal lesions accepted further treatment of endoscopic resection, surgical excision or puncture. The postoperative pathological diagnosis agreed with the preoperative MUPs diagnosis in 113 cases, thus the accuracy rate of the diagnosis by MUPs was 92.6%. Of the 162 patients with leiomyoma, 86 received either endoscopic resection or surgical excision. In 80 cases, the preoperative MUPs examination results were identical to the postoperative pathological diagnosis. However, the histological results of only 6 patients suffering from leiomyosarcoma (2 cases), gastric neurofibroma, esophageal tuberculosis granuloma, esophageal cyst gland retention, and colonic carcinoid were not consistent with the preoperative diagnoses by MUPs. The accuracy rate of the diagnosis by MUPs was 93%. Among the 146 patients with pseudo-submucosal lesions, 56 were diagnosed with polypus, 37 with inflammatory protruding and thickening of gastrointestinal mucosae, and 53 with extrinsic compression. The polypus and inflammatory protruding were confirmed by pathological biopsy, and the organs of extrinsic compression included spleen (15 cases), gallbladder (9 cases), aorta (8 cases), liver (6 cases), pancreas (4 cases), splenic vein (2 cases), lymph node (3 cases), thoracic vertebrae (2 cases) and mass with unknown nature (4 cases). Of the 11 patients with cholelithiasis, 7 were diagnosed with cholecystolithiasis, and 4 with choledocholith, which was not detected by surface type-B ultrasonography but was confirmed by surgical operation or ERCP. Among the 8 patients with chronic pancreatitis, 4 were diagnosed with pseudocyst of

pancreas, 1 with abscess of pancreas, 1 with distension of main pancreatic duct and 2 with pancreatic echo enhancement. Of the 8 patients, 4 were further confirmed by surgical operation or ERCP. The depth and healing of ulcer were verified by examination of EUS in 17 patients with peptic ulcer. According to the MUPs examination, 47 patients had normal stratification and structure of digestive tract. Of them, 5 patients were diagnosed with duodenal accessory papilla. In addition, some patients with gastrointestinal leiomyoma, lipoma, phlebangioma, cyst, inflammatory protruding or thickening were periodically followed up by MUPs, and the results of examinations showed no changes of these lesions in 1-2 years, but some lesions occurred such as inflammatory protruding, thickening and cyst shrank. All the patients could well tolerate this examination without serious complications such as bleeding, perforation and cardiac or pulmonary accident. No complications occurred in patients who received endoscopic resection or puncture.

DISCUSSION

The diameter of MUPs is small, so it can pass through the biopsy tube of a conventional endoscope and be placed anywhere inside the digestive tract to perform EUS. MUPs can reach or pass any small tubule or narrow space where the standard ultrasonic endoscope can not reach. MUPs do not cause compression on organ structures such as esophagus. MUPs can be easily operated. The frequency range of the probes was broad^[1]. The significance and experiences in using EUS with MUPs for the diagnosis and treatment of digestive tract diseases are as the following.

Value of MUPs in diagnosing gastrointestinal submucosal lesions

Studies have shown that EUS is the best diagnostic method of gastrointestinal submucosal lesions. EUS could not only confirm if the lesion is a true submucosal lesion, but also ascertain accurately the size, location, origin and nature of the lesion^[2-6]. We performed EUS with MUPs, and found 7.5-20 MHz MUPs was very important for the diagnosis of gastrointestinal true submucosal lesions. By this examination, we could

Table 1 MUPs diagnosis of 537 patients and histopathological diagnosis of 211 cases

Diseases	Esophagus	Stomach	Duodenum	Colon	Biliary tract	Pancreas	Total	Confirmation by pathological examination/operation
Leiomyoma	96	57	5	4			162	80/86
Leiomyosarcoma	3	4	1				8	8/8
Varicosis, Phlebangioma	27	13	2				42	3/3
Lipoma	1	4	1	2			8	3/3
Cyst	1	3	1	3			8	4/5
Brunner adenoma			5				5	4/4
Submucosal hematoma of esophagus	2						2	1/1
Ectopic pancreas		18					18	7/9
Lymphoma		3					3	3/3
Polyp	14	32	3	7			56	26/26
Inflammatory protruding and thickening	4	31	2				37	37/37
Pressure protruding lesions	10	38	3	2			53	8/8
Cancer	13	23		8		6	50	42/42
Cholecystolithiasis					11		11	11/11
Chronic pancreatitis						8	8	4/4
Peptic ulcer		16	1				17	
Achalasia	2						2	
Normal							47	
Total	173	242	24	26	11	14	537	211/220

determine the size, location, number and origin of the lesion. According to the ultrasonic characteristics of lesions, we could also distinguish the nature of different lesions^[7-11]. For example, scanned by MUPs, gastrointestinal leiomyoma presented homogeneous and hypoechoic lesions with a clear margin around the hyperechoic wrapping area, which was derived from muscularis mucosae or muscularis propria (Figure 1A). Gastrointestinal lipoma presented homogeneous and hyperechoic lesions with a distinct margin. The lesion often originated from submucosa (Figure 1B). Gastrointestinal cyst presented echoic lesions with a clear margin and enhancement behind. The lesion was often derived from submucosa (Figure 1C). Ectopic pancreas that often appeared in stomach or duodenum revealed non-homogeneous, middle-hyperechoic or patchy echoic lesions with a tubular structure and thickening of muscular layer. The lesions often originated from submucosa or muscularis propria (Figure 1D). Hemangioma and varicosis often appeared in gastric fundus and esophagus as echoic honeycomb-like lesions, and were easy to be deformed by compression. They mostly originated from mucosae or submucosae (Figure 1E). Our clinical research included not only these common submucosal lesions, but also leiomyosarcoma, lymphoma, carcinoid, neurofibroma, abscess, Brunner's adenoma and hematoma, etc. Leiomyoma was the most common benign tumor in gastrointestinal submucosal lesions, accounting for 64.3% of the total gastrointestinal submucosal lesions. According to our clinical and pathological study on gastrointestinal leiomyoma, leiomyoma mainly occurred in esophagus and stomach, and the incidence in small intestine and colon was much lower than that in esophagus and stomach. The size and layer of the origin of esophageal leiomyoma were obviously different from those of gastric leiomyoma. The majority of esophageal leiomyomas originated from muscularis mucosae, and the size was <1.0 cm. Whereas most of the gastric leiomyomas originated from muscularis propria, and the size was 1-2 cm. Almost all the patients with gastrointestinal leiomyoma only had a single lesion, which often progressed slowly or had no change^[12-14]. Among the 256 patients with gastrointestinal true submucosal lesions, 122 patients accepted further treatment of endoscopic resection, surgical excision, or puncture. The results showed that the size, layer, origin and number of the resected lesions were completely consistent with the diagnoses by MUPs. The nature of lesions was in agreement with preoperative diagnosis in 113 patients, and the diagnostic accuracy rate was 92.6%. Current studies with MUPs revealed its significant value in diagnosing gastrointestinal true submucosal lesions^[15-19]. In patients who were periodically followed, gastrointestinal leiomyoma, lipoma, ectopic pancreas, cyst and hemangioma remained unchanged within 1-2 years, and no obvious clinical symptoms were observed. This observation indicates that those who are old and can not or do not want to accept further treatment, with lesions located at unusual sites, should be regularly followed up.

Value of MUPs in diagnosing gastrointestinal pseudo-submucosal lesions

Scanning MUPs can display clearly the layer structure and adjacent organs of gastrointestinal tract, so that pseudo-submucosal or true submucosal protruding lesions could be accurately identified. According to our clinical experience, pseudo-submucosal lesions mainly included polypus, inflammatory protruding and pressure protruding lesions. Most gastrointestinal tract polypi and inflammatory protruding lesions could usually be diagnosed by conventional endoscopy. In a few patients, the color and structure of polypus or inflammatory prominence were similar to those of the surrounding normal mucosae, so we could not differentiate these lesions from submucosal lesions by conventional

endoscopy. By MUPs, according to the origin, layer structure, and changes of the lesion echoes, we could diagnose the lesions easily. As to some superficial and small lesions, we could not only locate them, but also show the layer structure and relationship of the lesions and gastrointestinal wall more clearly by changing probes with different frequencies. Gastrointestinal tract polypus and inflammatory prominences all originated from epithelia and mucosae. Polypus presented homogeneous or non-homogeneous, middle-hyperechoic lesions without envelope (Figure 1F). The latter manifested thickening or loss of epithelia and mucosae, but the layer, structure and echo of the lesions were all normal (Figure 1G). Our diagnostic accuracy rate of extrinsic compression by MUPs was 100%, the same as that reported by Cletti (1993) and Pfau (2002)^[20-21]. According to the complete layer and structure of gastrointestinal tract, the curved compression adventitia and the cross section images of surrounding tissues and structures, we could diagnose extrinsic compression easily by MUPs, just as by conventional ultrasonic endoscopy. At the same time, we could precisely distinguish most of the tissues and organs that caused the compression. Of the 537 patients, 53 were diagnosed with extrinsic compression, and the major organs that caused the compression were spleen (Figure 1H), gallbladder, aorta (Figure 1I), liver, pancreas, splenic vein, lymph node and thoracic vertebrae, etc. Furthermore, in most patients the compression was caused by the swelling and lesion of organs and tissues. So our clinical research confirmed the incomparable superiority of MUPs in diagnosing polypus, inflammatory protruding and extrinsic compression of gastrointestinal tract that are often difficult to be found out by conventional endoscopy.

Value of MUPs in diagnosing biliary-pancreatic diseases

When we performed EUS, we placed the ultrasonic probes in the gastrointestinal tract. Compared with surface ultrasonography, the probe closer to biliary tract and pancreas could avoid interference of duodenum and gas, so the images of biliary-pancreatic diseases (especially lesions of the lower middle part of common bile duct and ampulla) taken by EUS were clearer than those taken by surface ultrasonography. According to the literature, the diagnostic sensibility and specificity of EUS for choledocholith were 91% and 100% respectively, which were much higher than those of surface ultrasonography and common CT examination, and similar to those of ERCP, but the complications of EUS were much fewer than those of ERCP^[22,23]. In our study, 11 patients were diagnosed with cholelithiasis by a 7.5 MHz microprobe scan (Figure 1J, K). The calculi of the lower part of the common bile duct in 4 of the 11 patients were not detected by surface type B ultrasonography, but confirmed by ERCP or surgical operations. So MUPs are superior to surface ultrasonography and common CT for the diagnosis of calculus of the lower part of the common bile duct, and can greatly improve the diagnostic situations of common bile duct diseases. By MUPs, we could distinguish calculus from tumors in biliary tract by real-time observation and we could also observe the lesions of ampulla directly. Compared with surface ultrasonography, CT, and magnetic resonance cholangiopancreatography (MRCP), MUPs were much superior. Pancreas is deeply located, and its ultrasonic image may be influenced by abdominal gas, so ultrasonography has difficulty to examine it. By examinations with 7.5-12 MHz MUPs, 14 cases were diagnosed with pancreatic diseases. Of them, 8 cases had chronic pancreatitis, including 4 cases of pancreatic pseudocyst (Figure 1L), 1 case of abscess, 1 case of dilation of main pancreatic duct, and 2 cases of pancreatic echo enhancement. The results were consistent with those of spiral CT and ERCP. After examination by MUPs, 9 patients accepted surgical operations and the diagnoses were confirmed by pathologic examinations.

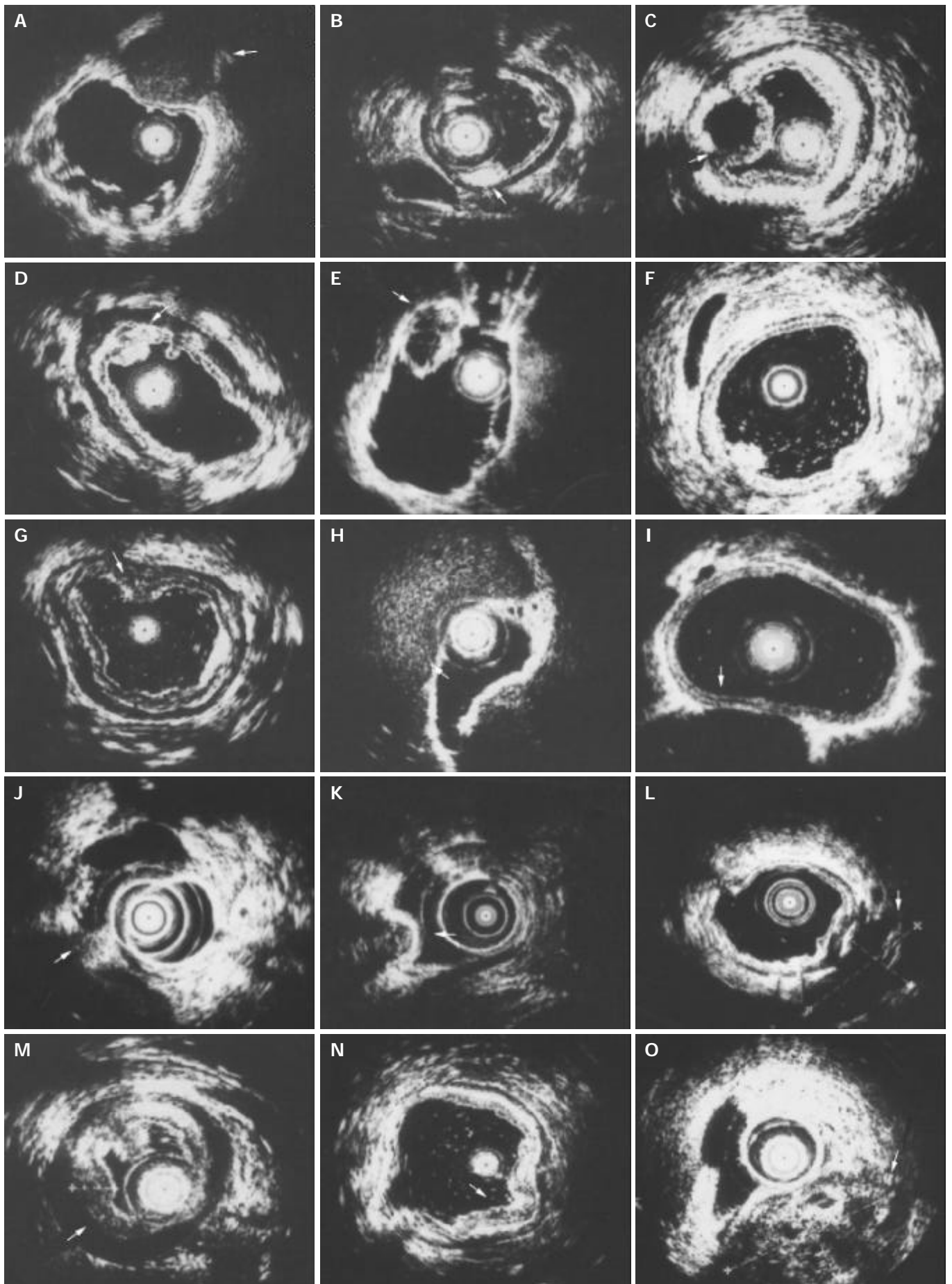


Figure 1 Lesions in digestive tract. A: Gastric leiomyoma, B: Gastric lipoma, C: Gastric cyst, D: Gastric ectopic pancreas, E: Gastric varicosis, F: Gastric polypi, G: Gastric inflammatory protruding, H: Gastric extrinsic compression (spleen), I: Esophageal extrinsic compression (aorta), J: Gallstone, K: Choledocholith, L: Pseudocyst of pancreas, M: Linitis plastica, N: Early gastric cancer, O: Pancreatic cancer.

On the basis of these results, we can make the conclusion that EUS with MUPs for pancreatic diseases is of diagnostic value. It can not only detect pancreatic duct, but also observe the changes of pancreatic parenchyma. Compared with ERCP, it was disadvantageous in displaying the full view of pancreatic duct, but it was advantageous in displaying the echo of pancreas, pancreatic calculus, and cyst. Furthermore, there were no ERCP-related complications in examinations by MUPs. So the diagnosis of pancreatic diseases by MUPs was effective, safe and convenient. Recently, there were reports about ultrasonography performed in biliary-pancreatic duct by MUPs^[1,24]. It can greatly improve the diagnostic situation of common bile duct and pancreatic parenchymal micro-lesions and has become the best diagnostic method for pancreatic endocrine tumors.

Value of MUPs in diagnosing and TNM staging of digestive tract cancer

TNM staging of digestive tract cancers by EUS is generally accepted. The sensitivity and specificity of EUS for TNM staging of digestive tract cancers were obviously higher than those of surface ultrasonography, conventional endoscopy, CT and MRI, etc, but EUS was inferior to CT and MRI in the diagnosis of stage M cancers^[25,26]. With 7.5-20 MHz microprobes, we researched the diagnosis, infiltrating depth and metastasis of surrounding lymph nodes in 50 patients with digestive tract cancers. The results showed the very important value of EUS with MUPs in diagnosing linitis plastica which could not be detected by conventional endoscopy. The growth pattern of this type of gastric cancer was unique. The cancer cells spread and infiltrated into submucosa. So it was hard to be detected by common biopsy. But it had special ultrasonic imaging changes which manifested obviously in diffuse thickening of gastric wall, loss of layer structure and hypoechoic lesion, etc. (Figure 1M). According to these ultrasonographic changes, 8 patients who were diagnosed with linitis plastica were confirmed by surgical operations. Investigations abroad have shown that the diagnostic accuracy rate of EUS for early stage gastrointestinal tract cancers was higher than that by any other examination^[24]. Our study also demonstrated that the depth of infiltration and surrounding lymph node metastasis in digestive tract cancers could be diagnosed by MUPs. 12-20 MHz microprobes could display the infiltrating depth of tumors in gastrointestinal wall clearly. A 7.5 MHz probe could show infiltrations in adjacent tissues, organs and lymph nodes, then we could judge whether the cancer lesion was in early stage (Figure 1N) or advanced stage (Figure 1O). The diagnoses by MUPs in 42 patients who received surgical operation or endoscopic resection were consistent with the pathological diagnoses. It is concluded that MUPs can be applied to TNM staging of digestive tract cancers. MUPs are superior to standard ultrasonic endoscopy because it can be inserted into the narrow gastrointestinal tract tumor infiltration or into other small tubules.

Value of MUPs in guiding treatment of digestive tract diseases

Our clinical research demonstrated that MUPs could not only diagnose digestive tract diseases, but also provide treatment plans for these diseases^[27-30]. MUPs had a very important diagnostic value in deciding the size, location, layer origin and nature of gastrointestinal submucosal lesions. By this examination, leiomyoma, lipoma and ectopic pancreas originating from above submucosae received endoscopic resection. Cysts derived from submucosa were treated by endoscopic puncture and aspiration. The procedure was effective, safe, economical and simple, and resulted in microtraumas only. Submucosal lesions originating from muscularis propria or adventitia were regarded as contraindications for endoscopic resection. The patients received

surgical operation or thoracoscopy or laparoscopy. Patients who did not undergo, or were unfavorable to undergo operations were followed up periodically; therefore, complications such as perforation were avoided. MUPs helped us in ascertaining the indications of endoscopic resection in patients with early stage gastrointestinal tract cancer. They also helped us in formulating scientific, reasonable treatment plans for patients with median or advanced stage of cancer. With the modality, hemangioma and varicosity in gastrointestinal tract were diagnosed, unnecessary biopsy and resection were avoided, and massive hemorrhage was prevented. The effective differentiation of inflammatory protruding from pressure protruding lesions helped formulate a correct treatment regimen and give up explorative operation. In addition, difficult biliary-pancreatic diseases could be diagnosed by MUPs; patients could be treated promptly and effectively. In conclusion, MUPs can greatly improve the accuracy rate of diagnosis and treatment of digestive tract diseases.

REFERENCES

- 1 **Menzel J**, Domschke W. Gastrointestinal miniprobe sonography: the current status. *Am J Gastroenterol* 2000; **58**: 605-616
- 2 **Varas Lorenzo MJ**, Maluenda MD, Pou JM, Abad R, Turro J, Espinos JC. The value of endoscopic ultrasonography in the study of submucosal tumors of the digestive tract. *Gastroenterol Hepatol* 1998; **18**: 121-124
- 3 **Rosch T**, Kaper B, Will U, Baronius W, Strobel M, Lorenz R, Ulm K. Accuracy of endoscopic ultrasonography in upper gastrointestinal submucosal lesions: a prospective multicenter study. *Scand J Gastroenterol* 2002; **37**: 856-862
- 4 **Shen EF**, Arnott ID, Plevris J, Penman ID. Endoscopic ultrasonography in the diagnosis and management of suspected gastrointestinal submucosal tumors. *Br J Surg* 2002; **89**: 231-235
- 5 **Gress F**, Schmitt C, Savides T, Faigel DO, Catalano M, Wassef W, Roubein L, Nickl N, Ciaccia D, Bhutani M, Hoffman B, Affronti J. Interobserver agreement for EUS in the evaluation and diagnosis of submucosal masses. *Gastrointest Endosc* 2001; **53**: 71-76
- 6 **Kameyama H**, Niwa Y, Arisawa T, Goto H, Hayakawa T. Endoscopic ultrasonography in the diagnosis of submucosal lesions of the large intestine. *Gastrointest Endosc* 1997; **46**: 406-411
- 7 **Massari M**, De Simone M, Cioffi U, Gabrielli F, Boccasanta P, Bonavina L. Endoscopic ultrasonography in the evaluation of leiomyoma and extramucosal cysts of the esophagus. *Hepatogastroenterology* 1998; **45**: 938-943
- 8 **Araki K**, Ohno S, Egashira A, Saeki H, Kawaguchi H, Ikeda K, Kitamura K, Sugimachi K. Esophageal hemangioma: a case report and review of the literature. *Hepatogastroenterology* 1999; **46**: 3148-3154
- 9 **Lu ZC**, Jing ZD. Submucosal tumors of the esophagus. Modern intraluminal ultrasonics. *Beijing: Science Press* 2000: 174-182
- 10 **Busarini E**, Stasi MD, Rossi S, Silva M, Giangregorio F, Adriano Z, Buscarini L. Endosonographic diagnosis of submucosal upper gastrointestinal tract lesions and large fold gastropathies by catheter ultrasound probe. *Gastrointest Endosc* 1999; **49**: 184-191
- 11 **Hizawa K**, Matsumoto T, Kouzuki T, Suekane H, Esaki M, Fujishima M. Cystic submucosal tumors in the gastrointestinal tract: endosonographic findings and endoscopic removal. *Endoscopy* 2000; **32**: 712-714
- 12 **Xu GQ**, Zhang BL, Li YM, Chen LH, Ji F, Chen WX, Cai SP. Diagnostic value of endoscopic ultrasonography for gastrointestinal leiomyoma. *World J Gastroenterol* 2003; **9**: 2088-2091
- 13 **Wang Y**, Sun Y, Liu Y, Wang Z. Transesophageal intraluminal ultrasonography in diagnosis and differential diagnosis of esophageal leiomyoma. *Zhonghua Yixue Zazhi* 2002; **82**: 456-458
- 14 **Zou XP**. Gastric leiomyoma. Modern Intraluminal Ultrasonics. *Beijing: Science Press* 2000: 202-205
- 15 **Xu GQ**, Li YM, Chen WX, Ji F, Huang HD. Diagnostic value of transendoscopic miniature ultrasonic probes on esophageal and gastric submucosal lesions. *Zhonghua Chaosheng Yingxiangxue Zazhi* 2002; **11**: 188-189
- 16 **Koch J**, Halvorsen RA Jr, Levenson SD, Cello JP. Prospective com-

- parison of catheter-based endoscopic sonography: evaluation of gastrointestinal-wall abnormalities and staging of gastrointestinal malignancies. *Clin Ultrasound* 2001; **29**: 117-124
- 17 **Catalano MF**. Endoscopic ultrasonography for esophageal and gastric mass lesions. *Gastroenterologist* 1997; **5**: 3-9
- 18 **Xu GQ**. Benign tumors of the esophagus. *Modern Esophagology. Shanghai: Shanghai Science And Technique Press* 1999: 268-273
- 19 **Futagami K**, Hata J, Haruma K, Yamashita N, Yoshida S, Tanaka S, Chayama K. Extracorporeal ultrasound is an effective diagnostic alternative to endoscopic ultrasound for gastric submucosal tumours. *Scand J Gastroenterol* 2001; **36**: 1222-1226
- 20 **Caletti G**, Fusaroli P. Endoscopic ultrasonography. *Endoscopy* 1993; **31**: 95-102
- 21 **Pfau PR**, Chak A. Endoscopic ultrasonography. *Endoscopy* 2002; **34**: 21-28
- 22 **Rosch T**, Meining A, Fruhmorgen S, Zillinger C, Schusdziarra V, Hellerhoff K, Classen M, Helmberger H. A prospective comparison of the diagnostic accuracy of ERCP, MRCP, CT and EUS in biliary strictures. *Gastrointest Endosc* 2002; **55**: 870-876
- 23 **Kohut M**, Nowakowska E, Marek T, Kaczor R, Nowak A. Accuracy of linear endoscopic ultrasonography in the evaluation of patients with suspected common bile duct stones. *Endoscopy* 2002; **34**: 299-303
- 24 **Nakazama S**. Recent advances in endoscopic ultrasonography. *J Gastroenterol* 2000; **35**: 257-260
- 25 **Wakelin SJ**, Deans C, Crofts TJ, Allan PL, Plevris JN, Paterson-Brown S. A comparison of computerized tomography, laparoscopic ultrasound and endoscopic ultrasound in the pre-operative staging of oesophagogastric carcinoma. *Eur J Radiol* 2002; **41**: 161-167
- 26 **Hunt GC**, Faigel DO. Assessment of EUS for diagnosing, staging and determining respectability of pancreatic cancer: a review. *Gastrointest Endosc* 2002; **55**: 232-237
- 27 **Izumi Y**, Inoue H, Kawano T, Tani M, Tada M, Okabe S, Takeshita K, Endo M. Endosonography during endoscopic mucosal resection to enhance its safety: a new technique. *Surg Endosc* 1999; **13**: 358-360
- 28 **kada N**, Higashino M, Osugi H, Tokuhara T, Kinoshita H. Utility of endoscopic ultrasonography in assessing the indications for endoscopic surgery of submucosal esophageal tumors. *Surg Endosc* 1999; **13**: 228-230
- 29 **Giovannini M**, Bernardini D, Moutardier V, Monges G, Houvenaeghel G, Seitz JF, Derlpero JR. Endoscopic mucosal resection (EMR): results and prognostic factors in 21 patients. *Endoscopy* 1999; **31**: 698-701
- 30 **Sun S**, Wang M, Sun S. Use of endoscopic ultrasound-guided injection in endoscopic resection of solid submucosal tumors. *Endoscopy* 2002; **34**: 82-85

Edited by Wang XL and Lei LM **Proofread by** Xu FM

Chronic liver disease questionnaire: Translation and validation in Thais

Abhasnee Sobhonslidsuk, Chatchawan Silpakit, Ronnachai Kongsakon, Patchareeya Satitpornkul, Chaleaw Sripetch

Abhasnee Sobhonslidsuk, Patchareeya Satitpornkul, Chaleaw Sripetch, Department of Medicine, Ramathibodi Hospital, Mahidol University, Bangkok, 10400, Thailand

Chatchawan Silpakit, Ronnachai Kongsakon, Department of Psychiatry, Ramathibodi Hospital, Mahidol University, Bangkok, 10400, Thailand

Correspondence to: Abhasnee Sobhonslidsuk, M.D., Department of Medicine, Ramathibodi hospital, 270 Praram 6 road, Bangkok 10400, Thailand. teasb@mahidol.ac.th

Telephone: +66-2-201 1387 **Fax:** +66-2-965 1769

Received: 2003-12-10 **Accepted:** 2004-01-16

Abstract

AIM: Quality of life (QOL) is a concept that incorporates many aspects of life beyond "health". The chronic liver disease questionnaire (CLDQ) was developed to evaluate the impact of chronic liver diseases (CLD) on QOL. The objectives of this study were to translate and validate a liver specific questionnaire, the CLDQ.

METHODS: The CLDQ was formally translated from the original version to Thai language with permission. The translation process included forward translation, back translation, cross-cultural adaptation and a pretest. Reliability and validity of the translated version was examined in CLD patients. Enrolled subjects included CLD and normal subjects with age- and sex-matched. Collected data were demography, physical findings and biochemical tests. All subjects were asked to complete the translated versions of CLDQ and SF-36, which was previously validated. Cronbach's alpha and test-retest were performed for reliability analysis. One-way Anova or non-parametric method was used to determine discriminant validity. Spearman's rank correlation was used to assess convergent validity. P -value <0.05 was considered statistically significant.

RESULTS: A total of 200 subjects were recruited into the study, with 150 CLD and 50 normal subjects. Mean ages (SD) were 47.3(11.7) and 49.1(8.5) years, respectively. The number of chronic hepatitis: cirrhosis was 76:74, and the ratio of cirrhotic patients classified as Child A:B:C was 37 (50%): 26(35%): 11(15%). Cronbach's alpha of the overall CLDQ scores was 0.96 and of all domains were higher than 0.93. Item-total correlation was >0.45 . Test-retest reliability done at 1 to 4 wk apart was 0.88 for the average CLDQ score and from 0.68 to 0.90 for domain scores. The CLDQ was found to have discriminant validity. The highest scores of CLDQ domains were in the normal group, scores were lower in the compensated group and lowest in the decompensated group. The significant correlation between domains of the CLDQ and SF-36 was found. The average CLDQ score was strongly correlated with the general health domain of SF-36. ($P=0.69$; $P=0.01$).

CONCLUSION: The translated CLDQ is valid and applicable in Thais with CLD. CLDQ reveals that QOL in these patients

is lower than that in normal population. QOL is more impaired in advanced stage of CLD.

Sobhonslidsuk A, Silpakit C, Kongsakon R, Satitpornkul P, Sripetch C. Chronic liver disease questionnaire: Translation and validation in Thais. *World J Gastroenterol* 2004; 10(13): 1954-1957

<http://www.wjgnet.com/1007-9327/10/1954.asp>

INTRODUCTION

The World Health Organization gave the definition of health as being not only the absence of disease and debility but also the presence of physical, mental and social well-being^[1]. Quality of life (QOL) is a concept that incorporates many aspects of an individual's experience, general well-being, satisfaction, social and physical function^[2]. By definition, QOL is subjective and multi-dimension. It can be influenced by socioeconomic factors, age, gender, presence of disease and treatment^[2]. QOL examines how patients experience and perceive. Its results provide a basis for holistic view of the patient and complements the organic outcomes. QOL has been evaluated in a large number of chronic medical and gastrointestinal conditions, such as dyspepsia, inflammatory bowel diseases, liver diseases, *etc.*^[3-7]. Well-developed and validated questionnaires have been used as instruments for QOL measurement. Generic and disease-specific instruments measure different aspects of QOL. It is encouraged to use both instruments in clinical research to gain substantial information^[5]. Since the development of the first liver-specific questionnaire, the chronic liver disease questionnaire (CLDQ)^[7], the QOL research in chronic liver diseases have been steadily reported^[6,8-12]. Previous studies in Western patients showed that chronic liver disease (CLD) had negative impact on QOL, and QOL worsened as the severity of disease increased^[8,9,12-14]. The study of QOL in gastrointestinal and liver diseases has hardly received attention in Asian population. Our study was aimed to translate and validate a disease specific questionnaire, the CLDQ, to be used in study of QOL in Thai population.

MATERIALS AND METHODS

Ethics

This study received ethics approval from the ethic committee of our hospital. All subjects provided written consent before participation.

Subjects

Between June 1 and September 31, 2003, 150 Thai patients with chronic liver diseases who attended gastroenterological clinic and 50 normal subjects were invited to participate in the study. Chronic liver diseases included chronic hepatitis and cirrhosis. Chronic hepatitis was defined by an elevation of serum transaminases above 1.5 times of upper normal limit for longer than 6 mo and cirrhosis by definition had biochemical and radiological findings consistent with cirrhosis^[15]. The staging of cirrhosis was categorized according to Child-Pugh classification: Child (class) A, B and C^[16]. Causes of chronic

liver disease were divided into viral hepatitis, alcohol, viral hepatitis combining with alcohol, non-alcoholic fatty liver (NAFLD) and others. Chronic liver disease due to alcohol was defined by the regular intake of alcohol (80 g/d in men, and 40 g/d in women)^[7]. History of other medical illness was taken from medical records. Exclusion criteria were concomitant presence of hepatic encephalopathy, other active medical diseases, malignancy, being treated with antiviral agents and those who refused to give consent.

QOL instruments

CLDQ The CLDQ is the first liver specific instrument developed by Younossi *et al.*^[7]. The CLDQ includes 29 items in the following domains: abdominal symptoms, fatigue, systemic symptoms, activity, emotional function and worry. The response of CLDQ results in 1 to 7 scales: ranging from “all of the time” to “none of the time”^[7]. The original CLDQ was shown to have constructed validity from the studies in chronic liver diseases^[7,12].

Translation of CLDQ After the translation permission was granted, the original version of CLDQ was translated into Thai according to the standardized guidelines proposed in 1993^[18]. Forward translation from the original English version was performed independently by two Thai native speakers. Reconciliation of both forward versions was done subsequently. A native English speaker living in Thailand who understood Thai language quite well and did not have knowledge about QOL carried out back translation. The semifinal version derived from reconciliation of the original, back translation and forward translation. A pretest in 10 patients with chronic liver diseases was performed. The final version was obtained after the step of cross-cultural adaptation.

Assessment of translated CLDQ The CLDQ and SF-36 questionnaires were administered in 150 patients with chronic liver diseases and in 50 normal subjects. The permission to use the SF-36, a generic questionnaire, in this study was granted from QualityMetric Inc. The study version of SF-36 was previously tested and validated in Thai population^[19]. CLDQ was repeated in 25 patients in 1-3 wk apart for test-retest analysis. Reliability was determined from Cronbach's alpha (reliability coefficient) and test-retest. One-way Anova or non-parametric method was used to determine discriminant validity of scores among different stages of liver diseases. Spearman's rank correlation was used to assess test-retest and convergent validity. A *P* value <0.05 was considered to be statistically significant.

RESULTS

Clinical and demographic data

One hundred and fifty patients with CLD and 50 normal subjects were enrolled into the study. Mean ages (SD) of CLD and controlled groups were 47.3(11.7) and 49.1(8.5) years (*P*=0.40). Of the 150 patients with CLD, 76(51%) had chronic

hepatitis and the remainder had cirrhosis. Summarized clinical and demographic data are shown in Table 1. Patients with cirrhosis were older, more unemployed and had lower education levels than those with chronic hepatitis. Viral hepatitis and regular alcohol drinking were the most common causes of CLD. Hepatitis B virus was the major cause of chronic viral hepatitis in this study (68.1%).

Table 1 Clinical and demographic data

Characteristics	Normal (n=50)	Chronic hepatitis (n=76)	Cirrhosis (n=74)	<i>P</i> -value
mean±SD, yr	49.1 (8.5)	43.1 (12.6)	51.6 (8.9)	0.00
Men, <i>n</i> (%)	28 (56)	49 (64.5)	47 (63.5)	0.60
Married, <i>n</i> (%)	40 (81.6)	46 (62.2)	52 (81.3)	0.01
Education, <i>n</i> (%) ¹				
≥Bachelor degree	20 (40)	29 (39.2)	10 (15.6)	0.004
Career, <i>n</i> (%) ¹				
- White collar	42 (91.3)	44 (69.8)	28 (50)	0.00
- Blue collar	1 (2.2)	4 (6.3)	9 (16)	
- Unemployed	3 (6.5)	15 (23.8)	19 (34)	
Financial burden (+), <i>n</i> (%) ¹	22 (44)	30 (40.5)	29 (45.3)	0.84
Etiologies, <i>n</i> (%)				
- Viral hepatitis		52 (68.4)	41 (55.4)	
- Alcohol		4 (5.3)	20 (27)	0.00
- Viral hepatitis and alcohol		2 (2.6)	7 (9.5)	
- Non-alcoholic fatty liver disease		11 (14.5)	2 (2.7)	
- Others		7 (9.2)	4 (5.4)	
Child-Pugh Classification, <i>n</i> (%)				
- Child A			37 (50)	
- Child B			26 (35)	
- Child C			11 (15)	

¹Incomplete data.

Reliability

Measurement of internal consistency Cronbach's alpha of overall scores was 0.96, which was above the acceptable level of 0.70 for comparison between groups^[20]. Cronbach's alpha of domains was higher than 0.93. Item-total correlation (omit that item) was above 0.45 (Table 2).

Test-retest Spearman's rank correlation of average CLDQ was 0.88 (*P*=0.00) and domains of CLDQ was higher than 0.67 (*P*=0.00).

Validity

Discriminant validity The various stages of liver diseases in this study were rearranged as normal, compensated (= chronic hepatitis + Child A cirrhosis) and decompensated (= Child B and Child C cirrhosis) groups. A comparison of domain scores in different groups was performed. All domain scores of CLDQ and SF-36 significantly decreased from normal group to

Table 2 Reliability of CLDQ

CLDQ domains	Mean score (SD)	Cronbach's alpha (if item deleted)	Test-retest reliability	
			Correlation coefficient	<i>P</i> -value
Abdominal symptoms	5.3 (1.3)	0.95	0.85	0.00
Fatigue	4.7 (1.2)	0.94	0.90	0.00
Systemic symptoms	5.3 (1.1)	0.94	0.77	0.00
Activity	5.3 (1.3)	0.94	0.68	0.00
Emotional function	5.2 (1.1)	0.94	0.80	0.00
Worry	5.3 (1.4)	0.94	0.78	0.00
Average CLDQ	5.2 (1.1)	0.93	0.88	0.00

Table 3 Discriminant validity among different groups of patients (mean±SD)

CLDQ domains	Normal (n=50)	Compensated group (n=113)	Decompensated group (n=37)	P-value
Abdominal symptoms	5.8 (1.2)	5.3 (1.1)	4.6 (1.6)	0.00
Fatigue	5.4 (1.0)	4.6 (1.1)	4.0 (1.4)	0.00
Systemic symptoms	5.9 (0.9)	5.2 (1.1)	4.7 (1.1)	0.00
Activity	5.9 (1.0)	5.4 (1.1)	4.4 (1.5)	0.00
Emotional function	5.7 (0.9)	5.1 (1.1)	4.8 (1.4)	0.001
Worry	6.3 (0.8)	5.2 (1.4)	4.4 (1.6)	0.00
Average CLDQ	5.8 (0.8)	5.2 (1.0)	4.5 (1.2)	0.00
SF-36 domains				
Physical function	79.4 (14.0)	74.1 (20.2)	59.1 (21.5)	0.00
Role physical	79.5 (34.5)	59.3 (41.1)	34.5 (42.2)	0.00
Bodily pain	76.0 (14.3)	69.4 (22.8)	57.7 (23.8)	0.001
General health	68.6 (19.1)	51.3 (24.2)	42.0 (22.9)	0.00
Vitality	66.1 (14.2)	63.3 (16.3)	57.2 (14.7)	0.03
Social function	85.5 (16.6)	77.5 (20.0)	74.3 (22.0)	0.02
Role emotion	78.0 (36.0)	59.3 (42.9)	39.6 (45.7)	0.00
Mental health	75.2 (15.4)	69.5 (17.7)	65.7 (17.9)	0.03

Table 4 Correlations between CLDQ and SF-36

CLDQ domains	SF-36 domains							
	Physical function	Role physical	Bodily pain	General health	Vitality	Social function	Role emotion	Mental health
Abdominal symptoms	0.28 ¹	0.32 ¹	0.48 ¹	0.49 ¹	0.45 ¹	0.35 ¹	0.38 ¹	0.53 ¹
Fatigue	0.44 ¹	0.52 ¹	0.49 ¹	0.61 ¹	0.58 ¹	0.54 ¹	0.63 ¹	0.59 ¹
Systemic symptoms	0.48 ¹	0.50 ¹	0.63 ¹	0.55 ¹	0.49 ¹	0.48 ¹	0.54 ¹	0.50 ¹
Activity	0.49 ¹	0.45 ¹	0.47 ¹	0.54 ¹	0.47 ¹	0.44 ¹	0.50 ¹	0.50 ¹
Emotional function	0.38 ¹	0.41 ¹	0.46 ¹	0.59 ¹	0.62 ¹	0.59 ¹	0.54 ¹	0.68 ¹
Worry	0.38 ¹	0.48 ¹	0.41 ¹	0.68 ¹	0.53 ¹	0.48 ¹	0.49 ¹	0.63 ¹
Average CLDQ	0.47 ¹	0.52 ¹	0.56 ¹	0.69 ¹	0.61 ¹	0.55 ¹	0.60 ¹	0.67 ¹

¹P=0.01.

compensated and decompensated groups (Table 3). The CLDQ was found to have good discriminant validity.

Convergen validity Each domain of CLDQ correlated with all domains of SF-36 with correlation coefficient (r) >0.27: P=0.01 as shown in Table 4. The average CLDQ score was strongly correlated with the general health domain of SF-36 (P=0.69: P=0.01).

Influence of disease severity on HRQOL

The CLDQ scores in Thai patients with CLD deteriorated as severity of chronic liver disease increased similarly to previous reports in Western patients^[8,9,12-14]. However, we found that average CLDQ, emotional function and activity scores in chronic hepatitis were lower than those in Child A cirrhosis (5.2(1.1) vs 5.7(1.2), 5.0(1.1) vs 5.5(1.0) and 5.0(0.9) vs 5.4(0.9), respectively; P-values were 0.04, 0.02 and 0.03.

DISCUSSION

The original CLDQ is a well-developed and validated disease-specific questionnaire for measuring QOL in CLD^[7]. It consists of 29 items which are a suitable number for exploring QOL in patients who have a brief visit to a clinic^[7]. It has 7 linkert scale type of answers^[7]. To find a standardized disease-specific questionnaire for researches involving QOL in CLD, we translated the CLDQ from the original English to Thai versions by following the proposed guideline^[18]. Simple translation of questionnaire from one language to the other without concerning language difference, culture context and lifestyle, jeopardizes the sensibility of the original version. The translated CLDQ used the language which even poorly educated Thais were able

to understand the questionnaire meaning, and it was aimed for conceptual and semantic equivalences with the original concept. After the translation and cross-cultural adaptation, the reliability and validity of the translated version were proved to be maintained. Reliability of the CLDQ was confirmed from internal consistency and test-retest. Cronbach's alpha of overall CLDQ was higher than 0.70, indicating that the translated version had acceptable reliability^[20]. Chronic liver diseases greatly impacted QOL, which was confirmed by both generic and disease-specific questionnaires. We arranged chronic hepatitis and cirrhosis Child A into "compensated" group, and Child B and C cirrhosis into "decompensated" group according to the reserved function of the liver. The results from generic and disease-specific questionnaires were in agreement with the fact that a markedly decrease of QOL was seen in advanced stages of chronic liver diseases. On the other hand, it showed that the average CLDQ, activity and emotion function domains in chronic hepatitis were significantly lower than those in Child A cirrhosis. This finding may point out that chronic hepatitis had impairment in some parts of QOL more than Child A cirrhosis which may be a more stable condition. We could not compare the QOL between Child B and C cirrhosis due to the small sample size in both groups. The CLDQ domains correlated significantly with every domain of SF-36. The strongest correlation was seen in the relationship between the average CLDQ score and the general health domain of SF-36. The effect of other demographic and clinical factors on QOL of CLD was inconsistently reported. From a previous study, old age was inversely correlated with physical function of SF-36^[8]. However, a subsequent study revealed that younger patients showed more impairment in QOL^[9]. Several studies

revealed that chronic viral hepatitis, especially viral hepatitis C-related decreased QOL greater than cholestatic or alcoholic liver disease^[8,12]. Other socioeconomic factors, e.g. education, career and financial status may affect QOL as well. The validated CLDQ is found to be a satisfactory tool for future research of QOL in Thai population.

ACKNOWLEDGEMENT

The authors would like to thank Thailand Research Fund (TRF) for the research grant, and Professor Anya Khanthavit for his guidance and comments.

REFERENCES

- 1 **WHO.** Constitution of the World Health Organization. In: World Health Organization. Handbook of basic documents. 5th ed. Geneva: Palais des Nations 1952: 3-20
- 2 **Glise H,** Wilklund I. Health-related quality of life and gastrointestinal disease. *J Gastroenterol Hepatol* 2002; **17**(Suppl): S72-S84
- 3 **Talley NJ,** Weaver AL, Zinsmeister AR. Impact of functional dyspepsia on quality of life. *Dig Dis Sci* 1995; **40**: 584-589
- 4 **Irvine EJ,** Feagan B, Rochon J, Archambault A, Fedorak RN, Groll A, Kinnear D, Saibil F, McDonald JW. Quality of life: a valid and reliable measure of therapeutic efficacy in the treatment of inflammatory bowel disease. *Gastroenterology* 1994; **106**: 287-296
- 5 **Younossi ZM,** Guyatt G. Quality-of-life assessments and chronic liver disease. *Am J Gastroenterol* 1998; **93**: 1037-1041
- 6 **Borgaonkar MR,** Irvine EJ. Quality of life measurement in gastrointestinal and liver disorders. *Gut* 2000; **47**: 444-454
- 7 **Younossi ZM,** Guyatt G, Kiwi M, Boparai N, King D. Development of a disease specific questionnaire to measure health related quality of life in patients with chronic liver disease. *Gut* 1999; **45**: 295-300
- 8 **Younossi ZM,** Boparai N, McCormick M, Price LL, Guyatt G. Assessment of utilities and health-related quality of life in patients with chronic liver disease. *Am J Gastroenterol* 2001; **96**: 579-583
- 9 **Marchesini G,** Bianchi G, Amodio P, Salerno F, Merli M, Panella C, Loguercio C, Apolone G, Niero M, Abbiati R. Factors associated with poor health-related quality of life of patients with cirrhosis. *Gastroenterology* 2001; **120**: 170-178
- 10 **Chong CA,** Gulamhussein A, Heathcote EJ, Lilly L, Sherman M, Naglie G, Krahn M. Health-state utilities and quality of life in hepatitis C patients. *Am J Gastroenterol* 2003; **98**: 630-638
- 11 **Bianchi G,** Loguercio C, Sgarbi D, Abbiati R, Brunetti N, De Simone T, Zoli M, Marchesini G. Reduced quality of life of patients with hepatocellular carcinoma. *Dig Liver Dis* 2003; **35**: 46-54
- 12 **Younossi ZM,** Boparai N, Price LL, Kiwi ML, McCormick M, Guyatt G. Health-related quality of life in chronic liver disease: the impact of type and severity of disease. *Am J Gastroenterol* 2001; **96**: 2199-2205
- 13 **Arguedas MR,** DeLawrence TG, McGuire BM. Influence of hepatic encephalopathy on health-related quality of life in patients with cirrhosis. *Dig Dis Sci* 2003; **48**: 1622-1626
- 14 **Cordoba J,** Flavia M, Jacas C, Sauleda S, Esteban JI, Vargas V, Estaban R, Guardia J. Quality of life and cognitive function in hepatitis C at different stages of liver disease. *J Hepatol* 2003; **39**: 231-238
- 15 **Leevy CM,** Sherlock S, Tygstrup N, Zetterman R. Disease of the liver and biliary tract. Standardization of nomenclature, diagnostic criteria and prognosis. *New York, Raven Press* 1994: 61-68
- 16 **Sherlock S,** Dooley J. Disease of the liver and biliary system. 10th ed. *Oxford: Blackwell Science* 1997: 135-180
- 17 **Sherlock S,** Dooley J. Disease of the liver and biliary system. 10th ed. *Oxford: Blackwell Science* 1997: 385-403
- 18 **Guillemin F,** Bombardier C, Beaton D. Cross-cultural adaptation of health-related quality of life measures: literature review and proposed guidelines. *J Clin Epidemiol* 1993; **46**: 1417-1432
- 19 **Kongsakon R,** Silpakit C. Thai version of the medical outcome study in 36 items short form health survey: an instrument for measuring clinical results in mental disorder patients. *Rama Med J* 2000; **23**: 8-19
- 20 **McDowell I,** Nevell C. Measuring health: a guide to rating scales and questionnaire. *New York: Oxford University Press* 1987

Edited by Wang XL Proofread by Xu FM

Comparison of three PCR methods for detection of *Helicobacter pylori* DNA and detection of *cagA* gene in gastric biopsy specimens

SI Smith, KS Oyedeji, AO Arigbabu, F Cantet, F Megraud, OO Ojo, AO Uwaifo, JA Otegbayo, SO Ola, AO Coker

SI Smith, Molecular Biology and Biotechnology Division, Nigerian Institute of Medical Research, P.M.B. 2013, Yaba, Lagos, Nigeria

KS Oyedeji, Microbiology Division, Nigerian Institute of Medical Research, P.M.B. 2013, Yaba, Lagos, Nigeria

AO Arigbabu, Department of Surgery, Obafemi Awolowo University Teaching Hospital Complex, Ile-Ife

F Cantet, F Megraud, Laboratoire de Bacteriologie, Bordeaux, Cedex, France

OO Ojo, AO Uwaifo, Department of Biochemistry, University of Ibadan, Ibadan, Nigeria

JA Otegbayo, SO Ola, Department of Medicine, University of Ibadan, Ibadan, Nigeria

AO Coker, College of Medicine, University of Lagos, Idi-Araba, Lagos, Nigeria

Supported by Inserm Fellowship, France, awarded to Dr. SI Smith

Correspondence to: Dr. SI Smith, Molecular Biology and Biotechnology Division, Nigerian Institute of Medical Research, P.M.B. 2013, Yaba, Lagos, Nigeria. stellaismith@yahoo.com

Fax: +2341-342-5171

Received: 2004-01-15 **Accepted:** 2004-04-14

Abstract

AIM: To comparatively evaluate PCR and other diagnostic methods (the rapid urease test and / or culture) in order to determine which of the three PCR methods (*ureA*, *glmM* and 26-kDa, *SSA* gene) was most appropriate in the diagnosis of *Helicobacter pylori* (*H pylori*) infection and also to evaluate the detection of a putative virulence marker of *H pylori*, the *cagA* gene, by PCR in biopsy specimens.

METHODS: One hundred and eighty-nine biopsy specimens were collected from 63 patients (three biopsies each) undergoing upper gastroduodenal endoscopy for various dyspeptic symptoms. The PCR methods used to detect *H pylori* DNA directly from biopsies were the *glmM*, 26-kDa, *ureA* and then *cagA* was used to compare the culture technique and CLO for urease with the culture technique being used as the gold standard.

RESULTS: Thirty-five percent of the biopsies were positive for *H pylori* DNA using the 3 PCR methods, while 68% of these were positive for the *cagA* gene. Twenty-four percent of the biopsies were negative for *H pylori* DNA in all PCR methods screened. The remaining 41% were either positive for *ureA* gene only, *glmM* only, 26-kDa only, or *ureA* + *glmM*, *ureA* + 26-kDa, *glmM* + 26-kDa. Out of the 35% positive biopsies, 41% and 82% were positive by culture and CLO respectively, while all negative biopsies were also negative by culture and *cagA*. *CagA* + infection was also predominantly found in *H pylori* DNA of the biopsies irrespective of the clinical diagnosis.

CONCLUSION: This method is useful for correctly identifying infections caused by *H pylori* and can be easily applied in our laboratory for diagnostic purposes.

Smith SI, Oyedeji KS, Arigbabu AO, Cantet F, Megraud F, Ojo OO, Uwaifo AO, Otegbayo JA, Ola SO, Coker AO. Comparison

of three PCR methods for detection of *Helicobacter pylori* DNA and detection of *cagA* gene in gastric biopsy specimens. *World J Gastroenterol* 2004; 10(13): 1958-1960

<http://www.wjgnet.com/1007-9327/10/1958.asp>

INTRODUCTION

Culture has been for long the method of choice to detect infectious agents. However, for some organisms that are growing slowly like *Helicobacter pylori* (*H pylori*), it may take several days to obtain a result. Furthermore, culture is very much dependent on infrastructure conditions and in developing countries may be jeopardized by shortage in electrical power supply.

Recently, assays based on PCR technology have been developed to detect the presence of microbial DNA, including *H pylori* DNA, by using several gene targets directly from the biopsies^[1-3]. The targets of these PCR methods include the urease A (*ureA*) gene^[4], the 26-kDa species-specific antigen (*SSA*) gene^[5] and the phosphosamine mutase (*glmM*) gene^[3] to mention a few. It can be standardized to diagnose different agents. With such methods, all the experiments are not lost in case of shortage of power supply as they can be easily repeated. A similar approach has been applied in difficult environments such as in Russia.

The present study was therefore aimed (i) to comparatively evaluate PCR and other diagnostic methods (the rapid urease test and / or culture) in order to determine which of the three PCR methods was most appropriate in the diagnosis of *H pylori* infection, and to evaluate the detection of a putative virulence marker of *H pylori*, the *cagA* gene, by PCR in biopsy specimens.

MATERIALS AND METHODS

Patients

A total of 189 specimens from 63 patients (three biopsies each) undergoing upper gastroduodenal endoscopy for various dyspeptic symptoms were included in this study and 3 biopsies each were taken from the antrum of the patients for CLO test, culture and DNA, respectively.

The specimens were obtained from four centres in Nigeria: Lagos University Teaching Hospital (LUTH), Lagos; Mount Pleasant Medical and Endoscopy clinic, Ojuelegba, Lagos; University College Hospital, Ibadan; and Obafemi Awolowo Teaching Hospital Complex (OAUTHC), Ile-Ife.

Bacterial strains

Twelve *H pylori* isolates were used in this study: one *cagA*-positive reference strain (26695), and 11 clinical isolates.

Other strains tested included local isolates of *Campylobacter jejuni* (4), *C. coli* (4) and *C. fetus* (3). The strains were tested by PCR to assess the specificity of the primers.

DNA extraction from biopsies was by the method of Marais *et al.*^[6]. Briefly, the biopsy samples were ground and centrifuged for 5 min at 10 000×g. The pellet was resuspended in 300 µL extraction buffer (20 mmol/L Tris-HCl, pH 8.0; 0.5% Tween 20) and proteinase K (0.5 mg/mL final concentration). The mixture was incubated at 56 °C for one hour after which

Table 1 Conditions for four different PCR methods

Target (reference), nucleotide (nt) positions amplified, and size of PCR products	Primer names and sequences	PCR conditions
26-kDa SSA gene (5), nt 474–776, 303 bp	Primer 3, 5' -TGGCGTGTCTATTGACAGCGAGC-3'	98 °C, 10 min (1cycle);
	Primer 4, 5' -CCTGCTGGGCATACTTCACCAG-3'	92 °C, 30 s; 68 °C, 1 min (37cycles); 92 °C, 30 s 68 °C, 1 min; 72 °C, 2 min (6 cycles)
Urease A gene (4), nt 304 – 714, 411 bp	HPU1, 5' -GCCAATGGTAAATTAGTT-3'	94 °C, 1 min; 45 °C, 1 min
<i>glmM</i> gene (3) nt 784–1 077, 294 bp	HPU2, 5' -CTCCTTAATTGTTTTTAC-3'	72 °C, 1 min (35 cycles)
	Forward primer, 5' -AAGCTTTTAGGGGTGTTAGGGGTTT-3'	93 °C, 1 min; 55 °C, 1 min;
CagA gene nt 394 bp	Reverse primer, 5' -AAGCTTACTTTCTAACACTAACGC-3'	72 °C, 1 min (35 cycles)
	Primer 1, 5' -CCATGAATTTTTGATCCGTTCCGG-3'	94 °C, 1 min, 58 °C, 1 min; 72 °C, 1 min (40 cycles)
	Primer 2, 5' -GATAACAGGCAAGCTTTTTGAGGGA-3'	

the enzyme was inactivated by boiling for 10 min.

Five µL of DNA was used as the template for each PCR. Each sample was examined by four different PCRs. Primers used in this study were from, 26-kDa SSA gene (303 bp), urease A gene (411 bp), *glmM* gene (294 bp) and the *cagA1* gene sequence (394 bp).

PCR reaction was carried out in a 50 µL volume in GeneAmp 9700 (Perkin Elmer). The primer sequences, conditions and sizes of these PCR methods are listed in Table 1.

Detection of amplified DNA products

A volume of seven µL of each PCR mixture was subjected to gel electrophoresis (1%) and ethidium -bromide staining for the detection of amplified DNA products.

RESULTS

Specificity of PCR assays with bacterial isolates

The specificity of PCR primers targeting *ureA*, *glmM*, 26-kDa and *cagA* gene was determined by testing 12 bacterial strains from related genus.

The 26-kDa PCR amplified the expected 303-bp fragment from the reference *H pylori* strain, while none from the other *Campylobacter* strains was amplified. Likewise, the *glmM* gene amplified the expected 294-bp fragment, *ureA*, 411-bp fragment and *cagA*, 394-bp fragment in *H pylori* reference and not in *Campylobacter* spp.

Detection of the three genes by PCR

Out of the 63 biopsies screened, 22(35%) were positive in all three PCR methods (26-kDa, *glmM*, *ureA*), 11 were positive for *ureA*, five for *glmM*, two for 26-kDa, two each for *ureA* and *glmM* and one each for *glmM*/ 26-kDa and *ureA* /26-kDa. Fifteen (24%) of the biopsies screened were negative for all three genes screened. Of these, 22 were positive for *H pylori* DNA, only nine (41%) were culture positive (Table 2). All negative biopsies from the 3 genes were negative by culture and CLO test. Two culture negative biopsies were positive in all three genes screened.

Detection of the *cagA* gene

Of the 22 biopsies that showed positive amplification in all three genes, 15(68%) were positive for the *cagA* gene. These comprised three biopsies from patients with cancer positive for the *cagA* gene. The patients with normal findings also had two out of three biopsies positive for the *cagA* gene. Out of the ten biopsies screened from patients with duodenitis or duodenal ulcer, only three (30%) were negative for the *cagA* gene (Table 3). All the biopsies that were positive for *cagA*

were also positive for their corresponding isolates. All negative biopsies were also negative for *cagA* gene.

Table 2 Results of three PCR methods and *cagA* gene for the detection of *H pylori* from gastric biopsy

Biopsy (n=63)	<i>ureA</i>	<i>glmM</i>	26-kDa	Cag A +	Culture	CLO
22	+	+	+	15	9+, 13-	18+, 4-
11	+	-	-	-	11-	3+, 8-
5	-	+	-	-	5 -	3+, 2-
2	-	-	+	-	2 -	2-
4	+	+	-	-	4 -	2-, 2+
2	+	-	+	-	1+, 1-	2 +
2	-	+	+	-	1+, 1-	2 +
15	-	-	-	-	15 -	15 -

–: negative, +: positive.

Table 3 Positive and negative predictive values of three different PCR methods

Value	Results [(%, No. of samples with value/total No.)] for PCR method		
	<i>ureA</i> gene	<i>glmM</i> gene	26-kDa gene
Positive predictive ¹	91 (10/11)	91 (10/11)	100 (11/11)
Negative predictive ²	44 (23/52)	56 (29/52)	67 (35/52)

¹Compared with 11 culture- positive samples, ²Compared with 52 culture- negative samples.

DISCUSSION

The *ureA* gene PCR had a very poor specificity in our study, as it amplified 29 of the 52 (npv=44%) culture negative biopsy specimens. This was contrary to the report by Lu *et al.*^[1], but they concluded that the sensitivity was unsatisfactory and could be due to sequence polymorphism in the loci.

However, the positive predictive value was 91%. The 26-kDa gene primer amplified all 100%(11/11) (ppv=100%) of *H pylori* culture positive biopsy samples and produced 17 false positive results on 52 culture negative specimens (npv=67%) (Table 2).

The *glmM* gene PCR amplified 10 out of the 11 culture positive biopsy specimens (ppv, 91%), with a low sensitivity, as 23 of 52 culture negative biopsy specimens (npv, 56%) were amplified.

Lage *et al.*^[2] however, reported in their study that there

were no false positive or negative biopsies amplified by the *glmM*. The reason for this is quite obvious as there are no problems of power outages in their environment and so it is easy to culture *H pylori* as a result of the steady power supply as opposed to our environment where constant power outages threaten the isolation of *H pylori*.

A comparison of the urease test using the CLO test kit (Delta West, Pty, Australia) showed that a total of 25 biopsies positive for urease test were negative by culture. This was possible as a result of the fact that the CLO test kit could detect the presence of *H pylori* even when they were very small, while when there was power outage the possibility of detecting the organism was small. In addition, occasionally the biopsy forcep could be contaminated during the passage of the endoscope in the stomach, resulting in growth of some other urease positive organisms from the biopsies^[7]. Another general explanation for the poor specificity of all tests compared to culture was as a result of incessant power outages in our country, thus decreasing the possibility of isolating *H pylori* (a fastidious organism) by culture.

Sixty-eight percent of the biopsies that were positive for all three PCR methods were positive for *cagA*. The presence of *cagA*, a virulence factor, was found to be common irrespective of the clinical diagnosis, similar to a previous study by Smith *et al.*^[8].

In conclusion, the 26-kDa gene, was found to be the most appropriate of the three different PCR methods for the detection of *H pylori* from biopsies. The study also showed that PCR had a potential value for studying *cagA* and possibly other virulent factors directly from biopsies, although it might not be important in rapidly detecting a patient that is at high risk of peptic ulcer since the frequency is similar to those of

non-ulcer dyspepsia and more importantly the method could be adapted for our environment, where there is constant power outage.

REFERENCES

- 1 **Lu JJ**, Perng CL, Shyu RY, Chen CH, Lou Q, Chong SKF, Lee CH. Comparison of five PCR methods for detection of *Helicobacter pylori* DNA in gastric tissues. *J Clin Microbiol* 1999; **37**: 772-774
- 2 **Lage A**, Godfroid E, Fauconnier A, Burette A, Butzler JP, Bollen A, Glupczynski Y. Diagnosis of *Helicobacter pylori* infection by PCR: comparison with other invasive methods. *J Clin Microbiol* 1995; **33**: 2752-2756
- 3 **Bickley J**, Owen RJ, Fraser AG, Pounder RE. Evaluation of the polymerase chain reaction for detecting the urease C gene of *Helicobacter pylori* in gastric biopsy samples and dental plaque. *J Med Microbiol* 1993; **39**: 338-344
- 4 **Clayton CL**, Kleanthous H, Coates PJ, Morgan DD, Tabaqchali S. Sensitive detection of *Helicobacter pylori* by using polymerase chain reaction. *J Clin Microbiol* 1992; **30**: 192-200
- 5 **Hammar M**, Tyszkiewicz T, Wadstrom T, O' Toole PW. Rapid detection of *Helicobacter pylori* in gastric biopsy material by polymerase chain reaction. *J Clin Microbiol* 1992; **30**: 54-58
- 6 **Marais A**, Monteiro L, Occhialini M, Pina M, Lamoliatte H, Megraud F. Direct detection of *Helicobacter pylori* resistance to macrolides by a polymerase chain reaction/DNA enzyme immunoassay in gastric biopsy specimens. *Gut* 1999; **44**: 463-467
- 7 **Smith SI**, Oyedeji KS, Arigbabu A, Anomneze EE, Chibututu CC, Atimomo CA, Atoyebi A, Adesanya A, Coker AO. Prevalence of *H pylori* in patients with gastritis and peptic ulcer in Western, Nigeria. *Biomedical Lett* 1999; **60**: 115-120
- 8 **Smith SI**, Kirsch C, Oyedeji KS, Arigbabu AO, Coker AO, Ekkehard B, Miehke S. Prevalence of *Helicobacter pylori vacA*, *cagA* and *iceA* genotypes in Nigerian patients with duodenal ulcer disease. *J Med Microbiol* 2002; **51**: 851-854

Edited by Wang XL and Xu FM

Frequencies of poor metabolizers of cytochrome P450 2C19 in esophagus cancer, stomach cancer, lung cancer and bladder cancer in Chinese population

Wei-Xing Shi, Shu-Qing Chen

Wei-Xing Shi, Department of Public Health, School of Medicine, Zhejiang University, Hangzhou 310031, Zhejiang Province, China

Shu-Qing Chen, Department of Biochemistry and Molecular Biology, College of Pharmaceutical Sciences, Zhejiang University, Hangzhou 310031, Zhejiang Province, China

Supported by Research funding from Health Bureau of Zhejiang Province (G20030697) and Research Fund from Hangzhou Tobacco Factory

Correspondence to: Dr Shu-Qing Chen, Department of Biochemistry and Molecular Biology, College of Pharmaceutical Sciences, Zhejiang University, Hangzhou 310031, Zhejiang Province, China. chenshuqing@zju.edu.cn

Telephone: +86-571-87217406 **Fax:** +86-571-87217406

Received: 2004-01-15 **Accepted:** 2004-02-12

Abstract

AIM: To investigate the association between cytochrome P450 2C19 (CYP2C19) gene polymorphism and cancer susceptibility by genotyping of CYP2C19 poor metabolizers (PMs) in cancer patients.

METHODS: One hundred and thirty-five cases of esophagus cancer, 148 cases of stomach cancer, 212 cases of lung cancer, 112 cases of bladder cancer and 372 controls were genotyped by allele specific amplification-polymerase chain reaction (ASA-PCR) for CYP2C19 PMs. The frequencies of PMs in cancer groups and control group were compared.

RESULTS: The frequencies of PMs of CYP2C19 were 34.1% (46/135) in the group of esophagus cancer patients, 31.8% (47/148) in the stomach cancer patients, 34.4% (73/212) in the group of lung cancer patients, only 4.5% (5/112) in the bladder cancer patients and 14.0% (52/372) in control group. There were statistical differences between the cancer groups and control group (esophagus cancer, $\chi^2=25.65$, $P<0.005$, $OR=3.18$, $95\%CI=2.005-5.042$; stomach cancer, $\chi^2=21.70$, $P<0.005$, $OR=2.86$, $95\%CI=1.820-4.501$; lung cancer, $\chi^2=33.58$, $P<0.005$, $OR=3.23$, $95\%CI=1.503-6.906$; bladder cancer, $\chi^2=7.50$, $P<0.01$, $OR=0.288$, $95\%CI=0.112-0.740$).

CONCLUSION: CYP2C19 PMs have a high incidence of esophagus cancer, stomach cancer and lung cancer, conversely they have a low incidence of bladder cancer. It suggests that CYP2C19 may participate in the activation of procarcinogen of esophagus cancer, stomach cancer and lung cancer, but may involve in the detoxification of carcinogens of bladder cancer.

Shi WX, Chen SQ. Frequencies of poor metabolizers of cytochrome P450 2C19 in esophagus cancer, stomach cancer, lung cancer and bladder cancer in Chinese population. *World J Gastroenterol* 2004; 10(13): 1961-1963

<http://www.wjgnet.com/1007-9327/10/1961.asp>

INTRODUCTION

Individuals vary widely in their susceptibility to carcinogens.

One attractive genetic mechanism to account for this variability is the activity of polymorphically expressed cytochrome P450 enzymes that activate procarcinogens or conversely detoxify carcinogens. Cytochrome P450 2C19 (CYP2C19) is a clinically important metabolic enzyme responsible for the metabolism of a number of therapeutic drugs, such as S-mephenytoin, omeprazole, diazepam, proguanil, propranolol and certain antidepressants^[1]. Recently, there were several papers concerning the CYP2C19 polymorphism and cancer susceptibility. Wadelius *et al.*^[2] found no association between CYP2C19 polymorphism and prostate cancer. Roddam *et al.*^[3] reported an increased risk of CYP2C19 poor metabolizers (PMs) to develop adult acute leukaemia and Sachse *et al.*^[4] found CYP2C19*2 had an decreased risk of colorectal cancer. Normally, Oriental people had a higher incidence of CYP2C19 poor metabolizers, which was usually about 13-16%, but in Caucasian people it was only 1-3% as well. So, for the purpose of investigating association between CYP2C19 polymorphism and cancer susceptibility, it is more easy to draw a conclusion in Oriental population. The aim of this study was to evaluate the relationship between CYP2C19 polymorphism and susceptibility to different kind of cancer by means of CYP2C19 genotyping among Chinese subjects.

MATERIALS AND METHODS

Reagents

Taq DNA polymerase, dNTPs, PCR buffer and 25 mmol/L MgCl₂ were purchased from Promega USA, Primers (Sangon, Shanghai), Igepal CA-630 (Sigma, USA), DNA Ladder (Huamei, Shanghai), Agarose (Pharmacia, Sweden), *Sma*I and *Hma*HI were obtained from MBI, USA. Other chemicals were of analytical grade.

Equipments

PCR machine (Hybaid, USA), electrophoresis apparatus (Pharmacia, Sweden), gel imaging system (Stratagene, USA), high speed centrifuge (Hitachi, Japan) and electro-balance (Mettler, France) were used.

Subjects

Cancer patients were from No 1 and No 2 hospitals affiliated to Zhejiang University. Healthy controls were recruited randomly around the same area. This study was approved by the Medical Institutional Review Board of the University and all subjects were provided informed consent prior to their participation. All the subjects were Chinese Han Nationality.

Methods

DNA extraction and detection of CYP2C19*2 and CYP2C19*3 A 5 mL blood sample was collected from each subject and DNA was extracted from blood for CYP2C19 genotyping according to Lahiri *et al.*^[5]. For the detection of CYP2C19*2, paired PCR reactions were set, one containing CYP2C19*2 primers and the other containing wild-type

primers (Table 1). Each PCR reaction (50 μ L) containing 10 mmol/L Tris-HCl, pH 8.3, 50 mmol/L KCl, 2.0 mmol/L MgCl₂, 0.2 mmol/L of each dNTPs, 0.2 μ mol/L of each primers and 50-1 000 ng of DNA template, 1 unit of Taq DNA polymerase was amplified through 35 cycles, each cycle consisting of denaturation at 94 °C for 1 min, primer annealing at 61 °C for 1 min, and extension at 72 °C for 1.5 min. Finally, a further extension was carried out at 72 °C for 10 min. The amplicon was analyzed on 20 g/L agarose gel electrophoresis. For detection of CYP2C19*3, paired PCR reactions were set, one containing CYP2C19*3 primers and the other containing wild-type primers (Table 2). Each PCR reaction (50 μ L) containing 10 mmol/L Tris-HCl pH 8.3, 50 mmol/L KCl, 2.0 mmol/L MgCl₂, 0.2 mmol/L of each dNTPs, 0.2 μ mol/L of each primers and 50-1 000 ng of DNA template, 1 unit of Taq DNA polymerase was amplified through 35 cycles, each cycle consisting of denaturation at 94 °C for 1 min, primer annealing at 58 °C for 1 min and extension at 72 °C for 30 s. Finally, a further extension was performed at 72 °C for 10 min. The amplicon was analyzed on 20 g/L agarose gel electrophoresis.

Table 1 Primers designed for detection of CYP2C19*2

Genotype		Sequences
Wild-type	Forward	5'-AATTAC AAC CAG AGA GCT TGG C-3'
	Reverse	5'-GTA ATT TGT TAT GGG TTC CC-3'
Mutant	Forward	5'-AAT TAC AAC CAG AGA GCT TGG C-3'
	Reverse	5'-GTA ATT TGT TAT GGG TTC CT-3'

Table 2 Primers designed for detection of CYP2C19*3

Genotype		Sequences
Wild-type	Forward	5'-TAT TAT TAT CTG TTA ACT AAT ATG A-3'
	Reverse	5'-AAC TTG GCC TTA CCT GGA TC-3'
Mutant	Forward	5'-TAT TAT TAT CTG TTA ACT AAT ATG A-3'
	Reverse	5'-AAC TTG GCC TTA CCT GGA TT-3'

The genotypes were judged by shown up of goal fragments in the paired PCR amplifications. For CYP2C19*2 allele, the goal fragment (139 bp band) could be seen only in the lane of CYP2C19*2 PCR reaction means homozygous CYP2C19*2 allele (*2/*2), only in the lane of wild-type reaction means homozygous wild-type (*1/*1), and in both reaction means heterozygous CYP2C19*2 (*1/*2). For CYP2C19*3 allele, the goal fragment (253 bp band) could be seen only in the lane of CYP2C19*3 PCR reaction means homozygous CYP2C19*3 allele (*3/*3), only in the lane of wild-type reaction means homozygous wild-type (*1/*1), and in both reaction means heterozygous CYP2C19*3 (*1/*3). In the consideration of both alleles, the other genotype could be *2/*3.

Quality control checks of PCR procedures indicated DNA samples genotyped in a double-blinded fashion yielded the same alleles as found during previous genotyping of DNA. The genotypes were checked for reliability by comparing with PCR-RFLP procedure^[6,7].

RESULTS

Genotyping of CYP2C19

Four pairs of primers were designed according to CYP2C19 wild-type sequence and the mutations in CYP2C19*2 and CYP2C19*3 by the principle of allele-specific amplification. PCR amplification conditions were tested to find the optimum annealing temperature and MgCl₂ concentration. The method was proved to be quick, accurate and less contamination (Figures 1, 2).

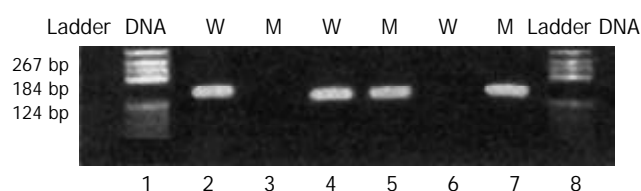


Figure 1 Typical electrophoresis pattern in detection of CYP2C19*2. Goal fragment was 139 bp. Lanes 1 and 8: DNA ladder; Lanes 2, 4 and 6: wild-type primers; Lanes 3, 5 and 7: mutant primers; Sample 1: homozygous wild-type (lanes 2 and 3); Sample 2: heterozygote (lanes 4 and 5); Sample 3: homozygous mutant (lanes 6 and 7).

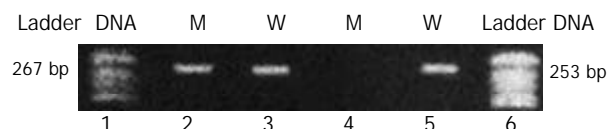


Figure 2 Typical electrophoresis pattern in detection of CYP2C19*3. Goal fragment was 253 bp. Lanes 1 and 6: DNA ladder; Lanes 2 and 4: mutant primers; Lanes 3 and 5: wild-type primers. Sample 1: heterozygote (lanes 2 and 3); Sample 2: homozygous wild-type (lanes 4 and 5); No homozygous mutant found in this study.

Frequency study of poor metabolizers in the cancer groups and the control group

The frequencies of poor metabolizers of CYP2C19 (genotypes of *2/*2 and *2/*3, no *3/*3 was found in this study) were of 34.1% (46/135) in the group of esophagus cancer patients, 31.8% (47/148) in the stomach cancer patients, 34.4% (73/212) in the group of lung cancer patients, only 4.5% (5/112) in the bladder cancer patients and 14.0% (52/372) in control group. There were statistical differences between cancer groups and control group (esophagus cancer, $\chi^2=25.65$, $P<0.005$, $OR=3.18$, $95\%CI=2.005-5.042$; stomach cancer, $\chi^2=21.70$, $P<0.005$, $OR=2.86$, $95\%CI=1.820-4.501$; lung cancer, $\chi^2=33.58$, $P<0.005$, $OR=3.23$, $95\%CI=1.503-6.906$; bladder cancer, $\chi^2=7.50$, $P<0.01$, $OR=0.288$, $95\%CI=0.112-0.740$). It was obviously that CYP2C19 PMs had a high incidence of esophagus cancer, stomach cancer and lung cancer, conversely CYP2C19 PMs had a low incidence of bladder cancer (Table 3).

Table 3 Frequencies of EMs and PMs in different cancer groups and control group

Group	Total cases	EMs (*1/*1, *1/*2, *1/*3)		PMs (*2/*2, *2/*3)	
		Cases	%	Cases	%
Esophagus cancer	135	89	65.9	46	34.1
Stomach cancer	148	101	68.2	47	31.8
Lung cancer	212	139	65.6	73	34.4
Bladder cancer	112	107	95.5	5	4.5
Control	372	320	86.0	52	14.0

Esophagus cancer, $\chi^2=25.65$, $P<0.005$, $OR=3.18$, $95\%CI=2.005-5.042$; Stomach cancer, $\chi^2=21.70$, $P<0.005$, $OR=2.86$, $95\%CI=1.820-4.501$; Lung cancer, $\chi^2=33.58$, $P<0.005$, $OR=3.23$, $95\%CI=1.503-6.906$; Bladder cancer, $\chi^2=7.50$, $P<0.01$, $OR=0.288$, $95\%CI=0.112-0.740$.

DISCUSSION

With the completion of the Human Genome Project, great opportunities exist to investigate the effects of genetic variation of the cancer susceptibility to environment exposure. It is known to all cigarette smoke can cause lung cancer, but the fact is not every smoker suffering from lung cancer. What is

the mechanism of which smoker is more susceptible to lung cancer, which smoker may not catch the disease. One of the answers may lie on the gene polymorphisms of drug metabolising enzymes. This rule may also apply to esophagus cancer, stomach cancer and bladder cancer.

Cytochrome P450s are the main drug metabolizing enzymes in human body, and are always found to participate in the metabolism of carcinogens or procarcinogens. Some are involved in the activation of procarcinogens, some may take part in the inactivation of carcinogens. That depends on what kind of carcinogens and what kind of cancers, and what kind of mechanism of carcinogenesis.

CYP2C19—one of the most important cytochrome P450s, is known as a key enzyme in the *in vivo* metabolism of a number of related hydantoins and barbiturates, as well as in the metabolism of structurally unrelated drugs such as omeprazole, lansoprazole, progulil, mephenytoin and citalopram^[1]. Individuals can be divided into two groups, poor metabolizers (PMs) and extensive metabolizers (EMs), depending on the hydroxylation ability of S-mephenytoin. There are two main enzyme deficient alleles called CYP2C19*2 (CYP2C19m1) and CYP2C19*3 (CYP2C19m2). CYP2C19*2 is a single base pair G₆₈₁→A mutation in exon 5 of CYP2C19 and accounts for 75% and 85% of Oriental and Caucasian mutant alleles, respectively^[6]. CYP2C19*3 is a single base pair G₆₃₆→A mutation in exon 4 of CYP2C19 which results in a premature stop codon^[7]. It accounts for 10–25% of Oriental mutant alleles and is rare in Caucasians. An individual who inherits two mutant CYP2C19 alleles, whatever same kind (*2/*2, *3/*3) or different kind (*2/*3), has a reduced capacity to metabolize CYP2C19 substrates and is a PM. Individuals who are homozygous (*1/*1) or heterozygous (*1/*2, *1/*3) for wild-type CYP2C19*1 have efficient enzyme to metabolize CYP2C19 substrates and are EMs. Although there are several other reports about rare enzyme defect alleles, it is recognized that the purpose of prediction of CYP2C19 phenotype can be achieved by genotyping CYP2C19 only with CYP2C19*2 and CYP2C19*3 in Chinese population^[8].

In this study, 135 esophagus cancer patients, 148 stomach cancer patients, 212 lung cancer patients, 112 bladder cancer patients and 372 controls were genotyped for CYP2C19. Among them, 34.1% of esophagus cancer patients, 31.8% of stomach cancer patients and 34.4% of lung cancer patients, but only 4.5% of bladder cancer patients and 14.0% of healthy controls were genotyped as CYP2C19 PMs. Statistical analysis of the frequencies of PMs in cancer groups and control group showed significant differences (Table 3). It means CYP2C19 PMs are more susceptible to esophagus cancer, stomach cancer and lung cancer, but it is unsusceptible to Bladder cancer.

Several studies on CYP2C19 polymorphism and its association with carcinogenesis have shown self-contradiction results^[2–4]. However, our data indicated that CYP2C19 polymorphism was associated with esophagus cancer, stomach cancer, lung cancer and bladder cancer. Furthermore, we found that CYP2C19 PMs had increased risk of esophagus cancer, stomach cancer and lung cancer, and a decreased risk of bladder cancer. However, Klose *et al.*^[9] reported that CYP2C19 was only expressed in liver and duodenum. How it functioned so differently in different organs remained a mystery. But from the organs listed above, it is deducible that CYP2C19 PMs are more susceptible to the cancers of upper or systemic organs, such as esophagus, stomach, lung and blood. And they are

unsusceptible to the cancers of lower organs, like bladder and colorectal cancers. Prostate cancer was another example which showed no relationship between CYP2C19 polymorphism and carcinogenesis. It implies that different type of cancers may have different oncological mechanisms.

The genetic background and living environment of an individual are most important factors for carcinogenesis^[10]. The relationship between genetic polymorphism of *CYP* genes^[11,12], ABO blood groups^[13] and well water pollution are widely recognized. But more efforts needed to elucidate the correlation of different types of cancer to so many different factors, the development of biochip technology may speed it up^[14].

REFERENCES

- 1 **Xie HG**, Kim RB, Wood AJ, Stein CM. Molecular basis of ethnic differences in drug disposition and response. *Annu Rev Pharmacol Toxicol* 2001; **41**: 815-850
- 2 **Wadelius M**, Autrup JL, Stubbins MJ, Andersson SO, Johansson JE, Wadelius C, Wolf CR, Autrup H, Rane A. Polymorphisms in NAT2, CYP2D6, CYP2C19 and GSTP1 and their association with prostate cancer. *Pharmacogenetics* 1999; **9**: 333-340
- 3 **Roddam PL**, Rollinson S, Kane E, Roman E, Moorman A, Cartwright R, Morgan GJ. Poor metabolizers at the cytochrome P450 2D6 and 2C19 loci are at increased risk of developing adult acute leukaemia. *Pharmacogenetics* 2000; **10**: 605-615
- 4 **Sachse C**, Smith G, Wilkie MJ, Barrett JH, Waxman R, Sullivan F, Forman D, Bishop DT, Wolf CR. A pharmacogenetic study to investigate the role of dietary carcinogens in the etiology of colorectal cancer. *Carcinogenesis* 2002; **23**: 1839-1849
- 5 **Lahiri DK**, Nurnberger JI Jr. A rapid non-enzymatic method for the preparation of HMW DNA from blood for RFLP studies. *Nucleic Acids Res* 1991; **19**: 5444
- 6 **de Morais SM**, Wilkinson GR, Blaisdell J, Meyer UA, Nakamura K, Goldstein JA. Identification of a new genetic defect responsible for the polymorphism of (S)-mephenytoin metabolism in Japanese. *Mol Pharmacol* 1994; **46**: 594-598
- 7 **de Morais SM**, Wilkinson GR, Blaisdell J, Nakamura K, Meyer UA, Goldstein JA. The major genetic defect responsible for the polymorphism of S-mephenytoin metabolism in humans. *J Biol Chem* 1994; **269**: 15419-15422
- 8 **Shu Y**, Zhou HH. Individual and ethnic differences in CYP2C19 activity in Chinese populations. *Acta Pharmacol Sin* 2000; **21**: 193-199
- 9 **Klose TS**, Blaisdell JA, Goldstein JA. Gene structure of CYP2C8 and extrahepatic distribution of the human CYP2Cs. *J Biochem Mol Toxicol* 1999; **13**: 289-295
- 10 **Yoshimura K**, Hanaoka T, Ohnami S, Kohno T, Liu Y, Yoshida T, Sakamoto H, Tsugane S. Allele frequencies of single nucleotide polymorphisms (SNPs) in 40 candidate genes for gene-environment studies on cancer: data from population-based Japanese random samples. *J Hum Genet* 2003; **48**: 654-658
- 11 **Bartsch H**, Nair U, Risch A, Rojas M, Wikman H, Alexandrov K. Genetic polymorphism of CYP genes, alone or in combination, as a risk modifier of tobacco-related cancers. *Cancer Epidemiol Biomarkers Prev* 2000; **9**: 3-28
- 12 **Ribeiro Pinto LF**, Teixeira Rossini AM, Albano RM, Felzenszwalb I, de Moura Gallo CV, Nunes RA, Andreollo NA. Mechanisms of esophageal cancer development in Brazilians. *Mutat Res* 2003; **544**: 365-373
- 13 **Su M**, Lu SM, Tian DP, Zhao H, Li XY, Li DR, Zheng ZC. Relationship between ABO blood groups and carcinoma of esophagus and cardia in Chaoshan inhabitants of China. *World J Gastroenterol* 2001; **7**: 657-661
- 14 **Landi S**, Gemignani F, Gioia-Patricola L, Chabrier A, Canzian F. Evaluation of a microarray for genotyping polymorphisms related to xenobiotic metabolism and DNA repair. *Biotechniques* 2003; **35**: 816-820

Allelotyping for loss of heterozygosity on chromosome 18 in gastric cancer

Jing-Cui Yu, Kai-Lai Sun, Buo Liu, Song-Bin Fu

Jing-Cui Yu, Department of Medical Genetics, China Medical University, Shenyang 110001, China; Department of Clinical Pharmacology, the Second Affiliated Hospital, Harbin Medical University, Harbin 150086, Heilongjiang Province, China

Song-Bin Fu, Laboratory of Medical Genetics, Harbin Medical University; Bio-pharmaceutical Key Laboratory of Heilongjiang Province, Harbin 150086, Heilongjiang Province, China

Kai-Lai Sun, Department of Medical Genetics, China Medical University, Shenyang 110001, Liaoning Province, China

Buo Liu, Chinese National Human Genome Center, Beijing 100176, China

Supported by the Teaching and Research Award Program for Outstanding Young Teachers in Higher Education Institutions by Ministry of Education of China and the National Natural Science Foundation, No. 30370783 and the Key Project of Science and Technology of Heilongjiang Province, No. GB03C601-1

Correspondence to: Dr. Song-Bin Fu, Laboratory of Medical Genetics, Harbin Medical University, Harbin 150086, Heilongjiang Province, China. fusb@ems.hrbmu.edu.cn

Telephone: +86-451-86674798 **Fax:** +86-451-86669576

Received: 2003-12-23 **Accepted:** 2004-02-01

Abstract

AIM: To investigate the association between loss of heterozygosity (LOH) on chromosome 18 and sporadic gastric cancer.

METHODS: Multiplex PCR was used to screen 14 highly polymorphic microsatellite markers on chromosome 18 in 45 cases of primary gastric cancer. PCR products were separated on polyacrylamide gels and the electrophoresis maps were analyzed with Genescan and Genotyper.

RESULTS: The LOH frequencies in gastric cancer at all 14 markers ranged from 10% to 58%. Eleven markers were found with over 20% LOH frequencies, in which 9 markers located in 18q, and 2 markers in 18p. Two overlapping deleted regions were identified: R1 between D18S61-D18S1161 at 18q22 (9cM) with 24% LOH frequency; R2 between D18S462-D18S70 at 18q22-23(6cM) with 32% LOH frequency.

CONCLUSION: LOH of chromosome 18 (18q and 18p) may be involved in gastric tumorigenesis. Two overlapping deleted fragments suggested that there might be unidentified tumor suppressor genes in those two regions.

Yu JC, Sun KL, Liu B, Fu SB. Allelotyping for loss of heterozygosity on chromosome 18 in gastric cancer. *World J Gastroenterol* 2004; 10(13): 1964-1966

<http://www.wjgnet.com/1007-9327/10/1964.asp>

INTRODUCTION

Inactivation of tumor suppressor genes (TSGs) has been considered to be one of the most important mechanisms during the human tumorigenesis^[1]. Earlier studies have shown that loss of heterozygosity (LOH) on specific chromosomal loci is related to the inactivation of TSGs. The Knudson "two-hit"

hypothesis has provided the rationale for identifying TSGs by mapping regions of LOH. Analysis of LOH has been developed and fully exploited for the detection of TSGs in a variety of tumors through comparison of copy number changes in tumor DNA with matched control DNA^[2]. Different chromosomal regions that are harboring putative TSGs can be found in tumors by searching for LOH markers. Furthermore, by identifying genetic distance between these markers and TSGs, the allelic loss regions can be narrowed step by step and the TSGs can be finally cloned.

Gastric cancer (GC) is one of the most frequent malignancies and remains a main cause of mortality in China^[3-5]. Many regions of LOH on different chromosomes have been found in GC^[6]. Allelic loss on the long arm of chromosome 18 (18q LOH) is highly related to GC^[7]. Little is known about allelic loss on the short arm of chromosome 18 (18pLOH) in GC, although a significant incidence of 18pLOH (specially 18q11) has been found in tumors of the lung, brain and breast^[8]. So in this paper, we chose fourteen highly polymorphic microsatellite markers spanning chromosome 18p and 18q and performed genome-wide allelotyping in 45 primary gastric cancers. We identified the chromosomal loci and overlapping regions that are frequently lost in GC for clarifying the roles of 18pLOH and 18qLOH in GC and providing evidences for finding new important TSGs.

MATERIALS AND METHODS

Sample collection and DNA extraction

Forty-five primary gastric tumors and corresponding non-tumorous tissue specimens were obtained at surgery from the First Hospital and the Second Hospital of Harbin Medical University. All the patients were confirmed by routine histologic examination and received no treatment before surgery. Each specimen was frozen immediately and stored at -80 °C until use. Genomic DNA was extracted using DNAzo1^R reagent-genomic DNA isolation reagent (Gibcol).

Fluorescent microsatellite analysis

Along chromosome 18, we chose 14 polymorphic microsatellite markers (5 markers at 18p, 9 markers at 18q) at a density of approximately one marker every 9 cM (<http://www.gdb.org>). The oligonucleotides were labeled with FAM, HEX and NED three different fluorescent dyes for allelotyping (primers were obtained from the ABI PRISM Linkage Mapping Set v. 2, Perkin-Elmer). Multiplex PCR was carried on in a Gene Amp^R PCR system 9600 (Perkin-Elmer) for amplifying matched pairs of normal and tumor DNAs. PCR reaction conditions were as follows: 5 µL final volume included 0.5 µL of 10×PCR buffer, 0.6 µL of 25 mmol/L MgCl₂, 0.1 µL of 10 mmol/L dNTP, 0.25 U of Hot-start tag polymerase, 0.04 µL of each primer and 50 ng of DNA. The following PCR run conditions were used: (a) an initial denaturation at 94 °C for 12 min; (b) 15 cycles each at 94 °C for 30 s, 63 °C for 1 min (0.5 °C decreased per cycle), 72 °C for 1 min 50 s; (c) 24 cycles each at 94 °C for 30 s, 56 °C for 1 min, 72 °C for 1 min 50 s; and (d) a final extension at 72 °C for 15 min. A portion of each PCR product (0.7 µL) was combined with 1 µL of the loading mix (ABI internal size standard and formamide loading buffer). After denaturation

at 95 °C for 5 min, products were electrophoresed on 4.5% polyacrylamide gels with 7 mol/L urea on ABI prism 377 DNA sequencer (Perkin-Elmer) for 2.5 h. The data were collected automatically and analyzed using ABI prism Genescan 3.1 and Genotyper 2.1 software. Two fragments amplified from normal DNA indicated heterozygote and alleles were defined as the two highest peaks within the expected size range of heterozygote. A ratio of $T_1:T_2/N_1:N_2$ (less than 0.67 or greater than 1.3) was scored as a LOH (Figure 1). A single fragment amplified from normal DNA (homozygote) and these PCR reactions in which fragments were not clearly amplified were scored as non-informative. The LOH frequency of a site was equal to the percentage of the number between allelic losses and informative cases.

RESULTS

LOH at various frequencies were found in GC patients, ranging

from 10% to 58%, with the highest rate at D18S70 (21/36, 58%). Of the 45 cases of GC studied, 36(80%) exhibited allelic losses at least at one site, 25 at over two sites. Figure 1 shows allelic losses in partial patients on several markers. Figure 2 shows LOH frequencies of 14 markers and cytogenetic locations. Eleven markers were found with over 20% LOH frequencies, including 2 markers at 18p and 9 markers at 18q. They were as follows: D18S59 (18p11.3, 28%), D18S452 (18p11.3, 24%), D18S478 (18q11.1-11.2, 37%), D18S1102 (18q12, 29%), D18S474 (18q21, 22%), D18S64 (18q21, 30%), D18S68 (18q21, 25%), D18S61 (18q22, 26%), D18S1161 (18q22, 21%), D18S462 (18q22-23, 29%) and D18S70 (18q23, 58%). Two overlapping deleted regions (Figure 2) were identified at 18q22 (between D18S61 and D18S1161, 9 cM or approximately 5 Mb DNA sequence, overlapping fragment LOH 24%) and 18q22-23 (between D18S462 and D18S70, 6 cM or approximately 3 Mb DNA sequence, overlapping fragment LOH 32%), respectively.

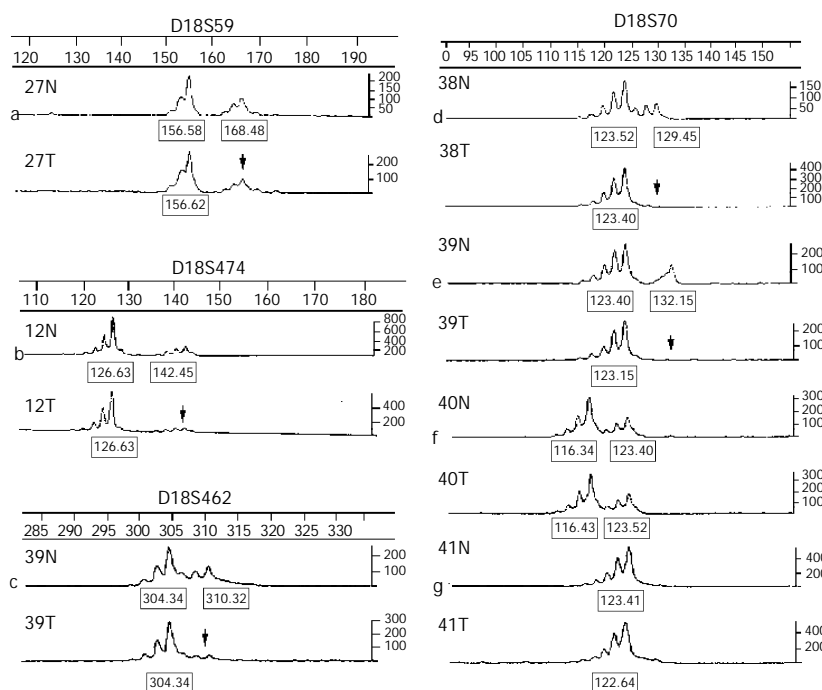


Figure 1 Representative LOH analysis of chromosome 18. The scales on the top and right side of each figure represent the size (bp) and the intensity, respectively; N: Nontumorous control; T: Tumor; Arrow: Informative case with allelic loss (a, b, c, d, e); f: An informative case without allelic loss (heterozygote); g: An non-informative case (homozygote).

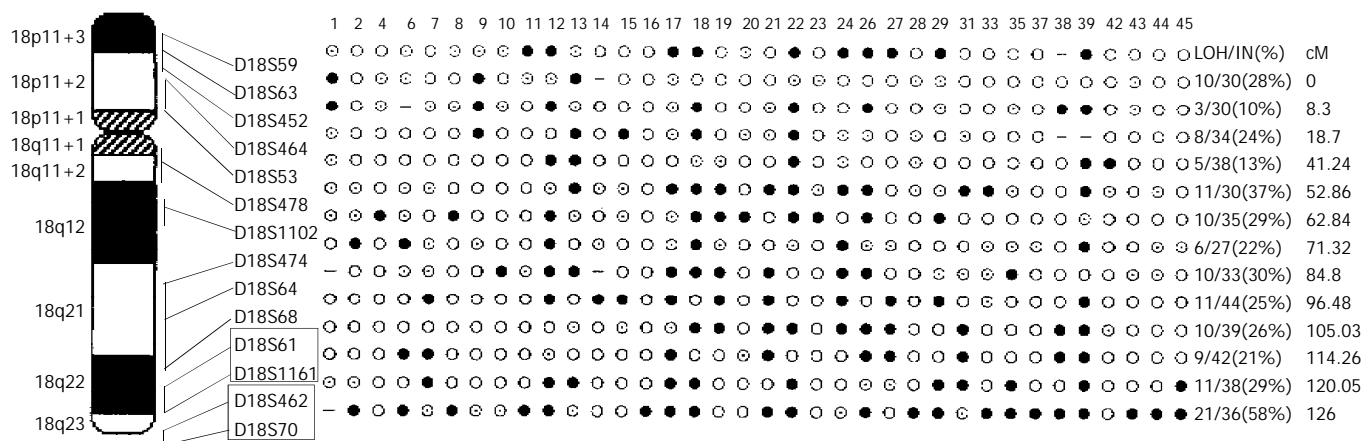


Figure 2 Results of analysis for LOH on chromosome 18. Top: the number of GC patient with LOH; Left: An ideogram of chromosome 18 with the physical order of 14 microsatellite markers according to Genome Database; Right: Allelotyping results from 36 GC patients; ●: Loss of heterozygosity (informative, IN); ○: Retention of heterozygosity (informative, IN); ⊙: Homozygote (non-informative); -: Not available; Black frame: Overlapping deleted region.

DISCUSSION

Genetic instability is often observed in tumor cells^[9]. Losses of fragments in some chromosomes may lead to allelic losses of TSGs. In the present study, more extensive genome screening was conducted on chromosome 18 in 45 cases of primary GC using 14 microsatellite markers (5 markers at 18p, 9 markers at 18q). Thirty-six out of 45 GC patients (80%) exhibited allelic losses at least one marker, allelic losses of over two markers were seen in 25 cases of GC patients. We found that two markers (D18S59 and D18S452) with over 20% LOH frequencies on chromosome band 18p11.3. DAL-1 gene (18p11.32) localizes between the two markers, which undergoes allelic losses in lung tumors and a significant proportion of ductal carcinomas *in situ* of the breast. It has been revealed that the DAL-1 protein suppresses the growth of MCF-7 breast cancer cell lines in part through the induction of apoptosis and that expression of DAL-1 increases attachment of these cells to a variety of extracellular matrices^[10]. DAL-1 plays a critical role in the suppression of lung tumor formation and metastasis^[11]. Our results support the role of DAL-1 gene in gastric carcinogenesis. Future investigations need to be carried on to understand the biological importance of the two putative loci and their clinical relevance in the pathogenesis of GC.

18qLOH is a frequent event in tumors, especially head and neck, colon, lung and gastric cancers^[12-14]. All of our 9 markers on this chromosomal arm have shown allelic loss frequencies exceeding 20%. D18S70 was the highest rate of LOH (21/36, 58%) marker on which frequent allelic loss has been reported in head and neck cancers^[15] and serous ovarian carcinoma^[16]. On the chromosome 18q22-23, Takebayashi *et al.* have identified three loci (D18S39, D18S61 and D18S70) which are lost in 70-75% of head and neck primary tumor cell lines. Lassus *et al.* observed that 59% of serous carcinomas have shown allelic loss at one or more sites and have been associated with tumor grade and poor survival. Moreover, they have identified two minimal common regions of loss at D18S465-D18S61 (18q22, 3.9 cM) and D18S462-D18S70 (18q23, 5.8 cM). Our data, together with these findings of others, suggest that D18S70 is a new putative tumor suppressor site in GC and support the existence of at least one candidate TSG near the site. Significant LOH of the two overlapping lost fragments identified by us appears novel for GC and no candidate TSGs have been reported in the two overlapping deleted regions so far. LOH frequencies of the two overlapping fragments suggest the presence of as yet unidentified TSGs. Although TSGs harboured in the two overlapping lost fragments have not been defined yet, the two regions are useful candidates for further allelotyping with higher-density microsatellite markers and may help us narrow the sites of frequent allelic loss in order to search for new critical TSGs involved in the development of GC.

The molecular genetic mechanisms of GC remain unclear. Investigators have postulated that, like other tumors, the multistep processes with a variety of factors are involved in GC. Step-wise accumulation of DNA damage from "normal" to tumor tissue serves as the basis of the tumor progression models^[17]. Our findings have shown that allelic losses are widespread on chromosome 18 and gastric tumorigenesis may be involved in synthetic effect of multiple TSGs.

ACKNOWLEDGEMENTS

We are grateful to Dr. Shen Yan (Chinese National Human Genome Center, Beijing) for his helpful advice.

REFERENCES

- 1 **Wang GS**, Wang MW, Wu BY, You WD, Yang XY. A novel gene, GCRG224, is differentially expressed in human gastric mucosa. *World J Gastroenterol* 2003; **9**: 30-34
- 2 **Tomlinson IPM**, Lambros MBK, Roylance RR. Loss of heterozygosity analysis: practically and conceptually flawed? *Genes Chromosomes Cancer* 2002; **34**: 349-353
- 3 **Wang GT**. Progress in studies of mechanism of gastric precancerous lesions, carcinogenesis and their reversion. *Shijie Huaren Xiaohua Zazhi* 2000; **8**: 1-4
- 4 **Deng DJ**, E Z. Overview on recent studies of gastric carcinogenesis: human exposure of N-nitrosamides. *Shijie Huaren Xiaohua Zazhi* 2000; **8**: 250-252
- 5 **Pan CJ**, Liu KY. Proliferation/apoptosis and expression of P53 and Bcl-2 in gastric carcinoma. *Shijie Huaren Xiaohua Zazhi* 2003; **11**: 526-530
- 6 **Du JJ**, Dou KF, Cao YX, Wang ZH, Wang WZ, Gao ZQ. CA11, a down-regulated gene in gastric cancer: a functional study. *Shijie Huaren Xiaohua Zazhi* 2002; **10**: 525-529
- 7 **Ren Q**, Wang ZN, Luo Y, Ao Y, Lu C, Jiang L, Xu HM, Zhang X. Loss of heterozygosity on chromosome 18 in microdissected gastric cancer cells. *Shijie Huaren Xiaohua Zazhi* 2003; **11**: 310-313
- 8 **Tran Y**, Benbatoul K, Gorse K, Rempel S, Futreal A, Green M, Newsham I. Novel regions of allelic deletion on chromosome 18p in tumors of the lung, brain and breast. *Oncogene* 1998; **17**: 3499-3505
- 9 **Lengauer C**, Kinzler KW, Vogelstein B. Genetic instability in colorectal cancers. *Nature* 1997; **386**: 623-627
- 10 **Charboneau AL**, Singh V, Yu T, Newsham IF. Suppression of growth and increased cellular attachment after expression of DAL-1 in MCF-7 breast Cancer Cells. *Int J Cancer* 2002; **100**: 181-188
- 11 **Yageta M**, Kuramochi M, Masuda M, Fukami T, Fukuhara H, Maruyama T, Shibuya M, Murakami Y. Direct association of TSLC1 and DAL-1, two distinct tumor suppressor proteins in lung cancer. *Cancer Res* 2002; **62**: 5129-5133
- 12 **Wu CL**, Kirley SD, Xiao H, Chuang Y, Chung DC, Zukerberg LR. Cables enhances cdk2 tyrosine 15 phosphorylation by weel, inhibits cell growth, and is lost in many human colon and squamous cancers. *Cancer Res* 2001; **61**: 7325-7332
- 13 **Tan D**, Kirley S, Li Q, Ramnath N, Slocum HK, Brooks JS, Wu CL, Zukerberg LR. Loss of cables protein expression in human non-small cell lung cancer: a tissue microarray study. *Hum Pathol* 2003; **34**: 143-149
- 14 **Candusso ME**, Luinetti O, Villani L, Alberizzi P, Klersy C, Fiocca R, Ranzani GN, Solcia E. Loss of heterozygosity at 18q21 region in gastric cancer involves a number of cancer-related genes and correlates with stage and histology, but lacks independent prognostic value. *J Pathol* 2002; **197**: 44-50
- 15 **Takebayashi S**, Ogawa T, Jung KY, Muallem A, Mineta H, Fisher SG, Grenman R, Carey TE. Identification of new minimally lost regions on 18q in head and neck squamous cell carcinoma. *Cancer Res* 2000; **60**: 3397-3403
- 16 **Lassus H**, Salovaara R, Aaltonen LA, Butzow R. Allelic analysis of serous ovarian carcinoma reveals two putative tumor suppressor loci at 18q22-q23 distal to SMAD4, SMAD2, and DCC. *Am J Pathol* 2001; **159**: 35-42
- 17 **Powell CA**, Klares S, O' Connor G, Brody JS. Loss of heterozygosity in epithelial cells obtained by bronchial brushing: clinical utility in lung cancer. *Clinical Cancer Research* 1999; **5**: 2025-2034

Effects of *Radix Puerariae* flavones on liver lipid metabolism in ovariectomized rats

Ji-Feng Wang, Yan-Xia Guo, Jan-Zhao Niu, Juan Liu, Ling-Qiao Wang, Pei-Heng Li

Ji-Feng Wang, Yan-Xia Guo, Jan-Zhao Niu, Juan Liu, Ling-Qiao Wang, Pei-Heng Li, Department of Biochemistry, Beijing University of Chinese Medicine, Beijing 100029, China

Supported by the National Natural Science Foundation of China, No. 30330220 and the Natural Science Foundation of Beijing, No. 7032024

Correspondence to: Professor Ji-Feng Wang, Department of Biochemistry, Beijing University of Chinese Medicine, Beijing 100029, China

Telephone: +86-10-64286995 **Fax:** +86-10-64286995

Received: 2003-09-15 **Accepted:** 2003-12-10

Abstract

AIM: To study the effects of *Radix Puerariae* flavones (RPF) on liver lipid metabolism in ovariectomized (OVX) rats.

METHODS: Forty adult female Wistar rats were randomly divided into four groups: OVX group; sham-OVX group; OVX+estrogen group and OVX+RPF group. One week after operation rats of the first two groups were treated with physiological saline, rats of OVX+estrogen group with estrogen (1 mg/kg·b.w.) and rats of OVX+RPF group with RPF (100 mg/kg·b.w.), respectively for 5 weeks. After the rats were killed, their body weight, the weight of the abdominal fat and uterus were measured, and the levels of total cholesterol (TC) and triglyceride (TG) in liver homogenate were determined.

RESULTS: Compared with the sham-OVX group, the body mass of the rats in OVX group was found increased significantly; more abdominal fat in store; TC and TG in liver increased and uterine became further atrophy. As a result, the RPF was found to have an inhibitive action on those changes of various degrees.

CONCLUSION: RPF has estrogen-like effect on lipid metabolism in liver and adipose tissue.

Wang JF, Guo YX, Niu JZ, Liu J, Wang LQ, Li PH. Effects of *Radix Puerariae* flavones on liver lipid metabolism in ovariectomized rats. *World J Gastroenterol* 2004; 10(13): 1967-1970
<http://www.wjgnet.com/1007-9327/10/1967.asp>

INTRODUCTION

Estrogen plays an important role not only in maintaining the reproductive function and the secondary sex characters of the female animals, but also in so-classical target tissues, such as the brain, bone, liver, kidney and the cardiovascular system^[1,2]. With the decreases of estrogen in postmenopausal women, the incidences of fracture in osteoporosis, cardiovascular and neurodegenerative diseases often increase^[3-5]. Estrogens replacement therapy is able to attenuate symptoms of menopausal syndrome and to reduce the incidence of above-mentioned diseases^[6-9].

Phytoestrogens are naturally occurring plant chemicals that

can produce an estrogen-like effect in the body, used as a natural alternative to hormone replacement therapy and to reduce menopausal symptoms. They are not chemically the same as the estrogens made in the body, but when digested and absorbed they can act somewhat as estrogen in the body^[10]. *Radix Puerariae* is the dried root of *Pueraria lobata* Ohwior *Pueraria thomsonii* Benth. Sweet in taste and neutral in nature, it can strengthen the spleen and stomach, invigorate the spleen and replenish *Qi*. Its main component is flavone. Recent research has found leguminous plants rich in flavone have a certain kind of estrogen-like effect^[11-13]. In this study extraction of *Radix Puerariae* was given to ovariectomized (OVX) rats and its estrogen-like effects were observed.

Previous studies in our laboratory have illustrated that when the female rats were OVX, the estrogen level in their body decreased, which might lead to the body weight gains, abdominal fat stores, increase of liver fat and atrophy of uterine^[12]. Therefore, the OVX rats can be used as models to reflect the pathologic changes in perimenopausal or postmenopausal women.

MATERIALS AND METHODS

Animals

All of the 40 female Wistar rats, 220±10 g in body mass, were purchased from the Experimental Animal Center of Chinese Academy of Medical Sciences. They were raised in an air-conditioned animal house at 25±1 °C with a light-dark cycle of 12 h, and fed with free forge and running water. The rats were randomly divided into four groups: OVX group; sham-OVX group; OVX+estrogen group and OVX+RPF group. After anesthetized with 15 g/L sodium pentobarbital intraperitoneally, the rats of OVX, OVX + estrogen and OVX+RPF groups were OVX. Rats from sham-OVX received only a squeeze in the connecting point between the ovary and the fallopian tube without having their ovary removed. Starting from the second week of the operation, the rats of OVX group and sham-OVX group were treated with saline, the rats of OVX+estrogen group were treated with estrogen (1 mg/kg·b.w.) and rats from OVX+RPF group were treated with RPF (100 mg/kg·b.w.) respectively for 5 wk. The average feed consumption and mass of the rats from various groups were measured once a week.

Drugs and reagents

The RPF, provided by Biochemistry Department of Beijing University of Chinese Medicine, was made into suspension of required concentration (10 g/L). The positive control drug was nilestriol (batch number: 20000403) provided by Beijing Four Rings Pharmaceutical Factory. TG and TC kit were provided by Beijing Zhong-Sheng High-Technology Bioengineering Company.

Instruments

The Semi-automatic Biochemistry Analyzer MD 100 was made in USA. The electronic analytical balance was produced by Shimadzu Co. in Japan and the high speed centrifuge TLLC

was manufactured by Beijing Sihuan Scientific Instrumental Company.

Collection and measurement methods of specimens

Five weeks after the operation, the animals were anesthetized with 15 g/L sodium pentobarbital and the liver, abdominal fat and uterus were taken weighed and frozen. Some liver specimens were collected after operation, fixed in 40 g/L formaldehyde, embedded in paraffin, sectioned and stained with hematoxylin and eosin for light microscopy. Some liver specimens were frozen stored at -20 °C. Liver triglyceride and total cholesterol concentration were measured with the TC kit and the TG kit on a MD100 Semi-automatic biochemistry analyzer respectively after lipid extraction.

Statistical analysis

Data were presented as mean±SD, and Student's *t* test was used to determine changes between different groups. *P*<0.05 was considered significant.

RESULTS

Effect of RPF on body weight of OVX rats

The mean body mass of the OVX group increased significantly after the operation, compared to the OVX group, RPF was found to have a long term effect on body weight gains (*P*<0.05). The mean body weight of the OVX group started to exceed that of the sham-OVX group significantly ever from the first week (*P*<0.05). The mean body mass of OVX+RPF group had a statistical difference from the mean body weight of OVX group after 3 wk (*P*<0.05). From the fifth week, the body mass of all rats began to drop, but the final data showed that RPF could control the weight gain caused by ovariectomy. During feeding, rats from the OVX+estrogen group were found with colporrhagia, magersucht, and anorexia, but no such symptoms found in the OVX+RPF group (Table 1).

Table 1 Effect of RPF on body mass of OVX rats

Group	<i>n</i>	Body mass after operation (g)	Body weight during recovery period (g)	Wk 1 (g)	Wk 2 (g)	Wk 3 (g)	Wk 4 (g)	Wk 5 (g)	Change rate
OVX	8	215±15	233±17	250±16	266±16 ^c	276±15 ^c	284±16 ^c	268±20 ^c	22.1%
Sham OVX	9	235±4.7	230±4	232±7	235±6	241±9	246±11	237±14	7.1%
OVX+estrogen	10	236±17	242.4±21	249±18	248±16 ^a	239±14 ^a	248±18 ^a	239±19 ^a	1.1%
OVX+RPF	10	216±15	233.3±16	243±17	251±20	249±16 ^a	246±19 ^a	245±17 ^a	5.6%

Results expressed as mean±SD. ^a*P*<0.05 vs OVX group, ^c*P*<0.05 vs sham-OVX.

Table 2 Effect of RPF on abdominal fat and fat factor of OVX rats

Group	<i>n</i>	Abdominal fat (g)	Compared with OVX (%)	Fat factor (%)	Compared with OVX (%)
OVX	8	13.2±2.1 ^c	—	5.1±0.4 ^c	—
Sham OVX	9	10.6±3.2	80.4	4.6±1.2	91.2
OVX+estrogen	10	6.8±3.6 ^a	52.1	3.1±1.6 ^a	60.1
OVX+RPF	10	8.5±2.5 ^a	64.4	3.7±1.2 ^a	72.1

Results expressed as mean±SD. ^a*P*<0.05 vs OVX group, ^c*P*<0.05 vs sham-OVX.

Table 3 Effect of RPF on liver lipid metabolism of OVX rats

Group	<i>n</i>	TC (mg/dL)	Compared with OVX (%)	TG (mg/dL)	Compared with OVX (%)
OVX	8	16.4±5.0 ^c	—	119±26 ^c	—
Sham-OVX	9	11.4±4.4	81±27	65±18	54±15
OVX+estrogen	10	10.2±1.7 ^a	62±10	54±31 ^a	45±26
OVX+RPF	10	10.2±2.0 ^a	76±15	46±24 ^a	39±20

Results expressed as mean±SD. ^a*P*<0.05 vs OVX group, ^c*P*<0.05 vs sham-OVX, OVX+estrogen and OVX+RPF group.

Effect of RPF on abdominal fat and fat factor of OVX rats

The mean weight of abdominal fat of the OVX group was obviously higher than that of the sham-OVX group (*P*<0.05). Both estrogen and RPF could inhibit the storing of abdominal fat caused by ovariectomy, the mean data was only 52.1% and 64.35% compared with OVX group, respectively (Table 2).

Effect of RPF on liver lipid metabolism of OVX rats

TC and TG in liver of the OVX group were 16.4±5.0 mg/dL and 119±26 mg/dL, respectively, which were significantly higher than other groups (*P*<0.05). In the sham-OVX group they were only 11.4±4.4 mg/dL and 65±18 mg/dL. The RPF was found to have a marked effect on controlling liver TC level, with TC 10.2±2.0 mg/dL and TG 46±24 mg/dL which were even lower than sham-OVX group and OVX+estrogen group (Table 3).

Effect of RPF on wet uterus weight of OVX rats

Six weeks after the operation, the uteri of the rats from the OVX group were found with severe atrophy with a quarter of the uterus weight of the sham OVX group. The uterus weight of the estrogen group was higher than the sham-OVX group (*P*<0.05). RPF has again been proved to have some effects on maintaining the uterus weight (*P*<0.05) in OVX group (Table 4).

Table 4 Effect of RPF on wet uterus weight of OVX rats

Group	<i>n</i>	Uterus (g)	Uterus factor (%)
OVX	8	0.11±0.02 ^c	0.40±0.10 ^c
Sham-OVX	9	0.39±0.14	1.70±0.60
OVX+estrogen	10	0.46±0.34 ^a	2.10±1.50 ^a
OVX+RPF	10	0.15±0.03 ^a	0.70±0.10 ^a

Results expressed as mean±SD. ^a*P*<0.05 vs OVX group, ^c*P*<0.05 vs sham-OVX.

DISCUSSION

Unlike the animal models that are often prepared by giving high fat diets for hyperlipemia study, the OVX rats were used in the present study. Results of the experiments showed that the animals with ovariectomy tended to have body weight gain, accumulated abdominal fat, increased TC and TG levels in liver and atrophied uterus, which are very similar to menopausal symptoms. Experience from our past studies has proved that animal models thus prepared are stable, which can be used in the study of lipid metabolic disturbance.

Current studies on phytoestrogen both at home and abroad are mainly focused on soy bean and its extracts, and there are very rare reports of *Radix Puerariae*, a plant from the leguminous family. In fact, the phytoestrogen content in *Radix Puerariae* is much higher than that in soy bean. The aim of the present research was to study the effects of extracts from *Radix Puerariae* on lipid metabolism in OVX rats, which mimicked the postmenopausal situation of the disorders of lipid metabolism. And we obtained a series of satisfactory results.

We found in the study that there was an obvious lipid metabolic disturbance in OVX rats. Five weeks after the operation, the TC concentration in liver in OVX group was found obviously higher than those in other groups. RPF could lower the TC concentration to the normal value. However, the mechanism for this change is not quite clear yet. The increased insulin concentration in OVX rats may accelerate the dephosphorylation effect of the hydroxymethylglutaryl CoA reductase (HMGCoA reductase), which is a rate-limiting enzyme of the composition of cholesterol. As a result, it accelerates the activity of the enzyme^[14-16]. Insulin could also induce the composition of the HMGCoA reductase directly to increase the composition of cholesterol^[17-19]. For the cholesterol metabolism *in vivo*, there are two transport pathways-the endogenous cholesterol transport and the reverse cholesterol transport. In the former, the cholesterol by exogenous absorption and synthesis in the liver is utilized when it, in the form of LDL-C, is combined with the receptors of the extra hepatic tissue, and the ligand combined with LDL receptors are mainly the apolipoprotein of apo B100 and apo E^[20-23]. In the latter, the extrahepatic cholesterol, in the form of HDL-C, is conveyed back to the liver and expelled out of the body after further metabolism^[24]. Some experiments have shown that estrogen can enhance the activity of the LDL receptors and promote the endogenous transport so as to lower the TC levels^[25]. In conclusion, the high insulin level in OVX rats may lead to a high level of cholesterol concentration, while, the low level of estrogen concentration may result in the low level of LDL-R concentration and activity, both of which can cause an accumulation of LDL. The increased production and decreased consumption together make a high level of cholesterol concentration in the body, followed by the hypercholeste and adiposis hepatica.

A high level of TG concentration was also found in the OVX rats. Extrinsic estrogen can be supplemented to reduce the TG accumulation in liver. It was found in our study that RPF had a similar effect. The histological sections revealed a great number of grease spots in the OVX group, while not so many in the estrogen treated group and RPF treated group. The mechanism may be as follows: First, glucose was promoted to change into TG by a high level of insulin concentration in OVX rats^[26]. Second, the high level of TC directly damaged the structure of hepatic sinusoid and chylomicrons that contained a high level of TG coming into the Disse's spaces without been treated. Therefore, the liver cell ingested a large amount of TG from the blood. Profound studies are still needed to further confirm its mechanisms.

We also noticed the side effects and risks of estrogen in this study. In clinic, the commonly encountered side effects of HRT are edema (fluid retention), nausea, breast tenderness,

and headache. Other side effects include rash, increased growth of facial hair, dizziness, and hypophrodisia. More serious potential health risks to consider of HRT are breast cancer, uterine cancer, blood clotting, and liver and gallbladder diseases^[27-29]. Today, selective estrogen receptor modulators (SERMs) have been used as an alternative approach to activate estrogen signaling pathways in a tissue-specific manner^[30,31]. Phytoestrogens have a similar chemical structure to estrogen, and could bind to the estrogen receptor (ER)-beta. Once they bind each other, the ER is occupied, and the real estrogen can not get in. Phytoestrogens then dispatch estrogen-like messages to the cells. Although it is a weak message, it is strong enough to produce some of the positive effects of estrogen but it is still too weak to stimulate the growth of cancer cells^[32,33]. When the estrogen levels are too high, this competition appears to reduce the effects of estrogen by replacing estrogen with the weaker phytoestrogen. When the estrogen levels are too low, it appears that phytoestrogen simulates the effects of estrogen and partially makes up for the deficiency^[34].

In conclusion, our data suggest that as a natural estrogen replacement, the RPF could regulate the lipid metabolic disturbance in liver in the OVX rats. Furthermore, there may be a possible protective action against cardiovascular diseases and osteoporosis caused by deficiency of estrogen in menopausal women. However, our data was limited. More work is still needed to confirm its profound pharmacological effects.

REFERENCES

- 1 **Diel P.** Tissue-specific estrogenic response and molecular mechanisms. *Toxicol Lett* 2002; **127**: 217-224
- 2 **Dubey RK,** Oparil S, Imthurn B, Jackson EK. Sex hormones and hypertension. *Cardiovasc Res* 2002; **53**: 688-708
- 3 **Diaz Lopez JB,** Rodriguez Rodriguez A, Ramos B, Caramelo C, Rodriguez Garcia M, Cannata Andia JB. Osteoporosis, estrogens, and bone metabolism. Implications for chronic renal insufficiency. *Nefrologia* 2003; **23**(Suppl 2): 78-83
- 4 **DeSoto MC.** Drops in estrogen levels affect brain, body and behavior: reported relationship between attitudes and menopausal symptoms. *Maturitas* 2003; **45**: 299-301
- 5 **Ahlborg HG,** Johnell O, Turner CH, Rannevik G, Karlsson MK. Bone loss and bone size after menopause. *N Engl J Med* 2003; **349**: 327-334
- 6 **Levine JP.** Long-term estrogen and hormone replacement therapy for the prevention and treatment of osteoporosis. *Curr Womens Health Rep* 2003; **3**: 181-186
- 7 **Miura S,** Tanaka E, Mori A, Toya M, Takahashi K, Nakahara K, Ohmichi M, Kurachi H. Hormone replacement therapy improves arterial stiffness in normotensive postmenopausal women. *Maturitas* 2003; **45**: 293-298
- 8 **Cohen LS,** Soares CN, Poitras JR, Prouty J, Alexander AB, Shifren JL. Short-term use of estradiol for depression in perimenopausal and postmenopausal women: a preliminary report. *Am J Psychiatry* 2003; **160**: 1519-1522
- 9 **Hodgin JB,** Maeda N. Minireview: estrogen and mouse models of atherosclerosis. *Endocrinology* 2002; **143**: 4495-4501
- 10 **Stark A,** Madar Z. Phytoestrogens: a review of recent findings. *J Pediatr Endocrinol Metab* 2002; **15**: 561-572
- 11 **Uesugi T,** Toda T, Tsuji K, Ishida H. Comparative study on reduction of bone loss and lipid metabolism abnormality in ovariectomized rats by soy isoflavones, daidzin, genistin, and glycitin. *Biol Pharm Bull* 2001; **24**: 368-372
- 12 **Wang JF,** Niu JZ, Li H, Zhang C, Liu LQ, Gao BH. Effects of soy extract on lipid metabolism in ovariectomized rats. *Zhongguo Zhongyao Zazhi* 2002; **27**: 285-288
- 13 **Boue SM,** Wiese TE, Nehls S, Burow ME, Elliott S, Carter-Wientjes CH, Shih BY, McLachlan JA, Cleveland TE. Evaluation of the estrogenic effects of legume extracts containing phytoestrogens. *J Agric Food Chem* 2003; **51**: 2193-2199
- 14 **Feoli AM,** Roehrig C, Rotta LN, Kruger AH, Souza KB, Kessler AM, Renz SV, Brusque AM, Souza DO, Perry ML. Serum and liver lipids in rats and chicks fed with diets containing different

- oils. *Nutrition* 2003; **19**: 789-793
- 15 **Jang I**, Hwang D, Lee J, Chae K, Kim Y, Kang T, Kim C, Shin D, Hwang J, Huh Y, Cho J. Physiological difference between dietary obesity-susceptible and obesity-resistant Sprague Dawley rats in response to moderate high fat diet. *Exp Anim* 2003; **52**: 99-107
- 16 **Colandre ME**, Diez RS, Bernal CA. Metabolic effects of trans fatty acids on an experimental dietary model. *Br J Nutr* 2003; **89**: 631-639
- 17 **Guerin M**, Egger P, Soudant C, Le Goff W, van Tol A, Dupuis R, Chapman MJ. Dose-dependent action of atorvastatin in type IIB hyperlipidemia: preferential and progressive reduction of atherogenic apoB-containing lipoprotein subclasses (VLDL-2, IDL, small dense LDL) and stimulation of cellular cholesterol efflux. *Atherosclerosis* 2002; **163**: 287-296
- 18 **Marino M**, Pallottini V, D'Eramo C, Cavallini G, Bergamini E, Trentalance A. Age-related changes of cholesterol and dolichol biosynthesis in rat liver. *Mech Ageing Dev* 2002; **123**: 1183-1189
- 19 **Dubrac S**, Parquet M, Blouquit Y, Gripois D, Blouquit MF, Souidi M, Lutton C. Insulin injections enhance cholesterol gallstone incidence by changing the biliary cholesterol saturation index and apo A-I concentration in hamsters fed a lithogenic diet. *J Hepatol* 2001; **35**: 550-557
- 20 **Demonty I**, Deshaies Y, Lamarche B, Jacques H. Interaction between dietary protein and fat in triglyceride metabolism in the rat: effects of soy protein and menhaden oil. *Lipids* 2002; **37**: 693-699
- 21 **Perrella J**, Berco M, Cecutti A, Gerulath A, Bhavnani BR. Potential role of the interaction between equine estrogens, low-density lipoprotein (LDL) and high-density lipoprotein (HDL) in the prevention of coronary heart and neurodegenerative diseases in postmenopausal women. *Lipids Health Dis* 2003; **2**: 4
- 22 **Stangl H**, Graf GA, Yu L, Cao G, Wyne K. Effect of estrogen on scavenger receptor BI expression in the rat. *J Endocrinol* 2002; **175**: 663-672
- 23 **Karjalainen A**, Heikkinen J, Savolainen MJ, Backstrom AC, Kesaniemi YA. Mechanisms regulating LDL metabolism in subjects on peroral and transdermal estrogen replacement therapy. *Arterioscler Thromb Vasc Biol* 2000; **20**: 1101-1106
- 24 **Bobkova D**, Poledne R. Lipid metabolism in atherogenesis. *Cesk Fysiol* 2003; **52**: 34-41
- 25 **Yoon M**, Jeong S, Lee H, Han M, Kang JH, Kim EY, Kim M, Oh GT. Fenofibrate improves lipid metabolism and obesity in ovariectomized LDL receptor-null mice. *Biochem Biophys Res Commun* 2003; **302**: 29-34
- 26 **Sugimoto T**, Kimura T, Fukuda H, Iritani N. Comparisons of glucose and lipid metabolism in rats fed diacylglycerol and triacylglycerol oils. *J Nutr Sci Vitaminol* 2003; **49**: 47-55
- 27 **Chlebowski RT**, Hendrix SL, Langer RD, Stefanick ML, Gass M, Lane D, Rodabough RJ, Gilligan MA, Cyr MG, Thomson CA, Khandekar J, Petrovitch H, McTiernan A. Influence of estrogen plus progestin on breast cancer and mammography in healthy postmenopausal women: the Women's Health Initiative Randomized Trial. *JAMA* 2003; **289**: 3243-3253
- 28 **Sidelmann JJ**, Jespersen J, Andersen LF, Skouby SO. Hormone replacement therapy and hypercoagulability. Results from the Prospective Collaborative Danish Climacteric Study. *BJOG* 2003; **110**: 541-547
- 29 **Gallus S**, Negri E, Chatenoud L, Bosetti C, Franceschi S, La Vecchia C. Post-menopausal hormonal therapy and gallbladder cancer risk. *Int J Cancer* 2002; **99**: 762-763
- 30 **Khosla S**. Estrogen, selective estrogen receptor modulators and now mechanism-specific ligands of the estrogen or androgen receptor? *Trends Pharmacol Sci* 2003; **24**: 261-263
- 31 **Fontana A**, Delmas PD. Selective estrogen receptors modulators in the prevention and treatment of postmenopausal osteoporosis. *Endocrinol Metab Clin North Am* 2003; **32**: 219-232
- 32 **Hu JY**, Aizawa T. Quantitative structure-activity relationships for estrogen receptor binding affinity of phenolic chemicals. *Water Res* 2003; **37**: 1213-1222
- 33 **Latonnelle K**, Fostier A, Le Menn F, Bennetau-Pelissero C. Binding affinities of hepatic nuclear estrogen receptors for phytoestrogens in rainbow trout (*Oncorhynchus mykiss*) and Siberian sturgeon (*Acipenser baeri*). *Gen Comp Endocrinol* 2002; **129**: 69-79
- 34 **Bolego C**, Poli A, Cignarella A, Paoletti R. Phytoestrogens: pharmacological and therapeutic perspectives. *Curr Drug Targets* 2003; **4**: 77-87

Edited by Zhu LH and Chen WW Proofread by Xu FM

Anti-cancer effects of COX-2 inhibitors and their correlation with angiogenesis and invasion in gastric cancer

Suo-Lin Fu, Yun-Lin Wu, Yong-Ping Zhang, Min-Min Qiao, Ying Chen

Suo-Lin Fu, Yun-Lin Wu, Yong-Ping Zhang, Min-Min Qiao, Ying Chen, Department of Gastroenterology, Ruijin Hospital, Shanghai Second Medical University, Shanghai 200025, China
Supported by the Science and Technology Development Foundation of Shanghai, No. 02ZB14042

Correspondence to: Professor Yun-Lin Wu, Department of Gastroenterology, Ruijin Hospital, Shanghai Second Medical University, Shanghai 200025, China. fusuolin@163.com
Telephone: +86-21-64370045-665246
Received: 2004-02-14 **Accepted:** 2004-03-04

Abstract

AIM: To observe the anti-cancer effects of COX-2 inhibitors and investigate the relationship between COX-2 inhibitors and angiogenesis, infiltration or metastasis in SGC7901 cancer xenografts.

METHODS: Thirty athymic mice xenograft models with human stomach cancer cell SGC7901 were established and divided randomly into 3 groups of 10 each. Sulindac, one non-specific COX inhibitor belonging to non-steroidal anti-inflammatory drugs (a series of COX inhibitors known as NSAIDs) and celecoxib, one selective COX-2 inhibitor (known as SCIs) were orally administered to mice of treatment groups. Immunohistochemistry was used to examine the expression of PCNA, CD44v6 and microvessel density (MVD). Apoptosis was detected by using TUNEL assay.

RESULTS: Tumors in sulindac and celecoxib groups were significantly smaller than those in control group from the second week after drug administration ($P < 0.01$). In treatment group, the cell proliferation index was lower ($P < 0.05$) and apoptosis index was higher ($P < 0.05$) than those in control groups. Compared with the controls, microvessel density was reduced ($P < 0.01$) and expression of CD44v6 on tumor cells was weakened ($P < 0.05$) in treatment groups.

CONCLUSION: COX-2 inhibitors have anticancer effects on gastric cancer. They play important roles in angiogenesis and infiltration or metastasis of stomach carcinoma. The anticancer effects of COX-2 inhibitors may include inducing apoptosis, suppressing proliferation, reducing angiogenesis and weakening invasiveness.

Fu SL, Wu YL, Zhang YP, Qiao MM, Chen Y. Anti-cancer effects of COX-2 inhibitors and their correlation with angiogenesis and invasion in gastric cancer. *World J Gastroenterol* 2004; 10(13): 1971-1974

<http://www.wjgnet.com/1007-9327/10/1971.asp>

INTRODUCTION

Gastric cancer is one of the commonest malignancies of human beings. The incidence of gastric cancer is typically high in China and as a result, more than 170 000 people die of it each

year. It has important significance if certain drugs are found to lower its incidence or prevent it.

Chemoprevention of NSAIDs against colorectal cancer has been observed for long^[1]. Since cyclooxygenase-2 (COX-2), one of the isoenzymes catalyzing the production of prostaglandins, was discovered in early 1990s^[2], its gene construction, biochemical property and biological role have been understood step by step. The discovery of COX-2 has enlightened people to pay more attention to its relation with neoplasm. More and more selective COX-2 inhibitors (SCIs) have been found out, further facilitating the cognition to COX-2^[3]. Although the roles COX-2 inhibitors play in various cancers and their mechanisms are being widely studied recently, few people have gone deep into *in vivo* experiments^[4]. Based on *in vitro* cytologic experiments^[5-7], this study went further into *in vivo* experiments so as to clarify the anti-cancer mechanisms of COX-2 inhibitors.

MATERIALS AND METHODS

Cell line

Human moderately differentiated gastric cancer cell line SGC7901 was cultured in RPMI 1640 medium at 37 °C in a humidified box (Hareus) with 50 mL/L CO₂ in our laboratory. When cells were amplified to a certain amount, they were dissociated, collected and suspended in PBS at a density of 5×10⁷/mL.

Animals

Thirty male athymic mice (BALB/c nu/nu, 6 wk old, 17-20 g) were purchased from Shanghai Experimental Animal Center of Chinese Academy of Sciences. Mice were maintained under specific pathogen-free conditions (Micro-FLO positive air supply rodent cage system) and fed with sterilized food and autoclaved water. Experiments were started after 3 d of acclimatization.

Agents

Gum arabic (50 mg/kg) was dissolved in sterilized water at a concentration of 10 mg/mL. Sulindac (8 mg/kg; Sigma inc.) and celecoxib (10 mg/kg) were agitated and suspended with gum arabic (50 mg/kg) in water at a same concentration, respectively, by using a homogenizer.

Animal experiment procedure

Each mouse was inoculated with a subcutaneous injection of SGC7901 cells (5×10⁶ in 0.1 mL PBS) into the right forelimb after weighed individually. Then these 30 mice were randomized into control, sulindac, and celecoxib groups. From the same day, the mice were orally administered different agents once daily (0.1 mL; according to mouse weight of 20 g): the controls with gum arabic, the sulindac group with sulindac, and the celecoxib group with celecoxib. Mice's diet, activity, stool, urine, and tumor growth were observed daily and shortest and longest diameters of xenografts were measured weekly. The tumor volume was deduced according to the formula^[8]: volume (mm³)=(the shortest diameter)²×(the longest diameter) /2. Both

body weight and tumor size of each mouse were measured again before they were killed by cervical dislocation on the 32 nd day. All tumors were dissected from the body and weighed, then divided along the longest diameter. Halves of the specimens were frozen in liquid nitrogen while the other halves were fixed in 40 g/L phosphate-buffered formaldehyde.

Immunohistochemical assays

The formalin-fixed tissues were embedded in paraffin, and sectioned at a thickness of 4 μ m. The sections were deparaffinized and hydrated gradually, and examined by histology of HE staining, immunohistochemistry, and TUNEL technique respectively. EnVision kits, the reagents of immunohistochemical assay, were purchased from GeneTech Co. Tests were performed according to the two step procedure. After incubated with 3% H_2O_2 for 10 min at room temperature and unmasked antigens by heat treatment, sections were covered with animal serum for 20 min. Specimens were then incubated with primary antibodies PCNA (PC10; 1/100; Santa Cruz), CD44v6 (ZM-0052; Beijing Zhongshan), or CD34 (BD) at 4 $^{\circ}C$ over night and further treated with EnVision kits for 30 min at room temperature. They were visualized by diaminobenzidin (DAB) and counter-stained by hematoxylin. TBS took the place of primary antibodies as a negative control. Sections were observed under microscope after mounted. The results of staining were analyzed and evaluated with American Image-Pro Plus software. The percentage of positive cells with PCNA staining in five 400 \times sights was counted as proliferation index (PI). The average of vessels with CD34 staining in three hot regions was calculated as MVD.

Apoptosis detection by TUNEL method

The reagent kit for apoptosis detection, TdT-FragEL DNA fragmentation detection kit was bought from ONCOGENE. Test procedures consisting of the following sections were provided in the brochure of the kit. The specimens were deparaffinized and hydrated gradually, and rinsed with 1 \times TBS, then incubated with proteinase K (20 μ g/mL in 10 mmol/L Tris-HCl) for 20 min. After immersed in 30 mL/L H_2O_2 at room temperature for 5 min and in TdT labeling reaction mixture at 37 $^{\circ}C$ for 1.5 h, specimens were covered with 1 \times conjugate for 30 min, visualized by DAB and counter-stained by hematoxylin afterwards. TBS took the place of primary antibodies as a negative control. After mounted, sections were observed under microscope. The results of staining were analyzed and evaluated with American Image-Pro Plus software. The percentage of positive cells with TUNEL staining in five 400 \times sights served as apoptosis index (AI).

Statistical analysis

Data were analyzed by software of SAS 6.12 and shown in a default form of mean \pm SD.

RESULTS

Animal experiments

During the experiment, the growth, diet, activity, *etc.* of mice were carefully observed, no hematuria and hematochezia were shown during experiment. Two mice died accidentally in the process however, which might be caused by the operation of enema clyster. The body weight among groups was not significantly different, nor did the weight change during the experiment. The growth of xenografts in treatment groups was significantly suppressed compared with the controls, but there was no difference between two treatment groups (Figure 1).

Difference of tumor growth in different groups was shown from the second week (Table 1).

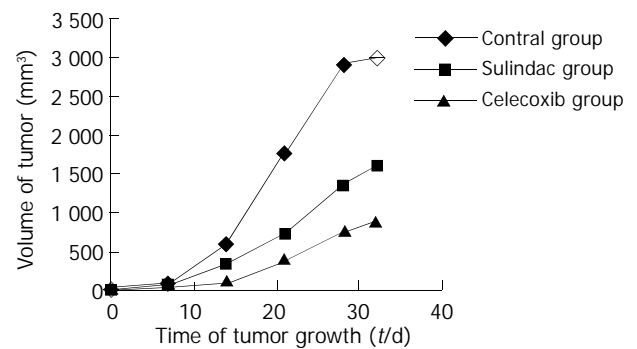


Figure 1 Effects of sulindac and celecoxib on the growth of human gastric cancer xenografts in athymic mice.

Table 1 Tumor volume of three groups (mean \pm SD)

Group	Date (d)				
	7	14	21	28	32
Control	45.2 \pm 35.5	609 \pm 289	1 779 \pm 366	2 920 \pm 776	2 984 \pm 589
Sulindac	78 \pm 137	351.5 \pm 227.0	723 \pm 514	1 370 \pm 832	1 590 \pm 1 009
Celecoxib	19.5 \pm 14.8	108 \pm 105	408 \pm 390	788 \pm 701	891 \pm 764
P	0.30	0.0002	0.0001	0.0001	0.0001

$F=27.95$, $P<0.01$ vs control group. No significant difference in volume was shown between sulindac group and celecoxib group.

In each group, five mice out of ten were picked out randomly and dissected with no obvious erosion, bleeding, or ulcer of stomach and no neoplasm metastasis.

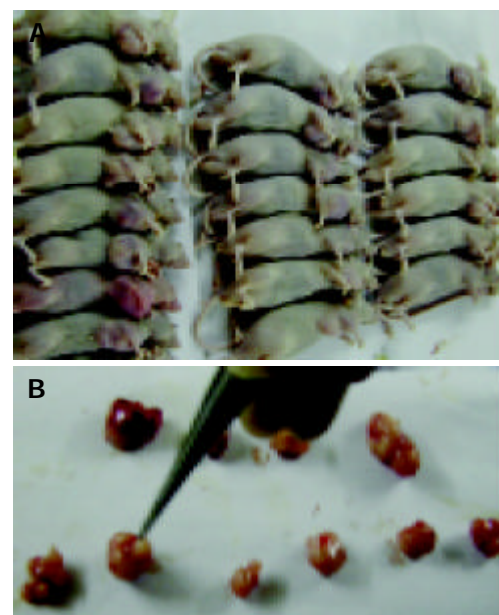


Figure 2 Histology of tumors. A: *In vivo* appearance of xenografts; B: *In vitro* appearance of xenografts.

Tumor histology

Xenograft took on an appearance of big globular neoplasia or cluster of several small neoplastic nodules (Figure 2). Necrosis could be seen comparatively common in cut of tumors, and the size of necrotic area seemed to be related to the volume of tumor. With regard to HE-stained sections, deeply stained tumor cells with big nuclei were arranged tightly with no cavum structure found under microscope, which coincided with the characteristics of tumor histology. Tumor cells among all groups showed no difference in morphology, while necrosis could be commonly seen under microscope.

Cell proliferation and apoptosis

PI of control group was significantly higher than that of sulindac group and celecoxib group ($P < 0.05$), but the difference was not notable between two treatment groups. AI in two treatment groups was higher than that in the control group ($P < 0.05$), while there was also no difference between the two groups. The AI/PI value was calculated and compared among all groups. Consequently, it was apparently larger in two treatment groups ($P < 0.01$), however no difference was shown between them.

Tumor angiogenesis

Immunohistochemical staining of CD34 revealed that celecoxib and sulindac could suppress angiogenesis of SGC7901 xenografts. MVD in sulindac and celecoxib groups was apparently lower than that in the control ($P < 0.01$). Although it was lower in celecoxib group, the difference is not notable.

Invasiveness of tumor cells

Membranes of tumor cells were stained brown by CD44v6 staining. By analysis of staining intensity and quantity of positive cells with Image-Pro Plus software, the expression of CD44v6 was markedly weakened by the treatment with sulindac and celecoxib ($P < 0.05$), but there was no apparent difference between sulindac and celecoxib groups.

DISCUSSION

COX-2 was successfully cloned and its structure has been clearly recognized more than ten years before^[9]. It is an inducible isoenzyme that catalyzes production of a series of prostaglandins. Participating in inflammatory reaction, COX-2 is expressed by a variety of tumor cells and correlated to tumorigenesis. Several researches have revealed the prophylactic effect of NSAIDs on colorectal carcinoma and their therapeutic effect on colon polyps^[10]. Here the mechanism of NSAIDs is considered as inhibiting COX-2. Non-specific COX inhibitors inhibit COX-1 at the same time, which may cause fatal side effects. As a result, they are not so ideal in long-term application for preventing tumorigenesis. Lately developed selective COX-2 inhibitors shed light on chemoprevention of neoplasms. Nevertheless a series of researches have to be carried out to confirm its effectiveness, reliability and virtues before extensive clinical application.

The expression of COX-2 also existed in gastric cancer while the positive rate might reach 61.4%^[11]. We have shown that human moderately differentiated gastric cancer cell SGC7901 can express COX-2. Its growth was suppressed *in vitro* after the treatment of sulindac, both proliferation and apoptosis were affected^[5]. This time we inoculated athymic mice with SGC7901 to observe the effects of sulindac and celecoxib, a clinically applied selective COX-2 inhibitor, on *in vivo* tumor by establishing animal models of gastric cancer. The results showed that both drugs had a notable inhibition on gastric cancer growth. Although the effect of celecoxib was better than of sulindac, no statistical difference was shown.

To explore the anticancer mechanisms of COX-2 inhibitors, we evaluated the influence of two drugs on tumor cell proliferation and apoptosis in xenografts by immunohistochemistry, which verified the results of *in vitro* researches. Administration of both sulindac and celecoxib increased apoptosis of cancer cells *in vivo*. The AI/PI, a value reflecting cytokinetics, showed a more significant difference.

The growth of tumor cells depends on nutrition supply, which largely relies on angiogenesis. Ischemia can induce tumor cell apoptosis, speeding up necrosis and cell extinction.

Many researches verified the relation between COX-2 and angiogenesis^[12] and the inhibition effects of NSAIDs on blood vessel endothelial cells^[13]. We observed that sulindac and celecoxib obviously decreased the blood vessel quantity of xenografts and reduced the MVD compared to that of the control group. COX-2 inhibitors realized their anti-cancer effects by repressing the expression of anti-apoptosis gene *Bcl-2*^[14] and reducing angiogenesis in stomach carcinoma, thereby impairing the nutrition supply of the tumor, further inhibiting proliferation and inducing apoptosis of gastric cancer cells. Our results were similar to those of Sawaoka *et al.*^[15].

Some studies suggested the expression of COX-2 was correlated to the clinicopathologic characteristics of gastric cancer, such as infiltration, lymphatic or hematogenous metastasis, prognosis, *etc*^[16]. As a cell surface adhesive molecule, CD44 was the receptor of hyaluronic acid and involved in cell-to-cell and cell-to-matrix interactions. Especially, the expression of its spliced variant 6 was closely correlated to cell movement, carcinogenesis, progress, incursion and metastasis of gastric carcinoma^[17]. In this study we evaluated COX-2 inhibitors' influence on the CD44v6 expression by using animal models, finding the positive cells of expressing CD44v6 (pigmented in membrane) often existed in the periphery of tumors with a tendency to surround blood vessels. The positivity of CD44v6 staining was strong in the control group and significantly weakened in two medication groups, which demonstrating that COX-2 inhibitors play a role in depressing invasiveness and reducing metastasis of gastric cancer, which could be one of their anti-cancer effects. No obvious metastasis was found by rough anatomy of mice in our study however. It requires improved experiment design.

In brief, the mechanisms of COX-2 inhibitors resisting the growth of gastric cancer might include suppressing cell proliferation, inducing apoptosis, reducing angiogenesis and weakening invasiveness. But selective COX-2 inhibitors were not observed obviously more effective than non-specific COX inhibitors. The former did not show any advantage in side effects either, such as gastrorrhagia, ulceration, and so on, which may be relevant to experiment animal model and short experiment duration. Further studies are required. This study also showed comparatively more necrosis of tumors, but its correlation to drug administration was unclear. In comparison, Japanese researchers discovered no relation between drug treatment of indomethacin or NS398 in MKN45 cell xenografts^[15].

This is the first part of a serial study, and we will verify the results afterwards using Western blotting, RT-PCR, *etc*.

REFERENCES

- 1 **Kune GA**, Kune S, Watson LF. Colorectal cancer risk, chronic illnesses, operations, and medications: case control results from the Melbourne Colorectal Cancer Study. *Cancer Res* 1988; **48**: 4399-4404
- 2 **Xie WL**, Chipman JG, Robertson DL, Erikson RL, Simmons DL. Expression of a mitogen-responsive gene encoding prostaglandin synthase is regulated by mRNA splicing. *Proc Natl Acad Sci U S A* 1991; **88**: 2692-2696
- 3 **Kawamori T**, Rao CV, Seibert K, Reddy BS. Chemopreventive activity of celecoxib, a specific cyclooxygenase-2 inhibitor, against colon carcinogenesis. *Cancer Res* 1998; **58**: 409-412
- 4 **Hahn KB**, Lim HY, Sohn S, Kwon HJ, Lee KM, Lee JS, Surh YJ, Kim YB, Joo HJ, Kim WS, Cho SW. *In vitro* evidence of the role of COX-2 in attenuating gastric inflammation and promoting gastric carcinogenesis. *J Environ Pathol Toxicol Oncol* 2002; **21**: 165-176
- 5 **Sun B**, Wu YL, Zhang XJ, Wang SN, He HY, Qiao MM, Zhang YP, Zhong J. Effects of Sulindac on growth inhibition and apoptosis induction in human gastric cancer cells. *Shijie Huaren Xiaohua Zazhi* 2001; **9**: 997-1002

- 6 **Wu YL**, Sun B, Zhang XJ, Wang SN, He HY, Qiao MM, Zhong J, Xu JY. Growth inhibition and apoptosis induction of Sulindac on Human gastric cancer cells. *World J Gastroenterol* 2001; **7**: 796-800
- 7 **Li JY**, Wang XZ, Chen FL, Yu JP, Luo HS. Nimesulide inhibits proliferation via induction of apoptosis and cell cycle arrest in human gastric adenocarcinoma cell line. *World J Gastroenterol* 2003; **9**: 915-920
- 8 **Ovejera AA**, Houchens DP, Barker AD. Chemotherapy of human tumor xenografts in genetically athymic mice. *Ann Clin Lab Sci* 1978; **8**: 50-56
- 9 **Hla T**, Neilson K. Human cyclooxygenase-2 cDNA. *Proc Natl Acad Sci U S A* 1992; **89**: 7384-7388
- 10 **Labayle D**, Fischer D, Vielh P, Drouhin F, Pariente A, Bories C, Duhamel O, Troussset M, Attali P. Sulindac causes regression of rectal polyps in familial adenomatous polyposis. *Gastroenterology* 1991; **101**: 635-639
- 11 **Joo YE**, Oh WT, Rew JS, Park CS, Choi SK, Kim SJ. Cyclooxygenase-2 expression is associated with well-differentiated and intestinal-type pathways in gastric carcinogenesis. *Digestion* 2002; **66**: 222-229
- 12 **Tsuji M**, Kawano S, Tsuji S, Sawaoka H, Hori M, DuBois RN. Cyclooxygenase regulates angiogenesis induced by colon cancer cells. *Cell* 1998; **93**: 705-716
- 13 **Sun B**, Wu YL, Zhang XJ, He HY, Wang SN, Qiao MM. Growth inhibition of Sulindac and Indomethacin on human umbilical vein endothelial cells ECV304. *Zhongliu* 2003; **23**: 370-372
- 14 **Sun B**, Wu YL, Wang SN, Zhang XJ, He HY, Qiao MM, Zhang J. The effects of sulindac on induction of apoptosis and expression of cyclooxygenase-2 and Bcl-2 in human hepatocellular carcinoma cells. *Zhonghua Xiaohua Zazhi* 2002; **22**: 338-340
- 15 **Sawaoka H**, Tsuji S, Tsuji M, Gunawan ES, Sasaki Y, Kawano S, Hori M. Cyclooxygenase inhibitors suppress angiogenesis and reduce tumor growth *in vivo*. *Lab Invest* 1999; **79**: 1469-1477
- 16 **Ohno R**, Yoshinaga K, Fujita T, Hasegawa K, Iseki H, Tsunozaki H, Ichikawa W, Nihei Z, Sugihara K. Depth of invasion parallels increased cyclooxygenase-2 levels in patients with gastric carcinoma. *Cancer* 2001; **91**: 1876-1881
- 17 **Joo M**, Lee HK, Kang YK. Expression of E-cadherin, beta-catenin, CD44s and CD44v6 in gastric adenocarcinoma: relationship with lymph node metastasis. *Anticancer Res* 2003; **23**: 1581-1588

Edited by Wang XL and Chen WW Proofread by Xu FM

Loss of heterozygosity on chromosome 10q22-10q23 and 22q11.2-22q12.1 and *p53* gene in primary hepatocellular carcinoma

Guang-Neng Zhu, Li Zuo, Qing Zhou, Su-Mei Zhang, Hua-Qing Zhu, Shu-Yu Gui, Yuan Wang

Guang-Neng Zhu, Li Zuo, Qing Zhou, Su-Mei Zhang, Hua-Qing Zhu, Shu-Yu Gui, Yuan Wang, Laboratory of molecular Biology and Department of Biochemistry, Anhui Medical University, Hefei 230032, Anhui Province, China

Li Zuo, Qing Zhou, Su-Mei Zhang, Hua-Qing Zhu, Shu-Yu Gui, Yuan Wang, Anhui Province Key Laboratory of Genomic Research, Hefei 230032, Anhui Province, China

Guang-Neng Zhu, Department of Biochemistry, Bengbu Medical College, Bengbu 233003, Anhui Province, China

Shu-Yu Gui, Department of Respiratory Disease, the First Affiliated Hospital of Anhui Medical University, Hefei 230032, Anhui Province, China

Supported by the Natural Science Foundation of Anhui Province, No.99044312 (YW), No.01043716(SYG) and Natural Science Foundation of Anhui Educational Commission, No.JL-97-077 (YW)

Correspondence to: Professor Yuan Wang, Laboratory of Molecular Biology and Department of Biochemistry, Anhui Medical University, Hefei 230032, Anhui Province, China. wangyuan@mail.hf.ah.cn

Telephone: +86-551-5161140

Received: 2003-09-09 **Accepted:** 2003-10-12

Abstract

AIM: To analyze loss of heterozygosity (LOH) and homozygous deletion on *p53* gene (exon2-3, 4 and 11), chromosome 10q22-10q23 and 22q11.2-22q12.1 in human hepatocellular carcinoma (HCC).

METHODS: PCR and PCR-based microsatellite polymorphism analysis techniques were used.

RESULTS: LOH was observed at D10S579 (10q22-10q23) in 4 of 20 tumors (20%), at D22S421 (22q11.2-22q12.1) in 3 of 20(15%), at TP53.A (*p53* gene exon 2-3) in 4 of 20 (20%), at TP53.B (*p53* gene exon 4) in 6 of 20(30%), and at TP53.G (*p53* gene exon 11) in 0 of 20(0%). Homozygous deletion was detected at 10q22-10q23(8/20; 40%), 22q11.2-22q12.1(8/20; 40%), *p53* gene exon 2-3(0/20;0%), *p53* gene exon 4(6/20; 30%), and *p53* gene exon 11(2/20; 10%).

CONCLUSION: There might be unidentified tumor suppressor genes on chromosome 10q22-10q23 and 22q11.2-22q12.1 that contribute to the pathogenesis and development of HCC.

Zhu GN, Zuo L, Zhou Q, Zhang SM, Zhu HQ, Gui SY, Wang Y. Loss of heterozygosity on chromosome 10q22-10q23 and 22q11.2-22q12.1 and *p53* gene in primary hepatocellular carcinoma. *World J Gastroenterol* 2004; 10(13): 1975-1978
<http://www.wjgnet.com/1007-9327/10/1975.asp>

INTRODUCTION

Hepatocellular carcinoma (HCC) is a primary liver malignancy with high mortality. It is among the most common malignancies worldwide, especially in Asia, Africa and Southern Europe^[1]. It has been generally accepted that HCC is highly associated with chronic hepatitis B virus (HBV) or hepatitis C virus (HCV)

infection or alcohol intake which induces cirrhosis^[2]. High intake of aflatoxin B found in many kinds of food is also reported to be a risk factor for HCC^[3,4]. Like other solid tumors, It has been proposed that hepatocarcinogenesis and metastasis of HCC is a multi-step process requiring the accumulation of genetic alterations, but the precise molecular pathogenesis is far from clear.

Loss of heterozygosity (LOH) analysis has become an effective way to identify informative loci and candidate tumor suppressor genes (TSGs). Molecular chromosomal studies of tumors by using polymerase chain reaction (PCR) -based polymorphic markers can detect small loci of anomalies that may harbor TSGs. Search for novel TSGs is based largely on the identification of common regions of deletion on chromosomes. LOH has been found in many types of tumors, including HCC. LOH in HCC has been detected on chromosomal arms 1p, 2q, 4p, 4q, 5q, 6q, 8p, 8q, 9p, 9q, 11p, 13q, 16p, 16q and 17p^[5-11]. However, deletion of 10q22-10q23, and 22q11.2-22q12.1 and *p53* gene exon 2-3 and 11 in HCC has not been investigated.

In the present study, we detected LOH and homozygous deletion on chromosome 10q, and chromosome 22q near the NF2 gene locus, and *p53* gene locus in 20 cases of HCC.

MATERIALS AND METHODS

Specimens

Surgical specimens of HCC were collected from the First Affiliated Hospital of Anhui Medical University and the Affiliated Hospital of Bengbu Medical College. The patients were born and grew in different places of Anhui Province, China. Both tumor and corresponding non-tumor liver tissues were immediately put into liquid nitrogen after separation and then stored at -80 °C until DNA extraction. Diagnosis of HCC was confirmed by pathological examination.

DNA extraction

Genomic DNA was extracted from tissues with the standard proteinase K-phenol/chloroform method. To each of the samples, 500 µL of DNA extraction buffer containing 200 mmol/L NaCl, 10 g/L sodium dodecyl sulfate, 2 mmol/L EDTA, 0.1 mol/L Tris-HCl was added during the process of homogenization. After 0.2 mg/mL proteinase K was added, the sample was shaken for 12 h at 37 °C. After phenol-chloroform extraction, DNA was precipitated with cold ethanol overnight at -20 °C. After centrifugation, the pellet was dried and resuspended in 50 µL TE buffer (Tris-EDTA buffer). DNA was stored at -20 °C until polymerase chain reaction (PCR) amplification was performed.

Pcr amplification

PCR amplification primer pairs for *p53* gene, 10q22-10q23 and 22q11.2-22q12.1 are as follows (Table 1).

Polyacrylamide gel electrophoresis

PCR product (12 µL) was mixed with 3 µL 950 g/L deionized formamide and 3 µL DNA loading buffer containing 2.5 g/L

Table 1 PCR amplification primer pairs for p53 gene, 10q22-10q23 and 22q11.2-22q12.1

Markers name	Forward	Reverse	Annealing (T °C)	Size (bp)
TP53.A1/TP53.A2 (p53 gene exon 2-3)	TGGATCCTCTTGCAGCAGCC	AACCCTTGTCTTACCAGAA	54	270
TP53.B1/TP53.B2 (p53 gene exon 4)	ATCTACAGTCCCCCTTGCCGGC	AACTGACCGTGCAAGTCA	57	296
TP53.G1/TP53.G2 (p53 gene exon 11)	TCTCTACAGCCACCTGAAG	CTGACGCACACCTATTGCAA	58	122
D10S579	CCGATCAATGAGGAGTGCC	ATACACCCAGCCAATGCTGC	60	260
D22S421	CTGCTGCCCTAACATATCAC	GGCCAGGAGTGTCTGAATTTTA	65	163
CDK4 ¹	GGAGGTCGGTACCAGAGTG	CATGTAGACCAGGACAGG	60	364

¹The aim of PCR amplification of CDK4 gene was to confirm that genomic DNA had been truly extracted from all samples. These primer sequences were retrieved from the Genome Database (<http://gdbwww.gdb.org>). PCR amplification was performed in a 50 µL reaction volume containing 400 ng template DNA, 0.2 mmol/L of each deoxynucleotide triphosphate, 20 mmol/L of each primer, 1.5 mmol/L MgCl₂, 1× reaction buffer and 2 U Taq DNA polymerase. The reaction mixture was denatured for 5 min at 94 °C. DNA was subsequently amplified for 35 cycles with 94 °C for 30 s, 54-65 °C for 30 s, 72 °C for 40 s, and a final extension at 72 °C for 8 min. PCR product (8 µL) was electrophoresed in a 20 g/L agarose gel, visualized by staining with ethidium bromide and ultraviolet illumination, and documented by a computer-linked camera. The target DNA fragments were confirmed by comparing to a 100 bp DNA ladder.

Table 2 Clinical and genetic features of 20 patients with HCC (*, LOH; △, homozygous deletion; O, no deletion; +, HBsAg positive; -, HBsAg negative)

Case No.	Age (yr)	Sex	HBsAg	TP53.A	TP53.B	TP53.G	D10S579	D22S421
1	49	M	+	*	*	O	*	O
2	55	M	+	O	△	O	O	△
3	39	M	+	O	△	O	△	△
4	55	F	+	*	O	O	O	*
5	72	F	+	O	*	△	△	O
6	40	M	+	O	O	O	O	O
7	34	F	+	O	*	O	△	△
8	56	M	+	O	O	O	O	O
9	27	F	-	O	*	O	△	O
10	50	M	+	O	O	O	O	△
11	48	M	+	O	△	O	△	△
12	52	M	+	O	O	O	△	O
13	63	F	+	O	△	△	△	△
14	60	M	+	O	△	O	*	△
15	65	M	+	O	O	O	*	O
16	34	M	+	O	*	O	O	O
17	64	M	+	*	*	O	*	*
18	52	F	+	O	O	O	△	O
19	32	F	+	O	△	O	O	△
20	38	M	+	*	O	O	O	*
LOH rate (%)				20	30	0	20	15
Homozygous deletion rate (%)				0	30	10	40	40

xylene cyanol FF, 2.5 g/L bromophenol blue, and 300 g/L glycerin. The mixture was denatured at 95 °C for 5 min, put onto ice for 10 min, loaded onto 80 g/L denaturing polyacrylamide gel containing 3.3 mol/L urea and then electrophoresed at 100 V for 2 h. The gel was silver-stained^[13]. LOH was determined by visual evaluation, which compared the allele bands from tumors and the corresponding non-tumor tissues. The complete loss of one polymorphic allele from those seen in the paired control DNA was scored as allelic loss by three independent observers. PCR reactions were performed twice to confirm LOH.

RESULTS

HCC tumor and corresponding non-tumor liver tissues of 20 patients were studied for LOH on 10q22-10q23 (D10S579), 22q11.2-22q12.1 (D22S421), and 17p13.1 by five microsatellite

markers, and the rate of LOH was 20% (4/20), 15% (3/20), 50% (10/20), respectively (Table 2). Homozygous deletion was observed in 8 of 20 cases (40%) for the marker D10S579, 8 of 20 cases (40%) for D22S421, 6 of 20 cases (30%) for TP53.B, 2 of 20 cases (10%) for TP53.G, and in 0 of 20 cases (0%) for the marker TP53.A.

Results of 20 g/L agarose gel electrophoresis are shown in Figure 1. LOH in tumor and corresponding non-tumor liver tissues are shown in Figure 2.

DISCUSSION

HCC is one of most malignant tumors. The mechanism of hepato-carcinogenesis is a multi-factor and multi-step process requiring the accumulation of genetic alterations, including chromosomal aberration, oncogene activation, inactivation of TSGs and abnormality of growth factors and growth factor

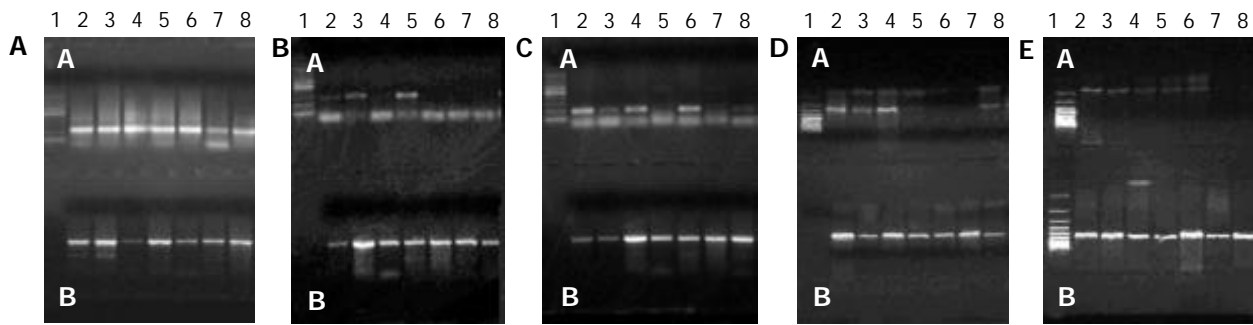


Figure 1 Agarose gel electrophoresis of PCR products of p53 gene exons 2-3, 4, 11, and chromosome 10q22-10q23 and 22q11.2-22q12. 1. A: PCR products of p53 exon 2-3. Lane 1, 100 bp DNA marker; Lanes 2-8, PCR products of p53 exon2-3 (A) and CDK4 gene (B, as a control) amplified from HCC genomic DNA. No homozygous deletion of p53 exon 2-3 was found in all HCC specimens. B: PCR products of p53 exon 4. Lane 1, 100 bp DNA marker; Lanes 2-8, PCR products of p53 exon4 (A) and CDK4 gene (B, as a control) amplified from HCC genomic DNA. Lines 4, 6-8, homozygous deletion. C: PCR products of p53 exon11. Line 1, 100 bp DNA ladder; Lanes 2-8, PCR products of p53 exon11 (A) and CDK4 gene (B, as a control) amplified from HCC genomic DNA. Lanes 5 and 7, homozygous deletion. D: PCR products of 10q22-10q23. Lane1, 100 bp DNA marker; Lanes 2-8, PCR products of 10q22-10q23 (A) and CDK4 gene (B, as a control) amplified from HCC genomic DNA. Lines 6 and 7, homozygous deletion. E: PCR products of 22q11.2-22q12.1. Lane 1, 100 bp DNA ladder; Lanes 2-8, PCR products of 22q11.2-22q12.1 (A) and CDK4 gene (B, as a control) amplified from HCC genomic DNA. Lanes 7 and 8, homozygous deletion.

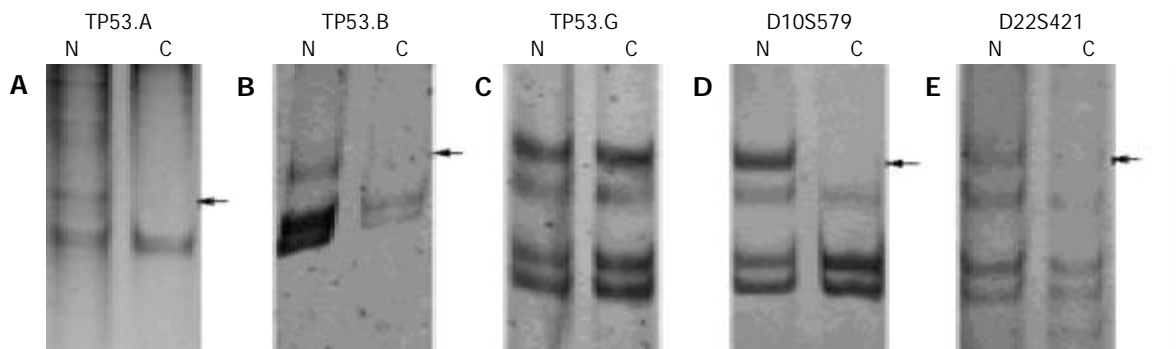


Figure 2 Representative illustrations of LOH detected with the microsatellite markers TP53.A, TP53.B, TP53.G, D10S579, D22S421 in human hepatocellular carcinomas (C) as compared to non-tumor liver tissues (N). The arrows show the location of the missing alleles. A: TP53.A (case 4); B: TP53.B (case 17); C: TP53.G (case 19, no LOH); D: D10S579 (case 17); E: D22S421 (case 20).

receptors. Of these factors, inactivation of TSGs is a very important factor.

Allelic loss on chromosome 17p is among the most common genetic abnormalities in many human cancers. *p53* gene is thought to be the gene associated with the genesis of these cancer types, including HCC^[12]. *p53* is activated in response to DNA damage, inducing either cell cycle arrest to permit DNA repair or apoptosis. Loss of *p53* function occurs mainly through allelic deletions at chromosome 17p13, where *p53* gene is located. In human HCC, LOH at chromosome 17p13 has been reported in 25-60% of tumors, and the worldwide prevalence of *p53* mutation is around 28% with, however, important geographic variations. In this study, LOH was observed at exon 2 and 3 (TP53.A) and exon 4 (TP53.B), of the gene in 20% and 30% of HCC cases, respectively, but not detected at exon 11 (TP53.G). In addition, all but one (19/20) patients were positive with HBsAg. These data also support the idea that LOH at *p53* gene and HBV infection are highly associated with the pathogenesis and development of HCC.

LOH on D10S579 has been reported in renal cell carcinoma (RCC)^[13]. We investigated 20 HCCs in the present study, and found four cases had LOH and eight cases had homozygous deletion on 10q22-10q23 (D10S579). Our finding suggests that on 10q22-10q23, there might be unidentified TSG(s) that plays an important role in the pathogenesis of hepatocellular carcinoma.

22q11.2-22q12.1 (D22S421) is near the locus of *NF2* gene. *NF2* (neurofibromatosis 2) gene, which is located on

chromosome 22q12.2-22q12.2, is postulated to be a tumor suppressor gene. It encodes for a protein with 595 amino acids, designated as merlin or schwannomin which belongs to a family of cytoskeletal proteins. The majority of *NF2* gene mutations are deletions, insertions, and point mutations, all of which lead to a nonfunctional, truncated protein^[14].

LOH at the *NF2* locus has been observed in many tumors, including schwannoma^[15], meningioma^[16], malignant mesothelioma^[17], gastrointestinal stromal tumor^[18], colorectal carcinoma^[19]. However, Handel-Fernandez *et al.*^[20] found that there was no LOH at *NF2* gene in pancreatic adenocarcinoma, but 37% of the cases had deletions which were clustered into two separate areas of chromosome 22 - one proximal and one distal to *NF2* gene. In the present study, we detected LOH on 22q11.2-22q12.1 in three of 20 HCCs and homozygous deletion on 22q11.2-22q12.1 in eight of 20 HCCs. Our finding suggests that 22q11.2-22q12.1 likely contains an unidentified tumor suppressor gene that contributes to the pathogenesis and the development of HCC, that the region plays an important role of cis-acting element similar to *NF2* gene, or that it acts the part of trans-acting factor similar to other TSGs, such as *p53* gene.

In conclusion, we have obtained important new information on LOH and homozygous deletion in chromosome 10q, 22q and 17p, in a subset of HCC. Inactivation of *p53* gene and unidentified tumor suppressor gene(s), present in regions of 10q22-10q23 and 22q11.2-22q12.1, may play an important role in the pathogenesis of HCC.

REFERENCES

- 1 **Simonetti RG**, Camma C, Fiorello F, Politi F, D' Amico G, Pagliaro L. Hepatocellular carcinoma. A worldwide problem and the major risk factors. *Dig Dis Sci* 1991; **36**: 962-972
- 2 **Harris CC**. Hepatocellular carcinogenesis: recent advances and speculations. *Cancer Cells* 1990; **2**: 146-148
- 3 **Yakicier MC**, Legoix P, Vaury C, Gressin L, Tubacher E, Capron F, Bayer J, Degott C, Balabaud C, Zucman-Rossi J. Identification of homozygous deletions at chromosome 16q23 in aflatoxin B1 exposed hepatocellular carcinoma. *Oncogene* 2001; **20**: 5232-5238
- 4 **Martins C**, Kedda MA, Kew MC. Characterization of six tumor suppressor genes and microsatellite instability in hepatocellular carcinoma in southern African blacks. *World J Gastroenterol* 1999; **5**: 470-476
- 5 **Fujimori M**, Tokino T, Hino O, Kitagawa T, Imamura T, Okamoto E, Mitsunobu M, Ishikawa T, Nakagama H, Harada H. Allelotyping study of primary hepatocellular carcinoma. *Cancer Res* 1991; **51**: 89-93
- 6 **Fujimoto Y**, Hampton LL, Wirth PJ, Wang NJ, Xie JP, Thorgeirsson SS. Alterations of tumor suppressor genes and allelic losses in human hepatocellular carcinomas in China. *Cancer Res* 1994; **54**: 281-285
- 7 **Hsu HC**, Peng SY, Lai PL, Sheu JC, Chen DS, Lin LI, Slagle BL, Butel JS. Allelotyping and loss of heterozygosity of p53 in primary and recurrent hepatocellular carcinomas. A study of 150 patients. *Cancer* 1994; **73**: 42-47
- 8 **Boige V**, Laurent-Puig P, Fouchet P, Flejou JF, Monges G, Bedossa P, Bioulac-Sage P, Capron F, Schmitz A, Olschwang S, Thomas G. Concerted nonsyntenic allelic losses in heperploid hepatocellular carcinoma as determined by a high-resolution allelotype. *Cancer Res* 1997; **57**: 1986-1990
- 9 **Nagai H**, Pineau P, Tiollais P, Buendia MA, Dejean A. Comprehensive allelotyping of human hepatocellular carcinoma. *Oncogene* 1997; **14**: 2927-2933
- 10 **Shao J**, Li Y, Li H, Wu Q, Hou J, Liew C. Deletion of chromosomes 9p and 17 associated with abnormal expression of p53, p16/MTS1 and p15/MTS2 gene protein in hepatocellular carcinomas. *Chin Med J* 2000; **113**: 817-822
- 11 **Herath NI**, Kew MC, Walsh MD, Young J, Powell LW, Leggett BA, MacDonald GA. Reciprocal relationship between methylation status and loss of heterozygosity at the p14^{ARF} locus in Australian and South African hepatocellular carcinomas. *J Gastroenterol Hepatol* 2002; **17**: 301-307
- 12 **Levine AJ**. p53, the cellular gatekeeper for growth and division. *Cell* 1997; **88**: 323-331
- 13 **Alimov A**, Li C, Gizatullin R, Fredriksson V, Sundelin B, Klein G, Zabarovsky E, Bergerheim U. Somatic mutation and homozygous deletion of PTEN/MMAC1 gene of 10q23 in renal cell carcinoma. *Anticancer Res* 1999; **19**(5B): 3841-3846
- 14 **Lasota J**, Fetsch JF, Wozniak A, Wasag B, Sciort R, Miettinen M. The neurofibromatosis type 2 gene is mutated in perineurial cell tumors: a molecular genetic study of eight cases. *Am J Pathol* 2001; **158**: 1223-1229
- 15 **Mohyuddin A**, Neary WJ, Wallace A, Wu CL, Purcell S, Reid H, Ramsden RT, Read A, Black G, Evans DG. Molecular genetic analysis of the NF2 gene in young patients with unilateral vestibular schwannomas. *J Med Genet* 2002; **39**: 315-322
- 16 **Leuraud P**, Marie Y, Robin E, Huguet S, He J, Mokhtari K, Cornu P, Hoang-Xuan K, Sanson M. Frequent loss of 1p32 region but no mutation of the p18 tumor suppressor gene in meningiomas. *J Neurooncol* 2000; **50**: 207-213
- 17 **Pylkkanen L**, Sainio M, Ollikainen T, Mattson K, Nordling S, Carpen O, Linnainmaa K, Husgafvel-Pursiainen K. Concurrent LOH at multiple loci in human malignant mesothelioma with preferential loss of NF2 gene region. *Oncol Rep* 2002; **9**: 955-959
- 18 **Fukasawa T**, Chong JM, Sakurai S, Koshiishi N, Ikeno R, Tanaka A, Matsumoto Y, Hayashi Y, Koike M, Fukayama M. Allelic loss of 14q and 22q, NF2 mutation, and genetic instability occur independently of c-kit mutation in gastrointestinal stromal tumor. *Jpn J Cancer Res* 2000; **91**: 1241-1249
- 19 **Sugai T**, Habano W, Nakamura S, Yoshida T, Uesugi N, Sasou S, Itoh C, Katoh R. Use of crypt isolation to determine loss of heterozygosity of multiple tumor suppressor genes in colorectal carcinoma. *Pathol Res Pract* 2000; **196**: 145-150
- 20 **Handel-Fernandez ME**, Nassiri M, Arana M, Perez MM, Fresno M, Nadji M, Vincek V. Mapping of genetic deletions on the long arm of chromosome 22 in human pancreatic adenocarcinomas. *Anticancer Res* 2000; **20**: 4451-4456

Edited by Xia HHX and Xu FM

Reversal of 5-fluorouracil resistance by adenovirus-mediated transfer of wild-type p53 gene in multidrug-resistant human colon carcinoma LoVo/5-FU cells

Zhi-Wei Yu, Peng Zhao, Ming Liu, Xin-Shu Dong, Ji Tao, Xue-Qin Yao, Xin-Hua Yin, Yu Li, Song-Bin Fu

Zhi-Wei Yu, Peng Zhao, Ming Liu, Xin-Shu Dong, Department of Abdominal Surgery, the Third Affiliated Hospital of Harbin Medical University, Harbin 150040, Heilongjiang Province, China

Ji Tao, Department of General Surgery, The fifth Hospital of Harbin Medical University, Harbin 150040, Heilongjiang Province, China

Xue-Qin Yao, Department of General Surgery, Nanfang Hospital, Guangzhou 510515, Guangdong Province, China

Xin-Hua Yin, Department of Geriatrics, the Second Affiliated Hospital of Harbin Medical University, Harbin 150096, Heilongjiang Province, China

Yu Li, Song-Bin Fu, Department of Molecular Biology, Harbin Medical University, Harbin 150057, Heilongjiang Province, China

Correspondence to: Zhi-Wei Yu, Department of Abdominal Surgery, the Third Affiliated Hospital of Harbin Medical University, Harbin 150040, Heilongjiang Province, China. yuzhiwei1974@163.com

Telephone: +86-451-6677580-2146

Received: 2003-07-04 **Accepted:** 2003-08-28

Abstract

AIM: To observe the reversal effects of wide-type p53 gene on multi-drug resistance to 5-FU (LOVO/5-FU).

METHODS: After treatment with Ad-p53, LOVO/5-FU sensitivity to 5-Fu was investigated using tetrazolium dye assay. Multidrug resistance gene-1 (MDR1) gene expression was assayed by semi-quantitative reverse transcription-polymerase chain reaction and the expression of p53 protein was examined by Western blotting.

RESULTS: The reversal activity after treatment with wide-type p53 gene was increased up to 4.982 fold at 48 h. The expression of MDR1 gene decreased significantly after treatment with wide-type p53 gene, and the expression of p53 protein lasted for about 5 d, with a peak at 48 h, and began to decrease at 72 h.

CONCLUSION: Wide-type p53 gene has a remarkable reversal activity for the high expression of MDR1 gene in colorectal cancers. The reversal effects seem to be in a time dependent manner. It might have good prospects in clinical application.

Yu ZW, Zhao P, Liu M, Dong XS, Tao J, Yao XQ, Yin XH, Li Y, Fu SB. Reversal of 5-fluorouracil resistance by adenovirus-mediated transfer of wild-type p53 gene in multidrug-resistant human colon carcinoma LoVo/5-FU cells. *World J Gastroenterol* 2004; 10(13): 1979-1983

<http://www.wjgnet.com/1007-9327/10/1979.asp>

INTRODUCTION

Resistance to cytotoxic agents is the major cause of failure of medical treatment of human cancer and it is known that tumor cells can become resistant to anticancer drugs by a variety of different mechanisms^[1]. MDR (multidrug-resistance) is a form

of drug resistance characterized by decreased cellular sensitivity to a broad range of chemotherapeutic agents and due significantly to the over expression of MDR1 mRNA and its product P-gp^[2,3]. As an integral membrane protein, the M_r 170 000 P-gp is thought to be an energy-dependent membrane pump involved in the excretion of toxins in normal cells^[4]. Elevated expression of P-gp in malignant cells results in increased efflux and therefore reduced intracellular accumulation of cytotoxic agents, such as 5-FU, anthracyclines, Vinca alkaloids, and epipodophyllotoxins, but is not cross-resistant to alkylating agents, antimetabolites, and cisplatin. This decrease is considered as the basic mechanism of the MDR phenomenon^[4-7]. While a number of pharmacological agents have been shown to partially reverse MDR *in vitro*^[8], there remains a need to identify more potent, more specific, and less toxic chemosensitizers for clinical use.

Inactivity of p53 gene by missense mutation or deletion is the most common genetic alteration in human cancers^[9]. The loss of p53 function has been reported to enhance cellular resistance to a variety of chemotherapeutic agents^[10-13]. Our preliminary experiments^[14] also showed that there was a strong relationship between the MDR1 gene expression and mutated p53 gene in colorectal cancers.

Thus, in light of the fact that MDR1 is over-expressed in colorectal cancer that often lacks a functional p53^[14], we ask whether p53 plays a role in the control of MDR1 gene. Therefore, we sought to determine whether the introduction of the wild - type p53 gene in LOVO/5-FU cells by an adenoviral vector could increase the sensitivity of cells to a DNA cross-linking agent 5-FU *in vitro* and *in vivo*.

MATERIALS AND METHODS

Cell culture

LoVo cells were derived from a human colon adenocarcinoma. 5-FU-resistant LoVo sub-line (LoVo/5-FU) was obtained from the LoVo cell line by selection with 5-FU^[15], and maintained in medium containing 5 ng/mL 5-FU as described previously. LoVo/5-FU cells were kindly provided by Dr. Xue-Qing Yao. Monolayer cultures of LoVo and LoVo/5-FU were maintained in RPMI 1640 medium supplemented with 150 g/L heat-inactivated fetal calf serum (Sigma Chemical Co), 10 mL/L of a 200 mmol/L glutamine solution, 100 U/mL penicillin, 100 µg/mL streptomycin, and 10 g/L vitamin solution for minimum essential Eagle's medium purchased from GIBICO-BRL (Gaithersburg, MD). Cell lines grown in the presence of agents were passed in drug-free medium 2 to 3 times prior to use. All cells were grown at 37 °C in a humidified atmosphere of 50 mL/L CO₂ and 950 mL/L air.

Adenovirus vectors

Construction and identification of Ad-p53 and Ad-LacZ were finished and kindly provide by Dr. Xin-Hua Yin. Briefly, recombinant p53 adenovirus, Ad5CMV-p53 containing cytomegalovirus promoter, wild-type p53 cDNA, and SV40

early lopyadenylation signal in a minigene cassette was inserted into the E1-deletion region of modified Ad5. p53 shuttle vector and recombinant plasmid pJM 17 were cotransfected into 293 cells (Ad-transformed human embryonic kidney cells) by a liposome-mediated technique. The culture supernatant of 293 cells showing the complete cytopathic effect was collected and used for subsequent infections. Control Ad-LacZ virus was generated in a similar manner. Viral titers were determined by plaque forming activity in 293 cells. Concentrated virus was dialyzed, aliquoted, and stored at -80 °C. Cells were harvested 36-40 h after infection, pelleted, resuspended in PBS, and lysed. Cell debris was removed by double cesium chloride gradient ultracentrifugation.

Transient transfections

Adherent cells were plated in the wells of a 12-well plate. After 24 h, Ad-LacZ was transfected into the cells in different diluting densities. Forty-eight transfection, the cells were washed twice with PBS and fixed for 2 h with 40 g/L formaldehyde solution at 4 °C, then washed twice again with PBS and stained with 1 g/L X-gal solution for about 8 h at 37 °C. Observed under the electron microscope, the cells with blue staining were positive cells with LacZ expression, and calculated to determine the transfection efficiency.

Drug sensitivity testing

Chemosensitizers in the various cell lines were determined by using the tetrazolium-based colorimetric assay (MTT [*i.e.*, 3-(4,5-dimethyl-2-thiazoly)-2-m-5-diphenyl-2H-tetrazolium bromide] assay). Cells (LoVo/5-FU/Ad-p53 cells, LoVo/5-FU cells, LoVo cells;) were seeded in a 96-well microtiter plate at a density of 1×10^5 cells/well and each well contained 200 μ L medium. Cells were exposed 24 h after plating to various concentrations of 5-FU for 4 h. After treatment, medium was removed and replaced with 200 μ L of drug-free medium. Plates were incubated for further 72 h. At this time, 15 μ L of MTT (4 mg/mL) solution was added to each well. After a 4-h incubation at 37 °C, the cellular supernatant was gently aspirated, and insoluble formazan crystals were dissolved by adding 180 μ L 1 000 g/L DMSO (dimethyl sulfoxide) to each well, then the plates were shaken for about 10 min. The absorbance of each well was determined by a spectrophotometry at the wavelength of 570 nm with a microculture plate reader. Inhibition of cell growth was determined as a percentage of absorbance of vehicle-treated control cultures. IC₅₀ was the concentration of drugs that reduced staining (A₅₇₀) to 50% of vehicle-treated controls.

The effect of chemosensitizers on drug resistance was studied by exposing cells to a range of concentrations of cytotoxic drugs in the absence or presence of concentrations of chemosensitizers. Dose-response curves were corrected for the inhibition of cell growth caused by chemosensitizers alone, and the "fold reversal" of MDR for 5-FU plus chemosensitizer combination was calculated as follows:

$$\text{Fold reversal} = \frac{\text{IC}_{50} \text{ drug alone}}{\text{IC}_{50} \text{ drug +chemosensitizer}}$$

Western blot analysis of wild-type p53 expression

Cells infected with the indicated adenovirus and MOI were grown to about 80% confluence in 10-cm plates. After washed with PBS, cells were scraped from the plate, washed once with ice-cold PBS containing 1 mmol/L phenylmethylsulfonyl fluoride, and centrifuged at 1 000 r/min for 4 min. The cell pellet was resuspended in ice-cold radioimmunoprecipitation assay buffer (1% NP40, 0.5% sodium deoxycholate, and 1 g/L SDS, 10 μ g/mL aprotinin, 10 μ g/mL leupeptin and 1 μ g/mL pepstatin A)

and sonicated. After centrifugation at 12 000 g at 4 °C for 20 min, the resulting supernatant was harvested as the total cell lysate. The protein was aliquoted and stored at -70 °C until use. Protein samples were electrophoresed through a 125 g/L polyacrylamide gel containing 1 g/L SDS and the gel was run at 30 mA for 3 h. Separated proteins were transferred onto nitrocellulose paper by electroblotting. After blocked with 50 mL/L blocking reagent, the nitrocellulose membrane was probed with a monoclonal antibody against human wild-type p53 from Oncogene Science. Detection was accomplished using ECL western blotting detection reagents from Amersham Pharmacia Corp.

Determination of MDR1 mRNA expression by RT-PCR

Expression of the MDR1 gene was determined by measuring the mRNA level from total RNA by SUPERSRIPT™ first-strand synthesis system (GIBCO BRL, Gaithersburg, MD), using MDR1-specific primer pairs. Briefly, total RNA was extracted from established lines with TRIzol reagent (Life Technologies, Inc.). Equal amounts of RNA, as determined by absorbance at 260 nm, were denatured and size was fractionated by electrophoresis through a 12 g/L agarose gel containing formaldehyde and 2 μ g/dL ethidium bromide (Figure 1). Equal amounts (1 μ g) of total RNA from each tissue were treated with RNase-free DNase I to remove any contaminated DNA. DNase-treated RNA was then used to synthesize single-strand cDNAs by AMV reverse transcriptase in the presence of random primers, followed by PCR amplification. The primers used for PCR reaction were: MDR1-1, GTA CCC ATC ATT GCA ATA GC and MDR1-2, CAA ACT TCT GCT CCT GAG TC. These two MDR1 primers bracketed the COOH-terminal region of the MDR1 cDNA and gave a PCR product of 147 bp. PCR amplification was performed by pre-denaturing at 95 °C for 3 min, and then running 30 cycles in the following conditions: denaturation at 94 °C for 40 s, annealing for 40 s at 55 °C, and extension at 72 °C for 50 s. As internal control, RT-PCR for β -actin was carried out using 5' CGT GGG CCG CCC TAG GCA CCA 3' (forward primer) and 5' TTG GCC TTA GGG TTC AGG GGG 3' (reverse primer) in the same conditions as described for MDR1, and showed a PCR product of 243 bp. The PCR products were electrophoresed in a 20 g/L agarose gel with 0.5 μ g/mL ethidium bromide and visualized under UV light. Quantitation of relative band volume counts was performed using Molecular analyst for windows software. To estimate MDR1 expression levels, a MDR1 index was designated as a band volume count ratio of MDR1 to constitutively expressed β -actin, because β -actin mRNA was expressed constitutively in cells. The higher the MDR1 index, the higher the expression level of MDR1 mRNA in cells.

RESULTS

Sensitivity of LoVo and LoVo/5-FU to 5-fluorouracil

The sensitivity of LoVo and LoVo/5-FU cells to 5-fluorouracil was evaluated using the MTT assay as shown in Table 1. Previous studies utilizing MTT assays have shown that the LoVo/5-FU cell line is 8.988-fold more resistant to 5-fluorouracil than parental LoVo cells. We found the two cell lines showed differences in sensitivity to 5-fluorouracil, too. The concentration inducing 50% inhibition of cell proliferation for 5-Fluorouracil was 0.82 μ g/mL for the parental line and 7.37 μ g/mL for the LoVo/5-FU cells.

Effect of wtp53 gene on cell growth in LoVo/5-FU cells

Figure 1 showed the effect of wild-type p53 on the LoVo/5-FU cells. It suggested that the dose of Ad-p53 for experiment didn't affect the growth rate of LoVo/5-FU cells during the six days after transfection.

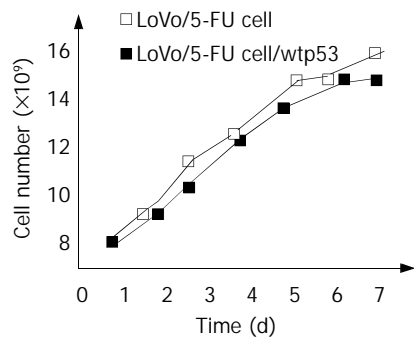


Figure 1 Effect of wild-type p53 on the growth rate of LoVo/5-FU cells.

Effect of wild-type p53 on LoVo/5-FU cells sensitivity to 5-fluorouracil

The effect of wild-type p53 on 5-fluorouracil sensitivity was examined using the MTT assay. A dose of 8.17×10^{10} pfu/mL Ad-p53 was chosen as the dose to modulate 5-fluorouracil sensitivity. For this study, cells were treated with wild-type p53 for 48 h, 5-fluorouracil was then added to the final concentration of 0.25 to 15 $\mu\text{g/mL}$ for 3 h, and then the medium was removed and replaced with a fresh medium without drugs and the incubation was continued. Cell growth was determined after an addition for 72 h. Treatment with wild-type p53 appeared to decrease the resistance of LoVo/5-FU cells to 5-fluorouracil (Table 1).

Table 1 Effect of wild-type p53 on LoVo/5-FU sensitivity to 5-fluorouracil

Cell lines	IC ₅₀ ($\mu\text{g/mL}$)	Resistant time	Reverse time
LoVo cells	0.82		
LoVo/5-FU cells	7.37	8.988	
LoVo/5-FU cells+wild-type p53	1.48 ^b	1.804	4.982

^b $P < 0.01$ compared with LoVo/5-FU cell control group.

Expression of wild-type p53 protein in cell lines

The X-gal staining suggested that the dilution of 1:20 for Ad-p53 could make about more than 80% cells infected successfully. LoVo/5-FU was transduced *in vitro* with the human wild-type p53 cDNA by exposing to Ad-p53 (1:20). To make sure that the constructed p53 expression vector, Ad-p53, efficiently expressed functional wild-type p53, we determined its protein expression and transactivating function. Western blot analysis showed a higher level of wild-type p53 protein expression as early as 48 h after infection with Ad-p53, and which lasted for 5 d, then decreased significantly on the sixth day. But no wild-type p53 was detected in parental (uninfected) cells or control cells infected with Ad-LacZ (data not shown), suggesting that the transfer and expression of p53 by Ad-p53 were highly efficient (Figure 2).

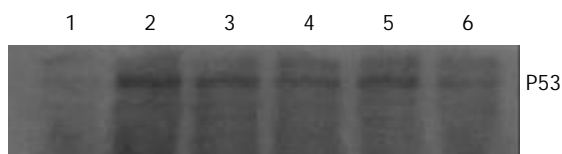


Figure 2 Western blot analysis of wild-type p53 in LoVo/5-FU cell line and LoVo/5-FU cells transiently transfected with p53 expression vector (Ad-p53). Lane 1: LoVo/5-FU cell line. Lanes 2, 3, 4, 5, 6: LoVo/5-FU cells transiently transfected with Ad-p53 for 2, 3, 4, 5, 6 d accordingly. Levels of wild-

type p53 protein (lanes 2-6) were determined by Western-blot analysis with an antibody which could detect wild-type forms of p53 protein.

Expression of wild-type p53 suppressed endogenous MDR1 gene expression

We asked whether wild-type p53 expression could indeed inhibit endogenous MDR1 gene expression in LoVo/5-FU cells. Successful generation of cell lines constantly expressing wild-type p53 was tested in human LoVo/5-FU cells transfected with Ad-p53 as above, and these cells constantly maintained wild-type p53 for about 6 d and provided a valuable reagent for studying drug sensitivity. As seen in Figure 2, vector-transfected LoVo/5-FU cells expressing wild-type p53, had a lower MDR1 mRNA expression than LoVo/5-FU cells without wild-type p53 expression, as determined by RT-PCR. There was a decrease in MDR1 transcripts compared with the empty vector-transfected cell line, suggesting that constitutive expression of p53 could inhibit endogenous MDR1 transcription in LoVo/5-FU cells, and this suppression showed a time-dependent mode (Figure 3, 4 and Tables 2, 3).

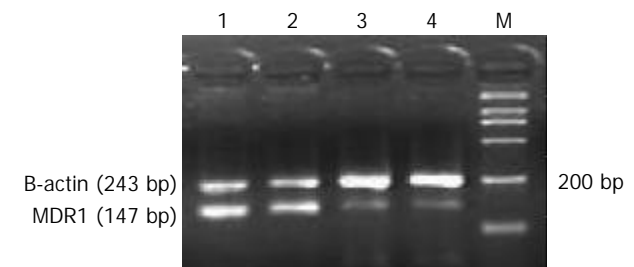


Figure 3 Results of RT-PCR for expression of MDR1 mRNAs in p53-null and wild-type p53 expressing LoVo/5-FU cells. M: marker; Lanes 1 and 2: results of untransfected LoVo/5-FU cells; Lanes 3 and 4: results of transfected LoVo/5-FU cells.

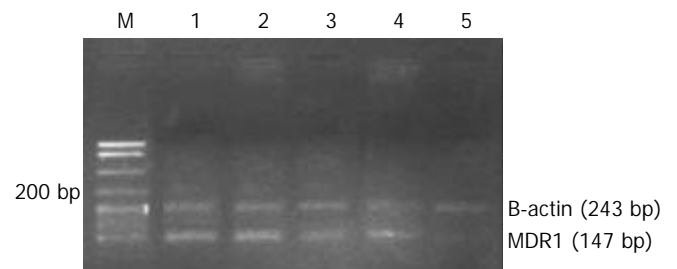


Figure 4 Results of RT-PCR for expression of MDR1 mRNAs of transfected LoVo/5-FU cells at different time. M: marker; Lanes 1, 2, 3, 4, 5: the cells transfected with Ad-p53 for 2, 3, 4, 5, 6 d accordingly.

Table 2 MDR1 expression in different cell lines

	Lane 1	Lane 2	Lane 3	Lane 4
MDR1/ β -actin	1.26	1.19	0.42	0.33

Table 3 MDR1 expression of LoVo/5-FU cells on different day after dealing with Ad-p53

Time/d	2	3	4	5	6
MDR1/ β -actin	1.22	1.24	1.06	0.86	0.42

DISCUSSION

Tumor cell resistance to chemotherapeutic drugs represents a major problem in clinical oncology; patients with colorectal

cancer are generally unresponsive to chemotherapy. The goal of our current cancer research was to find ways to improve the efficacy of gene replacement therapy for cancer by investigating interactions between the gene products and chemotherapeutic drugs.

Resistance to cytotoxic agents is the major cause of failure of medical treatment of human cancer and it is known that tumor cells could become resistant to anticancer drugs by a variety of mechanisms^[1]. In numerous *in vitro* models, this resistance has been shown to be mediated by MDR1 gene, whose product P-gp is thought to be an energy-dependent membrane pump involved in the excretion of toxins in normal cells. Elevated expression of P-gp in malignant cells could result in increased efflux and therefore reduced intracellular accumulation of cytotoxic agents. This decrease has been considered as the basic mechanism of the MDR phenomenon^[2-7].

LoVo/5-FU cells were selected from the LoVo parental cell line through culture in the presence of 5-fluorouracil and were resistant to 5-FU which was toxic to LoVo parental cells. LoVo/5-FU cells had cross-resistance to the drugs comprising the classical MDR phenotype^[15]. In this study, we found the resistance subline overexpressed MDR1 mRNA and no wild-type p53 protein was expressed.

An adenovirus system has potential advantages for gene delivery *in vivo*, such as easy production of high titer virus, high infection efficiency, and infectivity for many types of cells^[16-18]. The stability and duration of the expression of introduced gene are still controversial. For chemo-gene therapy, the expression levels and high infectivity may be more significant than the duration of expression because drugs can kill infected cells within several days. In our model, the expression of wild-type p53 gene was driven independently by the cytomegalovirus promoter contained in an Ad-p53 vector. The expression of wild-type p53 protein by Ad-p53 peaked after 48 h and decreased to a low level by the sixth day. This suggests that a transiently high level of wild-type p53 expression is sufficient to initiate the cytotoxic program in cancer cells.

We found that pretreatment of LoVo/5-FU cells with Ad-p53 was capable of restoring cell sensitivity to 5-fluorouracil. In the parental cell line, however, Ad-p53 did not potentiate 5-fluorouracil toxicity. The functional reversal of MDR by Ad-p53 in LoVo/5-FU cells appeared to be mediated by changes of the MDR1 gene expression.

Several agents have been described to affect MDR1 gene expression or the MDR phenotype in human or rodent cells, such as the Ca²⁺ channel blocker, verapamil, calmodulin inhibitor, trifluoperazine, which have been shown to reverse the MDR phenotype *in vitro* through direct competition with drugs for P-gp binding in the absence of changes in P-gp expression. Treatment with these agents could result in increased intracellular concentrations of cytotoxic drugs, which are thus a final common pathway in the reversal of the multidrug-resistant phenotype. They are presently used in clinical trials to patients with drug refractory tumors. However, they could induce significant cardiotoxicity, thus which limiting their clinical usefulness^[19,20]. The Ad-p53 concentrations reported here are active *in vivo* in the absence of significant toxicity.

Wild-type p53, a M_r 53 000 nuclear phosphoprotein involved in the control of cell growth and apoptosis is the most commonly altered gene in human tumors^[21]. Its role as a tumor suppressor has been well documented as its inactivation was strongly correlated with human cancer^[21-23]. p53 protein had different domains for DNA binding, transactivation, and tetramerization functions^[24,25]. After binding to consensus for DNA sequences, p53 could positively regulate the expression of downstream effector genes, including Gadd45, p21(WAF1/CIP1)^[26], and mouse muscle creatin kinase^[27]. In addition,

wild-type p53 could also negatively regulate a variety of genes that lack a p53 consensus binding site, including DNA topoisomerase II^[28], MDR1^[29-32], c-fos^[33], and other viral and cellular promoters. It has been suggested that transcriptional repression by p53 could result from its direct interactions with transcription factors, such as TATA-binding protein^[34,35], Sp1^[36,37] and CCAAT-binding factor^[28]. Taken together, these observations strongly imply that p53 acts directly with the transcription machinery to modulate MDR1 transcription.

Many tumors have no functional p53, and others express high levels of MDR1. Whether there is a direct connection has remained to be determined^[38]. However, our results suggested that restoration of wild-type p53 in tumor cells could overcome the uncontrolled up-regulation of MDR1 gene expression, and could add to the beneficial effect of wild-type p53 gene therapy that would restore cell growth inhibition and apoptosis pathway to facilitate drug-induced cell killing.

A variety of treatment protocols, including surgery, chemotherapy, and radiotherapy, have been tried for human colorectal cancer, but the long-term survival rate remains unsatisfactory. The combination therapy we present here might be effective as an adjuvant treatment to prevent local recurrence following primary tumor resection or as a treatment that could be given by intralesional injections in drug-resistant primary, metastatic, or locally recurrent colorectal cancer. Protocols are being developed to explore these clinical applications.

REFERENCES

- Zhu XH, Li JY, Xia XM, Zhu MQ, Geng MJ, Chen L, Zhang JQ. Multidrug resistance mechanisms in cell line HL-60/VCR. *Aizheng* 2002; **21**: 1310-1313
- Tsuruo T, Naito M, Tomida A, Fujita N, Mashima T, Sakamoto H, Haga N. Molecular targeting therapy of cancer: drug resistance, apoptosis and survival signal. *Cancer Sci* 2003; **94**: 15-21
- Tsuruo T. Molecular cancer therapeutics: recent progress and targets in drug resistance. *Intern Med* 2003; **42**: 237-243
- Fromm MF. The influence of MDR1 polymorphisms on P-glycoprotein expression and function in humans. *Adv Drug Deliv Rev* 2002; **54**: 1295-1310
- Johnstone RW, Ruefli AA, Smyth MJ. Multiple physiological functions for multidrug transporter P-glycoprotein? *Trends Biochem Sci* 2000; **25**: 1-6
- Shapiro AB, Ling V. Effect of quercetin on Hoechst 33342 transport by purified and reconstituted P-glycoprotein. *Biochem Pharmacol* 1997; **53**: 587-596
- Abu-Qare AW, Elmasry E, Abou-Donia MB. A role for P-glycoprotein in environmental toxicology. *J Toxicol Environ Health B Crit Rev* 2003; **6**: 279-288
- Thomas H, Coley HM. Overcoming multidrug resistance in cancer: an update on the clinical strategy of inhibiting p-glycoprotein. *Cancer Control* 2003; **10**: 159-165
- Tullo A, D' Erchia AM, Sbisa E. Methods for screening tumors for p53 status and therapeutic exploitation. *Expert Rev Mol Diagn* 2003; **3**: 289-301
- Chang BD, Swift ME, Shen M, Fang J, Broude EV, Roninson IB. Molecular determinants of terminal growth arrest induced in tumor cells by a chemotherapeutic agent. *Proc Natl Acad Sci U S A* 2002; **99**: 389-394
- Yazlovitskaya EM, DeHaan RD, Persons DL. Prolonged wild-type p53 protein accumulation and cisplatin resistance. *Biochem Biophys Res Commun* 2001; **283**: 732-737
- Yuan R, Meng Q, Hu H, Goldberg ID, Rosen EM, Fan S. P53-independent downregulation of p73 in human cancer cells treated with Adriamycin. *Cancer Chemother Pharmacol* 2001; **47**: 161-169
- Hawkins DS, Demers GW, Galloway DA. Inactivation of p53 enhances sensitivity to multiple chemotherapeutic agents. *Cancer Res* 1996; **56**: 892-898
- Yu ZW, Dong XS, Wang XH. The relationship between the mdr1 gene expression and mutations of p53 gene and ras gene in colorectal cancer. *Chin J Oncol* 2002; **24**: 480

- 15 **Yao XQ**, Qing SH, Yang Y. Establishment of multidrug-resistant human colorectal cancer cell line LoVo/5-FU: a preliminary study of biological characterization. *J First Mil Med Univ* 2001; **21**: 19-21
- 16 **Xu ZL**, Mizuguchi H, Mayumi T, Hayakawa T. Regulated gene expression from adenovirus vectors: a systematic comparison of various inducible systems. *Gene* 2003; **309**: 145-151
- 17 **Mohr L**, Geissler M. Gene therapy: new developments. *Schweiz Rundsch Med Praxis* 2002; **91**: 2227-2235
- 18 **Park J**, Ries J, Gelse K, Kloss F, von der Mark K, Wiltfang J, Neukam FW, Schneider H. Bone regeneration in critical size defects by cell-mediated BMP-2 gene transfer: a comparison of adenoviral vectors and liposomes. *Gene Ther* 2003; **10**: 1089-1098
- 19 **Durie BG**, Dalton WS. Reversal of drug-resistance in multiple myeloma with verapamil. *Br J Haematol* 1988; **68**: 203-206
- 20 **Epstein J**, Xiao HQ, Oba BK. P-glycoprotein expression in plasma cell myeloma is associated with resistance to VAD. *Blood* 1989; **74**: 913-917
- 21 **Vogelstein B**, Kinzler KW. p53 function and dysfunction. *Cell* 1992; **70**: 523-526
- 22 **Baker SJ**, Markowitz S, Fearon ER, Willson JK, Vogelstein B. Suppression of human colorectal carcinoma cell growth by wild-type p53. *Science* 1990; **249**: 912-915
- 23 **Zambetti GP**, Levine AJ. A comparison of the biological activities of wild-type p53 and mutant p53. *FASEB J* 1993; **7**: 855-865
- 24 **Cho Y**, Gorina S, Jeffrey PD, Pavletich NP. Crystal structure of a p53 tumor suppressor-DNA complex: understanding tumorigenic mutations. *Science* 1994; **265**: 346-355
- 25 **Wolcke J**, Reimann M, Klumpp M, Gohler T, Kim E, Deppert W. Analysis of p53 "latency" and "activation" by fluorescence correlation spectroscopy: Evidence for different modes of high affinity DNA binding. *J Biol Chem* 2003; **278**: 32587-32595
- 26 **Sowa Y**, Sakai T. Gene-regulating chemoprevention against cancer—as a model for "molecular-targeting prevention" of cancer. *Nippon Eiseigaku Zasshi* 2003; **58**: 267-274
- 27 **Zambetti GP**, Bargonetti J, Walker K, Prives C, Levine AJ. Wild-type p53 mediates positive regulation of gene expression through a specific DNA sequence element. *Genes Dev* 1992; **6**: 1143-1152
- 28 **Wang Q**, Zambetti GP, Suttle DP. Inhibition of DNA topoisomerase II alpha gene expression by the p53 tumor suppressor. *Mol Cell Biol* 1997; **17**: 389-397
- 29 **Chin KV**, Ueda K, Pastan I, Gottesman MM. Modulation of activity of the promoter of the human MDR1 gene by Ras and p53. *Science* 1992; **255**: 459-462
- 30 **Zastawny RL**, Salvino R, Chen J, Benchimol S, Ling V. The core promoter region of the P-glycoprotein gene is sufficient to confer differential responsiveness to wild-type p53 and mutant p53. *Oncogene* 1993; **8**: 1529-1535
- 31 **Thottassery JV**, Zambetti GP, Arimori K, Schuetz EG, Schuetz JD. P53-dependent regulation of MDR1 gene expression causes selective resistance to chemotherapeutic agents. *Proc Natl Acad Sci U S A* 1997; **94**: 11037-11042
- 32 **Bush JA**, Li G. Regulation of the Mdr1 isoforms in a p53-deficient mouse model. *Carcinogenesis* 2002; **23**: 1603-1607
- 33 **Elkeles A**, Juven-Gershon T, Israeli D, Wilder S, Zalcenstein A, Oren M. The c-fos proto-oncogene is a target for transactivation by the p53 tumor suppressor. *Mol Cell Biol* 1999; **19**: 2594-2600
- 34 **Seto E**, Usheva A, Zambetti GP, Momand J, Horikoshi N, Weinmann R, Levine AJ, Shenk T. Wild-type p53 binds to the TATA-binding protein and represses transcription. *Proc Natl Acad Sci U S A* 1992; **89**: 12028-12032
- 35 **Huang H**, Kaku S, Knights C, Park B, Clifford J, Kulesz-Martin M. Repression of transcription and interference with DNA binding of TATA-binding protein by C-terminal alternatively spliced p53. *Exp Cell Res* 2002; **279**: 248-259
- 36 **Borellini F**, Glazer RI. Induction of Sp1-p53 DNA-binding heterocomplexes during granulocyte/macrophage colony-stimulating factor-dependent proliferation in human erythroleukemia cell line TF-1. *J Biol Chem* 1993; **268**: 7923-7928
- 37 **Liedtke C**, Groger N, Manns MP, Trautwein C. The human caspase-8 promoter sustains basal activity through SP1 and ETS-like transcription factors and can be up-regulated by a p53-dependent mechanism. *J Biol Chem* 2003; **278**: 27593-27604
- 38 **Galmarini CM**, Kamath K, Vanier-Viorner A, Hervieu V, Peiller E, Falette N, Puisieux A, Ann Jordan M, Dumontet C. Drug resistance associated with loss of p53 involves extensive alterations in microtubule composition and dynamics. *Br J Cancer* 2003; **88**: 1793-1799

Edited by Wang XL and Xu FM

Influence of survivin and caspase-3 on cell apoptosis and prognosis in gastric carcinoma

Yun-Hong Li, Chen Wang, Kui Meng, Long-Bang Chen, Xiao-Jun Zhou

Yun-Hong Li, Department of Gastroenterology, Gulou Hospital, Medical College of Nanjing University, Nanjing 210008, Jiangsu Province, China

Chen Wang, Medical College of Nanjing University, Nanjing 210093, Jiangsu Province, China

Long-Bang Chen, Department of Oncology, Clinical School of Medical College of Nanjing University/Nanjing General Hospital of Nanjing Command, Nanjing 210002, Jiangsu Province, China

Kui Meng, Xiao-Jun Zhou, Department of Pathology, Clinical School of Medical College of Nanjing University/Nanjing General Hospital of Nanjing Command, Nanjing 210002, Jiangsu Province, China

Correspondence to: Dr. Yun-Hong Li, Department of Gastroenterology, Gulou Hospital, Medical College of Nanjing University, 321 Zhongshan Road, Nanjing 210008, Jiangsu Province, China. liyunhong37@vip.sina.com.cn

Telephone: +86-25-86522328 **Fax:** +86-25-83307016

Received: 2003-12-23 **Accepted:** 2004-01-15

Abstract

AIM: To evaluate the role of survivin and caspase-3 in apoptosis of gastric carcinoma, as well as in prognosis of patients with gastric carcinoma.

METHODS: Expressions of survivin and caspase-3 were investigated immunohistochemically in 80 gastric carcinoma patients without a history of chemo-radiation therapy. Tumor cell apoptosis was examined by TUNEL method.

RESULTS: Immunohistochemical analysis showed that survivin expression was positive in 61 of 80 patients (76%) with gastric carcinoma. In contrast, no expression of survivin in adjacent normal tissues was detected. Expression level of caspase-3 was higher in normal tissues than in carcinoma. Patients with higher expression of survivin had worse histological grades and pathological stages. Expression of caspase-3 was significantly associated with histological stages, but not with the pathological stages. Although survivin expression in carcinoma was not inversely related to caspase-3, patients with survivin (-) and caspase-3(+) had the maximum apoptosis index.

CONCLUSION: Expression level of survivin was associated with histological grades and pathological stages of the tumor, indicating that survivin may be a poor prognosis factor for gastric carcinoma. Unlike caspase-3, survivin (an apoptosis inhibitor) can markedly inhibit the apoptosis of tumor cells.

Li YH, Wang C, Meng K, Chen LB, Zhou XJ. Influence of survivin and caspase-3 on cell apoptosis and prognosis in gastric carcinoma. *World J Gastroenterol* 2004; 10(13): 1984-1988
<http://www.wjgnet.com/1007-9327/10/1984.asp>

INTRODUCTION

Abnormalities in cell death control are implicated as a cause or contributing factor in a range of diseases, including cancer,

autoimmunity, and degenerative disorders^[1]. This control involves several proteins that promote or inhibit apoptosis and an evolutionarily conserved multistep cascade^[2]. A number of proteins, such as Bcl-2, Fas and Bax affect upstream of the cascade^[3,4]. Survivin, a recently discovered inhibitor of apoptosis, may prolong cell survival by targeting the terminal effector caspase-3^[5,6]. Located at the end of cascade, caspase-3 acts as both initiators and executors in the apoptotic process. So survivin and caspase-3 have been the focus of debate regarding apoptosis.

In the last decade, molecular abnormalities of tumor cells have emerged as important prognostic indicators of gastric carcinoma. As a candidate molecule to influence the apoptosis balance, survivin has unique properties such as undetectable in normal adults tissues and overexpression in a variety of human cancers *in vivo*^[7]. Although studies indicated that survivin was a prognostic tumor marker^[8-13], little is known about its potential role in gastric carcinoma. In this study we sought to investigate the expression of survivin and caspase-3 in gastric carcinoma and to dissect their potential prognostic value, and discuss the relationship between survivin, caspase-3 and tumor cell apoptosis.

MATERIALS AND METHODS

Patients and samples

A total of 80 patients with gastric adenocarcinoma did not receive any treatment prior to surgery. Of them 56 were males and 24 were females, with a mean age of 60 years. Surgically resected specimens were fixed in 10% neutral formalin, embedded in paraffin, and stained by haematoxylin-eosin. Histological grades and pathological stages were conformed to the criteria of UICC (Figure 1). The subjects consisted of 17 cases in stage I, 34 cases in stage II, and 29 cases in stage III. Tumor tissues and normal tissues from every patient were detected.

Immunohistochemical staining for survivin and caspase-3

A pilot study using the anti-survivin antibody and anti-caspase-3 antibody was conducted on various neoplasms, including gastric carcinoma, lung cancer, breast cancer and non-Hodgkin's lymphoma to determine an appropriate dilution. The immunostaining was performed, and negative control slides processed without primary antibody were incubated for each staining. Paraffin-embedded slides were deparaffinized and put in 400 mL EDTA solution (0.001 mol/L, pH 6.0). Then the solution was heated in a pressure cooker and boiled for 2 min while maintaining the pressure. After cooling the slides were incubated with the primary antibody (mouse anti-human survivin or caspase-3 monoclonal antibody purchased from NEO MAEKERS) overnight at 4 °C and rinsed by PBS (0.01 mol/L, pH 7.4) three times. Then the slides were incubated with an anti-mouse conjugate containing horseradish peroxidase at 37 °C for 30 min and rinsed by PBS three times. Finally 3,3'-diaminobenzidine was used for color development and hematoxylin was used for counterstaining. The mean percentage of positive tumor cells was determined in at least five areas at 400-fold magnification and assigned to one of the following five categories^[14]: -, <5%; +, 5-25%; ++, 26-50%; +++, 51-75%; +++++, >75%.

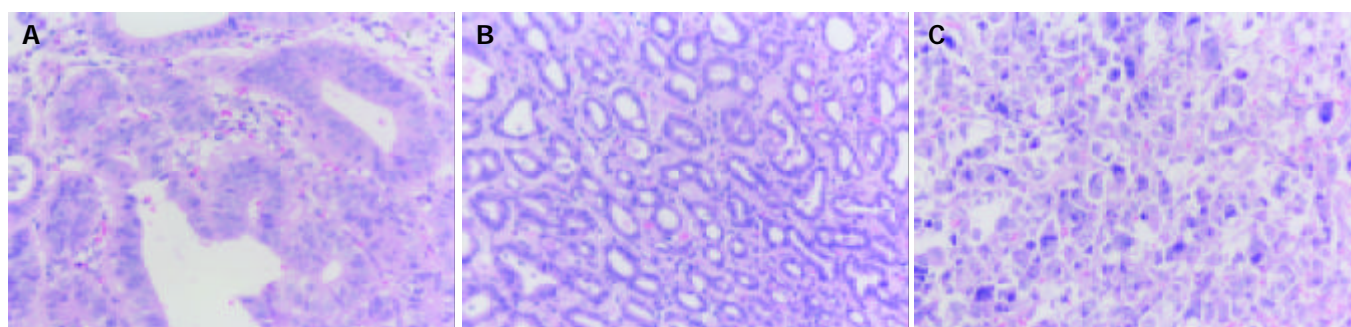


Figure 1 HE staining of gastric carcinoma. A: well differentiated gastric carcinoma; B: Moderately differentiated gastric carcinoma; C: Poorly differentiated gastric carcinoma (Original magnification: $\times 200$).

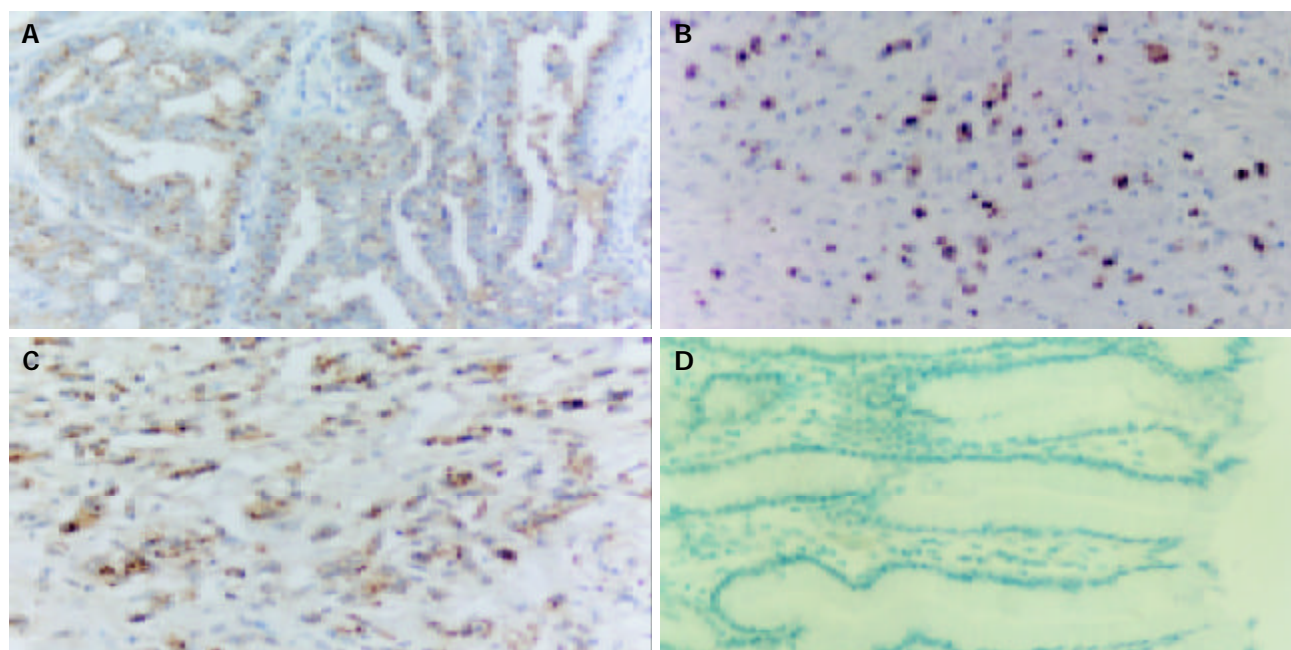


Figure 2 Survivin expression in gastric carcinoma. A: well differentiated gastric carcinoma; B: Moderately differentiated gastric carcinoma; C: Poorly differentiated gastric carcinoma; D: Substitution for antibody with PBS as negative control (Original magnification: $\times 200$).

Histochemical detection of apoptosis

All cases received detection of apoptosis except those with both survivin and caspase-3 negativities. Apoptotic cells and apoptotic bodies were detected by *in situ* labeling using a TUNEL kit purchased from Borriman Company. In brief, deparaffinized and rehydrated sections were digested with proteinase K for 20 min at room temperature and washed. After quenching in 30 mL/L hydrogen peroxide for 10 min and washing with PBS, terminal deoxynucleotidyl transferase enzyme was pipetted onto the sections, which were then incubated at 37 °C for 1 h. After stopping the reaction by putting sections in PBS and washing, anti-digoxin-peroxidase was added to the slides. Finally slides were washed with PBS, stained with 3,3-diaminobenzidine, and counterstained with hematoxylin. Substitution for terminal deoxynucleotidyl transferase with distilled water was used as negative control. Positive cells were determined according to the method described previously^[15]. In brief, positive cells had dark or dark brown nuclei and some morphological characteristics, including chromatin condensation, nuclear disintegration, and formation of crescent caps of condensed chromatin at the nuclear periphery. Counting method was the same as described previously.

Statistical analysis

Differences of positivity rates between different groups were assessed by *t*-test. Kruskal-Wallis' rank sum test was used to assess the differences between ranked data. Linear correlation

hypothesis test was used to evaluate the extent of correlation between two groups. All of the statistical analyses were performed with SAS statistical package.

RESULTS

Immunohistochemical staining revealed that anti-survivin mAb 8E2 specifically reacted with gastric carcinoma cells, with positive staining in cytoplasm and near the Golgi apparatus, whereas no expression of survivin was observed in adjacent normal tissues. A total of 61 cases of gastric carcinoma in this series were defined as positive staining (76%, Figure 2), with the mean percentage of 29.83%.

Of the 80 cases of gastric carcinomas, 75 cases (94%) of the adjacent normal tissues were positive for caspase-3, while 68 cases (85%) of the tumors were caspase-3 positive (Figure 3). Student's *t*-test showed that caspase-3 expressed higher in normal tissue than in carcinoma. Survivin and caspase-3 were not positive at the same position in cancer cells. Expression of survivin in carcinomas showed a negative but not linear correlation with that of caspase-3 ($r=-0.18$, $P>0.05$).

Through Kruskal-Wallis' rank sum test, we found that the expression of both survivin and caspase-3 had significant differences between tissues with different histological grades (Tables 1, 3). The expression of survivin was significantly associated with pathological stages, but caspase-3 was not (Tables 2, 4).

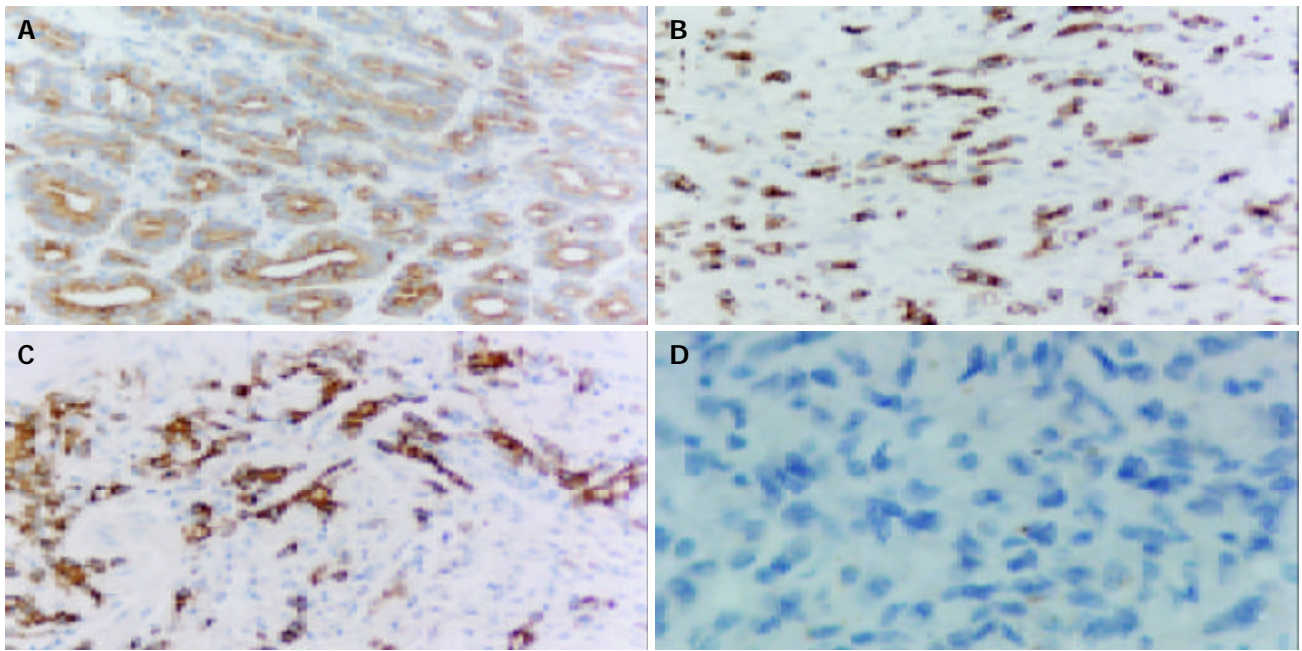


Figure 3 Expression of caspase-3 in gastric carcinoma. A: well differentiated gastric carcinoma; B: Moderately differentiated gastric carcinoma; C: Poorly differentiated gastric carcinoma; D: Substitution for antibody with PBS as negative control (Original magnification: $\times 200$).

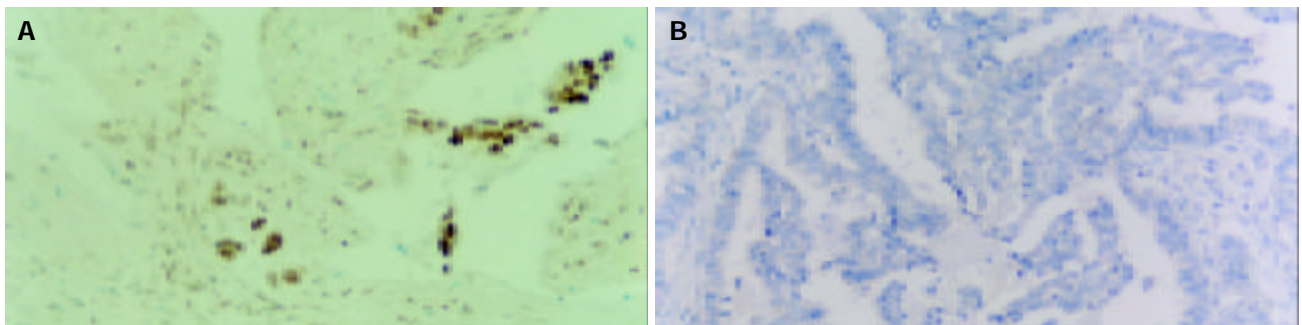


Figure 4 Apoptosis in gastric carcinoma. A: Positive; B: Substitution for terminal deoxynucleotidyl transferase with distilled water as negative control (Original magnification: $\times 200$).

Table 1 Correlation between histological grades and survivin expression

Positive degree	Poorly differentiated	Moderately differentiated	Well differentiated	Sum	Mean ranks
+	1	13	4	18	9.5
++	8	11	1	20	28.5
+++	10	5	1	16	46.5
++++	4	3	0	7	58
<i>n</i>	23	32	6	61	

$H_c=12.8, P<0.005$ between poorly, moderately and well differentiated gastric carcinomas.

Table 2 Correlation between pathological stages and expression of survivin

Positive degree	Stage I	Stage II	Stage III	Sum	Mean ranks
+	8	6	4	18	9.5
++	3	15	2	20	28.5
+++	1	3	12	16	46.5
++++	1	2	4	7	58
<i>n</i>	13	26	22	61	

$H_c=15.1, P<0.005$ between stages I, II and III.

Table 3 Correlation between histological grades and expression of caspase-3

Positive degree	Poorly differentiated	Moderately differentiated	Well differentiated	Sum	Mean ranks
+	6	2	0	8	3.5
++	10	14	1	25	17.5
+++	8	19	2	29	42.5
++++	1	1	4	6	63
<i>n</i>	25	36	7	68	

$H_c=11.7, P<0.005$ between poorly, moderately and well differentiated gastric carcinomas.

Table 4 Correlation between pathological stages and expression of caspase-3

Positive degree	Stage I	Stage II	Stage III	Sum	Mean ranks
+	1	5	2	8	4.5
++	7	7	11	25	21
+++	5	14	10	29	48
++++	3	2	1	6	65.5
<i>n</i>	16	28	24	68	

$H_c=0.54, P>0.75$ between stages I, II and III.

Apoptotic cells and apoptotic bodies were observed in gastric carcinoma by using *in situ* labeling (Figure 4). The mean apoptotic index (AI) of the 80 cases was 0.84%. The mean AI in survivin-positive tumors was 0.59%, which was significantly lower than the mean AI of 1.26% observed in survivin-negative tumors ($P < 0.005$). The mean AI in caspase-3-positive tumors (0.97%) was significantly higher than that in caspase-3-negative tumors (0.56%, $P < 0.05$). Tumors with survivin(-) and caspase-3 (+) had the highest AI of 1.58%.

DISCUSSION

Recently, several inhibitors of apoptosis (IAP) related to the baculovirus IAP gene have been identified in humans, mice, and *Drosophila*^[4]. Recombinant expressions of IAP proteins counteract various forms of apoptosis *in vivo*^[16] and *in vitro*^[17]. These molecules are thought to block an evolutionarily conserved step in apoptosis. At least in the case of X-linked IAP, this may involve direct inhibition of the terminal effectors caspase-3 and caspase-7 through a BIR-dependent recognition^[18]. Among the recently described IAP family, survivin is characterized by a unique structure with a single BIR and no-zinc-binding domain known as the RING finger^[19,20], and by the selective distribution in common human cancers^[4,7]. In this study, specific staining for survivin was detected in 61 cases (76%), with a variable proportion of positive tumor cells (10-85%). In contrast, the adjacent normal tissues or the infiltrating lymphocytes did not express survivin, consistent with similar studies^[13]. As the histological differentiation decreased and pathological stage increased, positivity rate and expression level of survivin were elevated. So survivin expression has prognostic value in human gastric carcinoma.

Alessandra^[21] reported that survivin was expressed in G₂-M phase of the cell cycle in a cell cycle-regulated manner and associated with mitotic spindle microtubules. In this study, survivin-positive patients had lower AI as compared with survivin-negative patients, suggesting that the overexpression of survivin in cancer might obliterate the checkpoint of the cell cycle and allow aberrant progression through the G₂-M phase checkpoint in gastric carcinoma.

In normal gastric tissues, caspase-3 was mainly expressed in gastric surface mucous cells, being in accord with the gastric cell turnover. Caspase-3 expression was increased in well differentiated tumors and apoptotic cells were increased in tumors with caspase-3 positivity, indicating that the expression of caspase-3 promoted apoptosis of tumor cells. It is well known that a number of genetic alterations are required for malignant transformation. Therefore we can speculate that abnormal differentiation leads to decreased expression of caspase-3 in tumor cells.

As a key effector molecule of apoptosis, caspase-3 can inactivate number proteins, which are associated with the structure and cycle of normal cells. Survivin showed an inversed function compared with caspase-3, which can be illustrated by the results that cases with survivin (-) and caspase-3 (+) had higher AI than cases with survivin (+) and caspase-3 (-). Then what we wanted to know was, if survivin inhibited directly the expression or function of caspase-3. Although our results indicated that expression of survivin was inversely associated with that of caspase-3, statistic analysis showed no linear correlation. So we think survivin did not inhibit the function of caspase-3 by directly inhibiting its expression. One of the relevant points to this issue was that survivin induced caspase-9 deactivation first^[22,23], and then caspase-3 could not be activated at the end of the cascade. Some other reports suggested that survivin inhibited caspase pathway of apoptosis, and controlled apoptosis and mitotic spindle checkpoint^[19,24]. We speculate that survivin mainly oppresses caspase-3

activation or possesses effect on the upstream promoter activity, but not its expression. Further studies are needed to confirm the process of how survivin inhibits caspase-3.

As long as survivin affects terminal effector of apoptosis and exists in tumor cells, it would be an ideal target of apoptosis-based therapy. One of the roles of chemotherapy is inducing apoptosis, and caspase-3 has been proved to participate in this process^[25], so acting on this target might also enhance sensitivity to chemotherapy or reduce the effect of drug-resistance. A recent *in vitro* study demonstrated that anti-survivin RNA down-regulated the expression of endogenous survivin in transformed cells and induced apoptotic cell death^[26]. Targeted antagonists of survivin may offer a new therapeutic method for gastric carcinoma. A homeland study^[27] revealed that antisense oligonucleotide targeting survivin induced decrease of survivin expression, increase of cell apoptosis, inhibition of cell proliferation in hepG2 cells. It also has been reported^[28] that survivin-based plasmids could induce apoptosis in gastric cancer cells and sensitize gastric cancer cells to chemotherapeutic agents. Gene therapy targeting survivin gene expression may offer a new approach to cancer therapy.

REFERENCES

- 1 **Cross M**, Dexter TM. Growth factors in development, transformation, and tumorigenesis. *Cell* 1991; **64**: 271-280
- 2 **Thompson CB**. Apoptosis in the pathogenesis and treatment of disease. *Science* 1995; **267**: 1456-1462
- 3 **Barinaga M**. Death by dozens of cuts. *Science* 1998; **280**: 32-34
- 4 **Tamm I**, Wang Y, Sausville E, Scudiero DA, Vigna N, Oltersdorf T, Reed JC. IAP-family protein survivin inhibits caspase activity and apoptosis induced by Fas (CD95), Bax, caspases, and anti-cancer drugs. *Cancer Res* 1998; **58**: 5315-5320
- 5 **Ambrosini G**, Adida C, Altieri DC. A novel anti-apoptosis gene, survivin, expressed in cancer and lymphoma. *Nat Med* 1997; **3**: 917-921
- 6 **Adida C**, Haioun C, Gaulard P, Lepage E, Morel P, Briere J, Dombret H, Reyes F, Diebold J, Gisselbrecht C, Salles G, Altieri DC, Molina TJ. Prognostic significance of survivin expression in diffuse large B-cell lymphomas. *Blood* 2000; **96**: 1921-1925
- 7 **Kawasaki H**, Altieri DC, Lu CD, Toyoda M, Tenjo T, Tanigawa N. Inhibition of apoptosis by survivin predicts shorter survival rates in colorectal cancer. *Cancer Res* 1998; **58**: 5071-5074
- 8 **Islam A**, Kageyama H, Hashizume K, Kaneko Y, Nakagawara A. Role of survivin, whose gene is mapped to 17q25, in human neuroblastoma and identification of a novel dominant-negative isoform, survivin-beta/2B. *Med Pediatr Oncol* 2000; **35**: 550-553
- 9 **Tanaka K**, Iwamoto S, Gon G, Nohara T, Iwamoto M, Tanigawa N. Expression of survivin and its relationship to loss of apoptosis in breast carcinomas. *Clin Cancer Res* 2000; **6**: 127-134
- 10 **Asanuma K**, Moriai R, Yajima T, Yagihashi A, Yamada M, Kobayashi D, Watanabe N. Survivin as a radioresistance factor in pancreatic cancer. *Jpn J Cancer Res* 2000; **91**: 1204-1209
- 11 **Lu CD**, Altieri DC, Tanigawa N. Expression of a novel antiapoptosis gene, survivin, correlated with tumor cell apoptosis and p53 accumulation in gastric carcinoma. *Cancer Res* 1998; **58**: 1808-1812
- 12 **Lu C**, Tanigawa N. Spontaneous apoptosis is inversely related to intratumoral microvessel density in gastric carcinoma. *Cancer Res* 1997; **57**: 221-224
- 13 **Duckett CS**, Nava VE, Gedrich RW, Clem RJ, Van Dongen JL, Gilfillan MC, Shiels H, Hardwick JM, Thompson CB. A conserved family of cellular genes related to the baculovirus iap gene and encoding apoptosis inhibitors. *EMBO J* 1996; **15**: 2685-2694
- 14 **Hay BA**, Wassarman DA, Rubin GM. *Drosophila* homologs of baculovirus inhibitor of apoptosis proteins function to block cell death. *Cell* 1995; **83**: 1253-1262
- 15 **Takahashi R**, Deveraux Q, Tamm I, Welsh K, Assa-Munt N, Salvesen GS, Reed JC. A single BIR domain of XIAP sufficient for inhibiting caspases. *J Biol Chem* 1998; **273**: 7787-7790
- 16 **Giodini A**, Kallio MJ, Wall NR, Gorbisky GJ, Tognin S, Marchisio PC, Symons M, Altieri DC. Regulation of microtubule stability

- and mitotic progression by survivin. *Cancer Res* 2002; **62**: 2462-2467
- 17 **Reed JC**. The Survivin saga goes *in vivo*. *J Clin Invest* 2001; **108**: 965-969
- 18 **Shi Y**. Survivin structure: crystal unclear. *Nat Struct Biol* 2000; **7**: 620-623
- 19 **Shankar SL**, Mani S, O' Guin KN, Kandimalla ER, Agrawal S, Shafit-Zagardo B. Survivin inhibition induces human neural tumor cell death through caspase-independent and -dependent pathways. *J Neurochem* 2001; **79**: 426-436
- 20 **Li F**, Ambrosini G, Chu EY, Plescia J, Tognin S, Marchisio PC, Altieri DC. Control of apoptosis and mitotic spindle checkpoint by survivin. *Nature* 1998; **396**: 580-584
- 21 **Sun XM**, MacFarlane M, Zhuang J, Wolf BB, Green DR, Cohen GM. Distinct caspase cascades are initiated in receptor-mediated and chemical-induced apoptosis. *J Biol Chem* 1999; **274**: 5053-5060
- 22 **Sasaki H**, Sheng Y, Kotsuji F, Tsang BK. Down-regulation of X-linked inhibitor of apoptosis protein induces apoptosis in chemoresistant human ovarian cancer cells. *Cancer Res* 2000; **60**: 5659-5666
- 23 **Hauser HP**, Bardroff M, Pyrowolakis G, Jentsch S. A giant ubiquitin-conjugating enzyme related to IAP apoptosis inhibitors. *J Cell Biol* 1998; **141**: 1415-1422
- 24 **Miller LK**. An exegesis of IAPs: salvation and surprises from BIR motifs. *Trends Cell Biol* 1999; **9**: 323-328
- 25 **Sun C**, Cai M, Gunasekera AH, Meadows RP, Wang H, Chen J, Zhang H, Wu W, Xu N, Ng SC, Fesik SW. NMR structure and mutagenesis of the inhibitor-of-apoptosis protein XIAP. *Nature* 1999; **401**: 818-822
- 26 **Kappler M**, Kotzsch M, Bartel F, Fussel S, Lautenschlager C, Schmidt U, Wurl P, Bache M, Schmidt H, Taubert H, Meye A. Elevated expression level of survivin protein in soft-tissue sarcomas is a strong independent predictor of survival. *Clin Cancer Res* 2003; **9**: 1098-1104
- 27 **Wang Y**, Wang JL. Antisense oligonucleotide targeting survivin inducing apoptosis of hepatic cancer cells. *Zhonghua Xiaohua Zazhi* 2003; **23**: 11-14
- 28 **Tan JH**, Tu SP, Zou B, Ma TL, Zhong J, Zhang CL, Qiao MM, Jiang SH. Experimental study on apoptosis induced by pcDNA3-survivin mutant in gastric cancer cell lines. *Zhonghua Xiaohua Zazhi* 2003; **23**: 199-202

Edited by Chen WW and Zhu LH **Proofread by** Xu FM

Enhanced antitumor efficacy on hepatoma-bearing rats with adriamycin-loaded nanoparticles administered into hepatic artery

Jiang-Hao Chen, Rui Ling, Qing Yao, Ling Wang, Zhong Ma, Yu Li, Zhe Wang, Hu Xu

Jiang-Hao Chen, Rui Ling, Qing Yao, Ling Wang, Zhong Ma, Department of Vascular and Endocrine Surgery, Xijing Hospital, Fourth Military Medical University, Xi'an 710033, Shaanxi Province, China

Yu Li, Department of Cell Biology, Fourth Military Medical University, Xi'an 710033, Shaanxi Province, China

Zhe Wang, Department of Pathology, Fourth Military Medical University, Xi'an 710033, Shaanxi Province, China

Hu Xu, Department of Orthopaedics, Xijing Hospital, Fourth Military Medical University, Xi'an 710033, Shaanxi Province, China

Correspondence to: Dr. Jiang-Hao Chen, Department of Vascular and Endocrine Surgery, Xijing Hospital, Fourth Military Medical University, Xi'an 710033, Shaanxi Province, China. chenjh@fmmu.edu.cn

Telephone: +86-29-83375271

Received: 2003-12-19 **Accepted:** 2004-01-15

Abstract

AIM: To investigate the antitumor activity of adriamycin (ADR) encapsulated in nanoparticles (NADR) and injected into the hepatic artery of hepatoma-bearing rats.

METHODS: NADR was prepared by the interfacial polymerization method. Walker-256 carcinomas were surgically implanted into the left liver lobes of 60 male Wistar rats, which were divided into 4 groups at random (15 rats per group). On the 7th day after implantation, normal saline (NS), free ADR (FADR), NADR, or ADR mixed with unloaded nanoparticles (ADR+NP) was respectively injected via the hepatic artery (i.a.) of rats in different groups. The dose of ADR in each formulation was 2.0 mg/kg body weight and the concentration was 1.0 mg/mL. Survival time, tumor enlargement ratio, and tumor necrosis degree were compared between each group.

RESULTS: Compared with the rats that received NS i.a., the rats that received FADR or ADR+NP acquired apparent inhibition on tumor growth, as well as prolonged their life span. Further significant anticancer efficacy was observed in rats that received i.a. administration of NADR. Statistics indicated that NADR brought on a more significant tumor inhibition and more extensive tumor necrosis, as compared to FADR or ADR+NP. The mean tumor enlargement ratio on the 7th day after NADR i.a. was 1.106. The mean tumor-bearing survival time was 39.50 days. Prolonged life span ratio was 109.22% as compared with rats that accepted NS.

CONCLUSION: Therapeutic effect of ADR on liver malignancy can be significantly enhanced by its nanoparticle formulation and administration via hepatic artery.

Chen JH, Ling R, Yao Q, Wang L, Ma Z, Li Y, Wang Z, Xu H. Enhanced antitumor efficacy on hepatoma-bearing rats with adriamycin-loaded nanoparticles administered into hepatic artery. *World J Gastroenterol* 2004; 10(13): 1989-1991
<http://www.wjgnet.com/1007-9327/10/1989.asp>

INTRODUCTION

Transhepatic arterial chemotherapy (TAC) is recognized as an efficient therapy for liver primary and metastatic tumors by increasing the drug concentration in tumor and improving the therapeutic effect subsequently. It was reported that administration of ADR via the hepatic artery (i.a.) was able to increase the drug concentration in tumor by 3-fold as compared to intravenous administration^[1]. In patients with cancers, the i.a. administration of ADR reduced the plasma AUC by about 30%^[2].

During recent years, nanoparticles have been extensively applied as carriers of antitumor drugs. *In vivo* studies have demonstrated that nanoparticles are specifically concentrated to the reticuloendothelial system (RES), especially to liver and spleen, after administered into body^[3]. On the basis of these experiences, we hypothesized that a further significant therapeutic effect could be expected by TAC in combination with nanoparticle techniques. We carried out a randomized control study to test it.

MATERIALS AND METHODS

NADR preparation and characterization

NADR was prepared by the interfacial polymerization method^[4]. α -polybutylcyanoacrylate (PBCA) was used as polymeric materials. The final product had an appearance of reddish, colloidal, semi-transparent solution. Under transmission electron microscopy (TEM), NADR showed a global, regular contour with a homogenous size and distribution. The diameter of particles ranged from 22 to 130 nm (mean, 93.1 nm). The drug-embedding ratio was 82.6%, the drug-loading ratio was 40.9%, and the effusion rate was less than 3% three months later.

Animals and anesthetic

Sixty male Wistar rats weighing 230-270 g (mean, 250 g) were provided by Laboratory Animal Center of our university and randomly divided into 4 groups, with 15 in each. Sumianxin (Changchun Agricultural Pastoral University) was used as anesthetic.

Establishment of hepatoma model

One mL of suspension containing 10⁷ Walker-256 (W256) carcinosarcoma cells (Shanghai Medical Industrial Institution) was injected into the thigh muscle of a carrier rat (not included in experimental rats). One week after inoculation, a palpable tumor generated at the injected site. Viable tumor tissue was excised under sterile conditions and soaked in 20 mL of Hanks balanced salt solution. Tissue was diced into approximately 1 mm×1 mm×1 mm fragments. Experimental rats were anesthetized with intramuscular injection of Sumianxin at 0.2 mL/kg. Median incision beneath the metasternum was made and the liver was exposed. The tumor fragment was implanted into the left liver lobe.

Administration i.a.

On the 7th day after tumor implantation, all animals received laparotomy again. The longest (a) and shortest (b) diameters of

the tumor were measured. The tumor volume was calculated as

$$\frac{a \times b^2}{2}$$

By cannulation method described previously^[5], normal saline (NS), free ADR (FADR), NADR, or ADR mixed with unloaded nanoparticles (ADR+NP) was injected into the hepatic artery of rats in groups 1-4 respectively. The dose of ADR in each formulation was 2.0 mg/kg body weight. The concentration of ADR was 1.0 mg/mL.

Assessment of therapeutic effect

Tumor growth inhibition Seven days later, all animals received the third laparotomy. The longest (a) and shortest (b) diameters of the tumor were measured again and the tumor volume after administration was calculated. The tumor volume ratio (TVR) was calculated as

$$\text{TVR} = \frac{\text{Tumor volume after administration}}{\text{Tumor volume before administration}}$$

Tumor necrosis degree Seven random rats in each group were killed and anatomized. Hepatoma was removed completely and fixed in 40 g/L formaldehyde. Three 5- μ m thick sections in each tumor were cut on the maximal transverse plane and mounted on glass slides overnight at room temperature. After HE staining, the sections were examined under microscope. According to the percentage of necrosis area, tumors were graded on the following criteria: I, 0-30%; II, 30-70%; III, 70-100%.

Increased life span Survival time of the remaining 8 rats in each group was recorded. The mean survival time of NS group was reckoned as control. Increased life span (%ILS) was calculated as

$$\% \text{ILS} = \left(\frac{\text{Mean survival of treated group}}{\text{Mean survival of control group}} - 1 \right) \times 100\%$$

Statistical analysis

SPSS 10.0 for windows was used for statistical analysis. Statistical significance was tested by ANOVA and Dunnett test for tumor growth inhibition, log rank test for survival time. $P < 0.05$ was considered statistically significant.

RESULTS

Tumor growth inhibition

No difference in tumor volume was found among groups before treatment ($P > 0.05$, Table 1). After treatment, the tumor grew rapidly in rats that received NS. The mean tumor volume was 31.55 times greater than that before treatment. Metastases were observed in about half of these rats. In contrast, the speed of tumor growth lowered apparently in rats that received FADR or ADR+NP ($P < 0.01$). No difference between FADR and ADR+NP was observed ($P > 0.05$). The slowest tumor growth was found in rats that received i.a. administration of NADR. Statistics indicated that NADR brought on a further significant tumor inhibition, as compared with FADR or ADR+NP ($P < 0.01$). In addition, no metastasis was found in rats that received NADR.

Tumor necrosis degree

Under microscope, W256 tumor cells in rats that received NS appeared active proliferation and extensive mitoses. Small areas of necroses were observed in the center of tumor tissue and accompanied with a few inflammatory cells (Table 2). Moderate to severe necroses were found in tumors of rats that

received FADR or ADR+NP. Grade III of tumor necroses was found in 5 of 7 tumors after administration of NADR, including 2 cases of complete tumor necrosis.

Increased life span

Compared with the survival time (18.88 d) in saline controls, the tumor-bearing survival time was greatly prolonged in animals that received NADR (mean, 39.50 d), or FADR (mean, 27.75 d), or ADR+NP (mean, 26.13 d) (Table 3). NADR prolonged the life span by 109.22%, which was longer than FADR (46.98%) and ADR+NP (38.40%) ($P < 0.05$).

Table 1 Tumor volume (V) and tumor volume ratio (TVR) after treatment (mean \pm SD)

Group	V (cm ³)		TVR
	Before treatment	After treatment	
NS	0.086 \pm 0.049	2.521 \pm 0.840	31.550 \pm 7.975
FADR	0.083 \pm 0.035	0.149 \pm 0.072	1.883 \pm 0.708 ^b
ADR+NP	0.079 \pm 0.036	0.161 \pm 0.105	1.896 \pm 0.565 ^b
NADR	0.079 \pm 0.033	0.087 \pm 0.038	1.106 \pm 0.275 ^d

^b $P < 0.01$, vs NS; ^d $P < 0.01$, vs FADR, ADR+NP.

Table 2 Tumor necrosis degree after treatment

Grade	NS	FADR	ADR+NP	NADR
I	6	2	1	0
II	1	3	5	2
III	0	2	1	5 ¹

¹Complete necrosis in 2 cases.

Table 3 Mean survival time and increased life span (%ILS) after treatment (mean \pm SD)

Group	Mean survival time (d)	%ILS
NS	18.88 \pm 2.80	-
FADR	27.75 \pm 6.34	46.98 ^b
ADR+NP	26.13 \pm 5.75	38.40 ^b
NADR	39.50 \pm 8.97	109.22 ^a

^a $P < 0.05$, vs FADR, ADR+NP; ^b $P < 0.01$, vs NS.

DISCUSSION

We did not include intravenous administration (i.v.) in the present experiment because the i.a. route was much more efficient than i.v. in the treatment of liver malignancies. Different from the liver parenchyma, which receives more than 70% of its blood supply from the portal vein and the rest from the hepatic artery, hepatoma receives approximately 90% of its blood supply from the hepatic artery. The speciality of liver blood supply determines the great difference between the two routes of administration. The difference did not warrant repeat comparison in our study.

The results of our experiments demonstrated that the antitumor activity of ADR could be markedly enhanced when the drug was encapsulated in nanoparticles and administered into the hepatic artery. Equivalent or similar effects could not be acquired using FADR or ADR+NP. Compared with FADR or ADR+NP, NADR produced a more significant tumor inhibition and more extensive tumor necrosis. The average tumor volume on the 7th day after treated with NADR was 0.087 cm³, nearly the half of 0.161 cm³ of the volume after treated with ADR+NP. The survival time of rats that received NADR was evidently increased. Compared with saline

controls, NADR prolonged the life span by 109.22%.

The likely explanations for the improved therapeutic activity in four aspects are as follows. First, it has been testified that the cytotoxic effect of ADR depends on the concentration and duration of exposure^[6]. Increasing ADR concentration in tumor cells or slowing its elimination could certainly enhance its antitumor efficacy. Secondly, encapsulating the drug into nanoparticles might modify its distribution pattern in tissues. After administered into body, nanoparticles were taken up selectively by RES, such as the liver, spleen, and bone marrow. Accumulation of biodegradable nanoparticles with associated drugs in Kupffer cells would create a gradient of drug concentration for a massive and prolonged diffusion of the free drug towards neoplastic tissues^[3]. Thirdly, *in vitro* studies reported that compared to FADR, NADR exhibited a 3-fold enhancement of cytotoxicity, as determined by cell growth inhibition and DNA synthesis, after continuous exposure to 0.02 and 0.04 $\mu\text{g}/\text{mL}$ ^[7]. Further studies showed that nanoparticulate pharmaceuticals were able to enter specifically certain types of tumor tissues or tumor cells^[8]. Fourthly, the tiny size of nanoparticle could increase its contact areas significantly, which would result in an apparent improvement in its bioavailability. A recent study compared carbendazim, a novel anticancer drug, with its nanoparticles. The result confirmed that nanoparticle formulation improved the drug bioavailability by 166%^[9].

Our experiments support the hypothesis that the therapeutic effect could be dramatically enhanced by TAC in combination with nanotechnology. We conclude that nanoparticles can be used as a promising drug carrier in TAC for the treatment of liver primary and metastatic tumors.

REFERENCES

- 1 **Ridge JA**, Collin C, Bading JR, Hancock C, Conti PS, Daly JM, Raaf JH. Increased adriamycin levels in hepatic implants of rabbits Vx-2 carcinoma from regional infusion. *Cancer Res* 1988; **48**: 4584-4587
- 2 **Eksborg S**, Cedermark BJ, Strandler HS. Intrahepatic and intravenous administration of adriamycin - a comparative pharmacokinetics study in patients with malignant liver tumours. *Med Oncol Tumor Pharmacother* 1985; **2**: 47-54
- 3 **Chiannilkulchai N**, Ammoury N, Caillou B, Devissaguet JP, Couvreur P. Hepatic tissue distribution of doxorubicin-loaded nanoparticles after i.v. administration in reticulosarcoma M 5076 metastasis-bearing mice. *Cancer Chemother Pharmacol* 1990; **26**: 122-126
- 4 **Andrieu V**, Fessi H, Dubrasquet M, Devissaguet JP, Puisieux F, Benita S. Pharmacokinetic evaluation of indomethacin nanocapsules. *Drug Des Deliv* 1989; **4**: 295-302
- 5 **Zou YY**, Ueno M, Yamagishi M, Horikoshi I, Yamashita I, Tazawa K, Gu XQ. Targeting behavior of hepatic artery injected temperature sensitive liposomal adriamycin on tumor-bearing rats. *Sel Cancer Ther* 1990; **6**: 119-127
- 6 **Rupniak HT**, Whelan RD, Hill BT. Concentration and time-dependent inter-relationships for antitumor drug cytotoxicities against tumour cells *in vitro*. *Int J Cancer* 1983; **32**: 7-12
- 7 **Astier A**, Doat B, Ferrer MJ, Benoit G, Fleury J, Rolland A, Leverage R. Enhancement of adriamycin antitumor activity by its binding with an intracellular sustained-release form polymethacrylate nanospheres, in U-937 cells. *Cancer Res* 1988; **48**: 1835-1841
- 8 **Jordan A**. Nanotechnology and consequences for surgical oncology. *Kongressbd Dtsch Ges Chir Kongr* 2002; **119**: 821-828
- 9 **Jia L**, Wong H, Wang Y, Garza M, Weitman SD. Carbendazim: disposition, cellular permeability, metabolite identification, and pharmacokinetic comparison with its nanoparticle. *J Pharm Sci* 2003; **92**: 161-172

Edited by Zhang JZ and Wang XL Proofread by Xu FM

Effect of glutamine on change in early postoperative intestinal permeability and its relation to systemic inflammatory response

Zhu-Fu Quan, Chong Yang, Ning Li, Jie-Shou Li

Zhu-Fu Quan, Chong Yang, Ning Li, Jie-Shou Li, Research Institute of General Surgery, Jinling Hospital, Medical College of Nanjing University, Nanjing 210002, Jiangsu Province, China

Correspondence to: Dr. Zhu-Fu Quan, Research Institute of General Surgery, Jinling Hospital, Medical College of Nanjing University, Nanjing 210002, Jiangsu Province, China. quanzhufu@hotmail.com
Telephone: +86-25-85137085 **Fax:** +86-25-84803956

Received: 2003-06-16 **Accepted:** 2003-09-18

Abstract

AIM: To study the effects of glutamine (Gln) on the change of intestinal permeability and its relationship to systemic inflammatory response in early abdominal postoperative patients.

METHODS: A prospective, randomized, double-blind and controlled trial was taken. Twenty patients undergoing abdominal surgery were randomized into Gln group (oral administration of glutamine, 30 g/d, for 7 d, $n=10$) and placebo group (oral administration of placebo, 30 g/d, for 7 d, $n=10$). Temperatures and heart rates of all patients were daily recorded. White blood cell counts (WBC) and biochemical variables were measured before operation and 4 and 7 d after drug administration. Serum concentrations of glutamine, endotoxin, diamine oxidase and malondialdehyde and urine lactulose/mannito (L/M) ratio were measured before and 7 d after drug administration.

RESULTS: The patients in the 2 groups were comparable prior to drug administration. Serum Gln concentration was significantly decreased in the placebo group and increased in the Gln group 7 d after drug administration. Urine L/M ratio was significantly increased in the placebo group and decreased in the Gln group. The serum concentration of endotoxin, diamine oxidase and malondialdehyde was significantly decreased in the Gln group compared with those in the placebo group. Temperatures, heart rates and WBC counts were significantly lower in the Gln group than those in the placebo group.

CONCLUSION: Gut is one of the sources of systemic inflammatory response in abdominal postoperative patients and glutamine can decrease intestinal permeability, maintain intestinal barrier and attenuate systemic inflammatory response in early postoperative patients.

Quan ZF, Yang C, Li N, Li JS. Effect of glutamine on change in early postoperative intestinal permeability and its relation to systemic inflammatory response. *World J Gastroenterol* 2004; 10(13): 1992-1994

<http://www.wjgnet.com/1007-9327/10/1992.asp>

INTRODUCTION

Gut has been considered as one of the central organs responding to stresses in surgical patients^[1]. In the last few years, animal experiments and clinical researches have proved that the

intestinal permeability increases during stresses, such as severe trauma, operation. Glutamine as a semi-essential amino acid is a special nutrient to intestinal mucosal cells. It can reduce the permeability of gut, but becomes increasingly exhausted after severe trauma or operation. In this research we studied the effects of glutamine on the change of intestinal permeability and its relationship to systemic inflammatory response in abdominal postoperative patients.

MATERIALS AND METHODS

Patient grouping

A prospective, randomized, double-blind and controlled trial was taken. Twenty abdominal surgical patients aged 18-65 years and without any severe disease in liver, kidney, cardiovascular system and hematopoietic system, were randomized into Gln group (oral administration of glutamine, 30 g/d, for 7 d, $n=10$) and placebo group (oral administration of placebo, 30 g/d, for 7 d, $n=10$). Their sex, age, body mass and operation type were similar (Tables 1, 2).

Table 1 General data of two groups

	Placebo group	Glutamine group
Age (yr)	48.3±12.2	48.3±10.8
Male/Female	7/3	6/4
Weight (kg)	54.2±11.1	56.7±12.1

Drug dose and administration

Glutamine was dissolved in warm water (1 g in 10 mL) and orally taken or by gastric tube (10 g one time, and 3 times per day) after operation for 7 d. Placebo was administered as glutamine.

Measurement

Temperature and heart rate of all patients were daily recorded from the day before operation to the end of drug administration.

Peripheral blood was sampled on the morning of the day before operation, the day before drug administration, 4 and 7 after drug administration. Liver and kidney functions were measured.

Peripheral blood was sampled on the morning of the day before and 7 d after drug administration for the measurement of the concentration of the serum glutamine (Gln)^[2], diamine oxidase (DAO)^[3] and malondialdehyde (MDA)^[4].

Peripheral blood was sampled before and 7 d after drug administration for the measurement of the concentration of serum endotoxin with an endotoxin detection kit (Shanghai Yihua Clinical Technology Company).

On the morning before and the 7th dafter administration, 6 h' s urine was collected after 50 mL lactulose/mannito (L/M) solution (lactulose 10 g and mannito 5 g) was taken for the measurement of the levels of lactulose and mannito with method of enzyme^[5,6] and calculation of the ratio of L/M.

Statistic method

Results were expressed as mean±SD and analyzed with Student *t*-test. $P<0.05$ was considered statistically significant.

Table 2 Detailed clinical data of patients in two groups

Group	Case(n)	Sex	Age(yr)	Diagnosis	Operation type
Gln group	1	Male	55	Cardiac orifice cancer	Total gastrectomy
	2	Male	30	Acute suppurative cholangitis	Cholecystectomy choledochostomy
	3	Female	40	Rectal cancer	Anterior resection of rectum
	4	Male	47	Sigmoid cancer	Sigmoidectomy
	5	Male	62	Cardiac orifice cancer	Proximal subtotal gastrectomy
	6	Female	28	Rectal cancer	Anterior resection of rectum
	7	Female	52	Cholecystolithiasis	Cholecystectomy
	8	Male	49	Gastric cancer	Subtotal gastrectomy
	9	Male	60	Gastric cancer	Subtotal gastrectomy
	10	Male	60	Cardiac orifice cancer	Proximal subtotal gastrectomy
Placebo group	1	Male	50	Pancreas pseudocyst	Cyst-jejunal Roux-en-y anastomosis
	2	Female	56	Ascending colon cancer	Right semi-colectomy
	3	Female	60	Rectal cancer	Anterior resection of rectum
	4	Female	54	Sigmoid cancer	Sigmoidectomy
	5	Male	48	Cardiac orifice cancer	Proximal subtotal gastrectomy
	6	Male	43	Ascending colon cancer	Right semi-colectomy
	7	Male	64	Gastric cancer	Proximal subtotal gastrectomy
	8	Female	29	Gastric cancer	Proximal subtotal gastrectomy
	9	Male	43	Sigmoid cancer	Sigmoidectomy
	10	Male	36	Acute biliary pancreatitis	Selective cholecystectomy

RESULTS

General condition

During the research, there were no complication and death in both Gln group and placebo group.

Temperature

The highest, average and lowest temperatures increased after operation. The highest and average temperatures from d 3 to 6 and the lowest temperatures from d 2 to 6 in the Gln group were significantly lower than those in the placebo group.

Heart rate

The highest, average and lowest heart rates increased after operation in patients of both groups. The highest and average heart rates on d 2, 3 and 5 and the lowest heart rates from d 2 to 5 were significantly lower in the Gln group than in the placebo group.

WBC count

WBC counts increased from the first day after operation in both groups with the maximum being above $12.0 \times 10^9/L$. WBC counts decreased to normal level 4 d later in the Gln group, but 7 d later in the placebo group.

Serum concentration of Gln

In the placebo group, the serum concentration of Gln decreased from $432.17 \pm 142.68 \mu\text{mol/L}$ to $250.78 \pm 77.10 \mu\text{mol/L}$ ($P < 0.05$), whereas in the Gln group the serum concentration of Gln increased from $361.17 \pm 161.25 \mu\text{mol/L}$ to $583.22 \pm 171.52 \mu\text{mol/L}$ ($P < 0.05$). The serum concentration of Gln in the Gln group was significantly higher than that in the placebo group ($P < 0.01$) (Table 3).

Table 3 Serum levels of Gln in two groups ($\mu\text{mol/L}$)

Group	Before drug administration	7 d after drug administration
Placebo group	432.17 ± 142.68	250.78 ± 77.10^b
Gln group	361.17 ± 161.25	583.22 ± 171.52^{ad}

^a $P < 0.05$, ^b $P < 0.01$, vs before drug administration; ^d $P < 0.01$, vs placebo group.

Serum DAO concentration

Serum DAO concentrations were not significantly different in the 2 groups before drug administration. Seven days after drug administration, serum DAO concentrations increased in the

placebo group and decreased in the Gln group ($P < 0.01$). The difference in serum DAO concentrations was very significant ($P < 0.01$) between the two groups (Table 4).

Table 4 Serum DAO levels in two groups (U/mL)

Group	Before drug administration	7 d after drug administration
Placebo group	2.06 ± 0.48	3.18 ± 1.13
Gln group	2.26 ± 0.63	1.25 ± 0.65^{bd}

^b $P < 0.01$ vs before administration; ^d $P < 0.01$ vs placebo group.

Serum MDA concentration

Serum MDA concentrations were not significantly different in the 2 groups before drug administration. Seven days after drug administration, they increased in the placebo group and decreased in the Gln group ($P < 0.01$). The serum MDA concentrations were significantly different between the two groups ($P < 0.01$) after drug administration (Table 5).

Table 5 Serum MDA levels in two groups (nmol/mL)

Groups	Before drug administration	7 d after drug administration
Placebo group	3.94 ± 0.56	4.85 ± 0.63^b
Gln group	4.46 ± 0.67	3.53 ± 0.59^{bd}

^b $P < 0.01$ vs before drug administration; ^d $P < 0.01$ vs placebo group.

Table 6 Levels of serum endotoxin in two groups (EU/mL)

Group	Before drug administration	7 d after drug administration
Placebo group	0.21 ± 0.07	0.25 ± 0.08
Gln group	0.23 ± 0.05	0.18 ± 0.06^{ab}

^a $P < 0.05$ vs before drug administration; ^b $P < 0.01$ vs placebo group.

Serum endotoxin concentration

Levels of serum endotoxin in the 2 groups were not significantly different before drug administration. After 7 d, the serum endotoxin concentrations increased in the placebo group significantly and decreased in the Gln group ($P < 0.05$) with a very significant difference between the two groups ($P < 0.01$, Table 6).

Ratio of urine L/M

The ratio of L/M was not significantly different in the 2 groups initially, which was 134.00 ± 18.48 in the placebo group and 146.102 ± 20.21 in the Gln group. After 7 d, the ratio of L/M significantly increased in the placebo group ($P < 0.01$), and significantly decreased in the Gln group ($P < 0.05$). Then, the ratio of L/M was significantly lower in the Gln group than in the placebo group ($P < 0.01$, Table 7).

Table 7 Changes of urine L/M ratio in two groups

Group	Before drug administration	7 d after drug administration
Placebo group	134.00 ± 18.48	194.83 ± 45.31^b
Gln group	146.10 ± 20.21	117.47 ± 25.68^{ad}

^a $P < 0.05$, ^b $P < 0.01$, vs before drug administration; ^d $P < 0.01$ vs placebo group.

DISCUSSION

Normally, besides digestion and absorption, the gut functions as a mucosal barrier to bacteria, endotoxin and some other toxins. Whether the mucosal barrier works well or not is closely related to intestinal permeability. To measure it, some material with large molecular weight was used as a probe. Lactulose/mannito was most often used^[7]. During the period of severe trauma or operation, the intestinal mucosal barrier was damaged, and therefore the intestinal permeability increased from which bacteria and endotoxin can easily transfer through the intestinal mucosa and invade tissue and blood, which is called bacterial translocation. Then the bacteria and endotoxin in blood would inversely affect the intestinal mucosal barrier and get it further damaged, thus forming a vicious circle. The more critical condition was that systemic inflammatory response syndrome (SIRS) and multiple organ dysfunction syndrome (MODS) could even occur^[8]. Therefore, how to maintain the function of intestinal mucosal barrier in severe trauma or postoperative patients and how to decrease the permeability and bacterial translocation to avoid the occurrence of SIRS and MODS have become a very important problem.

Brooks *et al.*^[9] took L/M as a molecular probe to measure the intestinal permeability in 25 cases of gastrointestinal tumor. The ratio of L/M was greatly increased in the placebo group. Li *et al.*^[10] measured 24 hours' urine ^{99m}T-DTPA taken orally in 8 cases of postoperative patients 7 d after operation. The excretory rate of ^{99m}T-DTPA was $13.71 \pm 4.85\%$, which almost doubly increased to that before operation ($6.64 \pm 3.95\%$). In this research, serum Gln concentration decreased by 41.97%, and increased by 61.48% in the Gln group after administration of Gln for 7 d, when compared with the level before administration. It was significantly higher in the Gln group than in the placebo group. The ratio of L/M was not significantly different in the two groups initially. After 7 d, the ratio of L/M significantly increased in the control group and significantly decreased in the Gln group. The ratio of L/M was significantly lower in the Gln group than in the placebo group. This result showed that supplement of ectogenetic Gln could significantly decrease the intestinal permeability. Jiang *et al.*^[11,12] also proved this in surgical patients. Supplement of alanyl-glutamine could increase serum Gln level and decrease urine L/M ratio.

Li *et al.*^[13-16] studied that measurement of serum DAO was helpful to determine the degree of intestinal mucous damage. In their research after administration of Gln, serum DAO level significantly increased in the placebo group and significantly

decreased in the Gln group compared with the level before drug administration. The change in serum endotoxin level was similar in the 2 groups. This change of serum endotoxin level was related to the fact that high serum Gln level could enhance the function of intestinal mucosal barrier. Low serum endotoxin level was helpful to reduce SIRS in patients. Some researches showed that endotoxin in early trauma could lead to the increase of production and release of cytokines such as TNF- α , IL-6, IL-8, which could take part in the generation of SIRS^[17].

Haga *et al.*^[18] studied the postoperative conditions of 292 gastrointestinal patients. The result was that 245 patients had SIRS early after operation, which was 83.9%. The possibility of postoperative complication and MODS in these patients was much higher than that in those without SIRS. The results in our study indicate that SIRS can be reduced in early postoperative patients.

REFERENCES

- 1 Wilmore DW, Smith RJ, O' Dwyer ST, Jacobs DO, Ziegler TR, Wang XD. The gut: a central organ after surgical stress. *Surgery* 1988; **104**: 917-923
- 2 You ZY, Yu B, Lei ZH, Zhao Y. The determination of Glu and Gln in plasma and tissue by RP-HPLC. *Disan Junyi Daxue Xuebao* 1995; **17**: 152-153
- 3 Hosoda N, Nishi M, Nakagawa M, Hiramatsu Y, Hioki K, Yamamoto M. Structural and functional alterations in the gut of parenterally or enterally fed rats. *J Surg Res* 1989; **47**: 129-133
- 4 Zhang JX, Gao SG. Malondialdehyde Kit for determining serum lipoperoxide. *Nanjing Tiedao Yixueyuan Xuebao* 1997; **16**: 63-64
- 5 Behrens RH, Docherty H, Elia M, Neale G. A simple enzymatic method for the assay of urinary lactulose. *Clin Chim Acta* 1984; **137**: 361-367
- 6 Lunn PG, Northrop CA, Northrop AJ. Automated enzymatic assays for the determination of intestinal permeability probes in urine. 2. Mannitol. *Clin Chim Acta* 1989; **183**: 163-170
- 7 Bjarnason I, MacPherson A, Hollander D. Intestinal permeability: an overview. *Gastroenterology* 1995; **108**: 1566-1581
- 8 Saadia R, Schein M, MacFarlane C, Boffard KD. Gut barrier function and the surgeon. *Br J Surg* 1990; **77**: 487-492
- 9 Brooks AD, Hochwald SN, Heslin MJ, Harrison LE, Burt M, Brennan MF. Intestinal permeability after early postoperative enteral nutrition in patients with upper gastrointestinal malignancy. *JPEN* 1999; **23**: 75-79
- 10 Li N, Liu FN, Li YS, Kang J, Li FJ, Li JS. The changes of plasma glutamine and its influence on intestinal permeability after abdominal surgery. *Changwai Yu Changnei Yingyang* 1998; **5**: 3-6
- 11 Jiang ZM, Wang LJ, Qi Y, Liu TH, Qiu MR, Yang NF, Wilmore DW. Comparison of parenteral nutrition supplemented with L-glutamine or glutamine dipeptides. *JPEN* 1993; **17**: 134-141
- 12 Bai MX, Jiang ZM, Liu YM, Wang WT, Li DM, Wilmore DW. Effects of alanyl-glutamine on gut barrier function. *Nutrition* 1996; **12**: 793-796
- 13 Li JY, Lu Y, Xue LB. The effect of oral administration of glutamine on free amino acids concentration in the plasma of scalded rat. *Anjisuan He Shengwuziyuan* 2000; **22**: 51-56
- 14 Lu Y, Li JY, Sun SR, Jin H, Jiang XG, Sun XQ, Sheng ZY. Relationship between change of plasma diamine oxidase activity and gut injury in rats during gut ischemia-reperfusion. *Anjisuan He Shengwuziyuan* 2000; **22**: 50-54
- 15 Li JY, Lu Y, Fu XB, Jin H, Hu S, Sun XQ, Sheng ZY. The significance of changes in diamine oxidase activity in intestinal injury after trauma. *Zhongguo Weizhongbing Jijiu Yixue* 2000; **12**: 482-484
- 16 Li JY, Lu Y, Hao J, Jin H, Xu HJ. Determination of diamine oxidase activity in intestinal tissue and blood using spectrophotometry. *Anjisuan He Shengwuziyuan* 1996; **18**: 28-30
- 17 Jiang JX, Tian KL, Chen HS, Zhu PF, Wang ZG. Changes of plasma cytokines in patients with severe trauma and their relationship with organ damage. *Zhonghua Waikao Zazhi* 1997; **35**: 406-407
- 18 Haga Y, Beppu T, Doi K, Nozawa F, Mugita N, Ikei S, Ogawa M. Systemic inflammatory response syndrome and organ dysfunction following gastrointestinal surgery. *Crit Care Med* 1997; **25**: 1994-2000

Safe major abdominal operations: Hepatectomy, gastrectomy and pancreatoduodenectomy in elder patients

Yu-Lian Wu, Jun-Xiu Yu, Bin Xu

Yu-Lian Wu, Jun-Xiu Yu, Bin Xu, Department of Surgery, 2nd Affiliated Hospital, School of Medicine, Zhejiang University, Hangzhou 310009, Zhejiang Province, China

Correspondence to: Dr. Yulian Wu, Department of Surgery, 2nd Affiliated Hospital, School of Medicine, Zhejiang University, Hangzhou 310009, Zhejiang Province, China. wuyulian@medmail.com.cn

Telephone: +86-571-87784604 **Fax:** +86-571-87784604

Received: 2003-12-10 **Accepted:** 2004-01-08

Abstract

AIM: To evaluate the impact of advanced age on outcome after hepatectomy, gastrectomy and pancreatoduodenectomy.

METHODS: Two hundreds and eleven patients undergone hepatectomy, gastrectomy and pancreatoduodenectomy from January 1998 to September 2002 were analyzed retrospectively. Clinicopathologic features and operative outcome of 83 patients aged 65 years or more were compared with that in 128 younger patients aged less than 65 years.

RESULTS: The nutritional state, such as pre-operation level of serum albumin and hemoglobin in the older patients was poorer than that in the younger patients. The older patients had higher comorbidities than the younger patients (48.2% vs 15.6%). No significant difference was observed in perioperative mortality, and complication rate between the older and younger patients (2.4% vs 1.6% and 22.9% vs 20.3%, respectively). Multivariate analysis demonstrated that pancreatoduodenectomy, hepatectomy with resection of more than 2 segments and comorbidities were independent predictors of postoperative complication, whereas age was not ($P=0.3172$).

CONCLUSION: It is safe for patients aged 65 years or more to undergo hepatic, pancreatic and gastric resection if great care is taken during perioperative period.

Wu YL, Yu JX, Xu B. Safe major abdominal operations: Hepatectomy, gastrectomy and pancreatoduodenectomy in elder patients. *World J Gastroenterol* 2004; 10(13): 1995-1997

<http://www.wjgnet.com/1007-9327/10/1995.asp>

INTRODUCTION

The number and proportion of the elderly in our population have increased progressively as a result of increased life expectancy. The population over the age of 65 years is growing at the fastest rate than any other age groups^[1]. But surgery for potentially curable disease frequently leaves elderly patients numerically de-represented^[2]. Worrying about surgical risks and morbidity may be one reason accounting for this phenomenon. There are different opinions about whether elderly surgical patients have poor outcome. Some studies suggested that elderly surgical patients had high morbidity and mortality^[3,4]. Other reports showed that there was no significant difference in the rate of complications and death between the

older and the younger surgical patients^[5,6]. Two hundreds and eleven patients undergone major abdominal operations, including hepatectomy, gastrectomy and pancreatoduodenectomy in recent 5 years were analyzed retrospectively to see whether the older patients face more risks than younger patients.

MATERIALS AND METHODS

Two hundreds and eleven patients who underwent hepatectomy, gastrectomy or pancreatoduodenectomy in our hospital from January 1998 to September 2002 were studied retrospectively. The patients were divided into two groups: older group (age ≥ 65 years) and younger group (age < 65 years). The patients' age and sex, diagnosis, comorbidities, preoperative laboratory values, type of operation, clinical and pathologic characteristics of local lesion, postoperative complications and death, operative blood loss and transfusion, relaparotomy, length of hospital stay were obtained from the operative records and medical notes. The primary carcinoma was divided into different stages according to TNM staging system defined by Union Internationale Contre le Cancer (UICC, 1997). The patients were considered to have comorbidity when treatment was required in additional organ systems. Complications were defined by the classification proposed by Clavien *et al.*^[7]. Because grade I complications (minor and were likely to resolve spontaneously) were difficult to collect due to retrospective audits, only grade IIa complications (requiring drug for treatment), grade IIb complications (requiring reoperation or invasive procedure), grade III complications (events with residual or lasting disability including organ resection), grade IV complications (death as a result of any complication) were included in this study. Mortality was defined as death from any cause within 30 days of the operation.

Data were analyzed with the SAS 8.0 statistical software. Differences were analyzed with the Chi-square test or Fisher's exact test for group contingency analysis and the Student's *t* test and Mann-Whitney non-parametric test for continuous variables. Using logistic regression, the influence of different variables on the complication was studied. Length of hospital stay of the two groups was compared with a nonparametric product-limit method analogous to a Kaplan-Meier survival analysis. $P < 0.05$ was considered statistically significant.

RESULTS

Of the 211 patients, 150 cases were men and 61 cases were women. The median age was 60 years (range, 18 to 88).

The older group consisted of 83 patients, including 51 cases (≥ 65 years), 21 cases (> 70 years), 6 cases (> 75 years), and 5 cases (> 80 years). Diagnosis included primary hepatic carcinoma (31 cases), hepatic adenoma (1 case), hepatic chronic granuloma (1 case), metastatic cancer in liver (5 cases), gastric carcinoma (30 cases), gastric carcinoid (1 case), pancreatic carcinoma (4 cases), periampullary cancer (8 cases), and chronic pancreatitis (2 cases).

The younger group consisted of 128 patients. Diagnosis included primary hepatic carcinoma (45 cases), hepatic malignant stroma (1 case), focal nodular hyperplasia of liver

(1 case), metastatic cancer in liver (1 case), gastric carcinoma (37 cases), gastric ulcer (1 case), gastric malignant stoma (1 case), pancreatic carcinoma (15 cases), periampullary cancer (23 cases), chronic pancreatitis (2 cases), and benign biliary stricture (1 case).

No difference in stage of primary cancer was seen between the older group and younger group, but the levels of serum albumin and hemoglobin in older group were lower than those in younger group (Table 1). A 48.2% of total patients in older group had one or more comorbidities, which was significantly higher than that in younger group (15.6%). There was no difference in the constitution of operative procedure in the older and younger group. Median operative blood loss and transfusion were similar in both groups (500 mL vs 500 mL and 2 units vs 2 units, Table 1).

Table 1 Comparison of clinicopathologic features between the two age groups

Clinicopathologic Features	Younger group (<65 yr)	Older group (≥ 65 yr)	P value
Age (median)	52	69	
Gender (n)			0.2142 ¹
Male	87	63	
Female	41	20	
Diagnosis (n)			0.1105 ²
Liver			
Hepatic carcinoma	45	31	
Others	3	7	
Stomach			
Gastric carcinoma	37	30	
Others	2	1	
Pancrea			
Pancreatic carcinoma	15	4	
Periampullary carcinoma	23	8	
Others	3	2	
Serum albumin (mean \pm SD, g/dL)	3.84 \pm 0.46	3.65 \pm 0.50	0.0045 ³
Hemoglobin (mean \pm SD, g/dL)	12.05 \pm 2.39	11.16 \pm 2.33	0.0082 ³
Stage of primary cancer (n)			0.5658 ¹
I	18	12	
II	32	13	
III	53	34	
IV	17	13	
Comorbidity	15.6% (20/128)	48.2% (40/83)	<0.0001 ¹

¹Chi-square test; ²Fisher's exact test; ³Student's *t* test.

Table 2 Comparison of therapeutic characteristics between the two age groups

Therapeutic characteristics	Younger group (<65 yr)	Older group (≥ 65 yr)	P value
Operative procedures			0.1708 ¹
Hepatectomy ≤ 2 segments	26	23	
Hepatectomy > 2 segments	22	15	
Gastrectomy-total/proximal	13	11	
Gastrectomy-distal	26	20	
Pancreatoduodenectomy	41	14	
Operative blood loss (median, mL)	500 (100-20 000)	500 (50-3 500)	0.6480 ³
Operative blood transfusion (median, units)	2 (0-36)	2 (0-13)	0.3395 ³
Rate of complications	20.3% (26/128)	22.9% (19/83)	0.6550 ¹
Reoperative rate	2.3% (3/128)	2.4% (2/83)	1.0000 ²
Perioperative mortality (within 30 d)	1.6% (2/128)	2.4 (2/83)	0.6470 ²
Hospital length of stay (median, d)	21 (4-128)	24 (8-147)	0.0241 ⁴

¹Chi-square test; ²Fisher's exact test; ³Mann-Whitney non-parametric test; ⁴Kaplan-Meier method.

There was no apparent difference in complication rates between the older and younger group (22.9% vs 20.3%, Table 2). The most common complications were wound infection. Other complications included pneumonia, bile leak, pancreatic fistula, delayed gastric emptying, gastrointestinal fistula, cerebrovascular accident, abdominal bleeding, gastric bleeding, DIC, hepatic encephalopathy, pleural effusion, and renal failure. Two patients (2.4%) were re-operated because of gastric bleeding and bile leak in older group. Three patients (2.3%) were re-operated because of intestinal fistula, abdominal bleeding and bile leak in younger group. There was no significant difference in the rate of the re-operation between the two groups (Table 2). In older group, one patient died of DIC and severe metabolic acidosis 4 d after operation, another patient died of pneumonia 24 d after operation. In younger group, two patients died of abdominal hemorrhage and hepatic encephalopathy 13 and 27 d, respectively, after operation. The older patients had almost same perioperative mortality rate as the younger patients (2.4% and 1.6%, respectively). The median hospital stay was 24 d (range, 8 to 147 d) in the older group, which was significantly longer than that in the younger group (median, 21 d, and range, 4 to 128 d) (Figure 1).

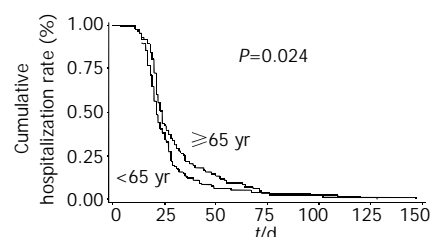


Figure 1 Length of hospital stay of the two age groups. Kaplan-Meier curves showed that the hospital stay in older group was significantly longer than that in younger group ($P=0.024$).

Table 3 Multivariate analysis of factors influencing major post-operative complications

Variables	Odds ratio	95% confidence interval	P value
Pancreatoduodenectomy	3.7736	1.7699-8.0145	0.0006
Hepatectomy > 2 segments	1.0858	1.0060-1.1834	0.0334
Comorbidity	3.2787	1.5361-6.9930	0.0021
Age (as continuous variable)	1.0173	0.9833-1.0537	0.3172

Logistic regression analysis showed pancreatoduodenectomy and hepatectomy with resection of more than 2 segments and comorbidities were independent factors for complications, whereas age was not.

The multivariate analysis by a stepwise logistic regression model identified three independent significant variables for postoperative complications in the both groups: pancreatoduodenectomy, hepatectomy with resection of more than 2 segments and comorbidities. Sex, reasons of operations, serum albumin, hemoglobin did not influence the morbidity as an independent factor. Calendaric age (in years) was not an independent predictor of complication ($P=0.3172$) (Table 3).

DISCUSSION

Our study suggests that there is no difference between the older patients and the younger patients in postoperative morbidities and mortalities. Similar results have been reported by others. Hodul *et al.*^[6] studied in 122 patients with pancreatoduodenectomy, including 48 patients aged over 70 years, and reported no significant difference between older group and younger group comparing the rate of complications, such as wound infection, abdominal abscess, pancreatic leak, and so on. A retrospective study carried out on 97 patients with a gastric tumor measuring 10 cm or more in diameter showed age was not the influencing factor of frequency of complications^[5]. Furthermore, analysis of extended hepatectomy (more than four liver segments) demonstrated age was not a contributor to in-hospital mortality^[8].

The improvement in perioperative management was a vital reason for reducing the morbidity and mortality^[9]. Developed guidelines for perioperative care may contribute the safety of operation for the elderly, for example, less use of nasogastric tubes can decrease the pulmonary complications, routine drainage being avoided in most cases or limited to a short period can facilitate early mobilization^[10]. Preoperative assessment of elderly and formulation of an effective anesthetic plan according the "individual principle" can decrease the risks of anesthesia^[11]. The surgeon's skill was enhanced due to specialization and made the major abdominal operation become safety. Special team including surgeons, physicians, anesthetists and nurses for unstable elderly patients can decrease the morbidity and mortality^[12]. The environment of operation room^[13] was improved, the operative instruments were updated, which could attenuate the stress of an operation. Positive and effective treatment in surgical intensive care unit (SICU) helps elderly patients live through the crisis after operation.

Older patients need more perioperative care. First, older patients have more comorbidities require to manage than younger patients. Blair *et al.*^[14] reported older cases had more comorbidities than the younger (49% vs 25%) in a series of 179 patients undergone gastrectomy and pancreatectomy. In our study, nearly half of older patients had one or more comorbidities, which were significantly higher than that in younger patients. Second, the nutrition of older patients is poorer than younger patients. Our study showed the level of serum albumin and hemoglobin in older group was lower than younger group. More comorbidities and poorer nutrition mean the older patients need more waiting time for operation and more time for postoperative management, which lead more length of hospital stay in the older cases. Thus, the median hospital stay was longer significantly in older group longer than that in younger group in our study.

In this study, the level of serum albumin and hemoglobin were not the independent predictors for complications, suggesting that short-term nutritional support before operation could improve the nutritional status and reduce the risks of the surgery and anesthesia^[15]. Comorbidity was an independent factor for complication in our study because the comorbidity

could not be controlled in short-term. Comorbidity must be treated during perioperative period, which is a positive measure to reduce perioperative morbidity and mortality.

The patients with complex major operation should receive more perioperative care. Pancreatoduodenectomy and hepatectomy with resection of more than 2 segments were independent predictors of complication in our study. The result was supported by more recent reports. Jarnagin *et al.*^[16] studied in 1803 consecutive cases with hepatic resection over the past decade, and reported that the number of hepatic segments resected and operative blood loss were the independent predictors of both perioperative morbidity and mortality. So, the authors figured out that the major operation has more complications than minor operation^[16].

In conclusion, the present data suggest that advanced age does not predict high morbidity and mortality after major abdominal operations. Surgeons should not advise against an operation just because the patient is old.

REFERENCES

- 1 **Etzioni DA**, Liu JH, Maggard MA, Ko CY. The aging population and its impact on the surgery workforce. *Ann Surg* 2003; **238**: 170-177
- 2 **Kmietowicz Z**. Call for greater care of elderly people in surgery. *BMJ* 1999; **319**: 1324B
- 3 **Pavlidis TE**, Galatianos IN, Papaziogas BT, Lazaridis CN, Atmatzidis KS, Makris JG, Papaziogas TB. Complete dehiscence of the abdominal wound and incriminating factors. *Eur J Surg* 2001; **167**: 351-354
- 4 **Saghir JH**, McKenzie FD, Leckie DM, McCourtney JS, Finlay IG, McKee RF, Anderson JH. Factors that predict complications after construction of a stoma: a retrospective study. *Eur J Surg* 2001; **167**: 531-534
- 5 **Yasuda K**, Shiraishi N, Adachi Y, Inomata M, Sato K, Kitano S. Risk factors for complications following resection of large gastric cancer. *Br J Surg* 2001; **88**: 873-877
- 6 **Hodul P**, Tansey J, Golts E, Oh D, Pickleman J, Aranha GV. Age is not a contraindication to pancreaticoduodenectomy. *Am Surg* 2001; **67**: 270-275
- 7 **Clavien PA**, Sanabria JR, Strasberg SM. Proposed classification of complications of surgery with examples of utility in cholecystectomy. *Surgery* 1992; **111**: 518-526
- 8 **Melendez J**, Ferri E, Zwillman M, Fischer M, DeMatteo R, Leung D, Jarnagin W, Fong Y, Blumgart LH. Extended hepatic resection: a 6-year retrospective study of risk factors for perioperative mortality. *J Am Coll Surg* 2001; **192**: 47-53
- 9 **Beliveau MM**, Multach M. Perioperative care for the elderly patient. *Med Clin North Am* 2003; **87**: 273-289
- 10 **Kehlet H**, Wilmore DW. Multimodal strategies to improve surgical outcome. *Am J Surg* 2002; **183**: 630-641
- 11 **Muravchick S**. Preoperative assessment of the elderly patient. *Anesthesiol Clin North America* 2000; **18**: 71-89
- 12 **Demetriades D**, Sava J, Alo K, Newton E, Velmahos GC, Murray JA, Belzberg H, Asensio JA, Berne TV. Old age as a criterion for trauma team activation. *J Trauma* 2001; **51**: 754-756
- 13 **Jin F**, Chung F. Minimizing perioperative adverse events in the elderly. *Br J Anaesth* 2001; **87**: 608-624
- 14 **Blair SL**, Schwarz RE. Advanced age does not contribute to increased risks or poor outcome after major abdominal operations. *Am Surg* 2001; **67**: 1123-1127
- 15 **Cohendy R**, Gros T, Arnaud-Battandier F, Tran G, Plaze JM, Eledjam J. Preoperative nutritional evaluation of elderly patients: the Mini Nutritional Assessment as a practical tool. *Clin Nutr* 1999; **18**: 345-348
- 16 **Jarnagin WR**, Gonen M, Fong Y, DeMatteo RP, Ben-Porat L, Little S, Corvera C, Weber S, Blumgart LH. Improvement in perioperative outcome after hepatic resection: analysis of 1 803 consecutive cases over the past decade. *Ann Surg* 2002; **236**: 397-406

Gastrointestinal decompression after excision and anastomosis of lower digestive tract

Wen-Zhang Lei, Gao-Ping Zhao, Zhong Cheng, Ka Li, Zong-Guang Zhou

Wen-Zhang Lei, Gao-Ping Zhao, Zhong Cheng, Ka Li, Zong-Guang Zhou, Department of Gastrointestinal Surgery, West China Hospital, Sichuan University, Chengdu 610041, Sichuan Province, China

Correspondence to: Dr. Gao-Ping Zhao, Department of Gastrointestinal Surgery, West China Hospital, Sichuan University, Chengdu 610041, Sichuan Province, China. zhgaoping@yahoo.com.cn

Telephone: +86-28-68126226 **Fax:** +86-28-68123364

Received: 2004-02-02 **Accepted:** 2004-02-24

Abstract

AIM: To discuss the clinical significance of postoperative gastrointestinal decompression in operation on lower digestive tract.

METHODS: Three hundred and sixty-eight patients with excision and anastomosis of lower digestive tract were divided into two groups, i.e. the group with postoperative gastrointestinal decompression and the group without postoperative gastrointestinal decompression. Clinical therapeutic outcome and incidence of complication were compared between two groups. Furthermore, an investigation on application of gastrointestinal decompression was carried out among 200 general surgeons.

RESULTS: The volume of gastric juice in decompression group was about 200 mL every day after operation. Both groups had a lower girth before operation than every day after operation. No difference in length of the first passage of gas by anus and defecation after operation was found between two groups. The overall incidence of complications was obviously higher in decompression group than in non-decompression group (28% vs 8.2%, $P < 0.001$). The incidence of pharyngolaryngitis was up to 23.1%. There was also no difference between two groups regarding the length of hospitalization after operation. The majority (97.5%) of general surgeons held that gastrointestinal decompression should be placed till passage of gas by anus, and only 2.5% of surgeons thought that gastrointestinal decompression should be placed for 2-3 d before passage of gas by anus. Nobody (0%) deemed it unnecessary for placing gastrointestinal decompression after operation.

CONCLUSION: Application of gastrointestinal decompression after excision and anastomosis of lower digestive tract cannot effectively reduce gastrointestinal tract pressure and has no obvious effect on preventing postoperative complications. On the contrary, it may increase the incidence of pharyngolaryngitis and other complications. Therefore, it is more beneficial to the recovery of patients without undergoing gastrointestinal decompression.

Lei WZ, Zhao GP, Cheng Z, Li K, Zhou ZG. Gastrointestinal decompression after excision and anastomosis of lower digestive tract. *World J Gastroenterol* 2004; 10(13): 1998-2001
<http://www.wjgnet.com/1007-9327/10/1998.asp>

INTRODUCTION

At present, gastrointestinal decompression after excision and anastomosis of lower digestive tract is still widely used in clinic. Although some researches regarding the application of gastrointestinal decompression after digestive tract operation were made, few researches related to the value of decompression after lower digestive tract have been carried out. Therefore, we performed a prospective randomized controlled study on 368 patients undergoing excision and anastomosis of lower digestive tract in West China Hospital, Sichuan University between July 2002 and October 2003. We also made an investigation in the application of gastrointestinal decompression among 200 general surgeons in China.

MATERIALS AND METHODS

Cases selection

Three hundred and sixty-eight cases underwent excision and anastomosis of lower digestive tract were divided into two groups. One group underwent gastrointestinal decompression after operation and the other group did not.

Clinical data

Of one hundred and eighty-six cases underwent postoperative gastrointestinal decompression, 109 were males and 77 were females, aged between 21-82 years with an average age of 56.8 years. Of the 182 cases in the group who did not undergo postoperative gastrointestinal decompression, 112 were males and 70 were females, aged between 23-84 years with a mean age of 57.2 years. In decompression group, there were 4 cases of small intestinal tumor, 6 cases of benign colon disease, 31 cases of carcinoma of colon and 145 cases of rectal cancer. In non-decompression group, there were 5 cases of small intestinal tumor, 8 cases of benign colon disease, 28 cases of carcinoma of colon and 141 cases of rectal cancer. Partial excision of small intestine was performed for small intestinal tumors. Patients with benign colon disease and colon carcinoma underwent partial or subtotal excision of colon, and those with rectal cancer received anterior resection.

Methods

A nasogastric tube was placed in all patients during operation. The tube was removed in the group with gastrointestinal decompression after passage of gas by intestines with continuous vacuum aspiration. The nasogastric tubes in the group without gastrointestinal decompression were immediately removed after operation. Then, the following procedures were carried out. The gastric juice of patients was collected and measured after operation, the postoperative girth was measured by circling umbilical region in the morning as a comparison value with preoperative one, the time for passage of gas by intestines and defecation, the length of hospitalization after operation and the incidence of complications and prognosis were observed and recorded. Those suffering from anastomotic leaks were subjected to treatments such as anti-infective treatment, nutrition support or colostomy. Correspondingly, acute dilatation of stomach was subjected

to gastrointestinal decompression and vacuum aspiration, pulmonary infection to anti-infective therapy, wound infection to local drainage, and cough and throat pain to oral nursing and fog inhalation therapy.

Clinical investigation

An investigation was carried out among 200 general surgeons from 18 hospitals by way of communication. The contents of investigation included the length of placing gastrointestinal decompression after excision and anastomosis of lower digestive tract by these surgeons and their cognition of the significance of placing gastrointestinal decompression.

Statistical analysis

SPSS 10.0 software was used to conduct statistical analysis.

RESULTS

General data

There were no significant differences between two groups in terms of sex ($P>0.05$), age ($P>0.05$). No statistical difference was found between two groups in case distributions ($P=0.892$).

Table 1 Girth of 368 cases before and after operation on lower digestive tract (mean \pm SD)

Girth	Decompression group (n=186)	Non-decompression group (n=182)	P value
Before operation (cm)	76.3 \pm 17.6 ^b	75.1 \pm 16.2 ^d	0.051
After operation (cm)			
Day 1	82.4 \pm 21.5	81.5 \pm 20.7	0.562
Day 2	82.8 \pm 19.8	83.6 \pm 21.8	0.367
Day 3	82.2 \pm 21.5	84.7 \pm 21.2	0.551

^b $P<0.001$, ^d $P<0.001$ vs the three initial days after operation.

Clinical observation

None of the 368 cases died due to operation. The volume of gastric juice in the group with gastrointestinal decompression was 10-520 mL every day after operation (146.5 \pm 87.4 mL on the 1st day, 204.9 \pm 92.5 mL on the 2nd day, and 205.3 \pm 107.1 mL on the 3rd day, respectively). The volume of gastric juice on the 1st day was lower than that on the 2nd and 3rd days ($P<0.001$). However, there was no statistical difference between the volumes on the 2nd and 3rd days ($P>0.05$). There was no significant difference between two groups in terms of girth before and after operation ($P>0.05$). However, the preoperative girth of two groups was less in comparison with the postoperative one ($P<0.001$) (Table 1). The time for passage of gas by anus was 3.2 \pm 1.1 d in the group with gastrointestinal decompression and 3.2 \pm 1.3 d in the group without gastrointestinal decompression ($P<0.05$). The time for the first defecation of the group with gastrointestinal decompression and the group without gastrointestinal decompression was 4.5 \pm 1.4 and 4.6 \pm 1.6 d, respectively ($P>0.05$). The time of hospitalization after operation was 9.0 \pm 4.5 d for the group with gastrointestinal decompression and 8.6 \pm 4.0 d for the group without gastrointestinal decompression ($P>0.05$). All patients

were completely recovered from such illnesses and discharged from hospital.

Incidence of complications

Table 2 shows the incidence of complications after operation. Symptoms as fever and leakage of intestinal contents were diagnosed as anastomotic leakage. There were 5 cases suffering from the lesion in the two groups. All the leakages occurred during excision and anastomosis of lower or ultra-lower rectal tumor and healed after clinical therapy. Those who suffered from abdominal distension, emesis and succussion splash of stomach were diagnosed with acute dilatation of stomach and then subjected to gastrointestinal decompression. Four cases of pulmonary infection were found in two groups by chest X-ray and cured through anti-inflammatory therapy. Any symptom with throat upset or pain was diagnosed as pharyngolaryngitis, 23.1% of patients suffered from pharyngolaryngitis in decompression group and only 4.4% in non-decompression group. Through statistical analysis, the incidence rate of pharyngolaryngitis in decompression group was obviously higher than that in non-decompression group ($P<0.001$). No statistical difference was found in terms of other complications ($P>0.05$). Compared with non-decompression group, the total incidence of complications in decompression group was evidently higher ($P<0.001$).

Investigation results

We conducted an investigation among 200 general surgeons in China, 97.5% (195/200) of surgeons routinely placed nasogastric tube for the passage of gas by anus after excision and anastomosis of lower digestive tract, while 2.5% (5/200) of surgeons discarded gastrointestinal decompression 2-3 d after operation before the passage of gas by anus. All patients of these surgeons underwent gastrointestinal decompression after operation and this kind of management was assumed as a matter of course by the surgeons investigated. Ninety-five percent of the surgeons (190/200) held that gastrointestinal decompression should be maintained till the passage of gas by anus, 4.5% (9/200) of surgeons thought it unnecessary for placing gastrointestinal decompression till passage of gas by anus.

DISCUSSION

Present status of application of gastrointestinal decompression after excision and anastomosis of lower digestive tract

At present, it is still generally believed that gastrointestinal decompression should be performed after operation on abdominal region. The monographs on operation pointed out that gastrointestinal decompression should be conducted for the passage of gas by anus^[1]. A randomized study on general surgeons showed that 72% of them performed routine gastrointestinal decompression after excision of small intestine and 49% of them performed routine gastrointestinal decompression after excision and anastomosis of large intestine^[2]. The present study revealed that 97.5% of surgeons thought gastrointestinal decompression should be performed for the passage of gas by anus after excision and anastomosis of lower digestive tract, suggesting that it has become a routine

Table 2 Complications of 368 cases after operation on lower digestive tract

Patient group	Anastomotic leakage (n, %)	Acute dilation of stomach (n, %)	Pulmonary infection (n, %)	Pharyngolaryngitis (n, %)	Wound infection (n, %)
Decompression group (n=186)	3(1.6)	1(0.5)	3(1.6)	43(23.1) ^b	2(1.1)
Non-decompression group (n=182)	2(1.1)	2(1.1)	1(0.5)	8(4.4)	1(0.5)

^b $P<0.001$ vs non-decompression group.

procedure after excision and anastomosis of lower digestive tract.

Effects of gastrointestinal decompression

Paralysis of intestine is a natural and transient physiological process after operation on abdominal region. Some researches^[3,4] regarding the relationship between such a phenomenon and gastrointestinal decompression have been made. However, there were few reports focusing on the theoretical basis of this field. It is well-known that the volume of secreted digestive juices was about 5 300-9 500 mL, and the gas secreted by deglutition and intestines was about 30-300 mL^[5]. Nevertheless, the volume extracted by gastrointestinal decompression every day was less than 10% of digestive juices. This study showed the volume extracted by gastrointestinal decompression every day was 200 mL. It is thus evident that gastrointestinal decompression could not effectively extract digestive juices. After operations on abdominal region, gastrointestinal motor function was reduced and the function of intestinal absorption was not greatly influenced. This research showed that the postoperative girth was increased as compared with preoperative girth, demonstrating that there exists paralysis of intestines after operation and paralysis of intestines is a normal and brief process. Clevers *et al.*^[3] reported that paralysis of intestine could not be alleviated by gastrointestinal decompression. The present study demonstrated that there were no significant differences between two groups in terms of passage of gas by anus and the length of defecation. The findings made it clear that gastrointestinal decompression could not get rid of paralysis of intestine or shorten the length of paralysis of intestine. There was no statistical difference between two groups in the increase of girth after operation, demonstrating that with the aid of gastrointestinal decompression, the liquid and gas were difficult to be extracted from intestines and there was no obvious effect upon postoperative abdominal distension. The above research results showed that gastrointestinal tract pressure could not be effectively reduced by means of gastrointestinal decompression.

Influence of gastrointestinal decompression upon postoperative complication

It is undoubtedly that the risk of incidence of anastomotic leakage would increase with the increased tract pressure after anastomosis. One of the purposes of gastrointestinal decompression was to reduce the inner pressure of gastrointestinal tract and the incidence rate of anastomotic leakage. This study revealed that there was no significant difference between two groups in the development of anastomotic leakage, which might be correlated with the fact that gastrointestinal decompression could not effectively reduce stoma pressure of gastrointestinal tract, and especially that gastrointestinal decompression played a small role in reducing the pressure of stoma of lower digestive tract. In the two groups, 3 cases suffered from acute dilation of stomach and no statistical difference was found between two groups. Of the 3 cases of acute dilation of stomach, 1 was from the non-decompression group and cured by the gastrointestinal decompression for 28 d. Although there was an increased probability of acute dilation of stomach without gastrointestinal decompression, its incident rate was lower and easily treated when it happened. In the two groups, there were 4 cases of pulmonary infection. Although gastrointestinal decompression was not the immediate cause for pulmonary infection, it could lead to cough and expectoration, and indirectly induce pulmonary infection. Owing to a low incidence rate of pulmonary infection, further researches for more cases need to be conducted. According to the report by Huerta *et al.*^[6], the incidence rate of pulmonary infection in those with gastrointestinal decompression after operation on

abdominal region was 10 times higher than that in those without gastrointestinal decompression. In addition, this report deemed that it was improper to perform gastrointestinal decompression as a routine procedure and that gastrointestinal decompression could be only used for the treatment of paralysis and dilation of stomach. Pharyngolaryngitis could be immediately induced by long-term irritation and compression of throat by gastrointestinal decompression tubes. Nathan *et al.*^[2] reported that the incidence rate of throat pain was greatly increased in gastrointestinal decompression group. This study revealed that the incidence rate of pharyngolaryngitis in decompression group was up to 23.1%, 5 times as high as in non-decompression group, showing that pharyngolaryngitis was related to nasogastric tubes. This kind of pharyngolaryngitis could be easily dealt with through treatments as fog inhalation therapy and oral nursing after removal of the tube. Michowitz *et al.*^[7] revealed that the incidence rate of complications was obviously increased in the group with gastrointestinal decompression after operations on abdominal region, and that postoperative hyperpyrexia and atelectasis were markedly enhanced. Another randomized research report showed that 70% of severe upsets were caused by gastrointestinal decompression^[8]. This study demonstrated that gastrointestinal decompression could not effectively prevent severe postoperative complications such as anastomotic leakage and instead, resulted in an increased incidence rate of pharyngolaryngitis.

Influence of gastrointestinal decompression upon prognosis

According to some research reports^[9,10], there were no increase in incidence rate of complications and no obvious influence upon prognosis by fluid feeding from the 1st day after operation on gastrointestinal tract without gastrointestinal decompression. Researches showed that it was unnecessary for gastrointestinal decompression after operation on abdominal region, which could reduce the incidence rate of pneumonia and recover the tract functions as early as possible^[11-16]. The present study showed that there was no obvious difference between two groups in terms of passage of gas by anus and length of defecation time, implying that there was no adverse influence upon recovery of intestinal functions without gastrointestinal decompression. Despite of no significant difference in the time of postoperative hospitalization, the total incidence rate of complications in decompression group was obviously higher than that in non-decompression group, demonstrating that it was more beneficial to the recovery of patients without gastrointestinal decompression.

In conclusion, gastrointestinal decompression following excision and anastomosis of lower digestive tract cannot reduce the pressure of gastrointestinal tract and has no obvious effects upon preventing of postoperative complications. Contrary to expectations, it may increase the incidence rate of pharyngolaryngitis and other complications. Therefore, it is more beneficial to the patients' recovery without gastrointestinal decompression.

REFERENCES

- 1 **Li JS**, Wu MC, Huang ZQ. The Complete works of surgery-general surgery volume. 1sted. Beijing: *People's Military Surgeon Press* 1996: 344-548
- 2 **Nathan BN**, Pain JA. Nasogastric suction after elective abdominal surgery: a randomised study. *Ann R Coll Surg Engl* 1991; **73**: 291-294
- 3 **Clevers GJ**, Smout AJ. The natural course of postoperative ileus following abdominal surgery. *Neth J Surg* 1989; **41**: 97-99
- 4 **Ying FM**. Reports on 112 cases with decompression operation on biliary tract without nasogastric tube. *Linchuang Waiké Zazhi* 1999; **7**: 104

- 5 **Tang YS**, Zhang XZ, Han DC. Human medical parameters and concepts. 1sted. *Jinnan: Jinan Press* 1995: 80-115
- 6 **Huerta S**, Arteaga JR, Sawicki MP, Liu CD, Livingston EH. Assessment of routine elimination of postoperative nasogastric decompression after Roux-en-Y gastric bypass. *Surgery* 2002; **132**: 844-848
- 7 **Michowitz M**, Chen J, Waizbard E, Bawnik JB. Abdominal operations without nasogastric tube decompression of the gastrointestinal tract. *Am Surg* 1988; **54**: 672-675
- 8 **Koukouras D**, Mastronikolis NS, Tzoracoleftherakis E, Angelopoulou E, Kalfarentzos F, Androulakis J. The role of nasogastric tube after elective abdominal surgery. *Clin Ter* 2001; **152**: 241-244
- 9 **Hoffmann S**, Koller M, Plaul U, Stinner B, Gerdes B, Lorenz W, Rothmund M. Nasogastric tube versus gastrostomy tube for gastric decompression in abdominal surgery: a prospective, randomized trial comparing patients' tube-related inconvenience. *Langenbecks Arch Surg* 2001; **386**: 402-409
- 10 **Gouzi JL**, Moran B. Nasogastric tubes after elective abdominal surgery is not justified. *J Chir* 1998; **135**: 273-274
- 11 **Colvin DB**, Lee W, Eisenstat TE, Rubin RJ, Salvati EP. The role of nasointestinal intubation in elective colonic surgery. *Dis Colon Rectum* 1986; **29**: 295-299
- 12 **Wolff BG**, Pemberton JH, van Heerden JA, Beart RW Jr, Nivatvongs S, Devine RM, Dozois RR, Ilstrup DM. Elective colon and rectal surgery without nasogastric decompression. A prospective, randomized trial. *Ann Surg* 1989; **209**: 670-673
- 13 **Racette DL**, Chang FC, Trekell ME, Farha GJ. Is nasogastric intubation necessary in colon operations? *Am J Surg* 1987; **154**: 640-642
- 14 **Dinsmore JE**, Maxson RT, Johnson DD, Jackson RJ, Wagner CW, Smith SD. Is nasogastric tube decompression necessary after major abdominal surgery in children? *J Pediatr Surg* 1997; **32**: 982-984
- 15 **Savassi-Rocha PR**, Conceicao SA, Ferreira JT, Diniz MT, Campos IC, Fernandes VA, Garavini D, Castro LP. Evaluation of the routine use of the nasogastric tube in digestive operation by a prospective controlled study. *Surg Gynecol Obstet* 1992; **174**: 317-320
- 16 **MacRae HM**, Fischer JD, Yakimets WW. Routine omission of nasogastric intubation after gastrointestinal surgery. *Can J Surg* 1992; **35**: 625-628

Edited by Wang XL and Chen WW Proofread by Xu FM

L-arginine-induced experimental pancreatitis

Péter Hegyi, Zoltán Rakonczay Jr, Réka Sári, Csaba Góg, János Lonovics, Tamás Takács, László Czakó

Péter Hegyi, Zoltán Rakonczay Jr, Réka Sári, Csaba Góg, János Lonovics, Tamás Takács, László Czakó, First Department of Medicine, Faculty of Medicine, University of Szeged, Szeged, H6722, Hungary
Péter Hegyi, Zoltán Rakonczay Jr, School of Cell and Molecular Biosciences, Medical School, University of Newcastle, Newcastle upon Tyne, NE2 4HH, United Kingdom

Supported by The Wellcome Trust, Grant No. 022618, and by the Hungarian Scientific Research Fund, No. D42188, T43066 and T042589

Correspondence to: Péter Hegyi, M.D., Ph.D., University of Szeged, Faculty of Medicine, First Department of Medicine, PO Box 469, H-6701, Szeged, Hungary. hep@in1st.szote.u-szeged.hu

Telephone: +36-62-545-200 **Fax:** +36-62-545-185

Received: 2003-11-12 **Accepted:** 2003-12-23

Abstract

Despite medical treatment, the lethality of severe acute pancreatitis is still high (20-30%). Therefore, it is very important to find good animal models to characterise the events of this severe disease. In 1984, Mizunuma *et al.* developed a new type of experimental necrotizing pancreatitis by intraperitoneal administration of a high dose of L-arginine in rats. This non-invasive model is highly reproducible and produces selective, dose-dependent acinar cell necrosis. Not only is this a good model to study the pathomechanisms of acute necrotizing pancreatitis, but it is also excellent to observe and influence the time course changes of the disease. By writing this review we illuminate some new aspects of cell physiology and pathology of acute necrotizing pancreatitis. Unfortunately, the reviews about acute experimental pancreatitis usually did not discuss this model. Therefore, the aim of this manuscript was to summarise the observations and address some challenges for the future in L-arginine-induced pancreatitis.

Hegyi P, Rakonczay Jr Z, Sári R, Góg C, Lonovics J, Takács T, Czakó L. L-arginine-induced experimental pancreatitis. *World J Gastroenterol* 2004; 10(14): 2003-2009
<http://www.wjgnet.com/1007-9327/10/2003.asp>

EFFECT OF EXCESSIVE DOSES OF L-ARGININE ON DIFFERENT TISSUES

Mizunuma *et al.* were the first who studied the effect of an excessive dose of L-arginine (Arg) on different tissues in rats^[1]. After a single intraperitoneal (ip.) injection of 500 mg/100 g body mass (bm) Arg, the liver cells showed slight vacuolar degeneration. The kidney contained eosinophilic compositions in some proximal convoluted tubules, but showed no degenerative changes. Adipose tissues around the pancreas showed fat necrosis. There were no changes in the weight of different organs (liver, kidney, spleen, thymus), except for the pancreas. Due to the effect of pancreatitis the weight of the pancreas nearly doubled by the end of the first 24 h. No evidence of pathophysiological lesions was observed in the lung, heart, intestine, testis, spleen and thymus^[1]. After the first observation Kishino *et al.* examined the pancreas by electron microscopy^[2]. They found that degeneration started with disorganization of the rough endoplasmic reticulum. The main changes in acinar cells after 24 h were partial distension of the endoplasmic

reticulum. At this time large sequestered areas in the cytoplasm contained disarranged rough endoplasmic reticulum and degraded zymogen granules. Forty-eight hours after Arg-injection, dissociation and necrosis of acinar cells were noted. Subsequently, the necrotic cells were replaced by interstitial tissue composed of leucocytes and fibroblasts. The early morphological changes of the acinar cells may be related to metabolic alterations associated with the endoplasmic reticulum. The final conclusion was that an excessive dose of arginine was toxic to the rat pancreas when injected intraperitoneally^[2]. Tani *et al.* continued this work by observing the effect of Arg on the pancreas^[3]. They clearly proved that excessive doses of Arg could cause a severe acute necrotizing pancreatitis. On the other hand, Delaney and Weaver showed that long term administration of Arg caused pancreatic atrophy with insufficiency, therefore high doses of Arg were also suitable for the induction of chronic pancreatitis^[4,5].

INDUCTION OF PANCREATITIS

Mizunuma *et al.* induced acute necrotizing pancreatitis by a high dose of Arg ip. (500 mg/100 g bm), which evoked selective pancreatic acinar cell damages without any morphological change in the Langerhans islets^[1]. After this first observation, researchers investigating Arg-induced pancreatitis usually modified the method of pancreatitis induction. Tani *et al.* tried to use higher doses of Arg, but found that Arg at the dose of more than 500 mg/100 g bm killed most of the treated rats within a few hours^[3]. When a single dose of 500 mg/100 g bm of Arg was injected, 70-80% of the pancreatic acinar cells were necrotized within 3 d^[3]. When rats were given additional 3 injections of 250 mg/100 g bm over 10 d, there was up to 90% acinar destruction^[4]. The longest treatment of Arg was performed by Weaver *et al.* Daily administration of 350 mg/100 g bm of Arg for 30 d resulted in severe pancreatic necrosis by wk 4, only isolated single acinar cells remained within a fibrous connective tissue matrix^[5]. Most of the authors, who studied the pathomechanisms of this pancreatitis used 250 mg/100 g bm of Arg twice at an interval of one hour^[6-8]. On the other hand, when the regenerative processes were studied after pancreatitis, a smaller dose of Arg (200 mg/100 g bm of Arg ip. twice at an interval of 1 h) was used^[9,10].

All in all, the dose- and time-dependency of the effects of Arg gives an excellent opportunity to study the different phases of pancreatitis. A higher dose of Arg is suggested to study the pathomechanism of acute pancreatitis, while a smaller dose of Arg seems more suitable to characterize the regenerative processes. Long-term administration of Arg is suggested to study chronic pancreatitis (Table 1).

PATHOMECHANISM OF L-ARGININE INDUCED PANCREATITIS

The mechanism by which Arg causes pancreatitis is not fully known. Accumulating evidence suggests that oxygen free radicals^[7,8,11-13], nitric oxide (NO)^[14], inflammatory mediators^[6,12,15,16] all have a key role in the development of the disease.

Changes in cytokine levels

We found that both serum tumor necrosis factor- α (TNF- α) and interleukin (IL)-6 level were already significantly increased

Table 1 Induction of pancreatitis: differences in methods

Dose of L-Arginine	Reference
Single dose	
500 mg/100 g bm ip.	Mizinuma <i>et al.</i> 1984, Kishino <i>et al.</i> 1984, Tani <i>et al.</i> 1990, Shields <i>et al.</i> 2000, Kihara <i>et al.</i> 2001, Tachibana <i>et al.</i> 1997, Tashiro <i>et al.</i> 2001
450 mg/100 g bm ip.	Tashiro <i>et al.</i> 2001
400 mg/100 g bm ip.	Tashiro <i>et al.</i> 2001, Rakonczay <i>et al.</i> 2002
300 mg/100 g bm ip.	Tashiro <i>et al.</i> 2001, Rakonczay <i>et al.</i> 2002
250 mg/100 g bm ip.	Pozsar <i>et al.</i> 1997
200 mg/100 g bm ip.	Tashiro <i>et al.</i> 2001
Double dose	
2×250 mg/100 g bm ip.	Takacs <i>et al.</i> 1996, Varga I. <i>et al.</i> 1997, Toma <i>et al.</i> 2000, Czako <i>et al.</i> 2000, Czako <i>et al.</i> 2000, Czako <i>et al.</i> 2000, Takacs <i>et al.</i> 2002, Toma <i>et al.</i> 2002
2×230 mg/100 g bm ip.	Takacs <i>et al.</i> 2002
2×200 mg/100 g bm ip.	Hegyi <i>et al.</i> 1997, Hegyi <i>et al.</i> 1999, Hegyi <i>et al.</i> 2000, Takacs <i>et al.</i> 2001
Multiple dose	
350 mg/100 g bm ip. daily from 1 to 4 wk	Weaver <i>et al.</i> 1994
a single 500 mg/100 g bm ip.	
and triple 250 mg/100 gbm ip.	Delaney <i>et al.</i> 1993
(d 4, 7, 10)	

Table 2 Changes of inflammatory mediator levels in Arg-induced acute pancreatitis

Mediator	Dose of Arg/100 g bm	Effect	Reference
MDA	2x250 mg	↑	Czakó <i>et al.</i> , 1998
NSG, MDA	300 mg	↑	Rakonczay <i>et al.</i> , 2003
Protein carbonyl	300 mg	↑	Rakonczay <i>et al.</i> , 2003
Mn-, Cu, Zn-SOD	2x250 mg	↓	Czakó <i>et al.</i> , 1998
Catalase	2x250 mg	↓	Czakó <i>et al.</i> , 1998
glutathione peroxidase	2x250 mg	↓ ↑	Czakó <i>et al.</i> , 1998
Serum TNF-α, IL-6	2x250 mg	↑	Czakó <i>et al.</i> , 2000
Serum TNF-α, IL-1, IL-6	2x230 mg	↑	Rakonczay <i>et al.</i> , 2002
Pancreatic IL-1β	300 and 400 mg	↑	Rakonczay <i>et al.</i> , 2003
Pancreatic TNF-α	300 and 400 mg	↑	Rakonczay <i>et al.</i> , 2003
Pancreatic cNOS	2x250 mg	↓ ↑	Takács <i>et al.</i> , 2002
Pancreatic iNOS	2x250 mg	↑	Takács <i>et al.</i> , 2002
CCK	2x250 mg	↑	Czakó <i>et al.</i> , 2000

↓ : decreased activity, ↑ : increased activity, Arg: L-arginine, MDA: malondialdehyde, NSG: nonprotein sulfhydryl group, SOD: superoxide dismutase, TNF: tumor necrosis factor, IL: interleukin, CCK: cholecystokinin-octapeptide.

at 12 h after administration of 2×250 mg/100 g bm Arg, and remained elevated at 48 h in Arg-treated animals *vs* controls (Table 2)^[6,12]. Increased serum TNF-α, IL-6 and IL-1 levels were demonstrated at 24 h after the induction of pancreatitis with 2×230 mg/100 g bm Arg^[15] (Table 2).

Later on, we showed that the pancreatic IL-1β level significantly decreased at 1 h after ip. administration of 300 or 400 g/100 g bm Arg^[15]. The IL-1β levels increased significantly at 12 h after Arg injection, peaked at 24 h and decreased thereafter (Table 2). The pancreatic TNF-α content increased significantly at 6 h, peaked at 18 h, and then remained elevated at a relatively constant level during pancreatitis (Table 2). Pretreatment with antioxidant pyrrolidine dithiocarbamate (PDTC) or methylprednisolone (MP) significantly decreased the pancreatic levels of these proinflammatory cytokines, ameliorated pancreatic oedema and exerted a beneficial effect on pancreatic morphological damage^[15]. It can be proposed that these cytokines are involved in the pathogenesis of Arg-induced acute pancreatitis.

Oxidative stress changes

In 1998, we demonstrated that the pancreatic malondialdehyde (MDA) level was significantly elevated at 24 h, and peaked at

48 h after administration of 2×250 mg/100 g bw Arg^[8]. Among the endogenous scavengers Mn-superoxide dismutase (SOD) and catalase activities decreased significantly throughout the entire study *vs* the control. Cu, Zn-SOD activity decreased only at 12 h, while the glutathione peroxidase activity decreased at 6 and 12 h after Arg injection (Table 2). Pretreatment with the xanthine oxidase inhibitor allopurinol (100 and 200 mg/kg) prevented the generation of reactive oxygen metabolites and ameliorated the severity of Arg-induced pancreatitis.

We also showed that 300 mg/100 g bm Arg significantly increased the pancreatic non-protein sulfhydryl group content, malondialdehyde and the protein carbonyl levels *vs* the control (Table 2)^[15]. Pretreatment with PDTC or MP significantly ameliorated these changes and reduced the severity of the disease.

These results suggest that generation of free radicals is an early and perhaps pivotal mechanism in the pathogenesis of Arg-induced acute pancreatitis.

Role of nitric oxide

NO, a highly reactive free radical, is generated from Arg by an enzymatic pathway (NO synthase: NOS) originally demonstrated in vascular endothelial cells^[17]. Under physiologic conditions,

constitutive NO synthase (cNOS) results in a low level of NO, while in different inflammatory processes inducible NO synthase (iNOS) produces larger quantities of NO in various cell types. The activity of NOS is specifically inhibited by structural analogues of L-arginine such as N^G-nitro-L-arginine methyl ester (L-NAME)^[17].

It was demonstrated that the cNOS activity was depleted at 6 h after onset of Arg-induced pancreatitis, it then gradually increased to a level significantly higher than that in controls and decreased thereafter at 48 h^[13]. The iNOS activity was significantly increased at 24 and 48 h *vs* control (Table 2). Treatment with L-NAME significantly reduced the amylase activity, pancreatic oedema, pancreatic vascular permeability and cNOS activity in the pancreas at 24 h after the onset of pancreatitis as compared with those in the control. L-NAME treatment reduced the iNOS activity, but not significantly, and did not exert any beneficial effect on the histological score^[14]. It can be concluded that both cNOS and iNOS play an important role in the development of Arg-induced acute pancreatitis in rats.

Endogenous cholecystokinin

Endogenous cholecystokinin (CCK) and CCK-A receptors have been suspected to play a role in the development of acute pancreatitis in rats^[18,19]. No significant differences in plasma CCK bioactivity were found between the pancreatic animals and the control group during the course of Arg-induced pancreatitis (Table 2). KSG-054, a CCK receptor antagonist did not exert any beneficial effect on the laboratory and morphologic changes observed in Arg-induced pancreatitis^[12]. These results suggest that endogenous CCK is not involved in the pathogenesis of Arg-induced pancreatitis.

Effect of nuclear factor-kappa B activation

Recent studies have established the critical role played by inflammatory mediators in acute pancreatitis^[14,20]. One of the most important transcription factors that control proinflammatory gene expression is nuclear factor kappa B (NF- κ B)^[21]. Therefore, we set out to investigate NF- κ B activation and proinflammatory cytokine synthesis in the pancreas during Arg-induced acute pancreatitis in rats^[15]. The dose-response (300 or 400 mg/100 g bm) and time-effect (0.5-96 h) curves related to the action of Arg on the pancreatic NF- κ B activation and IL-1 β , TNF- α , heat shock protein (HSP) 60 and HSP72 synthesis were evaluated. Also we wanted to establish whether PDTC or MP pretreatment could block the activation of pancreatic NF- κ B and their effects on the severity of Arg-induced acute pancreatitis. Our results showed that pancreatic NF- κ B and proinflammatory cytokine expressions were activated dose-dependently during Arg-induced acute pancreatitis in rats, although at a later stage as compared with other models. We have established that PDTC and MP pretreatment specifically and dose-dependently can block this NF- κ B activation in the pancreas. Furthermore, the inhibition of NF- κ B activation and proinflammatory cytokine synthesis has been found to be clearly associated with a protective effect against pancreatic damage^[15].

Apoptosis and gene expression of pancreatitis-associated protein

Pancreatitis-associated protein (PAP) is an acute phase secretory protein known to be overexpressed in acute pancreatitis^[22]. Motoo *et al.* examined the effects of arginine (1.25, 2.5, 5 or 10 mg/mL) on cellular morphology, PAP expression and apoptosis in rat pancreatic acinar AR4-2J cells^[23]. This *in vitro* experimental design allowed the study of acinar cells without the confounding effects of other cell types involved in acute pancreatitis (e.g. inflammatory cells). The growth of AR4-2J

cells was inhibited by Arg in a dose-dependent manner. This inhibition was due to Arg-induced apoptosis of cells which was shown by fluorescence staining, and DNA fragmentation assay. The DNA fragmentation was most prominent at 24 h when the PAP mRNA level was low, whereas it was not seen when the level was high. The expression of PAP mRNA was detected at 2 h and peaked at 6 h, it was highest at a dose of 2.5 mg/mL Arg. Motoo *et al.* speculated that PAP might inhibit the induction of apoptosis^[23].

Role of transforming growth factor beta 1

Mild acute pancreatitis is often followed by full recovery of pancreatic tissue structure and function once the primary cause is eliminated^[24]. Transforming growth factor beta (TGF- β) and the extracellular matrix are believed to play an important part in this process^[20]. TGF- β promotes regeneration in wounded tissues by attracting monocytes and leukocytes and inducing angiogenesis and fibroblast recruitment. Kihara *et al.* induced acute necrotizing pancreatitis by intraperitoneal injection of 500 mg/100 g bm Arg, and examined the expression of TGF- β 1, extracellular matrix proteins and metalloproteinases (degrading a variety of extracellular matrix components). TGF- β , procollagen types I, III, IV, and fibronectin mRNA expression reached a peak value on d 2.5-3 and gradually decreased thereafter to reach control levels on d 7. Matrix metalloproteinase-2 mRNA levels peaked on d 5, whereas the immunoreactivity was maximal on d 7. TGF- β immunoreactivity was detected in disrupted acinar cells on d 3 and 5. Immunoreactivity for fibronectin was detected around disrupted acinar cells and interstitial spaces on d 3 and maximally on d 5. The authors believe that the results suggest an important role of TGF- β in extracellular matrix production during the early phase of acute pancreatitis^[20].

Effect of endotoxaemia in Arg-induced pancreatitis

Systemic endotoxaemia is a common feature of severe acute pancreatitis^[25]. The effect of *E. coli* endotoxin was investigated by Pozsár *et al.* on the mortality rates and pancreatic histology of Arg-induced (250 mg/100 g bm) acute pancreatitis in rats^[26]. The mortality rates of rats treated with 5 and 10 mg/kg endotoxin were 10 % and 30%, respectively (no death was observed in the group with only Arg-induced pancreatitis). The extent of acinar cell necrosis, hemorrhage, oedema and leukocyte infiltration was significantly greater in the endotoxin-treated groups *vs* the control groups. The authors speculated that systemic endotoxaemia might exert its effect by stimulating proinflammatory cytokine synthesis in granulocytes. The animal experiments were closely related to similar observations made in humans. It was found that high serum endotoxin levels showed a positive correlation with disease severity^[26].

Expression of nerve growth factor

Nerve growth factor (NGF) is a known mediator of the inflammatory response^[27]. It is believed to play an important role in the pathogenesis of pain. NGF expression was investigated after injection of 250 mg/100 g bm Arg twice intraperitoneally^[28]. No significant differences in NGF mRNA levels were found between the Arg-injected and control rats before 3 d. However, NGF mRNA levels significantly increased on days 3 (10-18 fold) and 5 (3.2-6 fold). NGF protein levels were 2-fold higher than control levels on day 3, but this did not reach statistical significance. On d 5 there was a 4-fold increase in NGF protein levels. The cellular sites of increased NGF production were investigated by immunohistochemistry. In control rats NGF-immunoreactivity was localized to the islets of Langerhans. In Arg-induced pancreatitis, NGF was detected in the cytoplasm of exocrine pancreatic tissues, including acinar

and ductal cells at 2 and 6 h. On d of NGF was predominantly found in ductal cells. It was possible that this change in staining pattern represented a release of stored NGF from the islets to the parenchyma^[28].

Effect of Arg-induced pancreatitis on the cytoskeleton

Disruption of the cytoskeleton seems to be a common prominent early feature in acute pancreatitis. Actin cytoskeleton was investigated using rhodamin phalloidin and epifluorescence microscopy combined with Normanski images^[29]. In control tissue actin was primarily localised as an intense fluorescent band beneath the luminal membrane. Arg administration (200-500 mg/100 g bm) resulted in changes of the actin cytoskeleton, including reduced actin staining underneath the luminal and basolateral membranes and increased cytoplasmic staining in pancreatic acinar cells. Interestingly, the total actin content of cells was increased twofold at 24 h. The intermediate filaments were investigated by confocal microscopy. A single large dose arginine also induced the disruption of intermediate cytokeatin filaments, which were replaced by a few focal deposits or small aggregates. Sub-basolateral staining appeared with a lower intensity whereas cytoplasmic staining was not presenty^[29].

Role of heat shock proteins

Heat shock proteins (HSPs) are highly conserved cytoprotective proteins that are present in all species and have essential functions in protein folding, transport, translocation, assembly and degradation. HSP families have been categorized by their molecular mass. HSPs can be induced by a wide variety of conditions. Interestingly, cerulein pancreatitis has been reported to increase^[30-32] or decrease^[33-35] the synthesis of pancreatic HSP60 and HSP72. Arg-induced pancreatitis was accompanied with large increases in HSP27 and HSP70 levels, peaking at 24 h and localized to acinar cells^[36]. Moreover, HSP27 shifted to the phosphorylated forms during pancreatitis. There were smaller increases in HSP60 and HSP90, and no effect on GRP78. Interestingly, a lower dose of Arg induced less pancreatitis, but larger increases in HSP27 and HSP70 expression and phosphorylation of HSP27. The results of Tashiro *et al.* are in accordance with our findings^[36]. The smaller increases in the quantity of HSPs following 400 mg/100 g bm Arg were probably due to tissue necrosis, protein degradation and decreased gene activation. We believe that the increased levels of HSPs most probably act to limit the severity of the disease. In a recent study, Tashiro *et al.* have shown that hyperthermia and possibly HSPs confer significant protection against Arg-induced (400 mg/100 g bm) pancreatitis^[36]. More specifically, the degradation and disorganization of the actin cytoskeleton were prevented. These previous findings are in contrast with ours^[16]. We could only demonstrate decreases in the serum proinflammatory cytokine (TNF- α , IL-1, IL-6) levels after hot-water (and also cold-water) immersion pretreatment of rats with Arg-induced pancreatitis (2 \times 250 mg/100 g bm), but the biochemical and morphological parameters of the pancreas were not significantly different. The explanation of the discrepancies between the results of the two studies may lie in the different types of pretreatment and the differences in the dose of Arg and the strains of rats used.

Role of vacuole membrane protein 1

In vitro expression of vacuole membrane protein 1 (VMP1) promoted formation of cytoplasmic vacuoles which was followed by cell death^[37]. In order to test if VMP1 expression was related to the cytoplasmic vacuolization of acinar cells during acute pancreatitis, Vaccaro *et al.* studied the *in vivo* expression of the VMP1 gene during Arg-induced (500 mg/100 g

acute pancreatitis^[38]. Northern blot analysis showed that the maximal induction of VMP1 after 24 h remained high after 48 h of arginine administration. Significant increases in the number of apoptotic cells were found during those periods. Twenty-four and 48 h after arginine administration, light micrographs from thin plastic toluidine blue sections revealed numerous vacuoles in the cytoplasm of acinar cells. *In situ* hybridization studies showed a high expression of VMP1 in acinar cells with cytoplasmic vacuolization. VMP1 mRNA highly and significantly correlated with vacuole formation. The results suggest that VMP1 expression might be involved in the cytoplasmic vacuolization of acinar cells during the early stage of acute pancreatitis^[38].

EXTRAPANCREATIC MANIFESTATIONS OF L-ARGININE INDUCED PANCREATITIS

Whereas the mortality of interstitial pancreatitis was close to zero, patients with necrotizing pancreatitis had a considerable mortality. The extrapancreatic manifestations, such as circulatory, pulmonary, renal and hepatic failure (multi-organ failure) contributed significantly to the morbidity and mortality of this disease^[39-41]. This model seems to be an appropriate tool to study the extrapancreatic organ damage and its pathomechanisms.

We found that oxidative stress developed not only in the pancreas but also in remote organs during acute pancreatitis induced by 2 \times 250 mg/100 g bm Arg^[11]. The MDA concentration was significantly increased at 6 h after Arg treatment in the liver and at 24 h in the kidney. Among the endogenous scavengers, Mn-, and Cu, Zn-SOD and glutathione peroxidase were significantly reduced both in the liver and in the kidney during the course of Arg-induced pancreatitis. The catalase activity was significantly increased in the liver, whereas it was significantly decreased in the kidney. The prophylactic application of 200 mg/kg allopurinol significantly restrained the generation of free radicals in the liver. Histologic examination revealed vacuolar degeneration within hepatic cells and eosinophilic components in proximal convoluted tubules in the kidney.

Hypertonic saline (HTS) could restore the circulating volume in haemorrhagic shock by improving cardiac contractility and peripheral tissue perfusion^[42]. The aim of Shields^[43,44] was to investigate the effect of HTS resuscitation on the development of end-organ damage in Arg-induced pancreatitis. They demonstrated increased pulmonary endothelial permeability and increased myeloperoxidase activity at 72 h after pancreatitis induction by a single 500 mg/100 g bm Arg injection. Histological examination of the lung revealed marked interstitial congestion and hemorrhage. HTS injections (75 g/L NaCl, 2 mL/kg) were applied at 24 and 48 h after the administration of Arg. Pulmonary oedema, endothelial leak, enhanced neutrophil activity were all attenuated and the pancreatic and pulmonary histological scores were improved in animals treated with HTS.

REGENERATIVE PROCESS AFTER L-ARGININE-INDUCED PANCREATITIS

Time course changes

In the early phase of acute pancreatitis evoked by 200 mg/100 g bm Arg (d 1-3), the laboratory signs of acute pancreatic inflammation predominated in the Arg-treated rats^[9]. Pancreatitis revealed an intercellular edema with the infiltration of leukocytes, dilatation of the capillaries, and microfocal necroses in the parenchyma on d 1 after pancreatitis induction. Interestingly, acinar cells surrounding the Langerhans islets remained intact (Figure 1). Following the early acinar cell necrosis, histological examinations revealed a marked adipose tissue deposition at the end of the first week. Accumulation of adipose tissue was a sign of atrophy. The rest of the pancreas (not involved in Arg-induced cell

destruction) could be the site of pancreatic hypertrophy and hyperplasia. The pancreatic content of enzymes (amylase, trypsinogen and lipase) was decreased by d 7 as a sign of pancreatic acinar cell damage. After the first week regenerative processes dominated. Furthermore, by the end of the fourth week the pancreatic content of enzymes was significantly elevated^[9].

The mortality of this type of pancreatitis was 2.5%. The rats died between days 1-5 after pancreatitis induction. No mortality was found in the control group.

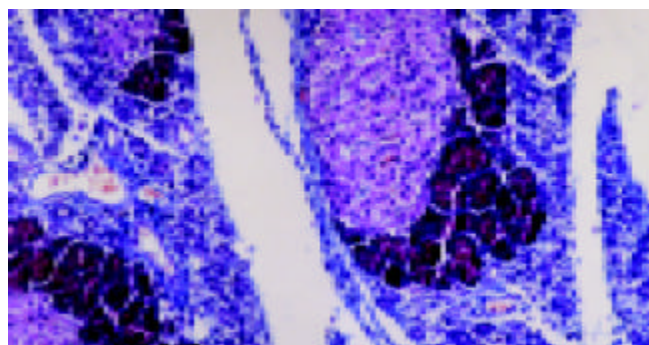


Figure 1 Histologic alterations in the pancreas following Arg-induced pancreatitis on d 3. The signs of acute inflammation and tubular complexes are visible. Segmental fibroses with blue stained fibroblast are observed. Intact pancreatic acinar cells are presented mainly around the Langerhans islets (Chrossmonn's trichrome staining $\times 100$).

Effect of exogenous CCK on the regenerative process

In the early phase of pancreatitis, administration of low doses of CCK-8 further deteriorated the laboratory and histologic parameters of acute pancreatitis^[9]. The mortality rate (15%) also demonstrated the harmful effect of CCK-8 in the early phase of this pancreatitis. Histologic sections demonstrated a more intense mitotic activity due to the effect of CCK-8 on d 7. Moreover, histologic examination revealed that the bulk of hypertrophized pancreatic acinar cells were found surrounding the enlarged Langerhans islets following CCK-8 administration. It appears that the closeness of the Langerhans islets protects acinar cells and accelerates the regenerative process during Arg-evoked pancreatic tissue damage. The reason for this might be the complex interaction of acinar and islet cells. The laboratory changes (such as pancreatic DNA and enzymes content) also proved the positive effect of CCK-8 during the recovery phase^[9].

Secretory changes

Experimental studies have revealed that, suggesting that pancreatic enzyme secretion is reduced after the induction of acute pancreatitis^[45-47]. We characterized the secretory changes in Arg-induced pancreatitis on d 1, 3, 7 and 14 following pancreatitis induction, when the rats were surgically prepared with pancreatic duct and femoral vein cannulae under urethane anesthesia^[48].

In pancreatitic rats, both the basal and the maximal pancreatic volumes were significantly increased *vs* controls on d 1 following the induction of pancreatitis. The basal output was still significantly higher *vs* controls on d 3 and 7, but the maximal output was significantly decreased *vs* the controls on d 7. No change in basal pancreatic fluid secretion was observed in pancreatitic rats, but the maximal output was significantly decreased on d 14. These results proved that there was a conversion from the acute inflammatory phase to the late regenerative phase on d 7. As far as the pancreatic protein secretion was concerned, in pancreatitis-group the basal secretory protein level was significantly diminished throughout

the experiment. The maximal pancreatic protein secretion was significantly decreased in a progressive manner on d 3, 7 and 14. In the pancreatitic rats, both the basal and the maximal pancreatic amylase secretion were significantly increased on d 1. The maximal output was significantly decreased only on d 14. Taken together, the pancreatic secretion in the early phase of Arg-induced pancreatitis is characterized by increases in the secretory volume and amylase level, with a simultaneous decrease in protein output. A progressive decrease in pancreatic secretory capacity was then detected confirming the acinar cell damage.

Effect of diabetes on Arg-induced pancreatitis

The interesting finding that periinsular acini remained intact during Arg-induced-pancreatitis prompted us to continue studies on the effects of diabetes in the process of pancreatic remodeling^[9]. An insulo-acinar correlation was also indicated by the morphological evidence. Acinar cells around the islets could be distinguished from teleinsular acini by their staining characteristics. These periinsular cells were larger, contained larger nuclei and nucleoli, and had more abundant zymogen granules^[49,50]. To achieve our aims, we used streptozotocin (STZ) to evoke diabetes^[51]. STZ was specifically toxic to the β -cells of the islets of Langerhans, which was irreversible and dose-dependent^[52]. When pancreatitis was induced in diabetic rats, the periinsular acini did not remain intact during Arg-induced-pancreatitis. We also found that in diabetic rats, the pancreatic regenerative processes (mitotic activity of acinar cells) in response to low doses of CCK-8 were markedly diminished. The lack of regenerative effect of CCK-8 may be due to the low insulin level. Furthermore, histological sections indicated no difference between the peri- and teleinsular acinar cell damage in diabetic rats. This is a morphological confirmation of the pivotal role of insulin in the regulation of the exocrine pancreatic structure. However, other islet cell hormones might also be involved in this process.

When Arg-induced pancreatitis was evoked in STZ-diabetic rats, the significant elevation in serum amylase level was not so obvious as that observed in pancreatitic rats. The explanation of this phenomenon is that a diabetic state (in rats without pancreatitis) appeared to shift the normal pancreatic enzyme content (decreased amylase and increased trypsinogen). These data are in accordance with those of Sofrankova *et al.*, who demonstrated a similar pancreatic enzyme pattern in a secretory study^[53].

Early increases were observed in the basal pancreatic fluid and amylase secretion in Arg-STZ-treated rats. However, no CCK-8-stimulated fluid secretory peak following pancreatitis induction was detected in diabetic animals, in contrast with the situation in non-diabetic rats, suggesting that diabetes could moderate the CCK-8-stimulated secretory changes in both the early and late phases of Arg-induced pancreatitis.

In order to clearly prove the effect of β -cells during the process of pancreatitis, we replaced the endogenous insulin with mixed exogenous insulin (2 IU s.c. twice daily, 30% short-acting and 70% intermediate-duration insulin), and found that simultaneous administration of exogenous insulin replaced the hypertrophic effect of low-doses of CCK-8^[54].

Late recovery in normal and diabetic rats

Six months after Arg-induced pancreatitis without diabetes, a major restitution of the pancreatic enzyme content was found^[55]. The lipase and trypsinogen contents of the pancreas were recovered, but amylase was significantly decreased *vs* the controls. In spite of this large-scale restitution of the pancreatic enzyme compositions, marked histologic alterations, periductal fibroses, adipose tissue and tubular complexes, were detected 6 mo following pancreatitis induction. No mitotic activity and centroacinar hyperplasia were observed at this time. When

pancreatitis was induced in STZ-diabetic rats, a very considerable recovery of the enzyme content was noted 6 mo following pancreatitis induction. Even at this time, however, the amylase content remained significantly decreased. This may be due to the combined effect of STZ-evoked decrease on amylase biosynthesis and the toxic damage caused by Arg to pancreatic acinar cells^[56]. So far as the pancreatic histologic structure was concerned, the morphologic changes were similar to those seen in Arg-induced pancreatic non-diabetic rats.

Effect of fibroblast growth factor-7 and fibroblast growth factor-10, and role of keratinocyte growth factor receptor

Keratinocyte growth factor (KGF) is a member of the rapidly growing fibroblast growth factor (FGF) family of mitogens^[57]. FGF-7 and FGF-10 show high structural homology and similar biological characteristics. Both are mainly synthesized by mesenchymal cells and stimulate epithelial cells via KGF receptor (KGFR) which is a splice variant of FGF receptor-2^[58].

In normal pancreas, FGF-7 is localized in alpha islet cells, but FGF-10 is not detected. KGFR is also localized in islet cells, ductal cells, and centroacinar cells in the normal pancreas. In the pancreatic tissues of rats with Arg-induced pancreatitis, FGF-7 was localized in alpha cells, whereas FGF-10 was expressed in vascular smooth muscle cells (VSMCs). KGFR was not expressed in centroacinar cells after Arg treatment. These findings suggest that FGF-7 and FGF-10 contribute to the regeneration and differentiation of acinar cells and angiogenesis in acute pancreatitis through KGFR^[58].

Expression of lumican proteins

Lumican is a member of a small leucine-rich proteoglycan family^[59]. It has been reported that lumican mRNA and its protein were ectopically and highly expressed in acinar cells in chronic pancreatitis (CP)-like lesions close to pancreatic cancer cells^[60]. CP-like lesions are characterized by acinar and ductal-ductular cell proliferation with expanding fibrosis. Immunohistochemically, the lumican proteins are localized in ductules and a few centroacinar cells in normal pancreas.

After administration of an excessive dose of Arg, an immature fibrosis with fragmented and loose collagen fibers was observed on d 4 after pancreatitis induction. Moreover, lumican immunoreactivity was also detected in the collagen fibers on d 4. Lumican mRNA was barely detected in islet cells in the normal pancreas, but it was strongly expressed in acinar and islet cells on d 1 following the induction of pancreatitis. Lumican mRNA was expressed in many proliferating fibroblasts on d 4. These findings indicate that lumican is transiently synthesized by acinar cells and fibroblasts during Arg-induced acute pancreatitis. Lumican proteins may contribute to immature and transient fibrosis of acute pancreatitis.

CONCLUSIONS AND PERSPECTIVES

We are just starting to understand the pathophysiology of acute necrotizing pancreatitis. By this review we tried to illuminate new aspects of cell physiology and pathology of acute necrotizing pancreatitis. Firstly, we explored the effects of high doses of Arg on different tissues. Then, we concentrated on the pancreas showing that Arg could cause a necrotizing acute pancreatitis. Finally we characterized the early and late phases of this model of acute experimental pancreatitis.

We believe that this review confirms the value of Arg-induced pancreatitis. In the past plenty of excellent observations were published on this necrotizing pancreatitis model. Many questions were answered concerning acute necrotizing pancreatitis using high doses of Arg. On the other hand, authors usually left the endocrine status of the pancreas unexamined. Using this model, we could highlight the importance of the insulo-acinar axis.

Despite our current knowledge, many hypotheses and questions remain unanswered concerning the effects of Arg. Therefore, it seems to be well worthwhile to continue to explore the pathomechanism of Arg-induced pancreatitis.

REFERENCES

- Mizunuma T**, Kawamura S, Kishino Y. Effects of injecting excess arginine on rat pancreas. *J Nutr* 1984; **114**: 467-471
- Kishino Y**, Kawamura S. Pancreatic damage induced by injecting a large dose of arginine. *Virchows Arch B Cell Pathol Incl Mol Pathol* 1984; **47**: 147-155
- Tani S**, Itoh H, Okabayashi Y, Nakamura T, Fujii M, Fujisawa T, Koide M, Otsuki M. New model of acute necrotizing pancreatitis induced by excessive doses of arginine in rats. *Dig Dis Sci* 1990; **35**: 367-374
- Delaney CP**, McGeeney KF, Dervan P, Fitzpatrick JM. Pancreatic atrophy: a new model using serial intra-peritoneal injections of L-arginine. *Scand J Gastroenterol* 1993; **28**: 1086-1090
- Weaver C**, Bishop AE, Polak JM. Pancreatic changes elicited by chronic administration of excess L-arginine. *Exp Mol Pathol* 1994; **60**: 71-87
- Takacs T**, Czako L, Jarmay K, Farkas G Jr, Mandi Y, Lonovics J. Cytokine level changes in L-arginine-induced acute pancreatitis in rat. *Acta Physiol Hung* 1996; **84**: 147-156
- Varga IS**, Matkovics B, Hai DQ, Kotorman M, Takacs T, Sasvari M. Lipid peroxidation and antioxidant system changes in acute L-arginine pancreatitis in rats. *Acta Physiol Hung* 1997; **85**: 129-138
- Czako L**, Takacs T, Varga IS, Tiszlavicz L, Hai DQ, Hegyi P, Matkovics B, Lonovics J. Involvement of oxygen-derived free radicals in L-arginine-induced acute pancreatitis. *Dig Dis Sci* 1998; **43**: 1770-1777
- Hegyi P**, Takacs T, Jarmay K, Nagy I, Czako L, Lonovics J. Spontaneous and cholecystokinin-octapeptide-promoted regeneration of the pancreas following L-arginine-induced pancreatitis in rat. *Int J Pancreatol* 1997; **22**: 193-200
- Takacs T**, Hegyi P, Jarmay K, Czako L, Gog C, Rakonczay Z Jr, Nemeth J, Lonovics J. Cholecystokinin fails to promote pancreatic regeneration in diabetic rats following the induction of experimental pancreatitis. *Pharmacol Res* 2001; **44**: 363-372
- Czako L**, Takacs T, Varga IS, Tiszlavicz L, Hai DQ, Hegyi P, Matkovics B, Lonovics J. Oxidative stress in distant organs and the effects of allopurinol during experimental acute pancreatitis. *Int J Pancreatol* 2000; **27**: 209-216
- Czako L**, Takacs T, Varga IS, Hai DQ, Tiszlavicz L, Hegyi P, Mandi Y, Matkovics B, Lonovics J. The pathogenesis of L-arginine-induced acute necrotizing pancreatitis: inflammatory mediators and endogenous cholecystokinin. *J Physiol Paris* 2000; **94**: 43-50
- Varga IS**, Matkovics B, Czako L, Hai DQ, Kotorman M, Takacs T, Sasvari M. Oxidative stress changes in L-arginine-induced pancreatitis in rats. *Pancreas* 1997; **14**: 355-359
- Takacs T**, Czako L, Morschl E, Laszlo F, Tiszlavicz L, Rakonczay Z Jr, Lonovics J. The role of nitric oxide in edema formation in L-arginine-induced acute pancreatitis. *Pancreas* 2002; **25**: 277-282
- Rakonczay Z**, Jarmay K, Kaszaki J, Mandi Y, Duda E, Hegyi P, Boros I, Lonovics J, Takacs T. NF-kappaB activation is detrimental in arginine-induced acute pancreatitis. *Free Radic Biol Med* 2003; **34**: 696-709
- Takacs T**, Rakonczay Z Jr, Varga IS, Ivanyi B, Mandi Y, Boros I, Lonovics J. Comparative effects of water immersion pretreatment on three different acute pancreatitis models in rats. *Biochem Cell Biol* 2002; **80**: 241-251
- Gross SS**, Wolin MS. Nitric oxide: pathophysiological mechanisms. *Annu Rev Physiol* 1995; **57**: 737-769
- Beglinger C**. Potential role of cholecystokinin in the development of acute pancreatitis. *Digestion* 1999; **60**(Suppl 1): 61-63
- Tachibana I**, Shirohara H, Czako L, Akiyama T, Nakano S, Watanabe N, Hirohata Y, Otsuki M. Role of endogenous cholecystokinin and cholecystokinin-A receptors in the development of acute pancreatitis in rats. *Pancreas* 1997; **14**: 113-121
- Kihara Y**, Tashiro M, Nakamura H, Yamaguchi T, Yoshikawa H, Otsuki M. Role of TGF-beta1, extracellular matrix, and matrix metalloproteinase in the healing process of the pancreas after

- induction of acute necrotizing pancreatitis using arginine in rats. *Pancreas* 2001; **23**: 288-295
- 21 **Abraham E.** NF-kappaB activation. *Crit Care Med* 2000; **28** (4 Suppl): N100-N104
 - 22 **Duseti NJ,** Frigerio JM, Fox MF, Swallow DM, Dagorn JC, Iovanna JL. Molecular cloning, genomic organization, and chromosomal localization of the human pancreatitis-associated protein (PAP) gene. *Genomics* 1994; **19**: 108-114
 - 23 **Motoo Y,** Taga K, Su SB, Xie MJ, Sawabu N. Arginine induces apoptosis and gene expression of pancreatitis-associated protein (PAP) in rat pancreatic acinar AR4-2J cells. *Pancreas* 2000; **20**: 61-66
 - 24 **Takacs T,** Czako L, Jarmay K, Hegyi P, Pozsar J, Marosi E, Pap A, Lonovics J. Time-course changes in pancreatic laboratory and morphologic parameters in two different acute pancreatitis models in rats. *Acta Med Hung* 1994; **50**: 117-130
 - 25 **Kivilaakso E,** Valtonen VV, Malkamaki M, Palmu A, Schroder T, Nikki P, Makela PH, Lempinen M. Endotoxaemia and acute pancreatitis: correlation between the severity of the disease and the anti-enterobacterial common antigen antibody titre. *Gut* 1984; **25**: 1065-1070
 - 26 **Pozsar J,** Schwab R, Simon K, Fekete L, Orgovan G, Pap A. Effect of endotoxin administration on the severity of acute pancreatitis in two experimental models. *Int J Pancreatol* 1997; **22**: 31-37
 - 27 **Dray A.** Inflammatory mediators of pain. *Br J Anaesth* 1995; **75**: 125-131
 - 28 **Toma H,** Winston J, Micci MA, Shenoy M, Pasricha PJ. Nerve growth factor expression is up-regulated in the rat model of L-arginine-induced acute pancreatitis. *Gastroenterology* 2000; **119**: 1373-1381
 - 29 **Tashiro M,** Schafer C, Yao H, Ernst SA, Williams JA. Arginine induced acute pancreatitis alters the actin cytoskeleton and increases heat shock protein expression in rat pancreatic acinar cells. *Gut* 2001; **49**: 241-250
 - 30 **Bhagat L,** Singh VP, Song AM, van Acker GJ, Agrawal S, Steer ML, Saluja AK. Thermal stress-induced HSP70 mediates protection against intrapancreatic trypsinogen activation and acute pancreatitis in rats. *Gastroenterology* 2002; **122**: 156-165
 - 31 **Ethridge RT,** Ehlers RA, Hellmich MR, Rajaraman S, Evers BM. Acute pancreatitis results in induction of heat shock proteins 70 and 27 and heat shock factor-1. *Pancreas* 2000; **21**: 248-256
 - 32 **Weber CK,** Gress T, Muller-Pillasch F, Lerch MM, Weidenbach H, Adler G. Supramaximal secretagogue stimulation enhances heat shock protein expression in the rat pancreas. *Pancreas* 1995; **10**: 360-367
 - 33 **Rakonczay Z Jr,** Ivanyi B, Varga I, Boros I, Jednakovits A, Nemeth I, Lonovics J, Takacs T. Nontoxic heat shock protein coinducer BRX-220 protects against acute pancreatitis in rats. *Free Radic Biol Med* 2002; **32**: 1283-1292
 - 34 **Strowski MZ,** Sparmann G, Weber H, Fiedler F, Printz H, Jonas L, Goke B, Wagner AC. Caerulein pancreatitis increases mRNA but reduces protein levels of rat pancreatic heat shock proteins. *Am J Physiol* 1997; **273**(4 Pt 1): G937-G945
 - 35 **Weber H,** Wagner AC, Jonas L, Merkord J, Hofken T, Nizze H, Leitzmann P, Goke B, Schuff-Werner P. Heat shock response is associated with protection against acute interstitial pancreatitis in rats. *Dig Dis Sci* 2000; **45**: 2252-2264
 - 36 **Tashiro M,** Ernst SA, Edwards J, Williams JA. Hyperthermia induces multiple pancreatic heat shock proteins and protects against subsequent arginine-induced acute pancreatitis in rats. *Digestion* 2002; **65**: 118-126
 - 37 **Duseti NJ,** Jiang Y, Vaccaro MI, Tomasini R, Azizi Samir A, Calvo EL, Ropolo A, Fiedler F, Mallo GV, Dagorn JC, Iovanna JL. Cloning and expression of the rat vacuole membrane protein 1 (VMP1), a new gene activated in pancreas with acute pancreatitis, which promotes vacuole formation. *Biochem Biophys Res Commun* 2002; **290**: 641-649
 - 38 **Vaccaro MI,** Grasso D, Ropolo A, Iovanna JL, Cerquetti MC. VMP1 expression correlates with acinar cell cytoplasmic vacuolization in arginine-induced acute pancreatitis. *Pancreatol* 2003; **3**: 69-74
 - 39 **Steinberg W,** Tenner S. Acute pancreatitis. *N Eng J Med* 1994; **330**: 1198-1220
 - 40 **Renner IG,** Savage WT, Pantoga JL, Renner VJ. Death due to acute pancreatitis. A retrospective analysis of 405 autopsy cases. *Dig Dis Sci* 1985; **10**: 1005-1008
 - 41 **Karomgani I,** Porter KA, Langevin RE, Banks PA. Prognostic factors in sterile pancreatic necrosis. *Gastroenterology* 1992; **103**: 1636-1640
 - 42 **Kramer GC,** Perron PR, Lindsey DC, Ho HS, Gunther RA, Boyle WA, Holcroft JW. Small-volume resuscitation with hypertonic saline dextran solution. *Surgery* 1986; **100**: 239-247
 - 43 **Shields CJ,** Sookhai S, Winter DC, Dowdall JF, Kingston G, Parfrey N, Wang JH, Kirwan WO, Redmond HP. Attenuation of pancreatitis-induced pulmonary injury by aerosolized hypertonic saline. *Surg Infect* 2001; **2**: 215-224
 - 44 **Shields CJ,** Winter DC, Sookhai S, Ryan L, Kirwan WO, Redmond HP. Hypertonic saline attenuates end-organ damage in an experimental model of acute pancreatitis. *Br J Surg* 2000; **87**: 1336-1340
 - 45 **Saluja A,** Saito I, Saluja M, Houlihan MJ, Powers RE, Meldolesi J, Steer ML. *In vivo* rat pancreatic acinar cell function during supramaximal stimulation with cerulein. *Am J Physiol* 1985; **249**: G702-G710
 - 46 **Manso MA,** San Roman JI, Dios I, Garcia LJ, Lopez MA. Cerulein-induced acute pancreatitis in the rat. Study of pancreatic secretion and plasma VIP and secretin levels. *Dig Dis Sci* 1992; **37**: 364-368
 - 47 **Niederer A,** Niederer M, Luthen R, Strohmeyer G, Ferrell LD, Grendel JH. Pancreatic exocrine secretion in acute experimental pancreatitis. *Gastroenterology* 1990; **99**: 1120-1127
 - 48 **Hegyi P,** Czako L, Takacs T, Szilvassy Z, Lonovics J. Pancreatic secretory responses in L-arginine-induced pancreatitis: comparison of diabetic and nondiabetic rats. *Pancreas* 1999; **19**: 167-174
 - 49 **Hellman B,** Wallgren A, Petersson B. Cytological characteristics of the exocrine pancreatic cells with regard to their position in relation to the islets of Langerhans. *Acta endocrinol* 1962; **93**: 465-473
 - 50 **Kramer MF,** Tan HT. The peri-insular acini of the pancreas of the rat. *Z Zellforsch* 1968; **86**: 163-170
 - 51 **Rakieten N,** Rakieten LM, Nadkarni MV. Studies on the diabetogenic action of streptozotocin. *Cancer Chemother* 1963; **29**: 91
 - 52 **Junod A,** Lambert AE, Orci L, Pictet R, Gonet AE, Renold AE. Studies on the diabetogenic action of streptozotocin. *Proc Soc Exp Biol Med* 1967; **126**: 201
 - 53 **Sofrankova A,** Dockray GJ. Cholecystokinin- and secretin-induced pancreatic secretion in normal and diabetic rats. *Am J Physiol* 1983; **244**: G370-G374
 - 54 **Hegyi P,** Rakonczay Z Jr, Sari R, Farkas N, Góg C, Nemeth J, Lonovics J, Takacs T. Insulin is necessary for the hypertrophic effect of CCK-8 following acute necrotizing experimental pancreatitis. *World J Gastroenterol* 2004; in press
 - 55 **Hegyi P,** Takacs T, Tiszlavicz L, Czako L, Lonovics J. Recovery of exocrine pancreas six months following pancreatitis induction with L-arginine in streptozotocin-diabetic rats. *J Physiol Paris* 2000; **94**: 51-55
 - 56 **Williams JA,** Goldfine ID. The insulin-acinar relationship. In: *The Exocrine Pancreas: Biology, Pathobiology and Diseases*. Edited by Go VLW *et al.* Raven Press, New York 1993; pp: 789-802
 - 57 **Werner S.** Keratinocyte growth factor: a unique player in epithelial repair processes. *Cytokine Growth Factor Rev* 1998; **9**: 153-165
 - 58 **Ishiwata T,** Naito Z, Lu YP, Kawahara K, Fujii T, Kawamoto Y, Teduka K, Sugisaki Y. Differential distribution of fibroblast growth factor (FGF)-7 and FGF-10 in L-arginine-induced acute pancreatitis. *Exp Mol Pathol* 2002; **73**: 181-190
 - 59 **Greiling H.** Structure and biological functions of keratan sulfate proteoglycans. *Review EXS* 1994; **70**: 101-122
 - 60 **Naito Z,** Ishiwata T, Lu YP, Teduka K, Fujii T, Kawahara K, Sugisaki Y. Transient and ectopic expression of lumican by acinar cells in L-arginine-induced acute pancreatitis. *Exp Mol Pathol* 2003; **74**: 33-39

Preparation of magnetic polybutylcyanoacrylate nanospheres encapsulated with aclacinomycin A and its effect on gastric tumor

Hong Gao, Ji-Yao Wang, Xi-Zhong Shen, Yong-Hui Deng, Wei Zhang

Hong Gao, Ji-Yao Wang, Xi-Zhong Shen, Department of Gastroenterology, Zhongshan Hospital, Fudan University, Shanghai 200032, China

Yong-Hui Deng, Department of Macromolecular Sciences, Fudan University, Shanghai 200032, China

Wei Zhang, Department of Gastroenterology, Huadong Hospital, Shanghai 200040, China

Supported by the National High Technology Research and Development Program of China 863 Program, No. 2001AA218011

Correspondence to: Dr. Xi-Zhong Shen, Associate Chief of Department of Gastroenterology, Zhongshan Hospital, Fudan University, Shanghai 200032, China. shenzx@zshospital.net

Telephone: +86-21-64041990-2070 **Fax:** +86-21-34160980

Received: 2004-02-02 **Accepted:** 2004-02-21

Abstract

AIM: To evaluate the effect of aclacinomycin A-loaded magnetic polybutylcyanoacrylate nanoparticles on gastric tumor growth *in vivo* and *in vitro*.

METHODS: Magnetic polybutylcyanoacrylate (PBCA) nanospheres encapsulated with aclacinomycin A (MPNS-ACM) were prepared by interfacial polymerization. Particle size, shape and drug content were examined. Female BABL/c nude mice were implanted with MKN-45 gastric carcinoma tissues subcutaneously to establish human gastric carcinoma model. The mice were randomly divided into 5 groups of 6 each: ACM group (8 mg/kg bm); group of high dosage of MPNS-ACM (8 mg/kg bm); group of low dosage of MPNS-ACM (1.6 mg/kg bm); group of magnetic PBCA nanosphere (MPNS) and control group (normal saline). Magnets (2.5 T) were implanted into the tumor masses in all of the mice one day before the therapy. Above-mentioned drugs were administered intravenously to the mice of every group on the first day and sixth day. When the mice were sacrificed, tumor weight was measured, and the assay of granulocyte-macrophage colony forming-unit (CFU-GM) was performed on semi-solid culture. White blood cell, alanine aminotransferase and creatine were examined. 3-[4-dimethylthiazol-2-yl]-2,5-diphenyltetrazolium bromide (MTT) was used to examine the viability of MKN-45 cells after incubation with different concentrations of ACM, MPNS and MPNS-ACM suspension respectively for 48 h.

RESULTS: Content of ACM in MPNS-ACM was 12.0% and the average diameter of the particles was 210 nm. The inhibitory rates of ACM (8 mg/kg bm), high dosage of MPNS-ACM (8 mg/kg bm), low dosage of MPNS-ACM (1.6 mg/kg bm) and MPNS on human gastric carcinoma in nude mice were 22.63%, 52.55%, 30.66% and 10.22%, respectively. There was a significant decrease in the number of CFU-GM of bone marrow in ACM group compared with control group, whereas no obvious change was observed in that of the nanosphere groups. The values of 50% inhibition concentration (IC50) of ACM, MPNS and MPNS-ACM were 0.09, 97.78 and 1.07 $\mu\text{g/mL}$, respectively.

CONCLUSION: The tumor inhibitory rate of MPNS-ACM was much higher than that of ACM under magnetic field and the inhibition on bone marrow was alleviated significantly compared with ACM group.

Gao H, Wang JY, Shen XZ, Deng YH, Zhang W. Preparation of magnetic polybutylcyanoacrylate nanospheres encapsulated with aclacinomycin A and its effect on gastric tumor. *World J Gastroenterol* 2004; 10(14): 2010-2013

<http://www.wjgnet.com/1007-9327/10/2010.asp>

INTRODUCTION

Cytotoxic medicine has extensively been employed in cancer chemotherapy. However, the usage of these drugs has been limited by the non-targeting towards cancer and serious toxicity to normal cells in the body. To enhance the therapeutic efficacy of anticancer drugs and reduce the toxicity to normal tissue of the body, targeted drug delivery systems at solid tumors have been developed.

Magnetic targeted drugs are the fourth generation of targeted reagents. The advantage of the magnetic targeted drug delivery systems over other drug targeting techniques is their ability to minimize the uptake by reticuloendothelial system (RES)^[1]. Some investigators have reported successful tumor remission in animal experiments upon the use of magnetically responsive anticancer drug carriers under magnetic fields, but in previous studies the majority of magnetically responsive drug carriers, which included magnetic albumin microspheres and magnetic liposomes had been administered intra-arterially to obtain highly efficient localized targeting during the first circulation passing through a strong magnetic field^[2,3]. However intra-arterial administration of these carriers is not considered to be suitable for the treatment of multiple systemic lesions and is inconvenient to apply. Accordingly, the treatment of solid tumors requires the development of magnetically responsive carriers that can be effectively delivered to any systemic site via intravenous administration. Yet the therapeutic efficacy of intravenously administered magnetically responsive carriers has not been established maturely to date.

Polyalkylcyanoacrylates (PACAs) were not employed as polymers until the early 1980s. However the corresponding monomers, alkylcyanoacrylates, have been extensively used as tissue adhesives for the closure of skin wounds^[4]. More recently, one application of the polymers is the use of PACAs as nanoparticulate drug carriers^[5-9]. This very exciting area of research has gained increasing interest in therapeutics, especially for cancer treatments. Other molecules of interest, including poorly stable compounds such as peptides and nucleic acids, have been combined with PACAs nanoparticles for targeting purposes^[10]. Today, PACAs nanoparticles are considered the most promising polymer colloidal for drug delivery system and are already in clinical development for cancer therapy^[11-15]. The main attraction of PACAs nanoparticles is their ability of tissue targeting and enhancing intracellular penetration of drugs^[16]. Among the species, polybutylcyanoacrylate (PBCA), as a polymer with medium-

length alkyl side chain, is of lower toxicity, proper degradation time. PBCA carrying drugs could increase the antibacterial efficacy^[17], elevate the anti-cancer effect^[18], enhance the relative bioavailability of insulin^[19] *etc.* So PBCA has recently been regarded as a kind of widely used, biocompatible, degradable, low-toxic drug carrier.

Employing supermagnetic iron oxide as the ferromagnetic material, aclacinomycin A (ACM) as the targeted fat soluble model drug and PBCA as the carrier, a kind of magnetically targeted polymer encapsulated with an anticancer drug, magnetic PBCA nanospheres encapsulated with ACM were designed and successfully prepared. The anticancer efficacy of the magnetically targeted system was investigated on gastric cancer *in vivo* and *in vitro*.

MATERIALS AND METHODS

Materials

Butylcyanoacrylate was supplied by Zhejiang Golden Roc. Chemicals Co. Inc. ACM was obtained from Shenzhen Main Luck Pharmaceuticals Inc. Human gastric cancer MKN-45 cell line and BALB/c nude mice (SPF, female) were kindly supplied by Shanghai Cancer Institute. Column NdFeB permanent magnets (surface field strength 2.5 T, diameter 1 mm, length 10 mm) were supplied by Shanghai Jieliang Magnetic & Device Co. Ltd. Semi-solid methylcellulose M3545 and Iscove's Modified Dulbecco's Medium (IMDM) were purchased from Stemcell Company, Canada.

Methods

Synthesis of magnetic colloidal nanoparticles Magnetic colloidal iron oxide nanoparticles were prepared with the method of coprecipitation as described before^[20]. Briefly, 10 mol/L sodium hydroxide was added into the mixture of solution of FeCl₂ and FeCl₃ (Fe²⁺/Fe³⁺ molar ratio 1/2) in a nitrogen atmosphere. The solution was stirred for 1 h at 20 °C, and heated at 90 °C for 1 h. The obtained iron oxide suspension was then stirred for 30 min at 90 °C with the addition of 100 mL trisodium citrate solution (0.3 mol/L). Subsequently, the iron oxide dispersion was cooled down to room temperature with continuous stir. The magnetic particles were washed with double distilled deionized water and collected with the help of a magnet. Finally, the ultrafine magnetic particles were redispersed in water and the suspensions were adjusted to 2.0% (w/w) for further use.

Preparation of ACM encapsulated magnetic PBCA nanoparticles (MPNS-ACM) Interfacial polymerization was applied to synthesize MPNS-ACM based on the methods used before^[21,22]. Briefly, 20 mg ACM dispersed in diluted hydrochloric acid and 2 mL magnetic fluid were mingled, then the mixture was added to 100 g hexane including 2 g Span 80 and 0.6 g polysorbate 80 which was stirred at 600 r/min. The fluid was stirred for 0.5-1 h to make it uniform and emulsive. Then 2 mL butylcyanoacrylate was added dropwise with constant stir at room temperature. After 6 h polymerization the particles were separated with the help of a magnet and washed with methanol for several times. Then the particles were washed with deionized water for several times. The particles were lyophilized and ⁶⁰Co irradiation (15 kGy) was performed to sterilize them. The preparation of magnetic PBCA nanoparticles (MPNS) is similar to the synthesis of MPNS-ACM except no ACM in HCl solution.

Characterization and measurements Transmission electron microscopy (TEM) was performed for MPNS (Hitachi HU-11B). Scanning electron microscopy (SEM, Philips XL30) was used to determine the size and morphology of MPNS. Dynamic light scattering (DLS, Malvern 4700) was used to measure the

hydrodynamic diameter of nanoparticles. The particles were treated with ammonia and then ACM was extracted with ethyl acetate. ACM concentration was determined with UV spectrophotometer at 259 nm. And then drug contents were calculated.

Human gastric carcinoma model of nude mice Human gastric carcinoma MKN-45 cells during exponential growth phase were adjusted to 5×10⁷/mL with RPMI 1640. Then 0.2 mL suspension of MKN-45 cells was inoculated subcutaneously near right forefoot in female BALB/c nude mice. Two weeks later, the solid tumors were taken out from the mice in which the tumors were well growing without necrosis. Tumor masses were cut into small pieces with the diameter of about 2 mm. One tiny piece was implanted into one mouse subcutaneously near right forefoot with a needle. The models were successfully produced after about 2 wk when the tumor grew up to 1 cm in diameter.

Tumor inhibition rate *in vivo* Thirty nude mice models were randomly divided into 5 groups of six each: ACM group (8 mg/kg bm), high dose of MPNS-ACM group (equivalent to ACM 8 mg/kg bm), low dose of MPNS-ACM group (equivalent to ACM 1.6 mg/kg bm), MPNS carrier group (equivalent to MPNS-ACM loaded with ACM 8 mg/kg bm) and control group (normal saline). Magnets (with surfacial field strength 2.5 T) were implanted into the center of the tumors one day before the administration. Above-mentioned agents were administrated intravenously on the first day and sixth day. The largest diameter (LD) and its vertical diameter (VD) of the tumors were measured with calipers every two days after the beginning of administration. The volume of tumor was equal to LD×VD²/2. The mice were sacrificed on the eleventh day after treatment. The tumors were taken out, weighed and the tumor inhibition rate (TIR) was calculated with the following formula: TIR(%)=(1-average tumor weight of experimental group/average tumor weight of control group)×100%.

Stem cells colony-forming unit assay of bone marrow was performed. White blood cell, serum alanine aminotransferase (ALT) and creatine of the mice were examined.

Assay of granulocyte-macrophage colony-forming unit (CFU-GM) of bone marrow The assay of CFU-GM was performed with semi-solid methylcellulose culture. The femoras of the mice were taken out under sterile condition. Both extremities of them were cut and the bones were immersed into Iscove's modified Dulbecco's medium (IMDM). The bone marrow was washed out and the concentration of the cells with nuclei was adjusted with IMDM to 2×10⁵/mL. Cell suspension 0.2 mL was added to 2 mL M3534 semi-solid culture. The mixture was added to a 12-well cell culture plate. The cells were cultured for 7 d at 37 °C with 50 mL/L CO₂ in air and >95% humidity. The number of colonies (>30 cells) were counted under inverted microscope^[23].

Anticarcinoma effect on gastric cancer cell line *in vitro* Gastric cancer cell line MKN-45 cells were trypsinized and suspended in RPMI 1640 with the concentration of 2×10⁵/mL. The cells were seeded onto 96-well culture plates with 190 μL per well and then were cultured at 37 °C with 50 mL/L CO₂ in air and >95% humidity for 24 h. Different concentrations of ACM, MPNS and MPNS-ACM in RPMI 1640 were added to the wells and the final concentrations were 0.001, 0.01, 0.1, 1.0, 10 and 100 μg/mL, respectively. The cells were cultured for another 48 h. Then, 10 μL of 5 mg/mL 3-(4,5-dimethylthiazol-2-yl)-2,5-diphenylterazolium bromide (MTT) was added to each well and the cells were cultured for 4 h at 37 °C. Then the culture medium was discarded, and 150 μL dimethylsulfoxide was added to each well and the absorbance at 570 nm (A₅₇₀) was measured with microplate reader.

Inhibition rate=(1-A₅₇₀ in treatment group/A₅₇₀ in control group)×100%.

Statistical analysis

The data were presented as mean±SD. One-Way ANOVA analysis was used to perform single factor multiple comparison in animal tests. The level of significance was set at $P<0.05$. Logistic regression was applied to analyze the inhibition rate of ACM, MPNS and MPNS-ACM in the *in vitro* study.

RESULTS

Characteristics of MPNS-ACM

The average particle size was 210 nm and the size distribution range was 100-400 nm with the most frequent size around 210 nm (Figure 1). A typical core-shell structure is shown under TEM (Figure 2), it indicated black Fe_3O_4 was surrounded by white polymer. SEM photograph shows uniform sphere. The drug content of MPNS-ACM was 12.0%.

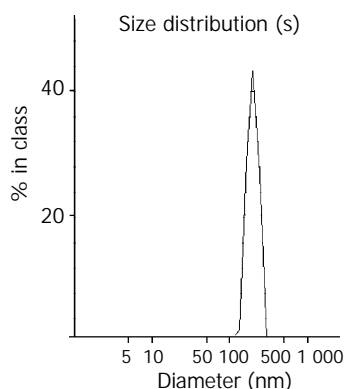


Figure 1 Size distribution of MPNS-ACM.

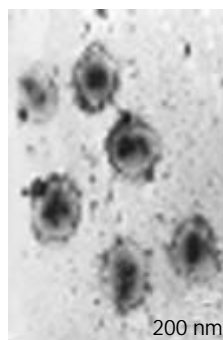


Figure 2 TEM photograph of MPNS-ACM.

Antitumor effect on human gastric carcinoma model of nude mice

The tumor mass and volume were significantly decreased in both ACM group and MPNS-ACM group than control group at the end of the therapy ($P<0.05$). The anti-tumor activity of high dosage of MPNS-ACM was higher than those of the other agents (Table 1).

Table 2 White blood cells, marrow CFU-GM, serum ALT and creatine ($n=6$, mean±SD)

Group	White blood cells ($\times 10^9/L$)	CFU-GM number ($/10^6$)	ALT (U/L)	Creatine ($\mu\text{mol/L}$)
ACM	76.67±17.32	74.75±21.91 ^b	30.67±16.51	12.17±1.17
High dosage of MPNS-ACM	70.00±8.74	107.83±14.75	29.17±14.36	12.50±1.05
Low dosage of MPNS-ACM	74.67±9.71	115.25±12.53	23.83±3.55	13.00±2.19
MPNS	79.00±11.23	117.50±12.75	20.83±4.71	12.00±1.55
Control	74.83±6.08	117.00±12.48	37.83±35.13	12.67±1.51

^b $P<0.001$ vs control group.

Table 1 Tumor mass on the 11th day and TIR of the five groups ($n=6$, mean±SD)

Group	Tumor mass (g)	TIR (%)
ACM	1.06±0.27 ^a	22.63
High dosage of MPNS-ACM	0.65±0.26 ^{ac}	52.55
Low dosage of MPNS-ACM	0.95±0.15 ^{ac}	30.66
MPNS	1.23±0.25	10.22
Control	1.37±0.21	//

^a $P<0.05$ vs control group; ^c $P<0.05$ vs ACM group; ^e $P<0.05$ vs group of low dosage MPNS-ACM; ^g $P<0.05$ vs MPNS group.

The TIR of ACM was 22.63%. The tumor mass of ACM group on the eleventh day (1.06±0.27 g) was much lower than that of control group (1.37±0.21 g) ($P<0.05$).

The TIR of high dosage of MPNS-ACM was 52.55%. The tumor mass on the eleventh day (0.65±0.26 g) was much lower than those of the same dosage of ACM group, low dosage of MPNS-ACM group (0.95±0.15 g), MPNS carrier group (1.23±0.25 g) and control group.

The TIR of low dosage of MPNS-ACM (1.6 mg/kg bm) group was 30.66%, which was higher than that of ACM group (8 mg/kg bm), but there was no statistical difference as to the tumor mass between the two groups ($P>0.05$). The tumor weight of low dosage of MPNS-ACM group was lower than those of MPNS group, and control group ($P<0.05$).

The TIR of MPNS carrier was 10.22%. The tumor weight (1.23±0.25 g) was similar to that of control group (1.37±0.21, $P>0.05$).

Side effects of the agents

The white blood cell counts, serum ALT and creatine of the mice in all the groups were similar ($P<0.05$) (Table 2). The number of CFU-GM of ACM group was much lower than those of the other four groups ($P<0.001$). The white blood cell counts in ACM group was lower than that in control group, yet the ones in MPNS carrier and MPNS-ACM groups were similar to that in control group ($P>0.05$, Table 2).

Anti-tumor effect on gastric cancer cell line in vitro

The IC₅₀ of ACM, MPNS and MPNS-ACM was 0.09, 97.78 and 1.07 (Table 3).

Table 3 Inhibition concentration of the drugs ($\mu\text{g/mL}$)

Group	IC ₁₀	IC ₅₀	IC ₉₀
ACM	0.006	0.09	1.53
MPNS	10.34	97.8	925
MPNS-ACM	0.19	1.07	6.03

DISCUSSION

Selective targeting agents are the trend of antineoplastic chemotherapy. However the production of the biodegradable agents of proper size, high targeting ability and good

bioconsistency is an ongoing challenge. Small-sized magnetic particles (<400 nm) can be extravasated into the tumor interstitium and retained there, owing to the enhanced permeability and retention effect of the tumor^[24]. Polymer carriers encapsulated with magnetite are difficult to prepare because of the different solubility of magnetite and polymers. Here, a kind of modified superparamagnetic iron oxide particles was introduced to prepare the magnetic targeting agents and the particle size could be controlled to 210 nm also, which was very important for the tolerance and efficacy of the agents.

There were two steps for preparation of MPNS-ACM: the preparation and modification of superparamagnetic iron oxide nanoparticles and the synthesis of magnetic polymer loaded with drug. Chemical coprecipitation was applied to synthesize the iron oxide nanoparticles. After modification with acid, well-suspended and stable magnetite fluid was successfully made. It can be stored as suspension for over one year at room temperature. The magnetite can be localized under magnetic field and redispersed when the magnetic force disappears. Interfacial polymerization was applied to the second step where the biodegradable macromolecular material butylcyanoacrylate reacted at the interface between oil and water. Magnetic nanoparticles and fat soluble ACM were encapsulated during the polymerization. The encapsulated ACM was more stable than the one by attachment. The lyophilization agent can be stored long-term at room temperature. After complete ultrasonication, the nanoparticles intravenously administered could locate at the tumor by magnetic force. ACM was slowly released to produce high efficacy and low toxicity with the degradation of polymer.

The results showed that the anti-tumor effect of MPNS-ACM *in vitro* without magnetic field was similar to that of MPNS carrier group (considering the drug content was 12% approximately), yet the anti-tumor test *in vivo* showed higher inhibitory efficacy of the magnetic carrier encapsulated with ACM on the gastric cancer model under magnetic field, which was based on the high targeting capacity of the system. TIR of targeted agent was higher than that of five-fold dosage of non-targeted drug. On the other hand, no toxicity to marrow, liver function and kidney function was found from targeted agents. The results show the high therapeutic efficacy on the tumor and the low toxicity to other organs of the magnetic targeted drug delivery system. It is a kind of safe chemotherapeutic agent.

Due to the difference between fat soluble drugs and water soluble drugs, different methods have been applied to encapsulate the drugs to the biopolymer carrier system with or without magnetite. The attempt to load ACM in to the carrier benefits the studies on other drugs including fat soluble drugs and water soluble drugs.

In conclusion, the magnetic targeted chemotherapy using MPNS-ACM has better tumor targeting, therapeutic efficacy and lower toxicity.

ACKNOWLEDGEMENT

We are grateful to Ming Yao and Shi-Ming Fan of Shanghai Cancer Institute for their kind help with the animal experiments.

REFERENCES

- Gupta PK**, Hung CT. Magnetically controlled targeted micro-carrier systems. *Life Sci* 1989; **44**: 175-186
- Widder KJ**, Morris RM, Poore GA, Howard DP, Senyei AE. Selective targeting of magnetic albumin microspheres containing low-dose doxorubicin: total remission in Yoshida sarcoma-bearing rats. *Eur J Cancer Clin Oncol* 1983; **19**: 135-139
- Rudge S**, Peterson C, Vessely C, Koda J, Stevens S, Catterall L. Adsorption and desorption of chemotherapeutic drugs from a magnetically targeted carrier (MTC). *J Control Release* 2001; **74**: 335-340
- King ME**, Kinney AY. Tissue adhesives: a new method of wound repair. *Nurse Pract* 1999; **24**: 66-74
- de Verdiere AC**, Dubernet C, Nemati F, Soma E, Appel M, Ferte J, Bernard S, Puisieux F, Couvreur P. Reversion of multidrug resistance with polyalkylcyanoacrylate nanoparticles: towards a mechanism of action. *Br J Cancer* 1997; **76**: 198-205
- Zhang ZR**, He Q. Study on liver targeting and hepatocytes permeable valaciclovir polybutylcyanoacrylate nanoparticles. *World J Gastroenterol* 1999; **5**: 330-333
- Ravi Kumar MN**. Nano and microparticles as controlled drug delivery devices. *J Pharm Pharm Sci* 2000; **3**: 234-258
- Soppimath KS**, Aminabhavi TM, Kulkarni AR, Rudzinski WE. Biodegradable polymeric nanoparticles as drug delivery devices. *J Control Release* 2001; **70**: 1-20
- Couvreur P**, Barratt G, Fattal E, Legrand P, Vauthier C. Nanocapsule technology: a review. *Crit Rev Ther Drug Carrier Syst* 2002; **19**: 99-134
- Kattan J**, Droz JP, Couvreur P, Marino JP, Boutan-Laroze A, Rougier P, Brault P, Vranckx H, Grognet JM, Morge X, Sancho-Garnier H. Phase I clinical trial and pharmacokinetic evaluation of doxorubicin carried by polyisohexylcyanoacrylate nanoparticles. *Invest. New Drugs* 1992; **10**: 191-199
- Stella B**, Arpicco S, Peracchia MT, Desmaele D, Hoebeke J, Renoir M, D' Angelo J, Cattel L, Couvreur P. Design of folic acid-conjugated nanoparticles for drug targeting. *J Pharm Sci* 2000; **89**: 1452-1464
- Brigger I**, Chaminade P, Marsaud V, Appel M, Besnard M, Gurny R, Renoir M, Couvreur P. Tamoxifen encapsulation within polyethylene glycol-coated nanospheres. A new antiestrogen formulation. *Int J Pharm* 2001; **214**: 37-42
- Calvo P**, Gouritin B, Chacun H, Desmaele D, D' Angelo J, Noel JP, Georgin D, Fattal E, Andreux JP, Couvreur P. Long-circulating PEGylated polycyanoacrylate nanoparticles as new drug carrier for brain delivery. *Pharm Res* 2001; **18**: 1157-1166
- Li YP**, Pei YY, Zhou ZH, Zhang XY, Gu ZH, Ding J, Zhou JJ, Gao XJ, Zhu JH. Stealth polycyanoacrylate nanoparticles as tumor necrosis factor- α carriers: pharmacokinetics and anti-tumor effects. *Biol Pharm Bull* 2001; **24**: 662-665
- Vauthier C**, Dubernet C, Fattal E, Pinto-Alphandary H, Couvreur P. Poly(alkylcyanoacrylates) as biodegradable materials for biomedical applications. *Adv Drug Deliv Rev* 2003; **55**: 519-548
- Skidan IN**, Gel' perina SE, Severin SE, Guliaev AE. Enhanced activity of rifampicin loaded with polybutyl cyanoacrylate nanoparticles in relation to intracellularly localized bacteria. *Antibiot Khimioter* 2003; **48**: 23-26
- Zhang ZR**, He Q, Liao GT, Bai SH. Study on the anticarcinogenic effect and acute toxicity of liver-targeting mitoxantrone nanoparticles. *World J Gastroenterol* 1999; **5**: 511-514
- Zhang Q**, Shen Z, Nagai T. Prolonged hypoglycemic effect of insulin-loaded polybutylcyanoacrylate nanoparticles after pulmonary administration to normal rats. *Int J Pharm* 2001; **218**: 75-80
- Deng Y**, Wang L, Yang W, Fu S, Elaissari A. Preparation of magnetic polymeric particles via inverse microemulsion polymerization process. *J Magnetism Magnetic Materials* 2003; **257**: 69-78
- Kreuter J**. Evaluation of nanoparticles as drug-delivery systems I: preparation methods. *Pharm Acta Helv* 1983; **58**: 196-209
- Sommerfeld P**, Schroeder U, Sabel BA. Long-term stability of PBCA nanoparticle suspensions suggests clinical usefulness. *Int J Pharm* 1997; **155**: 201-207
- Kuwata T**, Wang IM, Tamura T, Ponnampereuma RM, Levine R, Holmes KL, Morse HC III, De Luca LM, Ozato K. Vitamin A deficiency in mice causes a systemic expansion of myeloid cells. *Blood* 2000; **95**: 3349-3356
- Matsumura Y**, Maeda H. A new concept for macromolecular therapeutics in cancer chemotherapy: mechanism of tumoritropic accumulation of proteins and the antitumor agent smancs. *Cancer Res* 1986; **46**(12 Pt 1): 6387-6392
- Yuan F**, Dellian M, Fukumura D, Leunig M, Berk DA, Torchilin VP, Jain RK. Vascular permeability in a human tumor xenograft: molecular size dependence and cutoff size. *Cancer Res* 1995; **55**: 3752-3756

Clinical significance of serum vascular cell adhesion molecule-1 levels in patients with hepatocellular carcinoma

Joanna W. Ho, Ronnie T. Poon, Cindy S. Tong, Sheung Tat Fan

Joanna W. Ho, Ronnie T. Poon, Cindy S. Tong, Sheung Tat Fan,
Centre for the Study of Liver Disease and Department of Surgery,
University of Hong Kong, Pokfulam, Hong Kong, China

Supported by the Committee on Research and Conferences Grant of
the University of Hong Kong 2002-2003 and Sun CY Research
Foundation for Hepatobiliary and Pancreatic Surgery of the University
of Hong Kong, China

Correspondence to: Dr. Ronnie T. Poon, University of Hong Kong
Medical Centre, Department of Surgery, Queen Mary Hospital, 102
Pokfulam Road, Hong Kong, China. poontp@hkucc.hku.hk

Telephone: +852-28553635 **Fax:** +852-28175475

Received: 2004-02-06 **Accepted:** 2004-03-11

Abstract

AIM: To evaluate the correlation between serum vascular cellular adhesion molecule-1 (VCAM-1) levels and clinicopathological features in patients with hepatocellular carcinoma (HCC).

METHODS: Ninety-six patients who underwent HCC resection were recruited in the study. Preoperative serum levels of soluble VCAM-1 were measured by enzyme-linked immunosorbent assay.

RESULTS: Serum VCAM-1 level in HCC patients was inversely correlated with platelet count ($r=-0.431$, $P<0.001$) and serum albumin level ($r=-0.279$, $P<0.001$), and positively correlated with serum bilirubin level ($r=0.379$, $P<0.001$). Serum VCAM-1 level was not associated with tumor characteristics such as tumor size, venous invasion, presence of microsatellite nodules, tumor grade and tumor stage. Serum VCAM-1 level was significantly higher in HCC patients with cirrhosis compared with those without cirrhosis (median 704 vs 546 ng/mL, $P<0.001$). Furthermore, a significantly better disease-free survival was observed in HCC patients with low VCAM-1 level ($P=0.019$).

CONCLUSION: Serum VCAM-1 level appears to reflect the severity of underlying chronic liver disease rather than the tumor status in HCC patients, and low preoperative serum VCAM-1 level is predictive of better disease-free survival after surgery.

Ho JW, Poon RT, Tong CS, Fan ST. Clinical significance of serum vascular cell adhesion molecule-1 levels in patients with hepatocellular carcinoma. *World J Gastroenterol* 2004; 10 (14): 2014-2018

<http://www.wjgnet.com/1007-9327/10/2014.asp>

INTRODUCTION

Hepatocellular carcinoma (HCC) is a tumor characterized by a rich vasculature. The formation of rich vasculature depends on angiogenesis, which is a process that plays an important role in tumor progression, growth, and metastasis. Many angiogenic factors and mediators are involved in the control of angiogenesis.

Vascular cell adhesion molecule-1 (VCAM-1) is one of the adhesion molecules that have been implicated as a mediator of angiogenesis^[1]. As one of the cell adhesion molecules in the immunoglobulin superfamily, human VCAM-1 is M_r 100 000-110 000, type 1 transmembrane glycoprotein^[2-4]. VCAM-1 is transiently expressed on activated vascular endothelial cells in response to vascular endothelial growth factor (VEGF) and other cytokines, such as tumor necrosis factor α , interleukin 1β , and interferon γ ^[2,5-7]. Functionally, its expression plays a major role in adhesion of leukocytes to the endothelium in inflamed tissue and in the tumor site^[2]. It also plays an important role in providing attachment to the developing endothelium during angiogenesis^[8-10]. Furthermore, it may also exert its function as an adhesion molecule to facilitate metastasis^[2]. A previous study showed that VCAM-1 expression was associated with the metastasis of melanoma^[11].

VCAM-1 is a soluble molecule that can be detected in the circulation. Although the exact mechanism by which VCAM-1 is shredded into the bloodstream is unknown, it may involve both proteolytic processing and alternative splicing^[12,13]. Because VCAM-1 can be identified in bloodstream, it is potentially useful as a non-invasive biomarker for the monitoring of disease progression in cancer and other diseases^[14-16]. It has been reported that VCAM-1 is over-expressed in various diseases and cancers. Recent studies have demonstrated high serum levels of VCAM-1 in patients with colorectal cancer and gastric cancer^[16-17]. One study demonstrated that a high serum VCAM-1 level was significantly associated with advanced disease stage and the presence of distant metastasis in gastric cancer^[17]. A high serum VCAM-1 level has been shown to be associated with angiogenesis and poor prognosis in breast cancer^[18]. A study has also found that serum VCAM-1 was an independent prognostic marker in patients with Hodgkin's lymphoma^[19].

Up-regulated VCAM-1 expression in chronic liver disease has also been reported, suggesting that VCAM-1 may play a role in the pathogenesis of chronic hepatitis or cirrhosis^[20-26]. Serum VCAM-1 levels higher than normal have been consistently reported in several studies of chronic liver disease of various etiologies^[19-27]. However, the clinical significance of serum VCAM-1 in HCC patients has not yet been reported before. The majority of HCC patients have associated chronic hepatitis or cirrhosis. It is of interest to study serum VCAM-1 in HCC patients because VCAM-1 may be involved in the progression of both the tumor and the underlying chronic liver disease.

The objective of this study was to evaluate the levels of serum soluble VCAM-1 in HCC patients compared with cirrhotic patients without HCC and normal controls, and to analyze the correlation of serum VCAM-1 level with clinicopathological features in HCC patients.

MATERIALS AND METHODS

Patients

Ninety-six patients (71 men and 25 women; median age 55.5 years, range 16-79 years) who underwent resection of HCC in the Department of Surgery of the University of Hong Kong at Queen

Mary Hospital were studied. In the majority of cases (81%, $n=78$), HCC was related to hepatitis B viral infection. None of the 96 patients had received any preoperative treatment. The study was approved by the Ethics Committee of our institution and informed consent was obtained from the patients.

Preoperative serum was collected from the patients. Venous blood samples were drawn into a serum separator tube and centrifuged at 3 000 r/min for 10 min, then stored at -80°C until VCAM-1 levels were determined. Serum samples were also obtained from 19 healthy controls without evidence of any active disease and 23 patients with cirrhosis but no evidence of HCC on ultrasonography and alpha fetoprotein (AFP) surveillance. The majority of the 23 cirrhotic patients (74%, $n=17$) had cirrhosis related to hepatitis B viral infection.

Measurement of serum VCAM-1 level

Serum VCAM-1 levels were quantified using an enzyme-linked immunosorbent assay kit designed to quantitatively measure human soluble VCAM-1 concentration in serum (Human sVCAM-1 Immunoassay; R&D systems, Minneapolis, MN). This assay contains recombinant human VCAM-1 and antibodies against the recombinant factor. The assay can recognize both recombinant and natural human VCAM-1. Briefly, 100 μL of diluted VCAM-1 conjugate (antibody to recombinant VCAM-1 conjugated to horse-radish peroxidase) was added to each well that was pre-coated with monoclonal antibody specific for VCAM-1, after which, 100 μL of serially diluted recombinant VCAM-1 standards and serum samples were added to the wells and incubated at room temperature for 1.5 h. After the wells were washed with wash buffer 6 times to clear any unbound substances, tetramethylbenzidine was added to the wells for color development. The intensity of the developed color was measured by reading absorbance at 450 nm. Each measurement was made in duplicate and the serum VCAM-1 level was determined by extrapolation from a standard curve generated for each set of samples assayed. The sensitivity of the assay was 2 ng/mL, and the coefficients of variation of intraassay and interassay determination were in the range given by the manufacturer (4.3-5.9% and 8.5-10.2%, respectively).

Clinicopathologic and follow-up data

All clinicopathologic and follow-up data were prospectively collected and entered into a computerized database. Detailed preoperative blood tests such as complete blood count, coagulation profile, liver biochemistry, indocyanine green retention at 15 min (ICG_{15}), serum AFP level, and hepatitis viral serology were assessed for all patients. Histopathologic data including Edmonson grade^[28] (1-2 or 3-4), any venous invasion, tumor capsule, microsatellite lesion and pTNM stage^[29] (I/II or III/IVA) were collected. All patients had a computed tomography (CT) scan 1 mo after the hepatic resection to detect any tumor, which was considered a residual disease. Patients who had a positive margin or residual tumors in the 1-month CT scan were considered having a palliative resection.

Postoperative follow-up included monitoring for tumor recurrence by monthly serum AFP level and chest X-ray detection together with ultrasonography or computed tomography (CT) scan every 3 mo. Recurrence of disease was diagnosed by the detection of any intrahepatic or extrahepatic tumor with a typical enhancement pattern of HCC in contrast CT scan and elevation of serum AFP level on serial measurements. Percutaneous fine-needle aspiration cytology was performed to confirm the diagnosis of recurrence in uncertain cases. Disease-free survival was calculated from the date of hepatic resection to the date when recurrence was diagnosed or, in the absence of detectable recurrence, to the date of death or last follow-up.

Statistical analysis

Continuous data were expressed as median with range in parenthesis. For comparison between groups, Mann-Whitney U test was used for analysis of continuous variables, and Chi-square test (or the Fisher's exact test, where appropriate) was used for analysis of discrete variables. Correlation analysis was performed using the Spearman rank correlation test. Cumulative disease-free survival was computed using the Kaplan-Meier method and compared between groups by the log-rank test. Serum VCAM level was entered into a multivariate Cox regression analysis together with 7 other variables that were demonstrated to be of prognostic importance in previous studies from our center and others, namely, serum AFP level, tumor size, presence of venous invasion, presence of microsatellite nodules, presence of underlying cirrhosis and pTNM stage^[30,31]. All statistical analyses were performed using the SPSS statistical software (SPSS/PC+, SPSS Inc., Chicago, Illinois). $P<0.05$ was considered statistically significant.

RESULTS

Serum VCAM-1 levels

Figure 1 shows the distribution of serum VCAM levels in normal controls ($n=19$), patients with cirrhosis only ($n=23$) and HCC patients ($n=96$). The median serum VCAM-1 level in healthy individuals, patients with cirrhosis only, and patients with HCC was 631 ng/mL (449-1 103), 780 ng/mL (509-4 120), and 621 ng/mL (179-3 199), respectively. There was no significant difference in serum VCAM-1 levels between HCC patients and normal individuals ($P=0.447$). However, there were significant differences in serum VCAM-1 levels between cirrhotic patients without HCC and normal individuals ($P=0.010$), and between cirrhotic patients with and without HCC ($P<0.001$).

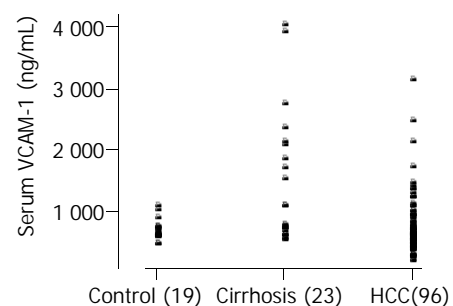


Figure 1 Scatter plot to illustrate the distribution of serum VCAM-1 level (ng/mL) in healthy control subjects ($n=19$), cirrhosis subjects without HCC ($n=23$), and HCC patients ($n=96$).

Correlation between serum VCAM-1 levels and clinicopathological features in HCC patients

Preoperative serum levels of VCAM-1 in the 96 patients with HCC were analyzed to identify any relationship with the clinicopathological parameters. When analyzed in relation to preoperative clinical parameters categorized as binary variables (Table 1), serum VCAM-1 level had no significant relationship with patients' sex, age, hepatitis B surface antigen status, serum AFP level or serum albumin level. However, serum VCAM-1 levels were significantly higher in patients with high ICG_{15} ($>10\%$), which signifies impaired liver function, and in patients with thrombocytopenia, which signifies the presence of significant hypersplenism. When correlated as continuous variables, serum VCAM-1 levels were positively correlated with serum bilirubin level ($r=0.379$, $P<0.001$) and negatively correlated with white cell count ($r=-0.226$, $P=0.027$), platelet count ($r=-0.431$, $P<0.001$) and serum albumin level ($r=-0.279$, $P<0.001$).

Table 1 Preoperative serum VCAM-1 levels categorized by clinical and laboratory variables

Variables	Median serum VCAM-1 (ng/mL)	P ¹
Gender		
Male (n=71)	623	0.381
Female (n=25)	594	
Age (yr)		
≤60 (n=56)	615	0.460
>60 (n=40)	639	
HBsAg		
Positive (n=78)	623	0.266
Negative (n=18)	592	
Serum AFP		
≤20 ng/mL (n=29)	608	0.737
>20 ng/mL (n=67)	623	
Serum albumin		
≤40 g/L (n=59)	614	0.228
>40 g/L (n=37)	634	
ICG ₁₅		
≤10% (n=45)	531	<0.001
>10% (n=51)	667	
Platelet count		
≤150 ×10 ⁹ /L (n=44)	728	<0.001
>150 ×10 ⁹ /L (n=52)	547	

HBsAg: Hepatitis B surface antigen; AFP: alpha-fetoprotein; ICG₁₅: indocyanine green retention at 15 min. ¹By Mann-Whitney U test.

Table 2 Preoperative serum VCAM-1 levels categorized by pathological variables

Variables	Median serum VCAM-1 (ng/mL)	P ¹
Background liver disease		
Normal (n=7)	462	0.084 ²
Chronic hepatitis (n=39)	548	
Cirrhosis (n=50)	704	<0.001 ^b
Cirrhotic liver		
Absent (n=46)	546	<0.001
Present (n=50)	704	
Tumor size		
≤5 cm (n=35)	686	0.158
>5 cm (n=61)	609	
Tumor capsule		
Absent (n=66)	597	0.015
Present (n=30)	736	
Venous invasion		
Absent (n=49)	643	0.248
Present (n=47)	574	
Microsatellite nodules		
Absent (n=50)	643	0.359
Present (n=46)	626	
Edmonson grade		
I/II (n=49)	634	0.629
III/IV (n=47)	642	
pTNM stage		
I/II (n=43)	649	0.134
III/IV (n=53)	592	

pTNM: Pathological tumor-node-metastasis. ¹By Mann-Whitney U test; ²Compared with normal nontumorous liver; ^bP<0.001 compared with both normal liver and chronic hepatitis.

Table 2 shows the relationship of serum VCAM-1 levels and histopathologic features of the resected HCC. There was no significant relationship with the tumor size ($P=0.185$), the presence of microsatellite tumor nodules ($P=0.359$) or venous invasion ($P=0.248$). Significantly higher serum VCAM-1 levels were observed with the presence of tumor capsule ($P=0.015$) and the presence of cirrhosis in adjacent non-tumor liver tissues ($P<0.001$). When categorized according to tumor pTNM staging or Edmonson grading, no significant differences in serum VCAM-1 levels were observed between different tumor stages or grades.

Serum VCAM-1 levels in HCC patients with or without cirrhosis

Fifty out of the 96 HCC patients had cirrhotic liver adjacent to the resected tumor. The median level of serum VCAM-1 in these cases of HCC with cirrhosis was 704 ng/mL (179-3 199), which was significantly higher than that in the HCC cases without cirrhosis (median 546 ng/mL, range 207-1 248, $P<0.001$), but it was significantly lower than that in the 23 patients with cirrhosis only ($P=0.034$). All patients with HCC and cirrhosis had Child's A liver function status, whereas among the 23 patients with cirrhosis only, 8 patients were Child's A, 7 patients were Child's B and 8 patients were Child's C. When compared with the healthy individuals, although the median level of serum VCAM-1 in HCC patients with cirrhosis was higher, the difference was not statistically different ($P=0.271$). In contrast, HCC patients without cirrhosis ($n=46$) had a significantly lower level of VCAM-1 when compared with healthy individuals ($P=0.008$). HCC patients with chronic hepatitis ($n=39$) had a higher serum VCAM-1 level than HCC patients with normal liver, but the difference was not statistically significant ($P=0.084$).

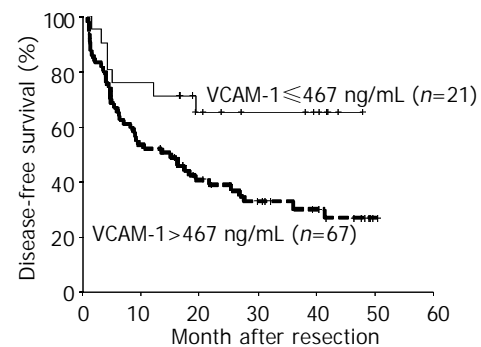


Figure 2 Disease-free survival analysis of HCC patients segregated into low (≤ 467 ng/mL, $n=21$) and high (>467 ng/mL, $n=67$) preoperative serum VCAM-1 levels ($P=0.019$).

Prognostic value of serum VCAM-1 levels on disease-free survival

Excluding 8 patients with hospital mortality or palliative resection, 88 patients were available for survival analysis to determine the prognostic influence of serum VCAM-1 levels. The median follow-up of the patients was 33 mo (range 15-52 mo). Because of the skewed distribution of serum VCAM-1 levels among the 88 patients, the 25 th percentile of VCAM-1 levels (467 ng/mL) was used as a cut-off point of high and low values of serum VCAM-1 levels in these patients^[32]. At the time of analysis, 52 of the 88 HCC patients had postoperative recurrence. The disease-free survival was compared between two groups of patients who were segregated in low ($n=21$) and high ($n=67$) serum VCAM-1 levels. Patients with low levels of VCAM-1 had significantly better disease-free survival than those with high levels of VCAM-1 (3-year disease-free survival 66.7% vs 32.8%, $P=0.019$, Figure 2). The overall survival was also better in the group with low serum VCAM-1 levels than in the group with high levels, but the difference was not statistically significant (3-year overall survival 75.0% vs 54.2%, $P=0.406$).

Serum VCAM-1 was entered into a Cox regression analysis of disease-free survival together with serum AFP ($>$ or ≤ 20 ng/mL), tumor size ($>$ or ≤ 5 cm), presence of venous invasion, presence of microsatellite lesions, presence of cirrhosis and tumor pTNM stage. Only pTNM stage (risk ratio 1.409, 95% confidence interval 1.080-1.840, $P=0.012$) and serum VCAM-1 (risk ratio 2.329, 95% confidence interval 1.045-5.191, $P=0.039$) were significant prognostic factors for disease-free survival.

DISCUSSION

Evaluation of angiogenic factors has shown important clinical implications in many types of cancer. In particular, the measurement of various circulating angiogenic factors might provide important prognostic values independent of conventional pathological factors in cancer patients^[33]. HCC is a highly vascularized malignancy, and angiogenesis has been known to be important for its development and metastasis^[34]. Hence, it is of great interest to evaluate the clinical significance of circulating angiogenesis-related markers in HCC patients. Serum VCAM-1 appears to be a promising circulating marker that might have a prognostic value in several types of cancer^[16-19]. To our knowledge, this is the first study that evaluated the clinical significance of serum VCAM-1 levels in HCC patients.

Although the median level of VCAM-1 in HCC patients appeared to be similar to that in normal subjects, within the group of HCC patients, those with underlying cirrhosis had a significantly higher VCAM-1 level than those with chronic hepatitis or normal nontumorous liver. Furthermore, high serum VCAM-1 levels in HCC patients correlated positively with serum bilirubin level and inversely with serum albumin level and platelet count. These findings suggested that high serum VCAM-1 levels were related to the severity of underlying chronic liver diseases. In contrast, there was no significant relationship between serum VCAM-1 levels and tumor size, pathological features of invasiveness or tumor stage. This finding in HCC patients was contrary to the findings of higher serum VCAM-1 levels associated with more advanced stage tumors in other cancers^[16-19]. Analysis of serum VCAM-1 levels in HCC patients is complicated by the fact that most cases of HCC are associated with chronic liver disease, which could also contribute to the serum VCAM-1 levels. The source of VCAM-1 in the circulation of HCC patients could come from activated endothelial cells in both the tumor and chronic hepatitis or cirrhosis in the nontumorous liver. Our study suggested that serum VCAM-1 level in HCC patients could reflect the severity of underlying chronic liver disease rather than the tumor status. Unlike the case of some other cancers, VCAM-1 may play a less important role as a mediator of angiogenesis or related pathological processes in HCC. One of the main functions of endothelial adhesion molecules in tumor is to facilitate the adhesion of leukocytes into tumor endothelium, which in turn could promote angiogenesis^[35]. Yoong *et al.*^[36] demonstrated that vascular adhesion protein-1 and intercellular adhesion molecule-1, rather than VCAM-1, supported adhesion of tumor infiltrating lymphocytes to tumor endothelium in HCC. In fact, the serum VCAM-1 levels of the 46 patients with HCC and noncirrhotic liver were significantly lower than those of normal controls, suggesting that VCAM-1 expression may be down-regulated in HCC patients. While most studies in other types of cancer reported the expression of serum VCAM-1 levels was up-regulated, down-regulation of VCAM-1 has also been reported in node positive breast cancer patients^[37].

The serum VCAM-1 levels in the 96 HCC patients in this study were significantly lower than those of 23 patients with cirrhosis only. Even when the 50 patients with HCC and background cirrhosis were separately analyzed, their serum

VCAM-1 levels were still significantly lower than those of the 23 patients with cirrhosis only. This is probably attributable to the fact that all cirrhotic patients with HCC who underwent hepatic resection had Child's A cirrhosis, whereas the majority of patients in the group with cirrhosis only had Child's B or C cirrhosis. Several previous studies have demonstrated that serum VCAM-1 levels were elevated in cirrhotic patients compared with normal controls, and that serum VCAM-1 level was higher with more severe impairment of liver function or more severe portal hypertension^[22,23,26,27]. Two studies demonstrated that serum VCAM-1 levels reflected the degree of fibrosis in hepatitis C related cirrhotic patients^[24,25]. Our study suggested a similar relationship between serum VCAM-1 level and severity of cirrhosis in a group of patients with predominantly hepatitis B virus related cirrhosis. VCAM-1 appears to play an important role in liver inflammation and fibrosis, probably by mediating interaction between lymphocytes and endothelium. Further studies to clarify the role of VCAM-1 in chronic liver disease may lead to a better understanding of the pathogenesis of cirrhosis and may provide a novel target of intervention to prevent progression of cirrhosis.

Although serum VCAM-1 level was not related to tumor invasiveness or stage, we observed a significantly better disease-free survival in HCC patients with low level of serum VCAM-1. Our study demonstrated that preoperative circulating level of VCAM-1 had a prognostic value in patients undergoing resection of HCC independent of conventional prognostic factors. The exact mechanism underlying the survival differences between patients with low and high serum VCAM-1 levels is unclear. In view of the relationship between serum VCAM-1 levels and the severity of underlying chronic liver disease or cirrhosis found in this study and other studies^[22-27], we speculate that the unfavorable prognostic influence of high serum VCAM-1 level is likely to be related to the underlying cirrhotic or fibrotic condition. The presence of cirrhosis or a higher degree of liver fibrosis has been shown to predispose to multicentric hepatocarcinogenesis and hence postoperative recurrence of HCC^[30,31]. An alternative possibility is that HCC with significantly down-regulated VCAM-1 expression may be associated with more favorable prognosis after resection. However, the exact mechanism for the reduction in serum VCAM-1 level in the presence of HCC observed in some patients is far from clear, and such a possibility seems less likely in view of the lack of association between serum VCAM-1 and tumor characteristics. Further studies that correlate serum VCAM-1 level with the expression of VCAM-1 in HCC tumor tissues and adjacent nontumorous liver may help clarify the mechanism underlying the prognostic significance of serum VCAM-1 levels in HCC patients. Irrespective of the underlying mechanism, the predictive value of serum VCAM-1 level might have potential clinical application in selecting patients with a higher risk of postoperative recurrence for some adjuvant therapy to reduce recurrence.

In conclusion, our data demonstrated that serum VCAM-1 levels in HCC patients correlated with the impairment of liver function and the presence of cirrhosis but not tumor size or features of tumor invasiveness. Hence, serum VCAM-1 levels appear to reflect the severity of underlying liver disease rather than the tumor status in HCC patients. A low serum VCAM-1 level predicts better disease-free survival after tumor resection in HCC patients. Further studies are merited to investigate the exact mechanisms involved in these observations and to explore the potential use of serum VCAM-1 level as a novel prognostic marker in HCC patients.

REFERENCES

- 1 **Koch AE**, Halloran MM, Haskell CJ, Shah MR, Polverini PJ.

- Angiogenesis mediated by soluble forms of E-selectin and vascular cell adhesion molecule-1. *Nature* 1995; **376**: 517-519
- 2 **Osborn L**, Hession C, Tizard R, Vassallo C, Luhowskyj S, Chi-Rosso G, Lobb R. Direct expression cloning of vascular cell adhesion molecule 1, a cytokine-induced endothelial protein that binds to lymphocytes. *Cell* 1989; **59**: 1203-1211
- 3 **Cybulsky MI**, Fries JW, Williams AJ, Sultan P, Eddy R, Byers M, Shows T, Gimbrone MA Jr, Collins T. Gene structure, chromosomal location, and basis for alternative mRNA splicing of the human VCAM1 gene. *Proc Natl Acad Sci U S A* 1991; **88**: 7859-7863
- 4 **Hession C**, Tizard R, Vassallo C, Schiffer SB, Goff D, Moy P, Chi-Rosso G, Luhowskyj S, Lobb R, Osborn L. Cloning of an alternate form of vascular cell adhesion molecule-1 (VCAM1). *J Biol Chem* 1991; **266**: 6682-6685
- 5 **Doukas J**, Pober JS. IFN-gamma enhances endothelial activation induced by tumor necrosis factor but not IL-1. *J Immunol* 1990; **145**: 1727-1733
- 6 **Thornhill MH**, Wellicome SM, Mahiouz DL, Lanchbury JS, Kyan-Aung U, Haskard DO. Tumor necrosis factor combines with IL-4 or IFN-gamma to selectively enhance endothelial cell adhesiveness for T cells. The contribution of vascular cell adhesion molecule-1-dependent and -independent binding mechanisms. *J Immunol* 1991; **146**: 592-598
- 7 **Fox SB**, Turner GD, Gatter KC, Harris AL. The increased expression of adhesion molecules ICAM-3, E- and P-selectins on breast cancer endothelium. *J Pathol* 1995; **177**: 369-376
- 8 **Imhof BA**, Dunon D. Leukocyte migration and adhesion. *Adv Immunol* 1995; **58**: 345-416
- 9 **Watt SM**, Gschmeissner SE, Bates PA. PECAM-1: its expression and function as a cell adhesion molecule on hemopoietic and endothelial cells. *Leuk Lymphoma* 1995; **17**: 229-244
- 10 **Patey N**, Vazeux R, Canioni D, Potter T, Gallatin WM, Brousse N. Intercellular adhesion molecule-3 on endothelial cells. Expression in tumors but not in inflammatory responses. *Am J Pathol* 1996; **148**: 465-472
- 11 **Langley RR**, Carlisle R, Ma L, Specian RD, Gerritsen ME, Granger DN. Endothelial expression of vascular cell adhesion molecule-1 correlates with metastatic pattern in spontaneous melanoma. *Microcirculation* 2001; **8**: 335-345
- 12 **Pigott R**, Dillon LP, Hemingway IH, Gearing AJ. Soluble forms of E-selectin, ICAM-1 and VCAM-1 are present in the supernatants of cytokine activated cultured endothelial cells. *Biochem Biophys Res Commun* 1992; **187**: 584-589
- 13 **Terry RW**, Kwee L, Levine JF, Labow MA. Cytokine induction of an alternatively spliced murine vascular cell adhesion molecule (VCAM) mRNA encoding a glycosylphosphatidylinositol-anchored VCAM protein. *Proc Natl Acad Sci U S A* 1993; **90**: 5919-5923
- 14 **Matsuda M**, Tsukada N, Miyagi K, Yanagisawa N. Increased levels of soluble vascular cell adhesion molecule-1 (VCAM-1) in the cerebrospinal fluid and sera of patients with multiple sclerosis and human T lymphotropic virus type-1-associated myelopathy. *J Neuroimmunol* 1995; **59**: 35-40
- 15 **Sudhoff T**, Wehmeier A, Kliche KO, Aul C, Schlomer P, Bauser U, Schneider W. Levels of circulating endothelial adhesion molecules (sE-selectin and sVCAM-1) in adult patients with acute leukemia. *Leukemia* 1996; **10**: 682-686
- 16 **Alexiou D**, Karayiannakis AJ, Syrigos KN, Zbar A, Kremmyda A, Bramis I, Tsigris C. Serum levels of E-selectin, ICAM-1 and VCAM-1 in colorectal cancer patients: correlations with clinicopathological features, patient survival and tumour surgery. *Eur J Cancer* 2001; **37**: 2392-2397
- 17 **Alexiou D**, Karayiannakis AJ, Syrigos KN, Zbar A, Sekara E, Michail P, Rosenberg T, Diamantis T. Clinical significance of serum levels of E-selectin, intercellular adhesion molecule-1, and vascular cell adhesion molecule-1 in gastric cancer patients. *Am J Gastroenterol* 2003; **98**: 478-485
- 18 **O'Hanlon DM**, Fitzsimons H, Lynch J, Tormey S, Malone C, Given HF. Soluble adhesion molecules (E-selectin, ICAM-1 and VCAM-1) in breast carcinoma. *Eur J Cancer* 2002; **38**: 2252-2257
- 19 **Christiansen I**, Sundstrom C, Enblad G, Totterman TH. Soluble vascular cell adhesion molecule-1 (sVCAM-1) is an independent prognostic marker in Hodgkin's disease. *Br J Haematol* 1998; **102**: 701-709
- 20 **Adams DH**, Burra P, Hubscher SG, Elias E, Newman W. Endothelial activation and circulating vascular adhesion molecules in alcoholic liver disease. *Hepatology* 1994; **19**: 588-594
- 21 **Haruta I**, Tokushige K, Komatsu T, Ikeda I, Yamauchi K, Hayashi N. Clinical implication of vascular cell adhesion molecule-1 and very late activation antigen-4 interaction, and matrix metalloproteinase-2 production in patients with liver disease. *Can J Gastroenterol* 1999; **13**: 721-727
- 22 **Lim AG**, Jazrawi RP, Levy JH, Petroni ML, Douds AC, Maxwell JD, Northfield TC. Soluble E-selectin and vascular cell adhesion molecule-1 (VCAM-1) in primary biliary cirrhosis. *J Hepatol* 1995; **22**: 416-422
- 23 **Pirisi M**, Fabris C, Falleti E, Soardo G, Toniutto P, Vitulli D, Gonano F, Bartoli E. Serum soluble vascular-cell adhesion molecule-1 (VCAM-1) in patients with acute and chronic liver diseases. *Dis Markers* 1996; **13**: 11-17
- 24 **Kaplanski G**, Farnarier C, Payan MJ, Bongrand P, Durand JM. Increased levels of soluble adhesion molecules in the serum of patients with hepatitis C. Correlation with cytokine concentrations and liver inflammation and fibrosis. *Dig Dis Sci* 1997; **42**: 2277-2284
- 25 **Lo Iacono O**, Garcia-Monzon C, Almasio P, Garcia-Buey L, Craxi A, Moreno-Otero R. Soluble adhesion molecules correlate with liver inflammation and fibrosis in chronic hepatitis C treated with interferon-alpha. *Aliment Pharmacol Ther* 1998; **12**: 1091-1099
- 26 **Yamaguchi N**, Tokushige K, Haruta I, Yamauchi K, Hayashi N. Analysis of adhesion molecules in patients with idiopathic portal hypertension. *J Gastroenterol Hepatol* 1999; **14**: 364-369
- 27 **Kobayashi H**, Horikoshi K, Long L, Yamataka A, Lane GJ, Miyano T. Serum concentration of adhesion molecules in post-operative biliary atresia patients: relationship to disease activity and cirrhosis. *J Pediatr Surg* 2001; **36**: 1297-1301
- 28 **Edmonson HA**, Steiner PE. Primary carcinoma of the liver: a study of 100 among 48 900 necropsies. *Cancer* 1954; **7**: 462-503
- 29 **Hermanek P**, Sobin LH, eds. TNM classification of malignant tumors. 4th ed. Berlin, Springer Verlag 1987
- 30 **Tung-Ping Poon R**, Fan ST, Wong J. Risk factors, prevention, and management of postoperative recurrence after resection of hepatocellular carcinoma. *Ann Surg* 2000; **232**: 10-24
- 31 **Lauwers GY**, Vauthey JN. Pathological aspects of hepatocellular carcinoma: a critical review of prognostic factors. *Hepatogastroenterology* 1998; **45**(Suppl 3): 1197-1202
- 32 **Kaplan EL**, Meier P. Nonparametric estimation from incomplete observations. *J Am Stat Assoc* 1958; **53**: 457-481
- 33 **Tung-Ping Poon R**, Fan ST, Wong J. Clinical implications of circulating angiogenic factors in cancer patients. *J Clin Oncol* 2001; **19**: 1207-1225
- 34 **Poon RT**, Fan ST, Wong J. Clinical significance of angiogenesis in gastrointestinal cancers: a target for novel prognostic and therapeutic approaches. *Ann Surg* 2003; **238**: 9-28
- 35 **Jain RK**, Koenig GC, Dellian M, Fukumura D, Munn LL, Melder RJ. Leukocyte-endothelial adhesion and angiogenesis in tumors. *Cancer Metastasis Rev* 1996; **15**: 195-204
- 36 **Yoong KF**, McNab G, Hubscher SG, Adams DH. Vascular adhesion protein-1 and ICAM-1 support the adhesion of tumor-infiltrating lymphocytes to tumor endothelium in human hepatocellular carcinoma. *J Immunol* 1998; **160**: 3978-3988
- 37 **Madhavan M**, Srinivas P, Abraham E, Ahmed I, Vijayalekshmi NR, Balaran P. Down regulation of endothelial adhesion molecules in node positive breast cancer: possible failure of host defence mechanism. *Pathol Oncol Res* 2002; **8**: 125-128

Effects of KAI1 gene on growth and invasion of human hepatocellular carcinoma MHCC97-H cells

Sui-Hai Si, Jian-Min Yang, Zhi-Hong Peng, Yuan-Hui Luo, Ping Zhou

Sui-Hai Si, Jian-Min Yang, Zhi-Hong Peng, Yuan-Hui Luo, Ping Zhou, Gastroenterology Research Center, Southwest Hospital, Third Military Medical University, Chongqing 400038, China
Supported by the National Natural Science Foundation of China, No. 30070348

Co-correspondents: Dr. Sui-Hai Si

Correspondence to: Professor Jian-Min Yang, Gastroenterology Research Center, Southwest Hospital, Third Military Medical University, Chongqing 400038, China. jianminyang@hotmail.com

Telephone: +86-23-68754678 **Fax:** +86-537-2903067

Received: 2003-08-06 **Accepted:** 2003-10-12

Abstract

AIM: To study the effects of sense and antisense KAI1 genes on the growth and invasion of human hepatocellular carcinoma (HCC) cell line MHCC97-H.

METHODS: KAI1 sense and antisense eukaryotic expression plasmids were constructed using subclone technique and transfected into MHCC97-H cells respectively by DOTAP liposome. After successful transfection was confirmed, *in vitro* growth curve, cell cycles, plate clone formation efficiency, invasive ability in Boyden Chamber assay and ultrastructural morphology were studied.

RESULTS: KAI1 sense and antisense genes had no significant effects on the cell growth curve and cell cycles. After transfection with sense KAI1 gene, decreased invasive ability in Boyden Chamber assay and decreased amount of mitochondria, but no significant changes of plate clone formation efficiency were observed in MHCC97-H-S cells. The plate clone formation efficiency and invasive ability in Boyden Chamber assay were significantly increased in MHCC97-H-AS cells, after transfection with antisense KAI1 gene. Furthermore, increased amount of mitochondria, rough endoplasmic reticulum, Golgi apparatus and expanded endoplasmic reticulum were also noted in MHCC97-H-AS cells.

CONCLUSION: Changes of KAI1 expression in HCC cells may alter their invasive and metastasis ability of the tumor.

Si SH, Yang JM, Peng ZH, Luo YH, Zhou P. Effects of KAI1 gene on growth and invasion of human hepatocellular carcinoma MHCC97-H cells. *World J Gastroenterol* 2004; 10 (14): 2019-2023

<http://www.wjgnet.com/1007-9327/10/2019.asp>

INTRODUCTION

Hepatocellular carcinoma (HCC) is one of the most common malignant tumors in China. Metastasis and recurrence are the most principal factors for the prognosis of patients with the tumor^[1]. KAI1 gene, isolated from human metastatic prostate tumor in 1995, was regarded as a new metastasis suppressor gene. Up to now, many researches on the relationship between

KAI1 gene and invasion, metastasis of malignant tumors have been reported, but most of them were made by histopathological and molecular pathological methods^[2-16]. In the present research, we studied the effects of KAI1 gene on the growth and invasion of human hepatocellular carcinoma (HCC) by subclone, gene transfection and antisense technology.

MATERIALS AND METHODS

Plasmid and vector

Plasmid pCMV-KAI1, with a full length of 8.2 kb, containing human a full-length of KAI1 structural cDNA gene, was a generous gift from Professor J. Carl Barrett and Dr. Dong of National Institute of Health of USA^[2]. Eukaryotic expression plasmid vector pCI-neo, with a full length of 4.7 kb, was purchased from Promega Corporation.

Gene recombination and identification

Sense and antisense KAI1 eukaryotic expression plasmids constructed by subclone technique, were confirmed and identified by restriction endonuclease *Sal* I and *Xba* I analysis.

Cell line and culture

MHCC97-H, a hepatocellular carcinoma cell line with highly metastatic potential^[17], purchased from Liver Cancer Institute, Zhongshan Hospital, Shanghai Fudan University, was used as target cells of gene transfection in the present study. The cell line was cultured in Dulbecco minimum essential medium (Hyclone, USA) containing 100 mL/L fetal calf serum (Hyclone, USA), 100 kU/L penicillin and 100 kU/L streptomycin at 37 °C in a 50 mL/L CO₂ incubator.

Gene transfection

Sense and antisense KAI1 eukaryotic expression plasmids were transfected into MHCC97-H cells respectively by DOTAP (Roche, USA) liposome transfection system similar to our previous report^[18]. Forty-eight hours after transfection, the cells were transfer-selection-cultured for two weeks under the pressure of 800 mg/L G418 (Pierces, USA) in the culture medium. Then the positive cell clones were mixed and the resistance cells were expanded to be cultured under the pressure of 250-600 mg/L G418. Enhanced culture, passaging and storage were performed until few cells were killed by G418.

Integration and expression of transfected genes

Gene integration was identified with amplification of neo genes^[19] by polymerase chain reaction (PCR). The primers, designed to amplify the neo genes in vector pCI-neo: forward (P1): 5' -CAA GAT GGA TTG CAC GCA GG-3', reverse (P2): 5' -CCC GCT CAG AAG AAC TCG TC -3', were synthesized by Shanghai Bioengineering Company, China. Theoretical length of PCR product was 790 bp. Western blot and immunocytochemistry were also performed to understand whether transfection was successful and the effects of transfected genes on KAI1 expression in MHCC97-H cells.

Ultrastructural morphology

Ultrastructural changes of the cells transfected with sense or antisense KAI1 gene were observed with transmission electron microscope.

Cell growth curve

Cells in exponential growth phase were trypsinized to develop single-cell suspension. Four $\times 10^4$ viable cells in 1 mL of medium were added to each well of the 24-well culture plates, which were incubated at 37 °C with 50 mL/L CO₂. Cell numbers in 4 wells were counted and averaged with blood counting chamber every 24 h for 10 consecutive days, and cell growth curve was plotted based on these results.

Cell cycles

Cell cycle analyses were performed by flow cytometry, and each group was examined for 3 times.

Plate clone formation test

Cells cultured (2×10^3) for 48 h were added to each well containing 1 mL of culture medium of a 6-well culture plate, each cell group contained 4 wells. Then the culture plate was gently swayed to disperse cells. The cells were incubated at 37 °C with 50 mL/L CO₂ for 12 d. Then the cells were washed twice with warm PBS, and stained with Giemsa solution. The number of colonies containing 50 cells or more was counted under a microscope.

In vitro invasion assay

In vitro invasive ability was tested by Boyden Chamber assay^[20,21] according to the kit directions. Invasion Chamber inserts (BD Biosciences, USA) with 8 μ m-pores in their PET membrane had been coated by matrigel. Before invasion assay, the invasion chambers were rehydrated with DMEM (serum-free) for 2 h in a humidified tissue culture incubator at 37 °C with 50 mL/L CO₂ atmosphere. DMEM with 100 mL/L fetal bovine serum was added to the lower compartment, and 1.5×10^5 tumor cells in serum-free DMEM were added to the upper compartment of the chamber. Each cell group was plated in 3 duplicate wells. After 48 h incubation, the matrigel was removed, and the filter was washed, cells were fixed and stained in Giemsa solution. Then the cells having migrated to the lower sides of the PET membrane in 5 random visual fields (200 \times) were counted under a light microscope.

Statistical analysis

Statistical analysis software package SPSS (V10.0) was used for data processing, and $P < 0.05$ was considered statistically significant.

RESULTS

KAI1 gene recombination and identification

Two fragments of 3 kb and 5.2 kb appeared after pCMV-KAI1 was digested by *Xba* I. According to the plasmid pCMV-KAI1 map, the 3 kb fragment containing human full-length structural KAI1 cDNA gene was extracted. The cleaved vector pCI-neo after digestion by *Xba* I and dephosphorylation by CIP was linked up with the 3 kb fragment. Two recombinant plasmids were extracted and digested by *Sal* I, the plasmid appearing 2 fragments of 2.25 kb and 6.22 kb after digestion was consistent with the expected sense KAI1 expression plasmid, and the other appearing two fragments of 0.75 kb and 7.72 kb was consistent with the expected antisense KAI1 expression plasmid (Figure 1A). Then the 2 recombinants were digested by *Xba* I to further confirm the insertion of target fragment into the vector. The results showed the two recombinants were respectively cleaved into the same two fragments 3 kb, 5.4 kb (Figure 1B),

and suggested subclone reconstruction was successfully performed.

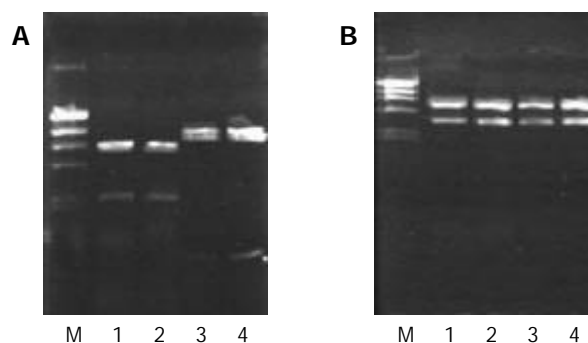


Figure 1 Identification of KAI1 recombinant plasmids digested by *Sal* I and *Xba* I. M: λ DNA/*Hind* III marker (23.13, 9.42, 6.56, 4.36, 2.32 and 2.02 kb), 1, 2: pCI-KAI1, 3, 4: pCI-anti-KAI1.

KAI1 gene transfection and identification

The recombinants containing sense or antisense KAI1 cDNA were respectively transfected into MHCC97-H cells by DOTAP liposome system. After stable cell clones were screened by G418, the cells transfected with sense KAI1 gene were renamed as MHCC97-H-S, the cells transfected with antisense KAI1 gene were renamed as MHCC97-H-AS, and the cells transfected with vector pCI-neo (vacant vector) were renamed as MHCC97-H-pCI. With amplification of the neo genes by PCR, a specific fragment with a length of 790 bp could be produced from MHCC97-H-S, MHCC97-H-AS and MHCC97-H-pCI cells, but none from MHCC97-H cells (Figure 2). It suggested that the recombinant genes were integrated into genomes of the target cells respectively.

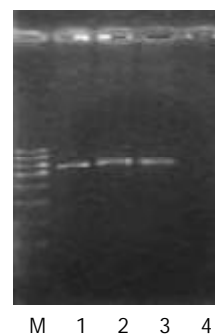


Figure 2 Identifications of gene integration by neo gene amplification. M: Ladder marker (1.0, 0.9, 0.8, 0.7, 0.6, 0.5, 0.4 and 0.3 kb), 1: MHCC97-H-S (790 bp), 2: MHCC97-H-AS (790 bp), 3: MHCC97-H-pCI (790 bp), 4: MHCC97-H.

Western blot and immunocytochemistry staining showed KAI1 protein expression was enhanced in MHCC97-H-S, but decreased in MHCC97-H-AS, and no obvious difference in MHCC97-H-pCI as compared with MHCC97-H cells (Figures 3, 4).

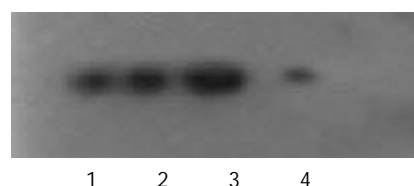


Figure 3 KAI1 protein expressions in different cells revealed by Western blot. 1: MHCC97-H, 2: MHCC97-H-pCI, 3: MHCC97-H-S, 4: MHCC97-H-AS.

Ultrastructural changes in transfected cells

Under electron microscope, the amount of mitochondria was decreased in MHCC97-H-S cells, but increased in MHCC97-H-AS cells. Furthermore, increased amount of rough endoplasmic reticulum (RER), Golgi apparatus, expanded endoplasmic reticulum and myelin-sheath-like changes of mitochondria were also noted in MHCC97-H-AS cells (Figure 5). However, there were no obvious differences in cell shape, superficial microvilli, karyotype and karyokinesis among MHCC97-H-S, MHCC97-H-AS and MHCC97-H cells.

Table 1 Cell cycle distribution of different cells revealed by flow cytometer (%)

Cell	G ₀ /G ₁	S	G ₂ /M
MHCC97-H-S	69.8±6.7	19.7±6.4	10.5±0.9
MHCC97-H-AS	72.1±7.2	19.0±6.3	8.9±0.9
MHCC97-H	73.1±2.0	16.4±1.4	10.5±1.5

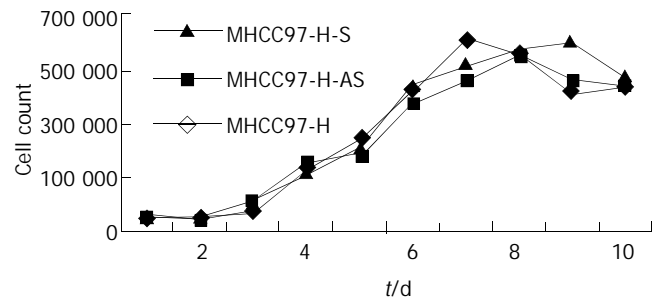


Figure 6 Growth curves of different cells.

Growth curve and cell cycles

No significant differences in growth curve and cell cycles were observed among MHCC97-H-S, MHCC97-H-AS, and MHCC97-H cells in 10 consecutive days (Figure 6, Table 1). The results demonstrated that KAI1 gene had no obvious effect on cell proliferation ability.

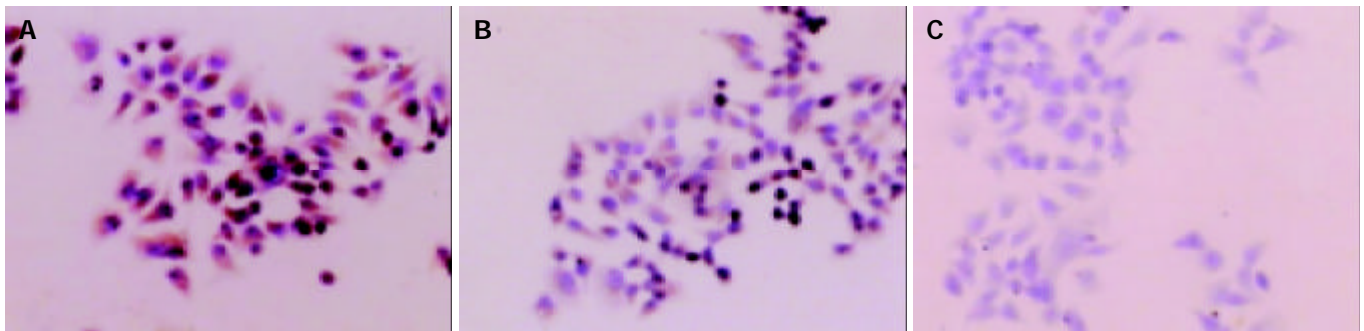


Figure 4 KAI1 protein expression in different cells revealed by immunocytochemistry (SP×400). A: MHCC97-H-S, B: MHCC97-H, C: MHCC97-H-AS.

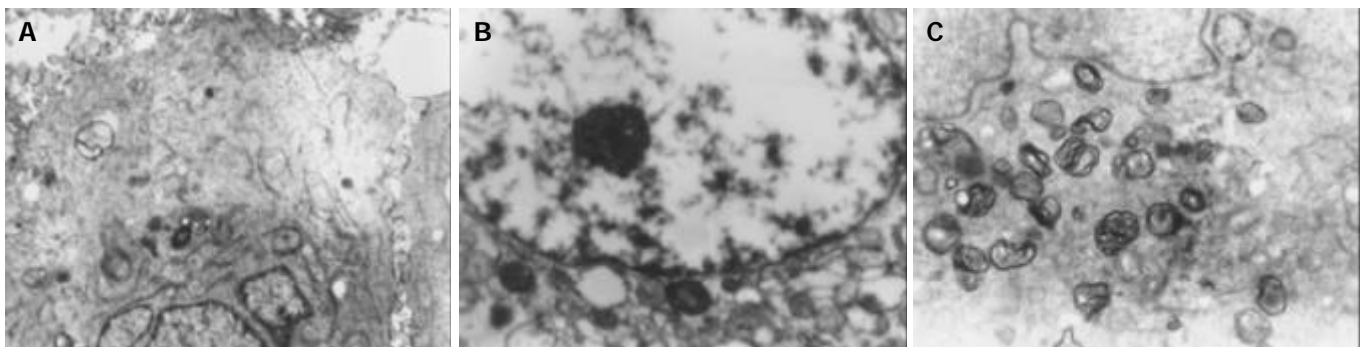


Figure 5 Ultrastructural changes in transfected cells. ×6 200. A: MHCC97-H-S cells, fewer RER and mitochondria, B: MHCC97-H-AS cells, more mitochondria, expanded endoplasmic reticulum, C: MHCC97-H-AS cells, myelin-sheath-like changes of mitochondria.

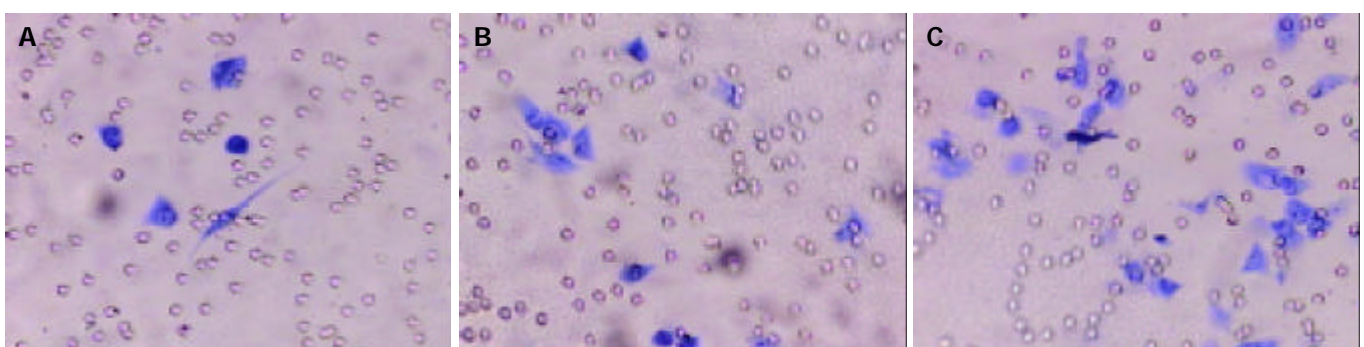


Figure 7 Penetrated cells (blue) in Boyden Chamber test. Giemsa×400. A: MHCC97-S, B: MHCC97-H, C: MHCC97-H-AS.

Plate clone formation efficiency

After two weeks of culture, the results of plate clone formation test showed no statistical difference in clone formation number between MHCC97-H-S (36.2 ± 3.3) and MHCC97-H (38.5 ± 1.9) ($P > 0.05$). However, MHCC97-H-AS (132.5 ± 2.9) showed more clone formation number ($P < 0.01$).

Cell invasive ability

Boyden Chamber assay showed that the cells penetrated the artificial basement membrane in MHCC97-H-S (59.7 ± 3.5) were fewer than in MHCC97-H (92.7 ± 1.5) ($P < 0.01$). However, more penetrated cells in MHCC97-H-AS (188.00 ± 4.5) were noted as compared with those in MHCC97-H ($P < 0.01$). These results suggested that sense KAI1 gene could decrease the invasive ability of MHCC97-H, while, antisense KAI1 gene could increase the invasive ability of MHCC97-H (Figure 7).

DISCUSSION

KAI1 is a newly discovered metastasis suppressor gene in human prostate cancer, which was mapped to chromosome 11p11.2 by Dr. Dong *et al.*^[2] of National Institute of Health, USA in 1995. KAI1 specifies a leukocyte surface glycoprotein of 267 amino acids with molecular mass of 29 610 u. KAI1 protein has been recognized as a structurally distinct family of membrane glycoproteins, transmembrane 4 superfamily^[22]. Recent researches showed the expression of KAI1 was down-regulated not only in human prostate cancer but also in a variety of human malignant tumors^[3,16], and these suggested KAI1 might be a broad-spectrum metastasis suppressor gene for human tumors.

Previous studies on the relationship between KAI1 gene and tumor invasion, metastasis were mostly based on the detection of KAI1 protein, DNA or RNA in tissue samples from surgical resections with immunopathological and molecular pathological methods in combination with analysis of clinical data. In the present study, we transfected full-length structural sense and antisense KAI1 genes from subclone recombinants into hepatocellular carcinoma MHCC97-H cell line with highly metastatic potential respectively. By observation of the changes of cell growth, invasion and ultrastructures of MHCC97-H before and after KAI1 transfection, we hoped to understand the effects of KAI1 gene on the capability of growth and invasion of hepatocellular carcinoma and to provide experimental evidences for the prevention and treatment of invasion and metastasis of this malignant tumor.

Restriction endonuclease analysis showed KAI1 full-length cDNA was respectively inserted into plasmid vector pCI-neo by two different directions, indicating that sense and antisense KAI1 genes eukaryon expression plasmids were successfully reconstructed. After KAI1 gene transfected into MHCC97-H by DOTAP liposome system, amplification of the neo gene in transfected cells was performed by PCR to confirm whether KAI1 gene was integrated into genomes of target MHCC97-H cells. Neo is a screening marker gene in the vector pCI-neo, and no sequence of this gene exists in the genomes of mammal cells, but it could stably exist in the genomes of mammal cells after transfection. Therefore, if the sequence could be amplified from the genomes of transfected cells by PCR, it could confirm the exogenous genes were integrated into genomes of MHCC97-H cells. PCR results showed sense and antisense KAI1 genes eukaryon expression plasmids were successfully integrated into genomes of MHCC97-H. Western blot and immunocytochemical staining were made to determine if the recombinant plasmids could expectantly express in the transfected cells. The results showed that sense KAI1 could up regulate the expression of KAI1 protein in MHCC97-H as compared with the control parental cells, but antisense KAI1 could down regulate the

expression of KAI1 protein, and no obvious difference between the cells transfected with pCI-neo and the control parental cells was noted. These results showed the transfected genes could produce expected effects, and vector pCI-neo itself had no obvious effects on the expression of KAI1. These suggested that the above cells transfected with genes could be used to explore the effects of KAI1 on the biological behaviors of HCC cells.

In the present study, our data indicated that KAI1 gene had no obvious effects on the *in vitro* cell growth and proliferation of hepatocellular carcinoma MHCC97-H cell line. These results were consistent with the studies in prostatic cancer, colon cancer cells by Dong and Takaoka *et al.*^[2,23]. In contrast with MHCC97-H control parent cells, the plate clone formation ability had no obvious reduction in MHCC97-H-S, but had obvious enhancement in MHCC97-H-AS cells. These data suggested down regulated expression of KAI1 could enhance motricity and aggregative abilities of MHCC97-H. Though the cells transfected with sense KAI1 expressed more KAI1 protein revealed by Western blot and immunocytochemical staining, their plate clone formation ability had no obvious reduction. This may be attributed to the small amount of KAI1 protein expression in MHCC97-H cells.

Invasion has been found to be one of the important and necessary properties for tumor metastasis formation^[24-29]. Boyden chamber assay, which imitates the invasion process of *in vivo* tumor cells, has also been found to be an ideal method for evaluating the invasive and metastatic abilities of tumor cells^[20,22]. Our data suggested that the invasive ability of HCC cells transfected with antisense KAI1 gene was increased, but the invasive ability of HCC cells transfected with sense KAI1 gene was partly inhibited. These indicated that different levels of KAI1 protein expression in HCC cells could affect their invasive and metastatic ability and that it might be an effective route to up regulate KAI1 expression for inhibiting the metastasis of HCC.

Under transmission electron microscope, we found that though KAI1 gene had no obvious effects on cell shape, superficial microvillus, karyotype and karyokinesis of MHCC97-H, sense KAI1 gene transfected into MHCC97-H resulted in reduction of the amount of mitochondria, however antisense KAI1 gene transfection resulted in increase of the amount of mitochondria, RER and Golgi apparatus with expanded endoplasmic reticulum and myelin-sheath-like changes of mitochondria. The biological function of these changes was unknown. It is still necessary to further study whether increased expression of KAI1 can inhibit invasion and metastasis of tumor cells by decreasing products of some organelles.

Though present researches have suggested KAI1 gene is important in preventing the development of metastases in a wide variety of human tumors, the mechanism of KAI1-mediated metastasis suppression remains unclear. The molecular structure of KAI1 protein indicates KAI1 functions in cell-cell interactions and cell-extracellular matrix interactions. These suggest that KAI1 may affect cell-cell adhesion and cell-extracellular matrix adhesion through some signaling pathways to inhibit tumor metastasis^[30,31].

REFERENCES

- 1 **Qin LX**, Tang ZY. The prognostic significance of clinical and pathological features in hepatocellular carcinoma. *World J Gastroenterol* 2002; **8**: 193-199
- 2 **Dong JT**, Lamb PW, Rinker-Schaeffer CW, Vukanovic J, Ichikawa T, Isaacs JT, Barrett JC. KAI1, a metastasis suppressor gene for prostate cancer on human chromosome 11p11.2. *Science* 1995; **268**: 884-886
- 3 **Huang CI**, Kohno N, Ogawa E, Adachi M, Taki T, Miyake M. Correlation of reduction in MRP-1/CD9 and KAI1/CD82 ex-

- pression with recurrences in breast cancer patients. *Am J Pathol* 1998; **153**: 973-983
- 4 **White A**, Lamb PW, Barrett JC. Frequent downregulation of the KAI1(CD82) metastasis suppressor protein in human cancer cell lines. *Oncogene* 1998; **16**: 3143-3149
 - 5 **Adachi M**, Taki T, Konishi T, Huang CI, Higashiyama M, Miyake M. Novel staging protocol for non-small-cell lung cancers according to MRP-1/CD9 and KAI1/CD82 gene expression. *J Clin Oncol* 1998; **16**: 1397-1406
 - 6 **Yu Y**, Yang JL, Markovic B, Jackson P, Yardley G, Barrett J, Russell PJ. Loss of KAI1 messenger RNA expression in both high-grade and invasive human bladder cancers. *Clin Cancer Res* 1997; **3**: 1045-1049
 - 7 **Houle CD**, Ding XY, Foley JF, Afshari CA, Barrett JC, Davis BJ. Loss of expression and altered localization of KAI1 and CD9 protein are associated with epithelial ovarian cancer progression. *Gynecol Oncol* 2002; **86**: 69-78
 - 8 **Liu FS**, Chen JT, Dong JT, Hsieh YT, Lin AJ, Ho ES, Hung MJ, Lu CH. KAI1 metastasis suppressor gene is frequently down-regulated in cervical carcinoma. *Am J Pathol* 2001; **159**: 1629-1634
 - 9 **Liu FS**, Dong JT, Chen JT, Hsieh YT, Ho ES, Hung MJ, Lu CH, Chiou LC. KAI1 metastasis suppressor protein is down-regulated during the progression of human endometrial cancer. *Clin Cancer Res* 2003; **9**: 1393-1398
 - 10 **Wu DH**, Liu L, Chen LH, Ding YQ. Expression of KAI1/CD82 in human colorectal tumor. *Diyi Junyi Daxue Xuebao* 2003; **23**: 714-715
 - 11 **Ito Y**, Yoshida H, Uruno T, Nakano K, Takamura Y, Miya A, Kobayashi K, Yokozawa T, Matsuzuka F, Kuma K, Miyauchi A. KAI1 expression in thyroid neoplasms: its linkage with clinicopathologic features in papillary carcinoma. *Pathol Res Pract* 2003; **199**: 79-83
 - 12 **Lee HS**, Lee HK, Kim HS, Yang HK, Kim WH. Tumour suppressor gene expression correlates with gastric cancer prognosis. *J Pathol* 2003; **200**: 39-46
 - 13 **Yang JL**, Jackson P, Yu Y, Russell PJ, Markovic B, Crowe PJ. Expression of the KAI1 metastasis suppressor gene in non-metastatic versus metastatic human colorectal cancer. *Anticancer Res* 2002; **22**: 3337-3342
 - 14 **Tozawa K**, Akita H, Kawai N, Okamura T, Sasaki S, Hayashi Y, Kohri K. KAI1 expression can be a predictor of stage A prostate cancer progression. *Prostate Cancer Prostatic Dis* 2001; **4**: 150-153
 - 15 **Imai Y**, Sasaki T, Shinagawa Y, Akimoto K, Fujibayashi T. Expression of metastasis suppressor gene (KAI1/CD82) in oral squamous cell carcinoma and its clinico-pathological significance. *Oral Oncol* 2002; **38**: 557-561
 - 16 **Muneyuki T**, Watanabe M, Yamanaka M, Shiraishi T, Isaji S. KAI1/CD82 expression as a prognostic factor in sporadic colorectal cancer. *Anticancer Res* 2001; **21**: 3581-3587
 - 17 **Li Y**, Tang ZY, Ye SL, Liu YK, Chen J, Xue Q, Chen J, Gao DM, Bao WH. Establishment of cell clones with different metastatic potential from the metastatic hepatocellular carcinoma cell line MHCC97. *World J Gastroenterol* 2001; **7**: 630-636
 - 18 **Yang JM**, Chen WS, Liu ZP, Luo YH, Liu WW. Effects of insulin-like growth factors-IR and -IIR antisense gene transfection on the biological behaviors of SMMC-7721 human hepatoma cells. *J Gastroenterol Hepatol* 2003; **18**: 296-301
 - 19 **Poggiali P**, Scoarughi GL, Lavitrano M, Donini P, Cimmino C. Construction of a swine artificial chromosome: a novel vector for transgenesis in the pig. *Biochimie* 2002; **84**: 1143-1150
 - 20 **Nawrocki-Raby B**, Gilles C, Polette M, Bruyneel E, Laronze JY, Bonnet N, Foidart JM, Mareel M, Birembaut P. Upregulation of MMPs by soluble E-cadherin in human lung tumor cells. *Int J Cancer* 2003; **105**: 790-795
 - 21 **Vehvilainen P**, Hyytiainen M, Keski-Oja J. Latent transforming growth factor-beta-binding protein 2 is an adhesion protein for melanoma cells. *J Biol Chem* 2003; **278**: 24705-24713
 - 22 **Dong JT**, Isaacs WB, Barrett JC, Isaacs JT. Genomic organization of the human KAI1 metastasis-suppressor gene. *Genomics* 1997; **41**: 25-32
 - 23 **Takaoka A**, Hinoda Y, Satoh S, Adachi Y, Itoh F, Adachi M, Imai K. Suppression of invasive properties of colon cancer cells by a metastasis suppressor KAI1 gene. *Oncogene* 1998; **16**: 1443-1453
 - 24 **Kurokawa H**, Katsube K, Podyma KA, Ikuta M, Iseki H, Nakajima M, Akashi T, Omura K, Takagi M, Yanagishita M. Heparanase and tumor invasion patterns in human oral squamous cell carcinoma xenografts. *Cancer Sci* 2003; **94**: 277-285
 - 25 **Wernicke M**, Pineiro LC, Caramutti D, Dorn VG, Raffo MM, Guixa HG, Telenta M, Morandi AA. Breast cancer stromal myxoid changes are associated with tumor invasion and metastasis: a central role for hyaluronan. *Mod Pathol* 2003; **16**: 99-107
 - 26 **Katayama M**, Sanzen N, Funakoshi A, Sekiguchi K. Laminin gamma2-chain fragment in the circulation: a prognostic indicator of epithelial tumor invasion. *Cancer Res* 2003; **63**: 222-229
 - 27 **Wells A**, Kassis J, Solava J, Turner T, Lauffenburger DA. Growth factor-induced cell motility in tumor invasion. *Acta Oncol* 2002; **41**: 124-130
 - 28 **Patarroyo M**, Tryggvason K, Virtanen I. Laminin isoforms in tumor invasion, angiogenesis and metastasis. *Semin Cancer Biol* 2002; **12**: 197-207
 - 29 **Nabeshima K**, Inoue T, Shimao Y, Sameshima T. Matrix metalloproteinases in tumor invasion: role for cell migration. *Pathol Int* 2002; **52**: 255-264
 - 30 **Lee B**, Jin K, Hahn JH, Song HG, Lee H. Metastasis-suppressor KAI1/CD82 induces homotypic aggregation of human prostate cancer cells through Src-dependent pathway. *Exp Mol Med* 2003; **35**: 30-37
 - 31 **Shibagaki N**, Hanada K, Yamashita H, Shimada S, Hamada H. Overexpression of CD82 on human T cells enhances LFA-1 / ICAM-1-mediated cell-cell adhesion: functional association between CD82 and LFA-1 in T cell activation. *Eur J Immunol* 1999; **29**: 4081-4091

Edited by Xu CT and Wang XL Proofread by Pan BR and Xu FM

Growth inhibition and apoptosis induction of tanshinone II-A on human hepatocellular carcinoma cells

Shu-Lan Yuan, Yu-Quan Wei, Xiu-Jie Wang, Fei Xiao, Sheng-Fu Li, Jie Zhang

Shu-Lan Yuan, Yu-Quan Wei, Xiu-Jie Wang, Fei Xiao, Sheng-Fu Li, Jie Zhang, Key Laboratory of Biotherapy of Human Diseases, Ministry of Education of China and Cancer Center, West China Hospital, West China Medical School, Sichuan University, Chengdu 610041, Sichuan Province, China

Supported by the Science Foundation of the Ministry of Health of China, No. 96-1-240 and the Applied Basic Research Programs of Science and Technology Commission Foundation of Sichuan Province, No.2000-135

Correspondence to: Shu-Lan Yuan, Key Laboratory of Biotherapy of Human Diseases, Ministry of Education of China and Cancer Center, West China Hospital, 37 Guo Xue Xiang, Chengdu 610041, Sichuan Province, China. tuyuan@mail.sc.cninfo.net

Telephone: +86-28-85423039 **Fax:** +86-28-85503246

Received: 2003-12-19 **Accepted:** 2004-01-08

Abstract

AIM: To evaluate the effects of tanshinone II-A on inducing growth inhibition and apoptosis of human hepatocellular carcinoma (HCC) cells.

METHODS: The human hepatocellular carcinoma cell line SMMC-7721 was used for the study. The cells were treated with tanshinone II-A at different doses and different times. Cell growth and proliferation were measured by MTT assay, cell count and colony-forming assay. Apoptosis induction was detected by microscopy, DNA ladder electrophoresis and flow cytometry.

RESULTS: In MTT assay, the inhibitory effect became gradually stronger with the passage of time, 24, 48, 72 and 96 h after treatment with tanshinone II-A, and the most significant effect was observed at 72 h. On the other hand, the increase of doses (0.125, 0.25, 0.5, 1.0 mg/L tanshinone II-A) resulted in enhanced inhibitory effect. The growth and proliferation of SMMC-7721 cells were obviously suppressed in a dose- and time-dependent manner. The results of cell count were similar to that of MTT assay. In colony-forming assay, the colony-forming rates were obviously inhibited by tanshinone II-A. In tanshinone II-A group, the morphology of cellular growth inhibition and characteristics of apoptosis such as chromatin condensation, crescent formation, margination and apoptotic body were observed under light and transmission electron microscopes. DNA ladder of cells was presented in electrophoresis. The apoptosis index (AI) was 16.9% (the control group was 4.6%) in flow cytometry. The cells were arrested in G₀/G₁ phase, and the expressions of apoptosis-related genes *bcl-2* and *c-myc* were down-regulated and *fas*, *bax*, *p53* up-regulated.

CONCLUSION: Tanshinone II-A could inhibit the growth and proliferation of HCC cell effectively *in vitro* by apoptosis induction, which was associated with up-regulation of *fas*, *p53*, *bax*, expression and down-regulation of *bcl-2* and *c-myc*.

Yuan SL, Wei YQ, Wang XJ, Xiao F, Li SF, Zhang J. Growth

inhibition and apoptosis induction of tanshinone II-A on human hepatocellular carcinoma cells. *World J Gastroenterol* 2004; 10(14): 2024-2028

<http://www.wjgnet.com/1007-9327/10/2024.asp>

INTRODUCTION

Hepatocarcinoma is one of the most common causes of malignancy-related death in China. Its therapy in clinic is a big challenge. New remedial method would possibly depend on advances in basic research^[1]. Recent evidence suggests that apoptosis of cell is closely related to occurrence, progress and metastasis of tumor^[2]. Study on induced apoptosis of tumor cells is an important field of tumor therapy and tumor molecular biology at present. Inducing apoptosis is a new therapeutic target of cancer research. New and promising anticancer drugs could be discovered by studies on apoptosis induction^[3-5]. Tanshinone II-A is an alcohol-extracted product from the root of the traditional Chinese medicine-*Salvia miltiorrhiza Bunge*, which is known to have anti-inflammatory, anti-oxidative and cytotoxic activities^[6-9]. Traditional Chinese medicines considered as potential drug in cancer treatment. Previous studies confirmed that tanshinone II-A could induce differentiation of human cervical carcinoma cell line (ME180) and leukemia cells (NB4, HL60 and K562), reverse malignant phenotype of human hepatocarcinoma cell line (SMMC-7721)^[10-16]. However, there were no studies about growth inhibition and apoptosis induction of tanshinone II-A in hepatocarcinoma cell. In this *in vitro* study, human hepatocarcinoma cell line SMMC-7721 was used. The growth inhibition and apoptosis induction of tanshinone II-A on SMMC-7721 cell were obviously exhibited. We conclude that the effect of growth inhibition of tanshinone II-A on hepatocarcinoma might be related to induction of cellular apoptosis through regulation of apoptosis-associated genes.

MATERIALS AND METHODS

Cell line culture and reagents

Human hepatocellular carcinoma SMMC-7721 cell line was provided by Shanghai Institute of Cancer Research^[17]. The cells were grown in RPMI 1640 (Gibco) supplemented with 100 ml/L fetal bovine serum (Huamei, Chengdu, China), penicillin (100 mg/L) and streptomycin (100 mg/L) in a humidified atmosphere of 50 mg/L CO₂ at 37 °C. Anti-*p53*, *fas*, *c-myc*, *bax* and *bcl-2* antibodies were obtained from Sigma. Other special chemicals were purchased from Sigma (St Louis, MO, USA).

Drugs and treatment

Tanshinone II-A (Tan II-A) was provided by Institute of Traditional Chinese Medicine (concentration 96%). It was dissolved in DMSO (final concentration 0.2 mL/L). The solution was filtered through a 0.22 μm micropore filter and stored at 4 °C.

SMMC-7721 cells were seeded in flasks or dishes. The Tan II-A group was treated with Tan II-A of different doses (0.125, 0.25, 0.5, 1.0 mg/L) for 24, 48, 72 and 96 h, respectively. The control group was added with equal concentration of DMSO

for negative control. The cells were measured after successive 96-h treatment.

MTT assay

SMMC-7721 cells were seeded in 96-well microtitre plates with 1×10^3 per well and incubated for 24 h in 100 μ L culture media. Then the cells were treated with 0.125, 0.25, 0.5, 1.0 mg/L of Tan II-A in the experimental group for 24, 48, 72, and 96 h respectively. MTT 100 μ L (5 g/L) was added to the cells and cultivated for another 4 h. After the supernatant fluid was removed, DMSO 100 μ L per well was added to the cells and shaken for 15 min. The absorbance at 570 nm was measured by an ELISA reader. At the same time, the SMMC-7721 cells without treatment were served as control. Each assay was repeated three times.

Cell count

SMMC-7721 cells were treated with Tan II-A (0.125, 0.25, 0.5, 1.0 mg/L) for 96 h, respectively, then condition of the cell growth was observed under an inverse and light microscope. Number and viability of the cells were assessed by trypan blue exclusion.

Cell colony-forming assay

Cells were seeded in a 6-well plate with 300 cells per well. After 24 h, the cells were treated with Tan II-A (0.125, 0.25, 0.5, 1.0 mg/L), and cultured in routine medium for 10 days continually. Then the cells were fixed by methanol, Giemsa staining. Finally, the sum of colony per group was counted. The inhibiting rate of colony-formation was calculated.

Light and transmission electron microscopy

SMMC-7721 cells were treated with DMSO (control group) or 0.5, 1.0 mg/L Tan II-A for 48 h. The cells were gently washed with serum-free medium, and observed by inverse and light microscopy after Giemsa staining. On the other hand, some other cells were fixed with 25 g/L glutaraldehyde in 0.1 mol/L of sodium cacodylate buffer, osmicated with 10 g/L osmium tetroxide. then cell block was stained, dehydrated in graded ethanol, infiltrated with propylene oxide, and embedded overnight and incubated in a 60 °C oven for 48 h. Silver sections were cut with an Ultracut E microtome, collected on a formvar and carbon-coated grid, stained with uranyl acetate and Reynold's lead citrate, and examined under a transmission electron microscope to identify the morphological changes of apoptosis.

DNA ladder detection

After induction of apoptosis, the cells (1×10^6 /group, both attached and detached cells) were washed by PBS, and fixed in ice-cold 700 mg/L ethanol for 24 h. After the ethanol was removed, the cells were rinsed in 0.2 mol/L Na_2HPO_4 and 0.1 mol/L citric acid (192:8, pH 7.8) for 60 min at room temperature. After being centrifuged (10 000 g), the supernatant was collected in Eppendorf tubes, 2.5 g/L NP-40 and 10 g/L RNase A were added at 37 °C for 30 min, then Protein K (1 g/L, Promega) was added at 50 °C for 30 min. Equal quantity of DNA was electrophoresed in 15 g/L agarose gels and stained with ethidium bromide (5 mL/L) for 2 h at 80 V. Ladder formation of oligonucleosomal DNA fragmentation was detected under ultraviolet light.

Flow cytometry measurement

The sample preparation and measurement followed the method described in reference^[15]. The cells were harvested, counted and fixed. The cell concentration was adjusted to 10^6 /mL. According to the routine method, cell frequency distribution of each phase in cell cycle was measured. Cellular *fas*, *p53*, *bax*, *bcl-2* and *myc* gene expressions were detected by immunohistochemical method on FACS-420 FCM. The results were shown with scanning figure and date.

Statistical analysis

Data were presented as the mean \pm SD error of the mean. Student's *t* test was used for comparison among different groups. A *P* value of less than 0.05 is considered statistically significant.

RESULTS

Cell growth and proliferation

Tan II-A exhibited a statistically significant dose-dependent growth-inhibitory effect on SMMC-7721 cell evaluated by MTT assay. The inhibiting rates of cell growth were 12.2%, 30.6%, 52.4% and 82.5%, respectively when treated with Tan II-A of different doses (0.125, 0.25, 0.5, 1.0 mg/L) for 96 h (Figure 1A). Moreover, the growth-inhibitory effect of Tan II-A on the cells was found to be time-dependent. The inhibiting rates were 12.5%, 38.2%, 47.6% and 58.7%, respectively when treated separately for 24, 48, 72 and 96 h with 0.5 mg/L of Tan II-A (Figure 2B). The inhibitory effect became gradually stronger with the passage of time after treatment, and the most significant effect was observed at 72 h. The cell growth and proliferation were obviously inhibited in a dose- and time-dependent manner. The same inhibitory effect was found by cell count. In colony-forming assay, the colony-forming rates of SMMC-7721 cell were 11.6%, 22.5%, 38.5%, 42.2% in Tan II-A group and 68.2% in control group, respectively, suggesting the obviously inhibiting effect of Tan II-A on cell proliferation.

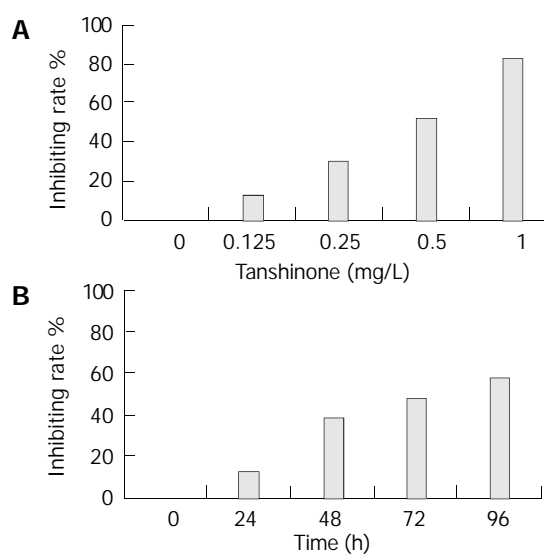


Figure 1 Growth-inhibitory effect of Tan II-A on SMMC-7721 cells detected by MTT. A: In a dose-dependent manner detected by MTT; B: In a time-dependent manner detected by MTT.

Morphological changes of apoptosis

As shown in Figure 2, Tan II-A-induced morphological changes were evident by 72 h of treatment in SMMC-7721 cell. Roundish, large and serried cells (in control group, Figure 2A) became polygonal, small, detached or sparse, membranous frothed and wizened (Tan II-A group, Figure 2B) in the dishes under light microscope. The ultrastructural characteristics of apoptosis such as chromatin condensation, crescent formation, margination and apoptotic bodies were observed by electron microscopy in the Tan II-A group (Figure 3), which were more obvious in the given experimental period than that in the control group.

DNA fragments

Agarose gel electrophoresis exhibited DNA ladder formation in SMMC-7721 cell after exposed to different concentration of Tan II-A for 96 h. Compared with control, the DNA ladder was

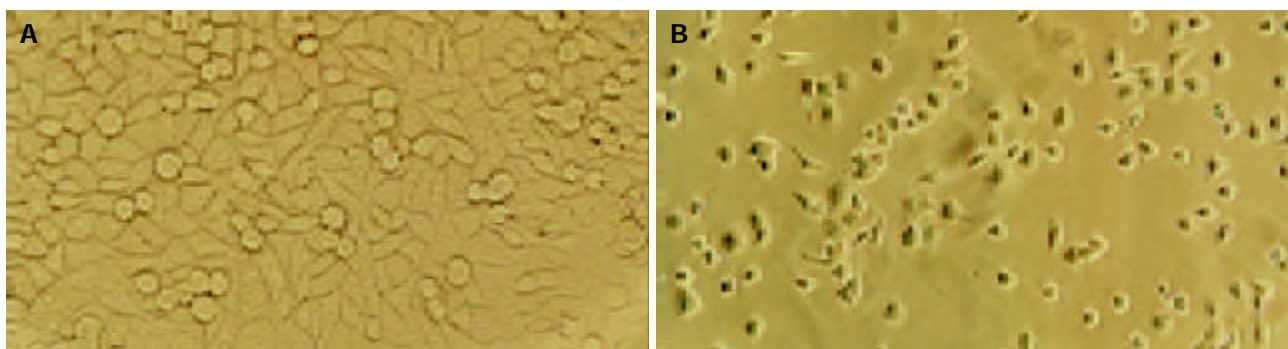


Figure 2 Morphological characteristics of SMMC-7721 cells before and after Tan II-A treatment. A: Roundish, large and serried SMMC-7721 cells (in control group); B: Polygonal, small, detached or sparse, membranous frothed and wizened SMMC-7721 cells (in Tan II A group).

more clearly observed by treatment with 0.5, 1.0 and 2.0 mg/L Tan II-A, while the DNA fragment induced by 0.125, 0.25 mg/L Tan II-A was not clear (Figure 4).

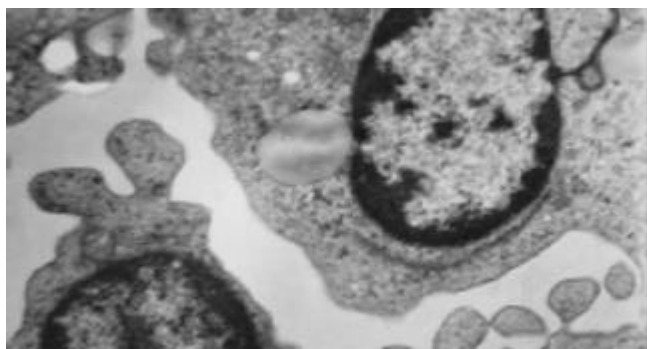


Figure 3 Ultrastructural changes of SMMC-7721 cells with 1.0 mg/L Tan II-A treatment for 96 h under TEM ($\times 10\,000$). The chromatin condensation, original margination were observed.

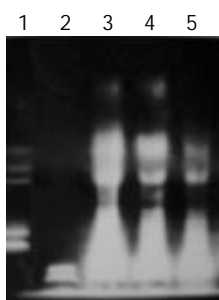


Figure 4 DNA agarose gel electrophoresis of SMMC-7721 cells with Tan II-A treatment for 96 h. Lane 1: Marker, Lane 2: Control, Lane 3: 2.0 mg.L⁻¹, Lane 4: 1.0 mg.L⁻¹, Lane 5: 0.5 mg.L⁻¹.

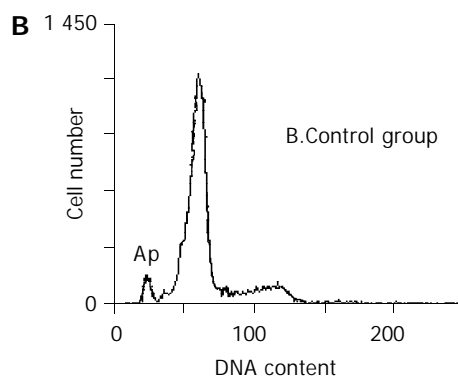
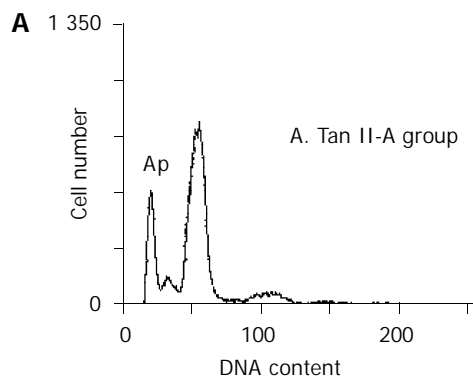


Figure 5 Flow cytometry analysis of apoptosis in SMMC-7721 cells treated with Tan II-A (A) and DMSO (B).

Cell cycle effect

In order to determine the effect of Tan II-A on proliferation and apoptosis in SMMC-7721 cell, the cells were exposed to 0.5 mg/L Tan II-A for 96 h. Cell cycle distribution, cell proliferation and apoptotic damage of DNA were determined on a flow cytometer. The result showed the accumulation of cells in G₀/G₁ and a corresponding reduction in percentages of cells in S and G₂/M phase, and decreased proliferation index (PI). The cells in sub-G₁ phase were increased. An apoptotic peak was detected (Table 1, Figure 5)

Table 1 Effect of Tan II-A on cell cycle distribution and apoptosis in SMMC-7721

Group	Cell cycle distribution (%)			PI %	AI %
	G ₀ /G ₁	S	G ₂ /M		
Control	71.3±2.3	9.8±0.6	18.9±1.6	28.7±2.6	4.9±0.4
Tan II-A	77.8±3.8 ^b	7.2±0.5 ^b	15.0±1.2 ^b	22.2±2.2 ^b	16.9±1.2

χ^2 test. ^bP<0.01 vs control group.

Table 2 Effect of Tan II-A on apoptosis associated gene expression of SMMC-7721

Group	Positive rate of protein expression (%)				
	fas	p53	bax	bcl-2	c-myc
Control	19.7±0.5	21.4±1.6	20.2±1.6	27.9±2.4	23.8±1.8
Tan II A	28.4±2.5 ^b	39.1±3.1 ^b	31.5±2.7 ^b	16.3±1.3 ^b	14.6±1.1 ^b

χ^2 test, ^bP<0.01 vs control group.

Apoptosis-associated genes expression

The expressions of apoptosis associated genes *fas*, *bax*, *p53* were up-regulated. The expressions of *bcl-2* and *c-myc* were

down-regulated (Table 2). The tabulated percentages were an average calculated on the results of three separate experiments. The values were presented as mean±SE ($n=3$).

DISCUSSION

Cellular proliferation and apoptosis in normal tissue maintain a balance. Unlimited growth and proliferation, but blocked apoptosis are main characteristics of malignant tumor cell. So inhibiting proliferation by apoptosis induction of cancer cell is a new method for cancer control and therapy^[18-20].

On the basis of previous studies, we chose different concentrations of non-cytotoxic Tan II-A to study Tan II-A induced-apoptosis *in vitro*. MTT, cell count assay and colony-forming assay showed that 0.25, 0.5, 1.0 mg/L Tan II-A obviously inhibited the growth and proliferation of SMMC-7721, and the inhibiting effect was in a dose- and time-dependent manner. The most significant effect was observed at 72 h by 1.0 mg/L Tan II-A. Flow cytometer showed that Tan II-A produced significant cell cycle arrest in G₀/G₁, decreased proliferation index (PI) as evidence of an antiproliferation effect. The cellular growth and inhibition could be observed by morphology. The morphological characteristics of cellular growth inhibition were also observed under light microscope. Our results demonstrated that Tan II-A inhibited growth and proliferation of SMMC-7721 cells^[21,22].

Apoptosis, or programmed cell death, has an essential role in controlling cell number in many developmental and physiological settings and in chemotherapy-induced tumour-cell killing. The execution of apoptosis may be initiated by many different signals, either from within or outside the cell involving ligand-receptor interactions, as has been shown for Fas/Fas-ligand, or potentially by more unspecific signals such as DNA damage. During the modulation phase of apoptosis many different genes such as *p53*, *c-myc* or *Bcl-2/Bax* have been shown to be able to shift the balance either to cellular proliferation or death. Cellular growth and proliferation are closely related to apoptosis^[23-25].

The detection of apoptotic cell by microscopy is based on several well-established morphological features. These features include condensation of chromatin and cytoplasm as well as fragmentation of the cells that lead to the appearance of membrane bound apoptotic bodies^[26]. Those ultrastructural characteristics apoptosis, the DNA ladder and increased cells in sub-G₁ phase were observed in SMMC-7721 cells treated with 0.5, 1.0 mg/L Tan II-A.

Apoptosis-associated genes play a major role in apoptosis, participating in the initiation and progress of programmed cell death. *Bcl-2* has been identified as an apoptosis inhibitor, and shown to cooperate with *c-myc* in immortalizing cells. Under certain conditions, constitutive expression of *c-myc* induces apoptosis and can be suppressed by *bcl-2*. It appears that the *c-myc* cooperating oncogenic activity of *bcl-2* is related to its inhibition of apoptotic pathways^[26]. Bax protein inhibits the function of *bcl-2* leading to increased apoptosis.

The tumor suppressor gene *p53*, a transcription factor, has been identified as a participant in the cellular DNA damage response. Upon DNA damage, *p53* up-regulation causes G₁ arrest. The apoptosis promoting capacity of *p53* is presumably due to its ability to activate *bax*, a gene that encodes an inhibitor of *bcl-2*. Fas (CD95/APO-1) is a death-promoting receptor that belongs to the tumor necrosis factor (TNF) receptor family, and induces apoptosis through different ways^[27].

In the present study, we observed down-regulation of *bcl-2* and *c-myc* expression, which is in keeping with the role of *bcl-2* in blocking apoptosis and *c-myc* in promoting proliferation. At the same time, the expressions of apoptosis

associated genes *fas*, *bax*, *p53* were up-regulated. These suggested that *Bcl-2*, *c-myc*, *fas*, *bax* and *p53* were involved in apoptosis of hepatocarcinoma cells induced by Tan II-A. Parts of these mechanisms were related to inhibition of cell growth. Some results of our study on inducing apoptosis in human hepatocellular carcinoma cell are consistent with other researches^[28].

Tan II-A inhibits growth and proliferation of hepatocarcinoma cells by inducing apoptosis. Tan II-A might have different mechanisms in inducing apoptosis and inhibiting proliferation of cancer cells. Other possible mechanisms of the action of Tan II-A need to be further investigated. We consider that Tan II-A could be a new prospective, highly effective and low toxic anticancer drug.

REFERENCES

- 1 **Kanzler S**, Galle PR. Apoptosis and the liver. *Semin Cancer Biol* 2000; **10**: 173-184
- 2 **Carson DA**, Ribeiro JM. Apoptosis and disease. *Lancet* 1993; **341**: 1251-1254
- 3 **Kerr JF**, Winterford CM, Harmon BV. Apoptosis. Its significance in cancer and cancer therapy. *Cancer* 1994; **73**: 2013-2026
- 4 **Thompson CB**. Apoptosis in the pathogenesis and treatment of disease. *Science* 1995; **267**: 1456-1462
- 5 **Lee SM**, Li ML, Tse YC, Leung SC, Lee MM, Tsui SK, Fung KP, Lee CY, Waye MM. Paenoniae Radix, a Chinese herbal extract, inhibit hepatoma cells growth by inducing apoptosis in a p53 independent pathway. *Life Sci* 2002; **71**: 2267-2277
- 6 **Li ZT**, Yang BJ, Ma GE. Chemical studies of *Salvia miltiorrhiza* f. *alba*. *Yaoxue Xuebao* 1991; **26**: 209-213
- 7 **Lin TJ**. Antioxidation mechanism of schizandrin and tanshinononic acid A and their effects on the protection of cardiotoxic action of adriamycin. *Shengli Kexue Jinzhan* 1991; **22**: 342-345
- 8 **Liang Y**, Yang YM, Yuan SL. Studies on Pharmic mechanism and clinic application of Tanshinone. *Traditional Herbal Drugs* 2000; **31**: 304-306
- 9 **Wu WL**, Chang WL, Chen CF. Cytotoxic activities of tanshinones against human carcinoma cell lines. *Am J Chin Med* 1991; **19**: 207-216
- 10 **Yuan S**, Huang G, Wang X. The differentiation-inducing effect of tanshinone and retinoic acid on human cervical carcinoma cell line *in vitro*. *Zhonghua Zhongliu Zazhi* 1995; **17**: 422-424
- 11 **Liang Y**, Yang Y, Yuang S, Liu T, Jia Y, Xu C, Niu T, Qin H, Qin P. Terminal differentiation of human acute promyelocytic leukemia (APL) cells induced by Tanshinone II A in primary culture. *Huaxi Yike Daxue Xuebao* 2000; **31**: 207-210
- 12 **Yoon Y**, Kim YO, Jeon WK, Park HJ, Sung HJ. Tanshinone IIA isolated from *Salvia miltiorrhiza* BUNGE induced apoptosis in HL60 human promyelocytic leukemia cell line. *J Ethnopharmacol* 1999; **68**: 121-127
- 13 **Sung HJ**, Choi SM, Yoon Y, An KS. Tanshinone IIA, an ingredient of *Salvia miltiorrhiza* BUNGE, induces apoptosis in human leukemia cell lines through the activation of caspase-3. *Exp Mol Med* 1999; **31**: 174-178
- 14 **Wang X**, Yuan S, Wang C. A preliminary study of the anti-cancer effect of tanshinone on hepatic carcinoma and its mechanism of action in mice. *Zhonghua Zhongliu Zazhi* 1996; **18**: 412-414
- 15 **Yuan S**, Wang Y, Chen X, Song Y, Yang Y. A study on apoptosis of nasopharyngeal carcinoma cell line induced by Tanshinone II A and its molecular mechanism. *Huaxi Yike Daxue Xuebao* 2002; **33**: 84-86
- 16 **Yuan SL**, Huang RM, Wang XJ, Song Y, Huang GQ. Reversing effect of Tanshinone on malignant phenotypes of human hepatocarcinoma cell line. *World J Gastroenterol* 1998; **4**: 317-319
- 17 **Ai ZW**. Reversing effect of retinoic acid on some phenotypes of human hepatocarcinoma cell line. *Zhonghua Zhongliu Zazhi* 1991; **13**: 9-12
- 18 **Marx J**. Cell death studies yield cancer clues. *Science* 1993; **259**:

- 760-761
- 19 **Sakuma H**, Yamamoto M, Okumura M, Kojima T, Maruyama T, Yasuda K. High glucose inhibits apoptosis in human coronary artery smooth muscle cells by increasing bcl-xL and bfl-1/A1. *Am J Physiol Cell Physiol* 2002; **283**: C422-428
- 20 **Tsuda H**, Sata M, Ijuuin H, Kumabe T, Uchida M, Ogou Y, Akagi Y, Shirouzu K, Hara H, Nakashima Y. A novel strategy for remission induction and maintenance in cancer therapy. *Oncol Rep* 2002; **9**: 65-68
- 21 **Hu W**, Kavanagh JJ. Anticancer therapy targeting the apoptotic pathway. *Lancet Oncol* 2003; **4**: 721-729
- 22 **Giridharan P**, Somasundaram ST, Perumal K, Vishwakarma RA, Karthikeyan NP, Velmurugan R, Balakrishnan A. Novel substituted methylenedioxy lignan suppresses proliferation of cancer cells by inhibiting telomerase and activation of c-myc and caspases leading to apoptosis. *Br J Cancer* 2002; **87**: 98-105
- 23 **Fimognari C**, Nusse M, Cesari R, Iori R, Cantelli-Forti G, Hrelia P. Growth inhibition, cell-cycle arrest and apoptosis in human T-cell leukemia by the isothiocyanate sulforaphane. *Carcinogenesis* 2002; **23**: 581-586
- 24 **Altieri DC**. Survivin, versatile modulation of cell division and apoptosis in cancer. *Oncogene* 2003; **22**: 8581-8589
- 25 **Suda T**, Takahashi T, Golstein P, Nagata S. Molecular cloning and expression of the Fas ligand, a novel member of the tumor necrosis factor family. *Cell* 1993; **75**: 1169-1178
- 26 **Barnhart BC**, Lee JC, Alappat EC, Peter ME. The death effector domain protein family. *Oncogene* 2003; **22**: 8634-8644
- 27 **Lyu SY**, Choi SH, Park WB. Korean mistletoe lectin-induced apoptosis in hepatocarcinoma cells is associated with inhibition of telomerase via mitochondrial controlled pathway independent of p53. *Arch Pharm Res* 2002; **25**: 93-101
- 28 **Rahman MA**, Dhar DK, Masunaga R, Yamanoi A, Kohno H, Nagasue N. Sulindac and exisulind exhibit a significant antiproliferative effect and induce apoptosis in human hepatocellular carcinoma cell lines. *Cancer Res* 2000; **60**: 2085-2089

Edited by Chen WW **Proofread by** Zhu LH and Xu FM

Prokaryotic expression and renaturation of engineering chimeric Fab antibody against human hepatoma

Jin-Liang Xing, Xiang-Min Yang, Xi-Ying Yao, Fei Song, Zhi-Nan Chen

Jin-Liang Xing, Xiang-Min Yang, Xi-Ying Yao, Fei Song, Zhi-Nan Chen, Cell Engineering Research Center, Faculty of Preclinical Medicine, Fourth Military Medical University, Xi'an 710032, Shaanxi Province, China

Supported by the National High Technology Research and Development Program of China (863 Program), No. 2001AA215101 and the National Natural Science Foundation of China, No. 3020330

Correspondence to: Professor Zhi-Nan Chen, Cell Engineering Research Center, Faculty of Preclinical Medicine, Fourth Military Medical University, Xi'an 710032, Shaanxi Province, China. chcerc2@fmmu.edu.cn

Telephone: +86-29-3374545 **Fax:** +86-29-3293906

Received: 2003-11-13 **Accepted:** 2004-01-15

Abstract

AIM: To express chimeric Fd (cFd) and chimeric light chain (cL) in *E.coli* respectively and refold them into chimeric Fab (cFab) antibody.

METHODS: cFd and cL genes were respectively inserted into the prokaryotic expression vector pET32a to construct recombinant vectors pET32a/cFd and pET32a/cL. Then, the competent *E.coli* cells were transformed by the recombinant vectors and induced by IPTG. Moreover, a large quantity of cFd and cL expression products were prepared and mixed with equal molar to refold into cFab by gradient dialysis. The refolded products were identified and analyzed by sodium SDS-PAGE, Western blotting, ELISA and HPLC.

RESULTS: High efficient prokaryotic expressions of both cFd and cL in the form of non-fusion protein were obtained with the expression levels of 28.3% and 32.3% of total bacteria proteins, respectively. Their relative molecular masses were all 24 ku or so, and both of them mainly existed in the form of inclusion bodies. In addition, cFd and cL were successfully refolded into cFab by gradient dialysis, with about 59.45% of recovery when the starting total protein concentration was 100 µg/mL. The renatured cFab could specifically bind to related antigen with high affinity.

CONCLUSION: The cFab antibody against human hepatoma was highly and efficiently expressed and refolded, which laid a solid foundation for studying its application in the treatment of hepatoma.

Xing JL, Yang XM, Yao XY, Song F, Chen ZN. Prokaryotic expression and renaturation of engineering chimeric Fab antibody against human hepatoma. *World J Gastroenterol* 2004; 10(14): 2029-2033

<http://www.wjgnet.com/1007-9327/10/2029.asp>

INTRODUCTION

The advent of monoclonal antibody (mAb) greatly promotes

application of antibodies in various fields^[1]. However, due to immunogenicity and comparatively high molecular mass, mouse derived complete antibody was more or less limited in the application of disease diagnosis and treatment^[2]. The cFab antibody is about 50 ku, only 1/3 of full-length IgG. Because of good penetrating ability, better characteristics of pharmaceutical kinetics and good antigen-binding activity, cFab antibody has been used more and more widely^[3-5]. Compared with complete antibody, the cFab has no Fc fragment so that non-specific binding is decreased greatly. In addition, the cFab could not produce antibody-dependent cellular cytotoxicity (ADCC) and complement-dependent cytotoxicity (CDC), so it was mostly used as the carrier for targeted delivery of drugs^[6]. It could also be further reconstructed into engineering cF(ab)₂ antibody^[7]. In this paper, based on cloned V_H and V_L genes of mAb HAb18 against human hepatoma^[8], we expressed cFd and cL in *E.coli* in the form of non-fusion protein and refolded them into cFab antibody. It was expected that a practical protocol could be established for the preparation of a large quantity of cFab against human hepatoma, which would lay a solid foundation for further studies of its application in hepatoma treatment.

MATERIALS AND METHODS

Materials

The pComb3/cFab vector containing cFd and cL genes of mAb HAb18 was previously constructed in our laboratory. Prokaryotic expression vector pET32a (+) and competent *E. coli JM109(DE3)* were purchased from Novagen Inc (USA). T vector, PCR reagents, restriction endonucleases and T4 DNA ligase were from Takara Inc. (DaLian, China). The mAb HAb18, chimeric IgG antibody chHAb18 and HRP-HAb18 were previously prepared in our laboratory. IPTG, FITC-labeled and HRP-labeled goat anti-human IgG were from SABC Inc. (Luo Yang, China). Protein G affinity column was purchased from Pharmacia Inc (USA). Hepatoma cell line HHCC was from ATCC (Shanghai, China).

Primer design and synthesis

According to gene sequences of HAb18 cFd and cL which were previously constructed in our laboratory, PCR primers were designed by computer software Primer Premier 5.0, and relative restriction endonuclease sites were introduced into primers for the construction of prokaryotic non-fusion expression vectors of cFd and cL. All PCR primers were synthesized by Shengong Inc. (Shanghai, China), and their sequences were as follows: cFd back: 5' GCGGAATTCATATGGTTAAGCTTGAAGAGTCTGGAGGAGGCTT 3'; cFd forward: 5' GGGGTCGACTCATTAAGTATTTGTGCAAGATTTGGGCT3'; cL back: 5' GCGGAATTCATATGAGTATTGTGATGACCCAGACTCCCA3'; cL forward: 5' GGGCCTCGAGTCATTAACATTCACCTCTGTTGAAGCTCT3'. Underlined sequences are restriction sites *Nde* I, *Sal* I and *Xho* I.

Construction of expression vectors

With the vector pComb3/cFab as template, cFd and cL genes were amplified using related primers. The PCR products were

purified by gel extraction. Then, the plasmid pET32a (+) and PCR amplified cFd or cL gene were digested by a pair of restriction endonucleases *Nde* I and *Sal* I or *Nde* I and *Xho* I. After the corresponding target fragments were purified by gel extraction, ligation, transformation and screening of the positive clones containing the recombinant vector pET32a/cFd or pET32a/cL were sequentially conducted. Finally, recombinant vectors were identified by restriction endonucleases digestion and DNA sequencing was completed by Shenggong Inc. (Shanghai, China).

Small-scale expression by IPTG induction

The *E. coli* cells containing pET32a/cFd or pET32a/cL or pET32a (+) were respectively inoculated with 1:100 into 5 mL LB medium containing ampicillin (100 µg/mL). When absorbance of $A_{600\text{nm}}$ was up to 0.8 or so, 1 mL *E. coli* cultures were obtained for further assay. Then, IPTG was added to left cultures with 1 mmol/L of final concentration and another 10 h induction of expression (250 r/min, 37 °C) was conducted. After being treated by boiling and centrifugation, all *E. coli* samples after and before induction were loaded onto 120 g/L SDS-PAGE gel for further analysis. At the same time, Western blotting was done by HRP-labeled goat anti-human IgG (H+L). In addition, *E. coli* cells containing pET32a/cFd and pET32a/cL after induction were collected and treated by repeated freezing and thawing. Then, the location of expression products was investigated by SDS-PAGE.

Renaturation of cFab antibody

A total of 500 mL cultures of *E. coli* containing pET32a/cFd or pET32a/cL were induced for the protein expression under the same condition as mentioned above. Inclusion body was isolated and solubilized by 8 mol/L urea^[9]. The total protein concentration was determined by bicinchoninic acid (BCA) assay^[10] and the expression percentages of cFd and cL were evaluated by SDS-PAGE. cFd and cL dissolved in urea were mixed with equal molar, and the total protein concentration was adjusted to 100 µg/mL by adding the lysis solution. Renaturation was conducted by gradient dialysis as described by Lee *et al.*^[11]. The renatured products were centrifuged, and the supernatant was collected, then the precipitation was dissolved in the lysis solution again. Protein recovery was determined by BCA assay. Single cFd and single cL were set as control at the same refolding condition when cFab was renatured. All samples above were detected by SDS-PAGE, Western blotting and HPLC.

Effect of total protein concentration on renaturation of cFab antibody

After the total protein concentration was respectively adjusted to 200 µg/mL and 400 µg/mL, cFab antibody was renatured according to the method described above. The protein concentration of all samples was detected by BCA assay and protein recovery was evaluated. In addition, all samples were loaded onto SDS-PAGE gel for further analysis.

Purification of renatured cFab antibody

After dialysis in PBS overnight at 4 °C, renatured cFab was purified by protein G affinity chromatography according to manufacturer's protocol.

Detection of antigen-binding activity of purified cFab antibody

Indirect ELISA GST-HAb18GE, GST-fusion expression product of extracellular region of HAb18G^[12] was the antigen of mAb HAb18, and the purified GST expression products were coated on the ELISA plates for detecting the antigen-binding activity of purified cFab antibody. Detailed protocol was described by Yan *et al.*^[13].

Competitive binding assay GST-HAb18GE was coated on

ELISA plates overnight at 4 °C. After blocking, the mixture of HRP-HAb18 (0.1 mg/L) and gradiently diluted cFab was added into ELISA plates. After incubation for 1 h at 37 °C, the unbound antibody was washed away by PBST, followed by TMB staining. Finally, A_{450} was detected by an ELISA plate reader (Bio-Rad, USA), and inhibition rate and comparative affinity were determined according to the following method: Inhibition rate (%) = $[(A_{450} \text{ of control group} - A_{450} \text{ of experimental group}) / A_{450} \text{ of control group}] \times 100\%$; comparative affinity (%) = $[\text{concentration of cFab when inhibition rate is } 50\% / \text{concentration of HRP-HAb18}(0.1 \text{ mg/L})] \times 100\%$.

FACS detection The single-cell suspension of hepatoma cell line HHCC overexpressing HAb18G was prepared. The cell density was adjusted to $5 \times 10^9 - 1 \times 10^{10}$ /L. HAb18 cFab diluted with horse serum was added into 50 µL HHCC single-cell suspension. Then, the mixture was incubated for 30 min at 4 °C. After washed twice by PBS, FITC-labeled rabbit anti-human IgG was added and the reaction mixture was incubated for 30 min at 4 °C. Then, washing and detecting were performed. In this assay, human IgG was set as negative control and PBS was set as blank control.

RESULTS

Construction of recombinant expression vectors

cFd and cL genes were successfully amplified using designed primers. Agarose gel electrophoresis showed that the sizes of cFd and cL genes were about 700 bp and 680 bp, respectively (lanes 2,5, Figure 1), which was in accordance with their expected sizes. The recombinant vectors pET32a/cFd and pET32a/cL digested by restrictive endonucleases (Figure 1) indicated that cFd and cL genes were correctly inserted into corresponding cloning sites. The results of DNA sequencing (results not provided) proved that cFd and cL genes inserted in expression vector had no base mutation and the codon reading frame was completely exact.

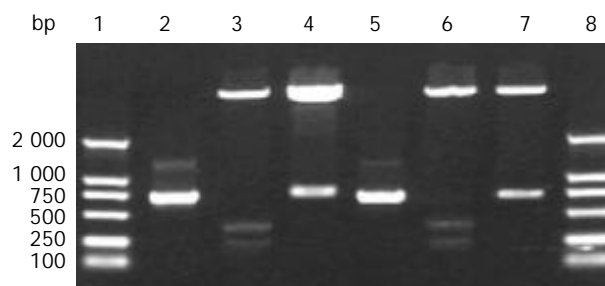


Figure 1 Analysis of recombinant non-fusion expression vectors pET32a/cFd and pET32a/cL digested by restrictive endonucleases. 1: DNA marker; 2: cFd; 3: pET32a/ *Nde* I+ *Sal* I; 4: pET32a/ cFd/ *Nde* I+ *Sal* I; 5: cL; 6: pET32a/ *Nde* I+ *Xho* I; 7: pET32a/ cL / *Nde* I+ *Xho* I; 8: DNA marker.

Expression induction and identification of cFd and cL

SDS-PAGE (Lanes 1-7, Figure 2) showed that a 21-ku new protein was expressed in *E. coli* transformed by control vector after induction, which is in accordance with the expression characteristics of the control vector, and that the recombinant cFd and cL with the same molecular weight of 24 ku were also successfully expressed after induced by IPTG. Scanning analysis by Smartview software indicated that the quantities of expressed cFd and cL were about 28.3% and 32.3% of the total bacterial protein, respectively. Western blotting (Lanes A-D, Figure 2) identified that both expressed cFd and cL were able to bind to anti-human IgG and the staining bands were at 24 ku. In addition, SDS-PAGE showed that the interested expression products existed in the form of insoluble inclusion body (Figure 3).

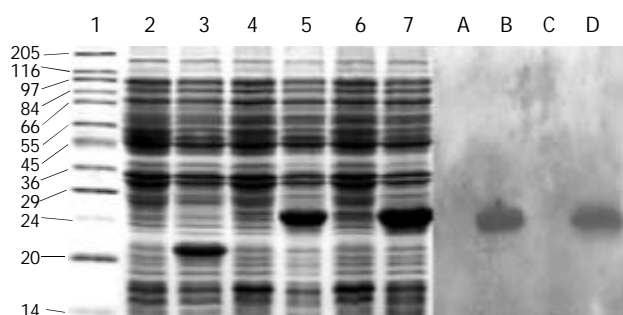


Figure 2 SDS-PAGE and Western blotting of the expressed products of cFd and cL. 1: High molecular mass marker; 2: Uninduced pET32a; 3: Induced pET32a; 4: Uninduced pET32a/cFd; 5: Induced pET32a/cFd; 6: Uninduced pET32a/cL; 7: Induced pET32a/cL; A: Uninduced pET32a/cFd; B: Induced pET32a/cFd; C: Uninduced pET32a/cL; D: Induced pET32a/cL.

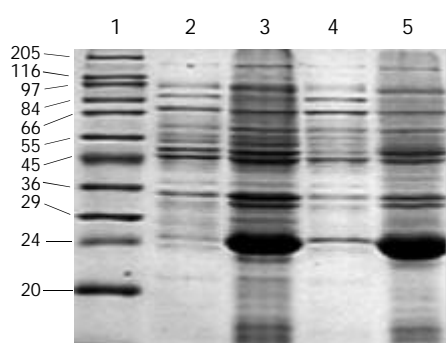


Figure 3 Location analysis of cFd and cL expression products on SDS-PAGE. 1: High molecular mass marker; 2: Supernatant of induced pET32a/cFd; 3: Inclusion body of induced pET32a/cFd; 4: Supernatant of induced pET32a/cL; 5: Inclusion body of induced pET32a/cL.

Renaturation of cFab antibody

The total protein concentrations of inclusion body solution in 8 mol/L urea containing cFd or cL determined by BCA assay were respectively 12.04 mg/mL and 9.66 mg/mL. The results (not provided) of SDS-PAGE analysis indicated that cFd and cL were up to 49.8% and 58.3% in the total protein of inclusion body solution, respectively. SDS-PAGE (Figure 4, lanes 1-7) also showed that the new 45-kDa protein band appeared under nonreduced condition after cFd and cL were mixed to refold. Western blotting (lanes A, B, Figure 4) also identified that the new protein bands could bind to anti-human IgG under reduced and nonreduced conditions. The recovery rate was about 75% when the starting concentration of total protein was 100 $\mu\text{g}/\text{mL}$. In addition, when the starting total protein concentration was separately increased to 200 $\mu\text{g}/\text{mL}$ and 400 $\mu\text{g}/\text{mL}$, recovery rate was respectively decreased to 70.5% and 61%. SDS-PAGE (Figure 5) demonstrated that precipitation rose rapidly with the increase of starting total protein concentration, and the percentage of elevated precipitation was more than that of increased starting total protein concentration. HPLC analysis (Figure 6) showed that two new elution peaks (1) and (2) emerged after cFd and cL were mixed to refold in comparison with single refolded cFd and cL. The largest absorbance value of elution peak (2) was at 260 nm, so it was possible that elution peak (2) was not protein peak. In addition, the position of elution peak (3) was the same as elution peak (4) of refolded cFd and elution peak (5) of refolded cL. ELISA (result not provided) demonstrated that only elution peak (1) had specific antigen-binding activity. The peak areas of elution peak (1) and (3) were 33.49% and 17.75%, respectively. Renaturation yield of cFab antibody was about 49% determined by the method described previously.

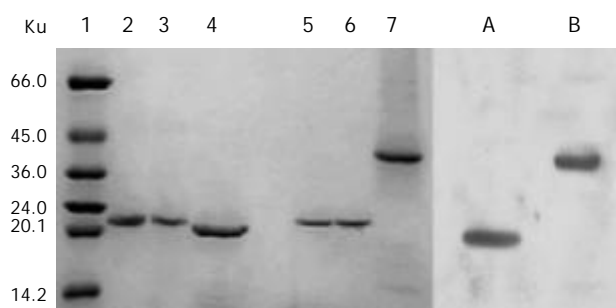


Figure 4 SDS-PAGE and Western blotting of renaturation of cFab antibody. 1: High molecular mass marker; 2: Reduced cFd; 3: Reduced cL; 4: Reduced cFab; 5: Unreduced cFd; 6: Unreduced cL; 7: Unreduced cFab; A: Western blotting of reduced cFab; B: Western blotting of unreduced cFab.

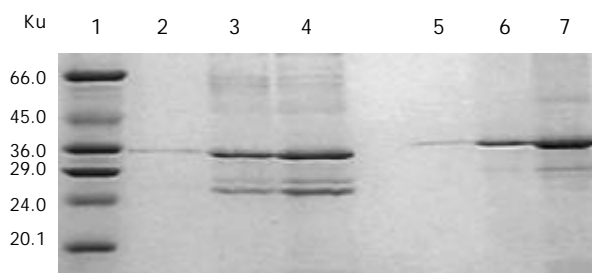


Figure 5 Relationship between the starting total protein concentration and denaturation analyzed by SDS-PAGE. 1: High molecular mass marker; 2, 3, 4: Precipitated proteins under reduced condition at starting total protein concentrations of 100, 200, 400 $\mu\text{g}/\text{mL}$, respectively; 5, 6, 7: Precipitated proteins under unreduced condition at starting total protein concentrations of 100, 200, 400 $\mu\text{g}/\text{mL}$, respectively.

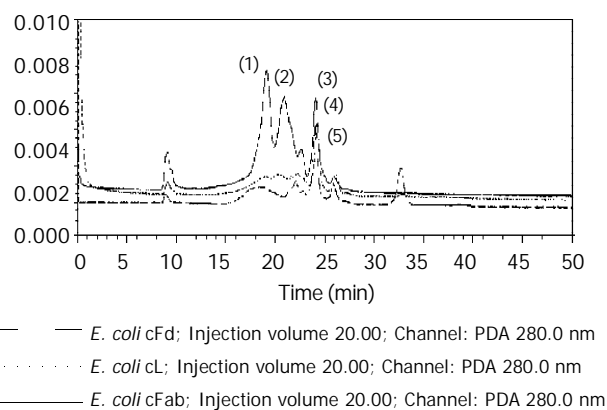


Figure 6 HPLC of cFd, cL and cFab after renaturation.

Analysis of antigen-binding activity of purified cFab antibody
 cFab 1 mL (80 $\mu\text{g}/\text{mL}$) was purified by protein G affinity chromatography. Indirect ELISA (Figure 7) showed that cFab was capable of specific binding to HAb18GE and the antigen-binding activity became higher with increasing concentration of cFab antibody. Competitive ELISA (Figure 8) indicated that the refolded cFab could competitively bind to the same antigen epitope as parental mouse antibody HAb18 and the binding ability improved with the increase of cFab antibody concentration. The affinity of cFab was evaluated to be 10% of parental mouse antibody HAb18 according to the concentration ratio of cFab and HAb18 when inhibition rate was 50%. FACS detection (Figure 9) demonstrated that cFab could bind specifically to hepatoma cell line HHCC and the binding capacity increased with the elevation of cFab antibody concentration.

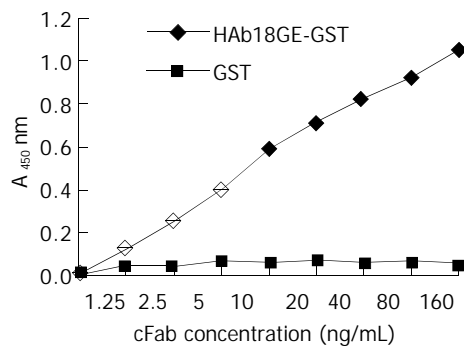


Figure 7 Detection of antigen-binding specificity of cFab by indirect ELISA.

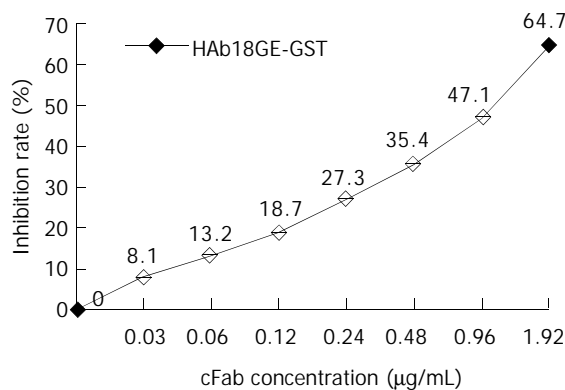


Figure 8 Detection of antigen-binding activity of cFab and HAB18 by competitive ELISA.

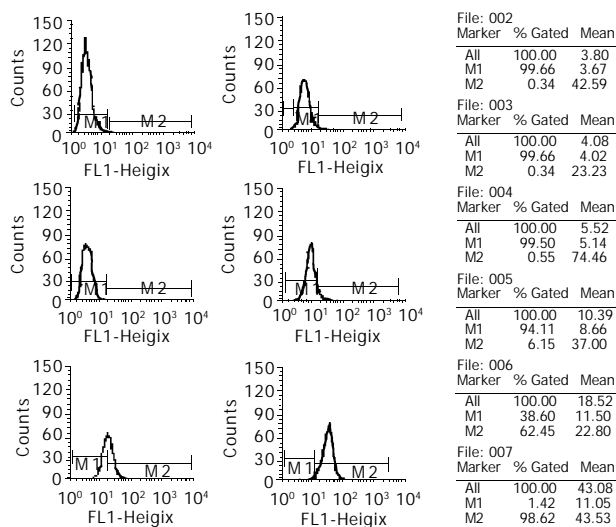


Figure 9 Detection of antigen-binding activity of cFab by FACS. 002: Negative control; 003: 0.008 µg/mL; 004: 0.04 µg/mL; 005: 0.2 µg/mL; 006: 1 µg/mL; 007: 5 µg/mL.

DISCUSSION

In a previous study, we successfully expressed cFab antibody gene in the periplasmic compartment of *E. coli*. However, the productivity was rather low. So, we tried to improve the expression level of cFab. We separately expressed cFd and cL without signal peptide in cytoplasm of *E. coli* in the form of inclusion body. The expression levels of different fragment of antibody genes in *E. coli* were greatly diverse, which mainly depended on the design of translation initiation site, the type of antibody fragment, antibody gene sequence, sensitivity to proteases of expression products and the class of host

bacterium, *etc*^[14]. But high efficient expression of antibody genes was relatively easy to be obtained using prokaryotic expression vector. We successfully constructed recombinant vectors pET32a/cFd and pET32a/cL by cloning cFd and cL genes into the pET32a expression vector, and achieved high expression level of cFd and cL in *E. coli*. The expression products mainly existed in the form of the inclusion body, with 28.3% and 32.3% of expression percentages of total bacterial protein, respectively. Expression proteins in inclusion body could avoid being digested by proteases and were easy to be isolated and purified. cFd and cL must be refolded together in order to get active cFab.

As we know, effectively promoting the correct formation of intramolecular or intermolecular disulfide bond and inhibiting the formation of aggregation were key to protein renaturation^[15]. In order to promote the refolded protein to form the correct disulfide bond, some reducers, such as β-sulphydryl ethanol and DTT, were added into detergent solution to unfold wrong disulfide bonds of expression proteins in inclusion body. These wrong disulfide bonds might be formed during the lysis of host bacterium or during the resolving process of expression protein. When the protein was renatured, correct disulfide bonds could be reformed only by air oxidation^[16]. In most cases, iron can promote the process of air oxidation^[17]. In addition, the repeated formation and unclosing of the disulfide bonds may increase the probability of obtaining protein with correct conformation. This process could be facilitated by some enzymes (such as disulfide isomerase)^[18] or oxidation-reduction response caused by the oxidation- and reduction-type sulphydryl mixture^[17] (such as glutathione). During the renaturation, the formation of aggregation was the most common reason resulting in lower renaturation efficiency. However, the mechanism of aggregation formation is still unclear. De Bern ardez Clark *et al.*^[19] suggested that the hydrophobic action among protein molecules was the most likely explanation for the aggregation formation facilitated by the formation of wrong disulfide bonds. In the experiment of mixed protein renaturation involving two or more proteins, small aggregation was first caused by the hydrophobic action, and then by the disulfide bonds formation from unpaired cystines that resulted in the formation of big heterogeneous aggregation. The formation of large quantities of aggregation would result in more protein precipitation, therefore, renaturation efficiency decreased greatly^[11]. The previous study on renaturation also showed that arginine, a kind of stable reagent promoting protein dissolving during renaturation, could facilitate the correct folding of proteins possibly by inhibiting the formation of bigger aggregation^[20].

In this study, we mixed cFd and cL with equal molar. The detergent was slowly removed from the mixture by gradient dialysis in the presence of a given concentration of arginine, while glutathione was added into the mixture to delete wrong reduced disulfide bonds. The results showed that this strategy for renaturation was successful. At the starting total protein concentration of 100 µg/mL, cFd and cL were refolded into cFab with 75% of protein recovery rate. Protein loss was mainly due to protein precipitation and adsorption onto dialysis belt. Replacing dialysis materials could reduce the latter loss. We identified the renatured cFab by SDS-PAGE, Western blotting and ELISA. The results proved that cFd and cL were successfully refolded into cFab. SDS-PAGE indicated that the molecular weight of renatured cFab was about 45 ku under the unreduced condition, less than 48 ku (cFd+cL), which revealed that the formation of intramolecular disulfide bond happened in the renatured protein^[15]. HPLC of renatured products revealed that the renatured cFab produced two very different elution peaks. ELISA demonstrated that only elution peak (1) had antigen-binding activity. In addition, the biggest absorbance value of elution peak (2) was at 260 nm, which

revealed that elution peak (2) might be nuclear acid existing in inclusion body. It was estimated by HPLC that the renaturation efficiency was up to 49%, which was quite desirable in comparison with the generally 10-40% of renaturation efficiency for antibody protein. The desirable renaturation efficiency was mainly explained by good renaturation strategy and special antibody sequences, which are in accordance with the viewpoint of Wibbenmeyer *et al.*^[21]. It was also estimated that dozens of milligrams of active cFab could be gained from 1 L of *E. coli* cultures under the experimental condition described above. Therefore, further optimizing the preparation protocol can increase the yield.

When preparing a large quantity of active protein by dialysis renaturation method, another important influence factor must be taken into consideration, namely the volume of renaturation protein solution. The speed of protein aggregating and precipitating was positively correlated with the protein concentration, so protein precipitation would be predominant course when protein concentration was up to the highest point. As a result, the starting total protein concentration was generally very low, which would inevitably result in excessively large sample volume to be dealt with otherwise more troubles would arise. In this study, in order to explore the optimal renaturation condition of preparing a large quantity of cFab antibody, we increased the starting total protein concentration for renaturation to 200 µg/mL and 400 µg/mL, respectively, and investigated the renaturation efficiency after the protein concentration was increased. The results revealed that protein precipitation promptly increased with the increase of starting protein concentration, and increased percentage was more than that of protein concentration increase, which indicated that a part of renaturation efficiency was surely sacrificed in order to reduce the treatment volume and increase the speed of preparation during the large-scale production of cFab.

In conclusion, we successfully obtained cFab antibody with good activity by prokaryotic expression technique, followed by dialysis, which laid a solid foundation for further application in hepatoma treatment. In addition, based on this achievement, we are planning to modify cFab genes to produce another kind of more useful engineering antibody, bivalent chimeric F(ab')₂^[22]. It is expected to replace murine-derived F(ab')₂ antibody produced by protease digestion, and reduce clinical cost and improve therapeutic efficacy.

REFERENCES

- 1 **Chen ZN**, Bian HJ, Jiang JL. Recent progress in anti-hepatoma monoclonal antibody and its application. *Huaren Xiaohua Zazhi* 1998; **6**: 461-462
- 2 **Hasholzner U**, Stieber P, Meier W, Lamerz R. Value of HAMA-determination in clinical practice-an overview. *Anticancer Res* 1997; **17**: 3055-3058
- 3 **Quinn MJ**, Plow EF, Topol EJ. Platelet glycoprotein IIb/IIIa inhibitors: recognition of a two-edged sword? *Circulation* 2003; **107**: E39-E39
- 4 **Lai ZZ**, Xiong DS, Fan DM, Peng H, Xu YF, Zhu ZP, Yang YZ. High expression of the chimeric antibody Fab against-CD₂₀ in *E. coli* and bioactivity determination. *Zhongguo Mianyixue Zazhi* 2000; **16**: 521-524
- 5 **Xia L**, Gu J, Zhang X, Liu Y, Wan H, Li P, Ruan C. Preparation of an antifibrin thrombus-specific murine/human chimeric monoclonal antibody Fab fragment in *Escherichia coli*. *Thromb Res* 1996; **8**: 477-484
- 6 **Better M**, Bernhard SL, Lei SP, Fishwild DM, Lane JA, Carroll SF, Horwitz AH. Potent anti-CD5 ricin A chain immunoconjugates from bacterially produced Fab' and F(ab')₂. *Proc Natl Acad Sci U S A* 1993; **90**: 457-461
- 7 **Humphreys DP**, Vetterlein OM, Chapman AP, King DJ, Antoniw P, Sutters AJ, Reeks DG, Parton TA, King LM, Smith BJ, Lang V, Stephens PE. F(ab')₂ molecules made from *Escherichia coli* produced Fab' with hinge sequences conferring increased serum survival in an animal model. *J Immunol Methods* 1998; **217**: 1-10
- 8 **Lou C**, Chen ZN, Bian HJ, Li J, Zhou SB. Pharmacokinetics of radioimmunotherapeutic agent of direct labeling mAb 188Re-HAb18. *World J Gastroenterol* 2002; **8**: 69-73
- 9 **Wu JY**, Jiang YH, Wang J, Zhang HB, Li M. Purification of recombinant human angiogenin. *Guangdong Yixue* 1999; **20**: 85
- 10 **Guo YJ**, Wu D, Chen RW, Sun SH. Purification and expression and cloning of porcine INF γ gene. *Shengwu Gongcheng Xuebao* 2001; **17**: 183-186
- 11 **Lee MH**, Kwak JW. Expression and functional reconstitution of a recombinant antibody (Fab') specific for human apolipoprotein B-100. *J Biotechnol* 2003; **101**: 189-198
- 12 **Xing JL**, Chen ZN, Mi L, Li Y, Feng Q. Establishment of CHO cell strain that can highly efficiently express hepatoma associate antigen HAb18G. *Zhongliu* 2001; **21**: 4-7
- 13 **Yan ZY**, Wang HL. Jingbian Fenzishengwuxue Shiyuan Zhinan [M]. *Beijing: Science Press* 1998
- 14 **Laden JC**, Philibert P, Torreilles F, Pugniere M, Martineau P. Expression and folding of an antibody fragment selected *in vivo* for high expression levels in *Escherichia coli* cytoplasm. *Res Microbiol* 2002; **153**: 469-474
- 15 **Middelberg AP**. Preparative protein refolding. *Trends Biotechnol* 2002; **20**: 437-443
- 16 **Anfinsen CB**, Haber E, Sela M, White FH Jr. The kinetics of formation of native ribonuclease during oxidation of the reduced polypeptide chain. *Proc Natl Acad Sci U S A* 1961; **47**: 1309-1314
- 17 **Saxena VP**, Wetlaufer DB. Formation of three-dimensional structure in proteins. I. Rapid nonenzymic reactivation of reduced lysozyme. *Biochemistry* 1970; **9**: 5015-5023
- 18 **Carmichael DF**, Morin JE, Dixon JE. Purification and characterization of a thiol: protein disulfide oxidoreductase from bovine liver. *J Biol Chem* 1977; **252**: 7163-7167
- 19 **De Bernardez Clark E**, Hevehan D, Szela S, Maachupalli-Reddy J. Oxidative renaturation of hen egg-white lysozyme. Folding vs aggregation. *Biotechnol Prog* 1998; **14**: 47-54
- 20 **Timasheff SN**, Arakawa T. Stabilization of protein structure by solvents. In: Creighton TE. Ed. *Protein Structure: A Practical Approach*, 2nd ed. Oxford: IRL Press 1997
- 21 **Wibbenmeyer JA**, Xavier KA, Smith-Gill SJ, Willson RC. Cloning, expression, and characterization of the Fab fragment of the anti-lysozyme antibody HyHEL-5. *Biochim Biophys Acta* 1999; **1430**: 191-202
- 22 **Rodrigues ML**, Snedecor B, Chen C, Wong WL, Garg S, Blank GS, Maneval D, Carter P. Engineering Fab' fragments for efficient F(ab)₂ formation in *Escherichia coli* and for improved *in vivo* stability. *J Immunol* 1993; **151**: 6954-6961

Edited by Chen WW Proofread by Zhu LH and Xu FM

Expression of cancer-testis antigens in hepatocellular carcinoma

Li Zhao, Dong-Cheng Mou, Xi-Sheng Leng, Ji-Run Peng, Wan-Xiang Wang, Lei Huang, Shu Li, Ji-Ye Zhu

Li Zhao, Xi-Sheng Leng, Ji-Run Peng, Wan-Xiang Wang, Lei Huang, Shu Li, Ji-Ye Zhu, Center of Hepatobiliary Surgery, People's Hospital, Peking University, Beijing 100044, China

Dong-Cheng Mou, Department of General Surgery, First Affiliated Hospital of Tsinghua University, Beijing 100016, China

Supported by the National Natural Science Foundation of China, No. 30200271, and the National Key Technologies Research and Development Program of China during the 9th Five-Year Plan Period, No. 2001BA703B04, and the Clinical Program of Ministry of Health of China (2001) and Center for Human Disease Genomics of Peking University (2001-6)

Co-first-authors: Li Zhao and Dong-Cheng Mou

Correspondence to: Dr. Xi-Sheng Leng, Center of Hepatobiliary Surgery, People's Hospital, Peking University, 11 XiZhimen Nandajie, West District, Beijing 100044, China. lengxs2003@yahoo.com.cn

Telephone: +86-10-68314422-3500

Received: 2004-02-02 **Accepted:** 2004-02-21

Abstract

AIM: To investigate the expression of cancer-testis (CT) antigens *MAGE-1*, *SSX-1*, *CTp11* and *HCA587* genes in hepatocellular carcinoma (HCC) and the possibility of applying these antigens as targets for specific immunotherapy for HCC.

METHODS: Expression levels of *MAGE-1*, *SSX-1*, *CTp11* and *HCA587* mRNA were detected with reverse transcription polymerase chain reaction (RT-PCR) in HCC tissues and corresponding adjacent non-cancerous tissues from 105 HCC patients, 40 samples of cirrhosis and normal liver tissues. Genes of five samples with positive PCR results were sequenced.

RESULTS: Of 105 HCC tissues, *MAGE1*, *SSX-1*, *CTp11* and *HCA587* mRNA expressions were detectable in 75.2%(79/105), 72.4%(76/105), 62.9%(66/105) and 56.2%(59/105) of HCC samples, respectively. About 93.3%(98/105), 72.4%(76/105), 48.6%(51/105) and 37.1%(39/105) of HCC tissues positively expressed at least one, two, three, and four members of CT antigens, respectively. Conversely, only *SSX-1* could be detectable in 2.9%(3/105) of the corresponding adjacent non-HCC tissues in which no metastatic lesion was found. Of the latter 3 patients, biopsy samples far from tumor were obtained in 2 patients and RT-PCR indicated no expression of *SSX-1* mRNA in these two samples. In addition, none of 40 samples of cirrhotic and normal liver tissues expressed CT antigen gene mRNA. DNA sequences confirmed that the RT-PCR products were true target cDNA. No relationship was found between expression of CT antigens and clinico pathological indicators such as age, gender, tumor size, degree of tumor differentiation, serum α -fetoprotein level and infection of hepatitis B virus or hepatitis C virus ($P>0.05$).

CONCLUSION: CT antigens genes (*MAGE-1*, *SSX-1*, *CTp11* and *HCA587*) are expressed with high percentage and specificity in HCC and their products are promising targets for antigen-specific immunotherapy of HCC. High frequent co-expression of multiple members of CT antigens in HCC

provides possibility of polyvalent vaccinations for HCC.

Zhao L, Mou DC, Leng XS, Peng JR, Wang WX, Huang L, Li S, Zhu JY. Expression of cancer-testis antigens in hepatocellular carcinoma. *World J Gastroenterol* 2004; 10(14): 2034-2038
<http://www.wjgnet.com/1007-9327/10/2034.asp>

INTRODUCTION

Hepatocellular carcinoma (HCC) is a common tumor with a poor prognosis, irrespective of a variety of treatment options^[1,2]. So, there is a need to develop additional therapeutic approaches for the management of this disease. A proposed strategy is immunotherapy, which has the potency to eradicate systemic tumor cells in multiple sites in the body and the specificity to discriminate between neoplastic and non-neoplastic cells^[3,4]. Genes or antigens, which are either exclusively or preferentially expressed in malignant tissues, are a prerequisite for antigen-specific cancer immunotherapy^[4,5].

Recently, the integration of molecular and immunological techniques has led to the identification of a new category of tumor-specific antigens called cancer-testis (CT) antigens, such as MAGE superfamily, SSX family, GAGE, BAGE, SCP-1, NY-ESO-1, CTp11 and HCA587^[6,7]. The CT antigens share several distinct features including: (1) CT antigen mRNA is expressed predominantly in tumors of different origins with various frequencies but not in normal tissues except for testis; and (2) the genes encoding CT antigens locate at the X chromosome^[8,9]. The combination of CT antigen peptides and human leukocyte antigen (HLA), when efficiently presented by antigen presenting cells to cytotoxic T lymphocytes (CTL), is capable of eliciting cellular immune responses in cancer patients^[10,11]. Also, some members of CT antigens are capable of inducing humoral immunity^[12,13]. Both cellular and humoral immune response can kill tumor cells specifically. The testis is an immune privileged organ because spermatogenic cells do not express HLA class I antigen at their surface. Concomitantly, the testis has a so-called blood-testis barrier, which limits contact between testicular and immune cells, in the seminiferous tubuli generated by the Sertoli cells^[7,14]. Because of these features, CT antigens have the potential to provide specific antitumor immunity directly to malignant cells without harm to normal cells. At present, the application of tumor antigenic peptide vaccine based on CT antigens for cancer immunotherapy has become a hot spot^[15,16].

The screening of tumor antigens recognized by autologous cytotoxic T cells led to the isolation of *MAGE-1*, which has been identified as a member of *MAGE-A* genes family^[17]. Clinical trials targeting *MAGE-1* antigen are in progress for malignant melanoma and have shown favorable curative effect^[18,19]. *SSX* genes and *HCA* genes were originally identified using serological analysis of recombinant cDNA expression libraries (SERAX). SEREX was to define B cell epitopes in antigens that were specifically recognized by antibodies in cancer sera, suggesting that *SSX* and *HCA* antigens were immunogenic and capable of inducing an antibody response^[6,20]. In a recent report, Li *et al.* have proved HCC patients were able to develop humoral immune response to HCA587 antigen. Based on representational difference analysis of cDNA, Zendman *et al.*^[21]

first identified the expression of *CTp11* in melanoma cell lines. In another study (unpublished data), our group predicted HLA-A2-restricted CTL epitopes of *CTp11* by peptide supermotif prediction combined with quantitative motif^[22,23] and found the potential HLA-A2-restricted CTL epitopes of *CTp11* antigen (*HLA-A2* is the most common *HLA-A* allele in Asian population, especially in Chinese, with an estimated frequency of more than 50%^[24,25]), suggesting the possibility of *CTp11* antigen to trigger cellular immunity and a new potential vaccine candidate for HCC immunotherapy.

Several studies reported high frequent expression of CT antigens in the HCC tissues, such as *MAGE-1*^[26,27] and *SSX-1*^[4,28]. However, the expression of CT antigens is heterogenous in a variety of human tumors, which may be a way for malignant cells to evade from immunosurveillance^[7,29-31]. Screening highly and specifically expressed multiple CT antigens in tumors and using them as targets for immunotherapy are promising means to overcome the heterogenous expression of tumor cells, thus expanding patients' opportunities for cancer specific immunotherapy and establishing the basis of polyvalent vaccinations^[29].

In an effort to improve the efficiency of tumour vaccines and prevent immune escape, we investigated the expression of CT antigens *MAGE1*, *SSX-1*, *CTp11* and *HCA587* in HCC tissues.

MATERIALS AND METHODS

Data of patients

From October 2000 to September 2003, 105 patients receiving operation for HCC, including hepatectomy or orthotopic liver transplantation, at the 2nd Hospital of Peking University Health Science Center, were enrolled in this study. There were 90 men and 15 women with a mean age of 47.2±8.4 years (range 18-75). The hepatitis B surface antigen was positive in 98 cases. Among 105 cases, anti-HCV was positive in 5 cases. The serum α -fetoprotein (α -FP) level was normal (<20 ng/mL) or elevated slightly (<40 ng/mL) in 35 patients. Histopathological examination indicated that 18 HCC samples were well differentiated, 61 moderately and 26 samples poorly differentiated, respectively. According to TNM classification of the International Union Against Cancer^[32], there were 13 cases at stage I, 30 at stage II, 12 at stage III and 50 at stage IV, respectively. Seventy-nine patients had large-sized tumors (>5 cm), while the tumor size of the other 26 patients was equal to or less than 5 cm (\leq 5 cm). The control samples included 20 tissues from cirrhosis patients and 20 normal liver tissues from patients without liver disease by surgical biopsy. Testis tissues (kindly provided by Urological Department of the 2nd Hospital of Peking University Health Science Centre) were used as the positive control. Each sample was immediately frozen in liquid nitrogen after a surgical resection and stored at -80 °C until the extraction of total RNA. Informed consent was obtained from each patient before the study was conducted. The Ethic Committee of Peking University approved the study protocol.

Total RNA extraction and synthesis of cDNA

Total RNA was extracted from frozen tissue specimens (50-100 mg) using TRIzol reagent (GIBCOL BRL) according to the protocol provided by the manufacturer. Total RNA (2.5 μ g) was primed with an Oligo (dT) 15 oligonucleotide (Promega) and reverse-transcribed according to manufacturer's instructions.

PCR amplification of CT antigens

The amplification reaction contained 5 μ L of a 1:5 dilution of reverse-transcribed products, 1 μ L each of 10 μ mol/L specific primers, 1 μ L 10 mmol/L dNTP mixture (dATP, dGTP, dCTP, dTTP), 2.5 U *Taq* DNA polymerase (Gibco BRL) and PCR-

buffer solution. The total volume was brought to 50 μ L using water. The PCR amplifications were performed in a UNO II thermocycler (Perkin-Elmer, USA) under the following conditions: After an initial denaturation for 5 min at 94 °C, samples were subjected to 35 cycles of amplification, followed by a final extension of 8 min at 72 °C. The length of PCR products was 421 base pair (bp) (*MAGE-1*), 422 bp (*SSX-1*), 297 bp (*CTp11*) and 238 bp (*HCA587*), respectively. To verify that the RNA had not degraded, a PCR assay with specific primers for the gene β_2 -microglobulin (*B₂-MG*) was performed on each cDNA sample under the following conditions: After an initial heating for 2 min at 94 °C, samples were subjected to 30 cycles of amplification, followed by a final extension of 8 min at 72 °C. The product size was 335 bp. The PCR conditions and specific primer sets for *MAGE-1*^[33], *SSX-1*^[4], *CTp11*^[21], *HCA587*^[34] and *B₂-MG*^[26] used in this study are shown in Table 1.

At last, 10 μ L of reaction product was analyzed by electrophoresis on a 20 g/L agarose gel (Promega, USA), followed by ethidium bromide staining and digital camera photographing (Korda D3.5, USA).

Sequence analysis of PCR products

To confirm the specificity of the RT-PCR products of the CT antigen genes, we performed the sequence analysis. In brief, purified PCR products were cloned into pGEM-T Easy Vector (Promega) by *T4* DNA ligase and amplified in *E. coli*, JM109. Five cases of positive colonies were selected and assessed using *EcoRI* digestion of mini-prepared DNA. The putative *MAGE-1*, *SSX-1*, *CTp11* and *HCA587* cDNA samples were sequenced with T7 sequencing primers in Sangon Co, Shanghai, China.

Statistical analysis

The statistical analysis was assessed using the chi-square test and the Fisher's exact test, and the significant level was set at $P < 0.05$.

RESULTS

Expression of CT antigen genes

Among the 105 HCC tissues investigated, *MAGE1*, *SSX-1*, *CTp11* and *HCA587* mRNA was expressed in 75.2% (79/105), 72.4% (76/105), 62.9% (66/105) and 56.2% (59/105) of tumor samples from HCC patients, respectively. At least one CT antigen mRNA was positive in 93.3% (98/105) of HCC tissues. Conversely, only *SSX-1* could be detected in 2.9% (3/105) of the corresponding adjacent non-HCC tissues in which no metastatic lesions were found. Of the latter 3 patients, biopsy samples far from tumor were obtained in 2 patients and RT-PCR indicated no expression of *SSX-1* mRNA was detectable in these 2 samples. No expression of *MAGE-1*, *CTP11* and *HCA587* was detected in the samples of corresponding adjacent non-cancerous tissues. In addition, none of 40 samples of cirrhosis and normal liver tissue expressed each CT antigen mRNA. In consistent with Chen *et al.*'s findings^[4], the electrophoretogram analysis revealed the intensities of PCR products varied considerably among different samples, indicating HCC cells expressing tumor antigens at mRNA level are heterogeneous. The typical electrophoresis of RT-PCR products amplified from cDNA of tissue samples of some HCC patients is shown in Figure 1.

Highly synchronous expression of multiple CT antigens in HCC samples

Highly frequent co-expression of multiple members of CT antigens was observed in HCC samples, with synchronous expression of at least two, three, and four of these gene in

Table 1 PCR amplification program

Gene	Temperature, duration of denaturation, annealing, extension	Primer sequence	Product size (bp)
MAGE-1	94 °C, 45 s	f: 5' -CGGCCGAAGGAACCTGACCCAG-3'	421
	65 °C, 45 s	s r: 5' -GCTGGAACCCCTACTGGGTTGCC-3'	
	72 °C, 45 s		
SSX-1	94 °C, 60 s	f: 5' -CTAAAGCATCAGAGAAGAGAAGC-3'	422
	57 °C, 60 s	r: 5' -AGATCTCTTATTAATCTTCTCAGAAA-3'	
	72 °C, 60 s		
CTp11	94 °C, 45 s	f: 5' -CTGCCCCAGACATTGAAGAA-3'	297
	57 °C, 60 s	r: 5' -TCCATGAATTCCTCCTCCTC-3'	
	72 °C, 90 s		
HCA587	94 °C, 30 s	f: 5' -AGGCGCGAATCA AGTTAG-3'	238
	60 °C, 30 s	r: 5' -CTCCTCTGCTGTGCTGAC-3'	
	72 °C, 30 s		
B ₂ -MG	94 °C, 45 s	f: 5' -CTCGCGCTACTCTCTCTTTCTGG-3'	335
	55 °C, 45 s	r: 5' -GCTTACATGTCGATCCCCTTA-3'	
	72 °C, 45 s		

f: Forward primer, r: Reverse primers.

Table 2 Expression of CT antigens and clinico pathological indicators

Group	n ¹	MAGE-1		SSX-1		CTp11		HCA587		CT ² (+)	
		+	-	+	-	+	-	+	-	+	-
Total number	105	79	26	76	29	66	39	59	46	98	7
Gender											
Male	90	70	20	66	24	57	33	48	42	85	5
Female	15	9	6	10	5	9	6	11	4	13	2
Tumor diameter											
≤5 cm	26	18	8	16	10	14	12	15	11	22	4
>5 cm	79	61	18	60	19	52	27	44	35	76	3
TNM stage											
I+II	43	29	14	31	12	27	16	22	21	39	4
III+IV	62	50	12	45	17	39	23	37	25	59	3
Hepatitis B virus											
HBV (+)	98	74	24	71	27	62	36	55	43	91	7
HBV (-)	7	5	2	5	2	4	3	4	3	7	0
Hepatitis C virus											
HCV (+)	5	5	0	4	1	4	1	4	1	5	0
HCV (-)	100	74	26	72	28	62	38	55	45	93	7
AFP (ng/mL)											
<40	35	28	7	22	13	20	15	18	17	32	3
≥40	70	51	19	54	16	46	24	41	29	66	4
Differentiation											
Well	18	13	5	12	6	12	6	9	9	16	2
Moderately	61	44	17	44	17	39	22	34	27	58	3
Poorly	26	22	4	20	6	15	11	16	10	24	2

n¹: Number of samples; CT²: At least one of these 4 CT antigen genes; No relationship is found between the expression of CT antigens and clinical indicators such as age, gender, degree of tumour differentiation, serum α-FP level, TNM classification, tumor size, infection of hepatitis B virus or hepatitis C virus ($P>0.05$).

72.4% (76/105), 48.6% (51/105) and 37.1% (39/105) of HCC tissues, respectively. We also analysed the cases with expression of neither *MAGE-1* nor *SSX-1* genes to determine targets for cancer immunotherapy other than *MAGE-1* and/or *SSX-1*. Among 18 HCC patients with expression of neither *MAGE-1* nor *SSX-1*, 61.1% (11/18) of HCC samples expressed *CTp11* and/or *HCA587*.

Sequence analysis of PCR products

Sequence analysis of PCR products verified the nucleotide

sequences of *MAGE-1*, *SSX-1*, *CTp11* and *HCA587* cDNA fragments were identical to that in the database of the GenBank. It confirmed that the RT-PCR products were true *MAGE-1*, *SSX-1*, *CTp11* and *HCA587* cDNA (data not shown).

Expression of CT antigens and clinical indicators

No relationship was found between the expression of CT antigens and clinico pathological indicators such as age, gender, differentiation degree of tumour, serum α-FP level, TNM classification, tumor size, infection of hepatitis B virus or

hepatitis C virus ($P > 0.05$). However, among 35 patients with the normal (< 20 ng/mL) or slightly elevated (< 40 ng/mL) serum α -FP level, 32 patients had *MAGE-1*, *SSX1*, *CTp11* or *HCA587* gene transcripts detected in their HCC tissues. The results are demonstrated in Table 2.

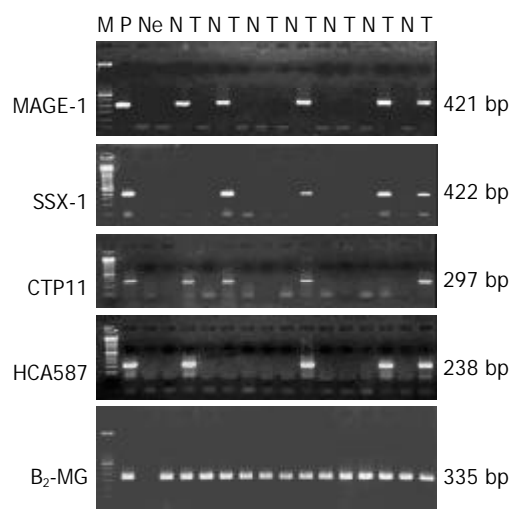


Figure 1 Electrophoresis of RT-PCR products amplified from cDNA of HCC tissues. M: Molecular marker, 100-bp DNA ladder (Gibco); P: Positive control, testis tissues; Ne: Negative control, PCR amplification in the absence of template; B₂-MG: 335-bp cDNA quality control; T: HCC tissues, arrows indicate the RT-PCR products of CT antigens; N: Corresponding adjacent non-tumor tissues. All the samples shown here except for the negative control are positive.

DISCUSSION

Tumor antigens should demonstrate high frequency expression in the tumor tissues and restricted expression in normal tissues, which is the prerequisite for being an ideal candidate antigen for antigen-specific cancer immunotherapy^[35]. The growing class of CT antigens is of particular interest for antitumor immunotherapy because of their specific expression on tumor cells. It has demonstrated high frequent expression of *MAGE-1* and *SSX-1* in HCC tissues, but little in nontumor tissues^[4,26-28]. However, the heterogeneous expression of *MAGE-1* and *SSX-1* antigens may cause problems for immunotherapy targeting these antigens, as tumor cases with a low percentage or negative expression of *MAGE-1* and/or *SSX-1* antigens may be less suitable for immunotherapy targeting these antigens. Furthermore, to our knowledge, so far little information is available on the *CTp11* and *HCA587* expression in HCC tissues. Therefore, we investigated the expression of CT antigens *MAGE1*, *SSX-1*, *CTp11* and *HCA587* in HCC tissues.

In the present study, we found highly positive rate of *MAGE-1*, *SSX-1*, *CTp11* and *HCA587* transcripts in HCC tissues (56.2-75.2%). No expression of *MAGE-1*, *CTP11* and *HCA587* was detected in the samples of corresponding adjacent non-cancerous tissues, while *SSX-1* mRNA could be detected in 2.9% (3/105) of the corresponding adjacent non-HCC tissues where no metastatic lesions were found, similar to Chen *et al.*'s findings^[4]. Of these 3 patients, biopsy samples far from tumor were obtained in 2 patients and RT-PCR indicated expression of *SSX-1* mRNA was not detectable in these two samples. The sensitivity of RT-PCR assay was much higher than that of conventional methods^[36], such as histochemistry and cytology, so we speculate that there might be micrometastasis in the adjacent non-tumor liver tissue. In addition, none of 40 samples of cirrhosis and normal liver tissues expressed each of these 4 CT antigen mRNAs. As *MAGE-1*, *SSX-1*, *CTp11* and *HCA587*

were expressed with a high percentage and specificity in HCC, their products might be ideal antigen targets for HCC immunotherapy. A high proportion (93.3%, 98/105) of the HCC tissue samples was positive for at least one of these 4 CT antigen genes, indicating using multiple CT antigens as targets will greatly increase the number of candidates for CT antigen-based HCC immunotherapy.

In the present study, we found relatively high frequency of expression of *CTp11* and *HCA587* mRNA, being 62.9% (66/105) and 56.2% (59/105) of tumor samples from HCC patients, respectively, while no expression of *CTP11* and *HCA587* was detected in the samples of corresponding adjacent non-cancerous tissues and control liver tissues, indicating their products may also be ideal antigen targets for HCC immunotherapy. Though frequency of expression of *CTp11* and *HCA587* mRNA was relative lower than that of *MAGE-1* and *SSX-1*, being 75.2% (79/105) and 72.4% (76/105), respectively, we found that samples with negative expression of *MAGE-1* and *SSX-1* showed expression of *CTp11* and *HCA587*. With respect to these HCC patients, vaccines based on *CTp11* and *HCA587* should be a desirable choice.

We also found a high frequency of synchronous expression of multiple CT antigens in HCC samples, with synchronous expression of at least two, three, and four of these genes in 72.4% (76/105), 48.6% (51/105) and 37.1% (39/105) of HCC tissues, respectively. High frequent co-expression of multiple members of CT antigens in HCC provides possibility of polyvalent vaccinations for HCC. The polyvalent vaccinations with multiple antigens, which avoid the heterogenous expression of tumor cells, might obtain better clinical results than a single antigen-based vaccination in cancer immunotherapy. Patients' opportunities for cancer specific immunotherapy can thus be expanded^[37]. However, our results showed no expression of CT antigens in 6.7% (7/105) of HCC tissues. For these patients, it is necessary to screen other CT antigens or tumor specific antigens serving as immune targets for HCC immunotherapy.

Concerning the issues of heterogenous expression of CT antigens and possibility of polyvalent vaccinations for HCC, Tahara *et al.*^[27] investigated the 10 CT antigens expression in HCC with RT-PCR and found that 86% (19/22) of HCC tissue samples expressed at least one CT antigen gene. Comparably, Luo *et al.*^[28] showed that 81% (17/21) of HCC tissue samples expressed at least one of the 10 CT genes. While in our present study, selecting just 4 CT antigens, we proved that 93.3% (98/105) of HCC patients were detectable of at least one positive CT antigen expression. Notably, the sample number of our study is 105, which is much more than the case number in the study of Tahara *et al.*^[27] (22 cases) or Luo *et al.*^[28] (22 cases), therefore our results should be more convincing.

Our previous report showed the prognostic value of *MAGE-1* and *MAGE-3* as tumor specific markers to detect blood dissemination of HCC cells after hepatectomy^[33]. In this study, our results indicated *SSX-1*, *CTp11* and *HCA587* were also expressed in HCC tissues with high percentage and sensitivity, and some cases with negative *MAGE* expression were positive for *SSX-1*, *CTp11* and/or *HCA587* transcripts. Therefore, we can combine *SSX-1*, *CTp11* and *HCA587* genes with *MAGE* genes and apply them as multiple-markers to detect hepatoma cells in circulation, which may improve the sensitivity of the assay.

In this study, the serum α -FP was normal (< 20 ng/mL) or slightly elevated (< 40 ng/mL) in 30.0% (35/105) of HCC patients. In these 35 patients, 32 had *MAGE-1*, *SSX1*, *CTp11* or *HCA587* transcripts in their HCC tissues, suggesting applying their mRNAs as tumour-specific markers to detect HCC cells in circulation might be an adjuvant diagnostic tool. This assay combined with the examination of serum α -FP level may improve the diagnosis of HCC patients.

REFERENCES

- 1 **Lai YC**, Shih CY, Jeng CM, Yang SS, Hu JT, Sung YC, Lin HT, Hou SM, Wu CH, Chen TK. Hepatic arterial infusion chemotherapy for hepatocellular carcinoma with portal vein tumor thrombosis. *World J Gastroenterol* 2003; **9**: 2666-2670
- 2 **Zhou Q**, He Q, Liang LJ. Expression of p27, cyclin E and cyclin A in hepatocellular carcinoma and its clinical significance. *World J Gastroenterol* 2003; **9**: 2450-2454
- 3 **Liu CL**, Fan ST. Nonresectional therapies for hepatocellular carcinoma. *Am J Surg* 1997; **173**: 358-365
- 4 **Chen CH**, Chen GJ, Lee HS, Huang GT, Yang PM, Tsai LJ, Chen DS, Sheu JC. Expressions of cancer-testis antigens in human hepatocellular carcinomas. *Cancer Lett* 2001; **164**: 189-195
- 5 **Tureci O**, Chen YT, Sahin U, Gure AO, Zwick C, Villena C, Tsang S, Seitz G, Old LJ, Pfreundschuh M. Expression of SSX genes in human tumors. *Int J Cancer* 1998; **77**: 19-23
- 6 **Wang Y**, Han KJ, Pang XW, Vaughan HA, Qu W, Dong XY, Peng JR, Zhao HT, Rui JA, Leng XS, Cebon J, Burgess AW, Chen WF. Large scale identification of human hepatocellular carcinoma-associated antigens by autoantibodies. *J Immunol* 2002; **169**: 1102-1109
- 7 **dos Santos NR**, Torensma R, de Vries TJ, Schreurs MW, de Bruijn DR, Kater-Baats E, Ruiter DJ, Adema GJ, van Muijen GN, van Kessel AG. Heterogeneous expression of the SSX cancer/testis antigens in human melanoma lesions and cell lines. *Cancer Res* 2000; **60**: 1654-1662
- 8 **Tajima K**, Obata Y, Tamaki H, Yoshida M, Chen YT, Scanlan MJ, Old LJ, Kuwano H, Takahashi T, Takahashi T, Mitsudomi T. Expression of cancer/testis (CT) antigens in lung cancer. *Lung Cancer* 2003; **42**: 23-33
- 9 **Yakirevich E**, Sabo E, Lavie O, Mazareb S, Spagnoli GC, Resnick MB. Expression of the MAGE-A4 and NY-ESO-1 cancer-testis antigens in serous ovarian neoplasms. *Clin Cancer Res* 2003; **9**: 6453-6460
- 10 **Sahin U**, Tureci O, Pfreundschuh M. Serological identification of human tumor antigens. *Curr Opin Immunol* 1997; **9**: 709-716
- 11 **Stockert E**, Jager E, Chen YT, Scanlan MJ, Gout I, Karbach J, Arand M, Knuth A, Old LJ. A survey of the humoral immune response of cancer patients to a panel of human tumor antigens. *J Exp Med* 1998; **187**: 1349-1354
- 12 **Chaux P**, Luiten R, Demotte N, Vantomme V, Stroobant V, Traversari C, Russo V, Schultz E, Cornelis GR, Boon T, van der Bruggen P. Identification of five MAGE-A1 epitopes recognized by cytolytic T lymphocytes obtained by *in vitro* stimulation with dendritic cells transduced with MAGE-A1. *J Immunol* 1999; **163**: 2928-2936
- 13 **Graff-Dubois S**, Faure O, Gross DA, Alves P, Scardino A, Chouaib S, Lemonnie FA, Kosmatopoulos K. Generation of CTL recognizing an HLA-A*0201-restricted epitope shared by MAGE-A1, -A2, -A3, -A4, -A6, -A10 and -A12 tumor antigens: implication in a broad-spectrum tumor immunotherapy. *J Immunol* 2002; **169**: 575-580
- 14 **Wang Z**, Zhang Y, Liu H, Salati E, Chiriva-Internati M, Lim SH. Gene expression and immunologic consequence of SPAN-Xb in myeloma and other hematologic malignancies. *Blood* 2003; **101**: 955-960
- 15 **Scanlan MJ**, Gure AO, Jungbluth AA, Old LJ, Chen YT. Cancer/testis antigens: an expanding family of targets for cancer immunotherapy. *Immunol Rev* 2002; **188**: 22-32
- 16 **Rosenberg SA**. Progress in human tumour immunology and immunotherapy. *Nature* 2001; **411**: 380-384
- 17 **van der Bruggen P**, Traversari C, Chomez P, Lurquin C, De Plaen E, Van den Eynde B, Knuth A, Boon T. A gene encoding an antigen recognized by cytolytic T lymphocytes on a human melanoma. *Science* 1991; **254**: 1643-1647
- 18 **Turner B**, Haendle I, Roder C, Dieckmann D, Keikavoussi P, Jonuleit H, Bend A, Maczek C, Schreiner D, von den Driesch P, Brocker EB, Steinman RM, Enk A, Kampgen E, Schuler G. Vaccination with mage-3A1 peptide-pulsed mature, monocyte-derived dendritic cells expands specific cytotoxic T cells and induces regression of some metastases in advanced stage IV melanoma. *J Exp Med* 1999; **190**: 1669-1678
- 19 **Hu X**, Chakraborty NG, Sporn JR, Kurtzman SH, Ergin MT, Mukherji B. Enhancement of cytolytic T lymphocyte precursor frequency in melanoma patients following immunization with the MAGE-1 peptide loaded antigen presenting cell-based vaccine. *Cancer Res* 1996; **56**: 2479-2483
- 20 **Gure AO**, Tureci O, Sahin U, Tsang S, Scanlan MJ, Jager E, Knuth A, Pfreundschuh M, Old LJ, Chen YT. SSX: a multigene family with several members transcribed in normal testis and human cancer. *Int J Cancer* 1997; **72**: 965-971
- 21 **Zendman AJ**, Cornelissen IM, Weidle UH, Ruiter DJ, van Muijen GN. CTp11, a novel member of the family of human cancer/testis antigens. *Cancer Res* 1999; **59**: 6223-6229
- 22 **Parker KC**, Bednarek MA, Coligan JE. Scheme for ranking potential HLA-A2 binding peptides based on independent binding of individual peptide side-chains. *J Immunol* 1994; **152**: 163-175
- 23 **Zhu B**, Chen Z, Cheng X, Lin Z, Guo J, Jia Z, Zou L, Wang Z, Hu Y, Wang D, Wu Y. Identification of HLA-A*0201-restricted cytotoxic T lymphocyte epitope from TRAG-3 antigen. *Clin Cancer Res* 2003; **9**: 1850-1857
- 24 **Shieh DC**, Lin DT, Yang BS, Kuan HL, Kao KJ. High frequency of HLA-A*0207 subtype in Chinese population. *Transfusion* 1996; **36**: 818-821
- 25 **Dong HL**, Sui YF, Ye J, Li ZS, Qu P, Zhang XM, Chen GS, Lu SY. Prediction synthesis and identification of HLA-A2-restricted cytotoxic T lymphocyte epitopes of the tumor antigen MAGE-n. *Zhonghua Yixue Zazhi* 2003; **83**: 1080-1083
- 26 **Chen H**, Cai S, Wang Y, Zhao H, Peng J, Pang X, Zhu J, Cong X, Rui J, Leng X, Du R, Wang Y, Vaughan H, Cebon J, Burgess AW, Chen W. Expression of the MAGE-1 gene in human hepatocellular carcinomas. *Chin Med J* 2000; **113**: 1112-1128
- 27 **Tahara K**, Mori M, Sadanaga N, Sakamoto Y, Kitano S, Makuuchi M. Expression of the MAGE gene family in human hepatocellular carcinoma. *Cancer* 1999; **85**: 1234-1240
- 28 **Luo G**, Huang S, Xie X, Stockert E, Chen YT, Kubuschok B, Pfreundschuh M. Expression of cancer-testis genes in human hepatocellular carcinomas. *Cancer Immunol* 2002; **2**: 11-16
- 29 **Mashion K**, Sadanaga N, Tanaka F, Yamaguchi H, Nagashima H, Inoue H, Sugimachi K, Mori M. Expression of multiple cancer-testis antigen genes in gastrointestinal and breast carcinomas. *Br J cancer* 2001; **85**: 713-720
- 30 **Jungbluth AA**, Stockert E, Chen YT, Kolb D, Iversen K, Coplan K, Williamson B, Altorki N, Busam KJ, Old LJ. Monoclonal antibody MA454 reveals a heterogeneous expression pattern of MAGE-1 antigen in formalin-fixed paraffin embedded lung tumours. *Br J cancer* 2000; **83**: 493-497
- 31 **Dhodapkar MV**, Osman K, Teruya-Feldstein J, Filippa D, Hedvat CV, Iversen K, Kolb D, Geller MD, Hassoun H, Kewalramani T, Comenzo RL, Coplan K, Chen YT, Jungbluth AA. Expression of cancer/testis (CT) antigens MAGE-A1, MAGE-A3, MAGE-A4, CT-7, and NY-ESO-1 in malignant gammopathies is heterogeneous and correlates with site, stage and risk status of disease. *Cancer Immunol* 2003; **3**: 9-14
- 32 **Peck-Radosavljevic M**, Pidlich J, Bergmann M, Ferenci P, Seelos C, Wichlas M, Lipinski E, Gnant M, Gangl A, Muhlbacher F. Pre-operative TNM-classification is a better prognostic indicator for recurrence of hepatocellular carcinoma after liver transplantation than albumin mRNA in peripheral blood. Liver Transplant Oncology Group. *J Hepatol* 1998; **28**: 497-503
- 33 **Mou DC**, Cai SL, Peng JR, Wang Y, Chen HS, Pang XW, Leng XS, Chen WF. Evaluation of MAGE-1 and MAGE-3 as tumour-specific makers to detect blood dissemination of hepatocellular carcinoma cells. *Br J Cancer* 2002; **86**: 110-116
- 34 **Lucas S**, De Plaen E, Boon T. MAGE-B5, MAGE-B6, MAGE-C2, and MAGE-C3: four new members of the MAGE family with tumor-specific expression. *Int J Cancer* 2000; **87**: 55-60
- 35 **Odunsi K**, Jungbluth AA, Stockert E, Qian F, Grnjatic S, Tammela J, Intengan M, Beck A, Keitz B, Santiago D, Williamson B, Scanlan MJ, Ritter G, Chen YT, Driscoll D, Sood A, Lele S, Old LJ. NY-ESO-1 and LAGE-1 cancer-testis antigens are potential targets for immunotherapy in epithelial ovarian cancer. *Cancer Res* 2003; **63**: 6076-6083
- 36 **Paterlini-Brechot P**, Vona G, Brechot C. Circulating tumorous cells in patients with hepatocellular carcinoma. Clinical impact and future directions. *Semin Cancer Biol* 2000; **10**: 241-249
- 37 **Sahin U**, Tureci O, Chen YT, Seitz G, Villena-Heinsen C, Old LJ, Pfreundschuh M. Expression of multiple cancer/testis (CT) antigens in breast cancer and melanoma: basis for polyvalent CT vaccine strategies. *Int J Cancer* 1998; **78**: 387-389

A DNA vaccine against extracellular domains 1-3 of flk-1 and its immune preventive and therapeutic effects against H22 tumor cell *in vivo*

Fan Lü, Zhao-Yin Qin, Wen-Bin Yang, Yin-Xin Qi, Yi-Min Li

Fan Lü, Zhao-Yin Qin, Wen-Bin Yang, Yin-Xin Qi, Yi-Min Li, Department of General Surgery, Second Hospital of Xi'an Jiaotong University, Xi'an 710004, Shaanxi Province, China

Supported by the Natural Science Foundation of Shaanxi Province, No. 2003C₂54

Correspondence to: Yi-Min Li, Department of General Surgery, Second Hospital of Xi'an Jiaotong University, Xi'an 710004, Shaanxi Province, China. liyiming@yahoo.com.cn

Telephone: +86-29-7679246

Received: 2004-02-06 Accepted: 2004-02-26

Abstract

AIM: To construct a DNA vaccine against extracellular domains 1-3 of fetal liver kinase-1 (flk-1), and to investigate its preventive and therapeutic effect against H22 cell *in vivo*.

METHODS: Flk-1 DNA vaccine was produced by cloning extracellular domains 1-3 of flk-1 and by inserting the cloned gene into pcDNA3.1 (+). Fifteen mice were divided into 3 groups and inoculated by vaccine, plasmid and saline respectively to detect specific T lymphocyte response. Thirty Mice were equally divided into preventive group and therapeutic group. Preventive group was further divided into V, P, and S subgroups, namely immunized by vaccine, pcDNA3.1 (+) and saline, respectively, and attacked by H22 cell. Therapeutic group was divided into 3 subgroups of V, P and S, and attacked by H22, then treated with vaccine, pcDNA3.1 (+) and saline, respectively. The tumor size, tumor weight, mice survival time and tumor latency period were compared within these groups. Furthermore, intratumoral microvessel density (MVD) was assessed by immunohistochemistry.

RESULTS: DNA vaccine pcDNA3.1 (+) flk-1-domains 1-3 was successfully constructed and could raise specific CTL activity. In the preventive group and therapeutic group, tumor latency period and survival time were significantly longer in vaccine subgroup than that in P and S subgroups ($P < 0.05$); the tumor size, weight and MVD were significantly less in vaccine subgroup than that in P and S subgroups ($P < 0.05$). The survival time of therapeutic vaccine subgroup was significantly shorter than that of preventive vaccine subgroup ($P < 0.05$); the tumor size, and MVD of therapeutic vaccine subgroup were significantly greater than that of preventive vaccine subgroup ($P < 0.05$).

CONCLUSION: DNA vaccine against flk-1 domains 1-3 can stimulate potent specific CTL activity; and has distinctive prophylactic effect on tumor H22; and also can inhibit the tumor growth *in vivo*. This vaccine may be used as an adjuvant therapy because it is less effective on detectable tumor.

Lü F, Qin ZY, Yang WB, Qi YX, Li YM. A DNA vaccine against extracellular domains 1-3 of flk-1 and its immune preventive and therapeutic effects against H22 tumor cell *in vivo*. *World*

J Gastroenterol 2004; 10(14): 2039-2044

<http://www.wjgnet.com/1007-9327/10/2039.asp>

INTRODUCTION

Extensive studies by many investigators established that angiogenesis has a central role in the invasion, growth and metastasis of solid tumors^[1-3]. The inhibition of tumor growth by attacking the tumor's vascular supply offers a primary target for anti-angiogenic intervention. There are several advantages of targeting proliferating endothelial cells in the tumor vasculature rather than directly to tumor cells. First, endothelial cells are genetically stable and do not down regulate MHC-class I and II antigens. Second, the therapeutic target is tumor-independent. Thus, killing of proliferating endothelial cells in the tumor microenvironment can be effective against a variety of malignancies and clones^[3,4]. Vascular endothelial growth factor (VEGF) plays a center role in tumor angiogenesis, while fetal liver kinase-1 (flk-1), which expressed exclusively on the endothelial cells, is the key receptor that binds VEGF^[5,6]. Blocking the VEGF-flk-1 pathway may inhibit tumor angiogenesis. Hence, we constructed a DNA vaccine to target the extracellular domain 1-3 of flk-1 and tested its preventive and therapeutic effect against H22 cell *in vivo* with the hope that the vaccine might be able to inhibit angiogenesis via targeting flk-1 and flk-1 expressing endothelial cell. This research has no parallel reports at home.

MATERIALS AND METHODS

Materials

Cell line Tumor cell H22 cell line, constructed by Dalian Medical University from the mouse ascite, was heterogeneous cells with higher declination to spread by lymph vessel. COS7 cell is derived from African green monkey kidney and preserved by our laboratory. Endothelial cells were primarily cultured from mouse vessel by our laboratory.

Animal BALB/c mice were bought from Laboratory Animal Center of the Fourth Military Medical University. All mice were male, specific pathogen free animals, with age of 6-8 wk and weight of 15-20 g.

Main reagents pcDNA3.1(+) was purchased from Invitrogen (U.S.). CD31 antibody was a product of Santa Cruz (U.S.). pMDT-18 Vector, T4 DNA ligase, Taq^{EX} DNA polymerase, *Hind* III, *Eco*R I, and dNTP were products of TaKaRa (Japan). *M-MLV* reverse transcriptase was purchased from Promega (U.S.). E.Z.N.A^R gel extraction kit was purchased from Omega Bio-tek (U.S.). Trizol, lipofectamine 2000, DMEM and G418 were purchased from Gibco (U.S.). Western blot luminescence kit was purchased from NEN (Britain). Micro BCA protein assay was purchased from Pierce (U.S.).

Methods

Culture of cells H22 cell was transferred in abdomen cavity of

BALB/c mouse. The ascites were taken from the mouse in the super clean bench and then diluted with DMEM to 1×10^7 /mL. A total of 0.2 mL of 1×10^7 H22 cells were inoculated subcutaneously at the right armpit of mouse to establish a tumor model. The interval between the ascites taking and the last mouse inoculation was less than 2 h. COS7 cell was cultured in DMEM containing 100 mL/L FCS and 50 mL/L CO₂ at 37 °C. Primary culture of endothelial cells (ECs) were performed as follow: the mouse thoracic aorta was sterile dissociated, and sheared into small pieces about 0.5 cm×0.5 cm, washed with Hank's fluid, its EC surface was stucked to 1.5% gelatin culture medium, and then DMEM containing 100 mL/L FCS and benzylpenicillin (100 U/mL) and streptomycin (100 U/mL) was slowly added, then cultured at 37 °C under humidified atmosphere containing 50 mL/L CO₂ until the cells form a single layer. Transfer of cell culture was performed (≤ 3 generations).

Construction of the expression vector encoding murine flk-1 domain 1-3 Total cellular RNA of mouse liver tissue was extracted using TRIZOL reagent and cDNA was prepared by random priming from 2 µg of total RNA using M-MLV according to the manufacturers' instructions. PCR was performed for 35 cycles as follows: denaturation at 94 °C for 30 s, annealing at 60 °C for 30 s and extension at 72 °C for 80 s. Oligonucleotide primers to amplify flk-1 domain 1-3 transcripts were designed on the mouse sequence: upstream primer: 5' -CGGATAACC TGGCTGACC-3' ; and downstream primer 5' -AGGGATT CGGACTTGACTGC-3. Then the cloned gene was inserted into the pMDT-18 vector, followed by cut out from pMDT-18 by *Eco*R I and *Hind* III and insertion into the pcDNA3.1 vector between the restriction sites *Eco*R I and *Hind* III generating pcDNA3.1 (+)-flk-1-Domain1-3. Reading frame and sequence were proved right by DNA sequencing.

Expression of the pcDNA3.1 (+)-flk-1-domain 1-3 in the COS7 cell COS7 cells were plated in antibiotic free growth medium and cultured until about 90% confluence at the time of transfection. A 4 µg of pcDNA3.1 (+)-flk-1-Domain1-3 was diluted and mixed in 250 µL of DMEM, 10 µL of lipofectamine™ 2000 was diluted and mixed in 250 µL of DMEM respectively. They were mixed together after 5 min of incubation at room temperature, and incubated for 20 min then poured into 35 mm wells plated with COS7. Mixed gently and incubated at 37 °C in 50 mL/L CO₂ incubator for 48 h. Cultured cells were incubated for 20 min and sonicated twice for 5 s in cold lysis buffer. Total extracts were cleared by centrifugation for 30 min at 4 °C at 14 000 g. Protein levels were quantified with Micro BCA protein assay. Samples were resolved by 120 g/L SDS-polyacrylamide gel electrophoresis (SDS-PAGE). In all gels, 80 µg of protein dissolved in sample buffer was loaded per lane. Immunoblotting was performed by electroblotting onto nitrocellulose membrane (0.2 mm) at 32 mA for 1 h using a semidry immunoblotter. Membranes were blocked for 2 h at room temperature with blocking buffer and subsequently incubated for 1 h at room temperature with anti-flk-1 polyclonal antibody at a 1:200 dilution with blocking buffer. The enhanced chemiluminescence system was used for the detection of bound antibody. Primary antibody-antibody-bound membranes were incubated for 1 h at room temperature with horseradish peroxidase conjugated antirabbit or antimouse IgG at a 1:1 000 dilution with blocking buffer. After washing with TBS and TBST, the membranes were treated with enhanced chemiluminescence reagents according to the manufacturer's protocol. The membranes were exposed to X-ray film for 2 min.

Analysis of specific cytolytic T lymphocyte (CTL) activity Fifteen mice were classified to three groups: vaccine group, plasmid group, and saline group, each group had 5 mice. Mice were injected with 100 µg of vaccine, 100 µg of plasmid, and 100 µg of saline respectively, at the concentration of 1 µg/µL once every 10 d. All the mice were killed on day 10 after the last

immunization and the spleen lymphocytes were separated and cultured in complete culture medium with interleukin-2 (1×10^5 U/L) and 100 mL/L FCS at saturated humidified atmosphere containing 50 mL/L CO₂ at 37 °C to induce the CTL. CTL and mouse ECs was mixed at 100:1 and 50:1 effector/target rate, respectively. In addition, there were a CTL control group, an ECs control group and a culture medium control group. The specimens of each group had 3 parallel wells on a 96-well culture plate and were cultured under conditions of saturated humidity at 37 °C containing 50 mL/L CO₂ for 48 h. Cell-mediated cytotoxicity was determined by using a standard ⁵¹Cr release assay. Briefly, target cells were pelleted and resuspended in 3.7 GBq of ⁵¹Cr per 10⁶ cells and incubated at 37 °C in a humidified 50 mL/L CO₂ incubator for 1 h. They were washed three times with media, resuspended to 5×10^4 /mL, and 0.1 mL was added to round-bottomed microtiter wells. Varying numbers of effector cells were added in 0.1-mL volume to achieve the desired E/T ratios. For a spontaneous ⁵¹Cr-release control, 0.1 mL of media was substituted for effector cells. Maximum release was determined by adding 0.1 mL of 1% NP-40 to the target cells. After 6 h at 37 °C, the plates were centrifuged at 1 200 r/min for 5 min, and 0.1 mL of supernatant was taken from each well and counted on a gamma counter. Data are presented as percent specific ⁵¹Cr-release = $100 \times [(\text{experimental group counts per minute (cpm)} - \text{spontaneous group cpm}) / (\text{maximum release cpm} - \text{spontaneous cpm})]$.

Preventive effect of pcDNA3.1 (+)-flk-1-domain1-3 against H22 Thirty BALB/c mice were randomly divided into V, P, and S subgroups, 10 mice in each subgroup, and immunized by 100 µg vaccine, plasmid, and saline, respectively, at concentration of 100 µg/µL, once every 10 d by intramuscular injection at left hip. Five days after the last immunization, all mice were injected with 1×10^7 of H22 cells at the right armpit subcutaneously. The mice weight, tumor formation, tumor size and mice survival time were recorded. Tumor volume was measured in 2 dimensions and calculated as follows: length/2×width². After mice death, tumor tissue was routinely fixed and embedded in paraffin and then performed CD31 staining. All mice were kept observation until death.

Therapeutic effect of pcDNA3.1 (+)-flk-1-domain1-3 against H22 Thirty BALB/c mice were randomly divided into V, P, and S subgroups, ten mice in each subgroup. All mice were injected with 1×10^7 of H22 tumor cell subcutaneously at right armpit. Four days later, tumor was formed in all mice, which demonstrated the successful construction of tumor model. Mice in different groups were treated with 100 µg of vaccine, plasmid, and saline, respectively, at the concentration of 1 µg/µL, two times every 5 d by intramuscular injection at left hip. The tumor weight and size were recorded each day. The mice weight, tumor formation, tumor size and survival period of mice were recorded. After mice death, tumor tissue was routinely fixed and embedded in paraffin for CD31 staining. All mice were kept observation until death.

Counting of microvessel density in H22 solid tumor Tumor tissue was washed with cold PBS, then fixed in 40 g/L buffered formaldehyde solution and embedded in paraffin. Tissue sections (4 µm thick) were preincubated for 30 min with PBS containing 3 mL/L hydrogen peroxide and then blocked with blocking solution containing 50 mL/L goat serum. CD31 staining was performed with a polyclonal rabbit anti-rat CD31 antibody diluted in PBS (1:50) supplemented with blocking solution for 24 h at 4 °C. Finally, sections were incubated with the biotinylated secondary antibody followed by streptavidin-horse-radish-peroxidase complex. Antibody binding was visualized with diaminobenzidine (DAB). Vessel counts within the tumor were assessed by light microscopy after CD31 staining. Based on the criteria of Weidner *et al.*^[7], a vessel lumen was not required for the identification of a microvessel.

The five areas with the highest number of discrete microvessels in each slide were identified by scanning tumor sections at low power. Then the number of microvessels were counted in these areas at 200 magnification (0.75 mm² area) to obtain accurate microvessel density. The average value of the five areas was counted as MVD.

Statistical analysis

Results were expressed as mean±SD. Data were analyzed by the method of ANOVA using SPSS 10.0 software. $P < 0.05$ was considered statistically significant.

RESULTS

Cloning of flk-1 domain1-3 and construction of pcDNA3.1 (+)-flk-1-domain1-3

A 1 250 bp gene part was cloned from mouse liver tissue using RT-PCR technique (Figure 1). DNA sequencing showed that pcDNA3.1 (+) flk-1-domain1-3 was the right reading frame and sequence. Western blotting of the lipotransfected COS7 cell showed that the expression of a M_r 44 000 protein in the cell after transfection of the pcDNA3.1 (+)-flk-1-domain1-3 (Figures 2, 3).

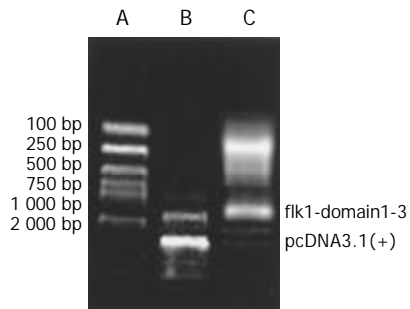


Figure 1 Clone of flk-1-domain1-3 and construction of expressing vector. A: DNA marker; B: PCR results.

Activity of spleen CTL

CTL activity of mice in vaccine subgroup was significantly higher than that of plasmid and saline subgroup (Figure 4, $P < 0.05$).

Protective effect of pcDNA3.1 (+)-flk-1-domain 1-3 against H22 in different subgroup

Observation of carcinogenesis Mice of different subgroups in immune preventive group were injected with H22 cells after 3 times inoculation, the tumor latent time, survival time of the vaccine subgroup were longer than that of plasmid subgroup and saline subgroup ($P < 0.05$); The tumor weight and tumor volume of vaccine subgroup was the lowest among the 3 subgroups ($P < 0.05$, Table 1, Figure 5). The tumor latent time, survival time, tumor volume and tumor weight of plasmid subgroup and saline subgroup have no statistical significance compared with each other.

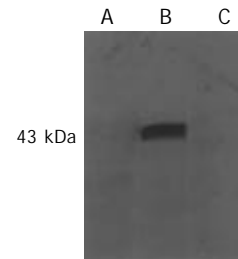


Figure 2 Functionality of the flk-1-domain 1-3 expressing vector. A: Western blotting of protein extracted from COS7 cell; B: Western blotting of protein from COS7 transfected with vaccine; C: Western blotting of protein from COS7 transfected with pcDNA3.1 (+).

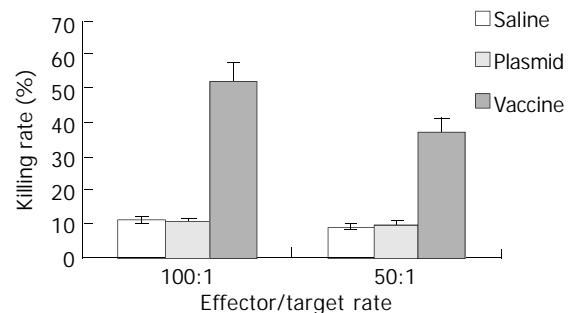


Figure 4 CTL activity of each group at different effector/target rate.

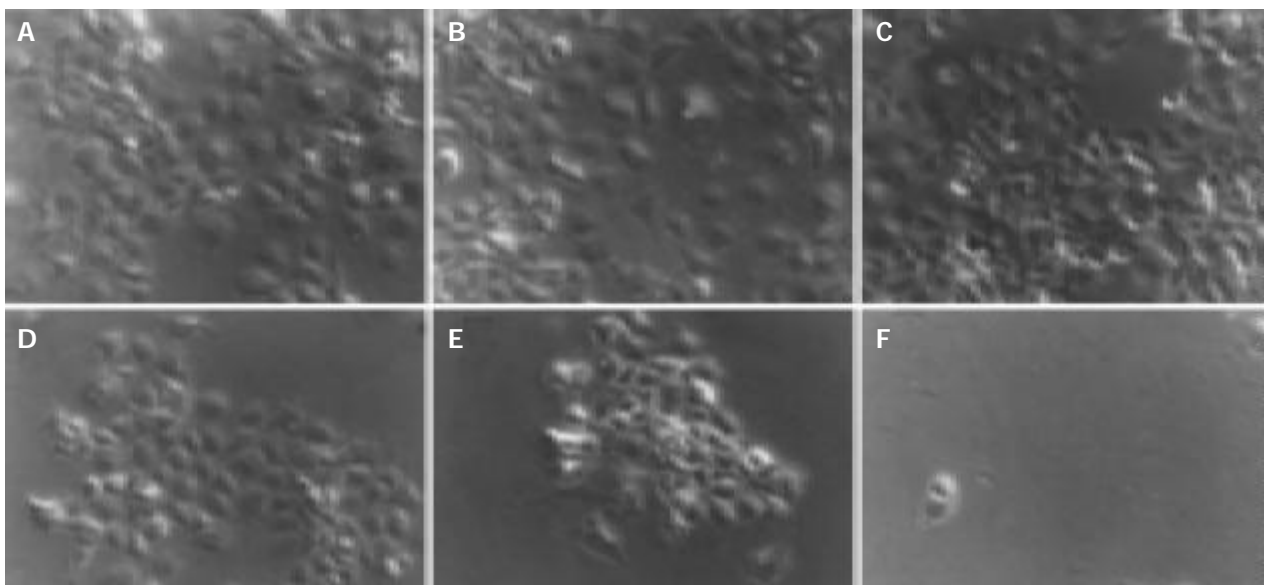
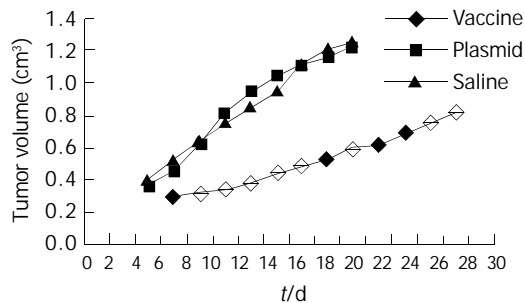


Figure 3 COS 7 cell before and after transfection with vaccine, plasmid and saline, respectively. A, D: One day before and 2 wk after transfection with vaccine; B, E: One day before and 2 wk after transfection with plasmid; C, F: One day before and 2 wk after transfection with saline.

Table 1 Protective effect of DNA vaccine against H22 tumor cell *in vivo* (mean±SD)

Group	n	Tumor latency time (d)	Survival time (d)	Microvessel density	Tumor weight (g)
Vaccine	10	5.20±0.86 ^a	24.47±3.23 ^c	10.10±1.66 ^e	1.41±0.13 ^g
Plasmid	10	4.00±0.67	14.70±2.63	27.30±3.34	1.79±0.16
Saline	10	3.80±0.63	14.30±2.00	25.30±4.64	1.82±0.16

^a $P<0.05$, ^c $P<0.05$, ^e $P<0.05$, ^g $P<0.05$ vs plasmid group and saline group.

**Figure 5** Curve of tumor growth in preventive group.

MVD of different subgroups Macroscopic structure showed the tumor tissue was hard and adhered to the surrounding tissue. MVD of vaccine subgroup was the lowest among the three subgroups ($P<0.05$). MVD of the plasmid subgroup and saline subgroup have no statistical significance compared with each other ($P>0.05$). This indicates that V subgroup has the lowest micro vessel density (Figure 6).

Therapeutic effect of pcDNA3.1 (+)-flk-1-domain1-3 against H22
Inhibitory effect of pcDNA3.1 (+)-flk-1-domain1-3 in carcinogenesis Treated with DNA vaccine pcDNA3.1 (+)-flk-1-domain1-3, plasmid and saline. The survival time of the vaccine subgroup were longer than that of plasmid subgroup and saline subgroup ($P<0.05$); The tumor weight and tumor volume of vaccine subgroup was the lowest among the 3 subgroups

($P<0.05$, Table 2, Figure 7). The survival time, tumor volume and tumor weight of plasmid subgroup and saline subgroup have no statistical significance compared with each other. But the survival times of therapeutic vaccine subgroup were significantly shorter than that of preventive vaccine subgroup ($P<0.05$); the tumor size, and MVD of therapeutic vaccine subgroup were significantly greater than that of preventive vaccine subgroup (Table 3).

MVD of different subgroups Macroscopic structure showed the tumor tissue was hard and adhered to the surrounding tissue. MVD of vaccine subgroup was the lowest among the 3 subgroups ($P<0.05$). MVD of the plasmid subgroup and saline subgroup had no statistical significance compared with each other (Figure 8).

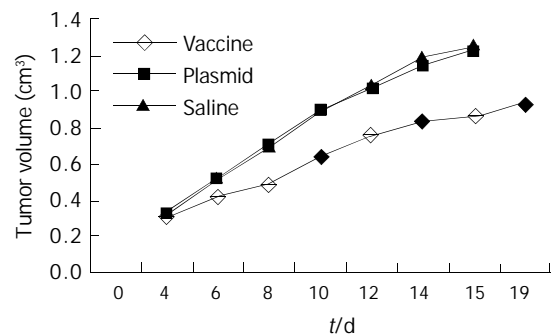
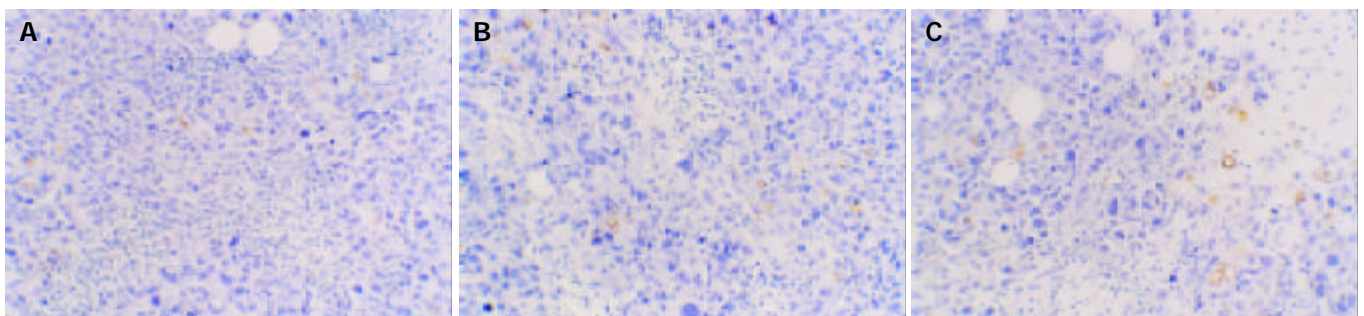
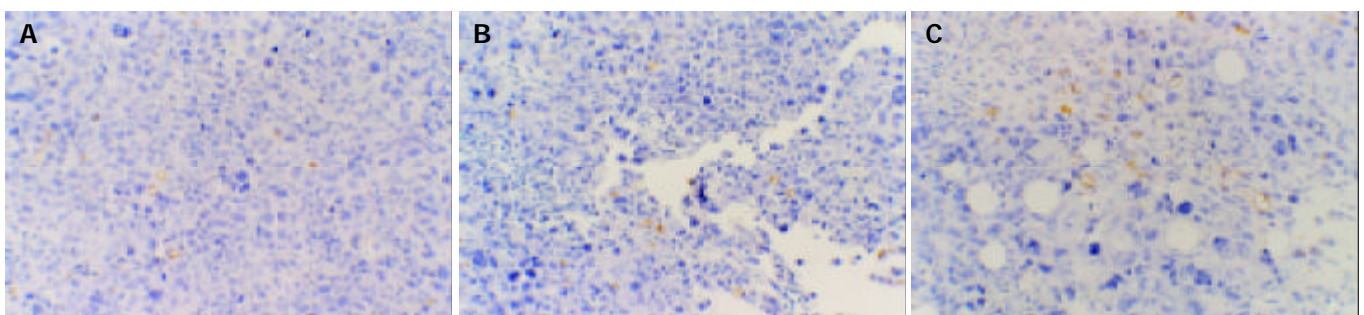
**Figure 7** Curve of tumor growth in therapeutic group.**Figure 6** Microvessel staining by anti-CD31 antibody in preventive Group (Original magnification: ×200). A: Vaccine subgroup; B: Plasmid control group; C: Saline control group.**Figure 8** Microvessel staining by anti-CD31 antibody in therapeutic group. A: Vaccine subgroup; B: Plasmid control group; C: Saline control group.

Table 2 Therapeutic effects of DNA vaccine against H22 tumor cell *in vivo* (mean±SD)

Group	n	Survival time (d)	Microvessel density	Tumor weight (g)
Vaccine	10	19.17±1.72 ^a	18.60±3.47 ^c	1.57±0.12 ^e
Saline	10	13.52±1.89	26.90±3.41	1.85±0.09
Plasmid	10	13.67±2.94	25.50±4.43	1.82±0.06

^aP<0.05, ^cP<0.05, ^eP<0.05 vs plasmid group and saline group.

Table 3 Comparison of therapeutic and preventive effects of DNA vaccine (mean±SD)

Group	n	Survival time (d)	Microvessel density	Tumor weight (g)
Protective vaccine subgroup	10	24.47±3.23 ^a	10.10±1.66 ^c	1.41±0.13 ^e
Therapeutic vaccine subgroup	10	19.17±1.72	18.60±3.47	1.57±0.12

^aP<0.05, ^cP<0.05, ^eP<0.05 vs therapeutic vaccine subgroup.

DISCUSSION

We successfully cloned the domains 1-3 of extracellular parts of flk-1, constructed the DNA vaccine pcDNA3.1 (+) flk-1-domains 1-3, which induced the immune response against endothelial cell, and finally blocked the growth of H22 tumor cells by blocking angiogenesis.

DNA sequencing and blast showed that the cloned gene completely matched the DNA sequence listed in GenBank. Western blot of lipotransfected COS7 showed that the cell transfected with vaccine could express a *M_r* 44 000 specific protein, which had no corresponding band in the control group, indicating that flk-1 could be expressed by the vaccine in eukaryotic cells. Standard 4-h ⁵¹Cr release test showed that the vaccine against domains 1-3 could generate specific immune response in mice through breaking tolerance to self-flk-1 antigen.

In the immune preventive group, mice were first inoculated with the vaccine and then challenged with tumor cells. The results showed that compared with the control group, the inoculated mice had a longer survival time, longer tumor latent period, lower tumor weight at death time and slower tumor growth rate. Furthermore, tumor in inoculated mice had low MVD. So we concluded that the vaccine inhibited tumor growth by its anti-angiogenic effects. In the therapeutic group, effects of the vaccine were supposed to investigate in the clinical conditions. The H22 cells were first injected to the mice and waited until tumor was well constructed, then the mice were treated with the vaccine. We found that, similar to the preventive group, the survival time, tumor weight at death time of mice and tumor growth rate all had significant difference compared with the control group. But compared with that of the preventive group, the vaccine was less effective in the therapeutic group. The MVD, survival time had significant difference between the vaccine subgroup of these groups, indicating that the vaccine might be less effective against well-structured tumors.

Recent advances in the understanding of the molecular control of angiogenesis have shown that this process is essential for tumor development and spread. VEGF is a highly specific mitogen for vascular endothelial cells, which can induce endothelial cell proliferation, promotes cell migration, and inhibits cell apoptosis and immune response against cancer^[8-11], and plays a central role in the tumor angiogenesis^[12-14].

Flk-1 is the main receptor through which VEGF could modulate tumor growth and metastasis^[15-18]. Flk-1 belongs to receptor

tyrosine kinases (RTKs) family and are expressed almost exclusively in endothelial cells and on various types of tumor cells^[19,20]. Flk-1 has a typical tyrosine kinase receptor structure with 7 immunoglobulin (Ig)-like domains in the extracellular region, as well as a long kinase insert in the tyrosine kinase domain^[20]. Evidence shows that IgG-like domains 2-3 are sufficient for tight binding, domain 1 is necessary for tight binding and domains 4-7 are not essential for signaling, and the residues within this region of domain 3 are critical for VEGF binding^[21, 22]. Various studies have shown that VEGF and flk-1 expression are significantly associated with advanced stage, high incidence of distant metastases after surgery, and less favorable prognosis in a number of malignancies^[23-28]. As it directly involved in tumor angiogenesis, flk-1 is an appropriate target for suppression of solid tumor growth^[6].

Several approaches have been used to block flk-1, including dominant-negative receptor mutants, germ-line disruption of VEGFR genes, monoclonal antibodies, dendritic cell vaccine, and a series of synthetic RTK inhibitors^[29-33]. They all achieved the goal of blocking VEGF-flk-1 signaling pathway and inhibiting angiogenesis, but they all have some common defects, such as requiring constant drug injection, only blocking VEGF pathway and high cost. Our strategy was to construct DNA vaccine target flk-1 in order to inhibit angiogenesis by blocking VEGF-flk-1 pathway and destructing endothelial cell that expresses flk-1. Compared with strategies mentioned above, DNA vaccines against flk-1 could achieve similar results and are simpler and cheaper to produce and can induce very long-lasting immune responses^[34,35]. Furthermore, the immune response not only blocks VEGF-flk-1 pathway, but also blocks other angiogenesis pathway by destruction of endothelial cells^[33]. Also it has been reported that liver cancer cells and various types of other tumor cells could express flk-1 receptor, but in our study we could not amplify flk-1 gene from cultured H22 tumor cells, so we could not evaluate whether or not the vaccine had direct effect on the tumor cells. Our research showed that the vaccine was less effective against well-formed tumors. This may be contributed to the immune escaping capacity of well-structured tumors. This result was in consistent with previous reports at home and abroad^[33, 36-38]. So we propose that the vaccine should be combined with other therapies, such as surgery, to prevent primary site from recurring and metastasis. Further research is needed in this direction.

In short, we constructed DNA vaccine against extracellular domain 1-3 of flk-1, and evaluated its immune preventive and immune therapeutic effects against H22 tumor cell, suggesting that the vaccine could inhibit tumor growth through its anti-angiogenic effect. Further research is needed to increase the effectiveness of this vaccine.

REFERENCES

- 1 **Bikfalvi A**, Bicknell R. Recent advances in angiogenesis, anti-angiogenesis and vascular targeting. *Trends Pharmacol Sci* 2002; **23**: 576-582
- 2 **Shibuya M**. Angiogenesis, anti-angiogenesis, and tumor suppression. *Nippon Yakurigaku Zasshi* 2002; **120**: 285-294
- 3 **Matter A**. Tumor angiogenesis as a therapeutic target. *Drug Discov Today* 2001; **6**: 1005-1024
- 4 **Bisacchi D**, Benelli R, Vanzetto C, Ferrari N, Tosetti F, Albini A. Anti-angiogenesis and angioprevention: mechanisms, problems and perspectives. *Cancer Detect Prev* 2003; **27**: 229-238
- 5 **Shibuya M**. Structure and function of VEGF/VEGF-receptor system involved in angiogenesis. *Cell Struct Funct* 2001; **26**: 25-35
- 6 **Shibuya M**. Vascular endothelial growth factor receptor-2: its unique signaling and specific ligand, VEGF-E. *Cancer Sci* 2003; **94**: 751-756
- 7 **Weidner N**, Folkman J, Pozza F, Bevilacqua P, Allred EN, Moore DH, Meli S, Gasparini G. Tumor angiogenesis: a new

- significant and independent prognostic indicator in early-stage breast carcinoma. *J Natl Cancer Inst* 1992; **84**: 1875-1887
- 8 **Graff BA**, Bjornæs I, Rofstad EK. Microvascular permeability of human melanoma xenografts to macromolecules: relationships to tumor volumetric growth rate, tumor angiogenesis, and VEGF expression. *Microvasc Res* 2001; **61**: 187-198
- 9 **Baek JH**, Jang JE, Kang CM, Chung HY, Kim ND, Kim KW. Hypoxia-induced VEGF enhances tumor survivability via suppression of serum deprivation-induced apoptosis. *Oncogene* 2000; **19**: 4621-4631
- 10 **Ohm JE**, Gabrilovich DI, Sempowski GD, Kisseleva E, Parman KS, Nadaf S, Carbone DP. VEGF inhibits T-cell development and may contribute to tumor-induced immune suppression. *Blood* 2003; **101**: 4878-4886
- 11 **Ohm JE**, Carbone DP. VEGF as a mediator of tumor-associated immunodeficiency. *Immunol Res* 2001; **23**: 263-272
- 12 **Yoshida S**, Amano H, Hayashi I, Kitasato H, Kamata M, Inukai M, Yoshimura H, Majima M. COX-2/VEGF-dependent facilitation of tumor-associated angiogenesis and tumor growth *in vivo*. *Lab Invest* 2003; **83**: 1385-1394
- 13 **Verheul HM**, Pinedo HM. The role of vascular endothelial growth factor (VEGF) in tumor angiogenesis and early clinical development of VEGF-receptor kinase inhibitors. *Clin Breast Cancer* 2000; **1**(Suppl 1): S80-84
- 14 **Werther K**, Nielsen HJ. Significance of vascular endothelial growth factor-VEGF-in tumor angiogenesis. Therapeutic possibilities in solid tumors. *Ugeskr Laeger* 2000; **162**: 4916-4920
- 15 **Yoshiji H**, Kuriyama S, Hicklin DJ, Huber J, Yoshii J, Miyamoto Y, Kawata M, Ikenaka Y, Nakatani T, Tsujinoue H, Fukui H. KDR/Flk-1 is a major regulator of vascular endothelial growth factor-induced tumor development and angiogenesis in murine hepatocellular carcinoma cells. *Hepatology* 1999; **30**: 1179-1186
- 16 **Brekken RA**, Overholser JP, Stastny VA, Waltenberger J, Minna JD, Thorpe PE. Selective inhibition of vascular endothelial growth factor (VEGF) receptor 2 (KDR/Flk-1) activity by a monoclonal anti-VEGF antibody blocks tumor growth in mice. *Cancer Res* 2000; **60**: 5117-5124
- 17 **Neufeld G**, Cohen T, Gengrinovitch S, Poltorak Z. Vascular endothelial growth factor (VEGF) and its receptors. *FASEB J* 1999; **13**: 9-22
- 18 **Xiang F**, Tanaka J, Takahashi J, Fukuda T. Expression of vascular endothelial growth factor (VEGF) and its two receptors in diffusely infiltrating astrocytomas and relationship to proliferative activity of tumor cells. *Brain Tumor Pathol* 2001; **18**: 67-71
- 19 **Kanno S**, Oda N, Abe M, Terai Y, Ito M, Shitara K, Tabayashi K, Shibuya M, Sato Y. Role of two VEGF receptors, Flt-1 and KDR, in the signal transduction of VEGF effects in human vascular endothelial cells. *Oncogene* 2000; **19**: 2138-2146
- 20 **McMahon G**. VEGF receptor signaling in tumor angiogenesis. *Oncologist* 2000; **5**(Suppl 1): 3-10
- 21 **Shinkai A**, Ito M, Anazawa H, Yamaguchi S, Shitara K, Shibuya M. Mapping of the sites involved in ligand association and dissociation at the extracellular domain of the kinase insert domain-containing receptor of vascular endothelial growth factor. *J Biol Chem* 1998; **273**: 31283-31288
- 22 **Lu D**, Kussie P, Pytowski B, Persaud K, Bohlen P, Witte L, Zhu Z. Identification of the residues in the extracellular region of KDR important for interaction with vascular endothelial growth factor and neutralizing anti-KDR antibodies. *J Biol Chem* 2000; **275**: 14321-14330
- 23 **Ryden L**, Linderholm B, Nielsen NH, Emdin S, Jonsson PE, Landberg G. Tumor specific VEGF-A and VEGFR2/KDR protein are co-expressed in breast cancer. *Breast Cancer Res Treat* 2003; **82**: 147-154
- 24 **Mukherjee T**, Kumar A, Mathur M, Chattopadhyay TK, Ralhan R. Ets-1 and VEGF expression correlates with tumor angiogenesis, lymph node metastasis, and patient survival in esophageal squamous cell carcinoma. *J Cancer Res Clin Oncol* 2003; **129**: 430-436
- 25 **Stockhammer G**, Obwegeser A, Kostron H, Schumacher P, Muigg A, Felber S, Maier H, Slavc I, Gunsilius E, Gastl G. Vascular endothelial growth factor (VEGF) is elevated in brain tumor cysts and correlates with tumor progression. *Acta Neuropathol* 2000; **100**: 101-105
- 26 **Wang S**, Xia T, Zhang Z, Kong X, Zeng L, Mi P, Xue Z. Expression of VEGF and tumor angiogenesis in bladder cancer. *Zhonghua Waikexue* 2000; **38**: 34-36
- 27 **Tamura M**, Ohta Y, Kajita T, Kimura K, Go T, Oda M, Nakamura H, Watanabe G. Plasma VEGF concentration can predict the tumor angiogenic capacity in non-small cell lung cancer. *Oncol Rep* 2001; **8**: 1097-1102
- 28 **Karademir S**, Sokmen S, Terzi C, Sagol O, Ozer E, Astarcioglu H, Coker A, Astarcioglu I. Tumor angiogenesis as a prognostic predictor in pancreatic cancer. *J Hepatobiliary Pancreat Surg* 2000; **7**: 489-495
- 29 **Becker CM**, Farnebo FA, Iordanescu I, Behonick DJ, Shih MC, Dunning P, Christofferson R, Mulligan RC, Taylor GA, Kuo CJ, Zetter BR. Gene therapy of prostate cancer with the soluble vascular endothelial growth factor receptor Flk1. *Cancer Biol Ther* 2002; **1**: 548-553
- 30 **Li Y**, Wang MN, Li H, King KD, Bassi R, Sun H, Santiago A, Hooper AT, Bohlen P, Hicklin DJ. Active immunization against the vascular endothelial growth factor receptor flk1 inhibits tumor angiogenesis and metastasis. *J Exp Med* 2002; **195**: 1575-1584
- 31 **Zhang W**, Ran S, Sambade M, Huang X, Thorpe PE. A monoclonal antibody that blocks VEGF binding to VEGFR2 (KDR/Flk-1) inhibits vascular expression of Flk-1 and tumor growth in an orthotopic human breast cancer model. *Angiogenesis* 2002; **5**: 35-44
- 32 **Shibuya M**. VEGF-receptor inhibitors for anti-angiogenesis. *Nippon Yakurigaku Zasshi* 2003; **122**: 498-503
- 33 **Li Y**, Wang MN, Li H, King KD, Bassi R, Sun H, Santiago A, Hooper AT, Bohlen P, Hicklin DJ. Active immunization against the vascular endothelial growth factor receptor flk1 inhibits tumor angiogenesis and metastasis. *J Exp Med* 2002; **195**: 1575-1584
- 34 **Haupt K**, Roggendorf M, Mann K. The potential of DNA vaccination against tumor-associated antigens for antitumor therapy. *Exp Biol Med* 2002; **227**: 227-237
- 35 **Henke A**. DNA immunization—a new chance in vaccine research? *Med Microbiol Immunol* 2002; **191**: 187-190
- 36 **Muehlbauer PM**. Anti-angiogenesis in cancer therapy. *Semin Oncol Nurs* 2003; **19**: 180-192
- 37 **Zogakis TG**, Libutti SK. General aspects of anti-angiogenesis and cancer therapy. *Expert Opin Biol Ther* 2001; **1**: 253-275
- 38 **Takahashi Y**, Mai M. Significance of angiogenesis and clinical application of anti-angiogenesis. *Nippon Geka Gakkai Zasshi* 2001; **102**: 381-384

Identification of 5' capped structure and 3' terminal sequence of hepatitis E virus isolated from Morocco

Guo-Bing Chen, Ji-Hong Meng

Guo-Bing Chen, Ji-Hong Meng, Department of Microbiology and Immunology, Southeast University School of Medicine, Nanjing 210009, Jiangsu Province, China

Supported by the Natural Scientific Foundation, No. 30271231; and the Natural Scientific Foundation of Jiangsu Province, No. BK2002053

Correspondence to: Professor Ji-Hong Meng, Department of Microbiology and Immunology, Southeast University School of Medicine, Nanjing 210009, Jiangsu Province, China. jihongmeng@263.net

Telephone: +86-25-3272454

Received: 2003-12-17 **Accepted:** 2004-01-08

Abstract

AIM: To examine 5' and 3' terminal sequences of hepatitis E virus (HEV) isolated from Morocco, to confirm 5' methylated cap structure of the genome, and to investigate whether the 3' UTR can be used to distinguish HEV genotypes instead of HEV complete genome sequence.

METHODS: RNA ligase-mediated rapid amplification of cDNA ends (RLM-RACE) was employed to obtain the 5' and 3' terminal sequences of HEV Morocco strain. The 3' UTR sequence of the Morocco strain was compared with that of the other 29 HEV strains using the DNASTar software.

RESULTS: The 5' PCR product was obtained only from the RLM-RACE based on the capped RNA template. The 5' UTR of the Morocco strain had 26 nucleotides, and the 3' UTR had 65 nucleotides upstream to the polyA. The 5' UTR between HEV strains had only point mutations of nucleotides. The phylogenetic tree based on the sequences of 3' UTR was not the same as that based on the complete sequences.

CONCLUSION: The genome of HEV Morocco strain was methylated cap structure. The 3' terminal sequence can not be used for distinguishing HEV genotype for all HEV strains in place of the whole HEV genome sequence.

Chen GB, Meng JH. Identification of 5' capped structure and 3' terminal sequence of hepatitis E virus isolated from Morocco. *World J Gastroenterol* 2004; 10(14): 2045-2049
<http://www.wjgnet.com/1007-9327/10/2045.asp>

INTRODUCTION

Hepatitis E virus (HEV) is an enterically transmitted agent that causes epidemic and sporadic cases of hepatitis predominantly in developing countries of Asia, Africa and North America^[1]. The disease generally affects young adults and has a high mortality rate, up to 20%, in infected pregnant women. Success in cloning and sequencing of the HEV genome allowed the elucidation of the HEV genetic organization^[2]. The HEV genome is a positive-sense, single-stranded, polyadenylated RNA of approximately 7.2 kb containing three open reading frames (ORFs). ORF1, located at the 5' end of the genome, is

about 5 kb in length and encodes for a putative nonstructural polyprotein that contains motifs characteristic for methyltransferase, papain-like protease, RNA helicase, and RNA-dependent RNA polymerase domains. ORF2 is about 2 kb in length and encodes for the structural protein(s). The small ORF3 of only 369 nucleotides overlaps ORF1 and ORF2 and encodes for a protein of unknown function^[3].

The genomes of several HEV strains from Asia and North America have been sequenced in their entirety^[4]. Partial sequences are also available for other strains from some of these geographic regions. In Africa, the HEV virus has been identified from Morocco, Tunisia, Algeria, Chad, Egypt, Nigeria and Namibia^[5-10]. However, only a few short isolated nucleotide sequences from African strains of HEV were available for analysis. In 1997, Chatterjee *et al.* isolated an HEV strain in Morocco^[5]. In 1999, Meng *et al.* obtained the nucleotide sequences of HEV Morocco strain that spanned the extreme 3' terminal region of ORF1, full length ORF2 and ORF3, and a part of the 3' noncoding region^[11,12]. Although more similar to the Asian strains than to the Mexico strain, partial HEV sequences from Morocco strains were, nonetheless, distinct from all known Asian strains. It is urgent to obtain the complete sequence of the Morocco strain to elucidate its biological function.

Although the genomic coding regions of several HEV strains have been sequenced completely, the sequence of the 5' UTR has been reported only for a limited number of HEV strains^[13]. The 5' UTR of HEV strains were usually determined either by cDNA cloning and sequencing or by classical 5' rapid amplification of cDNA ends (RACE)^[13]. However, there still exists the possibility that the 5' UTR sequences are not complete because neither method has a control to detect premature termination of cDNA synthesis. Furthermore, by coupling a reverse transcription polymerase chain reaction (RT-PCR) assay with immune-capture of genomic RNA based on the ability of a monoclonal antibody to recognize 7-methylguanosine showed that the genomic RNA of HEV is capped^[14]. It is not clear how this structure will have affected previous assays used to determine the 5' terminal nucleotides. For getting the complete sequence of HEV Morocco strain, we employed a RLM-RACE technique to obtain the 5' and 3' terminal sequences in our study, and confirmed that the genome of Morocco strain was capped.

Furthermore, how to distinguish the genotypes of HEV is still an issue. Based on the complete sequence analysis, Burma-1, Burma-2, China-1 to -6, Pak-1, Pak-2, India-1 to -4, Nepal and Morocco strains are included in genotype I; Mexico strain belongs to genotype II; Genotype III holds US-1, US-2, US-SW, Japan-1 to -7, Japan-SW and Canada-SW; China-T1 belongs to genotype IV^[15-17]. Considering the difficulties in obtaining the complete sequences of each strain, we attempted to evaluate whether the 3' UTR can be used to analyze the HEV genotype in this study.

MATERIALS AND METHODS

Sample

The sample was obtained from Professor Pillot, Pasteur Institute, France, and treated as described in references 16 and

17. Aliquots of virus stock were prepared and stored at -70°C .

Reagents

HEV RNA was extracted with TRIzol (GIBCO, USA). The 5' and 3' RLM-RACE was carried out with the GeneRacer kit (Invitrogen, USA). The nested PCR was carried out with high fidelity system DNA polymerase (Roche, USA). PCR products were purified with QIAquick PCR purification kit (Qiagen, German).

Primers

5' RACE primers: Two RNA 5' -adaptor primers supplied in the GenRacer kit were used as forward primers. The sequences of the reverse primers were: 5' -AGA AAA GGC CTA ACC ACC ACA GCA TTC G-3' (outer reverse primer) and 5' -CTA AAG CAG CCT GCT CAA TAG CAG TAG-3' (inner reverse primer).

3' RACE primers: Sequences of the forward primers were: 5' -GTT GTC TCA GCC AAT GGC GAG C-3' (outer forward primer) and 5' -AAG ATG AAG GTG GGT AAA ACT CGG GAG-3' (inner forward primer). Two RNA 3' -adaptor primers supplied in the GenRacer kit were used as reverse primers.

GenBank accession number and software

The GenBank accession number of 3' UTR sequence of HEV Morocco strain was AY220474. The 5' and 3' UTR sequence of Morocco strain were compared with that of other 29 strains, respectively, by the MegAlign in DNASTar software (DNASTAR Inc, USA). The phylogenetic trees of 3' and complete HEV sequences were also made with MegAlign in DNASTAR. The GenBank accession numbers of these sequences were: Jap-SW (AB073912)^[18], Japan-1 (AB074918), Japan-2 (AB074920)^[19], Japan-3 (AB089824)^[20], Japan-4 (AP003430)^[21], Japan-5 (AB074915), Japan-6 (AB074917)^[19], Japan-7 (AB080575)^[22], Nepal (AF051830)^[23], US-1 (AF060668), US-2 (AF060669)^[24,25], US-SW (AF082843)^[26], Canada-SW (AY115488)^[27], India-1 (X98292), India-2 (AF459438)^[28], India-3 (AF076239)^[29], India-4 (X99441), Pak-1 (M80581)^[30], Pak-2 (AF185822)^[31], Burma-1 (M73218)^[3], Burma-2 (D10330)^[32], China-1 (L25547), China-2 (L25595)^[33], China-3 (L08816), China-4 (M94177)^[34], China -5 (D11092)^[35], China-6 (D11093), Mexico (M74506)^[41] and China-T1 (AJ272108)^[36]. The RNA secondary structure was reconstructed with RNAstructure software (Isis Pharmaceuticals).

Extraction of HEV RNAs

One hundred microliters of the filtered supernatant of the Morocco strain was mixed with 400 μL of TRIzol reagent. The mixture was homogenized and incubated for 5 min at room temperature. One hundred microliters of chloroform was added and the mixture was vigorously shaken for 15 s and incubated at room temperature for 3 min. After centrifugation at 12 000 g for 15 min at 4°C , the aqueous phase was transferred to a fresh microfuge tube. The RNA from the aqueous phase was precipitated by incubating with an equal volume of isopropyl alcohol and 1 μL of glycogen (20 mg/mL) at room temperature for 15 min, and centrifuging at 12 000 g at 4°C for 15 min. After removing the supernatant, the RNA pellet was washed once with 800 μL of 750 mL/L ethanol and centrifuged again, dried, and then dissolved in 20 μL of diethylpyrocarbonate treated water.

5' RLM-RACE

The 5' RACE was carried out with the GeneRacer kit following the manufacture's instructions. Briefly, 14 μL of extracted RNA was treated with calf intestinal phosphatase (CIP) in a total 20 μL reaction mixture containing 2 μL of 10 \times CIP buffer

and 2 μL of CIP for 1 h at 50°C . After extracted with phenol/chloroform, RNA was resuspended in 6 μL of nuclease-free water. The 6 μL of CIP-treated RNA was treated with tobacco acid pyrophosphatase (TAP) in a 10 μL of reaction mixture containing 1 μL of 10 \times TAP buffer and 2 μL of TAP for 1 h at 37°C . Again after extracted with phenol/chloroform, the CIP/TAP-treated RNA was resuspended in 6 μL of nuclease-free water and ligated to 250 ng of RNA adaptor by T4 RNA ligase in a 10 μL reaction mixture for 1 h at 37°C . Then the CIP/TAP/Ligated-RNA was extracted with phenol/chloroform and resuspended in 20 μL nuclease-free water and reserved at -70°C . Another 6 μL non-treated RNA was ligated to 250 ng of RNA adaptor directly by T4 RNA ligase as a control. Ten microliters of the ligated RNA or control RNA was used as a template to synthesize cDNA with AMV reverse transcriptase for 1 h at 42°C . The outer reverse primer was used to prime the cDNA synthesis. The cDNA was then amplified by nested PCR with high fidelity system DNA polymerase. The PCR reaction mixture was incubated for 2 min at 94°C followed by 35 amplification cycles, comprising denaturation at 94°C for 30 s, annealing at 65°C for 30 s and extension at 72°C for 30 s. The reaction was extended for another 7 min at 72°C to insure the full extension. Based on our former work (data not shown), the expected size of the final PCR product was 100 bp or greater. PCR products were analyzed on 20 g/L agarose gel.

3' RACE

The 3' RACE was carried out with the GeneRacer kit following the manufacture's instructions. Ten microliters of the HEV RNA was used as a template to synthesize cDNA with AMV reverse transcriptase for 1 h at 42°C . The oligo (dT)-adaptor primer supplied with the kit was used to prime the cDNA synthesis. The cDNA was then amplified by nested PCR with high fidelity system DNA polymerase. The PCR reaction mixture was incubated for 2 min at 94°C , followed by 35 amplification cycles comprising denaturation at 94°C for 30 s, annealing at 65°C for 30 s, and extension at 72°C for 30 s. The reaction was extended for another 7 min at 72°C to ensure the full extension. Based on our former work (data not shown), the expected size of the final PCR product was 98 bp or greater. PCR products were analyzed on 20 g/L agarose gel.

Sequence analysis and comparison

PCR products were purified with QIAquick PCR purification kit and sequenced. The 5' and 3' UTR sequence of Morocco strain were compared with that of other 29 strains, respectively, using DNASTar software. The RNA secondary structure was reconstructed with RNAstructure software. The phylogenetic trees of 3' and complete HEV sequences were also made with DNASTAR.

RESULTS

5' UTR

As shown in Figure 1A, bands of the expected size were obtained. The band was obtained in 5' RLM-RACE reactions only when the template was CIP/TAP treated RNA.

The 5' terminus of Morocco had 26 nucleotides preceding the predicted start codon, including the 7-methylguanosine. The sequence of PCR product was: GGC AGA CCA CAT ATG TGG TCG ATG CC. A comparison of the 5' UTR sequence of 30 HEV strains was made as shown in Figure 2: there was a "T" at the position 4 preceding the predicted start codon in Morocco and other 25 strains while a "C" was found in other four strains; a "G" at the position 9 in the Morocco and other 28 strains turn out to be a "T" in US-SW strain; an "A" at the position 16 in Morocco and other 20 strains was replaced by a "G" or "C" in other nine strains; an additional

"A" at the terminus of eight strains except Morocco strain; and additional 9 nucleotides in the US-2 terminus.

As shown in Figure 3, the 26 nucleotides of 5' terminus could form a putative stem-loop structure. All single-nucleotide differences occurred within that loop structure.

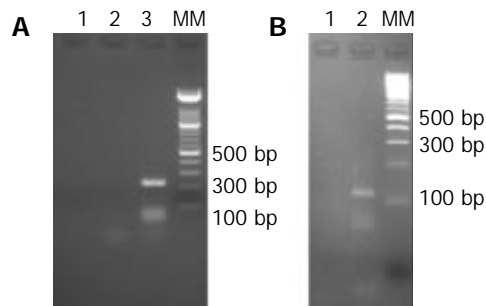


Figure 1 RT-PCR products of 5' and 3' RNA of HEV Morocco strain. A: Products of 5' RLM-RACE; Lane 1: negative control without template RNA; Lane 2: RNA template without CIP/TAP treated; Lane 3: RNA template treated with CIP and TAP. B: Products of 3' RACE; Lane 1: negative control without template RNA; Lane 2: products of 3' RACE; MM: 100 bp ladder.

Sequence Name	[]	< Pos =							
		35	30	25	20	15	10	5	1
Burma-1	[1]	-----	<u>GGCAGACCACATATGTGGTCGATGCCATG</u>						
Burma-2	[1]	-----	<u>GGCAGACCACATATGTGGTCGATGCCATG</u>						
Canada-3W	[3]	-----	<u>GGCAGACCACATATGTGGTCGATGCCATG</u>						
China-1	[1]	-----	<u>GGCAGACCACATATGTGGTCGATGCCATG</u>						
China-2	[1]	-----	<u>GGCAGACCACATATGTGGTCGATGCCATG</u>						
China-3	[1]	-----	<u>GGCAGACCACATATGTGGTCGATGCCATG</u>						
China-4	[1]	-----	<u>GGCAGACCACATATGTGGTCGATGCCATG</u>						
China-5	[1]	-----	<u>GGCAGACCACATATGTGGTCGATGCCATG</u>						
China-6	[1]	-----	<u>GGCAGACCACATATGTGGTCGATGCCATG</u>						
China-T1	[4]	-----	<u>GCAGACCACATATGTGGTCGATGCCATG</u>						
India-1	[1]	-----	<u>GGCAGACCACATATGTGGTCGATGCCATG</u>						
India-2	[1]	-----	<u>GGCAGACCACATATGTGGTCGATGCCATG</u>						
India-3	[1]	-----	<u>GGCAGACCACATATGTGGTCGATGCCATG</u>						
India-4	[1]	-----	<u>GGCAGACCACATATGTGGTCGATGCCATG</u>						
Japan-1	[3]	-----	<u>GCAGACCACATATGTGGTCGATGCCATG</u>						
Japan-2	[3]	-----	<u>GTCCGATGCCATG</u>						
Japan-3	[3]	-----	<u>GCAGACCACATATGTGGTCGATGCCATG</u>						
Japan-4	[3]	-----	<u>GGCAGACCACATATGTGGTCGATGCCATG</u>						
Japan-5	[4]	-----	<u>GTCCGATGCCATG</u>						
Japan-6	[4]	-----	<u>GTCCGATGCCATG</u>						
Japan-7	[4]	-----	<u>GCAGACCACATATGTGGTCGATGCCATG</u>						
Jap-3W	[3]	-----	<u>GCAGACCACATATGTGGTCGATGCCATG</u>						
Mexico	[2]	-----	<u>GCAGACCACATATGTGGTCGATGCCATG</u>						
MOROCCO	[1]	-----	<u>GGCAGACCACATATGTGGTCGATGCCATG</u>						
Nepal	[1]	-----	<u>GGCAGACCACATATGTGGTCGATGCCATG</u>						
Pak-1	[1]	-----	<u>GCAGACCACATATGTGGTCGATGCCATG</u>						
Pak-2	[1]	-----	<u>GCAGACCACATATGTGGTCGATGCCATG</u>						
US-1	[3]	-----	<u>ATG</u>						
US-2	[3]	<u>TCGACAGGGGGCAGACCACATATGTGGTCGATGCCATG</u>							
US-3W	[3]	-----	<u>ATCCGATGCCATG</u>						

Figure 2 Comparison of sequence in the 5' UTR of different HEV strains. The translation initiation codon is underlined. The number in brackets following the strain name is the genotype designation. Changes from the consensus sequence are boxed.

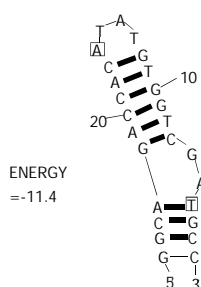


Figure 3 RNA secondary structure of HEV 5' terminal sequence. Changes among HEV strains are boxed.

3' UTR

As shown in Figure 1B, 3' RACE bands of the expected size were obtained. The 3' terminus of Morocco had 65 nucleotides upstream of the polyA (the GenBank accession is AY220474). The sequence of 3' UTR was: TTT ATT TGC TTG TGC CCT CCT TCT TTC TGT TGC TTA TTT CTC TTT TCT GCG TTT CGC GCT CCC TG. The comparison of the 3' UTR sequence with the corresponding regions of other 29 HEV strains from different parts of the world revealed that the Morocco strain was most similar to the genotype 1 strains (92.3-97.4%) (Table 1). The 3' UTR nucleotide sequences of the HEV genotypes II, III and IV strains shared a lower similarity with that of Morocco strain: 80%, 65.6-83.1% and 84.6-89.2%, respectively. The phylogenetic trees also showed that the HEV Morocco strain was grouped together with all genotype I strains as a separate branch (Figures 4 and 5). Based on the 3' UTR analysis, Japan-5, -6, -7 belonged to genotype III. But according to the complete sequence analysis, they were included in genotype IV.

Table 1 Percent identity of 3' UTR of HEV genotypes (%)

	I	II	III	IV
Mor	92.3-97.4	80	65.6-83.1	84.6-89.2
I	92.3-100	74.4-81.5	25.6-84.6	79.5-90.8
II	-	100	37.5-71.8	55.1-83.8
III	-	-	75.9-94.4	41.4-80.0
IV	-	-	-	77.9-94.3

I, II, III, IV: HEV Genotype; Mor: HEV Morocco strain; -: blank well.

DISCUSSION

Variations in the length of the 5' UTR have been observed. The Burma strain was reported to have 27 nucleotides in its 5' UTR, compared with 35 nucleotides in the 5' UTR of US-2 and 26 nucleotides in the most of other strains^[13]. It remains to be determined if the extra nucleotides are really present in functional genomes. Maybe they just represented artifacts generated because the presence of a cap structure was not recognized at the time some of those strains were sequenced, or because of the additional "A" with the non-proofreading DNA polymerase in the PCR action. What was more interesting, the US-2 strain had additional nine nucleotides at the 5' terminus. They were included in the GenBank sequence but had not been discussed elsewhere, so they were difficult to evaluate. Except the US-2, all HEV strains had a comparable 5' UTR sequence with only point change from each other, and the single-nucleotide differences occurred within the loop structure. This structure may play a very important role either in replication or translation. It needs to be verified experimentally.

The 5' UTR sequences obtained by the methods of cDNA cloning/sequencing or classical 5' rapid amplification of cDNA ends (RACE) may be incomplete because neither method has a control to detect premature termination of cDNA synthesis. The finding of a 7mGpppG cap allowed reevaluation of 5' UTR sequences with a modified RACE technique called RNA ligase-mediated RACE (RLM-RACE). In RLM-RACE, an RNA sample was first treated with calf intestinal phosphatase (CIP) to remove the 5' -phosphate from all RNA species except those with a cap structure. Tobacco acid pyrophosphatase (TAP) was then used to remove the cap structure from RNA, leaving a 5' -phosphate. Next, a synthetic RNA adaptor was ligated to the CIP/TAP treated RNA. Because the adaptor ligates only to RNA containing a 5' -phosphate, RLM-RACE ensures that cDNA was amplified from decapped RNA predominantly, starting at the ultimate 5' terminus. In 2001,

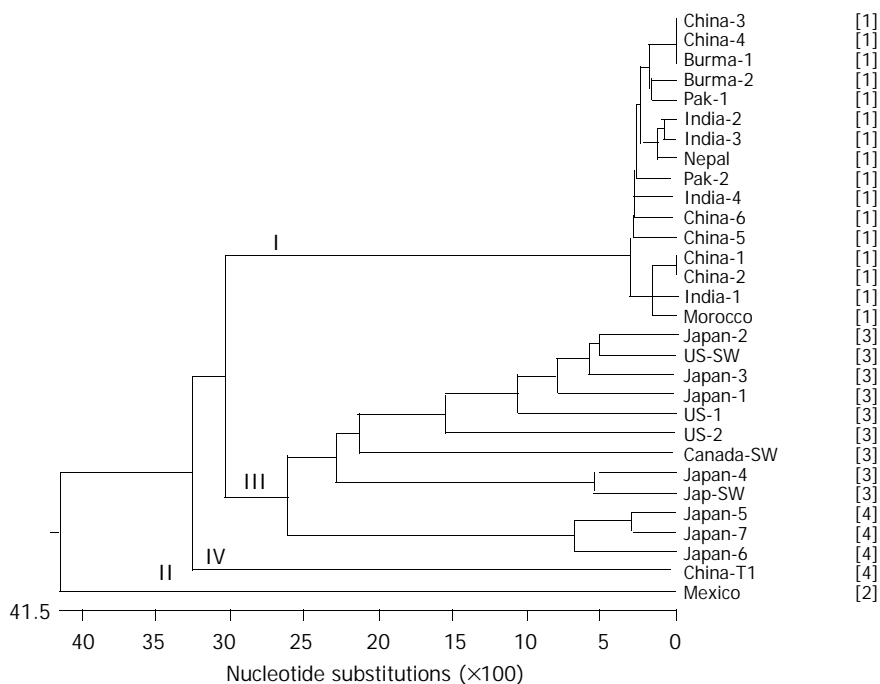


Figure 4 Proposed phylogenetic trees using 3' UTR sequences of Morocco and other 29 HEV strains. The Roman number in the tree represents the genotype designation based on the 3' UTR sequence. The number in brackets following the strain name represents the genotype designation based on the full genome sequence.

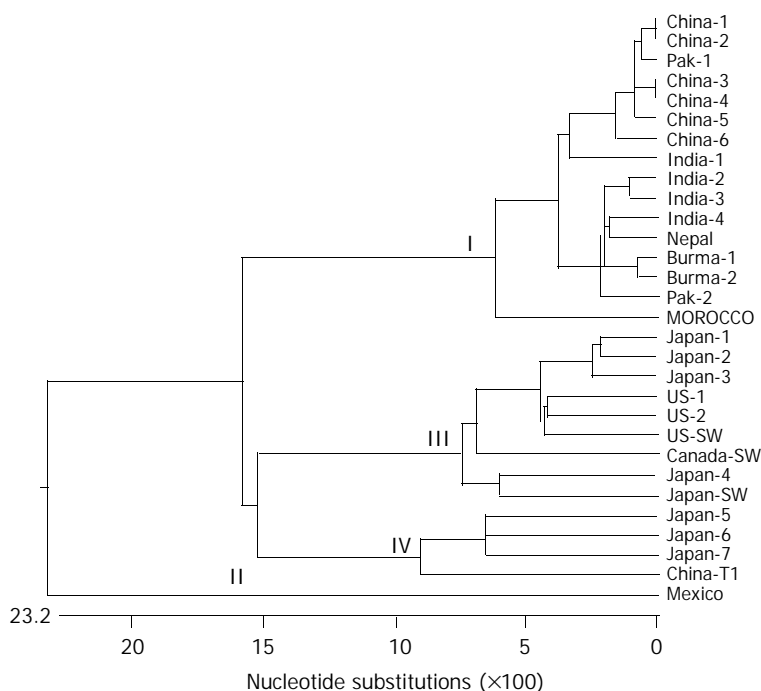


Figure 5 Proposed phylogenetic trees using full sequences of 30 HEV strains. The Roman number in the tree represents the genotype designation.

Zhang *et al.* used the RLM-RACE method to confirm the capped HEV genome and extended the 5' terminal sequence of Mexico and Pak-1 strains^[13]. In the current study to obtain the complete sequence of HEV Morocco strain, we used a sequence amplification procedure that required the presence of an internal pyrophosphatase sensitive linkage in the 5' termini of HEV genome. The results indicated that the Morocco strain was capped.

The comparison of the 3' UTR sequence with the corresponding regions of other 29 HEV strains and the phylogenetic trees of those complete sequences of 30 HEV strains revealed that the HEV Morocco strain was grouped together with all genotype

I strains as a separate branch. The distribution of 3' UTR of genotypes I, II and IV was as same as that obtained by the comparison of the complete genome sequence. However, three strains isolated from Japan, Japan-5, -6, -7, which were included in genotype IV according to complete sequences analysis, clustered together with the genotype III strains based on the 3' UTR sequences analysis. This suggests that the comparison of HEV 3' UTR sequence can not represent the divergence of complete genome sequence perfectly, although this region is regarded as containing the majority of genotype-specific nucleotide positions, and easily and efficiently to amplify. So, the 3' terminal sequence upstream the polyA can not be used

for phylogenetic genotyping analysis of the HEV genome optionally. Because of the difficulties to get the complete sequences, many scientists preferred to analyze the HEV genotypes based on the partial sequences they obtained. It remains uncertain whether the partial sequences can replace the complete genome in distinguishing the HEV genotypes. So, it is prudent to analyze the HEV genotypes based on complete sequences to date.

REFERENCES

- 1 **Worm HC**, van der Poel WH, Brandstatter G. Hepatitis E: an overview. *Microbes Infect* 2002; **4**: 657-666
- 2 **Reyes GR**, Purdy MA, Kim JP, Luk KC, Young LM, Fry KE, Bradley DW. Isolation of a cDNA from the virus responsible for enterically transmitted non-A, non-B hepatitis. *Science* 1990; **247**: 1335-1339
- 3 **Tam A W**, Smith MM, Guerra ME, Huang CC, Bradley DW, Fry KE, Reyes GR. Hepatitis E virus (HEV): molecular cloning and sequencing of the full-length viral genome. *Virology* 1991; **185**: 120-131
- 4 **Huang CC**, Nguyen D, Fernandez J, Yun KY, Fry KE, Bradley DW, Tam AW, Reyes GR. Molecular cloning and sequencing of the Mexico isolate of hepatitis E virus (HEV). *Virology* 1992; **191**: 550-558
- 5 **Chatterjee R**, Tsarev S, Pillot J, Coursaget P, Emerson SU, Purcell RH. African strains of Hepatitis E Virus that are distinct from Asian strains. *J Med Virol* 1997; **53**: 139-144
- 6 **Benjelloun S**, Bahbouhi B, Bouchrit N, Cherkaoui L, Hda N, Mahjour J, Benslimane A. Seroepidemiological study of an acute hepatitis E outbreak in Morocco. *Res Virol* 1997; **148**: 279-287
- 7 **Cuyck-Gandre H**, Zhang HY, Tsarev SA, Clements NJ, Cohen SJ, Caudill JD, Buisson Y, Coursaget P, Warren RL, Longer CF. Characterization of Hepatitis E virus (HEV) from Algeria and Chad by partial genome sequence. *J Med Virol* 1997; **53**: 340-347
- 8 **Tsarev SA**, Binn LN, Gomatos PJ, Arthur RR, Monier MK, Cuyck-Gandre H, Longer CF, Innis BL. Phylogenetic analysis of hepatitis E virus isolates from Egypt. *J Med Virol* 1999; **57**: 68-74
- 9 **Buisson Y**, Grandadam M, Nicand E, Cheval P, Cuyck-Gandre H, Innis B, Rehel P, Coursaget P, Teyssou R, Tsarev S. Identification of a novel hepatitis E virus in Nigeria. *J Gen Virol* 2000; **81**: 903-909
- 10 **Maila HT**, Bowyer SM, Swanepoel R. Identification of a new strain of hepatitis E virus from an outbreak in Namibia in 1995. *J Gen Virol* 2004; **85**: 89-95
- 11 **Meng J**, Cong M, Dai X, Pillot J, Purdy MA, Fields HA, Khudyakov YE. Primary structure of open reading frame 2 and 3 of the Hepatitis E Virus isolated from Morocco. *J Med Virol* 1999; **57**: 126-133
- 12 **Meng J**, Pillot J, Dai X, Fields HA, Khudyakov YE. Neutralization of different geographic strains of the hepatitis E virus with anti-hepatitis E virus-positive serum samples obtained from different sources. *Virology* 1998; **249**: 316-324
- 13 **Zhang M**, Purcell RH, Emerson SU. Identification of the 5' terminal sequence of the SAR-55 and MEX-14 strains of Hepatitis E Virus and confirmation that the genome is capped. *J Med Virol* 2001; **65**: 293-295
- 14 **Kabrane-Lazizi Y**, Meng XJ, Purcell RH, Emerson SU. Evidence that the genomic RNA of hepatitis E virus is capped. *J Virol* 1999; **73**: 8848-8850
- 15 **Schlauder GG**, Mushahwar IK. Genetic Heterogeneity of Hepatitis E Virus. *J Med Virol* 2001; **65**: 282-292
- 16 **Meng J**, Guinet R, Pillot J. Infection of PLC/PRF/5 cells with the hepatitis E virus. IN :Buisson Y, Coursaget P, Kane M, editors. Enterically-transmitted hepatitis viruses. Joue-les-Tours, France: *La Simarre* 1996: P336-345
- 17 **Meng J**, Dubreuil P, Pillot J. A new PCR-based seroneutralization assay in cell culture for diagnosis of hepatitis E. *J Clin Microbiol* 1997; **35**: 1373-1377
- 18 **Okamoto H**, Takahashi M, Nishizawa T, Fukai K, Muramatsu U, Yoshikawa A. Analysis of the complete genome of indigenous swine hepatitis E virus isolated in Japan. *Biochem Biophys Res Commun* 2001; **289**: 929-936
- 19 **Takahashi K**, Kang JH, Ohnishi S, Hino K, Mishiho S. Genetic heterogeneity of hepatitis E virus recovered from Japanese patients with acute sporadic hepatitis. *J Infect Dis* 2002; **185**: 1342-1345
- 20 **Tokita H**, Harada H, Gotanda Y, Takahashi M, Nishizawa T, Okamoto H. Molecular and serological characterization of sporadic acute hepatitis E in a Japanese patient infected with a genotype III hepatitis E virus in 1993. *J Gen Virol* 2003; **84**: 421-427
- 21 **Takahashi K**, Iwata K, Watanabe N, Hatahara T, Ohta Y, Baba K, Mishiho S. Full-genome nucleotide sequence of a hepatitis E virus strain that may be indigenous to Japan. *Virology* 2001; **287**: 9-12
- 22 **Takahashi M**, Nishizawa T, Yoshikawa A, Sato S, Isoda N, Ido K, Sugano K, Okamoto H. Identification of two distinct genotypes of hepatitis E virus in a Japanese patient with acute hepatitis who had not travelled abroad. *J Gen Virol* 2002; **83**: 1931-1940
- 23 **Gouvea V**, Snellings N, Popek MJ, Longer CF, Innis BL. Hepatitis E virus: complete genome sequence and phylogenetic analysis of a Nepali isolate. *Virus Res* 1998; **57**: 21-26
- 24 **Schlauder GG**, Dawson GJ, Erker JC, Kwo PY, Knigge MF, Smalley DL, Rosenblatt JE, Desai SM, Mushahwar IK. The sequence and phylogenetic analysis of a novel hepatitis E virus isolated from a patient with acute hepatitis reported in the United States. *J Gen Virol* 1998; **79**: 447-456
- 25 **Erker JC**, Desai SM, Schlauder GG, Dawson GJ, Mushahwar IK. A hepatitis E virus variant from the United States: molecular characterization and transmission in cynomolgus macaques. *J Gen Virol* 1999; **80**: 681-690
- 26 **Meng XJ**, Purcell RH, Halbur PG, Lehman JR, Webb DM, Tsareva TS, Haynes JS, Thacker BJ, Emerson SU. A novel virus in swine is closely related to the human hepatitis E virus. *Proc Natl Acad Sci U S A* 1997; **94**: 9860-9865
- 27 **Pei Y**, Yoo D. Genetic characterization and sequence heterogeneity of a Canadian isolate of swine hepatitis E virus. *J Clin Microbiol* 2002; **40**: 4021-4029
- 28 **Jameel S**, Zafarullah M, Chawla YK, Dilawari JB. Reevaluation of a North India isolate of hepatitis E virus based on the full-length genomic sequence obtained following long RT-PCR. *Virus Res* 2002; **86**: 53-58
- 29 **Panda SK**, Ansari IH, Durgapal H, Agrawal S, Jameel S. The *in vitro*-synthesized RNA from a cDNA clone of hepatitis E virus is infectious. *J Virol* 2000; **74**: 2430-2437
- 30 **Tsarev SA**, Emerson SU, Reyes GR, Tsareva TS, Legters LJ, Malik IA, Iqbal M, Purcell RH. Characterization of a prototype strain of hepatitis E virus. *Proc Natl Acad Sci U S A* 1992; **89**: 559-563
- 31 **van Cuyck-Gandre H**, Zhang HY, Tsarev SA, Warren RL, Caudill JD, Snellings NJ, Begot L, Innis BL, Longer CF. Short report: phylogenetically distinct hepatitis E viruses in Pakistan. *Am J Trop Med Hyg* 2000; **62**: 187-189
- 32 **Aye TT**, Uchida T, Ma X, Iida F, Shikata T, Ichikawa M, Rikihisa T, Win KM. Sequence and gene structure of the hepatitis E virus isolated from Myanmar. *Virus Genes* 1993; **7**: 95-109
- 33 **Yin S**, Purcell RH, Emerson SU. A new Chinese isolate of hepatitis E virus: comparison with strains recovered from different geographical regions. *Virus Genes* 1994; **9**: 23-32
- 34 **Bi SL**, Purdy MA, McCaustland KA, Margolis HS, Bradley DW. The sequence of hepatitis E virus isolated directly from a single source during an outbreak in China. *Virus Res* 1993; **28**: 233-247
- 35 **Aye TT**, Uchida T, Ma XZ, Iida F, Shikata T, Zhuang H, Win KM. Complete nucleotide sequence of a hepatitis E virus isolated from the Xinjiang epidemic (1986-1988) of China. *Nucleic Acids Res* 1992; **20**: 3512
- 36 **Wang Y**, Zhang H, Ling R, Li H, Harrison TJ. The complete sequence of hepatitis E virus genotype 4 reveals an alternative strategy for translation of open reading frames 2 and 3. *J Gen Virol* 2000; **81**: 1675-1686

Inhibition of human La protein by RNA interference downregulates hepatitis B virus mRNA in 2.2.15 cells

Qin Ni, Zhi Chen, Hang-Ping Yao, Zheng-Gang Yang, Ke-Zhou Liu, Ling-Ling Wu

Qin Ni, Zhi Chen, Hang-Ping Yao, Zheng-Gang Yang, Ke-Zhou Liu, Institute of Infectious Diseases, First Affiliated Hospital, School of Medicine, Zhejiang University, Hangzhou 310003, Zhejiang Province, China

Ling-Ling Wu, Department of Clinical Medicine, Medical College, Zhejiang University, Hangzhou 310031, Zhejiang Province, China

Supported by the Major Programs of Health Bureau of Zhejiang Province, No. 2002ZD007 and the National Natural Science Foundation of China, No. 30371270 and the Major Programs of Department of Science and Technology of Zhejiang Province, No. 2003C13015

Correspondence to: Dr. Zhi Chen, Institute of Infectious Diseases, First Affiliated Hospital, School of Medicine, Zhejiang University, Hangzhou 310003, Zhejiang Province, China. chen zhi@zju.edu.cn

Telephone: +86-571-87236579 **Fax:** +86-571-87068731

Received: 2004-02-20 **Accepted:** 2004-03-06

Abstract

AIM: To investigate the role of human La protein in HBV mRNA expression.

METHODS: Three human La protein (hLa) specific siRNA expression cassettes (SECs) containing U6+1 promoter were prepared via one-step overlapping extension PCR. After transfection with SECs into HepG2 cells, inhibition effects on hLa expression were analyzed by semi-quantitative RT-PCR and Western blotting. Then, effective SECs were screened out and transfected into 2.2.15 cells, a stable HBV-producing cell line. HBV surface antigen (HBsAg) and e antigen (HBeAg) secretions into culture media were detected by microparticle enzyme immunoassay (MEIA) and HBs and HBe mRNA levels were analyzed by semi-quantitative RT-PCR.

RESULTS: SEC products containing U6+1 snRNA promoter, and 3 sites of hLa mRNA specific siRNA were obtained successfully by one-step overlapping extension PCR and could be directly transfected into HepG2 cells, resulting in inhibition of La protein expression in both mRNA and protein levels, among which U6+1-hLa833 was the most efficient, which reduced 18.6-fold mRNA and 89% protein level respectively. In 2.2.15 cells, U6+1-hLa833 was also efficient on inhibition of hLa expression. Furthermore, semi-quantitative RT-PCR showed that HBs and HBe mRNA levels were significantly decreased by 8- and 66-fold in U6+1-hLa833 transfected cells compared to control. Accordingly, HBsAg and HBeAg secretions were decreased partly posttransfection with SECs.

CONCLUSION: PCR-based SECs can be used to mediate RNAi in mammalian cells and provide a novel approach to study the function of La protein. The inhibition of La protein expression can result in a significant decrease of HBV mRNA, which implies that the hLa protein is also involved HBV RNA metabolism as one of the HBV RNA-stabilizing factors in human cells.

Ni Q, Chen Z, Yao HP, Yang ZG, Liu KZ, Wu LL. Inhibition of human La protein by RNA interference downregulates hepatitis B virus mRNA in 2.2.15 cells. *World J Gastroenterol* 2004; 10(14): 2050-2054
<http://www.wjgnet.com/1007-9327/10/2050.asp>

INTRODUCTION

Human La protein is a 47-ku phosphoprotein predominantly localized in nuclei. La protein is a member of RNA-binding proteins containing RNA recognition motifs (RRM) and interacts with RNA polymerase III transcripts such as pre-tRNA by binding to a small stretch of uridines at the 3' -end common to these transcripts and might be necessary for proper processing of these precursors^[1-3]. In addition, La protein is known to interact with a variety of viral RNAs for stabilizing various RNAs^[4-7], and is required for viral internal ribosomal entry site (IRES) -mediated translation^[8-12].

La protein has been identified as a host factor potentially involved in the cytokine-induced post-transcriptional down-regulation of hepatitis B virus (HBV) RNA^[13]. A strong correlation between cytokine-mediated disappearance of HBV RNA and cytokine-induced processing of full-length mouse La protein (mLa) was observed. The mLa binding site was mapped to a predicted stem-loop structure within a region located at the 5' -end of the post-transcriptional regulatory element of HBV shared by all HBV RNAs^[5,6]. In addition, HBV RNA was accessible to endoribonucleolytic cleavage near this mLa binding site and HBV RNA substrates were more efficiently cleaved after induction of mLa processing^[7]. All these findings indicate that La protein might be an HBV RNA-stabilizing factor. Determination of the high affinity interaction between human La protein (hLa) and HBV RNA *in vitro*^[14], which is similar to that of mLa-HBV RNA interaction, implied that hLa might be involved in HBV RNA metabolism. But the role of human La protein (hLa) in HBV RNA metabolism *in vivo* is still unknown at present.

RNA interference (RNAi) is a process of sequence-specific post-transcriptional gene silencing via double-stranded RNA (dsRNA) present in plants and invertebrates^[15]. With the increasing findings that 21-23 nt RNA duplexes known as small interfering RNA (siRNA) can also specifically and effectively knock down target gene expression in mammalian cells but short enough to evade host response^[16], RNAi has been promptly developed into a powerful tool for studying protein function.

In this report, we utilized PCR-based siRNA strategy^[17-19] to obtain several hLa-specific siRNA expression cassettes (SECs) containing U6+1 snRNA promoter and to deplete the hLa expression by transfection with SECs into human cells. In a stable HBV-producing cell line 2.2.15 cells^[20], the inhibition of hLa expression resulted in a significant decrease of HBV mRNA and partly reduction of HBV antigen secretion. This result suggests that human La protein also plays an important role in HBV expression.

MATERIALS AND METHODS

Reagents and materials

Pyrobest DNA polymerase was obtained from Takara Biotech (Japan). TaqPlus DNA polymerase was purchased from Dingguo (China). QIAquick PCR purification kit was obtained from Qiagen (Germany). M-MuLV reverse transcriptase was obtained from MBI fermentas (Lithuania). G418 was from

Clontech (USA). Fetal calf serum was from Hyclone (USA). Trizol reagent and Lipofectamine 2000 were obtained from Invitrogen Lifetechnology (USA). Mouse monoclonal antibody against human La protein was purchased from BD Biosciences (USA). Rabbit polyclonal antibody against actin was from Wuhan Boster Biological Technology (China). Donkey anti-mouse and goat anti-rabbit horseradish peroxidase (HRP)-IgG were from SantaCruz (USA). *Re-Blot Plus* Western blot recycling kit was obtained from Chemicon (USA). SuperSignal west dura extended duration substrate ECL kit and CL-Xposure film were obtained from Pierce Biotech (USA). AxSYM and detective kits of HBsAg and HBeAg were purchased from ABBOTT (USA). Polyvinylidene difluoride (PVDF) membranes were obtained from Millipore (USA). All PCR primers were synthesized by Shanghai Sangon Biological Company (China).

Plasmids and cell lines

Plasmid pAVU6+27 was a gift of Dr. Paul D. Good (Engelke Laboratory, Department of Biological Chemistry). Plasmid pcDNA3.1 was obtained from Clontech (USA). HepG2, a human hepatoblastoma cell line, and 2.2.15 cells derived from HepG2 cells and stably transfected with HBV DNA^[20] were maintained in our laboratory.

Selection of siRNA and shRNA design

Target sites of siRNA were determined by using on-line tool from Ambion Company. Three sites for hLa located downstream of the start codon were selected, their sequences are as follows: coding region 347-357 (5' -AAGGCTTCCC AACTGATGC AA-3') for hLa347, 833-843 (5' -AAGCCAAG GAAGCAT TGGGTA-3') for hLa833, 911-921 (5' -AAGTACTAGAA GGAGAGGTGG-3') for hLa911. 5' -AAGGGCGAGG AGCTGTTACC-3' for EGFP10 siRNA site was used as control for studying the effect of hLa siRNA. Using 5' -TTCAAGAGA-3' as 9-nt loop, all short hairpin RNAs (shRNA) were designed according to the structure of siRNA sense strand-loop-siRNA antisense strand.

Preparation of SECs

U6+1 promoter was obtained from plasmid pAVU6+27 containing human U6 promoter. Oligonucleotides coding hairpin shRNA antisense were synthesized and used for PCR reaction as 3' specific extension primers. All extension primers have the 5' end 21-nt containing additional adaptor sequence and a stretch of 6 deoxyadenosines as transcription terminator. The 5' universal primer is complementary to 18 nt at the 5' end of the U6 snRNA promoter (bold italics) 5' -GGAAGA TCTGGATCCAAGGTCGGG-3' and the 3' universal primer is complementary to the first 21-nt at the 5' end of all extension primers 5' -CGGCT CTAGAGTTCAAAAAG-3'. Both universal primers were 5' -phosphorylated and could be used for all PCR reactions. SEC was constructed by using one specific extension primer and two universal primers via overlapping extension one-step PCR as depicted in Figure 1.

Using Pyrobest polymerase 30 cycles of PCR reactions were carried out, each at 94 °C for 30 s, at 58 °C for 30 s, and at 72 °C for 30 s. The PCR products were purified using QIAquick PCR purification kit (Qiagen) and stored at -20 °C prior to use.

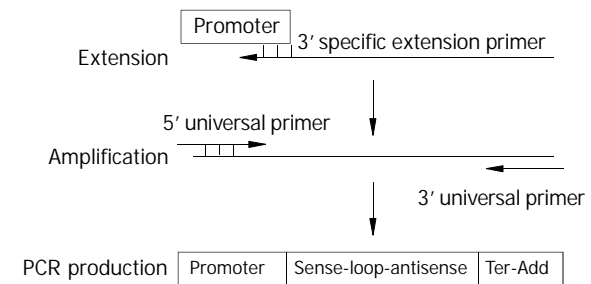


Figure 1 Schematic representation of one-step overlapping extension PCR strategy used to yield SECs.

Cell culture and cotransfection

HepG2 cells were maintained in Dulbecco's modified Eagle's minimal essential medium (DMEM) supplemented with 100 mL/L FCS, streptomycin (100 µg/mL) and penicillin (100 IU/mL) at 37 °C in a humidified atmosphere containing 50 mL/L CO₂. 2.2.15 cells were grown in DMEM with 100 mL/L FCS, 400 µg/mL G418. HepG2 and 2.2.15 cells were seeded into 24-well plates 24 h or 48 h prior to transfection. HepG2 cells at 50% confluence and 2.2.15 cells at 70% were prepared for transfection. For all co-transfections, a total of 0.05 µg pcDNA3.1+ (used as carrier DNA) and 0.2 µg SEC was delivered using Lipofectamine 2 000 according to the manufacturer's instructions. HepG2 cells were harvested for analysis of La mRNA and protein expression. 2.2.15 cells and supernatants were harvested for detection of HBV mRNA and antigen.

RNA extraction and semi-quantitative RT-PCR analysis

Total RNA was extracted from cells with Trizol reagent according to the manufacturer's instructions, 1.0 µg of total RNA was reverse transcribed to cDNA using oligo (dT) 18 as primer and Mu-MLV reverse transcriptase, and 0.5 µL of the cDNA template was separately used to amplify different mRNA. Information of primers is shown in Table 1. The PCR conditions for different target were as follows. A total of 28 cycles for GAPDH were performed, each at 94 °C for 30 s, at 60 °C for 30 s, and at 72 °C for 30 s. A total of 26 cycles for hLa were performed, each at 94 °C for 30 s, at 58 °C for 30 s, and at 72 °C for 30 s. A total of 26 cycles for HBs were performed, each at 94 °C for 30 s, at 56 °C for 30 s, and at 72 °C for 30 s. A total of 30 cycles for HBe were performed, each at 94 °C for 30 s, at 46 °C for 30 s, and at 72 °C for 45 s. After electrophoresis and scanning, all PCR product bands were analyzed by using the software Gel Pro analyzer32 and relative mRNA expression was estimated by normalization with GAPDH.

Table 1 PCR primers for amplification

Primer	GenBank accession No	Sequence of primer pair
GAPDH	BC023632 (26-260)	Sense: 5' -TGGGGAAGGTGAAGGTCGGA -3' Antisense: 5' -GGGATCTCGCTGCTCGAAGA -3'
hLa	BC001289 (871-1313)	Sense: 5' -GGATAGACTTCGTCAGAGGAGCA -3' Antisense: 5' -CTGGTCTCCAGCACCATTCTG -3'
HBs	U95551 (232-681)	Sense: 5' -CTCACAATACCGCAGAGTC -3' Antisense: 5' -TAAACTGAGCCAGGAGAAA -3'
HBe	U95551 (1816-2452)	Sense: 5' -ATGCAACTTTTTACCTC -3' Antisense: 5' -AACATTGAGGTTCCCGAG -3'

Western blot analysis

Cells were harvested and lysed in lysis buffer (0.1 mol/L Tris, pH 7.6, containing 0.15 mol/L NaCl, 2 mmol/L EDTA, 5 g/L Nonidet P-40, 5 g/L Triton X-100, 100 μmol/L sodium vanadate, 10 μg/mL aprotinin, and 20 μg/mL soybean trypsin inhibitor). The cell lysate (10-15 μg protein) was separated by sodium dodecyl sulfate-polyacrylamide (SDS-PAGE) gel electrophoresis and electrophoretically transferred onto PVDF membrane. After non-specific binding sites were blocked with 50 g/L non-fat milk, the membrane was incubated with mouse anti-hLa monoclonal antibody (1:600 dilution) overnight at 4 °C. After washed, the blot was incubated with HRP-conjugated anti-mouse IgG for 1 h at room temperature, and immunoreactive bands were visualized with the ECL reagent. After the blot was stripped with stripping solution, the blot was reprobed with rabbit anti-actin polyclonal antibody for comparison of protein load in each lane. Densitometric scanning of the X-ray film following chemiluminescence was done and La protein expression level was estimated after normalization with actin.

Microparticle enzyme immunoassay (MEIA) analysis

Supernatants of 2.2.15 cells were harvested on days 1, 2, 3, 6 and 9 posttransfection respectively in same wells. Each experiment well was performed in triplicate. A microparticle enzyme immunoassay (MEIA) method was applied for the detection of HBsAg and HBeAg according to the kit's instructions. Sample with S/N values great than or equal to 2.0 for HBsAg, and S/CO values great than or equal to 2.1 for HBeAg were considered reactive as described previously^[21].

RESULTS

RNAi inhibited hLa protein expression in cultured HepG2 cells

To determine whether siRNA specific to the hLa gene sequence could inhibit hLa expression, we screened the activity of three sites of hLa-specific siRNA by semi-quantitated RT-PCR of hLa mRNA in HepG2 cells 36 h posttransfection with SECs. Two of them, SEC U6+1-hLa347 and U6+1-hLa833 significantly decreased hLa mRNA levels by about 8.8- and 17.6-fold respectively as compared with the control (Figure 2A). However, SEC U6+1-hLa911 only slightly affected hLa mRNA expression (1.3-fold reduction). No significant inhibition of hLa mRNA expression was detected in cells transfected with SEC U6+1-EGFP10 (Figure 2A). Furthermore, we performed Western blot analysis to verify the inhibitory effects on hLa protein expression levels 72 h posttransfection with SEC U6+1-hLa347 and U6+1-hLa833. As shown in Figure 2B, hLa protein expression almost could not be detected in cells transfected with U6+1-hLa833. After normalized to actin, the level of hLa protein expression was reduced to approximately 11% and 49% of the control cells for U6+1-hLa833 and U6+1-hLa347 respectively, and no reduction was found for U6+1-EGFP10. These data demonstrated that SEC-mediated RNAi could effectively inhibit human La protein expression in cultured HepG2 cells and the down-regulation in hLa was sequence-specific and highly site-dependant.

RNAi inhibited hLa mRNA expression in cultured 2.2.15 cells

As SEC U6+1-hLa833 could greatly specific inhibit hLa mRNA and protein expressions in HepG2 cells, we then assessed its inhibitory effects on 2.2.15 cells derived from HepG2. As shown in Figure 3A, inhibition of hLa mRNA levels was detected with the reduction of about 22- and 3.4-fold on days 1 and 2 posttransfection, but no inhibitory effects were observed from days 3 to 9 posttransfection. In addition, no significant inhibition of hLa mRNA levels was detected in cells posttransfection with the SEC U6+1-EGFP-10 (Figure 3A).

This result indicates that SEC-mediated RNAi could also effectively inhibit hLa mRNA expression in cultured 2.2.15 cells, but the inhibitory effects could last only for a short time.

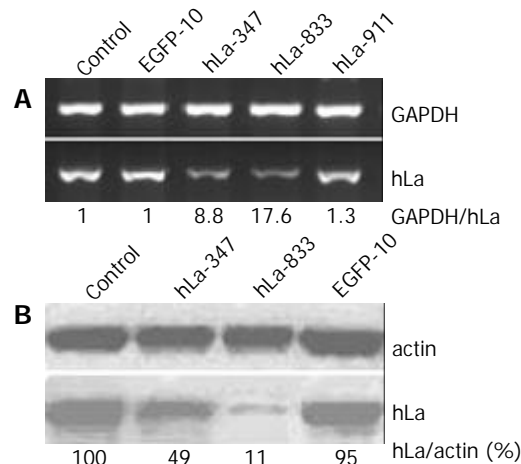


Figure 2 Effect of RNAi on hLa expression in HepG2 cells. A: Total RNA isolated from HepG2 cells transfected with various SECs for hLa and EGFP. The number was the ratio between the signal intensity for GAPDH and hLa mRNA amplified in parallel. B: Western blotting of total cell lysates harvested from SECs-transfected HepG2 cells 72 h posttransfection. Actin was used as loading control. The number was the percentage of the signal intensity of hLa and actin protein (%).

Inhibition of hLa expression led to reduction of HBV mRNA levels in cultured 2.2.15 cells

In order to investigate the relationship between hLa mRNA and HBV RNA expression, using the same samples, the levels of HBs and HBe mRNA expression in SEC-transfected 2.2.15 cells were detected by semi-quantitative RT-PCR. The HBs mRNA levels were also decreased about 8- and 2.8-fold in the first 2 d posttransfection, which were associated with a parallel reduction of hLa mRNA levels (Figure 3B). Moreover, HBe mRNA decreased dramatically, and almost could not be detected in the first 2 d and the inhibitory effect could last for at least 9 d (Figure 3C). In contrast, no significant changes in HBs and HBe mRNA levels were observed in cells posttransfection with SEC U6+1-EGFP-10 (Figures 3B and 3C). These results demonstrated that RNAi against hLa could lead to reduction of HBV mRNA levels in 2.2.15 cells.

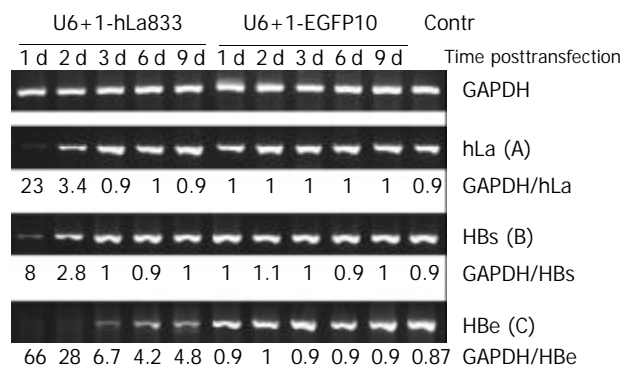


Figure 3 Effect of RNAi on hLa mRNA expression and levels of HBV mRNA expression in 2.2.15 cells. The number was the ratio between the signal intensity for hLa, HBs, HBe, and GAPDH mRNA amplified in parallel.

Inhibition of hLa expression affected HBsAg and HBeAg secretion in 2.2.15 cells

If the inhibition of hLa expression could affect HBs and HBe

mRNA expressions in 2.2.15 cells, HBsAg and HBeAg secretion would be affected accordingly. Supernatant of SEC-transfected and control cells was harvested in the same period of posttransfection, HBsAg and HBeAg concentrations in the culture media were measured by MEIA method. Figure 4A shows that transfection with SEC U6+1-hLa833 inhibited the secretion of HBsAg in 2.2.15 cells from days 3 to 9 posttransfection in comparison with that of SEC U6+1-EGFP10 ($P<0.05$). The maximal inhibitory effect on day 6 posttransfection was 40%, and returned to 26% on d 9. HBeAg secretion was inhibited 38% on d 3 posttransfection with SEC U6+1-hLa833 and remained 46% and 51% on d 6 and 9 respectively (Figure 4B). There was a significant difference ($P<0.05$) in HBeAg secretion between SEC U6+1-hLa833- and U6+1-EGFP10-transfected cells on d 3, 6 and 9 posttransfection.

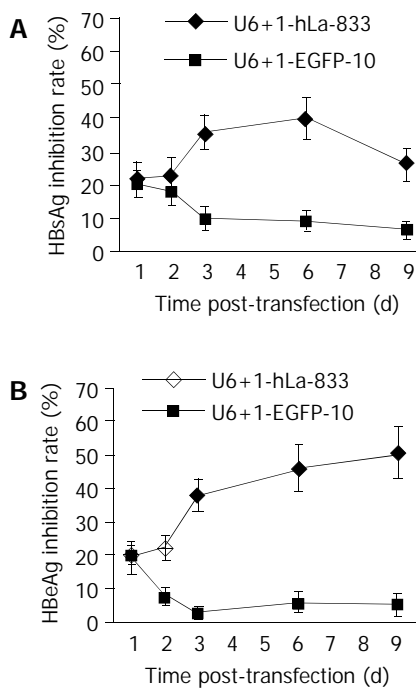


Figure 4 Time-efficiency inhibition course of SECs on HBsAg and HBeAg in 2.2.15 cells. The inhibition rate (IR) was calculated according to the following formula:

$$IR = \frac{X \text{ of wells for control} - X \text{ of wells for transfection}}{X \text{ of wells for control} - N} \times 100\%$$

X represents S/N or S/CO for HBsAg or HBeAg, and $n=2.0$ for HBsAg and 2.1 for HBeAg respectively.

DISCUSSION

Results showed here from studies in 2.2.15 cells using siRNA against human La protein revealed a significant reduction in hLa expression, that resulted in HBV mRNA level reduction simultaneously, especially the expression of HBe mRNA, which was markedly decreased in the first 3 d and maintained at a lower level on the 9th d after inhibition of hLa expression. Following HBV mRNA reduction, HBsAg and HBeAg secretions were decreased accordingly though reduction of HBV antigen was less significant than that of corresponding mRNA. The relevance of RNAi-mediated knockdown of hLa towards reduction of HBV mRNA level suggested that human La protein might also be involved in HBV RNA metabolism. Based on the previous findings of the high affinity interaction between human La protein (hLa) and HBV RNA *in vitro*^[14], and mouse La protein might be an HBV RNA-stabilizing factor in HBV-transgenic mouse model^[5,7]. Our results invited a

presumption that La protein might also play a role in stabilizing HBV RNA in human cells. However, HBsAg and HBeAg secretions could be affected slightly by hLa expression level, indicating that La protein is not a unique factor, and additional factors could contribute to viral RNA stability or HBV expression regulation. Therefore, using only hLa as targets for a novel antiviral strategy^[14] would not be practical. Experiments to investigate the role of other RNA-binding proteins in HBV RNA metabolism might gain better insights into this problem.

We also observed that downregulation of HBe seemed more significant than HBs, implying more abundant HBs mRNA could generate HBsAg than HBe in 2.2.15 cells, which was in accord with the redundant HBsAg expression and secretion from patients with HBV infection. So HBs might be poorly susceptible to interfering factors. In addition, the feature of overlapping reading frames made entire 2.1-kb mRNA sequence encode HBs that was contained in 3.5-kb mRNA sequence encoding Hbe^[22,23]. In fact, HBs mRNA level detected by RT-PCR in our experiments represented the total transcript level containing HBe and HBs. Therefore, instead of RT-PCR, Northern blot analysis should reflect the truth of all HBV transcripts in more detail.

As to siRNA application in RNAi technology, besides chemically synthesized 21-nt siRNA duplexes^[16], some approaches could generate siRNA for various needs, such as *in vitro* transcribed siRNA^[24,25], plasmid DNA expression vector-based siRNA^[26,27], viral vector-based siRNA^[28-30], and PCR-based siRNA expression cassette (SEC)^[17-19] which was proved to be a rapid, facile and cheap approach for identification of optimal siRNA-targets. In this report, we attempted to simplify the commonly used two-step PCR into overlapping-extension one-step PCR reaction by using three primers: a long specific extension primer and two universal primers, and also successfully prepared SECs targeting three sites of hLa mRNA. After transfection with these SECs into HepG2 cells, SEC U6+1-hLa833 demonstrated that strong RNAi effect was promptly screened out as optimal SEC to be used for further study. As a 347-bp in length of SEC DNA, it is often difficult to transfect them into mammalian cells, but using plasmid as carrier DNA, the efficiency of transfection seemed to be improved significantly (data not shown). On the other hand, stability of SEC DNA in cells should be considered. Despite SECs were phosphorylated for enhancing resistance to nuclease in cells, but target mRNA level still returned to normal on day 3 posttransfection, which maintained RNAi effect not as long as reported in application of vector-based siRNA^[26], indicating that SEC strategy should be just adapted to transient gene silencing at present and the better modification strategies should be developed for its stability.

To our knowledge, this is the first report that describes the role of human La protein in HBV expression in cultured human cells. Elucidating the mechanism of human La protein affecting HBV expression and replication will allow a deeper understanding of the interaction between host factors and HBV during HBV infection and clearance, and will provide useful clues for controlling HBV infection.

ACKNOWLEDGEMENTS

We thank Dr. Paul D. Good (Engelke Laboratory) for supplying plasmid pAVU6+27. We also thank Dr. Jian-Er Wo, Dr. Yu Chen and Dr. Jun-Bin Shao for technological support, and Dr. Edward Zumbika for English revision of this paper.

REFERENCES

- 1 **Chakshumathi G**, Kim SD, Rubinson DA, Wolin SL. A La protein requirement for efficient pre-tRNA folding. *EMBO J* 2003;

- 22: 6562-6572
- 2 **Wolin SL**, Cedervall T. The La protein. *Annu Rev Biochem* 2002; **71**: 375-403
 - 3 **Maraia RJ**. La Protein and the trafficking of nascent RNA polymerase iii transcripts. *J Cell Biol* 2001; **153**: F13-F18
 - 4 **Spangberg K**, Wiklund L, Schwartz S. Binding of the La autoantigen to the hepatitis C virus 3' untranslated region protects the RNA from rapid degradation *in vitro*. *J Gen Virol* 2001; **82**(Pt 1): 113-120
 - 5 **Heise T**, Guidotti LG, Cavanaugh VJ, Chisari FV. Hepatitis B virus RNA-binding proteins associated with cytokine-induced clearance of viral RNA from the liver of transgenic mice. *J Virol* 1999; **73**: 474-481
 - 6 **Heise T**, Guidotti LG, Chisari FV. La autoantigen specifically recognizes a predicted stem-loop in hepatitis B virus RNA. *J Virol* 1999; **73**: 5767-5776
 - 7 **Heise T**, Guidotti LG, Chisari FV. Characterization of nuclear RNases that cleave hepatitis B virus RNA near the La protein binding site. *J Virol* 2001; **75**: 6874-6883
 - 8 **Pudi R**, Abhiman S, Srinivasan N, Das S. Hepatitis C virus internal ribosome entry site-mediated translation is stimulated by specific interaction of independent regions of human La autoantigen. *J Biol Chem* 2003; **278**: 12231-12240
 - 9 **Ali N**, Puijn GJ, Kenan DJ, Keene JD, Siddiqui A. Human La antigen is required for the hepatitis C virus internal ribosome entry site-mediated translation. *J Biol Chem* 2000; **275**: 27531-27540
 - 10 **Cheung P**, Zhang M, Yuan J, Chau D, Yanagawa B, McManus B, Yang D. Specific interactions of HeLa cell proteins with Cocksackievirus B3 RNA: La autoantigen binds differentially to multiple sites within the 5' untranslated region. *Virus Res* 2002; **90**: 23-36
 - 11 **Ray PS**, Das S. La autoantigen is required for the internal ribosome entry site-mediated translation of Cocksackievirus B3 RNA. *Nucleic Acids Res* 2002; **30**: 4500-4508
 - 12 **De Nova-Ocampo M**, Villegas-Sepulveda N, del Angel RM. Translation elongation factor-1alpha, La, and PTB interact with the 3' untranslated region of dengue 4 virus RNA. *Virology* 2002; **295**: 337-347
 - 13 **Tsui LV**, Guidotti LG, Ishikawa T, Chisari FV. Posttranscriptional clearance of hepatitis B virus RNA by cytotoxic T lymphocyte-activated hepatocytes. *Proc Natl Acad Sci U S A* 1995; **92**: 12398-12402
 - 14 **Horke S**, Reumann K, Rang A, Heise T. Molecular characterization of the human La protein/hepatitis B virus RNA.B interaction *in vitro*. *J Biol Chem* 2002; **277**: 34949-34958
 - 15 **Hannon GJ**. RNA interference. *Nature* 2002; **418**: 244-251
 - 16 **Elbashir SM**, Harborth J, Lendeckel W, Yalcin A, Weber K, Tuschl T. Duplexes of 21-nucleotide RNAs mediate RNA interference in cultured mammalian cells. *Nature* 2001; **411**: 494-498
 - 17 **Castanotto D**, Li H, Rossi JJ. Functional siRNA expression from transfected PCR products. *RNA* 2002; **8**: 1454-1460
 - 18 **Gou D**, Jin N, Liu L. Gene silencing in mammalian cells by PCR-based short hairpin RNA. *FEBS Lett* 2003; **548**: 113-118
 - 19 **Zheng L**, Liu J, Batalov S, Zhou D, Orth A, Ding S, Schultz PG. An approach to genomewide screens of expressed small interfering RNAs in mammalian cells. *Proc Natl Acad Sci U S A* 2004; **101**: 135-140
 - 20 **Sells MA**, Chen ML, Acs G. Production of hepatitis B virus particles in HepG2 cells transfected with cloned hepatitis B virus DNA. *Proc Natl Acad Sci U S A* 1987; **84**: 1005-1009
 - 21 **Chen Y**, Wu W. Determination of low-level HBsAg in serum by microparticle enzyme immunoassay. *Hepatobiliary Pancreat Dis Int* 2002; **1**: 262-264
 - 22 **Moolla N**, Kew M, Arbuthnot P. Regulatory elements of hepatitis B virus transcription. *J Viral Hepat* 2002; **9**: 323-331
 - 23 **Seeger C**, Mason WS. Hepatitis B Virus Biology. *Microbiol Mol Biol Rev* 2000; **64**: 51-68
 - 24 **Anderson J**, Banerjee A, Planelles V, Akkina R. Potent suppression of HIV type 1 infection by a short hairpin anti-CXCR4 siRNA. *AIDS Res Hum Retroviruses* 2003; **19**: 699-706
 - 25 **Myers JW**, Jones JT, Meyer T, Ferrell JE Jr. Recombinant Dicer efficiently converts large dsRNAs into siRNAs suitable for gene silencing. *Nat Biotechnol* 2003; **21**: 324-328
 - 26 **Paul CP**, Good PD, Winer I, Engelke DR. Effective expression of small interfering RNA in human cells. *Nat Biotechnol* 2002; **20**: 505-508
 - 27 **Brummelkamp TR**, Bernards R, Agami R. A system for stable expression of short interfering RNAs in mammalian cells. *Science* 2002; **296**: 550-553
 - 28 **Liu CM**, Liu DP, Dong WJ, Liang CC. Retrovirus vector-mediated stable gene silencing in human cell. *Biochem Biophys Res Commun* 2004; **313**: 716-720
 - 29 **Rubinson DA**, Dillon CP, Kwiatkowski AV, Sievers C, Yang L, Kopinja J, Rooney DL, Ihrig MM, McManus MT, Gertler FB, Scott ML, Van Parijs L. A lentivirus-based system to functionally silence genes in primary mammalian cells, stem cells and transgenic mice by RNA interference. *Nat Genet* 2003; **33**: 401-406
 - 30 **Zhao LJ**, Jian H, Zhu H. Specific gene inhibition by adenovirus-mediated expression of small interfering RNA. *Gene* 2003; **316**: 137-141

Edited by Wang XL Proofread by Chen WW and Xu FM

Helicobacter pylori lipopolysaccharide: Biological activities *in vitro* and *in vivo*, pathological correlation to human chronic gastritis and peptic ulcer

Yi-Hui Luo, Jie Yan, Ya-Fei Mao

Yi-Hui Luo, Jie Yan, Ya-Fei Mao, Department of Medical Microbiology and Parasitology, College of Medical Science, Zhejiang University, Hangzhou 310031, Zhejiang Province, China

Supported by the Foundation of Ministry of Education of China for Distinguished Young Scholars

Correspondence to: Professor Jie Yan, Department of Medical Microbiology and Parasitology, College of Medical Science, Zhejiang University, 353 Yan An Road, Hangzhou 310031, Zhejiang Province, China. yanchen@mail.hz.zj.cn

Telephone: +86-571-87217385 **Fax:** +86-571-87217044

Received: 2003-12-23 **Accepted:** 2004-01-12

Abstract

AIM: To determine the biological activity of *Helicobacter pylori* (*H pylori*) lipopolysaccharide (H-LPS) and understand pathological correlation between H-LPS and human chronic gastritis and peptic ulcer.

METHODS: H-LPS of a clinical *H pylori* strain and LPS of *Escherichia coli* strain O55:B5 (E-LPS) were extracted by phenol-water method. Biological activities of H-LPS and E-LPS were detected by limulus lysate assay, pyrogen assay, blood pressure test and PBMC induction test in rabbits, cytotoxicity test in NIH 3T3 fibroblast cells and lethality test in NIH mice. By using self-prepared rabbit anti-H-LPS serum as the first antibody and commercial HRP-labeled sheep anti-rabbit sera as the second antibody, H-LPS in biopsy specimens from 126 patients with chronic gastritis (68 cases) or gastric ulcer (58 cases) were examined by immunohistochemistry.

RESULTS: Fibroblast cytotoxicity and mouse lethality of H-LPS were weaker than those of E-LPS. But the ability of coagulating limulus lysate of the two LPSs was similar (+/0.5 ng/mL). At 0.5 h after H-LPS injection, the blood pressures of the 3 rabbits rapidly declined. At 1.0 h after H-LPS injection, the blood pressures in 2 of the 3 rabbits fell to zero causing death of the 2 animals. For the other one rabbit in the same group, its blood pressure gradually elevated. At 0.5 h after E-LPS injection, the blood pressures of the three rabbits also quickly declined and then maintained at low level for approximately 1.0 h. At 0.5 h after injection with H-LPS or E-LPS, PBMC numbers of the rabbits showed a remarkable increase. The total positivity rate of H-LPS from 126 biopsy specimens was 60.3% (76/126). H-LPS positivity rate in the biopsy specimens from chronic gastritis (50/68, 73.5%) was significantly higher than that from gastric ulcer (26/58, 44.8%) ($\chi^2=10.77$, $P<0.01$). H-LPS positivity rates in biopsy specimens from chronic superficial gastritis (38/48, 79.2%) and chronic active gastritis (9/10, 90.0%) were significantly higher than that of the patients with atrophic gastritis (3/10, 30.0%) ($\chi^2=7.50-9.66$, $P<0.01$).

CONCLUSION: The biological activities of H-LPS were

weaker than those of E-LPS, the activities of H-LPS of lowering rabbit blood pressure and inducing rabbit PBMC were relatively stronger. H-LPS may play a critical role in inducing inflammatory reaction in human gastritis.

Luo YH, Yan J, Mao YF. *Helicobacter pylori* lipopolysaccharide: Biological activities *in vitro* and *in vivo*, pathological correlation to human chronic gastritis and peptic ulcer. *World J Gastroenterol* 2004; 10(14): 2055-2059

<http://www.wjgnet.com/1007-9327/10/2055.asp>

INTRODUCTION

Gastritis and peptic ulcer are the most prevalent gastric diseases. Gastric cancer is one of the malignant tumors with high morbidities in China^[1]. *Helicobacter pylori* (*H pylori*) is recognized as a human-specific gastric pathogen that colonizes the stomachs of at least half of the world's populations^[2]. Most infected individuals are asymptomatic. However, in some subjects, the infection causes acute, chronic gastritis or peptic ulceration, and plays an important role in the development of peptic ulcer and gastric adenocarcinoma, mucosa-associated lymphoid tissue lymphoma and primary gastric non-Hodgkin's lymphoma^[3-7].

H pylori is a microaerophilic Gram-negative bacillus. It is well known that lipopolysaccharide (LPS) is a common and essential component in outer membrane of most Gram-negative bacteria responsible for the toxicity of endotoxin. Some literatures revealed *H pylori* possesses LPS (H-LPS) with a lower virulence compared to the typical bacterial endotoxins such as *Escherichia coli* LPS (E-LPS)^[8-12]. However, some biological activities such as regulating blood pressure and inducing peripheral blood mononuclear cell (PBMC), which are clinically important in local tissue inflammation and injury, and pathological importance of H-LPS in human gastric diseases are still little understood. Besides, some previously published data demonstrated that different strains of the same bacterium and different extraction methods would significantly affect the biological activity of LPS^[13,14].

For measurement of the biological activities of H-LPS *in vivo* and *in vitro* compared to a typical LPS from *E. coli*, we used phenol-water method to extract LPS from a clinical isolated *H pylori* strain and applied routine assays for determining the endotoxin activity of H-LPS such as limulus lysate agglutination, rabbit pyrogenicity and mouse lethality. Furthermore, we also examined H-LPS activities on blood pressure regulation and PBMC inducement. To obtain direct evidence for the correlation of H-LPS and human chronic gastritis and peptic ulcer, we detected H-LPS in gastric biopsy specimens from patients with different gastric diseases.

MATERIALS AND METHODS

Bacterial strains and culture

A clinical *H pylori* strain named as Y06 was isolated from a

biopsy specimen of a male patient with chronic superficial gastritis and duodenal ulcer by using selected Columbia agar (bioMérieux) supplemented with 80 mL/L sheep blood, 5 g/L cyclodextrin, 5 mg/L trimethoprim, 10 mg/L vancomycin, 2.5 mg/L amphotericin B and 2 500 U/L cefsulodin. This strain was identified as *H pylori* based on its typical Gram staining morphology, positivity for both urease and oxidase, and agglutination with a commercial rabbit antibody against whole cell of *H pylori* (DAKO). *E. coli* strain O55:B5 was offered by the National Institute for the Control of Pharmaceuticals and Biological Products of China (NICBPB) and cultured with BL agar.

LPS extraction

H-LPS from *H pylori* strain Y06 and E-LPS from *E. coli* strain O55:B5 were extracted by phenol-water method. Briefly, the two bacteria collected from Columbia agar and BL agar were ultrasonically broken, respectively. Each of the broken bacterial solutions was added with an equal volume of pre-warmed phenol-water (9:1, V:V) and then vibrated for 30 min at 68-70 °C. The aqueous phase was collected after centrifugation at 3 000 r/min for 30 min. This extraction step was repeated for 3 times. All the aqueous phases were combined and then dialyzed against distilled water for 48 h. This rough LPS extract was concentrated to 1/6 of the original volume and then digested with RNase H and DNase I (Sigma) to both the final concentration of 50 µg/mL at 37 °C for 4 h. The digested extract was bathed in boiling-water for 15 min and then placed at 4 °C overnight. The supernatant obtained after centrifugation at 3 000 r/min for 30 min was dialyzed against distilled water for 48 h and then precipitated with 6-fold volumes of anhydrous alcohol at 4 °C for 12 h. The precipitate was collected by centrifugation at 5 000 r/min for 30 min and then re-suspended with distilled water and dialyzed against distilled water for 24 h to remove residual alcohol. The LPS extract was ultra-centrifuged at 110 000 g for 3 h (4 °C) and the pellet was dialysed in distilled water and freeze-dried. The purified H-LPS and E-LPS were dissolved in pyrogen-free water or normal saline prepared with pyrogen-free water just before different uses.

Limulus lysate assay

Limulus lysate assay was applied by using E-TOXATE Reagent Kit (Sigma) to detect the H-LPS and E-LPS preparations according to the manufacturer's instruction (Sensitivity = +, 1 ng/mL *E. coli* O55:B5 LPS). In this assay, *E. coli* O55:B5 LPS (Sigma) and pyrogen-free water were used as the positive and negative controls, respectively.

Rabbit pyrogen assay

Anal temperatures of normal New Zealand rabbits with 3.0±0.2 kg of body mass were detected for 3 times at an interval of 30 min before performing the test. A rabbit was suitable for the test if the fluctuant range of the three detected temperatures was ≤0.2 °C. The qualified rabbits were randomly divided into three groups and each group contained three animals. Each of the three rabbits in one group was injected with 0.5 mL normal saline containing H-LPS or E-LPS at the same dosage of 100 µg/kg through ear vein. Each of the three rabbits in the 3rd group was injected with an equal volume of pyrogen-free normal saline as a negative control. Anal temperature in each of the tested rabbits was detected at an interval of 30 min for 5 h after injection. The positive standard for rabbit pyrogen assay was described as following: body temperature for any one of the three rabbits in one group showed ≥0.6 °C elevation, or the total elevated body temperature for the three rabbits in one group was ≥1.4 °C.

Rabbit blood pressure regulation test

Normal New Zealand rabbits with 3.0±0.2 kg of body mass were ear-intravenously injected with 0.5 mL pyrogen-free normal saline. Then blood pressures of the animals were observed for three times at an interval of 30 min. A rabbit was suitable for this test if its blood pressure fluctuation was within 0.2 kPa. The qualified rabbits were divided into three groups and each contained three animals. Each of the three rabbits in one group was ear-intravenously injected with pyrogen-free saline containing H-LPS or E-LPS at the same dosage of 100 µg/kg and each of the three rabbits in the 3rd group were ear-intravenously injected with an equal volume of pyrogen-free saline as a negative control. The changes of blood pressure in the tested rabbits were observed.

PBMC inducement test

PBMC numbers in blood from ear vein of normal New Zealand rabbits with 3.0±0.2 kg of body mass were counted with hemacytometer twice at an interval of 30 min before performing the test. These rabbits were randomly divided into three groups and each contained 5 animals. Each of the five rabbits in one group was ear-intravenously injected with pyrogen-free saline containing H-LPS or E-LPS at the same dosage of 100 µg/kg and each of the five rabbits in the 3rd group were ear-intravenously injected with an equal volume of pyrogen-free saline as a negative control. The change of PBMC numbers for each of the tested rabbits was counted at an interval of 30 min after injection.

Cytotoxicity test

Microtiter plates were inoculated with 1×10⁴ mouse 3T3 fibroblast cells in RPMI 1640 medium containing 100 mL/L bovine serum per well and then incubated at 37 °C overnight in 50 mL/L CO₂ atmosphere. The medium in the plates was discarded and then added with 200 µL of fresh medium containing H-LPS or E-LPS with different double dilutions. For each of the dilutions, 3 wells were repeated and then incubated for 48 h under the same conditions as mentioned above. In this test, the other 5 wells added with the same volume of LPS-free medium were set up as a negative control. ³H-TdR per well (37 kBq) was added and then continuously incubated for 24 h. CPM value for each of the wells was detected by using ³H-TdR incorporation method to compare the cytotoxicity of H-LPS and E-LPS.

Mouse lethality test

NIH mice weighing 20±2 g were randomly divided into 7 groups and each contained 8 animals. For 6 of the 7 groups, each of the mice in one group was intraperitoneally injected with 0.2 mL pyrogen-free normal saline containing H-LPS or E-LPS at the different dosages of 0.25, 0.50 and 1.0 mg, respectively. Each of the mice in the last group was intraperitoneally injected with 0.2 mL pyrogen-free saline as a negative control. All the tested animals were observed for 7 d.

Detection of H-LPS in biopsy specimens from patients with chronic gastritis and gastric ulcer

Biopsy specimens with positive urease from 126 patients (86 male, 40 female, mean age: 40±18 years) with gastric diseases during January to September of 2003 were collected from three hospitals in Hangzhou. Among these patients, 68 suffered from chronic gastritis (48 cases with chronic superficial, 10 active and 10 atrophic gastritis) and 58 cases suffered from gastric ulcer (12 cases with gastric, 40 duodenal and 6 complex ulcer). The biopsy specimens were fixed with 50 g/L glutaraldehyde. Rabbit anti-H-LPS serum was prepared by using routine subcutaneous immunization. By using the

rabbit anti-H-LPS serum (1:200 dilution, self-prepared) as the first antibody and HRP-labeled sheep anti-rabbit serum (1:3 000 dilution, ImmunoResearch) as the second antibody, H-LPS in the biopsy specimens was detected by routine immunohistochemistry. Cells with at least one whole gastric gland in a biopsy section showing exactly brown color could be considered as positive.

RESULTS

Limulus lysate coagulation

The ability of coagulating limulus lysate of H-LPS was as low as 0.5 ng/mL, which was similar to E-LPS (Table 1).

Table 1 Results of limulus lysate assay of H-LPS and E-LPS

Group	LPS (ng/mL)							
	10.0	5.0	2.5	1.0	0.5	0.25	0.1	0.05
H-LPS	+	+	+	+	+	-	-	-
E-LPS	+	+	+	+	+	-	-	-
Pyrogen-free water	negative in two repeated samples							

Pyrogenic response

The rabbits injected with H-LPS or E-LPS showed a similar biphasic fever but E-LPS could induce a stronger pyrogenic response. The animal temperature reached a peak at 1.5 h after injection and then showed a slight fall. At 3 h after injection, the second fever peak occurred (Figure 1).

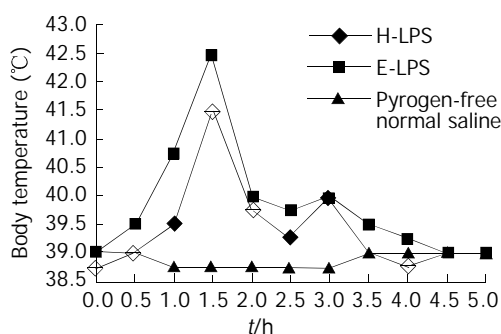


Figure 1 Fever curves of rabbits after injection with H-LPS or E-LPS.

Regulation of rabbit blood pressure

At 0.5 h after H-LPS injection, the blood pressures of the three rabbits rapidly declined from originally 11.331 ± 0.152 kPa to 5.999 ± 1.855 kPa. At 1.0 h after H-LPS injection, the blood pressures in two of the three rabbits fell to zero causing death of the two animals. For the other one rabbit in the same group, its blood pressure gradually elevated. At 0.5 h after E-LPS injection, the blood pressures of the three rabbits also quickly declined from originally 11.197 ± 0.163 kPa to 8.531 ± 2.424 kPa and then maintained the similar low blood pressure levels for approximately 1.0 h. At 2.5 h after injection, the blood pressures in all the three rabbits began to rise and returned to the original levels gradually.

PBMC inducement

At 0.5 h after injection with H-LPS or E-LPS, PBMC numbers of the rabbits showed a remarkable increase. From 1.0 h after injection with H-LPS or E-LPS, the PBMC numbers gradually and continuously decreased to low levels (Table 2).

Cytotoxicity to mouse fibroblast

Very low dosage of H-LPS or E-LPS (1 μ g/mL) could show

an obvious cytotoxicity to NIH 3T3 fibroblast. According to the counting per minute (CPM) of scintillation at the same concentrations, cytotoxicity of H-LPS seemed to be a little weaker than that of E-LPS (Table 3).

Table 2 PBMC number changes in the rabbits injected with H-LPS or E-LPS

Time (h)	PBMC (mean \pm SD, $\times 10^9$ /L)		
	H-LPS	E-LPS	Saline
Before injection	4.52 \pm 1.28	4.38 \pm 1.35	4.05 \pm 1.42
After injection			
0.5	12.51 \pm 0.54	8.22 \pm 0.68	4.25 \pm 1.28
1.0	2.55 \pm 0.87	2.23 \pm 1.32	4.40 \pm 1.19
1.5	1.56 \pm 1.33	1.58 \pm 1.27	4.08 \pm 1.24
2.0	1.62 \pm 0.93	1.64 \pm 0.89	4.05 \pm 1.06
2.5	1.65 \pm 1.12	1.60 \pm 1.34	4.35 \pm 1.17
3.0	1.56 \pm 1.45	1.52 \pm 1.10	4.16 \pm 1.22

Table 3 Cytotoxicity of H-LPS and E-LPS to mice fibroblast

Group	LPS (μ g/mL)	CPM (mean \pm SD)	t	P
H-LPS	1.0	7 722 \pm 819	3.74	<0.05
	5.0	4 724 \pm 726	7.29	<0.01
	10.0	4 328 \pm 1 194	6.56	<0.01
	50.0	3 618 \pm 434	9.27	<0.001
	100.0	2 963 \pm 764	9.20	<0.001
E-LPS	1.0	6 813 \pm 1 183	4.17	<0.05
	5.0	4 290 \pm 474	8.37	<0.005
	10.0	3 516 \pm 645	8.96	<0.001
	50.0	3 224 \pm 534	9.55	<0.001
	100.0	2 513 \pm 630	10.72	<0.001
Control	0	11 083 \pm 1 324		

Mouse lethality

H-LPS showed a significantly weaker virulence to mice than E-LPS. Although the injecting dosage was as high as 1 mg H-LPS per mouse, 2 of the 8 mice survived (Table 4).

Table 4 Toxicity test results in mice injected with H-LPS or E-LPS

Group	Number (n)	Dosage (mg/mouse)	Death/Survival (n/n)	Mortality (%)
H-LPS	8	0.25	0/8	0
	8	0.50	4/4	50.0
	8	1.00	6/2	75.0
E-LPS	8	0.25	2/6	25.0
	8	0.50	7/1	87.5
	8	1.00	8/0	100
	8	/	0/8	0

Positivity rate of H-LPS in biopsy specimens

The total positivity rate of H-LPS in the 126 biopsy specimens was 60.3% (Table 5). Totally 73.5% of the biopsy specimens from chronic gastritis patients (50/68) were H-LPS positive, which was significantly higher than that (44.8%) from gastric ulcer patients (26/58) ($\chi^2=10.77$, $P<0.01$). H-LPS positivity rate in biopsy specimens of the patients with chronic superficial gastritis (38/48, 79.2%) was similar to that of the patients with chronic active gastritis (9/10, 90.0%) ($\chi^2=0.63$, $P>0.05$), but both positivity rates were much higher than that of the patients with atrophic gastritis (3/10, 30.0%) ($\chi^2=7.50-9.66$, $P<0.01$). Among the biopsy specimens from patients with any one of

the three types of gastric ulcer, the H-LPS positive rates were similar to each other ($\chi^2=0.11-1.25$, $P>0.05$). A H-LPS positive biopsy specimen is shown in Figure 2.

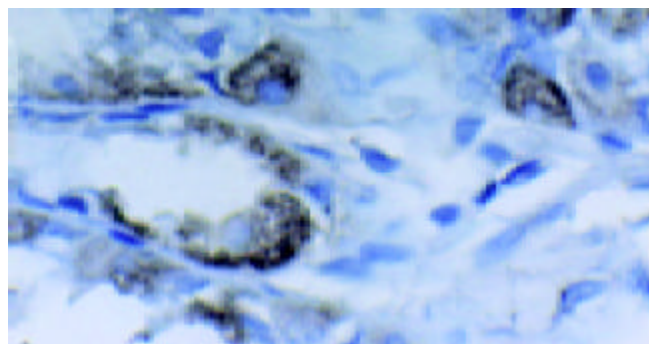


Figure 2 H-LPS positive biopsy specimen (Original magnification: $\times 600$).

Table 5 H-LPS detection rates in the biopsy specimens from patients with chronic gastritis and gastric ulcer

Group	Number (n)	Positivity (n)	Positive rate (%)
Chronic gastritis			
Superficial	48	38	79.2
Active	10	9	90.0
Atrophic	10	3	30.0
Gastric ulcer			
Gastric	12	7	58.3
Duodenal	40	16	40.0
Complex	6	3	50.0
Total	126	76	60.3

DISCUSSION

Bacterial endotoxin possesses broad biological activities and its toxicity is mainly dependent on lipid A^[15]. Among the biological activities of LPS, limulus amoebocyte lysate coagulation, rabbit pyrogen and mouse lethality are most typical and important^[16,17]. In some of the previously published data, H-LPS showed much lower activities of coagulating limulus lysate, pyrogenic response in rabbit and lethal potential in mice^[8,9]. In our study, we found that the effect of H-LPS on causing fever in rabbits, death in mice and its cytotoxicity to NIH 3T3 fibroblast were less compared to the LPS from *E. coli*. However, the ability of coagulating limulus lysate of H-LPS (+/0.5 ng/mL) was similar to that of E-LPS based on several repeated results. As mentioned in Introduction, LPS preparations might have various biological activities if different extraction methods were used^[13,14]. The result in limulus lysate assay of this study differed from the previously reported probably due to H-LPS from different strains and the distinction in LPS extraction methods.

Salgado *et al.* revealed that H-LPS from different strains could be divided into two types: One of low biological activity and one of high biological activity of inducing the mitogenicity and TNF- α synthesis of cells. And the strains with the high activity were demonstrated belonging to the low virulence genotypes with *cagA*⁻ and s1bm2 or s2m2 for *vacA*^[18]. To our surprise, at the same injected dosage (100 $\mu\text{g}/\text{kg}\cdot\text{b.w.}$) in our study, H-LPS caused death in two of the three tested rabbits in blood pressure regulation test but E-LPS did not. In addition, the ability of H-LPS of inducing PBMC at 0.5 h after injection ($12.51\pm 0.54\times 10^9/\text{L}$) was also stronger than that of E-LPS [$(8.22\pm 0.68)\times 10^9/\text{L}$]. These data, including the results reported

by Salgado *et al.*, indicated that the role of the LPS as a virulence factor from some *H. pylori* strains should be re-evaluated.

It was reported that H-LPS acted as a modulator of host-dependent gastritis through inducing both gastric epithelial cells and macrophages to secrete IL-1, TNF and IL-8^[19-21]. In this study, a high frequency of H-LPS in the biopsy specimens from chronic gastritis patients (73.5%) was found. However, the positivity rate of H-LPS in the biopsy specimens from gastric ulcer patients (44.8%) was relatively lower ($\chi^2=10.77$, $P<0.01$). Furthermore, the biopsy specimens from chronic superficial gastritis (79.2%) and chronic active gastritis (90.0%) showed significantly higher H-LPS positive rates compared to those from chronic atrophic gastritis (30.0%) ($\chi^2=7.50-9.66$, $P<0.01$). These data indicated that H-LPS might play a more important role in inducing human gastric inflammation than previously considered. It is well known that PBMC are a mixture of neutrophilic granulocytes, mononuclear macrophages and lymphocytes^[22-24]. Mononuclear macrophages and lymphocytes are the major cells to produce IL-1, TNF and IL-8^[25-27]. The result from our study showed that H-LPS had a stronger ability of inducing PBMC than E-LPS, suggesting the critical effect of H-LPS on inducing inflammatory reaction in human gastritis.

REFERENCES

- Zhang Z**, Yuan Y, Gao H, Dong M, Wang L, Gong YH. Apoptosis, proliferation and p53 gene expression of *H. pylori* associated gastric epithelial lesions. *World J Gastroenterol* 2001; **7**: 779-782
- Michetti P**, Kreiss C, Kotloff KL, Porta N, Blano JL, Bachmann D, Herranz M, Saldinger PF, Cortes-Theulaz I, Losonsky G, Nichols R, Simon J, Stolte M, Acherman S, Monath TP, Blum AL. Orally immunization with urease and *Escherichia coli* heat-labile enterotoxin is safe and immunogenic in *Helicobacter pylori*-infected adults. *Gastroenterology* 1999; **116**: 804-812
- Suganuma M**, Kurusu M, Okabe S, Sueoka N, Yoshida M, Wakatsuki Y, Fujiki H. *Helicobacter pylori* membrane protein 1: a new carcinogenic factor of *Helicobacter pylori*. *Cancer Res* 2001; **61**: 6356-6359
- Nakamura S**, Matsumoto T, Suekane H, Takeshita M, Hizawa K, Kawasaki M, Yao T, Tsuneyoshi M, Iida M, Fujishima M. Predictive value of endoscopic ultrasonography for regression of gastric low grade and high grade MALT lymphomas after eradication of *Helicobacter pylori*. *Gut* 2001; **48**: 454-460
- Uemura N**, Okamoto S, Yamamoto S, Matsumura N, Yamaguchi S, Yamakido M, Taniyama K, Sasaki N, Schlemper RJ. *Helicobacter pylori* infection and the development of gastric cancer. *N Engl J Med* 2001; **345**: 8298-8332
- Morgner A**, Miehle S, Fischbach W, Schmitt W, Muller-Hermelink H, Greiner A, Thiede C, Schetelig J, Neubauer A, Stolte M, Ehninger G, Bayerdorffer E. Complete remission of primary high-grade B-cell gastric lymphoma after cure of *Helicobacter pylori* infection. *J Clin Oncol* 2001; **19**: 2041-2048
- Kate V**, Ananthakrishnan N, Badrinath S. Effect of *Helicobacter pylori* eradication on the ulcer recurrence rate after simple closure of perforated duodenal ulcer: retrospective and prospective randomized controlled studies. *Br J Surg* 2001; **88**: 1054-1058
- Muotiala A**, Helander IM, Pyhala L, Kosunen TU, Moran AP. Low biological activity of *Helicobacter pylori* lipopolysaccharide. *Infect Immun* 1992; **60**: 1714-1716
- Ogawa T**, Suda Y, Kashiwara W, Hayashi T, Shimoyama T, Kusumoto S, Tamura T. Immunobiological activities of chemically defined lipid A from *Helicobacter pylori* LPS in comparison with Porphyromonas gingivalis lipid A and *Escherichia coli*-type synthetic lipid A (compound 506). *Vaccine* 1997; **15**: 1598-1605
- Matsuyama N**, Kirikae T, Kirikae F, Hashimoto M, Amanot K, Hayashi S, Hirai Y, Kubota T, Nakano M. Non-standard biological activities of lipopolysaccharide from *Helicobacter pylori*. *J Med Microbiol* 2001; **50**: 865-869
- Suda Y**, Kim YM, Ogawa T, Yasui N, Hasegawa Y, Kashiwara W, Shimoyama T, Aoyama K, Nagata K, Tamura T, Kusumoto S. Chemical structure and biological activity of a lipid A compo-

- nent from *Helicobacter pylori* strain 206. *J Endotoxin Res* 2001; **7**: 95-104
- 12 **Ogawa T**, Asai Y, Sakai Y, Oikawa M, Fukase K, Suda Y, Kusumoto S, Tamura T. Endotoxic and immunobiological activities of a chemically synthesized lipid A of *Helicobacter pylori* strain 206-1. *FEMS Immunol Med Microbiol* 2003; **36**: 1-7
- 13 **Venter P**, Lues JF. Extraction methods for lipopolysaccharides from *Escherichia coli* ATCC 25922 for quantitative analysis by capillary electrophoresis. *Int J Food Microbiol* 2003; **84**: 245-250
- 14 **Zherebylo OIe**, Moroz SM, Hvozdiak RI. Characteristics of bacterial lipopolysaccharides depending on extraction method. *Ukr Biokhim Zh* 2000; **72**: 51-55
- 15 **Mattsby-Baltzer I**, Mielniczuk Z, Larsson L, Lindgren K, Goodwin S. Lipid A in *Helicobacter pylori*. *Infect Immun* 1992; **60**: 4383-4387
- 16 **Skurnik M**. Molecular genetics, biochemistry and biological role of *Yersinia* lipopolysaccharide. *Adv Exp Med Biol* 2003; **529**: 187-197
- 17 **Luchi M**, Morrison DC. Comparable endotoxic properties of lipopolysaccharides are manifest in diverse clinical isolates of gram-negative bacteria. *Infect Immun* 2000; **68**: 1899-1904
- 18 **Salgado F**, Garcia A, Onate A, Gonzalez C, Kawaguchi F. Increased *in-vitro* and *in-vivo* biological activity of lipopolysaccharide extracted from clinical low virulence *vacA* genotype *Helicobacter pylori* strains. *J Med Microbiol* 2002; **51**: 771-776
- 19 **Pece S**, Giuliani G, Di Leo A, Fumarola D, Antonaci S, Jirillo E. Role of lipopolysaccharide and related cytokines in *Helicobacter pylori* infection. *Recenti Prog Med* 1997; **88**: 237-241
- 20 **Sakagami T**, Vella J, Dixon MF, O' Rourke J, Radcliff F, Sutton P, Shimoyama T, Beagley K, Lee A. The endotoxin of *Helicobacter pylori* is a modulator of host-dependent gastritis. *Infect Immun* 1997; **65**: 3310-3316
- 21 **Slomiany BL**, Slomiany A. Suppression of gastric mucosal inflammatory responses to *Helicobacter pylori* lipopolysaccharide by peroxisome proliferator-activated receptor gamma activation. *IUBMB Life* 2002; **53**: 303-308
- 22 **Valente JF**, Alexander JW, Li BG, Noel JG, Custer DA, Ogle JD, Ogle CK. Effect of *in vivo* infusion of granulocyte colony-stimulating factor on immune function. *Shock* 2002; **17**: 23-29
- 23 **Tsitsilonis OE**, Tsavaris NB, Kosmas C, Gouveris P, Papalambros E. Immune changes in patients with colorectal cancer treated by adjuvant therapy with monoclonal antibody 17-1A: a pilot study. *J Chemother* 2003; **15**: 387-393
- 24 **Yamamoto T**, Kimura T, Ueta E, Tatemoto Y, Osaki T. Characteristic cytokine generation patterns in cancer cells and infiltrating lymphocytes in oral squamous cell carcinomas and the influence of chemoradiation combined with immunotherapy on these patterns. *Oncology* 2003; **64**: 407-415
- 25 **Zhao D**, Pothoulakis C. Rho GTPases as therapeutic targets for the treatment of inflammatory diseases. *Expert Opin Ther Targets* 2003; **7**: 583-592
- 26 **Meeuwssen S**, Persoon-Deen C, Bsibsi M, Ravid R, Noort JM. Cytokine, chemokine and growth factor gene profiling of cultured human astrocytes after exposure to proinflammatory stimuli. *Glia* 2003; **43**: 243-253
- 27 **Xing L**, Remick DG. Relative cytokine and cytokine inhibitor production by mononuclear cells and neutrophils. *Shock* 2003; **20**: 10-16

Edited by Zhu LH and Chen WW Proofread by Xu FM

Gene distribution of *cagII* in *Helicobacter pylori*-infected patients of Zhejiang Province

Hai-Yan Liu, Ping-Chu Fang, Yun-Shui Jiang, Ran Tao, Jin Chen

Hai-Yan Liu, Ping-Chu Fang, Yun-Shui Jiang, Ran Tao, Jin Chen, Department of Medical Microbiology and Parasitology, School of Medicine, Zhejiang University, Hangzhou 310031, Zhejiang Province, China

Supported by the Project of China Medical Board, No.96-628, and the Natural Science Foundation of Zhejiang Province, No.302023

Correspondence to: Ping-Chu Fang, Department of Medical Microbiology and Parasitology, School of Medicine, Zhejiang University, 353 Yanan Road, Hangzhou 310031, Zhejiang Province, China. fangpc@cmm.zju.edu.cn

Telephone: +86-571-87217403

Received: 2003-12-19 **Accepted:** 2004-01-15

Abstract

AIM: To determine the prevalence of genotypes of *cagII* in *Helicobacter pylori* (*H pylori*)-infected patients in Zhejiang Province and investigate the relationship between these genotypes and the types of gastroduodenal diseases.

METHODS: One hundred and seventy one clinical isolates were collected from 70 chronic superficial gastritis, 31 chronic atrophic gastritis, 41 gastric ulcer, 21 duodenal ulcer, 3 gastric and duodenal ulcer, and 5 gastric adenocarcinoma patients. Polymerase chain reaction assays were performed for analysis of *cagT*, *ORF13* and *ORF10* genes in the *cagII* region.

RESULTS: Of 171 *H pylori* isolates from Zhejiang patients, 159(93.0%) were positive for all the three loci. One isolate (0.6%) was negative for all the three loci, and 11(6.4%) were partially deleted in *cagII*. The positive rates of *cagT*, *ORF13* and *ORF10* genes were 97.1%, 94.7% and 99.4%, respectively. In the strains isolated from the patients with diseases including chronic superficial gastritis, chronic atrophic gastritis, gastric ulcer and duodenal ulcer, the positive rates of *cagT* were 95.7%, 100.0%, 95.1% and 100.0%, respectively. The positive rates of *ORF13* were 94.3%, 93.5%, 95.1% and 100.0%, respectively. The positive rates of *ORF10* were 98.6%, 100.0%, 100.0% and 100.0%, respectively. The three genes were all positive in the three *H pylori* strains isolated from the patients with both gastric and duodenal ulcer. In the five strains isolated from the patients with gastric adenocarcinoma, only one isolate was negative for *ORF13*. There were no significant differences of the *cagT*, *ORF13* and *ORF10* genes among the different gastroduodenal diseases including chronic superficial gastritis, chronic atrophic gastritis, gastric ulcer, duodenal ulcer, both gastric and duodenal ulcer and gastric adenocarcinoma ($\chi^2=3.098$, $P>0.05$ for *cagT*; $\chi^2=3.935$, $P>0.05$ for *ORF13* and $\chi^2=6.328$, $P>0.05$ for *ORF10*).

CONCLUSION: The *cagII* is not a uniform and conserved entity. Although the genes in *cagII* are highly associated with the gastroduodenal diseases, the clinical outcome of *H pylori* infection is not reliably predicted by the three genes in *cagII* in patients from Zhejiang Province.

Liu HY, Fang PC, Jiang YS, Tao R, Chen J. Gene distribution of *cagII* in *Helicobacter pylori*-infected patients of Zhejiang Province. *World J Gastroenterol* 2004; 10(14): 2060-2062
<http://www.wjgnet.com/1007-9327/10/2060.asp>

INTRODUCTION

Although more than 50% of the world population are infected with *Helicobacter pylori* (*H pylori*), most of the carriers are asymptomatic^[1,2]. Only a minority of infected persons may develop serious gastroduodenal diseases. Though the pathogenesis of *H pylori* infection is not well understood, there are several putative virulence factors that may contribute to mucosal damage by *H pylori* infection such as the cytotoxin associated gene (*cag*) pathogenicity island (*PAI*)^[3]. The *cag PAI* was reported to be a major virulence factor of *H pylori*^[4,5]. The *cagII* is located on the left of *cag PAI*. There is growing evidence that genetic differences among strains determine the clinical outcome of infection^[6,7]. Some of the genes in *cagII* are believed to encode proteins that have similarities to recognized virulence factors in other bacteria. However in mainland China the distribution of these genes in *cagII* of *H pylori* and their relationship with gastroduodenal diseases remain unclear. In this work, we attempted to determine the structure of *cagII* of *H pylori* isolated from Zhejiang Province and the relationship between the genes in *cagII* and the types of the gastroduodenal diseases. The genes of *cagT*, *ORF13* and *ORF10* that have representative spacing sequences along the *cagII* were selected and amplified by polymerase chain reaction (PCR) to evaluate the *cagII* distribution in 171 isolates from *H pylori*-infected patients with different gastroduodenal diseases in Zhejiang Province.

MATERIALS AND METHODS

H pylori isolates

A total of 171 *H pylori* isolates were obtained from *H pylori*-infected adults who had undergone upper gastrointestinal endoscopy at the Second Affiliated Hospital of Zhejiang University and the Hospital of Daishan County in Zhejiang Province. The patients consisted of 115 men and 56 women with a mean age of 42.9 years (ranging from 16 to 71 years). The patients were classified into 6 groups of chronic superficial gastritis ($n=70$), chronic atrophic gastritis ($n=31$), gastric ulcer ($n=41$), duodenal ulcer ($n=21$), both gastric and duodenal ulcer ($n=3$) and gastric adenocarcinoma ($n=5$). The classification of patients was based on the results of endoscopic and histological examinations.

Culture of *H pylori*

Biopsy specimens were cultured on ECY-selective agar plates at 37 °C for 5 d under 100% humidity and microaerophilic conditions (50 mL/L O₂, 100 mL/L CO₂, and 850 mL/L N₂). *H pylori* was identified by the following criteria: characteristic of colony, rapid urease test, catalase test and morphology on Gram staining.

Genomic DNA extraction

H pylori genomic DNA was extracted by phenol/chloroform method.

Detection of *cagT*, *ORF13* and *ORF10* with PCR

For the detection of *cagT*, *ORF13* and *ORF10* genes, PCR was performed in a volume of 25 μ L containing 2.5 μ L of 10 \times buffer, 2 μ L of 25 mmol/L MgCl₂, 2.5 μ L of 2 mmol/L dNTPs, 0.2 μ L of *Taq* DNA polymerase, 0.5 μ L of 20 μ mol/L primer sets (Table 1), 1 μ L of genomic DNA, 15.8 μ L of water. The primers for *cagT*, *ORF13* and *ORF10* were synthesized as described in Table 1. The PCR amplification of *cagT*, *ORF13* and *ORF10* genes was as follows: initial denaturation at 95 $^{\circ}$ C for 3 min; 30 cycles of at 94 $^{\circ}$ C for 30 s, at 56 $^{\circ}$ C for 30 s and at 72 $^{\circ}$ C for 45 s; and a final extension at 72 $^{\circ}$ C for 7 min. PCR was performed in a thermal cycle (GeneAmp PCR system 9 600; Perkin-Elmer, Norwalk, Conn, USA). After amplification, 5 μ L of PCR products was electrophoresed on 17 g/L agarose gel and examined under UV illumination.

Table 1 PCR primers for amplification of *cagT*, *ORF13* and *ORF10*

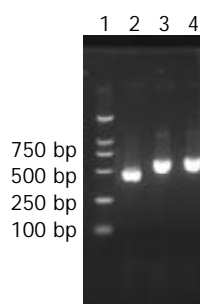
Gene	Strand	Primer sequence	Length (bp)
<i>cagT</i>	+	5' TCTAAAAAGATTACGCTCATAGGCG 3'	490
	-	5' CTTTGGCTTGCATGTTCAAGTTGCC 3'	
<i>ORF13</i>	+	5' CGTTCATGTTCCATACATCTTTGGC 3'	617
	-	5' GATTTATAGCGATCTAAGAAACCGC 3'	
<i>ORF10</i>	+	5' AATAGTGCTTCTTTAGGATTAGCG 3'	658
	-	5' CCGATTTAATCCTTTCGCTTATGTG 3'	

Statistical analysis

Statistical analysis was performed using the χ^2 test. Values of $P < 0.05$ were considered to be statistically significant.

RESULTS**Amplification of *cagT*, *ORF13* and *ORF10* genes**

After PCR amplification of the *cagT*, *ORF13* and *ORF10* genes, the products were electrophoresed on 1.7% agarose gels, and stained with ethidium bromide (Figure 1).

**Figure 1** Electrophoresis of *cagT*, *ORF13* and *ORF10* after PCR. Lane 1: 100 bp DNA ladder; Lane 2: *cagT* (490 bp); Lane 3: *ORF13* (617 bp); Lane 4: *ORF10* (658 bp).**Distribution of selected genes within *cagII* in *H pylori* isolates from patients with gastroduodenal diseases**

Of 171 *H pylori* isolates from Zhejiang Province, 159 (93.0%)

were positive for all the three loci. One isolate (0.6%) from a patient with chronic superficial gastritis was negative for all the three loci, and 11 (6.4%) were partially deleted in *cagII*. Among the latter 11 isolates, 6 were from chronic superficial gastritis, 2 from chronic atrophic gastritis, 3 from gastric ulcer and 1 from gastric adenocarcinoma. The positivity rates of *cagT*, *ORF13* and *ORF10* gene expression and their relationship with gastroduodenal diseases are listed in Table 2. There were no significant differences among the three selected genes in different gastroduodenal diseases ($\chi^2=3.098$, $P > 0.05$ for *cagT*; $\chi^2=3.935$, $P > 0.05$ for *ORF13* and $\chi^2=6.328$, $P > 0.05$ for *ORF10*).

DISCUSSION

H pylori is a Gram-negative, spiral-shaped, microaerophilic bacterium that infects human gastric mucosa and is recognized as a major cause of chronic active gastritis and most peptic ulcer diseases^[8,9]. It is also closely related with gastric adenocarcinoma, gastric mucosa-associated lymphoid tissue lymphoma and primary gastric non-Hodgkin's lymphoma^[10]. The *cag PAI* is an approximately 40-kb cluster of genes on the *H. pylori* chromosome^[3,11] and divided into two regions, *cagI* and *cagII*. There are 14 open reading frames in *cagII*. Some of the genes within *cagII* are believed to encode proteins, which have homologue of recognized virulence factors in other bacteria by amino acid database search and analysis. The protein encoded by *cagT* gene is similar to *Shigella flexnerii* 42-kDa surface antigen IPAC. It was reported that IPAC of *Shigella* was essential for initial bacterial entry into epithelial cells by interacting with beta-catenin and destabilizing the cadherin-mediated cell adhesion complex^[12], thus the epithelial cell-cell tight adhesion was disrupted. These events might facilitate the further basolateral invasion of bacteria through the disrupted space and/or modulate the cell-to-cell spread of *Shigella*. We propose that *cagT* may play a similar role in the pathogenesis of *H pylori*. Moreover the proteins encoded by *cagT*, *ORF13* and *ORF10* are similar to *virB7*, *virB10* and *virD4* of *Agrobacterium tumefaciens* that are needed for the transferring of the Ti plasmid DNA from the bacterium to the nucleus of the plant cell^[1, 13]. The products of the *virB7*, *virB10* and *virD4* genes are considered to be important components in type IV secretion system^[14]. Several lines of evidence suggest that the type IV secretion system encoded by the *cag PAI* of *H pylori* is recognized as a major virulence determinant, governing the translocation of the CagA protein to eukaryotic cells and inducing strongly the expression and secretion of IL-8 in gastric epithelial cells^[2,15,16]. Deletion of the *cagII* segment from strain 26695 reduced IL-8 synthesis to about 10-20% of the wild-type control. Inactivation of *ORF13* or *cagT* also caused similar reduction in IL-8 synthesis after infection. In addition, the products of *cagT*, *ORF13* and *ORF10* were absolutely essential for the translocation of CagA and tyrosine phosphorylation^[13,17,18]. IL-8, a potent neutrophil and T-cell chemoattractant and activator, is believed to play a key role in the pathogenesis of *H pylori*-induced tissue damage^[19,20]. These

Table 2 Relationship between *cagT*, *ORF13*, *ORF10* gene expression and clinical diagnosis in patients of Zhejiang Province

Group	n	<i>cagT</i> n	%	<i>ORF13</i> n	%	<i>ORF10</i> n	%
Chronic superficial gastritis	70	67	95.7	66	94.3	69	98.6
Chronic atrophic gastritis	31	31	100.0	29	93.5	31	100.0
Gastric ulcer	41	39	95.1	39	95.1	41	100.0
Duodenal ulcer	21	21	100.0	21	100.0	21	100.0
Both gastric and duodenal ulcer	3	3	-	3	-	3	-
Gastric adenocarcinoma	5	5	-	4	-	5	-
Total	171	166	97.1	162	94.7	170	99.4

results indicate that the genes in *cagII* participate in the translocation of CagA and induction of IL-8 synthesis and then a resultant severe inflammatory response. The presence of *cagII* is highly associated with the gastroduodenal diseases^[21].

In the present study, we have shown that the overall prevalence of the *cagT*, *ORF13* and *ORF10* is 97.1%, 94.7% and 99.4%, respectively. Although the genes in *cagII* are highly associated with the gastroduodenal diseases, the clinical outcome of *H pylori* infection is not reliably predicted by the genes of *cagT*, *ORF13* and *ORF10* in the *cag II* in Zhejiang Province. These results are in agreement with those of studies in Japanese and Taiwanese. The distribution of presence of *cagT*, *ORF13* and *ORF10* in Japan has been shown to be about 94%, 98.4% and 98.4%, respectively^[16]. In Taiwanese, all strains were positive for *cagT* and *ORF13* genes^[22]. However, in South Africa the overall positivity rate of *cagT* in clinical isolates was 81.7%, lower than our report. And the prevalence of *cagT* in patients with peptic ulceration and gastric adenocarcinoma was significantly higher than that in gastritis^[21]. In Europe the prevalence of *cagT*, *ORF13* and *ORF10* in clinical isolates was 79.5%, also lower than the one of our report^[23]. These results indicate that *H pylori* isolated from Asia is different from the ones isolated from South Africa and Europe. In the present study, of 171 *H pylori* isolates from Zhejiang patients, 159(93.0%) were positive for all the three loci. One isolate (0.6%) from a patient with chronic superficial gastritis was negative for all the three loci, and 11(6.4%) were partially deleted in *cagII*. It appears that the *cagII* is not a uniform, conserved entity.

In conclusion, we speculate that the distribution of *cagT*, *ORF13* and *ORF10* in Zhejiang Province is in accordance with those in other Asian countries. The clinical outcome of *H pylori* infection can not be reliably predicted by the genes of *cagT*, *ORF13* and *ORF10* in *cag II*. Many factors such as the genetic factors of both *H pylori* and the host cell and the circumstance may contribute to the clinical outcome of *H pylori* infection. Nevertheless, further work is required to illustrate pathogenesis of *cagII* in *H pylori* associated gastroduodenal diseases.

REFERENCES

- Covacci A, Telford JL, Del Giudice G, Parsonnet J, Rappuoli R. *Helicobacter pylori* virulence and genetic geography. *Science* 1999; **284**: 1328-1333
- Bhattacharyya A, Pathak S, Datta S, Chattopadhyay S, Basu J, Kundu M. Mitogen-activated protein kinases and nuclear factor-kappaB regulate *Helicobacter pylori*-mediated interleukin-8 release from macrophages. *Biochem J* 2002; **368**(Pt 1): 121-129
- Censini S, Lange C, Xiang Z, Crabtree JE, Ghiara P, Borodovsky M, Rappuoli R, Covacci A. *cag*, a pathogenicity island of *Helicobacter pylori*, encodes type I-specific and disease-associated virulence factors. *Proc Natl Acad Sci U S A* 1996; **93**: 14648-14653
- Ko JS, Seo JK. *cag* pathogenicity island of *Helicobacter pylori* in Korean children. *Helicobacter* 2002; **7**: 232-236
- Mizushima T, Sugiyama T, Kobayashi T, Komatsu Y, Ishizuka J, Kato M, Asaka M. Decreased adherence of *cagG*-deleted *Helicobacter pylori* to gastric epithelial cells in Japanese clinical isolates. *Helicobacter* 2002; **7**: 22-29
- Dubois A, Berg DE, Incecik ET, Fiala N, Heman-Ackah LM, Perez-Perez GI, Blaser MJ. Transient and persistent experimental infection of non-human primates with *Helicobacter pylori*: implications for human disease. *Infect Immun* 1996; **64**: 2885-2891
- Atherton JC, Peek RMJ, Tham KT, Cover TL, Blaser MJ. Clinical and pathological importance of heterogeneity in *vacA*, the vacuolating cytotoxin gene of *Helicobacter pylori*. *Gastroenterology* 1997; **112**: 92-99
- Zhang H, Fang DC, Wang RQ, Yang SM, Liu HF, Luo YH. Effect of *Helicobacter pylori* infection on expression of Bcl-2 family members in gastric adenocarcinoma. *World J Gastroenterol* 2004; **10**: 227-230
- Bai Y, Zhang YL, Wang JD, Lin HJ, Zhang ZS, Zhou DY. Conservative region of the genes encoding four adhesins of *Helicobacter pylori*: cloning, sequence analysis and biological information analysis. *Diyi Junyi Daxue Xuebao* 2002; **22**: 869-871
- Morgner A, Miehle S, Stolte M, Neubauer A, Alpen B, Thiede C, Klann H, Hierlmeier FX, Ell C, Ehninger G, Bayerdorffer E. Development of early gastric cancer 4 and 5 years after complete remission of *Helicobacter pylori* associated gastric low grade marginal zone B cell lymphoma of MALT type. *World J Gastroenterol* 2001; **7**: 248-253
- Tomb JF, White O, Kerlavage AR, Clayton RA, Sutton GG, Fleischmann RD, Ketchum KA, Klenk HP, Gill S, Dougherty BA, Reese K, Quackenbush J, Zhou L, Kirkness EF, Peterson S, Loftus B, Richardson D, Dodson R, Khalak HG, Glodek A, McKenney K, Fitzgerald LM, Lee N, Adams MD, Hickey EK, Berg DE, Gocayne JD, Utterback TR, Peterson JD, Kelley JM, Cotton MD, Weidman JM, Fujii C, Bowman C, Watthey L, Wallin E, Hayes WS, Borodovsky M, Karp PD, Smith HO, Fraser CM, Venter JC. The complete genome sequence of the gastric pathogen *Helicobacter pylori*. *Nature* 1997; **338**: 539-547
- Shaikh N, Terajima J, Watanabe H. IpaC of *Shigella* binds to the C-terminal domain of beta-catenin. *Microb Pathog* 2003; **35**: 107-117
- Akopyants NS, Clifton SW, Kersulyte D, Crabtree JE, Youree BE, Reece CA, Bukanov NO, Drazek ES, Roe BA, Berg DE. Analyses of the *cag* pathogenicity island of *Helicobacter pylori*. *Molecular Microbiology* 1998; **28**: 37-53
- Krall L, Wiedemann U, Unsin G, Weiss S, Domke N, Baron C. Detergent extraction identifies different VirB protein subassemblies of the type IV secretion machinery in the membranes of *Agrobacterium tumefaciens*. *Proc Natl Acad Sci U S A* 2002; **99**: 11405-11410
- Rohde M, Puls J, Buhrdorf R, Fischer W, Haas R. A novel sheathed surface organelle of the *Helicobacter pylori* *cag* type IV secretion system. *Mol Microbiol* 2003; **49**: 219-234
- Maeda S, Yoshida H, Ikenoue T, Ogura K, Kanai F, Kato N, Shiratori Y, Omata M. Structure of *cag* pathogenicity island in Japanese *Helicobacter pylori* isolates. *Gut* 1999; **44**: 336-341
- Fischer W, Puls J, Buhrdorf R, Gebert B, Odenbreit S, Haas R. Systematic mutagenesis of the *Helicobacter pylori* *cag* pathogenicity island: essential genes for CagA translocation in host cells and induction of interleukin-8. *Mol Microbiol* 2001; **42**: 1337-1348
- Selbach M, Moese S, Meyer TF, Backert S. Functional analysis of the *Helicobacter pylori* *cag* pathogenicity island reveals both VirD4-CagA-dependent and VirD4-CagA-independent mechanisms. *Infect Immun* 2002; **70**: 665-671
- Ogura K, Maeda S, Nakao M, Watanabe T, Tada M, Kyutoku T, Yoshida H, Shiratori Y, Omata M. Virulence factors of *Helicobacter pylori* responsible for gastric diseases in Mongolian gerbil. *J Exp Med* 2000; **192**: 1601-1609
- Yamaoka Y, Kita M, Kodama T, Sawai N, Tanahashi T, Kashima K, Imanishi J. Chemokines in the gastric mucosa in *Helicobacter pylori* infection. *Gut* 1998; **42**: 609-617
- Kidd M, Lastovica AJ, Atherton JC, Louw JA. Conservation of the *cag* pathogenicity island is associated with *vacA* alleles and gastroduodenal disease in South African *Helicobacter pylori* isolates. *Gut* 2001; **49**: 11-17
- Sheu SM, Sheu BS, Yang HB, Li C, Chu TC, Wu JJ. Presence of *iceA1* but not *cagA*, *cagC*, *cagE*, *cagF*, *cagN*, *cagT*, or *orf13* genes of *Helicobacter pylori* is associated with more severe gastric inflammation in Taiwanese. *J Formos Med Assoc* 2002; **101**: 18-23
- Jenks PJ, Megraud F, Labigne A. Clinical outcome after infection with *Helicobacter pylori* does not appear to be reliably predicted by the presence of any of the genes of the *cag* pathogenicity island. *Gut* 1998; **43**: 752-758

Effects of fucosylated milk of goat and mouse on *Helicobacter pylori* binding to Lewis b antigen

Hong-Tao Xu, Yao-Feng Zhao, Zheng-Xing Lian, Bao-Liang Fan, Zhi-Hui Zhao, Shu-Yang Yu, Yun-Ping Dai, Li-Li Wang, Hui-Ling Niu, Ning Li, Lennart Hammarström, Thomas Borén, Rolf Sjöström

Hong-Tao Xu, Zhi-Hui Zhao, Shu-Yang Yu, Yun-Ping Dai, Li-Li Wang, Hui-Ling Niu, Ning Li, State Key Laboratories for Agrobiotechnology, China Agriculture University, Beijing 100094, China

Yao-Feng Zhao, Lennart Hammarström, Center for Biotechnology, Karolinska Institute, Sweden

Zheng-Xing Lian, College of Animal Science and Technology, China Agriculture University, Beijing 100094, China

Bao-Liang Fan, Bio-tech Research Center of Shandong Academy of Agricultural Sciences, Jinan 250100, Shandong Province, China

Thomas Borén, Department of Odontology and Oral Microbiology, Umeå University, Sweden

Rolf Sjöström, Department of Odontology, Umeå University, Sweden

Correspondence to: Professor Ning Li, State Key Laboratories for Agrobiotechnology, China Agriculture University, Beijing 100094, China. ninglbau@public3.bta.net.cn

Telephone: +86-10-62893323 **Fax:** +86-10-62893904

Received: 2003-12-23 **Accepted:** 2004-01-08

Abstract

AIM: To evaluate the effects of animal milk containing fucosylated antigens on *Helicobacter pylori* (*H pylori*) binding to Lewis b antigen.

METHODS: A mammary gland expression vector containing human $\alpha 1$ -3/4-fucosyltransferase cDNA sequences was constructed. Transient expression of human $\alpha 1$ -3/4-fucosyltransferase cDNA in goat mammary cell and establishment of transgenic mice were performed. The adhesion inhibitory properties of milk samples were analyzed by using *H pylori*.

RESULTS: Goat milk samples were found to inhibit bacterial binding to Lewis b antigen. The highest inhibition was observed 42 h after injection of the plasmid. The binding activity of *H pylori* to Lewis b antigen reduced mostly, by 83%, however milk samples from transgenic mice did not inhibit *H pylori* binding to Lewis b antigen.

CONCLUSION: The use of "humanized" animal milk produced by the transgenic introduction of fucosylated antigen can perhaps provide an alternative therapy and preventive measure for *H pylori* infection.

Xu HT, Zhao YF, Lian ZX, Fan BL, Zhao ZH, Yu SY, Dai YP, Wang LL, Niu HL, Li N, Hammarström L, Borén T, Sjöström R. Effects of fucosylated milk of goat and mouse on *Helicobacter pylori* binding to Lewis b antigen. *World J Gastroenterol* 2004; 10(14): 2063-2066

<http://www.wjgnet.com/1007-9327/10/2063.asp>

INTRODUCTION

Helicobacter pylori (*H pylori*), a human specific gastric pathogen, was first isolated in 1983^[1]. Twenty years of research has found that *H pylori* infection is one of the major causes of upper gastrointestinal tract diseases, such as chronic active gastritis

and peptic ulcer disease^[2-6]. In chronic active gastritis, gastric ulcer and gastroduodenal ulcer, the incidences of *H pylori* infection are 71-94%, 72-100% and 73-100% respectively. In addition, *H pylori* infection has been linked with the development of gastric adenocarcinoma and mucosa-associated lymphoid tissue (MALT)^[7-13]. It has been defined as a Class I carcinogen by WHO^[14,15].

H pylori colonize human gastric mucosa by adhering both to the mucous epithelial cells and to the mucus layer^[16]. Specific receptor structures in combination with the unique tissue-specific distribution of receptors can restrict microbial colonization to a limited number of hosts, tissues and cell lineages^[17]. *H pylori* can bind tightly to epithelial cells using various bacterial surface components^[18-20]. The best characterized adhesin, BabA, is a 78-kD outer-membrane protein that binds to the fucosylated Lewis b (Le^b) blood group antigen^[21]. Accumulating evidence in animal models suggests that BabA is relevant to *H pylori*-associated diseases^[22]. Le^b antigen is one of the most important receptors, governing adhesion of *H pylori* to gastric mucosa. Boren *et al.* found that the fucosylated Lewis blood group antigens Le^b and H-1 were the carbohydrate structures that specifically mediated the adherence of *H pylori* to human gastric epithelial cells *in situ*.

Le^b antigen is a human blood group antigen. In human cells, the synthesis of Lewis antigens is regulated by a series of glycosyltransferases that act sequentially upon a precursor molecule. The fucosyltransferases are responsible for the final step in this process. Their function is to add a fucose residue to precursor molecules to form human blood antigens, such as Le^a, Le^b and H1 antigen (Figure 1). Addition of fucose to the terminal galactose residue of the lacto series core chain oligosaccharide results in the H1 antigen. Le^b antigen is formed by the addition of a "branched" fucose residue to H1-antigen, catalyzed by $\alpha 1$ -3/4-fucosyltransferase. The fucosylated blood group antigens, typically found on erythrocytes, are also expressed on the gastro-intestinal epithelium. Le^b is the dominant fucosylated blood group antigen expressed on the gastric surface mucous cells in the gastric epithelial lining. The fucosylated blood group antigens are also present in the mucins of the gastric mucus layer and, in addition, as natural "scavengers" or clearance factors in secretions such as saliva, tears, and human milk.

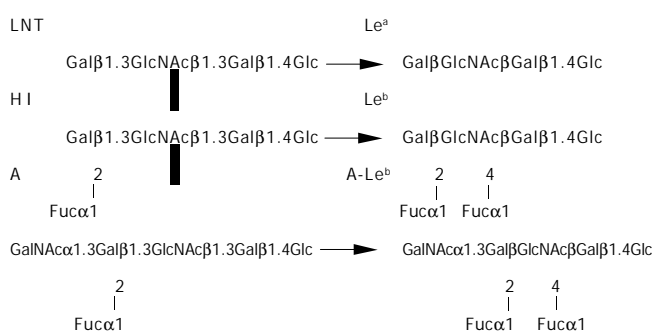


Figure 1 Formation of fucosylated blood group antigens.

H pylori infection is one of the most common infections in humans. Epidemiological data show that it affects about half of the human population. Without specific therapy, *H pylori* infection can persist for decades or even the host's lifetime. But only about 15% of *H pylori*-infected individuals actually have *H pylori*-associated diseases. It is likely to be associated with other additional factors such as genetic predisposition, age of infection, and the genotype of infective strain. The prevalence varies greatly among countries and among population groups within the same country. The overall prevalence of *H pylori* infection is strongly correlated with socioeconomic conditions. Eighty-five percent of *H pylori* can be eradicated by combination therapy in clinic, however, using antibiotics for several weeks may bring about other problems such as bacterial resistance. So many researchers are looking for other methods to prevent *H pylori* infection, such as preventing *H pylori* binding to or colonizing the gastric mucosa.

If we can add some *H pylori* specific receptor, for example, Le^b blood antigen or its analog to food, then *H pylori* binding to the human gastric mucosa may be prevented or reduced, and the bacteria will be excreted by the alimentary tract or destroyed by human antibody. Flak *et al.* reported that the α 1-3/4-fucosyltransferase was expressed in the gastric mucosa of mice and that *H pylori* could bind to the mice gastric mucosa. At present, there are no reports of α 1-3/4-fucosyltransferase being expressed in animal galactophore. Therefore, our aim was first to introduce human α 1-3/4-fucosyltransferase into animals and get them expressed in the animal mammary gland and thus produce Le^b antigen in milk. This kind of milk does not only have nutritional value, it is also a natural source of lectin, a molecule that can block *H pylori* binding to the human gastric mucosa, and therefore prevent *H pylori* infection and reduce the severity of the infectious process. In this way, people can prevent *H pylori* infection by drinking this kind of milk daily.

This paper describes the transient expression of human α 1-3/4-fucosyltransferase gene in goat mammary gland and the establishment of transgenic mouse model. A new test to prevent and cure *H pylori* infection and gastrointestinal diseases associated with *H pylori* infection is put forward in our study.

MATERIALS AND METHODS

Experimental animals

Kunming white mice were purchased from Beijing Laboratory Animal Research Center. Laoshan goats were provided by Beijing Sangao Corporation.

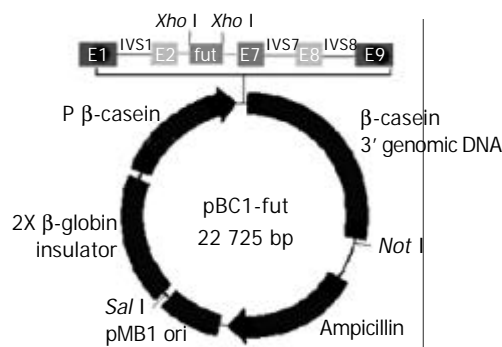


Figure 2 Map of expression vector: pBC1-fut.

Construction of expression vectors

A 1 115-bp α 1-3/4-fucosyltransferase cDNA encompassing the entire 1 086-nt coding region specifying the 361-AA transmembrane glycoprotein, containing an upstream Kozak consensus sequence and *Xho*I site, a downstream *Xho*I site,

was generated by PCR from a Fut/pCDM8 plasmid. The PCR product was then purified and digested by *Xho*I, and the digestion product was subcloned into pBC1 vector, which had been treated previously with *Xho*I, and transformed into *E. coli* DH5 α . pBC1 is a specific milk expression vector which contains the goat β -casein promoter and other proprietary DNA sequences. The positive transfected clone containing the properly oriented α 1-3/4-fucosyltransferase cDNA was screened by colony PCR. The expression vector, named pBC1-fut, allowed the α 1-3/4-fucosyltransferase cDNA to be placed in its downstream of the β -casein promoter (Figure 2).

Transient expression

pBC1-fut was purified using Qiagen Plasmid Maxi kit. About 1 mg pBC1-fut was injected into a lactating goat's right and left mammary glands from the goat glandular duct. Milk samples at different times were then collected over a 100-h (4 d) period from both right (R) and left (L) udders. Then, milk samples were analyzed in a dilution series (25-, 50-, 100- and 200-fold) for adhesion inhibition properties.

Transgenic mice production

The 16-kb DNA fragment inserted was isolated by agarose gel electrophoresis and recovered by electro-elution. To remove any contamination, products were spot dialyzed against 40 mL TE (10 mmol/L Tris, 0.1 mmol/L EDTA, pH7.4) for 30 min (VSWP02 500 membrane, Millipore). Purified DNAs were diluted to 2-3 ng/ μ L in TE buffer and microinjected into the pronuclei of fertilized eggs of Kunming white mice.

Genomic DNAs were isolated from the tails of transgenic mice using a standard method. A pair of primers was designed to screen for transgenic mice: upper primer: 5' - GATTGACAA GTAATACGCTGTTTCCTC-3' and downstream primer: 5' - CATCAGAAGTTAAACAGCACAGTTAG-3'. PCR reactions using genomic DNAs as template were performed under the following condition: 30 cycles of 94 °C for 1 min, 58 °C for 1 min, and 74 °C for 1 min. After PCR screening, transgenic mice were confirmed by Southern hybridization. The probe was created by ³²P labeling α 1-3/4-fucosyltransferase cDNA. Genomic DNA from transgenic mice and negative mouse as well as expression vector DNA were digested by *Bam*HI. Copies of the transgene were estimated by comparing the band density of the vector control with that in transgenic mice. Hybridizations were at 65 °C in Church (10 g/L BSA, 70 g/L SDS, 1 mmol/L EDTA, 0.5 mol/L sodium phosphate, pH 7.2). Final washes were in 2 \times SSC, 0.5 \times SDS at 65 °C. Signal from the membrane was detected using a Phosphor Screen (Molecular Dynamics, US).

Analysis of adhesion inhibitory properties of the milk

Goat milk was collected at different time points for 100 h from both right (R) and left (L) udders. The transgenic milk was collected at the 7 th day of lactation. The milk was centrifuged at 18 000 r/min for 1 h at 4 °C. The fat on the surface was removed and the clear part of the supernatant was put in a new tube and used as the sample. Le^b antigen was labeled with ¹²⁵I by the chloramine T method. Milk samples were analyzed in dilution series (25-, 50-, 100- and 200-fold). The samples were mixed with an *H pylori* strain (CCUG17875), which bound bind Le^b antigen efficiently, on a cradle for 17 h at room temperature. After this period, ¹²⁵I radioactivity in bacterial pellet was measured with a gamma counter.

Western blotting

After electrophoresis on 80 g/L SDS-PAGE, proteins were transferred to a nitrocellulose extra blotting membrane (Sartorius, Germany). Le^b monoclonal antibodies (Immucor, GA) and HRP-conjugated goat anti-rabbit-IgG (Cappel Laboratories, US) were used to detect Le^b antigen.

Table 1 Blocking effect on *H pylori* binding to Lewis b antigen by goat milk

Time	Bind/Free Le ^b (%)				Sample	Bind/Free Le ^b (%)			
	25×	50×	100×	200×		25×	50×	100×	200×
R 6 h	32.5	43.4	49.6	53.9	L 6 h	36.9	47.1	52.1	55.1
R 12h	28.2	41.7	49.4	53.0	L 12 h	34.7	45.3	51.3	53.4
R 18 h	25.5	40.5	49.4	53.1	L 18 h	29.4	42.3	49.2	53.2
R 23 h	16.8	32.3	43.9	50.6	L 23 h	22.1	37.3	46.5	51.7
R 30 h	15.0	31.0	43.1	49.4	L 30 h	25.6	37.1	46.3	51.9
R 36 h	11.9	28.7	41.2	48.3	L 36 h	20.0	35.4	45.1	50.8
R 42 h	11.2	27.0	40.1	48.0	L 42 h	17.2	33.3	43.6	49.7
R 54 h	16.6	32.3	43.4	49.5	L 54 h	20.3	35.1	44.9	50.4
R 60 h	20.2	35.9	45.1	50.5	L 60 h	25.9	38.7	47.6	51.7
R 66 h	24.6	38.3	45.8	51.0	L 66 h	22.6	36.2	44.9	50.6
R 78 h	35.2	45.6	51.6	54.2	L 78 h	31.9	43.1	50.2	53.3
R 84 h	37.8	46.2	51.7	56.0	L 84 h	36.3	45.9	51.1	54.0
R 90 h	37.1	46.5	51.9	54.8	L 90 h	38.5	46.3	51.3	54.8
R 102 h	42.6	49.4	54.1	57.1	L 102 h	38.8	46.3	51.3	55.0
Control 1	61.2	61.2	61.5	61.5	Control 2	61.0	60.8	61.1	61.2

R: Right udders; L: Left udders; Control 1: Milk from right udders of unimmunized goats; Control 2: Milk from left udders of unimmunized goats.

RESULTS

Transient expression

As shown in Table 1 and Figure 3, milk samples from experimental goats inhibited *H pylori* binding to Le^b antigen, and the time of the highest inhibition efficacy was at 42 h after DNA immunization. Furthermore, milk collected from both right (R) and left (L) udders had inhibitory effect on *H pylori* binding to Le^b. Unimmunized goat (the negative controls) did not inhibit bacterial binding. The binding activity of *H pylori* to Le^b antigen reduced mostly, 83 % in the 25-fold diluted milk samples.

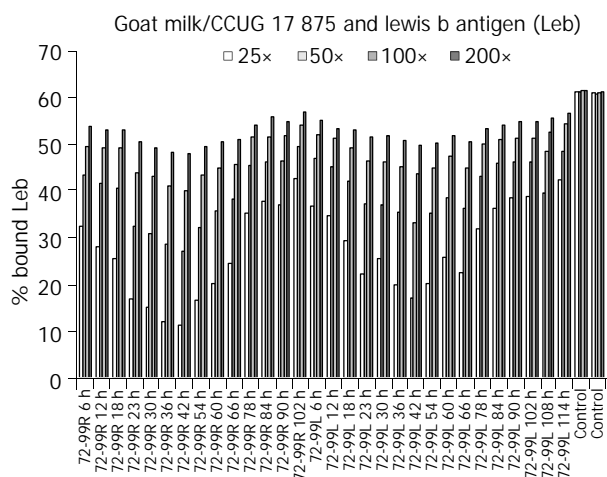


Figure 3 Blocking effect on *H pylori* binding to Lewis b antigen by goat milk. Abscissa: Goat milk collected at different time points and control milk. Ordinate: Rate of *H pylori* binding to Lewis b antigen.

Production of transgenic mice

Five of 84 mice including 2 males and 3 females were identified as being transgenic mice by PCR (Figure 4). The serial numbers of the positive mice were 15, 42, 47, 63 and 71. Efficiency of microinjection was about 6%, within the usual range of 5-20%. These transgenic mice were confirmed by using human α 1-3/4-fucosyltransferase cDNA as a probe in Southern blotting (Figure 5). Transgene copy numbers were also determined by Southern blotting. We analyzed three female's milk for the blocking effect on binding of *H pylori* to Le^b antigen, but no inhibitory activity was detected by our experimental system.

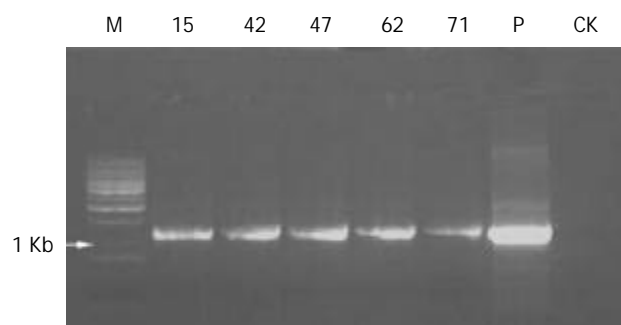


Figure 4 PCR results of transgenic mice. M: DNA ladder; P: pBC1-fut plasmid; CK: Non-transgenic mouse. 15, 42, 47, 62 and 71: Serial numbers of gene positive mice.

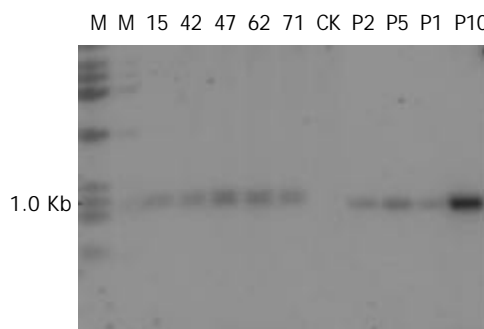


Figure 5 Southern blotting of transgenic mice. M: DNA ladder; CK: Non-transgenic mouse; P1, P2, P5 and P10: pBC1-fut plasmid equivalent to 1, 2, 5 and 10 gene copies, respectively. 15, 42, 47, 62 and 71: Serial numbers of gene positive mice.

Western blotting

We performed Western blotting and stained the membranes of the goat and transgenic mice milk protein with Le^b monoclonal antibody. The goat milk sample blot showed a beautiful, time-dependent induction of the blood group antigens secreted into milk (Figure 6). The band densities at different time points were consistent with the results of the transient expression described above. The band density was strongest at the 42 h after DNA immunization. But the transgenic mice milk did not give a positive signal, suggesting that this milk did not contain Le^b antigen or its analog.

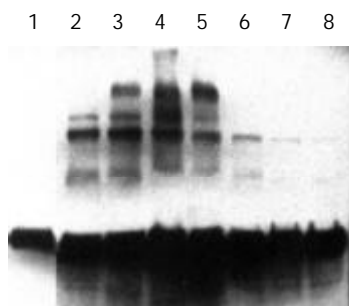


Figure 6 Western blotting of the transient expression milk of goat. Lanes 1-8: Milk collected at different time points of 6, 18, 30, 42, 60, 78, 90, 100 h postinjection, respectively.

DISCUSSION

In our experiment, goat milk could block *H pylori* binding to Le^b antigen, which is one of the most important receptors governing adhesion of *H pylori* to gastric mucosa. The activity of *H pylori* binding to Le^b antigen reduced as much as 83% in some samples. The result showed that some milk proteins might be fucosylated and structurally similar to human Le^b blood group antigen, so they were able to bind the bacteria. Goat milk fucosylated protein can bind *H pylori* *in vitro*. So “humanized” goat milk, in which human α 1-3/4-fucosyltransferase has been introduced into goat mammary gland, may be an alternative therapy and a prevention method for *H pylori* infection.

Unfortunately, the transgenic mice milk collected did not block *H pylori* binding to Le^b antigen. The reasons might be as follows: (1) Level of α 1-3/4-fucosyltransferase gene expression in mammary gland of mice was very low. Thus the quantity of Le^b antigen in the milk was so low that the milk could not effectively block *H pylori* binding to Le^b antigen. One way to increase the expression of α 1-3/4-fucosyltransferase would be to introduce the complete genomic sequence of the α 1-3/4-fucosyltransferase gene to mammary gland of mice. (2) There is no precursor of Le^b antigen in mice milk, so, even if α 1-3/4-fucosyltransferase was expressed in mouse galactophore, the transgenic glycosylation patterns that were generated by the activity of α 1-3/4-fucosyltransferase did not form epitopes that were recognized by the *H pylori* Le^b-binding adhesions. Therefore the milk could not block *H pylori* binding to Le^b antigen. Since other results have shown that α 1-3/4-fucosyltransferase expression in the gastric mucosa of mice can block the binding of *H pylori* to mouse gastric mucosa, it is possible that there might be differences between the carbohydrate core chains of the Le^b antigen in milk glands and gastric mucosa in mice.

Although the results for the transgenic mice were not positive, the successful introduction of α 1-3/4-fucosyltransferase cDNA into goat mammary cell and expression of Le^b antigen analog were an important finding. The “humanized” milk by the transgenic introduction of fucosylated antigens can be an alternative therapy and a prevention method for *H pylori* infection.

REFERENCES

- Warren JR, Marshall B. Unidentified curved bacilli on gastric epithelium in active chronic gastritis. *Lancet* 1983; **8336**: 1273-1275
- Parsonnet J, Hansen S, Rodriguez L, Gelb AB, Warnke RA, Jellum E, Orentreich N, Vogelman JH, Friedman GD. *Helicobacter pylori* infection and gastric lymphoma. *N Engl J Med* 1994; **330**: 1267-1271
- Hansson LE, Nyren O, Hsing AW, Bergstrom R, Josefsson S, Chow WH, Fraumeni JF Jr, Adami HO. The risk of stomach cancer in patients with gastric or duodenal ulcer disease. *New Engl J Med* 1996; **335**: 242-249
- Dooley CP, Cohen H, Fitzgibbons PL, Bauer M, Appleman MD, Perez-Perez GI, Blaser MJ. Prevalence of *Helicobacter pylori* infection and histologic gastritis in asymptomatic persons. *N Engl J Med* 1989; **321**: 1562-1566
- Eck M, Schmausser B, Haas R, Greiner A, Czub S, Muller-Hermelink HK. MALT-type lymphoma of the stomach is associated with *Helicobacter pylori* strains expressing the CagA protein. *Gastroenterology* 1997; **112**: 1482-1486
- Wang RT, Wang T, Chen K, Wang JY, Zhang JP, Lin SR, Zhu YM, Zhang WM, Cao YX, Zhu CW, Yu H, Cong YJ, Zheng S, Wu BQ. *H pylori* infection and gastric cancer: evidence from a retrospective cohort study and nested case-control study in China. *World J Gastroenterol* 2002; **8**: 1103-1107
- Eid R, Moss SF. *Helicobacter pylori* infection and the development of gastric cancer. *N Engl J Med* 2002; **346**: 65-67
- Parsonnet J, Isaacson PG. Bacterial infection and MALT lymphoma. *N Engl J Med* 2004; **350**: 213-215
- Forman D, Newell DG, Fullerton F, Yarnell JW, Stacey AR, Wald N, Sitas F. Association between infection with *Helicobacter pylori* and risk of gastric cancer: evidence from a prospective investigation. *BMJ* 1991; **302**: 1302-1305
- Fox JG. *Helicobacter* species and *in vivo* models of gastrointestinal cancer. *Aliment Pharmacol Ther* 1998; **12**(Suppl 1): 37-60
- Uemura N, Okamoto S, Yamamoto S, Matsumura N, Yamaguchi S, Yamakido M, Taniyama K, Sasaki N, Lehn P, R. *Helicobacter pylori* infection and the development of gastric cancer. *N Engl J Med* 2001; **345**: 784-789
- Wotherspoon AC. *Helicobacter pylori* infection and gastric lymphoma. *Br Med Bull* 1998; **54**: 79-85
- Wotherspoon AC. Gastric lymphoma of mucosa-associated lymphoid tissue and *Helicobacter pylori*. *Annu Rev Med* 1998; **49**: 289-299
- International Agency for Research on Cancer. Schistosomes, liver flukes and *Helicobacter pylori*. IARC Working Group on the Evaluation of Carcinogenic Risks to Humans. Lyon, 7-14 June 1994. *IARC Monogr Eval Carcinog Risks Hum* 1994; **61**: 1-241
- Bayardorffer E, Neubauer A, Rudolph B, Thiede C, Lehn N, Eidt S, Stolte M. Regression of primary gastric lymphoma of mucosa-associated lymphoid tissue type after cure of *Helicobacter pylori* infection. MALT Lymphoma Study Group. *Lancet* 1995; **345**: 1591-1594
- Karlsson KA. Animal glycosphingolipids as membrane attachment sites for bacteria. *Annu Rev Biochem* 1989; **58**: 309-350
- Boren T, Falk P, Roth KA, Larson G, Normark S. Attachment of *Helicobacter pylori* to human gastric epithelium mediated by blood group antigens. *Science* 1993; **262**: 1892-1895
- Mahdavi J, Sonden B, Hurtig M, Olfat FO, Forsberg L, Roche N, Angstrom J, Larsson T, Teneberg S, Karlsson KA, Altraja S, Wadstrom T, Kersulyte D, Berg DE, Dubois A, Petersson C, Magnusson KE, Norberg T, Lindh F, Lundskog BB, Arnqvist A, Hammarstrom L, Boren T. *Helicobacter pylori* SabA adhesin in persistent infection and chronic inflammation. *Science* 2002; **297**: 573-578
- Marshall B. *Helicobacter pylori*: 20 years on. *Clin Med* 2002; **2**: 147-152
- Odenbreit S, Faller G, Haas R. Role of the alpAB proteins and lipopolysaccharide in adhesion of *Helicobacter pylori* to human gastric tissue. *Int J Med Microbiol* 2002; **292**: 247-256
- Linden S, Nordman H, Hedenbro J, Hurtig M, Boren T, Carlstedt I. Strain- and blood group-dependent binding of *Helicobacter pylori* to human gastric MUC5AC glycoforms. *Gastroenterology* 2002; **123**: 1923-1930
- Guiruge JL, Falk PG, Lorenz RG, Dans M, Wirth HP, Blaser MJ, Berg DE, Gordon JI. Epithelial attachment alters the outcome of *Helicobacter pylori* infection. *Proc Natl Acad Sci U S A* 1998; **95**: 3925-3930

Microencapsulated hepatocytes and islets as *in vivo* bioartificial liver support system

Yue Gao, Jun Xu, Bei Sun, Hong-Chi Jiang

Yue Gao, Jun Xu, Bei Sun, Hong-Chi Jiang, Department of General Surgery, First Clinical Hospital, Harbin Medical University, Harbin 150001, Heilongjiang Province, China

Supported by the Natural Science Research Fund of Heilongjiang Province, D9746

Correspondence to: Dr. Yue Gao, Department of General Surgery, First Clinical Hospital of Harbin Medical University, 23 Youzheng Street, Nangang District, Harbin 150001, Heilongjiang Province, China. gaoyueee@163.com

Telephone: +86-451-88601563 **Fax:** +86-451-53600286

Received: 2004-01-15 **Accepted:** 2004-02-28

Abstract

AIM: To confirm the xenotransplantation of microencapsulated hepatocytes and islets as a temporary bioartificial liver support system for mice with acute liver failure (ALF).

METHODS: Mice were rendered ALF by a single intra-peritoneal injection of D-galactosamine (D-gal) and their tail blood was sampled to examine differences in blood ALT, albumin (ALB), total bilirubin (TB) and glucose (GLU) between 4 experimental groups. Rat hepatocytes and islets were collected and microencapsulated referring to both Sun's and Fritschy's methods. Mice were grouped into control group (CG), free hepatocyte group (FHG), microencapsulated hepatocyte group (MHG) and microencapsulated hepatocyte plus islet group (HIG). Tissue samples were subjected to microscopic and electron microscopic (EM) examinations.

RESULTS: The highest survival was observed in HIG, surprisingly at 100% (16/16), while the lowest was in CG at 12.5% (2/16), with inter-group statistical difference $P < 0.05$. ALT levels revealed no statistical difference between groups but the ALB level of HIG descended by the slightest margin $\{q = (0.54, 0.24, 1.33), P < 0.05\}$ at the time when it reached the lowest point in all groups. TB of HIG returned to normal reference range (NRR) statistically sooner than that of others after a fierce elevation. No statistical inter-group difference was observed in GLU levels. Fusion between hepatocytes and beta cells was demonstrated giving rise to theoretical assumptions.

CONCLUSION: Hepatocytes to be microencapsulated together with islets should be a preferred *in vivo* hepatic functional supporting system, which can dramatically prolong survival and improve living status.

Gao Y, Xu J, Sun B, Jiang HC. Microencapsulated hepatocytes and islets as *in vivo* bioartificial liver support system. *World J Gastroenterol* 2004; 10(14): 2067-2071

<http://www.wjgnet.com/1007-9327/10/2067.asp>

INTRODUCTION

Currently, temporary liver support is crucial to medical treatment for acute liver failure^[1,2]. In this point, hepatocyte transplantation as a kind of bioartificial liver holds a bright

prospect, but how to enhance graft functional status and neutralize immune rejection remains unsettled. Several authors have reported the "mutual benefit" between hepatocytes and pancreatic islets at co-transplantation^[3-5], whereas Lim and Sun's^[6] microencapsulating technique for immunoisolation opened a new era for cell transplantation. We suppose that hepatocytes and islets can be co-microencapsulated and transplanted to act as a bioartificial liver support system (BALSS), thus taking advantages of both the "mutual benefit" and the immunoisolation, simultaneously. If succeeded, this method would be a valuable alternative for *en bloc* organ transplantation and alleviate the donor shortage dilemma.

MATERIALS AND METHODS

Animals and ALF induction

Male Wistar rats weighing 150 g (as donor of hepatocytes) or 250 g (as donor of islets) and Kunming mice weighing 30-36 g served as donors and recipients, respectively. D-gal (Sigma) was dissolved in bacteriostatic normal saline and adjusted to pH 7.4 with 1 mol/L NaOH. The final concentration of the solution was 0.1 g/mL. Acute liver failure (ALF) mice was induced by a single intra-peritoneal injection of D-gal at a dose of 2 500 mg/kg without anesthesia, after which free access to aseptic water containing 100 g/L glucose was provided and models were fed on standard mouse chow.

Hepatocyte isolation

Donor hepatocytes were isolated by Seglen's *in situ* collagenase perfusion technique. Under pentobarbital anesthesia (35 mg/kg), the portal vein and the before-liver inferior vena cava (IVC) were cannulated and after liver IVC was ligated. The liver was perfused *in situ* first with 4 °C D-Hanks solution for 3 min and then with 37 °C Hanks solution containing 200 U/mL collagenase IV (Sigma) for 10 min at a flow rate of 20 mL/min until the effluent turned opaque. The perfusion route began at the portal vein and ended before liver IVC. The liver was removed, softly shattered and filtered through a hepatocyte dispersing instrument (containing a 105 µm stainless steel mesh) to produce a homogenous suspension. The hepatocytes were washed 3 times in 4 °C D-Hanks solution and centrifuged at 50 r/min for 2 min between washes, $(3.5-5.0) \times 10^8$ hepatocytes were obtained through this process. After the cell viability (82-93%) was determined by trypan blue exclusion test, the hepatocytes were cultured in 100 g/L fetal calf serum (FCS, Hyclone) enriched RPMI-1640 medium containing 10^{-7} mol/L insulin, 0.1 mg/mL streptomycin sulfate and 100 U/mL penicillin G at 37 °C in a humidified atmosphere (950 mL/L O₂ and 50 mL/L) awaiting transplantation.

Islet isolation

Donor islets of Langerhans were extracted by Sutton's method. The common bile duct (CBD) was cannulated and the rat was killed by a heart incision before the whole pancreas was distended uniformly with 4 mL 4 °C Hanks solution (buffered by 20 mmol/L HEPES at pH 7.8). The pancreas was removed, further distended by 16 mL 4 °C Hanks solution containing

2 mg/mL collagenase V (Sigma) and then put in an incubator at 38 °C for 8 min before the tissue was dispersed. The pelleted tissue was filtered through a steel mesh with 40 pores per inch and washed twice in 4 °C Hanks solution with centrifugation at 50 r/min for 1 min between washes. The last centrifugation was performed at 350 r/min for 2 min before the tissue was re-suspended in 25% Ficoll solution, on which 23%, 20% and 11% Ficoll densities were layered in sequence. The discontinuous density gradient containing the tissue pellets was spun at 800 r/min for 15 min at 4 °C. Islets from 20-23% interface were collected. 721 ± 153 islets could be isolated through this procedure with a purity higher than 87% and the ones with a diameter of 50-250 μm were handpicked and cultured in 100 g/L FCS enriched RPMI 1640 medium containing 0.1 mg/mL streptomycin sulfate and 100 U/mL penicillin G at 37 °C in a humidified atmosphere (950 g/L O_2 and 50 mL/L CO_2).

Microencapsulating procedure

Cells were microencapsulated according to Sun's and Fritschy's methods. The cells were centrifuged before re-suspension in 30 g/L alginate (ALG)-normal saline solution (pH 7.4) at a concentration of $1 \times 10^7/\text{mL}$ (according to hepatocytes). Then the mixture was put into the container of a bi-nozzle air-jet droplet generator and sprayed into 100 mmol/L calcium chloride solution (HEPES buffered, pH 7.4) under the disturbance of a co-axial oxygen flow at 4 L/min to form round droplets, which were then washed in 4 °C D-Hanks solution and reacted in sequence with 2 g/L poly-L-lysine (PLL) for 8 min, 2 g/L ALG for 4 min and 30 mmol/L sodium citrate for 8 min, all were kept at 4 °C and adjusted to pH 7.4. The microcapsules (MCs) with a diameter of 0.3-0.5 mm were cultured in aforementioned medium for 24 h. Every mouse received MCs equal to 3×10^6 hepatocytes and the ratio of hepatocytes to islets was $10^6/40$ at co-transplantation^[7]. Through a 12 G needle, the MCs were injected into the recipient's abdomen through a 3 mm incision under light ether anesthesia. All mice underwent the same procedure.

Experimental design

Sixty-four mice with ALF were randomly divided into 4 groups,

16 mice in each: CG, FHG, MHG and HIG. Each mouse in a certain group received only 1 mL sterilized normal saline in CG, 3×10^6 free hepatocytes transplantation in FHG, 3×10^6 microencapsulated hepatocytes in MHG, MCs containing 3×10^6 hepatocytes together with 120 islets in HIG.

Each group was randomly divided into 4 subgroups, 4 mice in each: ALT group, ALB group, TB group and GLU group so that every index was observed in 4 mice and documented by their average. Blood samples were collected from tail veins and indexes were recorded before and every 12 h after administration of D-gal (time "0") until the 4th d, then once on the 7th d and finally once on the 14th d. The body mass was measured daily.

Histological studies

All animals that died after D-gal injection were autopsied and those alive were sacrificed weekly until the 2nd mo. Then all the remaining ones were cervically dislocated to collect samples from livers, MC aggregates and floating MCs, which were fixed either in 100 g/L phosphate-buffered formaldehyde and stained with hematoxylin/eosin for histological examination or in 2.5% osmium tetroxide for transmission EM examination.

Statistical analysis

One-way ANOVA, *q* test and χ^2 test were used to establish inter-group difference and data were expressed as mean \pm SD.

RESULTS

Survival

Mice still alive after 72 h secured unlimited survival. Compared with CG, the survival rates of FHG, MHG and HIG were statistically higher ($P < 0.05$), while FHG held a survival rate significantly lower than MHG and HIG ($P < 0.05$), between which no statistical difference was observed ($P > 0.05$) (Figure 1A).

Biochemical findings

ALT in 4 groups similarly elevated to a peak of 1912 ± 344 U/L in 12 h, then dropped quickly to NRR (50.04 ± 7.72 U/L) in 48 h to 72 h. The sub-group of ALT in CG had only one mouse (1/4)

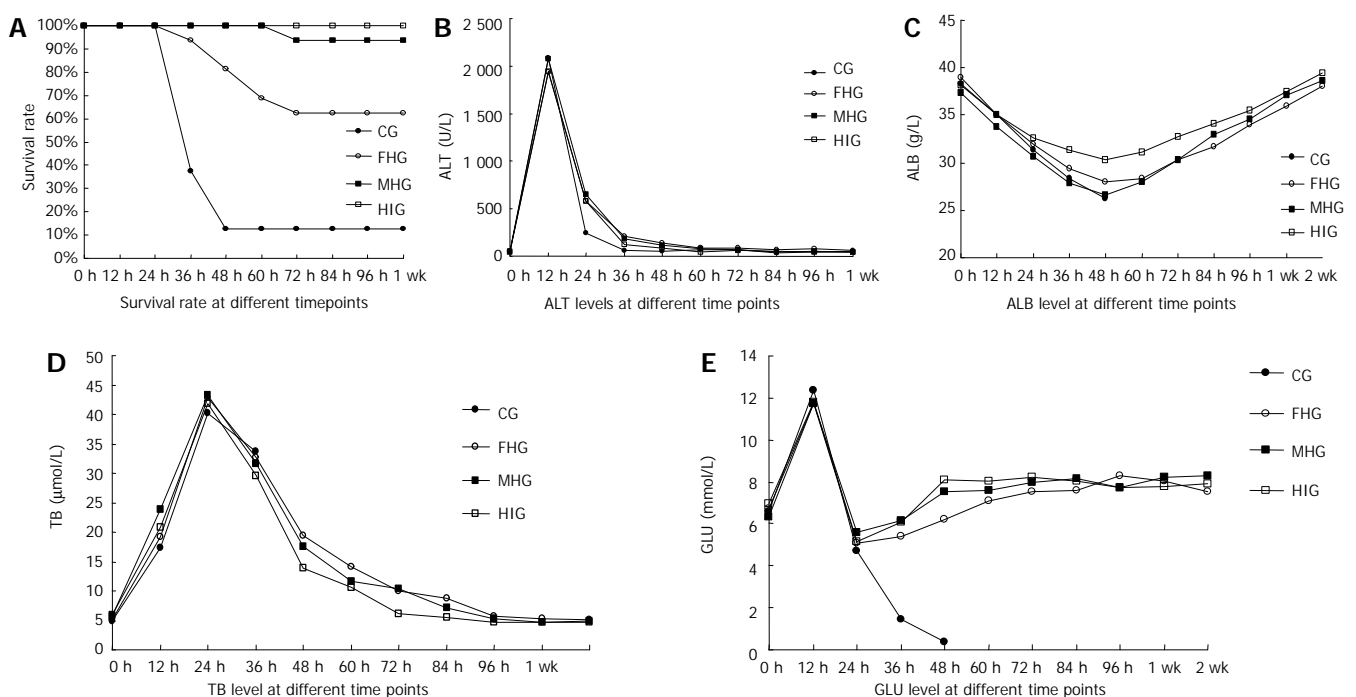


Figure 1 Survival rate, levels of ALT, ALB, TB and GLU at different time points. A: Survival rate; B: ALT level; C: ALB level; D: TB level; E: GLU level.

alive after 36 h. No relevant statistical difference was observed (Figure 1B).

Serum ALB gradually decreased after D-gal administration and reached the lowest point in 48 h, then stably returned to NRR of 38.19 ± 1.68 g/L in 96 h (Figure 1C). The maximum decrease in ALB of HIG was 7.85 ± 1.10 g/L, statistically smaller than that of other groups ($P < 0.05$). No statistical difference was found in ALB reduction between CG, FHG and MHG ($P > 0.05$).

TB in all groups ascended quickly after D-gal administration to the maximum of 36.64 ± 5.08 $\mu\text{mol/L}$ ($P > 0.05$) in 24 h, then began to descend. All the 4 mice in TB sub-group of CG died in 36 h bringing its curve to a stop, while TB of other groups continued to descend to NRR (5.42 ± 0.68 $\mu\text{mol/L}$) at different intervals. TB of HIG fell into NRR in 72 h, while FHG and MHG in 96 h (Figure 1D).

The non-fasting blood glucose of ALF mice temporarily elevated by 5.27 ± 1.56 mmol/L in 12 h after D-gal administration, then fell down to 5.14 ± 0.48 mmol/L at the 24th hour, when the mice underwent scheduled treatments. After 24 h, when the GLU of other groups began to increase, that of CG kept decreasing until all the four responsible mice died. The GLU of HIG ascended to NRR (8.31 ± 0.93 mmol/L) in 48 to 60 h, while that of FHG and MHG normalized after 72 h (Figure 1E). No statistical inter-group difference was observed at any time point ($P > 0.05$).

Liver destruction

Massive degenerative changes, ballooning and necrosis of the hepatic cells with vanishing nuclei were apparent under optical microscopy accompanied with closing sinusoids, widened Disse space and distorted hepatic lobules in tissue samples from mice died after administration of D-gal. Numerous bulbs, slightly distended mitochondria, shrinkage of nuclei and pigmentation of heterochromatin came under EM with cholangitis, exfoliation of microvilli and disappearance of tight junctions between adjacent hepatocytes dominating the view, as reported by Takenaka^[8] (Figure 2).

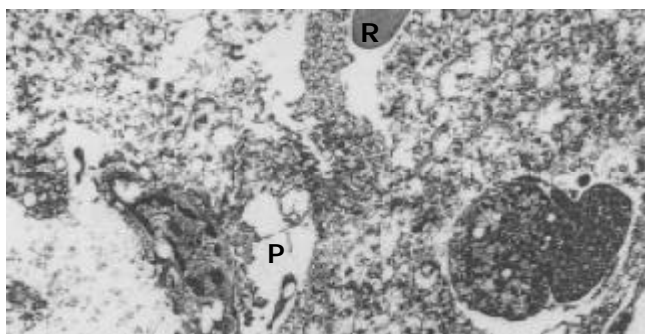


Figure 2 Transmigration of platelets (P) and red cells (R) into the Disse space.

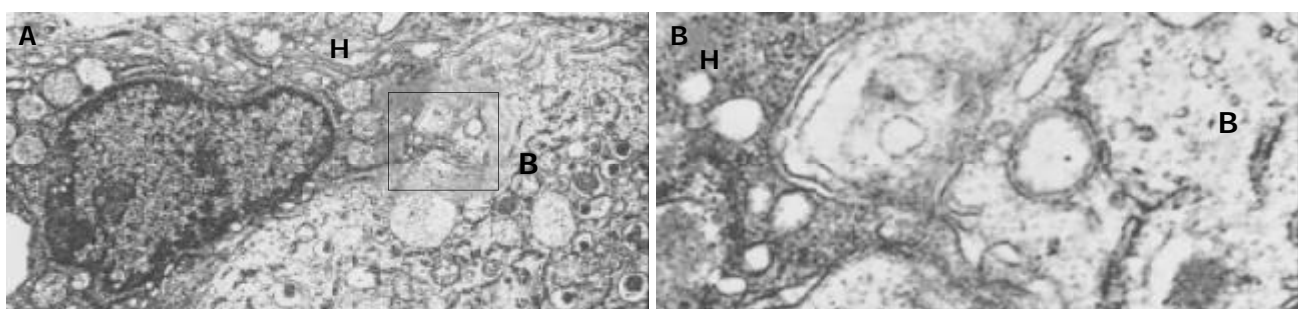


Figure 3 Association between hepatocytes (H) and a beta cells (B), and microvilli of hepatocytes (H) in beta cells (B). A: "Intimate association" between hepatocytes (H) and beta cells (B); B: Microvilli of hepatocytes (H) in beta cells (B).

Gross or microscopic microcapsules

Up to 90% of microcapsules remained free floating in 1 to 2 wk posttransplantation. Histological examination revealed smooth surface of most MCs, but mild fibroblasts were also observed on some MCs. Few hepatocytes were still alive inside the MCs from MHG, which were still free floating in the 4th week. Fewer free-floating MCs were observed in the HIG, blood vessels originated from the portal vein or the liver surface were easily seen with naked eyes polarizing huge aggregates of MCs attached to them. Till the 8th week, red aggregates of MCs were easily found in the vicinity of the portal vein in 67.5% (7/8) mice from HIG group. Though not abundant, aggregates attached to the diaphragmatic side of the liver, spleen or other organs were also seen. Smaller aggregates of MCs were seen on samples from MHG but without visible vascularization.

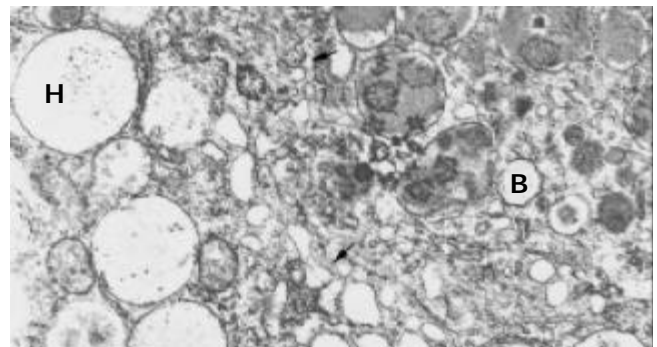


Figure 4 Connection of hepatocytes (H) and beta cells (B) by a network of plasmatic "bridges" formed by adjacent membranes of a string of vesicles (\rightarrow) lining up along their original border.

EM findings

Generally, the wall of the MCs was 6-8 μm thick and could be divided into 3 layers, but hepatocytes were always embedded in it de-homogenizing the thickness and disarranging the layers. Mostly, a very thin feather-like structure with a medium density formed the outer layer, inside was a section with a very high density and a thickness of approximately 0.5 μm , then a flocculent low density structure formed the inner layer. There was no clear boundary between the later two layers, instead, the density of the middle layer lowered until it changed into the inner one, to which the encapsulated hepatocytes attached with their microvilli. A small number of hepatocytes of MHG group survived inside the MCs until the 8th week but their microvilli shortened or disappeared and mitochondria distended. The MCs from HIG attached to the liver surface were totally covered by fibroblasts in the 8th week, but capillaries originated from the liver were seen encircling the MCs or entering them. Inside these MCs, living beta cells were found surrounded by transformed hepatocytes, whose many microvilli thrust deeply into the former and the membranes of

both cells morphologically vanished at some places where two plasmas mixed (Figures 3A, 3B). Some hepatocyte-like cells recognized by their big round mitochondria and glycogen had well formed insulin granules inside their plasma but with a smaller size (Figure 4). No desmosome mentioned by Ricordi was found. Several ball-shaped hepatocytes with long microvilli and normal organella were seen attached to the MC wall in distance of the aggregates of hepatocytes and beta cells.

DISCUSSION

Life sustaining is of the greatest importance to patients with ALF during life threatening period and patients with end stage chronic liver failure (CLF) awaiting proper donors, so liver function support in a limited period is crucial to the management of both ALF and CLF.

Based on this principle, many kinds of artificial liver were developed such as charcoal hemoperfusion or high porosity hemodialysis, but optimistically speaking, these methods could only partially substitute for the original liver because besides functioning living hepatocytes, any man-made device could provide but an incomplete liver function support^[9].

Artificial liver based on living hepatocytes has become a hot point of current researches aimed at substitution for liver function by hepatocytes. There are two kinds of BALSS currently in research: *ex vivo* bio-hemodialysis system and *in vivo* hepatocyte transplantation strategy. In recent years, great progress has been made in the *ex vivo* systems. Chen *et al.*^[10] demonstrated the successful application of BALSS to canine liver failure and Ding *et al.* reported their initial success on human patients. But, unfortunately, the viability of hepatocytes was hard to sustain extracorporeally and they gradually lost their original functions and de-differentiated in 1 to 2 wk *in vitro*^[11], so that frequent refreshing of the working hepatocytes is necessary to secure satisfactory efficiency, which adds extra-cost to the BALSS besides its already expensive electromechanical system. As for hepatocyte transplantation strategy, rejection aggressively reduced hepatocytic viability to almost zero in 1 wk^[12] after allo-transplantation. Great attention has been paid to the mechanism of hepatocytic rejection and a recent study showed that recombinant ribonuclease P remarkably reduced the expression of MHC-II molecules on transplanted hepatocytes, thus obviously alleviating rejection and prolonging hepatocytic survival. But before the entire truth of human genome is unveiled, no induction of gene or genetic products into human body would be ethically accepted and clinically approved. Genetic interference with transplantation may be preserved for far future. The microencapsulating technique initiated by Lim and Sun brought a bright new hope for artificial liver and hepatocyte transplantation. The microcapsules act as a selective barrier between the hepatocytes inside and the killing molecules such as antibodies outside, reserving the permeability of nutrients and small active cellular products such as albumin and insulin, so that cell transplantation under immunoisolation is realized. In addition, it has been proved that through some uncertain pathways islets could enhance the viability and function of isolated hepatocytes^[13,14]. We deem that microencapsulated hepatocytes and islets can be xenotransplanted to act as an *in vivo* BALSS, thus taking advantages of both the "mutual benefit" and the immunoisolation simultaneously. If succeeded, this method would be a valuable alternative for *en bloc* organ transplantation and alleviate the donor shortage dilemma.

In this work, we initially studied the feasibility of xenotransplantation of co-microencapsulated hepatocytes and islets between closely related species (Wistar rats to Kunming mice) and its therapeutic effects on D-gal induced ALF. Drug-induced ALF could better imitate clinical ALF, mostly toxic, than surgically induced ALF, since it presented with similar

pathological development^[15].

ALT is a sensitive index to hepatocytic destruction, which sharply ascended after administration of D-gal and peaked at the 12th hour but the amplitude greatly varied between individual mice. No significant influence upon ALT curve by cell transplant was observed in this study indicating that ALT could reflect the extent of cell destruction instead of the therapeutic effect of different interventions, as confirmed by Yu's studies^[16]. Anti-apoptotic agent etoposide was given prior to the administration of D-gal in Nakama's study^[17], which would possibly have changed the metabolism of D-gal in hepatocytes and the pathological process of hepatocytic destruction, preventing a considerable proportion of hepatocytes from apoptosis, so that a lowered ALT peak was documented. In fact, to give hepatocytic protective agents prior to the establishment of ALF model could only demonstrate the protecting effects of such agents instead of their therapeutic attributes, which has attracted much more attention from medical community since ALF patients would not take liver protective medications before they got trapped in ALF.

ALB is not a frequently used index to hepatic failure, but it changes with a steady pace giving concrete confirmation to the status of hepatic anabolism. In this study, ALB levels in HIG group decreased by a margin significantly smaller than those in other groups after administration of D-gal, indicating that under the influence of xenografted islets, at least the production of ALB of the remaining liver cells of the model mouse or the transplanted hepatocytes was improved. Wang *et al.*^[18] also confirmed the enhanced ALB synthesis in hepatocirrhotic rats after combined hepatocyte-islet transplantation.

TB level reflects the metabolic and detoxicating abilities of hepatocytes. It descended into NRR much earlier in HIG than in other groups, demonstrating a sooner recovery of hepatocellular metabolism in the existence of islets as stated by Wang *et al.*^[19].

Temporary increase of blood glucose after D-gal administration, was rarely reported because most researchers took rats as subjects and kept an interval between blood samplings as long as 24 h or more, missing this phenomenon. It might have resulted from the release of a great amount of glycogens at massive hepatocytic destruction, which was absent in studies adopting 90% partially hepatectomized models as in Demetriou's^[20]. Though curves in Figure 1E show a sooner extrication from hypoglycemia in HIG group than in MHG group, no statistical difference in GLU was noticed between experimental groups, which might have been the result of inadequate samples or large scale fluctuation of non-fasting blood glucose of ALF mice.

All mice in HIG group survived and the survival rate in MHG group was 93.75%, astonishingly higher than that in other reports, which used rat models. The first reason for such a high survival might be a larger amount of hepatocytes transplanted, say, 3×10^6 hepatocytes were nearly 3-5% of total hepatocytes per mouse liver and the second reason might be a much shorter hepatocytic regeneration cycle in mouse, which resulted in a quicker recovery of liver function and a shorter life threatening period. In this point of view, it may be conjectured that the shorter the hepatocytic regeneration cycle is, the better the therapeutic effect of bio-artificial liver can be expected, thus to shorten the regeneration cycle of liver cells by means of some genetic method may further enhance the survival rate after ALF.

A close functional relation between hepatocytes and islets has been proved both experimentally and clinically. An "intimate association" between hepatocytes and beta cells was discovered by Ricordi^[21] and then confirmed by others^[22]. In this study, an even closer relationship was proved morphologically inside the microcapsules 2 mo after hepatocyte-islet co-transplantation.

Under EM, the hepatocytes were easily recognized with their wheel-shaped mitochondria, smooth reticulum, rose-petal-

shaped glycogens and Golgi complexes while beta cells with their homogeneous eyeball-like insulin granules, which accommodated high-density crystalloids at the center with a wide vacuum space around. The hepatocytes abandoned their original hexagon or cubic shape and flattened to wrap on the beta cells thrusting numerous finger-like microvilli deeply into the latter. No matter how complicatedly the microvilli wound in three-dimensional space on a cross-section, we should see two layers of complete membrane separating these “fingers” from the plasma of the victim beta cells, but discontinuous membranes were noticed where direct exchange of cellular content was suspected. Much more interestingly, the boundary between some hepatocytes and beta cells was replaced by a complicated network of plasmatic “bridges” formed by adjacent membranes of a string of vesicles lining up along the original border. Meanwhile morphologically intact beta granules were found inside such hepatocytes in direct contact with their plasma, seemingly having been swallowed. Generally, this was a kind of “hybridization” between these two kinds of cells, as mentioned by Cossel^[23]. No desmosomes were found connecting these cells as mentioned by Ricordi. They might have functioned as anchors in the earlier stage (in 7 d as said by Ricordi) to immobilize cells giving rise to further interactions, then disappeared together with part of the membrane initiating hybridization in the later stage as found in our study. Direct plasmatic connection must be the best way for intercellular communication and exchange of substances, so contacting cells, which have close functional ties like hepatocytes and beta cells, would eventually establish such connections though neither the underlying mechanism nor its prognosis is clear. On the other hand, this phenomenon urges us to take good care of transplanted cells since it is still unknown whether such a “hybridization” produces pathogenic outcomes, say malignancies, or whether it undermines long-term effects of transplanted cells, though the outcome of such an association was fairly acceptable in our study. So that to separate transplanted cells by way of micro- or macro-encapsulation may be a good choice, which deprives them of direct contact with host cells and at the same time realizes functional support under immunoisolation.

In this study, we observed the hybridization between hepatocytes and beta cells inside microcapsules after co-transplantation. Better therapeutic effect of hepatocyte-islet co-transplantation than hepatocytes alone was also evidenced both histologically and biochemically. Though operative principles have not been fully established, co-transplantation of hepatocytes and islets by way of microencapsulation as a kind of BALSS holds a bright prospect.

ACKNOWLEDGEMENT

We are grateful to Wei Liu, Center of Scientific Research, 2nd Hospital of Harbin Medical University for sharing her expertise in cell bioengineering and to Wen-Jie Dai, National Center of Experimental Cell Transplantation for his administrative help during this project.

REFERENCES

- Fritschy WM**, Wolters GH, Van Schilfgaarde R. Effect of alginate-polylysine-alginate microencapsulation on *in vitro* insulin release from rat pancreatic islets. *Diabetes* 1991; **40**: 37-43
- Strain AJ**, Neuberger JM. A bioartificial liver—state of the art. *Science* 2002; **295**: 1005-1009
- Ricordi C**, Callery MP, Lacy PE, Flye MW. Pancreatic islets enhance hepatocellular survival in combined hepatocyte-islet-cell transplantation. *Transplant Proc* 1989; **21**(1 Pt 3): 2689-2690
- Genin B**, Anderegg E, Rubbia-Brandt L, Birraux J, Morel P, Le Coultre C. Improvement of the effect of hepatocyte isograft in the Gunn rat by cotransplantation of islets of Langerhans. *J Pediatr Surg* 1999; **34**: 321-324
- Kaufmann PM**, Sano K, Uyama S, Breuer CK, Organ GM, Schloo BL, Kluth D, Vacanti JP. Evaluation of methods of hepatotrophic stimulation in rat heterotopic hepatocyte transplantation using polymers. *J Pediatr Surg* 1999; **34**: 1118-1123
- Lim F**, Sun AM. Microencapsulated islets as bioartificial endocrine pancreas. *Science* 1980; **210**: 908-910
- Kaufmann PM**, Kneser U, Fiegel HC, Pollok JM, Kluth D, Izbicki JR, Herbst H, Rogiers X. Is there an optimal concentration of cotransplanted islets of langerhans for stimulation of hepatocytes in three dimensional matrices? *Transplantation* 1999; **68**: 272-279
- Takenaka K**, Sakaida I, Yasunaga M, Okita K. Ultrastructural study of development of hepatic necrosis induced by TNF- α and D-galactosamine. *Dig Dis Sci* 1998; **43**: 887-892
- Dixit V**, Darvasi R, Arthur M, Brezina M, Lewin K, Gitnick G. Restoration of liver function in Gunn rats without immunosuppression using transplanted microencapsulated hepatocytes. *Hepatology* 1990; **12**: 1342-1349
- Chen XP**, Xue YL, Li XJ, Zhang ZY, Li YL, Huang ZQ. Experimental research on TECA-I bioartificial liver support system to treat canines with acute liver failure. *World J Gastroenterol* 2001; **7**: 706-709
- Cai ZH**, Shi ZQ, Sherman M, Sun AM. Development and evaluation of a system of microencapsulation of primary rat hepatocytes. *Hepatology* 1989; **10**: 855-860
- Zhang YD**, Xu YM, Peng J. Viability and histological changes of encapsulated rat hepatocyte after transplantation. *Zhonghua Qiguan Yizhi Zazhi* 2001; **22**: 161-163
- Kaufmann PM**, Sano K, Uyama S, Schloo B, Vacanti JP. Heterotopic hepatocyte transplantation using three-dimensional polymers: evaluation of the stimulatory effects by portacaval shunt or islet cell cotransplantation. *Transplant Proc* 1994; **26**: 3343-3345
- Kaufmann PM**, Fiegel HC, Kneser U, Pollok JM, Kluth D, Rogiers X. Influence of pancreatic islets on growth and differentiation of hepatocytes in co-culture. *Tissue Eng* 1999; **5**: 583-596
- Papalois A**, Arkadopoulos N, Papalois B, Pataryas T, Papadimitriou J, Golematis B. Comparison of two experimental models for combined hepatocyte-islet transplantation. *Transplant Proc* 1994; **26**: 3473
- Yu CH**, Leng XS, Peng JR, Wei YH, Du RL. Morphology, structure and function of microencapsulated hepatocytes after intraperitoneal transplantation and its liver function support in acute hepatic failure rats. *Zhonghua Shiyian Waikē Zazhi* 1998; **15**: 441-443
- Nakama T**, Hirono S, Moriuchi A, Hasuike S, Nagata K, Hori T, Ido A, Hayashi K, Tsubouchi H. Etoposide prevents apoptosis in mouse liver with D-galactosamine/lipopolysaccharide-induced fulminant hepatic failure resulting in reduction of lethality. *Hepatology* 2001; **33**: 1441-1450
- Wang Y**, Xue J, Zhang Z, Zhou Y. The influence of intrahepatic transplantation of hepatocytes and insular cells on liver cirrhosis. *Zhonghua Waikē Zazhi* 1998; **36**: 179-181
- Wang XD**, Ar' Rajab A, Ahren B, Andersson R, Bengmark S. Improvement of the effects of intrasplenic transplantation of hepatocytes after 90% hepatectomy in the rat by cotransplantation with pancreatic islets. *Transplantation* 1991; **52**: 462-466
- Demetriou AA**, Reisner A, Sanchez J, Levenson SM, Moscioni AD, Chowdhury JR. Transplantation of microcarrier-attached hepatocytes into 90% partially hepatectomized rats. *Hepatology* 1988; **8**: 1006-1009
- Ricordi C**, Lacy PE, Callery MP, Park PW, Flye MW. Trophic factors from pancreatic islets in combined hepatocyte-islet allografts enhance hepatocellular survival. *Surgery* 1989; **105**(2 Pt 1): 218-223
- De Paepe ME**, Keymeulen B, Pipeleers D, Kloppel G. Proliferation and hypertrophy of liver cells surrounding islet grafts in diabetic recipient rats. *Hepatology* 1995; **21**: 1144-1153
- Cossel L**, Wohlrab F, Blech W, Hahn HJ. Morphological findings in the liver of diabetic rats after intraportal transplantation of neonatal isologous pancreatic islets. *Virchows Arch B Cell Pathol Incl Mol Pathol* 1990; **59**: 65-77

Contribution of C3d-P28 repeats to enhancement of immune responses against HBV-preS2/S induced by gene immunization

Li-Xin Wang, Wei Xu, Qing-Dong Guan, Yi-Wei Chu, Ying Wang, Si-Dong Xiong

Li-Xin Wang, Wei Xu, Qing-Dong Guan, Yi-Wei Chu, Ying Wang, Si-Dong Xiong, Department of Immunology, Shanghai Medical College of Fudan University, 138 Yi Xue Yuan Road, Shanghai 200032, China

Li-Xin Wang, Department of Microbiology and Immunology, School of Basic Medical Science of Southeast University, 87 Ding Jia Qiao Road, Nanjing 210009, Jiangsu Province, China

Supported by the Major State Basic Research Development Program of China, No. 2001CB510006; National Science Found for Distinguished Young Scholars from NSFC, No. 39925031 and Key Research Program of STCSM, No. 03DZ19229

Correspondence to: Dr. Si-Dong Xiong, Department of Immunology, Shanghai Medical College of Fudan University, 138 Yi Xue Yuan Road, Shanghai 200032, China. sdxiong@shmu.edu.cn

Telephone: +86-21-54237749 **Fax:** +86-21-54237749

Received: 2003-12-10 **Accepted:** 2004-02-01

Abstract

AIM: To investigate whether P28 derived from C3d can enhance the immune response to HBV-preS2/S induced by directly injection of naked plasmids containing variable repeats of P28 and HBV-preS2/S in fusion form.

METHODS: One to four copies of C3d-P28 coding gene, amplified by PCR and modified by restriction endonucleases digestion, were subcloned into a eukaryotic expression vector pVAON33 to construct pVAON33-P28, pVAON33-P28.2, pVAON33-P28.3 and pVAON33-P28.4 (pVAON33-P28.[1-4]). HBV-preS2/S coding sequence was then introduced into the pVAON33-P28.[1-4] and identified by both PCR and DNA sequencing. BALB/c mice were primed by intramuscular gene immunization with 100 µg different recombinant plasmids on day 0 and were boosted by subcutaneous inoculation with HBsAg protein (1 µg) 12 wk post-priming. The levels and avidity of specific IgG in sera collected at the indicated times from each group were determined by ELISA and NaSCN-displacement ELISA, respectively.

RESULTS: HBsAg specific antibody response was elicited in groups primed with plasmids pVAON33-S2/S-P28.[1-4] and pVAON33-S2/S. However, the response against HBsAg in the groups primed with pVAON33-S2/S-P28.[1-4] was significantly higher than that in pVAON33-S2/S group, the highest level of the specific antibody response was observed in the groups primed with pVAON33-S2/S-P28.4 ($P < 0.01$). After secondary immunization with specific antigen, the acceleration of antibody levels was significantly higher and faster in the mice primed with DNA expressing preS2/S-P28 fusions than that with DNA expressing preS2/S only ($P < 0.05$). Interestingly, mice primed with DNA expressing preS2/S-P28.4 fusions maintained the highest levels of anti-HBs antibodies in all animals. The avidity assay showed that the avidity index (AI) collected at 18 wk from mice primed with pVAON33-S2/S-P28.3 and pVAON33-S2/S-P28.4 were significantly higher than that from preS2/S-DNA vaccinated mice ($P < 0.01$).

CONCLUSION: Different repeats of C3d-P28 can enhance both humoral immune response and avidity maturation of specific antibodies induced by gene immunization, in which four copies of C3d-P28 may be necessary to achieve the most modest antibody response.

Wang LX, Xu W, Guan QD, Chu YW, Wang Y, Xiong SD. Contribution of C3d-P28 repeats to enhancement of immune responses against HBV-preS2/S induced by gene immunization. *World J Gastroenterol* 2004; 10(14): 2072-2077

<http://www.wjgnet.com/1007-9327/10/2072.asp>

INTRODUCTION

The third complement protein (C3) plays a major role in the complement activation pathway, the critical role of the cleavage fragments of C3 in the humoral immune response for both T-dependent and T-independent antigens was reported in studies performed over a quarter of a century ago^[1,2]. Complement's potential use as an adjuvant in vaccines was first suggested when Dempsey *et al.*^[2] demonstrated that mice, vaccinated with a genetically engineered construct containing three copies of mouse C3d fused to a model antigen, hen egg lysozyme, increased the efficiency of immunizations by more than 1 000-fold. Subsequent studies by Test *et al.*^[3] showed that covalent conjugates of C3d and the capsular polysaccharide of serotype 14 *streptococcus pneumoniae* (PPS14) elicited higher titers to PPS14 in mice than PPS14 only, and furthermore induced a class switch in anti-PPS14 from predominantly IgM to IgG1, which extended the adjuvant effects of C3d to T-independent antigen as well as T-dependent antigen. Recently, studies have further shown that gene immunization with C3d is an effective molecular adjuvant for inducing antibody responses to a range of viral pathogens, including influenza virus^[4,5], human immunodeficiency virus^[6], and measles virus^[7]. The mechanism, by which C3d increases antibody responses, has been hypothesized to reflect the binding of C3d to cluster of differentiation 21 (CD21) on the surface of B-cells or follicular dendritic cells (FDC)^[4,5,8,9].

The complement receptor 2 (CR2)-binding site on C3d was located, using chemical fragmentation and peptide mapping studies, between residues 1 199 and 1 210 of the complement C3 sequence (mature C3 numbering)^[10]. A synthetic peptide corresponding to the CR2-binding site on C3d, P28 (C3^{K1,187-A1,214,1187}KFLTTAKDKNRWEDPGKQLYNVEATSYA¹²¹⁴), as well as other C3d homologous, specifically binds to CR2 expressed on B cell lines, such as Raji cells^[10,11]. Binding of P28 stimulates the proliferation of peripheral resting B lymphocytes or CR2-positive B cell lines^[11-13]. In addition, the binding of CR2 to P28 peptides and the proliferative response of B cells by these peptides were dose dependent and could be inhibited by soluble C3d or anti-CR2 mAb^[12,14]. Furthermore, when a P16 peptide (equivalent to residues 1 195-1 210 of C3) was coupled to anti-idiotypic antibody, it induced a strong idiotype and antigen-specific response in mice^[15].

In present study, we selected this active C3d-P28 peptide as a molecular adjuvant according to its binding-ability to CR2

on the B-cells or FDC^[10-13,15], and HBV-preS2/S as a model antigen, to seek an enhanced anti-preS2/S antibody response following vaccination with DNA expressing fusions of HBV-preS2/S to variable copies of C3d-P28. Our results showed that immunizations with the preS2/S-P28 fusions DNA not only induced higher primary humoral responses as well as a faster and stronger memory reaction, but also accelerated the avidity maturation of anti-HBs compared with that resulting from immunization with preS2/S only. Our findings argue that four or more repeats of C3d-P28 may be necessary for efficient enhancement of antigen-specific immune responses.

MATERIALS AND METHODS

Plasmid

A eukaryotic expression vector pVAON33 was reconstructed from pVAX1, a kind gift from professor Zhongming Li (Food and Drug Administration, Bethesda, MD, USA). It contained the cytomegalovirus immediate-early (CMV-IE) promoter for initiating transcription of eukaryotic inserts and the bovine growth hormone polyadenylation signal [BGH poly(A)] for termination of transcription. It also contained pMB1 origin of replication for prokaryotic replication as well as the kanamycin resistance gene (*Kan^r*) for selection in antibiotic media. Moreover, a synthetic oligonucleotide (ON33) containing the Kozak's translation initiation sequence was inserted into pVAX1 for the convenience of cloning four tandem repeats of the C3d-P28 in-frame with the gene encoding HBV-preS2/S (Figure 1). Plasmid pTG825 (tPA-C3d₃) containing the encoding gene of C3d was a gift from Dr. Ted M. Ross (University of Pittsburgh, Pittsburgh, PA, USA). Plasmid pcDNA-preS2/S containing the encoding gene of HBV-preS2/S was constructed and conserved by our laboratory. pGEM-T vector was purchased from Huashun Biotechnology (Shanghai, China).

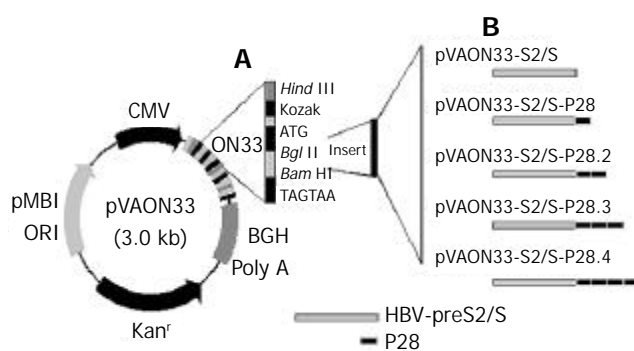


Figure 1 Schematic illustration representation of vector DNA vaccine constructs. A: A synthetic oligonucleotide (ON33) was inserted into the pVAX1 vector by the *Hind*III and *Bam*HI restriction endonuclease sites. Inserts were cloned into the vector using the *Bgl*II and *Bam*HI sites. B: The scheme represents constructs expressing fusions of HBV-preS2/S to variable copies of C3d-P28.

Cell lines

Human hepatocellular carcinoma cell lines SMMC-7721 was obtained from the Department of Biochemistry and Molecular Biology, Shanghai Medical College, Fudan University (Shanghai, China). SMMC-7721 cells were grown in RPMI 1640 medium (Gibco BRL) supplemented with 100 mL/L calf bovine serum (CBS), 100×10³ U/L penicillin and 100×10³ U/L streptomycin sulfate. *Escherichia coli* strain, DH5 α , was kept in our laboratory and maintained in LB medium.

Animals

Female BALB/c mice (H₂d, 6 to 8-week-old) were purchased

from the Center of Experimental Animal, Fudan University (Shanghai, China). They were randomly divided into 6 groups (6 mice per group) and fed with a standard laboratory diet under a specific pathogen-free (SPF) condition.

Main reagents

AMV reverse transcriptase, dNTP, Taq polymerase and PCR production-purified kits were purchased from Shanghai Biostar Co.. *Hind*III, *Bam*HI and *Bgl*II restriction endonuclease, T4 DNA ligase, DNA marker 2000 and RNase-free DNase I were purchased from MBI Co. (Ukraine). Horseradish peroxidase-labeled goat anti-mouse IgG were purchased from Southern Biotech (USA). Lipofectamine was purchased from the Invitrogen Co. (USA). The anion-exchange resin columns were purchased from Qiagen (Germany). The synthetic oligonucleotide (ON) and the PCR primers used were as follows: ON33, 5' -AGCTT GCCAC CATGA GATCT GGATC CTAGT AAG-3' (sense) and 5' -GATCT TACTA GGATC CAGAT CTCAT GGTGG CA-3' (antisense), which was used for reconstruction of the pVAX1 plasmid; C3d-P28, 5' -GAAGA TCTAA GTTTC TGAAC ACAGC-3' (sense) and 5' -CGGGA TCCGG CCTAG GATGT G-3' (antisense), which permitted the amplification of a 84-bp cDNA of C3d-P28; HBV-preS2/S, 5' -GGAAG ATCTC AGTGG AATTC CACAA C-3' (sense, bases 3 082 to 3 100) and 5' -GGAAG ATCTA ATGTA TACCC AAAGA CAA-3' (antisense, bases 706 to 688), which permitted the amplification of the entire coding region of HBV-preS2/s cDNA; T7 primers, 5' -CGATG AAGAT CTCT-3' (sense) and 5' -CGATG AAGAT CTCT-3' (antisense), which were used for identification of recombinant plasmids by PCR; GAPDH primers, 5' -CTGCA CCACC AACTG CTTAG-3' (sense) and 5' -CCACT GACAC GTTGG CAGTG-3' (antisense), which permitted the amplification of a 275-bp band corresponding to human GAPDH transcripts as described previously.

Construction of plasmid

The HBV-preS2/S gene was amplified by PCR from plasmid pcDNA-preS2/S. The gene encoding C3d-P28 amplified from plasmid pTG825 by PCR was cloned into the cloning vector-pGEM-T. Each gene was inserted into pVAON33 genetic immunization vector using standard molecular biological technology (Figure 1). Briefly, a 858 bp PCR-amplified preS2/S fragment was digested with *Bgl*II and ligated into the *Bgl*II restriction enzyme sites in the pVAON33. The vector expressing preS2/S-P28-fusion proteins was constructed by cloning four tandem repeats of the P28-encoding gene in-frame with preS2/S fragment and was designed based upon Dempsey *et al*^[2]. Potential proteolytic cleavage sites between the junctions of HBV-preS2/S and P28 and the junction of P28 were mutated by ligating *Bam*HI and *Bgl*II restriction endonuclease sites to replace an arginine codon with a glycine codon. All recombinant plasmids amplified in *Escherichia coli*, DH5 α , were verified by PCR, restricted endonucleases digestion and DNA sequencing, and then were purified using anion-exchange resin columns. Purity of DNA preparations was determined by optical density reading at 260 nm and 280 nm. All the plasmid DNA were stored at -20 °C in sterile saline at 1 mg/mL for experimental use.

Cell transfection and plasmid gene expression analysis

SMMC-7721 cells (5×10⁵ cells), a human hepatocellular carcinoma cell line, were transfected with 2 μ g of the different plasmids DNA mixed with 100 g/L lipofectamine according to the manufacturer's guidelines. Semiquantitative RT-PCR was used to analyze the transcription of HBV-preS2/S or preS2/S-P28 fusions and ensure the correct size of fusions containing variable copies of C3d-P28. Total RNA was extracted from the transfected cells (1×10⁶ cells) using

guanidinium isothiocyanate-based buffer system according to the manufacturer's instructions and then treated by RNase-free DNase I. First-strand cDNA was synthesized from 5 μ L of total cellular RNA with a GeneAmp PCR system 2400 cyclor (Perkin Elmer company, USA) using the following protocol: one cycle at 42 $^{\circ}$ C for 60 min and 70 for 10 min^[16]. The cDNA was subjected to 30 cycles of amplification using the appropriate primers: (1) sense and antisense of HBV-preS2/S, which permitted the amplification of the HBV-preS2/S cDNA; (2) HBV-preS2/S sense and C3d-P28 antisense, which permitted the amplification of the preS2/S-P28 fusions cDNA; (3) sense and antisense of GAPDH, which permitted the amplification of the GAPDH cDNA. After initiate denaturation at 94 $^{\circ}$ C for 5 min, the amplification conditions were as follows: denaturation at 94 $^{\circ}$ C for 1 min, primers annealing at 58 $^{\circ}$ C for 1 min, and extension at 72 $^{\circ}$ C for 2 min. Final PCR products were analyzed on 10 g/L agarose gel electrophoresis and the intensity of the preS2/S and GAPDH PCR products was assessed by densitometry and quantitated by using UV-2000 (Tanon Science and Technology Ltd., China); preS2/S mRNA expression was calculated as the ratio of the intensity of the preS2/S band to the GAPDH band. At the same time, direct PCR reaction was performed to exclude the contamination of potential plasmid DNA in the RNA extracted from the transfected cells.

Immunization

The quadriceps of mice were first injected with a total of 100 μ L of 2.5 g/L bupivacaine to enhance the cellular uptake of plasmid DNA one day before the first immunization. Then 100 μ g of each plasmid DNA dissolved in 100 μ L of normal saline was injected into the same region. Twelve weeks later, each mouse was boosted by subcutaneous injection with 1.0 μ g of purified HBsAg protein diluted in 100 μ L of sterile PBS. Sera were collected at 2-week intervals after primary immunization for antibody analysis.

Measurement of anti-HBs antibody levels

The anti-HBs antibody response elicited in mice was evaluated by ELISA. In brief, microtiter plates were coated with purified HBsAg protein (0.5 μ g/well). After incubation with 100 mL/L FBS in PBS for 60 min at 37 $^{\circ}$ C to prevent nonspecific binding, 1:10 dilution of mouse serum were added to the plates and incubated at 37 $^{\circ}$ C for an additional 60 min. After the samples were washed with PBS containing 0.5 g/L Tween-20, a horseradish peroxidase-labeled goat anti-mouse antibody was added at a dilution 1:5 000. After 60 min incubation, plates were washed, and substrate was added for color development. Absorbance (A_{490}) of each plate wells was read at 490 nm that indicated the levels of specific antibody.

Measurement of anti-HBs antibody avidity

Relative antibody avidity was determined by a modified elution ELISA that was similar to serum antibody determination ELISAs up to the addition of samples as previously described^[11,12]. Plates were washed 3 times with 0.5 g/L PBS-Tween 20. Sodium thiocyanate (NaSCN), a chaotropic compound that interferes with the antigen-antibody reaction, was added subsequently in concentrations ranging from 0.5 mol/L to 3.5 mol/L. Plates were allowed to left for 15 min at room temperature and then washed six times with PBS-Tween 20. Subsequent steps were performed similarly to the serum antibody determination ELISA. The avidity index (AI) corresponded to the effective concentration of NaSCN required to give a 50% reduction in absorbance at 490 nm.

Statistical analysis

Data were expressed as mean \pm SD. Experimental results were analyzed by variance analysis or *t* test with SPSS software. $P < 0.05$ were considered statistically significant.

RESULTS

Construction and identification of the recombinant plasmids

To test for an effect of C3d-P28 on the immune responses to a DNA vaccine, we selected plasmids encoding HBV envelope proteins as a model system. Then the genes encoding middle (preS2 plus S) HBV envelope proteins (858 bp) were cloned into a eukaryotic expression vector pVAON33. One to four tandem repeats of the C3d-P28 fragment were inserted into pVAON33 plasmid to construct the recombinant plasmids pVAON33-P28, pVAON33-P28.2, pVAON33-P28.3 and pVAON33-P28.4 (pVAON33-P28.[1-4]), respectively. HBV-preS2/S coding sequence was then introduced into the pVAON33-P28.[1-4], respectively. The results of identification by both PCR and DNA sequencing showed that the coding-codon of HBV-preS2/S coding gene, repeats of the P28-coding gene and their junctions were correct (data not shown).

Expression of plasmids

SMMC-7721 cells were transiently transfected with preS2/S and preS2/S-P28.4 protein expression vectors, with the plasmid pVAON33 serving as a negative control. At 2 d after transfection, the preS2/S mRNA could be detected in SMMC-7721 cells transfected with both plasmid pVAON33-S2/S and pVAON33-S2/S-P28.4, but not in mock plasmid (Figure 2). However, mRNA representing fusions of preS2/S to various copies of P28 could only be detected in SMMC-7721 cells transfected with pVAON33-S2/S-P28.4 plasmid. Digested with DNase I, RNA samples extracted from the cells transfected with both pVAON33-S2/S and pVAON33-S2/S-P28.4 were confirmed the exclusion of potential plasmid DNA contamination (Figure 2). These results suggested that various copies of P28 had fused with the HBV-preS2/S. Semiquantitative RT-PCR analysis showed that preS2/S expressed by pVAON33-S2/S-P28.4-DNA was 29.61% lower than that expressed by pVAON33-S2/S-DNA.

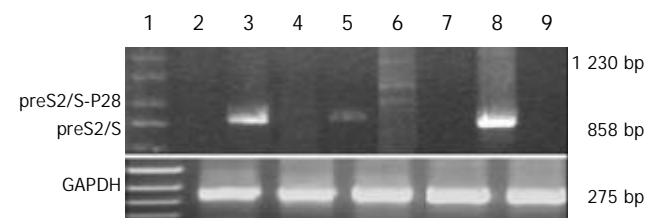


Figure 2 Semi-quantitative RT-PCR for expression of the preS2/S-P28 fusion proteins. Lane 1: DNA marker; Lanes 2,3 and 5: RT-PCR with preS2/Ss and preS2/Sa primers that amplified an entire coding region (858 bp) of preS2/S, using RNA extracted from pVAON33, pVAON33-S2/S and pVAON33-S2/S-P28.4 transfected-cells, respectively; Lanes 4 and 6: RT-PCR with preS2/Ss and P28a primers that amplified a 1 230 bp cDNA fragment of preS2/S-P28.4 fusion cDNA (the ladder showed the RT-PCR production due to 4 copies of P28), using RNA extracted from pVAON33-S2/S and pVAON33-S2/S-P28.4 transfected-cells, respectively; Lanes 7 and 9: RNA extracted from pVAON33-S2/S and pVAON33-S2/S-P28.4 transfected-cells was founded to exclude the potential contamination of potential plasmid DNA by PCR with preS2/Ss and preS2/Sa primers, respectively; and Lane 8: pVAON33-S2/S plasmid DNA was taken as positive control.

Anti-HBs IgG levels after primary immunization

The preS2/S-P28-expressing DNA plasmids showed higher levels of anti-HBs antibody than the preS2/S-expressing DNA (Figure 3). When sera were assayed on HBsAg-coated plates, there were various degrees of enhancement of anti-HBs IgG antibody levels in the mice with DNA expressing fusions of HBV-preS2/S to variable copies of P28 compared to the mice

primed with DNA expressing HBV-preS2/S only (Figure 3). Interestingly, at 12 wk after the primary immunization, the highest level of the specific antibody response (A_{490} , 1.049 ± 0.186) was observed in the groups primed with DNA expressing fusions of HBV-preS2/S to four copies of P28, which was not only significant higher than the level of antibody response from the group primed with preS2/S-expressing DNA (A_{490} , 0.621 ± 0.064 ; $P < 0.01$), but also obviously higher than the level of antibody response from the groups primed with preS2/S-P28.1-expressing DNA (A_{490} , 0.764 ± 0.143 ; $P < 0.01$), preS2/S-P28.2-expressing DNA (A_{490} , 0.915 ± 0.275 ; $P < 0.05$) and preS2/S-P28.3-expressing DNA (A_{490} , 0.696 ± 0.091 ; $P < 0.01$), respectively. It was suggested that P28, when fused with HBV-preS2/S, could enhance the specific antibody response against HBsAg following primary DNA immunization. Differences in the enhancement of the antibody levels raised by the fusions of preS2/S-P28 to variable repeats of P28 appeared to be determined by the different repeats of P28, in which four copies of P28 might be necessary to achieve the most modest antibody response.

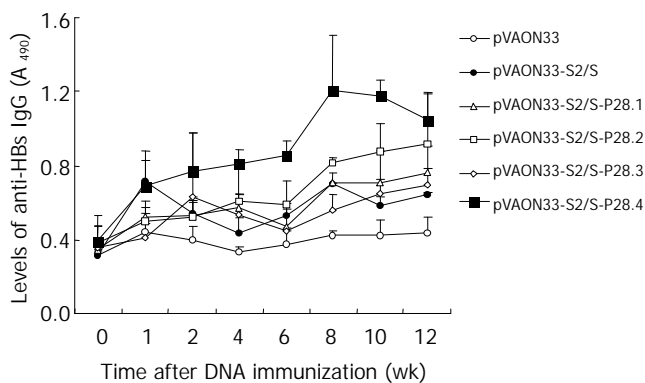


Figure 3 Determination of anti-HBs IgG of sera from mice primed by the plasmid vectors containing different copies of C3d-P28. BALB/c mice (6 animals per group) were primed im at week 0 with 100 μ g of mock DNA (O), pVAON33-S2/S plasmid (●), pVAON33-S2/S-P28 plasmid (Δ), pVAON33-S2/S-P28.2 plasmid (\square), pVAON33-S2/S-P28.3 plasmid (\diamond) and pVAON33-S2/S-P28.4 plasmid (\blacksquare), separately. Sera collected at the indicated weeks from each group were diluted 1:10 for determination of specific IgG levels by ELISA. Data were represented as the average for each group of mice. Error bars were represented as 95% CI of the geometric mean for each group of sera.

Anti-HBs IgG levels after secondary vaccination

To further observe the effects of P28 peptides on the memory responses against HBsAg, mice from each group were boosted subcutaneously with 1 μ g of HBsAg purified at the twelfth week after the primary immunization. The results showed that the mice of the groups vaccinated primarily with preS2/S-expressing DNA produced an increased levels of anti-HBs antibody compared to the mice immunized primarily with mock DNA after the second immunization with specific antigen (Figure 4). However, the acceleration of antibody levels was significantly higher and faster in the mice immunized with DNA expressing preS2/S-P28 fusions than that in the mice immunized with DNA expressing preS2/S only ($P < 0.05$). Interestingly, at the eighteenth week after the primary immunization, mice immunized primarily with DNA expressing preS2/S-P28.4 fusions maintained the highest levels of anti-HBs antibodies in all animals (A_{490} , 1.273 ± 0.106). It was suggested that the mice immunized with DNA expressing preS2/S-P28 fusions not only enhanced primary humoral responses against HBsAg, but also produced a quicker and stronger memory responses than that with DNA expressing

preS2/S only, in which four copies of P28 might also be necessary to obtain the most modest antibody memory reaction.

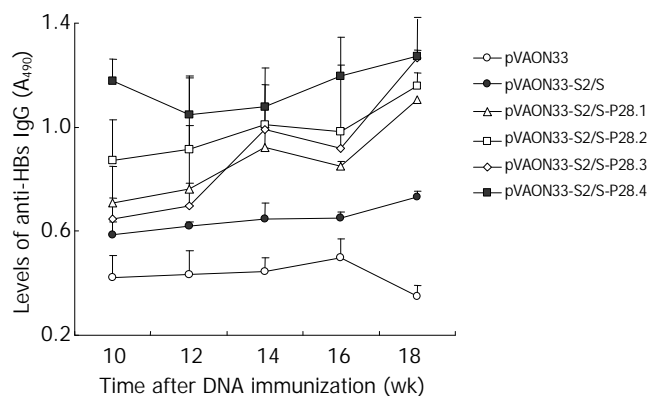


Figure 4 Determination of anti-HBs IgG of sera from mice primed by the different plasmid DNAs and boosted with HBsAg protein. Each group of mice ($n=6$) was primed im at week 0 with 100 μ g of mock DNA (O), pVAON33-S2/S plasmid (●), pVAON33-S2/S-P28 plasmid (Δ), pVAON33-S2/S-P28.2 plasmid (\square), pVAON33-S2/S-P28.3 plasmid (\diamond) and pVAON33-S2/S-P28.4 plasmid (\blacksquare), separately. And then boosted sc at week 12 with HBsAg (1 μ g per mouse). Sera collected at the indicated times from each group were diluted 1:10 for determination of specific IgG levels by ELISA.

Avidity of anti-HBs IgG

To observe whether P28 enhances the avidity maturation of the antibody response after immunization with P28-preS2/S fusions, NaSCN-displacement ELISA, a well-accepted approach, was used to evaluate the avidity of the anti-HBs antibodies^[11-13]. The results demonstrated that the AI collected at 18 weeks from mice immunized primarily with preS2/S-P28.3 and preS2/S-P28.4 expressing DNA, separately was significantly higher than that from preS2/S-DNA vaccinated mice (Figure 5, $P < 0.01$). However, no significant increases in the AI were found in either preS2/S-P28.1 expressing or preS2/S-P28.2 expressing DNA vaccinated mice compared to the mice immunized with DNA expressing preS2/S only. These results suggested that C3d-P28 could enhance the avidity maturation of antibodies against HBsAg following gene immunization with DNA expressing fusions of HBV-preS2/S to three or four repeats of C3d-P28.

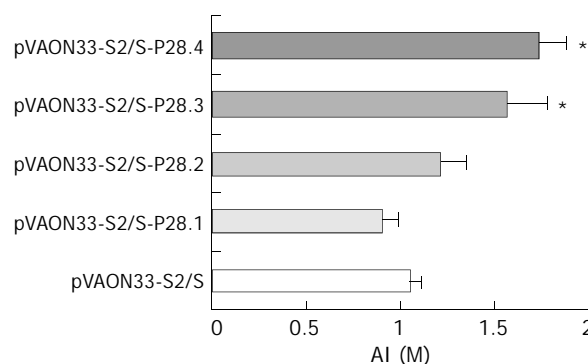


Figure 5 Determination of avidity of anti-HBs IgG of sera from immunized mice. Mice (six mouse per group) were primed im at week 0 with 100 μ g of different plasmid DNAs and then boosted sc at week 12 with HBsAg (1 μ g per mouse). Sera were obtained at week 18. The pooled serum samples from each mouse group were diluted 1:10 for determination of avidity of the anti-HBs IgG by an HBsAg-specific NaSCN-displacement ELISA. Data were represented as the average of three independent experiments plus standard errors (mean \pm SD).

DISCUSSION

Recently, several studies demonstrated that DNA vaccines encoding the small or middle viral envelope proteins of HBV elicited higher titer antibody, as well as cell-mediated immune responses compared with HBV subunit vaccines^[17-19]. Moreover, DNA immunization was able to break immune tolerance in the HBV transgenic mouse model^[20] and induces protective antibody responses in human non-responders to conventional vaccination^[17], indicating that DNA vaccines might be beneficial for immunotherapy for individuals with chronic HBV infections. DNA vaccines for HBV infection are efficacious, as well as inexpensive, and therefore, may be a promising tool in controlling the viral infections and liver diseases^[21].

However, one of the drawbacks that prevents the wide spread use of DNA vaccines is slower rise in humoral immunity compared with other vaccine strategies for HBV infection. This may be due to the low levels of antigen expression and presentation by inoculated DNA plasmids compared to the inoculation of HBsAg^[22]. In order to enhance the efficacy of antigens expression and presentation in the DNA immunization, several studies have shown that three copies of C3d, as a molecular adjuvant when fused to an antigen, could enhance the immune responses and accelerate the antibody avidity maturation^[2-7]. However, Suradhat *et al.*^[23] reported that fusions of one or two copies of C3d with either bovine rotavirus VP7 or bovine herpesvirus type 1 glycoprotein D inhibited the specific humoral response following DNA immunization, and suggested that using three or more copies of C3d molecule may be necessary for efficient enhance of antigen-specific immune responses following DNA immunization. These results indicated that different repeats of C3d in the fusions of target antigen to C3d might influence efficient enhancement of antigen specific immune response following DNA immunization^[2-7,23].

HBsAg is encoded by a single gene which is divided into S, preS2 and preS1 regions. preS vaccines have been most extensively applied in humans and shown to confer certain protective immunity. Recently more researches indicated that addition of the preS2 sequence could enhance the immunogenicity of the vaccines in human^[24,25]. Therefore in this study, we selected HBV-preS2/S as a model antigen and different repeats of P28 peptide, an active peptide corresponding to the CR2-binding site on C3d^[10-13], as a molecular adjuvant to explore enhancing effects on the immune response. As expected, mice vaccinated with DNA expressing fusions of preS2/S to P28 (one, two, three or four repeats) elicited a higher level of primary humoral response compared to mice vaccinated with DNA expressing only the preS2/S protein. Moreover, the mice immunized with DNA expressing preS2/S-P28 fusions produced a quicker and stronger memory responses than that with DNA expressing preS2/S only after second immunization. Interestingly, the results showed that the enhancing effect of various repeats of P28 in fusions of preS2/S to P28 on primary response as well as memory reaction was different, in which four copies of P28 might be necessary to achieve the most modest antibody response. It was indicated that the most modest antibody response appeared to be determined by the different repeats of P28. These results acquired here further explained the conflict between reports by Ross *et al.*^[4] and by Suradhat *et al.*^[23]. The increase in antibody response elicited by four copies of P28, similar to previous studies using antigen-C3d3 fusions^[3-7], was even more intriguing, since the preS2/S-expression at the mRNA level by preS2/S-P28.4-expressing plasmid was 29.61% lower than the expression by plasmid expressing HBV-preS2/S only. The most likely mechanism by which P28 increases antibody responses is similar to C3d, which has been hypothesized to reflect the binding of C3d to

CD21 on the surface of B-cells or follicular dendritic cells (FDC)^[3,4,8].

Surprisingly, immunization with the preS2/S-P28 fusions also resulted in enhanced avidity maturation of anti-HBs antibody. The results demonstrated that the AI of sera collected from mice immunized primarily with preS2/S-P28.3 and preS2/S-P28.4 expressing DNA, separately, was significantly higher than that from preS2/S-DNA vaccinated mice. Avidity is a term used to describe the strength of interaction between multivalent antigens and antibodies in serum and is dependent on the individual affinities of the polyclonal antibodies^[3]. Avidity maturation occurs in germinal centers where the somatic hypermutation of immunoglobulin results in a large repertoire of Ag-specific B cells that undergo inducing or selection for high-affinity B cell receptors by T helper cells or follicular dendritic cells (FDC)^[8,9,26-28]. The most likely mechanism by which P28 enhanced the avidity maturation of anti-HBs antibodies might relate to multiple interactions of cells responsible for humoral immunity, including B cells, T helper cells, and FDC. These interactions, coupled with the enhancing effects of CR2 ligation on germinal center formation^[29] and the enhancing effects of specific Th cells on somatic hypermutations of B cells^[30], could promote the selection of antigen-specific B cells with high-affinity B cell receptors, resulting in the avidity maturation of anti-HBs antibodies and the development and maintenance of memory B cells^[31].

Taken together, this is the first report to demonstrate that immunization with DNA expressing antigen-P28 fusions results in enhancing antibody response and enhancing antibody avidity maturation. These findings argue that four or more repeats of C3d-P28 may be necessary for efficient enhancement of antigen-specific immune responses, and thus C3d-P28, a short, active peptide derived from the CR2-binding site on complement C3d, may be another promising molecular adjuvant and may assist the future design of vaccines for health-threatening pathogens.

ACKNOWLEDGEMENTS

We sincerely thank Dr. T.M. Ross from University of Pittsburgh School of Medicine for helpful advice in this study and for providing the plasmid. We also thank Jin-Ping Zhang, Cong-Feng Xu, Huan-Bin Xu for their technical assistance.

REFERENCES

- 1 **Pepys MB.** Role of complement in induction of antibody production *in vivo*. Effect of cobra venom factor and other C3-reactive agents on thymus-dependent and thymus-independent antibody responses. *J Exp Med* 1974; **140**: 126-145
- 2 **Dempsey PW,** Allison MED, Akkaraju S, Goodnow CC, Fearon DT. C3d of complement as a molecular adjuvant: bridging innate and acquired immunity. *Science* 1996; **271**: 348-350
- 3 **Test ST,** Mitsuyoshi J, Connelly CC, Lucas AH. Increased immunogenicity and induction of class switching by conjugation of complement C3d to pneumococcal serotype 14 capsular polysaccharide. *Infect Immun* 2001; **69**: 3031-3040
- 4 **Ross TM,** Xu Y, Bright RA, Robinson HL. C3d enhancement of antibodies to Hemagglutinin accelerates protection against influenza virus challenge. *Nat Immunol* 2000; **1**: 127-131
- 5 **Mitchell JA,** Green TD, Bright RA, Ross TM. Induction of heterosubtypic immunity to influenza A virus using a DNA vaccine expressing hemagglutinin-C3d fusion proteins. *Vaccine* 2003; **21**: 902-914
- 6 **Ross TM,** Xu Y, Green TD, Montefiori DC, Robinson HL. Enhanced avidity maturation of antibody to human immunodeficiency virus envelope: DNA vaccination with gp120-C3d fusion proteins. *AIDS Res Hum Retroviruses* 2001; **17**: 829-835
- 7 **Green TD,** Newton BP, Rota PA, Xu Y, Robinson HL, Ross TM. C3d enhancement of neutralizing antibodies to measles

- hemagglutinin. *Vaccine* 2001; **20**: 242–248
- 8 **Tew JG**, Wu J, Qin D, Helm S, Burton GF, Szakal AK. Follicular dendritic cells and presentation of antigen and costimulatory signals to B cells. *Immunol Rev* 1997; **156**: 39–52
- 9 **Yellin MJ**, Sinning J, Covey LR, Sherman W, Lee JJ, Glickman-Nir E, Sippel KC, Rogers J, Cleary AM, Parker M, Chess L, Lederman S. T lymphocyte T cell-B cell-activating molecule/CD40-L molecules induce normal B cells or chronic lymphocytic leukemia B cells to express CD80 (B7/BB-1) and enhance their costimulatory activity. *J Immunol* 1994; **153**: 666–674
- 10 **Lambris JD**, Ganu VS, Hirani S, Müller-Eberhard HJ. Mapping of the C3d receptor (CR2)-binding site and a neoantigenic site in the C3d domain of the third component of complement. *Proc Natl Acad Sci U S A* 1985; **82**: 4235–4239
- 11 **Esparza I**, Becherer JD, Alsenz J, De la Hera A, Lao Z, Tsoukas CD, Lambris JD. Evidence for multiple sites of interaction in C3 for complement receptor type 2 (C3d/EBV receptor, CD21). *Eur J Immunol* 1991; **21**: 2829–2838
- 12 **Servis C**, Lambris JD. C3 synthetic peptides support growth of human CR2-positive lymphoblastoid B cells. *J Immunol* 1989; **142**: 2207–2212
- 13 **Frade R**, Hermann J, Barel M. A 16 amino acid synthetic peptide derived from human C3d triggers proliferation and specific tyrosine phosphorylation of transformed CR2-positive human lymphocytes and of normal resting lymphocytes-B. *Biochem Biophys Res Commun* 1992; **188**: 833–842
- 14 **Sarrias MR**, Franchini S, Canziani G, Argyropoulos E, Moore WT, Sahu A, Lambris JD. Kinetic analysis of the interactions of complement receptor 2 (CR2, CD21) with its ligands C3d, iC3b, and the EBV glycoprotein gp350/220. *J Immunol* 2001; **167**: 1490–1499
- 15 **Lou D**, Kohler H. Enhanced molecular mimicry of CEA using photoaffinity crosslinked C3d peptide. *Nat Biotechnol* 1998; **16**: 458–462
- 16 **Chow YH**, Chiang BL, Lee YL, Chi WK, Lin WC, Chen YT, Tao MH. Development of Th1 and Th2 populations and the nature of immune responses to hepatitis B virus DNA vaccines can be modulated by codelivery of various cytokine genes. *J Immunol* 1998; **160**: 1320–1329
- 17 **Rottinghaus ST**, Poland GA, Jacobson RM, Barr LJ, Roy MJ. Hepatitis B DNA vaccine induces protective antibody responses in human non-responders to conventional vaccination. *Vaccine* 2003; **31**: 4604–4608
- 18 **Kim SJ**, Suh D, Park SE, Park JS, Byun HM, Lee C, Lee SY, Kim I, Oh YK. Enhanced immunogenicity of DNA fusion vaccine encoding secreted hepatitis B surface antigen and chemokine RANTES. *Virology* 2003; **1**: 84–91
- 19 **Davis HL**, Mancini M, Michel ML, Whalen RG. DNA-mediated immunization to hepatitis B surface antigen: longevity of primary response and effect of boost. *Vaccine* 1996; **14**: 910–915
- 20 **Mancini M**, Hadchouel M, Davis HL, Whalen RG, Tiollais P, Michel ML. DNA-mediated immunization in a transgenic mouse model of the hepatitis B surface antigen chronic carrier state. *Proc Natl Acad Sci U S A* 1996; **93**: 12496–12501
- 21 **Hassett DE**, Whitton JL. DNA immunization. *Trends Microbiol* 1996; **4**: 307–312
- 22 **Robinson HL**, Pertmer TM. DNA vaccines for viral infections: basic studies and applications. *Adv Virus Res* 2000; **55**: 1–74
- 23 **Suradhat S**, Braun RP, Lewis PJ, Babiuk LA, Little-van den Hurk SD, Griebel PJ, Abca-Estrada ME. Fusion of C3d molecule with bovine rotavirus VP7 or bovine herpesvirus type 1 glycoprotein D inhibits immune responses following DNA immunization. *Vet Immunol Immunopathol* 2001; **83**: 79–92
- 24 **Davis HL**, Brazolot Millan CL. DNA-based immunization against hepatitis B virus. *Springer Semin Immunopathol* 1997; **19**: 195–209
- 25 **Jilg W**. Novel hepatitis B vaccines. *Vaccine* 1998; **16**: S65–S68
- 26 **Berek C**, Berger A, Apel M. Maturation of the immune response in germinal centers. *Cell* 1991; **67**: 1121–1129
- 27 **Jacob J**, Kelsoe G, Rajewsky K, Weiss U. Intracloonal generation of antibody mutants in germinal centres. *Nature* 1991; **354**: 389–392
- 28 **Fang Y**, Xu C, Fu YX, Holers VM, Molina H. Expression of complement receptors 1 and 2 on follicular dendritic cells is necessary for the generation of a strong antigen-specific IgG response. *J Immunol* 1998; **160**: 5273–5279
- 29 **Griffioen AW**, Rijkers GT, Janssens-Korpela P, Zegers BJM. Pneumococcal polysaccharides complexed with C3d bind to human B lymphocytes via complement receptor type 2. *Infect Immun* 1991; **59**: 1839–1845
- 30 **Razanajaona D**, van Kooten C, Lebecque S, Bridon JM, Ho S, Smith S, Callard R, Banchereau J, Briere F. Somatic mutations in human Ig variable genes correlate with a partially functional CD40-ligand in the X-linked hyper-IgM syndrome. *J Immunol* 1996; **157**: 1492–14928
- 31 **Fischer MB**, Goerg S, Shen L, Prodeus AP, Goodnow CC, Kelsoe G, Carroll MC. Dependence of germinal center B cells on expression of CD21/CD35 for survival. *Science* 1998; **280**: 582–585

Edited by Kumar M Proofread by Xu FM

Expression and *in vitro* cleavage activity of anti-caspase-7 hammerhead ribozymes

Wei Zhang, Qing Xie, Xia-Qiu Zhou, Shan Jiang, You-Xin Jin

Wei Zhang, Qing Xie, Xia-Qiu Zhou, Shan Jiang, Department of Infectious Disease, Ruijin Hospital, Shanghai Second Medical University, Shanghai 200025, China

You-Xin Jin, Shanghai Institute of Biochemistry, Chinese Academy of Sciences, Shanghai 200025, China

Supported by the National Natural Science Foundation of China, No. 30170850

Co-correspondents: Dr. You-Xin Jin

Correspondence to: Dr. Qing Xie, Department of Infectious Disease, Ruijin Hospital, Shanghai Second Medical University, Shanghai 200025, China. xieqing@sh163.net

Telephone: +86-21-64311242

Received: 2003-09-23 **Accepted:** 2004-01-12

Abstract

AIM: To prepare hammerhead ribozymes against mouse caspase-7 and identify their cleavage activity *in vitro*, in order to select a ribozyme with specific cleavage activity against mouse caspase-7 as a potential gene therapy for apoptosis-related diseases.

METHODS: Anti-caspase-7 ribozymes targeting sites 333 and 394 (named Rz333 and Rz394) were designed by computer software, and their DNA sequences encoding ribozymes were synthesized. Caspase-7 DNA sequence was acquired by RT-PCR. Ribozymes and caspase-7 DNA obtained by *in vitro* transcription were cloned into pBSKneo U6' and pGEM-T vectors, respectively. The cleavage activity of ribozymes against mouse caspase-7 was identified by cleavage experiments *in vitro*.

RESULTS: Rz333 and Rz394 were designed and their DNA sequences were synthesized respectively. The expression vector of caspase-7 and plasmids containing Rz333 and Rz394 were reconstructed successfully. Ribozymes and caspase-7 mRNA were expressed by *in vitro* transcription. *In vitro* cleavage experiment showed that 243-nt and 744-nt segments were produced after caspase-7 mRNA was mixed with Rz333 in equivalent, and the cleavage efficiency was 67.98%. No cleaved segment was observed when caspase-7 mRNA was mixed with Rz394.

CONCLUSION: Rz333 can site-specific cleave mouse caspase-7 mRNA, and it shows a potential for gene therapy of apoptosis-related diseases by down-regulating gene expression of caspase-7.

Zhang W, Xie Q, Zhou XQ, Jiang S, Jin YX. Expression and *in vitro* cleavage activity of anti-caspase-7 hammerhead ribozymes. *World J Gastroenterol* 2004; 10(14): 2078-2081 <http://www.wjgnet.com/1007-9327/10/2078.asp>

INTRODUCTION

Apoptosis, or programmed cell death, is characterized by a series of morphological features such as chromatin

condensation, nuclear fragmentation, and the appearance of membrane-enclosed apoptotic bodies, *etc.*^[1,2], most of which are caused by the activation of caspases, a family of aspartate-specific cysteine proteases^[3,4]. Caspases are constitutively present in cells as inactive zymogens and require proteolytic cleavage into the catalytic active heterodimer^[5]. All activated caspases are comprised of a large subunit with M_r 17 000-20 000 that contains a redox-sensitive cysteine at the active site and a small subunit with M_r 10 000 approximately. According to their function and sequence of activation, caspases can be grouped into three categories: Caspases that function primarily in cytokine maturation (such as caspases-1, -4, and -5); initiator caspases involved in the early steps of apoptotic signaling (caspases-8, -9, and -10) and effector proteases in the execution phase of apoptosis (caspases-3, -6, and -7). The initiator caspases lead to the activation of executioner caspases following characteristic apoptotic stimuli. The substrates of executioner caspases include many proteins, the cleavage of which causes the characteristic morphology of apoptosis^[6,7]. Because apoptosis is a regulated cellular process, it offers some opportunities for therapeutic intervention^[8,9]. Indeed, eliminating caspase activity, either through mutation or the use of small pharmacological inhibitors, will slow down or even prevent apoptosis.

Ribozymes are small RNA molecules that hybridize to the target RNA around the cleavage site, and catalyze site-specific cleavage of substrate. Cleaved mRNA is rapidly degraded, allowing ribozyme to react with new targets. Various ribozymes have been used to down-regulate gene expression in a sequence-specific manner. Among them the hammerhead ribozyme, composed of only 30 to 40 nucleotides, is the smallest and simplest one, and has been used extensively to down-regulate gene expression^[10-13].

Caspase-3 and caspase-7 are both important executioner caspases^[14]. Expression pattern of caspase-7 is distinguishable from that of caspase-3, suggesting that they may regulate apoptosis in disparate tissues, although they share strong homology. In the past years, many researches have been concentrated on interfering with the activity or expression of caspase-3 so as to intervene in apoptosis^[15-17]. Following its activation, caspase-7 was translocated into the microsomal and mitochondrial fractions, where it was responsible for the cleavage of specific substrates in those distinct subcellular compartments^[18]. Recent results suggested that as one of important executioner caspases, caspase-7 is also essential in apoptotic signaling^[19,20]. In this study, we designed and synthesized two hammerhead ribozymes against mouse caspase-7 at sites 333 and 394 (named Rz333 and Rz394), studied their *in vitro* transcription and cleavage activity, and selected the one that could site-specifically cleave caspase-7 mRNA as a hopeful gene therapy tool for apoptosis-related diseases.

MATERIALS AND METHODS

Materials

TRIzol reagent was product of Gibco. RT-PCR kit, T4 DNA ligase and restriction endonucleases were Takara products. *In vitro* transcription kit and pGEM-T vector were purchased from

Promega. pBSK neo-U6' was kindly donated by Dr. Youxin Jin. Plasmid extraction kit and gel purification kit were products of Shanghai Sangon Biotechnology Co.

Methods

Target mRNA secondary structure analysis and design of anti-caspase-7 ribozymes Caspase-7 gene sequence of BALB/c mouse searched in GenBank (gi: 6680849) was analyzed, and its secondary structure was simulated in computer. Ribozymes against caspase-7 mRNA were designed by software and DNA sequences encoding ribozymes were synthesized. A restriction site of *Xba*I was introduced into 5' end of sense strand. And a *Bam*H I restriction site was introduced into the 5' end of antisense strand. Two DNA strands were mixed at equal molar ratio after synthesis, and annealed by cooling to room temperature naturally after placed in boiling water for 2 min, then double strand DNA encoding ribozymes was obtained.

Ribozyme gene cloning Double-strand ribozyme DNAs designed by computer were inserted into pBSKneo U6' with T4 DNA ligase after pBSKneo U6' was cleaved by *Bam*H I and *Xba*I (Figure 1). The reconstructed plasmids containing ribozyme genes were identified by *Sal*I digestion and sequencing.

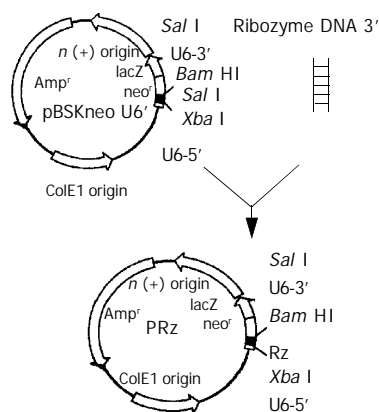


Figure 1 Ribozyme gene cloning.

Construction of caspase-7 expression vector Total RNA was extracted with TRIzol reagent from Balb/c mouse liver. Caspase-7 gene segment (841 bp) was amplified by RT-PCR with specific primers. The segment was cloned into pGEM-T vector downstream from T7 promoter, and the transformed clones selectively grew at 37 °C overnight in LB plate (Ampicillin resistance) containing IPTG and X-gal on plate's surface. Clones in blue were selected for sequencing. Caspase-7 primers were: P1 5' -GGATCCGAACGATGACCGATGATCAG-3', P2 5' -AAGCTTGTGAGCATGGACACCATAC-3'.

In vitro transcription of ribozyme and caspase-7 cDNAs Constructed caspase-7 plasmid was linearized with *Hind* III. Reconstructed ribozyme plasmid was considered as PCR template and a pair of primers containing T7 promoter was designed. P1 5' -TCTAGAGTAATACGACTCACTATAGG GCCTTCGGCAGCACATATAC-3', P2 5' -TATGGAACG CTTTCAGGAT-3' (The italic is T7 promoter sequence). Both caspase-7 linearized plasmid and pRz PCR product were phenol-chloroform extracted, and ethanol precipitated. *In vitro* transcription was performed using T7 RNA polymerase. Transcript of caspase-7 labeled with α -³²P-UTP was heated (2 min, 95 °C) before loading and electrophoresed on 6% polyacrylamide gel denatured by 8 mol/L urea. Transcript band was observed after autoradiography. *In vitro* transcription of ribozyme was not labeled with isotope. After electrophoresis on 60 g/L polyacrylamide gel, the transcript bands were observed

under ultraviolet. All transcript bands in gel, labeled with isotope or not, were cut and dipped into nucleic acid (0.5 mol/L NH₄Ac, 1 mmol/L EDTA, 1 g/L SDS), precipitated in ethanol and dissolved in DEPC-H₂O. Concentrations of substrate and ribozyme were calculated through cpm counting and A₂₆₀ measurement, respectively.

In vitro ribozyme cleavage assays Ribozymes and caspase-7 mRNA were incubated at equal molar ratio at 37 °C for 90 min in a system of 5–10 μ L containing 50 mmol/L Tris-HCl pH 7.5, 20 mmol/L MgCl₂, 20 mmol/L NaCl and 2 mmol/L EDTA. The products after cleavage were electrophoresed on 10% polyacrylamide gel, and the cleavage results were analyzed by autoradiography. Cleavage efficiency may be estimated according to cpm of both substrates (S) and cleaved products (P).

$$\text{Cleavage ratio} = [P/(S+P)] \times 100\%$$

RESULTS

Design of ribozymes

According to the results of computer simulation, triplet GUC at site 333 and GUA at site 394 of caspase-7 mRNA were chosen as the cleavage sites of ribozyme. So ribozymes targeting site 333 and site 394 (named Rz333 and Rz394) were designed to cleave the target mRNA. Both designed ribozymes were comprised of a catalytic core and two flanking sequences (Figure 2).

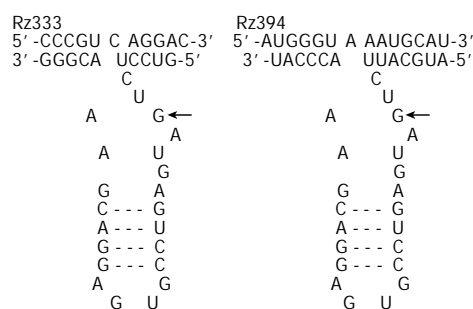


Figure 2 Sequences, structures and targets of ribozymes against caspase-7. Hammerhead ribozymes (bottom strand) binding to their targets (top strand) to form a typical three-stem structure that leads to the cleavage of caspase-7 RNA at the targets of GUC (Rz333) and GUA (Rz394).

Identification of reconstructed plasmid containing ribozyme

Reconstructed plasmids pU6Rz333 and pU6Rz394 were both incubated with *Sal*I at 37 °C for 2 h and then electrophoresed on 12 g/L agarose gel (Figure 3). Clones without 200 bp segment were sent for sequencing, and the results indicated that clones 2, 4 were correctly constructed.

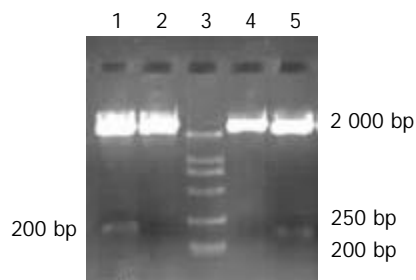


Figure 3 Restriction enzyme cleavage of reconstructed ribozyme plasmid. Lanes 1, 2: pU6Rz333 digested by *Sal*I; lanes 4, 5: pU6Rz394 digested by *Sal*I; lane 3: Marker (DL2000).

Caspase-7 DNA and its clone

Extracted total RNA was amplified by RT-PCR and a 891-bp caspase-7 DNA segment was seen on 20 g/L agarose gel (Figure 4).

It was cloned into pGEM-T vector, and white and blue monoclonal colonies were seen in LB medium after incubated at 37 °C overnight. Blue clones were selected and sent for sequencing.

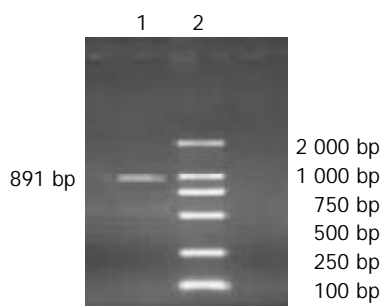


Figure 4 Agarose gel electrophoresis of RT-PCR products. Lane 1: A 891-bp caspase-7 gene segment; lane 2: Marker (DL2000).

In vitro transcription of target mRNA and ribozymes

Transcript of target mRNA was electrophoresed on 60 g/L polyacrylamide gel. After autoradiography, a black band of 987 nt was observed, including 891-nt caspase-7 mRNA and 96-nt U6 segment (Figure 5). *In vitro* transcripts of the two ribozymes were not labeled with isotope. The results of transcription were analyzed under ultraviolet. Black bands of 47 nt (Rz333) and 50 nt (Rz394) could be seen.

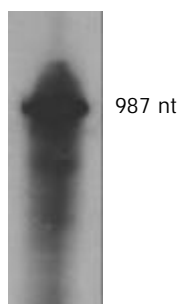


Figure 5 *In vitro* transcription of target RNA. The transcript is 987 nt.

In vitro cleavage of ribozymes

Products of cleavage assays were electrophoresed on 100 g/L polyacrylamide gel, and analyzed by autoradiography. Rz333 cleaved caspase-7 mRNA and produced two cleaved segments of 243 nt and 744 nt, with a cleavage efficiency of 67.98%. Rz394 could not cleave target RNA (Figure 6).

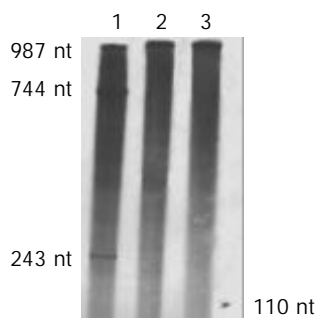


Figure 6 *In vitro* cleavage experiments of anti-caspase-7 ribozymes. Lane 1: Caspase-7 mRNA was mixed with Rz333 and two segments of 243 nt and 744 nt produced by cleavage reaction. Lane 2: Caspase-7 mRNA was mixed with Rz394 and no segment was seen after cleavage. Lane 3: Caspase-7 mRNA was mixed with neither Rz333 nor Rz394. The 110-nt marker is indicated by a short arrow.

DISCUSSION

RNA catalysis was first described by Altman and Cech with the discovery of RNase P and the group I intron, respectively^[21,22]. This makes RNA the only molecule with an information-carrying capacity and inherent catalytic activity. So far, several natural ribozyme motifs have been identified and their physical structure, biological and biochemical properties have been the subject of reviews^[23,24]. In general, however, natural ribozymes have been divided into groups based on their specialized catalytic properties. As the smallest one, the hammerhead ribozyme, with its capability of self-cleavage of a particular phosphodiester bond, has been studied extensively to understand the structure-activity relationship^[25-29]. It provides a very valuable tool for genetic therapy through its RNA-mediated inhibition of gene expression. Hammerhead ribozyme has been used extensively to down-regulate cellular and viral gene expression^[30,31], and recognized as a novel molecular therapeutic drug in the treatment of cancer or viral infection.

Apoptosis is essential to the normal development of multicellular organisms as well as physiologic cell turnover. In pathologic states, a failure to undergo apoptosis may cause abnormal cell overgrowth and malignancy, while excessive apoptosis may lead to organ injury. Apoptosis involves the activation of the caspases, which are hallmarks of apoptosis. Central to the execution phase of apoptosis are the two closely related caspase-3 and caspase-7, which share common substrate specificity and structure. Many cellular proteins are cleaved during the execution phase of apoptosis at a DXXD motif by the effector caspases-3 and -7. Caspase-3 has been extensively studied as gene therapeutic target. Caspase-7, as another crucial executioner caspase, has been chosen to be the gene therapy target of ribozyme.

In our experiment, we only discovered two sites (333 and 394) in caspase-7 gene suitable for hammerhead ribozymes to cleave, so Rz333 and Rz394 were synthesized and cloned. Caspase-7 gene segment (891 bp) was amplified by RT-PCR from total RNA of mouse liver, and was cloned into an expression plasmid. Ribozymes and substrate were both gained by *in vitro* transcription. The results of cleavage assays indicated that Rz333 could catalyze site-specific cleavage of caspase-7 mRNA, and produced 243-nt and 744-nt cleaved segments, but Rz394 could not cleave the substrate. This might be because the secondary structures of ribozymes and substrate simulated by computer could not reflect the real situation. Rz333 could site-specifically cleave caspase-7 mRNA with a cleavage efficiency of 67.98%. It may prevent apoptosis solely or in association with anti-caspase-3 ribozyme synthesized and selected in our previous study. Rz333 may become a candidate for gene therapy of apoptosis-related diseases.

REFERENCES

- 1 **Kuida K**, Zheng TS, Na S, Kuan CY, Yang D, Karasuyama H, Rakic P, Flavell RA. Decreased apoptosis in the brain and premature lethality in CPP32-deficient mice. *Nature* 1996; **384**: 368-372
- 2 **Woo M**, Hakem R, Soengas MS, Duncan GS, Shahinian DK, Hakem A, McCurrach M, Khoo W, Kaufman SA, Senaldi G, Howard T, Lowe SW, Mak TW. Essential contribution of caspase 3/CPP32 to apoptosis and its associated nuclear changes. *Genes Dev* 1998; **12**: 806-809
- 3 **Zimmermann KC**, Bonzon C, Green DR. The machinery of programmed cell death. *Pharmacol Ther* 2001; **92**: 57-70
- 4 **Xie Q**, Khaoustov VI, Chung CC, Sohn J, Krishnan B, Lewis DE, Yoffe B. Effect of tauroursodeoxycholic acid on endoplasmic reticulum stress-induced caspase-12 activation. *Hepatology* 2002; **36**: 592-601
- 5 **Hengartner MO**. The biochemistry of apoptosis. *Nature* 2000; **407**: 770-776

- 6 **Tozser J**, Bagossi P, Zahuczky G, Specht SI, Majerova E, Copeland TD. Effect of caspase cleavage-site phosphorylation on proteolysis. *Biochem J* 2003; **372**(Pt 1): 137-143
- 7 **Creagh EM**, Martin SJ. Caspases: cellular demolition experts. *Biochem Soc Trans* 2001; **29**(Pt 6): 696-702
- 8 **Katoch B**, Sebastian S, Sahdev S, Padh H, Hasnain SE, Begum R. Programmed cell death and its clinical implications. *Indian J Exp Biol* 2002; **40**: 513-524
- 9 **Ranganath RM**, Nagashree NR. Role of programmed cell death in development. *Int Rev Cytol* 2001; **202**: 159-242
- 10 **Lin JS**, Song YH, Kong XJ, Li B, Liu NZ, Wu XL, Jin YX. Preparation and identification of anti-transforming growth factor beta1 U1 small nuclear RNA chimeric ribozyme *in vitro*. *World J Gastroenterol* 2003; **9**: 572-577
- 11 **Langlois MA**, Lee NS, Rossi JJ, Puymirat J. Hammerhead ribozyme-mediated destruction of nuclear foci in myotonic dystrophy myoblasts. *Mol Ther* 2003; **7**(5 Pt 1): 670-680
- 12 **Hubinger G**, Wehnes E, Xue L, Morris SW, Maurer U. Hammerhead ribozyme-mediated cleavage of the fusion transcript NPM-ALK associated with anaplastic large-cell lymphoma. *Exp Hematol* 2003; **31**: 226-233
- 13 **Wang H**, Chen XP, Qiu FZ. Overcoming multi-drug resistance by anti-MDR1 ribozyme. *World J Gastroenterol* 2003; **9**: 1444-1449
- 14 **Sgorbissa A**, Benetti R, Marzinotto S, Schneider C, Brancolini C. Caspase-3 and caspase-7 but not caspase-6 cleave Gas2 *in vitro*: implications for microfilament reorganization during apoptosis. *J Cell Sci* 1999; **112**(Pt 23): 4475-4482
- 15 **Xu R**, Liu J, Zhou X, Xie Q, Jin Y, Yu H, Liao D. Activity identification of anti-caspase-3 mRNA hammerhead ribozyme in both cell-free condition and BRL-3A cells. *Chin Med J* 2001; **114**: 606-611
- 16 **Rajpal A**, Turi TG. Intracellular stability of anti-caspase-3 intrabodies determines efficacy in retargeting the antigen. *J Biol Chem* 2001; **276**: 33139-33146
- 17 **Xu R**, Liu J, Chen X, Xu F, Xie Q, Yu H, Guo Q, Zhou X, Jin Y. Ribozyme-mediated inhibition of caspase-3 activity reduces apoptosis induced by 6-hydroxydopamine in PC12 cells. *Brain Res* 2001; **899**: 10-19
- 18 **Chandler JM**, Cohen GM, MacFarlane M. Different subcellular distribution of caspase-3 and caspase-7 following Fas-induced apoptosis in mouse liver. *J Biol Chem* 1998; **273**: 10815-10818
- 19 **Germain M**, Affar EB, D' Amours D, Dixit VM, Salvesen GS, Poirier GG. Cleavage of automodified poly(ADP-ribose) polymerase during apoptosis. Evidence for involvement of caspase-7. *J Biol Chem* 1999; **274**: 28379-28384
- 20 **Sanceau J**, Hiscott J, Delattre O, Wietzerbin J. IFN-beta induces serine phosphorylation of Stat-1 in Ewing's sarcoma cells and mediates apoptosis via induction of IRF-1 and activation of caspase-7. *Oncogene* 2000; **19**: 3372-3383
- 21 **Guerrier Takada C**, Altman S. Catalytic activity of an RNA molecule prepared by transcription *in vitro*. *Science* 1984; **223**: 285-286
- 22 **Cech TR**, Zaug AJ, Grabowski PJ. *In vitro* splicing of the ribosomal RNA precursor of Tetrahymena: involvement of a guanosine nucleotide in the excision of the intervening sequence. *Cell* 1981; **27**(3 Pt 2): 487-496
- 23 **Cech TR**. The chemistry of self-splicing RNA and RNA enzymes. *Science* 1987; **236**: 1532-1539
- 24 **Symons RH**. Self-cleavage of RNA in the replication of small pathogens of plants and animals. *Trends Biochem Sci* 1989; **14**: 445-450
- 25 **Maniatis D**, Wood MJ, Phylactou LA. Hammerhead ribozymes reduce central nervous system (CNS)-derived neuronal nitric oxide synthase messenger RNA in a human cell line. *Neurosci Lett* 2002; **329**: 81-85
- 26 **Feng Y**, Kong YY, Wang Y, Qi GR. Intracellular inhibition of the replication of hepatitis B virus by hammerhead ribozymes. *J Gastroenterol Hepatol* 2001; **16**: 1125-1130
- 27 **Koizumi M**, Ozawa Y, Yagi R, Nishigaki T, Kaneko M, Oka S, Kimura S, Iwamoto A, Komatsu Y, Ohtsuka E. Design and anti-HIV-1 activity of hammerhead and hairpin ribozymes containing a stable loop. *Nucleosides Nucleotides* 1998; **17**: 207-218
- 28 **Hornes R**, Sczakiel G. The size of hammerhead ribozymes is related to cleavage kinetics: the role of substrate length. *Biochimie* 2002; **84**: 897-903
- 29 **Pley HW**, Flaherty KM, McKay DB. Three-dimensional structure of a hammerhead ribozyme. *Nature* 1994; **372**: 68-74
- 30 **Scott WG**, Finch JT, Klug A. The crystal structure of an all-RNA hammerhead ribozyme: a proposed mechanism for RNA catalytic cleavage. *Cell* 1995; **81**: 991-1002
- 31 **Fritz JJ**, Lewin A, Hauswirth W, Agarwal A, Grant M, Shaw L. Development of hammerhead ribozymes to modulate endogenous gene expression for functional studies. *Methods* 2002; **28**: 276-285

Edited by Chen WW Proofread by Zhu LH and Xu FM

Effects of octreotide on acute necrotizing pancreatitis in rabbits

László Czakó, Péter Hegyi, Tamás Takács, Csaba Góg, András Farkas, Yvette Mándy, Ilona Sz. Varga,
László Tiszlavicz, János Lonovics

László Czakó, Péter Hegyi, Tamás Takács, Csaba Góg, János Lonovics, First Department of Internal Medicine, University of Szeged, Szeged, Hungary

András Farkas, Second Department of Internal Medicine and Cardiological Center, University of Szeged, Szeged, Hungary

Yvette Mándy, Department of Microbiology, University of Szeged, Szeged, Hungary

Ilona Sz. Varga, Biological Isotope Laboratory, Attila József University, Szeged, Hungary

László Tiszlavicz, Department of Pathology, University of Szeged, Szeged, Hungary

Supported by the grant from the Hungarian Scientific Research Fund (OTKA No. D34004) the Hungarian Academy of Sciences (BÖ5/2003) and ETT SK503

Correspondence to: Dr. László Czakó M.D., Ph.D., First Department of Medicine, University of Szeged, Szeged, PO Box 469, H-6701, Hungary. czal@in1st.szote.u-szeged.hu

Telephone: +36-62-545201 **Fax:** +36-62-545185

Received: 2003-12-11 **Accepted:** 2004-01-17

Abstract

AIM: To assess the role of oxygen-derived free radicals and cytokines in the pathogenesis of taurocholic acid-induced acute pancreatitis, and to evaluate the preventive effects of octreotide towards the development of acute pancreatitis.

METHODS: Acute pancreatitis was induced in male New Zealand white rabbits by retrograde injection of 0.8 mL/kg·b.m. of 50 g/L sodium taurocholate (NaTC) in the pancreatic duct. Sham-operated animals served as control. Octreotide 1 mg/kg·b.m. was administered subcutaneously before the induction of pancreatitis. Blood was taken from the jugular vein before and at 1, 3, 6, 12 and 24 h after pancreatitis induction. Serum activities of amylase, IL-6 and TNF- α and levels of malonyl dialdehyde (MDA), glutathione (GSH), glutathione peroxidase (GPx), catalase and superoxide dismutase (Mn-, Cu-, and Zn-SOD) in pancreatic tissue were measured.

RESULTS: Serum TNF- α and IL-6 levels increased significantly 3 h after the onset of pancreatitis, and then returned to control level. The tissue concentration of MDA was significantly elevated at 24 h, while the GSH level and GP-x, catalase, Mn-SOD, Cu-, Zn-SOD activities were all significantly decreased in animals with pancreatitis as compared to the control. Octreotide pretreatment significantly reversed the changes in cytokines and reactive oxygen metabolites. Octreotide treatment did not alter the serum amylase activity and did not have any beneficial effects on the development of histopathological changes.

CONCLUSION: Oxygen-derived free radicals and proinflammatory cytokines are generated at an early stage of NaTC-induced acute pancreatitis in rabbits. Prophylactic octreotide treatment can prevent release of cytokines and generation of reactive oxygen metabolites, but does not have any beneficial effects on the development of necrotizing pancreatitis.

Czakó L, Hegyi P, Takács T, Góg C, Farkas A, Mándy Y, Varga IS, Tiszlavicz L, Lonovics J. Effects of octreotide on acute necrotizing pancreatitis in rabbits. *World J Gastroenterol* 2004; 10(14): 2082-2086

<http://www.wjgnet.com/1007-9327/10/2082.asp>

INTRODUCTION

Acute pancreatitis is clinically classified into mild and severe forms. Mild or edematous acute pancreatitis is a self-limiting disease with a low complication and mortality rate. However, severe necrotizing pancreatitis has an unacceptably high morbidity and mortality rate. Multiple therapeutic modalities have been suggested for acute pancreatitis, but none has been unambiguously proven to be effective yet. The major problem is that the pathophysiology of the disease is not fully understood and hence, there is no specific casual treatment yet. The treatment of acute pancreatitis to date is essentially supportive^[1-3].

Theories on the pathogenesis of acute pancreatitis suggest that autodigestion of the gland and peripancreatic tissues by activated digestive enzymes is a key component^[4,5]. Furthermore, stimulation of exocrine pancreatic secretion in experimental acute pancreatitis has been demonstrated to worsen the disease. Prevention of release and activation of enzymes by inhibition of pancreatic exocrine secretion has been therefore suggested as a specific treatment. Somatostatin and its long-acting analogue octreotide are potent inhibitors of pancreatic secretion^[6,7]. The efficacy of somatostatin and octreotide in the management of acute pancreatitis has been studied for decades, yet the data still remain inconclusive. Some experimental^[8,9] and clinical^[10] studies have shown beneficial results, but others^[11-14] demonstrated no benefit^[15,16].

Somatostatin and octreotide increase the tone of the sphincter of Oddi, which can be reversed by administration of glyceryl trinitrate^[17,18]. Furthermore, octreotide may trigger acute pancreatitis and worsen the disease^[19].

We studied the effects of octreotide on necrotizing pancreatitis in rabbits. In these animals the pancreatic duct enters the duodenum at its distal part, and is completely separated from the common bile duct. Therefore, we can exclude the effect of octreotide on the sphincter of Oddi. The present study was to assess the roles of oxygen-derived free radicals and cytokines in the pathogenesis of taurocholic acid-induced acute pancreatitis, and to evaluate the preventive effects of octreotide on the development of acute pancreatitis.

MATERIALS AND METHODS

Animals

New Zealand white rabbits weighing 2.5-3.5 kg were used. The animals were kept at a constant room temperature of 27 °C, and had free access to water and a standard laboratory chow [LATI, Gödöllő, Hungary]. The experimental protocol followed the principles of Laboratory Animal Care of the National Institute of Health, USA.

Experimental protocol

Overnight fasted animals were anesthetized with an intravenous

injection of pentobarbital 20 mg/kg and urethane 1 g/kg, and supplemented when needed. Four groups of animals were prepared through a midline incision; the pancreatic duct was cannulated transduodenally with a polyvinyl catheter. Acute pancreatitis was induced by retrograde intraductal infusion of 0.8 ml/kg·b.m. of 50 g/L sodium taurocholate (NaTc) (Reanal, Budapest) dissolved in 0.15 mol/L NaCl under steady manual pressure over a period of 30 s (Group I)^[20]. After infusion the catheter was removed, and the abdomen was closed in two layers. In control animals, laparotomy was performed with visualization of the pancreatic duct before closure of the abdomen [Group II]. Animals in which pancreatitis was induced by administration of NaTc were injected subcutaneously with 1 mg/kg·b.m. octreotide (SANDOSTATIN Novartis, Basel, Switzerland) before pancreatitis induction (Group III). In Group IV animals were treated with saline before induction of pancreatitis. The body temperatures and weights of the animals were measured every 6 h. Blood was taken from the jugular vein before and at 1, 3, 6, 12 and 24 h after pancreatitis induction. Physiologic saline was injected into the jugular vein during the experiment in order to avoid severe hypovolemia. Twenty-four hours after the abdominal operation, the animals were sacrificed by aorta exsanguination. The pancreas was removed.

Assays

Serum amylase activity was measured by the Phadebas test method^[21]. TNF- α levels were titrated in a bioassay on the WEHI-164 cell line^[22]. IL-6 concentrations were measured via their proliferative action on the IL-6-dependent mouse hybridoma cell line B-9^[23]. The activities were calibrated against recombinant TNF [Genzyme, Cambridge, UK] and recombinant IL-6 [Sigma-Aldrich, Munich, Germany].

The pancreata were homogenized. The homogenates were centrifuged at 3 000 r/min for 10 min and the supernatants were used for measurements.

Lipid peroxide MDA level was measured after reaction with thiobarbituric acid, according to the method of Placer *et al.*^[24], and was corrected for the protein content of the tissue.

Superoxide dismutase (SOD) activity was determined on the basis of the inhibition of epinephrine-adrenochrome autoxidation^[25]. Mn-SOD activity was measured by the autoxidation method in the presence of 5×10^{-3} mol/L KCN^[26]. Cu-, Zn-SOD activity resulted from the deduction of Mn-SOD from SOD activity.

Catalase activity was determined spectrophotometrically at 240 nm by the method of Beers *et al.*^[27] and expressed in Bergmeyer units (BU) (1 BU=decomposition of 1 g H₂O₂/min at 25 °C).

Glutathione (GSH) level was measured spectrophotometrically with Ellman's reagent from the supernatant, and was corrected for the protein content of the tissue^[28]. Glutathione peroxidase (GPx) activity was determined according to the 'chemical' method, using cumene hydroperoxide and reduced GSH as substrates of GPx^[29].

Protein concentration of the pancreatic tissue was determined by the method of Lowry *et al.*^[30].

Histologic examination

A portion of the pancreas was fixed overnight in a 6% neutral formaldehyde solution and embedded in paraffin. Tissue slices were subjected to hematoxylin and eosin staining and histologic study by light microscopy. Slides were coded and examined blind by the pathologist for the grading of histologic alterations. Grading of intestinal edema, vacuolization, inflammation, hemorrhage and acinar cell necrosis was performed on a scale of 1 to 4.

Statistical analysis

Results are expressed as mean \pm SE. Experiments were evaluated

statistically with two-way analysis of variance (ANOVA). *P* value less than 0.05 was statistically significant.

RESULTS

Seven animals died (2 within 1 h, 3 at 1 h, and 2 at 6 h after pancreatitis induction). Two of them were in the octreotide pretreatment (Group III), 2 in the saline pretreatment (Group IV), and 3 in the acute pancreatitis group (Group I). Thus, the results were the data on the surviving 32 animals (8 rabbits in each group). The results of Group III did not statistically differ from those of Group IV, therefore they were not depicted in figures and tables.

The body weights of the animals in the 3 groups did not change significantly during the experiments, indicating that the parenteral fluid supplementation during the observation period was sufficient.

The serum amylase activity was already increased significantly at 1 h, and increased gradually up to 24 h after the induction of pancreatitis in Group I as compared with the control group (5 678 \pm 881 vs 517 \pm 99 U/L) (Figure 1). Pretreatment of pancreatitic animals with octreotide (Group III) did not alter the serum amylase activity as compared with Group I at any time point. Since the amylase, TNF- α and IL-6 levels in Group IV did not differ significantly from those in Group III, they were not shown.

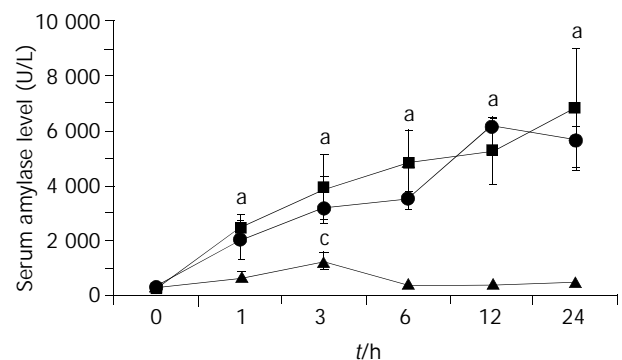


Figure 1 Effects of octreotide on serum amylase levels in rabbits with NaTc-induced acute pancreatitis. Group I: ●; Group II as control: ▲; Group III treated with octreotide: ■. ^a*P*<0.05 vs Group II; ^c*P*<0.05 vs Group I.

The serum TNF- α level increased significantly 3 h after the onset of pancreatitis in Group I (3 120 \pm 340 vs 85 \pm 15 U/L in Group II), and returned to the control level by 6 h (Figure 2). There was no significant serum TNF- α level elevation in the octreotide treated group.

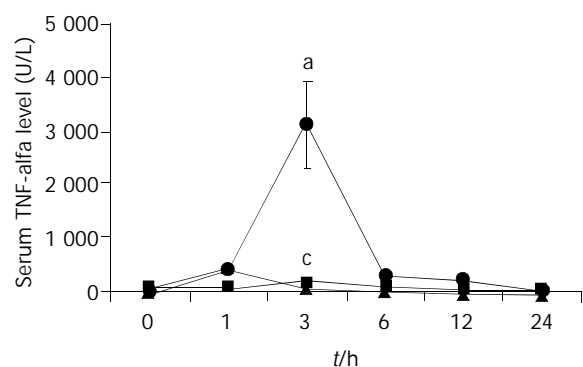


Figure 2 Effects of octreotide on serum TNF- α levels in rabbits with NaTc-induced acute pancreatitis. Group I: ●; Group II as control: ▲; Group III treated with octreotide: ■. ^a*P*<0.05 vs Group II; ^c*P*<0.05 vs Group I.

Table 1 Effects of octreotide on pancreatic level of MDA and endogenous scavengers in rabbits with NaTc-induced acute pancreatitis

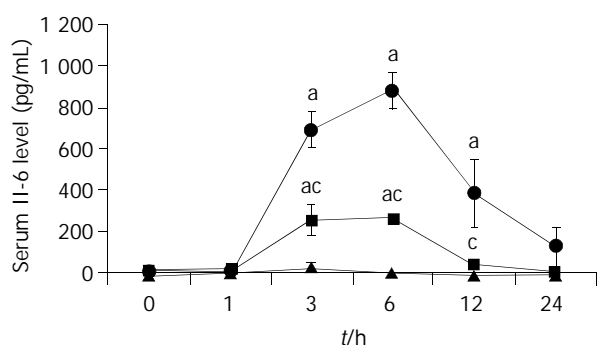
	Control	NaTc	NaTc+octreotide
MDA (nmol/mg protein)	2.24±0.51	7.52±1.05 ^a	4.14±0.86 ^{a,c}
GSH (nmol/mg protein ×10 ²)	2.76±0.45	1.68±0.24 ^a	2.23±0.48 ^{a,c}
GPx (U/mg protein ×10 ²)	1.18±0.34	0.53±0.08 ^a	0.82±0.16 ^{a,c}
Catalase (U/mg protein × 10 ⁴)	3.08±0.54	2.79±0.41 ^a	3.16±0.14 ^{a,c}
Mn-SOD (U/mg protein)	1.03±0.22	0.43±0.08 ^a	0.53±0.08 ^a
Zn-,Cu-SOD (U/mg protein)	4.96±0.76	3.34±0.56 ^a	4.12±0.84 ^{a,c}

^aP<0.05 vs control group; ^cP<0.05 vs NaTc treated group.

Table 2 Effects of octreotide on histologic score in rabbits with NaTc-induced acute pancreatitis

Group	Vacuolization	Edema	Necrosis	Inflammation	Congestion
Control	0	0	0	0	0
NaTc	1.12±0.16	2.00±0.35	2.37±0.42	3.15±0.48	1.57±0.33
NaTc+ somatostatin	1.57±0.45	2.14±0.32	2.43±0.58	3.05±0.36	1.50±0.25

The serum IL-6 level increased significantly 3 h after the onset of pancreatitis in Group I (690±88 vs 25±15 U/L in Group II), and returned to the control level by 24 h (Figure 3). Octreotide pretreatment attenuated the increase in IL-6 level throughout the study.

**Figure 3** Effects of octreotide on serum IL-6 levels in rabbits with NaTc-induced acute pancreatitis. Group I: ●; Group II as control: ▲; Group III treated with octreotide: ■. ^aP<0.05 vs Group II; ^cP<0.05 vs Group I.

The tissue concentration of MDA was elevated significantly at 24 h as compared to the control. Octreotide pretreatment prevented the increase in MDA level. The GSH level and the activities of endogenous scavengers (GPx, catalase, Mn-SOD and Cu-, Zn-SOD) were all decreased significantly in pancreatitis animals in comparison with the control. Octreotide treatment significantly reversed the decrease of GPx, catalase and Cu-, Zn-SOD, but not Mn-SOD activity in comparison with Group I (Table 1).

Histological examination revealed acinar cell necrosis, hemorrhage, inflammatory cell infiltration and edema. Octreotide pretreatment did not exert any beneficial effect on the histological score (Table 2).

DISCUSSION

The results of our study can be summarized as follows. In our model, a short-lasting infusion of taurocholic acid in the pancreatic duct of rabbits produced a rapidly evolving necrotizing pancreatitis with mortality, as described earlier^[20]. Proinflammatory cytokines were generated early in NaTc-induced acute pancreatitis. Tissue imbalance of the offense

system represented by MDA and the defense system represented by GSH, SOD, GPx and catalase was observed. Prophylactic octreotide treatment prevented the release of cytokines, the increase in MDA and the decrease in GSH, SOD, GPx and catalase activities, but did not reduce the serum amylase level, and did not have beneficial effects on the development of histopathological changes.

Oxygen-derived free radicals have been reported to play an important role in the pathogenesis of acute pancreatitis^[31,32]. In the present study, oxidative stress was assessed by measuring the MDA, a product of lipid peroxidation, the intracellular antioxidant GSH, and the endogenous scavengers SOD, GPx and catalase in pancreatic tissues, in order to elucidate the participation of free radicals in the process of NaTc-induced pancreatitis in rabbits. In agreement with previous studies made in other animals^[31,32], this study revealed that the elevation of MDA as an offense system, and lowered GSH, SOD, GPx and catalase activities as a defense system, might be one cause of pancreatic injury induced by NaTc in rabbits.

Published data suggest that activated pancreatic macrophages can release proinflammatory cytokines in response to local tissue damages. These cytokines may act locally to aggravate acute pancreatitis, and both locally and systemically to increase the capillary permeability and to promote leukocyte adherence and extravasation^[33, 34]. TNF- α , a major proinflammatory cytokine, is considered to be important in orchestrating the early events in the inflammatory cascade and contributes to the induction of systemic inflammatory response syndrome (SIRS) which is responsible for multiple organ failure in severe acute pancreatitis. IL-6 is the most potent inducer of acute-phase protein synthesis in the liver, and it has been shown that its level reflects the severity of acute pancreatitis^[35]. This study confirmed the observations of others in rabbits that TNF- α and IL-6 were released in the early phase of NaTc-induced pancreatitis.

There is a growing evidence that somatostatin could inhibit the production of different cytokines, especially TNF- α and IL-6^[36-38] and reduce the local generation of free radicals^[39]. Nuclear factor- κ B (NF- κ B) plays a pivotal role in inducing the expression of multiple genes involved in immune and inflammatory responses, such as cytokines. NF- κ B transcription pathway has been found to be activated by reactive oxygen species^[39]. Therefore, somatostatin may also reduce indirectly the production of cytokines by inhibiting the generation of reactive oxygen metabolites. Furthermore, somatostatin could exert a direct cyto- and organoprotective

action in several models of toxic organ injury and stimulate on the reticulo-endothelial system^[40-43].

In our study, octreotide completely reversed the pancreatitis-induced changes in cytokines, MDA, GSH, SOD, GPx and catalase activities. However, we were unable to detect a significant improvement both in the serum amylase level and in the histologic score in octreotide-treated group. This could be explained by severe chemical and mechanical destruction of the pancreatic gland induced by taurocholic acid. The severity of this local injury exceeded the pancreatic damage induced by inflammatory mediators. Overproduction of cytokines can lead to the development of SIRS, which is responsible for the mortality of the disease. However, reduction of cytokine production in octreotide-treated group did not result in a significant decrease in the morbidity or mortality. This suggests that liberation of other vasoactive and toxic mediators [e.g. phospholipase A2, platelet activating factor, nitric oxide, leukotrienes *etc*] by the necrotizing process plays an essential role in the development of SIRS. Therefore, blockade of one particular part of this complex inflammatory process is not beneficial.

Octreotide has been suggested for the treatment of acute pancreatitis on the basis of its inhibitory effect on pancreatobiliary secretion. However, a number of experimental studies have demonstrated that pancreatic enzyme secretion is almost abolished after induction of acute pancreatitis^[44-46]. Therefore, the use of drugs inhibiting exocrine pancreatic secretion does not have a beneficial effect on the progression and outcome of the disease. In contrast, the basal pancreatic fluid secretion was greatly increased during the early stages of acute experimental pancreatitis^[45, 46]. This fluid hypersecretion was resistant to cholecystokinin, secretin and cholinergic antagonists, and was probably caused by acinar cell proliferation^[46]. Fluid hypersecretion can wash out inflammatory mediators and activated pancreatic enzymes from the pancreas, thereby serving as a natural host protective mechanism after a pancreatic injury. Accordingly, it seems unnecessary to attempt to suppress the basal pancreatic enzyme secretion further since it is already blocked. If the fluid hypersecretion is interrupted after the onset of acute pancreatitis, this might exacerbate the inflammatory process.

Furthermore, somatostatin could reduce splanchnic blood flow and the impairment of pancreatic microcirculation could lead to further deterioration in acute pancreatitis^[47, 48].

Octreotide might worsen acute pancreatitis and even cause the disease by increasing the contractility of the sphincter of Oddi^[18,19]. The most commonly used animals to study the effects of octreotide in acute pancreatitis were rats, whereas rabbits have never been used. However, rabbits seem to be the excellent animals for this research. Since the pancreatic duct enters the duodenum at its distal part, and is completely separated from the common bile duct, we may avoid the harmful effect of octreotide on the sphincter of Oddi. However, we can not exclude the effect of octreotide on pancreatic sphincter.

In conclusion, proinflammatory cytokines are generated early in NaTc-induced acute pancreatitis in rabbits. Tissue imbalance of the offense system represented by MDA and the defense system represented by GSH, SOD, GPx and catalase was detected in the pancreas. Prophylactic octreotide treatment can prevent the release of cytokines, the increase in MDA and the decrease in GSH, SOD, GPx and catalase activities, but does not have any beneficial effects on the development of necrotizing pancreatitis. The pancreatic duct injection model in rabbit is a useful model to exclude the effect of sphincter of Oddi on the course of acute pancreatitis.

REFERENCES

- 1 **Yousaf M**, McCallion K, Diamond T. Management of severe acute pancreatitis. *Br J Surg* 2003; **90**: 407-420
- 2 **Banks PA**. Practice guidelines in acute pancreatitis. *Am J Gastroenterol* 1997; **92**: 377-386
- 3 Conservative therapeutic concepts in acute pancreatitis. In: Büchler MW, Uhl W, Friess H, Malfertheiner P eds. Acute pancreatitis. Novel concepts in biology and therapy. *Berlin: Blackwell* 1999: 291-344
- 4 **Saluja AK**, Steer MLP6. Pathophysiology of pancreatitis. Role of cytokines and other mediators of inflammation. *Digestion* 1999; **60**(Suppl 1): 27-33
- 5 Primary events in the initiation of acute pancreatitis. In: Büchler MW, Uhl W, Friess H, Malfertheiner P eds. Acute pancreatitis. Novel concepts in biology and therapy. *Berlin Blackwell* 1999: 1-48
- 6 **Robberecht P**, Deschodt-Lanckman M, De Neef P, Christophe J. Effects of somatostatin on pancreatic exocrine function. Interaction with secretin. *Biochem Biophys Res Commun* 1975; **67**: 315-323
- 7 **Guan D**, Maouyo D, Sarfati P, Morisset J. Effects of SMS 201-995 on basal and stimulated pancreatic secretion in rats. *Endocrinology* 1990; **127**: 298-304
- 8 **Baxter JN**, Jenkins SA, Day DW, Roberts NB, Cowel DC, Mackie CR, Shields R. Effects of somatostatin and a long-acting somatostatin analogue on the prevention and treatment of experimentally induced acute pancreatitis in the rat. *Br J Surg* 1985; **72**: 382-385
- 9 **Kaplan O**, Kaplan D, Casif E, Siegal A, Paran H, Graf E, Skornick Y. Effects of delayed administration of octreotide in acute experimental pancreatitis. *J Surg Res* 1996; **62**: 109-117
- 10 **Choi TK**, Mok F, Zhan WH, Fan ST, Lai EC, Wong J. Somatostatin in the treatment of acute pancreatitis: a prospective randomised controlled trial. *Gut* 1989; **30**: 223-227
- 11 **Lankisch PG**, Koop H, Winckler K, Folsch UR, Creutzfeldt W. Somatostatin therapy of acute experimental pancreatitis. *Gut* 1977; **18**: 713-716
- 12 **Murayama KM**, Drew JB, Joehl RJ. Does somatostatin analogue prevent experimental acute pancreatitis? *Arch Surg* 1990; **125**: 1570-1572
- 13 **McKay C**, Baxter J, Imrie C. A randomized, controlled trial of octreotide in the management of patients with acute pancreatitis. *Int J Pancreatol* 1997; **21**: 13-19
- 14 **Uhl W**, Buchler MW, Malfertheiner P, Beger HG, Adler G, Gaus W. A randomised, double blind, multicentre trial of octreotide in moderate to severe acute pancreatitis. *Gut* 1999; **45**: 97-104
- 15 **Greenberg R**, Haddad R, Kashtan H, Kaplan O. The effects of somatostatin and octreotide on experimental and human acute pancreatitis. *J Lab Clin Med* 2000; **135**: 112-121
- 16 **Uhl W**, Anghelacopoulos SE, Friess H, Buchler MW. The role of octreotide and somatostatin in acute and chronic pancreatitis. *Digestion* 1999; **60**(Suppl 2): 23-31
- 17 **Di Francesco V**, Angolini G, Bovo P, Casarini MB, Filippini M, Vaona B, Frulloni L, Rigo L, Brunori MP, Cavallini G. Effects of octreotide on sphincter of Oddi motility in patients with acute recurrent pancreatitis: a manometric study. *Dig Dis Sci* 1996; **41**: 2392-2396
- 18 **Veloso B**, Madácsy L, Szepes A, Pavics L, Csernay L, Lonovics J. The effects of somatostatin and octreotide on the human sphincter of Oddi. *Eur J Gastroenterol Hepatol* 1999; **11**: 897-901
- 19 **Bodemar G**, Hjortswang H. Octreotide-induced pancreatitis: an effect of increased contractility of Oddi sphincter. *Lancet* 1996; **348**: 1668-1669
- 20 **Gyongyosi M**, Takacs T, Czako L, Jambrik Z, Boda K, Farkas A, Forster T, Csanady M. Noninvasive monitoring of hemodynamic changes in acute pancreatitis in rabbits. *Dig Dis Sci* 1997; **42**: 955-961
- 21 **Ceska M**, Birath K, Brown B. A new and rapid method for the clinical determination of alpha-amylase activities in human serum and urine optimal conditions. *Clin Chem Acta* 1969; **26**: 437-444
- 22 **Espevik T**, Niessen-Meyer J. A highly sensitive cell line, WEHI 164 clone 13, for measuring cytotoxic factor/tumor necrosis factor from human monocytes. *J Immunol Methods* 1986; **95**: 99-105
- 23 **Aarden LA**, De Groot ER, Schaap OL, Lansdorp PM. Production of hybridoma growth factor by human monocytes. *Eur J Immunol* 1987; **17**: 1411-1416
- 24 **Placer ZA**, Cushman L, Johnson BC. Estimation of product of lipid peroxidation [malonyl dialdehyde] in biochemical systems. *Anal Biochem* 1966; **16**: 359-364

- 25 **Misra HP**, Fridovich I. The role of superoxide anion in the autoxidation of epinephrine and a simple assay for superoxide dismutase. *J Biol Chem* 1972; **247**: 3170-3175
- 26 **Beauchamp C**, Fridovich I. Superoxide dismutase: Improved assays and an assay applicable to acrylamide gels. *Anal Biochem* 1971; **44**: 276-287
- 27 **Beers RF Jr**, Sizer IW. A spectrophotometric method for measuring the breakdown of hydrogen peroxide by catalase. *J Biol Chem* 1952; **195**: 133-140
- 28 **Sedlak J**, Lindsay RH. Estimation of total, protein-bound, and nonprotein sulfhydryl groups in tissue with Ellman's reagent. *Anal Biochem* 1968; **25**: 192-205
- 29 **Chiu DT**, Stults FH, Tappel AL. Purification and properties of rat lung soluble glutathione peroxidase. *Biochim Biophys Acta* 1976; **445**: 558-566
- 30 **Lowry OH**, Rosenbrough NJ, Farr AL, Randall RJ. Protein measurement with the folin phenol reagent. *J Biol Chem* 1951; **193**: 265-275
- 31 **Schoenberg MH**, Birk D, Beger HG. Oxidative stress in acute and chronic pancreatitis. *Am J Clin Nutr* 1995; **62**(6 Suppl): 1306S-1314S
- 32 **Sweiry JH**, Mann GE. Role of oxidative stress in the pathogenesis of acute pancreatitis. *Scand J Gastroenterol Suppl* 1996; **219**: 10-15
- 33 **Norman JG**, Fink GW, Denham W, Yang J, Carter G, Sexton C, Falkner J, Gower WR, Franz MG. Tissue-specific cytokine production during experimental acute pancreatitis. A probable mechanism for distant organ dysfunction. *Dig Dis Sci* 1997; **42**: 1783-1788
- 34 **Norman J**. The role of cytokines in the pathogenesis of acute pancreatitis. *Am J Surg* 1998; **175**: 76-83
- 35 **Leser HG**, Gross V, Scheibenbogen C, Heinisch A, Salm R, Lausen M, Ruckauer K, Andreesen R, Farthmann EH, Scholmerich J. Elevation of serum interleukin-6 concentration precedes acute-phase response and reflects severity in acute pancreatitis. *Gastroenterology* 1991; **101**: 782-785
- 36 **Peluso G**, Petillo O, Melone MA, Mazzarella G, Ranieri M, Tajana GF. Modulation of cytokine production in activated human monocytes by somatostatin. *Neuropeptides* 1996; **30**: 443-451
- 37 **Karalis K**, Mastorakos G, Chrousos GP, Tolis G. Somatostatin analogues suppress the inflammatory reaction *in vivo*. *J Clin Invest* 1994; **93**: 2000-2006
- 38 **Balibrea JL**, Arias-Diaz J, Garcia C, Vara E. Effect of pentoxifylline and somatostatin on tumour necrosis factor production by human pulmonary macrophages. *Circ Shock* 1994; **43**: 51-56
- 39 **Arias-Diaz J**, Vara E, Torres-Melero J, Garcia C, Hernandez J, Balibrea JL. Local production of oxygen free radicals and nitric oxide in rat diaphragm during sepsis: effects of pentoxifylline and somatostatin. *Eur J Surg* 1997; **163**: 619-625
- 40 **Kim H**, Seo JY, Roh KH, Lim JW, Kim KH. Suppression of NF-kappaB activation and cytokines production by N-acetylcysteine in pancreatic acinar cells. *Free Radic Biol Med* 2000; **29**: 674-683
- 41 **Usadel KH**, Schwedes U, Wdowinski JM. Pharmacological effects of somatostatin in acute organ lesions. *Inn Med* 1982; **9**: 204-209
- 42 **Baxter JN**, Jenkins SA, Day DW, Shields R. Effects of a somatostatin analogue (SMS 201-995) on hepatic and splenic reticulo-endothelial function in the rat. *Br J Surg* 1985; **72**: 1005-1008
- 43 **Eliakim R**, Karmeli F, Okon E, Rachmilewitz D. Octreotide effectively decreases mucosal damage in experimental colitis. *Gut* 1993; **34**: 264-269
- 44 **Niederau C**, Niederau M, Luthen R, Strohmeyer G, Ferrell LD, Grendell JH. Pancreatic exocrine secretion in acute experimental pancreatitis. *Gastroenterology* 1990; **99**: 1120-1127
- 45 **Manso MA**, San Roman JI, de Dios I, Garcia LJ, Lopez MA. Cerulein-induced acute pancreatitis in the rat. Study of pancreatic secretion and plasma VIP and secretin levels. *Dig Dis Sci* 1992; **37**: 364-368
- 46 **Czako L**, Yamamoto M, Otsuki M. Pancreatic fluid hypersecretion in rats after acute pancreatitis. *Dig Dis Sci* 1997; **42**: 265-272
- 47 **Sonnenberg GE**, Keller U, Purruchud A, Burckhardt D, Gyr K. Effect of somatostatin on splanchnic hemodynamics in patients with cirrhosis of the liver and in normal subjects. *Gastroenterology* 1981; **80**: 526-532
- 48 **Schroder T**, Millard RW, Nakajima Y, Gabel M, Joffe SN. Microcirculatory effects of somatostatin in acute pancreatitis. *Eur Surg Res* 1988; **20**: 82-88

Edited by Wang XL and Chen WW Proofread by Xu FM

Changes of gut flora and endotoxin in rats with D-galactosamine-induced acute liver failure

Lan-Juan Li, Zhong-Wen Wu, Dang-Sheng Xiao, Ji-Fang Sheng

Lan-Juan Li, Zhong-Wen Wu, Dang-Sheng Xiao, Ji-Fang Sheng,
Department of Infectious Diseases, First Affiliated Hospital, College of Medicine, Zhejiang University, Hangzhou 310003, Zhejiang Province, China

Supported by the Foundation for Medical Research of Zhejiang Educational Bureau, No. 491010-G20252 and partially by National Basic Research Program of China, No. 2003CB515506

Correspondence to: Dr. Lan-Juan Li, Department of Infectious Diseases, First Affiliated Hospital, College of Medicine, Zhejiang University, 79 Qingchun Road, Hangzhou 310003, Zhejiang Province, China. ljli@mail.hz.zj.cn

Telephone: +86-571-87709001 **Fax:** +86-571-87236755

Received: 2003-11-17 **Accepted:** 2004-01-08

Abstract

AIM: To investigate the changes of gut microflora and endotoxin levels in rats with acute liver failure (ALF) induced by D-galactosamine (GalN).

METHODS: Flora and endotoxin levels in the jejunum, ileum and colon in normal rats (group A) and rats with GalN-induced ALF were determined at 24 h (group B) or 48 h (group C) after GalN injection, as well as the endotoxin level in portal venous blood (PVB) and right ventricle blood (RVB) were determined by chromogenic limulus amoebocyte assay.

RESULTS: Intestinal (jejunum, ileum, colon) *Lactobacillus* count was statistically reduced in group B compared with those in group A (3.4 ± 0.3 vs 4.9 ± 0.3 , 6.1 ± 0.4 vs 8.0 ± 0.3 , 8.1 ± 0.2 vs 9.3 ± 0.2 , $P < 0.001$, $P < 0.001$ and $P < 0.001$ respectively) and recovered partially in the group C compared with those in the group B, whereas the count of *Enterobacteriaceae* in the jejunum, ileum and colon in group B was increased markedly compared with those in the group A (5.1 ± 0.3 vs 3.6 ± 0.2 , 6.9 ± 0.5 vs 5.3 ± 0.3 , 8.7 ± 0.2 vs 7.6 ± 0.1 , $P < 0.001$, $P < 0.05$ and $P < 0.05$ respectively) and restored partially in the group C compared with those in the group B. The endotoxin level in ileum was increased in the group B compared with those in the group A (111.3 ± 22.8 vs 51.5 ± 8.9 , $P < 0.05$). In addition, the endotoxin level in PVB was obviously increased in group B compared with that in the group A (76.8 ± 9.1 vs 40.6 ± 7.3 , $P < 0.01$) and reduced to the baseline at 48 h (group C).

CONCLUSION: Severely disturbed gut flora in rats with GalN-induced acute liver failure plays an important role in the elevation of endotoxin level in PVB.

Li LJ, Wu ZW, Xiao DS, Sheng JF. Changes of gut flora and endotoxin in rats with D-galactosamine-induced acute liver failure. *World J Gastroenterol* 2004; 10(14): 2087-2090
<http://www.wjgnet.com/1007-9327/10/2087.asp>

INTRODUCTION

Patients with acute liver failure are prone to occurrence of

endotoxemia^[1], which is usually associated with Gram-negative infection. However, previous studies have showed that some patients with acute liver failure have a high level of endotoxin without clinical evidences of Gram-negative bacterial infection^[1,2]. Recent studies have proposed that the elevation of plasma endotoxin is related to the translocation of endotoxin from the gut^[3,4].

Gut contains numerous endotoxin, about 90% of which is released by aerobic Gram-negative bacteria, especially the family of enterobacteriaceae^[5]. Normally, intestinal anaerobic flora such as *Bifidobacterium* and *Bacteriodes* can prevent the adherence of potential pathogenic enteric bacilli and limit bacterial overgrowth by occupying the space closest to intestinal epithelial cells^[6], which is called microbial colonization resistance^[7]. Disrupted gut flora observed in severely disease, such as hepatic cirrhosis and hemorrhagic shock, resulted in decrease of microbial colonization resistance and subsequent bacterial overgrowth^[8,9]. Wang *et al.*^[10] showed the *Escherichia coli* overgrowth in the distal small intestine from 1 h onward after hepatectomy. Researchers suggested that impaired components of the gut barrier, including normal intestinal microflora, could translocate both endotoxin and bacteria from lumen to circulation or other distant organs^[6]. Moreover, manipulating gut contents with lactulose or neomycin sulfate with cefazolin could reduce the level of endotoxemia and enhance the survival of rat receiving partial hepatectomy^[11]. But to the author's knowledge, the relationship between the changes of gut flora and the fluctuations of the endotoxin levels both in intestine and plasma in rats with GalN-induced acute liver failure has not been reported. In the present study, the changes of gut flora and endotoxin level in the jejunum, ileum and colon, as well as the levels of endotoxin in PVB and RVB of rats with GalN-induced ALF were estimated at various time points.

MATERIALS AND METHODS

Animals and treatment

Male Sprague-Dawley rats weighing about 200-300 g provided by Zhejiang Academy of Medical Sciences, Hangzhou, China, were acclimated to the animal laboratory for 5 d before experiments. They were fed with standard rat chow and water *ad libitum*. All procedures were approved by the Institutional Review Board according to the Animal Protection Act of China.

Acute liver failure in the rats was induced according to the protocol described previously^[12]. Briefly, GalN (Chongqing Medical University, Chongqing, China) was dissolved in 0.5 mL of saline and adjusted to pH 6.8 with 1 mol/L NaOH. Then, 20 rats were intraperitoneally given 1.4 g/kg GalN twice at a 12-h interval, and fed with food and water after injection. Since the highest mortality of GalN-induced acute liver failure in rat is between 24 h and 48 h after drug administration^[12], and we ensure that the number of survival rat is more than 9^[13] at various time points after GalN administration, 40 rats were randomly divided into 3 groups according to the reported mortality^[12]: group A with 10 rats without administration of GalN was chosen as normal control, group B with 12 rats that were sacrificed 24 h after GalN injection and group C with 18 rats that were killed at

48 h after injection. Under light ether anesthesia and aseptic conditions, plasma was separated from the portal vein and right ventricle at various time points after laparotomy, then stored immediately at -80°C for analysis of endotoxin. The rats were killed by anaesthetic overdose after blood sampling, the segments of the jejunum, ileum and colon were removed as described by Wang *et al*^[10]. Briefly, the segments of the jejunum (5 cm in length, including intestinal wall) and ileum including intestinal wall 5 cm long as well as colon contents were immediately collected from the proximal intestine (5 cm distal of the ligament of Treitz), distal small intestine (5 cm proximal to the ileocecal valve), and descending colon, respectively. After weighting, the samples were placed in pyrogen-free saline (1:9 w/v) in an anaerobic chamber (Forma Scientific Co, USA), mixed by a vortex mixer, and aliquots of 1 mL of mixture were subsequently put into anaerobic solution A (1:9 v/v, decimal dilutions up to 10^{-8}). The remnant was kept at -80°C for detecting endotoxin.

Gut flora analysis

The specimens were cultured within 30 min after collection by modified Mitsuoaka's method^[14]. A total volume of 50 μL of the serial dilution (10^{-1} , 10^{-3} , 10^{-5} , 10^{-6} , 10^{-7} , 10^{-8}) was spread on 3 non-selective agar media: glucose blood liver (BL) (Nissui Pharmacy Co., Tokyo, Japan) agar with 60 mL/L defibrinated sheep blood for all lactic acid-producing bacteria; Eggerth Gagnon (EG) (Nissui Pharmacy Co.) agar with 60 mL/L defibrinated sheep blood for most obligate and facultative anaerobes; and trypticase soy (TS) agar (BioMerieux, Paris, France) with 60 mL/L defibrinated sheep blood for all aerobes and facultative anaerobes, and 4 selective agar media: neomycin sulfate-brilliant green-tetrahydrocholate-blood (NBGT) agar prepared with EG agar at our laboratory for members of the family *Bacteriodaceae*; MRS with vancomycin and bromocresol green (LAMVAB) medium^[15] for *Lactobacillus sp.*; eosin methylene blue (EMB) agar (Hangzhou microbiological Co., Hangzhou, China) for members of the family of *Enterobacteriaceae*; and *Enterococcus* (Ec) agar prepared at our laboratory for *Enterococcus sp.* The plates for the recovery of obligate anaerobes were incubated in an anaerobic chamber ($\text{N}_2:\text{CO}_2:\text{H}_2=8:1:1$) at 37°C for 48-72 h. The media used for the isolation of aerobes and facultative species were incubated in air for 48 h at 37°C . After incubation, morphologically distinct colonies were enumerated, isolated and identified. Identification was performed in most cases at family or genus levels using standard bacteriologic techniques^[16]. In our study, the lowest detection limit was 2×10^2 organisms per gram of the samples. The results were expressed as the \log_{10} of the number of bacteria per gram weight of the samples.

Chromogenic limulus amoebocyte assay for detecting endotoxin

Intestinal specimens were prepared for endotoxin detection according to the described method^[5]. The frozen specimens were thawed at room temperature. Limulus quantitative azo color (LQAC) test^[17] with limulus lysate reagent (Eihua Medical Co, Shanghai, China) was used.

Statistical analysis

Data were expressed as the mean \pm SE. One-way ANOVA was used to compare gut flora data among individual groups. Frequency data were compared using Chi-square test or the Fisher's exact test when necessary. $P < 0.05$ was considered statistically significant.

RESULTS

Degree of hepatic injury and mortality

To study the alterations in intestinal microflora and its relationship with plasma endotoxin, ALF model of rat was successfully established by GalN administration as mentioned

previously^[12]. The concentrations of alanine aminotransferase (ALT), aspartate aminotransferase (AST) and total bile acid (TBA) were increased significantly at 24 h and gradually decreased at 48 h, whereas those of alkaline phosphatase (AKP) and total bilirubin (TbIL) were increased continuously after GalN injection (Table 1). At the same time, the levels of serum total protein (TP) and albumin at 24 h after GalN administration were lowered markedly compared with those in control group ($P < 0.01$, respectively) (Table 1), and increased at 48 h without significance compared with those at 24 h. The mortality rate of group C was higher than group B ($P < 0.01$) (Table 1). The general conditions, such as activity and appetite, in survivors were restored partially after 48 h.

Table 1 Degree of hepatic injury and mortality in ALF rats at various time points after injection of GalN

	Group A (n=10)	Group B (n=11)	Group C (n=10)
TP (g/L)	62.6 \pm 1.3	48.9 \pm 1.2 ^d	51.0 \pm 3.1 ^d
Albumin (g/L)	34.3 \pm 0.7	27.8 \pm 0.7 ^d	30.3 \pm 1.1 ^d
Globulin (g/L)	28.6 \pm 0.8	21.1 \pm 1.1 ^d	21.5 \pm 2.6 ^d
ALT (U/L)	60.6 \pm 3.3	4 798 \pm 1 114 ^d	3 183 \pm 1 257 ^d
AST (U/L)	138.0 \pm 7.5	5 032 \pm 1 067 ^d	2 928 \pm 843 ^d
AKP (U/L)	272.0 \pm 18.6	639 \pm 60 ^d	747 \pm 133 ^d
TBA ($\mu\text{mol/L}$)	11.8 \pm 2.6	425 \pm 33 ^d	262 \pm 58 ^{da}
TbIL($\mu\text{mol/L}$)	7.0 \pm 0.4	40.6 \pm 8.2 ^d	63.2 \pm 18.4 ^d
Mortality	NO	8.33% (1/12)	44.44% (8/18) ^b

Values are expressed as mean \pm SE or frequency of occurrence (%). ^a $P < 0.05$, ^b $P < 0.01$ vs group B, ^d $P < 0.01$ vs group A.

Table 2 Alterations in gut flora in rats with ALF at various time points after GalN administration

Flora	Group A (n=10)	Group B (n=11)	Group C (n=10)
<i>Bacteriodaceae</i>			
Jejunum	ND	ND	ND
Ileum	4.0 \pm 0.3	5.0 \pm 0.5	4.6 \pm 0.7
Colon	9.3 \pm 0.3	9.5 \pm 0.3	9.7 \pm 0.4
<i>Lactobacillus</i>			
Jejunum	4.9 \pm 0.3	3.4 \pm 0.3 ^d	4.8 \pm 0.4 ^a
Ileum	8.0 \pm 0.3	6.1 \pm 0.4 ^f	6.2 \pm 0.3 ^f
Colon	9.3 \pm 0.2	8.1 \pm 0.2 ^f	8.5 \pm 0.2 ^d
<i>Enterobacteriaceae</i>			
Jejunum	3.6 \pm 0.2	5.1 \pm 0.3 ^f	4.3 \pm 0.3 ^b
Ileum	5.3 \pm 0.3	6.9 \pm 0.5 ^c	6.3 \pm 0.5
Colon	7.6 \pm 0.1	8.7 \pm 0.2 ^c	7.9 \pm 0.3 ^a
<i>Enterococcus</i>			
Jejunum	3.8 \pm 0.2	3.9 \pm 0.2	3.6 \pm 0.2
Ileum	4.9 \pm 0.3	5.8 \pm 0.3	5.2 \pm 0.5
Colon	6.8 \pm 0.2	5.8 \pm 0.4 ^c	6.7 \pm 0.3

Data are expressed as mean \pm SE. ND: Not detected; ^a $P < 0.05$, ^b $P < 0.01$ vs group B, ^c $P < 0.05$, ^d $P < 0.01$, ^f $P < 0.001$ vs group A.

Intestinal microflora analysis

To explore the variability in intestinal flora under ALF condition, we analyzed the microbiota from different intestinal segments including jejunum, ileum and colon of the rats at different time points. The count of *Enterobacteriaceae* in the jejunum, ileum and colon was significantly higher in the group A than that in control group ($P < 0.001$, $P < 0.05$, and $P < 0.05$, respectively), whereas the count of *Lactobacillus* in the jejunum, ileum and colon, and that of *Enterococcus* in colon were greatly decreased

($P < 0.01$, $P < 0.001$, $P < 0.001$, and $P < 0.05$, respectively) (Table 2). The count of *Enterobacteriaceae* in the jejunum and colon was lower in the group C than in the group B ($P < 0.01$ and $P < 0.05$, respectively), but the count of *Lactobacillus* in the jejunum in the group C was significantly elevated ($P < 0.05$) (Table 2). The count of *Lactobacillus* in the ileum and colon in the group C was decreased more evidently than that in the group A ($P < 0.001$ and $P < 0.01$, respectively). These results indicated that the disturbed gut flora existed in rat with ALF, and the extent of changes in flora was correlated with the severity of liver injury.

Changes of endotoxin in intestine, portal venous and right ventricle blood

Gut endotoxin is usually translocated into the portal vein. To determine the relations of the levels of endotoxin in blood and in gut in rats with ALF, we measured the endotoxin levels of the intestine, PVB and RVB at various time points after GalN by LQAC test (Table 3). The levels of endotoxin in the ileum and PVB in group B after administration of GalN were increased more significantly than those in the group A ($P < 0.05$ and $P < 0.01$, respectively). At the same time, the level of endotoxin in the colon was increased, but not significantly. The levels of endotoxin in the ileum and colon in the group C were increased more significantly than those in the group B, and higher than those in the group A ($P < 0.01$, respectively). The level of endotoxin in PVB in the group C was decreased significantly compared with those in the group B ($P < 0.05$). Although there was an increase of endotoxin level in RVB after GalN, no statistically significant difference was observed.

Table 3 Levels of endotoxin in intestine, PVB and RVB in rats with ALF at different time points after injection of GalN

	Group A (n=10)	Group B (n=11)	Group C (n=10)
Jejunum (ng/g)	67.8±13.0	56.7±18.6	88.1±15.2
Ileum (ng/g)	51.5±8.9	111.3±22.8 ^a	146.7±27.0 ^b
Colon (ng/g)	1 022±179	1 841±363	2 444±349 ^b
PVB (ng/L)	40.6±7.3	76.8±9.1 ^b	45.0±5.3 ^c
RVB (ng/L)	34.9±6.0	37.5±12.3	37.1±6.6

Data are expressed as mean±SE. ^a $P < 0.05$, ^b $P < 0.01$ vs group A; ^c $P < 0.05$ vs group B. PVB: Portal venous blood; RVB: Right ventricle blood.

DISCUSSION

The present study showed that the count of *Enterobacteriaceae* at 24 h after injection of GalN was significantly increased, whereas that of *Lactobacillus* was markedly lowered. The whole intestinal microflora trended to recover at 48 h after GalN administration. These results indicated that there were intestinal microbial disturbance and overgrowth of *Enterobacteriaceae* in the rats with ALF. The tendency of changes in flora from the jejunum and ileum was consistent with that from the colon, and the extent of imbalance of intestinal microflora was correlated with the severity of liver injury. The alterations of intestinal bacterial flora might be due to the diminished bile secretion and the impaired intestinal motility, which were usually observed in rats with acute liver failure^[18]. But the exact mechanisms need further study.

The level of endotoxin in the portal vein reflects the extent of translocation of endotoxin from gut^[19]. Our findings showed that the levels of endotoxin in the ileum and colon increased continuously after administration of GalN, and the level of endotoxin in the portal vein was significantly elevated at 24 h, but lowered to the baseline value at 48 h. Interestingly, the elevation of the endotoxin in PVB was accompanied by the imbalance of intestinal flora and the overgrowth of

Enterobacteriaceae, whereas a decrease of the level of endotoxin in PVB was paralleled with the partial restoration of disturbed flora. The present findings showed that an increase of endotoxin in PVB was closely related to the imbalance of intestinal flora in rats with ALF, and implied that ecological imbalance and bacterial overgrowth in ALF rats might play important roles in dysfunction of gut barrier, which could lead to translocation of endotoxin from gut. Our findings are supported by the previous study^[20] that gut bacterial overgrowth is one of the etiological factors of bacteria and endotoxin translocation from gut. Moreover, it has been reported that an increase in gut permeability is related to histamine released by intestinal mast cell in rat with GalN-induced acute liver injury^[21]. In addition, effect of bacterial proteases on microvillus membrane proteins contributes to the breakdown of the intestinal barrier^[22]. Another reason that should be considered is that edema of intestinal wall resulting from digestive congestion and hypoproteinemia in ALF can injure the function of gut barrier^[23]. In the present study, the levels of endotoxin in intestine increased continuously after GalN administration; this might be associated with the *Enterobacteriaceae* overgrowth^[5]. Nevertheless, our findings indicated that enlargement of gut endotoxin pool had no impact on endotoxin translocation. In addition, the present data suggested that restoration of the disturbed gut flora might play an important role in inhibiting the endotoxin translocation from gut.

The present data showed there was no significant change of the concentrations of endotoxin in RVB after GalN administration, which was in agreement with Nakao *et al.*^[24]. In contrast, the results by van Leeuwen *et al.*^[11] showed that arterial plasma endotoxin levels increased in rats with hepatic failure induced by two-third partial hepatectomy. The discrepancy between two types of ALF seemed that the count of Kupffer cell in the latter reduced significantly because of hepatectomy. Plasma endotoxin is removed primarily by the Kupffer cells. Then, GalN exerted a minor effect on the function of Kupffer cells, because the nucleotide contents of Kupffer cells were smaller than that those of hepatocytes^[25]. Logically, Kupffer cells in rats after GalN administration can phagocytose the gut-derived endotoxin.

At present, we could not measure the pretreatment effect of probiotics on endotoxin translocation for lack of *Lactobacillus* preparation suitable for rats. However, it was demonstrated that administration of the probiotics *Lactobacillus plantarum* could reduce the circulating antibody to endotoxin in patients with ulcerative colitis^[26]. Adawi *et al.*^[27] showed that administration of *Lactobacillus* could reduce bacterial translocation and hepatocellular damage in rats with acute liver injury. Moreover, our previous work demonstrated that administration of probiotics *Bifidobacterium* (DM8504) could decrease significantly the levels of plasma endotoxin in patients with chronic hepatitis B^[28].

In conclusion, severely disturbed intestinal flora disorders are observed in rats with GalN-induced acute liver failure, and related to the extent of injury of liver. Ecological imbalance of intestinal flora is one of the main causes of the translocation of endotoxin from lumen. Additionally, the present study implies that modulation of the intestinal flora using probiotics may be the optional treatment in preventing gut endotoxin translocation in patients with ALF.

ACKNOWLEDGEMENTS

We thank Dr. MH Wang (University of Colorado School of Medicine, USA) for revision the manuscript.

REFERENCES

- 1 **Rolando N**, Philpott-woward J, Williams R. Bacterial and fun-

- gal infection in acute liver failure. *Semin Liver Dis* 1996; **16**: 389-402
- 2 **Han DW**. Intestinal endotoxemia as a pathogenetic mechanism in liver failure. *World J Gastroenterol* 2002; **8**: 961-965
 - 3 **van Leeuwen PA**, Boermeester MA, Houdijk AP, Ferwerda CC, Cuesta MA, Meyer S, Wesdorp RI. Clinical significance of translocation. *Gut* 1994; **35**(1 Suppl): S28-S34
 - 4 **Camara DS**, Caruana JA Jr, Schwartz KA, Montes M, Nolan JP. D-galactosamine liver injury: absorption of endotoxin and protective effect of small bowel and colon resection in rabbits. *Proc Soc Exp Biol Med* 1983; **172**: 255-259
 - 5 **Goris H**, de Boer F, van der Waaij D. Kinetics of endotoxin release by gram-negative bacteria in the intestinal tract of mice during oral administration of *Bacitracin* and during *in vitro* growth. *Scand J Infect Dis* 1988; **20**: 213-219
 - 6 **Swank GM**, Deitch EA. Role of the gut in multiple organ failure: bacterial translocation and permeability changes. *World J Surg* 1996; **20**: 411-417
 - 7 **van der Waaij D**, Berghuis-de Vries JM, Lekkerkerk Lekkerkerk-v. Colonization resistance of the digestive tract in conventional and antibiotic-treated mice. *J Hyg* 1971; **69**: 405-411
 - 8 **Gunnarsdottir SA**, Sadik R, Shev S, Simren M, Simren M, Sjoval H, Stotzer PO, Abrahamsson H, Olsson R, Bjornsson ES. Small intestinal motility disturbances and bacterial overgrowth in patients with liver cirrhosis and portal hypertension. *Am J Gastroenterol* 2003; **98**: 1362-1370
 - 9 **Gordon DM**, Diebel LN, Liberati DM, Myers TA. The effects of bacterial overgrowth and hemorrhagic shock on mucosal immunity. *Am Surg* 1998; **64**: 718-721
 - 10 **Wang XD**, Ar' Rajab A, Andersson R, Soltesz V, Wang W, Svensson M, Bengmark S. The influence of surgically induced acute liver failure on the intestine in the rat. *Scand J Gastroenterol* 1993; **28**: 31-40
 - 11 **van Leeuwen PA**, Hong RW, Rounds JD, Rodrick ML, Wilmore D. Hepatic failure and coma after liver resection is reversed by manipulation of gut contents: the role of endotoxin. *Surgery* 1991; **110**: 169-174
 - 12 **Shito M**, Balis UJ, Tompkins RG, Yarmush ML, Toner M. A fulminant hepatic failure model in the rat: involvement of interleukin-1beta and tumor necrosis factor-alpha. *Dig Dis Sci* 2001; **46**: 1700-1708
 - 13 **Salminen S**, Salminen E. Lactulose, lactic acid bacteria, intestinal microecology and mucosal protection. *Scand J Gastroenterol Suppl* 1997; **222**: 45-48
 - 14 **Ohkusa T**, Ozaki Y, Sato C, Mikuni K, Ikeda H. Long-term ingestion of lactosucrose increases *Bifidobacterium sp.* in human fecal flora. *Digestion* 1995; **56**: 415-420
 - 15 **Hartemink R**, Rombouts FM. Comparison of media for the detection of bifidobacteria, lactobacilli and total anaerobes from faecal samples. *J Microbiol Methods* 1999; **36**: 181-192
 - 16 **Benno Y**, Endo K, Mizutani T, Namba Y, Komori T, Mitsuoka T. Comparison of fecal microflora of elderly persons in rural and urban areas of Japan. *Appl Environ Microbiol* 1989; **55**: 1100-1105
 - 17 **Li LJ**, Shen ZJ, Lu YL, Fu SZ. The value of endotoxin concentrations in expressed prostatic secretions for the diagnosis and classification of chronic prostatitis. *BJU Int* 2001; **88**: 536-539
 - 18 **Wang XD**, Soltesz V, Andersson R. Cisapride prevents enteric bacterial overgrowth and translocation by improvement of intestinal motility in rats with acute liver failure. *Eur Surg Res* 1996; **28**: 402-412
 - 19 **Deitch EA**. Bacterial translocation or lymphatic drainage of toxic products from the gut: what is important in human beings? *Surgery* 2002; **131**: 241-244
 - 20 **Barber AE**, Jones WG 2nd, Minei JP, Fahey TJ 3rd, Lowry SF, Shires GT. Bacterial overgrowth and intestinal atrophy in the etiology of gut barrier failure in the rat. *Am J Surg* 1991; **161**: 300-304
 - 21 **Stachlewitz RF**, Seabra V, Bradford B, Bradham CA, Rusyn I, Germolec D, Thurman RG. Glycine and uridine prevent D-galactosamine hepatotoxicity in the rat: role of Kupffer cells. *Hepatology* 1999; **29**: 737-745
 - 22 **Riepe SP**, Goldstein J, Alpers DH. Effect of secreted Bacteroides proteases on human intestinal brush border hydrolases. *J Clin Invest* 1980; **66**: 314-322
 - 23 **Hashimoto N**, Ohyanagi H. Effect of acute portal hypertension on gut mucosa. *Hepatogastroenterology* 2002; **49**: 1567-1570
 - 24 **Nakao A**, Taki S, Yasui M, Kimura Y, Nonami T, Harada A, Takagi H. The fate of intravenously injected endotoxin in normal rats and in rats with liver failure. *Hepatology* 1994; **19**: 1251-1256
 - 25 **Hofmann F**, Wagle SR, Decker K. Effect of d-galactosamine administration on nucleotide and protein metabolism in isolated rat Kupffer cells. *Hoppe Seylers Z Physiol Chem* 1976; **357**: 1395-1400
 - 26 **Garcia-Lafuente A**, Antolin M, Guarner F, Crespo E, Malagelada JR. Modulation of colonic barrier function by the composition of the commensal flora in the rat. *Gut* 2001; **48**: 503-507
 - 27 **Adawi D**, Ahrne S, Molin G. Effects of different probiotic strains of *Lactobacillus* and *Bifidobacterium* on bacterial translocation and liver injury in an acute liver injury model. *Int J Food Microbiol* 2001; **70**: 213-220
 - 28 **Li LJ**, Sheng JF. Effect of probiotics bifidobacterium (DM8504) on the plasma endotoxin in patients with chronic hepatitis B. *Chin J Microecol* 1996; **8**: 20-22

Edited by Kumar M and Chen WW Proofread by Xu FM

Effect of extracts of trichosanthes root tubers on HepA-H cells and HeLa cells

Chang-Ming Dou, Ji-Cheng Li

Chang-Ming Dou, Ji-Cheng Li, Institute of Cell Biology, Zhejiang University, Hangzhou 310031, Zhejiang Province, China

Supported by the Science and Technology Department of Zhejiang Province, No.2003C30057

Correspondence to: Dr. Ji-Cheng Li, Institute of Cell Biology, Zhejiang University, Department of Lymphology, Department of Histology and Embryology, Zhejiang University Medical College, Hangzhou 310031, Zhejiang Province, China. lijc@mail.hz.zj.cn

Telephone: +86-571-87217139 **Fax:** +86-571-87217139

Received: 2003-10-28 **Accepted:** 2003-12-08

Abstract

AIM: To investigate the cytotoxic activity of extracts of trichosanthes root tubers (EOT) on HepA-H cells and HeLa cells compared with trichosanthin (TCS), and to explore the possible mechanism of growth inhibitory effect of EOT on HeLa cells.

METHODS: Tumor cells were cultured *in vitro*, and then microculture tetrzoalium assay (MTT) was used to investigate drugs' cytotoxic activity. Scanning electron microscopy (SEM) and transmission electron microscopy (TEM) were used to observe ultrastructural changes of cells, and electrophoresis was performed to detect changes of biochemical characteristics of intercellular DNA.

RESULTS: TCS and EOT had no obvious effects on HepA-H cells ($P>0.05$), but had remarkable effects on HeLa cells in a time and dose dependent manner ($r>0.864$, $P<0.05$ or $P<0.01$). The inhibitory rate of EOT was much higher than that of TCS ($P<0.01$). Median inhibitory rates (IC50) of TCS and EOT on HeLa cells were 610.9 mg/L and 115.6 mg/L for 36 h, and 130.7 mg/L and 33.4 mg/L for 48 h respectively. Marked morphologic changes were observed including microvillus disappearance or reduction, cell membrane bleeding, cell shrinkage, condensation of chromosomes and apoptotic bodies with complete membranes. Meanwhile, apoptosis of HeLa cells was confirmed by DNA ladder formation on gel electrophoresis.

CONCLUSION: TCS and EOT have no obvious effects on HepA-H cells, but have significant inhibitory effects on HeLa cells, indicating that EOT is superior to TCS in anti-tumor activity.

Dou CM, Li JC. Effect of extracts of trichosanthes root tubers on HepA-H cells and HeLa cells. *World J Gastroenterol* 2004; 10(14): 2091-2094

<http://www.wjgnet.com/1007-9327/10/2091.asp>

INTRODUCTION

Trichosanthes Kirilowii Maximowii is a kind of liana of the Cucurbitaceae family, whose root tuber was a Chinese herbal medicine Tianhuafen (THF) that has been used to reset menstruation and expel retained placenta^[1]. In the 1980 s,

Trichosanthin (TCS) was isolated from the root tuber and proved to be the active component, a type I ribosome-inactivating protein (RIP) with 247 amino acids which inactivates eukaryotic ribosomes *via* its N-glycosidase activity. TCS has been used to induce mid-term abortion and to treat ectopic pregnancies, hydatidiform and trophoblastic moles in China^[2]. In recent years, TCS has also been found to possess various pharmacological properties including immunomodulatory, anti-tumor and anti-HIV activities^[3-6]. Clinical trials have also been performed. TCS has aroused extensive attention.

In the present study, we were interested in its anti-tumor activity *in vitro*. TCS has already been regarded as an effective anti-tumor agent highly specific to choriocarcinoma cells from trophoblasts^[7]. However, researches and clinical application about TCS on tumor are mainly on gastrointestinal tumor and seldom on others^[8]. TCS is an active anti-tumor component of *Trichosanthes*, yet there is no report of extracts of trichosanthes root tubers (EOT) on tumor cells. So in this study, we chose two tumor cell lines, HepA-H cells and HeLa cells, to investigate the growth inhibitory effect of EOT and TCS on the two cell lines and further compared their anti-tumor activity.

In recent years, screening of anti-tumor drugs from natural resource, especially from traditional Chinese medicines, has drawn worldwide research interest, and many exciting goals have been achieved^[9]. As a research focus of life science and medicine, apoptosis has revealed its promising future^[10-12]. Nowadays apoptosis has been considered as the most ideal path to conquer tumors. Therefore, in our study, we initially investigated the induction of apoptosis of HeLa cells by EOT. The present study may provide experimental bases for further researches and seeking novel anti-tumor agents.

MATERIALS AND METHODS

Drugs

TCS (1.2 mg/mL) was purchased from Jinshan Pharmacy Ltd, Shanghai. EOT was extracted from fresh root tubers of *Trichosanthes kirilowii* Maxim collected in Hangzhou^[13], Zhejiang Province in November 2002. SDS-PAGE (100 g/L) was performed to detect the components of EOT samples in comparison with TCS and protein marker. Gel was stained by Coomassie brilliant blue. After decoloring, the gel was visualized and photographed under gel imaging assay apparatus. Then straps in the gel were scanned to evaluate the content of relative proteins. Drugs were diluted with culture medium and sterilized before use.

Reagents and apparatus

RPMI-1640 and fetal calf serum (FCS) were from GIBCO, USA. 3-(4,5-dimethylthiazol-2-yl)-2,5-diphenyltetrazolium bromide (MTT), DMSO and all electrophoresis reagents were from Sigma Co., USA. Animal cell PCD ladder isolation kit was purchased from Dingguo Biological Products Ltd, Beijing. CO₂ incubator was the product of FORMA Company. TECNAI 10 TEM was from PHILIPS and STEREOSCAN 260 was from CAMBRIDGE Company. Electrophoresis apparatus was made by E-C Apparatus Corporation. Mini gel electrophoresis system was the product of Bio-Rad Company. Image analysis system was

purchased from Shanghai Tianneng Science and Technology Ltd.

Cell lines and cell culture

HepA-H and HeLa cells were preserved in our laboratory. The cell line of high lymphatic metastasis ascitic liver cancer was established and cultivated by professor Li and Yang^[14]. Cells were grown in RPMI-1640 culture medium containing 100 mL/L FCS, 100 U/mL penicillin and 100 U/mL streptomycin at 37 °C in a humidified atmosphere of 50 mL/L CO₂.

Cytotoxic activity

Growth inhibitory effects of HepA-H and HeLa cells with various treatments were determined by MTT assay. Cells at exponential phase were seeded into 96-well plates, 100 μL (1×10⁵/mL) per well. Then different concentrations of EOT and TCS in 100 μL culture medium were added and the final concentration in each well was 0.1 mg/L, 1 mg/L, 10 mg/L, 100 mg/L, and 500 mg/L respectively. Each treatment was tested in tetrad wells and the control group was given only culture medium containing no drug. All the above plates were placed in a 50 mL/L CO₂ humidified-atmosphere incubator at 37 °C for 24, 36 and 48 h. At the end of exposure, 20 μL MTT (5 g/L) was added to each well and the plates were incubated at 37 °C for 4 h. Then all culture medium supernatant was removed from wells and replaced with 100 μL DMSO. The plates were shaken for 15 min so that all the production of formazan reduced by MTT could be dissolved out from cells. Following thorough formation dissolved, the absorbance of each well was measured by standard enzyme-linked immunosorbant assay at 492 nm. The inhibition of tumor cell growth was calculated by the equation: Growth inhibitory rate=(1-A_{492 treated}/A_{492 control})×100%.

Based on the growth inhibitory rates of each group of drugs on cells, SPSS software was used to calculate 50% inhibitory concentrations (IC₅₀).

Specimens for electron microscope

HeLa cells at exponential phase were used and cultivated with various concentrations of EOT for 24 h. Then cells were harvested and fixed with 25 g/L glutaraldehyde in 0.1 mol/L phosphate buffer (pH 7.4) for 2 h at 4 °C. For TEM examination, the specimens were postfixed in 10 g/L osmium tetroxide in 0.1 mol/L phosphate buffer (pH 7.4) for 1 h at 4 °C. After dehydration in a graded series of ethanol and infiltration in propylene oxide, they were embedded in Epson 812. Fine sections were cut with an LKB 2088 ultramicrotome and stained with uranyl acetate and lead citrate. The sections were examined with a PHILIPS TECNAI 10 TEM at 60 kV. For SEM examination, the specimens were postfixed for 1 h in 10 g/L OsO₄, dehydrated in a graded series of alcohol, CO₂ critical-point dried, mounted on aluminum stubs and sputter-coated with gold. Specimens were examined with a STEREOSCAN 260 SEM at 25 kV.

Agarose gel electrophoresis of DNA

HeLa cells at exponential phase were exposed to different concentrations of EOT for 24, 36 and 48 h respectively. Then cells were harvested, washed twice with PBS, and DNA was extracted according to the directions of the kit. DNA was analyzed by electrophoresis at 75 mA on 8 g/L agarose gel containing 0.5 mg/L ethidium bromide. After about 1.5 h, the gel was visualized and photographed under transmission UV light.

Statistical analysis

Data were expressed as mean±SD. Statistics software package SPSS 11.5 was employed to process the data. Differences between groups were described by Student t test. *P* values less than 0.05 were considered statistically significant.

RESULTS

Protein electrophoresis of EOT and TCS

1 kg fresh trichosanthes root tubers was used in the present study and we got 0.83 g EOT. As the result of SDS-PAGE showed, sample EOT had an obvious major strap and several other minor straps. All the straps were scanned, sample EOT had a content of 70.93% of TCS and other unknown proteins. However, sample TCS had only a minor strap and its purity was 99.81%. Protein marker further conformed to protein TCS (Figure 1).

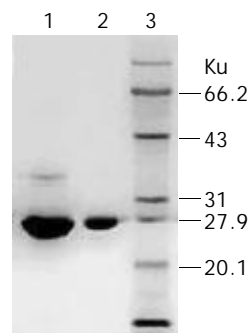


Figure 1 Analysis of EOT and TCS by SDS-PAGE. Lane 1: EOT, Lane 2: TCS, Lane 3: Protein Marker.

Cytotoxic activity of EOT and TCS in HepA-H and HeLa cells

After exposure to EOT and TCS, HepA-H cells had no growth arrest of significant importance. After 24 h, most growth of HepA-H cells was promoted, but the effect did not depend on the dose (*P*>0.05). After 36 h, all the cells were led to growth arrest, which also had no statistical relation with the dose. After 48 h, some were promoted, while the others were inhibited, and the relationship between the effect and dose was not found. All the three groups of data showed no statistical significance (*P*>0.05), suggesting HepA-H cells were not susceptible to EOT and TCS (Table 1).

Table 1 Cytotoxic activity of EOT and TCS in HepA-H cells (*n*=4, mean±SD)

Drug	Concentration (mg/L)	Inhibitory rate (%)		
		24 h	36 h	48 h
EOT	0.1	-3.1±2.9	19.1±2.6	15.7±0.8
	1.0	-3.6±8.1	7.9±11.5	5.1±2.6
	10	-25.0±1.7	6.8±0.1	3.8±3.6
	100	9.6±3.3	21.0±2.2	16.2±6.3
	500	7.6±7.6	17.0±3.0	13.4±0.7
TCS	0.1	-19.9±6.7	6.9±5.2	-3.7±4.9
	1.0	-6.1±6.4	4.7±0.6	7.4±2.7
	10	-16.1±19.1	0.7±2.4	-11.4±4.7
	100	-6.8±1.0	11.9±4.1	2.6±2.3
	500	-3.4±3.3	10.8±5.2	5.9±3.8

EOT and TCS had good effects on HeLa cells in a time and dose dependant manner (*r*>0.864). When the concentration of drugs was increased and the time was prolonged, the growth inhibitory rate increased gradually (*P*<0.01). EOT was superior to TCS in the effect on HeLa cells when the time and concentration were identical (*P*<0.01). The median inhibitory rates (IC₅₀) of TCS and EOT for HeLa cells were 610.9 mg/L and 115.6 mg/L after 36 h, and 130.7 mg/L and 33.4 mg/L after 48 h, respectively. The results suggested that EOT and TCS could inhibit the growth of HeLa cells, while EOT had much stronger cytotoxic activity (Table 2).

Table 2 Cytotoxic activity of EOT and TCS in HeLa cells (n=4, mean±SD)

Drug	Concentration (mg/L)	Inhibitory rate (%)		
		24 h	36 h	48 h
EOT	0.1	3.4±4.1	9.7±7.0	9.9±3.1
	1.0	4.5±3.7	11.1±2.0	11.3±1.9
	10	16.3±3.2	20.9±6.8	29.4±4.1
	100	36.7±4.0	44.2±1.7	54.6±3.0
	500	57.9±3.4	71.8±3.9	89.4±1.9
TCS	0.1	2.2±1.7	2.9±2.7	4.4±3.1
	1.0	2.9±2.0	5.5±1.2	6.0±2.7
	10	16.4±4.1	6.7±2.4	13.0±3.3
	100	26.3±2.5	29.3±3.9	47.9±5.2
	500	39.6±4.8	53.8±4.0	70.2±2.9

Morphological observation

After exposure to EOT for 24 h, HeLa cells were observed under SEM, typical apoptotic characteristics were found, including cell membrane blebbing, microvilli disappearance or reduction, and separated apoptotic bodies (Figure 2, A-B). Also treated HeLa cells were observed under TEM, and shrinkage of cells, condensation of chromosomes and apoptotic bodies with complete membrane were found (Figure 2, C-D).

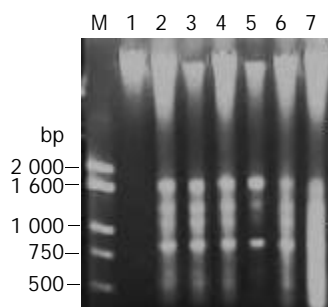


Figure 3 Analysis of DNA fragments of HeLa cells treated with EOT. M: DNA marker, lane 1: normal control, lane 2: 500 mg/L for 24 h, lane 3: 100 mg/L for 24 h, lane 4: 50 mg/L for 48 h, lane 5: 50 mg/L for 24 h, lane 6: 100 mg/L for 48 h, lane 7: 500 mg/L for 48 h.

DNA fragmentation

After HeLa cells were exposed to EOT 50 mg/L, 100 mg/L, 500 mg/L respectively for 24 h, DNA agarose gel electrophoresis showed the typical “DNA ladder” pattern of apoptosis. With time delayed, 48 h later, DNA ladder was much more obvious in the cells treated with EOT 50 mg/L, 100 mg/L, but DNA of cells treated with high concentration, 500 mg/L, took on a shape of smear, suggesting that cells underwent secondary necrosis (Figure 3). Results of DNA agarose gel electrophoresis further confirmed that EOT could induce HeLa cell apoptosis.

DISCUSSION

To our knowledge, researches of the effects of TCS on liver cancer arrived different conclusions, while studies on HeLa cells were scarcely reported^[15,16]. In the present work, we investigated and analyzed the effect of EOT and TCS on HepA-H and HeLa cells. We found that TCS and EOT had no significant effect on HepA-H cells but had remarkable effect on HeLa cells in a time and dose dependant manner. The data suggested EOT had a much higher anti-tumor effect on HeLa cells than TCS. After 48 h, the growth inhibitory rate of HeLa cells exposed to EOT and TCS (500 mg/L) was 89.4% and 70.2%, respectively. The median inhibitory rates (IC₅₀) were 610.9 mg/L and 115.6 mg/L after 36 h, and 130.7 mg/L and 33.4 mg/L after 48 h, respectively. SDS-PAGE showed, EOT contains 70.93% TCS and several other components. In contrast, TCS had a higher purity almost to 100%. It is generally believed TCS, a type I RIP, is the active component. So the results make us consider why EOT has a better inhibitory effect on the growth of tumor cells than TCS. Whether the good anti-tumor activity of EOT is correlated with the cooperation of other proteins or any other factors. As was reported, cytotoxicity of TCS was dependent on its intracellular concentration, and variation of cytotoxicity in different cells might be related to the mechanisms affecting its internalization^[17]. So there might be some active factors in EOT that promote internalization of TCS. Of course, the actual mechanism needs further researches to clarify.

It has been reported that TCS has strong effects on cytotoxicity and induction of apoptosis of gastric cancer cells, human choriocarcinoma cells and leukemia cells^[8,18,19]. Also relative genes inducing apoptosis have been isolated with their mechanism elucidated^[20]. In this study, we investigated

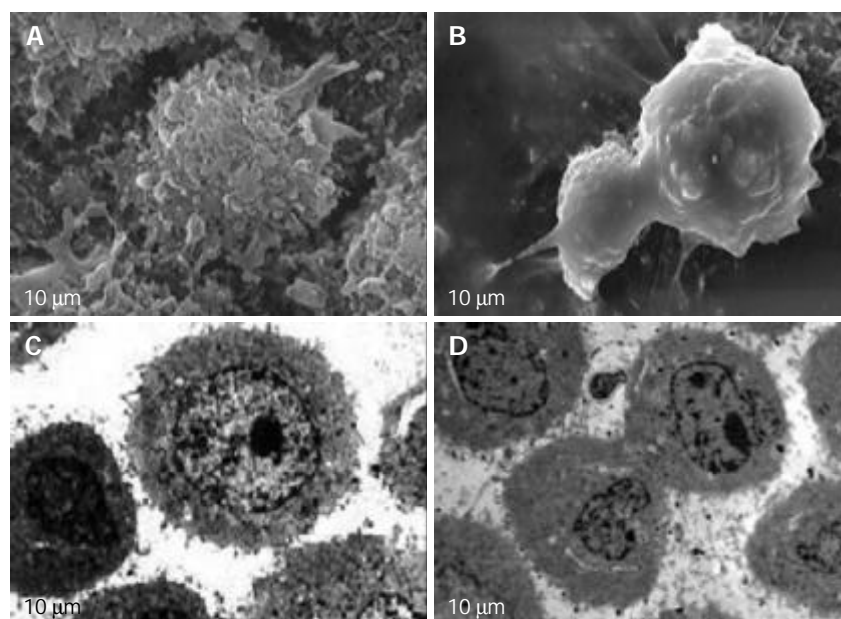


Figure 2 HeLa cells under SEM and TEM. A: HeLa cells under SEM in control group. B: HeLa cells under SEM treated with EOT (100 mg/L) for 24 h. C: HeLa cells under TEM in control group. D: HeLa cells under TEM treated with EOT (100 mg/L) for 24 h.

apoptosis of HeLa cells induced by EOT. Experiments on morphology and biochemistry revealed typical apoptotic characteristics, such as microvilli disappearance, cell membrane blebbing, apoptotic body and DNA ladder pattern. The results suggested that the anti-tumor effect of EOT on HeLa cells was related with the induction of apoptosis.

In conclusion, EOT has stronger anti-tumor effects and can induce apoptosis of HeLa cells. EOT would have a bright future in the treatment of tumors and further work may lead to relative anti-tumor agents to be used in clinic.

REFERENCES

- 1 **Chan SH**, Hung FS, Chan DS, Shaw PC. Trichosanthin interacts with acidic ribosomal proteins P0 and P1 and mitotic checkpoint protein MAD2B. *Eur J Biochem* 2001; **268**: 2107-2112
- 2 **Lu PX**, Jin YC. Trichosanthin in the treatment of hydatidiform mole. Clinical analysis of 52 cases. *Chin Med J* 1990; **103**: 183-185
- 3 **Chan SH**, Shaw PC, Mulot SF, Xu LH, Chan WL, Tam SC, Wong KB. Engineering of a mini-trichosanthin that has lower antigenicity by deleting its C-terminal amino acid residues. *Biochem Biophys Res Commun* 2000; **270**: 279-285
- 4 **Wang JH**, Nie HL, Huang H, Tam SC, Zheng YT. Independence of anti-HIV-1 activity from ribosome-inactivating activity of trichosanthin. *Biochem Biophys Res Commun* 2003; **302**: 89-94
- 5 **Wang JH**, Nie HL, Tam SC, Huang H, Zheng YT. Anti-HIV-1 property of trichosanthin correlates with its ribosome inactivating activity. *FEBS Lett* 2002; **531**: 295-298
- 6 **Cai X**, Yao G, Xu G, Yang C, Xu H, Lin Y, Yu J, Sun B. Identification of the amino acid residues in trichosanthin crucial for IgE response. *Biochem Biophys Res Commun* 2002; **297**: 510-516
- 7 **Chan WY**, Huang H, Tam SC. Receptor-mediated endocytosis of trichosanthin in choriocarcinoma cells. *Toxicology* 2003; **186**: 191-203
- 8 **Tu SP**, Jiang SH, Qiao MM, Cheng SD, Wang LF, Wu YL, Yuan YZ, Wu YX. Effect of trichosanthin on cytotoxicity and induction of apoptosis of multiple drugs resistance cells in gastric cancer. *Shijie Huanren Xiaohua Zazhi* 2000; **8**: 150-152
- 9 **Liu ZS**, Tang SL, Ai ZL. Effects of hydroxyapatite nanoparticles on proliferation and apoptosis of human hepatoma BEL-7402 cells. *World J Gastroenterol* 2003; **9**: 1968-1971
- 10 **Kerr JF**. History of the events leading to the formulation of the apoptosis concept. *Toxicology* 2002; **181**: 471-474
- 11 **Levy RR**, Cordonier H, Czyba JC, Guerin JF. Apoptosis in preimplantation mammalian embryo and genetics. *Ital J Anat Embryol* 2001; **106**(2 Suppl 2): 101-108
- 12 **Thatte U**, Bagadey S, Dahanukar S. Modulation of programmed cell death by medicinal plants. *Cell Mol Biol* 2000; **46**: 199-214
- 13 **Wang Q**. Trichosanthin. 2nd ed. Beijing: *Sci Pub* 2000: 21-28
- 14 **Yang ZR**, Li JC. Establishment and biological characteristics of two murine hepatocarcinoma substrains with different lymphatic metastatic ability. *Shiyan Shengwu Xuebao* 2003; **36**: 99-104
- 15 **Ru QH**, Luo GA, Liao JJ, Liu Y. Capillary electrophoretic determination of apoptosis of HeLa cells induced by trichosanthin. *J Chromatogr A* 2000; **894**: 165-170
- 16 **Wang Q**. Trichosanthin. 2nd ed. Beijing: *Sci Pub* 2000: 298-319
- 17 **Chan WL**, Zheng YT, Huang H, Tam SC. Relationship between trichosanthin cytotoxicity and its intracellular concentration. *Toxicology* 2002; **177**: 245-251
- 18 **Zhang C**, Gong Y, Ma H, An C, Chen D, Chen ZL. Reactive oxygen species involved in trichosanthin-induced apoptosis of human choriocarcinoma cells. *Biochem J* 2001; **355**(Pt 3): 653-661
- 19 **Kong M**, Ke YB, Zhou MY, Ke XY, Lu B, Nie HL. Study on Trichosanthin induced apoptosis of leukemia K562 cells. *Shiyan Shengwu Xuebao* 1998; **31**: 233-243
- 20 **Li XY**, Wang GQ, Ge HL, Wang Y, Li NL, Zhu Q, Chen YL, Chou GY. Isolation of a gene related to trichosanthin-induced apoptosis (GRETA). *Shiyan Shengwu Xuebao* 2000; **33**: 81-84

Edited by Wang XL and Xu CT Proofread by Xu FM

Role of COX-2 in microcirculatory disturbance in experimental pancreatitis

Wen-Wei Yan, Zong-Guang Zhou, You-Dai Chen, Hong-Kai Gao

Wen-Wei Yan, III Department of General Surgery, West China Hospital, Sichuan University, Chengdu 610041, Sichuan Province, China & Department of Organ Transplantation of Tianjin First Central Hospital, Tianjin 300052, China

Zong-Guang Zhou, III Department of General Surgery, West China Hospital, Sichuan University, Chengdu 610041, Sichuan Province, China
You-Dai Chen, Hong-Kai Gao, Institute of Digestive Surgery, West China Hospital, Sichuan University, Chengdu 610041, Sichuan Province, China

Supported by the National Natural Science Foundation of China, No. 39770722

Correspondence to: Dr. Zong-Guang Zhou, III Department of General Surgery, West China Hospital, Sichuan University, Chengdu 610041, Sichuan Province, China. zhou767@21cn.com

Telephone: +86-28-85422525 **Fax:** +86-28-85422484

Received: 2004-02-11 **Accepted:** 2004-02-18

Abstract

AIM: To elucidate the role of COX-2 in the development of capillary leakage in rats with acute interstitial pancreatitis.

METHODS: Rats with acute interstitial pancreatitis were induced by caerulein subcutaneous injection. Reverse transcription-polymerase chain reaction (RT-PCR) was used to determine the gene expression of COX-2 in pancreatic tissues, spectrophotometry was used to assay the parameters of acute pancreatitis such as the serum amylase and plasma myeloperoxidase, and determination of capillary permeability in the pancreas by quantifying the permeability index (PI) assisted response of pancreatic microvascular via intravital fluorescence microscope video image analysis system.

RESULTS: A significant increase of COX-2 expression, elevation of serum amylase, and plasma myeloperoxidase were detected in rats with acute edematous pancreatitis compared with control rats. The changes of pancreatic microvascular after caerulein injection were as following: (a) the decrease of pancreatic capillary blood flow (4th h, 0.56 ± 0.09 nL/min, $P < 0.05$; 8th h, 0.34 ± 0.10 nL/min, $P < 0.001$); (b) reduction of functional capillary density (4th h, 381 ± 9 cm⁻¹, $P > 0.05$; 8th h, 277 ± 13 cm⁻¹, $P < 0.001$); (c) irregular and intermittent capillary perfusion was observed at the 8th h and these vessels were also prone to permeation.

CONCLUSION: COX-2 plays an important role in mediating capillary permeability in pancreatitis, thereby contributing to capillary leakage.

Yan WW, Zhou ZG, Chen YD, Gao HK. Role of COX-2 in microcirculatory disturbance in experimental pancreatitis. *World J Gastroenterol* 2004; 10(14): 2095-2098
<http://www.wjgnet.com/1007-9327/10/2095.asp>

INTRODUCTION

Pancreatic microcirculatory disturbance has been considered as one of the possible and important causative factors for the

development of acute pancreatitis (AP)^[1-5], although the underlying mechanism is unclear. COX-2, known as prostaglandin endoperoxide synthase-2, is a rate-limiting enzyme in the production of prostaglandins and an important regulator of vascular function^[8,9]. Under resting conditions, the level of COX-2 was undetectable. COX-2 expression can be inducible by a wide range of extracellular and intracellular stimuli, including lipopolysaccharide, forskolin, interleukin-1 (IL-1), tumor necrosis factor (TNF), epidermal growth factor, interferon- γ , platelet activating factor and endothelin, suggesting that COX-2 plays a critical role in inflammatory disorder^[6,7]. Previous studies demonstrated that COX-2 was a classic example of immediate early or primary response gene activation and generally considered as a proinflammatory enzyme^[10-15], suggesting COX-2 may serve as one of triggering factors of inflammation. Studies showed that inducible cyclooxygenase (COX-2) might indirectly involve in the regulation of human vascular endothelial cells (HUVEC) inflammation^[16,17]. However, no further studies examined it. For the purpose of verification of the result, reverse transcription polymerase chain reaction (RT-PCR) and intravital fluorescence microscopy with fluorescein isothiocyanate (FITC) labeled erythrocytes were used to study COX-2 gene expression and pancreatic microvasculature, with the aim of consolidating the relevance between the gene expression of COX-2 and dysfunction of pancreatic local microvasculature during acute edematous pancreatitis (AEP).

MATERIALS AND METHODS

Animal

A total of 96 male Wistar rats (250-350 g) were starved 15 h prior to the experiments with water *ad libitum* and randomly divided into 2 groups: (1) AEP group ($n=72$), 24 rats for extraction of total RNA from pancreatic tissue and 3 mL blood samples of portal venous for assay of serum amylase (AMS) and plasma myeloperoxidase (MPO); 24 rats for studying pancreatic microvasculature by intravital fluorescence microscope with fluorescein FITC-RBC; 24 rats for accessing the pancreatic microvasculature permeability and water content. (2) Normal control group ($n=24$). The model of AEP was established by subcutaneous injection of caerulein (Sigma) as previously described^[1]. 1 h and 2 h after the beginning of experiment all experimental groups were injected caerulein 5.5 μ g/kg and 7.5 μ g/kg respectively, while control group received the same volume of 9 g/L sodium chloride.

Total RNA extraction from pancreatic tissue

After 2, 4, 8, 16 and 24 h of caerulein injection, the rats were anesthetized with intraperitoneal injection of 30 g/L barbitone sodium (35 mg/kg) and the sacrificed for extraction of total RNA. The isolation of total RNA was prepared from 100 mg pancreatic tissue, using Trizol reagent Kit (Gibco BRL). Yield and purity of RNA preparations were checked spectrophotometrically at 260 nm and 280 nm and quality was inspected visually on 13 g/L agarose gels after ethidium bromide staining.

Semi-quantitative RT-PCR analysis for COX-2 mRNA

RT-PCR was performed in combined one-tube reaction kits (Takara™) according to the manufacture's suggestions. β -actin was used as an internal control. The primers for control and COX-2 were as follows: β -actin (sense) 5' -GAT GGT GGG TAT GGG TCA GAA-3', (antisense) 5' -CTA GGA GCC AGG GCA GTA ATC-3'; COX-2 (sense) 5' -CTG TAT CCC GCC CTG CTG GT-3', (antisense) 5' -GAG GCA CTT GCG TTG ATG GT-3'. All the primers were synthesized by Life Technology (HongKong, China). RT-PCR was run in GeneAmp 9600 (Perkin-Elmer), following procedures: 50 °C for 30 min, 1 cycle; 94 °C for 2 min, 1 cycle; 94 °C for 30 s, 55 °C for 30 s, 72 °C for 40 s, 30 cycles; 72 °C for 10 min, 1 cycle. 5 μ L PCR products was placed onto 13 g/L agarose gels with ethidium bromide staining, using an ultraviolet illuminator, and the level of COX-2 mRNA was expressed as the quotient (Q) of the integrated optical density values (IOD) for the COX-2 and the β -actin bands ($Q = \text{IOD COX-2 band} / \beta\text{-actin band}$).

Assay of plasma myeloperoxidase (MPO)

The activity of MPO, an index of tissue leukocyte recruitment, is a marker of inflammation of tissue. The activity of MPO in the pancreatic tissues was determined following the method described by Calkins^[23] with minor modifications.

Response of pancreatic local microvessel

For studying response of pancreatic microvasculature we adopted erythrocytes (RBC) labeled by FITC using the approach as previously described. Briefly, washed RBC obtained from an experimental rat was incubated with PBS (137 mmol/L NaCl, 6.4 mmol/L Na_2HPO_4 , 2.7 mmol/L KCl, 1.5 mmol/L KH_2PO_4 , pH 7.8) solution containing 1 mg/mL FITC. The labeled cells were then washed twice with a saline solution containing 10 g/L bovine serum albumin (Sigma) to remove unconjugated fluorescent dye. The final volume percentage of the labeled cells was adjusted approximately to 50% by adding an isotonic saline solution, and an aliquot 91 mL/kg of these suspensions was injection through a tail vein of the rats to observe density and capillary perfusion by intravital fluorescence microscope (OLYMPUS X-70).

Assay for microvascular permeability

Half an hour before caerulein injection, the rats were given an intravenous injection of Evans blue (20 mg/kg) via a tail vein. Briefly, the lungs and pancreas were excised, weighted, and placed in 5 mL of formaldehyde solution and homogenized for 1 min. After incubated at room temperature for 16 h, the pancreas and lungs were measured at 650 nm in Beckman spectrophotometer. The concentration of Evans blue (EB) was determined by calculation against a standard curve. The blood was centrifuged at 600 r/min for 10 min and the concentration of EB in the serum was determined as described above. The permeability index (PI) = $\frac{[\text{Evans blue}]_{\text{tissue}}}{[\text{Evans blue}]_{\text{serum}}}$. Water mass fractions in the pancreas were used as a parameter of organ water accumulation after pancreatitis induction. The tissues were removed in a humidity chamber and the wet mass was measured immediately. The tissue was dried at 70 °C to a constant mass for the determination of dry mass. Organ edema was determined by calculating tissue water content according to the following formula: Water mass fraction (%) = $(1 - \text{dry mass/wet mass}) \times 100\%$.

Statistics analysis

All results were represented as mean \pm SD. The significance of changes were evaluated by means of a *F* test in comparisons of the same time point in two groups or by analysis of variance (Newman-Keuls) when different time points in the same group were compared. Differences were considered significant when the $P < 0.05$.

RESULTS

RT-PCR detection of COX-2 in the pancreas

COX-2 transcription remained at a low level in normal control (Figure 1). Whereas, after injection of caerulein, the expression of COX-2 mRNA in AEP was increased, with peaked at the 8th h, and kept at high level within 24 h. Setting the level of COX-2 expression at 2nd h as baseline, COX-2 expressions of the 4th h and 8th h in AEP were significant higher (2nd h, 0.23 ± 0.03 , $P < 0.05$; 4h, 1.55 ± 0.93 , 8th h, 4.04 ± 1.05 , 16th h, 3.73 ± 0.15 and 24th h, 3.37 ± 0.23 , $P < 0.01$ respectively). Compared with controls, this increase was also significant ($P < 0.01$).

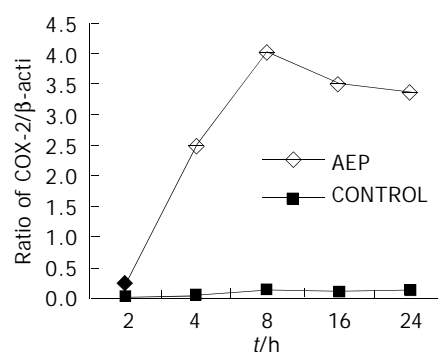


Figure 1 Time course of COX-2 gene expression in pancreas. After induction by caerulein, the expression of COX-2 mRNA in AEP was increased, which peaked at the 8th h and remained at a high level.

Inflammatory indicators for pancreatitis

The activity of serum AMS and MPO in AEP and controls are shown in Table 1.

Table 1 Levels of amylase (AMS) and myeloperoxidase (MPO) in AEP and control groups (mean \pm SD)

Group	n	MPO (U/mL)	AMS (U/dL)
Control (0 h)	24	0.32 \pm 0.13	40 \pm 37
AEP 2nd h	6	0.60 \pm 0.20	313 \pm 130 ^a
4th h	6	0.74 \pm 0.39 ^b	391 \pm 96 ^a
8th h	6	0.85 \pm 0.56 ^b	255 \pm 92 ^a
16th h	6	0.88 \pm 0.29 ^b	291 \pm 73 ^a
F		4.542	12.322

^a $P < 0.05$, ^b $P < 0.01$ vs control.

In vivo fluorescent microscopy

Compared with the control, the pancreatic microvasculature changes at the 4th, 6th and 8th h after caerulein were as follows: (a) the reduction of the density and velocity of FITC-RBC (4, 6 and 8th h $P < 0.001$); (b) the decrease of the pancreatic capillary blood flow (4, 6, and 8th h, $P < 0.001$); (c) diminution of functional capillary density (4th h, $P > 0.05$; 6th h, $P < 0.05$; 8th h, $P < 0.001$) and arterioles diameter (4th h, $P > 0.05$; 6th h and 8th h, $P < 0.05$); (d) insufficient capillary perfusion appeared at the 8th h; (e) arterioles of pancreatic lobules and capillary density at the 6th h experienced significant changes, while the calibers of venules and capillaries shown no marked change (Table 2).

Microvascular permeability in pancreas and lungs

The PI from rats of control were shown little changes before and after injection of 0.9% sodium chloride, while both pancreas and lungs showed a significant increase in microvasculature from the 4th h to 16th h in rats of AEP and the increase in the lungs was higher than that in the pancreas (Lungs, 8th and 16th h, $P < 0.001$, respectively; pancreas 8th and 16th h, $P < 0.01$,

Table 2 Response of pancreatic local microvascular in AEP and controls (mean±SD)

	4th h		6th h		8th h	
	NC	AIP	NC	AIP	NC	AIP
¹ Density of RBC /(±10 ⁹ cell/L)	113±5	85±9 ^a	104±4	68±7 ^a	96±6	59±9 ^a
² Velocity of RBC /(cell/min)	86±3	43±2 ^a	81±4	36±5 ^a	84±5	30±5 ^a
³ RBC flow (nL/L)	0.28±0.01	0.12±0.03 ^a	0.31±0.02	0.09±0.03 ^a	0.29±0.04	0.07±0.03 ^a
⁴ Blood flow	0.88±0.06	0.56±0.09 ^a	0.99±0.07	0.45±0.12 ^a	0.91±0.06	0.34±0.10 ^a
⁵ Diameter (arteriod)/μm	23.5±8.0	20.2±5.1 ^a	24.1±8.0	16.4±3.1 ^a	23.2±5.5	18.2±3.5 ^a
⁶ Diameter (venule)/μm	28±3.0	29.1±2.0 ^a	28±2.7	27.5±3.0 ^a	27.4±1.6	29±1.5 ^a
⁷ Diameter (capillary)/μm	6.7±1.5	7.0±1.4 ^a	6.9±1.5	6.0±0.3 ^a	7.3±1.0	5.2±0.3 ^a
⁸ Density (capillary)/cm	394±7	381±9 ^a	400±6	291±16 ^a	349±8	277±13 ^a

¹F=109.68, P<0.01; ²F=478.8, P<0.01; ³F=185.2, P<0.01; ⁴F=1.99, P<0.01; ⁵F=3.52, P<0.001; ⁶F=1.12, P>0.05; ⁷F=5.71, P<0.001; ⁸F=312.12, P<0.01; ^aP<0.05 vs control.

respectively) (Figure 2). The water mass fractions in the pancreas were increased after caerulein injection compared with controls (2ndh, 19.18±2.10; 4thh, 24.81±1.31; 8thh, 25.86±1.97; 16thh, 30.71±5.80, P<0.05), while the water mass fraction in normal remained relative stable.

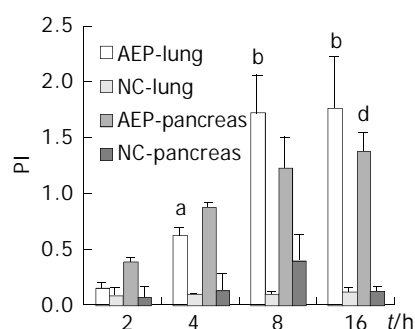


Figure 2 Microvascular permeability index (PI) in the pancreas and lungs in AEP and control group. The figures indicate the increase of PI in the lungs is higher than that in the pancreas ^aP<0.05 vs control; ^bP<0.001 vs control; ^dP<0.01 vs control.

DISCUSSION

Previous studies have discovered that COX-2 is the principal isoform of cyclooxygenase that participates in inflammation, while there is little COX-2 activity present in the stomach, kidney, or platelet. COX-2 is usually barely detectable during normal physiologic conditions. However, in response to several pro-inflammatory stimuli, the level of COX-2 expression can be rapidly induced to increase^[18-20]. In our study, we found that COX-2 transcription remains at a very low level in normal pancreatic tissue. In contrast, COX-2 expression was increased rapidly after induction of pancreatitis by caerulein. COX-2 may serve as one of factors of at the early phase of inflammation. During the active inflammation, the synthesis of PGE₂ (an important inflammatory mediator), the increase of vaso-permeability, sequestration of inflammatory cells and pyrogen are likely resulted from COX-2.

It has been reported that a strong correlation between the number of intra-vascular neutrophils and MPO existed. Thus these parameters were measured to quantify the total neutrophil

sequestration to the pancreas^[21-23]. In our previous study, we found the positive correlation between COX-2 and MPO in AEP ($r=0.5449$, P<0.05). From this study, the elevation of plasma myeloperoxidase was present in the experiment, suggesting MPO can serve as an indicator of AEP.

There is increasing evidence that the vascular endothelium, which is directly exposed to various fluid mechanical forces generated by pulsatile blood flow, can discriminate among these stimuli and transduce them into genetic regulatory events, as COX-2 gene can be upregulated by steady laminar shear stress stimulation^[25]. However little is known about the upregulation of COX-2 disturbing microcirculation. It is generally accepted that the dysfunction of pancreatic microcirculation serves as an important causative factor for the development of acute pancreatitis. The morphology of pancreatic microcirculation revealed that pancreatic lobule is supplied by a single intralobular arteriole, which is considered end-artery^[21,24-26]. This characteristic suggested that pancreatic lobules are susceptible to ischemic injury due to spasm of intralobular arterioles. In this study, we observed the responses of pancreatic microvascular after caerulein induction, which demonstrated that the enhanced COX-2 mRNA might involve in modulating the dynamical changes of the pancreatic microcirculation. The decrease of pancreatic capillary blood flow, the reduction of functional capillary density, and capillary perfusion irregular intermittent perfusion and capillary artery hypoperfusion were observed, especially at 8thh, which was coincident with the enhanced expression of COX-2 mRNA after AEP.

Based on the pathologic changes above, we postulate that COX-2 induce the inflammation of vascular endothelia, result in increase of vasopermeability, sequestration of leukocyte and water content in the pancreatic tissue. A functional role of the COX-2, mediating the changes of pancreatic microcirculation has several possible explanations: (1) it may be cooperated with inducible nitric oxide synthase (iNOS), and both mediators can activate platelets and leukocytes, promote the occurrence of microthrombus and affect microcirculatory stability^[27]; (2) it may be in linkage with the overexpression of adhesion molecules (e.g. ICAM-1, PCAM-1). Adhesion molecules are known to regulate partly the disturbance of microvascular barrier both *in vivo* and *in vitro*^[28,29]. Treatment with the monoclonal antibodies against ICAM-1, PECAM-1 to rats with gut barrier failure caused by intestinal ischemia and reperfusion (I/R) seemingly

most efficiently reduces the severity of I/R (i.e., enhanced capillary blood flow in the pancreas, reduced leukocyte rolling and stabilized capillary permeability)^[30,31]; (3) it may be feedback control of COX-2 expression through peroxisome proliferator-activated receptor- γ (PPAR- γ). PPAR- γ expressed in macrophages has been postulated as a negative regulator of inflammation^[9]. Additional investigation will be necessary to distinguish between these mechanisms of action.

REFERENCES

- Foitzik T**, Faulhaber J, Hotz HG, Kirchengast M, Buhr HJ. Endothelin receptor blockade improves fluid sequestration, pancreatic capillary blood flow and survival in severe experimental pancreatitis. *Ann Surg* 1998; **228**: 670-675
- Zhou ZG**, Chen YD. Influencing factors of pancreatic microcirculatory impairment in acute pancreatitis. *World J Gastroenterol* 2002; **8**: 406-412
- Menger MD**, Plusczyk T, Vollmar B. Microcirculatory derangements in acute pancreatitis. *J Hepatobiliary Pancreat Surg* 2001; **8**: 187-194
- Dembinski A**, Warzecha Z, Ceranowicz P, Stachura J, Tomaszewska R, Konturek SJ, Sendur R, Dembinski M, Pawlik WW. Pancreatic damage and regeneration in the course of ischemia-reperfusion induced pancreatitis in rats. *J Physiol Pharmacol* 2001; **52**: 221-235
- Jaffray C**, Yang J, Carter G, Mendez C, Norman J. Pancreatic elastase activates pulmonary nuclear factor kappa B and inhibitory kappa B, mimicking pancreatitis-associated adult respiratory distress syndrome. *Surgery* 2000; **128**: 225-231
- Heuser M**, Popken O, Kleiman I, Post S. Detrimental effects of octreotide on intestinal microcirculation. *J Surg Res* 2000; **92**: 186-192
- Yamanaka K**, Saluja AK, Brown GE, Yamaguchi Y, Hofbauer B, Steer ML. Protective effects of prostaglandin E₁ on acute lung injury of caerulein-induced acute pancreatitis in rats. *Am J Physiol* 1997; **272**: G23-G30
- Caughey GE**, Cleland LG, Gamble JR, James MJ. Up-regulation of endothelial cyclooxygenase-2 and prostanoid synthesis by platelets. Role of thromboxane A₂. *J Biol Chem* 2001; **276**: 37839-37845
- Crofford LJ**, Wilder RL, Ristimaki AP, Sano H, Remmers EF, Epps HR, Hla T. Cyclooxygenase-1 and 2 expression in rheumatoid synovial tissues. Effects of interleukin-1 β , phorbol ester, and corticosteroids. *J Clin Invest* 1994; **93**: 1095-1101
- Tamura M**, Sebastian S, Gurates B, Yang S, Fang Z, Bulun SE. Vascular endothelial growth factor upregulates Cyclooxygenase-2 expression in human endothelial cells. *J Clin Endocrinol Metab* 2002; **87**: 3504-3507
- Inoue H**, Tanabe T, Umesono K. Feedback control of Cyclooxygenase-2 expression through PPAR γ . *J Biol Chem* 2000; **275**: 28028-28032
- Chen JX**, Berry LC Jr, Christman BW, Tanner M, Myers PR, Meyrick BO. NO regulates LPS-stimulated cyclooxygenase gene expression and activity in pulmonary artery endothelium. *Am J Physiol Lung Cell Mol Physiol* 2001; **280**: L450-457
- Williams CS**, Dubois RN. Prostaglandin endoperoxide synthase: why two isoforms? *Am J Physiol* 1996; **270**: G393-400
- Crofford LJ**. Prostaglandin biology. *Gastroenterol Clin North Am* 2001; **30**: 863-876
- Colville-Nash PR**, Gilroy DW. COX-2 and the cyclopentenone prostaglandins-a new chapter in the book of inflammation? *Prostaglandins Other Lipid Media* 2000; **62**: 33-43
- Parfenova H**, Parfenov VN, Shlopov BV, Levine V, Falkos S, Pourcyrous M, Leffler CW. Dynamics of nuclear localization sites for COX-2 in vascular endothelial cells. *Am J Physiol* 2001; **81**: C166-C178
- Zabel-Langhennig A**, Holler B, Engeland K, Mossner J. Cyclooxygenase-2 transcription is stimulated and amylase secretion is inhibited in pancreatic acinar cells after induction of acute pancreatitis. *Biochem Biophys Res Commun* 1999; **265**: 545-549
- Inoue H**, Umesono K, Nishimori T, Hirata Y, Tanabe T. Glucocorticoid-mediated suppression of the promoter activity of the Cyclooxygenase-2 gene is modulated by expression of its receptor in vascular endothelial cells. *Biochem Biophys Res Commun* 1999; **254**: 292-298
- maszewska R**, Dembinski A, Warzecha Z, Ceranowicz P, Konturek SJ, Stachura J. The influence of epidermal growth factor on the course of ischemia-reperfusion induced pancreatitis in rats. *J Physiol Pharmacol* 2002; **53**: 183-198
- Calkins CM**, Barsness K, Bensard DD, Vasquez-Torres A, Raeburn CD, Meng X, McIntyre RC Jr. Toll-like receptor-4 signaling mediates pulmonary neutrophil sequestration in response to Gram-positive bacterial enterotoxin. *J Surg Res* 2002; **104**: 124-130
- Zhou ZG**, Gao XH, Wayand WU, Xiao LJ, Du Y. Pancreatic microcirculation in the monkey, with special reference to the blood drainage system of Langerhans islets: Light and scanning electron microscopic study. *Clin Anat* 1996; **9**: 1-9
- Peskar BM**, Maricic N, Gretzer B, Schuligoi R, Schmassmann A. Role of cyclooxygenase-2 in gastric mucosal defense. *Life Sci* 2001; **69**: 2993-3003
- Calkins CM**, Barsness K, Bensard DD, Vasquez-Torres A, Raeburn CD, Meng X, McIntyre RC. Toll-like receptor-4 signaling mediates pulmonary neutrophil sequestration in response to gram-positive bacterial enterotoxin. *J Surg Res* 2002; **104**: 124-130
- Dib M**, Zhao X, Wang XD, Andersson R. Role of mast cells in the development of pancreatitis-induced multiple organ dysfunction. *Br J Surg* 2002; **89**: 172-178
- Gimbrone MA**, Topper JN, Nagel T, Anderson KR, Garcia-Cardena G. Endothelial dysfunction, hemodynamic forces and atherogenesis. *Ann NY Acad Sci* 2002; **902**: 230-239
- Plusczyk T**, Bersal B, Westermann S, Menger M, Feifel G. ET-1 induces pancreatitis-like microvascular deterioration and acinar cell injury. *J Surg Res* 1999; **85**: 301-310
- Zhou ZG**, Zhang ZD, Yan LN, Shu Y, Cheng Z, Zhao JC, Lan P, Feng XM, Wang R. The feature of pancreatic microcirculatory impairment in caerulein induced acute pancreatitis. *Zhonghua Waike Zazhi* 1999; **37**: 138-140
- Gao HK**, Zhou ZG, Chen YQ, Han FH, Wang C. Expression of platelet endothelial cell adhesion molecule-1 between pancreatic microcirculation and peripheral circulation in rats with acute edematous pancreatitis. *Hepatobiliary Pancreat Dis Int* 2003; **2**: 463-466
- Zingarelli B**, Southan GJ, Gilad E, O'Connor M, Salzman AL, Szabo C. The inhibitory effects of mercaptoalkylguanidines on cyclo-oxygenase activity. *Br J Pharmacol* 1997; **120**: 357-366
- Sun Z**, Wang X, Lasson A, Bojesson A, Annborn M, Andersson R. Effects of inhibition of PAF, ICAM-1 and PECAM-1 on gut barrier failure caused by intestinal ischemia and reperfusion. *Scand J Gastroenterol* 2001; **36**: 55-65
- Frossard JL**, Saluja A, Bhagat L, Lee HS, Bhatia M, Hofbauer B, Steer ML. The role of intercellular adhesion molecule 1 and neutrophils in acute pancreatitis and pancreatitis-associated lung injury. *Gastroenterology* 1999; **116**: 694-701

Edited by Zhang JZ Proofread by Chen WW and Xu FM

Management of carbon tetrachloride-induced acute liver injury in rats by syngeneic hepatocyte transplantation in spleen and peritoneal cavity

Charalampos Pilichos, Despina Perrea, Maria Demonakou, Athena Preza, Ismini Donta

Charalampos Pilichos, Athena Preza, Third Department of Propaedeutic Surgery, University of Athens, Sotiria Hospital, Athens, Hellas

Despina Perrea, Ismini Donta, Laboratory of Experimental Surgery, University of Athens, Hellas

Maria Demonakou, Laboratory of Pathological Anatomy, Sismanogleion General Hospital, Athens, Hellas

Correspondence to: Dr. Charalampos Pilichos, Mpoumpoulinas 27-15341- Ag Paraskevi, Athens, Hellas (Greece). hpilichos@hotmail.com

Telephone: +30-210-6524097 **Fax:** +30-210-6524097

Received: 2004-01-02 **Accepted:** 2004-01-17

Abstract

AIM: Acute hepatitis may seldom have a fulminant course. In the treatment of this medical emergency, potential liver support measure must provide immediate and sufficient assistance to the hepatic function. The goal of our study was to study the adequacy of hepatocyte transplantation (HCTx) in two different anatomical sites, splenic parenchyma and peritoneal cavity, in a rat model of reversible acute hepatitis induced by carbon tetrachloride (CCl₄).

METHODS: After CCl₄ intoxication, 84 male Wistar rats used as recipients were divided in to four experimental groups accordingly to their treatment: Group A (n=24): intrasplenic transplantation of 10x10⁶ isolated hepatocytes, Group B (n=24): intraperitoneal transplantation of 20x10⁶ isolated hepatocytes attached on plastic microcarriers, Group C (n=18): intrasplenic injection of 1 mL normal saline (sham-operated controls), Group D (n=18): intraperitoneal injection of 2.5 mL normal saline (sham-operated controls). Survival, liver function tests (LFT) and histology were studied in all four groups, on d 2, 5 and 10 post-HCTx.

RESULTS: The ten-day survival (and mean survival) in the 4 groups was 72.2% (8.1±3.1), 33.3% (5.4±3.4), 0% (3.1±1.3) and 33.3% (5.4±3.6) in groups A, B, C, D, respectively ($P_{AB}<0.05$, $P_{AC}<0.05$, $P_{BD}=NS$). In the final survivors, LFT (except alkaline phosphatase) and hepatic histology returned to normal, independently of their previous therapy. Viable hepatocytes were identified within splenic parenchyma (in group A on d 2) and both in the native liver and the fatty tissue of abdominal wall (in group B on d 5).

CONCLUSION: A significantly better survival of the intrasplenically transplanted animals has been demonstrated. Intraperitoneal hepatocytes failed to promptly engraft. A different timing between liver injury and intraperitoneal HCTx may give better results and merits further investigation.

Pilichos C, Perrea D, Demonakou M, Preza A, Donta I. Management of carbon tetrachloride-induced acute liver injury in rats by syngeneic hepatocyte transplantation in spleen and peritoneal cavity. *World J Gastroenterol* 2004; 10(14): 2099-2102
<http://www.wjgnet.com/1007-9327/10/2099.asp>

INTRODUCTION

Acute hepatitis may seldom have a fulminant course. In the treatment of this medical emergency, potential liver support measure must provide immediate and sufficient assistance to the hepatic function. Hepatocyte transplantation (HCTx) is a mainly experimental and minimally invasive method for liver support, offering the opportunity for native liver regeneration in cases of reversible failure or serving as a "bridge" to whole liver transplantation in cases of irreversible damage. However, for the clinical implementation of this newly developed technique both theoretical and practical aspects have to be further elucidated.

Various anatomical sites for cell implantation such as native liver, spleen, peritoneal cavity, kidney, lung, pancreas and fat pads have been investigated by different teams since the introduction of the method, but their results are not conclusive due to the great methodological diversity^[1-7]. The spleen is considered as the most privileged anatomical site for HCTx. It is accessible by means of laparotomy. It can entrap a limited, but a sufficient number of hepatocytes within its sinusoids, providing conditions very similar to natural cell microenvironment. This process has been described by Mito in the early 1980' s, by the term "splenic hepatization"^[8]. On the other hand, peritoneal cavity is very promising as it can be accessed by minimally invasive means and allows the injection of a greater number of cells. However, the major disadvantage of intraperitoneal route was the inability of injected cells to promptly engraft and thus to receive an adequate vascular supply. This led to cell death in three days following transplantation^[9]. To overcome this limitation, Demetriou *et al.* introduced the technique of cell attachment on collagen-coated dextran-microcarriers, prior to transplantation^[10]. Since then, most experimental studies have relied on this concept. Microcarrier-attached hepatocytes can survive for a long time, forming neovascularized aggregates^[11].

The aim of our study was to study the adequacy of HCTx in two different anatomical sites, splenic parenchyma and peritoneal cavity, in a rat model of reversible acute hepatitis induced by carbon tetrachloride (CCl₄).

MATERIALS AND METHODS

Donors

Hepatocyte isolation Fifteen male Wistar rats (Institute Pasteur-Athens), weighing 300-450 g were used as donors of hepatocytes. For cell isolation, we used collagenase perfusion/incubation technique, which was previously described by our team^[12]. Aliquots were taken for cell count (Neubauer hemocytometer) and determination of cellular viability (Trypan Blue Exclusion Test).

Recipients

Development of acute hepatitis model In preliminary experiments, we tested a wide range of CCl₄ doses (0.5-4 mL/kg) given intraperitoneally in 35 controls. Total bilirubin, SGOT,

SGPT and ALP levels were measured before and after CCl₄ administration and correlated with the histological severity of liver damage. A single dose of 1 mL/kg CCl₄, dissolved in olive oil in a ratio of 1:5 v/v, resulted in approximately 10% mortality of acute hepatic injury within 24 h. This dosage allowed liver support measures to be initiated before animal death and was used for all experiments reported herein.

Experimental groups

One hundred male Wistar rats (Institute Pasteur-Athens) weighing 300-450 g were used as candidate recipients. They were maintained in a 48-h dark/light cycle, had free access to food and water and were given CCl₄ at the above-mentioned dose (d 0). Twenty-four hours later (d 1), 84 survivors were divided into 4 groups accordingly to their subsequent therapy: Group A (*n*=24): intrasplenic transplantation of 10×10⁶ isolated hepatocytes, Group B (*n*=24): intraperitoneal transplantation of 20×10⁶ isolated hepatocytes attached on plastic microcarriers, Group C (*n*=18): intrasplenic injection of 1 mL normal saline (sham-operated controls), Group D (*n*=18): intraperitoneal injection of 2.5 mL normal saline (sham-operated controls).

Transplantation technique

All rats were transplanted under ketamine and midazolame anesthesia. For intrasplenic HCTx, cell suspension was diluted in 1 mL of Hank's solution and injected after laparotomy using a 27G needle. Leakage was prevented with suture at the point of injection. Prior to intraperitoneal HCTx, cells were attached onto gelatin-coated plastic beads (Sigma, 1.5 g/10 g of liver tissue) by incubation at 37 °C for 45 min. Cell suspension was diluted in 2.5 mL of Hank's solution and subsequently injected using an 18G needle

Survival, liver function tests and histological study

Eighteen rats in groups A and B and nine rats in control groups C and D were observed for a 10-day period, in order to determine survival (survival rate and mean survival). Three animals from each group were sacrificed on d 2 and 5 respectively for biochemical and histological study. Final survivors were also sacrificed on day 10 for both biochemical and histological study. Sacrifice was achieved under general anesthesia according to the guidelines of the Hellenic National Research Council. Blood samples were taken directly from the left ventricle. Total bilirubin, SGPT, SGOT and alkaline phosphatase were measured in all groups. Liver, spleen and cell aggregates (when macroscopically visible) were taken for anatomical study. After fixation in buffered formaldehyde 40 g/L, they were stained with hematoxylin/eosin. The prepared sections were assessed systematically under code by one hepatopathologist, who was unaware of protocol features.

Determination of normal and baseline values

Normal and baseline values (24 h after CCl₄ administration) of liver function tests were measured in ten controls before and 24 h after CCl₄-intoxication.

Statistical analysis

For statistical analysis of mean survival and liver function tests we used Student's *t*-test. For statistical analysis of 10-day survival rate we used chi-square test. Statistical significance level was set at *P*<0.05.

RESULTS

Number and viability of isolated hepatocytes

A mean of approximately 250×10⁶ of liver cells was harvested from each donor, with a mean viability greater than 90%.

Survival rate

In all 4 groups, the 10-day survival rate was: 13/18 (72.2%), 6/18 (33.3%), 0/9 (0%) and 3/9(33.3%) in groups A, B, C, D, respectively. Furthermore, the mean survival was 8.1±3.1 d, 5.4±3.4 d, 3.1±1.3 d and 5.4±3.6 d in groups A, B, C, D, respectively (Figures 1 and 2). Statistically significant difference between transplanted groups (A and B) and their respective controls (C and D) was proven only for the intrasplenic HCTx (*P*_{AC}<0.05, *P*_{BD}=NS). Differences in 10-day survival rate and mean survival between groups A and B were also statistically significant (*P*_{AB}<0.05). All animals with a decreased survival time died within six days after CCl₄ poisoning.

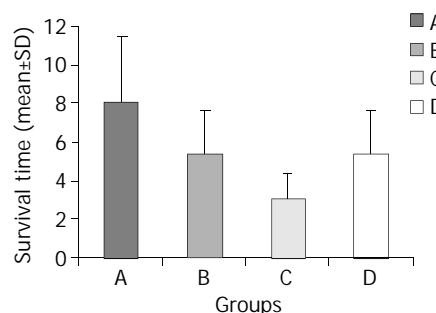


Figure 1 Mean survival in all four groups (*P*_{AC}<0.05, *P*_{BD}=NS, *P*_{AB}<0.05).

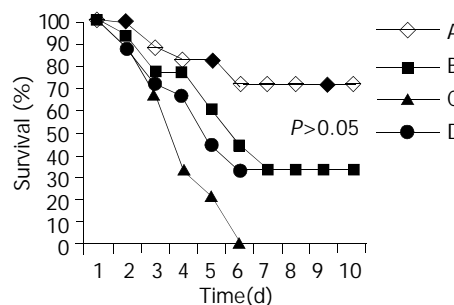


Figure 2 Survival curves in all four groups. Notice that all animal deaths occurred within the first 6 d after poisoning.

Table 1 Liver function tests during the 10-day observation period

		Day 2	Day 5	Day 10
Total Bilirubin (mg/dL)	A	0.53±0.05	0.33±0.05	0.35±0.10
	B	0.60±0.10	0.46±0.05	0.37±0.14
	C	0.86±0.10	0.76±0.10	¹
	D	0.86±0.15	0.66±0.15	0.20±0.10
SGPT (IU/L)	A	273±76.2	67.5±32.1	29.2±11
	B	400.3±155	61.6±27.7	54.8±25.0
	C	710±29.3	90.3±23.1	¹
	D	507.3±91.2	66±22.7	56.3±14.9
SGOT (IU/L)	A	380.6±63.4	68.3±24.1	84±13.3
	B	779.3±235.2	287.6±114	76.8±30.9
	C	1 088.3±131.7	610.6±148.6	¹
	D	836.6±171.2	250.6±139.6	112±63.2
Alkaline Phosphatase (IU/L)	A	469.3±157.5	427.6±129.5	343.1±180.5
	B	88.6±50	58.6±39	564.3±142.7
	C	123.6±50.5	116.3±37.4	¹
	D	104±31.1	129.3±41.7	792.3±246.5

All differences between final and baseline values were statistically significant. ¹All animals died before d 10. (Normal Values: Total Bilirubin: 0.18±0.07 mg/dL, SGPT: 44.1±24.8 IU/L, SGOT: 53.4±23.6 IU/L, Alk. Phosphatase: 86.8±49.6 IU/L -Baseline

Value: Total Bilirubin: 0.6±0.09 mg/dL, SGPT: 616.1±117.5 IU/L, SGOT: 1296.7±381.2 IU/L, Alk. Phosphatase: 91.4±63 IU/L).

Laboratory findings

After CCl₄ administration the rats responded with a marked increase in both serum aminotransferases, a moderate elevation in total bilirubin, while alkaline phosphatase was not affected. Table 1 summarizes the mean total bilirubin, SGPT, SGOT and alkaline phosphatase values during the whole period of the experimental observation.

On d10, in all experimental groups total bilirubin and aminotransferase levels were significantly lower than their pre-transplantation levels. In contrast, all final survivors presented significantly higher levels of alkaline phosphatase, independently of their previous therapy.

Histological findings

Twenty-four hours following CCl₄ intoxication, liver submassive necrosis affecting zone 3 of the hepatic lobule was the main histological finding. The type of cell injury leading to necrosis was more often ballooning degeneration and apoptosis. Normal hepatic histology was present in all final survivors. Viable hepatocytes were found within splenic parenchyma by d 2, forming structures similar to liver plates (Figure 3). Microcarrier-cell aggregates were macroscopically detected by d 5, within the native liver and the fatty tissue of the abdominal wall. The histological study of implants revealed presence of viable hepatocytes and formation of neo-vessels in the surrounding tissues (Figure 4).

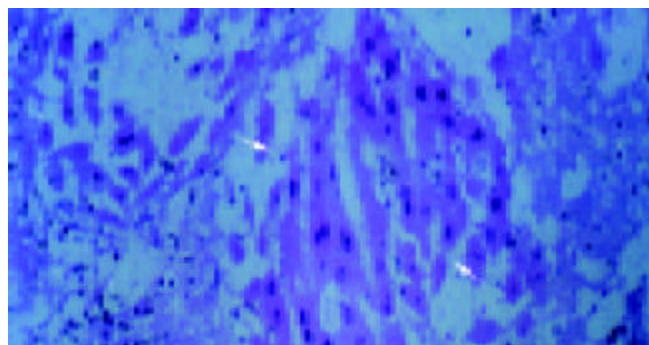


Figure 3 Viable hepatocytes within splenic parenchyma, forming structures similar to liver plates on d 2 (the so-called "splenic hepatization").

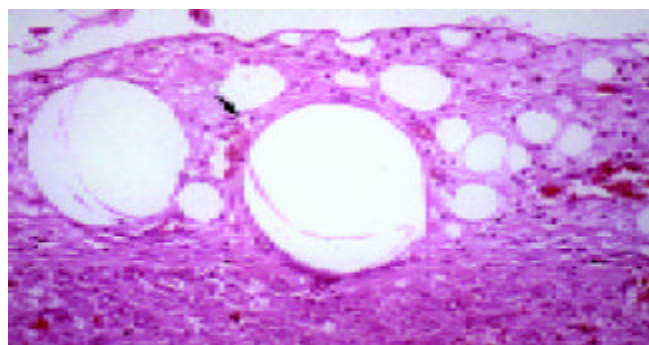


Figure 4 Microcarrier-cell aggregates within native liver parenchyma, Formation of neo-vessels in surrounding tissue on d 5.

DISCUSSION

To the best of our knowledge, this is the first experimental study, investigating two of the most popular anatomical sites for HCTx, in a model of chemically induced acute hepatic

injury. In their original work, te Velde *et al.* compared and found equivalent intrasplenic and intraperitoneal HCTx, in a model of liver ischemia-induced failure^[13]. However, liver ischemia based on liver devascularization in rodents is a model that induces massive hepatic necrosis within a few hours, but in contrast to hepatic failure in humans, the damage is always irreversible. Thus, we have chosen to work on CCl₄-induced acute hepatitis model, although it did not strictly meet the criteria of acute liver failure, because the induced liver damage was potentially reversible, mostly resembling the clinical course of the syndrome in humans and consequently was considered more realistic^[14,15].

A significantly better survival of intrasplenically transplanted animals has been demonstrated, suggesting the superiority of the spleen as a site for cell implantation in this experimental model. Intraperitoneal hepatocytes failed to promptly engraft and provided a delayed and probably useless liver support, indicating that the right timing between induction of liver injury and HCTx seems to be of major importance. Actually, Demetriou *et al.* observed that when microcarrier-attached hepatocytes were transplanted 3 d prior to 90% hepatectomy in rats, they induced a marked improvement in long term survival, whereas when they were transplanted after hepatectomy they did not^[16].

Furthermore, the rats succeeding to survive until d 6, remained alive for the whole 10-day period and their liver function tests and histology returned almost to normal, independently of their previous therapy. These survival data and laboratory findings are highly suggestive of the presence of a "crucial period" (extending from d 0 to d 6 in this experimental model), during which liver support measures must be initiated. Reversal of hepatic damage seems to be due initially to the direct action of engrafted hepatocytes during this "crucial period" and subsequently to the host liver recovery, taking place in all survivors beyond this period, independently of their initial treatment. Actually, the significant increase in alkaline phosphatase levels, occurring after d 5, could more possibly be attributed to the native liver regeneration than to a late cholestasis^[17].

In conclusion, intrasplenic HCTx has been proved effective on providing liver support, after CCl₄-intoxication. In contrast, a certain inability of intraperitoneally transplanted hepatocytes for immediate engraftment and vascularization, even after attachment onto microcarriers was observed in this experimental model. A different timing between liver injury and HCTx might give better results and merits further investigation. Theoretically, the intraperitoneal route has many advantages, such as easy accessibility and great capacity for cells implantation. To our opinion research should be encouraged towards this direction. It seems highly possible that the recent advances in various fields, such as the development of new biomaterials and especially the introduction of humoral factors accelerating the process of neovascularization, may overcome the current limitations of the intraperitoneal HCTx^[18,19].

REFERENCES

- 1 **Matas AJ**, Sutherland DE, Stefes MW, Mauer SM, Sowe A, Simmons RL, Najarian JS. Hepatocellular transplantation for metabolic deficiencies: decrease of plasma bilirubin in Gunn rats. *Science* 1976; **192**: 892-894
- 2 **Mito M**, Ebata H, Kusano M, Onishi T, Saito T, Sakamoto S. Morphology and function of isolated hepatocytes transplanted into rat spleen. *Transplantation* 1979; **28**: 499-505
- 3 **Sutherland DE**, Numata M, Matas AJ, Simmons RL, Najarian JS. Hepatocellular transplantation in acute liver failure. *Surgery* 1977; **82**: 124-132
- 4 **Ricordi C**, Flye MW, Lacy PE. Renal subcapsular transplantation of clusters of hepatocytes in conjunction with pancreatic islets. *Transplantation* 1988; **45**: 1148-1151

- 5 **Selden C**, Gupta S, Johnstone R, Hodgson HJ. The pulmonary vascular bed as a site for implantation of isolated liver cells in inbred rats. *Transplantation* 1984; **38**: 81-83
- 6 **Vroemen JP**, Buurman WA, van der Linden CJ, Visser R, Heirwegh KP, Kootstra G. Transplantation of isolated hepatocytes into the pancreas. *Eur Surg Res* 1988; **20**: 1-11
- 7 **Groth CG**, Arborgh B, Bjorken C, Sundberg B, Lundgren G. Correction of hyperbilirubinemia in the glucuronyltransferase-deficient rat by intraportal hepatocyte transplantation. *Transplant Proc* 1977; **9**: 313-316
- 8 **Mito M**, Ebata H, Kusano M, Onishi T, Hiratsuka M, Saito T. Studies on ectopic liver utilizing hepatocyte transplantation into the rat spleen. *Transplant Proc* 1979; **11**: 585-591
- 9 **Henne-Bruns D**, Kruger U, Sumpelmann D, Lierse W, Kremer B. Intraperitoneal hepatocyte transplantation: morphological results. *Virchows Arch A Pathol Anat Histopathol* 1991; **419**: 45-50
- 10 **Demetriou AA**, Whiting JF, Feldman D, Levenson SM, Chowdhury NR, Moscioni AD, Kram M, Chowdhury JR. Replacement of liver function in rats by transplantation of microcarrier-attached hepatocytes. *Science* 1986; **233**: 1190-1192
- 11 **Arkadopoulos N**, Rozga J, Petrovic L. Intraperitoneal transplantation of microcarrier-attached hepatocytes. In: Mito M, Sawa M ed. Hepatocyte transplantation. *Basel Karger* 1997; 98-106
- 12 **Fotiadis C**, Pilichos H, Preza A, Papalois A, Demonakou M, Perrea D, Xekouki P, Poussios D, Karampela E, Papadopoulou A, Grigoriou T, Karayannakos P, Sechas M. Transplantation of cultured allogeneic hepatocytes without immunosuppression. *Transplant Proc* 2001; **33**: 2400-2403
- 13 **te Velde AA**, Bosman DK, Oldenburg J, Sala M, Maas MA, Chamuleau RA. Three different hepatocyte transplantation techniques for enzyme deficiency disease and acute hepatic failure. *Artif Organs* 1992; **16**: 522-526
- 14 **Sommer BG**, Sutherland DE, Simmons RL, Najarian JS. Hepatocellular transplantation for experimental ischemic acute liver failure in dogs. *J Surg Res* 1980; **29**: 319-325
- 15 **Chamuleau RA**. Hepatocyte transplantation for acute liver failure. In: Mito M, Sawa M ed. Hepatocyte transplantation. *Basel Karger* 1997; 159-163
- 16 **Demetriou AA**, Reisner A, Sanchez J, Levenson SM, Moscioni AD, Chowdhury JR. Transplantation of microcarrier-attached hepatocytes into 90% partially hepatectomized rats. *Hepatology* 1988; **8**: 1006-1009
- 17 **Pelton JJ**, Hoffman JP, Eisenberg BL. Comparison of liver function tests after hepatic lobectomy and hepatic wedge resection. *Am Surg* 1998; **64**: 408-414
- 18 **Mooney DJ**, Kaufmann PM, Sano K, McNamara KM, Vacanti JP, Langer R. Transplantation of hepatocytes using porous, biodegradable sponges. *Transplant Proc* 1994; **26**: 3425-3426
- 19 **de Roos WK**, Borel Rinkes IH, Minnee P, Toet KH, Bouwman E, Kooistra T, Valerio D, Bruijn JA, Terpstra OT. Hepatocyte transplantation into solid supports in the rhesus monkey: the influence of acidic fibroblast growth factor on prevascularization and hepatocyte survival. *Transplant Proc* 1995; **27**: 633-634

Edited by Wang XL Proofread by Xu FM

Bridging PCR and partially overlapping primers for novel allergen gene cloning and expression insert decoration

Ai-Lin Tao, Shao-Heng He

Ai-Lin Tao, Shao-Heng He, Allergy and Inflammation Research Institute, Medical College, Shantou University, Shantou 515031, Guangdong Province, China

Supported by the Li Ka Shing Foundation, Hong Kong, China, No. C0200001 and Natural Science Foundation of Guangdong Province, No. 034617

Correspondence to: Professor Shao-Heng He, Allergy and Inflammation Research Institute, Medical College, Shantou University, 22 Xin-Ling Road, Shantou 515031, Guangdong Province, China. shoahenghe@hotmail.com

Telephone: +86-754-8900405 **Fax:** +86-754-8900192

Received: 2004-01-15 **Accepted:** 2004-03-02

Abstract

AIM: To obtain the entire gene open reading frame (ORF) and to construct the expression vectors for recombinant allergen production.

METHODS: Gene fragments corresponding to the gene specific region and the cDNA ends of pollen allergens of short ragweed (Rg, *Ambrosia artemisiifolia* L.) were obtained by pan-degenerate primer-based PCR and rapid amplification of the cDNA ends (RACE), and the products were mixed to serve as the bridging PCR (BPCR) template. The full-length gene was then obtained. Partially overlapping primer-based PCR (POP-PCR) method was developed to overcome the other problem, i.e., the non-specific amplification of the ORF with routine long primers for expression insert decoration. Northern blot was conducted to confirm pollen sources of the gene. The full-length coding region was evaluated for its gene function by homologue search in GenBank database and Western blotting of the recombinant protein Amb a 8 (D106) expressed in *Escherichia coli* pET-44 system.

RESULTS: The full-length cDNA sequence of Amb a 8(D106) was obtained by using the above procedure and deduced to encode a 131 amino acid polypeptide. Multiple sequence alignment exhibited the gene *D106* sharing a homology as high as 54-89% and 79-89% to profilin from pollen and food sources, respectively. The expression vector of the allergen gene *D106* was successfully constructed by employing the combined method of BPCR and POP-PCR. Recombinant allergen rAmb a 8(D106) was then successfully generated. The allergenicity was hallmarked by immunoblotting with the allergic serum samples and its RNA source was confirmed by Northern blot.

CONCLUSION: The combined procedure of POP-PCR and BPCR is a powerful method for full-length allergen gene retrieval and expression insert decoration, which would be useful for recombinant allergen production and subsequent diagnosis and immunotherapy of pollen and food allergy.

Tao AL, He SH. Bridging PCR and partially overlapping primers for novel allergen gene cloning and expression insert decoration. *World J Gastroenterol* 2004; 10(14): 2103-2108
<http://www.wjgnet.com/1007-9327/10/2103.asp>

INTRODUCTION

Atopic diseases such as asthma, rhinitis, eczema, pollen allergies and food allergies have been increasing in most industrialized countries of the world during the last 20 years^[1]. In the past years, we have improved our ability to recognize certain aspects of the pathogenesis of inflammatory bowel diseases, but our ability to effectively treat food and pollen allergy remains limited. The limitations for developing effective treatment regimens are due to some still unresolved and ambiguous aspects of the cross-reactivity of food and pollen allergy^[2]. Among the "cross-reactivity" food allergies, the so-called pollen-related food allergies are the most important. Patients with pollinosis have a high risk of developing a related food allergy, up to 70% of the patients are also allergic to fruits, vegetables or nuts^[3,4]. Short ragweed (Rg, *Ambrosia artemisiifolia* L.) is an important source of airborne allergens all over the world and has become an immunodominant allergen in China. Allergen-specific immunotherapy (SIT) represents one of the few curative approaches towards allergy^[5], for which a powerful method is to express the recombinant allergen proteins *in vitro*. Therefore, it is pivotal to obtain full-length allergen gene and to construct the expression vector. Generally, many full-length genes are acquired by prior acquisition of the specific fragments, and subsequently constructed in conception with computers by joining the amphi-end sequences obtained by rapid amplification of cDNA end (RACE)^[6]. In the process, a frequently occurred problem is the existence of alternatives in the amplification template. That is to say, though the length of amplified sequences is consistent with anticipation, the nucleotide compositions in different sequences are dramatically different and the existence of polymorphism is usually observed^[7-11]. Screening and detection of different clones obtained would account for the main expenditure of the prophase work of gene cloning. As for the expression vector construction, specific primers needed usually comprise two parts. One is the region for restriction recognition or the vector specific sequences for ligation-independent cloning (LIC), like newly developed pET-44 EK/LIC system. The other is the gene specific region for stringent polymerase chain reaction (PCR). The melting temperature (T_m) of such primers always goes beyond the ordinary limit of 72 °C, and the amplification specificity hence is reduced. It would be more disturbing when the GC content of the open reading frame (ORF) ends greatly deviates from 50%, which would usually occur in the 5' end of the ORF. To obviate the aforementioned problems, we have developed the *partially overlapping primer-PCR* (POP-PCR) method to surmount the non-specificity problem for long primers. This was then combined with bridging PCR (BPCR), which was coined for the PCR assay on joining two fragments containing a region of sequence similarity^[12,13], to conquer the difficulty in retrieving the full-length gene in cDNA pool that was originally used for gene fragments cloning. In the current study, we successfully constructed the expression vector and expressed the allergen protein from Rg pollens, and hallmarked the allergenicity on the purified fusion protein.

MATERIALS AND METHODS

Subjects

Eight selected sera of patients with a well-defined case history of Rg pollen allergy and specific IgE antibodies against Rg pollen allergen (higher than 3.5 kU_A/L) were taken in Allergy Clinics, Shenyang North Hospital, Shenyang, China and used in this study. Thirteen sera from non-allergic individuals were recruited from the First Affiliated Hospital of Medical College, Shantou University, Shantou, China and used as negative controls.

Preparation of PCR template

Pollens of Rg were harvested from Wuhan, one of the four pervasive areas of short ragweed in China, and immediately submerged in liquid nitrogen. Following powder-grinding, total RNA was extracted by using RNeasy Maxi kit (Qiagen Valencia, CA, USA) according to the manufacturer's instructions. Reverse transcription (2 µg total RNA per sample) was then performed by using ProtoScript first strand cDNA synthesis kit (New England Biolabs, Beverly, MA, USA) according to the manufacturer's instructions. Subsequently, the 5' end of the gene (gene fragment A, Figure 1) was obtained by RT-PCR with primer pair Sg1P5/S3D10 (Table 1). Whereas the 3' end (gene fragment B in Figure 1) was acquired by RACE (rapid amplification of the cDNA end) method^[6]. The cDNA pool, along with fragment A and fragment B would be used for the subsequent PCR templates.

Full-length gene cloning: BPCR

The amplification products A and B were mixed in equal volume and diluted 15-fold in distilled water. Bridging PCR (BPCR) outlined in Figure 1 was carried out by using 5 µL of the above diluents as template in 25 µL of the reaction mixture containing 1.25 U HotstarTaq DNA polymerase (Qiagen), 1×PCR buffer (Qiagen), 0.2 mmol/L dNTP, 0.4 µmol/L each of the primer pair Sg1P5 and RAC3 (Table 1). Thermal cycling was performed in a Peltier thermal cycler PTC-200 (MJ Research, Watertown, MA, USA) as follows. After an initial step at 95 °C for 15 min as recommended to activate the enzyme, the reaction temperature was decreased to 66 °C at the rate of -0.1 °C/s followed by an extension at 72 °C for 5 min, then 7 touchdown cycles were carried out at 94 °C for 45 s, at 68 °C for 30 s and at 72 °C for 30 s, with the annealing temperature decreased by 1 °C per cycle. Subsequently, the reaction mixture was subjected to 30 conventional cycles at 94 °C for 45 s, at 66 °C for 30 s, and at 72 °C for 2 min. Conventional PCR was also conducted as a control by using cDNA pool aliquot as template. As visualized on a 12 g/L

agarose gel, the target bands were recovered with a QIAquick™ gel extraction kit (Qiagen), cloned into pGEM-T easy vector (Promega Company, Madison, WI, USA), and transformed into *E. coli* strain JM109 (Promega). Sequencing of the positive clones was performed by BioAsia Biotechnology Co., Ltd (Shanghai, China). Sequence BLAST was performed in GenBank database.

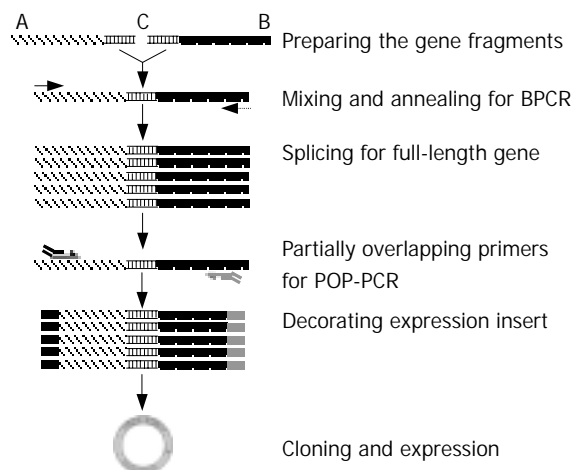


Figure 1 Experimental design and steps involved in bridging PCR (BPCR) and partially overlapping primer-based PCR (POP-PCR). Gene fragments A and B had the junction region C. Under specific temperature conditions, the fragments would anneal together to form the template molecule, thus triggering the amplification cascade. The partially overlapping primers at each site of the template ends contained two primers premixed in a certain molar ratio that had sequence identity but with different lengths. All the short primers located at the outward overhang region. The sequences of all primers used are shown in Table 1.

Expression insert decoration: POP-PCR

To decorate the expression insert, primers were designed according to the sequence of the gene-coding region and the specific sequence of the expression vector as recommended by the manufacturer's instructions. The melting temperature (T_m) of all primers was calculated by using the software Omega 2.0 (Oxford Molecular Ltd, Oxford, UK). Shorter overlapping primers were additionally designed for the long primers with the T_m beyond 72 °C (Table 1). The sequences of this kind of primers each were identical to the 5' terminal sequence of their corresponding longer ones. Pooling together the shorter and longer ones in different molar ratio formed the partially

Table 1 Primers used in bridging PCR (BPCR) and partially overlapping primer-PCR (POP-PCR)¹

Code	Definition	Sequence (5' 3')	T_m (°C)
Sg1P5	For fragment A and BPCR	ATGTCGTGGCAGGCCGTACGT	66.0
S3D10	For fragment A	GGACAATGCAACATGCTTGTGAGAGG	70.4
S5D106	For fragment B	GTGGAAGAAGGGAGCAGGAGG	66.4
RAC3	For fragment B and BPCR	GCTGTCAACGATACGCTACGTAACGG	68.4
DEN3	For ORF of D106	TAATTAGAAACCCGTTCGAGGAGATAGTCACC	68.4
POP51	For POP-PCR	GACGACGACAAG ATGTCGTGGCAGGCCGTACGT	80.8
POP52	For POP-PCR	GACGACGACAAG ATGTCGTGGCA	69.9
POP31	For POP-PCR	GAGGAGAAGCCCGG TTACATGCCCTGATCGATGAGAT	80.7
POP32	For POP-PCR	GAGGAGAAGCCCGG TTACATGCC	69.7

¹Fragments A and B were derived from allergen gene D106. The relationship thereof and the PCR steps are shown in Figure 1. The underlined oligonucleotides were for the specific sequences of the expression vector. Oligonucleotides in italic bold were gene specific sequences. Primers POP51 and POP52, POP31 and POP32 formed the partially overlapping primers, respectively, which were corresponding to the 5' and 3' end of the target gene.

overlapping primers (Figure 1). Pilot assays were conducted to optimize the molar ratio of the two primers in the partially overlapping primer pairs for PCR. The optimal proportion was subsequently chosen for partially overlapping primer PCR (POP-PCR), by using the product recovered from BPCR as a template. As a control, the cDNA pool, originally used for fragment gene cloning, was also used as the PCR template in parallel. The PCR mixture and the initial step were similar to those for BPCR, but with some changes in denaturing temperature and extension time. Following the initial denaturing step, 12 touchdown cycles at the initiative annealing step at 72 °C for 45 s, and an extension at 72 °C for 5 min were performed, followed by 30 extenuation cycles, which were initiated at 95 °C for 45 s, at 72 °C for 1 min and at 72 °C for 30 s, with the annealing time decreased by 1 s per cycle, and ended by a final extension at 72 °C for 10 min. The annealing temperature was usually adjusted according to the T_m of the primer being used in the reaction. The target bands visualized on the gel were purified and sequenced as described above. However, the plasmids were cloned into *E. coli* strain NovaBlue Singles™ cells (Novagen, Madison, WI, USA), according to the manufacturer's instruction.

Northern blot

Northern blot was performed according to the manufacturer's manual with a slight modification. Briefly, 20 µg RNAs from pollen and the mixture of calyx and pedicel was loaded on a formaldehyde-containing gel. After running at 40 volts for 3 h or so, the RNA bands were electrically transferred onto Nytran SuPerCharge nylon transfer membranes (Schleicher & Schull BioScience, Inc. New Hampshire, USA). Before stained with methylene blue [0.2 g/L in 0.3 mol/L sodium acetate (pH 5.5)] to investigate the transferring efficiency, RNA was UV cross-linked onto the membrane. After destaining, BrightStar™ Psoralen-biotin (Ambion Inc., Austin, TX, USA) labeled probe D106 was applied for hybridization in the ULTRhyb™ hybridization buffer (Ambion Inc., USA). Subsequent washing was performed twice with a buffer containing 2×SSC (0.3 mol/L NaCl, 0.03 mol/L sodium citrate) and 1 g/L SDS, before its probe was detected by Phototope star detection kit (Ambion). Finally, the filter was exposed to Fuji medical X-ray film at room temperature for several min.

Protein expression

After confirmation of the in-frame insertion, the positive clones were incubated overnight at 37 °C on an orbital shaker. The

plasmids therein were extracted by using QIAprep Miniprep kit (Qiagen) and transformed into *E. coli* strain BL21(DE3) (Novagen) for expression according to the manufacturer's instructions with a minor modification. Following overnight proliferation of the expression transformants, the cells were inoculated in liquid LB medium at the rate of 1%. After a further incubation for 4 h or so, expression of protein D106 was induced with 0.5 mmol/L isopropyl-*D*-thio-galactopyranoside (IPTG) for 2 h at 30 °C before harvest. The expression results were analyzed on 150 g/L SDS-PAGE.

Western blotting

After induced expression was confirmed, the recombinant allergen Amb a 8(D106) was purified with S-Tag thrombin purification kit (Novagen). Fifteen micrograms of fusion protein was resolved on 150 g/L SDS-PAGE and electrically transferred to PVDF membrane (Amersco, Solon, Ohio, USA). After the membrane was blocked overnight with 40 g/L BSA solution, Rg allergic serum (diluted 1:7) was added to each membrane strip for 8 h before addition of peroxidase conjugated goat anti-human IgE (Sigma-Aldrich, Inc., Saint Louis, MO, USA). The blotted band was visualized with DAB chromogenic substrate solution^[14] (Amersco).

RESULTS

Fragment gene cloning

Gene fragments A and B corresponding to the 5'- and 3'-ends of the gene were enriched by RT-PCR and subsequently inserted into the vector. The sequence analysis demonstrated that fragments A and B, sized 363 bp and 431 bp respectively, contained a common region of 126 bp, which would provide the junction region for BPCR. The theoretical full-length gene joined contained the stop codon, poly (A) tail and primer sequences (Figure 2). Bridging the two fragments produced a novel theoretical full-length gene, which can be available under GenBank Accession No AY268426. BLAST with the amino acid sequence deduced from the full-length cDNA sequence of *D106* retrieved a large number of homologous proteins corresponding to pollen, food and contact allergens from different species, all of which belonged to profilin family. The BLAST data also showed that Amb a 8(D106) shared a homology of 54-89% with pollen allergens and of 79-89% with food allergens, which could help to cluster Amb a 8(D106) into both pollen and food allergen groups with short distances (Figure 3).

```

1 ATGTCGTGGCAGGCGTACGTTGGATGACCACTTAATGTGCGAGATCGAGGGCAACCACCTTTCTGCCGCTGCCATCATCGGCCAC
M S W Q A Y V D D H L M C E I E G N H L S A A A I I G H
GACGGCGTGGTTGGGCTCAGTCAGCCACCTCCCTCAGGTCAAGCCAGAGGAAATAACTGGGATCATGAATGACTTTAATGA
D G V V W A Q S A T F P Q V K P E E I T G I M N D F N E
CCTGGCTCTCTGCACCGACTGGTTTATACCTTGGTGGTACCAAGTATATGGTTATTCAAGGCGAGCCAGGAGCTGTGATTCGA
P G S L A P T G L Y L G G T K Y M V I Q G E P 2 G A V I R
GGGAAAAAGGACCAGGAGGTGTTACTATTAAGACAACAATGTCTTGATCATTGGTATCTATGATGAACCCATGACTCCA
G K K G P G G V T I K K T T M S L I I G I Y D E P M T P
3 GGACAATGCAACATGCTTGTGGAGGCGCTGGTACTATCTCCTCGAACAGGTTTCTAAATTTACTTGTGGAAGCGATAGCGTA
G Q C N M L V E R P 4 G D Y L L E Q G F Stop
TTAGTAATTAAGCTCCTGGAGTTGTAAGCCAGGTGGTGGATGCTTGGATGAACAGTCTTTGAATTGATCAAATCCCTCCCTGTA
TTATCCTTCTCATGACAAAGTGTGATGGAAGTTCTTTTCTTTTGTAACTGGAGTGTATTTGATTATTTTTCAACGGTTTG
GTATTAATATAACACCTTTGCTTGTGTAATAAAAAAAAAAAAAACACTGTCATGCCGTTACGTAGCGTATCGTTGACAGC
5

```

Figure 2 cDNA sequence of novel allergen gene *D106* from short ragweed pollens. The five shadowed regions represent the primer sites, Sg1p5, S5D106, S3D10, DEN3 and RAC3.

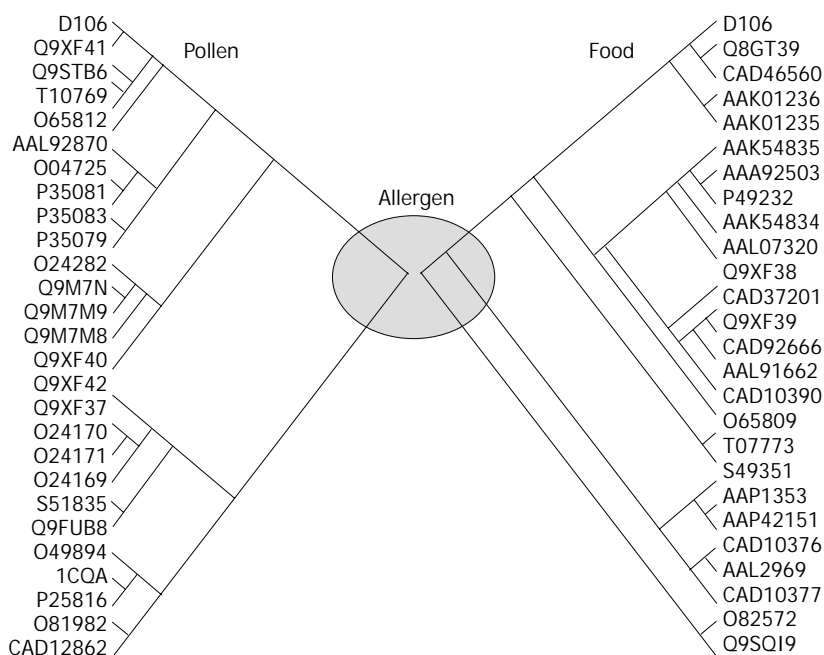


Figure 3 Phylogenetic relationships between newly obtained pollen allergen D106 (Amb a 8(D106)) and its cognates from GenBank as inferred from CLUSTAL W (1.82) alignment of the amino acid sequences. Amb a 8(D106) shared a homology as highly as 54-89% with different pollen allergens (from mugwort CAD12862 to apple Q9XF41) and as 79-89% with different food allergens (from peanut Q9SQI9 to peach Q8GT39).

Northern blot

To confirm the RNA derivation of cDNA of D106, Northern blot was performed. After blotting and UV-cross linking, methylene blue-staining of the membrane exhibited the sharp rRNA bands, suggesting the successful transferring and good quality of RNA. The sharp hybridization bands proved the pollen derivation of the cloned allergen cDNA (Figure 4). D106 could be detected both from pollen RNA and the RNA mixture from calyx and pedicel, which ruled out the PCR false derivation of D106.

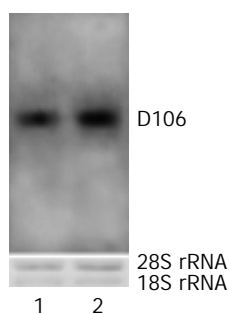


Figure 4 Northern blot profile confirming RNA derivation of cDNA of the newly obtained gene D106. Lane 1, total RNA from calyx and pedicel; Lane 2, total RNA from pollen. Both lanes exhibit obvious bands, suggesting the real RNA derivation of D106.

Enhanced amplification specificity

In order to clone the full-length gene coding region for expression vector construction, we first resorted to general PCR by using the cDNA pool as a template with the primers formerly used. However, no sharp bands of expected sizes were exhibited on the loaded agarose gel for general PCR, though a number of PCR conditions were applied. After the template was changed to the mixture of gene fragments A and B previously acquired, the bridging PCR (BPCR), as outlined in Figure 1, produced the optimal results with sharp bands and exact size observed (Figure 5). The gene sequence achieved was identical to that

spliced from gene fragments A and B, indicating that the ORF of the target gene D106 was contained.

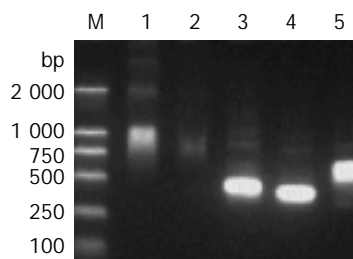


Figure 5 Agarose gel electrophoresis of PCR products. The PCR steps were depicted in Figure 1. Template in lanes 1, 2 and 5 is the mixture from gene fragments A and B; while template in lanes 3 and 4 is the BPCR product (lane 5). Lane 1, primer Sg1P5/RAC3; lane 2, primer POP51/POP31; lane 3, POP-PCR with primer POP51+POP52/POP31+POP32; lane 4, general PCR of the ORF of D106 with primer pair Sg1P5/DEN3; lane 5, BPCR of full-length D106 with primer Sg1P5/RAC3; M, molecular marker.

Decoration of expression insert

For comparison between conventional megaprimers and partially overlapping primers (POP), their amplification products were exhibited in parallel on the agarose gel (Figure 5). Longer primers and their relative shorter ones for POP-PCR listed in Table 1 were pre-mixed in a molar ratio of 1:1, 1:10, 1:50, 1:100. Hence 16 POP-pairs in different molar ratios were formed corresponding to both ends of the ORF of the gene, each of them was used for one reaction only. Comparison of the parallel PCR results showed that forward and reverse POPs in the molar ratios of 1:10 and 1:1 could produce the optimal amplification results, while conventional PCR exhibited the smear products with wrong sizes (Figure 5). The products recovered from target bands were successfully introduced into the expression vector pET-44 EK/LIC (Novagen) and transformed into *E. coli* strain NovaBlue Singles™ competent cells. Sequencing of the positive clones demonstrated that the

insert was in-frame and identical to those splices from gene fragments A and B and flanked by the vector specific sequence at both sides, indicating that the insertion was correct.

Protein expression and immunoblotting

Following proliferation of the clones selected, plasmids were extracted and successfully transformed into *E. coli* strain BL21 (DE3) for expression. SDS-PAGE analysis showed that the fusion protein was expressed mainly in a soluble form, with a molecular weight of 70 kDa as expected (Figure 6A). Immunoblotting result showed that the purified fusion protein could bind to IgE in the sera of allergic patients (Figure 6B), suggesting the allergenicity and the correct expression of the allergen protein.

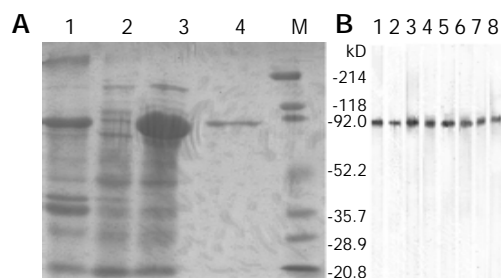


Figure 6 SDS-PAGE analysis (150 g/L) for expression (panel A) and immunoblot of fusion pollen allergen D106 (panel B). Panel A: 1. Lysate pellet of induced cells; 2. Cells without IPTG induction; 3. Supernatant of induced cell lysate; 4. Purified fusion pollen allergen D106; M. Broad range prestained SDS-PAGE standards (Bio-Rad, Hercules, CA, USA). Panel B: Fusion protein D106 was blotted with 8 serum samples from pollen allergic patients. Each strip represents one serum sample.

DISCUSSION

As industrialization developed, atopic diseases have been increasingly concerned in the past decades^[1]. It is known that pollen-allergic patients frequently present allergic symptoms after ingestion of several kinds of plant-derived foods. The majority of these reactions were caused by cross-reactive structures that are present in pollens^[2]. Allergic proteins containing these structures are often called 'panallergens'. Cloning the panallergen gene and expressing the recombinant protein would be one of the fewer prospective ways to pollen-food allergy diagnosis and immunotherapy^[15]. This study aiming this goal successfully cloned an allergen gene D106 from short ragweed pollens and expressed the recombinant protein. Interestingly, the newly cloned gene showed a high homology not only with other pollen-derived profilins but also with food-derived profilins from numerous species. The allergenicity of the recombinant protein was primarily detected by its binding to the serum IgE from the Rg pollen allergic patients, of which 20% of the chief complaints expressed the food allergy of different kinds. Based on the homology results and the widely accepted rule-of-thumb that 30% or 35% identity over aligned regions could suffice for the structural or functional deduction^[4,16,17], it is therefore tempting to speculate that the recombinant protein acquired in this study would be a useful tool both for pollen and food allergy study, and for diagnosis and immunotherapy.

The novel gene discovery by using suppression and subtractive hybridization (SSH)^[18,19] and/or reverse genetic method^[20] could clearly validate the overall strategy for the preparation of gene fragments. However, obtaining the full-length genes is needed for more investigations of gene functions. One of the pivotal steps in the process of obtaining the full-length genes is to generate the target genes from their

fragments. The most commonly used methods for this at present were to screen the cDNA library^[21-23], or back to the cDNA pool that was originally used for gene fragment detection^[23]. Numerous polymorphic clones obtained would render these methods to time-consuming, expensive and liable to produce the microheterogeneity of the genes. In BPCR, only if an appropriate length region of sequence similarity existed, the two fragments could be spliced together. Obviously, the spliced sequence would be faithfully identical to that of the fragments originally used. Therefore no more screening work was needed. In order to anneal the two fragments and form a template molecule, it is a key point to optimize the annealing temperature according to the T_m of the junction regions of two gene fragments to be spliced, with the primers used in the reaction. Following this principle, BPCR would splice any two gene fragments with homology junction. Notably for the junction sequences either coming from the nature, or intentionally synthesized (see below), exact identity is not necessary but it does require a certain degree of homology to anneal the two fragment genes. Therefore, two heterogeneity genes could be spliced by BPCR method to form a novel chimeric gene or hybrid gene, which would be useful for gene function study and disease treatment.

Introducing restriction site and/or the specific sequences of vector to the primers is considered as a crucial step for exact insertion of exogenous gene into the vector, through which relatively long primers could be produced. It was well known that these longer primers would be easier to enhance the chance of non-specific amplification. To eliminate the potential non-specific amplification, partially overlapping primer technique was developed in the current study. According to the outward overhang sequence of the longer primers, the shorter identical sequence was synthesized and mixed in an appropriate molar ratio with the longer ones, thus forming the partially overlapping primer mixture. With this technique, increased amplification specificity was achieved, and the tedious screening process of target clones was avoided. According to the protocol of the partially overlapping primer, POP-PCR can be used for the amplification assays that are relevant to the addition of a length of extending sequence. It is therefore tempting to suggest that any genes that have no sequence similarities can be accommodated with the junction sequence and spliced together with repeated use and reciprocal combination of BPCR and POP-PCR to form a novel gene (or full-length gene). As this is concerned, a relatively more complicated procedure but with different efficiencies and proposes has been recently developed^[24].

REFERENCES

- 1 **Miescher SM**, Vogel M. Molecular aspects of allergy. *Mol Aspects Med* 2002; **23**: 413-462
- 2 **Vieths S**, Scheurer S, Ballmer-Weber B. Current understanding of cross-reactivity of food allergens and pollen. *Ann N Y Acad Sci* 2002; **964**: 47-68
- 3 **Lorenz AR**, Scheurer S, Hausteiner D, Vieths S. Recombinant food allergens. *J Chromatogr B Biomed Sci Appl* 2001; **756**: 255-279
- 4 **Brusic V**, Petrovsky N, Gendel SM, Millot M, Gignonzac O, Stelman SJ. Computational tools for the study of allergens. *Allergy* 2003; **58**: 1083-1092
- 5 **Spangfort MD**, Mirza O, Ipsen H, Van Neerven RJ, Gajhede M, Larsen JN. Dominating IgE-binding epitope of Bet v 1, the major allergen of birch pollen, characterized by X-ray crystallography and site-directed mutagenesis. *J Immunol* 2003; **171**: 3084-3090
- 6 **Frohman MA**, Dush MK, Martin GR. Rapid production of full-length cDNAs from rare transcripts: amplification using a single gene-specific oligonucleotide primer. *Proc Natl Acad Sci U S A* 1988; **85**: 8998-9002
- 7 **Kruse S**, Kuehr J, Moseler M, Kopp MV, Kurz T, Deichmann

- KA, Foster PS, Mattes J. Polymorphisms in the IL 18 gene are associated with specific sensitization to common allergens and allergic rhinitis. *J Allergy Clin Immunol* 2003; **111**: 117-122
- 8 **Karjalainen J**, Hulkkonen J, Pessi T, Huhtala H, Nieminen MM, Aromaa A, Klaukka T, Hurme M. The IL1A genotype associates with atopy in nonasthmatic adults. *J Allergy Clin Immunol* 2002; **110**: 429-434
- 9 **Cookson W**. Genetics and genomics of asthma and allergic diseases. *Immunol Rev* 2002; **190**: 195-206
- 10 **Vailes LD**, Sun AW, Ichikawa K, Wu Z, Sulahian TH, Chapman MD, Guyre PM. High-level expression of immunoreactive recombinant cat allergen (Fel d 1): Targeting to antigen-presenting cells. *J Allergy Clin Immunol* 2002; **110**: 757-762
- 11 **Hales BJ**, Hazell LA, Smith W, Thomas WR. Genetic variation of Der p 2 allergens: effects on T cell responses and immunoglobulin E binding. *Clin Exp Allergy* 2002; **32**: 1461-1467
- 12 **Mehta RK**, Singh J. Bridge-overlap-extension PCR method for constructing chimeric genes. *Biotechniques* 1999; **26**: 1082-1086
- 13 **Liu S**, Thaler DS, Libchaber A. Signal and noise in bridging PCR. *BMC Biotechnol* 2002; **2**: 13
- 14 **Reindl J**, Rihs HP, Scheurer S, Wangorsch A, Hausteiner D, Vieths S. IgE reactivity to profilin in pollen-sensitized subjects with adverse reactions to banana and pineapple. *Int Arch Allergy Immunol* 2002; **128**: 105-114
- 15 **Ferreira F**, Wallner M, Breiteneder H, Hartl A, Thalhammer J, Ebner C. Genetic engineering of allergens: future therapeutic products. *Int Arch Allergy Immunol* 2002; **128**: 171-178
- 16 **Rost B**. Twilight zone of protein sequence alignments. *Protein Eng* 1999; **12**: 85-94
- 17 **Hileman RE**, Silvanovich A, Goodman RE, Rice EA, Holleschak G, Astwood JD, Hefle SL. Bioinformatic methods for allergenicity assessment using a comprehensive allergen database. *Int Arch Allergy Immunol* 2002; **128**: 280-291
- 18 **Diatchenko L**, Lau YF, Campbell AP, Chenchik A, Moqadam F, Huang B, Lukyanov S, Lukyanov K, Gurskaya N, Sverdlov ED, Siebert PD. Suppression subtractive hybridization: a method for generating differentially regulated or tissue-specific cDNA probes and libraries. *Proc Natl Acad Sci U S A* 1996; **93**: 6025-6030
- 19 **Sers C**, Tchernitsa OI, Zuber J, Diatchenko L, Zhumabayeva B, Desai S, Htun S, Hyder K, Wiechen K, Agoulnik A, Scharff KM, Siebert PD, Schafer R. Gene expression profiling in RAS oncogene-transformed cell lines and in solid tumors using subtractive suppression hybridization and cDNA arrays. *Adv Enzyme Regul* 2002; **42**: 63-82
- 20 **Yu CJ**, Lin YF, Chiang BL, Chow LP. Proteomics and immunological analysis of a novel shrimp allergen, Pen m 2. *J Immunol* 2003; **170**: 445-453
- 21 **Ding H**, Griesel C, Nimtz M, Conradt HS, Weich HA, Jager V. Molecular cloning, expression, purification, and characterization of soluble full-length, human interleukin-3 with a baculovirus-insect cell expression system. *Protein Expr Purif* 2003; **31**: 34-41
- 22 **Erez N**, Milyavsky M, Goldfinger N, Peles E, Gudkov AV, Rotter V. Falkor, a novel cell growth regulator isolated by a functional genetic screen. *Oncogene* 2002; **21**: 6713-6721
- 23 **Forestier M**, Banninger R, Reichen J, Solioz M. Betaine homocysteine methyltransferase: gene cloning and expression analysis in rat liver cirrhosis. *Biochim Biophys Acta* 2003; **1638**: 29-34
- 24 **Gao X**, Yo P, Keith A, Ragan TJ, Harris TK. Thermodynamically balanced inside-out (TBIO) PCR-based gene synthesis: a novel method of primer design for high-fidelity assembly of longer gene sequences. *Nucleic Acids Res* 2003; **31**: e143

Edited by Wang XL Proofread by Xu FM

Cloning and expression of mouse peroxiredoxin I in IEC-6 Cells

Bo Zhang, Yong-Ping Su, Tao Wang, Feng-Chao Wang, Guo-Ping Ai, Hui Xu, Jun-Ping Wang, Yue-Sheng Huang, Jian-Xin Jiang

Bo Zhang, Yong-Ping Su, Tao Wang, Feng-Chao Wang, Guo-Ping Ai, Hui Xu, Jun-Ping Wang, Yue-Sheng Huang, Jian-Xin Jiang, Institute of Combined Injury of PLA, State Key Laboratory of Trauma, Burns and Combined Injury, Third Military Medical University, Chongqing 400038, China

Supported by the National Natural Science Foundation of China, No. 30230360

Correspondence to: Professor Yong-Ping Su, Institute of Combined Injury of PLA, Third Military Medical University, Gaotanyan Street 30, Chongqing 400038, China. suyiping@yahoo.com

Telephone: +86-23-68752355 **Fax:** +86-23-68752279

Received: 2003-12-10 **Accepted:** 2004-02-01

Abstract

AIM: To clone and express mouse peroxiredoxin I in IEC-6 cells.

METHODS: Total RNAs were isolated from cultured IEC-6 cells, and the coding region of peroxiredoxin I was amplified by RT-PCR. After it was cloned into T-vector and sequenced, pSG5 was used to transiently express peroxiredoxin I in IEC-6 by liposome-mediated transfection, and the expression of peroxiredoxin I was evaluated by RT-PCR and Western blot.

RESULTS: A DNA fragment about 750 bp was amplified from total RNAs of IEC-6 cells using specific primers of peroxiredoxin I. The sequencing confirmed the coding region was successfully cloned into T-vector, which was completely coincident with the sequence in GeneBank. After the *EcoRI-BamHI* fragment of T-vector containing peroxiredoxin I was inserted into pSG5, the recombinant plasmid was transferred to IEC-6 cells. RT-PCR assay showed that a DNA fragment of 930 bp could be amplified, which indicated the transcription of pSG5-Prx. Western blot confirmed the expression of peroxiredoxin I in IEC-6 cells.

CONCLUSION: Mouse peroxiredoxin I can be successfully expressed in IEC-6 cells.

Zhang B, Su YP, Wang T, Wang FC, Ai GP, Xu H, Wang JP, Huang YS, Jiang JX. Cloning and expression of mouse peroxiredoxin I in IEC-6 Cells. *World J Gastroenterol* 2004; 10(14): 2109-2112

<http://www.wjgnet.com/1007-9327/10/2109.asp>

INTRODUCTION

Peroxiredoxin (Prx) is a novel defined protein family which plays a critical role in reducing hydrogen peroxide with hydrogen derived from NAD(P)H^[1-3]. The first member of this family was discovered as a 25 ku protein in yeast^[4]. All Prx proteins contain a conserved cysteine residue in the *N*-terminal region that is the active site of catalysis. In mammal cells, there are six isoforms of peroxiredoxin, which can be divided into two subgroups, termed as 1-Cys Prx (VI) and 2-Cys Prx (I-V)^[5,6]. The proteins of 2-Cys Prx subgroup contain another cysteine residue in the C-

terminal portion of the molecule. Prx isoforms are distributed differently within cells and therefore with different functions. Prx I and II are localized to the cytosol^[7,8], whereas Prx III has a mitochondrial-targeting signal and is localized in mitochondrion^[9]. Prx IV is secreted out of cells because of its *N*-terminal sequence for secretion. Prx V is found in mitochondrion as long form of this protein, but it also exists in peroxisome as short form^[10]. Same as Prx I and II, Prx VI is also found in cytosol^[11].

Prx I, which belongs to 2-Cys subgroup, is also known as MSP23, PAG and NEEF-A^[12-14]. Prx I is involved in redox regulation of the cell, such as reducing peroxides by reducing equivalents provided through the thioredoxin system but not from glutaredoxin. Prx I is found in abundance in the cytoplasm of cells as homodimers. Its cDNA was first cloned from mouse peritoneal macrophage encoding a protein of 23 ku. Now the antioxidative molecular mechanism of Prx I is elucidated by several researches on molecular structure has been performed. From the results of biochemical and physiological studies, Prx I has been implicated in a number of cellular functions, such as cell proliferation and differentiation, enhancement of the natural killer cell activity, and intracellular signaling, in addition to the antioxidant activity^[15-17]. Further studies have shown that the expression of Prx I is increased in cancer cells, indicating it may be related to cancer development or progression^[18]. We postulate that it may have an activity of anti-tumor development.

In our previous study, we found the expression of Prx I was up regulated by ionizing radiation in mouse intestinal epithelia^[19]. This was coincident with the results of other researchers^[20]. As a step to further study the biochemical functions of Prx I, we cloned the coding region of this gene and expressed it in IEC-6 cells. Our data showed that Prx I could be successfully expressed in this kind of cells.

MATERIALS AND METHODS

Materials

Male BALB/c mice, 58-62 d of age (weight 20-24 g), were purchased from Animal Center in Third Military Medical University, and housed in conventional cages with free access to drinking water and standard chow. Dulbecco's modified Eagle's medium (DMEM) and fetal bovine serum were purchased from Hyclone (Logan, USA). RNA PCR kit and T-vector were obtained from Takara (Dalian, China), and antibodies were from Santa Cruz (California, USA). Reagent for RNA isolation was from Roche Ltd. (Roche, USA). Plasmid pSG5 was a kindly gift from Dr. Chen Jian (Department of Biochemistry, Third Military Medical University). The specific primers were synthesized by Shanghai Shenyong Shengwu Jishu Corporation. Other chemicals not mentioned above were domestic made.

Isolation of total RNAs

Mouse intestinal epithelial cells were isolated as previously described^[21]. After the cell pipette washed with cold PBS (0.01 mol/L, pH7.4), the cells were lysed with Tripure solution. All performs were according to the manufacturer's instructions. The quality of isolated RNAs was checked by electrophoresis.

RT-PCR

The coding region of Prx I was amplified by RT-PCR with forward primer, 5' CGAATTCGTTCTCACGGCTCTTTCTGTTT3' (P1) and backward primer, 5' AGGATCCTTCTGGCTGCTCAATGC TGC3' (P2). One microgram of total RNAs was added into each reaction. After the reverse transcription was performed at 50 °C for 30 min, the amplification was carried out with one denaturing cycle of 3 min at 94 °C, then 28 cycles consisting of denaturation at 94 °C for 40 s, annealing at 58 °C for 40 s, and extension at 72 °C for 40 s, and one additional extension at 72 °C for 5 min. RT-PCR products were analyzed on 12 g/L agarose gel. To validate the transcription of recombinant plasmid, the mRNA of transfected IEC-6 cells was amplified by RT-PCR with primers P2 and P3 (5' AAAGCTGGATCGATCCTGAG3'). The procedure in details was performed according to the manufacturer's instructions.

Construction of expression vector

The amplified DNA was separated by electrophoresis and purified from gels. Then 1 μL of T-vector, 1 μL of T4 DNA ligase and 2 μL of 10×buffer were added to the purified RT-PCR product, and incubated at 16 °C overnight. Competent bacteria of *E. coli JM109* were transformed with the linkage product, and then spread on a LB agarose plate containing ampicillin and X-gal. The inserted DNA into T-vector of 3 random monoclonal colonies was sequenced, and the colony was termed as pT-Prx. To construct the recombinant expression vector, the *EcoRI-BamHI* fragment of pT-Prx was inserted into vector pSG5, which could transfect IEC-6 cells.

Cell culture and transfection

IEC-6 cells were cultivated at 37 °C in an atmosphere containing 100 mL/L CO₂ in air. The culture medium comprised of DMEM containing 100 mL/L fetal calf serum, penicillin (100 U/mL), and streptomycin (100 μg/mL). Exponentially growing cells were transferred to 100 mL culture dishes and cultured for 24 h to yield about 40% confluency at the time of transfection. Before transfection, 30 μg of DOTAP was diluted with 70 μL of HBS solution (20 mmol/L HEPES, 150 mmol/L NaCl, pH 7.4), and 5 μg of DNA was diluted to 0.1 μg/μL with the same solution. The mixture of DNA and DOTAP was prepared by gently mixing them together and incubated for 15 min at room temperature. To prepare cells for transfection, IEC-6 cells were washed twice with serum-free medium. After the cells were incubated with the mixture of DNA and DOTAP in 2 mL of serum-free medium for 4 h, the cells were washed with serum-free medium, followed by further culture for 16 h. Transfection was repeated one more time. At the time of 24 h after the second transfection, the cells were collected for RNA and proteins isolation.

Immunoblotting

IEC-6 cells were collected and washed with ice-cold PBS

(0.01 mol/L, pH 7.4) after transfection. Total proteins were isolated with RPI solution. The extraction mixture was centrifuged at 12 000 g at 4 °C for 20 min. The supernatants were transferred to a clean tube and stored at -70 °C as aliquots. The protein concentration was determined using Bradford dye-binding assay with bovine serum albumin as a standard. Total proteins were separated on 120 g/L SDS-polyacrylamide gel, and then transferred to nitrocellulose membranes. After being blocked for 1 h with the Tris/NaCl (50 mmol/L Tris-HCl, 200 mmol/L NaCl, 0.5 g/L Tween-20, pH 7.4) containing 20 g/L BSA, the membranes were probed with the goat anti-mouse Prx I polyclonal antibody. Immunoreactive bands were visualized with solution containing 1 mg/mL DAB and 0.1 mL/L H₂O₂. The expression of Prx I was normalized by that of GAPDH.

RESULTS

Amplification of the cDNA of Prx I

Total RNAs were isolated with 3 main bands appeared on agarose gels electrophoresis (Figure 1A). Message RNAs were smeared on the gel. After 28 cycles of RT-PCR, the products were run on 12 g/L agarose gel. A DNA band about 750 bp was visualized which was coincident with the length of the PrxI cDNA and could be cloned in the next step (Figure 1).

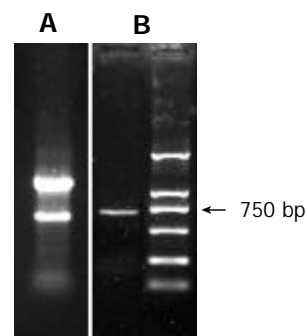


Figure 1 Amplification of Peroxiredoxin I by RT-PCR. A: total RNAs were isolated from mouse intestinal epithelia; three bands were visualized on agarose gel, which represented the main ribosome RNA of the cells. B: amplification of the coding region of peroxiredoxin I applying RT-PCR.

Cloning of Prx I

After the PCR product was ligated to T-vector, the linkage mixture transformed competent bacteria of JM109, and white colonies grew on LB plate containing ampicillin, X-gal and IPTG. Inserted DNA of 3 random colonies was sequenced, and the DNA was completely coincident with the sequence in GeneBank (data not shown). Then the inserted DNA of pT-Prx was digested with *EcoRI* and *BamHI*, purified, and inserted into

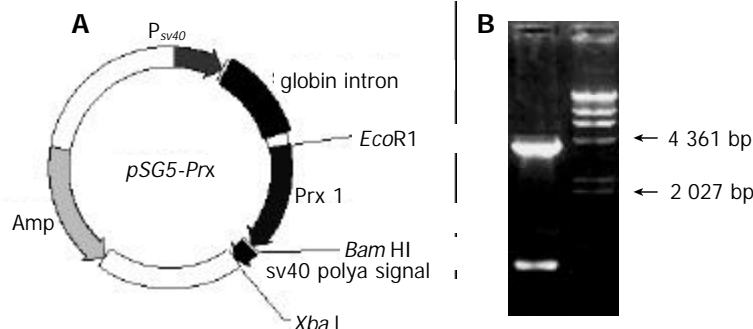


Figure 2 Recombinant expression vector pSG5-Prx. A: diagrams of the expression vector pSG5-Prx. B: electrophoresis map of this vector (*EcoRI* and *BamHI*). λ /*HindIII* marker was loaded to estimate the relative molecular weight of the expression vector.

vector pSG5. The recombinant expression vector was termed as pSG5-Prx (Figure 2). This recombinant plasmid was directly applied in cell transfection.

Transcription of pSG5-Prx in IEC-6 Cells by RT-PCR

We transfected IEC-6 cells with pSG5-Prx using pSG5 as a control. The cells grew very well during the period of transfection. Total RNAs of transfected IEC-6 cells were isolated after the second transfection using TriPure solution. Transcription of the recombinant plasmid was detected by applying RT-PCR with primers P2 and P3. The result showed that 2 DNA bands were visualized on agarose gel. Because the beta-globin intron (Figure 2A) in the primary transcript was spliced, the length of RT-PCR product based on mature mRNA was about 817 bp. However, the length of the other DNA band was about 1 399 bp, which was the PCR product using the recombinant plasmid as template (Figure 3).

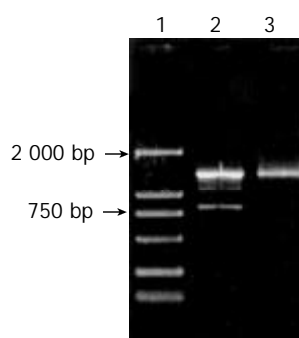


Figure 3 Detection of the transcription of recombinant vector pSG5-Prx by RT-PCR. Total RNAs isolated from transfected cells were applying for RT-PCR analysis with primers P2 and P3. Lane 1: DNA marker DL 2000, Lane 2: RT-PCR product, Lane 3: PCR product using purified recombinant vector as template.

Expression of Prx I in IEC-6 Cells

Total proteins of transfected IEC-6 cells were isolated after the second transfection and separated by SDS-PAGE. The blots were probed with specific antibodies against PrxI and GAPDH. Relative protein level was determined by quantitating the intensity of the bands with a densitometer. The ratio of the intensity of Prx I/GAPDH was automatically compared by Quantity One software (Bio-Rad Corp.). The result showed that the expression of Prx I was increased in pSG5-Prx transfected IEC-6 cells (50% more than the control cells) (Figure 4). This indicated that the recombinant plasmid could be transcribed and translated in IEC-6 cells.

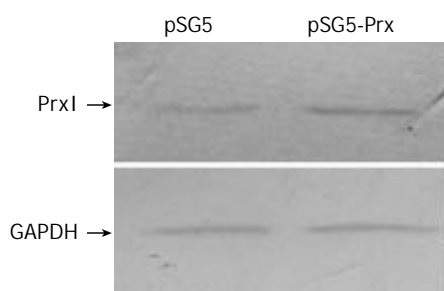


Figure 4 Immunoblotting of peroxiredoxin I of transfected and normal IEC-6 cell.

DISCUSSION

IEC-6 cell line was derived from normal rat intestinal epithelia.

Its living condition for stable passage was successfully established after trials. The cell line was testified to be the small intestinal epithelial cell by electron microscopy and immunohistochemistry, and has been applied to some related research work^[22]. It is rational to apply this cell line *in vitro* to mimic the intestinal epithelia *in vivo*.

To further study the biochemical and physiological function of Prx I, we cloned the coding region of this protein and over expressed it in IEC-6 cells in this study. The cDNA of Prx I was first cloned in 1994 applying differential hybridization technique, which was named as *MSP23*^[23]. Treatment with diethylmaleate or glucose/glucose oxidase markedly enhanced the induction of its transcription, and the amount of its protein in the cells rapidly increased. Moreover, the cDNAs corresponding to the thiol-specific antioxidant (TSA), which encoded a protein termed as Prx, has been cloned and sequenced in yeast and mammalian cells^[24]. From the results of biochemical and physiological studies, Prx I has been involved in association with a variety of diverse cellular functions including proliferation, differentiation, and immune response. However, the detailed pathophysiological functions of this protein remain unknown.

The most striking finding of Prx I was that it was increased in many kinds of tumor cells. Moreover, some researchers thought it might be a potential tumor marker^[25]. Prx I was over-expressed in human breast cancer tissues compared to normal tissues^[26]. Using comparative proteome analysis between human normal (BEAS 2B) and malignant (A549) lung epithelial cells, Chang *et al.*^[27] found that Prx I was increased more than twofold reproducibly. Additionally, Prx I expression levels in follicular neoplasm and thyroiditis group were significantly higher than that of the control group, though papillary carcinoma group did not show statistical significance^[25]. All these data suggested Prx I was involved in tumor development or progression, and it might be a new target for gene therapy of tumor cells.

It was suggested that Prx I was a radiation responsive gene. Lee *et al.*^[28] demonstrated, when the irradiated testis was examined, Prx I was found to be transiently up-regulated. Its highly homologous gene Prx II was increased in tissues isolated from the patients who did not respond to radiation therapy. However, treatment with a Prx II antisense decreased the expression of Prx II, enhancing the radiation sensitivity of cells^[29].

In this study, we found pSG5 was an efficient expression vector of mammal cells^[30]. Though it has no screen marker, the expression of recombinant plasmid can be easily verified at mRNA level applying RT-PCR technology owing to the globin intron of this vector. Because of the existence of the vector DNA in the sample purified by applying Tripure solution, two kinds of RT-PCR product were displayed on agarose gel, which represented different PCR template. After the second transfection, most of the cells expressed the exogenous vector, and the protein was accumulated in these cells, which could be detected by immunoblotting. We will further study the biochemical and physiological role in radiation response of this protein.

REFERENCES

- 1 **Rhee SG**, Kang SW, Chang TS, Jeong W, Kim K. Peroxiredoxin, a novel family of peroxidases. *IUBMB Life* 2001; **52**: 35-41
- 2 **Fujii J**, Ikeda Y. Advances in our understanding of peroxiredoxin, a multifunctional, mammalian redox protein. *Redox Rep* 2002; **7**: 123-130
- 3 **Butterfield LH**, Merino A, Golub SH, Shau H. From cytoprotection to tumor suppression: the multifactorial role of peroxiredoxins. *Antioxid Redox Signal* 1999; **1**: 385-402
- 4 **Kim K**, Kim IH, Lee KY, Rhee SG, Stadtman ER. The isolation and purification of a specific "protector" protein which inhibits enzyme inactivation by a thiol/Fe(III)/O₂ mixed-function

- oxidation system. *J Biol Chem* 1988; **263**: 4704-4711
- 5 **Chang TS**, Jeong W, Choi SY, Yu S, Kang SW, Rhee SG. Regulation of peroxiredoxin I activity by Cdc2-mediated phosphorylation. *J Biol Chem* 2002; **277**: 25370-25376
 - 6 **Rhee SG**, Chang TS, Bae YS, Lee SR, Kang SW. Cellular regulation by hydrogen peroxide. *J Am Soc Nephrol* 2003; **14**(8 Suppl 3): S211-215
 - 7 **Lee TH**, Yu SL, Kim SU, Lee KK, Rhee SG, Yu DY. Characterization of mouse peroxiredoxin I genomic DNA and its expression. *Gene* 1999; **239**: 243-250
 - 8 **Chung YM**, Yoo YD, Park JK, Kim YT, Kim HJ. Increased expression of peroxiredoxin II confers resistance to cisplatin. *Anticancer Res* 2001; **21**: 1129-1133
 - 9 **Choi JH**, Kim TN, Kim S, Baek SH, Kim JH, Lee SR, Kim JR. Overexpression of mitochondrial thioredoxin reductase and peroxiredoxin III in hepatocellular carcinomas. *Anticancer Res* 2002; **22**: 3331-3335
 - 10 **Seo MS**, Kang SW, Kim K, Baines IC, Lee TH, Rhee SG. Identification of a new type of mammalian peroxiredoxin that forms an intramolecular disulfide as a reaction intermediate. *J Biol Chem* 2000; **275**: 20346-20354
 - 11 **Chen JW**, Dodia C, Feinstein SI, Jain MK, Fisher AB. 1-Cys peroxiredoxin, a bifunctional enzyme with glutathione peroxidase and phospholipase A2 activities. *J Biol Chem* 2000; **275**: 28421-28427
 - 12 **Kawai S**, Takeshita S, Okazaki M, Kikuno R, Kudo A, Amann E. Cloning and characterization of OSF-3, a new member of the MER5 family, expressed in mouse osteoblastic cells. *J Biochem* 1994; **115**: 641-643
 - 13 **Shau H**, Butterfield LH, Chiu R, Kim A. Cloning and sequence analysis of candidate human natural killer-enhancing factor genes. *Immunogenetics* 1994; **40**: 129-134
 - 14 **Prosperi MT**, Apiou F, Dutrillaux B, Goubin G. Organization and chromosomal assignment of two human PAG gene loci: PAGA encoding a functional gene and PAGB a processed pseudogene. *Genomics* 1994; **19**: 236-241
 - 15 **Yang KS**, Kang SW, Woo HA, Hwang SC, Chae HZ, Kim K, Rhee SG. Inactivation of human peroxiredoxin I during catalysis as the result of the oxidation of the catalytic site cysteine to cysteine-sulfenic acid. *J Biol Chem* 2002; **277**: 38029-38036
 - 16 **Ishii T**, Itoh K, Sato H, Bannai S. Oxidative stress-inducible proteins in macrophages. *Free Radic Res* 1999; **31**: 351-355
 - 17 **Neumann CA**, Krause DS, Carman CV, Das S, Dubey DP, Abraham JL, Bronson RT, Fujiwara Y, Orkin SH, Van Etten RA. Essential role for the peroxiredoxin Prdx1 in erythrocyte antioxidant defence and tumour suppression. *Nature* 2003; **424**: 561-565
 - 18 **Crowley-Weber CL**, Payne CM, Gleason-Guzman M, Watts GS, Futscher B, Waltmire CN, Crowley C, Dvorakova K, Bernstein C, Craven M, Garewal H, Bernstein H. Development and molecular characterization of HCT-116 cell lines resistant to the tumor promoter and multiple stress-inducer, deoxycholate. *Carcinogenesis* 2002; **23**: 2063-2080
 - 19 **Wei YJ**, Zhang B, Su YP, Liu XH, Wang FC, Ai GP. Effect of ionizing radiation on the expression of Prx I and Prx VI gene in murine intestinal epithelial cells. *Chongqing Med J* 2003; **32**: 1343-1345
 - 20 **Chen WC**, McBride WH, Iwamoto KS, Barber CL, Wang CC, Oh YT, Liao YP, Hong JH, de Vellis J, Shau H. Induction of radioprotective peroxiredoxin-I by ionizing irradiation. *J Neurosci Res* 2002; **70**: 794-798
 - 21 **Zhang B**, Su YP, Ai GP, Liu XH, Wang FC, Cheng TM. Differentially expressed proteins of gamma-ray irradiated mouse intestinal epithelial cells by two-dimensional electrophoresis and MALDI-TOF mass spectrometry. *World J Gastroenterol* 2003; **9**: 2726-2731
 - 22 **Wood SR**, Zhao Q, Smith LH, Daniels CK. Altered morphology in cultured rat intestinal epithelial IEC-6 cells is associated with alkaline phosphatase expression. *Tissue Cell* 2003; **35**: 47-58
 - 23 **Ishii T**, Yamada M, Sato H, Matsue M, Taketani S, Nakayama K, Sugita Y, Bannai S. Cloning and characterization of a 23-kDa stress-induced mouse peritoneal macrophage protein. *J Biol Chem* 1993; **268**: 18633-18636
 - 24 **Chae HZ**, Rhee SG. A thiol-specific antioxidant and sequence homology to various proteins of unknown function. *BioFactors* 1994; **4**: 177-180
 - 25 **Yanagawa T**, Ishikawa T, Ishii T, Tabuchi K, Iwasa S, Bannai S, Omura K, Suzuki H, Yoshida H. Peroxiredoxin I expression in human thyroid tumors. *Cancer Lett* 1999; **145**: 127-132
 - 26 **Noh DY**, Ahn SJ, Lee RA, Kim SW, Park IA, Chae HZ. Overexpression of peroxiredoxin in human breast cancer. *Anticancer Res* 2001; **21**: 2085-2090
 - 27 **Chang JW**, Jeon HB, Lee JH, Yoo JS, Chun JS, Kim JH, Yoo YJ. Augmented expression of peroxiredoxin I in lung cancer. *Biochem Biophys Res Commun* 2001; **289**: 507-512
 - 28 **Lee K**, Park JS, Kim YJ, Soo Lee YS, Sook Hwang TS, Kim DJ, Park EM, Park YM. Differential expression of Prx I and II in mouse testis and their up-regulation by radiation. *Biochem Biophys Res Commun* 2002; **296**: 337-342
 - 29 **Park SH**, Chung YM, Lee YS, Kim HJ, Kim JS, Chae HZ, Yoo YD. Antisense of human peroxiredoxin II enhances radiation-induced cell death. *Clin Cancer Res* 2000; **6**: 4915-4920
 - 30 **Rose K**, Steinbuechel A. Construction and intergeneric conjugative transfer of a pSG5-based cosmid vector from *Escherichia coli* to the polyisoprene rubber degrading strain *Micromonospora aurantiaca* W2b. *FEMS Microbiol Lett* 2002; **211**: 129-132

Helicobacter pylori infection in patients with autoimmune thrombocytopenic purpura

Erdal Kurtoglu, Ertugrul Kayacetin, Aysegul Ugur

Erdal Kurtoglu, Department of Hematology, Selcuk University, Konya 42060, Turkey

Ertugrul Kayacetin, Department of Gastroenterology, Selcuk University, Konya 42060, Turkey

Aysegul Ugur, Department of Biochemistry, Selcuk University, Konya 42060, Turkey

Correspondence to: Dr. Erdal Kurtoglu, Feritpasa Mahallesi, Umit Bahadir Turk Sokak, No: 21/4 Girgic Apt, Konya 42060, Turkey. erdalkurtoglu@yahoo.com

Telephone: +90-332-323-2600 **Fax:** +90-332-324-4027

Received: 2004-02-02 **Accepted:** 2004-03-10

Abstract

AIM: To compare the prevalence of *Helicobacter pylori* (*H pylori*) infection in autoimmune thrombocytopenic purpura (AITP) patients with that of nonthrombocytopenic controls, and to evaluate the efficacy of the treatment in *H pylori*(+) and *H pylori*(-) AITP patients.

METHODS: The prevalence of gastric *H pylori* infection in 38 adult AITP patients (29 female and 9 male; median age 27 years; range 18-39 years) who consecutively admitted to our clinic was investigated.

RESULTS: *H pylori* infection was found in 26 of 38 AITP patients (68.5%). *H pylori* infection was found in 15 of 23 control subjects (65.2%). The difference in *H pylori* infection between the 2 groups was not significant. Thrombocyte count of *H pylori*-positive AITP patients was significantly lower than that of *H pylori*-negative AITP patients ($P<0.05$). Thrombocyte recovery of *H pylori*-positive group was less than that of *H pylori*-negative group ($P<0.05$).

CONCLUSION: *H pylori* infection should be considered in the treatment of AITP patients with *H pylori* infection.

Kurtoglu E, Kayacetin E, Ugur A. *Helicobacter pylori* infection in patients with autoimmune thrombocytopenic purpura. *World J Gastroenterol* 2004; 10(14): 2113-2115

<http://www.wjgnet.com/1007-9327/10/2113.asp>

INTRODUCTION

Autoimmune thrombocytopenic purpura (AITP) is an acquired bleeding disorder in which autoantibodies bind to platelet surface, leading to platelet destruction^[1,2]. The mechanism triggering the production of platelet autoantibodies are poorly understood^[2].

Helicobacter pylori (*H pylori*) is a spiral shaped bacterium that resides in the stomach mucosa. *H pylori* has been considered for years as the etiologic agent of gastritis, peptic ulcer, gastric cancer, and mucosa-associated lymphoid tissue (MALT) lymphoma^[3-5]. More recently, *H pylori* has been found to be associated with a number of autoimmune disorders, such as rheumatoid arthritis^[6], autoimmune thyroiditis^[7], Sjogren's syndrome^[8], Schonlein-Henoch purpura^[9], and AITP^[10,11].

There are data consistent with an association between *H pylori* infection and AITP^[12-14]. In addition a significant increase of platelet count following *H pylori* eradication has been reported in a proportion of AITP patients^[12]. AITP in adults is most often chronic, and up to 25% of cases of chronic AITP are refractory to standard therapy^[11]. However, although there is some evidence implicating *H pylori* in some autoimmune disorders, the association between AITP and *H pylori* infection is speculative.

The aim of this study was to compare the prevalence of *H pylori* infection in AITP patients with that of nonthrombocytopenic controls and to evaluate the efficacy of the treatment in *H pylori*(+) and *H pylori*(-) AITP patients.

MATERIALS AND METHODS

Between May 2001 and October 2003 we investigated the presence of gastric *H pylori* infection in 38 adult AITP patients (29 females, 9 males, median age: 27 years, range: 18-39 years) consecutively admitted to our clinic. AITP was diagnosed on the basis of the presence of isolated thrombocytopenia ($<100\times 10^9/L$) and megakaryocytic hyperplasia in bone marrow. Other causes of thrombocytopenia (drugs, pseudothrombocytopenia, hepatitis B and C virus infections, human immunodeficiency virus infection, malignancy) were excluded. Patients considered at bleeding risk who would require active treatment were also excluded. Age- and sex-matched 23 (18 females, 5 males, median age: 26 years, range: 18-35 years) nonthrombocytopenic patients without dyspeptic complaints were used as control group. None of the patients and controls had received antibiotics, proton pump inhibitors, and H₂-receptor blockers during 4 wk before the onset of AITP.

All patients underwent 1 mg/(kg.d) steroid therapy for 3 wk following diagnosis, and then the dose gradually tapered every week until withdrawal. Our second choice of therapy was intravenous immunoglobulin administration [400 mg/(kg.d) for 5 d], but we did not use it.

An agglutination method was used to detect anti-*H pylori* antibodies of IgG type in both patients and controls (Ridascreen® R-Biopharm, Darmstadt, Germany). Hemogram analysis was done by Coulter®STKS (Coulter Corporation, Miami, Florida, USA).

Although demonstration of *H pylori* in gastric biopsies is the gold standard of *H pylori* detection, we preferred blood antibody detection due to following reasons. Endoscopy might cause unexpected bleeding in thrombocytopenic patients especially in those whose thrombocyte counts were less than $50\times 10^9/L$. Urea breath test could not allow the detection of *H pylori* infection retrospectively. Both sensitivity and specificity of such kits were demonstrated in previous studies ($95\%<$)^[15].

Statistical analysis

Statistical analysis was performed using Kruskal-Wallis and Mann-Whitney *U* tests. Mean values were calculated for every variable in each group and compared between different groups. $P<0.05$ was considered as statistically significant.

RESULTS

There was no age or sex difference between controls and patients. *H pylori* infection was found in 26 of 38 patients with AITP (68.5%), and in 15 of 23 control subjects (65.2%). The difference between the 2 groups for *H pylori* infection was not significant (Table 1). Thrombocyte count of *H pylori*-positive AITP patients was lower than that of *H pylori*-negative AITP patients ($P < 0.05$). Thrombocyte recovery of *H pylori*-positive group was less than that of *H pylori*-negative group (Table 2) ($P < 0.05$).

Table 1 General characteristics of subjects in the study

Subjects	n	%	Mean age (range)	Sex (F/M)
<i>H pylori</i> -negative controls	8	(34.8)	25 (18-32)	6/2
<i>H pylori</i> -positive controls	15	(65.2)	27 (25-35)	12/3
<i>H pylori</i> -negative patients	12	(31.5)	29 (24-34)	8/4
<i>H pylori</i> -positive patients	26	(68.5)	26 (22-37)	21/5

Table 2 Platelet counts ($\times 10^9/L$) of AITP patients before and after steroid therapy

Parameters	<i>H pylori</i> -positive patients (n=26)	<i>H pylori</i> -negative patients (n=12)
Platelet counts ($\times 10^9/L$) (mean, range)	15 (10-22) ^a	29 (21-42)
Response to steroid (number, %)	17 (65) ^a	10 (83)
Post-treatment platelet counts ($\times 10^9/L$) (mean, range)	77 (61-112)	140 (124-180)

^a $P < 0.05$ vs *H pylori* negative patients.

DISCUSSION

AITP is an autoimmune disease caused by autoantibodies against platelets^[16]. Several lines of direct and indirect evidences suggest that infectious agents may influence the occurrence or the course of some autoimmune diseases^[17]. The role of some bacterial or viral agents in the pathogenesis of AITP is well known. It has been demonstrated that the mimicry of human antigens by infectious agents represents the mechanism underlying this phenomenon^[18].

H pylori is a ubiquitous Gram-positive bacterium involved in the pathogenesis of gastric and duodenal ulcers. Recently, the involvement of *H pylori* has also been suggested in various autoimmune diseases^[6-9]. *H pylori* has been shown to cause immunological responses to the production of large amounts of proinflammatory substances and mucosal damage through autoimmunity^[19]. Previous *in vitro* studies suggested that *H pylori* has the potential to initiate autoreactivity through molecular mimicry. Recently, a role of *H pylori* in the pathogenesis of AITP has been suggested because significant increases in thrombocyte count were reported after eradication of *H pylori*^[10,11]. Michel *et al.*^[2] and Jargue *et al.*^[14] found no evidence of an association between *H pylori* infection and AITP. But the role of *H pylori* in the pathogenesis of AITP is still controversial.

Regarding the association between *H pylori* and AITP, Gasbarrini *et al.*^[11] reported that 61% of 18 AITP cases were infected with *H pylori*. Emilia *et al.*^[10] then reported that 43% of 30 AITP patients were *H pylori* positive. Kohda *et al.*^[18] found that *H pylori* was positive in 62.5% of 40 AITP patients in Japan. The prevalence of *H pylori* in our series was 68.5%. The prevalence of *H pylori* infection in healthy population of Italy, where Gasbarrini's and Emilia's studies were held, was

about 63%^[20]. In Japan the prevalence of *H pylori* infection was about 25-45%^[21]. We found *H pylori* infection in 65.2% of healthy controls in Turkish population.

Steroid is considered as the most effective treatment for AITP in adults. But, most patients relapsed when steroids were withdrawn and only 10-30% of them maintained a long lasting remission^[22]. Kohda *et al.*^[18] and Michel *et al.*^[2] found that there was no significant difference regarding thrombocyte counts between *H pylori*-positive and *H pylori*-negative AITP patients. In our series the thrombocyte count of *H pylori*-positive group was higher than that of *H pylori*-negative group at the initial presentation, and the difference between two groups was significant ($P < 0.05$). Following treatment increase in the thrombocyte count of *H pylori*-positive patients was less than that of *H pylori*-negative patients. The difference was also significant ($P < 0.05$).

Although the pathogenetic mechanism underlying *H pylori*-induced thrombocytopenia remains obscure, *H pylori* has been presumed to induce the formation of autoantibodies by way of a chronic immunological stimulus or cross mimicry between itself and platelets^[23]. It has been demonstrated that autoantibodies against *H pylori* can also react with some extragastric tissues, such as glomerular capillary membrane, ductal cells of salivary glands, and renal tubular cells^[24]. Platelets may also be a target of such antibodies although there is no proof for this cross reactivity.

In conclusion, *H pylori* infection should be searched in all AITP patients, and we suggest that *H pylori* should be eradicated in *H pylori*-positive AITP patients.

REFERENCES

- George JN, el-Harake MA, Raskob GE. Chronic idiopathic thrombocytopenic purpura. *N Engl J Med* 1994; **331**: 1207-1211
- Michel M, Khellaf M, Desforgues L, Lee K, Schaeffer A, Godeau B, Bierling P. Autoimmune thrombocytopenic purpura and *Helicobacter pylori* infection. *Arch Intern Med* 2002; **162**: 1033-1036
- Suzuki H, Masaoka T, Nomura S, Hoshino Y, Kurabayashi K, Minegishi Y, Suzuki M, Ishii H. Current consensus on the diagnosis and treatment of *H pylori* associated gastroduodenal disease. *Keio J Med* 2003; **52**: 163-173
- Ando K, Shimamoto T, Tauchi T, Ito Y, Kuriyama Y, Gotoh A, Miyazawa K, Kimura Y, Kawai T, Ohyashiki K. Ca eradication therapy for *Helicobacter pylori* really improve the thrombocytopenia in idiopathic thrombocytopenic purpura? Our experience and a literature review. *Int J Hematol* 2003; **77**: 239-244
- Veneri D, Franchini M, Gottardi M, D'Adda M, Ambrosetti A, Krampera M, Zanetti F, Pizzolo G. Efficacy of *Helicobacter pylori* eradication in raising platelet count in adult patients with idiopathic thrombocytopenic purpura. *Haematologia* 2002; **87**: 1177-1179
- Zentilin P, Savarino V, Garnerio A, Accardo S, Serio B. Is *Helicobacter pylori* infection a risk factor for disease severity in rheumatoid arthritis? *Gastroenterology* 1999; **116**: 503-504
- De Luis DA, Varela C, de la Calle H. *Helicobacter pylori* infection is markedly increased in patients with autoimmune atrophic thyroiditis. *J Clin Gastroenterol* 1998; **26**: 259-263
- Figura N, Giordano N, Burrioni D, Macchia G, Vindigni C, Gennari C, Bayeli PF. Sjogren's syndrome and *Helicobacter pylori* infection. *European J Gastroenterol Hepatol* 1994; **6**: 321-322
- Reinauer S, Megahed M, Goertz G, Ruzicka T, Borchard F, Susanto F, Reinauer H. Schonlein-Henoch purpura associated with gastric *Helicobacter pylori* infection. *J Am Acad Dermatol* 1995; **33**: 876-879
- Emilia G, Longo G, Luppi M, Gandini G, Morselli M, Ferrara L, Amarri S, Cogossi K, Torelli G. *Helicobacter pylori* eradication can induce platelet recovery in idiopathic thrombocytopenic purpura. *Blood* 2001; **97**: 812-814
- Gasbarrini A, Franceschi F, Tartaglione R, Landolfi R, Pola P, Gasbarrini G. Regression of autoimmune thrombocytopenia after eradication of *Helicobacter pylori*. *Lancet* 1998; **352**: 878

- 12 **Hashino S**, Mori A, Suzuki S, Izumiyama K, Kahata K, Yonezumi M, Chiba K, Kondo T, Ota S, Toyashima N, Kato N, Tanaka J, Imamura M, Asaka M. Platelet recovery in patients with idiopathic thrombocytopenic purpura after eradication of *Helicobacter pylori*. *Int J Hematol* 2003; **77**: 188-191
- 13 **Hino M**, Yamane T, Park K, Tahubo T, Ohta K, Kitagawa S, Higuchi K, Arakawa T. Platelet recovery after eradication of *Helicobacter pylori* in patients with idiopathic thrombocytopenic purpura. *Ann Hematol* 2003; **82**: 30-32
- 14 **Jargue I**, Andreu R, Llopis I, De la Rubia J, Gomis F, Senent L, Jimenez C, Martin G, Martinez JA, Sanz GF, Ponce J, Sanz MA. Absence of platelet response after eradication of *Helicobacter pylori* infection in patients with chronic idiopathic thrombocytopenic purpura. *Br J Haematol* 2001; **115**: 1002-1003
- 15 **Feldman RA**, Deeks JJ, Evans SJ. For the *Helicobacter pylori* Serology Study Group Multi-laboratory comparison of eight commercially available *Helicobacter pylori* serology kits. *Eur J Clin Microbiol Infect Dis* 1995; **14**: 428-433
- 16 **McMillan R**. Autoantibodies and autoantigens in chronic immune thrombocytopenic purpura. *Semin Hematol* 2000; **37**: 239-248
- 17 **Benoist C**, Mathis D. Autoimmunity: the pathogen connection. *Nature* 1998; **394**: 227-228
- 18 **Kohda K**, Kuga T, Kogawa K, Kanisawa Y, Koike K, Kuroiwa G, Hirayama Y, Sato Y, Matsunaga T, Niitsu Y. Effect of *Helicobacter pylori* eradication on platelet recovery in Japanese patients with chronic idiopathic thrombocytopenic purpura and secondary autoimmune thrombocytopenic purpura. *Br J Hematol* 2002; **118**: 584-588
- 19 **Bamford KB**, Andersen L. Host response. *Current Opinion Gastroenterol* 1997; **13**(Suppl 1): 25-30
- 20 **Luzza F**, Imeneo M, Maletta M, Paluccio G, Nistico S, Perticone F, Foca A, Pallone F. Suggestion against an oral-oral route of transmission for *Helicobacter pylori* infection: a seroepidemiological study in a rural area. *Dig Dis Sci* 1998; **43**: 1488-1492
- 21 **Asaka M**, Kimura T, Kudo M, Tadeka H, Miyazaki T, Miki K, Garaham DY. Relationship of *Helicobacter pylori* to serum pepsinogens in an asymptomatic Japanese population. *Gastroenterology* 1992; **102**: 760-766
- 22 **George JN**, Woolf SH, Raskob GE, Wasser JS, Aledort LM, Ballem PJ, Blanchette VS, Bussel JB, Cines DB, Kelton JG, Lichtin AE, McMillan R, Okerbloom JA, Regan DH, Warrier I. Idiopathic thrombocytopenic purpura: a practice guideline developed by explicit methods for the American Society of Hematology. *Blood* 1996; **88**: 3-40
- 23 **Gasbarrini A**, Franceschi F. Autoimmune diseases and *Helicobacter pylori* infection. *Biomed Pharmacother* 1999; **53**: 223-226
- 24 **Ko GH**, Park HB, Shin MK, Park CK, Lee JH, Youn HS, Cho MJ, Lee WK, Rhee KH. Monoclonal antibodies against *Helicobacter pylori* cross react with human tissue. *Helicobacter* 1997; **2**: 210-215

Edited by Wang XL Proofread by Chen WW and Xu FM

Curative effects of interferon- α and HLA-DRB1 -DQA1 and -DQB1 alleles in chronic viral hepatitis B

Guo-Qing Zang, Min Xi, Ming-Liang Feng, Yun Ji, Yong-Sheng Yu, Zheng-Hao Tang

Guo-Qing Zang, Min Xi, Yong-Sheng Yu, Zheng-Hao Tang,
Department of Infectious Diseases, 6th People's Hospital of Shanghai
Jiaotong University, Shanghai 200233, China

Ming-Liang Feng, Yun Ji, Shanghai Blood Center, Shanghai
200051, China

Supported by the Foundation of Shanghai Municipal Health Bureau,
No. 01444

Correspondence to: Dr. Guo-Qing Zang, Department of Infectious
Diseases, 6th People's Hospital of Shanghai Jiaotong University,
Shanghai 200233, China

Telephone: +86-21-64369181

Received: 2003-11-26 **Accepted:** 2004-02-01

Abstract

AIM: To investigate the association between curative effects of interferon- α and partial human leucocyte antigen (HLA) II alleles in chronic viral hepatitis B.

METHODS: Sixty patients with chronic viral hepatitis B in Shanghai were treated with a standard course of treatment with interferon- α for 6 mo. HLA-DRB1, -DQA1, and -DQB1 alleles were detected by polymerase chain reaction-sequence specific primer (PCR-SSP) method.

RESULTS: Frequencies of HLA-DRB1*04 ($P < 0.025$) and HLA-DQA1*0303 ($P < 0.01$) in non-responders were significantly higher than those in partial and complete responders. Frequencies of HLA-DQA1*0505 ($P < 0.025$) and HLA-DQB1*0301 ($P < 0.005$) in partial and complete responders were significantly higher than those in non-responders.

CONCLUSION: Non-response to interferon- α therapy is positively correlated with HLA-DRB1*04 and HLA-DQA1*0303, and negatively correlated with HLA-DQA1*0505 and -DQB1*0301 in patient with chronic viral hepatitis B. HLA II genes of the identification alleles provide a method for evaluating outcome of interferon- α treatment.

Zang GQ, Xi M, Feng ML, Ji Y, Yu YS, Tang ZH. Curative effects of interferon- α and HLA-DRB1 -DQA1 and -DQB1 alleles in chronic viral hepatitis B. *World J Gastroenterol* 2004; 10(14): 2116-2118

<http://www.wjgnet.com/1007-9327/10/2116.asp>

INTRODUCTION

Chronic viral hepatitis B is a contagious disease with the higher infection and incidence rate in China, and approximately 0.3 million peoples died of chronic viral hepatitis B per year^[1]. Currently, it is mainly treated with interferon- α , lamivudine, etc. However, the effect of treatment is varying in different patients. Normally, complete response rate is about 30-40%, complete curability is less than 10%. What is the determinant of interferon- α curative effect on different individuals? Reports from domestic and overseas showed that individuals had

different endings after being infected by HBV and HCV^[2-3] and different response after being treated with interferon- α ^[4]. Researches indicated that these phenomenons were correlated with HLA alleles^[5]. HLA gene contributes to the host response against HBV. Individuals with different HLA alleles may differ in susceptibility or resistance to HBV^[6-8]. Our study tried to analyze HLA-DRB1, -DQB1, -DQA1 alleles in chronic viral hepatitis B to be treated with interferon- α for 6 mo, and study the association between curative effects of interferon- α and partial HLA alleles, which will help to direct the treating process of anti-virus in clinic.

MATERIALS AND METHODS

Research subjects and prescription

Sixty patients with chronic viral hepatitis B were enrolled in this study. The diagnosis of all the cases was made according to the criteria established on the Viral Hepatitis Conference held in 2000^[9]. All patients had abnormal serum transaminase levels. HBsAg, HBeAg, HBcAb in serum were detected by ELISA and HBV-DNA was detected by immunofluorescent semi-quantitative polymerase chain reaction. All patients' HAV, HCV, HDV and HEV in serum were negative, and did not have a history of using adrenal cortical hormone before. There were 41 male and 19 female patients with average age 35 \pm 8 years. They were all treated with 5.0 million units interferon- α daily for 2 wk and then every other day for an additional 22 wk. Liver function was detected every 2 wk. Hepatitis B viral marks were detected by Abbott Laboratories and HBV-DNA was determined by PCR at every 3-mo therapy.

Sampling and action

Five milliliter blood from each research subject was taken, and treated with EDTA for anti-coagulation. After mixed with 1 mL cell membrane cracking solution, the samples were centrifuged for 30 s, and then the supernatant was removed. Another 1 mL of cell membrane cracking solution was added after drying the test tube by bibulous paper. Centrifuged for 20 s and the top clear water was removed again. The cell mass at the bottom of the tube was vibrated and dissolved thoroughly. When mixed equally with 0.4 mL karyen cracking solution, separated out floccule DNA by adding 1 mL absolute ethanol. Supernatant was abandoned, and washed with 70% ethanol. After drying by blot paper, put it under room temperature to let ethanol volatilize. Then 0.1 double distilled water was added, and kept at -40 °C for testing.

Study method

HLA-DRB1, HLA-DQA1, and HLA-DQB1 alleles were detected by applying the PCR-SSP technique^[10]. PCR buffer solution was vibrated and mixed. Taq enzyme was put on the icebox. Distilled water 67 μ L and 1.8 μ L of Taq enzyme were added to the PCR buffer solution and vibrated. Then the solution was aspirated and added to the monitor hole. And 19 μ L of DNA samples were added to the spare mixing solution. Except negative contrast hole, the solution was added

to every hole. Color changed from yellow to pink. The reagent was sealed up, and sent to PCR apparatus for amplification. Sample solution 6 μ L was electrophoresed on 20 g/L agarose gel for 12 min under 150 V, and observed the under ultraviolet light.

Statistical analysis

HLA-DRB1, -DQA1, and -DQB1 alleles frequencies for the partial and complete responders were compared with those of the non-responders using the χ^2 test. $P < 0.05$ was considered statistically significant.

RESULTS

Based on the results of HBV markers and HBV-DNA after 6-mo therapy with interferon- α , patients were divided into 3 groups: (1) Complete response group: HBeAg and HBV-DNA were negative, while HBeAb was positive, and ALT was normal; (2) Partial response group: HBeAg and HBV-DNA level decreased, while ALT was normal; (3) Non-response group: HBeAg and HBV-DNA were stable. After inspection, it was found that the frequencies of HLA-DRB1*04 ($P < 0.025$) and HLA-DQA1*0303 ($P < 0.01$) in non-responders were significantly higher than those in partial and complete responders, and the frequencies of HLA-DQA1*0505 ($P < 0.025$) and HLA-DQB1*0301 ($P < 0.005$) in partial and complete responders were significantly higher than those in non-responders (Tables 1, 2 and 3).

Table 1 Comparison of frequency of HLA-DRB1 allele among non-responders and partial and complete responders

Allele	Partial and complete responders (n=34)	Non-responders (n=26)	χ^2
DRB1*10(+)	1	0	0.778
DRB1*11(+)	9	3	2.053
DRB1*4(+) ^a	1	6	2.053
DRB1*12(+)	9	7	0.002
DRB1*8(+)	4	5	0.644
DRB1*9(+)	15	11	0.020
DRB1*14(+)	4	4	0.167
DRB1*15(+)	8	10	1.564
DRB1*17(+)	1	2	0.700
DRB1*16(+)	3	0	2.415
DRB1*7(+)	4	0	3.277

^a $P < 0.025$.

Table 2 Comparison of HLA-DQA1 allele frequencies among non-responders and partial and complete responders

Allele	Partial and complete responders (n=32)	Non-responders (n=28)	χ^2
DQA1*0105(+)	1	0	0.890
DQA1*0505(+) ^a	12	3	5.714
DQA1*0303(+) ^b	0	6	7.619
DQA1*0601(+)	10	7	0.287
DQA1*0103(+)	9	7	0.075
DQA1*0302(+)	15	12	0.097
DQA1*0104(+)	4	4	0.041
DQA1*0102(+)	4	6	0.857
DQA1*0301(+)	1	4	2.435

^a $P < 0.025$, ^b $P < 0.01$.

Table 3 comparison of frequencies of HLA-DQB1 allele among non-responders and partial and complete responders

Allele	Partial and complete responders (n=32)	Non-responders (n=28)	χ^2
DQB1*0502(+)	6	1	3.338
DQB1*0301(+) ^a	20	7	8.485
DQB1*0401(+)	1	3	1.382
DQB1*0303(+)	15	12	0.097
DQB1*0503(+)	3	4	0.431
DQB1*0601(+)	6	9	1.429

^a $P < 0.005$.

DISCUSSION

Different individuals infected with HBV show different complicated symptoms. This is not only due to virus itself, but immunity itself^[11]. A great deal of evidences suggested that both cellular and humoral immunities were required for viral clearance. The latter is mainly subjected to major histocompatibility complex (MHC). HLA, the genetic offspring of MHC, is the first inherited system discovered to be associated with diseases definitely. Genes for HLA are located on the short arm of chromosome 6 with high polymorphism, and it is closely associated with immunoreactions of anti-HBV^[12]. Some special HLA genes may have influence on the rate of HBV infection and strength of immunoreactions^[13]. Patients who have successfully recovered from acute hepatitis B develop strong HLA classes I and II restricted T cell response, whereas these responses are weak or absent in patients with chronic hepatitis B^[14]. Jiang *et al.*^[15] found that HLA-DRB1*0301, -DQA1*0501 and -DQB1*0301 might be the susceptible genes, and HLA-DRB1*1101/1104 and -DQA1*0301 might be the resistant genes to chronic hepatitis B, and that host HLA class II gene was an important factor for determining the outcome of HBV infection. HLA spread on the cell surface through membrane protein with function of integrating with inner and outer antigen peptide and taking immune response when detected by CD4⁺ (cluster of differentiation) or CD8⁺ T cell on the surface of antigen presenting cells and target cells. Class II molecule, on the surface of antigen presenting cells, submits outer antigen including virus molecule group to the CD4⁺ T cell, which stimulates the releasing of the cell gene to take the effect of adjusting CD8⁺ cytotoxic T lymphocyte response and determine the antibody produce. Diepolder *et al.*^[16] found that people carrying HLA-DR13 had stronger CD4⁺ T cell response. That might be depended on the more accurate submission function of DR13, or associated with multiple peptide property of immunity adjusting gene chain near DR13. Thursz *et al.*^[17] discovered that DRB1*1302 possessed high frequency of clearance of hepatitis B virus in the Gambia people. Cotrina *et al.*^[5] also reported that predominance of the DRB1*1302 allele was observed in acute viral hepatitis B versus chronic viral hepatitis B in adult American. And the HLA-DRB1*0401 antigen was lower in the cases of chronic viral hepatitis B and C than that in the controls. Hohler *et al.*^[18] reported that the MHC class II allele DRB1*1301-02 was associated with protection from chronic viral hepatitis B in African Americans. Furthermore Bhimma *et al.*^[19] demonstrated that there was a high frequency of DQB1*0603 in subjects compared to controls in black children with hepatitis B virus-associated membranous nephropathy. Jiang *et al.*^[20] recently found that the possibility of fulminant hepatitis was increased in chronic hepatitis B with HLA-DRB1*1001. Tibbs *et al.*^[21] showed that the HLA-DQB1*0302 and HLA-DQA1*03 alleles conferred protection from chronic HCV-infection in Northern European

Caucasoid. These studies showed that HLA-II molecules were associated with clearance and prognosis of chronic viral hepatitis.

Currently, factors for forecasting interferon treating effect are as follows: ALT level before treatment; level of HBV-DNA; gene types of hepatitis B virus; sex of patients; and the duration of virus infection, etc. Interferon can induce the expression of IL-12 (interleukin-12) β_2 subpopulation, which induce Th0 (help T cell) cell to differentiate into Th1 cell. Previous studies showed that Th1 type response was beneficial for the clearance of chronically infected viruses^[7]. The balance of HBV differential antigen may influence the persistent HBV infection. Superiority of Th1 tends to occur acute hepatitis, while superiority of Th2 tends to occur persistent infection^[22]. There were fewer reports about association between curative effects of interferon- α with partial HLA allele. Qian *et al.*^[23] reported that the frequency of HLA-DRB1*07 in non-responders was higher than that in partial and complete responders in Guangdong Province of China, and the level of IL-4 and IFN- γ of each patient was higher than that of pre-treatment. It indicated that after treatment of chronic viral hepatitis B with IFN- γ , TH1 expression was relevant to the HLA-DRB1*07. Dincer *et al.*^[24] reported that in the HCV patient treated with interferon- α for 6 mo, the frequency of HLA-DRB1*13 was significantly higher in the non-responder group compared to the responder group. Our study showed that the frequency of HLA-DRB1*04 and HLA-DQA1*0303 in non-responders were obviously higher than those in partial and complete responders, and the frequency of HLA-DQA1*0505 and HLA-DQB1*0301 in partial and complete responders were markedly higher than those in non-responders. HLA-II molecules might be used for the treatment prognosis of interferon- α in patients with chronic hepatitis B.

REFERENCES

- World Health Organization, 1998. Hepatitis B fact sheet WHO/204. <http://www.who.int/inf-fs/en/fact203.html>
- van Hattum J, Schreuder GM, Schalm SW. HLA antigens in patients with various courses after hepatitis B virus infection. *Hepatology* 1987; **7**: 11-14
- Tong MJ, el-Farra NS, Reikes AR, Co RL. Clinical outcomes after transfusion-associated hepatitis C. *N Engl J Med* 1995; **332**: 1463-1466
- Miyaguchi S, Saito H, Ebinuma H, Morizane T, Ishii H. Possible association between HLA antigens and the response to interferon in Japanese patients with chronic hepatitis C. *Tissue Antigens* 1997; **49**: 605-611
- Cotrina M, Buti M, Jardi R, Rodriguez-Frias F, Campins M, Esteban R, Guardia J. Study of HLA-II antigens in chronic hepatitis C and B and in acute hepatitis B. *Gastroenterol Hepatol* 1997; **20**: 115-118
- Sobao Y, Sugi K, Tomiyama H, Saito S, Fujiyama S, Morimoto M, Hasuike S, Tsubouchi H, Tanaka K, Takiguchi M. Identification of hepatitis B virus-specific CTL epitopes presented by HLA-A*2402, the most common HLA class I allele in East Asia. *J Hepatol* 2001; **34**: 922-929
- Thimme R, Chang KM, Pemberton J, Sette A, Chisari FV. Degenerate immunogenicity of an HLA-A2-restricted hepatitis B virus nucleocapsid cytotoxic T-lymphocyte epitope that is also presented by HLA-B51. *J Virol* 2001; **75**: 3984-3987
- Shen JJ, Ji Y, Guan XL, Huang RJ, Sun YP. The association of HLA-DRB1*10 with chronic hepatitis B in Chinese patients. *Zhonghua Weishengwuxue He Mianyixue Zazhi* 1999; **19**: 58-59
- China physic association infectious disease & verminosis association liver disease sub-association viral hepatitis prevention & cure project. *Zhonghua Ganzangbing Zazhi* 2000; **8**: 324-329
- Olerup O, Zetterquist H. HLA-DR typing by PCR amplification with sequence-specific primers (PCR-SSP) in 2 hours: an alternative to serological DR typing in clinical practice including donor-recipient matching in cadaveric transplantation. *Tissue Antigens* 1992; **39**: 225-235
- Chen WN, Oon CJ. Mutation "hot spot" in HLA class I restricted T cell epitope on hepatitis B surface antigen in chronic carriers and hepatocellular carcinoma. *Biochem Biophys Res Commun* 1999; **262**: 757-761
- McDermott AB, Cohen SB, Zuckerman JN, Madrigal JA. Human leukocyte antigens influence the immune response to a pre-S/S hepatitis B vaccine. *Vaccine* 1999; **17**: 330-339
- McDermott AB, Madrigal JA, Sabin CA, Zuckerman JN, Cohen SB. The influence of host factors and immunogenetics on lymphocyte responses to hepatitis B vaccination. *Vaccine* 1999; **17**: 1329-1337
- Zhang SL, Liu M, Zhu J, Chai NL. Predominant Th₂ immune response and chronic hepatitis B virus infection. *Shijie Huaren Xiaohua Zazhi* 1999; **7**: 513-515
- Jiang YG, Wang YM, Liu TH, Liu J. Association between HLA class II gene and susceptibility or resistance to chronic hepatitis B. *World J Gastroenterol* 2003; **9**: 2221-2225
- Diepolder HM, Jung MC, Keller E, Schrant W, Gerlach JT, Gruner N, Zachoval R, Hoffmann RM, Schirren CA, Scholz S, Pape GR. A vigorous virus-specific CD4+ T cell response may contribute to the association of HLA-DR13 with viral clearance in hepatitis B. *Clin Exp Immunol* 1998; **113**: 244-251
- Thursz MR, Kwiatkowski D, Allsopp CE, Greenwood BM, Thomas HC, Hill AV. Association between an MHC class II allele and clearance of hepatitis B virus in the gambia. *New Engl J Med* 1995; **332**: 1065-1069
- Hohler T, Gerken G, Notghi A, Lubjuhn R, Taheri H, Protzer U, Lohr HF, Schneider PM, Meyer zum Buschenfelde KH, Rittner C. HLA-DRB1*1301 and *1302 protect against chronic hepatitis B. *J Hepatol* 1997; **26**: 503-507
- Bhimma R, Hammond MG, Coovadia HM, AdhiKari M, Connolly CA. HLA class I and II in black children with hepatitis B virus-associated membranous nephropathy. *Kidney Int* 2002; **61**: 1510-1515
- Jiang YG, Wang YM. Association between HLA-DRB1*1001 and severity of chronic hepatitis B. *Zhonghua Ganzangbing Zazhi* 2003; **11**: 256
- Tibbs C, Donaldson P, Underhill J, Thomson L, Manabe K, Williams R. Evidence that the HLA DQA1 *03 allele confers protection from chronic HCV-infection in northern european caucasoids. *Hepatology* 1996; **24**: 1342-1345
- Lee M, Lee SK, Son M, Cho SW, Park S, Kim HI. Expression of Th1 and Th2 type cytokines responding to HBsAg and HBxAg in chronic hepatitis B patient. *J Korean Med Sci* 1999; **14**: 175-181
- Qian Y, Zhang L, Hou JL. Association between non-response to interferon and HLA-DRB1*07 genes in chronic hepatitis B individuals. *Mianyixue Zazhi* 2002; **18**: 371-374
- Dincer D, Besisik F, Oguz F, Sever MS, Kaymakoglu S, Cakaloglu Y, Demir K, Turkoglu S, Carin M, Okten A. Genes of major histocompatibility complex class II influence chronic C hepatitis treatment with interferon in hemodialysis patients. *Int J Artiforgans* 2001; **24**: 212-214

Expansion and activation of natural killer cells from PBMC for immunotherapy of hepatocellular carcinoma

Bao-Gang Peng, Li-Jian Liang, Qiang He, Jie-Fu Huang, Ming-De Lu

Bao-Gang Peng, Li-Jian Liang, Qiang He, Jie-Fu Huang, Ming-De Lu, Department of Hepatobiliary Surgery, First Affiliated Hospital of Sun Yat-sen University, Guangzhou 510080, Guangdong Province, China
Supported by the Natural Science Foundation of Guangdong Province, No. 021889

Correspondence to: Dr. Bao-Gang Peng, Department of Hepatobiliary Surgery, First Affiliated Hospital of Sun Yat-sen University, 58 Zhongshan Road 2, Guangzhou 510080, Guangdong Province, China. pengbaogang@163.net

Telephone: +86-20-87335546 **Fax:** +86-20-87750632

Received: 2003-11-26 **Accepted:** 2004-01-15

Abstract

AIM: To induce efficient expansion of natural killer (NK) cells from peripheral blood mononuclear cells (PBMCs) using a culture of anchorage-dependent Wilms tumor cell lines, and to provide a reliable supply for adoptive immunotherapy of hepatocellular carcinoma.

METHODS: Culture expansion of NK cells was achieved using PBMCs cultured with Wilms tumor cells. Cytotoxicity was measured using a standard ⁵¹Cr release assay and crystal violet staining technique. The proportions of CD3+, CD4+, CD8+, CD16+, and CD56+ cells were determined by flow cytometry.

RESULTS: After PBMCs from healthy donors and hepatocellular carcinoma (HCC) were cultured with irradiated HFWT cells for 10-21 d, CD56+ CD16+ cells shared more than 50% of the cell population, and more than 80% of fresh HFWT cells were killed at an effector/target ratio of 2 over 24 h. NK-enriched lymphocyte population from HCC patients killed HCC-1 and 2 cells with sensitivities comparable to fresh TKB-17RGB cells. HCC cells proliferated 196-fold with the irradiated HFWT cells at 18 d. Stimulation by HFWT cells required intimate cell-cell interaction with PBMC. However, neither the soluble factors released from HFWT cells nor the fixed HFWT cells were effective for NK expansion. The lymphocytes expanded with IL-2 killed fresh HFWT target cells more effectively than the lymphocytes expanded with the 4-cytokine cocktail (IL-1 β , IL-2, IL-4 and IL-6). IL-2 was the sole cytokine required for NK expansion.

CONCLUSION: Wilms tumor is sensitive to human NK cells and is highly efficient for selective expansion of NK cells from PBMCs.

Peng BG, Liang LJ, He Q, Huang JF, Lu MD. Expansion and activation of natural killer cells from PBMC for immunotherapy of hepatocellular carcinoma. *World J Gastroenterol* 2004; 10 (14): 2119-2123

<http://www.wjgnet.com/1007-9327/10/2119.asp>

INTRODUCTION

Natural killer (NK) cells are CD3- CD56+ and/or CD16+ cytotoxic

lymphocytes that mediate first-line defense against various types of target cells without prior immunization^[1,2]. The regulation mechanism of human natural killer (NK) cell growth has not been well characterized despite the importance of NK cells in immune response^[3]. One reason is that the currently used culture system for human NK cells is relatively poor at inducing a strong growth response compared with culture systems for other lymphocytes, such as T cells.

Since K562 cells expressing scarcely MHC-class I on their surface are highly sensitive to natural killer (NK) cells, they have been widely used for the assay of NK killing activity^[4-6]. When K562 cells are killed by NK cells *in vitro*, apparent growth response of NK cells follows. The stimulation by K562 requires direct cell-cell contact and is not reconstituted by cell-free supernatants. However, the stimulation is not necessarily sufficient for the NK selective expansion in peripheral blood mononuclear cells (PBMCs) of every subject. Reports from Perussia *et al.*^[7] and Silva *et al.*^[8,9] suggested that human B lymphoblastoid cell lines and leukapheresed peripheral blood stem cell grafts were also useful for human NK cell expansion. Sekine *et al.*^[10] developed an alternative method for lymphocyte expansion from peripheral blood by cultivating cells with IL-2 and immobilized anti-CD3 monoclonal antibodies. Application of expensive anti-CD3, anti-CD16 bispecific antibodies may avoid the dilution of NK cells in the lymphocyte populations^[11]. Coculture of NK cells with dendritic cells (DCs) resulted in significant enhancement of NK cell cytotoxicity and IFN-gamma production^[12]. Coexpression of GM-CSF and B70 may enhance NK-mediated cytotoxicity, and then induce the antitumor immunity in hepatoma transplanted into nude mice^[13]. We consider that, for further use of the NK cells in adoptive immunotherapy of human tumors, clear separation of expanded NK cells and suspension cultured allogeneic EB virus-transformed cells that may have escaped from the killing by NK cells will be difficult.

In this study, we screened anchorage-dependent virus-free human tumor cell lines as an appropriate target in the NK cell expansion culture. We found that an anchorage-dependent cell line derived from Wilms tumor (HFWT) was sensitive to human NK cells.

MATERIALS AND METHODS

Cell lines and reagents

All the cell lines were from routine stock cultures in the RIKEN Cell Bank. Cell lines were maintained in basal medium containing 100 mL/L or 150 mL/L fetal bovine serum (FBS). Peripheral blood was taken from healthy volunteers and hepatocellular carcinomas (HCCs) were from patients who gave their informed consent. Recombinant human IL-1 β , -2, -4, -6, -7, -12, and -15 were purchased from Genzyme (Tokyo, Japan). Mouse anti-human-CD3, CD4, -CD8, CD56 and CD16 monoclonal antibodies were purchased from Nichirei Co., (Tokyo, Japan). ⁵¹Cr was purchased from NEN Life Science Products Inc. (Boston, USA).

Flow cytometry

Suspended cells (1×10^6) were washed three times with PBS, incubated for 30 min with monoclonal antibodies, 30 min with

FITC-labeled goat anti-mouse IgG polyclonal antibody. The cells were again washed with PBS containing 40 mL/L FBS. They were re-suspended in the same buffer at a concentration of 1×10^6 /mL and were immediately analyzed by FACS (Becton-Dickinson, Co.). The proportion of CD3+, CD4+, CD8+, CD16+, and CD56+ cells was detected with corresponding monoclonal antibodies.

Fixation of HFWT cells

HFWT cells (1×10^5 /mL, 1 mL) were plated in a 24-well plate and incubated overnight in a humidified 50 mL/L CO₂ incubator. The culture medium was replaced with PBS, and the cells were fixed with 0.5 mL of 40 g/L formaldehyde or 3:1 methanol-acetic acid mixture for 1 h, and then thoroughly washed with water.

HFWT cells were subjected to heat treatment at 100 °C for 2 s in a microwave oven after the replacement of the culture medium with PBS. The treated HFWT cell concentration was adjusted to 1×10^5 /well for the NK expansion experiments.

Expansion culture of NK cells

PBMCs were prepared from heparinized peripheral blood with the conventional preparation kit (Lymphoprep, Nycomed Pharma A.S., Norway). The cells were washed once with PBS, then once with RHAM alpha medium supplemented with 50 mL/L autologous plasma, and centrifuged at 1 400 r/min (240 g) for 10 min at room temperature. Before addition of PBMCs to the NK cell expansion cultures, the confluent target tumor cells maintained in a 24-well plate were irradiated with 50 Gy of X-rays. The PBMCs (1×10^6 /mL, approximately 1 mL/well) were then cultured with the tumor cells (at this stage, the responder/stimulator ratio was adjusted to 10 in the culture medium, i.e. the RHAM α medium was supplemented just before adding 50 mL/L autologous plasma and a 4-cytokine cocktail of IL-1 β (167 U/mL), IL-2 (67 U/mL), IL-4 (67 U/mL), and IL-6 (134 U/mL)). When IL-2 alone was used, the concentration was adjusted to 200 U/mL. IL-7, IL-12, and IL-15 were used at a concentration of 10 U/mL, 10 ng/mL, and 20 U/mL, respectively.

NK expansion culture was continued with appropriate changes of the medium, including addition of the indicated cytokines (at least half of the medium was changed every 2 d), until the adherent target cells disappeared. When K562 cells were the targets, this period was set at 7 d. The cell suspension was diluted to 5×10^5 /mL and the culture continued. Whenever the cell suspension reached 5×10^6 /mL, the dilution was repeated.

Cytotoxicity assay

A standard ⁵¹Cr release assay was performed in the 4-h co-culture of the effector lymphocytes and the target K562 cells as described^[14]. The crystal violet staining was also used^[15]. Briefly, the target cells, 1×10^4 /well suspended in 200 μ L RHAM α medium containing 50 mL/L plasma from the lymphocyte donor (or 50 mL/L PPF whenever the plasma was in short supply), were seeded in a 96-well plate and were pre-cultured overnight. The cultured target cells were washed once with PBS, then the cultured lymphocytes suspended in 200 μ L of RHAM α medium containing 50 mL/L autologous plasma (or 50 mL/L PPF) were added as effector cells to each well at the indicated effector/target (E/T) ratio. The cells were co-cultured for 4 or 24 h. Then, the wells were washed once gently with appropriate amounts of Dulbecco's PBS containing calcium and magnesium. The target cells remaining adhered were fixed for 1 h with 40 g/L formaldehyde (200 μ L/well), and then stained with crystal violet solution (4 g/L in water, 100 μ L/well) for 30 min at room temperature. The plate was washed with water and dried at room temperature. A 200 μ L of 800 mL/L methanol was added into each well and the absorbance at 570 nm (A_{570}) of each well was determined. As a 100% control, the A_{570} of the

target cells cultured in a separate plate was determined just before the addition of the effector cells.

Percentage of surviving target cells was defined as follows:

$$\text{Surviving target cells (\%)} = (A-B)/(C-D) \times 100\%$$

Where A is the A_{570} of the well containing the target cells and the effector cells, B is the A_{570} of the well containing only the effector cells which remained in the well after the washing with calcium- and magnesium-containing Dulbecco's PBS, C is the A_{570} of the 100% control target cells just before the addition of the effector cells, and D is the A_{570} of the well containing medium alone. The target cells cultured at an E/T ratio of 0 grew rapidly over the 24-h incubation period and, therefore, showed more than 100% survival.

RESULTS

Proportion of NK cells in the lymphocyte culture

Two hundred and forty kinds of human cell lines from RIKEN Cell Bank were screened for their expression of MHC-class I and class II surface molecules. Ten cell lines including leukemia cell line K562, HFWT (Wilms tumor), HMV-II (melanoma) and NB 19 (neuroblastoma) were found that weakly expressed MHC molecules of both.

Subsequently, PBMCs taken from healthy subjects were co-cultured with these cell lines after the target cells had been irradiated with 50 Gy of X-rays. HFWT cultures demonstrated a striking change in anchorage-dependent HFWT cells that were totally killed and disappeared after 13-14 d. CD3- CD56+ cells occupied 64.6%, 54.6%, and 75.9% of the lymphocyte population in the three experiments, respectively. However, K562 and HMV-II in experiments 2 and 3 only raised the proportion of CD3-CD56+ cells to 17.6% and 18.9%, respectively, though these proportions were higher than those (5.4-13.0%) in the control cultures containing no target cells. In contrast, irradiated TKB-17RGB cells increased CD3+CD56 T cells in the lymphocyte populations in the three experiments to 95.1%, 96.0%, and 84.8%, respectively as compared to 74.4%, 58.2% and 60.9% in controls.

Assay for NK cytotoxicity activity

Figure 1A depicts a typical dose-response curve for the 4-h ⁵¹Cr release assay. The NK-enriched population lysed 31.3% and 76.5% of the fresh HFWT cells at E/T ratios of 2 and 8, respectively. A mirror image of this curve was observed in crystal violet staining (Figure 1B). The target cells showed 100% survival in crystal violet staining and 20% lysis in the ⁵¹Cr release assay when E/T ratio was 1.

Effect of extending co-culture time to 24 h was also examined. The percentage of the surviving control target cells usually exceeded 100% (Figure 1C) at an E/T ratio of 0, but the shoulder portion of the dose-response curve in Figure 1B disappeared and fewer surviving target cells were observed at larger E/T ratios. Only 17.0% of the target cells remained at E/T ratio of 4, whereas 42.5% remained in the 4-h crystal violet staining. Therefore, for determination of killing activity, 24-h crystal violet staining had a higher sensitivity than 4-h crystal violet staining at low E/T ratios.

PBMCs grown on TKB-17RGB target cells could efficiently kill fresh TKB-17RGB cells but not fresh 17 RGB cells. Lymphocytes grown on the HFWT target cells could efficiently kill both fresh TKB-17RGB cells and fresh HFWT cells (Figure 2, 8 columns on the right), indicating that the lymphocytes contained nonspecific NK cells. The latter lymphocyte population, at an E/T ratio of 2 at 24 h, reduced TKB-17RGB target cells to 60.5% and HFWT target cells to 18.5% compared to the control tumor cells (E/T ratio of 0) that proliferated to 175-180% of starting levels.

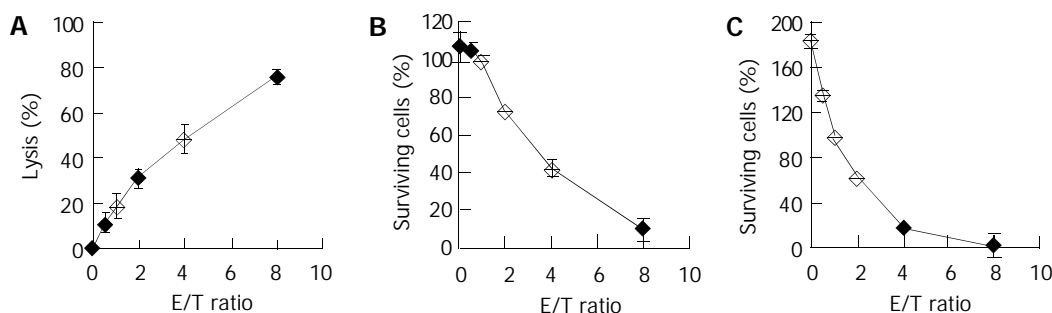


Figure 1 Dose-response relationships of ⁵¹Cr release assay and the two crystal violet staining assays. PBMCs were detected after 15-d culture with irradiated HFWT cells. A: ⁵¹Cr release assay, in which the effector lymphocytes and the fresh target cells pre-labeled with ⁵¹Cr were incubated for 4 h. B and C: crystal violet staining, in which effector lymphocytes and fresh target HFWT cells were incubated for 4 and 24 h, respectively. Each point and bar represent mean and SD (3-6 replicates), respectively.

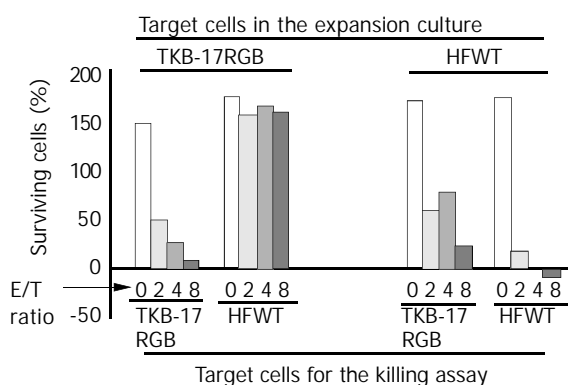


Figure 2 Killing by T cell- and NK-enriched lymphocytes. Lymphocytes derived from PBMC of the Subject-1 (taken from Experiment-1 of Table 1) were used in this 24-h crystal violet staining with various E/T ratios. Eight columns on left side are the results from assays of lymphocytes grown on irradiated TKB-17RGB cells (MHC class I positive). Major lymphocyte population was CD3+ CD56- (T cell-enriched, see Table 1). For the killing assay, fresh TKB-17RGB (left-end 4 columns) or cells (mid-left 4 columns) were submitted as the target. Right side 8 columns are the results from assays of lymphocytes grown on irradiated HFWT cells (MHC class I negative). Major lymphocyte population was CD3-CD56+ (NK-enriched, see Table 1). For the killing assay, fresh TKB-17RGB (mid-right 4 columns) or HFWT cells (right-end 4 columns) were used as the target. Each column represents the mean value of triplicate measurements.

Lymphocytes from PBMC of HCC patient were cultured on the irradiated cells and proliferated 196-fold at 18 d. This was about 6 times the proliferation of lymphocytes suspended with the irradiated K562 cells (data not shown) and the proliferation ceased after 14 d in the NK expansion culture. X-ray irradiated HCC-1 cells (MHC class I positive) and HCC-2 cells (MHC class I negative) obtained from the same hepatocellular carcinoma were used in place of HFWT cells, and neither of the two cell lines could support efficient growth of the lymphocytes from PBMC of HCC patient. NK-enriched lymphocyte population from HCC patient, however, killed HCC-1 and 2 cells with sensitivity comparable to fresh TKB-17RGB cells (Figure 3). About half of the control HCC-2 cells detached spontaneously

after 24-h incubation. The NK-enriched population derived from the patient and expanded on the irradiated HFWT cells could also kill fresh K562 cells with high efficiency (data not shown).

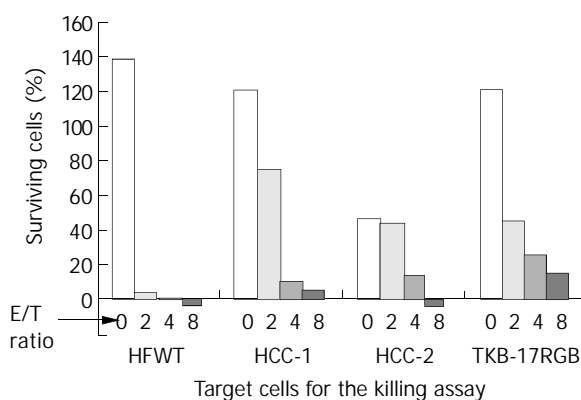


Figure 3 Killing activity of the NK-enriched population on MHC class I-positive and -negative cell lines. PBMCs of HCC patient were expanded on irradiated T cells and submitted to the 24-h crystal violet staining. Target cells were MHC class I-negative HFWT and HCC-2 cells, MHC class I-positive HCC-1 and TKB-17 RGB cells. HCC-1 and HCC-2 cells were derived from the same human hepatocellular carcinoma tissue.

In a separate experiment, the effect on NK expansion of HFWT and MHC class I-non-expressing HCC-2 cells were compared using a medium containing IL-2 (Table 1). After 10 d of co-culture with PBMCs from Subject 1, irradiated HFWT cells induced 72.0% concentration of CD3-CD56+ cells, whereas irradiated HCC-2 cells induced only 18.5% concentration of CD3-CD56+ cells. CD16+CD56+ cells co-cultured with HFWT grew to 72.7% of the lymphocyte population, whereas CD16+CD56+ cells co-cultured with HCC-2 grew to 22.8% of the lymphocyte population. All the other tumor cell lines showed lower similar efficiency for NK cell expansion.

Cell-cell interaction between PBMC and HFWT cells

After PBMCs from Subject 1 were grown for 10 d in direct-contact co-culture, the final proportion of CD16+ CD56+ cells reached 71.7%, but in the case of PBMCs separated from HFWT cells with a membrane filter, the final proportion reached only

Table 1 Proportion of CD16+ CD56+ cells compared to other cell groups after NK cell expansion cultures

Irradiated target cells used for expansion culture	Cell proportion in lymphocyte populations (%)			
	CD3+CD56-	CD3-CD56+	CD3+CD56+	CD16+CD56+
HFWT	15.2	72.0	12.3	72.7
HCC-2	49.7	18.5	31.1	22.8

Table 2 Proportion of CD16+CD56+ after co-culture of PBMC with irradiated HFWT cells with and without separation by a membrane filter

PBMCs and HFWT co-culture conditions	Cell proportion in the final lymphocyte populations (%)		
	CD3+CD56-	CD3-CD56+	CD16+CD56+
Without separation	13.4	78.2	71.7
Separated by a membrane filter	83.4	5.3	3.9

3.9% (Table 2). Most of the lymphocytes in the latter culture were T lymphocytes. These results demonstrate that direct cell-cell interaction is crucial for NK expansion.

Cytokine requirements for NK cell induction

The highest increase in lymphocyte number from Subject-2 reached 401-fold after 15 d in the expansion culture. Lymphocytes derived from both Subject-2 and Subject-3 expanded with IL-2-containing medium killed fresh HFWT target cells more effectively than the lymphocytes expanded with the 4-cytokine cocktail (data not shown). Without the presence of target HFWT cells, lymphokine activated killer (LAK) cells grew slower than those cultured on the target cells. Unlike IL-2, IL-12 inhibited and IL-15 stimulated the growth of lymphocytes cultured on target HFWT cells. IL-7 (10 U/mL) was not effective on lymphocyte growth. Without addition of IL-2 to the culture medium, the irradiated HFWT cells themselves could not support survival of the lymphocytes for several days.

We compared the effects of HFWT and MHC class I-non-expressing HCC-2 cells on NK cell expansion using IL-2-containing medium. For 10 d in the culture of PBMC from Subject-1, irradiated HFWT cells induced 72.0% of CD3-CD56+ cells, but irradiated HCC-2 cells could induce only 18.5% of CD3-CD56+ cells. CD16+ CD56+ cells shared 72.7% in the former lymphocyte population and, in the latter, 22.8%.

DISCUSSION

Expansion of human NK cells from PBMCs has long been investigated but large-scale expansions for adoptive immunotherapy of human tumors deserve further investigation. LAK cells have been applied to tumor immunotherapy. However, LAK cell expansion in culture for more than 2 wk usually resulted in the loss of killer cell activity. T cells without killing activity formed a major part of the resulting lymphocyte populations^[16]. Similar problems have been found in expansion cultures of tumor-infiltrating lymphocytes, in which cells bearing B cell, NK cell and macrophage markers disappeared early in the culture^[17].

The K562 cell line in suspension culture has long been adopted as the common target cell line for determination of the killing activity of human NK cells by the standard ⁵¹Cr release assay. For ecological reasons, a nonradioisotopic crystal violet staining assay was used in our experiments for determining the killing activity of CTLs against anchorage-dependent target tumor cells. The crystal violet staining assay is safe and amenable to coculturing effectors and targets for more than 4 h. Since HFWT cells disappeared completely during NK expansion culture described above, crystal violet staining using non-irradiated fresh T cells as the target, was considered as sensitive for assessment of the cytotoxic activity of the NK cells as the standard ⁵¹Cr release assay.

The results demonstrated that an anchorage-dependent Wilms tumor cell line is a highly efficient target for selective expansion of human NK cells from PBMCs. After culturing PBMCs from healthy donors for 10-21 d, the number of lymphocytes increased extensively. More than 50% of the resulting population consisted of CD16+ CD56+ NK cells that could efficiently kill the MHC class I-non-expressing K562.

Moreover, these expanded NK cells also appeared to kill MHC class I-expressing tumor cells (Figure 2, TKB-17 RGB target cells), suggesting the probability of using these highly active NK cells for adoptive immunotherapy of human tumors.

We have already repeated more than 20 times the 2-week cultures for NK expansion from PBMCs on HFWT cells. Under microscopic examination, we observed that anchorage-dependent target HFWT cells always disappeared completely, the advantage of which was adoptive immunotherapy with NK cells when compared to the methods of NK cell proliferation with suspension-cultured target tumor cells such as K562 and B lymphoblastoid cell lines.

For NK expansion, direct contact of PBMCs with HFWT cells was required (Table 2), suggesting that factors released from target cells do not contribute to NK cells expansion. The need for direct cell-cell contact had been noted in experiments using K562 cells^[18]. Growth stimulation through direct cell-cell contact might not be ascribed simply to molecules on the HFWT cell surface preserved after fixation, although Pierson *et al.*^[19] reported that NK cells plated directly on ethanol/acetic acid-fixed M2-10B4, which leaves stromal ligands (cell membrane components and ECM) intact, resulted in increased NK cells expansion compared with medium alone. The variety of the fixation methods used in the present experiments conserved, at least partially, reactivity of the surface molecules. Therefore, some interactions between the surface molecules of HFWT cells may contribute to NK expansion. In any case, contact between PBMCs and live HFWT cells were found to be a key requirement.

NK cells are cytotoxic to tumor and virus-infected cells that have lost surface expression of MHC class I proteins. Target cell expressing MHC class I proteins inhibits NK cytotoxicity through binding to inhibitory NK cell receptors^[20,21]. Therefore contrasting properties of NK cell inhibitory receptors compared to CTL T-cell receptors (MHC class I receptors that stimulate, rather than inactivate, the CTL cytotoxic response) are expected to provide complementarity in the cytotoxic response to tumor cells^[22,23]. In humans, natural killer (NK) cell function is regulated by a series of receptors and coreceptors with either triggering or inhibitory activity^[24].

HFWT cells were more effective targets for NK cell expansion than K562 cells. Since it has been reported that NK cells differentiate from CD34+ progenitor cells^[25,26], HFWT cells must stimulate NK cells differentiation from the progenitor cells included in PBMC but not in the CD3-CD56+ subset. Further investigation needs to be conducted to identify the NK precursor cells to which HFWT cells transmit the proliferative signal.

Since the present NK cell expansion culture started as one of variation of the human CTL induction culture from PBMC, the present study has shown that IL-2 is the sole cytokine required for the NK expansion on the T cell layer^[27]. In other reports, IL-15 was found to stimulate NK development from CD34+ hematopoietic progenitor cells^[28-30]; IL-7 as a cofactor during myelopoiesis, is capable of activating monocytes/macrophages and NK cells^[31]. IL-12 showed an inhibitory effect on NK cell growth^[32,33]; TGF β was reported to be similarly inhibitory^[34]. The present results suggest that expansion and activation of NK cells may provide an effective immunotherapy of hepatocellular carcinoma.

REFERENCES

- 1 **Souza SS**, Castro FA, Mendonca HC, Palma PV, Morais FR, Ferriani RA, Voltarelli JC. Influence of menstrual cycle on NK activity. *J Reprod Immunol* 2001; **50**: 151-159
- 2 **Luo DZ**, Vermijlen D, Ahishali B, Triantis V, Vanderkerken K, Kuppen PJ, Wisse E. Participation of CD45, NKR-P1A and ANK61 antigen in rat hepatic NK cell (pit cell) mediated target cell cytotoxicity. *World J Gastroenterol* 2000; **6**: 546-552
- 3 **Imai K**, Matsuyama S, Miyake S, Suga K, Nakachi K. Natural cytotoxic activity of peripheral-blood lymphocytes and cancer incidence: an 11-year follow-up study of a general population. *Lancet* 2000; **356**: 1795-1799
- 4 **Wong KH**, Simon JA. *In vitro* effect of gonadotropin-releasing hormone agonist on natural killer cell cytolysis in women with and without endometriosis. *Am J Obstet Gynecol* 2004; **190**: 44-49
- 5 **Malorni W**, Quaranta MG, Straface E, Falzano L, Fabbri A, Viora M, Fiorentini C. The Rac-activating toxin cytotoxic necrotizing factor 1 oversees NK cell-mediated activity by regulating the actin/microtubule interplay. *J Immunol* 2003; **171**: 4195-4202
- 6 **Guven H**, Gilljam M, Chambers BJ, Ljunggren HG, Christensson B, Kimby E, Dilber MS. Expansion of natural killer (NK) and natural killer-like T (NKT)-cell populations derived from patients with B-chronic lymphocytic leukemia (B-CLL): a potential source for cellular immunotherapy. *Leukemia* 2003; **17**: 1973-1980
- 7 **Perussia B**, Ramoni C, Anegon I, Cuturi MC, Faust J, Trinchieri G. Preferential proliferation of natural killer cells among peripheral blood mononuclear cells cocultured with B lymphoblastoid cell lines. *Nat Immun Cell Growth Regul* 1987; **6**: 171-188
- 8 **Silva MR**, Parreira A, Ascensao JL. Natural killer cell numbers and activity in mobilized peripheral blood stem cell grafts: conditions for *in vitro* expansion. *Exp Hematol* 1995; **23**: 1676-1681
- 9 **Porrata LF**, Inwards DJ, Lacy MQ, Markovic SN. Immunomodulation of early engrafted natural killer cells with interleukin-2 and interferon-alpha in autologous stem cell transplantation. *Bone Marrow Transplant* 2001; **28**: 673-680
- 10 **Sekine T**, Shiraiwa H, Yamazaki T, Tobisu K, Kakizoe T. A feasible method for expansion of peripheral blood lymphocytes by culture with immobilized anti-CD3 monoclonal antibody and interleukin-2 for use in adoptive immunotherapy of cancer patients. *Biomed Pharmacother* 1993; **47**: 73-78
- 11 **Malygin AM**, Somersalo K, Timonen T. Promotion of natural killer cell growth *in vitro* by bispecific (anti-CD3 x anti-CD16) antibodies. *Immunology* 1994; **81**: 92-95
- 12 **Yu Y**, Hagihara M, Ando K, Gansuvd B, Matsuzawa H, Tsuchiya T, Ueda Y, Inoue H, Hotta T, Kato S. Enhancement of human cord blood CD34+ cell-derived NK cell cytotoxicity by dendritic cells. *J Immunol* 2001; **166**: 1590-1600
- 13 **Kim KY**, Kang MA, Nam MJ. Enhancement of natural killer cell-mediated cytotoxicity by coexpression of GM-CSF/B70 in hepatoma. *Cancer Lett* 2001; **166**: 33-40
- 14 **Ucker DS**, Obermiller PS, Eckhart W, Apgar JR, Berger NA, Meyers J. Genome digestion is a dispensable consequence of physiological cell death mediated by cytotoxic T lymphocytes. *Mol Cell Biol* 1992; **12**: 3060-3069
- 15 **Liu SQ**, Saijo K, Todoroki K, Ohno T. Induction of human autologous cytotoxic T lymphocytes on formalin-fixed and paraffin-embedded tumour sections. *Nat Med* 1995; **1**: 267-271
- 16 **Zhang J**, Zhang JK, Zhuo SH, Chen HB. Effect of a cancer vaccine prepared by fusions of hepatocarcinoma cells with dendritic cells. *World J Gastroenterol* 2001; **7**: 690-694
- 17 **Haas GP**, Solomon D, Rosenberg SA. Tumor-infiltrating lymphocytes from nonrenal urological malignancies. *Cancer Immunol Immunother* 1990; **30**: 342-350
- 18 **Fink T**, Ebbesen P, Koppelhus U, Zachar V. Natural killer cell-mediated basal and interferon-enhanced cytotoxicity against liver cancer cells is significantly impaired under *in vivo* oxygen conditions. *Scand J Immunol* 2003; **58**: 607-712
- 19 **Pierson BA**, Gupta K, Hu WS, Miller JS. Human natural killer cell expansion is regulated by thrombospondin-mediated activation of transforming growth factor-beta 1 and independent accessory cell-derived contact and soluble factors. *Blood* 1996; **87**: 180-189
- 20 **Gumperz JE**, Parham P. The enigma of the natural killer cell. *Nature* 1995; **378**: 245-248
- 21 **Katz G**, Markel G, Mizrahi S, Arnon TI, Mandelboim O. Recognition of HLA-Cw4 but not HLA-Cw6 by the NK cell receptor killer cell Ig-like receptor two-domain short tail number 4. *J Immunol* 2001; **166**: 7260-7267
- 22 **Long EO**, Barber DF, Burshtyn DN, Faure M, Peterson M, Rajagopalan S, Renard V, Sandusky M, Stebbins CC, Wagtmann N, Watzl C. Inhibition of natural killer cell activation signals by killer cell immunoglobulin-like receptors (CD158). *Immunol Rev* 2001; **181**: 223-233
- 23 **Rolstad B**, Naper C, Lovik G, Vaage JT, Ryan JC, Backman-Petersson E, Kirsch RD, Butcher GW. Rat natural killer cell receptor systems and recognition of MHC class I molecules. *Immunol Rev* 2001; **181**: 149-157
- 24 **Bottino C**, Falco M, Parolini S, Marcenaro E, Augugliaro R, Sivori S, Landi E, Biassoni R, Notarangelo LD, Moretta L, Moretta A. NTB-A [correction of GNTB-A], a novel SH2D1A-associated surface molecule contributing to the inability of natural killer cells to kill Epstein-Barr virus-infected B cells in X-linked lymphoproliferative disease. *J Exp Med* 2001; **194**: 235-246
- 25 **Miller JS**, McCullar V, Punzel M, Lemischka IR, Moore KA. Single adult human CD34(+)/Lin-/CD38(-) progenitors give rise to natural killer cells, B-lineage cells, dendritic cells, and myeloid cells. *Blood* 1999; **93**: 96-106
- 26 **Mrozek E**, Anderson P, Caligiuri MA. Role of interleukin-15 in the development of human CD56+ natural killer cells from CD34+ hematopoietic progenitor cells. *Blood* 1996; **87**: 2632-2640
- 27 **Konjevic G**, Jovic V, Jurisic V, Radulovic S, Jelic S, Spuzic I. IL-2-mediated augmentation of NK-cell activity and activation antigen expression on NK- and T-cell subsets in patients with metastatic melanoma treated with interferon-alpha and DTIC. *Clin Exp Metastasis* 2003; **20**: 647-655
- 28 **Naora H**, Gougeon ML. Enhanced survival and potent expansion of the natural killer cell population of HIV-infected individuals by exogenous interleukin-15. *Immunol Lett* 1999; **68**: 359-367
- 29 **Carayol G**, Robin C, Bourhis JH, Bennaceur-Griscelli A, Chouaib S, Coulombel L, Caignard A. NK cells differentiated from bone marrow, cord blood and peripheral blood stem cells exhibit similar phenotype and functions. *Eur J Immunol* 1998; **28**: 1991-2002
- 30 **Lin SJ**, Yang MH, Chao HC, Kuo ML, Huang JL. Effect of interleukin-15 and Flt3-ligand on natural killer cell expansion and activation: umbilical cord vs adult peripheral blood mononuclear cells. *Pediatr Allergy Immunol* 2000; **11**: 168-174
- 31 **Appasamy PM**. Biological and clinical implications of interleukin-7 and lymphopoiesis. *Cytokines Cell Mol Ther* 1999; **5**: 25-39
- 32 **Liebau C**, Merk H, Schmidt S, Roesel C, Karreman C, Prisack JB, Bojar H, Baltzer AW. Interleukin-12 and interleukin-18 change ICAM-1 expression, and enhance natural killer cell mediated cytolysis of human osteosarcoma cells. *Cytokines Cell Mol Ther* 2002; **7**: 135-142
- 33 **Satoh T**, Saika T, Ebara S, Kusaka N, Timme TL, Yang G, Wang J, Mouraviev V, Cao G, Fattah el MA, Thompson TC. Macrophages transduced with an adenoviral vector expressing interleukin 12 suppress tumor growth and metastasis in a preclinical metastatic prostate cancer model. *Cancer Res* 2003; **63**: 7853-7860
- 34 **Billiau AD**, Sefrioui H, Overbergh L, Rutgeerts O, Goebels J, Mathieu C, Waer M. Transforming growth factor-beta inhibits lymphokine activated killer cytotoxicity of bone marrow cells: implications for the graft-versus-leukemia effect in irradiation allogeneic bone marrow chimeras. *Transplantation* 2001; **71**: 292-299

Intestinal colonization with *Candida albicans* and mucosal immunity

Xiao-Dong Bai, Xian-Hua Liu, Qing-Ying Tong

Xiao-Dong Bai, Department of Burn Surgery, General Hospital of Chinese People's Armed Police Force, Beijing 100039, China

Xian-Hua Liu, Central Laboratory, General Hospital of Chinese People's Armed Police Force, Beijing 100039, China

Qing-Ying Tong, Medical Affairs Department, General Hospital of Chinese People's Armed Police Force, Beijing 100039, China

Supported by the National Natural Science Foundation of China, No. 30100197

Correspondence to: Dr. Xiao-Dong Bai, Department of Burn Surgery, General Hospital of Armed Police Force, 69 Yong Ding Road, Hai Dian District, Beijing 100039, China. baixiaotmu@yahoo.com.cn

Telephone: +86-10-88276632

Received: 2003-11-27 **Accepted:** 2004-01-08

Abstract

AIM: To observe the relationship between intestinal lumen colonization with *Candida albicans* and mucosal secretory IgA (sIgA).

METHODS: A total of 82 specific-pathogen-free mice were divided randomly into control and colonization groups. After *Candida albicans* were inoculated into specific-pathogen-free mice, the number of *Candida albicans* adhering to cecum and mucosal membrane was counted. The lymphocyte proliferation in Peyer's patch and in lamina propria was shown by BrdU incorporation, while mucosal sIgA (surface membrane) isotype switch in Peyer's patch was investigated. IgA plasma cells in lamina propria were observed by immunohistochemical staining. Specific IgA antibodies to *Candida albicans* were measured with ELISA.

RESULTS: From d 3 to d 14 after *Candida albicans* gavage to mice, the number of *Candida albicans* colonizing in lumen and adhering to mucosal membrane was sharply reduced. *Candida albicans* translocation to mesenteric lymph nodes occurred at early time points following gavage administration and disappeared at later time points. Meanwhile, the content of specific IgA was increased obviously. Proliferation and differentiation of lymphocytes in lamina propria were also increased.

CONCLUSION: Lymphocytes in lamina propria play an important role in intestinal mucosal immunity of specific-pathogen-free mice when they are first inoculated with *Candida albicans*. The decreasing number of *Candida albicans* in intestine is related to the increased level of specific IgA antibodies in the intestinal mucus.

Bai XD, Liu XH, Tong QY. Intestinal colonization with *Candida albicans* and mucosal immunity. *World J Gastroenterol* 2004; 10(14): 2124-2126

<http://www.wjgnet.com/1007-9327/10/2124.asp>

INTRODUCTION

Candida albicans are the common opportunistic pathogens^[1];

one of their infection routes is overgrowth and translocation in intestinal lumen. So, inhibition of the translocation of *Candida* is an important way to prevent the deadly systemic infection. With the development of the study on mucosal immunity, local antibody production of sIgA has attracted much attention in preventing pathogen^[1] and bacterial translocation^[2,3]. It has been reported that *Candida albicans* infection of vaginal and oral mucus membrane was specifically inhibited by anti-*Candida albicans* sIgA. But, the mechanism still remains unclear. In the present study, by using *Candida*'s colonization model, we observed lymphocytes proliferation and differentiation in gut-associated lymphatic tissue (GALT) and the relationship between specific IgA and change of *Candida albicans* in the intestine, and further explored the mechanism of host defense against opportunistic pathogen and the effect of specific IgA against *Candida albicans* in intestinal lumen.

MATERIALS AND METHODS

Candida albicans

Candida albicans strain cmcc44104 provided by the Burn Institute of Southwest Hospital was amplified in the special selective culture medium. The *Candida albicans* suspension density was modulated to 1.5×10^9 cfu/mL, and stored below 4 °C.

Grouping of animals

A total of 82 specific-pathogen-free mice (BALB/c) were provided by the Animal Center of Third Military Medical University, and randomly divided into the control and colonization groups. Mice in colonization group were gavaged 0.5 mL *Candida albicans*, and killed on days 3, 7 and 14 after gavage by cervical dislocation. The control animals were treated in a similar way with a vehicle alone, and killed on day 14 after sham-treatment. The mesenteric lymph nodes, cecum and ileum of the mice were taken out.

Candida albicans adhering to ileum

Ilea of 10 cm were rinsed in PBS (0.01 mol/L, pH 7.2) three times until the ilea were translucent, then weighed and homogenized. Homogenized suspension (0.1 mL) was applied on the surface of the selective culture medium at 37 °C for 72 h.

Adherence result (cfu/g) = Colony-forming units × dilution / Ileum weight (g).

Quantity of *Candida albicans* in cecum

Ceca were weighed and homogenized in 5 mL PBS, then the suspension was cultured in the selective medium at 37 °C for 72 h. *Candida albicans* quantity (cfu/g) = Colony-forming units × dilution / Cecum weight (g).

Translocation of *Candida albicans*

Mesenteric lymph nodes (MLN) were taken to be weighed and homogenized and the suspension was applied on the selective medium at 37 °C for 72 h.

Lymphocytes proliferation in Peyer's patch and lamina propria

Mice were intraperitoneally injected 5-bromo-2'-deoxyuridine

(BrdU, 10 µg/g bm) at 12 h before cervical dislocation, the intestine and Peyer's patch (PP) were taken for immunohistochemistry staining. BrdU-positive cells in PP and in lamina propria (LP) of intestinal villi were counted.

Number of IgA plasma cell in LP

IgA plasma cells were counted after immunohistochemical stain as 40 villi/per mice and 5 mice/per time-point.

Expression of IgA of Peyer's patch lymphocyte

Peyer's patch lymphocytes were isolated, pooled, washed in RPMI 1640. Then IgA of lymphocytes was measured by flow cytometry.

Specific IgA to *Candida albicans* in intestinal mucus

Intestinal mucus (0.1 mL) was homogenized in 0.5 mL cold PBS, then centrifuged at 5 000 r/min for 5 min, the supernatant was taken as 1:1 mucus onto 96-well plates and coated by *Candida albicans* as immobilized antigen, which had been fixed in 40 g/L formaldehyde overnight at 4 °C for 72 h. Then plates were washed three times with PBS, and blocked by 5 g/L BSA for 0.5 h, the mucus samples were applied to ELISA plates for 1 h below 37 °C. After that, 96-well plates were washed with PBS, and goat anti-mouse IgA antibodies which coupled with horseradish-peroxidase were added to the wells, 100 µL/well and incubated at 37 °C for 1 h. Reaction was stopped by adding one drop of 2 mol/L H₂SO₄ and the result was shown by optical density (OD) at 492 nm.

Relative quantity of specific IgA^[4]

The specific IgA positive mucus measured before were serially diluted from 1:1 to 1:16, the content of specific IgA to *Candida albicans* in 1:1 mucus was regarded as 1 U/mL. The mucus was applied to ELISA in order to produce a standard curve. Specific IgA activity to *Candida albicans* was counted as follows:

$\text{IgA(U/mg)} = \text{IgA relative quantity (U/mL)} / \text{Protein content in the mucus (mg/mL)}$.

Statistic analysis

Data were analysed using analysis of variance (ANOVA).

RESULTS

Change of *Candida albicans*' adherence and translocation

In the colonization group, the total quantities of *Candida albicans* in intestine were larger on d 3 and 7 after gavage administration, about $(34-39) \times 10^5$ cfu/g, declined to 3.2×10^5 cfu/g on d 14. At the early phase after gavaging the mice, *Candida albicans* was found in the MLN, and then disappeared from day 7 to 14. Adherence also showed a declined tendency from the highest on day 3 to the lowest on d 14.

Proliferation of lymphocyte in PP and LP

BrdU incorporation of PP was found in both control and

colonization group. BrdU-positive cells were mainly at the verge sites of PP; there were no obvious changes in the colonization group compared with that in the control group. On d 14 after gavaging, LP lymphocytes proliferation in colonization group was significantly higher than that in the control mice (Table 1).

IgA plasma cell in LP

IgA plasma cells increased at all times, the highest was on day 14 (Table 1).

Flow cytometry of mucosal sIgA

There was no difference between the control and the colonization group in the level of mucosal sIgA (Table 1).

Specific IgA to *Candida albicans*

Specific anti-*Candida albicans* IgA contents on day 14 in colonization group were higher than that in the control group (Table 2).

Table 2 Specific IgA to *Candida albicans* in intestinal mucus membrane

Group	n	Positive rate	Content (U/mg)
Colonization			
3 d	20	5/20	33±8
7 d	18	3/18	36±13
14 d	25	10/25	69±25 ^a
Control	19	6/19	18.6±6.9

^aP<0.05 vs control.

DISCUSSION

Candida albicans is an opportunistic pathogen, which could survive in the intestine and keep the balance of body. sIgA prevents the body from some pathogen infection such as typhoid fever and cholera^[5,6], but its role in the balance between opportunistic pathogen and host is not clear yet^[7,8]. So we investigated the relationship between *Candida albicans* colonization and the change of local intestinal mucosal immunity by using SPF mice model, in order to understand the mechanism of the balance. We have found that in the early period of *Candida albicans* colonization, *Candida albicans* adherence was serious, while the specific IgA content was lower. Accompanying the increase of specific IgA to *Candida albicans*, quantity of *Candida albicans* adherence and in the cecum decreased, there was negative correlation between specific IgA and quantity of *Candida albicans* adherence, that is to say that specific IgA was the important factor to keep the balance between opportunistic pathogen and host^[9]. The colonization of *Candida albicans* could elicit a local mucosal immune reaction and finally limit *Candida albicans*' overgrowth^[10,11].

Table 1 Proliferation and differentiation of lymphocytes

Group	Number of BrdU-positive cells sIgA in PP			Positive rates	Number of IgA plasma cells in LP
	n	PP	LP		
Colonization					
3 d	5	75±12	0.30±0.46	7.7±1.2	0.68±0.37
7 d	5	58±20	1.05±1.00	7.7±2.5	0.67±0.54
14 d	5	37±10	3.34±2.35 ^a	ND	1.63±0.52 ^a
Control	5	70±15	0.78±1.04	10.3±1.8	0.35±0.15

^aP<0.05 vs control; PP: Peyer's patch; LP: Lamina propria; IgA plasma cells were counted after immunohistochemical stain as 40 villi/per mice and 5 mice/per time-point.

In the lamina propria, there was B lymphocyte clone that could secrete specific IgA against *Candida albicans*^[12], but the content was very lower. After *Candida albicans* were gavaged, stronger stimulation of *Candidas'* antigen induced specific B lymphocyte clone proliferation and differentiation, while the number of IgA plasma cell increased. Plenty of specific IgA against *Candida* secreted to the surface of intestinal mucus membrane and formed the antibody barrier. sIgA antibodies were thought to provide mucosal defense by immune exclusion^[13]; this refers to their ability to prevent contact between pathogens and epithelial surfaces through agglutination in the intestinal lumen, entrapment of immune complexes in mucus, and clearance by peristalsis. We could draw the conclusion that though *Candida albicans* infection is more common recently, it is possible to prevent *Candida albicans* infection by setting up a specific sIgA antibody barrier in the host.

REFERENCES

- 1 **Lamm ME**. Interaction of antigens and antibodies at mucosal surface. *Annu Rev Microbiol* 1997; **51**: 311-340
- 2 **Shu Q**, Gill H. Immune protection mediated by the probiotic *Lactobacillus rhamnosus* HN001 (DR20) against *Escherichia coli* O157: H7 infection in mice. *FEMS Immunol Med Microbiol* 2002; **34**: 59
- 3 **Nakasaka H**, Mitomi T, Tajima T, Ohnishi N, Fujii K. Gut bacterial translocation during panteral nutrition in experimental rats and its countermeasure. *Am J Surg* 1998; **175**: 38-43
- 4 **Coogan MM**, Sweet SP, Challacombe SJ. Immunoglobulin A. IgA1 and IgA2 antibodies to *Candida albicans* in whole and parotid saliva in human immunodeficiency virus infection and AIDS. *Infect Immun* 1994; **62**: 892-896
- 5 **Apter FM**, Michetti P, Winner LS 3rd, Mack JA, Mekalanos JJ, Neutra MR. Analysis of the roles of antilipo-polysaccharide and anti-cholera toxin immunoglobulinA (IgA) antibodies in protection against *Vibrio cholerae* and cholera toxin by use of monoclonal IgA antibodies *in vivo*. *Infect Immun* 1993; **61**: 5279-5285
- 6 **Maury G**, Pilette C, Sibille Y. Secretory immunity of the airways. *Rev Mal Respir* 2003; **20**: 928-939
- 7 **Schmucker DL**, Owen RL, Outenreath R, Thoreux K. Basis for the age-related decline in intestinal mucosal immunity. *Clin Dev Immunol* 2003; **10**: 67-72
- 8 **Hirsh M**, Dyugovskaya L, Bashenko Y, Krausz MM. Reduced rate of bacterial translocation and improved variables of natural killer cell and T-cell activity in rats surviving controlled hemorrhagic shock and treated with hypertonic saline. *Crit Care Med* 2002; **30**: 861-867
- 9 **Wozniak KL**, Wormley FL Jr, Fidel PL Jr. *Candida*-specific antibodies during experimental vaginal candidiasis in mice. *Infect Immun* 2002; **70**: 5790-5799
- 10 **Belazi M**, Fleva A, Drakoulakos D, Panayiotidou D. Salivary IgA and serum IgA and IgG antibodies to *Candida albicans* in HIV-infected subjects. *Int J STD AIDS* 2002; **13**: 373-377
- 11 **Bai X**, Xiao G, Tian X. The relationship between postburn gene expression of modulators in gut associated lymph tissue and the change in IgA plasma cells. *Zhonghua Shaoshang Zazhi* 2000; **16**: 108-110
- 12 **Koga-Ito CY**, Unterkircher CS, Watanabe H, Martins CA, Vidotto V, Jorge AO. Caries risk tests and salivary levels of immunoglobulins to *Streptococcus mutans* and *Candida albicans* in mouthbreathing syndrome patients. *Caries Res* 2003; **37**: 38-43
- 13 **Ren JM**, Zou QM, Wang FK, He Q, Chen W, Zen WK. PELA microspheres loaded *H pylori* lysates and their mucosal immune response. *World J Gastroenterol* 2002; **8**: 1098-1102

Edited by Chen WW Proofread by Zhu LH and Xu FM

Multidetector CT in evaluating blood supply of hepatocellular carcinoma after transcatheter arterial chemoembolization

Yong-Song Guan, Xiao-Hua Zheng, Xiang-Ping Zhou, Juan Huang, Long Sun, Xian Chen, Xiao Li, Qing He

Yong-Song Guan, Xiao-Hua Zheng, Xiang-Ping Zhou, Juan Huang, Long Sun, Xian Chen, Xiao Li, Qing He, Department of Radiology, Huaxi Hospital, Sichuan University, Chengdu 610041, Sichuan Province, China

Supported by the Medical Science Research Foundation of Sichuan Province, No. 200054

Correspondence to: Dr. Yong-Song Guan, Department of Radiology, Huaxi Hospital, Sichuan University, 37 Guoxuexiang, Chengdu 610041, Sichuan Province, China. yongsongguan@yahoo.com

Telephone: +86-28-85421008 **Fax:** +86-28-85421008

Received: 2003-12-12 **Accepted:** 2004-01-15

Abstract

AIM: To assess the value of multidetector-row computed tomography (MDCT) in choosing retreatment methods of hepatocellular carcinoma (HCC) through evaluating the blood supply of low-density area of HCC after transcatheter arterial chemoembolization (TACE).

METHODS: Thirty-two patients with HCC after TACE treatment were examined by plain scanning and hepatic multidetector-row CT. The location of low-density area on plain scanning and the enhancement patterns on dynamic contrast-enhanced scanning were observed. At the same time, three-dimensional CT (3D CT) models of the volume rendering, curved multiplanar reformations, surface shaded display and maximum intensity projection reconstruction of the hepatic artery and portal vein were performed in 6 cases.

RESULTS: In CT plain scanning data, low density areas of 32 cases of HCC after TACE treatment were divided into three types: peripheral, one-side-located and mixed types. In contrast-enhanced CT scans, the blood supply of low-density area was classified into four types: arterial blood supply (20 cases), portal blood supply (5 cases), arterial combined with portal blood supply (5 cases) and poor blood supply (2 cases). In 6 cases, the relationship between the low-density area and branches of hepatic artery as well as portal vein was shown by 3D CT.

CONCLUSION: Hepatic MDCT is an effective method for evaluating the blood supply of low-density area and therapeutic effect of HCC after TACE treatment. Types of blood supply is helpful for the selection of retreatment.

Guan YS, Zheng XH, Zhou XP, Huang J, Sun L, Chen X, Li X, He Q. Multidetector CT in evaluating blood supply of hepatocellular carcinoma after transcatheter arterial chemoembolization. *World J Gastroenterol* 2004; 10(14): 2127-2129

<http://www.wjgnet.com/1007-9327/10/2127.asp>

INTRODUCTION

Hepatocellular carcinoma (HCC) is one of the most common malignant neoplasms. In China, HCC was the second cancer

killer in rural areas, and ranked the third in urban areas and 110 000 patients were killed annually, accounting for 40% of the HCC deaths in the world^[1]. The majority of HCC patients are treated with palliative approaches because surgery is sometimes limited by poor liver function. Transcatheter arterial chemoembolization (TACE) has been one of the most common and effective palliative therapies^[2-11]. To evaluate the blood supply types of the low-density area of HCC pretreated by TACE and to explore its value in selecting appropriate retreatment, we studied MDCT and 3D CT image characteristics of 32 HCC cases pretreated with TACE.

MATERIALS AND METHODS

Patients

From January to November 2003, 32 consecutive patients with HCC who underwent TACE (28 men and 4 women, age range 15-61 years, mean age 37 years) were enrolled into this study. The diagnosis of HCC was based on the results of percutaneous needle biopsy ($n=13$) and operation ($n=2$) or test of serum alpha-fetoprotein level in combination with imaging appearance and follow-up images ($n=17$) according to the diagnostic criteria for HCC formulated by Chinese National Association of Anticancer Committee (1990).

TACE

TACE procedure was performed as follows: the focal segmental or sub-segmental artery was detected carefully by celiac arteriography, and variants were excluded by superior mesenteric arteriography and phrenic arteriography. When the tip of the catheter arrived at the appropriate focal artery, one or two anticancer agents were injected, followed by 8-15 mL iodized oil (Huaihai Pharmaceutical Factory, Shanghai, China) injected under fluoroscopic monitoring. Some patients were embolized with a gelatin sponge (1 mm ×1 mm ×10 mm) at the same time. TACE procedures were performed followed by MDCT within 4 to 6 wk.

MDCT

MDCT was performed with an MDCT scanner after TACE within 4 to 6 wk (Sensation16, Siemens Medical System, Germany). Multidetector row helical technique was applied to the scanning in cranial to caudal direction. Plain scanning of the liver was carried out. Then, after injection of the contrast media for hepatic arterial phase and portal venous phase image acquisition, enhanced scanning of 1.5 mm axial section was performed at 25 and 60 s, respectively. A total of 100 mL contrast medium (Ultravist 300, Schering Pharmaceutical Ltd., Guangzhou, China) was administered to each patient at a rate of 3.0 mL/s through a catheter placed in the peripheral vein of the antecubital fossa. Three dimensional CT models including the volume rendering technique, multiplanar reconstruction, shaded surface display and maximum intensity projection of the hepatic artery and portal vein were simultaneously completed in 6 cases.

Diagnostic criteria for low-density area

Diagnostic criteria for low-density area were the CT of 30 to 50 HU on non-enhanced CT.

Determination of low-density area and blood supply types

According to the location in CT plain scan, low-density area was divided into three types. The peripheral low-density area was the viable area around the portion that retained iodized oil. The one-side-located type was determined by the low-density area located in any one side of the lipiodol area. The mixed low-density area showed both peripheral and one-side-located types in which the lipiodol retention in the tumor was heterogeneous.

According to the showing time of low-density area on enhanced CT at biphasic MDCT, blood supply of low-density area was divided into four types. The arterial blood supply of low-density area could be enhanced early during contrast administration (during the hepatic arterial-dominant phase, HAP) as a hyperattenuating or a mixed attenuating area against a background of slightly enhanced liver parenchyma before the liver enhanced substantially from the portal venous delivery of contrast material. Furthermore, the area must be hypoattenuating during the portal venous-dominant phase (PVP). In the same way, the portal blood supplying low-density area could be enhanced during PVP as a hyperattenuating or a mixed attenuating area but hypoattenuating during HAP. If the low-density area was enhanced during both PVP and HAP, the type of arterial combined with portal blood supply was determined. The poor blood supply was defined as non-enhanced on biphasic MDCT.

Image analysis

MDCT of all the patients was retrospectively and blindly reviewed by two experienced radiologists. Image analysis included the presence/absence and patterns of low-density area at non-enhanced examination. After these results were recorded, the HAP and PVP images were reviewed. Lesions were categorized as hyperattenuating or hypoattenuating relative to adjacent liver parenchyma. If lesions exhibited in both hyper- and hypo-attenuating areas, they were categorized as having mixed attenuation.

RESULTS

Appearances and patterns of low-density area

Thirty-two patients with low-density area after TACE were divided into three types: sixteen patients were peripheral type; 5 were one-side location type and 11 were mixed type.

Types of blood supply

The appearances of the low-density area at each phase of imaging are shown in Table 1. According to the appearance of low-density area at biphasic MDCT, the cases of arterial blood supply, portal blood supply, arterial combined with portal blood supply and poor blood supply were 20, 5, 5, 2, respectively.

Table 1 Appearance of low-density area at biphasic MDCT

Phase of imaging	Appearance at MDCT (cases)		
	Hyperattenuating	Hypoattenuating	Mixed attenuating
HAP	17	7	8
PVP	4	22	6

HAP: hepatic arterial-dominant phase; PVP: portal venous-dominant phase.

DISCUSSION

Although surgery remains the best treatment of HCC, it is unsuitable for most of the cases who would be better treated with interventional therapy. However, as the blood supply of

HCC includes regular, variant, extrahepatic and collateral arterial blood supply, the portal vein is involved in some patients^[12,13]. Furthermore, the development of compensatory circulation after the occlusion of hepatic artery and the changes of the portal venous blood supply to tumor after TACE, will both result in incomplete tumor necrosis or recurrence^[14-18].

MDCT is a breakthrough in medical imaging examination technology. Equipped with a multidetector array, MDCT can perform multislice data acquisition simultaneously, which greatly reduces the time of volume scanning. Image quality is improved due to increased image resolution and clarity. MDCT could therefore provide a technique of thin-slice and dynamic enhancement scanning of liver at hepatic arterial phase and portal venous phase. In addition, multiplanar reformations, 3D renderings, and high-quality CT angiographic displays have opened a new vista in clinical applications. Its performance has been improved in several problem-solving tasks and become extremely valuable in image interpretation^[19,20].

The portion of tumor that retains iodized oil is necrotic. Pathologic specimens and the necrosis rate measured from CT image showed a good correlation between the portion of tumor that retained iodized oil and the portion of tumor necrotized. Lipiodol-negative but hypodense areas examined by X-ray proved to be necrotic or fibrotic with or without viable tumor islands. HCC with heterogeneous lipiodol uptake tended to recur at the site adjacent to the original tumors more frequently than HCC with homogeneous lipiodol uptake^[21-23]. HCC images that revealed a dense retention of lipiodol within the whole tumor or revealed no enhancement on contrast enhanced CT had a significantly higher necrotic rate. A lipiodol-negative but hypodense area with enhancement on dynamic MDCT was low-density area^[24-26]. According to the location, we divided it into three types: peripheral, one-side-located and mixed type. According to the time of enhancement of low-density area at biphasic MDCT, blood supply in low-density area was divided into four types: arterial blood supply, portal blood supply, arterial combined with portal blood supply and poor blood supply. The portal venous blood supply was mainly of tumor periphery distribution. After treatment of TACE, the portal venous blood supply to tumor periphery increased significantly, and some did have signs of enriched blood supply around the tumor^[17].

Evaluating the blood supply of low-density area with HCC after TACE has clinical significance in choosing the method and route of retreatment. When MDCT pictures revealed the patient of arterial blood supply type, repeated treatment with TACE was suggested. If it is necessary, subsegmental TACE should be performed because of its superior capability of achieving complete lipiodol accumulation. TACE showed a strong antitumor effect because of the overflow of excess iodized oil into the portal veins^[3]. Therefore, when the low-density area had two blood supply routes of arterial and portal veins, repeated treatment with TACE was also suggested. As portal venous blood supply to the tumor was affected by TACE treatment in portal blood supply group, interventional therapy via portal vein should be reasonable. Percutaneous ethanol injection and other non-vascular interventional therapy could be considered when the low-density area revealed poor blood supply^[27,28].

In short, MDCT plays important roles in evaluating the efficacy of chemoembolization. It is a practical, effective, and safe method for assessing the therapeutic effect of TACE. Evaluation of the blood supply of low-density area in MDCT is of practical significance for making retreatment plans.

REFERENCES

- 1 Ji XL, Liu YX, Wang YH, Zhao H. Histopathological study of hepatocellular carcinoma after transcatheter hepatic

- arterialembolization. *China Natl J New Gastroenterol* 1996; **2**: 79-81
- 2 **Fan J**, Ten GJ, He SC, Guo JH, Yang DP, Wang GY. Arterial chemoembolization for hepatocellular carcinoma. *World J Gastroenterol* 1998; **4**: 33-37
 - 3 **Oi H**. Liver intervention. *Nippon Igaku Hoshasen Gakkai Zasshi* 2000; **60**: 826-832
 - 4 **Okusaka T**, Okada S, Ueno H, Ikeda M, Yoshimori M, Shimada K, Yamamoto J, Kosuge T, Yamasaki S, Iwata R, Furukawa H, Moriyama N, Sakamoto M, Hirohashi S. Evaluation of the therapeutic effect of transcatheter arterial embolization for hepatocellular carcinoma. *Oncology* 2000; **58**: 293-299
 - 5 **Kim P**, Prapong W, Sze DY, So SK, Razavi MK. Treatment of hepatocellular carcinoma with sub-selective transcatheter arterial oily chemoinfusion. *Tech Vasc Interv Radiol* 2002; **5**: 127-131
 - 6 **Higashihara H**, Okazaki M. Transcatheter arterial chemoembolization of hepatocellular carcinoma: a Japanese experience. *Hepatogastroenterology* 2002; **49**: 72-78
 - 7 **Achenbach T**, Seifert JK, Pitton MB, Schunk K, Junginger T. Chemoembolization for primary liver cancer. *Eur J Surg Oncol* 2002; **28**: 37-41
 - 8 **Harris M**, Gibbs P, Cebon J, Jones R, Sewell R, Schelleman T, Angus P. Hepatocellular carcinoma and chemoembolization. *Intern Med J* 2001; **31**: 517-522
 - 9 **Poyanli A**, Rozanes I, Acunas B, Sencer S. Palliative treatment of hepatocellular carcinoma by chemoembolization. *Acta Radiol* 2001; **42**: 602-607
 - 10 **Zangos S**, Gille T, Eichler K, Engelmann K, Woitaschek D, Balzer JO, Mack MG, Thalhammer A, Vogl TJ. Transarterial chemoembolization in hepatocellular carcinomas: technique, indications, results. *Radiology* 2001; **41**: 906-914
 - 11 **Aguayo A**, Patt YZ. Nonsurgical treatment of hepatocellular carcinoma. *Semin Oncol* 2001; **28**: 503-513
 - 12 **Zheng XH**, Guan YS. The blood supply of hepatocellular carcinoma. *Fangshexue Shijian* 2002; **17**: 549-550
 - 13 **Huang J**, Zhou XP, Liu RB, Chen X, Xu CJ, Yan ZH, Xu JY. The spiral CT manifestations of the blood supply of primary hepatocellular carcinoma: correlation with pathologic findings. *Zhonghua Fangshexue Zazhi* 2000; **34**: 753-756
 - 14 **Tanaka K**, Nakamura S, Numata K, Okazaki H, Endo O, Inoue S, Takamura Y, Sugiyama M, Ohaki Y. Hepatocellular carcinoma: treatment with percutaneous ethanol injection and transcatheter arterial embolization. *Radiology* 1992; **185**: 457-460
 - 15 **Li C**, Guo Y, Tian G, Shi Z, Liu D, Zeng H, Jiang W, Li H, Zhou C. Extrahepatic arterial blood supply of hepatocellular carcinoma and interventional treatment. *Zhonghua Zhongliu Zazhi* 2002; **24**: 163-166
 - 16 **Honda H**, Tajima T, Kajiyama K, Kuroiwa T, Yoshimitsu K, Irie H, Aibe H, Shimada M, Masuda K. Vascular changes in hepatocellular carcinoma: correlation of radiologic and pathologic findings. *Am J Roentgenol* 1999; **173**: 1213-1217
 - 17 **Liu H**, Li D, Yang S, Wu Y, Luo J. Changes of blood supply from portal system after transcatheter arterial chemoembolization in huge hepatocellular carcinoma. *Hunan Yike Daxue Xuebao* 1998; **23**: 295-298
 - 18 **Imaeda T**, Yamawaki Y, Seki M, Goto H, Iinuma G, Kanematsu M, Mochizuki R, Doi H, Saji S, Shimokawa K. Lipiodol retention and massive necrosis after lipiodol-chemoembolization of hepatocellular carcinoma: correlation between computed tomography and histopathology. *Cardiovasc Intervent Radiol* 1993; **16**: 209-213
 - 19 **Mortelet KJ**, McTavish J, Ros PR. Current techniques of computed tomography. Helical CT, multidetector CT, and 3D reconstruction. *Clin Liver Dis* 2002; **6**: 29-52
 - 20 **Takahashi S**, Murakami T, Takamura M, Kim T, Hori M, Narumi Y, Nakamura H, Kudo M. Multi-detector row helical CT angiography of hepatic vessels: depiction with dual-arterial phase acquisition during single breath hold. *Radiology* 2002; **222**: 81-88
 - 21 **Arnold MM**, Kreel L, Wallace AC, Li AK. Distribution of Lipiodol and evidence for tumor necrosis in hepatocellular carcinoma. *Am J Clin Pathol* 1992; **97**: 405-410
 - 22 **Takayasu K**, Arii S, Matsuo N, Yoshikawa M, Ryu M, Takasaki K, Sato M, Yamanaka N, Shimamura Y, Ohto M. Comparison of CT findings with resected specimens after chemoembolization with iodized oil for hepatocellular carcinoma. *Am J Roentgenol* 2000; **175**: 699-704
 - 23 **Choi BI**, Kim HC, Han JK, Park JH, Kim YI, Kim ST, Lee HS, Kim CY, Han MC. Therapeutic effect of transcatheter oily chemoembolization therapy for encapsulated nodular hepatocellular carcinoma: CT and pathologic findings. *Radiology* 1992; **182**: 709-713
 - 24 **Kubota K**, Hisa N, Nishikawa T, Fujiwara Y, Murata Y, Itoh S, Yoshida D, Yoshida S. Evaluation of hepatocellular carcinoma after treatment with transcatheter arterial chemoembolization: comparison of Lipiodol-CT, power Doppler sonography, and dynamic MRI. *Abdom Imaging* 2001; **26**: 184-190
 - 25 **Ikeya S**, Takayasu K, Muramatsu Y, Moriyama N, Hasegawa H, Hirohashi S. Evaluation of the efficacy of oil chemoembolization for hepatocellular carcinoma by computed tomography: a proposal for altering the criteria to indicate the efficacy. *Gan No Rinsho* 1990; **36**: 985-992
 - 26 **Tan LL**, Li YB, Chen DJ, Li SX, Jiang JD, Li ZM. Helical dual-phase CT scan in evaluating blood supply of primary hepatocellular carcinoma after transcatheter hepatic artery chemoembolization with lipiodol. *Zhonghua Zhongliu Zazhi* 2003; **25**: 82-84
 - 27 **Murakami R**, Yoshimatsu S, Yamashita Y, Sagara K, Arakawa A, Takahashi M. Transcatheter hepatic subsegmental arterial chemoembolization therapy using iodized oil for small hepatocellular carcinomas. Correlation between lipiodol accumulation pattern and local recurrence. *Acta Radiol* 1994; **35**: 576-580
 - 28 **Palma LD**. Diagnostic imaging and interventional therapy of hepatocellular carcinoma. *Br J Radiol* 1998; **71**: 808-818

Edited by Chen WW and Zhu LH Proofread by Xu FM

Multiple gene differential expression patterns in human ischemic liver: Safe limit of warm ischemic time

Qi-Ping Lu, Ting-Jia Cao, Zhi-Yong Zhang, Wei Liu

Qi-Ping Lu, Ting-Jia Cao, Zhi-Yong Zhang, Wei Liu, Department of General Surgery, Wuhan General Hospital of Guangzhou Military Command, Wuhan 430070, Hubei Province, China

Supported by the National Natural Science Foundation of China, No. 30170928 and the Key Project of the Tenth-Five-year plan Foundation of PLA, No. 01MA040

Correspondence to: Qi-Ping Lu, Department of General Surgery, Wuhan General Hospital of Guangzhou Military Command, Wuhan 430070, Hubei Province, China

Telephone: +86-27-68878501

Received: 2004-02-11 **Accepted:** 2004-03-02

Abstract

AIM: To investigate the multiple gene differential expression patterns in human ischemic liver and to produce the evidence about the hepatic ischemic safety time.

METHODS: The responses of cells to hepatic ischemia and hypoxia at hepatic ischemia were analyzed by cDNA microarray representing 4 000 different human genes containing 200 apoptotic correlative genes.

RESULTS: There were lower or normal expression levels of apoptotic correlative genes during the periods of hepatic ischemia for 0-15 min, the maintenance homostatic genes were expressed significantly higher at the same time. But at the hepatic ischemia for 30 min, the expression levels of maintenance homeostatic genes were down-regulated, the expressions of many apoptotic correlative genes and nuclear transcription factors were activated and up-regulated.

CONCLUSION: HIF-1, APAF-1, PCDC10, FBX5, DFF40, DFFA XIAP, survivin may be regarded as the signal genes to judge the degree of hepatic ischemic-hypoxic injure, and the apoptotic liver cell injury due to ischemia in different time limits. The safe limit of human hepatic warm ischemic time appears to be generally less than 30 min.

Lu QP, Cao TJ, Zhang ZY, Liu W. Multiple gene differential expression patterns in human ischemic liver: Safe limit of warm ischemic time. *World J Gastroenterol* 2004; 10(14): 2130-2133

<http://www.wjgnet.com/1007-9327/10/2130.asp>

INTRODUCTION

The safety limit of human hepatic warm ischemic time is closely correlated with the recovery of hepatic function and the patient's prognosis after liver transplantation, serious hepatic injury and hepatectomy^[1-7]. Owing to the development in hepatic surgical operation techniques and perioperative period, numerous experts discovered that the safety limit of human hepatic warm ischemic time could be prolonged further. But the critical problem of what degree the safety limit should be generally controlled is drawing special attention of the whole hepatic surgery. The cell apoptosis we have found now is one

of the main cell death forms influencing visceral functions after the liver got ischemic injury^[8-12]. But because too many genes are involved in cell apoptosis, the expressions in differential ischemic safety time of the main controlling gene influencing the safety limit of human hepatic warm ischemic time remain unclear. For such a reason, by cDNA microarray, we investigated the multiple genes differential expression patterns in human ischemic liver for the purpose of producing some scientific evidence for the hepatic ischemic safety time.

MATERIALS AND METHODS

Tissue specimens

All the tissue specimens in question came from the hepatic tissues contributed by the unconscious patients dying of external brain injury whose other organic functions were normal (Table 1). Each group consisted of 5 specimens. The specimens were immediately stored in liquid N₂ after resection. All contributors had no hepatic disease, and the liver function remains normal before resection. The liver tissue construction was proved normal by pathologic examinations.

Table 1 Group division of tissue specimens

Group	Experiment group	Control group
Group 1	15 min ischemic tissue	Normal liver tissue
Group 2	30 min ischemic tissue	Normal liver tissue
Group 3	30 min ischemic tissue	15 min ischemic tissue

Chemicals and materials

TriZol and Script II reverse transcriptases were bought from American Life Technologies, Ltd. cDNA microarray containing 200 apoptotic correlative genes and biochip hybridization kit were from Shanghai Biotstar Gene chip, Ltd.

Total RNA extraction

Total RNA was extracted from human liver tissues in each group following the single step extraction (see details in the manual).

Probe preparation and hybridization

An equal volume of RNA was extracted from each group and 60 µg RNA was added into 50 µL reverse transcription system. The experiment group was labeled with Cy5-d CTP and the control group with Cy5-d CTP (see the way of labeling in the manual of the test kit). The chip was denatured and prehybridized for one time in advance. After denatured at 95 °C for 5 min, the probe mixture was added on the microarray and covered with a hyi slip. The slide was then placed in a constant temperature hybridization chamber for hybridization at 42 °C for 20 h. After hybridization, slides were washed 10 min in each of 2×SSC with 2 g/L GSDS, 0.1×SSC with 2 g/L GSDS, 0.1×SSC, then dried at room temperature. The hybridization in each group was replicated 3 times.

Fluorescent scanning and analysis

The chip was scanned by GenePix 4000B laser scanner at

2 wavelengths. The acquired image was analyzed by GenePix Pro 3.0 software. The intensity of each spot at the 2 wavelengths cut off the additional background signal represented the quantity of Cy3-dUTP and Cy5-dUTP respectively. Each ratio value of Cy3 to Cy5 was computed. The 2 overall intensities were normalized by a coefficient according to the ratio of the located 88 housekeeping genes, 43 negative control genes, 45 positive control genes and 3 blank locations. We defined two standards to screen out each differentially expressed gene. The ratio value >2 represented the level of the gene expression elevated significantly, the ratio value <0.5 represented the level of the significantly depressed gene expression. The data about the genes whose ratio value >2 or <0.5 were screened out in the comparisons of normal control group with 15 min ischemic group or 30 min ischemic group, then the variation of the ratio value was observed in the comparison of 15 min ischemic group with 30 min ischemic group and each “ ± 0.5 ” change in the ratio value was set as a “+”. All the data were input in the datasheet, and the biological functions of the target genes were analyzed.

RESULTS

Comparison of differential gene expressions between 15 min ischemic group and normal control group

Figure 1 (A and B) shows that the double-colored fluorescent labels in 15 min ischemic group and normal control group were overlapping. A total of 41 differentially expressed genes were identified by cDNA chip between the 15 min ischemic group and normal control group. Among them the ratio values of 33 genes were <0.5 , consisting of 22 genes correlated directly with cell apoptosis regulation, 9 congenic genes of stress-response protein relevant to cell apoptosis, and 3 genes correlated to metabolism regulation, 1 correlated to cell circle regulation, 1 correlated to the cell interpretation and synthesis. In the meantime, there were 8 differential expression genes whose ratio values were >2 , mainly about P43=mitochondrial elongation factor homolog (GenBank-ID: S75463), human ribosomal protein *S14* gene, complete cds (GenBank-ID: humrps 14), *H. sapiens* mRNA for squalene synthase

(GenBank-ID: hssqusyn), human sodium/potassium ATPase beta-2 subunit (*atpb2*) mRNA, complete cds (GenBank-ID: humatpbii), *H. sapiens* mRNA for H⁺-ATP synthase subunit b (GenBank-ID: hsatpsyn), and no gene relevant to apoptosis was highly expressed.

Comparison of differential gene expressions between 30 min ischemic group and normal control group

Figure 1 (C and D) shows that the double-colored fluorescent labels in 30 min ischemic group and normal control group were overlapping. A total of 9 differentially expressed genes were identified by cDNA chip between the 30 min ischemic group and normal control group. The ratio values of 3 genes of which were <0.5 , consisting of 2 genes correlated directly with cell apoptosis regulation (the congenic genes of survivin, AB028869 and X-linked inhibitor apoptosis protein, u45880 respectively), and 1 congenic gene (GenBank-ID: af004711) of TPKC1. In the meantime, there were 6 differential expression genes whose ratio values were >2 , of which 3 were the regulation genes correlated directly with cell apoptosis: APAF1 (GenBank-ID: NM-001160), PDCD10 (GenBank-ID: NM-007210) and an unnamed gene (GenBank-ID: AL031714), 1 was the congenic gene (GenBank-ID: AF050127) of HIF1, the functions of last 2 genes' were not clear.

Comparison of differential gene expressions between 15 min ischemic group and 30 min ischemic group

In the 200 genes, 35 genes were not expressed at the two time limits. The expressions of 167 genes in 30 min ischemic group differed from in 15 min ischemic group. One hundred and nineteen genes were expressed following the rising tendency, of which ratio values of 7 genes were $>“+++”$, 19 $>“++”$, 39 $>“+”$, and 55 genes only expressed the rising tendency but their ratio values were $\leq“+”$. There are 46 genes following the descending tendency, of which ratio values of 4 genes were $>“+++”$, 5 $>“++”$, 12 $>“+”$, and 25 genes only expressed the descending tendency but their ratio values were $\leq“+”$. In addition, 16 genes were expressed in 30 min ischemic group, but not in 15 min ischemic group, of which 11 genes were

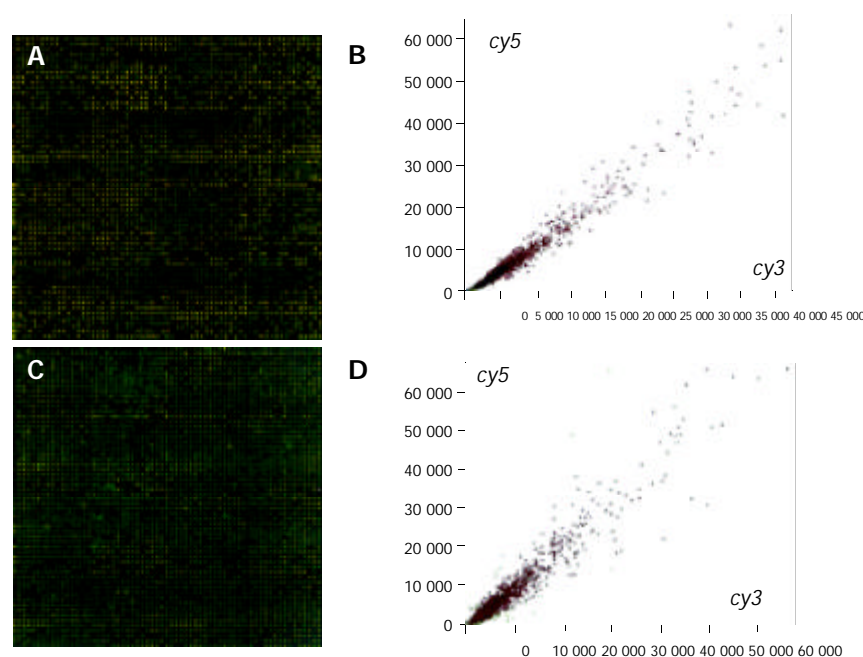


Figure 1 Double-colored fluorescent labels and scattered diagram of signal intensity of differential gene expressions in 15 min ischemic group and normal control group. Green: Down-regulation, Signal of cy3 is stronger; Red: Up-regulation, signal of cy5 is stronger. A, C: Double-colored fluorescent labels: In 15 min ischemic group and normal control group; B, D: Scatter diagram of signal intensity of differential gene expressions in 15 min ischemia group and normal control group.

correlated directly with cell apoptosis regulation, 5 genes were expressed in 15 min ischemic group, but not in 30 min ischemic group, of which only 1 gene was correlated directly with cell apoptosis regulation, namely XIAP (GenBank-ID: u45880).

DISCUSSION

Our data suggested that the apoptosis regulation gene at the hepatic ischemia for 0-30 min presented following features.

In hepatic ischemia for 0-15 min, the apoptosis regulation gene was expressed low or normally. The differentially expressed genes whose ratio values were >2 (namely, they were expressed following the rising tendency) were mainly the maintenance harmonious genes, such as genes regulate P43=mitochondrial elongation factor homolog (GenBank-ID: S75463), Human ribosomal protein S14 gene (GenBank-ID: humrps), *H. sapiens* mRNA for squalene synthase (GenBank-ID: hssqusyn), Na⁺/K⁺-ATPase activity α subunit (GenBank-ID: hsatpar) and β subunit (GenBank-ID: humatpbii), H⁺-ATPase activity (GenBank-ID: hsatpsyn). But they were not highly expressed with the congenic genes correlated directly with cell apoptosis regulation.

In hepatic ischemia for 15-30 min, the expression of apoptosis regulation genes changed greatly. One hundred and nineteen genes were expressed following the rising tendency, of which 59 genes were relevant to the apoptosis regulation. Although some anti-apoptosis genes [such as the congenic gene of *bcl-2* (GenBank-ID: AJ006288), the congenic gene of inhibitor apoptosis protein IEX-IL (GenBank-ID: AF071596)] which were expressed the low level, the majority of the higher expressed genes were the apoptotic genes, for example, the congenic gene of apoptotic protease activating factor-1 (APAF-1, GenBank-ID: NM-001160); Homo sapiens F-box protein 5, FBX5 (GenBank-ID: NM-012177); DNA fragmentation factor, 40 ku, subunit, DFF40 (GenBank-ID: AF064019); DNA fragmentation factor, 45 ku, alpha subunit, DFFA (GenBank-ID: NM-004401); p53-induced protein; PIG1 (GenBank-ID: NM-006034). Especially, APAF-1 was the only known human homologue of CED-4 and the nuclear element in the formation of apoptosis body^[13-16]. Now it is thought as the key element regulating cell apoptosis, and the ratio value of its expression in 30 min hepatic ischemia was an additional “+++” than that in 15 min hepatic ischemia. Meanwhile the ratio value of the congenic gene of PDCD10 (GenBank-ID: NM-007217) was also “++”. The significant rising of expression of the apoptotic genes showed that the unavoidable cell death after serious ischemic injury was a key expression of the serious cell injury. In 15 min hepatic ischemia, the congenic gene of the important X-linked inhibitor apoptosis protein, XIAP (GenBank-ID: u45880) changed from the normal expression to non-expression, following the obvious descending tendency. Compared with the normal group, the expression of the survivin congenic gene (GenBank-ID: AB028869) descended greatly with the ratio value <0.5. The codogenic genes (GenBank-ID: S75463, humrps, hssqusyn, hsatpar, humatpbii, hsatpsyn and so on) relevant to the internal circumstance and the organelle functions were expressed obviously in the period of 0-15 min hepatic ischemia, but in 15-30 min period their expression descended to “+”- “++”. The congenic gene of human hypoxia-inducible factor 1 HIF-1 alpha gene (GenBank-ID: AF050127) was expressed apparently (increased to “+++”). Lots of the regulation genes of nucleus translation factors were expressed notably for example, the codogenic gene of EIF4G2 (eukaryotic translation-induction factor 4 gamma, 2 (EIF4G2) mRNA, GenBank-ID: NM-001418), NF- κ B family, TNF receptor associated factor 6 (TRAF6) responsible for the existence and death of cells (GenBank-ID: hsu78798), increased to “++”. The latter was a transmission factor

participating in IL-1 signal transmission and activating the signal transmission about apoptosis of the nuclear factor NF- κ B^[17-20].

The data suggested that in 0-15 min hepatic ischemia, the gene regulation model inside of the cells was likely to better and maintain the harmonious of the internal circumstance to keep the wholeness of cell and organ functions even by controlling ion channel and organelle functions. At the same time, although acute ischemic-hypoxic injury changed the structure and functions of cells, the expression of each kind of genes relevant to apoptosis, according to the analysis of the level of gene regulation, remained on the low level, that is to say, the occurrence of apoptosis was not a main direction yet. With the time of ischemia and hypoxia passed, when hepatic ischemia lasted for 30 min, acute ischemic-hypoxic injury perhaps would lead to the significant rising of HIF-1, and the cell gene expression model responsible for the existence or death of the cells also was changed completely. The expressions of all kinds of regulation genes maintaining cells and the internal cellular circumstance descended obviously, while NF- κ B and many genes relevant to apoptosis were activated evidently and notably expressed. Therefore, it is suggested that cell death is unavoidable when hepatic ischemia lasts for 30 min. It is true that some experts deduced that the time of the human hepatic ischemia could be prolonged beyond the safe limit according to clinical experience in the progress after liver operation. Yet when dynamic changes of gene expressions after liver suffered ischemic injury are analyzed, it is suggested that the safe limit of one time hepatic ischemia should be less than 30 min, namely, when key death genes such as *APAF-1*, *PDCD10*, *FBX5*, *DFF40*, *DFFA* are activated evidently and expressed significantly, and before the obvious descending of inhibitor apoptosis genes such as XIAP, survivin. In the meantime it is suggested that HIF-1, APAF-1, PCDC10, XIAP, survivin may be regarded as the signal gene to judge the degree of hepatic ischemic-hypoxic injury, and the apoptotic liver cell injury due to ischemia in different time limits.

REFERENCES

- 1 **Makuuchi M**, Mori T, Gunven P, Yamazaki S, Hasegawa H. Safety of hemihepatic vascular occlusion during resection of the liver. *Surg Gynecol Obstet* 1987; **164**: 155-158
- 2 **Mori T**, Makuuchi M, Kobayashi J, Sukigara M, Yamasaki S, Hasegawa H. Clinical studies on changes in serum transaminase, lactate dehydrogenase, total bilirubin and alkaline phosphatase levels after hepatectomy with and without the hemihepatic vascular occlusion technique. *Nippon Geka Gakkai Zasshi* 1985; **86**: 837-845
- 3 **Gotoh M**, Monden M, Sakon M, Kanai T, Umeshita K, Nagano H, Mori T. Hilar lobar vascular occlusion for hepatic resection. *J Am Coll Surg* 1994; **178**: 6-10
- 4 **Wu CC**, Yeh DC, Ho WM, Yu CL, Cheng SB, Liu TJ, P'eng FK. Occlusion of hepatic blood inflow for complex central liver resections in cirrhotic patients: a randomized comparison of hemihepatic and total hepatic occlusion techniques. *Arch Surg* 2002; **137**: 1369-1376
- 5 **Liu DL**, Jeppsson B, Hakansson CH, Odselius R. Multiple-system organ damage resulting from prolonged hepatic inflow interruption. *Arch Surg* 1996; **131**: 442-447
- 6 **Emond J**, Wachs ME, Renz JF, Kelley S, Harris H, Roberts JP, Ascher NL, Lim RC Jr. Total vascular exclusion for major hepatectomy in patients with abnormal liver parenchyma. *Arch Surg* 1995; **130**: 824-830
- 7 **Scheele J**. Anatomical and atypical liver resections. *Chirurg* 2001; **72**: 113-124
- 8 **Yin XM**, Ding WX. Death receptor activation-induced hepatocyte apoptosis and liver injury. *Curr Mol Med* 2003; **3**: 491-508
- 9 **Jaeschke H**, Lemasters JJ. Apoptosis versus oncotic necrosis in hepatic ischemia/reperfusion injury. *Gastroenterology* 2003; **125**: 1246-1257

- 10 **Sass G**, Soares MC, Yamashita K, Seyfried S, Zimmermann WH, Eschenhagen T, Kaczmarek E, Ritter T, Volk HD, Tiegs G. Heme oxygenase-1 and its reaction product, carbon monoxide, prevent inflammation-related apoptotic liver damage in mice. *Hepatology* 2003; **38**: 909-918
- 11 **Berberat PO**, Katori M, Kaczmarek E, Anselmo D, Lassman C, Ke B, Shen X, Busuttill RW, Yamashita K, Csizmadia E, Tyagi S, Otterbein LE, Brouard S, Tobiasch E, Bach FH, Kupiec-Weglinski JW, Soares MP. Heavy chain ferritin acts as an antiapoptotic gene that protects livers from ischemia reperfusion injury. *FASEB J* 2003; **17**: 1724-1726
- 12 **Topaloglu S**, Abbasoglu O, Ayhan A, Sokmensuer C, Kilinc K. Antiapoptotic and protective effects of roscovitine on ischemia-reperfusion injury of the rat liver. *Liver Int* 2003; **23**: 300-307
- 13 **Zou H**, Henzel WJ, Liu X, Lutschg A, Wang X. Apaf-1, a human protein homologous to *C. elegans* CED-4, participates in cytochrome c-dependent activation of caspase-3. *Cell* 1997; **90**: 405-413
- 14 **Pan G**, O'Rourke K, Dixit VM. Caspase-9, Bcl-XL, and Apaf-1 form a ternary complex. *J Biol Chem* 1998; **273**: 5841-5845
- 15 **Shulache VP**. Cytochrome c in the apoptotic and antioxidant cascades. *FEBS Lett* 1998; **423**: 275-280
- 16 **Hu Y**, Benedict MA, Wu D, Inohara N, Nunez G. Bcl-XL interacts with Apaf-1 and inhibits Apaf-1-dependent caspase-9 activation. *Proc Natl Acad Sci U S A* 1998; **95**: 4386-4391
- 17 **Matsumura T**, Degawa T, Takii T, Hayashi H, Okamoto T, Inoue J, Onozaki K. TRAF6-NF-kappaB pathway is essential for interleukin-1-induced TLR2 expression and its functional response to TLR2 ligand in murine hepatocytes. *Immunol* 2003; **109**: 127-136
- 18 **Yoshida Y**, Yamashita U. Interleukin 1 signal transduction. *J UOEH* 2003; **25**: 237-248
- 19 **Takatsuna H**, Kato H, Gohda J, Akiyama T, Moriya A, Okamoto Y, Yamagata Y, Otsuka M, Umezawa K, Semba K, Inoue J. Identification of TIFA as an adapter protein that links tumor necrosis factor receptor-associated factor 6 (TRAF6) to interleukin-1 (IL-1) receptor-associated kinase-1 (IRAK-1) in IL-1 receptor signaling. *J Biol Chem* 2003; **278**: 12144-12150
- 20 **Kanamori M**, Kai C, Hayashizaki Y, Suzuki H. NF-kappaB activator Act1 associates with IL-1/Toll pathway adaptor molecule TRAF6. *FEBS Lett* 2002; **532**: 241-246

Edited by Wang XL Proofread by Chen WW and Xu FM

A report of 28 cases of 3-year follow-up after liver transplantation for advanced hepatocellular carcinoma

De-Chen Wang, Tong-Lin Zhang, Shi-Bing Song, Jiong Yuan, Dian-Rong Xiu, Xiao-Xia Yang

De-Chen Wang, Tong-Lin Zhang, Shi-Bing Song, Jiong Yuan, Dian-Rong Xiu, Xiao-Xia Yang, Department of General Surgery, Peking University Third Hospital, Beijing 100083, China
Correspondence to: Dr. De-Chen Wang, Department of General Surgery, Peking University Third Hospital, Beijing 100083, China. hepuzai@yahoo.com.cn
Telephone: +86-10-62017691 **Fax:** +86-10-62010334
Received: 2003-12-28 **Accepted:** 2004-01-08

Abstract

AIM: To investigate the therapeutic value of liver transplantation for advanced hepatocellular carcinoma (HCC).

METHODS: Twenty-eight patients with advanced HCC were treated by liver transplantation from August 2000 to October 2003 at Peking University Third hospital. All the patients were followed up to evaluate the result.

RESULTS: The longest follow-up duration was 3 years and 3 mo. Till the end of the follow-up period, 17 patients had already died and 11 were alive. Of those who died, 10 patients died of tumor recurrence, 4 died during the perioperative period, 2 died of variceal bleeding, and 1 died of biliary complication. According to life table method, the 1-, 2-, and 3-year survival rates were 87.5%, 52.5%, and 42.9%, respectively.

CONCLUSION: Liver transplantation provides a new treatment under the circumstance of lacking of an effective treatment for advanced HCC at present. Some patients can survive for a relatively long time free of tumor. In our country, if the patients can afford liver transplantation, advanced HCC without extrahepatic metastasis is an indication for liver transplantation at present.

Wang DC, Zhang TL, Song SB, Yuan J, Xiu DR, Yang XX. A report of 28 cases of 3-year follow-up after liver transplantation for advanced hepatocellular carcinoma. *World J Gastroenterol* 2004; 10(14): 2134-2135

<http://www.wjgnet.com/1007-9327/10/2134.asp>

INTRODUCTION

Hepatocellular carcinoma (HCC) is a common malignant tumor in China. The methods of treatment for advanced HCC are limited, and the prognosis is so poor. Peking University Third Hospital began to carry out liver transplantation since August 2000. Some of the patients suffered from advanced HCC. In our study, the result of treatment has been found to be somewhat accepted at present.

MATERIALS AND METHODS

Materials

Twenty-eight patients with advanced HCC were treated by liver transplantation from August 2000 to October 2003 at our

hospital. Of them, twenty-six patients were male. The average age was 46.3 years, ranging from 20 to 63 years. All the patients suffered from cirrhosis caused by hepatitis B. Child-Pugh classes A, B, and C patients were 13, 8, and 7, respectively. The diagnosis was made by ultrasound, computed tomography, magnetic resonance imaging, arteriography and serum alpha-fetoprotein levels. Postoperative pathologic examination confirmed that all the patients had HCC. The patients with extrahepatic spread were excluded by ultrasound, chest film and bone scan. All the patients met the following criteria: solitary tumor ≥ 5 cm or with multiple nodules and total diameter > 8 cm; and the mean diameter of single nodule was 10.3 cm, ranging from 3 cm to 20 cm. There were 12 patients with tumor involving bilateral hepatic lobes, 5 with positive porta hepatis nodes, and 18 with portal invasion.

Methods

All the patients underwent orthotopic liver transplantation (OLT) and were taken care of by the same medical team perioperatively. The donors were healthy male who had brain death with the age of 20-40 years. The initial 11 patients did not undergo formal chemotherapy postoperatively, and only the eighth patient underwent transarterial chemoembolization preoperatively (hot lipiodol 10 mL and cisplatin 100 mg). Seventeen patients underwent the formal intravenous chemotherapy postoperatively when the hepatic function was normal. The chemotherapy regime was: administration of adriamycin 40 mg, cisplatin 60 mg, calcium folinate-SF 200 mg and 5-Fluorouracil 1 000 mg on the first day, the same doses of calcium folinate-SF and 5-Fluorouracil from the second day to the fifth day. The course of chemotherapy was 5 d once a month, and there were 6 courses altogether. All the patients were followed up and the longest duration was 3 years and 3 mo.

Statistics

The survival rate was calculated according to the life table method. Patients who died of non-tumor and who stopped the follow-up in the intervals were listed into the lost.

RESULTS

Till the end of the follow-up period, 17 patients had already died, and 11 were alive. Of those dead patients (Table 1), 10 patients died of tumor recurrence, 4 died within perioperative period, 2 died of variceal bleeding, and 1 died of biliary complication. Among the patients who survived (Table 2), there were 1, 2, 2, and 3 patients survived for 8 mo, 1, 2, and 3 years free of tumor, respectively; and there were 1 and 2 patients survived for 8 mo and 1 year with tumor-recurrence, respectively. In the first year, 8 patients were lost, 3 were dead, and the 1-year survival rate was 87.5%. In the second year, 4 patients were lost, 6 were dead, and the 2-year survival rate was 52.5%. In the third year, 3 patients were lost, 1 was dead, and the 3-year survival rate was 42.9%.

Of the patients with single tumor of more than 10 cm, there was 1 patient who survived for more than 3 years. No patients with tumors involving many hepatic lobes could survive for more than 3 years, but there were 2 patients survived for more

than 2 years. There was 1 patient with positive portal lymph node survived for more than 3 years. Of the patients with portal invasion, 2 survived for more than 3 years, and 3 survived for more than 2 years. The cases were divided according to the different standards, and their survival time can be seen in Table 3.

Table 1 Causes and time of the death of patients

Cause	Peri-operatively	Variceal bleeding	Biliary complication	Tumor-recurrence		
				<1 yr	1-2 yr	>2 yr
Number	4	2 ¹	1 ²	3	6	1

¹2 years and 2 mo, and 6 mo after OLT, respectively, ²6 mo after OLT.

Table 2 Survival time of the patients

Time	<1 yr	1-2 yr	2-3 yr	>3 yr
Number	1+1 ¹	2+2 ¹	2	3

¹Survive with recurrence.

Table 3 Survival time of the different groups

Groups	<1 yr	12 yr	2-3 yr	>3 yr
Tumor diameter				
>10 cm	5	4	0	1
<10 cm	6	6	4	2
Portal invasion				
Yes	7	6	3	2
No	4	4	1	1

DISCUSSION

Among the surgical therapies of HCC, the dominant treatment is hepatic resection. A study showed that the 5-year survival rate is up to 50% after hepatic resection^[1]. But HCC always occurs in the presence of liver cirrhosis, hepatic resection is limited by the poor hepatic function and the presence of portal hypertension. In general, Child's C` stage is considered an absolute contraindication for any type of resection^[1].

According to the principle of tumor surgery, replacing an allograft after total hepatectomy is an ideal curative resection of HCC^[2]. Herrero *et al.* reported that in the patients with solitary HCC nodule less than 6 cm and those with 2-3 HCC nodules less than 5 cm in diameter, 1- and 3-year recurrence free survival rates were 87% and 79%, respectively^[3]. In the study by Yao *et al.*^[2], patients with HCC meeting the following criteria: solitary tumor ≤ 6.5 cm, or ≤ 3 nodules with the largest lesion ≤ 4.5 cm and total tumor diameter ≤ 8 cm, had survival rates of 90% and 75.2%, at 1 and 5 years after OLT, respectively. So they concluded that the current criteria for OLT based on tumor size might be modestly expanded while preserving excellent survival. Since OLT for early HCC is not fit for the situation of our country as well as the economic status, and the result of hepatic resection is good in our country, OLT is not accepted by the patients except that the patients having early HCC with serious cirrhosis can not tolerate hepatic resection.

The diagnosis of early HCC is achieved in around 30% of the cases^[4]. As to the unresectable HCC, the chief therapy is a

non-surgical treatment. But it always leads to poor prognosis for it is not a curative treatment. Now the generally accepted non-surgical treatment is transarterial chemoembolization. Lo *et al.* undertook a randomized controlled trial of transarterial chemoembolization for unresectable HCC^[5]. The patients were excluded if they had 1 or more of the following criteria: poor hepatic function (presence of hepatic encephalopathy, ascites not controlled by diuretics, history of variceal bleeding within last three months, a serum total bilirubin level over 50 $\mu\text{mol/L}$, a serum total albumin level below 28 g/L, or a prothrombin time of more than 4 s over the control); extrahepatic metastasis; main portal vein thrombosis *etc*^[5]. The chemoembolization group underwent transarterial chemoembolization, and the control group received only treatment for symptoms and complications. The estimated 1-, 2- and 3-year survival rates were 57%, 31% and 26% for the chemoembolization group, and 32%, 11%, and 3% for the control group, respectively.

There is no effective therapy for the patients with advanced HCC who do not meet the chemoembolization criteria, such as poor hepatic function and/or portal thrombosis, and they have poor prognosis even if there is no extrahepatic spread when the diagnosis of HCC is made. In the initial stage of OLT, the patients with advanced HCC were also treated by OLT in abroad, and the 3-year survival rate was 20-30%^[1]. Due to the poor prognosis and the shortage of donor, OLT for advanced HCC was abandoned in foreign countries. From the year of 2000, our hospital began to perform OLT and chose advanced HCC for the initial trial just as peers at home and abroad. Till now, 28 patients with advanced HCC underwent OLT at our hospital. We can not conclude that the result is excellent through the 3-year follow-up. Many patients who underwent OLT did not meet the chemoembolization criteria, but the total survival rate was higher than that of the chemoembolization group reported by Lo *et al.* Some patients survived for a relatively long time free of tumor after OLT. Thus, liver transplantation provides a new treatment under the circumstance of lacking of an effective treatment for HCC at present, and some patients have a chance to lengthen their lives. But the expense of liver transplantation is very high. In our country, if the patients can afford liver transplantation, advanced HCC without extrahepatic metastasis is an indication for liver transplantation at present.

REFERENCES

- 1 **Frilling A**, Malago M, Broelsch CE. Current status of liver transplantation for treatment of hepatocellular carcinoma. *Dig Dis* 2001; **19**: 333-337
- 2 **Yao FY**, Ferrell L, Bass NM, Watson JJ, Bacchetti P, Venook A, Ascher NL, Roberts JP. Liver transplantation for hepatocellular carcinoma: expansion of the tumor size limits does not adversely impact survival. *Hepatology* 2001; **33**: 1394-1403
- 3 **Herrero JI**, Sangro B, Quiroga J, Pardo F, Herraiz M, Cienfuegos JA, Prieto J. Influence of tumor characteristics on the outcome of liver transplantation among patients with liver cirrhosis and hepatocellular carcinoma. *Liver transplantation* 2001; **7**: 631-636
- 4 **Varela M**, Sala M, Llovet JM, Bruix J. Treatment of hepatocellular carcinoma: is there an optimal strategy? *Cancer Treat Rev* 2003; **29**: 99-104
- 5 **Lo CM**, Ngan H, Tso WK, Liu CL, Lam CM, Poon RTP, Fan ST, Wong J. Randomized controlled trial of transarterial lipiodol chemoembolization for unresectable hepatocellular carcinoma. *Hepatology* 2002; **35**: 1164-1171

Clinical features, diagnosis, treatment and prognosis of multiple primary colorectal carcinoma

Hong-Zhi Wang, Xin-Fu Huang, Yi Wang, Jia-Fu Ji, Jin Gu

Hong-Zhi Wang, Xin-Fu Huang, Yi Wang, Jia-Fu Ji, Jin Gu,
Department of Surgery, Beijing Cancer Hospital, School of Clinical
Oncology, Peking University, Beijing 100036, China

Correspondence to: Hong-Zhi Wang, Department of Surgery, Beijing
Cancer Hospital, School of Clinical Oncology, Peking University,
Beijing 100036, China. doctorwhz@163.com

Telephone: +86-10-88135234 **Fax:** +86-10-68518676

Received: 2004-02-02 **Accepted:** 2004-02-18

Abstract

AIM: To investigate the clinical features, diagnosis, treatment and prognosis of multiple primary colorectal carcinomas (MPCC).

METHODS: A retrospective analysis of 37 patients with MPCC from 1974 to 1998 was carried out.

RESULTS: The incidence of MPCC was 2.74%(37/1 348) in patients with primary colorectal carcinomas, 15 cases of them were patients with synchronous carcinomas (SC) and 22 cases were diagnosed as metachronous carcinomas (MC). Most tumors were located in the right colon and rectum. Fifty-five percent (12/22) of MC were diagnosed within 3 years after tumor resection and 41%(9/22) of MC occurred after 8 years. Radical resections were performed in all patients except for 1 case. The 5-year survival rate of SC was 72.7%(8/11) and that of MC after the first cancer and second cancer was 71.4%(15/21) and 38.9%(7/18), respectively.

CONCLUSION: The results indicate the importance of complete preoperative examination, careful intraoperative exploration and periodic postoperative surveillance. Early diagnosis and radical resection can increase survival rate of MPCC.

Wang HZ, Huang XF, Wang Y, Ji JF, Gu J. Clinical features, diagnosis, treatment and prognosis of multiple primary colorectal carcinoma. *World J Gastroenterol* 2004; 10(14): 2136-2139

<http://www.wjgnet.com/1007-9327/10/2136.asp>

INTRODUCTION

Multiple primary colorectal carcinoma (MPCC) refers to two or more primary colorectal carcinomas detected in a single individual simultaneously or consecutively. It is named synchronous carcinoma (SC) and metachronous carcinoma (MC) respectively. The prognosis of colorectal carcinoma is good compared with other carcinomas of the digestive organs. Along with increasing incidence of colorectal carcinomas and prolonged survival after radical resection, patients with MPCC have increased gradually. Generally, SC does not affect prognosis if it is recognized and treated in time, but if ignored, it may turn into more advanced MC. Therefore, after colorectal cancer surgery, occurrence of metachronous carcinoma is

regarded as a serious problem^[1]. Due to influence of doctor's recognition degree, missed and error diagnosis or inaccurate treatment appears frequently. The purpose of this review was to discuss the prevalence, preoperative diagnosis, postoperative follow-up and survival, in order to strengthen the acquaintance of MPCC.

MATERIALS AND METHODS

A total of 1 348 cases of primary colorectal carcinomas were treated at the Department of Surgery, Beijing Cancer Hospital from January 1, 1974 to December 31, 1998. MPCC was diagnosed according to the following criteria proposed by Moertel^[2]. Each tumor must have a definite pathologic picture of malignancy, metastasis or recurrence from another colorectal cancer was excluded, all cancers detected at the same time or within 6 mo were defined as SC, otherwise as MC, Tumors must be distinctly separated by at least 5 cm of an intact bowel wall from each other. MC must be more than 5 cm away from the normal anastomotic site of index cancer resection. MPCC originated from familial colonic polyposis or ulcerative colitis was excluded^[2].

Tumor locations were divided into 3 groups: (1) right colon which included appendix, cecum, ascending colon, hepatic flexure, and transverse colon; (2) left colon which included splenic flexure, descending colon and sigmoid colon; (3) rectum, upper boundary of which was 15 cm from the dentate line. It was considered as lost follow-up if a patient failed to come back to the Outpatient Department or could not be contacted by letter or telephone for more than one year.

Independent *t*-test and χ^2 -test were used to compare the factors in different groups. A *P* value less than or equal to 0.05 was considered statistically significant.

RESULTS

A total of 1 348 patients with colorectal carcinoma were treated during 25 years period. Fifteen cases had 2 SCs and 22 patients had 2(20 cases) or 4(1 case) or 5(1 case) MCs, respectively (Tables 1 and 2). No significant differences were noted among the groups in age and gender. The second MC appeared in 8-240 mo (mean: 68 mo), 55%(12/22) were diagnosed within 36 mo and 41%(9/22) after 96 mo. The interval of other one patient was 45 mo. Two patients had three times of MC, their interval was 15 years (one cancer), 19 years (two cancers) and 12 years (one cancer), 17 years (three cancers) respectively.

The distribution of MC and SC is shown in Table 2. Lesions were located at the adjacent intestinal segment in 6 of SC group (43%). In MC group, 20 patients had 2 lesions, 1 had 4 lesions and the other one had 5 lesions.

The clinical presentation was variable. All the 15 patients in SC group went to see doctors because of symptoms, such as bloody stool, abdominal pain, diarrhea, anemia and abdominal mass. The time of the development symptoms was more than 1 year. Thirteen cases (87%) were diagnosed by barium enema and/or colonoscopy before operation. And 2, 9 and 2 patients were staged as Dukes B, C and D, respectively. Other 2 patients of this group were diagnosed intraoperatively. In MC group,

3 of 22 cases (13.6%) were proved by routine postoperative colonoscopy (2: Dukes A, 1: Dukes B). Twenty-one patients went to see doctor owing to symptoms, 18(86%) were diagnosed preoperatively, 2 were diagnosed intraoperatively, and 1 was diagnosed by postoperative pathology.

Operation was the primary option. In SC group, 14 cases (93%) received radical resection. Among them, 5 cases received subtotal colectomy in combination with rectoileostomy, others received radical resection or combined radical resection of adjacent loop according to the cancer locations. One received by-pass due to severe local spread. In MC group, all the 22 cases with index cancer received radical resection. All secondary or third lesions except one underwent radical resection.

The histological types of all cancers are shown in Table 2. No significant differences were noted between the second cancer and SC with index cancer. There was a significant difference between the third cancer and index cancer.

The 5-year and 10-year survival rates are shown in Table 2. There was no significant difference between SC and index cancer of MC. The 5-year survival rate of the patients with secondary cancer could reach 39% after operation.

Table 1 Age and gender of patients with MPCC

	Group SC	Group MC
Number of patients	15	22
Age(yr)		
mean±SD	47±12	48±12
Range	27-71	30-68
P value		>0.1
Gender		
Male	11(73%)	16(73%)
Female	4(27%)	6(27%)
P value		>0.1

All statistical comparisons were with index cancer of MC by independent *t*-test or χ^2 -test.

DISCUSSION

MPCC is not uncommon in clinic. The estimated incidence rates

of SC and MC were 2.0-8.1% and 0.6-10.6% respectively^[3-10]. Such a significantly different result of these series may be due to several reasons. For example, the definition varied to allow diagnosis of a second carcinoma at a range of 6 mo to 3 years after the diagnosis of the index tumor. The patient number, observation period and follow-up time all could influence the final results. Bulow *et al.*^[9] followed up 501 patients younger than 40 years old with colorectal carcinoma for up to 41 years. In the first 10 years, only 12 cases developed MC. Since then, another 32 patients had developed MC in succession. Cali *et al.*^[1] reported that the calculated incidence for MC was 0.35 percent per year and the cumulative incidence at 18 years was 6.3 percent according to a group of 5 476 patients. In another larger group of 141 945 patients with histologically confirmed primary colorectal tumors within 14 years (mean follow-up of 4.72 years), 3 402(2.4%) and 1 526(1.1%) cases were diagnosed with SC and MC respectively^[8]. In our study, the incidence of MPCC was 2.74%(37/1348). The reported data showed that the occurrence of MPCC had a rising trend^[11].

Chen *et al.*^[12] reported that there was no difference in age of patients with SC, MC and single colorectal carcinoma. Oya *et al.*^[13] found the index lesions of synchronous cases did not differ from single lesions in age, size, differentiation, and location. However the male: female ratio was higher and distant metastasis was more frequent in synchronous cases than in single cases. Welch^[14] found that patients with synchronous tumors were older than those with single colon cancers or initial metachronous lesions. Our results showed that patients with SC or MC had similar age, gender, and location.

The time intervals between the diagnosis of index and metachronous cancers varied obviously. Kiefer *et al.* showed that early metachronous cancers (within 2 years) reached 40%^[15]. But others^[8] considered the “early” MC as an overlooked SC. The interval of MC could reach 41 years after the first tumor. Welch^[14] pointed out that the median interval between metachronous tumors was 9 years. The symptom duration was shorter before discovery of the second metachronous tumors. The occurrence of the second MC was 55% within 3 years and 41% after 8 years from index cancer resection in our series. The longest was 20 years. Therefore, early follow-up examination (within 3 years) was very important.

Table 2 Location, types, and survival rate in two groups

	MC			SC
	Index cancer	2nd cancer	3rd cancer	
No. of tumors	22	22	5	30
Location				
Right colon	9(41%)	7(32%)	2(40%)	7(23%)
Left colon	7(32%)	8(36%)	2(40%)	15(50%)
Rectum	6(27%)	7(32%)	1(20%)	8(27%)
P value		>0.1	>0.1	>0.1
Types				
AC	20(91%)	19(86%)	3(60%)	18(64%)
Mucoid AC	2(9)	1(5)		7(25)
Canceration (Adenoma/Polypus)		1(5%)	2(40%)	3(11%)
Ring cell C		1(5)		
P value		>0.1	<0.01	>0.05
Survival Rate				
5-yr	71%(15/21)	39%(7/18)		73%(8/11)
10-yr	53%(10/19)	19%(3/16)		63%(5/8)
P value				>0.1

A: Adenoid; C: Carcinoma. All statistical comparisons were with index cancer of MC by independent *t*-test or χ^2 -test.

The preoperative detection of SC not only can allow an appropriate surgical strategy to be carried out but also establish a logical policy for follow-up. It is stressed that a second tumor may present in large intestine during follow-up. Barium enema and/or colonoscopy should be given to patients in time. Examinations such as B-ultrasound, CT scan, CEA, fecal occult blood and fecal occult albumin may help to improve diagnosis, especially SC preoperatively. CEA, fecal occult blood and fecal occult albumin test were also used to detect the early stage colorectal cancer during mass screening for asymptomatic or follow-up for high risk populations^[16]. However, many results were still unsatisfactory^[5,12,17]. Finan *et al.*^[5] diagnosed only 42% of 59 SC patients preoperatively. Chen *et al.*^[12] reported that 66%(31/47) of SC were omitted during preoperative barium enema (46 patients) and/or colonoscopy (7 patients). But other report^[18] showed that the sensitivity of colonoscopy reached 76.7%(56/73) for detecting SC and 82%(14/17) of missed lesions were smaller than 1 cm polyps. In our group, although preoperative diagnostic rate of SC reached 87%, but 85% were Dukes C or D. The reason why multiple lesions could not be identified preoperatively was that the occluded distal lesions made it difficult to detect the proximal lesions. Therefore, we could not be satisfactory for diagnosis of one colorectal cancer and should examine the whole large bowel carefully pre- or postoperatively.

It is important to palpate the whole colon and to check pathological specimens carefully before the end of operation so that misdiagnosis of SC can be avoided. Even now, misdiagnosis is still existed. Chen's report^[12] showed that there were still 13 patients without detection of SC by operative palpation in the 31 preoperative undiagnosed cases. Intraoperative colonoscopy should be advised if necessary. We think that this technique should not be used as a routine one and could be performed early (within 6 mo) after surgery.

It is an effective measure to follow up with barium enema or colonoscopy periodically for diagnosing MC earlier. A previous report^[9] showed that surveillance colonoscopy once every three years after surgery, together with a fecal occult blood test, would be an efficient and appropriate way to detect MC. Some nonfamilial colorectal cancers have been reported to have microsatellite instability (MSI)^[19-23]. A research^[19] indicated the incidence of MC in MSI-positive group was significantly higher than that in MSI-negative. Logical analysis showed that MSI and coexistence of adenoma were significantly independent risk factors for the occurrence of MC. Studies^[20,21] showed the analysis of MSI and testing for replication errors at microsatellite loci in tumors might be helpful in predicting the development of MC in sporadic carcinomas of the distal colon and rectum. Others^[10,24] discovered the significant risk factor for developing MC was the presence of synchronous adenoma or carcinoma at the initial operation and the subsequent development of recurring metachronous adenomas. Therefore, colorectal cancer patients with MSI-positive and coexistence of adenoma should be given more rigorous surveillance. Togashi^[25] monitored 341 colorectal cancer cases with colonoscopy about 4.6 times in 6.2 years after operation. Twenty-two MCs were detected in 19 cases (5.6%), of these 17 MCs (77%) were less than 1 cm, 14 MCs (64%) occurred within 5 years and 71%(10/14) were early stage cancers. In our study, 12 MCs (55%) were diagnosed in 3 years, 3 MCs were discovered by routine colonoscopy (Dukes A: 2 patients, Dukes B: 1 case) and 9 MCs were diagnosed after the development of symptoms (Dukes B, C, D: 3, 2, 4 respectively). These results might prove that colonoscopy was important after surgery. We suggest that regular postoperative colonoscopic examinations should be performed annually during the first 5 years, then once every 3 years.

The treatment of SC or MC is the same as single colorectal carcinoma, with removal of enough intestines and cleaning of

local lymph node. It is suggested that subtotal colectomy with rectoileostomy should be performed for patients with far apart SC, combined with multiple adenomatoid polyps or a familial hereditary history if their general condition suits for operation. Fajobi *et al.*^[7] recommended that SC in different lymph drainage areas seemed a justifiable indication for subtotal colectomy. Easson *et al.*^[26] considered multiple colon cancer was an important factor for performing subtotal colectomy. While subtotal colectomy could eliminate the need for colonoscopic surveillance, however examining the rectum is still required.

Generally speaking, MPCC develops slowly and their prognosis is acceptable. Chen^[12] reported that the 5-year survivals of patients after radical resection for MPCC did not differ from that of patients with single colorectal cancer. The incidence rate was 54%, 60%, and 62% for "single", SC, MC respectively. Other reports^[8,27] displayed similar conclusions. Adloff^[3] found patients with SC or single lesions had similar 5-year survival, even when classified by Dukes' stage. Rennert *et al.*^[8] reported that survival time of patients with the second tumor in the rectum was shorter than that of a single tumor in the same stage and site. Only the stage of the second tumor was found to influence survival time of patients with metachronous tumors. Welch's result^[14] was quite worse. The overall uncorrected 5-year survival rate of MPCC was only 21 percent. In our study, there was no significant difference between SC and index cancer of MC in the 5-year or 10-year survival rate. The 5-year survival rate could reach 39% after second cancer resection. We consider early diagnosis with complete preoperative examination; careful intraoperative exploration and periodic postoperative surveillance and radical resection can increase the survival time of patients with MPCC.

REFERENCES

- 1 **Cali RL**, Pitsch RM, Thorson AG, Watson P, Tapia P, Blatchford GJ, Christensen MA. Cumulative incidence of metachronous colorectal cancer. *Dis Colon Rectum* 1993; **36**: 388-393
- 2 **Moortal CG**, Barga JA, Dockerty MB. Multiple carcinomas of the large intestine a review of the literature and a study of 261 cases. *Gastroenterology* 1958; **34**: 85-98
- 3 **Adloff M**, Arnaud JP, Bergamaschi R, Schloegel M. Synchronous carcinoma of the colon and rectum: prognostic and therapeutic implications. *Am J Surg* 1989; **157**: 299-302
- 4 **Lasser A**. Synchronous primary adenocarcinomas of the colon and rectum. *Dis Colon Rectum* 1978; **21**: 20-22
- 5 **Finan PJ**, Ritchie JK, Hawley PR. Synchronous and 'early' metachronous carcinomas of the colon and rectum. *Br J Surg* 1987; **74**: 945-947
- 6 **Cunliffe WJ**, Hasleton PS, Tweedle DE, Schofield PF. Incidence of synchronous and metachronous colorectal carcinoma. *Br J Surg* 1984; **71**: 941-943
- 7 **Fajobi O**, Yiu CY, Sen-Gupta SB, Boulos PB. Metachronous colorectal cancers. *Br J Surg* 1998; **85**: 897-901
- 8 **Rennert G**, Robinson E, Rennert HS, Neugut AI. Clinical characteristics of metachronous colorectal tumors. *Int J Cancer* 1995; **60**: 743-747
- 9 **Bulow S**, Svendsen LB, Mellemggaard A. Metachronous colorectal carcinoma. *Br J Surg* 1990; **77**: 502-505
- 10 **Yamazaki T**, Takii Y, Okamoto H, Sakai Y, Hatakeyama K. What is the risk factor for Metachronous colorectal carcinoma? *Dis Colon Rectum* 1997; **40**: 935-938
- 11 **Levin B**. "Multiple primary carcinomas of the large intestine" - 50 years later. *Cancer* 1998; **83**: 2425-2426
- 12 **Chen HS**, Sheen-Chen SM. Synchronous and "early" metachronous colorectal adenocarcinoma: analysis of prognosis and current trends. *Dis Colon Rectum* 2000; **43**: 1093-1099
- 13 **Oya M**, Takahashi S, Okuyama T, Yamaguchi M, Ueda Y. Synchronous colorectal carcinoma: clinico-pathological features and prognosis. *Jpn J Clin Oncol* 2003; **33**: 38-43
- 14 **Welch JP**. Multiple colorectal tumors. An appraisal of natural history and therapeutic options. *Am J Surg* 1981; **142**: 274-280

- 15 **Kiefer PJ**, Thorson AG, Christensen MA. Metachronous colorectal cancer. Time interval to presentation of a metachronous cancer. *Dis Colon Rectum* 1986; **29**: 378-382
- 16 **Zhang YL**, Zhang ZS, Wu BP, Zhou DY. Early diagnosis for colorectal cancer in China. *World J Gastroenterol* 2002; **8**: 21-25
- 17 **Tate JJ**, Rawlinson J, Royle GT, Brunton FJ, Taylor I. Pre-operative or postoperative colonic examination for synchronous lesions in colorectal cancer. *Br J Surg* 1988; **75**: 1016-1018
- 18 **Postic G**, Lewin D, Bickerstaff C, Wallace MB. Colonoscopic miss rates determined by direct comparison of colonoscopy with colon resection specimens. *Am J Gastroenterol* 2002; **97**: 3182-3185
- 19 **Shitoh K**, Konishi F, Miyakura Y, Togashi K, Okamoto T, Nagai H. Microsatellite instability as a marker in predicting metachronous multiple colorectal carcinomas after surgery: a cohort-like study. *Dis Colon Rectum* 2002; **45**: 329-333
- 20 **Masubuchi S**, Konishi F, Togashi K, Okamoto T, Senba S, Shitoh K, Kashiwagi H, Kanazawa K, Tsukamoto T. The significance of microsatellite instability in predicting the development of metachronous multiple colorectal carcinomas in patients with nonfamilial colorectal carcinoma. *Cancer* 1999; **85**: 1917-1924
- 21 **Horii A**, Han HJ, Shimada M, Yanagisawa A, Kato Y, Ohta H, Yasui W, Tahara E, Nakamura Y. Frequent replication errors at microsatellite loci in tumors of patients with multiple primary cancers. *Cancer Res* 1994; **54**: 3373-3375
- 22 **Thibodeau SN**, Bren G, Schaid D. Microsatellite instability in cancer of the proximal colon. *Science* 1993; **260**: 816-819
- 23 **Ionov Y**, Peinado MA, Malkhosyan S, Shibata D, Perucho M. Ubiquitous somatic mutations in simple repeated sequences reveal a new mechanism for colonic carcinogenesis. *Nature* 1993; **363**: 558-561
- 24 **Chen F**, Stuart M. Colonoscopic follow-up of colorectal carcinoma. *Dis Colon Rectum* 1994; **37**: 568-572
- 25 **Togashi K**, Konishi F, Ozawa A, Sato T, Shito K, Kashiwagi H, Okada M, Nagai H. Predictive factors for detecting colorectal carcinomas in surveillance colonoscopy after colorectal cancer surgery. *Dis Colon Rectum* 2000; **43**(10 Suppl): S47-53
- 26 **Easson AM**, Cotterchio M, Crosby JA, Sutherland H, Dale D, Aronson M, Holowaty E, Gallinger S. A population-based study of the extent of surgical resection of potentially curable colon cancer. *Ann Surg Oncol* 2002; **9**: 380-387
- 27 **Kaibara N**, Koga S, Jinnai D. Synchronous and metachronous malignancies of the colon and rectum in Japan with special reference to a coexisting early cancer. *Cancer* 1984; **54**: 1870-1874

Edited by Wang XL Proofread by Chen WW and Xu FM

Inhibition of growth and metastasis of human gastric cancer implanted in nude mice by *d*-limonene

Xiao-Guang Lu, Li-Bin Zhan, Bing-An Feng, Ming-Yang Qu, Li-Hua Yu, Ji-Hong Xie

Xiao-Guang Lu, Department of General Surgery, The Fourth Affiliated Hospital of Dalian Medical University, Dalian 116001, Liaoning Province, China

Li-Bin Zhan, Bing-An Feng, Ming-Yang Qu, Li-Hua Yu, Dalian Medical University Molecular Biological Laboratory for Chinese Traditional Medicine, Dalian 116027, Liaoning Province, China

Ji-Hong Xie, Dalian Medical Science Institute, Dalian 116001, Liaoning Province, China

Correspondence to: Dr. Xiao-Guang Lu, M.D. Department of General Surgery, Fourth Hospital of Dalian Medical University, Dalian 116001, Liaoning Province, China. dllxg@yahoo.com.cn

Telephone: +86-411-3039179 **Fax:** +86-411-4721582

Received: 2004-02-02 **Accepted:** 2004-02-21

Abstract

AIM: To investigate the effects and mechanism of *d*-limonene on the growth and metastasis of gastric cancer *in vivo*.

METHODS: Metastatic model simulating human gastric cancer was established by orthotopic implantation of histologically intact human tumor tissue into gastric wall of nude mice. One percent *d*-limonene was orally administered at dose of 15 ml/kg every other day for seven weeks. Eight weeks after implantation, tumor weight, inhibition rate, apoptotic index (AI), microvessel density (MVD), vascular endothelial growth factor (VEGF), variation of ultrastructure, and the presence of metastasis were evaluated, respectively, after the mice were sacrificed.

RESULTS: The tumor weight was significantly reduced in 5-FU group (2.55±0.28 g), *d*-limonene group (1.49±0.09 g) and combined treatment group (1.48±0.21 g) compared with the control group (2.73±0.23 g, $P < 0.05$). In 5-FU group, *d*-limonene group, combined treatment group, the inhibition rates were 2.60%, 47.58% and 46.84% and 0, respectively; AI was (3.31±0.33)%, (8.26±1.21)%, (20.99±1.84)% and (19.34±2.19)%, respectively; MVD was (8.64±2.81), (16.77±1.39), (5.32±4.26) and (5.86±2.27), respectively; VEGF expression was (45.77±4.79), (41.34±5.41), (29.71±8.92) and (28.24±8.55), respectively. The incidences of peritoneal metastasis also decreased significantly in 5-FU group (77.8%), *d*-limonene group (20.0%) and combined group (22.2%) compared with control group (100%) versus 62.5%, 30% and 22.2% ($P < 0.05$). Liver metastasis was also inhibited and the incidences decreased significantly in 5-FU group, *d*-limonene group and combined group than that in control group (87.5% vs 55.5%, 20.0% and 22.2% respectively) ($P < 0.05$). The incidence of ascites in control group, 5-FU group, *d*-limonene group and combined group was 25.0%, 22.2%, 0, 0, respectively and 12.5%, 11.1% 0, 0, with respect to the metastasis rate to other organs.

CONCLUSION: *d*-limonene has antiangiogenic and proapoptotic effects on gastric cancer, thereby inhibits tumor growth and metastasis. Combination of *d*-limonene with cytotoxic agents may be more effective.

Lu XG, Zhan LB, Feng BA, Qu MY, Yu LH, Xie JH. Inhibition of growth and metastasis of human gastric cancer implanted in nude mice by *d*-limonene. *World J Gastroenterol* 2004; 10 (14): 2140-2144

<http://www.wjgnet.com/1007-9327/10/2140.asp>

INTRODUCTION

d-limonene is a monoterpene compound. In recent years, it was used for prevention and cure of various animal tumor models induced by chemical carcinogen and was proved to have anti-cancer activities^[1-7]. Our previous study also suggested that *d*-limonene can inhibit the growth of human gastric cancer cell *in vitro* through a mechanism of inducing the apoptosis of tumor cells^[8]. To make a further understanding of the anti-cancer effects and mechanism of *d*-limonene *in vivo*, an orthotopic transplantation model of gastric cancer in nude mice was employed. The *d*-limonene emulsion was administered to investigate its inhibition effects on the growth and metastasis of gastric cancer dynamically, which will be the theoretical basis for the clinical application of *d*-limonene.

MATERIALS AND METHODS

Materials

Experimental animals Forty male BALB/c nu/nu nude mice, purchased from Chinese Medical University, were raised under the SPF (specific pathogen free) condition for a week to adapt the surroundings before the initiation of the experiment.

Tumor tissues Gastric cancer cell line BGC-823 was obtained from Cell Research Institute (Shanghai, China). A 0.2 mL of cell suspension (2×10^6 cells) was subcutaneously injected into the anterior axilla of nude mice to form the entity of cancer. When the tumor grew to a diameter of 2-2.5 cm, the mouse was sacrificed to dissect the neoplasm and the capsule of tumor was removed and kept in saline containing 100 U/mL penicillin, 100 U/mL streptomycin (pH 7.2). Pieces of fresh tumor tissue (1 mm³) near the margin were inoculated to another mouse by puncture method. The above procedure was repeated for 5 times and the last generation of the tumor tissue was used for orthotopic transplantation.

Animal model Before transplantation, mice bearing tumor were killed. Then the tumor was dissected and put into saline containing penicillin (100 U/mL) and streptomycin (100 U/mL) aseptically. Pieces of intact, fish-meat-like tumor tissue of 3 mm³ in diameter from margin were prepared after the removing of tumor capsule. Mice anesthetized by the thialisobumalnatium (40 mg/kg) injected into abdominal cavity were sterilized with caseiodine on skin of abdomen and a transverse incision was made in left upper quadrant. After the exposure of greater curvature of stomach, the serosa and muscular layer were incised. Then, tumor tissues were transplanted under serosa of stomach by means of suture and embedding. Stomach was brought into abdominal cavity; the incision in belly was sutured delaminatedly. The whole operation procedure followed the doctrine of aseptic manipulation.

Drugs and groups *d*-limonene with 97% purity (product

number: 183164) was purchased from Sigma Company (USA). It was prepared as 10 g/L lecithin emulsion by Dalian Medical Science Institute. Mice were randomly divided into 4 groups: control group, 5-FU group, *d*-limonene group, and *d*-limonene+5-FU group and administrated with saline (0.3 mL/d, gastric perfusion), 5-FU (30 mg/kg/d, intraabdominal injection), *D*-limonene (15 mL/kg/d, gastric perfusion), and 5-FU (30 mg/kg/d, intraabdominal injection)+ *d*-limonene (15 ml/kg.d, gastric perfusion), respectively for 7 wk. The body mass and abdominal circumstances were measured on the 7th, 14th, 21st, 28th, 35th, 42nd, 49th d after transplantation and the status of eating, drinking and defecation of mice were recorded. The dying mice were executed and necropsy was performed. In the 8th wk, all the mice were killed; the neoplasm was resected and weighted; and the occurrence of distant metastasis and ascites were examined.

Methods

The measurement of tumor weight and inhibition rate of tumor growth Mice were killed by dislocation of cervical vertebra, the tumor weight was measured and the tumor inhibition rate was calculated. inhibition rate=[(tumor weight of control group-tumor weigh of treated groups)/weight of control]×100%.

The occurrence of metastasis and ascites in nude mice The metastasis of gastric cancer was examined in abdominal cavity, peritoneum and liver. Tumor specimens were fixed in neutral formaldehyde, dehydrated by dimethylbenzene and embedded in paraffin for the hematoxylin and eosin (HE) staining and immunohistochemistry. The characters and volume of ascites were recorded.

Apoptotic index (AI) TUNEL method was used to detect the apoptosis of tumor cell. The sections were fixed and embedded as usual. TUNEL test kit was purchased from Roche Company. DNase I (1 mg/mL) was used to digesting the positive control specimen for 10 min before being put into TUNEL response mixture. Only label liquor was added into the negative control response mixture. Cells with brown or yellow nuclei were assumed as apoptotic cells. the number of apoptotic cells and total cancer cells were counted under light microscope at 400×magnification in 5 fields of vision and the average values were used for the calculation of apoptosis index (AI) according to the following formula: AI=(apoptotic cells/total cancer cells) ×100%.

Microvessel density assay The polyclonal antibody for factor \square -related antigen (F \square -Rag, Santa Cruz Biotechnology, Inc, USA) was selected to detect the microvessel density in paraffin embedded tumor sections by immunohistochemical method according to the manufacturer's instruction. Result determination: Sections were screened at 40× magnification under a light microscope to identify three regions with the highest MVD. Then, blood vessels stained brown by antibody for F \square -Rag was counted at 200×magnification. For the determination of microvessels, first of all, the hemorrhage area and marginal region were eliminated. Those brown-stained endothelial cells or cell cluster that had interspaces with microvessel, cancer cells and connective tissue were regarded as a micro vessels. The average value of the three regions was regarded as MVD.

Immunohistochemical assay of VEGF Immunohistochemical staining was performed with mouse monoclonal antibody specific for human VEGF (C1, Santa Cruz Biotechnology, Inc, USA) in a dilution of 1:100 according to SP method specification. The presence of brown or yellow granules in plasma or nucleus was regarded as positive staining for VEGF protein expression. The sum of positive cells number was calculated in five fields per slide at 200×magnification under light microscope. Results were ratified by fluorescence microscope and colorful microscopic figure analysis system (OLYMPUS BX51TR, Image-Pro Plus, Analysis Software).

Statistical analysis

Tumor weight, AI, MVD and VEGF were expressed as the mean±SD. Comparison between groups was performed using analysis of variance; Differences of the metastasis in peritoneum, liver and other organs and the occurrence of ascites were examined by χ^2 test ($P<0.05$ was considered statistically significant).

RESULTS

The influence of *d*-limonene on the general condition of tumor-bearing mice

At the end of the 7th wk, two mice-bearing tumor from control group, one from 5-FU group and one from combined group died of exhaustion while none from *d*-limonene group. During the whole process of the experiment, only one mouse in 5-FU group was found with loose stools, and no passage of bloody stools was found in any groups. Compared with the control and 5-FU group in which mice were found emaciation, inactive and lassitude, mice in *d*-limonene group and combined group had better appetite and increased body mass although statistically had no difference.

Influence of *d*-limonene on orthotopic transplanted tumor weight and tumor inhibition rate

At necropsy, xenografts of gastric cancer were found in each groups of nude mice. The transplanted tumor entity was pink in color, ellipse or round in shape, with nodosity in surface and necrosis in central parts, and was confirmed as adenocarcinoma by pathological section. Compared with the control group, the tumor weight of mice in *d*-limonene group and combined group were decreased significantly ($P<0.05$). Moreover, the inhibition effects of *d*-limonene or the combined effects of *d*-limonene and 5-FU on the growth of gastric cancer were more significant than that of 5-FU (Table 1).

Effects of *d*-limonene on tumor cell morphology and ultrastructure

Morphologically, tumor cells in the control group were bigger, ellipse, with red plasma and big, deep stained nuclei. A clear imbalance ratio of nucleus to plasma was found also. No significant difference was observed between the control and 5-FU group. While in *d*-limonene group and combined group, relatively small tumor cells with vacuoles in plasma and clouding nucleus were observed in which the ratio of nucleus to plasma was relatively normal.

Table 1 Inhibition effects of *d*-limonene on growth of orthotopic transplanted gastric tumor (mean±SD)

Groups	<i>n</i>	Tumor mass (g)	Inhibition rate (%)	AI (%)	MVD (<i>n</i>)	VEGF(%)
Control	8	2.69±0.32	0	3.31±1.44	18.64±2.81	45.77±4.79
5-FU	9	2.62±0.35	2.60	8.26±1.21 ^a	16.77±1.39	41.34±5.41
<i>d</i> -limonene	10	1.41±0.58 ^{ac}	47.58 ^{ac}	20.99±2.84 ^{ac}	5.32±4.26 ^{ac}	29.71±8.92 ^{ac}
Combined	9	1.43±0.51 ^{ad}	46.84 ^{ac}	19.34±3.19 ^{ac}	5.86±2.27 ^{ac}	28.24±8.55 ^{ac}

^a $P<0.05$ vs control group; ^c $P<0.05$ vs 5-FU group.

The major morphological changes of cancer cells in D-limonene and combined group were the shrinkage of cell, the condensation of cytoplasm, the aggregation of ribosome and mitochondrion, the occurrence of nuclear fragmentation, the peripheral masses of condensed chromatin. Apoptotic bodies derived from the shedding of condensed masses were found to be degraded by surrounding phagocytes and formed vacuoles in cytoplasm. Fusiform shape, morphological irregular and karyomegaly cancer cells were observed in control and 5-FU group with tight binding between cells, imbalance ratio of nucleus to plasma and the maldistribution of chromatin. But no obviously changes in cell morphology were detected.

Effects of d-limonene on apoptosis of cancer cell

Results of TUNEL demonstrated that apoptotic cells with yellow nucleus were seen occasionally in control group and 5-FU group while piles of apoptotic cells were observed in *d*-limonene and combined group. There was a significantly difference in AI in *d*-limonene and combined group compared to the control and 5-FU group ($P < 0.05$) (Table 1, Figures 1-4).

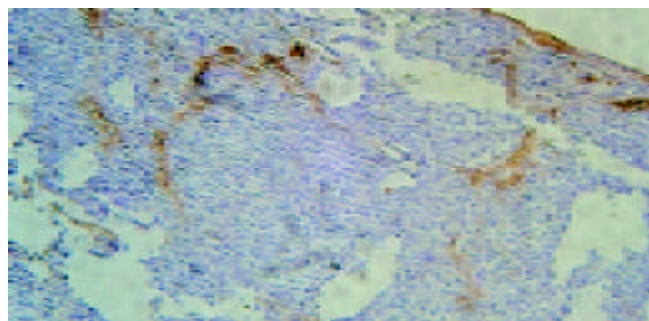


Figure 1 Control group FVIII-RAG with SP method. $\times 100$.

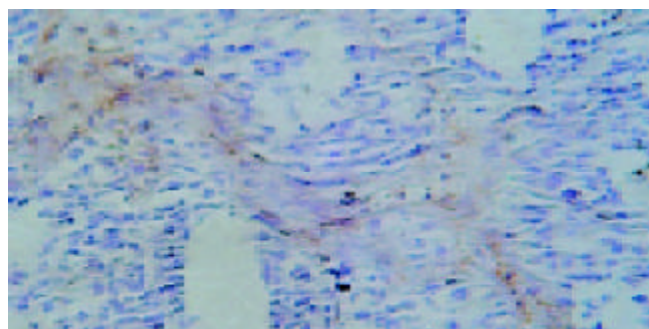


Figure 2 5-FU group FVIII-RAG with SP method. $\times 200$.

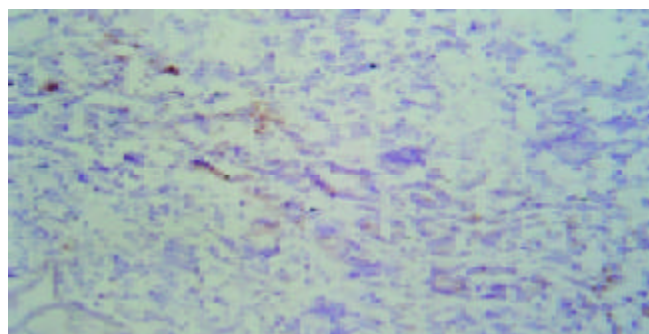


Figure 3 *d*-limonene group FVIII-RAG with SP method. $\times 100$.

The influence of d-limonene on MVD of orthotopic transplanted tumor

Under light microscope, the intensive brown-staining

microvessels on stomach wall was observed without integrated basement membrane in the control group. Compared with the control and 5-FU group, almost no microvessels was found in the tumor of *d*-limonene and combined group for the cancer cells were in dormancy status, and the MVD of those two groups was statistically lower than that of the control and 5-FU group (Table 1, Figures 5-8).

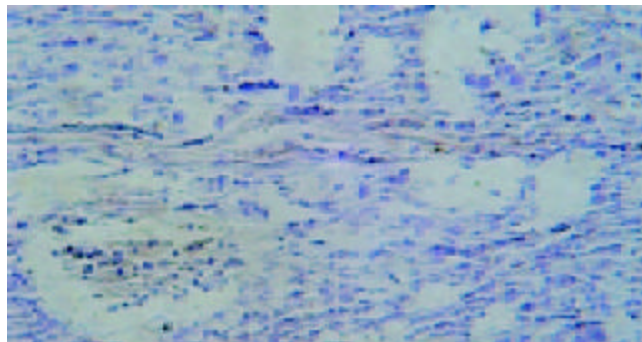


Figure 4 Combined group FVIII-RAG with SP method. $\times 100$.

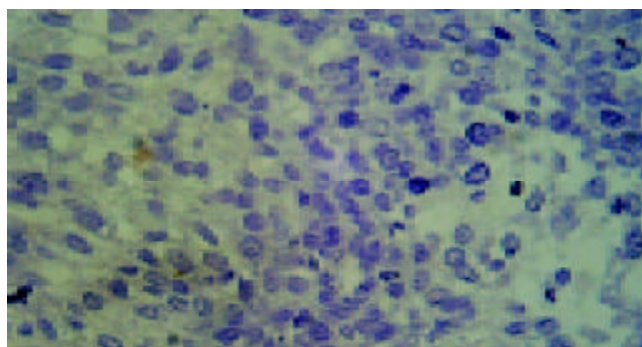


Figure 5 Control group TUNEL. $\times 400$.

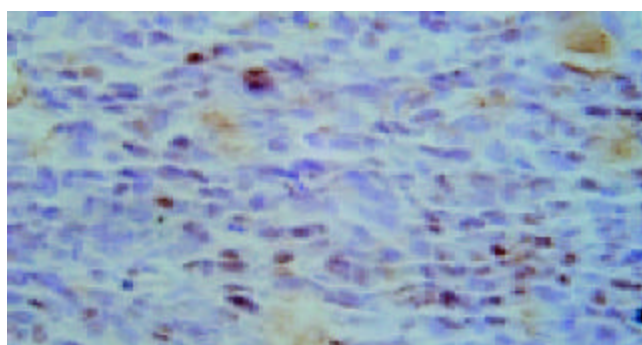


Figure 6 5-FU group TUNEL. $\times 400$.

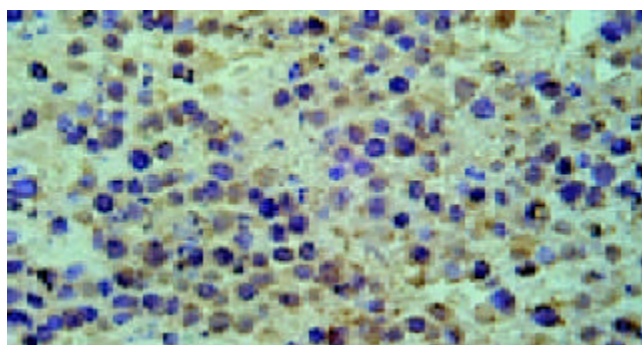


Figure 7 *d*-limonene group TUNEL. $\times 400$.

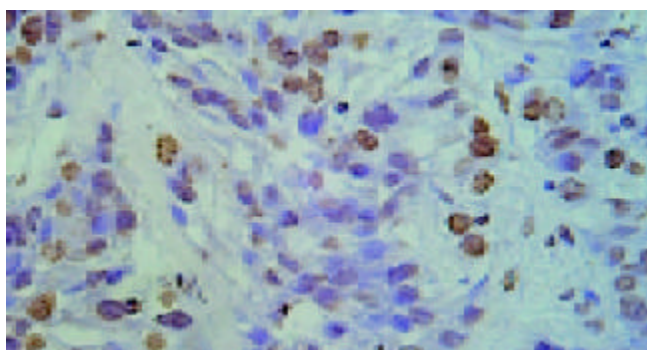


Figure 8 Combined group TUNEL. $\times 400$.

Inhibitory effects of d-limonene on metastasis of gastric cancer

The metastasis rate of gastric cancer to peritoneum (regional lymph node) was to 100% in the control group and the metastasis rates in other groups are displayed in Table 2. the metastasis to liver, peritoneum and other organs of gastric cancer and the formation of ascites were significantly inhibited in *d*-limonene and combined groups ($P < 0.05$) while no statistical inhibitory effects on the metastasis to liver and peritoneum were observed in 5-FU group ($P > 0.05$, Table 2).

Table 2 The Inhibitory effects of *d*-limonene on orthotopic transplanted gastric cancer (%)

Group	<i>n</i>	Peritoneum metastasis	Liver metastasis	Ascites	Metastasis to other organs
Control	8	8(100.0)	7(87.5)	2(25.0)	1(12.5)
5-FU	9	7(77.8)	5(55.5)	2(22.2)	1(11.1)
<i>D</i> -limonene	10	2(20.0) ^{ac}	2(20.0) ^{ac}	0 ^{ac}	0
Combined	9	3(33.3) ^{ac}	2(22.2) ^{ac}	0 ^{ac}	0

^a $P < 0.05$ vs control group; ^c $P < 0.05$ vs 5-FU group.

DISCUSSION

Gastric cancer is the most common malignant tumor in digestive system. The cure rate of gastric cancer was increased year by year with the progress of surgical technique, chemotherapy and other means. But a five-year survival rate is still wandered below 10%, especially in middle or late phase patients^[10]. Thus, to find an effective adjuvant chemotherapy drug became the focus of gastric cancer therapy besides emphasizing surgical operation.

Limonene (1-methyl-4-isopropyl-cyclohexene) is the essential component in citrus oil. *d*-limonene, the most common isomer of limonene, is a kind of monoterpene component. It has the ability of anti-oxygenation, anti-inflammation and drainage for gallstone. The anti-cancer activity of *d*-limonene was found recently. Therefore, *d*-limonene has been applied to precaution and treatment in chemical-induced animal model, such as colon cancer, breast cancer, gastric cancer, pancreatic cancer and hepatic cancer with promising results^[1-7]. Most of those studies focus in the chemoprophylaxis of tumor. Our results demonstrated that in *d*-limonene and combined group, the tumor weight of xenograft was decreased drastically, the metastasis to liver, peritoneum and the occurrence of ascites were inhibited significantly compared with the control group. Thus, an inhibition effect of *d*-limonene on the growth and metastasis of gastric cancer cells was ratified. Taking the results of TUNEL assay into consideration, we found the main mechanism underlying the inhibition effects of *d*-limonene was to induce the apoptosis of cancer cells.

At present, it is thought that a phenotype change from no-vascular period to angiogenesis stage exists during the growth

of tumor. In no-vascular period, the velocity of cancer cells apoptosis and proliferation maintain a dynamic balance and the tumor may survive for months or even years without the presence of metastasis. But the alterations of some important factors, such as heredity cause, over-expression of proangiogenic factors originated from cancer cells or down-regulation anti-angiogenic factors expressed by body tissues or cancer cells, the switch for tumor angiogenesis thereby activating and leading to vascularization of tumor. Once the tumor vascular is formed, the growth speed of tumor will be increased and the invasive growth and metastasis will be induced.

Microvessel density (MVD), is usually used to evaluate the vascularization level of tumor^[10]. A large amount of experiments and clinical research results showed that MVD had a close relationship with the prognosis of almost all malignant tumors, a higher MVD suggested the lower differentiation and the higher reoccurrence and metastasis incidence^[11]. We demonstrated that compared with control and 5-FU group, tumor MVD in *d*-limonene and combined group was decreased significantly, suggesting a inhibitive effect of *d*-limonene on tumor angiogenesis.

Although the mechanisms involved in tumor angiogenesis have not been understood exactly, the effect of VEGF on vascularization has been conformed. VEGF, a specific mitogen for vascular endothelial cells was isolated from follicular cell plasma of cattle and considered as the most important angiogenic factor of metastatic tumor^[12-14]. The expression of VEGF was found very low in normal adult tissues. Once initiated in pathologic status of tumor, the angiogenesis was induced and promoted drastically by VEGF and resulted in the increase of MVD. Among vascular growth factors, VEGF was the only one to stimulate the proliferation of tumor endothelial cell and to induce the vascularization of tumor directly^[15]. As the newly formed vessels may provide tumor with oxygen, nutrition, the growth of tumor will be invasive and uncontrollable^[16]. It was reported that the over expression of VEGF had close relationship with tumor metastasis and poor prognosis. The invasion of blood vessels and lymph nodes has been often observed in patients with enhanced VEGF expression, which will result in the rapidly malignant change of tumor, easily relapse and short survival period after surgical operation. Here we showed that relatively high level of VEGF in the tumor of control and 5-FU group, especially in the areas around vessels, while notably decreased expression of VEGF in *d*-limonene and combined group. Thus, a positive correlation of VEGF expression with increased MVD was ratified, suggesting the anti-angiogenic mechanism of *d*-limonene via down-regulation of VEGF. Moreover, we found that the anti-cancer target of 5-FU might not on the inhibition of neovascularization.

5-fluorouracil, an antimetabolite pyrimidine, has been used as traditional chemotherapeutic drug for more than 40 years. For the anti-cancer target of 5-FU lies in the inhibition of thymidylate synthetase to prevent DNA synthesis but not the interference of tumor angiogenesis^[17], no satisfied cure effect was obtained in our experiment. As to *d*-limonene, preventing tumor angiogenesis and increasing tumor cells apoptosis are the main anti-cancer mechanisms, which may diminish the incidence of drug resistance mutation for its character of physiological cell death. The effectiveness, non-toxicity, and lower drug resistance of *d*-limonene were ratified for a better eating, activity and living ability in *d*-limonene and combined groups than in control group within the 7-wk experiment. No statistical difference in body weight was observed among four groups for increased tumor weight and the formation of ascites in control and 5-FU group.

Further studies need to elucidate the apoptotic mechanisms of *d*-limonene before its clinical application.

REFERENCES

- 1 **Uedo N**, Tatsuta M, Iishi H, Baba M, Sakai N, Yano H, Otani T. Inhibition by D-limonene of gastric carcinogenesis induced by N-methyl-N'-nitro-N-nitrosoguanidine in Wistar rats. *Cancer Lett* 1999; **137**: 131-136
- 2 **Broitman SA**, Wilkinson J 4th, Cerda S, Branch SK. Effects of monoterpenes and mevinolin on murine colon tumor CT-26 *in vitro* and its hepatic "metastases" *in vivo*. *Adv Exp Med Biol* 1996; **401**: 111-130
- 3 **Kaji I**, Tatsuta M, Iishi H, Baba M, Inoue A, Kasugai H. Inhibition by d-limonene of experimental hepatocarcinogenesis in Sprague-Dawley rats does not involve p21(ras) plasma membrane association. *Int J Cancer* 2001; **93**: 441-444
- 4 **Witschi H**, Uyeminami D, Moran D, Espiritu I. Chemoprevention of tobacco-smoke lung carcinogenesis in mice after cessation of smoke exposure. *Carcinogenesis* 2000; **21**: 977-982
- 5 **Stratton SP**, Dorr RT, Alberts DS. The state-of-the-art in chemoprevention of skin cancer. *Eur J Cancer* 2000; **36**: 1292-1297
- 6 **Guyton KZ**, Kensler TW. Prevention of liver cancer. *Curr Oncol Rep* 2002; **4**: 464-470
- 7 **Nakaizumi A**, Baba M, Uehara H, Iishi H, Tatsuta M. d-limonene inhibits N-nitrosobis (2-oxopropyl) amine induced hamster pancreatic carcinogenesis. *Cancer Lett* 1997; **117**: 99-103
- 8 **Lu XG**, Feng BA, Zhan LB, Yu ZH. D-limonene induces apoptosis of gastric cancer cells. *Zhonghua Zhongliu Zazhi* 2003; **25**: 325-327
- 9 **Sun X**, Mu R, Zhou Y, Dai X, Qiao Y, Zhang S, Huangfu X, Sun J, Li L, Lu F. 1990-1992 mortality of stomach cancer in China. *Zhonghua Zhongliu Zazhi* 2002; **24**: 4-8
- 10 **Fanelli M**, Locopo N, Gattuso D, Gasparini G. Assessment of tumor vascularization: immunohistochemical and non-invasive methods. *Int J Biol Markers* 1999; **14**: 218-231
- 11 **El-Assal ON**, Yamanoi A, Soda Y, Yamaguchi M, Igarashi M, Yamamoto A, Nabika T, Nagasue N. Clinical significance of microvessel density and vascular endothelial growth factor expression in hepatocellular carcinoma and surrounding liver: possible involvement of vascular endothelial growth factor in the angiogenesis of cirrhotic liver. *Hepatology* 1998; **27**: 1554-1562
- 12 **Seo Y**, Baba H, Fukuda T, Takashima M, Sugimachi K. High expression of vascular endothelial growth factor is associated with liver metastasis and a poor prognosis for patients with ductal pancreatic adenocarcinoma. *Cancer* 2000; **88**: 2239-2245
- 13 **Shi H**, Xu JM, Hu NZ, Xie HJ. Prognostic significance of expression of cyclooxygenase-2 and vascular endothelial growth factor in human gastric carcinoma. *World J Gastroenterol* 2003; **9**: 1421-1426
- 14 **Ren J**, Dong L, Xu CB, Pan BR. The role of KDR in the interactions between human gastric carcinoma cell and vascular endothelial cell. *World J Gastroenterol* 2002; **8**: 596-601
- 15 **Risau W**. What, if anything, is an angiogenic factor? *Cancer Metastasis Rev* 1996; **15**: 149-151
- 16 **Folkman J**. The influence of angiogenesis research on management of patients with breast cancer. *Breast Cancer Res Treat* 1995; **36**: 109-118
- 17 **Rose MG**, Farrell MP, Schmitz JC. Thymidylate synthase: a critical target for cancer chemotherapy. *Clin Colorectal Cancer* 2002; **1**: 220-229

Edited by Kumar M and Xu FM

Clinical evaluation of radiotherapy for advanced esophageal cancer after metallic stent placement

You-Tao Yu, Guang Yang, Yan Liu, Bao-Zhong Shen

You-Tao Yu, Guang Yang, Yan Liu, Bao-Zhong Shen, Department of Radiotherapy, Tumor Hospital of Harbin University, Harbin 150040, Heilongjiang Province, China

Correspondence to: Bao-Zhong Shen, Department of Radiotherapy, Tumor Hospital of Harbin University, Harbin 150040, Heilongjiang Province, China. shenbzh@hotmail.com

Telephone: +86-451-88513575 **Fax:** +86-451-86623347

Received: 2003-11-12 **Accepted:** 2004-01-08

Abstract

AIM: To evaluate the therapeutic effect of radiotherapy for esophageal cancer after expandable metallic stent placement.

METHODS: Ten cases of advanced esophageal cancer were evaluated, 7 having complete obstruction and 3 with digestive-respiratory fistula. Ten nitinol stents were placed at the site of stenosis. Patients were treated with a total dose of 1 200 cGy divided into 3 fractions of 400 cGy 4-7 d after stents placement.

RESULTS: All the 10 stents were placed successfully at one time. After radiotherapy for advanced esophageal cancer, the survival period of the cases ranged from 14 to 22 mo, with a mean survival of 17 mo. No re-stenosis occurred among all the 10 cases.

CONCLUSION: Stent placement combined with radiotherapy for esophageal cancer is helpful to prolong patients' survival and reduce occurrence of re-stenosis.

Yu YT, Yang G, Liu Y, Shen BZ. Clinical evaluation of radiotherapy for advanced esophageal cancer after metallic stent placement. *World J Gastroenterol* 2004; 10(14): 2145-2146
<http://www.wjgnet.com/1007-9327/10/2145.asp>

INTRODUCTION

Radiotherapy for esophageal cancer is a relatively effective treatment. However, esophageal obstruction and esophageal stenosis due to inoperable cancer, as serious complications of esophageal cancer, are directly life-threatening and contraindicatory to radiotherapy for esophageal cancer. Inserting membrane-covered esophageal stents as an effective conservative and palliative treatment to expand the stent at the stenosis site due to cancer and obstruct the digestive fistulas is a currently widely-used therapy, which can dramatically alleviate obstruction and enhance patients' quality of life by enabling oral ingestion in patients with obstruction due to late cancer^[1-4]. With radiotherapy after membrane-covered esophageal stents placement for advanced esophageal cancer, we successfully overcame the contraindication of radiotherapy for esophageal cancer and achieved a quite satisfactory short-term effect^[5,6].

MATERIALS AND METHODS

Materials

Ten cases of esophageal cancer (8 males, 2 females, aging from

58 to 85 years) were studied. Esophagoscopy examination indicated that 9 of the cases were squamous carcinoma and one was adenocarcinoma. Barium contrast radiography and meglucamine diatrizoate radiography showed that the site of stenosis due to cancer ranged from 6 to 12 cm in length, with an average length of 8 cm, and the width of the esophageal lumen at the site of stenosis was less than 2 mm, which had been hard for liquid diet to pass for more than 2 wk. Seven of the cases had complete obstruction and 3 had digestive-respiratory fistulas. Physical examination showed that 9 of them had no carcinomatous distant metastasis and 1 case had carcinomatous metastasis to unilateral lung.

Methods

Stent placement Stents to be placed were homemade or imported silicone-covered nitinol memory alloy mesh stents, 2 cm in diameter and 8, 10, 12 cm in length, respectively, and bell-mouthed at one or both ends. Patients should take gentamicin orally, 160 000 units each time, 4-5 times per day before the therapy and stop eating and drinking 2 h before the placement. In accordance with the stenosis length shown by esophageal radiography, the stent of proper length was selected, placed and released along the site of stenosis by endoesophageal stent introducer under the guidance of the peroral guide wires, leaving both ends of the stent surpassing 1-2 cm respectively. After replacement, patient was advised to drink adequate warm water, making the stent expand properly. One week after the placement, a reexamination was carried out through upper digestive tract fluoroscopy with barium to see how unobstructed the stent was and an X-ray plane film was taken to locate the stent, measure its length and width, fix reference point, set irradiation dose and draw the related dose curve.

Endoesophageal irradiation Irradiation was performed 4-7 d after the stent was properly placed. First, the balloon catheter was inserted to the site of the lesion. Second, air was pumped into the sacculae to expand it and fix it inside the stent. Third, the location of the sacculae was confirmed through fluoroscopy and spot film. And finally, irradiation was performed according to the mark of the reference point fixed through measurement with the total dose of 1 200 cGy divided into three 400 cGy doses.

RESULTS

In all the 10 cases, the stents were all placed successfully once and fixed properly. Of all the 10 stents, 7 (four 8 cm, two 10 cm and one 12 cm in length) were homemade and 3 (two 10 cm and one 8 cm in length) were imported and all could expand properly, through which contrast medium could pass smoothly after placement. Esophageal fistulas in three cases were obstructed immediately after insertion and the patients could begin to take semiliquid diet 4 h afterwards. Reexaminations were performed through radiography 4 d after insertion, and it indicated that the contrast medium could go through the stents smoothly, that the stents did not displace and the esophageal fistulas were obstructed. So, patients could take food normally without dysphagia. After stents placement, 3 cases had retrosternal

foreign body sensation and retrosternal pain, which disappeared within 4-6 d. After endoesophageal radiotherapy, the survival period of the cases ranged from 14 to 22 mo, with a mean survival period of 17 mo. Of all the 10 cases, no endogenous stenosis recurred during the survival period.

DISCUSSION

Radiotherapy for esophageal cancer after esophageal stent placement effectively solved this contraindication of endoesophageal therapy and the problem of stenosis recurrence after stent placement. Esophageal stent insertion enhanced the life quality of patients with advanced esophageal cancer in a quick and effective way in that it remarkably improved the patients' nutrition absorption and constitution by enabling them to take food orally and it completely eliminated the symptoms such as coughing while eating or drinking by effectively obstructing the digestive-respiratory fistulas, which also alleviated the patients' psychological pressure and greatly comforted them. It enlarged the indication scope of radiotherapy for esophageal cancer by turning the former contraindication into indication. The stent inserted expanded the stenosis site and made it possible for brachytherapeutic treatment and radioactive source to pass easily and eventually dramatically prolonged the patients' survival period^[7,9-18]. No stenosis recurred in the 10 cases under our treatment during their survival period, which, in contrast to the 5% stenosis reoccurrence rate in other patients under our treatment who had stents placement without radiotherapy, marked a great decrease in occurrence of re-stenosis^[8]. Radiotherapy for esophageal cancer prevented the stents from being obstructed by the overgrowth of tumor, alleviated the patients' sufferings and raised their life quality. After the stents were properly placed, radiography was performed and film was spotted, through which the width of the stents expansion was measured. According to the width after calculation, the esophagus was expanded by the stents, the diameter of the balloon catheter and the reference point were fixed, and the optimal internal irradiation dose curve was designed. A comparison of the dose curves indicated that, after the expansion of the stents, the irradiation dosage over the esophageal mucosa was decreased, with the dose gradient homogeneous and small, which prevented the esophageal mucosa from being unnecessarily harmed while effectively inhibited the overgrowth of esophageal mucosa and the surface tumor, and insured the pathological center to receive therapeutic dose of irradiation. Experiments showed that the refraction and diffraction of the irradiation ray against the metallic stents could be neglected when the radioactive source was more than 5 mm away from the metallic stents. Our results of the clinical research seem to indicate that radiotherapy for esophageal cancer after esophageal stents placement is very helpful in treatment of advanced esophageal cancer.

REFERENCES

1 **Knyrim K**, Wagner HJ, Bethge N. A controlled trial of an expansile metal stent for palliation of esophageal obstruction

- due to inoperable cancer. *N Eng J Med* 1993; **329**: 1302-1303
- 2 **Nelson DB**, Axelrad AM, Fleischer DE, Koazarek RA, Silvis SE. Silicone-covered wallstent prototypes for palliation of malignant esophageal obstruction and digestive-respiratory fistulas. *Gastrointest Endosc* 1997; **45**: 31-37
- 3 **Decker P**, Lippler J, Decker D, Hirner A. Use of the Polyflex stent in the palliative therapy of esophageal carcinoma: results in 14 cases and review of the literature. *Surg Endosc* 2001; **15**: 1444-1447
- 4 **Morgan R**, Adam A. The radiologist's view of expandable metallic stents for malignant esophageal obstruction. *Gastrointest Endosc Clin N Am* 1999; **9**: 431-435
- 5 **Zhong J**, Wu Y, Xu Z, Liu X, Xu B, Zhai Z. Treatment of medium and late stage esophageal carcinoma with combined endoscopic metal stenting and radiotherapy. *Chin Med J* 2003; **116**: 24-28
- 6 **Funami Y**, Tokumoto N, Miyauchi H, Kuga K, Sato S. Improvement of oral ingestion in patients with inoperable esophageal cancer treated with radiotherapy, chemotherapy and insertion of a self-expanding nitinol stent. *Dis Esophagus* 1999; **12**: 289-292
- 7 **Bethge N**, Sommer A, Vakil N. Treatment of esophageal fistulas, with a new polyurethane-covered, self-expanding mesh stent: A prospective study. *Am J Gastroenterol* 1995; **90**: 2143-2146
- 8 **Schoefl R**, Winkelbauer F, Haefner M, Poetzi R, Gangl A, Lammer J. Two cases of fractured esophageal nitinol stents. *Endoscopy* 1996; **28**: 518-520
- 9 **Olsen E**, Thyregaard R, Kill J. Esophageal expanding stent in the management of patients with nonresectable malignant esophageal of cardiac neoplasm: a prospective study. *Endoscopy* 2001; **1**: 3-6
- 10 **Williamson JF**, Li Z. Monte Carlo aided dosimetry of the microelectron pulsed and high dose-rate ¹⁹²Ir sources. *Med Phys* 1995; **22**: 809-819
- 11 **Ciesielski B**, Reinstein LE, Wielopolski L, Meek A. Dose enhancement in buildup region by lead, aluminum and Lucite absorbers for 15 MV photon beam. *Med Phys* 1989; **16**: 609-613
- 12 **Kawrakow I**. Accurate condensed history Monte Carlo simulation of electron transport. I. EGSnrc, the new EGS4 version. *Med Phys* 2000; **27**: 485-498
- 13 **Knyrim K**, Wagner HJ, Bethge N, Keymling M, Vakil N. A controlled trial of an expansile metal stent for palliation of esophageal obstruction due to inoperable cancer. *N Engl J Med* 1993; **329**: 1302-1307
- 14 **Mayoral W**, Fleischer D, Salcedo J, Roy P, Al-Kawas F, Benjamin S. Nonmalignant obstruction is a common problem with metal stents in the treatment of esophageal cancer. *Gastrointest Endosc* 2000; **51**: 556-559
- 15 **Wang MQ**, Sze DY, Wang ZP, Wang ZQ, Gao YA, Dake MD. Delayed complications after esophageal stent placement for treatment of malignant esophageal obstructions and esophagorespiratory fistulas. *J Vasc Interv Radiol* 2001; **12**: 465-474
- 16 **Davies N**, Thomas HG, Eyre-Brook IA. Palliation of dysphagia from inoperable oesophageal carcinoma using Atkinson tubes or self-expanding metal stents. *Ann R Coll Surg Engl* 1998; **80**: 394-397
- 17 **Conio M**, Caroli-Bosc F, Demarquay JF, Sorbi D, Maes B, Delmont J, Dumas R. Self-expanding metal stents in the palliation of neo-plasms of the cervical esophagus. *Hepatogastroenterology* 1999; **46**: 272-277
- 18 **Sandha GS**, Marcon NE. Expandable metal stents for benign esophageal obstruction. *Gastrointest Endosc Clin N Am* 1999; **9**: 437-446

Edited by Chen WW Proofread by Zhu LH and Xu FM

Relationship between microvessel density and telomerase activity in hepatocellular carcinoma

Yun-Feng Piao, Min He, Yang Shi, Tong-Yu Tang

Yun-Feng Piao, Yang Shi, Tong-Yu Tang, Department of Gastroenterology, First Hospital of Jilin University, Changchun 130021, Jilin Province, China

Min He, Comprehensive Department of Infection, Changchun Infectious Hospital, Changchun 130021, Jilin Province, China

Correspondence to: Dr. Yang Shi, Department of Gastroenterology, First Hospital of Jilin University, No.1 Xinmin Road, Changchun 130021, Jilin Province, China. shiyangwhy@163.com

Telephone: +86-431-5612242 **Fax:** +86-431-5612542

Received: 2004-02-21 **Accepted:** 2004-03-12

Abstract

AIM: To study the relationship between microvessel density (MVD), telomerase activity and biological characteristics in hepatocellular carcinoma (HCC).

METHODS: S-P immunohistochemical method and telomeric repeat amplification protocol (TRAP) were respectively used to analyze the MVD and telomerase activity in 58 HCC and adjacent normal tissues.

RESULTS: The MVD in HCC with metastasis, lower differentiation or without intact capsule was significantly higher than that in HCC with intact capsule, higher differentiation, or without metastasis. While MVD had no relationship with tumor size, hepatic virus infection and other clinical factors. Telomerase activity was related to differentiation degree, but not to tumor size or histological grade. MVD in HCC with telomerase activity was higher than that in HCC without telomerase activity.

CONCLUSION: MVD and telomerase activity may serve as diagnostic criteria of HCC in earlier stage. Meanwhile, there may be a cooperative effect between MVD and telomerase on the growth and metastasis of HCC.

Piao YF, He M, Shi Y, Tang TY. Relationship between microvessel density and telomerase activity in hepatocellular carcinoma. *World J Gastroenterol* 2004; 10(14): 2147-2149

<http://www.wjgnet.com/1007-9327/10/2147.asp>

INTRODUCTION

Primary hepatocellular carcinoma (HCC) is a common malignant solid tumor, which is rich of blood. It has many characteristics, such as fast infiltrating growth, metastasis in early stage, high grade malignancy, poorly therapeutic efficacy. So it is important to study the angiogenesis of HCC. At present, it has been proved that MVD can serve as a prognostic criterion for relapse, metastasis and survival rate of all kinds of carcinoma^[1-6].

Telomerase is a reverse transcriptase. It can make up telomeres that lose 50-200 bp during each DNA replication so as to retain the telomere length and stabilize the cells. The expression of telomerase activity is important to cell proliferation, senescence, immortalization and carcinogenesis^[7-9]. It is known that telomerase activity can be detected in many carcinomas, but

not in most of normal tissues^[10-16].

MVD and telomerase activity can act as specific markers for malignant tumors, and are used to analyze the biologic characteristics, infiltration, metastasis and prognosis of tumors. But the relationship between them has not been reported. In this study, S-P immunohistochemistry method and telomeric repeat amplification protocol (TRAP) were used to respectively detect MVD and telomerase activity, so as to study their relationship and other clinical factors.

MATERIALS AND METHODS

Tissue specimens

Fifty-eight HCC and adjacent normal tissues specimens were obtained from Hepatobiliary Surgery Department of Changchun Infectious Hospital from December 2000 to December 2002. They were all proved as primary HCC. These patients did not receive radiotherapy, chemotherapy, or other therapies. Of them, 35 cases had liver cirrhosis, 52 cases had chronic hepatitis, 6 cases had carcinoma emboli in portal vein, 48 cases had positive marker of HBV, 4 cases had positive anti-HCV antibody, and 4 cases had negative marker of hepatitis virus. Each specimen was divided into two parts. One was stained by immunohistochemical method, and routinely fixed in formalin, embedded in paraffin, and then cut into 4-5 μ m thick sections. The other was frozen in liquid nitrogen and used to analyze telomerase activity by TRAP.

S-P Immunohistochemical method

UltraSensitive™ S-P kit, anti-VIII factor related antigen monoantibody (anti-FVIII RAG), and positive control were purchased from Fuzhou Maixin Biotechnology Development Company. The sections were deparaffinized in xylene and rehydrated in a serial gradient of ethanol solutions. Then S-P immunohistochemical method was used according to its manual. At last, they were restained with hematoxylin and observed. The negative control included empty control with normal rabbit IgG instead of primary antibodies or with the second antibody only. MVD was determined in triplicate in the area of the most intense vascularization (hot spot) of each tumor, and the average count was recorded.

Activity of telomerase assayed by TRAP silver staining

About 50-100 mg tissue was split. Then the supernatant was collected for analysis. The telomerase activity was detected using a TRAP kit following instructions of the manufacturer (Beijing Tiange Kangning Biotech Institute). The reaction system containing 25 μ L TRAP agent, 0.2 μ L *Taq* enzyme and 1 μ L cell extract was incubated for 30 min at 25 °C, then 0.5 μ L of primer was added and PCR was conducted for 30 cycles with denaturing at 94 °C for 30 s, annealing at 60 °C for 30 s, extending at 72 °C for 30 s. Fifteen microliter PCR product was loaded onto a 90 g/L non-degenerative SDS gel, resolved through the SDS-PAGE, demonstrated by a reaction in 2 g/L silver nitrate for 15 min, and visualized by incubation in 30 g/L anhydrous sodium carbonate containing formaldehydes (1 mL/L). The activity of telomerase was indicated by the presence of a 6 bp-DNA ladder. The cell extract inactivated by incubation at 75 °C for 10 min was used as negative control.

Statistical analysis

Result were expressed as mean±SD. Student's *t* test and χ^2 test were used. *P*<0.05 was considered statistically significant.

RESULTS

Relationship between MVD and some clinical factors

Observed with light microscope, venous endothelium but not lymphatic vessel endothelium was brown (Figure 1).

Table 1 shows that MVD in HCC tissues with metastasis within vein or liver was significantly higher than that in HCC without metastasis (*P*<0.05), MVD in HCC without intact capsule was higher than that in HCC with intact capsule (*P*<0.05). There was no significant difference in MVD between big (>5 cm) and small (≤5 cm) tumors.

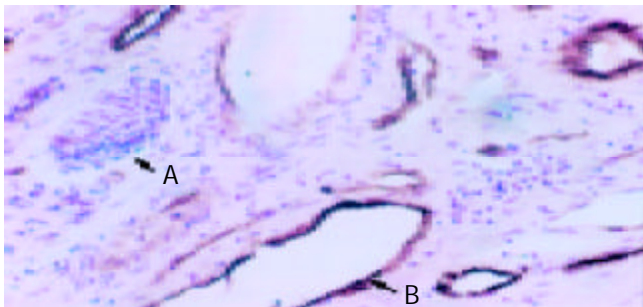


Figure 1 Immunohistochemical staining with anti-FVIII RAG (S-P, original magnification: ×400). A indicates the lymphatic vessel endothelium. B indicates the brown venous endothelium.

Table 1 Relationship between MVD and metastasis, capsular integrity, or size of tumor

Classification		Cases (n)	MVD(mean±SD)
Metastasis	+	36	39.3±9.6 ^a
	-	22	32.2±5.6
Capsular	-	38	38.8±9.3 ^a
	+	20	31.2±5.8
Integrity	>5 cm	42	37.3±8.8
Size	≤5 cm	16	36.9±8.7

^a*P*<0.05, vs corresponding group.

In this study, the distribution of MVD was different in various regions. MVD was higher in HCC with lower differentiation than that in HCC with higher differentiation (Table 2). MVD in

adjacent normal tissues (13.2±2.7) was mainly distributed in the area near the carcinoma tissues, especially around the pseudolobules with liver cirrhosis. It was reported that MVD in normal tissues was 11.8±0.2.

Table 2 MVD in HCC and adjacent normal liver tissues

Group	Cases (n)	MVD (mean±SD)
Adjacent normal tissue	58	13.2±2.7
HCC grade I	11	19.6±3.7
HCC grade II	22	29.7±6.1 ^a
HCC grade III	16	48.4±10.7 ^a
HCC grade IV	9	59.3±10.5 ^a

^a*P*<0.05 vs adjacent normal tissue.

Relationship between telomerase activity in HCC or adjacent normal tissues and some clinical factors

The results are shown in Figure 2. The positive rate of telomerase activity in HCC tissues (89.6%) was significantly higher than that in adjacent normal liver tissues (20.7%). The telomerase activity in HCC was related to differentiation grade of HCC, but was not related to HCC size, capsule integrity, number of liver nodules, metastasis, or hepatitis virus infection. While the telomerase activity in adjacent normal liver tissues was related to capsule integrity, number of liver nodules and hepatitis virus infection (Table 3).

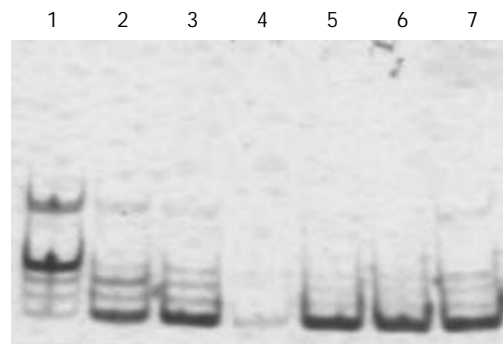


Figure 2 Telomerase activity of HCC tissues. Lane 1: Positive control. Lanes 2, 3: HCC tissue with low differentiation with a 6-bp interval ladder pattern. Lane 4: No ladder in adjacent normal tissues. Lanes 5, 6: HCC tissue with high differentiation with a 6-bp interval ladder pattern. Lane 7: HCC with moderate differentiation with a 6-bp interval ladder pattern.

Table 3 Relationship between telomerase activity in HCC or adjacent normal liver tissues and some clinical factors

Group		HCC			<i>P</i>	Adjacent normal tissues		
		Cases	Positive number	Positive rate(%)		Positive number	Positive rate(%)	<i>P</i>
Differentiation	High	11	6	54.4	<0.05	0	0	<0.05
	Middle	38	37	97.4		5	13.2	
	Low	9	9	100		7	77.8	
Size	≤5 cm	16	14	87.5	>0.05	3	18.8	>0.05
	>5 cm	42	38	90.9		9	21.4	
Capsule	-	20	16	80.0	>0.05	1	5.0	<0.05
Integrity	+	38	36	94.7		11	29.8	
Hepatitis virus	+	48	44	91.6		1	22.9	
Infection	-	10	8	80.0	>0.05	1	10.0	<0.05
Nod number	Mono-nod	15	12	80.0		1	6.7	
	Multi-nod	43	40	93.0		>0.05	>0.05	
Metastasis	+	36	34	94.4	>0.05	10	27.8	<0.05
	-	22	18	81.8		2	9.1	

Relationship between telomerase activity and MVD in HCC or adjacent normal tissue

Among the 58 HCC and adjacent normal liver tissues, MVD in those with positive telomerase activity was significantly higher than that in those with negative activity (Table 4).

Table 4 Relationship between telomerase activity and MVD in HCC or adjacent normal liver tissues

Group	HCC	Adjacent normal tissue
Group with positive telomerase activity	49.3±7.8 ^a	16.2±2.7 ^a
Group with negative telomerase activity	31.2±5.8	11.9±1.4

^a*P*<0.05 vs group with negative telomerase activity.

DISCUSSION

Carcinogenesis of HCC is a multi-factor, multi-step and complex process. Angiogenesis is necessary for solid tumors larger than 1 mm×1 mm. Or else the tumor would remain at dormancy phase and would not metastasize. As soon as it entered angiogenesis stage, the potency of metastasis exhibited at once^[17-20].

MVD is an important marker of angiogenesis in tumor and is valuable in prognosis of various carcinomas. In this study, S-P immunohistochemical staining was used to analyze MVD in 58 HCC and corresponding adjacent normal tissues. FVIII in cytoplasm of various vascular endothelium cells is synthesized in endothelial cells. FVIII-RAG is specific to endothelial cells so that it could be differentiated blood vessel from lymphatic vessel. The role of vascular genesis, development and distribution in occurrence, development, infiltration, metastasis and advancement of tumors has been studied^[21]. MVD in poorly differentiated HCC with metastasis in vein or liver, intact capsule was significantly higher than that in corresponding ones. This result was consistent with others, suggesting that HCC with higher MVD may obtain more nutrition from new blood vessels, so that it can grow faster and has the ability to infiltrate and metastasize. MVD might play a key role in development of HCC. There was no close relationship between MVD and tumor size, HBV infection. Maybe HBV infection is merely a carcinogenic factor, and is not related to the growth, infiltration and metastasis of HCC.

We also detected telomerase activity in 58 HCC and adjacent normal tissues by TRAP. Similar to Nouse's research, the expression of telomerase activity in HCC was negatively related to differentiation, but was not related to tumor size or histologic grade. Telomerase activity in adjacent normal tissues with middle or big size, multi-nods, unintegral capsule, positive HBsAg was higher than that in adjacent normal tissues without them, suggesting that there is some relationship between telomerase activity in adjacent normal tissue and prognosis of HCC. Hepatitis viruses, especially HBV, have been found to be an important factor in causing HCC. HBx, encoded by HBV, could block the function of p53, and make genome unstable. With the cell division, telomerase was activated. The cells with positive telomerase activity became immortalized and further developed to carcinoma cells. Histological examination in combination with detection of telomerase activity could increase the accuracy of diagnosis in early stage and improve the judgment on its prognosis.

In addition, there was some relationship between MVD and telomerase activity. Activation of telomerase could make liver cells immortalized, and MVD could offer nutrition for their growth and stimulate metastasis. These two factors would result in carcinogenesis at last.

In a word, MVD and telomerase activity have a key role in occurrence, development, infiltration and metastasis of HCC and have notable clinical values in diagnosing and treating HCC in early stage.

REFERENCES

- Du JR**, Jiang Y, Zhang YM, Fu H. Vascular endothelial growth factor and microvascular density in esophageal and gastric carcinomas. *World J Gastroenterol* 2003; **9**: 1604-1606
- Ding YB**, Chen GY, Xia JG, Zang XW, Yang HY, Yang L. Association of VCAM-1 overexpression with oncogenesis, tumor angiogenesis and metastasis of gastric carcinoma. *World J Gastroenterol* 2003; **9**: 1409-1414
- Moon WS**, Rhyu KH, Kang MJ, Lee DG, Yu HC, Yeum JH, Koh GY, Tarnawski AS. Overexpression of VEGF and angiotensin 2: a key to vascularity of hepatocellular carcinoma? *Mod Pathol* 2003; **16**: 552-557
- Takahashi R**, Tanaka S, Kitadai Y, Sumii M, Yoshihara M, Haruma K, Chayama K. Expression of vascular endothelial growth factor and angiogenesis in gastrointestinal stromal tumor of the stomach. *Oncology* 2003; **64**: 266-274
- Poon RT**, Ng IO, Lau C, Yu WC, Yang ZF, Fan ST, Wong J. Tumor microvessel density as a predictor of recurrence after resection of hepatocellular carcinoma: a prospective study. *J Clin Oncol* 2002; **20**: 1775-1785
- Ng IO**, Poon RT, Lee JM, Fan ST, Ng M, Tso WK. Microvessel density, vascular endothelial growth factor and its receptors Flt-1 and Flk-1/KDR in hepatocellular carcinoma. *Am J Clin Pathol* 2001; **116**: 838-845
- Blackburn EH**. Structure and function of telomeres. *Nature* 1991; **350**: 569-573
- Morin GB**. The human telomere terminal transferase enzyme is a ribonucleoprotein that synthesizes TTAGGG repeats. *Cell* 1989; **59**: 521-529
- Shay JW**, Wright WE. Ageing and cancer: the telomere and telomerase connection. *Novartis Found Symp* 2001; **235**: 116-125
- Kim NW**, Piatyszek MA, Prowse KR, Harley CB, West MD, Ho PL, Coviello GM, Wright WE, Weinrich SL, Shay JW. Specific association of human telomerase activity with immortal cells and cancer. *Science* 1994; **266**: 2011-2015
- Mu J**, Wei LX. Telomere and telomerase in oncology. *Cell Res* 2002; **12**: 1-7
- Masutomi K**, Yu EY, Khurts S, Ben-Porath I, Currier JL, Metz GB, Brooks MW, Kaneko S, Murakami S, DeCaprio JA, Weinberg RA, Stewart SA, Hahn WC. Telomerase maintains telomere structure in normal human cells. *Cell* 2003; **114**: 241-253
- Testorelli C**. Telomerase and cancer. *J Exp Clin Cancer Res* 2003; **22**: 165-169
- Yokota T**, Suda T, Igarashi M, Kuroiwa T, Waguri N, Kawai H, Mita Y, Aoyagi Y. Telomere length variation and maintenance in hepatocarcinogenesis. *Cancer* 2003; **98**: 110-118
- Mariani E**, Meneghetti A, Formentini I, Neri S, Cattini L, Ravaglia G, Forti P, Facchini A. Telomere length and telomerase activity: effect of ageing on human NK cells. *Mech Ageing Dev* 2003; **124**: 403-408
- Tomita M**, Matsuzaki Y, Onitsuka T. Effect of mast cells on tumor angiogenesis in lung cancer. *Ann thorac Surg* 2000; **69**: 1686-1690
- Lichtenbeld HH**, van Dam-Mieras MC, Hillen HF. Tumour angiogenesis: pathophysiology and clinical significance. *Neth J Med* 1996; **49**: 42-51
- Paweletz N**, Knierim M. Tumor-related angiogenesis. *Crit Rev Oncol Hematol* 1989; **9**: 197-242
- Desai SB**, Libutti SK. Tumor angiogenesis and endothelial cell modulatory factors. *J Immunother* 1999; **22**: 186-211
- Saaristo A**, Karpanen T, Alitalo K. Mechanisms of angiogenesis and their use in the inhibition of tumor growth and metastasis. *Oncogene* 2000; **19**: 6122-6129
- Ruiter DJ**, Schlingemann RO, Rietveld FJ, de Waal RM. Monoclonal antibody-defined human endothelial antigens as vascular markers. *J Invest Dermatol* 1989; **93**(2 Suppl): 25S-32S

Treatment of severe *Clonorchiasis sinensis* by endoscopic nasobiliary drainage and oral praziquantel

Fa-Chao Zhi, Xu-Ming Liu, Ze-Quan Liu, Yan Lin, Shu-Jian Chen

Fa-Chao Zhi, PLA Institute for Digestive Medicine, Nanfang Hospital, First Military Medical University, Guangzhou 510515, Guangdong Province, China

Xu-Ming Liu, Ze-Quan Liu, Yan Lin, Shu-Jian Chen, Department of Digestive Diseases, Hexian Hospital, Panyu, Guangzhou 511400, Guangdong Province, China

Correspondence to: Fa-Chao Zhi, PLA Institute for Digestive Medicine, Nanfang Hospital, First Military Medical University, Guangzhou 510515, Guangdong Province, China. zfc@fimmu.com

Telephone: +86-20-61641534 **Fax:** +86-20-87280770

Received: 2003-11-13 **Accepted:** 2004-01-12

Abstract

AIM: To assess the therapeutic value of endoscopic nasobiliary drainage (ENBD) and oral praziquantel for severe *Clonorchiasis sinensis* infection.

METHODS: Of the 84 *Clonorchiasis sinensis*-infected patients enrolled, 58 were treated with ENBD (as observing group, ENBD group), 26 received operations (control group, operation group). Both of the two groups were comparable in terms of patient's age, body mass index. Before and one week after treatment, the average diameters of common bile ducts were measured by ultrasound, and serum bilirubin, ALP, γ -GT and ALT were detected by biochemical methods. After ENBD or operation, the patients took praziquantel for two days.

RESULTS: Compared with the patients in operation group, ENBD patients in ENBD group had higher recovery rates of abdominal pain and fever as well as jaundice, quicker remission, smaller trauma, fewer complications and lower cost.

CONCLUSION: ENBD combined with oral praziquantel is an effective and safe method for the treatment of severe *Clonorchiasis sinensis*.

Zhi FC, Liu XM, Liu ZQ, Lin Y, Chen SJ. Treatment of severe *Clonorchiasis sinensis* by endoscopic nasobiliary drainage and oral praziquantel. *World J Gastroenterol* 2004; 10(14): 2150-2152

<http://www.wjgnet.com/1007-9327/10/2150.asp>

INTRODUCTION

Oral praziquantel is effective for the treatment of mild *Clonorchiasis sinensis*. As the parasitism of *Clonorchiasis sinensis* metacercaria can take more than 50 years in human body^[1], the therapy of *Clonorchiasis sinensis* is very difficult because of repeated infections. We have achieved effective results in treating 58 cases of severe *Clonorchiasis sinensis* infection from July 2000 to April 2003 by endoscopic nasobiliary drainage (ENBD) and oral praziquantel.

MATERIALS AND METHODS

Diagnostic criteria for severe *Clonorchiasis sinensis*

Criteria for severe *Clonorchiasis sinensis* are as follows: A

history of eating raw fish; spawn can be detected in feces or bile; obstructive jaundice or cholecystitis, biliary calculus in common bile duct, and suppurative cholangitis. All the 58 cases were in line with the above diagnostic standards.

Patients and treatments

There were 58 cases in ENBD group including 55 males and 3 females (aged from 29 to 76 with a mean age of 46.5 years). All cases had a history of eating raw fish. Among them, 36 cases had common bile duct dilatation, intrahepatic bile duct and gallbladder distention (6 of the 36 cases also had gallstones in common bile duct); 23 cases had mild dilatation in common bile duct. Nineteen cases were accompanied with fever and increased leukocyte counts. *Clonorchiasis sinensis* metacercaria were detected in feces of 39 cases. Laboratory examination results were as follows: Total bilirubin 86-280 $\mu\text{mol/L}$ with an average of 103 $\mu\text{mol/L}$, glutamic-pyruvic transaminase 60-360 U/L with an average of 98 U/L.

The 58 cases in ENBD group were treated according to the routine procedure^[2]. The instruments included duodenoscope, ducts, knives, guide wires, meshes, etc. The papilla of Vater and bile duct were examined for *Clonorchiasis sinensis* metacercaria. Then, endoscopic retrograde cholangiopancreatography (ERCP) was performed to diagnose the severity of the disease. Patients with mild inflammation without constriction were treated by nasobiliary drainage. Patients with obvious constriction were treated by nasobiliary drainage after sphincterotomy. If the common bile duct was full of *Clonorchiasis sinensis* metacercaria and purulent discharge, the ducts were first washed, and then nasobiliary drainage was performed. For the patients with biliary calculus in common bile ducts, stones were taken out by sphincterotomy followed by nasobiliary drainage. All the 58 patients took praziquantel orally 8-48 h after procedures. The dose was 3.6 g/d three times daily for 2 d.

There were 26 patients with *Clonorchiasis sinensis* infection proved by operations (operation group) including 25 males and 1 female aged 36 to 75 years with a mean age of 48.5 years. Preoperative diagnosis was as follows: Fifteen patients with cholecystitis, 5 with gallstones in common bile duct and 6 with duodenal ampulla carcinoma. Fifteen cases underwent cholecystectomy, 5 cases underwent choledocholithotomy, and 20 cases received operations for common bile duct dilatation. All the 26 cases had T-tube drainage. Laboratory examination results were as follows: Total bilirubin 76-123 $\mu\text{mol/L}$ with a mean of 94 $\mu\text{mol/L}$, glutamic-pyruvic transaminase 63-286 U/L with an average of 105 U/L.

The 26 cases were treated by exploratory laparotomy. The common bile duct was opened, and *Clonorchiasis sinensis* metacercaria and their purulent discharge were washed away with saline. Then, common bile duct was expanded with bougie. At last, T-tube was placed inside. Cholecystectomy followed by T-tube was performed for patients with cholelithiasis or cholecystitis. Choledocholithotomy followed by T-tube was performed for patients with gallstones in common bile ducts. All the 26 patients took praziquantel orally for 3-6 d after operation. The dose was 3.6 g/d three times daily for 2 d.

Table 1 Average diameter of common bile ducts, levels of serum total bilirubin, ALP, γ -GT and ALT one week after operation (mean \pm SD)

Group	Cases (n)	Therapy	Average diameter of common bile duct (mm)	Serum total bilirubin (μ mol/L)	ALP (U/L)	γ -GT (U/L)	ALT (U/L)
ENBD	58	Before	16 \pm 3	89 \pm 11	286 \pm 63	166 \pm 38	132 \pm 32
		After	9.6 \pm 2.2 ^b	29 \pm 9 ^b	108 \pm 23 ^b	86 \pm 22 ^b	60 \pm 12 ^b
Operation	26	Before	15.3 \pm 3.1	87 \pm 10	263 \pm 54	156 \pm 36	130 \pm 30
		After	9.5 \pm 2.1 ^d	27 \pm 8 ^d	98 \pm 25 ^d	87 \pm 22 ^d	57 \pm 11 ^d

^b P <0.01 vs markers before ENBD, ^d P <0.01 vs markers before operation.

Table 2 Therapeutic effects of two groups

Group	Cases (n)	Remission time of abdominal pain (d)	Complication (cases)	Average length of hospital stay (d)	Average cost (Yuan)
ENBD	58	1	13	9	6 503
Operation	26	6 ^b	10	20 ^b	16 300 ^b

^b P <0.01 vs ENBD group.

Observing parameters

The following parameters were measured before and one week after treatment. (1) Changes of the average diameter of common bile ducts, serum total bilirubin, ALP, γ -GT and ALT; (2) Complications, average length of hospital stay and the costs; (3) *Clonorchiasis sinensis* metacercaria in feces in follow-up patients.

Statistical analysis

All data were analysed by t test, and the significant level was set at P <0.05.

RESULTS

Therapeutic effects are shown in Tables 1 and 2. (1) ENBD group: Jaundice decreased in 72 h and disappeared in 3 wk. The average remission time of abdominal pain was 1 d after ENBD. Nineteen cases with fever returned to normal temperature 48 h after drainage. The dead polyp could be seen discharged from nasobiliary drainage 12 h after oral praziquantel. Peak time of dead polyp discharging was within 24-48 h after oral praziquantel and there was no dead polyp on the fifth day. (2) Operation group: The mean remission time of abdominal pain was 6 d after operation. Jaundice and fever began to decrease 2 d after operation. The dead polyp could be seen discharged from T-tube 12 h after oral praziquantel.

There were 8 cases with transient hyperamylasemia in ENBD group, who were cured in 48 h by fasting, anti-acid and anti-inflammation therapy. Two cases with bile duct retrograde infection after sphincterotomy accompanied with transient fever and chill were cured by anti-inflammation therapy. In all 58 cases, there was no case of bleeding and perforation, but 3 cases developed recurrent disease in 1-2 years and needed therapy again. In operation group, there were 8 cases with gallstone in common bile duct or cholangitis after operation, and 2 cases with intestinal adhesion.

Clonorchiasis sinensis metacercaria was found in feces of all the patients of the two groups 3, 6, 12, 18 and 24 mo after ENBD or operation. After oral praziquantel again, no *Clonorchiasis sinensis* metacercaria was found in feces.

DISCUSSION

Clonorchiasis sinensis is an amphixenosis parasitic disease threatening people's health. The average infectious rate was 21.1% in Pearl River Delta region, and up to 88.6% in certain

areas. Oral praziquantel is the first-line therapy drug; its effectiveness can be 98.8%^[3-5]. When *Clonorchiasis sinensis* infection is accompanied with obstructive jaundice^[6,7], obstruction remission and bile drainage should be the most important treatment target. The traditional method of obstruction remission is operation, but operation has some shortcomings, such as big trauma, high costs and recurrence. With the development of endoscopic intervention, the therapy of *Clonorchiasis sinensis* with endoscopic bile duct drainage has bright prospect^[8].

Our results showed that oral praziquantel after endoscopic nasobiliary drainage was a safe and effective way for the treatment of *Clonorchiasis sinensis* accompanied with obstructive jaundice. The two methods had equal effects (as shown in Tables 1 and 2), and no significant difference with regard to the remission time of jaundice and average diameter of common bile duct. However, endoscopic nasobiliary drainage did have some advantages, such as rapid remission of fever and abdominal pain, little trauma, rapid recovery, fewer complications, less length of hospital stay and less cost.

Sphincterotomy is required for patients with inflammatory papillary stenosis. Drainage is helpful for decreasing the restenosis after operation. Sphincterotomy is indicated in the following situations: Papilla opening is very small, stiff, and has no bile flow; it is difficult to inject contrast; contrast shows that inferior part of common bile duct is obviously narrow.

Generally, nasobiliary drainage should last 4-7 d and the bile duct should be washed by 5 g/L metronidazol 1-2 times daily. Once the drainage tube is out of place, it is not necessary to re-put drainage if there is no symptom of increasing stenosis, jaundice or fever. The causes of drainage dislocation included: Anterior extremity of nasobiliary drainage had no bents; the papilla opening was too big during sphincterotomy; some patients would pull out the nasobiliary drainage because of irritation and nausea; some patients had too much hiccupping and vomiting. Doctors should make more explanations to get patients' cooperation.

The main complication of endoscopic therapy was transient hyperamylasemia, which was associated with repeated pancreatic duct visualization during contrast imaging. This complication could be relieved by fasting, antacid and anti-inflammation therapy for 48 h. Once there was pancreatitis, the therapy was initiated for acute pancreatitis. In patients with moderate jaundice and good general condition, oral praziquantel could be taken 8 h after endoscopic drainage. Patients with

severe jaundice and severe impairment of hepatic function, should receive therapy to improve and protect hepatic function, and take oral praziquantel 2-3 d after drainage to decrease the damage to liver caused by the drugs.

On the whole, both ENBD and traditional operation are effective for the treatment of *Clonorchiasis sinensis* infection complicated with obstructive jaundice. However, ENBD has some advantages, such as rapid remission of fever and abdominal pain, little trauma, rapid recovery, fewer complications, less length of hospital stay and less cost.

REFERENCES

- 1 **Gao JS**, Liu YH, Wang XG, Yu DG, Shu Q. Experimental Observation of Praziquantel and Trichloro-benzodazole of Dog's Clonorchiasis. *Zhongguo Jishengchongbing Zazhi* 1998; **11**: 357-283
- 2 **Zhi FC**, Yan ZQ, Li XL, Zhu JX, Chen CL, Zhang XL, Zhou DY. Prospective study of diagnostic value of magnetic resonance cholangiopancreatography versus endoscopic retrograde cholangiopancreatography in cholangiopancreatic diseases. *Chin J Dig Dis* 2002; **3**: 124-126
- 3 **Huang XL**. 68 cases analysis of clonorchiasis. *Guangzhou Yixue* 2001; **32**: 45-50
- 4 **Yu SH**, Kawanaka M, Li XM, Xu LQ, Lan CG, Rui L. Epidemiological investigation on *Clonorchis sinensis* in human population in an area of South China. *Jpn J Infect Dis* 2003; **56**: 168-171
- 5 **Wang KX**, Zhang RB, Cui YB, Tian Y, Cai R, Li CP. Clinical and epidemiological features of patients with clonorchiasis. *World J Gastroenterol* 2004; **10**: 446-448
- 6 **Kim KH**, Kim CD, Lee HS, Lee SJ, Jeon YT, Chun HJ, Song CW, Lee SW, Um SH, Choi JH, Ryu HS, Hyun JH. Biliary papillary hyperplasia with clonorchiasis resembling cholangiocarcinoma. *Am J Gastroenterol* 1999; **94**: 514-517
- 7 **Lee SH**, Lee JI, Huh S, Yu JR, Chung SW, Chai JY, Hong ST. Secretions of the biliary mucosa in experimental clonorchiasis. *Korean J Parasitol* 1993; **31**: 13-20
- 8 **Zhi FC**, Li XL, Yang LC, He ZB, Cui XY, Qiu XL, Lin Y, Liu XM, Liang NL, Zhu JX. Diagnosis and treatment for clonorchiasis sinensis by endoscopic retrograde cholangiopancreatography and sphincterotomy. *Zhonghua Xiaohua Zazhi* 2003; **23**: 279-281

Edited by Chen WW and Zhu LH **Proofread by** Xu FM

Benign nontraumatic inflammatory stricture of mid portion of common bile duct mimicking malignant tumor: Report of two cases

Chiu-Yung Ho, Tseng-Shing Chen, Full-Young Chang, Shou-Dong Lee

Chiu-Yung Ho, Tseng-Shing Chen, Full-Young Chang, Shou-Dong Lee, Division of Gastroenterology, Department of Medicine, Taipei Veterans General Hospital, National Yang-Ming University School of Medicine, Taipei, Taiwan, China

Chiu-Yung Ho, Tao Yuang Veterans Hospital, Tao-Yuang, Taiwan, China

Correspondence to: Dr. Tseng-Shing Chen, Division of Gastroenterology, Department of Medicine, Taipei Veterans General Hospital, 201, Sec. 2, Shih-Pai Road, Taipei 112, Taiwan, China. tschen@vghtpe.gov.tw
Telephone: +886-2-2871-2121 **Fax:** +886-2-2873-9318

Received: 2004-03-06 **Accepted:** 2004-04-09

Abstract

Benign nontraumatic inflammatory stricture of the common bile duct (CBD) may result in obstructive jaundice, which can be misdiagnosed as a malignant tumor of the CBD preoperatively. Two cases with strictures of the mid portion of the common bile duct presenting with obstructive jaundice are reported herein. Preoperative radiological studies prompted us to confidently make the diagnosis of cholangiocarcinoma. However, the postoperative diagnosis on histological examination of the resected lesions was chronic inflammation and fibrosis. The complications of chronic duodenal ulcer are considered as the etiology of these two disorders.

Ho CY, Chen TS, Chang FY, Lee SD. Benign nontraumatic inflammatory stricture of mid portion of common bile duct mimicking malignant tumor: Report of two cases. *World J Gastroenterol* 2004; 10(14): 2153-2155

<http://www.wjgnet.com/1007-9327/10/2153.asp>

INTRODUCTION

Malignant bile duct strictures are mainly the result of cancer of the ampulla of Vater, pancreas, or bile duct, and account for most patients presenting with obstructive jaundice secondary to extra-hepatic bile duct stricture. Benign nontraumatic inflammatory strictures of the extra-hepatic bile duct are extremely rare with the exception of primary sclerosing cholangitis^[1-3]. Most benign strictures reported in the literature are located in the hepatic hilum^[4] or distal common bile duct (CBD). Here we report two cases of benign nontraumatic inflammatory strictures of the mid portion of the CBD with painless obstructive jaundice. They were confidently diagnosed as cholangiocarcinoma by radiological studies preoperatively.

CASE REPORT

Case 1

A 70 year-old male who had a 10-year history of hypertension and type 2 diabetes mellitus was presented to our hospital. He had tea-colored urine and yellowish skin discoloration for about 2 wk. No abdominal pain or body weight loss was reported. The physical examination was unremarkable except icteric sclera. A complete blood count was within normal limits.

Serum total bilirubin/direct bilirubin (TB/DB) 5.6/2.9 mg/dL (normal 0.2-1.6/0-0.3 mg/dL), alanine aminotransferase (ALT) 127 U/L (normal 0-40 U/L), aspartate aminotransferase (AST) 78 U/L (normal 5-45 U/L), alkaline phosphatase (ALK-P) 380 U/L (normal 10-100 U/L) and gamma-glutamyl transpeptidase (γ -GT) 333 U/L (normal 8-60 U/L) were noted. Abdominal sonography showed dilatation of the intrahepatic ducts and CBD. The contrast-enhanced abdominal CT scan disclosed similar findings. A PTCD tube was inserted and antegrade cholangiograms exhibited a segmental narrowing of the CBD about 2 cm below the insertion site of the cystic duct (Figure 1A). A segmental stricture about 1.5 cm in length over the CBD but below the cystic duct level and dilatation of the intrahepatic ducts were also demonstrated in the endoscopic retrograde cholangiopancreatogram (ERCP) (Figure 1B). The pancreatogram was normal. Three sets of bile fluid cytology were negative. Tumor markers CA19-9 and CEA were not elevated. A diagnosis of cholangiocarcinoma with CBD stricture was made. At surgery, stricture of the mid portion of the CBD was found. Cholecystectomy and choledocholithotomy with T-tube drainage were performed. Histological examination of the resected CBD showed chronic inflammation and fibrosis without malignant cells. No stone was detected in the gallbladder. Unfortunately, tea-colored urine and skin itching developed 3 years later. The laboratory evaluation revealed serum TB/DB 2.9/1.5 mg/dL, AST 111 U/L, ALT 125 U/L, ALK-P 427 U/L and γ -GT 676 U/L. Serum AMA, ASMA, IgG, IgM, IgA and ANA titers were within normal range. ERCP demonstrated segmental stricture of the common hepatic duct about 4 cm in length (Figure 1C) and choledochoduodenal fistula. The pancreatogram was normal. MR cholangiogram disclosed an annular mass lesion with enhancement at the proximal CBD, which caused segmental narrowing of the common hepatic duct and dilatation of the intrahepatic ducts (Figure 1D). Bile duct tumors such as cholangiocarcinoma were considered. At surgery, a firm and fixed tumor 4 cm \times 3 cm in size at the CBD was palpated. The duodenal bulb was adhered to the tumor and a choledochoduodenal fistula was found. Segmental resection of the CBD, hepaticojejunostomy and enteroenterostomy, end-to-side, were performed. Histological examination of the resected CBD showed chronic cholangitis with focal atypical epithelium.

Case 2

A 55 year-old male without significant past medical history was admitted because of painless jaundice for 1 mo. A double-contrast barium study of the upper gastrointestinal tract 2 years earlier demonstrated chronic duodenal ulcer with bulb deformity and prepyloric constriction (Figure 2). On examination, there was only icteric sclera. A complete blood count was within normal limits. Serum TB/DB 4.2/2.5 mg/dL, ALT 404 U/L, AST 293 U/L, ALK-P 357 and γ -GT 333 U/L were noted. Abdominal sonography showed dilatation of the intrahepatic ducts and CBD. A contrast-enhanced abdominal CT scan disclosed dilatation of the intrahepatic ducts and proximal CBD associated with distention of the gallbladder. ERCP failed. The MRI revealed an annular lesion about 3.5 cm

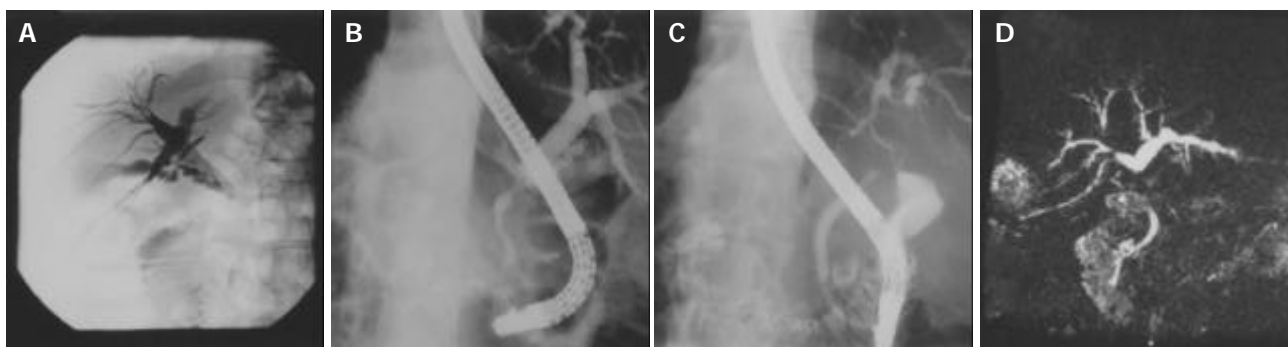


Figure 1 Segmental strictures of CBD demonstrated in percutaneous cholangiogram, ERCP and MR cholangiogram. A: Segmental narrowing of CBD below the insertion site of cystic duct in percutaneous cholangiogram; B: Segmental stricture of CBD with dilatation of intrahepatic bile ducts demonstrated in ERCP; C: Segmental stricture of CHD demonstrated in ERCP; D: Segmental narrowing of CHD and dilatation of the intrahepatic bile ducts demonstrated in MR cholangiogram.

in length in the mid portion of the CBD (Figure 3). Three sets of bile fluid cytology were negative. Tumor markers CA19-9 and CEA were not elevated. A diagnosis of cholangiocarcinoma was made. The patient had a laparotomy for resection of the tumor. A tumor over the middle third portion of the CBD with thickened wall was found. No stone was detected in the gallbladder or CBD. Resection of the tumor and Roux-en-Y choledochojejunostomy, end-to-side, was then performed. However, the postoperative histological examination of the lesion showed only chronic inflammation with marked fibrosis.

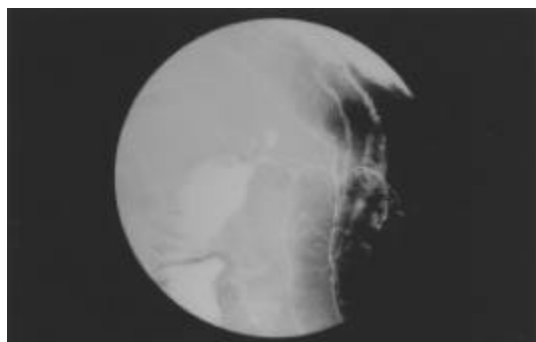


Figure 2 Chronic duodenal disease with bulb deformity and prepyloric constriction revealed in a double-contrast barium study.



Figure 3 Annular lesion in the mid portion of CBD disclosed in MRI (coronal view).

DISCUSSION

The clinical presentation and preoperative radiological studies without tissue or cytological proof led us to the diagnosis of malignant bile duct strictures in these 2 cases. It has been agreed that any localized extra-hepatic bile duct obstruction coexisting

with intra-hepatic bile duct dilatation should be considered as malignancies such as cancer of the ampulla of Vater, pancreas, or bile duct (cholangiocarcinoma) until proven otherwise^[5]. This agreement arose because of the difficulty in obtaining a tissue diagnosis in patients with obstructive jaundice caused by a bile duct stricture. Application of improved diagnostic methods, such as thin-section spiral CT and magnetic resonance cholangiopancreatography, can potentially increase the diagnostic accuracy, but neither could reliably differentiate malignant from benign lesions^[6,7]. Preoperative histological or cytological examination by means of biopsy or brush cytology was often difficult and liable to false-negative results with low sensitivity and could carry a potential risk of needle tract metastases^[8-12]. The lack of a tissue or cytological evidence might result in some patients being inappropriately treated as malignant disease when a benign stricture was present and vice versa. In the study of Gerhards *et al.*^[4] a false-positive preoperative diagnosis of malignancy resulted in a 15% resection rate of benign lesions in patients with suspicious hilar strictures. Careful review of all preoperative information and radiological images of our 2 cases yielded the initial diagnosis of a CBD tumor, although post-operative pathological examination revealed only inflammation and fibrosis. The decision to undertake resection of the strictures in these 2 cases was therefore not an error of judgment. Obviously, resection of the lesion and obtaining a tissue diagnosis are still the most reliable way to rule out malignancy. Therefore, resection of a benign stricture mimicking a malignant stricture in the extra-hepatic bile duct cannot be avoided completely. However, the lack of clinical constitutional symptoms such as body weight loss or abdominal pain and elevated tumor markers may implicate the possible benign entity of the disorder.

Benign, single, non-traumatic inflammatory strictures of the biliary tracts were infrequently reported with the exception of primary sclerosing cholangitis^[1-3]. Indeed, many benign nontraumatic inflammatory strictures of the common bile duct have been generally considered to be a variant of primary sclerosing cholangitis although Standfield *et al.*^[13] described 12 cases of benign strictures of unknown etiology, and differentiated them from the localized form of sclerosing cholangitis. Other inflammatory conditions of the CBD which are potential etiological factors included bacteria or virus infection, parasite infestation, abdominal trauma, congenital abnormality^[14], chronic pancreatitis^[15], inflammatory pseudotumors^[16], complication of chemotherapy^[17], complication of duodenal ulcer disease^[18-20], and sclerosing therapy of bleeding duodenal ulcer^[21]. Most benign segmental strictures of the extra-hepatic bile duct reported in the literature were located at the hilum or distal CBD. Few cases in the mid CBD have been reported.

The CBD strictures of these 2 patients were less likely due to biliary duct stones because the radiological studies and operative findings did not show the existence of stones. The normal pancreatogram excluded the possibility of chronic pancreatitis as the cause of mid CBD strictures. The radiological appearance, histological examination and the extremely rare incidence in this area made the diagnosis of primary sclerosing cholangitis less likely.

According to the clinical history and surgical findings, stricture of the CBD owing to fibrous encasement by chronic inflammatory changes due to an adjacent duodenal ulcer in these 2 cases was considered. Duodenal ulcer disease is a common disorder, and its associated complications such as hemorrhage, gastric outlet obstruction and perforation, are well known. However, the biliary complications of duodenal ulcer disease, such as biliary-enteric fistula or partial obstruction of the CBD were rare and less well-known^[18-20], especially after the worldwide use of effective antisecretory agents, H₂-receptor antagonists and proton pump inhibitors.

In conclusion, benign non-traumatic inflammatory strictures affecting the common bile duct can be mistaken for malignant tumors. Their existence should be considered in the differential diagnosis of any biliary strictures. The radiological documentation of these 2 cases is of interest to draw attention to the rare complication of obstructive jaundice secondary to duodenal ulcer disease. A tissue diagnosis should be obtained whenever possible as radiology alone is often insufficient to make a firm diagnosis of malignancy in biliary strictures.

REFERENCES

- Golematis B**, Giannopoulos A, Papachristou DN, Dreiling DA. Sclerosing cholangitis of the bifurcation of the common hepatic duct. *Am J Gastroenterol* 1981; **75**: 370-732
- Smadja C**, Bowley NB, Benjamin IS, Blumgart LH. Idiopathic localized bile duct strictures: relationship to primary sclerosing cholangitis. *Am J Surg* 1983; **146**: 404-408
- Panes J**, Bordas JM, Buguera M, Cortes M, Rhodes J. Localized sclerosing cholangitis? *Endoscopy* 1985; **17**: 121-122
- Gerhards MF**, Vos P, van Gulik TM, Rauws EAJ, Bosma A, Gauma DJ. Incidence of benign lesions in patients resected for suspicious hilar obstruction. *Br J Surg* 2001; **88**: 48-51
- Longmire WP Jr**, McArthur MS, Bastounis EA, Hiatt J. Carcinoma of the extrahepatic biliary tract. *Ann Surg* 1973; **178**: 333-345
- Feydy A**, Vilgrain V, Denys A, Sibert A, Belghiti J, Vuillierme MP. Helical CT assessment in hilar cholangiocarcinoma: correlation with surgical and pathologic findings. *Am J Roentgenol* 1999; **172**: 73-77
- Choi BI**, Han JK, Shin YM, Baek SY, Han MC. Peripheral cholangiocarcinoma: comparison of MRI with CT. *Abdom Imaging* 1995; **20**: 357-360
- Rabinovitz M**, Zajko AB, Hassanein T, Shetty B, Bron KM, Schade RR, Gavaler JS, Block G, Van Thiel DH, Dekker A. Diagnostic value of brush cytology in the diagnosis of bile duct carcinoma: a study of 65 patients with bile duct strictures. *Hepatology* 1990; **12**: 747-752
- Rustgi AK**, Kelsey PB, Guelrud M, Saini S, Schapiro RH. Malignant tumors of the bile ducts: diagnosis by biopsy during endoscopic cannulation. *Gastroint Endosc* 1989; **35**: 248-251
- Terasaki K**, Wittich GR, Lycke G, Walter R, Nowels K, Swanson D, Lucas D. Percutaneous transluminal biopsy of biliary strictures with a biptome. *Am J Roentgenol* 1991; **156**: 77-78
- Cope C**, Marinelli DL, Weinstein JK. Transcatheter biopsy of lesions obstructing the bile ducts. *Radiology* 1988; **169**: 555-556
- Andersson R**, Andren-Sandberg A, Lundstedt C, Tranberg KG. Implantation metastases from gastrointestinal cancer after percutaneous puncture or biliary drainage. *Eur J Surg* 1996; **162**: 551-554
- Standfield NJ**, Salisbury JR, Howard ER. Benign non-traumatic inflammatory strictures of the extrahepatic biliary system. *Br J Surg* 1998; **76**: 849-852
- Baggott BB**, Long WB. Annular pancreas as a cause of extrahepatic biliary obstruction. *Am J Gastroenterol* 1991; **86**: 224-226
- Littenberg G**, Afroudakis A, Kaplowitz N. Common bile duct stenosis from chronic pancreatitis: a clinical and pathologic spectrum. *Medicine* 1979; **58**: 385-412
- Hadjis NS**, Collier NA, Blumgart LH. Malignant masquerade at the hilum of the liver. *Br J Surg* 1985; **72**: 659-661
- Herrmann G**, Lorenz M, Kirkowa-Reiman M, Hottenrott C, Hubner K. Morphological changes after intra-arterial chemotherapy of the liver. *Hepatogastroenterology* 1987; **34**: 5-9
- Neiman JH**. Obstructive jaundice caused by duodenal ulcer. *J Am Med Assoc* 1953; **152**: 141
- Glick S**. Benign non-traumatic stricture of the common bile duct owing to penetrating duodenal ulcer. *Br J Surg* 1971; **58**: 918-920
- Fuller JW**, Christensen JA, Sherman RT. Common bile duct obstruction secondary to peptic ulcer. *Ann Surg* 1975; **41**: 640-642
- Luman W**, Hudson N, Choudari CP, Eastwood MA, Palmer KR. Distal biliary stricture as a complication of sclerosant injection for bleeding duodenal ulcer. *Gut* 1994; **35**: 1665-1667

Edited by Wang XL Proofread by Chen WW and Xu FM

Hepatitis E: An overview and recent advances in vaccine research

Ling Wang, Hui Zhuang

Ling Wang, Hui Zhuang, Department of Microbiology, Peking University Health Science Center, Beijing 100083, China

Supported by the National Major Projects of National Committee of Science and Technology (2502AA2Z3342), and the Beijing Municipal Committee of Science and Technology (H020920020190)

Correspondence to: Hui Zhuang, Professor of Department of Microbiology, Peking University Health Science Center, Beijing 100083, China. zhuanghu@publica.bj.cninfo.net

Telephone: +86-10-82802221 **Fax:** +86-10-82801617

Received: 2003-11-22 **Accepted:** 2004-01-08

Abstract

Hepatitis E virus (HEV) is an unclassified, small, non-enveloped RNA virus, as a causative agent of acute hepatitis E that is transmitted principally via the fecal-oral route. The virus can cause large water-borne epidemics of the disease and sporadic cases as well. Hepatitis E occurs predominantly in developing countries, usually affecting young adults, with a high fatality rate up to 15-20% in pregnant women. However, no effective treatment currently exists for hepatitis E, and the only cure is prevention. But so far there are no commercial vaccines for hepatitis E available in the world. Although at least four major genotypes of HEV have been identified to date, only one serotype of HEV is recognized. So there is a possibility to produce a broadly protective vaccine. Several studies for the development of an effective vaccine against hepatitis E are in progress and the best candidate at present for a hepatitis E vaccine is a recombinant HEV capsid antigen expressed in insect cells from a baculovirus vector. In this article, the recent advances of hepatitis E and the development of vaccine research for HEV including recombinant protein vaccine, DNA vaccine and the recombinant hepatitis E virus like particles (rHEV VLPs) are briefly reviewed.

Wang L, Zhuang H. Hepatitis E: An overview and recent advances in vaccine research. *World J Gastroenterol* 2004; 10(15): 2157-2162

<http://www.wjgnet.com/1007-9327/10/2157.asp>

INTRODUCTION

Hepatitis E previously known as enterically transmitted non-A, non-B hepatitis, is an infectious viral disease with clinical and epidemiological features of acute hepatitis. It is a water-borne disease, transmitted primarily by contaminated water. There is also a possibility of zoonotic spread of the virus, since several non-human primates, pigs, cows, sheep, goats and rodents are susceptible to the infection^[1,2]. Hepatitis E virus (HEV) is a principal cause of acute hepatitis in adults throughout much of Asia, Middle East and Northern Africa^[3] and transmitted from person-to-person through the fecal-oral route. HEV had provisionally been classified into the *caliciviridae* family from 1988 to 1998, but now it is classified into the separate genus *Hepatitis E-like viruses*^[4-6] because the phylogenetic analysis of non-structural regions of the virus did not support the classification of HEV into the *Caliciviridae* family^[7]. Although at least four major genotypes have been

identified, only one serotype of HEV is recognized^[8-10]. HEV infection is endemic in developing countries where sanitary conditions are not well maintained. Over 50 outbreaks have been reported in Southeast and Central Asia, the Middle East, northern and western parts of Africa, and Mexico^[11-15]. Most of hepatitis E cases in developed countries have been linked to travel to endemic areas. However, recent studies revealed that hepatitis E also occurred in patients who had never been abroad^[16-18]. China is one of the high epidemic areas and there have been 11 hepatitis E epidemics reported to date. The largest one in the world occurred in Xinjiang Uighur Autonomous Region, the Northwest of China, during 1986-1988, with a total number of 119 280 cases and more than 700 deaths^[19-20]. Hepatitis E accounts for more than 50% of acute viral hepatitis in young adults of developing countries, although only 1% to 3% of non-pregnant patients progress to fatal fulminant hepatitis, the case-fatality rate can be as high as 20% among pregnant patients^[21], constituting a serious public health problem and stressing the need for development of an effective vaccine. The development of an attenuated or killed vaccine is not currently possible because of lacking an efficient cell culture system for replication of HEV^[22-27], although some cell lines have been reported for culturing and isolating HEV *in vitro*^[28,29]. Therefore, either a nucleic acid-based vaccine or a recombinant protein vaccine is needed. Compared with gene engineering vaccine for hepatitis B, the study of hepatitis E recombinant vaccine was only a recent endeavor, but some progress has been made^[30].

HEV GENOME

HEV genome consists of a linear, single-stranded, positive-sense RNA of approximately 7.5 kb containing a 3' poly (A) tail and 3' noncoding (NC) regions, and contains three overlapping open reading frames (ORFs). All three coding frames are used to express different proteins^[31-33] (Figure 1). ORF1 begins at the 5' end of the viral genome after a 27-bp non-coding sequence and extends 5 079 nt to the 3' end. ORF1 encodes a polyprotein of about 1 690 amino acids (aa) consisting of non-structural proteins that are involved in viral genome replication and viral protein processing, as its sequence contains motifs characteristic of viral methyltransferases, papain-like cysteineproteases, helicases and RNA-dependent RNA polymerases. In addition, ORF1 has two regions called Y and X domains of unknown function. The very short 5' NTR at the 5' end of the viral genome of 27-35 nucleotides is consistent with a capped genome. The ability of a monoclonal antibody to recognize 7-methylguanosine in RNA extracted from virions of different HEV genotypes suggests that HEV RNAs are capped^[34,35]. ORF3 is 369 nt long, located at the end of ORF1 and overlaps ORF1 at its 5' end by only 1 nt, and overlaps ORF2 by 328 nt. It encodes for a 123-aa protein (pORF3), which is expressed intracellularly. The studies of the biology of HEV replication have shown that pORF3 may be capable of associating with the liver cell cytoskeleton and appears to serve as a cytoskeletal anchor site, where pORF2 and RNA can bind to begin the process of viral nucleocapsid assembly^[36].

The ORF2 is located between 5 147 and 7 127 nt, consists of 1 980 nt and encodes 660 aa (71-88 kDa) most likely representing one or more structural or capsid protein(s)^[2,29-31].

However, the size of the ORF2 protein in native virions is not known^[37]. *In vitro* assays suggest that the -88 kDa of glycoprotein is co-translationally translocated across the endoplasmic reticulum and is expressed intracellularly as well as on the cell surface^[38]. ORF2 contains important epitopes that can induce neutralizing antibodies and has been the focus of vaccine development^[39]. Major epitopes appear to exist near the carboxyl ends of ORF2 and ORF3. Epitopes contained in ORF2 are more conserved (90.5%) than epitopes contained in ORF3 (73.5%) in different strains. Many different ORF2 antigens have been shown to induce antibody (Table 1). There are a number of reports suggesting that truncated ORF2 peptide of shorter length might be more antigenic than the full-length protein^[40-44]. However, in the majority of cases, it has not been shown that the resulting antibodies are neutralizing and, therefore, it is not known whether these antigens could serve as vaccine candidates. Only three ORF2 antigens (trpE-C2, Burma 62 kDa, Pakistan 55 kDa) thus far have been shown to induce antibodies that neutralize the virus^[33].

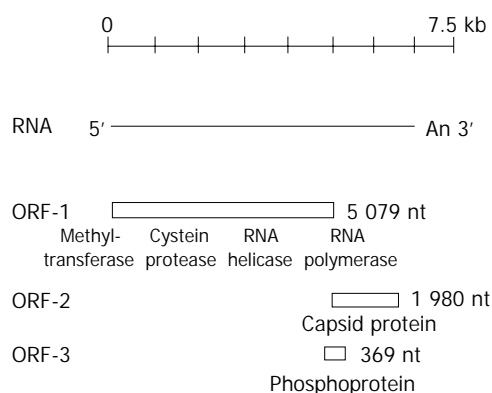


Figure 1 Genetic map of hepatitis E virus.

Table 1 HEV ORF2 antigenic peptides

HEV (origin)	Designation	Amino acid	
		N'	C'
Expressed in <i>E. coli</i>			
China	ORF2	1	660
Burma	TrpE-C2	221	660
Burma	SG3	328	654
China	ORF2.1	394	660
Mexico, Burma	3.2	612	654
Expressed in insect cells			
Burma	72 ku	1	660
Pakistan	63 ku	112	660
Burma	62 ku	112	636
Pakistan	55 ku	112	607
Pakistan	53 ku	112	578
Burma	50 ku	112	534
DNA vaccine			
Burma	pJHEV	1	660
China	pSVL-ORF3	1	123

HEV GENOTYPE

The genome sequence of HEV seems relatively stable^[45]. The genome of strains isolated from geographically distinct locations is generally more diverse. At present, no consensus exists on genotype classification. The detected HEV strains are currently genetically characterized in laboratories on the basis of ORFs regions^[32]. Recently, some research workers have

also started to characterize HEV strains antigenetically using specific antibodies produced by the recombinant expressed capsid proteins^[46,47]. On the basis of viruses having nucleotide divergence of not more than 20% of the nucleotides in the ORF2 region^[48], the genomes of several HEV strains from different parts of the world can be grouped into at least four major genotypes^[8,31,32,49]: Genotype 1 -including the isolates from South-East Asian (Burmese, some Indian strains), North and Central Asian (strains from China, Pakistan, Kyrgyzstan, and India), and North African strains; Genotype 2 -comprising the single North American (Mexico) isolate; Genotype 3 -consisting of the US and swine isolates; and Genotype 4 -including a subset of isolates from China and most isolates from Taiwan. Genetically heterogeneous isolates from several European countries have been designated new genotypes, but probably should be grouped with the US isolates into a large, heterogeneous group^[31,50]. Two novel isolates of HEV have recently been described in Argentina. Distinct from all previously described isolates, they represent two diverse subtypes of a new genotype of HEV^[51]. Despite the diversity of HEV genotype, no evidence has been found that heterogeneity results from the genetic diversity, thus HEV seems to exist as a single serotype^[8-10].

HEV VACCINE RESEARCHES

At present, no commercially available vaccines exist for the prevention of hepatitis E. However, several studies for the development of an effective vaccine against hepatitis E are in progress^[37,52-56]. Several lines of evidence have suggested the feasibility of a HEV vaccine. First, serum antibodies to HEV develop in response to naturally acquired and experimentally induced HEV infections in cynomolgus monkeys^[57]. Second, seroepidemiology of hepatitis E suggests that people previously infected with HEV are protected during epidemics of the disease^[58]. Finally, successful passive immune prophylaxis in animals indicated that effective vaccination against hepatitis E based on humoral immunity is possible^[59]. Although different geographical isolates of HEV have been identified, only one serotype has been recognized^[8]. So it may be possible to produce a broadly protective vaccine.

ORF2-encoded protein of HEV is the most promising subunit vaccine candidate because it possesses a good antigenicity. So far, HEV ORF2 gene or its fragments have been expressed in prokaryote cells^[56,60-64], insect cells^[37,65-68], yeast cells^[69-71], animal cells^[72], and plants (tomatoes)^[30], etc., and the expression products possess immunogenicity.

Expression in prokaryote cells

It was reported recently that the smallest fragment of ORF2, which is capable of combining the neutralizing antibody of HEV, is located between 452 and 617 aa. This fragment does not only induce neutralizing antibody, but also cross react to the antibody of other genotype^[22]. It was demonstrated that the 2/3 length of C-terminal region of HEV ORF2 contains epitopes, which are recognized by both acute-phase and convalescent-phase antibody to HEV and are likely to be associated with limited immunity to the infection, but these epitopes may be masked when larger portions of ORF2 are expressed as recombinant proteins^[64]. So far, many different length of ORF2 fragments have been expressed in *E. coli*^[56,63,64], but only a few expression products have been found with significant immunoactivity. The first candidate HEV vaccine was a recombinant fusion protein including 439 amino acids (221-660 aa). It comprised tryptophan synthetase and the carboxy terminal fragment of the ORF2 protein of the Burmese strain (genotype 1) and was expressed in *E. coli*. Two cynomolgus macaques were vaccinated with the fusion protein,

and neither of them developed hepatitis following experimental challenge. The animals challenged with the heterologous HEV, the Mexican strain (genotype 2), did get infected, but did not develop hepatitis^[73]. Another study also shows that the immunization with the bacterially expressed ORF2 peptide (pE2) corresponding to 394–607 aa, may prevent HEV infection in primates experimentally transmitted with the homologous strain of HEV^[56].

Expression in insect cells

It is thought that the best candidate at present for a hepatitis E vaccine is a recombinant HEV capsid antigen expressed in insect cells from a baculovirus vector^[25]. When ORF2 of genotype 1 strain is expressed from a baculovirus vector in insect cells, the initial 72-ku protein is quickly processed to smaller proteins, possibly via a protease encoded by the baculovirus^[66]. The most abundant proteins are 56 ku and 53 ku in size, respectively. However, the only neutralization epitope identified to date was mapped to a region of the ORF2 protein of Sar-55 between amino acids 578 and 607^[74]. Therefore, the 56 ku protein (112–607 aa) but not the 53 ku protein (112–578 aa) should contain this epitope. The recombinant 56 ku protein that is more soluble than the full-length protein was an efficient immunogen when adjuvanted with alum^[53,57]. Two 400 ng doses of the vaccine were injected to rhesus monkeys intramuscularly and high antibody titers (1:10 000) were achieved. The monkeys were protected against hepatitis E following intravenous challenge with 300 000 monkey infectious doses (MID₅₀) of the homologous (Sar-55) or 100 000 MID₅₀ of a heterologous HEV (Mexican 14)^[57]. To evaluate the immunogenicity and protective efficacy of the 53 kDa protein, the same research group immunized rhesus monkeys with the 53 ku vaccine, which was derived from processing of the ORF2 protein of Sar-55 and purified from the medium of recombinant baculovirus-infected insect cells and precipitated with alum. Two doses of vaccine containing 385 ng of alum-precipitated 53 ku protein were inoculated into the monkeys intramuscularly. The immunized monkeys were challenged with a high (1000 MID₅₀) or low (100 MID₅₀) dose of homologous virus. The result showed vaccination with the 53 ku protein greatly reduced virus shedding, but did not protect against hepatitis following the high dose challenge. Virus was not detected in the vaccinated animals following the low dose challenge, suggesting that sterilizing immunity might have been achieved. This study indicated that the 53 ku protein did not function as a better vaccine than did the 56 ku protein and actually appeared to have been less effective in preventing disease^[57]. The researches have shown that almost complete vaccine-induced protection lasts for at least 6 mo and partial protection persists for at least 1 year following vaccination^[75].

Expression in yeast and other cells

Recently, yeast expression system has been successfully used for production of vaccines, for example, the recombinant hepatitis B surface antigen^[76,77]. There are some advantages of using this expression system, such as the expression products similar to the natural protein, maintaining the biological activity of the production, to produce easily in large scale and so on^[78]. In recent studies, the ORF2 of HEV (69–660 aa and 112–660 aa) was successfully expressed in *pichia pastoris* and the expression products of recombinant protein (59 ku) was purified and immunized to rhesus monkeys. High titer of anti-HEV (1:8000) was detected in the immunized monkeys^[69–71,79]. Research on using plants for expression and delivery of oral vaccine has attracted much academic attention and has become a hot spot of study since 1990 when Curtiss *et al.*^[80] first reported the expression of *Streptococcus* mutants surface protein antigen A (SpaA) in tobacco, and great progress has

been made since then^[81]. In a recent study, the ORF2 partial gene of HEV named E2 (810 bp, 349–604 aa) was constructed into plasmid pCAMBIA1301 and yielded the reconstructed plant binary expression plasmid p1301E2^[62]. The p1301E2 was expressed in tomatoes and the recombinant antigen derived from them has normal immunoactivity. The transgenic tomatoes may hold a good promise for producing a new type of low-cost oral vaccine for hepatitis E^[30].

Subunit HEV vaccines

DNA immunization usually induces both cellular and antibody immune response. So it might provide a longer duration of protection. Therefore, it has become another focus of HEV vaccine research. Recombinant DNA vaccine is a recently developed new type of vaccine. Through directly injecting the recombinant plasmid DNA with the target gene into human or animals, the DNA will express the expected protein inside the host cells and therefore induce the immune responses to prevent and fight the disease. Recently, a new technology has been introduced for the development of subunit vaccines involving the direct injection of purified plasmid DNA containing protein coding sequences of interest and appropriate regulatory elements allowing expression in mammalian tissues. This novel technology has several potential advantages over other vaccine approaches^[82]. First, the antigens expressed in living cells are in their native form, improving processing and presentation and usually resulting in the activation of both arms of the immune system. Second, DNA can be made inexpensively, in large quantities, at high levels of purity, and is extremely stable. Third, the vector is unlikely to be, or to become, pathogenic, in contrast to live-virus vaccines, and there is little or no immune response to the vector.

In an early study, an HEV cDNA pSVL-ORF3 was constructed by inserting the full length of ORF3 fragment into prokaryotic expression vector pSVL. A total amount of 100 µg of the cDNA was injected to BALB/c mice intramuscularly and anti-HEV IgG was detected in 12 of the 16 immunized mice. However, no antibody was found in the mice injected with the empty vector. The result indicated that the recombinant HEV cDNA could induce the antibody response in mice^[83]. Later, another HEV cDNA pJHEV was constructed by inserting full length of ORF2 fragment. The HEV structural protein was expressed in Cos-7 cells under the control of a hCMV promoter. The successful construct was further tested in BALB/c mice for the induction of an ORF2 specific immune response. All the mice immunized with the cDNA were found seroconverted, but no anti-HEV responses induced in the mice of control group. Sera from the mice injected with pJHEV specifically recognized HEV ORF2 structural protein expressed in recombinant baculovirus in an enzyme-linked-immunosorbent assay (ELISA) and Western blot^[82]. Furthermore, it was also shown that the antiserum generated by the DNA vaccine could bind specifically to native HEV^[84]. Recently, a full-length HEV cDNA clone was constructed in a pSGI vector. The three ORFs were amplified separately and then reconstructed to the full-length clone. The *in vitro* transcribed RNA of the full-length cDNA clone was infective in a HepG2 tissue culture. Viral replication was detected for six passages with strand-specific PCR^[85].

The rHEV VLPs

In spite of the above vaccine candidates, recently the recombinant hepatitis E virus (rHEV) virus-like particles (VLPs) are also the focuses of vaccine research for hepatitis E. With 111 amino acids truncated at the N-terminal, when the capsid protein of HEV was expressed in the baculovirus expression system, it was spontaneously assembled into virus-like particles^[54]. Electron cryomicroscopy shows that these VLPs are formed with

60 copies of a 54 ku protein arranged in T=1 symmetry^[54, 86, 87]. As a mucosal immunogen, the VLPs have several advantages: they are composed of a single protein assembled into particles without nucleic acid, which makes them unable to replicate; they are easy to prepare and purify in large quantities, with a yield of approximately 1 mg /10⁷ insect cells; rHEV VLPs are antigenically similar to the native virions; they are highly immunogenic in experimental animals when injected parenterally; they are very stable at low pH such as in stomach; and oral delivery of rHEV VLPs could induce the same immune responses as occur in natural infection^[86,54].

In a previous study^[87], mice were orally inoculated with purified rHEV VLPs without adjuvant. Serum IgM response was obtained within 2 wk after the first administration. Serum IgG and IgA were detected by 4 wk, and the intestinal IgA response was found at 8 wk post-immunization. Therefore, the oral immunization of rHEV VLPs is capable of inducing both systemic and intestinal antibody responses. However, since mice are not susceptible to HEV, the same group recently immunized cynomolgus monkeys orally with 10 mg of purified rHEV VLPs, serum IgM, IgG, and IgA responses were observed. All these antibody responses were obtained without adjuvants. When the monkeys were challenged with native HEV by intravenous injection, they were protected against infection or developing hepatitis. These results suggested that rHEV VLPs could be a candidate for the oral hepatitis E vaccine^[88]. Some similar experiments have been described previously^[89-91].

PRE-CLINICAL AND CLINICAL TRIALS

So many vaccine candidates for hepatitis E have been explored as described above. But so far, there is only one HEV vaccine candidate progressed to the stage of clinical trials. That is the 56 ku (expressed in insect cells from a baculovirus vector) recombinant vaccine developed at the NIH, USA^[68]. In phase I trial, the vaccine was found to be safe and immunogenic in 88 American volunteers. A further phase I evaluation was performed in Nepal, where hepatitis E is endemic. Three doses of 5 µg and 20 µg, respectively, were injected into 22 Nepalese volunteers each at zero, one and six months. No serious adverse events were observed. By the second month, 43 of 44 volunteers had seroconverted to anti-HEV. By the 7th month, the remaining volunteers also developed antibody to HEV. The study indicated that the HEV vaccine candidate was safe and immunogenic. This same lot of vaccine is currently being used in phase II/III clinical trials in Nepal^[25], where as many as 90% of the jaundice cases are caused by HEV.

In recent pre-clinical trials, the vaccine used in the experiment was from the same lot that was prepared for the above clinical trials. The results indicated that two doses of HEV vaccine as small as 1 µg were highly effective in preventing not only hepatitis but also infection following intravenous administration of 10⁴ MID₅₀ of virulent virus. However, these doses of vaccine will not be sufficient for long-term protection. Other studies have shown that a third dose of vaccine at 6 or 12 mo following the first dose will enhance immunogenicity and/or efficacy^[75,92]. The study has also confirmed that the cross-protection against a Mexican genotype 2 isolate and extended the evidence for cross-protection to a US genotype 3 isolate of HEV. The results of this experiment have shown that the manufacture of a candidate hepatitis E vaccine can be scaled up to produce more clinical quality and that such a vaccine is highly immunogenic and effective for preventing hepatitis E in the pre-clinical trials. It is likely that protection against infection will be more effective following natural oral challenge with relatively small doses of HEV^[25].

CONCLUSIONS

Despite the achievements mentioned above, there are still many questions to be answered in future. For example, there is a study showing that acute hepatitis E can be induced by plasma transfusion from a donor with HEV viremia, which indicates the possibility of transfusion transmitted hepatitis E^[93]. Some similar studies also showed the possibility of post-transfusion hepatitis E^[94-97]. Therefore, effective measures for preventing post-transfusion hepatitis E must be taken. To achieve effective immunization, how should the HEV vaccine be given by, orally or intramuscularly? Will a monovalent vaccine protect against all HEV strains including HEV from animals and genotypes and provide a long-term immunity to hepatitis E? To facilitate vaccine development and to improve our knowledge about the mechanism of virus replication, an effective practical cell culture system should be established and demonstrated.

REFERENCES

- Harrison TJ. Hepatitis E virus-an update. *Liver* 1999; **19**: 171-176
- Aggarwal R, Krawczynski K. Hepatitis E: an overview and recent advances in clinical and laboratory research. *J Gastroenterol Hepatol* 2000; **15**: 9-20
- Perez-Gracia MT, Rodriguez-Iglesias M. Hepatitis E virus: current status. *Med Clin* 2003; **121**: 787-792
- Pringle CR. Virus taxonomy-San Diego 1998. *Arch Virol* 1998; **143**: 1449-1459
- Pringle CR. Virus taxonomy-1999. The universal system of virus taxonomy, updated to include the new proposals ratified by the International Committee on Taxonomy of Virus during 1998. *Arch Virol* 1999; **144**: 421-429
- Green KY, Ando T, Balayan MS, Berke T, Clarke IN, Estes MK, Matson DO, Nakata S, Neill JD, Studdert MJ, Thiel HJ. Taxonomy of the caliciviruses. *J Infect Dis* 2000; **181**(Suppl 2): S322-S330
- Berke T, Matson DO. Reclassification of the Caliciviridae into distinct genera and exclusion of hepatitis E virus from the family on the basis of comparative phylogenetic analysis. *Arch Virol* 2000; **145**: 1421-1436
- Schlauder GG, Mushahwar IK. Genetic heterogeneity of hepatitis E virus. *J Med Virol* 2001; **65**: 282-292
- Meng XJ, Purcell RH, Halbur PG, Lehman JR, Webb DM, Tsareva TS, Haynes JS, Thacker BJ, Emerson SU. A novel virus in swine is closely related to the human hepatitis E virus. *Proc Natl Acad Sci U S A* 1997; **94**: 9860-9865
- Wang Y, Zhang H, Ling R, Li H, Harrison TJ. The complete sequence of hepatitis E virus genotype 4 reveals an alternative strategy for translation of open reading frames 2 and 3. *J Gen Virol* 2000; **81**(Pt 7): 1675-1686
- Viswanathan R. A review of the literature on the epidemiology of infectious hepatitis. *Indian J Med Res* 1957; **45**(Suppl): 145-155
- Khuroo MS. Study of an epidemic of non-A, non-B hepatitis. Possibility of another human hepatitis virus distinct from post-transfusion non-A, non-B type. *Am J Med* 1980; **68**: 818-824
- Arora NK, Panda SK, Nanda SK, Ansari IH, Joshi S, Dixit R, Bathla R. Hepatitis E infection in children: study of an outbreak. *J Gastroenterol Hepatol* 1999; **14**: 572-577
- Naik SR, Aggarwal R, Salunke PN, Mehrotra NN. A large water-borne viral hepatitis E epidemic in Kanpur, India. *Bull World Health Organ* 1992; **70**: 597-604
- Velazquez O, Stetler HC, Avila C, Ornelas G, Alvarez C, Hadler SC, Bradley DW, Sepulveda J. Epidemic transmission of enterically transmitted non-A, non-B hepatitis in Mexico, 1986-1987. *JAMA* 1990; **263**: 3281-3285
- Schlauder GG, Dawson GJ, Erker JC, Kwo PY, Knigge MF, Smalley DL, Rosenblatt JE, Desai SM, Mushahwar IK. The sequence and phylogenetic analysis of a novel hepatitis E virus isolated from a patient with acute hepatitis reported in the United States. *J Gen Virol* 1998; **79**(Pt 3): 447-456
- Erker JC, Desai SM, Schlauder GG, Dawson GJ, Mushahwar IK. A hepatitis E virus variant from the United States: molecular characterization and transmission in cynomolgus macaques. *J Gen Virol* 1999; **80**(Pt 3): 681-690

- 18 **Takahashi K**, Iwata K, Watanabe N, Hatahara T, Ohta Y, Baba K, Mishiro S. Full-genome nucleotide sequence of a hepatitis E virus strain that may be indigenous to Japan. *Virology* 2001; **287**: 9-12
- 19 **Zhuang H**, Cao XY, Liu CB, Wang GM. Epidemiology of hepatitis E in China. *Gastroenterol Jpn* 1991; **26**(Suppl): 135-138
- 20 **Zhuang H**, Zhu WF, Li F, Zhu XJ, Li K, Cui YH, Zhu YH. Studies on hepatitis E. *Chin Med Sci J* 1999; **14**(Suppl): S47-50
- 21 **Skidmore S**. Overview of hepatitis E virus. *Curr Infect Dis Rep* 2002; **4**: 118-123
- 22 **Meng J**, Dai X, Chang JC, Lopareva E, Pillot J, Fieds HA, Khudyakov YE. Identification and characterization of the neutralization epitope(s) of the hepatitis E virus. *Virology* 2001; **288**: 203-211
- 23 **Schofield DJ**, Purcell RH, Nguyen HT, Emerson SU. Monoclonal antibodies that neutralize HEV recognize an antigenic site at the carboxyterminus of an ORF2 protein vaccine. *Vaccine* 2003; **22**: 257-267
- 24 **Meng J**, Dubreuil P, Pillot J. A new PCR-based seroneutralization assay in cell culture for diagnosis of hepatitis E. *J Clin Microbiol* 1997; **35**: 1373-1377
- 25 **Purcell RH**, Nguyen H, Shapiro M, Engle RE, Govindarajan S, Blackwelder WC, Wong DC, Prieels JP, Emerson SU. Pre-clinical immunogenicity and efficacy trial of a recombinant hepatitis E vaccine. *Vaccine* 2003; **21**: 2607-2615
- 26 **Zhang J**, Ge SX, Huang GY, Li SW, He ZQ, Wang YB, Zheng YJ, Gu Y, Ng MH, Xia NS. Evaluation of antibody-based and nucleic acid-based assays for diagnosis of hepatitis E virus infection in a rhesus monkey model. *J Med Virol* 2003; **71**: 518-526
- 27 **Grimm AC**, Fout GS. Development of a molecular method to identify hepatitis E virus in water. *J Virol Methods* 2002; **101**: 175-188
- 28 **Tam AW**, White R, Yarbough PO, Murphy BJ, McAttee CP, Lanford RE, Fuerst TR. *In vitro* infection and replication of hepatitis E virus in primary cynomolgus macaque hepatocytes. *Virology* 1997; **238**: 94-102
- 29 **Huang R**, Li D, Wei S, Li Q, Yuan X, Geng L, Li X, Liu M. Cell culture of sporadic hepatitis E virus in China. *Clin Diagn Lab Immunol* 1999; **6**: 729-733
- 30 **Ma Y**, Lin SQ, Gao Y, Li M, Luo WX, Zhang J, Xia NS. Expression of ORF2 partial gene of hepatitis E virus in tomatoes and immunoactivity of expression products. *World J Gastroenterol* 2003; **9**: 2211-2215
- 31 **Hepatitis E**. World health organization. *WHO/CDS/CSR/EDC/2001*: 12
- 32 **Worm HC**, van der Poel WH, Brandstatter G. Hepatitis E: an overview. *Microbes Infect* 2002; **4**: 657-666
- 33 **Emerson SU**, Purcell RH. Recombinant vaccines for hepatitis E. *Trends Mol Med* 2001; **7**: 462-466
- 34 **Magden J**, Takeda N, Li T, Auvinen P, Ahola T, Miyamura T, Merits A, Kaariainen L. Virus-specific mRNA capping enzyme encoded by hepatitis E virus. *J Virol* 2001; **75**: 6249-6255
- 35 **Kabrane-Lazizi Y**, Meng XJ, Purcell RH, Emerson SU. Evidence that the genomic RNA of hepatitis E virus is capped. *J Virol* 1999; **73**: 8848-8850
- 36 **Zafrullah M**, Ozdener MH, Panda SK, Jameel S. The ORF3 protein of hepatitis E virus is a phosphoprotein that associates with the cytoskeleton. *J Virol* 1997; **71**: 9045-9053
- 37 **Zhang M**, Emerson SU, Nguyen H, Engle RE, Govindarajan S, Gertin JL, Purcell RH. Immunogenicity and protective efficacy of a vaccine prepared from 53 kDa truncated hepatitis E virus capsid protein expressed in insect cells. *Vaccine* 2001; **20**: 853-857
- 38 **Zafrullah M**, Ozdener MH, Kumar R, Panda SK, Jameel S. Mutational analysis of glycosylation, membrane translocation, and cell surface expression of the hepatitis E virus ORF2 protein. *J Virol* 1999; **73**: 4074-4082
- 39 **Tam AW**, Smith MM, Guerra ME, Huang CC, Bradley DW, Fry KE, Reyes GR. Hepatitis E virus (HEV): molecular cloning and sequencing of the full-length viral genome. *Virology* 1991; **185**: 120-131
- 40 **Zhang Y**, McAttee P, Yarbough PO, Tam AW, Fuerst T. Expression, characterization, and immunoreactivities of a soluble hepatitis E virus putative capsid protein species expressed in insect cells. *Clin Diagn Lab Immunol* 1997; **4**: 423-428
- 41 **Ghabrah TM**, Tsarev S, Yarbough PO, Emerson SU, Strickland GT, Purcell RH. Comparison of tests for antibody to hepatitis E virus. *J Med Virol* 1998; **55**: 134-137
- 42 **Anderson DA**, Li F, Riddell M, Howard T, Seow HF, Torresi J, Perry G, Sumarsidi D, Shrestha SM, Shrestha IL. ELISA for IgG-class antibody to hepatitis E virus based on a highly conserved, conformational epitope expressed in *Escherichia coli*. *J Virol Methods* 1999; **81**: 131-142
- 43 **Li TC**, Zhang J, Shinzawa H, Ishibashi M, Sata M, Mast EE, Kim K, Miyamura T, Takeda N. Empty virus-like particle-based enzyme-linked immunosorbent assay for antibodies to hepatitis E virus. *J Med Virol* 2000; **62**: 327-333
- 44 **Obriadina A**, Meng J, Ulanova T, Trinta K, Burkov A, Fields H, Khudyakov Y. A new enzyme immunoassay for the detection of antibody to hepatitis E virus. *J Gastroenterol Hepatol* 2002; **17**(Suppl 3): S360-S364
- 45 **Arankalle VA**, Paranjape S, Emerson SU, Purcell RH, Walimbe AM. Phylogenetic analysis of hepatitis E virus isolates from India (1976-1993). *J Gen Virol* 1999; **80**(Pt 7): 1691-1700
- 46 **Riddell MA**, Li F, Anderson DA. Identification of immunodominant and conformational epitopes in the capsid protein of hepatitis E virus by using monoclonal antibodies. *J Virol* 2000; **74**: 8011-8017
- 47 **Wang Y**, Zhang H, Li Z, Gu W, Lan H, Hao W, Ling R, Li H, Harrison TJ. Detection of sporadic cases of hepatitis E virus (HEV) infection in China using immunoassays based on recombinant open reading frame 2 and 3 polypeptides from HEV genotype 4. *J Clin Microbiol* 2001; **39**: 4370-4379
- 48 **Anod T**, Noel JS, Fankhauser RL. Genetic classification of Norwalk-like viruses. *J Infect Dis* 2000; **181**(Suppl 2): S336-S348
- 49 **Wang Y**, Ling R, Erker JC, Zhang H, Li H, Desai S, Mushahwar IK, Harrison TJ. A divergent genotype of hepatitis E virus in Chinese patients with acute hepatitis. *J Gen Virol* 1999; **80**(Pt 1): 169-177
- 50 **Schlauder GG**, Desai SM, Zanetti AR, Tassopoulos NC, Mushahwar IK. Novel hepatitis E virus (HEV) isolates from Europe: evidence for additional genotypes of HEV. *J Med Virol* 1999; **57**: 243-251
- 51 **Schlauder GG**, Frider B, Sookoian S, Castano GC, Mushahwar IK. Identification of 2 novel isolates of hepatitis E virus in Argentina. *J Infect Dis* 2000; **182**: 294-297
- 52 **Purcell RH**, Emerson SU. Hepatitis E virus. In Knipe DM, Howley PM. *Fields Virology*, Fourth edition, V2 Lippincott and Wilkins, Philadelphia, PA 2001: 3051-3052
- 53 **Tsarev SA**, Tsareva TS, Emerson SU, Govindarajan S, Shapiro M, Gerin JL, Purcell RH. Recombinant vaccine against hepatitis E: dose response and protection against heterologous challenge. *Vaccine* 1997; **15**: 1834-1838
- 54 **Xing L**, Kato K, Li T, Takeda N, Miyamura T, Hammar L, Cheng RH. Recombinant hepatitis E capsid protein self-assembles into a dual-domain T=1 particle presenting native virus epitopes. *Virology* 1999; **265**: 35-45
- 55 **Yarbough PO**. Hepatitis E virus. Advances in HEV biology and HEV vaccine approaches. *Intervirology* 1999; **42**: 179-184
- 56 **Im SW**, Zhang JZ, Zhuang H, Che XY, Zhu WF, Xu GM, Li K, Xia NS, Ng MH. A bacterially expressed peptide prevents experimental infection of primates by the hepatitis E virus. *Vaccine* 2001; **19**: 3726-3732
- 57 **Tsarev SA**, Tsarva TS, Emerson SU, Govindarajan S, Shapiro M, Gerin JL, Purcell RH. Successful passive and active immunization of cynomolgus monkeys against hepatitis E. *Proc Natl Acad Sci U S A* 1994; **91**: 10198-10202
- 58 **Bryan JP**, Tsarev SA, Iqbal M, Ticehurst J, Emerson S, Ahmed A, Duncan J, Rafiqi AR, Malik IA, Purcell RH. Epidemic hepatitis E in Pakistan: patterns of serologic response and evidence that antibody to hepatitis E virus protects against disease. *J Infect Dis* 1994; **170**: 517-521
- 59 **Quiroga JA**, Cotonat T, Castillo I, Carreno V. Hepatitis E virus seroprevalence in acute viral hepatitis in a developed country confirmed by a supplemental assay. *J Med Virol* 1996; **50**: 16-19
- 60 **Zhang M**, Zhao H, Jiang Y. Expression of hepatitis E virus structural gene in *E. coli*. *Zhonghua Shiyan He Linchuang Bingduxue Zazhi* 1999; **13**: 130-132
- 61 **Bi S**, Lu J, Jiang L, Huang G, Pan H, Jiang Y, Zhang M, Shen X. Preliminary evidence that a hepatitis E virus (HEV) ORF2 recombinant protein protects cynomolgus macaques against challenge with wild-type HEV. *Zhonghua Shiyan He Linchuang Bingduxue Zazhi* 2002; **16**: 31-32
- 62 **Li SW**, Zhang J, He ZQ, Ge SX, Gu Y, Lin J, Liu RS, Xia NS. The

- study of aggregate of the ORF2 peptide of hepatitis E virus expressed in Escherichia coli. *Shengwu Gongcheng Xuebao* 2002; **18**: 463-467
- 63 **Li F**, Torresi J, Locarnini SA, Zhuang H, Zhu W, Guo X, Anderson DA. Amino-terminal epitopes are exposed when full-length open reading frame 2 of hepatitis E virus is expressed in Escherichia coli, but carboxy-terminal epitopes are masked. *J Med Virol* 1997; **52**: 289-300
- 64 **Li F**, Riddell MA, Seow HF, Takeda N, Miyamura T, Anderson DA. Recombinant subunit ORF2.1 antigen and induction of antibody against immunodominant epitopes in the hepatitis E virus capsid protein. *J Med Virol* 2000; **60**: 379-386
- 65 **Zhang M**, Yi Y, Zhan M, Liu C, Bi S. Expression of thermal stable, soluble hepatitis E virus recombinant antigen. *Zhonghua Shiyan He Linchuang Bingduxue Zazhi* 2002; **16**: 20-22
- 66 **Robinson RA**, Burgess WH, Emerson SU, Leibowitz RS, Sosnovtseva SA, Tsarev S, Purcell RH. Structural characterization of recombinant hepatitis E virus ORF2 proteins in baculovirus-infected insect cells. *Protein Expr Purif* 1998; **12**: 75-84
- 67 **McAtee CP**, Zhang Y, Yarbough PO, Fuerst TR, Stone KL, Samander S, Williams KR. Purification and characterization of a recombinant hepatitis E protein vaccine candidate by liquid chromatography-mass spectrometry. *J Chromatogr B Biomed Appl* 1996; **685**: 91-104
- 68 **Stevenson P**. Nepal calls the shots in hepatitis E virus vaccine trial. *Lancet* 2000; **355**: 1623
- 69 **Tong YP**, Bi SL, Jiang YZ, Zhan MY. Intracellular expression of hepatitis E virus ORF2 protein in *pichia pastoris* and its purification. *Bingdu Xuebao* 2001; **17**: 34-37
- 70 **Tong YP**, Bi SL, Zhang MC, Lu J, Zhan MY. Extracellular expression of hepatitis E virus ORF2 protein in *pichia pastoris*. *Zhonghua Shiyan He Linchuangbing Duxue Zazhi* 2000; **14**: 391-392
- 71 **Tong YP**, Lu J, Jian YZ, Bi SL, Zhan MY. The application of recombinant HEV ORF2 protein expressed in yeast cells to the diagnosis of hepatitis E. *Zhonghua Shiyan He Linchuang Bingduxue Zazhi* 2001; **15**: 189-190
- 72 **Jameel S**, Zafrullah M, Ozdener MH, Panda SK. Expression in animal cells and characterization of the hepatitis E virus structural proteins. *J Virol* 1996; **70**: 207-216
- 73 **Purdy MA**, McCaustland KA, Krawczynski K, Spelbring J, Reyes GR, Bradley DW. Preliminary evidence that a trpE-HEV fusion protein protects cynomolgus macaques against challenge with wild-type hepatitis E virus (HEV). *J Med Virol* 1993; **41**: 90-94
- 74 **Schofield DJ**, Glamann J, Emerson SU, Purcell RH. Identification by phage display and characterization of two neutralizing chimpanzee monoclonal antibodies to the hepatitis E virus capsid protein. *J Virol* 2000; **74**: 5548-5555
- 75 **Zhang M**, Emerson SU, Nguyen H, Engle R, Govindarajan S, Blasckwelder WC, Gerin J, Purcell RH. Recombinant vaccine against hepatitis E: duration of protective immunity in rhesus macaques. *Vaccine* 2002; **20**: 3285-3291
- 76 **Torres J**, Earnest-Silveira L, Deliyannis G, Edgtton K, Zhuang H, Locarnini SA, Fyfe J, Sozzi T, Jackson DC. Reduced antigenicity of the Hepatitis B virus HBsAg protein arising as a consequence of sequence changes in the overlapping polymerase gene that are selected by lamivudine therapy. *Virology* 2002; **293**: 305-313
- 77 **Zhang YX**, Dai L, Sun XM. Kinetic aspect of hepatitis B surface antigen production in recombinant *Saccharomyces cerevisiae* fermentation. *Process Biochemistry* 2003; **38**: 1593-1598
- 78 **Romanos M**. Advances in the use of *pichia pastoris* for high-level gene expression. *Curr Opin Biotechnol* 1995; **6**: 527-533
- 79 **Lu J**, Tong YP, Jiang YZ, Bi SL. The application of recombinant HEV ORF2 protein expressed in yeast cells to the detection of serum antibody in experimental rhesus monkeys. *Zhonghua Shiyan He Linchuang Bingduxue Zazhi* 2001; **15**: 382-383
- 80 **Curtiss R 3rd**, Galan JE, Nakayama K, Kelly SM. Stabilization of recombinant avirulent vaccine strains *in vivo*. *Res Microbiol* 1990; **141**: 797-805
- 81 **Gao Y**, Ma Y, Li M, Cheng T, Li SW, Zhang J, Xia NS. Oral immunization of animals with transgenic cherry tomatillo expressing HBsAg. *World J Gastroenterol* 2003; **9**: 996-1002
- 82 **He J**, Hoffman SL, Hayes CG. DNA inoculation with a plasmid vector carrying the hepatitis E virus structural protein gene induces immune response in mice. *Vaccine* 1997; **15**: 357-362
- 83 **Lu FM**, Zhuang H, Zhu YH, Zhu XI. A preliminary study on immune response to hepatitis E virus DNA vaccine in mice. *Chin Med J* 1996; **109**: 919-921
- 84 **He J**, Binn LN, Caudill JD, Asher LV, Longer CF, Innis BL. Antiserum generated by DNA vaccine binds to hepatitis E virus (HEV) as determined by PCR and immune electron microscopy (IEM): application for HEV detection by affinity-capture RT-PCR. *Virus Res* 1999; **62**: 59-65
- 85 **Panda SK**, Ansari IH, Durgapal H, Agrawal S, Jameel S. The *in vitro*-synthesized RNA from a cDNA clone of hepatitis E virus is infectious. *J Virol* 2000; **74**: 2430-2437
- 86 **Li TC**, Yamakawa Y, Suzuki K, Tatsumi M, Razak MA, Uchida T, Takeda N, Miyamura T. Expression and self-assembly of empty virus-like particles of hepatitis E virus. *J Virol* 1997; **71**: 7207-7213
- 87 **Li T**, Takeda N, Miyamura T. Oral administration of hepatitis E virus-like particles induces a systemic and mucosal immune response in mice. *Vaccine* 2001; **19**: 3476-3484
- 88 **Li TC**, Suzaki Y, Ami Y, Dhole TN, Miyamura T, Takeda N. Protection of cynomolgus monkeys against HEV infection by oral administration of recombinant hepatitis E virus-like particles. *Vaccine* 2004; **22**: 370-377
- 89 **Rose RC**, Lane C, Wilson S, Suzich JA, Rybicki E, Williamson AL. Oral vaccination of mice with human papillomavirus virus-like particles induces systemic virus-neutralizing antibodies. *Vaccine* 1999; **17**: 2129-2135
- 90 **Ball JM**, Hardy ME, Atmar RL, Conner ME, Estes MK. Oral immunization with recombinant Norwalk virus-like particles induces a systemic and mucosal immune response in mice. *J Virol* 1998; **72**: 1345-1353
- 91 **Estes MK**, Ball JM, Guerrero RA, Opekun AR, Gilger MA, Pacheco SS, Graham DY. Norwalk virus vaccine: Challenges and progress. *J Infect Dis* 2000; **181**(Suppl 2): S367-373
- 92 **Safary A**. Perspectives of vaccination against hepatitis E. *Intervirology* 2001; **44**: 162-166
- 93 **Xia NS**, Zhang J, Zheng YJ, Qiu Y, Ge SX, Ye XZ, Ou SH. Detection of hepatitis E virus on a blood donor and its infectivity to rhesus monkey. *Zhonghua Ganzangbing Zazhi* 2004; **12**: 13-15
- 94 **Nicand E**, Grandadam M, Teyssou R, Rey JL, Buisson Y. Viremia and faecal shedding of HEV in symptom-free carriers. *Lancet* 2001; **357**: 68-69
- 95 **Arankalle VA**, Chobe LP. Retrospective analysis of blood transfusion recipients: evidence for post-transfusion hepatitis E. *Vox Sang* 2000; **79**: 72-74
- 96 **Arankalle VA**, Chobe LP. Hepatitis E virus: can it be transmitted parenterally? *J Viral Hepat* 1999; **6**: 161-164
- 97 **Gao DY**, Peng G, Zhu JM, Sun L, Zheng YJ, Zhang J. Investigation of sub-clinical infection of hepatitis E virus in blood donors. *Zhonghua Ganzangbing Zazhi* 2004; **12**: 11-12

Clinicopathologic analysis of esophageal and cardiac cancers and survey of molecular expression on tissue arrays in Chaoshan littoral of China

Min Su, Xiao-Yun Li, Dong-Ping Tian, Ming-Yao Wu, Xian-Ying Wu, Shan-Ming Lu, Hai-Hua Huang, De-Rui Li, Zhi-Chao Zheng, Xiao-Hu Xu

Min Su, Xiao-Yun Li, Dong-Ping Tian, Ming-Yao Wu, Xian-Ying Wu, Xiao-Hu Xu, Department of Pathology, Shantou University Medical College, Shantou 515031, Guangdong Province, China
De-Rui Li, Tumor Hospital of Shantou University Medical College, Shantou 515031, Guangdong Province, China
Shan-Ming Lu, First Affiliated Hospital of Shantou University Medical College, Shantou 515031, Guangdong Province, China
Hai-Hua Huang, Zhi-Chao Zheng, Second Affiliated Hospital of Shantou University Medical College, Shantou 515031, Guangdong Province, China

Supported by the National Natural Science Foundation of China, No. 30210103904 and Key Natural Science Foundation of Guangdong Province, No. A1080203 and Medical Research Foundation of Guangdong Province and Elitist Foundation of Guangdong, No. Q02109 and Development Foundation of Shantou University and Sir Li Ka-Ching Foundation

Correspondence to: Professor Min Su, Department of Pathology, Shantou University Medical College, 22 Xinling Road, Shantou 515031, Guangdong Province, China. minsu@stu.edu.cn

Telephone: +86-754-8900429 **Fax:** +86-754-8900429

Received: 2003-12-28 **Accepted:** 2004-02-03

Abstract

AIM: To investigate clinical and pathologic data of esophageal carcinoma (EC) and cardiac carcinoma (CC) among residents in Chaoshan region of China.

METHODS: Clinical and pathologic data of 9 650 patients with EC and 4 173 patients with CC in the Chaoshan population were collected and analyzed. Moreover, Chaoshan esophageal carcinoma tissue arrays were made for high-throughput study.

RESULTS: Male to female ratio was 3:1 in patients with EC and 4.75:1 in CC. The average age of the occurrence of EC was 54.6 years, and of CC was 58.1 years. For both EC and CC, age at diagnosis was a little younger in Chaoshan region than in most other areas. The most commonly affected site of esophageal carcinoma was the middle third of esophagus (72.0%); the second was the lower third (15.3%). The main gross type of esophageal carcinoma was ulcerative type (41.50%); the medullary type was the second (39.6%). Squamous cell carcinoma accounted for the overwhelming majority of esophageal cancer (96.4%); adenocarcinoma accounted for the overwhelming majority of cardiac carcinoma (94.5%). Chaoshan esophageal carcinoma tissue arrays were easily for high-throughput study, and tissue cores with a diameter of 1.5 mm could better keep more structure for molecular expression study.

CONCLUSION: Both EC and CC are common in males. The average occurrence age of EC and CC is younger in Chaoshan than in most other regions of China. The most commonly affected site of esophageal carcinoma was the middle third of esophagus (72.0%). Squamous cell

carcinoma accounted for the overwhelming majority of esophageal cancer; adenocarcinoma accounted for the overwhelming majority of cardiac carcinoma. Tissue arrays technology is applicable for rapid molecular profiling of large numbers of cancers in a single experiment.

Su M, Li XY, Tian DP, Wu MY, Wu XY, Lu SM, Huang HH, Li DR, Zheng ZC, Xu XH. Clinicopathologic analysis of esophageal and cardiac cancers and survey of molecular expression on tissue arrays in Chaoshan littoral of China. *World J Gastroenterol* 2004; 10(15): 2163-2167

<http://www.wjgnet.com/1007-9327/10/2163.asp>

INTRODUCTION

Esophageal cancer (EC) ranks among the 10 most common cancers in the world, and is almost uniformly fatal. Chaoshan area is a unique littoral high-risk area of EC in China, within which Nanao island has the highest risk, the second being Jieyang county. According to the report from the Department of Public Health, Guangdong Province in 1993, the mortalities of EC in Nanao island were: $108.68 \pm 7.88/100\ 000$ in standardized Chinese population, $145.44 \pm 10.49/100\ 000$ in standardized world population, $261.16 \pm 25.01/100\ 000$ in standardized world population between the age of 35-64. The annual average incidence rates in males and females were $132.19/100\ 000$ and $69.20/100\ 000$ in Nanao island from 1987 to 1992^[1].

The predominant inhabitants of Chaoshan are offsprings of immigrants who hundreds or thousands of years ago came from the Central Plains of China, now a world well-known high risk region for EC. Chaoshan residents who have a high risk of EC and cardiac carcinoma (CC) are a relatively isolated population who have kept the old Chinese language (Chaoshan dialect) and customs. It is important to see if there is any evidence for the reducing incidence and mortality of EC and CC in Nanao island so far^[2] as the incidences of EC and CC present a downward trend in most other high risk regions. This unique society provides us an unparalleled base for the genetic and also environmental study of esophageal carcinoma. In the current study, we explored the clinical and pathologic features of EC and CC.

In addition, scholars have discovered that many genes and signaling pathways are involved in EC and CC development^[3-7]. However, genetic tumor markers have not gained in EC and CC diagnostics and prognosis prediction. Identification and evaluation of new molecular parameters are of utmost importance in cancer research. Here we present a high-throughput approach to rapidly identify relevant molecular expression changes in Chaoshan EC tissue arrays.

MATERIALS AND METHODS

Clinical data

Data about age, gender, and X-ray or pathological diagnoses of 13 823 patients with carcinoma of esophagus (9 650 cases) or

cardia (4 173 cases) were collected from the Tumor Hospital (1978-1998), First Affiliated Hospital (1989-1998), and Second Affiliated Hospital (1983-1998) of Shantou University Medical College, the Central Hospital of Shantou and the Hospital of Jieyang.

Sample collecting and EC tissues arrays construction

Seventy esophageal squamous carcinoma tissue specimens were selected from Department of Pathology, Shantou University Medical College in 2002. The specimens were fixed in 40 g/L neutrally buffered formaldehyde, embedded in paraffin. Sections of 5 μ m stained with hematoxylin and eosin were obtained to confirm the diagnosis and to identify different viable, representative areas of the specimen. From these defined areas core biopsies were taken with a precision instrument. Sixty-eight EC and para-cancerous tissue cores with a diameter of 1.5 mm from each specimen were punched and arrayed in 8 \times 9 on a recipient paraffin block. Five- μ m sections of the EC tissue array block was cut and placed on adhesive coated slides (cooperated with Cybrdi, Dr. Li Jun).

Immunohistochemistry

The expression of Erk1/Erk2 MAPK signaling protein was analyzed using Erk1/Erk2 Mouse derived anti-activated MAP kinase monoclonal antibody (1:400, Sigma), HistostainTM-SP kit and DAB visualization methods according to the manufacture's instruction (China Beijing Zhongshan Biological Technology CO., LTD.) And the expression of epidermal growth factor receptors were primarily analyzed using phosphor-EGFR (Tyr845) rabbit polyclonal antibodies and HRP-linked anti-rabbit IgG (Cell Signaling Technology, Inc. #2231, #7074). Four conventional normal esophageal epithelium tissues from autopsy were used as normal tissue controls. The human breast cancer tissue was used as positive control. Negative control was designed using phosphate-buffered saline (PBS) instead of primary antiserum. The detailed immunohistochemical process was carried out according to the manufacture's instructions.

Assessment of staining

The positive immunohistochemical staining of Erk1/Erk2 proteins was shown as brown signals in the nuclei; and the immunohistochemical signals of phosphor-EGFR (Tyr845) was in membrane and cytoplasm. The percentage of positive stained

cells was evaluated for each tissue sample by counting all cells at 5 high power fields of micrometric rule (5 mm \times 5 mm). The cases having positive cancer cells or epithelium accounting for more than 75% of all cancer cells or epithelium on the slide were defined as a score of +++, 50-74% were defined as a score of ++, 25-49% were defined as a score of +, 1-5% were defined as a score of \pm , less than 1% were defined as a score of -.

Statistical analysis

Data were stored in a computer data base (FoxPro, version 2.5 b) and analyzed using a computer (Pentium 4) spread sheet (Microsoft Excel 97) and professional statistical computer software (SPSS, version 11.0 and SAS, version 6.08). $P < 0.05$ was taken as significant. Immunoreactivity was classified as continuous data (undetectable levels or 0% to homogeneous staining or 100%) for all markers.

RESULTS

Gender and age

Genders of the patients were recorded in 9 635 cases. The 8 665 EC cases had age records, the youngest and the oldest were 17 years and 91 years respectively, and 3714 CC cases had age records. The male to female ratio and average age of morbidity for EC and CC in Chaoshan region are shown in Table 1. Constituent ratio of EC, CC in every age group is shown in the histogram (Figure 1).

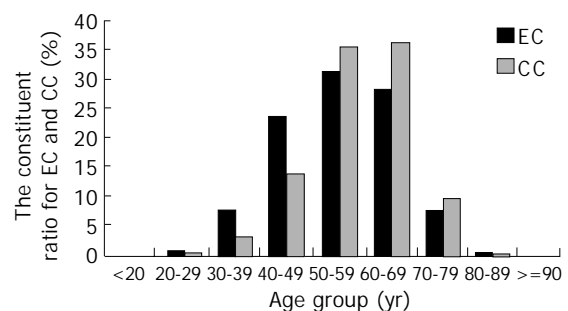


Figure 1 The histogram of the constituent ratio for EC and CC in Chaoshan region.

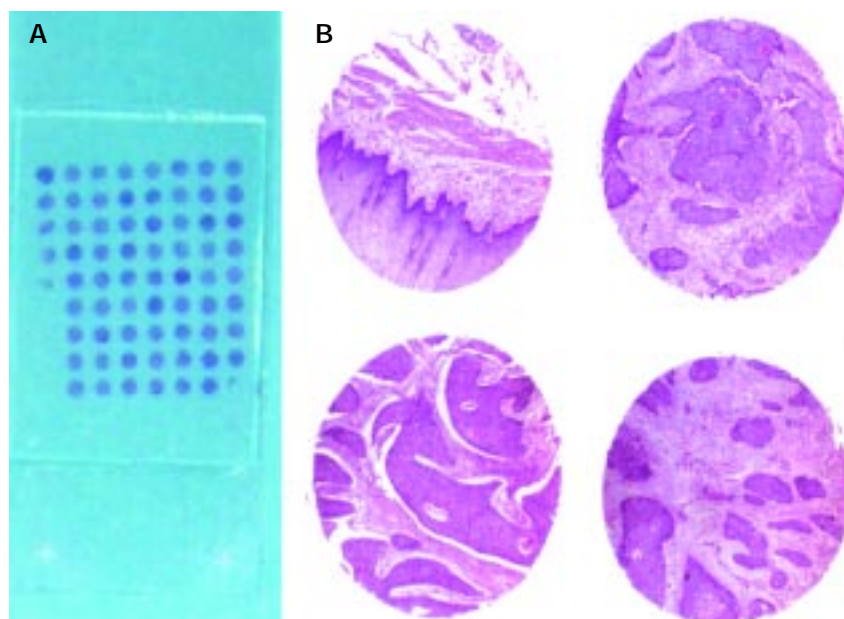


Figure 2 A: Overview of Chaoshan esophageal carcinoma tissue array (tissue cores with a diameter of 1.5 mm with 68 samples); B: Esophageal para-cancerous tissue and squamous carcinoma tissue (HE staining, original magnification: $\times 40$).

Table 1 Sex ratio, average age of morbidity for EC and CC in Chaoshan littoral region (mean±SD)

	<i>n</i>	Sex (male:female)	Age(yr)	<i>F</i>	<i>P</i>
EC	9 635	7 228:2 407(3.0:1)	54.61±10.73	103.24	<0.001
CC	4 167	3 442:725(4.75:1)	58.14±9.45		

EC:CC=2.31:1.

Pathology

The overwhelming majority of ECs were squamous cell carcinoma (96.4%); whereas CCs were composed mainly of adenocarcinomas (94.5%), and squamous cell carcinoma ranked second (4.4%). The detailed information of pathology is shown in Table 2.

Table 2 Pathology for EC and CC in Chaoshan littoral region (%)

	Site			Gross type				Histological type			
	U	M	L	UT	MT	ST	FT	SCA	ACA	UCA	O
EC	12.7	72.0	15.3	41.5	39.6	9.6	9.4	96.4	2.7	0.6	0.3
CC								4.4	94.5	0.9	0.2

Site (EC, *n*=6 384); Gross type (EC, *n*=1 193); Histological type (EC, *n*=7 272; CC, *n*=3 086); U: Upper third; M: Middle third; L: Lower third; UT: Ulcerative type; MT: Medullary type; ST: Scirrhus type; FT: Fungating type; SCA: Squamous cell carcinoma; ACA: Adenocarcinoma; UCA: Undifferentiated carcinoma; O: others.

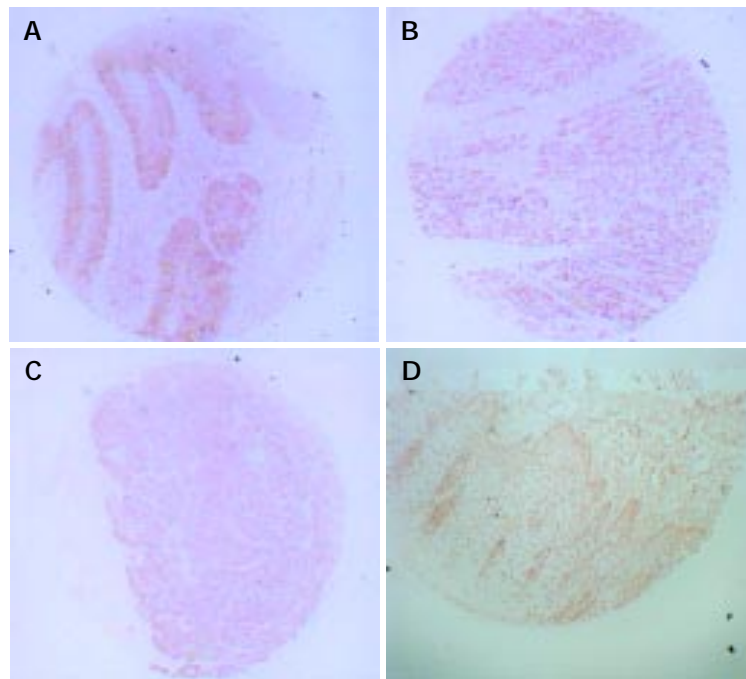


Figure 3 Phosphor-EGFR (Tyr845) expression on esophageal squamous carcinoma tissue (A, B, C) and esophageal para-cancerous tissue (D) (Cell Signaling Technology kit, original magnification: ×40).

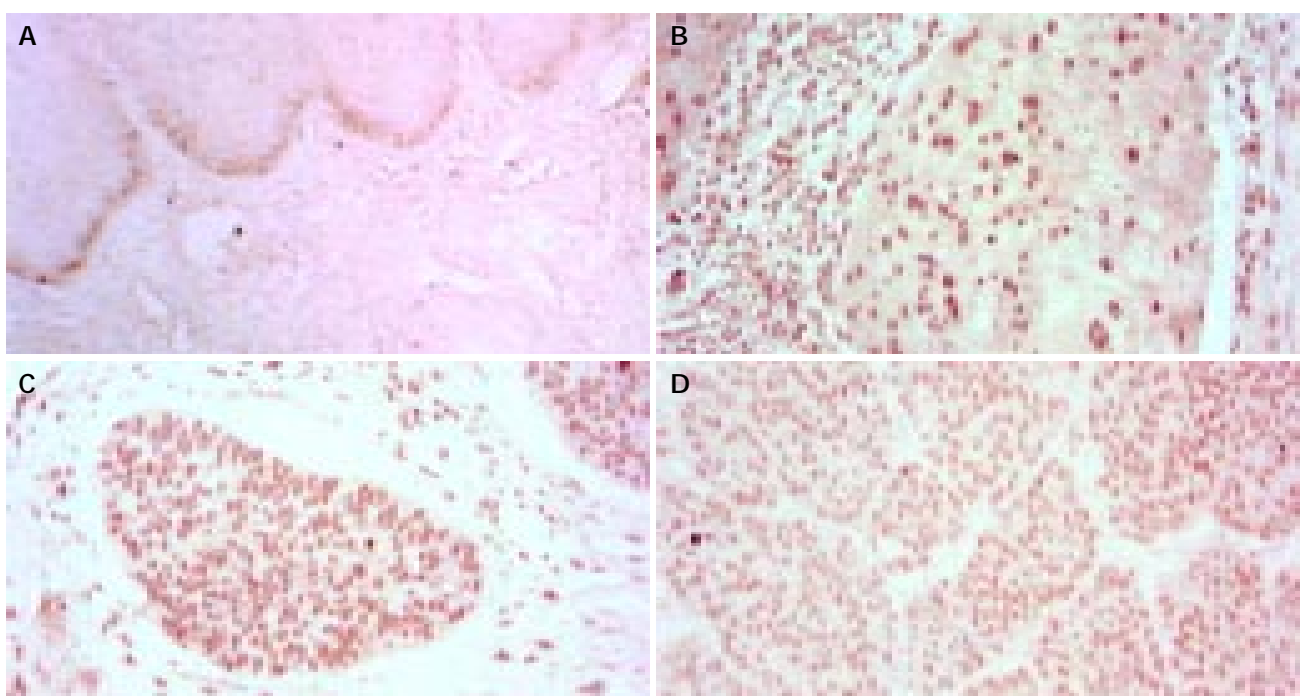


Figure 4 Erk1/Erk2 expression on normal esophageal squamous tissue (A, conventional tissue section, SP×100) and esophageal squamous carcinoma tissue (B, C, D tissue arrays) (SP×200).

Table 3 Expression of Erk1/Erk2 in esophageal squamous carcinoma tissue and para-cancerous tissue (% , mean±SD)

	Normal esophageal squamous cell (n=5)	Para-cancerous tissue (n=5)	Grade I (n=19)	Grade II (n=34)	Grade III (n=9)	F	P
Activated ERK1/ERK2	5.10±1.44	76.80±0.14	76.80±0.09	75.80±0.09	69.30±0.14	2.60	0.04

There was marked difference between normal esophageal epithelium and cancer tissues or para-cancerous tissue. But there was no marked difference among para-cancerous tissues and esophageal squamous carcinoma tissues ($F=1.463$, $P=0.236$).

Chaoshan EC tissues arrays and immunohistochemistry

Sections from tissue arrays were kept structure well for pathologic and immunohistochemical research (Figure 2). The expression of phosphor-EGFR(Tyr845) in esophageal squamous carcinoma tissue are relative diversity from \pm to $++++$, but no distinct differences among esophageal squamous carcinoma tissues according to grading (Figure 3). The expression of activated ERK in esophageal squamous carcinoma tissue and para-cancerous tissue are shown in Table 3 (Figure 4).

DISCUSSION

In data from Yangquan city of Shanxi Province (502 cases)^[8], the median age of EC patients was 59.17 years, 4.56 years older than that of Chaoshan EC patients. And also data from Linxian of Henan Province (2 601 cases)^[9], the proportion of EC patients from 20 to 30 years was 0.35%, from 30 to 40 was 5.19%; whereas both of the two proportions were lower than those from our data (0.70% and 7.70% respectively). In our data from Chaoshan region, the ulcerative type (41.5%) was the most common gross type of EC, which suggests that most EC patients were in the terminal stages when they arrived at hospitals.

Both preceding evidences indicated the average age of EC occurrence was younger in Chaoshan population than those in central plains of China. Synthetically analysis of two reports from Henan Province (1 045 cases and 1 332 cases respectively)^[9,10] showed the proportion of CC patients less than 50 years old was 15.56%, which was slightly lower than that from Chaoshan CC data (17.60%). The similar phenomena were seen in other papers^[11,12]. It might indicate that the age of incidence of cardiac cancer is also younger in Chaoshan region than in most other areas. Pathological analysis of 1 572 EC patients from Henan Province indicated histological type for the overwhelming majority of EC was squamous cell carcinoma (SCC), and the proportion of SCC (95.1%) was similar to that in our data (96.44%)^[13]. In comparison of the constituent ratios of histological types for cardiac carcinoma with data respectively from the Chinese Academy of Medical Science^[14], Erlangen - Nurnberg University in Germany^[15] and our data, it homoplasmically shows that adenocarcinoma accounts for the overwhelming majority of cardiac carcinoma, while the proportions of other histological types are relatively low.

Both data from Yangquan and Linxian^[16] also showed the middle third of esophagus was the most commonly affected site analogously, followed by the lower third and then the upper third, similar to our results.

Tissue array technology is applicable for rapid molecular profiling of large numbers of cancers in a single experiment. But a possible limitation of the tissue array technology is that the minute tissue samples acquired from the original tissues may not always be representative of the entire tumor, in light of the intratumor heterogeneity characteristic to most cancers. The comparisons between similarly acquired specimens from different stages of tumor progression placed on the same tissue microarray should be less problematic. If tumor arrays are used to investigate prevalence or prognostic significance of molecular changes, the critical issue is the extent to which minute tissue samples are representative of their donor tumors. The findings of this study suggest that significant results

can be obtained on tumor arrays issue cores with a diameter of 1.5 mm. Well and truly, one should consider the tumor tissue array technology as a rapid, high-throughput survey method to pinpoint the biologically most prevalent or clinically most promising genes and molecular markers for detailed studies combined with conventional tissue specimens.

The epidermal growth factor (EGF) peptide induces cellular proliferation through the epidermal growth factor receptor (EGFR), a M_r 170 000 single-pass transmembrane tyrosine kinase, which is believed to play important roles in the control of cell growth and differentiation. The EGFR activates ras and the MAP kinase pathway, ultimately causing phosphorylation of transcription factors such as c-Fos to create AP-1 and ELK-1 that contribute to proliferation. Gene amplification and overexpression of EGFR have been reported in various human tumors, including head and neck/oral cancer^[17-22].

Mitogen-activated protein kinase (MAPK) cascades have been shown to play a key role in transduction extracellular signals to cellular responses. Extracellular signal-regulated kinase (ERK) has been the best characterized MAPK and the Raf-MEK-ERK pathway represents one of the best characterized MAPK signaling pathway. The activated ERKs translocate to the nucleus and transactivate transcription factors, changing gene expression to promote growth, differentiation or mitosis^[23].

Our primary immunohistochemical study showed that phosphor-EGFR (Tyr845) and activated ERK were expressed in both para-cancerous and esophageal cancerous cells. The intensity of the expression was much higher in cancer than in normal tissue, suggesting that EGFR, Erk1/Erk2 MAPK signaling pathway might play an important role in the regulation of proliferation of esophageal cancer^[24,25].

In summary, Both EC and CC are common in males. The average age of occurrence is younger in Chaoshan than in most other regions of China. It is suggested that either genetic factors might play an important role in the pathogenesis of esophageal and cardiac cancers in Chaoshan or Chaoshan residents exposed themselves to some high risk environmental factors. Tissue microarrays technology is applicable for rapid molecular profiling of many tissue samples in a single experiment.

ACKNOWLEDGMENTS

The authors acknowledge the participation of the following members of the undergraduate scientific research group in Shantou University Medical College of China led by Professor Min Su: SM Ying, Y Ni, YS Gao, J Lin, JK Sun, BC Yuan, YF Li, XL Chen, JS X, Y F Chen, who helped us collect the case data of esophageal carcinoma and cardiac cancer. We express our special thanks to Professor Bruce AJ Ponder, Hutchison/MRC Research Centre, MRC Cancer Cell Unit and University of Cambridge, for his invaluable suggestions, Dr. John KL, for his kind assistance in the preparation of the grammatical structure of this paper.

REFERENCES

- 1 **Su M**, Lu SM, Tian DP, Zhao H, Li XY, Li DR, Zheng ZC. Relationship between ABO blood groups and carcinoma of esophagus and cardia in Chaoshan inhabitants of China. *World*

- J Gastroenterol* 2001; **7**: 657-661
- 2 **Li K**, Su M, Yu P. Mortality trends for malignancies in Nanao county of Guangdong province. *Zhongguo Zhongliu* 2001; **10**: 269-270
 - 3 **Su H**, Hu N, Shih J, Hu Y, Wang QH, Chuang EY, Roth MJ, Wang C, Goldstein AM, Ding T, Dawsey SM, Giffen C, Emmert Buck MR, Taylor PR. Gene expression analysis of esophageal squamous cell carcinoma reveals consistent molecular profiles related to a family history of upper gastrointestinal cancer. *Cancer Res* 2003; **63**: 3872-3876
 - 4 **Nie Y**, Liao J, Zhao X, Song Y, Yang GY, Wang LD, Yang CS. Detection of multiple gene hypermethylation in the development of esophageal squamous cell carcinoma. *Carcinogenesis* 2002; **23**: 1713-1720
 - 5 **Shinohara M**, Aoki T, Sato S, Takagi Y, Osaka Y, Koyanagi Y, Hatooka S, Shinoda M. Cell cycle-regulated factors in esophageal cancer. *Dis Esophagus* 2002; **15**: 149-154
 - 6 **Gibson MK**, Abraham SC, Wu TT, Burtness B, Heitmiller RF, Heath E, Forastiere A. Epidermal growth factor receptor, p53 mutation, and pathological response predict survival in patients with locally advanced esophageal cancer treated with preoperative chemoradiotherapy. *Clinical Cancer Research* 2003; **9**: 6461-6468
 - 7 **Arteaga CL**. Epidermal growth factor receptor dependence in human tumors: more than just expression? *The Oncologist* 2002; **7**(Suppl 4): 31-39
 - 8 **Li SK**, Mao XZ, Jia YT. Clinic analysis of 502 cases with esophageal carcinoma. *Zhongliu Yanjiu He Linchuang* 1996; **8**: 106-107
 - 9 **Wang LD**, Gao WJ, Yang WC, Li XF, Li J, Zou JX, Wang DC, Guo RX. Preliminary analysis of the statistics on 3933 cases with esophageal cancer and gastric cardia cancer from the subjects in the People's Hospital of Linzhou in 9 years. *J Henan Med Univ* 1997; **32**: 9-11
 - 10 Collaboration group of gastroscopy in some hospitals of Henan province. Occurrence condition of cardia carcinoma and endoscope classification of early cardia carcinoma in high and low incidence areas of esophageal carcinoma. *J Henan Med Collage* 1987; **22**: 207-210
 - 11 Collaboration group of endoscopy in Shanghai. Clinic analysis of 1451 cardia carcinomas diagnosed by gastroscopy. *Neijing* 1985; **2**: 32-34
 - 12 **Hansson LE**, Sparen P, Nyren O. Increasing incidence of carcinoma of the gastric cardia in Sweden from 1970 to 1985. *Br J Surg* 1993; **80**: 374-377
 - 13 **Xu JY**, Zhang JK, Wang RM. Control observation on esophageal carcinoma and esophagitis detected by endoscopy between high and low incidence areas of esophageal carcinoma. *Linchuang Xiaohuabing Zazhi* 1995; **7**: 101-103
 - 14 **Li L**, Pan GL, Huang GJ, Lu X. Pathomorphology characteristics of cardiac carcinoma. *Zhonghua Zhongliu Zazhi* 1984; **6**: 37-40
 - 15 **Husemann B**. Cardia carcinoma considered as a district clinical entity. *Br J Surg* 1989; **76**: 136-139
 - 16 **Liu FS**. Pathology of esophageal carcinoma. *Zhongliu Fangzhi Yanjiu* 1976; **3**: 234-238
 - 17 **Eriksen JG**, Steiniche T, Askaa J, Alsner J, Overgaard J. The prognostic value of epidermal growth factor receptor is related to tumor differentiation and the overall treatment time of radiotherapy in squamous cell carcinomas of the head and neck. *Int J Radiat Oncol Biol Phys* 2004; **58**: 561-566
 - 18 **Selvaggi G**, Novello S, Torri V, Leonardo E, De Giuli P, Borasio P, Mossetti C, Ardisson F, Lausi P, Scagliotti GV. Epidermal growth factor receptor overexpression correlates with a poor prognosis in completely resected non-small-cell lung cancer. *Ann Oncol* 2004; **15**: 28-32
 - 19 **Chan KS**, Carbajal S, Kiguchi K, Clifford J, Sano S, DiGiovanni J. Epidermal growth factor receptor-mediated activation of Stat3 during multistage skin carcinogenesis. *Cancer Research* 2004; **64**: 2382-2389
 - 20 **Shimizu M**, Suzui M, Deguchi A, Lim JT, Weinstein IB. Effects of acyclic retinoid on growth, cell cycle control, epidermal growth factor receptor signaling, and gene expression in human squamous cell carcinoma cells. *Clin Cancer Research* 2004; **10**: 1130-1140
 - 21 **Perez-Soler R**. HER1/EGFR targeting: refining the strategy. *Oncologist* 2004; **9**: 58-67
 - 22 **Dahlberg PS**, Ferrin LF, Grindle SM, Nelson CM, Hoang CD, Jacobson B. Gene expression profiles in esophageal adenocarcinoma. *Ann Thorac Surg* 2004; **77**: 1008-1015
 - 23 **Zhang W**, Liu HT. MAPK signal pathways in the regulation of cell proliferation in mammalian cells. *Cell Research* 2002; **12**: 9-18
 - 24 **Nemoto T**, Ohashi K, Akashi T, Johnson JD, Hirokawa K. Overexpression of protein tyrosine kinases in human esophageal cancer. *Pathobiology* 1997; **65**: 195-203
 - 25 **Trisciuglio D**, Iervolino A, Candiloro A, Fibbi G, Fanciulli M, Zangemeister-Wittke U, Zupi G, Del Bufalo D. Bcl-2 induction of urokinase plasminogen activator receptor expression in human cancer cells through Sp1 activation: involvement of ERK1/ERK2 activity. *J Biol Chem* 2004; **279**: 6737-6745

Edited by Zhu LH and Chen WW Proofread by Xu FM

Expression of cyclooxygenase-2 in human esophageal squamous cell carcinomas

Jian-Gang Jiang, Jiang-Bo Tang, Chun-Lian Chen, Bao-Xing Liu, Xiang-Ning Fu, Zhi-Hui Zhu, Wei Qu, Katherine Cianflone, Michael P. Waalkes, Dao-Wen Wang

Jian-Gang Jiang, Jiang-Bo Tang, Chun-Lian Chen, Bao-Xing Liu, Xiang-Ning Fu, Zhi-Hui Zhu, Dao-Wen Wang, Internal Medicine Department and Gene Therapy Center, Tongji Hospital, Tongji Medical College of Huazhong University of Science and Technology, Wuhan 430030, Hubei Province, China

Wei Qu, Michael P. Waalkes, Inorganic Carcinogenesis Section, Laboratory of Comparative Carcinogenesis, National Cancer Institute at the National Institute of Environmental Health Sciences, Research Triangle Park, North Carolina 27709, USA

Katherine Cianflone, Mike Rosenbloom Laboratory for Cardiovascular Research, McGill University Health Center, Montreal, Quebec H3A 1A1, Canada

Co-first-authors: Jian-Gang Jiang and Jiang-Bo Tang

Correspondence to: Dr. Dao-Wen Wang, Department of Internal Medicine and Gene Therapy Center, Tongji Hospital, Tongji Medical College of Huazhong University of Science and Technology, Wuhan 430030, Hubei Province, China. dwwang@tjh.tjmu.edu.cn

Telephone: +86-27-83662842 **Fax:** +86-27-83662842

Received: 2003-11-17 **Accepted:** 2004-01-08

Abstract

AIM: To determine whether cyclooxygenase-2 (COX-2) was expressed in human esophageal squamous cell carcinoma.

METHODS: Quantitative reverse transcription-polymerase chain reaction (RT-PCR), western blotting, immunohistochemistry and immunofluorescence were used to assess the expression level of COX-2 in esophageal tissue.

RESULTS: COX-2 mRNA levels were increased by >80-fold in esophageal squamous cell carcinoma when compared to adjacent noncancerous tissue. COX-2 protein was present in 21 of 30 cases of esophageal squamous cell carcinoma tissues, but was undetectable in noncancerous tissue. Immunohistochemistry was performed to directly show expression of COX-2 in tumor tissue.

CONCLUSION: These results suggest that COX-2 may be an important factor for esophageal cancer and inhibition of COX-2 may be helpful for prevention and possibly treatment of this cancer.

Jiang JG, Tang JB, Chen CL, Liu BX, Fu XN, Zhu ZH, Qu W, Cianflone K, Waalkes MP, Wang DW. Expression of cyclooxygenase-2 in human esophageal squamous cell carcinomas. *World J Gastroenterol* 2004; 10(15): 2168-2173 <http://www.wjgnet.com/1007-9327/10/2168.asp>

INTRODUCTION

Esophageal cancer is the fourth most prevalent malignancy in China. Although several factors have been implicated for the recent rise in the frequency of esophageal carcinoma, including diet, activation of *c-myc* oncogenes and inactivation of tumor suppressor genes (*p53*)^[1,2], the exact pathogenic mechanisms and promoting factors of this cancer remain to be

clarified. There is no effective strategy for treatment of this disease. Recently epidemiological studies suggest intake of nonsteroidal anti-inflammatory drugs (NSAIDs) such as aspirin and indomethacin can reduce the risk of colorectal cancer^[3,4]. Based on these findings, subsequent studies have addressed the role of COX enzyme as a target of these compounds.

COX is a rate-limiting enzyme involved in the conversion of arachidonic acid to prostaglandin H₂, the precursor of several molecules including prostaglandin (PG), prostacyclin, and thromboxane. Results from recent studies have established the presence of two distinct COX enzymes, a constitutive enzyme (COX-1) and an inducible form (COX-2). They share over 60% identity at the amino acid level and have similar enzymatic activities, but both isoforms are suggested to have different biological functions^[5-9]. COX-1 is constitutively expressed in most mammalian tissues and is thought to carry out "housekeeping" functions such as cytoprotection of the gastric mucosa, regulation of renal blood flow, and control of platelet aggregation. In contrast, COX-2 mRNA and protein are undetectable in normal tissues, but can be rapidly induced by proinflammatory or mitogenic stimuli including cytokines, endotoxins, interleukins, and phorbol ester^[10-12].

Multiple lines of experimental evidence have also suggested that COX-2 is involved in carcinogenesis. For example, COX-2 is up-regulated in transformed cells^[13] and in various forms of cancer^[14-17], whereas levels of COX-1 are relatively stable. Moreover, COX-2 knockout mice develop 75% fewer chemically-induced skin papillomas than control mice. Recently, it has been shown that selective COX-2 inhibitors may significantly suppress experimentally-induced colon carcinogenesis^[18,19]. Epidemiological studies have shown that intake of aspirin was associated with up to a 90% decreased risk of developing esophageal cancer^[20,21], and in induced esophageal carcinomas, indomethacin had antitumor activity^[22,23].

Here we investigated whether COX-2 was up-regulated in esophageal squamous cell carcinomas from Chinese patients. Our data show that levels of COX-2 are markedly increased in esophageal squamous cell carcinomas, which raises the possibility that selective inhibitors of COX-2 may be useful in the prevention or treatment of this important disease.

MATERIALS AND METHODS

Samples

We examined 30 cases of esophageal squamous cell carcinoma. Both tumor tissue and surrounding normal tissue were obtained from surgical patients with esophageal squamous cell carcinoma at Tongji Hospital during operations. The age of the patients was 57±9 years (mean±SD; range, 37 to 75 years). Of the patients, 23 were men and 7 were women. A small portion from each tissue sample was immediately frozen in liquid nitrogen and stored at -80 °C. Tissue samples were fixed in 40 g/L neutral buffered formaldehyde, processed through graded ethanol solutions, and embedded in paraffin and immunostained for COX-2. A subset of paired tumor tissues and surrounding normal tissue was further examined by RT-PCR and Western blotting.

RNA extraction

Protein and total RNA were extracted using TriZol Reagent (Life Technologies, GIBCO BRL). RT-PCR kit was purchased from Takara Bio Co., Ltd. COX-2 affinity-purified polyclonal antibodies were obtained from Santa Cruz Biotechnology, Inc. Rabbit anti-goat IgG conjugated with horse-radish peroxidase (HRPO) was obtained from KPL, Inc., USA. ImmunoResearch Lab Enhanced chemiluminescence assay was purchased from PIERCE, Inc. SDS-PAGE standard was obtained from Bio-Rad, Inc.

Western blotting for detection of COX-2

Protein in the various samples were extracted and purified by TriZol Reagent, and the protein concentration was evaluated by Bradford method. A portion of protein (20 μ g) extracted from each tissue sample was subjected to electrophoresis in 80 g/L polyacrylamide slab gels. After transfer to PVDF membrane and blocking with fat free milk powder, blots were probed with COX-2 antibodies (1:750), followed by incubation with HRPO-conjugated secondary antibody (rabbit anti-goat 1:800). COX-2 proteins were visualized by enhanced chemiluminescence.

Semi-quantitative RT-PCR

Total RNA was isolated and purified by TriZol Reagent, and the RNA concentration was determined. Semi-quantitative analysis of the expression of COX-2 mRNA was performed using the multiplex RT-PCR technique. In this assay, we used a housekeeping gene, glyceraldehyde-3-phosphate dehydrogenase (GAPDH), as an internal standard. A sample (1 μ g) of total RNA was reverse-transcribed using the Takara Bio RT-PCR kit according to the manufacturer's protocol. PCR was performed in a 25 μ L reaction mixture containing 5 μ L of cDNA template, 1 \times PCR buffer, 1.5 mmol/L MgCl₂, 0.8 mmol/L dNTPs, 100 nmol/L of each primer for COX-2 (sense primer, 5'-CCGAGGTGTATGTATGAGTG-3'; antisense primer, 5'-AGGAGAGGTTAGAGAAGG-3') or 100 nmol/L GAPDH (sense primer, 5'-CCTTGCCTCTCAGACAATGC-3'; antisense primer, 5'-CCACGACATACTCAGCAC-3') and 1 U of *Taq* DNA polymerase. The PCR primers used for detection of COX-2, and GAPDH yielded cDNA products of 314-bp and 340-bp, respectively. The conditions for PCR were one cycle of denaturing at 94 $^{\circ}$ C for 5 min, followed by 35 cycles of at 94 $^{\circ}$ C for 45 s, 56 $^{\circ}$ C for 45 s, 72 $^{\circ}$ C for 1 min with a final extension at 72 $^{\circ}$ C for 7 min. The electrophoresed PCR products were scanned by densitometry and the ratio of COX-2 to GAPDH was calculated in each sample.

Immunohistochemistry

Tissue sections (4 μ m thick) were deparaffinized in xylene and rehydrated. Heat antigen retrieval was performed as described previously^[24]. Slides were then processed for immunohistochemistry. In the primary antibody reaction step, slides were incubated with the COX-2 antibody (final concentration 5 μ g/mL) for 1 h at room temperature. For positive controls, sections of colon cancer expressing the COX-2 protein were included in each staining procedure. For negative controls, nonimmunized rabbit IgG or Tris-buffered saline was substituted for the primary antibody to distinguish false positive responses from nonspecific binding to IgG or the secondary antibody. In addition, preabsorbed antibody with an excess amount of immunogen abolished the staining. Staining was repeated twice to avoid possible technical errors and similar results were obtained in all cases.

Evaluation of COX-2 immunohistochemistry

All immunostained sections were coded and evaluated without

prior knowledge of the clinical or pathological parameters. In each section, five high-power fields were selected at random and a total number of at least 700 cells were evaluated. The results were expressed as the intensity of staining. The intensity of staining was judged relative to smooth muscle cells in the sample, and estimated on a scale 0-3 (0 negative; 1 weak; 2 moderate; and 3 strong). All slides were interpreted by two investigators on three different occasions. Their evaluations were similar and <10% disagreement between the investigators was noted. In case of major disagreement, the final evaluation of such sections was determined by consensus using a multihead microscope.

Immunofluorescence assay

Tissue samples were cut into 6 μ m crystal-sections, and processed with COX-2 specific antibody and fluorescein labeled secondary antibodies and all the sections were observed immediately under fluorescence microscope.

Statistical analysis

Statistical analysis was performed using SAS software. Results of immunohistochemistry were analyzed by Fisher's exact test. The correlation of RT-PCR and western blotting was analyzed by logistic regression analysis. $P < 0.05$ was considered statistically significant.

RESULTS

COX-2 mRNA expression in esophageal squamous cell carcinoma by semi-quantitative RT-PCR

To examine the level of COX-2 mRNA, RT-PCR was performed to estimate the expression of COX-2 in tumor tissues relative to that in the matched normal tissues, which was expressed as COX-2/GAPDH ratio. GAPDH was used as an internal control. Semiquantitative RT-PCR indicated that COX-2 mRNA was found in 21 of 30 esophageal squamous cell carcinomas. In surrounding normal tissue of esophageal squamous cell carcinoma, COX-2 mRNA could not be detected (Figure 1). In the 21 esophageal squamous cell carcinoma tissues, the COX-2/GAPDH ratios ranged from 0.6 to 1.0, levels of COX-2 mRNA were increased by >80-fold compared to adjacent noncancerous tissue.

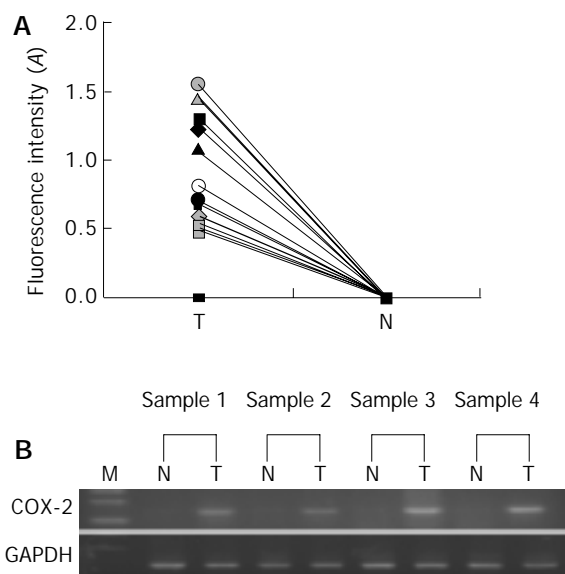


Figure 1 Semiquantitative result of RT-PCR analysis of COX-2 mRNA expression in squamous carcinoma tissues and matched normal tissues of the esophagus. A: Data are expressed as the fluorescence values of COX-2 band in tumor and nontumorous

tissue samples from 30 patients with esophageal squamous cell carcinoma. B: Representative results of semiquantitative RT-PCR, indicated COX-2 mRNA was found in esophageal squamous cell carcinoma samples (T), while in surrounding normal tissue (N), COX-2 mRNA could not be detected. The coamplified GAPDH gene served as an internal control. PCR product sizes are 314 bp for COX-2 and 340 bp for GAPDH. M indicates DNA marker. The samples in lanes 1N and 1T, 2N and 2T, 3N and 3T, 4N and 4T are paired samples from 4 patients, respectively.

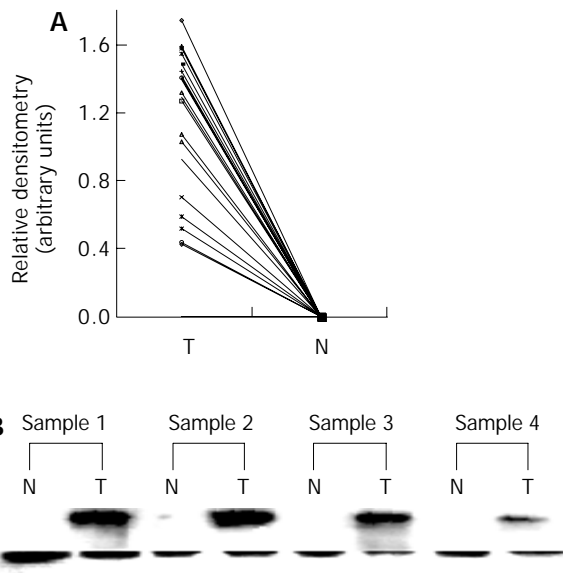


Figure 2 Western blot analysis of COX-2 in squamous carcinoma tissues and matched normal tissues of the esophagus. COX-2 expressions in representative tumor (T) and nontumorous (N) are shown. A: Data are expressed as the absorbency values of COX-2 band in tumor and nontumorous tissue samples from 30 patients with esophageal squamous cell carcinoma. B: Representative result of Western blot analysis. COX-2 protein was detected in tumor tissue but was undetectable in nontumorous tissue in the same patients. β -actin was used as an internal control. The samples in lanes 1N and 1T, 2N and 2T, 3N and 3T, 4N and 4T are paired samples from 4 patients, respectively.

Western blotting

To determine whether levels of COX-2 protein were also increased in esophageal squamous cell carcinomas, western blot analysis of paired tumorous and nontumorous tissue was performed. COX-2 protein was detected in tumor tissue from 21 of 30 patients but was undetectable in nontumorous tissue in the same patients. β -actin was used as an internal control

(Figure 2). Furthermore, the results of western blot analysis paralleled those of mRNA RT-PCR analysis. There was a significant positive correlation between western blot analysis and RT-PCR analysis results ($r=0.708$, $P<0.01$) (Figure 3).

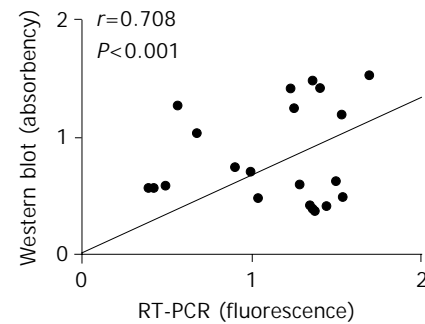


Figure 3 Correlation between western blot analysis and RT-PCR analysis results. The results showed that the expression of COX-2 in cancer tissues (western blot analysis) was highly correlated with by RT-PCR analysis (r value=0.708, $P<0.001$).

Table 1 Expression of COX-2 in esophageal squamous cell carcinomas detected by immunohistochemistry

	Intensity				
	0	1	2	3	
Tumor tissue	10	2	12	6	$P<0.05$
Normal tissue	27	3	0	0	

The intensity of staining was estimated on a scale 0–3. (0, negative; 1, weak; 2, moderate; and 3, strong).

COX-2 expression in esophageal squamous cell carcinoma by immunohistochemistry

Immunohistochemistry was performed to directly indicate cell specific COX-2 protein expression. In nontumorous tissue specimens, a weak COX-2 staining or no COX-2 staining was detected. In contrast, a moderate to strong expression of COX-2 was noted in many esophageal squamous cell carcinomas of the same patients. Specifically, a strong expression of COX-2 protein was present in 6 of 30 (20%) esophageal squamous cell carcinomas, moderate expression was present in 12 of 30 (40%), and weak expression was present in 2 of 30 (15%). The level of COX-2 expression in esophageal squamous cell carcinomas was significantly higher than that in surrounding normal tissue (Table 1). Expression of COX-2 was localized to tumor cells, not to surrounding stromal cells or infiltrating inflammatory cells (Figure 4).

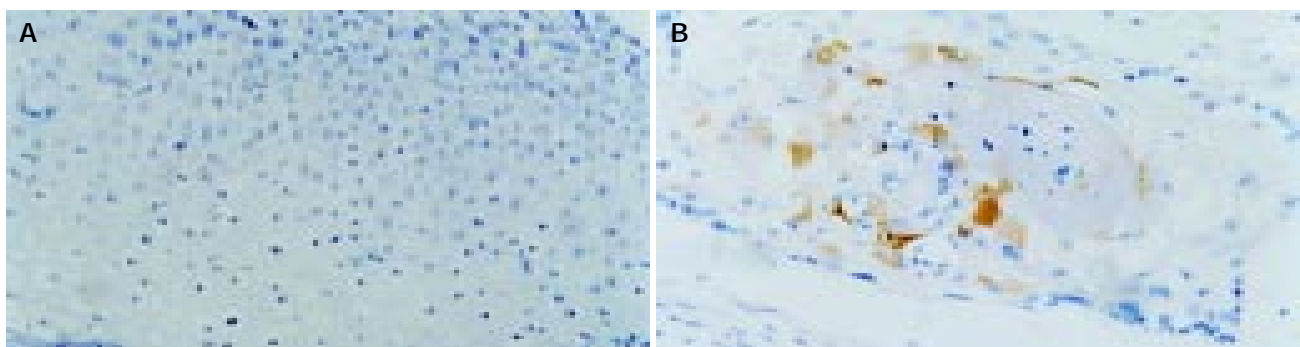


Figure 4 Representative results of immunohistochemical analysis of COX-2 in squamous carcinoma tissues and matched normal tissues of the esophagus from the same patient (Magnification x200). In normal esophageal tissue there is no positive staining for COX-2 (A) but in esophageal squamous cell carcinoma tissue, carcinoma cells display a strong staining for COX-2, which indicate COX-2 expression specifically in cancer tissues (B).

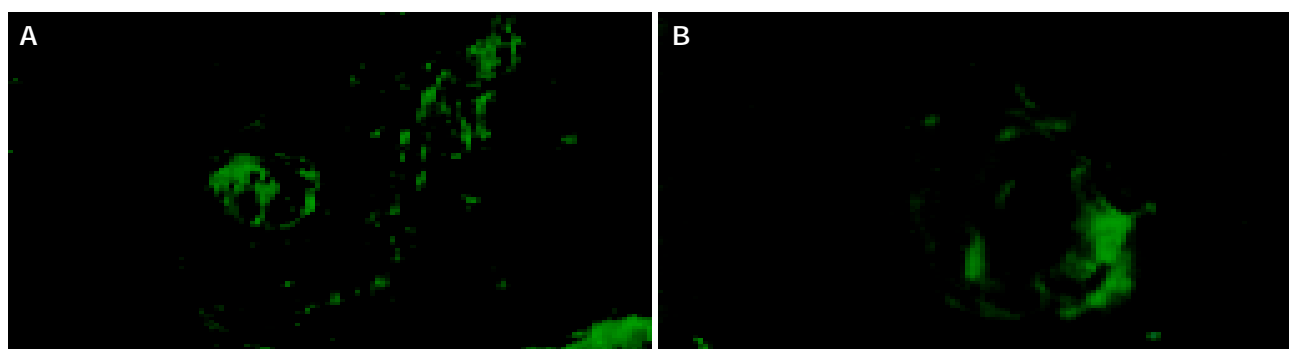


Figure 5 Immunofluorescence analysis of COX-2 in squamous carcinoma tissues (Magnification, x400). A and B are from 2 different patients with esophageal squamous cell carcinoma, Both display a strong green fluorescence staining for COX-2 in cancer-nests.

COX-2 expression in esophageal squamous cell carcinoma by immunofluorescence

Immunofluorescence was performed to directly indicate whether COX-2 protein was expressed in esophageal cancer. COX-2 expression was detected in esophageal squamous cell carcinomas. Immunofluorescence in esophageal squamous cell carcinomas displayed a cancer-nest structure (Figure 5).

DISCUSSION

Epidemiological studies indicate that the administration of nonsteroidal anti-inflammatory drugs (NSAIDs) results in a marked reduction in adenoma size and number and, not infrequently, leads to a complete regression of colonic polyps in patients with familial adenomatous polyposis^[25-27]. NSAIDs also reduce the risk of sporadic colorectal, breast, and lung cancers^[28,29]. These effects of NSAIDs on the inhibition of carcinogenesis have also been demonstrated in animal experiments, including pancreatic tumor model induced by N-nitrosobis (2-oxopropyl) amine in hamsters^[30]. Several lines of evidence indicate that the antitumor effects of NSAIDs may be due in part to the inhibition of COX-2 activity^[19,31-33]. Indeed, in carcinomas of the colon and lung and also in gastric and esophageal carcinomas, the level of COX-2 expression is significantly increased. These findings suggest that up-regulation of this enzyme might be a common mechanism for carcinogenesis of cells of an epithelial origin. Indeed, in the present large sampled study we found that COX-2 expression was increased at both the RNA and protein levels in a large proportion of esophageal squamous cell carcinoma compared with paired normal surrounding esophageal tissues by RT-PCR and Western blot analyses. RT-PCR analyses indicated that 21 of 30(70%) esophageal squamous cell carcinoma cases displayed increased COX-2 mRNA. Furthermore, the results of mRNA analysis paralleled those of western blot and immunohistochemistry. Thus, approximately 67% of the carcinoma samples exhibited positive staining of COX-2 protein, whereas paired normal tissues showed little or no COX-2 staining. Up to 60% of carcinoma cases showed moderate to strong COX-2 immunostaining (intensity 2 or 3). Also, immunofluorescence demonstrated the expression of COX-2 in esophageal squamous cell cancer-nests. These findings suggest that COX-2 may also be a marker for the malignant potential of esophageal squamous cell carcinoma, although this function remains to be clarified. Taken into consideration of the limited number of specimens, a conservative interpretation of the increased COX-2 mRNA and protein expression is necessary. Examination of a larger number of paired samples of tumor tissue and nonmalignant mucosa from esophageal cancer patients, as well as normal mucosa from persons without esophageal cancer in future studies will be necessary to more clearly determine the status of COX-2 in normal esophageal mucosa and in

esophageal cancer. Because COX-2 was up-regulated at the transcriptional level, which can increase COX-2 protein expression, subsequent determination of COX-2 protein synthesis and bioactivity at the protein level is important. It is also important to study the possible link between the known genetic alterations and COX-2 in esophageal cancer. However, the present results indicate COX-2 is elevated in esophageal cancer in a fashion similar to that in intestinal tumors.

COX-2 could potentially cause carcinogenesis via multiple mechanisms, and the role of COX-2 in tumor development and progression *in vivo* is not known. The most obvious possibility is that overexpression of COX-2 leads to high levels of prostaglandins (PGs) in tumor tissue. This hypothesis is supported by the finding of elevated levels of PGs in cancer tissues, compared with corresponding normal tissues^[34,35]. PGs produced by COX-2 may subsequently facilitate tumor progression by acting as differentiation and growth factors, immunosuppressors and angiogenic agents^[36-38]. Additionally, it has been shown that elevated PGE₂ levels in COX-2 overexpression cancer cells correlate with the metastatic potential of the cancer cells, and can be reduced in a dose-dependent manner by COX inhibitors^[39]. On the other hand, there is also evidence that NSAIDs might exert their antineoplastic effect by a PG-independent pathway, and the COX-2 enzyme itself may promote cancer development and progression^[40]. Thus, NSAIDs suppressed proliferative activity in colon cancer cells devoid of cyclooxygenase and PGs^[31]. Moreover, in extrahepatic tissues in which cytochrome P450 content is low, COX may be important for generation of carcinogens. For example, several classes of chemical carcinogens, e.g., dihydrodiol derivatives of polycyclic aromatic hydrocarbons, aromatic amines and heterocyclic amines, are activated to mutagenic derivatives by COX^[41]. The generation of carcinogens by COX-2 may be important, therefore, for understanding the link between cigarette smoking or consumption of grilled or fried meat and esophageal cancer^[42]. Additional studies are needed to determine which of these mechanisms are more important in esophageal squamous cell carcinoma.

Selective inhibition of COX-2 in esophageal cancer cells induces apoptotic cell death and reduces proliferative activity and these effects correlate with the inhibition of PG synthesis. Similar results have been reported^[43-45]. The significance of COX-2 likely varies between different classes of tumors. We cannot conclude from this and other published data whether the antiproliferative and proapoptotic effects of COX-2 inhibition on esophageal cancer cells are exclusively mediated through the inhibition of PG synthesis or if other mechanisms are also involved. However, our data provide a theoretical basis for evaluation of long-term intake of COX inhibitors on reduction of the incidence of esophageal cancer. Defining actual response of individual tumors to COX-2 inhibitors *in vivo*, however,

awaits further evaluation, especially since the level of COX-2 expression varies substantially between different tumors. Based on our data, a more thorough study on COX-2 expression is needed in patients with esophageal squamous cell carcinoma. Patients with a high COX-2 expression may benefit from specific or nonspecific COX-2 inhibitor medication, such as aspirin, for potential carcinogenic prevention of these cancers. Long-term intake of COX-2 inhibitors may be recommended for family members, especially with a positive family history of esophageal squamous cell carcinoma.

Taken together, our study suggests that COX-2 may play a role in esophageal squamous cell carcinoma development and/or progression and COX-2 inhibitors may be potential agents for the prevention or treatment of human invasive esophageal squamous cell carcinoma. Therefore, long-term intake of NSAIDs, such as aspirin, might reduce the risk of esophageal squamous cell carcinoma. To verify this hypothesis studies to evaluate the efficacy of COX-2 inhibitors in relevant animal models of esophageal squamous cell carcinoma are needed. In addition, studies to define the possible role of COX-2 in esophageal squamous cell carcinoma and the mechanisms by which COX-2 inhibitors exert antitumor activity are essential.

ACKNOWLEDGEMENTS

We thank Drs. Fan Zhang and Chun-Xia Zhao for their technical assistance.

REFERENCES

- Ishizuka T, Tanabe C, Sakamoto H, Aoyagi K, Maekawa M, Matsukura N, Tokunaga A, Tajiri T, Yoshida T, Terada M, Sasaki H. Gene amplification profiling of esophageal squamous cell carcinomas by DNA array CGH. *Biochem Biophys Res Commun* 2002; **296**: 152-155
- Kajiyama Y, Hattori K, Tomita N, Amano T, Iwanuma Y, Narumi K, Udagawa H, Tsurumaru M. Histopathologic effects of neoadjuvant therapies for advanced squamous cell carcinoma of the esophagus: multivariate analysis of predictive factors and p53 overexpression. *Dis Esophagus* 2002; **15**: 61-66
- Greenberg ER, Baron JA, Freeman DH Jr, Mandel JS, Haile R. Reduced risk of large-bowel adenomas among aspirin users. *J Natl Cancer Inst* 1993; **85**: 912-916
- Giovannucci E, Egan KM, Hunter DJ, Stampfer MJ, Colditz GA, Willett WC, Speizer FE. Aspirin and the risk of colorectal cancer in women. *N Engl J Med* 1995; **333**: 609-614
- Hla T, Neilson K. Human cyclooxygenase-2 cDNA. *Proc Natl Acad Sci U S A* 1992; **89**: 7384-7388
- Kennedy BP, Chan CC, Culp SA, Cromlish WA. Cloning and expression of rat prostaglandin endoperoxide synthase (cyclooxygenase)-2 cDNA. *Biochem Biophys Res Commun* 1993; **197**: 494-500
- Feng L, Sun W, Xia Y, Tang WW, Chanmugam P, Soyoola E, Wilson CB, Hwang D. Cloning two isoforms of rat cyclooxygenase: differential regulation of their expression. *Arch Biochem Biophys* 1993; **307**: 361-368
- Smith WL, Meade EA, DeWitt DL. Pharmacology of prostaglandin endoperoxide synthase isozymes-1 and -2. *Ann N Y Acad Sci* 1994; **714**: 136-142
- Williams CS, DuBois RN. Prostaglandin endoperoxide synthase: why two isoforms? *Am J Physiol* 1996; **270**(3 Pt 1): G393-400
- DuBois RN, Tsujii M, Bishop P, Awad JA, Makita K, Lanahan A. Cloning and characterization of a growth factor-inducible cyclooxygenase gene from rat intestinal epithelial cells. *Am J Physiol* 1994; **266**(5 Pt 1): G822-G827
- Hempel SL, Monick MM, Hunninghake GW. Lipopolysaccharide induces prostaglandin H synthase-2 protein and mRNA in human alveolar macrophages and blood monocytes. *J Clin Invest* 1994; **93**: 391-396
- Prescott SM, White RL. Self-promotion? Intimate connections between APC and prostaglandin H synthase-2. *Cell* 1996; **87**: 783-786
- Subbaramaiah K, Telang N, Ramonetti JT, Araki R, DeVito B, Weksler BB, Dannenberg AJ. Transcription of cyclooxygenase-2 is enhanced in transformed mammary epithelial cells. *Cancer Res* 1996; **56**: 4424-4429
- Eberhart CE, Coffey RJ, Radhika A, Giardiello FM, Ferrenbach S, DuBois RN. Up-regulation of cyclooxygenase 2 gene expression in human colorectal adenomas and adenocarcinomas. *Gastroenterology* 1994; **107**: 1183-1188
- Ristimaki A, Honkanen N, Jankala H, Sipponen P, Harkonen M. Expression of cyclooxygenase-2 in human gastric carcinoma. *Cancer Res* 1997; **57**: 1276-1280
- Wilson KT, Fu S, Ramanujam KS, Meltzer SJ. Increased expression of inducible nitric oxide synthase and cyclooxygenase-2 in Barrett's esophagus and associated adenocarcinomas. *Cancer Res* 1998; **58**: 2929-2934
- Hida T, Yatabe Y, Achiwa H, Muramatsu H, Kozaki K, Nakamura S, Ogawa M, Mitsudomi T, Sugiura T, Takahashi T. Increased expression of cyclooxygenase 2 occurs frequently in human lung cancers, specifically in adenocarcinomas. *Cancer Res* 1998; **58**: 3761-3764
- Reddy BS, Rao CV, Seibert K. Evaluation of cyclooxygenase-2 inhibitor for potential chemopreventive properties in colon carcinogenesis. *Cancer Res* 1996; **56**: 4566-4569
- Kawamori T, Rao CV, Seibert K, Reddy BS. Chemopreventive activity of celecoxib, a specific cyclooxygenase-2 inhibitor, against colon carcinogenesis. *Cancer Res* 1998; **58**: 409-412
- Thun MJ, Namboodiri MM, Calle EE, Flanders WD, Heath CW Jr. Aspirin use and risk of fatal cancer. *Cancer Res* 1993; **53**: 1322-1327
- Funkhouser EM, Sharp GB. Aspirin and reduced risk of esophageal carcinoma. *Cancer* 1995; **76**: 1116-1119
- Rubio CA. Antitumoral activity of indomethacin on experimental esophageal tumors. *J Natl Cancer Inst* 1984; **72**: 705-707
- Rubio CA. Further studies on the therapeutic effect of indomethacin on esophageal tumors. *Cancer* 1986; **58**: 1029-1031
- Ciaparrone M, Yamamoto H, Yao Y, Sgambato A, Cattoretti G, Tomita N, Monden T, Rotterdam H, Weinstein IB. Localization and expression of p27KIP1 in multistage colorectal carcinogenesis. *Cancer Res* 1998; **58**: 114-122
- Giardiello FM, Hamilton SR, Krush AJ, Piantadosi S, Hylind LM, Celano P, Booker SV, Robinson CR, Offerhaus GJ. Treatment of colonic and rectal adenomas with sulindac in familial adenomatous polyposis. *N Engl J Med* 1993; **328**: 1313-1316
- Labayle D, Fischer D, Vielh P, Drouhin F, Pariente A, Bories C, Duhamel O, Troussat M, Attali P. Sulindac causes regression of rectal polyps in familial adenomatous polyposis. *Gastroenterology* 1991; **101**: 635-639
- Tonelli F, Valanzano R. Sulindac in familial adenomatous polyposis. *Lancet* 1993; **342**: 1120
- Thun MJ, Namboodiri MM, Heath CW Jr. Aspirin use and reduced risk of fatal cancer. *N Engl J Med* 1991; **325**: 1593-1596
- Schreinemachers DM, Everson RB. Aspirin use and lung, colon, and breast cancer incidence in a prospective study. *Epidemiology* 1994; **5**: 138-146
- Takahashi M, Furukawa F, Toyoda K, Sato H, Hasegawa R, Imaida K, Hayashi Y. Effects of various prostaglandin synthesis inhibitors on pancreatic carcinogenesis in hamsters after initiation with N-nitrosobis(2-oxopropyl)amine. *Carcinogenesis* 1990; **11**: 393-395
- Levy GN. Prostaglandin H synthases, nonsteroidal anti-inflammatory drugs, and colon cancer. *FASEB J* 1997; **11**: 234-247
- Takahashi M, Fukutake M, Yokota S, Ishida K, Wakabayashi K, Sugimura T. Suppression of azoxymethane-induced aberrant crypt foci in rat colon by nimesulide, a selective inhibitor of cyclooxygenase 2. *J Cancer Res Clin Oncol* 1996; **122**: 219-222
- Sano H, Kawahito Y, Wilder RL, Hashimoto A, Mukai S, Asai K, Kimura S, Kato H, Kondo M, Hla T. Expression of cyclooxygenase-1 and -2 in human colorectal cancer. *Cancer*

- Res* 1995; **55**: 3785-3789
- 34 **Bennett A**, Tacca MD, Stamford IF, Zebro T. Prostaglandins from tumours of human large bowel. *Br J Cancer* 1977; **35**: 881-884
- 35 **Maxwell WJ**, Kelleher D, Keating JJ, Hogan FP, Bloomfield FJ, MacDonald GS, Keeling PW. Enhanced secretion of prostaglandin E2 by tissue-fixed macrophages in colonic carcinoma. *Digestion* 1990; **47**: 160-166
- 36 **Marnett LJ**. Aspirin and the potential role of prostaglandins in colon cancer. *Cancer Res* 1992; **52**: 5575-5589
- 37 **Hla T**, Ristimaki A, Appleby S, Barriocanal JG. Cyclooxygenase gene expression in inflammation and angiogenesis. *Ann N Y Acad Sci* 1993; **696**: 197-204
- 38 **Qiao L**, Kozoni V, Tsioulas GJ, Koutsos MI, Hanif R, Shiff SJ, Rigas B. Selected eicosanoids increase the proliferation rate of human colon carcinoma cell lines and mouse colonocytes *in vivo*. *Biochim Biophys Acta* 1995; **1258**: 215-223
- 39 **Tsujii M**, Kawano S, DuBois RN. Cyclooxygenase-2 expression in human colon cancer cells increases metastatic potential. *Proc Natl Acad Sci U S A* 1997; **94**: 3336-3340
- 40 **Hanif R**, Pittas A, Feng Y, Koutsos MI, Qiao L, Staiano-Coico L, Shiff SJ, Rigas B. Effects of nonsteroidal anti-inflammatory drugs on proliferation and on induction of apoptosis in colon cancer cells by a prostaglandin-independent pathway. *Biochem Pharmacol* 1996; **52**: 237-245
- 41 **Eling TE**, Thompson DC, Foureman GL, Curtis JF, Hughes MF. Prostaglandin H synthase and xenobiotic oxidation. *Annu Rev Pharmacol Toxicol* 1990; **30**: 1-45
- 42 **Ahlgren JD**. Epidemiology and risk factors in pancreatic cancer. *Semin Oncol* 1996; **23**: 241-250
- 43 **Gierse JK**, Hauser SD, Creely DP, Koboldt C, Rangwala SH, Isakson PC, Seibert K. Expression and selective inhibition of the constitutive and inducible forms of human cyclo-oxygenase. *Biochem J* 1995; **305**(Pt 2): 479-484
- 44 **Ogino K**, Hatanaka K, Kawamura M, Katori M, Harada Y. Evaluation of the pharmacological profile of meloxicam as an anti-inflammatory agent, with particular reference to its relative selectivity for cyclooxygenase-2 over cyclooxygenase-1. *Pharmacology* 1997; **55**: 44-53
- 45 **Klein T**, Nusing RM, Wiesenber-Boettcher I, Ullrich V. Mechanistic studies on the selective inhibition of cyclooxygenase-2 by indanone derivatives. *Biochem Pharmacol* 1996; **51**: 285-290

Edited by Zhu LH Proofread by Chen WW and Xu FM

Gastric malignancies in Northern Jordan with special emphasis on descriptive epidemiology

Kamal E. Bani-Hani, Rami J. Yaghan, Hussein A. Heis, Nawaf J. Shatnawi, Ismail I. Matalaka, Amjad M. Bani-Hani, Kamal A. Gharaibeh

Kamal E. Bani-Hani, Rami J. Yaghan, Hussein A. Heis, Nawaf J. Shatnawi, Amjad M. Bani-Hani, Kamal A. Gharaibeh, Department of Surgery Princess Basma Teaching Hospital, Faculty of Medicine, Jordan University of Science & Technology, Irbid- Jordan

Ismail I. Matalaka, Department of Pathology, Princess Basma Teaching Hospital, Faculty of Medicine, Jordan University of Science & Technology, Irbid- Jordan

Correspondence to: Kamal E. Bani-Hani, Associate Professor of Surgery, Department of Surgery, Faculty of Medicine, Jordan University of Science and Technology, PO Box 3030, Irbid 22110, Jordan. banihani60@yahoo.com

Telephone: +962-79-5500014 **Fax:** +962-2-7060300

Received: 2004-02-06 **Accepted:** 2004-02-24

Abstract

AIM: To study the epidemiology of gastric malignancies in Jordan as a model for Middle East countries where such data is scarce.

METHODS: Pertinent epidemiological and clinicopathological data for 201 patients with gastric malignancy in north of Jordan between 1991 and 2001 were analyzed.

RESULTS: Male: female ratio was 1.8:1. The mean age was 61.2 years, and 8.5% of the patients were younger than 40 years of age. The overall age-adjusted incidence was 5.82/100 000 population/year. The age specific incidence for males raised from 1.48 in those aged 30-39 years to 72.4 in those aged 70-79 years. Adenocarcinomas, gastric lymphomas, malignant stromal tumors, and carcinoids were found in 87.5%, 8%, 2.5%, and 2% respectively. There was an average of 10.1-month delay between the initial symptoms and the diagnosis. Only 82 patients underwent "curative" gastrectomy. Among adenocarcinoma groups, Lauren intestinal type was the commonest (72.2%) and the distal third was the most common localization (48.9%). The mean follow up for patients with gastric adenocarcinoma was 25.1 mo (range 1-132 mo). The 5-year survival rates for stages I ($n=15$), II ($n=41$), III ($n=59$), and IV ($n=53$) were 67.3%, 41.3%, 5.7%, and 0% respectively ($P=0.0001$). The overall 5 year survival was 21.1%.

CONCLUSION: Despite low incidence, some epidemiological features of gastric cancer in Jordan mimic those of high-risk areas. Patients are detected and treated after a relatively long delay. No justification in favor of a possible gastric cancer screening effort in Jordan is supported by our study; rather, the need of an earlier diagnosis and subsequent better care.

Bani-Hani KE, Yaghan RJ, Heis HA, Shatnawi NJ, Matalaka II, Bani-Hani AM, Gharaibeh KA. Gastric malignancies in Northern Jordan with special emphasis on descriptive epidemiology. *World J Gastroenterol* 2004; 10(15): 2174-2178
<http://www.wjgnet.com/1007-9327/10/2174.asp>

INTRODUCTION

Gastric cancer (GC) is one of the most prevalent cancers and, today, is the second cause of cancer death worldwide^[1,2]. The pattern and incidence of GC vary widely between different parts of the world. Costa Rica and Japan have the first and second highest rates in the world with a death rate of 77.5 and 50.5 /100 000 population, respectively^[2,3]. In the United States 12 100 deaths from GC were expected during 2003 with a death rate of 6.8/100 000, and it was estimated that 224 00 (13 400 in men) new cases of GC were diagnosed in the same year^[4]. The risk of developing GC was relatively lower in the Middle East and North Africa compared to those of western countries^[1,5].

The epidemiology of GC has been widely studied in the Western world as well as in Japan^[6-12]. However, only few scattered reports from the developing world have been published^[13-17]. There is a lack of good descriptive data on GC from the Middle East countries, where both cancer registration and prevalence of risk factors are relatively unknown. Because of the decreasing trend that took place in the Western world as a result of possibly, socio-economic development and its consequences, it is important to gain an insight into what is happening in other parts of the world such as in the Middle East. This prompted us to report on the epidemiological and clinicopathological features of gastric malignancy in Jordan in comparison to other countries whenever possible. This could assist in the better understanding of the important risk factors, which contribute to the development of GC. This will also give a clue about whether or not screening programs are needed in our region.

MATERIALS AND METHODS

Patients

This is a retrospective study of gastric malignancy in the north of Jordan over an eleven-year period (Jan 1991 to Dec 2001). The population of Irbid province (north of Jordan) as determined in the last official census conducted in Jordan in 1994 was 745 774 out of which 385 264 (51.66%) were males. Fifty percent of the Jordanian population are below the age of 16 years^[18]. A total of 76% of the population live in cities and towns.

Initial data were obtained from the computer database at the Department of Pathology at Jordan University of Science and Technology. This is the only pathology center serving the area. Histologically confirmed primary gastric malignancy was found in 201 patients, including 176 patients with adenocarcinoma, 16 patients with primary gastric lymphoma (PGL), 5 patients with malignant gastric stromal tumors, and 4 patients with gastric carcinoids. Further information was obtained from the medical records of these patients at Princess Basma Teaching Hospital and Prince Rashed Teaching Hospital, the only two tertiary centers in Northern Jordan. All available endoscopy reports were reviewed. Patients and/or family members were contacted whenever possible.

A single pathologist reviewed all the histological slides. Gastric adenocarcinoma was classified into intestinal (IT), diffuse (DT), or mixed types according to the histological criteria

of Lauren^[19]. The site of the tumor was assessed pathologically in the resected specimens and endoscopically in the remaining cases, and was defined as that part of the stomach harboring the bulk of the tumor. Tumor staging in each patient was based on clinical information, preoperative radiological investigations, operative findings, and pathological examination. The staging was made in accordance with the TNM system endorsed by the Union Internationale Contre Le Cancer (UICC)^[20].

Vital status of patients was ascertained from death certificates or from families who were contacted.

All deaths within 30 d of surgery were considered surgical mortality. The incidence rates were adjusted to the world population. Our hospital based incidence data were matched with the Jordanian National Cancer Registry (JNCR) data only for the period 1996-2001, since the Registry was established in 1996. The survival rate was analyzed for each stage by the Kaplan-Meier method, and the survival curves were compared by the log-rank test using the Statistical Package for the Social Sciences Software Program (SPSS®, Inc., Chicago, Illinois, USA). Differences were considered statistically significant at $P < 0.05$.

RESULTS

During the study period 201 patients with primary gastric malignancy were identified, 128 (63.7%) patients were males with a male: female ratio of 1.8:1.

Sixty-five percent of the patients (131/202) were diagnosed during the second half of the study period. Analyses of the data from the JNCR, which was established in 1996, showed that all the 131 study patients diagnosed with gastric malignancy between 1st January 1996 and 31st December 2001 appeared in the registry and there were no additional patients from northern Jordan in the registry not identified by our study.

The overall age-adjusted incidence (world population) was 5.82/100 000 per year. Table 1 shows the age specific incidence

rate (ASIR) per 100 000 population by gender. The peak incidence was in the age group 60-69 years (39.8%), followed by the age group 70-79 (22.9%). Approximately 8.5% of the patients were younger than 40 years of age. The mean age for the whole group was 61.2 years (SD±12.3, range 24-91 years).

Presenting features for our patients are summarized in Table 2. Acute presentation was seen in 59 (29.4%) patients; 37 patients (18.4%) presented with upper gastrointestinal bleeding, 17 (8.5%) with gastric outlet obstruction, and in the remaining 5 (2.5%) patients perforation was the mode of presentation.

Table 2 Presenting features of patients with gastric malignancy

	Number of patients	%
Abdominal pain	144	71.6
Weight loss and/or anemia	130	64.7
Dyspepsia	98	48.8
Nausea, vomiting	96	47.8
Abdominal mass	62	30.8
Anorexia	58	28.9
Dysphagia	44	21.9
Gastrointestinal bleeding	37	18.4
Obstruction	17	8.5
Perforation	5	2.5

There was an average of 10.1-month delay (range 2-17 mo) between the initial symptoms and the diagnosis. In 119 patients this was a result of reluctance in seeking medical advice and/or delay in referring patients for endoscopy. However, in five patients the delay was caused by a false negative upper gastrointestinal endoscopy.

Table 3 shows the distribution of the different histological types according to age and sex. The histologic subtypes of the

Table 1 Age specific incidence rate per 100 000 population/year by age and gender

Age (yr) group	Male			Female		
	Population	No. of cancers ¹	ASIR ²	Population	No. of cancers ¹	ASIR ²
0-9	113 142	0	0	106 465	0	0
10-19	092 899	0	0	087 629	0	0
20-29	076 938	0	0	071 445	1	0.13
30-39	043 068	7	1.48	038 967	9	2.1
40-49	024 175	11	4.14	023 480	6	2.32
50-59	019 763	21	9.66	017 526	9	4.67
60-69	010 157	53	47.44	009 009	27	27.25
70-79	003 641	29	72.4	004 264	17	36.24
80	001 481	7	43	001 725	4	21.08
Total	385 264	128	3.02	360 510	73	1.84

¹Number of cancers during the 11-year study. ²Age specific incidence rate per 100 000 population/year.

Table 3 Histopathological distribution of gastric malignancies according to age and sex (%)

Histopathologic diagnosis	Age (yr)		Sex		Total
	Mean	Range	Male	Female	
Intestinal type adenocarcinoma	62.7	35-91	90(70.9)	37(29.1)	127(63.2)
Diffuse type adenocarcinoma	51.9	24-75	9(31)	20(69)	29(14.4)
Mixed type adenocarcinoma	64.3	51-72	11(57.9)	8(42.1)	19(9.5)
Adenosquamous carcinoma	82	82	1	-	1(0.5)
Primary gastric lymphoma	57.9	41-82	12(75)	4(25)	16(8)
Carcinoid	66	41-81	2(50)	2(50)	4(2)
Malignant stromal tumors	69.4	43-84	3(60)	2(40)	5(2.5)
Total	61.2	24-91	128(63.7)	73(36.3)	201(100)

Table 4 Distribution of gastric adenocarcinoma according to site (%)

Histopathological type	Proximal third	Middle third	Distal third	Entire stomach	Total
Intestinal type adenocarcinoma	22(17.3)	30(23.6)	70(55.1)	5(3.9)	127
Diffuse type adenocarcinoma	6(20.7)	7(24.1)	7(24.1)	9(31)	29
Mixed type adenocarcinoma	3(15.8)	5(26.3)	8(42.1)	3(15.8)	19
Adenosquamous carcinoma	-	-	1	-	1
Total	31(17.6)	42(23.9)	86(48.9)	17(9.7)	176

82 patients who had gastrectomy were correctly diagnosed in pre-gastrectomy endoscopic biopsies except in 2 cases, which were diagnosed as IT adenocarcinoma and turned out to be of the DT in subsequent examinations of the resected specimens. Pathological examination of the 65 resected IT and mixed adenocarcinomas revealed that 51 of the cancers were moderately differentiated, 10 were poorly differentiated and four were well differentiated.

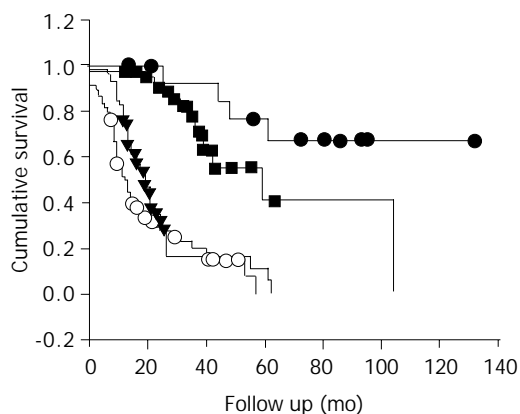
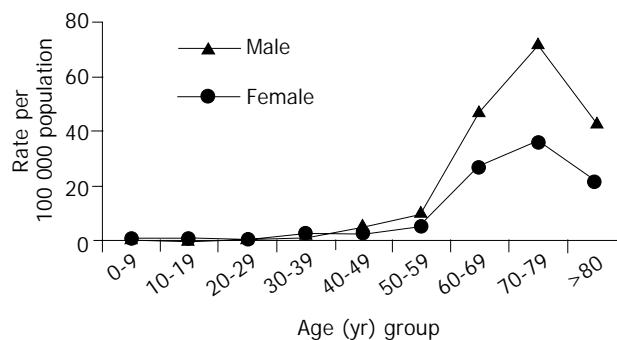
Table 4 shows the distribution of various histologic types of gastric adenocarcinoma according to the sites affected.

For gastric adenocarcinoma, using the TNM staging, 15 patients had stage I, 41 patients had stage II, 59 patients had stage III, and 53 patients had stage IV disease. In the remaining 8 patients, the stage could not be determined due to insufficient data (stage X).

Gastrectomy was performed for 82 patients (D1 in 63 and D2 in 19 patients). Palliative resection or bypass procedures were done for 95 patients, while 3 patients with PGL had chemotherapy only. The remaining 21 patients were too frail to be treated. No patients had D3 gastrectomy. None of the patients with adenocarcinoma was given adjuvant therapy. Postoperative morbidity occurred in 25.4% (45/177) of the patients. Eight patients died during the postoperative period giving a surgical mortality of 4.5% (8/177).

For the 176 patients with adenocarcinoma, the mean follow up until December 2002 was 25.1 mo (range 1-132 mo). At that time, vital status was available for 163 patients (92.6%). The remaining 13 patients (mean age 59.6 years; 11 males and 2 females) were lost to follow up at a mean of 28.2 mo (range 7-86 mo). The stages of the disease for these 13 patients were I, II, III, IV, and X in 1, 2, 4, 4, and 2 patients respectively.

Survival analysis included the 8 early postoperative deaths and the later non-cancer deaths. The median survival for stages II, III, and both stages IV and X was 59, 19, and 13 mo respectively. Figure 1 demonstrates the survival curves for stages I-IV using Kaplan-Meier method. The 5-year survival rates for stages I, II, III, and IV were 67.3%, 41.3%, 5.7%, and 0% respectively ($P=0.0001$). The overall 5 year survival was 21.1%.

**Figure 1** Survival rate of gastric adenocarcinoma patients according to stage using Kaplan-Meier analysis. (●) Stage I; $n=15$, (■) Stage II; $n=41$, (▼) Stage III; $n=59$, (○) Stage IV and X; $n=61$.**Figure 2** Age specific incidence rate per 100 000 population/year by gender.

DISCUSSION

There was consistency between our study and the data of the JNCR. The incidence was calculated and corrected for age in relation to the world population. The age-adjusted incidence of gastric malignancy in this study was 5.82/100 000 per year, which was significantly lower than those of developed countries but rather similar to most other Middle East countries^[1,2]. However, this incidence would rise sharply when the ASIR is calculated because of the specific pyramidal age distribution of our population where approximately 50% of our population are below the age of 16 years (1994 census). The ASIR for males per 100 000 population raised from 1.48 in those aged 30-39 years to 72.4 in those aged 70-79 years (Figure 2). Similarly, figures from the JNCR showed that during 1997, the ASIR raised sharply from 3.3 to 108 for the same gender and age groups^[18]. During the same year GC was the eighth commonest cancer, representing 4% of all cancer cases, and it accounted for 22% of all primary gastrointestinal tract cancers.

It is well known that the incidence of GC is decreasing globally. The apparent increase in diagnosing GC during the second half of the study period most likely reflects a better diagnostic yield after the relatively recent introduction of endoscopic services throughout the country rather than an actual increase in the incidence. Still the following two factors may play a role in this increasing trend. First, the rapid change in dietary habits Jordan is witnessing might constitute a risk factor. Vitamin C-rich fresh vegetables and fruits, starch, and natural unprocessed wheat products were the major constituents of Jordanian food. However, canned food, hot spices, pickles, and animal proteins are now dominating the Jordanian menu. It is known that the environmental risk factors for GC could be dietary in origin^[21,22]. Second, the already high prevalence of *Helicobacter pylori* in Jordan is increasing and the exposure time is also increasing with the improvement in life expectancy among Jordanians^[23,24]. It is proposed that Lauren's IT of GC is related to chronic *Helicobacter pylori* infection. Among our study group IT adenocarcinoma was the commonest histological subtype (63.2%).

Most resections were done with palliative intent. The low rate of gastrectomy with "curative" intent could be explained by the high proportion of patients with advanced GC at

presentation. However, we believe that surgical undertreatment might be a contributing factor. Our patients tended to present late as evidenced by the facts that there was a long interval between onset of symptoms and presentation, 29.4% presented acutely, and that only 40.8% (82/201) of them underwent D1 or D2 gastrectomy. This is not only due to insufficiency of current endoscopic services, but also due to the fact that many people in Jordan who have non-specific dyspeptic symptoms will seek the advice of non-physician personnel who will either prescribe herbal medicine for long term treatment or induce patches of second or third degree burns to the epigastric region using hot metals in order to ameliorate the deep seated pain! Subsequently some of these patients in whom the cause of dyspepsia is cancer will present to the hospital with late stage GC or one of its complications. In addition, the elderly people usually fail to make use of the available medical services due to inadequacy of primary health care in Jordan.

Some GC patterns in north of Jordan were similar to those reported from high-risk regions worldwide^[3,25]. In particular, the mean age was in the seventh decade, male to female ratio was 1.8:1, IT adenocarcinoma was more common than DT (4.4:1), and distal location was more frequent than proximal one (2.5:1). Since the demographic features among Jordanians are homogenous, we believe that these trends apply to whole Jordan. In contrary, in a low-risk area, such as Kenya, the DT is the commonest subtype^[26].

In our study, DT adenocarcinoma occurred in younger patients with a mean age of 51.9 years and was commoner in females with a male to female ratio of 0.45:1 (Table 3). Similar findings of diffuse tumors prevailing among young patients and women were reported from Sweden, Finland, Mexico and Taiwan^[6,8,16,17], but not from neighboring Saudi Arabia^[14,15].

Our survival rate for stages I and II is consistent with the rate reported in the Western literature^[27,28]. However, this rate was much lower for our patients with more advanced stages probably reflecting undertreatment at our institute. After the introduction of a specialized upper gastrointestinal unit at our hospital in January 2001, we have adopted a more radical approach.

In Western countries, PGL represented only 2% to 5% of gastric malignancies^[29], while it represented 8% of our series, which was similar to the 9% figure from neighboring Iraq^[30], but different from the 14-22% figure reported from Saudi Arabia^[14,15]. During the past three decades the site of PGL in the Middle East has changed^[31]. Small intestinal involvement became less common, and gastric involvement more frequent. This varying pattern seemed to be environmental in origin^[31]. Although the ratio of PGL to gastric adenocarcinoma among our patients was higher than in western series, a recent study from Jordan demonstrated that other patterns of PGL were mimicking those of the west^[32]. The stomach was the commonest site of involvement, accounting for 62% of all cases^[32].

Our rates for the gastric malignant stromal tumors and carcinoids are consistent with rates reported elsewhere^[33]. The survival rate for these patients was not calculated due to the small number of patients.

At the end of this discussion, we would like to highlight some of the shortcomings in our study. First, the incidence figures were calculated only after histological confirmation by endoscopy or surgery. In Jordan, hospital postmortem is rarely performed because of religious or social grounds. Additionally, only half of deaths are attended by medical workers personals. This means that some patients with GC were certainly not included in the incidence calculation. The limitation to histologically confirmed cases increases specificity but lowers the sensitivity in identifying cases to be included in the incidence figures. Cases admitted to hospitals with a suspicion of GC or deceased with a diagnosis of GC but without histological

confirmation were not considered in the estimation of incidence rates. Additionally as one third of our patients presented with an abdominal mass, and there was a 10-mo delay in diagnosis so the estimated incidence was lower than the real incidence because many patients did not reach the hospitals. Second, Lauren classification is known to be affected by a quite low reproducibility^[34]. Specifically, mixed cases might be classified as intestinal or as diffuse type, depending on the examined tissue areas endoscopically biopsied or from the surgical specimens.

In conclusion, the incidence of GC in Jordan is low, but increases appreciably with age. This, in addition to the fact that 50% of the Jordanian population are below the age of 16 years, shows that it does not seem justified introducing a screening program. However, general practitioners should be more liberal in referring patients for endoscopy and resist the temptation to treat dyspeptic patients with anti-ulcer therapy without an endoscopy. Open access endoscopy, greater efforts in patient education and improvement of the diagnostic technical skills may raise the chance of detecting GC early. Some patterns of GC in Jordan (age, sex, tumor location, and histological type) are similar to features from high-risk areas. Although this study clearly highlights the pertinent epidemiological and clinicopathological features of gastric malignancy in Jordan, further studies are needed to evaluate the treatment outcomes.

REFERENCES

- 1 **Parkin DM**, Pisani P, Ferlay J. Estimates of the worldwide incidence of 25 major cancers in 1990. *Int J Cancer* 1999; **80**: 827-841
- 2 **Parkin DM**, Pisani P, Ferlay J. Global cancer statistics. *CA Cancer J Clin* 1999; **49**: 33-64
- 3 **Sasagawa T**, Solano H, Mena F. Gastric cancer in Costa Rica. *Gastrointest Endosc* 1999; **50**: 594-595
- 4 **Jemal A**, Murray T, Samuels A, Ghafoor A, Ward E, Thun MJ. Cancer statistics, 2003. *CA Cancer J Clin* 2003; **53**: 5-26
- 5 **Pisani P**, Parkin DM, Bray F, Ferlay J. Estimates of the worldwide mortality from 25 cancers in 1990. *Int J Cancer* 1999; **83**: 18-29
- 6 **Ekstrom AM**, Hansson LE, Signorello LB, Lindgren A, Bergstrom R, Nyren O. Decreasing incidence of both major histologic subtypes of gastric adenocarcinoma—a population-based study in Sweden. *Br J Cancer* 2000; **83**: 391-396
- 7 **Kaneko S**, Yoshimura T. Time trend analysis of gastric cancer incidence in Japan by histological types, 1975-1989. *Br J Cancer* 2001; **84**: 400-405
- 8 **Lauren PA**, Nevalainen TJ. Epidemiology of intestinal and diffuse types of gastric carcinoma. A time-trend study in Finland with comparison between studies from high- and low-risk areas. *Cancer* 1993; **71**: 2926-2933
- 9 **Haugstvedt TK**, Viste A, Eide GE, Maartmann-Moe H, Myking A, Soreide O. Is Lauren's histopathological classification of importance in patients with stomach cancer? A national experience. Norwegian Stomach Cancer Trial. *Eur J Surg Oncol* 1992; **18**: 124-130
- 10 **Stelzner S**, Emmrich P. The mixed type in Lauren's classification of gastric carcinoma. Histologic description and biologic behavior. *Gen Diagn Pathol* 1997; **143**: 39-48
- 11 **Leocata P**, Ventura L, Giunta M, Guadagni S, Fortunato C, Discepoli S, Ventura T. Gastric carcinoma: a histopathological study of 705 cases. *Ann Ital Chir* 1998; **69**: 331-337
- 12 **Monferrer Guardiola R**, Peiro Gomez AM, Galiana Gil R, Montes Rotgla A, Lillo Sanchez A, Cuevas Campos A. Incidence of gastric cancer in the 02 health area of Castellon. *An Med Interna* 1996; **13**: 68-72
- 13 **Johnson O**, Ersumo T, Ali A. Gastric carcinoma at Tikur Anbessa Hospital, Addis Ababa. *East Afr Med J* 2000; **77**: 27-30
- 14 **Hamdi J**, Morad NA. Gastric cancer in southern Saudi Arabia. *Ann Saudi Med* 1994; **14**: 195-197
- 15 **Al-Mofleh IA**. Gastric cancer in upper gastrointestinal endos-

- copy population: prevalence and clinicopathological characteristics. *Ann Saudi Med* 1992; **12**: 548-551
- 16 **Mohar A**, Suchil-Bernal L, Hernandez-Guerrero A, Podolsky-Rapoport I, Herrera-Goepfert R, Mora-Tiscareno A, Aiello-Crocifoglio V. Intestinal type: diffuse type ratio of gastric carcinoma in a Mexican population. *J Exp Clin Cancer Res* 1997; **16**: 189-194
- 17 **Wu CW**, Tsay SH, Hsieh MC, Lo SS, Lui WY, P'eng FK. Clinicopathological significance of intestinal and diffuse types of gastric carcinoma in Taiwan Chinese. *J Gastroenterol Hepatol* 1996; **11**: 1083-1088
- 18 **Al-Kayed S**, Hijawi B. Cancer incidence in Jordan 1997 report. National Cancer Registry. The hashemite kingdom of Jordan. *Amman (HKJ), Ministry of Health* 1999
- 19 **Lauren P**. The two histological main types of gastric carcinoma: diffuse and so-called intestinal type carcinoma. *Acta Path Microbiol Scan* 1965; **64**: 31-49
- 20 Hermanek P, Sobin L. TNM classification of malignant tumors. 4th ed. *Berlin: Springer Verlag* 1987
- 21 **Ngoan LT**, Mizoue T, Fujino Y, Tokui N, Yoshimura T. Dietary factors and stomach cancer mortality. *Br J Cancer* 2002; **87**: 37-42
- 22 **Palli D**. Epidemiology of gastric cancer: an evaluation of available evidence. *J Gastroenterol* 2000; **35**: 84-89
- 23 **Bani-Hani KE**, Hammouri SM. Prevalence of *Helicobacter pylori* in Northern Jordan. Endoscopy-based study. *Saudi Med J* 2001; **22**: 843-847
- 24 **Latif AH**, Shami SK, Batchoun R, Murad N, Sartawi O. *Helicobacter pylori*: a Jordanian study. *Postgrad Med J* 1991; **67**: 994-998
- 25 **Correa P**. Clinical implications of recent developments in gastric carcinoma pathology and epidemiology. *Semin Oncol* 1985; **12**: 2-10
- 26 **Ogutu EO**, Lule GN, Okoth F, Musewe AO. Gastric carcinoma in the Kenyan African population. *East Afr Med J* 1991; **68**: 334-339
- 27 **Davis PA**, Sano T. The difference in gastric cancer between Japan, USA and Europe: what are the facts? what are the suggestions? *Crit Rev Oncol Hematol* 2001; **40**: 77-94
- 28 **Fuchs CS**, Mayer RJ. Gastric carcinoma. *N Engl J Med* 1995; **333**: 32-41
- 29 **Hertzer NR**, Hoerr SO. An interpretive review of lymphomas of the stomach. *Surg Gynecol Obstet* 1976; **143**: 113-124
- 30 **Al-Bahrani Z**, Al-Mondhiry H, Bakir F, Al-Saleem T, Al-Eshaiker M. Primary gastric lymphoma. Review of 32 cases from Iraq. *Ann R Coll Surg Engl* 1982; **64**: 234-237
- 31 **Taleb N**, Chamseddine N, Abi Gergis D, Chahine A. Non-Hodgkin's lymphoma of the digestive system. General epidemiology and epidemiological data concerning 100 Lebanese cases seen between 1965 and 1991. *Ann Gastroenterol Hepatol* 1994; **30**: 283-286
- 32 **Almasri NM**, al-Abbadi M, Rewaily E, Abulkhail A, Tarawneh MS. Primary gastrointestinal lymphomas in Jordan are similar to those in Western countries. *Mod Pathol* 1997; **10**: 137-141
- 33 **Hamilton SR**, Aaltonen LA, eds. World Health Organization classification of tumours. Pathology and genetics of tumours of the digestive system. *Lyon IARC Press* 2000
- 34 **Palli D**, Bianchi S, Cipriani F, Duca P, Amorosi A, Avellini C, Russo A, Saragoni A, Todde P, Valdes E. Reproducibility of histologic classification of gastric cancer. *Br J Cancer* 1991; **63**: 765-768

Edited by Zhu LH and Xu FM

Identification of tumor markers using two-dimensional electrophoresis in gastric carcinoma

Kai-Juan Wang, Run-Tian Wang, Jian-Zhong Zhang

Run-Tian Wang, Department of Epidemiology and Biostatistics, School of Public Health, Peking University, Beijing 100083, China

Kai-Juan Wang, Department of Epidemiology, School of Public Health, Zhengzhou University, Zhengzhou 450052, Henan Province, China

Jian-Zhong Zhang, National Institute for Communicable Disease Control and Prevention, Chinese Center for Disease Control and Prevention, Beijing 102206, China

Supported by the National Natural Science Foundation of China, No. 30070671

Correspondence to: Professor Run-Tian Wang, Department of Epidemiology and Biostatistics, School of Public Health, Peking University, Beijing 100083, China. kjwang@163.com

Telephone: +86-10-82801525

Received: 2004-02-20 **Accepted:** 2004-03-02

Abstract

AIM: To study the differential expression of proteins in normal and cancerous gastric tissues, and further identify new molecular markers for diagnosis and prognosis of gastric carcinoma, as well as develop new therapeutic targets of the disease.

METHODS: Matched pairs of tissues from 6 gastric cancer patients were analyzed for their two-dimensional electrophoresis (2DE) profiles. Soluble fraction proteins from human normal and cancerous gastric tissue were separated in the first dimension by isoelectric focusing on immobilized pH gradient (IPG, pH3-10) strips, and by 125 g/L sodium dodecyl sulfate polyacrylamide gel electrophoresis (SDS-PAGE) in the second dimension with silver nitrate staining. Protein differential expression was analyzed by use of image analysis software to find out candidates for gastric cancer-associated proteins.

RESULTS: Nine protein spots overexpressed in tumor tissues as compared with noncancerous regions. In the next step, 9 tumor-specific spots were cut off from Coomassie Brilliant Blue staining gels, digested in gel with L-1-tosylamide-2-phenylethyl chloromethyl ketone (TPCK)-trypsin. Protein identification was done by peptide mass fingerprinting with matrix assisted laser desorption/ionization-time of flight-mass spectrometry (MALDI-TOF-MS). In total, 5 tumor-specific protein spots corresponding to 5 different polypeptide chains were identified, including annexin V, carbonic anhydrase, prohibitin, fibrin beta and fibrinogen fragment D. Among these 5 spots, the potential significance of the differential expressions is discussed.

CONCLUSION Differential expression analysis of proteomes may be useful for the development of new molecular markers for diagnosis and prognosis of gastric carcinoma.

Wang KJ, Wang RT, Zhang JZ. Identification of tumor markers using two-dimensional electrophoresis in gastric carcinoma. *World J Gastroenterol* 2004; 10(15): 2179-2183
<http://www.wjgnet.com/1007-9327/10/2179.asp>

INTRODUCTION

Gastric cancer is a prevalent tumor worldwide. It is a multistage process involving multiple factors in aetiology and many gene-environment interactions. It is important to emphasize the heterogeneity of the histological background on which the tumor develops. Methods have been developed to identify tumor associated antigens such as molecular cloning in expression system or using a biochemical strategy based on the extraction of antigenic peptides bound to major histocompatibility complex class I molecules from tumor cells. These methods have allowed the recognition of certain human tumor antigens^[1]. Several tumor markers of gastric cancer have been identified^[2-4], including Lewis antigen, sulfomucin, CA50. However, no evidence has been obtained indicating that the detection of these markers precedes clinical diagnosis of gastric cancer. Proteomics studies of clinical tumor samples have led to the identification of cancer-specific protein markers, which provides a basis for developing new methods for early diagnosis and early detection of cancers as well as clues to understanding the molecular mechanism of cancer progression^[5]. In order to identify proteins that elicit humoral responses in gastric cancer patients, proteome-based approach was used. A number of proteins from gastric tumor tissues were separated by 2DE and identified by using mass spectrometry. It includes the systematic cataloging of protein expression on a large scale. Such studies could help elucidate the molecular mechanism of cellular events associated with cancer progression, such as cellular signaling^[6,7].

MATERIALS AND METHODS

Tissue samples and preparation^[8]

Six pairs of primary, and advanced poorly differentiated gastric adenocarcinoma tissues and corresponding adjacent noncancerous gastric tissues were obtained with informed consent from patients who underwent gastrectomy at the First Affiliated Hospital of Zhengzhou University and Beijing Cancer Hospital. Cancer samples were obtained from the "core" part of the tumor to avoid the adjacent noncancerous tissue. For each of the normal tissues, surface epithelium was selectively procured by dissection with special care for minimal contamination of nonepithelial cells, and samples were immediately snap-frozen in liquid nitrogen. They were classified histologically according to Lauren's classification after H & E staining.

Fragments of normal and malignant tissues were sharp dissected and homogenized with a homogenizer in 2 mL fresh lysis buffer [2 g/L dithiothreitol (Amersham Bioscience, USA), 200 mL/L trichloroacetic acid (Sigma, USA) and 800 g/L acetone], then placed into tubes at 4-8 °C for 8-10 h. The mixture was centrifuged at 1 000 r/min for 5 min to remove tissue and cell debris, then centrifuged in a Beckman TL-100 table top ultracentrifuge at 430 000 g in a TLA-100.2 rotor for 30 min at 4 °C. The supernatant was taken as soluble fraction. Protein was lyophilized, resuspended in isoelectric focusing gel rehydration solution {7 mol/L urea, 2 mol/L thiourea, 40 g/L 3-([3-cholamidopropyl] dimethylammonio)-1-propanesulfonate

(CHAPS), 50 mmol/L dithiothreitol, 20 g/L IPG buffer pH 3-10, L} and stored at -80 °C until use. These were used as the 2DE samples for the soluble fraction. Protein concentration of 2-DE samples was estimated according to a commercial Bradford reagent. BSA was used as standard.

2DE with IPG strips

First-dimension bioelectric focusing was carried out on Multiphor II system basically as described by the manufacturer Amersham Bioscience Inc. Samples containing up to 200 µg protein for analytical gels were diluted to up to 450 µL with dehydration solution (8 mol/L urea, 20 g/L CHAPS, 100 mol/L dithiothreitol, 5 g/L IPG buffer). Pre-cast Immobilized pH gradient (IPG) strip (24 cm, pH 3-10, linear gradient) was used for the first-dimensional separation. Strips were applied by overnight rehydration at 50 V, and for 1 h at 1 000 V. Then a gradient was applied from 1 000 to 8 000 V for 8 h to give a total of 180 000 Vh. All IEF steps were carried out at 20 °C. After the first-dimensional IEF, IPG gel strips were placed in an equilibration solution (6 mol/L urea, 200 g/L SDS, 300 g/L glycerol, 50 mol/L Tris-HCl, pH 8.8) containing 10 g/L dithiothreitol and shaken for 15 min. The gels were then transferred to the equilibration solution containing 25 g/L iodoacetamide to alkylate thiols and shaken for a further 15 min before being placed on a 125 g/L polyacrylamide gel slab. Separation in the second dimension was carried out using Tris-glycine buffer containing 1 g/L SDS, at a current setting of 5 mA/gel for the initial 0.5 h and 18 mA/gel thereafter and a temperature of 20 °C.

For silver staining, gels were immersed in ethanol: acetic acid: water (35:7:58) for 1.5 h, followed by washed twice in deionized water for 20 min. Gels were pretreated for 1 min in a solution of 0.2 g/L Na₂S₂O₃ and followed by 3 of 1-min washes in deionized water. Proteins were stained in a solution containing 2 g/L AgNO₃ and 0.075% formalin (37 g/L formaldehyde in water) for 20 min, and washed twice in deionized water for 1 min. Subsequently, gels were developed in a solution of 0.6 g/L formaldehyde, 20 g/L Na₂S₂O₃ and 0.004 g/L Na₂S₂O₃. When the desired intensity was attained, the developer was discarded and reaction stopped by 10 g/L EDTA-Na₂. For Coomassie Brilliant Blue staining of gels, gels were equilibrated in a solution containing 500 mL/L methanol, 50 mL/L acetic acid and 25 g/L Coomassie Brilliant Blue R-250. Gels were rinsed in 300 mL/L ethanol containing 70 mL/L acetic acid.

Protein patterns in the gels after silver staining were recorded as digitalized images using a high-resolution scanner. Gel image matching was done with PDQuest software.

In-gel protein digestion

Protein spots on Coomassie blue stained gel was performed essentially as described. After the completion of staining, the gel slab was washed twice with water for 10 min. The spots of interest were excised with a scalpel and put into 1.5 mL micro-tubes. The particles were washed twice with water and then twice with water/acetonitrile (1:1) for 15 min. The solvent volumes were about twice that of the gel. Liquid was removed, acetonitrile was added to the gel particles and the mixture was left for 2 h. After that, liquid was removed and the particles were rehydrated in 25 mmol/L NH₄HCO₃ for 5 min. Acetonitrile was added to produce a 1:1 mixture of 25 mmol/L NH₄HCO₃ / acetonitrile and the mixture was incubated for 15 min. All liquid was removed. Gel particles were dried in a vacuum centrifuge, reswelled in 10 mmol/L of dithiothreitol and 25 mmol/L of NH₄HCO₃, and incubated for 30 min at 56 °C to reduce the peptides. After chillness of tubes to room temperature and removal of the liquid, 55 mmol/L iodoacetamide in 25 mmol/L NH₄HCO₃ was added. The tubes were incubated for 30 min at room temperature in the dark to S-alkylate the peptides. Then

iodoacetamide solution was removed, the particles were washed with 25 mmol/L NH₄HCO₃ and acetonitrile, dried in a vacuum centrifuge, rehydrated in digestion buffer containing 50 mmol/L NH₄HCO₃ and 12.5 ng/µL trypsin (TPCK-treated, proteomics grade, Sigma, USA), incubated for 8-12 h at 37 °C. After digestion, 25 mmol/L NH₄HCO₃ was added, and the tube was incubated for 15 min. Acetonitrile was added and the tube was incubated for another 15 min. The supernatant was recovered, and the extraction was repeated twice with 50 g/L TFA/acetonitrile (1:1). The three extracts were pooled and dried in a vacuum centrifuge.

MALDI-TOF-MS analysis

One µL sample with 1 µL matrix solution CCA (α-cyano-4-hydroxycinnamic acid) was spotted on the target and dried. Dried spots were analyzed in an REFLEX-III (Bluker) MALDI-TOF mass spectrometer. The spectrometer was run in positive ion mode and in reflector mode with the setting: accelerating voltage, 20 kV; grid voltage, 76%; guide wire voltage, 0.01%; and a delay time of 150 ns. The low mass gate was set at 500 m/z.

Proteins were identified by peptide mass fingerprinting with the search programs Mascot (<http://www.matrixscience.com/cgi/index.pl?page=.1>). The following search parameters were applied: SWISS-PROT and NCBI were used as the protein sequence databases, a mass tolerance of 50 ppm and one incomplete cleavage were allowed; acetylation of the N-terminus, alkylation of lysine by carboxyamidomethylation were considered as possible modifications^[9].

RESULTS

Evaluation of the reproducibility

Mini 2DE gels (7 cm, pH3-10) were used to evaluate the reproducibility of the soluble protein preparations and to quantify the protein extracts for 2DE gel analysis. To ensure quality and reproducibility of results, 2DE maps (24 cm) were established from each sample based on silver staining of at least three independent gels, pairs of gels were run simultaneously with the same power supply and subjected to subsequent image analysis. Protein extracts prepared from tissues were compared in this way and found to be highly reproducible and similar amounts of total soluble protein were yielded when analyzed on the gels.

Overview analysis of the protein expression profiles of paired samples

2DE Gel separation of proteins from 6 pairs of normal and cancerous epithelial cells was procured from the same gastric carcinoma specimen respectively. A series of 2DE maps were constructed for the soluble fraction proteins of human gastric tissue. A representative 2DE gel images following silver staining of cancer tissues (Figure 1A) and normal tissues (Figure 1B) were produced in a 2DE imageMaster. Comparison of the differential protein expression between cancer and normal tissues shown in 2DE images was carried out using the AutoDetect Spots menu of PDQuest software. Figure 1A (from cancer tissues) contains a total of 356 spots, whereas Figure 1B (from normal tissues) contains a total of 382 spots. A total of 323 spots from cancer tissues could be matched to those from normal tissues. In total, we were able to identify 9 cancer-specific spots in 2DE gels. The positions of the identified proteins are shown in Figure 1A. These differences were observed in other cancerous samples. Because all of the identified spots were detectable with Coomassie Blue staining, they could be considered as abundant proteins.

Protein identification

The resulting spot identification was mapped onto the analytical

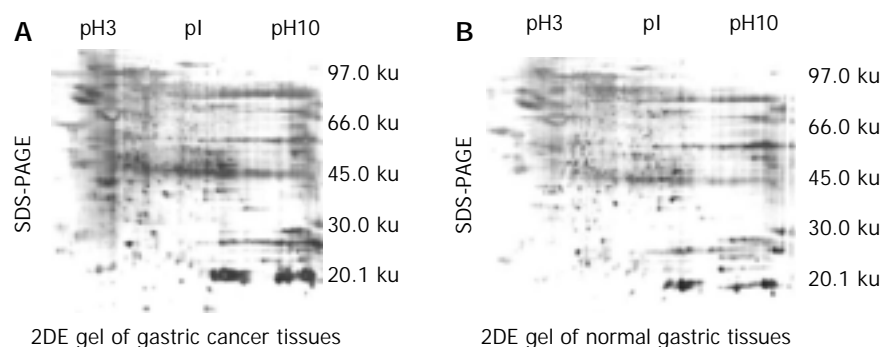


Figure 1 2DE maps of human gastric tissue from No.5 patient. A: was from gastric cancer. B: from normal gastric sample of the same patient. Proteins were separated on pH 3-10 linear IPG strip in the first dimension and 125 g/L SDS-PAGE in the second dimension, gels were silver stained. All labeled spots were tumor-specific.

gels stained by Coomassie Brilliant Blue. On the map, 9 cancer-specific spots were excised and subjected to in-gel digestion followed by peptide mass fingerprinting for protein identification. Figure 2 shows the identification of the spot No. 18 as an example. We identified proteins by peptide mass fingerprinting, MS-Fit of UCSF.

The criteria used to accept identifications included the extent of sequence coverage, the number of peptides matched, the probability score, and whether human protein appeared as the top candidates in the first pass search where no restriction was applied to the species of origin.

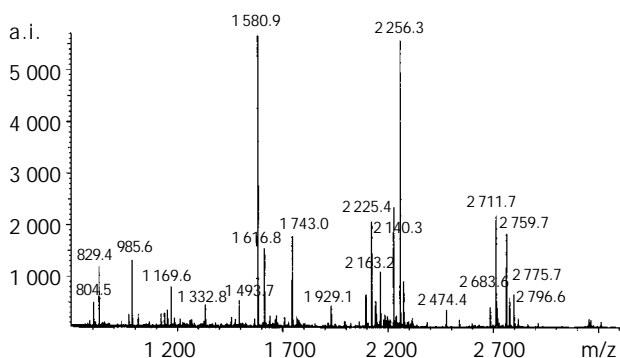


Figure 2 MALDI-TOF MS of tryptic digests of protein spot No. 18 resolved on 2DE gel, REFLEX III (BLUker). The data were collected on positive ion and reflector mode. Experimentally determined mass values are labeled on peptides. Spot 10 matched peptide 11; amino acid coverage, 60%; the spot was identified as carbonic anhydrase I.

The results of identification are summarized in the Appendix Table 1. For identified protein, probability based score greater than 73 was significant ($P < 0.05$). For example, in the case of annexin V, the protein score is 163. Some of these proteins, such as carbonic anhydrase I; chain B, crystal structure of fibrinogen fragment D; fibrin beta and prohibitin, have already been detected in gastric cancer tissues.

DISCUSSION

Proteome based profiling employs the measurement of protein expression pattern for the identification of individual proteins and clusters of proteins that mediate particular aspects in a physiological and pathophysiological process. The measurement of protein expression patterns of normal and disease tissues or cell populations will lead to the characterization of diagnostic and prognostic markers, and it can be further employed for the analysis of the disease stage which might also have an impact on the therapy. Thus, preferably small clusters of proteins represent the ideal diagnostic markers enabling an easier and more accurate diagnosis of diseases for better therapy^[10].

This study was based on an ongoing proteomic analysis of gastric cancer aiming at screening the protein markers in the proteome for diagnosis of gastric cancer. With the availability of high-throughput 2DE gels and initial screening by using automated procedures, identification of changes in the proteome in various tissues will be possible. The approach we described in this study has shown that high-throughput analysis will be a valuable tool. An effort is currently being made using proteome based techniques^[11]. 2DE pattern of normal and diseased tissues revealed a number of polypeptides

Table 1 Protein spots in GC searched by PeptIdent software in the SWISS-PROT database

Spot ID	SWISS-PROT ID	Peptide matched	Top score	Theoretic pI	Theoretic M_r	Sequence covered rate (%)	Protein name
17	gi999937	17/31	163	4.98	35 839	63	Annexin V
10	gi515109	11/24	116	6.63	28 778	60	Carbonic anhydrase I
5	gi2781208	15/43	105	5.84	38 081	55	Chain B, crystal structure of fibrinogen fragment D
12	gi223002	12/33	92	7.95	51 358	42	Fibrin beta
19	gi4505773	11/46	75	5.57	29 843	55	Prohibitin
4	gi2781208	9/31	67	5.84	38 081	37	Chain B, crystal structure of fibrinogen fragment D
18	gi15192925	8/29	63	6.90	31 032	46	Alcohol dehydrogenase
16	gi15895617	9/31	58	9.01	42 229	34	Sugar transaminase, involved in dTDP-4, 6-dideoxyglucose biosynthesis
11	gi1586816	10/35	55	9.33	42 071	27	Jerky gene

associated with gastric cancer, which were expressed in gastric cancer tissues, but absent in normal gastric tissues. Some of them might possibly be identified and serve as diagnostic and prognostic markers in gastric cancer.

In the preparation of 2DE maps presented in this study, tissue samples from different individuals were used without pooling of samples. The total homogenate was fractionated by ultracentrifugation into soluble fraction^[12]. In order to minimize the influence of the methodology, we attempted, when possible, to make protocols for 2DE PAGE alike. Our initial analyses of six normal tissue samples indicated the overall protein pattern remained very similar across the samples.

We identified nine protein spots which were expressed in cancerous tissues but absent in normal gastric tissues. Of the 9 position identifications, spots 4, and 5 were found as multiple spots on the 2DE gels. Those included the subunits of the proteins, both of which focused in several pI positions but had the same molecular mass. It indicated that these gene products were present as isoforms with post-translation modification^[13].

Annexins are Ca²⁺ and phospholipid binding proteins forming an evolutionarily conserved multigene family. For some annexins, it appears that they participate in the regulation of membrane organization and membrane traffic and the regulation of ion (Ca²⁺) currents across membranes or Ca²⁺ concentrations within cells. Some members of the family have been identified extracellularly where they can act as receptors for serum proteases on the endothelium as well as inhibitors of neutrophil migration and blood coagulation^[14]. Annexin V is used widely as a marker for apoptotic cells, the annexin V mutants showed defective homotypic cell adhesion and resistance to Ca²⁺-dependent apoptotic agents without exhibiting any changes in the generation of cytosolic Ca²⁺ fluxes^[15]. Annexin V also known as calphobindindin I, has been shown to be an endogenous inhibitor of protein kinase C, a key enzyme in cellular signal transduction. The inhibition of protein kinase C by annexin V is presumed to be ultimately related to carcinogenesis and studies have demonstrated that a decrease in the production of annexin V may lead to the dysregulated protein kinase C^[16,17]. Annexin V has been found in other cancer tissues or cell lines^[18,19], but its presence in gastric cancer has not be documented.

Carbonic anhydrase (CA) is the zinc-containing metalloenzyme that catalyzes the reversible hydration of CO₂. The role of the enzyme has been thoroughly investigated. The main functions of the enzyme are to produce HCO₃⁻ for the intermediate metabolism and to maintain pH, water, and ion equilibrium in the body^[20]. CAs show various levels of catalytic activity and binding to inhibitors. They have considerable diversity in tissue distribution and cellular localization, and they perform a variety of biological functions. CAI protein is associated with cell growth. It is likely expressed by rapidly proliferating tumor cells or cells that are about to enter the proliferative state, because the CA domain and other elements of the molecule take part in the regulation of cell growth in certain tumor cell types^[21].

The presence of fibrin (ogen) within the tumor stroma likely affects the progression of tumor cell growth and metastasis^[22]. The deposition of fibrin (ogen), along with other adhesive glycoproteins, into the extracellular matrix serves as a scaffold to support binding of growth factors and to promote the cellular responses of adhesion, proliferation, and migration during angiogenesis and tumor cell growth. Inappropriate synthesis and deposition of extracellular matrix constituents are linked to altered regulation of cell proliferation, leading to tumor cell growth and malignant transformation^[23,24]. Fibrin deposition occurs within the stroma of a majority of tumor types. Fibrin (ogen) content was significantly higher in malignant tumor patients than that in benign disease patients, significant

reduction was observed after treatment and became elevated again when there was recurrence or metastasis^[25]. Biggerstaff *et al.*^[26] suggested that coagulation activation and the subsequent increase in circulating fibrin may enhance platelet adhesion to circulating tumor cells and thereby facilitate metastatic spread. Assessment of fibrin (ogen) not only helps to diagnose cancers but also evaluates the therapeutic effect and prognosis^[27].

Prohibitin proteins have been implicated in cell proliferation, ageing and the maintenance of mitochondria integrity^[28], prohibitins are present in the inner mitochondrial membrane and always bound to each other. They are expressed during development and their expression levels are indicative of a role in mitochondrial metabolism^[29]. High level expression of the proteins is consistently seen in primary human tumors. The prohibitin protein has been found having various functions, including cell cycle regulation, apoptosis, assembly of mitochondrial respiratory chain enzymes and ageing. We are currently trying to identify the additional proteins whose expression is significantly altered in cancerous tissue.

This study also confirms that proteomic analysis is a powerful tool for the discovery of such molecular markers. Proteomic analysis allows the characterization of picoquantities of proteins with MS and changes in the levels inherent to the pathophysiology of any cell type, tissue, or whole organism. It is hoped that the identification of protein markers by this approach could discriminate cancerous from normal cells. As demonstrated here, proteomic analysis may be efficiently used to identify new indicators for the diagnosis and prognosis of cancer progression.

In conclusion, the differences of the proteins between normal gastric epithelial cell and malignant cells are complex. Our data only show a few of the highly expressed spots. Further basic and clinical investigation will be needed to demonstrate if these proteins could be markers for GC and to evaluate other non-constant spots in relation to the clinical condition of the patient.

ACKNOWLEDGEMENTS

The authors would like to thank Dr. Bo-Qing Li and Qing-Hua Zhou at Chinese Center for Disease Control and Prevention for their assistance in the experiments.

REFERENCES

- 1 **Lawrie LC**, Fothergill JE, Murray GI. Spot the differences: proteomics in cancer research. *Lancet Oncol* 2001; **2**: 270-277
- 2 **Zhang M**, Martin KJ, Sheng SJ, Sager R. Expression genetics: a different approach to cancer diagnosis and prognosis. *Trends Biotechnol* 1998; **16**: 66-71
- 3 **Torrado J**, Plummer M, Vivas J, Garay J, Lopez G, Peraza S, Carillo E, Oliver W, Muñoz N. Lewis antigen alterations in a population at high risk of stomach cancer. *Cancer Epidemiol Biomarkers Prev* 2000; **9**: 671-674
- 4 **Xu CT**, Pan BR, Zhang LZ, Li XX, Wang J. Significance of serum tumor markers CA50 and CEA in gastric cancer. *China J New Gastroenterol* 1996; **2**: 16-19
- 5 **Macgregor PF**, Squire JA. Application of microarrays to the analysis of gene expression in cancer. *Clin Chem* 2002; **48**: 1170-1177
- 6 **Gygi SP**, Corthals GL, Zhang Y, Rochon Y, Aebersold R. Evaluation of two-dimensional gel electrophoresis-based proteome analysis technology. *Proc Natl Acad Sci* 2000; **97**: 9390-9395
- 7 **Ni XG**, Zhao P, Liu Y, Zhao XH. Application of proteomic approach for solid tumor marker discovery. *Aizheng* 2003; **22**: 664-667
- 8 **Emmert-Buck MR**, Gillespie JW, Pawletz CP, Ornstein DK, Basrur VB, Appella E, Wang QH, Huang J, Hu N, Taylor P, Petricoin III EF. An approach to proteomic analysis of human tumors. *Mol Carcinog* 2000; **27**: 158-165
- 9 **Gorg A**, Obermaier C, Boguth G, Harder A, Scheibe B,

- Wildgruber R, Weiss W. The current state of two-dimensional electrophoresis with immobilized pH gradients. *Electrophoresis* 2000; **21**: 1037-1053
- 10 **Yu YL**, Yang PY, Fan HZ, Huang ZY, Rui YC, Yang PY. Protein expressions in macrophage-derived foam cells: comparative analysis by two-dimensional gel electrophoresis. *Acta Pharmacol Sin* 2003; **24**: 873-877
- 11 **Becamel C**, Galeotti N, Poncet J, Jouin P, Dumuis A, Bockaert J, Marin P. A proteomic approach based on peptide affinity chromatography, 2-dimensional electrophoresis and mass spectrometry to identify multiprotein complexes interacting with membrane-bound receptors. *Biol Proced Online* 2002; **4**: 94-104
- 12 **Mikami S**, Kishimoto T, Hori H, Mitsui T. Technical improvement to 2D-PAGE of rice organelle membrane proteins. *Biosci Biotechnol Biochem* 2002; **66**: 1170-1173
- 13 **Steel LF**, Shumpert D, Trotter M, Seeholzer SH, Evans AA, London WT, Dwek R, Block TM. A strategy for the comparative analysis of serum proteomes for the discovery of biomarkers for hepatocellular carcinoma. *Proteomics* 2003; **3**: 601-609
- 14 **Katayanagi K**, Van de Water J, Kenny T, Nakanuma Y, Ansari AA, Coppel R, Gershwin ME. Generation of monoclonal antibodies to murine bile duct epithelial cells: identification of annexin V as a new marker of small intrahepatic bile ducts. *Hepatology* 1999; **29**: 1019-1025
- 15 **Nimmo MC**, Carter CJ. The antiphospholipid antibody syndrome: A riddle wrapped in a mystery inside an enigma. *Clinical Applied Immunol Rev* 2003; **4**: 125-140
- 16 **Karube A**, Shidara Y, Hayasaka K, Maki M, Tanaka T. Suppression of calphobindin I (CPB I) production in carcinoma of uterine cervix and endometrium. *Gynecol Oncol* 1995; **58**: 295-300
- 17 **Shibata S**, Sato H, Ota H, Karube A, Takahashi O, Tanaka T. Involvement of annexin V in antiproliferative effects of gonadotropin-releasing hormone agonists on human endometrial cancer cell line. *Gynecol Oncol* 1997; **66**: 217-221
- 18 **Seow TK**, Ong SE, Liang RC, Ren EC, Chan L, Ou K, Chung MC. Two-dimensional electrophoresis map of the human hepatocellular carcinoma cell line, HCC-M, and identification of the separated proteins by mass spectrometry. *Electrophoresis* 2000; **21**: 1787-1813
- 19 **Xin W**, Rhodes DR, Ingold C, Chinnaiyan AM, Rubin MA. Dysregulation of the annexin family protein family is associated with prostate cancer progression. *Am J Pathol* 2003; **162**: 255-261
- 20 **Ivanov S**, Liao SY, Ivanova A, Danilkovitch-Miagkova A, Tarasova N, Weirich G, Merrill MJ, Proescholdt MA, Oldfield EH, Lee J, Zavada J, Waheed A, Sly W, Lerman MI, Stanbridge EJ. Expression of hypoxia-inducible cell-surface transmembrane carbonic anhydrases in human cancer. *Am J Pathol* 2001; **158**: 905-919
- 21 **Nogradi A**. The role of carbonic anhydrases in tumors. *Am J Pathol* 1998; **153**: 1-4
- 22 **Palumbo JS**, Kombrinck KW, Drew AF, Grimes TS, Kiser JH, Degen JL, Bugge TH. Fibrinogen is an important determinant of the metastatic potential of circulating tumor cells. *Blood* 2000; **96**: 3302-3309
- 23 **Stewart DA**, Cooper CR, Sikes RA. Changes in extracellular matrix (ECM) and ECM-associated proteins in the metastatic progression of prostate cancer. *Reprod Biol Endocrinol* 2004; **2**: 2
- 24 **Sahni A**, Odrlic T, Francis CW. Binding of basic fibroblast growth factor to fibrinogen and fibrin. *J Biol Chem* 1998; **273**: 7554-7559
- 25 **Holmbeck K**, Bianco P, Birkedal-Hansen H. MT1-mmp: a collagenase essential for tumor cell invasive growth. *Cancer Cell* 2003; **4**: 83-84
- 26 **Biggerstaff JP**, Seth NB, Meyer TV, Amirkhosravi A, Francis JL. Fibrin monomer increases platelet adherence to tumor cells in a flowing system: a possible role in metastasis? *Thromb Res* 1998; **92**: S53-S58
- 27 **Kim HK**, Lee KR, Yang JH, Yoo SJ, Lee SW, Jang HJ, Park SJ, Moon YS, Park JW, Kim CM. Plasma levels of D-dimer and soluble fibrin polymer in patients with hepatocellular carcinoma: a possible predictor of tumor thrombosis. *Thromb Res* 2003; **109**: 125-129
- 28 **McClung JK**, Jupe ER, Liu XT, Dell'Orco RT. Prohibitin: potential role in senescence, development, and tumor suppression. *Exp Gerontol* 1995; **30**: 99-124
- 29 **Nijtmans LGJ**, de Jong L, Artal Sanz M, Coates PJ, Berden JA, Back JW, Muijsers AO, van der Spek H, Grivell LA. Prohibitins act as a membrane-bound chaperone for the stabilization of mitochondrial proteins. *EMBO J* 2000; **19**: 2444-2451

Edited by Zhu LH Proofread by Chen WW and Xu FM

Therapeutic effects and prognostic factors in three-dimensional conformal radiotherapy combined with transcatheter arterial chemoembolization for hepatocellular carcinoma

De-Hua Wu, Li Liu, Long-Hua Chen

De-Hua Wu, Long-Hua Chen, Department of Radiation Oncology, Nanfang Hospital, First Military Medical University, Guangzhou 510515, Guangdong Province, China

Li Liu, Department of Pathology, First Military Medical University, Guangzhou 510515, Guangdong Province, China

Supported by the Natural Science Foundation of Guangdong Province, No. 013056

Correspondence to: Dr. Long-Hua Chen, Department of Radiation Oncology, Nanfang Hospital, First Military Medical University, Guangzhou 510515, Guangdong Province, China. flch@fimmu.com

Telephone: +86-20-61642136 **Fax:** +86-20-61642131

Received: 2003-12-10 **Accepted:** 2004-02-01

Abstract

AIM: To evaluate the therapeutic efficacy of three-dimensional conformal radiotherapy (3D-CRT) combined with transcatheter arterial chemoembolization (TACE) on the patients with hepatocellular carcinoma (HCC).

METHODS: Between 1998 and 2001, 94 patients with HCC received 3D-CRT combined with TACE. A total 63 patients had a Okuda stage I lesion and 31 patients had stage II. The median tumor size was 10.7 cm (range 3.0-18 cm), and liver cirrhosis was present in all the patients. There were 43 cases of class A and 51 class B. TACE was performed using lipiodol, 5-fluorouracil, cisplatin, doxorubicin hydrochloride and mitomycin, followed by gelatin sponge cubes. Fifty-nine patients received TACE only one time, while the others 2 to 3 times. 3D-CRT was started 3-4 wk after TACE. All patients were irradiated with a stereotactic body frame and received 4-8 Gy single high-dose radiation for 8-12 times at the isocenter during a period of 17-26 d (median 22 d).

RESULTS: The median follow-up was 37 mo (range 10-48 mo) after diagnosis. The response rate was 90.5%. The overall survival rate at 1-, 2-, and 3- year was 93.6%, 53.8% and 26.0% respectively, with the median survival of 25 mo. On univariate analysis, age ($P=0.026$), Child-Pugh classification for cirrhosis of liver ($P=0.010$), Okuda stage ($P=0.026$), tumor size ($P=0.000$), tumor type ($P=0.029$), albuminemia ($P=0.035$), and radiation dose ($P=0.000$) proved to be significant factors for survival. On multivariate analysis, age ($P=0.024$), radiation dose ($P=0.001$), and tumor size ($P=0.000$) were the significant factors.

CONCLUSION: 3D-CRT combined with TACE is an effective and feasible approach for HCC. Age, radiation dose and tumor size were found to be significant prognostic factors for survival of patients with HCC treated by 3D-CRT combined with TACE. Further study for HCC is needed to improve the treatment efficacy.

Wu DH, Liu L, Chen LH. Therapeutic effects and prognostic factors in three-dimensional conformal radiotherapy combined with transcatheter arterial chemoembolization for

hepatocellular carcinoma. *World J Gastroenterol* 2004; 10 (15): 2184-2189

<http://www.wjgnet.com/1007-9327/10/2184.asp>

INTRODUCTION

Hepatocellular carcinoma (HCC) is a major health threat in Africa and China where rates of hepatitis B infection have always been high^[1]. Although early diagnosis and curative surgical resection can achieve the best prognosis, the number of patients who could undergo resection is still limited, even for those with small tumors because of the unique characteristics of this tumor, such as multifocality, early vascular invasion, and concurrent liver cirrhosis^[2]. Nonsurgical therapies, such as percutaneous ethanol injection, transcatheter arterial chemoembolization (TACE), have been tried for unresectable HCC^[3,4]. TACE has achieved improved survival; however, the antitumor effect of TACE alone has frequently been incomplete, even after repeated treatments^[5,6]. Radiotherapy used for HCC has been attempted for more than 4 decades. Early trials adopted whole liver irradiation but the radiation dose was inadequate^[7]. Because of the unsatisfactory results obtained with this low-dose whole liver irradiation, doctors have not long applied it in their treatment of HCC. The advanced technique of three-dimensional conformal radiotherapy (3D-CRT), however, has made it possible to deliver a higher dose of radiation to part of the liver accurately without a significant dose increase in the other intra-abdominal critical structures. Several studies reported that 3D-CRT could tolerate higher radiation levels with a substantial tumor response^[8-17]. Their findings indicate that 3D-CRT can be an effective component of the treatment strategy for HCC. The principle for 3D-CRT was to escalate the radiation dose in an attempt to elevate the rate of tumor response without damaging the normal liver cells. Stereotactic radiosurgery or hypofractionated radiotherapy has 80-90% local control rate, even for so-called radioresistant tumors, such as renal cell carcinoma and melanoma^[18,19]. Because of its success, small-volume radiotherapy has been applied to extracranial lesions, such as lung and liver tumors^[20,21]. Although the role of 3D-CRT in the management of HCC has been increasingly recognized, there are still several questions to be solved, one of which involves the identification of prognostic factors so as to improve the therapeutic effects of the management for HCC after 3D-CRT combined with TACE. Another is how to assess the exact effectiveness and toxicity of 3D-CRT combined with TACE. In our department, 3D-CRT combined with TACE has been actively applied for the treatment of HCC since the 1998. In this retrospective study, we aimed to analyze the effects and prognostic factors affecting survival in 94 HCC patients treated with this therapy.

MATERIALS AND METHODS

Patients

The diagnosis of HCC was based on histological features or

on radiologic findings (liver tumor CT scan, as well as hypervascular mass in hepatic angiography) and on a serum alpha-fetoprotein (AFP) level exceeding 400 ng/mL. All tumors with an AFP less than 400 ng/mL underwent a biopsy for diagnosis. The exclusion criteria included were as follows: (1) the presence of extrahepatic metastasis; (2) liver cirrhosis of Child-Pugh class C; (3) tumors occupying more than two-thirds of the liver; and (4) a score of Karnofsky performance status of less than 60.

Table 1 Patient data before initiation of radiotherapy (*n*=94)

Data	<i>n</i> (%)
Age (yr)	
<60	78(83.0)
60	16(17.0)
Gender	
Male	84(89.4)
Female	10(10.6)
Alpha-fetoprotein	
>400 ng/mL	64 (68.1)
400 ng/mL	30(31.9)
Child-Pugh classification for cirrhosis of liver	
Class A	43(45.7)
Class B	51(54.3)
Karnofsky performance score	
>70	90(95.7)
<70	4(4.3)
Okuda stage	
I	63(67.0)
II	31(33.0)
Tumor size (cm)	
<5	17(18.1)
5-10	40(42.6)
>10	37(39.3)
Tumor type	
Massive	66(70.2)
Multinodular	28(29.8)
PVT	
Yes	12(12.8)
No	82(87.2)
Albuminemia	
<3 g/dL	15(16.0)
>3 g/dL	79(84.0)
Bilirubinemia	
<3 mg/dL	29(30.9)
>3 mg/dL	65(69.1)
Chronic hepatitis in serum virology	
Type B	90(95.7)
Type C	4(4.3)
Radiation dose	
60 Gy	34(36.2)
56 Gy	34(36.2)
48 Gy	26(27.6)
TACE	
1 fraction	59(62.8)
>1 fraction	35(37.2)

Ninety-four patients (84 male and female) who received 3D-CRT combined with TACE in our department between August 1998 and August 2001 were enrolled in this study. The patient data are shown in Table 1. Their median age was 51.5 years (range 23–73 years). Sixty-four patients had an serum AFP level >400 ng/mL. Liver cirrhosis was present in all patients, with 43 patients of Child-Pugh class's A. Most patients had good

performance status, and 90 patients had a Karnofsky performance score (KPS) of more than 70. The Okuda stage I was in 66 patients and II in 28 patients. The tumor size was calculated according to the mean of three orthogonal diameters on CT. It was <5 cm in 7 patients, 5-10 cm in 30 patients, and >10 cm in 57 patients, with the median tumor size of 10.7 cm (range 3.0-18 cm). The massive tumor was the most frequent type, which was found in 82 patients (87.2%). Portal vein thrombosis (PVT) was present in 12 patients (12.8%). Chronic hepatitis in serum virology was present in 90 patients with type B (95.7%), and in 4 patients with type C (4.3%).

TACE procedures

TACE was performed with the infusion of a mixture of 5–20 mL of iodized oil contrast medium (Lipiodol, Huaihai Pharmaceutical Factory, Shanghai, China), 1.0 g of 5-fluorouracil (5-Fu, Xudong Haipu Pharmaceutical Inc., Shanghai, China) and 40-60 mg of cisplatin (CDDP, Qilu Pharmaceutical Factory, Jinan, China) or 30-50 mg of doxorubicin hydrochloride (Adriamycin, Main Luck Pharmaceutical Inc., Shenzhen, China), and 10 mg of mitomycin (Mytomycin-C C, Kyowa Hakko Kogyo, Tokyo, Japan), followed by 1 mm×1 mm×10 mm of gelatin sponge cubes (Gelfoam, the 3rd Pharmaceutical Factory of Nanjing, Nanjing, China) embolization. To preserve liver function as much as possible, we performed superselective TACE for the feeding arteries of each intrahepatic tumor. When there was an arterial portal shunt or main branch PVT, we performed TACE without lipiodol to prevent severe damage to the normal liver. TACE procedures were performed with a 4-wk interval, and the patients received 1 to 3 times.

Radiotherapy

Radiation treatment was given to patients placed in a supine position, with both arms raised above the head and the head in a natural position. The patients were immobilized in this position using a vacuum pillow (TN-1, TOPSLANE, Shanghai, China) with an oxygen mask (3 000–5 000 cc/min) for respiratory suppression for CT simulator (PQS 2000, Picker, USA). CT data were all transferred to a 3D-radiation treatment planning system (STP 3.0, Leibinger, Freiburg, Germany) by the network. The hepatic tumor, liver, kidneys, spinal cord, and gastroduodenal intestine of each patient were contoured and reconstructed to form a 3D representation. The radiation treatment volumes and treatment angles were designed according to the beam's-eye view technique to minimize critical organ injury. Each beam's shape was designed using a multileaf collimator or custom-made block. Three-dimensional CT-based computerized treatment planning was used to determine the best combination of coplanar and noncoplanar portals. A dose-volume histogram (DVH) was generated from the stereotactic treatment planning system for each patient. Gross tumor volume (GTV) was defined as the hepatic tumor volume, visualized by three-dimensional computation of contrast CT-defined contours. Clinical target volume (CTV) was defined as GTV plus a 0.5 cm margin. Planning target volume (PTV) was defined as CTV plus a 0.5 cm margin at medial/lateral/ventral/dorsal sides, but plus a 1.5-2 cm margin at cranial/caudal sides to account for daily setup error and respiratory organ motion. Dose inhomogeneity of PTV should be within ±7% of isocenter dose. Normal liver was defined as the total liver volume minus the GTV. The average volume of GTV for these 94 patients was 979±623 mL. The average volume of whole liver was 1 790±645 mL. The number of portals used for radiation treatment ranged from 2 to 6, with a median of 5. Ultimately, the radiotherapy volume involved a portion of the liver, and whole liver radiation was always avoided. 3D-CRT was started within 3-4 wk after TACE using a 6-MV linear accelerator (CLINAC 600C/D, Varian Assoc, USA).

A dose of 4-8 Gy was applied each time and 3 times a week to deliver a total dose of 48-60 Gy. The total dose was determined by the fraction of the nontumorous liver receiving >50% of the isocenter dose. The guidelines were as follows: if <25% of the nontumorous liver received >50% of the isocenter dose, the total dose was increased to 60 Gy with 7.5 Gy each time; if 25-50%, the dose was 54 Gy with 6 Gy each time; if 50-75%, the dose was 48 Gy with 4 Gy each time; and if >75%, no treatment was given. This guideline was more strictly followed after the application of three-dimensional planning. The total radiation dose ranged from 48 to 60 Gy, and the median tumor dose was 56 Gy. During treatment, patients were monitored weekly with complete blood counts and liver function tests and AFP test.

Evaluation

The evaluation of tumor response was based on the change in mean tumor size (calculated according to the mean of three orthogonal diameters) on serial CT scans which are first started 4-6 wk after treatment completion and then performed at 1-, 3-mo interval. The evaluation of the change in tumor size was done at 3 mo after the treatment. Complete disappearance of the tumor was considered a complete response (CR), a decrease of >50% in tumor size was defined as a partial response (PR), a decrease of <50% in tumor size or no change was defined as stable disease (SD), and progression was defined as progressive disease (PD). CR and PR were considered to be responsible, whereas SD or PD not to be responsible. Acute toxicity was that occurred during treatment and 1 mo after the treatment. Subacute or chronic toxicity was defined as that occurring from 1 mo after radiotherapy.

Statistics

Statistical analysis was performed using SPSS 10.0. Overall survival was estimated from the date of diagnosis according to the Kaplan-Meier method. Log-rank statistics were used to identify the prognostic factors important for survival. Cox proportional models using enter stepwise regression were applied to all potentially significant variables for the multivariate analysis. $P < 0.05$ was considered statistically significant.

RESULTS

Tumor response

As shown in Table 2, tumor response (CR+PR) was evaluated by the change in mean tumor size on CT 3 mo after treatment completion.

Table 2 CT response of HCC to 3D-CRT combined with TACE

Response	No of patients (%)
Complete	12(12.8)
Partial	73(77.7)
Stable disease	6(6.4)
Progressive disease	3(3.1)

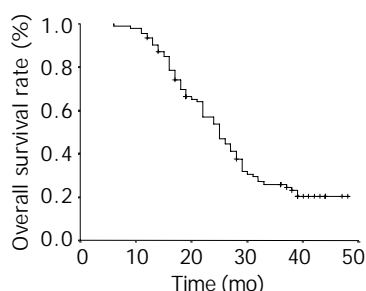


Figure 1 Actuarial survival of 94 patients treated with 3D-CRT combined with TACE.

Overall survival

The median follow-up was 37 mo (range 10-48 mo) after diagnosis. The overall survival rates of 1-, 2-, and 3-year were 93.6%, 53.8%, and 25.9%, respectively (median survival 25 mo, Figure 1).

Factors affecting overall survival

The results of univariate and multivariate analyses of prognosis factors for overall survival are shown in Table 3. On univariate analysis, age ($P=0.026$, Figure 2), Child-Pugh classification for cirrhosis of liver ($P=0.01$, Figure 3), Okuda stage ($P=0.008$, Figure 4), tumor size ($P=0.000$, Figure 5), tumor type ($P=0.029$, Figure 6), albuminemia ($P=0.035$, Figure 7), and radiation dose ($P=0.000$, Figure 8) were shown as significant factors. Multivariate regression identified the following independent favorable prognostic factors: younger age ($P=0.024$), high radiation dose ($P=0.001$), and small tumor size ($P=0.000$).

Table 3 Univariate and multivariate analyses of prognosis factors for overall survival

Univariate analysis	Multivariate analysis		
	P	R (95% CI)	P
Age (yr)	0.026	2.377	0.024
Tumor size	0.000	6.183	0.000
Radiation dose	0.000	0.491	0.001
Child-Pugh classification for cirrhosis of liver	0.010		
Karnofsky performance status	0.913		
Okuda stage	0.008		
Gender	0.202		
Tumor type	0.029		
PVT	0.235		
Albuminemia	0.035		
Bilirubinemia	0.305		
Chronic hepatitis in serum virology	0.060		
Alpha-fetoprotein	0.861		
TACE	0.892		

HR: Hazard ratio; 95% CI: Confidence interval.

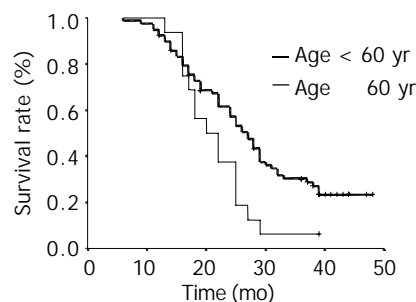


Figure 2 Univariate analysis of age on survival of patients treated with 3D-CRT combined with TACE.

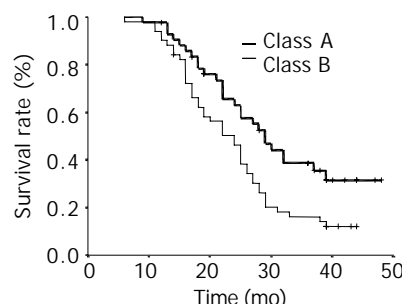


Figure 3 Univariate analysis of Child-Pugh classification on survival of patients treated with 3D-CRT combined with TACE.

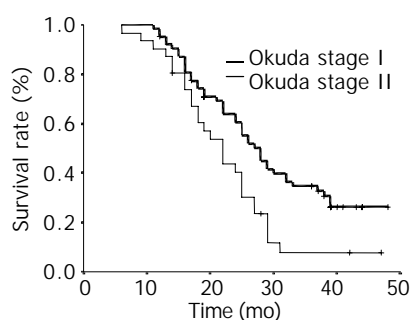


Figure 4 Univariate analysis of Okuda stage on survival of patients treated with 3D-CRT combined with TACE.

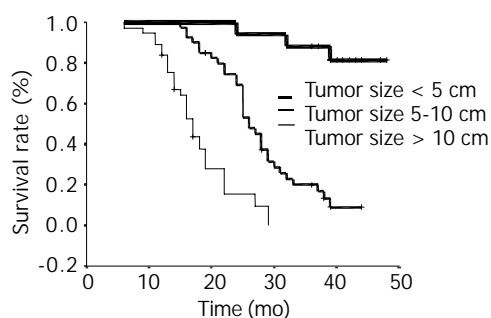


Figure 5 Univariate analysis of tumor size on survival of patients treated with 3D-CRT combined with TACE.

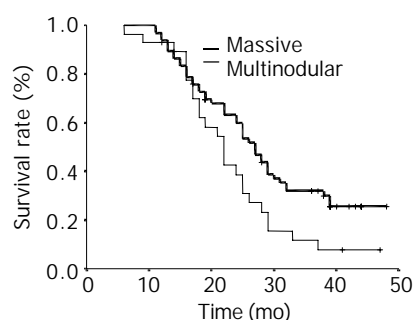


Figure 6 Univariate analysis of tumor type on survival of patients treated with 3D-CRT combined with TACE.

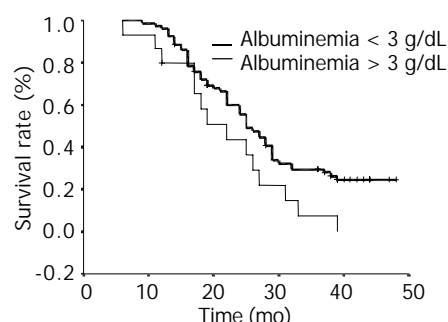


Figure 7 Univariate analysis of albuminemia on survival of patients treated with 3D-CRT combined with TACE.

Toxicity

In terms of acute toxicity, alterations in the liver function test (23 patients, 24.5%) and fever (51 patients, 54.3%) were frequently found in patients during the early time after TACE. These effects were transient and most patients recovered within 1-2 wk. Hematologic toxicity involved thrombocytopenia (platelets $<50\,000/\text{mm}^3$) in 13 patients and leucopenia (white blood cells $<2\,000/\text{mm}^3$) in 2 patients. Subacute and chronic toxicity involved radiation-induced liver disease (RILD) in

12 patients, 4 of whom died from RILD, and gastroduodenal ulcer in 5 patients. The patients other than the 4 victims of RILD were treated conservatively, and no death was found related to the treatment.

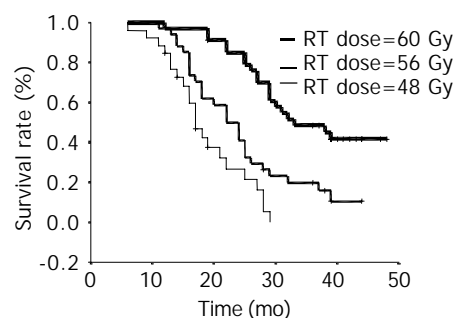


Figure 8 Univariate analysis of radiation dose on survival of patients treated with 3D-CRT combined with TACE.

DISCUSSION

Although TACE has been proved to be effective in treating HCC, and selectively and repeatedly used for patients with unresectable HCC, no survival benefits have been observed in at least two randomized trials of TACE^[22,23]. TACE is not a curative method and its limitation has also been well documented. After TACE, the tumor cells remain viable, especially in and around the capsule, and tumors may recur by the blood supply from the collateral circulation or portal vein or recanalization of the originally embolized artery^[6,24,25]. In advanced HCC, it is almost impossible to achieve a measurable response with TACE^[26].

Local radiotherapy can be an effective adjunct to the palliative treatment of HCC, even with portal vein thrombosis. Some studies of local radiotherapy, however, as either combination therapy with TACE or salvage therapy following TACE, have not shown a survival benefit, despite tumor response^[4-17]. This is because HCC eradication requires at least 50 Gy of radiation^[1,2]; but 33 Gy is a sufficient dose to induce RILD for whole liver radiation. With three-dimensional radiation planning, conformal radiotherapy can minimize scattering, limit unnecessary exposure of normal tissue, and deliver higher doses (40-80 Gy) to tumors^[27,28]. Therefore, it can be a feasible approach in the treatment of HCC with high dosage of radiation.

3D-CRT has been reported by a few studies to be effective in treatment of primary and metastatic tumors of lung and liver^[20, 21], but it has not been common to be applied in the treatment of HCC. The common therapy for HCC has been reported to be a daily dose of 1.8-2 Gy, 5 fractions per week, to a total delivered dose of 40-60 Gy^[4-17]. In our study of the 94 cases of HCC, we suggested that employing 3D-CRT could be beneficially combined with TACE with the following considerations.

Firstly, the combination of 3D-CRT with TACE may remedy the limitation of each alone and has synergistic effects. Secondly, tumor shrinkage after TACE allows the use of smaller irradiation fields, which permits higher tumor doses and improves the normal liver tolerance. Thirdly, combination therapy may also serve the purpose of eliminating residual cancer cells after TACE. Furthermore, the anticancer drug retained in the tumor may have a documented radiosensitizing effect^[6,29]. The anticancer drug, when mixed with lipiodol, has been reported to maintain relatively high concentrations in tumors as long as 27 d and decrease to a trace level after 47 d^[30]. Guo *et al.*^[6] reported that TACE followed by irradiation was a promising approach for large HCC and confirmed that TACE combined with radiotherapy was more effective than TACE alone.

In discussing the factors affecting the prognosis, we are not going to deal with the commonly known ones, which were also found in our study, such as age, Child-Pugh classification for cirrhosis of liver, Okuda stage, tumor size and type, and albuminemia. Only radiation dose is to be discussed, for it is of clinical importance in exploration of a better therapeutic method for HCC. In our present study, the radiation dose started at 60 Gy in 8 fractions within 17 d in cases with <25% of the nontumorous liver receiving >50% of the isocenter dose, at 56 Gy in 9 fractions within 19 d in cases with 25-50%, and 48 Gy in 12 fractions within 26 d in cases with 50-75%. Using the linear quadratic model, the biologic effective dose (BED) was here defined to be $nd(1+d/\alpha/\beta)$ in Gray, where n is the fractionation number, d is the daily dose, and α/β ratio is assumed to be 10 for tumors. The BEDs for our 3 different dose groups were equivalent respectively to those for 87.5 Gy total doses, 72 Gy total dose and 56 Gy total dose with a daily fraction of 2 Gy. The univariate and multivariate analyses of prognosis factors for overall survival showed that radiation dose is closely related to the prognosis. It seems clear that our virtually high total doses resulted in better response rates and overall survival. In our study, the radiologically documented response rates were 90.5%, our survival rates at 1-, 2-, and 3-year were 93.6%, 53.8%, and 25.9%, respectively, and our median survival rate was 25.0 mo. Besides better survival effect, hypofractionated 3D-CRT offers advantages of a shorter treatment course than a conventional radiotherapy and higher acceptance on the part of the patients without increasing side effects.

It has been reported that if less than 25% of the normal liver is treated with radiotherapy, then there may be no upper limit on dose associated with RILD; if 33%, 67%, or the whole liver is under uniform irradiation of 90 Gy, 47 Gy, or 31 Gy, respectively, there may be 5% risk of RILD associated with the treatment^[31]. In analyzing the correlation of RILD with patient-related and treatment-related dose-volume factors, Cheng *et al.*^[15] showed that after 3D-CRT, 12 of 68 patients developed RILD which was not found to be associated with their tumor volume. Compared with the documented ones, our results showed no increased toxicity in spite of the increased dose per fraction. This indicated that 3D-CRT played a critical role in the treatment of HCC.

In conclusion, 3D-CRT hypofractionated combined with TACE is a very safe and effective treatment method in higher tumor control and similar normal-tissue toxicity to conventional radiotherapy for HCC.

ACKNOWLEDGEMENTS

We thank Professor Liang Ping for his revision of the English version and An Sheng-li for his help in statistical analysis in the present study.

REFERENCES

- 1 **Oberfield RA**, Steele G Jr, Gollan JL, Sherman D. Liver cancer. *CA Cancer J Clin* 1989; **39**: 206-218
- 2 **Tang ZY**. Small hepatocellular carcinoma: current status and prospects. *HePatobiliary Pancreat Dis Int* 2002; **1**: 349-353
- 3 **Mok KT**, Wang BW, Lo GH, Liang HL, Liu SI, Chou NH, Tsai CC, Chen IS, Yeh MH, Chen YC. Multimodality management of hepatocellular carcinoma larger than 10 cm. *J Am Coll Surg* 2003; **197**: 730-738
- 4 **Qian J**, Feng GS, Vogl T. Combined interventional therapies of hepatocellular carcinoma. *World J Gastroenterol* 2003; **9**: 1885-1891
- 5 **Seong J**, Park HC, Han KH, Chon CY, Chu SS, Kim GE, Suh CO. Clinical results of 3-dimensional conformal radiotherapy combined with transarterial chemoembolization for hepatocellular carcinoma in the cirrhotic patients. *HePatol Res* 2003;

- 27: 30-35
- 6 **Guo WJ**, Yu EX, Liu LM, Li J, Chen Z, Lin JH, Meng ZQ, Feng Y. Comparison between chemoembolization combined with radiotherapy and chemoembolization alone for large hepatocellular carcinoma. *World J Gastroenterol* 2003; **9**: 1697-1701
- 7 **Stillwagon GB**, Order SE, Guse C, Klein JL, Lechner PK, Leibel SA, Fishman EK. 194 hepatocellular cancers treated by radiation and chemotherapy combinations: Toxicity and response: A Radiation Therapy Oncology Group Study. *Int J Radiat Oncol Biol Phys* 1989; **17**: 1223-1229
- 8 **Seong J**, Park HC, Han KH, Chon CY. Clinical results and prognostic factors in radiotherapy for unresectable hepatocellular carcinoma: a retrospective study of 158 patients. *Int J Radiat Oncol Biol Phys* 2003; **55**: 329-336
- 9 **Cheng JC**, Wu JK, Huang CM, Liu HS, Huang DY, Tsai SY, Cheng SH, Jian JJ, Huang AT. Dosimetric analysis and comparison of three-dimensional conformal radiotherapy and intensity-modulated radiation therapy for patients with hepatocellular carcinoma and radiation-induced liver disease. *Int J Radiat Oncol Biol Phys* 2003; **56**: 229-234
- 10 **Yamada K**, Izaki K, Sugimoto K, Mayahara H, Morita Y, Yoden E, Matsumoto S, Soejima T, Sugimura K. Prospective trial of combined transcatheter arterial chemoembolization and three-dimensional conformal radiotherapy for portal vein tumor thrombus in patients with unresectable hepatocellular carcinoma. *Int J Radiat Oncol Biol Phys* 2003; **57**: 113-119
- 11 **Li B**, Yu J, Wang L, Li C, Zhou T, Zhai L, Xing L. Study of local three-dimensional conformal radiotherapy combined with transcatheter arterial chemoembolization for patients with stage III hepatocellular carcinoma. *Am J Clin Oncol* 2003; **26**: E92-99
- 12 **Park HC**, Seong J, Han KH, Chon CY, Moon YM, Suh CO. Dose-response relationship in local radiotherapy for hepatocellular carcinoma. *Int J Radiat Oncol Biol Phys* 2002; **54**: 150-155
- 13 **Seong J**, Park HC, Han KH, Lee DY, Lee JT, Chon CY, Moon YM, Suh CO. Local radiotherapy for unresectable hepatocellular carcinoma patients who failed with transcatheter arterial chemoembolization. *Int J Radiat Oncol Biol Phys* 2000; **47**: 1331-1335
- 14 **Yamada K**, Soejima T, Minami T, Yoden E, Watanabe Y, Takenaka D, Imai M, Okayama T, Fujii M, Sugimura K. Three-dimensional treatment planning using electrocardiographically gated multi-detector row CT. *Int J Radiat Oncol Biol Phys* 2003; **56**: 235-239
- 15 **Cheng JC**, Wu JK, Huang CM, Liu HS, Huang DY, Cheng SH, Tsai SY, Jian JJ, Lin YM, Cheng TI, Horng CF, Huang AT. Radiation-induced liver disease after three-dimensional conformal radiotherapy for patients with hepatocellular carcinoma: dosimetric analysis and implication. *Int J Radiat Oncol Biol Phys* 2002; **54**: 156-162
- 16 **Chia-Hsien Cheng J**, Chuang VP, Cheng SH, Lin YM, Cheng TI, Yang PS, Jian JJ, You DL, Horng CF, Huang AT. Unresectable hepatocellular carcinoma treated with radiotherapy and/or chemoembolization. *Int J Cancer* 2001; **96**: 243-252
- 17 **Guo WJ**, Yu EX. Evaluation of combined therapy with chemoembolization and irradiation for large hepatocellular carcinoma. *Br J Radiol* 2000; **73**: 1091-1097
- 18 **Aoyama H**, Shirato H, Onimaru R, Kagei K, Ikeda J, Ishii N, Sawamura Y, Miyasaka K. Hypofractionated stereotactic radiotherapy alone without whole-brain irradiation for patients with solitary and oligo brain metastasis using noninvasive fixation of the skull. *Int J Radiat Oncol Biol Phys* 2003; **56**: 793-800
- 19 **Vesagas TS**, Aguilar JA, Mercado ER, Mariano MM. Gamma knife radiosurgery and brain metastases: local control, survival, and quality of life. *J Neurosurg* 2002; **97**(5 Suppl): 507-510
- 20 **Kelsey CR**, Schefter T, Nash R, Russ P, Baron AE, Zeng C, Gaspar LE. Retrospective clinicopathologic correlation of gross tumor size of hepatocellular carcinoma: implications for extracranial stereotactic radiosurgery. *Int J Radiat Oncol Biol Phys* 2003; **57**(2 Suppl): S283
- 21 **Onimaru R**, Shirato H, Shimizu S, Kitamura K, Xu B, Fukumoto S, Chang TC, Fujita K, Oita M, Miyasaka K,

- Nishimura M, Dosaka-Akita H. Tolerance of organs at risk in small-volume, hypofractionated, image-guided radiotherapy for primary and metastatic lung cancers. *Int J Radiat Oncol Biol Phys* 2003; **56**: 126-135
- 22 **Pelletier G**, Roche A, Ink O, Anciaux ML, Derhy S, Rougier P, Lenoir C, Attali P, Etienne JP. A randomized trial of hepatic arterial chemoembolization in patients with unresectable hepatocellular carcinoma. *J Hepatol* 1990; **11**: 181-184
- 23 Groupe d'Etude et de Traitement du Carcinome Hepatocellulaire. A comparison of lipiodol chemoembolization and conservative treatment for unresectable hepatocellular carcinoma. *N Engl J Med* 1995; **332**: 1256-1261
- 24 **Ernst O**, Sergent G, Mizrahi D, Delemazure O, Paris JC, L'Herminie C. Treatment of hepatocellular carcinoma by transcatheter arterial chemoembolization: comparison of planned periodic chemoembolization and chemoembolization based on tumor response. *Am J Roentgenol* 1999; **172**: 59-64
- 25 **Yu YQ**, Xu DB, Zhou XD, Lu JZ, Tang ZY, Mack P. Experience with liver resection after hepatic arterial chemoembolization for hepatocellular carcinoma. *Cancer* 1993; **71**: 62-65
- 26 **Seong J**, Keum KC, Han KH, Lee DY, Lee JT, Chon CY, Moon YM, Suh CO, Kim GE. Combined transcatheter arterial chemoembolization and local radiotherapy of unresectable hepatocellular carcinoma. *Int J Radiat Oncol Biol Phys* 1999; **43**: 393-397
- 27 **Aguayo A**, Patt YZ. Nonsurgical treatment of hepatocellular carcinoma. *Semin Oncol* 2001; **28**: 503-513
- 28 **McGinn CJ**, Ten Haken RK, Ensminger WD, Walker S, Wang S, Lawrence TS. Treatment of intrahepatic cancers with radiation doses based on a normal tissue complication probability model. *J Clin Oncol* 1998; **16**: 2246-2252
- 29 **Seong J**, Kim SH, Suh CO. Enhancement of tumor radioresponse by combined chemotherapy in murine hepatocarcinoma. *J Gastroenterol Hepatol* 2001; **16**: 883-889
- 30 **Raoul JL**, Heresbach D, Bretagne JF, Ferrer DB, Duvauferrier R, Bourguet P, Messner M, Gosselin M. Chemoembolization of hepatocellular carcinomas. A study of the biodistribution and pharmacokinetics of doxorubicin. *Cancer* 1992; **70**: 585-590
- 31 **Dawson LA**, Ten Haken RK, Lawrence TS. Partial irradiation of the liver. *Semin Radiat Oncol* 2001; **11**: 240-246

Edited by Kumar M and Chen WW **Proofread by** Xu FM

Transfection of IL-2 and/or IL-12 genes into spleen in treatment of rat liver cancer

Tian-Geng You, Hong-Shun Wang, Jia-He Yang, Qi-Jun Qian, Rui-Fang Fan, Meng-Chao Wu

Tian-Geng You, Hong-Shun Wang, Jia-He Yang, Qi-Jun Qian, Rui-Fang Fan, Meng-Chao Wu, Eastern Hepatobiliary Hospital, Second Military Medical University, 225 Changhai Road, Shanghai 200433, China

Supported by the National Natural Science Foundation of China, No. 30271476 and No. 39970838 and the Shanghai Science and technology Key Problem Foundation, No. 034119837

Correspondence to: Professor Jie-He Yang, Department of Comprehensive Treatment III, Eastern Hepatobiliary Hospital, Second Military Medical University, Changhai Road 225, Shanghai 200433, China. tgyou59@hotmail.com

Telephone: +86-21-25070769 **Fax:** +86-21-65562400

Received: 2004-02-02 **Accepted:** 2004-02-21

Abstract

AIM: To test the efficacy of gene therapy in rat liver tumor.

METHODS: A retroviral vector GCIL12EIL2PN encoding human IL-2 (hIL-2) and mouse IL-12 (mIL-12) fused gene and its packaging cell were constructed. The packaging cell lines contained of IL-2 and/or IL-12 genes were injected intrasplenically to transfect splenocyte at different time. The therapeutic effect, immune function and toxic effect were evaluated.

RESULTS: The average survival times of the 4 groups using IL genes at days 1, 3, 5 and 7 after tumor implantation were 53.3±3.7, 49.3±4.2, 31.0±2.1 and 24.3±1.4 d respectively in IL-2/IL-12 fused gene group, 25.0±2.5, 23.5±2.0, 18.3±2.4 and 12.0±1.8 d respectively in IL-2 gene treatment group, and 39.0±4.8, 32.0±3.9, 23.0±2.5 and 19.4±2.1 d respectively in IL-12 gene treatment group ($P<0.01$, $n=10$). In the IL-12/IL-2 fused gene treatment group, 30% of rats treated at days 1 and 3 survived more than 60 d and serum mIL-12 and hIL-2 levels were still high at day 3 after treatment. Compared with IL alone, NK cell activity was strongly stimulated by IL-2/IL-12 gene. Microscopy showed that livers were infiltrated by a number of lymphocytes.

CONCLUSION: IL-2 and/or IL-12 genes injected directly into spleen increase serum IL-2 and IL-12 levels and enhance the NK cell activity, which may inhibit the liver tumor growth. The therapy of fused gene IL-2/IL-12 is of low toxicity and relatively high NK cell activity. Our data suggest that IL-2/IL-12 fused gene may be a safe and efficient gene therapy for liver tumor. The gene therapy should be administrated as early as possible.

You TG, Wang HS, Yang JH, Qian QJ, Fan RF, Wu MC. Transfection of IL-2 and/or IL-12 genes into spleen in treatment of rat liver cancer. *World J Gastroenterol* 2004; 10(15): 2190-2194

<http://www.wjgnet.com/1007-9327/10/2190.asp>

INTRODUCTION

Gene therapy to liver cancer is limited by both number and

duration of died cancer cells being treated^[1,2]. Interleukin 2 (IL-2) and interleukin 12 (IL-12) were secreted mainly by mononuclear cell and B cell^[3], which play a prominent role in immune response to tumor. These cytokines are stimulated by antigens, for instance virus, bacteria and tumor cells. Others have shown that IL-2 and IL-12 were inhibited by colon cancer^[4] and both can up-regulated the T-cell and NK cell to kill tumor cell after administration of exogenous ILs.

The conditions under which the gene therapies of IL-2 and IL-12 are cytotoxic to liver tumor in an animal model have not been clear yet. Understanding the role and the mechanism of IL-2 and IL-12 in the induction of anti-tumor cytotoxic factors is relevant to both the long-term expression of IL and the safety of gene drug in liver tumor gene therapy.

IL-2, a glycoprotein consisted of 133 amino acids, through promotion of growth and proliferation of T cell, can induce either LAK cell or NK cell. IL-2 also induces immunocyte to produce interferon (INF) and tumor necrosis factor (TNF). Immunoreaction mediated by IL-2 increases therapeutic efficacy of colon cancer^[4,5]. Secretion of IL-2 and reaction to IL-2 are decreased in tumor patients by as yet unknown reasons. Previous report has demonstrated that metastases are related to the IL-2 level, and the tumor immune mediated by IL is decreased in favor of carcinogenesis, growth, diffusion and metastasis of tumor^[6-10].

IL-12 has p35 subunit and p40 subunit localized respectively on chromosome 3 and chromosome 5. The single subunit has no biological activity, and p35 gene and p40 gene are expressed simultaneously to have activity. IL-12 activates NK cell and LAK cell, promotes generation and differentiation of T cell and induces NK cell to express a small amount of TNF- β .

Primary liver cancer is common malignant tumors in China. The surgical treatment of the cancer is a main choice, but it is not ideal therapy because of high recurrence. Gene therapy is the new way for some diseases such as diabetes and tumors. Our previous work was to treat liver cancer with IL-12 gene alone, by which tumor growth was inhibited compared with control. Now we constructed the fused gene of IL-2/IL-12. However, little is known on liver cancer treatment with combination of IL-2/IL-12 gene therapy.

We hypothesized that the immunologic regulation to liver cancer following fused gene therapy of IL-2/IL-12 would be dependent upon the production and duration of the cytokines. The toxic effect of IL-2 and IL-12 would be dependent upon approach of drug delivery. In this study, using the model of implanted hepatoma of rats, we have shown that the liver tumors are reduced after IL-2 and/or IL-12 gene are injected into spleen and the cytokines are transferred into liver and blood circulation by porta vein.

MATERIALS AND METHODS

Construction of retrovirus vector of packaging mIL-12 gene and hIL-2 gene

Aprotinin, leupeptin, pepstatin, fetal calf serum and protein standard mixture were from Sigma. Plasmid pGCp35IRESp40 containing both p35 subunit and p40 subunit of mIL-12 gene was a gift from Professor Xin-Huan Liu. Plasmid pLIL2SN

containing hIL-2 gene was constructed by our laboratory. Cellular strains of hepatoma CBRH3 were provided kindly by Professor Hong Xie (Shanghai Institute of Biochemistry and Cell Biology, Chinese Academy of Sciences). Monotropic packaging cell PE501, amphiphilic packaging cell PA317 and cell NIH3T3 were provided by our laboratory. All other chemicals were of analytical grade and obtained from Merck or Sigma.

To amplify full length *p35* and *p40* genomes, PCR fragment was generated from downstream primer of mL-12 *p35* subunit and upstream primer of mL-12 *p40* subunit that templated with pGCp35IRESp-40SN. The products derived from PCR were harvested after 1% agarose gel electrophoresis. According to pLIL2PN templation, hIL-2 genome was then amplified and harvested. Fragments of mL-12 *p35* and *p40* derived from PCR were templated to amplify with downstream primer of *p35* and upstream primer of *p40* by PCR, which contain linker sequence. The mL-12 fused gene was harvested by electrophoresis^[11,12]. The mL-12 and hIL-2 gene fragments were connected respectively with pGEMTM-Teasy vector (Promega, USA) by T4 ligase (Boehringer Mannheim, Germany). The vector was transfected into *E. coli* TG1 competence cell and the positive clone was screened by PCR. Plasmid DNA was extracted from positive clone after partial exonuclease III digestion of PCR product, resulting in constructing GCILEXPn polyclonal sites after endonuclease (*Not I* and *Sal I*) (Promega, USA) that containing GCIL12EXPn of mL-12 gene, GCXEIL2PN of hIL-2 gene and GCIL12EIL2PN of mL-12 and hIL-2 fused gene.

Retrovirus packaging, identification, titer determination and expression

Reverse transcript virus was transfected into PE501 cell by electroporation. The clones were screened by G418 after 48 h. PA317 cell was infected by filtered supernatant 10-14 d late. G418 was screen after 3 d. Viral supernatants were harvested after amplifying 6 monoclonal from every groups for 2-3 wk. Stock cells were frozen at -80 °C.

Recombined reverse transcript viral vector was identified by RT-PCR. Titers of viral supernatants were determined with NIH3T3 cell. The packaging cells with highest viral titer that contain GCIL12EXPn, GCXEIL2PN and GCIL12EIL2PN were named as PA317-GCIL12EXPn, PA317-GCXEIL2PN and PA317-GCIL12EIL2PN, respectively. Protein expression of mL-12 and hIL-2 was determined by ELISA. ELISA kits (human IL-2 DuoSet and mouse IL-2 DuoSet) were from R&D Systems.

Implanted liver cancer in rats

Male Wister rats (200-250 g bm) were obtained from Animal Center of Chinese Academy of Sciences. Animals were maintained on a standard diet. Hepatoma CBRH3 cells were injected into abdominal cavity of rat. Rats were sacrificed and tumors were removed from abdominal cavity 7-9 d late. Tumors were cut into pieces of 0.05-0.75 cm and then were implanted into rat liver for one or more locations respectively. The tumors were grown up to 0.6-1 cm in diameter after 7-10 d of implantation.

Experimental procedure

Rats were anaesthetized with diethylether. The effects of IL-2 and/or IL-12 on liver cancer were studied in a total of 75 animals for 5 groups that contained 15 rats in every group: 1. Physiological saline control: 0.8 mL 9 g/L NaCl was injected into spleen following implanted liver cancer at day 1; 2. Blank vector control: 1×10^7 packaging cells of PA317-GCXEPN was injected into spleen of rat; 3. mL-12 gene group: 1×10^7 packaging cell PA317-GCIL12EXPn was injected into rat spleen after implanted rat liver cancer on days 1, 3, 5 and 7 thereafter; 4. hIL-12 gene group: 1×10^7 packing cell PA317-GCxeILPN was injected into

rat spleen after implanted rat liver cancer on days 1, 3, 5 and 7 respectively; 5. hIL-2 and mL-12 fused gene group: 1×10^7 packing cell PA317-GCIL12EIL2PN was injected into rat spleen after implanted rat liver cancer on days 1, 3, 5 and 7 thereafter. In addition, when rat survived over 2 mo, rats were named long term survivors and the liver cancer tissues were implanted into liver once more in order to observe cancer growth.

CT imaging and pathology

CT imaging was observed before and after treatment. The survival time and drug toxicity were observed. To observe the tumor cell and lymphocyte infiltration, the pathologic examination was performed following 5 and 7 d of treatment. The serum IL-2 and IL-12, according to the protocol of R&D Systems, were measured on d 1 before treatment and on d 3, 7, 30 and 60 thereafter.

Analysis of NK cytotoxic activity

NK target cell YAC-1 was obtained from the American Type Culture Collection (Bethesda, MD). The cytotoxicity of spleen NK cell was analyzed as follows^[13]. A single-cell suspension of spleen cells was centrifuged at 400 r/min for 30 min. The lymphocyte layers were harvested. For the preparation of targeted cells, YAC-1 was labeled with $^{51}\text{Cr}[\text{Na}_2\text{CrO}_4]$ and mixed with various numbers of spleen cell in a total volume of 200 μL of DMEM. The experimental radioactivity released (ER) in 100 μL samples of cell-free supernatants was determined. The amounts of radioactivity released in wells containing YAC-1 cells alone with and without 0.01% Triton X-100 were designated the total release (TR) and the spontaneous release (SR), respectively. The percentage of specific ^{51}Cr release was calculated by $[(\text{ER} - \text{SR}) / (\text{TR} - \text{SR})] \times 100$.

Statistical analysis

All results were expressed as the mean \pm SD of at least 10 individual measurements. A one-way analysis of variance (ANOVA) was first carried out to test for any differences in mean values between experimental and respective control group. If differences were established, the values were compared by two-tailed unpaired *t* test. The values were considered to significant difference if $P < 0.05$.

RESULTS

Identification of packing cell strain

The total RNA of packaging cell strains (PA317-GCIL12EXPn, PA317-GCXEIL2PN and PA317-GCIL12EIL2PN) was extracted. The RNA was amplified by RT-PCR and the product was harvested by electrophoresis. The sequence showed that PA317-GCXEIL2PN and PA317-GCIL12EIL2PN packaging cell strains contained the mL-12 sequence, and PA317-GCXEIL2PN and PA317-GCIL12EIL2PN packaging cell strains contained the hIL-2 sequence. The target genes were inserted into viral genomes and the packaging cell strains were transfected by IL gene.

Determination of titer of virus and protein expression

The highest virus titer of packaging cell was 2×10^6 CFU/mL of PA317-GCIL12EXPn, 2.4×10^6 CFU/mL of PA317-GCXEIL2PN and 1.4×10^6 CFU/mL of PA317-GCIL12EIL2PN respectively. Protein expression was measured by ELISA on these 3 packaging cell strains: 1. mL-12 fused protein: PA317-GCIL12EXPn expressed mL-12 fused protein 150 ng/ 10^6 /48 h and PA317-GCIL12EIL2PN expressed mL-2 fused protein 45.8 ng/ 10^6 /48 h; 2. hIL-2 protein: PA317-GCEXIL2PN expressed hIL-2 protein 7.5 ng/ 10^6 /48 h and PA317-GCIL12EIL2PN expressed hIL-2 protein 6.7 ng/ 10^6 /48 h.

Table 1 Average survival time (day) of rat ($n=0$, mean \pm SD)

Group	Injection on d 1	Injection on d 3	Injection on d 5	Injection on d 7
Physiologic saline control	10.7 \pm 1.5	-	-	-
Blank vector control	11.4 \pm 1.3	-	-	-
IL-2 gene therapy	25.0 \pm 2.5 ^b	23.5 \pm 2.0 ^b	18.3 \pm 2.4 ^b	12.0 \pm 1.8
IL-12 gene therapy	39.0 \pm 4.8 ^b	32.0 \pm 3.9 ^b	23.0 \pm 2.5 ^b	19.4 \pm 2.1 ^a
IL-12-IL-2 fused gene therapy	53.3 \pm 3.7 ^c	49.3 \pm 4.2 ^c	31.0 \pm 2.1 ^c	24.3 \pm 1.4 ^c

^a $P<0.05$ and ^b $P<0.01$ vs physiologic saline control and blank vector control; ^c $P<0.05$ vs IL-2 group or IL-12 group.

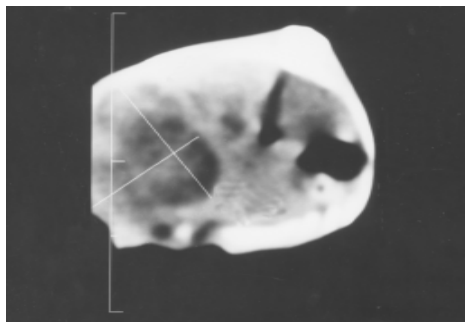
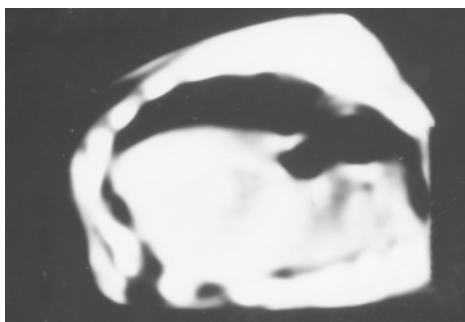
Average survival time by IL gene therapy

Table 1 shows the average survival time of rat. All rats were died within 15 d after implanting liver cancer in both physiologic saline control and blank vector control. Compared with control, the survival time of rat was prolonged significantly by treatment with IL-2 or IL-12 ($P<0.01$). The rat survival time of treatment with fused gene of IL-2/IL-12 was lengthened markedly compared with IL treatment alone ($P<0.05$). Moreover, the survival time of early treatment was much longer than that of later treatment with IL ($P<0.01$). In addition, 6 rats treated early with fused gene of IL-2/IL-12 were lived more than 60 d, but there were 3 rats treated with IL-12 that lived more than 60 d.

When the tumor was undetectable by abdominal pathologic biopsy in the rats that lived more than 60 d, the 4 rats were implanted tumor piece again. It was interested that there were no tumor growths in abdominal cavities 7 d late.

Imaging features

The liver tumor was detected by CT on day 7 after implantation in control (Figure 1). The 6 of 10 rats administrated early with IL-2/IL-12 fused gene showed that the liver tumors were reduced after 2 mo (Figure 2).

**Figure 1** CT scan of the liver cancer 7 d after implantation.**Figure 2** CT scan of the tumor treated with IL-2/IL-12 fused gene after 2 mo.

Pathologic features

A number of lymphocyte infiltrations in liver tumor were

observed significantly after 5 d of treatment with IL-2/IL-12 fused gene and 7 d of treatment with IL-2 gene or IL-12 gene (Figure 3).

**Figure 3** Pathological changes of implanted liver cancer (HE staining, original magnification: $\times 200$). There are numerous lymphocytes in tumor tissues.

Serum mIL-12 and hIL-2 levels

Compared with control, both IL-2 and IL-12 in serum were increased significantly in rats treated with IL gene on day 1 (Table 2). After the injection of IL-2/IL-12 fused gene, both IL-2 and IL-12 in serum reached the highest level on day 3, then decreased stepwise and maintained at a lower level for 2 mo (Table 3).

Table 2 Determination of serum hIL-2 or mIL-12 3 d after administration of IL gene (ng/mL)

Group	HIL-2	MIL-12
Physiologic saline control	<0.8	<0.8
Blank vector control	<0.8	<0.8
IL-2 gene therapy	19.4 \pm 1.8	<0.8
IL-12 gene therapy	<0.8	22 \pm 2.5
IL-12-IL-2fused gene therapy	18.5 \pm 2.4	20.5 \pm 2.5

Table 3 Determination of serum hIL-2 and mIL-12 on fused gene group (ng/mL)

Group	HIL-2	MIL-12
Control	<0.8	<0.8
On d 3 after therapy	18.5 \pm 2.4	20.5 \pm 2.5
On d 7 after therapy	10.2 \pm 2.5	11.5 \pm 2.5
One mo after therapy	5.3 \pm 1.2	6.2 \pm 1.4
Two mo after therapy	<0.8	<0.8

IL increases NK cell activity

IL-2 and IL-12 have been reported to increase NK cell activity. To determine if the IL-2/IL-12 fused gene could induce NK cell activation, rats were treated as described above with IL-2 and/or IL-12. The rats were sacrificed on day 7, and the spleen lymphocytes were assayed for the ability to kill ⁵¹Cr-labeled

YAC-1 target cells. There was a significant increase in NK activity after rats were injected with IL-2 or IL-12 alone ($P < 0.01$). Compared with IL alone, treatment with IL-2/IL-12 fused gene markedly enhanced NK cell activity ($P < 0.05$).

Toxicity of IL

Three rats (30%) in IL-2 group and 1 (10%) in IL-2/IL-12 group showed anorexia after administration of IL. The symptom was recovered 3-5 d late (Figure 4).

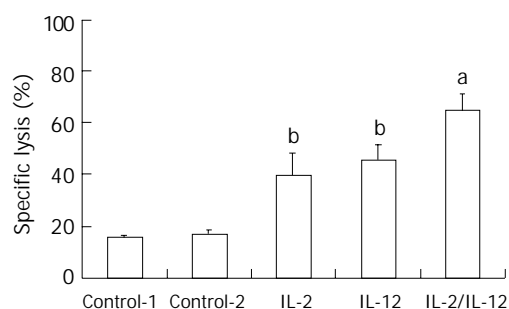


Figure 4 Activation of NK cell activity after administration of IL-2 and/or IL-12 ($n=5$). ^b $P < 0.01$ vs control; ^a $P < 0.05$ vs IL-2 group or IL-12 group.

DISCUSSION

The establishment of DNA recombination and transfection allowed us to utilize gene therapy for killing or inhibiting the tumor cells^[14]. The utility of recombinant adenoviral vectors for gene therapy is limited by the low transduction efficiency and lack of specificity for target cells^[15,16]. Spread of the virus throughout the cells maximizes the percent of cells within a cell expressing the gene of interest, and should improve the antitumor response. This may be significant for gene delivery expressing cytokines, tumor antigens or enzymes. One limitation of the transduction system is the inefficiency of the combined cytokines expression system. The initial work in this study was to construct the IL-2/IL-12 fused gene vector that was then injected into spleen, in which splenic cells, probably including liver cells, were transduced to express IL-2 and IL-12 simultaneously.

The active IL-12 is a heterogeneous dimer, which contains p35 subunit and p40 subunit, so that both subunits express simultaneously in cells if used to treat disease. Using PCR technique based on the subunit characterization of different gene sequences, we constructed the active IL-2/IL-12 fused gene and a linker sequence was incorporated into subunits of IL-12, so that the gene could correctly express protein. In present study, the IL-2 and IL-12 levels were not significantly different in serum.

The single gene therapy for the liver cancer is not ideal because it is resulted from multi-factors^[17]. Chen *et al.* suggested recently that TRAIL and chemotherapeutic agents or anticancer cytokines combination might be a novel strategy for the treatment of liver cancer. Combination of IL-2/IL-12 results in stable antitumor effect, which induces the cytotoxic T lymphocyte and NK cell^[18]. IL-2 and IL-12 have synergetic effect such as immunoregulatory^[19,20]. The antitumor immunologic effect from IL-2 and IL-12 depends on available concentration of IL-2 and IL-12. IL-2 and IL-12 also cause a long term antitumor immunologic memory^[21]. In present study, retrovirus vector containing IL-2/IL-12 genes was constructed, in which gene products of IL-2 and IL-12 were expressed simultaneously in the liver. We treated rat liver cancer with IL-2 and/or IL-12 gene. The liver cancer rats treated with IL-2 or IL-12 survived longer than those in control ($P < 0.01$). Compared with IL alone,

combination of IL-2/IL-12 gene showed a longer survival of 14-28 d in early treatment group and 5-12 d in late treatment group.

Spleen is the biggest immune organ that has a lot of immunocytes and produces antibodies and cytokines. Spleen is also the main organ of inducing immunoresponsiveness to heterologous antigen. The retrovirus packaging cell strain was injected into spleen, which expresses the high level of cytokine in order to activate immunocytes. In other hand, the retrovirus packaging cells would be transferred from spleen to liver by splenic veins and the liver cells would be infected by packaging cells resulting in enhanced anti-tumor immunity. In present study, the IL gene was injected into spleen and the blood concentration of IL was the highest on day 3. The IL concentration maintained at a level for 2 mo. Authors from Spain reported that gutless adenoviral vector encoding hIL-2 and mL-12 was injected into animals and IL was expressed by hepatocytes. The peak concentration of IL-12 was at 10 h and it completely disappeared by 72 h. If the vectors were administrated continually, the serum IL-12 would maintain at least for 48 wk^[22,23]. The rats received the splenic gene therapy survived longer than those in control. When combination of IL-2/IL-12 gene was injected into spleen, the high concentration of IL was determined from blood until day 3 and the rats survived a longer time compared with IL therapy alone.

Moreover, early gene treatment is better than late therapy. In this study, 6 rats (30%) with combined gene therapy on early stage survived a long term and the tumor nodes in liver was not detected by CT imaging and pathologic observation, in which the IL-2 and IL-12 kept a high concentration at least for 2 mo. As same as other therapy for cancer, the IL gene therapy should administrate as early as possible. In present study, the liver cancer rats treated with IL-2 or IL-12 on day 1 survived more than 8 d or 13 d respectively compared with that treated on d 7 (Table 1). The combined IL gene therapy has the similar result.

IL-2 or IL-12 produced significant toxic reaction if they were administrated enough dosage to maintain a high blood concentration. When IL-2 or IL-12 was injected into rat liver, some rats showed acute toxic reaction such as anorexia, convulsion and bleeding shock (unpublished data). In present study, when IL genes were injected into spleen, the severe acute toxic reaction was not observed in all groups.

A mechanism of IL gene treatment may be due to enhancement of NK cell activation and production of cytokines including IL^[24]. Several investigators have shown that NK cells are a relative smaller cell population in peripheral lymphoid organs but are abundant in the liver. An initial response to tumor cell may involve the innate arm of the immune response resulting in killing of mutant cell strain by NK cell^[25,26]. The findings in this study are novel since IL-2/IL-12 fused gene expresses IL-2 and IL-12 simultaneously that result in further stimulation of NK cells. We propose that liver tumor is inhibited because of IL production, such as IL-2 and IL-12, which is stimulated by IL gene therapy.

It is interesting that serum IL-2 and IL-12 levels do not change in IL-2/IL-12 gene therapy compared with IL alone, but NK cell activity is enhanced significantly compared with IL alone. We propose that the NK cell activity is strongly stimulated by both IL-2 and IL-12 at the same time, which was caused by IL-2/IL-12 fused gene expression^[27-30].

In summary, treatment with IL-2 and/or IL-12 gene increases serum IL-2 and IL-12 levels and enhances the NK cell activity, which may inhibit the liver tumor growth. The fused gene therapy of IL-2/IL-12 is of low toxicity and relatively high NK cell activity. We suggest that IL-2/IL-12 fused gene therapy may be a safe and efficient method for the treatment of liver cancer. For IL gene therapy, early intervention is better than late one.

REFERENCES

- 1 **Yang Y**, Wilson JM. Clearance of adenovirus-infected hepatocytes by MHC class I-restricted CD4⁺ CTLs *in vivo*. *J Immunol* 1995; **155**: 2564-2570
- 2 **Shi M**, Wang FS, Wu ZZ. Synergetic anticancer effect of combined quercetin and recombinant adenoviral vector expressing human wild-type p53, GM-CSF and B7-1 genes on hepatocellular carcinoma cells *in vitro*. *World J Gastroenterol* 2003; **9**: 73-78
- 3 **Rissoan MC**, Soumelis V, Kadowaki N, Grouard G, Briere F, Waal Malefyt R, Liu YJ. Reciprocal control of T helper cell and dendritic cell differentiation. *Science* 1999; **283**: 1083-1086
- 4 **Nakamori M**, Iwahashi M, Nakamura M, Ueda K, Zhang X, Yamaue H. Intensification of antitumor effect by T helper 1-dominant adoptive immunogene therapy for advanced orthotopic colon cancer. *Clin Cancer Res* 2003; **9**: 2357-2365
- 5 **Chi CH**, Wang YS, Lai YS, Chi KH. Anti-tumor effect of *in vivo* IL-2 and GM-CSF electrogene therapy in murine hepatoma model. *Anticancer Res* 2003; **23**: 315-321
- 6 **Taketo MM**. Cyclooxygenase-2 inhibitors in tumorigenesis. *J Natl Cancer Inst* 1998; **90**: 1529-1536
- 7 **Milanovich MR**, Snyderman CH, Wagner R, Johnson JT. Prognostic significance of prostaglandin E2 production by mononuclear cells and tumor cells in squamous cell carcinomas of the head and neck. *Laryngoscope* 1995; **105**: 61-65
- 8 **Arvind P**, Papavassiliou ED, Tsioulis GJ, Qiao L, Lovelace CI, Ducean B, Rigas B. Prostaglandin E2 down-regulates the expression of HLA-DA antigen in human colon adenocarcinoma cell lines. *Biochemistry* 1995; **34**: 5604-5609
- 9 **Pavlidis N**, Nicolaidis C, Bairaktari E, Kalef-Ezra J, Athanassiadis A, Seferiadis C, Fountzilias G. Soluble interleukin-2 receptors in patients with advanced colorectal carcinoma. *Int J Bio Markers* 1996; **11**: 6-11
- 10 **Satomi A**, Murakami S, Ishida K, Mastuki M, Hashimoto T, Sonoda M. Significance of increased neutrophils in patients with advanced colorectal cancer. *Acta Oncol* 1995; **34**: 69-73
- 11 **Merchinsky M**, Moss B. Resolution of vaccinia virus DNA concatemer junctions requires late-gene expression. *J Virol* 1989; **63**: 1595-1603
- 12 **Gnant MF**, Noll LA, Irvine KR, Puhlmann M, Terrill RE, Alexander HR Jr, Bartlett DL. Tumor-specific gene delivery using recombinant vaccinia virus in a rabbit model of liver metastases. *J Natl Cancer Inst* 1999; **91**: 1744-1750
- 13 **Zhang HG**, Xie J, Xu L, Yang P, Xu X, Sun S, Wang Y, Curiel DT, Hsu HC, Mountz JD. Hepatic DR5 induces apoptosis and limits adenovirus gene therapy product expression in the liver. *J Virol* 2002; **76**: 5692-5700
- 14 **Abo T**, Kawamura T, Watanabe H. Physiological responses of extrathymic T cells in the liver. *Immunol Rev* 2000; **174**: 135-149
- 15 **Khuri FR**, Nemunaitis J, Ganly I, Arseneau J, Tannock IF, Romei L, Gore M, Ironside J, MacDougall RH, Heise C, Randlev B, Gillenwater AM, Brusco P, Kaye SB, Hong WK, Kirn DH. A controlled trial of intratumoral ONYX-015, a selectively 3-replicating adenovirus, in combination with cisplatin and 5-fluorouracil in patients with recurrent head and neck cancer. *Nat Med* 2000; **6**: 879-885
- 16 **Walker JR**, McGeagh KG, Sundaresan P, Jorgensen TJ, Rabkin SD, Martuza RL. Local and systemic therapy of human prostate adenocarcinoma with the conditionally replicating herpes simplex virus vector G207. *Hum Gene Ther* 1999; **10**: 2237-2243
- 17 **Salazar-Mather TP**, Hamilton TA, Biron CA. A chemokine-to-cytokine-to-chemokine cascade critical in antiviral defense. *J Clin Invest* 2000; **105**: 985-993
- 18 **Gillies SD**, Lan Y, Brunkhorst B, Wong WK, Li Y, Lo KM. Bi-functional cytokine fusion proteins for gene therapy and antibody-targeted treatment of cancer. *Cancer Immunol Immunother* 2002; **51**: 449-460
- 19 **Dietrich A**, Kraus K, Brinckmann U, Friedrich T, Muller A, Liebert UG, Schonfelder M. Complex cancer gene therapy in mice melanoma. *Langenbecks Arch Surg* 2002; **387**: 177-182
- 20 **Li D**, Shugert E, Guo M, Bishop JS, O'Malley BW Jr. Combination nonviral interleukin 2 and interleukin 12 gene therapy for head and neck squamous cell carcinoma. *Arch Otolaryngol Head Neck Surg* 2001; **127**: 1319-1324
- 21 **Wigginton JM**, Wiltout RH. IL-12/IL-2 combination cytokine therapy for solid tumours: translation from bench to bedside. *Expert Opin Biol Ther* 2002; **2**: 513-524
- 22 **Wang L**, Hernandez-Alcoceba R, Shankar V, Zabala M, Kochanek S, Sangro B, Kramer MG, Prieto J, Qian C. Prolonged and inducible transgene expression in the liver using gutless adenovirus: a potential therapy for liver cancer. *Gastroenterology* 2004; **126**: 278-289
- 23 **Sobota V**, Bubenik J, Simova J, Jandlova T. Intratumoral IL-12 gene transfer improves the therapeutic efficacy of IL-12 but not IL-19. *Folia Biol* 2000; **46**: 191-193
- 24 **Tanaka M**, Saijo Y, Sato G, Suzuki T, Tazawa R, Satoh K, Nukiwa T. Induction of antitumor immunity by combined immunogene therapy using IL-2 and IL-12 in low antigenic Lewis lung carcinoma. *Cancer Gene Ther* 2000; **7**: 1481-1490
- 25 **Chen B**, Timiryasova TM, Haghighat P, Andres ML, Kajioka EH, Dutta-Roy R, Gridley DS, Fodor I. Low-dose vaccinia virus-mediated cytokine gene therapy of glioma. *J Immunother* 2001; **24**: 46-57
- 26 **Satoh Y**, Esche C, Gambotto A, Shurin GV, Yurkovetsky ZR, Robbins PD, Watkins SC, Todo S, Herberman RB, Lotze MT, Shurin MR. Local administration of IL-12-transfected dendritic cells induces antitumor immune responses to colon adenocarcinoma in the liver in mice. *J Exp Ther Oncol* 2002; **2**: 337-349
- 27 **Sangro B**, Qian C, Schmitz V, Prieto J. Gene therapy of hepatocellular carcinoma and gastrointestinal tumors. *Ann N Y Acad Sci* 2002; **963**: 6-12
- 28 **Sato T**. Locoregional immuno(bio)therapy for liver metastases. *Semin Oncol* 2002; **29**: 160-167
- 29 **Martinet O**, Divino CM, Zang Y, Gan Y, Mandeli J, Thung S, Pan PY, Chen SH. T cell activation with systemic agonistic antibody versus local 4-1BB ligand gene delivery combined with interleukin-12 eradicate liver metastases of breast cancer. *Gene Ther* 2002; **9**: 786-792
- 30 **Yoshida H**, Katayose Y, Unno M, Suzuki M, Kodama H, Takemura S, Asano R, Hayashi H, Yamamoto K, Matsuno S, Kudo T. A novel adenovirus expressing human 4-1BB ligand enhances antitumor immunity. *Cancer Immunol Immunother* 2003; **52**: 97-106

Edited by Zhang JZ and Chen WW Proofread by Xu FM

Combined gene therapy of endostatin and interleukin 12 with polyvinylpyrrolidone induces a potent antitumor effect on hepatoma

Pei-Yuan Li, Ju-Sheng Lin, Zuo-Hua Feng, Yu-Fei He, He-Jun Zhou, Xin Ma, Xiao-Kun Cai, De-An Tian

Pei-Yuan Li, Ju-Sheng Lin, He-Jun Zhou, Xin Ma, Xiao-Kun Cai, De-An Tian, Institute of Liver Diseases, Tongji Hospital, Tongji Medical College, Huazhong University of Science and Technology, Wuhan 430030, Hubei Province, China

Zuo-Hua Feng, Yu-Fei He, Department of Biochemistry and Molecular Biology, Tongji Medical College, Huazhong University of Science and Technology, Wuhan 430030, Hubei Province, China

Supported by the Major State Basic Research Development Program of China 973 Program, No. 2002CB513100

Correspondence to: Ju-Sheng Lin, Institute of Liver Diseases, Tongji Hospital, Tongji Medical College, Huazhong University of Science and Technology, Wuhan 430030, Hubei Province, China. linjusheng2001@163.com

Telephone: +86-27-83662578 **Fax:** +86-27-83662578

Received: 2003-10-20 **Accepted:** 2003-12-16

Abstract

AIM: To study the antitumor effect of combined gene therapy of endostatin and interleukin 12 (IL-12) with polyvinylpyrrolidone (PVP) on mouse transplanted hepatoma.

METHODS: Mouse endostatin eukaryotic plasmid (pSecES) with a mouse Igk signal sequence inside and mouse IL-12 eukaryotic plasmid (pmIL-12) were transfected into BHK-21 cells respectively. Endostatin and IL-12 were assayed by ELISA from the supernatant and used to culture endothelial cells and spleen lymphocytes individually. Proliferation of the latter was evaluated by MTT. H22 cells were inoculated into the leg muscle of mouse, which was injected intratumorally with pSecES/PVP, pmIL-12/PVP or pSecES+pmIL-12/PVP repeatedly. Tumor weight, serum endostatin and serum IL-12 were assayed. Tumor infiltrating lymphocytes, tumor microvessel density and apoptosis of tumor cells were also displayed by HE staining, CD31 staining and TUNEL.

RESULTS: Endostatin and IL-12 were secreted after transfection, which could inhibit the proliferation of endothelial cells or promote the proliferation of spleen lymphocytes. Tumor growth was highly inhibited by 91.8% after injection of pSecES+pmIL-12/PVP accompanied by higher serum endostatin and IL-12, more infiltrating lymphocytes, fewer tumor vessels and more apoptosis cells compared with injection of pSecES/PVP, pmIL-12/PVP or vector/PVP.

CONCLUSION: Mouse endostatin gene and IL-12 gene can be expressed after intratumoral injection with PVP. Angiogenesis of hepatoma can be inhibited synergistically, lymphocytes can be activated to infiltrate, and tumor cells are induced to apoptosis. Hepatoma can be highly inhibited or eradicated.

Li PY, Lin JS, Feng ZH, He YF, Zhou HJ, Ma X, Cai XK, Tian DA. Combined gene therapy of endostatin and interleukin 12 with polyvinylpyrrolidone induces a potent antitumor effect on hepatoma. *World J Gastroenterol* 2004; 10(15): 2195-2200 <http://www.wjgnet.com/1007-9327/10/2195.asp>

INTRODUCTION

Liver cancer is one of the most common neoplasms worldwide. In some parts of Asia and Africa the prevalence is more than 100/100 000 population^[1]. Treatments often come to failure because of its high resistance to chemotherapy or radiotherapy and the severe side-effects induced^[1]. At present the only curative options are partial hepatectomy or total hepatectomy with liver transplantation. But the chance for surgery is very limited. The effects of some other treatments such as intratumoral injection of ethanol or acetic acid, transarterial catheter embolization, and thermal destruction or microwave coagulation were also very poor due to the high incidence of tumor recurrence and hepatic failure^[1-3]. Now combined treatments including biotherapy have been regarded as the most promising methods to cure liver cancer^[4,5].

Among the biotherapies, antiangiogenic therapies have recently attracted an intense interest for their broad-spectrum action, low toxicity, and in direct endothelial targeting, the absence of drug resistance^[6]. Antiangiogenic therapy induced by endostatin could specifically inhibit endothelial proliferation and potently inhibit angiogenesis and tumor growth accompanied by apoptosis in tumor cells^[7-9]. Repeated cycles of antiangiogenic therapy were even followed by prolonged tumor dormancy without further therapy^[10].

More and more learners have begun to realize that the occurrence of tumors is a complex course induced by multiple genes and multiple steps. Interference of single factor on tumor often can not get satisfactory results. Although primary tumors were regressed to dormant microscopic lesions after endostatin therapy, tumor cells were not eradicated at all^[7,10]. Conventional chemotherapy or radiotherapy can do little on residual tumor cells, accurate recognition and clearance of which depends on the immune system of host^[11]. IL-12 is among the most potent cytokines in stimulating antitumor immunity^[12-14], which also showed significant inhibitory activity on angiogenesis^[15].

So antiangiogenesis therapy by endostatin in combination with antitumor immunotherapy by IL-12 has become an attractive approach. On one hand synergistically antiangiogenic effect may be achieved to induce tumor dormancy. On the other hand, residual tumor cells may be also eradicated by antitumor immunotherapy induced by IL-12. Due to the problems such as bioactive protein production in large quantities, high costs and daily administration of endostatin^[10,16], and the severe side-effects of system administration of IL-12^[17,18], local gene therapy has proved to be very effective and nontoxic at the same time^[19-24]. In this study combined intratumoral gene therapy of endostatin and IL-12 was observed in treatment of mouse hepatoma.

MATERIALS AND METHODS

Plasmid and host

Mouse endostatin eukaryote expression plasmid pSecES was constructed in our laboratory (data not shown). The expression of endostatin was under the control of *cytomegalovirus* (CMV) promoter. A mouse Igk signal peptide sequence was located upstream of endostatin sequence to lead endostatin to secrete out. Mouse IL-12 eukaryote expression plasmid (pmIL-12) was

a gift from Professor David M. Mahvi in Wisconsin University, USA. Both *M*, 35 000 light chain gene and *M*, 40 000 heavy chain gene linked by an internal ribosome entrance site were put downstream of CMV promoter^[25]. Empty plasmid pcDNA3.1, pcDNA3.1-lacZ and *E. coli* DH5 α were from the collection of our laboratory. DH5 α bacteria containing the plasmids were grown in LB medium to mid-log phase. The plasmids were then purified with Qiagen columns (Qiagen). An analytical gel of each plasmid (cut and uncut) was done to ensure that there was no contamination with other nucleic acids. The A_{260}/A_{280} ratios ranged from 1.8 to 2.0. Also each plasmid was confirmed to be free of endotoxin. For gene therapy, concentrated plasmid stock solution was made by lyophilizing and rehydrating with water. Then it was formulated into a solution containing 1 g/L plasmid, 50 g/L polyvinylpyrrolidone (PVP, K30, *M*, 40 000, from Sigma), 150 mmol/L NaCl before use.

Cell culture and animals

BHK-21, human umbilical vein endothelial cell line (HUVEC) ECV304 and mouse hepatoma cell line H22 were purchased from China Center for Type Culture Collection. All the cell lines were maintained in RPMI 1640 medium (GibcoBRL) supplemented with 100 mL/L fetal bovine serum (FBS), 10^5 U/L penicillin and 100 mg/L streptomycin. Cells were cultured at 37 with 50 mL/L CO₂. Six to 8-wk-old male BALB/c mice of specific-pathogen-free (SPF) grade (purchased from Hubei Experimental Animals Center, China) were maintained in a standard SPF animal's room. All animal studies were performed in accordance with acceptable animal use guidelines.

Secretion and activity of endostatin plasmid and IL-12 plasmid

In 6-well plate, 5×10^5 BHK-21 cells per well were transfected with 1 μ g pSecES or 1 μ g pmIL-12, 3 μ L LipoGen (InvivoGen) in accordance with directions of the manufacturer. Forty-eight hours after transfection, 0.1 mL ECV304 cells (2×10^7 /L) cultured in RPMI 1640 additionally supplemented with 2 μ g/L recombinant human basic fibro growth factor (rhbFGF) (PeproTech, UK) was inoculated to a 96-well plate. 0.1 mL supernatant of BHK-21 cells transfected with pSecES was added to ECV304 cells per well. Seventy-two hours later, 20 μ L 5 g/L MTT was added per well. After 4 h, the supernatant was discarded and 150 μ L DMSO was added. Absorbency at 570 nm was assayed. Forty-eight hours after transfection, mouse spleen cells were also produced by routine protocols and cultured in RPMI 1640 medium supplemented with 100 mL/L FBS for 2 h. Then the suspending lymphocytes were adjusted to 1×10^8 /L and seeded to a 24-well plate (0.5 mL per well). Also 0.5 mL supernatant of BHK-21 cells transfected with pmIL-12 was added per well. Forty-eight hours later, the proliferation was evaluated by MTT assay as above. The supernatant of BHK-21 transfected with pcDNA3.1-lacZ was used as control. Also transfection rate was evaluated by X-gal staining of BHK-21 transfected with pcDNA3.1-lacZ 48 h later. All the three kinds of supernatant was stored at -20°C for further assay.

Combined gene therapy of endostatin and IL-12 for H22 hepatoma in vivo

In 0.1 mL PBS, 10^5 H22 cells were inoculated i.m. into the hind limb of BALB/c mice. Then the mice were randomly divided into five groups (6 per group): PVP/NaCl (untreated), pcDNA3.1 (empty vector), pSecES, pmIL-12, pSecES+pmIL-12. Another 6 mice were not inoculated for further assay of basic serum endostatin. From the next day after inoculation, 100 μ g pSecES/PVP and/or pmIL-12/PVP, 100 μ g pcDNA3.1/PVP or 100 μ L PVP/NaCl solution was injected into the inoculation site respectively with a 26 G needle every three days. After inoculation for 21 days, tumors were removed and weighed.

Before tumor dissection, mouse blood was collected and stored at 4°C overnight. Then the serum was stored at -20°C for further assay after centrifugation. The data were analyzed statistically by SPSS 10.0 procedure.

Assay of mouse endostatin and IL-12 (p70) in supernatant or serum

The frozen supernatant of BHK-21 transfected with pSecES, pmIL-12 or pcDNA3.1-lacZ and the frozen serum were thawed to room temperature. Then mouse endostatin and IL-12 (p70) were assayed according to the directions of CytELISA mouse endostatin kit (CytImmune, USA) and mouse IL-12 (p70) ELISA kit (Shengzhen Jingmei Biotech, China).

Detection of MVD, TILs and apoptosis of H22 hepatoma

Paraffin sections (5 μ m) of tumor tissues were stained with rat anti-mouse CD31 antibody (eBioscience). Then the primary antibody was detected by biotinylated secondary rabbit anti-rat IgG and SABC immunohistochemistry kit (Wuhan Boster Biotech, China) according to directions of its manufacturer. Paraffin sections were also stained with HE to reveal tumor infiltrating lymphocytes (TILs). Apoptosis of tumors was displayed by TdT-mediated dUTP nick end labeling (TUNEL) staining with an *in situ* cell death detection kit (Boehringer Mannheim, Germany) in accordance with the guideline of its manufacturer.

Tumor microvessel density (MVD) was counted as previously described^[26,27]. The CD31 staining sections were scanned in 40 \times microscope and "hot spots" (area with greatest vasculature) were found, from which 3 random fields of 200 \times microscope were selected. The average vascular number of the three fields was looked as MVD. For HE and TUNEL staining sections, 5 random nonnecrotic tissue fields in 400 \times microscope was selected. The average number of TILs or apoptotic cells was counted. The data were analyzed statistically by SPSS 10.0 procedure.

RESULTS

Secretion and activity of endostatin plasmid and IL-12 plasmid

β -galactosidase expression was assessed by X-gal staining 48 h post-transfection. The transfection efficiency was about 30%. No endostatin or IL-12 was detected in the supernatant of BHK-21 transfected with pcDNA3.1-lacZ. Endostatin secreted by BHK-21 transfected with pSecES was 65.5 ± 10.9 ng/ 10^6 cells. When this supernatant was added to ECV304 stimulated by rhbFGF, the proliferation of the latter was inhibited by 29.2% 72 h later (inhibitory efficiency = 1 - A of endostatin group/A of control group, $P < 0.01$). Also 221.8 ± 44.4 ng/ 10^6 cells IL-12 (p70) was detected in the supernatant of BHK-21 transfected with pmIL-12. It could promote mouse spleen lymphocytes to proliferate by 15.2% (proliferation efficiency = A of IL-12 group/A of control group - 1, $P < 0.05$). The results are displayed in Figure 1.

Antitumor effect of combined gene therapy of endostatin and IL-12 for H22 hepatoma in vivo

On the next day after inoculation, the mice received gene therapy. No skin lesions were found in the injection sites. On d 21 after inoculation, tumors were dissected and weighed. Big tumors could be found in all mice of PVP/NS group and pcDNA3.1 group. In pSecES group, all mice formed tumors, some of which were much smaller. Four mice formed tumors in pmIL-12 group and only two mice formed small tumors in pSecES+pmIL-12 group. The average tumor weight of pSecES group was much lower than that of PVP/NS group or pcDNA3.1 group ($P < 0.01$) (Figure 2). The inhibitory rate was 56.4% (inhibitory efficiency = 1 - tumor weight of pSecES group/tumor

weight of pcDNA3.1 group). For pmIL-12 group, the inhibitory rate was 85.7%. When pSecES gene therapy and pmIL-12 gene therapy were used in combination, tumor growth was inhibited by 91.8% ($P<0.01$).

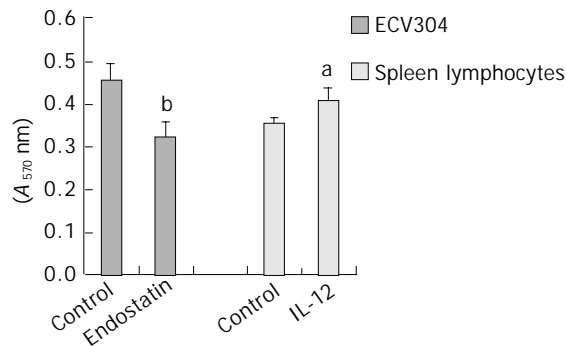


Figure 1 Proliferation of ECV304 inhibited by the supernant of BHK-21 transfected with pSecES and proliferation of spleen lymphocytes stimulated by the supernant of BHK-21 transfected with pmIL-12. Each bar represents A value of ECV304 or spleen lymphocytes, and mean \pm SD for 5 wells. ^a $P<0.05$ vs control, ^b $P<0.01$ vs control.

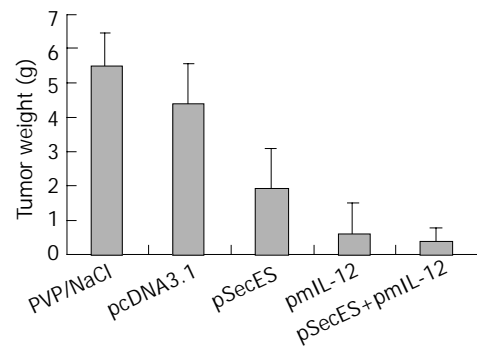


Figure 2 Hepatoma formation and growth inhibited by gene therapy of endostatin and IL-12. Each bar represents tumor weight of mice treated with PVP/NaCl, pcDNA3.1/PVP, pSecES/PVP, pmIL-12/PVP or pSecES+pmIL-12/PVP, and mean \pm SD for six mice. $P<0.01$ by ANOVA analysis.

Serum endostatin and IL-12 levels after gene therapy

When gene therapy was finished, the serum endostatin and IL-12 levels were evaluated by ELISA. The serum endostatin level in pSecES group was 117.1 ± 12.8 $\mu\text{g/L}$, which was much higher than that in pcDNA3.1 group (87.7 ± 6.1 $\mu\text{g/L}$) or the basic level

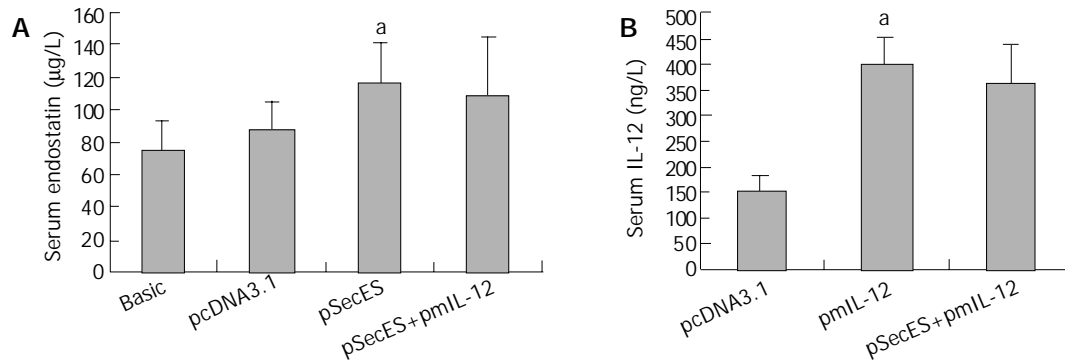


Figure 3 Increase of mice serum endostatin levels or IL-12 levels after gene therapy. A: Serum endostatin levels of mice treated with pcDNA3.1/PVP, pSecES/PVP, pSecES+pmIL-12/PVP or not inoculated with H22 cells (basic levels). Each bar represents mean \pm SD for six mice. ^a $P<0.05$ vs pcDNA3.1 group. B: Serum IL-12 levels of mice treated with pcDNA3.1/PVP, pmIL-12/PVP, pSecES+pmIL-12/PVP. Each bar represents mean \pm SD for six mice. ^a $P<0.05$ vs pcDNA3.1 group.

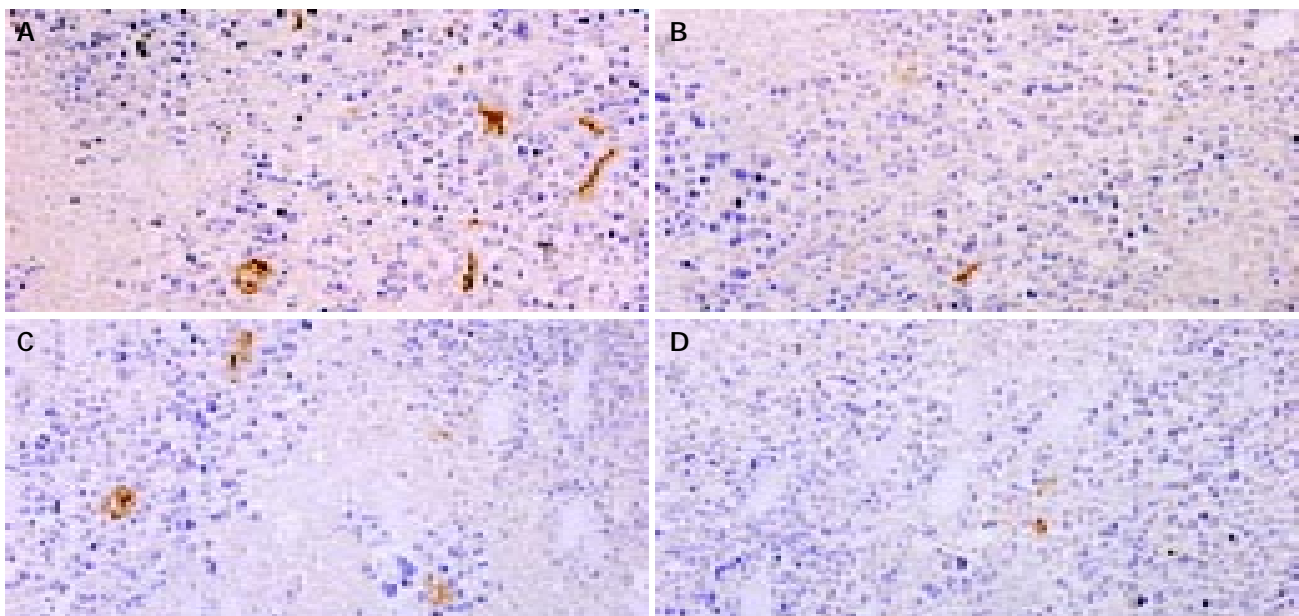


Figure 4 Hepatoma angiogenesis inhibited by gene therapy of endostatin and IL-12. MVD (CD31staining, 200 \times) of hepatoma treated with pSecES/PVP (7.3 ± 1.2) (B), pmIL-12/PVP (10.0 ± 1.7) (C) or pSecES+pmIL-12/PVP (3.7 ± 1.2) (D) was less than that treated with pcDNA3.1/PVP (22.7 ± 3.1 , $P<0.05$) (A).

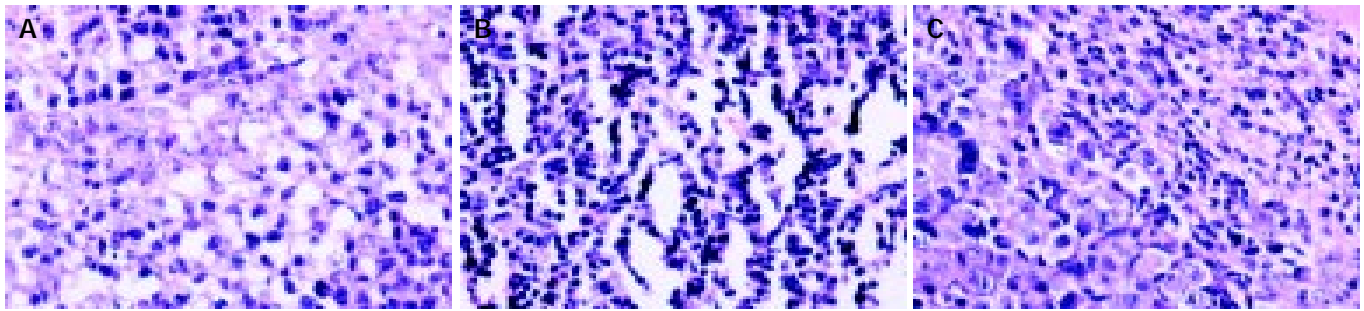


Figure 5 Lymphocytes infiltration into hepatoma promoted by gene therapy of IL-12. TILs (HE staining, 400 \times) of hepatoma treated with pmIL-12/PVP (146.2 \pm 24.6) (B) and pSecES+pmIL-12/PVP (123.2 \pm 21.4) (C) were more than that treated with pcDNA3.1/PVP (45.2 \pm 11.8, P <0.01) (A).

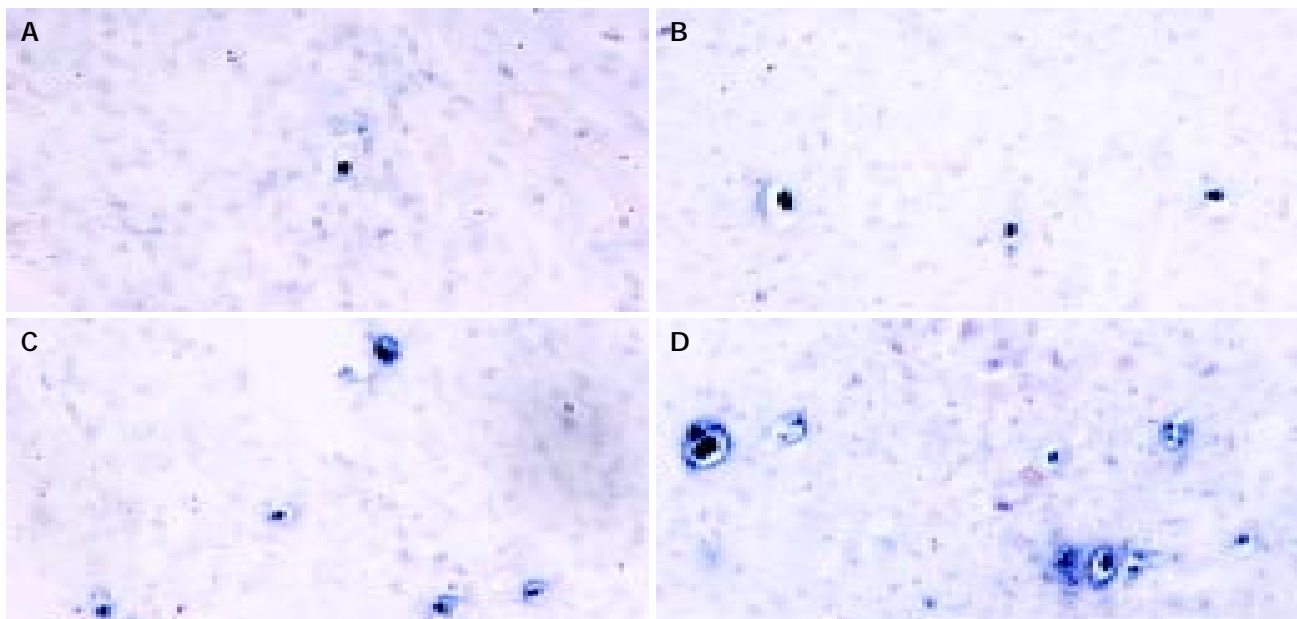


Figure 6 Apoptosis of hepatoma cells induced by gene therapy of endostatin and IL-12. Apoptotic tumor cells (TUNEL, 400 \times) treated with pSecES/PVP (11.2 \pm 2.3) (B), pmIL-12/PVP (14.4 \pm 3.5) (C) or pSecES+pmIL-12/PVP (24.8 \pm 4.8) (D) were more than those treated with pcDNA3.1/PVP (1.4 \pm 1.7, P <0.05) (A).

(75.8 \pm 6.6 μ g/L) (P <0.05). Also, after pmIL-12 gene therapy, the serum IL-12 level was higher in pmIL-12 group (401.0 \pm 51.6 ng/L) than in pcDNA3.1 group (154.8 \pm 25.8 ng/L) (P <0.05) (Figure 3).

MVD, TILs and apoptosis of H22 hepatoma after gene therapy

MVD were counted after CD31 staining in tumor sections. Compared with pcDNA3.1 group, MVD of hepatoma treated with pSecES/PVP or pmIL-12/PVP were much less. And in pSecES+pmIL-12 group, MVD were less than any single gene therapy group (P <0.05) (Figure 4).

Tumor sections were stained by HE, then TILs were evaluated. After pmIL-12/PVP or pSecES+pmIL-12/PVP gene therapy, TILs in hepatoma were more than that treated with pcDNA3.1/PVP (P <0.01). The results are displayed in Figure 5.

Also, tumor apoptosis was displayed by TUNEL staining. Figure 6 shows that there were only a few apoptotic tumor cells dispersed in 400 \times random scopes in pcDNA3.1 group. But in pSecES group or pmIL-12 group, apoptotic tumor cells increased. In pSecES+pmIL-12 group, apoptotic tumor cells were much more than any group (P <0.05).

DISCUSSION

Despite the progress in early diagnosis of liver cancer, its prognosis remains poor. In average, the mean life span was less than a year after diagnosis^[1]. How to prevent or cure the recurrence of remained tumor cells after partial hepatectomy

and how to inhibit tumor infiltrating in liver cancer patients in advanced stage are urgent challenges for liver cancer therapy. Now antiangiogenic therapy and immunotherapy have been paid more and more attention and many promising conclusions have been drawn^[28-31]. But in clinical trails, few satisfactory results were obtained by single biotherapy^[17,18,32]. Whether synergistic effects of antiangiogenesis therapy in combination with immunotherapy could be achieved is worthy to be researched.

Studies showed that angiogenesis played a very important role in the course of growth and metastasis of solid tumors including liver cancer. When the tumor size was beyond 2-3 mm³, oxygen and nutrition were not enough by simple diffusion. Then new vessels must be formed for further growth^[33]. However, angiogenesis was dependent on the cooperation of pro-angiogenesis factors and anti-angiogenesis factors^[34]. Among many inhibitors, endostatin, the C terminal of collagen X VIII, which is a *M*, 20 000 protein with 184 amino acids in primary structure, has the strongest antiangiogenesis and antitumor effect. It was identified from the medium of a murine hemangioendothelioma (EOMA) cell line in 1997^[7]. Researchers indicated that both natural and recombinant endostatin could markedly inhibit endothelial cell proliferation *in vitro* and angiogenesis in chick chorioallantoic membrane, but had no effect on non-endothelial cells. When endostatin was administrated subcutaneously, primary tumors were regressed to dormant microscopic lesions and metastasis was inhibited. Repeated cycles of endostatin therapy showed prolonged tumor dormancy without further therapy^[7,10]. In our previous study, subcutaneous

injection of 10 mg/(kg.d) endostatin produced by gene engineering showed a potent inhibitory effect on the formation and growth of mouse H22 hepatoma^[35]. Also the clinical trial of endostatin has been carried out^[32]. But to obtain both high quantity and high quality of endostatin was necessary for optimal therapeutic benefit^[36]. It was indicated that the activity of endostatin expressed in mammalian cells was 1 000 times than recombinant protein extracted from *E.coli*^[37]. So gene therapy of endostatin has become a very good solution and many studies suggested that gene therapy of endostatin showed a powerful inhibition on liver cancer^[21,22].

When H22 hepatoma cells, derived from Balb/c mouse liver cancer in 1940 s, were inoculated into the leg muscle of mice, solid tumors formed quickly, which were easy to touch and easy for injection. Compared with viral vectors, non-viral vectors bore some advantages such as easy to handle, high capacity for DNA sequences, low toxicity, and non-immunogenic thus permitting repeated vector administrations^[38]. So we constructed endostatin eukaryotic plasmid pSecES, inside which a mouse Igk signal peptide sequence was put upstream endostatin sequence to let endostatin secrete out. *In vitro* high-levels endostatin with inhibitory activity on the proliferation of endothelial cells could be detected from the supernatant after transfection. And *in vivo*, for lower degradation of input DNA by endosomes and/or lysosomes and higher transfection efficiency, non-toxic PVP was used to enhance gene expression according to previous reports^[39,40]. Plasmid/PVP was injected intratumorally and repeatedly for a higher local concentration. After endostatin gene therapy, mice serum endostatin levels were consistently 2-3-fold higher than basic levels. Compared with controls, tumors formed slowly with less MVD and more apoptosis cells. The average tumor weight inhibitory rate was 56.4%. It was indicated that pro-angiogenic factors such as VEGF were induced when tumor vessels formed gradually, and antiangiogenic factors such as endostatin increased for a negative regulation^[41,42]. This opinion was also confirmed by our study that serum endostatin levels in mice burdened with big tumors after vector injection were increased compared with basic levels. When more endostatin were added by gene therapy, the balance would be broken and angiogenesis was inhibited.

Immunocytokines which were important in the regulation of the immune system could overcome immune tolerance against tumor antigens, thus tumor rejection was facilitated. It was benefic for prevention of recurrence of micro tumor cells and advanced tumors which could not accept operation or chemotherapy^[11,13]. Different cytokines (IL-2, IL-4, IL-12, INF- γ , TNF- α , GM-CSF) have been used to modulate the host's immune response either *in vitro* or *in vivo*. The activation and proliferation of immunocytes and antitumor immunity were induced more or less^[13]. IL-12 is among the most potent cytokines in stimulating antitumor immunity. It is a disulfide-linked heterodimeric cytokine. IL-12 acts by inducing a TH1 type of response, activating natural killer cells and cytotoxic T lymphocytes, enhancing expression of adhesion molecules on endothelial cells, thus facilitating the traffic of lymphocytes to the tumor, and inducing a potent antiangiogenic effect. In previous researches, the antitumor effect of IL-12 was established in various *in vivo* systems^[12-14]. However, the latter was reported to cause fatal toxicity in a clinical trial^[17], which led investigators to local administration of this cytokine by gene therapy or gene gun, that proved to be very effective and nontoxic at the same time^[23,24]. In our study, active IL-12 (p70) was expressed *in vitro* and *in vivo*. Tumors did not formed in 30% mice that received IL-12 gene therapy. The formed tumors were also highly inhibited with more TILs, less MVD and more apoptotic tumor cells. Moreover, the inhibitory effect of IL-12 gene therapy on H22 hepatoma was much better than that of endostatin plasmid ($P < 0.05$).

When combined gene therapy of endostatin and IL-12 was used, its antitumor effect was much better than others. Tumor formation was not observed in 66.7% mice. The average tumor weight inhibitory rate was 91.8%. But in mice that received endostatin gene therapy, no tumor regressed. The average tumor weight inhibitory rate was 56.4%. No tumor was formed in 33.3% mice after they received IL-12 gene therapy. The average tumor weight inhibitory rate was 85.7%. It was suggested that synergistic antitumor effect was achieved after combined gene therapy of endostatin and IL-12. The proposed mechanism of the combined gene therapy maybe a synergistic cooperation of an antiangiogenesis effect induced by endostatin and IL-12 in combination with an immune rejection induced by IL-12. On one hand, endostatin and IL-12, which were expressed locally in combination with increased serum levels after gene delivery mediated by plasmid with PVP, could inhibit angiogenesis of hepatoma synergistically. This was convinced by that MVD in pSecES+pmIL-12 group was much less than any single gene therapy group. But now the antiangiogenesis mechanism of endostatin and IL-12 was still not very clear. Through this way, H22 hepatoma cells came to apoptosis or necrosis due to lack of blood supply. On the other hand, more TILs (including activated CTL, NK, TH1 etc.) were observed in tumors that received IL-12 gene therapy or combined gene therapy, which maybe an indication of activated immune response on H22 hepatoma cells. Antitumor immune rejection induced by IL-12 through immunocytes or cytokines also promoted apoptosis of tumor cells. So there were much more apoptotic tumor cells in combined gene therapy group than any single one. Due to these factors, formation and growth of transplanted H22 hepatoma was prevented synergistically.

Combined gene therapies for liver cancer were also reported previously. Learners have focused on combined genes of two or three immunocytokines, or on suicide gene therapy in combination with genetic immunotherapy^[25,30,31,43]. Biotherapy in combination with chemotherapy for lymphoma was also studied^[44]. Before our reports, combined treatment with type 5 adenovirus vectors expressing murine angiostatin and IL-12 showed an antitumor effect on a murine breast cancer^[45]. Our report is the first to demonstrate the potent antitumor effect of combined gene therapy of endostatin and interleukin 12 with polyvinylpyrrolidone on hepatoma.

In conclusion, active target protein can be expressed by repeated local injections of plasmid with PVP. Through this way, a short-term course of combined gene therapy of endostatin and IL-12 can effectively prevent the formation and development of transplanted H22 hepatoma in mice. Antiangiogenic therapy in combination with immunotherapy may be used to regress or to eradicate other solid tumors.

ACKNOWLEDGEMENT

We thank Xiao-Yan Yang and Dong-Po Song for their expert technical assistance in animal experiments and Peng-Cheng Zhu for his help in histopathological analysis in this study.

REFERENCES

- 1 **Badvie S.** Hepatocellular carcinoma. *Postgrad Med J* 2000; **76**: 4-11
- 2 **Zibari GB,** Riche A, Zizzi HC, McMillan RW, Aultman DF, Boykin KN, Gonzalez E, Nandy I, Dies DF, Gholson CF, Holcombe RF, McDonald JC. Surgical and nonsurgical management of primary and metastatic liver tumors. *Am Surg* 1998; **64**: 211-220
- 3 **Okuda K.** Hepatocellular carcinoma. *J Hepatol* 2000; **32**(1 Suppl): 225-237
- 4 **Kamohara Y,** Kanematsu T. Treatment of liver cancer: current status and future prospectives. *Ganto Kagaku Ryoho* 2000; **27**: 987-992
- 5 **Sorokin P.** New agents and future directions in biotherapy. *Clin J Oncol Nurs* 2002; **6**: 19-24

- 6 **Zogakis TG**, Libutti SK. General aspects of anti-angiogenesis and cancer therapy. *Expert Opin Biol Ther* 2001; **1**: 253-275
- 7 **O'Reilly MS**, Boehm T, Shing Y, Fukai N, Vasios G, Lane WS, Flynn E, Birkhead JR, Olsen BR, Folkman J. Endostatin: an endogenous inhibitor of angiogenesis and tumor growth. *Cell* 1997; **88**: 277-285
- 8 **Huang X**, Wong MKK, Zhao Q, Zhu Z, Wang KZQ, Huang N, Ye C, Gorelik E, Li M. Soluble recombinant endostatin purified from *Escherichia coli*: antiangiogenic activity and antitumor effect. *Cancer Res* 2001; **61**: 478-481
- 9 **Sorensen DR**, Read TA, Porwol T, Olsen BR, Timpl R, Sasaki T, Iversen PO, Benestad HB, Sim BK, Bjerkvig R. Endostatin reduces vascularization, blood flow, and growth in a rat gliosarcoma. *Neuro Oncol* 2002; **4**: 1-8
- 10 **Boehm T**, Folkman J, Browder T, O'Reilly MS. Antiangiogenic therapy of experimental cancer does not induce acquired drug resistance. *Nature* 1997; **390**: 404-407
- 11 **Musiani P**, Modesti A, Giovarelli M, Cavallo F, Colombo MP, Lollini PL, Forni G. Cytokine, tumor-cell death and immunogenicity: a question of choice. *Immunol Today* 1997; **18**: 32-36
- 12 **Pham-Nguyen KB**, Yang W, Saxena R, Thung SN, Woo SL, Chen SH. Role of NK and T cells in IL-12-induced anti-tumor response against hepatic colon carcinoma. *Int J Cancer* 1999; **81**: 813-819
- 13 **Ruiz J**, Qian C, Drozdzik M, Prieto J. Gene therapy of viral hepatitis and hepatocellular carcinoma. *J Viral Hepat* 1999; **6**: 17-34
- 14 **Schmitz V**, Qian C, Ruiz J, Sangro B, Melero I, Mazzolini G, Narvaiza I, Prieto J. Gene therapy for liver diseases: recent strategies for treatment of viral hepatitis and liver malignancies. *Gut* 2002; **50**: 130-135
- 15 **Yao L**, Sgadari C, Furuke K, Bloom ET, Teruya-Feldstein J, Tosato G. Contribution of natural killer cells to inhibition of angiogenesis by interleukin-12. *Blood* 1999; **93**: 1612-1621
- 16 **Dhanabal M**, Ramchandran R, Volk R, Stillman IE, Lombardo M, Iruela-Arispe ML, Simons M, Sukhatme VP. Endostatin: yeast production, mutants, and antitumor effect in renal cell carcinoma. *Cancer Res* 1999; **59**: 189-197
- 17 **Leonard JP**, Sherman ML, Fisger GL, Buchanan LJ, Larsen G, Atkins MB, Sosman JA, Dutcher JP, Vogelzang NJ, Ryan JL. Effects of single-dose interleukin-12 exposure on interleukin-12-associated toxicity and interferon- γ production. *Blood* 1997; **90**: 2541-2548
- 18 **Lotze MT**, Zitvogel L, Campbell R, Robbins PD, Elder E, Haluszczak C, Martin D, Whiteside TL, Storkus WJ, Tahara H. Cytokine gene therapy of cancer using interleukin-12: murine and clinical trials. *Ann N Y Acad Sci* 1996; **795**: 440-454
- 19 **Peroulis I**, Jonas N, Saleh M. Antiangiogenic activity of endostatin inhibits c6 glioma growth. *Int J Cancer* 2002; **97**: 839-845
- 20 **Jin X**, Bookstein R, Wills K, Avanzini J, Tsai V, LaFace D, Terracina G, Shi B, Nielsen LL. Evaluation of endostatin antiangiogenesis gene therapy *in vitro* and *in vivo*. *Cancer Gene Ther* 2001; **8**: 982-989
- 21 **Li X**, Fu GF, Fan YR, Shi CF, Liu XJ, Xu GX, Wang JJ. Potent inhibition of angiogenesis and liver tumor growth by administration of an aerosol containing a transferrin-liposome-endostatin complex. *World J Gastroenterol* 2003; **9**: 262-266
- 22 **Wang X**, Liu FK, Li X, Li JS, Xu GX. Retrovirus-mediated gene transfer of human endostatin inhibits growth of human liver carcinoma cells SMMC7721 in nude mice. *World J Gastroenterol* 2002; **8**: 1045-1049
- 23 **Barajas M**, Mazzolini G, Genove G, Bilbao R, Narvaiza I, Schmitz V, Sangro B, Melero I, Qian C, Prieto J. Gene therapy of orthotopic hepatocellular carcinoma in rats using adenovirus coding for interleukin-12 (IL-12). *Hepatology* 2001; **33**: 52-61
- 24 **Zheng S**, Xiao ZX, Pan YL, Han MY, Dong Q. Continuous release of interleukin 12 from microencapsulated engineered cells for colon cancer therapy. *World J Gastroenterol* 2003; **9**: 951-955
- 25 **Oshikawa K**, Shi F, Rakhmievich AL, Sondel PM, Mahvi DM, Yang NS. Synergistic inhibition of tumor growth in a murine mammary adenocarcinoma model by combinational gene therapy using IL-12, pro-IL-18, and IL-1 β converting enzyme cDNA. *Proc Natl Acad Sci U S A* 1999; **96**: 13351-13356
- 26 **Weidner N**. Current pathologic methods for measuring intratumoral microvessel density within breast carcinoma and other solid tumors. *Breast Cancer Res Treat* 1995; **16**: 169-180
- 27 **Yamashita YI**, Shimada M, Hasegawa H, Minagawa R, Rikimaru T, Hamatsu T, Tanaka S, Shirabe K, Miyazaki JJ, Sugimachi K. Electroporation-mediated interleukin-12 gene therapy for hepatocellular carcinoma in the mice model. *Cancer Res* 2001; **61**: 1005-1012
- 28 **Cao Y**. Endogenous angiogenesis inhibitors and their therapeutic implications. *Int J Biochem Cell Biol* 2001; **33**: 357-369
- 29 **Ryan CJ**, Wilding G. Angiogenesis inhibitors. New agents in cancer therapy. *Drugs Aging* 2000; **17**: 249-255
- 30 **Wang Z**, Qiu SJ, Ye SL, Tang ZY, Xiao X. Combined IL-12 and GM-CSF gene therapy for murine hepatocellular carcinoma. *Cancer Gene Ther* 2001; **8**: 751-758
- 31 **Putzer BM**, Stiewe T, Rodicker F, Schildgen O, Ruhm S, Dirsch O, Fiedler M, Damen U, Tennant B, Scherer C, Graham FL, Roggendorf M. Large nontransplanted hepatocellular carcinoma in woodchucks: treatment with adenovirus-mediated delivery of interleukin 12/B7.1 genes. *J Natl Cancer Inst* 2001; **93**: 472-479
- 32 **Mundhenke C**, Thomas JP, Wilding G, Lee FT, Kelzc F, Chappell R, Neider R, Sebree LA, Friedl A. Tissue examination to monitor antiangiogenic therapy: a phase I clinical trial with endostatin. *Clin Cancer Res* 2001; **7**: 3366-3374
- 33 **Folkman J**, Watson K, Ingber D, Hanahan D. Induction of angiogenesis during the transition from hyperplasia to neoplasia. *Nature* 1989; **339**: 58-62
- 34 **Cavallaro U**, Christofori G. Molecular mechanisms of tumor angiogenesis and tumor progression. *J Neurooncol* 2000; **50**: 63-70
- 35 **Li PY**, Feng ZH, Zhang GM, Zhang H, Xue SL, Huang B, Lin JS. Inhibitory effect of recombinant endostatin on angiogenesis and tumor growth of hepatoma. *J Huazhong Univ Sci Tech [Med Sci]* 2003; **23**: 223-226
- 36 **Chen CT**, Lin J, Li Q, Phipps SS, Jakubczak JL, Stewart DA, Skripchenko Y, Forry-Schaudies S, Wood J, Schnell C, Hallenbeck PL. Antiangiogenic gene therapy for cancer via systemic administration of adenoviral vectors expressing secreted endostatin. *Hum Gene Ther* 2000; **11**: 1983-1996
- 37 **Yamaguchi N**, Anand-Apte B, Lee M, Sasaki T, Fukai N, Shapiro R, Que I, Lowik C, Timpl R, Olsen BR. Endostatin inhibits VEGF-induced endothelial cell migration and tumor growth independently of zinc binding. *EMBO J* 1999; **18**: 4414-4423
- 38 **Prince HM**. Gene transfer: A review of methods and applications. *Pathology* 1998; **30**: 335-347
- 39 **Mumper RJ**, Duguid JG, Anwer K, Barron MK, Nitta H, Rolland AP. Polyvinyl derivatives as novel interactive polymers for controlled gene delivery to muscle. *Pharm Res* 1996; **13**: 701-709
- 40 **Quezada A**, Horner MJ, Loera D, French M, Pericle F, Johnson R, Perrard J, Jenkins M, Coleman M. Safety toxicity study of plasmid-based IL-12 therapy in Cynomolgus monkeys. *J Pharm Pharmacol* 2002; **54**: 241-248
- 41 **Lai R**, Estey E, Shen Y, Despa S, Kantarjian H, Beran M, Maushouri T, Quackenbush RC, Keating M, Albitar M. Clinical significance of plasma endostatin in acute myeloid leukemia/myelodysplastic syndrome. *Cancer* 2002; **94**: 14-17
- 42 **Suzuki M**, Iizasa T, Ko E, Baba M, Saitoh Y, Shibuya K, Sekine Y, Yoshida S, Hiroshima K, Fujisawa T. Serum endostatin correlates with progression and prognosis of non-small cell lung cancer. *Lung Cancer* 2002; **35**: 29-34
- 43 **Sakai Y**, Kaneko S, Nakamoto Y, Kagaya T, Mukaida N, Kobayashi K. Enhanced anti-tumor effects of herpes simplex virus thymidine kinase/ganciclovir system by codelivering monocyte chemoattractant protein-1 in hepatocellular carcinoma. *Cancer Gene Ther* 2001; **8**: 695-704
- 44 **Bertolini F**, Fusetti L, Mancuso P, Gobbi A, Corsini C, Ferrucci PF, Martinelli G, Pruneri G. Endostatin, an antiangiogenic drug, induces tumor stabilization after chemotherapy or anti-CD20 therapy in a NOD/SCID mouse model of human high-grade non-Hodgkin lymphoma. *Blood* 2000; **96**: 282-287
- 45 **Gyorffy S**, Palmer K, Podor TJ, Hitt M, Gaudie J. Combined treatment of a murine breast cancer model with type 5 adenovirus vectors expressing murine angiostatin and IL-12: a role for combined anti-angiogenesis and immunotherapy. *J Immunol* 2001; **166**: 6212-6217

Analysis of clinical effect of high-intensity focused ultrasound on liver cancer

Chuan-Xing Li, Guo-Liang Xu, Zhen-You Jiang, Jian-Jun Li, Guang-Yu Luo, Hong-Bo Shan, Rong Zhang, Yin Li

Chuan-Xing Li, Guo-Liang Xu, Jian-Jun Li, Guang-Yu Luo, Hong-Bo Shan, Rong Zhang, Yin Li, Department of HIFU, Cancer Center, Sun Yat-sen University, Guangzhou 510060, Guangdong Province, China

Zhen-You Jiang, Medical College, Jinan University, Guangzhou 510632, Guangdong Province, China

Correspondence to: Chuan-Xing Li, Department of HIFU, Cancer Center, Sun Yat-sen University, Guangzhou 510060, Guangdong Province, China. lichx@163.net

Telephone: +86-20-87343381 **Fax:** +86-20-87342737

Received: 2003-12-10 **Accepted:** 2004-01-15

Abstract

AIM: To evaluate the clinical effect of high-intensity focused ultrasound (HIFU) in the treatment of patients with liver cancer.

METHODS: HIFU treatment was performed in 100 patients with liver cancer under general anesthesia and by a targeted ultrasound. Evaluation of efficacy was made on the basis of clinical symptoms, liver function tests, AFP, MRI or CT before and after the treatment.

RESULTS: After HIFU treatment, clinical symptoms were relieved in 86.6%(71/82) of patients. The ascites disappeared in 6 patients. ALT (95±44) U/L and AST (114±58) U/L before HIFU treatment were reduced to normal in 83.3%(30/36) and 72.9%(35/48) patients, respectively, after the treatment. AFP was lowered by more than 50% in 65.3%(32/49) patients. After HIFU treatment, MRI or CT findings indicated coagulation necrosis and blood supply reduction or disappearance of tumor in the target region.

CONCLUSION: HIFU can efficiently treat the patients with liver cancer. It will offer a significant noninvasive therapy for local treatment of liver tumor.

Li CX, Xu GL, Jiang ZY, Li JJ, Luo GY, Shan HB, Zhang R, Li Y. Analysis of clinical effect of high-intensity focused ultrasound on liver cancer. *World J Gastroenterol* 2004; 10(15): 2201-2204

<http://www.wjgnet.com/1007-9327/10/2201.asp>

INTRODUCTION

Since 1942, Lynn *et al.*^[1] firstly brought forward the conception of HIFU, i.e. high intensity focused ultrasound. Fry^[2] applied HIFU technology to experimentally treat nervous system diseases, and suggested the potential of HIFU in surgical operations. As a result, he found that ultrasound beam could form a preferable focal field at a special depth inside body, and destroy target tissue through focus pointing without damaging neighboring tissues. In 1956, Burov proposed that effect of short-time high-intensity ultrasound irradiation was better than low-intensity ultrasound. With research progress on HIFU technology, this technology has been used in clinic over the

years^[3-6]. The present study makes an assessment on clinic effect of HIFU in treating liver cancer.

MATERIALS AND METHODS

Materials

We performed HIFU treatments in 100 patients (80 male, 20 female, ranging 30-74 years with mean age of 56 years) with liver cancer from July 2001 to July 2003, totally 130 HIFU treatments, 1.30 times per patient. Patients included 62 primary liver cancers and 38 metastatic liver cancers. Sixty-eight patients were with single nodule, 22 with two nodules, 10 with three nodules. Totally 36 tumor nodules with a diameter less than 5 cm, 76 with a diameter between 5-10 cm, 30 with a diameter more than 10 cm were involved. All cases were investigated and verified by pathohistology or an obvious increase of serum AFP and positive imaging, and conformed to diagnostic standard of National Cooperation Conference and Hepatic Carcinoma Prevention and Treatment in 1997. Eighteen patients were in stage I, 48 patients in stage II, and 34 patients in stage III.

Instrument

JC type focused ultrasound tumor therapeutic system was designed by Chongqing HIFU Technology Co, Ltd. Chongqing, China. It includes two main parts, i.e. ultrasound real-time orientation monitor device and HIFU three-dimensional combination scanning therapeutic device. Under the control of a computer, it can orient to preassigned tumor target zone automatically, determine range of therapy.

The main parameters included therapy frequency 0.8 MHz, mean diameter of focal field 1.1 mm, length of focal field 9.8 mm, focus distance 135 mm, therapy power 140-240 W.

Methods

Routine examinations and preoperative preparation were conducted according to the principle of surgery. Based on the result of image and ultrasound examination, the therapeutic scheme of HIFU was constituted. HIFU treatment was performed with patient fixed properly. The tumor position and size, therapeutic layers and therapeutic range of every layer were determined by ultrasound diagnostic probe. Then the therapeutic probe treated tumor tissue of every layer from outside body, and in terms of order of layer, from spot to line, and from line to area, leading whole tumor to coagulation necrosis. During the therapeutic process, through changes of graphics of target field and echo of tissue between before and after therapy at every layer, real-time estimate of HIFU therapeutic effect by computer processing image system was carried out, and with feedback, ultrasound therapeutic dosage estimated in the therapy scheme was controlled according to changes of ultrasound photograph. The therapeutic method was divided into complete coverage and local coverage. Twenty-eight cases used complete coverage, including whole tumor focus and normal liver tissue within 2 cm away from edge of tumor, the other cases used local coverage due to reasons, such as large tumor volume, rib overlap or close-by, or involvement of liver tube or cholecyst, *etc.*

Observatory parameters

The following aspects were observed: Improvement of clinic symptoms; changes of liver function 2 d and 2 wk before and after therapy; changes of AFP 2 wk before and after therapy; changes in range and blood supply of coagulation necrosis of tumor focus, also shrink of tumor through re-examination of MRI or CT before and after therapy.

RESULTS

One hundred liver cancer patients were treated by using HIFU in this group, of which 82 exhibited clinic symptoms. Seventy-one patients were improved obviously after HIFU treatment: appetite increased, weight gained, discomfort or pain on liver region relieved. Remission rate for symptoms was 86.6% (71/82). For 6 patients who had had mild ascites, ascites disappeared after HIFU treatment. For patients with abnormal liver function

(ALT 95 ± 44 U/L, AST 114 ± 58 U/L), 2 d after HIFU treatment, liver enzymes rose slightly, but no obvious statistic difference was found compared with pre-treatment. The patients' liver enzymes fell to normal level after 2 wk, respectively, ALT 83.3% (30/36), AST 72.9% (35/48). For the patients whose AFP was increased, AFP was 50% less than original level 2 wk after HIFU treatment, in 65.3% (32/49), only one patient's AFP rose continuously after HIFU treatment, and multi-bone metastases were found by ECT examination. Self-comparison of MRI showed that T₁-weighted images and T₂-weighted images of tumor therapeutic region were high signal and low signal respectively after HIFU treatment. Enhanced MRI did not show enhanced signal, indicating that coagulation necrosis had occurred in the tumor therapeutic region, blood supply of tumor was diminished or eliminated, tumor of some patients had shrunk obviously after countercheck MRI (Figures 1-3).

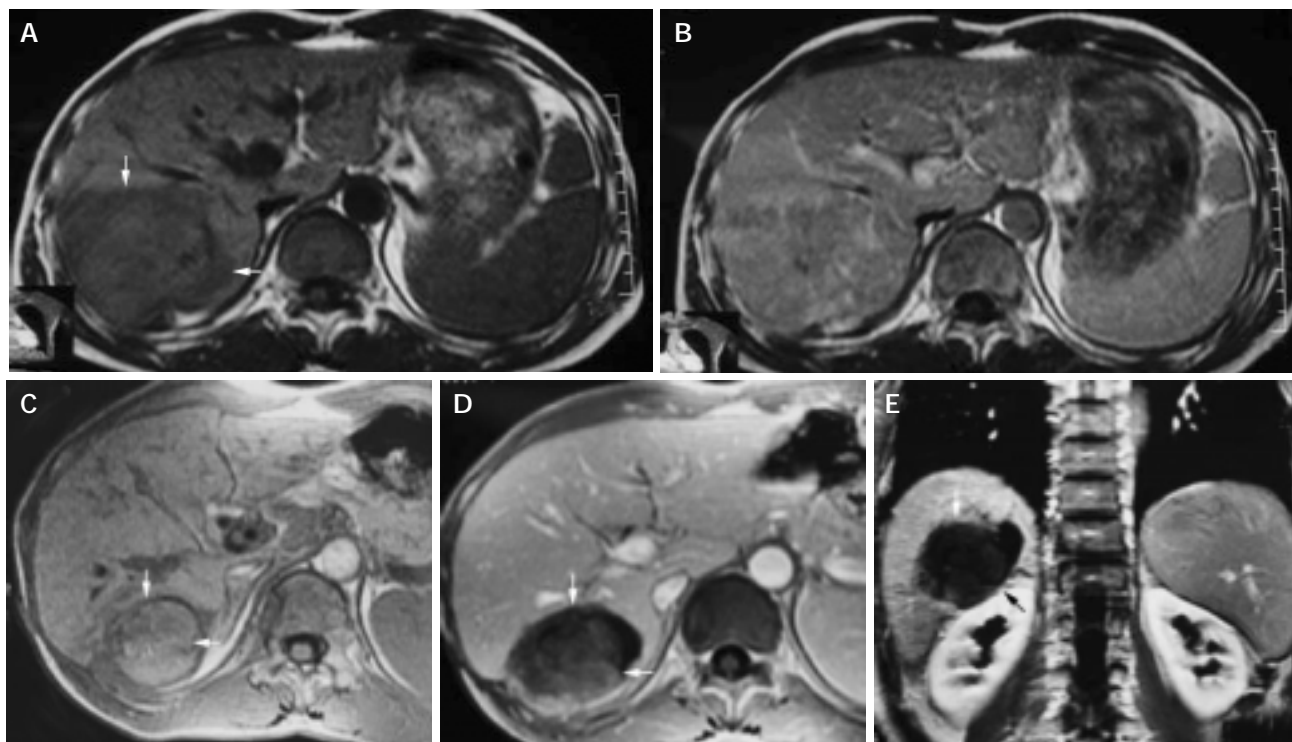


Figure 1 A 42-year-old male with hepatocellular carcinoma. A: MRI T₁-weighted images before HIFU treatment showed that liver tumor of right-posterior lobe was 115 mm×100 mm×66 mm; B: MRI enhanced imaging before HIFU revealed that enhancement of mass in liver right-posterior lobe was higher than that of surrounding normal liver tissues; C: MRI T₁-weighted imaging 11 mo after HIFU revealed that liver tumor of right-posterior lobe obviously decreased in size (50 mm×55 mm×60 mm); D, E: MRI enhanced imaging (cross section and coronal section) 11 mo after HIFU revealed that liver tumor had shrunk obviously, blood supply of tumor was eliminated, the tumor therapeutic region had coagulation necrosis.

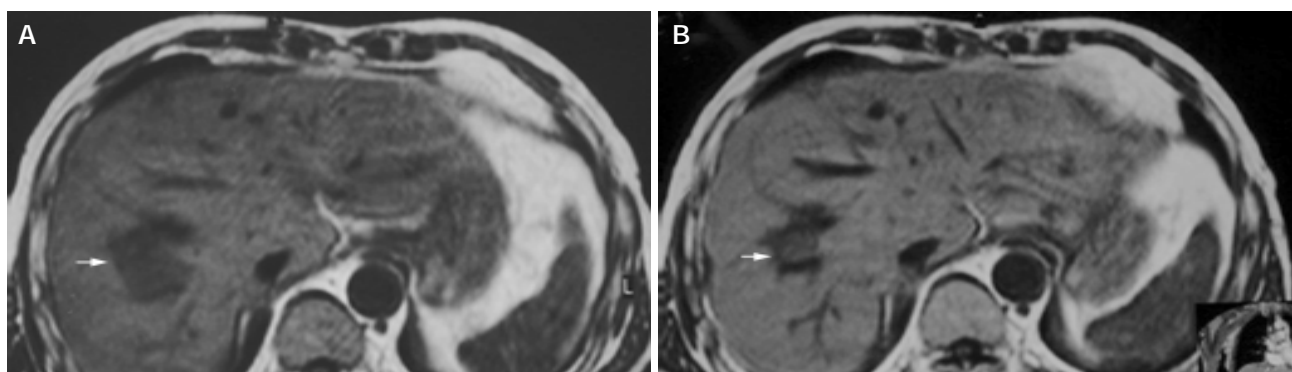


Figure 2 A 55-year-old man with metastatic hepatocarcinoma in sigmoid cancer postoperation. A: MRI images before HIFU treatment showed that liver tumor of right-posterior lobe was 40 mm×30 mm×30 mm; B: MRI images 2 wk after HIFU revealed that liver tumor of right-posterior lobe obviously decreased in size (20 mm×20 mm×15 mm).

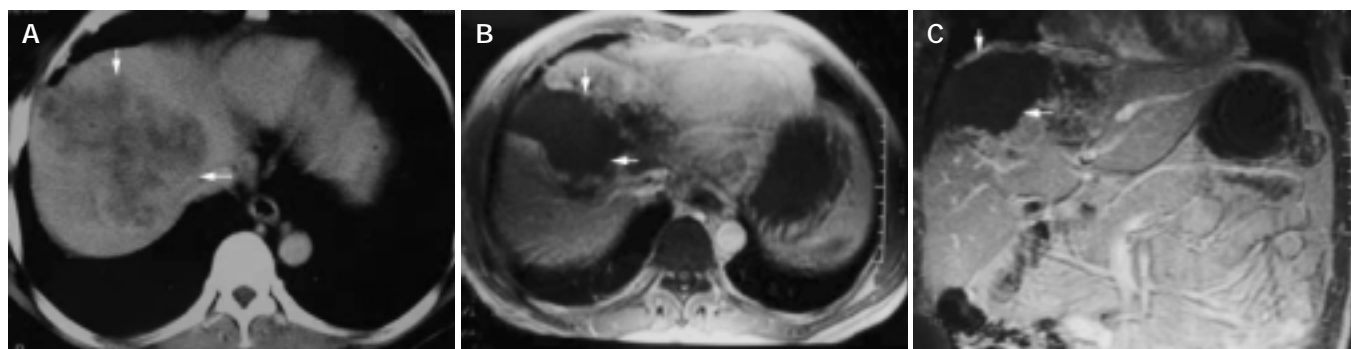


Figure 3 A 54-year-old man with primary carcinoma of liver in right lobe. A: CT enhanced imaging before HIFU treatment revealed that enhancement of mass in liver right-posterior lobe was higher than that of surrounding normal liver tissues (AFP: 5516 $\mu\text{g/L}$); B, C: MRI enhanced imaging (cross section and coronal section) 2 mo after HIFU revealed that necrotic tissue in the therapeutic region of the tumor was not enhanced (AFP: 183 $\mu\text{g/L}$).

DISCUSSION

HIFU is a high-tech developed successfully in the 1990's, a local way of treating tumor without any damages. It utilizes the physics characteristics of ultrasound beam with assemble and penetration, to focus low energy outside body on inner tumor target field, through instantaneous high temperature effect, cavitate effect, making tumor target tissue of focal zone coagulation necrosis, without destroying surrounding tissues^[7-14].

HIFU has the following characteristics in therapy of malignant tumors. Firstly, noninvasiveness. HIFU treats inner tumor without damaging outside body. Previous research on animal angiography indicated that after treating liver tumor of Morris rat using HIFU, nourishing blood vessels which diameter was less than 200 μm of irradiation zone closed, but they were normal for blood vessels which diameter was more than 200 μm ^[15]. Secondly, accuracy. HIFU can pass through tissues and accurately damage target tissues inside organisms. The boundary between therapy zone and un-therapy zone is clear, tissue beyond target zone is hardly destroyed or without damage^[16,17]. Ultrasound Therapy Section of London Emperor Hospital, Britain found that only six cells existed between cells killed completely and cells without damage^[18]. Thirdly, real-time therapy. For whole process of therapy, it is a real-time targeting and monitoring process, real-time estimating therapeutic effect and adjusting dosage^[19]. Fourthly, suitable therapy. According to the size and shape of tumor, it determines therapy range of tumor target zone, overlays tumor target zone. Therefore, treatment of malignant tumor using HIFU has many advantages such as less pain, no damage, fewer influences on splanchnic function, faster recovery for body and no increase of tumor metastasis chance^[20], *etc.*

It is shown that in this research, 100 liver cancer patients had obvious improvement in symptoms and signs after being treated by using HIFU. Short-term effect of HIFU therapy was obvious and affirmative in liver cancer. But for liver cancer patients who had huge block or multifocal big nodules, to make tumor completely occur coagulation necrosis, to gain the purpose of "ablation" tumor integrity, we performed treatment for two or three times. Firstly, we treated deeper tumor parts, to induce coagulation necrosis of the tumor, so as to make it easy to treat remaining superficial parts next time. Conversely, if at first, it makes superficial parts occur coagulation necrosis, and then treats deep tumor tissue, because of change of the impedance dispersion and absorb coefficient of sound, the attenuation of penetrating tissue with ultrasound will aggravate. Meanwhile, focus energy in focal field can not reach ideal degree, as a result it takes more time to make tumor tissue coagulation necrosis.

If tumor locates on the edge of liver with poor blood supply, during therapy of HIFU, We estimate every therapeutic effect by using real-time ultrasound imaging to monitor the change of

gray value. If gray value is changed, it indicates that tumor tissue must occur coagulation necrosis. However, tissues with coagulation necrosis do not always exhibit changes of gray value. For tumor in deep part, during real-time monitor, most changes of gray value are not distinct or lightly increased with suffusion. Through quantitative analysis and comparison of gray value of ultrasound imaging before and after therapy, we can find that the difference of gray rank before and after therapy is obvious. This indicates that local tumor tissues have no reversible coagulation necrosis.

For liver cancer patients with abundant blood supply relatively, we should first perform transcatheter arterial chemoembolization before using HIFU, so as to make inner tumor tissue have more iodised oil deposition, which not only is convenient to ultrasound orientation, but also changes the impedance dispersion and absorb coefficient of sound of tumor zone. Accordingly, it is convenient to energy sediment of focal zone, exerts cooperative function of raising temperature, excites high temperature to get to purpose of destruct therapy at local and makes tumor tissue coagulation necrosis^[21,22].

Yang *et al.*^[15] used HIFU to treat Morris rat hepatoma implanted in the liver. Treatment was administered with a lens-focused 4-MHz transducer that created a focused beam of 550 W/cm^2 at peak intensity. One hundred and twelve rats with liver tumors were divided into two groups of 56 each. Group 1 received HIFU therapy while group 2 (the control group) did not. All rats were killed immediately or 1, 3, 7, 14, 21, 28 d after treatment. Eight rats in each group were killed at each interval for pathologic and biochemical studies. Significant inhibition of the tumor growth was seen in the HIFU-treated group, with tumor growth inhibition rates of 65.4-93.1% from on d 3 to 28 after treatment. Ultrasound-treated tumors showed direct thermal cytotoxic necrosis and fibrosis. An additional 56 ACl rats with liver tumors were divided into 4 groups of 14 each. Group 1 received doxorubicin hydrochloride intraperitoneally and HIFU therapy; group 2, HIFU therapy; group 3, doxorubicin hydrochloride; and group 4 (the control group), neither HIFU nor doxorubicin hydrochloride. Significantly improved survival rates were noted in HIFU-treated animals (groups 1 and 2) compared with those of groups 3 and 4.

Research results of home and abroad using animals showed that HIFU can safely and effectively destroy inner liver tissue or liver transplant tumor^[23-30]. Clinic results showed that HIFU can also treat liver cancer securely and effectively^[11,31,32].

HIFU is a new method with definite therapeutic effect on tumor without damage and poisonous to normal tissues. With improvement of HIFU technology, accumulation of clinic application experience and further research on mechanism of HIFU, HIFU, as a new local therapy, would be applied more extensively to treat liver cancer.

REFERENCES

- 1 **Lynn JG**, Putnam TJ. Histological and cerebral lesions produced by focused ultrasound. *Am J Pathol* 1944; **20**: 637-649
- 2 **Fry WJ**, Fry FJ. Fundamental neurological research and human neurosurgery using intense ultrasound. *IRE Trans Med Electron* 1960; **7**: 166-181
- 3 **Chen W**, Wang Z, Wu F, Bai J, Zhu H, Zou J, Li K, Xie F, Wang Z. High intensity focused ultrasound alone for malignant solid tumors. *Zhonghua Zhongliu Zazhi* 2002; **24**: 278-281
- 4 **Wu F**, Chen WZ, Bai J, Zou JZ, Wang ZL, Zhu H, Wang ZB. Tumor vessel destruction resulting from high-intensity focused ultrasound in patients with solid malignancies. *Ultrasound Med Biol* 2002; **28**: 535-542
- 5 **Yang R**, Sanghvi NT, Rescorla FJ, Kopecky KK, Grosfeld JL. Liver cancer ablation with extracorporeal high-intensity focused ultrasound. *Eur Urol* 1993; **23**: 17-22
- 6 **Kennedy JE**, Ter Haar GR, Cranston D. High intensity focused ultrasound: surgery of the future? *Br J Radiol* 2003; **76**: 590-599
- 7 **Ter Haar GR**. High intensity focused ultrasound for the treatment of tumors. *Echocardiography* 2001; **18**: 317-322
- 8 **Paek BW**, Vaezy S, Fujimoto V, Bailey M, Albanese CT, Harrison MR, Farmer DL. Tissue ablation using high-intensity focused ultrasound in the fetal sheep model: potential for fetal treatment. *American J Obstetrics Gynecol* 2003; **189**: 702-705
- 9 **Wang Z**, Bai J, Li F, Du Y, Wen S, Hu K, Xu G, Ma P, Yin N, Chen W, Wu F, Feng R. Study of a "biological focal region" of high-intensity focused ultrasound. *Ultrasound Med Biol* 2003; **29**: 749-754
- 10 **Ter Haar G**. High intensity ultrasound. *Semin Laparosc Surg* 2001; **8**: 77-89
- 11 **Wu F**, Chen WZ, Bai J, Zou JZ, Wang ZL, Zhu H, Wang ZB. Pathological changes in human malignant carcinoma treated with high-intensity focused ultrasound. *Ultrasound Med Biol* 2001; **27**: 1099-1106
- 12 **Bailey MR**, Couret LN, Sapozhnikov OA, Khokhlova VA, Ter Haar G, Vaezy S, Shi X, Martin R, Crum LA. Use of overpressure to assess the role of bubbles in focused ultrasound lesion shape *in vitro*. *Ultrasound Med Biol* 2001; **27**: 695-708
- 13 **Prat F**, Ponchon T, Berger F, Chapelon JY, Gagnon P, Cathignol D. Hepatic lesions in the rabbit induced by acoustic cavitation. *Gastroenterology* 1991; **100**(5 Pt 1): 1345-1350
- 14 **Huo YM**, Chen YZ. Comparative study of ultrasound transducers in HIFU. *Zhongguo Yaoli Xuebao* 2000; **24**: 97-101
- 15 **Yang R**, Reilly CR, Rescorla FJ, Fauth PR, Sanahvi NT, Frv FJ, Franklin TD Jr, Lumena L, Grosfeld JL. High-intensity focused ultrasound in the treatment of experimental liver cancer. *Arch Surg* 1991; **126**: 1002-1009
- 16 **Wang ZB**, Wu F, Wang ZL, Zhang Z, Zou JZ, Liu C, Liu YG, Cheng G, Du YH, He ZC, Gu ML, Wang ZG, Feng R. Targeted damage effects of high intensity focused ultrasound (HIFU) on liver tissues of Guizhou Province miniswine. *Ultrason Sonochem* 1997; **4**: 181-182
- 17 **Yang R**, Sanghvi NT, Rescorla FJ, Galliani CA, Fry FJ, Griffith SL, Grosfeld JL. Extracorporeal liver ablation using sonography-guided high-intensity focused ultrasound. *Invest Radiol* 1992; **27**: 796-803
- 18 **Dorr LN**, Hynynen K. The effects of tissue heterogeneities and large blood vessels on the thermal exposure induced by short high-power ultrasound pulses. *Int J Hyperthermia* 1992; **8**: 45-59
- 19 **Vaezy S**, Shi X, Martin RW, Chi E, Nelson PI, Bailey MR, Crum LA. Real-time visualization of high-intensity focused ultrasound treatment using ultrasound imaging. *Ultrasound Med Biol* 2001; **27**: 33-42
- 20 **Oosterhof GO**, Conel EB, Smits GA, Debryne FM, Schalken JA. Influence of high-intensity focused ultrasound on the development of metastases. *Eur Urol* 1997; **32**: 91-95
- 21 **Jin CB**, Wu F, Wang ZB, Chen WZ, Zhu H. High intensity focused ultrasound therapy combined with transcatheter arterial chemoembolization for advanced hepatocellular carcinoma. *Zhonghua Zhongliu Zazhi* 2003; **25**: 401-403
- 22 **Zhao J**, Wang Z, Guo D, Yu C, Xie W, Li G. CT appearance and its diagnosis value in liver cancer after transcatheter oily chemoembolization combining with high intensity focused ultrasound therapy. *Zhonghua Ganzangbing Zazhi* 2001; **9**: 61-63
- 23 **Sibille A**, Prat F, Chapelon JY, abou el Fadil F, Henry L, Theilliere Y, Ponchon T, Cathignol D. Characterization of extracorporeal ablation of normal and tumor-bearing liver tissue by high intensity focused ultrasound. *Ultrasound Med Biol* 1993; **19**: 803-813
- 24 **Adams JB**, Moore RG, Anderson JH, Strandberg JD, Marshall FF, Davoussi LR. High-intensity focused ultrasound ablation of rabbit kidney tumors. *J Endourol* 1996; **10**: 71-75
- 25 **Sibille A**, Prat F, Chapelon JY, Abou-el-Fadil F, Henry L, Theilliere Y, Ponchon T, Cathignol D. Extracorporeal ablation of liver tissue by high-intensity focused ultrasound. *Oncology* 1993; **50**: 375-379
- 26 **Righetti R**, Kallel F, Stafford RJ, Price RE, Krouskop TA, Hazle JD, Ophir J. Elastographic characterization of HIFU-induced lesions in canine livers. *Ultrasound Med Biol* 1999; **25**: 1099-1113
- 27 **Gignoux BM**, Scoazec JY, Curiel L, Beziat C, Chapelon JY. High intensity focused ultrasonic destruction of hepatic parenchyma. *Ann Chir* 2003; **128**: 18-25
- 28 **Yang R**, Kopecky KK, Rescorla FJ, Galliani CA, Wu EX, Grosfeld JL. Sonographic and computed tomography characteristics of liver ablation lesions induced by high-intensity focussed ultrasound. *Invest Radiol* 1993; **28**: 796-801
- 29 **Cheng SQ**, Zhou XD, Tang ZY, Yu Y, Wang HZ, Bao SS, Qian DC. High-intensity focused ultrasound in the treatment of experimental liver tumour. *J Cancer Res Clinical Oncol* 1997; **123**: 219-223
- 30 **Ishikawa T**, Okai T, Sasaki K, Umemura S, Fujiwara R, Kushima M, Ichihara M, Ichizuka K. Functional and histological changes in rat femoral arteries by HIFU exposure. *Ultrasound Med Biol* 2003; **29**: 1471-1477
- 31 **Li CX**, Xu GL, Li JJ, Luo GY. High intensity focused ultrasound for liver cancer. *Zhonghua Zhongliu Zazhi* 2003; **25**: 94-96
- 32 **Wu F**, Wang Z, Chen W. Pathological study of extracorporeally ablated hepatocellular carcinoma with high-intensity focused ultrasound. *Zhonghua Zhongliu Zazhi* 2001; **23**: 237-239

Edited by Zhu LH and Chen WW Proofread by Xu FM

Honokiol induces apoptosis through p53-independent pathway in human colorectal cell line RKO

Tao Wang, Fei Chen, Zhe Chen, Yi-Feng Wu, Xiao-Li Xu, Shu Zheng, Xun Hu

Tao Wang, Fei Chen, Zhe Chen, Xiao-Li Xu, Shu Zheng, Xun Hu, Cancer Institute, Second Hospital of Medicine College of Zhejiang University, Hangzhou 310009, Zhejiang Province, China

Yi-Feng Wu, Life Science College of Zhejiang University, Hangzhou 310009, Zhejiang Province, China

Supported by the Cheung Kong Scholars Program, National Ministry of Education of China, and Li Ka Shing Foundation, Hong Kong

Co-first-authors: Tao Wang and Fei Chen

Correspondence to: Professor Xun Hu, Cancer Institute Second Hospital of Medicine College of Zhejiang University, Hangzhou 310009, Zhejiang Province, China. huxun@zju.edu.cn

Telephone: +86-571-87783868 **Fax:** +86-571-87214404

Received: 2004-02-21 **Accepted:** 2004-03-12

Abstract

AIM: To investigate the signal pathway of honokiol-induced apoptosis on human colorectal carcinoma RKO cells and to evaluate whether p53 and p53-related genes were involved in honokiol-treated RKO cells.

METHODS: Cell cycle distribution and subdiploid peak were analyzed with a flow cytometer and DNA fragment with electrophoresis on agarose gels. Transcriptional level of Bax, Bcl-2, Bid and Bcl-xl was accessed by RT-PCR. Western blotting was used to measure p53 protein expression and other factors related to apoptosis. Proliferation inhibition of two cell lines (RKO, SW480) with high expression of p53 and one cell line with p53 negative expression (LS180) was monitored by MTT assay.

RESULTS: Honokiol induced RKO cell apoptosis in a dose-dependent manner. The mRNA expression level and protein level of Bid were up-regulated while that of Bcl-xl was down-regulated, but no changes in Bax and Bcl-2 were observed. Western blotting showed p53 expression had no remarkable changes in honokiol-induced RKO cell apoptosis. LS180 cells treated with honokiol exhibited apparent growth inhibition like RKO cells and Sw480 cells.

CONCLUSION: Honokiol can induce RKO cells apoptosis through activating caspase cascade by p53-independent pathway.

Wang T, Chen F, Chen Z, Wu YF, Xu XL, Zheng S, Hu X. Honokiol induces apoptosis through p53-independent pathway in human colorectal cell line RKO. *World J Gastroenterol* 2004; 10(15): 2205-2208

<http://www.wjgnet.com/1007-9327/10/2205.asp>

INTRODUCTION

Honokiol is a major active constituent extracted from the bark of *Magnolia officianlis* (Chinese name for *Houpu*) (Figure 1). It has a variety of pharmacological effects, such as anti-inflammatory^[1], antithrombosis^[2], anti-arrhythmic^[3], antioxidant^[4] and anxiolytic effects^[5]. Recently, honokiol has been reported to exhibit a

potent cytotoxic activity by inducing cell apoptosis in some cell lines^[6-8]. Honokiol-triggered apoptotic process is accompanied with down-modulation of Bcl-XL, release of mitochondrial cytochrome C in CH27 cells^[9].

Cells undergoing apoptosis are characterized by distinct biochemical and morphological changes. Many of the biochemical and morphological events of apoptosis are a direct result of caspase-mediated cleavage of specific substrates^[10,11]. Together with caspase, Bcl-2 family is involved in inducing cell apoptosis and identified as essential components of the intracellular apoptotic signaling pathways. Cell viability versus death is determined by the relative abundance of various members of the Bcl-2 family, acting in concert with other proteins in the death pathway^[12,13].

In many tumor cells, wild-type p53 is considered to participate in apoptosis in response to DNA damage^[14]. P53 may transactivate apoptotic regulators, such as Bcl-2^[15-17] and Bax^[18,19]. Recent studies have shown that p53 plays a role in apoptosis by the mitochondrial-mediated apoptotic pathway^[20]. Activation of p53 upregulates Bax^[19] and increases the ratio of Bax:Bcl-2, releases cytochrome C and other polypeptides from the intermembrane space of mitochondria into cytoplasm. Cytochrome C activates caspase cascade^[12,13].

It is well known that a broad range of agents can induce tumor cell apoptosis through p53-regulated manner by Bax/mitochondria/caspase-9 pathway. But up to now, it is not clear that whether wild-type p53 takes part in honokiol-induced apoptosis. In this present study we examined whether wild-type p53 and p53-related gene were involved in honokiol-treated RKO cells.

MATERIALS AND METHODS

Materials

RPMI 1640 medium was obtained from Gibco BRL. Newborn bovine serum was supplied by Sijiqing Biotechnology Co. (Hangzhou, China). Monoclonal antibodies to Bax, Bcl-xl, Bid, Bcl-2, β -actin and p53 were purchased from NeoMarkers, Fremont, CA, USA. Honokiol was got from the National Institute for Pharmaceutical and Biological Products, Beijing, China. The drug was dissolved in DMSO with the stock concentration of 10 mg/mL. It was further diluted in culture medium with the final DMSO concentration <1%. 3-(4, 5-dimethylthiazol-2-yl)-2, 5-diphenyltetrazolium bromide (MTT) and propidium iodide (PI) were purchased from Sigma Chemical Corporation, USA.

Cell culture

Human colorectal cell lines RKO, SW480 and LS180 were provided by Cancer Institute of Zhejiang University. Three cells were maintained in RPMI 1640 medium (Gibco BRL) supplemented with 100 mL/L heat-inactivated fetal bovine serum (Si-Ji-Qing Biotechnology Co, Hangzhou, China), 100 U/mL penicillin and 100 μ g/mL streptomycin at 37 °C in a 50 mL/L CO₂ atmosphere.

Detection of DNA fragmentation

To detect DNA fragments, RKO cells were collected and lysed with lysis buffer containing 50 mmol/L Tris-HCl (pH 7.5),

20 mmol/L EDTA, and 10 g/L NP-40. Then 10 g/L SDS and RNase (5 µg/mL) were added to the supernatants, and incubated at 56 °C for 2 h, followed by incubation with proteinase K (2.5 µg/mL) at 37 °C for 2 h. After DNA was precipitated by addition of both ammonium acetate (3.3 mol/L) and ethanol (995 mL/L) dissolved in a loading buffer, DNA fragmentation was detected by electrophoresis on 15 g/L agarose gels and visualized with ethidium bromide staining.

Cell cycle analysis by FCM

Honokiol-treated RKO cells (5, 10, 15 µg/mL) and vehicle were fixed with 700 mL/L alcohol for 15 min at 4 °C, then stained with 1.0 µg/mL propidium iodide (PI, Sigma, USA). The red fluorescence of DNA-bound PI in individual cells was measured at 488 nm with a FACSCalibur (Becton Dickinson, USA) and the results were analyzed using ModFit 3.0 software. Ten thousand events were analyzed for each sample.

RT-PCR assay

RKO cells 1×10^5 were seeded on 24-well plate. After 24-h culture, cells were treated with 5, 10 µg/mL honokiol and vehicle for 48 h. Total RNA from RKO cells was extracted using Trizol (Invitrogen, USA). In RT-PCR, cDNA synthesis was performed using a RNA PCR kit (TaKaRa Biomedicals, Osaka, Japan) with the supplied oligo dT primer (Table 1). Reverse transcription was performed using a thermal program of 92 °C for 2 min, then 38 cycles of annealing for 30 s at 55 °C, extension for 90 s at 72 °C. As an internal control, semiquantitative analysis of β-actin was also amplified. This primer pair of β-actin had an optimal annealing temperature of 55 °C with 20 cycles and yielded a 350-bp PCR product. Samples were separated on 20 g/L agarose gel and visualized with ethidium bromide staining under UV light.

Western blotting

RKO cells (5×10^6) treated with 5, 10 µg/mL honokiol and vehicle respectively for 24 h were lysed by 4 g/L trypsin containing 0.2 g/L EDTA, then collected after washed twice with phosphate-buffered saline (PBS, pH 7.4). Total protein extract from RKO cells was prepared using cell lysis buffer [150 mmol/L NaCl, 0.5 mol/L Tris-HCl (pH 7.2), 0.25 mol/L EDTA (pH 8.0), 10 g/L Triton X-100, 50 mL/L glycerol, 12.5 g/L SDS]. The extract (30 µg) was electrophoresed on 12 g/L SDS-PAGE and electroblotted onto polyvinylidene difluoride membrane (PVDF, Millipore Corp., Bedford, MA) for 2 h in a buffer containing 25 mmol/L Tris-HCl (pH 8.3), 192 mmol/L glycine and 200 mL/L methanol. The blots were blocked with 50 g/L nonfat milk in TBST washing buffer for 2 h at room temperature and then incubated at 4 °C overnight with antibodies. All antibodies were diluted in TBST according to the manufacturer's instructions. After washed at room temperature with washing buffer, the blots were labeled with peroxidase-conjugated secondary antibodies.

Cell proliferation assay

RKO cells, SW480 and LS180 cells (1×10^4 in 100 µL) were seeded on 96-well plates in triplicate respectively. Following a 24-h culture at 37 °C, the medium was replaced with fresh medium containing vehicle control or various concentrations of honokiol

in a final volume of 200 µL. Cells were incubated at 37 °C for 68 h. Then 50 µL of MTT (2 mg/mL in PBS) was added to each well, incubated for an additional 4 h, the plate was centrifuged at 1 000 r/min for 10 min, then the medium was removed. The MTT formazan precipitate was dissolved in 100 µL DMSO, shaken mechanically for 10 min and then read immediately at 570 nm by a plate reader (Opsys MR, Denex Technology, USA).

Statistics

Statistical significance was determined by Student's *t*-test. A *P* value of 0.05 or less was considered significant.

RESULTS

DNA fragmentation detection in RKO cells

In honokiol-treated RKO cells, a degradation of chromosomal DNA into small internucleosomal fragments was evidenced by the formation of 180-200 bp DNA ladder on agarose gels (Figure 2), hallmark of cells undergoing apoptosis. No DNA ladders were detected in the samples isolated from control cultures. These results indicated that honokiol induced an apoptotic cell death in RKO cells

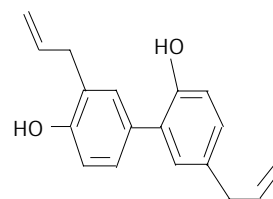


Figure 1 Chemical structure of honokiol (C₁₈H₁₈O₂, M_r 266.33).

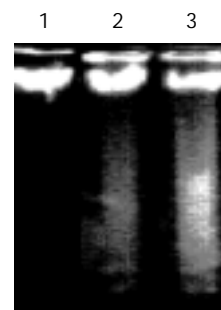


Figure 2 Differences in vehicle and honokiol induced apoptotic DNA laddering of RKO cells. Lane 1: Vehicle; Lane 2: 5 µg/mL; Lane 3: 10 µg/mL.

Effect of honokiol on cell cycle phase distribution

RKO cells were exposed to the increased concentrations of honokiol (5-15 µg/mL) for 48 h, and the cell growth was analyzed using flow cytometry. In the absence of honokiol, the cell populations were at G₁, S, and G₂/M phases (Figure 3), accompanied with increased concentrations of honokiol by a concomitant increase of the G₁ phase (Table 2). From Figure 3, we considered the peak areas of subdiploid were up at the

Table 1 Expected size of PCR amplification product with each apoptosis modulator primer pair

Apoptosis modulator	Upstream primer (5'-3')	Downstream primer (5'-3')	Size (bp)
Bax	ACCAAGAAGCTGAGCGAGTGT	ACAAACATGGTCACGGTCTGC	332
Bcl-xl	GGAGCTGGTGGTTGACTTTCT	CCGGAAGAGTTCATTCACTAC	379
Bid	GAC CCG GTG CCT CAG GA	ATG GTC ACG GTC TGC CA	586
Bcl-2	TTGTGGCCTTCTTTGAGTTCG	TACTGCTTAGTGAACCTTTT	332
β-actin	AGCCAACCGCGAGAAGATGACC	GAAGTCCAGGGCGACGTAGCAC	350

increased concentrations of honokiol. This observation led to a suggestion of G1 arrest. When the cells were exposed to honokiol at 10 $\mu\text{g}/\text{mL}$ and above, subdiploid peak was significantly increased and the percentage of apoptotic cells in 10 000 cells was 14.1% and 20.31% respectively (Table 2).

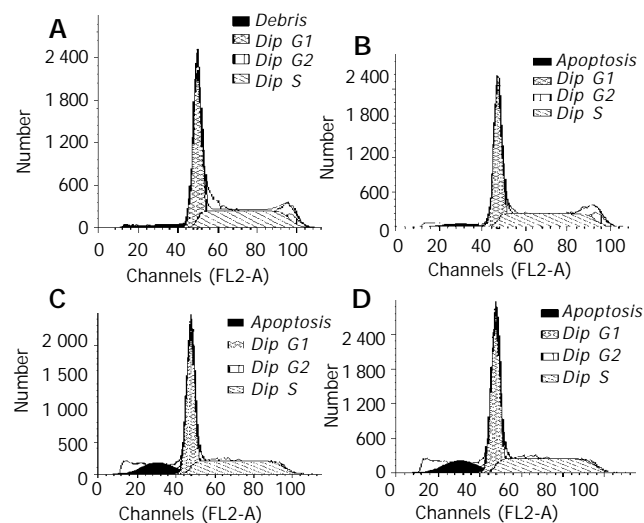


Figure 3 Apoptosis of RKO cells detected by FCM. A: Vehicle; B: 5 $\mu\text{g}/\text{mL}$ honokiol; C: 10 $\mu\text{g}/\text{mL}$ honokiol; D: 15 $\mu\text{g}/\text{mL}$ honokiol.

Table 2 Effect of honokiol on cell cycle distribution and apoptosis in RKO cells

Treatment ($\mu\text{g}/\text{mL}$)	Cell cycle distribution (%)			Apoptosis (%)
	G0/G1	S	G2/M	
Control	44.76	45.09	10.14	0.21
5	48.03	42.37	9.60	4.51
10	54.04	40.30	5.66	14.10 ^b
15	58.94	39.36	1.70	20.31 ^d

Cell cycle distribution was determined after 48 h of treatment in each group. The tabulated percentages were an average calculated on the results of three separate experiments. ^b $P < 0.01$, ^d $P < 0.01$ vs corresponding control group.

Semi-quantification of Bid, Bax, Bcl-2 and Bcl-xl mRNA expression

mRNA expression of apoptosis-related genes in response to different levels of honokiol was assessed. The Bcl-xl mRNA expression was significantly reduced in RKO cells exposed to honokiol, while Bid mRNA expression was remarkably up-regulated. No apparent changes of Bax and Bcl-2 were observed (Figure 4).

Effect of honokiol on expression of p53-related gene and p53

p53 and p53-related gene were found to be importantly involved in apoptosis induced by many agents. To study their role in honokiol-treated RKO, we monitored Bax, Bcl-2, Bcl-xl, Bid and p53 protein levels. Results in Figure 5 shows that no significant changes of Bax, Bcl-2 and p53 were found compared with vehicle. The level of Bcl-xl was decreased to vehicle level, while the level of Bid was increased remarkably after treated with 5 and 10 $\mu\text{g}/\text{mL}$ honokiol respectively. The protein levels were measured by quantitative Western blot analysis after normalized with β -actin content.

Inhibition of proliferation in RKO, Sw480 and LS180 cells

RKO cells had positively expressed of high wild-type p53 and SW480 cells had positive expression of high mutant p53, while LS180 had negative p53 antigen expression^[20-22]. Cells treated with various concentrations of honokiol resulted in a dose-

dependent cytotoxicity in three cells. As shown in Figure 6, honokiol-treated LS180 exhibited apparent growth inhibition like RKO cells and Sw480. Honokiol-mediated cytotoxicity occurred at the concentration of 5 $\mu\text{g}/\text{mL}$ and above. A significant decrease in cell number was seen at 10 $\mu\text{g}/\text{mL}$. The concentration leading to a 50% decrease in cell number (IC₅₀) was approximate 10.33, 12.98, 11.16 $\mu\text{g}/\text{mL}$ in RKO, SW480 and LS180 cells respectively.

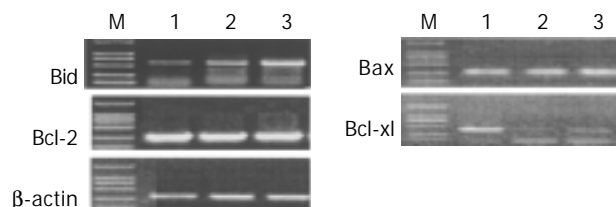


Figure 4 Analysis of Bcl-2, Bax, Bid and Bcl-xl mRNA by RT-PCR. M: DNA mark; Lane 1: Vehicle; Lane 2: 5 $\mu\text{g}/\text{mL}$ honokiol; Lane 3: 10 $\mu\text{g}/\text{mL}$ honokiol.

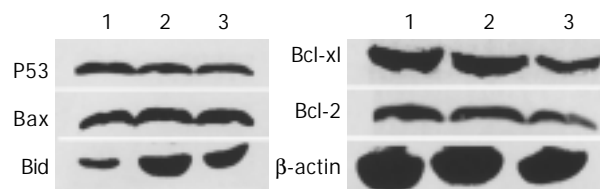


Figure 5 Western blotting of honokiol- and vehicle-induced Bax, Bcl-2, Bcl-xl, Bid and p53 protein levels in RKO cell line. Lane 1: Vehicle; Lane 2: 5 $\mu\text{g}/\text{mL}$; Lane 3: 10 $\mu\text{g}/\text{mL}$.

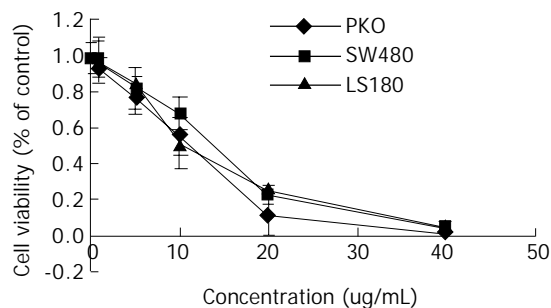


Figure 6 Concentration-dependent inhibition of RKO, SW480 and LS180 cells exposed to the various concentrations of honokiol shown by MTT assay.

DISCUSSION

p53 is a crucial protein in cellular stress response. p53-dependent arrest of cells in the G1 phase of the cell cycle was an important component of the cellular response to stress^[23]. Wild-type p53 was considered to participate in apoptosis in response to DNA damage in many tumor cells^[14,24]. When cells received UV or ionizing radiation and were exposed to anticancer drugs, p53 protein was accumulated^[25,26]. The increased p53 could transactivate its downstream target genes to induce cell cycle arrest, DNA repair, and apoptosis^[27,28]. p53-dependent apoptosis was also observed *in vivo*^[29]. However, p53-independent apoptotic cascades after administration of anticancer drugs or r-irradiation have been described.

In the present study, honokiol-treated RKO cells could induce apoptosis in a concentration-dependent manner, with the ratio of G1 phase increased. The agent also caused an increase of the expression of caspase-3 and caspase-7 in a dose-dependent manner, did not cause the significant increase

of caspase-9 (data not shown). In CH27 cells it promoted to release cytochrome C and activate caspase 3^[9].

p53-dependent apoptosis was activated by the Bax/mitochondrial/caspase-9 pathway. Bcl-2 and Bax expression were regulated by p53 both *in vitro* and *in vivo*, and Bax was a direct target of p53 transcriptional activation^[30]. Bax, a proapoptotic member of the Bcl-2 family, was located in the outer membrane of mitochondria^[25]. Increased in the ratio of Bax/Bcl-2 could cause changes in the membrane potential of mitochondria, consequently, cytochrome C and other polypeptides were released from the intermembrane space of mitochondria into cytoplasm. Once released, cytochrome C could activate procaspase-9 by self-cleavage^[12,13] and then other caspases^[12].

According to previous data, honokiol led to cell G1 arrest and cytochrome C release like p53. Thus it is necessary to evaluate the mRNA and protein expression of Bax and Bcl-2. Our results showed that honokiol-induced apoptosis of RKO cells was accompanied with up-regulation of Bid and down-modulation of Bcl-xl, but did not involve the regulation of Bcl-2 or Bax protein expression. Since pro-apoptotic Bax is a p53 downstream target, the lack of change of Bax and Bcl-xl supports the view that honokiol probably does not trigger the p53/Bax-mediated apoptosis pathway. Next we examined the expression of p53 in honokiol-treated RKO cells. We found that no significant change of p53 was observed (Figure 5). Finally we analyzed honokiol-induced apoptosis of the three cells with different p53 expression. Our data showed that honokiol-treated LS180 and SW480 cells exhibited apparent growth inhibition like RKO cells.

These results suggest that honokiol-induced caspase activation and cell apoptosis are entirely controlled by the p53-independent pathway.

REFERENCES

- 1 **Liou KT**, Shen YC, Chen CF, Tsao CM, Tsai SK. The anti-inflammatory effect of honokiol on neutrophils: mechanisms in the inhibition of reactive oxygen species production. *Eur J Pharmacol* 2003; **475**: 19-27
- 2 **Teng CM**, Chen CC, Ko FN, Lee LG, Huang TF, Chen YP, Hsu HY. Two antiplatelet agents from *Magnolia officinalis*. *Thromb Res* 1988; **50**: 757-765
- 3 **Liou KT**, Lin SM, Huang SS, Chih CL, Tsai SK. Honokiol ameliorates cerebral infarction from ischemia-reperfusion injury in rats. *Planta Med* 2003; **69**: 130-134
- 4 **Lo YC**, Teng CM, Chen CF, Chen CC, Hong CY. Magnolol and honokiol isolated from *Magnolia officinalis* protect rat heart mitochondria against lipid peroxidation. *Biochem Pharmacol* 1994; **47**: 549-553
- 5 **Watanabe K**, Watanabe H, Goto Y, Yamaguchi M, Yamamoto N, Hagino K. Pharmacological properties of magnolol and honokiol extracted from *Magnolia officinalis*: central depressant effects. *Planta Med* 1983; **49**: 103-108
- 6 **Hirano T**, Gotoh M, Oka K. Natural flavonoids and lignans are potent cytostatic agents against human leukemic HL-60 cells. *Life Sci* 1994; **55**: 1061-1069
- 7 **Hibasami H**, Achiwa Y, Katsuzaki H, Imai K, Yoshioka K, Nakanishi K, Ishii Y, Hasegawa M, Komiya T. Honokiol induces apoptosis in human lymphoid leukemia Molt 4B cells. *Int J Mol Med* 1998; **2**: 671-673
- 8 **Nagase H**, Ikeda K, Sakai Y. Inhibitory effect of magnolol and honokiol from *Magnolia obovata* on human fibrosarcoma HT-1080. Invasiveness *in vitro*. *Planta Med* 2001; **67**: 705-708
- 9 **Yang SE**, Hsieh MT, Tsai TH, Hsu SL. Down-modulation of BCL-XL, release of cytochrome c and sequential activation of caspases during honokiol-induced apoptosis in human squamous lung cancer CH27 cells. *Biochem Pharmacol* 2002; **63**: 1641-1651
- 10 **Miyashita T**, Krajewski S, Krajewska M, Wang HG, Lin HK, Liebermann DA, Hoffman B, Reed JC. Tumor suppressor p53 is a regulator of bcl-2 and bax gene expression *in vitro* and *in vivo*. *Oncogene* 1994; **9**: 1799-1805
- 11 **Miyashita T**, Harigai M, Hanada M, Reed JC. Identification of a p53-dependent negative response element in the bcl-2 gene. *Cancer Res* 1994; **54**: 3131-3135
- 12 **Li P**, Nijhawan D, Budihardjo I, Srinivasula SM, Ahmad M, Alnemri ES, Wang X. Cytochrome c and dATP-dependent formation of Apaf-1/caspase-9 complex initiates an apoptotic protease cascade. *Cell* 1997; **91**: 479-489
- 13 **Stennicke HR**, Deveraux QL, Humke EW, Reed JC, Dixit VM, Salvesen GS. Caspase-9 can be activated without proteolytic processing. *J Biol Chem* 1999; **274**: 8359-8362
- 14 **Lowe SW**, Bodis S, McClatchey A, Remington L, Ruley HE, Fisher DE, Housman DE, Housman DE, Jacks T. p53 status and the efficacy of cancer therapy *in vivo*. *Science* 1994; **266**: 807-810
- 15 **Haldar S**, Negrini M, Monne W, Sabbioni S, Croce CM. Down-regulation of bcl-2 by p53 in breast cancer cells. *Cancer Res* 1994; **54**: 2095-2097
- 16 **Beham A**, Marin MC, Fernandez A, Herrmann J, Brisbay S, Tari AM, Lopez-Berestein G, Lozano G, Sarkiss M, McDonnell TJ. Bcl-2 inhibits p53 nuclear import following DNA damage. *Oncogene* 1997; **15**: 2767-2772
- 17 **Marin MC**, Hsu B, Meyn RE, Donehower LA, el-Naggar AK, McDonnell TJ. Evidence that p53 and bcl-2 are regulators of a common cell death pathway important for *in vivo* lymphomagenesis. *Oncogene* 1994; **9**: 3107-3112
- 18 **Miyashita T**, Krajewski S, Krajewska M, Wang HG, Lin HK, Liebermann DA, Hoffman B, Reed JC. Tumor suppressor p53 is a regulator of bcl-2 and bax gene expression *in vitro* and *in vivo*. *Oncogene* 1994; **9**: 1799-1805
- 19 **Selvakumaran M**, Lin HK, Miyashita T, Wang HG, Krajewski S, Reed JC, Hoffman B, Liebermann D. Immediate early up-regulation of bax expression by p53 but not TGF-beta1: a paradigm for distinct apoptotic pathways. *Oncogene* 1994; **9**: 1791-1798
- 20 **Smith ML**, Chen IT, Zhan Q, O'Connor PM, Fornace AJ Jr. Involvement of the p53 tumor suppressor in repair of u.v.-type DNA damage. *Oncogene* 1995; **10**: 1053-1059
- 21 **Rodrigues NR**, Rowan A, Smith ME, Kerr IB, Bodmer WF, Gannon JV, Lane DP. p53 mutations in colorectal cancer. *Proc Natl Acad Sci U S A* 1990; **87**: 7555-7559
- 22 **Xu LH**, Deng CS, Zhu YQ, Liu SQ, Liu DZ. Synergistic antitumor effect of TRAIL and doxorubicin on colon cancer cell line SW480. *World J Gastroenterol* 2003; **9**: 1241-1245
- 23 **Luu Y**, Bush J, Cheung KJ Jr, Li G. The p53 Stabilizing Compound CP-31398 induces apoptosis by activating the intrinsic Bax/mitochondrial/caspase-9 pathway. *Exp Cell Res* 2002; **276**: 214-222
- 24 **Schuler M**, Bossy-Wetzel E, Goldstein JC, Fitzgerald P, Green DR. p53 induces apoptosis by caspase activation through mitochondrial cytochrome c release. *J Biol Chem* 2000; **275**: 7337-7342
- 25 **Li G**, Bush JA, Ho VC. p53-dependent apoptosis in melanoma cells after treatment with camptothecin. *J Invest Dermatol* 2000; **114**: 514-519
- 26 **Li G**, Ho VC, Mitchell DL, Trotter MJ, Tron VA. Differentiation-dependent p53 regulation of nucleotide excision repair in keratinocytes. *Am J Pathol* 1997; **150**: 1457-1464
- 27 **Green DR**, Reed JC. Mitochondria and apoptosis. *Science* 1998; **281**: 1309-1312
- 28 **Li G**, Ho VC. p53-dependent DNA repair and apoptosis respond differently to high- and low-dose ultraviolet radiation. *Br J Dermatol* 1998; **139**: 3-10
- 29 **Tron VA**, Trotter MJ, Tang L, Krajewska M, Reed JC, Ho VC, Li G. P53-regulated apoptosis is differentiation dependent in ultraviolet B-irradiated mouse keratinocytes. *Am J Pathol* 1998; **153**: 579-585
- 30 **Liebermann DA**, Hoffman B, Steinman RA. Molecular controls of growth arrest and apoptosis: p53-dependent and independent pathways. *Oncogene* 1995; **11**: 199-210

Natural history of chronic hepatitis C in patients on hemodialysis: Case control study with 4-23 years of follow-up

Kunio Okuda, Osamu Yokosuka

Kunio Okuda, Osamu Yokosuka, Department Medicine and Clinical Oncology, Graduate School of Medicine, Chiba University, Chiba 260-8670, Japan

Correspondence to: Osamu Yokosuka, M.D., Department of Medicine and Clinical Oncology, Graduate School of Medicine, Chiba University, Chiba 260-8670, Japan. yokosukao@faculty.chiba-u.jp

Telephone: +81-43-226-2083 **Fax:** +81-43-226-2088

Received: 2004-03-05 **Accepted:** 2004-04-09

Abstract

AIM: Hepatitis C virus (HCV) infection is very common among end-stage kidney disease patients on hemodialysis, but its natural history is not known.

METHODS: In this study, 189 dialysis patients (case) positive for HCV antibodies who were followed up for more than 4 years were compared with twice as many sex/age matched controls with chronic hepatitis C who were diagnosed in the same month as the case and followed up for comparable periods. The longest follow-up was 23 years in dialysis cases. The disease activities were graded into "asymptomatic" if ALT was less than 40 (35 in cases) IU/L, "low activities" if ALT was 40 (35)-79 IU/L, and "high activities" if ALT was above 80 IU/L during the last or latest 4 year period.

RESULTS: All 25 dialysis cases who were followed up for more than 15 years were asymptomatic and 15 of them were negative for HCV RNA. Of the 50 controls followed up for more than 15 years, 34 had high activities, and none cleared HCV RNA. There were 60 controls who were asymptomatic, but they were all positive for HCV RNA, while 22.3% of asymptomatic dialysis cases were RNA negative. No dialysis patients with chronic hepatitis C progressed to cirrhosis, whereas the disease progressed to cirrhosis in more than one quarter of the controls. These differences were highly significant ($P < 0.0001$).

CONCLUSION: Chronic hepatitis C among hemodialysis patients is mild in disease activity, and is not progressive, perhaps due to immunological abnormalities in these patients. Hepatic C virus is frequently cleared in asymptomatic dialysis patients during a long course. A possible mechanism for viral clearance is viral particle destruction on the surface of the dialyzer membrane.

Okuda K, Yokosuka O. Natural history of chronic hepatitis C in patients on hemodialysis: Case control study with 4-23 years of follow-up. *World J Gastroenterol* 2004; 10(15): 2209-2212
<http://www.wjgnet.com/1007-9327/10/2209.asp>

INTRODUCTION

Hepatitis C virus (HCV) infection is very common among patients on hemodialysis for chronic renal failure with global anti-HCV prevalence of up to 91%^[1], because of the frequent past blood transfusions and nosocomial infections^[2,3]. Although

at the clinical setting, dialysis patients with HCV infection seem to have a mild disease, reports on the natural history of hepatitis C in hemodialysis patients vary^[4]. Sterling *et al.*^[5] compared 50 consecutive patients with end-stage renal disease and HCV infection to HCV-positive controls. Ninety-six percent of patients on dialysis had normal alanine-aminotransferase (ALT) and low necroinflammatory score on biopsy. Despite minimal biochemical evidence of disease, some dialysis patients were more likely to have bridging hepatic fibrosis. Another cohort study^[6] showed that the crude relative risk of death comparing HCV positive to negative dialysis patients was not significant. However, adjustment for age, transplantation, and other factors raised the relative risk somewhat. Akpolat *et al.*^[7] compared liver histology between 9 dialysis patients and 37 patients with normal renal function, and found less active and progressive chronic hepatitis C in the former. They admitted that the number of patients was too small for conclusion. Thus, more information is required on the natural history of chronic HCV infection in hemodialysis patients. This study was designed to compare end-stage kidney disease patients who were positive for HCV antibodies and control patients infected with HCV but not on dialysis.

MATERIALS AND METHODS

At the end of 2001, 603 patients with renal failure were dialyzed with 221 consoles at Sanai Amalgamated Dialysis Center, Chiba, which consists of Sanai Memorial Hospital, Sanai Soga Hospital and Ichihara Dialysis Clinic. Of these 603 patients, 142 were tested positive for HCV antibodies. Many of these patients had chronic non-A, non-B hepatitis and were subsequently found to have HCV antibody positive. Dialysis patients commonly had cardiovascular, intracranial and other complications, and they died while on dialysis. At this center, about 55 patients on average died per year. As yet, none of these anti-HCV positive patients turned antibody negative during the observation period after 1991 when C100-3 antibody kit became available at the hospital. The antibody kit was subsequently changed to the 2nd and 3rd generation test. All dialysis patients underwent periodic blood tests that included ALT and aspartate-aminotransferase (AST) every 4 wk. In this study, 189 patients who were anti-HCV positive and followed up for more than 4 years to the end of 2001 constituted the study (case) subjects. Twenty-five patients were followed for more than 15 years (longest 23 years), 94 patients were followed for 10-15 years and 70 for 4-10 years (Table 1). Ten patients were treated with interferon^[8] and they were excluded. Currently 3 patients had cirrhosis, they were positive for both HBV and HCV. They were not included. The three patients had cirrhosis when dialysis was started at this hospital.

One patient with renal failure started on dialysis in 1978, 11 in 1983, 5 in 1984, 4 in 1985, 8 in 1986, 13 in 1987, 18 in 1988, 14 in 1989, 21 in 1990, 24 in 1991, 22 in 1992, 14 in 1993, 18 in 1994, 10 in 1995, and 6 in 1996. There were 137 male dialysis patients whose age ranged from 21 to 75 years, averaged 48.6±11.8 years, and 52 females whose age ranged 24 to 83 years, averaged 51.7±11.1 years.

The control group consisted of anti-HCV positive patients with chronic hepatitis who were diagnosed and followed up at the Liver Center of the Chiba University Hospital. The patients who were treated with interferon and had sustained virological response were excluded. At this center, approximately 1 200 HCV positive patients were followed up at an interval of 1 to 3 mo, and about 20-30 new patients were found per month. Out of these patients, two control patients for each dialysis case were chosen who were age (± 5 years) and sex matched, and found to be HCV positive in the same month and subsequently followed up for a similar period of time. All these patients were followed up for more than 4 years, and the disease activities were recorded in the last 4 years before death or in the latest 4 year period.

Diagnosis of cirrhosis was made on the basis of liver biopsy, imaging, blood chemistry and physical signs. Imaging findings suggestive of cirrhosis included ascites, liver surface irregularity, splenomegaly, enlarged left gastric vein, enlarged paraumbilical vein, obtuse liver edge, enlarged caudate lobe, excessively large left lobe compared to the right lobe, splenorenal or gastrosplenic shunt by ultrasound and CT, and esophago-gastric varices by endoscopy. The patients with past or currently elevated ALT in the absence of these features were diagnosed as having chronic hepatitis C.

Serum HCV RNA was measured using the branch DNA method and subsequently by Amplicor test (Nippon Roche, Tokyo). Viral load was measured twice at an interval of 2 or more years in dialysis patients to see the change in viral load. Beside the routine liver tests, 7S domain type IV collagen was measured as an indirect indicator of hepatic fibrosis in dialysis cases^[9,10].

The disease activities were graded into three categories: "asymptomatic" if ALT levels remained below 40 IU/L for the control group and below 35 IU/L for dialysis cases, the difference in the upper normal limit was due to normally low ALT and AST in dialysis patients^[11,12]; "low activities" if ALT fluctuated between 35 (40 in control) and 79 IU/L; and "high activities" if ALT levels exceeded 80 IU/L during the last 4 year period.

Statistical analyses were made by the χ^2 test and ANOVA.

RESULTS

The disease activities in these dialysis cases who were divided into three groups according to the length of dialysis (more than 15 years, 10-15 years and 4-10 years) are given in Table 1. All the 25 patients on dialysis for more than 15 years were asymptomatic, and only 3 of 50 controls were asymptomatic. The remainder of the controls all had disease activities. Of the 94 patients on dialysis for 10-15 years, 81 (85%) were asymptomatic and 6 (6.4%) had high activities. Whereas in the controls, only 26 (13.8%) of 188 were asymptomatic and 109 (58.0%) had high activities. Of the 70 patients on dialysis for 4-10 years, 58 (83%) were asymptomatic and 5 (7.1%) had high activities. The corresponding figures were 22.1% and 52.1%, respectively, in the controls. These differences were highly significant ($P < 0.001$). Table 1 also lists the number of patients in parentheses in whose serum HCV RNA levels were PCR negative or below the quantifiable level by Amplicor. Of the 25 long (more than 15 years) follow-up dialysis cases, RNA was negative or below the quantifiable level in 15 (60%). However, RNA was negative in only one of 14 dialysis cases with low disease activities, the remaining 13 cases were positive. All high activities cases were positive, while none of the control patients was negative for HCV RNA.

The clinical course of these 189 patients was uneventful from the point of view of liver disease. Many of these patients died from liver unrelated diseases, but the liver disease progressed to cirrhosis in none of them. The three cases of HCV positive

cirrhosis who were followed up had already had cirrhosis when they came to our hospital. All cases who were followed up for more than 15 years were asymptomatic by the end of the follow-up (Table 1). More dialysis cases who were follow-up for a shorter period of time had disease activities. Thus, chronic hepatitis C among dialysis patients seemed to slowly improve and seldom worsen. In contrast, the disease was progressive in most control patients. In the 50 control patients who were followed up for more than 15 years, the disease progressed to cirrhosis in 18 during the follow-up. In the 228 controls who were followed up for 10-15 years, cirrhosis developed in 62. In the 140 controls who were followed up for 4-10 years, 29 developed cirrhosis.

Table 1 Clinical evaluation of dialysis (case) and control patients in recent 4 years or last 4 years before liver unrelated death

Group	Number	Disease activities			
		Asymptomatic	Low	High	
Follow-up: <15 yr					
Case	Male	14(5)	14(5)	0	0 ^b
	Female	11(10)	11(10)	0	0 ^d
Control	Male	28(0)	0	8(0)	20 ^b (0)
	Female	22(0)	3(0)	5(0)	14 ^d (0)
Follow-up: 10-15 yr					
Case	Male	70(15)	58(14)	7(1)	5 ^b (0)
	Female	24(0)	23(10)	0	1 ^d (0)
Control	Male	140(0)	16(0)	29(0)	95 ^b (0)
	Female	48(0)	10(0)	24(0)	14 ^d (0)
Follow-up: 4-10 yr					
Case	Male	53(5)	41(5)	7(0)	5 ^b (0)
	Female	17(9)	17(9)	0	0 ^d
Control	Male	106(0)	24(0)	23(0)	59 ^b (0)
	Female	34(0)	7(0)	13(0)	14 ^d (0)

(): HCV RNA, PCR negative or below quantifiable level by Amplicor ^b $P < 0.001$, ^d $P < 0.001$ by χ^2 test.

Table 2 Serum HCV RNA in dialysis patients in the study

Range (KIU/mL)	Group		
	Asymptomatic	Low activities	High activities
<0.5	53	2	0
0.6-100	32	2	1
101-400	48	4	1
401->850 ¹	21	6	9
Total	154	14	11

¹Includes values above 1 000 by Amplicor Version I. Values by branched DNA method were converted to Amplicor values. $P < 0.001$ by χ^2 test.

Table 3 Comparison of the first and second measurements of HCV RNA at intervals longer than 2 years in dialysis patients

Change	Group		
	Asymptomatic	Low activities	High activities
Unchanged (change <50%)	44	1	2
Increased (+ >50%)	25	3	2
Decreased (- >50%)	36	5	2
Total	105	9	6

The initial serum levels of HCV RNA in 179 dialysis patients are given in Table 2. Of the 154 asymptomatic cases, the RNA

level was negative or below the quantifiable level in 53 (34.4%) and below 100 KIU/mL in 32 (20.8%), but the remaining 69 patients had RNA levels greater than 101 KIU/mL. All the 11 dialysis patients with high activities had high levels of RNA. Thus, differences among the three activity groups were significant by the χ^2 test ($P < 0.001$). Serum RNA could be measured twice at an interval of 2 years or longer in 120 patients. The change was less than 50% of the initial level (unchanged) in 44 (41.9%), increased by more than 50% in 25 (23.8%) and decreased by more than 50% in 36 (41.0%) (Table 3). Serum RNA clearly reflected the absence or presence of disease activities. Serum 7S fragment of type IV collagen was measured in 143 dialysis patients (Table 4). The values ranged from 1.8 to 12.0 $\mu\text{g/mL}$ with a mean of 5.59 ng/mL. The mean \pm SD for the asymptomatic group was 5.05 \pm 1.59 ng/mL, 6.21 \pm 1.94 ng/mL for the low activities group and 6.92 \pm 2.63 ng/mL for the high activity group. The differences were significant ($P < 0.05$) by ANOVA.

Table 4 Serum 7S fragment of type IV collagen in dialysis patients

Group	Number of patients	7S IV collagen (ng/mL)
Asymptomatic	118	5.05 \pm 1.59 ^{a,c}
Low activities	14	6.21 \pm 1.94 ^a
High activities	11	6.92 \pm 2.63 ^c
Total	143	5.59

^a $P < 0.05$, ^c $P < 0.05$ by ANOVA.

DISCUSSION

In this study, 189 dialysis patients with HCV infection were followed up for more than 4 years in comparison with 378 sex/age matched nondialysis control patients who were diagnosed as chronic hepatitis C. Disease activities were divided into three grades: asymptomatic, low activities (ALT not exceeding 80 IU/L) and high activities (ALT exceeding 80 IU/L) during the last or latest 4 year period. Of the 189 dialysis patients, 25 were followed up for more than 15 years. They all became asymptomatic after a varying period of elevated and fluctuating ALT, and 15 were HCV RNA negative. In a distinct contrast, the majority of controls who were followed up for a comparable period remained to have high activities (Table 1), and none lost HCV RNA, one quarter to one third of them progressed to cirrhosis. Serum type IV collagen 7S domain was measured in dialysis patients, and the results suggested that fibrogenetic activities increased with high disease activities. These results clearly showed that patients on hemodialysis became much better than nondialysis patients with chronic hepatitis C. No dialysis patients progressed to cirrhosis in this series.

The question is why there is such a distinct difference in the natural history of chronic hepatitis C between dialysis and nonuremic patients. It has been suggested that liver injury caused by HCV infection is mainly through immunologic processes^[13] rather than the virus that is directly cytopathic^[14]. It has been well established that patients with end-stage renal disease and on maintenance hemodialysis have severe immunologic abnormalities with reduced immune responsiveness^[15].

Some of our dialysis patients had a high viral load. RNA levels did not show direct correlation with disease activities, but more asymptomatic cases were RNA negative, and RNA levels tended to decrease in more patients when studied at an interval of 2 years or longer. There have been several studies on viral load in hemodialysis patients, but the results were not consistent. According to Umlauf *et al.*^[16], HCV viremia fluctuated with the time of undetectable RNA. Whereas in the

study of Fabrizi *et al.*^[17], HCV load was low and relatively stable. HCV RNA levels decreased in dialysis patients in another report^[18].

In 1996, we first described the phenomenon in which the number of HCV viral particles decreased after each dialysis procedure and restored to the previous level at the next dialysis^[19]. Subsequently it was found that viral particles were adsorbed onto the dialyzer membrane and destroyed^[20]. Our observations have since been confirmed. According to Furusyo *et al.*^[18], HCV RNA levels were significantly lower in 98 dialysis patients (0.4 mEq/mL) compared with 228 nonuremic patients (2.0 mEq/mL). The dialysis procedure itself might contribute to the reduction of viral load in the long run. Another possible explanation for viral load reduction in dialysis patients was coinfection with another hepatotropic virus^[21]. However, our earlier study in this dialysis center, the rates of infection with hepatitis G virus^[22] and TT virus^[23] were very low. Yokosuka *et al.*^[24] followed up 320 patients with chronic type C liver disease and found that no chronic hepatitis patients were seroconverted, seronegative conversion occurred in 2%, only in end stage cirrhotic patients with or without hepatocellular carcinoma. The difference in the temporal virus load between dialysis and non-dialysis patients was so remarkable that it required biological explanation. It is not known whether C-viruses are able to replicate in liver cells of immunologically compromised dialysis patients as in immunologically competent individuals. Hepatocytes of the dialysis patients might not have normal metabolic and synthetic capabilities under the influence of uremic state, as exemplified by very low AST and ALT levels in serum^[11,12]. Replication of viral particles within hepatocytes might be reduced for the same reason. It seems that the most plausible explanation would be the negative balance between mechanical destruction of viral particles by membrane dialysis procedure and viral replication.

ACKNOWLEDGMENT

The authors express sincere thanks to Dr. Irie Y for his help and support in preparing this manuscript.

REFERENCES

- 1 **Wasley A**, Alter MJ. Epidemiology of hepatitis C: geographic differences and temporal trends. *Semin Liver Dis* 2000; **20**: 1-16
- 2 **Zeldis JB**, Depner TA, Kuramoto IK, Gish RG, Holland OV. The prevalence of hepatitis C virus antibodies among hemodialysis patients. *Ann Intern Med* 1990; **112**: 958-960
- 3 **Okuda K**, Hayashi H, Kobayashi S, Irie Y. Mode of hepatitis C infection not associated with blood transfusion among chronic hemodialysis patients. *J Hepatol* 1995; **23**: 28-31
- 4 **Zacks SL**, Fried MW. Hepatitis B and C and renal failure. *Infect Dis Clin North Am* 2001; **15**: 877-899
- 5 **Sterling RK**, Sanyal AJ, Luketic VA, Stravitz RT, King AL, Post AB, Mills AS, Contos MJ, Shiffman ML. Chronic hepatitis C infection in patients with end stage renal disease. Characterization of liver histology and viral load in patients awaiting renal transplantation. *Am J Gastroenterol* 1999; **94**: 3576-3582
- 6 **Stehman-Breen CO**, Emerson S, Gretch D, Johnson RJ. Risk of death among chronic dialysis patients infected with hepatitis C virus. *Am J Kidney Dis* 1998; **32**: 629-534
- 7 **Akopolat I**, Ozyilkan E, Karagoz F, Akpolat T, Kandemir B. Hepatitis C in haemodialysis and nonuraemic patients: a histopathological study. *Int Urol Nephrol* 1998; **30**: 349-355
- 8 **Okuda K**, Hayashi H, Yokozeki K, Kondo T, Kashima T, Irie Y. Interferon treatment for chronic hepatitis C in haemodialysis patients: suggestions based on a small series. *J Gastroenterol Hepatol* 1995; **10**: 616-620
- 9 **Murawaki Y**, Ikuta Y, Koda M, Kawasaki H. Serum type III procollagen peptide, type IV collagen 7S domain, central triple-

- helix of type IV collagen and tissue inhibitor of metalloproteinase in patients with chronic viral liver disease: relation to liver histology. *Hepatology* 1994; **20**: 780-787
- 10 **Ishibashi K**, Kashiwagi T, Ito A, Tanaka Y, Nagasawa M, Toyama T, Ozaki S, Naito M, Azuma M. Changes in serum fibrogenesis markers during interferon therapy for chronic hepatitis type C. *Hepatology* 1996; **24**: 27-31
- 11 **Wolf PL**, Williams D, Coplon N, Coulson AS. Low aspartate transaminase activity in serum of patients undergoing hemodialysis. *Clin Chim* 1972; **18**: 567-568
- 12 **Yasuda K**, Okuda K, Endo N, Ishiwatari Y, Ikeda R, Hayashi H, Yokozeki K, Kobayashi S, Irie Y. Hypoaminotransferasemia in patients undergoing long-term hemodialysis; clinical and biochemical appraisal. *Gastroenterology* 1995; **109**: 1295-1300
- 13 **Rehermann B**. Interaction between the hepatitis C virus and the immune system. *Semin Liver Dis* 2000; **20**: 127-141
- 14 **Ballardini G**, Groff P, Pontisso P, Giostra F, Francesconi R, Lenzi M, Zauli D, Alberti A, Bianchi FB. Hepatitis C virus (HCV) genotype, tissue HCV antigens hepatocellular expression of HLA-A,B,C, and intercellular adhesion-1 molecules. Clues to pathogenesis of hepatocellular damage, and response to interferon treatment in patients with chronic hepatitis C. *J Clin Invest* 1995; **95**: 2067-2075
- 15 **Decamps-Latscha B**, Herbelin A. Long-term dialysis and cellular immunity: a critical survey. *Kidney Int* 1993; **43**: S135-S142
- 16 **Umlauf F**, Gruenewald K, Weiss G, Kessler H, Urbanek M, Haun M, Santner B, Koenig P, Keeffe EB. Patterns of hepatitis C viremia in patients receiving hemodialysis. *Am J Gastroenterol* 1997; **92**: 73-78
- 17 **Fabrizi F**, Martin P, Dixit V, Brezina M, Cole MJ, Vinson S, Mousa M, Gitnick G. Biological dynamics of viral load in hemodialysis patients with hepatitis C virus. *Am J Kidney Dis* 2000; **35**: 122-129
- 18 **Furusyo N**, Hayashi J, Ariyama I, Sawayama Y, Etoh Y, Shigematsu M, Kashiwagi S. Maintenance hemodialysis decreases serum hepatitis C virus (HCV) RNA levels in hemodialysis patients with chronic HCV infection. *Am J Gastroenterol* 2000; **95**: 490-496
- 19 **Okuda K**, Hayashi H, Yokozeki K, Irie Y. Destruction of hepatitis C virus particles by hemodialysis. *Lancet* 1996; **347**: 909-910
- 20 **Hayashi H**, Okuda K, Yokosuka O, Kobayashi S, Yokozeki K, Ohtake Y, Irie Y. Adsorption of hepatitis C virus particles onto the dialyzer membrane. *Artif Organs* 1997; **21**: 1056-1059
- 21 **Janusz Kiewicz-Lewandowska D**, Wysocki J, Rembowska J, Lewandowski K, Nowak T, Pernak M, Nowak J. Hepatitis G virus co-infection may affect the elimination of hepatitis C virus RNA from the peripheral blood of hemodialysis patients. *Acta Virol* 2001; **45**: 261-263
- 22 **Okuda K**, Kanda T, Yokosuka O, Hayashi H, Yokozeki K, Ohtake Y, Irie Y. GB virus-C infection among chronic haemodialysis patients: clinical implications. *J Gastroenterol Hepatol* 1997; **12**: 766-770
- 23 **Ikeuchi T**, Okuda K, Yokosuka O, Kanda T, Kobayashi S, Murata M, Hayashi H, Yokozeki K, Ohtake Y, Kashima T, Irie Y. Superinfection of TT virus and hepatitis C virus among chronic haemodialysis patients. *J Gastroenterol Hepatol* 1999; **14**: 796-800
- 24 **Yokosuka O**, Kojima H, Imazeki F, Tagawa M, Saisho H, Tamatsukuri S, Omata M. Spontaneous negativation of serum hepatitis C virus RNA is a rare event in type C chronic liver diseases: analysis of HCV RNA in 320 patients who were followed for more than 3 years. *J Hepatol* 1999; **31**: 394-399

Edited by Wang XL and Xu FM

Initial steroid-free immunosuppression after liver transplantation in recipients with hepatitis c virus related cirrhosis

Perdita Wietzke-Braun, Felix Braun, Burckhart Sattler, Giuliano Ramadori, Burckhardt Ringe

Perdita Wietzke-Braun, Giuliano Ramadori, Abteilung für Gastroenterologie und Endokrinologie, Georg-August-Universität, 37075 Göttingen, Germany

Felix Braun, Burckhardt Ringe, Georg-August-Universität, 37075 Göttingen, Germany

Burckhart Sattler, Zentrum Pathologie, Georg-August-Universität, 37075 Göttingen, Germany

Correspondence to: Dr. Perdita Wietzke-Braun, Abteilung für Gastroenterologie und Endokrinologie, Georg-August Universität, Robert-Koch-Str. 40, 37075 Göttingen, Germany. gramado@med.uni-goettingen.de

Telephone: +49-551-39-6301 **Fax:** +49-551-39-8596

Received: 2003-12-09 **Accepted:** 2004-02-24

Abstract

AIM: Steroids can increase hepatitis C virus (HCV) replication. After liver transplantation (LTx), steroids are commonly used for immunosuppression and acute rejection is usually treated by high steroid dosages. Steroids can worsen the outcome of recurrent HCV infection. Therefore, we evaluated the outcome of HCV infected liver recipients receiving initial steroid-free immunosuppression.

METHODS: Thirty patients undergoing LTx received initial steroid-free immunosuppression. Indication for LTx included 7 patients with HCV related cirrhosis. Initial immunosuppression consisted of tacrolimus 2×0.05 mg/kg·d po and mycophenolate mofetil (MMF) 2×15 mg/kg·d po. The tacrolimus dosage was adjusted to trough levels in the target range of 10-15 µg/L during the first 3 mo and 5-10 µg/L thereafter. Manifestations of acute rejection were verified histologically.

RESULTS: Patient and graft survival of 30 patients receiving initial steroid-free immunosuppression was 86% and 83% at 1 and 2 years. Acute rejection occurred in 8/30 patients, including 1 HCV infected recipient. All HCV-infected patients had HCV genotype II (1b). HCV seropositivity occurred within the first 4 mo after LTx. The virus load was not remarkably increased during the first year after LTx. Histologically, grafts had no severe recurrent hepatitis.

CONCLUSION: From our experience, initial steroid-free immunosuppression does not increase the risk of acute rejection in HCV infected liver recipients. Furthermore, none of the HCV infected patients developed serious chronic liver diseases. It suggests that it may be beneficial to avoid steroids in this particular group of patients after LTx.

Wietzke-Braun P, Braun F, Sattler B, Ramadori G, Ringe B. Initial steroid-free immunosuppression after liver transplantation in recipients with hepatitis c virus related cirrhosis. *World J Gastroenterol* 2004; 10(15): 2213-2217

<http://www.wjgnet.com/1007-9327/10/2213.asp>

INTRODUCTION

Liver diseases related to chronic viral hepatitis are the leading

indication for liver transplantation (LTx) worldwide^[1]. Hepatitis B virus and hepatitis C virus (HCV) infection account for the majority of liver diseases related to chronic viral hepatitis. In Europe, 8 422 patients received a liver graft for virus related cirrhosis between January 1988 to December 2000^[2]. Posttransplantation HCV infection is a relatively benign condition during the short-term follow-up and liver recipients reach survival rates similar to other indications. However, the natural history of posttransplantation HCV reinfection is variable. Almost all recipients became HCV seropositive during the first year after LTx. At 5 years posttransplantation, up to 30% of the recipients developed cirrhosis^[3,12]. The patients' immune status seems to be an important factor regarding the progression of fibrosis. The immunosuppressed liver recipients had a higher rate of fibrosis progression per year compared to patients without immunosuppression^[4].

The role of immunosuppressive treatment in the occurrence and severity of HCV reinfection has been discussed controversially^[5]. Since the first liver transplantation performed by Starzl in 1963, corticosteroids have been used traditionally for immunosuppression after organ transplantation due to the lack of other available immunosuppressive drugs^[6]. Nowadays, a variety of potent and selective immunosuppressive drugs are available, thus allowing avoidance of immunosuppressive drugs with unselective mode of action or unfavorable side effects^[7]. Corticosteroids have a well described spectrum of adverse effects including metabolic changes and an increased risk of cardio-vascular diseases. Also, corticosteroids have an unselective immunosuppressive mode of action. Furthermore, corticosteroids increased HCV replication *in vitro* and *in vivo*^[8-10]. After liver transplantation, high early HCV-RNA levels could be associated with more severe recurrence of hepatitis^[11]. Prieto *et al.* reported positive relationships between the number of rejection episodes, methylprednisolone (MP) boluses, treatment of rejection, cumulative dose of steroids and the development of HCV cirrhosis^[12]. These findings implicated that prevention of acute cellular rejection and avoidance of high-dose or maintenance steroids could be beneficial^[5], however, the experience with completely steroid-free immunosuppression after LTx is still limited.

Recently, we published a series of 30 patients receiving steroid-free immunosuppression that consisted of tacrolimus and mycophenolate mofetil (MMF)^[13]. Since the hypothesis that steroid-free immunosuppression might be particularly beneficial in HCV infected liver recipients, we analyzed this subgroup of liver recipients with regard to the risk of acute rejection, and development of serious HCV related liver disease in the graft.

MATERIALS AND METHODS

Patients

Thirty adult patients underwent LTx between June 1996 and January 1999. The detailed characteristics have been previously described^[13]. The indications for LTx included hepatitis C virus related cirrhosis in seven recipients. The HCV patients included 4 females and 3 males with a median (range) age of 58(43-62) years. HCV-RNA was seropositive prior to transplantation with a

median (range) viral load of $10^4(10^3-10^5)$ genome equivalent/mL. The serum HCV-specific RNA was detected by reverse transcription (RT)/polymerase chain reaction (PCR) as previously described by Mihm *et al.*^[14]. HCV genotype was classified as II (1b) in all seven patients according to Okamoto *et al.* and Simmonds *et al.*^[15,16]. Child-Turcotte-Pugh Score prior to LTx was Child A in 2, Child B in 2 and Child C in 3 patients. Four of the patients had a coexisting hepatocellular carcinoma.

Methods

Apart from an intravenous (IV) bolus of 500 mg MP before reperfusion of the graft, recipients received no further steroids. Tacrolimus (Prograf, Fujisawa GmbH, München, Germany) was started 6 h after reperfusion at an oral dosage of 2×0.05 mg/kg-d. Thereafter, tacrolimus dosages were adjusted to a target range of 10-15 μ g/L during the first three months and 5-10 μ g/L after the third month after LTx. Tacrolimus trough levels were measured by a microparticle enzyme immunoassay (Prograf-MEIA II, Abbott Laboratories, Chicago, IL, USA). MMF (Cell Cept, Hoffmann-La Roche, Grenzach-Wyhlen, Germany) was given orally starting from the first postoperative day (pod) at a body mass adjusted dosage of 2×15 mg/kg-d. Liver biopsies were performed routinely on d 7, after 6 mo, every year, and whenever clinically indicated. Acute rejection was defined as abnormal liver function tests, histological changes as graded by the Banff classification, and the necessity for therapy^[12]. Treatment of acute rejection consisted of IV-MP boluses of 500 mg over a period of 3-5 d with or without additional prednisolone tapering. Combined antiviral therapy consisting of interferon alfa and "low-dose" ribavirin was used in patients with HCV reinfection accompanied by chronic active hepatitis as described previously by Wietzke *et al.*^[17,18].

Statistical analysis

Actual survival was calculated by the Kaplan-Meier method.

RESULTS

Patient and graft survival

Twenty-two of the 30 patients receiving initial steroid-free immunosuppression have been alive after a median (range) follow-up of 1 386(44-2 037) d. Actual patient survival was 86.7% at 2 years and 73.3% at 5 years (Figure 1A). The actual patient survival of HCV-infected recipients was 85.7% at 2 years and 57.1% at 5 years, the difference was not statistically significant (Log-rank test (Cox-Mantel): $P=0.33$) (Figure 1B).

At present, four of the seven HCV infected liver recipients have been alive with a median (range) follow-up of 47(46-60)

mo after LTx. None of the deaths in the HCV patients was related to HCV reinfection. The causes of the 3 deaths were chronic graft dysfunction (CDF) on pod 164, heart failure due to preexisting toxic cardiomyopathy on pod 774, and a *de-novo* ovarian carcinoma on pod 950. One of the seven patients with HCV-related cirrhosis underwent successful retransplantation for primary nonfunction (PNF) on day 5 (Table 1).

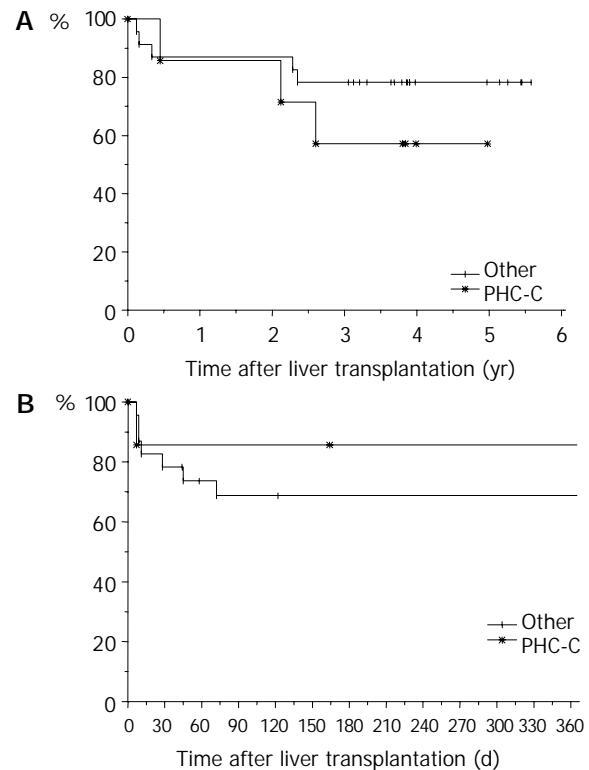


Figure 1 A: Actual patient survival according to primary indication (HCV related cirrhosis vs others) of liver recipients receiving steroid-free immunosuppression. B: Actual rejection free interval according to primary indication (HCV related cirrhosis vs others) during the first year after LTx in liver recipients receiving steroid-free initial immunosuppression.

Acute rejection episodes and immunosuppression

In total, 8 of the 30 liver recipients (26.2%) had an episode of acute rejection. The onset of acute rejection was between pod 7 and 72. The median (range) grade of acute rejection was 5.5(3-8) according to Banff classification. Low tacrolimus trough levels associated with diarrhea were observed in five of the eight recipients with acute rejection. Also, diarrhea was

Table 1 Characteristics of liver recipients with HCV-infection receiving initial steroid-free immunosuppression

#	Gender (M/F)	Rge (yr)	Child Class	HCC	HCV genotype	HCV viral load				Liver histology	Outcome (pod)
						prior	1 mo	4 mo	1 yr		
5	f	60	C	no	II (1b)	10^4	10^5	10^4	10^5		died (950), ovarian-ca
9	f	62	B	no	II (1b)	10^5	10^5	10^6	10^5	AR, hepatitis (+/-)	alive (1817), reLTx (5)
12	m	57	A	yes	II (1b)	10^5	10^5	10^4			died (774), heart failure
13	f	59	C	yes	II (1b)	10^5	10^5	10^5		hepatitis (+/-), fibrosis (+)	alive (1456)
19	m	58	B	yes	II (1b)	10^4	10^3		10^4	hepatitis (+)	alive (1402)
20	m	46	A	yes	II (1b)	10^3		10^4	10^4		alive (1389)
25	f	43	C	no	II (1b)	10^4	10^4	10^5			died, CDF (164)

Abbreviations: # (patient number), HCC (hepatocellular carcinoma), HCV (hepatitic C virus), pod (postoperative day), yr (year), mo (mo), prior (prior to LTx), AR (acute rejection), +/-/+/-/+/-/+/- (minimal/moderate/severe/reversed), reLTx (liver retransplantation), CDF (chronic graft dysfunction).

the predominant adverse effect when tacrolimus and MMF were given simultaneously. All acute rejection episodes completely resolved after IV-MP boluses and four of the patients with rejection episodes received additional steroid taper. In the further postoperative course, there was no graft loss due to rejection and all of these patients have been alive. Only one of the eight patients with acute rejection had HCV-related cirrhosis. This patient underwent retransplantation on pod 5 for PNF. Until retransplantation, immunosuppression was temporarily discontinued and the patient suffered from diarrhea, thus tacrolimus trough levels were low.

Only 3 of the 7 HCV patients received steroids after LTx, two in conjugation with tacrolimus first and then cyclosporine (CyA), and one for acute rejection. One patient was reconverted to tacrolimus after suspicion of CDF. MMF was intermittently discontinued in all 7 patients and withdrawn in 5 patients. The cause of MMF withdrawal was diarrhea in 3 patients and conversion to CyA in 2 patients. Maintenance immunosuppression in the HCV infected recipients consisted of tacrolimus monotherapy in 3 patients, tacrolimus/MMF in 2 patients, tacrolimus/prednisolone in 1 patient, and CyA/prednisolone in 1 patient.

HCV reinfection

All 7 HCV infected patients had HCV genotype II (1b). Recurrence of HCV-RNA in serum occurred within 4 mo after LTx in all seven liver recipients with HCV-related cirrhosis. Prior to LTx the median viral load was 10^4 (10^3 - 10^5) genome equivalent/mL. During the first four months, the viral load ranged from 10^3 to 6.5×10^5 genome equivalent/mL. The virus load was not markedly increased during the first year after LTx (Figure 2). Histologically, only 1 HCV patient had suspicion of minimal portal hepatitis in the most recent biopsy that occurred 15 mo after LTx and transaminases were within normal values (Table 1). Five months after LTx, another recipient had elevated transaminases (AST 55, ALT 109 U/L), suspicion of portal hepatitis and mild fibrosis in the graft. Combination therapy with subcutaneous interferon alfa-2a 3 MU three times per week and oral ribavirin 10 mg/kg body mass in three divided doses per day was given for 6 mo. At the end of treatment, the patient had transaminases within normal values (AST 9, ALT 12 U/L), and histological improvement without fibrosis, but positive serum HCV-RNA. A third recipient developed suspicion of minimal portal hepatitis and fibrosis associated with a reduction of small bile ducts. Liver histology improved after reintroduction of MMF. Initially, this patient underwent retransplantation for PNF and acute rejection was resolved.

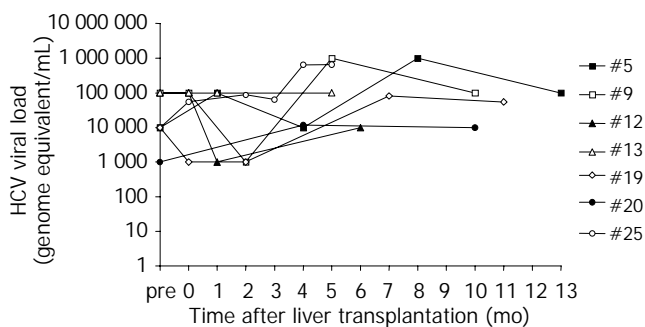


Figure 2 Serum virus concentration in seven HCV infected recipients during the first year after LTx. All patients received initial steroid-free immunosuppression.

DISCUSSION

Although steroids are known to increase HCV replication^[8],

they are given routinely for prophylaxis and treatment of rejection after solid organ transplantation. The potential risk of acute rejection must be faced against the benefit of steroid withdrawal. After LTx, HCV infection has been clearly identified as a risk factor for the development of early acute rejection^[19]. On the other hand, the presence, number, and treatment of acute rejections were found to be associated with the histologic recurrence of HCV infection after LTx^[20,21]. In 96 liver recipients, histologic recurrence of HCV infection occurred in 18% without acute rejection, 42% with one acute rejection episode, and 70% with more than one episode of acute rejection^[21]. In liver recipients, MP treatment for acute rejection was found to increase serum HCV RNA between 4 to 100 fold^[8]. OKT3, used for treatment of steroid-resistant rejection after LTx, was associated with more severe recurrences^[20]. The mutual relation between treatment of acute rejection and recurrence of HCV-infection after LTx sets the stage for a completely steroid-free immunosuppressive protocol.

Recently, it was clearly demonstrated that steroid-free immunosuppression after LTx was feasible and safe^[13,22-24]. The different immunosuppressive regimens consisted of CyA/azathioprine (Aza)^[23], CyA or tacrolimus monotherapy^[22], CyA/rapamycin, rapamycin monotherapy^[24], and tacrolimus/MMF^[13]. The reported rates of acute rejection were 65% for CyA and 66% for tacrolimus monotherapy^[22]. The combination of CyA/Aza resulted in 80% of acute rejection, but only 9% of acute rejections required treatment. Compared to patients receiving CyA/Aza/prednisone, the incidence and severity of rejection were similar in both groups but the dynamics of virus replication of HCV-RNA was faster among those treated with prednisone. The 2 year survival rate was 70.2% with prednisone and 78.3% without prednisone^[23]. The rate of acute rejection using rapamycin/CyA was 28% and with sirolimus monotherapy 75%^[24].

We reported that complete avoidance of corticosteroids after LTx could be performed without an increased risk of mortality, morbidity, and severe acute rejection. The rate of acute rejection with the use of tacrolimus in combination with MMF was only 26.2%^[13]. This rate of acute rejections might even be reduced, if underimmunosuppression were avoided. Low tacrolimus trough levels were observed in patients with diarrhea when tacrolimus and MMF were given simultaneously. Diarrhea could be avoided after introduction of a two hour dosing interval between tacrolimus and MMF administration^[13,25]. Therefore, the rate of acute rejections might be lower if tacrolimus and MMF are administered with a dosing interval.

In our present study, only 1 HCV patient developed acute rejection. This patient had a complicated clinical course with PNF, retransplantation, temporary discontinuation of immunosuppression, acute rejection, and received MP boluses as well as intermittent steroids until pod 255. Reinfection with HCV was noticed in all seven patients. Within 4 mo after LTx, all seven patients were HCV seropositive. Compared to the pretransplant HCV load, there was no significant increase during the first year after LTx. Also, liver histology was completely unsuspecting in 4 HCV patients. Three patients had suspicion of minimal portal hepatitis which was followed up by frequent biopsies in one patient. Another patient with supposed minimal portal hepatitis and additional mild fibrosis received combination therapy which improved transaminases and histology^[17]. Also, one patient with previous retransplantation developed portal hepatitis and fibrosis. MMF was reintroduced for reduction of small bile ducts, minimal portal hepatitis and fibrosis and resulted in histological improvement. None of the HCV infected patients developed serious chronic liver disease. However, one patient died of CDF which was related to underimmunosuppression after conversion to CyA for

suspicion of tacrolimus induced neurotoxicity. From our limited experience with the small number of patients, the avoidance of steroids did not alter the posttransplant HCV reinfection in serum and the histological alterations were mild despite all patients had HCV genotype II (1b). Feray *et al.* reported that HCV genotype II (1b) was a risk factor for recurrent hepatitis^[26,27]. However, the influence of HCV genotype II (1b) has been controversial. Gordon *et al.* reported a similar frequency of recurrent hepatitis with all HCV genotypes, but HCV genotype II (1b) was associated with a higher rate of cirrhosis^[28]. Thus, the avoidance of steroids seems to be beneficial for liver recipients with HCV genotype II (1b).

Hitherto, it remains unclear which immunosuppressive regimen is best for HCV liver recipients. MMF was discussed controversially in liver transplant recipients with HCV^[29]. In a recent prospective randomized trial comparing tacrolimus/prednisolone with tacrolimus/MMF/prednisolone in liver recipients with HCV, MMF had no impact on patient and graft survival, rejection or rate of HCV recurrence^[30]. However, MMF might reduce the frequency of acute rejection and therefore exposure to steroids^[31]. Our intention was to use a safe steroid-free immunosuppressive regimen. Tacrolimus is a potent immunosuppressive drug, but impairment of renal function might limit the use of tacrolimus especially during the early phase after LTx. Thus, we used a combination of tacrolimus and MMF which resulted in a low frequency of acute rejection^[13]. However, the combination of tacrolimus and MMF could cause diarrhea or other side effects that often required discontinuation or withdrawal of MMF. Thus, therapeutic drug monitoring of tacrolimus is an essential requirement for the combination of tacrolimus and MMF. Alternatively, anti-IL-2 receptor antibodies might have potential in steroid-free regimens. The use of anti-IL-2 receptor antibodies reduces the frequency of acute rejection after LTx, but there has been limited experience with HCV infection when anti-IL-2 receptor antibodies are given for induction of immunosuppression. Most recently, two immunosuppressive protocols using daclizumab have been reported with controversial results regarding HCV infection. Tacrolimus/MMF was compared with daclizumab/tacrolimus/MMF in a randomized open-label study and corticosteroids were eliminated 24 h after LTx in both arms. Steroids could be avoided safely after pod 1 and HCV recurrence was documented in 2 patients who did not receive daclizumab^[32]. In a group of 21 HCV infected liver recipients receiving daclizumab, MMF, and steroids for induction of immunosuppression, patients with HCV infection administered daclizumab were more likely to have an earlier onset of hepatitis, jaundice and greater histological activity compared with a well-matched HCV control group. Also, recurrent hepatitis progressed more rapidly in the daclizumab group. Nelson *et al.* concluded that daclizumab in combination with MMF might be associated with early recurrence of HCV and more rapid histological progression of disease in the early period after LTx^[33]. Also, triple and double immunosuppressive regimens had a higher rate of fibrosis and cirrhosis in HCV infected patients compared to monotherapy^[34,35]. These findings implicate that strenuous induction protocols should be avoided in HCV infected liver recipients.

As proposed by some centers, early withdrawal or avoidance of steroids in HCV infected patients could be beneficial. From our experience with the limited number of HCV infected liver recipients, initial steroid-free immunosuppression is safe, has a low risk of acute rejection without a need for high-dose steroids and high cumulative steroid dosages, which are likely to induce less severe HCV reinfection. Furthermore, none of the HCV infected patients developed serious chronic liver diseases. Therefore, it is high time to seriously reconsider the use of any steroids in liver transplantation especially for HCV-

infection patients and to prove this approach in a large randomized controlled trial.

REFERENCES

- Rosen HR. Hepatitis B and C in the liver transplant recipient: current understanding and treatment. *Liver Transplant* 2001; **7** (11 Suppl 1): S87-98
- European Liver Transplant Registry. <http://www.eltr.org>
- Gane EJ, Naoumov NV, Qian KP. A longitudinal analysis of hepatitis C virus replication following liver transplantation. *Gastroenterology* 1996; **110**: 167-177
- Berenguer M, Ferrell L, Watson J. HCV-related fibrosis progression following liver transplantation: increase in recent years. *J Hepatol* 2000; **32**: 673-684
- Samuel D, Feray C. Recurrence of hepatitis C virus infection after liver transplantation. *J Hepatol* 1999; **31**(Suppl 1): 217-221
- Starzl TE, Waddell WR, Marchioro TL. Reversal of rejection in human renal homografts with subsequent development of homograft tolerance. *Surg Gyn Obst* 1963; **117**: 385
- Braun F, Lorf T, Ringe B. Update of current immunosuppressive drugs used in clinical organ transplantation. *Transplant Int* 1998; **11**: 77-81
- Gane EJ, Portmann BC, Naoumov NV. Long-term outcome of hepatitis C infection after liver transplantation. *N Engl J Med* 1996; **334**: 815-820
- Magy N, Cribier B, Schmitt C. Effects of corticosteroids on HCV infection. *Int J Immunopharmacol* 1999; **21**: 253-261
- McHutchinson JG, Ponnudurai R, Bylund DL. Prednisone withdrawal followed by interferon alpha for treatment of chronic hepatitis C infection. *J Clin Gastroenterol* 2001; **32**: 133-137
- Sreekumar R, Gonzalez-Koch A, Maor-Kendler Y. Early identification of recipients with progressive histologic recurrence of hepatitis C after liver transplantation. *Hepatology* 2000; **32**: 1125-1130
- Prieto M, Berenguer M, Rayón JM. High incidence of allograft cirrhosis in hepatitis C virus genotype 1b following transplantation: relationship with rejection episodes. *Hepatology* 1999; **29**: 250-256
- Ringe B, Braun F, Schütz E. A novel management strategy of steroid-free immunosuppression after liver transplantation: efficacy and safety of tacrolimus and mycophenolate mofetil. *Transplantation* 2001; **71**: 508-515
- Mihm S, Hartmann H, Ramadori G. A reevaluation of the association of hepatitis C virus replication intermediates with peripheral blood cells including granulocytes by a tagged reverse transcription/polymerase chain reaction technique. *J Hepatol* 1996; **24**: 491-497
- Okamoto H, Tokita H, Sakamoto M, Horikita M, Kojima M, Iizuka H. Characterization of the genomic sequence of type V (or 3a) hepatitis C virus isolates and PCR primer for specific detection. *J Gen Virol* 1993; **74**: 2385-2390
- Simmonds P, Mc Omish F, Yap PL, Chan SW, Lin CK, Duscheiko G. Sequence variability in the 5'-noncoding region of hepatitis C virus: identification of a new virus type and restrictions on sequence diversity. *J Gen Virol* 1993; **74**: 661-668
- Wietzke P, Braun F, Ringe B, Ramadori G. Interferon alpha-2a and ribavirin therapy for hepatitis C recurrence after liver transplantation. *Transplant Proc* 2000; **32**: 2539-2542
- Wietzke-Braun P, Meier V, Braun F, Ramadori G. Combination of "low-does" ribavirin and interferon alpha-2a therapy followed by interferon alpha-2a monotherapy in chronic HCV-infected non-responders and relapsers after interferon alpha-2a monotherapy. *World J Gastroenterol* 2001; **7**: 222-227
- Gómez-Manero N, Herrero JI, Quiroga J, Sangro B, Pardo F, Cienfuegos JA, Prieto J. Prognostic model for early acute rejection after liver transplantation. *Liver Transplantation* 2001; **7**: 246-254
- Rosen HR, Shackleton CR, Higa L. Use of OKT3 is associated with early and severe recurrence of hepatitis C after liver transplantation. *Am J Gastroenterol* 1997; **92**: 1453
- Sheiner PA, Schwartz ME, Mor E. Severe or multiple rejection episodes are associated with early recurrence of hepatitis C after orthotopic liver transplantation. *Hepatology* 1995; **21**: 30

- 22 **Rolles K**, Davidson BR, Burrhoughs AK. A pilot study of immunosuppressive monotherapy in liver transplantation: tacrolimus versus microemulsified cyclosporin. *Transplantation* 1999; **68**: 1195
- 23 **Tisone G**, Angelico M, Palmieri G. A pilot study on the safety and effectiveness of immunosuppression without prednisone after liver transplantation. *Transplantation* 1999; **67**: 1308-1313
- 24 **Watson CJE**, Friend PJ, Jamieson NV, Frick TW, Alexander G, Gimson AE, Calne R. Sirolimus: A potent new immunosuppressant for liver transplantation. *Transplantation* 1999; **67**: 505-509
- 25 **Braun F**, Canelo R, Schütz E. How to handle Mycophenolate Mofetil in combination with Tacrolimus? *Transplant Proc* 1998; **30**: 4094-4095
- 26 **Feray C**, Caccamo L, Graeme J. European collaborative study on factors influencing outcome after liver transplantation for hepatitis C. *Gastroenterology* 1999; **117**: 619
- 27 **Feray C**, Gigou M, Samuel D. Influence of the genotypes of hepatitis C virus on the severity of recurrent liver disease after liver transplantation. *Gastroenterology* 1995; **108**: 1088
- 28 **Gordon FD**, Poterucha JJ, Germer J. Relationship between hepatitis C genotype and severity of recurrent hepatitis C after liver transplantation. *Transplantation* 1997; **63**: 1419
- 29 **Charlton MR**. Mycophenolate and hepatitis C: salve on a wound or gasoline on a fire? *Liver Transplant* 2002; **8**: 47-49
- 30 **Jain A**, Kashyap R, Demetris AJ, Eghstesad B, Pokharna R, Fung JJ. A prospective randomized trial of mycophenolate mofetil in liver transplant recipients with hepatitis C. *Liver Transplant* 2002; **8**: 40-46
- 31 **Wiesner RH**, Rabkin J, Klintmalm G. A randomized double-blind comparative study of mycophenolate mofetil and azathioprine in combination with cyclosporine and corticosteroids in primary liver transplant recipients. *Liver Transplant* 2001; **7**: 442-450
- 32 **Washburn K**, Speeg KV, Esterl R. Steroid elimination 24 hours after liver transplantation using daclizumab, tacrolimus, and mycophenolate mofetil. *Transplantation* 2001; **72**: 1675-1679
- 33 **Nelson DR**, Soldevila-Pico C, Reed A. Anti-Interleukin-2 receptor therapy in combination with mycophenolate mofetil is associated with more severe hepatitis C recurrence after liver transplantation. *Liver Transpl* 2001; **7**: 1064-1070
- 34 **Papatheodoridis GV**, Davies S, Dhillon AP. The role of different immunosuppression in the long-term histological outcome of HCV reinfection after liver transplantation for HCV cirrhosis. *Transplantation* 2001; **72**: 412-418
- 35 **International Panel**. Banff schema for grading liver allograft rejection. *Hepatology* 1997; **25**: 658-63

Edited by Zhu LH Proofread by Xu FM

Genotype and phylogenetic characterization of hepatitis B virus among multi-ethnic cohort in Hawaii

Mayumi Sakurai, Fuminaka Sugauchi, Naoky Tsai, Seiji Suzuki, Izumi Hasegawa, Kei Fujiwara, Etsuro Orito, Ryuzo Ueda, Masashi Mizokami

Mayumi Sakurai, Fuminaka Sugauchi, Seiji Suzuki, Izumi Hasegawa, Kei Fujiwara, Masashi Mizokami, Department of Clinical Molecular Informative Medicine, Nagoya City University Graduate School of Medical Sciences, Nagoya 467-8601, Japan

Etsuro Orito, Ryuzo Ueda, Department of Clinical Internal Medicine and Molecular Science, Nagoya City University Graduate School of Medical Sciences, Nagoya 467-8601, Japan

Naoky Tsai, Division of Gastroenterology, John A. Burns School of Medicine, University of Hawaii, USA

Correspondence to: Dr. Masashi Mizokami, Department of Clinical Molecular Informative Medicine, Nagoya City University Graduate School of Medical Sciences, Kawasumi, Mizuho, Nagoya 467-8601, Japan. mizokami@med.nagoya-cu.ac.jp

Telephone: +81-52-853-8292 **Fax:** +81-52-842-0021

Received: 2003-10-08 **Accepted:** 2004-04-15

Abstract

AIM: Hepatitis B virus (HBV) genomes in carriers from Hawaii have not been evaluated previously. The aim of the present study was to evaluate the distribution of HBV genotypes and their clinical relevance in Hawaii.

METHODS: Genotyping of HBV among 61 multi-ethnic carriers in Hawaii was performed by genetic methods. Three complete genomes and 61 core promoter/precore regions of HBV were sequenced directly.

RESULTS: HBV genotype distribution among the 61 carriers was 23.0% for genotype A, 14.7% for genotype B and 62.3% for genotype C. Genotypes A, B and C were obtained from the carriers whose ethnicities were Filipino and Caucasian, Southeast Asian, and various Asian and Micronesian, respectively. All cases of genotype B were composed of recombinant strains with genotype C in the precore plus core region named genotype Ba. HBeAg was detected more frequently in genotype C than in genotype B (68.4% vs 33.3%, $P < 0.05$) and basal core promoter (BCP) mutation (T1762/A1764) was more frequently found in genotype C than in genotype B. Twelve of the 38 genotype C strains possessed C at nucleotide (nt) position 1858 (C-1858). However there was no significant difference in clinical characteristics between C-1858 and T-1858 variants. Based on complete genome sequences, phylogenetic analysis revealed one patient of Micronesian ethnicity as having C-1858 clustered with two isolates from Polynesia with T-1858. In addition, two strains from Asian ethnicities were clustered with known isolates in carriers from Southeast Asia.

CONCLUSION: Genotypes A, B and C are predominant types among multi-ethnic HBV carriers in Hawaii, and distribution of HBV genotypes is dependent on the ethnic background of the carriers in Hawaii.

Sakurai M, Sugauchi F, Tsai N, Suzuki S, Hasegawa I, Fujiwara K, Orito E, Ueda R, Mizokami M. Genotype and phylogenetic characterization of hepatitis B virus among multi-ethnic cohort

in Hawaii. *World J Gastroenterol* 2004; 10(15): 2218-2222
<http://www.wjgnet.com/1007-9327/10/2218.asp>

INTRODUCTION

Hepatitis B virus (HBV) is one of the major causes of chronic liver diseases including chronic hepatitis, liver cirrhosis (LC) and hepatocellular carcinoma (HCC)^[1]. HBV has been classified into 7 genotypes from A to G based on a sequence divergence of 8% or greater of the entire genome sequences^[2-5]. The genotypes of HBV have distinct geographical distributions, which have been associated with anthropologic history^[6,7].

Recently, genotypes of HBV have been reported to be an influential factor in the clinical manifestation of chronic liver disease in the host. Genotype A is associated with chronic liver disease more frequently than genotype D in Europe^[8]. Genotype C induces more severe liver disease than genotype B found in Asia^[9,10]. Furthermore, it was reported that genotype B had two subgroups^[11], and these subgroups influence the clinical manifestations of liver disease in these patients^[12].

Hawaii has a large Asian American and Pacific Islander population. Many people have emigrated from various countries in Asia and the Pacific Basin, where HBV infection is endemic. Indeed, the estimated rate of HBV carriers in Hawaii ranges from 1.7% to 3%^[13,14], higher than 0.5% of the mainland of United States. However, there has been no information on genotype distribution and sequences of HBV in multi-ethnic carriers in Hawaii.

The aim of this study was to evaluate the HBV genotypes among 61 multi-ethnic carriers in Hawaii by genetic method, and to determine the influences of HBV genotypes on the clinical characteristics.

MATERIALS AND METHODS

Patients

A total of 61 serum samples with HBsAg-positive were collected from patients with HBV infection who admitted St. Francis Medical Center in Honolulu, Hawaii between 1995 and 2000. All the patients were classified into 4 clinical groups: a symptomatic carriers (ASC) ($n=14$) who had no subjective symptoms and had consistently normal serum alanine aminotransferase (ALT) levels for at least 1 year, patients ($n=39$) with chronic liver disease and persistently elevated serum ALT levels, such as those with chronic hepatitis (CH); patients with liver cirrhosis (LC) ($n=4$), and patients with hepatocellular carcinoma (HCC) ($n=4$). A clinical diagnosis was made on the basis of serum biochemical examination, ultrasonography, computerized tomography and liver biopsy performed as required. Patients coinfecting with hepatitis C virus or human immunodeficiency virus were excluded. No patients received antiviral treatment during the follow-up period. The study protocol was approved by the Ethics Committees of the participating institutions in accordance with the 1975 Declaration in Helsinki. Informed consent was obtained from each patient prior to any study related procedures.

Genotyping of HBV

The serum samples were stored at -20 °C until assay was performed. Serum DNA was extracted from 100 µL of serum using a DNA extractor kit (Genome Science Laboratory, Fukushima, Japan). The genotypes of HBV were determined by enzyme-linked immunosorbent assay (ELISA) (HBV GENOTYPE EIA, Institute of Immunology Co., Ltd., Tokyo, Japan) with monoclonal antibodies that are type-specific to epitope in the preS2-region product^[15]. If the result of ELISA was indeterminate, the genotypes were detected by restriction fragment length polymorphism (RFLP), as previously described^[16]. Genotype B was classified into 2 subgroups, “Ba” which has a recombinant sequence of genotype C in the precore/core region, or “Bj” which does not have it, by the method reported previously^[12]. Genotype G of HBV was detected by PCR with hemi-nested primers deduced from the unique insertion of 36 nucleotides (nt) in the core gene that is specific to this genotype^[17].

Sequencing of HBV genome

Three complete genomes and 61 core promoter/precore regions of HBV were amplified by polymerase chain reaction with several primer sets, as previously described^[18]. Amplified HBV DNA fragments were sequenced directly by dideoxy sequencing using a Taq Dye Deoxy Terminator cycle sequencing kit with a fluorescent 3100 DNA sequencer (Applied Biosystems, Foster City, CA, USA). These nucleotide sequences were deposited in the DDBJ/EMBL/GenBank databases under the accession numbers AB105172- AB105174.

Molecular evolutionary analysis of HBV

The pairwise nucleotide sequences were aligned using the CLUSTAL W program^[19]. The genetic distances were calculated with the 6-parameter method, and the phylogenetic tree was constructed by the neighbor-joining method^[20] using

ODEN program (version 1.1.1)^[21]. To confirm the reliability of the phylogenetic tree, bootstrap resampling tests were performed 1 000 times. Reference sequences of HBV, shown as accession numbers, were obtained from the DDBJ/EMBL/GenBank database.

Statistical analyses

Statistical differences were evaluated using the Mann-Whitney nonparametric test, the Fisher's exact probability test and the Student's *t*-test where appropriate. Differences were considered significant for a *P*-value less than 0.05.

RESULTS

Genotypes of HBV

The distribution of HBV genotypes among 61 multi-ethnic carriers in Hawaii was 14(23.0%) for genotype A, 9(14.7%) for genotype B and 38(62.3%) for genotype C. All the 9 genotype B strains were found to be Ba that has a recombinant sequence of genotype C in precore/core region. Genotypes D, E, F and G were not found in this study.

Comparison with clinical characteristics among HBV genotypes

Clinical and serological characteristics were compared among the patients infected with genotypes A, B and C (Table 1). Patients with HBV genotype A were of Filipino (*n*=10), Caucasian (*n*=3) and Polynesian (*n*=1) ethnicities. Genotype B was found in patients of Chinese (*n*=4), Taiwanese (*n*=2), Vietnamese (*n*=2), and Hawaiian/Chinese (*n*=1) ethnicities. Genotype C was found in the patients whose ethnic backgrounds were various Asian (*n*=33), Micronesian (*n*=3), and Caucasian (*n*=2). There were no significant differences in terms of the age, gender, serum AST, ALT, ALP, γ -GTP and the clinical stages of liver disease among them. The proportion of HBeAg positive-phenotype in patients with genotypes A, B

Table 1 Comparison of clinical backgrounds in carriers with HBV genotypes A, B and C

Features	Genotype <i>n</i> (%)			
	A (<i>n</i> =14)	B (<i>n</i> =9)	C (<i>n</i> =38)	
Age (mean±SD, yr)	49.1±14.5	46.9±13.0	43.0±11.9	
Gender (male:female)	10:4	4:5	21:17	
Race	Asian			
	Mainland Chinese	0(0)	5(33)	10(67)
	Philippine	10(83)	0(0)	2(17)
	Taiwanese	0(0)	2(50)	2(50)
	Hong Kong	0(0)	0(0)	8(100)
	Vietnamese	0(0)	2(40)	3(60)
	Korean	0(0)	0(0)	7(100)
	Japanese	0(0)	0(0)	1(100)
	Micronesian	0(0)	0(0)	3(100)
	Polynesian	1(100)	0(0)	0(0)
Caucasian	3(60)	0(0)	2(40)	
Liver disease	ASC	2(14)	3(33)	9(24)
	CH	10(71)	5(56)	24(63)
	LC	2(14)	1(11)	1(3)
	HCC	0(0)	0(0)	4(11)
	HBeAg (+)	8(57)	3(33) ^a	26(68) ^a
Laboratory finding	AST (U/L)	63.3±42.2	56.6±58.7	54.7±81.9
	ALT (U/L)	41.4±31.6	34.8±27.0	37.3±59.7
	ALP (U/L)	359.9±139.4	287.3±140.2	328.0±166.2
	γ -GTP (U/L)	121.0±121.3	55.9±37.2	66.8±103.0

^a*P*<0.05 between genotypes B and C. ASC: Asymptomatic carrier; CH: Chronic hepatitis; LC: Liver cirrhosis; HCC: Hepatocellular carcinoma; ALT: Alanine aminotransferase; AST: Aspartate aminotransferase; ALP: Alkaline phosphatase; γ -GTP: γ -glutamyl transpeptidase.

and C was 57.1%, 33.3% and 68.4% respectively, with a significant difference observed between genotypes B and C ($P < 0.05$). HCC was found in 10.5% of patients with genotype C.

Comparison with core promoter/precore sequences

The frequency of mutation in core promoter (nt 1762/1764) and precore (nt 1858 and nt 1896) region was compared among genotypes A, B and C (Table 2). No significant differences in the frequency of the core promoter mutants were found among genotypes A, B and C (21.4%, 44.4%, and 57.9% respectively). Precore stop mutation (A-1896) was detected in genotypes B and C (33.3% and 21.1%) but not detected in genotype A. Sequence analysis of the mutation at nt 1858 in the precore region showed that all genotype B strains and 68% of genotype C strains possessed a T nucleotide (T-1858). In contrast, all genotype A strains had a C nucleotide in this region (C-1858).

HBV genotype C with C-1858 or T-1858

In order to clarify the significance of nucleotide variety (C or T) at nt 1858 in clinical and virological characteristics, 12 genotype C strains with C-1858 were compared to that of 26 strains of

genotype C with T-1858 (Table 3). All strains of both groups were obtained only from carriers whose ethnic background is Asian. HBeAg positive-phenotype was more frequent in genotype C patients with C-1858 than in those with T-1858 (83.3% vs 61.5%). The precore stop mutation (A-1896) was found in 30.8% (8/26) of those with genotype C with nucleotide T-1858, but not in those subjects with the C-1858 nucleotide. There were no significant differences in frequencies in terms of the age, gender, serum AST, ALT, ALP, γ -GTP and the clinical stages of liver disease and BCP mutation between them.

Phylogenetic analysis

To clarify the phylogenetic characterization of genotype C with C-1858, the complete genome of three HBV strains in carriers was sequenced. These subjects were from Micronesia (HI-1), Hong Kong (HI-2) and Vietnam (HI-3). Molecular evolutionary analysis was also conducted (Figure 1). Of them, one strain (HI-1) was clustered into a subgroup of genotype C with T-1858 from Polynesian with significant bootstrap values. The HI-2 and HI-3 strains were clustered into a subgroup of genotype C from Thailand and Vietnam, and separated from

Table 2 Comparison of core promoter/precore sequences between genotypes A, B and C

Mutation		Genotype <i>n</i> (%)		
		A (<i>n</i> =14)	B (<i>n</i> =9)	C (<i>n</i> =38)
CP mutation	Double mutation	3(21)	4(44)	22(58%)
PC mutation	nt 1858	Cytosine (C)	14(100)	0(0)
		Thymine (T)	0(0)	9(100)
	nt 1896	Guanine (G)	14(100)	6(67)
		Adenine (A)	0(0)	3(33)

CP: Core promoter; PC: Precore; nt: Nucleotide.

Table 3 Clinical and virological characteristics in carriers of genotype C with C-1858 or T-1858

		Mutation <i>n</i> (%)		
		C-1858 (<i>n</i> =12)	T-1858 (<i>n</i> =26)	
Age (mean±SD, yr)		41.7±13.0	43.5±11.6	
Gender (male:female)		9:3	12:14	
Race	Asian			
	Mainland Chinese	3(30)	7(70)	
	Filipino	0(0)	2(100)	
	Taiwanese	0(0)	2(100)	
	Hong Kong	3(38)	5(63)	
	Vietnamese	2(67)	1(33)	
	Korean	1(14)	6(86)	
	Japanese	0(0)	1(100)	
	Micronesian	2(100)	0(0)	
	Polynesian	0(0)	0(0)	
	Caucasian	1(50)	1(50)	
	Liver disease	ASC	2(17)	10(29)
		CH	8(67)	21(60)
LC		1(8)	1(3)	
HCC		1(8)	3(9)	
Laboratory finding		HBeAg (+)	10(83)	16(62)
	AST (U/L)	34.9±17.0	63.8±97.6	
	ALT (U/L)	23.2±11.2	43.8±71.3	
	ALP (U/L)	334.6±186.3	324.9±157.0	
	γ -GTP (U/L)	87.8±167.3	57.2±48.4	
CP mutation	Double mutation	6(50)	16(62)	
PC mutation	A-1896	0(0)	8(31)	

ASC: Asymptomatic carrier; CH: Chronic hepatitis; LC: Liver cirrhosis; HCC: Hepatocellular carcinoma; ALT: Alanine aminotransferase; AST: Aspartate aminotransferase; ALP: Alkaline phosphatase; γ -GTP: γ -glutamyl transpeptidase; CP: Core promoter; PC: Precore.

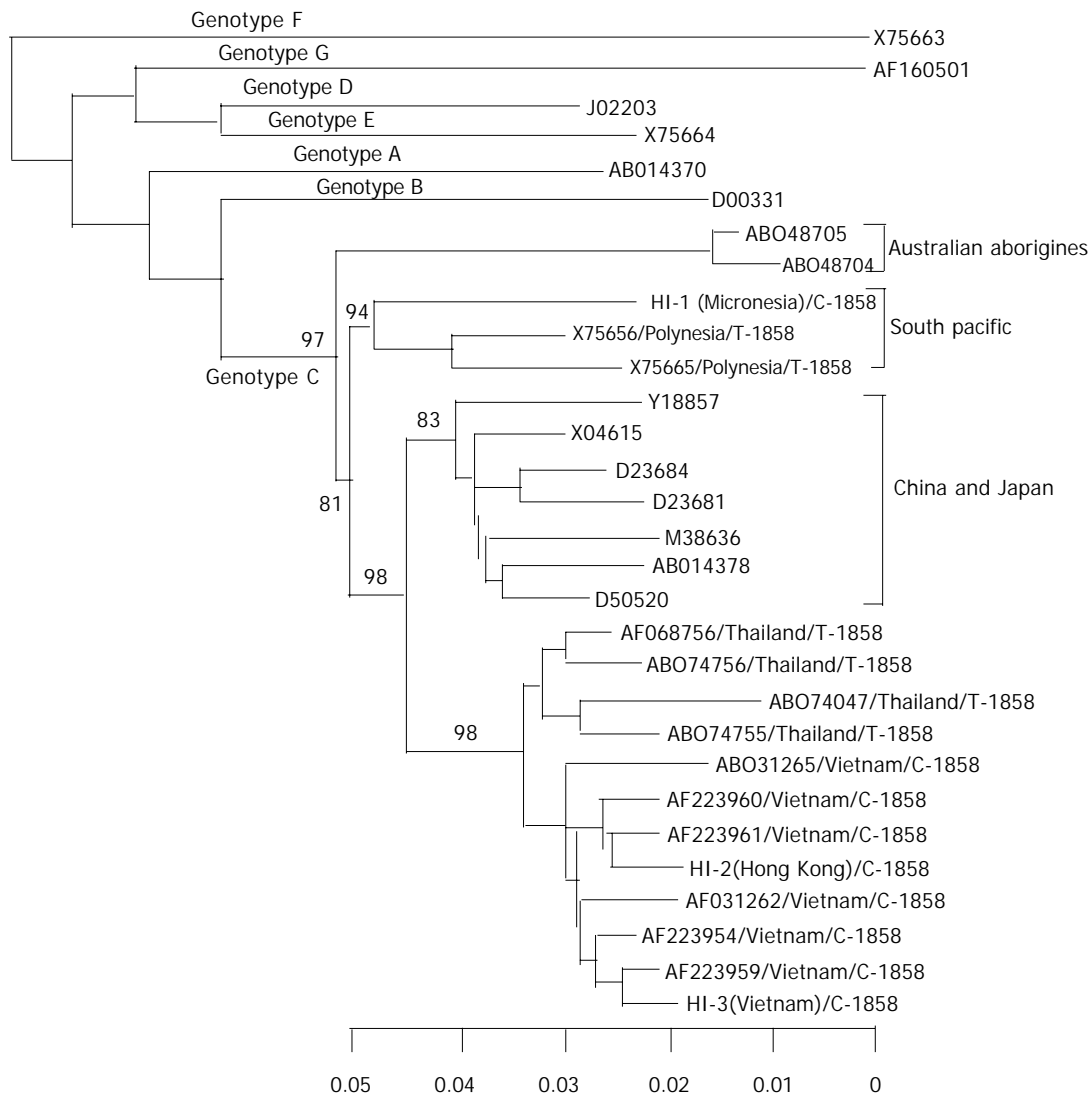


Figure 1 A phylogenetic tree based on the complete genome sequences of hepatitis B virus with 27 reference strains. Isolate names of HI-1, HI-2 and HI-3 were sequenced in this study. The length of the horizontal bar indicates the number of nucleotide substitutions per site. Numbers beside the main roots are the results of bootstrap analysis.

those strains of China and Japan. Moreover, the strains from Thailand and Vietnam had separate branches, and Hawaiian strains were clustered into the branch with Vietnam strains. Interestingly, all strains from Vietnam had C-1858, and those from Thailand had T-1858.

DISCUSSION

The findings of the present study indicate that HBV genotypes A, B and C are prevalent in Hawaii, and genotype C is the major genotype. Most cases of genotype A were found in immigrants from the Philippines and countries known to be prevalent regions for genotype A^[6]. Genotype B was found only in immigrants from Asian regions where genotype B was endemic. In addition, genotype C was obtained from immigrant who came from various Asian countries, where genotype C was prevalent^[22]. These results indicate that the distribution of HBV genotypes in Hawaii is associated with their respective ethnic background.

Recently, it was reported that genotype B could be classified into the Bj (j standing for Japan) and Ba (a standing for Asia) subgroups. Ba shared a genomic sequence with genotype C in the precore/core region, which was prevalent in Asian countries. Bj was restricted to Japan, and did not have this recombination^[11]. It was shown that Ba induces more severe liver disease than Bj

due to delayed seroconversion of HBeAg^[12]. In this study, we found that genotype B, prevalent in Hawaii, was classified as Ba because they were all obtained from carriers with Asian ethnicity (excluding Japanese). In addition, the rate of positive HBeAg (33.3%) and basal core promoter (BCP) mutation (44.4%) in patients of Hawaii infected with genotype B were higher than those in Japanese patients with genotype B^[9]. This result is also consistent with a previous report.

The double mutation in the core promoter, A-to-T mutation at nt 1762 and G-to-A mutation at nt 1764, was associated with reduced synthesis of precore mRNA^[23,24]. In addition, it has been reported that the BCP mutation was associated with the progression of liver disease^[25]. In this study, although it was not significant, BCP mutation was detected more frequently in genotype C than in genotype B. This result supports our previous observation that the BCP mutation was significantly more frequent in genotype C patients than in genotype B patients^[9]. In addition, the present study demonstrated that the proportion of HBeAg positivity in genotype C was significantly higher than that in genotype B (68.4% vs 33.3%). However, our study could not show the clinical difference between genotypes B and C most likely due to the small number of patients studied. In the future, a case-controlled study in multi-ethnic carriers with larger samples is required to confirm

if genotype C could induce more severe liver disease than genotype B^[9,10].

Interestingly, we detected 12 strains of genotype C possessing C-1858 in Hawaii. HBV strain with C-1858 could prevent the A-1896 precore mutation from shutting off the synthesis of HBeAg^[26]. This C-1858 variant was frequently found in genotypes A and F^[26]. In genotype C, the C-1858 variant was observed in Southeast Asian patients, and the phylogenetic origin of genotype C with C-1858 variant has been reported from Vietnam recently. In this study, the complete genomes of 3 genotype C strains with C-1858 were sequenced. One strain obtained from a Micronesian patient with C-1858 was clustered with previously reported Polynesian strains with T-1858. This indicates that both the C-1858 and T-1858 strains of genotype C are endemic to South Pacific countries. Two other strains obtained from patients with Hong Kong and Vietnamese ethnicities were clustered with the strains of genotype C from Southeast Asian countries. This result is consistent with geographic distribution of HBV genotype^[18]. Interestingly, in this subgroup, there were 2 variants of strains, one had C-1858, prevalent in Vietnam, and the other had T-1858, prevalent in Thailand.

The clinical significance of C-1858 or T-1858 among genotype C is not well known. In this study, we compared the clinical and laboratory characteristics between C-1858 and T-1858 variant, but there were no significant differences between them. The number of patients was not enough to clarify the importance of this variation, and its significance for clinical characteristics remains unknown. Further studies would be required using larger numbers of samples.

In conclusion, genotypes A, B and C are the predominant types among multi-ethnic HBV carriers in Hawaii, and the distribution of these genotypes is dependent on the ethnic origin of the carriers in Hawaii. The influence of these genotypes on the clinical manifestations of these HBV carriers in Hawaii is not well defined due to the current small sample size. Case-controlled study with larger cohorts from our unique community is needed.

REFERENCES

- 1 Lee WM. Hepatitis B virus infection. *N Engl J Med* 1997; **337**: 1733-1745
- 2 Okamoto H, Tsuda F, Sakugawa H, Sastrosowignjo RI, Imai M, Miyakawa Y, Mayumi M. Typing hepatitis B virus by homology in nucleotide sequence: comparison of surface antigen subtypes. *J Gen Virol* 1998; **69**: 2575-2583
- 3 Nordor H, Hammas B, Lofdahl S, Courouce AM, Magnus LO. Comparison of the amino acid sequences of nine different serotypes of hepatitis B surface antigen and genomic classification of the corresponding hepatitis B virus. *J Gen Virol* 1992; **73**: 1201-1208
- 4 Nordor H, Courouce AM, Magnus LO. Complete genome, phylogenetic relatedness, and structural protein of six strains of the hepatitis B virus, four of which represent two new genotypes. *Virology* 1994; **198**: 489-503
- 5 Stuyver L, De Gendt S, Van Geyt C, Zoulim F, Fried M, Schinazi RF, Rossau R. A new genotype of hepatitis B virus: Complete genome and phylogenetic relatedness. *J Gen Virol* 2000; **81**: 67-74
- 6 Nordor H, Hammas B, Lee SD, Bile K, Courouce AM, Mushahwar IK, Magnus LO. Genetic relatedness of hepatitis B viral strains of diverse geographical origin and natural variations in the primary structure of the surface antigen. *J Gen Virol* 1993; **74**: 1341-1348
- 7 Orito E, Ichida T, Sakugawa H, Sata M, Horiike N, Hino K, Okita K, Okanoue T, Iino S, Tanaka E, Suzuki K, Watanabe H, Hige S, Mizokami M. Geographic distribution of hepatitis B virus (HBV) genotype in patients with chronic HBV infection in Japan. *Hepatology* 2001; **34**: 590-594
- 8 Mayerat C, Mantegani A, Frei PC. Does hepatitis B virus (HBV) genotype influence the clinical outcome of HBV infection. *J Viral Hepat* 1999; **6**: 299-304
- 9 Orito E, Mizokami M, Sakugawa H, Michitaka K, Ishikawa K, Ichida T, Okanoue T, Yotsuyanagi H, Iino S. A case-control study for clinical and molecular biological differences between hepatitis B viruses of genotypes B and C. *Hepatology* 2001; **33**: 218-223
- 10 Kao JH, Chen PJ, Lai MY, Chen DS. Hepatitis B genotypes correlate with clinical outcomes in patients with chronic hepatitis B. *Gastroenterology* 2000; **118**: 554-559
- 11 Sugauchi F, Orito E, Ichida T, Kato H, Sakugawa H, Kakumu S, Ishida T, Chutaputti A, Lai CL, Ueda R, Miyakawa Y, Mizokami M. Hepatitis B virus of genotype B with or without recombination with genotype C over the precore region plus the core gene. *J Virol* 2002; **76**: 5985-5992
- 12 Sugauchi F, Orito E, Ichida T, Kato H, Sakugawa H, Kakumu S, Ishida T, Chutaputti A, Lai CL, Gish RG, Ueda R, Miyakawa Y, Mizokami M. Epidemiological and virological characteristics of hepatitis B virus genotype B having the recombination with genotype C. *Gastroenterology* 2003; **124**: 925-932
- 13 Ching N, Lumeng J, Pang R, Pang G, Or FW, Ching N, Ching C. Long term low dose interferon alpha-2b in multi-ethnic patients in Hawaii. *Hawaii Med J* 1996; **55**: 201-203
- 14 Pon EW, Ren H, Margolis H, Zhao Z, Schatz GC, Diwan A. Hepatitis B virus infection in Honolulu students. *Pediatrics* 1993; **92**: 574-578
- 15 Usuda S, Okamoto H, Iwanari H, Baba K, Tsuda F, Miyakawa Y, Mayumi M. Serological detection of hepatitis B virus genotypes by ELISA with monoclonal antibodies to type-specific epitopes in the preS2-region product. *J Virol Methods* 1999; **80**: 97-112
- 16 Mizokami M, Nakano T, Orito E, Tanaka Y, Sakagawa H, Mukaide M, Robertson BH. Hepatitis B virus genotype assignment using restriction fragment length polymorphism patterns. *FEBS Lett* 1999; **450**: 66-71
- 17 Kato H, Orito E, Sugauchi F, Ueda R, Gish RG, Usuda S, Miyakawa Y, Mizokami M. Determination of hepatitis B virus genotype G by polymerase chain reaction with hemi-nested primers. *J Virol Methods* 2001; **98**: 153-159
- 18 Sugauchi F, Mizokami M, Orito E, Ohno T, Kato H, Suzuki S, Kimura Y, Ueda R, Butterworth LA, Cooksley WG. A novel variant genotype C of hepatitis B virus identified in isolates from Australian Aborigines: Complete genome sequence and phylogenetic relatedness. *J Gen Virol* 2001; **82**: 883-892
- 19 Thompson JD, Higgins DG, Gibson TJ. CLUSTAL W: improving the sensitivity of progressive multiple sequence alignment through sequence weighting, position-specific gap penalties and weight matrix choice. *Nucleic Acids Res* 1994; **22**: 4673-4680
- 20 Saitou N, Nei M. The neighbor-joining method: a new method for reconstructing phylogenetic trees. *Mol Biol Evol* 1987; **4**: 406-425
- 21 Ina Y. ODEN: a program package for molecular evolutionary analysis and database search of DNA and amino acid sequences. *Comput Appl Biosci* 1994; **10**: 11-12
- 22 Kao JH. Hepatitis B viral genotypes: clinical relevance and molecular characteristics. *J Gastroenterol Hepatol* 2002; **17**: 643-650
- 23 Okamoto H, Tsuda F, Akahane Y, Sugai Y, Yoshihara M, Moriyama K, Tanaka T, Miyakawa Y, Mayumi M. Hepatitis B virus with mutations in the core promoter for an e antigen-negative phenotype in carriers with antibody to e antigen. *J Virol* 1994; **68**: 8102-8110
- 24 Buckwold VE, Xu Z, Chen M, Yen TS, Ou JH. Effects of a naturally occurring mutation in the hepatitis B virus basal core promoter on precore gene expression and viral replication. *J Virol* 1996; **70**: 5845-5851
- 25 Takahashi K, Aoyama K, Ohno N, Iwata K, Akahane Y, Baba K, Yoshizawa H, Mishiro S. The precore/core promoter mutant (T1762A1764) of hepatitis B virus: clinical significance and an easy method for detection. *J Gen Virol* 1995; **76**: 3159-3164
- 26 Li JS, Tong SP, Wen YM, Vitvitski L, Zhang Q, Trepo C. Hepatitis B virus genotype A rarely circulates as an HBe-minus mutant: possible contribution of a single nucleotide in the precore region. *J Virol* 1993; **67**: 5402-5410

HCV NS5A abrogates p53 protein function by interfering with p53-DNA binding

Guo-Zhong Gong, Yong-Fang Jiang, Yan He, Li-Ying Lai, Ying-Hua Zhu, Xian-Shi Su

Guo-Zhong Gong, Yong-Fang Jiang, Yan He, Li-Ying Lai, Ying-Hua Zhu, Xian-Shi Su, Center for Liver Diseases, Second Xiangya Hospital, Central South University, Changsha 410011, Hunan Province, China

Supported by the National Natural Science Foundation of China, No. 3967067

Correspondence to: Dr. Guo-Zhong Gong, Center for Liver Diseases, Second Xiangya Hospital, Central South University, 86 Renmin Zhong Road, Changsha 410011, Hunan Province, China. guozhong_gong@hotmail.com

Telephone: +86-731-5524222 **Fax:** +86-731-5533525

Received: 2003-12-12 **Accepted:** 2004-01-08

Abstract

AIM: To evaluate the inhibition effect of HCV NS5A on p53 transactivation on p21 promoter and explore its possible mechanism for influencing p53 function.

METHODS: p53 function of transactivation on p21 promoter was studied with a luciferase reporter system in which the luciferase gene is driven by p21 promoter, and the p53-DNA binding ability was observed with the use of electrophoretic mobility-shift assay (EMSA). Lipofectin mediated p53 or HCV NS5A expression vectors were used to transfect hepatoma cell lines to observe whether HCV NS5A could abrogate the binding ability of p53 to its specific DNA sequence and p53 transactivation on p21 promoter. Western blot experiment was used for detection of HCV NS5A and p53 proteins expression.

RESULTS: Relative luciferase activity driven by p21 promoter increased significantly in the presence of endogenous p53 protein. Compared to the control group, exogenous p53 protein also stimulated p21 promoter driven luciferase gene expression in a dose-dependent way. HCV NS5A protein gradually inhibited both endogenous and exogenous p53 transactivation on p21 promoter with increase of the dose of HCV NS5A expression plasmid. By the experiment of EMSA, we could find p53 binding to its specific DNA sequence and, when co-transfected with increased dose of HCV NS5A expression vector, the p53 binding affinity to its DNA gradually decreased and finally disappeared. Between the Huh 7 cells transfected with p53 expression vector alone or co-transfected with HCV NS5A expression vector, there was no difference in the p53 protein expression.

CONCLUSION: HCV NS5A inhibits p53 transactivation on p21 promoter through abrogating p53 binding affinity to its specific DNA sequence. It does not affect p53 protein expression.

Gong GZ, Jiang YF, He Y, Lai LY, Zhu YH, Su XS. HCV NS5A abrogates p53 protein function by interfering with p53-DNA binding. *World J Gastroenterol* 2004; 10(15): 2223-2227
<http://www.wjgnet.com/1007-9327/10/2223.asp>

INTRODUCTION

Hepatitis C virus (HCV) is recognized as a major causative agent leading to chronic hepatitis and cirrhosis^[1-3], which have a close relationship with the development of hepatocellular carcinoma (HCC)^[4,5]. HCV is a positive single-stranded RNA virus belonging to the Flaviridae family, and its genome only contains a single long open reading frame encoding a large polyprotein precursor that is thereafter processed by a combination of cellular and viral proteases into several mature proteins, including three or four structural proteins (core, E1, E2/P7) and at least 6 nonstructural proteins (NS): NS2, NS3, NS4A, NS4B, NS5A, NS5B^[6]. HCV NS5A as a nonstructural protein does not assemble into the HCV particles, but still has a lot of functions in the HCV replication and the development of chronic liver disease and hepatocellular carcinoma. Recent studies showed that HCV NS5A could interact with a number of cellular proteins including PKR, p53, Grb2 and Cdk1^[7-10], and enhance expression of some genes related to cell proliferation such as PCNA, NF- κ B, Stat-3, SRCAP and IL-8^[11-14], indicating that HCV NS5A has a critical role in promoting cell proliferation and malignant transformation. HCV NS5A prevents p53 and TNF- α mediated apoptosis^[15-17], and possibly perturbs the DNA repair when cells are treated with DNA damage agents including viruses, toxins or physical damage. HCV NS5A is important for the HCV replication. It can form a complex with an SNARE-like protein, hVAP-33 and HCV NS5B^[18] and can associate with ER and Golgi complex, and the amphipathic helix (AH) of the HCV NS5A is necessary for this membrane localization and for HCV RNA replication^[19,20]. Interaction of HCV NS5A with La protein can also maintain and benefit HCV RNA replication and HCV protein translation^[21,22]. Sequence mutation in HCV NS5A might be a reason for the responsiveness in the patient who received IFN treatment^[23-25]. The patients with wild type of interferon sensitive-determining region (ISDR) in HCV NS5A usually have a lower responsive rate to the IFN therapy, and the mechanism is that the wild type ISDR can bind PKR, which is induced by IFN and has an anti-viral activity, and can disrupt PKR function^[7,26,27]. The tumor suppressor p53 protein has been reported to possess a number of important functions. Activated p53 can transactivate a lot of target genes, maintain normal cell cycle through inducing apoptosis and repairing damaged DNA, and suppressing oncogenic transformation. In this study we explored the interaction between HCV NS5A and p53 and the mechanism by which the HCV NS5A abrogated the p53 transactivation.

MATERIALS AND METHODS

Cell lines and plasmids

P^{C53-NS3}, P^{wwp-luc} and P^{wwp-mut-luc} were kind gifts from Professor Vogelstein (The Johns Hopkins University). P^{C53-NS3} is an eukaryotic expression vector that is constructed by cloning normal human p53 cDNA into p^{CMV} plasmid. P^{wwp-luc} carries luciferase reporter gene driven by p21 promoter that contains the specific consensus DNA sequence binding to p53 protein. P^{wwp-mut-luc} is approximately the same vector as P^{wwp-luc} except for deletion mutation introduced in the p53 binding sequence

of p21 promoter. P^{CNS5A} is made in Dr. Siddiqui's laboratory (University of Colorado, USA) through inserting of HCV NS5A cDNA into P^{CMV} plasmid^[12]. The liver carcinoma cell lines Huh7 with p53 gene mutation and HepG2 with wild-type p53 gene were from ATCC(USA) and maintained in Dulbecco's Modified Eagle Medium (Life Technologies, USA) complemented with 100 mL/L fetal calf serum. The cells were transfected by the individual plasmids with Lipofectin reagent (Life Technologies, USA) when they became 60-70% confluent. Forty-eight hours after transfection, the cells were harvested for the analysis of relative luciferase activity and electrophoretic mobility shift assay (EMSA).

Relative luciferase activity assay

After 48 h of transfection, cells in the plates were washed two times with PBS, and then 750 μ L lysis buffer (0.1 mmol/L K₂HPO₄, pH 7.8, 10 mmol/L DTT, 5 g/L NP-40) was added onto plates. The plates were then placed on ice for 15 min and then cells were transferred into a clean 1.5-mL Eppendorf tube. After centrifugation at 15 000 g for 10 min, the supernatants were collected for further experiment. For relative luciferase activity assay, 0.4 mL determination buffer (0.1 mmol/L K₂HPO₄, pH 7.8, 0.15 mmol/L MgSO₄, 10 mmol/L DTT, 0.5 mmol/L ATP) and the different volumes of supernatant containing equivalent protein were put into 5-mL glass tube to observe the times of luminescence within 10 s using a luminometer (Optocomp II, MGM, USA). The experiment was repeated three times and each in triplicate.

Electrophoretic mobility-shift assay (EMSA)

In this experiment, we investigated the ability of p53 binding to the specific consensus DNA sequence, and studied if the binding could be influenced by HCV NS5A. Briefly, this experiment was done as following: (1) Labeling of DNA probe: 50 pmol chemically synthesized oligonucleotide 5' - GGACATGCCCGG GCATGTCC -3' which is the specific consensus DNA sequence to bind p53, 2 μ L γ -P³² ATP (74 000 GBq/mmol), 20 U T₄ polynucleotide kinase, 2 μ L reaction buffer and incubated for 30 min at 37 °C, then 60 μ L dH₂O was added to the mixture and the labeled oligonucleotides were purified from the free γ -P³² ATP by use of Sephadex-G25. The purified P³²-labeled DNA probe was stored at -20 °C until use. (2) Nuclear protein isolation: After transfection with different plasmids for 48 h, cells were washed 3 times with PBS and scrapped down from the plates and then transferred into 1.5-mL Eppendorf tubes and washed 3 times again with PBS. Lysis buffer 30 μ L (20 mmol/L Hepes, pH 7.9, 10 mmol/L KCl, 10 mmol/L Na₃VO₄, 1 mmol/L ETDA, 100 mL/L glycerol, 1 mmol/L PMSF, 3 g/L aprotinin, 1 g/L leupeptin, 1 mmol/L DTT, 2 g/L NP-40, 20 mmol/L NaF) was added to suspend the cells. After 15 min on ice, and centrifugation at 15 000 \times g for 1 min, the supernatant was discarded and the pellet resuspended in 20 μ L nuclear extract buffer (20 mmol/L Hepes, pH 7.9, 10 mmol/L KCl, 420 mmol/L NaCl, 10 mmol/L Na₃VO₄, 1 mmol/L ETDA, 200 mL/L glycerol, 1 mmol/L PMSF, 3 g/L aprotinin, 1 g/L leupeptin, 1 mmol/L DTT, 20 mmol/L NaF). After incubation at 4 °C for 30 min. with mild agitation, and centrifugation at 15 000 g for 5 min, aliquot supernatants were collected and stored at -70 °C until use. (3) Assessment of p53 binding to DNA probe: For each reaction tube, the followings were added: 2 μ g nuclear extraction protein, 2 μ L labeled probe containing p53 binding sequence, 1.5 μ L EMSA reaction buffer (50 mmol/L NaCl, 0.5 mmol/L ETDA, 40 mL/L glycerol, 1 mmol/L MgCl₂, 1 mmol/L DTT, 10 mmol/L Tris-Cl, pH 7.5, 0.05 g/L poly (dI-dC)) and dH₂O to a total volume of 15 μ L. After incubation for 30 min on ice, 20 μ L of samples was loaded onto 60 g/L undenatured PAGE and run at 160 V for approximately 6 h. The gel was dried and autoradiographed at -70 °C for about 16 h.

Western blotting to detect p53 and HCV NS5A protein expression

Cell lysates of Huh7 cells transfected with P^{C53-NS3} or co-transfected with P^{CNS5A} were made by routine method. The same amount of total protein from the cell lysate was used to load onto 120 g/L PAGE, and then transferred onto PV (polyvinylidene difluoride) membrane. After blocked in block solution (20 mmol/L Tris-HCl, pH 7.5, 150 mmol/L NaCl, 3 g/L PVP, 5 g/L Tween 20) for 2 h, the membrane was probed by anti-HCV NS5A or anti-p53, washed and incubated with the second enzyme-labeled antibody, and then observed by using an ECL kit (Boehringer Mannheim Co., Germany).

Statistical analysis

Statistical significance of differences between the 2 groups was determined by applying Student's *t* test or two-sample *t* test. Statistical significance of differences in more than 3 groups was determined by applying one-way ANOVA. A *P* value less than 0.05 was considered significant.

RESULTS

HCV NS5A protein inhibited the transactivation of endogenous p53 on p21 promoter

Relative luciferase activities in P^{wpp-luc}-transfected HepG2 cells (3.95×10^5) were significantly higher than that in P^{wpp-mut-luc} group (0.60×10^5 , $t=5.92$, $P<0.01$). Compared to P^{wpp-luc}-transfected HepG2 cells, the relative luciferase activities in the HepG2 cells co-transfected with P^{wpp-luc} and P^{CNS5A} decreased in a P^{CNS5A} dose- dependent manner ($F=20.71$, $P<0.01$), suggesting that HCV NS5A protein can inhibit the transactivation of endogenous p53 on p21 promoter. In contrast, the relative luciferase activities of the HepG2 cells co-transfected with P^{wpp-mut-luc} and P^{CNS5A} had little change ($F=0.76$, $P>0.05$) in comparison with P^{wpp-mut-luc}-transfected HepG2 cells. Those results indicated that endogenous p53 has a transactivation on p21 promoter, and HCV NS5A down-regulated p21 promoter activity through inhibiting endogenous p53 activity (Table 1).

Table 1 HCV NS5A inhibits the transactivation of endogenous p53 on p21 promoter

Group	Relative luciferase activity	<i>F</i>	<i>P</i>
P ^{wpp-luc} (1 μ g)			
+ P ^{CNS5A} (0 μ g)	3.49×10^{5b}	20.71	<0.01
+ P ^{CNS5A} (0.5 μ g)	2.69×10^5		
+ P ^{CNS5A} (1.0 μ g)	1.62×10^5		
+ P ^{CNS5A} (2.0 μ g)	0.58×10^5		
P ^{wpp-mut-luc} (1.0 μ g)			
+ P ^{CNS5A} (0 μ g)	0.60×10^5	0.76	>0.05
+ P ^{CNS5A} (0.5 μ g)	0.65×10^5		
+ P ^{CNS5A} (1.0 μ g)	0.62×10^5		
+ P ^{CNS5A} (2.0 μ g)	0.64×10^5		

^b $t=5.92$, $P<0.01$.

HCV NS5A protein abrogated exogenous p53 transactivation on p21 promoter

The mean of relative luciferase activity in the Huh7 cells individually transfected with P^{wpp-luc} and P^{wpp-mut-luc} was 0.47×10^5 and 0.45×10^5 respectively and there were no statistically differences between these two groups ($t=1.16$, $P>0.05$). This might be because p53 gene in Huh7 cells has been mutated and p53 protein has lost its normal transactivation function, therefore, no matter what happened to p21 promoter (wild type or mutated), the expression of p21 promoter driven luciferase gene was not affected. When P^{wpp-luc} or P^{wpp-mut-luc} was co-

transfected with $P^{C53-NS3}$ into Huh7 cells, respectively, the relative luciferase activities in the $P^{wpp-luc} + P^{C53-NS3}$ group greatly increased ($\chi=5.63 \times 10^5$), but the relative luciferase activities in the $P^{wpp-mut-luc} + P^{C53-NS3}$ group only mild increased ($\chi=0.50 \times 10^5$), and a remarkable variance between the two groups existed ($t=10.12$, $P<0.01$). These results indicated that exogenous p53 should have a strong transactivation on p21 promoter. In order to see if HCV NS5A protein has any effect on the exogenous p53 transactivation, we used P^{CNS5A} , $P^{C53-NS3}$ and $P^{wpp-luc}$ to co-transfect Huh7 cells, and the result showed that the relative luciferase activities in the $P^{CNS5A}+P^{C53-NS3}+P^{wpp-luc}$ group cells decreased in a P^{CNS5A} dose-dependent way ($F=24.23$, $P<0.01$). P^{CNS5A} and $P^{wpp-luc}$ were also used to transfect Huh7 cells to find out if HCV NS5A had a direct effect on p21 promoter. The result showed that HCV NS5A did not increase or decrease the relative luciferase activity. From those experiments we proposed that HCV NS5A down-regulated p21 promoter activity by inhibiting exogenous p53 activity, and not by HCV NS5A's direct effect on p21 promoter (Tables 2, 3).

Table 2 HCV NS5A inhibits exogenous p53 transactivation on p21 promoter

Group	Relative luciferase activity	F	P
$P^{wpp-luc}$ (1 μ g)	0.47×10^{5ab}	24.23	<0.01
+ $P^{C53-NS3}$ (1 μ g)	5.63×10^{5b}		
+ P^{CNS5A} (0.5 μ g)	1.61×10^5		
+ P^{CNS5A} (1.0 μ g)	0.69×10^5	0.69	>0.05
$P^{wpp-mut-luc}$ (1 μ g)	0.45×10^{5a}		
+ $P^{C53-NS3}$ (1 μ g)	0.50×10^5		
+ P^{CNS5A} (0.5 μ g)	0.43×10^5		
+ P^{CNS5A} (1.0 μ g)	0.48×10^5		

^a $t=1.16$, $P>0.05$; ^b $t=10.12$, $P<0.01$.

Table 3 HCV NS5A and p21 promoter activity

Group	Relative luciferase activity	F	P
$P^{wpp-luc}$ (1.0 μ g)	0.44×10^5	0.52	>0.05
+ P^{CNS5A} (0.5 μ g)	0.46×10^5		
+ P^{CNS5A} (1.0 μ g)	0.43×10^5		
$P^{wpp-luc}$ (1.0 μ g)	0.56×10^5	28.16	<0.01
+ P^{C53-NS} (0.5 μ g)	2.68×10^5		
+ P^{C53-NS} (1.0 μ g)	4.84×10^5		

HCV NS5A inhibited p53 protein transactivation through abrogation of p53 binding to the specific DNA

Through EMSA, the band of specific p53 and DNA probe complex was found in the nuclear lysates prepared from Huh7 cells transfected with $P^{C53-NS3}$, and verified by the appearance of the supershift after addition of the monoclonal anti-p53 (a generous gift of Dr. Harris, USA) or polyclonal anti-HCV NS5A antibody (a generous gift of Professor Rice, USA) in the EMSA mixtures. This p53-probe complex band did not occur in the nuclear lysates prepared from Huh7 cells untransfected with plasmids or only transfected with P^{CNS5A} , suggesting there is wild-type p53 protein expressed in these cells. In the next experiment, we used different doses of P^{CNS5A} and constant amount (1 μ g) of $P^{C53-NS3}$ to co-transfect Huh7 cells. The p53-probe band became gradually weakened and finally disappeared with increasing doses of P^{CNS5A} , suggesting that HCV NS5A could inhibit p53 transactivation through disruption of the binding of p53 to its specific consensus DNA (Figure 1).

HCV NS5A had no effect on p53 protein expression

p53 protein was expressed at about the same level between the Huh7 cells transfected with p53 expression vector and the Huh7

cells co-transfected with P^{CNS5A} and p53 expression vectors (Figure 2). This result indicates that HCV NS5A does not affect p53 protein expression.

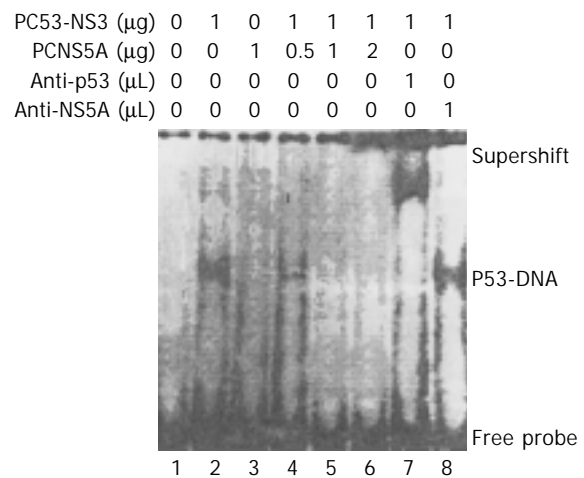


Figure 1 HCVNS5A inhibits p53 binding to its specific DNA probe. Lane 1: Negative control; Lane 2: Transfected with pC53-NS3 only; Lane 3: Transfected with pCNS5A only; Lanes 4-6: Co-transfected with pC53-NS3 (1 μ g) and different dose of pCNS5A; Lanes 7-8: Transfected with pC53-NS3, and anti-p53, antiNS5A anti-bodies were added to the reaction mixture individually.

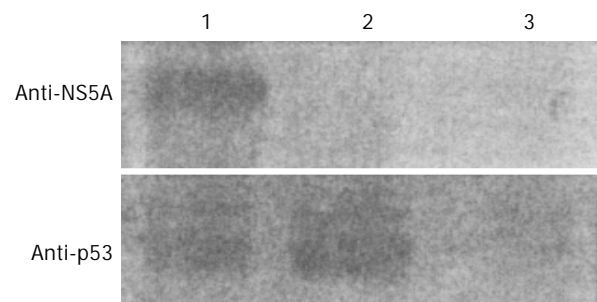


Figure 2 Western blotting for the expression of NCV NS5A and p53 proteins. Lane 1: Huh 7 cells co-transfected with $P^{C53-NS3}$ and P^{CNS5A} ; Lane 2: Huh 7 cells transfected with $P^{C53-NS3}$; Lane 3: Huh 7 cells untransfected.

DISCUSSION

HCV NS5A is a phosphoprotein that exists in two different forms of M_r 56 000 and 58 000 with modifications of serine residues, and M_r 58 000 form is produced by additional phosphorylation of the M_r 56 000 form^[28-30]. Initial studies found that HCV NS5A contains acidic and proline-rich amino acids in its carboxyl-terminal, and this structure feature resembles eukaryotic transcription activator^[31,32]. Later studies showed that the HCV NS5A with amino-terminal deleted (1-146) mutant did have a strong transcriptional activation, but the whole length HCV NS5A showed no apparent transcriptional activity^[33]. The potential transactivation of HCV NS5A has attracted great attention and become the research focus of the nonstructural proteins of HCV due to its important role in the pathogenesis of chronic liver disease and even hepatocellular carcinoma. Clinical observations suggested the responsiveness of patients to IFN treatment might be related to HCV NS5A ISDR sequence mutations^[23-25]. Several experiments from Katze's laboratory and others confirmed that HCV NS5A could repress RNA dependent protein kinase (PKR) function, by which HCV can escape the effect of IFN, and also inhibit apoptosis and promote cell proliferation^[7,26,27]. When PKR is dysfunctional, sustained

expression of eIF-2 α in cells results in cell growth and differentiation, and induces malignant transformation and the development of tumors in nude mice. ISDR of HCV NS5A can bind the domain of PKR and prevent the PKR dimerizing which is the critical process to activate PKR function. Mapping studies found that ISDR and the adjacent C-terminal 26 amino acids can form a heterodimer with PKR. The effect of HCV NS5A on the protection of apoptosis induced by TNF- α and p53 was further identified^[16,17]. In the present study, we explored the possible effect of HCV NS5A on the transactivation of p53. Luciferase reporter gene driven by p21 promoter was used in this experiment, which showed that both endogenous and exogenous p53 protein could transactivate p21 promoter as expected. But, when HCV NS5A protein was introduced, by transfection or co-transfection with HCV NS5A expressing vector, the p21 promoter function activated by p53 was greatly depressed. This finding is in agreement with previous reports^[8,11]. To further understand the mechanism of interaction between HCV NS5A and p53, we did an EMSA experiment for p53 binding to its consensus DNA probe, to see if HCV NS5A could disturb the binding reaction. The result showed that HCV NS5A disrupted p53 binding to its DNA probe, and with the increase of dosage of HCV NS5A expressing vector transfected, inhibition of the binding seemed more remarkable. All the above results suggested HCV NS5A depressed the p53 transactivation by interrupting the binding between p53 and its specific DNA. Recent studies also evidenced that HCV NS5A could physically associate with p53 and form a complex, which might be the reason why p53 binding to its DNA was disrupted^[8,34]. Further, we wanted to know whether p53 protein expression was affected by the presence of HCV NS5A. Through western blot, we found that after co-transfection of HCV NS5A expressing vector, the level of p53 protein expression in the cells did not show any change compared to empty vector transfected cells. This result was also similarly found in another report^[11]. In summary, according to our experiments and previous reports by others, HCV NS5A represses p53 transactivation function by disrupting p53 binding to its specific DNA through HCV NS5A and p53 complex formation, not by the disturbance of the p53 protein expression. HCV NS5A can interact with many cellular factors in the host cells such as PKR, p53, Bcl2 and disrupt their functions^[7,8,26,27,34,35], which are related to the processes of apoptosis. HCV NS5A can also interact with unknown cellular factors and induce the expression of genes such as SRCAP, NF- κ B and PCNA^[11-13], which are related to the promotion of cell proliferation. HCV NS5A seems to be a very active protein interacting with host cellular proteins and taking a major part in modulating cell growth and death, as well as in the development of hepatocellular carcinoma.

ACKNOWLEDGEMENTS

We would like to thank Dr. A Siddiqui and G Waris from University of Colorado School of Medicine for their help in this study.

REFERENCES

- 1 **Choo QL**, Kuo G, Weiner AJ, Overby LR, Bradley DW, Houghton M. Isolation of a cDNA clone derived from a blood-borne non-A, non-B viral hepatitis genome. *Science* 1989; **244**: 359-362
- 2 **Kuo G**, Choo QL, Alter HJ, Gitnick GL, Redeker AG, Purcell RH, Miyamura T, Dienstag JL, Alter MJ, Stevens CE. An assay for circulating antibodies to a major etiologic virus of human non-A, non-B hepatitis. *Science* 1989; **244**(3 Suppl): 362-364
- 3 **Seeff LB**. Natural history of hepatitis C. *Hepatology* 1997; **26**: 21S-28S
- 4 **Saito I**, Miyamura T, Ohbayashi A, Harada H, Katayama T, Kikuchi S, Watanabe Y, Koi S, Onji M, Ohta Y, Choo QL, Houghton M, Kuo G. Hepatitis C virus infection is associated with the development of hepatocellular carcinoma. *Proc Natl Acad Sci U S A* 1990; **87**: 6547-6549
- 5 **Di Bisceglie AM**, Lyra AC, Schwartz M, Reddy RK, Martin P, Gores G, Lok AS, Hussain KB, Gish R, Van Thiel DH, Younossi Z, Tong M, Hassanein T, Balart L, Fleckenstein J, Flamm S, Blei A, Befeler AS. Hepatitis C virus-related hepatocellular carcinoma in the United States: influence of ethnic status. *Am J Gastroenterol* 2003; **98**: 2060-2063
- 6 **Clarke B**. Molecular virology of hepatitis C virus. *J Gen Virol* 1997; **78**(Pt 10): 2397-2410
- 7 **Gale M Jr**, Blakely CM, Kwieciszewski B, Tan SL, Dossett M, Tang NM, Korth MJ, Polyak SJ, Katze MG. Control of PKR protein kinase by hepatitis C virus nonstructural 5A protein: molecular mechanisms of kinase. *Mol Cell Biol* 1998; **18**: 5308-5319
- 8 **Majumder M**, Ghosh AK, Steele R, Ray R. Hepatitis C virus NS5A physically associates with p53 and regulates p21/waf1 gene expression in a p53-dependent manner. *J Virol* 2001; **75**: 1401-1407
- 9 **Tan SL**, Nakao H, He Y, Vijaysri S, Neddermann P, Jacobs BL, Mayer BJ, Katze MG. NS5A, a nonstructural protein of hepatitis C virus, binds growth factor receptor-bound protein 2 adaptor protein in a Src homology3 domain/ligand-dependent manner and perturbs mitogenic signaling. *Proc Natl Acad Sci U S A* 1999; **96**: 5533-5538
- 10 **Arima N**, Kao CY, Licht T, Padmanabhan R, Sasaguri Y, Padmanabhan R. Modulation of cell growth by the hepatitis C virus nonstructural protein NS5A. *J Biol Chem* 2001; **276**: 12675-12684
- 11 **Ghosh AK**, Steele R, Meyer K, Ray R, Ray RB. Hepatitis C virus NS5A protein modulates cell cycle regulatory genes and promotes cell growth. *J Gen Virol* 1999; **80**(Pt 5): 1179-1183
- 12 **Gong G**, Waris G, Tanveer R, Siddiqui A. Human hepatitis C virus NS5A protein alters intracellular calcium level, induces oxidative stress, and activates STAT-3 and NF- κ B. *Proc Natl Acad Sci U S A* 2001; **98**: 9599-9604
- 13 **Ghosh AK**, Majumder M, Steele R, Yaciuk P, Chrivia J, Ray R, Ray RB. Hepatitis C virus NS5A protein modulates transcription through a novel cellular transcription factor SRCAP. *J Biol Chem* 2000; **275**: 7184-7188
- 14 **Polyak SJ**, Khabar KS, Paschal DM, Ezelle HJ, Duverlie G, Barber GN, Levy DE, Mukaida N, Gretch DR. Hepatitis C virus nonstructural 5a protein induces interleukin-8 leading to partial inhibition of the interferon-induced antiviral response. *J Virol* 2001; **75**: 6095-6106
- 15 **Lan KH**, Sheu MI, Hwang SJ, Yen SH, Chen SY, Wu JC, Wang YJ, Kato N, Omata M, Chang FY, Lee SD. HCV NS5A interacts with p53 and inhibits p53-mediated apoptosis. *Oncogene* 2002; **21**: 4801-4811
- 16 **Majumder M**, Ghosh AK, Steele R, Zhou XY, Phillips NJ, Ray R, Ray RB. Hepatitis C virus NS5A protein impairs TNF-mediated hepatic apoptosis, but not by an anti-fas antibody, in transgenic mice. *Virology* 2002; **294**: 94-105
- 17 **Ghosh AK**, Majumder M, Steele R, Meyer K, Ray R, Ray RB. Hepatitis C virus NS5A protein protects against TNF-alpha mediated apoptotic cell death. *Virus Res* 2000; **67**: 173-178
- 18 **Tu H**, Gao L, Shi ST, Taylor DR, Yang T, Mircheff AK, Wen Y, Gorbalenya AE, Hwang SB, Lai MM. Hepatitis C virus RNA polymerase and NS5A complex with a SNARE-like protein. *Virology* 1999; **263**: 30-41
- 19 **Elazar M**, Cheong KH, Liu P, Greenberg HB, Rice CM, Glenn JS. Amphipathic helix-dependent localization of NS5A mediates hepatitis C virus RNA replication. *J Virol* 2003; **77**: 6055-6061
- 20 **Brass V**, Bieck E, Montserret R, Wolk B, Hellings JA, Blum HE, Penin F, Moradpour D. An amino-terminal amphipathic alpha-helix mediates membrane association of hepatitis C virus nonstructural protein 5A. *J Biol Chem* 2002; **277**: 8130-8139
- 21 **Houshmand H**, Bergqvist A. Interction of hepatitis C virus NS5A with la protein revealed by T7 phage display. *Biochem Biophys Res Commun* 2003; **309**: 695-701
- 22 **He Y**, Tan SL, Tareen SU, Vijaysri S, Langland JO, Jacobs BL, Katze MG. Regulation of mRNA translation and cellular sig-

- naling by hepatitis C virus nonstructural protein NS5A. *J Virol* 2001; **75**: 5090-5098
- 23 **Schiappa DA**, Mittal C, Brown JA, Mika BP. Relationship of hepatitis C genotype 1 NS5A sequence mutations to early phase viral kinetics and interferon effectiveness. *J Infect Dis* 2002; **185**: 868-877
- 24 **Hung CH**, Lee CM, Lu SN, Wang JH, Tung HD, Chen TM, Hu TH, Chen WJ, Changchien CS. Mutations in the NS5A and E2-PePHD region of hepatitis C virus type 1b and correlation with the response to combination therapy with interferon and ribavirin. *J Viral Hepat* 2003; **10**: 87-94
- 25 **Watanabe H**, Enomoto N, Nagayama K, Izumi N, Marumo F, Sato C, Watanabe M. Number and position of mutations in the interferon (IFN) sensitivity-determining region of the gene for nonstructural protein 5A correlate with IFN efficacy in hepatitis C virus genotype 1b infection. *J Infect Dis* 2001; **183**: 1195-1203
- 26 **Tan SL**, Katze MG. How hepatitis C virus counteracts the interferon response: the jury is still out on NS5A. *Virology* 2001; **284**: 1-12
- 27 **Gale M Jr**, Kwieciszewski B, Dossett M, Nakao H, Katze M. Antiapoptotic and oncogenic potentials of hepatitis C virus are linked to interferon resistance by viral repression of the PKR protein kinase. *J Virol* 1999; **73**: 6506-6516
- 28 **Kaneko T**, Tanji Y, Satoh S, Hijikata M, Asabe S, Kimura K, Shimotohno K. Production of two phosphoproteins from the NS5A region of the hepatitis C viral genome. *Biochem Biophys Res Commun* 1994; **205**: 320-326
- 29 **Hirota M**, Satoh S, Asabe S, Kohara M, Tsukiyama-Kohara K, Kato N, Hijikata M, Shimotohno K. Phosphorylation of nonstructural 5A protein of hepatitis C virus: HCV group-specific hyperphosphorylation. *Virology* 1999; **257**: 130-137
- 30 **Tanji Y**, Kaneko T, Satoh S, Shimotohno K. Phosphorylation of hepatitis C virus-encoded nonstructural protein NS5A. *J Virol* 1995; **69**: 3980-3986
- 31 **Chung KM**, Song OK, Jang SK. Hepatitis C virus nonstructural protein 5A contains potential transcriptional activator domain. *Mol Cells* 1997; **7**: 661-667
- 32 **Tanimoto A**, Ide Y, Arima N, Sasaguri Y, Padmanabhan R. The amino terminal deletion mutants of Hepatitis C virus nonstructural protein NS5A function as transcriptional activators in yeast. *Biochem Biophys Res Commun* 1997; **236**: 360-364
- 33 **Kato N**, Lan KH, One-Nia SK, Shiratori Y, Omata M. Hepatitis C virus nonstructural region 5A protein is a potent transcriptional activator. *J Virol* 1997; **71**: 8856-8859
- 34 **Qadri I**, Iwahashi M, Simon F. Hepatitis C virus NS5A protein binds TBP and p53, inhibiting their DNA binding and p53 interactions with TBP and ERCC3. *Biochim Biophys Acta* 2002; **1592**: 193-204
- 35 **Chung YL**, Sheu ML, Yen SH. Hepatitis C virus NS5A as a potential viral Bcl-2 homologue interacts with Bax and inhibits apoptosis in hepatocellular carcinoma. *Int J Cancer* 2003; **107**: 65-73

Edited by Zhu LH and Chen WW Proofread by Xu FM

Early diagnosis of bacterial and fungal infection in chronic cholestatic hepatitis B

Xiong-Zhi Wu, Dan Chen, Lian-San Zhao, Xiao-Hui Yu, Mei Wei, Yan Zhao, Qing Fang, Qian Xu

Xiong-Zhi Wu, Lian-San Zhao, Xiao-Hui Yu, Yan Zhao, Qing Fang, Qian Xu, Infectious Disease Center, West China Hospital of Sichuan University, Chengdu 610041, Sichuan Province, China
Dan Chen, Mei Wei, Luzhou Medical College, Luzhou 646000, Sichuan Province, China

Correspondence to: Xiong-Zhi Wu, Infectious Disease Center, West China Hospital of Sichuan University, Chengdu 610041, Sichuan Province, China. ilwxz@163.com

Telephone: +86-28-85422650 **Fax:** +86-28-85423783

Received: 2004-01-02 **Accepted:** 2004-01-12

Abstract

AIM: To investigate the early diagnostic methods of bacterial and fungal infection in patients with chronic cholestatic hepatitis B.

METHODS: One hundred and one adult in-patients with chronic hepatitis B were studied and divided into 3 groups: direct bilirubin (DBil)/total bilirubin (TBil) ≥ 0.5 , without bacterial and fungal infection (group A, $n=38$); DBil/TBil < 0.5 , without bacterial and fungal infection (group B, $n=23$); DBil/TBil ≥ 0.5 , with bacterial or fungal infection (group C, $n=40$). The serum biochemical index and pulse rate were analyzed.

RESULTS: Level of TBil, DBil, alkaline phosphatase (ALP) and DBil/ALP in group A increased compared with that in group B. The level of ALP in group C decreased compared with that in group A, whereas the level of TBil, DBil and DBil/ALP increased (ALP: 156 ± 43 , 199 ± 68 , respectively, $P < 0.05$; TBil: 370 ± 227 , 220 ± 206 , respectively, $P < 0.01$; DBil: 214 ± 143 , 146 ± 136 , respectively, $P < 0.01$; DBil/ALP: 1.65 ± 1.05 , 0.78 ± 0.70 , respectively, $P < 0.001$). The level of DBil and infection affected DBil/ALP. Independent of the effect of DBil, infection caused DBil/ALP to rise ($P < 0.05$). The pulse rate in group A decreased compared with that in group B (63.7 ± 6.4 , 77.7 ± 11.4 , respectively, $P < 0.001$), and the pulse rate in group C increased compared with that in group A (81.2 ± 12.2 , 63.7 ± 6.4 , respectively, $P < 0.001$). The equation (infection = 0.218 pulse rate + 1.064 DBil/ALP - 16.361), with total accuracy of 85.5%, was obtained from stepwise logistic regression. Pulse rate (< 80 /min) and DBil/ALP (< 1.0) were used to screen infection. The sensitivity was 62.5% and 64.7% respectively, and the specificity was 100% and 82.8% respectively.

CONCLUSION: Bacterial and fungal infection deteriorate jaundice and increase pulse rate, decrease serum ALP and increase DBil/ALP. Pulse rate, DBil/ALP and the equation (infection = 0.218 pulse rate + 1.064 DBil/ALP - 16.361) are helpful to early diagnosis of bacterial and fungal infection in patients with chronic cholestatic hepatitis B.

Wu XZ, Chen D, Zhao LS, Yu XH, Wei M, Zhao Y, Fang Q, Xu Q. Early diagnosis of bacterial and fungal infection in chronic cholestatic hepatitis B. *World J Gastroenterol* 2004; 10(15): 2228-2231
<http://www.wjgnet.com/1007-9327/10/2228.asp>

INTRODUCTION

Patients with chronic hepatitis are known to be abnormally susceptible to infection as a result of multiple immunologic defects^[1-6]. The incidence of bacteremia in chronic liver disease is 5- to 7- fold higher than that found in other hospitalized patients^[7]. Infection is often associated with systemic inflammatory response syndrome and multiple organ dysfunction syndrome that is easy to develop into liver failure^[8,9]. Infection can prove fatal either directly or by precipitation of encephalopathy, gastrointestinal hemorrhage, hepatic hemodynamic derangement, portal hypertension, or renal failure^[9-17]. About 33% mortality in bacteremic patients with chronic liver disease has been noted^[18]. Considering the low positivity rate and lengthy bacterial culture, severe chronic liver disease patients with clinical diagnosis of infection should get the antibiotic treatment immediately to improve the survival opportunity before pathogen diagnosis^[19-24]. However, clinical diagnosis is made more difficult by the absence of the typical clinical feature of infection - that is, fever, leucocytosis, and localized symptoms^[9,21]. Clinically apparent focus of infection could not be found in 20% to 60% of bacteremic patients with chronic liver disease^[9,25,26]. No specific site is identified in one third to one half of the infections, in which case the only clue may be deterioration of hepatic precoma or coma or renal function. The preventive antibiotic treatment is often applied to serious patients who have the liability to infection (such as the protein in ascites < 10 g/L, gastrointestinal hemorrhage, and previous spontaneous bacterial peritonitis), and in the meantime it might increase the risk of drug resistance^[19,27-30]. The early diagnostic methods of secondary bacterial and fungal infection in patients with chronic hepatitis B have not been studied. To reduce infection related mortality, the development of new methods for early diagnosis is of great significance.

MATERIALS AND METHODS

Patients

One hundred and one adult in-patients with chronic icteric hepatitis B in West China Hospital from October 2002 to March 2003 were studied and divided into three groups: direct bilirubin (DBil)/total bilirubin (TBil) ≥ 0.5 , without bacterial or fungal infection (group A, $n=38$); DBil/TBil < 0.5 , without bacterial or fungal infection (group B, $n=23$); DBil/TBil ≥ 0.5 , with bacterial and fungal infection (group C, $n=40$).

Inclusion criteria

All patients in the study met with the following criteria: positive HBsAg or HBVDNA; TBil > 17.1 mmol/L; age between 14 to 65 years. In addition, the patients in group C had the following features: leukocytes $\geq 10 \times 10^9$ /L or neutrophils $\geq 7 \times 10^9$ /L or the ratio of neutrophil $\geq 70\%$ in blood; leukocytes in urine ≥ 5 per visual field under high power microscope; leukocytes $\geq 0.5 \times 10^9$ /L or neutrophils $\geq 0.25 \times 10^9$ /L in ascites; bacterial culture of blood, urine, phlegm or ascites was positive.

Exclusion criteria

The patient who had one of the followings was excluded from

group A and group B: infected with other pathogens rather than HBV; complicated with other diseases which had not relation with hepatitis B; recently occurring gastrointestinal hemorrhage. The patient who had one of the followings was excluded from group C: infected with other virus; complicated with other liver diseases which had not relation with hepatitis B; recently occurring gastrointestinal hemorrhage; leukocytes in urine 5 per visual field under high power microscope but normal in routine blood test in female patients who were in menstruation or in patient who had non-inflammatory nephrosis.

Investigation indexes

Blind tests for TBil, DBil, indirect bilirubin (IBil), DBil/IBil, alanine aminotransferase (ALT), aspartate aminotransferase (AST), AST/ALT, serum total protein (TP), albumin (ALB), globulin (GLOB), ALB/GLOB, γ -glutamyltransferase (GGT), alkaline phosphatase (ALP), DBil/ALP, lactate dehydrogenase (LDH), cholinesterase (ChE), serum total bile acid (TBA) and pulse rate were performed. The first liver biochemical test of group A and B after hospitalization and the first liver biochemical test of group C after confirmation of infection were done, and pulse rate of all patients were measured after 15-min bed rest.

Statistical analysis

All data were presented as mean \pm SE. Analysis of variance and covariance was used to determine whether there were significant differences among the three groups. Data with significant difference were entered into a stepwise logistic regression analysis. Statistical calculations were performed by SPSS (Version: 11.0, Chicago, USA).

RESULTS

Clinical features of infection

Fifteen percent of patients in group C showed a rise in leukocyte or neutrophil in blood, 55% of patients showed a rise in the ratio of neutrophil in blood lightly, and 12.5% of patients showed an increase in leukocyte or neutrophil in ascites. Eleven patients showed a leukocyte rise in urine (in these cases, 5 patients showed an increase in leukocyte or neutrophil in blood or in the ratio of neutrophil, 5 patients had a history of fever, 2 patients showed spontaneous bacterial peritonitis). Fifteen patients presented with the localized symptoms of infection. Sixteen patients had a history of fever (the fever was light and persisted shortly in most patients). Positivity rate of bacterial culture was 25% (3/12).

Table 1 Comparison of serum bilirubin

Group	Case	Tbil ($\mu\text{mol/L}$)	DBil ($\mu\text{mol/L}$)	IBil ($\mu\text{mol/L}$)	DBil/TBil
A	38	220 \pm 206	146 \pm 136	73 \pm 72	0.660 \pm 0.078
B	23	59 \pm 33 ^b	22 \pm 12 ^d	38 \pm 23	0.361 \pm 0.105 ^d
C	40	370 \pm 227 ^{bf}	214 \pm 143 ^{bf}	136 \pm 92 ^{df}	0.631 \pm 0.840 ^f

^b P <0.01 vs group A; ^d P <0.001 vs group A; ^f P <0.001 vs group B.

Table 2 Comparison of TBA, ALP, DBil/ALP and pulse rate (mean \pm SE)

Group	<i>n</i>	TBA($\mu\text{mol/L}$)	<i>n</i>	ALP(U/L)	<i>n</i>	DBil/ALP	<i>n</i>	Pulse rate(times/min)
A	22	148 \pm 89	29	199 \pm 68	29	0.78 \pm 0.70	38	63.7 \pm 6.4
B	16	31 \pm 17 ^d	18	149 \pm 50 ^a	18	0.14 \pm 0.06 ^b	23	78 \pm 11 ^d
C	22	140 \pm 60 ^f	34	156 \pm 43 ^{ac}	34	1.65 \pm 1.05 ^{df}	40	81 \pm 12 ^d

^a P <0.05 vs group A; ^c P <0.05 vs group B; ^b P <0.01 vs group A; ^d P <0.001 vs group A; ^f P <0.001 vs group B.

Analysis of variance

Level of TBil, DBil, ALP and DBil/ALP in group A increased significantly compared with that in group B (P <0.01, P <0.01, P <0.05, P <0.01, respectively). The level of ALP in group C decreased compared with that in group A (156 \pm 43, 199 \pm 68, respectively, P <0.05), whereas the level of TBil, DBil and DBil/ALP increased significantly (TBil: 370 \pm 227, 220 \pm 206, respectively, P <0.01; DBil: 214 \pm 143, 146 \pm 136, respectively, P <0.01; DBil/ALP: 1.65 \pm 1.05, 0.78 \pm 0.70, respectively, P <0.001). The level of IBil in group C decreased compared with that in group A (P <0.001) (Tables 1, 2).

The pulse rate in group A decreased significantly compared with that in group B (63.7 \pm 6.4, 77.7 \pm 11.4, P <0.001). The pulse rate in group C increased compared with that in group A and normal adults (81.2 \pm 12.2, 63.7 \pm 6.4, 72, P <0.001), but decreased compared with that in infectious patients without hepatitis (81.2 \pm 12.2, 90, P <0.001) (Table 2, Figure 1).

The level of ALT, AST, AST/ALT, TP, ALB, GLOB, ALB/GLOB, GGT, LDH, and ChE showed no significant difference among the three groups (data not shown).

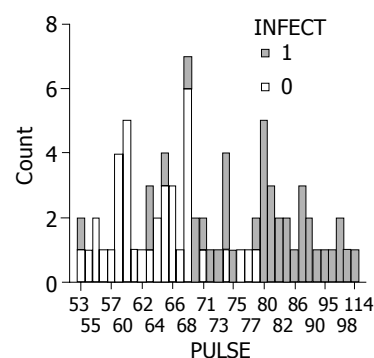


Figure 1 Pulse rate in cholestatic patients. 1: With bacterial or fungal infection; 0: Without bacterial and fungal infection.

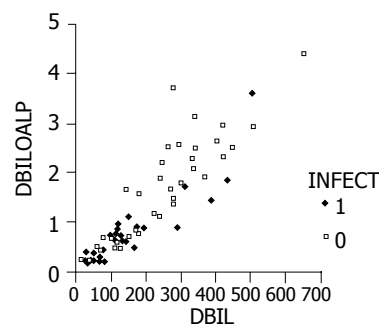


Figure 2 DBil/ALP and DBil in cholestatic patients. 1: With bacterial or fungal infection, 0: Without bacterial and fungal infection.

Analysis of covariance

There was linear correlation between DBil and DBil/ALP in groups A and C, and the distribution of DBil between the two groups was closely similar (Figure 2). The level of DBil and infection affected DBil/ALP (P <0.05, P <0.001, respectively)

(Table 3). Independent of the effect of DBil, infection caused DBil/ALP to rise ($P<0.05$) (Table 4).

Table 3 Tests of between-subjects effects (dependent variable: DBil/ALP)

Source	Type III sum of squares	Df	Mean square	F	P
Corrected model	50.025	2	25.012	129.672	<0.001
Infection	1.172	1	1.172	6.074	0.017
DBil	38.709	1	38.709	200.682	<0.001

Table 4 Pairwise comparisons (dependent variable: DBil/ALP)

Infection I	Infection J	Mean difference(I-J)	SE	P	95% CI
1	2	-0.293 ¹	0.119	0.017	-0.531 -0.055
2	1	0.293 ¹	0.119	0.017	0.0551 0.531

¹The mean difference is significant at the 0.05 level.

Logistic regression

The stepwise logistic regression was used to establish the best statistical model to early diagnose infection, and the equation (infection=0.218 pulse rate+1.064 DBil/ALP -16.361, $P<0.001$) was obtained. Its overall accuracy was 85.5%, and accuracy for diagnosing infection and noninfection were 85.7% and 85.3%, respectively (Table 5).

Table 5 Logistic analysis of bacterial and fungal infection

	B	SE	Wald	Df	P	Exp (B)
Pulse rate	0.218	0.059	13.468	1	<0.001	1.244
DBil/ALP	1.064	0.447	5.657	1	0.017	2.899
Constant	-16.361	4.251	14.815	1	<0.001	<0.001

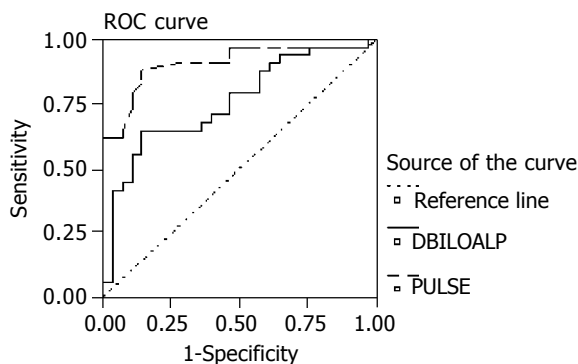


Figure 3 Receiver operator characteristic curve of pulse rate and DBil/ALP.

Screening test

Because the diagnostic index of pulse rate at 80/min to screen infection was the greatest, the cut off point was selected at 80/min (Figure 3). The sensitivity (Sen), specificity (Spe), diagnostic index (DI), false positive rate (α), false negative rate (β), Youden's index (γ), crude accuracy (CA), adjusted agreement (AA), positive predictive value (PV+) and negative predictive value (PV-) were 62.5%, 100%, 1.625, 100%, 71.7%,

62.5%, 80.8%, 83.6%, 0% and 37.5%, respectively. Area under the curve (A_z)=0.889 ($P<0.001$) (Table 6). Because the diagnostic index of DBil/ALP at 1.0 was the greatest, the cut off point was selected at 1.0 (Figure 3). Sen, Spe, DI, α , β , γ , CA, AA, PV+ and PV- were 64.7%, 82.8%, 1.475, 81.5%, 66.7%, 47.5%, 73.0%, 73.9%, 17.8% and 35.3%, respectively. A_z =0.7373 ($P<0.001$) (Table 6). Pulse rate was a better index than DBil/ALP ($P<0.001$).

DISCUSSION

Bacterial and fungal infections are the common complications of chronic hepatitis, frequently aggravating hepatitis. Since the bacterium culture in chronic hepatitis patients is often negative, clinical diagnosis plays a major role. However, a large number of patients do not often present with the typical clinical features of infection. In a prospective study, fever was initially absent in 45% of cases, and leukocytosis was absent in 25% of cases^[10]. Urinary tract infection is the common type of infection and the source of bacteremia in up to 50% of patients with cirrhosis, and 20% of episodes of spontaneous bacterial peritonitis^[10-30]. However, patients with urinary tract infection often do not have localized symptoms or physical findings^[10,11]. Careful urinalysis is important to exclude infection in patients with chronic liver disease^[10]. In our study, the leukocyte or neutrophil in blood rose in 15% of infected patients, and the ratio of neutrophil rose lightly in 55% of patients. Leukocyte or neutrophil in ascites increased in 5 patients, and leukocyte in urine rose in 11 patients. Sixteen patients had a history of fever (the fever was mild and short-lasting in most patients). Only 37.5% of patients presented localized symptoms of infection. The positivity rate of bacterial culture was 25%(3/12). Therefore, early diagnosis of bacterial and fungal infection is difficult in chronic hepatitis.

The level of ALP frequently rises in cholestatic patients. However, in serious liver disease, along with the increase of serum TBil and DBil, sometimes ALP decreased. Hadjis discovered that the synthesis of ALP decreased in the case of widespread hepatocyte necrosis. As well as ALT and AST, it is a marker of disease aggravation. In our study, the level of TBil and DBil in cholestatic patients with infection increased compared with that without infection, but ALP in infection patients decreased compared with that without infection.

In order to characterize the contrary alteration of DBil and ALP in infection patients, we introduced a new index -that is the ratio of DBil to ALP. The level of DBil/ALP showed significant difference between the three groups (0.7829±0.7002, 0.1377±0.0652, 1.6468±1.0500, respectively, $P<0.01$). Analysis of covariance showed that the level of DBil and infection affected DBil/ALP, and independent of the effect of DBil, infection led to DBil/ALP increase ($P<0.05$).

To test whether DBil/ALP could be used to screen infection, a screening test was performed. Its sensitivity, specificity, positive predictive value and negative predictive value were 64.7%, 82.8%, 81.5% and 66.7%, respectively (the cut off point at 1.0). Therefore, we hypothesize that DBil/ALP can be used as an "infection index" to diagnose infection early in chronic cholestatic hepatitis B. If DBil/ALP is greater than 1.0, the probability of infection is 82.8%.

The mean pulse rate in normal adults is 72/min, but it frequently increases in infection, often above 90/min. Because the vagus's excitement increased in cholestatic patient, the

Table 6 Screening test of bacterial and fungal infection

Diagnosis		Sensitivity	Specificity	Diagnostic Index	A_z	Z	P
Pulse rat	80/min	0.625	1.000	1.625	0.889	20.372	<0.001
DBil/ALP	1.0	0.647	0.828	1.475	0.7373	4.022	<0.001

pulse rate decreased compared with that in normal adults (63.7 ± 6.4 , 72 , $P < 0.001$). Although the pulse rate in cholestatic patient increased after infection (81.2 ± 12.2 , 63.7 ± 6.4 , $P < 0.001$), it was slower compared with that in infection patients without cholestasis (81.2 ± 12.2 , 90 , $P < 0.001$). That is why alteration of pulse rate in those patients is likely to be neglected in clinic.

To test whether pulse rate could be used to screen infection, a screening test was done. Its sensitivity, specificity, positive predictive value and negative predictive value were 62.5%, 100%, 100% and 71.7%, respectively (the cut off point at 80/min). Pulse rate was better for screening infection than DBil/ALP ($P < 0.001$).

In order to establish the best statistical model to diagnose infection early, the equation (infection = 0.218 pulse rate + 1.064 DBil/ALP - 16.361 , $P < 0.001$) was obtained from the stepwise logistic regression. Its total accuracy, the accuracy of diagnosing infection and noninfection was 85.5%, 85.7% and 85.3%, respectively.

It is interesting that there is notable relationship between the logistic equation and screening test. Among the 18 indexes that we studied, only pulse rate and DBil/ALP could affect the logistic equation. The equation can be described approximately as "infection = 0.2 pulse rate + DBil/ALP - 16 ". As 0.2 multiplied by 80 is 16 , if pulse rate 80 /min, the equation = 0 obviously. But if pulse rate < 80 /min, DBil/ALP significantly affects the equation. For severe chronic cholestatic hepatitis B, if pulse rate 80 /min, perhaps the antibiotic treatment should be applied immediately before pathogen diagnosis to improve the survival opportunity. If DBil/ALP > 1.0 but pulse rate < 80 /min, the equation is helpful to estimate the probability of infection. If DBil/ALP < 1.0 and pulse rate < 80 /min, the equation is useful to exclude infection. It is a sensitive, quick, simple and economical method to diagnose infection early and possibly improve the survival opportunity of severe chronic cholestatic hepatitis B.

REFERENCES

- Rimola A, Soto R, Bory F, Arroyo V, Perra C, Rodes J. Reticuloendothelial system phagocytic activity in cirrhosis and its relation to bacterial infections and prognosis. *Hepatology* 1984; **4**: 53-58
- Larcher VF, Wyke RJ, Mowat AP, Williams R. Bacterial and fungal infection in children with fulminant hepatic failure: possible role of opsonisation and complement deficiency. *Gut* 1982; **23**: 1037-1043
- Wyke RJ, Yousif-Kadaru AG, Rajkovic IA, Eddleston AL, Williams R. Serum stimulatory activity and polymorphonuclear leucocyte movement in patients with fulminant hepatic failure. *Clin Exp Immunol* 1982; **50**: 442-449
- Wyke RJ, Rajkovic IA, Williams R. Impaired opsonization by serum from patients with chronic liver disease. *Clin Exp Immunol* 1983; **51**: 91-98
- Wyke RJ, Rajkovic IA, Eddleston AL, Williams R. Defective opsonisation and complement deficiency in serum from patients with fulminant hepatic failure. *Gut* 1980; **21**: 643-649
- Inamura T, Miura S, Tsuzuki Y, Hara Y, Hokari R, Ogawa T, Teramoto K, Watanabe C, Kobayashi H, Nagata H, Ishii H. Alteration of intestinal intraepithelial lymphocytes and increased bacterial translocation in a murine model of cirrhosis. *Immunol Lett* 2003; **90**: 3-11
- Graudal N, Milman N, Kirkegaard E, Korner B, Thomsen AC. Bacteremia in cirrhosis of the liver. *Liver* 1986; **6**: 297-301
- Iber FL. Patients with cirrhosis and liver failure are at risk for bacterial and fungus infection. *Am J Gastroenterol* 1999; **94**: 2001-2003
- Rolando N, Wade J, Davalos M, Wendon J, Philpott-Howard J, Williams R. The systemic inflammatory response syndrome in acute liver failure. *Hepatology* 2000; **32**(4 Pt 1): 734-739
- Wyke RJ, Canalese JC, Gimson AE, Williams R. Bacteraemia in patients with fulminant hepatic failure. *Liver* 1982; **2**: 45-52
- Ruiz-del-Arbol L, Urman J, Fernandez J, Gonzalez M, Navasa M, Monescillo A, Albillos A, Jimenez W, Arroyo V. Systemic, renal, and hepatic hemodynamic derangement in cirrhotic patients with spontaneous bacterial peritonitis. *Hepatology* 2003; **38**: 1210-1218
- Navasa M, Follo A, Filella X, Jimenez W, Francitorra A, Planas R, Rimola A, Arroyo V, Rodes J. Tumor necrosis factor and interleukin-6 in spontaneous bacterial peritonitis in cirrhosis: relationship with the development of renal impairment and mortality. *Hepatology* 1998; **27**: 1227-1232
- Poddar U, Thapa BR, Prasad A, Sharma AK, Singh K. Natural history and risk factors in fulminant hepatic failure. *Arch Dis Child* 2002; **87**: 54-56
- Zhao C, Chen SB, Zhou JP, Xiao W, Fan HG, Wu XW, Feng GX, He WX. Prognosis of hepatic cirrhosis patients with esophageal or gastric variceal hemorrhage: multivariate analysis. *Hepatobiliary Pancreat Dis Int* 2002; **1**: 416-419
- De Mattos AA, Coral GP, Menti E, Valiatti F, Kramer C. Bacterial infection in cirrhotic patients. *Arq Gastroenterol* 2003; **40**: 11-15
- De las Heras D, Fernandez J, Gines P, Cardenas A, Ortega R, Navasa M, Barbera JA, Calahorra B, Guevara M, Bataller R, Jimenez W, Arroyo V, Rodes J. Increased carbon monoxide production in patients with cirrhosis with and without spontaneous bacterial peritonitis. *Hepatology* 2003; **38**: 452-459
- Perdomo Coral G, Alves de Mattos A. Renal impairment after spontaneous bacterial peritonitis: incidence and prognosis. *Can J Gastroenterol* 2003; **17**: 187-190
- Barnes PF, Arevalo C, Chan LS, Wong SF, Reynolds TB. A prospective evaluation of bacteremic patients with chronic liver disease. *Hepatology* 1988; **8**: 1099-1103
- Chu CM, Chang KY, Liaw YF. Prevalence and prognostic significance of bacterascites in cirrhosis with ascites. *Dig Dis Sci* 1995; **40**: 561-565
- Runyon BA, Hoefs JC. Culture-negative neutrocytic ascites: a variant of spontaneous bacterial peritonitis. *Hepatology* 1984; **4**: 1209-1211
- Rimola A, Garcia-Tsao G, Navasa M, Piddock LJ, Planas R, Bernard B, Inadomi JM. Diagnosis, treatment and prophylaxis of spontaneous bacterial peritonitis: a consensus document. International Ascites Club. *J Hepatol* 2000; **32**: 142-153
- Navasa M, Rimola A, Rodes J. Bacterial infections in liver disease. *Semin Liver Dis* 1997; **17**: 323-333
- Fernandez J, Bauer TM, Navasa M, Rodes J. Diagnosis, treatment and prevention of spontaneous bacterial peritonitis. *Baillieres Best Pract Res Clin Gastroenterol* 2000; **14**: 975-990
- Evans LT, Kim WR, Poterucha JJ, Kamath PS. Spontaneous bacterial peritonitis in asymptomatic outpatients with cirrhotic ascites. *Hepatology* 2003; **37**: 897-901
- Javaloyas de Morlius M, Ariza Cardenal J, Gudiol Munte F. Bacteremia in patients with hepatic cirrhosis. Etiopathogenic analysis and prognosis of 92 cases. *Med Clin* 1984; **82**: 612-616
- Jones EA, Sherlock S, Crowley N. Bacteraemia in association with hepatocellular and hepatobiliary disease. *Postgrad Med J* 1967; **43**: 7-11
- Sort P, Gines P, Navasa M, Arroyo V. Current treatment of ascites and spontaneous bacterial peritonitis in Spain: analysis of a survey of gastroenterologists and hepatologists. *Gastroenterol Hepatol* 1997; **20**: 437-441
- Navasa M, Follo A, Llovet JM, Clemente G, Vargas V, Rimola A, Marco F, Guarner C, Forne M, Planas R, Banares R, Castells L, Jimenez De Anta MT, Arroyo V, Rodes J. Randomized, comparative study of oral ofloxacin versus intravenous cefotaxime in spontaneous bacterial peritonitis. *Gastroenterology* 1996; **111**: 1011-1017
- Salmeron JM, Tito L, Rimola A, Mas A, Navasa MA, Llach J, Gines A, Gines P, Arroyo V, Rodes J. Selective intestinal decontamination in the prevention of bacterial infection in patients with acute liver failure. *J Hepatol* 1992; **14**: 280-285
- Rolando N DRA. Treatment and prevention of bacterial and mycotic infection in acute liver failure. *Rev Gastroenterol Peru* 1997; **17**(Suppl 1): 100-106

Increased oxidative DNA damage, inducible nitric oxide synthase, nuclear factor κ B expression and enhanced antiapoptosis-related proteins in *Helicobacter pylori*-infected non-cardiac gastric adenocarcinoma

Chi-Sen Chang, Wei-Na Chen, Hui-Hsuan Lin, Cheng-Chung Wu, Chau-Jong Wang

Chi-Sen Chang, Wei-Na Chen, Division of Gastroenterology, Chung Shan Medical University, Taichung, Taiwan, china

Chi-Sen Chang, Wei-Na Chen, Division of Gastroenterology, Taichung Veterans General Hospital, Taichung, Taiwan, china

Cheng-Chung Wu, Division of General Surgery, Taichung Veterans General Hospital, Taichung, Taiwan, china

Chi-Sen Chang, Wei-Na Chen, Hui-Hsuan Lin, Chau-Jong Wang, Institute of Biochemistry, Chung Shan Medical University, Taichung, Taiwan, china

Cheng-Chung Wu, National Young-Min Medical University, Taipei, Taiwan, china

Correspondence to: Chau-Jong Wang, Institute of Biochemistry, College of Medicine, Chung Shan Medical University, No. 110, Sec. 1, Chien Kuo North Road, 402, Taichung, Taiwan, china. wjg@csmu.edu.tw

Telephone: +886-4-24730022 **Fax:** +886-4-23248167

Received: 2004-03-15 **Accepted:** 2004-04-09

Abstract

AIM: Several epidemiological studies have demonstrated a close association between *Helicobacter pylori* (*H Pylori*) infection and non-cardiac carcinoma of the stomach. *H pylori* infection induces active inflammation with neutrophilic infiltrations as well as production of oxygen free radicals that can cause DNA damage. The DNA damage induced by oxygen free radicals could have very harmful consequences, leading to gene modifications that are potentially mutagenic and/or carcinogenic. The aims of the present study were to assess the effect of *H pylori* infection on the expression of inducible nitric oxidative synthase (iNOS) and the production of 8-hydroxy-deoxyguanosine (8-OHdG), a sensitive marker of oxidative DNA injury in human gastric mucosa with and without tumor lesions, and to assess the possible factors affecting cell death signaling due to oxidative DNA damage.

METHODS: In this study, 40 gastric carcinoma specimens and adjacent specimens were obtained from surgical resection. We determined the level of 8-OHdG formation by HPLC-ECD, and the expression of iNOS and mechanism of cell death signaling [including nuclear factor- κ B (NF κ B), MEKK-1, Caspase 3, B Cell lymphoma leukemia-2 (Bcl-2), inhibitor of apoptosis protein (IAP) and myeloid cell leukemia-1 (Mcl-1)] by Western-blot assay.

RESULTS: The concentrations of 8-OHdG, iNOS, NF κ B, Mcl-1 and IAP were significantly higher in cancer tissues than in adjacent non-cancer tissues. In addition, significantly higher concentrations of 8-OHdG, iNOS, NF κ B, Mcl-1 and IAP were detected in patients infected with *H pylori* compared with patients who were not infected with *H pylori*. Furthermore, 8-OHdG, iNOS, NF κ B, Mcl-1 and IAP concentrations were significantly higher in stage 3 and 4 patients than in stage 1 and 2 patients.

CONCLUSION: Chronic *H pylori* infection induces iNOS expression and subsequent DNA damage as well as enhances anti-apoptosis signal transduction. This sequence of events supports the hypothesis that oxygen-free radical-mediated damage due to *H pylori* plays a pivotal role in the development of gastric carcinoma in patients with chronic gastritis.

Chang CS, Chen WN, Lin HH, Wu CC, Wang CJ. Increased oxidative DNA damage, inducible nitric oxide synthase, nuclear factor κ B expression and enhanced antiapoptosis-related proteins in *Helicobacter pylori*-infected non-cardiac gastric adenocarcinoma. *World J Gastroenterol* 2004; 10 (15): 2232-2240

<http://www.wjgnet.com/1007-9327/10/2232.asp>

INTRODUCTION

Helicobacter pylori (*H pylori*) infection is associated with an increased risk of both peptic ulcer and gastric cancer^[1] Chronic gastritis induced by *H pylori* significantly increases the risk for non-cardiac gastric cancer^[2,3], and host responses that may affect the threshold for carcinogenesis include alteration of epithelial cell proliferation and apoptosis. Although the linkage between *H pylori* infection and gastric cancer is convincing, the molecular mechanism or mechanisms responsible are unclear, and both bacterial and host factors are implicated. One possible factor is that increased inflammation generates reactive oxygen and nitrogen intermediates that have been shown to damage DNA directly^[4].

Mucosal hyperproliferation has been reproducibly demonstrated in *H pylori*-infected human^[5-7] and rodent gastric tissue^[8-10], and proliferation scores normalize following successful eradication in humans^[5-7]. However, maintenance of tissue integrity requires that enhanced cell production is accompanied with increased rates of cell loss consequently, studies have also examined the effect of *H pylori* on apoptosis. In contrast to hyperproliferation, *H pylori* has been associated with increased^[11-14], unchanged^[15], or even decreased^[16] levels of apoptosis *in vivo*, and within a particular population, substantial heterogeneity exists among apoptosis scores^[11-14]. These observations suggest that increases in proliferation that are not balanced by concordant increases in apoptosis over years of colonization may heighten the retention of mutated cells, ultimately enhancing the risk for gastric malignancy in certain populations. Alteration of epithelial cell proliferation and apoptosis is a manifestation of *H pylori*-induced gastritis. However, the precise mechanisms underlying these effects remain incompletely clarified. In this study, we aimed to assess the effect *H pylori* infection on the expression of iNOS and the production of 8-OHdG, a sensitive marker of oxidative DNA injury in human gastric mucosa with and without tumor lesions, as well as the possible factors affecting cell death signaling due to oxidative DNA damage.

MATERIALS AND METHODS

Patients

In this study, 40 patients (aged 68.3±11.4 years, range 39–84 years, M/F: 26/14) with non-cardiac gastric adenocarcinoma were included. Specimens from tumor site and adjacent non-tumor site were obtained from surgical resection. By TNM staging according to the criteria described by the International Union Against Cancer^[17], there were 2 cases in stage 1, 6 cases in stage 2, 8 cases in stage 3 and 24 cases in stage 4 (Table 1). *H. pylori* infection was assessed by the following three methods: histology (haematoxylin and eosin staining or Giemsa staining, rapid urease test (CLO test, Delta West Pty Ltd, Perth, Australia) and serum *H. pylori* ELISA IgG assays (Trinity Biotech USA, Jamestown, NY). A patient was considered *H. pylori* positive if one or more of the diagnostic methods applied were positive, and *H. pylori* negative if all methods were negative. There were 29 patients (72.5%) with *H. pylori* infection and 11 patients (27.5%) without *H. pylori* infection. We determined the level of 8-OHdG formation by HPLC-ECD, and the expression of iNOS and cell death signaling, including NFκB, MEKK1, Caspase 3, Bcl-2, Mcl-1 and IAP by Western-blot assay.

Table 1 Characteristics of all patients

Case No	Stage	<i>H. pylori</i> infection	Case No	Stage	<i>H. pylori</i> infection
1	II	+	21	III	+
2	IV	+	22	IV	+
3	IV	+	23	IV	+
4	III	+	24	IV	+
5	IV	+	25	IV	-
6	IV	+	26	IV	+
7	IV	+	27	I	+
8	III	-	28	I	-
9	III	+	29	IV	-
10	III	+	30	II	+
11	IV	+	31	IV	+
12	IV	-	32	IV	+
13	IV	-	33	IV	+
14	IV	+	34	III	+
15	IV	+	35	II	+
16	II	+	36	III	+
17	III	-	37	IV	-
18	IV	+	38	IV	+
19	IV	+	39	IV	+
20	II	-	40	II	-

DNA extraction and digestion

DNA was extracted with Dneasy tissue kit (QIAGEN) according to the protocol of Dahlhaus and Apple^[18] with minor modifications as described previously^[19]. Briefly, one volume of nuclear fraction obtained from surgical tissue was mixed with ten volumes of extraction buffer (1 mol/L NaCl, 10 mmol/L Tris-HCl, 1 mmol/L EDTA, 5 g/L SDS, pH 7.4) and one volume of chloroform:isoamylalcohol (12:1 v/v). After vigorous shaking, the aqueous phase was separated by centrifugation. This step was repeated three times before DNA was precipitated with absolute ethanol (-70 °C). DNA pellet was dissolved in TE buffer (10 mmol/L Tris-HCl, 1 mmol/L EDTA, pH 7.4), and then incubated with RNase A to remove RNA. After incubation, DNA was extracted with chloroform:isoamylalcohol, and precipitated with absolute ethanol again. The DNA pellet was dissolved in 10 mmol/L Tris-HCl (pH 7.0) and hydrolyzed according to the previous procedure^[20]. Briefly, 200 µg DNA in 200 µL 10 mmol/L Tris-HCl (pH 7.0) was first denatured at 95 °C for 3 min. The digestion was carried out at 37 °C for 1 h with 100 units DNase I (from bovine pancreas, Sigma) in a buffer containing 10 mmol/L MgCl₂, followed by incubation with 5 units nuclease P₁ (from penicillium citrinum, Sigma) in

100 µmol/L ZnCl₂ for an additional hour. The mixture was incubated finally with 3 units alkaline phosphatase (from *Escherichia coli*, Sigma) at 37 °C for 1 h. The incubation was terminated with acetone (HPLC grade, Merck, Germany) to precipitate proteins. After 12 000 g centrifugation for 15 min, the supernatant was dried under vacuum in a rotary evaporator (Eyela, Tokyo, Japan) and DNA was dissolved in distilled H₂O.

8-OHdG assay

8-OHdG levels were determined by HPLC/ECD consisting of a BAS PM-80 pump (Bioanalytical Systems, West Lafayette, IN, USA), a CMA-200 microautosampler (CAM/Microdialysis, Stockholm, Sweden), a BAS-4C amperometric detector (Bioanalytical Systems, West Lafayette, IN, USA), a microbore reversed-phase column (Inertsil-2, 5-µm ODS, 1.0×150 mm I.D. G.L. Sciences, Tokyo, Japan) Beckman I/O 406 interface, and Beckman system gold data analysis software (Beckman Instruments). A potential of +0.6 V was selected for the glassy carbon working electrode which corresponded to a silver/silver chloride reference electrode. The mobile phase consisted of 12.5 mmol/L citric acid, 30 mmol/L NaOH, 25 mmol/L sodium acetate, 10 mmol/L acetic acid glacial and 50 mL/L methanol (pH 5.3). The flow rate was set at 1 mL/min. Under these conditions, the retention time of 8-OHdG was 8.49 min with a significantly higher signal than background noise.

Immunoblot analysis

Cancerous and non-cancerous tissue samples were homogenized with ten volumes of homogenization buffer (50 mmol/L Tris, 5 mmol/L EDTA, 150 mmol/L sodium chloride, 10 g/L Nonidet P-401 g/L SDS, 5 g/L deoxycholic acid, 1 mmol/L sodium orthovanadate, 170 µg/mL leupeptin, 100 µg/mL phenylsulfonyl fluoride; pH 7.5). After 30 min of mixing at 4 °C, the mixture was centrifuged at 800 r/min for 10 min, and the supernatant was collected. The protein content of the samples was determined with the Bio-Rad protein assay reagent using BSA as a standard. For Western blotting analysis, 50 µg protein from both cancerous and non-cancerous tissue samples was resolved on 100 g/L SDS-PAGE gels along with prestained protein molecular weight standards (Bio-Rad). The separated proteins were then blotted onto NC membrane (0.45 µm, Bio-Rad) and reacted with primary antibodies (against iNOS, NFκB, MEKK1, Caspase 3, Bcl-2, Mcl-1 and IAP). After washed, the blots were incubated with peroxidase-conjugated goat anti-mouse antibody. Immunodetection was carried out using the enhanced chemiluminescence (ECL) Western blotting detection kit (Amersham Corp., UK). Relative protein expression levels were quantified by densitometric measurement of ECL reaction bands and normalized with values of tubulin. Finally, enhanced chemiluminescence (ECL) was used to detect the membrane, and then the membrane was exposed to X-ray film to observe results. All the immunoblot results were determined by Alpha Imager 2000 documentation & analysis system (Alpha Innotech Corporation).

Statistical analysis

Each parameter expressed by fold of increase of the data from cancer tissue was compared to the adjacent non-cancer tissue. The results were reported as mean±SE from individual magnitudes. Data were analyzed with Student's *t*-test. Statistical differences were considered significant when *P*<0.05.

RESULTS

To assess the effect of *H. pylori* infection on each determined parameter, the results were expressed by fold of increase comparing the data of cancer tissue with those of the adjacent non-cancer tissue. The concentrations of 8-OHdG were analyzed by HPLC/ECD. There were significantly higher concentrations

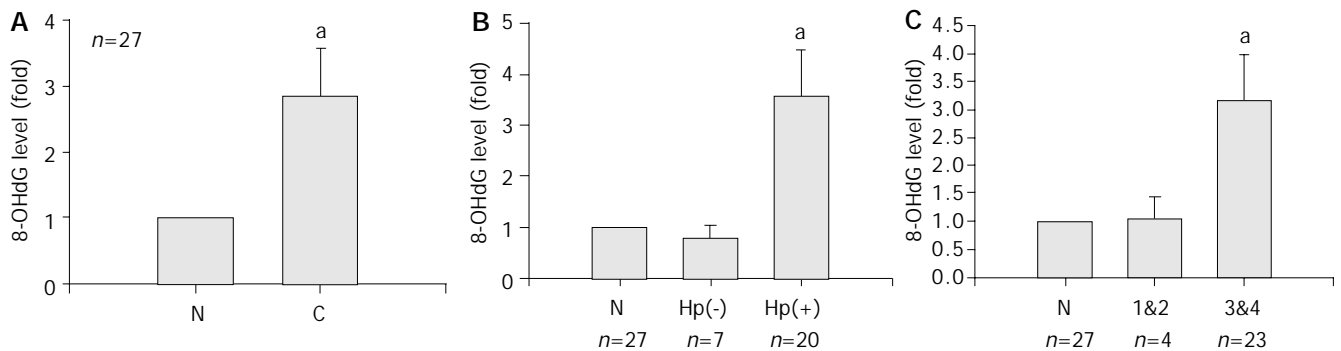


Figure 1 Concentrations of 8-OHdG. A: Higher concentration of 8-OHdG in cancer tissues compared with adjacent non-cancer tissues. B: Higher concentration of 8-OHdG in cancer tissues of patients with and without *H pylori* infection. C: Significantly higher 8-OHdG concentrations in stage 3 and 4 patients ^a $P < 0.05$, N: non-cancer tissue, Hp(-): without *H pylori* infection, Hp(+): with *H pylori* infection, 1&2: gastric cancer stages 1 and 2, 3&4: gastric cancer stages 3 and 4.

of 8-OHdG in cancer tissues than in adjacent non-cancer tissues (Figure 1). In addition, significantly higher concentrations of 8-OHdG were detected in patients infected with *H pylori* than in those without *H pylori* infection. 8-OHdG levels were also significantly higher in stage 3 and 4 patients than in stage 1 and 2 patients.

Immunoblot analysis of several factors affecting cell death signaling related to oxidative DNA damage showed increased concentrations of iNOS and NFκB in patients infected with *H pylori* compared to patients who were tested negative for *H pylori* (Figure 2A-B). Furthermore, iNOS and NFκB concentrations were significantly higher in stage 3 and 4 patients than in stage 1 and 2 patients.

Although there were some increases in the concentrations of MEKK1 and Caspase-3 in the cancer tissue (Figure 2C-D), these changes were not statistically significant. In addition, no significant increases of MEKK1 and Caspase-3 in patients infected with *H pylori* were noted. The concentrations of Caspase-3 in stage 1 and 2 patients were significantly lower than those in stage 3 and 4 patients.

Among the anti-apoptosis-related proteins, there were some increases in the concentrations of Bcl-2 in the cancer tissue (Figure 2E). However, the changes were not statistically significant. In addition, no significant increase of Bcl-2 in patients infected with *H pylori* was noted. The concentrations of Bcl-2 in stage 1 and 2 patients were significantly lower than those in stage 3 and 4 patients. Mcl-1 and IAP concentrations were significantly higher in the cancer tissues than in the adjacent non-cancer tissues (Figure 2F-G). In addition, Mcl-1 and IAP concentrations were significantly higher in *H pylori*-positive patients than in *H pylori*-negative patients. Stage 3 and 4 patients had significantly higher concentrations of Mcl-1 and IAP than stage 1 and 2 patients.

Table 2 8-oHdG, iNOS, NFκB, Mel-1 and IAP Concentrations in cancer and adjacent non-cancer tissues

	Cancer tissue	<i>H pylori</i> (+)	Stages I & II	Stages III & IV
8-OHdG	a	a	-	a
iNOS	b	b	-	b
NF-κB	a	a	-	a
MEKK1	-	-	-	-
Caspase 3	-	-	b	-
Bcl-2	-	-	b	-
Mcl-1	a	a	-	a
IAP	a	a	-	a

: increase, : decrease, -: no significant change, ^a $P < 0.05$, ^b $P < 0.01$ compared with control, by one sample *t*-test and independent *t*-test, respectively.

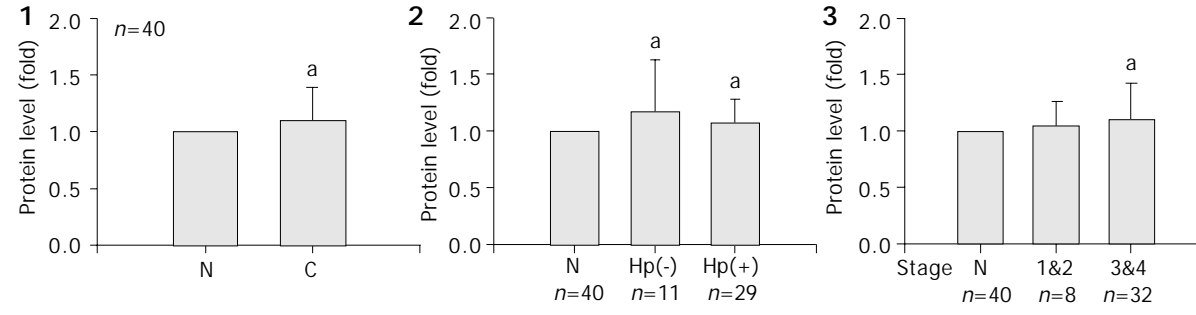
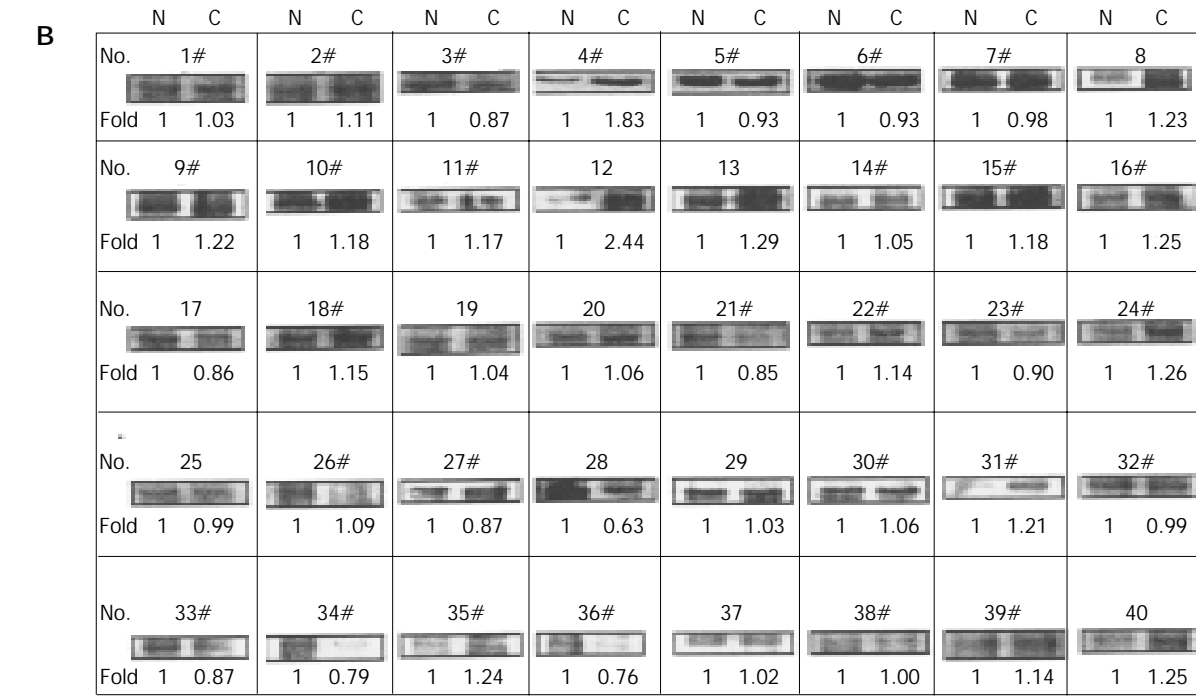
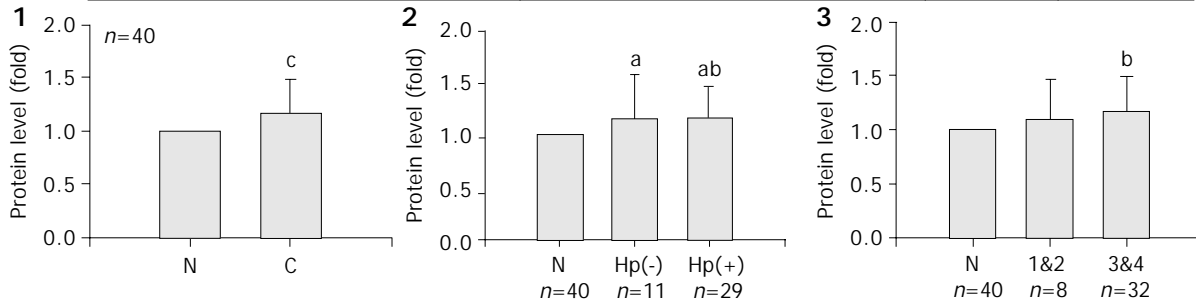
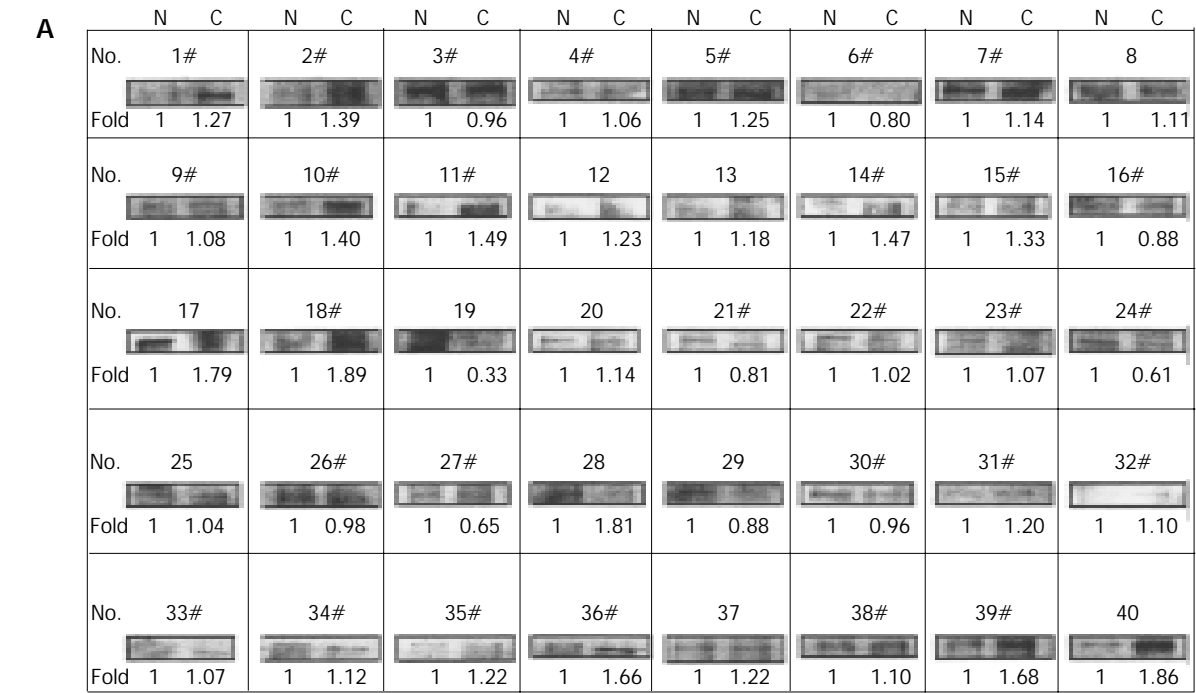
In summary, 8-OHdG, iNOS, NFκB, Mcl-1 and IAP concentrations were significantly higher in cancer tissues than in adjacent non-cancer tissues (Table 2). In addition, significantly higher concentrations of 8-OHdG, iNOS, NFκB, Mcl-1 and IAP were detected in patients infected with *H pylori* compared to patients who were not infected with *H pylori*.

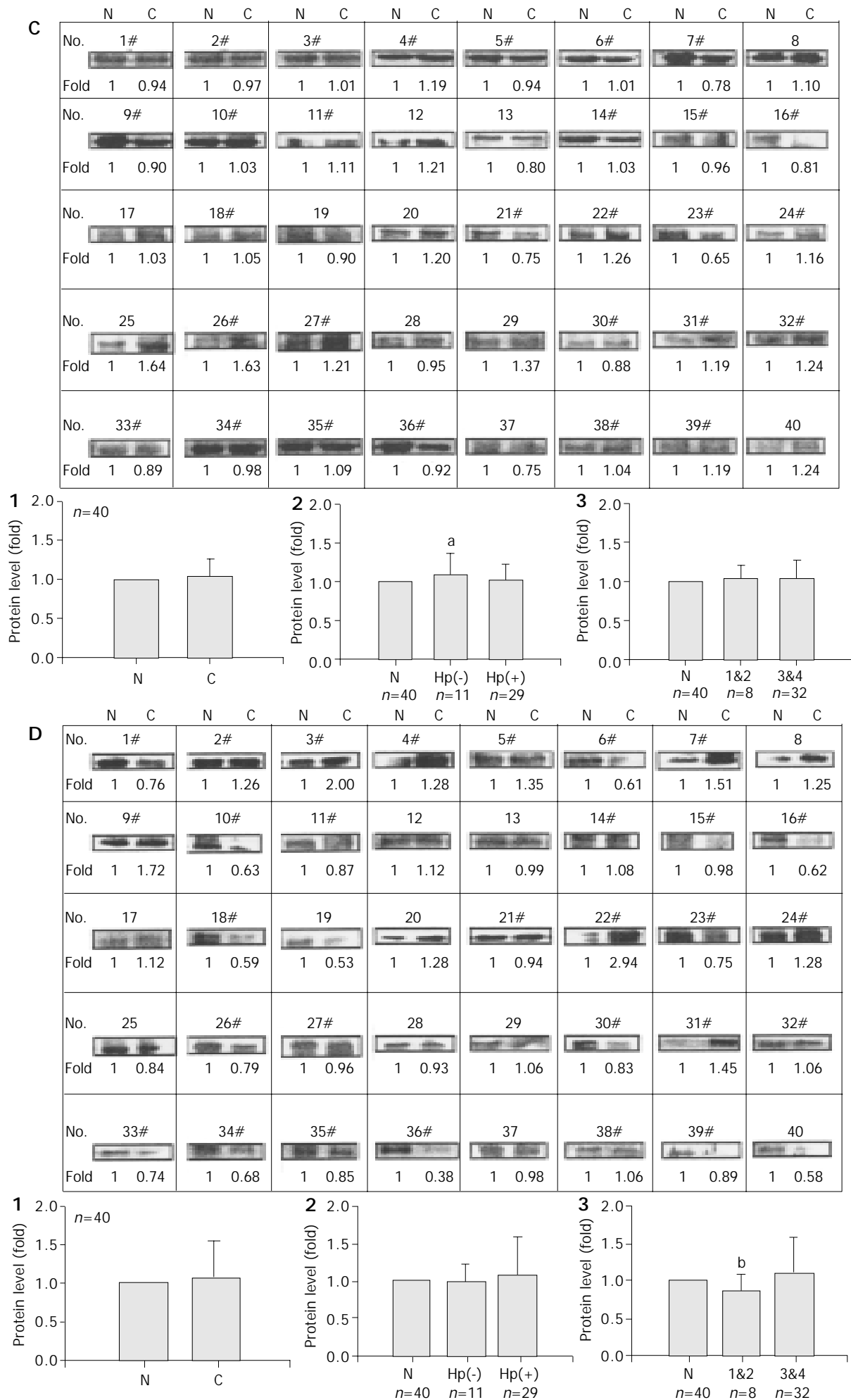
Furthermore, 8-OHdG, iNOS, NFκB, Mcl-1 and IAP concentrations were significantly higher in stage 3 and 4 patients than in stage 1 and 2 patients.

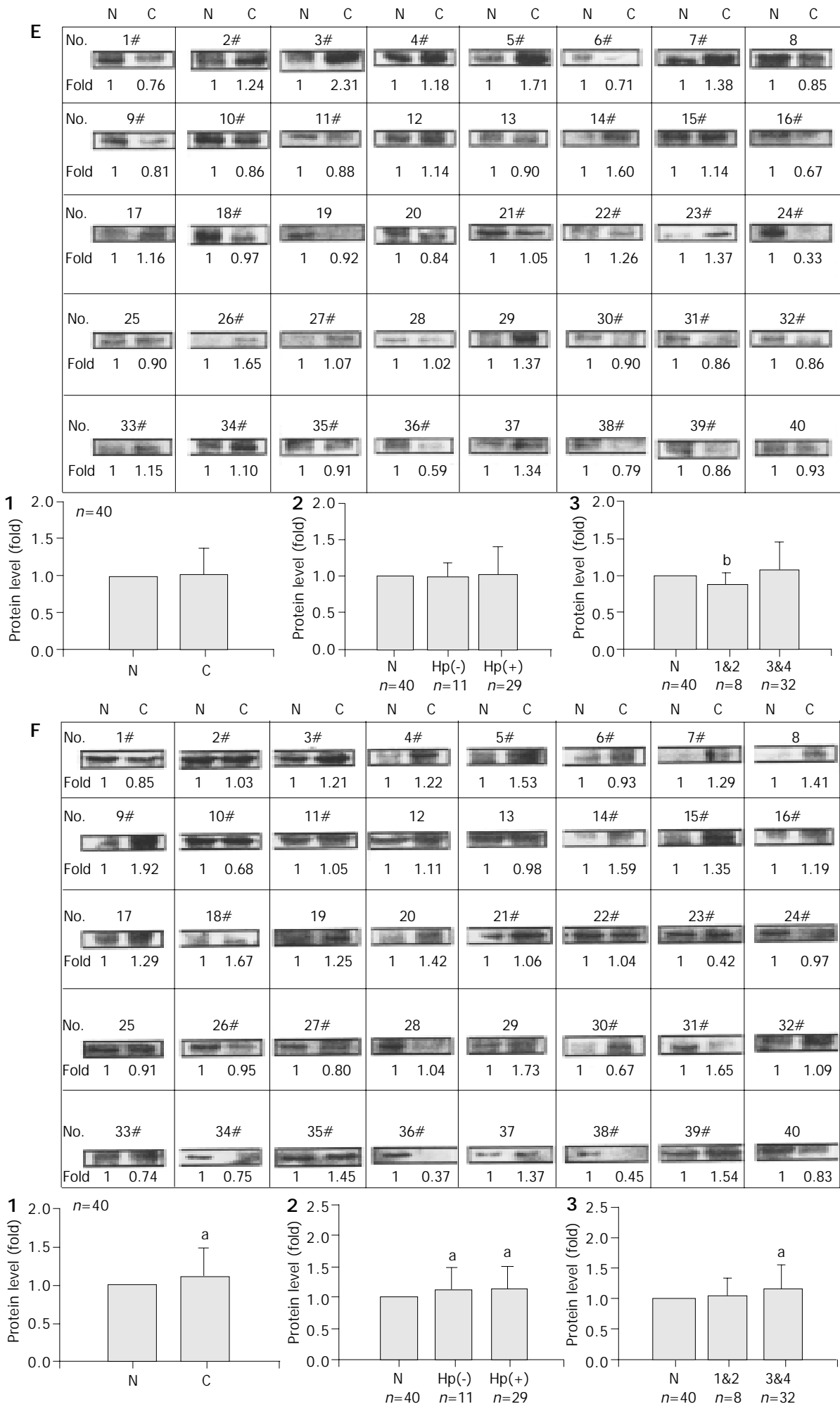
DISCUSSION

H pylori infection may influence the progression from chronic gastritis to adenocarcinoma of the distal stomach by a multifactorial, multistep process, in which chronic inflammation plays a major role. Free radical mediated oxidative DNA damage was involved in this process^[21-23]. The DNA damage provoked by oxygen free radicals can have very harmful consequences, leading to gene modifications that are potentially mutagenic and/or carcinogenic. Recently, 8-OHdG has been accepted as a sensitive marker for oxidative DNA damage in affected organs. Chronic gastritis due to *H pylori* infection is characterized by the accumulation of oxidative DNA damage measured by concentrations of 8-OHdG, indicating mutagenic and carcinogenic potential^[24]. In this study, we demonstrated an increase in the concentrations of 8-OHdG in cancer tissues. Furthermore, the increase was significantly higher in patients infected with *H pylori* as well as in patients with advanced gastric cancer. The increased level of oxidative DNA damage suggested a mechanistic link between *H pylori* infection and gastric carcinoma^[25,26].

H pylori-associated inflammation related to DNA damage is indicated by increased levels of oxidative DNA damage, increased occurrence of apoptosis, as well as increased expression of iNOS, which seemed to provide the mechanistic links between *H pylori* infection and gastric carcinogenesis^[27,28]. Upregulation of iNOS expression might contribute to the oxidative DNA damage observed during *H pylori* infection^[25]. Recent studies have shown that nitric oxide (production of iNOS) reacts rapidly with superoxide anions produced by *H pylori*-infected gastric tissues to form peroxynitrate, which could induce oxidative damage^[29]. This may increase the mutation rate in infected hyperproliferative gastric mucosa. In addition, the expressions of iNOS are closely related to tumor angiogenesis, and involved in progression of the disease as well as lymph node metastasis. Thus the expressions of iNOS might serve as indexes for evaluating staging of gastric carcinoma. In this study, we observed significantly higher increases in the concentrations of iNOS in patients infected with *H pylori* and in patients with advanced gastric cancer, compared with *H pylori*-negative patients and low stage gastric cancer patients, respectively.







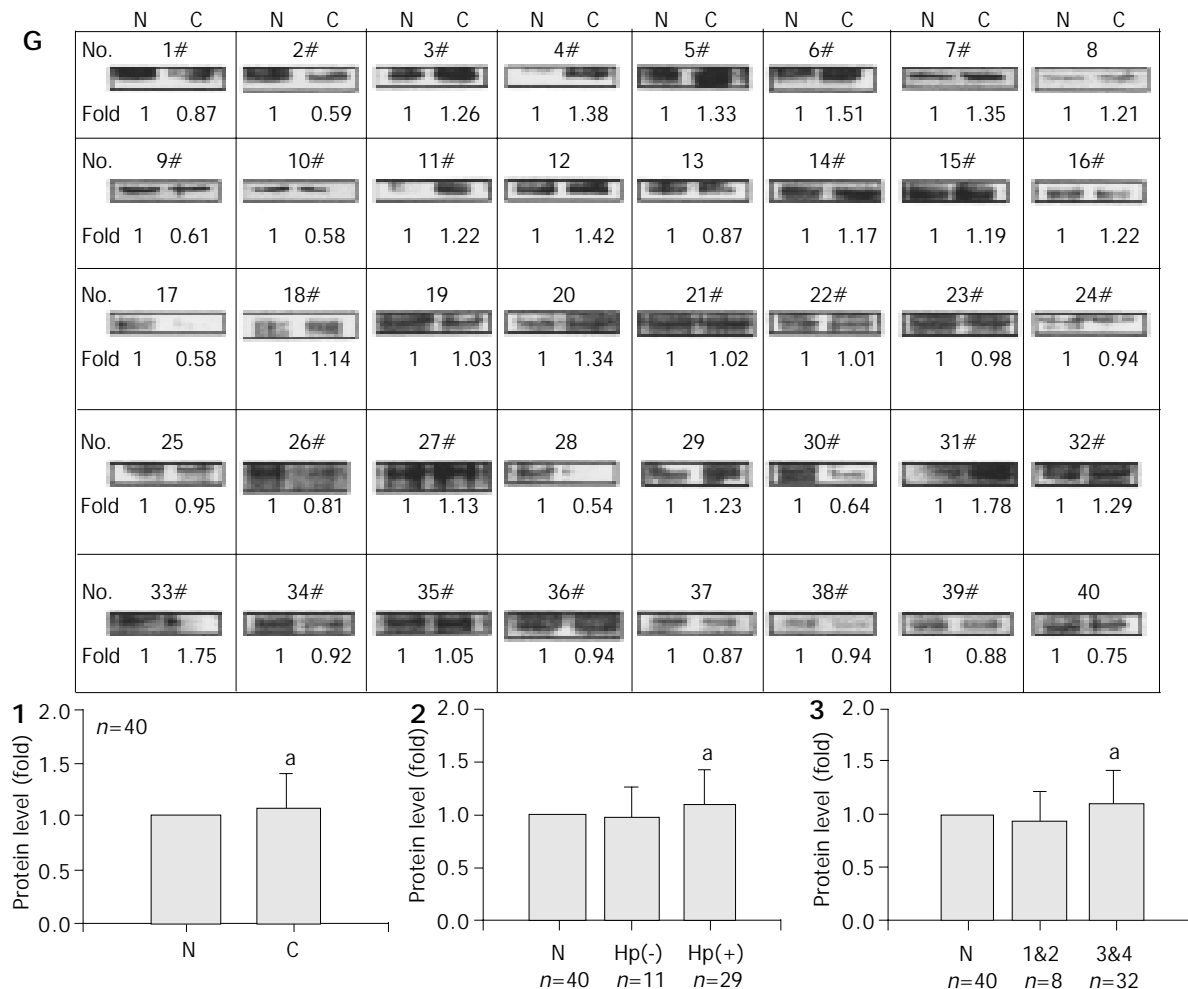


Figure 2 Immunoblot analysis of factors affecting cell death. A: Immunoblot analysis of iNOS. 1: Significantly higher concentrations of iNOS in cancer tissues compared with adjacent non-cancer tissues. 2: Significantly higher concentrations of iNOS in cancer tissues of patients with and without *H pylori* infection. 3: Significantly higher iNOS concentrations in stage 3 and 4 patients. #=*H pylori* infected, ^a $P<0.05$, ^b $P<0.01$, N: non-cancer tissue, C: cancer tissue, Hp(-): without *H pylori* infection, Hp(+): with *H pylori* infection, 1&2: gastric cancer stages 1 and 2, 3&4: gastric cancer stages 3 and 4. B: Immunoblot analysis of NF κ B. 1: Significantly higher concentrations of NF κ B in cancer tissues in comparison with adjacent non-cancer tissues. 2: Significantly higher concentrations of NF κ B in cancer tissues of patients with and without *H pylori* infection. 3: Significantly higher NF κ B concentrations in stage 3 and 4 patients #=*H pylori* infected, $P<0.05$, N: non-cancer tissue, C: cancer tissue, Hp(-): without *H pylori* infection, Hp(+): with *H pylori* infection, 1&2: gastric cancer stages 1 and 2, 3&4: gastric cancer stages 3 and 4. C: Immunoblot analysis of MEKK1. 1: Concentrations of MEKK1 in cancer tissues and adjacent non-cancer tissues. 2: Significantly higher concentrations of MEKK1 in cancer tissues of patients without *H pylori* infection. 3. No differences in MEKK1 concentrations in cancer tissues with different stages. #=*H pylori* infected, ^a $P<0.05$, N: non-cancer tissue, C: cancer tissue, Hp(-): without *H pylori* infection, Hp(+): with *H pylori* infection, 1&2: gastric cancer stages 1 and 2, 3&4: gastric cancer stages 3 and 4. D: Immunoblot analysis of Caspase 3. 1: Similar concentrations of Caspase 3 in cancer tissues and adjacent non-cancer tissues. 2: Similar concentrations of Caspase 3 in cancer tissues of patients with and without *H pylori* infection. 3: Significantly lower Caspase 3 concentrations in stage 1 and 2 patients. #=*H pylori* infected, ^b $P<0.01$, N: non-cancer tissue, C: cancer tissue, Hp(-): without *H pylori* infection, Hp(+): with *H pylori* infection, 1&2: gastric cancer stages 1 and 2, 3&4: gastric cancer stages 3 and 4. E: Immunoblot analysis of Bcl-2. 1: Similar concentrations of Bcl-2 in cancer tissues and adjacent non-cancer tissues. 2: No differences in concentrations of Bcl-2 in cancer tissues of patients with and without *H pylori* infection. 3: Significantly higher Bcl-2 concentrations in stage 1 and 2 patients. #=*H pylori* infected, ^b $P<0.01$, N: non-cancer tissue, C: cancer tissue, Hp(-): without *H pylori* infection, Hp(+): with *H pylori* infection, 1&2: gastric cancer stages 1 and 2, 3&4: gastric cancer stages 3 and 4. F: Immunoblot analysis of Mcl-1. 1: Significantly higher concentrations of Mcl-1 in cancer tissues in comparison with adjacent non-cancer tissues. 2: Significantly higher concentration of Mcl-1 in cancer tissues of patients with and without *H pylori* infection. 3: Significant higher Mcl-1 concentrations in stage 3 and 4 patients than #=*H pylori* infected, ^a $P<0.05$, N: non-cancer tissue, C: cancer tissue, Hp(-): without *H pylori* infection, Hp(+): with *H pylori* infection, 1&2: gastric cancer stages 1 and 2, 3&4: gastric cancer stages 3 and 4. G: Immunoblot analysis of IAP. 1: Significantly higher concentrations of IAP in cancer tissues compared with adjacent non-cancer tissues, 2: Significantly higher concentrations of IAP in cancer tissues with *H pylori* infection, 3: Significantly higher IAP concentrations in stage 3 and 4 patients #=*H pylori* infected, ^a $P<0.05$, N: non-cancer tissue, C: cancer tissue, Hp(-): without *H pylori* infection, Hp(+): with *H pylori* infection, 1&2: gastric cancer stages 1 and 2, 3&4: gastric cancer stages 3 and 4.

NF κ B has been found to be a critical regulator of genes involved in inflammation, cell proliferation, and apoptosis^[30]. Recent studies suggested that NF κ B might play a critical role in protecting cells against apoptosis^[31,32]. The magnitude of the stimulus and the cell type involved may determine whether

NF κ B leads to cell survival or cell death. Maeda *et al.* reported cag PAI positive *H pylori* was capable of inducing apoptotic effects mainly through the mitochondrial pathway. Antiapoptotic effects mediated by NF κ B activation were also observed by Maeda *et al.*^[33]. In this study, we revealed an

increase in the concentrations of NF κ B in cancer tissues. In addition, the increase was significantly higher in patients infected with *H pylori* as well as in patients with advanced gastric cancer compared with *H pylori*-negative patients and low stage gastric cancer patients, respectively.

Recent investigations implicated mitogen-activated protein kinases (MAPK) as additional mediators of *H pylori*-dependent NF κ B activation and IL-8 expression. Studies have demonstrated the presence of cross-talk between the MAPK and NF κ B pathways^[21-34]. MAPK cascades are signal transduction networks that target transcription factors and thus participate in a diverse array of cellular functions including cytokine production. In this study, there was an increase in the concentrations of MEKK1, a member of the MAPK signaling cascade in cancer tissues. However, the increase was not significant in all the studied patient groups.

Kanai *et al.* noted that transforming growth factor- α played an anti-apoptotic role in gastric mucosal cells by enhancing the expression of Bcl-2 family proteins via an NF κ B-dependent pathway^[35]. NF κ B is now known to upregulate transcription of several anti-apoptotic genes, including a cellular inhibitor of apoptosis, a Bcl-2 homolog, and cyclooxygenase-2, as well as pro-apoptotic genes, such as bax and p53. Tumor cells can have abnormal expression levels of factors such as Bcl-2 family proteins that slow the progression of apoptosis and elevate NF κ B-regulated transcription, which can inhibit TNF- α -induced apoptosis. However, in this study, no significant changes in the concentrations of Bcl-2 in cancer tissues or patients infected with *H pylori* were noted. Furthermore, upregulation of anti-apoptotic gene mcl-1 might play a role in interleukin-6-mediated protection of gastric cancer cells from the apoptosis induced by hydrogen peroxide^[36]. The anti-apoptotic role played by NF κ B also involves the ability of this transcriptional factor to induce expression of genes that promote cell survival, such as the genes coding for TRAF1, TRAF2, and the cellular inhibitors of apoptosis 1 and 2 (c-IAP1, c-IAP2)^[37]. In this study, we demonstrated an increase in the concentrations of IAP and Mcl-1, anti-apoptosis related proteins in cancer tissues. Furthermore, the increase was significantly higher in patients infected with *H pylori* as well as in patients with advanced gastric cancer, compared with *H pylori*-negative and non-advanced gastric patients, respectively. Therefore, enhanced antiapoptosis-related protein expression may contribute to disease progression.

Caspase3 is a member of the cell death effector (CED)-3 family, which is involved in the induction of apoptosis. Hoshi *et al.* reported Caspase 3 was involved in the development or regulation of apoptotic cell death in cell turnover of normal and neoplastic mucosa of the human stomach^[38]. These results indicate that gastric adenocarcinoma is associated with an inhibition of apoptosis and the augmentation of proliferative activity of tumor cells when compared to non-neoplastic gastric mucosa. However, in this study, there was no difference of increase in Caspase 3 between patients with or without *H pylori* infection or patients with or without advanced gastric cancer.

In conclusion, chronic *H pylori*-induced iNOS expression and subsequent DNA damage as well as signal transduction appear to make an important contribution to *H pylori*-related gastric carcinogenesis. This sequence of events found in this study supports the hypothesis that oxygen-free radical-mediated damage induced by *H pylori* plays a vital role in the development of gastric carcinoma in patients with chronic gastritis.

ACKNOWLEDGEMENT

The authors would like to thanks the Biostatistics Task Force of Taichung Veterans General Hospital for their help with the statistical analyses performed in this study.

REFERENCES

- 1 **Wang KX**, Wang XF, Peng JL, Cui YB, Wang J, Li CP. Detection of serum anti-*Helicobacter pylori* immunoglobulin G in patients with different digestive malignant tumors. *World J Gastroenterol* 2003; **9**: 2501-2504
- 2 **Nomura A**, Stemmermann GN, Chyou PH, Kato I, Perez-Perez GI, Blaser MJ. *Helicobacter pylori* infection and gastric carcinoma among Japanese Americans in Hawaii. *N Engl J Med* 1991; **325**: 1132-1136
- 3 **Parsonnet J**, Friedman GD, Vandersteen DP, Chang Y, Vogelman JH, Orentreich N, Sibley RK. *Helicobacter pylori* infection and the risk of gastric carcinoma. *N Engl J Med* 1991; **325**: 1127-1131
- 4 **Van Antwerp DJ**, Martin SJ, Kafri T, Green DR, Verma IM. Suppression of TNF- α induced apoptosis by NF- κ B. *Science* 1996; **274**: 787-789
- 5 **Correa P**, Ruiz B, Shi TY, Janney A, Sobhan M, Torrado J, Hunter F. *Helicobacter pylori* and nucleolar organizer regions in the gastric antral mucosa. *Am J Clin Pathol* 1994; **101**: 656-660
- 6 **Fraser AG**, Sim R, Sankey EA. Effect of eradication of *Helicobacter pylori* on gastric epithelial cell proliferation. *Aliment Pharmacol Ther* 1994; **8**: 167-173
- 7 **Lynch DA**, Mapstone NP, Clarke AM, Sobala GM, Jackson P, Morrison L, Dixon MF, Quirke P, Axon AT. Cell proliferation in *Helicobacter pylori* associated gastritis and the effect of eradication therapy. *Gut* 1995; **36**: 346-350
- 8 **Fox JG**, Dangler CA, Taylor NS, King A, Koh TJ, Wang TC. High-salt diet induces gastric epithelial hyperplasia and parietal cell loss, and enhances *Helicobacter pylori* colonization in C57BL/6 mice. *Cancer Res* 1999; **59**: 4823-4828
- 9 **Peek R**, Wirth HP, Moss SF, Yang M, Abdalla AM, Tham KT, Zhang T, Tang LH, Modlin IM, Blaser MJ. *Helicobacter pylori* alters gastric epithelial cell cycle events and gastrin secretion in Mongolian gerbils. *Gastroenterology* 2000; **118**: 48-59
- 10 **Israel DA**, Salama N, Arnold CN, Moss SF, Ando T, Wirth HP, Tham KT, Camorlinga M, Blaser MJ, Falkow S, Peek RM Jr. *Helicobacter pylori* strain-specific differences in genetic content, identified by microarray, influence host inflammatory responses. *J Clin Invest* 2001; **107**: 611-620
- 11 **Moss SF**, Calam J, Agarwal B, Wang S, Holt PR. Induction of gastric epithelial apoptosis by *Helicobacter pylori*. *Gut* 1996; **38**: 498-501
- 12 **Mannick EE**, Bravo LE, Zarama G, Realpe JL, Zhang XJ, Ruiz B, Fonham ET, Mera R, Miller MJ, Correa P. Inducible nitric oxide synthase, nitrotyrosine and apoptosis in *Helicobacter pylori* gastritis: effects of antibiotics and antioxidants. *Cancer Res* 1996; **56**: 3238-3243
- 13 **Jones NL**, Shannon PT, Cutz E, Yeager H, Sherman PM. Increase in proliferation and apoptosis of gastric epithelial cells early in the natural history of *Helicobacter pylori* infection. *Am J Pathol* 1997; **151**: 1695-1703
- 14 **Rudi J**, Kuck D, Strand S, von Herbay A, Mariani SM, Krammer PH, Galle PR, Stremmel W. Involvement of the CD95 (APO-1/Fas) Receptor and Ligand System in *Helicobacter pylori*-induced Gastric Epithelial Apoptosis. *J Clin Invest* 1998; **102**: 1506-1514
- 15 **Anti M**, Armuzzi A, Iascone E, Valenti A, Lippi ME, Covino M, Vecchio FM, Pierconti F, Buzzi A, Pignataro G, Bonvicini F, Gasbarrini G. Epithelial-cell apoptosis and proliferation in *Helicobacter pylori*-related chronic gastritis. *Ita J Gastroenterol Hepatol* 1998; **30**: 153-159
- 16 **Hirasawa R**, Tatsuta M, Iishi H, Yano H, Baba M, Uedo N, Sakai N. Increase in apoptosis and decrease in ornithine decarboxylase activity of the gastric mucosa in patients with atrophic gastritis and gastric ulcer after successful eradication of *Helicobacter pylori*. *Am J Gastroenterol* 1999; **94**: 2398-2402
- 17 International Union Against Cancer; Sobin L and Wittekind C, eds. TNM Classification of Malignant Tumors. 6th ed. New York, USA: Wiley-Liss 2002: 65-68
- 18 **Dahlhaus M**, Appel KE. N-Nitrosodimethylamine, N-nitrosodiethylamine, and N-nitrosomorpholine fail to generate 8-hydroxy-2'-deoxyguanosine in liver DNA of male F344 rats. *Mutat Res* 1993; **285**: 295-302
- 19 **Shen HM**, Ong CN, Lee BL, Shi CY. Aflatoxin B1-induced 8-hydroxydeoxyguanosine formation in rat hepatic DNA. *Car-*

- cinogenesis* 1995; **16**: 419-422
- 20 **Yermilov V**, Rubio J, Becchi M, Friesen MD, Pignatelli B, Ohshima H. Formation of 8-nitroguanine by the reaction of guanine with peroxyxynitrite *in vitro*. *Carcinogenesis* 1995; **16**: 2045-2050
- 21 **Mercurio F**, Zhu H, Murray BW, Shevchenko A, Bennett BL, Li J, Young DB, Barbosa M, Mann M, Manning A, Rao A. IKK-1 and IKK-2: cytokine-activated I κ B kinases essential for NF κ B activation. *Science* 1997; **278**: 860-866
- 22 **Yu J**, Russell RM, Salomon RN, Murphy JC, Palley LS, Fox JG. Effect of *Helicobacter mustelae* infection on ferret gastric epithelial cell proliferation. *Carcinogenesis* 1995; **16**: 1927-1931
- 23 **Peek RM Jr**, Moss SF, Tham KT, Perez-Perez GI, Wang S, Miller GG, Atherton JC, Holt PR, Blaser MJ. *Helicobacter pylori* cagA⁺ strains and dissociation of gastric epithelial cells proliferation from apoptosis. *J Natl Cancer Inst* 1997; **89**: 863-868
- 24 **Farinati F**, Cardin R, Degan P, Rugge M, Mario FD, Bonvicini P, Naccarato R. Oxidative DNA damage accumulation in gastric carcinogenesis. *Gut* 1998; **42**: 351-356
- 25 **Baik SC**, Youn HS, Chung MH, Lee WK, Cho MJ, Ko GH, Park CK, Kasai H, Rhee KH. Increased oxidative DNA damage in *Helicobacter pylori*-infected human gastric mucosa. *Cancer Res* 1996; **56**: 1279-1282
- 26 **Papa A**, Danese S, Sgambato A, Ardito R, Zannoni G, Rinelli A, Vecchio FM, Gentiloni-Silveri N, Cittadini A, Gasbarrini G, Gasbarrini A. Role of *Helicobacter pylori* CagA⁺ infection in determining oxidative DNA damage in gastric mucosa. *Scand J Gastroenterol* 2002; **37**: 409-413
- 27 **Hahm KB**, Lee KJ, Kim JH, Cho SW, Chung MH. *Helicobacter pylori* infection, oxidative DNA damage, gastric carcinogenesis, and reversibility by rebamipide. *Dig Dis Sci* 1998; **43**(Suppl 9): 72S-77S
- 28 **Koh E**, Noh SH, Lee YD, Lee HY, Han JW, Lee HW, Hong S. Differential expression of nitric oxide synthase in human stomach cancer. *Cancer Lett* 1999; **146**: 173-180
- 29 **Tamir S**, Tannenbaum S. The role of nitric oxide in the carcinogenic process. *Biochim Biophys Acta* 1996; **1288**: F31-36
- 30 **Baldwin AS Jr**. The NF- κ B and I κ B proteins: new discoveries and insights. *Annu Rev Immunol* 1996; **14**: 649-683
- 31 **Wang CY**, Mayo MW, Baldwin AS Jr. TNF- and cancer therapy-induced apoptosis: potentiation by inhibition of NF- κ B. *Science* 1996; **274**: 784-787
- 32 **Beg AA**, Baltimore D. An essential role for NF- κ B in preventing TNF α -induced cell death. *Science* 1996; **274**: 782-784
- 33 **Maeda S**, Yoshida H, Mitsuno Y, Hirata Y, Ogura K, Shiratori Y, Omata M. Analysis of apoptotic and antiapoptotic signaling pathways induced by *Helicobacter pylori*. *Gut* 2002; **50**: 771-778
- 34 **Malinin NL**, Boldin MP, Kovalenko AV, Wallach D. MAP3K-related kinase involved in NF- κ B induction by TNF, CD95 and IL-1. *Nature* 1997; **385**: 540-544
- 35 **Dumont A**, Hehner SP, Hofmann TG, Ueffing M, Droge W, Schmitz ML. Hydrogen peroxide-induced apoptosis is CD95-independent, requires the release of mitochondria-derived reactive oxygen species and the activation of NF- κ B. *Oncogene* 1999; **18**: 747-757
- 36 **Lin MT**, Juan CY, Chang KJ, Chen WJ, Kuo ML. IL-6 inhibits apoptosis and retains oxidative DNA lesions in human gastric cancer AGS cells through up-regulation of anti-apoptotic gene mcl-1. *Carcinogenesis* 2001; **22**: 1947-1953
- 37 **Wang CY**, Mayo MW, Korneluk RG, Goeddel DV, Baldwin AS Jr. NF- κ B antiapoptosis: induction of TRAF1 and TRAF2 and c-IAP1 and c-IAP2 to suppress caspase-8 activation. *Science* 1998; **281**: 1680-1683
- 38 **Hoshi T**, Sasano H, Kato K, Yabuki N, Ohara S, Konno R, Asaki S, Toyota T, Tateno H, Nagura H. Immunohistochemistry of Caspase3/ CPP32 in human stomach and its correlation with cell proliferation and apoptosis. *Anticancer Res* 1998; **18**: 4347-4353

Edited by Wang XL Proofread by Xu FM

Japanese herbal medicine, *Saiko-keishi-to*, prevents gut ischemia/reperfusion-induced liver injury in rats via nitric oxide

Yoshinori Horie, Mikio Kajihara, Shuka Mori, Yoshiyuki Yamagishi, Hiroyuki Kimura, Hironao Tamai, Shinzo Kato, Hiromasa Ishii

Yoshinori Horie, Mikio Kajihara, Shuka Mori, Yoshiyuki Yamagishi, Hiroyuki Kimura, Hironao Tamai, Shinzo Kato, Hiromasa Ishii, Department of Internal Medicine, School of Medicine, Keio University, Tokyo 160-8582, Japan

Supported by the Grants from Tsumura Co. Ltd

Correspondence to: Yoshinori Horie, M.D., Department of Internal Medicine, School of Medicine, Keio University, 35 Shinanomachi Shinjuku-ku, Tokyo 160-8582, Japan. yhorie@sc.itc.keio.ac.jp

Telephone: +81-3-5363-3789 **Fax:** +81-3-3356-9654

Received: 2004-02-06 **Accepted:** 2004-03-16

Abstract

AIM: To determine whether *Saiko-keishi-to* (TJ-10), a Japanese herbal medicine, could protect liver injury induced by gut ischemia/reperfusion (I/R), and to investigate the role of NO.

METHODS: Male Wistar rats were exposed to 30-min gut ischemia followed by 60 min of reperfusion. Intravital microscopy was used to monitor leukocyte recruitment. Plasma tumor necrosis factor (TNF) levels and alanine aminotransferase (ALT) activities were measured. TJ-10 1 g/(kg·d) was intragastrically administered to rats for 7 d. A NO synthase inhibitor was administered.

RESULTS: In control rats, gut I/R elicited increases in the number of stationary leukocytes, and plasma TNF levels and ALT activities were mitigated by pretreatment with TJ-10. Pretreatment with the NO synthase inhibitor diminished the protective effects of TJ-10 on leukostasis in the liver, and the increase of plasma TNF levels and ALT activities. Pretreatment with TJ-10 increased plasma nitrite/nitrate levels.

CONCLUSION: TJ-10 attenuates the gut I/R-induced hepatic microvascular dysfunction and sequential hepatocellular injury via enhancement of NO production.

Horie Y, Kajihara M, Mori S, Yamagishi Y, Kimura H, Tamai H, Kato S, Ishii H. Japanese herbal medicine, *Saiko-keishi-to*, prevents gut ischemia/reperfusion-induced liver injury in rats via nitric oxide. *World J Gastroenterol* 2004; 10(15): 2241-2244
<http://www.wjgnet.com/1007-9327/10/2241.asp>

INTRODUCTION

Herbal medicines that have been used in China for thousands of years are now being manufactured in Japan as drugs containing ingredients of standardized quality and quantity. The clinical efficacy of these medicines has been utilized by Japanese Western-medicine practitioners for more than 20 years and is well recognized. One of the herbal medicines, *Saiko-keishi-to* (TJ-10) (Chinese name; *Chai-Hu-Gui-Zhi-Tang*), is a common drug to treat duodenal ulcer, pancreatitis, and chronic liver disease in Japan. It is an oral medicine and consists of 9 herb components: *Bupleurum* root, *Pinellia tuber*, *Scutellaria*

root, *Jujube* fruit, *Ginger rhizome*, ginseng root, cinnamon bark, peony root and *Glycyrrhiza* root. Another common herbal medicine, Sho-saiko-to (TJ-9), consists of 7 components of them: *Bupleurum* root, *Pinellia tuber*, *Scutellaria* root, jujube fruit, ginger rhizome, ginseng root, and *Glycyrrhiza* root. In a double-blind multicenter clinical trial, TJ-9 was reported to reduce the elevated serum activities of aspartate transaminase, alanine transaminase (ALT), and glutamyl transpeptidase in chronic active hepatitis patients^[1]. TJ-9 has been shown to improve liver function as well as the symptoms associated with chronic liver disease including digestive discomfort^[2]. Although TJ-10 has been often administered to patients with chronic liver disease as well as TJ-9, there are few epidemiological reports^[3], and little is known about mechanisms of its cytoprotective effects on liver damage. Recently, because of its major pharmaceutical effects, TJ-10 is presumed to gradually improve biological defense mechanisms. One of the components of TJ-10, *Saikosaponin*, has been reported to inhibit hepatocyte necrosis induced by galactosamine^[4], and *Saikosaponin-d* has been shown to reduce microsomal lipid peroxidation induced by NADPH and CCl₄^[5]. However, its mode of action has not been fully elucidated.

Nitric oxide (NO) has been found to be a modulator of the adhesive interactions between leukocytes, platelets, and endothelial cells^[6-9] as well as an important modulator of tissue blood flow, arterial pressure, and neurotransmission^[8], and NO-dependent cell-cell interactions have been demonstrated in tissues exposed to ischemia and reperfusion (I/R), an injury process in which leukocyte-endothelial cell adhesion plays a critical role. A role of NO in the pathobiology of I/R injury has been supported by observations that inhibition of NO biosynthesis could elicit most of the microvascular alterations observed in tissues exposed to I/R^[7,10], and NO-donating compounds have been shown to provide significant protection against the microvascular dysfunction that is normally associated with I/R^[7]. We developed a murine model of leukocyte-dependent hepatocellular dysfunction that was elicited by gut I/R^[11-13]. The model allows *in vivo* assessment of the effects of I/R on leukocyte sequestration in sinusoids of different regions of the liver lobule, leukocyte adherence in postsinusoidal venules, and the number of perfused sinusoids. Using this model, we have recently demonstrated that inhibition of both NO synthase and supplementation with exogenous NO could affect the leukocyte rolling, leukocyte adhesion, and sinusoidal perfusion elicited in the liver by gut I/R^[14-16].

Some herbal medicines have been reported to have an inducing effect on NO production by non-stimulated macrophages^[17]. We have recently reported that TJ-9 could attenuate the gut I/R-induced hepatic microvascular dysfunction and sequential hepatocellular injury via NO^[18]. However, little is known about the effect of TJ-10 on plasma NO levels and I/R injury *in vivo*. TJ-9 is contraindicated for liver cirrhosis, because of its side-effect, causing lung fibrosis. Since TJ-10 has 30% less *Saikosaponin* compared to TJ-9, it seems to be safer. Therefore, frequency and importance of TJ-10 are expected to increase in Japan. In the present study, we investigated whether TJ-10 modulated the gut I/R-induced microvascular dysfunction in the liver, and the role of NO in the responses by inhibiting NO synthase.

MATERIALS AND METHODS

Animals and surgical procedure

Male Wistar rats (200-250 g) were fed a standard rat chow for 2 wk, and TJ-10 (1 g/kg in saline) or saline alone was then administered for 7 d intragastrically through a tube. Experiments below were performed 18 h after the final dose of TJ-10 or saline. The rats were fasted for 18 h prior to each experiment, and then intraperitoneally anesthetized with pentobarbital sodium (35 mg/kg). The left carotid artery was cannulated, and a catheter was positioned in aortic arch to monitor blood pressure. The left jugular vein was cannulated for drug administration. All experiments were performed according to the criteria outlined in the National Research Council Guide.

Intravital microscopy

After laparotomy, one lobe of the liver was examined through an inverted intravital microscope (TMD-2S, Diaphoto, Nikon, Tokyo, Japan) and images were recorded with a silicon intensified target (SIT) camera (C-2400-08, Hamamatsu photonicus, Shizuoka, Japan). The liver was placed on an adjustable Plexiglas microscope stage and covered with a nonfluorescent coverslip that allowed observation of a 2 cm² segment of tissue. The liver was carefully positioned to minimize the influence of respiratory movements, and its surface was moistened and covered with cotton gauze soaked with saline. Images of microcirculation at the surface of the liver were observed through consecutive microfluorographs of hepatic microcirculation, that is, those of rhodamine-6G-labeled leukocytes in the sinusoids, were observed at 90 min after the onset of SMA occlusion and recorded on a digital video recorder. The number of stationary leukocytes was determined off-line during playback of videotape images. A leukocyte was considered to be stationary within the microcirculation (sinusoids) if it remained stationary for more than 10 s. The lobule, which had the fewest stationary leukocytes, was selected for observation at the basal condition. Stationary leukocytes were quantified in both the midzonal and pericentral regions of the liver lobule and expressed as the number per field of view (2.1×10⁵ μm²). The percentage of non-perfused sinusoids was calculated as the ratio of the number of non-perfused sinusoids to the total number of sinusoids per microscopic field.

Experimental protocols

We observed the surface of liver for 10 min before ligating the superior mesenteric artery to ensure that all parameters measured on-line were in a steady state. The superior mesenteric artery was then ligated for 0 (sham) or 30 min with a snare created from a polyethylene tube. At the end of the ischemic period, the ligation was gently removed. Leukocyte accumulation and the number of non-perfused sinusoids (NPS) were measured before ischemia, immediately following reperfusion, and every 15 min for 1 h thereafter. In one set of experiments, 7 untreated animals, and 5 TJ-10-treated animals in the control groups (sham gut I/R) and gut I/R groups were used. In another set of experiments in which TJ-10 was administered, the rats were given a NO synthase (NOS) inhibitor, N^G-monomethyl-L-arginine (L-NMMA; Sigma, St. Louis, MO) (0.5 mg/kg, i.v.) 30 min before the onset of ischemia. These experiments were performed with 5 animals in each group. In some experiments, the rats were given dexamethasone (2 mg/kg, Sigma, St. Louis, MO) with or without L-NMMA (0.5 mg/kg, i.v.) 30 min before the onset of ischemia. These experiments were performed with 5 animals in each group.

Tumor necrosis factor and endotoxin assay

Sixty min after the onset of reperfusion, blood plasma samples

for tumor necrosis factor (TNF) detection were collected from the inferior vena cava at a point proximal to the hepatic vein. Plasma TNF concentration was determined in a microtiter plate using a TNF immunoassay kit (BioSource International, Camarillo, CA) based on enzyme-linked immunosorbent assay (ELISA) as described in our previous study^[19]. Plasma endotoxin levels were measured by endospecy (an endotoxin-specific chromogen. Seikagaku Co., Tokyo, Japan) according to our previous report^[20].

Enzyme and nitrite/nitrate assay

Blood samples for enzyme activities were collected from the carotid artery 6 h after the onset of reperfusion. Serum ALT activity was determined by conventional UV methods as previously described^[21]. Blood samples for nitrite/nitrate assay were collected from the inferior vena cava 16 h after the last administration of TJ-10 (saline as control). The combined levels of nitrite and nitrate in plasma were determined by a previously reported method^[22]. Five separate experiments were performed.

Statistical analysis

The data were analyzed by standard statistical methods, i.e., ANOVA and Scheffe's (post hoc) test. All values were reported as mean±SD. *P*<0.05 was considered statistically significant.

RESULTS

Figure 1A shows the effects of TJ-10 and/or L-NMMA on the gut I/R induced leukostasis in sinusoids of the midzonal and pericentral (including the terminal hepatic venule [THV]) regions of the liver lobule (panel A), and the entire liver lobule (sinusoids + THV, panel B). In control rats, gut I/R elicited significant increases in the number of stationary leukocytes compared to basal values. Pretreatment with TJ-10 blunted the gut I/R-induced leukostasis in the midzonal (untreated+I/R: 9.6±0.6, TJ-10+I/R: 3.6±0.6, per field) and the pericentral regions (untreated+I/R: 6.0±0.7, TJ-10+I/R: 3.6±0.5, per field). L-NMMA diminished the protective effect of TJ-10 in the pericentral region (5.6±0.2, per field), but did not significantly affect the gut I/R-induced leukostasis in the midzonal region or the entire liver lobule.

Figure 1B shows the effect of TJ-10 and/or L-NMMA on the gut I/R-induced elevation of plasma TNF levels. In the control rats, gut I/R elevated the plasma TNF-α levels. Pretreatment with TJ-10, however, blunted the gut I/R-induced elevation of plasma TNF-α levels (untreated+I/R: 140.8±12.6, TJ-10+I/R: 61.7±22.5 ng/L). L-NMMA diminished the protective effects of TJ-10 (113.2±13.7 ng/L).

Figure 1C shows the effect of TJ-10 and/or L-NMMA on the gut I/R-induced elevation of serum endotoxin levels. In the control rats, gut I/R elevated the serum endotoxin levels. Pretreatment with TJ-10, however, blunted the gut I/R-induced elevation of serum endotoxin levels (untreated+I/R: 39.2±8.1, TJ-10+I/R: 11.1±3.3 ng/L). L-NMMA diminished the protective effects of TJ-10 (34.7±5.3 ng/L).

Figure 1D illustrates the effect of TJ-10 and/or L-NMMA on the gut I/R-induced elevation of plasma ALT activities. In the control rats, gut I/R elevated the plasma ALT activities. Pretreatment with TJ-10, however, blunted the gut I/R-induced elevation of plasma ALT levels (untreated+I/R: 146.6±13.0, TJ-9+I/R: 76.0±7.0 IU/L). L-NMMA diminished the protective effects of TJ-10 (123.2±11.9 IU/L).

Table 1 shows the effects of TJ-9 and TJ-10 on plasma nitrite/nitrate levels. Pretreatment with TJ-10 increased the plasma nitrite/nitrate levels as well as TJ-9.

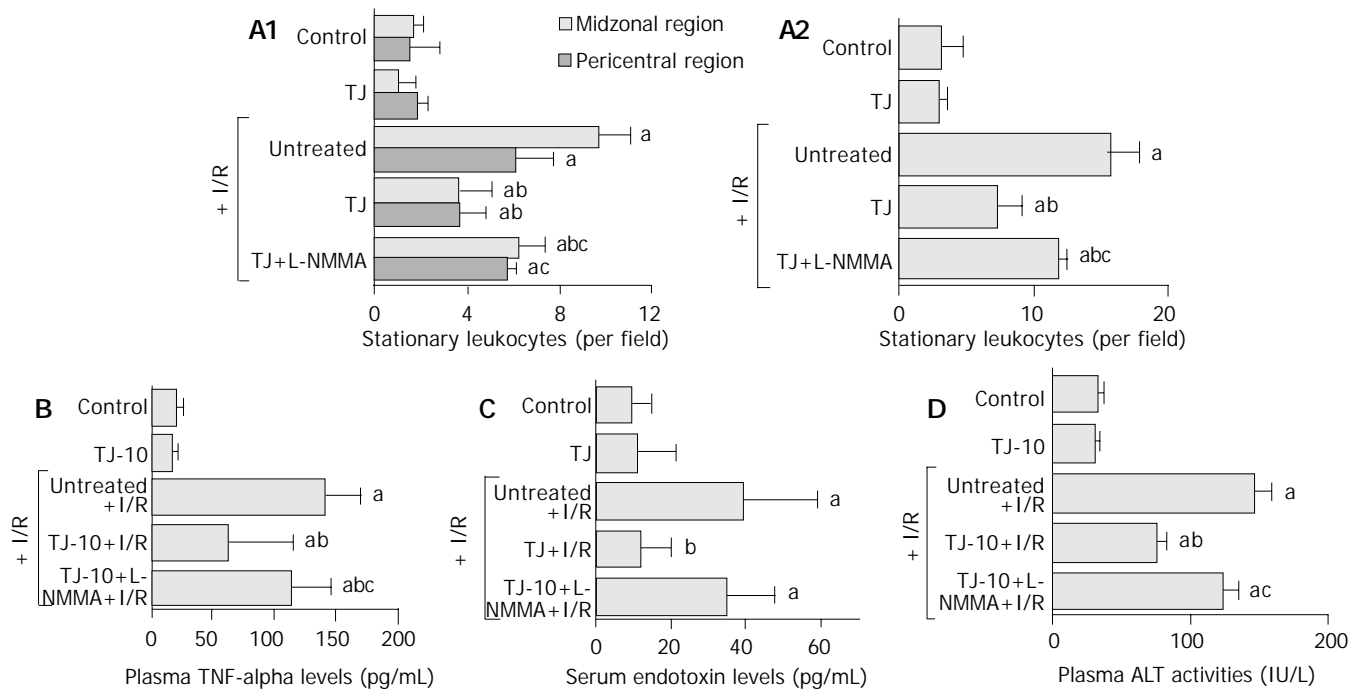


Figure 1 Effects of Saiko-keishi-to (TJ-10) and/or an NO synthase inhibitor (N^G-monomethyl-L-arginine, L-NMMA) on the number of stationary leukocytes, plasma TNF- α levels, serum endotoxin levels, and plasma ALT activities. A: In each region (the midzonal and pericentral regions) (panel A) and the entire (combined) liver lobule (panel B) after 30 min of gut ischemia and 60 min of reperfusion; B: Plasma TNF- α levels at 60 min after gut I/R; C: Serum endotoxin levels at 60 min after gut I/R; D: Plasma ALT activities at 6 h after gut I/R.

Table 1 Effects of Sho-saiko-to (TJ-9) and Saiko-keishi-to (TJ-10) on plasma nitrite/nitrate levels ($n = 5$)

Group	Plasma nitrite/nitrate levels
Control	17.1 \pm 2.9
TJ-9	35.8 \pm 4.3 ^a
TJ-10	39.0 \pm 4.0 ^a

^a $P < 0.05$ vs control.

DISCUSSION

Herbal medicines are widely used in Japan. The clinical efficacy of these medicines has been utilized by Japanese Western-medicine practitioners for more than 20 years and is well recognized. In cases of gastroenterological and hepatological diseases, they are often used for patients with chronic liver disease as well as gastrointestinal functional disorder. Although TJ-9 has been the most famous herbal medicine for chronic liver disease in Japan, TJ-10 is another common drug to treat duodenal ulcer, pancreatitis, and chronic liver disease. TJ-10 has effectiveness for more kinds of diseases rather than TJ-9. Indeed, the components of TJ-10 include all of the 7 components of TJ-9. Although TJ-10 has been often administered to patients with chronic liver disease as well as TJ-9, there were few epidemiological reports^[3], and little is known about mechanisms of the cytoprotective effects on liver damage.

Previously published work has demonstrated that reperfusion of the ischemic small intestine could elicit an acute inflammatory response both in the intestine and in distant organs, such as the liver^[11,12,23] and lung^[23,24]. In the liver, the response was characterized by leukocyte plugging of sinusoids, leukocyte adherence in postcapillary venules, a reduction in the number of perfused sinusoids, hepatocellular hypoxia, and leakage of enzymes (ALT) from hepatocytes^[11,12,23,25]. Recently, we have reported that TJ-9 could attenuate the gut I/R-induced responses in the liver^[18]. In the present study, it was demonstrated that TJ-10 had a similar effect to TJ-9 on the gut

I/R-induced responses in the liver. NO has been found to be a modulator of the adhesive interactions between leukocytes, platelets, and endothelial cells^[6-9], and NO-dependent cell-cell interactions have been demonstrated in tissues exposed to ischemia and reperfusion (I/R), an injury process in which leukocyte-endothelial cell adhesion plays a critical role. Depletion and/or inactivation of NO has been implicated as a key event in the recruitment of leukocytes in tissues exposed to I/R^[26-28]. We previously demonstrated that treatment with L-NMMA resulted in exaggerated leukostasis and cellular injury in the murine liver after gut I/R and that increased delivery/generation of NO in the liver via a NO donor attenuated the inflammatory responses and microvascular dysfunction elicited in the liver by gut I/R^[13]. These results suggest a protective effect of NO on the gut I/R-induced responses in the rat liver. The finding in the present study that L-NMMA diminished the protective effect of TJ-10 on the increase in plasma TNF- α and serum endotoxin levels, leukostasis in the liver, and plasma ALT activities, suggested that TJ-10 could prevent the gut I/R-induced cytokine production and microvascular dysfunction in the liver by elevating sinusoidal NO level. NO could modulate leukocyte- and/or platelet-endothelial cell interactions^[6,9,13,14]. Since pretreatment with TJ-10 actually increased plasma nitrite/nitrate levels in the present study, the increase in NO production by hepatocytes and macrophages after treatment with TJ-10 appeared to be involved in the cytoprotective effects of TJ-10.

In the present study, L-NMMA diminished the protective effect of TJ-10 on the increase in plasma TNF- α and serum endotoxin levels, leukostasis in the liver, and plasma ALT activities. While, in the previous study^[18], L-NMMA did not affect the protective effect of TJ-9 on the increase in leukostasis in the midzonal region, the total number of stationary leukocytes, or the plasma ALT activity. One likely interpretation is that a mechanism other than the increase in NO production mediates the protective effects of TJ-9. Steroids have been known to prevent reperfusion injury^[29]. The evidence in our previous study^[18] that L-NMMA did not affect either TJ-9- or dexamethasone-induced decrease in the gut I/R-elevated plasma

ALT activities, raises a possibility that TJ-9-increased blood corticosterone level may prevent the gut I/R-induced microvascular and hepatocellular injury. Since L-NMMA diminished the protective effect of TJ-10 on the gut I/R-induced increase in plasma ALT activities, corticosteroid effect was not involved in the prevention of gut I/R-induced hepatocellular injury by TJ-10. *Kampo* (herbal medicines) prescriptions affect as the complex. For example, though one of the components in TJ-10, cinnamon bark, which is not included in TJ-9, had a very strong anti-oxidant effect, there was no significant difference between TJ-9 and 10 in the potential for anti-oxidation^[30]. Thus, our results suggest that TJ-10 has different characteristics from TJ-9, even including all components of TJ-9.

Recently, the importance of the way of traditional diagnosis "Sho" in the use of *Kampo* prescriptions has come to be widely described even in package insert drug information pamphlets of *Kampo* prescriptions. "Sho" is judged comprehensively by a complex of subjective and objective symptoms at a certain point of illness. The process is generally complicated, but we sometimes diagnose by tonus felt on the abdomen. Namely, hypertonus is "Jitsu Sho", and hypotonus is "Kyo Sho". General fatigue, sleepiness, sleepless, appetite loss, tiredness of eyes, easily catching cold, dizziness, looking pale, and so on are symptoms of "Kyo Sho". TJ-10 suits for "Kyo Sho" rather than TJ-9. Moreover, most patients with chronic hepatitis have "Kyo Sho". TJ-10 prevents microvascular dysfunction in the liver increase in NO production. Symptoms of "Kyo Sho" described above seem to be caused by microvascular dysfunction. Taken together, TJ-10 is recommended for chronic hepatitis patients with "Kyo Sho".

Although further studies are required to clarify the mechanisms of the protective effects of TJ-10 on reperfusion injury, this study has demonstrated the protective effect of TJ-10 on reperfusion injury via NO.

REFERENCES

- Hirayama C, Okumura M, Tanikawa K, Yano M, Mizuta M, Ogawa N. A multicenter randomized controlled clinical trial of *Shosaiko-to* in chronic active hepatitis. *Gastroenterol Jpn* 1989; **24**: 715-719
- Fujiwara K, Ohta Y, Ogata I, Oka Y, Hayashi S, Oka H. Treatment trial of traditional oriental medicine in chronic viral hepatitis. In: Ohta Y ed. *New Trends in Peptic Ulcer and Chronic Hepatitis: Part II chronic hepatitis*. Tokyo: *Excerpta Medica* 1987: 141-146
- Itoh T, Shibahara N, Mantani N, Tahara E, Shimada Y, Terasawa K. Effect of *kampo* treatment on chronic viral hepatitis. *J Trad Med* 1997; **14**: 204-210
- Abe H, Sakaguchi M, Yamada M, Arichi S. Pharmacological actions of saikosaponins isolated from *Bupleurum falcatum*. I. Effects of *Saikosaponin* on liver function. *Planta Medica* 1980; **40**: 366-372
- Abe H, Orita M, Konishi H, Arichi S, Odashima S. Effects of *Saikosaponin*-d on enhanced CCl₄-hepatotoxicity by phenobarbitone. *J Pharm Pharmacol* 1985; **37**: 555-559
- Kurose I, Kubes P, Suzuki M, Wolf R, Anderson DC, Paulson J, Miyasaka M, Granger DN. Inhibition of nitric oxide production mechanisms of vascular albumin leakage. *Circ Res* 1993; **73**: 164-171
- Kurose I, Wolf R, Grisham MB, Granger DN. Modulation of ischemia/reperfusion-induced microvascular dysfunction by nitric oxide. *Circ Res* 1994; **74**: 376-382
- Moncada S, Palmer RM, Higgs EA. Nitric oxide: Physiology, pathophysiology, and pharmacology. *Pharmacol Rev* 1991; **43**: 109-142
- Radomski MW, Palmer RM, Moncada S. Endogenous nitric oxide inhibits human platelet adhesion to vascular endothelium. *Lancet* 1987; **2**: 1057-1058
- Granger DN, Kurose I, Kubes P. Nitric oxide: A modulator of cell-cell adhesion and protein exchange in postcapillary venules. In: Shock, Sepsis, and Organ Failure-Nitric Oxide. G. Schlang, H. Redl, eds. *Springer, Heidelberg, Germany* 1994: 121-136
- Horie Y, Wolf R, Miyasaka M, Anderson DC, Granger DN. Leukocyte adhesion and the hepatic microvascular responses to intestinal ischemia-reperfusion. *Gastroenterology* 1996; **111**: 666-673
- Horie Y, Wolf R, Anderson DC, Granger DN. Hepatic leukostasis and hypoxic stress in adhesion molecule-deficient mice after gut ischemia-reperfusion. *J Clin Invest* 1997; **99**: 781-788
- Horie Y, Ishii H. Liver dysfunction elicited by gut ischemia-reperfusion. *Pathophysiology* 2001; **8**: 11-20
- Horie Y, Wolf R, Granger DN. Role of nitric oxide in gut ischemia reperfusion-induced hepatic microvascular dysfunction. *Am J Physiol* 1997; **273**: G1007-G1013
- Horie Y, Wolf R, Anderson DC, Granger DN. Nitric oxide modulates gut ischemia/reperfusion-induced P-selectin expression in murine liver. *Am J Physiol* 1998; **275**: H520-H526
- Horie Y, Yamagishi Y, Kato S, Kajihara M, Kimura H, Ishii H. Low-dose ethanol attenuates gut ischemia/reperfusion-induced liver injury in rats via nitric oxide production. *J Gastroenterol Hepatol* 2003; **18**: 211-217
- Fukuda K. Modulation of nitric oxide production by crude drugs and *Kampo* medicines. *J Traditional Med* 1998; **15**: 22-32
- Horie Y, Kajihara M, Yamagishi Y, Kimura H, Tamai H, Kato S, Ishii H. A Japanese herbal medicine, *Sho-Saiko-To*, prevents Ischemia/reperfusion-induced hepatic microvascular dysfunction in rats. *J Gastroenterol Hepatol* 2001; **16**: 1260-1266
- Horie Y, Wolf R, Russell J, Shanley TP, Granger DN. Role of Kupffer cells in gut ischemia-reperfusion-induced hepatic microvascular dysfunction in mice. *Hepatology* 1997; **26**: 1499-1505
- Tamai H, Kato S, Horie Y, Ohki E, Yokoyama H, Ishii H. Effect of acute ethanol administration on the intestinal absorption of endotoxin in rats. *Alcohol Clin Exp Res* 2000; **24**: 390-394
- Horie Y, Kato S, Ohki E, Hamamatsu H, Fukumura D, Kurose I, Suzuki H, Suematsu M, Miura S, Ishii H. Effect of lipopolysaccharides on erythrocyte flow velocity in rat liver. *J Gastroenterol* 1997; **32**: 783-790
- Horie Y, Kimura H, Kato S, Ohki E, Tamai H, Yamagishi Y, Ishii H. Role of nitric oxide in endotoxin-induced hepatic microvascular dysfunction in rats chronically fed ethanol. *Alcohol Clin Exp Res* 2000; **24**: 845-851
- Hill J, Lindsay T, Rusche J, Valeri CR, Shepro D, Hechman HB. A Mac-1 antibody reduces liver and lung injury but not neutrophil sequestration after intestinal ischemia-reperfusion. *Surgery* 1992; **112**: 166-172
- Carden DL, Young JA, Granger DN. Pulmonary microvascular injury after intestinal ischemia-reperfusion: role of P-selectin. *J Appl Physiol* 1993; **75**: 2529-2534
- Simpson R, Alon R, Kobzik L, Valeri CR, Shepro D, Hechtman HB. Neutrophil and nonneutrophil-mediated injury in intestinal ischemia reperfusion. *Ann Surg* 1993; **218**: 444-454
- Kubes P, Suzuki M, Granger DN. Nitric oxide: an endogenous modulator of leukocyte adhesion. *Proc Natl Acad Sci U S A* 1991; **88**: 4651-4655
- Ma XL, Weyrich AS, Lefer DJ, Lefer AM. Diminished basal nitric oxide release after myocardial ischemia and reperfusion promotes neutrophil adherence to coronary endothelium. *Circ Res* 1993; **72**: 403-412
- Siegrfried MR, Erhardt J, Rider T, Ma XL, Lefer AM. Cardioprotection and attenuation of endothelial dysfunction by organic nitric oxide donors in myocardial ischemia-reperfusion. *J Pharmacol Exp Ther* 1991; **260**: 668-675
- Valen G, Kawakami T, Tahepold P, Starkopf J, Kairane C, Dumitrescu A, Lowbeer C, Zilmer M, Vaage J. Pretreatment with methylprednisolone protects the isolated rat heart against ischemic and oxidative damage. *Free Radic Res* 2000; **33**: 31-43
- Yoshikawa T. Free radical and *Kampo* medicines. *Kyoto University Kampo Seminar* 1995; **4**: 24-37

KAI1 gene expression in colonic carcinoma and its clinical significances

De-Hua Wu, Li Liu, Long-Hua Chen, Yan-Qing Ding

De-Hua Wu, Long-Hua Chen, Department of Radiation Oncology, Nanfang Hospital, First Military Medical University, Guangzhou 510515, Guangdong Province, China

Li Liu, Yan-Qing Ding, Department of Pathology, First Military Medical University, Guangzhou 510515, Guangdong Province, China
Supported by the National Natural Science Foundation, No. 30370649

Correspondence to: Dr. Yang-Qing Ding, Department of Pathology, First Military Medical University, Guangzhou 510515, Guangdong Province, China. dyq@fimmu.com

Telephone: +86-20-61642148 **Fax:** +86-20-61642148

Received: 2003-12-12 **Accepted:** 2004-02-01

Abstract

AIM: To investigate *KAI1* gene expression in the progression of human colonic carcinoma and its clinical significances.

METHODS: *KAI1* expression was detected by *in situ* hybridization and immunohistochemistry in the 4 established cell lines of colorectal carcinoma with different metastatic potentials, and in 80 specimens of colonic carcinoma, 21 colonic carcinoma specimens with lymphatic metastasis and 20 controls of normal colonic mucosa.

RESULTS: The expressions of *KAI1* in HT29 and SW480 cell lines were higher than those in LoVo and SW620. The expression of *KAI1* gene was significantly higher in colorectal carcinoma compared with normal colonic mucosa and lymphatic metastasis ($\chi^2=46.838$, $P<0.01$). The expression of *KAI1* gene had no relationship with histological grade. The *KAI1* expressions in Dukes A and B carcinoma were higher at both mRNA and protein levels compared to Dukes C carcinoma ($\chi^2=16.061$, $P<0.05$). The expression of *KAI1* in colonic carcinoma specimens with lymphatic metastasis was almost lost. The results of *in situ* hybridization were in concordance with immunohistochemistry.

CONCLUSION: *KAI1* is highly related to the metastasis of colonic carcinoma and may be a useful indicator of metastasis in colonic carcinoma.

Wu DH, Liu L, Chen LH, Ding YQ. *KAI1* gene expression in colonic carcinoma and its clinical significances. *World J Gastroenterol* 2004; 10(15): 2245-2249

<http://www.wjgnet.com/1007-9327/10/2245.asp>

INTRODUCTION

Colorectal carcinoma is one of the most common forms of malignancy, and metastasis is the major cause of mortality in human population. Timely and precise identification of the occurrence of metastasis and its contributive factors are very important in the enhancement of prognosis and effects of treatment. *KAI1* gene was first identified in human prostate carcinoma and mapped to human chromosome 11p11.2^[1]. It encodes 267 amino acids belonging to plasma membrane glycoprotein, which consists of 4 transmembrane domains and

1 large and 1 small extracellular domains. The extracellular domains have 3 potential N-glycosylation sites. According to its special structure, it may be predicted that the function of *KAI1* gene may come down to cell-cell adherence and cell-matrix connection^[2]. The role of *KAI1* in tumor progression may not be limited to prostatic cancer. It was reported to be important in preventing the development of metastases in a wide variety of human tumor types, including cervical^[3], breast^[4], pancreatic^[5], esophageal^[6], bladder^[7], and ovarian cancers^[8]. In the present study, the expression of *KAI1* was detected by *in situ* hybridization in 4 cell lines of colorectal carcinoma, and in paraffin-embedded normal colonic epithelium, carcinoma, and lymphatic metastasis. The purpose was to explore the relationship between *KAI1* expression and colonic carcinoma metastasis and its clinical significances.

MATERIALS AND METHODS

Cell lines and culture conditions

LoVo and HT29 cell lines were cultured in RPMI 1640 supplemented with 100 mL/L heat-inactivated fetal bovine serum (FBS) and 100 U/mL penicillin/streptomycin. SW480 and SW620 were cultured in DMEM medium supplemented with the 100 mL/L FBS. All cells were grown in 50 mL/L CO₂ humidified atmosphere at 37 °C.

Tissue specimens

A total of 80 colonic carcinoma specimens, 20 normal colonic mucosa samples and 20 lymphatic metastasis samples were obtained from Nanfang Hospital. All the samples were routinely fixed in 40 g/L formaldehyde solution, embedded in paraffin, and cut into 4 μm thick sections. Samples were selected according to the pathological diagnosis and reviewed by a pathologist to confirm the diagnosis.

In situ hybridization (ISH) assays

The digoxigenin-labeled *KAI1*-cDNA probe for *in situ* hybridization was prepared as described in one of our previous papers^[9]. The ISH was performed according to the instruction of the enhanced sensitive ISH detection kit (purchased from Boster Biotechnology Company). Briefly, the sections were deparaffinized with xylene, dehydrated with graded ethanol and incubated in 30 mL/L H₂O₂ to block endogenous peroxidases for 30 min at room temperature. After being treated for 10 min with Triton X-100 and for 40 s with 3% pepsin, the sections were prehybridized for 3 h and hybridized overnight at 37 °C. The final concentrations of the labeled probes were 0.15 ng/μL. After hybridization, excess probes were removed through rinsing in 2×SSC (1×SSC is 0.15 mol/L NaCl plus 0.015 mol/L sodium citrate pH 7.0), 0.5×SSC, 0.2×SSC, respectively. The sections were incubated with an antidigoxigenin antibody conjugated biotin for 120 min at room temperature and then added strept-avidin biotin complex for 30 min. For color reaction, diaminobenzidine (DAB) was used. If the ISH signals were present, the cytoplasm would be full of brown granules. For ISH of the four colorectal carcinoma cell lines, the cells were incubated and grown on cover slip for 24 h, fixed with 950 mL/L

ethanol and washed with PBS (phosphate-buffered saline pH 7.2) 3 times, and then carried out ISH as described above. For negative controls, the digoxigenin-labeled KAI1-cDNA probe was replaced by prehybridized solution.

Immunohistochemical assays

To confirm the results of *KAI1* gene expression on *in situ* hybridization, immunohistochemical studies were performed as described previously^[9,10]. Briefly, the fixed cells and sections were subjected to immunostaining by using an ultrasensitive streptavidin-peroxidase technique (Maixin Biotechnology Company). Endogenous peroxidases were blocked by incubating with 5 mL/L H₂O₂ for 30 min at room temperature. The cells and sections were subsequently treated for 10 min with Triton X-100 and for 40 s with 30 g/L pepsin. The cells and sections were incubated for 30 min at 37 °C with normal nonimmune serum before overnight incubation at 4 °C with specific monoclonal KAI1-antibody (BD pharmingen technical company) at a dilution of 1:100. The cells and sections were then treated with biotin-conjugated second antibody before adding streptavidin-peroxidase. For color reaction, diaminobenzidine was used. If the positive signals were present, the cytoplasm and membrane were stained brown. For negative controls, the monoclonal KAI1 antibody was replaced by PBS.

Review and scoring of the section

The stained sections were reviewed and scored independently by two pathologists under Olympus microscope. The different degrees of intensity of staining were graded on a scale of 0 to 3 as follows: 0 indicated that the number of positive cells was less than 10%; 1 indicated weak positive and the number of positive cells more than 10%, but less than 30%; 2 indicated positive and the number of positive cells more than 30% but less than 50%; 3 indicated strong positive and the number of positive cells more than 50%.

Statistical analysis

Fisher's exact probability test was adopted to examine the relationship between the variables. A *P* value <0.05 was considered statistically significant.

RESULTS

KAI1 gene expression in colorectal carcinoma cell lines

HT29 and SW480 cell lines were derived from primary colorectal adenocarcinoma. SW620 and LoVo cell lines were established from metastatic colorectal carcinoma. Especially, SW620 cell line was isolated from the same case as was SW480 cell line. The expressions of KAI1 mRNA and protein in HT29 and SW480 cells were positive, whereas those in SW620 and LoVo cells were negative (Figures 1, 2).

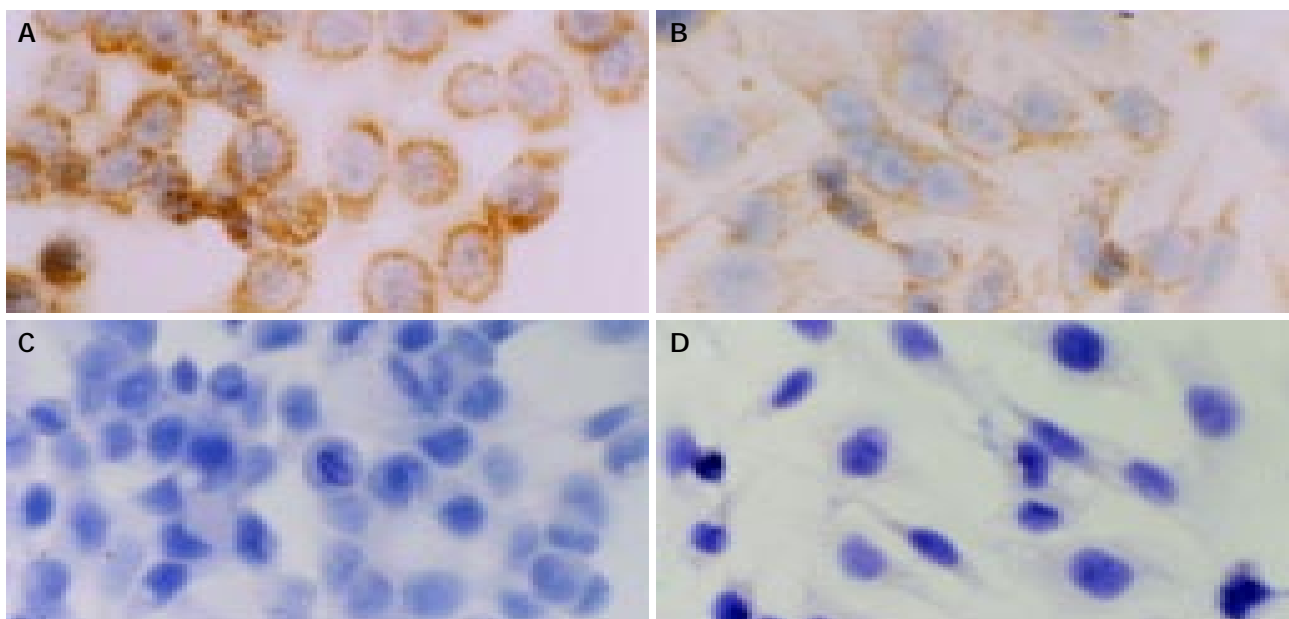


Figure 1 *In situ* hybridization detection of expression of KAI1 mRNA in colorectal carcinoma cell lines (Original magnification: $\times 400$). A: In HT29 cells, the positive expression (brown granule) was located in cytoplasm; B: In SW480 cells, the positive expression was located in cytoplasm; C: In SW620 cells, the expression of KAI1 mRNA was negative; D: In LoVo cells, the expression of KAI1 mRNA was negative.

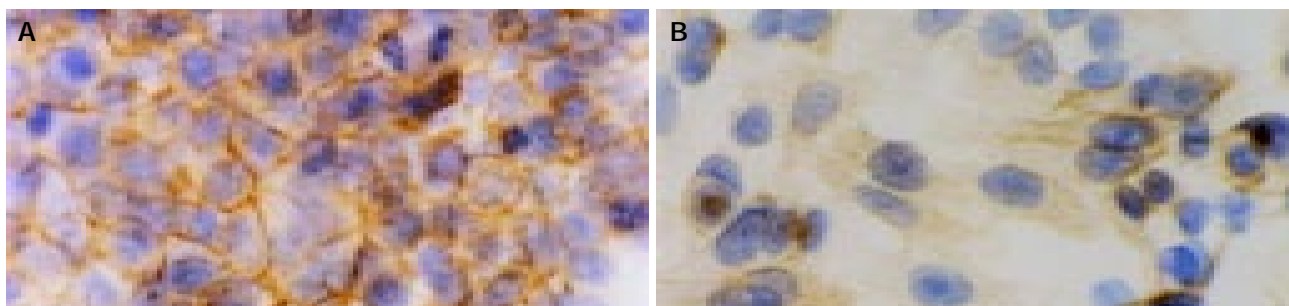


Figure 2 Expression of KAI1 protein detected by immunohistochemistry in colorectal carcinoma cell lines (Original magnification: $\times 400$). A: In HT29 cells, the positive expression located in cytoplasm and membrane; B: In SW480 cells, the positive expression located in cytoplasm and membrane.

Heterogeneous expression of *KAI1* mRNA in colonic carcinoma tissue

Of the 80 colonic carcinoma specimens, 56(70%) were classified as *KAI1* positive (Figure 3). There were 4 cases (20%) with positive *KAI1* mRNA expression in normal colonic mucosa and 2 cases (10%) in lymphatic metastasis. The results are shown in Table 1. The positivity ratio was significantly higher in colonic carcinoma than that in normal colonic mucosa and in lymphatic metastasis ($\chi^2=46.838$, $P<0.01$). The expression in lymphatic metastasis was almost lost.

To further investigate the relationship between the expression of *KAI1* and the clinical pathology, we sorted the colonic carcinomas based on histological grades and Dukes stages. Histological grade I means well differentiated adenocarcinoma, II means moderately differentiated and III means poorly differentiated. The results indicated that *KAI1* expression had no relationship with histological grades ($\chi^2=3.887$, $P>0.05$). The expression in Dukes A and B carcinoma was markedly higher in comparison with Dukes C carcinoma ($\chi^2=16.061$, $P<0.01$).

KAI1 protein expression analyzed by immunohistochemistry

There were 52(65%) cases with positive *KAI1* protein expressions in the colonic carcinomas (Figure 3). The positive ratios of normal colonic mucosa and lymphatic metastasis were 25% and 10%, respectively. The *KAI1* expressions in 3 groups were significantly different ($\chi^2=28.298$, $P<0.01$). Overall, the immunohistochemical results agreed well with those from the *in situ* hybridization assays.

DISCUSSION

Loss of the function of metastasis suppressor genes is an important step in the progression of a tumor type. Several candidate antimetastasis or anti-invasion genes have been studied in colorectal carcinoma, including nm23^[11], E-cadherin^[12], and CD44^[13], but inconsistent findings have been reported. For example, in separate studies, nm23 expression has been found to be directly correlated, not to be correlated, or inversely correlated with metastatic potential in colorectal cancer^[14-16]. *KAI1* has been thought to be one of such metastasis suppressor genes, because it was shown to suppress the ability of human prostatic cancer cells to metastasize when the tumor was transplanted into nude mice^[1] and because *KAI1* mRNA expression was reduced in advanced pancreatic cancer^[17] so that the pancreatic cancer cells spread to lymph nodes and distant organs. Furthermore, the transfer of the *KAI1* gene into mammary cancer cells has been shown to lead to suppression of their metastatic potential, whereas their primary tumor growth has not been affected^[18-20].

KAI1 is a member of the transmembrane-4 superfamily (TM4SF), many of which, including *KAI1*, are CD antigens present on the surface of leukocytes^[21,22]. At least three TM4SF members are implicated in metastasis, including CD9/MRP-1, CD63/ME491, and CD82/*KAI1*^[23]. *KAI1* and other TM4SF members, such as integrins and E-cadherin, have been demonstrated to bind to each other and relay extracellular signals to signal transduction pathways that are important in cellular adhesion, invasive motility, and metastasis^[24-27].

In our previous studies, we transfected the *KAI1* cDNA

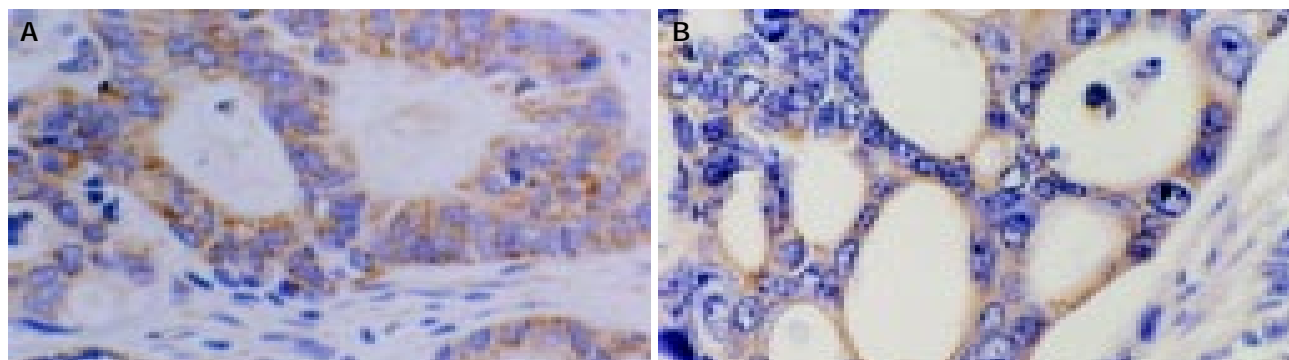


Figure 3 *In situ* hybridization and immunohistochemical detection of *KAI1* mRNA and protein in colonic carcinoma (Original magnification: $\times 400$). A: *In situ* hybridization detection found that strong *KAI1* mRNA staining was located in cytoplasm (brown granule); B: Detection by immunohistochemistry showed strong *KAI1* protein staining was in cytoplasm and membrane.

Table 1 *KAI1* gene expression in normal colonic mucosa, colonic carcinoma and lymphatic metastasis *n* (%)

Tissue	KAI1/CD82 expression				Total
	0	1	2	3	
Normal colonic mucosa	16(80.0)	3(15.0)	1(5.0)	0	20
Colonic carcinoma					
Histological grade					
I	6(23.1)	2(7.7)	12(46.2)	6(23.1)	26
II	10(26.3)	12(31.6)	14(36.8)	2(5.3)	38
III	8(50.0)	6(37.5)	2(12.5)	0	16
Dukes stage					
Dukes A	1(4.3)	6(26.1)	9(39.1)	7(30.4)	23
Dukes B	3(17.6)	6(35.3)	5(29.4)	3(17.6)	17
Dukes C	20(50.0)	10(25.0)	8(20.0)	2(5.0)	40
Lymphatic metastasis	18(90.0)	2(10.0)	0	0	20

into a colorectal carcinoma cell line, LoVo, and found that the KAI1 transfectant exhibited significantly increased homotypic cell adhesion and suppressed invasion and metastasis^[9]. Our findings were consistent with those in the studies of prostatic cancer^[2] and breast cancer^[18] cells.

In this study, we first investigated KAI1 mRNA expression in 4 colorectal carcinoma cell lines and found *KAI1* gene expression was much higher in HT29 and SW480 cell lines than in SW620 and LoVo cell lines. SW480 was isolated from a high-grade primary colonic tumor, and SW620 was isolated from a metastatic lymph node from the same patient 1 year later at the time of clinical relapse. KAI1 protein expression was high in SW480 but reduced in SW620. The colonic cancer cell line derived from metastatic lesions, LoVo, hardly exhibited any expression. In our observation we found that *KAI1* gene expressions both at mRNA and protein level, were inversely correlated with the metastatic potential of some established colorectal carcinoma cell lines.

We next examined KAI1 expression in normal colonic mucosa, carcinoma and lymphatic metastasis by *in situ* hybridization. The results indicated that KAI1 gene was highly expressed in colonic carcinoma compared with normal colonic epithelium and lymphatic metastasis. We found that although the expression had no relationship with histological grades, it was significantly correlated with Dukes stages. This indicates that the KAI1 mRNA expression may be positively related with the Dukes stages. The data shown in Table 1 demonstrate that KAI1 expression increases at an earlier tumor stage of colonic carcinoma, while decreases at advanced stages, and is possibly lost in metastases. That is to say, the expression of KAI1 has a reverse correlation with metastasis in colorectal carcinoma.

How does reduced TM4SF expression cause changes of invasive ability of tumor cells? It was hypothesized that tetraspanins might be implicated in the assembly of integrin-contained signaling complexes, thus modulating the function of integrin receptors in cell migration^[24]. Some results indicated that integrin-tetraspanin protein complexes played an important role in regulating protrusive activity of the tumor cells and contributed to extracellular matrix-induced production of matrix metalloproteinase 2 (MMP-2), and as a consequence, the invasive ability of cells^[28].

KAI1 has been extensively studied for its involvement in the progression of different human cancers. The mechanism of down-regulation of KAI1 has also been analyzed, however, much debate still exists. Recent study found a putative p53 consensus-binding site within the promoter region of KAI1 and demonstrated that the loss of p53 function, which was commonly observed in many types of cancer, led to the down-regulation of the *KAI1* gene, which might result in the progression of metastasis^[29]. But other data suggested that the down-regulation of KAI1 was not associated with either mutation, allelic loss, methylation of the promoter, or p53 regulation^[30]. Our previous study also demonstrated that mutation of the KAI1 gene, methylation of CpG islands and the abnormality of p53 were not related to low expression of KAI1.

In conclusion, KAI1 expression increases in an earlier tumor stage of colonic carcinoma, decreases in advanced stages, and is possibly lost in lymphatic metastases. The loss of KAI1 expression is correlated with higher stage, a surrogate marker for metastatic potential. The down-regulation of KAI1 in Dukes C and loss in metastasis demonstrate that loss of KAI1 expression occurs in cancer progression. The selection of cells that have the ability to spread from the primary tumor to the metastasis may favor those cells that have lost KAI1 expression. Those cells would be expected to be less adhesive, more invasive, and more motile^[31], and these characteristics are necessary for metastasis.

REFERENCES

- Dong JT**, Lamb PW, Rinker-Schaeffer CW, Vukanovic J, Ichikawa T, Isaacs JT, Barrett JC. KAI1, a metastasis suppressor gene for prostate cancer on human chromosome 11p11.2. *Science* 1995; **268**: 884-886
- Dong JT**, Isaacs WB, Barrett JC, Isaacs JT. Genomic organization of the human KAI1 metastasis-suppressor gene. *Genomics* 1997; **41**: 25-32
- Liu FS**, Chen JT, Dong JT, Hsieh YT, Lin AJ, Ho ES, Hung MJ, Lu CH. KAI1 metastasis suppressor gene is frequently down-regulated in cervical carcinoma. *Am J Pathol* 2001; **159**: 1629-1634
- Debies MT**, Welch DR. Genetic basis of human breast cancer metastasis. *J Mammary Gland Biol Neoplasia* 2001; **6**: 441-451
- Friess H**, Guo XZ, Tempia Caliera AA, Fukuda A, Martignoni ME, Zimmermann A, Korc M, Buchler MW. Differential expression of metastasis-associated genes in papilla of vater and pancreatic cancer correlates with disease stage. *J Clin Oncol* 2001; **19**: 2422-2432
- Miyazaki T**, Kato H, Shitara Y, Yoshikawa M, Tajima K, Masuda N, Shouji H, Tsukada K, Nakajima T, Kuwano H. Mutation and expression of the metastasis suppressor gene KAI1 in esophageal squamous cell carcinoma. *Cancer* 2000; **89**: 955-962
- Jackson P**, Kingsley EA, Russell PJ. Inverse correlation between KAI1 mRNA levels and invasive behaviour in bladder cancer cell lines. *Cancer Lett* 2000; **156**: 9-17
- Liu FS**, Dong JT, Chen JT, Hsieh YT, Ho ES, Hung MJ. Frequent down-regulation and lack of mutation of the KAI1 metastasis suppressor gene in epithelial ovarian carcinoma. *Gynecol Oncol* 2000; **78**: 10-15
- Liu L**, Wu DH, Li ZG, Yang GZ, Ding YQ. Effects of KAI1/CD82 on biological behavior of human colorectal carcinoma cell line. *World J Gastroenterol* 2003; **9**: 1231-1236
- Wu DH**, Liu L, Chen LH, Ding YQ. Expression of KAI1/CD82 in human colorectal tumor. *Diyi Junyi Daxue Xuebao* 2003; **23**: 714-715
- Dursun A**, Akyurek N, Gunel N, Yamac D. Prognostic implication of nm23-H1 expression in colorectal carcinomas. *Pathology* 2002; **34**: 427-432
- El-Bahrawy MA**, Poulson R, Jeffery R, Talbot I, Alison MR. The expression of E-cadherin and catenins in sporadic colorectal carcinoma. *Hum Pathol* 2001; **32**: 1216-1224
- Wong K**, Rubenthiran U, Jothy S. Motility of colon cancer cells: modulation by CD44 isoform expression. *Exp Mol Pathol* 2003; **75**: 124-130
- Forte A**, D'Urso A, Gallinaro LS, Lo Storto G, Soda G, Bosco D, Bezzi M, Vietri F, Beltrami V. NM23 expression as prognostic factor in colorectal carcinoma. *G Chir* 2002; **23**: 61-63
- Heys SD**, Langlois N, Smith IC, Walker LG, Eremin O. NM23 gene product expression does not predict lymph node metastases or survival in young patients with colorectal cancer. *Oncol Rep* 1998; **5**: 735-739
- Cheah PY**, Cao X, Eu KW, Seow-Choen F. NM23-H1 immunostaining is inversely associated with tumour staging but not overall survival or disease recurrence in colorectal carcinomas. *Br J Cancer* 1998; **77**: 1164-1168
- Guo X**, Friess H, Graber HU, Kashiwagi M, Zimmermann A, Korc M, Buchler MW. KAI1 expression is up-regulated in early pancreatic cancer and decreased in the presence of metastases. *Cancer Res* 1996; **56**: 4876-4880
- Yang X**, Wei LL, Tang C, Slack R, Mueller S, Lippman ME. Overexpression of KAI1 suppresses *in vitro* invasiveness and *in vivo* metastasis in breast cancer cells. *Cancer Res* 2001; **61**: 5284-5288
- Ono M**, Handa K, Withers DA, Hakomori S. Motility inhibition and apoptosis are induced by metastasis-suppressing gene product CD82 and its analogue CD9, with concurrent glycosylation. *Cancer Res* 1999; **59**: 2335-2339
- Takaoka A**, Hinoda Y, Sato S, Itoh F, Adachi M, Hareyama M, Imai K. Reduced invasive and metastatic potentials of KAI1-transfected melanoma cells. *Jpn J Cancer Res* 1998; **89**: 397-404
- White A**, Lamb PW, Barrett JC. Frequent downregulation of

- the KAI1(CD82) metastasis suppressor protein in human cancer cell lines. *Oncogene* 1998; **16**: 3143-3149
- 22 **Okochi H**, Mine T, Nashiro K, Suzuki J, Fujita T, Furue M. Expression of tetraspans transmembrane family in the epithelium of the gastrointestinal tract. *J Clin Gastroenterol* 1999; **29**: 63-67
- 23 **Adachi M**, Taki T, Konishi T, Huang CI, Higashiyama M, Miyake M. Novel staging protocol for non-small-cell lung cancers according to MRP-1/CD9 and KAI1/CD82 gene expression. *J Clin Oncol* 1998; **16**: 1397-1406
- 24 **Rubinstein E**, Le Naour F, Lagaudriere Gesbert C, Billard M, Conjeaud H, Boucheix C. CD9, CD63, CD81, and CD82 are components of a surface tetraspan network connected to HLA-DR and VLA integrins. *Eur J Immunol* 1996; **26**: 2657-2665
- 25 **Bienstock RJ**, Barrett JC. KAI1, a prostate metastasis suppressor: prediction of solvated structure and interactions with binding partners; integrins, cadherins, and cell-surface receptor proteins. *Mol Carcinog* 2001; **32**: 139-153
- 26 **Hiroki H**, Arimichi T, Takahiro T, Toshihiko T, Toshihiko T, Keiichi K, Nobuoki K, Yoshio Y, Masayuki M. Integrin alpha3 expression as a prognostic factor in colon cancer: association with MRP-1/CD9 and KAI1/CD82. *Int J Cancer* 2002; **97**: 518-525
- 27 **Hemler ME**, Mannion BA, Berditchevski F. Association of TM4SF proteins with integrins: relevance to cancer. *Biochim Biophys Acta* 1996; **1287**: 67-71
- 28 **Muneyuki T**, Watanabe M, Yamanaka M, Shiraishi T, Isaji S. KAIL/CD82 expression as a prognostic factor in sporadic colorectal cancer. *Anticancer Res* 2001; **21**: 3581-3587
- 29 **Mashimo T**, Watabe M, Hirota S, Hosobe S, Miura K, Tegtmeyer PJ, Rinker-Shaeffer CW, Watabe K. The expression of the KAI1 gene, a tumor metastasis suppressor, is directly activated by p53. *Proc Natl Acad Sci* 1998; **95**: 11307-11311
- 30 **Uzawa K**, Ono K, Suzuki H, Tanaka C, Yakushiji T, Yamamoto N, Yokoe H, Tanzawa H. High prevalence of decreased expression of KAI1 metastasis suppressor in human oral carcinogenesis. *Clin Cancer Res* 2002; **8**: 828-835
- 31 **Geradts J**, Maynard R, Birrer MJ, Hendricks D, Abbondanzo SL, Fong KM, Barrett JC, Lombardi DP. Frequent loss of KAI1 expression in squamous and lymphoid neoplasms. An immunohistochemical study of archival tissues. *Am J Pathol* 1999; **154**: 1665-1671

Edited by Kumar M Proofread by Chen WW and Xu FM

Influence of serum from liver-damaged rats on differentiation tendency of bone marrow-derived stem cells

Hai Hong, Jian-Zhi Chen, Feng Zhou, Ling Xue, Guo-Qiang Zhao

Hai Hong, Jian-Zhi Chen, Feng Zhou, Ling Xue, Guo-Qiang Zhao, Department of Pathology, Medical School of Sun Yat-Sen University, Guangzhou 510080, Guangdong Province, China
Supported by the National Natural Science Foundation of China, No. 30170473

Correspondence to: Professor Guo-Qiang Zhao, Department of Pathology, Medical School of Sun Yat-Sen University, 74 Zhongshan 2nd Rd., Guangzhou 510080, Guangdong Province, China. gqzhao@gzsums.edu.cn

Telephone: +86-20-87331075 **Fax:** +86-20-87331236

Received: 2003-12-10 **Accepted:** 2004-01-07

Abstract

AIM: Recent studies in both rodents and humans indicated that bone marrow (BM)-derived stem cells were able to home to the liver after they were damaged and demonstrated plasticity in becoming hepatocytes. However, the question remains as to how these stem cells are activated and led to the liver and where the signals initiating the mechanisms of activation and differentiation of stem cells originate. The aim of this study was to investigate the influence of serum from liver-damaged rats on differentiation tendency of bone marrow-derived stem cells.

METHODS: Serum samples were collected from rats treated with a 2-acetylaminofluorene (2-AAF)/carbon tetrachloride (CCl₄) program for varying time points and then used as stimulators of cultured BM stem cells. Expression of M₂- and L-type isozymes of rat pyruvate kinase, albumin as well as integrin-β1 were then examined by reverse transcription polymerase chain reaction (RT-PCR) to estimate the differentiation state of BM stem cells.

RESULTS: Expression of M₂-type isozyme of pyruvate kinase (M₂-PK), a marker of immature hepatocytes, was detected in each group stimulated with experimental serum, but not in controls including mature hepatocytes, BM stem cells without serum stimulation, and BM stem cells stimulated with normal control serum. As a marker expressed in the development of liver, the expression signal of integrin-β1 was also detectable in each group stimulated with experimental serum. However, expression of L-type isozyme of pyruvate kinase (L-PK) and albumin, marker molecules of mature hepatocytes, was not detected in groups stimulated with experimental serum.

CONCLUSION: Under the influence of serum from rats with liver failure, BM stem cells begin to differentiate along a direction to hepatocyte lineage and to possess some features of immature hepatocytes.

Hong H, Chen JZ, Zhou F, Xue L, Zhao GQ. Influence of serum from liver-damaged rats on differentiation tendency of bone marrow-derived stem cells. *World J Gastroenterol* 2004; 10 (15): 2250-2253

<http://www.wjgnet.com/1007-9327/10/2250.asp>

INTRODUCTION

Recent studies in both rodents and humans indicated that bone marrow (BM) stem cells were able to home to the liver after they were damaged, and demonstrated plasticity in becoming hepatocytes^[1-4]. Questions remain as to how BM stem cells are activated and led to the liver and where the signals initiating the mechanisms of activation and differentiation of stem cells originate. Transfused oval cells (hepatic stem cells) that had a selective tropism for the liver in an animal model of liver-damage suggested that "signal molecules" were present in serum of this animal model and played an important role in mediating both hepatic and non-hepatic stem cell activation^[5]. However, the influence of these putative signal molecules in serum on the differentiation state of bone marrow-derived stem cells is yet unclear. The purposes of the present work were to confirm the existence of signaling molecules in serum of liver-damaged rats and to observe its effects on the differentiation of BM stem cells into hepatocytes.

MATERIALS AND METHODS

Establishment of animal model of liver-damage

Male Sprague-Dawley (SD) rats, 6-week-old, were used for the establishment of an animal model of liver-damage. The model was made by means of a 2-AAF/CCl₄ program according to Petersen^[1]. In experimental group, 2-acetylaminofluorene (2-AAF, Sigma), 2.5 g/L in earthnut oil, was administered to stomach of rats everyday for 7 d. On the 7th d of 2-AAF administration, an Ld50 dose of CCl₄ was given by intraperitoneal injection. Animal blood was taken at the time points of 2, 4, 8, 12, and 24 h after CCl₄ injection. Experimental serum was prepared on standby. The serum from normal animals was used as control.

Isolation and culture of bone marrow stromal cells

The SD rats were sacrificed by means of ether asphyxia. Bone marrow was collected from tibiae and BM cells were suspended in Dulbecco's modified Eagle's medium (DMEM) with fetal bovine serum. After centrifugation and re-suspension, the cells were seeded in a culture flask and cultured under a routine condition (37 °C, 50 mL/L CO₂). The solution of medium was changed every 4 d while the cells floating on the medium were discarded. The cells adhering to bottom of the flask (so-called BM stromal cells) were cultured sequentially for 12-14 d. After 3 population doublings, the purified cells were harvested and used in the following stimulating culture with experimental serum.

Stimulating culture of BM stromal cells with experimental serum

BM stromal cells were cultured sequentially in a specialized medium (DMEM-F12) containing 3 ml/L experimental rat serum. In the control group, the culture medium contained 3 mL/L normal rat serum instead of experimental rat serum. Cultures were grown and submerged for 12 d. The cells were harvested on the 13th culture day for ribonucleic acid (RNA) isolation.

Table 1 Primer pairs for RT-PCR

Marker genes	Primer pairs	PCR fragments
M ₂ -PK	5'ccatctaccacttgagttatcga3' / 5'tcatggtacaggcactacacgc3'	431 bp
L-PK	5'acctctgccttctggatactgact3' / 5'tgcaagactccggttcgtatct3'	322 bp
Albumin	5'gagccccgaaagaacgagtgtt3' / 5'ggggaatctctggctcatcacg3'	389 bp
INT-β1	5'tacttcagactccgcattgg3' / 5'cagtgactgcaaaaatcgctcg3'	488 bp
GAPDH	5'ccatggagaaggctggg3' / 5'caaagttgcatggtgatgacc3'	180 bp

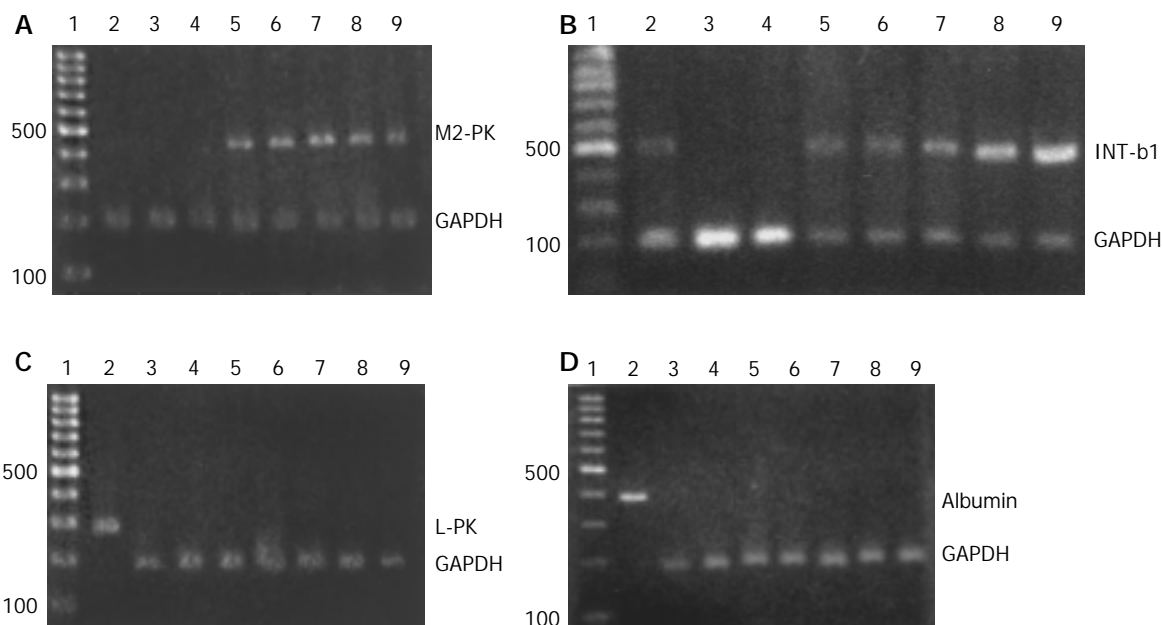


Figure 1 Expressions of M₂-PK, Integrin-β1, L-PK and albumin in BM stem cells. A: Expression of M₂-PK in BM stem cells. Lane 1, 100 bp DNA marker; Lane 2, Hepatocytes; Lane 3, BM stem cells without stimulation; Lane 4, BM stem cells stimulated with control serum; Lane 5, BM stem cells stimulated with experimental serum for 2 h; Lane 6, BM stem cells stimulated with experimental serum for 4 h; Lane 7, BM stem cells stimulated with experimental serum for 8 h; Lane 8, BM stem cells stimulated with experimental serum for 12 h; Lane 9, BM stem cells stimulated with experimental serum for 24 h. B: Expression of Integrin-β1 in BM stem cells. Lane 1, 100 bp DNA marker; Lane 2, Hepatocytes; Lane 3, BM stem cells without stimulation; Lane 4, BM stem cells stimulated with control serum; Lane 5, BM stem cells stimulated with experimental serum for 2 h; Lane 6, BM stem cells stimulated with experimental serum for 4 h; Lane 7, BM stem cells stimulated with experimental serum for 8 h; Lane 8, BM stem cells stimulated with experimental serum for 12 h; Lane 9, BM stem cells stimulated with experimental serum for 24 h. C: Expression of L-PK in BM stem cells. Lane 1, 100 bp DNA marker; Lane 2, Hepatocytes; Lane 3, BM stem cells without stimulation; Lane 4, BM stem cells stimulated with control serum; Lane 5, BM stem cells stimulated with experimental serum for 2 h; Lane 6, BM stem cells stimulated with experimental serum for 4 h; Lane 7, BM stem cells stimulated with experimental serum for 8 h; Lane 8, BM stem cells stimulated with experimental serum for 12 h; Lane 9, BM stem cells stimulated with experimental serum for 24 h. D: Expression of albumin in BM stem cells. Lane 1, 100 bp DNA marker; Lane 2, Hepatocytes; Lane 3, BM stem cells without stimulation; Lane 4, BM stem cells stimulated with control serum; Lane 5, BM stem cells stimulated with experimental serum for 2 h; Lane 6, BM stem cells stimulated with experimental serum for 4 h; Lane 7, BM stem cells stimulated with experimental serum for 8 h; Lane 8, BM stem cells stimulated with experimental serum for 12 h; Lane 9, BM stem cells stimulated with experimental serum for 24 h.

Isolation of RNA

RNA was extracted from the cells collected from the cultures described above, according to the protocol of QIAGEN RNA easy mini kit. RNA samples were then stored at -80 °C.

Primers selection

Genes of M₂-type and L-type isozymes of rat pyruvate kinase (M₂-PK, L-PK), albumin and integrin-β1 (INT-β1) were selected as the markers representing different differentiation stages of hepatocyte lineage. The gene of glyceraldehyde-3-phosphate-dihydrogenase (GAPDH) was used as an internal control for RT-PCR reactions. Primer pairs used for RT-PCR are shown in Table 1.

RT-PCR reactions

RNA samples were first reversely transcribed into cDNA, and then used as templates in the following PCR reactions. The

reaction cocktails (containing 1 μg template cDNA, 50 μmol/L dNTPs, 400 μmol/L primers, 1×PCR buffer, 2.5 mmol/L MgCl₂, 1 U Taq-polymerase, add H₂O to 50 μL of total volume) were run on GeneAmp® PCR System 9600 (AB) with a combined program of program 1 (at 94 °C for 5 min), program 2 (at 95 °C for 1 min, at 60 °C for 1 min, at 72 °C for 1 min; 30 cycles), and program 3 (at 95 °C for 1 min, at 60 °C for 1 min, at 72 °C for 5 min). The PCR products were electrophoresed in 12 g/L agarose gel, stained with ethidium bromide, and photographed.

RESULTS

M₂-PK, as a marker of immature hepatocytes, was used to estimate the differentiation state of BM stem cells stimulated by the experimental serum. The results showed that the expression signals of M₂-PK were detected in each group

stimulated with experimental serum, but not in the control group of normal BM stem cells that had no stimulation, BM stem cells stimulated with control serum, and normal mature hepatocytes (Figure 1A). Integrin- β 1 is a marker expressed during the development of liver. In this study, its expression signals were also detectable in each group stimulated with experimental serum as those observed in the positive control of hepatocytes (Figure 1B). L-PK and albumin, as marker molecules of mature hepatocytes, were used to estimate the terminal differentiation state of BM stem cells under the influence of experimental serum. However, no signals were detected in the experimental groups, except for the positive control of hepatocytes (Figure 1C, D).

DISCUSSION

The existence of liver stem cells had been widely proved in both rodents and humans^[1-4,6-9]. By extension, liver stem cells could be divided into three groups: (1) mature hepatocytes that proliferate during normal liver tissue renewal and after less severe liver damage, (2) oval cells that are activated to proliferate when the liver damage is extensive and chronic, and (3) exogenous liver stem cells that may derived from bone marrow cells and respond to severe liver damage^[10]. However, in a narrow sense, the concept of liver stem cells is usually limited to hepatic oval cells and non-hepatic bone marrow stem cells.

A phenomenon that was often observed both in experimental animal models and in clinics was that the proliferation of liver stem cells occurred most often in conditions of severe liver damages or chronic liver diseases^[11-15]. Maybe it is the reason that stem cells were seldom detected in healthy livers. Thus it can be understood that liver-damage is an important prerequisite for activation of liver stem cells. This suggests that the signals initiating activation of hepatic or non-hepatic stem cells might originate from damaged livers. This hypothesis had been partially proved by our previous experimental work^[5]. In our previous experiments, oval cells isolated from male SD rats were transfused, through caudal vein into the circulatory system of a female rat with liver damage. Sex-determining gene *sry* that was located on Y chromosome was then examined respectively by PCR and *in situ* hybridization technique in the liver, kidney and spleen of experimental animals. The results of cell-transplant experiments showed that *sry* gene was detectable only in the liver but not in the spleen and kidney of rats with liver damages and that no signals could be detected in control animals, neither in the liver, spleen nor in the kidney. It could be also morphologically observed that some exogenous cells with *sry* marker migrated into the parenchyma of liver and settled there, suggesting that transfused oval cells had a selective tropism for damaged liver. These results also suggested that signaling molecules existed in the serum of animals with liver damage and might play a role in mediating stem cell activation.

In the present study, an animal model of liver-damage was established with a 2-AAF/CCl₄ program. In this model, the capacity of hepatocyte self-regeneration was first impaired by 2-AAF and then the liver was damaged severely by CCl₄. In this status, the damaged liver would likely produce a signal to initiate the activation of stem cells in the bone marrow. The results of the present study showed that the expression of M₂-PK, a marker of immature hepatocyte^[16-22], could be detected in each group stimulated with experimental serum, but not in any of the control groups. Integrin- β 1 is a marker expressed during the development of liver. Its expression could be detected in fetal hepatocyte as early as at 8th wk of gestation^[30]. In the present results, the expression signal of integrin- β 1 was also detectable in each group stimulated with experimental

serum. Thus, the functional state of BM-derived stem cells was changed under the influence of experimental serum, thus differentiating toward the direction of a hepatocyte lineage. Although the markers of a mature hepatocyte, L-PK and albumin were not detectable in stimulated BM stem cells, the leap from an undetermined state to a determined state was a marker of entry into the process of programmed differentiation. A variety of possibilities could account for the lack of detectable signals for L-PK and albumin in stimulated BM stem cells. Among the possibilities, one could be the deficiency in intensity and time of stimulation, while another could, by reasoning, be that the postulated "signal molecules" existing in the experimental serum were involved only in the early activation and determination of BM stem cells, while the terminal differentiation of the cells into hepatocytes might still need other signals.

The results in the present study indicated that the driving force promoting differentiation of BM stem cells to hepatocytes was certainly generated from the serum of rats treated by 2-AAF/CCl₄. It has been further testified that some "signal molecules" were existed in the circulation of rats treated by 2-AAF/CCl₄ and that they might play an important role in the initiation of activation of stem cell. It would be helpful for understanding the mechanisms of stem cell differentiation if the "signal molecules" could be further identified and isolated.

Recent studies have convincingly demonstrated that adult bone marrow contains cells capable of differentiating into hepatocyte-like cells. Nevertheless, what type of cell population are the ancestor cells for hepatocytes still remains a question. In the vast majority of reports, hematopoietic cells were considered to be capable of "transdifferentiating" into hepatocytes^[2,4,23-28]. However, Wagers (2002) deemed that there was little evidence for transdifferentiation of adult hematopoietic stem cells^[29]. The present study showed that bone marrow stromal cells demonstrated the plasticity in changing into hepatocytes. By this token, the debate about origin of liver stem cells will keep on.

REFERENCES

- 1 **Petersen BE**, Bowen WC, Patrene KD, Mars WM, Sullivan AK, Murase N, Boggs SS, Greenberger JS, Goff JP. Bone marrow as a potential source of hepatic oval cells. *Science* 1999; **284**: 1168-1170
- 2 **Lagasse E**, Connors H, Al Dhalimy M, Reitsma M, Dohse M, Osborne L, Wang X, Finegold M, Weissman IL, Grompe M. Purified hematopoietic stem cells can differentiate into hepatocytes *in vivo*. *Nat Med* 2000; **6**: 1229-1234
- 3 **Theise ND**, Nimmakayalu M, Gardner R, Illei PB, Morgan G, Teperman L, Henegariu O, Krause DS. Liver from bone marrow in humans. *Hepatology* 2000; **32**: 11-16
- 4 **Alison M**, Poulsom R, Jeffery R, Dhillon AP, Quaglia A, Jacob J, Novelli M, Prentice G, Williamson J, Wright NA. Hepatocytes from non-hepatic adult stem cells. *Nature* 2000; **406**: 257
- 5 **Chen JZ**, Hong H, Xiang J, Xue L, Zhao GQ. A selective tropism of transfused oval cells for liver. *World J Gastroenterol* 2003; **9**: 544-546
- 6 **Crosby HA**, Hubscher S, Fabris L, Joplin R, Sell S, Kelly D, Strain AJ. Immunolocalization of putative human liver progenitor cells in livers from patients with end-stage primary biliary cirrhosis and sclerosing cholangitis using the monoclonal antibody OV-6. *Am J Pathol* 1998; **152**: 771-779
- 7 **Lowes KN**, Brennan BA, Yeoh GC, Olynyk JK. Oval cell numbers in human chronic liver diseases are directly related to disease severity. *Am J Pathol* 1999; **154**: 537-541
- 8 **Theise ND**, Saxena R, Portmann BC, Thung SN, Yee H, Chiriboga L, Kumar A, Crawford JM. The canals of Hering and hepatic stem cells in humans. *Hepatology* 1999; **30**: 1425-1433
- 9 **Malhi H**, Irani AN, Gagandeep S, Gupta S. Isolation of human progenitor liver epithelial cells with extensive replication capacity and differentiation into mature hepatocytes. *J Cell Sci* 2002; **115**: 2679-2688

- 10 **Sell S.** The role of progenitor cells in repair of liver injury and in liver transplantation. *Wound Repair Regen* 2001; **9**: 467-482
- 11 **Roskams T,** Yang SQ, Koteish A, Durnez A, DeVos R, Huang X, Achten R, Verslype C, Diehl AM. Oxidative stress and oval cell accumulation in mice and humans with alcoholic and nonalcoholic fatty liver disease. *Am J Pathol* 2003; **163**: 1301-1311
- 12 **Lowes KN,** Croager EJ, Olynyk JK, Abraham LJ, Yeoh GC. Oval cell-mediated liver regeneration: Role of cytokines and growth factors. *J Gastroenterol Hepatol* 2003; **18**: 4-12
- 13 **Fausto N,** Campbell JS. The role of hepatocytes and oval cells in liver regeneration and repopulation. *Mech Dev* 2003; **120**: 117-130
- 14 **Oh SH,** Hatch HM, Petersen BE. Hepatic oval 'stem' cell in liver regeneration. *Semin Cell Dev Biol* 2002; **13**: 405-409
- 15 **Faris RA,** Konkin T, Halpert G. Liver stem cells: a potential source of hepatocytes for the treatment of human liver disease. *Artif Organs* 2001; **25**: 513-521
- 16 **Tian YW,** Smith PG, Yeoh GC. The oval-shaped cell as a candidate for a liver stem cell in embryonic, neonatal and precancerous liver: identification based on morphology and immunohistochemical staining for albumin and pyruvate kinase isoenzyme expression. *Histochem Cell Biol* 1997; **107**: 243-250
- 17 **Tee LB,** Kirilak Y, Huang WH, Smith PG, Morgan RH, Yeoh GC. Dual phenotypic expression of hepatocytes and bile ductular markers in developing and preneoplastic rat liver. *Carcinogenesis* 1996; **17**: 251-259
- 18 **Steinberg P,** Klingelhoffer A, Schafer A, Wust G, Weisse G, Oesch F, Eigenbrodt E. Expression of pyruvate kinase M2 in preneoplastic hepatic foci of N-nitrosomorpholine-treated rats. *Virchows Arch* 1999; **434**: 213-220
- 19 **Hacker HJ,** Steinberg P, Bannasch P. Pyruvate kinase isoenzyme shift from L-type to M2-type is a late event in hepatocarcinogenesis induced in rats by a choline-deficient/DL-ethionine-supplemented diet. *Carcinogenesis* 1998; **19**: 99-107
- 20 **Tee LB,** Kirilak Y, Huang WH, Morgan RH, Yeoh GC. Differentiation of oval cells into duct-like cells in preneoplastic liver of rats placed on a choline-deficient diet supplemented with ethionine. *Carcinogenesis* 1994; **15**: 2747-2756
- 21 **Scott RJ,** English V, Noguchi T, Tanaka T, Yeoh GC. Pyruvate kinase isoenzyme transitions in cultures of fetal rat hepatocytes. *Cell Differ Dev* 1988; **25**: 109-118
- 22 **Vessey CJ,** de la Hall PM. Hepatic stem cells: a review. *Pathology* 2001; **33**: 130-141
- 23 **Wang X,** Ge S, McNamara G, Hao QL, Crooks GM, Nolte JA. Albumin-expressing hepatocyte-like cells develop in the livers of immune-deficient mice that received transplants of highly purified human hematopoietic stem cells. *Blood* 2003; **101**: 4201-4208
- 24 **Fiegel HC,** Lioznov MV, Cortes-Dericks L, Lange C, Kluth D, Fehse B, Zander AR. Liver-specific gene expression in cultured human hematopoietic stem cells. *Stem Cells* 2003; **21**: 98-104
- 25 **Austin TW,** Lagasse E. Hepatic regeneration from hematopoietic stem cells. *Mech Dev* 2003; **120**: 131-135
- 26 **Mallet VO,** Mitchell C, Mezey E, Fabre M, Guidotti JE, Renia L, Coulombel L, Kahn A, Gilgenkrantz H. Bone marrow transplantation in mice leads to a minor population of hepatocytes that can be selectively amplified *in vivo*. *Hepatology* 2002; **35**: 799-804
- 27 **Avital I,** Inderbitzin D, Aoki T, Tyan DB, Cohen AH, Ferrarasso C, Rozga J, Arnaout WS, Demetriou AA. Isolation, characterization, and transplantation of bone marrow-derived hepatocyte stem cells. *Biochem Biophys Res Commun* 2001; **288**: 156-164
- 28 **Mitaka T.** Hepatic stem cells: from bone marrow cells to hepatocytes. *Biochem Biophys Res Commun* 2001; **281**: 1-5
- 29 **Wagers AJ,** Sherwood RI, Christensen JL, Weissman IL. Little evidence for developmental plasticity of adult hematopoietic stem cells. *Science* 2002; **297**: 2256-2259
- 30 **Couvelard A,** Bringuier AF, Dauge MC, Nejjari M, Darai E, Benifla JL, Feldmann G, Henin D, Scoazec JY. Expression of integrins during liver organogenesis in humans. *Hepatology* 1998; **27**: 839-847

Edited by Wang XL and Qin D Proofread by Xu FM

Pathophysiological significance of a reaction in mouse gastrointestinal tract associated with delayed-type hypersensitivity

Wan-Gui Yu, Ping Lin, Hui Pan, Lan Xiao, En-Cong Gong, Lin Mei

Wan-Gui Yu, Department of Physiology, Medical College of Yangtze University, Jingzhou 434000, Hubei Province, China

Ping Lin, Department of Physiology, Medical School of Hubei Institute for Nationalities, Enshi, 445000, Hubei Province, China

Hui Pan, Lan Xiao, Lin Mei, Department of Physiology and Pathophysiology, Peking University Health Science Center, Beijing, 100083, China

En-Cong Gong, Department of Pathology, Peking University Health Science Center, Beijing, 100083, China

Supported by the National Natural Science Foundation of China, No. 30170419

Correspondence to: Dr. Lin Mei, Department of Physiology and Pathophysiology, Peking University Health Science Center, Beijing, 100083, China. linmei@bjmu.edu.cn

Telephone: +86-10-82801477 **Fax:** +86-10-82801746

Received: 2003-12-17 **Accepted:** 2004-01-08

Abstract

AIM: To explore the pathophysiological significance of delayed type hypersensitivity (DTH) reaction in mouse gastrointestinal tract induced by an allergen 2,4-dinitrochlorobenzene (DNCB).

METHODS: BALB/c mice were randomly divided into control and DTH₁₋₆ groups. After sensitized by DNCB smeared on the abdominal skin, the mice were challenged with DNCB by gavage or enema. The weight, stool viscosity and hematochezia were observed and accumulated as disease active index (DAI) score; the gastrointestinal motility was represented by active charcoal propulsion rate; the colon pathological score was achieved by macropathology and HE staining of section prepared for microscopy; and the leukocyte migration inhibitory factor (LMIF) activity was determined by indirect capillary assay of the absorbance (A) of migrated leukocytes.

RESULTS: Active charcoal propulsion rates of small intestine in the DNCB gavages groups were significantly higher than that in the control group ($P < 0.01$). The DAI scores and pathological score in DNCB enema groups were also higher than that in the control group ($P < 0.05$), and there were significant rises in LMIF activity in DNCB enema groups as compared with control groups ($P < 0.01$).

CONCLUSION: Mouse gastrointestinal DTH reaction could be induced by DNCB, which might facilitate the mechanism underlying the ulcerative colitis.

Yu WG, Lin P, Pan H, Xiao L, Gong EC, Mei L. Pathophysiological significance of a reaction in mouse gastrointestinal tract associated with delayed-type hypersensitivity. *World J Gastroenterol* 2004; 10(15): 2254-2258
<http://www.wjgnet.com/1007-9327/10/2254.asp>

INTRODUCTION

The gastrointestinal tract (GI) is not only an important organ in digestion and endocrine, but also the largest peripheral

immunological organ in the body^[1]. The secretory immunoglobulin A (s-IgA) and T cell are responsible for developing mucosa vaccines and producing oral tolerance^[2,3]. Furthermore, the manifestation of T cell mediated reaction in GI tract was most often in the way of delayed-type hypersensitivity (DTH), thereby resulting in ulcerative colitis^[4,5]. 2,4-dinitrochlorobenzene (DNCB), a chemical compound of low molecular weight, could combine with tissue protein to function as a full antigen in activating T cell mediated DTH reaction, such as skin DTH^[6] and colon inflammation/ulcer^[5,7,8]. Gastrointestinal DTH (or colitis) induced by DNCB in rabbit, guinea pig and rat has been reported^[5,7,8], but that in mice has not been reported. In this study, DNCB-induced DTH in mice GI tract were found, and its pathophysiological significance was discussed.

MATERIALS AND METHODS

Animals

Healthy male BALB/c mice weighing 18-21 g (supplied by the Department of Experimental Animals, Peking University Health Science Center) were used. Animals were fed with a standard diet and allowed free access to water.

Preparation of major chemicals

DNCB solution For DNCB sensitization, 330 mg DNCB (Beijing Chemical Reagent Company, Beijing, P.R. China) was dissolved in 10 mL of acetone-olive oil (1:1) vehicle. For DNCB gavage, 300 mg DNCB was first mixed with a minimum volume of polysorbate 80, and a minimum volume of ethanol was added until the mixture was completely dissolved, followed by the addition of olive oil to achieve a final DNCB concentration of 6.6 g/L. The ratios of polysorbate 80-ethanol-olive oil in this vehicle were 6.6%, 8.8% and 84.6%, respectively. Then the 6.6% solution was diluted to 1.3 g/L and 0.3 g/L DNCB solution. For DNCB enema, DNCB was dissolved in 600 mL/L ethanol to achieve 4 g/L, 2 g/L, and 1 g/L DNCB solution, separately. All these DNCB solutions were stored at 4 °C.

Activated charcoal suspension The suspension was made according to Qi *et al.*^[9] with a little modification. A total of 6 g activated charcoal (Tianjin 6th Chemical Reagent Company, Tianjin, China) and 2 g astragalum gum (Beijing Chemical Reagent Company, China) were dissolved in 50 mL of normal saline (NS) just before intragastric use.

RPMI 1640 One milliliter of RPMI 1640 culture medium contained 100 IU penicillin and 100 µg streptomycin, and then the pH was adjusted to 6.8-7.2.

Phytohemagglutinin (PHA) A 100 mg PHA was dissolved in 10 mL incomplete RPMI1640, and then sterilized and preserved at -20 °C.

Ammonium chloride solution (erythrocyte lytic fluid) A total of 1.03 g Tris and 3.735 g NH₄Cl were dissolved in 500 mL distilled water.

Induction of DTH response in GI tract

Grouping Ninety-six BALB/c mice were randomly divided into 10 groups, including DTH₁₋₆, DTH negative (DTH₋) group and control group.

Sensitization On the first day of experiment, mouse fur on abdomen (2.5 cm diameter) was shaved. A total of 50 μ L of 33 g/L DNCB was smeared on the shaved skin once a day for 1 or 4 d. Mice in the DTH₍₋₎ and control groups were smeared with acetone-olive oil vehicle.

Gavage All the mice were fasted for 6 h before gavage. On the second day of experiment the mice in DTH₁, DTH₂ and DTH₃ groups were gavaged with 0.8 mL of 0.3 g/L, 1.3 g/L and 6.6 g/L DNCB, respectively. The DTH₍₋₎ group was gavaged 1.3 g/L DNCB and the control group was gavaged polysorbate 80-ethanol-olive oil vehicle. On the third day, 0.8 mL of activated charcoal was gavaged to each mouse. Twenty minutes later, the mice were killed by decapitation for determination of gastrointestinal motility.

Enema On the 5 th day, a silica-gel tube with 10 mm diameter was inserted into the colons of the mice, its tip being 3-3.5 cm far from the anus. The mice in DTH₄, DTH₅ and DTH₆ groups were intracolonicly administered 1 g/L, 2 g/L and 4 g/L DNCB (2 μ L/g) once a day for 4 d. DTH₍₋₎ group was administered 2 g/L DNCB and the control group was administered 600 mL/L ethanol vehicle.

Evaluation of the animals

Gastrointestinal motility After each mouse was killed, the whole small intestine was taken out, rinsed with NS quickly, and the intestinal wall was cut open longitudinally, laid and unfolded on a flat plate for estimation of the active charcoal migration distance (cm). The gastrointestinal motility was expressed by charcoal propulsion rate by using the formula: charcoal propulsion rate = migration distance of active charcoal / the distance from pylorus-duodenum junction to ileocecum $\times 100\%$.

Body mass and stool By using disease activity index (DAI) score^[10], the body mass and stool were scored as follows: Body mass: score 0-normal; score 1-1-5% lower than normal; score 2-6-10% lower than normal; score 3-11-15% lower than normal; and score 4-above 15% lower than normal. Stool viscosity: score 0-normal; score 2-fluffy; and score 4-diarrhea. Stool hemorrhage: score 0-normal; and score 2-apparent hemorrhage.

Pathological score On the 9 th d, all the mice received enema were killed by cervical dislocation. The colon was cut open longitudinally along the attachments of mesenteries and was first macropathologically observed. Then specimens were taken from inflammatory/ulcerative colon and were fixed in 40 g/L formaldehyde. Paraffin-embedded 5- μ m thick section was made for HE staining. The macropathological score and microscopy score were obtained by adopting Dr. Murano's method^[10] with slight modification as follows: Macropathological score: score 0-no cementation (colon was easily detached from other tissues) and no inflammation in colon; score 1-moderate cementation or local congestion; score 2-severe cementation with one ulcer (<1 cm); score 3- more than one ulcer (<1 cm) with inflammation; and score 4-more than one ulcer (>1 cm) with inflammation.

Microscopy: score 0-normal colon mucosa or slight congestion; score 1-mucosa hyperemia, infiltration of chronic inflammatory cells and decrease of the number of goblet cell in colon mucosa; score 2-mucosa hyperemia, infiltration of chronic inflammatory cells and local superficial erosion; and score 3-atrophic change with ulcer and serious infiltration of chronic inflammatory cells in colon mucosa.

Measurement of leukocyte migration inhibitory factor (LMIF) activity

LMIF preparation By following our previous method^[11], the spleen lymphocytes (2×10^6 /mL) of mice received enema were cultured in PHA (60 μ g/mL) for 72 h. Then the supernatant containing LMIF component was collected by centrifugation

(1 500 r/min, 15 min), followed by lyophilization. The lyophilized powder was stored at -20 . Working solution (LMIF solution) was prepared by dissolving the lyophilized powder in RPMI-1640 to one third of its original volume before using.

Preparation of peripheral leukocytes A suspension of indicator cells (migrated leukocytes) was prepared from the anti-coagulated whole blood of guinea pigs. Three percent gelatin of 1/3 volume of the blood was added to the blood before culturing the sample at 37 for 30 min. The upper layer rich in leukocytes was taken out and centrifuged (1 000 r/min) for 10 min. Then the sediment was washed twice with Hanks' solution free of Mg²⁺ and Ca²⁺, and again centrifuged (1 000 r/min) for 10 min. Finally, the sediment was used as the indicator cell and was adjusted to a concentration of $(1.6-1.8) \times 10^7$ cells/mL RPMI 1640.

Detection of leukocyte absorbance By following our previous work^[11] with a little improvement, the leukocyte was injected into a capillary tube of 80 μ L volume. After heat-sealing one end of the tube and spinning at 1 000 r/min for 10 min, the tubes were cut at the liquid-cell interface. The portion containing the cells was placed inside each chamber of a 24-well plate filled with 210 μ L LMIF solution for culture. Twelve hours later, 200 μ L solution was taken out from each chamber and was put in an well of a 96-well plate, followed by an addition of 20 μ L methylthiazolotetrazolium, MTT) was added into each well before the plate was incubated at 37 for 4 h. Then the supernatant was removed, 200 μ L of DMSO was added into each well and the plate was shaken for 10 min. The absorbance (A value) of the migration cells was determined in Micro plate Reader at a wavelength of 570 nm. The average of A values of 3 wells was regarded as a mean A value. The above processes were repeated for 9 times.

Statistical analysis

Data were expressed as mean \pm SE. Analysis of variance (ANOVA) and student's *t* test were used for comparison among the groups and between paired data. $P < 0.05$ was considered to be statistically significant.

RESULTS

Gastrointestinal motility

Active charcoal propulsion rates of small intestine in the DTH₁ (0.3 g/L DNCB) and DTH₂ (1.3 g/L DNCB) groups were significantly higher than that in the control group ($P < 0.01$) and DTH₍₋₎ groups ($P < 0.05$ or $P < 0.01$), whereas there was no significant difference between the control group and DTH₍₋₎ group (Figure 1). All the mice in DTH₃ group died after the 0.66% DNCB gavage.

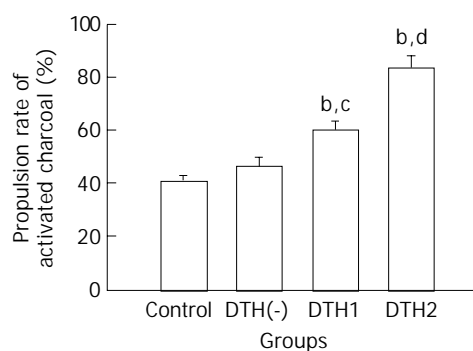


Figure 1 Effect of DNCB gavage on gastrointestinal motility in sensitized mice. ^b $P < 0.01$ vs control, ^c $P < 0.05$ vs DTH₍₋₎, ^d $P < 0.01$ vs DTH₍₋₎ and DTH₁, $n = 8$ in control; $n = 7$ in DTH₍₋₎, DTH₁ and DTH₂ groups.

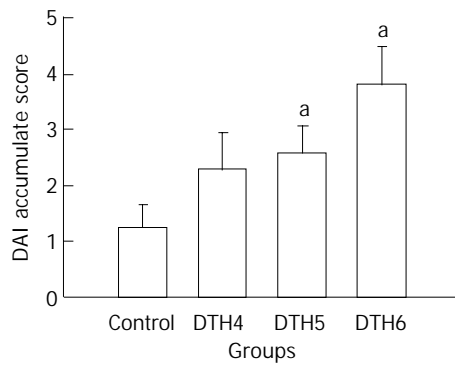


Figure 2 Effect of DNCB enema on DAI score in sensitized mice. ^a $P < 0.05$ vs control. $n = 16$ in control group and DTH₄ group; $n = 11$ in DTH₅ group; $n = 17$ in DTH₆ group.

DAI score and pathological score

Diarrhea was first found in the mice 24 h after DNCB enema, and weight loss was found 3 d later. Serious weight loss and obvious diarrhea were seen in the 4 g/L DNCB group, 24% of whom died. DAI scores are shown in Figure 2.

Pathologically, the control and DTH₍₋₎ groups had normal histological structures and glands, no ulcer was found except

for occasional slight mucosa congestion (Figure 3A). In DTH₄ (1 g/L DNCB) group, there was slight colic edema, mucosa congestion, infiltration of lymphocytes and a decrease in the number of glands and goblet cells (Figure 3B). In DTH₅ (2 g/L DNCB) group, intestinal adhesion and flatulence were found. A more disturbing array of glands, local erosion, dramatic decrease in goblet cells and diffuse inflammatory cellular infiltration were found (Figure 3C). In DTH₆ (4 g/L DNCB) group, more extensive colic cementation, expansion of the proximal intestinal cavity, some white exudates, mucosa congestion, necrosis and multiple ulcers were found. Under the microscope, mucosa atrophy, decrease of glands and disturbance of tissue structure were observed (Figure 3D), moreover, erosion, hemorrhage, necrosis as well as deeper/extensive ulcers were easily seen (Figure 3E). The pathological score in each group is shown in Figure 4.

The LMIF activities and its relationship with colitis

With the increased DNCB doses in enema, which exacerbated colonic tissue damage, we could see an increase of the LMIF activity (A value decreased). The LMIF activity was significantly increased in the DTH₅ and DTH₆ groups as compared with the control group ($P < 0.01$, student's t -test) (Table 1). There were also significant differences in LMIF activity ($P < 0.01$) among DTH₄, DTH₅ and DTH₆ groups (ANOVA).

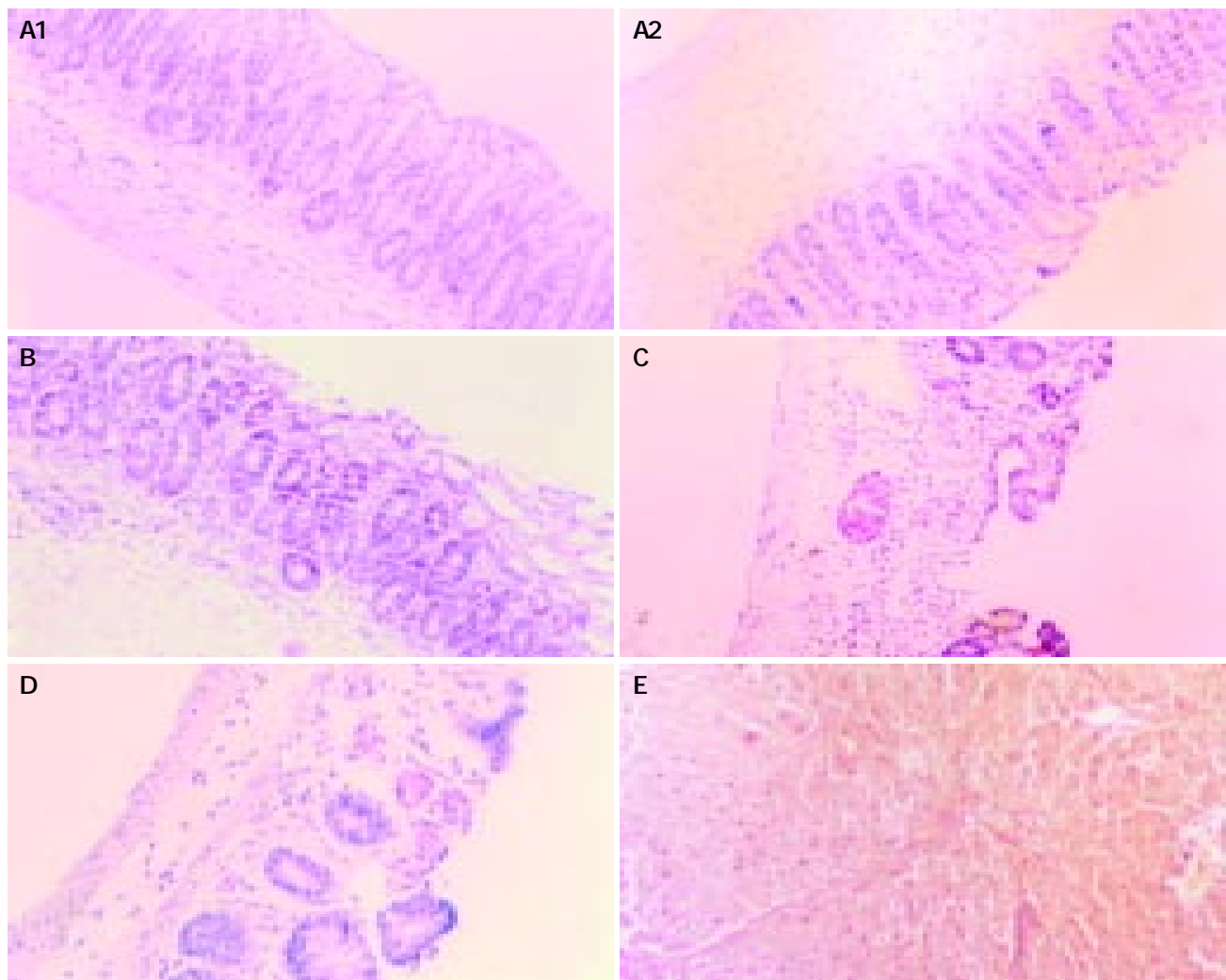


Figure 3 The pathological change of colon by DNCB enema in sensitized mice. A1: control 600 mL/L ethanol, normal histological structures. A2: DTH₍₋₎, only slight mucosa congestion. B: 1 g/L DNCB, hyperemia, infiltration of chronic inflammatory cells, decrease of the number of goblet cell in colon mucosa. C: 2 g/L DNCB, superficial erosion, chronic inflammation of colon mucosa. D: 4 g/L DNCB, atrophic changes of colon mucosa with chronic inflammation. E: 4 g/L DNCB, ulcer and hemorrhage in colon mucosa (HE, $\times 200$).

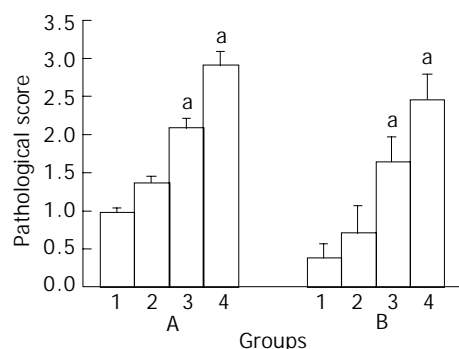


Figure 4 Pathological score in the mice received DNCB enema after sensitization. 4A: macropathology; 4B: microscopically observation. group 1: control (600 mL/L ethanol, $n=16$); group 2: DTH₄ (1 g/L DNCB, $n=17$); group 3: DTH₅ (2 g/L DNCB, $n=17$); and group 4: DTH₆ (4 g/L DNCB, $n=17$)^a $P<0.05$ vs group 4A1 and 4B1, respectively.

Table 1 Effect of DNCB enema on LMIF activity in sensitized mice

Group	Skin smearing (50 μ L/mouse)	Enema (2 μ L/g bm)	A value (mean \pm SE)
Control	Acetone-olive oil	600 mL/L ethanol	0.426 \pm 0.009
DTH _(c)	Acetone-olive oil	2 g/L DNCB	0.401 \pm 0.007
DTH ₄	33 g/L DNCB	1 g/L DNCB	0.383 \pm 0.038
DTH ₅	33 g/L DNCB	2 g/L DNCB	0.220 \pm 0.012 ^b
DTH ₆	33 g/L DNCB	4 g/L DNCB	0.139 \pm 0.019 ^d

^b $P<0.01$ when compared with the control and DTH_(c) (student's t -test). ^d $P<0.01$ between DTH₄, DTH₅ and DTH₆ groups (ANOVA); $n=9$ in each group. A, the absorbance of migration leukocytes. The skin smearing and enema were completed daily for 4 d.

DISCUSSION

For the first time, here, we reported DTH response of mice GI tract by intra-gastrointestinal administration of DNCB. The evidence of gastrointestinal DTH response were as follows: DNCB-sensitized mouse showed increased GI motility, diarrhea, hematochezia and colitis after DNCB challenge; and the activity of LMIF released from sensitized T-lymphocyte was significantly increased after DNCB enema. The mechanism of the DTH phenomenon might be the same as that of the ear skin DTH reaction in our previous study^[6].

What is the pathophysiological significance of GI DTH reaction? Early in the 1960's, Bicks *et al.* found that inflammation and ulcer could be induced by DNCB enema in guinea pigs^[4], which he thought as being a cellular immune induced by DNCB that resulted in a DTH reaction in GI tract. Later, several other researchers explored the relations between DNCB-activated cellular immune and GI disorder, but they either indirectly inferred the possibility of GI being influenced by DTH skin tests^[12] or only focused on the pathological relation of DNCB-colitis with human ulcerative colitis (UC)^[5,7,8]. Comparing with previous DNCB-colitis in rat, guinea pig and rabbit by other researchers, our work here not only successfully created DNCB-colitis model in mouse, but also found a more convenient and more sensitive animal model for DTH study^[13]. In our study, we proved, using the specific DTH index of LMIF^[14,15], that DNCB could induce DTH in mouse GI tract, and this kind of DTH might be the essence of UC.

MIF is one of the cytokines released from sensitized T cell after subjecting the allergen again^[14,15]. According to the target cell, LMIF can be classified as LMIF and MMIF^[16]. There was a dramatic positive correlation between LMIF activity and the

gravity of DTH response^[17]. We found that the ConA-stimulated lymphocytes from mesenteric lymph node of DNCB-treated mouse showed higher LMIF activity than the control, and LMIF activity increased as DNCB concentration increased (Table 1), whereas in DTH_(c) group, neither higher LMIF activity nor colon inflammation/ulcer was found, indicating a possible relations among GI DTH response, LMIF activity and UC. Secondly, we know that the main clinical manifestations of UC are diarrhea and pus hematochezia, which result from an irritated intestinal peristaltic and inflectional ulcer^[18,19]. Our results were in accordance with the clinical manifestations of UC (Figures 1-4), indicating that colitis in mouse caused by DNCB was basically similar to human UC in pathology. Finally, two representatives but separate works by Bartnik *et al.*^[20] and Murakami *et al.*^[21] support the hypothesis that the essence of UC is gastrointestinal DTH response. Bartnik *et al.* reported that patients with severe or moderate ulcerative colitis showed LMIF release, which was significantly greater than that observed in patients with other large bowel diseases^[20]; and Murakami *et al.* reported that the number of MIF expressing cells increased at the colonic mucosa in patients with ulcerative colitis, and MIF induced significant levels of IL-1 and IL-8 in monocytes and dendrite cells in UC patients, indicating a role of MIF in the induction and/or perpetuation of the inflammatory environment in UC^[21]. Comparing with all the other cytokines reported in UC^[22], we think that the distinctive (unique) significance of LMIF in UC and its pivotal role in connecting DTH with UC have been showed by Bartnik and Murakami.

To sum up, we have enough reasons to conclude that the GI DTH in mouse may provide not only experimental models of human UC, but also insight into pathogenic mechanisms of the UC, an inflammatory bowel disease (IBD) of unknown etiology.

REFERENCES

- 1 Takahashi I, Kiyono H. Gut as the largest immunologic tissue. *J Parenter Enteral Nutr* 1999; **23**(5 Suppl): S7-12
- 2 Czerkinsky C, Anjuere F, McGhee JR, George-Chandy A, Holmgren J, Kieny MP, Fujiyoshi K, Mestecky JF, Pierrefite-Carle V, Rask C, Sun JB. Mucosal immunity and tolerance: relevance to vaccine development. *Immunol Rev* 1999; **170**: 197-222
- 3 Galliaerde V, Desvignes C, Peyron E, Kaiserlian D. Oral tolerance to haptens: intestinal epithelial cells from 2,4-dinitrochlorobenzene-fed mice inhibit hapten-specific T cell activation *in vitro*. *Eur J Immunol* 1995; **25**: 1385-1390
- 4 Bicks RO, Rosenberg EW. A chronic delayed hypersensitivity reaction in the guinea pig colon. *Gastroenterology* 1964; **46**: 543-549
- 5 Rabin BS, Rogers SJ. A cell-mediated immune model of inflammatory bowel disease in the rabbit. *Gastroenterology* 1978; **75**: 29-33
- 6 Mei L, Li LQ, Li YF, Deng YL, Sun CW, Ding GF, Fan SG. Conditioned immunosuppressive effect of cyclophosphamide on delayed-type hypersensitivity response and a preliminary analysis of its mechanism. *Neuroimmunomodulation* 2000; **8**: 45-50
- 7 Glick ME, Falchuk ZM. Dinitrochlorobenzene-induced colitis in the guinea-pig: studies of colonic lamina propria lymphocytes. *Gut* 1981; **22**: 120-125
- 8 Zhang YB, Zou YH, Lian ZC, Chen WQ. Experimental model of ulcerative colitis in rat and its abnormality of colonic electricity. *Laboratory Animal Science Administration* 2002; **19**: 5-7
- 9 Qi HB, Luo JY, Liu X. Effect of enterokinetic prucalopride on intestinal motility in fast rats. *World J Gastroenterol* 2003; **9**: 2065-2067
- 10 Murano M, Maemura K, Hirata I, Toshina K, Nishikawa T, Hamamoto N, Sasaki S, Saitoh O, Katsu K. Therapeutic effect of intracolonic administered nuclear factor kappa B (p65) antisense oligonucleotide on mouse dextran sulphate sodium

- (DSS)-induced colitis. *Clin Exp Immunol* 2000; **120**: 51-58
- 11 **Mei L**, Li LQ, Fan SG, Ding GF. An assay of leukocyte migration inhibitory factor (LMIF) and the conditioned suppression effect on LMIF. *Chin J Microbiol Immunol* 1998; **18**: 474-478
- 12 **Shell-Duncan B**, Wood JW. The evaluation of delayed-type hypersensitivity responsiveness and nutritional status as predictors of gastro-intestinal and acute respiratory infection: a prospective field study among traditional nomadic Kenyan children. *J Trop Pediatr* 1997; **43**: 25-32
- 13 **Gold D**. Delayed-type hypersensitivity to *Entamoeba histolytica* in mice and hamsters: a comparison. *Parasitol Res* 1989; **75**: 335-342
- 14 **Bloom BR**, Bennett B. Mechanism of a reaction *in vitro* associated with delayed-type hypersensitivity. *Science* 1966; **153**: 80-82
- 15 **Wolberg WH**, Goelzer ML. *In vitro* assay of cell mediated immunity in human cancer: Definition of leukocyte migration inhibitory factor. *Nature* 1971; **229**: 632-634
- 16 **Matsui Y**, Oshima S. Migration inhibition and stimulation factors produced from peripheral blood lymphocyte cultures of sensitized guinea pigs. *Asian Pac J Allergy Immunol* 1985; **3**: 151-155
- 17 **Malorny U**, Goebeler M, Gutwald J, Roth J, Sorg C. Difference in migration inhibitory factor production by C57Bl/6 and BALB/c mice in allergic and irritant contact dermatitis. *Int Arch Allergy Appl Immunol* 1990; **92**: 356-360
- 18 **Soffer EE**. Diarrhea and malabsorption In: Stoller JK, Ahmad M, Longworth DL, eds. The Cleveland clinic intensive review of internal medicine. *New York Lippincott Williams Wilkins* 2000: 730-732
- 19 **Stenson WF**. Inflammatory bowel disease In: Yamada T, Apers DH, Laine L, Owyang C, Powell DW, eds. Textbook of gastroenterology. *New York Lippincott Williams Wilkins* 1999: 1782-1783
- 20 **Bartnik W**, ReMine SG, Shorter RG. Leukocyte migration inhibitory factor (LMIF) release by human colonic lymphocytes. *Arch Immunol Ther Exp* 1981; **29**: 397-405
- 21 **Murakami H**, Akbar SM, Matsui H, Horiike N, Onji M. Macrophage migration inhibitory factor activates antigen-presenting dendritic cells and induces inflammatory cytokines in ulcerative colitis. *Clin Exp Immunol* 2002; **128**: 504-510
- 22 **Zhou T**, Lin P, Pan H, Mei L. Ulcerative colitis: a review in its pathogenesis and immune mechanisms. *Shijie Huaren Xiaohua Zazhi* 2003; **11**: 1782-1786

Edited by kumar M and Xu FM

Hepatitis B virus X gene induces human telomerase reverse transcriptase mRNA expression in cultured normal human cholangiocytes

Sheng-Quan Zou, Zhen-Liang Qu, Zhan-Fei Li, Xin Wang

Sheng-Quan Zou, Zhan-Fei Li, Xin Wang, Department of Surgery, Tongji Hospital of Tongji Medical College, Huazhong University of Science and Technology, Wuhan 430030, Hubei Province, China
Zhen-Liang Qu, Department of General Surgery, the 254th Military Hospital, Tianjin 300142, China

Supported by the National High Technology Research and Development Program of China, 863 Program, No. 2002AA214061

Correspondence to: Dr. Sheng-Quan Zou, Department of Surgery, Tongji Hospital of Tongji Medical College, Huazhong University of Science and Technology, Wuhan 430030, Hubei Province, China. sqzou@tjh.tjmu.edu.cn

Telephone: +86-27-83662398

Received: 2003-10-20 **Accepted:** 2003-12-29

Abstract

AIM: To study the transcriptional regulation of human telomerase reverse transcriptase (hTERT) mRNA in normal human cholangiocytes (HBECs) after hepatitis B virus X (HBx) gene transfection and to elucidate the possible mechanism of HBV infection underlying cholangiocarcinoma.

METHODS: HBECs were cultured *in vitro* and co-transfected with a eukaryotic expression vector containing the HBx coding region and a cloning vector containing coding sequences of enhanced green fluorescent protein (EGFP) using lipid-mediated gene transfer. The transfection efficiency was determined by the expression of EGFP. The expressions of hTERT mRNA and HBx protein in HBECs were detected by RT-PCR and immunocytochemical stain, respectively.

RESULTS: The transfection efficiencies were about 15% for both HBx gene expression plasmid and empty vector. No hTERT mRNA was expressed in HBECs when transfected with OPTI-MEM medium and empty vector, but a dramatic increase was observed for hTERT mRNA expression in HBECs when transfected with HBx expression vector. HBx protein was only expressed in HBECs when transfected with HBx expression vector.

CONCLUSION: HBx transfection can activate the transcriptional expression of hTERT mRNA. Cis-activation of hTERT mRNA by HBx gene is the primary mechanism underlying the proliferation, differentiation and tumorigenesis of biliary epithelia.

Zou SQ, Qu ZL, Li ZF, Wang X. Hepatitis B virus X gene induces human telomerase reverse transcriptase mRNA expression in cultured normal human cholangiocytes. *World J Gastroenterol* 2004; 10(15): 2259-2262

<http://www.wjgnet.com/1007-9327/10/2259.asp>

INTRODUCTION

Telomeres make up the ends of chromosomes of eukaryote and progressively shorten with each cell cycle. Critically short

telomeres induce cellular senescence and death^[1]. Telomere lengths become stabilized by the activation of telomerase in most tumor cells, highly proliferative cells and human somatic cells. The activation of telomerase is a crucial step in tumorigenesis and cellular senescence^[2]. The most important catalytic protein subunit of telomerase ribonucleoprotein is hTERT whose expression parallels telomerase activity^[3]. It is known that hTERT expression is regulated mainly at the transcriptional level and that the core promoter of hTERT encompasses numerous transcription factor binding sites. All these factors, which regulate hTERT promoter region individually or coordinately, comprise a complex regulation system^[4]. A recent study has shown that HBV DNA integration locates upstream to the hTERT promoter and that HBV enhancer can cis-activate the transcriptional expression of hTERT gene in hepatocarcinoma cell lines^[5]. HBx gene also activates the expression of telomerase^[6]. All these findings provide a new mechanism of HBV in liver carcinogenesis. There is a prominent expression of HBx protein in tissues of both intrahepatic^[7,8] and extrahepatic cholangiocarcinomas^[9]. So far, it is not clear whether HBV infection involves in the tumorigenesis of cholangiocarcinoma and if HBx gene can regulate the expression of telomerase gene. In order to determine the possible correlation of HBV infection and cholangiocarcinogenesis, we transferred HBx gene into human normal cholangiocytes (HBECs) and assayed the expression of hTERT mRNA by RT-PCR.

MATERIALS AND METHODS

Cell and culture

HBECs, isolated from normal human bile ducts^[10], were kindly provided by Dr. Ludwik K. Trejdosiewicz (ICRF Cancer Medical Research Unit, St James's University Hospital, Leeds, UK). HBECs were maintained as adherent monolayers in "HBEC medium" comprising a 1:1 mixture of Ham's F12 and DMEM (Gibco BRL[®]), supplemented with 50 g/L fetal bovine serum (Gibco BRL[®]), 5 ng/mL epidermal growth factor (Intergen Company), 0.4 µg/mL hydrocortisone hemisuccinate, 2 nmol/L triiodothyronine and 5 µg/mL insulin (all from Sigma) and 10 ng/mL human recombinant hepatocyte growth factor (R&D Systems,). Cells were seeded in 25 cm² tissue culture flasks and propagated at 37 °C in a humidified atmosphere of 550 mL/L CO₂ in air and monolayers passaged approximately once a week at or before confluence by incubation in trypsin-versene for approximately 5 min until the cells were shrunken. Trypsin activity was quenched by addition of fresh medium containing FBS and cells were seeded at 1/2 split ratio.

Plasmids and transfection

The plasmids pcDNA3, pCMV-X and pEGFP were the gifts from Professor Xiao-Dong Zhang (Institute for Molecular Biology, Nankai University, China). The empty pcDNA3 vector, a eukaryotic expression vector, was used as negative control. pCMV-X was constructed by inserting the entire HBx

coding region (HBV nucleotides 1 372-1 833 465 bp) into the *EcoRI/EcoRV* sites of the pCDNA3 vector^[11]. Cloning vector pEGFP carried an enhanced green fluorescent protein (EGFP) gene that was cloned between the two MCS of the pPD16.43. EGFP encoded by pEGFP could emit bright green fluorescence in eukaryotic cells. All the plasmids contained ampicillin resistance genes for propagation and selection in *E. coli*.

Transient transfection of plasmids into HBECs was performed using Lipofectamine (Gibco BRL[®]) according to the protocol recommended by the manufacturer. The day before transfection, cells were trypsinized and seeded in 6-well plates. On the day of transfection, cells reached 60% confluence. 2.9 μ g pCDNA3 DNA or pCMV-X DNA and 0.1 μ g pEGFP DNA were diluted with OPTI-MEM medium (Invitrogen) and then mixed with Lipofectamine. A total of 1 mL transfection medium was added to the cells after the cells were washed one time by OPTI-MEM medium. The cells were incubated at 37 $^{\circ}$ C in a humidified atmosphere of 50 mL/LCO₂ in air for 3 h. After 3 h incubation, the transfection medium was replaced with fresh complete medium containing serum and the cells were incubated for another 36 h. Then the cells were harvested and extracted. The expression of transfected gene was examined by immunocytochemistry. The cells transfected with OPTI-MEM medium were used as blank control and transfected with pCDNA3 vector as empty vector control, co-transfected pEGFP as a marker for transfection efficiency^[12].

RT-PCR of hTERT mRNA

Total cellular RNAs were extracted from different groups by TRIzol reagent (Gibco BRL[®]). A 2 μ g of extracted RNA was reverse transcribed into cDNA first-strand with 200 units of Moloney murine leukemia virus reverse transcriptase (Promega) and 1 μ g of oligo (dT)₁₅ primer (Promega) in a final volume of 25 μ L of enzyme buffer for 60 min at 42 $^{\circ}$ C. hTERT cDNA analysis was performed by PCR amplification of a 145 bp fragment using primer pairs 5'-CGGAAGAGTGTCTG GAGCAA-3' (sense) and 5'-GGATGAAGCGGAGTCTGGA-3' (antisense) as described previously^[13]. A 320 bp fragment of GAPDH gene was amplified as an internal control. The primers for GAPDH were 5'GGAAGCTTGTCATCAATGG 3' (sense) and 5'CTGTGGTCATGAGTCCTTC 3' (antisense). PCR was performed with 5 μ L of cDNA first-strand in a 50 μ L reaction mixture containing 2 mmol/L MgCl₂, 1 mmol/L dNTPs, 0.4 μ mol/L of each primer, and 2.5 units of *Taq* DNA polymerase (Promega). The reaction mixture was heated at 94 $^{\circ}$ C for 5 min, then 33 cycles of PCR were performed. Each cycle included denaturation at 94 $^{\circ}$ C for 40 s, annealing at 60 $^{\circ}$ C for 40 s and extension at 72 $^{\circ}$ C for 90 s. A 10 μ L PCR products was assessed by 15 g/L agarose electrophoresis and ethidium bromide staining (0.5 μ g/mL), visualized under ultraviolet light and analyzed by NIH Image software.

Immunocytochemistry

Cells in different groups were cultured on coverslips and fixed with acetone and methanol. Detection of HBx protein expression in the transfected cells was performed by the ultrasensitive immunocytochemistry kit (Maixin Company, Fuzhou, China) according to the manufacturer's instructions. Rabbit anti-human HBx polyclonal antibody (1:800) was provided by Dr. Wen-Liang Wang (The 4th Military Medical University, Xi'an, China).

RESULTS

Transfection efficiency

Under fluorescence microscope, EGFP can only be observed in the HBx gene transfected cell cultures and the cells of empty

vector control (Figure 1). There was no such green fluorescence in the cells of the blank control. Transfection efficiency was estimated by counting the percentage of EGFP-expressing cells in at least 3 fields of vision under fluorescence microscope. For the HBx gene transfected cell cultures and empty vector control, the transfection efficiency was about 15%.

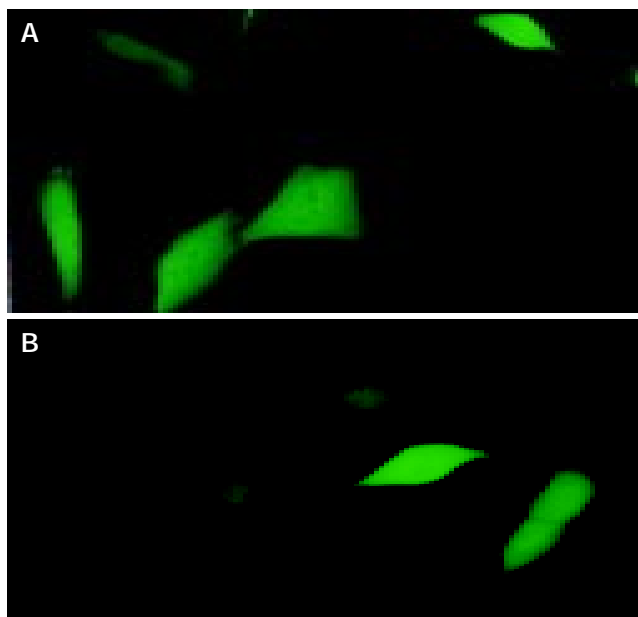


Figure 1 Transfection efficiency evaluated by EGFP-expressing cells in the HBx gene transfected cell cultures and empty vector control. pEGFP 0.1 μ g and pCMV-X (or pCDNA3) 2.9 μ g were co-transfected into HBECs by Lipofectamine. Thirty-eight hours after transfection. EGFP-expressing cells were visible under fluorescence microscope in the HBx gene transfected cell cultures (A) and empty vector control (B), but not in the blank control (Under fluorescence microscope $\times 200$).

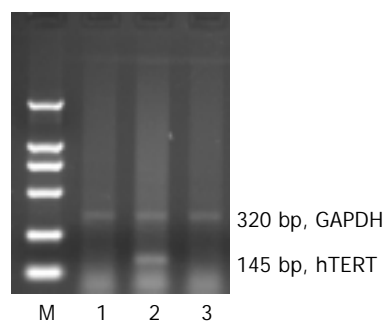


Figure 2 Analysis of hTERT mRNA expression by RT-PCR. RT-PCR was performed on total RNA extracted from HBECs transfected with OPTI-MEN medium (1), pCMV-X (2) and pCDNA3 (3), respectively. M: DL2000 Marker.

hTERT mRNA expression

To examine the effects of HBx gene on hTERT transcription, pCMV-X expression vector was co-transfected with pEGFP into HBECs. The expression of human GAPDH RNA in all of the samples was quantitatively measured and used as an internal control. After RT-PCR analysis, a prominent level of hTERT transcript was detected in the HBx gene transfected cell cultures. In contrast, as shown in Figure 2, hTERT mRNA of HBECs in the blank control and empty vector control were undetectable. The relative expression level of hTERT mRNA was determined by measuring band intensities of both hTERT transcript and GAPDH transcript and calculating the ratio of hTERT to GAPDH. As shown in Figure 3, after transferred with HBx

gene, the HBECs exhibit more distinct hTERT mRNA expression in contrast to those transfected with blank control and empty vector.

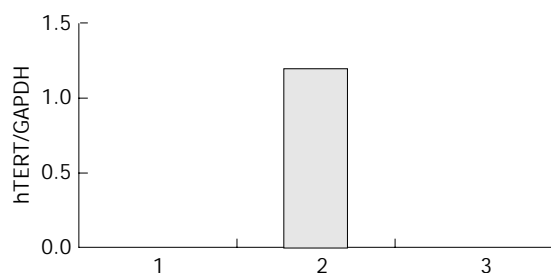


Figure 3 Quantitative and relative changes of hTERT mRNA expression analyzed by NIH Image software. Dramatic expression of hTERT mRNA was observed in HBECs when transferred with pCMV-X vector (lane 2), but there was no hTERT mRNA expression in HBECs when transferred with OPTI-MEM medium (lane 1) and empty vector (lane 3).

HBx protein expression in HBECs

HBx protein expression in transferred HBECs was identified by immunocytochemistry. Positive signals could be observed sporadically in the HBx gene transfected cell cultures (Figure 4B). As for the HBECs in the blank control and empty vector control, there are no such observable positive signals (Figures 4A, C).

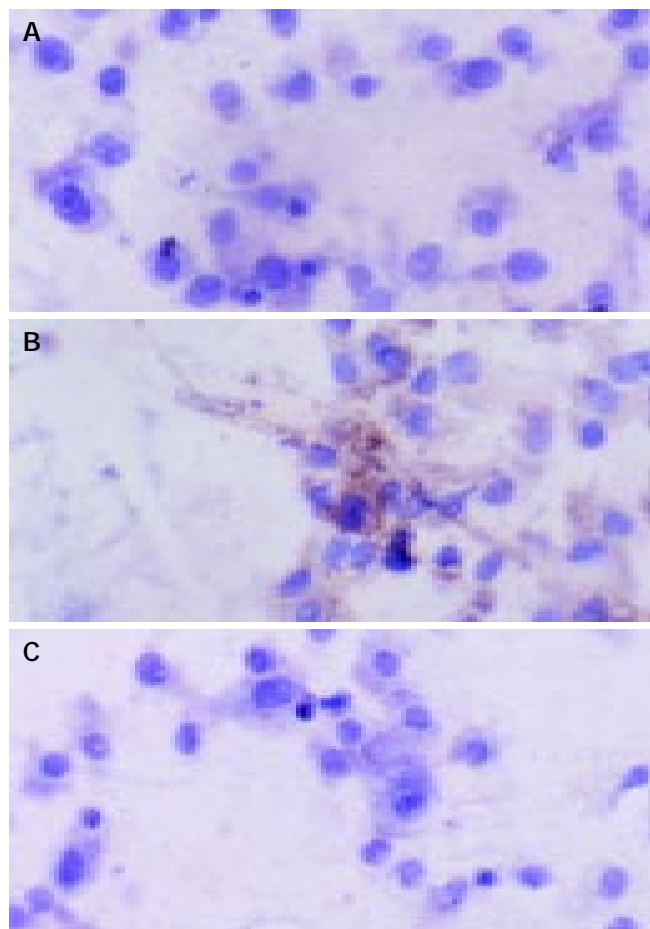


Figure 4 HBx protein expression in transferred HBECs assayed by ultrasensitive immunocytochemistry. The blank vector and OPTI-MEM transfected HBECs showed no expression of HBx protein (A, C), but pale brown positive signals scattered in pCMV-X vector transfected HBECs (B). Immunocytochemistry (S-P methods, $\times 200$).

DISCUSSION

HBECs were isolated from normal human bile duct epithelia and cultured *in vitro*. As no retroviral transduction with SV-40 large T antigen cDNA was performed, the cells were not immortalized. They were really primary culture cells and would only grow for a few passages before becoming senescent, the cells simply stopped dividing and died eventually. Though there was expression of telomerase endogenous genes (such as the telomerase RNA component gene) in this kind of finite cell lines, telomerase was inactivated as the expression of hTERT was repressed. The inhibition of hTERT expression originated from the presence of numerous transcription factors in the core promoter of hTERT. Transcriptional repressors such as p53^[14,15], Mad1^[16,17] and myeloid-specific zinc finger protein 2^[18], could specifically inhibit the transcriptional expression of hTERT mRNA in normal human somatic cells. Our results confirmed this hypothesis. When we transferred the empty vector and OPTI-MEM medium into the HBECs, we could not assay the expression of hTERT mRNA. Dramatic hTERT mRNA expression in HBECs transfected with HBx gene showed that HBx gene could cis-activate transcriptional expression of hTERT gene. An early study also showed that normal human cells could restore the telomerase activity in the presence of other oncogenic viruses^[19]. It has been reported that HBV genome was integrated into the promoter region of hTERT both in HuH-4 human hepatocellular carcinoma-derived cell line^[5] and in liver tumor tissues^[20]. The integration of HBV enhancer upstream of the hTERT promoter cis-activated hTERT gene transcription in HuH-4 cells^[5]. It is known that the up-regulation of telomerase activity could be observed in hepatocellular carcinoma cell line HepG2 after transferred with X gene^[6]. Together with our results, this was a most important demonstration of transcriptional regulation of telomerase gene through HBx gene in carcinogenesis of both human hepatocarcinomas and cholangiocarcinomas. The precise mechanism of such an action is still unknown.

It has been well known that HBx protein encoded by HBx gene, is a potential oncogenic factor and mainly acts as a transcriptional co-activator involving in multiple gene regulation and signaling pathway^[21]. Up-regulation of telomerase gene expression may be another major role of HBx at the stage of carcinogenesis^[22]. Our early study found that higher expression levels of HBx protein and mRNA could be assayed in the tissues of cholangiocarcinomas^[9,23]. Based on our present finding that HBx protein expression could be detected in HBECs transfected with HBx gene, we could suggest that HBV infection and its genome integration might involve in the pathogenesis of cholangiocarcinomas^[24]. HBx protein, which has long been studied as the major causative factor for hepatocarcinogenesis^[25,26], might still play more important role in the carcinogenesis of cholangiocarcinomas than other proteins encoded by other genes of HBV^[27]. As for the mechanism for HBx protein' carcinogenic action, we deduced there should be a binding site for HBx protein in the core promoter region of hTERT gene although this motif has not been identified. Another notion derived from our study is that HBx protein may recruit some cis-action elements (such as c-Myc^[28], AP-2^[29]) or repress other factors (like p53^[30], E2F1^[31]) in mediating the transcriptional regulation of hTERT gene. When exogenous HBx gene was transferred into HBECs, HBx protein translation was achieved in some of HBECs. It is the expression of HBx protein in the transfected cells that be responsible for cis-activation of hTERT mRNA directly or indirectly.

In summary, HBECs do not show the expression of hTERT mRNA and a dramatic high expression of hTERT mRNA can be observed in HBECs transfected with HBx gene. The cis-activation of hTERT gene by HBx is the primary mechanism

underlying proliferation, differentiation and tumorigenesis of biliary epithelia.

ACKNOWLEDGMENTS

We thank Dr. Ludwik K. Trejdosiewicz for kindly providing us HBECs and Professor Xiao-Dong Zhang for providing us three kinds of plasmids.

REFERENCES

- Aragona M**, Maisano R, Panetta S, Giudice A, Morelli M, La Torre I, La Torre F. Telomere length maintenance in aging and carcinogenesis. *Int J Oncol* 2000; **17**: 981-989
- Kim NW**, Piatyszek MA, Prowse KR, Harley CB, West MD, Ho PL, Coviello GM, Wright WE, Weinrich SL, Shay JW. Specific association of human telomerase activity with immortal cells and cancer. *Science* 1994; **266**: 2011-2015
- Dhaene K**, Van Marck E, Parwaresch R. Telomeres, telomerase and cancer: an up-date. *Virchows Arch* 2000; **437**: 1-16
- Poole JC**, Andrews LG, Tollefsbol TO. Activity, function, and gene regulation of the catalytic subunit of telomerase (hTERT). *Gene* 2001; **269**: 1-12
- Horikawa I**, Barrett JC. Cis-Activation of the human telomerase gene (hTERT) by the hepatitis B virus genome. *J Natl Cancer Inst* 2001; **93**: 1171-1173
- Zhou WP**, Shen QH, Gu BY, Ren H, Zhang DH. Effects of hepatitis B virus X gene on apoptosis and the activity of telomerase in HepG2 cells. *Zhonghua Ganzhangbing Zazhi* 2000; **8**: 212-214
- Wang WL**, Gu GY, Hu M. Expression and significance of HBV genes and their antigens in human primary intrahepatic cholangiocarcinoma. *World J Gastroenterol* 1998; **4**: 392-396
- Wang W**, Gu G, Hu M. Expression and significance of hepatitis B virus genes in human primary intrahepatic cholangiocarcinoma and its surrounding tissue. *Zhonghua Zhongliu Zazhi* 1996; **18**: 127-130
- Qu ZL**, Zou SQ, Zhen SL, Wu XZ, Cui NQ. The expression and significance of hepatitis B virus X protein in extrahepatic bile duct carcinomas and the surrounding noncancerous tissues. *Zhonghua Shiyan Waike Zazhi* 2002; **19**: 401-402
- Cruickshank SM**, Southgate J, Selby PJ, Trejdosiewicz LK. Inhibition of T cell activation by normal human biliary epithelial cells. *J Hepatol* 1999; **31**: 1026-1033
- Gottlob K**, Fulco M, Levrero M, Graessmann A. The hepatitis B virus HBx protein inhibits caspase 3 activity. *J Biol Chem* 1998; **273**: 33347-33353
- Jaiswal M**, LaRusso NF, Shapiro RA, Billiar TR, Gores GJ. Nitric oxide-mediated inhibition of DNA repair potentiates oxidative DNA damage in cholangiocytes. *Gastroenterology* 2001; **120**: 190-199
- Nakamura TM**, Morin GB, Chapman KB, Weinrich SL, Andrews WH, Lingner J, Harley CB, Cech TR. Telomerase catalytic subunit homologs from fission yeast and human. *Science* 1997; **277**: 955-959
- Kanaya T**, Kyo S, Hamada K, Takakura M, Kitagawa Y, Harada H, Inoue M. Adenoviral expression of p53 represses telomerase activity through down-regulation of human telomerase reverse transcriptase transcription. *Clin Cancer Res* 2000; **6**: 1239-1247
- Xu D**, Wang Q, Gruber A, Bjorkholm M, Chen Z, Zaid A, Selivanova G, Peterson C, Wiman KG, Pisa P. Downregulation of telomerase reverse transcriptase mRNA expression by wild type p53 in human tumor cells. *Oncogene* 2000; **19**: 5123-5133
- Oh S**, Song YH, Yim J, Kim TK. Identification of Mad as a repressor of the human telomerase (hTERT) gene. *Oncogene* 2000; **19**: 1485-1490
- Gunes C**, Lichtsteiner S, Vasserot AP, Englert C. Expression of the hTERT gene is regulated at the level of transcriptional initiation and repressed by Mad1. *Cancer Res* 2000; **60**: 2116-2121
- Fujimoto K**, Kyo S, Takakura M, Kanaya T, Kitagawa Y, Itoh H, Takahashi M, Inoue M. Identification and characterization of negative regulatory elements of the human telomerase catalytic subunit (hTERT) gene promoter: possible role of MZF-2 in transcriptional repression of hTERT. *Nucleic Acids Res* 2000; **28**: 2557-2562
- Baega AC**, Berger A, Schlegel R, Veldman T, Schlegel R. Cervical epithelial cells transduced with the papillomavirus E6/E7 oncogenes maintain stable levels of oncoprotein expression but exhibit progressive, major increases in hTERT gene expression and telomerase activity. *Am J Pathol* 2002; **160**: 1251-1257
- Gozuacik D**, Murakami Y, Saigo K, Chami M, Mugnier C, Lagorce D, Okanoue T, Urashima T, Brechot C, Paterlini-Brechot P. Identification of human cancer-related genes by naturally occurring hepatitis B virus DNA tagging. *Oncogene* 2001; **20**: 6233-6240
- Murakami S**. Hepatitis B virus X protein: a multifunctional viral regulator. *J Gastroenterol* 2001; **36**: 651-660
- Horikawa I**, Barrett JC. Transcriptional regulation of the telomerase hTERT gene as a target for cellular and viral oncogenic mechanisms. *Carcinogenesis* 2003; **24**: 1167-1176
- Qu ZL**, Zou SQ, Wei GH, Sun ZC, Wu XZ. *In situ* nucleic acid detection of HBV X gene in extrahepatic biliary tract carcinomas and its clinicopathological significance. *Zhonghua Waike Zazhi* 2004; **42**: 88-91
- Liu X**, Zou S, Qiu F. Pathogenesis of hilar cholangiocarcinoma and infection of hepatitis virus. *Zhonghua Waike Zazhi* 2002; **40**: 420-422
- Diao J**, Garces R, Richardson CD. X protein of hepatitis B virus modulates cytokine and growth factor related signal transduction pathways during the course of viral infections and hepatocarcinogenesis. *Cytokine Growth Factor Rev* 2001; **12**: 189-205
- Guo SP**, Wang WL, Zhai YQ, Zhao YL. Expression of nuclear factor-kappa B in hepatocellular carcinoma and its relation with the X protein of hepatitis B virus. *World J Gastroenterol* 2001; **7**: 340-344
- Wang WL**. Expression of five different antigens of HBV in human intrahepatic cholangiocarcinoma and cholangiohepatocarcinoma. *Zhonghua Zhongliu Zazhi* 1993; **15**: 252-255
- Su F**, Theodosis CN, Schneider RJ. Role of NF-kappaB and myc proteins in apoptosis induced by hepatitis B virus HBx protein. *J Virol* 2001; **75**: 215-225
- Kekule AS**, Lauer U, Weiss L, Lubber B, Hofschneider PH. Hepatitis B virus transactivator HBx uses a tumour promoter signalling pathway. *Nature* 1993; **361**: 742-745
- Kwon JA**, Rho HM. Transcriptional repression of the human p53 gene by hepatitis B viral core protein (HBc) in human liver cells. *Biol Chem* 2003; **384**: 203-212
- Choi M**, Lee H, Rho HM. E2F1 activates the human p53 promoter and overcomes the repressive effect of hepatitis B viral X protein (Hbx) on the p53 promoter. *IUBMB Life* 2002; **53**: 309-317

Edited by Chen WW and Wang XL Proofread by Xu FM

In vitro anti-coxsackievirus B₃ effect of ethyl acetate extract of Tian-hua-fen

Zhen-Hong Li, Bao-Ming Nie, Hong Chen, Shu-Yun Chen, Ping He, Yang Lu, Xiao-Kui Guo, Jing-Xing Liu

Zhen-Hong Li, Bao-Ming Nie, Hong Chen, Shu-Yun Chen, Ping He, Yang Lu, Xiao-Kui Guo, Jing-Xing Liu, Department of Microbiology and Parasitology, Shanghai Second Medical University, Shanghai 200025, China

Supported by Project of National Nature Science Foundation of China, No. 39970691 and Project from Education Commission of Shanghai, China, No. 2000B04

Correspondence to: Jing-Xing Liu, Department of Microbiology and Parasitology, Shanghai Second Medical University, Shanghai 200025, China. lee1217@citiz.net

Telephone: +86-21-64453285 **Fax:** +86-21-64453285

Received: 2003-11-12 **Accepted:** 2004-02-01

Abstract

AIM: To investigate the anti-coxsackievirus B₃ (CVB_{3m}) effect of the ethyl acetate extract of Tian-hua-fen on HeLa cells infected with CVB_{3m}.

METHODS: HeLa cells were infected with CVB_{3m} and the cytopathic effects (CPE) were observed through light microscope and crystal violet staining on 96-well plate and A₆₀₀ was detected using spectrophotometer. The protective effect of the extract to HeLa cells and the mechanism of the effect were also evaluated through the change of CPE and value of A₆₀₀.

RESULTS: The extract had some toxicity to HeLa cells at a higher concentration while had a marked inhibitory effect on cell pathological changes at a lower concentration. Consistent results were got through these two methods. We also investigated the mechanism of its anti-CVB_{3m} effect and the results indicated that the extract represented an inhibitory effect through all the processes of CVB_{3m} attachment, entry, biosynthesis and assemble in cells.

CONCLUSION: The results demonstrate that the ethyl acetate extract of Tian-hua-fen has a significant protective effect on HeLa cells infected with CVB_{3m} in a dose-dependent manner and this effect exists through the process of CVB_{3m} attachment, entry, biosynthesis and assemble in cells, suggesting that the ethyl acetate extract of Tian-hua-fen can be developed as an anti-virus agent.

Li ZH, Nie BM, Chen H, Chen SY, He P, Lu Y, Guo XK, Liu JX. *In vitro* anti-coxsackievirus B₃ effect of ethyl acetate extract of Tian-hua-fen. *World J Gastroenterol* 2004; 10(15): 2263-2266 <http://www.wjgnet.com/1007-9327/10/2263.asp>

INTRODUCTION

Tian-hua-fen is the dried root of *Trichosanthes kirilowii Maxim* or *Trichosanthes japonica Regel*. The major component of it is mass starch, various amino acids, phytohemagglutinin, saccharide, saponin and some other things^[1]. Tian-hua-fen was mentioned in Compendium of Materia Medica written by Li Shizhen in the late 14th Century as a drug to reset menstruation

and facilitating the expulsion of retained placenta. For a long time, Tian-hua-fen had been used in the powdered form in conjunction with other Chinese herbal medicines to induce abortion^[2]. Clinical applications over the years proved that Tian-hua-fen had multiple pharmacological effects, such as termination of pregnancy, anti-tumor, anti-inflammation, anti-virus and immunoregulation and so on^[3-5]. The anti-virus, especially anti-HIV-1, effect of trichosanthin (TCS) has been known to us. But to the author's knowledge research about the non-protein parts of Tian-hua-fen is rare. Coxsackievirus B is the major pathogen of viral myocarditis and now there is no effective therapeutic drug. In the process of screening anti-virus agents from Chinese medicinal herb we found that the nonprotein parts of Tian-hua-fen had a notable anti-virus effect *in vitro* and *in vivo*.

MATERIALS AND METHODS

Preparation of the ethyl acetate extract of Tian-hua-fen

A total amount of 200 g Tian-hua-fen powder (Shanghai drug store) was macerated with 2 L 750 mL/L ethanol overnight, then was boiled in water under reflux for 3 h and the boiled fluid was filtered. The filtrate was evaporated under reduced pressure to gain a residue. The residue was suspended in water and partitioned with petroleum ether, ethyl acetate and n-BuOH (Analytical pure, Shanghai chemical company Ltd) successively. The four fractions were evaporated under reduced pressure to give petroleum ether fraction (0.56 g), ethyl acetate fraction (0.82 g), n-BuOH fraction (0.85 g) and aqueous fraction (12.7 g), respectively.

Preparation of HeLa cells and titration of virus titer

HeLa cells were stored in liquid nitrogen with 100 g/L dimethyl sulphoxide (DMSO) and 900 mL/L fetal calf serum (FCS) and maintained in culture flasks in complete RPMI 1640 medium (Gibcol, BRL America). Subculture was carried out every 2-3 d after it had formed a confluent monolayer. CVB_{3m} (Stored by our laboratory) was serially diluted to 10⁻¹⁰ with non-FCS RPMI1640 culture medium. On 40-well plate, 0.025 mL CVB_{3m} with variable dilution and 0.025 mL non-FCS RPMI1640 culture medium were added to each well. Finally, 0.05 mL viable HeLa cells (3×10⁵/mL) were added. Each dilution was quadrupled and normal HeLa cells co-cultured only with RPMI1640 containing 10 mL/L FCS were prepared as negative control at the same time. Then the cells were incubated at 37 °C with 50 mL/L CO₂ for 72 h. The cytopathic effects (CPE) were observed under light microscope. The titer at which cells appeared 50% CPE was designated 1 TCID₅₀ (50% tissue culture infectious doses). A 100 TCID₅₀ was used as the infectious titer in the following experiment.

Assay of the toxicity of the extract to HeLa cells

A total of 5 mg extract was dissolved in 5 μL DMSO, then 2.5 mL deionized water was added and the liquid was sterilized at 115 °C for 20 min. After cooling to 55 °C, 2.5 mL 2×RPMI 1640 culture medium (without FCS) was added to make the end concentration of the extract (1 mg/mL). The original liquid

was diluted with non-FCS RPMI 1640 culture medium serially from 1:2 to 1:1 024. A total of the 0.025 mL sample with various concentration and 0.025 mL of the same culture medium were added to each well on 96-well plate. Finally 0.05 mL viable HeLa cells (3×10^5 /mL) were added. Each concentration of the sample was quadrupled. Two controls, HeLa cells co-cultured only with RPMI1640 (containing 100 mL/L FCS) and 1 g/L DMSO respectively were prepared synchronously. Cells were incubated at 37 °C with 50 mL/L CO₂ for 72 h. CPE was observed under light microscope and the concentration at which cells appeared <50% CPE (compared with that of extract-free cultures) was regarded as the lowest toxic concentration. In addition, cells were stained with 5 g/L crystal violet (Ameresco) and A₆₀₀ was detected using spectrophotometer.

Assay of the anti-CVB_{3m} effect of the extract

The extract was diluted serially from 1:256 at which it had no toxicity to HeLa cells to 1:8 192 with non-FCS RPMI 1640 culture medium. Then 0.025 mL extract with variable concentration was added to each well of 96-well plate. Then 0.025 mL 100 TCID₅₀CVB_{3m} was overlaid. After incubation at 37 °C with 50 mL/L CO₂ for 1 h, 0.05 mL viable HeLa cells (3×10^5 /mL) were added. Each concentration was quadrupled and three controls, normal HeLa cells co-cultured only with RPMI1640 (containing 100 mL/L FCS), 100 TCID₅₀CVB_{3m} and the extract (1:256 mg/mL), respectively were prepared synchronously. Cells were grown for 3 days and then CPE was observed under light microscope. Later, the cells were stained with 5 g/L crystal violet and A₆₀₀ was measured using spectrophotometer.

Primary study on the mechanism of anti-CVB_{3m} effect of the extract^[6]

The extract was diluted with non-FCS RPMI1640 culture medium from 1:256 to 1:8 192. HeLa cells (1.5×10^4 /well) were seeded onto three 96-well plates and allowed to attach to the well bottom. When the cells were confluent the culture medium was discarded and the cells were rinsed twice with the same culture medium. The cells on three plates were treated respectively as follows: The first plate: 0.025 mL 100TCID₅₀CVB_{3m} and 0.025 mL extract of variable concentration were added to each well. After incubation at 37 °C with 50 mL/L CO₂ for 1 h, the mixture was substituted with 0.1 mL non-FCS RPMI1640 culture medium; the second plate: 0.025 mL 100TCID₅₀CVB_{3m} and 0.025 mL extract of variable concentration were added. The plate was incubated at 37 °C with 50 mL/L CO₂ for 1 h. Then the mixture was substituted with 0.025 mL extract of

variable concentration and 0.075 mL non-FCS RPMI1640 culture medium; the third plate: 0.025 mL 100TCID₅₀CVB_{3m} and 0.025 mL non-FCS RPMI1640 culture medium were added first. After incubation at 37 °C with 50 mL/L CO₂ for 1 h the mixture was discarded and 0.025 mL extract of variable concentration and 0.075 mL non-FCS RPMI1640 culture medium were overlaid. Three controls, HeLa cells co-cultured only with RPMI1640 containing 100 mL/L FCS, 100TCID₅₀CVB_{3m} and extract (1:256 mg/mL) respectively were prepared synchronously and each extract concentration was quadrupled. At last all plates were incubated at 37 °C with 50 mL/L CO₂. When the cells treated with CVB_{3m} appeared 100% CPE, the cells were stained with 5 g/L crystal violet and A₆₀₀ was detected using spectrophotometer.

RESULTS

Titration of CVB_{3m} titers

The incubation was terminated after 72 h and CPE was observed under light microscope. The results showed the cells in all quadrupled wells treated with CVB_{3m} at titer of 10⁻¹-10⁻⁶ appeared 100% CPE. About the cells treated with CVB_{3m} at titer of 10⁻⁷, the cells in two wells appeared 100% CPE while the others appeared 50% CPE. In regards to the cells co-cultured with CVB_{3m} at titer of 10⁻⁸-10⁻¹⁰, the cells in four wells appeared no CPE completely. Then TCID₅₀ was calculated as 10⁻⁷ according to Reed-Muench method^[7].

Assay of toxicity of ethyl acetate extract to HeLa cells

After incubation for 72 h, CPE induced by the extract was observed under light microscope. The results showed the cells co-cultured with extract at concentration from 1:2-1:128 mg/mL appeared CPE of different degrees, while the cells co-cultured with extract at concentration from 1:256 to 1:8 192 mg/mL appeared no CPE. The 50% toxic concentration was 1:128 mg/mL according to Reed-Muench method. The value of A₆₀₀ also indicated that the extract had no toxicity to HeLa cells from 1:256 mg/mL. The cells co-cultured with 1 g/L DMSO appeared no CPE, which showed that DMSO at this concentration had no toxicity to HeLa cells (Table 1).

Assay of the anti-CVB_{3m} effect of the extract

From 1:256 to 1:8 192 mg/mL the extract showed various protective effects to HeLa cells and the effect was decreased with the increased dilution. The protective effect was best at concentration from 1:256 to 1:1 024 mg/mL. The minimal effective inhibitory concentration (EIC) was 1:8 192. The value

Table 1 Cytotoxicity of ethyl acetate extract to HeLa cells shown in the value of A₆₀₀

Dilution	1:2	1:4	1:8	1:16	1:32	1:64	1:128	1:256	1:512	1:1 024
Value of A ₆₀₀	0.20±0.029	0.22±0.030	0.32±0.022	0.29±0.069	0.38±0.043	0.59±0.035	0.69±0.075	1.30±0.069	1.23±0.061	1.29±0.056

The A₆₀₀ value of the cells co-cultured with the extract at concentration from 1:2 to 1:128 mg/mL was lower than that of normal HeLa cells (1.32±0.034), which showed that the extract had some toxicity to HeLa cells at these concentrations. From 1:256 mg/mL the A₆₀₀ value became close to that of normal HeLa cells, which indicated that from 1:256 mg/mL the extract had no toxicity to HeLa cells again.

Table 2 Protective effect of ethyl acetate extract on HeLa cells shown in the value of A₆₀₀

Dilution	1:256	1:512	1:1 024	1:2 048	1:4 096	1:8 192
Value of A ₆₀₀	1.09±0.017	1.02±0.122	0.89±0.060	0.91±0.039	0.83±0.048	0.77±0.028

The A₆₀₀ value of the cells co-cultured only with RPMI1640 was 1.32±0.02; the A₆₀₀ value of the cells co-cultured only with 10⁻⁵ CVB_{3m} was 0.22±0.026; and the A₆₀₀ value of the cells co-cultured only with extract at concentration of 1:256 mg/mL was 1.21±0.042. As shown in the table the value of A₆₀₀ of the cells treated with extract is higher than that of the cells infected with CVB_{3m} while not treated with the extract (^bP<0.01), indicating the protective effect of the extract on HeLa cells from CVB_{3m} infection.

Table 3 Protective effect of ethyl acetate extract on HeLa cells shown in percentage (A_{600} value of cells protected with the extract/ A_{600} value of normal HeLa cells)

Dilution	1:256	1:512	1:1 024	1:2 048	1:4 096	1:8 192	10 ⁻⁵ CVB _{3m}
The ratio of A_{600}	88.56±0.032	79.46±0.008	73.07±0.057	65.57±0.023	61.83±0.038	56.1±0.015	16.7±0.027

The percentage of vital cells protected with the extract accounted for compared with normal HeLa cells decreased with the increased extract dilution, and it was preferable from concentration 1:256 mg/mL to 1:1 024 mg/mL. ^b $P < 0.01$ vs group of 10⁻⁵ CVB_{3m}.

Table 4 The value of A_{600} obtained from various infective phase

Dilution/ A_{600}	1:256	1:512	1:1 024	1:2 048	1:4 096	1:8 192
First group	0.45±0.041	0.56±0.011	0.63±0.036	0.65±0.043	0.37±0.076	0.38±0.029
Second group	0.72±0.022	0.96±0.013	0.69±0.009	65.00±0.025	0.78±0.056	0.73±0.054
Third group	0.53±0.030	0.48±0.036	0.40±0.049	0.39±0.066	0.39±0.077	0.32±0.015

The A_{600} value of the cells co-cultured only with RPMI1640, cells co-cultured only with 10⁻⁵ CVB_{3m} and cells co-cultured only with extract (1:256 mg/mL) was 1.29±0.011, 0.24±0.023 and 1.20±0.029, respectively. The value of A_{600} of the cells treated with extract of variable concentration at different time of CVB_{3m} infection was higher than that of the cells infected with CVB_{3m} and not treated with the extract, which indicated the protective effect of the extract existed through all the processes of CVB_{3m} attachment, entry, biosynthesis and assemble in cells.

of A_{600} obtained using crystal violet staining showed that starting from 1:256 mg/mL, the value of A_{600} decreased with the increased dilution. There was a negative correlation between them ($r=0.8525$, $P < 0.01$, Tables 2-3, Figure 1).

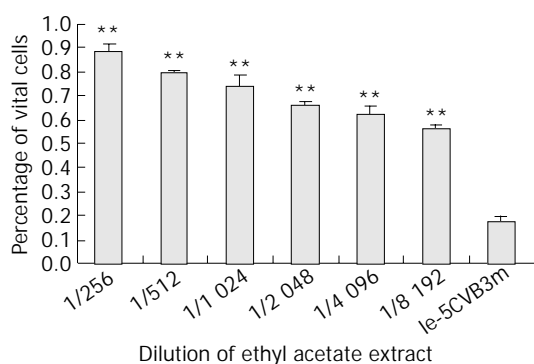


Figure 1 The protective effect of the extract on HeLa cells expressed in column figure. The value of A_{600} obtained using crystal violet staining decreased with the increased dilution of the extract. From 1:256 to 1:8 192 mg/mL the extract showed various protective effects on HeLa cells and the effect was decreased with the increased dilution of the extract. The protective effect was best at concentration of 1:256 to 1:1 024 mg/mL.

Primary study on the mechanism of anti-CVB_{3m} effect of the extract *in vitro*

In the first group, the extract was added in the process of virus adsorption. In second group, the extract was added in the process of virus adsorption and also after adsorption while in the third one, the extract was added after virus adsorption. The value of A_{600} of the three groups were obtained. Among all three groups, A_{600} obtained from the cells treated with extract from 1:256 to 1:8 192 mg/mL was higher than that treated with 100TCID₅₀ CVB_{3m}, and that of the second group was the highest. This suggested the extract exerted anti-CVB_{3m} effect through all the processes of the virus infection (Table 4).

DISCUSSION

Proliferation of virus primarily depends on the biosynthesis system of host cells because virus deficit the enzymes needed for their proliferation. Virus proliferation was similar to nucleotide replication of host cells and there is also great similarity between its products such as nucleotide and proteins

and that of host cells. So the demand for killing virus while not infecting the normal physiological function of host cells brings us great difficulty to design and synthesize effective anti-virus drug. The development of anti-virus drugs is very slow compared with that of anti-bacteria drugs in the last one hundred years since the discovery of virus. Though it is an important way to synthesize anti-virus drugs using chemical methods, it is very slow and time-consuming. In recent years, many countries are paying more and more attention to look for anti-virus agents from Chinese medicinal herbs. Tian-hua-fen is a traditional Chinese medicinal herb. It has been used in Chinese for centuries to induce mid-term abortion. And there were many records about its biological efficacy. In the 70 s, the active ingredient of Tian-hua-fen, TCS, a protein from the root tuber of the Chinese medicinal herb *Trichosanthes kirilowii Maxim* was found and purified. It is a monomeric protein with a pI (isoelectric point) of 9.4 and an apparent molecular weight of 24 kDa. There are no cysteine residues in the molecule^[8]. TCS is a member of type 1 ribosome-inactivating protein (RIP) family^[7-9]. RIP is a group of cytotoxic proteins acting on eukaryotic ribosomes. They can inactivate 60S ribosomal subunits by only hydrolyzing a single phosphodiester bond between the guanosine residue at position 4 325(G4 325) and the adenosine residue at position 4 326(A4 326) in 28S rRNA. TCS can inactivate eukaryotic ribosomes through its N-glycosidase activity by hydrolyzing the N-C glycosidic bond of adenylic acid at 4 324 site in 28S rRNA of rat liver^[10]. Thus cell protein synthesis was inhibited. Clinical application over the years showed TCS had multiple pharmacological effects. The research about TCS was once popular since McGrath *et al.*^[11,12] reported it could inhibit HIV-1 for the first time. But the sever side effect prevented its more extensive clinical application^[13]. There are some other components such as polysaccharide, phytohemagglutinin, sterol and palmitic acid and so on in Tian-hua-fen besides TCS^[14]. Polysaccharide in Tian-hua-fen had marked immunoregulation effect^[1]. The galactose-binding lectin from Tian-hua-fen stimulated the incorporation of D-[3-3H]glucose into lipids in isolated rat epididymal adipocytes^[15]. In the process of screening anti-virus agents, we found the ethyl acetate extract of Tian-hua-fen had obvious preventive effect on HeLa cells from CVB_{3m} infection. This showed the potential anti-virus effect of the ethyl acetate extract of Tian-hua-fen. In this study, Tian-hua-fen was treated with chemical reagents and then was extracted with organic reagents. Finally, four kinds of extract were obtained. The anti-CVB_{3m} effect of the four fractions was tested and the results showed

ethyl acetate fraction had the best preventive effect on HeLa cells from CVB_{3m} infection. The preventive effect decreased as the extract dilution increased. There was an obvious correlation between them. The ethyl acetate fraction was further chromatographed on silica gel column and their anti-virus effect was also tested. The results suggested that toxicity of the further extract to HeLa cells was decreased compared with the former one and there also existed a negative correlation between the preventive effect and the dilution.

Many methods have been developed for determining the antiviral activities of compounds in cell culture. For viruses that cause discernable cytopathic effects (CPE) microscopically in cells, visual scoring of CPE inhibition is performed most frequently because it is rapid, and allows a number of compounds to be evaluated using 96-well microplates^[16]. Since solely relying on visual scoring was inaccurate for assessing the cytotoxicities, the use of a dye or stain is very important. The results indicated that methods using bisbenzimidazole, crystal violet, fluorescein diacetate, MTT, neutral red, or rhodamine 6G were similar to visual scoring for determining anti-influenza virus activity in cell culture. Rapid staining (15 min) methods could be done with crystal violet and rhodamine 6G, and rhodamine 6G gave a high background in microwells containing only water (no cells or virus) which had to be subtracted^[17], whereas other methods for determining antiviral activity of test substances may be much more tedious, requiring more microplates, compound, and/or time than the above methods. These include the plaque reduction assay^[18], virus yield reduction assay^[19], determining drug effect by counting the number of infected cells stained by fluorescent antibody^[20] and [³H]TdR incorporation^[21]. For this reason, we preferred crystal violet staining in our study in order to quantitatively screen anti-virus agents.

We also did some primary study on the anti-CVB_{3m} mechanism of the extract. The extract was added before virus adsorption, during adsorption and after adsorption and then the cells were stained with crystal violet and A₆₀₀ was measured. The value of A₆₀₀ of the three groups was higher than that of the cells infected with virus. This indicated the three kinds of treatment had preventive effect on HeLa cells from CVB_{3m} infection at different levels and suggested that the extract could act through virus adsorption, penetration and synthesis in cells.

Our results showed that the ethyl acetate extract of Tian-hua-fen had marked anti-CVB_{3m} effect *in vitro*. Some questions still remained to be answered. Which component play key role in the process of anti-virus? Which has the better anti-virus effect between the crude extract and the further extract? What is the anti-virus mechanism of it? To answer these questions needs more and further research. Anyway it is sure that the ethyl acetate extract of Tian-hua-fen has marked anti-virus effect. The answers to the above questions will help to wide the range of virus that Tian-hua-fen resists and also help to make Tian-hua-fen a clinical-used drug.

REFERENCES

- 1 Wang Y. Trichosanthin. Second Edition, Beijing. *China Science Press* 2000; **18**: 81
- 2 Shaw PC, Chan WL, Yeung HW, Ng TB. Minireview: trichosanthin-a protein with multiple pharmacological properties. *Life Sci* 1994; **55**: 253-262
- 3 Wu L, LaRosa G, Kassam N, Gordon CJ, Heath H, Ruffing N, Chen H, Humblias J, Samson M, Parmentier M, Moore JP, Mackay CR. Interaction of chemokine receptor CCR5 with its ligands: multiple domains for HIV-1 gp120 binding and a single domain for chemokine binding. *J Exp Med* 1997; **186**: 1373-1381
- 4 Zheng YT, Chan WL, Chan P, Huang H, Tam SC. Enhancement of the anti-herpetic effect of trichosanthin by acyclovir and interferon. *FEBS Lett* 2001; **496**: 139-142
- 5 Fan ZS, Ma BL. IL-10 and trichosanthin inhibited surface molecule expression of antigen processing cells and T-cell proliferation. *Zhongguo Yaoli Xuebao* 1999; **20**: 353-357
- 6 Carlucci MJ, Sclaro LA, Errea MI, Matulewicz MC, Damonte EB. Antiviral activity of natural sulphated galactans on herpes virus multiplication in cell culture. *Planta Med* 1997; **63**: 429-432
- 7 Krah DL. Receptors for binding measles virus on host cells and erythrocytes. *Biologicals* 1991; **19**: 223-227
- 8 Maraganore JM, Joseph M, Bailey MC. Purification and characterization of trichosanthin. Homology to the ricin A chain and implications as to mechanism of abortifacient activity. *J Biol Chem* 1987; **262**: 11628-11633
- 9 Barbieri L, Battelli MG, Stirpe F. Ribosome-inactivating proteins from plants. *Biochim Biophys Acta* 1993; **1154**: 237-282
- 10 Zhang C, Gong Y, Ma H, An C, Chen D, Chen ZL. Reactive oxygen species involved in trichosanthin-induced apoptosis of human choriocarcinoma cells. *Biochem J* 2001; **355**(Pt 3): 653-661
- 11 McGrath MS, Hwang KM, Caldwell SE, Gaston I, Luk KC, Wu P, Ng VL, Crowe S, Daniels J, Marsh J. GLQ223: an inhibitor of human immunodeficiency virus replication in acutely and chronically infected cells of lymphocyte and mononuclear phagocyte lineage. *Proc Natl Acad Sci U S A* 1989; **86**: 2844-2848
- 12 McGrath MS, Santulli S, Gaston I. Effects of GLQ223 on HIV replication in human monocyte/macrophages chronically infected *in vitro* with HIV. *AIDS Res Hum Retroviruses* 1990; **6**: 1039-1043
- 13 Byers VS, Levin AS, Malvino A, Waites L, Robins RA, Baldwin RW. A phase II study of effect of addition of trichosanthin to zidovudine in patients with HIV disease and failing antiretroviral agents. *AIDS Res Hum Retroviruses* 1994; **10**: 413-420
- 14 Wu AM, Wu JH, Tsai MS, Herp A. Carbohydrate specificity of an agglutinin isolated from the root of *Trichosanthes kirilowii*. *Life Sci* 2000; **66**: 2571-2581
- 15 Ng TB, Wong CM, Li WW, Yeung HW. Effect of *Trichosanthes kirilowii* lectin on lipolysis and lipogenesis in isolated rat and hamster adipocytes. *Ethnopharmacol* 1985; **14**: 93-98
- 16 Sidwell RW, Huffman JH. Use of disposable micro tissue culture plates for antiviral and interferon induction studies. *Appl Microbiol* 1971; **22**: 797-801
- 17 Smee DF, Morrison AC, Barnard DL, Sidwell RW. Comparison of colorimetric, fluorometric, and visual methods for determining anti-influenza (H1N1 and H3N2) virus activities and toxicities of compounds. *J Virol Methods* 2002; **106**: 71-79
- 18 Desideri N, Conti C, Mastromarino P, Mastropaolo F. Synthesis and anti-rhinovirus activity of 2-styrylchromones. *Antivir Chem Chemother* 2000; **11**: 373-381
- 19 Semple SJ, Pyke SM, Reynolds GD, Flower RL. *In vitro* antiviral activity of the anthraquinone chrysophanic acid against poliovirus. *Antiviral Res* 2001; **49**: 169-178
- 20 Smee DF, Sidwell RW, Barnett BB, Spendlove RS. Bioassay system for determining ribavirin levels in human serum and urine. *Chemotherapy* 1981; **27**: 1-11
- 21 Baba M, Pauwels R, Balzarini J, Arnout J, Desmyter J, De Clercq E. Mechanism of inhibitory effect of dextran sulfate and heparin on replication of human immunodeficiency virus *in vitro*. *Proc Nat Acad Sci U S A* 1998; **85**: 6132-6136

FR167653 attenuates murine immunological liver injury

Hong-Wei Yao, Jun Li, Ji-Qiang Chen

Hong-Wei Yao, Ji-Qiang Chen, Zhejiang Respiratory Drugs Research Laboratory of State Food and Drug Administration of China, School of Medicine, Zhejiang University, Hangzhou 310031, Zhejiang Province, China

Jun Li, Institute of Clinical Pharmacology, Anhui Medical University, Hefei 230032, Anhui Province, China

Correspondence to: Dr. Hong-Wei Yao, Zhejiang Respiratory Drugs Research Laboratory of State Food and Drug Administration of China, School of Medicine, Zhejiang University, Hangzhou 310031, Zhejiang Province, China. yhgwei@hotmail.com

Telephone: +86-571-87217150

Received: 2003-12-19 **Accepted:** 2004-01-13

Abstract

AIM: To study the effect of FR167653 on immunological liver injury (ILI) in mice.

METHODS: ILI was established by tail vein injection of 2.5 mg *Bacillus Calmette-Guerin* (BCG), and 10 d later with 10 mg lipopolysaccharide (LPS) in 0.2 mL saline (BCG plus LPS). Alanine aminotransferase (ALT), aspartate aminotransferase (AST) in sera and malondialdehyde (MDA), glutathione peroxidase (GSHpx) contents in liver homogenates were assayed by spectrophotometry. The levels of tumor necrosis factor- α (TNF- α) and nitric oxide (NO) levels in sera were determined using ELISA. Interleukin-1 (IL-1) produced by peritoneal macrophages was determined by the method of ^3H -infiltrated cell proliferation. The nuclear factor-kappa B (NF- κB) p65 in liver tissue was analyzed with reverse transcription polymerase chain reaction (RT-PCR). Liver samples collected were stained with hematoxylin and eosin.

RESULTS: FR167653 (50, 100, 150 mg/kg) could significantly decrease the serum transaminase (ALT, AST) activity and MDA content in liver homogenate, and improve reduced GSHpx level of liver homogenate. Liver histopathological examination showed FR167653 (100, 150 mg/kg) significantly reduced inflammatory cells infiltration and liver cells necrosis. FR167653 (50, 100, 150 mg/kg) significantly lowered TNF- α and NO levels in serum, and IL-1 produced by peritoneal macrophages. Moreover, expression of NF- κB mRNA in liver tissue of ILI induced by BCG plus LPS was significantly reduced by FR167653.

CONCLUSION: All results showed that FR167653 had significant inhibitory action on ILI in mice.

Yao HW, Li J, Chen JQ. FR167653 attenuates murine immunological liver injury. *World J Gastroenterol* 2004; 10(15): 2267-2271 <http://www.wjgnet.com/1007-9327/10/2267.asp>

INTRODUCTION

It has been demonstrated that tissue inflammation plays a critical role in liver pathology via induction of cellular injury. The infiltration of mononuclear phagocytes into the liver has been shown to correlate with the severity of liver injury. Kupffer

cells (KCs) are among the first cells that respond to endotoxins, including lipopolysaccharides (LPS), and are considered to be the primary macrophages involved in the clearance of gut-derived bacteria or bacterial toxins. High portal level of LPS can lead to a pronounced secretion of proinflammatory mediators by KCs and ultimately to endotoxin-induced liver injury^[1,2]. Moreover, proinflammatory cytokines such as tumor necrosis factor- α (TNF- α) and interleukin-1 (IL-1) β have been linked to liver injury^[3-5], and shown to be early and important mediators of liver injury^[6-8]. Thus, inhibition of KCs activity and proinflammatory cytokines production would be beneficial to alleviate liver injury.

FR167653, 1-[7-(4-fluorophenyl)-1,2,3,4-tetrahydro-8-(4-pyridyl)pyrazolo[5,1-c][1,2,4]triazin-2-yl]-2-phenylethanedione sulfate monohydrate, was first discovered to be a potent dual inhibitor of IL-1 and TNF- α production in LPS-stimulated human monocytes and phytohemagglutinin-stimulated human lymphocytes^[9]. Takahashi *et al.*^[10] and Kawano *et al.*^[11] also confirmed the inhibitory effect of FR167653 on cytokine production. FR167653 ameliorated endotoxin shock in rabbits and intravascular coagulation in rats^[9,12], and also ameliorated cardiac dysfunction caused by chronic infusion of LPS in rats^[13]. Furthermore, FR167653 protected lung, liver, and heart against ischemia-reperfusion injury in dogs^[14-17], and the protection against liver ischemia-reperfusion injury was associated with inhibition of proinflammatory cytokines from KCs^[18, 19]. Recent studies suggest that FR167653 inhibits IL-1 β and TNF- α production via specific inhibition of p38 MAPK activity^[12,17,20-22]. Because effective therapy has not been established for liver injury, development of an anti-inflammatory compound is urgently needed. From this viewpoint, it is worthwhile to assess the anti-inflammatory and immunomodulatory effect of FR167653. In the current study, we administered FR167653 to a murine model of *Bacillus Calmette Guerin* (BCG) and LPS-induced liver injury and assessed histopathological changes and its effects on cytokine production.

MATERIALS AND METHODS

Animals and reagents

Male Kunming strain mice weighing 18-22 g were purchased from Animal Center of Anhui Medical University. Mice were allowed to access to food and tap water *ad libitum*, and acclimated to facilities for at least 1 wk before any treatments. 1, 1, 3, 1-tetraethoxypropane (TEP) and 5, 5'-dithiobis-(2-nitrobenzoic acid) (DTNB) were purchased from FLUKA Co., Switzerland. BCG was purchased from Institute of Shanghai Biological Products. ConA, LPS from *Escherichia coli*, and TNF- α ELISA kit were purchased from Sigma Co., St. Louis, USA. The primers of NF- κB and β -actin were synthesized by BIOASIA Biotech Co. Shanghai. FR167653 supplied by the Fujisawa Pharmaceutical Co. Ltd. (Tokyo, Japan), was dissolved to 20 mL/L with 5 g/L methylcellulose solution. To obtain the dose of 50, 100, or 150 mg/kg body mass (BM), 2.5, 5, or 7.5 $\mu\text{L/g}\cdot\text{bm}$. of 20 mL/L FR167653 solution was injected subcutaneously.

Model of BCG and LPS-induced immunological liver injury (ILI) and treatment^[23]

Each mouse was injected with 2.5 mg BCG (viable bacilli) in 0.2 mL saline via tail vein, and 10 d later with 10 mg LPS in 0.2 mL

saline. At 4, 8, and 12 h post-injection of LPS, animals received FR167653 at 50, 100, and 150 mg/kg, s.c., respectively. The control group was subcutaneously administered the same volume of 5 g/L methylcellulose solution. The mice were anesthetized with ether, then sacrificed by cervical dislocation 16 h after LPS injection and blood was collected, and centrifuged at 1 500 r/min for 10 min at room temperature. Serum was aspirated and stored at -70 °C until assayed as described below. The liver was also removed and stored at -70 °C until required.

Measurement of ALT, AST

Serum ALT, and AST were determined using commercial kits purchased from Institute of Shanghai Biological Products affiliated to the Ministry of Health.

Measurement of MDA and GSHpx in liver homogenate

Livers were thawed, weighed and homogenized with Tris-HCl buffer (5 mmol/L, containing 2 mmol/L EDTA, pH 7.4). Homogenates were centrifuged at 1 000 r/min for 10 min at room temperature and the supernatant was used immediately for the assays of MDA and GSHpx. MDA was measured by the thiobarbituric acid method according to standard techniques. The content of MDA was expressed as nmol per gram liver tissue. GSHpx was measured by the DTNB method, and its content was expressed as U per milligram protein.

Measurement of TNF- α , IL-1, and nitric oxide (NO)

Serum TNF- α and NO were measured using commercial kits produced by Sigma Co. and Beijing Biotinge-Tech Co. Ltd, and their levels were expressed as pg/mL and μ mol/L respectively. IL-1 produced by peritoneal macrophages was measured according to the method of 3 H-infiltrated cell proliferation.

RT-PCR assay for NF- κ B p65 mRNA in liver tissue

Liver tissue RNA was extracted using RNA easy kit (Invitrogen, USA). To test the efficacy of reverse transcriptase, RT-PCR was performed for β -actin mRNA. Briefly, the first strand of cDNA was synthesized by reverse transcriptase and pooled. The resulting cDNA samples were adjusted to PCR buffer conditions and run for PCR simultaneously. The primers for NF- κ B p65 were 5'-GCG GCC AAG CTT AAG ATC TGC CGA GTA AAC-3', and 5'-CGC TGC TCT AGA GAA CAC AAT GGC CAC TTG CCG-3'. The primers for β -actin were 5'-TGG AAT CCT GTG GCA TCC ATG AA-3', and 5'-TAA AAC GCA GCT CAG TAA CAG TC-3'. The amplifications of NF- κ B p65 and β -actin genes are expected to generate 198 bp and 348 bp fragments, respectively. Amplification was performed for 30 cycles, each of which consisted of 1 min of denaturation at 94 °C, 1 min of annealing at 58 °C, and 3 min of primer extension at 72 °C. Ten μ L of reaction mixture was loaded to 10 g/L agarose gel containing 0.5 μ g/mL ethidium bromide for electrophoresis, the gel was then placed under ultraviolet light for semi-quantitative detection.

Histological examination of liver specimens

Formalin-fixed liver specimens were embedded in paraffin and

stained with hematoxylin and eosin for conventional morphological evaluation.

Statistical analysis

All values were expressed as mean \pm SD. The significance of differences between groups was determined by ANOVA followed by Student's *t* test. *P* value of less than 0.05 was considered significant.

RESULTS

Effects of FR167653 on ILI induced by BCG plus LPS in mice

The levels of ALT and AST in plasma and MDA content in liver homogenate were significantly increased after the sequential injection of BCG and LPS. Meanwhile, the GSHpx level in liver homogenate was sharply decreased (Figures 1, 2). FR167653 (50, 100, 150 mg/kg, s.c.) could not only significantly decrease ALT, AST, and MDA levels, but also evidently increase GSHpx level in mice with ILI (Figures 1, 2). Liver histopathologic examination showed extensive inflammatory cells infiltration and liver cells necrosis. FR167653 (100, 150 mg/kg) significantly reduced inflammatory cells infiltration and liver cells necrosis (Figure 3).

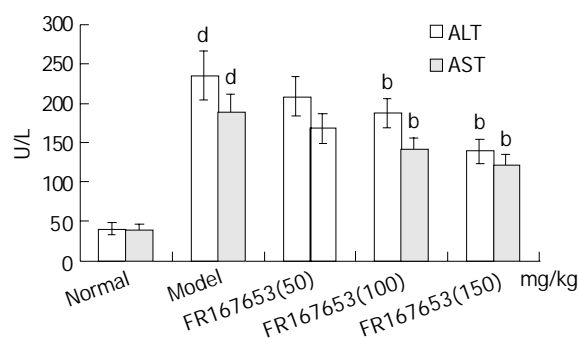


Figure 1 Effect of FR167653 on serum ALT and AST activities in ILI mice. *n*=8, mean \pm SD, ^b*P*<0.01 vs model group; ^d*P*<0.01 vs normal group.

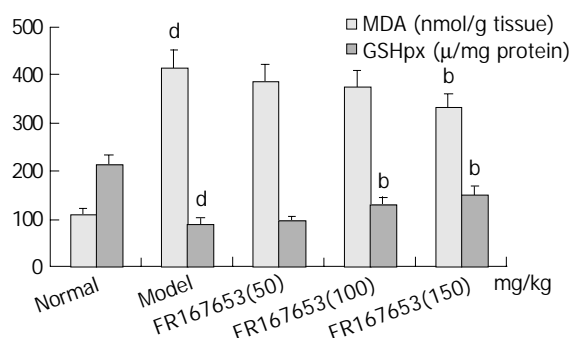


Figure 2 Effect of FR167653 on MDA and GSHpx contents in liver homogenates of ILI mice. *n*=8, mean \pm SD, ^b*P*<0.01 vs model group; ^d*P*<0.01 vs normal group.

Table 1 Effect of FR167653 on serum TNF- α , NO and IL-1 from peritoneal macrophages in ILI mice

Group	Dose (mg/kg)	TNF- α (pg/mL)	NO (μ mol/L)	IL-1 (10^3 /min)
Normal	-	Under detection limit	15.7 \pm 4.3	6.4 \pm 1.42
Model	-	523.1 \pm 28.6 ^d	117.8 \pm 10.7 ^d	21.5 \pm 5.04 ^d
FR167653	50	491.8 \pm 20.5 ^a	109.3 \pm 10.5	17.4 \pm 3.81
	100	404.9 \pm 18.5 ^b	95.4 \pm 8.9 ^b	14.7 \pm 3.05 ^b
	150	341.8 \pm 19.1 ^b	84.3 \pm 8.7 ^b	11.9 \pm 2.85 ^b

n=8, mean \pm SD, ^a*P*<0.05, ^b*P*<0.01 vs model group; ^d*P*<0.01 vs normal group.

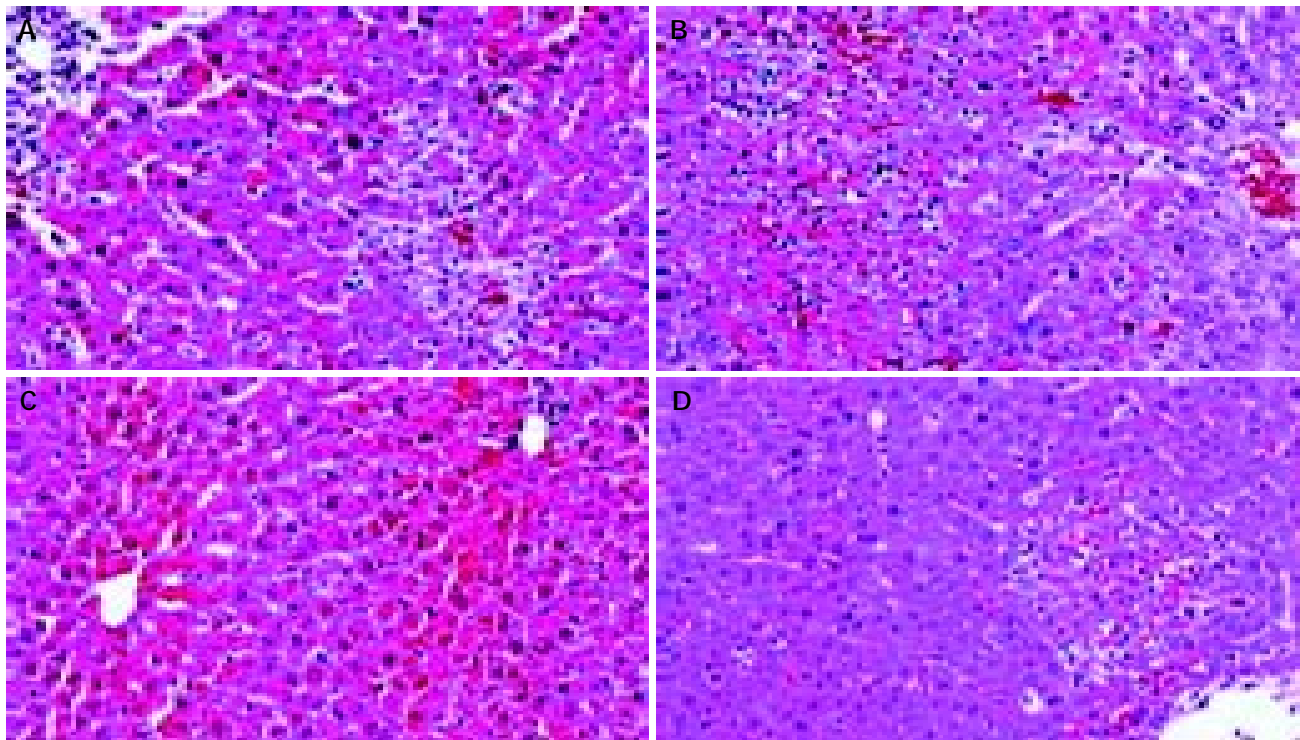


Figure 3 Effect of FR167653 on liver histopathology of ILI mice. A: Normal group; B: Model group; C: Model plus FR167653 (100 mg/kg); D: Model plus FR167653 (150 mg/kg). All sections were stained with hematoxylin and eosin (200 \times).

Effects of FR167653 on TNF- α , IL-1, and NO

The levels of TNF- α and NO were elevated significantly in mice injected with BCG and then challenged with LPS. Likewise, IL-1 excreted by peritoneal macrophages was also significantly increased in the model group (Table 1). FR167653 (50, 100, 150 mg/kg) obviously counteracted the increase of TNF- α and NO levels in sera. IL-1 produced by peritoneal macrophages was also significantly inhibited by FR167653 (Table 1).

Effects of FR167653 on NF- κ B p65 expression in liver tissue

Gel electrophoresis and semi-quantitative analysis showed that FR167653 significantly reduced expression of NF- κ B mRNA in liver tissue of ILI induced by BCG plus LPS compared with model group (Figure 4).

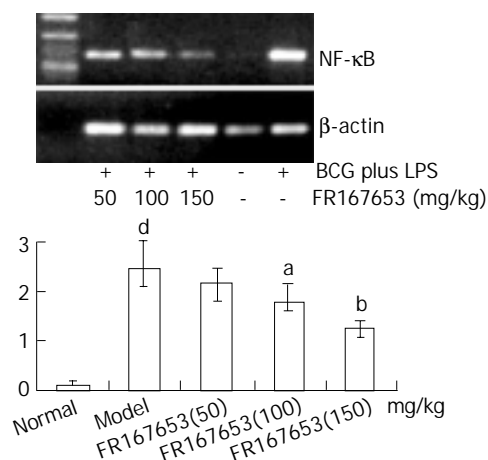


Figure 4 Effect of FR167653 on NF- κ B mRNA in liver tissue of ILI mice. $n=3$, mean \pm SD. ^a $P<0.05$. ^b $P<0.01$ vs model group; ^d $P<0.01$ vs normal group.

DISCUSSION

It has been demonstrated that severe hepatitis could be induced

by injecting a small dose of bacterial LPS into BCG-pretreated mice^[23]. In the present study, ILI was successfully induced by BCG plus LPS. On this basis, FR167653 (50, 100, 150 mg/kg) could significantly lower the increased plasma transaminase levels and MDA contents in liver homogenate. Meanwhile, GSHpx levels were increased significantly. Histopathologic examination showed FR167653 significantly reduced inflammatory cells infiltration and liver cells necrosis.

Although several parameters of the inflammatory response contribute to liver injury^[24], one well-studied pathway is the production of TNF- α . In a number of liver injury models, elevated TNF- α levels were present and correlated with liver injury^[23,25,26]. Inhibition of TNF- α activity can decrease liver injury. The addition of soluble TNF receptors that diminished the biological effect of TNF- α could significantly decrease liver enzyme levels, improve liver histology, and reduce mortality immediately after acute carbon tetrachloride administration. Similar results were seen in chronic alcohol-induced liver disease in rats. In humans, elevated levels of TNF- α are seen in hepatitis and are associated with increased mortality^[27]. Furthermore, TNF- α might act as the first mediator of liver injury, its elevation would result in release of a number of proinflammatory mediators including IL-1, NO, IL-6, IL-8^[3,28], further deteriorating the liver injury. In the present study, TNF- α in the sera and IL-1 produced by peritoneal macrophages were significantly increased in mice with ILI compared with control. FR167653, a potent inhibitor of TNF- α and IL-1, suppressed elevated TNF- α and IL-1 levels, which was consistent with previous observations^[29]. As potent producers of inflammatory cytokines such as TNF- α and IL-1, KCs have been implicated in the pathway leading to liver injury^[30]. Whether inhibition of FR167653 on TNF- α production was associated with diminished KCs proliferation, and decreased inflammatory cells infiltration needs to be further clarified.

A growing body of evidence suggests that sustained production of NO resulting from up-regulation of inducible NOS (iNOS) after LPS challenge may cause hepatocellular injury, either directly^[31,32], or indirectly, by forming reactive nitrogen

intermediates^[33]. Menezes *et al.*^[34,35] demonstrated that a NO scavenger, NOX, decreased hepatocellular injury and improved survival after hemorrhagic shock. As reported previously, the synthesis of NO was regulated by various factors including TNF- α , IL-1, and NF- κ B. The inhibition of NF- κ B led to a decrease in the inducible isoform of NO and the transcription of TNF- α in KCs^[36-38]. Moreover, synthetic double-stranded oligodeoxynucleotides (ODN) transfer with a high affinity to NF- κ B (NF- κ B/decoy/ODN) *in vivo* effectively suppressed endotoxin-induced fatal liver injury in mice^[39]. In our study, we observed significant suppression of NF- κ B p65 mRNA in liver tissue and NO in sera of BCG plus LPS - induced ILI by FR167653. It indicated that inhibition of FR167653 on liver injury might be related with decreased NO production through inhibiting NF- κ B transcription. Recent studies suggested that p38 MAPK inhibitor, SB203580, diminished phosphorylation of the transactivation domain of the p65 subunit of NF- κ B^[40]. Moreover, the pharmacological characteristics and chemical structure of FR167653 resemble SB203580^[41,42]. Therefore, inhibition of FR167653 on liver injury was associated with reduced expression of NF- κ B via p38 MAPK, and led to down-regulation of TNF- α , IL-1, and NO.

REFERENCES

- 1 Enomoto N, Ikejima K, Yamashina S, Hirose M, Shimizu H, Kitamura T, Takei Y, Sato And N, Thurman RG. Kupffer cell sensitization by alcohol involves increased permeability to gut-derived endotoxin. *Alcohol Clin Exp Res* 2001; **25**(6 Suppl): 51S-54S
- 2 Lukkari TA, Jarvelainen HA, Oinonen T, Kettunen E, Lindros KO. Short-term ethanol exposure increases the expression of Kupffer cell CD14 receptor and lipopolysaccharide binding protein in rat liver. *Alcohol Alcohol* 1999; **34**: 311-319
- 3 Shito M, Balis UJ, Tompkins RG, Yarmush ML, Toner M. A fulminant hepatic failure model in the rat: involvement of interleukin-1beta and tumor necrosis factor-alpha. *Dig Dis Sci* 2001; **46**: 1700-1708
- 4 Nishioji K, Okanou T, Mori T, Sakamoto S, Itoh Y. Experimental liver injury induced by *Propionibacterium acnes* and lipopolysaccharide in macrophage colony stimulating factor-deficient osteopetrotic (*op/op*) mice. *Dig Dis Sci* 1999; **44**: 1975-1984
- 5 Bradham CA, Plumpe J, Manns MP, Brenner DA, Trautwein C. Mechanisms of hepatic toxicity I. TNF-induced liver injury. *Am J Physiol* 1998; **275**: G387-392
- 6 Spitzer JA, Zheng M, Kolls JK, Vande Stouwe C, Spitzer JJ. Ethanol and LPS modulate NF-kappaB activation, inducible NO synthase and COX-2 gene expression in rat liver cells *in vivo*. *Front Biosci* 2002; **7**: a99-108
- 7 Wang JH, Redmond HP, Wu QD, Bouchier-Hayes D. Nitric oxide mediates hepatocyte injury. *Am J Physiol* 1998; **275**: G1117-1126
- 8 Hoek JB, Pastorino JG. Ethanol, oxidative stress, and cytokine-induced liver cell injury. *Alcohol* 2002; **27**: 63-68
- 9 Yamamoto N, Sakai F, Yamazaki H, Nakahara K, Okuhara M. Effect of FR167653, a cytokine suppressive agent, on endotoxin-induced disseminated intravascular coagulation. *Eur J Pharmacol* 1996; **314**: 137-142
- 10 Takahashi S, Shigeta J, Inoue H, Tanabe T, Okabe S. Localization of cyclooxygenase-2 and regulation of its mRNA expression in gastric ulcers in rats. *Am J Physiol* 1998; **275**: G1137-1145
- 11 Kawano T, Ogushi F, Tani K, Endo T, Ohmoto Y, Hayashi Y, Sone S. Comparison of suppressive effects of a new anti-inflammatory compound, FR167653, on production of PGE₂ and inflammatory cytokines, human monocytes, and alveolar macrophages in response to endotoxin. *J Leukoc Biol* 1999; **65**: 80-86
- 12 Yamamoto N, Sakai F, Yamazaki H, Sato N, Nakahara K, Okuhara M. FR167653, a dual inhibitor of interleukin-1 and tumor necrosis factor-alpha, ameliorates endotoxin-induced shock. *Eur J Pharmacol* 1997; **327**: 169-174
- 13 Gardiner SM, Kemp PA, March JE, Bennett T. Influence of FR167653, an inhibitor of TNF-alpha and IL-1, on the cardiovascular responses to chronic infusion of lipopolysaccharide in conscious rats. *J Cardiovasc Pharmacol* 1999; **34**: 64-69
- 14 Kamoshita N, Takeyoshi I, Ohwada S, Iino Y, Morishita Y. The effects of FR167653 on pulmonary ischemia-reperfusion injury in dogs. *J Heart Lung Transplant* 1997; **16**: 1062-1072
- 15 Kobayashi J, Takeyoshi I, Ohwada S, Iwanami K, Matsumoto K, Muramoto M, Morishita Y. The effects of FR167653 in extended liver resection with ischemia in dogs. *Hepatology* 1998; **28**: 459-465
- 16 Koyano T, Takeyoshi I, Takahashi T, Hasegawa Y, Sato Y, Ishikawa S, Matsumoto K, Morishita Y. Effect of FR167653 on ischemia-reperfusion injury of the canine heart: ultrastructural study. *Transplant Proc* 1998; **30**: 3370-3371
- 17 Kobayashi M, Takeyoshi I, Yoshinari D, Matsumoto K, Morishita Y. P38 mitogen-activated protein kinase inhibition attenuates ischemia-reperfusion injury of the rat liver. *Surgery* 2002; **131**: 344-349
- 18 Hashimoto K, Nishizaki T, Yoshizumi T, Uchiyama H, Okano S, Ikegami T, Yanaga K, Sugimachi K. Beneficial effect of FR167653 on cold ischemia/reperfusion injury in rat liver transplantation. *Transplantation* 2000; **70**: 1318-1322
- 19 Minami S, Furui J, Kanematsu T. Role of carcinoembryonic antigen in the progression of colon cancer cells that express carbohydrate antigen. *Cancer Res* 2001; **61**: 2732-2735
- 20 Kobayashi M, Takeyoshi I, Yoshinari D, Koibuchi Y, Koyama T, Kawashima Y, Ohwada S, Matsumoto K, Morishita Y. FR167653 ameliorates ischemia-reperfusion injury of the rat liver through P38 mitogen-activated protein kinase pathway. *Transplant Proc* 2001; **33**: 865
- 21 Takahashi S, Keto Y, Fujita T, Uchiyama T, Yamamoto A. FR167653, a p38 mitogen-activated protein kinase inhibitor, prevents *Helicobacter pylori*-induced gastritis in Mongolian gerbils. *J Pharmacol Exp Ther* 2001; **296**: 48-56
- 22 Lasky JA, Ortiz LA, Tonthat B, Hoyle GW, Corti M, Athas G, Lungarella G, Brody A, Friedman M. Connective tissue growth factor mRNA expression is upregulated in bleomycin-induced lung fibrosis. *Am J Physiol* 1998; **275**: L365-371
- 23 Wang GS, Liu GT. Influences of Kupffer cell stimulation and suppression on immunological liver injury in mice. *Zhongguo Yaoli Xuebao* 1997; **18**: 173-176
- 24 Moulin F, Copple BL, Ganey PE, Roth RA. Hepatic and extrahepatic factors critical for liver injury during lipopolysaccharide exposure. *Am J Physiol Gastrointest Liver Physiol* 2001; **281**: G1423-1431
- 25 Zhang XL, Quan QZ, Sun ZQ, Wang YJ, Jiang XL, Wang D, Li WB. Protective effects of cyclosporine A on T-cell dependent ConA-induced liver injury in Kunming mice. *World J Gastroenterol* 2001; **7**: 569-571
- 26 Zang GQ, Zhou XQ, Yu H, Xie Q, Zhao GM, Wang B, Guo Q, Xiang YQ, Liao D. Effect of hepatocyte apoptosis induced by TNF-alpha on acute severe hepatitis in mouse models. *World J Gastroenterol* 2000; **6**: 688-692
- 27 Madhotra R, Gilmore IT. Recent developments in the treatment of alcoholic hepatitis. *Q J Med* 2003; **96**: 391-400
- 28 Muntane J, Rodriguez FJ, Segado O, Quintero A, Lozano JM, Siendones E, Pedraza CA, Delgado M, O'Valle F, Garcia R, Montero JL, De La Mata M, Mino G. TNF-alpha dependent production of inducible nitric oxide is involved in PGE₁ protection against acute liver injury. *Gut* 2000; **47**: 553-562
- 29 Hou Z, Yanaga K, Kamohara Y, Eguchi S, Tsutsumi R, Furui J, Kanematsu T. A new suppressive agent against interleukin-1beta and tumor necrosis factor-alpha enhances liver regeneration after partial hepatectomy in rats. *Hepatology* 2003; **26**: 40-46
- 30 Luckey SW, Petersen DR. Activation of Kupffer cells during the course of carbon tetrachloride-induced liver injury and fibrosis in rats. *Exp Mol Pathol* 2001; **71**: 226-240
- 31 Engin A, Bozkurt BS, Altan N, Memi L, Bukan N. Nitric oxide-mediated liver injury in the presence of experimental bile duct obstruction. *World J Surg* 2003; **27**: 253-255
- 32 Nadler EP, Dickinson EC, Beer-Stolz D, Alber SM, Watkins SC, Pratt DW, Ford HR. Scavenging nitric oxide reduces hepatocellular injury after endotoxin challenge. *Am J Physiol*

- Gastrointest Liver Physiol* 2001; **281**: G173-181
- 33 **Fintelmann S**, Jung M, Weidenbach H, Steinle AU, Beger HG, Nussler AK. Effect of cellular growth factors on hepatocytes in experimental infection—regulation of NF-kappa B and glutathione homeostasis. *Langenbecks Arch Chir Suppl Kongressbd* 1998; **115**(Suppl 1): 405-408
- 34 **Menezes J**, Hierholzer C, Watkins SC, Lyons V, Peitzman AB, Billiar TR, Twardy DJ, Harbrecht BG. A novel nitric oxide scavenger decreases liver injury and improves survival after hemorrhagic shock. *Am J Physiol* 1999; **277**: G144-151
- 35 **Hierholzer C**, Billiar TR, Twardy DJ, Harbrecht B. Reduced hepatic transcription factor activation and expression of IL-6 and ICAM-1 after hemorrhage by NO scavenging. *Arch Orthop Trauma Surg* 2003; **123**: 55-59
- 36 **Shimohashi N**, Nakamuta M, Uchimura K, Sugimoto R, Iwamoto H, Enjoji M, Nawata H. Selenoorganic compound, ebselen, inhibits nitric oxide and tumor necrosis factor-alpha production by the modulation of jun-N-terminal kinase and the NF-kappaB signaling pathway in rat Kupffer cells. *J Cell Biochem* 2000; **78**: 595-606
- 37 **Cao Q**, Mak KM, Lieber CS. Dilinoleoylphosphatidylcholine decreases acetaldehyde-induced TNF-alpha generation in Kupffer cells of ethanol-fed rats. *Biochem Biophys Res Commun* 2002; **299**: 459-464
- 38 **Lin M**, Rippe RA, Niemela O, Brittenham G, Tsukamoto H. Role of iron in NF-kappa B activation and cytokine gene expression by rat hepatic macrophages. *Am J Physiol* 1997; **272** (6 Pt 1): G1355-1364
- 39 **Ogushi I**, Iimuro Y, Seki E, Son G, Hirano T, Hada T, Tsutsui H, Nakanishi K, Morishita R, Kaneda Y, Fujimoto J. Nuclear factor kappa B decoy oligodeoxynucleotides prevent endotoxin-induced fatal liver failure in a murine model. *Hepatology* 2003; **38**: 335-344
- 40 **Wilms H**, Rosenstiel P, Sievers J, Deuschl G, Zecca L, Lucius R. Activation of microglia by human neuromelanin is NF-kappaB dependent and involves p38 mitogen-activated protein kinase: implications for Parkinson's disease. *Faseb J* 2003; **17**: 500-502
- 41 **Cuenda A**, Rouse J, Doza YN, Meier R, Cohen P, Gallagher TF, Young PR, Lee JC. SB 203580 is a specific inhibitor of a MAP kinase homologue which is stimulated by cellular stresses and interleukin-1. *FEBS Lett* 1995; **364**: 229-233
- 42 **Lee JC**, Laydon JT, McDonnell PC, Gallagher TF, Kumar S, Green D, McNulty D, Blumenthal MJ, Heys JR, Landvatter SW. A protein kinase involved in the regulation of inflammatory cytokine biosynthesis. *Nature* 1994; **372**: 739-746

Edited by Zhu LH Proofread by Chen WW and Xu FM

Therapeutic plasma exchange in patients with hyperlipidemic pancreatitis

Jui-Hao Chen, Jiann-Horng Yeh, Hsin-Wen Lai, Chao-Sheng Liao

Jui-Hao Chen, Hsin-Wen Lai, Chao-Sheng Liao, Department of Gastroenterology, Shin kong Wu-Ho-Su Memorial Hospital, Taipei, Taiwan, china

Jiann-Horng Yeh, Department of Neurology, Shin kong Wu-Ho-Su Memorial Hospital, Taipei, Taiwan, china

Correspondence to: Jui-Hao Chen, Department of Gastroenterology, Shin kong Wu-Ho-Su Memorial Hospital, 95 Wenchang Road, Shih-Lin District, Taipei, Taiwan, china. m000723@ms.skh.org.tw

Telephone: +886-2-28332211 **Fax:** +886-2-28389335

Received: 2004-02-20 **Accepted:** 2004-04-09

Abstract

AIM: To clarify the effectiveness of plasma exchange by comparing the mortality and morbidity before and after the intervention of plasma exchange.

METHODS: Plasma exchange has been available as an optional therapy for hyperlipidemic pancreatitis since August 1999 in our hospital. The patients were assorted into 2 groups (group I: before August 1999 and group II: after August 1999). Group I consisted of 34 patients (before the availability of plasma exchange). Group II consisted of 60 patients (after the availability of plasma exchange). Twenty patients in group II received plasma exchange after giving their consent. The mortality and morbidity were compared between group I and group II. Furthermore, the patients with severe hyperlipidemic pancreatitis (Ranson's score = 3) were analyzed separately. The mortality and morbidity were also compared between those receiving plasma exchange (group A) and those who did not receive plasma exchange (group B).

RESULTS: There was no statistical difference in the mortality, systemic and local complications between group I and group II. When the patients with severe hyperlipidemic pancreatitis were analyzed separately, there was no statistical difference between group A and group B.

CONCLUSION: Plasma exchange can not ameliorate the overall mortality or morbidity of hyperlipidemic pancreatitis. The time of plasma exchange might be the critical point. If patients with hyperlipidemic pancreatitis can receive plasma exchange as soon as possible, better result may be predicted. Further study with more cases is needed to clarify the role of plasma exchange in the treatment of hyperlipidemic pancreatitis.

Chen JH, Yeh JH, Lai HW, Liao CS. Therapeutic plasma exchange in patients with hyperlipidemic pancreatitis. *World J Gastroenterol* 2004; 10(15): 2272-2274
<http://www.wjgnet.com/1007-9327/10/2272.asp>

INTRODUCTION

Hypertriglyceridemia (HTG) is a rare cause of pancreatitis. Hyperlipidemic pancreatitis (HLP) secondary to HTG presents

typically as an episode of acute pancreatitis or recurrent acute pancreatitis or rarely as chronic pancreatitis^[1]. The typical clinical profile of HLP is a patient with preexisting lipid abnormality along with the presence of secondary factors (such as poorly controlled diabetes mellitus, alcohol abuse, pregnancy, or a medication) that can induce HTG^[1]. It is generally accepted that a TG level more than 1 000 mg/dL is needed to precipitate an episode of acute pancreatitis^[2]. It is postulated that hydrolysis of TG by pancreatic lipase into free fatty acid is toxic to pancreatic endothelium and acinar cells^[3]. In an animal study, hyperlipidemia could intensify the course of acute edematous pancreatitis and necrotizing pancreatitis^[3].

Plasmapheresis has been claimed to reduce triglyceride level rapidly in HLP^[4-11] and is believed to halt the progression of HLP^[8-10]. Actually, experiences of plasmapheresis in HLP are limited and only sporadic cases were reported^[5-11]. There was no control study in the past concerning whether plasmapheresis could improve the mortality or morbidity of HLP. Our aim was to analyze the benefits of plasma exchange by comparing the mortality and morbidity of HLP patients with those without receiving such an intervention.

MATERIALS AND METHODS

Patient characteristics

From September 1992 to June 2003, a total of 862 patients with acute pancreatitis were reviewed and 94 patients were consistent with hyperlipidemic pancreatitis (HLP). As plasma exchange has been available as an optional therapy of HLP since August 1999 in our hospital, the patients were assorted into 2 groups (group I: before August 1999 and group II: after August 1999). Group I consisted of 34 patients (before the availability of plasmapheresis) and group II consisted of 60 patients (after the availability of plasmapheresis). Twenty of 60 patients in group II received plasma exchange after giving their consents. The Ranson's score was used for assessment of the severity of pancreatitis. Half of the patients receiving plasma exchange were severe cases (Ranson's score = 3). The anatomical change of acute pancreatitis was assessed according to the Balthazar's grading. The enrolled criteria of plasma exchange in HLP were as followings: (1) overt symptoms of acute pancreatitis, (2) pancreatitis proved by CT, ultrasound or elevation of pancreatic enzymes, (3) triglyceride (TG) >1 000 mg/dL and lactescent serum, (4) exclusion of other causative conditions, such as gall stone, trauma or neoplasm, (5) patient's agreement. The mortality and morbidity between group I and group II were compared.

Furthermore, the patients with severe HLP (Ranson's score = 3) were analyzed separately. We divided the patients with severe HLP (a total of 29 patients) into 2 groups. Group A received plasma exchange, while group B did not receive the intervention. The mortality and morbidity between group A and group B were also compared.

The secondary factors inducing HTG in our patients included diabetes mellitus (46 patients), alcoholic consumption (32 patients) and oral contraceptive (one patient). The median time for starting plasma exchange was 3 d after symptom onset (range, 2-6 d).

Apheresis

Plasma exchange was carried out using membrane filtration in a KM 8800 membrane plasmapheresis monitor (Kuraray, Osaka, Japan) with a Plasmacure plasma separator (Kuraray, Osaka, Japan) to separate plasma from blood. One calculated plasma volume was processed during each session of plasma exchange. One course of plasma exchange treatment consisted of one or two daily sessions based on the doctor's decision, single session in 13 patients and two sessions in 7. Heparin was used as the anticoagulant. Either a double lumen catheter in a central vein (fifteen patients) or a dialysis catheter in an antecubital vein (five patients) was used for vascular access. Replacement fluid was given with fresh frozen plasma (FFP) in 8 patients and isovolumetric 5% albumin solution in 12 patients.

Statistical analysis

t-test and chi-square test were used for statistical analysis. $P < 0.05$ was considered statistically significant.

RESULTS

The demographic characteristics of all the patients are summarized in Table 1. The mean age and sex distribution were similar in both groups. The initial mean TG level was around 1900 in both groups. The severity of pancreatitis was predicted by the Ranson's criteria. Severe pancreatitis (Ranson's score ≥ 3) was 20.6% in group I and 36.7% in group II ($P = 0.105$). The anatomical change of pancreatitis was assessed according to the Balthazar's grading system and 54.2% of group I and 41.3% of group II were belonged to Balthazar grade D or E ($P = 0.305$).

The mortality rate, systemic and local complications of both groups are demonstrated in the Table 2. The systemic complication was defined by the Atlanta definition^[12]: (1) pulmonary insufficiency, $\text{PaO}_2 < 8$ kPa, (2) renal insufficiency, $\text{Cr} > 2$ mg/dL, (3) shock, $\text{SBP} < 12$ kPa, (4) UGI bleeding > 500 mL/24 h. The local complications included abscess and pseudocyst formation. There was no significant difference between group I and group II in mortality and complications. Further comparison of individual items of systemic and local complications between the two groups revealed no statistical differences (Tables 3, 4).

Table 1 Demographic characteristics

	Group I (n=34)	Group II (n=60)	P value
Age (yr)	40.8±6.8	42.3±8.9	0.394
Initial TG	1922±1287	1913±612	0.966
DM (%)	38(13/34)	55(33/60)	0.118
Alcohol (%)	44(15/34)	28.3 (17/60)	0.121
Ranson > 3 (%)	20.6(7/34)	36.7(22/60)	0.105
Balthazar D, E (%)	54.2(13/24)	41.3(19/46)	0.305

Table 2 Comparison of mortality and morbidity between patients before and after availability of plasma exchange

	Group I (%, n=34)	Group II (%, n=60)	P value
Mortality (%)	5.9(2/34)	6.7(4/60)	0.881
Systemic complications (%)	17.6(6/34)	18.3(11/60)	0.934
Local complications (%)	11.8(4/34)	6.7(4/60)	0.395

When severe hyperlipidemic pancreatitis (Ranson's score ≥ 3) was analyzed separately (Table 5), the mortality rate, systemic and local complications of group A (with plasmapheresis) and group B (without plasmapheresis) were not statistically different ($P = 0.369, 0.153, 0.454$, respectively).

The mean serum concentration of TG and lipase fell significantly after plasma exchange. The serum TG level declined

from 2019 ± 780 mg/dL to 691 ± 331 mg/dL (65.8% reduction) and the serum lipase level declined from 4007 ± 355 U/L to 447 ± 35 U/L (88.8% reduction).

Table 3 Comparison of systemic complications between patients before and after the availability of plasma exchange

	Group I (%, n=34)	Group II (%, n=60)	P value
ARF	17.6(6/34)	10(6/60)	0.286
UGI bleeding	0(0/34)	8.3(5/60)	0.084
Shock	8.8(3/34)	10(6/60)	0.852
ARDS	11.8(4/34)	10(6/60)	0.790

ARF: Acute renal failure; ARDS: Acute respiratory distress syndrome.

Table 4 Comparison of local complications between patients before and after availability of plasma exchange

	Group I (%, n=34)	Group II (%, n=60)	P value
Abscess	17.6(6/34)	10(6/60)	0.286
Pseudocyst	0(0/34)	8.3(5/60)	0.084

Table 5 Comparison of patients with severe hyperlipidemic pancreatitis receiving plasma exchange and not receiving plasma exchange

	Group A: PE(+) (%, n=10)	Group B: PE(-) (%, n=19)	P value
Ranson > 3			
Mortality	30(3)	15.8(3)	0.369
Systemic complications	70(7)	42.1(8)	0.153
Local complications	10(1)	21.1(4)	0.454

PE (+): With plasma exchange; PE (-): Without plasma exchange.

DISCUSSION

The association between hyperlipidemia and acute pancreatitis was first described by Speck in 1865^[1]. Studies on patients with familial HTG and their longterm follow-up have shown that extreme elevation of TG occurred during episode of acute pancreatitis^[13]. It has been generally believed that a TG level of more than 1000 mg/dL was needed to precipitate an acute pancreatitis^[2]. The hypothesis of hyperlipidemic pancreatitis is that pancreatic damage was resulted from toxic injury to the capillary endothelium and the damage of pancreatic acinar cells was caused by free fatty acids liberated by pancreatic lipase^[3]. Conservative treatment (fasting, lipid lowering drugs, insulin or fluid restoration) might decrease TG level slowly in a time span of days to weeks^[14]. In contrast, plasmapheresis might remove excessive lipid from serum in about 2 h^[4,6]. Sporadic reports about plasmapheresis used in hyperlipidemic pancreatitis were seen in the past^[4-10]. They all concluded that plasmapheresis was helpful for treating or preventing acute hyperlipidemic pancreatitis. However, no control study to assess the value of plasmapheresis in the treatment of hyperlipidemic pancreatitis is available.

Different methods have been used in plasmapheresis. Plasma exchange is superior to double filtration in the removal of excessive TG because the membrane of plasma separator was usually blocked by the larger particles of chylomicron^[6]. We used plasma exchange with replacement of albumin or fresh frozen plasma (FFP) in the treatment of HLP in this study. FFP could supply lipoprotein lipase and apolipoprotein from the healthy donor^[13]. Lipoprotein lipase and apolipoprotein were essential for the catabolism of TG^[13].

In our study, plasma exchange could remove TG effectively

from turbid plasma in a short time (about 2 h). TG declined from $2\,019\pm 780$ mg/dL to 691 ± 331 mg/dL (65.8% reduction). It was also postulated that plasmapheresis could remove circulating activated enzymes and inflammatory mediators^[15], but its beneficial effects in pancreatitis has not been proved^[10]. The serum lipase level declined from $4\,007\pm 355$ U/L to 447 ± 35 U/L (88.8% reduction) after plasma exchange in our patients.

Despite the marked reduction in TG and lipase after plasma exchange, we could not achieve statistically significant improvement in the mortality and morbidity after the intervention of plasma exchange. The mortality was 5.9% before the intervention (group I) and 6.7% after the intervention (group II). The rate of systemic complications (acute renal failure, UGI bleeding, shock, or pulmonary insufficiency) was 17.6% in group I and 18.3% in group II. The rate of local complications (abscess or pseudocyst) was 11.8% in group I and 6.7% in group II. While individual items of complications were considered, there were still no statistical differences between the two groups.

When the patients with severe HLP (Ranson's score ≥ 3) were analyzed separately, the mortality rate was 30% in group A (with plasma exchange) and 15.8% in group B (without plasma exchange). The mortality in severe HLP was not decreased by plasma exchange. The rate of systemic complication was 70% in group A and 42.1% in group B ($P=0.153$). The rate of local complication was 10% in group A and 21.1% in group B ($P=0.454$). Again, plasma exchange was not able to alter the complication rate significantly.

Why could plasma exchange not improve the mortality and morbidity in HLP? We proposed that the time of plasmapheresis might be the critical point. If patients with HLP could receive plasma exchange as soon as possible, better result might be expected^[5].

In conclusion, plasma exchange fails to improve the overall mortality and morbidity of HLP in our study. Further study with more cases is needed to clarify the role of plasmapheresis in the treatment of HLP.

REFERENCES

- 1 **Yadav D**, Pitchumoni CS. Issues in hyperlipidemic pancreatitis. *J Clin Gastroenterol* 2003; **36**: 54-62
- 2 **Toskes PP**. Hyperlipidemic pancreatitis. *Gastroenterol Clin North Am* 1990; **19**: 783-791
- 3 **Hofbauer B**, Friess H, Weber A, Baczako K, Kisling P, Schilling M, Uhl W, Dervenis C, Buchler MW. Hyperlipaemia intensifies the course of acute oedematous and acute necrotising pancreatitis in the rat. *Gut* 1996; **38**: 753-758
- 4 **Yeh JH**, Chen JH, Chiu HC. Plasmapheresis for hyperlipidemic pancreatitis. *J Clin Apheresis* 2003; **18**: 181-185
- 5 **Furuya T**, Komatsu M, Takahashi K, Hashimoto N, Hashizume T, Wajima N, Kubota M, Itoh S, Soeno T, Suzuki K, Enzan K, Matsuo S. Plasma exchange for hypertriglyceridemic acute necrotizing pancreatitis: report of two cases. *Ther Apher* 2002; **6**: 454-458
- 6 **Yeh JH**, Lee MF, Chiu HC. Plasmapheresis for severe lipidemia: comparison of serum-lipid clearance rates for the plasma-exchange and double-filtration variants. *J Clin Apheresis* 2003; **18**: 32-36
- 7 **Piolot A**, Nadler F, Cavallero E, Coquard JL, Jacotot B. Prevention of recurrent acute pancreatitis in patients with severe hypertriglyceridemia: value of regular plasmapheresis. *Pancreas* 1996; **13**: 96-99
- 8 **Valbonesi M**, Occhini D, Frisoni R, Malfanti L, Capra C, Gualandi F. Cyclosporin-induced hypertriglyceridemia with prompt response to plasma exchange therapy. *J Clin Apheresis* 1991; **6**: 158-160
- 9 **Lennertz A**, Parhofer KG, Samtleben W, Bosch T. Therapeutic plasma exchange in patients with chylomicronemia syndrome complicated by acute pancreatitis. *Ther Apher* 1999; **3**: 227-233
- 10 **Saravanan P**, Blumenthal S, Anderson C, Stein R, Berkelhammer C. Plasma exchange for dramatic gestational hyperlipidemic pancreatitis. *J Clin Gastroenterol* 1996; **22**: 295-298
- 11 **Bildirici I**, Esinler I, Deren O, Durukan T, Kabay B, Onderoglu L. Hyperlipidemic pancreatitis during pregnancy. *Acta Obstet Gynecol Scand* 2002; **81**: 468-470
- 12 **Bradley EL**. A clinically based classification system for acute pancreatitis. *Arch Surg* 1993; **128**: 586-590
- 13 **Athyros VG**, Giouleme OI, Nikolaidis NL, Vasiliadis TV, Bouloukos VI, Kontopoulos AG, Eugenidis NP. Long-term follow-up of patients with acute hypertriglyceridemia-induced pancreatitis. *Clin Gastroenterol* 2002; **34**: 472-475
- 14 **Fortson MR**, Freedman SN, Webster PD 3rd. Clinical assessment of hyperlipidemic pancreatitis. *Am J Gastroenterol* 1995; **90**: 2134-2139
- 15 **Heinisch A**, Balle C, Kadow R. Plasmapheresis in severe acute pancreatitis-a new therapeutic option? *Gastroenterology* 1995; **108**: 359

Edited by Wang XL Proofread by Chen WW and Xu FM

Insulin is necessary for the hypertrophic effect of cholecystokinin-octapeptide following acute necrotizing experimental pancreatitis

Péter Hegyi, Zoltán Rakonczay Jr, Réka Sári, László Czakó, Norbert Farkas, Csaba Góg, József Németh, János Lonovics, Tamás Takács

Péter Hegyi, Zoltán Rakonczay Jr, Réka Sári, László Czakó, Norbert Farkas, Csaba Góg, József Németh, János Lonovics, Tamás Takács, First Department of Medicine, Faculty of Medicine, University of Szeged Szeged H6722, Hungary
Péter Hegyi, Zoltán Rakonczay Jr, School of Cell and Molecular Biosciences, Medical School, University of Newcastle, Newcastle upon Tyne, NE2 4HH, United Kingdom
Supported by The Wellcome Trust Grant No. 022618, and by the Hungarian Scientific Research Fund D42188, T43066 and T042589
Correspondence to: Péter Hegyi, M.D., Ph.D., University of Szeged, Faculty of Medicine, First Department of Medicine, PO Box 469, H-6701, Szeged, Hungary. hep@in1st.szote.u-szeged.hu
Telephone: +36-62-545-200 **Fax:** +36-62-545-185
Received: 2003-08-26 **Accepted:** 2003-09-05

Abstract

AIM: In previous experiments we have demonstrated that by administering low doses of cholecystokinin-octapeptide (CCK-8), the process of regeneration following L-arginine (Arg)-induced pancreatitis is accelerated. In rats that were also diabetic (induced by streptozotocin, STZ), pancreatic regeneration was not observed. The aim of this study was to deduce whether the administration of exogenous insulin could in fact restore the hypertrophic effect of CCK-8 in diabetic-pancreatic rats.

METHODS: Male Wistar rats were used for the experiments. Diabetes mellitus was induced by administering 60 mg/kg body mass of STZ intraperitoneally (i.p.), then, on d 8, pancreatitis was induced by 200 mg/100 g body mass Arg i.p. twice at an interval of 1 h. The animals were injected subcutaneously twice daily (at 7 a.m. and 7 p.m.) with 1 µg/kg of CCK-8 and/or 2 IU mixed insulin (300 g/L short-action and 700 g/L intermediate-action insulin) for 14 d after pancreatitis induction. Following this the animals were killed and the serum amylase, glucose and insulin levels as well as the plasma glucagon levels, the pancreatic mass/body mass ratio (pm/bm), the pancreatic contents of DNA, protein, amylase, lipase and trypsinogen were measured. Pancreatic tissue samples were examined by light microscopy on paraffin-embedded sections.

RESULTS: In the diabetic-pancreatic rats treatment with insulin and CCK-8 significantly elevated pm/bm and the pancreatic contents of protein, amylase and lipase vs the rats receiving only CCK-8 treatment. CCK-8 administered in combination with insulin also elevated the number of acinar cells with mitotic activities, whereas CCK-8 alone had no effect on laboratory parameters or the mitotic activities in diabetic-pancreatic rats.

CONCLUSION: Despite the hypertrophic effect of CCK-8 being absent following acute pancreatitis in diabetic-rats, the simultaneous administration of exogenous insulin

restored this effect. Our results clearly demonstrate that insulin is necessary for the hypertrophic effect of low-doses of CCK-8 following acute pancreatitis.

Hegyi P, Rakonczay Jr Z, Sári R, Czakó L, Farkas N, Góg C, Németh J, Lonovics J, Takács T. Insulin is necessary for the hypertrophic effect of cholecystokinin-octapeptide following acute necrotizing experimental pancreatitis. *World J Gastroenterol* 2004; 10(15): 2275-2277
<http://www.wjgnet.com/1007-9327/10/2275.asp>

INTRODUCTION

We have previously demonstrated that the administration of low doses of cholecystokinin-octapeptide (CCK-8) accelerated the processes of regeneration following L-arginine (Arg)-induced pancreatitis^[1] and this was not observed in rats that were also diabetic^[2]. The most significant difference in the regeneration was observed after two wk of CCK-8 treatment^[1]. In addition, the histologic examination revealed that the majority of hypertrophized pancreatic acinar cells were found surrounding the enlarged islets of Langerhans following CCK-8 administration. It appears that the close proximity of the islets of Langerhans functions to protect the acinar cells as well as accelerate the regenerative process during Arg-evoked pancreatic tissue damage. A reason for this may be due to the interaction of acinar and islet cells. The exocrine and endocrine pancreas possesses a multitude of complex anatomical and functional interrelations^[3]. It is well documented that intact islets of Langerhans are necessary for normal pancreatic exocrine function^[4], and so we set out to investigate whether the administration of exogenous insulin could restore the hypertrophic effect of CCK in diabetic-pancreatic rats.

MATERIALS AND METHODS

Male Wistar rats weighing 250-300 g were divided into five groups. The animals were kept at a constant room temperature of 25 °C with a 12-h light-dark cycle, and were allowed free access to water and standard laboratory chow (Biofarm, Zagyvaszántó, Hungary). Rats in group D (diabetic -control group) were injected with 60 mg/kg body mass of streptozotocin (Zanosar®, The Upjohn Company, Kalamazoo, MI) intraperitoneally (i.p.). In group DP (diabetic and pancreatic) the rats received STZ as in group D, and on d 8, pancreatitis was induced by 200 mg/100 g body mass Arg (Sigma, St. Louis, MO) i.p. twice at an interval of 1h. In group DPC, apart from being given Arg and STZ, the rats were also administered 1 µg/kg of CCK-8 (synthesized by Botond Penke, Department of Medical Chemistry University of Szeged) subcutaneously (s.c.) twice daily (at 7 a.m. and 7 p.m.). In group DPI, besides being administered Arg and STZ, the rats received 2 IU mixed insulin (300 g/L short-action and 700 g/L intermediate-action insulin, HUMULIN M3®, Lilly Hungária Kft, Hungary) s.c. twice

Table 1 Laboratory parameters changes in diabetic-pancreatic rats due to a 14 d administration of insulin and/or CCK-8

	Serum glucose	Serum insulin	pm/bm	Pancreatic DNA	Pancreatic protein	Pancreatic amylase	Pancreatic trypsinogen	pancreatic lipase
Insulin treatment				-	-		-	-
CCK-8 treatment	-	-	-	-	-	-	-	-
Insulin and CCK-8 treatment				-				-

CCK-8: cholecystokinin-octapeptide, pm/bm: pancreatic weight/body weight ratio. increased or decreased activity/ level, - no change, significantly larger increase of activity compared with the sign. All changes are given in comparison to the untreated diabetic-pancreatic rats (group DP).

daily (at 7 a.m. and 7 p.m.). In group DPCI, diabetes and pancreatitis were induced as in group DP and the rats were administered CCK-8 and mixed insulin as mentioned before. The animals were killed in the morning by exsanguination through the abdominal aorta 14 d after pancreatitis induction. The serum amylase, glucose, insulin and plasma glucagon levels, pancreatic mass/body mass ratio (pm/bm), the pancreatic contents of DNA, protein, amylase, lipase and trypsinogen were measured^[2]. Pancreatic tissue samples were examined by light microscopy on paraffin-embedded sections. Results were expressed as mean±SE. Statistical analysis was performed by using ANOVA. *P* values <0.05 were accepted as significant.

RESULTS

In diabetic groups D, DP, and DPC, the serum glucose levels (22.5±1.5 mmol/L, 29.5±0.8 mmol/L and 29.0±0.7 mmol/L respectively) were significantly elevated and the insulin levels (0.70±0.30 U/l, 0.35±0.09 U/l and 0.20±0.05 U/l, respectively) were significantly lower vs those in insulin-treated groups DPI and DPCI (14.5±2.3 mmol/L and 12.9±2.8 mmol/L; 401±38 U/L and 138±35 U/L, respectively). These results clearly indicated the presence of diabetes mellitus in the animals studied and the efficacy of insulin treatment. There were no significant differences in plasma glucagon and serum amylase levels in group D as compared with any of the other groups. In groups DPI and DPCI, pm/bm (2.98±0.21 mg/g, 3.58±0.11 mg/g, respectively) was significantly elevated vs group DP (2.09±0.26 mg/g). However, no significant differences were observed in pm/bm between group DPC and group DP (2.62±0.26 mg/g and 2.09±0.26 mg/g, respectively). In group DPCI (insulin- and CCK-8-treated diabetic-pancreatic rats), the pancreatic protein content (250±35 mg/p) was significantly elevated vs groups DP and DPC (147±10 mg/p and 148±10 mg/p, respectively). In groups DPI and DPCI (insulin-treated rats), the pancreatic amylase content (3 948±1 288 U/p, 10 502±2 935 U/p, respectively) was significantly elevated vs groups DP and DPC (158±5 U/p and 182±25 U/p, respectively). In group DPCI, pancreatic amylase content (10 502±2 935 U/p) was significantly elevated vs group DPI (3 948±1 288 U/p). No significant differences were found in the pancreatic DNA and lipase contents between group D and any other groups. In group DPCI, the pancreatic trypsinogen content was significantly elevated vs group DPI (976±132 IU/p and 592±63 IU/p, respectively). However, no significant differences were observed in the pancreatic trypsinogen content between group DPC (655±36 IU/p) and DP (776±48 IU/p). Histological examination revealed signs of chronic inflammation in diabetic-pancreatic rats, where acute inflammatory cells had been replaced by interstitial tissues, mononuclear cells and fibroblasts. Histological examination did not show any differences between groups DPC and DP. In group DPCI, a more intense mitotic activity was observed vs group DPC due to the effect of insulin (Table 1).

DISCUSSION

The intraperitoneal administration of high doses of Arg induces selective pancreatic acinar cell damage without any morphological change to the islets of Langerhans^[5]. STZ has been reported to be specifically toxic to the β-cells of the islets of Langerhans and to induce a dose-dependent and irreversible diabetes in rats without any morphological change to the exocrine pancreas^[6]. These models seemed to be suitable for studying the correlation between diabetes mellitus and pancreatitis. The role of insulin in the process of spontaneous and CCK-8-promoted pancreatic regeneration following acute pancreatitis has not yet been characterised in detail. The interesting finding which showed that periinsular acini remained intact during Arg-induced-pancreatitis as well as a lack of the hypertrophic effect of CCK in diabetic rats prompted us to continue studies on the effects of insulin in the process of pancreatic remodelling. Our hypothesis stated that insulin was necessary for the regenerative effect of CCK-8, therefore, we evoked diabetes and pancreatitis in rats as described earlier^[2] and then, in the diabetic rats insulin was administered by s.c. injections. The elevation of serum insulin level and the diminution of serum glucose level, clearly showed the efficacy of the insulin treatment. CCK-8 could only elevate pw/bw, the pancreatic contents of protein, amylase and lipase in the presence of insulin. Moreover, CCK-8 could also increase the number of acinar cells with mitotic activity when insulin was administered, but CCK-8 alone had no effect on the laboratory parameters or the mitotic activity in diabetic-pancreatic rats. Lines of evidence demonstrate that both pancreatic secretory and growth processes are (at least partially) under the control of pancreatic islet hormones. Hypoinsulinemia was known to cause pancreatic atrophy and fat infiltration of the exocrine pancreas in guinea pigs^[7]. In contrast to this, endogenous and exogenous insulin evoked an increase in pancreatic enzyme synthesis and growth^[8]. These direct (via acinar insulin receptors) and indirect (influence on CCK receptors) effects of insulin are well understood. It was also demonstrated that insulin binding to its receptors on the pancreatic acini could be correlated with the subsequent stimulation of protein synthesis^[9]. Another indirect observation was that anti-insulin serum completely blocked the CCK-8-stimulated pancreatic secretion in rats^[10]. It further suggests that endogenous insulin is necessary for the stimulatory action of CCK-8 on pancreatic exocrine secretion and growth^[10]. The present study proves our hypothesis that insulin is indeed necessary for the hypertrophic effect of CCK-8 following acute necrotizing experimental pancreatitis.

REFERENCES

- Hegy P, Takacs T, Jarmay K, Nagy I, Czako L, Lonovics J. Spontaneous and cholecystokinin-octapeptide-promoted regeneration of the pancreas following L-arginine-induced pancreatitis in rat. *Int J Pancreatol* 1997; **22**: 193-200

- 2 **Takacs T**, Hegyi P, Jarmai K, Czako L, Gog C, Rakonczay Z, Nemeth J, Lonovics J. CCK fails to promote pancreatic regeneration in diabetic rats following the induction of experimental pancreatitis. *Pharm Res* 2001; **44**: 363-372
- 3 **Williams JA**, Goldfine ID. The insulin-acinar relationship. In: Go VLW et al. eds. *The Exocrine Pancreas: Biology, Pathobiology and Diseases*. New York: *Raven Press* 1993: 789-802
- 4 **Moessner J**, Logsdon CD, Williams JA, Goldfine ID. Insulin, via its own receptor, regulates growth and amylase synthesis in pancreatic acinar AR42J cells. *Diabetes* 1985; **34**: 891-897
- 5 **Tani S**, Itoh H, Okabayashi Y, Nakamura T, Fujii M, Fujisawa T, Koide M, Otsuki M. New model of acute necrotizing pancreatitis induced by excessive doses of arginine in rats. *Dig Dis Sci* 1990; **35**: 367-374
- 6 **Junod A**, Lambert AE, Orci L, Pictet R, Gonet AE, Renold AE. Studies on the diabetogenic action of streptozotocin. *Proc Soc Exp Biol Med* 1967; **126**: 201
- 7 **Balk MW**, Lang CM, White WJ, Munger BL. Exocrine pancreatic dysfunction in guinea pigs with diabetes mellitus. *Lab Invest* 1975; **32**: 28-32
- 8 **Saito A**, Williams JA, Kanno T. Potentiation of cholecystokinin-induced exocrine secretion by both exogenous and endogenous insulin in isolated and perfused rat pancreata. *J Clin Invest* 1980; **65**: 777-782
- 9 **Sankaran H**, Iwamoto Y, Korc M, Williams JA, Goldfine ID. Insulin action in pancreatic acini from streptozotocin-treated rats. II. Binding of ¹²⁵I-insulin to receptors. *Am J Physiol* 1981; **240**: G63-G68
- 10 **Lee KY**, Zhou LU, Ren XS, Chang TM, Chey WY. An important role of endogenous insulin on exocrine pancreatic secretion in rats. *Am J Physiol* 1990; **258**(2 Pt 1): G268-G274

Edited by Zhu LH **Proofread by** Xu FM

Effects of terlipressin on systolic pulmonary artery pressure of patients with liver cirrhosis: An echocardiographic assessment

Engin Altintas, Necdet Akkus, Ramazan Gen, M. Rami Helvacı, Orhan Sezgin, Dilek Oguz

Engin Altintas, Orhan Sezgin, Division of Gastroenterology, Mersin University, School of Medicine, Mersin, Turkey

Necdet Akkus, Cardiology Department, Mersin University, School of Medicine, Mersin, Turkey

Ramazan Gen, M. Rami Helvacı, Internal Medicine Department, Mersin University, School of Medicine, Mersin, Turkey

Dilek Oguz, Gastroenterology Department, Türkiye Yüksek İhtisas Hospital, Ankara, Turkey

Correspondence to: Dr. Engin Altintas, Mersin Üniversitesi Tıp Fakültesi Hastanesi İç Hastalıkları A.D., 33079 Mersin, Türkiye. enginaltintas@mersin.edu.tr

Telephone: +90-324337 43 00 **Fax:** +90-324336 7117

Received: 2004-03-03 **Accepted:** 2004-04-09

Abstract

AIM: Portopulmonary hypertension is a serious complication of chronic liver disease. Our aim was to search into the effect of terlipressin on systolic pulmonary artery pressure among cirrhotic patients.

METHODS: Twelve patients (6 males and 6 females) with liver cirrhosis were recruited in the study. Arterial blood gas samples were obtained in sitting position at rest. Contrast enhanced echocardiography and measurements of systolic pulmonary artery pressure were performed before and after the intravenous injection of 2 mg terlipressin.

RESULTS: Of 12 patients studied, the contrast enhanced echocardiography was positive in 5, and the positive findings in contrast enhanced echocardiography were reversed to normal in two after terlipressin injection. The mean systolic pulmonary artery pressure was 25.5 ± 3.6 mmHg before terlipressin injection, and was 22.5 ± 2.5 mmHg after terlipressin ($P=0.003$). The systolic pulmonary artery pressure was above 25 mmHg in seven of these 12 patients. After the terlipressin injection, systolic pulmonary artery pressure was <25 mmHg in four of these cases (58.3% vs 25%, $P=0.04$).

CONCLUSION: Terlipressin can decrease the systolic pulmonary artery pressure in patients with liver cirrhosis.

Altintas E, Akkus N, Gen R, Helvacı MR, Sezgin O, Oguz D. Effects of terlipressin on systolic pulmonary artery pressure of patients with liver cirrhosis: An echocardiographic assessment. *World J Gastroenterol* 2004; 10(15): 2278-2280
<http://www.wjgnet.com/1007-9327/10/2278.asp>

INTRODUCTION

The spectrum of pulmonary vascular disorders in liver disease and portal hypertension ranges from hepatopulmonary syndrome characterized by intrapulmonary vascular dilatations (IPVD) to pulmonary hypertension (portopulmonary hypertension), in which pulmonary vascular resistance is elevated^[1].

Hepatopulmonary syndrome (HPS) is incurable but resolves over time after liver transplantation^[2]. In patients with cirrhosis, 1% pulmonary hypertension is developed^[2,3]. Portopulmonary hypertension (PPH) is irreversible and there is no effective treatment^[4]. Mortality of liver transplantation in patients with PPH ranges from 50% to 100%^[4]. The common causes of HPS and PPH are portal hypertension and portosystemic shunting, indicating that vasoactive and angiogenic factors originating from the liver can control pulmonary circulation^[4].

So far, observational studies have examined several drugs^[5-8]. No clearly effective medical therapies for PPH have been found. In the present study, we investigated the effects of terlipressin that was used in the treatment of variceal hemorrhage on systolic pulmonary artery pressure (SPAP) among cirrhotic patients.

MATERIALS AND METHODS

Patients

Twelve cirrhotic patients without any malignancy, heart failure, renal failure (serum creatinin >20 mg/L), chronic obstructive lung disease, pneumonia, and anemia (hemoglobin level <100 mg/L) were studied. All patients had portal hypertension. The presence of hepatic dysfunction or portal hypertension was assessed by the following: (1) clinical history of complications related to liver disease and portal hypertension (ascites, hepatic encephalopathy, esophagogastric varices, variceal bleeding and spontaneous bacterial peritonitis); (2) liver function tests (aspartate and alanine aminotransferase, alkaline phosphatase, total bilirubin, prothrombin time, and albumin); and (3) abdominal ultrasound evidences of cirrhosis and portal hypertension (small, nodular liver, hepatofugal portal venous flow, portosystemic collateral circulation, splenomegaly, and ascites). The severity of hepatic dysfunction was stratified according to the Pugh-Child's criteria.

Methods

Chest X-ray and electrocardiogram were performed for all patients. Blood samples were obtained to calculate the score of Pugh-Child in the morning of study day. Arterial blood gas samples were obtained from a single radial artery puncture while the patient was breathing room air in sitting position at rest.

Transthoracic contrast-enhanced echocardiography (CEE) was performed to investigate the intrapulmonary vascular dilations. CEE was performed after the administration of 10 mL of hand-agitated normal saline solution in the supine position via an upper extremity peripheral vein. Positive results were qualitatively defined as any visual opacification of the left heart chamber more than three cardiac cycles after appearance of microbubbles in the right ventricle^[9]. These findings suggested intrapulmonary passage of microbubbles through either dilated precapillary and capillary vessels or direct arteriovenous communications. Echocardiographic assessments were carried out with Wingmed system five 1.7 MHz electronic probe by an experienced cardiologist. Left lateral position was used during measurements. Left atrium, left ventricular diastolic and systolic dimensions were calculated with standard M-mode echocardiographic pictures in parasternal long axis view. Wall motions and wall thickness were also evaluated. Fractional

shortening was studied at level of chordae tendinae (left ventricular end diastolic dimension-left ventricular end systolic dimension/left ventricular end diastolic dimension $\times 100$). Each parameter represented the mean value of three successive measurements. Maximum flow rates with continuous wave Doppler (CW) at level of tricuspid valves were used to calculate SPAP (modified Bernoulli equation: $\Delta p=4V^2$). SPAPs were computed by adding estimated right atrial pressure (5 mmHg) to pressure gradient calculated by modified Bernoulli equation.

CEE and measurements of SPAP were performed before and after the intravenous injection of 2 mg terlipressin (Glypressin® 1 mg flacon, ERKIM Ilac AS, Istanbul, Turkey).

All statistical calculations were done using the SPSS 11.0 software. The measurements were given as the mean values. The paired sample test, Cochran's Q test, and Friedman's test were used to determine the difference of SPAP, the frequency of CEE, and the frequency of patients whose SPAP ≥ 25 mmHg respectively before and after terlipressin injection. $P < 0.05$ was accepted as statistically significant.

RESULTS

The clinical and demographical characteristics of patients are shown in Table 1. A total of 12 patients, six males and six females were studied, with a mean age of 52 years. The mean score of Pugh-Child was 5.08, and the mean value of arterial pO_2 was 77.83 mmHg. Ascites was detected in two patients. Two patients suffered from dyspnea. In two patients, chest X ray films showed bilaterally reticulonodular densities at the basal areas.

Before the injection of terlipressin intravenously, a positive CEE was detected in 5 patients, and two of them were disappeared after the drug was injected. Three of the patients who had evident hypoxemia suffered dyspnea, and CEE was positive in these patients. After terlipressin injection, CEE was negative in two of the three patients. Arterial pO_2 was high in the rest two patients with CEE (+), after terlipressin injection CEE positivity was continued. There was not any difference before and after the drug injection according to the frequency of the positivity of CEE (5/12 vs 3/12, $P=0.15$ according to Cochran's Q test). This meaningless result might be due to the small number of patients. The SPAP value was ≥ 25 mmHg in four of five patients with positive CEE. Two patients with a negative CEE after the drug injection had the lowest SPAP value in this group, 24 mmHg and 27 mmHg respectively.

Although the value of SPAP was 25.5 ± 3.6 mmHg before the drug injection, it was decreased to 22.5 ± 2.5 mmHg after

terlipressin injection ($P=0.003$). The value of SPAP was above the level of 25 mmHg as the limit of pulmonary hypertension in seven patients. After the injection of terlipressin, it continued to be higher above this level in three patients [7/12 (58.3%) patients versus 3/12 (25%) patients]. This difference was statistically significant ($P=0.04$). CEE was positive in one of the three patients whose SPAP was >25 mmHg after terlipressin injection. The positivity of CEE disappeared after terlipressin injection in one patient who had a SPAP value lower than 25 mmHg.

DISCUSSION

The association of pulmonary hypertension with portal hypertension, also known as portopulmonary hypertension (PPH), is a complication of chronic liver disease that has been associated with high morbidity and mortality at the time of liver transplantation^[2-4]. PPH has been defined as mean pulmonary artery pressure >25 mmHg in the presence of a normal pulmonary capillary wedge pressure and portal hypertension^[2-4].

The presence of intrapulmonary vascular dilatations can be confirmed using one of the three imaging modalities: contrast-enhanced echocardiography, perfusion lung scan - technetium 99 m-labeled macroaggregated albumin scanning, and pulmonary arteriography^[9,10]. A Doppler echocardiogram is a highly sensitive and noninvasive diagnostic modality for both measuring PAP and determining IPVD. Therefore, it should be considered as the first screening method of choice^[11].

Heretofore, therapy for chronic management of PPH is lacking. Recently, continuous intravenous infusion of epoprostenol has been demonstrated to improve symptomatology and survival in the general population of patients with PPH^[5]. Anecdotal reports suggested that long-term epoprostenol therapy given by continuous infusion might be effective for patients with portopulmonary hypertension, but the efficacy of epoprostenol has not been rigorously studied in this subgroup of patients^[5-7]. Kuo *et al.*^[5] reported the use of epoprostenol in the more specific instance of PPH. Over a period of 6-14 mo, epoprostenol (10-28 ng/kg.min) therapy was associated with a 29-46% decrease in mean pulmonary artery pressure, a 22-71% decrease in pulmonary vascular resistance, and a 25-75% increase in cardiac output in a group of four patients^[5]. These results suggest that effective chronic therapy for PPH is available. In combination with inhaled nitric oxide as acute intraoperative therapy, epoprostenol infusion represented an additional therapeutic option for treatment of PPH in the liver transplant candidate^[5].

Table 1 Characteristics of patients. PBS: primary biliary cirrhosis, HBV: hepatitis B virus, HCV: hepatitis C virus, N: Normal, BB-Nod: bilateral basillary nodularity, (-): absent, (+): present, PAP: pulmonary artery pressure and, CEE: contrast enhanced echocardiography

Sex	Age (yr)	Etiology	Pugh-Child Score	pO_2 (mmHg)	Ascites	Dyspnea	Chest X-ray	PAP-0 (mmHg)	PAP-1 (mmHg)	CEE-0	CEE-1
F	60	PBS	5	89	(-)	(-)	N	28	26	(+)	(+)
F	55	HBV	4	85	(-)	(-)	N	24	24	(-)	(-)
M	54	Alcohol	4	65	(-)	(+)	BB-Nod	27	21	(+)	(-)
F	48	Cryptogenic	5	60	(-)	(+)	N	24	20	(+)	(-)
M	58	HCV	4	63	(-)	(+)	N	28	24	(+)	(+)
M	56	HBV	4	73	(-)	(-)	N	25	25	(-)	(-)
M	52	HBV	5	88	(-)	(-)	N	30	22	(+)	(+)
F	50	HBV	10	90	(+)	(+)	BB-Nod	31	26	(-)	(-)
M	48	HCV	5	85	(-)	(-)	N	21	22	(-)	(-)
M	60	HBV	7	80	(+)	(-)	N	20	19	(-)	(-)
F	55	HCV	4	71	(-)	(-)	N	27	22	(-)	(-)
F	39	HBV	4	85	(-)	(-)	N	21	19	(-)	(-)

There are no long-term studies or guidelines on the use of pharmacotherapy in PPH. In view of the rarity of this disease, much of the traditional treatment of this disease has been empirical. Inhaled NO could decrease the pulmonary artery pressures in some patients with PPH and might have some promise for long-term treatment of this disease^[12]. Other medications have been reported to cause amelioration of pulmonary hypertension in patients with portal hypertension including beta-blockers, nitrates, calcium-channel blockers, prostacyclin and prostacyclin analogs, phosphodiesterase inhibitors (sildenafil), L-arginine, and, endothelin antagonists^[3]. In view of the decreased incidence of variceal bleeding in patients taking beta-blockers and nitrates, we encourage the use of these medications in patients with PPH. Beta-blocking agents, which are used in the treatment for portal hypertension may have deleterious effects on the setting of pulmonary hypertension because they decrease cardiac output and increase pulmonary vascular resistance. Vasodilators are usually ineffective and poorly tolerated because these patients usually have a decreased systemic vascular resistance. Most patients with porto-pulmonary hypertension do not receive anticoagulants because the risk of bleeding is deemed to be elevated, especially when esophageal varices are present.

In patients with hepatopulmonary syndrome, supplemental oxygen and liver transplantation were the usual treatments of choice^[2]. Pharmacologic approaches were limited in improving hypoxemia^[2]. Outcome following liver transplantation was variable, increased cardiopulmonary mortality occurred in patients with moderate to severe pulmonary hypertension. Although a few reports have demonstrated improvement of pulmonary hypertension after liver transplantation, this procedure was a very risky one in patients with markedly increased pulmonary artery pressures^[13]. Report about combined liver-lung transplantation might open a perspective for selected patients with porto-pulmonary hypertension^[14].

Terlipressin is a long-acting vasopressin analogue that has been proved useful in the treatment of variceal hemorrhage. Terlipressin could reduce portal pressure in cirrhotic patients mainly through intense splanchnic vasoconstriction that decreases portal venous inflow^[15]. Hepatic blood flow might also be reduced by terlipressin^[15]. The systemic haemodynamic response to terlipressin was moreover associated with the decrease in portal pressure^[16]. After administration of terlipressin, the azygos blood flow decreased significantly^[17]. In patients with cirrhosis, a single injection of 2 mg terlipressin significantly and markedly reduced portal pressure and azygos blood flow for up to 4 h^[17]. The azygos blood flow (superior porto-systemic collateral circulation) correlated strongly with portal venous flow in patients with portal hypertension^[17]. It could be expected that terlipressin could reverse the vasodilatation of dilated intrapulmonary arteries with HPS and PPH. It can also decrease SPAP by reducing the increased blood flow that may facilitate pulmonary arterial hypertension. In our study, it reduced SPAP from 25.5±3.6 mmHg to 22.5±2.5 mmHg and, this result was statistically meaningful. CEE that showed intrapulmonary vascular dilatation was positive in 5 patients, and it was reversed to normal in 2 patients after terlipressin injection. However, more studies are needed to decide whether this result is meaningful or not.

Chronic terlipressin therapy in combination with a multidisciplinary, well-planned evaluation and treatment plan, may be the answer to a heretofore untreatable disease. This one is a prestudy, because more and detailed studies are

required to show its efficiency. In the context of persisting uncertainty about the cause and treatment of PPH, future studies must focus on the pathophysiology of PPH, predicting reversibility after liver transplantation, and identifying other treatment options.

REFERENCES

- 1 **Hervé P**, Lebrec D, Brenot F, Simonneau G, Humbert M, Sitbon O, Duroux P. Pulmonary vascular disorders in portal hypertension. *Eur Respir J* 1998; **11**: 1153-1166
- 2 **Krowka MJ**. Hepatopulmonary syndrome and portopulmonary Hypertension. *Curr Treat Options Cardiovasc Med* 2002; **4**: 267-273
- 3 **Budhiraja R**, Hassoun PM. Portopulmonary hypertension; A tale of two circulations. *Chest* 2003; **123**: 562-576
- 4 **Naeye R**. Hepatopulmonary syndrome and portopulmonary hypertension. *Swiss Med Wkly* 2003 Mar 22; **133**: 163-169
- 5 **Kuo PC**, Johnson LB, Plotkin JS, Howell CD, Bartlett ST, Rubin LJ. Continuous intravenous infusion of epoprostenol for the treatment of portopulmonary hypertension. *Transplantation* 1997; **63**: 604-606
- 6 **Rafanan AL**, Maurer J, Mehta AC, Schilz R. Progressive portopulmonary hypertension after liver transplantation treated with epoprostenol. *Chest* 2000; **118**: 1497-1500
- 7 **Schroeder RA**, Rafii AA, Plotkin JS, Johnson LB, Rustgi VK, Kuo PC. Use of aerosolized inhaled epoprostenol in the treatment of portopulmonary hypertension. *Transplantation* 2000; **70**: 548-550
- 8 **Krowka MJ**, Plevak DJ, Findlay JY, Rosen CB, Wiesner RH, Krom RA. Pulmonary hemodynamics and perioperative cardiopulmonary-related mortality in patients with portopulmonary hypertension undergoing liver transplantation. *Liver Transpl* 2000; **6**: 443-450
- 9 **Krowka MJ**, Tajik AJ, Dickson ER, Wiesner RH, Cortese DA. Intrapulmonary vascular dilatations in liver transplant candidates: screening by two-dimensional contrast enhanced echocardiography. *Chest* 1990; **97**: 1165-1170
- 10 **Lange PA**, Stoller JK. The hepatopulmonary syndrome. *Ann Intern Med* 1995; **22**: 521-529
- 11 **Torregrosa M**, Genesca J, Gonzalez A, Evangelista A, Mora A, Margarit C, Esteban R, Guardia J. Role of Doppler echocardiography in the assessment of portopulmonary hypertension in liver transplantation candidates. *Transplantation* 2001; **71**: 572-574
- 12 **Findlay JY**, Harrison BA, Plevak DJ, Krowka MJ. Inhaled nitric oxide reduces pulmonary artery pressures in portopulmonary hypertension. *Liver Transpl Surg* 1999; **5**: 381-387
- 13 **Krowka MJ**, Plevak DJ, Findlay JY, Rosen CB, Wiesner RH, Krom RA. Pulmonary hemodynamics and perioperative cardiopulmonary-related mortality in patients with portopulmonary hypertension undergoing liver transplantation. *Liver Transpl* 2000; **6**: 443-450
- 14 **Pirene J**, Verleden G, Nevens F, Delcroix M, Van Raemdonck D, Meyns B, Herijgers P, Daenen W, De Leyn P, Aerts R, Coosemans W, Decaluwe H, Koek G, Vanhaecke J, Schetz M, Verhaegen M, Cicalese L, Benedetti E. Combined liver and (heart-) lung transplantation in liver transplant candidates with refractory portopulmonary hypertension. *Transplantation* 2002; **73**: 140-142
- 15 **Oberti F**, Veal N, Kaassis M, Pilette C, Rifflet H, Trouve R, Cales P. Hemodynamic effects of terlipressin and octreotide administration alone or in combination in portal hypertensive rats. *J Hepatol* 1998; **29**: 103-111
- 16 **Moller S**, Hansen EF, Becker U, Brinch K, Henriksen JH, Bendtsen F. Central and systemic haemodynamic effects of terlipressin in portal hypertensive patients. *Liver* 2000; **20**: 51-59
- 17 **Escorsell A**, Bandi JC, Moitinho E, Feu F, Garcia-Pagan JC, Bosch J, Rodes J. Time profile of the haemodynamic effects of terlipressin in portal hypertension. *J Hepatol* 1997; **26**: 621-627

Empirical antibiotic treatment with piperacillin-tazobactam in patients with microbiologically-documented biliary tract infections

Gabrio Bassotti, Fabio Chistolini, Francis Sietchiping-Nzepa, Giuseppe de Roberto, Antonio Morelli

Gabrio Bassotti, Fabio Chistolini, Francis Sietchiping-Nzepa, Giuseppe de Roberto, Antonio Morelli, Gastrointestinal and Hepatology Section, Department of Clinical and Experimental Medicine, University of Perugia, Italy

Correspondence to: Dr. Gabrio Bassotti, Strada del Cimitero, 2/a, San Marco 06131 Perugia, Italy. gabassot@tin.it

Fax: +39-75-5847570

Received: 2003-11-26 **Accepted:** 2004-01-17

Abstract

AIM: To report our experience with empiric antimicrobial monotherapy (piperacillin/tazobactam, of which no data are available in such specific circumstances) in microbiologically-documented infections in patients with benign and malignant conditions of the biliary tract.

METHODS: Twenty-three patients, 10 with benign and 13 with malignant conditions affecting the biliary tree and microbiologically-documented infections were recruited and the efficacy of empirical antibiotic therapy was assessed.

RESULTS: The two groups featured similar demographic and clinical data. Overall, the infective episodes were most due to Gram negative agents, more than 60% of such episodes (mostly in malignant conditions) were preceded by invasive instrumental maneuvers. Empirical antibiotic therapy with a single agent (piperacillin/tazobactam) was effective in more than 80% of cases. No deaths were reported following infections.

CONCLUSION: An empiric therapeutic approach with piperacillin/tazobactam is highly effective in biliary tract infections due to benign or malignant conditions.

Bassotti G, Chistolini F, Sietchiping-Nzepa F, de Roberto G, Morelli A. Empirical antibiotic treatment with piperacillin-tazobactam in patients with microbiologically-documented biliary tract infections. *World J Gastroenterol* 2004; 10(15): 2281-2283
<http://www.wjgnet.com/1007-9327/10/2281.asp>

INTRODUCTION

The common causes of intra-abdominal infections are those related to the biliary tract^[1]. However, to obtain a microbiological diagnosis in biliary tract infections (BTI) is not easy, due to the difficulty of sampling bile and the low incidence of positive blood cultures. Therefore, antimicrobial therapy is often empirical^[2], and the choice of an appropriate regimen depends on the knowledge of the most common causative bacteria and the reported efficacy of antimicrobial drugs in BTI. Moreover, the paucity of randomized clinical trials for BTI treatment probably justifies the fact that there is no standardized approach to these infections^[2].

The present study was to report our experience with empirical single antibiotic treatment with piperacillin-tazobactam of BTI in patients with benign and malignant diseases of the biliary tract, since there are no specific data on this compound in the treatment of such infections.

MATERIALS AND METHODS

Twenty-three consecutive patients (15 men, 8 women, age range 22-88 years) with microbiologically documented BTI entered the study. Underlying disease and causative organisms were assessed. Empirical treatment (4.5 g t.i.d) was started immediately after obtaining samples (blood and/or bile) for microbiological cultures, and concordance with antibiogram and its efficacy were also evaluated. The treatment was judged effective when fever and clinical symptoms of infection resolved within 72 h, whereas the persistence of fever beyond 72 h from the start of treatment, the deterioration of clinical conditions or the death as a result of the primary infection was considered as failure.

RESULTS

Overall, records were obtained from 10 patients with benign and 13 patients with malignant conditions affecting the biliary tree. Table 1 shows the clinical characteristics of the two groups. In more than 60% of patients, BTI were preceded by an invasive procedure on the biliary tree, and this was less frequent in benign than in malignant conditions (50% vs 77%).

Table 1 Demographic and clinical variables of 23 patients with BTI

	Benign conditions	Malignant conditions
No (%)	10/23(43.5)	13/23(56.5)
Average duration of treatment (d)	7±1	10±1
Underlying condition (No.)	Cholelithiasis (7) Acute cholecystitis (2) Iatrogenic stenosis (1)	Cholangiocarcinoma (6) Pancreatic carcinoma (4) Gallbladder carcinoma (2) Infiltrating hepatoma (1)
Previous instrumental invasive maneuvers (No.)	None (5) PTD (3) ERCP (2)	None (3) PTD (10)

Abbreviations: BTI=biliary tract infections; ERCP=endoscopic retrograde cholangio-pancreatography; PTD=percutaneous transhepatic drainage.

Table 2 Microbiological variables in 23 patients with BTI

	Benign conditions (10 patients)	Malignant conditions (13 patients)
Insulation medium (No.)	Blood (7) Bile (3)	Blood (6) Bile (7)
Polymicrobial infections	1 (4%)	7 (30%)
Isolated pathogens (No. cases)	<i>E.coli</i> (4) Enterococcus spp (3) Pseudomonas spp (3) Enterobacter spp (2) Streptococcus spp (2) Klebsiella spp (1) Candida spp (1)	Enterococcus spp (6) Staphylococcus spp (6) Candida spp (5) <i>E.coli</i> (2) Pseudomonas spp (2) Proteus spp (1) Enterobacter spp (1) Salmonella spp (1)

Table 2 shows the microbiological characteristics of the pathogens isolated in both groups. As expected, most infections were caused by Gram negative agents, and 30% of them (almost exclusively found in malignant conditions) were polymicrobial. *Candida spp* were always isolated from bile in polymicrobial infections. In 19(82.6%) patients there was no need of modifying the empiric therapeutic schedule, whereas in the remaining 4 the antibiotic regimen was modified according to the antibiogram showing resistance or insensitivity to piperacillin/tazobactam. In all patients with BTI due to benign conditions, decrease of fever and improvement of clinical conditions were observed within 3-18 h. A slower trend was observed in patients with BTI due to malignant conditions (improvement within 8-24 h), probably due to more polymicrobial infections and resistances to the empiric regimen. After the results from the antibiogram were obtained, these latter patients treated with more targeted antibiotic regimens, had the disappearance of fever and improvement of the clinical conditions. No deaths were reported attributable to BTI.

DISCUSSION

In this study, we reported our experience with an empiric antibiotic regimen in BTI, and showed that a monotherapy with piperacillin/tazobactam (that, to the best of our knowledge has still not been assessed in such circumstances) might be effective in more than 80% of cases. The organisms more commonly cultured in our patients, in both benign and malignant conditions, were Gram negative bacteria, the pathogens were more frequently associated with obstructive conditions of the biliary tree^[3,4]. Several infective episodes followed invasive instrumental procedures, especially percutaneous drainage (that also gave a discrete yield for bile culture, as previously shown for this procedure^[5]), and were mostly represented by polymicrobial infections.

A preferred therapeutic schedule for BTI, until recently, was usually a combination of a penicillin (usually ampicillin) and an aminoglycoside^[6-9]. This combination had limited anaerobic coverage, frequent resistance (to ampicillin) of Gram negative bacteria, and the risks of renal damage (aminoglycoside, significantly increased in patients with cholestasis)^[10]. However, other antibiotics (such as the ureidopenicillins) exhibited a broad spectrum of activity, that included many anaerobes, *enterococci* and *P.aeruginosa*, in addition to Gram negative bacilli^[11], so that they may result in appealing for use as single agents. Actually, it has been shown that monotherapy with a ureidopenicillin (mezlocillin, piperacillin) is equally or more effective than the traditional approach with ampicillin/aminoglycoside for treatment of BTI^[12-14], although in patients undergoing nonsurgical invasive procedure of the biliary tree and/or with suspected increased risk of *P.aeruginosa* the association of ureidopenicillin/aminoglycoside has been still

justifiable^[15,16]. On the other hand, the combination of piperacillin with the beta-lactamase inhibitor tazobactam (that displays a substantial elimination in bile^[17,18]) might be a reasonable alternative when the local resistance pattern featured a high incidence of ureidopenicillin-resistant *E.coli* or *Klebsiella spp*^[2,19], as also shown by its effectiveness as single empiric agent in high-risk, febrile neutropenic patients with cancer^[20].

Experience with quinolones for treatment of BTI was still limited^[2,21]. However, there is good evidence that monotherapy with these compounds might be as effective as combination therapy for treatment of BTI^[22-24].

To date, the combination of piperacillin/tazobactam has been demonstrated clinically- and cost-effective in both uncomplicated and complicated intraabdominal infections^[25-27], although no specific data on BTI are available. Therefore, we feel that our experience might be a useful adjunct to the therapeutic armamentarium.

In conclusion, empiric antibiotic treatment with piperacillin/tazobactam is frequently effective in BTI due to benign and malignant conditions. Of course, in such circumstances an early operative drainage of the biliary tree is always mandatory, regardless of the presence or absence of suppuration in the common bile duct^[28], to prevent relapses and septic complications.

REFERENCES

- 1 **Lea AS**, Feliciano DV, Gentry DO. Intra-abdominal infections -an update. *J Antimicrob Chemother* 1982; **9**(Suppl A): 107-113
- 2 **Westphal JF**, Brogard JM. Biliary tract infections. A guide to drug treatment. *Drugs* 1999; **57**: 81-91
- 3 **Leung JW**, Ling TK, Chan RC, Cheung SW, Lai CW, Sung JJ, Chung SC, Cheng AF. Antibiotics, biliary sepsis, and bile duct stones. *Gastrointest Endosc* 1994; **40**: 716-721
- 4 **Carpenter HA**. Bacterial and parasitic cholangitis. *Mayo Clin Proc* 1998; **73**: 473-478
- 5 **Brody LA**, Brown KT, Getrajdman GI, Kannegieter LS, Brown AE, Fong Y, Blumgart LH. Clinical factors associated with positive bile cultures during primary percutaneous biliary drainage. *J Vasc Interv Radiol* 1998; **9**: 572-578
- 6 **Boey JH**, Way LW. Acute cholangitis. *Ann Surg* 1980; **191**: 264-270
- 7 **Thompson JE**, Tomkins RK, Longmire WP. Factors in management of acute cholangitis. *Ann Surg* 1982; **195**: 137-145
- 8 **Munro R**, Sorrell TC. Biliary sepsis: reviewing treatment options. *Drugs* 1986; **31**: 449-454
- 9 **Chang WT**, Lee KT, Wang SR, Chuang SC, Kuo KK, Chen JS, Sheen PC. Bacteriology and antimicrobial susceptibility in biliary tract disease: an audit of 10-year's experience. *Kaohsiung J Med Sci* 2002; **18**: 221-228
- 10 Desai TK, Tsang TK. Aminoglycoside nephrotoxicity in obstructive jaundice. *Am J Med* 1988; **85**: 47-50
- 11 **Eliopoulos GM**, Moellering RC. Azlocillin, mezlocillin and piperacillin: new broad spectrum penicillins. *Ann Intern Med* 1982; **97**: 755-760

- 12 **Muller EL**, Pitt HA, Thompson JE, Doty JE, Mann LL, Manchester B. Antibiotics in infections of the biliary tract. *Surg Gynecol Obstet* 1987; **165**: 285-292
- 13 **Gerecht WB**, Henry NK, Hoffman WW, Muller SM, LaRusso NF, Rosenblatt JE, Wilson WR. Prospective randomized comparison of mezlocillin therapy alone with combined ampicillin and gentamicin therapy for patients with cholangitis. *Arch Intern Med* 1989; **149**: 1279-1284
- 14 **Thompson JE**, Pitt HA, Doty JE, Coleman J, Irving C. Broad spectrum penicillins as an adequate therapy for acute cholangitis. *Surg Gynecol Obstet* 1990; **171**: 275-282
- 15 **Levine JG**, Botet J, Kurtz RC. Microbiological analysis of sepsis complicating non-surgical biliary drainage in malignant obstruction. *Gastrointest Endosc* 1990; **36**: 364-368
- 16 **Demediuk B**, Speer AG, Hellyar A. Induced antibiotic resistant bacteria in cholangitis with biliary sepsis. *Aust N Z J Surg* 1996; **66**: 778-780
- 17 **Sörgel F**, Kinzig M. Pharmacokinetic characteristics of piperacillin/tazobactam. *Intensive Care Med* 1994; **20**: S14-S20
- 18 **Westphal JF**, Brogard JM, Caro-Sampara F, Adloff M, Blickle JF, Monteil H, Jehl F. Assessment of the biliary excretion of piperacillin-tazobactam in humans. *Antimicrob Agents Chemother* 1997; **41**: 1636-1640
- 19 **Chamberland S**, L'Ecuyer J, Lessard C, Bernier M, Provencher P, Bergeron MG. Antibiotic susceptibility profiles of 941 gram-negative bacteria isolated from septicemic patients throughout Canada. *Clin Infect Dis* 1992; **15**: 615-628
- 20 **Del Favero A**, Menichetti F, Martino P, Bucaneve G, Micozzi A, Gentile G, Furno P, Russo D, D'Antonio P, Ricci P, Martino B, Mandelli F. A multicenter, double-blind, placebo-controlled trial comparing piperacillin-tazobactam with and without amikacin as empiric therapy for febrile neutropenia. *Clin Infect Dis* 2001; **33**: 1295-1301
- 21 **Westphal JF**, Blicklé JF, Brogard JM. Management of biliary tract infections: potential role of quinolones. *J Antimicrob Chemother* 1991; **28**: 486-490
- 22 **Sung JJ**, Lyon DJ, Suen R, Chung SC, Co AL, Cheng AF, Leung JW, Li AK. Intravenous ciprofloxacin as treatment for patients with acute suppurative cholangitis: a randomized, controlled clinical trial. *J Antimicrob Chemother* 1995; **35**: 855-864
- 23 **Karachalios GN**, Nasiopoulou DD, Bourlinou PK, Reppa A. Treatment of acute biliary tract infections with ofloxacin: a randomized, controlled clinical trial. *Int J Clin Pharmacol Ther* 1996; **34**: 555-557
- 24 **Rekhnimitr R**, Fogel EL, Kalayci C, Esber E, Lehman GA, Sherman S. Microbiology of bile in patients with cholangitis or cholestasis with and without plastic biliary endoprosthesis. *Gastrointest Endosc* 2002; **56**: 885-889
- 25 **Cohn SM**, Lipsett PA, Buchman TG, Cheadle WG, Milsom JW, O'Marro S, Yellin AE, Jungerwirth S, Rochefort EV, Haverstock DC, Kowalsky SF. Comparison of intravenous/oral ciprofloxacin plus metronidazole versus piperacillin/tazobactam in the treatment of complicated intraabdominal infections. *Ann Surg* 2000; **232**: 254-262
- 26 **Dietrich ES**, Schubert B, Ebner W, Daschner F. Cost efficacy of tazobactam/piperacillin versus imipenem/cilastatin in the treatment of intra-abdominal infection. *Pharmacoeconomics* 2001; **19**: 79-94
- 27 **Holzheimer RG**, Dralle H. Antibiotic therapy in intra-abdominal infections - a review on randomised clinical trials. *Eur J Med Res* 2001; **30**: 277-291
- 28 **Connor MJ**, Schwartz ML, McQuarrie DG, Sumer HW. Acute bacterial cholangitis: an analysis of clinical manifestations. *Arch Surg* 1982; **117**: 437-444

Edited by Wang XL Proofread by Xu FM

Determination of glycosylated hemoglobin in patients with advanced liver disease

Theresa Lahousen, Karin Hegenbarth, Rottraut Ille, Rainer W. Lipp, Robert Krause, Randie R. Little, Wolfgang J. Schnedl

Karin Hegenbarth, Rainer W. Lipp, Robert Krause, Wolfgang J. Schnedl, Department of Internal Medicine, School of Medicine, Medical University Graz, Auenbruggerplatz 15, A-8063 Graz, Austria
Theresa Lahousen, Rottraut Ille, Department of Psychiatry, School of Medicine, Medical University Graz, Auenbruggerplatz 31, A-8063 Graz, Austria

Randie R. Little, University of Missouri School of Medicine, Department of Pathology and Child Health, One Hospital Drive, Columbia, MO 65212, USA

Correspondence to: Dr. Wolfgang J. Schnedl, Department of Internal Medicine, Medical University Graz, Auenbruggerplatz 15, A-8036 Graz, Austria. wolfgang.schnedl@meduni-graz.at

Telephone: +43-316-385-81801 **Fax:** +43-316-385-3062

Received: 2004-02-23 **Accepted:** 2004-04-09

Abstract

AIM: To evaluate the glycosylated hemoglobin (HbA_{1c}) determination methods and to determine fructosamine in patients with chronic hepatitis, compensated cirrhosis and in patients with chronic hepatitis treated with ribavirin.

METHODS: HbA_{1c} values were determined in 15 patients with compensated liver cirrhosis and in 20 patients with chronic hepatitis using the ion-exchange high performance liquid chromatography and the immunoassay methods. Fructosamine was determined using nitroblue tetrazolium.

RESULTS: Forty percent of patients with liver cirrhosis had HbA_{1c} results below the non-diabetic reference range by at least one HbA_{1c} method, while fructosamine results were either within the reference range or elevated. Twenty percent of patients with chronic hepatitis (hepatic fibrosis) had HbA_{1c} results below the non-diabetic reference range by at least one HbA_{1c} method. In patients with chronic hepatitis treated with ribavirin, 50% of HbA_{1c} results were below the non-diabetic reference using at least one of the HbA_{1c} methods.

CONCLUSION: Only evaluated in context with all liver function parameters as well as a red blood count including reticulocytes, HbA_{1c} results should be used in patients with advanced liver disease. HbA_{1c} and fructosamine measurements should be used with caution when evaluating long-term glucose control in patients with hepatic cirrhosis or in patients with chronic hepatitis and ribavirin treatment.

Lahousen T, Hegenbarth K, Ille R, Lipp RW, Krause R, Little RR, Schnedl WJ. Determination of glycosylated hemoglobin in patients with advanced liver disease. *World J Gastroenterol* 2004; 10(15): 2284-2286

<http://www.wjgnet.com/1007-9327/10/2284.asp>

INTRODUCTION

Measurement of glycosylated hemoglobin (HbA_{1c}) is used for routine evaluation and management of patients with diabetes mellitus. Concentrations of HbA_{1c} provide a means of assessing

long-term glycemic status and correlate well with development of complications related to diabetes mellitus^[1,2]. The liver plays a major role in regulating glucose metabolism because it is the main source of endogenous glucose and a major site involved in insulin metabolism. Because liver disease is associated with an increased prevalence of impaired glucose tolerance and diabetes mellitus, there is a need for tools to measure its long-term glycemic control^[3]. Previous studies indicated that both HbA_{1c} and fructosamine measurement should not be used in patients with liver cirrhosis, although the reason for this was unclear^[4-6]. Shortened erythrocyte life span as in hemolytic anemia is known to cause clinically and analytically low HbA_{1c} values independent of glycemia^[7], but measurement of fructosamine, which has been used to document glycemic status over a period of 2-4 wk, should not be affected by erythrocyte life span. This study described the determination of HbA_{1c} and fructosamine as well as parameters of liver disease and anemia in patients with advanced liver disease.

MATERIALS AND METHODS

Blood samples were collected, with and without EDTA, from 15 consecutive patients with compensated liver cirrhosis and 20 patients with chronic hepatitis and fibrosis of the liver. Diagnostic liver biopsies were performed routinely in all patients during the course of treatment in the Division of Gastroenterology and Hepatology, Department of Internal Medicine, Medical University in Graz. Liver cirrhosis was histologically defined as a diffuse process characterized by fibrosis and the conversion of normal liver architecture into structurally abnormal nodules^[8,9]. Of 15 patients with compensated liver cirrhosis Child-Pugh class A (total bilirubin <2 mg/dL, serum albumin >3.5 g/dL, prothrombin time 1-4 s prolonged, no hepatic encephalopathy and no ascites), 6 were tested positive for hepatitis C, 8 had alcoholic liver disease and 1 had primary biliary cirrhosis. Of the 20 patients with chronic hepatitis and fibrosis, 19 were tested positive for hepatitis C and 1 suffered from alcoholic liver disease. Ten of these patients with chronic hepatitis C were treated with interferon- α plus the antiviral drug ribavirin that can cause reversible hemolytic anemia^[10]. None of the patients included in the study had a history of impaired glucose tolerance or diabetes mellitus.

HbA_{1c} was measured within 3 d of collection using the Hi-Auto A_{1c} HA-8140 HPLC (Menarini Diagnostics, Florence, Italy), the DCA 2000 immunoassay method (Bayer, Vienna, Austria) and the Roche Cobas Integra immunoassay method (Roche, Vienna, Austria). Each of these HbA_{1c} methods was certified by the National Glycohemoglobin Standardization Program (NGSP)^[11]. Routine hematological data were determined with a Coulter counter (Beckman, Vienna, Austria). Blood glucose was determined with a hexokinase/glucose-6-phosphate dehydrogenase colorimetric method (Gluco-Quant; Roche, Vienna, Austria) and used as mean of 4-6 measurements on separate days during the preceding 1 mo. The relationship of blood glucose and HbA_{1c} was calculated according to MBG (mmol/L)=(1.98·HbA_{1c})-4.29^[12]. Fructosamine was determined with a colorimetric test that uses nitroblue tetrazolium in alkaline solution (Unimate FRA; Roche, Vienna, Austria). Reference

ranges were provided by each manufacturer and in most cases represented the mean \pm 2SD of a population without known diabetes. All determinations were analyzed blindly and the procedures were in accordance with the declaration of Helsinki and the local ethics committee recommendations.

RESULTS

Forty percent (6/15) of the patients with liver cirrhosis had HbA_{1c} levels below the non-diabetic reference range with at least one HbA_{1c} method, while fructosamine concentrations were either within the reference range ($n=10$) or elevated ($n=5$) (Figure 1). Twenty percent (2/10) of the patients with chronic hepatitis had HbA_{1c} levels below the non-diabetic reference range with at least one HbA_{1c} method. Fructosamine concentrations of all the 10 patients with chronic hepatitis were below the non-diabetic reference range. In patients with chronic hepatitis treated with ribavirin, 50% (5/10) of HbA_{1c} levels were below the non-diabetic reference range detected by at least one of the HbA_{1c} methods (Figure 1). One patient in this group demonstrated a fructosamine concentration within the diabetic range.

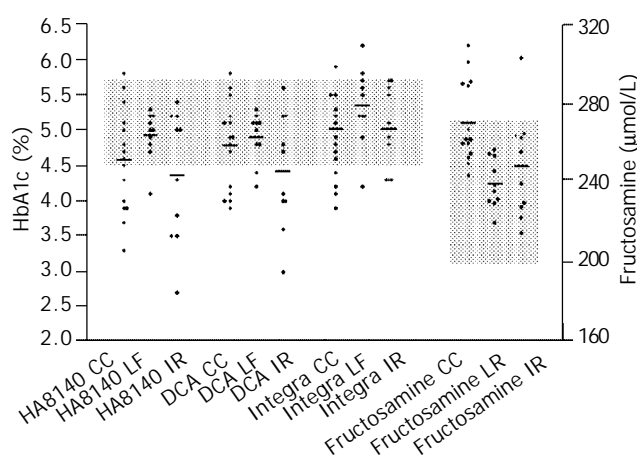


Figure 1 HbA_{1c} level and fructosamine concentration in patients with liver disease. CC: Compensated cirrhosis; LF: Chronic hepatitis (liver fibrosis); IR: Chronic hepatitis with interferon and ribavirin treatment. Shaded areas represent the mean \pm 2SD reference range for each test (HbA_{1c}: 4.5-5.7%; fructosamine: 200-272 μ mol/L).

Table 1 shows the percentage of patients in each group

(cirrhosis, chronic hepatitis, chronic hepatitis with interferon and ribavirin treatment) that the levels of erythrocyte, hematocrit and hemoglobin were below the normal range, and reticulocyte counts above the normal range. Although 30-53% of the patients with cirrhosis and chronic hepatitis demonstrated moderate anemia, none had a reticulocyte count within normal. All of those with low HbA_{1c} also demonstrated anemia but some patients with anemia did not have low HbA_{1c}. Seventy to eighty percent of the patients with chronic hepatitis treated with ribavirin demonstrated moderate anemia and 30% also had high reticulocyte counts (Table 1). All of those with high reticulocyte counts, as well as some of those with anemia and normal reticulocyte counts, had below-normal HbA_{1c}. This study showed elevated reticulocytes, which might be a sign of shortened erythrocyte life span, in only 3 patients with chronic hepatitis and ribavirin treatment. In these patients HbA_{1c} was below the non-diabetic reference range on all methods. We also found HbA_{1c} values below the non-diabetic reference range in up to 40% of the patients with liver cirrhosis and in 50% of the patients with chronic hepatitis treated with ribavirin as measured by at least one of the HbA_{1c} methods. In these groups of patients the HbA_{1c} levels were negatively correlated to the percentage of reticulocytes (Pearson correlation, $r=-0.55$ to -0.79 depending on method, $P<0.05$ for all methods). There was no significant relationship between HbA_{1c} and reticulocyte count in the patients with chronic hepatitis and no ribavirin therapy.

We performed an one-sample *t*-test comparing mean blood glucose calculated of HbA_{1c} results (MBG (mmol/L) = $(1.98 \cdot \text{HbA}_{1c}) - 4.29$) and measured blood glucose as the actual value. HbA_{1c} results of the HPLC Menarini HA-8140 and the immunoassay method DCA 2000 were used to calculate a desired blood glucose value because in Pearson correlation they did not correlate with blood glucose. In patients with chronic hepatitis treated with ribavirin the one sample *t*-test for measured blood glucose and calculated blood glucose resulted in a significant difference ($t_{9\text{Menarini}}=7.68$, $P<0.05$; $t_{9\text{DCA}}=6.67$, $P<0.05$). In patients with liver cirrhosis calculated blood glucose was up to 1 mmol/L lower than measured blood glucose but a high standard deviation (Table 2) caused no statistical difference.

No correlation was found for all 3 groups between HbA_{1c} results and hepatic serum parameters as -glutamyl transferase (GGT), glutamate-oxalate transaminase (GOT) and glutamyl-pyruvic transaminase (GPT). In all 3 patient groups total protein measured in serum was within normal and albumin was normal in all patients with chronic hepatitis. Three patients with compensated cirrhosis had serum albumin below normal. There was no correlation found in all 3 patient groups between

Table 1 Percentage of patients outside the reference range for parameters of anemia

Group	Patients below normal (%) (Reference range)			Patients above normal (%) Reticulocytes (5-20%)
	Erythrocytes (4.5-5.9 T/L)	Hct (40-50%)	Hb (13-17 g/dL)	
Cirrhosis ($n=15$)	46	53	40	0
Chronic hepatitis ($n=10$)	30	30	30	0
Chronic hepatitis /ribavirin ($n=10$)	80	80	70	30

Hct: Hematocrit; Hb: Hemoglobin.

Table 2 Values of measured blood glucose (mean \pm SD) and calculated mean blood glucose values [MBG (mmol/L) = $(1.98 \cdot \text{HbA}_{1c}) - 4.29$]

	Measured MBG (mmol/L)	Menarini HA-8140 Calculated MBG (mmol/L)	DCA 2000 Bayer Calculated MBG (mmol/L)
Cirrhosis ($n=15$)	5.8 \pm 1.9	4.8	5.1
Chronic hepatitis ($n=10$)	5.1 \pm 0.3	5.4	5.4
Chronic hepatitis /Ribavirin ($n=10$)	5.2 \pm 0.4	4.3	4.5

MBG: Mean blood glucose.

fructosamine results and total protein or albumin. In patients with hepatic cirrhosis, mean fructosamine was within the high non-diabetic reference range. In patients with chronic hepatitis, fructosamine was close to the middle of the non-diabetic reference range. Five patients with cirrhosis and one patient with chronic hepatitis treated with ribavirin had high fructosamine levels even though they had normal blood glucose values.

DISCUSSION

The liver plays a major role in regulating glucose metabolism because it is the main source of endogenous glucose and a major site involved in insulin metabolism. The most common pathogenic agents in liver disease are alcohol abuse and infectious hepatitis that may cause disturbed erythropoiesis and decreased red cell survival. Macrocytic anemia is a common feature in liver disease but is still incompletely understood^[13]. The antiviral drug ribavirin has been widely used in combination with interferon in the treatment of chronic hepatitis C and a major side effect of ribavirin is a reversible hemolytic anemia^[10].

Glycated hemoglobin (GHb) measured as HbA_{1c} in diabetic patients, is used for evaluating long-term control of diabetes mellitus. GHb is the result of irreversible non-enzymatic glycation at one or both NH₂-terminal valines of the hemoglobin's α -chain. The extent of glycation and the relative involvement of the hemoglobin's α - and β -chains still remain unclear. Depending on the determination method used the concentration of HbA_{1c} is approximately 4-6% in healthy non-diabetic patients. Glycated hemoglobin most accurately reflects the previous 2-3 mo of glycemic control. Diabetic patients could present with abnormal liver chemistries, representing findings from benign hepatic steatosis to severe cirrhosis of the liver. Some medications to treat diabetes mellitus have an effect on liver metabolism or could even cause hepatotoxic reactions. Liver cirrhosis promotes glucose intolerance and diabetes through various mechanisms including insulin resistance and impaired insulin secretion. Sixty to 80% of patients with liver disease have glucose intolerance and 10-15% eventually develop overt diabetes.

In this study we demonstrated HbA_{1c} values below the non-diabetic reference range in up to 40% of the patients with liver cirrhosis while fructosamine results were either within the reference range or elevated in the diabetic range. However, protein metabolism was normal in our patients and although fructosamine results depend on glycation of serum proteins the results might be altered by reduced hepatic protein synthesis due to impairment of liver function. In 50% of the patients with chronic hepatitis treated with ribavirin, HbA_{1c} values were below the non-diabetic reference range as measured by at least one of the HbA_{1c} methods. In these groups of patients the HbA_{1c} results were negatively correlated to the percentage of reticulocytes that might be caused by disturbed erythropoiesis and decreased red cell survival. In patients with liver cirrhosis and chronic hepatitis treated with ribavirin, the HbA_{1c} calculated value of mean blood glucose was up to 1 mmol/L (18 mg/dL) lower than measured mean blood glucose. This underlines that impairment of liver function has influence on results of HbA_{1c} determination. Fructosamine may be a more reasonable marker for long term glucose control in patients with liver disease, but based on our findings we recommend frequent blood glucose monitoring as a measure for glucose control in patients with advanced liver disease.

We conclude that only evaluated in context with all liver function parameters as well as a red blood count including reticulocytes, HbA_{1c} should be used in patients with liver disease. Although the pathophysiologic reasons have still not

been confirmed, our data demonstrate that HbA_{1c} and fructosamine measurements should be used with caution when evaluating long-term glucose control in patients with hepatic cirrhosis or in patients with chronic hepatitis with ribavirin treatment. This interference may be due to alterations in erythrocyte lifespan and altered protein metabolism, but further investigations are needed to elucidate the exact cause of the interference in patients with liver disease.

ACKNOWLEDGEMENTS

We kindly acknowledge the determination of HbA_{1c} by the following laboratories: Institute of Chemical and Laboratory Diagnostics, Medical University Graz and Laboratory of the County Hospital in Wagna, Austria. Determination of fructosamine was performed in the Laboratory of the Department of Gynecology, Medical University Graz, Austria.

REFERENCES

- 1 Diabetes Control and Complications Trial Research Group: The effect of intensive treatment of diabetes on the development and progression of long-term complications in insulin-dependent diabetes mellitus. *N Engl J Med* 1993; **329**: 977-986
- 2 Turner RC, Cull CA, Frighi V, Holman RR. Glycemic control with diet, sulfonylurea, metformin, or insulin in patients with type 2 diabetes mellitus: progressive requirement for multiple therapies (UKPDS 49). UK Prospective Diabetes Study (UKPDS) Group. *JAMA* 1999; **281**: 2005-2012
- 3 Shetty A, Wilson S, Kuo P, Laurin JL, Howell CD, Johnson L, Allen EM. Liver transplantation improves cirrhosis-associated impaired oral glucose tolerance. *Transplantation* 2000; **69**: 2451-2454
- 4 Trenti T, Cristani A, Cioni G, Pentore R, Mussini C, Ventura E. Fructosamine and glycated hemoglobin as indices of glycemic control in patients with liver cirrhosis. *Ric Clin Lab* 1990; **20**: 261-267
- 5 Cacciatore L, Cozzolino G, Giardina MG, De Marco F, Sacca L, Esposito P, Francica G, Lonardo A, Matarazzo M, Varriale A. Abnormalities of glucose metabolism induced by liver cirrhosis and glycosylated hemoglobin levels in chronic liver disease. *Diabetes Res* 1988; **7**: 185-188
- 6 Nomura Y, Nanjo K, Miyano M, Kikuoka H, Kuriyama S, Maeda M, Miyamura K. Hemoglobin A₁ in cirrhosis of the liver. *Diabetes Res* 1989; **11**: 177-180
- 7 Jiao Y, Okumiya T, Saibara T, Park K, Sasaki M. Abnormally decreased HbA_{1c} can be assessed with erythrocyte creatine in patients with shortened erythrocyte age. *Diabetes Care* 1998; **21**: 1732-1735
- 8 Bravo AA, Sheth SG, Chopra S. Current concepts: liver biopsy. *N Engl J Med* 2001; **344**: 495-500
- 9 Oberti F, Valsesia E, Pilette C, Rousselet MC, Bedossa P, Aube C, Gallois Y, Rifflet H, Maiga MY, Penneau-Fontbonne D, Cales P. Noninvasive diagnosis of hepatic fibrosis or cirrhosis. *Gastroenterology* 1997; **113**: 1609-1616
- 10 De Franceschi L, Fattovich G, Turrini F, Ayi K, Brugnara C, Manzato F, Noventa F, Stanzial AM, Solero P, Corrocher R. Hemolytic anemia induced by ribavirin therapy in patients with chronic hepatitis C infection: role of membrane oxidative damage. *Hepatology* 2000; **31**: 997-1004
- 11 Little RR, Rohlfing CL, Wiedmeyer HM, Myers GL, Sacks DB, Goldstein DE. The national glycohemoglobin standardization program: a five-year progress report. *Clin Chem* 2001; **47**: 1985-1992
- 12 Rohlfing C, Wiedmeyer HM, Little RR, England JD, Tennill A, Goldstein DE. Defining the relationship between plasma glucose and HbA_{1c}. *Diabetes Care* 2002; **25**: 275-278
- 13 Maruyama S, Hirayama C, Yamamoto S, Koda M, Udagawa A, Kadowaki Y, Inoue M, Sagayama A, Umeki K. Red blood cell status in alcoholic and non-alcoholic liver disease. *J Lab Clin Med* 2001; **138**: 332-337

Expression and localization of c-Fos and NOS in the central nerve system following esophageal acid stimulation in rats

Xiao-Wei Shuai, Peng-Yan Xie

Xiao-Wei Shuai, Peng-Yan Xie, Department of Gastroenterology, First Hospital of Peking University, Beijing 100034, China

Supported by the Beijing Natural Science Foundation, No.7042030

Correspondence to: Dr. Peng-Yan Xie, Department of Gastroenterology, First Hospital of Peking University, Beijing 100034, China. pengyanx2002@yahoo.com

Telephone: +86-10-66551122-2581

Received: 2004-01-02 **Accepted:** 2004-02-09

Abstract

AIM: To determine the distribution of neurons expressing c-Fos and nitric oxide synthase (NOS) in the central nerve system (CNS) following esophageal acid exposure, and to investigate the relationship between c-Fos and NOS.

METHODS: Twelve Wistar rats were randomly divided into two equal groups. Hydrochloric acid with pepsin was perfused in the lower part of the esophagus for 60 min. As a control, normal saline was used. Thirty minutes after the perfusion, the rats were killed and brains were removed and processed for c-Fos immunohistochemistry and NADPH-d histochemistry. Blood pressure (BP), heart rate (HR), and respiratory rate (RR) during the experimental procedures were recorded every 10 min.

RESULTS: There were no significant differences in BP, HR and RR between the two groups. c-Fos immunoreactivity was significantly increased in rats receiving acid plus pepsin perfusion in amygdala (AM), paraventricular nucleus (PVN), parabrachial nucleus (PBN), nucleus tractus solitarius and dorsal motor nucleus of vagus (NTS/DMV), nucleus ambiguus (NA), reticular nucleus of medulla (RNM) and area postrema (AP). NOS reactivity in this group was significantly increased in PVN, PBN, NTS/DMV, RNM and AP. c-Fos and NOS had significant correlation between PVN, PBN, NTS/DMV, RNM and AP.

CONCLUSION: Acid plus pepsin perfusion of the esophagus results in neural activation in areas of CNS, and NO is likely one of the neurotransmitters in some of these areas.

Shuai XW, Xie PY. Expression and localization of c-Fos and NOS in the central nerve system following esophageal acid stimulation in rats. *World J Gastroenterol* 2004; 10(15): 2287-2291
<http://www.wjgnet.com/1007-9327/10/2287.asp>

INTRODUCTION

Reflux esophagitis (RE) is a common gastrointestinal motility disorder. Esophageal reflux occurs when gastric contents move in a retrograde direction into the esophagus, and esophagitis develops by prolonged exposure to gastric contents. This happens when the lower esophageal sphincter fails to provide an adequate mechanical barrier, when the esophageal peristaltic

contractions fail to provide adequate clearance of the gastric contents, and/or when gastric contents exist for a prolonged time due to gastroparesis^[1]. Esophageal motility is controlled by a variety of factors of which the nerve system is the most important one. Locally, motility disorder caused by esophagitis is usually due to the decreased release of acetylcholine^[2,3], signal transduction failure^[4], and/or decreased intracellular Ca²⁺^[5]. In CNS, little has been known about the distribution of activated neurons after esophageal acid exposure^[6].

It is reported that *c-fos* is the most well characterized IEGs (immediate early genes) in neurons; the *c-fos* message is induced within minutes of stimuli and the protein is expressed within 1-3 h^[7-10]. The expression of *c-fos* in CNS is considered to be a marker of neuronal activity following an appropriate stimulus, and the site of central expression of c-Fos in response to a stimulus is used as a means of elucidating the course of the response^[11-16]. Nitric oxide (NO) acts as an intercellular messenger in CNS. As a highly diffusible and short-lived gas, NO is always studied by means of nitric oxide synthase (NOS)^[17]. Studies have shown that NOS-containing neurons are identical to those selectively stained for NADPH diaphorase^[18]. The present study was designed to determine the distribution of neurons expressing c-Fos and NOS in CNS following esophageal acid exposure, and to investigate the relationship between c-Fos and NOS.

MATERIALS AND METHODS

Animals

Twelve male Wistar rats weighing 220-260 g were housed in standard home cages under conditions of controlled illumination (12:12 h light/dark cycle), humidity, and temperature (18-26 °C) for at least 7 d prior to the experimental procedure. They were fed a standard rat diet and tap water. The animals were deprived of food but not water 12-16 h before each experiment. They were randomly divided into two equal groups. All procedures were approved by the Committee for Animal Care and Usage for Research and Education of the Peking University.

Methods

Rats were anaesthetized with an intraperitoneal injection of urethane (1.0 g/kg). After a rat reached a complete state of anesthesia, the abdominal wall and gastric wall were incised, and a drainage cannula was inserted in the gastric cardia to collect run-off solution from the esophagus. The anesthetized rat, strapped supine to an animal board, was then positioned with its head elevated at a slight angle (20-30°). A single lumen clear vinyl tube (ID 0.05 mm, A 0.8 mm) was passed by mouth into the esophagus. The tip of the cannula was located 3 cm above the esophagogastric junction. The cannula was then positioned and connected to a continuous perfusion pump (Medical Equipment Ltd. Zhejiang University, Hangzhou, China). A solution containing hydrochloric acid (HCl 0.1 mol/L) and pepsin (2 000-4 000 U/mL) (pH 1.5) was perfused continuously at a rate of 10 mL/h for 60 min. As a control, normal saline was used. Blood pressure (BP), heart rate (HR) and respiratory rate

(RR) during the experimental procedures were recorded every 10 min. After perfusion, the rat was left undisturbed for another 30 min before being deeply anesthetized with urethane (1.5 g/kg i.p.). The animal then was transcardially perfused with 9 g/L saline followed by 40 g/L paraformaldehyde in 0.1 mol/L phosphate buffer saline (PBS, pH 7.3). The brain was removed and postfixed in the same fixative overnight and cryoprotected by immersion in 200 g/L sucrose for 72 h. Coronal sections (40 μ m) of the brain were cut in a cryostat. Every fourth section was used to reveal c-Fos immunoreactivity and NADPH-diaphorase (NADPH-d) staining, and the second set of sections was used as a control for the immunohistochemical reaction.

The sections were collected and rinsed in 0.01 mol/L PBS containing 3 g/L Triton X-100 (PBST). Then they were incubated at 37 $^{\circ}$ C for 2 h in a solution containing 1 mmol/L NADPH (Biomol, London, UK), 0.5 mmol/L nitroblue tetrazolium (Biomol), Tris-HCl 50 mmol/L, and Triton X-100 2 g/L. After a rinse in PBST, sections were placed into a 50 g/L goat serum for 30 min at room temperature (RT), and incubated overnight at RT in primary antibody c-Fos (1:200, Santa Cruz Biotechnology, California, USA). After washing for 15 min with PBST, the sections were incubated in biotinylated anti-rabbit IgG (Zymed, South San Francisco, Canada) diluted 1:300 in PBST at RT for 2 h, and then incubated in peroxidase-conjugated streptavidin (1:300 dilution, Zymed) for 2 h at RT. The immunoreactivity was visualized by incubating with 0.05 mol/L Tris-HCl buffer containing 0.1 g/L 3,3'-diaminobenzidine, and 0.3 mL/L H₂O₂ for 10-20 min at RT. The stained sections were mounted on APES-coated glass slides, dehydrated and coverslipped.

Statistical analysis

BP, HR and RR recorded every 10 min during the 90-min experimental procedures were averaged per animal and then per experimental group, respectively. The distribution of c-Fos and NADPH-d positive cells was detected under a microscope (Olympus, Tokyo, Japan), and the cells were counted on LEICA Q550CW system (Leica Microsystems Imaging Solutions Ltd, Wetzlar, Germany). The numbers of cells containing c-Fos immunoreactivity and NADPH-d were counted unilaterally in specific nuclei in several sections; 5 sections for amygdala

(AM), nucleus tractus solitarius and dorsal motor nucleus of vagus (NTS/DMV), nucleus ambiguus (NA) and reticular nucleus of medulla (RNM) and 4 sections for paraventricular nucleus (PVN), supraoptic nucleus (SON), parabrachial nucleus (PBN) and area postrema (AP). The average number of c-Fos or NADPH-d positive neurons per section for each rat was calculated, respectively, by dividing the total number of c-Fos or NADPH-d positive cells obtained from all sections by the number of sections taken for each brain nucleus. Data were expressed as mean \pm SD of the respective brain areas. Statistical analyses were performed by SPSS 12.0 using the *t*-test, and a *P* value of less than 0.05 was considered statistically significant. The relationship between c-Fos and NADPH-d positive cells was performed by the correlation analysis.

RESULTS

BP, HR and RR to acid-pepsin perfusion

Esophageal acid perfusion did not change BP (18.03 \pm 1.07 vs 17.26 \pm 0.62 kPa, *F*=2.663, *P*=0.134), HR (275.30 \pm 14.43 vs 265.00 \pm 22.12 beats/min, *F*=1.343, *P*=0.273), and RR (92.00 \pm 10.41 vs 94.56 \pm 9.46 breathes/min, *F*=0.078, *P*=0.785) compared with control group.

c-Fos and NADPH-d staining in CNS

The c-Fos positive cell nuclei of activated cells showed the characteristic dark brown staining of oxidized DAB. In both groups of rats, c-Fos expression was observed in several brain regions. In telencephalon and diencephalon, c-Fos positive cells were mainly located in AM (Figure 1A, B), PVN (Figure 1C, D), SON and the numbers of the former two areas increased significantly in the acid-pepsin perfusion group (Table 1). Esophageal exposure to acid and pepsin also stimulated a significantly greater number of c-Fos-labeled neurons in areas of brain stem including PBN, NTS/DMV, NA (Figure 2A, D), RNM and AP (Table 1). NADPH-d activity was visualized as a vibrant blue color within perikarya, dendrites and axons. Acid-pepsin perfusion significantly increased the numbers of NADPH-d stained cells in PVN (Figure 1C, D), PBN, NTS/DMV, RNM and AP (Table 1). There were some coexistence of Fos

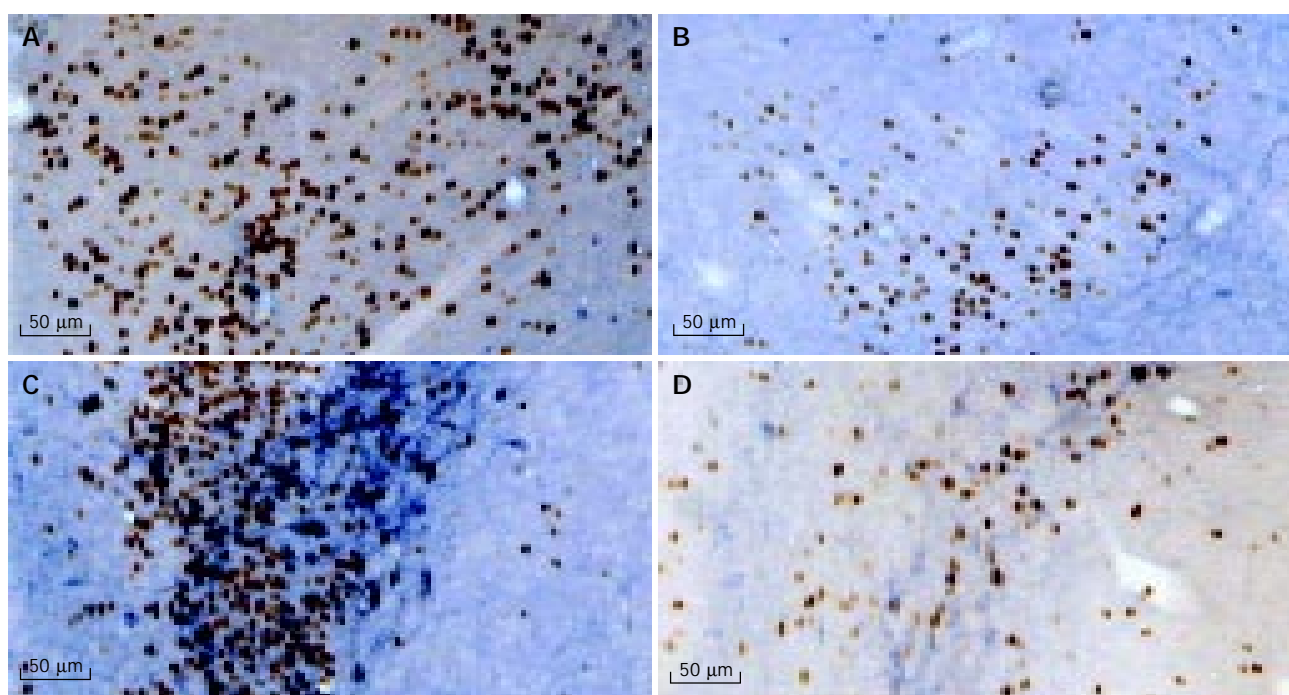


Figure 1 Photomicrographs showing c-Fos and NOS positive neurons in amygdala (A and B), paraventricular nucleus (C and D). A and C were taken from rats with acid-pepsin perfusion, while B and D were taken from rats with saline perfusion. (3V: the third ventricle).

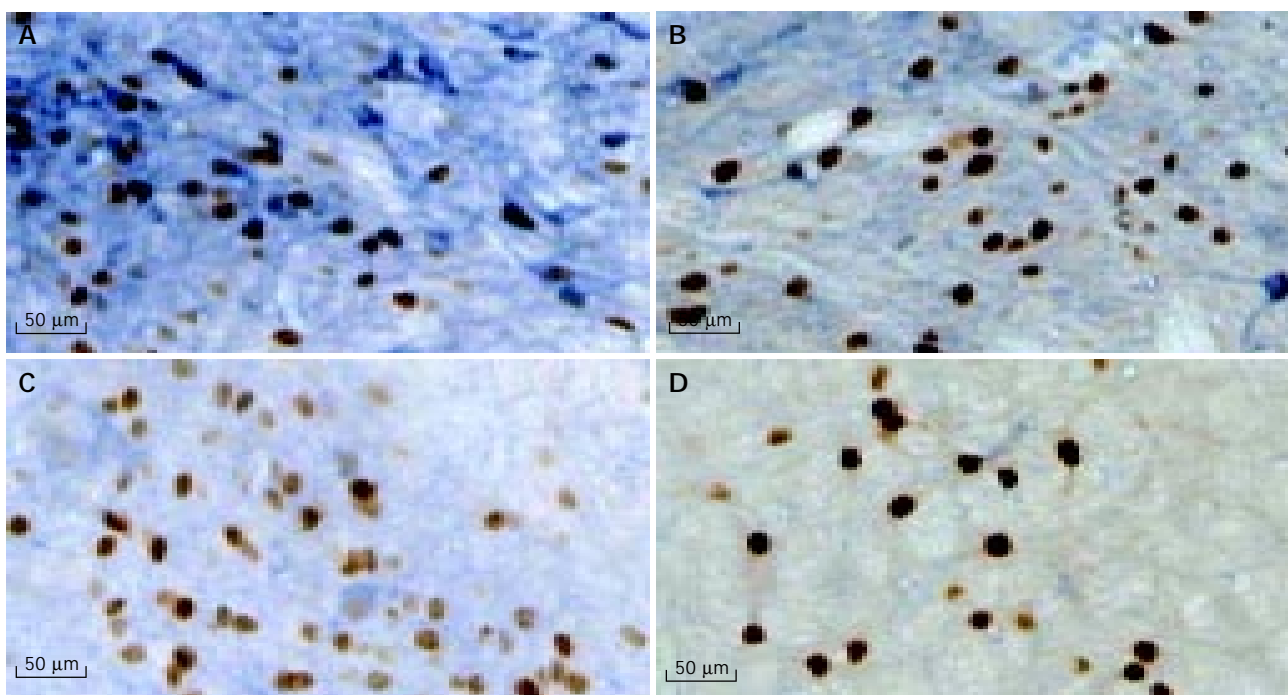


Figure 2 Photomicrographs showing c-Fos and NOS positive neurons in nucleus tractus solitarius (A and B), nucleus ambiguus (C and D). A and C were taken from rats with acid-pepsin perfusion, while B and D were taken from rats with saline perfusion.

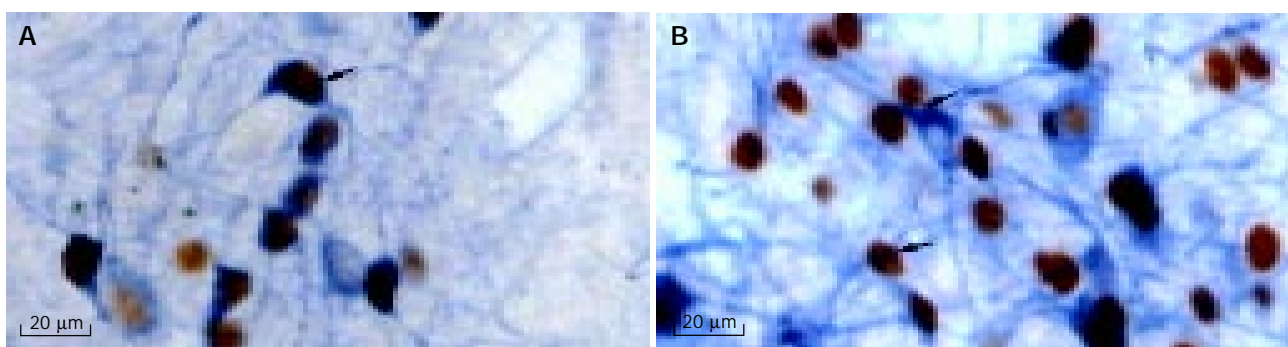


Figure 3 Photomicrographs showing the coexistence of c-Fos and NADPH-d positive staining, i.e. colocalization (left) and close proximity (right).

Table 1 Effects of esophageal acid-pepsin perfusion on c-Fos and NOS expression in brain nuclei, as determined by the average of number of c-Fos or NADPH-d positive neurons/section

Nuclei	Acid-pepsin perfusion			Saline perfusion		
	c-Fos	NOS	c-Fos&NOS	c-Fos	NOS	c-Fos&NOS
AM	341.3±13.7 ^b	8.0±2.0	1.7±0.7	166.2±2.7	6.5±0.5	1.9±0.4
PVN	551.1±11.6 ^b	151.8±48.5 ^b	127.6±34.1 ^b	232.2±12.9	66.9±1.5	64.1±4.4
SON	181.0±3.5	96.2±2.4	66.0±7.0	183.3±5.8	95.3±4.2	64.9±2.1
PBN	103.0±4.1 ^b	17.1±1.8 ^b	2.9±1.0 ^b	79.7±2.6	3.4±0.6	1.1±0.5
NTS/DMV	161.1±6.9 ^b	48.8±6.8 ^b	32.3±4.7 ^b	75.0±0.8	23.7±0.7	8.4±1.5
NA	42.7±0.8 ^b	2.1±0.4	1.0±0.2	25.0±1.5	2.0±0.6	1.0±0.2
RNM	77.4±7.6 ^b	15.1±1.5 ^b	7.6±1.1 ^b	32.9±0.4	5.1±0.5	1.9±0.3
AP	190.1±11.1 ^b	6.0±2.3 ^b	2.3±1.1 ^a	107.2±2.1	1.9±0.6	0.9±0.3

Data are expressed as mean±SD. ^a*P*<0.05, acid-pepsin perfusion vs saline perfusion. ^b*P*<0.01, acid-pepsin perfusion vs saline perfusion. c-Fos, c-Fos positive neurons; NOS, NADPH-d positive neurons.

and NADPH-d positive staining (Figure 3). The coexistence included colocalization that was visualized as blue-stained perikarya (NADPH-d activity) containing a clearly visible dark brown nucleus (c-Fos protein), and close proximity that was visualized as c-Fos positive nucleus being within

neuronal processes of NADPH-d, and that was the presence of NADPH-d positive staining within 3 μm from c-Fos-positive nucleus. Both of them have been adopted as a criterion of close proximity^[19,20]. The coexisting cells were mainly observed in PVN, SON and NTS/DMV.

Correlation between c-Fos and NADPH-d positive cells

There was a high correlation between c-Fos and NADPH-d positive cells in PVN, PBN, NTS/DMV, RNM and AP. The correlation coefficient (r) was 0.805, 0.943, 0.923, 0.947, 0.869 (all $P < 0.01$) respectively. There was no correlation between c-Fos and NADPH-d expression in AM, SON, and NA.

DISCUSSION

Acid, in combination with pepsin, was chosen to be the stimulant in this rat model of gastroesophageal reflux. This combination has been shown to cause esophagitis in experimental models^[21,22].

The nerve supply to esophagus is composed of extrinsic and intrinsic components. The extrinsic innervation is mainly through the autonomic nervous system, which is divided into sympathetic and parasympathetic components. The parasympathetic innervation of esophagus is supplied by the vagus nerves. Three types of vagal afferent fibers are classified on the basis of their sensitivity to mechanical stimulation: those responding to mucosal stroking (mucosal receptors), those responding to circular tension (tension receptors) and those responding to mucosal stroking and circular tension (tension/mucosal receptors)^[23]. Sensory afferents from the esophagus usually travel to NTS. DMV, which contains preganglionic motor neurons, has efferent fibers. The dorsal vagal complex (DVC) comprising NTS and DMV is the center of the integration of vagal control of esophagus^[24,25]. Exposing the subdiaphragmatic vagus nerves (SDV) to horseradish peroxidase (HRP), Norgren *et al.* found that retrogradely labeled neurons occurred within NA and the reticular formation caudal to NA, and DMV whereas anterograde HRP reaction product occurred in NTS and AP^[26]. Besides, connections of NTS with the medullary reticular formation and AP existed^[27]. They were reported to take part in some visceral reflexes. In the present study, c-Fos positive neurons were seen in NTS, DMV, NA, RNM, and AP. In comparison with the controls, the number was greater in the acid-pepsin group. In this context, the present results confirm those reports mentioned above. During the esophageal exposure to acid, a cascade of chemoreceptors that lie along the passage is stimulated. Some of these signals are carried by vagal afferents to NTS in brainstem. From there, visceral information is disseminated to various brain sites, where it affects regulatory functions by engaging endocrine, autonomic, and some other effector mechanisms. But how all these different pathways interconnect within subnuclei is still unknown. It has been reported that PBN is related to noxious information from the visceral organs^[14]. Esophageal acid exposure also induces high density of c-Fos expression in PBN.

A significantly increased number of c-Fos positive nuclei was observed in AM and PVN. Although many of c-Fos staining cells were seen in SON, there was no significant increase in this area in response to acid-pepsin perfusion. PVN is immediate beneath the ependyma of the third ventricle. The afferent connections of PVN are from hippocampal formation, septal nuclei, locus ceruleus, AM, and NTS. The efferent connections appear, in part, to be reciprocal to the afferent systems. The AM has reciprocal connections with locus ceruleus, substantia nigra, NTS, DMV, PBN, reticular formation, and nuclei of the hypothalamus. The present study showed that only some of those areas expressed c-Fos immunoreactivity, which suggests that those activated neurons are related to esophageal innervation. In order to exclude the potential contribution of the pressor response to the induction of c-Fos in NTS and other nuclei, BP, HR, and RR were recorded during the experimental procedures. There were no significant changes in BP, HR, and RR between the two groups.

It has been reported that NOS exists in neurons of DVC.

The premotoneurons in NTS express NOS, and NO acting in the NA takes part in the esophageal peristalsis^[28]. The present study showed that many NADPH-d positive neurons were seen in PBN, NTS/DMV, RNM, and that some were seen in NA and AP. This suggests that NO release may modulate characteristics of the activated neurons in these nuclei that are evoked by esophageal acid stimulus. It has been reported that NOS inhibitor, N-nitro-L-arginine methyl ester (L-NAME), reduces the spontaneous discharge rate of the NTS neurons *in vivo* and *in vitro*, which confirms that NO has the excitatory effect on NTS^[29]. L-NAME also reduces the c-Fos expression in DVC, suggesting that c-Fos expression is, in part, related to NO release in DVC. Little has been known about the neurotransmitters in telencephalon and diencephalon. In the present study, many NADPH-d positive cells were observed in PVN and SON, but only few were found in AM.

The present study observed the coexistence of c-Fos and NADPH-d positive staining. It is possible that the neuronal cells containing NOS are activated during esophageal acid exposure, which may cause NO release to themselves or to other brain regions in modulating the esophageal reflux.

In conclusion, acid-pepsin exposure to lower part of the esophagus stimulates the mucosal receptors, which in turn activates the neurons of NTS through vagal afferent fibers, and finally the neurons in DMV and NA to modulate the esophageal peristalsis. The possible nuclei involved in these procedures are AM, PVN, PBN, RNM, and AP. Double labeled staining of c-Fos and NADPH-d suggests that NO is one of the neurotransmitters in PVN, PBN, NTS/DMV, RNM and AP.

REFERENCES

- Zarling EJ. A review of reflux esophagitis around the world. *World J Gastroenterol* 1998; **4**: 280-284
- Biancani P, Sohn UD, Rich HG, Harnett KM, Behar J. Signal transduction pathways in esophageal and lower esophageal sphincter circular muscle. *Am J Med* 1997; **103**(5A): 23S-28S
- Cao Y, Xie P, Xing Y. Role of endogenous cholinergic nerve in esophageal dysmotility with reflux esophagitis. *Zhonghua Neike Zazhi* 2001; **40**: 670-672
- Kim N, Sohn UD, Mangannan V, Rich H, Jain MK, Behar J, Biancani P. Leukotrienes in acetylcholine-induced contraction of esophageal circular smooth muscle in experimental esophagitis. *Gastroenterology* 1997; **112**: 1548-1558
- Rich H, Sohn UD, Behar J, Kim N, Biancani P. Experimental esophagitis affects intracellular calcium stores in the cat lower esophageal sphincter. *Am J Physiol* 1997; **272**(6 Pt 1): G1523-G1529
- Suwanprathes P, Ngu M, Ing A, Hunt G, Seow F. c-Fos immunoreactivity in the brain after esophageal acid stimulation. *Am J Med* 2003; **115**(Suppl 3A): 31S-38S
- Hughes P, Dragunow M. Induction of immediate-early gene and the control of neurotransmitter-regulated gene expression within the nervous system. *Pharmacol Rev* 1995; **47**: 133-178
- Muller R, Bravo R, Burckhardt J, Curran T. Induction of c-fos gene and protein by growth factors precedes activation of c-myc. *Nature* 1984; **312**: 716-720
- Sonnenberg JL, Macgregor-Leon PF, Curran T, Morgan JJ. Dynamic alterations occur in the levels and composition of transcription factor AP-1 complexes after seizure. *Neuron* 1989; **3**: 359-365
- Sheng M, Greenberg ME. The regulation and function of c-fos and other immediate early genes in the nervous system. *Neuron* 1990; **4**: 477-485
- Yamamoto T, Sawa K. C-Fos-like immunoreactivity in the brainstem following gastric loads of various chemical solutions in rats. *Brain Res* 2000; **866**: 135-143
- Schicho R, Schemann M, Pabst MA, Holzer P, Lippe IT. Capsaicin-sensitive extrinsic afferents are involved in acid-induced activation of distinct myenteric neurons in the rat stomach. *Neurogastroenterol Motil* 2003; **15**: 33-44
- Tong C, Ma W, Shin SW, James RL, Eisenach JC. Uterine cervi-

- cal distension induces cFos expression in deep dorsal horn neurons of the rat spinal cord. *Anesthesiology* 2003; **99**: 205-211
- 14 **Monnikes H**, Ruter J, Konig M, Grote C, Kobelt P, Klapp BF, Arnold R, Wiedenmann B, Tebbe JJ. Differential induction of *c-fos* expression in brain nuclei by noxious and non-noxious colonic distension: role of afferent C-fibers and 5-HT₃ receptors. *Brain Res* 2003; **966**: 253-264
- 15 **Tada H**, Fujita M, Harris M, Tatewaki M, Nakagawa K, Yamamura T, Pappas TN, Takahashi T. Neural mechanism of acupuncture-induced gastric relaxations in rats. *Dig Dis Sci* 2003; **48**: 59-68
- 16 **de Medeiros MA**, Canteras NS, Suchecki D, Mello LE. Analgesia and c-Fos expression in the periaqueductal gray induced by electroacupuncture at the Zusanli point in rats. *Brain Res* 2003; **973**: 196-204
- 17 **Bredt DS**, Hwang PM, Snyder SH. Localization of nitric oxide synthase indicating a neural role for nitric oxide. *Nature* 1990; **347**: 768-770
- 18 **Dawson TM**, Bredt DS, Fotuhi M, Hwang PM, Snyder SH. Nitric oxide synthase and neuronal NADPH diaphorase are identical in brain and peripheral tissues. *Proc Natl Acad Sci USA* 1991; **88**: 7797-7801
- 19 **Li J**. Nitric oxide synthase (NOS) coexists with activated neurons by skeletal muscle contraction in the brainstem of cats. *Life Sci* 2002; **71**: 2833-2843
- 20 **Tassorelli C**, Joseph SA. NADPH-diaphorase activity and Fos expression in brain nuclei following nitroglycerin administration. *Brain Res* 1995; **695**: 37-44
- 21 **Lanas A**, Royo Y, Ortego J, Molina M, Sainz R. Experimental esophagitis induced by acid and pepsin in rabbits mimicking human reflux esophagitis. *Gastroenterology* 1999; **116**: 97-107
- 22 **Pursnani KG**, Mohiuddin MA, Geisinger KR, Weinbaum G, Katzka DA, Castell DO. Experimental study of acid burden and acute oesophagitis. *Br J Surg* 1998; **85**: 677-680
- 23 **Page AJ**, Blackshaw LA. An *in vitro* study of the properties of vagal afferent fibres innervating the ferret oesophagus and stomach. *J Physiol* 1998; **512**(Pt 3): 907-916
- 24 **Hornby PJ**, Abrahams TP. Central control of lower esophageal sphincter relaxation. *Am J Med* 2000; **108**(Suppl 4a): 90S-98S
- 25 **Sang Q**, Goyal RK. Swallowing reflex and brain stem neurons activated by superior laryngeal nerve stimulation in the mouse. *Am J Physiol Gastrointest Liver Physiol* 2001; **280**: G191-G200
- 26 **Norgren R**, Smith GP. Central distribution of subdiaphragmatic vagal branches in the rat. *J Comp Neurol* 1988; **273**: 207-223
- 27 **Herbert H**, Moga MM, Saper CB. Connections of the parabrachial nucleus with the nucleus of the solitary tract and the medullary reticular formation in the rat. *J Comp Neurol* 1990; **293**: 540-580
- 28 **Beyak MJ**, Xue S, Collman PI, Valdez DT, Diamant NE. Central nervous system nitric oxide induces oropharyngeal swallowing and esophageal peristalsis in cat. *Gastroenterology* 2000; **119**: 377-385
- 29 **Ma S**, Abboud FM, Felder RB. Effect of L-arginine-derived nitric oxide synthesis on neuronal activity in nucleus tractus solitarius. *Am J Physiol* 1995; **268**(2 Pt 2): R487-R491

Edited by Xia HHX and Chen WW Proofread by Xu FM

Effect of octreotide on human pancreatic cancer cells after transfected with somatostatin receptor type 2 gene

Zheng-Ren Liu, Ren-Yi Qin, Gao-Song Wu, Qing Chang, Da-Yu Wang, Sheng-Quan Zou, Fa-Zu Qiu

Zheng-Ren Liu, Ren-Yi Qin, Gao-Song Wu, Qing Chang, Da-Yu Wang, Sheng-Quan Zou, Fa-Zu Qiu, Department of General Surgery, Tongji Hospital, Tongji Medical College, Huazhong University of Science and Technology, Wuhan 430030, Hubei Province, China

Supported by the Natural Science Foundation of Hubei Province, No. 2000J068

Correspondence to: Professor Ren-Yi Qin, Department of General Surgery, Tongji Hospital, Tongji Medical College, Huazhong University of Science and Technology, Wuhan 430030, Hubei Province, China. ryqin@tjh.tjmu.edu.cn

Telephone: +86-27-83662389

Received: 2003-10-27 **Accepted:** 2003-12-16

Abstract

AIM: To observe the effect of octreotide on apoptosis rate of human pancreatic cancer cells PC-3 after transfected with somatostatin receptor type 2 (SST2) gene.

METHODS: SST2 plasmid was transfected into PC-3 cells by liposome. Result of transfection was detected by immunocytochemical staining and Western blotting. Apoptosis rates of PC-3 cells under different dosages of octreotide were measured by MTT assay and flow cytometry (FCM).

RESULTS: Apoptosis rate caused by octreotide of transfected PC-3 cells was $7.56 \pm 1.06\%$ at the dosage of $0.20 \mu\text{g/mL}$, $9.25 \pm 1.73\%$ at the dosage of $0.40 \mu\text{g/mL}$ and $14.18 \pm 2.71\%$ at the dosage of $0.80 \mu\text{g/mL}$. Apoptosis rate caused by octreotide of non-transfected PC-3 cells was $5.76 \pm 0.75\%$ at the dosage of $0.20 \mu\text{g/mL}$, $6.69 \pm 0.80\%$ at the dosage of $0.40 \mu\text{g/mL}$ and $7.26 \pm 1.28\%$ at the dosage of $0.80 \mu\text{g/mL}$. Transfected PC-3 cells growth inhibition rate caused by octreotide was $9.36 \pm 1.34\%$ at the dosage of $0.20 \mu\text{g/mL}$, $12.03 \pm 1.44\%$ at the dosage of $0.40 \mu\text{g/mL}$ and $20.23 \pm 4.21\%$ at the dosage of $0.80 \mu\text{g/mL}$. Non-transfected PC-3 cells growth inhibition rate caused by octreotide was $6.44 \pm 0.66\%$ at the dosage of $0.20 \mu\text{g/mL}$, $7.65 \pm 0.88\%$ at the dosage of $0.40 \mu\text{g/mL}$ and $9.29 \pm 1.32\%$ at the dosage of $0.80 \mu\text{g/mL}$. We found that octreotide caused higher apoptosis rate and inhibition rate in transfected groups than in non-transfected groups ($P < 0.05$) at the tested dosages (0.20 , 0.40 and $0.80 \mu\text{g/mL}$).

CONCLUSION: Deficiency of SST2 was probably the major reason why octreotide had little effect on PC-3 cells. Transfecting SST2 gene could strengthen the ability of octreotide of killing PC-3 cells. It provided an experimental evidence for using both octreotide and transfection with SST2 gene on clinical treatment of pancreatic cancer.

Liu ZR, Qin RY, Wu GS, Chang Q, Wang DY, Zou SQ, Qiu FZ. Effect of octreotide on human pancreatic cancer cells after transfected with somatostatin receptor type 2 gene. *World J Gastroenterol* 2004; 10(15): 2292-2294
<http://www.wjgnet.com/1007-9327/10/2292.asp>

INTRODUCTION

Octreotide, the artificial synthetic somatostatin analogue, which possesses the advantage of relative specificity, long lasting and small ill effect, has already been applied to clinical therapy extensively. Its anti-tumor mechanism mainly depends on the expression of somatostatin receptor, especially SST2^[1-3]. Most tumors highly express SST2, but some do not express or low express. For example, 90% human pancreatic cancer cells have lost the ability of expressing SST2, which leads to the unsatisfactory treatment effect in pancreatic cancer^[4]. We did the experiment to explore octreotide's effect on the apoptosis rate of pancreatic cancer (PC-3) cells after transfected with SST2 gene.

MATERIALS AND METHODS

Materials

PC-3 cells were a gift from China Medical University. RPMI 1640, fetal calf serum, Liposome 2000 Reagent were purchased from Gibco Co. USA. Octreotide was kindly presented by Novartis Co. Swiss. MTT, DMSO and G418 were purchased from Sigma Co. USA. Goat-anti-human SST2 monoclonal antibody was purchased from Santa Cruz Co. USA. Rabbit-anti-goat and DAB were purchased from Zhongshan Biotechnology Co. Beijing, China. ECL kit was purchased from Amersham Pharmacia Biotechnology Inc. ABC test kit was purchased from Huamei Co. China. Human SST2 plasmid was kindly presented by Junbo Hu of Maryland University, USA.

Methods

SST2 plasmid amplification and transfection We adopted colon bacillus (DH-5 α) to amplify and extract the human SST2 plasmid, which was identified by endonuclease. We cultured the PC-3 cells with RPMI 1640 supplemented with 100 mL/L fetal calf serum. When PC-3 cells were in exponential growth phase, the human SST2 plasmid was transfected into PC-3 cells mediated by Liposome 2000 reagent and screened with culture medium with 600 mg/L G418.

Immunocytochemical staining Transfective effect was detected by immunocytochemical staining. ABC test kit was adopted to stain the cells crawling on the slides with immunocytochemical staining. Goat-anti-human SST2 monoclonal antibody was diluted to 1:100. Blank groups used PBS instead of goat-anti-human antibody.

Western blotting Expression of SST2 was detected by western-blot. Transfected cells were collected and lysed with the cell-lysis to extract protein. Goat-anti-human SST2 monoclonal antibody (1:1 000) was used. The signals were developed with the ECL kit.

FCM Apoptosis rate was detected by flow cytometry. When the PC-3 cells were in exponential growth phase, octreotide at different dosages (0.05 , 0.10 , 0.20 , 0.40 , $0.80 \mu\text{g/mL}$) was added. After 24 h, culture medium was renewed and octreotide added according to the above dosages. Cells in the culture medium were collected and preserved in 700 mL/L alcohol at -20°C . Cells were collected after 48 h; the apoptosis rate was detected by flow cytometry.

MTT assay MTT assay was adopted to detect the sensitivity of PC-3 cells *in vitro* after using different dosages of octreotide. We divided them into three groups: blank groups (no cells), control groups (no drug) and octreotide groups. Octreotide treated cells were divided into five groups according to the dosages (0.05, 0.10, 0.20, 0.40, 0.80 $\mu\text{g}/\text{mL}$). Then the transfected PC-3 cells and non-transfected cells were inoculated into the 96-well culture panel, about $3 \times 10^6/\text{L}$ in each well. Each panel had 10 replicate wells. After 24-h culture, octreotide was added and then cultivated for another 48 h. The sensitivity of PC-3 cells was detected with MTT assay and inhibition rate was measured by detecting the value of the A ($\lambda=550 \text{ nm}$). Inhibition rate of PC-3 cells growth = $[(A_{\text{control group}} - A_{\text{blank group}}) - (A_{\text{experiment group}} - A_{\text{blank group}})] / (A_{\text{control group}} - A_{\text{blank group}}) \times 100\%$.

Statistical analysis

t-test and SPSS software were employed to analyze data. $P < 0.05$ indicates significant difference.

RESULTS

Expression of SST2 in transfected and non-transfected PC-3 cells

Cells crawling on the slides were stained by immunocytochemical staining. SST2 gene expressing PC-3 cells would present brown particles spreading mainly in the cytoplasm and cell membrane (Figure 1). PC-3 cells non-transfected were negative-expression (Figure 2). We proved that PC-3 cells did not express SST2. In contrast, they could express SST2 after transfected with SST2 gene. And it also proved that the transfection was effective and accorded with the requirement of our experiments.

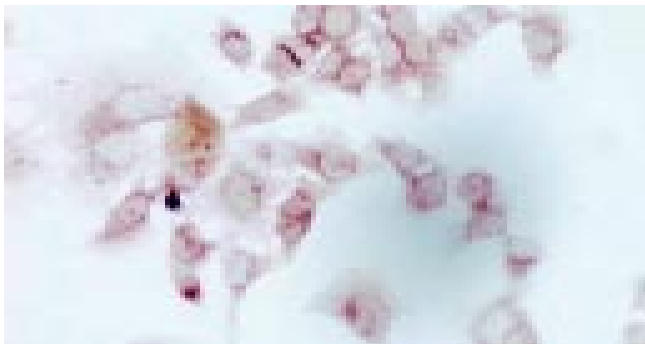


Figure 1 SST2 expressed in the transfected PC-3 cells (10 \times 40).



Figure 2 SST2 did not express in non-transfected PC-3 cells (10 \times 40).

Western blotting of SST2 expression

Protein of transfected PC-3 cells was extracted and the expression of SST2 was detected by Western blotting. SST2 in transfected PC-3 cells was detected (Figure 3), the M_r is about

40 000. It also proved that the transfection was effective at protein level. This was the base of our next experiments.

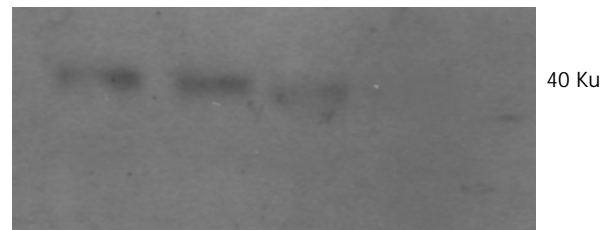


Figure 3 SST2 could be detected in the transfected PC-3 cells.

Analysis of PC-3 cell inhibition rate by MTT assay

Inhibition rate was detected by MTT assay. Growth inhibition rate of transfected PC-3 cells caused by octreotide was $3.45 \pm 0.91\%$ at the dosage of 0.05 $\mu\text{g}/\text{mL}$, $5.18 \pm 1.21\%$ at the dosage of 0.10 $\mu\text{g}/\text{mL}$, $9.36 \pm 1.34\%$ at the dosage of 0.20 $\mu\text{g}/\text{mL}$, $12.03 \pm 1.44\%$ at the dosage of 0.40 $\mu\text{g}/\text{mL}$ and $20.23 \pm 4.21\%$ at the dosage of 0.80 $\mu\text{g}/\text{mL}$. The inhibition rate caused by octreotide for non-transfected PC-3 cells was $3.28 \pm 0.54\%$ at the dosage of 0.05 $\mu\text{g}/\text{mL}$, $4.08 \pm 0.45\%$ at the dosage of 0.10 $\mu\text{g}/\text{mL}$, $6.44 \pm 0.66\%$ at the dosage of 0.20 $\mu\text{g}/\text{mL}$, $7.65 \pm 0.88\%$ at the dosage of 0.40 $\mu\text{g}/\text{mL}$ and $9.29 \pm 1.32\%$ at the dosage of 0.80 $\mu\text{g}/\text{mL}$. After using octreotide (0.05-0.80 $\mu\text{g}/\text{mL}$) for 48 h, we found that it caused a higher inhibition rate in transfected groups than in non-transfected groups ($P < 0.05$) at different dosages (0.20, 0.40 and 0.80 $\mu\text{g}/\text{mL}$). It proved that the expression of SST2 could enhance octreotide's effect on the inhibition of PC-3 cells (Figure 4).

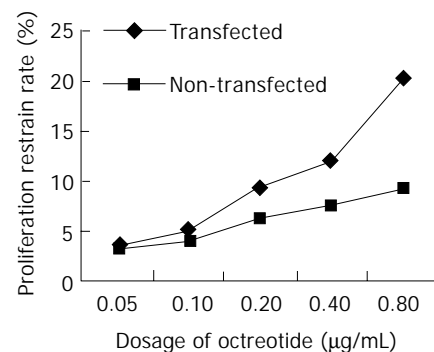


Figure 4 Transfected PC-3 cells growth inhibition rate under octreotide.

Flow cytometric analysis of PC-3 cell apoptosis rate

When 0.05-0.80 $\mu\text{g}/\text{mL}$ octreotide was added and incubated for 48 h, the PC-3 cells would show the typical apoptosis peak measured by flow cytometry. Moreover, the higher the drug dosage was, the higher the apoptosis rate was. Higher dosages (0.20, 0.40 and 0.80 $\mu\text{g}/\text{mL}$) of octreotide caused a greater increase of inhibition in PC-3 cells transfected groups than in non-transfected groups ($P < 0.05$) (Table 1).

Table 1 Apoptosis rate of PC-3 cells transfected and non-transfected with SST2 gene under different dosages of octreotide (mean \pm SD)

Dosage of octreotide ($\mu\text{g}/\text{mL}$)	Apoptosis rate of transfected PC-3 cells (%)	Apoptosis rate of non-transfected PC-3 cells (%)	<i>P</i>
0.05	3.65 \pm 0.66	2.77 \pm 0.33	>0.05
0.10	4.45 \pm 0.78	3.23 \pm 0.57	>0.05
0.20	7.56 \pm 1.06	5.76 \pm 0.75	<0.05
0.40	9.25 \pm 1.73	6.69 \pm 0.80	<0.05
0.80	14.18 \pm 2.71	7.26 \pm 1.28	<0.05

DISCUSSION

At present, somatostatin has been widely used in therapy of various tumors especially endocrine tumors. In a majority of cases, favorable effect has been noted. In combined treatment with classical chemotherapeutic drugs, such as 5-fluorouracil, somatostatin has synergistic action of killing tumor cells^[5]. The mechanism of somatostatin's anti-tumor effect *in vitro* lies in combining with its receptor. Somatostatin receptor belongs to a protein G coupled receptor family^[6]. According to the similarity of structure and difference in affinity to somatostatin, somatostatin receptors are classified into two categories: (1) having strong affinity to somatostatin, including SST2A, SST2B, SST3 and SST5; (2) having weak affinity to somatostatin, including SST1 and SST4^[7,8]. It is known that somatostatin receptors are extensively distributed in human central nervous system and other tissues. The category and amount of somatostatin receptor expression is different in various tumors. Somatostatin receptor, especially SST2 is usually highly expressed in many tumor tissues. SST2 may play a role in anti-tumor effect of somatostatin (It is considered as a tumor suppressing gene)^[9-11]. The mechanisms of somatostatin's anti-tumor action are as follows: (1) direct negative effect on tumor growth; (2) inhibiting the growth of tumors by interfering with synthesis of growth factors, which are produced via paracrine and autocrine of tumor cells; (3) anti-tumor effects by inhibiting excretion of somatotropin, insulin, gastrin and other hormones or depressing insulin-like growth factor-I (IGF-I), epidermal growth factor (EGF) and other growth factors; (4) interference with DNA synthesis of tumor cells; (5) suppression of angiogenesis of tumors^[12].

Substantial evidence has shown that loss or low expression of SST2 was observed in primary pancreatic cancer^[9,13-15]. Our previous research results have also shown that expression of SST2 was detected in 12.5 % of primary pancreatic cancers. These results suggest that expression of SST2 was deficient in a majority of pancreatic cancer tissues, which may be the main reason why somatostatin and somatostatin analogues were nearly inefficacious in the treatment of pancreatic cancer. But it is interesting that expression of SST2 was observed in the majority of adjacent histologically noncancerous pancreas, which was beneficial for somatostatin and somatostatin analogues to suppress fast invasion and growth of tumor cells. These results also suggest that if expression of SST2 in pancreatic cancer and adjacent histologically noncancerous pancreas was reduced; somatostatin and somatostatin analogues were nearly inefficacious in the treatment of pancreatic cancer. But if expression of SST2 in both pancreatic cancer and adjacent histologically noncancerous pancreas were observed, somatostatin and somatostatin analogues were efficacious^[11,1]. Therefore, different expression of SST2 in pancreatic cancer and adjacent histologically noncancerous pancreas is bound to result in different effects of treatment, which may be the main reason why reports of effects of somatostatin and somatostatin analogues treatment on pancreatic cancer are inconsistent at the present time. We believe that it is very important to make clear whether SST2 is expressed in pancreatic cancer and adjacent histologically noncancerous pancreas before somatostatin and somatostatin analogues are used in treatment of pancreatic cancer. We have demonstrated that transfecting SST2 gene into human pancreatic cancer cells which lack SST2 could markedly up-regulate SST2 expression, increase apoptosis rate of human pancreatic cancer cells and

enhance somatostatin analogue octreotide to inhibit growth of human pancreatic cancer cells and induce apoptosis. These results suggest that it may be an exciting molecular biological therapy for human pancreatic cancer deficiency of SST2 gene via transfection with SST2 gene and combination with somatostatin analogue.

REFERENCES

- 1 **Guillermet J**, Saint-Laurent N, Rochaix P, Cuvillier O, Levade T, Schally AV, Pradayrol L, Buscail L, Susini C, Bousquet C. Somatostatin receptor subtype 2 sensitizes human pancreatic cancer cells to death ligand-induced apoptosis. *Proc Natl Acad Sci U S A* 2003; **100**: 155-160
- 2 **Moneta D**, Richichi C, Aliprandi M, Dournaud P, Dutar P, Billard JM, Carlo AS, Viollet C, Hannon JP, Fehlmann D, Nunn C, Hoyer D, Epelbaum J, Vezzani A. Somatostatin receptor subtypes 2 and 4 affect seizure susceptibility and hippocampal excitatory neurotransmission in mice. *Eur J Neurosci* 2002; **16**: 843-849
- 3 **Hofland LJ**, Lamberts SW. Somatostatin receptor subtype expression in human tumors. *Ann Oncol* 2001; **12**(Suppl 2): S31-36
- 4 **Raderer M**, Hamilton G, Kurtaran A, Valencak J, Haberl I, Hoffmann O, Kornek GV, Vorbeck F, Hejna MH, Virgolini I, Scheithauer W. Treatment of advanced pancreatic cancer with the long-acting somatostatin analogue lanreotide: *in vitro* and *in vivo* results. *Br J Cancer* 1999; **79**: 535-537
- 5 **Weckbecker G**, Raulf F, Tolcsvai L, Bruns C. Potentiation of the anti-proliferative effects of anti-cancer drugs by octreotide *in vitro* and *in vivo*. *Digestion* 1996; **57**(Suppl 1): 22-28
- 6 **Burchett SA**, Flanary P, Aston C, Jiang L, Young KH, Uetz P, Fields S, Dohlman HG. Regulation of stress response signaling by the N-terminal dishevelled/EGL-10/pleckstrin domain of Sst2, a regulator of G protein signaling in *Saccharomyces cerevisiae*. *J Biol Chem* 2002; **277**: 22156-22167
- 7 **Prevost G**, Veber N, Viollet C, Roubert V, Roubert P, Benard J, Eden P. Somatostatin-14 mainly binds the somatostatin receptor subtype 2 in human neuroblastoma tumors. *Neuroendocrinology* 1996; **63**:188-197
- 8 **Hoyer D**, Bell GI, Berelowitz M, Epelbaum J, Feniuk W, Humphrey PP, O'Carroll AM, Patel YC, Schonbrunn A, Taylor JE. Classification and nomenclature of somatostatin receptors. *Trends Pharmacol Sci* 1995; **16**: 86-88
- 9 **Rochaix P**, Delesque N, Esteve JP, Saint-Laurent N, Voight JJ, Vaysse N, Susini C, Buscail L. Gene therapy for pancreatic carcinoma: local and distant antitumor effects after somatostatin receptor sst2 gene transfer. *Hum Gene Ther* 1999; **10**: 995-1008
- 10 **Hofland LJ**, Lamberts SW. Somatostatin analogs and receptors. Diagnostic and therapeutic applications. *Cancer Treat Res* 1997; **89**: 365-382
- 11 **Paillard F**. Somatostatin receptor gene transfer induces bystander effects. *Hum Gene Ther* 1999; **10**: 857-859
- 12 **Zaki M**, Harrington L, McCuen R, Coy DH, Arimura A, Schubert ML. Somatostatin receptor subtype 2 mediates inhibition of gastrin and histamine secretion from human, dog, and rat antrum. *Gastroenterology* 1996; **111**: 919-924
- 13 **Froidevaux S**, Hintermann E, Torok M, Macke HR, Beglinger C, Eberle AN. Differential regulation of somatostatin receptor type 2 (sst2) expression in AR4-2J tumor cells implanted into mice during octreotide treatment. *Cancer Res* 1999; **59**: 3652-3657
- 14 **Delesque N**, Buscail L, Esteve JP, Saint-Laurent N, Muller C, Weckbecker G, Bruns C, Vaysse N, Susini C. sst2 somatostatin receptor expression reverses tumorigenicity of human pancreatic cancer cells. *Cancer Res* 1997; **57**: 956-962
- 15 **Buscail L**, Saint-Laurent N, Chastre E, Vaillant JC, Gespach C, Capella G, Kalthoff H, Lluis F, Vaysse N, Susini C. Loss of sst2 somatostatin receptor gene expression in human pancreatic and colorectal cancer. *Cancer Res* 1996; **56**: 1823-1827

Inhibitory effect of *Huangqi Zhechong* decoction on liver fibrosis in rat

Shuang-Suo Dang, Xiao-Li Jia, Yan-An Cheng, Yun-Ru Chen, En-Qi Liu, Zong-Fang Li

Shuang-Suo Dang, Xiao-Li Jia, Yan-An Cheng, Yun-Ru Chen,
Department of Infectious Diseases, Second Hospital of Xi'an Jiaotong University, Xi'an 710004, Shaanxi Province, China

En-Qi Liu, Center of Experimental Animal, Xi'an Jiaotong University, Xi'an 710004, Shaanxi Province, China

Zong-Fang Li, Department of Surgery, Second Hospital of Xi'an Jiaotong University, Xi'an 710004, Shaanxi Province, China

Supported by the Science and Technology Foundation of Shaanxi Province, No. 2002k11-G7

Correspondence to: Shuang-Suo Dang, Department of Infectious Disease, Second Hospital of Xi'an Jiaotong University, Xi'an 710004, Shaanxi Province, China. shuang suo640212@sohu.com

Telephone: +86-29-83036998

Received: 2003-12-19 **Accepted:** 2004-01-15

Abstract

AIM: To assess the inhibitory effect of *Huangqi Zhechong* decoction on hepatic fibrosis in rats induced by CCl₄ plus alcohol and high fat low protein diet.

METHODS: Male SD rats were randomly divided into hepatic fibrosis model group, control group and 3 treatment groups consisting of 12 rats in each group. Except for the normal control group, all the rats were subcutaneously injected with CCl₄ at a dosage of 3 mL/kg. In 3 treated groups, either high-dose group (9 mL/kg), or medium-dose group (6 mL/kg), or low-dose group (3 mL/kg) was daily gavaged with *Huangqi Zhechong* decoction, and saline vehicle was given to model and normal control rats. Enzyme-linked immunosorbent assay (ELISA) and biochemical examinations were used to determine the changes of alanine aminotransferase (ALT), aspartate aminotransferase (AST), hyaluronic acid (HA), laminin (LN), type-III-procollagen-N-peptide (PIIIP), and type IV collagen content in serum, and hydroxyproline (Hyp) content in liver after sacrificing the rats. Pathologic changes, particularly fibrosis were examined by hematoxylin and eosin (HE) and Van Gieson staining.

RESULTS: Compared with the model control group, serum ALT, AST, HA, LN, PIIIP and type IV collagen levels dropped markedly in *Huangqi Zhechong* decoction groups, especially in the medium-dose *Huangqi Zhechong* decoction group (1 954±576 U/L vs 759±380 U/L, 2 735±786 U/L vs 1 259±829 U/L, 42.74±7.04 ng/mL vs 20.68±5.85 ng/mL, 31.62±5.84 ng/mL vs 14.87±1.45 ng/mL, 3.26±0.69 ng/mL vs 1.47±0.46 ng/mL, 77.68±20.23 ng/mL vs 25.64±4.68 ng/mL, respectively) ($P<0.05$). The Hyp content in liver tissue was also markedly decreased (26.47±11.24 mg/mgprot vs 9.89±3.74 mg/mgprot) ($P<0.01$). Moreover, the stage of the rat liver fibrosis in *Huangqi Zhechong* decoction groups was lower than that in model group, and more dramatic drop was observed in medium-dose *Huangqi Zhechong* decoction group ($P<0.01$).

CONCLUSION: *Huangqi Zhechong* decoction can inhibit hepatic fibrosis resulted from chronic liver injure, retard the development of cirrhosis, and notably ameliorate the liver

function. It may be a safe and effective therapeutic drug for patients with fibrosis.

Dang SS, Jia XL, Cheng YA, Chen YR, Liu EQ, Li ZF. Inhibitory effect of *Huangqi Zhechong* decoction on liver fibrosis in rat. *World J Gastroenterol* 2004; 10(15): 2295-2298

<http://www.wjgnet.com/1007-9327/10/2295.asp>

INTRODUCTION

Liver fibrosis is common in most chronic liver diseases regardless of the etiology^[1-8]. Although new therapeutic approaches have recently been proposed, there is no established therapy for liver fibrosis^[9]. *Huangqi Zhechong* decoction is a traditional Chinese medicine. The aim of the present study was to investigate the protective effects of *Huangqi Zhechong* decoction on liver fibrosis in rats of CCl₄-induced cirrhosis.

MATERIALS AND METHODS

Reagents

CCl₄ (Xi'an Chemical Factory) was diluted into 400 g/L in olive oil (Xi'an Chemical Factory). *Huangqi Zhechong* decoction was self-made by the Pharmaceutical Department of the Second Hospital, Xi'an Jiaotong University. The kit for Hyp was bought from Nianjing Jiancheng Biological Institute. Kits for HA, LN, PIIIP and type IV collagen were bought from Senxiong Company, Shanghai.

Animals

Sixty adult male SD rats weighing 150-200 g were provided by the Laboratory Animal Center of the College of Medicine, Xi'an Jiaotong University. The rats were randomly divided into 5 groups of 12 each: control group; model group; and 3 treatment groups. Except for the control rats, all rats were subcutaneously injected with 400 g/L CCl₄ (CCl₄:Olive oil 2:3), 3 mL/kg·b.w., at every 3 d for 6 wk, and fed with high fat low protein diet (75% pure maize plus 20% lard and 0.5% cholesterol) and 300 mL/L alcohol as drinks. In the 3 treatment groups, *Huangqi Zhechong* decoction was administered daily via gastric tube to high-dose, medium-dose and low-dose groups at a dosage of 9 mL/kg, 6 mL/kg and 3 mL/kg for 6 wk, respectively. After 6 wk, except the dead, all the rats were anesthetized with 200 g/L urethane (5 mL/kg, abdominal injection). Blood was taken from abdominal aorta, centrifuged at 4 °C, and plasma were kept at -20 °C for assays.

Pathological observations

Hepatic tissues were fixed in 40 g/L solutions of formaldehyde in 0.1% mol/L phosphate-buffered saline (pH 7.4), and embedded in paraffin. Five-micrometer thick section slides were prepared. All the sections stained with HE and standard van Gieson staining (VG) were coded and scored by blind reading. Van Gieson's method was used to detect collagen fibers^[10]. Liver condition was classified according to the standard formulated by China Medical Association in 1995^[11],

and fibrosis was graded from 0 to 4 (0: no fibrosis; 1: portal area fibrosis; 2: fibrotic septa between portal tracts; 3: fibrosis septa and structure disturbance of hepatic lobule; and 4: cirrhosis).

Statistical analysis

Results were expressed as mean±SD. Quantitative data were analyzed by using ANOVA in statistical software SPSS 11.0. A value of $P<0.05$ was considered statistically significant. Redit test was used for statistical analysis of the qualitative data.

RESULTS

Hyp content in liver tissues

Liver Hyp level was significantly lower in rats treated with CCl_4 and *Huangqi Zhechong* decoction compared to the rats treated with CCl_4 alone ($P<0.01$). And the liver Hyp level of rat in 3 *Huangqi Zhechong* decoction treatment groups has no significant difference from control group (Table 1).

Plasma levels of ALT and AST

Plasma levels of ALT and AST in model group were higher than those in the controls ($P<0.01$), while the *Huangqi Zhechong* decoction treatment groups showed significant lower

ALT and AST levels than the model group. Furthermore, among the 3 treatment groups the medium-dose group showed the best effect and the levels of ALT and AST in serum showed no difference compared with the normal group (Table 1).

Table 1 Level of serum ALT, AST and liver Hyp

Group	<i>n</i>	ALT (U/L)	AST (U/L)	Liver Hyp (μg/mgprot)
Control	12	86.0±17.7	329±40	10.02±1.05
Model	11	1 954±576 ^d	2 735±786 ^d	26.47±11.24 ^d
High-dose group	9	989±576 ^{ad}	1 584±988 ^c	15.01±7.59 ^b
Medium-dose group	10	759±380 ^{bc}	1 259±829 ^a	9.89±3.74 ^b
Low-dose group	10	1 003±530 ^{ad}	1 650±928 ^c	10.06±2.58 ^b

^a $P<0.05$, ^b $P<0.01$ vs model group; ^c $P<0.05$, ^d $P<0.01$ vs control group.

HA, LN, PIIP and type IV collagen levels in serum

Serum levels of HA, LN, PIIP and type IV collagen in model group, compared with the controls, were all markedly increased ($P<0.01$). And compared with the model group, the serum levels of HA, LN, PIIP and type IV collagen were significant decreased in the 3 treatment groups ($P<0.01$) (Table 2).

Table 2 Serum levels of HA, LN, PIIP and type IV collagen

Group	<i>n</i>	PIIP (ng/mL)	Type IV collagen (ng/mL)	LN (ng/mL)	HA (ng/mL)
Control	12	0.34±0.67	18.47±3.43	10.07±1.74	17.96±5.86
Model	11	3.26±0.69 ^d	77.68±20.23 ^d	31.62±5.84 ^d	42.74±7.04 ^d
High-dose group	9	2.01±0.40 ^{bd}	39.14±4.97 ^{bd}	16.32±2.73 ^{bd}	21.71±5.69 ^b
Medium-dose group	10	1.47±0.46 ^{bd}	25.64±4.68 ^b	14.87±1.45 ^{bd}	20.68±5.85 ^b
Low-dose group	10	1.84±0.27 ^{bd}	29.09±2.78 ^b	17.02±2.74 ^{bd}	24.18±7.89 ^b

^a $P<0.05$, ^b $P<0.01$ vs model group; ^c $P<0.05$, ^d $P<0.01$ vs control group.

Table 3 Pathological observation of liver condition

Group	<i>n</i>	Liver condition					<i>U</i>
		0	I	II	III	IV	
Model	11	0	0	0	3	8	
High-dose group	9	0	2	3	3	1	2.98 ^a
Medium-dose group	10	0	4	4	2	0	4.01 ^b
Low-dose group	10	0	2	4	3	1	3.75 ^b

^a $P<0.05$, ^b $P<0.01$ vs model group; The value of *U* represents the Redit value of the two groups, $U>1.96$ means $P<0.05$, $U>2.58$ means $P<0.01$.



Figure 1 Liver tissue under light microscope. A: Normal liver tissue in control group (HE staining, original magnification: ×400); B: Liver fibrosis tissue in model group, more fibrous tissue was formed in liver. A large amount of inflammatory cells soaked into the intralobular and the interlobular (van Gieson staining, original magnification: ×200); C: Liver fibrosis tissue in *Huangqi Zhechong* decoction group. The pathological change of liver was rather lighter compared with the model (van Gieson staining, original magnification: ×200).

Pathological assay

At the end of the study, the liver of control rats had no appreciable alterations (Figure 1A). In the model group, the margin of liver was uneven; more fibrous tissues formed and extended into the hepatic lobules to separate them incompletely; a large amount of inflammatory cells infiltrated in the intralobular and the interlobular regions; the liver structure was disordered with some displacement of central veins, and there were more necrotic and degenerated liver cells compared with the control (Figure 1B). While in the 3 treatment groups, especially in the medium-dose group, the pathological changes of liver was rather milder, showing less fibrous tissue proliferation and inflammatory cell infiltration in the interlobular space; the hepatic cell cords arranged radially with less displacement of central veins and less degenerated or necrosis hepatic cells, without any pseudolobule observed (Figure 1C). Compared with the model group, the liver condition of the rats was significantly improved in *Huangqi Zhechong* decoction groups (Table 3).

DISCUSSION

The incidence rate of chronic hepatopathy in China is high, which afflicts the patients by progressively developing irreversible cirrhosis^[12,13]. Hepatic fibrosis is the intermediate and crucial stage of this process, characterized by reversibility. If treated properly in this stage, cirrhosis could be successfully prevented^[14]. But it remains a problem to prevent cirrhosis or to control its progression in patients with a chronic liver disease^[15]. Great efforts have been made to find safe and effective drugs. Recent clinical and experimental observations have demonstrated that Chinese medicines might be of some preventive and therapeutic values against fibrosis^[16-18].

Of *Huangqi Zhechong* decoction, the Chinese traditional medicine, the *Astragalus* has the effects of activating blood circulation to relieve stasis, strengthening "spleen", supplementing and smoothening "qi" to eliminate fullness, reinforcement body's immunological function. It also could preserve the integrity of hepatocytes, eliminate toxic free radicals, inhibit lipid peroxidation of cytomembrane, relieve necrosis of hepatocytes, and obviously antifibrosis^[19-23]. *Thoroughfare* is mainly used to activate blood circulation, remove stasis, and dredge the liver^[24].

Huangqi Zhechong decoction has been used in clinic for many years to prevent liver fibrosis and shown good effect. However, its effect and the associated mechanisms need further experimental evidence. CCl₄ is a super-hepatotoxin, with which the CCl₃ free radical is produced during metabolic processes and acts on liver cells to covalently conjugate with the membranous unsaturated lipid to cause lipid peroxidation and necrosis of hepatocytes^[25-27]. For this reason, CCl₄ was used to induce liver fibrosis.

We started to treat the rats with *Huangqi Zhechong* decoction at the same time of subcutaneous injection with CCl₄. After 6 wk, the histological features showed that there were no appreciable alterations in control group. But pathological evaluation showed that the rats in model group almost had integrity fibrosis septum, and pseudolobular could be seen in nearly every section. While the rats received *Huangqi Zhechong* decoction had less fibrosis, the reticular fibrosis in the interlobular septum was limited remarkably, and no pseudolobular could be seen. In addition, *Huangqi Zhechong* decoction, especially the medium-dose administration could decrease the scores of hepatic fibrosis grading.

ALT and AST are indexes to describe liver functions. Most part of ALT is presented in the cytoplasm of liver cell, discharged in blood when degeneration, hyper permeability and necrosis of liver cells occur. So the increase of ALT level in serum reflects the degree of liver cell injury. Our study

showed that the *Huangqi Zhechong* decoction could decrease serum levels of ALT and AST in rats with hepatic injury caused by CCl₄. It indicates that *Huangqi Zhechong* decoction may work through protecting the liver cells.

HA, LN, PIIIP and type IV collagen are good serum markers of hepatic fibrosis. In this study, the serum contents of these 4 markers in the model group were much higher than those of the controls ($P < 0.01$). And the *Huangqi Zhechong* decoction groups had significantly low HA, LN, PIIIP and type IV collagen levels in serum than those in the controls, which indicated that *Huangqi Zhechong* decoction could successfully prevent hepatic fibrosis.

Hyp content in liver is another important index to react the hepatic fibrosis. In fibrotic liver, collagen fibers increase, which induced the rise of Hyp content in liver^[28]. So Hyp level could provide the information about the degree and variant process of cirrhosis. In this study, we observed that the liver Hyp level in the model group was much higher than that of the controls and *Huangqi Zhechong* decoction groups.

In summary, *Huangqi Zhechong* decoction may play a role in antifibrotic therapy. It can protect the liver cells and inhibit the deposition of collagen fibers in liver. It may provide a safe and effective strategy for inhibition of cirrhosis in clinic use.

REFERENCES

- 1 **Ma X**, Qiu DK, Peng YS. Immunohistochemical study of hepatic oval cells in human chronic viral hepatitis. *World J Gastroenterol* 2001; **7**: 238-242
- 2 **Reshetnyak VI**, Sharafanova TI, Ilchenko LU, Golovanova EV, Poroshenko GG. Peripheral blood lymphocytes DNA in patients with chronic liver diseases. *World J Gastroenterol* 2001; **7**: 235-237
- 3 **McCaughan GW**, Gorrell MD, Bishop GA, Abbott CA, Shackel NA, McGuinness PH, Levy MT, Sharland AF, Bowen DG, Yu D, Slaitini L, Church WB, Napoli J. Molecular pathogenesis of liver disease: an approach to hepatic inflammation, cirrhosis and liver transplant tolerance. *Immunol Rev* 2000; **174**: 172-191
- 4 **Okazaki I**, Watanabe T, Hozawa S, Arai M, Maruyama K. Molecular mechanism of the reversibility of hepatic fibrosis: with special reference to the role of matrix metalloproteinases. *J Gastroenterol Hepatol* 2000; **15**(Suppl): D26-32
- 5 **Jung SA**, Chung YH, Park NH, Lee SS, Kim JA, Yang SH, Song IH, Lee YS, Suh DJ, Moon IH. Experimental model of hepatic fibrosis following repeated periportal necrosis induced by allyl alcohol. *Scand J Gastroenterol* 2000; **35**: 969-975
- 6 **Plummer JL**, Ossowicz CJ, Whibley C, Ilsley AH, Hall PD. Influence of intestinal flora on the development of fibrosis and cirrhosis in a rat model. *J Gastroenterol Hepatol* 2000; **15**: 1307-1311
- 7 **Croquet V**, Moal F, Veal N, Wang J, Oberti F, Roux J, Vuillemin E, Gallois Y, Douay O, Chappard D, Cales P. Hemodynamic and antifibrotic effects of losartan in rats with liver fibrosis and/or portal hypertension. *J Hepatol* 2002; **37**: 773-780
- 8 **Marcellin P**, Asselah T, Boyer N. Fibrosis and disease progression in hepatitis C. *Hepatology* 2002; **36**(5 Suppl 1): S47-56
- 9 **Friedman SL**. Molecular regulation of Hepatic fibrosis, an integrated cellular response to tissue injury. *J Biol Chem* 2000; **275**: 2247-2250
- 10 **Zhu H**, Zeng L, Zhu D, Yuan Y. The role of TGF-beta 1 in mice hepatic fibrosis by Schistosomiasis Japonica. *J Tongji Med Univ* 2000; **20**: 320-321
- 11 China Medical Association infectious branch. The standard of grading and staging of viral hepatitis. *Zhonghua Chuanranbing Zazhi* 1995; **13**: 241-247
- 12 **Lamireau T**, Desmouliere A, Bioulac-Sage P, Rosenbaum J. Mechanisms of hepatic fibrogenesis. *Arch Pediatr* 2002; **9**: 392-405
- 13 **Brenner DA**, Waterboer T, Choi SK, Lindquist JN, Stefanovic B, Burchard E, Yamauchi M, Gillan A, Rippe RA. New aspects of hepatic fibrosis. *J Hepatol* 2000; **32**(1 Suppl): 32-38
- 14 **Riley TR 3rd**, Bhatti AM. Preventive strategies in chronic liver disease: part II. Cirrhosis. *Am Fam Physician* 2001; **64**: 1735-1740
- 15 **Murphy F**, Arthur M, Iredale J. Developing strategies for liver

- fibrosis treatment. *Expert Opin Investig Drugs* 2002; **11**: 1575-1585
- 16 **Liu C**, Jiang CM, Liu CH, Liu P, Hu YY. Effect of Fuzhenghuayu decoction on vascular endothelial growth factor secretion in hepatic stellate cells. *Hepatobiliary Pancreat Dis Int* 2002; **1**: 207-210
- 17 **Liu P**, Liu CH, Wang HN, Hu YY, Liu C. Effect of salivianolic acid B on collagen production and mitogen-activated protein kinase activity in rat hepatic stellate cells. *Acta Pharmacol Sin* 2002; **23**: 733-738
- 18 **Kusunose M**, Qiu B, Cui T, Hamada A, Yoshioka S, Ono M, Miyamura M, Kyotani S, Nishioka Y. Effect of Sho-saiko-to extract on hepatic inflammation and fibrosis in dimethylnitrosamine induced liver injury rats. *Biol Pharm Bull* 2002; **25**: 1417-1421
- 19 **Wang RT**, Shan BE, Li QX. Extracorporeal experimental study on immuno-modulatory activity of Astragalus membranaceus extract. *Zhongguo Zhongxiyi Jiehe Zazhi* 2002; **22**: 453-456
- 20 **Chu DT**, Lin JR, Wong W. The *in vitro* potentiation of LAK cell cytotoxicity in cancer and aids patients induced by F3—a fractionated extract of Astragalus membranaceus. *Zhonghua Zhongliu Zazhi* 1994; **16**: 167-171
- 21 **Zhang YD**, Shen JP, Zhu SH, Huang DK, Ding Y, Zhang XL. Effects of astragalus (ASI, SK) on experimental liver injury. *Yaoxue Xuebao* 1992; **27**: 401-406
- 22 **Tan YW**, Yin YM, Yu XL. Influence of Salvia miltiorrhizae and Astragalus membranaceus on hemodynamics and liver fibrosis indexes in liver cirrhotic patients with portal hypertension. *Zhongguo Zhongxiyi Jiehe Zazhi* 2001; **21**: 351-353
- 23 **Fu QL**. Experimental study on yiqi-huoxue therapy of liver fibrosis. *Zhongguo Zhongxiyi Jiehe Zazhi* 1992; **12**: 228-229
- 24 **Chen H**, Weng L. Comparison on efficacy in treating liver fibrosis of chronic hepatitis B between Astragalus Polygonum anti-fibrosis decoction and jinshuibao capsule. *Zhongguo Zhongxiyi Jiehe Zazhi* 2000; **20**: 255-257
- 25 **Kanta J**, Dooley S, Delvoux B, Breuer S, D'Amico T, Gressner AM. Tropoelastin expression is up-regulated during activation of hepatic stellate cells and in the livers of CCl₄-cirrhotic rats. *Liver* 2002; **22**: 220-227
- 26 **Yan JC**, Ma Y, Chen WB, Xu CJ. Dynamic observation on vascular diseases of liver tissues of rats induced by CCl₄. *Shijie Huaren Xiaohua Zazhi* 2000; **8**: 42-45
- 27 **Yan JC**, Chen WB, Ma Y, Xu CJ. Immunohistochemical study on hepatic vascular forming factors in liver fibrosis induced by CCl₄ in rats. *Shijie Huaren Xiaohua Zazhi* 2000; **8**: 1238-1241
- 28 **Garcia L**, Hernandez I, Sandoval A, Salazar A, Garcia J, Vera J, Grijalva G, Muriel P, Margolin S, Armendariz-Borunda J. Pirfenidone effectively reverses experimental liver fibrosis. *J Hepatol* 2002; **37**: 797-805

Edited by Kumar M and Chen WW Proofread by Xu FM

Transanal approach in repairing acquired rectovestibular fistula in females

Ya-Jun Chen, Ting-Chong Zhang, Jin-Zhe Zhang

Ya-Jun Chen, Ting-Chong Zhang, Jin-Zhe Zhang, Beijing Children's Hospital, Capital University of Medical Sciences, Beijing 100045, China

Correspondence to: Dr. Ya-Jun Chen, Beijing Children's Hospital, Capital University of Medical Sciences, Beijing 100045, China. chen-yajun@hotmail.com

Telephone: +86-10-63296188 **Fax:** +86-10-68011503

Received: 2003-12-17 **Accepted:** 2004-01-13

Abstract

AIM: To summarize the operative experience of the transanal approach in acquired rectovestibular fistula repair.

METHODS: Ninety-six cases of acquired rectovestibular fistula in young females were analyzed retrospectively. The etiology and operative procedure were discussed. Operative essential points were, the patient was laid in prone frog position, with the knees and hips flexed at 90°; the perineum was elevated; and the anal opening was exposed. Four stay sutures were applied to the margin of the fistular orifice in the anal opening at points 3, 6, 9 and 12 o'clock. A circular incision of mucosa surrounding the stay sutures was made. The fistula was dissected from its anal opening to its vestibular opening. The wound of vestibule was sutured, and the rectoanal wound was then sutured transversely.

RESULTS: All the 96 patients recovered uneventfully from operation with a successful rate of 93.75%.

CONCLUSION: The transanal approach in the treatment of the acquired rectovestibular fistula is a simple and feasible technique.

Chen YJ, Zhang TC, Zhang JZ. Transanal approach in repairing acquired rectovestibular fistula in females. *World J Gastroenterol* 2004; 10(15): 2299-2300

<http://www.wjgnet.com/1007-9327/10/2299.asp>

INTRODUCTION

Acquired rectovestibular fistula in small girls is a common anorectal disease. Its etiology is still indefinite. Some of pediatric surgeons described it as a kind of congenital malformation. In China, most thought it as an acquired disease caused by the infection of crypts of *Morgagni*^[1-7]. There are two main surgical procedures that are commonly adopted, transanal and perineal approach^[8-13].

MATERIALS AND METHODS

Patients

Ninety-six patients with an average age of four years and two mo, ranging from 6 mo to 14 years, were admitted and operated. Most patients came with the complaint of passing stool or flatus through vagina. Half of them had a history of perineal inflammation at the early life of 2-3 mo. An external opening

was usually found in the vestibule, a little bit right or left to the vaginal opening, while the internal opening was always found at the mid-point of the dentate line on the anterior anorectal wall. The diameter of fistula orifice ranged from 2 to 8 mm.

Preoperative preparation

Metronidazole tablet (30 mg/kg per day, divided t.i.d) and oral garamycina (15 mg/kg per day, divided t.i.d) were given before operation for 3 d. Nothing but water by mouth was allowed for 1 d before operation day. Enema was performed at the night before operation day and on the morning of the operation day.

Operative methods

Under general anesthesia, patient was laid in prone frog position, with knees and hips flexed at 90° fixed at the caudal end of the operation table, with a soft pillow placed under the pubis. Almost half roll of sterile bandage was inserted into rectum to prevent rectal discharge. The tail of bandage might be soaked with iodophor before being sent deeply into the rectum, and it was tied by a long heavy silk, which was left outside the anal orifice in order to make the removal of the bandage easily after operation. The anal opening was widely stretched bilaterally to expose the inner opening of fistula, four stay sutures were applied to four points at 3, 6, 9 and 12 o'clock respectively. The stay sutures were pulled, and a circular incision of mucosa around the inner opening of fistula was made by Bovie. The fistula was dissected toward the outer opening in the vestibule and resected. The wound of vestibule was sutured interruptedly with 5-0 Dexon. Usually fistula was about 0.8 cm long. The levator ani muscle was approximated longitudinally to abolish the dead space anterior to the rectum. The anorectal wall was freed proximally for about 1.0 cm to make the wound closed without tension. The packing bandage in rectum was pulled out after operation.

Postoperative treatment

Nothing but water by mouth was provided for 3 d after operation, and intravenous antibiotics were given 3 to 5 d. Perianal area was kept clean and dry by warm ventilation 3 to 5 times every day for some 5 d.

RESULTS

Six cases, about 6.25% of all patients, had recurrence of fistula. However, three of them healed spontaneously 2 to 3 wk later without any specific treatment except sitz bath with 30 g/L boric acid.

DISCUSSION

Bryndorf and Madsen reported rectovestibular fistula, a fistulous tract between the bowel and the low female genital tract, in 1960^[14]. The disease is more common in Asian than in Europeans. There were two controversial opinions about its etiology, the congenital or the acquired. Chatterjee *et al.*^[1-5] described rectovestibular fistula with normal anus in females as a kind of congenital malformation, double terminal of the alimentary tract. The family history, coexisting anomalies as

anal stenosis or sacral vertebrae abnormality and the stratified squamous epithelium lining of fistular wall were the basis favouring the congenital consideration. The inflammatory changes of fistula might be secondary.

Most doctors in China believe that the development of rectovestibular fistula with normal anus in small girls was similar to the inflammatory fistula-in-ano in males^[6-8]. The inflammation started by the infection of crypts of Morgagni, perianal abscess formation followed, and finally it ruptured through the vestibule. On the other hand, some deep crypts or anal glands cystoid dilatation as well as infantile hypoergic immunity of the rectoanal mucosa make the rectum mucosa barrier imperfect^[15-17]. All these might play a role in anal fistula formation. Certainly it was not the congenital double termination of the alimentary tract. None of patients had a definite history of fistula at birth, and neither did a surgical specimen show normal histology of mucosa, submucosa and continuous smooth muscle in the fistula tract.

Ninety-six females with acquired rectovestibular fistula were treated by transanal approach in the last 10 years with a satisfactory result. The main experience may be concluded as: (1) Rectal bandage packing may prevent stool contamination during operation. (2) Fistula should be dissected completely by Bovie to make a bloodless operation field. (3) Rectum and vagina should be separated clearly. (4) Anterior rectal wall should be sutured perfectly without tension. (5) Dead space anterior to rectum should be eliminated by suturing the levator ani muscles and central body.

The favorite age for operation ought to be 3 to 5 years in order to wait for the improvement of the symptoms and also for better development of perianal structures of the child.

Recurrence of fistula, if happened, often occurred about 7 d after operation, and its symptoms included perineal inflammation, followed by passing of stool or flatus through the sutured incision. By sitz bath in 30 g/L boric acid and waiting for inflammation subsiding, half of the patients with early recurrent fistula healed spontaneously.

Diverting colostomy provides a clean operation area for anal fistula repair^[11,12], but it needs at least three operations. We believe that a careful preoperative, operative and postoperative treatment offers a satisfactory result without a diverting colostomy.

REFERENCES

- 1 **Chatterjee SK**. Double termination of the alimentary tract-a second look. *J Pediatr Surg* 1980; **15**: 623-627
- 2 **Bagga D**, Chadha R, Malhotra CJ, Dhar A. Congenital H-type vestibuloanorectal fistula. *Pediatr Surg Int* 1995; **10**: 481-484
- 3 **Rintala RJ**, Mildh L, Lindahl H. H-type anorectal malformations: incidence and clinical characteristics. *J Pediatr Surg* 1996; **31**: 559-562
- 4 **Bianchini MA**, Fava G, Cortese MG, Vinardi S, Costantino S, Canavese F. A rare anorectal malformation: a very large H-type fistula. *Pediatr Surg Int* 2001; **17**: 649-651
- 5 **Yazici M**, Etensel B, Gürsoy H, Özksaçk S. Congenital H-type anovestibular fistula. *World J Gastroenterol* 2003; **9**: 881-882
- 6 **Zhang JZ**. Etiological and pathological study of fistula-in-ano in children. *Zhonghua Xiaerwaike Zazhi* 1988; **9**: 111-112
- 7 **Sun L**, Wang YX, Liu Y. Histopathological study of fistula-in-ano in female. *Zhonghua Xiaerwaike Zazhi* 1995; **16**: 136-137
- 8 **Chen YJ**, Niu ZY, Zhang JZ, Liu YT, Li L, Wang DY. Transperineal approach to repair acquired rectovestibular fistula in female. *Shiyong Erkelin Chuang Zazhi* 2001; **16**: 242-243
- 9 **Tsugawa C**, Nishijima E, Muraji T, Satoh S, Kimura K. Surgical repair of rectovestibular fistula with normal anus. *J Pediatr Surg* 1999; **34**: 1703-1705
- 10 **Kulshrestha S**, Kulshrestha M, Prakash G, Gangopadhyay AN, Sarkar B. Management of congenital and acquired H-type anorectal fistulae in girls by anterior sagittal anorectovaginoplasty. *J Pediatr Surg* 1998; **33**: 1224-1228
- 11 **Mirza I**, Zia-ul-Miraj M. Management of perineal canal anomaly. *Pediatr Surg Int* 1997; **12**: 611-612
- 12 **Ismail A**. Perineal canal: a simple method of repair. *Pediatr Surg Int* 1994; **9**: 603-604
- 13 **Rao KL**, Choudhury SR, Samujh R, Narasimhan KL. Perineal canal-repair by a new surgical technique. *Pediatr Surg Int* 1993; **8**: 449-450
- 14 **Bryndorf J**, Madsen CM. Ectopic anus in the female. *Acta Chir Scand* 1960; **118**: 466-478
- 15 **Watanabe Y**, Todani T, Yamamoto S. Conservative management of fistula in ano in infants. *Pediatr Surg Int* 1998; **13**: 274-276
- 16 **Festen C**, van Harten H. Perianal abscess and fistula-in-ano in infants. *J Pediatr Surg* 1998; **33**: 711-713
- 17 **Rosen NG**, Gibbs DL, Soffer SZ, Hong A, Sher M, Pena A. The nonoperative management of fistula-in-ano. *J Pediatr Surg* 2000; **35**: 938-939

Edited by Zhu LH and Chen WW Proofread by Xu FM

Hepatitis B virus reactivation in a patient undergoing steroid-free chemotherapy

Daisuke Shimizu, Kenichi Nomura, Yosuke Matsumoto, Kyoji Ueda, Kanji Yamaguchi, Masahito Minami, Yoshito Itoh, Shigeo Horiike, Masuji Morita, Masafumi Taniwaki, Takeshi Okanoue

Daisuke Shimizu, Kenichi Nomura, Yosuke Matsumoto, Kyoji Ueda, Shigeo Horiike, Masafumi Taniwaki, Molecular Hematology and Oncology, Kyoto Prefectural University of Medicine Graduate School of Medical Science, Kyoto 602-0841, Japan

Kanji Yamaguchi, Masahito Minami, Yoshito Itoh, Takeshi Okanoue, Molecular Gastroenterology and Hepatology, Kyoto Prefectural University of Medicine Graduate School of Medical Science, Kyoto 602-0841, Japan

Masuji Morita, School of Nursing, Kyoto Prefectural University of Medicine Graduate School of Medical Science, Kyoto 602-0841, Japan

Masafumi Taniwaki, Clinical Molecular Genetics and Laboratory Medicine, Kyoto Prefectural University of Medicine Graduate School of Medical Science, Kyoto 602-0841, Japan

Correspondence to: Dr. Kenichi Nomura, Molecular Hematology and Oncology, Kyoto Prefectural University of Medicine Graduate School of Medical Science, Kawaramachi-Hirokoji, Kamigyo-Ku, Kyoto 602-0841, Japan. nomuken@sun.kpu-m.ac.jp

Telephone: +81-75-251-5521 **Fax:** +81-75-251-0710

Received: 2004-03-15 **Accepted:** 2004-04-09

Abstract

A 62-year-old Japanese man who was positive for hepatitis B surface antigen (HBsAg) and anti-HBe antibody, underwent chemotherapy for non-Hodgkin's lymphoma (NHL). Mutations were detected in the precore region (nt1896) of HBV. Because steroid-containing regimen may cause reactivation of hepatitis B virus (HBV) and hepatitis may progress to be fulminant after its withdrawal, we administered CHO (CPA, DOX and VCR) therapy and the patient obtained complete response. However, he developed acute exacerbation of hepatitis due to HBV reactivation. Recovery was achieved with lamivudine (100 mg/d) and plasma exchange. The present case suggests that acute exacerbation of hepatitis can occur with steroid-free regimen. Because the efficacy of the prophylactic use of lamivudine has been reported and the steroid enhances curability of malignant lymphoma, the steroid containing regimen with prophylaxis of lamivudine should be evaluated further.

Shimizu D, Nomura K, Matsumoto Y, Ueda K, Yamaguchi K, Minami M, Itoh Y, Horiike S, Morita M, Taniwaki M, Okanoue T. Hepatitis B virus reactivation in a patient undergoing steroid-free chemotherapy. *World J Gastroenterol* 2004; 10(15): 2301-2302

<http://www.wjgnet.com/1007-9327/10/2301.asp>

INTRODUCTION

CHOP regimen consisting of cyclophosphamide (CPA), doxorubicin (DOX), vincristine (VCR), and prednisolone (PSL) is performed as the first line therapy for non-Hodgkin's lymphoma (NHL) because of its high response rate and less incidence of side effect. However, CHOP regimen for hepatitis B virus (HBV) carrier may cause reactivation of HBV due to prednisolone and hepatitis may progress to be fulminant after its withdrawal. On the other hand, it has already been proven

that steroid containing-regimens show higher complete response and survival rate than steroid free regimens^[1]. Thus, it is difficult to choose which chemotherapeutic regimen for NHL carrying HBV.

We described an asymptomatic HBV carrier patient with NHL who received CHO therapy. Although he achieved complete response, hepatitis acutely exacerbated. Lamivudine and plasma exchange improved hepatic failure.

CASE REPORT

A 62-year-old man complained of tonsil swelling, redness and sore throat. He was referred to our hospital in August 2003. Needle biopsy from tonsil revealed him as having NHL (diffuse large B-cell lymphoma). He was admitted to our hospital on August 21 because tonsil swelling developed rapidly. Two enlarged cervical lymph nodes were palpable and right tonsil swelled. Hematological studies showed WBC 5 600/mL, Hb 15.4 g/dL and platelet $7.2 \times 10^4/\text{mm}^3$, LDH 167 IU/L, GOT 25 IU/L, GPT 15 IU/L, ALP 392 IU/L, Ch-E 163 IU/L, T-bil 1.82 mg/dL, prothrombin time (PT) 14.7 s, IL-2 receptor 564 U/mL, indocyanine green test (ICG) 25%. Serological tests showed HBsAg (+), HBeAg (-), HBeAb (+). HBV-DNA level was 4.7 LGE/mL (TMA method). Mutant virus having mutation at precore and core promoter region was detected by enzyme-linked mini-sequence assay (Smitest HBV Pre-C ELMA, Roche Diagnostics, Tokyo, Japan) and enzyme-linked specific probe assay (Smitest HBV core promoter mutation detection kit, Genome Science Laboratory, Tokyo, Japan). Ultrasonography revealed cirrhotic pattern of liver and mild splenomegaly. Neck magnetic resonance imaging revealed swelling of right tonsil and two cervical lymph nodes. Computed tomography scanning revealed no lymph node swelling in chest and abdomen. Bone marrow aspiration revealed involvement of abnormal lymphocytes. Thus, we diagnosed he was at stage IV.

He received first course of CHO regimen on August 22. Although tonsil swelling improved, liver dysfunction gradually developed after the third course. After the fourth course, liver dysfunction got severe, as serum LDH level was 499 IU/L, GOT 650 IU/L, GPT 422 IU/L, T-bil 1.49 mg/dL, PT 25.9 s and HBV-DNA level increased 6.2 LGE/mL. We diagnosed it as acute exacerbation of HBV and started both lamivudine (100 mg/d) and plasma exchange. Liver dysfunction improved gradually. In January 2004, hematological data improved as LDH 328 IU/L, GOT 98 IU/L, GPT 54 IU/L, T-bil 3.66 mg/dL, PT 19.6 s, HBV DNA 2.8 LGE/mL. He was following good clinical course and remained complete response for NHL.

DISCUSSION

It has been reported that steroid may induce exacerbation of hepatitis after cessation of steroid therapy or during tapering of steroid. Cheng *et al.* reported that 50 NHL patients carrying HBV were randomized to receive either ACE (epirubicin, CPA and etoposide) or PACE (prednisolone+ACE). The cumulative incidence of HBV reactivation was 38% and 73%, respectively. On the other hand, it is clear that PACE chemotherapy was

more effective than ACE arm in the treatment of NHL, because CR rate was 46% and 35%, overall survival rate at 46 mo was 68% and 36%, respectively^[1]. Thus, there is no consensus regarding the best therapy for NHL with HBV.

Regarding to HBV-DNA, cases with a point mutation from G to A at nucleotide 1896 of the precore region of HBV tended to develop fulminant hepatitis with steroid containing treatment^[2-5]. Because we detected the mutant HBV in peripheral blood before chemotherapy, we performed CHO regimen and obtained CR for NHL. However, hepatitis acutely exacerbated.

Recently, several reports have shown promising results for the prophylactic use of lamivudine in cancer patients before chemotherapy^[6-8]. However, we did not administer prophylaxis of lamivudine in the present patient, because (1) he was an asymptomatic HBV-carrier, (2) lamivudine-resistant virus might appear after lamivudine treatment or acute exacerbation after discontinuation of lamivudine, and (3) in Japan, adefovir dipivoxil was not available. Theoretically, the steroid containing regimen with lamivudine prophylaxis for NHL patients carrying HBV may be the best therapy. To prove the efficacy of this therapy, further studies are required.

REFERENCES

- 1 **Cheng AL**, Hsiung CA, Su JJ, Chen PJ, Chang MC, Tsao CJ, Kao WY, Uen WC, Hsu CH, Tien HF, Chao TY, Chen LT, Whang-Peng J. Steroid-free chemotherapy decreases risk of hepatitis B virus (HBV) reactivation in HBV-carriers with lymphoma. *Hepatology* 2003; **37**: 1320-1328
- 2 **Carman WF**, Jacyna MR, Hadziyannis S, Karayiannis P, McGarvey MJ, Makris A, Thomas HC. Mutation preventing formation of hepatitis B e antigen in patients with chronic hepatitis B infection. *Lancet* 1989; **2**: 588-591
- 3 **Sato T**, Kato J, Kawanishi J, Kogawa K, Ohya M, Sakamaki S, Niitsu Y. Acute exacerbation of hepatitis due to reactivation of hepatitis B virus with mutations in the core region after chemotherapy for malignant lymphoma. *J Gastroenterol* 1997; **32**: 668-671
- 4 **Dai MS**, Lu JJ, Chen YC, Perng CL, Chao TY. Reactivation of precore mutant hepatitis B virus in chemotherapy-treated patients. *Cancer* 2001; **92**: 2927-2932
- 5 **Skrabs C**, Muller C, Agis H, Mannhalter C, Jager U. Treatment of HBV-carrying lymphoma patients with Rituximab and CHOP: a diagnostic and therapeutic challenge. *Leukemia* 2002; **16**: 1884-1886
- 6 **Persico M**, De Marino F, Russo GD, Morante A, Rotoli B, Torella R, De Renzo A. Efficacy of lamivudine to prevent hepatitis reactivation in hepatitis B virus-infected patients treated for non-Hodgkin lymphoma. *Blood* 2002; **99**: 724-725
- 7 **Silvestri F**, Ermacora A, Sperotto A, Patriarca F, Zaja F, Damiani D, Fanin R, Baccarani M. Lamivudine allows completion of chemotherapy in lymphoma patients with hepatitis B reactivation. *Br J Haematol* 2000; **108**: 394-396
- 8 **Rossi G**, Pelizzari A, Motta M, Puoti M. Primary prophylaxis with lamivudine of hepatitis B virus reactivation in chronic HBsAg carriers with lymphoid malignancies treated with chemotherapy. *Br J Haematol* 2001; **115**: 58-62

Edited by Wang XL Proofread by Chen WW and Xu FM

Alverine citrate induced acute hepatitis

Mehmet Arhan, Seyfettin Köklü, Aydın S Köksal, Ömer F Yolcu, Senem Koruk, Irfan Koruk, Ertugrul Kayacetin

Mehmet Arhan, Seyfettin Köklü, Aydın S Köksal, Ömer F Yolcu, Senem Koruk, Irfan Koruk, Ertugrul Kayacetin, Kavaklik mah, Ahmet Apaydin cad, Sultan Apartment, No 39/7, Sahinbey 27060, Gaziantep, Turkey

Correspondence to: Dr. Irfan Koruk, Kavaklik mah, Ahmet Apaydin cad, Sultan Apartment, No 39/7, Sahinbey 27060, Gaziantep, Turkey. irfan_koruk@yahoo.com

Telephone: +90-342-3397615 **Fax:** +90-312-3124120

Received: 2004-02-20 **Accepted:** 2004-03-13

Abstract

Alverine citrate is a commonly used smooth muscle relaxant agent. A MEDLINE search on January 2004 revealed only 1 report implicating the hepatotoxicity of this agent. A 34-year-old woman was investigated because of the finding of elevated liver function tests on biochemical screening. Other etiologies of hepatitis were appropriately ruled out and elevated enzymes were ascribed to alverine citrate treatment. Although alverine citrate hepatotoxicity was related to an immune mechanism in the first case, several features such as absence of predictable dose-dependent toxicity of alverine citrate in a previous study and absence of hypersensitivity manifestations in our patient are suggestive of a metabolic type of idiosyncratic toxicity.

Arhan M, Köklü S, Köksal AS, Yolcu ÖF, Koruk S, Koruk I, Kayacetin E. Alverine citrate induced acute hepatitis. *World J Gastroenterol* 2004; 10(15): 2303-2304

<http://www.wjgnet.com/1007-9327/10/2303.asp>

INTRODUCTION

Toxic hepatitis is a liver injury caused by drugs and chemicals. The severity varies from nonspecific changes in liver functions such as abnormalities in liver enzymes to fulminant hepatic failure and cirrhosis. Its incidence has been increased over the past several decades. Drugs have been estimated to be responsible for 15-20% of all cases of fulminant and subfulminant hepatitis in Western countries and 18% of acute liver failure in the United States^[1,2].

Alverine citrate is a smooth muscle relaxant agent, commonly used in patients with irritable bowel syndrome in association with simethicone. Hepatotoxicity of alverine citrate is extremely rare and has been reported only in 1 patient before^[3]. Herein we report a new case of alverine citrate-induced hepatotoxicity occurred in a middle-aged woman that resolved completely after discontinuation of the drug.

CASE REPORT

On July 24, 2003, a 34-year-old woman was admitted to the Outpatient Clinic of Gastroenterology Department of Yuksek Ihtisas Hospital with the chief complaint of dyspepsia lasting for 2 years. She described bloating after meals and sometimes had gastroesophageal reflux symptoms. She did not have any chronic disease states. Physical examination was completely normal. Her biochemical tests including liver enzymes (AST, ALT, ALP and GGT) were all within normal limits. Upper

gastrointestinal endoscopy was performed showing grade I esophagitis and pangastritis. On July 29, omeprazole PO 20 mg bid, liquid alginate acid (Gaviscon) PO 10 mL qid (30 min after meal and at bedtime) and meteospasmyl (a tablet containing 60 mg alverine citrate and 300 mg simethicone) PO tid (before meals) were prescribed. Till the 14th d after prescription she told that she used all of the drugs as recommended. At that time omeprazole was ceased and she continued to medical treatment with Gaviscon and meteospasmyl.

She was admitted to another hospital because of arthralgia lasting for years on August 18, 2003, but therapy was managed on an outpatient basis. Amitriptyline 25 mg PO bid was added to Gaviscon and Meteospasmyl and a gastroenterology consultation was requested because of the finding of abnormal liver function test values on biochemical screening. On August 18, serum liver enzymes were as follows: ALT: 319 IU/L, AST: 211 IU/L (N: 40 IU/L for both); ALP: 184 IU/L (N: 35-129), GGT: 116 IU/L (N: 5-40) and normal direct and indirect bilirubin levels. She began to take amitriptyline on August 23 and readmitted to our hospital on August 26. Her ALT and AST levels were 1119 IU/L and 853 IU/L, respectively. Other biochemical tests such as, hemoglobin level, white blood cell count, platelet count, and prothrombin time were within normal limits. Hepatobiliary imaging with ultrasonography was normal. Viral markers for hepatitis including hepatitis A, B and C viruses, cytomegalovirus, Epstein-Barr virus, and herpes simplex virus were all negative. Autoantibodies (antinuclear, antimitochondrial, anti-smooth-muscle, anti-liver-kidney microsomal enzymes and anti-soluble liver antigen) were also negative. She denied taking any other medications and using alcohol or any herbal and folk remedies anytime. There were no known environmental issues that could be contributing.

Liver enzyme elevations were thought to be drug induced. Amitriptyline, Gaviscon and Meteospasmyl were all immediately discontinued on August 26. The ALT and AST values decreased to 597 IU/L and 237 IU/L 8 d after withdrawal of all drugs and became completely normal 18 d after cessation. The time course of liver function tests is presented in Table 1. Liver biopsy was not performed, and rechallenge with Meteospasmyl was not attempted because of ethical reasons. Since she had continuing mild symptoms related to gastroesophageal reflux, she continued to take Gaviscon and omeprazole without any increase in biochemical parameters.

Table 1 Time course of liver function tests

Date	AST (IU/L)	ALT (IU/L)	GGT (IU/L)	ALP (IU/L)
7/24/2003	30	32	21	162
8/18	211	319	116	184
8/26	853	1119	-	-
9/3	237	597	-	229
10/2	22	21	35	75

Omeprazole, alginate acid, and alverine citrate were started on 7/30/2003. Omeprazole was ceased on 8/10/2003. Amitriptyline was added to alginate acid and alverine citrate on 8/23/2003 and all medications were discontinued on 8/26/2003. ALP: Alkaline phosphatase; ALT: Alanine aminotransferase; AST: Aspartate aminotransferase; GGT: γ -glutamyl transferase.

DISCUSSION

Meteospasmyl is a most widely used drug for irritable bowel syndrome. It contains 60 mg alverine citrate and 300 mg simethicone. Simethicone has been used as an antifoaming agent and considered as an inert one^[4]. It is excreted via feces without any metabolizing in the gastrointestinal system. It has been widely used in patients with gastrointestinal gas and for the improvement of visibility during radiologic examination^[5]. To our knowledge, no systemic side effect regarding simethicone was reported in the literature.

Alverine is one of the papaverine congeners. Its antispasmodic effects are mediated by processes involving smooth muscle cells, extrinsic nervous system, and calcium channels^[6]. In humans, the drug is completely absorbed by the gastrointestinal tract and mainly metabolised in the liver, with negligible amounts excreted in the urine^[3]. Side effects such as flushing on the face and neck, nausea, headache, dizziness, and allergic skin eruptions may be observed. To our knowledge, hepatotoxicity associated with alverine use was reported once in the literature. Hepatotoxicity was not reported for the other papaverine derivatives other than trimebutine^[7].

In our patient increase in liver enzymes was ascribed to alverine treatment due to several reasons. There was a temporal relationship between alverine treatment and hepatitis. Liver function tests were normal before treatment and increases appeared three weeks after the start of alverine treatment. The timeline of exposure to alverine and initial observation of increase in liver function tests were consistent with drug-induced liver disease^[8]. Liver function tests completely normalized three weeks after withdrawal of the drug. Furthermore other etiologies of hepatitis (alcohol, steatohepatitis, autoimmune hepatitis and viral hepatitis) were appropriately ruled out. Omeprazole was not thought to be responsible for our patient's hepatitis in view of her prior uses of this drug without adverse effects. Neither chemical nor clinical side effects were seen in her consequent follow-up after alginic acid and omeprazole were started again. We therefore classified our case as probable alverine-induced hepatotoxicity according to the Naranjo probability scale^[9].

Drugs cause liver injury either via intrinsic toxicity (dose-dependent or predictable) or host idiosyncrasy (dose-independent or unpredictable). Idiosyncratic hepatotoxicity may be in metabolic or immunoallergic form. Metabolic-type idiosyncratic injury develops as a result of the susceptibility of rare individuals to hepatotoxicity from a drug that is usually safe at conventional doses. In this pattern, reactions would occur among susceptible individuals who possess an isolated genetic enzymatic alteration not expressed under normal conditions, which would become clinically apparent following the

administration of certain drugs^[10]. The mechanism of alverine induced liver disease is unknown. In the first case described in the literature alverine hepatotoxicity was related to immune mechanisms due to the presence of transient hypereosinophilia, eosinophil polymorphonuclear cells in the liver inflammatory infiltrates, and antinuclear autoantibodies. In our patient autoantibodies were negative and there was no hypereosinophilia in the peripheral blood smear. Several features such as the absence of predictable dose-dependent toxicity of alverine and fever, rash, and arthralgia (hypersensitivity manifestations) in our patient were consistent with a metabolic type of idiosyncratic toxicity.

In conclusion, alverine is a smooth muscle relaxant drug. This report presents the second case of alverine-associated possible liver toxicity. Alverine citrate should be included in the list of drugs causing toxic hepatitis.

REFERENCES

- 1 **Bernuau J**, Benhamou JP. Fulminant and subfulminant liver failure. In: Bircher J, Benhamou JP, McIntyre N, Rizzetto M, Rodes J, eds. Oxford Textbook of Clinical Hepatology, 2nd ed. Oxford: Oxford University Press 1999: 1341-1372
- 2 **Ostapowicz G**, Fontana RJ, Schiodt FV, Larson A, Davern TJ, Han SH, McCashland TM, Shakil AO, Hay JE, Hynan L, Crippin JS, Blei AT, Samuel G, Reisch J, Lee WM. U.S. Acute Liver Failure Study Group. Results of a prospective study of acute liver failure at 17 tertiary care centers in the United States. *Ann Intern Med* 2002; **137**: 947-954
- 3 **Malka D**, Pham B, Courvalin JC, Corbic M, Pessayre D, Erlinger S. Acute hepatitis caused by alverine associated with anti-lamin A and C autoantibodies. *J Hepatol* 1997; **27**: 399-403
- 4 **Brečević L**, Bosan KI, Strajnar F. Mechanism of antifoaming action of simethicone. *J Appl Toxicol* 1994; **14**: 207-211
- 5 **Sudduth RH**, DeAngelis S, Sherman KE, McNally PR. The effectiveness of simethicone in improving visibility during colonoscopy when given with a sodium phosphate solution: a double-blind randomized study. *Gastrointest Endosc* 1995; **42**: 413-415
- 6 **Lemann M**, Coffin B, Chollet R, Jian R. Gut sensitivity: methodology for study in man and pathophysiological implications. *Gastroenterol Clin Biol* 1995; **19**: 270-281
- 7 **Bacq Y**, Vaillant L, Moneqier du Sorbier C. Severe erythema multiforme and hepatitis during treatment with trimebutine. *Gastroenterol Clin Biol* 1989; **13**: 522-523
- 8 **Lewis JH**. Drug-induced liver disease. *Med Clin of North Am* 2000; **84**: 1275-1311
- 9 **Naranjo CA**, Busto U, Sellers EM, Sandor P, Ruiz I, Roberts EA. A method for estimating the probability of adverse drug reactions. *Clin Pharmacol Ther* 1981; **30**: 239-245
- 10 **Farrell GC**. Liver disease caused by drugs, anesthetics, and toxins. In: Feldman M, Scharschmidt BF, Sleisenger MH, eds. Sleisenger and Fordtran's gastrointestinal and liver disease. 6th ed. Philadelphia: W.B. Saunders Company 1998: 1221-1253

Edited by Wang XL Proofread by Chen WW and Xu FM

Pregnant woman with fulminant hepatic failure caused by hepatitis B virus infection: A case report

Yue-Bo Yang, Xiao-Mao Li, Zhong-Jie Shi, Lin Ma

Yue-Bo Yang, Xiao-Mao Li, Zhong-Jie Shi, Lin Ma, Department of Obstetrics and Gynecology, Third Affiliated Hospital, Sun Yat-sen University, Guangzhou 510630, Guangdong Province, China

Correspondence to: Professor Xiao-Mao Li, Department of Obstetrics and Gynecology, Third Affiliated Hospital, Sun Yat-sen University, Guangzhou 510630, Guangdong Province, China. tigerlee777@163.net

Telephone: +86-20-85515609 **Fax:** +86-20-87565575

Received: 2004-02-21 **Accepted:** 2004-03-04

Abstract

AIM: To report the experience in successfully treating pregnant women with severe hepatitis.

METHODS: Comprehensive medical treatments were performed under strict monitoring.

RESULTS: Pregnant woman with severe hepatitis was successfully rescued.

CONCLUSION: Vital measures taken in the treatment of pregnant women with severe hepatitis include termination of the pregnancy at a proper time and control of various complications, such as disseminated intravascular coagulation (DIC), hepatorenal syndrome, hepatic encephalopathy and infection.

Yang YB, Li XM, Shi ZJ, Ma L. Pregnant woman with fulminant hepatic failure caused by hepatitis B virus infection: A case report. *World J Gastroenterol* 2004; 10(15): 2305-2306
<http://www.wjgnet.com/1007-9327/10/2305.asp>

INTRODUCTION

Hepatitis B virus (HBV) infection is common in China^[1], and it is one of the most common causes of severe hepatitis in pregnancy, with a high mortality rate of 43-80%^[2]. In this paper, we reported a pregnant woman with severe hepatitis B infection complicated by postpartum massive hemorrhage, hepatorenal syndrome, hepatic encephalopathy, spontaneous bacterial peritonitis and infection of biliary tract. Under strict monitoring, we applied comprehensive medical treatments. Both the mother and the child were discharged in healthy condition.

CASE REPORT

A 33-year-old pregnant woman was admitted in our hospital on April 15, 2003, presenting with a 38-week pregnancy, 10-d puffiness and yellow urine, and 3-d deep jaundice. She had a history of HBsAg(+), HBeAg(+) and HBcAb(+) for about 10 years, but her liver function had been normal until she got pregnant. The last menstrual period (LMP) was 2002-7-22. The expected date of confinement (EDC) was 2003-4-29. Physical examination showed she had normal vital signs, an urgent and painful looking, clear mind, icteric sclera and xanthochromia, bulbar conjunctiva edema, normal heart and

lung on auscultation, absence of abdominal tenderness or rebound tenderness, no detection of liver or spleen and no shifting dullness on palpation, moderate edema of both legs. Obstetrical conditions were as follows: she had left occipitoanterior position (LOP) of fetus, the height of fundus was 36 cm, the abdomen circumference was 99 cm, fetal heart rate (FHR) was 120 beats/min. No dilatation of cervix was found. Laboratory findings were as follows: aspartate transaminase (AST) was 125.0 U/L, alanine transaminase (ALT) was 138.0 U/L, albumin (ALB) was 32.5 g/L; total bilirubin (TB) was 383.9 μmol/L, blood urea nitrogen (BUN) was 36.03 mmol/L, creatinine (CREAT) was 402.6 μmol/L, white blood cell count (WBC) was 21.60×10⁹/L, hemoglobin (Hb) was 82 g/L, prothrombin time (PT) was 24 s, uric protein was (+++). β-ultrasonography showed her liver was in a chronic hepatitis state, and moderate ascites and a little liquid in both sides of thoracic cavity were also found. Markers of series of hepatitis virus were negative for hepatitis A, C, D and E, but positive for HBsAg (+), HBeAg (+) and HBcAb (+). Therefore she was diagnosed as pregnancy associated with hepatitis B infection and fulminant hepatic failure of pregnancy (FHFP).

After admission, the pregnant woman received supportive treatments. Later, because of "fetal distress", she received a cesarean section plus hysterectomy under general anesthesia. During the operation, we found yellow ascites of about 1 500 mL, and the same color of amniotic fluid was also found. The newborn was a mature male baby with normal vital signs, and transmitted to pediatrics department and given hepatitis B virus (HBV) specific immunoglobulin (HBIG) and HBV vaccine. After the delivery of placenta and membrane, there was no sign of uterine contraction, and massive hemorrhage occurred (about 2 000 mL). So hysterectomy was performed. The liver was obviously small, which was about the palm size and a little harder than normal.

After operation, the patient developed a clinical course of exacerbation. She developed hepatic encephalopathy of degree III, hepatorenal syndrome, spontaneous bacterial peritonitis, infection of biliary tract, secondary fungal infection, septicemia and prolonged healing of the wound. The comprehensive and well-designed rescue measures were taken and her condition was under control on June 25. After a hospitalization of 104 d, the patient and her newborn were discharged in generally good conditions.

DISCUSSION

Generally, a pregnant woman with fulminant hepatic failure refers to failure of liver function caused by viral hepatitis. Often the complications included disseminated intravascular coagulation (DIC) that presents a hemorrhage trend^[3,4], hepatic encephalopathy, hepatorenal syndrome, toxic intestinal tympanites, cerebral edema and infection of biliary tract, and so on. A pregnant woman with severe hepatitis often had hypodynamia, deep jaundice, hypocoagulability, hypoproteinemia, coma and acute renal failure. It was reported that many viruses including hepatitis virus (HAV, HBV, HCV, HDV, HEV, HGV, and so forth^[5,6]), cytomegalovirus (CMV), TTV^[7] and herpes virus^[8], could cause severe hepatitis. But HEV and HBV

infections were most frequent^[9-12]. Clinically, about 0.2-0.5% of total patients with hepatitis would develop into severe hepatitis. The prognosis of severe hepatitis during late pregnancy was so poor that it could be listed among the causes of maternity and parity mortality. In this report, the patient with a 10-year history of hepatitis had a 38-wk pregnancy. She developed severe hepatic dysfunction with hypocoagulability, hepatic encephalopathy and hepatorenal syndrome. She was positive for HBsAg, HBeAg, and HBcAb. Therefore the diagnosis of pregnancy associated with severe hepatitis and HBV infection was confirmed^[13,14]. Under strict monitoring, we took comprehensive therapeutic measures and got a successful result. The key points of rescuing the patient were as follows.

The general treatment included: (1) The patient was asked to have an absolute rest in bed with a diet low in lipid and protein^[15] and rich in fiber and vitamins. The total energy should be controlled at 1 500 kcal. Intra-gastrointestinal food could not only neutralize gastric acid, promote gastro-intestinal movement, but also reduce the incidence of toxic intestinal tympanites, endotoxemia, infection of biliary tract, peritonitis or even septicemia. (2) Protecting liver function, gastric membrane and preventing gastrointestinal hemorrhage. (3) Using antibiotics to prevent and treat infections, gamma globulin to promote immune state and neutralize endotoxins. HBIG, which can neutralize HBV and is relatively safe for gestational period, should also be used. (4) Maintaining the balance of body fluid and electrolytes and using dexamethasone for a short period of time (3-5 d) to improve the toxic symptoms and the maturity of fetal lung, thus getting ready for planned delivery.

To terminate pregnancy at a proper time, internal carotid artery cesarean was performed and a tube placed to detect the central vein pressure and determine the amount of transfusion, thus preventing the incidence of cerebral edema or pulmonary edema. Before cesarean section, colocolysis and atropine were used. But sedatives such as luminal were not taken into consideration. General anesthesia instead of epidural anesthesia was to avoid epidural hematoma^[16], and during cesarean section^[17], we chose longitudinal incision. After cesarean section, we performed hysterectomy and placed an absorbable hemostatic gauze on the cervical stump to reduce hemorrhage during and after operation. We also detected the size of liver during operation to make a general evaluation of its condition of direct prognosis. We perfused the abdomen cavity with iodophors to reduce abdominal infection. We remained a gastric tube during operation to prevent intestinal tympanites and to put in medicines that could improve the movement of intestine. After operation, we remained a drainage tube in abdomen to facilitate the expulsion of ascites and to inspect whether there was continuous hemorrhage.

To prevent and cure complications, measures were taken to reduce possible motivations such as using none or as few as sedatives and narcotics, to avoid too much or too fast diuretics or relieving of ascites, to prevent constipation or mass hemorrhage or infection, to adjust intestinal environment by lactulose towards pH<7 to reduce absorption of NH₃ and endotoxin which would exacerbate the condition of hepatic encephalopathy, to take metronidazole and norfloxacin to compress intestinal bacteria which could produce NH₃, to use colocolysis to accelerate the expulsion of intestinal bacteria and endotoxin and NH₃-removing medicines, to keep normal neurotransmitter by applying L-dopa or aceglutamide, to inject hepat amine intravenously to keep amino-acid balance, to use Chinese formulated medicines such as *Angong niuhuang wan*. Heparin in low dose was used to prevent dissipation of large amount of plot and thrombin factors and to improve clotting mechanism. Thrombin factors such as fresh frozen plasma,

plot, cryoprecipitate, pro- thrombin complex, and fibrinogen were used in a great quantity. Hepatorenal syndrome was treated by restricting the infusion of fluid, correcting hypoproteinemia and hypovolemia in time. Diuretics such as furosemide, diuretics complex (furosemide + dopamine + phentolamine) or mannitol + furosemide were used.

To promote regeneration of hepatocytes, glucagon and insulin were used to trigger the synthesis of hepatocyte DNA, human albumin was used to neutralize indirect bilirubin, stimulate regeneration of hepatocytes and prevent further necrosis of hepatocytes.

Blood routine, clotting function, liver function and biochemical indices, especially ALT, AST, alkaline phosphatase (AKP), acetylcholine esterase (CHE), alpha fetoprotein (AFP) and glucose (GLU) were monitored. Intensive nursing and sterile operation were performed, regular mouth care and clean of incision and perineum were maintained. 50% glucose + insulin was used to promote wound healing.

Before labor, HBIG or anti-HBV medicines (safe for both maternity and fetus) were given to interrupt intrauterine HBV infection^[1]. The newborn was also given HBIG and HB vaccine^[18] to build up active and passive immunity.

REFERENCES

- 1 **Li XM**, Yang YB, Hou HY, Shi ZJ, Shen HM, Teng BQ, Li AM, Shi MF, Zou L. Interruption of HBV intrauterine transmission: a clinical study. *World J Gastroenterol* 2003; **9**: 1501-1503
- 2 **Liu LC**, Shi JF, Feng PQ. Treatment for digestive emergencies. Beijing: *China Med Sci Technol Publish House* 1996: 162
- 3 **Tank PD**, Nandanwar YS, Mayadeo NM. Outcome of pregnancy with severe liver disease. *Int J Gynaecol Obstet* 2002; **76**: 27-31
- 4 **Xu H**. Analysis of 18 cases of postpartum haemorrhagic shock in pregnancy with virus hepatitis. *Zhonghua Fuchanke Zazhi* 1992; **27**: 150-152
- 5 **Khuroo MS**, Kamili S. Aetiology, clinical course and outcome of sporadic acute viral hepatitis in pregnancy. *J Viral Hepat* 2003; **10**: 61-69
- 6 **Duff P**. Hepatitis in pregnancy. *Semin Perinatol* 1998; **22**: 277-283
- 7 **Yan J**, Chen LL, Luo YH, Mao YF, He M. High frequencies of HGV and TTV infections in blood donors in Hangzhou. *World J Gastroenterol* 2001; **7**: 637-641
- 8 **Fink CG**, Read SJ, Hopkin J, Peto T, Gould S, Kurtz JB. Acute herpes hepatitis in pregnancy. *J Clin Pathol* 1993; **46**: 968-971
- 9 **Smith JL**. A review of hepatitis E virus. *J Food Prot* 2001; **64**: 572-586
- 10 **Coursaget P**, Buisson Y, N'Gawara MN, Van Cuyck-Gandre H, Roue R. Role of hepatitis E virus in sporadic cases of acute and fulminant hepatitis in an endemic area (Chad). *Am J Trop Med Hyg* 1998; **58**: 330-334
- 11 **Hussaini SH**, Skidmore SJ, Richardson P, Sherratt LM, Cooper BT, O'Grady JG. Severe hepatitis E infection during pregnancy. *J Viral Hepat* 1997; **4**: 51-54
- 12 **Molinie C**, Desrame J. Viral hepatitis E. *Med Trop* 1996; **56**: 285-288
- 13 **Hamid SS**, Jafri SM, Khan H, Shah H, Abbas Z, Fields H. Fulminant hepatic failure in pregnant women: acute fatty liver or acute viral hepatitis? *J Hepatol* 1996; **25**: 20-27
- 14 **Ochs A**. Acute hepatopathies in pregnancy: diagnosis and therapy. *Schweiz Rundsch Med Prax* 1992; **81**: 980-982
- 15 **Wienbeck M**. The treatment of hepatic emergencies. *Fortschr Med* 1979; **97**: 189-193
- 16 **Sato T**, Hashiguchi A, Mitsuse T. Anesthesia for cesarean delivery in a pregnant woman with acute hepatic failure. *Anesth Analg* 2000; **91**: 1441-1442
- 17 **Zhang ZJ**. Cesarean section in pregnancy complicated by severe hepatitis and heart disease. *Zhonghua Fuchanke Zazhi* 1990; **25**: 12-14
- 18 **Murata R**, Isshiki G, Yoshioka H, Chiba Y, Tada H, Koike M, Kimura M. Prevention of vertical transmission of hepatitis B virus by yeast recombinant hepatitis B vaccine. *Acta Paediatr Jpn* 1989; **31**: 180-185

ISI journal citation reports 2003 – GASTROENTEROLOGY AND HEPATOLOGY

Rank	Abbreviated journal title	ISSN	2003 Total cites	Impact factor	Immediacy index	2003 Articles	Cited Half-life
1	GASTROENTEROLOGY	0016-5085	46 174	12.718	2.810	316	6.9
2	HEPATOLOGY	0270-9139	30 844	9.503	1.574	296	5.5
3	SEMIN LIVER DIS	0272-8087	2 524	6.524	0.810	42	4.7
4	GUT	0017-5749	20 612	5.883	1.147	307	6.5
5	J HEPATOL	0168-8278	11 111	5.283	0.879	281	5.0
6	LIVER TRANSPLANT	1527-6465	2 944	4.242	0.621	211	2.9
7	AM J GASTROENTEROL	0002-9270	17 923	4.172	0.678	391	5.1
8	ALIMENT PHARM THERAP	0269-2813	60 32	3.529	0.573	372	3.9
9	AM J PHYSIOL-GASTR L	0193-1857	11 047	3.421	0.634	268	5.9
10	GASTROINTEST ENDOSC	0016-5107	10 047	3.328	1.798	331	4.8
11	WORLD J GASTROENTERO	1007-9327	2 387	3.318	0.345	632	2.4
12	J VIRAL HEPATITIS	1352-0504	1 320	3.258	0.386	70	4.0
13	ENDOSCOPY	0013-726X	4 238	3.227	0.349	152	5.5
14	INFLAMM BOWEL DIS	1078-0998	1 278	3.023	0.625	40	3.8
15	HELICOBACTER	1083-4389	798	2.624	0.426	68	3.6
16	NEUROGASTROENT MOTIL	1350-1925	848	2.500	0.333	66	3.7
17	DIS COLON RECTUM	0012-3706	8 130	2.343	0.191	256	7.6
18	SCAND J GASTROENTERO	0036-5521	7 271	2.140	0.118	238	7.6
19	LIVER	0106-9543	1 337	2.076		0	5.4
20	J GASTROINTEST SURG	1091-255X	1 236	1.881	0.430	142	3.6
21	PANCREAS	0885-3177	2 271	1.855	0.364	140	5.8
22	INT J COLORECTAL DIS	0179-1958	1 167	1.848	0.373	83	6.4
23	GASTROENTEROL CLIN N	0889-8553	1 517	1.684	0.019	54	6.7
24	PANCREATOLOGY	1424-3903	240	1.596	0.115	52	2.2
25	EUR J GASTROEN HEPAT	0954-691X	3 163	1.578	0.367	177	4.6
26	J CLIN GASTROENTEROL	0192-0790	3 215	1.564	0.484	155	7.2
27	J GASTROEN HEPATOL	0815-9319	3 171	1.530	0.254	193	4.5
28	DIGEST LIVER DIS	1590-8658	637	1.463	0.151	159	2.5
29	J PEDIATR GASTR NUTR	0277-2116	3 963	1.402	0.257	183	6.1
30	DIGESTION	0012-2823	2 193	1.399	0.091	55	7.7
31	DIGEST DIS SCI	0163-2116	9 149	1.387	0.144	347	7.9
32	CAN J GASTROENTEROL	0835-7900	813	1.265	0.134	82	3.9
33	J GASTROENTEROL	0944-1174	1 625	1.179	0.319	191	4.5
34	DIGEST DIS	0257-2753	534	1.151	0.031	32	5.7
35	Z GASTROENTEROL	0044-2771	918	1.076	0.112	116	5.4
36	ABDOM IMAGING	0942-8925	1 190	0.996	0.194	124	5.0
37	BEST PRACT RES CL GA	1521-6918	342	0.992	0.000	66	3.4
38	HEPATOL RES	1386-6346	406	0.991	0.168	155	2.6
39	GASTROEN CLIN BIOL	0399-8320	1 497	0.884	0.235	153	6.3
40	HEPATO-GASTROENTEROL	0172-6390	3 886	0.837	0.044	544	5.0
41	DIS ESOPHAGUS	1120-8694	354	0.809	0.027	75	4.7
42	ACTA GASTRO-ENT BELG	0001-5644	345	0.670	0.065	31	5.2
43	DIGEST SURG	0253-4886	548	0.619	0.114	79	4.2
44	CURR OPIN GASTROEN	0267-1379	300	0.598	0.050	60	3.9
45	REV ESP ENFERM DIG	1130-0108	255	0.348	0.211	57	6.0
46	CHIR GASTROENTEROL	0177-9990	74	0.157	0.039	76	
47	LIVER INT	1478-3231	4		0.053	75	

Citation indexes of Chinese scientific journals in 2003 (ISI JCR 2004)

Rank	Abbreviated journal title	2003 total cites	Impact factor	Index immediacy	2003 articles	Cited half-life
1	WORLD J GASTROENTERO	2 387	3.318	0.345	632	2.4
2	CHINESE J ASTRON AST	229	1.768	0.065	62	2.2
3	CELL RES	354	1.729	0.192	52	3.2
4	FUNGAL DIVERS	207	1.437	0.189	53	2.5
5	CHINESE PHYS	855	1.347	0.193	233	2.3
6	ACTA PHYS SIN ¹	2 410	1.130	0.172	586	2.9
7	CHINESE PHYS LETT	1 955	1.095	0.173	664	2.4
8	ACTA PETROL SIN ¹	444	1.078	0.067	89	4.0
9	ASIAN J ANDROL	188	1.064	0.140	57	2.6
10	ACTA GEOL SIN	467	1.040	0.457	46	4.4
11	EPISODES	411	1.020	0.056	36	7.0
12	ACTA PHARMACOL SIN	1 586	0.884	0.120	208	4.8
13	SCI CHINA SER D	737	0.801	0.272	151	3.8
14	CHEM J CHINESE U ¹	2 391	0.796	0.093	569	3.7
15	COMMUN THEOR PHYS	727	0.666	0.242	310	2.3
16	ACTA CHIM SINICA	1 375	0.643	0.105	381	3.9
17	BIOMED ENVIRON SCI	387	0.609	0.043	47	6.7
18	CHINESE SCI BULL	2 302	0.593	0.136	544	4.7
19	CHINESE J CHEM	578	0.592	0.118	255	2.7
20	ACTA MECH SINICA	270	0.587	0.043	70	6.2
21	CHINESE J STRUC CHEM ¹	319	0.548	0.039	152	3.3
22	CHINESE J CATAL	396	0.542	0.083	180	3.6
23	SCI CHINA SER B	838	0.541	0.069	72	9.2
24	CHINESE J INORG CHEM ¹	481	0.535	0.075	281	3.0
25	ACTA BIOCH BIOPH SIN ¹	386	0.524	0.053	190	3.7
26	CHINESE J ORG CHEM ¹	430	0.497	0.069	246	3.3
27	J RARE EARTH	263	0.486	0.049	144	3.6
28	ACTA PHYS-CHIM SIN ¹	516	0.468	0.093	257	3.2
29	ADV ATMOS SCI	231	0.449	0.069	101	4.3
30	SCI CHINA SER C	228	0.440	0.029	68	4.3
31	J UNIV SCI TECHNOL B	145	0.437	0.087	104	2.7
32	CHINA OCEAN ENG	95	0.413	0.119	59	
33	CHINESE MED J	1 245	0.393	0.081	431	6.0
34	ACTA MECH SOLIDA SIN	115	0.389	0.021	47	4.0
35	CHINESE J GEOPHYS ¹	278	0.375	0.038	133	4.4
36	CHEM RES CHINESE U	175	0.370	0.054	112	3.6
37	CHINESE J CHEM	172	0.357	0.062	145	3.0
38	J WUHAN UNIV TECHNOL	139	0.356	0.037	81	3.1
39	SCI CHINA SER E	210	0.355	0.028	72	3.8
40	ACTA POLYM SIN ¹	410	0.351	0.055	146	4.4
41	CHINESE ANN MATH B	169	0.343	0.019	52	5.4
42	CHINESE CHEM LETT	717	0.342	0.028	394	3.8
43	PROG NAT SCI	360	0.335	0.136	154	3.6
44	RARE METAL MAT ¹	435	0.329	0.149	262	3.1
45	T NONFERR METAL SOC	413	0.322	0.026	348	3.6
46	ACTA BOT SIN	712	0.321	0.063	222	5.3
47	PROG CHEM	121	0.319	0.045	66	3.9
48	J CENT SOUTH UNIV T	80	0.299	0.000	75	
49	SPECTROSC SPECT ANAL ¹	427	0.298	0.020	352	3.4
50	ACTA MATH SIN	327	0.297	0.041	49	6.6
51	HIGH ENERG PHYS NUC ¹	293	0.285	0.105	238	3.0
52	J MATER SCI TECHNOL	318	0.275	0.026	190	3.7
53	ALGEBR COLLOQ	106	0.274	0.038	52	5.9
53	RARE METALS	98	0.274	0.033	61	
55	J ENVIRON SCI-CHINA	137	0.255	0.014	140	4.3
56	APPL MATH MECH	422	0.251	0.086	152	5.1
57	SCI CHINA SER A	722	0.247	0.024	85	7.3
57	ACTA METALL SIN	569	0.247	0.097	258	4.8
57	J INORG MATER ¹	346	0.247	0.030	234	4.0
60	J IRON STEEL RES INT	40	0.245	0.000	43	
61	PROG BIOCHEM BIOPHYS ¹	206	0.241	0.048	145	3.0
62	CHINESE J ANAL CHEM ¹	971	0.224	0.036	389	5.2
63	J INFRARED MILLIM W	107	0.160	0.019	105	3.5
64	J COMPUT MATH	188	0.153	0.013	79	>10.0
65	CHINESE ASTRON ASTR	57	0.149	0.000	57	
66	J COMPUT SCI TECHNOL	50	0.140	0.040	99	
67	ACTA MATH SCI	119	0.127	0.000	50	>10.0

¹Chinese.

Impact factors and citation times of Chinese scientific journals covered by ISI JCR (2000-2003)

Abbreviated journal title	Impact factor				Citation time			
	2000	2001	2002	2003	2000	2001	2002	2003
ACTA BIOCH BIOPH SIN ¹	0.289	0.399	0.596	0.524	150	217	377	386
ACTA BOT SIN	0.434	0.284	0.376	0.321	698	516	1 336	712
ACTA CHIM SINICA ¹	0.435	0.530	0.536	0.643	844	990	1 298	1 375
ACTA GEOL SIN	1.000	0.271	0.531	1.040	323	234	316	467
ACTA MATH SCI			0.104	0.127			108	119
ACTA MATH SIN	0.234	0.324	0.407	0.297	212	275	299	327
ACTA MECH SINICA	0.575	0.734	0.726	0.587	180	242	265	270
ACTA MECH SOLIDA SIN	0.215	0.191	0.226	0.389	68	70	78	115
ACTA METALL SIN				0.247				569
ACTA PETROL SINICA ¹			0.534	1.078			289	444
ACTA PHARMACOL SIN	0.485	0.631	0.688	0.884	854	958	1 575	1 586
ACTA PHYS SIN ¹		0.657	1.182	1.130		1 227	2 277	2 410
ACTA PHYS SIN	0.210	0.369			100	176		
ACTA PHYS-CHIM SIN ¹	0.192	0.269	0.361	0.468	119	283	350	516
ACTA POLYM SIN		0.377	0.288	0.351		314	358	410
ADV ATMOS SCI		0.327	0.288	0.449		146	172	231
ALGEBR COLLOQ	0.089	0.188	0.150	0.274	25	84	94	106
APPL MATH MECH	0.166	0.155	0.199	0.251	250	267	354	422
ASIAN J ANDROL			0.827	1.064			99	188
BIOMED ENVIRON SCI	0.400	0.437	0.500	0.609	359	332	390	387
CELL RES		2.102	1.958	1.729		244	308	354
CHEM J CHINESE U ¹	0.590	0.904	0.830	0.796	1 421	1 959	2 189	2 391
CHEM RES CHINESE U	0.260	0.223	0.229	0.370	125	106	131	175
CHINA OCEAN ENG	0.137	0.206	0.196	0.413	24	46	41	95
CHINESE ANN MATH B	0.153		0.296	0.343	116		146	169
CHINESE ASTRON ASTR	0.164	0.144	0.181	0.149	49	47	60	57
CHINESE CHEM LETT	0.229	0.289	0.347	0.342	536	603	733	717
CHINESE J ANAL CHEM ¹		0.288	0.240	0.224		992	949	971
CHINESE J ASTRON AST			0.879	1.768		1	65	229
CHINESE J CATAL				0.542				396
CHINESE J CHEM	0.707	0.663	0.558	0.592	318	369	413	578
CHINESE J CHEM	0.124	0.223	0.222	0.357	55	101	117	172
CHINESE J GEOPHYS ¹	0.097	0.155	0.122	0.375	13	34	45	278
CHINESE J INORG CHEM ¹		0.301	0.494	0.535		141	280	481
CHINESE J ORG CHEM ¹		0.294	0.377	0.497		271	338	430
CHINESE J STRUCT CHEM ¹		0.184	0.324	0.548		168	260	319
CHINESE MED J ¹	0.107	0.108	0.182	0.393	752	807	909	1 245
CHINESE PHYS		0.828	1.185	1.347	39	200	542	855
CHINESE PHYS LETT	0.638	0.813	1.036	1.095	761	1 215	1 644	1 955
CHINESE SCI BULL	0.414	0.511	0.570	0.593	1 321	1 628	2 030	2 302
COMMUN THEOR PHYS	0.302	0.397	0.453	0.666	350	479	577	727
EPISODES				1.020				411
FUNGAL DIVERS				1.437				207
HIGH ENERG PHYS NUC ¹	0.264	0.324	0.248	0.285	225	271	248	293
J ASIAN NAT PROD RES	0.294	0.508			16	54		
J CENT SOUTH UNIV T			0.052	0.299			6	80
J COMPUT MATH	0.250	0.168	0.135	0.153	175	155	173	188
J COMPUT SCI TECHNOL			0.154	0.140			53	50
J ENVIRON SCI-CHINA				0.255				137
J INFRARED MILLIM W ¹	0.146	0.198	0.121	0.160	39	68	85	107
J INORG MATER ¹		0.131	0.222	0.247		77	260	346
J IRON STEEL RES INT	0.195	0.171	0.083	0.245	18	21	31	40
J MATER SCI TECHNOL	0.241	0.269	0.239	0.275	164	220	271	318
J RARE EARTH	0.125	0.236	0.287	0.486	57	117	147	263
J UNIV SCI TECHNOL B	0.118	0.099	0.397	0.437	38	37	100	145
J WUHAN UNIV TECHNOL	0.185	0.140	0.376	0.356	41	56	119	139
PROG BIOCHEM BIOPHYS ¹	0.077	0.112	0.160	0.241	95	109	140	206
PROG CHEM				0.319				121
PROG NAT SCI	0.249	0.288	0.264	0.335	167	279	309	360
RARE METAL MAT ENG ¹	0.242	0.319	0.225	0.329	103	151	223	435
RARE METALS		0.142	0.284	0.274		60	69	98
SCI CHINA SER A	0.309	0.340	0.295	0.247	528	627	682	722
SCI CHINA SER B	0.751	0.840	0.702	0.541	799	925	895	838
SCI CHINA SER C	0.291	0.396	0.358	0.440	155	171	180	228
SCI CHINA SER D	0.475	0.610	0.688	0.801	236	369	580	737
SCI CHINA SER E	0.309	0.376	0.412	0.355	91	140	197	210
SPECTROSC SPECT ANAL ¹		0.250	0.293	0.298		280	377	427
T NONFERR METAL SOC	0.294	0.340	0.293	0.322	221	306	374	413
WORLD J GASTROENTERO	0.993	1.445	2.532	3.318	327	722	1 535	2 387
TOTAL					13 557	20 957	28 866	35 842

¹Chinese.

Drug therapy for ulcerative colitis

Chang-Tai Xu, Shu-Yong Meng, Bo-Rong Pan

Chang-Tai Xu, Editorial Department, Journal of Fourth Military Medical University, Fourth Military Medical University, Xi'an 710032, Shaanxi Province, China

Shu-Yong Meng, Department of Thoracic and Oncology Surgery, Shaanxi Provincial Textile Hospital, Xi'an 710038, Shaanxi Province, China

Bo-Rong Pan, Department of Oncology, Xijing Hospital, Fourth Military Medical University, Xi'an 710032, Shaanxi Province, China
Supported by the Science Foundation of Health Bureau of Shaanxi province, No.04D26

Correspondence to: Chang-Tai Xu, Editorial Department, Journal of Fourth Military Medical University, Fourth Military Medical University, 17 Changle West Road, Xi'an 710032, Shaanxi Province, China. xuct2001@163.com

Telephone: +86-29-83373804 **Fax:** +86-29-83374499

Received: 2004-03-23 **Accepted:** 2004-04-29

Abstract

Ulcerative colitis (UC) is an inflammatory destructive disease of the large intestine occurred usually in the rectum and lower part of the colon as well as the entire colon. Drug therapy is not the only choice for UC treatment and medical management should be as a comprehensive whole. Azulfidine, Asacol, Pentasa, Dipentum, and Rowasa all contain 5-aminosalicylic acid (5-ASA), which is the topical anti-inflammatory ingredient. Pentasa is more commonly used in treating Crohn's ileitis because Pentasa capsules release more 5-ASA into the small intestine than Asacol tablets. Pentasa can also be used for treating mild to moderate UC. Rowasa enemas are safe and effective in treating ulcerative proctitis and proctosigmoiditis. The sulfa-free 5-ASA agents (Asacol, Pentasa, Dipentum and Rowasa) have fewer side effects than sulfa-containing Azulfidine. In UC patients with moderate to severe disease and in patients who failed to respond to 5-ASA compounds, systemic (oral) corticosteroids should be used. Systemic corticosteroids (prednisone, prednisolone, cortisone, *etc.*) are potent and fast-acting drugs for treating UC, Crohn's ileitis and ileocolitis. Systemic corticosteroids are not effective in maintaining remission in patients with UC. Serious side effects can result from prolonged corticosteroid treatment. To minimize side effects, corticosteroids should be gradually reduced as soon as the disease remission is achieved. In patients with corticosteroid-dependent or unresponsive to corticosteroid treatment, surgery or immunomodulator is considered. Immunomodulators used for treating severe UC include azathioprine/6-MP, methotrexate, and cyclosporine. Integrated traditional Chinese and Western medicine is safe and effective in maintaining remission in patients with UC.

Xu CT, Meng SY, Pan BR. Drug therapy for ulcerative colitis. *World J Gastroenterol* 2004; 10(16): 2311-2317
<http://www.wjgnet.com/1007-9327/10/2311.asp>

INTRODUCTION

Ulcerative colitis (UC) is an inflammatory destructive disease of the large intestine characterized by motility and secretion

disorders. Inflammation usually occurs in the rectum and lower part of the colon, but it may affect the entire colon^[1-4]. UC rarely affects the small intestine except for the end section, called the terminal ileum. UC may also be called colitis or proctitis^[4,5].

Inflammation makes the colon empty frequently, causing diarrhea. Ulcers formed in places where the inflammation has killed the cells of colon, bleeding ulcers and pus discharge. UC is an inflammatory bowel disease (IBD) that causes inflammation in the small intestine and colon. UC can be difficult to diagnose because its symptoms are similar to other intestinal disorders and another type of IBD called Crohn's disease (CD). CD differs from UC because it causes deeper inflammation within the intestinal wall^[5-7]. Also, CD usually occurs in the small intestine, although it can also occur in the mouth, esophagus, stomach, duodenum, large intestine, appendix, and anus. UC may occur in people of any age, but most often it starts between ages 15 and 30, or less frequently between ages 50 and 70. Children and adolescents sometimes develop the disease. UC affects men and women equally and appears to run in some families.

UC CHARACTERISTICS

Of the estimated two million Americans suffer from IBD, CD is far less common than UC, but currently the incidences of each are estimated to be about equal. The incidence may vary depending on gender, age, and geography^[4-6]. Men and women have an equal risk for UC. IBD is diagnosed most often in young people between the ages of 10 and 19, but it can occur at any age. A smaller peak onset occurs between 50 and 80 years. About 2% of IBD cases appear in children below age 10. UC is most common among people of European descent. People of African descent have a lower incidence than Caucasians. Low incidence regions include Asia and South America. Ethnically, Jewish people have a higher risk. UC may disproportionately affect people of higher socioeconomic classes, but evidence for this is inconclusive.

UC shares certain characteristics^[4-8]: (1) Symptoms usually appear in young adults. (2) Symptoms can develop gradually or suddenly. (3) Both are chronic. The symptoms may flare up (relapse) after symptom-free periods (remission) or symptoms may be continuous without treatment. (4) The disease can be mild or very severe and disabling. (5) The severity of symptoms and relapse rates of both UC and DC vary with seasons, with the highest risk in winter and autumn and lowest in summer.

Factors associated with UC

Smokers have lower than average rates of UC (but higher than average rates of CD). In fact, it has been reported that some patients with UC had disorders after they gave up smoking, and many studies have stressed the association between smoking and protection against UC. This information is certainly no encouragement to smoke. Rather, patients should ask their physician about trials using nicotine replacement aids. Breast feeding also appears to be associated with lower risk of UC. Left-handed people have a significantly higher risk for both IBDs and other diseases associated with immune abnormalities. A 2001 study reported that patients with UC were more likely to have a history of depression or anxiety than those without IBD. Some researchers suggested that depression might alter the immune system and make people more susceptible to UC^[3,4].

Symptoms of UC

General symptoms Fever may occur with severe attacks, usually a low-grade. Spiking fever and chills indicate complications. Loss of appetite, weight loss and impaired growth in children are usually not evidence of mild or moderate or severe UC. Increased frequency, a feeling of incomplete evacuation, tenesmus (a painful urge for a bowel movement even if the rectum is empty) and fecal incontinence may occur in mild or severe stage. Anal ulcers and fistulae, channels that can burrow between organs, loops of intestine or between intestines and skin, may be early symptoms. Recurrent diarrhea is very common, but the onset may be very gradual and mild or silent. Feces may also contain mucus. Recurrent diarrhea is prevalent in developing countries, particularly in tropical regions^[6-8]. Blood is always present in stools, it may be readily visible or visible only using a microscope (so-called occult blood). Constipation can be a symptom of UC but not as common as diarrhea. It can occur during flare-ups, and when the inflamed rectum triggers a reflex response in the colon that causes it to retain the stool. But constipation in CD is usually a symptom of obstruction in the small intestine.

Abdominal symptoms Pain is not a prominent symptom but can vary. Vague discomfort may occur in the lower abdomen, an ache around the top of the hipbone, or cramps in the middle of the abdomen. Severe pain can occur during flare-ups. Recurrent episodes of pain in the lower right part of the abdomen or above the pubic bone often precede and are relieved by defecation. Bloating, nausea, and vomiting may also occur. Intestinal pain may also be an indication of serious conditions, such as an abscess, or a perforation of the intestinal wall.

Complications of UC Patients with UC limited to the rectum (proctitis) or colitis limited to the end of the left colon (proctosigmoiditis) usually do quite well. Short periodic treatments using oral medications or enemas may be sufficient. Serious complications are rare in these patients. In those with a more extensive disease, blood loss from the inflamed intestines can lead to anemia, and may require treatment with iron supplements or even blood transfusions. Rarely, the colon can acutely dilate to a large size when the inflammation becomes very severe. This condition is called toxic megacolon. Patients with toxic megacolon are extremely ill with fever, abdominal pain and distention, dehydration, and malnutrition. Unless the patient improves rapidly with medication, surgery is usually necessary to prevent colon rupture^[3-5,7,8].

Colon cancer is a recognized complication of chronic UC. The risk for cancer begins to rise significantly after 8 to 10 years of colitis. The risk of a patient with UC developing colon cancer is also related to the location and the extent of the disease. Patients with only ulcerative proctitis probably do not have increased colon cancer risk compared to the general population. Among patients with active pancolitis of 10 years or longer, their risk of colon cancer is 10-20 times higher than that of the general population. In patients with chronic left-sided colitis, the risk of colon cancer is increased but not as high as in patients with chronic pancolitis.

Since these cancers have a more favorable outcome when treated at an earlier stage, yearly colon examination is recommended after 8 years of a known extensive disease. During these examinations, samples of tissue (biopsies) should be taken to search for precancerous lesions in the lining cells of the colon. When precancerous lesions are found, removal of the colon may be necessary to prevent colon cancer.

Complications of UC involve other parts of the body. Ten percent of the patients can develop inflammation of the joints (arthritis). Some patients have low back pain due to arthritis of the sacroiliac joints. Rarely, patients may develop painful and red skin nodules (erythema nodosum). Yet others can have painful and red eyes (uveitis, episcleritis). Because these

particular complications are a permanent risk in vision impairment, eye pain or redness is symptoms that require a physician's evaluation. Diseases of the liver and bile ducts may associate with UC. For example, in rare patients with a condition called sclerosing cholangitis, repeated infections and inflammation in the bile ducts can lead to recurrent fever, yellowing of skin (jaundice), cirrhosis, and the need for a liver transplant.

DRUG TREATMENT

Both medications and surgery have been used to treat UC^[7-21]. However, surgery is reserved for those with severe inflammation and life-threatening complications. There is no medication that can cure UC. Patients with UC will typically experience periods of relapse (worsening of inflammation) followed by periods of remission lasting for months to years. During relapses, symptoms of abdominal pain, diarrhea, and rectal bleeding can worsen patients' quality of life. During remissions, these symptoms subside. Remissions usually occur because of treatment with medications or surgery, but occasionally they occur spontaneously.

Since UC cannot be cured by medications, the goals of treatment with medications are to induce remissions, maintain remissions, minimize side effects of treatment, and improve the quality of life. The treatment of UC with medications is similar, though not always identical, to the treatment of CD^[9-11,16-20].

Medications treating UC include anti-inflammatory agents such as 5-ASA compounds, systemic and topical corticosteroids, and immunomodulators.

Anti-inflammatory medications that decrease intestinal inflammation are analogous to arthritis medications that decrease joint inflammation (arthritis). The anti-inflammatory medications used in the treatment of UC are topical 5-ASA compounds such as sulfasalazine (Azulfidine), olsalazine (Dipentum), and mesalamine (Pentasa, Asacol, Rowasa enema) that need direct contact with the inflamed tissues in order to be effective. Systemic corticosteroids can decrease the inflammation throughout the body without direct contact with the inflamed tissue. Systemic corticosteroids have predictable side effects in long-term treatment. Immunomodulators are medications that suppress the body's immune system either by reducing the cells that are responsible for immunity, or by interfering with proteins that are important in promoting inflammation. Immunomodulators are increasingly becoming important for patients with severe UC who do not respond adequately to anti-inflammatory agents. Examples of immunomodulators include 6-mercaptopurine (6-MP), azathioprine, methotrexate, and cyclosporine.

A somewhat curious new treatment is nicotine. It has long been observed that the risk of UC appears to be higher in nonsmokers and in ex-smokers. In certain circumstances, patients could improve clinically when treated with nicotine while they failed to respond to other medications.

5-ASA compounds (azulfidine, asacol, pentasa, dipentum)

5-ASA (5-aminosalicylic acid), also called mesalamine, is chemically similar to aspirin. Aspirin (acetylsalicylic acid) has been used for many years in treating arthritis, bursitis, and tendinitis (conditions of tissue inflammation). Aspirin, however, is not effective in treating UC. On the other hand, 5-ASA is effective in treating UC if the drug can be delivered directly (topically) onto the inflamed colon lining^[17-21]. For example, Rowasa for enema is a 5-ASA solution that is effective in treating inflammation in and near the rectum (ulcerative proctitis and ulcerative proctosigmoiditis). However, the enema solution cannot reach high enough to treat inflammation in the upper colon. Therefore, for most patients with UC, 5-ASA must be taken orally. When pure 5-ASA is taken orally, however, the

stomach and upper small intestine absorb most of the drug before it reaches the colon. Therefore, to be effective as an oral agent for UC, 5-ASA has to be modified chemically to escape absorption by the stomach and upper intestines. These modified 5-ASA compounds are sulfasalazine (Azulfidine), mesalamine (Pentasa, Asacol), and olsalazine (Dipentum).

Azulfidine

Sulfasalazine (Azulfidine)^[22] has been used successfully for many years in inducing remission among patients with mild to moderate UC. Inducing remission means decreasing intestinal inflammation and relieving symptoms of abdominal pain, diarrhea, and rectal bleeding. Sulfasalazine has also been used for prolonged periods of time to maintain remissions.

Sulfasalazine consists of a 5-ASA molecule linked chemically to a sulfapyridine molecule. (Sulfapyridine is a sulfa antibiotic). Connecting the two molecules together prevents absorption by the stomach and upper intestines prior to reaching the colon. When sulfasalazine reaches the colon, bacteria in the colon will break the linkage between the two molecules. After breaking away from 5-ASA, sulfapyridine is absorbed into the body and then excreted in the urine. Most of the active 5-ASA, however, remains in the colon to treat colitis.

Most of the side effects of sulfasalazine are due to the sulfapyridine molecule. These side effects include nausea, heartburn, headache, anemia, skin rashes, and in rare instances, hepatitis and kidney inflammation. In men, sulfasalazine can reduce the sperm count which sperm count is reversible, and the count usually returns to normal after discontinuing sulfasalazine or by changing to a different 5-ASA compound.

The benefits of sulfasalazine generally are dose related. Therefore, high doses of sulfasalazine may be necessary to induce remission. Some patients cannot tolerate high doses because of nausea and stomach upset. To minimize stomach upset, sulfasalazine is generally taken after or with meals. Some patients find it easier to take Azulfidine-EN (enteric-coated form of sulfasalazine). Enteric-coating helps decrease stomach upset. The newer 5-ASA compounds do not have the sulfapyridine component and have fewer side effects than sulfasalazine.

Asacol

Asacol is a tablet consisting of 5-ASA compound, mesalamine, surrounded by an acrylic resin coating (Asacol is sulfa free)^[22,23]. The resin coating prevents 5-ASA from being absorbed as it passes through the stomach and small intestine. When the tablet reaches the terminal ileum and colon, the resin coating dissolves, thus releasing 5-ASA into the colon.

Asacol is effective in inducing remissions in patients with mild to moderate UC. It is also effective when used for prolonged periods of time to maintain remissions. The recommended dose of Asacol to induce remission is two 400-mg tablets three times daily (total of 2.4 g/d). Two tablets of Asacol twice daily (1.6 g/d) are recommended for maintaining remission. Occasionally, the maintenance dose should be higher. As Azulfidine, the benefits of Asacol are dose-related. If patients do not respond to 2.4 g/d of Asacol, the dose is frequently increased to 3.6 g/d (and sometimes even higher) to induce remission. If patients fail to respond to the higher doses of Asacol, then alternatives such as corticosteroids are recommended.

Pentasa

Pentasa is a capsule consisting of 5-ASA compound mesalamine inside controlled-release spheres. Like Asacol, it is sulfa free. As the capsule travels down the intestines, 5-ASA inside the spheres is slowly released into the intestines. Unlike Asacol, mesalamine in Pentasa is released into the small intestine as well as colon. Therefore, Pentasa can be effective in treating inflammation in the small intestine and colon. Pentasa is

currently the most logical 5-ASA compound for treating mild to moderate CD involving the small intestine. Pentasa is also used to induce remission and maintain remission among patients with mild to moderate UC^[23,24].

Olsalazine (Dipentum)

Olsalazine (Dipentum) consists of two 5-ASA molecules linked together^[24,25]. It is sulfa free. The linked 5-ASA molecules travel through the stomach and the small intestine unabsorbed. When the drug reaches the terminal ileum and the colon, normal bacteria in the intestine break the linkage and release the active drug into the colon and terminal ileum. Olsalazine has been used in treating UC and maintaining remissions. A side effect unique to olsalazine is secretory diarrhea (diarrhea resulting from excessive production of fluid in the intestines). This condition occurs in 5-10% of patients, and diarrhea sometimes can be severe.

Colazal

Colazal (balsalazide) is a capsule in which 5-ASA is linked by a chemical bond to another molecule that is inert (without effect on the intestine) and prevents 5-ASA from being absorbed^[25-29]. This drug is able to travel through the intestine unchanged until it reaches the end of the small bowel (terminal ileum) and colon. There, intestinal bacteria break apart 5-ASA and the inert molecule, releasing 5-ASA. Because intestinal bacteria are most abundant in the terminal ileum and colon, Colazal is used to treat inflammation predominantly localized to the colon. Colazal recently has been approved by FDA for use in United States of America.

More clinical trials are needed to compare the effectiveness of Colozal to other mesalamine compounds such as Asacol in treating UC. Therefore in United States of America, 5-ASA, has to be individualized^[27,28]. Colozal should be prescribed for patients who cannot tolerate or fail to respond to Asacol, also for patients with predominantly left sided colitis, since some studies seem to indicate that Colozal is effective in treating left sided colitis.

Rowasa enema

Rowasa is 5-ASA compound mesalamine in enema form and is effective in the treatment of ulcerative proctitis and ulcerative proctosigmoiditis (two conditions where active 5-ASA drugs taken as enemas can easily reach the inflamed tissues directly)^[29,30]. Each Rowasa enema contains 4 g of mesalamine in 60 mL of fluid. The enema is usually administered at bedtime, and patients are encouraged to retain the enema through the night.

The enema contains sulfite and should not be used by patients with sulfite allergy. Otherwise, Rowasa enemas are safe and well tolerated.

Rowasa also comes in suppository form for treating limited proctitis. Each suppository contains 500 mg of mesalamine and usually is administered twice daily. While some patients improve within several days after using Rowasa, the usual course of treatment is 3-6 wk. Some patients may need even longer courses of treatment for optimal benefit. In patients who do not respond to Rowasa, oral 5-ASA compounds (such as Asacol) can be added. Some studies have reported increased effectiveness in treating ulcerative proctitis and proctosigmoiditis by combining oral 5-ASA compounds with Rowasa enemas. Oral 5-ASA compounds are also used to maintain remission in ulcerative proctitis and proctosigmoiditis^[30].

Another alternative for patients who fail to respond to Rowasa or who cannot use Rowasa is cortisone enemas (Cortenema). Cortisone is a corticosteroid that is a potent anti-inflammatory agent. Oral corticosteroids are systemic drugs with serious and predictable long-term side effects. Cortenema is a topical corticosteroid that is less absorbed into the body than oral corticosteroids, and therefore, it has fewer and less side effects.

Side effects of 5-ASA compounds

Sulfa-free 5-ASA compounds have fewer side effects than sulfasalazine and also do not impair male fertility. In general, they are safe medications for long-term use and well tolerated^[23-28]. Patients allergic to aspirin should avoid 5-ASA compounds because they are chemically similar to aspirin. In a few occasions kidney inflammation has been reported due to the use of 5-ASA compounds. These compounds should be used with caution in patients with known kidney disease. It also is recommended that blood tests of kidney function are obtained before and during the treatment.

A rare instance of acute worsening of diarrhea, cramps, and abdominal pain may occur at times and may be accompanied by fever, rash, and malaise. This reaction is believed to represent an allergy to 5-ASA compounds.

Corticosteroids for UC

Corticosteroids (prednisone, prednisolone, hydrocortisone, etc.) have been used for many years in the treatment of patients with moderate to severe CD and UC or who fail to respond to optimal doses of 5-ASA compounds^[31-34]. Unlike 5-ASA compounds, corticosteroids do not require direct contact with inflamed intestinal tissues to be effective. Oral corticosteroids are potent anti-inflammatory agents. After absorption, corticosteroids exert prompt anti-inflammatory action throughout the body. Consequently, they are used in treating Crohn's enteritis, ileitis, and ileocolitis, as well as UC and Crohn's colitis. In critically ill patients, intravenous corticosteroids (such as hydrocortisone) can be given in the hospital. Corticosteroids are faster acting than 5-ASA compounds. Patients frequently experience improvement in their symptoms within days after using starting corticosteroids. Corticosteroids, however, do not appear to be useful in maintaining remissions in UC^[22-24].

Proper use of corticosteroids

Once the decision is made to use oral corticosteroids, treatment usually is initiated with prednisone, 40-60 mg daily. The majority of patients with UC respond with an improvement in symptoms. Once symptoms improve, prednisone is reduced by 5-10 mg per wk until the dose of 20 mg per day is reached. The dose then is tapered at a slower rate until prednisone ultimately is discontinued. Gradually reducing corticosteroids not only minimizes the symptoms of adrenal insufficiency, but also reduces the chances of abrupt relapse of colitis.

Many doctors use 5-ASA compounds at the same time as corticosteroids. In patients who achieve remission with systemic corticosteroids, 5-ASA compounds such as Asacol are often continued to maintain remissions^[10,17-19]. In patients whose symptoms return during reduction of the dose of corticosteroids, the dose of corticosteroids is increased slightly to control the symptoms. Once the symptoms are under control, the reduction can resume at a slower pace. Some patients become corticosteroid dependent and consistently develop symptoms of colitis whenever the corticosteroid dose is below a certain level. In patients who are corticosteroid dependent or unresponsive to corticosteroids, other anti-inflammatory medications, immunomodulator medications or surgery are considered. The management of patients who are corticosteroid dependent or patients with a severe disease which responds poorly to medications is complex. Doctors who are experienced in treating inflammatory bowel disease and in using immunomodulators should evaluate these patients.

Side effects of corticosteroids

Side effects of corticosteroids depend on the dose and duration of treatment. Short courses of prednisone, for example, usually are well tolerated with few and mild side effects. Long term high

doses of corticosteroids usually produce predictable and potentially serious side effects. Common side effects include rounding of the face (moon face), acne, increased body hair, diabetes, weight gain, high blood pressure, cataracts, glaucoma, increased susceptibility to infections, muscle weakness, depression, insomnia, mood swings, personality changes, irritability, and thinning of bones (osteoporosis) with an accompanying increased risk of compression fractures of the spine. Children on corticosteroids can experience stunted growth.

The most serious complication of long-term corticosteroid use is aseptic necrosis of the hip joints. Aseptic necrosis means death of bone tissue. It is a painful condition that can ultimately lead to the need for surgical replacement of the hips. Aseptic necrosis also has been reported in knee joints. It is unknown how corticosteroids cause aseptic necrosis. The estimated incidence of aseptic necrosis among corticosteroid users is 3-4%. Patients on corticosteroids who develop pain in hips or knees should report the pain to their doctors promptly. Early diagnosis of aseptic necrosis with cessation of corticosteroids has been reported in some patients to decrease the severity of the disease and possibly help avoid hip replacement.

Prolonged use of corticosteroids can depress the ability of adrenal glands to produce cortisol (a natural corticosteroid necessary for proper functioning of the body). Abruptly discontinuing corticosteroids can cause symptoms due to a lack of natural cortisol (a condition called adrenal insufficiency). Symptoms of adrenal insufficiency include nausea, vomiting, and even shock. Withdrawing corticosteroids too quickly can also produce symptoms of joint aches, fever, and malaise. Therefore, corticosteroids need to be gradually reduced rather than abruptly stopped. Even after corticosteroids are discontinued, the ability of adrenal glands to produce cortisol can remain depressed for months to two years. The depressed adrenal glands may not be able to produce enough cortisol to help the body handle stresses such as accidents, surgery, and infections. These patients will need treatment with corticosteroids (prednisone, hydrocortisone, etc.) during stressful situations to avoid developing adrenal insufficiency. Because corticosteroids are not useful in maintaining remission in UC and CD and because they have predictable and potentially serious side effects, these drugs should be used for the shortest possible time.

Preventing corticosteroid-induced osteoporosis

Long-term use of corticosteroids such as prednisolone or prednisone can cause osteoporosis, because corticosteroids could decrease calcium absorption from intestines and increase loss of calcium from the kidneys and bones. Increasing dietary calcium intake is important but alone cannot halt corticosteroid-induced bone loss. Management of patients on long-term corticosteroids should include adequate calcium (1 000 mg/d if premenopausal, 1 500 mg/d if postmenopausal) and vitamin D (800 U/d) intake, needs for continued corticosteroid treatment and the lowest effective dose, a bone density study to measure the extent of bone loss in patients taking corticosteroids for more than 3 mo, regular weight-bearing exercise and stopping cigarette smoking, discussion with the doctor regarding the use of alendronate (Fosamax) or risedronate (Actonel) in prevention and treatment of corticosteroid induced osteoporosis.

Immunomodulator medications

Immunomodulators are medications that weaken the body's immune system, which is composed of immune cells and cell-produced proteins. These cells and proteins serve to defend the body against harmful bacteria, viruses, fungi, and other foreign invaders. Activation of the immune system causes

inflammation within the tissues where the activation occurs. Normally, the immune system is activated only when the body is exposed to harmful invaders. In patients with CD and UC, however, the immune system is abnormally and chronically activated in the absence of any known invaders. Immunomodulators decrease tissue inflammation by reducing the population of immune cells and/or by interfering with their production of proteins that promote immune activation and inflammation. Generally, the benefits of controlling moderate to severe UC outweigh the risks of infection due to weakened immunity. Examples of immunomodulators include azathioprine (Imuran), 6-mercaptopurine (6-MP, Purinethol), cyclosporine (Sandimmune), and methotrexate^[31-37].

Azathioprine (imuran) and 6-MP (purinethol)

Azathioprine and 6-mercaptopurine (6-MP) are medications that weaken the body's immunity by reducing the population of a class of immune cells called lymphocytes^[31]. Azathioprine and 6-MP are related chemically. Specifically, azathioprine is converted into 6-MP inside the body. In high doses, these two drugs are useful in preventing rejection of transplanted organs and in treating leukemia. In low doses, they are used to treat patients with moderate to severe CD and UC. Azathioprine and 6-MP are increasingly recognized by doctors as valuable drugs in treating CD and UC. Some 70% of patients with moderate to severe disease benefit from these drugs. Because of the slow onset of action and the side effects, 6-MP and azathioprine are used mainly in the following situations^[31-34], UC and CD patients with severe diseases not responding to corticosteroids, patients experiencing undesirable corticosteroid-related side effects, patients dependent on corticosteroids and unable to discontinue them without developing relapses.

When azathioprine and 6-MP are added to corticosteroids in the treatment of UC patients who do not respond to corticosteroids alone, they may have an improved response to smaller doses, and shorter courses of corticosteroids may be used. Some patients can discontinue corticosteroids without experiencing relapses. The ability to reduce corticosteroid use has earned the reputation of 6-MP and azathioprine as "steroid-sparing" medications^[32-34]. In severe UC patients with severe disease who suffer frequent relapses, 5-ASA may not be sufficient, and more potent azathioprine and 6-MP will be necessary to maintain remissions. In the doses used for treating UC and CD, the long-term side effects of azathioprine and 6-MP are less serious than long-term oral corticosteroids or repeated courses of oral corticosteroids.

Side effects of 6-MP and azathioprine

Side effects of 6-MP and azathioprine include increased vulnerability to infections, inflammation of the liver (hepatitis) and pancreas (pancreatitis), and bone marrow toxicity (interfering with the formation of cells that circulate in the blood)^[31-37].

The goal of treatment with 6-MP and azathioprine is to weaken the body's immune system in order to decrease the intensity of inflammation in intestines. However, weakening the immune system increases the vulnerability to infections. For example, in a group severe CD patients unresponsive to standard doses of azathioprine, raising the dose of azathioprine helped to control the disease, but two patients developed cytomegalovirus (CMV) infection.

Azathioprine and 6-MP-induced inflammation of the liver (hepatitis) and pancreas (pancreatitis) is rare. Pancreatitis typically causes severe abdominal pain and sometimes vomiting. Pancreatitis due to 6-MP or azathioprine occurs in 3-5% of patients, usually during the first several wk of treatment. Patients who develop pancreatitis should not receive either of these two medications again^[38,39]. Azathioprine and 6-MP also

suppress the bone marrow where red blood cells, white blood cells, and platelets are made. Actually, a slight reduction in white blood cell count during treatment is desirable since it indicates that the dose of 6-MP or azathioprine is high enough to have an effect. However, excessively low red or white blood cell counts indicate bone marrow toxicity. Therefore, patients on 6-MP and azathioprine should have periodic detection of blood counts (usually every two wk initially and then every 3 mo during maintenance) to monitor the effect of the drugs on their bone marrow. 6-MP can reduce the sperm count in men. When the partners of male patients on 6-MP conceive, there is a higher incidence of miscarriages and vaginal bleeding. There also are respiratory difficulties in the newborn. Therefore, it is recommended that whenever feasible, male patients should stop 6-MP and azathioprine for 3 mo before conception. Patients on long-term high dose azathioprine to prevent rejection of the kidney after kidney transplantation have an increased risk of lymphoma. There is no evidence at present that long-term use of azathioprine and 6-MP in low doses used in IBD increases the risk of lymphoma, leukemia or other malignancies^[6,40].

6-MP characteristics

One problem with 6-MP and azathioprine is their slow onset of action. Typically, 3 mo or a longer time is required to achieve the full benefit of these drugs. During this time, corticosteroids frequently have to be maintained at high levels to control inflammation^[33].

The reason for this slow onset of action is partly due to the way prescribed 6-MP by doctors. Typically, 6-MP is started at a dose of 50 mg/d. The blood count is then checked 2 wk later. If the white blood cell count (specifically the lymphocyte count) is not reduced, the dose is increased. This cautious, stepwise approach helps prevent severe bone marrow and liver toxicity, but delays benefit from the drug.

Studies have shown that giving higher doses of 6-MP early can speed up the benefit of 6-MP without increasing toxicity in most patients, but some patients do develop severe bone marrow toxicity. Therefore, the dose of 6-MP has to be individualized. Scientists now believe that an individual's vulnerability to 6-MP toxicity is genetically inherited. Blood tests can be performed to identify those individuals with increased vulnerability to 6-MP toxicity. In these individuals, lower initial doses can be used. Blood tests can also be performed to measure the levels of certain by-products of 6-MP^[32-34]. The levels of these by-products in the blood help doctors more quickly determine whether the dose of 6-MP is right for the patient.

6-MP maintained treatment

Patients on maintenance with 6-MP or azathioprine for years have not any important long-term side effects. Their doctors, however, should closely monitor their patients on long-term 6-MP. There are data suggesting that patients on long-term maintenance with 6-MP or azathioprine fared better than those who stopped these medications. Those who stopped 6-MP or azathioprine were more likely to experience relapses, more likely to need corticosteroids or undergo surgery^[22-24,40].

Methotrexate

Methotrexate is an immunomodulator and anti-inflammatory medication. Methotrexate has been used for many years in the treatment of severe rheumatoid arthritis and psoriasis, and is helpful in treating patients with moderate to severe CD who neither respond to 6-MP and azathioprine nor tolerate these two medications. Methotrexate may also be effective in patients with moderate to severe UC who do not respond to corticosteroids or 6-MP and azathioprine. It can be given orally or by weekly

injections under the skin or into the muscles. It is more reliably absorbed with the injections^[35-39]. One major complication of methotrexate is the development of liver cirrhosis when the medication is given over a prolonged period of time (years). The risk of liver damage is higher in patients who also abuse alcohol or have morbid (severe) obesity. Generally, periodic liver biopsies are recommended for a patient who has received a cumulative (total) methotrexate dose of 1.5 g and higher^[38-40].

Other side effects of methotrexate include low white blood cell counts and inflammation of the lungs.

Methotrexate should not be used in pregnancy.

Cyclosporine

Cyclosporine (Sandimmune) is a potent immunosuppressant used in preventing organ rejection after transplantation. It has also been used to treat patients with severe UC and CD. Because of the approval of infliximab (Remicade) for treating severe CD, cyclosporine will probably be used primarily in severe UC. Cyclosporine is useful in fulminant UC and severely ill patients who do not respond to systemic corticosteroids. Cyclosporine is available as an oral medication, but the relapse rate with oral cyclosporine is high. Therefore, cyclosporine seems most useful when administered intravenously in acute situations^[33-37].

Side effects of cyclosporine include high blood pressure, renal function impairment, and tingling sensations in the extremities. More serious side effects include anaphylactic shock and seizures.

Traditional Chinese medicine

A total of 10 218 patients with UC reported in Chinese medical literature and the cases diagnosed were analyzed according to the diagnostic criteria of Lennard-Jones from 1981 to 2000. The number of cases increased by 3.08 times over the past 10 years (2 506 patients were diagnosed from 1981 to 1990 while 7 512 patients were diagnosed from 1991 to 2000). Lesion range was described in 7 966 patients, 5 592 (70.2%) were proctosigmoiditis or proctitis, 1 792 (22.5%) left-sided colitis, 582 (7.3%) pancolitis. Among the 8 122 patients, 2 826 (34.8%) had first episode, 4 272 (52.6%) had chronic relapse, 869 (10.7%) were of chronic persistent type, 154 (1.9%) were of acute fulminant type. The course of the illness was described in 5 867 patients, 4 427 (75.5%) were less than 5 years, 910 (15.5%) between 5 and 10 years, 530 (9.1%) more than 10 years. Six hundred and sixteen patients (6.1%) had extraintestinal manifestations. The mean age at the diagnosis was 40.7 years (range 6-80 years, and the peak age 30-49 years). The male to female ratio was 1.09. Among the 270 patients diagnosed in our hospital, 36 had histories of smoking, there was no negative association between the severity of UC and smoking ($P>0.05$), 21 smokers were followed up for one year, 15 of them had given up smoking when the disease was diagnosed, and one year later, 7 patients relapsed, another 6 patients continued smoking, and one year later, 2 patients relapsed. Among the 270 UC patients diagnosed in our hospital, 4 patients (1.5%) from 2 families had a familial history of UC. Treatment was done in 6 859 patients, only 5-ASA and/or corticosteroid only in 1 276 patients (18.6%), Chinese herbs alone in 1 377 patients (20.1%), combined Chinese and Western medicine in 4 056 patients (59.1%), surgery was performed in 87 patients (1.3%), other treatments in 63 patients (0.9%). In China, the number of UC patients increased significantly in the past 10 years. Lesions were commonly located to the left side colon. The course was short with rare extraintestinal manifestations. The age of onset was relatively high. Males and females were nearly equally affected. No negative relation was found between smoking and severity of the disease. Familial relatives were rarely involved. Traditional Chinese medicine (TCM) was widely used in the treatment of UC^[33].

Langmead *et al.*^[41] reported that herbal remedies for the treatment of IBD included slippery elm, fenugreek, devil's claw, Mexican yam, tormentil and *Wei tong ning*, a traditional Chinese medicine. Reactive oxygen metabolites produced by inflamed colonic mucosa may be pathogenic. Aminosalicylates (5-ASA) are antioxidant and other such agents could be therapeutic. Luminol-enhanced chemiluminescence in a xanthine/xanthine oxidase cell-free system was used to detect superoxide scavenging by herbs and 5-ASA. Fluorimetry was used to define peroxy radical scavenging by using a phycoerythrin degradation assay. Chemiluminescence was used to detect herbal effects on generation of oxygen radicals by mucosal biopsies from patients with active UC. All materials tested scavenged peroxy dose-dependently. Oxygen radical release from biopsies was reduced after incubation in all herbs except Mexican yam. All six herbal remedies have antioxidant effects. Fenugreek is not a superoxide scavenger, while Mexican yam does not inhibit radical generation of inflamed biopsies. Slippery elm, fenugreek, devil's claw, tormentil and *Wei tong ning* are novel drugs in IBD.

A total of 118 patients with UC were treated by integration of traditional Chinese and Western medicine^[42-44]. Another 86 cases of UC were treated by simple Western drugs as controls. The therapeutic effects on both groups were observed and compared after two therapeutic courses of 40 consecutive days. As a result, 39 cases were cured, 60 cases improved and 19 cases failed, with a total effective rate of 84% in the treatment group. In the control group, 15 cases were cured, 37 cases improved and 34 cases failed, with a total effective rate of 60.5%. Statistically, the difference was very significant ($P<0.01$). It can be concluded that treatment of UC by the integrated method is superior to that by simple Western drugs^[40].

Treatment of chronic UC by traditional Chinese and Western medicine is safe and effective in maintaining remission^[41-44].

REFERENCES

- 1 **Daperno M**, Sostegni R, Scaglione N, Ercole E, Rigazio C, Rocca R, Pera A. Outcome of a conservative approach in severe ulcerative colitis. *Dig Liver Dis* 2004; **36**: 21-28
- 2 **Hurlstone DP**, McAlindon ME, Sanders DS, Koegh R, Lobo AJ, Cross SS. Further validation of high-magnification chromoscopic-colonoscopy for the detection of intraepithelial neoplasia and colon cancer in ulcerative colitis. *Gastroenterology* 2004; **126**: 376-378
- 3 **Diculescu M**, Ciocirlan M, Ciocirlan M, Pitigoi D, Becheanu G, Croitoru A, Spanache S. Folic acid and sulfasalazine for colorectal carcinoma chemoprevention in patients with ulcerative colitis: the old and new evidence. *Rom J Gastroenterol* 2003; **12**: 283-286
- 4 **van Staa TP**, Cooper C, Brusse LS, Leufkens H, Javaid MK, Arden NK. Inflammatory bowel disease and the risk of fracture. *Gastroenterology* 2003; **125**: 1591-1597
- 5 **Winther KV**, Jess T, Langholz E, Munkholm P, Binder V. Survival and cause-specific mortality in ulcerative colitis: follow-up of a population-based cohort in Copenhagen County. *Gastroenterology* 2003; **125**: 1576-1582
- 6 **Thuraisingam A**, Leiper K. Medical management of ulcerative colitis. *Hosp Med* 2003; **64**: 703-707
- 7 **Raychaudhuri SP**, Raychaudhuri SK. Role of NGF and neurogenic inflammation in the pathogenesis of psoriasis. *Prog Brain Res* 2004; **146**: 433-437
- 8 **Lichtenstein GR**. Evaluation of bone mineral density in inflammatory bowel disease: current safety focus. *Am J Gastroenterol* 2003; **98**(12 Suppl): S24-S30
- 9 **Solem CA**, Loftus EV, Tremaine WJ, Sandborn WJ. Venous thromboembolism in inflammatory bowel disease. *Am J Gastroenterol* 2004; **99**: 97-101
- 10 **Kane SV**, Bjorkman DJ. The efficacy of oral 5-ASAs in the treatment of active ulcerative colitis: a systematic review. *Rev Gastroenterol Disord* 2003; **3**: 210-218

- 11 **Teml A**, Kratzer V, Schneider B, Lochs H, Norman GL, Gangl A, Vogelsang H, Reinisch W. Anti-Saccharomyces cerevisiae antibodies: a stable marker for Crohn's disease during steroid and 5-aminosalicylic acid treatment. *Am J Gastroenterol* 2003; **98**: 2226-2231
- 12 **Gionchetti P**, Rizzello F, Habal F, Morselli C, Amadini C, Romagnoli R, Campieri M. Standard treatment of ulcerative colitis. *Dig Dis* 2003; **21**: 157-167
- 13 **Sutherland L**, MacDonald JK. Oral 5-aminosalicylic acid for induction of remission in ulcerative colitis. *Cochrane Database Syst Rev* 2003; CD000543
- 14 **Toubanakis C**, Batziou E, Sipsas N, Galanopoulos G, Tzivras M, Archimandritis A. Acute pancreatitis after long-term therapy with mesalazine, and hyperamylasaemia associated with azathioprine in a patient with ulcerative colitis. *Eur J Gastroenterol Hepatol* 2003; **15**: 933-934
- 15 **Ustun S**, Dagci H, Aksoy U, Guruz Y, Ersoz G. Prevalence of amebiasis in inflammatory bowel disease in Turkey. *World J Gastroenterol* 2003; **9**: 1834-1835
- 16 **Diculescu M**, Ciocirlan M, Ciocirlan M, Pitigoi D, Becheanu G, Croitoru A, Spanache S. Folic acid and sulfasalazine for colorectal carcinoma chemoprevention in patients with ulcerative colitis: the old and new evidence. *Rom J Gastroenterol* 2003; **12**: 283-286
- 17 **Russinko PJ**, Agarwal S, Choi MJ, Kelty PJ. Obstructive nephropathy secondary to sulfasalazine calculi. *Urology* 2003; **62**: 748
- 18 **Norgard B**, Puhø E, Pedersen L, Czeizel AE, Sorensen HT. Risk of congenital abnormalities in children born to women with ulcerative colitis: a population-based, case-control study. *Am J Gastroenterol* 2003; **98**: 2006-2010
- 19 **Aqel B**, Bishop M, Krishna M, Cangemi J. Collagenous colitis evolving into ulcerative colitis: a case report and review of the literature. *Dig Dis Sci* 2003; **48**: 2323-2327
- 20 **Moum B**. 5-aminosalicylic acid in the treatment of ulcerative colitis and Crohn's disease. *Tidsskr Nor Laegeforen* 2003; **123**: 2565-2567
- 21 **Wong JM**, Wei SC. Efficacy of Pentasa tablets for the treatment of inflammatory bowel disease. *J Formos Med Assoc* 2003; **102**: 613-619
- 22 **Loftus EV Jr**, Kane SV, Bjorkman D. Systematic review: short-term adverse effects of 5-aminosalicylic acid agents in the treatment of ulcerative colitis. *Aliment Pharmacol Ther* 2004; **19**: 179-189
- 23 **Chourasia MK**, Jain SK. Pharmaceutical approaches to colon targeted drug delivery systems. *J Pharm Pharm Sci* 2003; **6**: 33-66
- 24 **Edmond LM**, Hopkins MJ, Magee EA, Cummings JH. The effect of 5-aminosalicylic acid-containing drugs on sulfide production by sulfate-reducing and amino acid-fermenting bacteria. *Inflamm Bowel Dis* 2003; **9**: 10-17
- 25 **Foster RA**, Zander DS, Mergo PJ, Valentine JF. Mesalamine-related lung disease: clinical, radiographic, and pathologic manifestations. *Inflamm Bowel Dis* 2003; **9**: 308-315
- 26 **Farrell RJ**. Epidermal growth factor for ulcerative colitis. *N Engl J Med* 2003; **349**: 395-397
- 27 **Christodoulou D**, Katsanos K, Baltayannis G, Tzabouras N, Tsianos EV. A report on efficacy and safety of azathioprine in a group of inflammatory bowel disease patients in northwest Greece. *Hepatogastroenterology* 2003; **50**: 1021-1024
- 28 **Sinha A**, Nightingale J, West KP, Berlanga-Acosta J, Playford RJ. Epidermal growth factor enemas with oral mesalamine for mild-to-moderate left-sided ulcerative colitis or proctitis. *N Engl J Med* 2003; **349**: 350-357
- 29 **Paoluzi P**, D'Albasio G, Pera A, Bianchi Porro G, Paoluzi OA, Pica R, Cottone M, Miglioli M, Prantera C, Sturmiolo G, Ardizzone S. Oral and topical 5-aminosalicylic acid (mesalazine) in inducing and maintaining remission in mild-moderate relapse of ulcerative colitis: one-year randomized multicentre trial. *Dig Liver Dis* 2002; **34**: 787-793
- 30 **Ebinger M**, Leidl R, Thomas S, Von Tirpitz C, Reinshagen M, Adler G, Konig HH. Cost of outpatient care in patients with inflammatory bowel disease in a German University Hospital. *J Gastroenterol Hepatol* 2004; **19**: 192-199
- 31 **Card T**, West J, Hubbard R, Logan RF. Hip fractures in patients with inflammatory bowel disease and their relationship to corticosteroid use: a population based cohort study. *Gut* 2004; **53**: 251-255
- 32 **Quondamcarlo C**, Valentini G, Ruggeri M, Forlini G, Fenderico P, Rossi Z. Campylobacter jejuni enterocolitis presenting as inflammatory bowel disease. *Tech Coloproctol* 2003; **7**: 173-177
- 33 **Reffitt DM**, Meenan J, Sanderson JD, Jugdaohsingh R, Powell JJ, Thompson RP. Bone density improves with disease remission in patients with inflammatory bowel disease. *Eur J Gastroenterol Hepatol* 2003; **15**: 1267-1273
- 34 **Katz S**. Update in medical therapy of ulcerative colitis: a practical approach. *J Clin Gastroenterol* 2002; **34**: 397-407
- 35 **Keven K**, Sahin M, Kutlay S, Sengul S, Erturk S, Ersoz S, Erbay B. Immunoglobulin deficiency in kidney allograft recipients: comparative effects of mycophenolate mofetil and azathioprine. *Transpl Infect Dis* 2003; **5**: 181-186
- 36 **Corominas H**, Baiget M. Clinical utility of thiopurine s-methyltransferase genotyping. *Am J Pharmacogenomics* 2004; **4**: 1-8
- 37 **Menachem Y**, Gotsman I. Clinical manifestations of pyoderma gangrenosum associated with inflammatory bowel disease. *Isr Med Assoc J* 2004; **6**: 88-90
- 38 **Schroder O**, Blumenstein I, Schulte-Bockholt A, Stein J. Combining infliximab and methotrexate in fistulizing Crohn's disease resistant or intolerant to azathioprine. *Aliment Pharmacol Ther* 2004; **19**: 295-301
- 39 **Feagan BG**. Maintenance therapy for inflammatory bowel disease. *Am J Gastroenterol* 2003; **98**(12 Suppl): S6-S17
- 40 **Hanauer SB**, Present DH. The state of the art in the management of inflammatory bowel disease. *Rev Gastroenterol Disord* 2003; **3**: 81-92
- 41 **Langmead L**, Dawson C, Hawkins C, Banna N, Loo S, Rampton DS. Antioxidant effects of herbal therapies used by patients with inflammatory bowel disease: an *in vitro* study. *Aliment Pharmacol Ther* 2002; **16**: 197-205
- 42 **Chen Q**, Zhang H. Clinical study on 118 cases of ulcerative colitis treated by integration of traditional Chinese and Western medicine. *J Tradit Chin Med* 1999; **19**: 163-165
- 43 **Meng M**. TCM differential treatment of 57 cases of chronic gastritis complicated by ulcerative colitis. *J Tradit Chin Med* 1999; **19**: 10-15
- 44 **Wang B**, Ren S, Feng W, Zhong Z, Qin C. Kui jie qing in the treatment of chronic non-specific ulcerative colitis. *J Tradit Chin Med* 1997; **17**: 10-13

Edited by Chen WW and Wang XL Proofread by Xu FM

Construction and selection of subtracted cDNA library of mouse hepatocarcinoma cell lines with different lymphatic metastasis potential

Li Hou, Jan-Wu Tang, Xiao-Nan Cui, Bo Wang, Bo Song, Lei Sun

Li Hou, Jan-Wu Tang, Xiao-Nan Cui, Bo Wang, Bo Song, Lei Sun, Department of Pathology, Dalian Medical University, Dalian 116027, Liaoning Province, China

Supported by the Natural Science Foundation of Liaoning Province, No. 20022122

Correspondence to: Dr. Jian-Wu Tang, Department of Pathology, Dalian Medical University, Dalian 116027, Liaoning Province, China. houli72@163.net

Telephone: +86-411-4720610

Received: 2003-06-05 **Accepted:** 2003-07-30

Abstract

AIM: In order to elucidate the molecular mechanism of lymphatic metastasis of hepatocarcinoma, we detected the difference of gene expression between mouse hepatocarcinoma cell lines Hca-F and Hca-P with different lymphatic metastasis potential.

METHODS: cDNA of Hca-F cells was used as a tester and cDNA of Hca-P cells was used as a driver. cDNAs highly expressed in Hca-F cells were isolated by the suppression subtractive hybridization (SSH) method. The isolated cDNA was cloned into T/A cloning vector. The ligation products were transformed into DH5 α competent cells. Individual clones were randomly selected and used for PCR amplification. Vector DNA from positive clones was isolated for sequencing.

RESULTS: There were 800 positive clones in amplified subtracted cDNA library. Random analysis of 160 clones with PCR showed that 95% of the clones contained 100-700 bp inserts. Analysis of 20 sequenced cDNA clones randomly picked from the SSH library revealed 4 known genes (mouse heat shock protein 84 ku, DNA helicase, ribosomal protein S13, ethanol induced 6 gene) and 3 expressed sequence tags (ESTs). Four cDNAs showed no homology and presumably represent novel genes.

CONCLUSION: A subtracted cDNA library of differentially expressed genes in mouse hepatocarcinoma cell lines with different lymphatic metastasis potential was successfully constructed with SSH and T/A cloning techniques. The library is efficient and lays a solid foundation for searching new lymphatic metastasis related genes. The expression of mouse heat shock protein gene, DNA helicase and other 4 novel gene may be different between mouse hepatocarcinoma cell lines with different lymphatic metastasis potential.

Hou L, Tang JW, Cui XN, Wang B, Song B, Sun L. Construction and selection of subtracted cDNA library of mouse hepatocarcinoma cell lines with different lymphatic metastasis potential. *World J Gastroenterol* 2004; 10(16): 2318-2322 <http://www.wjgnet.com/1007-9327/10/2318.asp>

INTRODUCTION

Metastasis is the most lethal attribute of malignant tumors^[1].

Ninety percent of malignant tumors are carcinomas, and lymph nodes are often the first organ to develop metastasis^[2]. Lymph node metastases form a bridgehead for further metastatic spread. But its molecular mechanism remains poorly understood. A mouse hepatocarcinoma cell line named Hca-F with high lymphogenous metastatic potential and its syngeneic cell line named Hca-P^[3] with low lymphogenous metastatic potential have been isolated from hepatocarcinomas in mice. The biological phenotypes between different cells are based on the difference between their phenotypes of gene expression. In this study, we constructed a subtracted cDNA library of differentially expressed genes in these two hepatocarcinoma cell lines using the suppressive subtractive hybridization (SSH)^[4-6], which can detect the difference in gene expression between different cells.

MATERIALS AND METHODS

Animals and cell lines

Hepatocarcinoma cell lines, Hca-F and Hca-P, were obtained from our department. Twenty inbred 615-mice maintained in our laboratory were equally divided into 2 groups. Hca-F and Hca-P cells (2×10^6 cells/mouse) were respectively inoculated in 10 mice in each group. On the 28th day post inoculation, the mice were killed and their lymph nodes were collected and stained by HE and examined under microscope. Therefore, the lymph node metastasis rate was calculated.

Isolation of RNA and mRNA

Total RNA was isolated from Hca-F and Hca-P cells (10^8 cells) respectively using Trizol reagent (Gibco BRL, USA). And mRNA was isolated from total RNA using the OligotexTM mRNA kit (Qiagen, USA) according to its manufacturer's instructions. The integrity of RNA and mRNA was checked on a 1% agarose gel.

Suppression subtractive hybridization (SSH)

Analysis of differentially expressed genes in Hca-F and Hca-P cells was performed by the suppression subtractive hybridization (SSH) using the CLONTECH PCR-SelectTM cDNA subtraction kit (Clontech, USA). In brief^[7,8], 2 μ g of mRNA from Hca-F and Hca-P cells was used for double strand cDNA synthesis, and the resulting cDNA was digested with Rsa I. The digested cDNA of Hca-F cells (as a Tester) was split into two groups and ligated to either adaptor I or adaptor 2R. Subtractive hybridization was performed by annealing an excess of Hca-P cDNAs (as a Driver) with each sample of adaptor ligated tester cDNAs. The cDNAs were heat denatured and incubated at 68°C for 8 h. After the first hybridization, the two samples were mixed together and hybridized again with freshly denatured driver cDNAs for 20 h at 68°C. The two rounds of hybridization would generate a normalized population of tester specific cDNA with different adaptors on each end. After filling in the end, two rounds of PCR amplification were performed to enrich desired cDNAs containing both adaptors by exponential amplification of these products. The optimized cycles for the first and second PCR were 30 and 20, respectively, to increase representation and reduce redundancy of subtracted cDNA libraries. Secondary PCR products were used as templates for

PCR amplification of G3PDH at 20, 25, 30, 35 cycles to assure subtracted efficiency.

Cloning of subtracted cDNA libraries

Products from the secondary PCR were T-A cloned into a T vector (Takara, China). The ligation products were transformed into DH5 α competent cells. The transformed cells were plated on LB plates containing ampicilin, X-Gal and IPTG, which allowed for color selection of colonies. Randomly selected individual white clones were grown for 8 h and then used for PCR amplification of clones.

Sequencing and BLAST homology search

Twenty candidate positive clones from subtracted cDNA library were selected for sequencing. Sequencing was performed by Takara Biotech using a M13 primer. The BLAST program was used to search for the cDNA sequence homology of isolated clones in GeneBank.

RESULTS

The analysis of integrity of RNA and mRNA

The A_{260}/A_{280} of RNA and mRNA from Hca-F and Hca-P was 1.9, which showed extracted RNA and mRNA were pure. Agarose gel electrophoresis showed that RNA was not destroyed by ribonucleases (Figure 1).

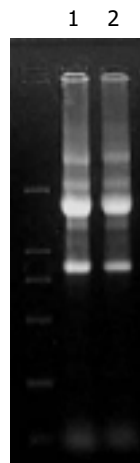


Figure 1 Total RNA from Hca-F and Hca-P cells. Lane 1: RNA from Hca-F cells, Lane 2: RNA from Hca-P cells.

Rsa I digestion

The size of digested cDNA molecular was smaller than undigested in agarose gel electrophoresis, indicating that tester cDNA and driver cDNA were completely digested.

Subtracted cDNA library construction by SSH

In this study, SSH was performed to identify differentially expressed genes among cDNAs of hepatocarcinoma cell lines, Hca-F and Hca-P. One subtracted F-P cDNA library was constructed using Hca-F with high lymphogenous metastatic potential as a tester and its syngeneic cell line named Hca-P with low lymphogenous metastatic potential as a driver. The subtracted cDNA library after secondary PCR amplification looked like smears (Figure 2).

Subtraction efficiency analysis showed that the abundance of non-differentially expressed genes was effectively reduced. In no subtracted cDNA library, the PCR products of housekeeping gene G3PDH were visible after 25 cycles. However, 35 cycles were required in the subtracted cDNA library for G3PDH to be detected (Figure 3).

The subtraction cDNA library contained 800 positive (white) clones. Random analysis of 160 clones with PCR showed that 95% of positive clones contained 100-700 bp inserts (Figure 4).

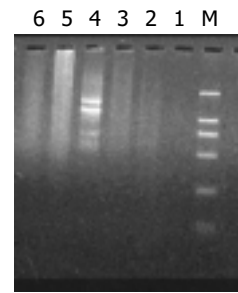


Figure 2 Results of secondary PCR amplification. Lanes 1-3: Product of primary PCR amplification, Lane 4: Secondary PCR amplification product of PCR control cDNA, Lane 5: Secondary PCR amplification product of unsubtracted cDNA, Lane 6: Secondary PCR amplification product of subtracted cDNA.

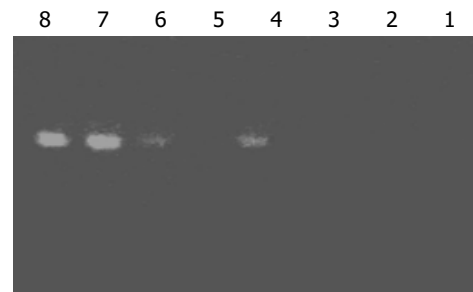


Figure 3 Analysis of subtraction effect. PCR was performed on subtracted (Lanes 1-4) or unsubtracted (Lanes 5-8) secondary PCR product with G3PDH 5'-Primer and 3'-primer. Lanes 1, 5: 20 cycles, Lanes 2, 6: 25 cycles, Lanes 3, 7: 30 cycles, Lanes 4, 8: 35 cycles.

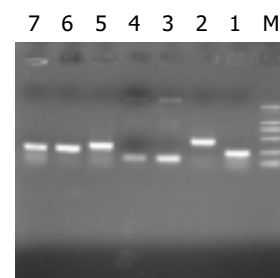


Figure 4 Results of clone PCR amplification. There was a average insert size of 0.1-0.7 kb.

ACCTGATTACGAATTCGAGCTCGGTACCCGGGGATCCTCTAGAG
 ATTGGCCGCCCCGGGCAGGTCTATAGGGCTCGAGCGGCCG
 CCCGGGCAGGTACCATGGTCTAGAGTCTGACTAAGTAGGTA
 ACTCGAGCTGCAGGTCTAGATCAGAAAACTCGAGCCTGCA
 GGTCTAGATCAGAAAAAACTCGAGCCTGCAGG
 TCTAGATGGCATCGATGAAGATGAGGTCCTGCAGAGGAGC
 CCAGTGTCTGTTCTGATGATCCCCCTCTGGAAGGGGATG
 AGGATGCCTCGCGCATGGAAGAGGTGGATTAAGCCTCCTG
 GAAGAAGCCCTGCCCTCTGTATAGTATCCCCGTTGGCTCCCAGCA
 GCCCTGACCCACTGACTCTCTGCTCATGTCTACAAGAATCTTCT
 ATCCCTGCTGTCCTTAAGGCAGGAAGATCCCCCTCCACAGAAT
 AGCAGGGTTGGGTGTTATGTATTGTGTTTTTTTGTCTTAT
 TTTGTTCTAAAATTAAGTATGCAAAATAAAGAAGATGCA
 GTTTCAAAAAACTCGAGCCTGCAGGTCTAGATCA
 GCGCGTGGTACCTCGGCCGACACGCTAATCGTTCGACCT
 GCAGGCATGCAAGCT

Figure 5 Sequence of clone 10-3.

Sequencing and homology search

Automatic sequencing proved that most clones were isolated no more than two times (Figures 5-7). BLAST homology search revealed that some sequences were homologous with known gene fragments and others were possibly novel genes, showing few sequence homologies with any known sequences in the GenBank. The results of homology search are shown in Table 1.

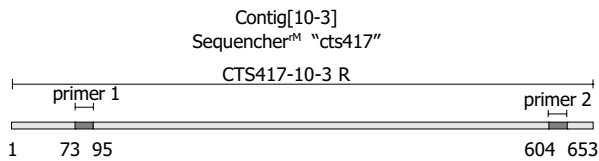


Figure 6 Gene structure of clone 10-3. Both nested primer 1 and nested primer 2R in the cDNA sequence were contained in subtracted library, indicating that only cDNA with both 2 adaptors could be amplified by PCR.

Table 1 Homologue searching of sequenced cDNA fragments from SSH library

Clone number	Size(bp)	Sequence identity
10-3	508	Mus musculus heat shock protein, 84 ku 1 (Hsp84-1)
2-2	385	Mus musculus ribosomal protein S13 (Rps13)
6-2	323	Mouse mRNA for DNA helicase
18-4	226	Mouse, similar to ethanol induced 6, clone MGG51351
11-7	363	Mouse 10 d embryo whole body cDNA, RIKEN full-length enrich library, clone 2610102k11
16-3	403	Mouse 2 d neonate thymus thymic cells cDNA RIKEN full-length library enriched library, clone E430002F13
7-1	570	Mouse chromosome 2 clone RP 24-322M5
15-7	460	Mouse chromosome 12 clone RP23-210N16
1-8	200	EST-mouse
5-8	159	EST-mouse
6-8	216	EST-mouse
2-6	61	Unknown
1-3	132	Unknown
1-6	241	Unknown
16-8	240	Unknown

Analysis of metastasis rate of Hca-F and Hca-P cells

The lymphatic metastasis rate was 80% (8/10) and 10% (1/10), respectively, for Hca-F cells and Hca-P cells.

DISCUSSION

Cancer is the most important cause of death of humans. There is no technique that can selectively kill cancer cells. A wide range of Metastasis leads to the failure of treatment and the death of patients. Therefore, investigation of cancer metastasis, particular the mechanisms, is important in order to improve the efficacy of the treatment. Metastasis^[9] is a complex process, which is made up of several steps. However, the molecular mechanism of lymphatic metastasis remains poorly understood because of lack of lymphatic metastasis models. A mouse hepatocarcinoma cell line named Hca-F with a metastasis rate over 70% and its syngeneic cell line named Hca-P with a metastasis rate less than 30% have been separated from hepatocarcinomas in mice. The difference in their metastasis potential might be based on the difference in their phenotypes of gene expression. Many different techniques could be used to isolate differentially expressed genes, such as expressed sequencing tag (EST)^[10], serial analysis of gene expression (SAGE)^[11], subtractive hybridization, mRNA differential display (DD-RT-PCR)^[12], cDNA representative difference analysis (RDA)^[13], suppression subtractive hybridization (SSH), and cDNA microarray^[14].

The novel technique named SSH^[15-18] has become an ideal subtractive system that combines high subtraction efficiency with normalized representation of differentially expressed genes, and is based on suppression PCR that permits exponential amplification of genes differing in abundance, but suppresses the amplification of sequences of identical abundance genes in two cells at the same time. Therefore, differentially expressed genes of low abundance can be cloned, while differentially expressed genes of high abundance are not excessively isolated. It has been reported that SSH can achieve more than 1 000-fold enrichment of low abundance genes, but only requires 2 µg mRNA instead of the 5-20 µg required in other methods. This method has been successfully used to isolate significant genes in many researches^[19-23]. Von Stein *et al.* observed a 94% positive rate in their study, and suggested that confirmation of differential expression by Northern blot analysis for each clone obtained was unnecessary^[24].

In the present study, we reported the efficiency of SSH

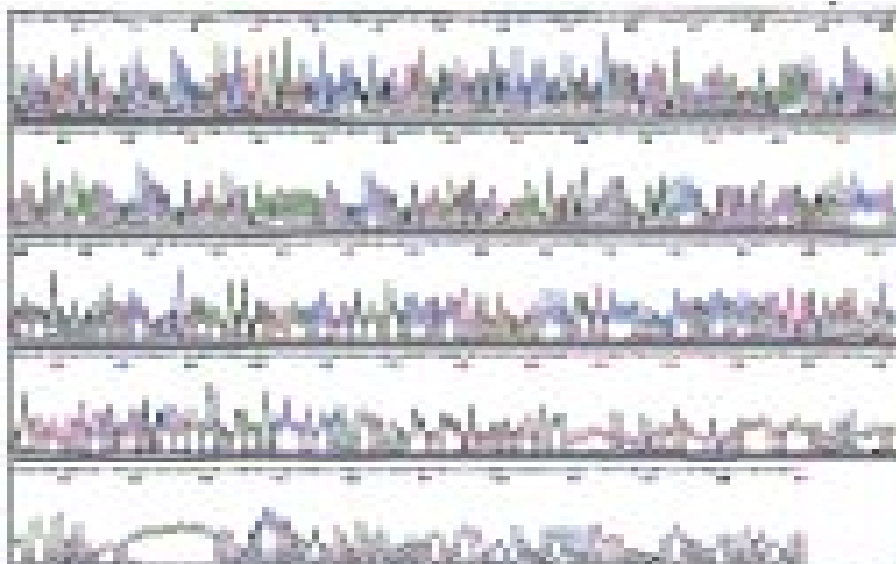


Figure 7 Result of clone 10-3 sequencing.

technique in identifying differentially expressed genes in Hca-F and Hca-P. PCR analysis showed that the subtraction efficiency after subtractive hybridization was effectively reduced. We constructed a subtracted cDNA library between Hca-F cells and Hca-P cells. There were 800 positive clones in the amplified subtracted cDNA library. Random analysis of 160 clones with PCR showed that 95% of clones contained 100-700 bp inserts. After sequencing and BLAST homology search, these clones could be divided into three groups: known genes preciously reported to be related to metastasis and carcinogenesis, known genes never described to be related to metastasis and carcinogenesis, and unknown genes. The identification of the first group of known genes attested to the validity of this method. The library is efficient and lays a solid foundation for searching new lymphatic metastasis related genes.

The No. 10-3 clone obtained in the present study showed homology with mouse heat shock proteins (HSPs). HSPs^[25-27] have been found to be ubiquitous molecules expressed in response to stress in all living organisms. The three important roles^[28] in regard to cancer development are regulation of apoptosis, modulation of immune response and drug resistance. HSPs are cytoplasmic proteins that could act as molecular chaperones for protein molecules in various intra-cellular processes^[29,30]. They are called "heat shock proteins" since they were first discovered in cells exposed to high temperatures. HSPs were also expressed in hepatocarcinoma (HCC)^[31-34], and up-regulated in early stage of HCC compared with noncancerous liver tissue. King *et al.*^[33] reported that HSPs expressed in HCC (45/58), and its expression was stronger in HCC than in noncancerous liver tissue. HSPs were related to metastasis^[35-38]. HSP expression was found in 54 out of 86 (62.7%) gastric carcinomas and was significantly related to more than six metastatic lymph nodes^[35]. Over expression of HSPs was related to tumor configuration, lymph node metastasis, and lymphatic vessel invasion in esophageal squamous cell carcinoma^[36]. So far, there has no report concerning HSP expression and lymphatic metastasis of HCC. In the present study, we found that HSP expression was different between mouse HCC cell lines Hca-F and Hca-P, indicating that HSP expression might be related to HCC metastasis.

The No. 6-2 clone obtained showed homology with mouse helicase. It has been found that DNA helicases^[39-41], because they unwound duplex DNA, have important roles in cellular DNA events such as replication, recombination, repair and transcription. The change in helicases expression could be found in human carcinomas^[42], lymphoma^[43], leukemia and so on. Helicases were also related to metastasis^[44]. B16-F10 and B16-BL6 are B16 mouse melanoma sublines that preferentially metastasize to the lung and their metastasis potential is different. Helicases and ribosomal protein (L37) showed higher expression in B16-BL6 cells than in B16-F10 cells^[45]. There has been no report on the association between helicase up-regulation and HCC metastasis. Thus, further investigations are required to elucidate the role of helicase in HCC metastasis.

Besides, two clones obtained in the present study showed homology to mouse ribosomal protein S13 and ethanol induced 6 gene. To our knowledge, there have been no reports on their relation to metastasis. Whether ribosomal protein S13 and ethanol induced 6 gene can be considered as candidate gene of metastasis related gene remains unclear. Clone 11-7 showed homology with mouse of 10-d embryo whole body cDNA library clone 2610102k11, It is important to study the correlation between metastasis and embryo gene expression. Clone 7-1 showed homology with mouse chromosome 2 clone RP 24-322M5 and clone 15-7 showed homology with mouse chromosome 12 clones RP23-210N16. Whether there are candidate metastasis-related genes on chromosome 2 and

chromosome 12 needs further investigation. The other three clones showed homology with three EST sequence.

In addition to the known genes, four clones showed no homology with any known sequences, indicating that they were novel genes, although the full-length sequence of these new genes and their function in lymphatic metastasis remain to be determined.

In conclusion, differentially expressed genes in mouse hepatocarcinoma cell lines with different lymphatic metastasis potential can be isolated by SSH method. Comprehensive study of these genes can help understand the molecular mechanism of lymphatic metastasis.

REFERENCES

- 1 **Yoshida BA**, Sokoloff MM, Welch DR, Rinker-Schaeffer CW. Metastasis-suppressor genes: a review and perspective on an emerging field. *J Natl Cancer Inst* 2000; **92**: 1717-1730
- 2 **Sleeman JP**. The lymph node as a bridgehead in the metastatic dissemination of tumors. *Recent Results Cancer Res* 2000; **157**: 55-81
- 3 **Hou L**, Li Y, Jia YH, Wang B, Xin Y, Ling MY, Lü S. Molecular mechanism about lymphogenous metastasis of hepatocarcinoma cells in mice. *World J Gastroenterol* 2001; **7**: 532-536
- 4 **Ahmed FE**. Molecular techniques for studying gene expression in carcinogenesis. *J Environ Sci Health Part C Environ Carcinog Ecotoxicol Rev* 2002; **20**: 77-116
- 5 **Li J**, Han BL, Huang GJ, Qian GS, Liang P, Yang TH, Chen J. Screening and identification for cDNA of differentially expressed genes in human primary hepatocellular carcinoma. *Zhonghua Yixue Yichuanxue Zazhi* 2003; **20**: 49-52
- 6 **Petersen S**, Petersen I. Expression profiling of lung cancer based on suppression subtraction hybridization (SSH). *Methods Mol Med* 2003; **75**: 189-207
- 7 **Luo M**, Kong XY, Liu Y, Zhou RH, Jia JZ. cDNA libraries construction and screening in gene expression profiling of disease resistance in wheat. *Yichuan Xuebao* 2002; **29**: 814-819
- 8 **Liu Y**, Cheng J, Lu YY, Wang G, Mou JS, Li L, Zhang LX, Chen JM. Cloning of genes transactivated by hepatitis B virus X protein. *Zhonghua Ganzhangbing Zazhi* 2003; **11**: 5-7
- 9 **Poste G**, Fidler IJ. The pathogenesis of cancer metastasis. *Nature* 1980; **283**: 139-146
- 10 **Adams MD**, Kelley JM, Gocayne JD, Dubnick M, Polymeropoulos MH, Xiao H, Merril CR, Wu A, Olde B, Moreno RF, Kerlavage AR, McCombie WR, Verlavage JC. Complementary DNA sequencing: expressed sequence tags and human genome project. *Science* 1991; **252**: 1651-1656
- 11 **Velculescu VE**, Zhang L, Vogelstein B, Kinzler KW. Serial analysis of gene expression. *Science* 1995; **270**: 484-487
- 12 **Liang P**, Pardee AB. Differential display of eukaryotic messenger RNA by means of the polymerase chain reaction. *Science* 1992; **257**: 967-971
- 13 **Lisitsyn N**, Wigler M. Cloning the differences between two complex genomes. *Science* 1993; **259**: 946-951
- 14 **Schena M**, Shalon D, Davis RW, Brown PO. Quantitative monitoring of gene expression patterns with a complementary DNA microarray. *Science* 1995; **270**: 467-470
- 15 **Ai JK**, Huang X, Wang YJ, Bai Y, Lu YQ, Ye XJ, Xin DQ, Na YQ, Zhang ZW, Guo YL. Screening of novel genes differentially expressed in human renal cell carcinoma by suppression subtractive hybridization. *Aizheng* 2002; **21**: 1065-1069
- 16 **Li JY**, Boado RJ, Pardridge WM. Blood-brain barrier genomics. *J Cereb Blood Flow Metab* 2001; **21**: 61-68
- 17 **Chen I**, Hsieh T, Thomas T, Safe S. Identification of estrogen-induced genes downregulated by AhR agonists in MCF-7 breast cancer cells using suppression subtractive hybridization. *Gene* 2001; **262**: 207-214
- 18 **Wang H**, Zhan Y, Xu L, Feuerstein GZ, Wang X. Use of suppression subtractive hybridization for differential gene expression in stroke: discovery of CD44 gene expression and localization in permanent focal stroke in rats. *Stroke* 2001; **32**: 1020-1027
- 19 **Zhou J**, Wang H, Lu A, Hu G, Luo A, Ding F, Zhang J, Wang X, Wu M, Liu Z. A novel gene, NMES1, downregulated in human

- esophageal squamous cell carcinoma. *Int J Cancer* 2002; **101**: 311-316
- 20 **Saito A**, Fujii G, Sato Y, Gotoh M, Sakamoto M, Toda G, Hirohashi S. Detection of genes expressed in primary colon cancers by *in situ* hybridisation: overexpression of RACK 1. *Mol Pathol* 2002; **55**: 34-39
- 21 **Miyasaka Y**, Enomoto N, Nagayama K, Izumi N, Marumo F, Watanabe M, Sato C. Analysis of differentially expressed genes in human hepatocellular carcinoma using suppression subtractive hybridization. *Br J Cancer* 2001; **85**: 228-234
- 22 **Roberts D**, Williams SJ, Cvetkovic D, Weinstein JK, Godwin AK, Johnson SW, Hamilton TC. Decreased expression of retinol-binding proteins is associated with malignant transformation of the ovarian surface epithelium. *DNA Cell Biol* 2002; **21**: 11-19
- 23 **Stassar MJ**, Devitt G, Brosius M, Rinnab L, Prang J, Schradin T, Simon J, Petersen S, Kopp-Schneider A, Zoller M. Identification of human renal cell carcinoma associated genes by suppression subtractive hybridization. *Br J Cancer* 2001; **85**: 1372-1382
- 24 **von Stein OD**, Thies WG, Hofmann M. A high throughput screening for rarely transcribed differentially expressed genes. *Nucleic Acids Res* 1997; **25**: 2598-2602
- 25 **Piura B**, Rabinovich A, Yavelsky V, Wolfson M. Heat shock proteins and malignancies of the female genital tract. *Harefuah* 2002; **141**: 969-972
- 26 **Friedman EJ**. Immune modulation by ionizing radiation and its implications for cancer immunotherapy. *Curr Pharm Des* 2002; **8**: 1765-1780
- 27 **Parmiani G**, Castelli C, Dalerba P, Mortarini R, Rivoltini L, Marincola FM, Anichini A. Cancer immunotherapy with peptide-based vaccines: what have we achieved? Where are we going? *J Natl Cancer Inst* 2002; **94**: 805-818
- 28 **Lebret T**, Watson RW, Fitzpatrick JM. Heat shock proteins: their role in urological tumors. *J Urol* 2003; **169**: 338-346
- 29 **Srivastava P**. Roles of heat-shock proteins in innate and adaptive immunity. *Nat Rev Immunol* 2002; **2**: 185-194
- 30 **Candido EP**. The small heat shock proteins of the nematode *Caenorhabditis elegans*: structure, regulation and biology. *Prog Mol Subcell Biol* 2002; **28**: 61-78
- 31 **Chuma M**, Sakamoto M, Yamazaki K, Ohta T, Ohki M, Asaka M, Hirohashi S. Expression profiling in multistage hepatocarcinogenesis: identification of HSP70 as a molecular marker of early hepatocellular carcinoma. *Hepatology* 2003; **37**: 198-207
- 32 **Yin Y**, Qin Q, Zhang W, Zhao J, Zhang C, Yu J. Overexpression of heat shock protein 70 and spontaneous cancer cell apoptosis in hepatocellular carcinoma. *Zhonghua Ganzangbing Zazhi* 2001; **9**: 84-85
- 33 **King KL**, Li AF, Chau GY, Chi CW, Wu CW, Huang CL, Lui WY. Prognostic significance of heat shock protein-27 expression in hepatocellular carcinoma and its relation to histologic grading and survival. *Cancer* 2000; **88**: 2464-2470
- 34 **Osada T**, Sakamoto M, Nishibori H, Iwaya K, Matsuno Y, Muto T, Hirohashi S. Increased ubiquitin immunoreactivity in hepatocellular carcinomas and precancerous lesions of the liver. *J Hepatol* 1997; **26**: 1266-1273
- 35 **Kapranos N**, Kominea A, Konstantinopoulos PA, Savva S, Artelaris S, Vantoros G, Sotiropoulou-Bonikou G, Papavassiliou AG. Expression of the 27-kDa heat shock protein (HSP27) in gastric carcinomas and adjacent normal, metaplastic, and dysplastic gastric mucosa, and its prognostic significance. *J Cancer Res Clin Oncol* 2002; **128**: 426-432
- 36 **Noguchi T**, Takeno S, Shibata T, Uchida Y, Yokoyama S, Muller W. Expression of heat shock protein 70 in grossly resected esophageal squamous cell carcinoma. *Ann Thorac Surg* 2002; **74**: 222-226
- 37 **Sagol O**, Tuna B, Coker A, Karademir S, Obuz F, Astarcioglu H, Kupelioglu A, Astarcioglu I, Topalak O. Immunohistochemical detection of pS2 protein and heat shock protein-70 in pancreatic adenocarcinomas. Relationship with disease extent and patient survival. *Pathol Res Pract* 2002; **198**: 77-84
- 38 **Mese H**, Sasaki A, Nakayama S, Yoshioka N, Yoshihama Y, Kishimoto K, Matsumura T. Prognostic significance of heat shock protein 27 (HSP27) in patients with oral squamous cell carcinoma. *Oncol Rep* 2002; **9**: 341-344
- 39 **Ishiguro H**, Shimokawa T, Tsunoda T, Tanaka T, Fujii Y, Nakamura Y, Furukawa Y. Isolation of HELAD1, a novel human helicase gene up-regulated in colorectal carcinomas. *Oncogene* 2002; **21**: 6387-6394
- 40 **Fuchsova B**, Novak P, Kafkova J, Hozak P. Nuclear DNA helicase II is recruited to IFN-alpha-activated transcription sites at PML nuclear bodies. *J Cell Biol* 2002; **158**: 463-473
- 41 **Furuichi Y**. Premature aging and predisposition to cancers caused by mutations in RecQ family helicases. *Ann N Y Acad Sci* 2001; **928**: 121-131
- 42 **Mohaghegh P**, Hickson ID. DNA helicase deficiencies associated with cancer predisposition and premature ageing disorders. *Hum Mol Genet* 2001; **10**: 741-746
- 43 **Kaneko H**, Morimoto W, Fukao T, Kasahara K, Kondo N. Telomerase activity in cell lines and lymphoma originating from Bloom syndrome. *Leuk Lymphoma* 2001; **42**: 757-760
- 44 **Takagi Y**, Suyama E, Kawasaki H, Miyagishi M, Taira K. Mechanism of action of hammerhead ribozymes and their applications *in vivo*: rapid identification of functional genes in the post-genome era by novel hybrid ribozyme libraries. *Biochem Soc Trans* 2002; **30**(Pt 6): 1145-1149
- 45 **Ishiguro T**, Nakajima M, Naito M, Muto T, Tsuruo T. Identification of genes differentially expressed in B16 murine melanoma sublines with different metastatic potentials. *Cancer Res* 1996; **56**: 875-879

COX-2 expression and tumor angiogenesis in colorectal cancer

Ai-Wen Wu, Jin Gu, Zhen-Fu Li, Jia-Fu Ji, Guang-Wei Xu

Ai-Wen Wu, Jin Gu, Jia-Fu Ji, Guang-Wei Xu, Department of Surgery, Beijing Cancer Hospital, Beijing Institute for Cancer Research, School of Oncology, Peking University, Beijing 100036, China

Zhen-Fu Li, Department of Biochemistry, Beijing Cancer Hospital, Beijing Institute for Cancer Research, School of Oncology, Peking University, Beijing 100036, China

Correspondence to: Dr. Guang-Wei Xu, Department of Surgery, Beijing Cancer Hospital, Beijing Institute for Cancer Research, School of Oncology, Peking University, 52 Fucheng Road, Haidian District, Beijing 100036, China. gwx@caca.edu.cn

Telephone: +86-10-88122452 **Fax:** +86-10-88122452

Received: 2003-11-17 **Accepted:** 2003-12-22

Abstract

AIM: Cyclooxygenase-2 (COX-2) is one of the rate-limiting enzymes in metabolism of arachidonic acid, and COX-2 inhibitors demonstrate preventive effects on cancer, especially on colorectal cancer. The underlying mechanism remains unclear. The aim of this study was to illustrate the relationship between angiogenesis and COX-2 in carcinogenesis of colorectal cancer.

METHODS: One hundred and seventy patients with colorectal cancer were enrolled in our study from January 1993 to September 2001 in School of Oncology, Peking University. COX-2 and VEGF expression were detected with the immunohistochemistry (IHC) technique. IHC assays were carried out with the aid of tissue microarray (TMA) procedure. Specimens from 35 of these patients were examined with reverse transcriptase PCR (RT-PCR).

RESULTS: COX-2 and VEGF expressions were stronger in colorectal cancer than those in the corresponding normal tissues, at both protein and mRNA levels. One hundred patients were eligible for analysis after IHC assay of COX-2 and VEGF. The positive rate of VEGF was much higher in COX-2 positive group (47/85) than in COX-2 negative group ($\chi^2 = 4.181$, $P = 0.041$). The result was further verified by the result of RT-PCR ($\chi^2 = 8.517$, $P = 0.003$). Correlation coefficient was 0.409 after Spearman correlation analysis ($P = 0.015$).

CONCLUSION: COX-2 may be involved in the course of tumor angiogenesis of colorectal cancer and acts through VEGF.

Wu AW, Gu J, Li ZF, Ji JF, Xu GW. COX-2 expression and tumor angiogenesis in colorectal cancer. *World J Gastroenterol* 2004; 10(16): 2323-2326

<http://www.wjgnet.com/1007-9327/10/2323.asp>

INTRODUCTION

Cyclooxygenase (COX) is one of the rate-limiting enzymes in metabolism of arachidonic acid, which catalyzes arachidonic acid into a series of products such as prostaglandins and other eicosanoids. It has two isoforms, COX-1 and COX-2. COX-2 acts as superoxidants and transforms arachidonic acid into

PGG₂, and then into PGH₂. COX-2 is inducibly expressed in many human tissues by cytokines, oncogenes, and tumor promoters^[1-3]. Recent clinical epidemiological studies have demonstrated the preventive effect of COX inhibitors on cancer, especially on colorectal cancer^[4-6]. Cellular and animal experimental studies have also indicated its relevance to tumor invasion, metastasis, cell apoptosis, cell cycle, and body immunity^[7], and the role of COX-2 in the development of colorectal cancer.

Angiogenesis is among the most important characteristics of tumors and plays an important role in the course of cancer invasion and metastasis. Recent studies have confirmed the hypothesis of tumor growth, which is generally dependent on tumor angiogenesis. Any significant increase in tumor mass must be preceded by an increase in vascular supply to deliver nutrients and oxygen to the tumor^[8]. Experimental studies from Seed and Tsujii^[9,10] suggested that COX-2 might be involved in angiogenesis. Few reports on the role of COX-2 in tumor angiogenesis of colorectal cancer in clinical settings are available.

MATERIALS AND METHODS

Patients and tissues

A total of 170 patients after surgical treatment in School of Oncology, Peking University, from January 1993 to September 2001 were studied retrospectively. Specimens from these patients were prepared as tissue microarray and then underwent immunohistochemical assays. Specimens from thirty-five patients were prepared for reverse transcriptase PCR (RT-PCR), including 22 male patients and 13 female patients.

Tissue array preparation and immunohistochemical staining

Formalin-fixed and paraffin-embedded tissues were subjected to routine sectioning of 3-5 μ m thickness and HE staining. Tissue array block was completed for subsequent sectioning according to the predetermined scheme described before^[11]. Two-step immunohistochemical staining was used for COX-2 and VEGF detection. The titer of COX-2 (Cayman Chemical, USA) and VEGF (Zhongshan Biological Inc., Beijing, China) antibody were 1:200 and 1:50 respectively. Human colon adenocarcinoma with strong COX-2 staining served as a positive control, whereas PBS instead of antibody served as a negative control. Two pathologists independently reviewed slides with immunohistochemical staining. Microscopically, the slides with no staining in the negative control and the specific dark yellow staining of cytoplasm and nuclear membrane in the positive control were eligible for a further analysis. Semiquantitative scoring system was adopted according to the staining intensity: 0 for no staining, 1 for weak yellow, 2 for dark yellow, and 3 for brown staining with granular distributions. The mean score was used for statistical analysis and the threshold for positivity was 2^[11].

Specimen preparation and RT-PCR

Tumor tissues and the corresponding normal mucosae at least 10 cm away were collected 30 min after removal of the specimens. The tissues were then stored under -70 °C for RNA extraction. Total RNA was prepared from the specimens with Trizol reagent

(Gibco BRL Co.) according to the manufacturer's instructions. cDNA synthesis was carried out with 1 μ g of total RNA. Sense and antisense primers of 0.5 μ L were mixed with 11 μ L dd H₂O, 5 μ L PCR buffer, 3 μ L MgCl₂ (25 mmol/L), 2 μ L dNTP (10 mmol/L), 2 μ L cDNA, and 0.8 μ L Taq DNA polymerase for PCR. The primers for PCR were 5' TTC AAA TGA GAT TGT GGG AAA AT 3' (sense primer) and 5' AGA TCA TCT CTG CCT GAG TAT CTT 3' (antisense primer). PCR reactions were processed in a PTC 100 thermocycler under the following conditions: at 94 °C for 5 min, at 94 °C for 30 s, extension at 55 °C for 30 s, then at 72 °C for 30 s for 40 cycles, and then at 72 °C for 5 min. The RT-PCR products were then analyzed on 15 g/L agarose gels. Colon cancer cell line HT-29 and β -actin served as a positive and inner control, respectively. PCR reactions without cDNA were used as blank controls.

Statistical analysis

All statistical analyses were carried out with the SPSS software, 10.0, USA. The relationship between COX-2 expression and categorical variables was compared with χ^2 test or Fisher two-sided exact test. Continuous variables were analyzed with *t* test and *P* < 0.05 was considered statistically significant. Correlation analysis was processed via the Spearman method.

RESULTS

Expression of COX-2 protein in colorectal cancer tissues

Of the 170 colorectal cancer patients, 139 were eligible for analysis after COX-2 immunohistochemical assays. Immunohistochemical assays demonstrated that COX-2 protein was located in cytoplasm and nuclear membrane. The staining was weak yellow, dark yellow, and brown at a low-power field and diffuse or granular staining at a high-power field under a microscope (Figure 1A). A weak staining of COX-2 was observed in normal tissue with a positive rate of 24.1% (7/29). COX-2 expression was much stronger in tumor cells with dark yellow or brown staining with occasional granular distributions than in normal tissues. The positive rate of COX-2 in colorectal cancer was 84.9% (118/139).

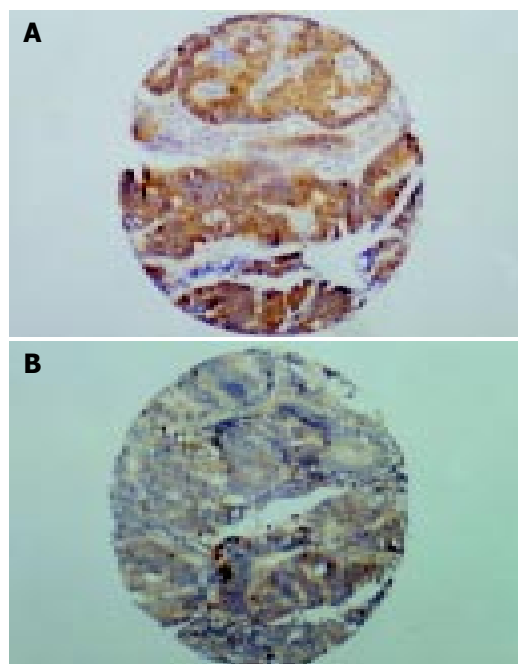


Figure 1 COX-2 and VEGF expressions in colorectal cancer tissues (IHC assay). A: Well-differentiated colonic adenocarcinoma, COX-2 immunostaining, $\times 100$. B: Well-differentiated colonic adenocarcinoma, VEGF immunostaining, $\times 100$.

Expression of VEGF protein in colorectal cancer tissues

For some reasons, only 100 colorectal cancer patients were eligible for further analysis after immunohistochemical assays. VEGF protein was located in cytoplasm of tumor cells and endothelial cells (Figure 1B). About 51.0% (51/100) of the tumors presented with strong VEGF staining, and the rate was much higher than that of normal tissues.

Expression of COX-2 and VEGF mRNA in colorectal cancer tissues

In consistent with the results of IHC assay, RT-PCR revealed stronger expressions of COX-2 and VEGF in tumors than in corresponding normal tissues (Figure 2). Among the 35 paired specimens of colorectal cancer tissues undergoing RT-PCR assays, 27 (77.1%) and 28 (80.0%) were positive with VEGF and COX-2, respectively, compared with 9 (25.7%) and 11 (31.4%) in normal tissues (*P* < 0.01).



Figure 2 COX-2 and VEGF expressions in colorectal cancer tissues (RT-PCR assay). N: normal T: tumor IC: internal control M: marker. The Arabic number represents the number of samples. The marker has six lanes from 100 bp to 600 bp. The left four lanes stand for the 304 bp products of COX-2 while the right two lanes are the VEGF products of 541 and 408 bp respectively. The internal control of β -actin produced a 496 bp product.

Correlation between COX-2 and VEGF expression in colorectal cancer tissues

For the reason of TMA, a total of 100 cases were eligible for IHC analysis. Among these, 47 COX-2 positive cases presented with a positive VEGF staining (55.3%). The positive rate of VEGF was much higher than that in COX-2 negative group (26.7%). The difference between two groups had a statistical significance ($\chi^2 = 4.181$, *P* = 0.041). Among the 27 cases with COX-2 mRNA expression, 25 had a strong VEGF expression while only 2 in COX-2 negative group ($\chi^2 = 8.517$, *P* = 0.003) (Table 1). COX-2 and VEGF expression demonstrated a tendency to having a positive correlation with correlation coefficient of 0.409 (*P* = 0.015).

Table 1 Expression of COX-2 and VEGF in colorectal cancer tissue (RT-PCR/IHC)¹

VEGF expression	COX-2 positive	COX-2 negative	Total
Positive	25 / 47	2 / 4	27 / 51
Negative	3 / 38	5 / 11	8 / 49
Total	28 / 85	7 / 15	35 / 100

¹Fisher double-side exact test (*P* = 0.003/0.041).

DISCUSSION

It has been documented that COX-2 plays an important role in the development of human tumors^[12-16]. COX-2 could promote the growth and invasion of tumors^[17,18] and increase invasiveness and potential of tumor metastasis^[19,20]. Recent research results indicated that COX-2 could also induce tumor angiogenesis and was correlated with hematogenous metastasis of tumors^[10,21].

Tumor angiogenesis is one of the important characteristics of tumors involving their growth and metastasis. The formation of primary or metastatic lesions and even their further development are dependent on tumor angiogenesis. Newly-formed vessels were in need of nutrition and oxygen when the tumor grew to 2-3 mm in size^[8].

It had been found many factors are involved in tumor angiogenesis including bFGF, aFGF, PGE₁, PGE₂, VEGF, TGF α , TGF β , and TNF^[22]. The most important is vessel endothelial growth factor (VEGF), a highly specific mitogen of vessel endothelial cells. The biological functions of VEGF included selective promotion of mitosis of endothelial cells, stimulation of their proliferation and angiogenesis, an increase in vessel transparency and extravasculization of plasma large molecules^[23-26]. It was reported that COX-2 might interact with VEGF^[27,28]. Therefore, the relationship of COX-2 and angiogenesis (VEGF as the marker of angiogenesis) was then investigated at protein and mRNA levels.

The positive rate of COX-2 mRNA and COX-2 protein were 80% (28/35) and 84.9% in colorectal cancer. Both were much higher than those in normal tissues ($P < 0.01$), which indicated the role of COX-2 in carcinogenesis of colorectal cancer. The expressions of COX-2 and VEGF were studied through RT-PCR and IHC assays. The result of RT-PCR showed that 25 were VEGF positive among the 28 COX-2 positive patients, and only 2 were VEGF positive in the COX-2 negative group. Correspondingly, of the 85 patients with COX-2 positive staining, 47 (55.3%) expressed VEGF while only 26.7% in the COX-2 negative group, indicating the correlation between the expressions of COX-2 and VEGF, which was further verified by the Spearman correlation analysis. Cianchi^[28] recently found a close correlation between COX-2 and VEGF as well as microvessel density (MVD) in their studies on 31 colorectal cancer patients by Western blot and Northern blot analysis, and immunohistochemical assays, which was consistent with our results.

The mechanism underlying the role of COX-2 in tumor angiogenesis has been unclear^[29]. Preliminary results showed that angiogenesis occurred when endothelial cells were cultured with cancer cells over-expressing COX-2^[10]. It could be inhibited by selective COX-2 inhibitors in endothelial cells *in vitro*^[29]. It was proved that the activity of COX-2 in interstitial cells was necessary for secretion of VEGF, proliferation of endothelial cells and new vessel formation^[30]. These experimental results suggested that such metabolic products might induce the expression of VEGF via pathways of paracrine, autocrine or intracrine, and stimulate proliferation of vessel endothelial cells and formation of tumor vessels^[29].

The regulatory effect of COX-2 on VEGF production and tumor angiogenesis suggested that COX-2 expression might be an upstream event in tumor angiogenesis^[10,29]. We also found that COX-2 expression was positively correlated with expression of VEGF, one of the most important factors for tumor angiogenesis. The expression rate of VEGF was high in patients with positive COX-2 expression (25/28) while low in COX-2 negative patients (2/7). In addition, staining intensity of COX-2 was correlated with that of VEGF. Management of the murine animal model of lung and prostate cancers with the gene knockout technique or COX-2 inhibitor resulted in not only tumor shrinkage but also inhibition of tumor angiogenesis. Endothelial cells were scattered without formation of an ordered tubular structure. The MVD of tumor and expression of VEGF were significantly decreased, further suggesting the role of COX-2 on VEGF expression and tumor angiogenesis^[31,32].

Great progresses have been made in the research of tumor angiogenesis. Trials on targeted therapy against angiogenesis have been ongoing to block or postpone tumor angiogenesis so as to cure cancer^[33,34]. More than twenty drugs are in their

phase I or II and even III clinical trials in the United States of America. Though preliminary results were promising, there is still a long way to go. Therefore, as an upper-stream event, COX-2 might be a potential target of the cancer gene therapy worthy of further research.

REFERENCES

- 1 **Williams CS**, Mann M, DuBios RN. The role of cyclooxygenases in inflammation, cancer, and development. *Oncogene* 1999; **18**: 7908-7916
- 2 **Egil F**. Biochemistry of cyclooxygenase (COX-2) inhibitors and molecular pathology of COX-2 in neoplasia. *Crit Rev Clin Lab Sci* 2000; **37**: 431-502
- 3 **Subbaramaiah K**, Dannenberg AJ. Cyclooxygenase 2: a molecular target for cancer prevention and treatment. *Trends Pharmaco Sci* 2003; **24**: 96-102
- 4 **Thun MJ**, Hennekenn CH. Aspirin and other non-steroidal anti-inflammatory drugs and the risk of cancer development. In: DeVitt VT, Hellman S, Rosenberg SA. Cancer: principles and practice of oncology. 6th edition. Philadelphia: *Lippincott Williams Wilkins Press U S A* 2001: 601-607
- 5 **Kawamori T**, Rao CV, Seibert K, Reddy BS. Chemopreventive activity of celecoxib, a specific cyclooxygenase-2 inhibitor, against colon carcinogenesis. *Cancer Res* 1998; **58**: 409-412
- 6 **Reddy BS**, Rao CV, Seibert K. Evaluation of cyclooxygenase-2 inhibitor for potential chemopreventive properties in colon carcinogenesis. *Cancer Res* 1996; **56**: 4566-4569
- 7 **Dannenberg AJ**, Zakim D. Chemoprevention of colorectal cancer through inhibition of cyclooxygenase-2. *Semin Oncol* 1999; **26**: 499-504
- 8 **Folkman J**. What is the evidence that tumors are angiogenesis dependent? *J Natl Cancer Inst* 1990; **82**: 4-6
- 9 **Seed MP**, Brown JR, Freemantle CN, Papwoeth JL, Colville-Nash PR, Willis D, Somerville KW, Asculai S, Willoughby DA. The inhibition of colon-26 adenocarcinoma development and angiogenesis by topical diclofenac in 2.5% hyaluronan. *Cancer Res* 1997; **57**: 1625-1629
- 10 **Tsujii M**, Kawano S, Tsuji S, Sawaoka H, Hori M, DuBios RN. Cyclooxygenase regulates angiogenesis induced by colon cancer cells. *Cell* 1998; **93**: 705-716
- 11 **Wu AW**, Gu J, Ji JF, Li ZF, Xu GW. Role of COX-2 in carcinogenesis of colorectal cancer and its relationship with tumor biological characteristics and patients' prognosis. *World J Gastroenterol* 2003; **9**: 1990-1994
- 12 **Eberhart CE**, Coffey RJ, Radhika A, Giardiello FM, Ferrenbach S, DuBois RN. Up-regulation of cyclooxygenase 2 gene expression in human colorectal adenomas and adenocarcinomas. *Gastroenterology* 1994; **107**: 1183-1188
- 13 **Ohno R**, Yoshinaga K, Fujita T, Hasegawa K, Iseki H, Tsunozaki H, Ichikawa W, Nihei Z, Sugihara K. Depth of invasion parallels increased cyclooxygenase-2 levels in patients with gastric carcinoma. *Cancer* 2001; **91**: 1876-1881
- 14 **Saukkonen K**, Nieminen O, van Rees B, Vilkkki S, Harkonen M, Juhola M, Mecklin JP, Sipponen P, Ristimaki A. Expression of cyclooxygenase-2 in dysplasia of the stomach and in intestinal-type gastric adenocarcinoma. *Clin Cancer Res* 2001; **7**: 1923-1931
- 15 **Wolff H**, Saukkonen K, Anttila S, Karjalainen A, Vainio H, Ristimaki A. Expression of cyclooxygenase-2 in human lung carcinoma. *Cancer Res* 1998; **58**: 4997-5001
- 16 **Shamma A**, Yamamoto H, Doki Y, Okami J, Kondo M, Fujiwara Y, Yano M, Inoue M, Matsuura N, Shiozaki H, Monden M. Up-regulation of cyclooxygenase-2 in squamous carcinogenesis of the esophagus. *Clin Cancer Res* 2000; **6**: 1229-1238
- 17 **Tsujii M**, Kawano S, DuBois RN. Cyclooxygenase-2 expression in human colon cancer cells increases metastatic potential. *Proc Natl Acad Sci U S A* 1997; **94**: 3336-3340
- 18 **Attiga FA**, Fernandez PM, Weeraratna AT, Manyak MJ, Patierno SR. Inhibitors of prostaglandin synthesis inhibit human prostate tumor cell invasiveness and reduce the release of matrix metalloproteinases. *Cancer Res* 2000; **60**: 4629-4637
- 19 **Tomazawa S**, Nagawa H, Tsuno NH, Hatano K, Osada T, Kitayama J, Osada T, Saito S, Tsuruo T, Shibata Y, Nagawa H.

- Inhibition of haematogenous metastasis of colon cancer in mice by a selective COX-2 inhibitor, JTE-522. *Br J Cancer* 1999; **81**: 1274-1279
- 20 **Tomozawa S**, Tsuno NH, Sunami E, Hatano K, Kitayama J, Osada T, Saito S, Tsuruo T, Shibata Y, Nagawa H. Cyclooxygenase-2 overexpression correlates with tumour recurrence, especially haematogenous metastasis, of colorectal cancer. *Br J Cancer* 2000; **83**: 324-328
- 21 **Masunaga R**, Kohno H, Dhar DK, Ohno S, Shibakita M, Kinugasa S, Yoshimura H, Tachibana M, Kubota H, Nagasue N. Cyclooxygenase-2 expression correlates with tumor neovascularization and prognosis in human colorectal carcinoma patients. *Clin Cancer Res* 2000; **6**: 4064-4068
- 22 **Fidler IJ**. Molecular biology of cancer: invasion and metastasis. In: DeVita SH, Rosenberg SA, eds. *Cancer: Principles and Practice of Oncology*, 5th edition. Philadelphia: *Lippincott Raven Publishers* 1997: 135-152
- 23 **Yancopoulos GD**, Klagsbrun M, Folkman J. Vasculogenesis, angiogenesis, and growth factors: ephrins enter the fray at the border. *Cell* 1998; **93**: 661-664
- 24 **Krishnan J**, Kirkin V, Steffen A, Hegen M, Weih D, Tomarev S, Wilting J, Sleeman JP. Differential *in vivo* and *in vitro* expression of vascular endothelial growth factor (VEGF)-C and VEGF-D in tumors and its relationship to lymphatic metastasis in immunocompetent rats. *Cancer Res* 2003; **63**: 713-722
- 25 **Furudoi A**, Tanaka S, Haruma K, Kitadai Y, Yoshihara M, Chayama K, Shimamoto F. Clinical significance of vascular endothelial growth factor C expression and angiogenesis at the deepest invasive site of advanced colorectal carcinoma. *Oncology* 2002; **62**: 157-166
- 26 **Li CY**, Shan S, Huang Q, Braun RD, Lanzen J, Hu K, Lin P, Dewhirst MW. Initial stages of tumor cell-induced angiogenesis: evaluation via skin window chambers in rodent models. *J Natl Cancer Inst* 2000; **92**: 143-147
- 27 **Leung WK**, To KF, Go MY, Chan KK, Chan FK, Ng EK, Chung SC, Sung JJ. Cyclooxygenase-2 upregulates vascular endothelial growth factor expression and angiogenesis in human gastric carcinoma. *Int J Oncol* 2003; **23**: 1317-1322
- 28 **Cianchi F**, Cortesini C, Bechi P, Fantappie O, Messerini L, Vannacci A, Sardi I, Baroni G, Boddi V, Mazzanti R, Masini E. Up-regulation of cyclooxygenase 2 gene expression correlates with tumor angiogenesis in human colorectal cancer. *Gastroenterology* 2001; **121**: 1339-1347
- 29 **Prescott SM**. Is cyclooxygenase-2 the alpha and the omega in cancer? *J Clin Invest* 2000; **105**: 1511-1513
- 30 **Tsujii M**, DuBois RN. Alterations in cellular adhesion and apoptosis in epithelial cells overexpressing prostaglandin endoperoxide synthase 2. *Cell* 1995; **83**: 493-501
- 31 **Williams CS**, Tsujii M, Reese J, Dey SK, DuBois RN. Host cyclooxygenase-2 modulates carcinoma growth. *J Clin Invest* 2000; **105**: 1589-1594
- 32 **Liu XH**, Kirschenbaum A, Yao S, Lee R, Holland JF, Levine AC. Inhibition of cyclooxygenase-2 suppresses angiogenesis and the growth of prostate cancer *in vivo*. *J Urol* 2000; **164**(3 Pt1): 820-825
- 33 **Ruggeri B**, Singh J, Gingrich D, Angeles T, Albom M, Chang H, Robinson C, Hunter K, Dobrzanski P, Jones-Bolin S, Aimone L, Klein-Szanto A, Herbert JM, Bono F, Schaeffer P, Casellas P, Bourie B, Pili R, Isaacs J, Ator M, Hudkins R, Vaught J, Mallamo J, Dionne C. CEP-7055: a novel, orally active pan inhibitor of vascular endothelial growth factor receptor tyrosine kinases with potent antiangiogenic activity and antitumor efficacy in preclinical models. *Cancer Res* 2003; **63**: 5978-5991
- 34 **Ellis LM**. A targeted approach for antiangiogenic therapy of metastatic human colon cancer. *Am Surg* 2003; **69**: 3-10

Edited by Wang XL and Chen ZR Proofread by Xu FM

• VIRAL HEPATITIS •

New serum biomarkers for detection of HBV-induced liver cirrhosis using SELDI protein chip technology

Xiao-Dong Zhu, Wei-Hua Zhang, Cheng-Lin Li, Yang Xu, Wei-Jiang Liang, Po Tien

Xiao-Dong Zhu, Wei-Jiang Liang, Po Tien, Department of Molecular Virology, Institute of Microbiology, Chinese Academy of Sciences, Beijing 100080, China

Wei-Hua Zhang, Yang Xu, CIPHERGEN Biosystems, Inc., Beijing, China

Cheng-Lin Li, Department of Pathology, Beijing You' an Hospital, Beijing 100054, China

Supported by the Major State Basic Research Development Program of China (973 Program), No. 2001CB510001

Co-first-authors: Xiao-Dong Zhu and Wei-Hua Zhang

Correspondence to: Professor Po Tien, Department of Molecular Virology, Institute of Microbiology, Chinese Academy of Sciences, Zhongguancun Beiyitiao, Beijing 100080, China. tienpo@sun.im.ac.cn

Telephone: +86-10-62554247 **Fax:** +86-10-62622101

Received: 2003-12-12 **Accepted:** 2004-02-18

Abstract

AIM: To find new serum biomarkers for liver cirrhosis (LC) in chronic carriers of hepatitis B virus (HBV).

METHODS: Surface enhanced laser desorption/ionization time-of-flight (SELDI-TOF) mass spectrometry was used to discover biomarkers for differentiating HBV induced LC from non-cirrhotic cohorts. A training population of 25 patients with HBV-induced LC, 20 patients with HCC, and 25 closely age-matched healthy men, was studied.

RESULTS: Two biomarkers with M_r 7 772 and 3 933 were detected in sera of non-cirrhotic cohorts, but not in patients with HBV-induced LC. A sensitivity of 80% for all LC patients, a specificity of 81.8% for all non-cirrhotic cohorts and a positive predictive value of 75% for the study population were obtained.

CONCLUSION: These two serum biomarkers for HBV-induced LC might be used for diagnosis and assessment of disease progression.

Zhu XD, Zhang WH, Li CL, Xu Y, Liang WJ, Tien P. New serum biomarkers for detection of HBV-induced liver cirrhosis using SELDI protein chip technology. *World J Gastroenterol* 2004; 10(16): 2327-2329

<http://www.wjgnet.com/1007-9327/10/2327.asp>

INTRODUCTION

Liver cirrhosis (LC), the end-stage of liver fibrosis, is generally irreversible. Patients with LC caused by chronic infection of HBV are at high risks of hepatocellular carcinoma and high death rate^[1,2]. Although some serum assays are on the way to differentiate chronic HBV infection or LC from HCC, pretreatment liver biopsy has been considered as the "gold standard" for assessing the grade of liver injury and stage of liver fibrosis. Clinicians relying on liver biopsy are able to correctly diagnose the stage of fibrosis or presence of cirrhosis in 80% patients^[3]. However, liver biopsy can be associated with significant expense, manpower issues, and risk of patient

injury. As a result, we still need to identify noninvasive tests that could replace liver biopsy.

Protein profiles might reflect the pathological state of HBV infection. The relationship between protein profile and disease progression could be achieved by analyzing the complex serum proteomic patterns^[4,5]. We used a protein biochip surface-enhanced laser desorption/ionization time-of-flight (SELDI-TOF) mass spectrometry coupled with an artificial intelligence learning algorithm to differentiate HBV induced LC from non-cirrhotic cohorts. A blinded test was used to determine the sensitivity and specificity of the established pattern.

MATERIALS AND METHODS

Samples

Of the 107 serum samples selected, 40 were from patients with HBV-induced LC and 30 from patients with HCC from You' an Hospital, Beijing, China, 37 from healthy men provided by Center of Cancer Prevention and Treatment, Zhongshan University, China. All HBV infected patients with LC were examined by ELISA and were HBeAg positive in serum. The final diagnoses were pathologically confirmed and specimens were obtained before treatment. All samples were fresh and stored at -70 °C and closely age-matched.

Protein chip array analysis

Three different chip chemistries (cationic, anionic, and Cu metal binding, CIPHERGEN Biosystems, Inc, Fremont, CA) were tested to determine which provided the best serum profiles in terms of number and resolution of protein peaks. It showed that WCX2 weak cationic chip gave the best result. A total of 10 μ L of each sample was diluted into 20 μ L with U9 buffer (1 \times PBS, 9 mol/L urea, 1% CHAPS) and mixed. The mixing step was repeated several times on ice for a total of 30 min. An eight-spot WCX chip was washed with 50 mmol/L sodium acetate (pH 4.0) twice. Then sodium acetate buffer was added to U9-treated sample to make a further 1:13 dilution. The diluted serum mixture (100 μ L) was applied to a protein chip array and incubated for 1 h on a shaker. After washing with the same sodium acetate buffer three times followed by a quick water rinse, 0.5 μ L of saturated sinapinic acid (SPA) solution was applied onto each spot and allowed to air-dry. Then chips were performed on Protein Biological System II(c) mass spectrometer reader (PBSII, CIPHERGEN Biosystems, Inc).

Bioinformatics and biostatistics

Classification model was built up with Biomarker Pattern's Software (BPS, CIPHERGEN Biosystems, Inc). Training data set consisted of 70 serum samples (25 from patients with LC, 20 from patients with liver cancer, and 25 from healthy individuals). A classification tree was set up to divide the data set into two bins based on the intensities of peaks. At each bin a peak intensity threshold was set. If the peak intensity of a sample was lower than or equal to the threshold, this sample would go to the left-side bin. Otherwise, the sample would go to the right-side bin. The process would go on until a blind sample entered a final bin, either labeled at Con (control sample) or LC (LC serum). Peaks selected by the process to form the model

were the ones that yielded the least classification error when they were combined to use.

Data set from double-blind trials consisted of 37 serum samples (15 from patients with LC, 10 from patients with liver cancer, and 12 from healthy individuals) and was used to test the model.

Specificity and sensitivity were respectively calculated as the proportion of the number of non-cirrhotic samples correctly identified to the total number of non-cirrhotic samples. Positive predictive value gives the probability of disease if a test result is positive.

RESULTS

Evaluation of SELDI protein chip

As various chip array chemistries provided different serum protein profiles in terms of number and resolution of protein peaks, WCX2, SAX2 and IMAC3-Cu metal binding chip arrays were tested, respectively. WCX2 binding chip was observed to give the best results. To demonstrate the reproducibility of the mass spectra, 8 independently obtained spectra of a serum sample of a healthy man were performed by between-run assay. We calculated that the coefficient of variance for seven selected M/Z peaks whose relative intensities were above 25 with the highest amplitude <10%. As shown in Figure 1, serum spectra from patients and healthy men do not show large variations. Therefore, small variations between different sample groups could be used for biomarker discovery. SELDI-TOF spectra of randomly selected serum samples of patients with HBV induced LC, patients with HCC, and healthy individuals are shown in Figures 1 and 2. Two proteins of M_r 7 772 and 3 933 were down-regulated in LC or up-regulated in non-cirrhotic group (healthy/HCC).

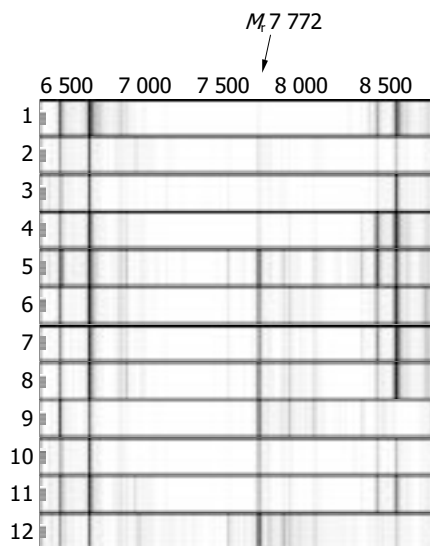


Figure 1 SELDI-TOF mass spectra. Spectra 1-4 from HBV-induced LC patients, 5-8 from healthy men, and 9-12 from HCC patients. A biomarker of M_r 7 772 was present in non-cirrhotic group, but not in LC serum samples.

Data analysis

Peak labeling was performed with Biomarker Wizard of Ciphergen ProteinChip software 3.1.1. The peak intensities were then transferred to Biomarker Pattern's software. Totally 35 peaks from M_r 2 000 to 30 000 were selected to construct the classification model. Figure 3 shows the tree structure and sample distribution. Two peaks, M_r 7 772 and 3 933, were chosen to set up the decision tree, respectively. At Node 1, samples of M_r 7 772 with peak intensities lower than or equal to 7.514 went

to Terminal Node 1, which had 9 control samples and 21 LC samples. Otherwise, samples entered Node 2, which had 40 samples. At Node 2, samples of M_r 3 933 with peak intensities lower than or equal to 8.217 went to Terminal Node 2, which had 1 control sample and 3 LC samples. The other samples entered Terminal Node 3, which had 35 control samples and 1 LC sample. The model identified 70 samples, 36 in control and 34 in LC, and yielded a sensitivity of 96% and specificity of 77.8%. When the double-blind sample data set was used to challenge the model, the model predicted a sensitivity of 80% and specificity of 81.8%. The positive predictive value was 75%.

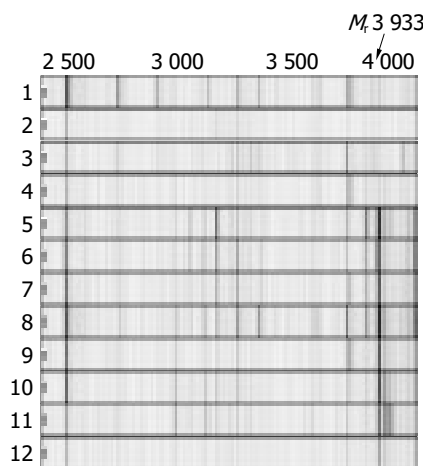


Figure 2 SELDI-TOF mass spectra. Spectra 1-4 from HBV-induced LC patients, 5-8 from healthy men, and 9-12 from HCC patients. A biomarker of M_r 3 933 was present in non-cirrhotic group, but not in LC serum samples.

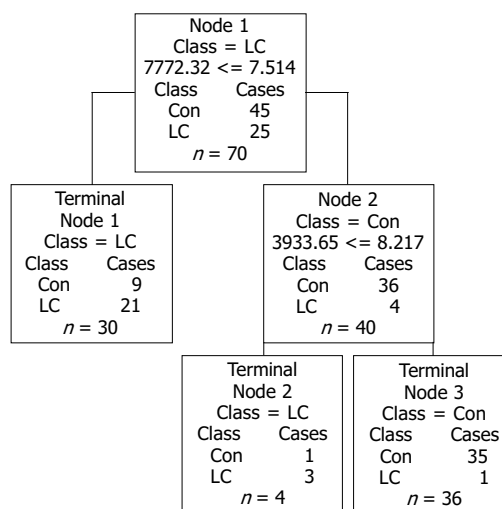


Figure 3 Tree structure and sample distribution. The root node and descendant nodes are indicated in gray, and the terminal nodes are shown in black. Peaks with M_r 7 772 and 3 933 were chosen to set up the decision tree.

DISCUSSION

HBV infection often leads to a prolonged active viral replication, HBV DNA integration and eventually LC^[6]. About 55-85% of LC patients will develop hepatocellular carcinoma, which always has bad prognosis. It is estimated that HCC may be responsible for more than 1 million deaths annually and it is the fifth most frequent cause of cancer death worldwide^[7]. Liver biopsy has remained the gold standard for identification of patients with liver diseases. However, the differential diagnosis between HCC

and LC is sometimes difficult and new biochemical markers for HCC are required. In recent years, several non-invasive serum biomarkers have been considered to diagnose LC associated with HBV, including hyaluronic acid (HA)^[8,9], type III procollagen peptide, laminin and type IV collagen^[10].

Among the non-invasive serum biomarkers for liver fibrosis and cirrhosis, HA was reported to be the best marker for diagnosis^[11]. HA with a molecular mass of several million is present in most tissues as a component of the extracellular matrix. Elevated levels of serum HA have been reported in various diseases including liver diseases. Increases in serum HA correspond to the progression of liver diseases, including viral and non-viral diseases. Ding *et al.* demonstrated that the elevated serum HA levels were closely related to the severity of liver fibrosis, particularly in LC^[12]. In addition, Procollagen III peptide, laminin, and type IV collagen with molecular masses of 45 000, 400 000 and 67 000, respectively, are also extracellular matrix glycoproteins and have been reported to be correlated to necrosis and inflammation as well as fibrosis in patients with chronic hepatitis and LC^[13]. However, the diagnostic value, i.e. sensitivity and specificity, of these markers for patients with cirrhosis has not been satisfactory so far. Use of multiple markers led to 90% sensitivity at most in diagnosing cirrhosis, but variable specificity was about 60%^[14].

SELDI-TOF mass spectrometry is a recently described affinity-based mass spectrometric method that combines chromatography and mass spectrometry. This novel technology has been used for protein or peptide biomarker identification, biomolecular interactions and post-translational modifications. Protein chip technology has proven to be useful in the discovery of potential diagnostic markers for prostate^[15-17], bladder^[18], ovarian^[19], breast^[20-22], lung cancers^[23], and pancreatic ductal adenocarcinoma. However, using it to discover new biomarkers of HBV induced diseases has not been addressed before. To identify potential biomarkers that can detect HBV induced LC, protein profiles of serum samples from LC patients were compared with those from the non-cirrhotic controls. Biomarker Pattern's Software was used to identify two peaks differentially presented in control healthy and HCC serum samples compared with LC samples. The top-scored two peaks with M_r 7 772 and 3 933 were finally selected. These two proteins generated a sensitivity of 96% and specificity of 77.8%. It is difficult to find a good single marker associated with diseases because of the differences among patients' age, gender, diet and genes. Furthermore, double-blind test was used to determine the sensitivity and specificity of the model. A sensitivity of 80%, specificity of 81.8% and positive predictive value of 75% for the study population were obtained when comparing LC versus non-cirrhotic (HCC/healthy men) groups. The low-molecular-mass serum proteins are apparently different from known non-invasive serum biomarkers for LC in many aspects and might be acceptable for diagnosis and assessment of HBV associated LC.

REFERENCES

- 1 **Lai CL**, Lok A, Wu PC, Ng M. Risk factors and hepatocellular cancer. *Lancet* 1985; **2**: 329-330
- 2 **Colombo M**, de Franchis R, Del Ninno E, Sangiovanni A, De Fazio C, Tommasini M, Donato MF, Piva A, Di Carlo V, Dioguardi N. Hepatocellular carcinoma in Italian patients with cirrhosis. *N Engl J Med* 1991; **325**: 675-680
- 3 **Poniachik J**, Bernstein DE, Reddy KR, Jeffers LJ, Coelho-Little ME, Civantos F, Schiff ER. The role of laparoscopy in the diagnosis of cirrhosis. *Gastrointest Endosc* 1996; **43**: 568-571
- 4 **Issaq HJ**, Veenstra TD, Conrads TP, Felschow D. The SELDI-TOF MS approach to proteomics: protein profiling and biomarker identification. *Biochem Biophys Res Commun* 2002; **292**: 587-592
- 5 **He QY**, Lau GK, Zhou Y, Yuen ST, Lin MC, Kung HF, Chiu JF. Serum biomarkers of hepatitis B virus infected liver inflammation: a proteomic study. *Proteomics* 2003; **3**: 666-674
- 6 **Torbenson M**, Thomas DL. Occult hepatitis B. *Lancet Infect Dis* 2002; **2**: 479-486
- 7 **Yu AS**, Keefe EB. Management of hepatocellular carcinoma. *Rev Gastroenterol Disord* 2003; **3**: 8-24
- 8 **Xiang Y**, Qian L, Wang B. Reversion of HBV-related liver fibrosis and early cirrhosis by baicao rougan capsule. *Zhongguo Zhongxiyi Jiehe Zazhi* 1999; **19**: 709-711
- 9 **Kozłowska J**, Loch T, Jablonska J, Cianciara J. Biochemical markers of fibrosis in chronic hepatitis and liver cirrhosis of viral origin. *Przeegl Epidemiol* 2001; **55**: 451-458
- 10 **Chang TT**, Lin HC, Lee SD, Tsai YT, Lee FY, Jeng FS, Wu JC, Yeh PS, Lo KJ. Clinical significance of serum type-III procollagen aminopropeptide in hepatitis B virus-related liver diseases. *Scand J Gastroenterol* 1989; **24**: 533-538
- 11 **Luo R**, Yang S, Xie J, Zhao Z, He Y, Yao J. Diagnostic value of five serum markers for liver fibrosis. *Zhonghua Ganzhangbing Zazhi* 2001; **9**: 148-150
- 12 **Ding H**, Chen Y, Feng X, Liu D, Wu A, Zhang L. Correlation between liver fibrosis stage and serum liver fibrosis markers in patients with chronic hepatitis B. *Zhonghua Ganzhangbing Zazhi* 2001; **9**: 78-80
- 13 **Castera L**, Hartmann DJ, Chapel F, Guettier C, Mall F, Lons T, Richardet JP, Grimbert S, Morassi O, Beaugrand M, Trinchet JC. Serum laminin and type IV collagen are accurate markers of histologically severe alcoholic hepatitis in patients with cirrhosis. *J Hepatol* 2000; **32**: 412-418
- 14 **Oh S**, Afdhal NH. Hepatic fibrosis: are any of the serum markers useful? *Curr Gastroenterol Rep* 2001; **3**: 12-18
- 15 **Qu Y**, Adam BL, Yasui Y, Ward MD, Cazares LH, Schellhammer PF, Feng Z, Semmes OJ, Wright GL Jr. Boosted decision tree analysis of surface-enhanced laser desorption/ionization mass spectral serum profiles discriminates prostate cancer from noncancer patients. *Clin Chem* 2002; **48**: 1835-1843
- 16 **Adam BL**, Qu Y, Davis JW, Ward MD, Clements MA, Cazares LH, Semmes OJ, Schellhammer PF, Yasui Y, Feng Z, Wright GL Jr. Serum protein fingerprinting coupled with a pattern-matching algorithm distinguishes prostate cancer from benign prostate hyperplasia and healthy men. *Cancer Res* 2002; **62**: 3609-3614
- 17 **Banez LL**, Prasanna P, Sun L, Ali A, Zou Z, Adam BL, McLeod DG, Moul JW, Srivastava S. Diagnostic potential of serum proteomic patterns in prostate cancer. *J Urol* 2003; **170**: 442-446
- 18 **Adam BL**, Vlahou A, Semmes OJ, Wright GL Jr. Proteomic approaches to biomarker discovery in prostate and bladder cancers. *Proteomics* 2001; **1**: 1264-1270
- 19 **Petricoin EF**, Ardekani AM, Hitt BA, Levine PJ, Fusaro VA, Steinberg SM, Mills GB, Simone C, Fishman DA, Kohn EC, Liotta LA. Use of proteomic patterns in serum to identify ovarian cancer. *Lancet* 2002; **359**: 572-577
- 20 **Li J**, Zhang Z, Rosenzweig J, Wang YY, Chan DW. Proteomics and bioinformatics approaches for identification of serum biomarkers to detect breast cancer. *Clin Chem* 2002; **48**: 1296-1304
- 21 **Paweletz CP**, Trock B, Pennanen M, Tsangaris T, Magnant C, Liotta LA, Petricoin EF 3rd. Proteomic patterns of nipple aspirate fluids obtained by SELDI-TOF: potential for new biomarkers to aid in the diagnosis of breast cancer. *Dis Markers* 2001; **17**: 301-307
- 22 **Coombes KR**, Fritsche HA Jr, Clarke C, Chen JN, Baggerly KA, Morris JS, Xiao LC, Hung MC, Kuerer HM. Quality control and peak finding for proteomics data collected from nipple aspirate fluid by surface-enhanced laser desorption and ionization. *Clin Chem* 2003; **49**: 1615-1623
- 23 **Xiao XY**, Tang Y, Wei XP, He DC. A preliminary analysis of non-small cell lung cancer biomarkers in serum. *Biomed Environ Sci* 2003; **16**: 140-148

Association of interleukin-12 *p40* gene 3'-untranslated region polymorphism and outcome of HCV infection

Li-Min Yin, Wan-Fu Zhu, Lai Wei, Xiao-Yuan Xu, De-Gui Sun, Yan-Bin Wang, Wen-Mei Fan, Min Yu, Xiu-Lan Tian, Qi-Xin Wang, Yan Gao, Hui Zhuang

Li-Min Yin, Wan-Fu Zhu, Wen-Mei Fan, Hui Zhuang, Department of Microbiology, School of Basic Medical Sciences, Peking University, Beijing 100083, China

Xiao-Yuan Xu, Min Yu, Xiu-Lan Tian, Department of Infectious Disease, First Hospital, Peking University, Beijing 100034, China

Lai Wei, Qi-Xin Wang, Yan Gao, Hepatology Institute, People's Hospital, Peking University, Beijing 100044, China

De-Gui Sun, Gu'an Station of Disease Prevention and Control, Gu'an 102700, Hebei Province, China

Yan-Bin Wang, Beijing Ditan Hospital, Beijing 100730, China

Supported by the National Key Technologies Research and Development Program of China during the 10th Five-Year Period, No. 2001BA705B06

Correspondence to: Professor Wan-Fu Zhu, Department of Microbiology, School of Basic Medical Sciences, Peking University, Beijing 100083, China. zhuwanfu@sun.bjmu.edu.cn

Telephone: +86-10-82801599 **Fax:** +86-10-82801599

Received: 2004-01-15 **Accepted:** 2004-02-21

Abstract

AIM: To investigate the effect of interleukin-12 *p40* gene (*IL12B*) 3'-untranslated region polymorphism on the outcome of HCV infection.

METHODS: A total of 133 patients who had been infected with HCV for 12-25 (18.2±3.8) years, were enrolled in this study. Liver biochemical tests were performed with an automated analyzer and HCV RNA was detected by fluorogenic quantitative polymerase chain reaction. B-mode ultrasound was used for liver examination. Polymerase chain reaction-restriction fragment length polymorphism (PCR-RFLP) was used for the detection of *IL12B* (1188A/C) polymorphism.

RESULTS: Self-limited infection was associated with AC genotype (OR = 3.48; *P* = 0.001) and persistent infection was associated with AA genotype (OR = 0.34; *P* = 0.014) at site 1188 of *IL12B*. In patients with persistent HCV infection, no significant differences were found regarding the age, gender, duration of infection and biochemical characteristics (*P* > 0.05). According to B-mode ultrasound imaging and clinical diagnosis, patients with persistent infection were divided into groups based on the severity of infection. No significant differences were found in the frequency of IL-12 genotype (1188A/C) between different groups (*P* > 0.05).

CONCLUSION: The polymorphism of *IL12B* (1188A/C) appears to have some influence on the outcome of HCV infection.

Yin LM, Zhu WF, Wei L, Xu XY, Sun DG, Wang YB, Fan WM, Yu M, Tian XL, Wang QX, Gao Y, Zhuang H. Association of interleukin-12 *p40* gene 3'-untranslated region polymorphism and outcome of HCV infection. *World J Gastroenterol* 2004; 10(16): 2330-2333

<http://www.wjgnet.com/1007-9327/10/2330.asp>

INTRODUCTION

Hepatitis C virus (HCV) is the major cause of post-transfusion hepatitis. As is estimated by WHO, approximately 170 million people globally may have been infected with HCV^[1]. Although chronic HCV infections are often clinically silent for decades, an estimated 85% of individuals infected with HCV develop persistent infection, and these patients are likely to end up with cirrhosis and liver cancer^[1-3]. HCV infection persists despite the presence of specific humoral and cellular immune responses, and the factors leading to viral clearance or persistence are poorly understood. But some researches showed that the outcome might already be determined at an early time point following infection^[4-7]. Patients with acute HCV infection presenting a self-limited acute hepatitis develop a strong Th1 response. In contrast, patients developing a chronic infection show a predominant Th2 response, but a weak Th1 response. These findings suggest that the imbalance or skewness between responses of Th1 and Th2 cells is involved in disease progression and in the incapability to eradicate HCV^[8-10]. Interleukin 12 (IL-12) is a key cytokine presented with the initiation of immune response, which is one of the most clearly defined factors determining Th1 and Th2 differentiation^[11,12]. IL-12 might, therefore, play an important role in the pathogenesis of HCV infection by affecting the Th1/Th2 balance. Single nucleotide polymorphism (SNP) (1188A/C) was identified at position 1188 in the 3'-untranslated region (UTR) of IL-12 *p40* gene (*IL12B*) and was found to correlate with many diseases^[13-15].

In this study, we proposed that some genotypes of SNP (1188A/C) might associate with either disease outcome or the state of illness in chronic HCV infection. To test this hypothesis, we determined the frequency of genotypes at the SNP site using polymerase chain reaction-restriction fragment length polymorphism (PCR-RFLP) in HCV infected patients, as well as the relationship between *IL12B* and outcome of HCV infection.

MATERIALS AND METHODS

Subjects

A total of 133 patients with confirmed diagnoses of HCV infection in Gu'an County, Hebei Province, China, who had been infected with HCV for 12-25 (18.2±3.8) years, were enrolled in this study. All the patients were investigated in January 2002. There were 61 (45.9%) male and 72 (54.1%) female patients ranging from 30 to 69 years old (mean age, 46.5±8.3 years). All subjects had no access to antiviral treatment.

Laboratory examination

Venous blood was drawn from each individual and genomic DNA was extracted from clotted blood with a protocol by using silica (Sigma, S-5631). Genotyping of SNP (1188A/C) was carried out by PCR-RFLP according to Hall *et al.*^[13]. Liver biochemistry tests including alanine aminotransferase (ALT), aspartate aminotransferase (AST), γ -glutamyltransferase (γ -GT), alkaline phosphatase (ALP), total bilirubin (TBil), direct bilirubin (DBil), total protein (Tp), albumin (ALB) and serum albumin/globulin ratio (A/G) were measured with HITACHI 7170 automatic

biochemistry analyzer. The B-mode ultrasound was performed for liver examination. HCV RNA was detected with quantitative fluorogenic PCR.

Statistical analysis

Data were expressed as mean±SD. Student's *t*-test, one-way analysis of variance and Chi-square tests were used for statistical analysis according to the data obtained. Logistic regression was used to assess the impact of variables on the odds of the outcome of HCV infection. Multivariate analysis of variance was used to analyze the difference of clinical characteristics among patients with persistent infection. All univariate and multivariable calculations, including odds ratios (OR), 95% confidence intervals (95% CI), and *P* values were calculated using the SPSS (version 10).

RESULTS

Of 133 cases investigated in this study, 91 (68.4%) were HCV RNA positive and 42 (31.6%) were HCV RNA negative. SNP typing of DNA samples from all the subjects is shown in Table 1. The proportions of male subjects were 31.0% in self-limited infection and 52.7% in persistent infection. Female gender was closely related to self-limited infection ($P < 0.05$). All patients were HCV infected as a consequence of plasma donation. The mean durations of infection were 17.76 and 18.44 years for patients with self-limited infection and matched patients with persistent infection, respectively. HCV genotype 1b was found in all the patients except two. In addition, the two groups were indistinguishable with respect to age, source of infection, duration of infection and HCV genotype ($P > 0.05$).

Table 1 Features of subjects enrolled in the study

Group	<i>n</i>	Gender (male/female)	Age (yr)	Duration of infection (yr)
Self-limited infection	42	13/29	45.71±7.68	17.76±3.82
Persistent infection	91	48/43	46.85±8.56	18.44±3.82

Agarose gel electrophoresis result of three genotypes of SNP (1188A/C) is shown in Figure 1. Genotype frequencies at SNP (1188A/C) are listed in Table 2. There was significant difference in genotype distribution between subjects with self-limited infection and subjects with persistent infection ($P < 0.01$). The distribution of genotype showed a good fit to Hardy-Weinberg equilibrium. At SNP (1188A/C) locus, the AC homozygous genotype was found more frequently in subjects with self-limited infection compared to those with persistent infection: 64.3% vs 34.1% (OR = 3.48; 95% CI: 1.52-8.10; $P = 0.001$). The AA genotype was more frequent in individuals with persistent infection compared to those with self-limited infection: 40.7% vs 19.0% (OR = 0.34; 95% CI: 0.12-0.87; $P = 0.014$).

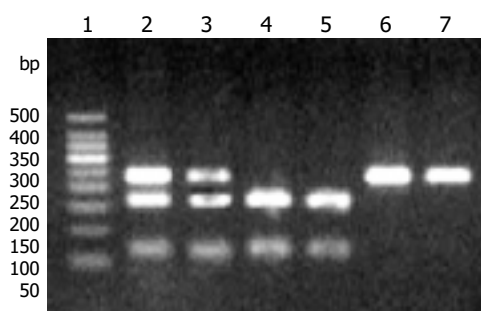


Figure 1 2% agarose gel electrophoresis of restriction enzyme digested products. Lane 1: 50 bp DNA ladder; lanes 2 and 3: AC genotype; lanes 4 and 5: CC genotype; lanes 6 and 7: AA genotype.

Table 2 Genotype frequencies of 1188A/C SNP of *IL12B* in patients

Genotype	Self-limited infection (%) <i>n</i> = 42	Persistent infection (%) <i>n</i> = 91	OR	95% CI	<i>P</i>
AA	8 (19.0)	37 (40.7)	0.34	0.12-0.87	0.014
CC	7 (16.7)	23 (25.3)	0.59	0.20-1.61	0.270
AC	27 (64.3)	31 (34.1)	3.48	1.52-8.10	0.001

Comparisons of genotype distribution using chi square test showed significant difference between self-limited infection and persistent infection ($P = 0.004$).

Effects of variables on the outcome of HCV infection were investigated by means of binary logistic regression analysis (Table 3). Both genotypes of SNP (1188A/C) and gender were independently associated with the outcome of HCV infection (OR 0.43, $P = 0.001$; OR 0.41, $P = 0.029$, respectively).

Table 3 Multivariate analysis of the effects of variables on the outcome of HCV infection

Variable	<i>P</i>	Multivariate odds ratio (95% CI)
Genotype	0.001	0.43 (0.27-0.70)
Gender	0.029	0.41 (0.18-0.91)
Duration of infection	NS	-

The general features, biochemical characteristics and HCV RNA levels in patients with persistent infection grouped by the genotype of SNP (1188A/C) of *IL12B* were analyzed (Table 4). No significant differences were found in age, gender or the duration of infection between three groups. And no significant differences were found in ALT, AST, γ -GT, ALP, TBil, DBil, Tp, ALB, A/G or HCV RNA levels between three groups ($P > 0.05$). According to the result from B-mode ultrasound and clinical diagnosis, patients with persistent infection were divided into groups based on severity. No significant differences were found in genotype frequencies between different groups ($P > 0.05$). Multivariate analysis of variance was used to analyze the different biochemical characteristics between three groups, and no difference was found ($P > 0.05$) (data not shown).

Table 4 Characteristics of patients with different SNP (1188A/C) genotypes during persistent infection

Characteristics	AA <i>n</i> = 38	CC <i>n</i> = 23	AC <i>n</i> = 30
Age (yr)	46.9±8.2	46.7±9.7	46.8±8.4
Gender (male/female)	21/17	12/11	15/15
Duration of disease (yr)	18.0±3.8	18.8±4.0	18.1±3.8
ALT (U/L)	51±44	51±60	44±26
AST (U/L)	50±30	51±34	47±20
γ -GT (U/L)	24±26	35±33	28±34
ALP (U/L)	88±26	92±28	93±22
Tbil (μ mol/L)	29±11	8.95±2.59	10.1±4.2
Dbil (μ mol/L)	5.8±2.0	5.3±2.2	5.4±2.4
Tp (g/L)	75.3±3.9	72.24±5.95	75.0±5.8
ALB (g/L)	44.4±2.3	43.8±2.3	44.5±2.6
A/G	1.46±0.21	1.59±0.32	1.51±0.30
HCV RNA ¹	5.07±1.49	4.95±1.52	5.58±1.24

¹Values are expressed as log₁₀ RNA copies per mL.

DISCUSSION

For the first time, we investigated here the polymorphism of

SNP (1188A/C) of *IL12B* in patients with HCV infection and demonstrated that AA genotype decreased and AC genotype increased in self-limited infection. Although there was no significant difference in allele distribution between patients with self-limited infection and patients with persistent infection, A allele tended to be decreased and C genotype to be increased in self-limited infection. In this study, however, there was no association between genotype of SNP (1188A/C) of *IL12B* and biochemical characteristics of subjects with persistent infection. And no association was found between genotype of SNP (1188A/C) and the severity of subjects with persistent infection.

HCV infection is characterized by a broad spectrum of possible outcomes. Infection is self-limited in a fortunate minority, while the majority of patients develop persistent infection^[16,17]. Patients with acute HCV infection presenting a self-limited acute hepatitis and with eradication of the virus develop a strong Th1 response but a weak or absent Th2 response. In contrast, patients developing a chronic infection show a predominant Th2 response, but a weak Th1 response. These observations suggest that Th1 cytokine effect is essential for protection against HCV infection, while the production of Th2 cytokine seems to have an inhibiting effect on the patient's immunological system^[8,10]. IL-12 is a key regulator of the polarization of immune responses to T helper 1 or 2 categories and plays a role in autoimmune and infectious diseases^[11,12,18]. IL-12 might, therefore, have effects on the pathogenesis of HCV infection by affecting Th1/Th2 balance.

IL-12 is comprised of two disulphide-linked protein subunits designated p35 and p40, which are encoded by two different genes, *IL12A* and *IL12B*^[19,20]. IL-12 p40 expression is restricted to the production of p70 because p35 is expressed ubiquitously and constitutively at low levels. Thus, secretion of the biologically active p70 heterodimer appears to be predominantly regulated at the level of *IL12B*^[12]. IL-12 is secreted mainly by antigen-presenting cells and plays a key role in innate resistance and adaptive immunity. IL-12 acts on T cells and NK cells by enhancing generation and activity of cytotoxic lymphocytes and inducing proliferation and production of cytokines, especially IFN- γ . IL-12 is also the major cytokine responsible for differentiation of T helper 1 cells, which are potent producers of IFN- γ ^[12,19]. And IFN- γ plays important roles in the immune response to HCV infection. Some studies have been reported that the deletions of IL-12 p40 lead to serious impairment of immunity to intracellular bacteria^[21]. The SNP at position 1188 in the untranslated region of IL-12 p40 gene mapped to chromosome 5q31-33. Although SNP is located in UTR and does not alter the coding sequence, some researches showed that this SNP site was associated with immune-mediated disease^[13,22].

Many studies showed that there was close relationship between IL-12 and hepatitis C. Nelson *et al.* reported that patients with chronic HCV infection had elevated IL-12, which correlated with serum ALT and intrahepatic HCV-specific CTL activity. These data indicate that IL-12 is involved in the immunopathogenesis of chronic HCV infection, especially in cell-mediated immunity, which might be important in spontaneous or interferon mediated viral clearance^[23,24]. Another study reported the impairment in allostimulatory capacity of peripheral blood dendritic cells in HCV-infected individuals, which is likely due to low IL-12 expression and restored by endogenous IL-12^[25]. Some studies have found that IL-12 can produce lower HCV-RNA level^[26-31].

Studies on functional characteristics of this polymorphism suggest that they influence the secretion of cytokines. Morahan *et al.* reported the 3'-UTR alleles showed different levels of *IL12B* mRNA expression in cell lines. They identified EBV-transformed cell lines homozygous for each allele. Expression of *IL12B* mRNA was significantly reduced in the C/C genotype cell line in contrast to the A/A line^[32]. But Seegers *et al.* found that a TaqI polymorphism (C/C) in IL12 p40 3'-UTR correlated

with increased IL-12 p70 *in vitro*^[33]. The results were complicated and the functional characteristics of this polymorphism still need to be evaluated. Currently our group is working on the IL-12 mRNA and protein levels of three different genotypes to clarify how SNP (1188A/C) influences the course of hepatitis C.

In summary, we have reported that the frequency of A/A genotype of *IL12B* 3'-UTR SNP was decreased in self-limited HCV infection. It suggests that this SNP is associated with different outcomes of HCV infection, presumably by affecting Th1/Th2 balance. Nevertheless, since the outcome of HCV infection is a complicated polygenic trait, the interactive effects between SNP (1188A/C) of *IL12B* and other factors involved in the outcome of hepatitis C still need to be evaluated.

ACKNOWLEDGEMENT

We are very grateful to Professor Shu-Lin Liu for his critical revision of this paper.

REFERENCES

- 1 Global surveillance and control of hepatitis C. Report of a WHO Consultation organized in collaboration with the Viral Hepatitis Prevention Board, Antwerp, Belgium. *J Viral Hepat* 1999; **6**: 35-47
- 2 Villano SA, Vlahov D, Nelson KE, Cohn S, Thomas DL. Persistence of viremia and the importance of long-term follow-up after acute hepatitis C infection. *Hepatology* 1999; **29**: 908-914
- 3 Alter HJ, Seeff LB. Recovery, persistence, and sequelae in hepatitis C virus infection: a perspective on long-term outcome. *Semin Liver Dis* 2000; **20**: 17-35
- 4 Thimme R, Bukh J, Spangenberg HC, Wieland S, Pemberton J, Steiger C, Govindarajan S, Purcell RH, Chisari FV. Viral and immunological determinants of hepatitis C virus clearance, persistence, and disease. *Proc Natl Acad Sci U S A* 2002; **99**: 15661-15668
- 5 Alberti A, Chemello L, Benvenuto L. Natural history of hepatitis C. *J Hepatol* 1999; **31**(Suppl 1): 17-24
- 6 Diepolder HM, Zachoval R, Hoffmann RM, Jung MC, Gerlach T, Pape GR. The role of hepatitis C virus specific CD4+ T lymphocytes in acute and chronic hepatitis C. *J Mol Med* 1996; **74**: 583-588
- 7 Lechner F, Wong DK, Dunbar PR, Chapman R, Chung RT, Dohrenwend P, Robbins G, Phillips R, Klenerman P, Walker BD. Analysis of successful immune responses in persons infected with hepatitis C virus. *J Exp Med* 2000; **191**: 1499-1512
- 8 Montano-Loza A, Meza-Junco J, Remes-Troche JM. Pathogenesis of hepatitis C virus infection. *Rev Invest Clin* 2001; **53**: 561-568
- 9 Boyer N, Marcellin P. Pathogenesis, diagnosis and management of hepatitis C. *J Hepatol* 2000; **32**(1 Suppl): 98-112
- 10 Pape GR, Gerlach TJ, Diepolder HM, Gruner N, Jung M, Santantonio T. Role of the specific T-cell response for clearance and control of hepatitis C virus. *J Viral Hepat* 1999; **6**(Suppl 1): 36-40
- 11 Trinchieri G. Interleukin-12 and the regulation of innate resistance and adaptive immunity. *Nat Rev Immunol* 2003; **3**: 133-146
- 12 Watford WT, Moriguchi M, Morinobu A, O'Shea JJ. The biology of IL-12: coordinating innate and adaptive immune responses. *Cytokine Growth Factor Rev* 2003; **14**: 361-368
- 13 Hall MA, McGlinn E, Coakley G, Fisher SA, Boki K, Middleton D, Kaklamani E, Moutsopoulos H, Loughran TP Jr, Ollier WE, Panayi GS, Lanchbury JS. Genetic polymorphism of IL-12 p40 gene in immune-mediated disease. *Genes Immun* 2000; **1**: 219-224
- 14 Tsunemi Y, Saeki H, Nakamura K, Sekiya T, Hirai K, Fujita H, Asano N, Kishimoto M, Tanida Y, Kakinuma T, Mitsui H, Tada Y, Wakugawa M, Torii H, Komine M, Asahina A, Tamaki K. Interleukin-12 p40 gene (IL12B) 3'-untranslated region polymorphism is associated with susceptibility to atopic dermatitis and psoriasis vulgaris. *J Dermatol Sci* 2002; **30**: 161-166
- 15 Davoodi-Semiromi A, Yang JJ, She JX. IL-12 p40 is associated with type 1 diabetes in Caucasian-American families. *Diabetes* 2002; **51**: 2334-2336

- 16 **Alter MJ**, Margolis HS, Krawczynski K, Judson FN, Mares A, Alexander WJ, Hu PY, Miller JK, Gerber MA, Sampliner RE. The natural history of community-acquired hepatitis C in the United States. The Sentinel Counties Chronic non-A, non-B Hepatitis Study Team. *N Engl J Med* 1992; **327**: 1899-1905
- 17 **Zhu WF**, Yin LM, Li P, Huang J, Zhuang H. Pathogenicity of GB virus C on virus hepatitis and hemodialysis patients. *World J Gastroenterol* 2003; **9**: 1739-1742
- 18 **Romani L**, Puccetti P, Bistoni F. Interleukin-12 in infectious diseases. *Clin Microbiol Rev* 1997; **10**: 611-636
- 19 **Trinchieri G**. Interleukin-12: a proinflammatory cytokine with immunoregulatory functions that bridge innate resistance and antigen-specific adaptive immunity. *Annu Rev Immunol* 1995; **13**: 251-276
- 20 **Gately MK**, Renzetti LM, Magram J, Stern AS, Adorini L, Gubler U, Presky DH. The interleukin-12/interleukin-12-receptor system: role in normal and pathologic immune responses. *Annu Rev Immunol* 1998; **16**: 495-521
- 21 **Altare F**, Lammas D, Revy P, Jouanguy E, Doffinger R, Lamhamedi S, Drysdale P, Scheel-Toellner D, Girdlestone J, Darbyshire P, Wadhwa M, Dockrell H, Salmon M, Fischer A, Durandy A, Casanova JL, Kumararatne DS. Inherited interleukin 12 deficiency in a child with bacille Calmette-Guerin and Salmonella enteritidis disseminated infection. *J Clin Invest* 1998; **102**: 2035-2040
- 22 **Alloza I**, Heggarty S, Goris A, Graham CA, Dubois B, McDonnell G, Hawkins SA, Carton H, Vandebroek K. Interleukin-12 p40 polymorphism and susceptibility to multiple sclerosis. *Ann Neurol* 2002; **52**: 524-525
- 23 **Nelson DR**, Marousis CG, Ohno T, Davis GL, Lau JY. Intrahepatic hepatitis C virus-specific cytotoxic T lymphocyte activity and response to interferon alfa therapy in chronic hepatitis C. *Hepatology* 1998; **28**: 225-230
- 24 **Quiroga JA**, Martin J, Navas S, Carreno V. Induction of interleukin-12 production in chronic hepatitis C virus infection correlates with the hepatocellular damage. *J Infect Dis* 1998; **178**: 247-251
- 25 **Kanto T**, Hayashi N, Takehara T, Tatsumi T, Kuzushita N, Ito A, Sasaki Y, Kasahara A, Hori M. Impaired allostimulatory capacity of peripheral blood dendritic cells recovered from hepatitis C virus-infected individuals. *J Immunol* 1999; **162**: 5584-5591
- 26 **Zeuzem S**, Hopf U, Carreno V, Diago M, Shiffman M, Grune S, Dudley FJ, Rakhit A, Rittweger K, Yap SH, Koff RS, Thomas HC. A phase I/II study of recombinant human interleukin-12 in patients with chronic hepatitis C. *Hepatology* 1999; **29**: 1280-1287
- 27 **O'Brien CB**, Moonka DK, Henzel BS, Caufield M, DeBruin MF. A pilot trial of recombinant interleukin-12 in patients with chronic hepatitis C who previously failed treatment with interferon-alpha. *Am J Gastroenterol* 2001; **96**: 2473-2479
- 28 **Pockros PJ**, Patel K, O'Brien C, Tong M, Smith C, Rustgi V, Carithers RL, McHutchison JG, Olek E, DeBruin MF. A multicenter study of recombinant human interleukin 12 for the treatment of chronic hepatitis C virus infection in patients nonresponsive to previous therapy. *Hepatology* 2003; **37**: 1368-1374
- 29 **Zeuzem S**, Carreno V. Interleukin-12 in the treatment of chronic hepatitis B and C. *Antiviral Res* 2001; **52**: 181-188
- 30 **Barth H**, Klein R, Berg PA, Wiedenmann B, Hopf U, Berg T. Analysis of the effect of IL-12 therapy on immunoregulatory T-cell subsets in patients with chronic hepatitis C infection. *Hepatogastroenterology* 2003; **50**: 201-206
- 31 **Lee JH**, Teuber G, von Wagner M, Roth WK, Zeuzem S. Antiviral effect of human recombinant interleukin-12 in patients infected with hepatitis C virus. *J Med Virol* 2000; **60**: 264-268
- 32 **Morahan G**, Huang D, Ymer SI, Cancilla MR, Stephen K, Dabadghao P, Werther G, Tait BD, Harrison LC, Colman PG. Linkage disequilibrium of a type 1 diabetes susceptibility locus with a regulatory IL12B allele. *Nat Genet* 2001; **27**: 218-221
- 33 **Seegers D**, Zwiers A, Strober W, Pena AS, Bouma G. A TaqI polymorphism in the 3'UTR of the IL-12 p40 gene correlates with increased IL-12 secretion. *Genes Immun* 2002; **3**: 419-423

Edited by Chen WW Proofread by Zhu LH and Xu FM

• *H pylori* •

Helicobacter pylori enhances tumor necrosis factor-related apoptosis-inducing ligand-mediated apoptosis in human gastric epithelial cells

Yi-Ying Wu, Hwei-Fang Tsai, We-Cheng Lin, Ai-Hsiang Chou, Hui-Ting Chen, Jyh-Chin Yang, Ping-I Hsu, Ping-Ning Hsu

Yi-Ying Wu, Hwei-Fang Tsai, We-Cheng Lin, Ai-Hsiang Chou, Hui-Ting Chen, Ping-Ning Hsu, Graduate Institute of Immunology, College of Medicine, National Taiwan University, Taiwan, China
Jyh-Chin Yang, Ping-I Hsu, Department of Internal Medicine, National Taiwan University Hospital, Taipei, Taiwan, China
Supported by the Grants from the National Health Research Institute, Taiwan, NHRI-GI-EX89S942C and the National Science Council, NSC-90-2314B-075B003, NSC 91-2320B-002 and the National Taiwan University Hospital, NTUH 89S2011

Correspondence to: Dr. Ping-Ning Hsu, Graduate Institute of Immunology, College of Medicine, National Taiwan University, No. 1, Sec. 1, Jen-Ai Road, Taipei, Taiwan, China. phsu@ha.mc.ntu.edu.tw
Telephone: +886- 223123456 Fax: +886- 223217921

Received: 2004-03-15 Accepted: 2004-04-15

Abstract

AIM: To investigate the relations between tumor necrosis factor-related apoptosis-inducing ligand (TRAIL) and *Helicobacter pylori* (*H pylori*) infection in apoptosis of gastric epithelial cells and to assess the expression of TRAIL on the surface of infiltrating T-cells in *H pylori*-infected gastric mucosa.

METHODS: Human gastric epithelial cell lines and primary gastric epithelial cells were co-cultured with *H pylori* *in vitro*, then recombinant TRAIL proteins were added to the culture. Apoptosis of gastric epithelial cells was determined by a specific ELISA for cell death. Infiltrating lymphocytes were isolated from *H pylori*-infected gastric mucosa, and expression of TRAIL in T cells was analyzed by flow cytometry.

RESULTS: The apoptosis of gastric epithelial cell lines and primary human gastric epithelial cells was mildly increased by interaction with either TRAIL or *H pylori* alone. Interestingly, the apoptotic indices were markedly elevated when gastric epithelial cells were incubated with both TRAIL and *H pylori* (Control vs TRAIL and *H pylori*: 0.51 ± 0.06 vs 2.29 ± 0.27 , $P = 0.018$). A soluble TRAIL receptor (DR4-Fc) could specifically block the TRAIL-mediated apoptosis. Further studies demonstrated that infiltrating T-cells in gastric mucosa expressed TRAIL on their surfaces, and the induction of TRAIL sensitivity by *H pylori* was dependent upon direct cell contact of viable bacteria, but not CagA and VacA of *H pylori*.

CONCLUSION: *H pylori* can sensitize human gastric epithelial cells and enhance susceptibility to TRAIL-mediated apoptosis. Modulation of host cell sensitivity to apoptosis by bacterial interaction adds a new dimension to the immunopathogenesis of *H pylori* infection.

Wu YY, Tsai HF, Lin WC, Chou AH, Chen HT, Yang JC, Hsu PI, Hsu PN. *Helicobacter pylori* enhances tumor necrosis factor-related apoptosis-inducing ligand-mediated apoptosis in

human gastric epithelial cells. *World J Gastroenterol* 2004; 10(16): 2334-2339

<http://www.wjgnet.com/1007-9327/10/2334.asp>

INTRODUCTION

Helicobacter pylori (*H pylori*), which infects about 50% of the world's population, is the leading cause of chronic gastritis and peptic ulcer diseases. Recent studies have shown that apoptosis of gastric epithelial cells is increased during *H pylori* infection^[1-4]. The enhanced gastric epithelial cell apoptosis in *H pylori* infection has been suggested to play an important role in the pathogenesis of chronic gastritis, peptic ulcer and gastric neoplasia. There are a number of mechanisms that may be involved, including the direct cytotoxic effects of the bacteria, as well as inflammatory responses elicited by the infection^[4-7]. Recent studies have suggested that T helper type 1 (Th1) cells are selectively increased during *H pylori* infection^[8-11]. Th1 cytokines, such as gamma interferon (IFN-) and tumor necrosis factor alpha (TNF-), can increase the release of proinflammatory cytokines, augmenting apoptosis induced by *H pylori*^[7]. *H pylori* infection could also induce gastric mucosa damage by increasing expression of Fas in gastric epithelial cells, leading to gastric epithelial cell apoptosis through Fas/FasL interaction with infiltrating T cells^[6,12]. These findings suggest a role for immune-mediated apoptosis of gastric epithelial cells during *H pylori* infection.

TRAIL, a novel TNF superfamily member with strong homology to FasL, is capable of inducing apoptosis in a variety of transformed cell lines *in vitro*^[13,14]. Recent studies indicated that TRAIL-induced apoptosis occurred through a caspase signaling cascade^[15-17]. It has been shown that T cells can kill target cells via TRAIL/TRAIL receptor interaction^[18-23], suggesting that TRAIL might serve as a cytotoxic effector molecule in activated T cells *in vivo*. In addition to its role in inducing apoptosis by binding to death receptors, TRAIL itself can stimulate T cells and augment IFN- secretion^[24]. These findings have led us to hypothesize that TRAIL/TRAIL receptor interaction was involved in the apoptosis of gastric epithelial cells in *H pylori* gastritis. We therefore designed the study to investigate the interactions between TRAIL and *H pylori* in apoptosis of human gastric epithelial cells. Additionally, we assessed the expression of TRAIL on the surface of infiltrating T-cells in *H pylori*-infected gastric mucosa.

MATERIALS AND METHODS

Bacterial strains, cell lines, and media

H pylori standard strain ATCC43504 (CagA+, VacA+) and the mutant strain ATCC51932 (CagA-, VacA-), obtained from American Type Culture Collections (ATCC) were used. *H pylori* strain NTUH-C1 (CagA+, VacA+) was isolated from a patient with duodenal ulcer in National Taiwan University Hospital. Before each experiment, *H pylori* was passaged on 5% sheep blood agar plates by incubation in an atmosphere consisting

of 5% O₂, 15% CO₂, and 80% N₂ for 2–4 d at 37 °C. Bacteria were cultured in Brucella broth (Difco Labs, Inc. Detroit, MI) supplemented with 5% FBS, vancomycin and amphotericin B under the same conditions for 30 h at 37 °C with agitation (80–100 rpm/min). Cells were then pelleted and resuspended in phosphate-buffered saline at a concentration of 10⁸ CFU/mL. Human gastric adenocarcinoma cell line AGS was obtained from ATCC and maintained in DMEM, supplemented with 10% FBS.

Generation of *cagA* or *vacA* gene knock out *H pylori* mutant strains

For generation of *H pylori* isogenic mutant strains with *cagA* or *vacA* gene defect, we introduced mutations into *cagA* or *vacA* gene in *H pylori* strain NTUH-C1. *cagA* and *vacA* genes were amplified by PCR with the following primer pairs, *cagA*: 5'-ATGACTAACGAACTATTGATCAAACA-3' and 5'-AGATTTTTGGAAACCACCTT TTGTATTA-3'; *vacA*: 5'-GCTGGGATTGGGGGAATG-3' and 5'-TTGCGCGCTA TTGGGTGG-3'. The PCR fragments were purified and then cloned on pGEM-T easy vector by a TA cloning kit (Promega, Madison, WI, USA). The cloned *cagA* or *vacA* gene was digested with *Nhe* I, after which the chloramphenicol resistant marker (CAT cassette) was ligated with recombinant *Nhe* I sites at both ends. The plasmid pGEM-T Easy Vector with *cagA* or *vacA* inserted by the CAT cassette was used for the natural transformation of *H pylori* strain NTUH-C1. The *cagA* gene or *vacA* gene isogenic knockout mutants were selected by the BHI agar plate with 40 ppm chloramphenicol and confirmed with PCR.

Expression and purification of recombinant TRAIL protein and soluble TRAIL receptor (DR4-Fc)

Recombinant TRAIL proteins were expressed in *E. coli* expression system and purified with Ni column as described^[24]. In brief, the coding portion of the extracellular domain of TRAIL (amino acid 123–314) was PCR amplified, subcloned into pRSET B vector (Invitrogen, Groningen, the Netherlands) and expressed in *E. coli* expression system. Purification of recombinant His-TRAIL fusion protein was performed by metal chelate column chromatography using Ni-NTA resin according to the manufacturer's recommendations (Qiagen, Hilden, Germany). His-TRAIL was quantified by the Bradford method and protein assay reagent (BioRad, Richmond, CA, USA). To generate soluble recombinant DR4-Fc fusion molecules, the coding sequence for the extracellular domain of human DR4 was isolated by RT-PCR using the forward primer, CGGATTTTCATGGCGCCACCACCA, and the reverse primer, GAAGATCTATTATGTCCATTGCC. The amplified product was ligated in-frame into *Bam*HI-cut pUC19-IgG1-Fc vector containing the human IgG1 Fc coding sequence. The fusion gene was then subcloned into pBacPAK9 vector (Clontech, Palo Alto, CA). DR4-Fc fusion protein was recovered from the filtered supernatants of the recombinant virus-infected Sf21 cells using protein G-sepharose beads (Pharmacia, Piscataway, NJ). The bound DR4-Fc protein was eluted with glycine buffer (pH 3) and dialyzed into PBS. The DR4-Fc is a soluble TRAIL receptor, which could bind to TRAIL and block its effect.

Culture of primary human gastric epithelial cells

The culture of human gastric epithelial cells was adapted from the methods described by Smoot *et al.*^[25]. Gastric biopsies were obtained from patients undergoing gastric endoscopy in National Taiwan University Hospital for dyspepsia with informed consents. Specimens were collected in Leibowitz's L-15 medium (Life Technologies, Grand Island, NY). Gastric cells were isolated enzymatically after mechanically mincing the tissue, into pieces less than or equal to 1 mm in size. The tissue was then pelleted by centrifugation at 1 500 rpm for five

minutes at 4 °C, the collagenase/dispase was discarded, then the tissue was washed once in 10 mL of PBS and pelleted again by centrifugation. The cells were resuspended in the cell culture medium. The gastric epithelial cells obtained above were suspended in 2 mL of Ham's F12 cell culture medium (Life Technologies, Grand Island, NY) with 10% FBS and placed into a 6-well tissue culture cluster well.

Apoptosis assay

A sensitive ELISA which detects cytoplasmic histone-associated DNA fragments was performed according to the manufacturer's protocol (Cell Death Detection ELISA^{PLUS}; Roche Mannheim Biochemicals, Mannheim Germany). Human gastric epithelial cells were cultured in a 96-well plate (10⁴ cells/well) overnight, then treated with TRAIL recombinant protein, harvested by centrifugation at 200 g. The cells were lysed by incubation with lysis buffer for 30 min, followed by centrifugation at 200 g for 10 min at room temperature. The supernatant was collected and incubated with immunoreagent pre-prepared for 2 h. After washed gently, the supernatant was pipetted into each well with a substrate solution and kept in the dark until development of the color was sufficient for photometric analysis. The reaction was determined in a spectrophotometer at 405 nm.

Effects of TRAIL and *H pylori* on apoptosis in human gastric epithelial cells

AGS cells or primary human gastric epithelial cells 5×10⁴/well were incubated with *H pylori* (ATCC strain 43504 or strain 51932) under the concentration of 4×10⁷ CFU for 12 h. Recombinant TRAIL proteins were added into the culture at the concentration of 1.0 g/mL for 4 h in the absence or presence of soluble TRAIL receptor, DR4-Fc (30 g/mL), which could block the function of TRAIL proteins. Apoptosis of gastric epithelial cells was determined by a specific ELISA as described.

Effects of lipopolysaccharide (LPS) and *Campylobacter jejuni* on induction of TRAIL sensitivity in human gastric epithelial cells

To exclude the possibility that the effect of induction of TRAIL sensitivity in AGS cells by *H pylori* was a general phenomenon in Gram-negative bacteria, possibly via interaction with LPS on cell wall, we further studied the TRAIL-mediated apoptosis in AGS cells following contact with LPS and *Campylobacter jejuni*. AGS cells were incubated with LPS from *E. coli*, *Campylobacter jejuni*, and *H pylori* (domestic strain NTUH-C1) for 12 h. Recombinant TRAIL proteins were added into the culture. Apoptosis was measured with ELISA as described.

Effects of direct cell contact of bacteria on TRAIL-mediated apoptosis of epithelial cells

AGS cells were incubated with *H pylori* (ATCC strain 43504; CagA+, VacA+) concentrated culture supernatant or with live bacteria separated by a membrane filter (Nunc Tissue Culture; Nunc, Roskilde, Denmark) under the concentration of 4×10⁷ CFU/5×10⁴ cells for 12 h. Recombinant TRAIL proteins were added into the culture. Cell death was measured with ELISA as described.

Effects of *CagA* and *VacA* on TRAIL-mediated apoptosis of epithelial cells

AGS cells (5×10⁴ cells) were incubated with a CagA-negative and VacA-negative *H pylori* mutant strain (ATCC strain 51932) as well as the *cagA* or *vacA* gene defect NTUH-C1 isogenic mutant strains for 12 h. Recombinant TRAIL proteins were then added into the culture. Apoptosis was measured with ELISA assay as described.

Expressions of TRAIL on surface of T-lymphocytes in gastric mucosa

For isolation of gastric infiltrating lymphocytes from endoscopic biopsy specimens, the collected tissues were immediately placed in ice-cold RPMI 1640 complete medium (GIBCO BRL, Gaithersburg, MD, USA) containing 10% fetal calf serum (FCS) supplemented with penicillin (50 IU/mL), streptomycin (50 mg/mL), L-glutamine (2 mmol/L) and sodium pyruvate (1 mmol/L). The tissues were washed, diced into 1 mm³ pieces and treated with collagenase (Type I, 5 g/mL; Sigma Co. St. Louis, MO) and heparin (5 U/mL) in RPMI 1640 complete medium at 37 °C for 60 min. After the samples were washed twice with RPMI 1640 medium, mononuclear cells were collected and then stained with anti-CD3 and anti-TRAIL mAb. The expression of TRAIL on the surface of T cells was detected by flow cytometry according to our previous study^[24].

Statistical analysis

The values of apoptosis assay were presented as mean±SD. The results were compared by Student's *t* test. A *P* value less than 0.05 was regarded as statistically significant.

RESULTS

Effects of TRAIL and *H pylori* on apoptosis in human gastric epithelial cell line

Figure 1 shows the effects of *H pylori* and TRAIL on apoptosis in AGS cells. The apoptosis of AGS cells was slightly increased by TRAIL proteins or *H pylori* alone. Interestingly, the apoptotic index was dramatically increased when AGS cells were incubated with both TRAIL and *H pylori* (*P*<0.01 as compared with control medium, TRAIL or *H pylori* alone). Further studies disclosed that TRAIL-induced apoptosis in AGS cells was increased by *H pylori* in a dose-dependent manner (data not shown).

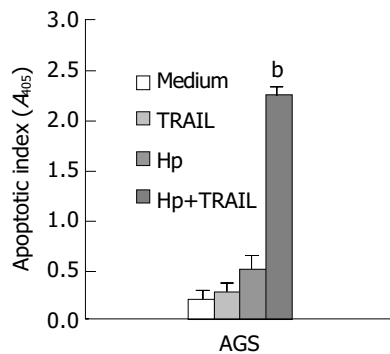


Figure 1 Effects of TRAIL and *H pylori* on apoptosis in human gastric epithelial cell line AGS (^b*P*<0.01 when compared with medium control, TRAIL or *H pylori* alone).

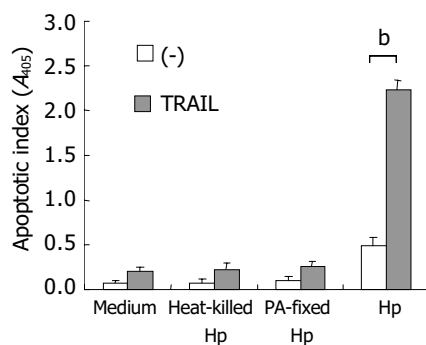


Figure 2 AGS cells incubated with heat killed, paraformaldehyde-fixed (PA-fixed) or live *H pylori* (ATCC strain 43504) under the concentration of 4×10⁷ CFU/5×10⁴ cells for 12 h. Open bar: without TRAIL; filled bar: with TRAIL (^b*P*<0.01).

Figure 2 shows that the TRAIL-induced apoptosis depended on viable *H pylori* because exposure of the host cells to heat-killed *H pylori* and paraformaldehyde-fixed *H pylori* did not induce sensitivity to TRAIL-mediated apoptosis.

Impacts of TRAIL and *H pylori* on apoptosis in primary human gastric epithelial cells

We further isolated and cultured primary human gastric epithelial cells from 23 different human cases (*H pylori*-positive: 12 cases; *H pylori*-negative: 11 cases) to investigate the effects of *H pylori* and TRAIL on apoptosis. The apoptosis of primary human gastric epithelial cells was mildly elevated by either TRAIL or *H pylori* alone (Table 1). However, the apoptotic indices were markedly elevated when the primary gastric epithelial cells were incubated with both *H pylori* and TRAIL. The apoptosis induced by *H pylori* and TRAIL was specifically blocked by adding soluble TRAIL receptor, DR4-Fc, indicating that the cell death was resulted from interaction between TRAIL and TRAIL receptor on the cell surface. Figure 3 shows the representative responses of four cases. All the gastric epithelial cells tested were sensitive to TRAIL after interaction with *H pylori* *in vitro*.

Table 1 Effects of TRAIL and *H pylori* on apoptosis in primary human gastric epithelial cells

	Apoptotic index ¹ (n=23)	<i>P</i> value ²
Medium	0.512±0.064	-
TRAIL	0.812±0.109	0.425
HP	0.684±0.085	0.779
HP+TRAIL	2.286±0.268	0.018
HP+TRAIL+DR4	0.816±0.129	0.216

¹mean±SD; ²Compared with medium alone samples.

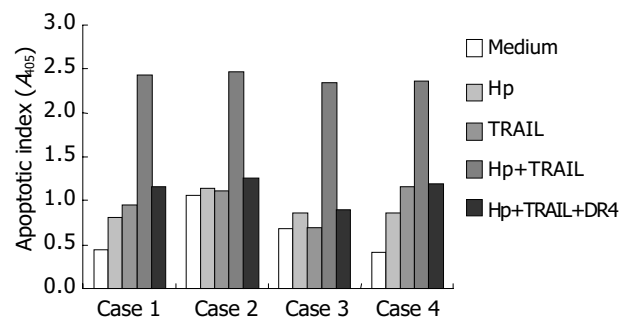


Figure 3 Enhancement of TRAIL-mediated apoptosis by *H pylori* in primary human gastric epithelial cells.

Effects of LPS and *Campylobacter jejuni* on induction of TRAIL sensitivity in human gastric epithelial cells

To exclude the possibility that the effect of induction of TRAIL sensitivity by *H pylori* was a general phenomenon in Gram-negative bacteria, possible via interaction with lipopolysaccharide (LPS) on cell walls, we further studied the induction of sensitivity to TRAIL-mediated apoptosis in AGS cells after interaction with LPS from *E. coli* and with *Campylobacter jejuni*, a Gram-negative bacterial pathogen in gastrointestinal tract. The results in Figure 4 demonstrate that *H pylori* enhanced TRAIL-mediated apoptosis in AGS cells. However, neither LPS from *E. coli* nor *Campylobacter jejuni* was able to induce TRAIL-sensitivity. Moreover, similar to ATCC strains, domestic *H pylori* strain NTUH-C1 was also capable of inducing TRAIL-sensitivity in AGS cells (Figure 4). These results indicated the ability to sensitize human gastric epithelial cells to TRAIL-induced apoptosis was *H pylori*-specific and not a general phenomenon in Gram-negative bacteria.

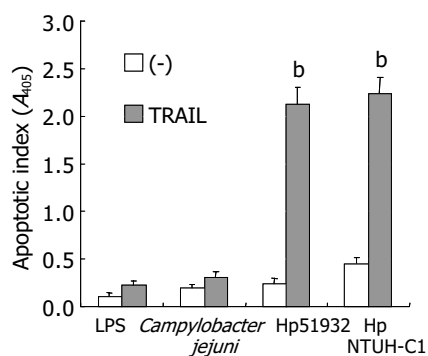


Figure 4 Induction of TRAIL sensitivity specific for *H pylori* in human gastric epithelial cells ($^bP < 0.01$ when compared with *H pylori* alone without adding TRAIL samples).

Effects of direct cell contact of bacteria on TRAIL-mediated apoptosis of gastric epithelial cells

To investigate the effects of direct bacteria-epithelial cell contact in induction of TRAIL sensitivity by *H pylori*, AGS cells and bacteria were separated by a membrane filter (Nunc Tissue Culture; Nunc, Roskilde, Denmark). Figure 5 shows the effects of direct cell contact of bacteria on TRAIL-mediated apoptosis in human gastric epithelial cells. The enhancement of TRAIL sensitivity by *H pylori* was abrogated when AGS cells were separated by the filter without direct bacteria-cell contact or co-cultured with concentrated *H pylori* culture supernatant without viable bacteria, indicating that direct contact with viable bacteria was required for induction of TRAIL sensitivity by *H pylori*.

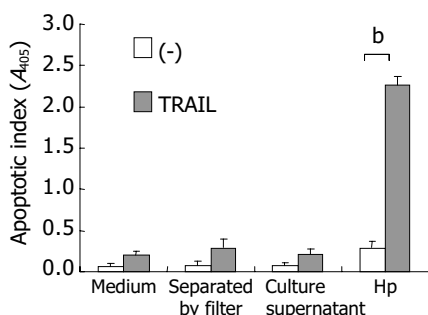


Figure 5 Enhancement of direct bacteria-cell contact dependent TRAIL sensitivity by *H pylori* ($^bP < 0.01$).

Effects of *cagA* and *vacA* on TRAIL-mediated apoptosis of epithelial cells

To exclude the possibility that the death of gastric epithelial

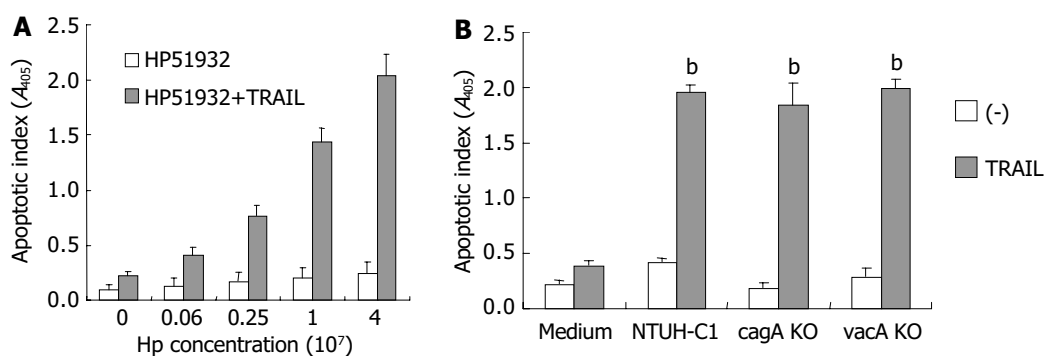


Figure 6 Effects of *vacA* and *cagA* on induction of TRAIL sensitivity by *H pylori*. A: AGS cells (5×10^4 cells) were incubated with a different concentration of *H pylori* (ATCC strain 51932) for 12 h. B: AGS cells were incubated with *H pylori* NTUH-C1 and its *cagA*, *vacA* gene knock out mutant strains (*cagA* KO, *vacA* KO) in the concentration of 4×10^7 CFU/ 5×10^4 cells for 12 h ($^bP < 0.01$ when compared with *H pylori* alone without adding TRAIL samples).

cells induced by TRAIL was related with *vacA* cytotoxin of *H pylori*, and to elucidate the role of *cagA* gene products in onset of the apoptotic process, we examined the abilities to enhance TRAIL-mediated apoptosis in *H pylori* mutant strain, ATCC 51932, which is deficient of cytotoxin *vacA* and *cagA*, and *H pylori* NTUH-C1 *cagA*, *vacA* gene knock out isogenic mutant strains. Figure 6 shows the effects of *CagA*-negative and *VacA*-negative *H pylori* strains on TRAIL-mediated apoptosis in gastric epithelial cells. *H pylori* strain 51932 significantly enhanced sensitivity to TRAIL-mediated apoptosis in gastric epithelial cell lines in a dose-dependent manner. *cagA* or *vacA* gene knock out NTUH-C1 mutant strain was also capable of inducing TRAIL sensitivity in gastric epithelial cells. Taken together, these results suggested that *vacA* and *cagA* proteins of *H pylori* were not required for induction of TRAIL-sensitivity in human gastric epithelial cells.

Expression of TRAIL on surface of T-lymphocytes in gastric mucosa

To confirm the expression of TRAIL in gastric infiltrating lymphocytes, gastric biopsy specimens were collected from subjects and examined by flow cytometry. Figure 7 demonstrates the expression of TRAIL on surface of T-lymphocytes isolated from gastric mucosa. Flow cytometry confirmed the presence of TRAIL on the surface of gastric infiltrating T-lymphocytes.

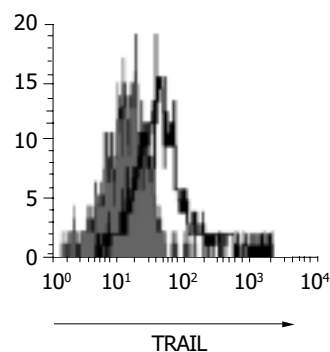


Figure 7 Expression of TRAIL on surface of T cells isolated from gastric mucosa.

DISCUSSION

In this study, we investigated the effects of *H pylori* and TRAIL on apoptosis in human gastric epithelial cells. The apoptosis of primary human gastric epithelial cells was mildly increased after incubated with either *H pylori* or TRAIL alone. Interestingly, the apoptotic indices of gastric epithelial cells were markedly increased when the primary gastric epithelial cells were incubated with both TRAIL and *H pylori*. The

induction of TRAIL-mediated apoptosis by *H pylori* was specifically blocked by adding soluble TRAIL receptor, DR4-Fc. The results implicated that *H pylori* could directly trigger apoptosis in gastric epithelial cells as previously described^[26-28]. Additionally, the microorganism was also capable of enhancing TRAIL sensitivity in gastric epithelial cells. Most of the apoptosis in gastric epithelial cells after exposure to both *H pylori* and TRAIL was resulted from interaction between TRAIL and TRAIL receptor on the surface of gastric epithelial cells, but not due to direct cytotoxicity induced by *H pylori*.

To confirm the expression of TRAIL in infiltrating T-lymphocytes of gastric mucosa, we isolated the gastric infiltrating lymphocytes from gastric biopsy specimens of *H pylori*-infected subjects. Our data confirmed that TRAIL was expressed on the surface of gastric infiltrating T-cells. This important finding further supports the hypothesis that TRAIL/TRAIL-R interaction is involved in epithelial cell damage during *H pylori* infection. Furthermore, it implicates that infiltrating T-cells in gastric mucosa may play a crucial role in the sequential changes of *H pylori*-related chronic gastritis.

In this study, we also demonstrated that neither *Campylobacter jejuni* nor LPS from *E. coli* was able to induce TRAIL-sensitivity in AGS cells. In contrast, *H pylori* standard strain ATCC43504 (CagA+, VacA+), mutant strain ATCC51932 (CagA-, VacA-) and our domestic strain NTUH-C1 (CagA+, VacA+) were capable of inducing TRAIL-sensitivity in AGS cells. The results indicate the ability to enhance TRAIL sensitivity of gastric epithelial cells is specific for *H pylori* and not a general phenomenon of Gram-negative Bacteria.

It has been demonstrated recently that *H pylori* could directly trigger cell death by cytotoxins after interaction with gastric epithelial cells^[26,27,29]. Other reports have shown that *H pylori* could secrete *cagA* into gastric epithelial cells by Type IV secretion, thus inducing intracellular protein phosphorylation in host cells^[30-33]. To elucidate the role of *cagA* gene products and *vacA* in TRAIL-mediated apoptosis, we examined the ability to induce TRAIL of a CagA-negative and *vacA*-negative *H pylori* mutant strain, ATCC 51932 as well as *cagA*, *vacA* gene knock out mutants of NTUH-C1 strain. All the *H pylori* wild type and mutant strains significantly enhanced sensitivity to TRAIL-mediated apoptosis in gastric epithelial cell lines. These findings suggest that expression of *cagA* and *vacA* is not mandatory for induction of TRAIL-sensitivity in gastric epithelial cells.

To investigate the effects of direct bacteria-epithelial cell contact in induction of TRAIL sensitivity by *H pylori*, AGS cells were separated by the filter without direct bacteria-cell contact or co-cultured with concentrated *H pylori* culture supernatant without viable bacteria. The enhanced TRAIL sensitivity was only observed when AGS cells were co-cultured with viable *H pylori*, but not with bacteria culture supernatant or with viable bacteria separated by a permeable membrane, indicating that direct contact with viable bacteria is necessary for induction of TRAIL sensitivity of gastric epithelial cells.

We demonstrated here that human gastric epithelial cells sensitized to *H pylori* conferred susceptibility to TRAIL-mediated apoptosis. Although the induction of TRAIL sensitivity by *H pylori* in gastric epithelial cells was independent of *H pylori* virulent factors CagA and VacA, the degree of apoptosis was linked to the presence of *H pylori* and the associated inflammatory response. Therefore, the degree of mucosal damage was also determined by the inflammatory response induced by *H pylori* within gastric epithelium. Our results suggest a role for immune-mediated apoptosis of gastric epithelial cells by infiltrating T cells during *Helicobacter* infection.

In conclusion, *H pylori* enhance susceptibility of gastric epithelial cells to TRAIL-mediated apoptosis. The induction of TRAIL sensitivity by *H pylori* is dependent upon direct contact

of viable bacteria with gastric epithelial cells, but independent of expression of *H pylori* virulent factors *vacA* and *cagA*. Gastric infiltrating T-lymphocytes can express TRAIL on their cell surfaces. Modulation of host cell apoptosis by bacterial interaction adds a new dimension to the immune pathogenesis in chronic *Helicobacter* infection.

ACKNOWLEDGEMENTS

We thank Dr. N Sutkowski for the critical review of the manuscript, Dr. SB Wang and JM Wong (Department of Medicine, National Taiwan University Hospital) for supporting endoscopic biopsy specimens, Ms. WI Tsai and WH Wu for assistance with *H pylori* cultures.

REFERENCES

- 1 Jones NL, Shannon PT, Cutz E, Yeger H, Sherman PM. Increase in proliferation and apoptosis of gastric epithelial cells early in the natural history of *Helicobacter pylori* infection. *Am J Pathol* 1997; **151**: 1685-1703
- 2 Mannick EE, Bravo LE, Zarama G, Realpe JL, Zhang XJ, Ruiz B, Fonham ET, Mera R, Miller MJ, Correa P. Inducible nitric oxide synthase, nitrotyrosine and apoptosis in *Helicobacter pylori* gastritis: effect of antibiotics and antioxidants. *Cancer Res* 1996; **56**: 3238-3243
- 3 Moss SF, Calam J, Agarwal B, Wang S, Holt PR. Induction of gastric epithelial apoptosis by *Helicobacter pylori*. *Gut* 1996; **38**: 498-501
- 4 Rudi J, Kuck D, Strand S, von Herbay A, Mariani SM, Krammer PH, Galle PR, Stremmel W. Involvement of the CD95 (APO-1/Fas) receptor and ligand system in *Helicobacter pylori*-induced gastric epithelial apoptosis. *J Clin Invest* 1998; **102**: 1506-1514
- 5 Fan X, Crowe SE, Behar S, Gunasena H, Ye G, Haeberle H, Van Houten N, Gourley WK, Ernst PB, Reyes VE. The effect of class II major histocompatibility complex expression on adherence of *Helicobacter pylori* and induction of apoptosis in gastric epithelial cells: a mechanism for T helper cell type 1-mediated damage. *J Exp Med* 1998; **187**: 1659-1669
- 6 Jones NL, Day AS, Jennings HA, Sherman PM. *Helicobacter pylori* induces gastric epithelial cell apoptosis in association with increased Fas receptor expression. *Infect Immun* 1999; **67**: 4237-4242
- 7 Wagner S, Beil W, Westermann J, Logan RP, Bock CT, Trautwein C, Bleck JS, Manns MP. Regulation of epithelial cell growth by *Helicobacter pylori*: evidence for a major role of apoptosis. *Gastroenterology* 1997; **113**: 1836-1847
- 8 Bamford KB, Fan X, Crowe SE, Leary JF, Gourley WK, Luthra GK, Brooks EG, Graham DY, Reyes VE, Ernst PB. Lymphocytes in the human gastric mucosa during *Helicobacter pylori* have a T helper cell 1 phenotype. *Gastroenterology* 1998; **114**: 482-492
- 9 D'Elia MM, Manghetti M, De Carli M, Costa F, Baldari CT, Burroni D, Telford JL, Romagnani S, Del Prete G. T helper 1 effector cells specific for *Helicobacter pylori* in gastric antrum of patients with peptic ulcer disease. *J Immunol* 1997; **158**: 962-967
- 10 Karttunen R, Karttunen T, Ekre HP, MacDonald TT. Interferon gamma and interleukin 4 secreting cells in the gastric antrum in *Helicobacter pylori* positive and negative gastritis. *Gut* 1995; **36**: 341-345
- 11 Lindholm C, Quiding-Jarbrink M, Lonroth H, Hamlet A, Svennerholm AM. Local cytokine response in *Helicobacter pylori*-infected subjects. *Infect Immun* 1998; **66**: 5964-5971
- 12 Wang J, Fan X, Lindholm C, Bennett M, O'Connell J, Shanahan F, Brooks EG, Reyes VE, Ernst PB. *Helicobacter pylori* modulates lymphoepithelial cell interactions leading to epithelial cell damage through Fas/Fas Ligand interactions. *Infect Immun* 2000; **68**: 4303-4311
- 13 Wiley SR, Schooley K, Smolak PJ, Din WS, Huang CP, Nicholl JK, Sutherland GR, Smith TD, Rauch C, Smith CA. Identification and characterization of a new member of the TNF family that induces apoptosis. *Immunity* 1995; **3**: 673-682
- 14 Griffith TS, Lynch DH. TRAIL: a molecule with multiple re-

- ceptors and control mechanisms. *Curr Opin Immunol* 1998; **10**: 559-563
- 15 **Sheridan JP**, Marsters SA, Pitti RM, Gurney A, Skubatch M, Baldwin D, Ramakrishnan L, Gray CL, Baker K, Wood WI, Goddard AD, Godowski P, Ashkenazi A. Control of TRAIL-induced apoptosis by a family of signaling and decoy receptors. *Science* 1997; **277**: 818-821
- 16 **Pan G**, Ni J, Wei YF, Yu G, Gentz R, Dixit VM. An antagonist decoy receptor and a death domain-containing receptor for TRAIL. *Science* 1997; **277**: 815-818
- 17 **LeBlanc H**, Lawrence D, Varfolomeev E, Totpal K, Morlan J, Schow P, Fong S, Schwall R, Sinicropi D, Ashkenazi A. Tumor-cell resistance to death receptor-induced apoptosis through mutational inactivation of the proapoptotic Bcl-2 homolog Bax. *Nat Med* 2002; **8**: 274-281
- 18 **Kayagaki N**, Yamaguchi N, Nakayama M, Eto H, Okumura K, Yagita H. Type I interferons (IFNs) regulate tumor necrosis factor-related apoptosis-inducing ligand (TRAIL) expression on human T cells: A novel mechanism for the antitumor effects of type I IFNs. *J Exp Med* 1999; **189**: 1451-1460
- 19 **Kayagaki N**, Yamaguchi N, Nakayama M, Kawasaki A, Akiba H, Okumura K, Yagita H. Involvement of TNF-related apoptosis-inducing ligand in human CD4+ T cell-mediated cytotoxicity. *J Immunol* 1999; **162**: 2639-2647
- 20 **Thomas WD**, Hersey P. TNF-related apoptosis-inducing ligand (TRAIL) induces apoptosis in Fas ligand-resistant melanoma cells and mediates CD4 T cell killing of target cells. *J Immunol* 1998; **161**: 2195-2200
- 21 **Nieda M**, Nicol A, Koezuka Y, Kikuchi A, Lapteva N, Tanaka Y, Tokunaga K, Suzuki K, Kayagaki N, Yagita H, Hirai H, Juji T. TRAIL expression by activated human CD4(+)/V alpha 24NKT cells induces *in vitro* and *in vivo* apoptosis of human acute myeloid leukemia cells. *Blood* 2001; **97**: 2067-2074
- 22 **Kaplan MJ**, Ray D, Mo RR, Yung RL, Richardson BC. TRAIL (Apo2 ligand) and TWEAK (Apo3 ligand) mediate CD4+ T cell killing of antigen-presenting macrophages. *J Immunol* 2000; **164**: 2897-2904
- 23 **Dorr J**, Waiczies S, Wendling U, Seeger B, Zipp F. Induction of TRAIL-mediated glioma cell death by human T cells. *J Neuroimmunol* 2002; **122**: 117-124
- 24 **Chou AH**, Tsai HF, Lin LL, Hsieh SL, Hsu PI, Hsu PN. Enhanced proliferation and increased IFN-gamma production in T cells by signal transduced through TNF-related apoptosis-inducing ligand. *J Immunol* 2001; **167**: 1347-1352
- 25 **Smoot DT**, Sewchand J, Young K, Desbordes BC, Allen CR, Naab T. A method for establishing primary cultures of human gastric epithelial cells. *Methods Cell Sci* 2000; **22**: 133-136
- 26 **Kuck D**, Kolmerer B, Iking-Konert C, Krammer PH, Stremmel W, Rudi J. Vacuolating cytotoxin of *Helicobacter pylori* induces apoptosis in the human gastric epithelial cell line AGS. *Infect Immun* 2001; **69**: 5080-5087
- 27 **Le'Negrate G**, Ricci V, Hofman V, Mograbi B, Hofman P, Rossi B. Epithelial intestinal cell apoptosis induced by *Helicobacter pylori* depends on expression of the cag pathogenicity island phenotype. *Infect Immun* 2001; **69**: 5001-5009
- 28 **Domek MJ**, Netzer P, Prins B. *Helicobacter pylori* induces apoptosis in human epithelial gastric cells by stress activated protein kinase pathway. *Helicobacter* 2001; **6**: 110-115
- 29 **Domek MJ**, Netzer P, Prins B, Nguyen T, Liang D, Wyle FA, Warner A. Induction of gastric epithelial cell apoptosis by *Helicobacter pylori* vacuolating cytotoxin. *Cancer Res* 2003; **63**: 951-957
- 30 **Odenbreit S**, Puls J, Sedlmaier B, Gerland E, Fischer W, Haas R. Translocation of *Helicobacter pylori* CagA into gastric epithelial cells by type IV secretion. *Science* 2000; **287**: 1497-1501
- 31 **Asahi M**, Azuma T, Ito S, Ito Y, Suto H, Nagai Y, Tsubokawa M, Tohyama Y, Maeda S, Omata M, Suzuki T, Sasakawa C. *Helicobacter pylori* CagA protein can be tyrosine phosphorylated in gastric epithelial cells. *J Exp Med* 2000; **191**: 593-602
- 32 **Stein M**, Rappuoli R, Covacci A. Tyrosine phosphorylation of the *Helicobacter pylori* CagA antigen after cag-driven host cell translocation. *Proc Natl Acad Sci U S A* 2000; **97**: 1263-1268
- 33 **Higashi H**, Tsutsumi R, Muto S, Sugiyama T, Azuma T, Asaka M, Hatakeyama M. SHP-2 Tyrosine phosphatase as an intracellular target of *Helicobacter pylori* CagA. *Science* 2002; **295**: 683-686

Edited by Wang XL Proofread by Chen WW and Xu FM

Antigen epitope of *Helicobacter pylori* vacuolating cytotoxin A

Xiu-Li Liu, Shu-Qin Li, Chun-Jie Liu, Hao-Xia Tao, Zhao-Shan Zhang

Xiu-Li Liu, Shu-Qin Li, Chun-Jie Liu, Hao-Xia Tao, Zhao-Shan Zhang, Beijing Institute of Biotechnology, Beijing 100071, China
Supported by the National High Technology Research and Development Program of China (863 Program), No. 2001AA215161
Correspondence to: Zhao-Shan Zhang, Beijing Institute of Biotechnology, 20 Dongdajie Street, Fengtai District, Beijing 100071, China. zhangzs@nic.bmi.ac.cn
Telephone: +86-10-66948834 **Fax:** +86-10-63833521
Received: 2004-02-11 **Accepted:** 2004-02-24

Abstract

AIM: To construct and select antigen epitopes of vacuolating cytotoxin A (VacA) for nontoxic VacA vaccine against *Helicobacter pylori* (*H pylori*) infection.

METHODS: Eleven VacA epitopes were predicted according to VacA antigenic bioinformatics. Three candidates of VacA epitope were constructed through different combined epitopes. The candidate was linked with *E. coli* heat-labile enterotoxin B (LTB) by a linker of 7 amino acids, and cloned into plasmid pQE-60 in which fusion LTB-VacA epitope was efficiently expressed. To test the antigenicity of the candidate, 6 BALB/c mice were treated with the fusion LTB-VacA epitope through intraperitoneal injection. To explore the ability of inhibiting the toxicity of VacA, antiserum against the candidate was used to counteract VacA that induced HeLa cells to produce cell vacuoles *in vitro*.

RESULTS: Serum IgG against the candidate was induced in the BALB/c mice. *In vitro*, the three antisera against the candidate efficiently counteracted the toxicity of VacA, and decreased the number of cell vacuoles by 14.17%, 20.20% and 30.41% respectively.

CONCLUSION: Two of the three candidates, LZ-VacA1 and LZ-VacA2, can be used to further study the mechanism of vacuolating toxicity of VacA, and to construct nontoxic VacA vaccine against *H pylori* infection.

Liu XL, Li SQ, Liu CJ, Tao HX, Zhang ZS. Antigen epitope of *Helicobacter pylori* vacuolating cytotoxin A. *World J Gastroenterol* 2004; 10(16): 2340-2343
<http://www.wjgnet.com/1007-9327/10/2340.asp>

INTRODUCTION

Pathogenic strains of *Helicobacter pylori* (*H pylori*) release a M_r 95 000 protein toxin in the growth medium. Growing evidence indicates that VacA is a major virulence factor in *H pylori* long-term infection leading to gastroduodenal ulcers^[1-5]. This toxin induces formation of vacuoles in the cytosol of cells, therefore it has been named vacuolating toxin^[6-11]. VacA is thus considered as a therapeutic vaccine for individuals infected with *H pylori*. The VacA gene encodes a protoxin approximately M_r 140 000, which belongs to the family of secreted proteins. During the process of VacA secretion, a M_r 95 000 mature toxin is exported.

A large oligomeric complex appear as 'flower' with M_r 900 000 which is composed of 6-7 VacA monomers^[12-15]. When exposed to the acidic situation, the oligomeric complexes were assembled into monomers and the toxicity of VacA was enhanced^[16-18]. After VacA exerted its effect on the cells for 90 min, vacuoles were formed^[19]. The vacuoles induced by VacA were acidic. Intracellular vacuolation is believed to induce cell damage and eventually apoptosis, which might lead to release of necrotic factors *in vivo* and therefore contribute to the establishment of a chronic inflammatory response. Because vacuolating cytotoxin A is difficult to express, purify and construct the combined vaccine, we studied the antigen epitopes to reduce the toxin.

MATERIALS AND METHODS

E. coli JM109, pFS2.2 and HeLa cell were preserved in our laboratory; pQE-60 was a gift of professor Hou-Chu Zhu, Beijing Institute of Biotechnology, Beijing, China; *H pylori* Sydney strain (*HP SSI*), was a gift of professor Min-Hu Chen, Sun Yat-sen University, Guangzhou, China.

*Bam*H I, *Eco*R V, *Nco* I, *Hind* III, Pyrobest Taq DNA polymerase and T₄ DNA ligase were purchased from TaKaRa Biotechnology corporations.

Isopropyl β -D-thiogalactoside (IPTG), Freund's adjuvant and sheep anti-mouse IgG-HRP were purchased from Sigma corporations, RPMI 1640 and newborn calf serum were purchased from Hyclone corporations.

BALB/c female mice: 6-8 wk old, SPF.

Bioinformatic analysis and design for candidates of VacA antigen epitope

According to the protein characteristics of hydrophilicity, hydrophobicity, secondary structure, accessibility, flexibility and antigenicity, 9 VacA antigen epitopes in the amino acid site of 34-810 were predicted by the antigen-analyzing software GOLDKEY (Table 1).

Table 1 Site and amino acid sequences of predicted VacA epitopes

Site of amino acid	Amino acid sequences of predicted epitopes
35-46	AEEANKTPDKPD
61-66	PHKEYD
146-154	KDSADRTTR
297-317	GYKDKPKDKPSNTTQNNANN
335-338	NSAQ
446-450	TDTKN
566-568	SGE
734-737	NNNR
746-748	TDD
766-768	DNY
799-806	TPTENGGN

Three candidates of VacA antigen epitope were designed by combining part of 9 predicted epitopes. The candidate LZ-VacA1 was composed of amino acids 35-36 and 146-154, LZ-VacA2 included amino acids 297-317, and LZ-VacA3 contained

aminoacids 61-66, 446-450, 734-737, 746-748, 766-768, and 799-806. The gene sequence of candidate epitope was fused with a 7-amino acid linker (YPQDPSS). The nucleotide acid and amino acid sequences of three candidate epitopes were as following.

The sequence of LZ-VacA1 was:

```
TAC CCT 5'---CAG GAT CCG TCT TCC gcc gaa gaa gcc
Y P Q D P S S A E E A
aat aaa acc cca gat aaa ccc gat aag gat agt gct gat
N K T P D K P D K D S A D
cgc acc acg aga GAT---3'
R T T R D
```

The sequence of LZ-VacA2 was

```
TAC CCT 5'---CAG GAT CCG TCT TCC ggt tat aag gat
Y P Q D P S S G Y K D
aaa cct aag gat aaa cct agt aac acc acg caa aat aat
K P K D K P S N T T Q N N
gct aat aat aac GAT---3'
A N N N D
```

The sequence of LZ-VacA3 was

```
TAC CCT 5'---CAG GAT CCG TCT TCC cct cac aag gaa
Y P Q D P S S P H K E
tac gac acg gat acc aaa aac aac aat aac cgc act gat
Y D T D T K N N N N R T D
gac gac aat tac acg cct act gag aat ggt ggc aat GAT---3'
D D N Y T P T E N G G N D
```

Synthesis of DNA sequence of candidate epitopes and insertion of plasmid pFS2.2

Two splicing sequences were designed according to the nucleotide acid sequences of the candidate epitope and linker. These sequences were synthesized artificially and spliced by PCR reaction. PCR reaction solution containing 5 μ L 10 \times PCR buffer, 0.25 μ L pyrobest Taq polymerase (5 U/ μ L), 1 μ L P1 and P2 primer (50 ng/ μ L), 4 μ L dNTP, H₂O to 50 μ L. Five PCR cycles were performed, each at 95 °C for 30 s, at 60 °C for 30 s, at 72 °C for 15 s.

LZ-VacA1 primer sequence was P1: 5'--cag gat ccg tet tcc gcc gaa gaa gcc aat aaa acc cca gat aaa ccc gat aag--3', P2: 5'---atc tct cgt ggt gcg atc agc act atc ctt atc ggg ttt atc tgg gg---3'.

LZ-VacA2 primer sequence was P1: 5'--cag gat ccg tet tcc ggt tat aag gat aaa cct aag gat aaa cct agt aac acc--3', P2: 5'---atc gtt att att agc att att ttg cgt ggt gtt act agg ttt atc c---3'.

LZ-VacA3 primer sequence was, P1: 5'--cag gat ccg tet tcc cct cac aag gaa tac gac acg gat acc aaa aac aac aat aac cgc act gat--3', P2: 5'---atc att gcc acc att ctc agt agg ggt gta att gtc gtc atc agt cgc gtt att gtt gt---3'.

The DNA sequences of the candidate epitope and plasmid pFS2.2 containing LTB, were digested with restriction endonucleases *Bam*HI and *Eco*RV, and ligated with T₄ ligase. The recombinant plasmid, which included LTB-VacA gene was transformed to JM109. The positive clones were screened and named them as pLZ-SV1, pLZ-SV2 and pLZ-SV3, respectively.

Construction of expression vector and purification of LTB-VacA protein

To improve the efficiency of expression, two primers with the cloning sites *Nco*I and *Hind*III were designed to construct plasmid pQE-60 with LTB-VacA gene. The recombinant plasmid was transformed to JM109. The positive clones were screened and named them as pLZ-QV1, pLZ-QV2 and pLZ-QV3 respectively.

The primers was

P1 5'---cagccatggGTGAATAAAGTAAAATG---3'

*Nco*I

P2 5'---ggcaagcctGCTCGGTACTAATTAATTAG---3'

*Hind*III

The strain with recombinant plasmid was cultured in the Luria-Bertani broth for 3 h, induced by IPTG for 4 h, and then harvested. The targeted protein of LTB-VacA was an inclusion body by SDS-PAGE test. The inclusion body was denatured with 6 mol/L guanidine hydrochloride, and natured with dialysis. LTB-VacA infused protein was purified through the anti-LTB antibody affinity chromatography.

Immunization

Twenty-four female BALB/c mice were randomly and averagely divided into control (LTB), LTB-VacA1, LTB-VacA2 and LTB-VacA3 groups. The mice of each group were immunized through intraperitoneal injection of 200 μ L (100 μ g protein) LTB, LTB-VacA1, LTB-VacA2 or LTB-VacA3 on days 0, 14 and 28. On days 7, 21 and 35, blood of each mouse was collected and antibody titer was determined.

Cell Vacuolization test

VacA was purified from *H. pylori* strain SS1 culture supernatant with ammonia sulfate precipitation. The preliminary experiment was performed to show the amount of *H. pylori* strain SS1 culture supernatant was added when cell vacuoles were formed. HeLa cells were cultured as monolayers in flasks in RPMI 1640 containing NCS under 50 mL/L CO₂ at 37 °C. Twenty-four hours before experiment, the cells were released with trypsin/EDTA and seeded in 96-well plates in 10³/well. After the VacA protein was incubated with antibody to LTB-VacA1, 2, 3 and LTB for 4 h at 37 °C, we added the fixture and VacA protein onto the cell surface for 6 h. Then we calculated the total cell number and cell number of vacuolization.

Statistical analysis

Data are presented as mean \pm SD. Analysis of variance with a two-tailed students *t*-test was used to identify significant differences. *P*<0.05 was considered statistically significant.

RESULTS

Construction of recombinant plasmid

Recombinant plasmids pLZ-VacA1, 2, 3 encoded the infused gene of LTB and VacA1, 2, 3. It was shown from the digestion map of restriction endonucleases *Nco*I and *Hind*III, the infused gene was successfully cloned to pQE-60 (Figure 1). LTB-VacA1 had the nucleotide acid number of 465 bp (LTB387+LZ-VacA1 78). LTB-VacA2 had the nucleotide acid number of 465 bp (LTB387+LZ-VacA2 78). LTB-VacA3 had the nucleotide acid number of 489 bp (LTB387+LZ-VacA3 102). The amino acids of three LTB-VacA were deduced from the nucleotide acid sequences. LTB-VacA1 and LTB-VacA2 had 155 amino acids, and the *M_r* was about 17 000. LTB-VacA3 had 163 amino acids, and the molecular weight was about 17 900. The sequences of the three genes were correct by sequencing analyses.

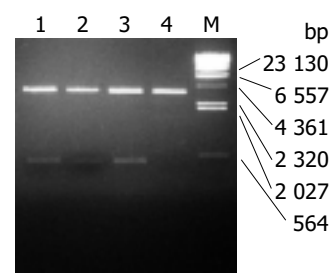


Figure 1 Digestion of recombinant plasmid. M: λ DNA/ *Hind* III; Lane 1: pLZ-QV3/ *Nco*I+*Hind* III; Lane 2: pLZ-QV2/ *Nco*I+*Hind* III; Lane 3: pLZ-QV1/ *Nco*I+*Hind* III; Lane 4: pQE-60/ *Nco*I+*Hind* III.

Expression and purification of infused protein

The LTB-VacA1, 2, 3 proteins were expressed in the JM109 strain. In the SDS-PAGE, the three proteins were 14.13%, 15.51% and 14.79% of the total protein respectively. After purification with anti-LTB antibody affinity chromatography, the percentage of three proteins in the total proteins was improved to 69.26%, 70.18% and 75.35% respectively (Figure 2).

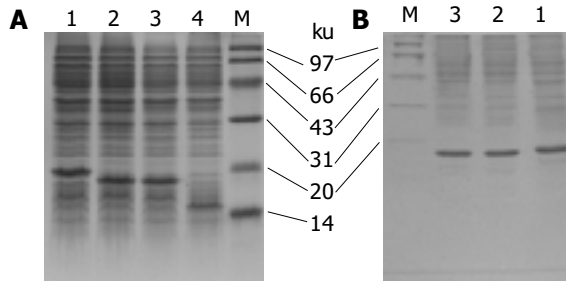


Figure 2 SDS-PAGE of LTB-VacA protein. M: Marker; Lane 1: LTB-VacA3; Lane 2: LTB-VacA2; Lane 3: LTB-VacA1; Lane 4: LTB. A: LTB-VacA proteins were expressed in the JM109; B: Purification with anti-LTB antibody affinity chromatography.

Serum antibody levels in infused protein

Intraperitoneal immunization with the infused protein and Freund's adjuvant resulted in a marked elevation of serum IgG antibody in all the 6 mice after three immunizations (Figure 3).

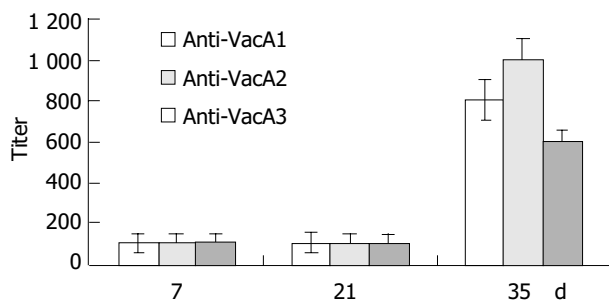


Figure 3 IgG against VacA induced by different LTB-VacA.

Seven days after the first immunization, the Level of antibody was lower. The titer of the antibody was about 1:100. Seven days after the second immunization, the titer of the antibody had no remarkable changes. But 14 d after the third immunization, the titer of the anti-LTB-VacA1 antibody, the titer of the anti-LTB-VacA2 antibody and the titer of the anti-LTB-VacA1 antibody was increased to 1:800, 1:1 000 and 1:600 respectively. The biggest value of positive and negative in the three antibodies was 3.8, 4.2 and 3.2.

HeLa cell vacuolization

The preliminary experimental results showed when we added 10, 30, 40, 80 and 100 μ L culture supernatant, the cell vacuolization was produced. Because the space of wells in flasks well was limited, 100 μ L VacA protein was added into the culture medium. The ratio of cell vacuolization after we added 100 μ L protein was 49.52% (Figure 4).

The control serum, anti-VacA1 serum, anti-VacA2 serum and anti-VacA1 serum were incubated with 100 μ L VacA antigen for 4 h. Then we added the fixture and VacA protein in the flasks wells for 6 h. The result showed the control serum and 100 μ L VacA antigen could not reduce the ratio of cell vacuolization, but anti-VacA1 serum, anti-VacA2 serum, anti-VacA3 serum could decrease the ratio of cell vacuolization. The change rate of cell vacuolization is 30.41%, 20.20% and 14.17% respectively (Table 2).

Table 2 Inhibition of anti-LTB-VacA antibody on VacA toxin

Group	HeLa cells with vacuoles in total cells (%)	Change rate (%)
VacA toxin	49.52 \pm 2.77	0
Anti-LTBantibody (Control)	47.51 \pm 1.31	-4.05 \pm 1.61
Anti-LTB-VacA1 antibody	34.47 \pm 1.97	-30.41 \pm 2.41 ^b
Anti-LTB-VacA2 antibody	39.52 \pm 1.69	-20.20 \pm 2.07 ^b
Anti-LTB-VacA3 antibody	42.51 \pm 1.84	-14.17 \pm 2.27 ^a

^a P <0.05, ^b P <0.01 vs control.

DISCUSSION

Many methods could predict the epitopes of protein known as the primary structure, for example hydrophilicity scheme^[20], accessibility scheme^[21], antigenicity scheme^[22], flexibility scheme^[23,24] and secondary structure scheme^[17]. The antigenic epitopes are correlated with the characteristics, number, sequence of amino acid and protein conformation. Because the different prediction methods emphasize different biological information of antigens, several methods are considered in practice. In this study we chose the GOLDKEY software developed by the Experimental Group led by professor Jia-Jin Wu to analyse the characteristics of VacA protein including hydrophilicity, hydrophobicity, secondary structure, accessibility, flexibility and antigenicity. This software could predict the liner B epitope. At last we got 11 VacA candidate epitopes.

Due to the small molecular weight and the weakness of antigenicity of the antigen epitopes, the carrier or adjuvant must be linked to the epitopes^[25,26]. Several epitopes were joined in series and at last got 3 VacA candidate epitopes. LTB is an excellent protein adjuvant to facilitate the organism to produce the antibody epitopes, so we chose LTB to link the 3 epitopes.

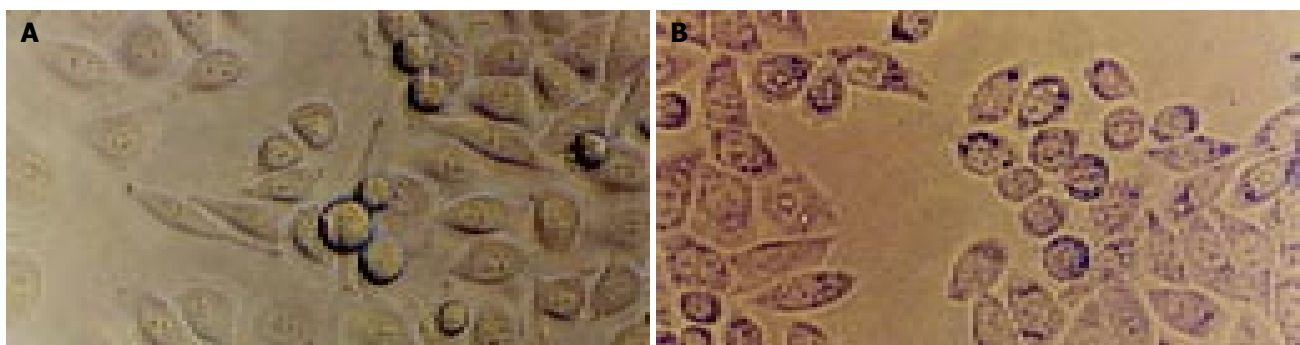


Figure 4 Microscopy of large vacuoles induced by VacA in HeLa cells. A: Normal HeLa cells; B: Vacuolated HeLa cells (Original magnification: \times 400).

The experiment of Schodel enucleate that plasmid pFS2.2 was a carrier in which *LTB* gene could express soluble LTB and carry outer polypeptides. The experiment of Zhang showed that 21-bp nucleotide acids between LTB and the epitopes could enhance the antigenicity of the epitopes. In our study, 7 peptides were used as a linker to join LTB with the epitopes.

At the beginning, LTB-VacA was cloned into plasmid pFS2.2, but the gene could not express these proteins, and then the genes were cloned into plasmid pET22b (+) again. There was a signal peptide in plasmid pET22b (+) in which the gene could express the soluble protein and secrete the protein into periplasm. The soluble proteins would be purified through the anti-LTB antibody affinity chromatography. Contrary to our wishes, the proteins in pFS2.2 were not expressed as expected. Finally, infused proteins were cloned into plasmid pQE-60 and expressed in JM109, but the expressed proteins were inclusion bodies. The inclusion bodies were denatured with guanidine hydrochloride and nated with dialysis, and LTB-VacA was purified through the anti-LTB antibody affinity chromatography.

Protein vacuolating toxin A is the only known virulence factor of *H. pylori*. Ninety minutes after VacA activation, the acidic vacuoles were induced in cells. Scientific researches showed that VacA was integrated with receptors in membranes to form an anionic channel. This channel could change the permeation characteristics of the membranes, so that the cells were damaged would undergo apoptosis. In this study, all the 3 antigen epitopes of VacA could induce antibody in mice. Although the antibody could inhibit the vacuolation of HeLa cells at a certain extent, they did not inhibit the vacuoles entirely. There are two reasons for this result. First, these epitopes were a part of the neutralized epitopes of VacA, antibody to these epitopes combined with VacA did not destroy the toxicity of VacA, only suppressed the toxin partly. Second, the titer of the antibody was not enough to neutralize the toxin of VacA. Next we are going to settle the problem. First, these epitopes will be joined in series for several copies so that the titer of the antibody will be improved to inhibit the toxin of VacA. Second, we will construct deficient mutations to farther verify the neutralized epitopes of VacA.

REFERENCES

- 1 Telford JL, Ghiara P, Dell'Orco M, Comanducci M, Burroni D, Bugnoli M, Tecce MF, Censini S, Covacci A, Xiang Z. Gene structure of the *Helicobacter pylori* cytotoxin and evidence of its key role in gastric disease. *J Exp Med* 1994; **179**: 1653-1658
- 2 van Amsterdam K, van Vliet AH, Kusters JG, Feller M, Dankert J, van der Ende A. Induced *Helicobacter pylori* vacuolating cytotoxin VacA expression after initial colonisation of human gastric epithelial cells. *FEMS Immunol Med Microbiol* 2003; **39**: 251-256
- 3 Inui T, Mizuno S, Takai K, Nakagawa M, Uchida M, Fujimiya M, Asakawa A, Inui A. *Helicobacter pylori* cytotoxin: a novel ligand for receptor-like protein tyrosine phosphatase beta. *Int J Mol Med* 2003; **12**: 917-921
- 4 Cho SJ, Kang NS, Park SY, Kim BO, Rhee DK, Pyo S. Induction of apoptosis and expression of apoptosis related genes in human epithelial carcinoma cells by *Helicobacter pylori* VacA toxin. *Toxicon* 2003; **42**: 601-611
- 5 Toro Rueda C, Garcia-Samaniego J, Casado Farinas I, Rubio Alonso M, Baquero Mochales M. Clinical importance of the CagA and VacA proteins and of the host factors in the development of peptic ulcer in patients infected by *Helicobacter pylori*. *Rev Clin Esp* 2003; **203**: 430-433
- 6 Parsonnet J, Hansen S, Rodriguez L, Gelb AB, Warnke RA, Jellum E, Orentreich N, Vogelstein JH, Friedman GD. *Helicobacter pylori* infection and gastric lymphoma. *N Engl J Med* 1994; **330**: 1267-1271
- 7 Yuan JP, Li T, Shi XD, Hu BY, Yang GZ, Tong SQ, Guo XK. Deletion of *Helicobacter pylori* vacuolating cytotoxin gene by introduction of directed mutagenesis. *World J Gastroenterol* 2003; **9**: 2251-2257
- 8 Gebert B, Fischer W, Weiss E, Hoffmann R, Haas R. *Helicobacter pylori* vacuolating cytotoxin inhibits T lymphocyte activation. *Science* 2003; **301**: 1099-1102
- 9 Qiao W, Hu JL, Xiao B, Wu KC, Peng DR, Atherton JC, Xue H. cagA and vacA genotype of *Helicobacter pylori* associated with gastric diseases in Xi'an area. *World J Gastroenterol* 2003; **9**: 1762-1766
- 10 Caputo R, Tuccillo C, Manzo BA, Zarrilli R, Tortora G, Blanco Cdel V, Ricci V, Ciardiello F, Romano M. *Helicobacter pylori* VacA toxin up-regulates vascular endothelial growth factor expression in MKN 28 gastric cells through an epidermal growth factor receptor-, cyclooxygenase-2-dependent mechanism. *Clin Cancer Res* 2003; **9**: 2015-2021
- 11 Wang J, van Doorn LJ, Robinson PA, Ji X, Wang D, Wang Y, Ge L, Telford JL, Crabtree JE. Regional variation among vacA alleles of *Helicobacter pylori* in China. *J Clin Microbiol* 2003; **41**: 1942-1945
- 12 Cover TL, Blaser MJ. Purification and characterization of the vacuolating toxin from *Helicobacter pylori*. *J Biol Chem* 1992; **267**: 10570-10575
- 13 Lupetti P, Heuser JE, Manetti R, Massari P, Lanzavecchia S, Bellon PL, Dallai R, Rappuoli R, Telford JL. Oligomeric and subunit structure of the *Helicobacter pylori* vacuolating cytotoxin. *J Cell Biol* 1996; **133**: 801-807
- 14 Nguyen VQ, Caprioli RM, Cover TL. Carboxy-terminal proteolytic processing of *Helicobacter pylori* vacuolating toxin. *Infect Immun* 2001; **69**: 543-546
- 15 Lanzavecchia S, Bellon PL, Lupetti P, Dallai R, Rappuoli R, Telford JL. Three-dimensional reconstruction of metal replicas of the *Helicobacter pylori* vacuolating cytotoxin. *Struct Biol* 1998; **121**: 9-18
- 16 Cover TL, Hanson PI, Heuser JE. Acid-induced dissociation of VacA, the *Helicobacter pylori* vacuolating cytotoxin, reveals its pattern of assembly. *J Cell Biol* 1997; **138**: 759-769
- 17 Yahiro K, Niidome T, Kimura M, Hatakeyama T, Aoyagi H, Kurazono H, Imagawa K, Wada A, Moss J, Hirayama T. Activation of *Helicobacter pylori* VacA toxin by alkaline or acid conditions increases its binding to a 250-kDa receptor protein-tyrosine phosphatase beta. *J Biol Chem* 1999; **274**: 36693-36699
- 18 McClain MS, Cao P, Cover TL. Amino-terminal hydrophobic region of *Helicobacter pylori* vacuolating cytotoxin (VacA) mediates transmembrane protein dimerization. *Infect Immun* 2001; **69**: 1181-1184
- 19 Cover TL, Halter SA, Blaser MJ. Characterization of HeLa cell vacuoles induced by *Helicobacter pylori* broth culture supernatant. *Hum Pathol* 1992; **23**: 1004-1010
- 20 Hopp TP, Woods KR. Prediction of protein antigenic determinants from amino acid sequences. *Proc Natl Acad Sci U S A* 1981; **78**: 3824-3828
- 21 Scott JK, Smith GP. Searching for peptide ligands with an epitope library. *Science* 1990; **249**: 386-390
- 22 Welling GW, Weijer WJ, van der Zee R, Welling-Wester S. Prediction of sequential antigenic regions in proteins. *FEBS Lett* 1985; **188**: 215-218
- 23 Zhao S, Goodsell DS, Olson AJ. Analysis of a data set of paired uncomplexed protein structures: new metrics for side-chain flexibility and model evaluation. *Proteins* 2001; **43**: 271-279
- 24 Kolibal SS, Brady C, Cohen SA. Definition of epitopes for monoclonal antibodies developed against purified sodium channel protein: implications for channel structure. *J Membr Biol* 1998; **165**: 91-99
- 25 Thomson SA, Sherritt MA, Medveczky J, Elliott SL, Moss DJ, Fernando GJ, Brown LE, Suhrbier A. Delivery of multiple CD8 cytotoxic T cell epitopes by DNA vaccination. *J Immunol* 1998; **160**: 1717-1723
- 26 Mateo L, Gardner J, Chen Q, Schmidt C, Down M, Elliott SL, Pye SJ, Firat H, Lemonnier FA, Cebon J, Suhrbier A. An HLA-A2 polyepitope vaccine for melanoma immunotherapy. *J Immunol* 1999; **163**: 4058-4063

4-hydroxy-2, 3-nonenal activates activator protein-1 and mitogen-activated protein kinases in rat pancreatic stellate cells

Kazuhiro Kikuta, Atsushi Masamune, Masahiro Satoh, Noriaki Suzuki, Tooru Shimosegawa

Kazuhiro Kikuta, Atsushi Masamune, Masahiro Satoh, Noriaki Suzuki, Tooru Shimosegawa, Division of Gastroenterology, Tohoku University Graduate School of Medicine, Sendai 980-8574, Japan
Supported by Grant-in-Aid for Encouragement of Young Scientists from Japan Society for the Promotion of Science (to A.M.), by Pancreas Research Foundation of Japan (to A.M.), and by the Kanae Foundation for Life and Socio-Medical Science (to A. M.)

Correspondence to: Atsushi Masamune, M. D., Division of Gastroenterology, Tohoku University Graduate School of Medicine, 1-1 Seiryō-cho, Aoba-ku, Sendai 980-8574, Japan. amasamune@int3.med.tohoku.ac.jp

Telephone: +11-81-22-717-7171 **Fax:** +11-81-22-717-7177

Received: 2004-02-06 **Accepted:** 2004-02-21

mitogen-activated protein kinases in rat pancreatic stellate cells. *World J Gastroenterol* 2004; 10(16): 2344-2351
<http://www.wjgnet.com/1007-9327/10/2344.asp>

INTRODUCTION

In 1998, star-shaped cells in the pancreas, namely pancreatic stellate cells (PSCs), were identified and characterized^[1,2]. They are morphologically similar to the hepatic stellate cells that play a central role in inflammation and fibrogenesis of the liver^[3]. In normal pancreas, stellate cells are quiescent and can be identified by the presence of vitamin A-containing lipid droplets in the cytoplasm. In response to pancreatic injury or inflammation, they are transformed (“activated”) from their quiescent phenotype into highly proliferative myofibroblast-like cells which express the cytoskeletal protein α -smooth muscle actin (α -SMA), and produce type I collagen and other extracellular matrix components. Many of the morphological and metabolic changes associated with the activation of PSCs in animal models of fibrosis also occur when these cells are grown in serum-containing medium in culture on plastic. There is accumulating evidence that PSCs, like hepatic stellate cells, are responsible for the development of pancreatic fibrosis^[1,2,4]. It has also been suggested that PSCs may participate in the pathogenesis of acute pancreatitis^[4,5]. In view of their importance in pancreatic fibrosis and inflammation, it is of particular importance to elucidate the molecular mechanisms underlying their activation. The activation of signaling pathways such as p38 mitogen-activated protein (MAP) kinase^[6] and Rho-Rho kinase pathway^[7] is likely to play a central role in PSC activation. However, the precise intracellular signaling pathways in PSCs are largely unknown.

The role of oxidative stress in the development of acute and chronic pancreatitis has been clarified^[8,9]. Reactive oxygen species and aldehydic end-products of lipid peroxidation, such as 4-hydroxy-2,3-nonenal (HNE), could act as mediators affecting signal transduction pathways, proliferation, and functional responses of target cells^[10-12]. HNE is a specific and stable end product of lipid peroxidation. It could be produced in response to oxidative insults^[13], and has been regarded to be responsible for many of the effects during oxidative stress *in vivo*^[13,14]. It reacts with DNA and proteins, generating various forms of adducts (cysteine, lysine, and histidine residues) that are capable of inducing cellular stress responses such as cell signaling and apoptosis^[14]. It has been shown that alcoholic chronic pancreatitis is characterized by the co-localization of evident lipid peroxidation, as assessed by immunoreactivity of HNE inside acinar cells, and the deposition of collagen type I in the fibrous septa and fibrotic stroma surrounding the pancreatic acini^[15]. The stronger HNE immunoreactivity at the periphery of acini raised the possibility that HNE might affect the cell functions of PSCs, but the effects of HNE on the signaling pathways and the regulation of cell functions in PSCs are unknown. We here report that HNE at physiologically relevant and non-cytotoxic concentrations activated activator protein-1 (AP-1) and three classes of MAP kinases in PSCs. In addition, HNE increased type I collagen production from PSCs. Specific

Abstract

AIM: Activated pancreatic stellate cells (PSCs) are implicated in the pathogenesis of pancreatic inflammation and fibrosis, where oxidative stress is thought to play a key role. 4-hydroxy-2,3-nonenal (HNE) is generated endogenously during the process of lipid peroxidation, and has been accepted as a mediator of oxidative stress. The aim of this study was to clarify the effects of HNE on the activation of signal transduction pathways and cellular functions in PSCs.

METHODS: PSCs were isolated from the pancreas of male Wistar rats after perfusion with collagenase P, and used in their culture-activated, myofibroblast-like phenotype unless otherwise stated. PSCs were treated with physiologically relevant and non-cytotoxic concentrations (up to 5 μ mol/L) of HNE. Activation of transcription factors was examined by electrophoretic mobility shift assay and luciferase assay. Activation of mitogen-activated protein (MAP) kinases was assessed by Western blotting using anti-phosphospecific antibodies. Cell proliferation was assessed by measuring the incorporation of 5-bromo-2'-deoxyuridine. Production of type I collagen and monocyte chemoattractant protein-1 was determined by enzyme-linked immunosorbent assay. The effect of HNE on the transformation of freshly isolated PSCs in culture was also assessed.

RESULTS: HNE activated activator protein-1, but not nuclear factor κ B. In addition, HNE activated three classes of MAP kinases: extracellular signal-regulated kinase, c-Jun N-terminal kinase, and p38 MAP kinase. HNE increased type I collagen production through the activation of p38 MAP kinase and c-Jun N-terminal kinase. HNE did not alter the proliferation, or monocyte chemoattractant protein-1 production. HNE did not initiate the transformation of freshly isolated PSCs to myofibroblast-like phenotype.

CONCLUSION: Specific activation of these signal transduction pathways and altered cell functions such as collagen production by HNE may play a role in the pathogenesis of pancreatic disorders.

Kikuta K, Masamune A, Satoh M, Suzuki N, Shimosegawa T. 4-hydroxy-2, 3-nonenal activates activator protein-1 and

activation of these signal transduction pathways and altered cell functions such as collagen production by HNE may play a role in the pathogenesis of pancreatic disorders.

MATERIALS AND METHODS

Materials

3-(4, 5-dimethylthiazole-2-yl)-2, 5-diphenyltetrazolium bromide (MTT) was obtained from Dojindo (Kumamoto, Japan). Poly (dI.dC)-poly (dI.dC) and [γ - 32 P] ATP were purchased from Amersham Biosciences UK, Ltd. (Buckinghamshire, England). Collagenase P and recombinant human interleukin (IL)-1 β were from Roche Applied Science (Mannheim, Germany). Double-stranded oligonucleotide probes for AP-1 and nuclear factor κ B (NF- κ B) were purchased from Promega (Madison WI). Rat recombinant platelet-derived growth factor (PDGF)-BB was from R&D Systems (Minneapolis, MN). Rabbit antibodies against phosphospecific MAP kinases, total MAP kinases, and inhibitor of NF- κ B (I κ B- α) were purchased from Cell Signaling Technologies (Beverly, MA). Rabbit antibody against glyceraldehyde-3-phosphate dehydrogenase (G3PDH) was from Trevigen (Gaithersburg, MD). HNE, SB203580, SP600125, and U0126 were from Calbiochem (La Jolla, CA). All other reagents were from Sigma-Aldrich (St. Louis, MO) unless specifically described.

Cell culture

All animal procedures were performed in accordance with the National Institutes of Health Animal Care and Use Guidelines. Rat PSCs were prepared from the pancreas tissues of male Wistar rats (Japan SLC Inc., Hamamatsu, Japan) weighing 200–250 g as previously described using the Nycodenz solution (Nycomed Pharma, Oslo, Norway) after perfusion with 0.3 g/L collagenase P^[16]. The cells were resuspended in Ham's F-12 containing 100 mL/L heat-inactivated fetal bovine serum (ICN Biomedicals, Aurora, OH), penicillin sodium, and streptomycin sulfate. Cell purity was always more than 90% as assessed by a typical star-like configuration and by detecting vitamin A autofluorescence. All experiments were performed using cells between passages two and five except for those using freshly isolated PSCs. Unless otherwise stated, we incubated PSCs in serum-free medium for 24 h before the addition of experimental reagents.

Cell viability assay

Cell viability was assessed by the MTT assay as previously described^[17]. After treatment with HNE for 24 h, MTT solution was added to the cells at a final concentration of 500 μ g/mL and the incubation continued at 37 °C for 4 h. After the incubation period, the medium was aspirated and the formazan product was solubilized with dimethylsulfoxide. Cell viability was determined by the differences in absorbance at wavelengths of 570 nm and 690 nm.

Intracellular peroxide production assay

Intracellular peroxide production was examined as previously described^[14]. Briefly, cells were incubated with 2', 7'-dichlorofluorescein diacetate (DCF-DA) at 50 μ mol/L for 30 min at 37 °C, and then treated with experimental reagents for an additional 30 min at 37 °C. After chilled on ice, cells were washed with ice-cold PBS, scraped from the plate, and resuspended at 1 \times 10⁶ cells/mL in PBS containing 10 mmol/L EDTA. The fluorescence intensities of 2', 7'-dichlorofluorescein formed by the reaction of DCF-DA with peroxides of more than 10 000 viable cells from each sample were analyzed by FACSCaliber flow cytometer (Becton Dickinson Co. Ltd., Tokyo, Japan) with excitation and emission settings of 488 and 525 nm, respectively. Prior to data collection, propidium iodide was added to the

sample to gate out dead cells. Experiments were repeated at least twice with similar results. The data are expressed as one representative histogram.

Cell proliferation assay

Serum-starved PSCs (approximately 80% density) were treated with HNE at the indicated concentrations in the absence or presence of PDGF-BB (25 ng/mL). Cell proliferation was assessed using a commercial kit (Cell proliferation ELISA, BrdU; Roche Applied Science) according to the manufacturer's instruction. This is colorimetric immunoassay based on the measurement of 5-bromo-2'-deoxyuridine (BrdU) incorporation during DNA synthesis^[18]. After 24-hour-incubation with experimental reagents, cells were labeled with BrdU for 3 h at 37 °C, fixed, and incubated with peroxidase-conjugated anti-BrdU antibody. Then the peroxidase substrate 3,3',5,5'-tetramethylbenzidine was added, and BrdU incorporation was quantitated by differences in absorbance at wavelength 370 nm and 492 nm.

Nuclear extracts preparation and electrophoretic mobility shift assay

Nuclear extracts were prepared and electrophoretic mobility shift assay was performed as previously described^[19]. Double-stranded oligonucleotide probes for AP-1 (5'-CGCTTGATGAGT CAGCCGGA-3') and NF- κ B (5'-AGTTGAGGGGACTT TCCCAGGC-3') were end-labeled with [γ - 32 P]ATP. Nuclear extracts (approximately 5 μ g) were incubated with the labeled oligonucleotide probe for 20 min at 22 °C, and electrophoresed through a 40 g/L polyacrylamide gel. Gels were dried, and autoradiographed at -80 °C overnight. A 100-fold excess of unlabeled oligonucleotide was incubated with nuclear extracts for 10 min prior to the addition of the radiolabeled probe in the competition experiments.

Luciferase assay

Luciferase assays were performed as previously described^[20] using luciferase expression vectors containing two consensus AP-1 binding sites (TGACTCA), or two consensus NF- κ B binding sites (GGGACTTTCC), which were kindly provided by Dr. Naofumi Mukaida (Kanazawa University, Japan). Approximately 1 \times 10⁶ PSCs were transfected with 2 μ g of each luciferase expression vector, along with 40 ng of pRL-TK vector (Promega) as an internal control, using the FuGENE6 reagent (Roche Applied Science). After 24 h, the transfected cells were treated with HNE at 1 μ mol/L for an additional 24 h. At the end of the incubation, cell lysates were prepared using Pica Gene kit (Toyo Ink Co., Tokyo, Japan), and the light intensities were measured using a model Lumat LB9507 Luminescence Reader (EG&G Berthold, Bad Wildbad, Germany).

Western blot analysis

Activation of MAP kinases was examined by Western blot analysis using anti-phosphospecific MAP kinase antibodies as previously described^[21]. Cells were treated with HNE, and lysed in sodium dodecyl sulfate buffer (62.5 mmol/L Tris-HCl at pH 6.8, 20 g/L sodium dodecyl sulfate, 100 mL/L glycerol, 50 mmol/L dithiothreitol, 1 g/L bromophenol blue) for 15 min on ice. The samples were then sonicated for 2 s, heated for 5 min, and centrifuged at 12 000 g for 5 min to remove insoluble cell debris. Whole cell extracts (approximately 100 μ g) were fractionated on a 100 g/L sodium dodecyl sulfate-polyacrylamide gel. They were transferred to a nitrocellulose membrane (Bio-Rad, Hercules, CA), and the membrane was incubated overnight at 4 °C with rabbit antibodies against phosphorylated MAP kinases (extracellular signal-regulated kinase (ERK)1/2, c-Jun N-terminal kinase (JNK), or p38 MAP kinase). After incubation with peroxidase-conjugated goat anti-rabbit secondary

antibody for 1 h, proteins were visualized by using an ECL kit (Amersham Biosciences UK, Ltd.). Levels of total MAP kinases, I κ B- α , α -SMA, and G3PDH were examined in a similar manner.

Enzyme-linked immunosorbent assay

After a 24-h incubation, cell culture supernatants were harvested and stored at -80 °C until the measurement. Monocyte chemoattractant protein-1 (MCP-1) levels in the culture supernatants were measured by enzyme-linked immunosorbent assay (Pierce Biotechnology, Rockford, IL) according to the manufacturer's instructions.

Collagen assay

PSCs were incubated with HNE in serum-free medium for 48 h. Type I collagen released into the culture supernatant was quantified by enzyme-linked immunosorbent assay, as previously described^[22]. Briefly, immunoassay plates (Becton Dickinson, Franklin Lakes, NJ) were coated with diluted samples overnight at 4 °C. After blocking with 50 g/L dry milk in PBS, plates were incubated with goat anti-rat type I collagen antibody (SouthernBiotech, Birmingham, AL). After washing of the plate, rabbit anti-goat IgG antibody conjugated with alkaline phosphatase was added, and incubated. Finally, P-nitrophenylphosphate was added as a substrate, and the collagen levels were determined by differences in absorbance at wavelength 405 min 690 nm. Rat tail collagen type I was used as a standard. The collagen levels in each sample were normalized to the cellular DNA content, which was determined by a fluorometric assay, according to the method of Brunk *et al.*^[23]. The results are expressed as a percentage of the untreated control.

Activating effect of HNE on PSCs in culture

Freshly isolated PSCs were incubated with HNE (at 1 μ mol/L) in serum-free medium or 50 mL/L fetal bovine serum-containing medium. After 7-d incubation, morphological changes characteristic of PSC activation were assessed after staining with glial acidic fibrillary protein (GFAP) as previously described^[24] using a streptavidin-biotin-peroxidase complex detection kit (Histofine Kit; Nichirei, Tokyo, Japan). Briefly, cells were fixed with 100 mL/L methanol for 5 min at -20 °C, and then endogenous peroxidase activity was blocked by incubation in methanol with 3 mL/L hydrogen peroxide for 5 min. After immersion in normal goat serum for 1 h, the slides were incubated with rabbit anti-GFAP antibody at a dilution of 1:100 overnight at 4 °C. The slides were incubated with biotinylated goat anti-rabbit antibody for 45 min, followed by peroxidase-conjugated streptavidin for 30 min. Finally, color was developed by incubating the slides for several minutes with diaminobenzidine (Dojindo, Kumamoto, Japan). In addition, total cellular proteins (approximately 25 μ g) were prepared, and the levels of α -SMA and G3PDH were determined by Western blotting.

Statistical analysis

The results were expressed as mean \pm SD. Luminograms and autoradiograms are representative of at least three experiments. Differences between experimental groups were evaluated by the two-tailed unpaired Student's *t* test. A *P*-value less than 0.05 was considered statistically significant.

RESULTS

HNE was cytotoxic at high concentrations

Because HNE has been shown to be cytotoxic at high concentrations in several types of cells^[25], we first examined the effect of HNE on the cell viability of PSCs. PSCs were incubated with increasing concentrations of HNE for 24 h, and the cell viability was assessed by MTT assay. HNE up to 5 μ mol/L

did not alter the cell viability, but above 5 μ mol/L, HNE was cytotoxic (Figure 1). The results were also confirmed by trypan blue dye exclusion test (data not shown). Based on these results, we used HNE up to 5 μ mol/L in the subsequent experiments.

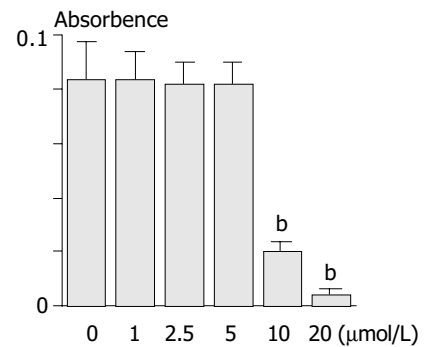


Figure 1 PSCs were incubated with HNE at the indicated concentrations in serum-free medium for 24 h. Cell viability was determined by the MTT assay, and the absorbance at 570 min 690 nm ("A.") of the sample is given. Data are shown as mean \pm SD (*n* = 6). ^a*P*<0.05 vs control, ^b*P*<0.01 vs control.

HNE was a potential inducer of oxidative stress

We examined the production of pro-oxidants using a peroxide-sensitive fluorescent probe, DCF-DA. This chemical is freely permeable to cells. Once inside the cells, it is hydrolyzed to DCF and trapped intracellularly. In the presence of peroxides, especially hydrogen peroxide, DCF is oxidized to fluorescent 2',7'-dichlorofluorescein, which can then be readily detected by flow cytometry^[14]. Treatment with HNE (at 5 μ mol/L) increased the peroxide-activated fluorescence intensity, indicating that HNE was a potential inducer of intracellular oxidative stress in PSCs (Figure 2).

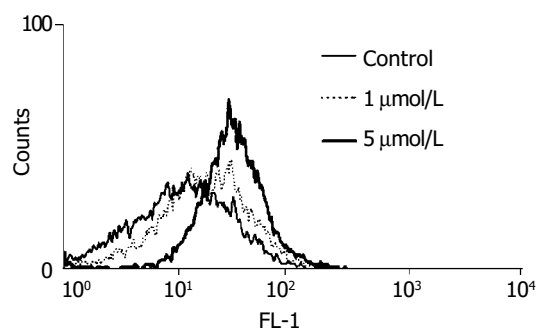


Figure 2 PSCs were incubated with DCF-DA (at 50 μ mol/L) for 30 min and then treated with HNE (at 1 or 5 μ mol/L) for 30 min. The fluorescence intensity of more than 10 000 cells was analyzed using a flow cytometer.

HNE increased AP-1, but not NF- κ B binding activity

We next examined the effects of HNE on the activation of the transcription factors NF- κ B and AP-1. These transcription factors are important regulators of gene expression in response to many stimuli including proinflammatory cytokines and growth factors^[26,27]. PSCs were incubated with HNE, or IL-1 β for 1 h. Nuclear extracts were prepared, and the specific binding activities of AP-1 and NF- κ B were examined by electrophoretic mobility shift assay. HNE, as well as IL-1 β , increased the AP-1 binding activity (Figure 3A). The specificity of AP-1-specific DNA binding activity was demonstrated by the addition of a 100-fold molar excess of unlabeled AP-1 oligonucleotide, but not by unrelated NF- κ B oligonucleotide in competition assays (data not shown). In contrast, NF- κ B binding activity was induced by IL-1 β , but not by HNE (Figure 3B).

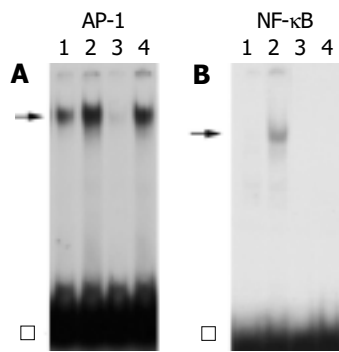


Figure 3 PSCs were treated with IL-1 β (at 2 ng/mL, lane 2) or HNE (at 5 μ mol/L, lane 4) in serum-free medium for 1 h. Nuclear extracts were prepared and subjected to electrophoretic mobility shift assay using AP-1 (panel A) or NF- κ B (panel B) oligonucleotide probes. Arrows denote specific inducible complexes competitive with cold double-stranded oligonucleotide probes (lane 3). Lane 1: control (serum-free medium only). \square : free probe.

HNE increased AP-1, but not NF- κ B dependent transcriptional activity

To confirm that AP-1 activation observed by electrophoretic mobility shift assay was functional, the effect of HNE on AP-1 dependent transcriptional activity was examined. PSCs were transiently transfected with NF- κ B- or AP-1-luciferase gene reporter constructs and assayed for the luciferase activity. As shown in Figure 4, HNE increased AP-1-dependent, but not NF- κ B-dependent luciferase activity. Phosphorylation and degradation of the inhibitory protein I κ B- α , and subsequent dissociation of this protein from NF- κ B were thought to be necessary for the activation^[26]. We also examined the effect of HNE on the degradation of I κ B- α by Western blotting. IL-1 β , but not HNE, induced transient degradation of I κ B- α , further supporting that HNE did not activate NF- κ B (Figure 4B).

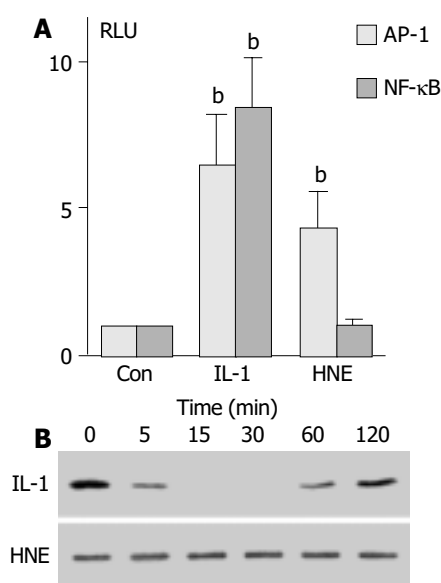


Figure 4 HNE increased AP-1, but not NF- κ B, -dependent transcriptional activity. A: PSCs were transfected with the luciferase vectors (2 X AP-1 or 2 X NF- κ B) along with pRL-TK vector as an internal control. After 24 h, the transfected cells were treated with IL-1 β (at 2 ng/mL) or HNE (at 1 μ mol/L). After another 24-h incubation, intracellular luciferase activities were determined. The data represent mean \pm SD, calculated from three independent experiments as fold induction compared with the activity observed in control (serum-free medium only, "Con"). ^b P <0.01 vs control. RLU: relative light

units. B: PSCs were treated with IL-1 β (at 2 ng/mL) or HNE (at 1 μ mol/L) in serum-free medium for the indicated times. Total cell lysates were prepared, and the level of I κ B- α was determined by Western blotting.

HNE activated MAP kinases

Induction of the expression of AP-1 components c-Fos and c-Jun by a variety of stimuli such as growth factors and cytokines is mediated by the activation of three distinct MAP kinases: ERK1/2, JNK, and p38 MAP kinase^[27,28]. Activation of these kinases occurs through phosphorylation^[27,28]. We determined the activation of these MAP kinases in HNE-treated cells by Western blotting using anti-phosphospecific MAP kinase antibodies. These antibodies recognize only phosphorylated forms of MAP kinases, thus allowing the assessment of activation of these kinases. HNE activated these three classes of MAP kinases in a time-dependent manner with peaking around 5 to 15 min (Figure 5).

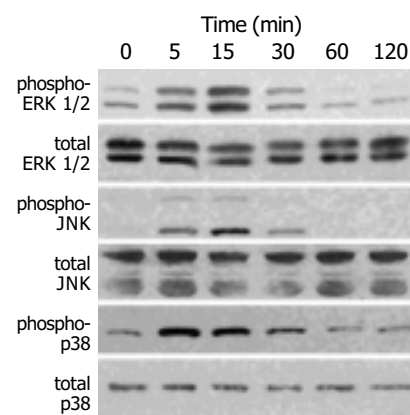


Figure 5 PSCs were treated with HNE (at 1 μ mol/L) for the indicated times. Total cell lysates (approximately 100 μ g) were prepared, and the levels of activated, phosphorylated MAP kinases were determined by Western blotting using anti-phosphospecific antibodies. Levels of total MAP kinases were also determined.

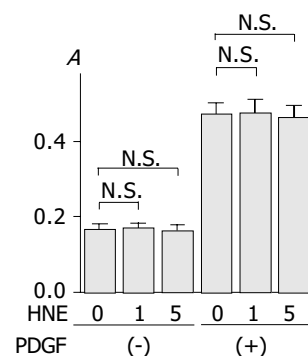


Figure 6 PSCs were treated with HNE (at 0, 1, or 5 μ mol/L) in the absence or presence of PDGF (at 25 ng/mL) in serum-free medium. After 24-h incubation, cells were labeled with BrdU for 3 h. Cells were fixed, and incubated with peroxidase-conjugated anti-BrdU antibody. Then the peroxidase substrate 3,3',5,5'-tetramethylbenzidine was added, and BrdU incorporation was quantitated by differences in absorbance at wavelength 370 nm 492 nm ("A.", optical density). Data are shown as mean \pm SD (n = 6). ^b P <0.01 versus control (serum-free medium only), N.S.: not significant.

HNE did not alter basal and PDGF-BB-induced proliferation

We then examined the effects of HNE on basal and PDGF-induced proliferation. As previously reported^[16], PDGF-BB significantly increased proliferation. HNE did not affect either

basal or PDGF-BB-induced proliferation of PSCs (Figure 6).

HNE did not induce MCP-1 production

Activated PSCs acquired the proinflammatory phenotype; they might modulate the recruitment and activation of inflammatory cells through the expression of MCP-1^[29]. IL-1 β induced MCP-1 production, but HNE did not (Figure 7).

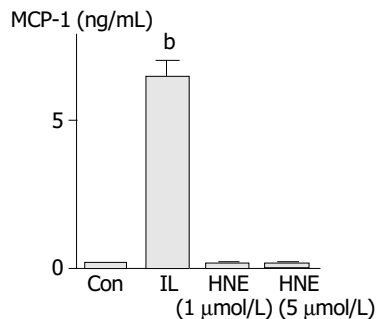


Figure 7 PSCs were treated with IL-1 β (2 ng/mL, "IL") or HNE (at 1 or 5 μ mol/L) in serum-free medium. After 24 h, culture supernatant was harvested, and the MCP-1 level was determined by enzyme-linked immunosorbent assay. Data shown are expressed as mean \pm SD ($n = 6$). ^b $P < 0.01$ versus control ("Con", serum-free medium only).

HNE increased type I collagen production

It has been shown that culture-activated PSCs express α -SMA and produce type I collagen. Indeed, α -SMA expression has been accepted as a marker of PSC activation^[1], and *in situ* hybridization techniques showed that α -SMA-positive cells were the principal source of collagen in the fibrotic pancreas^[4]. HNE increased the production of type I collagen (Figure 8). Our previous finding that ethanol and acetaldehyde induced collagen production through p38 MAP kinase^[30] prompted us to examine the role of MAP kinases in HNE-induced type I collagen production. Thus we employed specific inhibitors to block these pathways. A selective p38 MAP kinase inhibitor SB203580^[31], and a JNK inhibitor SP600125^[32] decreased type I collagen production. In contrast, U0126, a specific inhibitor of MAP kinase kinase activation and consequent ERK1/2 activation^[33], did not affect the collagen production. These results suggested that HNE induced type I collagen production through the activation of p38 MAP kinase and JNK, but not ERK pathway.

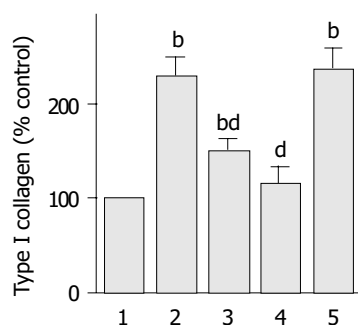


Figure 8 PSCs were treated with HNE (at 1 μ mol/L, lane 2) in the absence or presence of SB203580 (at 25 mmol/L, lane 3), SP600125 (at 10 μ mol/L, lane 4), or U0126 (at 5 μ mol/L, lane 5). After 48-h incubation, type I collagen released into the culture supernatant was quantified by enzyme-linked immunosorbent assay. The collagen levels in each sample were normalized to the cellular DNA content. The results are expressed as a percentage of the untreated control ("Con"). Data are shown as

mean \pm SD ($n = 6$). ^b $P < 0.01$ vs control (serum-free medium only, lane 1). ^d $P < 0.01$ vs HNE only (lane 2).

HNE did not initiate the transformation of freshly isolated PSCs to activated phenotype

Finally, we examined whether HNE initiated the transformation of PSCs from quiescent to myofibroblast-like phenotype in culture. Freshly isolated PSCs were incubated with HNE in serum-free medium or 50 mL/L serum-containing medium for 7 d. Morphological changes characteristic of PSC activation were assessed after staining with GFAP. After 7 d, PSCs cultured with 50 mL/L serum showed transformation into cells with a myofibroblast-like phenotype (Figure 9A). In contrast, PSCs treated with HNE were small and circular, with lipid droplets presenting in many cells and slender dendritic processes (Figure 9B), as PSCs treated with serum-free medium only (Figure 9C). In agreement with the morphological changes, significant expression of α -SMA was observed on d 7 in serum-treated PSCs, whereas HNE did not induce α -SMA expression.

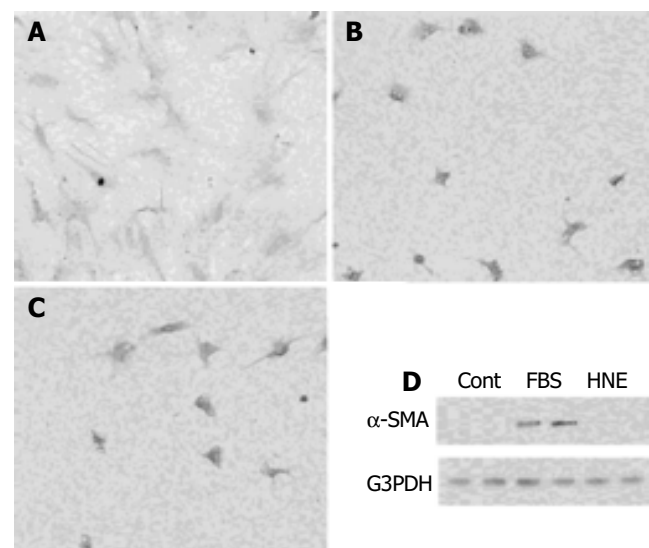


Figure 9 A,B,C: Freshly isolated PSCs were incubated with 50 mL/L serum (panel A), HNE (at 1 μ mol/L, panel B), or serum-free medium (panel C) for 7 d. Morphological changes characteristic of PSC activation were assessed after staining with GFAP. Original magnification: $\times 10$ objective. D: Total cell lysates (approximately 25 μ g) were prepared from cells treated with serum-free medium ("Cont"), 50 mL/L serum ("FBS"), or HNE (at 1 μ mol/L) for 7 d, and the levels of α -SMA and G3PDH were determined by Western blotting.

DISCUSSION

It has been established that oxidative stress plays a critical role in the pathogenesis of both acute and chronic pancreatitis^[8,9]. HNE, an aldehydic end product of lipid peroxidation, is believed to be largely responsible for pathological effects observed during oxidative stress^[13]. The major effects of HNE produced during oxidative stress are believed to be damage to cellular components such as glutathione and proteins. However, recent studies have revealed that HNE at non-cytotoxic levels could potentially activate a stress response mechanism^[14]. In this study, we have shown for the first time that HNE, at non-cytotoxic concentrations, activated AP-1, but not NF- κ B, in PSCs. This selective pattern of activation was distinct from that elicited by IL-1 β and tumor necrosis factor- α , which also activated NF- κ B^[5]. In addition, HNE activated three classes of MAP kinases (ERK1/2, JNK, and p38 MAP kinase). HNE-induced type I collagen production was inhibited by SB203580, a p38 MAP kinase inhibitor, and by SP600125, a JNK inhibitor, suggesting

a role of p38 MAP kinase and JNK in the type I collagen production. The concentrations of HNE used in this study (up to 5 $\mu\text{mol/L}$) could be easily reached *in vivo* in conditions of mild to moderate oxidative stress, and were considered to be physiologically relevant^[13].

It has been shown that ethanol increased HNE protein adduct accumulation in the pancreas of rats^[34]. During pancreatic injury *in vivo*, PSCs might be exposed to HNE via two pathways: (1) exogenous exposure as a result of the generation of HNE by surrounding cells (e.g. acinar cells and inflammatory cells) or (2) endogenous exposure as a result of the generation of HNE within the cells. Casini *et al.*^[15] have shown that stronger HNE immunoreactivity was observed at the periphery of acini in chronic alcoholic pancreatitis. Under such a circumstance, it is likely that PSCs exogenously expose to HNE. Our present study is exclusively concerned with the effect of exogenously-delivered HNE on cell biology, and it remains to be clarified how results of this study correlated with the potential effect of HNE formed endogenously in the cell. It is likely that PSCs were exposed to endogenous HNE during ethanol consumption, because PSCs, in addition to pancreatic acinar cells^[35], had the capacity to metabolize ethanol to acetaldehyde via alcohol dehydrogenase-mediated oxidation of ethanol^[36].

Activated PSCs acquire the proinflammatory phenotype; they may modulate the recruitment and activation of inflammatory cells. We have reported that activated PSCs expressed MCP-1^[29] in response to IL-1 β and tumor necrosis factor- α *in vitro*. Indeed, MCP-1 expression by activated PSCs was shown to be increased in fibrous tissue sections from patients with chronic pancreatitis^[37]. In this study, HNE failed to induce NF- κ B activation and consequent MCP-1 production. The failure of HNE to induce MCP-1 expression is not surprising because the activation of NF- κ B has been shown to play a central role in MCP-1 expression in PSCs^[29]. This is in contrast to human endothelial cells where the AP-1 proteins c-Fos and c-Jun directly induce MCP-1 expression independently of the NF- κ B pathway^[38]. The effects of HNE on the activation of NF- κ B and AP-1 appeared to depend on the types of cells. In a similar manner to PSCs, HNE activated AP-1, but not NF- κ B, in murine and human macrophages^[39] and human hepatic stellate cells^[40]. On the other hand, HNE did not activate AP-1, but did attenuate IL-1 β - and phorbol ester-induced NF- κ B activation in human monocytic THP-1 cells^[41]. The inhibition of NF- κ B activation was mediated through the inhibition of I κ B phosphorylation and subsequent proteolysis^[41]. Recent reviews^[42,43] have emphasized that redox-dependent activation of NF- κ B was cell and stimulus specific as opposed to the concept that oxidative stress was a common mediator of diverse NF- κ B activators. Li and Karin^[42] reported that when a redox-regulated effect on NF- κ B was observed, it appeared to occur downstream from the I κ B kinase, at the level of ubiquitination and/or degradation of I κ B.

In this study, HNE activated three classes of MAP kinases in PSCs. This is in agreement with the previous study showing that HNE activated these three classes of MAP kinases in rat liver epithelial RL34 cells^[14]. In human hepatic stellate cells, Parola *et al.*^[40] reported that HNE formed adducts with the p46 and p54 isoforms of JNK, leading to the nuclear translocation and activation of these signaling molecules, and, in turn, the induction of the transcription factors c-jun and AP-1. Unlike human hepatic stellate cells, we showed that HNE induced phosphorylation of p46 and p54 JNK in rat PSCs. On the other hand, we have shown that activation of ERK played a central role in PDGF-BB-induced proliferation of PSCs^[16]. In spite of the ability to activate ERK, HNE failed to alter the proliferation regardless of the presence or absence of PDGF-BB, suggesting that activation of ERK is required but not sufficient for the proliferation of PSCs. This is in agreement with the concept

that activation of ERK, although necessary, may not be sufficient to justify the mitogenic properties of an agonist^[44].

We here showed that HNE did not initiate the transformation of quiescent PSCs. This is in disagreement with the previous reports showing that ethanol and acetaldehyde activated quiescent PSCs through the generation of oxidative stress^[36]. However, it should be noted that previous studies examining the effects of oxidative stress on the activation of hepatic stellate cells have reported conflicting results. Lee *et al.*^[45] reported that quiescent hepatic stellate cells were activated upon exposure to the pro-oxidant compound ascorbate/ferrous sulfate or the lipid peroxidation product malondialdehyde. Maher *et al.*^[46] reported that stimulatory effects of malondialdehyde only occurred after hepatic stellate cells had been preactivated by culture on plastic. Olynyk *et al.*^[47] reported that malondialdehyde and HNE decreased α -SMA expression in hepatic stellate cells at d 3 when compared to controls not incubated with the compounds. Previous studies have suggested that cytokines and growth factors such as transforming growth factor- β 1 and tumor necrosis factor- α induced the transformation of quiescent PSCs^[48,49]. These mediators were released or produced from inflammatory cells, platelets, and pancreatic acinar cells, during the course of pancreatitis^[48,49], leading to the activation of PSCs. Once activated, PSCs were sensitive to HNE, and showed profibrogenic responses, thus playing a role in the pathogenesis of pancreatic fibrosis.

In agreement with the previous study in human hepatic stellate cells^[40], HNE increased type I collagen production in PSCs. Lee *et al.*^[45] reported that oxidative stress-induced collagen synthesis in hepatic stellate cells was associated with induction of transcription factors NF- κ B and c-myb^[45]. In rat PSCs, the role of NF- κ B was unlikely because HNE failed to activate NF- κ B. Although the molecular mechanisms by which HNE increased type I collagen production in hepatic stellate cells were not further pursued, we have shown that HNE-induced type I collagen production was mediated by the activation of JNK and p38 MAP kinase. Along this line, it has been reported that malondialdehyde increased α 2 (I) collagen gene activity through JNK activation in hepatic stellate cells^[50]. It should be noted that the biological action of HNE may result in multiple effects within the complex network of events occurring in the process of fibrosis following reiterated pancreatic injury, with the resulting overall biological effects being influenced by the actual HNE concentration, the target cell or cells available, and the presence of growth factors and other mediators in the microenvironment. Nevertheless, our findings that HNE induced type I collagen production suggest possible links between oxidant stress, aldehyde-adduct formation, and pancreatic fibrosis. Very recently, it has been reported that HNE acted as a potent pro-fibrogenic stimulus in the expression of genes involved in extracellular matrix deposition in activated hepatic stellate cells^[51]. Indeed, we have found that HNE increased the transcriptional activity of prolyl 4-hydroxylase (α), a key enzyme that catalyzes the formation of 4-hydroxyproline (Satoh *et al.* manuscript in preparation). Elucidation of the functions of PSCs would provide better understanding and rational approaches for the control of pancreatic inflammation and fibrosis.

ACKNOWLEDGEMENT

The authors thank Dr. Naofumi Mukaida for the luciferase vectors.

REFERENCES

- 1 Apte MV, Haber PS, Applegate TL, Norton ID, McCaughan GW, Korsten MA, Pirola RC, Wilson JS. Periacinar stellate

- shaped cells in rat pancreas: identification, isolation, and culture. *Gut* 1998; **43**: 128-133
- 2 **Bachem MG**, Schneider E, Gross H, Weidenbach H, Schmid RM, Menke A, Siech M, Beger H, Grunert A, Adler G. Identification, culture, and characterization of pancreatic stellate cells in rats and humans. *Gastroenterology* 1998; **115**: 421-432
- 3 **Friedman SL**. Molecular regulation of hepatic fibrosis, an integrated cellular response to tissue injury. *J Biol Chem* 2000; **275**: 2247-2250
- 4 **Haber PS**, Keogh GW, Apte MV, Moran CS, Stewart NL, Crawford DH, Pirola RC, McCaughan GW, Ramm GA, Wilson JS. Activation of pancreatic stellate cells in human and experimental pancreatic fibrosis. *Am J Pathol* 1999; **155**: 1087-1095
- 5 **Masamune A**, Sakai Y, Kikuta K, Satoh M, Satoh A, Shimosegawa T. Activated rat pancreatic stellate cells express intercellular adhesion molecule-1 (ICAM-1) *in vitro*. *Pancreas* 2002; **25**: 78-85
- 6 **Masamune A**, Satoh M, Kikuta K, Sakai Y, Satoh A, Shimosegawa T. Inhibition of p38 mitogen-activated protein kinase blocks activation of rat pancreatic stellate cells. *J Pharmacol Exp Ther* 2003; **304**: 8-14
- 7 **Masamune A**, Kikuta K, Satoh M, Satoh K, Shimosegawa T. Rho kinase inhibitors block activation of pancreatic stellate cells. *Br J Pharmacol* 2003; **140**: 1292-1302
- 8 **Sanfey H**, Bulkley GB, Cameron JL. The pathogenesis of acute pancreatitis. The source and role of oxygen-derived free radicals in three different experimental models. *Ann Surg* 1985; **201**: 633-639
- 9 **Braganza JM**. The pathogenesis of chronic pancreatitis. *QJM* 1996; **89**: 243-250
- 10 **Droge W**. Free radicals in the physiological control of cell function. *Physiol Rev* 2002; **82**: 47-95
- 11 **Hensley K**, Robinson KA, Gabbita SP, Salsman S, Floyd RA. Reactive oxygen species, cell signaling, and cell injury. *Free Radic Biol Med* 2000; **28**: 1456-1462
- 12 **Uchida K**. 4-Hydroxy-2-nonenal: a product and mediator of oxidative stress. *Prog Lipid Res* 2003; **42**: 318-343
- 13 **Esterbauer H**, Schaur RJ, Zollner H. Chemistry and biochemistry of 4-hydroxynonenal, malonaldehyde and related aldehydes. *Free Rad Biol Med* 1991; **11**: 81-128
- 14 **Uchida K**, Shiraiishi M, Naito Y, Torii Y, Nakamura Y, Osawa T. Activation of stress signaling pathways by the end product of lipid peroxidation. 4-hydroxy-2-nonenal is a potential inducer of intracellular peroxide production. *J Biol Chem* 1999; **274**: 2234-2242
- 15 **Casini A**, Galli A, Pignatola P, Frulloni L, Grappone C, Milani S, Pederzoli P, Cavallini G, Surrenti C. Collagen type I synthesized by pancreatic periacinar stellate cells (PSC) co-localizes with lipid peroxidation-derived aldehydes in chronic alcoholic pancreatitis. *J Pathol* 2000; **192**: 81-89
- 16 **Masamune A**, Kikuta K, Satoh M, Kume K, Shimosegawa T. Differential roles of signaling pathways for proliferation and migration of rat pancreatic stellate cells. *Tohoku J Exp Med* 2003; **199**: 69-84
- 17 **Mosmann T**. Rapid colorimetric assay for cellular growth and survival: application to proliferation and cytotoxicity assays. *J Immunol Methods* 1983; **65**: 55-63
- 18 **Porstmann T**, Ternynck T, Avrameas S. Quantitation of 5-bromo-2-deoxyuridine incorporation into DNA: an enzyme immunoassay for the assessment of the lymphoid cell proliferative response. *J Immunol Methods* 1985; **82**: 169-179
- 19 **Masamune A**, Igarashi Y, Hakomori S. Regulatory role of ceramide in interleukin(IL)-1 beta-induced E-selectin expression in human umbilical vein endothelial cells. Ceramide enhances IL-1 beta action, but is not sufficient for E-selectin expression. *J Biol Chem* 1996; **271**: 9368-9375
- 20 **Masamune A**, Shimosegawa T, Masamune O, Mukaida N, Koizumi M, Toyota T. *Helicobacter pylori*-dependent ceramide production may mediate increased interleukin 8 expression in human gastric cancer cell lines. *Gastroenterology* 1999; **116**: 1330-1341
- 21 **Masamune A**, Satoh K, Sakai Y, Yoshida M, Satoh A, Shimosegawa T. Ligands of peroxisome proliferator-activated receptor-gamma induce apoptosis in AR42J cells. *Pancreas* 2002; **24**: 130-138
- 22 **Moshage H**, Casini A, Lieber CS. Acetaldehyde selectively stimulates collagen production in cultured rat liver fat-storing cells but not in hepatocytes. *Hepatology* 1990; **12**(3 Pt1): 511-518
- 23 **Brunk CF**, Jones KC, James TW. Assay for nanogram quantities of DNA in cellular homogenates. *Anal Biochem* 1979; **92**: 497-500
- 24 **Masamune A**, Satoh M, Kikuta K, Suzuki N, Shimosegawa T. Establishment and characterization of a rat pancreatic stellate cell line by spontaneous immortalization. *World J Gastroenterol* 2003; **9**: 2751-2758
- 25 **Kruman I**, Bruce-Keller AJ, Bredesen D, Waeg G, Mattson MP. Evidence that 4-hydroxynonenal mediates oxidative stress-induced neuronal apoptosis. *J Neurosci* 1997; **17**: 5089-5100
- 26 **Grilli M**, Chiu JJ, Lenardo MJ. NF-kappa B and Rel: participants in a multifunctional transcriptional regulatory system. *Int Rev Cytol* 1993; **143**: 1-62
- 27 **Karin M**, Liu Z, Zandi E. AP-1 function and regulation. *Curr Opin Cell Biol* 1997; **9**: 240-246
- 28 **Robinson MJ**, Cobb MH. Mitogen-activated protein kinase pathways. *Curr Opin Cell Biol* 1997; **9**: 180-186
- 29 **Masamune A**, Kikuta K, Satoh M, Sakai Y, Satoh A, Shimosegawa T. Ligands of peroxisome proliferator-activated receptor-gamma block activation of pancreatic stellate cells. *J Biol Chem* 2002; **277**: 141-147
- 30 **Masamune A**, Kikuta K, Satoh M, Satoh A, Shimosegawa T. Alcohol activates activator protein-1 and mitogen-activated protein kinases in rat pancreatic stellate cells. *J Pharmacol Exp Ther* 2002; **302**: 36-42
- 31 **Cuenda A**, Rouse J, Doza YN, Meier R, Cohen P, Gallagher TF, Young PR, Lee JC. SB 203580 is a specific inhibitor of a MAP kinase homologue which is stimulated by cellular stresses and interleukin-1. *FEBS Lett* 1995; **364**: 229-233
- 32 **Bennett BL**, Sasaki DT, Murray BW, O'Leary EC, Sakata ST, Xu W, Leisten JC, Motiwala A, Pierce S, Satoh Y, Bhagwat SS, Manning AM, Anderson DW. SP600125, an anthrapyrazolone inhibitor of Jun N-terminal kinase. *Proc Natl Acad Sci U S A* 2001; **98**: 13681-13686
- 33 **Favata MF**, Horiuchi KY, Manos EJ, Daulerio AJ, Stradley DA, Feese WS, Van Dyk DE, Pitts WJ, Earl RA, Hobbs F, Copeland RA, Magolda RL, Scherle PA, Trzaskos JM. Identification of a novel inhibitor of mitogen-activated protein kinase kinase. *J Biol Chem* 1998; **273**: 18623-18632
- 34 **McKim SE**, Uesugi T, Raleigh JA, McClain CJ, Arteel GE. Chronic intragastric alcohol exposure causes hypoxia and oxidative stress in the rat pancreas. *Arch Biochem Biophys* 2003; **417**: 34-43
- 35 **Haber PS**, Apte MV, Applegate TL, Norton ID, Korsten MA, Pirola RC, Wilson JS. Metabolism of ethanol by rat pancreatic acinar cells. *J Lab Clin Med* 1998; **132**: 294-302
- 36 **Apte MV**, Phillips PA, Fahmy RG, Darby SJ, Rodgers SC, McCaughan GW, Korsten MA, Pirola RC, Naidoo D, Wilson JS. Does alcohol directly stimulate pancreatic fibrogenesis? Studies with rat pancreatic stellate cells. *Gastroenterology* 2000; **118**: 780-794
- 37 **Saurer L**, Reber P, Schaffner T, Buchler MW, Buri C, Kappeler A, Walz A, Freiss H, Mueller C. Differential expression of chemokines in normal pancreas and in chronic pancreatitis. *Gastroenterology* 2000; **118**: 356-367
- 38 **Wang N**, Verna L, Hardy S, Forsayeth J, Zhu Y, Stemberman MB. Adenovirus-mediated overexpression of c-Jun and c-Fos induces intercellular adhesion molecule-1 and monocyte chemoattractant protein-1 in human endothelial cells. *Arterioscler Thromb Vasc Biol* 1999; **19**: 2078-2084
- 39 **Camandola S**, Scavazza A, Leonarduzzi G, Biasi F, Chiarpotto E, Azzi A, Poli G. Biogenic 4-hydroxy-2-nonenal activates transcription factor AP-1 but not NF-kappa B in cells of the macrophage lineage. *Biofactors* 1997; **6**: 173-179
- 40 **Parola M**, Robino G, Marra F, Pinzani M, Bellomo G, Leonarduzzi G, Chiarugi P, Camandola S, Poli G, Waeg G, Gentilini P, Dianzani MU. HNE interacts directly with JNK isoforms in human hepatic stellate cells. *J Clin Invest* 1998; **102**:

- 1942-1950
- 41 **Page S**, Fischer C, Baumgartner B, Haas M, Kreusel U, Loidl G, Hayn M, Ziegler-Heitbrock HW, Neumeier D, Brand K. 4-Hydroxynonenal prevents NF-kappaB activation and tumor necrosis factor expression by inhibiting IkappaB phosphorylation and subsequent proteolysis. *J Biol Chem* 1999; **274**: 11611-11618
- 42 **Li N**, Karin M. Is NF-kappaB the sensor of oxidative stress? *FASEB J* 1999; **13**: 1137-1143
- 43 **Bowie A**, O'Neill LA. Oxidative stress and nuclear factor-kappaB activation: a reassessment of the evidence in the light of recent discoveries. *Biochem Pharmacol* 2000; **59**: 13-23
- 44 **Blenis J**. Signal transduction via the MAP kinases: proceed at your own RSK. *Proc Natl Acad Sci U S A* 1993; **90**: 5889-5892
- 45 **Lee KS**, Buck M, Houglum K, Chojkier M. Activation of hepatic stellate cells by TGF alpha and collagen type I is mediated by oxidative stress through c-myb expression. *J Clin Invest* 1995; **96**: 2461-2468
- 46 **Maher JJ**, Tzagarakis C, Gimenez A. Malondialdehyde stimulates collagen production by hepatic lipocytes only upon activation in primary culture. *Alcohol Alcohol* 1994; **29**: 605-610
- 47 **Olynyk JK**, Khan NA, Ramm GA, Brown KE, O'Neill R, Britton RS, Bacon BR. Aldehydic products of lipid peroxidation do not directly activate rat hepatic stellate cells. *J Gastroenterol Hepatol* 2002; **17**: 785-790
- 48 **Apte MV**, Haber PS, Darby SJ, Rodgers SC, McCaughan GW, Korsten MA, Pirola RC, Wilson JS. Pancreatic stellate cells are activated by proinflammatory cytokines: implications for pancreatic fibrogenesis. *Gut* 1999; **44**: 534-541
- 49 **Schneider E**, Schmid-Kotsas A, Zhao J, Weidenbach H, Schmid RM, Menke A, Adler G, Waltenberger J, Grunert A, Bachem MG. Identification of mediators stimulating proliferation and matrix synthesis of rat pancreatic stellate cells. *Am J Physiol Cell Physiol* 2001; **281**: C532-C543
- 50 **Anania FA**, Womack L, Jiang M, Saxena NK. Aldehydes potentiate alpha(2)(I) collagen gene activity by JNK in hepatic stellate cells. *Free Radic Biol Med* 2001; **30**: 846-857
- 51 **Zamara E**, Novo E, Marra F, Gentilini A, Romanelli RG, Caligiuri A, Robino G, Tamagno E, Aragno M, Danni O, Autelli R, Colombatto S, Dianzani MU, Pinzani M, Parola M. 4-Hydroxynonenal as a selective pro-fibrogenic stimulus for activated human hepatic stellate cells. *J Hepatol* 2004; **40**: 60-68

Edited by Zhu LH and Xu FM

Structure prediction and activity analysis of human heme oxygenase-1 and its mutant

Zhen-Wei Xia, Wen-Pu Zhou, Wen-Jun Cui, Xue-Hong Zhang, Qing-Xiang Shen, Yun-Zhu Li, Shan-Chang Yu

Zhen-Wei Xia, Yun-Zhu Li, Shan-Chang Yu, Department of Pediatrics, Rui Jin Hospital, Shanghai Second Medical University, Shanghai 200025, China

Wen-Pu Zhou, Wen-Jun Cui, Xue-Hong Zhang, College of Life Science and Biotechnology, Shanghai Jiaotong University & Chinese Academy of Sciences, Shanghai Branch, Shanghai 200030, China

Qing-Xiang Shen, Shanghai Institute of Planned Parenthood Research, Shanghai 200032, China

Supported by the National Natural Science Foundation of China, No. 30170988, Shanghai Municipal Education Commission Foundation, No.2000B06, and Shanghai Jiaotong University-Shanghai Second Medical University Cooperative Foundation

Correspondence to: Dr. Xia Zhen Wei, Department of Pediatrics, Rui Jin Hospital, Shanghai Second Medical University, 197 Rui Jin Er Road, Shanghai 200025, China. xzw63@hotmail.com

Telephone: +86-21-64333414 **Fax:** +86-21-64333414

Received: 2004-01-02 **Accepted:** 2004-02-03

Abstract

AIM: To predict wild human heme oxygenase-1 (whHO-1) and hHO-1 His25Ala mutant (Δ hHO-1) structures, to clone and express them and analyze their activities.

METHODS: Swiss-PdbViewer and Antheptot 5.0 were used for the prediction of structure diversity and physical-chemical changes between wild and mutant hHO-1. hHO-1 His25Ala mutant cDNA was constructed by site-directed mutagenesis in two plasmids of *E. coli* DH5 α . Expression products were purified by ammonium sulphate precipitation and Q-Sepharose Fast Flow column chromatography, and their activities were measured.

RESULTS: rHO-1 had the structure of a helical fold with the heme sandwiched between heme-heme oxygenase-1 helices. Bond angle, dihedral angle and chemical bond in the active pocket changed after Ala25 was replaced by His25, but Ala25 was still contacting the surface and the electrostatic potential of the active pocket was negative. The mutated enzyme kept binding activity to heme. Two vectors pBHO-1 and pBHO-1(M) were constructed and expressed. Ammonium sulphate precipitation and column chromatography yielded 3.6-fold and 30-fold higher purities of whHO-1, respectively. The activity of Δ hHO-1 was reduced 91.21% after mutation compared with whHO-1.

CONCLUSION: Proximal His25 ligand is crucial for normal hHO-1 catalytic activity. Δ hHO-1 is deactivated by mutation but keeps the same binding site as whHO-1. Δ hHO-1 might be a potential inhibitor of whHO-1 for preventing neonatal hyperbilirubinemia.

Xia ZW, Zhou WP, Cui WJ, Zhang XH, Shen QX, Li YZ, Yu SC. Structure prediction and activity analysis of human heme oxygenase-1 and its mutant. *World J Gastroenterol* 2004; 10(16): 2352-2356

<http://www.wjgnet.com/1007-9327/10/2352.asp>

INTRODUCTION

Heme oxygenase (HO) is responsible for the physiological breakdown of heme into equimolar amounts of biliverdin, carbon monoxide, and iron. Three isoforms (HO-1, HO-2, and HO-3) have been identified. HO-1 is ubiquitous, its mRNA levels and activity can be increased several-fold by heme, other metalloporphyrins, transition metals, and stress-inducing stimuli. In contrast, HO-2 is present chiefly in brain and testes and is virtually uninducible. HO-3 has very low activity; its physiological functions probably include heme binding. The HO system has been strongly highlighted for its potential significance in maintaining cellular homeostasis. Nevertheless the physiological correlations of the three isoforms and their reciprocal interrelation have been poorly understood^[1-4].

HO-1 regulates the levels of serum bilirubin as the rate-limiting enzyme in heme degradation pathway. Recent reports showed that HO-1 was identified as an ubiquitous stress protein and it had important physiological roles. Overexpression of HO-1 gene resulted in protection from cytokine-induced oxidative stress^[5], inflammation^[6-9], apoptosis^[10-17] and proliferation^[18-25].

It has been reported that histidine (His) residues at positions 25, 84, 119 and 132 in HO-1 sequence are conserved in rat, human, mouse and chicken. These histidines may be important for heme-binding^[26]. His25 and His132 mutants were reported for the proximal heme iron ligand in rat heme oxygenase-1 (rHO-1)^[27]. The unambiguous spectroscopic demonstration that His25 is the proximal iron ligand leaves the role of His132 uncertain. His 25 is essential for heme degradation activity of the enzyme. The research on human HO-1 (hHO-1) structure has been shown that hHO-1 embodies a novel protein fold that consists primarily of α -helices, and the heme is held between two of these helices^[28].

It is unclear whether hHO-1 mutant has the same characteristics and displays catalytic inactivity but binding heme as Ala replacing His 25. In this study, the characteristics of wild hHO-1 (whHO-1) and its mutant were predicted by bioinformatics method. On the basis of the results, the truncated hHO-1 cDNA mutant was constructed by site-directed mutagenesis. Two expression plasmids, pBHO-1 and pBHO-1 (M) containing whHO-1 and hHO-1 His25Ala mutant (Δ hHO-1), respectively, were constructed and expressed in *E. coli*, and then isolated, purified and analyzed of their activities analysis.

MATERIALS AND METHODS

Materials

Swiss-PdbViewer and Antheptot 5.0 were from GlaxoSmithKline R&D and the Swiss Institute of Bioinformatics and CBI, BeiJin University respectively. Plasmid pBHO-1 was provided by Lightning and Ortiz de Montellano (Department of Pharmaceutical Chemistry, University of California). Mutation primer was synthesized by Boya Company. Anti-HO-1 antibody, RNase and DNase were purchased from Sigma. Restriction endonucleases were from Haojia Company, Q-Sepharose Fast Flow Anion exchange column was from Amersham Pharmacia. pBS II KS⁺/-, pGEM3Z and *E. coli* strain DH5 α were stored in author's laboratory.

Methods

Structure analysis of hHO-1 and its mutant Swiss-PdbViewer and Antheprot 5.0 were used to analyze the structure diversity and physical-chemical changes between whHO-1 and Δ hHO-1. Then the prime structure was refined by energy minimization. Gromos96 was used as force field. The molecular surfaces and electrostatic potential were calculated. The rationality of the resulted model was validated by Ramachandran plot.

Construction of Δ hHO-1 expression vector pBHO-1 (M) *EcoRI/SalI* digested fragment of pBHO-1, which is from expression vector containing the truncated hHO-1 cDNA (804 bp), was cloned into the *EcoRI/SalI* sites of plasmid pBSKS II to construct plasmid pBSHO-1. hHO-1 His25Ala mutant cDNA could be amplified by PCR using pBSHO-1 as template. The mutation primer (5'-GACAGCATGCCCCAGGATTTGTCAGAGGCCCTGAAGGAGGCCACCAAGGAGGTGGCCACCC-3') and reverse primer (5'-AACAGCTATGACCATG-3') were chosen, which have changed the His 25 codon CAC into Ala codon GCC. The reaction conditions were: at 94 °C for 5 min, followed by 94 °C for 1 min, at 55 °C for 1 min, 72 °C for 2 min, with amplification repeated for 30 cycles, and finally at 72 °C for 10 min. The mutant cDNA was gel-purified and digested with *SphI/SalI* and then cloned into *SphI/SalI* sites of plasmid pGEM3Z. hHO-1 His25Ala mutant cDNA was screened by restriction digestion and confirmed by sequencing in pGEM3ZHO-1(M). Verified hHO-1 mutant cDNA was obtained from *SphI/SalI* digested fragment of pGEM3ZHO-1 (M) and then cloned into pBHO-1, thus the expression vector containing Δ hHO-1 was designated as pBHO-1 (M) (Figure 1).

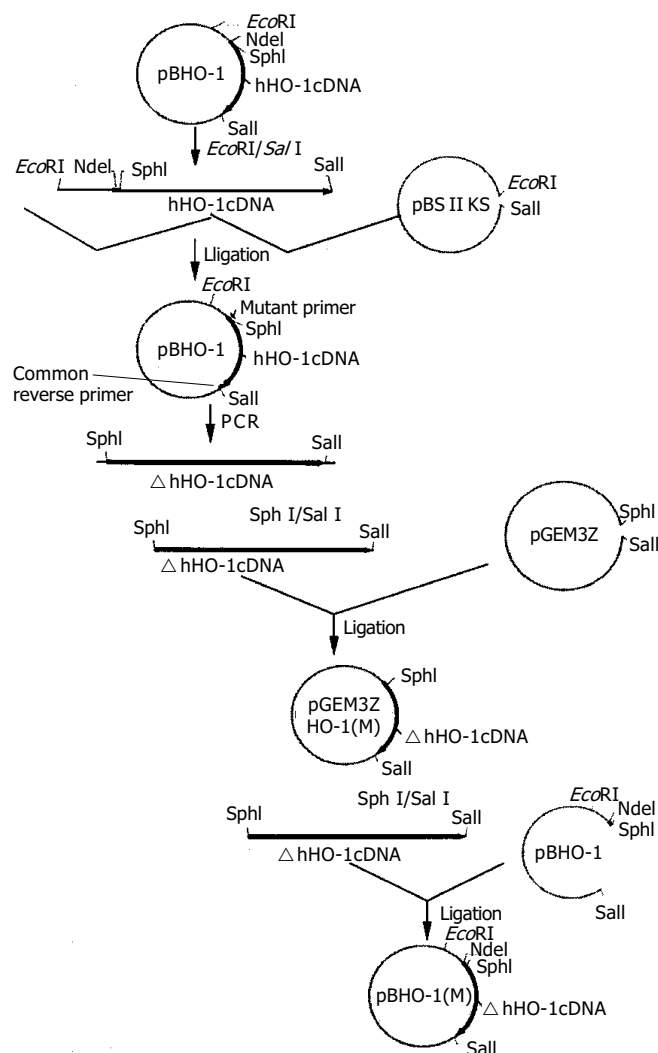


Figure 1 Construction of expression vector pBHO-1(M).

Expression and purification of whHO-1 and Δ hHO-1 A total of 5.0 mL inoculum was set up from plates with fresh colonies of transformed *E. coli* DH5 α and incubated at 37 °C for 12-16 h. From the fresh cultures 400 μ L was used to inoculate into 40 mL cultures of the same media. The cells were grown at 37 °C until A_{600} reached 0.3-0.5, then added with 0.5 mmol/L IPTG for 18 h. The expression products were harvested and analyzed with sodium dodecyl sulfate-polyacrylamide gel (SDS-PAGE) and Western blotting at the time points of 7, 9 and 11 h, respectively, after addition of IPTG. Then 500 mL inoculum in medium was incubated under same condition. The harvested cells were centrifuged at 6 000 r/min for 20 min at 4 °C, washed once in PBS, and then centrifuged at 6 000 r/min for 10 min at 4 °C. The cells were lysed in 50 mmol/L Tris buffer (pH 8.0) containing 1 mmol/L dithiothreitol, 1 mmol/L EDTA, 1 mmol/L phenylmethanesulfonyl fluoride (PMSF) and sonicated for 10 min. Then the cells were centrifuged at 13 000 r/min for 1 h at 4 °C. The supernatant was collected and ammonium sulfate was added to a final concentration of 30%, and the solution was stirred for 60 min. Following centrifugation (13 000 r/min for 20 min), ammonium sulfate concentration was raised to 60% of saturation. The pellets precipitated by ammonium sulfate were collected and resuspended in 0.1 mol/L potassium phosphate (pH 7.4) and then dialyzed against 1 g/L NH_4HCO_3 for 4 h ($\times 4$ -times). Protein 130 mg was applied to a Q-Sepharose Fast Flow anion column and eluted with a step gradient of 50 mmol/L Tris-HCl (pH 7.4) (buffer A) containing 0-0.5 mol/L NaCl (buffer B). The fractions containing hHO-1 protein were pooled together and applied to Q-Sepharose Fast Flow anion column again. The protein was eluted with a step gradient of 50 mmol/L Tris-HCl (pH 8.4) (buffer C) containing 0-0.5 mol/L NaCl (buffer B). The gradient was increased linearly from 0-100% buffer B. Fractions containing hHO-1 protein were pooled and dialyzed against 1 g/L NH_4HCO_3 for 4 h ($\times 4$ -times).

Western blotting Blot analysis was carried out as previously described^[29]. Microsomal protein samples were fractionated by SDS-PAGE under denaturing conditions. The separated proteins were electrophoretically transferred to a nitrocellulose membrane. Western blotting was carried out using monoclonal antibody to hHO-1 and the immunoreactive bands were visualized by staining (1 mol/L Tris-HCl pH 9.5, 1 mol/L MgCl_2 , 0.1 mg/mL nitro-blue tetrazolium, 0.1 mg/mL 5-bromo-4-chloro-3-indolylphosphate-toluidine salt).

Analysis of whHO-1 and Δ hHO-1 activities Protein samples were incubated with heme (50 μ mol/L), rat liver cytosol (5 mg/mL), MgCl_2 (2 mmol/L), glucose-6-phosphate dehydrogenase (1 unit), glucose-6-phosphate (2 mmol/L), and NADPH (0.8 mmol/L) in 0.5 mL of 0.1 mol/L potassium phosphate buffer (pH 7.4), for 60 min at 37 °C. Reaction was stopped by putting the tubes on ice, and reaction solution was extracted with chloroform. The rate of bilirubin formation was monitored at 464 nm by a spectrophotometer and then calculated using an extinction coefficient of 40.0 $\text{mmol}/(\text{L}\cdot\text{cm})$ ^[29].

RESULTS

Whole structure comparison between whHO-1 and Δ hHO-1

In heme-heme oxygenase-1 complex, heme is sandwiched in whHO-1. When Ala 25 replaces His 25, the complex structure does not change. In the heme-binding pocket, Ala 25 loses contacting with heme as His 25 does. The molecular surface has a catalytic reaction pocket, which includes Thr 21, His 25, Ala 28, Glu 29, Gly 139, Asp140, Gly 143. After binding heme, His 25 still lies on the surface but Gly139, Asp140 and Gly143 are covered by heme. When Ala 25 replaces His 25, Ala 25 still lies in the surface (Figure 2). In activity domain, the bond angle, dihedral angle and chemical bond appear differently after Ala 25 replacing His 25 (Table 1, Figure 3).

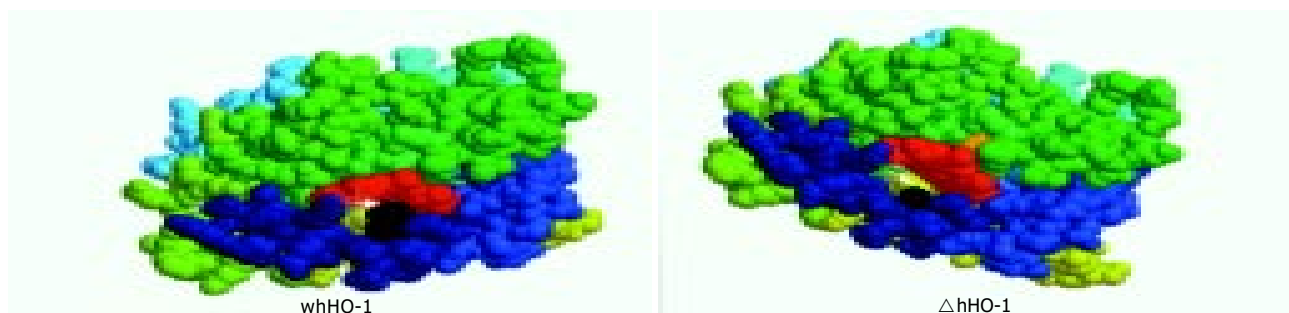


Figure 2 Prime simulated structure of whHO-1 and Δ hHO-1. Red: heme; Black: His 25 and Ala 25. Ala 25 loses contacting with heme as His 25 does in the heme-binding pocket.



Figure 3 Changes of bond angle, dihedral angle and chemical bond.



Figure 4 Molecular surfaces and electrostatic potential of whHO-1 and Δ hHO-1. The electrostatic potential of active pocket is -1.800 .

Table 1 Bond angle, dihedral angle and the distance between atoms of Δ hHO-1

		Prime simulation	Optimized simulation
Bond angle	C24-N-CA	119.12	121.79
	CA-C-N26	115.92	115.12
Distance between atoms	CB-FE	5.55	5.58
	CA-FE	6.28	6.26
Dihedral angle	ω	175.40	175.61
	ϕ	-40.78	-34.45
	ψ	-60.70	-62.89

Though Ala 25 replaces His 25, the molecular surfaces and electrostatic potential changed little (Figure 4). The electrostatic potential of active pocket was still negative. The mutagenesis had no apparent effect on molecular surface. Ramachandran plot showed that dihedral angles ϕ (-33.98) and ψ (-64.46) were in rational range.

Antheprot 5.0 analysis also showed that there was no alteration in the secondary structure between whHO-1 and Δ hHO-1. Garnier, Gibrat, DPM and homology predicted the same results. Physical-chemical characteristics showed somewhat alteration. Hydrophobicity increased, while hydrophilicity decreased. There was no change in antigenicity, helical membranous regions and solvent accessibility.

Construction of pBHO-1(M) containing Δ hHO-1

hHO-1 cDNA was site mutated at His 25 (to Ala) by PCR with pBSHO-1 as the template. The 866-bp PCR product showed that nucleotide 3-773 sequences encoded hHO-1 domain from 25-265 AA. The mutant cDNA was cloned into the *SphI/SalI* sites of plasmid pGEM3Z for constructing plasmid pGEM3ZHO-1 (M). hHO-1 His25Ala mutant cDNA was confirmed by sequencing in pGEM3ZHO-1 (M). The verified hHO-1 mutant cDNA from the *SphI/SalI* digested fragment of pGEM3ZHO-1 (M) was cloned into pBHO-1, thus the expression vector containing Δ hHO-1 was designated as pBHO-1 (M) (Figure 1). Both whHO-1 and Δ hHO-1 cDNAs equally encoded the proteins containing 265 amino acids with a M_r 30 500.

Expression and identification of whHO-1 and Δ hHO-1 in *E. coli* DH5 α

E. coli DH5 α was transformed by pBHO-1 and pBHO-1 (M), respectively, and treated with 0.5 mmol/L IPTG for 18 h at 37 °C. Equal quantities of cells transformed with different expression vectors were lysed by protein electrophoresis buffer. Untransformed *E. coli* sample was used as the negative control. As shown in Figure 5, *E. coli* DH5 α transformed pBHO-1 or pBHO-1 (M) highly expressed whHO-1 and Δ hHO-1 with a M_r 30 500. Meanwhile, *E. coli* DH5 α not treated with IPTG also expressed whHO-1 and Δ hHO-1, but its expression yield

was significantly lower than that of transformed cells. Analysis of cell lysates showed that whHO-1 and Δ hHO-1 were mainly present in the supernatants.

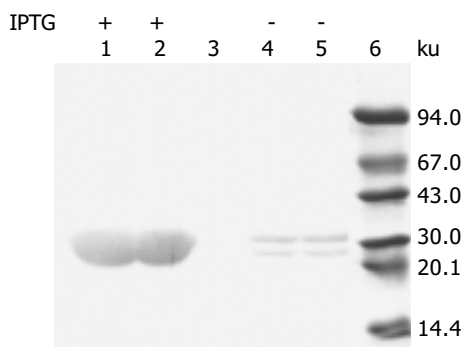


Figure 5 Western blotting of whHO-1 and Δ hHO-1 expressed in DH5 α . Lanes 1, 2: Expression products of pBHO-1 and pBHO-1(M) in DH5 α induced with IPTG; lane 3: Control; lanes 4, 5: Expression products of pBHO-1 and pBHO-1(M) in DH5 α not treated with IPTG; lane 6: Marker.

Purification of whHO-1 and Δ hHO-1

The protein with a M_r 30 500 was purified by 30-60% ammonium sulphate precipitation and analyzed by SDS-PAGE.

After precipitated with ammonium sulphate, whHO-1 sample was applied to Q-Sepharose Fast Flow anion column (pH 7.4). The first peak containing whHO-1 (No. 1-3 tubes) was collected (Figure 6A) and loaded on Q-Sepharose Fast Flow anion column (pH 8.4) again. whHO-1 was shown to be eluted in the second peak (No. 49-63 tubes) (Figure 6B). All samples were analyzed by SDS-PAGE and Western blotting in order to identify the separation efficiency. The activity of whHO-1 after purification was 30-fold higher than that in the initial lysates (Table 2).

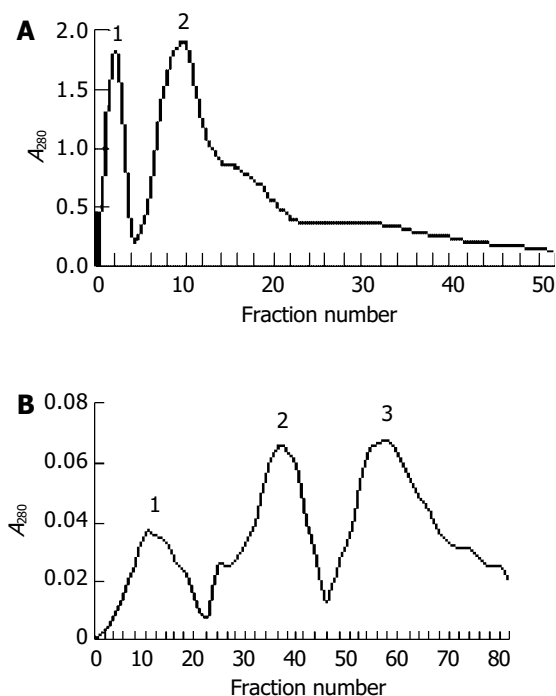


Figure 6 Q-Sepharose Fast Flow column chromatography. A: pH 7.4 buffer; B: pH 8.4 buffer.

Precipitated Δ hHO-1 was further purified in the same way as described above. One purified protein's M_r was 30 500. The purified whHO-1 and Δ hHO-1 are shown on SDS-PAGE (Figure 7).

Table 2 whHO-1 activities after different purification

	Supernatant of DH5 α lysates	30-60% (NH ₄) ₂ SO ₄	Q-Sepharose fast flow
whHO-1 activity (U·mg ⁻¹ ·h ⁻¹)	0.5	1.8	15
Purification fold	1.0	3.6	30

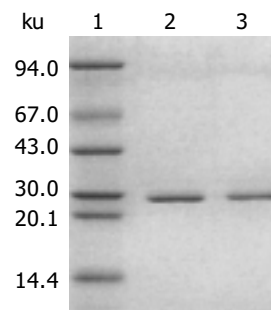


Figure 7 SDS-PAGE analysis of purified whHO-1 and Δ hHO-1. Lane 1: Marker; lane 2: whHO-1; lane 3: Δ hHO-1.

DISCUSSION

An understanding of the structure and function of hHO-1 is of importance in the context of human diseases, but due to limited accessibility and difficulties associated with their purification from microsomal membranes, little direct information has been available until the expression of rHO-1 in *E. coli* was achieved. The protein thus obtained is soluble, easily purified, and fully active. Encouraged by this result, the research on HO-1 including hHO-1 has been thriving.

hHO-1 is anchored to the endoplasmic reticulum membrane via a stretch of hydrophobic residues at the C-terminus. While full-length hHO-1 consists of 288 residues, a truncated version with residues 1-265 has been expressed as a soluble active enzyme in *E. coli*. This recombinant enzyme precipitated from ammonium sulfate solution but without a high purity for studies^[30].

In the present studies, we acquired the structures of hHO-1 with residues 1-265 and its mutant using Swiss-PdbViewer. Due to the high similarity between hHO-1 and its mutant, the hHO-1 structure was used as template. Through homology modeling, template selection and target-template alignment, a molecular backbone and side chains were built in one step. Results demonstrated that the refined model, as well as the entire assay, was valid. Predictions of the structure showed that hHO-1 and its mutant had similar electrostatic potential suggesting that they have similar affinity to heme in electrostatic potential. Ala is a hydrophobic amino acid without chemical activity, and its side chain is short. So it has no interference with binding through steric hindrance.

Rat His25Ala HO-1 provides a new approach to construct hHO-1 mutant. hHO-1 mutants were prepared in which residue His25 was replaced by Ala using site-directed mutagenesis to understand the role of hHO-1 His25 in keeping the activity of this enzyme. In this study, the synthesized forward primer was applied in which His25 codon was replaced by the Ala codon. This cDNA was cloned into the expression vector pBHO-1, then pBHO-1 and pBHO-1(M) were transformed into *E. coli*, which were used to express whHO-1 and Δ hHO-1. Although the endogenous protein expression of *E. coli* could disturb the measurement of whHO-1 and its mutants by SDS-PAGE, hHO-1 and its mutant expression could be detected by anti-HO-1 antibody in Western blotting.

Our study shows that precipitation with ammonium sulfate can enrich whHO-1 and Δ hHO-1 in the lysates. Compared with the whHO-1 activity, Δ hHO-1 activity was reduced by

91.21%. It suggests that His25 is crucial for the catalytic activity of hHO-1, the proximal His25 ligand is critically required for normal hHO-1 catalysis. The results are similar to previous reports^[31-35].

hHO-1 has anti-inflammatory^[6-9], antiapoptotic^[10-17], and antiproliferative^[18-25] effects, and salutary effects on neonatal hyperbilirubinemia^[36]. The results show a valid way to control the concentration of bilirubin in human, since hHO-1 is the rate-limiting enzyme in the catabolic reaction of heme, which ultimately produces bilirubin in human body. High-level bilirubin in newborns, patients with the Crigler-Najjar type I syndrome and certain hepatic disorders can result in hyperbilirubinemia, especially in patients whose bilirubin is impaired for developmental or genetic reasons. Currently clinical methods are only to eliminate formed bilirubin. There is no effective way to inhibit bilirubin production, and Δ hHO-1 would be a potential inhibitor for bilirubin production.

REFERENCES

- 1 Elbirt KK, Bonkovsky HL. Heme oxygenase: recent advances in understanding its regulation and role. *Proc Assoc Am Physicians* 1999; **111**: 438-447
- 2 Scapagnini G, D'Agata V, Calabrese V, Pascale A, Colombrita C, Alkon D, Cavallaro S. Gene expression profiles of heme oxygenase isoforms in the rat brain. *Brain Res* 2002; **954**: 51-59
- 3 Montellano PR. The mechanism of heme oxygenase. *Curr Opin Chem Biol* 2000; **4**: 221-227
- 4 Chu GC, Katakura K, Zhang X, Yoshida T, Ikeda-Saito M. Heme degradation as catalyzed by a recombinant bacterial heme oxygenase (Hmu O) from *Corynebacterium diphtheriae*. *J Biol Chem* 1999; **274**: 21319-21325
- 5 Immenschuh S, Ramadori G. Gene regulation of heme oxygenase-1 as a therapeutic target. *Biochem Pharmacol* 2000; **60**: 1121-1128
- 6 Kushida T, Li Volti G, Quan S, Goodman A, Abraham NG. Role of human heme oxygenase-1 in attenuating TNF-alpha-mediated inflammation injury in endothelial cells. *J Cell Biochem* 2002; **87**: 377-385
- 7 Alcaraz MJ, Fernandez P, Guillen MI. Anti-inflammatory actions of the heme oxygenase-1 pathway. *Curr Pharm Des* 2003; **9**: 2541-2551
- 8 Wagener FA, van Beurden HE, von den Hoff JW, Adema GJ, Figdor CG. The heme-heme oxygenase system: a molecular switch in wound healing. *Blood* 2003; **102**: 521-528
- 9 Chok Mk, Senechal M, Dorent R, Mallat Z, Leprince P, Bonnet N, Pavie A, Ghossoub JJ, Gandjbakhch I. Apoptosis and expression of heme oxygenase-1 in heart transplant recipients during acute rejection episodes. *Transplant Proc* 2002; **34**: 3239-3240
- 10 Rothfuss A, Speit G. Overexpression of heme oxygenase-1 (HO-1) in V79 cells results in increased resistance to hyperbaric oxygen (HBO)-induced DNA damage. *Environ Mol Mutagen* 2002; **40**: 258-265
- 11 Takata K, Kitamura Y, Kakimura J, Shibagaki K, Taniguchi T, Gebicke-Haerter PJ, Smith MA, Perry G, Shimohama S. Possible protective mechanisms of heme oxygenase-1 in the brain. *Ann N Y Acad Sci* 2002; **977**: 501-506
- 12 Katori M, Busuttil RW, Kupiec-Weglinski JW. Heme oxygenase-1 system in organ transplantation. *Transplantation* 2002; **74**: 905-912
- 13 Cornelussen RN, Knowlton AA. Heme-oxygenase-1: versatile sentinel against injury. *J Mol Cell Cardiol* 2002; **34**: 1297-1300
- 14 Ke B, Shen XD, Zhai Y, Gao F, Busuttil RW, Volk HD, Kupiec-Weglinski JW. Heme oxygenase 1 mediates the immunomodulatory and antiapoptotic effects of interleukin 13 gene therapy *in vivo* and *in vitro*. *Hum Gene Ther* 2002; **13**: 1845-1857
- 15 Abraham NG, Kushida T, McClung J, Weiss M, Quan S, Lafaro R, Darzynkiewicz Z, Wolin M. Heme oxygenase-1 attenuates glucose-mediated cell growth arrest and apoptosis in human microvessel endothelial cells. *Circ Res* 2003; **93**: 507-514
- 16 Colombrita C, Lombardo G, Scapagnini G, Abraham NG. Heme oxygenase-1 expression levels are cell cycle dependent. *Biochem Biophys Res Commun* 2003; **308**: 1001-1008
- 17 Pandya HC, Snetkov VA, Twort CH, Ward JP, Hirst SJ. Oxygen regulates mitogen-stimulated proliferation of fetal human airway smooth muscle cells. *Am J Physiol Lung Cell Mol Physiol* 2002; **283**: L1220-1230
- 18 Perrella MA, Yet SF. Role of heme oxygenase-1 in cardiovascular function. *Curr Pharm Des* 2003; **9**: 2479-2487
- 19 Morse D. The role of heme oxygenase-1 in pulmonary fibrosis. *Am J Respir Cell Mol Biol* 2003; **29**(3 Suppl): S82-86
- 20 Stanford SJ, Walters MJ, Hislop AA, Haworth SG, Evans TW, Mann BE, Motterlini R, Mitchell JA. Heme oxygenase is expressed in human pulmonary artery smooth muscle where carbon monoxide has an anti-proliferative role. *Eur J Pharmacol* 2003; **473**: 135-141
- 21 Li L, Grenard P, Nhieu JT, Julien B, Mallat A, Habib A, Lotersztajn S. Heme oxygenase-1 is an antifibrogenic protein in human hepatic myofibroblasts. *Gastroenterology* 2003; **125**: 460-469
- 22 Bauer I, Rensing H, Florax A, Ulrich C, Pistorius G, Redl H, Bauer M. Expression pattern and regulation of heme oxygenase-1/heat shock protein 32 in human liver cells. *Shock* 2003; **20**: 116-122
- 23 Hancock WW, Buelow R, Sayegh MH, Turka LA. Antibody-induced transplant arteriosclerosis is prevented by graft expression of anti-oxidant and anti-apoptotic genes. *Nat Med* 1998; **4**: 1392-1396
- 24 Zhang M, Zhang BH, Chen L, An W. Overexpression of heme oxygenase-1 protects smooth muscle cells against oxidative injury and inhibits cell proliferation. *Cell Res* 2002; **12**: 123-132
- 25 Soares MP, Lin Y, Anrather J, Cszizmadia E, Takigami K, Sato K, Grey ST, Colvin RB, Choi AM, Poss KD, Bach FH. Expression of heme oxygenase-1 can determine cardiac xenograft survival. *Nat Med* 1998; **4**: 1073-1077
- 26 Liu Y, Moenne-Loccoz P, Hildebrand DP, Wilks A, Loehr TM, Mauk AG, Ortiz de Montellano PR. Replacement of the proximal histidine iron ligand by a cysteine or tyrosine converts heme oxygenase to an oxidase. *Biochemistry* 1999; **38**: 3733-3743
- 27 Ito-Maki M, Ishikawa K, Matera KM, Sato M, Ikeda-Saito M, Yoshida T. Demonstration that histidine 25, but not 132, is the axial heme ligand in rat heme oxygenase-1. *Arch Biochem Biophys* 1995; **317**: 253-258
- 28 Schuller DJ, Wilks A, Ortiz de Montellano PR, Poulos TL. Crystal structure of human heme oxygenase-1. *Nat Struct Biol* 1999; **6**: 860-867
- 29 Xia Z, Shao J, Shen Q, Wang J, Li Y, Chen S, Yu S. The preparation of rat heme oxygenase-1 mutant to reduce the level of bilirubin. *Chin Med J* 2001; **114**: 348-351
- 30 Schuller DJ, Wilks A, Ortiz de Montellano P, Poulos TL. Crystallization of recombinant human heme oxygenase-1. *Protein Sci* 1998; **7**: 1836-1838
- 31 Auclair K, Moenne-Loccoz P, Ortiz de Montellano PR. Roles of the proximal heme thiolate ligand in cytochrome p450 (cam). *J Am Chem Soc* 2001; **123**: 4877-4885
- 32 Wilk A, Medzihradsky KF, Ortiz de Montellano PR. Heme oxygenase active-site residues identified by heme-protein cross-linking during reduction of CBrC13. *Biochemistry* 1998; **37**: 2889-2896
- 33 Lad L, Schuller DJ, Shimizu H, Friedman J, Li H, Ortiz de Montellano PR, Poulos TL. Comparison of the heme-free and -bound crystal structures of human heme oxygenase-1. *J Biol Chem* 2003; **278**: 7834-7843
- 34 Foresti R, Motterlini R. The heme oxygenase pathway and its interaction with nitric oxide in the control of cellular homeostasis. *Free Radic Res* 1999; **31**: 459-475
- 35 Chang SH, Barbosa-Tessmann I, Chen C, Kilberg MS, Agarwal A. Glucose deprivation induces heme oxygenase-1 gene expression by a pathway independent of the unfolded protein response. *J Biol Chem* 2002; **277**: 1933-1940
- 36 Maines MD. The heme oxygenase system: a regulator of second messenger gases. *Annu Rev Pharmacol Toxicol* 1997; **37**: 517-554

Effect of SNPs in protein kinase *Cz* gene on gene expression in the reporter gene detection system

Zhuo Liu, Hong-Xia Sun, Yong-Wei Zhang, Yun-Feng Li, Jin Zuo, Yan Meng, Fu-De Fang

Zhuo Liu, Hong-Xia Sun, Yong-Wei Zhang, Yun-Feng Li, Jin Zuo, Yan Meng, Fu-De Fang, National Laboratory of Medical Molecular Biology, Institute of Basic Medical Sciences, Chinese Academy of Medical Sciences & Peking Union Medical College, Beijing 100005, China

Supported by the National High Technology Research and Development Program of China, No. 2002BA711A05, No. 2002BA711A10-02 and the National Natural Science Foundation of China, No. 30170441, No. 30370668 and the Natural Science Foundation of Beijing, No. 7032033 and the Foundation of Ministry of Education of China, No. 20030023020, No. 20010023024

Co-first-authors: Zhuo Liu and Yong-Wei Zhang

Co-correspondents: Yan Meng and Fu-De Fang

Correspondence to: Fu-De Fang, National Laboratory of Medical Molecular Biology, Institute of Basic Medical Sciences, Chinese Academy of Medical Sciences & Peking Union Medical College, Beijing 100005, China. fangfd@public3.bta.net.cn

Telephone: +86-10-65253005 **Fax:** +86-10-65253005

Received: 2003-12-10 **Accepted:** 2004-01-12

Abstract

AIM: To investigate the effects of the SNPs (rs411021, rs436045, rs427811, rs385039 and rs809912) on gene expression and further identify the susceptibility genes of type 2 diabetes.

METHODS: Ten allele fragments (49 bp each) were synthesized according to the 5 SNPs mentioned above. These fragments were cloned into luciferase reporter gene vector and then transfected into HepG2 cells. The activity of the luciferase was assayed. Effects of the SNPs on RNA splicing were analyzed by bioinformatics.

RESULTS: rs427811T allele and rs809912G allele enhanced the activity of the reporter gene expression. None of the 5 SNPs affected RNA splicing.

CONCLUSION: SNPs in protein kinase *Cz* (*PKCZ*) gene probably play a role in the susceptibility to type 2 diabetes by affecting the expression level of the relevant genes.

Liu Z, Sun HX, Zhang YW, Li YF, Zuo J, Meng Y, Fang FD. Effect of SNPs in protein kinase *Cz* gene on gene expression in the reporter gene detection system. *World J Gastroenterol* 2004; 10(16): 2357-2360

<http://www.wjgnet.com/1007-9327/10/2357.asp>

INTRODUCTION

Type 2 diabetes is a highly heterogeneous chronic disease characterized by metabolic disorder of blood glucose, its onset involves a number of susceptibility genes. Since 1996, locating and cloning the predisposing genes of type 2 diabetes, as well as the functional investigation, has become one of the hot spots worldwide in type 2 diabetes research. Based on genomic screening technology, it was reported firstly among Western population in succession that type 2 diabetes susceptibility

genes located on different chromosomes^[1-23]. The susceptibility genes were localized on chromosome 9 in Chinese population^[24]. According to the case-control analysis in the region of 1p36.33-1p36.23, our research group found that one SNP locus, rs436045 in protein kinase *Cz* (*PKCZ*) gene, was linked to type 2 diabetes in Chinese population, and the haplotype block has been identified. While analyzing the haplotype which consists of the 5 SNPs (rs411021, rs436045, rs427811, rs385039, rs809912), we noticed that, in the case group, the haplotype CGTAG showed a significantly higher frequency than that in control group, whereas the frequency of haplotype TAGGA decreased significantly ($P < 0.01$, OR = 1.625), it implied that the changes of those haplotypes related to the onset of type 2 diabetes in Chinese^[25]. However, it is still unclear whether haplotypes play a role during the episode of the disease.

To determine the biological function of those haplotypes, we investigated their influence on gene expression by bioinformatics approach and reporter gene activity determination system, which would provide a basis for further research.

In the previous work, we found that the 5 SNPs at the introns of *PKCZ* gene located in the same haplotype block in case group, and the haplotype they formed was clearly associated with type 2 diabetes mellitus. In order to determine the susceptibility loci associated with type 2 diabetes, we performed functional analysis on 5 SNPs.

MATERIALS AND METHODS

Identification of SNPs in the coding region of *PKCZ* gene

Coding region (from exon 4 to exon 13 or from rs1878745 to rs262642) of *PKCZ* gene was investigated for SNPs (cSNP) by sequencing. Ten unrelated type 2 diabetic patients and 10 control subjects from Han population in China were enrolled in a case-control study. Primers were designed by Primer 3.0 program (http://zeno.well.ox.ac.uk:8080/gitbin/primer3_www.cgi) and each PCR product was limited within about 500 base pairs. The sequencing results from ABI377 sequencer were analyzed through PhredPhrap/consed program to identify functional SNPs.

Analysis of the effect of 5 intron SNPs on mRNA splicing

The distance from the SNP to the splicing point in exon was determined based on the published genome sequence. According to this information, we preliminarily estimated whether the SNP site influences gene splicing.

Search of the information on PKC family member

The location and sequence of other PKC family members were obtained by means of bioinformatics. Then, different spliceosomes from other family members residing in the sequence of *PKCZ* were analyzed.

Analysis of the introns where 5 SNPs located

Each SNP and the intron sequence around the loci were compared with the data in cDNA database (www.sanbi.ac.za) to reveal the sequence homology. The open reading frames in this sequence were analyzed, and then the amino acid was

blast using the (www.ncbi.nlm.nih.gov) protein database in search of the sequence homology.

Effects of SNPs on gene expression by transient transfection

Ten alleles corresponding to the 5 SNPs in *PKCZ* gene were cloned into pGL3-promoter vector in the direction from 5' to 3' (Table 1). Meanwhile, HepG2 cells were cultured with DMEM (Gibco, LOS angeles, USA) containing 100 mL/L fetal bovine serum. Then, the cells (1.5×10^5 - 2×10^6) were transfected with pGL3-promoter vector (1 uL) or recombinant vector with Lipofectamine transfection reagent (Promega, madison, USA). The transfection rate was assayed by using pRL-SV40 DNA (100 ng, Promega, madison, USA) as an internal control. Forty-eight hours post transfection, the luciferase activity was determined by the Dual-Luciferase[®] Reporter Assay System using pRL-SV40 as an internal control.

Table 1 Sequence of ten 49-bp fragments containing each allele of 5 SNPs

Fragment name	Sequence
rs809912G-forward	5' ggggtaccagccatctccacc c gccattctccatcc 3'
rs809912G-reverse	3' gtcggtaggaggtgg g cgggtaagaggtaggttctagaag 5'
rs809912A-forward	5' ggggtaccagccatctccacc t gccattctccatcc 3'
rs809912A-reverse	3' ggggtaccagccatctccacc a gccattctccatcc 5'
rs436045A-forward	5' ggggtaccagcagtgctctcag a ttgttccaagcagt 3'
rs436045A-reverse	3' tcgtcacggacagtc t aaaccaggttcgctactctagaag 5'
rs436045G-forward	5' ggggtaccagcagtgctctcag g ttgttccaagcagt 3'
rs436045G-reverse	3' tcgtcacggacagtc c aaaccaggttcgctactctagaag 5'
rs427811T-forward	5' ggggtaccgctcagtgctctctt t gagaaggtataggtg 3'
rs427811T-reverse	3' gagtcacaggagaaa a ctctccatcatcacatctagaag 5'
rs427811G-forward	5' ggggtaccgctcagtgctctctt g gagaaggtacaggtg 3'
rs427811G-reverse	3' gagtcacaggagaaa c ctctccatcatcacatctagaag 5'
rs385039G-forward	5' ggggtacctgtttacagaagctac g ttgtaaacctgctc 3'
rs385039G-reverse	3' caaatgtctcagat c aacattgtggacgagatctagaag 5'
rs385039A-forward	5' ggggtacctgtttacagaagctac a ttgtaaacctgctc 3'
rs385039A-reverse	3' caaatgtctcagat t aacattgtggacgagatctagaag 5'
rs411021C-forward	5' ggggtaccgggggttcggtgagc c gagattgtgccactg 3'
rs411021C-reverse	3' cccaacgccactcg c ctctaacacggtgacctctagaag 5'
rs411021T-forward	5' ggggtaccgggggttcggtgagc t gagattgtgccactg 3'
rs411021T-reverse	3' cccaacgccactcg a ctctaacacggtgacctctagaag 5'

RESULTS

SNPs in the coding region of *PKCZ* gene

While seeking for functional SNPs by sequencing the exons around the 13 intron SNPs discovered in the previous work, we found no new ones except for the rs1878745 corresponding to NCBI database. It suggested that the disease loci probably did not exist in the coding region.

Influence of positive SNP on the *PKCZ* gene expression

To locate the disease SNP, we investigated the effect of the 5 positive SNPs (rs411021, rs436045, rs427811, rs385039, and rs809912) lying in the same haplotype block on *PKCZ* gene expression. The influence of the 5 SNPs over RNA splicing was evaluated since all the 5 SNPs lay in the introns. The distance of the SNPs from the upstream and downstream of the splicing site are respectively as the following: rs411021 (3 535 bp, 5 283 bp), rs436045 (4 770 bp, 4 048 bp), rs427811 (8 729 bp, 89 bp), rs385039 (1 629 bp, 57 bp), and rs809912 (>2 kb, 2 057 bp). Those are comparatively long distant to 5' splice donor site, 3' receptor site and the internal vertex, suggesting that they have little association with pre-mRNA splicing. In addition, we estimated if differential splicing occurs between *PKCZ* gene and other PKC family members. Although there are at least 11 family

members besides *PKCZ*, none of them locate on chromosome 1, which negates the 'differential splicing supposition'. The location of introns where 5 SNPs located was analyzed. As a first step, we compared the intron sequence around the loci of each of the 5 SNPs with the data in cDNA database (www.sanbi.ac.za) in order to reveal the sequence homology. Result showed that the introns had no coding function because neither cDNA sequence homology nor protein sequence homology by ORF analysis was found. But this result needs to be further confirmed by Northern blotting. And finally, the effects of the SNPs on gene expression were investigated. Transfected HepG2 cell containing pGL3-promoter reporter gene vector was used to detect the activity of the reporter gene that could reflect indirectly whether the fragment inserted affected gene expression. Statistical analysis showed a significant difference between the two SNPs of rs427811 and rs809912. In rs427811, the reporter gene activity of T allele was 1.5 times that of the G allele, while in rs809912, in G allele it was 1.7 times that of A allele (Table 2). Therefore, these two SNPs will probably affect the expression level of *PKCZ* gene.

Table 2 Transcriptional regulatory activity of each construct of *PKCZ* in HepG2 cells

Construct	Relative luciferase activity	P
pGL3-promoter	0.3533±0.040	
pGL3-rs411021C	0.5167±0.064	
pGL3-rs411021T	0.5100±0.102	0.928
pGL3-rs436045A	0.3433±0.051	
pGL3-rs436045G	0.3767±0.023	0.363
pGL3-rs427811T	0.6233±0.064 ^a	
pGL3-rs427811G	0.4433±0.068	0.029
pGL3-rs385039A	0.3500±0.044	
pGL3-rs385039G	0.3467±0.015	0.907
pGL3-rs809912A	0.1800±0.017 ^a	
pGL3-rs809912G	0.3033±0.042	0.009

^aP<0.05 in comparison between construct and pGL3-promoter vector.

DISCUSSION

PKCZ is a member of serine/threonine protein kinase family, belonging to atypical PKC, and independent of both calcium and diacylglycerol (DAG)^[26]. It is insensitive to PKC inhibitors and cannot be activated by phorbol ester. *PKCZ* protein is thought to function downstream of phosphatidylinositol 3-kinase (PI 3-kinase) in insulin signaling pathway and plays a role in promoting the translocation and activation of GluT4 from the cytosol to membranes which will accelerate the glucose transport in skeletal muscle and adipocytes^[27-30]. In addition, *PKCZ* can induce negative feedback to the signaling pathway through phosphorylating IRS-1^[31,32]. Insulin-stimulated glucose transport is defective in type 2 diabetes mellitus, and this defect can be ameliorated via correcting PRKC-zeta/lambda activation defect^[33], suggesting that the transport deficiency is at least partly associated with the activation defect of *PKCZ*. Our previous research showed that *PKCZ* is related to susceptibility to type 2 diabetes mellitus in Chinese population. If so, whether genetic polymorphism of *PKCZ* gene will influence the pathways associated with blood glucose regulation by affecting its gene expression, and increase the susceptibility to this disease ultimately? Based on bioinformatics research and reporter gene activity determination system, our data provide first evidence that intron SNP loci in *PKCZ* gene affect gene expression. Horikawa^[34] has reported that gene expression was under the influence of the 3 intron SNPs in *CAPN10* gene, the

susceptibility gene of type 2 diabetes in Mexican American. Such kind of result was also reported by other groups, for example, an SNP in *COL1N1* gene can change the binding site of transcription factor Sp1 thereby influencing the gene expression, resulting in the decline of bone density as well as osteoporosis^[35].

In our experiment, we found the two alleles (rs427811T and rs809912G) that had a relatively high frequency in type 2 diabetic patients could improve the reporter gene expression, apparently in conflict with our predicted result. This phenomenon might be explained by the hypothesis that *PKCZ* gene was involved in other signaling pathways and its relation to the disease was more complicated than we had estimated. Till now, there have been no reports that *PKCZ* gene expression is changed in the tissues of type 2 diabetic patients. But PED/PEA-15, a substrate of PKC, was reported to increase *PKCZ* gene expression in the patient's tissues^[36], which inhibited insulin stimulated glucose transportation. Thus, the high expression of PED/PEA-15 gene probably plays a role in insulin resistance of type 2 diabetes. Our next goals are to determine whether *PKCZ* interacts with PED/PEA-15 in insulin signaling pathway, and whether PED/PEA-15 or its analogue is involved in the inhibition of the insulin stimulated glucose transport via another signal pathway.

REFERENCES

- 1 **Hanis CL**, Boerwinkle E, Chakraborty R, Ellsworth DL, Concannon P, Stirling B, Morrison VA, Wapelhorst B, Spielman RS, Gogolin-Ewens KJ. A genome-wide search for human non-insulin-dependent (type 2) diabetes genes reveals a major susceptibility locus on chromosome 2. *Nat Genet* 1996; **13**: 161-166
- 2 **Mahtani MM**, Widen E, Lehto M, Thomas J, McCarthy M, Brayer J, Bryant B, Chan G, Daly M, Forsblom C, Kanninen T, Kirby A, Kruglyak L, Munnely K, Parkkonen M, Reeve-Daly MP, Weaver A, Brettin T, Duyk G, Lander ES, Groop LC. Mapping of a gene for type 2 diabetes associated with an insulin secretion defect by a genome scan in Finnish families. *Nat Genet* 1996; **14**: 90-94
- 3 **Ghosh S**, Watanabe RM, Hauser ER, Valle T, Magnuson VL, Erdos MR, Langefeld CD, Balow J Jr, Ally DS, Kohtamaki K. Type 2 diabetes: evidence for linkage on chromosome 20 in 716 Finnish affected sib pairs. *Proc Natl Acad Sci U S A* 1999; **96**: 2198-2203
- 4 **Vionnet N**, Hani El H, Dupont S, Gallina S, Francke S, Dotte S, De Matos F, Durand E, Lepretre F, Lecoeur C, Gallina P, Zekiri L, Dina C, Froguel P. Genomewide search for type 2 diabetes-susceptibility genes in French whites: evidence for a novel susceptibility locus for early-onset diabetes on chromosome 3q27-qter and independent replication of a type 2-diabetes locus on chromosome 1q21-q24. *Am J Hum Genet* 2000; **67**: 1470-1480
- 5 **Elbein SC**, Hoffman MD, Teng K, Leppert MF, Hasstedt SJ. A genome-wide search for type 2 diabetes susceptibility genes in Utah Caucasians. *Diabetes* 1999; **48**: 1175-1182
- 6 **Watanabe RM**, Ghosh S, Langefeld CD, Valle TT, Hauser ER, Magnuson VL, Mohlke KL, Silander K, Ally DS. The Finland-United States investigation of non-insulin-dependent diabetes mellitus genetics (FUSION) study. II. An autosomal genome scan for diabetes-related quantitative-trait loci. *Am J Hum Genet* 2000; **67**: 1186-1200
- 7 **Wiltshire S**, Hattersley AT, Hitman GA, Walker M, Levy JC, Sampson M, O'Rahilly S, Frayling TM, Bell JI, Lathrop GM, Bennett A, Dhillon R, Fletcher C, Groves CJ, Jones E, Prestwich P, Simecek N, Rao PV, Wishart M, Bottazzo GF, Foxon R, Howell S, Smedley D, Cardon LR, Menzel S, McCarthy MI. A genomewide scan for loci predisposing to type 2 diabetes in a U.K. population (the Diabetes UK Warren 2 Repository): analysis of 573 pedigrees provides independent replication of a susceptibility locus on chromosome 1q. *Am J Hum Genet* 2001; **69**: 553-569
- 8 **Permutt MA**, Wasson JC, Suarez BK, Lin J, Thomas J, Meyer J, Lewitzky S, Rennich JS, Parker A, DuPrat L, Maruti S, Chayen S, Glaser B. A genome scan for type 2 diabetes susceptibility loci in a genetically isolated population. *Diabetes* 2001; **50**: 681-685
- 9 **Lindgren CM**, Mahtani MM, Widen E, McCarthy MI, Daly MJ, Kirby A, Reeve MP, Kruglyak L, Parker A, Meyer J, Almgren P, Lehto M, Kanninen T, Tuomi T, Groop LC, Lander ES. Genomewide search for type 2 diabetes mellitus susceptibility loci in Finnish families: the Botnia study. *Am J Hum Genet* 2002; **70**: 509-516
- 10 **Busfield F**, Duffy DL, Kesting JB, Walker SM, Lovelock PK, Good D, Tate H, Watego D, Marczak M, Hayman N, Shaw JTE. A genomewide search for type 2 diabetes-susceptibility genes in indigenous Australians. *Am J Hum Genet* 2002; **70**: 349-357
- 11 **Demenais F**, Kanninen T, Lindgren CM, Wiltshire S, Gaget S, Dandrieux C, Almgren P, Sjogren M, Hattersley A, Dina C, Tuomi T, McCarthy MI, Froguel P, Groop LC. A meta-analysis of four European genome screens (GIFT Consortium) shows evidence for a novel region on chromosome 17p11.2-q22 linked to type 2 diabetes. *Hum Mol Genet* 2003; **12**: 1865-1873
- 12 **Lakka TA**, Rankinen T, Weisnagel SJ, Chagnon YC, Rice T, Leon AS, Skinner JS, Wilmore JH, Rao DC, Bouchard C. A quantitative trait locus on 7q31 for the changes in plasma insulin in response to exercise training: the HERITAGE Family Study. *Diabetes* 2003; **52**: 1583-1587
- 13 **Daimon M**, Ji G, Saitoh T, Oizumi T, Tominaga M, Nakamura T, Ishii K, Matsuura T, Inageda K, Matsumine H, Kido T, Htay L, Kamatani N, Muramatsu M, Kato T. Large-scale search of SNPs for type 2 DM susceptibility genes in a Japanese population. *Biochem Biophys Res Commun* 2003; **302**: 751-758
- 14 **Laivuori H**, Lahermo P, Ollikainen V, Widen E, Haiva-Mallinen L, Sundstrom H, Laitinen T, Kaaja R, Ylikorkala O, Kere J. Susceptibility loci for preeclampsia on chromosomes 2p25 and 9p13 in Finnish families. *Am J Hum Genet* 2003; **72**: 168-177
- 15 **Thameem F**, Yang X, Permana PA, Wolford JK, Bogardus C, Prochazka M. Evaluation of the microsomal glutathione S-transferase 3 (MGST3) locus on 1q23 as a Type 2 diabetes susceptibility gene in Pima Indians. *Hum Genet* 2003; **113**: 353-358
- 16 **Reynisdottir I**, Thorleifsson G, Benediktsson R, Sigurdsson G, Emilsson V, Einarsdottir AS, Hjorleifsdottir EE, Orlygssdottir GT, Bjornsdottir GT, Saemundsdottir J, Halldorsson S, Hrafnkelsdottir S, Sigurjonsdottir SB, Steinsdottir S, Martin M, Kochan JP, Rhee BK, Grant SF, Frigge ML, Kong A, Gudnason V, Stefansson K, Gulcher JR. Localization of a susceptibility gene for type 2 diabetes to chromosome 5q34-q35.2. *Am J Hum Genet* 2003; **73**: 323-335
- 17 **van Tilburg JH**, Sandkuijl LA, Strengman E, van Someren H, Rigters-Aris CA, Pearson PL, van Haeften TW, Wijmenga C. A genome-wide scan in type 2 diabetes mellitus provides independent replication of a susceptibility locus on 18p11 and suggests the existence of novel Loci on 2q12 and 19q13. *J Clin Endocrinol Metab* 2003; **88**: 2223-2230
- 18 **Duggirala R**, Almasy L, Blangero J, Jenkinson CP, Arya R, DeFronzo RA, Stern MP, O'Connell P. American Diabetes Association GENNID Study Group. Further evidence for a type 2 diabetes susceptibility locus on chromosome 11q. *Genet Epidemiol* 2003; **24**: 240-242
- 19 **Frayling TM**, Wiltshire S, Hitman GA, Walker M, Levy JC, Sampson M, Groves CJ, Menzel S, McCarthy MI, Hattersley AT. Young-onset type 2 diabetes families are the major contributors to genetic loci in the Diabetes UK Warren 2 genome scan and identify putative novel loci on chromosomes 8q21, 21q22, and 22q11. *Diabetes* 2003; **52**: 1857-1863
- 20 **Duggirala R**, Almasy L, Blangero J, Jenkinson CP, Arya R, DeFronzo RA, Stern MP, O'Connell P. American Diabetes Association GENNID Study Group. Further evidence for a type 2 diabetes susceptibility locus on chromosome 11q. *Genet Epidemiol* 2003; **24**: 240-242
- 21 **Hsueh WC**, St Jean PL, Mitchell BD, Pollin TI, Knowler WC, Ehm MG, Bell CJ, Sakul H, Wagner MJ, Burns DK, Shuldiner AR. Genome-wide and fine-mapping linkage studies of type 2

- diabetes and glucose traits in the Old Order Amish: evidence for a new diabetes locus on chromosome 14q11 and confirmation of a locus on chromosome 1q21-q24. *Diabetes* 2003; **52**: 550-557
- 22 **Kim SH**, Ma X, Klupa T, Powers C, Pezzolesi M, Warram JH, Rich SS, Krolewski AS, Doria A. Genetic modifiers of the age at diagnosis of diabetes (MODY3) in carriers of hepatocyte nuclear factor-1alpha mutations map to chromosomes 5p15, 9q22, and 14q24. *Diabetes* 2003; **52**: 2182-2186
- 23 **Sellick GS**, Garrett C, Houlston RS. A novel gene for neonatal diabetes maps to chromosome 10p12.1-p13. *Diabetes* 2003; **52**: 2636-2638
- 24 **Luo TH**, Zhao Y, Li G, Yuan WT, Zhao JJ, Chen JL, Huang W, Luo M. A genome-wide search for type II diabetes susceptibility genes in Chinese Hans. *Diabetologia* 2001; **44**: 501-506
- 25 **Li YF**, **Sun HX**, Wu GD, Du WN, Zuo J, Shen Y, Qiang BQ, Yao ZJ, Wang H, Huang W, Chen Z, Xiong MM, Meng Y, Fang FD. Protein kinase C/zeta (*PRKCZ*) gene is associated with type 2 diabetes in Han population of North China and analysis of its haplotypes. *World J Gastroenterol* 2003; **9**: 2078-2082
- 26 **Nishizuka Y**. Protein kinase C and lipid signaling for sustained cellular responses. *FASEB J* 1995; **9**: 484-496
- 27 **Standaert ML**, Galloway L, Karnam P, Bandyopadhyay G, Moscat J, Farese RV. Protein kinase C-zeta as a downstream effector of phosphatidylinositol 3-kinase during insulin stimulation in rat adipocytes. Potential role in glucose transport. *J Biol Chem* 1997; **272**: 30075-30082
- 28 **Standaert ML**, Bandyopadhyay G, Perez L, Price D, Galloway L, Poklepovic A, Sajan MP, Cenni V, Sirri A, Moscat J, Toker A, Farese RV. Insulin activates protein kinases C-zeta and C-lambda by an autophosphorylation-dependent mechanism and stimulates their translocation to GLUT4 vesicles and other membrane fractions in rat adipocytes. *J Biol Chem* 1999; **274**: 25308-25316
- 29 **Etgen GJ**, Valasek KM, Broderick CL, Miller AR. *In vivo* adenoviral delivery of recombinant human protein kinase C-zeta stimulates glucose transport activity in rat skeletal muscle. *J Biol Chem* 1999; **274**: 22139-22142
- 30 **Tremblay F**, Lavigne C, Jacques H, Marette A. Defective insulin-induced GLUT4 translocation in skeletal muscle of high fat-fed rats is associated with alterations in both Akt/protein kinase B and atypical protein kinase C (zeta/lambda) activities. *Diabetes* 2001; **50**: 1901-1910
- 31 **Ravichandran LV**, Esposito DL, Chen J, Quon MJ. Protein kinase C-zeta phosphorylates insulin receptor substrate-1 and impairs its ability to activate phosphatidylinositol 3-kinase in response to insulin. *J Biol Chem* 2001; **276**: 3543-3549
- 32 **Liu YF**, Paz K, Herschkovitz A, Alt A, Tennenbaum T, Sampson SR, Ohba M, Kuroki T, LeRoith D, Zick Y. Insulin stimulates PKCzeta-mediated phosphorylation of insulin receptor substrate-1 (IRS-1). A self-attenuated mechanism to negatively regulate the function of IRS proteins. *J Biol Chem* 2001; **276**: 14459-14465
- 33 **Kanoh Y**, Bandyopadhyay G, Sajan MP, Standaert ML, Farese RV. Rosiglitazone, insulin treatment, and fasting correct defective activation of protein kinase C-zeta/lambda by insulin in vastus lateralis muscles and adipocytes of diabetic rats. *Endocrinology* 2001; **142**: 1595-1605
- 34 **Horikawa Y**, Oda N, Cox NJ, Li X, Orho-Melander M, Hara M, Hinokio Y, Lindner TH, Mashima H, Schwarz PE, del Bosque-Plata L, Horikawa Y, Oda Y, Yoshiuchi I, Colilla S, Polonsky KS, Wei S, Concannon P, Iwasaki N, Schulze J, Baier LJ, Bogardus C, Groop L, Boerwinkle E, Hanis CL, Bell GI. Genetic variation in the gene encoding calpain-10 is associated with type 2 diabetes mellitus. *Nat Genet* 2000; **26**: 163-175
- 35 **Uitterlinden AG**, Burger H, Huang Q, Yue F, McGuigan FE, Grant SF, Hofman A, van Leeuwen JP, Pols HA, Ralston SH. Relation of alleles of the collagen type Ialpha1 gene to bone density and the risk of osteoporotic fractures in postmenopausal women. *N Engl J Med* 1998; **338**: 1016-1021
- 36 **Condorelli G**, Vigliotta G, Iavarone C, Caruso M, Tocchetti CG, Andreozzi F, Cafieri A, Tecce MF, Formisano P, Beguinot L, Beguinot F. PED/PEA-15 gene controls glucose transport and is overexpressed in type 2 diabetes mellitus. *EMBO J* 1998; **17**: 3858-3866

Edited by Zhu LH and Chen WW Proofread by Xu FM

Prolongation of liver allograft survival by dendritic cells modified with NF- κ B decoy oligodeoxynucleotides

Ming-Qing Xu, Yu-Ping Suo, Jian-Ping Gong, Ming-Man Zhang, Lü-Nan Yan

Ming-Qing Xu, Jian-Ping Gong, Ming-Man Zhang, Lü-Nan Yan, Department of General Surgery, West China Hospital, Sichuan University, Chengdu 610041, Sichuan Province, China

Yu-Ping Suo, West China Second University Hospital, Sichuan University, Chengdu 610041, Sichuan Province, China

Supported by the Postdoctoral Science Foundation of China, No. 2003033531

Correspondence to: Professor Lü-Nan Yan, Department of General Surgery, West China Hospital, Sichuan University, Chengdu 610041, Sichuan Province, China. xumingqing0018@163.com

Telephone: +86-28-85582968

Received: 2003-07-04 **Accepted:** 2003-09-25

Abstract

AIM: To induce the tolerance of rat liver allograft by dendritic cells (DCs) modified with NF- κ B decoy oligodeoxynucleotides (ODNs).

METHODS: Bone marrow (BM)-derived DCs from SD rats were propagated in the presence of GM-CSF or GM-CSF+IL-4 to obtain immature DCs or mature DCs. GM-CSF+IL-4-propagated DCs were treated with double-strand NF- κ B decoy ODNs containing two NF- κ B binding sites or scrambled ODNs to ascertain whether NF- κ B decoy ODNs might prevent DC maturation. GM-CSF-propagated DCs, GM-CSF+NF- κ B decoy ODNs or scrambled ODNs-propagated DCs were treated with LPS for 18 h to determine whether NF- κ B decoy ODNs could prevent LPS-induced IL-12 production in DCs. NF- κ B binding activities, costimulatory molecule (CD40, CD80, CD86) surface expression, IL-12 protein expression and allostimulatory capacity of DCs were measured with electrophoretic mobility shift assay (EMSA), flow cytometry, Western blotting, and mixed lymphocyte reaction (MLR), respectively. GM-CSF-propagated DCs, GM-CSF+IL-4-propagated DCs, and GM-CSF+NF- κ B decoy ODNs or scrambled ODNs-propagated DCs were injected intravenously into recipient LEW rats 7 d prior to liver transplantation and immediately after liver transplantation. Histological grading of liver graft rejection was determined 7 d after liver transplantation. Expression of IL-2, IL-4 and IFN- γ mRNA in liver graft and in recipient spleen was analyzed by semiquantitative RT-PCR. Apoptosis of liver allograft-infiltrating cells was measured with TUNEL staining.

RESULTS: GM-CSF-propagated DCs, GM-CSF+NF- κ B decoy ODNs-propagated DCs and GM-CSF+ scrambled ODNs-propagated DCs exhibited features of immature DCs, with similar low level of costimulatory molecule(CD40, CD80, CD86) surface expression, absence of NF- κ B activation, and few allocostimulatory activities. GM-CSF+IL-4-propagated DCs displayed features of mature DCs, with high levels of costimulatory molecule (CD40, CD80, CD86) surface expression, marked NF- κ B activation, and significant allocostimulatory activity. NF- κ B decoy ODNs completely abrogated IL-4-induced DC maturation and allocostimulatory activity as well as LPS-induced NF- κ B activation and IL-12

protein expression in DCs. GM-CSF+NF- κ B decoy ODNs-propagated DCs promoted apoptosis of liver allograft-infiltrating cells within portal areas, and significantly decreased the expression of IL-2 and IFN- γ mRNA but markedly elevated IL-4 mRNA expression both in liver allograft and in recipient spleen, and consequently suppressed liver allograft rejection, and promoted liver allograft survival.

CONCLUSION: NF- κ B decoy ODNs-modified DCs can prolong liver allograft survival by promoting apoptosis of graft-infiltrating cells within portal areas as well as down-regulating IL-2 and IFN- γ mRNA and up-regulating IL-4 mRNA expression both in liver graft and in recipient spleen.

Xu MQ, Suo YP, Gong JP, Zhang MM, Yan LN. Prolongation of liver allograft survival by dendritic cells modified with NF- κ B decoy oligodeoxynucleotides. *World J Gastroenterol* 2004; 10(16): 2361-2368

<http://www.wjgnet.com/1007-9327/10/2361.asp>

INTRODUCTION

Dendritic cells (DC) play a critical role in the initiation and regulation of immune response and are instrumental in the induction and maintenance of tolerance^[1-7]. The function of DCs is regulated by their state of maturation. Immature DCs resident in nonlymphoid tissues such as normal liver are deficient at antigen capture and progressing^[8,9], whereas mature DCs, resident in secondary lymphoid tissues, are potent antigen-presenting cells (APC), which can induce naive T-cell activation and proliferation^[9-13]. The ability of DCs to initiate immune responses is determined by their surface expression of major histocompatibility complex (MHC) gene products and costimulatory molecules (CD40, CD80, CD86), and the secretion of the immune regulator, interleukin (IL)-12^[9-18]. Immature DCs that express surface MHC class II, but deficient in surface costimulatory molecules and few expressions of IL-12, can induce T-cell anergy^[8,19,20], and inhibit immune reactivity^[21,22].

Immature donor-derived DCs that are deficient in surface costimulatory molecules freshly isolated from commonly transplanted organs, can induce alloAg-specific T cell anergy *in vitro*^[23]. These DCs prolong survival of fully allogeneic grafts in rodents, in some cases, indefinitely^[24,25]. In addition, pharmacologic inhibition of DC maturation in nonhuman primates is associated with the induction of organ transplant tolerance^[26]. Moreover, immature human DCs have been shown to induce T regulatory cells *in vitro*^[27] and to promote Ag-specific T cell tolerance in healthy volunteers^[28]. Thus, DCs offer potential both for therapy of allograft rejection and promotion of transplant tolerance.

The inherent ability of DCs to traffic exquisitely to T cell areas of secondary lymphoid tissues^[8,29] and to regulate immune responses makes them attractive targets for manipulation with genes encoding immunosuppressive molecules, such as IL-4, IL-10, CTLA4lg, Fas ligand (CD95L), or transforming growth factor (TGF)- β 1, that suppress T cell response by various

mechanisms. A potential obstacle to the successful use of genetically engineered DCs for therapeutic immunosuppression is their maturation/activation *in vivo* following interactions with proinflammatory factors that may overcome the desired effect of transgene products. Recent studies showed that both DC maturation and immunostimulatory ability depended on NF- κ B-dependent gene transcription^[29-34], inhibition of NF- κ B activation could suppress DC maturation/activation induced by IL-4 or LPS stimulation^[29,34,35], and DCs treated with NF- κ B decoy oligodeoxynucleotides (ODNs) containing specific NF- κ B binding sites could induce tolerance of cardiac allograft^[29,34].

Although genetically engineered DCs have been used in tolerance induction of cardiac allograft, there are few evidences that genetically engineered DCs can be used to induce tolerance of liver allograft. In the present study, whether NF- κ B decoy ODNs-treated DCs could prolong liver allograft survival in rats was studied.

MATERIALS AND METHODS

NF- κ B decoy ODNs

Double-stranded NF- κ B decoy ODNs or scrambled ODNs (as a control for NF- κ B decoy ODNs) were generated using equimolar amounts of single-stranded sense and antisense phosphorothioate-modified oligonucleotide containing two NF- κ B binding sites (sense sequence 5'-AGGGACTTTCCGCTG-GGGACTTCC-3', NF- κ B binding sites bold lines and underlined)^[34] and scrambled oligonucleotide (sense sequence 5'-TTGCCGTACCTGACTTAGCC-3')^[36]. Sense and antisense strands of each oligonucleotide were mixed in the presence of 150 mmol/L PBS, heated to 100 °C, and allowed to cool to room temperature to obtain double-stranded DNA.

Propagation of bone marrow-derived DC populations

Bone marrow cells harvested from femurs of normal SD rats were cultured in 24-well plates (2×10^6 per well) in 2 mL of RPMI 1640 complete medium supplemented with antibiotics, 10 mL/L fetal calf serum (FCS) and 4.0 ng/mL recombinant rat GM-CSF to obtain immature DCs. In addition to GM-CSF, 10 ng/mL recombinant rat IL-4 was added to cultures to obtain mature DCs. To select plates, 10 μ mol/L NF- κ B decoy or scrambled ODNs was added at the initiation of culture of DCs^[34] to test the ability of NF- κ B decoy ODNs to inhibit IL-4-induced DC maturation. Cytokine-enriched medium was refreshed every 2 d, after gentle swirling of the plates, half of the old medium was aspirated and an equivalent volume of fresh, cytokine-supplemented medium was added. Thus, nonadherent granulocytes were depleted without dislodging clusters of developing DC attached loosely to a monolayer of plastic-adherent macrophages. Nonadherent cells released spontaneously from the clusters were harvested after 7 d. In certain experiments, after propagation for 7 d, GM-CSF-propagated DCs, GM-CSF+NF- κ B decoy ODNs-propagated DCs and GM-CSF+scrambled ODNs-propagated DCs were cultured with 10 μ g/mL LPS for 18 h to test the ability of NF- κ B decoy ODNs to prevent LPS-induced IL-12 production in DCs.

Phenotypical features of DCs

Expression of cell surface molecules was quantitated by flow cytometry as described in our previous study. Aliquots of 2×10^5 DCs propagated for 7 d *in vitro* were incubated with the following primary mouse anti-rat mAbs against CD40, CD80, CD86, or rat IgG as an isotype control for 60 min on ice [1 μ g/mL diluted in PBS/(10 mL/L FCS)]. Cells were washed with PBS/(10 mL/L FCS) and labeled with FITC-conjugated goat anti-mouse IgG, diluted 1/50 in PBS/(10 mL/L FCS) for 30 min on ice. At the end of this incubation, the cells were washed, propidium iodide/PBS were added, and the cells were subsequently analyzed by a FACS-

4 200 flow cytometer.

DCs allostimulatory capacity

One-way mixed leukocyte reactions (MLR) were performed in 96-well, round-bottomed microculture plates. Graded doses of γ -irradiated (20Gy) allogeneic (SD) stimulator cells (DCs) were added to 2×10^5 nylon wool-eluted LEW rat splenic T cells (responders) and maintained in complete medium for 72 h in 50 mL/L CO₂ in air at 37 °C. [³H]thymidine (1 μ Ci/well) was added for the last 18 h of culture. Cells were harvested onto glass fiber mats using an automatic system, and [³H]thymidine incorporation was determined by a liquid scintillation counter. Results were expressed as mean \pm SD.

Isolation of nuclear proteins

Nuclear proteins were isolated from DC extract by placing the sample in 0.9 mL of ice-cold hypotonic buffer [10 mmol/L HEPES (pH 7.9), 10 mmol/L KCl, 0.1 mmol/L EDTA, 0.1 mmol/L ethylene glycol tetraacetic acid, 1 mmol/L DTT, protease inhibitors (aprotinin, pepstatin, and leupeptin, 10 mg/mol/L each)]. Homogenates were incubated on ice for 20 min, vortexed for 20 s after adding 50 μ L of 100 g/L Nonidet P-40, and then centrifuged for 1 min at 4 °C in an Eppendorf centrifuge. Supernatants were decanted, nuclear pellets after a single wash with hypotonic buffer without Nonidet-P40 were suspended in an ice-cold hypertonic buffer [20 mmol/L HEPES (pH 7.9), 0.4 mol/L NaCl, 1 mmol/L EDTA, 1 mol/L DTT, protease inhibitors], incubated on ice for 30 min at 4 °C, mixed frequently, and centrifuged for 15 min at 4 °C. Supernatants were collected as nuclear extracts and stored at -70 °C. Concentrations of total proteins in the samples were determined according to the method of Bradford.

Electrophoretic mobility shift assay (EMSA) for NF- κ B activation of DCs

NF- κ B binding activity was performed in a 10- μ L binding reaction mixture containing 1 \times binding buffer [50 mg/L of double-stranded poly (dI-dC), 10 mmol/L Tris-HCl (pH 7.5), 50 mmol/L NaCl, 0.5 mmol/L EDTA, 0.5 mmol/L DTT, 1 mmol/L MgCl₂, and 100 mL/L glycerol], 5 μ g of nuclear protein, and 35 fmol of double-stranded NF- κ B consensus oligonucleotide (5'-AGT TGAGGGGACTTT CCCAGGC-3') that was endly labeled with γ -³²P (111 TBq/mmol at 370 GBq⁻¹) using T4 polynucleotide kinase. The binding reaction mixture was incubated at room temperature for 20 min and analyzed by electrophoresis on 70 g/L nondenaturing polyacrylamide gels. After electrophoresis, the gels were dried by a gel-drier and exposed to Kodak X-ray films at -70 °C.

Western blotting for IL-12 protein expression in DCs stimulated with LPS

GM-CSF-propagated DCs, GM-CSF+NF- κ B decoy ODNs-propagated DCs and GM-CSF+scrambled ODNs-propagated DCs were cultured with 10 μ g/mL LPS for 18 h. DCs were starved in serum-free medium for 4 h at 37 °C. These cells were washed twice with cold PBS, resuspended in 100 μ L lysis buffer (1 mL/L Nonidet P-40, 20 mmol/L Tris-HCl, pH 8.0, 137 mmol/L NaCl, 100 mL/L glycerol, 2 mmol/L EDTA, 10 μ g/mL leupeptin, 10 μ g/mL aprotinin, 1 mmol/L PMSF, and 1 mmol/L sodium orthovanadate), and total cell lysates were obtained. Homogenates were centrifuged at 10 000 g for 10 min at 4 °C. Cell lysates (20 μ g) were electrophoresed on SDS-PAGE gels, and transferred to PVDC membranes for Western blot analysis. Briefly, PVDC membranes were incubated in a blocking buffer for 1 h at room temperature, then incubated for 2 h with Abs against IL-12 p35 and IL-12 p40 and IL-12 p70. Membranes were washed and incubated for 1 h with HRP-labeled horse anti-goat or goat anti-rabbit IgG. Immunoreactive bands were visualized by ECL detection reagents. The binding bands were quantified by a

scanning the densitometer of a bio-image analysis system. The results were expressed as a relative optical density.

Liver transplantation

Sixty male LEW rats and sixty male SD rats weighing 250–300 g were used in all experiments. Allogeneic liver transplantation model was established using a combination of SD rats with LEW rats. All operations were performed under ether anesthesia in sterile conditions. Orthotopic liver transplantation was performed according to the method described in our previous study. Normal saline (group A), 1×10^7 GM-CSF-propagated DCs (group B), 1×10^7 GM-CSF+IL-4-propagated DCs (group C), and 1×10^7 GM-CSF+ NF- κ B decoy ODNs or scrambled ODNs-propagated DCs (group D or group E) were injected intravenously through the penile vein into recipient LEW rats 7 d prior to liver transplantation and immediately after liver transplantation, respectively. Liver graft tissues and recipient spleen samples ($n = 8$) were harvested 7 d after liver transplantation and immediately frozen in liquid nitrogen and kept at -80°C until use. Part of the liver graft tissues was sectioned and preserved in 40 g/L formaldehyde.

Histology

Part of liver tissues was sectioned and preserved in 40 g/L formaldehyde, embedded in paraffin, and stained with hematoxylin and eosin. Histological grading of rejection was determined according to the criteria described by Williams.

Apoptosis of liver graft-infiltrating cells (GIC)

Apoptotic cells in tissue sections were detected with the *in situ* cell death detection kit. Liver graft tissue sections were dewaxed and rehydrated according to standard protocols. Tissue sections were incubated with proteinase K (20 $\mu\text{g}/\text{mL}$ in 10 mmol/L Tris/HCl, pH 7.4–8.0) for 15 to 30 min at $21\text{--}37^\circ\text{C}$. Endogenous peroxidase activity was quenched with blocking solution (3 mL/LH₂O₂ in methanol) for 30 min at room temperature before exposure to TUNEL reaction mixture at 37°C for 60 min. After washed in stop wash buffer, peroxidase (POD) was added to react for 30 min at 37°C . DAB-substrate was used for color development, and the sections were counterstained with Harris' hematoxylin. TUNEL staining was mounted under glass coverslip and analysed under a light microscope.

Semiquantitative RT-PCR assay for expression of IL-2, IL-4 and IFN- γ mRNA in liver graft and spleen

IL-2, IL-4 and IFN- γ mRNA expression was determined by semiquantitative RT-PCR amplification in contrast with house-keeping gene β -actin, respectively. Total RNA from 10 mg liver allograft and recipient spleen tissue was extracted using Tripure™ reagent. First-strand cDNA was transcribed from 1 μg RNA using AMV and an Oligo(dT)₁₅ primer. PCR was performed in a 25 μL reaction system containing 10 μL cDNA, 2 μL 10 mmol/L dNTP, 2.5 μL 10 \times buffer, 2.5 μL 25 mmol/L MgCl₂, 2 μL specific primer, 5 μL water and 1 μL Taq (35 cycles: at 95°C for 60 s, at 59°C for 90 s, and at 72°C for 10 s). Primers^[37–39] used in PCR reactions were as follows: IL-2, 5' primer 5'-CAT GTA CAGCA TGCAGCTCGCATCC-3', 3' primer 5'-CCACCACAGTTGCTG GCTCATCATC-3', to give a 410-bp PCR product; IL-4, 5' primer 5'-TGATGGGCTCAGCCCCACCTTGC-3', 3' primer 5'-CTT TCAGTGTGTTGTGAGCGTGGACTC-3', to give a 378-bp PCR product; IFN- γ , 5' primer 5'-AAGACAACCAGGCCATCAGCA-3', 3' primer 5'-AGCCACAGTGTGAGTTTCATC-3', to give a 547-bp product; β -actin, 5' primer 5'-ATGCCATCC TGCGT CTGGACCTGGC-3', 3' primer 5'-AGCATTGCGGTGCAC GATGGAGGG-3', to give a 607-bp product. PCR products of each sample were subjected to electrophoresis in a 15 g/L agarose gel containing 0.5 mg/L ethidium bromide. Densitometrical

analysis using NIH image software was performed for semiquantification of PCR products, and mRNA expression was evaluated by the band-intensity ratio of IL-2, IL-4 and IFN- γ to β -actin, and presented as percent of β -actin (%).

Statistical analysis

Statistic analysis of data was performed using the *t*-test and rank sum test, $P < 0.05$ was considered statistically significant.

RESULTS

NF- κ B decoy ODNs inhibited IL-4 or LPS - induced NF- κ B activation in DCs

To confirm whether NF- κ B decoy ODNs might specifically bind to NF- κ B, analysis of NF- κ B activity was performed with nuclear extracts obtained from GM-CSF-propagated DCs, GM-CSF+IL-4-propagated DCs, GM-CSF+LPS-propagated DCs, GM-CSF+IL-4+ODNs-propagated DCs and GM-CSF+LPS+ODNs-propagated DCs by EMSA. As shown in Figure 1, EMSA analysis showed no NF- κ B activation in GM-CSF-propagated DCs but significant NF- κ B activation in IL-4 or LPS-stimulated DCs. NF- κ B decoy ODNs completely inhibited IL-4 or LPS-induced NF- κ B activation in DCs, whereas scrambled ODNs had little effect on inhibition of IL-4 or LPS-induced NF- κ B activation in DCs.

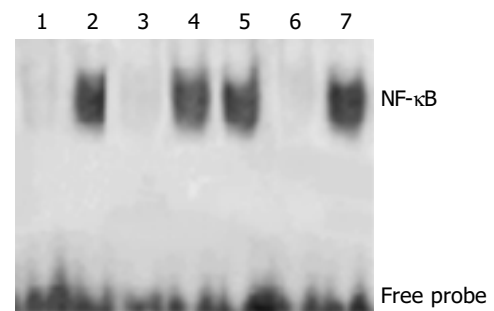


Figure 1 Inhibition of IL-4 or LPS-induced NF- κ B activation in DCs by NF- κ B decoy ODNs. Nuclear proteins of GM-CSF DCs, GM-CSF + IL-4 DCs, GM-CSF+IL-4 + NF- κ B decoy ODNs DCs, GM-CSF+IL-4 + scrambled ODNs DCs, GM-CSF + LPS DCs, GM-CSF+LPS+ NF- κ B decoy ODNs DCs and GM-CSF+LPS+ scrambled ODNs DCs were measured by EMSA (lanes 1–7).

NF- κ B decoy ODNs inhibited IL-4 - induced costimulatory molecule surface expression in DCs

Functional maturation of DCs was associated with up-regulation of costimulatory molecules (CD40, CD80, and CD86). To test the ability to inhibit DC maturation, NF- κ B decoy ODNs or scrambled ODNs were added at the initiation of culture of GM-CSF+IL-4-stimulated SD rat BM-derived DCs. After culture for 7 d, surface expression of CD40, CD80, and CD86 was analyzed by flow cytometry. Figure 2 shows the effects of ODNs on phenotype of the cultured DCs in the presence of GM-CSF+IL-4. Flow cytometric analysis showed GM-CSF-propagated DCs exhibited immature phenotypical features with very low levels of CD40, CD80 and CD86 surface expression, GM-CSF+IL-4-propagated DCs displayed mature phenotypical features with high level of CD40, CD80, and CD86 surface expression. NF- κ B decoy ODNs prevented IL-4-induced DCs maturation, and maintained DCs in the immature state, with low levels of surface costimulatory molecule expression. Whereas the scrambled ODNs could not prevent IL-4-induced DCs maturation, and maintained DCs in the mature state, with similar high levels of surface costimulatory molecule expression compared with GM-CSF+IL-4-propagated DCs (data not shown).

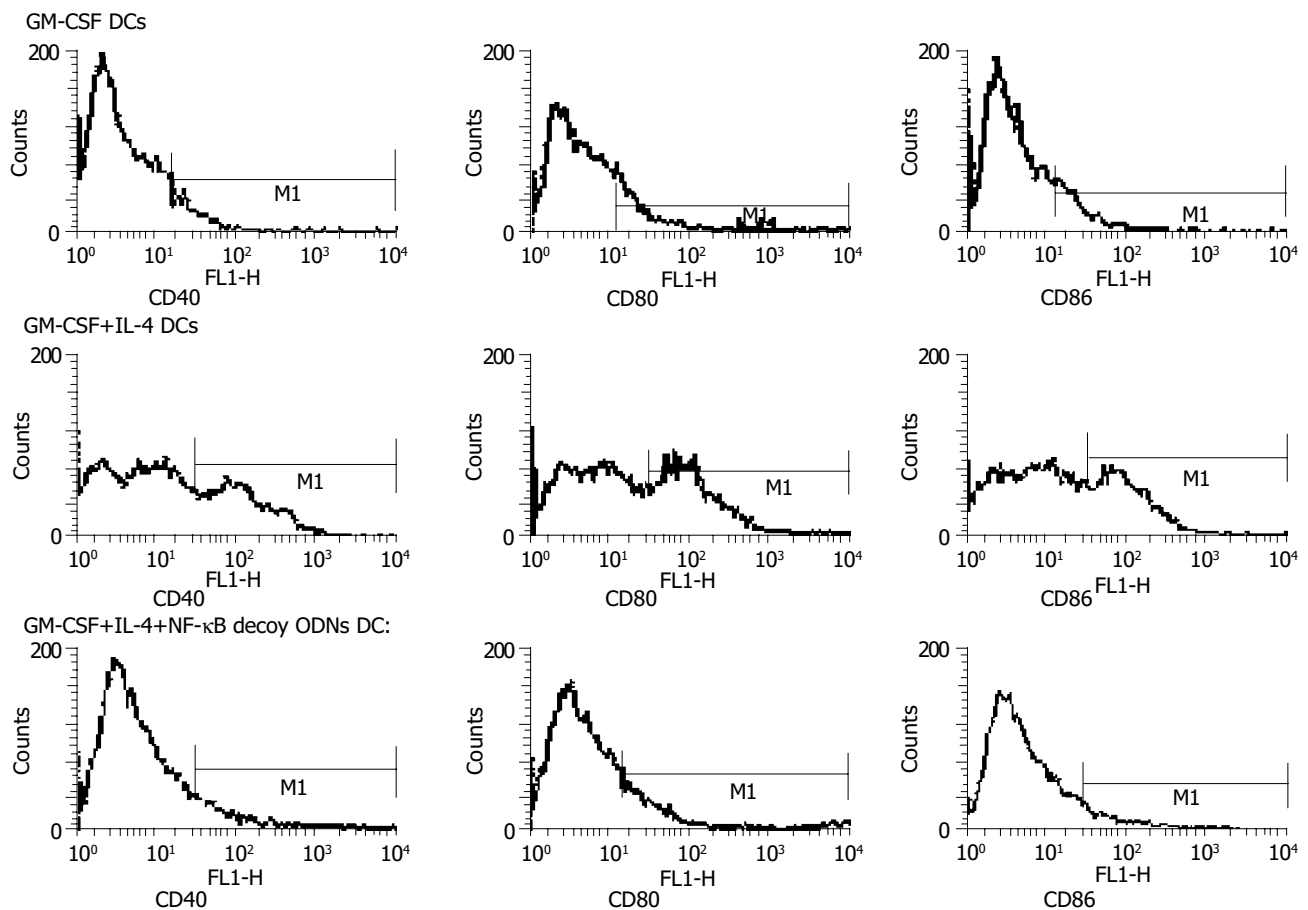


Figure 2 Suppression of IL-4-induced costimulatory molecule expression in DCs by NF- κ B decoy ODNs.

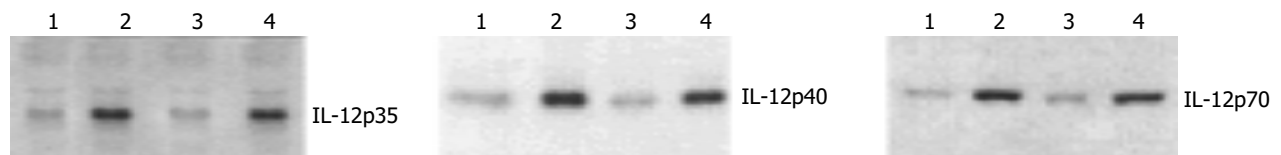


Figure 3 Suppression of IL-12 protein expression in LPS-stimulated DCs by NF- κ B decoy ODNs. Protein extracts from GM-CSF DCs, GM-CSF+LPS DCs, GM-CSF+LPS +NF- κ B decoy ODNs DCs and GM-CSF+LPS +scrambled ODNs DCs were measured by Western blot (lane 1-4).

NF- κ B decoy ODNs abrogated LPS-induced IL-12 protein expression in DCs

Previous studies showed that IL-12 protein expression was significantly up-regulated in mature DCs^[10,17,19,40]. To further confirm whether NF- κ B decoy ODNs might prevent DC maturation, LPS-induced IL-12 protein (p35, p40 and p70) expression in DCs was measured. As shown in Figure 3, very low level of IL-12 protein was detected in GM-CSF DCs, and markedly high level of IL-12 protein was detected in LPS-stimulated DCs ($P < 0.001$). NF- κ B decoy ODNs completely abrogated the LPS-induced production of IL-12 protein in DCs, whereas scrambled ODNs had almost no effect on down-regulation of LPS-induced IL-12 protein expression in DCs.

DCs allostimulatory capacity was inhibited by NF- κ B decoy ODNs

The effect of NF- κ B decoy ODNs on DCs immunostimulatory activity was evaluated by *in vitro* MLR. Graded number of γ -irradiated DCs (SD) was cultivated for 72 h with a fixed number of allogeneic (LEW) splenic T cells in MLR. The results of a representative experiment are shown in Figure 4. In comparison with IL-4 stimulated mature DCs or IL-4 + scrambled ODNs-propagated DCs, which were potent inducers of DNA synthesis and consistent with their mature surface phenotype, IL-4+NF- κ B

decoy ODNs-propagated DCs induced only a minimal T cell proliferation. The poor stimulatory capacity of IL-4 +NF- κ B decoy ODNs DCs remained unchanged after a longer incubation with allogeneic T cells (4- or 5-d MLR, data not shown). The results suggested that allostimulatory capacity of DCs was inhibited by NF- κ B decoy ODNs.

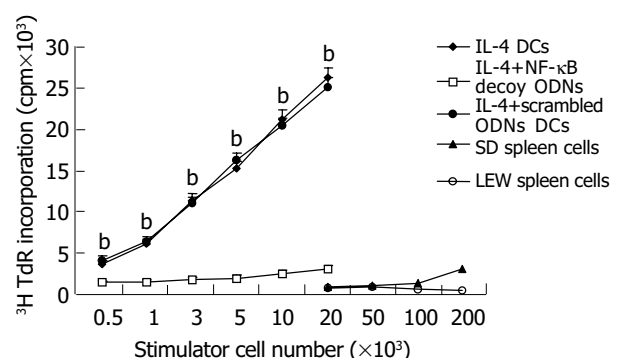


Figure 4 Suppression of allostimulatory function of IL-4-stimulated DCs by NF- κ B decoy ODNs. ^b $P < 0.001$ vs IL-4+NF- κ B decoy ODNs-propagated DCs.

NF-κB decoy ODNs- treated DCs prolonged donor-specific liver allograft survival

To examine the effect of NF-κB decoy ODNs-treated DCs on liver allograft survival *in vivo*, 1×10^7 unmodified immature bone marrow-derived DCs from SD rats (GM-CSFDCs), GM-CSF+IL-4-propagated mature DCs, and GM-CSF+NF-κB decoy ODNs or scrambled ODNs-propagated immature DCs were injected intravenously through the penile vein into recipient LEW rats 7 d prior to liver transplantation and immediately after liver transplantation, respectively. Table 1 and Figure 5 show the effect of DCs on liver allograft rejection and recipient survival. GM-CSF+IL-4-propagated mature DCs accelerated the liver allograft rejection and shortened the survival time of recipient animals. Immature donor DCs (GM-CSF or GM-CSF+scrambled ODNs-propagated DCs) significantly suppressed liver allograft rejection and prolonged graft survival compared with untreated controls. In comparison with GM-CSF or GM-CSF +scrambled ODNs-propagated DCs, NF-κB decoy ODNs-treated DCs exerted a marked effect on liver allograft rejection and recipient survival, and significantly suppressed the liver allograft rejection and prolonged survival time of recipient animals.

Table 1 Rejection stages of liver allografts

Rejection stages	Group A (n)	Group B (n)	Group C (n)	Group D (n)	Group E (n)
0	0	1	0	6	2
1	2	6	0	2	6
2	6	1	2	0	0
3	0	0	6	0	0

Group B vs group A, $u = 2.475, P < 0.05$; Group C vs group A, $u = 2.951, P < 0.01$; Group D vs group A, $u = 3.298, P < 0.01$; Group D vs group B, $u = 2.416, P < 0.05$; Group E vs group A, $u = 0.901, P > 0.05$.

NF-κB decoy ODNs-treated DCs promoted apoptosis of liver allograft-infiltrating cells in portals

Although the precise mechanisms remain unclear, spontaneous acceptance of liver grafts in mice has been associated with high levels of apoptosis in GIC population^[41]. In contrast, FL liver glografts that were rejected acutely showed reduced apoptotic activity in GIC within portal areas and enhanced apoptosis of hepatocytes^[42]. These data suggested a critical immunoregulatory role of apoptosis in determining the outcome of hepatic allografts. To determine whether the prolongation of

liver allografts survival induced by NF-κB decoy ODNs-treated DCs was associated with enhanced apoptosis of GIC, apoptotic activity in the graft was examined by TUNEL staining with immunohistochemistry analysis. *In situ* TUNEL staining of liver graft sections revealed that a certain level of apoptosis of GIC was induced by immature DCs (GM-CSF or GM-CSF+scrambled ODNs-propagated DCs), and mature DCs appeared to protect GIC from apoptosis. The greatest degree of apoptosis of GIC within portal areas of liver grafts was induced by NF-κB decoy ODNs-treated DCs (Figure 6). These data strongly suggested that augmentation of apoptosis of activated GIC within portal areas of liver grafts might be critical in promoting the tolerance of liver allografts.

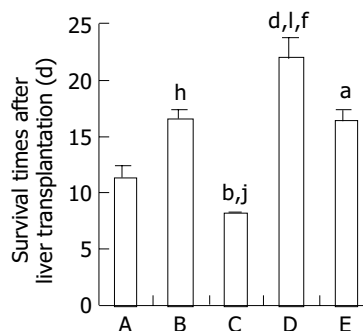


Figure 5 Prolongation of survival of liver allograft recipient by NF-κB decoy ODNs-treated DCs. ^b $P < 0.001$ vs group A, ^d $P < 0.001$ vs group A, ^f $P < 0.001$ vs group C, ^h $P < 0.001$ vs group A, ^l $P < 0.001$ vs group B, ^a $P > 0.05$ vs group B.

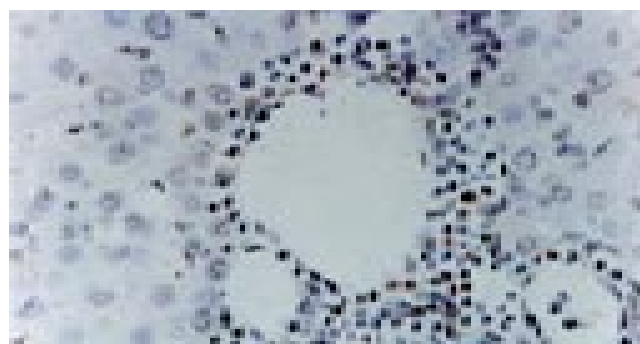


Figure 6 Augmentation of apoptosis of liver allograft-infiltrating cells in portals. by NF-κB decoy ODNs-treated DCs (×400).

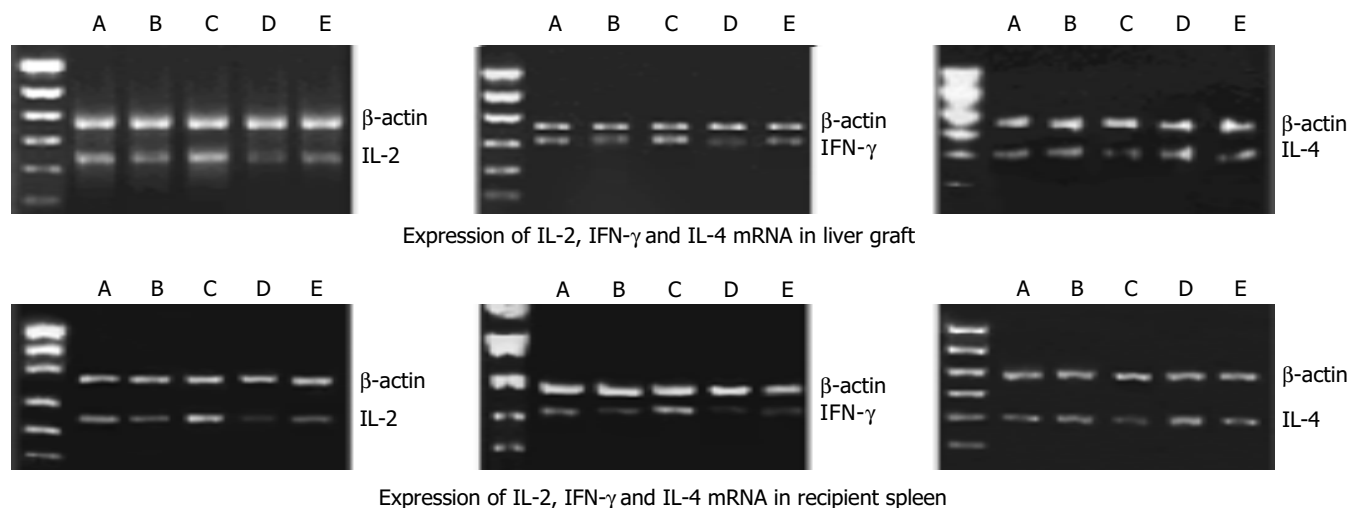


Figure 7 Suppression of IL-2 and IFN-γ mRNA expression and up-regulation of IL-4 mRNA expression both in liver graft and in recipient spleen by NF-κB decoy ODNs-modified DCs.

NF- κ B decoy ODNs-treated DCs suppressed IL-2 and IFN- γ mRNA but elevated IL-4 mRNA expression both in liver graft and in recipient spleen

To determine the relationship of specific cytokine production to the outcome of liver transplantation, cytokine mRNA expression in liver graft and recipient spleen 7 d after liver transplantation was examined by RT-PCR assay. IL-2, IL-4 and IFN- γ mRNA were readily detected both in liver graft and in recipient spleen 7 d after liver transplantation in animals from group A. Administration of immature DCs (group B and group E) partially down-regulated IL-2 mRNA and INF- γ mRNA expression and partially up-regulated IL-4 mRNA expression in liver graft and recipient spleen. Administration of IL-4 stimulated mature DCs (Group C) significantly up-regulated expression of IL-2 and IFN- γ mRNA but markedly down-regulated IL-4 mRNA expression in liver graft and recipient spleen ($P < 0.001$ vs group A, B, D, E. Statistic data not shown). However, administration of NF- κ B decoy ODNs-modified DCs (group D) significantly suppressed expression of IL-2 and IFN- γ mRNA and significantly elevated expression of IL-4 mRNA both in liver grafts and in recipient spleen ($P < 0.001$ vs group A, B, C, E. Statistic data not shown). Taken together, these results suggested that prolongation of liver allograft survival induced by NF- κ B decoy ODNs-modified DCs might be associated with down-regulation of IL-2 and IFN- γ production and up-regulation of IL-4 production in liver graft and recipient lymphoid tissue.

DISCUSSION

It is accepted that both donor and recipient DCs mediate the rejection of graft in organ transplantation. Thus, conversion of these two sets of DCs to specifically inactivate recipient alloreactive T cells should allow the long-term acceptance of graft in the absence of continuous immunosuppression. In the present study, we showed that stably immature DCs modified with NF- κ B decoy ODNs markedly suppressed the rejection of liver allograft and prolonged liver allograft survival.

The ability of DCs to traffic to T cell areas of secondary lymphoid tissues and subsequently direct immune responses makes them ideal candidates for cell-based therapies of allograft rejection. Several studies showed that immature donor DCs, deficient in surface costimulatory molecules, could induce T-cell hyporesponsiveness^[20-22] and prolong graft survival in unmodified hosts^[43,44].

Several strategies have been used to arrest the maturation of DCs and to potentiate their tolerogenicity. While some have shown their promising, all have significant disadvantages. CsA could inhibit DC function, but its effect was weak and temporary, easily to be overcome by cytokines such as IL-4^[45]. CsA may inhibit DC maturation *in vivo*, but also interferes with signal transduction through the T cell receptor complex, thus impairing the development of antigen-specific tolerance. Indeed, CsA interferes with T cell maturation and selection and can lead to generation of autoreactive T cells. Additionally, CsA is associated with significant toxicity. Antibodies to fusion proteins specific for cell-surface molecules (anti-CD40, CTLA4Ig) could prevent DC costimulation of T cells^[46]. However, antibodies and fusion proteins have a limited half-life. Late up-regulation of DC costimulatory molecules upon encountering the host microenvironment requires treatment of multiple antibodies. Expression of immunosuppressive gene products such as IL-10, TGF- β and CTLA4-Ig by DCs could result in further inhibition of alloimmune responses *in vitro*^[20,29,47,48]. However, adenoviral vectors used to efficiently deliver transgene expression could simultaneously activate DCs^[20,29]. Thus, transgene expression was overcome by the vigorous upregulation of costimulatory molecules on the transfected DC surface. Antisense oligodeoxynucleotides to molecules such as ICAM-1

could prolong kidney and heart allograft survival^[49]. However, effects were not donor specific, nor did grafts survive indefinitely. To date, strategies using genetically DCs alone in experimental organ transplantation have failed to induce tolerance. In the setting of transplantation, proinflammatory cytokines and other factors were capable of promoting DC maturation around within recipient tissues. Thus, late maturation and inherent T cell stimulatory potential of genetically engineered DCs may overcome the effects of localized immunosuppressive transgene expression. However, our and other data indicated that preconditioning donor DCs *in vitro* with ODN to block NF- κ B nuclear translocation were sufficient to stably suppress the up-regulation of costimulatory molecules and IL-12 production in response to potent activating stimuli, such as LPS and IL-4.

NF- κ B is an important transcriptional regulator of the immune response in a variety of cell types, but its precise function in DCs has not been extensively evaluated. Nonetheless, interference with its actions, either by CsA or using ODN decoy approach, could result in significant suppression of immune function at the level of cytokine production, effector function, and costimulation capacity.

Although long-term allograft survival has been achieved after infusion of costimulatory molecule-deficient DCs in a few specific mouse strain combinations, the ability of immature DCs to prolong allograft survival in most models is still not satisfactory.

In this study, by targeting the NF- κ B pathway in DCs with short NF- κ B decoy ODNs, DCs were maintained in an immature phenotype associated with significantly reduced allostimulatory capacity *in vitro*. More importantly, with administration of NF- κ B decoy ODNs-treated donor DCs, significant suppression of liver allograft rejection and marked prolongation of recipient survival were achieved in the absence of immunosuppression. *In vivo*, only the effect of NF- κ B decoy ODNs-treated donor DCs on liver allograft survival was maximal, although some suppression of liver allograft rejection and survival prolongation were observed in recipients injected with immature DCs without NF- κ B decoy ODNs modification.

The mechanisms by which NF- κ B decoy ODNs-treated DCs prolong survival of liver allografts are unclear. We found *in vitro* and *in vivo* evidence that stably immature NF- κ B decoy ODNs-treated DCs could suppress T cell allostimulatory ability, promote apoptosis of graft-infiltrating cells, and inhibit Th1 immunostimulatory cytokines such as IL-2 and IFN- γ mRNA expression and increase Th2 cytokine (IL-4) mRNA expression both in liver graft and in recipient spleen. Apoptosis of alloreactive T cells appears to be an important mechanism underlying the survival prolongation of organ graft, apoptosis of immunoreactive T cells within the graft and host secondary lymphoid tissue plays a pivotal role in determining the balance between liver transplant tolerance and rejection. Previous studies showed that blockade of costimulation by donor-derived DCs markedly promoted apoptosis of alloreactive T cells in host lymphoid tissue and prolonged organ graft survival^[50,51]. However, prevention of apoptosis of alloreactive T cells could block the induction of peripheral transplant tolerance^[42,52]. In the present study, *in situ* TUNEL staining of liver grafts from NF- κ B decoy ODNs-modified DCs-treated recipients showed the greatest degree of apoptosis of lymphocytes within portal areas of liver grafts. The result strongly suggested that the enhanced apoptosis of liver allograft-infiltrating lymphocytes might be an important mechanism for survival prolongation of liver allograft induced by NF- κ B decoy ODNs-treated DCs.

Another important mechanism by which NF- κ B decoy ODNs-treated DCs prolong survival of liver allografts may be the alteration of immunoregulatory cytokines (such as IL-2, IL-4 and IFN- γ) mRNA expression both in liver graft and in recipient spleen. In the present study, high level expression of IL-2, IL-4 and IFN- γ mRNA was observed in grafts and recipient spleen

of untreated recipient animals, which was consistent with immune activation. Administration of immature DCs (GM-CSF DCs or GM-CSF + scrambled ODNs DCs) partially down-regulated IL-2 mRNA and IFN- γ mRNA expression and partially up-regulated IL-4 mRNA expression both in liver graft and in recipient spleen. NF- κ B decoy ODNs-treated DCs appeared to skew cytokine expression toward Th2 cytokines (IL-4), and significantly suppressed Th1 cytokines (INF- γ and IL-2) mRNA expression both in liver graft and in recipient spleen. The suppressed expression of IFN- γ and IL-2 mRNA both in liver graft and in spleen might be associated with the enhanced apoptosis of T cells and the skewing toward Th2. Although there is evidence that IL-10 could exacerbate organ allograft rejection and its neutralization could modestly prolong transplant survival^[53,54], the predominant expression of Th2 cytokines, such as IL-4 and IL-10, was implicated in long term survival of the allograft in general. In contrast to Th2 cytokines, expression of Th1 cytokines, especially IFN- γ , in graft models has been shown to be associated with acute rejection^[29,50,55]. Thus, significantly decreased expression of Th1 cytokines such as IL-2 and IFN- γ mRNA, as well as the relatively high level of IL-4 mRNA both in liver allograft and in recipient spleen may be an important mechanism underlying the tolerance of liver allograft induced by NF- κ B decoy ODNs-treated DCs.

REFERENCES

- Zhang JK, Chen HB, Sun JL, Zhou YQ. Effect of dendritic cells on LPAK cells induced at different times in killing hepatoma cells. *Shijie Huaren Xiaohua Zazhi* 1999; 7: 673-675
- Li MS, Yuan AL, Zhang WD, Chen XQ, Tian XH, Piao YT. Immune response induced by dendritic cells induce apoptosis and inhibit proliferation of tumor cells. *Shijie Huaren Xiaohua Zazhi* 2000; 8: 56-58
- Luo ZB, Luo YH, Lu R, Jin HY, Zhang PB, Xu CP. Immunohistochemical study on dendritic cells in gastric mucosa of patients with gastric cancer and precancerous lesions. *Shijie Huaren Xiaohua Zazhi* 2000; 8: 400-402
- Li MS, Yuan AL, Zhang WD, Liu SD, Lu AM, Zhou DY. Dendritic cells *in vitro* induce efficient and specific anti-tumor immune response. *Shijie Huaren Xiaohua Zazhi* 1999; 7: 161-163
- Wang FS, Xing LH, Liu MX, Zhu CL, Liu HG, Wang HF, Lei ZY. Dysfunction of peripheral blood dendritic cells from patients with chronic hepatitis B virus infection. *World J Gastroenterol* 2001; 7: 537-541
- Banchereau J, Briere F, Caux C, Davoust J, Lebecque S, Liu YJ, Pulendran B, Palucka K. Immunobiology of dendritic cells. *Annu Rev Immunol* 2000; 18: 767-811
- Banchereau J, Steinman RM. Dendritic cells and the control of immunity. *Nature* 1998; 392: 245-252
- Khanna A, Morelli AE, Zhong C, Takayama T, Lu L, Thomson AW. Effects of liver-derived dendritic cell progenitors on Th1- and Th2-like cytokine responses *in vitro* and *in vivo*. *J Immunol* 2000; 164: 1346-1354
- Morelli AE, O'Connell PJ, Khanna A, Logar AJ, Lu L, Thomson AW. Preferential induction of Th1 responses by functionally mature hepatic (CD8 α - and CD8 α +) dendritic cells: association with conversion from liver transplant tolerance to acute rejection. *Transplantation* 2000; 69: 2647-2657
- Mehling A, Grabbe S, Voskort M, Schwarz T, Luger TA, Beissert S. Mycophenolate mofetil impairs the maturation and function of murine dendritic cells. *J Immunol* 2000; 165: 2374-2381
- Stuart LM, Lucas M, Simpson C, Lamb J, Savill J, Lacy-Hulbert A. Inhibitory effects of apoptotic cell ingestion upon endotoxin-driven myeloid dendritic cell maturation. *J Immunol* 2002; 168: 1627-1635
- Ismaili J, Rennesson J, Aksoy E, Vekemans J, Vincart B, Amraoui Z, Van Laethem F, Goldman M, Dubois PM. Monophosphoryl lipid A activates both human dendritic cells and T cells. *J Immunol* 2002; 168: 926-932
- Sato K, Nagayama H, Enomoto M, Tadokoro K, Juji T, Takahashi TA. Autocrine activation-induced cell death of T cells by human peripheral blood monocyte-derived CD4⁺ dendritic cells. *Cell Immunol* 2000; 199: 115-125
- Zheng H, Dai J, Stoilova D, Li Z. Cell surface targeting of heat shock protein gp96 induces dendritic cell maturation and anti-tumor immunity. *J Immunol* 2001; 167: 6731-6735
- Morel Y, Truneh A, Sweet RW, Olive D, Costello RT. The TNF superfamily members LIGHT and CD154 (CD40 ligand) costimulate induction of dendritic cell maturation and elicit specific CTL activity. *J Immunol* 2001; 167: 2479-2486
- Kobayashi M, Azuma E, Ido M, Hirayama M, Jiang Q, Iwamoto S, Kumamoto T, Yamamoto H, Sakurai M, Komada Y. A pivotal role of Rho GTPase in the regulation of morphology and function of dendritic cells. *J Immunol* 2001; 167: 3585-3591
- Hertz CJ, Kiertscher SM, Godowski PJ, Bouis DA, Norgard MV, Roth MD, Modlin RL. Microbial lipopeptides stimulate dendritic cell maturation via Toll-like receptor 2. *J Immunol* 2001; 166: 2444-2450
- Thoma-Uszynski S, Kiertscher SM, Ochoa MT, Bouis DA, Norgard MV, Miyake K, Godowski PJ, Roth MD, Modlin RL. Activation of toll-like receptor 2 on human dendritic cells triggers induction of IL-12, but not IL-10. *J Immunol* 2000; 165: 3804-3810
- Hirano A, Luke PP, Specht SM, Fraser MO, Takayama T, Lu L, Hoffman R, Thomson AW, Jordan ML. Graft hyporeactivity induced by immature donor-derived dendritic cells. *Transpl Immunol* 2000; 8: 161-168
- Lee WC, Zhong C, Qian S, Wan Y, Gauldie J, Mi Z, Robbins PD, Thomson AW, Lu L. Phenotype, function, and *in vivo* migration and survival of allogeneic dendritic cell progenitors genetically engineered to express TGF-beta. *Transplantation* 1998; 66: 1810-1817
- Hayamizu K, Huie P, Sibley RK, Strober S. Monocyte-derived dendritic cell precursors facilitate tolerance to heart allografts after total lymphoid irradiation. *Transplantation* 1998; 66: 1285-1291
- Khanna A, Steptoe RJ, Antonysamy MA, Li W, Thomson AW. Donor bone marrow potentiates the effect of tacrolimus on nonvascularized heart allograft survival: association with microchimerism and growth of donor dendritic cell progenitors from recipient bone marrow. *Transplantation* 1998; 65: 479-485
- Lu L, McCaslin D, Starzl TE, Thomson AW. Bone marrow-derived dendritic cell progenitors (NLDC 145+, MHC class II+, B7-1dim, B7-2-) induce alloantigen-specific hyporesponsiveness in murine T lymphocytes. *Transplantation* 1995; 60: 1539-1545
- Fu F, Li Y, Qian S, Lu L, Chambers F, Starzl TE, Fung JJ, Thomson AW. Costimulatory molecule-deficient dendritic cell progenitors (MHC class II+, CD80dim, CD86-) prolong cardiac allograft survival in nonimmunosuppressed recipients. *Transplantation* 1996; 62: 659-665
- Lutz MB, Suri RM, Niimi M, Ogilvie AL, Kukutsch NA, Rossner S, Schuler G, Austyn JM. Immature dendritic cells generated with low doses of GM-CSF in the absence of IL-4 are maturation resistant and prolong allograft survival *in vivo*. *Eur J Immunol* 2000; 30: 1813-1822
- Thomas JM, Contreras JL, Jiang XL, Eckhoff DE, Wang PX, Hubbard WJ, Lobashevsky AL, Wang W, Asiedu C, Stavrou S, Cook WJ, Robbin ML, Thomas FT, Neville DM Jr. Peritransplant tolerance induction in macaques: early events reflecting the unique synergy between immunotoxin and deoxyspergualin. *Transplantation* 1999; 68: 1660-1673
- Jonuleit H, Schmitt E, Schuler G, Knop J, Enk AH. Induction of interleukin 10-producing, nonproliferating CD4(+) T cells with regulatory properties by repetitive stimulation with allogeneic immature human dendritic cells. *J Exp Med* 2000; 192: 1213-1222
- Dhodapkar MV, Steinman RM, Krasovsky J, Munz C, Bhardwaj N. Antigen-specific inhibition of effector T cell function in humans after injection of immature dendritic cells. *J Exp Med* 2001; 193: 233-238
- Bonham CA, Peng L, Liang X, Chen Z, Wang L, Ma L, Hackstein H, Robbins PD, Thomson AW, Fung JJ, Qian S, Lu L. Marked prolongation of cardiac allograft survival by dendritic cells genetically engineered with NF-kappa B oligodeoxyribonucleotide decoys and adenoviral vectors encoding CTLA4-Ig. *J Immunol* 2002; 169: 3382-3391
- Ouaaz F, Arron J, Zheng Y, Choi Y, Beg AA. Dendritic cell

- development and survival require distinct NF- κ B subunits. *Immunity* 2002; **16**: 257-270
- 31 **Rescigno M**, Martino M, Sutherland CL, Gold MR, Ricciardi-Castagnoli P. Dendritic cell survival and maturation are regulated by different signaling pathways. *J Exp Med* 1998; **188**: 2175-2180
- 32 **Verhasselt V**, Vanden Berghe W, Vanderheyde N, Willems F, Haegeman G, Goldman M. N-acetyl-L-cysteine inhibits primary human T cell responses at the dendritic cell level: association with NF- κ B inhibition. *J Immunol* 1999; **162**: 2569-2574
- 33 **Mann J**, Oakley F, Johnson PW, Mann DA. CD40 induces interleukin-6 gene transcription in dendritic cells: regulation by TRAF2, AP-1, NF- κ B, AND CBF1. *J Biol Chem* 2002; **277**: 17125-17138
- 34 **Giannoukakis N**, Bonham CA, Qian S, Chen Z, Peng L, Harnaha J, Li W, Thomson AW, Fung JJ, Robbins PD, Lu L. Prolongation of cardiac allograft survival using dendritic cells treated with NF- κ B decoy oligodeoxynucleotides. *Mol Ther* 2000; **1**(5 Pt 1): 430-437
- 35 **Nouri-Shirazi M**, Guinet E. Direct and indirect cross-tolerance of alloreactive T cells by dendritic cells retained in the immature stage. *Transplantation* 2002; **74**: 1035-1044
- 36 **Abeyama K**, Eng W, Jester JV, Vink AA, Edelbaum D, Cockerell CJ, Bergstresser PR, Takashima A. A role for NF- κ B-dependent gene transactivation in sunburn. *J Clin Invest* 2000; **105**: 1751-1759
- 37 **Sun J**, McCaughan GW, Matsumoto Y, Sheil AG, Gallagher ND, Bishop GA. Tolerance to rat liver allografts. I. Differences between tolerance and rejection are more marked in the B cell compared with the T cell or cytokine response. *Transplantation* 1994; **57**: 1394-1357
- 38 **McKnight AJ**, Barclay AN, Mason DW. Molecular cloning of rat interleukin 4 cDNA and analysis of the cytokine repertoire of subsets of CD4+ T cells. *Eur J Immunol* 1991; **21**: 1187-1194
- 39 **Ikejima K**, Enomoto N, Iimuro Y, Ikejima A, Fang D, Xu J, Forman DT, Brenner DA, Thurman RG. Estrogen increases sensitivity of hepatic Kupffer cells to endotoxin. *Am J Physiol* 1998; **274**(4 Pt 1): G669-G676
- 40 **Stober D**, Schirmbeck R, Reimann J. IL-12/IL-18-dependent IFN- γ release by murine dendritic cells. *J Immunol* 2001; **167**: 957-965
- 41 **Qian S**, Lu L, Fu F, Li Y, Li W, Starzl TE, Fung JJ, Thomson AW. Apoptosis within spontaneously accepted mouse liver allografts: evidence for deletion of cytotoxic T cells and implications for tolerance induction. *J Immunol* 1997; **158**: 4654-4661
- 42 **Qian S**, Lu L, Fu F, Li W, Pan F, Steptoe RJ, Chambers FG, Starzl TE, Fung JJ, Thomson AW. Donor pretreatment with Flt-3 ligand augments antidonor cytotoxic T lymphocyte, natural killer, and lymphokine-activated killer cell activities within liver allografts and alters the pattern of intra-graft apoptotic activity. *Transplantation* 1998; **65**: 1590-1598
- 43 **Lu L**, Li W, Zhong C, Qian S, Fung JJ, Thomson AW, Starzl TE. Increased apoptosis of immunoreactive host cells and augmented donor leukocyte chimerism, not sustained inhibition of B7 molecule expression are associated with prolonged cardiac allograft survival in mice preconditioned with immature donor dendritic cells plus anti-CD40L mAb. *Transplantation* 1999; **68**: 747-757
- 44 **Lutz MB**, Suri RM, Niimi M, Ogilvie AL, Kukutsch NA, Rossner S, Schuler G, Austyn JM. Immature dendritic cells generated with low doses of GM-CSF in the absence of IL-4 are maturation resistant and prolong allograft survival *in vivo*. *Eur J Immunol* 2000; **30**: 1813-1822
- 45 **Lee JI**, Ganster RW, Geller DA, Burckart GJ, Thomson AW, Lu L. Cyclosporine A inhibits the expression of costimulatory molecules on *in vitro*-generated dendritic cells: association with reduced nuclear translocation of nuclear factor kappa B. *Transplantation* 1999; **68**: 1255-1263
- 46 **Yin D**, Ma L, Zeng H, Shen J, Chong AS. Allograft tolerance induced by intact active bone co-transplantation and anti-CD40L monoclonal antibody therapy. *Transplantation* 2002; **74**: 345-354
- 47 **Takayama T**, Kaneko K, Morelli AE, Li W, Tahara H, Thomson AW. Retroviral delivery of transforming growth factor-beta1 to myeloid dendritic cells: inhibition of T-cell priming ability and influence on allograft survival. *Transplantation* 2002; **74**: 112-119
- 48 **Takayama T**, Nishioka Y, Lu L, Lotze MT, Tahara H, Thomson AW. Retroviral delivery of viral interleukin-10 into myeloid dendritic cells markedly inhibits their allostimulatory activity and promotes the induction of T-cell hyporesponsiveness. *Transplantation* 1998; **66**: 1567-1574
- 49 **Stepkowski SM**, Wang ME, Condon TP, Cheng-Flournoy S, Stecker K, Graham M, Qu X, Tian L, Chen W, Kahan BD, Bennett CF. Protection against allograft rejection with intercellular adhesion molecule-1 antisense oligodeoxynucleotides. *Transplantation* 1998; **66**: 699-707
- 50 **Li W**, Lu L, Wang Z, Wang L, Fung JJ, Thomson AW, Qian S. IL-12 antagonism enhances apoptotic death of T cells within hepatic allografts from Flt3 ligand-treated donors and promotes graft acceptance. *J Immunol* 2001; **166**: 5619-5628
- 51 **Li W**, Lu L, Wang Z, Wang L, Fung JJ, Thomson AW, Qian S. Costimulation blockade promotes the apoptotic death of graft-infiltrating T cells and prolongs survival of hepatic allografts from FLT3L-treated donors. *Transplantation* 2001; **72**: 1423-1432
- 52 **Li Y**, Li XC, Zheng XX, Wells AD, Turka LA, Strom TB. Blocking both signal 1 and signal 2 of T-cell activation prevents apoptosis of alloreactive T cells and induction of peripheral allograft tolerance. *Nat Med* 1999; **5**: 1298-1302
- 53 **Li W**, Fu F, Lu L, Narula SK, Fung JJ, Thomson AW, Qian S. Differential effects of exogenous interleukin-10 on cardiac allograft survival: inhibition of rejection by recipient pretreatment reflects impaired host accessory cell function. *Transplantation* 1999; **68**: 1402-1409
- 54 **Li W**, Fu F, Lu L, Narula SK, Fung JJ, Thomson AW, Qian S. Systemic administration of anti-interleukin-10 antibody prolongs organ allograft survival in normal and presensitized recipients. *Transplantation* 1998; **66**: 1587-1596
- 55 **Shirwan H**, Barwari L, Khan NS. Predominant expression of T helper 2 cytokines and altered expression of T helper 1 cytokines in long-term allograft survival induced by intrathymic immune modulation with donor class I major histocompatibility complex peptides. *Transplantation* 1998; **66**: 1802-1809

Grey scale enhancement of rabbit liver and kidney by intravenous injection of a new lipid-coated ultrasound contrast agent

Ping Liu, Yun-Hua Gao, Kai-Bin Tan, Zheng Liu, Song Zuo

Ping Liu, Yun-Hua Gao, Kai-Bin Tan, Zheng Liu, Song Zuo, Department of Ultrasound, Xinqiao Hospital, Third Military Medical University, Chongqing 400037, China

Supported by the National Natural Science Foundation of China, No. 30270384

Correspondence to: Professor Yun-hua Gao, Department of Ultrasound, Xinqiao Hospital, Third Military Medical University, Chongqing 400037, China. gaoyunhua116@hotmail.com

Telephone: +86-23-68774698 Fax: +86-23-68755631

Received: 2003-12-12 Accepted: 2004-01-15

Abstract

AIM: To assess the grey scale enhancement of a new lipid-coated ultrasound contrast agent in solid abdominal organs as liver and kidney.

METHODS: Size distribution and concentration of the lipid-coated contrast microbubbles were analyzed by a Coulter counter. Two-dimensional (2D) second harmonic imaging of the hepatic parenchyma, the inferior vena cava and the right kidney of the rabbits were acquired before and after contrast agent injection. Images were further quantified by histogram in Adobe Photoshop 6.0. Time-intensity curves of hepatic parenchyma, inferior vena cava and renal cortex were generated from the original grey scale.

RESULTS: The 2D images of hepatic parenchyma and cortex of the kidney were greatly enhanced after injection and the peak time could last more than 50 min.

CONCLUSION: This new lipid ultrasound contrast agent could significantly enhance the grey scale imaging of the hepatic parenchyma and the renal cortex for more than 50 min.

Liu P, Gao YH, Tan KB, Liu Z, Zuo S. Grey scale enhancement of rabbit liver and kidney by intravenous injection of a new lipid-coated ultrasound contrast agent. *World J Gastroenterol* 2004; 10(16): 2369-2372

<http://www.wjgnet.com/1007-9327/10/2369.asp>

INTRODUCTION

New ultrasound contrast consisting of perfluorocarbon microbubbles could enhance grey scale images of parenchymal organs. It provided a new method in diagnosis^[1-10]. The development of new ultrasound contrast agent (UCA) has become one of the most promising fields in ultrasound medicine. So far, several UCAs, like Optison^[11,12] and Definity^[13], have been approved for treatment and become commercially available; many others are still in clinical trials^[14-16]. Based on the chemical components of bubble film, UCAs could be divided into four different types: Surfactants^[17-19], human albumin^[20,21], polymer^[22] and lipids^[23-25]. The lipids are superior to the others in many aspects: no risk of blood transmitted infection, excellent stability and some tissue-specific targeting, like the reticuloendothelial

system. This study was aimed to investigate the effectiveness, reproducibility of a new lipid contrast agent in the enhancement of abdominal parenchymal organs. All the protocols were approved by IRB (Internal Review Board) of Xinqiao Hospital.

MATERIALS AND METHODS

Preparation and analysis of lipid-coated microbubble agent

Liposome, which consists of two kinds of phospholipids and polyethylene glycol, was prepared by lyophilization. Then the lipids were rehydrated with certain media, like glucose and deionized water. The resultant suspension was sonicated by an ultrasound sonicator (YJ 92-II Xinzhi Corp. Hang-zhou, Zhejiang Province). The perfluoropropane was introduced into the suspension during sonication, then it was kept still, until it was separated into two layers, the upper layer was still in white colloid whereas the lower layer was slowly defecated. Then the upper layer of the agent was extracted and analyzed. To acquire size distribution data of the new contrast agent, the milky microbubbles suspension was analyzed by Sysmex KX-21 (Sysmex Corporation, Japan). The surface electric potential and pH of UCA were measured by Zeta 3 000 (Malvern Ltd., United Kingdom).

Animal models

Ten healthy rabbits, weighing 2.0-2.2 kg, were enrolled in this study. The body hair at experimental region was removed for liver and renal scan. Rabbits were anesthetized by intramuscular injection of "Xu Mian Xing" (mainly consisted of haloperidol and made by Changchun University of Agriculture and Prologue) at the dose of 0.15 mL/kg bm, and the intravenous infusion was set up through ear veins. Lipid contrast agent was injected at 0.01 mL/kg bm, and followed by 1 mL saline flush.

Settings of ultrasound equipment

A Siemens Sequoia 512 (Siemens Acuson Co., Mountain View, California) ultrasound system was used in this study. The second harmonic imaging of 6L3 probe at 3.0/6.0 MHz was used. The mechanic index and output power were set at 0.11 and -24 dB, respectively. All the other parameters, like gain, depth, TGC, compress and focus, were kept constant during experiment. Experimental images were digitally recorded. Overall, baseline and 60 min contrast images were acquired. All images were transformed from original DICOM files into JPEG format by Viewpro (Acuson Co.). Grey scale was calculated by histogram in Adobe Photoshop 6.0 (Adobe Co.). Sample area used in the histogram had 1 088 pixels in an ellipse. Time-density curve was generated based on the mean pixel grey scale of hepatic parenchyma and renal cortex.

Pathological examination

All animals were sacrificed by intravenous injection of 10% potassium chloride. The liver, kidney and lung tissues were autopsied and fixed in 40 g/L formaldehyde for H&E stain. All tissue slides were reviewed by pathologists.

Statistical analysis

The grey scale data acquired from liver, inferior vena cava and

renal cortex were expressed as mean \pm SD. Pre- and post-contrast of liver's and kidney's grey scale data were compared by paired two-tailed Student's *t* test in SPSS 8.0 program. *P* critical value less than 0.05 was considered to be statistically significant.

RESULTS

Contrast agent

The visual appearance of the newly made liposome contrast agent was an opaque milky suspension, and it was slowly delaminated. The microbubble concentration was (7-8) \times 10⁹/mL, and the size distribution was 2 to 10 μ m. About 90% of the microbubbles were less than 8 μ m (Figure 1). The surface electric potential was -71.2 mV and the pH was 6.42.

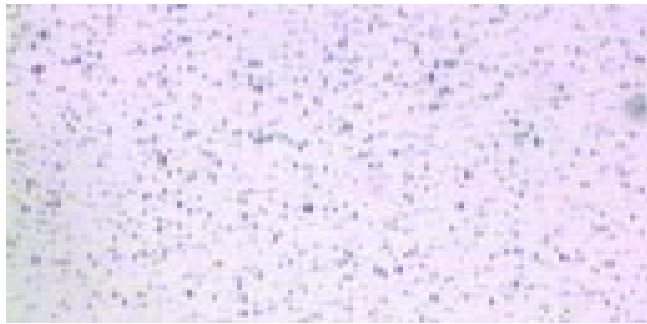


Figure 1 Microbubbles in 400-fold diluted saline (original magnification: \times 100).

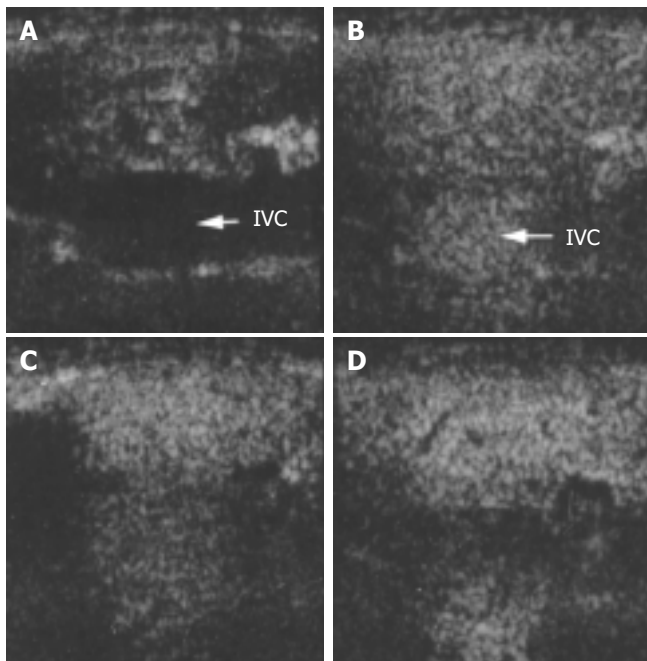


Figure 2 Ultrasound images of liver parenchyma and inferior vena cava (IVC) before and after the injection of microbubbles. A: before injection; B: 30 s after injection; C: 1 min after injection; D: 2 min after injection.

Grey scale enhancement of liver and kidney

The images of both hepatic parenchyma and renal cortex were visually significantly enhanced after intravenous injection of the contrast agent (Figures 2-5). Time-intensity curves of both liver and cortex were elevated and kept at a high level. The grey scale of liver parenchyma (61.2 \pm 3.1) 30 s after contrast injection was significantly higher than that of baseline image (38.0 \pm 3.0, *P*<0.05). At the time point of 180 s after injection, the grey scale of liver parenchyma reached 83.2 \pm 1.8 which was significantly

higher than baseline (*P*<0.01). And 54 min after the injection, the liver enhancement remained at 57.8 \pm 1.4. One hour after contrast injection, the grey scale dropped to 45.2 \pm 1.0, which had no statistical significance. Similar results were observed in the contrast enhancement of renal cortex, and the grey scales were 18.1 \pm 3.8 at baseline, 48.8 \pm 3.3 (*P*<0.01) 10 s after injection, 27.4 \pm 4.1 (*P*<0.01) 56 min after injection, 26.1 \pm 3.9 60 min after injection (*P*<0.05). These results confirmed that this lipid microbubbles contrast agent could effectively enhance hepatic parenchyma and renal cortex at a relatively long time.

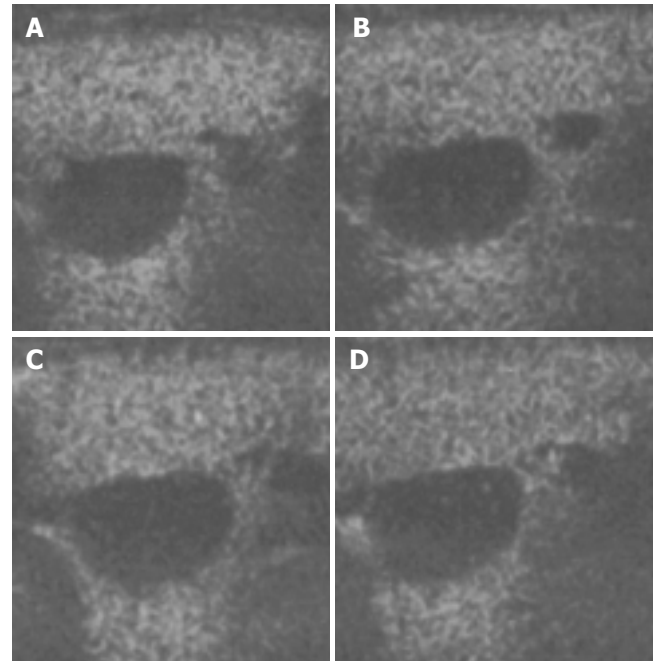


Figure 3 Ultrasound images of liver parenchyma and inferior vena cava (IVC) before and after the injection of microbubbles. A: 15 min after injection; B: 25 min after injection; C: 30 min after the injection; D: 40 min after the injection.

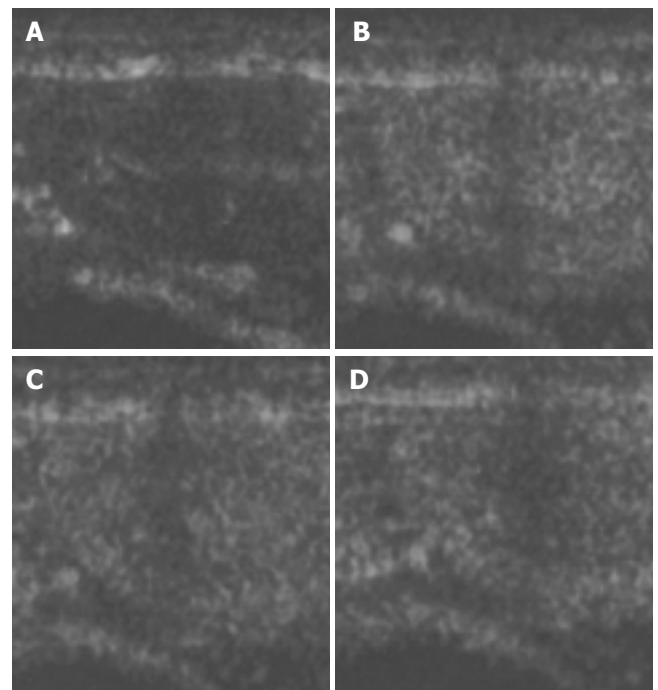


Figure 4 Ultrasound images of renal cortex before and after the injection of microbubbles. A: before injection; B: 30 s after injection; C: 1 min after injection; D: 2 min after injection.

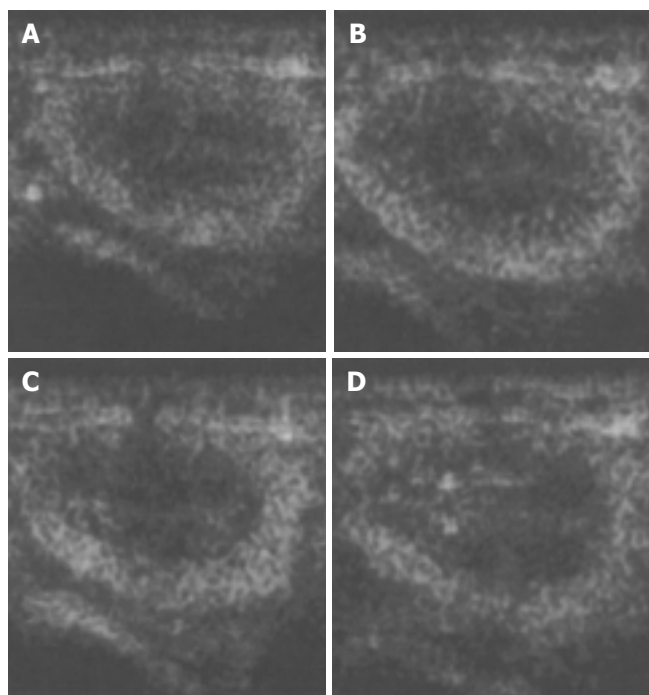


Figure 5 Ultrasound images of the renal cortex after injection of microbubbles. A: 5 min after injection; B: 10 min after injection; C: 30 min after injection; D: 40 min after injection.

At inferior vena cava (IVC), the time-intensity curve was different from that of hepatic parenchyma and renal cortex. The grey scale of IVC significantly rose to 52.5 ± 2.9 20 s after contrast injection which was higher compared with baseline (5.8 ± 1.6). The significant enhancement lasted only 120 s after injection, then diminished gradually and disappeared at 240 s after contrast injection. IVC contrast intensity dropped back to baseline 27 min after injection (17.0 ± 5.2).

Pathological results

All tissues from liver, lung, and kidney were normal in histology, and there was no sign of air embolism or infarction spot.

DISCUSSION

Lipid-coated microbubbles were mainly composed of several biocompatible phospholipids that had excellent stability and non-bioactive components. The lipids had been widely used in the preparation of ultrasound contrast agent, liposome and other drugs. In this study, a new ultrasound contrast agent based on lipids was prepared and showed excellent stability in the enhancement of hepatic parenchyma and renal cortex at a minimal dose of 0.01 mL/kg bm. Grey scale enhancement could last more than 50 min from both visual assessment and quantitative statistical analysis. This enhancement was longer than some previous reports, which were about 5-15 min^[19,25,26]. Also, the time-intensity curves of hepatic parenchyma and renal cortex were quite different from that of inferior vena cava. These microbubbles tended to be stable in parenchyma, rather than in circulation, as the time-density curve from IVC showed a 200-s wash-in and wash-out enhancement.

According to some reports^[27,28] and our experiment^[29], we assumed that the prolonged enhancement was due to the uptake of microbubbles by the reticuloendothelial system in liver. But this could not explain the prolonged enhancement in the kidney, which is not rich of reticuloendothelial system. There might be some other reasons. Since the peak contrast intensities of liver parenchyma and cortex appeared much later than that of inferior vena cava, they were 12 min, 6 min and 30 s,

respectively, it indicated that after the peak contrast in circulation there was another peak contrast in solid organs, and it was presumed to be the accumulation of microbubbles in hepatic sinusoids or capillary bed in cortex. As we know, hepatic parenchyma is consisted of hepatic sinusoids and renal cortex is mostly consisted of glomeruli. They are both rich in capillaries. Meanwhile, the blood flow in hepatic sinusoids and glomeruli is much slower than that in inferior vena cava. So, the microbubbles could easily be accumulated in capillary bed, which resulted in the prolonged enhancement of liver and kidney.

As IVC grey scale at 27 min postinjection was lower than that before injection, the hepatic parenchyma might block ultrasound transmission to IVC by condensed bubble's attenuation, and this could produce visually lower IVC echo.

In this study, the new lipids ultrasound contrast agent was long-term stable in enhancement of liver parenchyma and renal cortex. The mean size of the microbubbles was less than 8 μm , which was smaller than that of red blood cell, and thereby it was safe for intravenous injection. Pathologically, all the tissues from liver, lung, and kidney were normal in histology, and there were no signs of air embolism or infarction spot.

In comparison with other lipid-coated microbubbles^[30], this contrast agent had a higher bubble concentration and a longer stability in parenchymal organs. The reason for this might attribute to the reconstituted membrane of the microbubbles. Polyethylene glycol could protect phagocytosis from Kupffer cell, and it could exist in hepatic sinusoid longer. Tween 80, a kind of surfactant, which has never been used in other lipid microbubbles contrast agent, may increase the bubbles or microbubbles concentration.

Although this new lipid-based contrast agent exhibited a prolonged enhancement, the true reason has not been clarified. Further studies are needed to investigate the mechanism of long-lasting enhancement.

REFERENCES

- 1 **Lindner JR**, Song J, Christiansen J, Klibanow AL, Xu F, Ley K. Ultrasound assessment of inflammation and renal tissue injury with microbubbles targeted to P-Selectin. *Circulation* 2001; **104**: 2107-2112
- 2 **Bang N**, Nielsen MB, Rasmussen AN, Osterhammel PA, Pedersen JF. Hepatic vein transit time of an ultrasound contrast agent: simplified procedure using pulse inversion imaging. *Br J Radiol* 2001; **74**: 752-755
- 3 **Ramarine KV**, Kyriakopoulou K, Gordon P, McDicken NW, McArdle CS, Leen E. Improved characterisation of focal liver tumours: dynamic power Doppler imaging using NC100100 echo-enhancer. *Eur J Ultrasound* 2000; **11**: 95-104
- 4 **Marelli C**. Preliminary clinical experience in cardiology with sonazoid. *Am J Cardiol* 2000; **86**(Suppl): 10G-13G
- 5 **Albrecht T**, Blomley MJK, Cosgrove DO, Taylor-Robinson SD, Jayaram V, Eckersley R, Urbank A, Butler-Barnes J, Patel N. Non-invasive diagnosis of hepatic cirrhosis by transit-time analysis of an ultrasound contrast agent. *Lancet* 1999; **353**: 1579-1583
- 6 **Du WH**, Yang WX, Wang X, Xiong XQ, Zhou Y, Li T. Vascularity of hepatic VX2 tumors of rabbits: Assessment with conventional power Doppler US and contrast enhanced harmonic power Doppler US. *World J Gastroenterol* 2003; **9**: 258-261
- 7 **Lindner JR**. Detection of inflamed plaques with contrast ultrasound. *Am J Cardiol* 2002; **90**(Suppl): 32L-35L
- 8 **Wang WP**, Ding H, Qi Q, Mao F, Xu ZZ, Kudo M. Characterization of focal hepatic lesions with contrast-enhanced C-cube gray scale ultrasonography. *World J Gastroenterol* 2003; **9**: 1667-1674
- 9 **Eyding J**, Wilkening W, Postert T. Brain perfusion and ultrasonic imaging techniques. *Eur J Ultrasound* 2002; **16**: 91-104
- 10 **Feril LB**, Kondo T, Zhao QL, Ogawa R, Tachibana K, Kudo N, Fujimoto S, Nakamura S. Enhancement of ultrasound-induced

- apoptosis and cell lysis by echo-contrast agents. *Ultrasound Med Biol* 2003; **29**: 331-337
- 11 **Yamaya Y**, Niizeki K, Kim J, Entin PL, Wagner H, Wagner PD. Effects of optison® on pulmonary gas exchange and hemodynamics. *Ultrasound Med Biol* 2002; **28**: 1005-1013
 - 12 **Masugara H**, Peters B, Lafittc S, Strachan MG, Ohmori K, DcMarin AN. Quantitative assessment of myocardial perfusion during graded coronary stenosis by real-time myocardial contrast echo refilling curves. *J Am Coll Cardiol* 2001; **37**: 262-269
 - 13 **Kitzman DW**, Goldman ME, Gillam LD, Cohen JL, Aurigemma GP, Gottdiener JS. Efficacy and safety of the novel ultrasound contrast agent perflutren (definity) in patients with suboptimal baseline left ventricular echocardiographic images. *Am J Cardiol* 2000; **86**: 669-674
 - 14 **Driven HA**, Rasmussen H, Johnson H, Videm S, Walday P, Grant D. Intestinal and hepatic lesions in mice, rats, and other laboratory animals after intravenous administration of gas-carrier contrast agents used in ultrasound imaging. *Toxicol Appl Pharmacol* 2003; **188**: 165-175
 - 15 **Moran CM**, Anderson T, Pye SD, Sboros V, McDicken WN. Quantification of microbubble destruction of three fluorocarbon-filled ultrasonic contrast agents. *Ultrasound Med Biol* 2000; **26**: 629-639
 - 16 **Moran CM**, Watson RJ, Fox KAA, McDiken WN. *In vitro* acoustic characterisation of four intravenous ultrasonic contrast agents at 30MHz. *Ultrasound Med Biol* 2002; **28**: 785-791
 - 17 **Marelli C**. Preliminary clinical experience in cardiology with Sonazoid. *Am J Cardiol* 2000; **86**(Suppl): G10-13
 - 18 **Yokoyama N**, Schwarz KQ, Chen X, Steinmetz SD, Becher H, Schimpky C, Schlieff R. The effect of echo contrast agent on doppler velocity measurements. *Ultrasound Med Biol* 2003; **29**: 765-770
 - 19 **Basude R**, Duckworth JW, Wheatley MA. Influence of environmental conditions on a new surfactant-based contrast agent: ST68. *Ultrasound Med Biol* 2000; **26**: 621-628
 - 20 **Porter TR**, Xie F, Kricsfeld A, Kilzer K. Noninvasive identification of acute myocardial ischemia and reperfusion with contrast ultrasound using intravenous perfluoropropane-exposed sonicated dextrose albumin. *J Am Coll Cardiol* 1995; **26**: 33-40
 - 21 **Bekeredjian R**, Behrens S, Ruef J, Dinjus E, Unger E, Baum M, Kuecherer HF. Potential of gold-bound microtubules as a new ultrasound contrast agent. *Ultrasound Med Biol* 2002; **28**: 691-695
 - 22 **Wei K**, Crouse L, Weiss J, Villanueva F, Schiller NB, Naqvi TZ, Siegel R, Monaghan M, Goldman J, Aggarwal P, Feigenbaum H, Demaria A. Comparison of usefulness of dipyridamole stress myocardial contrast echocardiography to technetium-99m sestamibi single-photon emission computed tomography for detection of coronary artery disease (PB127 Multicenter Phase 2 Trial results). *Am J Cardiol* 2003; **91**: 1293-1298
 - 23 **Bjerknes K**, Braenden JU, Smistad G, Agerkvist I. Evaluation of different formulation studies on air-filled polymeric microcapsules by multivariate analysis. *Inter J Pharma* 2003; **257**: 1-14
 - 24 **Basilico R**, Blomley MJK, Harvey CJ, Filippone A, Heckemann RA, Eckersley RJ, Cosgrove DO. Which continuous US scanning mode is optimal for the detection of vascularity in liver lesions when enhanced with a second generation contrast agent? *Euro J Radiol* 2002; **41**: 184-191
 - 25 **Bokor D**. Diagnostic efficacy of SonoVue. *Am J Cardiol* 2000; **86**(Suppl): 19G-24G
 - 26 **Totaro R**, Baldassarre M, Sacco S, Marini C, Carolei A. Prolongation of TCD-enhanced doppler signal by continuous infusion of levovist. *Ultrasound Med Biol* 2002; **28**: 1555-1559
 - 27 **Quaia E**, Blomley MJK, Patel S, Harvey CJ, Padhani A, Price P, Cosgrove DO. Initial observations on the effect of irradiation on the liver-specific uptake of Levovist. *Eur J Radiol* 2002; **41**: 192-199
 - 28 **Heckemann RA**, Harvey CJ, Blomley MJK, Eckersley RJ, Butler-Barnes J, Jayaram V, Cosgrove D. Enhancement characteristics of the microbubble agent Levovist: reproducibility and interaction with aspirin. *Eur J Radiol* 2002; **41**: 179-183
 - 29 **Liu P**, Gao YH, Tan KB, Zuo S, Liu Z. Enhanced imaging of the rabbit liver using the self-made liposome contrast agent: an earlier experimental study. *Zhongguo Chaosheng Yixue Zazhi* 2003; **19**: 4-6
 - 30 **Bouakaz A**, Krenning BJ, Vletter WB, Cate FJ, Jong ND. Contrast superharmonic imaging: A feasibility study. *Ultrasound Med Biol* 2003; **29**: 547-553

Edited by Chen WW Proofread by Zhu LH and Xu FM

Intestinal barrier damage caused by trauma and lipopolysaccharide

Lian-An Ding, Jie-Shou Li, You-Sheng Li, Nian-Ting Zhu, Fang-Nan Liu, Li Tan

Lian-An Ding, Jie-Shou Li, You-Sheng Li, Nian-Ting Zhu, Fang-Nan Liu, Li Tan, Jinling Hospital, Nanjing University Medical School, Nanjing 210002, Jiangsu Province, China

Correspondence to: Lian-An Ding, Associate Professor, Jinling Hospital, Nanjing University Medical School, 305 East Zhongshan Road, Nanjing 210002, Jiangsu Province, China. dlahaolq@hotmail.com

Telephone: +86-532-2911324 **Fax:** +86-532-2911840

Received: 2003-08-05 **Accepted:** 2003-10-27

Abstract

AIM: To investigate the intestinal barrier function damage induced by trauma and infection in rats.

METHODS: Experimental models of surgical trauma and infection were established in rats. Adult Sprague-Dawley rats were divided into 4 groups: control group ($n = 8$), EN group ($n = 10$), PN group ($n = 9$) and Sep group ($n = 8$). The rats in PN and Sep groups were made into PN models that received isonitrogenous, isocaloric and isovolumic TPN solution during the 7-d period. Rats in EN and Sep groups received laparotomy and cervical catheterization on day 1 and received lipopolysaccharide injection intraperitoneally on d 7. On the 7th day all the animals were gavaged with lactulose and mannitol to test the intestinal permeability. Twenty-four hours later samples were collected and examined.

RESULTS: The inflammatory responses became gradually aggravated from EN group to Sep group. The mucosal structure of small intestine was markedly impaired in PN and Sep groups. There was a low response in IgA level in Sep group when compared with that of EN group. Lipopolysaccharide injection also increased the nitric oxide levels in the plasma of the rats. The intestinal permeability and bacterial translocation increased significantly in Sep group compared with that of control group.

CONCLUSION: One wk of parenteral nutrition causes an atrophy of the intestinal mucosa and results in a moderate inflammatory reaction in the rats. Endotoxemia aggravates the inflammatory responses that caused by laparotomy plus TPN, increases the production of nitric oxide in the body, and damages the intestinal barrier function.

Ding LA, Li JS, Li YS, Zhu NT, Liu FN, Tan L. Intestinal barrier damage caused by trauma and lipopolysaccharide. *World J Gastroenterol* 2004; 10(16): 2373-2378

<http://www.wjgnet.com/1007-9327/10/2373.asp>

INTRODUCTION

Severe infection is still the main cause of death in critical illnesses such as severe trauma, burns and in massive use of immunosuppressive medicines. The endotoxin produced by *G*-bacilli is the important factor for the impairment of tissues and cells of the body. It could damage the systemic immunity, impair the intestinal barrier function, increase the mucosal permeability, and hence cause enterogenous infection, a phenomenon known as bacteria translocation^[1,2]. The impairments aggravate the

primary infection, which might cause multiple organ dysfunction syndrome (MODS), and even death. The alterations in pathophysiology and immunology when endotoxemia occurs, are very important for us to evaluate the impaired gut barrier function.

In routine clinical practice, some patients would complicate with infections after operation and trauma. Most of them can be cured, but a few of these infections would last for a longer time. Based on the consideration of the latter being a phenomenon of bacterial translocation as a result of the damage of intestinal barrier function, we conducted this animal experiment so as to investigate if there were gut barrier damage and bacterial translocation in such instances.

MATERIALS AND METHODS

Experimental animals and grouping

Adult, healthy male Sprague-Dawley rats, with body mass of 150-180 g (supplied by Shanghai Experimental Animal Center, Chinese Academy of Sciences) were used. The rats were fed for over 1 wk in our laboratory for adaptation and then put into metabolic cages for 5-7 d. The temperature in the animal rooms was 17-21°C with proper humidity (about 60%) and illumination of 12 h/d (6:00-18:00). During the adaptation period all the rats were fed with regular rat chow and tap water *ad libitum*. When the rat's body mass reached 200-300 g, 33 rats were chosen randomly and divided into 4 groups: (1) control group ($n = 8$), which were fed rat chow and tap water freely; (2) EN group ($n = 10$), in which a central venous catheter was inserted into animals' superior vena cava through right jugular vein under anaesthesia, and connected to the swivel apparatus. The rats also received laparotomy and were fed the chow freely; (3) PN group ($n = 9$), which were infused with a whole nutrients solution through a central venous catheter, and with drinking water *ad libitum*; (4) Sep group ($n = 8$) in which an exploratory laparotomy and central venous catheterization served as the trauma. After this, TPN was their sole nutrition source plus drinking water *ad lib*. On the 7th day 5 mg/kg of lipopolysaccharide was injected intraperitoneally for EN and SEP groups. PN and Sep Groups received isonitrogenous, isocaloric and isovolumic TPN solution during the 7-d period. All the protocols and procedures were approved by our University Committee of Animal Experiment Administration.

Intravenous nutrients and other relevant chemicals

TPN ingredients About 11.4% compound amino acids injection (Novamin), 20% medium-long chain fat emulsion (Lipovenoes MCT), multivitamin mixture (Soluvit, Vitalipid) and a trace element mixture (Addamel) were purchased from Sino-Sweden and Fresenius Pharmaceutical Corp. LTD.

Chemicals and reagents Lipopolysaccharide (LPS, from *E. coli*, 055: B5) was purchased from Sigma Co.; NO Test Kit was purchased from Promega Co., USA. Immunohistochemistry (T cell subgroups measurement) reagents were purchased from Serotec Ltd., Germany and IgA, Bethyl Co., USA.

Experimental model

Operation procedures Under anaesthesia with 100 mg/kg of ketamin injected into the animals intraperitoneally, the TPN model was established and a rotary transfusion apparatus was

used for TPN infusion^[3]. For surgical trauma, after shaving the hair on the abdomen, an incision (about 4 cm in length) was made and the whole abdominal cavity was explored and examined for about 5 min from the epigastrium to the pelvic cavity. The incision was sutured in double layers with silk suture No. 1. The operation was done under aseptic conditions. **TPN solution** The rats were put in the metabolic cages after surgical recovery. Each rat received 230 kcal/kg body mass of calories and 1.42 g nitrogen/kg each day in 50 mL of TPN solution. The ratio of glucose to lipid in this solution is 2:1, and nonprotein calorie to nitrogen (kcal/g), 137:1. Multivitamins, electrolytes, trace elements and 500 units of heparin were also included in the TPN solution. All the nutrient solutions were prepared under aseptic conditions daily and the infusion was done with an injecting micropump continuously and uniformly during 24 h each day. TPN infusion was started immediately after recovery from the laparotomy. On the first and last days of the experiment, each rat was given half of the total calories without any changes of other TPN ingredients.

Induction of endotoxemia On the 7th d of the experiment, 5 mg/kg of LPS in 5 mL of sterile distilled water was injected into the animals' peritoneal cavity to cause a sepsis state.

Lactulose/mannitol solution gavage On the 7th d of the experiment, 66 mg of lactulose and 50 mg of mannitol dissolved in 2 mL of normal saline were gavaged. Twenty-four hour urine was collected, the volume recorded and 0.2 mL of mercury salicylosulfide added. Then 5 mL of the urine specimen was stored at -20 °C until measurement.

Sample preparation and measurements

Twenty-four hours after gavaging with lactulose and mannitol and injecting endotoxin, 100 mg/kg of ketamine was injected intraperitoneally as an anesthetic. After the laparotomy was done, tissue and blood samples were collected and gross and laboratory examinations were performed.

Bacteriological test Blood 0.5 mL from the portal vein was drawn for culture. One gram of anterior lobe liver tissue and about 0.2-0.5 g mesenteric lymph nodes were excised. Each sample was put in a tissue homogenizer and 1.5 mL of normal saline was added before they were homogenized. The specimens were sent to a microbiological laboratory for aerobic culture and bacterial identification by morphological and bacteriological analyzer.

Bacterial culture (1) 10 µL homogenates of the lymph nodes and liver were separately taken and put on blood agar plates. Another 10 µL lymph nodes and liver homogenates were mixed with 10 mL saline for a dilution and the diluted samples were inoculated also on blood agar plates. (2) 0.5 mL of portal vein blood was inoculated into 4.5 mL of common broth for bacterial enrichment 16-18 h, then 20 µL of the enrichment solution was inoculated on blood agar plates. (3) The cultured media were put in a CO₂ incubator at 35 °C for 24-48 h. If there was no bacterial growth, they would be regarded as negative; but if there was growth, it would be further identified.

Identification of bacteria First, Gram-stained smears were made to determine whether they were cocci or bacilli and G⁺ or G⁻. Second, identifications were made using bacteriological analyzer of Vitek-32 (Bio Merieux Vitek, Inc., USA). Gram-positive cocci were tested with GPI card, Gram-negative bacilli, with GNI card, and fungi, YBC card.

Preparation of small intestine specimens The whole small intestine below the Treitz ligament was excised and immediately placed on ice cold of 9 g/L saline. The intestine was opened longitudinally and the contents of the intestine were washed out with icy saline. Two cm of proximal jejunum and distal ileum were cut and put into a 40 g/L neutral formaldehyde solution promptly and sent to be examined histologically. About 5 cm intestine segments from the upper, middle and lower sections

were resected and then the surfaces of the mucosa were dried with cotton swabs. The mucous membrane of the icy specimens was scraped, weighed and divided into two equal parts. They were immediately put into liquid nitrogen and then stored at -70 °C. **Histological examination of the intestinal mucosa** Specimens were embedded in paraffin, 4 µm sections were cut and stained with H.E., analyzed with an HPIAS-1000 Multimedia Color Analysis System. Three low power (10×10) fields in each section were observed. The lengths of 5 villi, the depth of 5 crypts and the thickness of the mucosa at 5 sites were analyzed. The average value was calculated and documented. All the calculation was done double-blindly by two experienced pathologists.

Immunohistochemical analysis of T cell subpopulation^[4] Specimens were embedded in paraffin, 4 µm sections were cut and stained with H.E., T cell subsets were examined by immunohistochemical SP method. The total T lymphocyte and its positive stained subpopulations (CD3, CD4, CD8) were counted in 10 whole villi in each section. The ratios and rates were then calculated. All the calculation was done double-blindly by two experienced pathologists.

Blood sampling Three milliliter blood from the right cardiac ventricle was drawn and 1 250 u heparin added. The blood was centrifuged and the serum stored at -70 °C. Then the animals were sacrificed by exsanguination.

Lactulose/mannitol test The lactulose and mannitol concentrations in the preserved urine sample were measured by a high-performance liquid chromatograph (Waters Co., USA). The ion-exchange column used was purchased from Transgenomic Co., USA. The ratio between the two sugars was then calculated. The test was to measure the amount of excreted dual sugars in urine of 24 h. Because these two kinds of saccharide nearly neither metabolize nor synthesize in the body, amounts of the two sugars being excreted from urine reflect the "leaking" degree of the intestine, or permeable extent of the intestine. The molecular weight of these two saccharides is different. The test error can be reduced when using two sugars of different molecular weight than using one only for the test. If the ratio of the two sugars' percentage in tested group was significantly bigger than that of normal control group, it could be concluded that the intestinal permeability in tested animals increased.

Determination of IgA The frozen samples of blood plasma and mucosa of the small intestine were melted to room temperature and 1 mL normal saline was then added to the melted 100 mg of mucosa before the homogenates were made, and then the concentration of IgA in their supernatants after centrifugation below 4 °C was measured. The results were shown as IgA µg/mL of blood plasma and IgA µg/g of small intestine mucosa.

Determination of NO The frozen samples of blood plasma and mucosa of the small intestine were melted to room temperature and concentration of NO in them was measured with the enzymatic method (Griess Reaction)^[5]. The results were shown as NO µmol/L of blood plasma and NO µmol/g of small intestine mucosa.

Statistical analysis

All the values were expressed as the mean±SE. One-way ANOVA was used to check the differences between groups. Chi-square test was used to check the differences of bacterial translocation rates between groups. When *P* was less than 0.05, the difference was considered statistically significant. The degree of correlation was described using Pearson correlation coefficient. Software SPSS10.0 was used in all statistical tests.

RESULTS

General animal manifestation

All the rats except those in the normal group appeared to have

symptoms in different degrees, such as lethargy, idleness, ruffling of hair, stop drinking and grossly concentrated urine. Some rats appeared very slow in their responses to sound stimulations and also had diarrhea. Their eyes appeared glazed with crusting exudates. These symptoms were prominent during the 5 to 15 h following LPS injection. There was no statistical difference in mortality within 24 h after LPS injection between EN and Sep groups.

Complete blood cell count

The total number of leukocytes and the number of neutrophils in PN group $[(14.97 \pm 2.704) \times 10^9/L$ and $(6.82 \pm 2.254) \times 10^9/L]$ was more than those of control group $[(7.59 \pm 0.379) \times 10^9/L$ and $(2.34 \pm 0.568) \times 10^9/L]$. On the contrary, Sep group rats showed a low response in cell count $[(8.9 \pm 0.82) \times 10^9$ and $(4.35 \pm 0.92) \times 10^9/L]$. Platelet count in groups of EN, PN and Sep $[(586.5 \pm 65.03) \times 10^9$, $(483.33 \pm 94.62) \times 10^9$ and $(277.5 \pm 44.87) \times 10^9/L$ respectively] decreased markedly as compared with that of control group $[(928.7 \pm 33.89) \times 10^9/L]$.

Body weight

At the beginning of the experiment there was no difference in the body mass of the animals. At the end of the experiment, the body mass increase was 32.38 ± 3.39 g in the control group. The body mass of other three groups decreased; it was 33.88 ± 3.19 g of loss in Sep group, the greatest among them.

Morphology and morphometry of small intestinal mucous membrane

The degree of damage of the villi and crypts and the thinning of the mucous membrane in jejunum and ileum were most significant in Sep group among the animals (Figures 1, 2).

Concentrations of NO in blood plasma and small intestinal mucosa

Concentrations of NO in blood plasma increased significantly after LPS injection (groups EN and SEP), whereas it was not evident in mucous membrane of small intestine (Table 1).

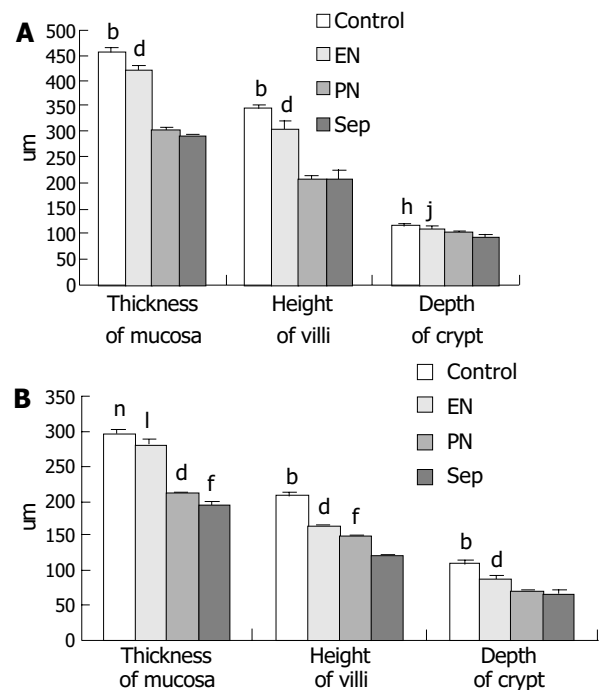


Figure 2 Morphometry for structure of small intestine mucosa (mean \pm SE). ^b $P < 0.001$ vs EN, PN and Sep gorups; ^d $P < 0.001$ vs PN and Sep gorups; ^f $P < 0.01$ vs Sep gorup; ^h $P < 0.005$ vs PN and Sep gorups; ^j $P < 0.001$ vs Sep group; ⁿ $P < 0.01$ vs EN gorup; ^l $P < 0.001$ vs PN and Sep groups.

IgA levels in plasma and small intestinal mucosa

IgA level was highest in blood plasma and intestinal mucosa in EN group among the animals (Table 2).

CD3 lymphocyte and CD4/CD8 ratio

There was no difference in CD3 population among the groups

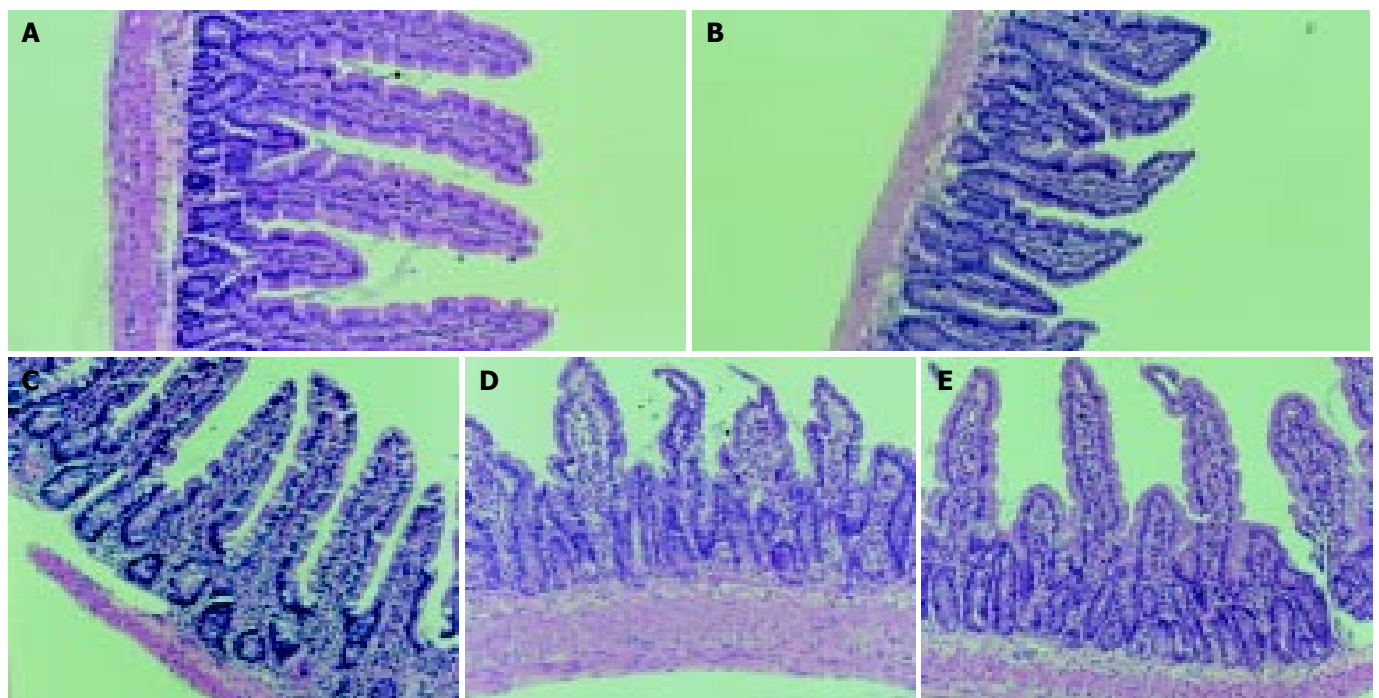


Figure 1 Alterations in architecture of small intestinal mucosa. (HE staining, original magnification: $\times 100$). A: Normal mucous membrane of jejunum in control rats. B: Normal mucous membrane of ileum in control rats. C: Histological changes of jejunal mucosa of group T1 rats. The villi become sparser than those in control. The height and shape of villi are normal on the whole. D: Histological changes of ileal mucosa in PN group rats. The section shows a severe atrophy in mucosal structure. The villi become shorter, blunt and swollen. E: Histological changes of jejunal mucosa of Sep group. The villi are sparse and shorter than those of control group.

but CD4/CD8 ratio in EN and PN groups was higher than that of control group. There was no significant difference in ratio of CD4 to CD8 between Sep group and control group.

Table 1 Concentrations of NO in blood plasma and in intestinal mucosa

Group	n	BP($\mu\text{mol/L}$)	SIM($\mu\text{mol/g}$) ¹
Control	8	38.63 \pm 8.75 ^b	39.19 \pm 2.68
EN	10	103.39 \pm 10.18	67.19 \pm 6.67
PN	9	63.06 \pm 23.33 ^a	66.90 \pm 6.25
Sep	8	113.33 \pm 30.47	53.10 \pm 2.16

Values are expressed as mean \pm SE; BP, blood plasma; SIM, mucous membrane of small intestine; ^b P <0.01 vs EN group and Sep group; ^a P <0.05 vs Sep group; ¹There was no statistical significance in NO levels in mucous membrane of small intestine among groups; $r = 0.485$, $P = 0.515$, there was no correlation of NO concentration in mucous membrane with that in blood plasma.

Table 2 IgA levels in blood plasma and small intestinal mucosa

Group	n	Blood plasma IgA ($\mu\text{g/mL}$)	Mucosa tissue IgA ($\mu\text{g/g}$)
Con	8	146.73 \pm 18.03 ^a	507.48 \pm 59.18 ^a
EN	10	260.37 \pm 38.54 ^b	733.51 \pm 81.42 ^b
PN	9	133.94 \pm 21.47	489.38 \pm 14.27
Sep	8	194.52 \pm 39.31	511.89 \pm 52.33

Data are expressed as mean \pm SE; ^a P <0.05 vs EN group; ^b P <0.01 vs PN group; $r = 0.998$, $P = 0.002$, P <0.003, there was a positive correlation in IgA level in blood plasma with that in intestinal mucosa.

Lactulose/mannitol (L/M) test

The L/M ratio showed a significant increment in all rats except those in control group animals (Table 3).

Table 3 Dual sugar (lactulose/mannitol) test

Group	n	Rate of lactulose	Rate of mannitol	Ratio of L/M
Control	8	0.0097 \pm 0.0027	0.0202 \pm 0.0026	0.4789 \pm 0.1001
EN	10	0.0213 \pm 0.0035	0.0283 \pm 0.0020	0.7981 \pm 0.1559
PN	9	0.0981 \pm 0.0374	0.0723 \pm 0.0285	1.4494 \pm 0.2670
Sep	8	0.1466 \pm 0.0572	0.0361 \pm 0.0089	4.0088 \pm 0.8893 ^b

Data are expressed as mean \pm SE. Rate of lactulose (or mannitol): denotes the rate of lactulose (mannitol) amount excreted in urine with that gavaged; Ratio of L/M denotes the ratio of the above two rates. ^b P <0.01 vs control, EN and PN groups.

Table 4 Examination of bacterial translocation

Group	n	MLN	Liver	PVB	RBT	Log ₁₀ TB \pm SD
Control	8	3/8	0/8	0/8	12.5% (3/24)	0.5414 \pm 0.288
EN	10	4/10	2/10	3/10	30.0% (9/30)	1.6444 \pm 0.349
PN	9	5/9	4/9	4/9	48.15% (13/27) ^b	2.3279 \pm 0.433 ^b
Sep	8	6/8	7/8	7/8	83.33% (20/24) ^d	3.2815 \pm 0.483 ^d

Values are expressed as mean \pm SE; MLN: Mesenteric lymph node; PVB: Portal venous blood; RBT: Rate of bacterial translocation; TB: Translocated bacteria; 3/8: Numerator represents the positive samples of bacteria culture; denominator represents the number of animals enrolled. ^b P <0.01 vs Control; ^d P <0.01 vs control, EN and PN groups; $r = 0.979$, $P = 0.021$, P <0.03, there was a positive correlation of rate of bacterial translocation with the value of Log₁₀ translocated bacteria.

Bacterial identification and bacterial translocation

The results of bacterial culture were labeled as positive when the CFU found per gram of tissue (or mL of blood) was more than or equaled to 10³[6]. In Sep group the rate of bacterial translocation was the highest. The logarithm of the number of translocated bacteria correlated positively with the rate of bacterial translocation (Table 4). The bacteria translocated, in order of frequency, were proteus, *E. coli*, enterococcus and other Gram-negative bacteria. One or two, even three bacterial groups were usually recovered from the same organ when translocation was present.

DISCUSSION

Recent studies have shown that the gastrointestinal tract is not only an organ for nutrient digestion and absorption, but also an organ for systemic immunity and at the same time performs a barrier function. It prevents bacteria and endotoxin in the lumen of the GI tract from entering the blood circulation (bacterial/endotoxin translocation). At the time when body and/or organ tissues are injured by trauma, burns, infection, ischemia/reperfusion and surgical operation strikes, the intestinal barrier malfunction occurs and enterogenous infection ensues. Thus, it aggravates the original illness and makes it persistent, causing multiple organ dysfunction syndrome (MODS) and even death^[1,2,6-9]. Based on these, Wilmore named the GI tract as "a central organ after surgical stress"^[3].

Most infections that take place in abdominal surgery are commonly caused by G⁻ bacilli or polyinfection, which brings harm to body through endotoxin. Endotoxin (LPS) plays a very important role during stress. *In vivo* and *in vitro* studies in animals and humans indicated that LPS could cause damage to the intestinal barrier function and cause bacterial translocation^[1,3,6]. The aim of the experiment was to mimic the clinical cases above. In the experiment, we had laparotomy plus parenteral nutrition as trauma. Sick manifestations emerged after a few days' parenteral nutrition. One wk parenteral nutrition was obviously an inflammatory stimulus to rats. Laparotomy was a minor injury, whereas it was an intermediate degree of impairment when administering laparotomy plus 1-wk parenteral nutrition to rats. Clinical manifestations in rats confirmed the point of view. We injected lipopolysaccharide to rats intraperitoneally after 1-wk parenteral nutrition so as to mimic infested clinical situations after trauma. There were two main harmful stimuli, parenteral nutrition and LPS injection, included in our experiment. We have had another two control groups, the group of parenteral nutrition (PN) and the group of LPS injection with enteral feeding (EN) except the normal control one so as to investigate and compare the damage degree of different injury stimuli to gut barrier.

Investigations have reported the relation of TPN with bacterial translocation. Qin and his colleagues^[10] discovered that parenteral feeding in a 7-d period in experimental pancreatitis of dogs caused a significant damage of intestinal mucosa and bacterial translocation (BT) when compared with that of given isonitrogenous and isocaloric enteral feeding. Similar results were reported by other scholars^[11,12]. A study even revealed that 2-d TPN resulted in BT in SD rats^[13]. In their investigation patients underwent thoracic esophagectomy, Takagi *et al.* presented that in patients receiving TPN from 1 wk before operation to 2 wk after operation, serum levels of IL-6, IL-10 and endotoxin were higher than that of receiving isonitrogenous and isocaloric TEN. The result suggested that TPN could increase the endotoxin translocation from the bowel^[14].

Our investigation achieved similar results and showed that feeding rats with TPN for 1 wk led to a remarkable atrophy of the intestinal mucous membrane; hence an increase in intestinal permeability and bacterial translocation ensued. The rats were

in a state of systemic inflammatory response, which was shown by clinical manifestations of the animals and analysis of their blood cells. It is known that the cause of increment in intestinal permeability in animals fed with TPN is mainly the atrophy of the intestinal mucous membrane^[15,16]. Parenteral nutrition could meet the needs of other organs and tissues of the body, but not that of the intestinal mucosa. Seventy percent of the nutrients that intestinal epithelia need is absorbed directly from the intestinal lumen by mucosa cells^[17]. Enteral feeding could prevent the intestinal mucous membrane from atrophy and avoid increment of intestinal permeability^[10-12]. Likewise, it could also prevent gut associated lymphatic tissue (GALT) from atrophy, which could increase the intestinal mucosal immunity^[16,17]. It could be seen from our investigation that the damage of intestinal mucous membrane in EN rats was greatly attenuated. Enteral feeding led to a better immune reaction in these rats than others. The increase of gut permeability was avoided and the rate of bacterial translocation alleviated. It was shown from the analysis of complete blood cell count in the rats that the total number of leukocytes and the number of neutrophils increased following the stimulus of TPN in PN group, whereas there was a low reaction in Sep group, which suffered from more severe stress injury than PN group. The falling of platelet count may be related to a greater depletion of platelets that was caused by an intravascular coagulation due to the systemic inflammatory reaction^[1,18].

A series of symptoms appeared after injecting LPS into laparotomised TPN-rats in our experiment: lethargy, idleness, ruffling of hair, stopping drinking and grossly concentrated urine *etc.* Some rats appeared to have very low reactions to sound and other stimulations and also had diarrhea. Some eyes appeared glazed with crusting exudates. These symptoms were prominent during the 5 to 15 h following LPS injection, and the manifestations were alleviated gradually thereafter. These were in accordance with other reports^[1,3,6,18-20]. No statistical difference was found in the mortality within 24 h after LPS injection between the two groups (there were 1 and 3 deaths for EN and Sep groups respectively).

The animals in Sep group responded acutely after being injected with LPS intraperitoneally. LPS aggravated the impairment of the intestinal mucosal barrier and bacterial translocation that was caused by TPN. The aggravation of impairment of the mucosal barrier function might be related to nitric oxide (NO), which was shown by an increased NO level in blood plasma after LPS injection. Some scholars considered that high output of NO after surgical stress could damage the oxygenation metabolism in mitochondria of the intestinal epithelia^[3,21].

The increment of intestinal permeability caused by endotoxin is very complicated. It may relate to many inflammatory mediators such as cytokines, vasoactive amines and oxygen free radicals^[22,23]. Among them, NO, one of the main oxygen free radicals in the body, is an important inflammatory mediator causing impairment of the intestinal barrier^[3,18,24]. Generally, the body could only secrete small amounts of NO under the effects of constructive NO synthase (cNOS) and endothelial NO synthase (eNOS). This low level of NO has protective effects on the body^[20], whereas a higher concentration of NO being produced under the effect of inducible NO synthase (iNOS) when the body suffered from harmful stimulations, would impair the functions of cells and tissues of the body, including the intestinal barrier function. It was concluded from a great number of studies that a lower NO level was beneficial and a higher NO level was harmful to the body^[3,23,25], and using NO inhibitor when stress occurred could reduce the damage of gut barrier^[26,27]. The results from our investigation were in accordance with this hypothesis.

The intestinal immunity is very important in maintaining

intestinal barrier function. It is known that the digestive tract is the largest immune organ in the human body. About 80% of humoral immunity and 50% of cellular immunity locate in the digestive tract^[25,28]. Intestinal mucosal IgA is the first defense line of the intestinal barrier. It has an important function in preventing bacterial adherence and translocation from intestinal lumens^[21]. The IgA secretion in our EN group increased after LPS stimulation, but it had a low reaction in PN group when compared with that of EN group. The ratio of CD4 to CD8 in mucous membrane of small intestine in Sep group was lower than that in groups EN and PN, reflecting a low cellular immune response. This is in accordance with other reports that LPS could stimulate the increment of suppressive T lymphocytes^[22]. IgA level in blood plasma is positively correlated with that in the intestinal mucosa, and this accords with a previous report^[29]. Our results indicated that the increase of bacterial translocation was not only caused by an increased intestinal permeability, but also by an impairment of the whole intestinal barrier function^[16,30]. The kinds and groups of translocated bacteria and the phenomenon that there were 1 to 3 kinds of translocated bacteria in the same organ found in our experiment were in accordance with other reports^[3,31].

In summary, one week of parenteral nutrition caused an extreme atrophy of intestinal mucosa and an impairment of intestinal barrier function in SD rats. LPS aggravated this damage and also damaged the systemic immunity of the animals. The aggravation was related to the increased NO produced by the stimulation of LPS.

ACKNOWLEDGEMENT

We would like to thank Professor Hai-Feng Shao and Professor Gen-Bao Xu for their technical guidance and advice; we are grateful to the staff of the Animal Laboratory and the Institute of General Surgery of Nanjing University Medical School for their generous support and assistance to our study.

REFERENCES

- 1 **van Deventer SJ**, ten Cate JW, Tytgat GN. Intestinal endotoxemia. Clinical significance. *Gastroenterology* 1988; **94**: 825-831
- 2 **Yu P**, Martin CM. Increased gut permeability and bacterial translocation in *Pseudomonas pneumonia*-induced sepsis. *Crit Care Med* 2000; **28**: 2573-2577
- 3 **Dickinson E**, Tuncer R, Nadler E, Boyle P, Alber S, Watkins S, Ford H. NOX, a novel nitric oxide scavenger, reduces bacterial translocation in rats after endotoxin challenge. *Am J Physiol* 1999; **277**(6 Pt 1): G1281-1287
- 4 **Whiteland JL**, Nicholls SM, Shimeld C, Easty DL, Williams NA, Hill TJ. Immunohistochemical detection of T-cell subsets and other leukocytes in paraffin-embedded rat and mouse tissues with monoclonal antibodies. *J Histochem Cytochem* 1995; **43**: 313-320
- 5 **Green LC**, Wagner DA, Glogowski J, Skipper PL, Wishnok JS, Tannenbaum SR. Analysis of nitrate, nitrite, and [15N]nitrate in biological fluids. *An Biochem* 1982; **126**: 131-138
- 6 **O' Dwyer ST**, Michie HR, Ziegler TR, Revhaug A, Smith RJ, Wilmore DW. A single dose of endotoxin increases intestinal permeability in healthy humans. *Arch Surg* 1988; **123**: 1459-1464
- 7 **Wilmore DW**, Smith RJ, O'Dwyer ST, Jacobs DO, Ziegler TR, Wang XD. The gut: a central organ after surgical stress. *Surgery* 1988; **104**: 917-923
- 8 **Berg RD**. Bacterial translocation from the gastrointestinal tract. *Trends Microbiol* 1995; **3**: 149-154
- 9 **Swank GM**, Deitch EA. Role of the gut in multiple organ failure: bacterial translocation and permeability changes. *World J Surg* 1996; **20**: 411-417
- 10 **Qin HL**, Su ZD, Hu LG, Ding ZX, Lin QT. Effect of early intrajejunal nutrition on pancreatic pathological features and

- gut barrier function in dogs with acute pancreatitis. *Clin Nutr* 2002; **21**: 469-473
- 11 **Mosenthal AC**, Xu D, Deitch EA. Elemental and intravenous total parenteral nutrition diet-induced gut barrier failure is intestinal site specific and can be prevented by feeding nonfermentable fiber. *Crit Care Med* 2002; **30**: 396-402
 - 12 **Li J**, Langkamp-Henken B, Suzuki K, Stahlgren LH. Glutamine prevents parenteral nutrition-induced increases in intestinal permeability. *J Parenter Enterol Nutr* 1994; **18**: 303-307
 - 13 **Pscheidl E**, Schywalsky M, Tschaikowsky K, Boke-Prols T. Fish oil-supplemented parenteral diets normalize splanchnic blood flow and improve killing of translocated bacteria in a low-dose endotoxin rat model. *Crit Care Med* 2000; **28**: 1489-1496
 - 14 **Takagi K**, Yamamori H, Toyoda Y, Nakajima N, Tashiro T. Modulating effects of the feeding route on stress response and endotoxin translocation in severely stressed patients receiving thoracic esophagectomy. *Nutrition* 2000; **16**: 355-360
 - 15 **Sugiura T**, Tashiro T, Yamamori H, Takagi K, Hayashi N, Itabashi T, Toyoda Y, Sano W, Nitta H, Hirano J, Nakajima N, Ito I. Effects of total parenteral nutrition on endotoxin translocation and extent of the stress response in burned rats. *Nutrition* 1999; **15**: 570-575
 - 16 **MacFie J**. Enteral versus parenteral nutrition: the significance of bacterial translocation and gut-barrier function. *Nutrition* 2000; **16**: 606-611
 - 17 **van der Hulst RR**, von Meyenfeldt MF, van Kreel BK, Thunnissen FB, Brummer RJ, Arends JW, Soeters PB. Gut permeability, intestinal morphology, and nutritional depletion. *Nutrition* 1998; **14**: 1-6
 - 18 **Fish RE**, Spitzer JA. Continuous infusion of endotoxin from an osmotic pump in the conscious, unrestrained rat: a unique model of chronic endotoxemia. *Circ Shock* 1984; **12**: 135-149
 - 19 **Wichterman KA**, Baue AE, Chaudry IH. Sepsis and septic shock—a review of laboratory models and a proposal. *J Surg Res* 1980; **29**: 189-201
 - 20 **Schmidt H**, Secchi A, Wellmann R, Bach A, Bohrer H, Gebhard MM, Martin E. Effect of endotoxemia on intestinal villus microcirculation in rats. *J Surg Res* 1996; **61**: 521-526
 - 21 **Unno N**, Wang H, Menconi MJ, Tytgat SH, Larkin V, Smith M, Morin MJ, Chavez A, Hodin RA, Fink MP. Inhibition of inducible nitric oxide synthase ameliorates endotoxin-induced gut mucosal barrier dysfunction in rats. *Gastroenterology*, 1997; **113**: 1246-1257
 - 22 **Marshall JC**, Christou NV, Meakins JL. Small-bowel bacterial overgrowth and systemic immunosuppression in experimental peritonitis. *Surgery* 1988; **104**: 404-411
 - 23 **Mishima S**, Xu D, Deitch EA. Increase in endotoxin-induced mucosal permeability is related to increased nitric oxide synthase activity using the Ussing chamber. *Crit Care Med* 1999; **27**: 880-886
 - 24 **Forsythe RM**, Xu DZ, Lu Q, Deitch EA. Lipopolysaccharide-induced enterocyte-derived nitric oxide induces intestinal monolayer permeability in an autocrine fashion. *Shock* 2002; **17**: 180-184
 - 25 **Nadler EP**, Ford HR. Regulation of bacterial translocation by nitric oxide. *Pediatr Surg Int* 2000; **16**: 165-168
 - 26 **Hsu CM**, Liu CH, Chen LW. Nitric oxide synthase inhibitor ameliorates oral total parenteral nutrition-induced barrier dysfunction. *Shock* 2000; **13**: 135-139
 - 27 **Deitch EA**, Shorshtein A, Houghton J, Lu Q, Xu D. Inducible nitric oxide synthase knockout mice are resistant to diet-induced loss of gut barrier function and intestinal injury. *J Gastrointest Surg* 2002; **6**: 599-605
 - 28 **Hulsewe KW**, van Acker BA, von Meyenfeldt MF, Soeters PB. Nutritional depletion and dietary manipulation: effects on the immune response. *World J Surg* 1999; **23**: 536-544
 - 29 **Brandtzaeg P**, Halstensen TS, Kett K, Krajci P, Kvale D, Rognum TO, Scott H, Sollid LM. Immunobiology and immunopathology of human gut mucosa: humoral immunity and intraepithelial lymphocytes. *Gastroenterology* 1989; **97**: 1562-1584
 - 30 **Deitch EA**, Ma WJ, Ma L, Berg RD, Specian RD. Protein malnutrition predisposes to inflammatory-induced gut-origin septic states. *Ann Surg* 1990; **211**: 560-567
 - 31 **Naaber P**, Smidt I, Tamme K, Liigant A, Tapfer H, Mikelsaar M, Talvik R. Translocation of indigenous microflora in an experimental model of sepsis. *J Med Microbiol* 2000; **49**: 431-439

Edited by Zhang JZ and Chen WW Proofread by Zhu LH and Xu FM

DA-9601 for erosive gastritis: Results of a double-blind placebo-controlled phase III clinical trial

Sang Yong Seol, Myung Hwan Kim, Jong Sun Ryu, Myung Gyu Choi, Dong Wook Shin, Byoung Ok Ahn

Sang Yong Seol, Department of Gastroenterology, Inje University of Medicine, Busan, Korea

Myung Hwan Kim, Department of Gastroenterology, Ulsan University of Medicine, Seoul, Korea

Jong Sun Ryu, Department of Gastroenterology, Chunnam University of Medicine, Gwangju, Korea

Myung Gyu Choi, Department of Gastroenterology, Catholic University of Medicine, Seoul, Korea

Dong Wook Shin, Byoung Ok Ahn, Dong-A Pharmaceutical Research Institute, Yongin, Korea

Correspondence to: Byoung Ok Ahn, Dong-A Pharmaceutical Research Institute, 47-5, Sanggal-ri, Kiheung-up, Yongin-shi, Kyunggi-do 449-905, Korea. ahnbo@donga.co.kr

Telephone: +82-31-2801394 **Fax:** +82-31-2828564

Received: 2004-02-06 **Accepted:** 2004-03-02

Abstract

AIM: To determine the efficacy and safety of DA-9601 on erosive gastritis versus cetraxate as a standard drug by gastrointestinal endoscopy.

METHODS: Five hundred and twelve patients with erosive gastritis were divided into three groups. The groups received 180 mg or 360 mg of DA-9601, or 600 mg of cetraxate (Neuer™) t.i.d. for 2 wk, respectively. Endoscopic observations were performed before and 2 wk after the treatment, and the cure and improvement rates were investigated.

RESULTS: Of the 512 intention-to-treat (ITT) population, 457 patients comprised the per protocol (PP) analysis. Endoscopic cure rate was significantly higher in the DA-9601 group than in the cetraxate group in both the PP (56%, 58% vs 36%; DA-9601 180 mg, 360 mg and cetraxate, respectively) and ITT (52%, 51% vs 35%) populations. Two DA-9601 groups (180 and 360 mg) had significantly higher endoscopic improvement rates than the cetraxate group in both the PP (67%, 65% vs 46%) and ITT (63%, 58% vs 45%) populations. The percentage of symptom relief over the 2 wk was found not significantly different between groups. During the study, both DA-9601 and cetraxate produced no treatment-associated adverse events.

CONCLUSION: From these results, it appears that DA-9601 has excellent efficacy on erosive gastritis. This study also confirms the safety profile of DA-9601.

Seol SY, Kim MH, Ryu JS, Choi MG, Shin DW, Ahn BO. DA-9601 for erosive gastritis: Results of a double-blind placebo-controlled phase III clinical trial. *World J Gastroenterol* 2004; 10(16): 2379-2382

<http://www.wjgnet.com/1007-9327/10/2379.asp>

INTRODUCTION

Gastritis is a heterogeneous pathological condition, and is one of the most frequent reasons for medical consultation in Asian

countries, including Korea and Japan. However, in Western countries, these conditions are diagnosed as non-ulcer dyspepsia (NUD), which affects approximately one in five Americans^[1-4]. Gastritis, the “precursor” lesion to mucosal ulceration is both an important clinical entity and an important cause of abdominal pain in children^[5]. Inflammation of the gastric mucosa is the end result of an imbalance between mucosal defensive and aggressive factors (i.e., disturbances in gastric acidity and the mucus-bicarbonate barrier), and recently a great deal of attention has been focused on gastric hormones, specifically gastrin, and pepsinogens I and II^[6,7].

Gastritis can be classified into acute or chronic forms based upon Sydney System, and chronic gastritis can be subclassified as nonatrophic, atrophic, and special types^[8,9]. Using this Sydney pathologic classification as a guide, Chen *et al.*^[10] reported a simplified classification for gastritis based on practical radiologic evaluation, including erosive gastritis (acute and chronic), *Helicobacter pylori* (*H pylori*) gastritis, chronic nonspecific gastritis, hyperplastic gastritis, and miscellaneous types (including granulomatous, phlegmonous, eosinophilic, corrosive, other infectious types and rare types).

At present, the exact pathophysiology of this syndrome is poorly understood. However, current evidence suggests that *H pylori* infection, changes in lifestyles, eating behaviors, and nonsteroidal anti-inflammatory drug (NSAID) ingestion are causative factors in the pathogenesis of gastric mucosal injury in humans^[11]. *H pylori* is known to be a particularly important pathogen in gastric and duodenal inflammation by producing excessive mucosal-reactive oxygen species (ROS), which damage the cell membrane and deplete gastric antioxidants^[12].

The current rationale for drug treatment in gastritis is similar to other gastrointestinal disorders (eg., non-ulcer dyspepsia), and depends mainly on symptomatic relief using gastroprotective agents (e.g., rebamipide, teprenone, ecabet sodium, sofalcone, cetraxate, *etc.*), H₂ receptor antagonists (e.g., cimetidine, ranitidine, famotidine, *etc.*), and antacids^[13]. However, despite many efforts, the pharmacological treatment of patients with gastritis usually achieves only partial symptomatic relief in the majority of cases.

DA-9601 (Stillen™), a phytopharmaceutical derived from *Artemisia asiatica*, has been reported to possess antioxidative and cytoprotective actions in various models of gastric mucosal damage^[14-16]. Though the mode of action of DA-9601 has not been fully elucidated, this new antioxidative drug scavenges superoxide and hydroxyl radicals, possesses potent anti-inflammatory activities, regenerates mucosal epithelial cells, and enhances the cytoprotective cytokines^[17-19].

The present study was designed to assess the therapeutic effects and safety of DA-9601 on gastritis. Cetraxate, which has been shown to have therapeutic effects on gastritis was selected as the standard drug for comparative purposes.

MATERIALS AND METHODS

Patients

The patients examined in this study consisted of 550 erosive gastritis patients who were diagnosed endoscopically between

August 2000 and December 2001. All patients gave their written consent to this study. Out of 550 initially enrolled patients, 512 completed the study. Those 512 patients were subsequently randomized, of whom 326 were allocated to DA-9601 (186 had 180 mg and 140 had 360 mg daily) and 186 to cetraxate 600 mg. The exclusion criteria were: a history of peptic ulcer disease and reflux esophagitis; the presence of a malignant tumor in the digestive tract; the use of drugs capable of interfering with digestive mucosal integrity, gastric secretion or gastrointestinal motility, including H₂ receptor antagonists, NSAIDs, muscarinic antagonists, gastroprotective agents (within the previous 14 d); thrombotic patients (cerebral thrombosis, myocardial infarction, thrombophlebitis, etc.); consumption coagulopathy patients; a history of hypersensitivity to drugs (rash, fever, itching, etc.); the presence of major hematological, renal, cardiac, pulmonary, or hepatic abnormalities.

Methods

The study was performed as a randomized, double-blind, placebo-controlled, multicenter trial. Subjects were recruited at the following five Korean centers; Inje University of Medicine (Busan), Ulsan University of Medicine (Seoul), Chunnam University of Medicine (Gwangju), Catholic University of Medicine (Seoul), and Ajou University of Medicine (Suwon). Gastrointestinal endoscopies were performed in all patients before starting therapy, and 2 wk later. Patients diagnosed with erosive gastritis were included and divided into 3 groups following initial symptom assessment, and either treated with DA-9601 180 or 360 mg, or cetraxate 600 mg t.i.d. for 2 wk. After completing the therapy, endoscopic examinations were conducted according to the following grades: score 1, no erosions; score 2 (mild), erosion number between 1 and 2; score 3 (moderate), erosion number between 3 and 5; score 4 (severe), erosion number more than 6, for the evaluation of cure rate and improvement rate (Table 1). In addition, all patients completed a standardized subjective assessment questionnaire, according to Table 2. Safety surveillance was done at the end of therapy, based on responses to a complaint questionnaire, results of physical examinations and laboratory tests. Blood samples were obtained at the end of therapy to determine concentrations of GPT, GOT, and bilirubin. Complaint questionnaires were recorded for the appreciable harmful or unpleasant reactions experienced by a patient as a result of drug therapy.

Table 1 Evaluation of efficacy based on endoscopic observations

Score	Number of erosions
1 (none)	0
2 (mild)	1-2
3 (moderate)	3-5
4 (severe)	6<

Table 2 Evaluation of efficacy in individual symptom

Score	Criteria
1 (none)	No symptom
2 (weak)	Symptoms occurred once a week
3 (moderate)	The symptoms did not affect their life and occurred more than twice a week
4 (strong)	The symptoms affected their everyday life and occurred daily

Statistics analysis

Endoscopic efficacy was analyzed on an intention-to-treat (ITT) and per protocol (PP) basis. Both subjective and objective

criteria were analyzed using Duncan's multiple test. Comparisons between treatment groups were performed using the chi-square test. Data were considered to be significant when $P < 0.05$.

RESULTS

A total of 512 patients completed the trial. Baseline characteristics of the study populations are detailed in Table 3, which shows that the study groups were comparable with respect to demographics and disease-specific characteristics.

Table 3 Base-line characteristics of the patients (n, %)

Characteristic	DA-9601 180 mg (n = 186)	DA-9601 360 mg (n = 140)	Cetraxate 600 mg (n = 186)
Male sex	89 (47.9)	72 (51.4)	92 (49.5)
Age(yr)	45.9±11.2	44.6±12.1	46.4±11.5
History	<1 wk	3 (1.6)	1 (0.7)
	1-4 wk	31 (16.7)	28 (20.0)
	>4 wk	98 (52.7)	27 (19.3)
	Unknown	54 (29.0)	84 (60.0)
Type	Erosion	186 (100)	140 (100)
	Bleeding	8 (4.3)	4 (2.9)
	Redness	51 (27.4)	47 (33.6)
	Edema	2 (1.1)	10 (7.1)
Grade	Mild	14 (7.5)	18 (12.9)
	Moderate	50 (26.9)	40 (28.6)
	Severe	122 (65.6)	82 (58.6)

Data values are mean±SD.

Table 4 Number of patients for ITT and PP assays

	Number of patients		
	DA-9601 180 mg	DA-9601 360 mg	Cetraxate 600 mg
ITT analysis	186	140	186
PP analysis	171	120	166

Efficacy evaluation

The ITT population was composed of 512 patients (186 in the DA-9601 180 mg group, 140 in the DA-9601 360 mg group, and 186 in the cetraxate 600 mg group) (Table 4). Endoscopic cure rates in DA-9601 180 mg, 360 mg, and cetraxate 600 mg groups were 52.2%, 51.4%, and 35%, respectively (Figure 1). A significant difference was found between the DA-9601 and cetraxate groups ($P < 0.05$), however, no difference in cure rates was found between the DA-9601 groups.

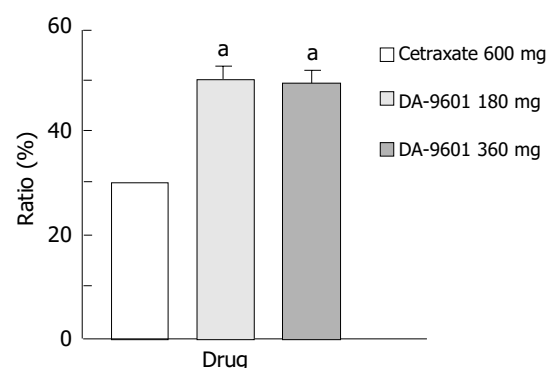


Figure 1 Estimated cure rates of erosive gastritis by intention-to-treat (ITT) analysis among patients treated with DA-9601 (180 mg or 360 mg, t.i.d.) or cetraxate (600 mg, t.i.d.) for 2 wk. * $P < 0.05$ vs 600 mg of cetraxate.

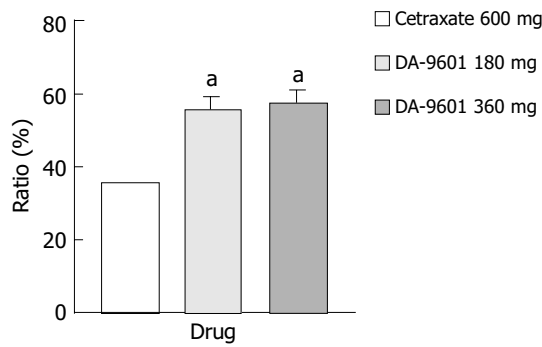


Figure 2 Estimated cure rates of erosive gastritis by per protocol (PP) analysis among patients treated with DA-9601 (180 mg or 360 mg, t.i.d.) or cetraxate (600 mg, t.i.d.) for 2 wk. ^a*P*<0.05 vs 600 mg of cetraxate.

The PP assay population comprised 457 patients (171 in the DA-9601 180 mg group, 120 in the DA-9601 360 mg group, and 166 in the cetraxate 600 mg group) (Table 4). The estimated cure rates of erosive gastritis by PP analysis in DA-9601 180 mg, 360 mg, and cetraxate 600 mg groups were 55.6% (95/171), 57.5% (69/120), and 35.5% (59/166), respectively (Figure 2). The cure rates between the DA-9601 and cetraxate groups (*P*<0.05) were significantly different, however, no difference was found between the DA-9601 groups.

Estimated improvement rates by ITT analysis of erosive gastritis patients treated with cetraxate (600 mg) and DA-9601 (180 or 360 mg) showed statistically significant differences (*P*<0.05); however, no difference was observed between the DA-9601 treated populations (Figure 3). The improvement rates of those treated with DA-9601 180 mg, 360 mg and cetraxate 600 mg were 63.4% (118/186), 57.9% (81/140), and 44.6% (83/186), respectively.

The estimated improvement rates by PP analysis for erosive gastritis treated with DA-9601 or cetraxate were statistically different (*P*<0.05) (Figure 4). However, no difference was found between the DA-9601 treated groups. The estimated improvement rates were 67.3% (115/171), 65.0% (78/120), and 46.4% (77/166) in the DA-9601 180 mg, DA-9601 360 mg, cetraxate 600 mg treated groups.

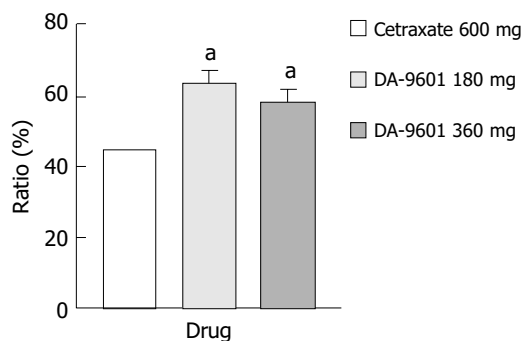


Figure 3 Estimated improvement rates of erosive gastritis by intention-to-treat (ITT) analysis among patients treated with DA-9601 (180 mg or 360 mg, t.i.d.) or cetraxate (600 mg, t.i.d.) for 2 wk. ^a*P*<0.05 vs 600 mg of cetraxate.

Symptom relief rates

The symptom relief rates determined by the ITT and PP methods showed no statistically significant difference between the study populations. The overall degrees of symptom reduction by the ITT method in the DA-9601 180 mg, 360 mg, and cetraxate 600 mg groups were 77.4% (144/186), 75.0% (105/140), and 73.1% (136/186), respectively (Figure 5), and by PP analysis these were 81.3% (139/171), 81.7% (98/120), and 76.5% (127/166).

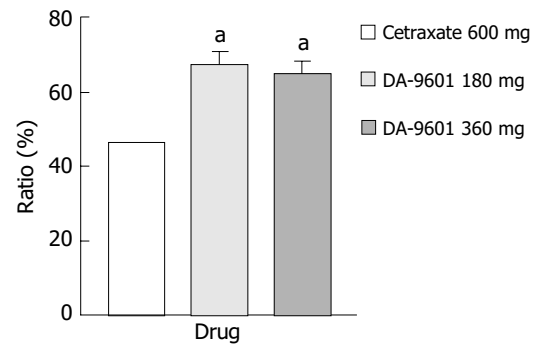


Figure 4 Estimated improvement rates of erosive gastritis by per protocol (PP) analysis among patients treated with DA-9601 (180 mg or 360 mg, t.i.d.) or cetraxate (600 mg, t.i.d.) for 2 wk. ^a*P*<0.05 vs. 600 mg of cetraxate.

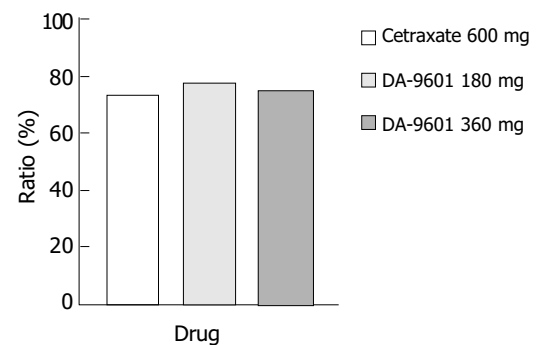


Figure 5 Overall reduction rates of symptoms among patients treated with cetraxate (600 mg, t.i.d.) or DA-9601 (180 mg and 360 mg, t.i.d.) for 2 wk.

Table 5 Incidence of adverse events (n, %)

	DA-9601 180 mg	Cetraxate 600 mg
Gastrointestinal		
Dyspepsia	2 (1.08)	0
Nausea	2 (1.08)	0
Diarrhea	2 (1.08)	0
Heartburn	1 (0.54)	1 (0.54)
Abdominal pain	1 (0.54)	1 (0.54)
Acid reflux	0	1 (0.54)
Vomiting	1 (0.54)	1 (0.54)
CNS and ANS		
Dizziness	1 (0.54)	0
Headache	1 (0.54)	1 (0.54)
Skin		
Itching	1 (0.54)	1 (0.54)
Skin redness	1 (0.54)	1 (0.54)
Facial edema	0	1 (0.54)
Liver		
sGPT elevation	1 (0.54)	1 (0.54)
sGOT elevation	0	1 (0.54)
Bilirubin elevation	0	1 (0.54)
Total	14 (7.53)	11 (5.91)

Safety

Serious adverse reactions were not encountered during this study. Of the 186 cetraxate 600 mg treated patients, the incidence of adverse effects was 7.5% (11 cases); including heartburn, abdominal pain, acid reflux, headache, itching, skin redness, facial edema, *etc.* Mild adverse events were observed in 14 of 186 patients treated with DA-9601 180 mg (Table 5). In the case of DA-9601 360 mg group, no notable change was observed

either in subjective assessment questionnaire or in clinical examination at the end of the study as compared to DA-9601 180 mg or cetraxate groups. No statistically significant difference was observed between the cetraxate and DA-9601 treated groups.

DISCUSSION

Although gastritis is the most common complication in the digestive tract, the definition of gastritis is not consensual due to differences in diagnostic criteria. It has been postulated that gastritis contributes to the natural history of ulcer development due to the decreased protection offered by the mucosal barrier lining the stomach, and increased epithelial cell exposure to hydrochloric acid.

The aim of this study was to demonstrate the efficacy and safety of DA-9601 versus cetraxate, a widely used anti-ulcer drug, for the treatment of erosive gastritis. Cetraxate, which has a mucosal protective effect, was first introduced in 1976 as an anti-ulcer drug^[20]. It is widely used clinically in Japan and other Asian countries. The mode of action of cetraxate is ascribed to an increased gastric mucosal blood flow through enhanced nitric oxide synthase activity, and the prevention of a decrease in the mucosal prostaglandin content^[21]. The results of the present randomized, double-blind, placebo-controlled, multicenter study demonstrate that orally administered DA-9601 is both effective and well-tolerated in the treatment of erosive gastritis of various etiologies.

Adverse reactions were seen in 7.5% (14/186) of the patients in DA-9601 180 mg treated group and in 5.9% (11/186) of patients in the cetraxate 600 mg treated group. In both groups, the main adverse reactions were vomiting, abdominal pain, headache, skin rash, itching, and sGPT elevation. However, in DA-9601 360 mg treated group, no obvious adverse reactions were observed (0%, 0/140). Therefore, we concluded that there was no drug treatment related adverse reaction based on the lack of dose-response relationship. In the previous four-wk oral toxicity study of DA-9601 in rats at doses of 120, 500, and 2 000 mg/kg.d, no treatment related alternations, including changes in blood biochemistry were observed^[22]. In animal experiments, DA-9601 prevented acetaminophen, and CCl₄-induced hepatic GSH depletion and CCl₄-induced increased hepatic MDA (a parameter of lipid peroxidation) in a dose-dependent manner^[23,24]. In addition, sGPT and sGOT levels showed a tendency to fall to below the normal range in DA-9601 treated patients (unpublished data).

Conclusively, the present study indicates that DA-9601 has an excellent efficacy and safety profile. Therefore, we believe that DA-9601 is a highly attractive option for the treatment of erosive gastritis, in which a balance between aggressive and defensive factors plays a significant role.

REFERENCES

- 1 Talley NJ. Dyspepsia: how to manage and how to treat? *Aliment Pharmacol Ther* 2002; **16**(Suppl 4): 95-104
- 2 Talley NJ. Therapeutic options in nonulcer dyspepsia. *J Clin Gastroenterol* 2001; **32**: 286-293
- 3 Talley NJ, Stanghellini V, Heading RC, Koch KL, Malagelada JR, Tytgat GN. Functional gastroduodenal disorders. *Gut* 1999; **45**: II37-II42

- 4 Kurata JH, Haile BM. Epidemiology of peptic ulcer disease. *Clin Gastroenterol* 1984; **13**: 289-307
- 5 Blecker U, Gold BD. Gastritis and peptic ulcer disease in childhood. *Eur J Pediatr* 1999; **158**: 541-546
- 6 Taylor IL. Gastrointestinal hormones in the pathogenesis of peptic ulcer disease. *Clin Gastroenterol* 1984; **13**: 355-382
- 7 Defize J, Meuwissen SG. Pepsinogens: an update of biochemical, physiological, and clinical aspects. *J Pediatr Gastroenterol Nutr* 1987; **6**: 493-508
- 8 Dixon MF, Genta RM, Yardley JH, Correa P. Classification and grading of gastritis. The updated Sydney System. International Workshop on the Histopathology of Gastritis, Houston 1994. *Am J Surg Pathol* 1996; **20**: 1161-1181
- 9 Whitehead R. The classification of chronic gastritis: current status. *J Clin Gastroenterol* 1995; **21**(Suppl 1): S131-S134
- 10 Chen MY, Ott DJ, Clark HP, Gelfand DW. Gastritis: classification, pathology, and radiology. *South Med J* 2001; **94**: 184-189
- 11 Yoshikawa T, Naito Y. The role of neutrophils and inflammation in gastric mucosal injury. *Free Rad Res* 2000; **33**: 785-794
- 12 Kashiwagi H. Ulcers and gastritis. *Endoscopy* 2003; **35**: 9-14
- 13 Talley NJ. Update on the role of drug therapy in non-ulcer dyspepsia. *Rev Gastroenterol Disord* 2003; **3**: 25-30
- 14 Oh TY, Ryu BK, Yang JI, Kim WB, Park JB, Oh TY, Lee SD, Lee EB. Studies on antiulcer effects of DA-9601, an *Artemisia herba* extract against experimental gastric ulcers and its mechanism. *J Appl Pharmacol* 1996; **4**: 111-121
- 15 Lee EB, Kim WB, Ryu BK, Ahn BO, Oh TY, Kim SH. Studies on protective effect of DA-9601, an *Artemisiae Herba* extract, against ethanol-induced gastric mucosal damage and its mechanism. *J Appl Pharmacol* 1997; **5**: 202-210
- 16 Oh TY, Ryu BK, Ko JI, Ahn BO, Kim SH, Kim WB, Lee EB, Jin JH, Hahm KB. Protective effect of DA-9601, an extract of *Artemisiae Herba*, against naproxen-induced gastric damage in arthritic rats. *Arch Pharm Res* 1997; **20**: 414-419
- 17 Lee JJ, Han BG, Kim MN, Chung MH. The inhibitory effect of eupatilin on *Helicobacter pylori*-induced release of leukotriene D₄ in the human neutrophils and gastric mucosal cells. *Korean J Physiol Pharmacol* 1997; **1**: 573-580
- 18 Oh TY, Lee JS, Ahn BO, Cho H, Kim WB, Kim YB, Surh YJ, Cho SW, Lee KM, Hahm KB. Oxidative stress is more important than acid in the pathogenesis of reflux oesophagitis in rats. *Gut* 2001; **49**: 364-371
- 19 Oh TY, Lee JS, Ahn BO, Cho H, Kim WB, Kim YB, Surh YJ, Cho W, Hahm KB. Oxidative damage are critical in pathogenesis of reflux esophagitis: implication of antioxidants in its treatment. *Free rad Biol Med* 2001; **30**: 905-915
- 20 Suzuki Y, Hayashi M, Ito M, Yamagami I. Anti-ulcer effects of 4'-(2-carboxyethyl) phenyl trans-4-aminomethyl cyclohexanecarboxylate hydrochloride (cetraxate) on various experimental gastric ulcers in rats. *Jpn J Pharmacol* 1976; **26**: 471-480
- 21 Tachi K, Goto H, Hayakawa T, Sugiyama S. Prevention of water immersion stress-induced gastric lesions through the enhancement of nitric oxide synthase activity in rats. *Aliment Pharmacol Ther* 1996; **10**: 97-103
- 22 Kim OJ, Kang KK, Kim DH, Baik NG, Ahn BO, Kim WB, Yang I. Four-week oral toxicity study of DA-9601, an antiulcer agent of *Artemisia* spp. Extract, in rats. *J Appl Pharmacol* 1996; **4**: 354-363
- 23 Ryu BK, Ahn BO, Oh TY, Kim SH, Kim WB, Lee EB. Studies on protective effect of DA-9601, *Artemisia asiatica* extract, on acetaminophen- and CCl₄-induced liver damage in rats. *Arch Pharm Res* 1998; **21**: 508-513
- 24 Cheong JY, Oh TY, Lee KM, Kim DH, Ahn BO, Kim WB, Kim YB, Yoo BM, Hahm KB, Kim JH, Cho SW. Suppressive effects of antioxidant DA-9601 on hepatic fibrosis in rats. *Korean J Hepatol* 2002; **8**: 436-447

• CLINICAL RESEARCH •

Impaired gallbladder motility and delayed orocecal transit contribute to pigment gallstone and biliary sludge formation in β -thalassemia major adults

Piero Portincasa, Antonio Moschetta, Massimo Berardino, Agostino Di Ciaula, Michele Vacca, Giuseppe Baldassarre, Anna Pietrapertosa, Rosario Cammarota, Nunzia Tannoia, Giuseppe Palasciano

Piero Portincasa, Antonio Moschetta, Massimo Berardino, Michele Vacca, Giuseppe Palasciano, Section of Internal Medicine, Department of Internal Medicine and Public Medicine (DIMIMP), University Medical School, Bari, Italy

Agostino Di Ciaula, Division of Internal Medicine, Hospital of Bisceglie, Italy

Giuseppe Baldassarre, Division of Geriatrics, Hospital "Miulli", Acquaviva delle Fonti, Bari, Italy

Anna Pietrapertosa, Rosario Cammarota, Nunzia Tannoia, Chair of Hematology II, University of Bari, Italy

Correspondence to: Professor Piero Portincasa, Section of Internal Medicine, Department of Internal and Public Medicine (DIMIMP), University Medical School of Bari, P.zza G. Cesare 11, 70124 Bari, Italy. p.portincasa@semeiotica.uniba.it

Telephone: +39-80-5478227 **Fax:** +39-80-5478232

Received: 2004-02-02 **Accepted:** 2004-03-13

Abstract

AIM: Gallbladder and gastrointestinal motility defects exist in gallstones patients and to a lesser extent in pigment gallstone patients. To investigate the role of gallbladder and gastrointestinal motility disorders in pigment gallstone formation in β -thalassemia major.

METHODS: Twenty-three patients with β -thalassemia major (16 females; age range 18-37 years) and 70 controls (47 females, age range 18-40 years) were studied for gallbladder and gastric emptying (functional ultrasonography), orocecal transit (OCTT, H₂-breath test), autonomic dysfunction (sweat-spot, cardiorespiratory reflex tests), bowel habits, gastrointestinal symptoms and quality of life (all with questionnaires). Gallbladder content (ultrasonography) was examined before and during 8-12 mo follow-up.

RESULTS: Gallstones and/or biliary sludge were found in 13 (56%) patients. β -thalassemia major patients had increased fasting (38.0±4.8 mL vs 20.3±0.7 mL, $P = 0.0001$) and residual (7.9±1.3 mL vs 5.1±0.3 mL, $P = 0.002$) volume and slightly slower emptying (24.9±1.7 min vs 20.1±0.7 min, $P = 0.04$) of the gallbladder, together with longer OCTT (132.2±7.8 min vs 99.7±2.3 min, $P = 0.00003$) than controls. No differences in gastric emptying and bowel habits were found. Also, patients had higher dyspepsia (score: 6.7±1.2 vs 4.9±0.2, $P = 0.027$), greater appetite ($P = 0.000004$) and lower health perception ($P = 0.00002$) than controls. Autonomic dysfunction was diagnosed in 52% of patients (positive tests: 76.2% and 66.7% for parasympathetic and sympathetic involvement, respectively). Patients developing sludge during follow-up (38%, 2 with prior stones) had increased fasting and residual gallbladder volume.

CONCLUSION: Adult β -thalassemia major patients have gallbladder dysmotility associated with delayed small intestinal transit and autonomic dysfunction. These

abnormalities apparently contribute together with haemolytic hyperbilirubinemia to the pathogenesis of pigment gallstones/sludge in β -thalassemia major.

Portincasa P, Moschetta A, Berardino M, Di Ciaula A, Vacca M, Baldassarre G, Pietrapertosa A, Cammarota R, Tannoia N, Palasciano G. Impaired gallbladder motility and delayed orocecal transit contribute to pigment gallstone and biliary sludge formation in β -thalassemia major adults. *World J Gastroenterol* 2004; 10(16): 2383-2390

<http://www.wjgnet.com/1007-9327/10/2383.asp>

INTRODUCTION

Patients with cholesterol gallstones have impaired gallbladder emptying^[1] and may show dyspeptic symptoms with functional defects of both upper and lower gastrointestinal tract^[2-4]. Recently, we reported that gallbladder emptying was also defective in patients with black pigment stones and such defect was less severe than in patients with cholesterol stones^[2].

β -thalassemia is one of the most widespread single-gene disorders with 3-6% of the world's population carrying the gene. The disease represents a major public health problem in the Mediterranean area, the Middle East, the India subcontinent and the Far East^[5]. Increased production of bilirubin from chronic hemolysis is a prerequisite for formation of pigment gallstones^[6,7], and black pigment gallstones often accompany thalassemia major^[6]. However, despite similar biochemical and clinical features, many β -thalassemia major patients with marked hemolysis did not develop gallstones. One might hypothesize that gallbladder stasis and functional gastrointestinal disorders could contribute to gallstone pathogenesis in β -thalassemia major. In the present study, we investigated for the first time the role of gallbladder and gastrointestinal motility in adult β -thalassemia major patients in relation to gallstone/sludge formation. Autonomic neuropathy and gastrointestinal symptoms were also evaluated.

MATERIALS AND METHODS

Subjects

β -thalassemia major patients ($n = 23$) Age 26±1 years (mean±SE, range 18-37 years), body mass index (BMI) of 21.4±0.6 kg/m². Sixteen were women. Patients attended regular review from October 2001 until June 2003 at the Referral Center of the University Hospital of Bari. All the patients were homozygous for a mutation β^0 or β^+ or double heterozygous for a mutation β^0 or β^+ . The genetic characteristics of the patients seen in Bari have been previously reported^[8]. As β -thalassemia major requires regular blood transfusions and chelating therapy to alleviate the harmful accumulation of iron, all patients were on a program consisting of one or two monthly blood transfusion of packed red blood cells and desferrioxamine given as 40-60 mg/(kg·d) subcutaneously overnight using syringe pumps. The program

lasted for 5 nights per week. Mean length of desferrioxamine treatment was 19.2 ± 0.6 years. All patients had various stages of liver involvement, as confirmed by ultrasonography (*e.g.* liver steatosis, hyperechoic parenchyma) and/or liver biopsy (ranging from active/chronic siderotic and fibrotic hepatitis to definite liver cirrhosis, $n = 1$). The analysis of organ involvement confirmed that splenomegaly, hypothyroidism, and heart disease were the most frequent conditions with a prevalence of 39%, 35% and 18%, respectively. Hypogonadism was present in 35% of the patients. Type I insulin-dependent diabetes and a positive oral glucose tolerance test were present in 9% and 22% of the patients, respectively.

Healthy subjects ($n = 70$) Age 28 ± 1 years (range 18-40 years), BMI 22.0 ± 0.3 kg/m². Forty-seven were women. They were recruited from local staff members, students, and family practices. None of the healthy subjects complained of gastrointestinal symptoms or had previous gastrointestinal diseases or surgery. All had a negative abdominal ultrasound.

No significant difference existed in age, BMI and gender distribution between the patients and the normal controls. As expected^[9], patients had shorter stature than their matched controls (males: 168 ± 2 cm vs 178 ± 7 cm, $P = 0.0006$ and females: 158 ± 0.01 cm vs 167 ± 6 cm, $P = 0.00005$). All subjects gave their informed consent and the study was approved by the University of Bari Human Subjects Committee.

Study design

After the outpatient clinic evaluation consisting of history, physical examination, and serum analyses, subjects were scheduled for the motility studies and tests for autonomic neuropathy. A clinical and ultrasonographic follow-up was planned within the next 8-12 mo. Ultrasonography was chosen because it was a non-invasive and validated technique allowing to study both gallbladder^[1,10] and gastric^[11-16] emptying, simultaneously^[17]. We also developed a novel, one-day test for studying the upper gastrointestinal motility by simultaneous assessment of gallbladder, stomach, and small bowel transit^[18].

Gallbladder and gastric emptying

The gallbladder was studied for content, wall, shape, and motility with standardized methodology^[17]. Gallstones were diagnosed by the presence of mobile high-level echoes with acoustic shadows in the gallbladder, and sludge by the presence of mildly echogenic intraluminal sediment in the

absence of acoustic shadows^[19]. All gallstone patients had a small gallstone burden (*i.e.* less or equal to 20% of fasting gallbladder volume)^[20] and a thin gallbladder wall (*i.e.* less than 3 mm in the fasting state) delimiting a regularly pear-shaped organ^[17]. Gallbladder motility was assessed by monitoring gallbladder volumes before and at 5-15 min intervals over 2 h after ingestion of a liquid test meal.

Gastric emptying was assessed by monitoring antral areas at the same time points as for the gallbladder^[11,13]. The equipment consisted of an Esaote AUC50 equipped with a 3.5 MHz convex probe. The test meal consisted of 200 mL liquid formula containing fat 11.6 g (35%), protein 12 g (16%) and carbohydrate 36.8 g (49%) with a total of 300 kcal, 1 270 kJ, 445 mOsm/L (*Nutridrink*[®], Nutricia S.p.A., Lainate Milano, Italy).

Orocecal transit time

Orocecal transit time was measured at the time when ultrasonographic studies were performed by the hydrogen breath test with a portable, previously validated device (EC60-Gastrolyzer, Bedford, USA)^[18,21]. The substrate consisted of 10 g lactulose (Duphalac Dry[®], Solvay Pharma, Belgium) which was added directly to the standard liquid test meal. The accuracy of the detector was ± 2 p.p.m. A rise of 10 p.p.m. above baseline on two consecutive measurements was considered as orocecal transit time and expressed in minute^[22].

Autonomic neuropathy

Symptoms and signs of autonomic dysfunction were evaluated by taking the clinical history according to Rangari *et al.*^[23]. The questionnaire was scored as "normal", "mild" and "severe" for the presence of orthostatic hypotension, gastric symptoms, bowel disorders, sweating disorders, bladder dysfunction and in males, impotence. A combination of tests including the Sweat-spot-test (SST)^[22,24,25] and cardiorespiratory reflex tests^[26], were employed as sensitive methods to assess the presence of autonomic neuropathy^[27]. The SST was used to investigate the involvement of cholinergic sympathetic fibers by analyzing sweat abnormalities on the dorsum of the foot. An example of positive and negative test is shown in Figure 1.

A portable device was used to measure the "beat-to-beat" modifications of the R-R interval using skin electrodes connected to *Cardionomic*[®] (Lifescan, Italy). Lying-to-standing and standing-to-lying tests were used for sympathetic involvement. Valsalva maneuver, deep-breathing, cough test, and postural hypotension test were used for parasympathetic

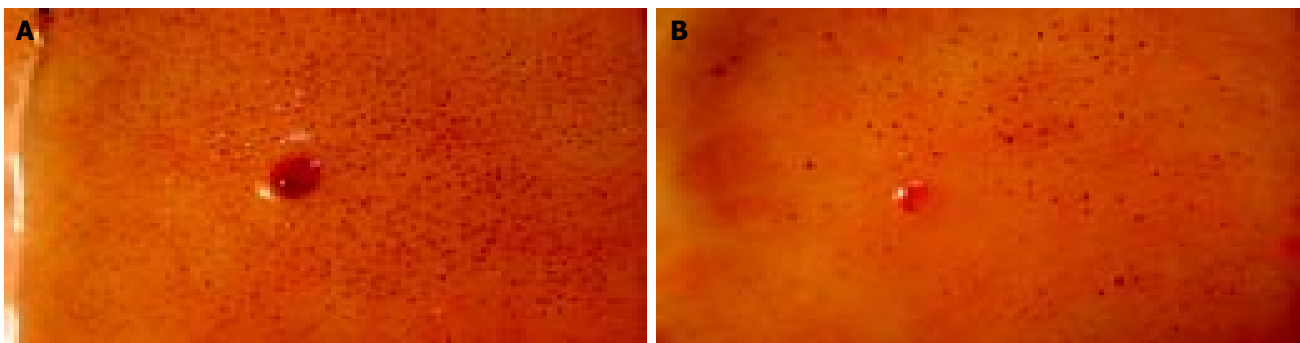


Figure 1 Sweat spot test (SST) for assessment of sympathetic autonomic nervous system^[22,24,25]. The skin is coated with iodine and a fine emulsion of starch in arachis oil. Sweat is stimulated by intra-dermal injection of 0.1 mL acetylcholine (the red dot indicates the point of injection). Denervated glands do not respond to the acetylcholine injection. A colorimetric reaction between starch and iodine is triggered by the sweat from stimulated glands, so that each pore appears as a small black dot after 2-5 min. A digital photo is taken and transferred to a magnifying software to measure the number and distribution of dots appearing in a standard squared grid of 529 mm² divided into 64 squared subareas. A normal SST implied a score 12 dots/subarea and/or <8% of abnormal subareas (each square of the grid having less than 6 dots) according to Ryder^[24] and to our group^[25]. Only patients with both indices (SST score and % abnormal subareas) outside normal limits were considered to have a positive test. A: Normal and even distribution of sweating glands seen as black dots; B: Defective response in a β -thalassemia major patient with sympathetic autonomic neuropathy.

involvement. The results of each test were scored as normal, borderline or abnormal, according to age-controlled values. The overall results for autonomic neuropathy were therefore normal (all tests normal), early involvement (one abnormal test or two borderline abnormal), definite involvement (two or more abnormal tests)^[23].

Questionnaires

On the same day of the motility studies, subjects were asked to complete the following questionnaires under the supervision of one operator.

Bristol stool scale form^[28] This is a semi-quantitative score to assess the quality of bowel movements. The weekly frequency of evacuations over a time span of one mo was also assessed.

Dyspepsia score^[29] This is a semi-quantitative score from four symptoms such as epigastric pain, burning, belching/burping, postprandial fullness. Maximum score was equal to 48 with the upper normal limit equal to 8 and estimated from the mean \pm 2SD of healthy control values.

Visual analogue scales (VAS) of upper gastrointestinal perception^[18,30] These are self-assessed 100 mm horizontal lines of upper gastrointestinal perception monitoring appetite, satiety, nausea, abdominal fullness and upper abdominal (epigastric) pain or discomfort. Scores in mm were obtained at baseline (*i.e.* time 0) and at 15, 30, 45, 60, 90 and 120 min postprandially.

Rome criteria for biliary pain^[31] Patients with gallstones or sludge were considered "symptomatic" with a history of one or more episodes of colicky pain during the last 12 mo.

Health survey SF-36^[18,32,33] This is a short form of questionnaires assessing health-related quality of life (HRQOL). The SF36 includes 36 items which measure eight multi-item variables: general health, physical function, role physical, role emotional, social function, mental health, body pain, and vitality. Healthy subjects in this setting had a HRQOL profile remarkably similar to that derived from subjects across different cultures in USA and UK^[34].

Statistical analysis

Results are expressed as mean \pm SE. Demographic data, as well as baseline characteristics were checked for normal distribution (Kolmogorov-Smirnov goodness of fit test). Statistical significance in contingency tables was evaluated using χ^2 -test or Fisher's exact test when appropriate. Comparison of continuous variables among groups was performed with unpaired Student's *t*-test or Mann-Whitney rank sum test when appropriate. Comparison between multiple groups was assessed using one-way analysis of variance (ANOVA) or the Kruskal-Wallis non parametric ANOVA on ranks. *Post-hoc* multiple pair wise comparisons were calculated with the Fisher's LSD test. Linear regression analysis was performed by the method of least square and Pearson's coefficient. A multivariate analysis was constructed to study the effect on appetite of motility variables. The variables showing significant correlations in univariate analysis were included in a stepwise multiple regression analysis. All statistical calculations were performed with the NCSS2004 software (Kaysville, UT, USA). Statistical tests were conducted as a two-sided alpha level of 0.05^[35,36].

RESULTS

Gallbladder sludge and stones were found in 13 (56%) patients, all asymptomatic for previous episodes of biliary pain. Sludge was detected in 6 (26%) patients, while gallstones were observed in 7 (30%) patients, solitary and small in size (5-9 mm). The other 10 patients (44%) were gallstone/sludge-free.

Routine biochemical analysis

There was no difference in laboratory biochemistry among the

three subgroups of thalassemia patients, according to gallbladder content (Table 1). There was a statistically significant relationship between levels of ferritin and AST and ALT in the serum ($0.73 < r < 0.77$; $P > 0.00002$, $P < 0.00007$).

Table 1 Laboratory biochemistry in β -thalassemia major patients with gallstones, biliary sludge and gallstone-free

	Gallstones	Sludge	Gallstone/ sludge-free	P
No. of subjects	7	6	10	
Total bilirubin (mg/dL)	2.3 \pm 0.4	1.4 \pm 0.4	1.8 \pm 0.3	NS
AST (U/L)	50.9 \pm 11.5	32.8 \pm 12.5	44.9 \pm 9.7	NS
ALT (U/L)	76.7 \pm 17.7	42.7 \pm 19.1	59.8 \pm 14.8	NS
Ferritin (mg/dL)	1 922 \pm 445	1 165 \pm 481	1 900 \pm 372	NS
Hb (g/dL)	9.3 \pm 0.1	9.5 \pm 0.2	9.5 \pm 0.1	NS
Iron (mg/dL)	186.8 \pm 16.8	189.6 \pm 8.4	156.5 \pm 16.8	NS
Total proteins (g/dL)	7.8 \pm 0.2	7.9 \pm 0.2	7.4 \pm 0.2	NS
GGT (U/L)	34.4 \pm 5.6	18.3 \pm 6.0	19.4 \pm 4.7	NS
Alk. Phosphatase (U/L)	1.15 \pm 0.2	0.98 \pm 0.2	0.9 \pm 0.2	NS
LDH (U/L)	331.3 \pm 46.7	293.7 \pm 36.7	310.7 \pm 28.4	NS
Cholesterol (mg/dL)	98.3 \pm 10.2	129.4 \pm 12.1	96.9 \pm 9.0	NS
Tryglicerides (mg/dL)	114.9 \pm 23.5	71.6 \pm 27.9	84.4 \pm 22.0	NS

Data are expressed as mean \pm SE; NS: Not significant; AST: Aspartate transaminase; ALT: Alanine transaminase; GGT: Gamma-glutamyl transpeptidase; LDH: Lactate dehydrogenase.

Ultrasonographic studies

The study of gallbladder emptying showed that β -thalassemia major patients had increased fasting gallbladder volume (38.0 \pm 4.8 mL vs 20.3 \pm 0.7 mL, $P = 0.0001$), and residual volume (7.9 \pm 1.3 mL vs 5.1 \pm 0.3 mL, $P = 0.002$), decreased percent residual volume (20.3 \pm 1.5% vs 24.6 \pm 1.0%, $P = 0.03$) and slightly slower emptying (24.9 \pm 1.7 min vs 20.1 \pm 0.7 min, $P = 0.04$) than controls, as also suggested by the analysis of the gallbladder emptying curves (Figure 2).

Although all subgroups compared to controls had a significantly greater fasting gallbladder volume, only patients with biliary sludge and normal gallbladder had increased residual volume and delayed emptying. Indeed, relative gallbladder contraction (percent residual volume) was increased in patients with gallstones. β -thalassemia patients and controls showed comparable fasting and postprandial indices of gastric emptying (Table 2).

Orocecal transit time

Mean OCTT was longer in β -thalassemia patients than in controls (132.2 \pm 7.8 min vs 99.7 \pm 2.3 min, $P = 0.00003$) (Figure 3). Seven patients (30.4%) but none of controls had OCTT above the upper normal value of 140 min (*i.e.* mean \pm 2SD) derived from the control group ($P = 0.000026$, χ^2 -test). Similar results were found among different subgroups (Table 2).

Autonomic neuropathy

Twenty-one patients agreed to undergo the tests. Symptoms and signs of autonomic dysfunction were found in 11 patients (52%), which were mild in all but 2 cases (asymptomatic). Early or definitive parasympathetic and sympathetic involvement was present in 76.2% and 66.7% of cases, respectively. Early involvement was more frequent in the cases of parasympathetic AN system than those of sympathetic AN system (81.3% vs 28.6%, $P = 0.00037$). Overall, there were 3 (14%), 5 (24%), and 13 (62%) patients with normal tests, early involvement (mainly parasympathetic), and definitive involvement (both parasympathetic and sympathetic), respectively. All 5 patients with type I insulin-dependent diabetes or impaired oral glucose tolerance test and all 7 patients with thyroid involvement had

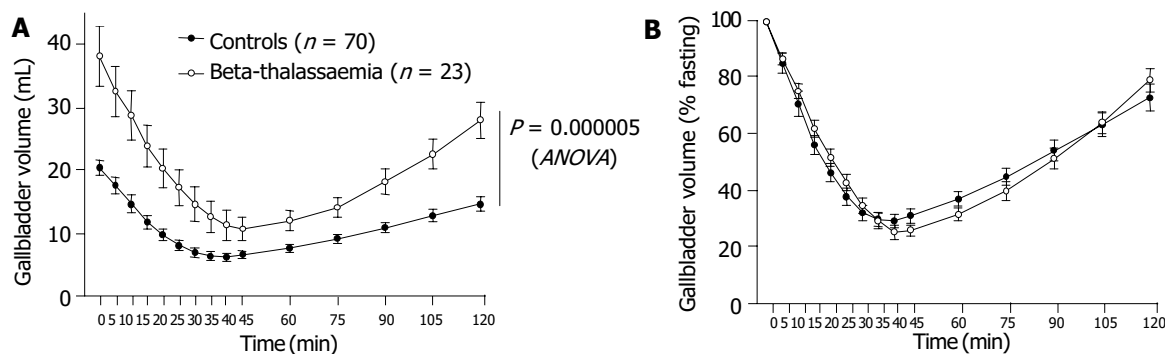


Figure 2 Time-course of fasting and postprandial gallbladder volumes in 23 β -thalassaemia major patients and 70 controls and expressed as mL (panel A) or percent fasting gallbladder volume (panel B). Symbols indicate means, while vertical lines indicate SEM. Patients had impaired gallbladder emptying, with significantly increased fasting and postprandial volumes at each time point (panel A), in spite of similar contraction (panel B), compared to controls.

Table 2 Dyspeptic symptoms, bowel habits and gastrointestinal motility indices (gallbladder, stomach, small bowel) in β -thalassaemia major patients with or without gallstone/sludge and in controls

	Gallstones	Sludge	GS/sludge-free	Controls	P
No. of subjects	7	6	10	70	
Dyspepsia (Buckley score)	5.0 \pm 1.0	6.8 \pm 2.2	7.8 \pm 2.5 ^a	4.9 \pm 0.2	0.046
Bowel habits (Bristol score)	3.5 \pm 0.21	3.4 \pm 0.6	3.8 \pm 0.2	3.5 \pm 0.07	NS
Stomach					
Fasting antral area (cm ²)	2.8 \pm 0.2	2.9 \pm 0.2	3.4 \pm 0.3	3.2 \pm 0.1	NS
Postprandial maximal area (cm ²)	10.4 \pm 0.2	10.7 \pm 0.5	10.9 \pm 0.4	11.5 \pm 0.2	NS
Postprandial minimal area (%)	0.9 \pm 0.5	0.3 \pm 0.3	0.4 \pm 0.7	2.1 \pm 0.4	NS
Postprandial minimal (cm ²)	2.9 \pm 0.2	3.0 \pm 0.2	3.3 \pm 0.2	3.4 \pm 0.1	NS
Half-emptying time (min)	28 \pm 2	31 \pm 2	28 \pm 2	27 \pm 1	NS
Gallbladder					
Fasting volume (mL)	30.1 \pm 3.8 ^a	42.9 \pm 10.3 ^a	40.6 \pm 8.9 ^a	20.3 \pm 0.7	0.000001
Postprandial residual volume (mL)	4.4 \pm 0.9	10.0 \pm 2.7 ^{ac}	9.1 \pm 2.3 ^{ac}	5.1 \pm 0.3	0.00030
Postprandial residual volume (%)	14.7 \pm 1.6 ^a	23.0 \pm 2.7	22.6 \pm 2.4	24.6 \pm 1.0	0.023
Half-emptying time (min)	21 \pm 1	27 \pm 5 ^a	26 \pm 2 ^a	20 \pm 1	0.009
Small bowel					
Orocecal transit Time (min)	128.6 \pm 13.4 ^a	30.0 \pm 15.0 ^a	136.0 \pm 13.6 ^a	99.7 \pm 2.3	0.000002

Data are expressed as mean \pm SE; GS: Gallstones; ^a P <0.05 vs controls; ^c P <0.05 vs gallstones (ANOVA and Fisher's LSD multiple-comparison test); NS: Not significant.

evidence of autonomic neuropathy. Neither age nor mean duration of desferrioxamine therapy was significantly different in patients with or without autonomic neuropathy (data not shown). Patients with autonomic neuropathy compared with those without it ($n=3$, scant number might imply a type 2 error), showed a trend towards longer OCTT (132 \pm 9 min vs 117 \pm 3 min, $P=0.06$), increased fasting volume (39.5 \pm 5.7 mL vs 19.7 \pm 4.3 mL, $P=0.07$) and decreased contraction (residual volume 8.6 \pm 1.6 vs 3.2 \pm 0.7 mL, $P=0.044$).

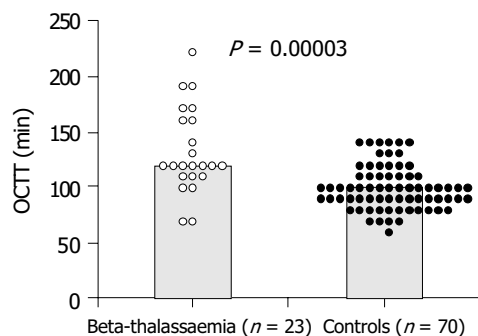


Figure 3 Orocecal transit time (OCTT) by lactulose H₂-breath test in β -thalassaemia major patients and controls. Patients had significantly longer OCTT than controls. Data are expressed as

individual points and means (bars).

Questionnaires

Overall, bowel habits were comparable in controls and patients (overall: 3.5 \pm 0.01 vs 3.6 \pm 0.2, respectively), while the score for dyspepsia was slightly higher (and statistically significant) in patients than in controls (6.7 \pm 1.2 vs 4.9 \pm 0.2, $P=0.027$) (Table 2).

The results of VAS for satiety and appetite (as postprandial AUC) showed that the two feelings were strongly and negatively correlated in both patients ($r=-0.87$, $P<0.0001$, $n=23$) and controls ($r=-0.03$, $P<0.0001$, $n=70$). Profiles for both appetite and satiety, however, were different in patients and controls. Fasting and postprandial appetite scores were invariably greater in patients than in controls. In particular, VAS for appetite was increased at baseline and showed a rapid decrease followed by a rapid and marked postprandial increase, compared to controls (Figure 4). Whereas univariate analysis suggested an inverse relation between appetite and OCTT, gallbladder contraction (as residual volume in percent) and gallbladder half emptying time, multiple regression analysis identified gallbladder half-emptying time as the only predictor ($P<0.002$) of time-related changes of appetite perception in patients. The relationship is shown in Figure 5.

There was no difference in nausea, fullness and abdominal pain between patients and controls either at baseline or postprandially (data not shown).

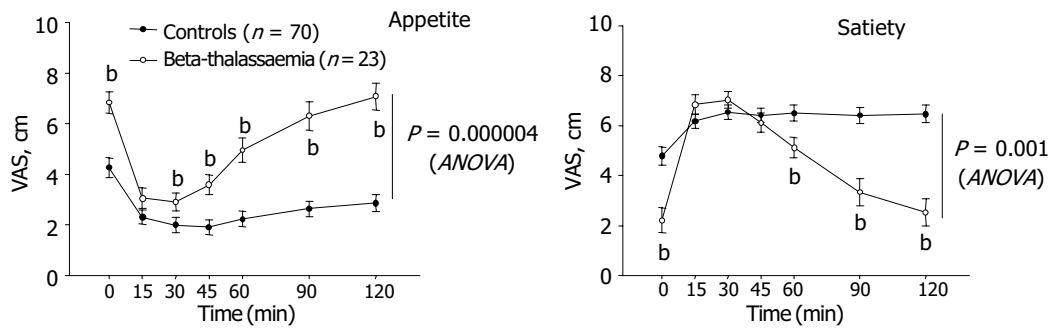


Figure 4 Time-course of visual analogue scale (VAS) for appetite and satiety in β -thalassemia major patients and controls. Data are mean \pm SE. On the X-axis time “0” is before ingestion of test meal. Asterisks indicate significant differences of controls vs patients (0.0001 < P < 0.001, at various time-points and overall ANOVA).

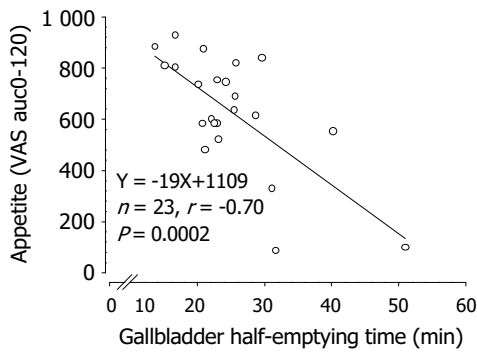


Figure 5 Correlation between appetite sensation (area under curve during 120 min of visual analogues scale) and speed of gallbladder emptying (half-emptying time) in β -thalassemia major patients.

Quality of life

Patients showed a significant deterioration in general health and a lower score than controls (51.7 \pm 4 vs 73.1 \pm 2, P = 0.00002, ANOVA). All other domains were similar between the two groups.

Follow-up

The follow up was completed after 8-12 mo in 16 out of 23 (69.6%) patients (2 patients were lost at follow-up because one died and the other moved to a different city). All patients remained asymptomatic for biliary symptoms. Gallbladder ultrasound was utilized to identify three subgroups of patients according to gallbladder content: (1) patients with a still anechoic gallbladder bile (n = 5), (2) patients who developed biliary sludge alone (n = 4) and (3) patients with prior sludge/gallstones who had unchanged gallbladder content (n = 5) or had stones and developed additional sludge (n = 2) during follow-up.

Table 3 Prior gallbladder motility indices in β -thalassemia major patients according to ultrasonographic appearance of the gallbladder during 8-12 mo follow-up

	Still anechoic	Developed sludge	Prior sludge/gallstones
No. of subjects	5	4	7
Fasting volume (mL), basal	29.2 \pm 7.3	60 \pm 17 ^a	29.2 \pm 4.2
Residual volume (mL), basal	5.5 \pm 1.4	14.7 \pm 4.6 ^a	4.9 \pm 0.9
Fasting volume at follow-up (mL)	30.9 \pm 6.5	72.8 \pm 20.1 ^{a,c}	36.7 \pm 5.1

Data are expressed as mean \pm SE; ^aP < 0.017 vs still anechoic group; ^cP < 0.05 vs prior sludge/gallstones group (ANOVA and Fisher’s LSD multiple comparison test).

Variations in individual fasting gallbladder volumes for each subgroup are depicted in Figure 6. Major changes were evident in patients developing biliary sludge (panel A), also when gallbladder volume was expressed as percent increase (panel B). Interestingly, maximum percent increase in fasting gallbladder volume was observed in 2 patients (89% and 130%) who developed sludge in a gallbladder which previously contained only stones and showed normal fasting volume (*i.e.* < cut-off value of 32 mL). These two patients had clinical evidence of diabetes mellitus (and autonomic neuropathy) and hypothyroidism.

Furthermore, patients who developed sludge during follow-up had also significant changes in postprandial gallbladder volume (Table 3), with a trend towards decreased gallbladder contraction (residual volume: 25.6 \pm 4.7% vs 19.5 \pm 2.8% vs 17.9 \pm 3.0%), and longer transit time (OCTT: 150 \pm 15.8 vs 108 \pm 9.7 vs 126 \pm 12.9 min) when compared with the other two subgroups.

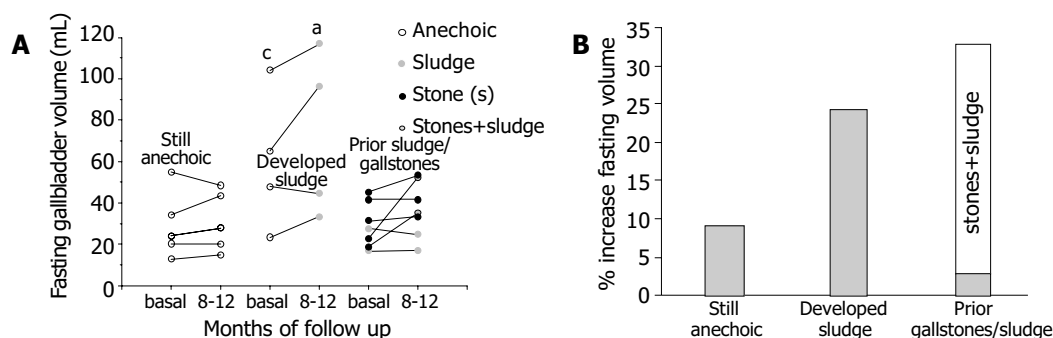


Figure 6 Variations in individual fasting gallbladder volumes for each subgroup in β -thalassemia major patients. A: Major changes in patients who developed biliary sludge: asterisks indicate significant differences, compared to the other two groups of patients (^aP < 0.05 vs prior sludge/gallstones group and ^cP < 0.017 vs still anechoic group). B: Percent increased fasting gallbladder volume in the three groups of patients. The last bar represents those gallbladders with stones that developed additional sludge (n = 2).

DISCUSSION

The present study examined the role of gallbladder and gastrointestinal motility in a well characterized group of adult β -thalassemia major patients in their 3rd decade of life, in relation with the presence of gallstones/biliary sludge. The results suggested the coexistence of impaired gallbladder motility, delayed small intestinal transit, and high prevalence of autonomic neuropathy in β -thalassemia major patients. These abnormalities might contribute, together with haemolytic hyperbilirubinemia to the pathogenesis of gallstones/sludge in β -thalassemia major.

As for other hemolytic disorders including sickle hemoglobinopathy^[37], both hyperbilirubinemia and bilirubin overload/precipitation in bile were definite predisposing factors for pigment gallstone in β -thalassemia major patients during chronic hemolysis^[6]. Indeed, in this study gallstones and/or biliary sludge were found in 56% of β -thalassemia major patients at entry, increasing to over 80% during follow-up (8-12 mo). A previous study^[7] in young patients reported a prevalence of 11.8% and 29.4% for gallstones and sludge, respectively. However, the mean age of β -thalassemia major patients in the present series was 26 years, while it was 12 years in the above mentioned study.

Several pathways might be involved in the pathogenesis of sludge and pigment stones in β -thalassemia. Glucuronidation of excess bilirubin was a predisposing factor in chronic haemolytic diseases^[38]. After injection of desferroxamine, both fecal and urinary excretion were observed and there was formation of iron-desferroxamine complex^[39] which might potentially interfere with the gallbladder microenvironment, already enriched in calcium bilirubinate. Moreover, increased secretion of glycoproteins by epithelial cells was seen after iron-induced stimulation in the guinea pig gallbladder^[40], and this might also take place in β -thalassemia major patients who developed sludge. However, since not all β -thalassemia patients with hemolytic hyperbilirubinemia had gallstones, other pathogenetic mechanisms underlying gallstone formation in β -thalassemia major may play a role.

The present study for the first time suggested that bile stasis and intestinal dysmotility might be key factors in the pathogenesis of pigment gallstones in β -thalassemia major. Pigment stones were common in patients with cirrhosis^[41,42], chronic hemolysis^[37,43,44], ileal Crohn's disease^[45], and conditions associated with impaired gallbladder kinetics^[37,44,46-48]. A recent study by our group found a certain degree of impaired motorfunction of the gallbladder also in non-hemolytic pigment stone patients^[1]. Compared with controls, there was about 100% increase of fasting gallbladder volume across 3 β -thalassemia major subgroups: *i.e.* patients with stones, sludge and stone-sludge free. Increased fasting gallbladder volume seems to be common in hemolytic conditions leading to pigment stones. Everson *et al.* found a volume of about 27 mL in adolescents and young adults with sickle hemoglobinopathy^[37]. Nevertheless, we found that adult "symptomatic" pigment (non hemolytic) stone patients had a fasting volume comparable to controls^[2]. In general, fasting gallbladder volume increased with body size^[49] and obesity^[49,50]. In this respect, the finding of increased fasting gallbladder volume was even more striking if one considered that β -thalassemia major patients had reduced growth with short stature, compared with matched controls^[9]. The increment in fasting gallbladder volume in β -thalassemia major, therefore, represents a true phenomenon and seems to point to defective interprandial (fasting) gallbladder motility. It has been found that fluctuations in fasting gallbladder volume (leading to 20-30% contraction) are normally synchronized with the intestinal migrating motor complex (MMC) and release of the intestinal hormone motilin^[51]. Patients with cholesterol gallstones had frequently increased fasting gallbladder volume^[1] with abnormal MMC and motilin release pattern. Interdigestive gallbladder emptying was reduced, contributing to gallstone formation^[52,53].

A similar derangement of fasting gallbladder motility might also develop in β -thalassemia major patients, and contribute to stasis and sludge/stone formation. A mechanical effect on fasting volume due to the physical presence of gallstones in the gallbladder lumen in β -thalassemia major was unlikely since fasting volume was larger in patients with sludge than in those with stones and also greater in patients without gallstone/sludge than in controls. Also, patients were all asymptomatic for biliary colicky pain (excluding an impacted stone within the cystic duct and/or acute cholecystitis). Our data indicate that postprandial gallbladder motility in β -thalassemia major patients is deranged. Not only fasting, but also residual volume was increased and emptying speed was somewhat slower (although still in the normal range) in sludge or gallstone/sludge-free patients, compared to both patients with gallstones and controls. The large residual gallbladder volume might be the consequence of a greater starting fasting volume^[1,50,54-58]. By contrast, we found that "crude" contraction was preserved (*i.e.* similar or even smaller percent residual volume than in controls, Table 2). Thus, findings in the present study mimicked those seen in sickle hemoglobinopathy^[37], with a smaller contraction index characteristic of β -thalassemia major patients (without mentioning gallbladder emptying speed). Differences in patients' characteristics, age and study protocol might partly account for the discrepancies across studies. Why in our study those patients with gallstones had better gallbladder contraction than controls, remains to be elucidated. Prospective observations are needed to see if, at *equilibrium* (*i.e.* after stone have formed), the gallbladder adapts to a smaller fasting volume and therefore better contraction (smaller residual volume). According to Laplace's law, in fact, the smaller the radius of a given shape (*i.e.* the gallbladder), the smaller the wall tension (from smooth muscle contraction) required to withstand a given internal fluid pressure^[59]. It is highly unlikely that release of endogenous cholecystokinin was deranged in this series of pigment gallstone patients, as seen during total parenteral nutrition^[60]. Whereas in cholesterol gallstone patients excess biliary cholesterol might alter cholecystokinin smooth muscle receptors^[61,62], resulting in secondary impaired gallbladder motility. This possibility has been ruled out in β -thalassemia major patients. In fact, biliary cholesterol saturation did not increase in pigment stone patients and gallbladder smooth muscle contractility *in vitro* was normal^[63].

We also found that OCTT was slightly delayed in β -thalassemia major patients, evidently across all subgroups. A clear explanation of the finding is not readily available, but a condition secondary to bacterial overgrowth or delayed colonic transit was highly unlikely, since there was no evidence of bacterial translocation with H₂-breath test and all patients had normal weekly bowel habits and a stool scale form. Small bowel dysmotility might accompany abnormal intestinal migrating motor complexes, as seen in a subgroup of patients with irritable bowel^[64] and functional dyspepsia^[65]. Also, intestinal mucosal changes have been described in β -thalassemia major patients^[66] and might influence some motility patterns in the small bowel. Others have found that small bowel inflammation and/or malabsorption are not more frequent in β -thalassemia major patients^[67]. Patients with ileal disease, bypass, or resection were at increased risk for developing pigment gallstones, so were patients with ileal Crohn's disease. Increased bilirubin levels in bile of patients with Crohn disease were caused by lack of functional ileum^[45]. One might speculate that delayed OCTT in β -thalassemia major patients might lead to increase of enterohepatic cycling of bilirubin^[68], therefore predisposing to pigment gallstone formation.

Autonomic neuropathy might be associated with gastrointestinal dysmotility. As expected, all β -thalassemia major patients with diabetes or abnormal oral glucose tolerance test had impaired tests for autonomic neuropathy (*i.e.* 23% of all patients).

Surprisingly abnormal tests of sympathetic and parasympathetic system were found in 86% of the patients. Potential causes for autonomic neuropathy in β -thalassemia major patients were the coexistence of diabetes mellitus, neurotoxicity of desferroxamine ad iron overload (or both)^[69,70] (for example, visual and auditory neurotoxicity were found in 1 patient of this series). The presence of hemolysis might also contribute to neuropathy, as abnormal autonomic cardiovascular response was described in patients with sickle cell anemia^[71]. Last but not least, the presence of autonomic dysfunction was also a feature in patients with different types and stages of chronic liver disease,^[72] and this might also the case in chronic liver disease of β -thalassemia major patients. Further studies are needed to clarify if the presence of autonomic dysfunction is a useful tool for the prediction of prognosis and outcome of patients with β -thalassemia major.

Positive tests for autonomic neuropathy tended to relate to abnormal gallbladder and small bowel motility. Interestingly, we found delayed OCTT with increased bowel movements in chronic alcoholic patients during abstinence, was associated with dysfunction of autonomic nervous system. A form of subclinical autonomic neuropathy might predispose to a diffuse disorder of smooth muscle, suggesting the multi-organic involvement of the gastrointestinal tract. In the determination of altered OCTT a possible role for dysfunction of autonomic nervous system has been suggested in other series of patients^[22] and might deserve further investigations also in β -thalassemia major patients.

In conclusion, the present study shows for the first time that in β -thalassemia major patients in the 3rd decade of life, increased volume and deranged motility of the gallbladder are associated with delayed small intestinal transit and mild dyspeptic symptoms. Such functional abnormalities apparently contribute together with haemolytic hyperbilirubinemia to the pathogenesis of gallstones/sludge in β -thalassemia major.

REFERENCES

- 1 **Portincasa P**, Di Ciaula A, Baldassarre G, Palmieri VO, Gentile A, Cimmino A, Palasciano G. Gallbladder motor function in gallstone patients: sonographic and *in vitro* studies on the role of gallstones, smooth muscle function and gallbladder wall inflammation. *J Hepatol* 1994; **21**: 430-440
- 2 **Portincasa P**, Di Ciaula A, Vendemiale G, Palmieri VO, Moschetta A, vanBerge-Henegouwen GP, Palasciano G. Gallbladder motility and cholesterol crystallization in bile from patients with pigment and cholesterol gallstones. *Eur J Clin Invest* 2000; **30**: 317-324
- 3 **Portincasa P**, Di Ciaula A, Palmieri VO, Velardi A, vanBerge-Henegouwen GP, Palasciano G. Impaired gallbladder and gastric motility and pathological gastro-esophageal reflux in gallstone patients. *Eur J Clin Invest* 1997; **8**: 653-661
- 4 **van Erpecum KJ**, vanBerge-Henegouwen GP. Gallstones: an intestinal disease? *Gut* 1999; **44**: 435-438
- 5 **Rodgers GP**. Hemoglobinopathies: The Thalassemias. In: Goldmann L, Bennett JC, editors. Cecil. Textbook of Medicine. Philadelphia: W.B. Saunders Company 2000
- 6 **Sherlock S**, Dooley J. Diseases of the liver and biliary system. *Oxford Blackwell Science* 2002
- 7 **Kalayci AG**, Albayrak D, Gunes M, Incesu L, Agac R. The incidence of gallbladder stones and gallbladder function in beta-thalassemic children. *Acta Radiol* 1999; **40**: 440-443
- 8 **Leoni GB**, Rosatelli C, Vitucci A, Addis M, Loi A, Tannoia N, Cao A. Molecular basis of beta-thalassemia intermedia in a southern Italian region (Puglia). *Acta Haematol* 1991; **86**: 174-178
- 9 **Wonke B**. Clinical management of beta-thalassemia major. *Semin Hematol* 2001; **38**: 350-359
- 10 **Everson GT**, Braverman DZ, Johnson ML, Kern F Jr. A critical evaluation of real-time ultrasonography for the study of gallbladder volume and contraction. *Gastroenterology* 1980; **79**: 40-46
- 11 **Hveem K**, Jones KL, Chatterton BE, Horowitz M. Scintigraphic measurement of gastric emptying and ultrasonographic assessment of antral area: relation to appetite. *Gut* 1996; **38**: 816-821
- 12 **Wedmann B**, Schmidt G, Wegener M, Coenen C, Ricken D, Althoff J. Effects of age and gender on fat-induced gallbladder contraction and gastric emptying of a caloric liquid meal: a sonographic study. *Am J Gastroenterol* 1991; **86**: 1765-1770
- 13 **Bolondi L**, Bortolotti MSV, Calleti T, Gaiani S, Labo' G. Measurement of gastric emptying by real-time ultrasonography. *Gastroenterology* 1985; **89**: 752-759
- 14 **Ricci R**, Bontempo I, Corazziari E, La Bella A, Torsoli A. Real-time ultrasonography of the gastric antrum. *Gut* 1993; **34**: 173-176
- 15 **Bergmann JF**, Chassany O, Petit A, Triki R, Caulin C, Segrestaa JM. Correlation between echographic gastric emptying and appetite: influence of psyllium. *Gut* 1992; **33**: 1042-1043
- 16 **Darwiche G**, Almer LO, Bjorgell O, Cederholm C, Nilsson P. Measurement of gastric emptying by standardized real-time ultrasonography in healthy subjects and diabetic patients. *J Ultrasound Med* 1999; **18**: 673-682
- 17 **Portincasa P**, Colecchia A, Di Ciaula A, Larocca A, Muraca M, Palasciano G, Roda E, Festi D. Standards for diagnosis of gastrointestinal motility disorders. *Ultrasonography. Dig Liver Dis* 2000; **32**: 160-172
- 18 **Portincasa P**, Moschetta A, Baldassarre G, Altomare DF, Palasciano G. Pan-enteric dysmotility, impaired quality of life and alexithymia in a large group of patients meeting the Rome II criteria for irritable bowel syndrome. *World J Gastroenterol* 2003; **9**: 2293-2299
- 19 **Gallinger S**, Taylor RD, Harvey PRC, Petrunka CN, Strasberg SM. Effects of mucous glycoprotein on nucleation time of human bile. *Gastroenterology* 1985; **89**: 648-658
- 20 **Portincasa P**, Di Ciaula A, Palmieri VO, Vendemiale G, Altomare E, Palasciano G. Sonographic evaluation of gallstone burden in humans. *Ital J Gastroenterol Hepatol* 1994; **26**: 141-144
- 21 **Mann NS**, Condon DS, Leung JW. Colonic preparation correlates with fasting breath hydrogen in patients undergoing colonoscopy. *Hepatogastroenterology* 2003; **50**: 85-86
- 22 **Altomare DF**, Portincasa P, Rinaldi M, Di Ciaula A, Martinelli E, Amoroso AC, Palasciano G, Memeo V. Slow-transit constipation: a solitary symptom of a systemic gastrointestinal disease. *Dis Colon Rectum* 1999; **42**: 231-240
- 23 **Rangari M**, Sinha S, Kapoor D, Mohan JC, Sarin SK. Prevalence of autonomic dysfunction in cirrhotic and noncirrhotic portal hypertension. *Am J Gastroenterol* 2002; **97**: 707-713
- 24 **Ryder RE**, Marshall R, Johnson K, Ryder AP, Owens DR, Hayes TM. Acetylcholine sweatspot test for autonomic denervation. *Lancet* 1988; **1**: 1303-1305
- 25 **Altomare D**, Pilot MA, Scott M, Williams N, Rubino M, Ilincic L, Waldron D. Detection of subclinical autonomic neuropathy in constipated patients using a sweat test. *Gut* 1992; **33**: 1539-1543
- 26 **Vespasiani G**, Bruni M, Meloncelli I, Clementi L, Amoretti R, Branca S, Carinci F, Lostia S, Nicolucci A, Romagnoli F, Verga S, Benedetti MM. Validation of a computerised measurement system for guided routine evaluation of cardiovascular autonomic neuropathy. *Comput Methods Programs Biomed* 1996; **51**: 211-216
- 27 **Diem P**, Laederach-Hofmann K, Navarro X, Mueller B, Kennedy WR, Robertson RP. Diagnosis of diabetic autonomic neuropathy: a multivariate approach. *Eur J Clin Invest* 2003; **33**: 693-697
- 28 **O'Donnell MR**, Virjee J, Heaton KW. Detection of pseudo diarrhoea by simple assessment of intestinal transit rate. *Br Med J* 1990; **300**: 439-440
- 29 **Buckley MJ**, Scanlon C, McGurgan P, O'Morain C. A validated dyspepsia symptom score. *Ital J Gastroenterol Hepatol* 1997; **29**: 495-500
- 30 **Portincasa P**, Altomare DF, Moschetta A, Baldassarre G, Di Ciaula A, Venneman NG, Rinaldi M, Vendemiale G, Memeo V, vanBerge-Henegouwen GP, Palasciano G. The effect of acute oral erythromycin on gallbladder motility and on upper gastrointestinal symptoms in gastrectomized patients with and without gallstones: a randomized, placebo-controlled ultrasonographic study. *Am J Gastroenterol* 2000; **95**: 3444-3451
- 31 **Schoenfield LJ**, Carulli N, Dowling RH, Sama C, Wolpers C. Asymptomatic gallstones: definition and treatment. *Gastroenterol International* 1989; **2**: 25-29
- 32 **Ware JE**, Snow KK, Kosinski M. SF-36 health survey. Manual

- and interpretation guide. Boston: The Health Institute: *New England Medical Center* 1993
- 33 **Stewart AL**, Greenfield S, Hays RD, Wells K, Rogers WH, Berry SD, McGlynn EA, Ware JE Jr. Functional status and well-being of patients with chronic conditions. Results from the Medical Outcomes Study. *JAMA* 1989; **262**: 907-913
- 34 **Hahn BA**, Yan S, Strassels S. Impact of irritable bowel syndrome on quality of life and resource use in the United States and United Kingdom. *Digestion* 1999; **60**: 77-81
- 35 **Armitage P**, Berry G. Statistical methods in medical research. 3rd ed. *Oxford Blackwell Science Ltd* 1994
- 36 **Dawson B**, Trapp RG. Basic & Clinical Biostatistics. 3rd ed. *New York McGraw Hill* 2001
- 37 **Everson GT**, Nemeth A, Kourourian S, Zogg D, Leff NB, Dixon D, Githens JH, Pretorius D. Gallbladder function is altered in sickle hemoglobinopathy. *Gastroenterology* 1989; **96**: 1307-1316
- 38 **Feverly J**, Verwilghen R, Tan TG, de Groote J. Glucuronidation of bilirubin and the occurrence of pigment gallstones in patients with chronic haemolytic diseases. *Eur J Clin Invest* 1980; **10**: 219-226
- 39 **Faa G**, Crisponi G. Iron chelating agents in clinical practice. *Coodination Chemistry Reviews* 1999; **184**: 291-310
- 40 **Hale WB**, Turner B, LaMont JT. Oxygen radicals stimulate guinea pig gallbladder glycoprotein secretion *in vitro*. *Am J Physiol* 1987; **253**: G627-G630
- 41 **Alvaro D**, Angelico M, Gandin C, Ginanni Corradini S, Capocaccia L. Physico-chemical factors predisposing to pigment gallstone formation in liver cirrhosis. *J Hepatol* 1990; **10**: 228-234
- 42 **Sakata R**, Ueno T, Sata M, Sujacu K, Tamaki S, Torimura T, Tanikawa K. Formation of black pigment gallstone in a hamster model of experimental cirrhosis. *Eur J Clin Invest* 1997; **27**: 840-845
- 43 **Carey MC**. Pathogenesis of gallstones. *Am J Surg* 1993; **165**: 410-419
- 44 **Trotman BW**. Pigment gallstone disease. *Gastroenterol Clin North Am* 1991; **20**: 111-126
- 45 **Brink MA**, Slors JF, Keulemans YC, Mok KS, De Waart DR, Carey MC, Groen AK, Tytgat GN. Enterohepatic cycling of bilirubin: a putative mechanism for pigment gallstone formation in ileal Crohn's disease. *Gastroenterology* 1999; **116**: 1420-1427
- 46 **Kurihara N**, Ide H, Omata T, Yonamine S, Mashima Y, Tanno M, Chiba K, Yamada H. Evaluation of gallbladder emptying in patients with chronic liver disease by 99 mTc-EHIDA hepatobiliary scintigraphy. *Radioisotopes* 1989; **38**: 269-274
- 47 **Pompili M**, Rapaccini GL, Caturelli E, Curro D, Montuschi P, D'Amato M, Aliotta A, Grattagliano A, Cedrone A, Anti M. Gallbladder emptying, plasma levels of estradiol and progesterone, and cholecystokinin secretion in liver cirrhosis. *Dig Dis Sci* 1995; **40**: 428-434
- 48 **Acalovschi M**, Dumitrascu DL, Csakany I. Gastric and gall bladder emptying of a mixed meal are not coordinated in liver cirrhosis - a simultaneous sonographic study. *Gut* 1997; **40**: 412-417
- 49 **Palasciano G**, Serio G, Portincasa P, Palmieri VO, Fanelli M, Velardi ALM, Calo' Gabrieli B, Vinciguerra V. Gallbladder volume in adults and relationship to age, sex, body mass index and gallstones: a sonographic population study. *Am J Gastroenterol* 1992; **87**: 493-497
- 50 **Portincasa P**, Di Ciaula A, Palmieri VO, vanBerge-Henegouwen GP, Palasciano G. Effects of cholestyramine on gallbladder and gastric emptying in obese and lean subjects. *Eur J Clin Invest* 1995; **25**: 746-753
- 51 **Portincasa P**, Peeters TL, Berge-Henegouwen GP, Van Solinge WW, Palasciano G, van Erpecum KJ. Acute intraduodenal bile salt depletion leads to strong gallbladder contraction, altered antroduodenal motility and high plasma motilin levels in humans. *Neurogastroenterol Motil* 2000; **12**: 421-430
- 52 **Stolk MF**, van Erpecum KJ, Peeters TL, Samsom M, Smout AJ, Akkermans LM, vanBerge-Henegouwen GP. Interdigestive gallbladder emptying, antroduodenal motility, and motilin release patterns are altered in cholesterol gallstone patients. *Dig Dis Sci* 2001; **46**: 1328-1334
- 53 **Xu QW**, Scott RB, Tan DTM, Shaffer EA. Altered migrating myoelectrical complex in an animal model of cholesterol gallstone disease: the effect of erythromycin. *Gut* 1998; **43**: 817-822
- 54 **Palasciano G**, Portincasa P, Belfiore A, Baldassarre G, Cignarelli M, Paternostro A, Albano O, Giorgino R. Gallbladder volume and emptying in diabetics: the role of neuropathy and obesity. *J Intern Med* 1992; **231**: 123-127
- 55 **Portincasa P**, Di Ciaula A, Palmieri VO, vanBerge-Henegouwen GP, Palasciano G. Ultrasonographic study of gallbladder and gastric dynamics in obese people after oral cholestyramine. *Dordrecht Kluwer Academic Publisher* 1994: 323-327
- 56 **Portincasa P**, Di Ciaula A, Palmieri VO, Baldassarre G, Palasciano G. Enhancement of gallbladder emptying in gallstone patients after oral cholestyramine. *Am J Gastroenterol* 1994; **89**: 909-914
- 57 **Festi D**, Frabboni R, Bazzoli F, Sangermano A, Ronchi M, Rossi L, Parini P, Orsini M, Primerano AM, Mazzella G, Aldini R, Roda E. Gallbladder motility in cholesterol gallstone disease. Effect of ursodeoxycholic acid administration and gallstone dissolution. *Gastroenterology* 1990; **99**: 1779-1785
- 58 **van de Meeberg PC**, Portincasa P, Wolfhagen FH, van Erpecum KJ, vanBerge-Henegouwen GP. Increased gall bladder volume in primary sclerosing cholangitis. *Gut* 1996; **39**: 594-599
- 59 **Shaffer EA**. Abnormalities in gallbladder function in cholesterol gallstone disease: bile and blood, mucosa and muscle—the list lengthens. *Gastroenterology* 1992; **102**: 1808-1812
- 60 **Sitzmann JV**, Pitt HA, Steinborn PA, Pasha ZR, Sanders RC. Cholecystokinin prevents parenteral nutrition induced biliary sludge in humans. *Surg Gynecol Obstet* 1990; **170**: 25-31
- 61 **Upp JR Jr**, Nealon WH, Singh P, Fagan CJ, Jonas AS, Greeley GH Jr, Thompson JC. Correlation of cholecystokinin receptors with gallbladder contractility in patients with gallstones. *Ann Surg* 1987; **205**: 641-648
- 62 **Xu QW**, Shaffer EA. The potential site of impaired gallbladder contractility in an animal model of cholesterol gallstone disease. *Gastroenterology* 1996; **110**: 251-257
- 63 **Behar J**, Lee KY, Thompson WR, Biancani P. Gallbladder contraction in patients with pigment and cholesterol stones. *Gastroenterology* 1989; **97**: 1479-1484
- 64 **Pfeiffer A**, Schmidt T, Holler T, Herrmann H, Pehl C, Wendl B, Kaess H. Effect of trospium chloride on gastrointestinal motility in humans. *Eur J Clin Pharmacol* 1993; **44**: 219-223
- 65 **Jebbink HJ**, Berge-Henegouwen GP, Bruijjs PP, Akkermans LM, Smout AJ. Gastric myoelectrical activity and gastrointestinal motility in patients with functional dyspepsia. *Eur J Clin Invest* 1995; **25**: 429-437
- 66 **Awwad S**, Khalifa AS, Abdel-Fattah S, Mousa S, Sabry F, Eid S. Intestinal mucosal changes in thalassaemia major. *Gaz Egypt Paediatr Assoc* 1975; **23**: 261-265
- 67 **Sinniah D**, Nagalingam I. D-xylose absorption in B-thalassaemia major. *J Trop Med Hyg* 1978; **81**: 185-187
- 68 **Vitek L**, Carey MC. Enterohepatic cycling of bilirubin as a cause of 'black' pigment gallstones in adult life. *Eur J Clin Invest* 2003; **33**: 799-810
- 69 **Triantafyllou N**, Fisis M, Sideris G, Triantafyllou D, Rombos A, Vrettou H, Mantouvalos V, Politi C, Malliara S, Papageorgiou C. Neurophysiological and neuro-otological study of homozygous beta-thalassaemia under long-term desferrioxamine (DFO) treatment. *Acta Neurol Scand* 1991; **83**: 306-308
- 70 **Zafeiriou DI**, Kousi AA, Tsantali CT, Kontopoulos EE, Augoustidou-Savvopoulou PA, Tsoubaris PD, Athanasiou MA. Neurophysiologic evaluation of long-term desferrioxamine therapy in beta-thalassaemia patients. *Pediatr Neurol* 1998; **18**: 420-424
- 71 **Romero-Vecchione E**, Perez O, Wessolosky M, Rosa F, Liberatore S, Vasquez J. Abnormal autonomic cardiovascular responses in patients with sickle cell anemia. *Sangre* 1995; **40**: 393-399
- 72 **Oliver MI**, Miralles R, Rubies-Prat J, Navarro X, Espadaler JM, Sola R, Andreu M. Autonomic dysfunction in patients with non-alcoholic chronic liver disease. *J Hepatol* 1997; **26**: 1242-1248

• CLINICAL RESEARCH •

Clinical features of human intestinal capillariasis in Taiwan

Ming-Jong Bair, Kao-Pin Hwang, Tsang-En Wang, Tai-Cherng Liou, Shee-Chan Lin, Chin-Roa Kao,
Tao-Yeuan Wang, Kwok-Kuen Pang

Ming-Jong Bair, Department of Gastroenterology, Mackay Memorial Hospital, Taitung Branch, Taiwan, China

Kao-Pin Hwang, Department of Pediatrics, Kaohsiung Medical College, Taipei, China

Tsang-En Wang, Tai-Cherng Liou, Shee-Chan Lin, Chin-Roa Kao, Department of Gastroenterology, Mackay Memorial Hospital, Taipei, China

Tao-Yeuan Wang, Department of Pathology, Mackay Memorial Hospital, Taipei, China

Kwok-Kuen Pang, Department of Radiology, Mackay Memorial Hospital, Taitung Branch, Taiwan, China

Correspondence to: Dr. Ming-Jong Bair, Department of Gastroenterology, Mackay Memorial Hospital, Taitung Branch, 1, Lane 303 Chang-Sha St. Taitung, Taiwan, China. library@ttms.mmh.org.tw

Telephone: +886-89-310150 **Fax:** +886-89-321240

Received: 2003-09-15 **Accepted:** 2003-11-06

Abstract

Human intestinal capillariasis is a rare parasitosis that was first recognized in the Philippines in the 1960 s. Parasitosis is a life threatening disease and has been reported from Thailand, Japan, South of Taiwan (Kaoh-Siung), Korea, Iran, Egypt, Italy and Spain. Its clinical symptoms are characterized by chronic diarrhea, abdominal pain, borborygmus, marked weight loss, protein and electrolyte loss and cachexia. Capillariasis may be fatal if early treatment is not given. We reported 14 cases living in rural areas of Taiwan. Three cases had histories of travelling to Thailand. They might have been infected in Thailand while stayed there. Two cases had the diet of raw freshwater fish before. Three cases received emergency laparotomy due to peritonitis and two cases were found of enteritis cystica profunda. According to the route of transmission, freshwater and brackish-water fish may act as the intermediate host of the parasite. The most simple and convenient method of diagnosing capillariasis is stool examination. Two cases were diagnosed by histology. Mebendazole or albendazole 200 mg orally twice a day for 20-30 d is the treatment of choice. All the patients were cured, and relapses were not observed within 12 mo.

Bair MJ, Hwang KP, Wang TE, Liou TC, Lin SC, Kao CR, Wang TY, Pang KK. Clinical features of human intestinal capillariasis in Taiwan. *World J Gastroenterol* 2004; 10(16): 2391-2393
<http://www.wjgnet.com/1007-9327/10/2391.asp>

INTRODUCTION

Capillaria species parasitize many classes of vertebrates, although only 4 species described have been found in humans, namely *Capillaria philippinensis*, *Capillaria plica*, *Capillaria aerophila*, and *Capillaria hepatica*^[1]. *C. philippinensis* is a tiny nematode that was first described in the 1960 s as the causative agent of severe diarrheal syndromes in humans. In 1962, the first case of human intestinal capillariasis occurred in a previously healthy young man from Luzon (Philippines) who subsequently died. At autopsy, a large number of worms, later

described as *C. philippinensis*, were found in the large and small intestines^[2]. The disease was first reported by Chitwood *et al.* in 1964^[3]. During the Philippine epidemic from 1967 to 1968, more than 1300 persons acquired the illness and 90 patients with parasitologically confirmed infections died^[4]. In late 1978 and early 1979, another small outbreak was identified in northeastern Mindanao, the Philippines, and about 50 persons acquired the infection^[4]. Sporadic cases continued to appear in northern Luzon as well as in other areas where epidemics had occurred. The disease is also endemic in Thailand, and was first reported in 1973^[5]. Sporadic cases have also been found in Iran^[6], Egypt^[7,8], Taiwan^[9], Japan^[10,11], Indonesia^[12], Korea^[13], Spain (probably acquired in Colombia)^[14] and Italy (acquired in Indonesia)^[15], indicating that this infection is widespread. Because the infection can result in a severe disease with a high mortality when untreated, early diagnosis is very important. Here we described 14 cases of human intestinal capillariasis found in Taiwan from 1983 to 2001.

MATERIALS AND METHODS

Since 1983, 14 cases have been diagnosed as intestinal capillariasis in Taiwan, all with the symptoms of chronic diarrhea, abdominal pain, borborygmus and marked weight loss. All patients were hospitalized for examination and treatment. Their diagnosis was confirmed by eggs and/or larvae and/or adult *C. philippinensis* found in the feces of 5 patients. Two cases were recognized by a pathologist by histology of jejunum or ileum (Figures 1, 2) with negative stool examination. Bacterial cultures of stool specimens were negative in all patients. The stool specimens were examined by formalin-ether concentration method. *C. philippinensis* eggs were peanut-shaped with flattened bipolar plugs, 20×40 μm in size (Figure 3).

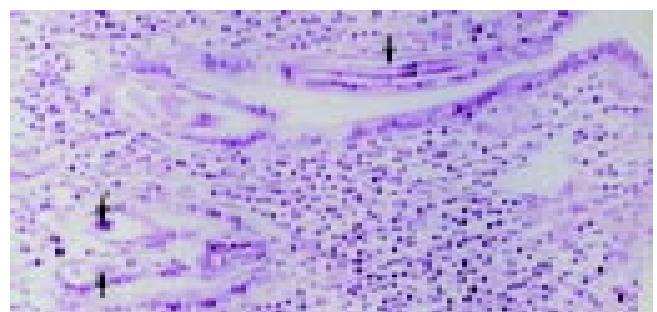


Figure 1 *C. philippinensis* worms embedded in intestinal mucosa (arrow). Hematoxylin and eosin, ×200.

RESULTS

Fourteen cases, nine males and five females, were 36 to 76 years old when they were diagnosed as intestinal capillariasis (Tables 1, 2). Three lived in Kaohsiung County and eleven in Taitung County. Seven of them were aborigines and two were brother and sister. Two of them had histories of travelling to Thailand. Two patients had history of eating raw or insufficiently cooked fresh-water fish. Four of 14 patients had mixed infection with *Clonorchis sinensis* or *Strongyloides stercoralis* whose eggs were also found in the feces.

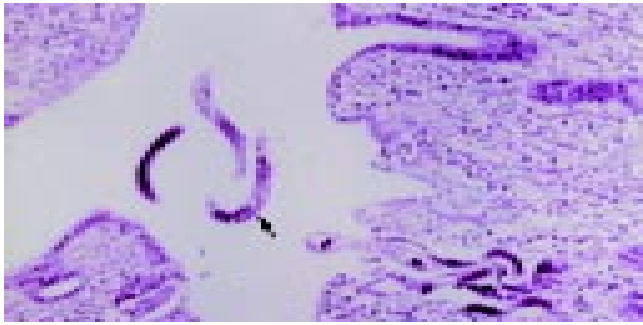


Figure 2 Multiple longitudinal sections of *C. philippinensis* on mucosal surface and lumen. The longitudinal sections shows a row of stichocytes (arrow). Hematoxylin and eosin, $\times 200$.

Three cases received emergency laparotomy due to peritonitis and two of them were found to have jejunitis cystica profunda. Small bowel series and colonoscopic study revealed mild dilatation and thickened mucosa of jejunum and ileum, which suggested malabsorption. Laboratory findings revealed anemia, malabsorption of fats and carbohydrates and low serum levels of potassium, sodium, calcium and total protein. Mebendazole 200 mg twice a day for 20 d was given to 12 patients, while albendazole was given to the other two patients. All of them were cured and relapses were not observed within 12 mo following chemotherapy and supportive treatment.

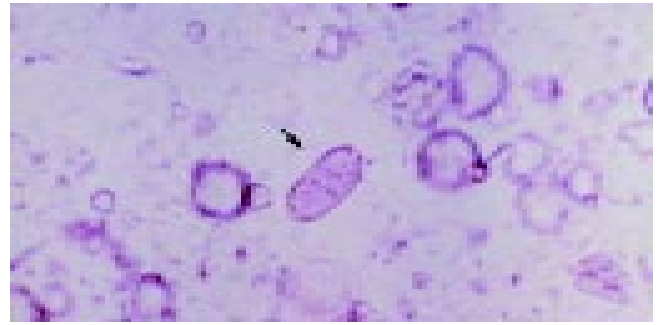


Figure 3 Peanut-shaped eggs of *C. philippinensis* in feces with flattened bipolar plugs. $\times 160$.

DISCUSSION

Capillaria species parasitize many classes of vertebrates, although only 4 species have been found in humans, namely *C. philippinensis*, *C. plica*, *C. aerophila*, and *C. hepatica*^[1]. *C. philippinensis* is a tiny nematode first described in the 1960s as a pathogen inducing severe diarrheal syndromes in humans. In 1962, the first reported case of human intestinal capillariasis occurred in a previously healthy young man from Luzon in the Philippines, who subsequently died. At autopsy, a large number of worms were found in the large and small intestines^[2]. Chitwood *et al.* described this case in 1964^[3]. There was an epidemic of

Table 1 Characteristics of seven patients with intestinal capillariasis reported in Tai-tung

Case No.	Year Occurred	Occupation	Age (yr)	Sex	Travel history	Associated parasite	Treatment	Outcome
1	1983	Farmer	76	M	-	<i>Clonorchis sinensis</i>	Albendazole	Cure
2	1987	Merchant	46	M	-	-	Albendazole	Cure
3	1988	Housewife	58	F	Thailand	-	Mebendazole	Cure
4	1990	Housewife	41	F	-	-	Mebendazole	Cure
5	1991	Housewife	36	F	-	-	Mebendazole	Cure
6	1991	Farmer	62	M	-	<i>Clonorchis sinensis</i>	Mebendazole	Cure
7	1991	Housewife	46	F	-	-	Mebendazole	Cure
8	1992	Merchant	53	M	Thailand	-	Mebendazole	Cure
9	1992	Farmer	45	M	-	-	Mebendazole	Cure
10	1995	Farmer	61	M	-	-	Mebendazole	Cure
11	1995	Housewife	45	F	-	<i>Strongyloides stercoralis</i>	Mebendazole	Cure
12	1999	Farmer	39	M	-	-	Mebendazole	Cure
13	2000	Fisher-man	69	M	-	-	Mebendazole	Cure
14	2001	Farmer	50	M	-	<i>Clonorchis sinensis</i>	Mebendazole	Cure

Table 2 Clinical features and diagnostic method of seven patients with intestinal capillariasis reported in Tai-tung

Case No.	Duration of onset to diagnosis	Diagnostic method	Chronic diarrhea	Abdominal Pain	Abdominal borborygmi	Body weight loss	Anemia	Hypoalbuminemia
1	119 d	Stool ova	+	+	+	+	+	+
2	2Y7 M	Stool ova	+	+	+	+	+	+
3	6 M	Stool ova	+	+	+	+	+	+
4	1Y3 M	Histology	+	+	+	+	+	+
5	120 d	Histology	+	+	+	+	+	+
6	70 d	Stool ova	+	-	-	+	-	+
7	7 d	Stool ova	+	+	-	-	+	+
8	65 d	Stool ova	+	+	+	+	+	+
9	34 d	Stool ova	+	+	+	+	+	-
10	103 d	Stool ova	+	+	+	-	+	+
11	66 d	Stool ova	+	+	+	-	-	+
12	37 d	Histology	+	+	+	+	-	+
13	25 d	Histology	+	-	-	+	-	+
14	17 d	Stool ova	+	+	+	+	-	+

the disease in the Philippines from 1967 to 1968, more than 1 300 persons acquired the illness, and 90 patients with parasitologically confirmed infection died^[4]. In late 1978 and early 1979, another small outbreak was identified in northeastern Mindanao, Philippines, with about 50 persons infected^[4]. Sporadic cases continued to appear in northern Luzon and also in other areas where epidemics had occurred. The disease is endemic in Thailand, where it was first reported in 1973^[5]. Sporadic cases have also been found in Iran^[6], Egypt^[7,8], Taiwan^[9], Japan^[10,11], Indonesia^[12], Korea^[13], Spain (probably acquired in Colombia)^[14], and Italy (acquired in Indonesia)^[12]. The parasite thus appears to be widespread. Because infection may result in severe disease with a high mortality when untreated, early diagnosis is very important. Infection with *C. philippinensis* should be considered in the differential diagnosis of malabsorption syndrome^[15]. There was often a delay in diagnosis, averaging 4 mo and even longer in Taiwan, especially in non-endemic areas^[16]. The delay was over a year in our cases.

It has been found that *Capillaria* species are closely related to *Trichuris* and *Trichinella* species^[1], and the eggs of *Trichuris trichiura* and *C. philippinensis* are similar in appearance, although they can be differentiated by experienced observers^[17]. Some individuals could be infected with both parasites, which further confuse the picture. In fact, 10 of the 11 patients described by Whaler *et al.*^[18] were infected with both *T. trichiura* and *C. philippinensis*. An inexperienced observer might confuse the eggs of *Capillaria* with those of *T. trichiura*^[1], although a correct parasitologic diagnosis could be made by finding characteristic peanut-shaped eggs with flattened bipolar plugs^[2].

The source of *C. philippinensis* infection in our two patients was unclear, particularly as they had no travel history. In Thailand and the Philippines, the infection has been attributed to eating raw or insufficiently cooked fish harboring the larvae^[2,19]. Hakka Chinese in Taiwan like to eat raw, freshwater fish, so they might be expected to have a significant incidence of infection if freshwater fish in Taiwan commonly host *C. philippinensis*. This is not the case, however. Our two patients lived in the southeastern part of Taiwan, closest to Luzon, so it was possible that the fish imported from the Philippines were the source of infection. Fish in markets in Taitung County, southeastern Taiwan, have been examined for *C. philippinensis* infection, but the results were negative. Recent findings suggested that fishing-eating birds might be the natural definitive hosts^[20], including *Bulbulcus ibis*, *Nycticorax nycticorax*, and *Ixobrychus sinensis*, all of which have been found in Taiwan^[21]. Therefore, the possibility of human infection acquired in Taiwan by direct or indirect ingestion of fresh-water fish with a larval stage of the parasite cannot be discounted.

Enteritis cystica profunda is a disorder with mucin-filled cystic spaces lined by non-neoplastic columnar epithelium in the wall of small intestine, predominantly the submucosa. The histology has been found to simulate mucinous carcinoma^[22]. It has also been shown to occur in the esophagus^[23] and stomach^[24,25]. The irregular distribution of the glands and cysts with normal-appearing glandular epithelium containing mucus and Paneth's cells were features suggestive of its benign nature^[26].

Albendazole was presently considered the drug of choice for the treatment of human intestinal capillariasis because it was effective against eggs, larvae, and adult worms^[1,26]. However, for a major infection, mebendazole (200 mg orally twice a day for 20 d) was recommended as the treatment of choice. Attempts to reduce the standard schedule of mebendazole treatment (400 mg daily for 3 wk) have failed in Thailand. Our patients responded well to a standard course of mebendazole and had no evidence of relapse.

Convenient international travel and commercial globalization

have facilitated the wide dissemination of infectious diseases, whether they are carried by human hosts or non-human vectors. Intestinal capillariasis needs to be considered in the differential diagnosis of patients with chronic diarrhea, borborygmus, abdominal pain, and marked weight loss.

REFERENCES

- 1 Cross JH. Intestinal capillariasis. *Clin Microbiol Rev* 1992; **5**: 120-129
- 2 Cross JH. Intestinal capillariasis. *Parasitol Today* 1990; **6**: 26-28
- 3 Chitwood MB, Valasquez C, Salazar NG. *Capillaria philippinensis* sp. N. (Nematoda: Trichinellida) from the intestine of man in the Philippines. *J Parasitol* 1968; **54**: 368-371
- 4 Cross JH, Singson CN, Battad S, Basaca-Sevilla V. Intestinal capillariasis: epidemiology, parasitology and treatment. *Proc R Soc Med Int Cong Symp Ser* 1979; **24**: 81-86
- 5 Pradatsundarasar A, Pecharanond K, Chintanawongs C, Ungthavorn P. The first case of intestinal capillariasis in Thailand. *Southeast Asian J Trop Med Pub Health* 1973; **4**: 131-134
- 6 Hoghooghi-Rad N, Maraghi S, Narenj-Zadeh A. *Capillaria philippinensis* infection in Khoozestan Province, Iran: case report. *Am J Trop Med Hyg* 1987; **37**: 135-136
- 7 Youssef FG, Mikhail EM, Mansour NS. Intestinal capillariasis in Egypt: a case report. *Am J Trop Med Hyg* 1989; **40**: 195-196
- 8 Mansour NS, Anis MH, Mikhail EM. Human intestinal capillariasis in Egypt. *Trans R Soc Trop Med Hyg* 1990; **84**: 114
- 9 Chen CY, Hsieh WC, Lin JT, Liu MC. Intestinal capillariasis: report of a case. *J Formosa Med Assoc* 1989; **88**: 617-620
- 10 Mukai T, Shimizu S, Yamamoto M. A case of intestinal capillariasis. *Jpn Arch Int Med* 1983; **3**: 163-169
- 11 Nawa Y, Imai JI, Abe T, Kisanuki H, Tsuda K. A case report of intestinal capillariasis. The second case found in Japan. *Jpn J Parasitol* 1988; **37**: 113-118
- 12 Chichino G, Bernuzzi AM, Bruno A. Intestinal capillariasis (*Capillaria philippinensis*) acquired in Indonesia: a case report. *Am J Trop Med Hyg* 1992; **47**: 10-12
- 13 Lee SH, Hong ST, Chai JY. A case of intestinal capillariasis in the Republic of Korea. *Am J Trop Med Hyg* 1993; **48**: 542-546
- 14 Drona F, Chaves F, Sanz A, Lopez-Velez R. Human intestinal capillariasis in an area of nonendemicity: case report and review. *Clin Infect Dis* 1993; **17**: 909-912
- 15 Paulino GB, Wittenberg J. Intestinal capillariasis: a new cause of a malabsorption pattern. *Am J Roentgenol Radiother Nucl Med* 1973; **117**: 340-345
- 16 Hwang KP. Human intestinal capillariasis in Taiwan. *Acta Paed Sin* 1998; **39**: 82-85
- 17 Zaman V, Keong LA. Helminths in: Handbook of medical parasitology. 2nd ed. *Edinburgh: Churchill Livingstone* 1990: 87-217
- 18 Whalen GE, Rosenberg EB, Strickland GT. Intestinal capillariasis: a new disease in man. *Lancet* 1969; **1**: 13-16
- 19 Bhahulaya M, Indra-Ngarm S, Anathapruit M. Freshwater fishes of Thailand as experimental intermediate host for *Capillaria philippinensis*. *Int J Parasitol* 1979; **9**: 105-108
- 20 Bhaibulaya M, Indra-Ngarm S. *Amaurornis phoeniceus* and *ardeola bacchus* as experimental definite hosts for *capillaria philippinensis* in Thailand. *Int J Parasitol* 1979; **9**: 321-322
- 21 Cross JH, Basaca-Sevilla V. Experimental transmission of capillaria philippinensis to birds. *Trans R Soc Trop Med Hyg* 1983; **77**: 511-514
- 22 Kyriakos M, Condon SC. Enteritis cystica profunda. *Am J Clin Pathol* 1978; **69**: 77-85
- 23 Volrol MW, Welsh RA, Genet EF. Esophagitis cystica. *Am J Gastroenterol* 1973; **59**: 446-453
- 24 Oberman HA, Lodmell JG, Sower ND. Diffuse heterotopic cystic malformation of the stomach. *N Engl J Med* 1963; **269**: 909-911
- 25 Fonde EC, Rodning CB. Gastritis cystica profunda. *Am J Gastroenterol* 1986; **81**: 459-464
- 26 Anderson NJ, Rivera ES, Flores DJ. Peutz-Jeghers syndrome with cervical adenocarcinoma and enteritis cystica profunda. *West J Med* 1984; **141**: 242-244

• CLINICAL RESEARCH •

Accuracy of indocyanine green pulse spectrophotometry clearance test for liver function prediction in transplanted patients

Chung-Bao Hsieh, Chung-Jueng Chen, Teng-Wei Chen, Jyh-Cherng Yu, Kuo-Liang Shen, Tzu-Ming Chang, Yao-Chi Liu

Chung-Bao Hsieh, Chung-Jueng Chen, Teng-Wei Chen, Jyh-Cherng Yu, Kuo-Liang Shen, Yao-Chi Liu, Division of General Surgery, Department of Surgery, Tri-Service General Hospital, National Defense Medical Center, Taipei, Taiwan, China

Tzu-Ming Chang, Department of Surgery, Tungs' Taichung Metroharbor Hospital, Taichung, Taiwan, China

Correspondence to: Dr. Chung-Bao Hsieh, 325, sec 2, Cheng-Kung Rd, Taipei, Taiwan, China. albert0920@yahoo.com.tw

Telephone: +886-2-87927191 **Fax:** +866-2-87927372

Received: 2003-11-12 **Accepted:** 2003-12-16

Abstract

AIM: To investigate whether the non-invasive real-time Indocyanine green (ICG) clearance is a sensitive index of liver viability in patients before, during, and after liver transplantation.

METHODS: Thirteen patients were studied, two before, three during, and eight following liver transplantation, with two patients suffering acute rejection. The conventional invasive ICG clearance test and ICG pulse spectrophotometry non-invasive real-time ICG clearance test were performed simultaneously. Using linear regression analysis we tested the correlation between these two methods. The transplantation condition of these patients and serum total bilirubin (T. Bil), alanine aminotransferase (ALT), and platelet count were also evaluated.

RESULTS: The correlation between these two methods was excellent ($r^2=0.977$).

CONCLUSION: ICG pulse spectrophotometry clearance is a quick, non-invasive, and reliable liver function test in transplantation patients.

Hsieh CB, Chen CJ, Chen TW, Yu JC, Shen KL, Chang TM, Liu YC. Accuracy of indocyanine green pulse spectrophotometry clearance test for liver function prediction in transplanted patients. *World J Gastroenterol* 2004; 10(16): 2394-2396 <http://www.wjgnet.com/1007-9327/10/2394.asp>

INTRODUCTION

Monitoring of liver function is important in patients undergoing liver transplantation. Exact liver function and the extent of the remaining liver function at end-stage liver disease can indicate the appropriate timing of liver transplantation^[1-3]. During liver transplantation, immediate liver function evaluation can resolve primary non-functioning of the liver and technical complications^[4]. Moreover, post-transplantation early liver function evaluation can detect delayed graft malfunction or acute/chronic graft rejection.

Indocyanine green (ICG) is a synthetic dye that has been used for many years to measure hepatic blood flow and as a test of liver function^[5]. It was also used by Makuuchi and his colleagues, based on their experience, as a guide for selecting

the type of resection to be performed^[6,7]. During liver transplantation, ICG clearance rate has been used for evaluation of the recipient liver^[3,8], the donor liver^[9,10] and the post-transplant liver graft^[3]. Conventional ICG clearance is determined by measuring the rate of elimination using 3 mL venous samples at 0, 5, 10, 15, and 20 min after administering ICG. This invasive technique produces patient discomfort through repeated peripheral venous sampling at exact time intervals. Pulse spectrophotometry is an infrared-based non-invasive technique originally developed for monitoring tissue oxygenation. It has been previously used for the measurement of hepatic ICG concentration by Shinohara *et al.*^[11]. In a recent case report, infrared spectrophotometry was sufficiently sensitive to measure the ICG clearance in surgical patients^[12].

Even though the ICG clearance test has been used worldwide to predict liver function, there are some limitations for end-stage liver disease in patients with hyperbilirubinemia, intrahepatic shunt or capillarization^[13].

ICG pulse spectrophotometry (LiMON) has not been tested in transplanted patients previously.

The aim of this study was to determine the accuracy of ICG spectrophotometry, compared with the conventional invasive method, in predicting liver function in waiting and transplanted patients.

MATERIALS AND METHODS

Thirteen patients who underwent liver transplantation and follow-up at the Tri-Service General Hospital were evaluated in the current study. Eleven male patients were transplanted for chronic liver disease of various etiologies (1 hepatitis C, 2 hepatitis B, and 8 hepatitis B with hepatoma) and 2 patients with end-stage liver disease awaiting transplantation. Patients 7 and 11 were studied in acute rejection during follow up (d36 and 90) and proved by liver biopsy. Patients 3, 4 and 13 were studied immediately post-liver transplantation (within 24, 27 and 12 h) (Table 1).

Invasive ICG measurement

An intravenous (IV) bolus of 0.5 mg/kg ICG was injected rapidly through a central venous catheter or large peripheral venous line, and samples were obtained from another peripheral venous line at 0, 5, 10, 15, 20 min thereafter and kept in an EDTA-treated tube at room temperature until centrifuged at 3 000 r/min for 10 min. Absorbance was measured by a Perkin Elmer spectrophotometer at 805 nm. Direct ICG retention rate at 15 min (ICG_{15D}) and the elimination rate constant ($ICG(K)_D$) values were calculated using a commercial computer program (V-500 Spectra Manager, Jasco, Japan).

ICG pulse spectrophotometry

Pulse-dye densitometry (LiMON, Stahigruberring, Munich, Germany) was used to measure the blood ICG concentration non-invasively in real time. This apparatus makes such measurements possible by continuously monitoring the optical absorption at 805 nm and 890 nm, via an optical probe attached to the patient's finger. During the first 5-10 min after

Table 1 The demographic data of all patients

Diagnosis	Condition (d)	T. Bil	ALT	Cr.	PLT	ICG _{15D}	ICG _{15E}	ICG(K) _D	ICG(K) _E	
1	Alcoholism	Waiting	1.6	121	0.8	16.4	27.2	28.4	0.05	0.08
2	HBV+HCC	Waiting	1.4	47	0.9	12.6	36	38.3	0.03	0.06
3	HBV	During-OLT-(2)	1.6	126	0.8	7.4	3	3.9	0.24	0.22
4	HBV	During-OLT-(2)	1.1	102	1.0	11.8	1	2.5	0.28	0.29
5	HCV+HCC	Post-OLT (43)	0.7	233	2.3	15.1	4	3.7	0.18	0.22
6	HBV	Post-OLT (212)	0.5	8	2.9	12.1	1	2.3	0.35	0.29
7	HBV	Post-OLT (36)	9.1	131	1.6	7.2	26	24	0.10	0.10
	Ac. rejection									
8	HBV+HCC	Post-OLT (142)	0.8	15	1.3	11	6.5	6.8	0.21	0.25
9	HBV+HCC	Post-OLT. (166)	1.1	37	0.7	24.9	2	4	0.32	0.23
10	HBV+HCC	Post-OLT (312)	0.5	16	1.0	18.8	4	4.5	0.24	0.21
11	HBV+HCC	Post-OLT (90)	2.0	50	2.2	11.5	18	13.7	0.16	0.13
	Ac. rejection									
12	HBV+HCC	Post-OLT (367)	1.3	46	3.4	6.4	10	11.2	0.28	0.27
	Ac. renal failure									
13	HBV+HCC	During OLT (1)	3.6	213	3.4	8.5	5.1	5.4	0.31	0.33

HBV: Hepatitis B virus; HCV: Hepatitis C virus; HCC: Hepatocellular carcinoma; OLT: Orthotopic liver transplantation; Ac.: Acute; T. Bil: Total bilirubin; ALT: Alanine aminotransferase; Cr.: Creatinine; PLT: Platelet.

Table 2 The transplanted condition and laboratory data

Patients condition (n)	T. Bil	ICG _{15D}	ICG _{15E}	ICG(K) _D	ICG(K) _E
ESLD (2)	1.50±0.10	29.6±4.4	34.4±4.9	0.04±0.01	0.07±0.01
During-OLT (3)	1.35±0.25	2.0±1.0	3.2±0.7	0.26±0.02	0.25±0.04
Post-OLT (6)	0.86±0.30	3.6±2.1	3.9±0.8	0.26±0.08	0.24±0.03
Acute rejection (2)	5.60±3.60	22.0±4.0	18.9±5.2	0.13±0.03	0.12±0.02

ESLD: End-stage liver disease on waiting list; During-OLT: immediately after liver transplantation within seven days; Post-OLT: > one month after liver transplantation in stable condition; Acute rejection: proved by liver biopsy; the number in brackets means the case number.

ICG was injected, blood ICG concentrations were monitored at every pulse interval via pulse spectrophotometry. The elimination rate constant ICG(K)_E was calculated automatically by the time course of blood ICG concentration. The estimated ICG₁₅ retention rate (ICG_{15E}) was obtained via pulse spectrophotometry computer analysis during the first 5-10 min. As the usual measurement time of the Limon is between 5 and 10 min, the (ICG_{15E}) is simply calculated from the ICG plasma disappearance rate^[14].

Statistical analysis

Linear regression analysis was used to test the correlation. Statistical significance was considered at $P < 0.05$. The statistic software was S-Plus®2000 for Windows (CANdiensten, Amsterdam, The Netherlands).

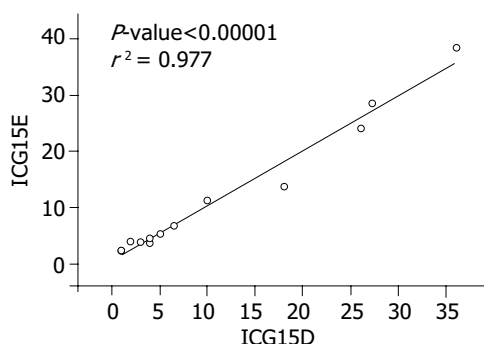


Figure 1 Correlation between the ICG_{15E} and ICG_{15D}. The correlation is excellent, $r^2 = 0.977$.

RESULTS

The correlation between ICG_{15D}, ICG_{15E}, ICG(K)_D, ICG(K)_E values for ICG₁₅ and ICG(K) by these two methods was excellent ($r^2 = 0.977, 0.855$) (Figures 1, 2). Two patients had poor liver function, elevated T. Bil, and higher ICG₁₅ retention rates, and were on the waiting list for transplantation. Three patients who had good liver function immediately post-liver transplantation showed elevated T. Bil, and lower ICG₁₅ retention rates. Two patients who were in acute rejection had poor liver function with elevated ALT and higher ICG₁₅ retention rates. Five patients, who were in a stable condition with good liver function post-liver transplantation, had low T. Bil, and better ICG₁₅ retention rates.

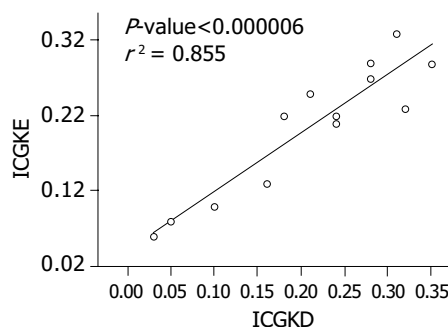


Figure 2 Correlation between ICG(K)_E and ICG(K)_D. The correlation is excellent, $r^2 = 0.855$.

DISCUSSION

ICG is a water-soluble tricarboyanine dye that is extracted by

hepatic parenchyma cells and excreted almost entirely into bile. Hepatic clearance of ICG occurs by two major processes: by uptake across the sinusoidal plasma membrane with a high extraction ratio; and by removal from the hepatocytes via cytoplasmic transport and exclusive biliary excretion with neither intrahepatic conjugation nor enterohepatic circulation^[15]. The concentration in the plasma can be measured by spectrophotometry and its rate of elimination has been widely used as a measure of liver blood flow and liver function^[16]. Most of the studies assessing liver function before hepatectomy and the postoperative outcome were carried out using the ICG clearance test^[17].

Pulse spectrophotometry has been developed in recent years to enable the blood ICG concentration to be measured easily, less invasively, and continuously. The previous method for measuring the ICG concentration by spectrophotometry did not show sufficient accuracy. The new approach, based on pulse spectrophotometry, is able to continuously measure the arterial ICG concentration because of its ability to detect the pulse wave, greatly improving its accuracy.

Pulse spectrophotometry measurements of ICG concentration with each pulse could provide information on ICG liver uptake and excretion. From the concentration, a time curve of the ICG uptake and excretion rates were calculated under different experimental conditions. The experimental study by El-Desoky *et al.*^[5] showed the sensitivity of measurement of ICG uptake and excretion rates in hepatic artery occlusion, portal vein occlusion, ischemia-reperfusion injury, hepatic microcirculation, colchicines treatment, and bile duct ligation.

Assessment of liver function remains difficult in transplanted patients because of etiological complexity. The differential diagnosis includes primary non-function of the graft, rejection, virus re-infection, drug intoxication, and thrombosis of hepatic blood vessels. After liver transplantation, liver function tests are often difficult to interpret and non-specific. The diagnosis at present relies on a combination of biochemical, hemodynamic, clinical markers, and occasionally liver biopsy. However, serial observations up to 72 h are required. Measurement of ICG clearance appears to be a simple and safe test to assess early liver graft function. The development of non-invasive pulse spectrophotometry has enabled bedside assessment of the elimination of ICG with immediate results, therefore increasing its clinical usefulness.

A study by Jalan *et al.* showed the ICG measured at 24 h after liver transplantation accurately reflected graft function and predicted graft survival and outcome. In other studies, ICG excretion was a sensitive index of ischemia/reperfusion injury during the early stages post-liver transplantation^[17].

The traditional ICG clearance test is invasive and labor-dependent. The whole procedure requires more than 30 min at the bedside for loading dosage and venous puncture. Failure may occur as a result of the patient's underlying disease and medication such as gout, arthritis, and anti-TB drugs. Technical failure may be due to blood hemolysis or laboratory errors. The real-time pulse spectrophotometry ICG clearance test is non-invasive and machine-dependent. Technical failure may be due to detecting probe malpositioning, and patient movement.

In this study, we have chosen two ICG clearance test methods to measure end-stage liver disease, immediately post-liver transplantation or in acute rejection patients. In patients with hyperbilirubinemia, before and after successful liver transplantation, the ICG₁₅ clearance test may be very useful in

evaluating the new liver's function. ICG pulse spectrophotometry appears to be a sensitive and specific test to predict graft function in ischemia/reperfusion and acute rejection patients. The correlations between ICG(K) and ICG₁₅ using these two methods were excellent.

In conclusion, in this study, the correlation between conventional and pulse spectrophotometry ICG clearance tests is excellent in transplanted patients. The ICG pulse spectrophotometry clearance test is a quick, non-invasive, easy, inexpensive, and reliable liver function test in transplantation patients.

REFERENCES

- 1 Miyagawa S, Makuuchi M, Kawasaki S, Kakazu T. Criteria for safe hepatic resection. *Am J Surg* 1995; **169**: 589-594
- 2 Oellerich M, Burdelski M, Lautz HU, Rodeck B, Duewel J, Schulz M, Schmidt FW, Brodehl J, Pichlmayr R. Assessment of pretransplant prognosis in patients with cirrhosis. *Transplant* 1991; **51**: 801-806
- 3 Tsubono T, Todo S, Jabbour N, Mizoe A, Warty V, Demetris AJ, Staez TE. Indocyanine green elimination test in orthotopic liver recipients. *Hepatology* 1996; **24**: 1165-1171
- 4 Plevris JN, Jalan R, Bzeizi KI, Dollinger MM, Lee A, Garden OJ, Hayes PC. Indocyanine green clearance reflects reperfusion injury following liver transplantation and is an early predictor of graft function. *J Hepatol* 1999; **30**: 142-148
- 5 El-Desoky A, Seifalian AM, Cope M, Delpy DT, Davidson BR. Experimental study of liver dysfunction evaluated by direct indocyanine green clearance using near infrared spectroscopy. *Br J Surg* 1999; **86**: 1005-1011
- 6 Lau H, Man K, Fan ST, Yu WC, Lo CM, Wong J. Evaluation of preoperative hepatic function in patients with hepatocellular carcinoma undergoing hepatectomy. *Br J Surg* 1997; **84**: 1255-1259
- 7 Parks RW, Garden OJ. Liver resection for cancer. *World J Gastroenterol* 2001; **7**: 766-771
- 8 Niemann CU, Yost CS, Mandell S, Henthorn TK. Evaluation of the splanchnic circulation with indocyanine green pharmacokinetics in liver transplant patients. *Liver Transplant* 2002; **5**: 476-481
- 9 Seifalian AM, Mallet SV, Rolles K, Davidson BR. Hepatic microcirculation during human orthotopic liver transplantation. *Br J Surg* 1997; **84**: 1391-1395
- 10 Koneru B, Leevy CB, Klein KM, Zweil P. Clearance of indocyanine green in the evaluation of liver donors. *Transplantation* 1994; **58**: 729-731
- 11 Shinohara H, Tanaka A, Kitai T, Yanabu N, Inomoto T, Satoh S, Hatano E, Yamaoka Y, Hirao K. Direct measurement of hepatic indocyanine green clearance with near-infrared spectroscopy: separate evaluation of uptake and removal. *Hepatology* 1996; **23**: 137-144
- 12 Mandell MS, Wachs M, Niemann CU, Henthorn TK. Elimination of indocyanine green in the perioperative evaluation of donor liver function. *Anesth Analg* 2002; **95**: 1182-1184
- 13 Ott P, Clemmesen O, Keiding S. Interpretation of simultaneous measurements of hepatic extraction fractions of indocyanine green and sorbitol. Evidence of hepatic shunts and capillarization? *Dig Dis Sci* 2000; **45**: 359-365
- 14 Sakka SG, Meier-Hellmann A. Non-invasive liver function monitoring by indocyanine green plasma disappearance rate in critically ill patients. *International J Intensive Care* 2002; **66**-72
- 15 Wheeler HO, Cranston WI, Meltzer JI. Hepatic uptake and biliary excretion of indocyanine green in the dog. *Proc Soc Exp Biol Med* 1958; **99**: 11-20
- 16 Caesar J, Shaldon S, Chiandussi L, Guevara L, Sherlock S. The use of indocyanine green in the measurement of hepatic blood flow and as a test of hepatic function. *Clin Sci* 1961; **21**: 43-47
- 17 Kawasaki S, Makuuchi M, Miyagawa S, Kakazu T, Hayashi K, Kasai H, Milva S, Hui AM, Nishimaki K. Results of hepatic resection for hepatocellular carcinoma. *World J Surg* 1995; **19**: 31-34

Prevalence of subclinical hepatic encephalopathy in cirrhotic patients in China

Yu-Yuan Li, Yu-Qiang Nie, Wei-Hong Sha, Zheng Zeng, Fu-Ying Yang, Li Ping, Lin Jia

Yu-Yuan Li, Yu-Qiang Nie, Wei-Hong Sha, Zheng Zeng, Li Ping, Lin Jia, Department of Gastroenterology, First Municipal People's Hospital of Guangzhou 510180, Guangdong Province, China

Fu-Ying Yang, Department of Neurology, First Municipal People's Hospital of Guangzhou 510180, Guangdong Province, China

Supported by Research Funds from Guangzhou Medical College, and Bureau of Public Health of Guangdong Province, China

Correspondence to: Dr. Yu-Yuan Li, Department of Gastroenterology, First Municipal People's Hospital of Guangzhou, #1 Panfu Road, Guangzhou 510180, Guangdong Province, China. liyiyiyi@163.net

Telephone: +86-20-81045208 **Fax:** +86-20-81045937

Received: 2003-11-12 **Accepted:** 2003-12-08

Abstract

AIM: Subclinical hepatic encephalopathy (SHE) is a common complication of liver diseases. The aim of this study was to find out the normal value of psychometric test and to investigate the prevalence of SHE in Chinese patients with stabilized hepatic cirrhosis.

METHODS: Four hundred and nine consecutive cirrhotic patients without overt clinical encephalopathy were screened for SHE by using number connection test part A (NCT-A) and symbol digit test (SDT). SHE was defined as presence of at least one abnormal psychometric test. The age-corrected normal values were defined as the mean \pm 2 times standard deviation (2SD), and developed in 356 healthy persons as normal controls. Four hundred and sixteen patients with chronic viral hepatitis were tested as negative controls to assess the diagnostic validity of this test battery.

RESULTS: There was no significant difference in NCT scores and SDT quotients between healthy controls and chronic hepatitis group ($P>0.05$). In all age subgroups, the NCT and SDT measurements of cirrhotic patients differed significantly from those of the controls ($P<0.05$). When mean \pm 2SD of SDT and NCT measurements from healthy control group was set as the normal range, 119 cirrhotic patients (29.1%) were found to have abnormal NCT-A and SDT tests, 53 (13.0%) were abnormal only in SDT and 36 (8.8%) only in NCT-A. Taken together, SHE was diagnosed in 208 (50.9%) cirrhotic patients by this test battery. The prevalence of SHE increased from 39.9% and 55.2% in Child-Pugh's grade A and B groups to 71.8% in Child-Pugh's grade C group ($P<0.05$). After the adjustment of age and residential areas required from the tests, no correlation was found in the rate of SHE and causes of cirrhosis, education level and smoking habit.

CONCLUSION: Psychometric tests are simple and reliable indicators for screening SHE among Chinese cirrhotic patients. By using a NCT and SDT battery, SHE could be found in 50.9% of cirrhotic patients without overt clinical encephalopathy. The prevalence of SHE is significantly correlated with the severity of liver functions.

Li YY, Nie YQ, Sha WH, Zeng Z, Yang FY, Ping L, Jia L.

Prevalence of subclinical hepatic encephalopathy in cirrhotic patients in China. *World J Gastroenterol* 2004; 10(16): 2397-2401

<http://www.wjgnet.com/1007-9327/10/2397.asp>

INTRODUCTION

Subclinical hepatic encephalopathy (SHE) has been defined as a condition in which patients with cirrhosis regardless of its etiology, demonstrates neuro-psychiatric and neuro-physiological defects, yet, having a normal mental and neurological status through global clinical examination^[1-3]. SHE could have some disadvantageous influence on patients' daily life, and could be a preceding stage of manifested hepatic encephalopathy (HE) clinically. The prevalence of SHE was reported to vary from 10% to 84%, depending on the diagnostic techniques used and patients selected for the studies^[1-10]. Many diagnostic techniques including psychometric test, electro-encephalogram, evoked potentials (EP), have been used to detect SHE. Among these tests, only psychometric test can be administered easily in epidemiological studies. In a variety of psychometric tests listed in the medical literature, SDT and NCT part A (NCT-A) were reported to have the advantages of simplicity and reliability^[1,11-15]. The combination of these two tests was commonly applied in epidemiological studies. We evaluated a battery of SDT and NCT tests in a pilot study in Chinese patients with good results^[16]. Therefore, it was selected in this big sample size study. By definition, SHE can only be found in cirrhotic patients. In this study, besides the healthy control group for the establishment of normal values of SDT and NCT, we also set up a chronic hepatitis group as negative control to assess the reliability of SDT and NCT test battery. In recent years, studies on the prevalence of SHE have been greatly increased in Western literature, but those from Chinese patients have not been fully documented. The aim of the present study was to establish the normal value of psychometric tests for Chinese people, to determine the prevalence of SHE in stable cirrhotic patients in China by using this test battery, and to explore the features of SHE in these patients.

MATERIALS AND METHODS

Subjects

Four hundred and nine consecutive cirrhotic patients attending the Department of Gastroenterology of Guangzhou Municipal First People's Hospital for screening of SHE from June 1, 1998 to March 31, 2002 were included in the study. Inclusion criteria were: no neurological or mental diseases, no attack of HE in the past or present, no use of sedative or other psychotropic drugs two wk prior to the tests. The following patients were excluded. Those who had portosystemic shunt operation, those who had alcohol consuming more than 150 g daily within 1 wk prior to the study, those who had gastrointestinal bleeding 4 wk previously, those whose hemoglobin level was less than 90 g/L, those who had dehydration or electrolyte imbalance, those whose body temperature was higher than 37.5 °C, those who had severe cardiac or pulmonary or renal or cerebrovascular

diseases or diabetes mellitus, and those who were illiterates.

Diagnosis of cirrhosis was made according to the criteria revised in 1990 National Symposium on Cirrhosis in China^[17]. In this study, 10 patients had liver biopsy. The Child-Pugh's scores were used to assess the severity of liver disease. Special attention was paid to the exclusion of stage 1 HE. The symptoms in this stage included abnormal behavior (exaggeration of normal behavior, euphoria or depression), sleeping disorders (hypersomnia, insomnia or inversion of sleeping pattern), neuromuscular activity (muscular incoordination, impaired handwriting) and changes in mental function (declined alertness or memory, subtle disorientation or impaired calculation). The etiology of the 409 cirrhotic patients consisted of chronic hepatitis B in 322 (78.7%), chronic hepatitis C in 28 (6.9%), and chronic alcoholics in 59 (14.4%). According to the Child-Pugh's grading of liver function, 188 (46.0%) were grade A, 143 (35.0%) grade B and 78 (19.0%) grade C. Two hundred and fourteen patients (52.3%) had no ascites, 72 (17.6%) had mild ascities and 123 (30.1%) had severe ascities. One hundred and sixty-nine patients (41.3%) had normal levels of serum albumin, 102 (24.9%) had mild hypoalbuminemia (30-35 g/L) and 138 (38.8%) had severe hypoalbuminemia (<30 g/L). One hundred and twenty-three patients (30.1%) had normal prothrombin time (PT), 152 (37.2%) had mildly prolonged PT (14-18 s) and 134 (32.7%) severely prolonged PT (>18 seconds). Under endoscopic examination, 28 patients (6.8%) had severe esophageal varices, 152 (37.2%) had mild varices and 229 (56.0%) had no varices.

Normal values of the psychometric tests were obtained from 356 consecutive healthy subjects undergoing routine physical check-up in the hospital between June 1 and July 1, 1998. All of them had no physical and psychological disorders, no neurological or mental diseases and no history of sedatives or alcohol consumption. The negative control group consisted of 416 consecutive outpatients with chronic viral hepatitis in Division of Infectious Diseases of our hospital in the same period. The diagnostic criteria were in accordance with the Chinese National Standards of Viral Hepatitis^[18]. Among the 416 cases, 384 (92.3%) had hepatitis B, 32 (7.7%) hepatitis C.

The study was approved by the Ethics Committee of the First Municipal People's Hospital of Guangzhou, Guangzhou Medical College, with written consent from each patient and subject.

Questionnaire

Questionnaire was given to each subject. It included the following items, namely age, sex, smoking habit (smoking cigarette daily, yes/no), alcohol (drinking alcohol daily, yes/no), education (<6 years, 6-12 years, >12 years), residential area (urban/rural), occupation, history of liver diseases, concomitant illness.

Psychometric assessment

Symbol digit test (SDT) was in Chinese version of Wechsler adult intelligence scale revised (WAIS-RC) by Gong^[19]. The individuals were given a list of digits from 1 to 9 associated with symbols and asked to fill in blanks with symbols that corresponded to each number. An initial demonstration was performed to familiarize the subjects with the test. The test scores were the total number of correctly sequential matched symbols to the number within a 90-seconds interval. The score was only 0.5, if the symbol was placed upside down. According to age, the total score of each subject was transformed to a quotient from an equivalent form, the subjects were divided into two groups according to their residential areas, either rural or urban area.

In the number connection test (NCT) part A, the subjects were asked to connect the numbers printed on the paper

consecutively from 1 to 25 as quickly as possible^[20]. After explanation to the subjects, demonstrative tests were given to ensure a correct understanding and then the test was carried on. The test scores included the time required for the test and for correcting the errors.

These two psychometric tests were performed by the patients and subjects with help from medical staffs without awareness of the diagnosis.

Statistical analysis

Student's *t* test and Chi-square test were used to assess the differences among the groups. Multivariate logistic analysis was used to evaluate the influence of the variables in the prevalence. $P < 0.05$ was considered statistically significant. Normal cut-off values of SDT and NCT were set at the mean \pm 2SD from the normal control arm, with a low value indicating a poor performance in SDT test and a higher score indicating a poor performance in NCT test. The diagnosis of SHE was made when one or both SDT and NCT appeared abnormal.

RESULTS

The demographic data of three arms are shown in Table 1. There was no significant difference ($P > 0.05$) among all variables from the three arms. The results of SDT and NCT in different age subgroups from the three arms are shown in Table 2 and Table 3. In both tests, no significant difference was found between healthy controls and chronic hepatitis arms ($P > 0.05$). However, the results in the cirrhotic arm differed significantly from those of the two control arms ($P < 0.05$). This finding supported that the Chinese version of SDT and NCT tests could clearly distinguish the neuro-psychiatric defects in SHE. The values of SDT and NCT tests from the healthy control arm could be good parameters for the establishment of normal values of these two tests.

Table 1 Demography in 3 groups

	Control <i>n</i> = 356	Hepatitis <i>n</i> = 416	Cirrhosis <i>n</i> = 409
Age (yr)	44.4 \pm 12.7	36.8 \pm 18.6	53.4 \pm 11.9
Male/female	207/149	330/86	248/161
Education (yr)			
>6	69 (19.4)	69 (16.9)	82 (20.0)
6-12	168 (47.2)	215 (51.7)	190 (46.5)
> 12	119 (33.4)	132 (31.7)	137 (33.5)
Smoking	65 (18.3)	99 (23.8)	88 (21.5)
Alcohol	39 (10.9)	48 (11.5)	123 (30.1)

The influence of the variables on the results of SDT and NCT is shown in Table 4. No significant difference was found in sex, smoking and alcohol drinking habits, and the etiology of cirrhosis ($P > 0.05$), but the difference was related to age, education and Child-Pugh's grade ($P < 0.05$). However, after adjustment of age and residential areas required for SDT and NCT tests, Child-Pugh's grade was the only risk factor of SHE ($P < 0.05$).

The relationships between Child-Pugh's grade and SDT/NCT are shown in Table 5. Although the rate of SHE between Child's grades A and B of liver disease was not significantly different ($P > 0.05$), significance was found between grades A and C, and grades B and C ($P < 0.05$). One hundred and nineteen patients (29.1%) were abnormal in both NCT and SDT, 53 (13.0%) abnormal in SDT only and 36 (8.8%) in NCT-A only. Taken together, the two-test battery gave the diagnostic rate of SHE in 50.9% of 208 patients.

Table 2 Results of SDT in 3 groups

Age (yr)	Control		Hepatitis		Cirrhosis	
	<i>n</i>	mean±SD	<i>n</i>	mean±SD	<i>n</i>	mean±SD
</=34	82	12.5±2.2	176	12.7±3.1	52	10.8±2.8 ^a
35-44	76	11.9±1.7	114	12.3±3.5	73	9.4±2.7 ^a
45-54	74	12.8±2.3	71	12.3±2.2	107	8.9±2.5 ^a
55-64	69	11.9±2.1	35	11.5±1.6	87	7.8±2.5 ^a
>/=65	54	12.7±2.4	20	9.0±2.2	90	6.7±2.3 ^a
Tota	356	12.2±2.3	416	12.2±3.1	409	8.5±2.8 ^a

^a*P*<0.05 vs normal control and chronic hepatitis.**Table 3** Results of NCT in 3 groups

Age (yr)	Control		Hepatitis		Cirrhosis ^a	
	<i>n</i>	mean±SD	<i>n</i>	mean±SD	<i>n</i>	mean±SD
</=34	82	26.7±8.8	176	27.0±6.9	52	46.1±19.2
35-44	76	34.2±12.7	114	35.8±20.3	73	51.4±26.5
45-54	74	39.8±13.8	71	41.9±12.7	107	59.3±30.8
55-64	69	52.7±13.5	35	54.3±7.3	87	71.1±41.8
>/=65	55	69.9±14.8	20	80.1±12.1	90	102.3±48.8
Total	356	47.8±13.2	416	36.8±18.6	409	68.2±41.2

^a*P*<0.05 vs cirrhosis versus normal control and chronic hepatitis.**Table 4** Multivariate logistic analysis for risk factors in cirrhotic group

	<i>n</i>	NCT	DST	SHE(%)	p2	OR
Sex					0.494	0.9
Male	344	67.4±42.1	8.6±2.8	51.2		
Female	65	72.4±36.0	8.7±2.6	52.3		
p1		0.367	0.266	0.866		
Smoking					0.903	1.0
Yes	288	6.2±38.7	8.6±2.6	51.0		
No	121	67.8±46.4	8.3±2.9	52.1		
p1		0.145	0.358	0.850		
Etiology					0.430	0.8
Alcohol	59	71.3±40.1	8.0±2.6	54.2		
Non-alcohol	350	67.7±41.4	8.6±2.9	51.0		
p1		0.541	0.153	0.646		
Education (yr)					0.390	0.9
< 6	72	92.8±50.0	6.9±2.4	51.4		
6-12	199	69.6±41.1	8.2±2.6	55.3		
> 12	138	53.3±27.6	9.7±2.9	45.3		
p1		0.001	0.001	0.221		
Age (yr)					0.779	1.0
< 35	52	46.1±19.2	10.8±2.8	51.9		
35-44	73	51.4±26.5	9.4±2.7	52.1		
45-54	107	59.3±30.8	8.9±2.5	49.5		
55-64	87	71.1±41.8	7.8±2.5	50.0		
> 65	90	102.3±48.8	6.7±2.3	57.8		
p1		0.001	0.001	0.617		
Child-Pugh					0.001	2.0
A	188	58.5±34.9	9.3±2.8	39.9%		
B	143	72.8±41.2	8.1±2.8	55.2%		
C	78	83.1±49.1	7.4±2.6	71.8%		
p1		0.001	0.001	0.001		

p1: *P* value within groups. p2: *P* value among groups in logistic analysis.

Table 5 Relationships between psychometric tests and Child-Pugh's grade

	Child's A	Child's B	Child's C	Total (n,%)
<i>n</i>	188	143	78	409
Abnormal in SDT	23	20	10	53 (13.0)
Abnormal in NCT	16	10	10	36 (8.8)
Abnormal in SDT and NCT	35	48	36	119 (29.1)
Total (%)	74 (39.4)	78 (54.5)	56 (71.9) ^a	208 (50.9)

^a*P*<0.05.

DISCUSSION

The reasons why we selected SDT and NCT part A out of a variety of psychometric tests from the medical literature in this study are as follows. (1) NCT and SDT were simple, inexpensive and sensitive tests and have been well used in many SHE studies on its prevalence, prognosis and treatment^[1-15]. NCT part A alone has been shown to be sufficient in detection of SHE in the majority of patients^[3,12]. (2) The patients with SHE exhibited selective deficits in reactivity and fine motor skills, with preservation of general intelligence, memory and language speaking. Therefore, it was reasonable to select WAIS performance subtests such as SDT^[11,12]. (3) Both SDT and NCT were easy to perform and reproduce in minutes at the outpatient clinics. Moreover more complicated tests would increase the patients' fatigue and mental burden and affect their performance efficiency^[11]. In order to evaluate the reliability of SDT/NCT test battery, two control groups were set up. Normal data of each age subgroup in the two tests were obtained from healthy subjects and then assessed with the data from chronic hepatitis negative control and cirrhosis positive control. The corresponding scores of the tests from healthy and chronic hepatitis control groups were very close. By using the normal range drawn from healthy subjects, the total abnormal rate of SDT and NCT in chronic hepatitis group was 5.5% and 7.2% respectively, near marginally statistical range. The results supported that SDT and NCT test battery was a sensitive and specific method for detection of SHE.

Whether or not the patients with alcoholic cirrhosis have a higher prevalence of SHE is still controversial. The higher prevalence of SHE in patients with alcoholic cirrhosis was mostly reported from the studies using EP or electroencephalogram^[21], suggesting a diffuse neurological disturbance in alcoholic cirrhotic patients. In China, most cirrhotic patients were caused by chronic hepatitis B. No significant difference in various etiologies was found among the subgroups in this investigation, probably due to the application of psychometric measures only. Some reports supposed that the elder and educational levels might influence the results of psychometric tests^[22,23]. No significant correlation was found between the different subgroups in age and education in the present study, since we used age-related normal values to correct the findings.

The selected subjects in this study reflected the real spectrum of cirrhotic patients in Guangzhou. The detected SHE prevalence was 50.9%, with its rate increased from 39.4% in Child-Pugh's grade A to 54.5% and 71.9% in grades B and C. These results agreed well with the data reported from Western literature. The patients with worse liver functions assessed by Child-Pugh's grade had a higher rate of SHE. Child-Pugh's scores were based on patients' symptoms (HE and ascites) and laboratory tests (serum levels of albumin, bilirubin, prothrombin). Patients with HE were excluded from this study. We also observed that the patients who had more or severer symptoms and poorer laboratory parameters of cirrhosis whether or not including in Child-Pugh's grade might tend to develop SHE.

Patients with SHE appeared to have no clinical symptoms. However, they might be at risk when they performed complex

motor activities as operating a heavy machinery or driving an automobile^[24]. They might have abnormal behaviors such as altered sleeping pattern and impaired cognitive function^[25,26]. Patients with SHE were vulnerable to HE^[27-29]. However, medical treatment and dietary management in these patients could improve the psychometric tests^[28-30]. Early diagnosis and treatment of SHE seem extremely important in China, because of the big population and high prevalence of liver diseases in this country. A high prevalence of SHE in cirrhotic patients should lead us to pay attention to these important findings frequently encountered in our medical practice.

REFERENCES

- 1 Ferenci P, Lockwood A, Mullen K, Tarter R, Weissenborn K, Blei AT. Hepatic encephalopathy- definition, nomenclature, diagnosis, and quantification: final report of the working party at the 11th World Congress of Gastroenterology, Vienna, 1998. *Hepatology* 2002; **35**: 716-721
- 2 Rikkers L, Jenko P, Rudman D, Freides D. Subclinical hepatic encephalopathy: detection, prevalence and relationship to nitrogen metabolism. *Gastroenterology* 1978; **75**: 462-469
- 3 Watanabe A, Sakai T, Sato S, Imai F, Ohto M, Arakawa Y, Toda G, Kobayashi K, Muto Y, Tsujii T, Kawasaki H, Okita K. Clinical efficacy of lactulose in cirrhotic patients with and without subclinical hepatic encephalopathy. *Hepatology* 1997; **26**: 1410-1414
- 4 Das A, Dhiman RK, Saraswat VA, Verma M, Naik SR. Prevalence and natural history of subclinical hepatic encephalopathy in cirrhosis. *J Gastroenterol Hepatol* 2001; **16**: 531-535
- 5 Zeng Z, Li YY, Nie YQ. An epidemiological survey of subclinical hepatic encephalopathy. *Chinese J Hepatol* 2003; **11**: 680-682
- 6 Yoo HY, Edwin D, Thuluvath PJ. Relationship of the model for end-stage liver disease (MELD) scale to hepatic encephalopathy, as defined by electroencephalography and neuropsychometric testing, and ascites. *Am J Gastroenterol* 2003; **98**: 1395-1399
- 7 Kramer L, Bauer E, Gendo A, Funk G, Madl C, Pidlich J, Gangl A. Neurophysiological evidence of cognitive impairment in patients without hepatic encephalopathy after tranjugular intrahepatic portosystemic shunts. *Am J Gastroenterol* 2002; **97**: 162-166
- 8 Scotinoti IA, Lucey MR, Metz DC. *Helicobacter pylori* infection is not associated with subclinical hepatic encephalopathy in stable cirrhotic patients. *Dig Dis Sci* 2001; **46**: 2744-2751
- 9 Romero-Gomez M, Boza F, Garcia-Valdecasas MS, Garcia E, Aguilar-Reina J. Subclinical hepatic encephalopathy predicts the development of overt hepatic encephalopathy. *Am J Gastroenterol* 2001; **96**: 2718-2723
- 10 Hartmann JJ, Groeneweg M, Quero JC, Beijeman ST, de Man RA, Hop WC, Schalm SW. The prognostic significance of subclinical hepatic encephalopathy. *Am J Gastroenterol* 2000; **95**: 2029-2034
- 11 McCrea M, Cordoba J, Vessey G, Blei AT, Randolph C. Neuropsychological characterization and detection of subclinical hepatic encephalopathy. *Arch Neurol* 1996; **53**: 758-763
- 12 Amodio P, Del Piccolo F, Marchetti P, Angeli P, Iemmolo R, Caregari L, Merkel C, Gerunda C, Gatta A. Clinical features and survival of cirrhotic patients with subclinical cognitive alteration detected by the number connection test and computerized psychometric tests. *Hepatology* 1999; **29**: 1662-1667
- 13 Gitlin N, Lewis D, Hinkley L. The diagnosis and prevalence of

- subclinical hepatic encephalopathy in apparently healthy, ambulant non-shunted patients with cirrhosis. *J Hepatol* 1986; **3**: 75-82
- 14 **Gilberstadt SJ**, Gilberstadt H, Zieve L, Buegel B, Collier R Jr, McClain CJ. Psychometric performance defects in cirrhotic patients without overt encephalopathy. *Arch Intern Med* 1980; **140**: 519-521
- 15 **Sood GK**, Sarin SK, Mahaptra J, Broor SL. Comparative efficacy of psychometric tests in detection on subclinical hepatic encephalopathy in nonalcoholic cirrhotics: search for a rational approach. *Am J Gastroenterol* 1989; **84**: 156-159
- 16 **Jia L**, Li YY. Subclinical hepatic encephalopathy. *Chinese J Intern Med* 1996; **36**: 495-497
- 17 **Wang JY**. Summary of national symposium on cirrhosis in China. *Zhonghua Xiaohua Bingxue Zazhi* 1991; **11**: 290-291
- 18 **Wang JY**. Consensus of viral hepatitis prevention and treatment. *Zhonghua Chuanran Bingxue Zazhi* 1995; **13**: 241-247
- 19 **Gong YX**. Wechsler Adult Intelligence-Revised in China (WAIS-RC). 1st edition, Changsha, China Hunan Atlas Press 1992: 52-53
- 20 **Dhiman RK**, Saraswat VA, Verma M, Naik SR. Figure connection: A universal test for assessment of mental state. *J Gastroenterol Hepatol* 1995; **10**: 14-23
- 21 **Schenker S**, Butterworth R. NMR spectroscopy in portal systemic encephalopathy: are we there yet? *Gastroenterology* 1997; **112**: 1758-1761
- 22 **Davies AD**. The influence of age on trail making test performance. *J Clin Psychol* 1968; **24**: 96-98
- 23 **Zeneroli ML**, Cioni G, Ventura P, Russo AM, Venturini I, Casalgrandi G, Ventura E. Interindividual variability of the number connection test. *J Hepatol* 1992; **15**: 263-264
- 24 **Schomerus H**, Hanster W, Blunck H, Reinhard U, Mayer K, Dolle W. Latent portasystemic encephalopathy, I, Nature of cerebral functional defects and their effect on fitness to drive. *Dig Dis Sci* 1981; **26**: 622-630
- 25 **Tarter RE**, Hegedus AM, Vanthiel DH, Schade RR, Gavaler JS, Starzl TE. Non-alcoholic cirrhosis associated with neuropsychological dysfunction in the absence of overt evidence of hepatic encephalopathy. *Gastroenterology* 1984; **86**: 1421-1427
- 26 **Cordoba J**, Cabrera J, Lataif L, Penev P, Zee P, Blei AT. High prevalence of sleep disturbance in cirrhosis. *Hepatology* 1998; **27**: 339-345
- 27 **Yen CL**, Liaw YF. Somatosensory evoked potentials and number connection test in the detection of subclinical hepatic encephalopathy. *Heptogastroenterology* 1990; **37**: 332-334
- 28 **Zeng Z**, Li YY. Effects of lactulose treatment on the course of subclinical hepatic encephalopathy. *Zhonghua Yixue Zazhi* 2003; **83**: 1126-1129
- 29 **Saxena N**, Bhatia M, Joshi YK, Garg PK, Dwivedi SN, Tandon RK. Electrophysiological and neuropsychological tests for the diagnosis of subclinical hepatic encephalopathy and prediction for overt encephalopathy. *Liver* 2002; **22**: 190-197
- 30 **Dhiman RK**, Sawhney MS, Chawla YK, Das G, Ram S, Dilawari JB. Efficacy of lactulose in cirrhotic patients with subclinical hepatic encephalopathy. *Dig Dis Sci* 2000; **45**: 1549-1552

Edited by Wu XN and Wang XL Proofread by Xu FM

• CLINICAL RESEARCH •

Prevalence of a newly identified SEN virus in China

Shi-Jie Mu, Juan Du, Lin-Sheng Zhan, Hai-Ping Wang, Rui Chen, Quan-Li Wang, Wen-Ming Zhao

Shi-Jie Mu, Wen-Ming Zhao, School of Life Sciences and Technology, Xi'an Jiaotong University, Xi'an 710049, Shaanxi Province, China

Juan Du, Lin-Sheng Zhan, Hai-Ping Wang, Quan-Li Wang, Institute of Field Transfusion Medicine, Academy of Military Medical Sciences, Beijing 100850, China

Rui Chen, Department of Blood Transfusion, Xijing Hospital, Fourth Military Medical University, Xi'an 710032, Shaanxi Province, China
Supported by the Innovation Foundation of Academy of Military Medical Sciences, No.200104

Correspondence to: Shi-Jie Mu, School of Life Sciences and Technology, Xi'an Jiaotong University, Xi'an 710049, Shaanxi Province, China. musj@nwblood.com

Telephone: +86-29-83375465 **Fax:** +86-29-83244952

Received: 2003-12-23 **Accepted:** 2004-01-08

Abstract

AIM: To establish nested-PCR methods for the detection of SENV-D and SENV-H and to investigate the epidemiology of SEN virus in China.

METHODS: According to published gene sequences, primers from the conserved region were designed. Then, 135 samples from healthy voluntary blood donors and 242 samples from patients with various forms of liver disease were detected by nested-PCR of SENV-D/H. Some PCR products were cloned and sequenced.

RESULTS: By sequencing, the specificity of genotype-specific PCR was confirmed. SENV-D/H DNA was detected in 31% of the blood donors, which was higher than those in America and Italy (2%), and in Japan and Taiwan (15-20%). The prevalence of SENV-D/H viremia was significantly higher in patients with hepatitis B and hepatitis C than in blood donors (59-85% vs 31%, $P < 0.05$). The prevalence among patients with non-A-E hepatitis was significantly higher than among blood donors (68% vs 31%, $P < 0.01$), and equivalent to that among patients with hepatitis B and C.

CONCLUSION: Nested-PCR with genotype-specific primers could serve as a useful SENV screening assay. SENV has the same transmission modes as HBV and HCV. The high prevalence in patients with non-A-E hepatitis may attribute to the transmission modes, and SENV may not serve as the causative agents.

Mu SJ, Du J, Zhan LS, Wang HP, Chen R, Wang QL, Zhao WM. Prevalence of a newly identified SEN virus in China. *World J Gastroenterol* 2004; 10(16): 2402-2405

<http://www.wjgnet.com/1007-9327/10/2402.asp>

INTRODUCTION

Recently, a novel DNA virus designated SEN virus (SENV) was discovered in the serum of a human immunodeficiency virus type 1 (HIV-1)-infected patient^[1]. Phylogenetic analysis^[2] showed 8 strains (A-H) of SENV. To date, the ninth genotype (SENV-I) has been identified^[3]. Among them, 2 SENV strains

(SENV-D and SENV-H) were significantly associated with transfusion-associated non-A-E hepatitis^[4]. SENV-D and SENV-H were also detected more frequently in patients with chronic liver disease and hepatocellular carcinoma (HCC) than in healthy adults^[5,6]. However, the association of SENV infection with liver cell damage is far from clear, and further studies are needed to investigate the clinical relevance of SENV infection worldwide.

The purpose of this study was to develop a nested polymerase chain reaction (nPCR) method for the detection of SENV-D and SENV-H DNA in serum and elucidate its specificity. The presence of SENV-D and SENV-H viremia in patients with various forms of liver diseases and the possible role of SENV infection in non-A-E hepatitis were investigated.

MATERIALS AND METHODS

Patients

A total of 377 serum samples from March 1999 to April 2003 were studied in Xijing Hospital. They were divided into 5 groups as follows: 135 blood donors; 55 patients with acute hepatitis A virus (HAV); 126 with chronic hepatitis B; 20 with chronic hepatitis C; 41 with non-A-E hepatitis defined as negative control for known serologic markers, including I gM anti-HAV, I gM antibody to hepatitis B core antigen (anti-HBc), hepatitis B surface antigen (HBsAg), and antibodies to HCV, HDV and HEV.

Detection of SENV DNA

Viral DNA was extracted from 100 μ L serum with the QIAamp blood kit (Qiagen) and resuspended in 20 μ L elution buffer. PCR mixture of 20 μ L contained 0.4 μ mol/L sense primer SENV-P2 (5' -CC[C/G]AAA CTG TTT GAA GAC [C/A]A-3') (designed by ourselves), 0.4 μ mol/L antisense primer Lucky2AS (5' -CCT CGG TT[G/T] [C/G]AA A[G/T]G T[C/T]T GAT AGT-3')^[1], 200 μ mol/L of each dNTP, 2 μ L DNA sample, and 1 U *Taq* DNA polymerase. The reactions consisted of preheating at 94 $^{\circ}$ C for 3 min, 30 cycles of denaturation at 94 $^{\circ}$ C for 1 min, annealing at 50 $^{\circ}$ C for 1 min, extension at 72 $^{\circ}$ C for 40 s, and final incubation at 72 $^{\circ}$ C for 5 min. The second PCR step was carried out with a 20 μ L PCR reaction mixture containing 2 μ L of the first-step amplification product, the same PCR buffer used for the first PCR step, 0.4 μ mol/L sense primer D10s (5' -GTA ACT TTG CGG TCA ACT GCC-3')^[1] and antisense primer Lucky2AS for SENV-D; 0.4 μ mol/L sense primer C5s (5' -GGT GCC CCT [A/T] GT [C/T]AG TTG GCG GTT-3') (designed by ourselves) and antisense primer Lucky2AS for SENV-H, 200 μ mol/L of each dNTP, and 1 U *Taq* DNA polymerase, PCR consisted of preheating at 94 $^{\circ}$ C for 1 min, annealing at 58 $^{\circ}$ C for 1 min, extension at 72 $^{\circ}$ C for 40 s, and final incubation at 72 $^{\circ}$ C for 5 min.

Determination of SENV genotypes

Amplicons containing polyA tails and producing visible bands on agarose gel were excised from the gel and ligated to the pGEM vector. DNA extracted from transformed *Escherichia Coli* was sequenced. The sequences excluding primer sequences were aligned with Cluster W to all SENV genotypes, representative of TTV (TA278) and TLMV isolates. The genotype of SENV was determined by the phylogenetic trees.

Table 1 Prevalence of SENV infection in different hepatitis groups in China

Disease	n	Single SENV-D	Single SENV-H	Combined SENV-D/-H	Total n (%)
Acute hepatitis A	55	2 (3.6)	12 (21)	6 (11)	20 (36)
Chronic hepatitis B	126	17 (13)	16 (12)	41 (32)	74 (59) ^b
Chronic hepatitis C	20	4 (20)	4 (20)	9 (45)	17 (85) ^b
Acute+chronic non-A-E	41	10 (24)	7 (17)	11 (27)	28 (68) ^b
Blood donors	135	9 (6.7)	7 (5)	26 (19)	42 (31)

^b $P < 0.01$ vs Blood donors.

Statistical analysis

Data were analyzed by χ^2 test with Yates' correction or Fisher's exact test; $P < 0.05$ was considered to be statistically significant.

RESULTS

Genotype-specific PCR with specific primers

PCR products were detected by 20 g/L agarose gel. The results showed that there was a 230-bp band in the gel (Figure 1). The PCR products were inserted into pGEM-T vectors and sequenced. A phylogenetic tree of the SENV-D sequences (Figure 2A) from 8 blood donors (B7, B11, B13, B14, B28, B29, B31 and B33) and 7 patients with non-A-E hepatitis (N4, N9, N10, NC, NF, NG and NK) was constructed. To determine a root of the phylogenetic tree, TLMV was used as an out-group. SENV-D DNA sequences from study subjects clustered in a monophyletic group with the SENV-D prototype sequences. A phylogenetic tree of the SENV-H sequences (Figure 2B) from 7 blood donors (B1, B4, B11, B12, B28, B29 and B30) and 5 patients with non-A-E hepatitis (N4, N8, N10, NA and NF) was constructed. SENV-H DNA sequences from study subjects clustered in a monophyletic group with the SENV-H prototype sequences with the exception of 2 outliers (B1 and B28), which had closer homology to SENV-C.

The specificity of genotype-specific PCR was confirmed by sequencing. Here, all 15 patients diagnosed as SENV-D by the genotype-specific PCR had homology to SENV-D (Figure 2A), while 10 of 12 patients (83%) diagnosed as SENV-H by the genotype-specific PCR had homology to SENV-H, the other 2 had homology to SENV-C which was of the same genotype as SENV-H (Figure 2B).

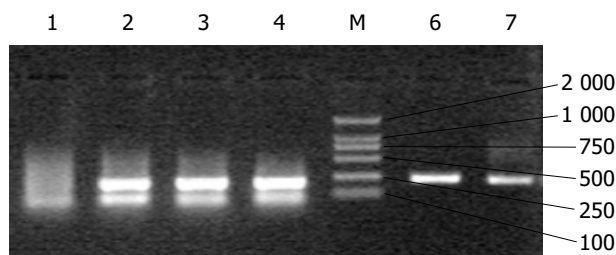


Figure 1 Electrophoresis of PCR products. Lane 1: Negative control; lane 2: Positive control; lanes 3, 4: SENV-D; lane 5: Marker DL2000; lanes 6, 7: SENV-H.

SENV prevalence in patients with liver diseases and in blood donors

SENV-D and/or SENV-H (SENV-D/H) DNAs were positive in 31% of healthy Chinese adults. SENV viremia was identified in 20 (36%) of 55 patients with acute or chronic hepatitis A, in 74 (59%) of 126 patients with chronic hepatitis B, in 17 (85%) of 20 patients with chronic hepatitis C, in 28 (68%) of 41 patients with acute or chronic non-A-E hepatitis. Compared with healthy blood donors, SENV infection was found more frequently in patients with hepatitis B, hepatitis C and non-A-E hepatitis

(59-85% vs 31%, $P < 0.01$, Table 1). However, the prevalence was comparable among patients with acute hepatitis A and healthy adults (31% vs 36%). The prevalence of SENV-H was 2-fold higher than that of SENV-D in patients with acute hepatitis A. Mixed SENV-D/H infection was common (Table 1).

DISCUSSION

Viral hepatitis is a worldwide disease^[7] and imperils human health gravely. To date, 5 hepatitis viruses from HAV to HEV^[8], which account for 8% to 90% hepatitis cases, have been discovered. But we could not find any hepatitis viruses in the left 10% to 20% cases that have typical viral hepatitis manifestations. Scientists speculated that the virus TTV was correlated with non-A-E hepatitis. Chinese scholars studied infection rate of TTV in different populations and its pathogenicity in liver^[9-12], and found that TTV had no pathogenicity^[13-15]. Afterwards, Primi *et al.*^[11] found that SENV and TTV had similar structure. SENV has homogeneity of 55% at nucleotide level with TTV, but they only have homogeneity of 37% at amino acid level^[2]. SENV appears to belong to a family of small, circular, non-enveloped, single-stranded DNA viruses that have been designated as circoviruses^[16,17]. Phylogenetic analysis of SENV has shown the existence of 8 different variants (A-H). Among them, only SENV-D and SENV-H have higher prevalence ratios, and they are found in 2% of blood donors and >50% of persons with transfusion-associated non-A-E hepatitis in Italy and the United States. Although a strong association of SENV-D/H with transfusion-associated non-A-E hepatitis has been reported, whether SENV-D/H serves as a causative agent of post-transfusion hepatitis remains unknown^[18-20].

The results of our present study indicate that nPCR amplified with genotype-specific primers could serve as a useful SENV screening assay. Moreover, because all components of the assay are readily available (specific antibodies are not required), viral testing can be performed in most laboratories that perform PCR. Our recent study indicated that 31% of healthy Chinese adults were positive for SENV-D/H DNA, a rate comparable to that of blood donors in Japan (10-20%)^[5,21] and Taiwan (14-20%)^[6] (age-specific prevalence), but higher than that of blood donors in the United States and Italy (2%)^[22,23]. Co-infection with SENV has been frequently observed in 22-67% of patients with chronic hepatitis B^[5,6] and 20-76% of patients with chronic hepatitis C^[4-6,24,25]. Our study showed that the prevalence of SENV-D/H infection in patients with chronic hepatitis B and C were 59% and 85% respectively, implying that HCV, HBV and SENV may share common modes of transmission. Our study also indicated that compared with blood donors (31%), SENV-D/H infection was more frequent in patients with non-A-E hepatitis (68%), but comparable to those in patients with chronic hepatitis C and B (85% and 59%, respectively). These results can not support a causal role for SENV-D/H in the development of non-A-E hepatitis. Otherwise, we also documented that the prevalence of SENV-H was comparable to that of SENV-D in different subjects, such as blood donors, patients with chronic

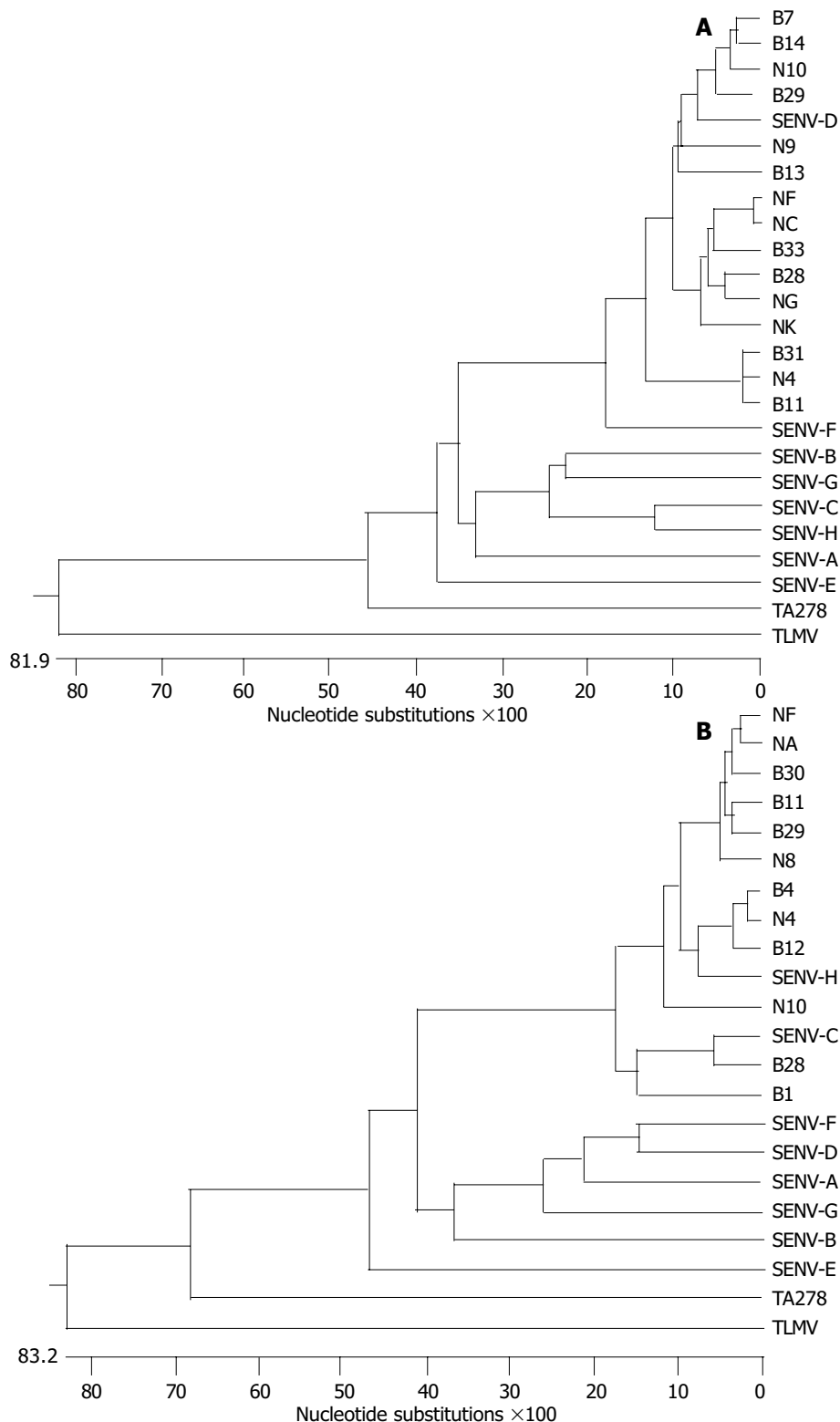


Figure 2 Phylogenetic tree of SENV by neighbor-joining method. A: The tree constructed on basis of 1 prototype TTV isolate (TA278), 1 TTV variant, 8 SEN virus isolates (A-H) and 15 SENV-D Chinese isolates. B: The tree constructed on basis of 1 prototype TTV isolate (TA278), 1 TTV variant, 8 SEN virus isolates (A-H) and 12 SENV-H Chinese isolates.

hepatitis B or C, and patients with non-A-E hepatitis, but among patients with acute hepatitis A, SENV-H was more prevalent than SENV-D ($P < 0.05$). This phenomenon awaits further prospective studies.

In summary, the results of this study suggest that SENV has the same transmission modes as HBV and HCV^[26]. The high prevalence in patients with non-A-E hepatitis may attribute to the transmission modes, and SENV may not serve as the causative agents. At present, SENV and the larger group of human circoviruses have no established pathogenicity, but

they may have disease associations that have not been identified, or they may serve as commensal organisms that have some beneficial role in maintaining homeostasis in the host. They are worthy of more attention, even in the absence of confirmed disease associations.

REFERENCES

- 1 **Primi D, Fiordalisi G.** Identification of SENV Genotypes. International patent number WO0028039 (<http://ep.espacenet.com/>)

- 2 **Tanaka Y**, Primi D, Wang RY, Umemura T, Yeo AE, Mizokami M, Alter HJ, Shih JW. Genomic and molecular evolutionary analysis of a newly identified infectious agent (SEN virus) and its relationship to the TT virus family. *J Infect Dis* 2001; **183**: 359-367
- 3 **Kojima H**, Kaita KD, Zhang M, Giulivi A, Minuk GY. Genomic analysis of a recently identified virus (SEN virus) and genotypes D and H by polymerase chain reaction. *Antiviral Res* 2003; **60**: 27-33
- 4 **Umemura T**, Yeo AE, Sottini A, Moratto D, Tanaka Y, Wang RY, Shih JW, Donahue P, Primi D, Alter HJ. SEN virus infection and its relationship to transfusion-associated hepatitis. *Hepatology* 2001; **33**: 1303-1311
- 5 **Shibata M**, Wang RY, Yoshida M, Shih JW, Alter HJ, Mitamura K. The presence of a newly identified infectious agent (SEN virus) in patients with liver diseases and in blood donors in Japan. *J Infect Dis* 2001; **184**: 400-404
- 6 **Kao JH**, Chen W, Chen PJ, Lai MY, Chen DS. Prevalence and implication of a newly identified infectious agent (SEN Virus) in Taiwan. *J Infect Dis* 2002; **185**: 389-392
- 7 **Zheng RQ**, Wang QH, Lu MD, Xie SB, Ren J, Su ZZ, Cai YK, Yao JL. Liver fibrosis in chronic viral hepatitis: An ultrasonographic study. *World J Gastroenterol* 2003; **9**: 2484-2489
- 8 **Chang JH**, Wei L, Du SC, Wang H, Sun Y, Tao QM. Hepatitis G virus infection in patients with chronic non-A-E hepatitis. *China Nati J New Gastroenterol* 1997; **3**: 143-146
- 9 **Liu YL**, Zhu YM, Chen HS, Wang Y. Prevalence and pathogenicity of TT virus infection in patients with liver diseases. *Shijie Huaren Xiaohua Zazhi* 2002; **10**: 1143-1148
- 10 **Zhang JH**, Chen SZ. An epidemiological study on transfusion transmitted virus infection in China. *Shijie Huaren Xiaohua Zazhi* 2001; **9**: 1384-1390
- 11 **Zhao Y**, Wang JB. Epidemiological survey on TTV infection and the association with other viral liver diseases in Changchun area. *Shijie Huaren Xiaohua Zazhi* 2001; **9**: 747-750
- 12 **Fu EQ**, Bai XF, Pan L, Li GY, Yang WS, Tang YM, Wang PZ, Sun JF. Investigation of TT virus infection in groups of different people in Xi'an. *Shijie Huaren Xiaohua Zazhi* 1999; **7**: 967-969
- 13 **Abe K**, Inami T, Asano K, Miyoshi C, Masaki N, Hayashi S, Ishikawa K, Takebe Y, Win KM, El-Zayadi AR, Han KH, Zhang DY. TT virus infection is widespread in the general populations from different geographic regions. *J Clin Microb* 1999; **37**: 2703-2705
- 14 **Ikeuchi T**, Yokosuka O, Kanda T, Imazeki F, Seta T, Saisho H. Roles of TT virus infection in various types of chronic hepatitis. *Intervirology* 2001; **44**: 219-223
- 15 **Kadayifci A**, Guney C, Uygun A, Kubar A, Bagci S, Dagalp K. Similar frequency of TT virus infection in patients with liver enzyme elevations and healthy subjects. *Int J Clin Pract* 2001; **55**: 434-436
- 16 **Adair BM**. Immunopathogenesis of chicken anemia virus infection. *Dev Comp Immunol* 2000; **24**: 247-255
- 17 **Takahashi K**, Iwasa Y, Hijikata M, Mishiro S. Identification of a new human DNA virus (TTV-like mini virus, TLMV) intermediately related to TT virus and chicken anemia virus. *Arch Virol* 2000; **145**: 979-993
- 18 **Umemura T**, Tanaka Y, Kiyosawa K, Alter HJ, Shih JW. Observation of positive selection within hypervariable regions of a newly identified DNA virus (SEN virus)(1). *FEBS Lett* 2002; **510**: 171-174
- 19 **Wilson LE**, Umemura T, Astemborski J, Ray SC, Alter HJ, Strathdee SA, Vlahov D, Thomas DL. Dynamics of SEN virus infection among injection drug users. *J Infect Dis* 2001; **184**: 1315-1319
- 20 **Schroter M**, Laufs R, Zollner B, Knodler B, Schafer P, Sterneck M, Fischer L, Feucht HH. Prevalence of SENV-H viraemia among healthy subjects and individuals at risk for parenterally transmitted diseases in Germany. *J Viral Hepat* 2002; **9**: 455-459
- 21 **Umemura T**, Yeo AET, Shih J, Matsumoto A, Orii K, Tanaka E. The presence of SEN Virus infection in Japanese patients with viral hepatitis and liver disease. *Hepatology* 2000; **32**: 381A
- 22 **Mushahwar IK**. Recently discovered blood-borne viruses: are they hepatitis viruses or merely endosymbionts? *J Med Virol* 2000; **62**: 399-404
- 23 **Bowden S**. New hepatitis viruses: contenders and pretenders. *J Gastroenterol Hepatol* 2001; **16**: 124-131
- 24 **Rigas B**, Hasan I, Rehman R, Donahue P, Wittkowski KM, Lebovics E. Effect on treatment outcome of coinfection with SEN viruses in patients with hepatitis C. *Lancet* 2001; **358**: 1961-1962
- 25 **Umemura T**, Alter HJ, Tanaka E, Orii K, Yeo AE, Shih JW, Matsumoto A, Yoshizawa K, Kiyosawa K. SEN virus: response to interferon alfa and influence on the severity and treatment response of coexistent hepatitis C. *Hepatology* 2002; **35**: 953-959
- 26 **Tang W**, Peng XM, Zhang Y, Wang H, Jiang XL, Zhou BP. Establishment and application of polymerase chain reaction for detecting D and H subtypes of SEN virus. *Shijie Huaren Xiaohua Zazhi* 2003; **11**: 1540-1543

Edited by Chen WW Proofread by Zhu LH and Xu FM

• CLINICAL RESEARCH •

E-cadherin and calretinin as immunocytochemical markers to differentiate malignant from benign serous effusions

Dong-Nan He, Hua-Sheng Zhu, Kun-He Zhang, Wen-Jian Jin, Wei-Ming Zhu, Ning Li, Jie-Shou Li

Dong-Nan He, School of Medicine, Nanjing University, Nanjing 210093, Jiangsu Province, China

Hua-Sheng Zhu, Department of General Surgery, Shanghai Meishan Hospital, Nanjing 210039, Jiangsu Province, China

Kun-He Zhang, Wen-Jian Jin, Digestive Disease Institute of Jiangxi Medical College, Nanchang 330006, Jiangxi Province, China

Wei-Ming Zhu, Ning Li, Jie-Shou Li, Department of General Surgery, Jingling Hospital, Clinical School of Nanjing University, Nanjing 210002, Jiangsu Province, China

Correspondence to: Kun-He Zhang, Digestive Disease Institute of Jiangxi Medical College, Nanchang 330006, Jiangxi Province, China. yfyzkh@sina.com

Telephone: +86-791-8692695

Received: 2003-12-12 **Accepted:** 2004-01-08

Abstract

AIM: To investigate the expressions of E-cadherin and calretinin in exfoliated cells of serous effusions and evaluate their values in distinguishing malignant effusions from benign ones.

METHODS: Fresh serous effusion specimens were centrifuged and exfoliated cells were collected. Cells were then processed with a standardized procedure, including paraformaldehyde fixation, BSA-PBS solution washing and smears preparation. E-cadherin and calretinin were detected by immunocytochemistry (ICC).

RESULTS: In the exfoliated cells of serous effusions, most of carcinoma cells only expressed E-cadherin, and most of mesothelial cells only expressed calretinin, and benign cells (lymphocytes and granulocytes) did not express either of them. For E-cadherin, 85.7% (30/35) of malignant effusions and 8.1% (3/37) of benign fluids were ICC-positive ($P < 0.001$). The sensitivity of E-cadherin ICC in the diagnosis of malignant effusions was 85.7%, specificity 91.9%, and diagnostic rate 88.9%. For calretinin, 94.6% (35/37) of benign effusions and 11.4% (4/35) of malignant effusions were ICC-positive ($P < 0.001$). The sensitivity of calretinin ICC in the diagnosis of benign effusions was 94.6%, specificity 88.6%, and diagnostic rate 91.7%. For diagnosis of benign and malignant effusions by combining E-cadherin ICC and calretinin ICC, the specificities were up to 100% and 97.1%, respectively.

CONCLUSION: E-cadherin ICC and calretinin ICC are sensitive and specific in differential diagnosis of benign and malignant serous effusion specimens and specificities are evidently improved when both markers are combined.

He DN, Zhu HS, Zhang KH, Jin WJ, Zhu WM, Li N, Li JS. E-cadherin and calretinin as immunocytochemical markers to differentiate malignant from benign serous effusions. *World J Gastroenterol* 2004; 10(16): 2406-2408

<http://www.wjgnet.com/1007-9327/10/2406.asp>

INTRODUCTION

Serous effusions are common in clinical practice and some cases

are caused by metastasis of malignant tumors (malignant effusions). Distinguishing malignant from benign tumors is very important, but sometimes very difficult^[1]. Some studies have shown that immunocytochemistry (ICC) of exfoliated cells is valuable in differentiating malignant effusions from benign ones^[2-6]. However, the diagnostic value of a single marker was limited, and a panel of markers were more useful^[7,8]. Recently, several studies have shown that E-cadherin, an epithelial adhesion molecule, was a useful marker for identifying the carcinoma cells in effusions^[9,10], and calretinin, a calcium-binding protein, was a useful marker for identifying the mesothelial cells^[11,12]. It is well known that the differentiation between cancer cells and reactive mesothelial cells is the main problem in cytological diagnosis of effusions. In the present study, both E-cadherin and calretinin were used as markers in immunocytochemical staining of exfoliated cells in serous effusions, and their diagnostic values were evaluated.

MATERIALS AND METHODS

Patients and specimens

Seventy-two patients with serous effusions were enrolled in this study (35 male, 37 female, age 14-77 years with an average of 51.8 years). All patients were from the First Affiliated Hospital of Jiangxi Medical College from 2001 to 2002. Effusion specimens were collected and divided into two groups, benign and malignant, according to cytological results. Of these specimens, there were 45 pleural effusions, 24 peritoneal effusions, and 3 malignant pericardial effusions. In the 23 cases of benign pleural effusions, there were 13 cases of tuberculous pleuritis, 2 cases of liver cirrhosis, 1 pulmonary tuberculosis, 1 chyle pleural effusion, and 6 unknown causes. In the 22 cases of malignant pleural effusion, there were 11 cases of lung cancer, 1 submaxillary gland cancer, 1 gastric cancer, 1 primary liver cancer, and 8 cases of unknown origin. In the 14 cases of benign peritoneal effusions, there were 8 cases of liver cirrhosis, 3 tuberculous peritonitis, 1 hepatitis B, 1 Budd-Chiari syndrome, 1 unknown cause. In the 10 cases of malignant peritoneal effusions, there were 4 cases of ovarian cancer, 2 primary liver cancers, 1 gastric cancer, 1 colonic cancer, 1 duodenal papilla cancer, and 1 unknown origin. Three cases of malignant pericardial effusions included 1 case of lung cancer, 1 metastatic squamous cancer and 1 unknown origin.

Specimen processing

About 100 mL fresh effusion was centrifuged at 2 000 r/min for 10 min, and cell pellets were collected. When the effusion was bloody, erythrocytes were destroyed with isotonic ammonium chloride solution (NH₄Cl 4.5 g, KHCO₃ 0.5 g, EDTA 0.0186 g, solved in 400 mL distilled water, then distilled water add to a total volume of 500 mL). Same volume of the solution was added to dissolve the cell pellets, which were stirred for 5 min at room temperature, centrifuged at 2 000 r/min for 10 min, and the supernatants removed. Two cell smears were prepared for cytological diagnosis. The remaining cells were processed with a "standardized" procedure^[13]: fixed in 40 g/L paraformaldehyde-PBS solution, washed in 10 g/L BSA-PBS solution, the cell concentration was adjusted to 2×10^6 /mL, and finally several

cell smears were prepared. The smears were air-dried and stored in a freezer (-85 °C).

Immunocytochemistry and evaluation

Reagents for immunocytochemical staining were provided by Beijing Zhongshan Biotechnology Co. Ltd. Mouse anti-human E-cadherin monoclonal antibody (1:100 dilution) or rabbit anti-human calretinin polyclonal antibody (1:50 dilution) was used as the primary antibody. Biotinylated goat anti-mouse/rabbit IgG was used as the second antibody. The reaction products were visualized by using the streptavidin-horseradish peroxidase and diaminobenzidine. The smears were counterstained with hematoxylin. PBS was used instead of the primary antibodies as negative control.

In E-cadherin ICC, positive cells were stained at cytomembrane, especially in the areas surrounding the cells. In calretinin ICC, whole cells were stained with a "fried eggs" staining pattern. One hundred cells (carcinoma and/or non-carcinoma) were counted under a high power microscope, and the percentage of positive cells was calculated. ICC-positive cells $\geq 80\%$ were defined as strong expression (+++), 20-79% as moderate expression (++), 6-19% as weak expression (+), 0-5% as negative expression (-). Specimens with expressions (+)-(++) were regarded as ICC-positive, and expression (-) as ICC-negative.

Statistical analysis

Qualitative data were analysed with chi-square test, and rank data were tested with rank sum test. Diagnostic values of ICC results were calculated in contrast to that of the cytological results. Diagnostic values of the combination of E-cadherin and calretinin ICC results were calculated in series ways.

RESULTS

E-cadherin expression of exfoliated cells in serous effusions

E-cadherin expression in carcinoma cells was usually strong, with obvious staining at cytomembrane and sometimes in cytoplasm (Figure 1). The areas surrounding the cells had densely stained lines in the clusters of carcinoma cells, but single carcinoma cell was weakly stained. Mesothelial cells were stained occasionally, and no lymphocytes and granulocytes were stained. Thirty of 35 malignant effusion specimens were ICC-positive for E-cadherin (85.7%), and most of them were strong (93.3% was +++). Only 3 of 37 benign effusions were ICC-positive for E-cadherin (8.1%), in which a few mesothelial cells were weakly stained in cytoplasm. The differences in positivity rates and expression intensities between two groups were significant ($P < 0.001-0.0001$) (Table 1).

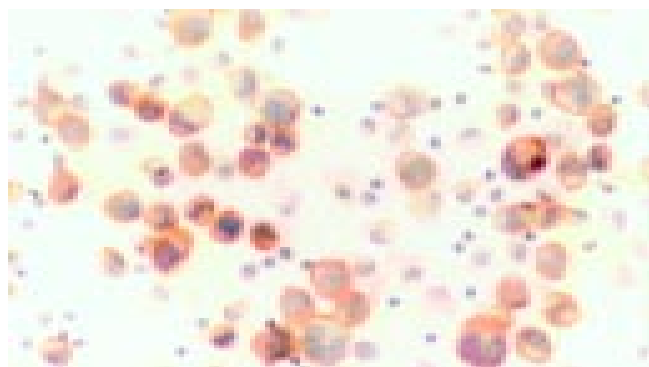


Figure 1 Immunocytochemistry of E-cadherin in the cells from a malignant ascites specimen. Carcinoma cells were mainly stained at cell membranes. Inflammatory cells without staining were as control (Original magnification, $\times 400$).

Table 1 E-cadherin expression in exfoliated cells of serous effusions

Effusion group	n	Positivity (%)	Expression intensity			
			-	+	++	+++
Malignant	35	30 (85.7)	5	2	21	7
Benign	37	3 (8.1)	34	1	2	0

$\chi^2 = 43.633$, $P < 0.001$ between the two groups, $H = 42.744$, $P < 0.0001$ between the two groups.

Calretinin expression of exfoliated cells in serous effusions

Calretinin expression in mesothelial cells was usually high, stained in whole cells (Figure 2). The typical cells looked like "fried eggs". Carcinoma cells were occasionally stained weakly, and no lymphocytes and granulocytes were stained. Thirty-five of 37 benign effusions were ICC-positive for calretinin (94.6%), and all of them were strong positive (+++). Only 4 of 35 malignant effusion specimens were ICC-positive for calretinin (11.4%), with a few carcinoma cells stained weakly. Differences of positivity rates and expression intensities between the two groups were significant ($P < 0.001-0.0001$) (Table 2).

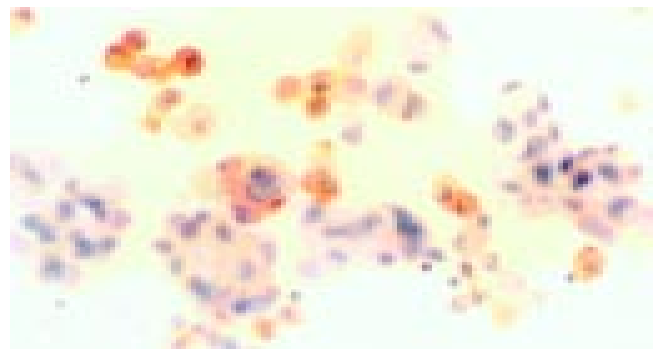


Figure 2 Immunocytochemistry of calretinin in the cells from a malignant ascites specimen. Mesothelial cells were stained strongly and some of them like "fried eggs". Carcinoma cells and inflammatory cells without staining were as control (Original magnification, $\times 400$).

Table 2 Calretinin expression in exfoliated cells of serous effusions

Effusion group	n	Positivity (%)	Expression intensity			
			-	+	++	+++
Malignant	35	4 (11.4)	31	1	3	0
Benign	37	35 (94.6)	2	0	0	35

$\chi^2 = 50.109$, $P < 0.001$ between the two groups, $H = 59.576$, $P < 0.0001$ between the two groups.

Table 3 Diagnostic values of E-cadherin or/and calretinin ICC for serous effusions

Index	Malignant effusion (%)		Benign effusion (%)	
	E-cadherin	E(+) + C(-)	Calretinin	E(-) + C(+)
Sensitivity	85.7	77.1	94.6	86.5
Specificity	91.9	100	88.6	97.1
PV+	90.9	100	89.7	97.0
PV-	87.2	82.2	93.9	87.2
DAR	88.9	88.9	91.7	91.7

E (+)/E (-): E-cadherin (+)/(-); C (+)/C (-): Calretinin (+)/(-); PV+: ICC-positive predictive value; PV-: ICC-negative predictive value; DAR: Accordance rate.

Diagnostic values of E-cadherin ICC or/and calretinin ICC for serous effusions

The diagnostic values (sensitivity, specificity) of both E-cadherin ICC and calretinin ICC for malignant effusions were $\geq 90\%$. Combination analysis of E-cadherin ICC and calretinin ICC could improve the specificities (up to 97.1-100%), while the sensitivities maintained at an acceptable level (Table 3).

DISCUSSION

Serous effusions are common clinical syndromes and can be simply divided into benign and malignant. Differentiation between two kinds of effusions is very important for diagnosis, treatment and prognostic evaluation. The cytological examination is a simple and reliable method for the diagnosis of malignant effusions, but its sensitivity is only 40-60%^[14], even lower in clinical practice. Cytological examinations are based on the cellular morphology, which may raise difficulties in distinguishing carcinoma cells from reactive mesothelial cells. Sometimes, carcinoma cells without typical morphological changes or enough number could not be diagnosed cytologically. How to identify the metastatic carcinoma cells and differentiate them from reactive mesothelial cells is key to diagnosing malignant effusions^[15]. In the past decade, immunocytochemistry seemed to be a valuable tool in solving the problem, with a complementary value for cytological diagnosis of malignant effusions^[16].

The cadherin family consists of more than 16 kinds of molecules that make up a group of phylogenetically and structurally related molecules, with M_r 120 000^[17]. E-cadherin, one member of a family of intracellular calcium-dependent adhesion molecules, is a transmembrane protein expressed in epithelial cells. Its extracellular amino terminal binds to the same structure of neighboring homotypic cells when calcium ion exists, mediating the epithelial cell-cell adhesion. Theoretically, only the exfoliated cells originating from epithelial tissues can express E-cadherin, so detection of E-cadherin expression is helpful for determining cells from epithelia. Because no epithelial cells were in benign effusions, the appearance of epithelial cells in effusions means a metastasis of carcinoma developed from epithelia. Our results showed that E-cadherin ICC of the exfoliated cells were valuable for the diagnosis of malignant effusions, with a sensitivity, specificity, positive predictive value, negative predictive value, and diagnostic rate near or over 90% respectively, similar to other studies^[1,18]. However, when epithelial cells transformed into malignant cells, E-cadherin expression might decrease to some extent^[19,20]. That is the reason why a few carcinoma cells showed weak or negative E-cadherin expression in effusions.

Calretinin is a calcium adhesion protein with M_r 29 000 and mainly expresses in nerve system. Lately, it was found that calretinin selectively expressed in mesotheliomas^[21,22], with powerful ability to differentiate mesothelial cells from other cells in effusions^[1,5,11,22]. Our results showed that calretinin expression in mesothelial cells was evident, but not in non-mesothelial cells, therefore it is useful in determining the cells from mesothelium, with a sensitivity, specificity, positive predictive value, negative predictive value, and diagnostic rate all near or over 90%. The "fried eggs" staining pattern made calretinin ICC more valuable in differentiating mesothelial cells from carcinoma cells^[1].

E-cadherin is an epithelial cell marker, and calretinin is a mesothelial cell marker. Our results showed that the combination of both markers significantly increased their differential diagnostic value with specificities up to 97.1% in serous effusions and 100% in benign and malignant effusions.

REFERENCES

- 1 **Chhieng DC**, Yee H, Schaefer D, Cangiarella JF, Jagirdar J, Chiriboga LA, Jagirdar J, Chiriboga LA, Cohen JM. Calretinin staining pattern aids in the differentiation of mesothelioma from adenocarcinoma in serous effusions. *Cancer* 2000; **90**: 194-200
- 2 **Ascoli V**, Scalzo CC, Taccogna S, Nardi F. The diagnostic value of thrombomodulin immunolocalization in serous effusions. *Arch Pathol Lab Med* 1995; **119**: 1136-1140
- 3 **Ascoli V**, Carnovale-Scalzo C, Taccogna S, Nardi F. Utility of HBME-1 immunostaining in serous effusions. *Cytopathology* 1997; **8**: 328-335
- 4 **Morgan RL**, De Young BR, McGaughy VR, Niemann TH. MOC-31 aids in the differentiation between adenocarcinoma and reactive mesothelial cells. *Cancer* 1999; **87**: 390-394
- 5 **Zimmerman RL**, Fogt F, Goonewardene S. Diagnostic utility of BCA-225 in detecting adenocarcinoma in serous effusions. *Anal Quant Cytol Histol* 2000; **22**: 353-357
- 6 **Afify AM**, Al-Khafaji BM, Paulino AF, Davila RM. Diagnostic use of muscle markers in the cytologic evaluation of serous fluids. *Appl Immunohistochem Mol Morphol* 2002; **10**: 178-182
- 7 **Davidson B**, Risberg B, Kristensen G, Kvalheim G, Emilsen E, Bjamer A, Berner A. Detection of cancer cells in effusions from patients diagnosed with gynaecological malignancies. Evaluation of five epithelial markers. *Virchows Arch* 1999; **435**: 43-49
- 8 **Ko EC**, Jhala NC, Shultz JJ, Chhieng DC. Use of a panel of markers in the differential diagnosis of adenocarcinoma and reactive mesothelial cells in fluid cytology. *Am J Clin Pathol* 2001; **116**: 709-715
- 9 **Schofield K**, D'Aquila T, Rimm DL. The cell adhesion molecule, E-cadherin, distinguishes mesothelial cells from carcinoma cells in fluids. *Cancer* 1997; **81**: 293-298
- 10 **Schofield K**, D'Aquila T, Rimm DL. E-cadherin expression is a sensitive and specific method for detection of carcinoma cells in fluid specimens. *Diagn Cytopathol* 2000; **22**: 263-267
- 11 **Barberis MC**, Faleri M, Veronese S, Casadio C, Viale G. Calretinin. A selective marker of normal and neoplastic mesothelial cells in serous effusions. *Acta Cytol* 1997; **41**: 1757-1761
- 12 **Wieczorek TJ**, Krane JF. Diagnostic utility of calretinin immunohistochemistry in cytologic cell block preparations. *Cancer* 2000; **90**: 312-319
- 13 **Kuonen-Boumeester V**, van Loenen P, de Bruijn EM, Henzen-Logmans SC. Quality control of immunocytochemical staining of effusions using a standardized method of cell processing. *Acta Cytol* 1996; **40**: 475-479
- 14 **Fenton KN**, Richardson JD. Diagnosis and management of malignant pleural effusions. *Am J Surg* 1995; **170**: 69-74
- 15 **Bedrossian CW**. Diagnostic problems in serous effusions. *Diagn Cytopathol* 1998; **19**: 131-137
- 16 **Delahaye M**, Van der Ham F, Van der Kwast TH. Complementary value of five carcinoma markers for the diagnosis of malignant mesothelioma, adenocarcinoma metastasis, and reactive mesothelium in serous effusions. *Diagn Cytopathol* 1997; **17**: 115-120
- 17 **Harrington KJ**, Syrigos KN, Harrington KJ. The role of E-cadherin-catenin complex: more than an intercellular glue? *Ann Surg Oncol* 2000; **7**: 783-788
- 18 **Simsir A**, Fetsch P, Mehta D, Zakowski M, Abati A. E-cadherin, N-cadherin, and calretinin in pleural effusions: the good, the bad, the worthless. *Diagn Cytopathol* 1999; **20**: 125-130
- 19 **Wijnhoven BP**, Dinjens WN, Pignatelli M. E-cadherin-catenin cell-cell adhesion complex and human cancer. *Br J Surg* 2000; **87**: 992-1005
- 20 **Cai KL**, Wang GB, Xiong LJ. Effects of carbon dioxide and nitrogen on adhesive growth and expressions of E-cadherin and VEGF of human colon cancer cell CCL-228. *World J Gastroenterol* 2003; **9**: 1594-1597
- 21 **Gotzos V**, Vogt P, Celio MR. The calcium binding protein calretinin is a selective marker for malignant pleural mesotheliomas of the epithelial type. *Pathol Res Pract* 1996; **192**: 137-147
- 22 **Dogliani C**, Tos AP, Laurino L, Iuzzolino P, Chiarelli C, Celio MR, Viale G. Calretinin: a novel immunocytochemical marker for mesothelioma. *Am J Surg Pathol* 1996; **20**: 1037-1046

Assessment of correlation between serum titers of hepatitis c virus and severity of liver disease

Bhupinder S. Anand, Maria Velez

Bhupinder S. Anand, Maria Velez, Department of Medicine, V. A. Medical Center and Baylor College of Medicine, Houston, Texas 77030, USA

Correspondence to: Bhupinder S. Anand, MD, Digestive Diseases Section (111D), VA Medical Center, 2002 Holcombe Blvd. Houston, Texas 77030, USA. ana0@flash.net

Telephone: +713-794-7273 **Fax:** +713-794-7687

Received: 2003-08-11 **Accepted:** 2004-03-04

Abstract

AIM: The significance of hepatitis C virus (HCV) serum titers has been examined in several clinical situations. There is much evidence that patients with a lower viral load have better response rates to anti-viral therapy compared to those with higher levels. Moreover, a direct association has been observed between serum titers of HCV and transmission rates of the virus. The aim of the present study was to determine if there was any correlation between HCV viral load and the severity of liver disease.

METHODS: Fifty patients with HCV infection were included in the study. These comprised of 34 subjects with a history of alcohol use and 16 non-alcoholics. Quantitative serum HCV RNA assay was carried out using the branched DNA (bDNA) technique. Linear regression analysis was performed between serum viral titers and liver tests. In addition, for the purpose of comparison, the subjects were divided into two groups: those with low viral titers (≤ 50 genome mEq/mL) and high titers (> 50 mEq/mL).

RESULTS: All subjects were men, with a mean \pm SD age of 47 ± 7.8 years. The mean HCV RNA level in the blood was $76.3\times 10^5 \pm 109.1$ genome equivalents/mL. There was no correlation between HCV RNA levels and age of the patients ($r = 0.181$), and the history or amount (g/d) of alcohol consumption ($r = 0.07$). Furthermore, no correlation was observed between serum HCV RNA levels and the severity of liver disease as judged by the values of serum albumin ($r = 0.175$), bilirubin ($r = 0.217$), ALT ($r = 0.06$) and AST ($r = 0.004$) levels. Similarly, no significant difference was observed between patients with low viral titers and high titers with respect to any of the parameters.

CONCLUSION: Our results indicate that the severity of liver disease is independent of serum levels of hepatitis C virus. These findings are important since they have a direct impact on the current debate regarding the role of direct cytopathic effect of hepatitis C virus versus immune-mediated injury in the pathogenesis of HCV-related liver damage.

Anand BS, Velez M. Assessment of correlation between serum titers of hepatitis c virus and severity of liver disease. *World J Gastroenterol* 2004; 10(16): 2409-2411

<http://www.wjgnet.com/1007-9327/10/2409.asp>

INTRODUCTION

Hepatitis C virus (HCV) is a bloodborne pathogen that is

endemic in most parts of the world, with an estimated overall prevalence of nearly 3%^[1]. Approximately 80% patients with hepatitis C virus develop chronic infection, and progression to cirrhosis occurs in nearly 20% of these subjects^[2]. Moreover, patients with HCV-related cirrhosis are at an increased risk of developing hepatocellular carcinoma, which is estimated to occur at the rate of 1.5% to 4% per year^[2]. In most individuals, liver disease progresses slowly over several decades, but the rate of progression is highly variable^[3-5]. Whereas some patients develop cirrhosis and end-stage liver disease within one to two years of exposure, others may die of old age or an entirely unrelated cause^[6]. Although it is mostly unclear why some patients progress more rapidly than others, several factors have been identified as having a role in disease severity. HCV patients co-infected with hepatitis B virus (HBV) have an increased risk of developing cirrhosis and decompensated liver disease^[7] as well as hepatocellular carcinoma^[8]. Several researches have noted more severe clinical and histological abnormalities in HCV infected chronic alcoholics compared to non-alcoholics with HCV infection^[9-12]. Other factors associated with a more rapid course of liver disease include age at acquisition of HCV infection, gender of the patient and presence of immunodeficiency states^[5,6].

Several studies have assessed the correlation between serum HCV viral titers and different clinical and laboratory parameters. Perinatal transmission of HCV from mothers to infants has been found to be related to maternal HCV titers. The risk of HCV transmission was found to be significantly higher (36%) among infants born to women with HCV RNA titers of at least 10^6 per mL compared to none if the titers were $< 10^6$ per mL^[13]. HCV titers have been found to be associated with responses to anti-viral treatment. Patients with a baseline HCV viral load of $\leq 2\times 10^6$ copies per mL have significantly better responses to anti-viral therapy compared to those with higher viral titers^[14]. Patients with HCV genotype 1 have been found in some studies to have higher viral loads than those with HCV genotype 2^[15,16], although other studies have failed to observe such an association^[17-19]. Previous attempts to assess the effect of viral titers on the severity of liver disease have produced conflicting results and the present study was designed to examine this issue in more detail.

MATERIALS AND METHODS

Patients with chronic hepatitis C virus infection diagnosed on the basis of a positive recombinant immunoblot assay (Riba) were included in the study. All patients were negative for other causes of chronic liver disease including hepatitis B virus infection. Patients were interviewed with respect to alcohol use, and in those with a positive history an assessment was made of the duration of alcohol abuse and amount of daily consumption. Physical findings and results of laboratory tests were recorded. All patients were treatment-naïve and were tested before the administration of anti-viral therapy.

Quantitative HCV analysis

Quantitative assay of hepatitis C virus levels was performed by the branched-chain DNA (bDNA) technique (Quantiplex

HCV-RNA; Chiron Corporation, Emeryville, USA). The bDNA assay incorporates a series of steps involving viral nucleic acid hybridizations to obtain signal amplification. This technique is unlike the polymerase chain reaction (PCR)-based assays in which the viral genome is amplified. The results of viral RNA titers in clinical samples are expressed as viral or genome milliequivalents per mL (mEq/mL). When the study was first initiated, only the initial version of the bDNA assay (Quantiplex 1.0), which had a lower limit of detection of 350 000 viral mEq/mL, was available commercially. Subsequently, the Chiron Corporation upgraded the technique and the latest version of the assay (Quantiplex 2.0) was employed which has a lower limit of detection of 200 000 viral mEq/mL.

Statistical analysis

Descriptive statistical analyses were performed, and the results are presented as mean±SD. Comparison of quantitative measurements between groups was performed using Wilcoxon Rank Sum Test. The Students' *t*-test was used to assess changes in HCV RNA levels in the same individual. Linear regression analysis was employed to examine the presence of any correlation between serum HCV RNA levels and different laboratory and clinical parameters including the amount of daily alcohol consumption.

RESULTS

A total of 50 patients were included in the study. These comprised of 34 patients with a history of alcohol use and 16 non-alcoholics. All subjects were men, with a mean±SD age of 47±7.8 years. The mean HCV-RNA level in the blood was $76.3 \times 10^5 \pm 109.1$ genome equivalents/mL. There was no correlation between HCV RNA levels and the age of the patients ($r = 0.181$), a history of alcohol use or the amount (g/day) of alcohol consumption ($r = 0.07$). Furthermore, no correlation was observed between HCV RNA levels and the severity of liver disease as judged by the values of serum albumin ($r = 0.175$), bilirubin ($r = 0.217$), ALT ($r = 0.06$) and AST ($r = 0.004$) levels.

To further assess the effects of viral titers on the severity of liver disease, the study subjects were arbitrarily divided into two groups: patients with low viral titers (≤ 50 genome mEq/mL) and those with high titers (> 50 genome mEq/mL). The results are shown in Table 1. Again, no difference was observed between the two groups with respect to any of the parameters examined.

Table 1 Comparison of patients with low and high hepatitis C virus serum titers

Parameter	Low HCV RNA level (≤ 50 genome mEq/L) <i>n</i> = 28	High HCV RNA level (> 50 genome mEq/L) <i>n</i> = 22	<i>P</i> value
Age (yr)	48±8.8	45±6	0.35
Alcohol use (g/d)	221±110	274±170	0.27
ALT (U/mL)	77±56	75±41	0.76
AST (U/L)	79±58	93±100	0.96
Albumin (g %)	3.70±0.76	3.90±0.43	0.44
Bilirubin (mg %)	1.35±1.2	0.88±0.32	0.55

Results are expressed as mean±SD.

DISCUSSION

Several factors have been incriminated in predicting the rate of progression of HCV-related chronic liver disease. These include age at acquisition of HCV infection, gender of the patient, alcohol abuse and co-infection with HBV and HIV infections^[5-12]. Studies assessing the relationship between serum viral titers and the severity of biochemical and histological abnormalities

have produced conflicting results. Some found no correlation between HCV viral loads, and serum ALT values and the extent of histological damage^[16,17,19-21]. On the other hand, Kato *et al.* observed significantly higher HCV RNA titers in patients with chronic active hepatitis and cirrhosis compared to those with milder histological abnormalities such as chronic persistent hepatitis^[22]. Similarly, Fanning *et al.* in a study on Irish women who acquired their HCV infection through the administration of contaminated anti-D immunoglobulin, obtained a significant correlation between serum HCV viral loads and the degree of hepatic inflammation in liver biopsy specimens^[23].

In the present study, we further assessed the association between serum HCV RNA titers and several clinical and laboratory factors. Linear regression analysis showed a complete lack of correlation between the viral loads and age at presentation of the patients and the extent of alcohol consumption. Moreover, none of the laboratory tests showed any correlation with HCV viral count. For the purposes of statistical analysis, we subdivided the patients into those with low (≤ 50 genome mEq/L) and high (> 50 genome mEq/L) viral loads. Again, there was no correlation between any of the clinical and laboratory parameters and HCV viral loads (Table 1).

Our results indicate that the severity of liver disease is independent of serum levels of hepatitis C virus. The precise mechanism by which hepatitis C virus damages the liver remains poorly understood. Until recently, a direct cytopathic effect of the virus was considered as the primary form of liver injury caused by the virus. It has been suggested that the degree of liver damage is the result of a complicated interaction between the virus and immune response of the host^[24]. Immune mediated liver damage is believed to be initiated by HCV-specific T cells and is enhanced by HCV-induced HLA-A, B and C and intracellular adhesion molecules^[25,26]. The results of the present study are important since they argue against a direct cytopathic effect of HCV and support the hypothesis that the pathogenesis of HCV-related liver damage is immune-mediated.

REFERENCES

- 1 Wasley A, Alter MJ. Epidemiology of hepatitis C: Geographical differences and temporal trends. *Sem Liv Dis* 2000; **20**: 1-16
- 2 Alter MJ. The epidemiology of hepatitis C virus in the west. *Semin Liv Dis* 1995; **15**: 5-14
- 3 Kiyosawa D, Soeyama T, Tanaka E. Interrelationship of blood transfusion non-A, non-B hepatitis and hepatocellular carcinoma: analysis by detection of antibody to hepatitis C virus. *Hepatology* 1990; **12**: 671-675
- 4 Tong MJ, El-Farra NS, Reikes AR, Co RL. Clinical outcomes after transfusion-associated hepatitis C. *N Engl J Med* 1995; **332**: 1463-1466
- 5 Poynard T, Bedossa P, Opolon P. Natural history of liver fibrosis progression in patients with chronic hepatitis C the OBSVIRC, METAVIR, CLINIVIR, and DOSVIRC groups. *Lancet* 1997; **349**: 825-832
- 6 Hoofnagle JH. Hepatitis C: The clinical spectrum of disease. *Hepatology* 1997; **26**(Suppl 1): 15S-20S
- 7 Chuang WL, Chang WY, Lu SN. The role of hepatitis C virus in chronic hepatitis B virus infection. *Gastroenterol Jpn* 1993; **28**(Suppl 5): 23-27
- 8 Di Bisceglie AM. Hepatitis C and hepatocellular carcinoma. *Hepatology* 1997; **26**(Suppl 1): 34S-38S
- 9 Coelho-Little ME, Jeffers LJ, Bernstein DE, Goodman JJ, Reddy KR, de Medina M, Li X. Hepatitis C virus in alcoholic patients with and without clinically apparent liver disease. *Alcohol. Clinical Expt Res* 1995; **19**: 1173-1176
- 10 Rosman AS, Waraich A, Galvin K, Casiano J, Paronetto F, Lieber CS. Alcoholism is associated with hepatitis C but not hepatitis B in an urban population. *Am J Gastroenterol* 1996; **91**: 498-505
- 11 Brillanti S, Masci C, Siringo S, Di Febo G, Miglioli M, Barbara L. Serological and histological aspects of hepatitis C virus in-

- fection in alcoholic patients. *J Hepatol* 1991; **13**: 347-350
- 12 **Zarski JP**, Thelu MA, Moulin C, Rachail M, Seigneurin JM. Interest of the detection of hepatitis C virus RNA in patients with alcoholic liver disease. *J Hepatol* 1993; **17**: 10-14
- 13 **Ohto H**, Terazewa S, Sasaki N. Transmission of hepatitis C virus from mothers to infants. *N Engl J Med* 1994; **330**: 744-750
- 14 **McHutchison JG**, Gordon SC, Schiff ER, Shiffman ML, Lee WM, Rustgi VK, Goodman ZD. Interferon alfa-2b alone or in combination with ribavirin as initial treatment for chronic hepatitis C. *N Engl J Med* 1998; **339**: 1485-1492
- 15 **Lau JYN**, Mizokami M, Kolberg JA, Davis GL, Prescott LE, Ohno T, Perrillo RP. Application of six hepatitis C virus genotyping systems to sera from chronic hepatitis C patients in the United States. *J Infect Dis* 1995; **171**: 281-289
- 16 **Kao JH**, Lai MY, Chen PJ, Hwang LH, Chen W, Chen DS. Clinical significance of serum hepatitis C virus titers in patients with chronic type C hepatitis. *Am J Gastroenterol* 1996; **91**: 506-510
- 17 **Nousbaum JB**, Pol S, Nalpas B, Landais P, Berthelot P, Brechot C. Collaborative Study Group. Hepatitis C virus type 1b (II) infection in France and Italy. *Ann Intern Med* 1995; **122**: 161-168
- 18 **Lau JYN**, Davis GL, Prescott LE, Maertens G, Lindsay KL, Qian K, Mizokami M. Distribution of hepatitis C virus genotypes determined by line probe assay in patients with chronic hepatitis C seen at a tertiary referral center in the United States. *Ann Intern Med* 1996; **124**: 868-876
- 19 **Zeuzem S**, Franke A, Lee JH, Herrmann G, Ruster B, Roth WK. Phylogenetic analysis of hepatitis C virus isolates and their correlation to viremia, liver function tests, and histology. *Hepatology* 1996; **24**: 1003-1009
- 20 **Lau JY**, Davis GL, Kniffen J, Qian KP, Urdea MS, Chan CS, Mizokami M. Significance of serum hepatitis C virus RNA levels in chronic hepatitis C. *Lancet* 1993; **341**: 1501-1504
- 21 **McCormick SE**, Goodman ZD, Maydonovitch CL, Sjogren MH. Evaluation of liver histology, ALT elevation, and HCV RNA titer in patients with chronic hepatitis C. *Am J Gastroenterol* 1996; **91**: 1516-1522
- 22 **Kato NK**, Hosoda K, Ito Y, Ohto M, Omata M. Quantification of hepatitis C virus by competitive reverse transcription - polymerase chain reaction: increase of the virus in advanced liver disease. *Hepatology* 1993; **18**: 16-20
- 23 **Fanning L**, Kenny E, Sheehan M, Cannon B, Whelton M, O'Connell J, Collins JK, Shanahan F. Viral load and clinicopathological features of chronic hepatitis C (1b) in a homogeneous population. *Hepatology* 1999; **29**: 904-907
- 24 **Rehermann B**. Interaction between the hepatitis C virus and the immune system. *Semin Liv Dis* 2000; **20**: 127-141
- 25 **Ballardini G**, Groff P, Pontisso P. Hepatitis C virus (HCV) genotype, tissue HCV antigens, hepatocellular expression of HLA-A, B, C, and intracellular adhesion-1 molecules. *J Clin Invest* 1995; **95**: 2967-2975
- 26 **Nelson DR**, Marousis CG, Davis GL. The role of hepatitis C virus-specific cytotoxic T lymphocytes in chronic hepatitis C. *J Immunol* 1997; **158**: 1473

Edited by Zhu LH Proofread by Xu FM

Hypertrophied anal papillae and fibrous anal polyps, should they be removed during anal fissure surgery?

Pravin J. Gupta

Pravin J. Gupta, Proctologist, Gupta Nursing Home, D/9, Laxminagar, NAGPUR- 440022, India

Correspondence to: Pravin J. Gupta, M.S., Proctologist, Gupta Nursing Home, D/9, Laxminagar, NAGPUR- 440022, India. drpjg@nagpur.dot.net.in

Received: 2003-07-12 **Accepted:** 2004-03-04

Abstract

AIM: Hypertrophied anal papillae and fibrous anal polyps are not given due importance in the proctology practice. They are mostly ignored being considered as normal structures. The present study was aimed to demonstrate that hypertrophied anal papillae and fibrous anal polyps could cause symptoms to the patients and that they should be removed in treatment of patients with chronic fissure in anus.

METHODS: Two groups of patients were studied. A hundred patients were studied in group A in which the associated fibrous polyp or papillae were removed by radio frequency surgical device after a lateral subcutaneous sphincterotomy for relieving the sphincter spasm. Another group of a hundred patients who also had papillae or fibrous polyps, were treated by lateral sphincterotomy alone. They were followed up for one year.

RESULTS: Eighty-nine percent patients from group A expressed their satisfaction with the treatment in comparison to only 64% from group B who underwent sphincterotomy alone with the papillae or anal polyps left untreated. Group A patients showed a marked reduction with regard to pain and irritation during defecation ($P=0.0011$), pricking or foreign body sensation in the anus ($P=0.0006$) and pruritus or wetness around the anal verge ($P=0.0008$).

CONCLUSION: Hypertrophied anal papillae and fibrous anal polyps should be removed during treatment of chronic anal fissure. This would add to effectiveness and completeness of the procedure.

Gupta PJ. Hypertrophied anal papillae and fibrous anal polyps, should they be removed during anal fissure surgery? *World J Gastroenterol* 2004; 10(16): 2412-2414
<http://www.wjgnet.com/1007-9327/10/2412.asp>

INTRODUCTION

Hypertrophied anal papillae are essentially skin tags that project up from the dentate line, or the junction between the skin and the epithelial lining of the anus^[1]. They are often found as part of the classic triad of a chronic fissure, namely the fissure itself, hypertrophied papilla above and a skin tag below^[2,3]. They are also found in isolation, maybe firm and palpable on a digital examination of the anus. In this situation, they must be differentiated from polyps, hemorrhoids, or other growths. Endoscopically they could be differentiated from an adenomatous

polyp by their white appearance and their origin from the lower (squamous) aspect of the dentate line in the anal canal. They are usually a symptomatic but occasionally grow large enough to be felt by the patient or are likely to prolapse. Hypertrophied anal papilla should be included in the differential diagnosis of a smooth mass located near the anal verge, especially in a patient with a history of chronic anal irritation or infection^[2].

With passage of time, papillae continue to grow in size. A papilla is liable to acquire considerable fibrous thickening over a period of time when it gets a rounded expanded tip, which is known as a fibrous polyp. This is due to piling up and consolidation of chronic inflammatory tissues at the proximal part of the fissure at the dentate line. As many as 16% of the patients having chronic fissure in anus recorded the presence of papillae that turned into fibrous polyps^[4]. These papillae are presumed to be caused by edema and low-grade infection.

A fibrosed-hypertrophied papilla is also frequently found at the upper part of a chronic anal fissure or guarding the internal opening of fistula in anus. In the later case however, the symptoms may completely dominate and distort the clinical findings. Dilated veins, white areas, and a large hypertrophied anal papilla are often found in prolapsing types of hemorrhoids^[5].

In the past, these structures were not given any importance and were left untreated. Those patients, in whom, the fissure in anus was treated but the concomitant papillae or polyps were left untouched, continued to complain of pruritus, wetness, or an intermittent pricking sensation in the anus. Those with fibrous polyps felt incompletely treated due to a feeling of *something* projecting from the anus. Even a case of giant hypertrophied anal papilla complicated with a massive anal bleeding and prolapse was reported^[6].

This study was aimed to assess the impact and utility of attending to these two conditions concurrently while dealing with cases of fissure in ano.

MATERIALS AND METHODS

This study was carried out at Gupta Nursing Home, Nagpur, India, between July 2000 and December 2001.

Two hundred patients suffering from chronic fissure in ano associated with hypertrophied anal papillae or fibrous polyps were selected for the study. All these patients had primarily reported symptoms and complaints of chronic anal fissure. The papillae and polyps were diagnosed preoperatively by using a pediatric anoscope to avoid discomfort during examination. The number of papillae ranged from two to four. However, the fibrous polyp was found to be single in all those patients who were having this pathology.

Only those patients who came for a follow-up after 12 mo of the procedure were included in the study.

Exclusion criteria

Patients having fissure in ano with sentinel tags or hemorrhoids and those who had not signed the informed consent were not included in the study.

The patients were divided into two groups viz: group A and B.

Group A consisted of one hundred patients in whom the anal papillae, anal polyp, or both were treated by radio frequency

procedure along with the fissure. Another hundred patients (group B) were treated only for the fissure and the papillae or polyps were left untreated. The randomization was done by a sealed envelope, which was opened by the operation room nurse upon patient's arrival for the procedure.

An informed consent was obtained from all patients under study. The study was approved by the local ethical committee and was done in accordance with the Declaration of Helsinki. No special pre-operative preparation was carried out. All the patients received a dose of laxative on the prior night. The patient description is given in Table 1.

Table 1 Patient demographic data

Patient characteristics	Group A	Group B
No. of patients	100	100
Mean age yr	37	39
Male: Female	64:36	66:34
Hypertrophied papillae (No. of patients)	100	100
Fibrous anal polyp (No. of patients)	11	8

Statistical analysis

Unpaired Student's *t* test was used to measure postoperative parameters. The level of statistical significance between groups was set at 5 per cent.

Procedures

The procedure was carried out under a short general anesthesia with a muscle relaxant. A lateral subcutaneous sphincterotomy was performed to relieve the sphincter spasm. This was followed by insertion of the anoscope with a proximal illumination. The anal canal was cleaned off the collection. The papillae or polyps were located and were dealt with through a radio frequency surgical technique.

Radio frequency surgery aims at cutting or coagulation of tissues by using a high frequency alternate current. The radiofrequency device performs a simultaneous function of cutting and coagulating of the tissues. The effect of cutting, known as high frequency section, is executed without pressuring or crushing the tissue cells. This is due to the result of heat produced by the tissues' resistance to the passage of the high frequency wave set to motion by the equipment. The heat makes the intracellular water boil, thereby increasing the inner pressure of the cell to the point of breaking it from inside to outside (explosion). This phenomenon is called cellular volatilization^[7].

In this procedure, we used the radio frequency generator known as Ellman Dual Frequency 4MHz by Ellman International, Hewlett, N.Y. This instrument produces an electromagnetic wave of a very high frequency that reaches 4 megahertz. The unit is supplied with a handle to which different interchangeable electrodes could be attached to suit the exact requirement^[8]. In our study, we used the ball electrode for coagulation and a round loop electrode for shaving off the desired tissues.

The papillae were directly coagulated with a ball electrode with the radio frequency unit kept on coagulation mode, which resulted in shrinkage and disappearance of the papillae in no time.

For the fibrous anal polyp, we initially coagulated its base circumferentially by a ball electrode and then shaved off the mass by using the round loop electrode. The minor bleeding encountered in some cases was coagulated by touching the bleeding points with the ball electrode. The whole procedure took around 7-10 min to complete.

The patients were prescribed analgesics for one wk and a stool softener for a period of 1 mo.

The first follow up was made after 30 d. The fissures were healed and there was no sphincter spasm in any of the patients from either group. During examination of patients from group A, anoscopies showed total absence of the papillae. Patients who were treated for fibrous polyps did have some amount of edema and mild elevation at the site of destruction. However, patients had fewer complaints of pruritus, pricking, heaviness and a sense of incomplete evacuation as compared to patients from group B.

Follow up on completion of 12 mo of treatment

An independent observer blinded to the procedures made the observations during the follow up. He noted down all the symptoms in a prescribed format specially prepared for the study. The findings are given in Table 2.

RESULTS

The patients from group A who were treated by sphincterotomy followed by radio frequency surgical procedures for removal of hypertrophied anal papillae or fibrous polyps felt far more comfortable as compared to patients in group B who were subjected only to sphincterotomy for treatment of fissure and in whom, as per the prevailing practice, the papillae or anal polyps were left untouched. The other visible advantages experienced by the patients in group A were: a relief of pain and irritation during defecation, absence of pricking or foreign body sensation in the anus and disappearance of pruritus or wetness around the anal verge.

Table 2 One-yr follow-up findings of patients with removal or no removal of hypertrophied anal papillae and fibrous anal polyps (Student's unpaired *t* test)

Findings based on complaints of	Group A	Group B	<i>P</i>
Pruritus ani	7 (7%)	32 (32%)	0.0008
Anal pain and irritation	5 (5%)	26 (26%)	0.0011
Discharge per anus	2 (2%)	34 (36%)	0.0005
Sense of incomplete evacuation	5 (5%)	22 (22%)	0.0008
Crawling sensation in anus	8 (8%)	48 (48%)	0.0002
Pricking or foreign body sensation in anus	3 (3%)	32 (32%)	0.0006
Prolapsed per rectum	Nil	4 (4%)	N
Sepsis in the wound	1 (1%)	8 (8%)	0.0044
Recurrence of papillae or polyps	Nil	Not applicable	N
Recurrence of fissure	Nil	Nil	N
Overall satisfaction from the procedures	89%	64%	0.0004

N, not studied.

DISCUSSION

Anal papillae were found in almost 50-60% patients examined by us in regular practice. Usually, they were small, caused no symptoms, and could be regarded as normal structures^[9]. However, if it is a case of hypertrophy and the papillae start projecting in the anal canal, it not only requires attention but calls for a suitable treatment also. In such cases, there are chances of increase in the mucus leak resulting in increased anal moisture. These are liable to get traumatized and inflamed during the passage of stool. In addition, on being converted into a fibrous polyp, they tend to project at the anal orifice during defecation, often requiring to be digitally replaced. These polyps are considered as one of the differential diagnoses of rectal prolapse^[10]. The patients also reported symptoms like pruritus^[11], a foreign body sensation, pricking, a nagging sense of incomplete evacuation and heaviness in the anal region.

As a routine practice, these pathologies were not given any importance^[12]. There is very brief reference to this entity in the standard textbooks and other references. Secondary goals of fissure surgery sometimes required the removal of hypertrophied papilla and skin tag as well as the removal of inflammatory and fibrotic tissues surrounding the fissure^[13]. Customarily, in the symptomatic papillae or polyps, their removal by crushing of the bases, excision after ligation or electrocauterization has been suggested. All these procedures are time consuming and are associated with complications at times. The use of radio frequency devices to deal with these pathologies has been found to be a quick, easy and significant complication free procedure^[14]. The device can ablate the papillae instantly, while the fibrous polyps can be excised after coagulation of the bases and thereafter the pedicles. In the present study, we have specifically excluded those patients of chronic fissure in ano who had sentinel tags or piles, as they were known to cause few of the similar symptoms that were associated with hypertrophied papillae or fibrous anal polyps.

Hypertrophied anal papillae and fibrous anal polyps are important anal pathologies associated with chronic anal fissure and are responsible for symptoms like pruritus, a pricking sensation, heaviness, etc. Their removal should be made an essential part of treatment of chronic fissures in ano. Persistence of these structures leaves behind a sense of incomplete treatment and thereby reducing the overall satisfaction on the

part of the patient. radio frequency procedures have been found useful in successfully eradicating these concomitant pathologies of chronic fissure in ano. This procedure should be given a fair chance to prove its utility and long-term efficacy.

REFERENCES

- 1 **Lenhard B.** Guideline on the disease picture of hypertrophic anal papilla. *Hautarzt* 2002; **53**: 104-105
- 2 **Heiken JP, Zuckerman GR, Balfe DM.** The hypertrophied anal papilla: recognition on air-contrast barium enema examinations. *Radiology* 1984; **151**: 315-318
- 3 **Schwartz SI.** In Principles of Surgery, McGraw-Hill international book company, Singapore, 4th Edition 1984: 1225
- 4 **Thomson JPS, Nicholls RJ, Williams CB.** In colorectal diseases, William Heinemann Medical Book Limited, London, Page 312 1981
- 5 **Sadahiro S, Mukai M, Tokunaga N, Tajima T, Makuuchi H.** A new method of evaluating hemorrhoids with the retroflexed fiberoptic colonoscope. *Gastrointest Endosc* 1998; **48**: 272-275
- 6 **Kusunoki M, Horai T, Sakanoue Y, Yanagi H, Yamamura T, Utsunomiya J.** Giant hypertrophied anal papilla. *Case Report Eur J Surg* 1991; **157**: 491-492
- 7 **Pfenninger JL.** Modern treatments for Internal Hemorrhoids. *BMJ* 1997; **314**: 1211-1212
- 8 **Goldberg SN, Gazelle GS, Dawson SL.** Tissue ablation with radiofrequency: effect of probe size, gauge, duration and temperature on lesion volume. *Acad Radiol* 1995; **2**: 399-404
- 9 **Golighar J, Duthie H, Nixon H.** Surgery of the anus rectum and colon. *Fifth Edition Bailliere Tindal, London* 1992: 151
- 10 **Euro K W, Seow-Choen F.** Functional problems in adult rectal prolapse and controversies in surgical treatment. *Br J Surg* 1997; **84**: 904-911
- 11 **Sabiston DC.** In Textbook of Surgery, WB Saunders Company, London, 12th Edition 1981: 1130
- 12 **Jensen SL.** A randomized trial of simple excision of non-specific hypertrophied anal papillae versus expectant management in patients with chronic pruritus ani. *Ann R Coll Surg Engl* 1988; **70**: 348-349
- 13 **Weaver RM, Ambrose NS, Alexander-Williams J, Keighley MR.** Manual dilatation of the anus vs. lateral subcutaneous sphincterotomy in the treatment of chronic fissure-in-ano: results of a prospective, randomized, clinical trial. *Dis Colon Rectum* 1987; **30**: 420-423
- 14 **Brown JS.** Radio frequency surgery- Minor surgery a text and atlas. *Chap Hall Med* 1997; **42**: 300-326

Edited by Zhu LH Proofread by Xu FM

Lack of evidence for leukocyte maternal microchimerism in primary biliary cirrhosis

Kenichi Nomura, Yoshio Sumida, Takaharu Yoh, Atsuhiko Morita, Yosuke Matsumoto, Sawako Taji, Naohisa Yoshida, Masahito Minami, Yoshito Itoh, Shigeo Horiike, Keisho Kataoka, Masafumi Taniwaki, Takeshi Okanoue

Kenichi Nomura, Yosuke Matsumoto, Shigeo Horiike, Keisho Kataoka, Masafumi Taniwaki, Molecular Hematology and Oncology, Kyoto Prefectural University of Medicine Graduate School of Medical Science, Kyoto 602-0841, Japan

Yoshio Sumida, Department of Internal Medicine, National Nara Hospital, Nara 630-8305, Japan

Takaharu Yoh, Department of Internal Medicine, Aiseikai Yamashina Hospital, Kyoto 607-8086, Japan

Atsuhiko Morita, Ayabe city Hospital, Kyoto 623-0011, Japan

Naohisa Yoshida, Sawako Taji, Masahito Minami, Yoshito Itoh, Takeshi Okanoue, Molecular Gastroenterology and Hepatology, Kyoto Prefectural University of Medicine Graduate School of Medical Science, Kyoto 602-0841, Japan

Masafumi Taniwaki, Clinical Molecular Genetics and Laboratory Medicine, Kyoto Prefectural University of Medicine Graduate School of Medical Science, Kyoto 602-0841, Japan

Supported by the grants of the Ministry of Education, Science, Sports, and Culture of Japan, No.15790497

Correspondence to: Dr. Kenichi Nomura, Molecular Hematology and Oncology, Kyoto Prefectural University of Medicine Graduate School of Medical Science, Kawaramachi-Hirokoji, Kamigyo-ku, Kyoto 602-0841, Japan. nomuken@sun.kpu-m.ac.jp

Telephone: +81-75-251-5521 **Fax:** +81-75-251-0710

Received: 2004-03-11 **Accepted:** 2004-04-09

Abstract

AIM: It is reasonable to assume that microchimerism could also be involved in the induction of primary biliary cirrhosis (PBC). However, previous reports investigated only fetus-microchimerism in women patients. Maternal microchimerism has not been investigated until now. The current study aimed to clear either maternal microchimerism was involved in the pathogenesis of PBC or not.

METHODS: We used fluorescence *in situ* hybridization on paraffin-embedded tissue (We called "Tissue-FISH".) to determine whether maternal cells infiltrated in male patients who were diagnosed as having PBC. Tissue-FISH was performed by using both X and Y specific probes on the biopsy liver sample of 3 male PBC patients.

RESULTS: Infiltrating lymphocytes demonstrated both X and Y signals in all 3 male patients.

CONCLUSION: Maternal microchimerism does not play a significant role in PBC. PBC may not relate to fetus and maternal microchimerism.

Nomura K, Sumida Y, Yoh T, Morita A, Matsumoto Y, Taji S, Yoshida N, Minami M, Itoh Y, Horiike S, Kataoka K, Taniwaki M, Okanoue T. Lack of evidence for leukocyte maternal microchimerism in primary biliary cirrhosis. *World J Gastroenterol* 2004; 10(16): 2415-2416

<http://www.wjgnet.com/1007-9327/10/2415.asp>

INTRODUCTION

Molecular biological techniques have shown that fetal cells can be detected in maternal peripheral blood in most pregnancies^[1-3]. On this observation, the radical hypothesis of autoimmune disease, proposed in 1996, may be caused by fetal cells that are retained after pregnancies^[4]. In systemic sclerosis, it was reported that fetal antimaternal graft-versus-host reactions might be involved in the pathogenesis of systemic sclerosis in some women^[5,6]. Thus, the hypothesis that microchimerism might cause the primary biliary cirrhosis (PBC) is very fascinating^[7], because it may explain clinical similarities between PBC and chronic graft-versus-host disease (GVHD) in liver after bone marrow transplantation. Some previous reports hypothesized that fetal microchimerism may also play a role in the pathogenesis of PBC^[8-11]. However, they concluded that fetal microchimerism was not important in the development of PBC.

Although there is a possibility that PBC may be developed by maternal microchimerism, not fetal microchimerism in female patients, maternal microchimerism has not been considered until now. Thus, we produced one hypothesis that maternal microchimerism might cause PBC.

To test the hypothesis, we investigated 3 male PBC patients by fluorescence *in situ* hybridization (FISH) on paraffin-embedded tissues.

MATERIALS AND METHODS

Patients

Three male patients with PBC were studied after giving informed consent. They were diagnosed at Kyoto Prefectural University of Medicine by liver biopsy and the positivity of serum antimitochondrial antibody (AMA). All patients were compatible with the feature of PBC. None of these patients had scleroderma. They had no experience of blood transfusion.

Methods

We reported tissue-FISH method previously^[12-14]. Sections from paraffin-embedded tissues were placed on silane-coated glass slides. The slides were deparaffinized immediately in 2 rinses of 1 000 g/L xylene for 10 min each. Each slide was rehydrated in an ethanol series for 5 min. The slides were then treated with 0.2 mol/L HCl for 20 min, followed by 2×SSC (0.3 mol/L sodium chloride and 0.03 mol/L sodium citrate) for 20 min at 80 °C, treated with 0.05 mg/mL proteinase K in TEN (0.05 mol/L Tris-HCl, pH 7.8, 0.01 mol/L EDTA, and 0.01 mol/L sodium chloride) for 10 min at 37 °C, and placed in 40 g/L formaldehyde in PBS for 10 min. Both FISH probes and target DNA were denatured simultaneously for 10 min at 90 °C, and the slides were incubated overnight at 42 °C, placed in 2×SSC for 10 min at 42 °C, washed twice in 2×SSC/500 g/L formaldehyde formamide for 5 min each at 42 °C, washed 2×SSC for 5 min at 42 °C, and counterstained in 2×SSC/0.03 µg/mL DAPI.

RESULTS

It was easy to recognize the architecture of liver tissues by

fluorescence microscope BX40-RF (Olympus, Tokyo, Japan). The lymphocytes aggregated at the portal zone (Figure 1). We assessed only non-overlapping nuclei having XY or XX signals. Almost infiltrating lymphocytes at septa revealed the XY chromosome pattern (Figure 2). The frequency of nuclei having XY in 3 patients is 96%, 98%, and 97%, respectively. ($P < 0.01$).

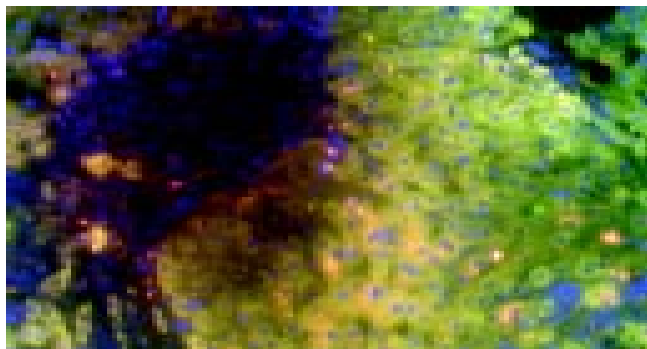


Figure 1 Aggregated lymphocytes at the portal zone.

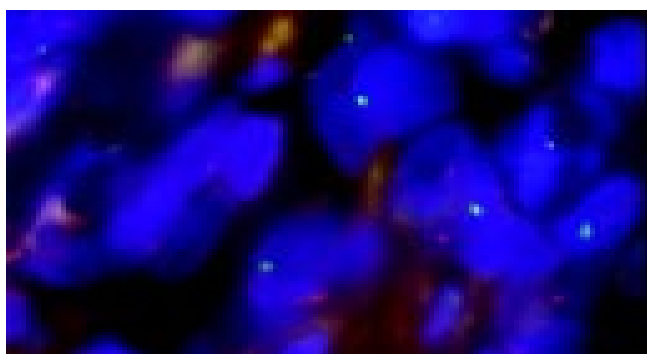


Figure 2 Infiltrating lymphocytes revealed XY chromosome pattern (X; Green, Y; Orange).

DISCUSSION

The hypothesis that fetal microchimerism causing PBC is fascinating. However, this hypothesis does not explain why some cases with PBC were fetal microchimerism negative and why even males and nulliparous women were suffering from PBC. On the other hand, the hypothesis that maternal microchimerism causes PBC is more fascinating, because it resolves the above questions. Every one has the risk of maternal microchimerism, because it has been already established that maternal cells persist for a long-term in immunocompetent offsprings^[15]. However, this hypothesis could not be resolved by polymerase chain reaction (PCR), because PCR can only detect the Y-chromosome specific DNA.

To clear whether infiltrating lymphocytes derived from either maternal or fetal cells in male PBC patients, we performed tissue-FISH. Tissue-FISH is able to distinguish infiltrating lymphocytes from hepatocytes, because this method preserves the architecture of liver tissues and the shapes of cells. Tissue-FISH revealed that almost infiltrating lymphocytes were male cells in the liver sample of male patients. These results showed that maternal

microchimerism did not play an important role in introducing and maintaining primary biliary cirrhosis.

In conclusion, we were unable to provide the evidence of maternal microchimerism in PBC patients. Although PBC shows the similar histological features with GVHD, PBC may be different from GVHD in etiology.

REFERENCES

- 1 **Lo YM, Patel P, Sampietro M, Gillmer MD, Fleming KA, Wainscoat JS.** Detection of single-copy fetal DNA sequence from maternal blood. *Lancet* 1990; **335**: 1463-1464
- 2 **Thomas MR, Williamson R, Craft I, Yazdani N, Rodeck CH.** Y chromosome sequence DNA amplified from peripheral blood of women in early pregnancy. *Lancet* 1994; **343**: 413-414
- 3 **Bianchi DW.** Prenatal diagnosis by analysis of fetal cells in maternal blood. *J Pediatr* 1995; **127**: 847-856
- 4 **Nelson JL.** Maternal-fetal immunology and autoimmune disease: is some autoimmune disease auto-alloimmune or allo-autoimmune? *Arthritis Rheum* 1996; **39**: 191-194
- 5 **Artlett CM, Smith JB, Jimenez SA.** Identification of fetal DNA and cells in skin lesions from women with systemic sclerosis. *N Engl J Med* 1998; **338**: 1186-1191
- 6 **Nelson JL, Furst DE, Maloney S, Gooley T, Evans PC, Smith A, Bean MA, Ober C, Bianchi DW.** Microchimerism and HLA-compatible relationships of pregnancy in scleroderma. *Lancet* 1998; **351**: 559-562
- 7 **McDonnell WM.** Is primary biliary cirrhosis a complication of pregnancy? *Hepatology* 1998; **28**: 593-594
- 8 **Tanaka A, Lindor K, Gish R, Batts K, Shiratori Y, Omata M, Nelson JL, Ansari A, Coppel R, Newsome M, Gershwin ME.** Fetal microchimerism alone does not contribute to the induction of primary biliary cirrhosis. *Hepatology* 1999; **30**: 833-838
- 9 **Rubbia-Brandt L, Philippeaux MM, Chavez S, Mentha G, Borisch B, Hadengue A.** FISH for Y chromosome in women with primary biliary cirrhosis: lack of evidence for leukocyte microchimerism. *Hepatology* 1999; **30**: 821-822
- 10 **Invernizzi P, De Andreis C, Sirchia SM, Battezzati PM, Zuin M, Rossella F, Perego F, Bignotto M, Simoni G, Podda M.** Blood fetal microchimerism in primary biliary cirrhosis. *Clin Exp Immunol* 2000; **122**: 418-422
- 11 **Corpechot C, Barbu V, Chazouilleres O, Poupon R.** Fetal microchimerism in primary biliary cirrhosis. *J Hepatol* 2000; **33**: 696-700
- 12 **Nomura K, Sekoguchi S, Ueda K, Nakao M, Akano Y, Fujita Y, Yamashita Y, Horiike S, Nishida K, Nakamura S, Taniwaki M.** Differentiation of follicular from mucosa-associated lymphoid tissue lymphoma by detection of t(14;18) on single-cell preparations and paraffin-embedded sections. *Genes Chromosomes Cancer* 2002; **33**: 213-216
- 13 **Nomura K, Yoshino T, Nakamura S, Akano Y, Tagawa H, Nishida K, Seto M, Nakamura S, Ueda R, Yamagishi H, Taniwaki M.** Detection of t(11;18) (q21;q21) in marginal zone lymphoma of mucosa-associated lymphocytic tissue type on paraffin-embedded tissue sections by using fluorescence *in situ* hybridization. *Cancer Genet Cytogenet* 2003; **140**: 49-54
- 14 **Matsumoto Y, Nomura K, Matsumoto S, Ueda K, Nakao M, Nishida K, Sakabe H, Yokota S, Horiike S, Nakamine H, Nakamura S, Taniwaki M.** Detection of t(14;18) in follicular lymphoma by dual-color fluorescence *in situ* hybridization on paraffin-embedded tissue sections. *Cancer Genet Cytogenet* 2004; **150**: 22-26
- 15 **Maloney S, Smith A, Furst DE, Myerson D, Rupert K, Evans PC, Nelson JL.** Microchimerism of maternal origin persists into adult life. *J Clin Invest* 1999; **104**: 41-47

Gastrointestinal stromal tumor: Computed tomographic features

Chi-Ming Lee, Hsin-Chi Chen, Ting-Kai Leung, Ya-Yen Chen

Chi-Ming Lee, Hsin-Chi Chen, Ting-Kai Leung, Ya-Yen Chen,
Department of Diagnostic Radiology, Taipei Medical University
Hospital, Taipei, Taiwan, China

Correspondence to: Chi-Ming Lee, M.D., 252, WuHsing Street,
110, Taipei, Taiwan, China. yayen0220@yahoo.com.tw

Telephone: +886-2-27372181 Ext. 1131 **Fax:** +886-2-23780943

Received: 2004-01-10 **Accepted:** 2004-02-24

Abstract

AIM: Gastrointestinal stromal tumor (GIST) is a rare type of cancer. Computed tomography (CT) is an imaging modality of choice for diagnosing GIST. The aim of this retrospective study was to review the CT imaging features of 17 GIST patients.

METHODS: From 1995 to 2003, there were 47 patients with pathologically proven GISTs at our hospital. Of these, 17 patients underwent preoperative CT. We collected and analyzed these CT images. The CT imaging features included tumor diameter, number and location, tumor margin, location of metastasis, hounsfield units of tumor and effect of contrasts. In addition, we also recorded the surgical findings, including complications, tumor size and location for comparative analysis.

RESULTS: The results showed that 12 (70%) tumors were located in the stomach and five (30%) were located in the jejunum mesentery. GISTs were extraluminal in 12 (70%) patients. The tumor margins of 13 (76%) tumors were well defined and irregular in four (24%). The effect of contrast enhancement on GIST CT imaging was homogenous enhancement in 13 (76%) and heterogeneous enhancement in four (24%). The hounsfield units (HU) were 30.41 ± 5.01 for precontrast images and postcontrast hounsfield units were 51.80 ± 9.24 .

CONCLUSION: The stomach was the commonest site of GIST occurrence among our patients. The CT features of GIST were well-defined tumor margins, homogenous enhancement on postcontrast CT images.

Lee CM, Chen HC, Leung TK, Chen YY. Gastrointestinal stromal tumor: Computed tomographic features. *World J Gastroenterol* 2004; 10(16): 2417-2418
<http://www.wjgnet.com/1007-9327/10/2417.asp>

INTRODUCTION

The term gastrointestinal stromal tumor (GIST) has traditionally been used as a descriptive term for soft tissue tumors of the gastrointestinal tract. Although their exact incidence is still somewhat unclear, it is now estimated that between 5 000 and 10 000 people each year develop GISTs in the world; men and women are equally affected^[1]. GISTs were previously thought to be smooth muscle neoplasms, and most were classified as leiomyosarcoma. With the advent of immunohistochemistry and electron microscopy, it has become apparent that GIST may have myogenic features (smooth muscle GIST), neural

attributes (gastrointestinal autonomic nerve tumor), characteristics of both muscle and nerve (mixed GIST) or may lack differentiation (GIST not otherwise specified)^[2]. GISTs are often discovered incidentally at surgery and should be completely excised. The increasing use of computed tomography (CT) and endoscopy of the upper gastrointestinal tract is a non-or minimally invasive means for the detection of asymptomatic GISTs^[3].

In this retrospective study, we analyzed our experience with 17 patients with GISTs who were presurgically investigated by using CT and described the anatomic distribution and imaging features of GIST.

MATERIALS AND METHODS

Patients' data

From 1995 to 2003, there were 47 patients with pathologically proven GISTs at Taipei Medical University Hospital (TMUH) and Wan Fang Hospital (WFH). Of these, 17 (8 males, 9 females, with ages ranging from 33 to 91 years, mean age: 64 years) underwent preoperative CT. We collected and analyzed these CT images.

The abdominopelvic CT scans (HiSpeed CT/I; GE Medical Systems, Milwaukee, WI, USA) were typically obtained after oral administration of 1 000 mL 40 g/L iohalamate meglumine (Mallinckrodt, USA) and intravenous administration of 100 mL (350 mg/mL) iohexol (Nycoveien, Norway) at a flow rate of 2 mL/s, with a section thickness of 10 mm and a pitch of 1.5. The CT imaging features included tumor diameter, number and location, tumor margin (well defined, irregular or clearly invasive), location of metastasis, hounsfield units of tumor and effect of contrast. These characteristics were reviewed blindly by three radiology diplomates. In addition, we also recorded the surgical findings, including complications, tumor size and location for comparison.

RESULTS

The CT imaging findings showed that 14 (82%) patients had one tumor and 3 (18%) patients had two tumors. GIST size ranged from 2 to 19 cm (5.4 ± 1.8 cm). Tumors were located in the stomach in 12 (70%) patients and 5 (30%) patients had tumor located in the jejunal mesentery. GISTs were extraluminal in 12 (70%) patients and intraluminal in 5 (30%). GISTs caused intraluminal bowel obstruction in two patients.

The mean precontrast hounsfield units were 30.41 ± 5.01 and the mean postcontrast hounsfield units were 51.80 ± 9.24 . The effect of contrast enhancement on GIST CT imaging was slight enhancement (Figure 1). Thirteen (76%) showed homogenous enhancement and 4 (24%) showed heterogeneous enhancement.

Tumors were well defined in 13 (76%) patients and irregular in 4 (24%) patients. There was no clearly invasive or vascular encasement of tumors among our patients. Three (18%) patients had metastasis, two to the liver and one to the lung. Twelve patients underwent follow-up CT (range of follow-up period from date of diagnosis, 2-40 mo, mean, 22 mo). No patients relapsed.

Operative findings showed that 14 (82%) patients had one tumor and 3 (18%) patients had two tumors. The smallest GIST was 2 cm×2 cm×1.8 cm and the largest was 19 cm×16 cm×8.5 cm in size. The commonest complications among our patients were gastrointestinal tract chronic inflammation, diarrhea and wound

infection. In addition, 17 patients all underwent lymphadenectomies but no metastasis to the lymph nodes was found.

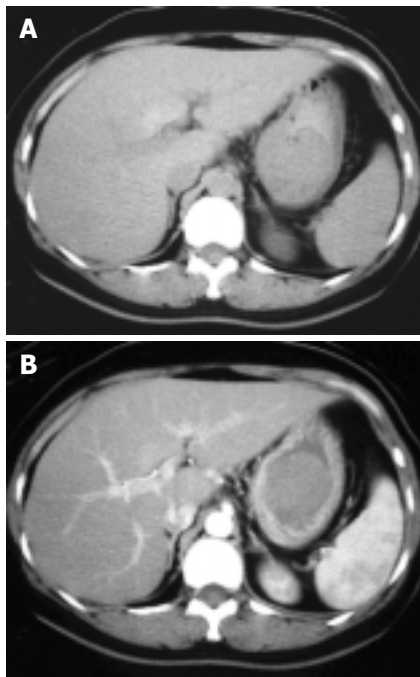


Figure 1 Precontrast and postcontrast CT scans of tumor. A: A precontrast CT scan shows a well-defined intragastric tumor with slightly lower density than the liver. The hounsfield units are 38.77. B: A postcontrast CT scan shows homogenous enhancement of the tumor, with a hounsfield unit of 57.58.

DISCUSSION

The distribution of 725 malignant smooth muscle tumors of the gastrointestinal tract was 47.3% in the stomach, 35.4% in the small intestine, 4.6% in the colon and 7.4% in the rectum, according to Skandalak and Gray^[4]. In the report by Akwari *et al.*^[5], 68.3% of GISTs were in the stomach, 25.4% were in the small intestine, 2.6% were in the colon and 3.7% were in the rectum. According to a previous study^[6], GIST can also occur in the omental and mesenteric tissues, the duodenum and other sites of the gastrointestinal tract. In our study, 12 (70%) patients had tumors located in stomach and five (30%) patients had tumors located in the jejunal mesentery, a distribution more similar to that reported by Akwari *et al.*^[5].

According to our results, the precontrast hounsfield units of the tumors were 30.41 ± 5.01 and the postcontrast hounsfield units were 51.80 ± 9.24 . The postcontrast hounsfield units were 70% higher than the precontrast hounsfield units. Suster^[7] reported hounsfield units of 33.2 ± 1.25 on precontrast imaging and 55.32 ± 5.22 on postcontrast imaging, with 68% enhancement. Ludwig^[8] reported hounsfield units of 34.21 ± 1.33 on precontrast imaging and 56.29 ± 3.12 on postcontrast imaging, with 67% enhancement. We believe that precontrast hounsfield units of 30 to 35 and postcontrast hounsfield units of 50 to 60 are indicative of GISTs on CT.

We analyzed the correlation of contrast type and tumor size. Of the 17 patients, 4 (24%) had heterogeneous contrast enhancement and 13 (76%) had homogenous contrast enhancement. The mean tumor diameter of the heterogeneous tumors was 11.6 ± 2.1 cm and that of the homogenous tumors was 3.8 ± 1.3 cm. We found that large tumor sizes appeared to be related to heterogeneous enhancement. Our result is similar to that of Conlon *et al.*^[9]. In addition, we found tumors in 13 (76%)

of our patients were well-defined, and in Lee's study^[10], more than two-thirds of patients also had well-defined GISTs. Thus, well-defined tumors appear to be a feature of GISTs on CT imaging.

Licht *et al.*^[11] proposed that the relationship between multiple tumors and metastasis needed further investigation. In our study, we had three patients with multiple tumors and also had three patients with metastases. Only one patient with liver metastasis had multiple tumors; the other two patients with metastasis had only single tumor. Our data appear to indicate that there is no evident correlation between multiple tumors and metastasis. Additionally, 3 (18%) of our patients had metastasis compared to other studies^[12,13] in which 20% to 35% of patients had metastasis, but this difference was not statistically significant. Fong *et al.*^[13] reported that the metastasis percentage was related to the degree of lymph node involvement. Based on our surgical findings, all the patients who had metastasis had no lymph node involvement. Thus, our results differed from those reported by Fong.

In conclusion, the stomach was the commonest site of GIST tumor location among our patients, with a mean tumor diameter of 5.4 ± 1.8 cm. The CT features of GISTs included well-defined tumor margins and predominantly homogenous contrast enhancement, with precontrast hounsfield units of 30 to 35 and postcontrast hounsfield units of 50 to 60. According to the percentage presented above, we also found a "4 seventy rule" in our GIST images review: 70% tumors were located in the stomach, 70% tumors were extraluminal, 76% tumor margins were well defined, 76% GIST CT imagings were homogenous enhancement. In addition, metastasis was not related to the degree of lymph node involvement or tumor number in our study.

REFERENCES

- Miettinen M, Monihan JM, Sarlamo-Rikala M. Gastrointestinal stromal tumors/smooth muscle tumors (GISTs) primary in the omentum and mesentery: clinicopathologic and immunohistochemical study of 26 cases. *Am J Surg Pathol* 1999; **23**: 1109-1118
- Mazur M, Clark HB. Gastric stromal tumors: Reappraisal of histogenesis. *Am J Surg Pathol* 1983; **7**: 507-519
- Pidhorecky I, Cheney RT, Kraybill WG, Gibbs JF. Gastrointestinal stromal tumors: current diagnosis, biologic behavior, and management. *Ann Surg Oncol* 2000; **7**: 705-712
- Skandalakis JE, Gray SW. Smooth muscle tumors of the alimentary tract. In: Ariel IM, ed. *Progress in Clinical Cancer*. New York: Grune and Stratton 1965: 692-708
- Akwari OE, Dozois RR, Weiland LH, Beahrs OH. Leiomyosarcoma of the small and large bowel. *Cancer* 1978; **42**: 1375-1384
- Lewis JJ, Leung D, Woodruff JM, Brennan MF. Retroperitoneal soft-tissue sarcoma: analysis of 500 patients treated and followed at a single institution. *Ann Surg* 1998; **228**: 355-365
- Suster S. Gastrointestinal stromal tumors. *Semin Diag Pathol* 1996; **13**: 297-313
- Ludwig DJ, Traverso LW. Gut stromal tumors and their clinical behavior. *Am J Surg* 1997; **173**: 390-394
- Conlon KC, Casper ES, Brennan MF. Primary gastrointestinal sarcomas: analysis of prognostic variables. *Ann Surg Oncol* 1995; **2**: 26-31
- Lee YT. Leiomyosarcoma of the gastrointestinal tract: general pattern of metastasis and recurrence. *Cancer Treat Rev* 1983; **10**: 91-101
- Licht JD, Weissmann LB, Antman K. Gastrointestinal sarcomas. *Semin Oncol* 1988; **15**: 181-188
- Lindsay PC, Ordonez N, Raaf JH. Gastric leiomyosarcoma: clinical and pathological review of fifty patients. *J Surg Oncol* 1981; **18**: 399-421
- Fong Y, Coit DG, Woodruff JM, Brennan MF. Lymph node metastasis from soft tissue sarcoma in adults. Analysis of data from a prospective database of 1772 sarcoma patients. *Ann Surg* 1993; **217**: 72-77

Effect of parenteral and enteral nutrition combined with octreotide on pancreatic exocrine secretion of patients with pancreatic fistula

Huan-Long Qin, Zhen-Dong Su, Yang Zou, You-Ben Fan

Huan-Long Qin, Zhen-Dong Su, Yang Zou, You-Ben Fan,
Department of Surgery, Sixth People's Hospital, Shanghai Jiaotong University, Shanghai 200233, China

Supported by the Shanghai Science Foundation for Distinguished Young Scholars, No.99QB14010

Correspondence to: Huan-Long Qin, Department of Surgery, Sixth People's Hospital, Shanghai Jiaotong University, Shanghai 200233, China. jiaqc@online.sh.cn

Telephone: +86-21-64368920 **Fax:** +86-21-64368920

Received: 2003-12-10 **Accepted:** 2004-01-15

Abstract

AIM: To evaluate the effect of parenteral and enteral nutrition combined with octreotide on pancreatic exocrine secretion of the patients with pancreatic fistula.

METHODS: Pancreatic juice, drained directly from the pancreatic fistula, was collected, and the volume, protein, amylase, HCO_3^- , K^+ , Na^+ and Cl^- were determined on d 1, 4 and 7 before and after 7-d treatment with octreotide, respectively.

RESULTS: No differences in exocrine pancreatic secretion were observed during the enteral and parenteral nutrition period ($t = 2.03$, $P > 0.05$); there were significant decreases in pancreatic juice secretion volume, protein, amylase, HCO_3^- , K^+ , Na^+ and Cl^- after parenteral and enteral nutrition combined with octreotide compared with octreotide pretreatment ($t = 4.14$, $P < 0.05$).

CONCLUSION: There is no stimulatory effect on the pancreatic secretion by intrajejunal nutrition and parenteral nutrition. Octreotide is effective on the reduction of pancreatic fistula output.

Qin HL, Su ZD, Zou Y, Fan YB. Effect of parenteral and enteral nutrition combined with octreotide on pancreatic exocrine secretion of patients with pancreatic fistula. *World J Gastroenterol* 2004; 10(16): 2419-2422

<http://www.wjgnet.com/1007-9327/10/2419.asp>

INTRODUCTION

Since the 1960 s, parenteral nutrition (PN) has been the dominant mode for administering postoperative nutritional support. PN and enteral nutrition (EN) have been successfully used to treat varied severe diseases^[1,2]. But in patients who are recovering from pancreatitis or who have a pancreatic fistula, efforts should be made to avoid stimulation of pancreatic secretion. More recent experimental studies and clinical findings about small intestinal motility and absorption, the development of needle-catheter jejunostomy, and the appearance of new diets have given impetus to the use of enteral feeding for early postoperative nutritional support and the use of octreotide to inhibit pancreatic fistula^[3-5]. During application of enteral feeding, the question arises. How the pancreatic secretion was influenced by EN

administered into the second jejunal loop? Can the more expensive and less physiological PN be replaced by this method^[2]? Since the exocrine function of the pancreas is stimulated by the vagus nerve and the release of gastrointestinal hormones in response to food, there might be no significant increase in the exocrine activity of the pancreas. Animal experiments supported this supposition^[6,7]; however, perfusion of distal jejunum with essential amino acids in human and infusion of carbohydrate into the ileum in human and dog enhanced pancreatic enzyme secretion. The present study was to evaluate the effect of parenteral and EN combined with octreotide on pancreatic secretion of the patients with pancreatic fistula by determining the levels of pancreatic secretion, amylase and electrolytes.

MATERIALS AND METHODS

Patients and groups

Seventeen patients (12 male and 5 female; mean age 43 years, range 27 to 71 years) with pancreatic fistula after abdominal injury or operation from July 1997 to March 2003 were recruited and randomly divided into PN group ($n = 9$) and EN group ($n = 8$). It included pancreatic fistula after pancreas injury in 8 cases, pancreatic body and tail tumor resection in 5 cases, pancreatoduodenectomy in 4 cases.

Parenteral nutritional support

Nine cases with pancreatic fistula 3-5 d postoperatively were supported by PN for 2 wk. In the first wk, they received only PN. In the second week they received PN and octreotide. The target of nutritional therapy was to provide 20-25 kcal/(kg·d) non-protein diet and 0.12-0.15 g protein/(kg·d), the ratio of calories to nitrogen was (100-120):1. PN was given through continuous infusion (14 h/d) of a mixture of 200 mL/L Intralipid or 200 mL/L Lipofundin (B. Braun), 500 g/L glucose and 70 g/L Vamin and branched-chain amino acid. Seizure energy index of glucose to fat emulsion was 1:1. Multivitamins and electrolytes were also administered into total PN (TPN) solutions. Insulin was supplemented into PN at a ratio of glucose vs insulin 6:1. Six patients received TPN through right subclavian vein, 3 cases through right jugular vein. TPN was infused initially at a rate of 40 mL/h and was increased by 20 mL/h every 4 h. Antibiotics were infused by another peripheral vein. The liver and renal function, bicarbonate, serum glucose, fat metabolism were measured every other day. Human albumin, plasma and fresh blood were infused according to the patient's condition. Octreotide 0.3 mg/500 mL saline was infused continuously for 8 h in the second wk and 0.1 mg octreotide was injected subcutaneously at 8:00 pm per day for 7 d.

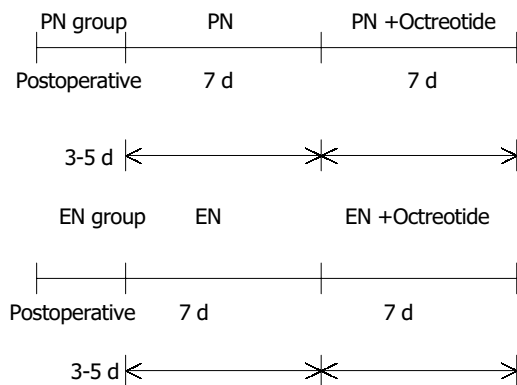
EN

Eight cases with pancreatic fistula were administered EN 3-5 d postoperatively. Nutrison (Nutricia) was used. Enteral feeding included 2 cases of nasoduodenal tube feeding, 4 cases of jejunectomy, and 2 cases of endoscopically placed nasojejunal tube. The jejunum through jejunostomy catheter was infused 250 mL Nutrison and 500 mL 9 g/L saline during days 1-3; Nutrison 500-1 000 mL and 500 mL milk or vegetable soup were infused for 10-14 d. The infusion rate was controlled by a

microcomputer-pump (Nutricia). During EN, inadequate calories and nitrogen were supplemented by partial PN. Octreotide 0.3 mg/500 mL saline was continuously infused for 8 h in the second week, 0.1 mg octreotide was injected subcutaneously at 8:00 pm per day for 7 d.

Observation samples

Pancreatic juice was collected on ice from the fistula during PN or EN and on d 1, 4, 7 before and after using octreotide, respectively. Samples were stored at -20 until amylase and protein content of the fractions were measured by established methods. Experimental procedures are shown as below.



Statistical analysis

Data were collected by two persons blinded to the patients and presented as mean±SD. Statistical significance was evaluated using *t* test by SPSS 10.0 statistical-software, and a *P* value less than 0.05 was considered significant.

RESULTS

Effect of PN and/or EN on pancreatic juice, protein and amylase secretion

Though pancreatic juice, protein and amylase in EN group were slightly increased as compared with PN group, there were no significant changes between the two groups at the first wk (*P*>0.05). During the second wk, the pancreatic juice, protein, amylase decreased markedly from 79.6 mL/d to 60.8 mL/d, 31 mg/L to 22.8 mg/L and 4 220 U/L to 3 270 U/L, respectively, and there was a significant statistical difference as compared with

that of pre-using octreotide in PN group (*P*<0.05). During EN combined with octreotide, the pancreatic juice, protein, amylase secretion decreased significantly from 87.9 mL/d to 65.3 mL/d, 36 mg/L to 29.1 mg/L, and 4 440 U/L to 3670 U/L, respectively, and there is a statistical difference as compared with that of pre-using octreotide (*P*<0.05); but there was no statistical difference between two groups after using octreotide (*P*>0.05).

Effect of PN and/or EN combined with octreotide on HCO₃⁻, K⁺, Na⁺, Cl⁻ secretion in pancreatic juice

During the first wk, there were no differences in HCO₃⁻, K⁺, Na⁺ and Cl⁻ secretion in pancreatic juice between the two groups. After PN combined with octreotide, HCO₃⁻, K⁺, Na⁺, and Cl⁻ secretion decreased markedly, from 71 mmol/d to 45 mmol/d, 30 mmol/L to 21 mmol/L, 130 mmol/L to 87 mmol/L, and 60 mmol/L to 45 mmol/L, respectively, and there was a statistical difference as compared with that of pre-using octreotide, respectively (*P*<0.05). During EN supporting, there were no differences in HCO₃⁻, K⁺, Na⁺ and Cl⁻ secretion in pancreatic juice as compared with PN. During the second wk, HCO₃⁻, K⁺, Na⁺, and Cl⁻ secretion in EN group decreased significantly, from 79 mmol/d to 52 mmol/d, 35 mmol/L to 25 mmol/L, 135 mmol/L to 94 mmol/L, and 74 mmol/L to 54 mmol/L, respectively, there was a statistical difference as compared with that of pre-using octreotide (*P*<0.05); but there was no statistical difference between two groups after using octreotide (*P*>0.05).

DISCUSSION

As many as 50-70% of patients underwent enterocutaneous pancreatic fistulas after operation^[5]. High-out fistulas (more than 200 mL daily) result in significant loss of fluid, alteration in acid-base status and malnutrition. In addition, digestive enzymes, often of extreme pH, can cause inflammation and soft tissue or skin destruction along the fistula tract. These increase the risk of infection and hemorrhage, prolong the time required for spontaneous fistula closure and increase postoperative mortality rates. Conservative management of enterocutaneous pancreatic fistula, including TPN, skin care and infection control, succeeds in a spontaneous closure rate of 24-73%^[5-10]. However, such treatment is often of long duration (2-3 mo) and high cost, and is associated with considerable morbidity. In cases in which maximal medical treatment has failed, re-operation for fistula closure is required.

Table 1 Effect of PN and/or EN combined with octreotide on pancreatic juice, protein and amylase secretion

Group	n	Pancreatic juice (mL/d)			Protein (mg/L)			Amylase (U/L)		
		d 1	d 4	d 7	d 1	d 4	d 7	d 1	d 4	d 7
PN	9	86±35	77±49	81±31	34±17	30±17	29±17	4 268±1 361	4 026±1 131	4 468±1 487
PN+Oc- treotide	9	64±21 ^a	58±19 ^a	60±23 ^a	25±17 ^a	21±17 ^a	23±17 ^a	3 268±1 031 ^a	3 342±1 116 ^a	3 081±1 213 ^a
EN	8	91±73	81±73	93±73	36±24	37±24	35±24	4 761±987	4 361±1 023	4 276±912
EN+Oc- treotide	8	67±29 ^c	61±39 ^a	66±34 ^a	27±12 ^a	31±17	30±10	3 963±1 104 ^a	3 566±1 001 ^a	3 363±1 221 ^a

Oct: Octreotide; ^a*P*<0.05 vs PN group; ^c*P*<0.05 vs EN group.

Table 2 Effect of PN and/or EN combined with octreotide on HCO₃⁻, K⁺, Na⁺ and Cl⁻ secretion in pancreatic juice (mmol/L)

Group	n	HCO ₃ ⁻			K ⁺			Na ⁺			Cl ⁻		
		d 1	d 4	d 7	d 1	d 4	d 7	d 1	d 4	d 7	d 1	d 4	d 7
PN	9	73±37	69±31	71±32	32±19	28±12	31±17	123±33	133±31	126±43	61±34	63±31	58±24
PN+Oct	9	54±34 ^a	57±24 ^a	59±31 ^a	22±11 ^a	19±9 ^a	21±17 ^a	87±53 ^a	78±67 ^a	93±55 ^a	49±13 ^a	42±21 ^a	49±17 ^a
EN	8	79±44	81±35	83±47	37±17	36±13	34±19	131±44	129±33	139±28	73±37	71±43	68±31
EN+Oct	8	65±23 ^c	61±33 ^c	57±37 ^c	25±15 ^c	28±11 ^c	28±13	101±63 ^c	95±79 ^c	91±73 ^c	51±15 ^c	49±21 ^c	53±35 ^c

Oct: Octreotide; ^a*P*<0.05 vs PN group; ^c*P*<0.05 vs EN group.

In theory, reduction of fistula output should promote the chances of spontaneous closure. This is usually achieved by restriction of oral intake, sometimes supplemented with nasogastric suction in order to relieve the burden of gut and pancreas. Pharmacological attempts to decrease intestinal secretions involve using drugs such as somatostatin, loperamide, atropine or pirenzepine, and H₂ blockers such as omeprazole. Although the effectiveness of such treatments has yet to be confirmed^[7]. In clinics, PN or EN is usually considered, and they may play an important role in the spontaneous closure of pancreatic fistula, but there is some controversy over their effectiveness and safety.

Effect of PN on pancreatic exocrine secretion

TPN with complete gut rest has been proposed as adjuvant therapy in the treatment of severe acute pancreatitis, to meet metabolic demands and relieve pancreas. A decrease in volume of pancreatic secretion and, in particular, its enzymatic content would likely have a beneficial effect on patient's clinical course. That TPN decreases pancreatic activity is supported by several animal studies. Hamilton *et al.* documented a marked decrease in pancreatic secretions of the normal dog pancreas stimulated maximally by secretion and pancreozymin with the institution of TPN. The volume of pancreatic secretion decreased by 50% and amylase secretion decreased by 71%, but there was a slight increase in bicarbonate excretion. Adler, in 1975, demonstrated that intravenous administration of hypertonic solutions including 50% dextrose resulted in a 24% decrease in pancreatic secretion and a 69% decrease in biliary secretion in a maximally secretin- and pancreozymin-stimulated dog model. PN for patients with pancreatitis has, in general, shown no adverse or beneficial effects on the course of pancreatitis but has provided adequate nutritional support.

The use of intravenous lipid formulations in patients with pancreatic fistula remains controversial despite the evidence that they are not harmful. Kelly and Nahrwold^[11] compared the exocrine pancreatic secretory response to intravenous saline and PN in dogs with chronic gastric fistula and found that the latter produced a small but significant increase in the mean volume of pancreatic juice (2.4 vs 1.8 mL per 15 min; $P < 0.05$) with a slight increase in mean protein and bicarbonate secretions. These differences are minimal compared with the changes found in dogs receiving an intraduodenal infusion of an enteral diet. Hamiloon reported that PN could ameliorate stimulation to the pancreas. The output of the pancreatic juice decreased by 50%, that of amylase by 71% and that of glucose slightly increased. Another canine with chronic pancreatic fistula and stomach ectomy received fat emulsion infusion. Meanwhile, the canine received stimulation of secretin. The results showed that pancreatic juice, protein enzyme, total protein and HCO₃⁻ did not change during infusion of fat emulsion^[12]. Patients with pancreatic fistula postoperative of gastrectomy received PN by administration of 640 mL or 840 mL 100 g/L Liposym for 8 d, the pancreatic juice, protein and HCO₃⁻ did not increase^[13]. Klein *et al.*^[14] believed that the effects of different PN contents on the pancreatic juice, HCO₃⁻ and amylase secretion were different. Intralipid could increase pancreatic juice from 33 mL/h to 39 mL/h, HCO₃⁻ from 44.5 mmol/L to 54.5 mmol/L, amylase from 25 000 U/L to 32 000 U/L. They held that fat emulsion should be used to supplement essential fatty acid. In the present study, 250 mL 200 mL/L Intralipid or 200 mL/L Lipofundin per day was used as fat energy sources for 2 wk. The results showed that pancreatic juice, protein, amylase, HCO₃⁻, K⁺, Na⁺ and Cl⁻ secretion did not change. It suggested that PN could not stimulate pancreatic secretion, and supplemental fat emulsion was safety.

Effect of EN on pancreatic secretion

The presence of food in the stomach and duodenum elicits

gastropancreatic and duodenopancreatic reflexes that result in stimulation of pancreatic exocrine secretion. However, these effects are not pronounced when nutrients are delivered directly into jejunum.

A study^[15] in dogs showed that intragastric delivery of nutrients caused an increase in the volume, and protein and bicarbonate content of pancreatic secretions compared with those in saline-infused controls. Intraduodenal feeding increased the volume of pancreatic secretions but did not affect protein or bicarbonate secretion. Other studies^[16] in dogs also showed that the intraduodenal administration of elemental diets or pure amino acid solutions significantly increased pancreatic secretions, suggesting that the amino acid content of elemental diets is responsible for the stimulatory effects. In contrast, intrajejunal delivery of nutrients was not associated with a significant change in the volume, or protein or bicarbonate content of pancreatic secretions compared with controls. These authors also found in one human subject that avoidance of cephalic, gastric, and duodenal stimuli by jejunal tube feeding of acids did not result in pancreatic stimulation. Another canine study^[17], in which an elemental diet was fed into the proximal jejunum, demonstrated a brisk pancreatic secretory response. However, the pancreatic juice collected was watery and low in enzyme. They concluded that bypassing the stomach minimized acid secretion, which played an important role in keeping the pancreas at rest. Bodoky *et al.*^[18] randomized 12 patients undergoing pylorus-preserving pancreaticoduodenectomy for chronic pancreatitis to receive EN via a needle catheter feeding jejunostomy (7 patients) or PN (5 patients). A catheter placed during operation in the pancreatic duct was used to collect pancreatic secretions. The authors believed that the disease was mainly in the pancreatic head and that the function of the pancreatic remnant was nearly normal. They did not find any difference in the volume of pancreatic secretions or the content of bicarbonate, protein, chymotrypsin or amylase between the two groups.

In the present study, 8 patients received EN for 2 wk, during which the volume of pancreatic juice, protein, amylase and bicarbonate in EN group had a small but not significant increase as compared with PN group. Although there is a paucity of human studies on the effects of oral feeding and EN on pancreatic secretion, one might reasonably conclude from available evidence from human and canine studies that oral, intragastric and intraduodenal feeding produce a significant stimulation of pancreatic secretions. In contrast, intrajejunal feeding has much fewer stimulatory effects and is therefore the route of choice for enteral feeding in pancreatic diseases.

Effect of octreotide on pancreatic juice exocrine secretion

Discovered in 1972, somatostatin is a naturally occurring tetradecapeptide with a wide spectrum of inhibitory biological actions. Within the gastrointestinal tract, somatostatin has been found in the pancreas, stomach, intestinal mucosa and mesenteric neurons. Because of its inhibitory actions, it has been used in the management of upper gastrointestinal haemorrhage, secretory diarrhoea, dumping syndrome and peptide-secreting tumors. Since the mid-1980 s, somatostatin has been advocated as an adjuvant therapy in the conservative treatment of patients with enterocutaneous pancreatic fistula^[19,20]. However, its short half-life (1.1-3.0 min) mandates continuous administration. Long-acting somatostatin analogues, such as octreotide acetate and lanreotide, have been developed. Octreotide has a biological half-life of 90-120 min and can be administered subcutaneously two or three times per day. Compared with somatostatin, it not only significantly reduces the secretions of the pancreas and stomach, but also has a more selective range of targets. Both somatostatin and octreotide have been described as effective treatments for

enteric fistulas in adults, with few severe short-term side-effects (mostly diarrhoea, flushing and abdominal pain). These preparations have, therefore, the potential benefit of cutting the cost of treatment and reducing the discomfort of patients by shortening the length of hospital stay. Since 1990, several groups have described favourable results using somatostatin or octreotide for the "conservative" management of enterocutaneous pancreatic fistula. Administration of such drugs has been reported to result in rapid and significant reduction of fistula output (often within 24 h of treatment) and acceleration of fistula closure (from as early as day 2)^[21-25].

Martineau *et al.*^[4] reviewed the role of octreotide for the management of established enterocutaneous pancreatic fistulas by summarizing the results of 4 randomized trials and 8 case series. They concluded that octreotide significantly decreased enterocutaneous pancreatic fistula output, but did not significantly improve the rate of spontaneous fistula closure. Furthermore, octreotide did not seem to reduce the output, or hasten the time or rate of closure, in fistula of recent onset (less than 8 d). Recently, Berberat *et al.*^[8] reviewed six randomized controlled trials and one open randomized trial, and assessed the efficacy of octreotide on preventing postoperative complications in patients underwent major pancreatic operations. They concluded that prophylactic use of octreotide could significantly reduce the complication rate. Sitges-Serra^[9] reported that 20 cases with pancreatic fistula received octreotide 10 µg/8 h for 20 d (*n* = 13). The output of pancreatic juice decreased from 725 mL/24 h to 151 mL/24 h, the rate of spontaneous fistula closure was 78%. Another group (*n* = 7) used octreotide 100 µg/8 h for 7 d. The output of pancreatic juice increased from 218 mL/24 h to 436 mL/24 h. Torres^[26] reported 33 patients with pancreatic fistula received octreotide 75-100 µg/8 h for 10 d, and then stopped. It resulted in increase of pancreatic juice secretion from 228 mL/24 h to 498 mL/24 h. After 6 h, octreotide was used again. Output of pancreatic juice decreased from 828 mL/24 h to 247 mL/24 h, the rate of spontaneous fistula closure was 79%. The time of spontaneous fistula closure of octreotide group was 2-10 d shorter than that of control group. In the present study, the patients with pancreatic fistula received octreotide combined with PN and EN, the secretion of pancreatic juice, protein and amylase was decreased, and secretion of HCO₃⁻, K⁺, Na⁺ and Cl⁻ was inhibited. These results showed that octreotide can inhibit pancreatic juice, amylase secrete, and maybe beneficial to pancreatic fistula self-repair.

We conclude that administration of nutrient solutions into second jejunal loop does not overstimulate the exocrine function of pancreas, while it produces equivalent results to parenteral administration of nutrients. The enteral feeding combined with octreotide could be effective and safe to reduce pancreatic fistula output.

REFERENCES

- 1 **Kalfarentzos FE**, Karavias DD, Karatzas TM, Alevizatos BA, Androulakis JA. Total parenteral nutrition in severe acute pancreatitis. *J Am Coll Nutr* 1991; **10**: 156-162
- 2 **Buchman AL**, Moukarzel AA, Bhutta S, Belle M, Ament ME, Eckhart CD, Hollander D, Gornbein J, Kopple JD, Vijayaraghavan SR. Parenteral nutrition is associated with intestinal morphologic and functional changes in humans. *J Parenter Enteral Nutr* 1995; **19**: 453-460
- 3 **Dorta G**. Role of octreotide and somatostatin in the treatment of intestinal fistulae. *Digestion* 1999; **60**(Suppl 2): 53-56
- 4 **Martineau P**, Shwed JA, Denis R. Is octreotide a new hope for enterocutaneous and external pancreatic fistulas closure? *Am J Surg* 1996; **172**: 386-395

- 5 **De Graef J**, Woussen-Colle MC. Physiological control and pharmacological inhibition of digestive secretions. *Acta Chir Belg* 1985; **85**: 149-153
- 6 **Qin HL**, Su ZD, Hu LG, Ding ZX, Lin QT. Effect of early intrajejunal nutrition on pancreatic pathological features and gut barrier function in dogs with acute pancreatitis. *Clin Nutr* 2002; **21**: 469-473
- 7 **Qin HL**, Su ZD, Hu LG, Ding ZX, Lin QT. Parenteral versus early intrajejunal nutrition: Effect on pancreatic natural course, entero-hormones release and its efficacy on dogs with acute pancreatitis. *World J Gastroenterol* 2003; **9**: 2270-2273
- 8 **Berberat PO**, Friess H, Uhl W, Buchler MW. The role of octreotide in the prevention of complications following pancreatic resection. *Digestion* 1999; **60**(Suppl 2): 15-22
- 9 **Sitges-Serra A**, Guirao X, Pereira JA, Nubiola P. Treatment of gastrointestinal fistulas with Sandostatin. *Digestion* 1993; **54**(Suppl 1): 38-40
- 10 **Voss M**, Ali A, Eubanks WS, Pappas TN. Surgical management of pancreaticocutaneous fistula. *J Gastrointest Surg* 2003; **7**: 542-546
- 11 **Kelly GA**, Nahrwold DL. Pancreatic secretion in response to an elemental diet and intravenous hyperalimentation. *Surg Gynecol Obstet* 1976; **143**: 87-91
- 12 **Burns GP**, Stein TA. Pancreatic enzyme secretion during intravenous fat infusion. *J Parenter Enteral Nutr* 1987; **11**: 60-62
- 13 **Edelman K**, Valenzuela JE. Effect of intravenous lipid on human pancreatic secretion. *Gastroenterology* 1983; **85**: 1063-1066
- 14 **Klein E**, Shnebaum S, Ben-Ari G, Dreiling DA. Effects of total parenteral nutrition on exocrine pancreatic secretion. *Am J Gastroenterol* 1983; **78**: 31-33
- 15 **Ragins H**, Levenson SM, Signer R, Stamford W, Seifter E. Intrajejunal administration of an elemental diet at neutral pH avoids pancreatic stimulation. Studies in dog and man. *Am J Surg* 1973; **126**: 606-614
- 16 **Wolfe BM**, Keltner RM, Kaminski DL. The effect of an intraduodenal elemental diet on pancreatic secretion. *Surg Gynecol Obstet* 1975; **140**: 241-245
- 17 **Cassim MM**, Allardyce DB. Pancreatic secretion in response to jejunal feeding of elemental diet. *Ann Surg* 1974; **180**: 228-231
- 18 **Bodoky G**, Harsanyi L, Pap A, Tihanyi T, Flautner L. Effect of enteral nutrition on exocrine pancreatic function. *Am J Surg* 1991; **161**: 144-148
- 19 **Gray M**, Jacobson T. Are somatostatin analogues (octreotide and lanreotide) effective in promoting healing of enterocutaneous fistulas? *J Wound Ostomy Continence Nurs* 2002; **29**: 228-233
- 20 **Voss M**, Pappas T. Pancreatic fistula. *Curr Treat Options Gastroenterol* 2002; **5**: 345-353
- 21 **Li-Ling J**, Irving M. Somatostatin and octreotide in the prevention of postoperative pancreatic complications and the treatment of enterocutaneous pancreatic fistulas: a systematic review of randomized controlled trials. *Br J Surg* 2001; **88**: 190-199
- 22 **Takacs T**, Hajnal F, Nemeth J, Lonovics J, Pap A. Stimulated gastrointestinal hormone release and gallbladder contraction during continuous jejunal feeding in patients with pancreatic pseudocyst is inhibited by octreotide. *Int J Pancreatol* 2000; **28**: 215-220
- 23 **Duerksen DR**, Bector S, Yaffe C, Parry DM. Does jejunal feeding with a polymeric immune-enhancing formula increase pancreatic exocrine output as compared with TPN? A case report. *Nutrition* 2000; **16**: 47-49
- 24 **Stabile BE**, Borzatta M, Stubbs RS. Pancreatic secretory responses to intravenous hyperalimentation and intraduodenal elemental and full liquid diets. *J Parenter Enteral Nutr* 1984; **8**: 377-380
- 25 **Grant JP**, Davey-McCrae J, Snyder PJ. Effect of enteral nutrition on human pancreatic secretions. *J Parenter Enteral Nutr* 1987; **11**: 302-304
- 26 **Torres AJ**, Landa JJ, Moreno-Azcoita M, Arguello JM, Silecchia G, Castro J, Hernandez-Merlo F, Jover JM, Moreno-Gonzales E, Balibrea JL. Somatostatin in the management of gastrointestinal fistulas. A multicenter trial. *Arch Surg* 1992; **127**: 97-99

Risk factors for alcoholic liver disease in China

Xiao-Lan Lu, Jin-Yan Luo, Ming Tao, Yan Gen, Ping Zhao, Hong-Li Zhao, Xiao-Dong Zhang, Nei Dong

Xiao-Lan Lu, Jin-Yan Luo, Ping Zhao, Hong-Li Zhao, Xiao-Dong Zhang, Nei Dong, Department of Gastroenterology, Second Hospital of Xi'an Jiaotong University, Xi'an 710004, Shaanxi Province, China
Ming Tao, Department of Epidemiology, Medical College of Xi'an Jiaotong University, Xi'an 710061, Shaanxi Province, China
Yan Gen, Department of Clinical Laboratory, Second Hospital of Xi'an Jiaotong University, Xi'an 710004, Shaanxi Province, China
Supported by the Scientific Foundation of Ministry of Health of China, No.98-1-236

Correspondence to: Dr. Xiao-Lan Lu, Department of Gastroenterology, Second Hospital of Xi'an Jiaotong University, 157 Xiwulu, Xi'an 710004, Shaanxi Province, China. xiaolan-lu@163.com

Telephone: +86-29-87768926 **Fax:** +86-29-87678758

Received: 2003-11-13 **Accepted:** 2003-03-29

Abstract

AIM: To examine the association of daily alcohol intake, types of alcoholic beverage consumed, drinking patterns and obesity with alcoholic liver disease in China.

METHODS: By random cluster sampling and a 3-year follow-up study, 1 270 alcohol drinkers were recruited from different occupations in the urban and suburban areas of Xi'an City. They were examined by specialists and inquired for information on: Medical history and family medical history, alcohol intake, types of alcoholic beverage consumed, drinking patterns by detailed dietary questionnaires. Routine blood tests and ultrasonography were done.

RESULTS: Multivariate analysis showed that: (1) The risk threshold for developing alcoholic liver disease was ingestion of more than 20 g alcohol per day, keeping on drinking for over 5 years in men. The highest OR was at the daily alcohol consumption ≥ 160 g, the occurrence rate of ALD amounted to 18.7% ($P < 0.01$). No ALD occurred when ingestion of alcohol was less than 20 g per day. (2) 87.9% of all drank only at mealtimes. The cumulative risk of developing ALD was significantly higher in those individuals who regularly drank alcohol without food than in those who drank only at mealtimes, especially for those who regularly drank hard liquors only and multiple drinks ($P < 0.05$). (3) The alcohol consumption in those with BMI ≥ 25 was lower than in those with BMI < 25 , but the risk increased to 11.5%, significantly higher than that of general population, 6.5% ($P < 0.01$). (4) Abstinence and weight reduction could benefit the liver function recovery.

CONCLUSION: In the Chinese population the ethanol risk threshold for developing ALD is 20 g per day, and this risk increases with increased daily intake. Drinking 20 g of ethanol per day and for less than 5 years are safe from ALD. Drinking alcohol outside mealtimes and drinking hard liquors only and multiple different alcohol beverages both increase the risk of developing ALD. Obesity also increases the risk. Abstinence and weight reduction will directly affect the prognosis of ALD. Doctor's strong advice might influence the prognosis indirectly.

Lu XL, Luo JY, Tao M, Gen Y, Zhao P, Zhao HL, Zhang XD, Dong N. Risk factors for alcoholic liver disease in China. *World J Gastroenterol* 2004; 10(16): 2423-2426

<http://www.wjgnet.com/1007-9327/10/2423.asp>

INTRODUCTION

Alcoholic liver disease (ALD) is a major health and economic problem in the Western world^[1-5]. Over 14 million Americans are alcohol abusers or alcohol dependent. The problem in China is not as serious as that in Western world. But in recent years, along with the improved living standard and increased alcohol consumption, the morbidity of ALD has risen quickly. Among drinkers, the morbidity has reached 6.1%^[6]. Therefore, ALD has become an increasingly serious disease risk in health care. However, not all drinkers are ALD patients, and there is different susceptibility to damage by alcohol in individuals^[5]. As a common problem, some of its risk factors have been reported in Western countries, but recent analyses have confirmed that geographic and racial variations are evident. In China, however, there is no such study to confirm the main risk factors of ALD, such as cumulative alcohol intake, drinking patterns, types of alcoholic beverage ingested and obesity. In the present study, we aimed to analyze these factors according to random cluster sampling data and a 3-year follow-up study.

MATERIALS AND METHODS

Subjects

We recruited 1 270 drinkers from different occupations in the urban and suburban areas of Xi'an City by random cluster sampling. Every participant was examined by medical staff and received detailed inquiry at his or her home. The medical staff members were trained before the beginning of the study in order to be able to administer the questionnaire uniformly. The questions included: (1) An extensive medical history, including previous diagnosis of chronic liver disease and family medical history. (2) Evaluation of alcohol intake, including detailed questions on the use of alcoholic beverages, types of alcoholic beverage consumed, drinking patterns, the duration of use and the time of drinking (at mealtimes or without food). All the questions were also validated by cross-checking with family members. (3) A detailed physical examination, the body mass index (BMI) and ultrasonography were also performed and recorded. (4) Blood samples were taken to check serum alanine aminotransferase (ALT), serum aspartate aminotransferase (AST), γ -glutamyl transferase (GGT), hepatitis B (HBsAg) and anti-hepatitis C virus (anti-HCV). (5) Three years later, all the patients were investigated again, including detailed inquiry about their relevant diseases and alcohol intake in the past 3 years. Meanwhile, the BMI, ultrasonography and blood samples were taken again.

Diagnosis

The diagnosis of ALD was confirmed according to the published data^[6].

Statistical analysis

Statistical analysis was performed with SPSS 10.0 statistical

package. A logistic-regression model was used in the multivariate modeling of associations. All the factors for which the *P* value of univariate and discriminant analysis was less than 0.05 were entered in the model. Odds ratios (ORs) and 95% confidence intervals (CI) were also calculated.

RESULTS

Study population

Of the 1 270 drinkers, 83 were ALD patients including 72 cases of alcoholic fatty liver, 6 cases of alcoholic hepatitis, and 4 cases of alcoholic cirrhosis. Only one woman was excluded from the study. None of the patients took any medicine in latest 3 mo. Anti-HCV and HBsAg were all negative. Three years later, 66 of 82 ALD subjects were reinvestigated, constituting 80.5% of all. Of the 66 ALD, 19 subjects had BMI \geq 25 and 47 subjects had BMI less than 25.

Daily alcohol consumption and ALD

Analysis of the data showed that the risk of having ALD was significant with a daily alcohol intake higher than 20 g (Table 1) and the mean duration of drinking longer than 5 years. Above this threshold, the OR for ALD increased proportionally with daily alcohol consumption. The highest OR (10.7, $P < 0.01$) occurred when daily consumption exceeded 160 g. At this highest level of alcohol intake, the percentage of subjects with ALD was 18.7%, significantly higher than that of the lowest level of alcohol intake of less than 20 g/d. Among these subjects whose daily alcohol consumption was less than 20 g and the duration of drinking was less than 5 years, no ALD occurred. So we can assume that daily intake of 20 g alcohol for 5 years is the risk threshold. With longer duration of drinking (more than 10-15 years), a few cases occurred even though the daily intake was less than 20 g, but the morbidity was very low, only 2.2%.

Table 1 Average daily alcohol intake and duration of drinking

Alcohol intake (g/d)	<i>n</i>	<5 yr	\geq 5-9 yr	\geq 10-14 yr	\geq 15-19 yr	\geq 20 yr	Total	OR (95% CI)
<20	780	0	1	3	5	8	17 (2.2%)	—
\geq 20-39	217	1	2	6	6	10	25 (11.4%)	5.5 (2.9-12.3)
\geq 40-79	149	1	6	4	3	6	20 (13.5%)	7.1 (3.5-13.6)
\geq 80-159	76	1	3	2	1	4	11 (14.6%)	8.4 (4.1-17.3)
\geq 160	48	1	1	2	1	4	9 (18.7%)	10.7 (5.2-23.4)
Total	1 270	4 (1.5%)	13 (4.4%)	17 (6.9%)	16 (11.3%)	32 (9.4%)	82 (6.5%)	

$P < 0.01$, vs group of alcohol intake < 20 g/d.

Table 2 Different drinking habits and types of alcoholic beverage

Type of beverage	<i>n</i>	With meals only			At any time			χ^2
		Daily intake (g)	<i>n</i> (%)	Patients (%)	Daily intake (g)	<i>n</i> (%)	Patients (%)	
Beer	390	6.1 \pm 3.7	351 (90.0)	2 (0.57)	8.9 \pm 4.3	39 (10.0)	0 (0.00)	
Wine	132	10.8 \pm 5.3	118 (89.4)	1 (0.84)	19.2 \pm 9.6	14 (10.6)	1 (7.1)	3.32
Hard liquor	491	45.2 \pm 15.9	417 (84.9)	46 (11.0)	67.7 \pm 21.1	74 (15.1)	14 (18.9)	3.65
Multiple	257	29.4 \pm 11.5	231 (89.9)	14 (6.1)	42.8 \pm 13.2	26 (10.9)	4 (15.4)	3.12
Total	1 270		1 117 (87.9)	63 (5.6)		153 (12.1)	19 (12.4)	

$P < 0.05$, vs Beer.

Table 3 Relationship between BMI and ALD

BMI	<i>n</i>	ALD	Years	Daily intake (g)	OR	<i>P</i>
\geq 25	203	24	13.5 \pm 6.2	26.4 \pm 13.7	5.6 (3.02-6.21)	< 0.01
< 25	1 067	58	16.3 \pm 5.8	35.7 \pm 18.1		

Drinking habits and ALD

In our population, beer or wine drinkers were 41.1%, and their alcohol daily intake was less than others. Rural people tended to drink hard liquors. Multiple drinkers were 20.2%, 87.9% of the drinkers consumed alcohol only at mealtimes, the daily alcohol intake was significantly lower than that of alcohol consumed at any time (with and without food) ($P < 0.05$). Daily alcohol intake of only hard liquors, also without food was significantly higher than that of all other categories of drinkers, the morbidity of ALD was also the highest, 2.7 times that of drinkers who drank only wine or beer at mealtimes (Table 2).

Obesity and ALD

Among the 1 270 drinkers, 203 had BMI more than 25. Although their average daily alcohol intake was lower than those with BMI less than 25, the ALD morbidity was 11.5%, more than twice that of normal body mass, significantly higher than the average 6.5%. There were no significant differences in drinking habits between the two groups. Multivariate analysis of the data showed that obesity was a risk factor for ALD, (OR: 5.6, $P < 0.01$). The difference was significant (Table 3).

Retrospective results

A 3-year follow-up indicated that among 19 cases with BMI \geq 25, only 3 cases had a body mass of 20% higher than before, and an increased BMI. Their serum ALT and AST were more than twice the upper normal level. The ultrasonography of the liver also indicated typical alcoholic fatty liver. In 9 of the 19 cases with a significant loss of body weight, their BMI also reduced to below 25. The ultrasonography of liver in several cases also became nearly normal. ALT and AST level was below the upper normal level. Of the remaining 7 subjects, their BMI was the same as before, the "liver function" became nearly normal. Ultrasonography findings became normal in 2 of 7 cases, and

remained the same in the other 5. All these 19 subjects except 3 who drank a little occasionally have already abstained.

Among 47 cases with BMI<25, their body mass did not change significantly. Eleven of them who kept on drinking had ALT and AST more than twice the upper normal level. The ultrasonography of liver revealed no improvement. Of the remaining who abstained from drinking, more than 85% of them had nearly normal "liver function", and better ultrasonographic findings. The percentage of "liver function" recovery was significantly higher than those who went on drinking ($P<0.01$).

DISCUSSION

Alcohol abuse has been claimed as one important factor leading to chronic liver diseases, as known in other diseases^[7-12]. The natural history of alcoholic liver disease ranges from asymptomatic indolent to end stage liver disease. Most patients lack specific clinical features^[13,14]. Diagnosis of alcoholic fatty liver and alcoholic steatohepatitis, like non-alcoholic fatty liver, without confirmatory laboratory tests, may involve the history of drinking, ultrasonography and liver biopsy^[15-18].

ALD is not only associated with genetic factors, but also involves other factors such as sex, body weight, BMI, the type and pattern of alcoholic beverage consumed, the habit of drinking hard liquors and of consuming alcohol without food, the duration of drinking^[19-21]. Yet, as to the risk threshold, in terms of daily alcohol intake and years of duration that can induce alcohol liver damage, there is no uniformed conclusion: with the wide range between 30 g/d and 80 g/d^[13]. Great differences between Western and Eastern countries exist: geographic variations must be present^[22,23], especially in China.

Our data suggested that the risk threshold of daily alcohol intake was 20 g; the duration was 5 years for Chinese men. Below the threshold, drinking seldom induced liver damage. If the daily intake exceeded 40 g and the duration was longer than 5 years, the liver damage occurred more frequently. However, with a daily intake higher than 160 g, in some cases the prevalence of alcoholic liver disease was only 18.7%. It means there is significantly different susceptibility among different individuals^[24]. It is commonly believed that prevalence of ALD in general population is up to about 15%, and rises with increased alcoholic intake. Our result was a little higher than that, maybe because our subjects were all men. In China, women drinkers are few, and their alcohol consumption is low, so few women develop ALD. There was only one woman case in our data. In spite of that, we believe that there is a great hepatic susceptibility to damage by alcohol in women.

The types of alcoholic beverage and the different drinking and dietary habits are closely related with ALD. Yet, a dose-effect relation between alcohol intake and alcohol-induced hepatic and other organ functional impairment has been demonstrated.

We were able to demonstrate for the first time in China that the habit of drinking hard liquors without food and the consumption of multiple types of drinks were risk factors of alcohol-induced liver damage. Those who drank only wine and beer were at lower risk for ALD. Fortunately, 90% of the Chinese drink wine or alcohol at mealtimes with food. Drinking without food might differentially affect the intragastric metabolism of ethanol by decreasing gastric alcohol dehydrogenase and hepatic glutathione and by accelerating gastric emptying, as it occurs in rats.

Recent studies confirm that the prevalence of alcohol-induced liver disease in obesity is high and serious. Obesity may be a co-risk factor for ALD and accelerate liver damage^[25,26]. It is reported that if the body weight is 20% above normal, the risk for ALD will be twice as great as in normal weight one. This is similar to our result. Among those obese patients whose

weight was above normal for more than 10 years, the risk for ALD was 2.5-3 times higher. At the same time, the liver damage increases with the increased BMI^[27,28]. However, the mechanism is not clear.

All of the patients in this study whose Anti-HCV and HBsAg were negative and with no recent medication history were "pure" ALD. Multivariate analysis showed that each factor was independent of the other variables.

Besides abstaining, which directly affects the prognosis of ALD^[29], BMI can also affect the progress of ALD^[30]. For the overweight cases, weight loss is an important treatment^[31]. Our data have another indication that "education" is also very important for changing patients' lifestyle^[32]. Because all the subjects with BMI \geq 25 had been told that alcohol and overweight would cause bad prognosis of ALD and strongly recommended complete alcohol abstinence and weight reduction, none of these cases went on drinking heavily. On the other hand, among the men with BMI<25, some did not take the risk of drinking seriously, nearly 15% of them went on drinking during the 3 years, resulting in progress of their ALD.

From the present data we can conclude that the minimum alcohol intake and the duration of years associated with a significant increase in the prevalence of alcohol-related liver disease was 20 g per day and 5 years for men. This risk increases in a dose-related pattern. However, the most striking result is that not only the quantity of alcohol consumed, but also the patterns of drinking are an important determinant of the risk of having ALD. Drinking only hard liquors or multiple types of alcoholic beverages without food, independent of the amount, is associated with an increased prevalence of alcohol-related liver disease. Obesity is also an independent risk factor for ALD. Abstinence and weight loss directly affect the prognosis of ALD. Therefore, we suggest reducing alcohol intake, avoiding drinking outside of mealtimes and consuming only wine or beer, especially for obese people.

REFERENCES

- 1 **Kerr WC**, Fillmore KM, Marvy P. Beverage-specific alcohol consumption and cirrhosis mortality in a group of English-speaking beer-drinking countries. *Addiction* 2000; **95**: 339-346
- 2 **Menon KV**, Gores GJ, Shah VH. Pathogenesis, diagnosis, and treatment of alcoholic liver disease. *Mayo Clin Proc* 2001; **76**: 1021-1029
- 3 **Campollo O**, Martinez MD, Valencia JJ, Segura-Ortega J. Drinking patterns and beverage preferences of liver cirrhosis patients in Mexico. *Subst Use Misuse* 2001; **36**: 387-398
- 4 **O'Keefe C**, McCormick PA. Severe acute alcoholic hepatitis: an audit of medical treatment. *Ir Med J* 2002; **95**: 108-109
- 5 **Monzoni A**, Masutti F, Saccoccio G, Bellentani S, Tiribelli C, Giacca M. Genetic determinants of ethanol-induced liver damage. *J Mol Med* 2001; **7**: 255-262
- 6 **Lu XL**, Tao M, Luo JY, Gen Y, Zhao P, Zhao HL. Epidemiology of alcoholic liver diseases in Xi'an. *Shijie Huaren Xiaohua Zazhi* 2003; **11**: 719-722
- 7 **Crews FT**, Braun CJ. Binge ethanol treatment causes greater brain damage in alcohol-preferring P rats than in alcohol-nonpreferring NP rats. *Alcohol Clin Exp Res* 2003; **27**: 1075-1082
- 8 **Schuckit MA**, Smith TL, Danko GP, Isacescu V. Level of response to alcohol measured on the self-rating of the effects of alcohol questionnaire in a group of 40-year-old women. *Am J Drug Alcohol Abuse* 2003; **29**: 191-201
- 9 **Hezode C**, Lonjon I, Roudot-Thoraval F, Pawlotsky JM, Zafrani ES, Dhumeaux D. Impact of moderate alcohol consumption on histological activity and fibrosis in patients with chronic hepatitis C, and specific influence of steatosis: a prospective study. *Aliment Pharmacol Ther* 2003; **17**: 1031-1037
- 10 **Rehm J**, Sempos CT, Trevisan M. Alcohol and cardiovascular disease-more than one paradox to consider. Average volume of alcohol consumption, patterns of drinking and risk of coronary heart disease-a review. *J Cardiovasc Risk* 2003; **10**: 15-20

- 11 **Lip GY**, Beevers DG. Alcohol and cardiovascular disease-more than one paradox to consider. Alcohol and hypertension-does it matter? *J Cardiovasc Risk* 2003; **10**: 11-14
- 12 **Dal Maso L**, La Vecchia C, Polesel J, Talamini R, Levi F, Conti E, Zambon P, Negri E, Franceschi S. Alcohol drinking outside meals and cancers of the upper aero-digestive tract. *Int J Cancer* 2002; **102**: 435-437
- 13 **Gordon H**. Detection of alcoholic liver disease. *World J Gastroenterol* 2001; **7**: 297-302
- 14 **Vaquero J**, Blei AT. Etiology and management of fulminant hepatic failure. *Curr Gastroenterol Rep* 2003; **5**: 39-47
- 15 **Skelly MM**, James PD, Ryder SD. Findings on liver biopsy to investigate abnormal liver function tests in the absence of diagnostic serology. *J Hepatol* 2001; **35**: 195-199
- 16 **Angelico F**, Del Ben M, Conti R, Francioso S, Feole K, Maccioni D, Antonini TM, Alessandri C. Non-alcoholic fatty liver syndrome: a hepatic consequence of common metabolic diseases. *J Gastroenterol Hepatol* 2003; **18**: 588-594
- 17 **Hourigan KJ**, Bowling FG. Alcoholic liver disease: a clinical series in an Australian private practice. *J Gastroenterol Hepatol* 2001; **16**: 1138-1143
- 18 **Jarque-Lopez A**, Gonzalez-Reimers E, Rodriguez-Moreno F, Santolaria-Fernandez F, Lopez-Lirola A, Ros-Vilamajo R, Espinosa-Villarreal JG, Martinez-Riera A. Prevalence and mortality of heavy drinkers in a general medical hospital unit. *Alcohol Alcohol* 2001; **36**: 335-338
- 19 **Thurman RG**. Sex-related liver injury due to alcohol involves activation of Kupffer cells by endotoxin. *Can J Gastroenterol* 2000; **14**(Suppl D): 129D-135D
- 20 **Walsh K**, Alexander G. Alcoholic liver disease. *Postgrad Med J* 2000; **76**: 280-286
- 21 **Ropero Gradilla P**, Villegas Martinez A, Fernandez Arquero M, Garcia-Agundez JA, Gonzalez Fernandez FA, Benitez Rodriguez J, Diaz-Rubio M, de la Concha EG, Ladero Quesada JM. C282Y and H63D mutations of HFE gene in patients with advanced alcoholic liver disease. *Rev Esp Enferm Dig* 2001; **93**: 156-163
- 22 **Stewart SH**. Racial and ethnic differences in alcohol-associated aspartate aminotransferase and gamma-glutamyltransferase elevation. *Arch Intern Med* 2002; **162**: 2236-2239
- 23 **Naveau S**, Giraud V, Ganne N, Perney P, Hastier P, Robin E, Pessione F, Chossegros P, Lahmek P, Fontaine H, Ribard D, Dao T, Filoche B, El Jammal G, Seyrig JA, Dramard JM, Chousterman M, Pillegand B. Patients with alcoholic liver disease hospitalized in gastroenterology. Anational multicenter study. *Gastroenterol Clin Biol* 2001; **25**: 131-136
- 24 **Diehl AM**. Liver disease in alcohol abusers: clinical perspective. *Alcohol* 2002; **27**: 7-11
- 25 **Brunt EM**, Ramrakhiani S, Cordes BG, Neuschwander-Tetri BA, Janney CG, Bacon BR, Di Bisceglie AM. Concurrence of histologic features of steatohepatitis with other forms of chronic liver disease. *Mod Pathol* 2003; **16**: 49-56
- 26 **Clouston AD**, Powell EE. Interaction of non-alcoholic fatty liver disease with other liver diseases. *Best Pract Res Clin Gastroenterol* 2002; **16**: 767-781
- 27 **Ioannou GN**, Weiss NS, Kowdley KV, Dominitz JA. Is obesity a risk factor for cirrhosis-related death or hospitalization? a population-based cohort study. *Gastroenterology* 2003; **125**: 1053-1059
- 28 **Mulhall BP**, Ong JP, Younossi ZM. Non-alcoholic fatty liver disease: an overview. *J Gastroenterol Hepatol* 2002; **17**: 1136-1143
- 29 **Serra MA**, Escudero A, Rodriguez F, del Olmo JA, Rodrigo JM. Effect of hepatitis C virus infection and abstinence from alcohol on survival in patients with alcoholic cirrhosis. *J Clin Gastroenterol* 2003; **36**: 170-174
- 30 **Bellentani S**, Saccoccio G, Masutti F, Croce LS, Brandi G, Sasso F, Cristanini G, Tiribelli C. Prevalence of and risk factors for hepatic steatosis in Northern Italy. *Ann Intern Med* 2000; **132**: 112-117
- 31 **Angulo P**, Lindor KD. Treatment of non-alcoholic steatohepatitis. *Best Pract Res Clin Gastroenterol* 2002; **16**: 797-810
- 32 **Xie X**, Mann RE, Smart RG. The direct and indirect relationships between alcohol prevention measures and alcoholic liver cirrhosis mortality. *J Stud Alcohol* 2000; **61**: 499-506

Edited by Zhu LH Proofread by Chen WW and Xu FM

Receptor binding characteristics and cytotoxicity of insulin-methotrexate

Xiao-Hong Ou, An-Ren Kuang, Zheng-Lu Liang, Xian Peng, Yu-Guo Zhong

Xiao-Hong Ou, An-Ren Kuang, Zheng-Lu Liang, Department of Nuclear Medicine, West China Hospital of Sichuan University, Chengdu 610041, Sichuan Province, China

Xian Peng, Yu-Guo Zhong, Department of Pharmacy, Sichuan University, Chengdu 610041, Sichuan Province, China

Supported by the National Natural Science Foundation of China, No. 30270415

Correspondence to: Anren Kuang, Department of Nuclear Medicine, West China Hospital of Sichuan University, Chengdu 610041, Sichuan Province, China. ouxiaohong2002@xinhuanet.com

Telephone: +86-28-85422696 **Fax:** +86-28-85422696

Received: 2003-09-06 **Accepted:** 2003-10-07

Abstract

AIM: To characterize the receptor binding affinity and cytotoxicity of insulin-methotrexate (MTX) for the potential utilization of insulin as carriers for carcinoma target drugs.

METHODS: MTX was covalently linked to insulin. Insulin-MTX conjugate was purified by Sephadex G-25 column and analyzed by high performance liquid chromatography. Hepatocellular carcinoma cell membrane fractions were isolated by sucrose density gradient centrifugation. Competitive displacement of ^{125}I -insulin with insulin and insulin-MTX binding to insulin receptors were carried out. Cyto-reductive effect of insulin-MTX on human hepatoma BEL7402 cells and human hepatocyte cell line HL7702 was evaluated using the MTT assay.

RESULTS: Insulin-MTX competed as effectively as insulin with ^{125}I -insulin for insulin receptors. The values of Kd for insulin-MTX and insulin were 93.82 ± 19.32 nmol/L and 5.01 ± 1.24 nmol/L, respectively. The value of Kd for insulin-MTX was significantly increased in comparison with insulin ($t=7.2532$, $n=4$, $P<0.005$). Insulin-MTX inhibited the growth of human hepatoma cells (BEL7402) almost as potently as MTX. The inhibitory effect reached a peak on the 5th day when the growth of cells was inhibited by 79% at a concentration of 5.0 $\mu\text{g/mL}$ insulin-MTX. Treatment with 5.0 $\mu\text{g/mL}$ of MTX and 5.0 $\mu\text{g/mL}$ of insulin-MTX merely resulted in inhibition of HL7702 cells by 31.5% and 7.8% on the 5th day.

CONCLUSION: Insulin-MTX specifically recognizes insulin receptors and inhibits the growth of BEL7402 cells. These results suggest that insulin can be used as a carrier in receptor mediated carcinoma-targeting therapy.

Ou XH, Kuang AR, Liang ZL, Peng X, Zhong YG. Receptor binding characteristics and cytotoxicity of insulin-methotrexate. *World J Gastroenterol* 2004; 10(16): 2430-2433
<http://www.wjgnet.com/1007-9327/10/2430.asp>

INTRODUCTION

Methotrexate (MTX), a folic acid analog, is a widely used

antimetabolite in cancer chemotherapy. It inhibits dihydrofolate reductase, an enzyme necessary for purine and pyrimidine synthesis. However, MTX also acts on other rapidly dividing cells such as trophoblast cells, which comprise the implantation site of early gestation. Other toxic effects include depression of the bone marrow and damage to the epithelium of the gastrointestinal tract. Selective targeting of therapeutic and diagnostic agents may improve MTX's efficacy and reduce its adverse effects. Existing methods for selective targeting are usually based upon chemical conjugation of agents to cell-specific targeting molecules (e.g. ligands, antibodies).

Receptor mediated endocytosis may provide a pathway by which exogenous molecules are transported into the interior of target cells. In recent years a number of receptors have been used for DNA delivery via receptor-mediated endocytosis, including asialoglycoprotein^[1-4], transferrin^[5-7], epidermal growth factor (EGF) peptides^[8-10], as well as insulin receptor^[11-13]. It has been shown that expression of insulin receptor is increased on a variety of malignant tumor cells^[14-17]. Insulin can be internalized into nuclei of cells possessing insulin receptors^[18-21]. These facts indicate that insulin may be an attractive candidate carrier for anticancer drugs in target therapy of carcinomas.

To reduce side effects and increase safety, we planned to deliver MTX via insulin receptor-mediated endocytosis. In the present study, we conjugated MTX to insulin and characterized the binding activity and cytotoxicity of insulin-MTX complex. Our results suggest that insulin is a suitable candidate carrier for anticancer drugs.

MATERIALS AND METHODS

Radioiodination of insulin

Porcine insulin was radioiodinated using the Ch-T method and purified by polyacrylamide gel electrophoresis. Radiochemical purity of the ^{125}I -insulin was measured by thin layer chromatogram (TLC).

The radiochemical purity of ^{125}I -insulin was 98% and remained over 95% 14 d after stored at -20°C .

Preparation of insulin-MTX

Insulin-MTX was synthesized by the Department of Pharmacy, Sichuan University. Briefly, MTX (50 mg), EDC (100 mg) and HOBt (50 mg) were dissolved in 3 mL of phosphate-buffered saline (pH = 8.9) and mixed with 1 mL of phosphate-buffered saline (pH = 8.9) containing 25 mg of insulin. The mixture was stirred at 4°C for 48 h. The precipitation was removed by filtration and pH of the solvent was adjusted to 5.5 with 0.5 mol/L HCL. The reaction mixture was kept at 4°C overnight. Thereafter, the solution was filtered through a 0.25 μm membrane (Millipore, Germany) and the filtrate was evaporated under vacuum. The products were purified over a 3 cm \times 45 cm Sephadex G-25 column eluted with 2% ammonium carbonate, and fractions which had the maximal absorbance at 276 nm were collected.

Isolated insulin-MTX was analyzed by analytical HPLC (Beckman) with a 4 mm \times 200 mm ODS column. The mobile phase was 270 mL/L acetonitrile and 730 mL/L 0.1 mol/L NaH_2PO_4 (pH = 0.3) at a flow rate of 0.5 mL/min.

SDS-polyacrylamide gel electrophoresis (SDS-PAGE) was performed in 150 g/L polyacrylamide gel to calculate the molecular weight of insulin-MTX.

Preparation of cell membrane

Hepatocellular carcinoma specimens were obtained from six patients during surgery whose diagnoses were confirmed by histopathology and immediately frozen at -70°C . Cell membrane fractions were prepared according to established techniques. Tissues were cut into pieces, put into Tris-HCL buffer (pH 7.5) and homogenized. The cell membrane fractions purified by centrifugation in a discontinuity sucrose density gradient were stored at -70°C . The protein concentration was determined according to Lowry method.

Receptor binding assay

The conditions of the assay system were modified according to the method reported earlier. In saturation experiments, the cell membrane fractions (80 μg protein) were incubated with increasing concentrations (5×10^3 - 5×10^5 cpm) of ^{125}I -insulin in the absence (total binding) or presence of the same unlabeled insulin (4.3 nmol/L, nonspecific binding). In competition experiment, the cell membrane fractions (80 μg protein) were incubated with 5 nmol/L ^{125}I -insulin in the absence (total binding) and presence of increasing concentrations (10^{-12} - 10^{-7} mol/L) of the unlabeled insulin or insulin-MTX. After incubation for 20 h at 4°C , free ligands were removed by centrifugation at 2000 r/min for 10 min after addition of 0.1 mL of 3 g/L bovine γ -globulin and 0.8 mL of 15.8% PEG. Radioactivity of the membrane pellets was determined in a gamma counter for 1 min as the total binding. Specific bindings were obtained by subtracting nonspecific bindings from total bindings.

Cell culture

Human hepatoma BEL7402 cells and human hepatocyte HL7702 cells were grown at 37°C in a humidified incubator with 50 mL/L CO_2 atmosphere in RPMI1640 (GIBCO BRL) medium containing 100 mL/L of deplemented FBS, penicillin (100 U/mL) and streptomycin (100 U/mL).

Cell treatment and MTT assay

BEL7402 cells and HL7702 cells were seeded at a density of 10^4 cells per well into 96-well plates. After overnight growth, the medium was removed and RPMI containing different concentrations of insulin-MTX or MTX was added. At given time points, 20 μL of MTT (50 mg/mL) was added to each well. After incubation for 4 h at 37°C in a humidified 50 mL/L CO_2 atmosphere, the medium was removed and 0.2 mL of DMSO was added. Then, the absorbency at 570 nm was read.

Data calculation and statistical analysis

Binding data were calculated with receptor binding analysis software. Values were presented as mean \pm SD. Statistical

comparisons between the means were made with paired *t*-test at a confidence level of 95%.

RESULTS

Analysis of insulin-MTX

The recovery of insulin-MTX was around 71.5%. HPLC assay indicated that isolated insulin-MTX (retention time 12.08 min) yield was approximately 94% (Figure 1). The rest contained insulin (8.81 min) and MTX (4.16 min).

The calculated molecular weight of insulin-MTX was 6779 u according to its relative position to the molecular mass marker in SDS-PAGE pattern.

Receptor binding

The binding of insulin receptors to unlabelled insulin and the insulin-MTX conjugate derivative were determined by their ability to compete with free radioactively labelled insulin for receptor sites on cell membranes of hepatocellular carcinoma. We first established the normal binding characteristics of ^{125}I -insulin to cell membranes. Binding took place rapidly in the first 2 h, then slowed down and reached its maximum at approximately 18 h. For all subsequent binding experiments, the incubation time was 20 h at 4°C . As the concentration of ^{125}I -insulin increased, the binding mounted up and plateaued rapidly.

Similar to insulin, the conjugate competed for the binding sites with ^{125}I -insulin on the insulin receptor in a dose-dependent manner (Figure 2). Binding of ^{125}I -insulin (5 nmol/L) was reduced to 50% in the presence of 5.01 ± 1.24 nmol/L of unlabelled insulin or 93.82 ± 19.32 nmol/L of insulin-MTX, respectively. In contrast, MTX did not compete for binding (data not shown).

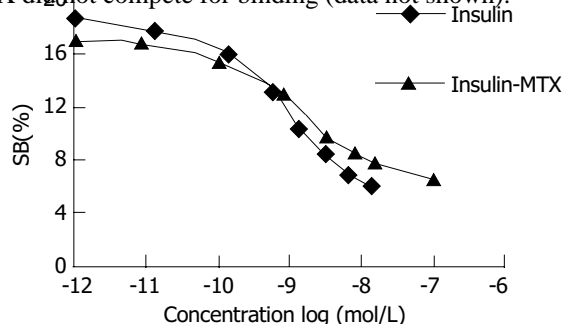


Figure 2 Competitive binding curves of ^{125}I -insulin against insulin-MTX or insulin. The concentration of ^{125}I -insulin was 5 nmol/L. The binding assay was described in the *MATERIALS AND METHODS*.

Inhibition of insulin-MTX complex on cell proliferation

Dose-response curves of insulin-MTX and MTX on BEL7402 and HL7702 cells are shown in Figure 3. Viability was expressed as a percentage of control by dividing the absorbance of each treated well by the average of untreated control. BEL7402 cells

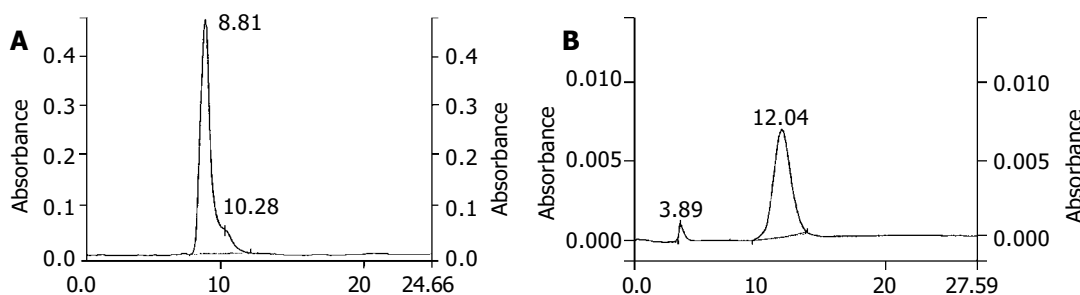


Figure 1 HPLC analysis of insulin and insulin-MTX. The condition was described in *MATERIALS AND METHODS*. Retention time of insulin was 8.81 min. Retention time of insulin-MTX was 12.16 min. A: HPLC analysis of insulin. B: HPLC analysis of insulin-MTX.

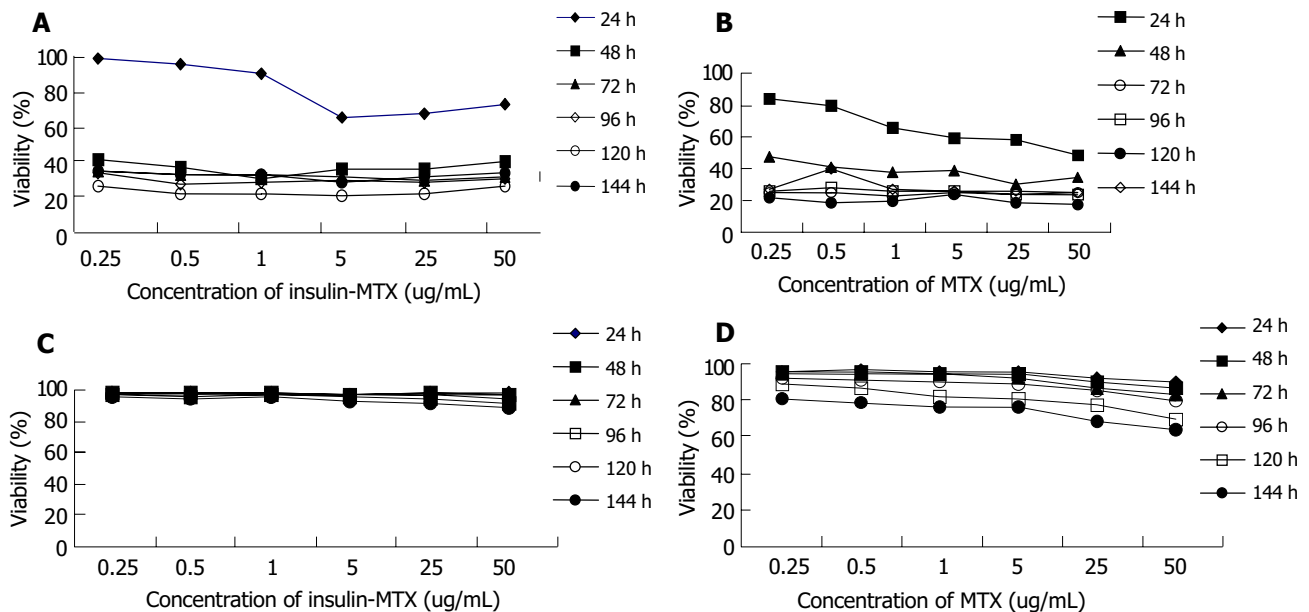


Figure 3 Concentrations of MTX and insulin-MTX in BEL7402 and HL7702 cells. BEL7402 cells and HL7702 cells having cultured overnight were exposed to insulin-MTX or MTX at the indicated concentration for 24 h, 48 h, 72 h, 96 h, 120 h and 144 h respectively. Cell viability was assessed using MTT assay. Viability was expressed as a percentage of control by dividing the absorbance of each treated well by the average of the untreated control. A: Viability of BEL7402 cells treated with insulin-MTX (mean±SD, $n = 3$), B: Viability of BEL7402 cells treated with MTX (mean±SD, $n = 3$), C: Viability of HL7702 cells treated with insulin-MTX (mean±SD, $n = 3$), D: Viability of HL7702 cells treated with MTX (mean±SD, $n = 3$).

were sensitive to both insulin-MTX and MTX. Cyto-reductive effect of MTX and insulin-MTX on BEL7402 cells was concentration-dependent. As early as 24 h, 5.0 $\mu\text{g/mL}$ of insulin-MTX inhibited BEL7402 cell growth by 34.3%, which was relatively lower as compared with 40.6% by 5.0 $\mu\text{g/mL}$ of MTX. The effect reached its peak on the 5th d, and BEL7402 cells were inhibited by 79% at a concentration of 5.0 $\mu\text{g/mL}$ insulin-MTX and 82.1% at 5.0 $\mu\text{g/mL}$ MTX, respectively. In contrast, treatment with 5.0 $\mu\text{g/mL}$ of MTX and 5.0 $\mu\text{g/mL}$ of insulin-MTX merely resulted in the inhibition of HL7702 cells by 31.5% and 7.8% on the 5th d.

DISCUSSION

The molecule of insulin has sufficient hydroxys and carboxyls that can be used for conjugation with other small molecules. Exploration of the efficiency and specificity of cell entry offered by insulin receptor mediated endocytosis has been proposed previously^[22,23]. Here we demonstrated that cross-linking MTX to insulin produced a soluble molecule capable of both specific recognition of the insulin receptors and inhibition of growth of tumor cells, thereby providing a possible tool for target transporting anticancer drugs. The use of insulin as a carrier might offer two advantages. First, most of insulin-MTX could go to tumor cells which overexpress insulin receptors, thus rapidly dividing normal tissues would not be damaged by the drug. Second, tumor cells could develop MTX-resistance frequently via various mechanisms. One of them was due to decreased membrane transport^[24-28]. The use of insulin as a carrier might offer an increased MTX transportation into drug-resistant tumor cells.

Since laboratory iodination of insulin with ¹²⁵I could incur oxidation damage and brings about indiscriminate labelling of tyrosine residues leading to decreased biological activity including aberrant receptor binding, polyacrylamide gel electrophoresis was used to purify monoiodo [¹²⁵I-Tyr^{A14}] insulin, which was fully active in receptor binding assays^[29]. Receptor binding analysis showed that insulin-MTX could specifically bind to insulin receptors on human hepatocellular carcinoma.

The increased K_d indicated a decreased affinity for receptors, indicating that linking MTX to insulin molecule did interfere with the affinity of insulin-receptor binding. High affinity is one of the most important criteria of tumor-target agents. Decrease in affinity of insulin-MTX for insulin receptors may result from conjugation of MTX with A13 and B17 positions of insulin molecules. These positions are located in the hexamer-forming surface and on the opposite side of the classical binding site, and constitute a second domain of the molecule important for receptor binding^[30]. Further studies to improve the affinity of insulin-MTX by modifying the method of conjugation would be needed.

Insulin receptor was considered to play a role in the regulation of hepatocellular carcinoma^[31] and there have been reports showing increased insulin receptors expressed on these cells^[29,32]. Therefore human hepatoma BEL7402 cell line was selected to measure the cyto-reductive effect of insulin-MTX. Our studies showed that BEL7402 cells were sensitive to both insulin-MTX and MTX. However, the molecular weight of insulin-MTX complex was far greater than that of MTX. It was observed that 0.375 nmoL (1.5×10^{-6} mol/L \times 0.25 mL) of MTX conjugated to insulin inhibited the growth of BEL7402 cells as effectively as 2.5 nmoL (1×10^{-5} mol/L \times 0.25 mL) of MTX. HL7702 cells appeared to be less sensitive to both insulin-MTX and MTX, especially to insulin-MTX, when compared with BEL7402 cells. Treatment with 5.0 $\mu\text{g/mL}$ of insulin-MTX resulted in about 10-fold higher toxicity on BEL7402 cells than on HL7702 cells. This may result from the elevated proliferation and the increased expression of insulin receptors of BEL7402 cells. These results indicated that conjugation of insulin could enhance the cytotoxicity of MTX to hepatocarcinoma cells.

Our results showed that the new construct could bind specifically to insulin receptors, but its effect on glucose metabolism depended on the residues with which MTX molecule interacted. An unparalleled relationship of receptor binding and glucose uptake was observed in other insulin analogues and mutants^[33,34]. Therefore, it is necessary to test the biological activity of insulin-MTX in glucose metabolism in order to understand its effects on plasma glucose levels. In our study,

SDS-polyacrylamide agarose gel electrophoresis showed the molecular weight of insulin-MTX was 6 779 u, which equaled the mass of one molecule of insulin ($M_r = 5\ 800$) and two molecules of MTX ($M_r = 454.5$). The ratio of insulin molarity to the MTX was estimated to be 1:2. On the basis of this molar ratio, only 20-200 μmol insulin is required to obtain a high plasma concentration (10-100 $\mu\text{mol/L}$). Besides, the dose may be reduced because of the targeting ability of insulin-MTX. Even if the conjugates have partial bioactivity in glucose uptake, there is little probability that administration of such a low dose in therapy would result in adverse effects of hypoglycemia.

In the present study, we demonstrated that insulin-MTX complex could specifically bind to insulin receptors and efficiently inhibit the growth of human hepatoma BEL7402 cells, although the affinity needs to be improved. Receptor-mediated endocytosis has a tremendous potential for delivery of carcinoma target drugs because of the overexpression of insulin receptors on carcinoma tissues.

REFERENCES

- 1 Wu J, Nantz MH, Zern MA. Targeting hepatocytes for drug and gene delivery: emerging novel approaches and applications. *Front Biosci* 2002; 7: d717-725
- 2 Yang Y, Park Y, Man S, Liu Y, Rice KG. Cross-linked low molecular weight glycopeptide-mediated gene delivery: relationship between DNA metabolic stability and the level of transient gene expression *in vivo*. *J Pharm Sci* 2001; 90: 2010-2022
- 3 Ren T, Zhang G, Liu D. Synthesis of galactosyl compounds for targeted gene delivery. *Bioorg Med Chem* 2001; 9: 2969-2978
- 4 Han J, Il Yeom Y. Specific gene transfer mediated by galactosylated poly-L-lysine into hepatoma cells. *Int J Pharm* 2000; 202: 151-160
- 5 Qian ZM, Li H, Sun H, Ho K. Targeted drug delivery via the transferrin receptor-mediated endocytosis pathway. *Pharmacol Rev* 2002; 54: 561-587
- 6 Li X, Fu GF, Fan YR, Shi CF, Liu XJ, Xu GX, Wang JJ. Potent inhibition of angiogenesis and liver tumor growth by administration of an aerosol containing a transferrin-liposome-endothelin complex. *World J Gastroenterol* 2003; 9: 262-266
- 7 Li H, Qian ZM. Transferrin/transferrin receptor-mediated drug delivery. *Med Res Rev* 2002; 22: 225-250
- 8 Blessing T, Kurka M, Holzhauser R, Kircheis R, Wagner E. Different strategies for formation of pegylated EGF-conjugated PEI/DNA complexes for targeted gene delivery. *Bioconjug Chem* 2001; 12: 529-537
- 9 Xu B, Wiehle S, Roth JA, Cristiano RJ. The contribution of poly-L-lysine, epidermal growth factor and streptavidin to EGF/PLL/DNA polyplex formation. *Gene Ther* 1998; 5: 1235-1243
- 10 Gaidamakova EK, Backer MV, Backer JM. Molecular vehicle for target-mediated delivery of therapeutics and diagnostics. *J Control Release* 2001; 74: 341-347
- 11 Reddy JA, Low PS. Folate-mediated targeting of therapeutic and imaging agents to cancers. *Crit Rev Ther Drug Carrier Syst* 1998; 15: 587-627
- 12 Sobolev AS, Rosenkranz AA, Smirnova OA, Nikitin VA, Neugodova GL, Naroditsky BS, Shilov IN, Shatski IN, Ernst LK. Receptor-mediated transfection of murine and ovine mammary glands *in vivo*. *J Biol Chem* 1998; 273: 7928-7933
- 13 Zhang Y, Boado RJ, Pardridge WM. Marked enhancement in gene expression by targeting the human insulin receptor. *J Gene Med* 2003; 5: 157-163
- 14 Kalli KR, Falowo OI, Bale LK, Zschunke MA, Roche PC, Conover CA. Functional insulin receptors on human epithelial ovarian carcinoma cells: implications for IGF-II mitogenic signaling. *Endocrinology* 2002; 143: 3259-3267
- 15 Vella V, Sciacca L, Pandini G, Mineo R, Squatrito S, Vigneri R, Belfiore A. The IGF system in thyroid cancer: new concepts. *Mol Pathol* 2001; 54: 121-124
- 16 Maune S, Gorogh T. Detection of overexpression of insulin receptor gene in laryngeal carcinoma cells by using differential display method. *Inotologie* 2000; 79: 438-441
- 17 Frittitta L, Vignori R, Stampfer MR, Goldfine ID. Insulin receptor overexpression in 184B5 human mammary epithelial cells induces a ligand-dependent transformed phenotype. *J Cell Biochem* 1995; 57: 666-669
- 18 Shah N, Zhang S, Harada S, Smith RM, Jarett L. Electron microscopic visualization of insulin translocation into the cytoplasm and nuclei of intact H35 hepatoma cells using covalently linked Nanogold-insulin. *Endocrinology* 1995; 136: 2825-2835
- 19 Radulescu RT, Doklea ED, Kehe K, Muckter H. Nuclear colocalization and complex formation of insulin with retinoblastoma protein in HepG2 human hepatoma cells. *J Endocrinol* 2000; 166: R1-4
- 20 Harada S, Smith RM, Jarett L. Mechanisms of nuclear translocation of insulin. *Cell Biochem Biophys* 1999; 31: 307-319
- 21 Zacksenhaus E, Jiang Z, Hei YJ, Phillips RA, Gallie BL. Nuclear localization conferred by the pocket domain of the retinoblastoma gene product. *Biochim Biophys Acta* 1999; 1451: 288-296
- 22 Zhang Y, Jeong Lee H, Boado RJ, Pardridge WM. Receptor-mediated delivery of an antisense gene to human brain cancer cells. *J Gene Med* 2002; 4: 183-194
- 23 Ivanova MM, Rosenkranz AA, Smirnova OA, Nikitin VA, Sobolev AS, Landa V, Naroditsky BS, Ernst LK. Receptor-mediated transport of foreign DNA into preimplantation mammalian embryos. *Mol Reprod Dev* 1999; 54: 112-120
- 24 Nestle FO, Alijagic S, Gilliet M, Sun Y, Grabbe S, Dummer R, Burg G, Schadendorf D. Vaccination of melanoma patients with peptide- or tumor lysate-pulsed dendritic cells. *Nat Med* 1998; 4: 328-332
- 25 Thurner B, Haendle I, Roder C, Dieckmann D, Keikavoussi P, Jonuleit H, Bender A, Maczek C, Schreiner D, von den Driesch P, Brocker EB, Steinman RM, Enk A, Kampgen E, Schuler G. Vaccination with mage-3A1 peptide-pulsed mature, monocyte-derived dendritic cells expands specific cytotoxic T cells and induces regression of some metastases in advanced stage IV melanoma. *J Exp Med* 1999; 190: 1669-1678
- 26 Wu TC, Guarnieri FG, Staveley-O'Carroll KF, Viscidi RP, Levitsky HI, Hedrick L, Cho KR, August JT, Pardoll DM. Engineering an intracellular pathway for major histocompatibility complex class II presentation of antigens. *Proc Natl Acad Sci U S A* 1995; 92: 11671-11675
- 27 Asai S, Miyachi H, Kobayashi H, Takemura Y, Ando Y. Large diversity in transport-mediated methotrexate resistance in human leukemia cell line CCRF-CEM established in a high concentration of leucovorin. *Cancer Sci* 2003; 94: 210-214
- 28 Sierra EE, Goldman ID. Recent advances in the understanding of the mechanism of membrane transport of folates and antifolates. *Semin Oncol* 1999; 26(2 Suppl 6): 11-23
- 29 Kurtaran A, Li SR, Raderer M, Leimer M, Muller C, Pidlich J, Neuhold N, Hubsch P, Angelberger P, Scheithauer W, Virgolini I. Technetium-99m-galactocyl-neoglycoalbumin combined with iodine-123-Tyr-(A14) insulin visualizes human hepatocellular carcinomas. *J Nucl Med* 1995; 36: 1875-1880
- 30 Beavis RC, Kneirman MD, Sharknas D, Heady MA, Frank BH, DeFelippis MR. A novel protein cross-linking reaction in stressed Neutral Protamine Hagedorn formulations of insulin. *J Pharm Sci* 1999; 88: 331-336
- 31 Scharf JG, Dombrowski F, Ramadori G. The IGF axis and hepatocarcinogenesis. *Mol Pathol* 2001; 54: 138-144
- 32 Spector SA, Olson ET, Gumbs AA, Friess H, Buchler MW, Seymour NE. Human insulin receptor and insulin signaling proteins in hepatic disease. *J Surg Res* 1999; 83: 32-35
- 33 Guo ZY, Shen L, Gu W, Wu AZ, Ma JG, Feng YM. *In vitro* evolution of amphioxus insulin-like peptide to mammalian insulin. *Biochemistry* 2002; 41: 10603-10607
- 34 Liao ZY, Tang YH, Xu MH, Feng YM, Zhu SQ. B9-serine residue is crucial for insulin actions in glucose metabolism. *Acta Pharmacol Sin* 2001; 22: 939-943

Analysis of multiple factors of postsurgical gastroparesis syndrome after pancreaticoduodenectomy and cryotherapy for pancreatic cancer

Ke Dong, Bo Li, Quan-Lin Guan, Tao Huang

Ke Dong, Bo Li, Quan-Lin Guan, Tao Huang, Department of General Surgery, West China Hospital, Sichuan University, Chengdu 610041, Sichuan Province, China

Supported by the Research Foundation of Department of Health of Sichuan Province, No. 000050

Correspondence to: Dr. Bo Li, Department of General Surgery, West China Hospital, Sichuan University, Chengdu 610041, Sichuan Province, China. cdlibo@medmail.com

Telephone: +86-28-85422476

Received: 2003-11-21 **Accepted:** 2004-02-01

Abstract

AIM: To explore the etiology, pathogenesis, diagnosis, and treatment of postsurgical gastroparesis syndrome (PGS) after pancreatic cancer cryotherapy (PCC) or pancreaticoduodenectomy (PD), and to analyze the correlation between the multiple factors and PGS caused by the operations.

METHODS: Clinical data of 210 patients undergoing PD and 46 undergoing PCC were analyzed retrospectively.

RESULTS: There were 31 (67%, 31/46) patients suffering PGS in PCC group, including 29 with pancreatic head and uncinate tumors and 2 with pancreatic body and tail tumors. Ten patients (4.8%, 10/210) developed PGS in PD group, which had a significantly lower incidence of PGS than PCC group ($\chi = 145$, $P < 0.001$). In PCC group, 9 patients with PGS were managed with non-operative treatment (drugs, diet, nasogastric suction, etc.), and one received reoperation at the 16th day, but the symptoms were not relieved. In PD group, all the patients with PGS were managed with non-operative treatment. The PGS in patients undergoing PCC had close association with PCC, tumor location, but not with age, gender, obstructive jaundice, hypoproteinemia, preoperative gastric outlet obstruction and the type and number of gastric biliary tract operations. The mechanisms of PGS caused by PD were similar to those of PGS following gastrectomy. The damage to interstitial cells of Cajal might play a role in the pathogenesis of PGS after PCC, for which multiple factors were possibly responsible, including ischemic and neural injury to the antropyloric muscle and the duodenum after freezing of the pancreaticoduodenal regions or reduced circulating levels of motilin.

CONCLUSION: PGS after PCC or PD is induced by multiple factors and the exact mechanisms, which might differ between these two operations, remain unknown. Radiography of the upper gastrointestinal tract and gastroscopy are main diagnostic modalities for PGS. Non-operative treatments are effective for PGS, and reoperation should be avoided in patients with PGS caused by PCC.

Dong K, Li B, Guan QL, Huang T. Analysis of multiple factors of postsurgical gastroparesis syndrome after pancreaticoduodenectomy and cryotherapy for pancreatic cancer. *World J Gastroenterol* 2004; 10(16): 2434-2438
<http://www.wjgnet.com/1007-9327/10/2434.asp>

INTRODUCTION

Postsurgical gastroparesis syndrome (PGS) is a complex disorder characterized by postprandial nausea, vomiting, and gastric atony in the absence of mechanical gastric outlet obstruction. Patients frequently suffer marked weight loss and malnutrition that require hospitalization and prolonged parenteral nutrition (PN). These symptoms can be disabling and often fail to be alleviated by drug therapy, for which gastric reoperations usually prove unsuccessful. An identified cause for PGS has not been available, nor is its mechanism quite clarified. PGS after gastrectomy or pancreaticoduodenectomy (PD) has been reported in a number of literatures^[1-5]. Based on the results of clinical investigations^[6-9], cryosurgery targeting at the pancreaticoduodenal region was considered safe and effective for unresectable pancreatic cancer. However, PGS caused by cryotherapy for pancreatic cancer (PCC), to our knowledge, has not been reported. As a unique complication of PCC, gastric stasis occurs in the early postoperative period in most of cases receiving PCC (67%), resulting in long-term loss of a large amount of gastric juice and delayed recovery of oral food intake, and occasionally, excessive gastric juice loss leads to body fluid deficit and metabolic alkalosis. To define the factors contributing to the development of PGS following PD or PCC, we performed this study to retrospectively examine the clinical data of 210 patients undergoing PD and 46 undergoing PCC.

MATERIALS AND METHODS

Subjects

From January 1990 to June 2003, 210 patients (147 male and 63 female patients, aged 35 to 75 years with a mean of 53.6 years) received PD in our hospital for pancreatic cancer or periampullary adenocarcinoma. None of the patients were preoperatively identified to have mechanical gastric outlet obstruction, but 95 had obstructive jaundice and 15 had hypoproteinemia.

During the period between January 1995 to March 2003, another 46 patients (including 31 male and 15 female patients, aged between 39 and 78 years with a mean of 54 years) underwent PCC for unresectable advanced pancreatic cancer, located in the pancreatic head in 21 cases, in the uncinate process in 15 cases, and in the pancreatic body and tail in 10 cases. All the tumors were identified by preoperative helical computed tomography (CT) scan and by intraoperative exploration, including 31 tumors with local involvement and 15 metastatic tumors. Preoperatively, 34 patients were identified to have obstructive jaundice and 6 had hypoproteinemia. All the patients, excluding the 8 with preoperative duodenal obstruction, were free of preoperative mechanical gastric outlet obstruction. Gastrojejunostomy was performed in 37 cases, and cholecystojejunostomy or choledochojejunostomy done in 32 cases during PCC for relief or prevention of the common bile duct and gastric outlet obstruction. Four patients also had concurrent splanchicectomy with ethanol.

Endoscopy or radiography was employed to identify and exclude cases of mechanical gastric outlet obstruction, and also to detect such problems of anastomotic stricture, efferent

limb obstruction, and jejuno gastric intussusception *etc.*, as well as food retention after a 4- to 8-h fast, for validating the diagnosis of gastroparesis.

Diagnostic criteria for PGS

At present, consensus has not been reached on the criteria for diagnosis of PGS. Stanciu^[10] suggested using gastric scintigraphy with ⁹⁹Tc-labeled low-fat meal as the gold standard for diagnosing delayed gastric emptying, which utilized gamma camera imaging of the abdomen following the ingestion of a radiolabeled meal, performed at regular intervals of 2 to 4 h to quantify the meal emptying in terms of percentages. Typically, meal emptying of over 50% within 2 h was considered normal, whereas delayed gastric emptying was indicated if gastric retention greater than 10% at 4 h. In this study, we formulated practical diagnostic criteria for PGS after consultation of the previous documentations in the literature^[5-7,10], as the following: (1) Absence of mechanical gastric outlet obstruction identified by one or more medical examination modalities; (2) A volume of gastric juice aspirate exceeding 800 mL/d that sustained for more than 10 d; (3) No abnormalities in water, electrolytes, or acid-alkali balance. (4) Absence of underlying diseases causing gastroparesis, such as diabetes, chorionitis, hypothyroidism, *etc.* (5) No history of using such agents as morphine, atropine, *etc.* that affected contraction function of the smooth muscle.

Surgical procedures

In PD group, the organs resected during PD included the gallbladder, common bile duct, head of the pancreas, the entire duodenum, with also subtotal gastrectomy. Proximal jejunum of 10 to 15 cm was also resected. The alimentary and biliary tracts were reconstructed with methods of Child or Whipple.

In patients of PCC group that defied surgical resection of the tumor, cryoprobes were deployed directly into the tumor for freezing to -196 °C twice, lasting for 10-15 min (using LCS 2000 cryogenic surgical system), with the common bile duct, stomach, and jejunum protected by dry cotton pads. Subsequent gastroenteroanastomosis, cholecystojejunostomy, or choledochojejunostomy were performed to reconstruct the alimentary and biliary tracts, according to the findings by intraoperative exploration. Care was taken to avoid freezing of the duodenal wall or causing other iatrogenic injuries such as damage to the biliary system or gastroduodenal artery. Jejunostomy was performed in some cases highly suspected of gastroparesis after PCC for postoperative enteral nutrition (EN) support.

Statistical analysis

The incidence of PGS in the two groups was compared and multiple factors were analyzed using χ^2 test. A *P* value less than 0.05 was considered statistically significant.

RESULTS

No serious complications took place in the PCC group, nor did operative death or complications occur in relation to the anastomosis. None of the patients developed fistula or pancreatitis. There was only transient elevation of amylase following the operation and the liver function and blood sugar remained normal. In PD group, in contrast, 4 patients developed serious complications after PD, including leakage at the pancreatojejunostomy in 2, bleeding at the anastomosis in 2 cases, stenosis of the anastomosis in 1 and stress peptic ulcer in 1 case. The mortality rate of PD in the perioperative period was 1.5%.

Ten of the 210 patients in PD group presented PGS within 5-10 d postoperatively. PGS developed in 31 of the 46 patients in PCC group, occurring within 5-7 d after the operation, including 29 patients with pancreatic head and uncinate tumors

and 2 with pancreatic body and tail tumors. In PD group, 14 patients with PGS received non-operative treatment such as medication, diet therapy, and nasogastric suction *etc.*, and 1 patient underwent reoperation on postoperative day 16, which, however, failed to relieve the symptoms. All patients with PGS in PCC group received non-operative treatment. Altogether 41 patients developed PGS in the two groups according to our diagnostic criteria, 15 of these cases were identified 4-7 d after withdrawal of the nasogastric tube and 10 were found to have a gradually increasing volume of gastric juice aspirate to 800 mL/d till 3-7 d after operation. Twenty of the 40 patients developed PGS 2-3 d after intake of liquid or semiliquid diet. Furthermore, the volume of gastric juice suction exceeded 2 000 mL/d in 4 cases following PCC and persisted for ten or more days (Table 1).

PGS following cryosurgery was closely associated with PCC, tumor location, but not with age, gender, obstructive jaundice, hypoproteinemia, preoperative gastric outlet obstruction or the type and number of gastric biliary tract operations (Table 2). PGS following PD was related with age, hypoproteinemia, preoperative gastric outlet obstruction and the type and number of gastric operations performed. Patients undergoing PCC were more likely to develop PGS than those undergoing PD (67% vs 4.8%, $\chi = 145$, $P < 0.001$).

DISCUSSION

Many debates over the etiology and pathophysiology of PGS remain unresolved. Clinically, the frequency of this complication varies in close association with the type and number of gastric operations performed. Donahue *et al.*^[11] reported a 26% incidence of chronic morbidity in patients after truncal vagotomy and antrectomy compared with a 5% incidence after highly selective vagotomy. There also appears to be a greater incidence of PGS associated with antrectomy and Roux-en-Y reconstruction compared with more conventional Billroth I and Billroth II reconstructions. Therefore, the main factor contributing to PGS is denervation and the consequent atony of the gastric remnant rather than disruption of the pacemaker activity in the Roux limb.

The exact mechanisms responsible for PGS after gastric surgery remain unclear but are likely to be multifactorial. The loss of gastric parasympathetic control resulted from vagotomy contributes to PGS via several mechanisms. In the proximal stomach, loss of vagal control leads to accelerated emptying of liquids by disrupting the late-stage tonic contractions responsible for relaxation and accommodation of the gastric fundus. In the distal stomach, vagotomy weakens antral peristaltic contraction responsible for breakdown of chyme. When coupled with the observed decrease in intestinal secretion of prokinetic hormones seen after truncal vagotomy, this leads to delayed emptying of solid substances. Also, the loss of vagal suppression of the ectopic intestinal pacemakers may cause dissociation of the antral pressure waves from the duodenal waves. The consequent disruption of wave sequence prolongs the lag phase of solid food digestion during which food is broken down into small particles by retropulsion and further delays the digestive process^[12,13].

Recently, it has been recognized that interstitial cells of Cajal generate electrical pacemaker activity and mediate motor neurotransmission in the stomach. The interstitial cells of Cajal are located in the muscular wall of the gastric corpus and antrum. Gastric dysrhythmias (tachygastrias and bradygastrias) are disturbances of the normal gastric pacesetter potentials and are associated with such symptoms as nausea, epigastric fullness, bloating and delayed gastric emptying. Ordog *et al.*^[14] suggest that damage to interstitial cells of Cajal may play a key role in the pathogenesis of diabetic gastropathy. Meanwhile, Zarate *et al.*^[15] reported that histological and immunohistochemical

Table 1 Clinical data of the PGS cases

Patient No	Gender	Age (yr)	Operation type	Mean volume of gastric juice aspirate/d (mL)	Period of nasogastric tube aspirate(d)	Period of recovery (d)	Outcome
1	M	53	PCC+A+B	2 200	56	70	Recovery
2	F	39	PCC+B	1 200	13	28	Recovery
3	F	62	PCC+A+C	1 000	10	14	Recovery
4	M	60	PCC+A+C	1 000	21	21	Recovery
5	M	51	PCC+A	850	10	30	Recovery
6	M	61	PCC+A+B	1 250	15	26	Recovery
7	M	62	PCC+A+C	1 200	13	35	Recovery
8	F	60	PCC+C	1 300	11	43	Recovery
9	F	40	PCC+A+B	2 000	25	25	Recovery
10	F	61	PCC +C	1 200	19	14	Recovery
11	M	64	PCC+A+B	1 200	18	Death on d 13 for diabetes complication	Death
12	F	78	PCC	1 500	19	Discharged on d 24 ¹	Recovery
13	M	50	PCC+A+C	1 050	12	49	Recovery
14	M	50	PCC+A+C	1 400	15	Transferred to another hospital on d 16	Recovery
15	M	42	PCC	1 450	17	14	Recovery
16	M	46	PCC+A+C	2 000	18	21	Recovery
17	M	43	PCC+A+B	1 200	13	20	Recovery
18	M	73	PCC +B	800	10	19	Recovery
19	M	46	PCC	1 350	14	18	Recovery
20	M	62	PCC+A+B+D	900	11	19	Recovery
21	M	40	PCC+A+C	1 300	15	20	Recovery
22	F	50	PCC +C	2 050	24	32	Recovery
23	F	61	PCC+A+C	1 200	15	20	Recovery
24	M	39	PCC+A+B	1 000	12	Discharged on d 16 ¹	Recovery
25	M	53	PCC+A	1 050	13	17	Recovery
26	F	42	PCC+A+B	900	11	18	Recovery
27	M	60	PCC+A+C	1 800	19	25	Recovery
28	M	62	PCC	1 700	20	30	Recovery
29	M	60	PCC+A+C	1 050	12	20	Recovery
30	M	40	PCC+A+C	1 250	12	17	Recovery
31	F	64	PCC+A+B	1 300	13	31	Recovery
32	M	75	PD	1 200	12	16	Recovery
33	F	42	PD	850	10	15	Recovery
34	F	35	PD	1 050	10	19	Recovery
35	M	45	PD	1 250	11	Death on d 16 for complications	Death
36	F	48	PD	1 050	11	17	Recovery
37	M	56	PD	1 450	16	21	Recovery
38	M	60	PD	1 400	14	20	Recovery
39	F	65	PD	1 500	15	20	Reoperation at 16 th d
40	M	47	PD	1 250	13	18	Recovery
41	M	63	PD	1 600	16	21	Recovery
mean±SD		53.8±13		1 180±310	15.5±6	23.1±9	

A: Gastroenteroanastomosis; B: Cholecystojejunostomy; C: Choledochojejunostomy; D: Chemical splanchnicectomies. ¹Discharged on request by the patient.

study of the resected specimen showed hypoganglionosis, neuronal dysplasia, and marked reduction in both myenteric and intramuscular interstitial cells of Cajal in patients with idiopathic gastroparesis.

Certainly, PGS after gastric surgery also can be due to

muscular, neural, or humoral abnormalities. Hypothyroidism and diabetes^[4] have been identified as contributing factors to gastroparesis in some patients. In patients without an identified cause, the gastroparesis is labeled as idiopathic. The mechanisms of PGS following PD is similar to that after gastrectomy.

Table 2 Correlation between multiple factors and PGS after PCC

Group	Age (yr)		Gender		Hypoproteinemia		Jaundice		Surgical procedure		Tumor location		Outlet obstruction	
	60	<60	M	F	Y	N	Y	N	PCC+A (or B, C, D)	PCC	Head and uncinate	Body and tail	Y	N
PGS	15	16	21	10	2	29	22	9	27	4	29	2	5	26
NO PGS	7	8	10	5	4	11	12	3	12	3	7	8	3	12
<i>P</i>	NS		NS		NS		NS		NS		<0.05		NS	

NS: No-significant.

The results of our observations suggest no significant direct relation of PGS following PCC with the types of gastric operations or the loss of gastric parasympathetic control, nor was it related to the patients' age or presence of hypoproteinemia or preoperative gastric outlet obstruction (Table 2), which, however, might be the factors contributing to PGS after gastrectomy or PD^[1-5]. We therefore suggest that the mechanism of PGS after PCC may differ, at least partially, from that underlying the PGS following gastrectomy or PD.

Patients with tumors located in the pancreatic head and uncinate process are at higher risk to develop PGS following PCC than those with tumors in the pancreatic body and tail (Table 2). The interstitial cells of Cajal in the muscular wall of the gastric corpus and antrum are exposed to likely damage during the freezing of the pancreatico-duodenal area, which offers a possible explanation for the pathogenesis of PGS after PCC.

Pylorus-preserving pancreatoduodenectomy (PPPD) frequently results in gastric stasis^[12,16], which occurs in 20% to 50% of the patients during the early postoperative period. As the duodenum has proved to be important in the initiation and consolidation of phase III activity of the migrating motor complex (MMC) of the stomach, its removal severely undermines the gastric phase III, hence gastric stasis may occur. On the basis of their findings that patients undergoing PPPD had slower recovery of gastric phase III and lower plasma motilin concentrations than those undergoing duodenum-preserving pancreatic head resection, Matsunaga *et al.*^[16] concluded that PGS after PPPD might be attributed, at least in part, to delayed recovery of gastric phase III activity due to lowered concentrations of plasma motilin after resection of the duodenum. However, resection of the pancreas does not seem to affect gastrointestinal motility. Malfertheiner and Sarr^[17] reported that even a total pancreatectomy failed to obviously affect the motor activity of the entire upper gastrointestinal tract in dogs.

We found in this study that PGS developed in 67% of all patients after PCC through multifactorial mechanisms, which could be at least partially in common with those underlying the PGS resulted from PPPD. The possible factors responsible for PGS after PCC include ischemic and neural injury to the antropyloric muscles and the duodenum after freezing of the pancreatico-duodenal area (but not to direct freezing of the duodenal pacemaker) and reduced circulating levels of motilin originally produced by the enterochromaffin cells in the duodenum and proximal jejunum. The peak plasma motilin concentration occurs in line with phase III activity of the interdigestive MMC in the stomach and duodenum. The phase III starts in the gastroduodenal region and migrates downward along the small intestine, hence its nickname the "housekeeper". The housekeeper function of phase III may be important to empty the gastric juice in the postoperative period after PCC. As the duodenum plays a role in the initiation and consolidation of gastric phase III, the injury of the duodenum by freezing -and thus the interruption of gastric phase III- may be one of the several possible causes of PGS after PCC. But still, the above hypotheses currently have to remain hypothetical, and the exact mechanisms of PGS caused by PCC must await

further investigation.

Patients with PGS have non-specific symptoms of early satiety, postprandial bloating, nausea, and vomiting, and the volume of gastric juice suction in most of them can increase gradually during early postoperative period. The diagnosis of PGS is often difficult to confirm. In the absence of identifiable anatomic problems such as anastomotic stricture, efferent limb obstruction, or jejuno gastric intussusception, other causes of gastric dystonia must be carefully examined. Hypothyroidism has been identified as a contributing factor to gastroparesis in some patients. Gastroparesis can also occur in patients with diabetes^[18,19]. Several complementary diagnostic modalities may be used to confirm the diagnosis of PGS. Fiberoptic endoscopy or radiography of the upper gastrointestinal tract should be performed routinely to exclude anatomical causes of gastric outlet obstruction. Radionuclide GESs can also be necessary, for clinical evaluation and conventional radiographic studies are often unreliable. If endoscopy and radionuclide scintigraphy are inconclusive, a small bowel contrast study should be performed to rule out possible mechanical lesions and/or generalized gut hypomotility. Although not routinely available^[20], electromyography of the gastrointestinal tract may provide valuable assistance in the diagnosis of patients with complex motility disturbances.

As the treatment of gastroparesis is far from ideal, nonconventional approaches and nonstandard medications might be of use. Traditional medical therapy consists of behavioral and diet modification, nasogastric tube suction and the use of prokinetic drugs such as bethanecol, metoclopramide, erythromycin and the more recent cisapride^[10]. Dietary measures and prokinetic drugs may help relieve the symptoms in most patients, while some patients with severe nausea and vomiting require antiemetic medications. A few patients fail medical therapy and continue to have debilitating symptoms of gastroparesis, who may benefit from a venting gastrostomy^[18] or jejunostomy performed surgically, endoscopically, or fluoroscopically^[20]. Near-completion gastrectomy (NCG) has proved useful in small series of patients^[21], but data on long-term follow-up has been lacking. Gastric electrical stimulation can be of value in the management of gastroparesis^[22-24], in which the patients with PGS received continuous high-frequency/low-energy gastric electrical stimulation via electrodes deposited in the muscular wall of the antrum and connected to a neurostimulator in an abdominal wall pocket. This method produced entrainment of the intrinsic slow wave and promoted contractions in phase III with the normal slow wave. This is why a suitable stimulation to the stomach during gastroscopic examination is also helpful for the remission of PGS^[3-5]. In this study, 5 patients received gastroscopic examination and the symptoms were markedly relieved. Ten patients with PGS were treated with acupuncture, and the effects were satisfactory.

According to our experience, all patients of PGS caused by PD or PCC need to undergo a long period of nasogastric suction till the clinical symptom relief or recovery occurs. The patients may experience epigastric fullness, nausea, or even vomiting, if

the nasogastric tube is withdrawn too early. Therefore, almost all of the patients with PGS in this study received the gastric juice suction over an average period of 2.2 wk, with the longest exceeding 8 wk. Because of long-term absence of food intake, these patients required nutritional support with a feeding jejunostomy tube or underwent a period of parenteral nutrition. The jejunostomy tube, as we believe, is safe, economic and practical for nutrition support in such patients, because their small intestinal peristaltic contractions and absorption function were normal in spite of PGS. Clinically, almost all of the patients had a concurrent jejunostomy during cryosurgery, considering the likeliness of these patients to develop delayed gastric emptying and for administration of postoperative enteral nutrition support. We consider that the non-operative treatments are effective for PGS after PCC or PD, and gastric reoperations should be avoided.

REFERENCES

- Naritomi G, Tanaka M, Matsunaga H, Yokohata K, Ogawa Y, Chijiwa K, Yamaguchi K. Pancreatic head resection with and without preservation of the duodenum: Different postoperative gastric motility. *Surgery* 1996; **120**: 831-837
- Toyota N, Takada T, Yasuda H, Amano H, Yoshida M, Isaka T, Hijikata H, Takada K. The effects of omeprazole, a proton pump inhibitor, on early gastric stagnation after a pylorus-preserving pancreaticoduodenectomy: results of a randomized study. *Hepatogastroenterology* 1998; **45**: 1005-1010
- Cai YT, Qin XY. Clinical analysis of 15 cases with gastroparesis after radical gastrectomy. *Zhongguo Shiyong Waikē Zazhi* 1999; **19**: 338-340
- Qin XY, Lei Y. Functional delayed gastric emptying after gastrectomy. *Zhongguo Weichang Waikē Zazhi* 2000; **3**: 7-9
- Lui FL, Qin XY. Clinical analysis of 20 cases with postsurgical gastroparesis syndrome after radical subtotal gastrectomy. *Zhonghua Weichang Waikē Zazhi* 2002; **5**: 245-248
- Kovach SJ, Hendrickson RJ, Cappadona CR, Schmidt CM, Groen K, Koniaris LG, Sitzmann JV. Cryoablation of unresectable pancreatic cancer. *Surgery* 2002; **131**: 463-464
- Patiutko IuI, Barkanov AI, Kholikov TK, Lagoshnyi AT, Li LI, Samoilenko VM, Afrikian MN, Savel'eva EV. The combined treatment of locally disseminated pancreatic cancer using cryosurgery. *Vopr Onkol* 1991; **37**: 695-700
- Li B. The current status of combined treatment for pancreatic carcinoma. *Zhongguo Puwai Jichu Yu Linchuang Zazhi* 2000; **7**: 390-392
- Chen XL, Wang D, Yan LN, Li B, Wang XY, Yang BY. Experimental study of cryosurgery for isolated pancreano-duodinal area: a possible therapy for pancreano-duodinal neoplasm. *Zhongguo Puwai Jichu Yu Linchuang Zazhi* 1998; **5**: 324-325
- Stanciu GO. Gastroparesis and its management. *Rev Med Chir Soc Med Nat Iasi* 2001; **105**: 451-456
- Donahue PE, Bombeck CT, Condon RE, Nyhus LM. Proximal gastric vagotomy versus selective vagotomy with antrectomy: Results of a prospective, randomized clinical trial after four to twelve years. *Surgery* 1984; **96**: 585-590
- Horowitz M, Dent J, Fraser R, Sun W, Hebbard G. Role and integration mechanisms controlling gastric emptying. *Dig Dis Sci* 1994; **39**(Suppl 12): 7S-13S
- Schirmer BD. Gastric atony and the Roux syndrome. *Gastroenterol Clin North Am* 1994; **23**: 327-343
- Ordog T, Takayama I, Cheung WK, Ward SM, Sanders KM. Remodeling of networks of interstitial cells of Cajal in a murine model of diabetic gastroparesis. *Diabetes* 2000; **49**: 1731-1739
- Zarate N, Mearin F, Wang XY, Hewlett B, Huizinga JD, Malagelada JR. Severe idiopathic gastroparesis due to neuronal and interstitial cells of Cajal degeneration: pathological findings and management. *Gut* 2003; **52**: 966-970
- Matsunaga H, Tanaka M, Takahata S, Ogawa Y, Naritomi G, Yokohata K, Yamaguchi K, Chijiwa K. Manometric evidence of improved early gastric stasis by erythromycin after pylorus-preserving pancreaticoduodenectomy. *World J Surg* 2000; **24**: 1236-1242
- Malfertheiner P, Sarr MG, Dimagno EP. Role of the pancreas in the control of interdigestive gastrointestinal motility. *Gastroenterology* 1989; **96**: 200-205
- Watkins PJ, Buxton-Thomas MS, Howard ER. Long-term outcome after gastrectomy for intractable diabetic gastroparesis. *Diabet Med* 2003; **20**: 58-63
- Lehmann R, Honegger RA, Feinle C, Fried M, Spinass GA, Schwizer W. Glucose control is not improved by accelerating gastric emptying in patients with type 1 diabetes mellitus and gastroparesis. A pilot study with cisapride as a model drug. *Exp Clin Endocrinol Diabetes* 2003; **111**: 255-261
- Koch KL. Electrogastrography: physiological basis and clinical application in diabetic gastropathy. *Diabetes Technol Ther* 2001; **3**: 51-62
- Jones MP, Maganti K. A systematic review of surgical therapy for gastroparesis. *Am J Gastroenterol* 2003; **98**: 2122-2129
- Abell T, Lou J, Tabbaa M, Batista O, Malinowski S, Al-Juburi A. Gastric electrical stimulation for gastroparesis improves nutritional parameters at short, intermediate, and long-term follow-up. *J Parenter Enteral Nutr* 2003; **27**: 277-281
- Lin Z, Forster J, Sarosiek I, McCallum RW. Treatment of gastroparesis with electrical stimulation. *Dig Dis Sci* 2003; **48**: 837-848
- Lawlor PM, McCullough JA, Byrne PJ, Reynolds JV. Electrogastrography: a non-invasive measurement of gastric function. *Ir J Med Sci* 2001; **170**: 126-131

Edited by Chen WW Proofread by Zhu LH and Xu FM

Simultaneous detection of HBV and HCV by multiplex PCR normalization

Ning Wang, Xue-Qin Gao, Jin-Xiang Han

Ning Wang, Xue-Qin Gao, Jin-Xiang Han, Shandong Medicinal Biotechnological Center, Shandong Academy of Medical Sciences; Key Laboratory for Biotechdrugs, Ministry of Public Health, Jinan 250062, Shandong Province, China

Supported by the National Key Technology Research and Development Program of China during the 9th Five-Year Plan Period, No. 96C020117

Correspondence to: Professor Jin-Xiang Han, Shandong Medicinal Biotechnological Center, Shandong Academy of Medical Sciences; Key Laboratory for Biotechdrugs, Ministry of Public Health, Jinan 250062, Shandong Province, China. jxhan@sdu.edu.cn

Telephone: +86-531-2919888

Received: 2003-08-23 **Accepted:** 2003-10-07

Abstract

AIM: To design and establish a method of multiplex PCR normalization for simultaneously detecting HBV and HCV.

METHODS: Two pairs of primers with a 20 bp joint sequence were used to amplify the target genes of HBV and HCV by two rounds of amplification. After the two rounds of amplification all the products had the joint sequence. Then the joint sequence was used as primers to finish the last amplification. Finally multiplex PCR was normalized to a single PCR system to eliminate multiplex factor interference. Four kinds of nucleic acid extraction methods were compared and screened. A multiplex PCR normalization method was established and optimized by orthogonal design of 6 key factors. Then twenty serum samples were detected to evaluate the validity and authenticity of this method.

RESULTS: The sensitivity, specificity, diagnostic index and efficiency were 83.3%, 70%, 153.3% and 72.2%, respectively for both HBsAg and anti-HCV positive patients, and were 78.6%, 80%, 258.6% and 79.2%, respectively for HBsAg positive patients, and were 75%, 90%, 165% and 83.3%, respectively for anti-HCV positive patients.

CONCLUSION: The multiplex PCR normalization method shows a broad prospect in simultaneous amplification of multiple genes of different sources. It is practical, correct and authentic, and can be used to prevent and control HBV and HCV.

Wang N, Gao XQ, Han JX. Simultaneous detection of HBV and HCV by multiplex PCR normalization. *World J Gastroenterol* 2004; 10(16): 2439-2443

<http://www.wjgnet.com/1007-9327/10/2439.asp>

INTRODUCTION

Multiplex PCR uses several pairs of primers that target different genes to simultaneously amplify several different target sequences at a high speed and with a high efficiency. As many amplification factors may interact and produce non-specific amplification, its clinical use is limited. According to the characteristics of a small fragment that did not complement to

the genes of PCR primers, we established a multiplex PCR normalization method (This method has been patented in the Chinese Patent Agency). By creating a primary reaction that was appropriate to all target templates, the multiplex was normalized to a single target PCR. This method could overcome the difficulties in establishing and optimizing the multiplex reaction system. In this article the practicality and effectiveness of multiplex PCR were validated by simultaneous detection of HBV and HCV.

MATERIALS AND METHODS

Specimen collection

Twenty-eight serum samples were collected from Jinan Central Hospital and Jinan Infectious Disease Hospital. The samples were all validated by ELISA method, in which 14 cases were HBsAg (+), 8 were anti-HCV (+), and 6 were positive for both HBsAg and anti-HCV. Ten cases were negative for both HBsAg and anti-HCV and used as control.

Reagents and instruments

HBV PCR kits and HCV PCR kits were purchased from Institutes of Liver Diseases, Peking University Medical College. dNTPs, AMV, proteinase K, isothiocyanate guanidine and Triton X-100 were products of TAKARA. PCR Amplification Minicycler™ was from MJ Research, USA. Innotech Imager™ 2200 was from Alpha Innotech Incorporation.

Extraction of virus nucleic acids

Method 1^[1]: Proteinase K (10 mg/mL) was added to 150 µL serum and incubated at 50 °C for 2 h. RNA and DNA were extracted with phenol-chloroform at pH4.0 and 8.0 respectively, and then nucleic acids were precipitated with Isopropyl alcohol. The final pellets were dissolved in 10 µL RNase free water and stored at -70 °C.

Method 2^[2]: 200 µL guanidine isothiocyanate and 20 µL glass powder were added to 200 µL serum and incubated at ambient temperature for 90 min and centrifuged at 12 000 g. The supernatant was removed and the pellet was washed and dissolved in reverse transcription buffer PCR detection.

Method 3^[3]: 90 µL lytic buffer (120 g GUSCN, 100 mL 0.1 mol/L Tris-HCl, pH6.4), 0.2 mol/L EDTA (20 µL, pH8.0) and glass powder were added to 50 µL serum and incubated at room temperature for 10 min, mixed and centrifuged at 12 000 g for 15 s, washed 2 times with washing solution (120 g GUSCN, 100 mL 0.1 mol/L Tris-HCl, pH 6.4, 2.6 g Triton ×100), and further washed with 700 mL/L ethanol and acetone. Then acetone was removed and dried at 56 °C for 10 min and TE buffer was added to the pellets and incubate at 56 °C for 2 min and then centrifuged for 2 min. The supernatant was transferred to another tube for further amplification.

Method 4^[4]: 200 µL lytic buffer [6 mol/L guanidine hydrochloride, 10 mmol/L Tris-HCl (pH 7.5), 200 g/L Triton X-100 (pH 4.4)], and 10 mmol/L urea, were added to 200 µL serum, proteinase K 40 µL, glass powder 10 µg, and incubated in 72 °C water bath for 10 min, then 100 µL Isopropyl alcohol was added and centrifuged at 8 000 r/min for 1 min. The supernatant was removed, and washed with 100 µL washing solution [20 mmol/L NaCl, 20 mmol/L Tris-HCl (pH7.5) and 1 000 mL/L ethanol] and

centrifuged at 8 000 r/min for 1 min. The supernatant was removed and washed and centrifuged at 8 000 r/min for 1 min and 13 000 g for 10 s, dried and dissolved in 50 μ L RNase free water.

Primer design

The primers for the first round of PCR: HBV reverse primer: 5'-GAT GAT GGG ATG GGA ATA CA-3' (position: 2 566-2 586 of P gene), HBV RT primer: 5'-GCT GGT TCA CAT TGT GAG GGG AGT CTA GAC TCG TGG TGG A-3' with the former 20 bp as the joint sequence, and the latter 20 bp in the position of the overlap of genome P region and Pre-S region (position 2 921-2 941). There was a 395 bp between R and RT primers. HCV reverse primer: 5'-ATC ACT CCC CTG TGA GGA A-3' which was located between 47-65 bp. RT-PCR primer: 5'-GCT GGT TCA CAT TGT GAG GGC TAC GAG ACC TCC CGG GGC A-3'. The former 20 bp was the joint sequence, the latter 20 bp was in 313-332 of HBV genome. The product between R and RT primers was a 315 bp fragment. The second round primers: N primer sequence was 5'-GCT GGT TCA CAT TGT GAG GG TAG AGG ACA AAC GGG CAA CA3', the former 20 bp was the joint sequence, and the latter 20 bp was in 2 703-2 723 of HBV genome. RT-PCR primer was the same as that of the first round, the amplification product was a 278 bp fragment between N and RT. The HCV N primer was 5'-GCT GGT TCA CAT TGT GAG GGG GAG GCC AT AGT GGT CTG-3', the former 20 bp was the joint sequence, and the latter 20 bp was located between 132-151 of HCV. RT primers were the same as the first round of amplification and the product was a 241 bp fragment. After two rounds of amplification, the third round was amplified with the common primers T: 5'-GCT GGT TCA CAT TGT GAG GG3'. The primers were synthesized by phosphoamidite method with 391 DNA synthesizer. The synthesized primers were purified with OPC column^[5].

Quality evaluation parameters of designed diagnostic assay

Sensitivity indicated the percent of positive cases by the diagnostic assay in the patient group. It was calculated according to the following formula.

$$\text{Sensitivity} = \frac{\text{True positivity}}{\text{True positive} + \text{false negative}} \times 100\%$$

The sensitivity should be 100% for a perfect diagnostic assay.

Specificity indicated the percent of negative cases determined by the diagnostic assay in control group. It was calculated according to the following equation.

$$\text{Specificity} = \frac{\text{True negativity}}{\text{False positivity} + \text{true negativity}} \times 100\%$$

The specificity should be 100% for a perfect diagnostic assay.

Diagnostic index was a combined parameter to evaluate the sensitivity and specificity. It was the sum of sensitivity and specificity. The perfect diagnostic index should be 200%, and

it should not be lower than 100%.

Agreement rate indicated the ability of a diagnostic assay to correctly discern the patients and control cases. It was calculated by the following method. The perfect agreement rate of a diagnostic assay should be 100%.

$$\text{Agreement rate} = \frac{\text{TP} + \text{TN}}{\text{TP} + \text{FP} + \text{TN} + \text{FN}} \times 100\%$$

(TP: true positivity; TN: true negativity; FP: false positivity; FN: false negativity).

Positive predictive value (PPV) indicated the percent of patients in the positive results of diagnostic assay. It was calculated according to the following equation.

$$\text{PPV} = \frac{\text{TP}}{\text{TP} + \text{FP}} \times 100\%$$

Negative predictive value (NPV) indicated the percent of non-patients in the negative results of diagnostic assay. It was calculated according to the following equation.

$$\text{NPV} = \frac{\text{TN}}{\text{FN} + \text{TN}} \times 100\%$$

(NPV: negative predictive value; TN: true negativity; FN: false negativity; TN: true negativity).

RESULTS

Screening extraction methods for HBV DNA from HBsAg positive serum

Four methods were used to extract HBV DNA from HBsAg positive sera of patients. The results of amplification were compared to that of ELISA (Table 1).

The positive amplification rates were 20%, 60%, 85% and 95% for methods 1 to 4 respectively.

Screening the extracting methods of HCV RNA from anti-HCV positive serum

Fifteen anti-HCV positive sera were extracted with the four methods and the results were compared with ELISA (Table 2).

The positive amplification rates were 6%, 6%, 30% and 95% for methods 1 to 4, respectively compared to the ELISA.

Establishment of simultaneous extraction method of HBVDNA and HCV RNA

Six samples positive for both HBsAg and anti-HCV were extracted and amplified, the simultaneous extraction positive rate was 100% for HBV and 83% for HCV, respectively.

Establishment of RT and first round of amplification method

Orthogonal method was used to select the six common factors

Table 1 Amplification results of HBV DNA from 20 HBsAg positive sera

Method	Sample number																			
	1	2	3	4	5	6	7	8	9	10	11	12	13	14	15	16	17	18	19	20
ELISA	+	+	+	+	+	+	+	+	-	+	+	+	+	+	+	+	+	+	+	+
Method 1	-	-	+	+	+	-	+	-	-	-	-	+	-	-	-	-	-	-	-	-
Method 2	+	-	-	+	+	+	+	+	+	-	+	+	+	-	-	-	+	+	-	-
Method 3	+	+	+	+	+	+	+	+	+	-	-	+	+	+	+	-	+	+	+	+
Method 4	+	+	+	+	+	+	+	+	+	+	+	+	+	+	+	-	+	+	+	+

Note: + represents positive amplification; - represents negative amplification.

Table 2 Amplification results of HCV RNA from 15 anti-HCV positive sera

Method	Sample number														
	1	2	3	4	5	6	7	8	9	10	11	12	13	14	15
ELISA	+	+	+	+	+	+	+	+	+	+	+	+	+	+	+
Method 1	-	-	-	-	-	-	-	-	+	-	-	-	-	-	-
Method 2	-	-	-	+	-	-	-	-	-	-	-	-	-	-	-
Method 3	-	+	+	+	-	-	-	-	+	+	-	-	+	-	-
Method 4	+	+	+	+	+	+	+	+	+	+	-	+	+	+	+

Note: + represents positive amplification; - represents negative amplification.

affecting the amplification, which were the concentrations of dNTPs, Mg²⁺, Taq polymerase, AMV and primers (including HBV and HCV). Five levels were designed for each factor. The pattern of orthogonal was L 25^[5,6]. The PCR reaction was as follows: HBV, 8 μL HCV template, 5 μL 10×buffer, 40 U RNase inhibitor, and other components and finally ddH₂O was added to make the total volume 50 μL. Twenty-five kinds of amplification system were available. After paraffin oil was added, reactions were performed at 50 °C for 30 min, at 95 °C for 2 min, and 30 cycles at 95 °C for 30 s, at 55 °C for 30 s, at 72 °C for 1 min. Then 10 μL amplification product was identified by 15 g/L agarose electrophoresis. The results showed under the condition of protocol 13, that both HBV and HCV targets were successfully amplified, therefore protocol 13 was chosen as the first round protocol. The amplification program was at 50 °C for 30 min, at 95 °C for 2 min, and at 95 °C for 30 s, at 55 °C for 30 s and at 72 °C for 1 min for a total of 30 cycles.

Screening of the second round of amplification reaction condition

According to the orthogonal method and experience, 6 protocols were designed. The reaction condition was at 95 °C for 30 s, at 55 °C for 30 s, and at 72 °C for 45 s for a total of 10 cycles. The results showed that the two target bands of HBV and HCV were successfully separated in protocol 1. Therefore the protocol 1 was chosen as the final optimal protocol.

Screening of the third round of amplification reaction

According to the results of the above two rounds of amplification, 7 protocols were designed for the third round of amplification. All the amplification reactions were done at 95 °C for 30 s, at 55 °C for 30 s, at 72 °C for 1 min for a total of 30 cycles. The results showed that the HBV and HCV target bands were discerned more obviously under the condition of protocol 2, which was therefore determined as the optimal protocol.

Comparison of normalized PCR detection results with ELISA method

Twenty-eight samples were detected with both normalized PCR method and ELISA method. In the 14 samples positive for HBsAg, the results of the six antibody-positive amplifications are shown in Figure 1. The concordance of PCR with ELISA was 78.8%. Eight anti-HCV positive samples detected with multiplex PCR had a coincidence rate of 75% compared with ELISA method. When it was used to detect samples positive for both HBsAg and anti-HCV, the coincidence rate was 83.3%. Ten control cases negative for both HBsAg and anti-HCV were also detected with normalized PCR, of which 2 were positive for HBV and 1 for HCV.

Quality evaluation of simultaneous PCR detection of HBV and HCV

Fourteen patients with HBV infection were detected with normalized PCR method. The results showed that the true positivity was 11 and the false negativity was 3 (Table 3).

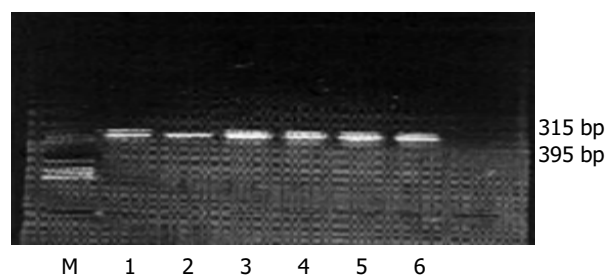


Figure 1 Normalized PCR amplification for patients with both HBsAg and anti-HCV antibodies. M represents X174-hae III marker. Lanes 1 to 6 represent amplification results of six patients who were positive for HBsAg and anti-HCV. Only lane 2 is negative for HCV.

Of the eight HCV patients detected with normalized method, 6 were positive and 2 were negative. Six patients with both HBV and HCV infection were also detected, of which 5 were positive and 1 was negative (Figure 1 and Table 4). Ten patients without HBsAg and anti-HCV infection were also detected with our method, of which 8 were negative for HBV and 2 were positive for HBV (false positivity), 9 were negative for HCV and 1 positive for HCV (false positivity) (Tables 3, 4).

Evaluation of validity and diagnostic power of normalized PCR for detecting HBV DNA

The sensitivity of this method for the detection of HBV DNA was 78.6% (11/14). The specificity was 80% (8/10). The diagnostic index was 158.6% (78.6% plus 80%) and the agreement rate was 79.2%. The positive predictive value was 84.6% (11/13). The negative predictive value was 72.7% (8/11) (Table 3).

Table 3 Evaluation of validity and diagnostic power of normalized PCR for detecting HBV DNA

	HBV patient	Non-HBV control	Total
Positive	11	2	13
Negative	3	8	11
Total	14	10	24

Table 4 Evaluation of validity and diagnostic power of normalized PCR for detecting HCV RNA

	HCV patients	Non-HCV control	Total
Positive	6	1	7
Negative	2	9	11
Total	8	10	18

Quality evaluation of validity and diagnostic power of normalized PCR for detecting HCV RNA

The sensitivity of this method for the detection of HCV RNA

was 75% (6/8). The specificity was 90% (9/10). The diagnostic index was 165% (75% plus 90%) and the diagnostic efficiency was 83.3%. The positive predictive value was 85.7% (6/7). The negative predictive value was 81.8% (9/11) (Table 4).

Evaluation of validity and diagnostic power of normalized PCR for detection of both HBV DNA and HCV RNA

The sensitivity of this method for the detection of superinfection of HBV DNA and HCV RNA was 83.3% (5/6). The specificity was 70% (7/10). The diagnostic index was 153.3% (83.3% plus 70%) and the diagnostic efficiency was 72.2%. The positive predictive value was 62.5%. The negative predictive value was 87.5% (Table 5).

Table 5 Evaluation of validity and diagnostic power of normalized method for detecting HBV and HCV double infection

	HBV(+)and anti-HCV(+)	HBV(-) and anti-HCV(-)	Total
Positive	5	8	13
Negative	1	2	3
Total	6	10	16

DISCUSSION

Virus particles of HBV and HCV are rare in blood and HCV RNA is easily to degrade, therefore selecting protein denaturing agents to quickly dissolve the membrane protein is very important in the process of simultaneous extraction of HBV and HCV nucleic acids. Our results showed that method 4 was the most effective among the four extraction methods. The effective extraction rate was 95% for both HBsAg and anti-HCV positive serum. In method 4, hydrochloride guanine was a potent protein denaturant, it could dissolve the protein and destruct its secondary structure and cell structure, and mad it possible to separate nucleotide protein from nucleic acids. Urea and Triton X-100 are non-detergents and could dissolve cell membrane and precipitate the protein. Proteinase K could further degrade protein. Glass powder had absorptive effect on nucleic acids and therefore could absorb nucleic acids on its surface. Isopropyl alcohol could precipitate nucleic acids and finally the low ion potential solution could elute nucleic acids from the glass powder. This method was confirmed to be effective and authentic, suitable for the separation of virus RNA and DNA. In practice, it was a simple, fast, stable and reproducible method.

Theoretically, there is no limit on the number of target sequences simultaneously amplified by multiplex PCR. But the stringency of specific conditions restricted the number of target sequences amplified. In order to overcome these limits, we established a multiplex normalized amplification method. First a nested PCR amplification was performed with 2 pairs of primers with a joint sequence. Then a normalized amplification was done with joint primers. The effects of competition of primers were the lowest, so that the multiplex PCR became a single target PCR. These measurements could overcome the difficulties in establishing and optimizing the conditions of multiplex PCR. The success of this method has shed some lights on the development of PCR techniques. We used the orthogonal method for the design of experiment^[6], and divided the key factors of PCR reaction such as primer concentration, dNTPs, Taq polymerase, AMV and magnesium chloride concentration into different grades, and a factor table was set up. This included all possible arrangements and combination of factors. The results showed that the coordination of proportion of the 6 factors was very important. If the proportion of HBV and HCV primers was not appropriate, and sometimes one of the amplifications was superior to another and only one band could

be identified by electrophoresis.

ELISA is a method to detect antibody for the purpose of diagnosis of virus infection. The antibody was only detected 1 to 2 wk after infection, which reflected the immune response of the host, but could not explain the virus replication. PCR method could directly detect the virus nucleic acids. It could reflect the state of virus replication. When the virus was cleaned up, only the antibody was positive, the nucleic acids could not be detected. That is why the detection rate of PCR was lower when ELISA was used as a golden standard. In this study, 1/8 of the anti-HCV patients were negative for HCV RNA, and 1/6 patients were positive for both HBsAg and HCV, which were undetectable by our method. This is partly because the patients were in the state of convalescence, and the virus was already cleaned up or was false positive for ELISA due to hyperimmunoglobulinemia, rheumatoid factor and superoxide dismutase. The detection of HCV RNA in non-hepatitis patients could be explained by the fact that the patients might be in the early stage of acute hepatitis, and the antibody had not been produced yet. A close follow-up is needed for the early diagnosis and treatment after the possibility of false positive is excluded.

Currently, the super-infection rate of HBV and HCV was very high, and it was 13.64% to 27.27% reported by Xu^[7]. It is important to establish methods that can simultaneously detect combined virus infection. Konomi *et al.*^[8] reported a multiplex polymerase chain reaction (PCR) method for simultaneous detection of hepatitis B, C, and G viral genomes. The levels of concordance with the data obtained by conventional single PCR method were 100% for single infection, 98-100% for double infection, and 92% for triple infection. Meng Q and his colleagues^[9] established an automatic multiplex system for simultaneously screening hepatitis B virus (HBV), hepatitis C virus (HCV), and human immunodeficiency virus type 1 (HIV-1) in blood donations. The detection limits (95% confidence interval) were 22 to 60 copies/mL for HBV, 61 to 112 IU/mL for HCV, and 33 to 66 copies/mL for HIV-1, using a specimen input volume of 0.2 mL. The AMPLINAT MPX assay could detect a broad range of genotypes or subtypes for all three viruses and had a specificity of 99.6% for all three viruses with sero-negative specimens. In an evaluation of sero-conversion panels, the AMPLINAT MPX assay detected HBV infection an average of 24 d before the detection of HBsAg by enzyme immunoassay. HCV RNA was detected an average of 31 d before HCV antibody appeared. HIV-1 RNA was detected an average of 14 d before HIV-1 antibody and an average of 9 d before p24 antigen. A Chinese group has designed a visual gene-detecting technique using nanoparticle-supported gene probes. With the aid of gold nanoparticle-supported 3'-end-mercapto-derivatized oligonucleotide serving as a detection probe, and 5'-end -amino-derivatized oligonucleotide immobilized on glass surface acting as a capturing probe, target DNA was detected visually by sandwich hybridization based on highly sensitive "nano-amplification" and silver staining. Different genotypes of hepatitis B and C viruses in serum samples from infected patients were detected using home made HBV, HCV, and HBV/HCV gene chips by the gold/silver nanoparticle staining amplification method. The present visual gene-detecting technique might avoid limitations of the reported methods due to for its high sensitivity, good specificity, simplicity, speed, and cheapness^[10].

Multiplex PCR assay has been used for the simultaneous detection of many different genes of pathogens including genes related with antibiotic resistance genes in *Staphylococcus aureus*^[11]. A multiplex reverse transcriptase polymerase chain reaction (RT-PCR) was also applied for the simultaneous detection of hepatitis A virus (HAV), poliovirus (PV) and simian rotavirus (RV-SA11), and compared with specific primers for

each genome sequence. Three amplified DNA products representing HAV (192 bp), PV (394 bp) and RV (278 bp) were identified when positive controls were used^[12]. A multiplex RT-PCR method was described for the simultaneous detection of all four viruses in combination with a plant mRNA specific internal control which could be used as an indicator of the effectiveness of the extraction and RT-PCR. The upper detection limit for the four viruses was at an extract dilution of 1/200^[13]. A multiplex semi-nested PCR was developed for the simultaneous detection and differentiation among porcine circovirus 1 (PCV1), PCV2, and porcine parvovirus (PPV) from boar semen. Primers of PCV1, PCV2 and PPV were specific and did not react with other viruses respectively. Twenty (20.4%) and 42 (42.9%) out of 98 whole semen samples were found to be positive for PCV and PPV using conventional multiplex and semi-nested PCR respectively^[14]. Multiplex method for HBV/HCV/HIV-1 has been used for screening 6 805 010 units of serologically negative donation and 112 HBV DNA-positives, 25 HCV RNA positives and 4 HIV-1 RNA positives were screened out and prevented transfusion of the positive blood^[15,16].

The sensitivity of our multiplex normalized PCR method was 78.6%, 75% and 83.3% for the detection of HBVDNA, HCV RNA, and super-infection of HBV and HCV respectively. The specificity was 80%, 90% and 70%, respectively. These are good enough for a diagnostic assay. It can detect both DNA and RNA simultaneously and can be completed in one day. It is not only suitable for clinical diagnosis, but also suitable for the screening of HBV and HCV from blood donors to prevent the transmission of these diseases. It can also be used for an epidemiological study. In these respects it needs to be further studied in a large-scale population.

REFERENCES

- 1 **Hu KQ**, Yu CH, Lee S, Villamil FG, Vierling JM. Simultaneous detection of both hepatitis B virus DNA and hepatitis C virus RNA using a combined one-step polymerase chain reaction technique. *Hepatology* 1995; **21**: 901-907
- 2 **Yamada O**, Matsumoto T, Nakashima M, Hagari S, Kamahora T, Ueyama H, Kishi Y, Uemura H, Kurimura T. A new method for extracting DNA or RNA for polymerase chain reaction. *J Virol Methods* 1990; **27**: 203-209
- 3 **Boom R**, Sol CJ, Salimans MM, Jansen CL, Wertheim-van Dillen PM, van der Noordaa J. Rapid and simple method for purification of nucleic acids. *J Clin Microbiol* 1990; **28**: 495-503
- 4 **Vogelstein B**, Gillespie D. Preparative and analytical purification of DNA from agarose. *Proc Natl Acad Sci U S A* 1979; **76**: 615-619
- 5 **Han JX**, Zhang C, Yang XC, Tang TH, Wang ML. Investigation on the purification and synthesizing of DNA fragments by OPC methods. *Shandong Yike Daxue Xuebao* 1995; **33**: 173-174
- 6 **Fang JQ**, Fu CZ, Liao RR. Regression methods of pair-wise data. *Zhongguo Weisheng Tongji* 1996; **13**: 1-5
- 7 **Xu ZF**, Xu KC, Meng XY. Investigation on the double infection of HBV and HCV. *Nantong Yixueyuan Xuebao* 1994; **14**: 162-165
- 8 **Konomi N**, Yamaguchi M, Naito H, Aiba N, Saito T, Arakawa Y, Abe K. Simultaneous detection of hepatitis B, C, and G viral genomes by multiplex PCR method. *Jpn J Infect Dis* 2000; **53**: 70-72
- 9 **Meng Q**, Wong C, Rangachari A, Tamatsukuri S, Sasaki M, Fiss E, Cheng L, Ramankutty T, Clarke D, Yawata H, Sakakura Y, Hirose T, Impraim C. Automated multiplex assay system for simultaneous detection of hepatitis B virus DNA, hepatitis C virus RNA, and human immunodeficiency virus type 1 RNA. *J Clin Microbiol* 2001; **39**: 2937-2945
- 10 **Wang YF**, Pang DW, Zhang ZL, Zheng HZ, Cao JP, Shen JT. Visual gene diagnosis of HBV and HCV based on nanoparticle probe amplification and silver staining enhancement. *J Med Virol* 2003; **70**: 205-211
- 11 **Strommenger B**, Kettlitz C, Werner G, Witte W. Multiplex PCR assay for simultaneous detection of nine clinically relevant antibiotic resistance genes in *Staphylococcus aureus*. *J Clin Microbiol* 2003; **41**: 4089-4094
- 12 **Coelho C**, Vinatea CE, Heinert AP, Simoes CM, Barardi CR. Comparison between specific and multiplex reverse transcription-polymerase chain reaction for detection of hepatitis A virus, poliovirus and rotavirus in experimentally seeded oysters. *Mem Inst Oswaldo Cruz* 2003; **98**: 465-468
- 13 **Thompson JR**, Wetzel S, Klerks MM, Vaskova D, Schoen CD, Spak J, Jelkmann W. Multiplex RT-PCR detection of four aphid-borne strawberry viruses in *Fragaria* spp. in combination with a plant mRNA specific internal control. *J Virol Methods* 2003; **111**: 85-93
- 14 **Kim J**, Han DU, Choi C, Chae C. Simultaneous detection and differentiation between porcine circovirus and porcine parvovirus in boar semen by multiplex seminested polymerase chain reaction. *J Vet Med Sci* 2003; **65**: 741-744
- 15 **Ohnuma H**, Tanaka T, Yoshikawa A, Murokawa H, Minegishi K, Yamanaka R, Lizuka HY, Miyamoto M, Satoh S, Nakahira S, Tomono T, Murozuka T, Takeda Y, Doi Y, Mine H, Yokoyama S, Hirose T, Nishioka K. The first large-scale nucleic acid amplification testing (NAT) of donated blood using multiplex reagent for simultaneous detection of HBV, HCV, and HIV-1 and significance of NAT for HBV. *Microbiol Immunol* 2001; **45**: 667-672
- 16 **Mine H**, Emura H, Miyamoto M, Tomono T, Minegishi K, Murokawa H, Yamanaka R, Yoshikawa A, Nishioka K. High throughput screening of 16 million serologically negative blood donors for hepatitis B virus, hepatitis C virus and human immunodeficiency virus type-1 by nucleic acid amplification testing with specific and sensitive multiplex reagent in Japan. *J Virol Methods* 2003; **112**: 145-151

Edited by Wang XL and Zhang JZ. Proofread by Xu FM

Role of endoscopic miniprobe ultrasonography in diagnosis of submucosal tumor of large intestine

Ping-Hong Zhou, Li-Qing Yao, Yun-Shi Zhong, Guo-Jie He, Mei-Dong Xu, Xin-Yu Qin

Ping-Hong Zhou, Guo-Jie He, Xin-Yu Qin, Department of General Surgery, Zhongshan Hospital, Fudan University, Shanghai 200032, China

Li-Qing Yao, Yun-Shi Zhong, Mei-Dong Xu, Endoscopic Center, Zhongshan Hospital, Fudan University, Shanghai 200032, China

Correspondence to: Dr. Ping-Hong Zhou, Department of General Surgery, Zhongshan Hospital, Fudan University, Shanghai 200032, China. chow@zshospital.net

Telephone: +86-21-64043947 **Fax:** +86-21-64038472

Received: 2003-12-10 **Accepted:** 2004-02-01

Abstract

AIM: To evaluate the role of miniprobe ultrasonography under colonoscope in the diagnosis of submucosal tumor of the large intestine, and to determine its imaging characteristics.

METHODS: Thirty-five patients with submucosal tumors of the large intestine underwent miniprobe ultrasonography under colonoscope. The diagnostic results of miniprobe ultrasonography were compared with pathological findings of specimens by biopsy and surgical resection.

RESULTS: Lipomas were visualized as hyperechoic homogeneous masses located in the submucosa with a distinct border. Leiomyomas were visualized as hypoechoic homogeneous mass originated from the muscularis propria. Leiomyosarcomas were shown with inhomogeneous echo and irregular border. Carcinoids were presented as submucosal hypoechoic masses with homogenous echo and distinct border. Lymphangiomas were shown as submucosal hypoechoic masses with cystic septal structures. Malignant lymphomas displayed as hypoechoic masses from mucosa to muscularis propria, while pneumatosis cystoides intestinalis originated from submucosa with a special sonic shadow. One large leiomyoma was misdiagnosed as leiomyosarcoma.

CONCLUSION: Endoscopic miniprobe ultrasonography can provide precise information about the size, layer of origin, border of submucosal tumor of the large intestine and has a high accuracy in the diagnosis of submucosal tumor of the large intestine. Pre-operative miniprobe ultrasonography under colonoscope may play an important role in the choice of therapy for submucosal tumor of the large intestine.

Zhou PH, Yao LQ, Zhong YS, He GJ, Xu MD, Qin XY. Role of endoscopic miniprobe ultrasonography in diagnosis of submucosal tumor of large intestine. *World J Gastroenterol* 2004; 10(16): 2444-2446

<http://www.wjgnet.com/1007-9327/10/2444.asp>

INTRODUCTION

Due to the development of colonoscope and CT, the reported number of submucosal tumor (SMT) of the large intestine has been increased. SMT of the large intestine includes lipoma,

lymphangioma, leiomyoma, carcinoid, metastatic tumor, *etc.* Previous diagnosis depended mainly on barium enema and colonoscope, but none of them could make clear the histological features of SMT, and it was also difficult to differentiate SMT from extramural compression. In the 1980 s, the development of endoscopic ultrasonography (EUS) significantly improved the accuracy of diagnosis of the digestive tract diseases^[1]. EUS can provide detailed information about gastrointestinal wall structure and adjacent organs. EUS is highly accurate in the visualization of submucosal lesions and their sonographic layer of origin within gastrointestinal wall. Concerning SMT of the digestive tract, several studies have been published mainly in upper digestive tract^[2-4], but there have been few studies on SMT of the lower digestive tract. The aim of this study was to assess the value of EUS in the diagnosis of SMT of the large intestine and determine their imaging characteristics.

MATERIALS AND METHODS

Patients

EUS was performed in 35 patients with elevated lesions which had normal mucosal vision under colonoscope between January 2001 and November 2003. The patient group comprised 19 men and 16 women with a mean age of 54.6 years (range, 32-72 years). The diameter of lesions ranged 0.5-4.2 cm. Of the 35 lesions, 28 were confirmed histologically by endoscopic biopsy and surgical resection, and the histological findings were compared with ultrasonographic imagings. The other 7 patients were observed without resection. The lesion that caused extramural compression of intestinal wall was excluded from this study, which could easily be confused with SMT clinically.

Instruments

A ultrasonic miniprobe (Olympus UM-2R, 12MHz; UM-3R, 20 MHz, Tokyo, Japan) was introduced under electronic colonoscope (Olympus CF-Q240, Tokyo, Japan), as well as an endoscopic ultrasonography system (Olympus EU-M30, Tokyo, Japan). The video image was recorded by ultrasonography image recorder (Sony UP-890, Tokyo, Japan).

Operative procedures

Patients undergoing EUS were prepared with the same method as for conventional colonoscopy. Five mg midazolam was administered intramuscularly and 10 mg scopolamine butylbromide was injected intravenously for sedation before the procedure. When an elevated lesion with normal mucosa was observed endoscopically, the tip of the colonoscope was placed at the distal end of the lesion. The lumen was filled with 100-200 mL water to achieve acoustic coupling between the transducer and the intestinal wall. Subsequently, the miniprobe was introduced through the working channel of the colonoscope and advanced beyond the lesion. The lesion was assessed by real-time ultrasonography while the miniprobe was moved over the lesion region^[4].

The layer of origin of SMT was determined according to the continuity between the lesion and adjacent normal colonic wall. The nature of SMT was assessed by its size, layer of origin, border characteristic and internal echogenicity.

Statistical analysis

Values were presented as mean±SD. Analysis of variance with *t* test was used for statistical analysis. $P</=0.05$ was considered statistically significant.

RESULTS

EUS was performed successfully in all 35 patients. The normal wall of the large intestine was displayed in 5 layers (Figure 1). The first 2 layers represented the mucosa (m). The third layer stood for the submucosa (sm). The muscularis propria (mp) was depicted by the 4th layer. Adventitia or serosa (sa) was sometimes displayed as the 5th layer. As the lower part of rectum below the peritoneal reflection had no serosa, the pericolic fat and the mural outer layer constituted the hyperechoic layer. SMT was mostly visualized as hyperechoic, hypoechoic, anechoic lesions within the colorectal wall (Figure 1). The EUS characteristics of SMT are summarized in Table 1.

Lipomas, the most common SMT of the large intestine (accounting for 1/3 in our study), were visualized as hyperechoic homogeneous masses located in the third layer (sm) with a distinct border. Leiomyomas were visualized as hypoechoic homogeneous mass originated from the 4th layer(mp). Two

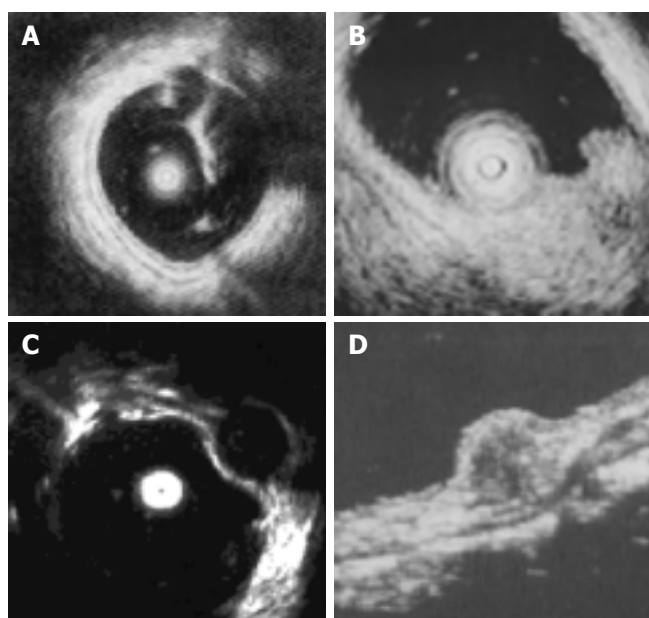


Figure 1 EUS imagines of normal wall and SMT of the large intestine. A: The normal wall was displayed in 5 layers; B: Lipoma imagine showed a hyperechoic homogeneous mass located in the third layer; C: Leiomyoma imagine showed a hypoechoic homogeneous mass originated from the 4th layer; D: Rectal carcinoid imagine showed a submucosal hypoechoic mass with a homogenous echo.

Table 1 EUS characteristics of SMT of the large intestine

Diagnosis (No.of patients)	EUS findings					
	Size (mm)	Shape	Border	Layer of origin	Echogenicity	Internal echo
Lipoma (n = 12)	15±3.1	Round	Regular	Third	Hyperechoic	Homogeneous
Leiomyoma (n = 8)	17±4.3	Round	Regular	Fourth	Hypoechoic	Homogeneous
Lymphangioma (n = 6)	14±2.3	Round	Regular	Third	Anechoic	Multilocular
Leiomyosarcoma (n = 2)	38±2.8	Round Lobulated	Regular	Fourth	Hypoechoic	Inhomogeneous
Carcinoid (n = 3)	14±4.2	Round	Regular	Third	Hypoechoic	Homogeneous
Malignant lymphoma (n = 2)		Irregular	Irregular	Second to fourth	Hypoechoic	Inhomogeneous
Pneumatosis cystoid intestinalis (n = 2)	17±3.6	Irregular	Irregular	Third	Hypoechoic	Inhomogeneous

^a $P<0.05$ vs leiomyoma.

leiomyosarcomas with a mean diameter of 38 mm, inhomogeneous and irregular border were confirmed histologically by surgical resection. One large leiomyoma was misdiagnosed as leiomyosarcoma. Carcinoid was presented as a submucosal hypoechoic mass with a homogenous echo and distinct border. All 3 carcinoids were located in rectus, of which 2 were less than 10 mm in diameter, submucosal continuity was not disrupted, and were resected under colonoscope. Another one was resected by surgery because of large diameter (1.8 cm) and disrupted submucosal continuity. Lymphangiomas were shown with EUS as submucosal anechoic masses with cystic septal structures. Malignant lymphoma displayed as hypoechoic mass from mucosa to mp depending on stage of the disease, while pneumatosis cystoides intestinalis, not real tumor, originated from sm with a special sonic shadow behind mass.

DISCUSSION

Barium enema and colonoscopy are the main widely used examinations in the diagnosis of submucosal lesions of the large intestine. Takada *et al.*^[3] classified colonic SMT into five types on the basis of barium enema studies. Typical endoscopic feature of the colonic SMT is an elevated lesion with normal mucosa, and each has its own endoscopic morphologic features. However, it is difficult to determine the real size, layer of the origin and histologic nature of SMT with these procedures alone. In addition, lesions smaller than 10 mm cannot be detected.

Under these circumstances, the development of EUS has provided a brand new dimension in the diagnosis of colorectal lesions^[5-11]. EUS can image the entire structure of the colonic wall which corresponds to the histologic layer structure. Normal colonic wall is presented as five-layered structure. By placing high frequency miniprobe on the elevated spot, the layer of the origin of SMT is generally determined by demonstrating continuity between the tumor and the colonic wall. Extraluminal compression is easily differentiated from SMT by EUS. Our study found lipoma, lymphangioma and carcinoid were originated from the third layer (sm). Myogenic tumors were found to be originated from the fourth layer (mp). According to literature, some myogenic tumors were from muscularis mucosa^[12].

The size of SMT can be measured with EUS. The biggest SMT we detected in this study was 4.2 cm in diameter. Because of the high frequency employed in this study, it was difficult for miniprobe to observe big lesions. In general, the lower the frequency employed, the better the depth of US penetration and the clearer the image. Therefore, 20 MHz is suitable for clear images of superficial lesions. On the other hand, 12 MHz and 7.5 MHz are more suitable for the evaluation of the big lesions and contiguous tissues. The smallest SMT we detected was 5 mm in diameter, while Sun *et al.*^[13] reported that the smallest size detectable was 2 mm in diameter histologically.

The nature of SMT can be determined by the internal echogenicity. In this study, all lipomas were hyperechoic

homogeneous and lymphangiomas were anechoic with cystic septal structures^[14]. The other SMTs were mostly visualized as hypochoic masses. Therefore, the former findings are strongly suggestive of lipomas and lymphangiomas.

Leiomyosarcoma of the large intestine is extremely rare, only accounting for 0.1% of colonic malignancy^[12]. With regard to differential diagnosis of leiomyomas and leiomyosarcomas, it is suggested to distinguish according to the size and the internal ultrasonic characteristics of the tumor in literature. For the lesion which has the diameter <30 mm, homogenous resonance and clear borderline, the benign is considered. In contrast, if the lesion has a diameter >30 mm, inhomogeneous resonance and irregular border, it may be diagnosed as malignant. But one case in our study with a diameter of 3.2 cm was eventually diagnosed as leiomyoma by pathology. Endoscopic ultrasonography guided fine needle aspiration (FNA) can further help to diagnose the submucosal masses^[15].

EUS is useful in determining the therapy for SMT of the large intestine^[16]. Lipoma and lymphangioma are easy to be diagnosed by EUS, and these lesions can be removed endoscopically or observed without resection. Although leiomyoma and leiomyosarcoma are difficult to differentiate, leiomyosarcoma should be strongly suspected, and surgery should be considered when the tumor is over 30 mm in diameter and has an inhomogeneous internal echo. Although myogenic tumor diagnosed by EUS is an indication for surgery at our department, patients are followed up by EUS according to a strict protocol when the size of tumor is smaller than 20 mm and the patient declines surgery.

In conclusion, EUS can provide precise information about the size, layer of origin, and echogenicity of the SMT of the large intestine. It is useful in the diagnosis of SMT of the large intestine and can have an important role in the choice of therapy.

ACKNOWLEDGEMENT

We thank Eisai Cho and Kenjiro Yasuda of the Department of Gastroenterology of Kyoto Second Red Cross Hospital (Japan) for their technical support to this study.

REFERENCES

- 1 **Stergiou N**, Haji-Kermani N, Schneider C, Menke D, Kockerling F, Wehrmann T. Staging of colonic neoplasms by colonoscopic miniprobe ultrasonography. *Int J Colorectal Dis* 2003; **18**: 445-449
- 2 **Waxman I**, Saitoh Y, Raju GS, Watari J, Yokota K, Reeves AL, Kohgo Y. High-frequency probe EUS-assisted endoscopic mucosal resection: a therapeutic strategy for submucosal tumors of the GI tract. *Gastrointest Endosc* 2002; **55**: 44-49
- 3 **Takada N**, Higashino M, Osugi H, Tokuhara T, Kinoshita H. Utility of endoscopic ultrasonography in assessing the indications for endoscopic surgery of submucosal esophageal tumors. *Surg Endosc* 1999; **13**: 228-230
- 4 **Xi WD**, Zhao C, Ren GS. Endoscopic ultrasonography in pre-operative staging of gastric cancer: determination of tumor invasion depth, nodal involvement and surgical resectability. *World J Gastroenterol* 2003; **9**: 254-257
- 5 **Roseau G**, Dumontier I, Palazzo L, Chapron C, Dousset B, Chaussade S, Dubuisson JB, Couturier D. Rectosigmoid endometriosis: endoscopic ultrasound features and clinical implications. *Endoscopy* 2000; **32**: 525-530
- 6 **Shimizu S**, Myojo S, Nagashima M, Okuyama Y, Sugeta N, Sakamoto S, Kutsumi H, Otsuka H, Suyama Y, Fujimoto S. A patient with rectal cancer associated with ulcerative colitis in whom endoscopic ultrasonography was useful for diagnosis. *J Gastroenterol* 1999; **34**: 516-519
- 7 **Gast P**, Belaiche J. Rectal endosonography in inflammatory bowel disease: differential diagnosis and prediction of remission. *Endoscopy* 1999; **31**: 158-166
- 8 **Lew RJ**, Ginsberg GG. The role of endoscopic ultrasound in inflammatory bowel disease. *Gastrointest Endosc Clin N Am* 2002; **12**: 561-571
- 9 **Polkowski M**, Regula J, Wronska E, Pachlewski J, Rupinski M, Butruk E. Endoscopic ultrasonography for prediction of postpolypectomy bleeding in patients with large nonpedunculated rectosigmoid adenomas. *Endoscopy* 2003; **35**: 343-347
- 10 **Bhutani MS**, Nadella P. Utility of an upper echoendoscope for endoscopic ultrasonography of malignant and benign conditions of the sigmoid/left colon and the rectum. *Am J Gastroenterol* 2001; **96**: 3318-3322
- 11 **Mo LR**, Tseng LJ, Jao YT, Lin RC, Wey KC, Wang CH. Balloon sheath miniprobe compared to conventional EUS in the staging of colorectal cancer. *Hepatogastroenterology* 2002; **49**: 980-983
- 12 **Xu GQ**, Zhang BL, Li YM, Chen LH, Ji F, Chen WX, Cai SP. Diagnostic value of endoscopic ultrasonography for gastrointestinal leiomyoma. *World J Gastroenterol* 2003; **9**: 2088-2091
- 13 **Sun S**, Wang M, Sun S. Use of endoscopic ultrasound-guided injection in endoscopic resection of solid submucosal tumors. *Endoscopy* 2002; **34**: 82-85
- 14 **Watanabe F**, Honda S, Kubota H, Higuchi R, Sugimoto K, Iwasaki H, Yoshino G, Kanamaru H, Hanai H, Yoshii S, Kaneko E. Preoperative diagnosis of ileal lipoma by endoscopic ultrasonography probe. *J Clin Gastroenterol* 2000; **31**: 245-247
- 15 **Kinoshita K**, Isozaki K, Tsutsui S, Kitamura S, Hiraoka S, Watabe K, Nakahara M, Nagasawa Y, Kiyohara T, Miyazaki Y, Hirota S, Nishida T, Shinomura Y, Matsuzawa Y. Endoscopic ultrasonography-guided fine needle aspiration biopsy in follow-up patients with gastrointestinal stromal tumours. *Eur J Gastroenterol Hepatol* 2003; **15**: 1189-1193
- 16 **Ouchi J**, Araki Y, Chijiwa Y, Kubo H, Hamada S, Ochiai T, Harada N, Nawata H. Endosonographic probe-guided endoscopic removal of colonic pedunculated leiomyoma. *Acta Gastroenterol Belg* 2000; **63**: 314-316

Edited by Kumar M and Zhu LH Proofread by Xu FM and Chen WW

Gastrointestinal autonomic nerve tumors: A surgical point of view

Anton Stift, Josef Friedl, Michael Gnant, Friedrich Herbst, Raimund Jakesz, Etienne Wenzl

Anton Stift, Josef Friedl, Michael Gnant, Friedrich Herbst, Raimund Jakesz, Etienne Wenzl, Department of General Surgery, Medical University of Vienna, Vienna, Austria

Correspondence to: Dr. Anton Stift, Department of General Surgery, Medical University of Vienna, Waehringerquertel 18-20, A-1090 Vienna, Austria. a.stift@akh-wien.ac.at

Telephone: +43-1-40400-5621 **Fax:** +43-1-40400-6932

Received: 2003-11-12 **Accepted:** 2003-12-16

Abstract

AIM: Gastrointestinal autonomic nerve tumors are uncommon stromal tumors of the intestinal tract. Their histological appearance is similar to that of other gastrointestinal stromal tumors. We report two cases and performed an analysis of the literature by comparing our findings with the available case reports in the medical literature.

METHODS: Two patients were admitted with abdominal tumor masses. One occurred in the stomach with large multiple liver metastases and the second originated in Meckel's diverticulum. The latter site has never been reported previously. Both patients underwent surgery. In one patient gastrectomy, right liver resection and colon transversum resection were performed to achieve aggressive tumor debulking. In the other patient the tumor bearing diverticulum was removed.

RESULTS: Postoperative recovery of both patients was uneventful. Histological examination, immunohistochemical analysis and electron microscopy revealed the diagnosis of a gastrointestinal autonomic nerve tumor. The patient with the tumor in Meckel's diverticulum died 6 mo after surgery because of pneumonia. The patient with liver metastases has been alive 13 years after initial tumor diagnosis and 7 years after surgery with no evidence of tumor progression. In light of our results, we performed a thorough comparison with available literature reports.

CONCLUSION: Radical surgical resection of gastrointestinal autonomic nerve tumors seems to be the only available curative approach to date, and long term survival is possible even in large metastasized tumors.

Stift A, Friedl J, Gnant M, Herbst F, Jakesz R, Wenzl E. Gastrointestinal autonomic nerve tumors: A surgical point of view. *World J Gastroenterol* 2004; 10(16): 2447-2451
<http://www.wjgnet.com/1007-9327/10/2447.asp>

INTRODUCTION

Gastrointestinal autonomic nerve tumors (GANTs) were first described by Herrera *et al.* in 1984. The authors used the term plexosarcoma to describe this entity^[1]. In the last decade several investigators have recognized the distinct characteristics of this type of tumor^[2-6]. It consists of a subgroup of gastrointestinal stromal tumors (GISTs) with a specific ultrastructural appearance, suggesting that it originates from neurons of the

enteric plexus. Histologically, GANTs are usually low-grade spindle-cell neoplasms but cannot be definitely distinguished from stromal tumors or other neurogenic tumors by histological or immunohistochemical features. To date, the diagnosis of GIST is strongly suggested by immunostaining for the transmembrane tyrosine kinase receptor CD117 and c-kit gene mutations^[7,8]. Partly based on these findings GISTs have been defined as tumors of the interstitial cells of Cajal^[9]. Because GANTs also often showed CD117 staining some authors considered GISTs to be identical to GANTs^[10]. Eyden *et al.* have recently studied 82 gastrointestinal stromal tumors in terms of their cellular differentiation by using electron microscopy. They demonstrated that electron microscopy was needed to establish the diagnosis of GANTs and to exclude other gastrointestinal stromal tumors^[6]. We performed an analysis of the literature to compare our patients with the published data. The literature search yielded more than 120 published cases of GANTs, including the two cases presented in this report^[1-6,11-38].

CASE REPORT

Case 1

This female patient was 22-year-old when she first noted fatigue, loss of appetite and epigastric discomfort in 1990. On physical examination she had a palpable epigastric mass. Upper gastrointestinal series and computed tomography (CT) suggested that the mass was a large gastric tumor. Endoscopy revealed several large masses protruding into the stomach without erosion of the overlying mucosa. Laparotomy showed that the entire stomach was infiltrated with nodular masses. In addition, the liver demonstrated multiple nodules. Intraoperatively obtained frozen sections revealed a leiomyosarcoma. Due to the poor prognosis of the disease and the extensive tumor burden the surgeon decided not to remove any tumor mass. The patient was discharged without any further treatment. Histological features and immunohistochemical characteristics were determined and found to be analogous to the results obtained six years later. Ultrastructural examination was not performed. At the time this case was diagnosed, only 10 GANTs had been documented in the literature.

Six years later the patient was still alive and was admitted to our hospital after an extensive weight loss (she weighed 38 kg at the time of admission). The patient complained of progressive abdominal discomfort and dyspnea. On physical examination the abdominal wall was extremely distended by a large palpable epigastric mass. Diagnostic studies including CT scan confirmed the known abdominal tumor. On the CT image the liver foci were partly solid and partly liquid (Figure 1).

Again, a laparotomy was performed. The intraoperative findings were similar to those obtained 6 years earlier. By then, the gastric tumor invaded the transverse mesocolon. Maximum debulking was achieved by total gastrectomy, transverse colon resection and right hepatectomy, leaving only small tumor deposits in the left liver. The resected gastric tumor mass measured approximately 40 cm×25 cm×20 cm in aggregate and the liver foci covered 25 cm×12 cm×12 cm (Figures 2, 3). After an uneventful recovery the patient was discharged after 3 wk and returned to work 5 wk later. CT series obtained 3, 6 and 12 mo after the operation showed no measurable expansion of the remaining foci in the left liver. A CT scan performed 24 mo

after the operation revealed spontaneous partial regression of the metastatic liver foci. Seven years after surgery, the patient was still in excellent clinical condition and free of discomfort. In addition, the patient delivered a healthy boy in 1997.

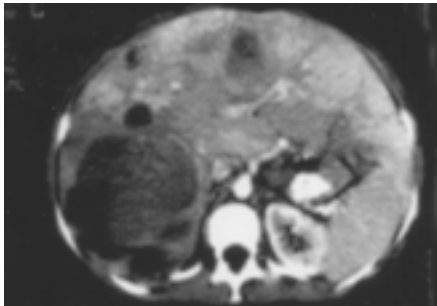


Figure 1 Preoperative CT-scan of diseased liver and stomach.



Figure 2 Stomach with infiltrating nodular masses.



Figure 3 Right liver containing multiple metastatic nodules.

Microscopically, the resected gastric tumor chiefly consisted of plump spindle cells with distinct nuclear pleomorphism. In some areas 15 mitotic figures per 10 high power fields were identified. Immunohistochemical studies showed positive staining with antibodies to neuron specific enolase (NSE) and vimentin. There was also a weak focal staining for S 100 and HSL-19. No detectable staining for chromogranin A, 1 A 4, HHF 35, EMA, MNF 116, CAM 5.2, JC 70a and CD117 was observed. Just a small part of the tumor mass showed positive staining with an antibody to CD 34. Microscopically, the resected metastatic liver tumor also mainly consisted of plump spindle cells. In contrast to the original tumor mass, immunohistochemical studies showed 100 percent positive staining for CD 34 but negative staining for CD 117. CD 117 staining was performed a few weeks ago in order to take into account newest drug developments like tyrosine kinase inhibitors as a potential treatment option. Approximately 80% of the sampled tumors were necrotic. Ultrastructural examination showed neuron-like cells with long cytoplasmatic processes and dense core neurosecretory granules. Thus, the diagnosis of a gastrointestinal autonomic nerve tumor (GANT) was made.

Case 2

A 68-year-old man was admitted to the hospital with a one month history of fever and weight loss of 4 kg. No abnormal findings were registered on physical examination. Computerized tomography showed a decaying liver tumor. The Mendel-Mantoux reaction was highly positive. Therefore the liver focus was considered to be tuberculotic. Tuberculostatic triple-drug therapy was administered for 6 mo. After 12 mo, a CT scan of the abdomen and upper gastrointestinal series showed a normal liver with no pathological signs. An additional new finding was suggestive of a tumor of the ileum. Laparotomy revealed neoplastic nodular masses (9 cm×6 cm) originating from Meckel's diverticulum. The tumor was resected along with an ileal segment. The patient had an uneventful recovery and was discharged 10 d postoperatively. Light microscopy revealed that the tumor was composed of interlacing fascicles of plump, pleomorphic spindle cells, partly showing a storiform and epithelioid pattern. Less than one mitotic figure per 10 high-power fields was identified. Immunohistochemical stainings for vimentin, S-100 and neuron specific enolase (NSE) were positive, whereas staining for Lu 5, CAM 5.2, MNF 116, EMA, desmin, chromogranin, 1A4, Q-BENT10, JC70A, HMB-45, PGM1, HHF35 and CD117 was negative.

Ultrastructural examination showed neuron-like cells with long branching cytoplasmatic processes. Dense-core granules were scarce. No basal lamina, dense bodies, or pinocytotic vesicles were found.

Six months later the patient died of a severe pneumonia. A post-mortem examination showed no intestinal abnormalities or recurrence of disease.

DISCUSSION

Gastrointestinal autonomic nerve tumors represent a rare distinct subcategory of gastrointestinal stromal tumors. First described by Herrera *et al.* in 1984 as plexosarcoma supposedly originating from the enteric autonomic plexus, more than 120 cases including our own have been documented in the literature^[1-6,11-38]. These tumors were found in patients of a wide age range (10 to 85 years) with a median age of 58 years. Seventy-nine per cent of patients were older than 50 years. The tumors were found slightly more often in males (62 males vs 58 females). The reported clinical signs and symptoms are shown in Table 1. In the majority of cases, the primary site of the tumor was the stomach, duodenum, jejunum and ileum, but the esophagus^[21,22], rectum^[26,34], bladder^[30] or colon^[31] have also been reported in some cases (Table 2).

Table 1 Clinical symptoms of 78 reported GAN tumors

Clinical symptoms	No. of patients	Percent of patients
Abdominal pain	32	41
Meaena	19	24
Abdominal mass	10	13
Weight loss	10	13
Vomiting	9	12
Fatigue	7	9
Fever	5	6
Anemia	4	5
Obstructive jaundice	2	2
No clinical symptoms	5	6

On imaging studies, the tumor often presents as a large and lobulated solid mass, with areas of necrosis. It is locally invasive. Radiological techniques did not permit a distinction between GANTs and other gastrointestinal stromal tumors^[28,33].

The greatest dimension of the tumor was determined in 81

cases, and ranged from 1.5 cm to 40 cm (median 10.4 cm). Eighty per cent was larger than 5 cm and 37% had one dimension larger than 10 cm. The bulky tumor masses were predominantly cystic and necrotic. In two cases an abscess was present in the tumor^[17,29]. Some of these GANTs were observed in patients with Carney's triad (3 cases)^[16,17], neurofibromatosis (3 cases)^[15,20,25], and adrenal ganglioneuroma (1 case)^[20].

Table 2 Anatomic sites of the primary tumors (*n* = 120)

Location	No. of patients	Percent of patients
Stomach	45	37.5
Jejunum	26	22.0
Ileum	21	17.5
Duodenum	12	10.0
Retroperitoneum	4	3.3
Mesentery	3	2.5
Esophagus	2	1.6
Peritoneum	2	1.6
Rectum	2	1.6
Colon	1	0.8
Bladder	1	0.8
Omentum	1	0.8

The tumors were usually intramuscular-intramural, well demarcated, but not encapsulated, unilocated or multilocated masses of variable consistency, with or without haemorrhage and necrosis.

Histologically, the reported tumors showed a variety of patterns, none of which was specifically diagnostic. Most lesions were spindle cell tumors with features resembling either smooth muscle tumors or neurogenic tumors. Epithelioid cells were also detected, usually as a minor population. The cellular arrangement was either whorled, patternless, fascicular, palisaded or storiform. Generally, the tumor cells had an eosinophilic cytoplasm. Pleomorphism was not significant and mitosis ranged from 1 to 23/10 high-power fields.

Results of immunohistochemical studies demonstrated that the tumor was most often reactive to vimentin and other markers of nerve tissues such as neuron-specific enolase (NSE), synaptophysin, S-100 protein, neurofilament, and chromogranin A (Table 3). These proteins are normally expressed by neurons from the autonomic enteric nerve plexus, supporting a histogenesis of GANTs from enteric autonomic plexuses of Meissner or Auerbach. The muscle marker desmin and muscle-specific actin could not be demonstrated, although focal alpha-SMA positivity was seen in 7 reported cases^[24,27]. Except for one study (2 cases) focal staining for cytokeratins (CAM5.2) was found to be negative^[26]. GANTs usually lacked smooth muscle cell features^[1,2,11].

Table 3 Summary of immunohistochemical findings of 120 cases

Antigens	No. of cases studied	No. positive cases	Percent of positivity
Vimentin	103	95	92
Neuron-specific Enolase	117	105	90
Chromogranin A	92	10	11
Synaptophysin	105	33	31
S-100 protein	117	44	38
Neurofilaments	87	14	16
Vasoactive intestinal peptide	25	5	20

Over the last two years GANTs were also tested for CD117 and almost all of them were positive^[10].

Ultrastructural studies of all the reported cases revealed features suggestive of myenteric plexus in origin. The diagnostic ultrastructural features included the presence of long, closely opposed cell processes containing intermediate filaments, dense-core neurosecretory granules, microtubules, and synapse-like structures with variable numbers of neurosecretory granules and small vesicles. The essential ultrastructural criteria applied for the diagnosis of GANT in all reported cases included neurosecretory granules and intermediate filaments. It should be noted that five reported GANTs showed weak signs of smooth-muscle morphology. Therefore, the presence of smooth muscle cell features might also suggest GANT^[6].

The primary therapy in almost all reported cases was surgical resection or debulking, in 2 cases preceded by radiotherapy, and in nine cases preceded by chemotherapy. Three patients received chemotherapy alone. There was no evidence of clinical response using chemotherapy or radiation. As demonstrated in our report, aggressive tumor debulking without any further treatment could also be considered suitable in terms of prolonged survival and quality of life.

According to published reports, 8 patients out of 67 (12%) had metastases at clinical presentation and 18 patients (27%) developed metastases during follow up (Table 4). The estimated survival curve of the clinically documented cases (*n* = 67) is shown in Figure 4.

Table 4 Metastases of reported GANT cases (*n* = 67)

Location	Metastases at clinical presentation		Metastases in clinical follow up		
	No. of patients	%	No. of patients	%	
Liver	7	10	Liver	6	9
Lymph node	2	3	Retroperitoneal	4	6
			Local recurrence	5	7
Omentum	2	3	Omentum	3	4
			Mesentery	2	3
			Peritoneum	2	3

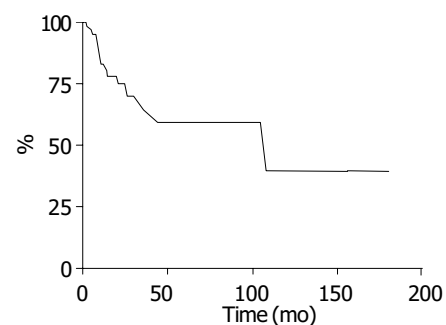


Figure 4 Estimated Kaplan-Meier survival curve of 67 reported patients.

Gastrointestinal autonomic nerve tumors occurred with an estimated frequency of 1% of all malignant gastrointestinal tumors and up to 25% of gastrointestinal stromal tumors^[6]. In retrospective studies of collected pathological specimens, several investigators found that light microscopic studies yielded ambiguous results and ultrastructural examination was required in order to establish an accurate diagnosis of gastrointestinal autonomic nerve tumor^[6,20,26].

Based on these observations we believe that GANTs are probably more common than previously thought. The rarity of GANT may therefore be a consequence of the unavailability of routine electron microscopic analysis. The exact biological behavior of GANTs is not fully elucidated because of the limited

number of reported cases, but it appears that, despite their low grade malignant histological appearance, most GANTs had an uncertain and a poor prognosis in case of metastases. With respect to one of our patients long term survival was possible even with metastatic diseases. Preliminary data indicated no significant correlation between treatment, tumor site and clinical outcomes^[2,15].

Some authors suggested that GANTs should be regarded as a type of GISTs because of their mostly identical c-kit mutations^[10,39]. Others argued that this common feature might not justify considering GIST and GANT as the same entity because of the neuronal nature of GANT^[6]. The recent observation that most GANTs were CD117 positive could have an important clinical impact, since tyrosine kinase inhibitors have yielded good responses in other CD117 positive tumor entities. To date there are no reports on the use of tyrosine kinase inhibitors in CD 117 positive GANTs, but promising data for c-kit positive GISTs which were successfully treated with tyrosine kinase inhibitors have recently been published^[39].

Radical surgical resection appears to be the most promising and solely curative treatment regimen for gastrointestinal autonomic nerve tumors. However, as demonstrated in case 1, patients with metastases might also survive for a long time. Some studies in the literature report had similar findings. We therefore suggest that even in cases of large tumor masses, non-curative, aggressive surgical tumor debulking is potentially useful to improve the patient's quality of life. For metastatic CD117 positive tumors tyrosine kinase inhibitors might be an appropriate palliative treatment approach. As demonstrated in case 2, GAN tumors could also involve unusual anatomic sites like Meckel's diverticulum.

To gain more information about this distinct type of GISTs, careful ultrastructural and immunohistochemical studies of all GIST cases would be beneficial. We are aware that ultrastructural examination is not available at every clinical pathology unit. However, we propose that pathologists harvest small specimens of the tumor for analysis at specialized institutions. An accurate histological diagnosis seems to be essential in order to ensure that all patients receive adequate and timely treatment and furthermore to learn more about this tumor and its biological behavior especially with respect to newly developed drugs like tyrosine kinase inhibitors. To date there is no difference in the surgical treatment of GANTs and GISTs. But there is some evidence that these tumors are from different origins and may therefore exhibit distinct biological behaviors. However, due to the limited number of reported GANTs further investigations would be necessary to fully characterize these tumors with respect to future treatment decisions.

ACKNOWLEDGMENT

We thank Christine Brostjan, PhD for critical review of the manuscript.

REFERENCES

- Herrera GA, Pinto de Moraes H, Grizzle WE, Han SG. Malignant small bowel neoplasm of enteric plexus derivation (plexosarcoma). Light and electron microscopic study confirming the origin of the neoplasm. *Dig Dis Sci* 1984; **29**: 275-284
- Herrera GA. Small bowel neoplasm. *Dig Dis Sci* 1985; **30**: 698
- Walker P, Dvorak AM. Gastrointestinal autonomic nerve (GAN) tumor. Ultrastructural evidence for a newly recognized entity. *Arch Pathol Lab Med* 1986; **110**: 309-316
- Tortella BJ, Matthews JB, Antonioli DA, Dvorak AM, Silen W. Gastric autonomic nerve (GAN) tumor and extra-adrenal paraganglioma in Carney's triad. A common origin. *Ann Surg* 1987; **205**: 221-225
- Dvorak AM. Gut autonomic nerve (GAN) tumors. In: Watanabe S, Wolf M, Sommers SC, eds. Digestive disease pathology. Vol 2. Philadelphia WB Saunders 1989: 49-66
- Eyden B, Chorneyko KA, Shanks JH, Menasce LP, Banerjee SS. Contribution of electron microscopy to understanding cellular differentiation in mesenchymal tumors of the gastrointestinal tract: a study of 82 tumors. *Ultrastruct Pathol* 2002; **26**: 269-285
- Miettinen M, Sobin LH, Sarlomo-Rikala M. Immunohistochemical spectrum of GISTs at different sites and their differential diagnosis with a reference to CD117 (KIT). *Mod Pathol* 2000; **13**: 1134-1142
- Schmid S, Wegmann W. Gastrointestinal pacemaker cell tumor: clinicopathological, immunohistochemical, and ultrastructural study with special reference to c-kit receptor antibody. *Virchows Arch* 2000; **436**: 234-242
- Kindblom LG, Remotti HE, Aldenborg F, Meis-Kindblom JM. Gastrointestinal pacemaker cell tumor (GIPACT): gastrointestinal stromal tumors show phenotypic characteristics of the interstitial cells of Cajal. *Am J Pathol* 1998; **152**: 1259-1269
- Lee JR, Joshi V, Griffin JW Jr, Lasota J, Miettinen M. Gastrointestinal autonomic nerve tumor: immunohistochemical and molecular identity with gastrointestinal stromal tumor. *Am J Surg Pathol* 2001; **25**: 979-987
- Herrera GA, Cerezo L, Jones JE, Sack J, Grizzle WE, Pollack WJ, Lott RL. Gastrointestinal autonomic nerve tumors. 'Plexosarcomas'. *Arch Pathol Lab Med* 1989; **113**: 846-853
- Walsh NM, Bodurtha A. Auerbach's myenteric plexus. A possible site of origin for gastrointestinal stromal tumors in von Recklinghausen's neurofibromatosis. *Arch Pathol Lab Med* 1990; **114**: 522-525
- MacLeod CB, Tsokos M. Gastrointestinal autonomic nerve tumor. *Ultrastruct Pathol* 1991; **15**: 49-55
- Pinedo Moraleda F, Martinez Gonzalez MA, Ballestin Carcavilla C, Vargas Castrillon J. Gastrointestinal autonomic nerve tumours: a case report with ultrastructural and immunohistochemical studies. *Histopathology* 1992; **20**: 323-329
- Lauwers GY, Erlandson RA, Casper ES, Brennan MF, Woodruff JM. Gastrointestinal autonomic nerve tumors. A clinicopathological, immunohistochemical, and ultrastructural study of 12 cases. *Am J Surg Pathol* 1993; **17**: 887-897
- Perez-Atayde AR, Shamberger RC, Kozakewich HW. Neuroectodermal differentiation of the gastrointestinal tumors in the Carney triad. An ultrastructural and immunohistochemical study. *Am J Surg Pathol* 1993; **17**: 706-714
- Thomas JR, Mrak RE, Libuit N. Gastrointestinal autonomic nerve tumor presenting as high-grade sarcoma. Case report and review of the literature. *Dig Dis Sci* 1994; **39**: 2051-2055
- Segal A, Carello S, Caterina P, Papadimitriou JM, Spagnolo DV. Gastrointestinal autonomic nerve tumors: a clinicopathological, immunohistochemical and ultrastructural study of 10 cases. *Pathology* 1994; **26**: 439-447
- Kodet R, Snajdauf J, Smelhaus V. Gastrointestinal autonomic nerve tumor: a case report with electron microscopic and immunohistochemical analysis and review of the literature. *Pediatr Pathol* 1994; **14**: 1005-1016
- Dhimes P, Lopez-Carreira M, Ortega-Serrano MP, Garcia-Munoz H, Martinez-Gonzalez MA, Ballestin C. Gastrointestinal autonomic nerve tumours and their separation from other gastrointestinal stromal tumours: an ultrastructural and immunohistochemical study of seven cases. *Virchows Arch* 1995; **426**: 27-35
- Lam KY, Law SY, Chu KM, Ma LT. Gastrointestinal autonomic nerve tumor of the esophagus. A clinicopathologic, immunohistochemical, ultrastructural study of a case and review of the literature. *Cancer* 1996; **78**: 1651-1659
- Shek TW, Luk IS, Loong F, Ip P, Ma L. Inflammatory cell-rich gastrointestinal autonomic nerve tumor. An expansion of its histologic spectrum. *Am J Surg Pathol* 1996; **20**: 325-331
- Ojanguren I, Ariza A, Navas-Palacios JJ. Gastrointestinal autonomic nerve tumor: further observations regarding an ultrastructural and immunohistochemical analysis of six cases. *Hum Pathol* 1996; **27**: 1311-1318
- Shanks JH, Harris M, Banerjee SS, Eyden BP, Joglekar VM, Nicol A, Hasleton PS, Nicholson AG. Mesotheliomas with deciduoid morphology: a morphologic spectrum and a variant

- not confined to young females. *Am J Surg Pathol* 2000; **24**: 285-294
- 25 **Sakaguchi N**, Sano K, Ito M, Baba T, Fukuzawa M, Hotchi M. A case of von Recklinghausen's disease with bilateral pheochromocytoma-malignant peripheral nerve sheath tumors of the adrenal and gastrointestinal autonomic nerve tumors. *Am J Surg Pathol* 1996; **20**: 889-897
- 26 **Erlandson RA**, Klimstra DS, Woodruff JM. Subclassification of gastrointestinal stromal tumors based on evaluation by electron microscopy and immunohistochemistry. *Ultrastruct Pathol* 1996; **20**: 373-393
- 27 **Matsumoto K**, Min W, Yamada N, Asano G. Gastrointestinal autonomic nerve tumors: immunohistochemical and ultrastructural studies in cases of gastrointestinal stromal tumor. *Pathol Int* 1997; **47**: 308-314
- 28 **Jain KA**, Gerscovich EO, Goodnight JJ. Malignant autonomic nerve tumor of the duodenum. *Am J Roentgenol* 1997; **168**: 1461-1463
- 29 **Honda K**, Mikami T, Ohkusa T, Takashimizu I, Fujiki K, Araki A, Shimoi K, Enomoto Y, Ariake K, Miyasaka N, Nihei Z, Oda K, Terada T. Gastrointestinal autonomic nerve tumor with giant abscess. A case report and literature review. *J Clin Gastroenterol* 1997; **24**: 280-285
- 30 **Reid I**, Suvarna SK, Wagner BE, Rogers K. Plexosarcoma of the bladder. *Eur J Surg Oncol* 1997; **23**: 463-465
- 31 **Donner LR**. Gastrointestinal autonomic nerve tumor: a common type of gastrointestinal stromal neoplasm. *Ultrastruct Pathol* 1997; **21**: 419-424
- 32 **Minni F**, Casadei R, Santini D, Verdirame F, Zanelli M, Vesce G, Marrano D. Gastrointestinal autonomic nerve tumor of the jejunum. Case report and review of the literature. *Ital J Gastroenterol Hepatol* 1997; **29**: 558-563
- 33 **Rueda O**, Escribano J, Vicente JM, Garcia F, Villeta R. Gastrointestinal autonomic nerve tumors (plexosarcomas). Is a radiological diagnosis possible? *Eur Radiol* 1998; **8**: 458-460
- 34 **Lev D**, Kariv Y, Messer GY, Isakov J, Gutman M. Gastrointestinal autonomic nerve (GAN) tumor of the rectum. *J Clin Gastroenterol* 2000; **30**: 438-440
- 35 **Kerr JZ**, Hicks MJ, Nuchtern JG, Saldivar V, Heim-Hall J, Shah S, Kelly DR, Cain WS, Chintagumpala MM. Gastrointestinal autonomic nerve tumors in the pediatric population: a report of four cases and a review of the literature. *Cancer* 1999; **85**: 220-230
- 36 **Tornoczky T**, Kalman E, Hegedus G, Horvath OP, Sapi Z, Antal L, Jakso P, Pajor L. High mitotic index associated with poor prognosis in gastrointestinal autonomic nerve tumour. *Histopathology* 1999; **35**: 121-128
- 37 **Giessler U**, Puffer E, Ludwig K. Gastrointestinal autonomic nerve tumor (GANT)—a rare tumor of the ileum. *Chirurg* 2001; **72**: 600-602
- 38 **Beck A**, Jonas J, Frenzel H, Bahr R. Gastrointestinal autonomic nerve tumor. *Zentralbl Chir* 2001; **126**: 702-706
- 39 **Joensuu H**, Fletcher C, Dimitrijevic S, Silberman S, Roberts P, Demetri G. Management of malignant gastrointestinal stromal tumours. *Lancet Oncol* 2002; **3**: 655-664

Edited by Wang XL Proofread by Zhu LH and Xu FM

Granular cell tumor of colon: Report of a case and review of literature

Dae-Kyung Sohn, Hyo-Seong Choi, Yeon-Soo Chang, Jin-Myeong Huh, Dae-Hyun Kim, Dae-Yong Kim, Young-Hoon Kim, Hee-Jin Chang, Kyung-Hae Jung, Seung-Yong Jeong

Dae-Kyung Sohn, Hyo-Seong Choi, Yeon-Soo Chang, Jin-Myeong Huh, Dae-Hyun Kim, Dae-Yong Kim, Young-Hoon Kim, Hee-Jin Chang, Kyung-Hae Jung, Seung-Yong Jeong, Research Institute and Hospital, National Cancer Center, Goyang, Gyeonggi 411-769, Korea

Correspondence to: Dr. Seung-Yong Jeong, Center for Colorectal Cancer, Research Institute and Hospital, National Cancer Center, 809 Madu-dong, Ilsan-gu, Goyang, Gyeonggi 411-769, Korea. syjeong@ncc.re.kr

Telephone: +82-31-920-1632 **Fax:** +82-31-920-0002

Received: 2004-03-15 **Accepted:** 2004-04-09

Abstract

Granular cell tumor (GCT) is uncommon in the colon and rectum. Here we report a case of GCT in the transverse colon. A 48-year-old male patient underwent a screening colonoscopy. A yellowish sessile lesion, about 4 mm in diameter, was found in the transverse colon. An endoscopic snare resection was performed without complication. Histological examination revealed the tumor consisted of plump neoplastic cells with abundant granular eosinophilic cytoplasm containing acidophilic periodic acid Schiff-positive, diastase-resistant granules. Immunohistochemical analysis showed the tumor cells expressed S-100 protein and neuron-specific enolase. Thus, the resected tumor was diagnosed as a GCT. Since GCTs are usually benign, endoscopic resection constitutes an easy and safe treatment. Colonoscopists should consider the possibility of GCT in the differential diagnosis of submucosal tumors of the colon.

Sohn DK, Choi HS, Chang YS, Huh JM, Kim DH, Kim DY, Kim YH, Chang HJ, Jung KH, Jeong SY. Granular cell tumor of colon: Report of a case and review of literature. *World J Gastroenterol* 2004; 10(16): 2452-2454
<http://www.wjgnet.com/1007-9327/10/2452.asp>

INTRODUCTION

Granular cell tumor (GCT) is relatively rare soft tissue tumor that can be located anywhere in the body. It commonly occurs in oral cavities and subcutaneous tissues, but is uncommon in

the colon and rectum^[1,2]. In the gastrointestinal tract, the most common site for GCT is the esophagus, followed by the duodenum, anus and stomach^[3,4]. This usually benign tumor appears as a submucosal nodule, measuring less than 2 cm in diameter, and is often found incidentally during colorectal examinations^[2-6]. Here we report a case of a 48-year-old man diagnosed with a GCT arising in the transverse colon and treated by endoscopic resection.

CASE REPORT

A 48-year-old man was admitted for a screening colonoscopy. He had been healthy without specific complaints, family or past medical history. At the time of colonoscopy, a yellowish, hemispheric nodule 4 mm in diameter, was found in the transverse colon. It was a firm nodule covered by intact mucosa (Figure 1). The patient underwent an endoscopic snare resection, was observed for 30 min, and then discharged. There was no immediate or delayed complication.



Figure 1 A hemispheric, yellowish submucosal tumor with intact mucosa, about 4 mm in diameter in transverse colon revealed by endoscopy.

Histological examination of the resected tissue revealed a submucosal tumor composed of solid masses of plump histiocyte-like tumor cells with abundant granular eosinophilic cytoplasm containing acidophilic periodic acid Schiff (PAS)-positive, diastase-resistant granules (Figure 2). Immunohistochemical analysis showed the tumor cells

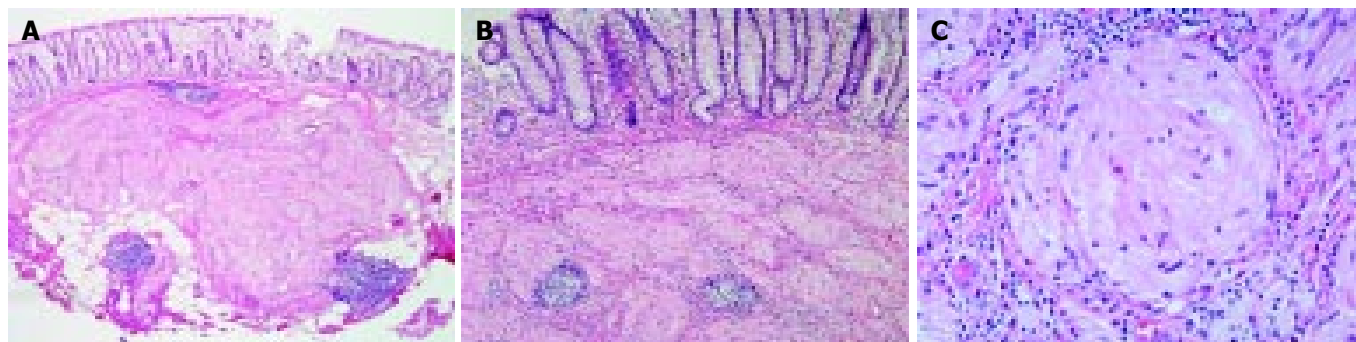


Figure 2 A submucosal tumor revealed by histological examination in resected tissue. A: Resected lesion showing a submucosal tumor covered with normal mucosa (HE staining, $\times 40$). B: Higher magnification view of the tumor (HE staining, left: $\times 100$; right: $\times 200$).

Table 1 Summary of 7 cases of colorectal granular cell tumor reported in Korea

N	Year	Author	Sex/Age	Location	Size (cm)	Treatment
1	1982	Kim <i>et al.</i> ¹²	F/44	Cecum	1.5×1.5	Surgery
2	1983	Lee <i>et al.</i> ¹³	F/31	Cecum	1.0	Surgery
3	1991	Choi <i>et al.</i> ¹⁴	F/39	A-colon	0.9×0.8	Polypectomy
4	2000	Kim <i>et al.</i> ¹⁵	M/40	Appendix	0.7	Polypectomy
5	2003	Lee <i>et al.</i> ¹⁶	F/36	A-colon	1.5×0.6	Polypectomy
6	2003	Kim <i>et al.</i> ¹⁷	M/49	Rectum	0.7	Polypectomy
7	The present case		M/48	T-colon	0.4×0.3	Polypectomy

expressed S-100 protein and neuron-specific enolase (NSE) (Figure 3), but were negative for desmin and cytokeratin. The resected tumor was diagnosed as a GCT occurring in the transverse colon.

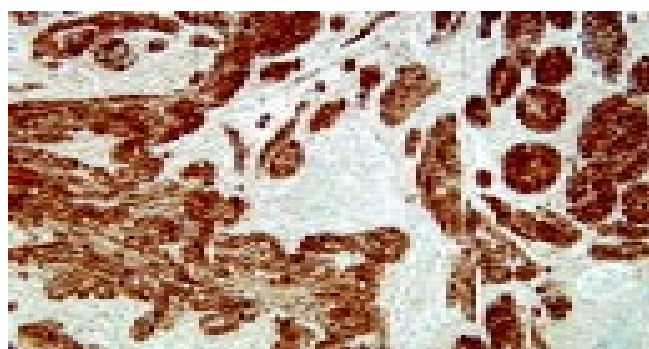


Figure 3 Diffuse and strong expression of S-100 protein in tumor shown by immunohistochemical examination (Original magnification: ×100).

DISCUSSION

GCT, first described by Abrikossoff in 1926^[7], may arise virtually anywhere in the body, but was seldomly found in the gastrointestinal tract^[1,2]. In most cases, gastrointestinal GCTs were found incidentally during endoscopy, and appeared as small, round submucosal nodules covered by normal mucosa^[1-5,8-10]. GCTs have also been detected in the muscle layer of the gastrointestinal tract and in subserosal areas, although such findings were uncommon^[2,4,11].

Endo *et al.*^[10] reported 33 cases of colorectal GCT in Japan, and Rossi *et al.*^[8] reported 55 patients diagnosed with GCTs of the colon. To date, 7 cases of colonic GCT have been reported in Korean literature (Table 1). This excludes two cases of perianal GCT which may have arisen from perianal skin rather than anal mucosa. Except for one rectal case, all 6 colonic GCTs reported in Korea were located in the proximal colon - ascending colon, transverse colon and cecum including the appendix. The male-to-female ratio was 1:1.3 and the mean age was 41.0±6.5 years (range 31-49 years). Bowel resection was the treatment administered for the 2 cases diagnosed before 1985, while endoscopic removal of the tumor was performed in the later cases. Advances in endoscopic diagnosis and resection probably led to the alteration in treatment approach for the latter cases.

GCT could seldomly be diagnosed based on macroscopic and endoscopic examination due to both its small size and its shape resembling a diminutive polyp^[1]. Recently, endoscopic ultrasound has been frequently used for determining the depth of tumor invasion in the gastrointestinal wall, and is also useful for evaluating gastrointestinal submucosal tumors^[9,10,18]. However, in the present case, it was difficult to suspect GCT because the endoscopic features of the tumor resembled those of a small sessile polyp. We performed one-stage endoscopic

snare polypectomy during screening colonoscopy.

The final diagnosis of GCT depends on pathological findings. The histological markers for GCT are: (1) plump histiocyte-like, bland-looking neoplastic cells with abundant granular eosinophilic cytoplasm containing acidophilic, PAS-positive, diastase-resistant granules; (2) small, uniform nuclei, in which mitotic figures are absent; (3) neural markers, including S-100 protein or NSE expressed uniformly^[6,11,23]. In the present patient, the histological findings on the resected specimen were typical of a GCT.

Although GCTs are usually benign, some malignant GCT cases have been reported. Malignancy has been found to correlate with tumor size, more than 60% of metastatic GCTs were larger than 4 cm in diameter^[6,11,23]. However, in most colonic GCTs, the tumor size was less than 2 cm and the tumor was well separated from the muscularis propria. Since this tumor is considered to be usually benign, endoscopic removal has been the most appropriate choice of treatment for colonic GCT^[2,8,10,24].

In conclusion, we report a case of GCT in the transverse colon. The tumor was removed by endoscopic resection and the patient was discharged without complication. GCTs of the colon can be found incidentally during colonoscopy, and endoscopic removal of the tumor is the safest and most feasible treatment. Colonoscopists should consider the possibility of GCT in the differential diagnosis of submucosal tumors of the colon.

REFERENCES

- Lack EE, Worsham GF, Callihan MD, Crawford BE, Klappenbach S, Rowden G, Chun B. Granular cell tumor: a clinicopathological study of 110 patients. *J Surg Oncol* 1980; **13**: 301-316
- Yasuda I, Tomita E, Nagura K, Nishigaki Y, Yamada O, Kachi H. Endoscopic removal of granular cell tumors. *Gastrointest Endosc* 1995; **41**: 163-167
- Melo CR, Melo IS, Schmitt F, Fagundes R, Amendola D. Multicentric granular cell tumor of the colon: report of a patient with 52 tumors. *Am J Gastroenterol* 1993; **88**: 1785-1787
- Yamaguchi K, Maeda S, Kitamura K. Granular cell tumor of the stomach coincident with two early gastric carcinomas. *Am J Gastroenterol* 1989; **84**: 656-659
- Kulaylat MN. Granular cell tumor of the colon [letter]. *Dis Colon Rectum* 1996; **39**: 711
- Jardines L, Cheung L, LiVolsi V, Hendrickson S, Brooks JJ. Malignant granular cell tumors: report of a case and review of the literature. *Surgery* 1994; **116**: 49-54
- Abrikossoff A. Über myoma ausgehend von der quergestreiften willkürlichen muskulatur. *Virchows Arch Pathol Anat* 1926; **260**: 215-233
- Rossi GB, de Bellis M, Marone P, De Chiara A, Losito S, Tempesta A. Granular cell tumors of the colon: report of a case and review of the literature. *J Clin Gastroenterol* 2000; **30**: 197-199
- Nakachi A, Miyazato H, Oshiro T, Shimoji H, Shiraishi M, Muto Y. Granular cell tumor of the rectum: a case report and review of the literature. *J Gastroenterol* 2000; **35**: 631-634
- Endo S, Hirasaki S, Doi T, Endo H, Nishina T, Moriwaki T, Nakauchi M, Masumoto T, Tanimizu M, Hyodo I. Granular cell tumor occurring in the sigmoid colon treated by endo-

- scopic mucosal resection using a transparent cap (EMR-C). *J Gastroenterol* 2003; **38**: 385-389
- 11 **Uzoaru I**, Firfer B, Ray V, Hubbard-Shepard M, Rhee H. Malignant granular cell tumor. *Arch Pathol Lab Med* 1992; **116**: 206-208
- 12 **Kim MJ**, Oh SH, Moon YM, Choi HJ, Kim BR, Park CI. A case of granular cell tumor of the colon. *J Korean Med Assoc* 1982; **25**: 765-769
- 13 **Lee SR**, Park EB. Granular cell myoblastoma of the colon. *Korean J Gastrointest Endosc* 1983; **3**: 103-107
- 14 **Choi JK**, Choi MG, Choi KY, Chung IS, Cha SB, Chung KW, Sun HS, Kim BS, Choi YJ, Lee AH. A case of colonoscopically removed granular cell tumor in the ascending colon. *Korean J Gastrointest Endosc* 1991; **11**: 383-386
- 15 **Kim HS**, Cho KA, Hwang DY, Kim KU, Kang YW, Park WK, Yoon SG, Lee KR, Lee JK, Lee JD, Kim KY. A case of granular cell tumor in the appendix. *Kor J Gastroenterol* 2000; **36**: 404-407
- 16 **Lee SH**, Kim SH, Kim BR, Kim HJ, Bhandari S, Jung IS, Hong SJ, Ryu CB, Kim JO, Cho JY, Lee JS, Lee MS, Shim CS, Kim BS, Jin SY. Granular cell tumor of the ascending colon: report of a case. *Intestinal Research* 2003; **1**: 59-63
- 17 **Kim DH**, Kim YH, Kwon NH, Song BG, Jung JH, Kim MH, Rhee PL, Kim JJ, Rhee JC. A case of granular cell tumor in the rectum. *Korean J Gastrointest Endosc* 2003; **27**: 88-91
- 18 **Orlowska J**, Pachlewski J, Gugulski A, Butruk E. A conservative approach to granular cell tumors of the esophagus: four case reports and literature review. *Am J Gastroenterol* 1993; **88**: 311-315
- 19 **Azzopardi JC**. Histogenesis of the granular cell "myoblastoma". *J Pathol* 1957; **71**: 85-94
- 20 **Joshi A**, Chandrasoma P, Kiyabu M. Multiple granular cell tumors of the gastrointestinal tract with subsequent development of esophageal squamous carcinoma. *Dig Dis Sci* 1992; **37**: 1612-1618
- 21 **Armin A**, Connelly EM, Rowden G. An immunoperoxidase investigation of S-100 protein in granular cell myoblastomas: evidence for Schwann cell derivation. *Am J Clin Pathol* 1983; **79**: 37-44
- 22 **Lisato L**, Bianchini E, Reale D. Granular cell tumor of the rectum: description of a case with unusual histological features. *Pathologica* 1995; **87**: 175-178
- 23 **Matsumoto H**, Kojima Y, Inoue T, Takegawa S, Tsuda H, Kobayashi A, Watanabe K. A malignant granular cell tumor of the stomach: report of a case. *Surg Today* 1996; **26**: 119-122
- 24 **Kawamoto K**, Yamada Y, Furukawa N, Utsunomiya T, Haraguchi Y, Mizuguchi M, Oiwa T, Takano H, Masuda K. Endoscopic submucosal tumorectomy for gastrointestinal submucosal tumors restricted to the submucosa: a new form of endoscopic minimal surgery. *Gastrointest Endosc* 1997; **46**: 311-317

Edited by Wang XL Proofread by Chen WW and Xu FM

• CASE REPORT •

A case of leptospirosis simulating colon cancer with liver metastases

Alessandro Granito, Giorgio Ballardini, Marco Fusconi, Umberto Volta, Paolo Muratori, Vittorio Sambri, Giuseppe Battista, Francesco B. Bianchi

Alessandro Granito, Giorgio Ballardini, Marco Fusconi, Umberto Volta, Paolo Muratori, Francesco B. Bianchi, Departments of Internal Medicine, Cardioangiology, Hepatology, Alma Mater Studiorum - University of Bologna, Italy

Vittorio Sambri, Department of Clinical and Experimental Medicine, Section of Microbiology, Alma Mater Studiorum - University of Bologna, Italy

Giuseppe Battista, Department of Radiology, Alma Mater Studiorum - University of Bologna, Italy

Correspondence to: Alessandro Granito, MD, Dipartimento di Medicina Interna, Cardioangiologia, Epatologia, Policlinico S.Orsola-Malpighi, via Massarenti, 9, 40138 Bologna, Italy. gralex@libero.it

Telephone: +39-51-6363631 **Fax:** +39-51-340877

Received: 2003-12-10 **Accepted:** 2004-03-04

Abstract

We report a case of a 61-year-old man who presented with fatigue, abdominal pain and hepatomegaly. Computed tomography (CT) of the abdomen showed hepatomegaly and multiple hepatic lesions highly suggestive of metastatic diseases. Due to the endoscopic finding of colon ulcer, colon cancer with liver metastases was suspected. Biochemically a slight increase of transaminases, alkaline phosphatase and gammaglutamyl transpeptidase were present; α -fetoprotein, carcinoembryogenic antigen and carbohydrate 19-9 antigen serum levels were normal. Laboratory and instrumental investigations, including colon and liver biopsies revealed no signs of malignancy. In the light of spontaneous improvement of symptoms and CT findings, his personal history was reevaluated revealing direct contact with pigs and their tissues. Diagnosis of leptospirosis was considered and confirmed by detection of an elevated titer of antibodies to leptospira. After two mo, biochemical data, CT and colonoscopy were totally normal.

Granito A, Ballardini G, Fusconi M, Volta U, Muratori P, Sambri V, Battista G, Bianchi FB. A case of leptospirosis simulating colon cancer with liver metastases. *World J Gastroenterol* 2004; 10(16): 2455-2456
<http://www.wjgnet.com/1007-9327/10/2455.asp>

INTRODUCTION

Leptospirosis is a zoonosis caused by spirochetes of the genus *Leptospira*. Humans are infected only occasionally by direct contact with infected animals or through contaminated water and soil. The clinical presentation ranges from occult infection to Weil's disease with fatal complications as hepatorenal failure. It remains underdiagnosed largely due to the broad spectrum of symptoms and signs.

CASE REPORT

A 61 year-old male farmer, non-smoker without a history of alcohol abuse or cancer, was admitted to a local hospital due to fatigue and pain in the right upper abdominal quadrant with discovery of enlarged liver over the past three days. Ultrasonography (US) showed many hypoechoic lesions scattered in all hepatic

segments. A computed tomography (CT) scan of the abdomen showed substitution of the whole liver by multiple low-density lesions with mild ring enhancement highly suggestive of metastatic disease (Figure 1) and retroperitoneal small (< 1 cm) lymph nodes. Upper gastrointestinal endoscopy was negative and colonoscopy disclosed an ulcer of the transverse colon which histologically revealed edema and necro-inflammatory damage without signs of malignancy.



Figure 1 Contrast-enhanced abdominal CT scan (portal phase): multiple lesions appearing hypodense compared with normal liver parenchyma and showing mild ring enhancement.

Ultrasound guided liver biopsy of one of the lesions taken 10 d after admission excluded malignancy and was consistent with mild portal hepatitis and cholestasis. Laboratory tests showed alanine aminotransferase (ALT) 130 IU/l (normal <40), aspartate aminotransferase (AST) 76 IU/l (normal <37), alkaline phosphatase (ALP) 359 MU/mL (normal <280), gammaglutamyl transpeptidase (γ -GT) 252 MU/mL (normal <50). Normal serum levels of α -fetoprotein, carcinoembryogenic antigen (CEA) and carbohydrate 19-9 antigen (CA 19-9) were present. The patient refused further investigations and was discharged with the suspicion of misdiagnosed neoplastic disease. Four wk later, on admission to our Unit, the patient was in good general condition and denied a weight loss and gastrointestinal symptoms. Physical examination revealed only a mild indolent hepatomegaly. Laboratory investigations showed only ALP 443 MU/mL and γ -GT 77 MU/mL. Ultrasonography and abdominal CT scan (Figure 2) revealed a dramatic decrease both in number and volume of the hepatic lesions with unmodified vascularization pattern. Chest X-ray was unremarkable. Colonoscopy revealed an ulcer of the right colon (Figure 3) characterized under histological profile by edema and necro-inflammatory cells. Viral, autoimmune and metabolic liver diseases were excluded by appropriate tests as well as metastatic tumors, primary hepatoma, pyogenic liver abscess, parasitic liver and colon lesions and colon cancer. Due to spontaneous improvement of symptoms and CT findings, his personal history was reevaluated. A direct contact with pigs and their tissues three days before the onset of symptoms was reported (the patient, living in rural areas, butchered a domestic pig). On specific request, transient hematuria before admittance was reported. The hypothesis of leptospirosis was considered and confirmed by the positive result of indirect immunofluorescence on cultured leptospira (*Leptospira interrogans* serovar icterohaemorrhagiae), which showed a high titer of antibodies

to leptospira (titer 1:1024). No cross-reaction with other spirochetes (*Treponema* and *Borrelia*) was seen. In two wk' time biochemical alterations were almost subsided. Despite spontaneous recovery, treatment with tetracyclines was started and the patient was dismissed. Two mo later US, CT and colonoscopy were totally normal and after a 2-year follow-up the patient has been fine.



Figure 2 Contrast-enhanced abdominal CT scan (portal phase): after 46 d both number and volume of hepatic lesions were considerably decreased.



Figure 3 Endoscopic view of right colon showing an ulcerated lesion without signs of bleeding. A series of biopsies of the ulcer revealed only necro-inflammatory cells.

DISCUSSION

Leptospirosis is a worldwide zoonotic infection that commonly occurs in tropical and subtropical regions and in both urban and rural contexts. Human disease is acquired by contact with urine or tissues of an infected animal or through contaminated water and soil, whereas human-to-human transmission is rare. Diagnosis of leptospirosis is based either on isolation of the organism from the patient or on seroconversion. Antibodies generally do not appear until the second week of illness. The pathogenesis of leptospirosis is incompletely understood but it is well known that all forms of leptospire can damage small blood vessels, lead to vasculitis and spread to all organs^[1]. The clinical presentation ranges from occult infection to Weil's disease with fatal complications as hepatorenal failure. The severity of disease reflects the severity of the underlying vasculitis. As a result of its protean clinical manifestations and non-specific presentations, leptospirosis has been underdiagnosed and frequently misdiagnosed as other diseases such as influenza, viral hepatitis, encephalitis, pneumonitis and acute renal failure^[1-3]. The great majority of cases, as in this patient, were of mild severity (anicteric leptospirosis) and resolution coincided with the appearance of antibodies. Icteric leptospirosis, occurring between 5 and 10 % of patients, was a severe disease and often very rapidly progressive with multi-organ failure^[4,5]. Treatment of leptospirosis depends on the severity of infection. Anicteric leptospirosis often requires

hospital admission and close observation. Streptomycin, penicillins, cephem and tetracyclines are all effective anti-leptospirotic antibiotics^[4,5]. Radiological abnormalities, in particular pulmonary localization on high resolution CT (nodular densities, ground glass opacities, areas of consolidation) possibly related to haemorrhage, have been described in severe forms^[6-8]. Although hepatomegaly is usual, CT evidence of multiple hepatic lesions, to our knowledge, has not yet been described in patients with leptospirosis. The histopathology of the liver in the course of leptospirosis was characterized by intrahepatic cholestasis, centrilobular necrosis with hypertrophy and hyperplasia of Kupffer cells but the architecture of parenchyma was not significantly disrupted and severe hepatic necrosis was not usual^[4]. The presence of multiple hypoattenuated nodules in the liver was the most interesting feature of this case. The differential diagnosis of this CT appearance included hypovascular metastases, abscess, especially by angioinvasive organisms or lymphoma. However, the absence of a mass effect on the surrounding hepatic structures would be helpful in suggesting the possibility of an abscess correlated with damage of small blood vessels. The pathologic basis for this hypoattenuation may be correlated with a coagulative necrosis of the hepatic tissues caused by vasculitis of the hepatic vessels.

Gastrointestinal involvement with haemorrhage has been reported, mainly in the severe form of leptospirosis^[2]. Interestingly, in this patient a colon ulcer was found at two different sites without any symptoms and signs of bleeding. The endoscopic and histological patterns of these colon lesions were consistent with ischemic colitis. Vascular disease of diverse etiologies and in particular vasculitis could be a cause of ischemic colitis^[9].

In this patient, according to our experience, liver lesions were correlated with the endoscopic findings of colon ulcer therefore primary colon cancer with liver metastases was suspected initially. On the other hand, the CT pattern when seen in the appropriate clinical setting reduced the diagnostic suppositions of infectious disease.

In conclusion, this case, initially misdiagnosed as colon cancer with liver metastases, confirms clinical polymorphism of leptospirosis and high lights the role of a good knowledge of personal history and epidemiological data in the diagnosis of leptospirosis, especially in areas of relatively low endemicity as in western countries, where domestic animal contact is prominent sources of infection. This report also suggests that a diagnosis of leptospirosis should be considered in patients with laboratory and CT findings of liver involvement and a relevant history.

REFERENCES

- 1 **Plank R**, Dean D. Overview of the epidemiology, microbiology, and pathogenesis of *Leptospira* spp. In humans. *Microbes Infect* 2000; **2**: 1265-1276
- 2 **Lecour H**, Miranda M, Magro C, Rocha A, Goncalves V. Human leptospirosis-a review of 50 cases. *Infection* 1989; **17**: 8-12
- 3 **Katz AR**, Ansdell VE, Effler PV, Middleton CR, Sasaki DM. Assessment of the clinical presentation and treatment of 353 cases of laboratory-confirmed leptospirosis in Hawaii, 1974-1998. *Clin Infect Dis* 2001; **33**: 1834-1841
- 4 **Levett PN**. Leptospirosis. *Clin Microbiol Rev* 2001; **14**: 296-326
- 5 **Kobayashi Y**. Clinical observation and treatment of leptospirosis. *J Infect Chemother* 2001; **7**: 59-68
- 6 **Lee RE**, Terry SI, Walker TM, Urquhart AE. The chest radiograph in leptospirosis in Jamaica. *Br J Radiol* 1981; **54**: 939-943
- 7 **Henk CB**, Kramer L, Schoder M, Bankier AA, Ratheiser K, Mostbeck GH. Weil disease: importance of imaging findings for early diagnosis. *J Comput Assist Tomogr* 1996; **20**: 609-612
- 8 **Yiu MW**, Ooi GC, Yuen KY, Tsang KW, Lam WK, Chan FL. High resolution CT of Weil's disease. *Lancet* 2003; **362**: 117

Acute esophageal necrosis and liver pathology, a rare combination

Amir Maqbul Khan, Rangit Hundal, Vijaya Ramaswamy, Mark Korsten, Sunil Dhuper

Amir Maqbul Khan, Rangit Hundal, Vijaya Ramaswamy, Mark Korsten, Sunil Dhuper, North Central Bronx and Veterans Affairs Hospital, New York 10710, USA

Correspondence to: Amir Maqbul Khan, 59 Beaumont Circle #3 Yonkers, NY 10710, USA. dramirkhan@hotmail.com

Telephone: +1-718-5849000 Ext. 6753

Received: 2003-12-12 **Accepted:** 2004-02-18

Abstract

Acute esophageal necrosis (AEN) or "black esophagus" is a clinical condition found at endoscopy. It is a rare entity the exact etiology of which remains unknown. We describe a case of 'black esophagus', first of its kind, in the setting of liver cirrhosis and hepatic encephalopathy.

Khan AM, Hundal R, Ramaswamy V, Korsten M, Dhuper S. Acute esophageal necrosis and liver pathology, a rare combination. *World J Gastroenterol* 2004; 10(16): 2457-2458
<http://www.wjgnet.com/1007-9327/10/2457.asp>

INTRODUCTION

Endoscopic discovery of a 'black esophagus' or 'acute esophageal necrosis' (AEN) that is unrelated to ingestion of caustic or corrosive agents is quite exceptional. It has been described only a few times in the past. Lacey *et al.* in 1991 reported 25 cases^[1]. A similar report by Benoit *et al.*^[2] in 1999 cited 27 cases after an extensive review of the literature. Since then there have been sporadic case reports. It is difficult to estimate its true incidence as we think this disease is largely underreported. The exact etiology of 'black esophagus' still remains unknown. We describe a case of 'black esophagus', first of its kind, in the setting of liver cirrhosis and hepatic encephalopathy.

CASE REPORT

A 59-year-old hispanic male with a known past medical history of hypertension, chronic alcohol abuse, liver cirrhosis, chronic pancreatitis and depression was admitted to the psychiatry service for aggressive behaviours, depression and suicidal ideation. On d 2, he was transferred to the medical floor after evaluation for a change in mental status with confusion, disorientation and impulsive behaviours.

A detailed history was elicited on further interrogation. Patient was known to have hypertension for 10 years for which he required monopropril, metoprolol and clonidine. The history also revealed alcohol abuse for 45 years, still an active abuser, alcoholic liver cirrhosis diagnosed for 4 years and negative hepatitis B and C serologies. He had multiple previous admissions for hepatic encephalopathy and earlier in the same year underwent chemotherapy for a biopsy proven hepatocellular carcinoma. He denied smoking and illicit drug abuse.

On examination the patient was drowsy but arousable, responding to verbal commands, oriented to 'place and person', but not 'time'. He was afebrile and hemo-dynamically stable. General physical examination was normal. Cardiac, pulmonary, abdominal and neurological examinations did not show any abnormalities. Rectal examination was normal with a negative

guaiac test.

Laboratory data on admission were: WBC 5.1 n/L with 48% granulocytes, hemoglobin (H)/ hematocrit (Hct) of 10.3/ 31, MCV of 80.3 fl, RDW of 15.4%, platelets of 174 /n.

Na 141 mE, K 4.5 mE, Cl 108 mE, CO₂ 26.1 mE, BUN 32 mg/dL, Creatinine 2.1 mg, Gluc 134 mg, Total bili 0.6 (0.3 direct), albumin 2.8 gm, proteins 6.7 gm, alkaline phosph 217 U/L, SGOT 50 U/L, SGPT 39U/L, LD 225 U/L, PT 11.4, aPTT 27.6 s and INR 1.05 s, Ammonia 139.8 um.

Ethanol on admission was 56.2, serum Osm 312, normal TSH, syphilis(-), ferritin 593, TIBC 168, total iron 58 and iron saturation 35%, B12/folate 226/22.7. CT scan of the head was negative for bleed/metastasis or any mass. CT scan of the abdomen revealed a few scattered diverticuli and accessory spleen.

A diagnosis of hepatic encephalopathy, anemia and intravascular volume depletion was established based on the clinical and laboratory data. Hydration with normal saline at 125 cc/h and treatment with lactulose 445 cc qid (titrated to bowel movement) were given. The rest of the management included administration of resperidal, thiamine, folate and ativan (prn). His anti-hypertensive medications were continued and patient was placed under close observation for alcohol withdrawal.

During the following 2 d (d 4 and 5) the patient's mental status improved to full orientation without any signs of confusion, agitation and/or suicidal ideation. Ammonia level dropped to 85 um. A drop in H/Hct (9.7/29.7) was related to intravascular volume depletion.

On d 6 of admission, the patient's clinical status deteriorated with a recurrence of confusion and lethargy. Patient was found to have tachycardia (heart rate of 120/min), a blood pressure of 105/70, a positive stool guaiac test, BUN/Creatinine of 68/3, ammonia of 105 um and a drop in his H/Hct (7.8/22). His management at this point included continuous intravenous hydration, blood transfusion with 3 units of packed red blood cells and intravenous proton pump inhibitors. His anti-hypertensive medications were held. The patient was transferred to a monitored setting for further observation and an esophageal gastro-duodenoscopy (EGD) was scheduled.

EGD revealed a continuous segment (15-35 cm) of necrosis with exudates, ulcerations and friable mucosa in the middle and distal parts of the esophagus. The gastro-esophageal (GE) junction showed no evidence of varices, stomach and duodenum linings were normal. A biopsy taken from the necrotic area confirmed the findings of fibrinoid necrotic debris with hemosiderin deposits and acute inflammatory cells on pathological examination of the specimen. An ultrasound of the abdomen revealed a medical renal disease without obstruction, liver texture consistent with cirrhosis with reversal of portal venous flow and mild ascites.

The patient made an uneventful recovery over the next 3 d. He was transferred to the medical floor from where he was discharged with a follow up in the outpatient clinic. No recurrences of any GI symptoms were reported in his 3-month follow-up.

DISCUSSION

'Black esophagus' has been described primarily in post-mortem studies^[3,4]. Goldenberg *et al.*^[5] gave us a detailed endoscopic description of 2 cases in the early 1990s. In a one-year prospective study conducted in Rouen University Hospital,

France, 8 (0.2%) cases of 'acute esophageal necrosis' were identified among the 3 900 patients who underwent EGD^[6]. Since then there have been only a handful of case reports. The numbers reported in the literature may highly underestimate the real incidence of this condition as suggested by this prospective trial. Acute esophageal bleeding is the most common presentation. The condition is generally seen in the elderly and those having co-morbid conditions.

A variety of mechanisms have been proposed to account for the development of this condition, and low systemic perfusion seems to play the dominant role. Other mechanisms cited include direct toxic effect^[7,8], as well as indirect mucosal breakdown and acid effect^[9], however, none of these have been proved. The frequent involvement of distal 1/3 esophagus^[10], absence of gastric lesions, presence of necrosis of mucosal/submucosal necrosis, presence of thrombus microscopically and rapid regression of disease after hemodynamic stability were similar to ischemic colitis^[11,12] and strongly support the ischemic basis for the insult.

Other conditions associated with this disease entity were prolonged hypertension^[13], ischemia^[5,14], hyperglycemia^[1], hypersensitivity to antibiotics^[15], herpetic infection^[16], gastric volvulus^[17], posterior mediastinal haematoma and aortic dissection^[3,18], anti-cardiolipin antibodies^[19] and Steven Johnson syndrome^[20]. In short, a multi-factorial etiology to absence of any disease (idiopathic) is possible. The pathogenesis of ischemic insult in our case can be accounted for by the low systemic perfusion with reversal of portal venous flow and worsening of hepatic encephalopathy.

Diagnosis is established with endoscopy with or without biopsy. The differential diagnosis included melanosis^[21], pseudo-melanosis^[22], and acanthosis nigrans^[23].

The main reported complications of AEN were esophageal stenosis and stricture formation^[1,2]. Lacy *et al.*^[1] reported a 15% complication rate, whereas other case series have reported very low to none. Recurrence was less than 10%^[6,24] and mortality ranged between 0-33%^[1,6,25]. The prognosis depends on the patient's general status rather than the extent of local esophageal necrotic lesions.

Generally there is no standardized treatment but the overall consensus favours conservative treatment with intra-venous proton pump inhibitors and short-term parenteral nutrition. The main aim is to avoid extension of insult with time for a spontaneous and aided recovery.

In short, AEN is still uncommon with exact etiology and pathogenesis largely unclear. The majority do not have any long-term sequel, only a few develop strictures and stenosis. Prognosis varies, and a majority recover with conservative treatment with death being an uncommon outcome.

REFERENCES

1 Lacy BE, Toor A, Benson SP, Rothstein RI, Maheshwari Y. Acute esophageal necrosis: report of two case ans a review of the literature. *Gastrointestinal Endoscopy* 1999; **49**: 527-532

- 2 Benoit R, Grobost O. Oesophage noir en rapport avec une nécrose aigue oesophagienne: un nouveau cas [French]. *Presse Med* 1999; **28**: 1509-1512
- 3 Lee KR, Stark E, Shaw FE. Esophageal infarction complicating spontaneous rupture of the thoracic aorta. *J AMA* 1977; **237**: 1233-1234
- 4 Brennan JL. Case of extensive necrosis of the esophageal mucosa following hypothermia. *J Clin Pathol* 1967; **20**: 581-584
- 5 Goldenberg SP, Wain SL, Marignani P. Acute necrotising esophagitis. *Gastroenterology* 1990; **98**: 493-496
- 6 Emmanuel ES, Savoye G, Hochain P, Herve S, Antonietti M, Lemoine F, Ducrotte P. Acute esophageal necrosis: a 1 year prospective study. *Gastrointestinal Endoscopy* 2002; **56**: 213-217
- 7 Orlando RC, Powell DW, Carney CN. Pathophysiology of acute acid injury in rabbit esophageal epithelium. *J Clin Invest* 1981; **68**: 286-293
- 8 Tobey NA, Orlando RC. Mechanisms of acid injury to rabbit esophageal epithelium: role of basolateral cell membrane acidification. *Gastroenterology* 1991; **101**: 1220-1228
- 9 Bass BL, Schweitzer EJ, Harmon JW, Kraimer J. H+back diffusion interferes with intrinsic reactive regulation of the esophageal mucosal blood flow. *Surgery* 1984; **96**: 404-413
- 10 Swigart LL, Siekert RG, Hambley WC, Anson BJ. The esophageal arteries: an anatomic study of 150 specimens. *Surg Gynecol Obstet* 1950; **90**: 234-243
- 11 Marston A, Pheils MT, Thomas ML, Morson BC. Ischaemic colitis. *Gut* 1966; **7**: 1-15
- 12 Ottinger LW. Mesenteric ischemia. *N Engl J Med* 1982; **307**: 535-537
- 13 Haviv YS, Reinus C, Zimmerman J. Black esophagus: a rare complication of shock. *Am J Gastroenterol* 1996; **91**: 2432-2434
- 14 Goldenberg SP, Wain SL, Marignani P. Acute necrotising esophagitis [letter]. *Gastroenterology* 1991; **101**: 281-282
- 15 Mangan TF, Colley AT, Wytock DH. Antibiotic-associated acute necrotising esophagitis [letter]. *Gastroenterology* 1990; **99**: 900
- 16 Cattan P, Cuillerier E, Cellier C. Black esophagus associated with herpes esophagitis. *Gastrointestinal Endoscopy* 1999; **49**: 105-107
- 17 Kram M, Gorenstein L, Eisen D, Cohen D. Acute esophageal necrosis associated with gastric volvulus. *Gastrointestinal Endoscopy* 2000; **51**: 610-612
- 18 Minatoya K, Okita Y, Tagusari O, Imakita M, Yutani C, Kitamura S. Transmural necrosis of the esophagus secondary to acute aortic dissection. *Ann Thorac Surg* 2000; **69**: 1584-1586
- 19 Cappell MS. Esophageal necrosis and perforation associated with the anticardiolipin antibody syndrome. *Am J Gastroenterol* 1994; **89**: 1241-1245
- 20 Mahe A, Keita S, Blanc L, Bobin P. Esophageal necrosis in the Stevens-Johnson syndrome. *J Am Acad Derm* 1993; **29**: 103-104
- 21 Sharma S, Venkateswaran S, Chacko A, Mathan M. Melanosis of the esophagus. *Gastroenterology* 1991; **100**: 13-16
- 22 Kimball MW. Pseudomelanosis of the esophagus. *Gastrointest Endosc* 1978; **24**: 121-122
- 23 Geller A, Aguilar H, Burgart L, Gostout CJ. The black esophagus. *Am J Gastroenterol* 1995; **90**: 2210-2212
- 24 Nayyar AK, Royston C, Slater D, Bardhan KD. Pseudomembranous esophagitis. *Gastrointestinal Endoscopy* 2001; **54**: 730-735
- 25 Moreto M, Ojembarrena E, Zaballa M, Tanago JG, Ibanez S. Idiopathic acute esophageal necrosis: not necessarily a terminal event. *Endoscopy* 1993; **25**: 534-536

Dysphagia lusorium in elderly: A case report

Bulent Kantarceken, Ertan Bulbuloglu, Murvet Yuksel, Ali Cetinkaya

Bulent Kantarceken, Division of Gastroenterology, Medical Faculty, Sutcu Imam University, Kahramanmaras, Turkey

Ertan Bulbuloglu, Department of General Surgery, Medical Faculty, Sutcu Imam University, Kahramanmaras, Turkey

Murvet Yuksel, Department of Radiodiagnostic, Medical Faculty, Sutcu Imam University, Kahramanmaras, Turkey

Ali Cetinkaya, Department of Internal Medicine, Medical Faculty, Sutcu Imam University, Kahramanmaras, Turkey

Correspondence to: Bulent Kantarceken, Yenisehir Mah. 22. Sokak Ahenk Apt.No;17/5, Kahramanmaras, Turkey. bkantarceken@inonu.edu.tr

Telephone: +90-344-2210915 **Fax:** +90-344-2212371

Received: 2004-03-09 **Accepted:** 2004-04-09

Abstract

AIM: Late onset of dysphagia due to vascular abnormalities is a rare condition. We aimed to present a case of right subclavian artery abnormalities caused dysphagia in the elderly.

METHODS: A 68-year-old female was admitted with dysphagia seven months ago. Upper endoscopic procedures and routine examinations could not demonstrate any etiology. Multislice computed thorax tomography was performed for probable extra- esophageal lesions.

RESULTS: Multislice computed thorax tomography showed right subclavian artery abnormality and esophageal compression with this aberrant artery.

CONCLUSION: Causes of dysphagia in the elderly are commonly malignancies, strictures and/or motility disorders. If routine examinations and endoscopic procedures fail to show any etiology, rare vascular abnormalities can be considered in such patients. Multislice computed tomography is a usefull choice in such conditions.

Kantarceken B, Bulbuloglu E, Yuksel M, Cetinkaya A. Dysphagia lusorium in elderly: A case report. *World J Gastroenterol* 2004; 10(16): 2459-2460

<http://www.wjgnet.com/1007-9327/10/2459.asp>

INTRODUCTION

Dysphagia Lusoria was first described by Bayford in 1794 in a 62 year-old woman^[1]. Postmortem examination of this case showed the abnormal origination of right subclavian artery from aortic arch and compression on the esophagus. Abnormalities of the thoracic aorta and great vessels are not uncommon and can result in esophageal compression and dysphagia. The most common congenital abnormality of the aorta is an isolated aberrant right subclavian artery^[2]. Usually this abnormality does not lead to symptoms. However, sometimes dysphagia (dysphagia lusoria) develops. Mass effect on the esophagus can cause dysphagia. A right aortic arch with an aberrant left subclavian artery is less common but may also result in esophageal compression^[3]. A pulmonary sliding occurs when an aberrant left pulmonary artery arises from the right pulmonary artery and passes between trachea and esophagus. Compression

on both trachea and esophagus can occur. This abnormality can also be reliably detected with contrast-enhanced CT. We aimed to present a 68-year-old woman who had late onset dysphagia due to such a rare condition.

CASE REPORT

A 68-year-old female was admitted to our hospital with dysphagia nearly for seven months. Dysphagia was occurring both solid and liquids. There were no clear symptoms except dysphagia, such as loss of weight, fever, sweating at night, diarrhea, hematemesis, melena or hematochesia. She complained about odinophagia, bloating, regurgitation and epigastric pain especially after analgesic using. She also had chest pain radiating to the left arm with effort. She had a history of operation for discal hernia, ischemic heart disease and diabetes mellitus. She was using anti-ischemic drugs, analgesics (Including aspirin), beta blockers and diuretics.

In physical examination her general condition was good, thyroid was palpable. She had mild epigastric pain with palpation and no other signs. Hgb was 136 g/L, WBC (White blood cell count) was 77 000 μ L, PLT was 290 000 μ L in laboratory tests. Erythrocyte sedimentation rate was 10 /h, SGOT was 57 U/L, SGPT was 84 U/L, ALP was 245 U/L. Other biochemical parameters were normal (BUN, creatinine, glucose, etc). Markers for hepatitis A,B,C were negative. Thyroid function tests were normal. She had esophagus graphy with radiopaque two months ago showing slight compression on esophagus in lower levels. Esophagogastroduodenoscopy (EGD) 5 mo ago showed minimal hiatus hernia, reflux esophagitis and antral gastritis. Some drugs were given to the patient for these findings but her dysphagia symptoms did not relieve. EGD 3 mo after, only showed antral gastritis. Other drugs (PPIs, antiacids) were given also, but dysphagia of the patient did not relieve. After admission to our clinic, the major complaint of the patient was persistent dysphagia despite the treatments. Thorax CT was performed (Multislice spiral CT) to exclude thoracic lesion-dysphagia, it showed right subclavian artery abnormality and esophageal compression on this aberrant artery (Figures 1A, B). Multislice computed thorax tomography (MCT) showed the right subclavian artery originating from the posterior wall of the aortic arch as its last branch distal to the origin of the left subclavian artery and it passed obliquely between esophagus and vertebral column and then coursed upwards on the right side.

DISCUSSION

Dysphagia is a common problem that lowers quality of life for the elderly and a symptom that may originate from many different causes. Esophageal dysphagia could be caused by esophageal carcinoma, esophageal stricture and webs, achalasia, diffuse esophageal spasm and scleroderma, caustic esophagitis and infectious esophagitis^[4]. The other rare cause of dysphagia in the elderly is vascular compression on the esophagus (Dysphagia lusoria). Based on autopsy findings, the lusorian artery had a prevalence of 0.7% in the general population^[5]. Recently Fockens *et al.* found a prevalence of 0.4% in 1 629 patients who underwent endoscopy for various reasons^[6]. Dysphagia lusoria might be seen in young adults^[7], and in middle and/or elder ages as in our case^[8]. Why it gives symptoms in

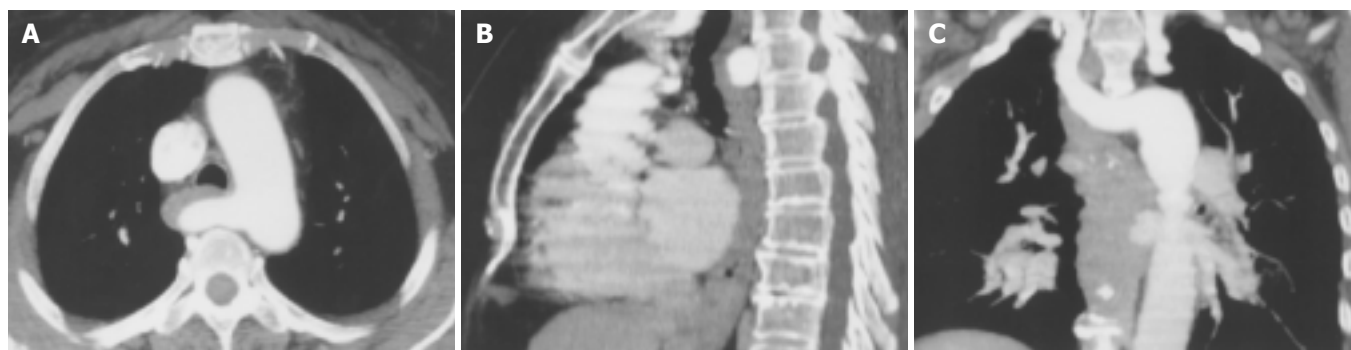


Figure 1 Axial (A) coronal (B) sagittal (C) MIP multislice CT images from the arterial phase showing right subclavian artery originating from the posterior wall of aortic arch, and compression with antero-right lateral displacement of esophagus by this right subclavian artery.

elderly is not clear. Some theories have been suggested, such as increased rigidity of the esophagus itself or the vessel wall, aneurysm formation, especially in the presence of a Kommerell's diverticulum^[9], elongation of the aorta, and the combination of an aberrant artery and a truncus bicaroticus^[10]. Interestingly in our patient, she had a history of dysphagia for 7 mo. She had not any lesion except minimal esophagitis in EGD. Reflux esophagitis can explain dysphagia sometimes. After the treatment of esophagitis with proton pump inhibitors (PPI), our patient's dysphagia symptom did not relieve. The late onset of dysphagia in our patient could be explained by the changes in vertebral column. Retrosternal goitre which may be responsible for dysphagia was not found in CT. Radiopaque graphy of the esophagus could be used to show the compression of aberrant artery on esophagus, but CT scanning and/or angiography can usually confirm the diagnosis of dysphagia lusoria. Aberrant artery could be shown with multislice CT as three dimension angiographic images were non-invasive without the need of invasive angiography^[11]. Here, we also presented the multislice computed tomography angiography images of the patient with a symptomatic aberrant retro-esophageal subclavian artery compression (Figure 2).

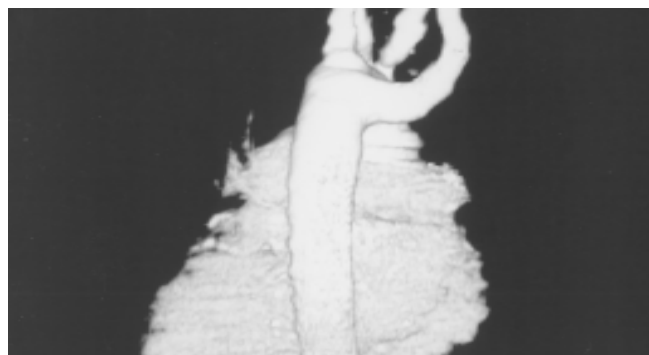


Figure 2 Volume-rendered three-dimensional image by computed tomography demonstrating aberrant artery right subclavian artery originating from the posterior wall of aortic arch.

We showed the aberrant right subclavian artery abnormality and compression on the esophagus clearly. That is why we did not repeat the radiopaque graphy of the esophagus. Coronary angiography was planned but the patient refused this procedure. So the patient was referred to a cardiovascular surgeon.

In conclusion, dysphagia in an elder patient can be caused by a rare abnormality of the subclavian artery insertion. Multislice CT can reveal this abnormality.

REFERENCES

- 1 **Bayford D.** An account of singular case of obstructed deglutition. *Memoires Med Soc London* 1794; **2**: 275-286
- 2 **McLoughlin MJ,** Weisbrod G, Wise DJ, Yeung HP. Computed tomography in congenital anomalies of the aortic arch and great vessels. *Radiology* 1981; **138**: 399-403
- 3 **Jaffe RB.** Radiographic manifestations of congenital anomalies of the aortic arch. *Radiol Clin North Am* 1991; **29**: 319-334
- 4 **Barloon TJ,** Bergus GR, Lu CC. Diagnostic imaging in the evaluation of dysphagia. *Am Fam Physician* 1996; **53**: 535-546
- 5 **Molz G,** Burri B. Aberrant subclavian artery (arteria lusoria): Sex differences in the prevalence of various forms of the malformations. Evaluation of 1378 observations. *Virch Arch A Pathol Anat Histol* 1978; **380**: 303-315
- 6 **Fockens P,** Kisman K, Tytgat GNJ. Endosonographic imaging of an aberrant right subclavian (lusorian) artery. *Gastrointest Endosc* 1996; **43**: 419
- 7 **Ballotta E,** Bardini R, Bottio T. Aberrant right subclavian artery. An original median cervical approach. *J Cardiovasc Surg* 1996; **37**: 571-573
- 8 **Cullen DM,** Kirk RK, Joseph IM. Late-onset dysphagia lusoria. *Ann Thorac Surg* 2001; **71**: 710-712
- 9 **Brown DL,** Chapman WC, Edwards WH, Coltharp WH, Stoney WS. Dysphagia lusoria: Aberrant right subclavian artery with a Kommerell's diverticulum. *Am Surg* 1993; **59**: 582-586
- 10 **Janssen M,** Baggen MG, Veen HF, Smout AJ, Bekkers JA, Jonkman JG, Ouwendijk RJ. Dysphagia lusoria: clinical aspects, manometric findings, diagnosis, and therapy. *Am J Gastroenterol* 2000; **95**: 1411-1416
- 11 **Gareth J MH,** Owens PE, Roobottom CA. Aberrant right subclavian artery and dysphagia lusoria. *N Engl J Med* 2002; **347**: 1532

Minute gastric carcinoid tumor with regional lymph node metastasis: A case report and review of literature

Shu-Duo Xie, Lin-Bo Wang, Xiang-Yang Song, Tao Pan

Shu-Duo Xie, Lin-Bo Wang, Xiang-Yang Song, Tao Pan,
Department of Oncologic Surgery, Sir Run Run Shaw Hospital, College of Medical Science, Zhejiang University, Hangzhou 310016, Zhejiang Province, China

Correspondence to: Dr. Shu-Duo Xie, Department of Oncologic Surgery, Sir Run Run Shaw Hospital, College of Medical Science, Zhejiang University, 3 Qingchun East Road, Hangzhou 310016, Zhejiang Province, China. jamestse@netease.com

Telephone: +86-571-86959492

Received: 2003-12-12 **Accepted:** 2004-02-18

Abstract

We have encountered an unusual case of gastric carcinoid tumor. Gastroscopic examination of this 32-year-old male patient showed a smooth protrusion at the greater curvature of the gastric body with a central depression, identified by subsequent biopsy as carcinoma. The patient had a normal serum gastrin level and was negative for anti-parietal cell antibody. Histological examination of the resected gastric tissues showed that the tumor was a carcinoid, 0.3 cm×0.3 cm in size with only one regional lymph node metastasis. We reviewed the pathogenesis, clinical presentation, diagnosis and treatment of gastric carcinoids and raise the possibility of being a lymph vessel-related metastasis even for a minute carcinoid tumor. Sentinel lymph node biopsy is recommended for surgery of minute carcinoid tumors.

Xie SD, Wang LB, Song XY, Pan T. Minute gastric carcinoid tumor with regional lymph node metastasis: A case report and review of literature. *World J Gastroenterol* 2004; 10 (16): 2461-2463

<http://www.wjgnet.com/1007-9327/10/2461.asp>

INTRODUCTION

Carcinoid tumors represent an unusual and complex disease spectrum with protean clinical manifestations. Gastric carcinoids account for 3 of every 1 000 gastric neoplasms. Gastric carcinoids types I and II generally follow a benign course, with 9% to 30% developing metastases, usually multiple and small characterized by infiltration restricted to the mucosa and submucosa. The third type of gastric carcinoids (type III, sporadic tumors) occurs without hypergastrinemia but often progresses in an aggressive course, 54% to 66% of which may develop metastases. Approximately 50% of these often large, single tumors have atypical histology, and some patients may develop carcinoid syndrome; but except for rare cases, carcinoid tumor of the stomach less than 1 cm in size generally does not give rise to regional metastasis.

CASE REPORT

The patient in question was male, aged 32 years old, admitted for upper gastric discomfort after dinner for six mo, which worsened in the past two mo prior to admission. The patient complained of epigastric distention, but this did not affect his

normal diet. He had no vomiting, abdominal pain, melena or regurgitation. The symptoms waxed and waned, but clearly worsened in the last two mo. Physical examination revealed no obvious anemia, the lung and heart sounds were normal, the abdomen was soft and flat, and no hepatomegaly or splenomegaly was noted, nor was an abdominal mass palpated; rectal examination found no abnormalities, and no enlargement of the superficial lymph nodes was present. The patient was free of symptoms of hypergastrinemia or carcinoid. Gastroscopy identified a nodule on the greater curvature of the stomach, 0.6 cm by 0.6 cm in size, with erosive lesion above the nodule. Biopsy was done and the results indicated carcinoid. The patient received subsequently laparotomy in which a node was found near the pylorus, yellowish in color and 0.5 cm by 0.5 cm in size. The node was extensively resected along with the marginal area 2 cm in width. One enlarged lymph node below the pylorus was also resected. Post-operative histology revealed a 0.3 cm node, gray-white or gray-red, beneath the mucosa. Under microscope, tumor cells were seen in the submucosa and mucosa propria, uniform in shape and arranged in cribiform nests. A radical distal subtotal gastrectomy was subsequently performed, and the post-operative histology reported no residual cancer or additional metastasis in the 23 lymph nodes. The patient was then discharged and followed up for one year without findings indicative of recurrence or distant metastasis.

DISCUSSION

Carcinoid is also known as chromaffin cell carcinoma and belongs to an unusual type of tumor with relatively low malignant potential. The most frequent sites for carcinoid tumors in human are the gastrointestinal (GI) tract (74%) and the bronchopulmonary system (25%). Within the GI tract, most carcinoid tumors occur in the small bowel (29%), appendix (19%), and rectum (13%)^[1]. However, the frequency of gastric carcinoid tumors has increased markedly due to endoscopic screening, performed in patients with chronic atrophic gastritis. In Japan, mass endoscopic screening for gastric lesions is common, which results in an identified frequency of gastric carcinoid tumor as high as 41% of all carcinoid tumors^[2]. Zhen *et al.* reviewed 26 reports of carcinoid in China and reported 126 cases of carcinoid in the stomach from a total of 1 080 cases of GI tract carcinoid. Most gastric carcinoids occur in 40- to 60-year-old patients, irrespective of genders. Recently, a classification system was proposed to distinguish gastric carcinoid tumors into three types, namely, tumors associated with chronic atrophic gastritis (type I), tumors associated with Zollinger-Ellison syndrome (ZES, type II), and biologically more aggressive, sporadic lesions (type III)^[3,4]. Currently little is known about the factors that may induce or promote the malignant growth of carcinoids^[5]. For some gastric carcinoids, studies show that gastrin is an important growth factor^[6], and an increased incidence of gastric carcinoids can be expected in disease states (pernicious anemia, atrophic gastritis, Zollinger-Ellison syndrome) that result in hypergastrinemia. In pernicious anemia and atrophic gastritis, 4% to 11% of the patients develop gastric carcinoids^[7,8]. Patients with Zollinger-Ellison syndrome

also develop gastric carcinoids, although they are much more frequent in the subgroup with MEN 1^[9]. Studies suggest that other important growth factors in some carcinoid tumors include transforming growth factor alpha (TGF- α) and TGF- β ^[10,11], insulin-like growth factor-1 (IGF-1)^[7,11], trefoil peptides (TFF1, TFF2, TFF3)^[7], platelet-derived growth factor^[10], vascular endothelial growth factor^[12], acidic and basic fibroblast growth factor, and epidermal growth factor^[10,11]. Mutations in common oncogenes, such as *K-ras*, are uncommon in GI carcinoids. Over amplification of *HER2/neu*, *c-myc*, and *c-jun* have been described in some cell lines derived from GI endocrine tumors and some carcinoids^[13]. Alterations in the common tumor suppressor gene *p53* are also uncommon in carcinoids. MEN 1 has been shown to be due to defects in the 10-exon gene on chromosome 11q13 that encodes a 610-amino acid nuclear protein^[14,15]. Loss of heterozygosity at this locus has been reported to occur in 26% to 78% of cases of carcinoids, and mutations in the MEN I gene in 18%^[16-18]. Microsatellite instability is rare in carcinoids^[19]; however, by comparative genomic hybridization, both frequent gains (of chromosome 5, 14, 17q, 7) and losses (especially of chromosome 9p) are reported^[20].

Gastric carcinoids originate from parachromaffin cells of the gastric mucosa. Tumor cells can occur virtually anywhere in the stomach, but mostly occur in the antrum. Gastric carcinoid is often difficult to diagnose due to the absence of specific symptoms or signs, especially in the early stage. When the tumor protrudes into the gastric cavity, the patient usually feels epigastric pain, suffers bloody vomiting, melena, epigastric burning, nausea or other digestive disorders. Carcinoid syndrome is seen in only a few gastric carcinoid cases where extensive dissemination or liver metastasis can be present. Gastric carcinoid in its early stage frequently escapes detection, and is usually found by gastroscopy. When the tumor grows to more than 2 cm, barium meal will help the diagnosis. The patient in this report was a young man who had only non-specific symptoms like epigastric distension without carcinoid syndrome and the tumor was near the antrum only 0.5 cm in size. The pathology was typical carcinoid. This patient did not have chronic gastritis or Zollinger-Ellison syndrome and the lesion was single, which belonged therefore to type III.

Surgical resection is the major strategy for treatment of gastric carcinoid, and chemotherapy and radiotherapy have not proved to produce obvious effects. For gastric carcinoids, the treatment is generally decided on the basis of the presence of hypergastrinemia^[21-25]. Most researchers recommend that in patients with type I or II, in which hypergastrinemia is present with small lesions of less than 1 cm, the carcinoid should be removed endoscopically^[22,24,25], while when the tumor exceeds 2 cm or local invasion is present, disputes over total gastrectomy^[26] or only resection with antrectomy arise for type I (pernicious anemia) lesions^[21]. For type I or II lesions of 1 to 2 cm, no agreement has been reached on the treatment. Some recommend that these lesions should be treated surgically^[21], whereas others urge endoscopic treatment^[25]. In type III gastric carcinoids not associated with hypergastrinemia, which tend to be larger and more aggressive, excision and regional lymph node clearance is recommended when the tumor grows to larger than 2 cm^[21-23,25]. Some researchers prefer a similar approach for any carcinoid larger than 1 cm, whereas others consider such a resection be reserved for tumors in this size range showing histologic invasion. Most tumors smaller than 1 cm can be treated endoscopically. Tumors less than 1 cm in size are called minute carcinoids, which seldom give rise to regional lymph node metastasis, especially tumors less than 0.5 cm in size. But very rarely, minute carcinoids do have lymph node metastasis, as reported by a Japanese researcher Naitoh^[27]. Such a case has not previously been reported in China. The

case reported in this paper is similar to the case reported in Japan. The post-operative pathology showed only a single lesion 0.3 cm in size invading the submucosa. There was just one lymph node metastasis, which is also uncommon. Local resection of the stomach was done in the first operation, and one enlarged lymph node was resected that was identified as metastasis by histology, so subtotal gastrectomy and lymph node dissection were done in the second operation. The other lymph nodes were normal, however, we regarded this approach was appropriate.

Sentinel lymph node biopsy has been used widely for surgery of melanoma^[28,29] and is currently receiving intensive study on its application for other malignant tumors such as breast, rectal and gastric cancer^[30,31]. The sentinel node is the most likely lymph node that harbors metastasis. A negative sentinel lymph node (SLN) would suggest that metastatic disease has not occurred, whereas a positive SLN would indicate possible involvement of other nodes in the same basin. Therefore sentinel lymph node biopsy may be attempted in operations for minute carcinoid. If the sentinel lymph node is positive, excision and regional lymph node clearance is needed, otherwise, local resection of the stomach is sufficient.

The prognosis of gastric carcinoid is favorable and patients may expect long postoperative survival. In patients with localized disease, 5-year survival rate may reach 64%, and it was 40% for regional involvement. Postoperative chemotherapy or radiotherapy was not performed in this particular case and the one-year follow-up found no recurrence or distant metastasis.

REFERENCES

- 1 **Modlin IM**, Sandor A. An analysis of 8305 cases of carcinoid tumors. *Cancer* 1997; **79**: 813-829
- 2 **Mizuma K**, Shibuya H, Totsuka M, Hayasaka H. Carcinoid of the stomach: a case report and of 100 cases reported in Japan. *Ann Chir Gynaecol* 1983; **72**: 23-27
- 3 **Soreide JA**, van Heerden JA, Thompson GB, Schleck C, Ilstrup DM, Churchward M. Gastrointestinal carcinoid tumors: long-term prognosis for surgically treated patients. *World J Surg* 2000; **24**: 1431-1436
- 4 **Modlin IM**, Gilligan CJ, Lawton GP, Tang LH, West AB. Gastric carcinoids-the Yale experience. *Arch Surg* 1995; **130**: 250-256
- 5 **Oberg K**. Biology, diagnosis, and treatment of neuroendocrine tumors of the gastrointestinal tract. *Curr Opin Oncol* 1994; **6**: 441
- 6 **Rindi G**, Bordi C, Rappel S, La Rosa S, Stolte M, Solcia E. Gastric carcinoids and neuroendocrine carcinomas: pathogenesis, pathology, and behavior. *World J Surg* 1996; **20**: 168
- 7 **Modlin IM**, Tang LH. Cell and tumor biology of the gastric enterochromaffin-like cell. *Ital J Gastroenterol Hepatol* 1999; **31**: S117
- 8 **Kokkola A**, Sjoblom SM, Haapiainen R, Sipponen P, Puolakkainen P, Jarvinen H. The risk of gastric carcinoma and carcinoid tumours in patients with pernicious anaemia. *Scand J Gastroenterol* 1998; **33**: 88
- 9 **Lehy T**, Cadiot G, Mignon M, Ruzsniowski P, Bonfils S. Influence of multiple endocrine neoplasia type 1 on gastric endocrine cells in patients with the Zollinger-Ellison syndrome. *Gut* 1992; **33**: 1275
- 10 **Oberg K**. Expression of growth factors and their receptors in neuroendocrine gut and pancreatic tumors, and prognostic factors for survival. *Ann N Y Acad Sci* 1994; **733**: 46
- 11 **Wulbrand U**, Wied M, Zofel P, Goke B, Arnold R, Fehmann H. Growth factor receptor expression in human gastroenteropancreatic neuroendocrine tumours. *Eur J Clin Invest* 1998; **28**: 1038
- 12 **Terris B**, Scoazec JY, Rubbia L, Bregeaud L, Pepper MS, Ruzsniowski P, Belghiti J, Flejou J, Degott C. Expression of vascular endothelial growth factor in digestive neuroendocrine tumours. *Histopathology* 1998; **32**: 133
- 13 **Evers BM**, Rady PL, Tying SK, Sanchez RL, Rajaraman S, Townsend CM Jr, Thompson JC. Amplification of the HER-

- 2/neu protooncogene in human endocrine tumors. *Surgery* 1992; **112**: 211
- 14 **Guru SC**, Goldsmith PK, Burns AL, Marx SJ, Spiegel AM, Collins FS, Chandrasekharappa SC. Menin, the product of the MEN1 gene, is a nuclear protein. *Proc Natl Acad Sci U S A* 1998; **95**: 1630
- 15 **Chandrasekharappa SC**, Guru SC, Manickam P, Olufemi SE, Collins FS, Emmert-Buck MR, Debelenko LV, Zhuang Z, Lubensky IA, Liotta LA, Crabtree JS, Wang Y, Roe BA, Weisemann J, Boguski MS, Agarwal SK, Kester MB, Kim YS, Heppner C, Dong Q, Spiegel AM, Burns AL, Marx SJ. Positional cloning of the gene for multiple endocrine neoplasia-type 1. *Science* 1997; **276**: 404
- 16 **Jakobovitz O**, Nass D, DeMarco L, Barbosa AJ, Simoni FB, Rechavi G, Friedman E. Carcinoid tumors frequently display genetic abnormalities involving chromosome 11. *J Clin Endocrinol Metab* 1996; **81**: 3164
- 17 **Gortz B**, Roth J, Krahenmann A, de Krijger RR, Muletta-Feurer S, Rutimann K, Saremaslani P, Speel EJ, Heitz PU, Komminoth P. Mutations and allelic deletions of the MEN1 gene are associated with a subset of sporadic endocrine pancreatic and neuroendocrine tumors and not restricted to foregut neoplasms. *Am J Pathol* 1999; **154**: 429
- 18 **D'Adda T**, Keller G, Bordi C, Hofler H. Loss of heterozygosity in 11q13-14 regions in gastric neuroendocrine tumors not associated with multiple endocrine neoplasia type 1 syndrome. *Lab Invest* 1999; **79**: 671
- 19 **Ghimenti C**, Lonobile A, Campani D, Bevilacqua G, Caligo MA. Microsatellite instability and allelic losses in neuroendocrine tumors of the gastro-entero-pancreatic system. *Int J Oncol* 1999; **15**: 361
- 20 **Terris B**, Meddeb M, Marchio A, Danglot G, Flejou JF, Belghiti J, Ruszniewski P, Bernheim A. Comparative genomic hybridization analysis of sporadic neuroendocrine tumors of the digestive system. *Genes Chromosomes Cancer* 1998; **22**: 50
- 21 **Ahlman H**, Kolby L, Lundell L, Olbe L, Wangberg B, Granerus G, Grimelius L, Nilsson O. Clinical management of gastric carcinoid tumors. *Digestion* 1994; **55**: 77
- 22 **Gilligan CJ**, Lawton GP, Tang LH, West AB, Modlin IM. Gastric carcinoid tumors: the biology and therapy of an enigmatic and controversial lesion. *Am J Gastroenterol* 1995; **90**: 338
- 23 **Akerstrom G**. Management of carcinoid tumors of the stomach, duodenum, and pancreas. *World J Surg* 1996; **20**: 173
- 24 **Bordi C**, Falchetti A, Azzoni C, D'Adda T, Canavese G, Guariglia A, Santini D, Tomassetti P, Brandi ML. Aggressive forms of gastric neuroendocrine tumors in multiple endocrine neoplasia type I. *Am J Surg Pathol* 1997; **21**: 1075
- 25 **Ahlman H**. Surgical treatment of carcinoid tumours of the stomach and small intestine. *Ital J Gastroenterol Hepatol* 1999; **31**: S198
- 26 **Shi W**, Buchanan KD, Johnston CF, Larkin C, Ong YL, Ferguson R, Laird J. The octreotide suppression test and [¹¹¹In-DTPA-D-Phe]-octreotide scintigraphy in neuroendocrine tumours correlate with responsiveness to somatostatin analogue treatment. *Clin Endocrinol* 1998; **48**: 303
- 27 **Kumashiro R**, Naitoh H, Teshima K, Sakai T, Inutsuka S. Minute gastric carcinoid tumor with regional lymph node metastasis. *Int Surg* 1989; **74**: 198-200
- 28 **Shen J**, Wallace AM, Bouvet M. The role of sentinel lymph node biopsy for melanoma. *Semin Oncol* 2002; **29**: 341-352
- 29 **Leong SP**. Selective sentinel lymphadenectomy for malignant melanoma. *Surg Clin North Am* 2003; **83**: 157-185
- 30 **Tafra L**. Sentinel node biopsy for breast cancer. *Minerva Chir* 2002; **57**: 425-435
- 31 **Lin KM**, Rodriguez F, Ota DM. The sentinel node in colorectal carcinoma. Mapping technique, pathologic assessment, and clinical relevance. *Oncology* 2002; **16**: 567-575

Edited by Chen WW Proofread by Zhu LH and Xu FM